Scientific and Technical Aerospace Reports

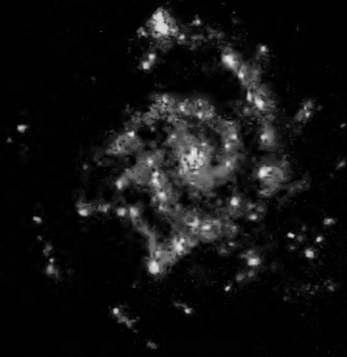

An Abstract Journal

Volume 32, Number 6
June 1994
N94-22702 to N94-25542

The NASA STI Program ... in Profile

Since its founding, NASA has been dedicated to the advancement of aeronautics and space science. The NASA Scientific and Technical Information (STI) Program plays a key part in helping NASA maintain this important role.

The NASA STI Program provides access to the NASA STI Database, the largest collection of aeronautical and space science STI in the world. The Program is also NASA's institutional mechanism for disseminating the results of its research and development activities.

Specialized services that help round out the Program's diverse offerings include creating custom thesauri, translating material to or from 34 foreign languages, building customized databases, organizing and publishing research results ... even providing videos.

For more information about the NASA STI Program, you can:

- **Phone** the NASA Access Help Desk at (301) 621-0390
- **Fax** your question to the NASA Access Help Desk at (301) 621-0134
- **E-mail** your question via the **Internet** to help@sti.nasa.gov
- **Write** to:

NASA Access Help Desk
NASA Center for AeroSpace Information
800 Elkridge Landing Road
Linthicum Heights, MD 21090-2934

Scientific and Technical Aerospace Reports

STAR

Scientific and Technical Aerospace Reports (STAR), is published each month as a major product of the NASA Scientific and Technical Information (STI) Program.

Inside this issue you will find:

- **Front Matter** containing a typical citation and abstract sample explaining the standard format, including codes for ordering reports
- **An Abstract Section** containing citations and abstracts of reports and publications that provide comprehensive coverage of worldwide aerospace-related topics including aeronautics and space science technology. *STAR* lists published and publicly available reports entered into the NASA STI Database during the four weeks preceding publication of this issue. These citations and abstracts are listed by subject categories.
- **An Index Section**
  - Subject
  - Personal author
  - Corporate source
  - Contract number
  - Report number
- **An Appendix** containing a guide for ordering cited reports, registering with the NASA STI Program, and using the available products and services. Additionally, price schedules, phone numbers, and addresses are included in this information packed section.

NASA also sponsors the companion journal, *NASA Open Volumes on Aerospace (NOVA)*, which lists abstracts of the open literature on aerospace subjects available worldwide. *NOVA* is for internal NASA use only, available from the NASA Center for AeroSpace Information (CASI).

Entries found in *STAR* are available through the NASA online retrieval service, RECON, and through DIALOG as the Aerospace Database.

The NASA STI Program gathers information through national and international agreements and exchanges and makes this information available to the NASA community and to the public in many forms through various outlets.

For additional information on the NASA STI Program, call the NASA Access Help Desk at (301) 621-0390, or write to:

NASA Center for AeroSpace Information
800 Elkridge Landing Road
Linthicum Heights, Maryland 21090-2934

US ISSN 0036-8741

This publication was prepared by the NASA Center for AeroSpace Information,
800 Elkridge Landing Road, Linthicum Heights, MD 21090-2934, (301) 621-0390.

Volume 32 Number 6 / June 1994

TABLE OF CONTENTS

AERONAUTICS For related information see also *Astronautics.*

01 AERONAUTICS (GENERAL) **2153**

02 AERODYNAMICS **2165**
Includes aerodynamics of bodies, combinations, wings, rotors, and control surfaces; and internal flow in ducts and turbomachinery. For related information see also 3*4 Fluid Mechanics and Heat Transfer.*

03 AIR TRANSPORTATION AND SAFETY **2172**
Includes passenger and cargo air transport operations; and aircraft accidents. For related information see also *16 Space Transportation* and *85 Urban Technology and Transportation.*

04 AIRCRAFT COMMUNICATIONS AND NAVIGATION **2174**
Includes digital and voice communication with aircraft; air navigation systems (satellite and ground based); and air traffic control. For related information see also *17 Space Communications, Spacecraft Communications, Command and Tracking* and *32 Communications and Radar.*

05 AIRCRAFT DESIGN, TESTING AND PERFORMANCE **2176**
Includes aircraft simulation technology. For related information see also *18 Spacecraft Design, Testing and Performance* and *39 Structural Mechanics.* For land transportation vehicles see *85 Urban Technology and Transportation.*

06 AIRCRAFT INSTRUMENTATION **2186**
Includes cockpit and cabin display devices; and flight instruments. For related information see also *19 Spacecraft Instrumentation* and *35 Instrumentation and Photography.*

07 AIRCRAFT PROPULSION AND POWER **2186**
Includes prime propulsion systems and systems components, e.g., gas turbine engines and compressors; and onboard auxiliary power plants for aircraft. For related information see also *20 Spacecraft Propulsion and Power, 28 Propellants and Fuels,* and *44 Energy Production and Conversion.*

08 AIRCRAFT STABILITY AND CONTROL **2190**
Includes aircraft handling qualities; piloting; flight controls; and autopilots. For related information see also *05 Aircraft Design, Testing and Performance.*

09 RESEARCH AND SUPPORT FACILITIES (AIR) **2192**
Includes airports, hangars and runways; aircraft repair and overhaul facilities; wind tunnels; shock tubes; and aircraft engine test stands. For related information see also *14 Ground Support Systems and Facilities (Space).*

ASTRONAUTICS For related information see also *Aeronautics.*

12 ASTRONAUTICS (GENERAL) **2194**
For extraterrestrial exploration see *91 Lunar and Planetary Exploration.*

13 ASTRODYNAMICS **2195**
Includes powered and free-flight trajectories; and orbital and launching dynamics.

14 GROUND SUPPORT SYSTEMS AND FACILITIES (SPACE) **2196**
Includes launch complexes, research and production facilities; ground support equipment, e.g., mobile transporters; and simulators. For related information see also *09 Research and Support Facilities (Air).*

15 LAUNCH VEHICLES AND SPACE VEHICLES **2198**
Includes boosters; operating problems of launch/space vehicle systems; and reusable vehicles. For related information see also *20 Spacecraft Propulsion and Power.*

16 SPACE TRANSPORTATION **2199**
Includes passenger and cargo space transportation, e.g., shuttle operations; and space rescue techniques. For related information see also *03 Air Transportation and Safety* and *18 Spacecraft Design, Testing and Performance.* For space suits see *54 Man/System Technology and Life Support.*

17 SPACE COMMUNICATIONS, SPACECRAFT COMMUNICATIONS, COMMAND AND TRACKING.... **2201**
Includes telemetry; space communications networks; astronavigation and guidance; and radio blackout. For related information see also *04 Aircraft Communications and Navigation* and *32 Communications and Radar.*

N.A.—No abstracts were assigned to this category for this issue.

18 SPACECRAFT DESIGN, TESTING AND PERFORMANCE 2203
Includes satellites; space platforms; space stations; spacecraft systems and components such as thermal and environmental controls; and attitude controls. For life support systems see *54 Man/System Technology and Life Support.* For related information see also *05 Aircraft Design, Testing and Performance, 39 Structural Mechanics,* and *16 Space Transportation.*

19 SPACECRAFT INSTRUMENTATION 2208
For related information see also *06 Aircraft Instrumentation* and *35 Instrumentation and Photography.*

20 SPACECRAFT PROPULSION AND POWER 2209
Includes main propulsion systems and components, e.g., rocket engines; and spacecraft auxiliary power sources. For related information see also *07 Aircraft Propulsion and Power, 28 Propellants and Fuels, 44 Energy Production and Conversion,* and *15 Launch Vehicles and Space Vehicles.*

CHEMISTRY AND MATERIALS

23 CHEMISTRY AND MATERIALS (GENERAL) 2222

24 COMPOSITE MATERIALS 2226
Includes physical, chemical, and mechanical properties of laminates and other composite materials. For ceramic materials see *27 Nonmetallic Materials.*

25 INORGANIC AND PHYSICAL CHEMISTRY 2231
Includes chemical analysis, e.g., chromatography; combustion theory; electrochemistry; and photochemistry. For related information see also *77 Thermodynamics and Statistical Physics.*

26 METALLIC MATERIALS 2238
Includes physical, chemical, and mechanical properties of metals, e.g., corrosion; and metallurgy.

27 NONMETALLIC MATERIALS 2252
Includes physical, chemical, and mechanical properties of plastics, elastomers, lubricants, polymers, textiles, adhesives, and ceramic materials. For composite materials see *24 Composite Materials.*

28 PROPELLANTS AND FUELS 2264
Includes rocket propellants, igniters and oxidizers; their storage and handling procedures; and aircraft fuels. For related information see also *07 Aircraft Propulsion and Power, 20 Spacecraft Propulsion and Power,* and *44 Energy Production and Conversion.*

29 MATERIALS PROCESSING 2266
Includes space-based development of products and processes for commercial application. For biological materials see *55 Space Biology:*

ENGINEERING For related information see also *Physics.*

31 ENGINEERING (GENERAL) 2267
Includes vacuum technology; control engineering; display engineering; cryogenics; and fire prevention.

32 COMMUNICATIONS AND RADAR 2273
Includes radar; land and global communications; communications theory; and optical communications. For related information see also *04 Aircraft Communications and Navigation* and *17 Space Communications, Spacecraft Communications, Command and Tracking.* For search and rescue see *03 Air Transportation and Safety,* and *16 Space Transportation.*

33 ELECTRONICS AND ELECTRICAL ENGINEERING 2306
Includes test equipment and maintainability; components, e.g., tunnel diodes and transistors; microminiaturization; and integrated circuitry. For related information see also *60 Computer Operations and Hardware* and *76 Solid-State Physics.*

34 FLUID MECHANICS AND HEAT TRANSFER 2315
Includes boundary layers; hydrodynamics; fluidics; mass transfer and ablation cooling. For related information see also *02 Aerodynamics* and *77 Thermodynamics and Statistical Physics.*

35 INSTRUMENTATION AND PHOTOGRAPHY 2342
Includes remote sensors; measuring instruments and gauges; detectors; cameras and photographic supplies; and holography. For aerial photography see *43 Earth Resources and Remote Sensing.* For related information see also *06 Aircraft Instrumentation* and *19 Spacecraft Instrumentation.*

36 LASERS AND MASERS 2347
Includes parametric amplifiers. For related information see also *76 Solid-State Physics.*

37 MECHANICAL ENGINEERING 2351
Includes auxiliary systems (nonpower); machine elements and processes; and mechanical equipment.

38 QUALITY ASSURANCE AND RELIABILITY 2371
Includes product sampling procedures and techniques; and quality control.

39 STRUCTURAL MECHANICS 2374
Includes structural element design and weight analysis; fatigue; and thermal stress. For applications see *05 Aircraft Design, Testing and Performance* and *18 Spacecraft Design, Testing and Performance.*

GEOSCIENCES For related information see also *Space Sciences.*

42 GEOSCIENCES (GENERAL) 2381

43 EARTH RESOURCES AND REMOTE SENSING 2381
Includes remote sensing of earth resources by aircraft and spacecraft; photogrammetry; and aerial photography. For instrumentation see *35 Instrumentation and Photography.*

44 ENERGY PRODUCTION AND CONVERSION 2389
Includes specific energy conversion systems, e.g., fuel cells; global sources of energy; geophysical conversion; and windpower. For related information see also *07 Aircraft Propulsion and Power, 20 Spacecraft Propulsion and Power,* and *28 Propellants and Fuels.*

45 ENVIRONMENT POLLUTION 2396
Includes atmospheric, noise, thermal, and water pollution.

46 GEOPHYSICS 2400
Includes aeronomy; upper and lower atmosphere studies; ionospheric and magnetospheric physics; and geomagnetism. For space radiation see *93 Space Radiation.*

47 METEOROLOGY AND CLIMATOLOGY 2407
Includes weather forecasting and modification.

48 OCEANOGRAPHY 2417
Includes biological, dynamic, and physical oceanography; and marine resources. For related information see also *43 Earth Resources and Remote Sensing.*

LIFE SCIENCES

51 LIFE SCIENCES (GENERAL) 2420

52 AEROSPACE MEDICINE 2423
Includes physiological factors; biological effects of radiation; and effects of weightlessness on man and animals.

53 BEHAVIORAL SCIENCES 2427
Includes psychological factors; individual and group behavior; crew training and evaluation; and psychiatric research.

54 MAN/SYSTEM TECHNOLOGY AND LIFE SUPPORT 2429
Includes human engineering; biotechnology; and space suits and protective clothing. For related information see also *16 Space Transportation.*

55 SPACE BIOLOGY 2444
Includes exobiology; planetary biology; and extraterrestrial life.

MATHEMATICAL AND COMPUTER SCIENCES

59 MATHEMATICAL AND COMPUTER SCIENCES (GENERAL) 2444

60 COMPUTER OPERATIONS AND HARDWARE 2444
Includes hardware for computer graphics, firmware, and data processing. For components see *33 Electronics and Electrical Engineering.*

61 COMPUTER PROGRAMMING AND SOFTWARE 2447
Includes computer programs, routines, algorithms, and specific applications, e.g., CAD/CAM.

62 COMPUTER SYSTEMS 2465
Includes computer networks and special application computer systems.

63 CYBERNETICS **2469**
Includes feedback and control theory, artificial intelligence, robotics and expert systems. For related information see also *54 Man/System Technology and Life Support.*

64 NUMERICAL ANALYSIS **2478**
Includes iteration, difference equations, and numerical approximation.

65 STATISTICS AND PROBABILITY **2493**
Includes data sampling and smoothing; Monte Carlo method; and stochastic processes.

66 SYSTEMS ANALYSIS **2497**
Includes mathematical modeling; network analysis; and operations research.

67 THEORETICAL MATHEMATICS **2523**
Includes topology and number theory.

PHYSICS For related information see also *Engineering.*

70 PHYSICS (GENERAL) **2523**
For precision time and time interval (PTTI) see *35 Instrumentation and Photography*; for geophysics, astrophysics or solar physics see *46 Geophysics, 90 Astrophysics*, or *92 Solar Physics.*

71 ACOUSTICS **2525**
Includes sound generation, transmission, and attenuation. For noise pollution see *45 Environment Pollution.*

72 ATOMIC AND MOLECULAR PHYSICS **2530**
Includes atomic structure, electron properties, and molecular spectra.

73 NUCLEAR AND HIGH-ENERGY PHYSICS **2540**
Includes elementary and nuclear particles; and reactor theory. For space radiation see *93 Space Radiation.*

74 OPTICS **2541**
Includes light phenomena and optical devices. For lasers see *36 Lasers and Masers.*

75 PLASMA PHYSICS **2548**
Includes magnetohydrodynamics and plasma fusion. For ionospheric plasmas see *46 Geophysics.* For space plasmas see *90 Astrophysics.*

76 SOLID-STATE PHYSICS **2555**
Includes superconductivity. For related information see also *33 Electronics and Electrical Engineering* and *36 Lasers and Masers.*

77 THERMODYNAMICS AND STATISTICAL PHYSICS **2568**
Includes quantum mechanics; theoretical physics; and Bose and Fermi statistics. For related information see also *25 Inorganic and Physical Chemistry* and *34 Fluid Mechanics and Heat Transfer.*

SOCIAL SCIENCES

80 SOCIAL SCIENCES (GENERAL) **2571**
Includes educational matters.

81 ADMINISTRATION AND MANAGEMENT **2585**
Includes management planning and research.

82 DOCUMENTATION AND INFORMATION SCIENCE **2588**
Includes information management; information storage and retrieval technology; technical writing; graphic arts; and micrography. For computer documentation see *61 Computer Programming and Software.*

83 ECONOMICS AND COST ANALYSIS **2595**
Includes cost effectiveness studies.

84 LAW, POLITICAL SCIENCE AND SPACE POLICY .... **N.A.**
Includes NASA appropriation hearings; aviation law; space law and policy; international law; international cooperation; and patent policy.

85 URBAN TECHNOLOGY AND TRANSPORTATION **2596**
Includes applications of space technology to urban problems; technology transfer; technology assessment; and surface and mass transportation. For related information see *03 Air Transportation and Safety, 16 Space Transportation,* and *44 Energy Production and Conversion.*

SPACE SCIENCES For related information see also *Geosciences.*

88 SPACE SCIENCES (GENERAL) .... N.A.

89 ASTRONOMY 2598
Includes radio, gamma-ray, and infrared astronomy; and astrometry.

90 ASTROPHYSICS 2601
Includes cosmology; celestial mechanics; space plasmas; and interstellar and interplanetary gases and dust. For related information see also *75 Plasma Physics.*

91 LUNAR AND PLANETARY EXPLORATION 2605
Includes planetology; and manned and unmanned flights. For spacecraft design or space stations see *18 Spacecraft Design, Testing and Performance.*

92 SOLAR PHYSICS 2623
Includes solar activity, solar flares, solar radiation and sunspots. For related information see also *93 Space Radiation.*

93 SPACE RADIATION 2629
Includes cosmic radiation; and inner and outer earth's radiation belts. For biological effects of radiation see *52 Aerospace Medicine.* For theory see *73 Nuclear and High-Energy Physics.*

GENERAL

Includes aeronautical, astronautical, and space science related histories, biographies, and pertinent reports too broad for categorization; histories or broad overviews of NASA programs.

99 GENERAL 2630

SUBJECT INDEX I-1

PERSONAL AUTHOR INDEX I-185

CORPORATE SOURCE INDEX I-207

CONTRACT NUMBER INDEX I-239

REPORT NUMBER INDEX I-245

APPENDIX A-1

TYPICAL CITATION AND ABSTRACT

NASA SPONSORED
ON MICROFICHE
↓↓

ACCESSION NUMBER → **N94-12270*#** United Technologies Corp., West Palm Beach, FL. Pratt and Whitney. ← **CORPORATE SOURCE**

TITLE → **ADVANCED CONTROL FOR AIRBREATHING ENGINES, VOLUME 1: PRATT AND WHITNEY**

AUTHOR → J. A. Ralph Jul. 1993 83 p ← **PUBLICATION DATE**

CONTRACT OR GRANT → (Contract NAS3-25952; RTOP 505-62-61)

REPORT NUMBERS → (NASA-CR-189203; E-8006; NAS 1.26:189203) Avail: CASI HC A05/MF A01 ← **AVAILABILITY SOURCE AND PRICE CODE**

The application of advanced control concepts to air breathing engines may yield significant improvements in aircraft/engine performance and operability. Screening studies of advanced control concepts for air breathing engines were conducted by three major domestic aircraft engine manufacturers to determine the potential impact of concepts on turbine engine performance and operability. The purpose of the studies was to identify concepts which offered high potential yet may incur high research and development risk. A target suite of proposed advanced control concepts was formulated and evaluated in a two phase study to quantify each concept's impact on desired engine characteristics. To aid in the evaluation specific aircraft/engine combinations were considered: a Military High Performance Fighter mission, a High Speed Civil Transport mission, and a Civil Tiltrotor mission. Each of the advanced control concepts considered in the study are defined and described. The concept potential impact on engine performance was determined. Relevant figures of merit on which to evaluate the concepts are determined. Finally, the concepts are ranked with respect to the target aircraft/engine missions. A final report describing the screening studies was prepared by each engine manufacturer. Volume 1 of these reports describes the studies performed by Pratt & Whitney. Author (revised)

VOLUME 32 NUMBER 6 / June 1994

Scientific and Technical Aerospace Reports

A Monthly Publication of the National Aeronautics and Space Administration

01 AERONAUTICS (GENERAL)

N94-23553*# Sverdrup Technology, Inc., Brook Park, OH.
UNSTEADY JET FLOW COMPUTATION TOWARDS NOISE PREDICTION Final Report
Woo-Yung Soh Jan. 1994 17 p Presented at the 32nd Aerospace Sciences Meeting, Reno, NV, 10-13 Jan. 1994; sponsored by AIAA
(Contract NAS3-25266; RTOP 537-02-22)
(NASA-CR-194449; E-8329; NAS 1.26:194449; AIAA Paper 94-0138)
Avail: CASI HC A03/MF A01

An attempt has been made to combine a wave solution method and an unsteady flow computation to produce an integrated aeroacoustic code to predict far-field jet noise. An axisymmetric subsonic jet is considered for this purpose. A fourth order space accurate Pade compact scheme is used for the unsteady Navier-Stokes solution. A Kirchhoff surface integral for the wave equation is employed through the use of an imaginary surface which is a circular cylinder enclosing the jet at a distance. Information such as pressure and its time and normal derivatives is provided on the surface. The sound prediction is performed side by side with the jet flow computation. Retarded time is also taken into consideration since the cylinder body is not acoustically compact. The far-field sound pressure has the directivity and spectra show that low frequency peaks shift toward higher frequency region as the observation angle increases from the jet flow axis.
Author

N94-23711* National Aeronautics and Space Administration, Washington, DC.
AERONAUTICAL ENGINEERING: A CONTINUING BIBLIOGRAPHY WITH INDEXES (SUPPLEMENT 298)
Dec. 1993 102 p
(NASA-SP-7037(298); NAS 1.21:7037(298)) Avail: CASI HC A06

This bibliography lists 328 reports, articles, and other documents recently introduced into the NASA scientific and technical information system. Subject coverage includes the following areas: design, construction, and testing of aircraft and aircraft engines; aircraft components, equipment, and systems; ground support systems; and theoretical and applied aspects of aerodynamics and general fluid dynamics. Author

N94-23973* National Aeronautics and Space Administration, Washington, DC.
AERONAUTICAL ENGINEERING: A CONTINUING BIBLIOGRAPHY WITH INDEXES (SUPPLEMENT 299)
Jan. 1994 75 p
(NASA-SP-7037(299); NAS 1.21:7037(299)) Avail: CASI HC A04

This bibliography lists 244 reports, articles, and other documents introduced into the NASA scientific and technical information system in Jan. 1994. Subject coverage includes: design, construction and testing of aircraft and aircraft engines; aircraft components, equipment, and systems; ground support systems; and theoretical and applied aspects of aerodynamics and general fluid dynamics. Author

N94-24100*# National Aeronautics and Space Administration. Lewis Research Center, Cleveland, OH.
ROLES, USES, AND BENEFITS OF GENERAL AVIATION AIRCRAFT IN AEROSPACE ENGINEERING EDUCATION
Dennis P. ODonoghue (Sverdrup Technology, Inc., Brook Park, OH.) and Robert C. McKnight Jan. 1994 15 p Presented at the 32nd Aerospace Sciences Meeting and Exhibit, Reno, NV, 10-13 Jan. 1994; sponsored by AIAA
(Contract NAS3-25266)
(NASA-TM-106463; E-8326; NAS 1.15:106463; AIAA Paper 94-0852)
Avail: CASI HC A03/MF A01

Many colleges and universities throughout the United States offer outstanding programs in aerospace engineering. In addition to the fundamentals of aerodynamics, propulsion, flight dynamics, and air vehicle design, many of the best programs have in the past provided students the opportunity to design and fly airborne experiments on board various types of aircraft. Sadly, however, the number of institutions offering such 'airborne laboratories' has dwindled in recent years. As a result, opportunities for students to apply their classroom knowledge, analytical skills, and engineering judgement to the development and management of flight experiments on an actual aircraft are indeed rare. One major reason for the elimination of flight programs by some institutions, particularly the smaller colleges, is the prohibitive cost of operating and maintaining an aircraft as a flying laboratory. The purpose of this paper is to discuss simple, low-cost, relevant flight experiments that can be performed using readily available general aviation aircraft. This paper examines flight experiments that have been successfully conducted on board the NASA Lewis Research Center's T-34B aircraft, as part of the NASA/AIAA/University Flight Experiment Program for Students (NAUFEPS) and discusses how similar experiments could be inexpensively performed on other general aviation aircraft.
Author (revised)

N94-24241 Israel Society of Aeronautics and Astronautics, Tel Aviv.
THE 33RD ISRAEL ANNUAL CONFERENCE ON AVIATION AND ASTRONAUTICS
Alexander Burcat (Technion - Israel Inst. of Tech., Haifa.) 25 Feb. 1993 523 p Conference held in Tel-Aviv, Israel, February 24-25, 1993 Convened by Israel Society of Aeronautics and Astronautics, Tel-Aviv; Technion - Israel Institute of Technology, Haifa; Tel-Aviv University, Ramat Aviv, Israel; Ben-Gurion University of the Negev, Beersheva, Israel; RAFAEL - Armament Development Auth
(ITN-94-85227) Copyright Avail: Issuing Activity (Israel Society of Aeronautics and Astronautics, c/o Faculty of Engineering, Tel-Aviv Univ., Ramat Aviv 69978, Israel)

Subjects covered by the 48 papers include: aircraft design and development technology; satellite and spacecraft design and testing; unmanned aerial vehicle technology; shock and blast studies; propellant, combustion and engine performance; space systems, spacecraft and satellites; space and aircraft structures, structural materials and damage control; aircraft control and spacecraft control; particle combustion; fracture mechanics and fatigue; structural dynamics; and spray combustion. For individual titles, see N94-24242 through N94-24289.

N94-24242 Jet Propulsion Lab., California Inst. of Tech., Pasadena.
THE JET PROPULSION LABORATORY SPACE EXPLORATION: PAST, PRESENT AND FUTURE c12
Josette Bellan *In* Israel Society of Aeronautics and Astronautics, The 33rd Israel Annual Conference on Aviation and Astronautics 25 Feb. 1993 p 1-26 (For primary document see N94-24241 06-01)
Copyright Avail: Issuing Activity (Israel Society of Aeronautics and Astronautics, c/o Faculty of Engineering, Tel-Aviv Univ., Ramat Aviv 69978, Israel)

The most recent scientific results from space exploration carried out by the Jet Propulsion Laboratory (JPL) are discussed. To aid understanding of these results, a brief background of JPL's history is presented, followed by a description of the Deep Space Network, JPL's system of antennas which communicates with spacecraft. The results from the missions of Voyager 1 and Voyager 2 are described. The atmosphere, rings, satellites and magnetospheres of Jupiter, Saturn, Uranus and Neptune are discussed with particular emphasis on novelty of the discoveries and the challenges encountered in explaining them. A brief discussion of the impact of spray research upon space exploration follows. This is because most recently launched missions used liquid fueled rockets to escape Earth's gravity. A summary of future missions and the National Aeronautics and Space Administration's new policies is presented in the conclusion. ISA

N94-24243 In-Space Propulsion Ltd., Sacramento, CA.

LIQUID ROCKET PROPULSION: RETROSPECTIVE AND PROSPECTS c20

Sanders D. Rosenberg *In* Israel Society of Aeronautics and Astronautics, The 33rd Israel Annual Conference on Aviation and Astronautics 25 Feb. 1993 p 27-36 (For primary document see N94-24241 06-01)

Copyright Avail: Issuing Activity (Israel Society of Aeronautics and Astronautics, c/o Faculty of Engineering, Tel-Aviv Univ., Ramat Aviv 69978, Israel)

Rocket propulsion has made a fundamental contribution to change in the human condition during the second half of the 20th Century. This paper presents a survey of the basic elements of and future prospects for liquid rocket propulsion systems, with emphasis placed on their bipropellant engines, which have contributed profoundly to the successes of this 'aerospace century.' Many technologies had to reach maturity simultaneously to enable our current progress: materials, electronics, guidance and control, systems engineering, and propulsion, made major contributions. However, chemical propellants and the engine systems required to extract and control their propulsive power successfully are at the heart of all that humankind has accomplished through space flight and the use of space for the betterment of all. And it is a fascinating story to tell. ISA

N94-24244 California Univ., Los Angeles. Mechanical, Aerospace and Nuclear Engineering Dept.

AEROELASTIC, AEROMECHANICAL AND VIBRATION PROBLEMS IN HELICOPTERS c08

Peretz P. Friedmann *In* Israel Society of Aeronautics and Astronautics, The 33rd Israel Annual Conference on Aviation and Astronautics 25 Feb. 1993 p 37-81 (For primary document see N94-24241 06-01)

Copyright Avail: Issuing Activity (Israel Society of Aeronautics and Astronautics, c/o Faculty of Engineering, Tel-Aviv Univ., Ramat Aviv 69978, Israel)

This paper describes and emphasizes the fundamental advances, achieved during the last two decades, in three important areas which have a central role in modern rotorcraft design. The topics considered are: (1) helicopter aeroelasticity, (2) aeromechanical problems, and (3) vibration and its alleviation using active controls. Each topic contains background to provide the reader with a certain perspective, illustrative examples and speculation on future research needs. ISA

N94-24245 Israel Aircraft Industries Ltd., Ben-Gurion Airport.

UAV CURRENT TECHNOLOGY AND FUTURE TRENDS c05

D. Harari *In* Israel Society of Aeronautics and Astronautics, The 33rd Israel Annual Conference on Aviation and Astronautics 25 Feb. 1993 p 83-88 (For primary document see N94-24241 06-01)

Copyright Avail: Issuing Activity (Israel Society of Aeronautics and Astronautics, c/o Faculty of Engineering, Tel-Aviv Univ., Ramat Aviv 69978, Israel)

The operational value of unmanned air vehicles (UAV) was clearly demonstrated by the use of the Pioneer UAV during the recent Gulf War. After sifting through operational data from Desert Storm, U.S. Army, Navy, Marine and Air Force planners agree that there is a validated requirement for future battlefield doctrine and tactics, that employ unmanned aerial vehicle systems. These systems will be deployed to help different users by determining enemy positions and, equally important, accurately tracking fast moving friendly troops. Emerging technologies such as artifical intelligence, data fusion, long range communications will influence the design and operation of future UAV systems. The presentation will try to present future UAV developments in the postwar environment of the Operation Desert Storm from operational and technology aspects. ISA

N94-24246 MacNeal-Schwendler Corp., Gouda (Netherlands).

THE PLASTIC RESPONSE OF A CYLINDRICAL SHELL SUBJECTED TO AN INTERNAL BLAST WAVE WITH A FINITE WIDTH SHOCK FRONT c39

Y. Kivity, C. Florie, and H. Lenselink *In* Israel Society of Aeronautics and Astronautics, The 33rd Israel Annual Conference on Aviation and Astronautics 25 Feb. 1993 p 89-102 (For primary document see N94-24241 06-01)

Copyright Avail: Issuing Activity (Israel Society of Aeronautics and Astronautics, c/o Faculty of Engineering, Tel-Aviv Univ., Ramat Aviv 69978, Israel)

This paper considers the plastic deformation of a thin cylindrical shell subjected to an internal explosion. It is assumed that the explosive charge is placed on the axis of symmetry of the shell so that an axisymmetric blast wave is produced. The shell response is calculated assuming an elastic-perfectly plastic material. The plastic response is evaluated for two types of loads. In the first type, the blast is assumed to have an ideal shock front with a discontinuous jump to the peak pressure. In the second type of loading, the shock front has a finite rise-time. This type of loading was introduced to study the effect of finite width shock fronts. Such finite width shock fronts are typical of hydrocode calculations when simulating problems involving blast waves and their interactions with adjacent structures. It is found that for equal impulse loads, the numerical rise-time reduces the shell plastic response significantly. Numerical calculations with a three-dimensional hydrocode are presented to illustrate the analytical results. A generalization of the analysis is given which may be used to determine the required mesh resolution of a hydrocode calculation in order to obtain a prescribed accuracy in the shell response. ISA

N94-24247 Instituto de Estudos Avancados, Sao Jose dos Campos (Brazil).

AN INVESTIGATION ON A NEW TECHNIQUE TO IMPROVE THE PERFORMANCE OF THE SHOCK TUBE/TUNNEL TESTING IN THE EQUILIBRIUM INTERFACE CONDITION c09

Marco A. S. Minucci, Marco A. C. Nascimento, and Henry T. Nagamatsu (Rensselaer Polytechnic Inst., Troy, NY.) *In* Israel Society of Aeronautics and Astronautics, The 33rd Israel Annual Conference on Aviation and Astronautics 25 Feb. 1993 p 103-113 (For primary document see N94-24241 06-01)

Copyright Avail: Issuing Activity (Israel Society of Aeronautics and Astronautics, c/o Faculty of Engineering, Tel-Aviv Univ., Ramat Aviv 69978, Israel)

A 0.3-m diameter hypersonic shock tunnel has been designed and constructed to investigate the effect of a thin layer of a separating gas on the performance of the tunnel when operating in the equilibrium interface condition. The separating gas is placed between the drive gas, He, and the test gas, air. Preliminary experiments employing He, Ar and SF6 as the separating gases indicate a strong dependence of the final equilibrium interface pressure on the kind of gas used. These experiments showed that when SF6 is used, the highest equilibrium pressure is attained and that the time required to reach this pressure is the shortest when compared with the other two gases tested. It was observed that the separating gas acts as a gaseous piston enhancing the compression provided by the moving He/air interface. Tests involving the CO2 laser radiation absorption in SF6 were also conducted. These tests revealed not only the arrival of the gaseous piston at a given shock tunnel station but also the existence of SF6 leakage through the boundary layer. ISA

N94-24248 Technion - Israel Inst. of Tech., Haifa. Faculty of Aerospace Engineering.

STABILITY OF HYPERSONIC FLOW OF A DETONABLE GAS MIXTURE IN THE STAGNATION REGION OF A BLUNT BODY AND A FORWARD FACING STEP c34

Genadi Tivanov and Joseph Rom *In* Israel Society of Aeronautics and Astronautics, The 33rd Israel Annual Conference on Aviation and Astronautics 25 Feb. 1993 p 114-124 (For primary document see N94-24241 06-01)

Copyright Avail: Issuing Activity (Israel Society of Aeronautics and Astronautics, c/o Faculty of Engineering, Tel-Aviv Univ., Ramat Aviv 69978, Israel)

The time-dependent characteristics of the hypersonic flow of a detonable gas mixture in the stagnation region of a blunt-nosed body and blunt face of a forward facing step are studied using approximations based on inviscid analysis. In this investigation the approximation that at hypersonic speeds the flow in the stagnation region, behind the normal shock wave which is established in front of the blunt face of the model, can be considered to be at 'constant density' is used. Both of these approximations may be justified for very high Reynolds number flow at hypersonic speeds. In this analysis, it is shown that using the time-dependent flow equations which include the heat addition due to the chemical reactions, it is possible to develop a second-order differential equation for the instantaneous temperature. The stability characteristics of this governing equation are analyzed for the zero-order and first-order chemical reaction cases so as to determine the stability boundaries of the detonation phenomena in terms of the flow and the chemical reaction parameters. These dynamic characteristics are studied by the examination of the phase diagrams. The stability characteristics are determined by the analysis of the linearized equations. The calculated eigenvalues of the solutions are used to define both the stability boundaries and the oscillation frequencies. ISA

N94-24249 Israel Aircraft Industries Ltd., Tashan. Aerodynamics Dept.

NEW FEATURES IN COMPUTATIONAL FLUID DYNAMICS (CFD) TECHNOLOGY AT THE TASHAN ENGINEERING CENTER AT IAI c34

B. Epstein *In* Israel Society of Aeronautics and Astronautics, The 33rd Israel Annual Conference on Aviation and Astronautics 25 Feb. 1993 p 125-132 (For primary document see N94-24241 06-01)

Copyright Avail: Issuing Activity (Israel Society of Aeronautics and Astronautics, c/o Faculty of Engineering, Tel-Aviv Univ., Ramat Aviv 69978, Israel)

The presentation gives an overview of CFD (computational fluid dynamics) activities at the TASHAN Engineering Center of Israel Aircraft Industries (TECIAI), emphasizing new features in CFD technology. The first part starts with the description of purposes of industrial CFD at TECIAI. It then introduces the main codes developed 'in-house' during 1977-92, and explains the use of CFD codes in a typical cycle of CFD-aided aircraft design. The second part is devoted to state-of-the-art CFD technology with a number of typical applications given. Applications include complete aircraft analysis by a Multigrid Euler Code and incompressible 2-D Navier-Stokes calculations. ISA

N94-24250 Israel Aircraft Industries Ltd., Tashan. Wind Tunnels Center.

ON THE EFFECT OF THE DAMPING COEFFICIENTS ON THE TRAJECTORIES OF SYMMETRIC AND NON-SYMMETRIC STORES c05

Moshe Zilberman and Alex Cazes *In* Israel Society of Aeronautics and Astronautics, The 33rd Israel Annual Conference on Aviation and Astronautics 25 Feb. 1993 p 133-141 (For primary document see N94-24241 06-01)

Copyright Avail: Issuing Activity (Israel Society of Aeronautics and Astronautics, c/o Faculty of Engineering, Tel-Aviv Univ., Ramat Aviv 69978, Israel)

The effect of the damping coefficients of stores, being released from a parent aircraft, on their trajectories was quantitatively analyzed. Trajectories which were obtained at the Israel Aircraft Industries (IAI) four-foot trisonic wind tunnel by using the Captive Trajectory System (CTS), were recalculated for various dynamic coefficients. Three types of stores were tested. The first store was an M117, which has an axisymmetric shape and is statically stable. The second type was a Multiple Ejection Rack (MER), which was asymmetrically loaded, and the third type of store was an MER which was loaded symmetrically. Two methods were utilized to recalculate the trajectories. The Zero-Order Correction (ZOC), in which the static coefficients were not corrected, and the First-Order Correction (FOC), in which the static loads were linearly extrapolated according to the corrected positions of the store. The main objectives of this study were threefold: (1) to study the effect of a particular damping coefficient on a trajectory which was obtained by the CTS; (2) to characterize the effect of the damping coefficients with respect to the nature of the store, namely, symmetric or non-symmetric, and (3) to compare the off-line correction, ZOC and FOC, with the original trajectories which were obtained by the CTS. Finally, the influence of the damping coefficients on the clearance in separation is quantitatively examined by a parametric study of the 6-degrees-of-freedom (6DOF) equations. ISA

N94-24251 Technion - Israel Inst. of Tech., Haifa. Turbo and Jet Engine Laboratory.

THRUST VECTORING THEORY, LABORATORY AND FLIGHT TESTS c07

Benjamin Gal-Or and Valery Sherbaum *In* Israel Society of Aeronautics and Astronautics, The 33rd Israel Annual Conference on Aviation and Astronautics 25 Feb. 1993 p 142-153 (For primary document see N94-24241 06-01)

Copyright Avail: Issuing Activity (Israel Society of Aeronautics and Astronautics, c/o Faculty of Engineering, Tel-Aviv Univ., Ramat Aviv 69978, Israel)

Fundamental concepts of thrust-vectored fighter aircraft are defined and represented by novel designs of roll-yaw-pitch vectoring nozzles designed for maximized Post-Stall (PST) agility. The concepts are employed to formulate a unified mathematical phenomenology of PST, thrust-vectoring-induced supermaneuverability and to define standard agility comparison maneuvers in the PST domain. New dynamic scale rules generate an unorthodox methodolgy which combines full-scale jet-engine laboratory tests of new vectorable nozzles and inlets with flying 1/7-scale vectored models of F-22, F-15, F-16 and other, tailless, stealth, vectored models. A general vectoring control rate control rule is also defined. ISA

N94-24252 Soreq Research Establishment, Israel Atomic Energy Commission, Yavneh.

BURNING RATE OF DOUBLE-BASE PROPELLANT IN THE PRESENCE OF PLASMA c28

S. Rozen, D. Saphier, and E. Sher (Ben Gurion Univ. of the Negev, Beersheva, Israel.) *In* Israel Society of Aeronautics and Astronautics, The 33rd Israel Annual Conference on Aviation and Astronautics 25 Feb. 1993 p 154-158 (For primary document see N94-24241 06-01)

Copyright Avail: Issuing Activity (Israel Society of Aeronautics and Astronautics, c/o Faculty of Engineering, Tel-Aviv Univ., Ramat Aviv 69978, Israel)

A combustion model for the burning of double-base propellants in the presence of hot plasma has been developed and used to predict burning rates at high ambient pressures. The theoretical model has been developed in order to gain some understanding of the experimental results obtained with a new gun design in which plasma is injected into the propellant cartridge in order to improve its ballistic performance. The hot plasma is introduced and mixed instantaneously with the products of combustion while increasing their temperature, thus augmenting the heat flux to the solid propellant and accelerating its burning rate. Based on the results of the present study, a numero-empirical model has been proposed to correlate the regression rate and the pressure by a simple form of the Vielle equation: dx/dt = A.p(exp n). The parameters A and n were found to be strong functions of the temperature. ISA

N94-24253 Ben Gurion Univ. of the Negev, Beersheva (Israel). Dept. of Mechanical Engineering.

THE EFFECT OF HIGH ALTITUDE PRESSURE ON THE POWER AND EFFICIENCY OF AN AIRBORNE TWO-STROKE ENGINE c07

R. Harari and E. Sher *In* Israel Society of Aeronautics and Astronautics, The 33rd Israel Annual Conference on Aviation and Astronautics 25 Feb. 1993 p 159-165 (For primary document see N94-24241 06-01)

Copyright Avail: Issuing Activity (Israel Society of Aeronautics and Astronautics, c/o Faculty of Engineering, Tel-Aviv Univ., Ramat Aviv 69978, Israel)

The effect of ambient pressure on the torque and fuel consumption characteristics of a crankcase-scavenged spark-ignition two-stroke engine has been investigated. The study includes an experimental part and a theoretical part. In the experimental part, the engine was tested under high-altitude conditions by using a simulator chamber where both the pressure at the inlet manifold and the pressure at the exhaust pipe were controlled separately. The influence of the simulation system on the engine performance has been investigated at sea level (s.l.) and the effect of the ambient pressure on the engine performance has been investigated in the range of 100 to 44 kPa, where the low pressure corresponds to a standard altitude of 21,000 feet (7 km). In the theoretical part a detailed computer program has been used to simulate the engine cycle under low ambient pressure. The computer program has been calibrated by using the s.l. experimental results. Very good agreement between the results of the theoretical model and the measurements under low ambient pressure conditions has been found over the entire range of operating conditions (100 to 44 kPa). An empirical correlation for the correction factor of the engine power has been suggested. The correction factor was found to be proportional to the ambient pressure raised to the power 1.5: ip/ip(sub s)= (P/P(sub s))(exp 1.5) Previous studies have suggested a power of 9/8 (1.125), but their validity was limited to a minimum ambient pressure of 70 kPa. ISA

N94-24254 Technion - Israel Inst. of Tech., Haifa. Faculty of Aerospace Engineering.

DESIGN CONSIDERATIONS OF HYBRID ROCKETS c20

Adela Ben-Yakar *In* Israel Society of Aeronautics and Astronautics, The 33rd Israel Annual Conference on Aviation and Astronautics 25 Feb. 1993 p 166-174 (For primary document see N94-24241 06-01)

Copyright Avail: Issuing Activity (Israel Society of Aeronautics and Astronautics, c/o Faculty of Engineering, Tel-Aviv Univ., Ramat Aviv 69978, Israel)

The design procedure of hybrid engines which can meet mission requirements at optimized performance is presented. Multi-port grains are considered, and the effects of key operating and geometrical parameters on overall performance and on variations during engine operation are discussed. Excellent performance with an average specific impulse as high as 99% of the peak specific impulse, while keeping the thrust within 5% of the nominal value, in spite of the large geometrical variations during the grain combustion, are demonstrated for a LOX/HTPB system. ISA

N94-24255 Rafael Armament Development Authority, Haifa (Israel).

ALTITUDE SIMULATION FACILITY FOR TESTING LARGE SPACE MOTORS c14

U. Katz, J. Lustig, Y. Cohen, and I. Malkin *In* Israel Society of Aeronautics and Astronautics, The 33rd Israel Annual Conference on Aviation and Astronautics 25 Feb. 1993 p 175-184 (For primary document see N94-24241 06-01)

Copyright Avail: Issuing Activity (Israel Society of Aeronautics and Astronautics, c/o Faculty of Engineering, Tel-Aviv Univ., Ramat Aviv 69978, Israel)

This work describes the design of an altitude simulation facility for testing the AKM motor installed in the 'Ofeq' satellite launcher. The facility, which is controlled by a computer, consists of a diffuser and a single-stage ejector fed with preheated air. The calculations of performance and dimensions of the gas extraction system were conducted according to a one-dimensional analysis. Tests were carried out on a small-scale model of the facility in order to examine the design concept, then the full-scale facility was constructed and operated. There was good agreement among the results obtained from the small-scale facility, from the full-scale facility, and from calculations. ISA

N94-24256 Academy of Sciences (USSR), Alma-Ata. Mechanical Engineering Research Institute.

NEARLY UNIFORM DEPLOYMENT/RETRIEVAL STRATEGY FOR SPACE TETHER SYSTEMS c18

E. M. Levin *In* Israel Society of Aeronautics and Astronautics, The 33rd Israel Annual Conference on Aviation and Astronautics 25 Feb. 1993 p 185-195 (For primary document see N94-24241 06-01)

Copyright Avail: Issuing Activity (Israel Society of Aeronautics and Astronautics, c/o Faculty of Engineering, Tel-Aviv Univ., Ramat Aviv 69978, Israel)

The nearly uniform deployment/retrieval strategy is advantageously applicable to the deployment or retrieval of many types of prospective space tether systems that include two satellites connected with a long flexible thread (tether). The basic idea of this strategy is to control the tether tension in such a way as to maintain a desired deployment rate. Normally, after a short initial transient process, the rate of deployment or retrieval approaches a 'cruising speed' which is then maintained up to the beginning of the final transient process. Under perturbations of a different nature (unexpected internal friction, non-gravitational external forces, etc.), the rate of deployment or retrieval is automatically adjusted in such a way as to compensate for the additional dynamic loads introduced. To generate the command tension, one has to know only the instantaneous deployed length of the tether and the rate of deployment or retrieval. In addition, the tension control of the same type is capable of damping out undesired in-plane and out-of-plane oscillations during stationkeeping. ISA

N94-24257 Centro Tecnico Aerospacial, San Jose dos Campos (Brazil). Instituto de Aeronautica e Espaco - IAE.

MODAL TEST OF THE BRAZILIAN SATELLITE LAUNCHER (VLS) CONFIGURATION BURN-OUT OF THE FIRST STAGE c15

R. L. R. Carmona, R. Pirk, D. D. daSilveira, D. J. Strafacci, and E. Barros *In* Israel Society of Aeronautics and Astronautics, The 33rd Israel Annual Conference on Aviation and Astronautics 25 Feb. 1993 p 196-202 (For primary document see N94-24241 06-01)

Copyright Avail: Issuing Activity (Israel Society of Aeronautics and Astronautics, c/o Faculty of Engineering, Tel-Aviv Univ., Ramat Aviv 69978, Israel)

A modal survey was performed on the Brazilian Satellite Launcher Vehicle, in four different configurations, to validate the theoretical finite element model. This paper describes the methodology and related techniques used in the experimental modal analysis, namely the burn-out of the first stage. ISA

N94-24258 Technion - Israel Inst. of Tech., Haifa. Faculty of Aerospace Engineering.

SATELLITE AUTONOMOUS NAVIGATION AND ORBIT DETERMINATION USING MAGNETOMETERS c13

G. Shorshi and Itzhack Y. Bar-Itzhack *In* Israel Society of Aeronautics and Astronautics, The 33rd Israel Annual Conference on Aviation and Astronautics 25 Feb. 1993 p 203-212 (For primary document see N94-24241 06-01)

Copyright Avail: Issuing Activity (Israel Society of Aeronautics and Astronautics, c/o Faculty of Engineering, Tel-Aviv Univ., Ramat Aviv 69978, Israel)

This paper presents near earth (less than 1000 km altitude) satellite autonomous navigation and orbit determination method, using measurements of the earth magnetic field. An orbit state vector comprised of six Keplerian elements enables the estimation of the instantaneous orbital elements by a relatively simple extended Kalman filter algorithm. The satellite position and velocity are computed as a function of the estimated orbital elements. The basic algorithm uses a 'measurement' of the magnetic field magnitude. Consequently, this algorithm is independent of altitude information. Simulation tests yielded an accurate Keplerian element estimation and a few kilometers of position estimation error. More complicated algorithms, which estimate drag and/or utilize altitude information, were tested. The basic algorithm was successfully applied to Earth Radiation Budget Satellite (ERBS) real data, and a modified version of this algorithm was applied to Gamma Ray Observatory (GRO) magnetometer readings to yield orbital elements, position, and velocity estimation. In both cases of real satellite navigation, the position was estimated within a few tens of kilometers. ISA

N94-24259 Israel Aircraft Industries Ltd., Ben-Gurion Airport. LAHAV Engineering Dept.

REPAIR OF CRACKED ALUMINUM AIRCRAFT STRUCTURE WITH COMPOSITE PATCHES c05

N. Sasson, A. Simon, H. Leibovich (Israel Aircraft Industries Ltd., Tashan.), and A. K. Green (Israel Aircraft Industries Ltd., Tashan.) *In* Israel Society of Aeronautics and Astronautics, The 33rd Israel Annual Conference on Aviation and Astronautics 25 Feb. 1993 p 213-224 (For primary document see N94-24241 06-01)

Copyright Avail: Issuing Activity (Israel Society of Aeronautics and Astronautics, c/o Faculty of Engineering, Tel-Aviv Univ., Ramat Aviv 69978, Israel)

The concept of repairing cracked aluminum aircraft structures with composite patches was investigated both analytically and experimentally. Coupon tests provided basic mechanical properties of composite patches obtained using a repair procedure. A new surface treatment for bonding patches was developed and optimized. The damage repair process was substantiated by element and beam testing. Crack growth predictions were made using analytical stress intensity factors for the patched structure, and excellent correlation was obtained between observed and predicted values. Patches were very effective in reducing the crack growth rate. Cracks of unpatched element specimens which propagated to failure during random spectrum fatigue loading survived without failure for much longer lifetimes (approximately 3.5 times) under all tested environmental conditions. The process was substantiated by repairing and testing a defective beam element. ISA

N94-24260 Israel Aircraft Industries Ltd., Ben-Gurion Airport.

POST BUCKLING BEHAVIOUR OF STIFFENED COMPOSITE PANELS LOADED IN CYCLIC COMPRESSION AND SHEAR **c39**

A. Segal, Y. Frostig, D. Shalev, T. Weller (Technion - Israel Inst. of Tech., Haifa.), and Y. Sheinman (Technion - Israel Inst. of Tech., Haifa.) *In* Israel Society of Aeronautics and Astronautics, The 33rd Israel Annual Conference on Aviation and Astronautics 25 Feb. 1993 p 225-236 (For primary document see N94-24241 06-01)

Copyright Avail: Issuing Activity (Israel Society of Aeronautics and Astronautics, c/o Faculty of Engineering, Tel-Aviv Univ., Ramat Aviv 69978, Israel)

This paper presents the summary of a multiphase experimental - analytical study of the post-buckling mechanical behavior of a graphite/epoxy integrally stiffened panel. The first phase of the study included cyclic compression tests in the post-buckling regime of flat panels stiffened by either 'I' or 'J' shaped stiffeners. Static residual strength of the panels after 250,000 cycles was greater than the reference strength; however, some stiffness loss was observed. A series of tests of individual stiffeners, identical to those in the panels, was also carried out and the results showed the same trends as had been observed in the panels. There were no cases of early failure during the cyclic tests. The second phase included an experimental study of the post-buckling behavior of cylindrical panels integrally stiffened in the axial and transverse directions. Panels were tested in cyclic compression, cyclic torsion, and in combinations of both. The panels were stressed through 40,000 cycles, damage was inflicted, and an additional 40,000 cycles were imposed. No damage development was observed. The third phase of the study included an analytical effort for the development of a computer code, PBCOMP, for the buckling and post-buckling analysis of stiffened laminated flat and curved panels. The results of this study clearly show a great potential for the safe use of stiffened graphite/epoxy panels in aircraft structures. ISA

N94-24261 Israel Aircraft Industries Ltd., Tashan.

DEVELOPMENT OF A DAMAGE TOLERANCE TOOL TO ANALYZE MULTIPLE-SITE DAMAGE IN AIRCRAFT STRUCTURE **c05**

A. Brot and A. Nathan *In* Israel Society of Aeronautics and Astronautics, The 33rd Israel Annual Conference on Aviation and Astronautics 25 Feb. 1993 p 237-245 (For primary document see N94-24241 06-01)

Copyright Avail: Issuing Activity (Israel Society of Aeronautics and Astronautics, c/o Faculty of Engineering, Tel-Aviv Univ., Ramat Aviv 69978, Israel)

A multiple site damage (MSD) analytical model is presented that predicts the crack growth behavior of a series of cracks at a row of open holes. A coupon test program is described that serves to verify the accuracy of the analytical model. For both equal and unequal sized initial cracks, the analysis predicted lives that were 10-14% longer than the average test result. The results also show that, if MSD effects were to be neglected, a non-conservative error of nearly 100% would result. The results of a parametric study are presented that demonstrate when MSD effects are most significant. ISA

N94-24262 Israel Aircraft Industries Ltd., Tashan.

COMPUTER BASED EXPERT SYSTEM FOR BATTLE DAMAGE REPAIR OF COMPOSITE STRUCTURES **c61**

S. Gali, Z. Karuchro, D. Naor, I. Kressel, H. Lebovitz, J. Baron (Israeli Air Force, Zahal.), and J. Gerrassy (Israeli Air Force, Zahal.) *In* Israel Society of Aeronautics and Astronautics, The 33rd Israel Annual Conference on Aviation and Astronautics 25 Feb. 1993 p 246-250 (For primary document see N94-24241 06-01)

Copyright Avail: Issuing Activity (Israel Society of Aeronautics and Astronautics, c/o Faculty of Engineering, Tel-Aviv Univ., Ramat Aviv 69978, Israel)

The computerized system, REPCOMP, developed for damage repair of composite structures, is an expert system for the design of damage repair. REPCOMP provides detailed repair instructions and drawings, taking into consideration strength and stiffness requirements as well as aerodynamics, weight, and other design considerations. The REPCOMP expert system is being developed for the two major paths in damage repair of composite structures, which are: permanent damage repair, suitable for long-term use in civil and military aircraft, and A/C battle damage repair (ABDR), suitable for field repair of military aircraft during battle. REPCOMP operates on a portable computer (pc), using the Microsoft Windows graphical environment. It is an independent system and can be used in any field repair base. Currently the program handles the ABDR path. ISA

N94-24263 Eidgenoessische Technische Hochschule, Zurich (Switzerland). Measurement and Control Laboratory.

A MIXED MAP/VARIABLE STRUCTURE OBSERVER FOR TARGET TRACKING **c63**

S. A. R. Hepner, Luca L. Bagnaschi, and H. P. Geering *In* Israel Society of Aeronautics and Astronautics, The 33rd Israel Annual Conference on Aviation and Astronautics 25 Feb. 1993 p 251-262 (For primary document see N94-24241 06-01)

Copyright Avail: Issuing Activity (Israel Society of Aeronautics and Astronautics, c/o Faculty of Engineering, Tel-Aviv Univ., Ramat Aviv 69978, Israel)

Simultaneous state and input estimation is often mandatory in control systems with output feedback in the presence of unknown, systematic input signals. Guidance loops are a typical example for such systems. It has been shown in the literature that state and input estimation can be performed by switched observers for processes that satisfy a certain matching condition. There are, however, two major difficulties associated with this result: the matching condition is satisfied by only a few systems of practical importance, and the extension of the switched observer concept to the case of measurements which are corrupted by stochastic measurement noise is still an open question. In this paper, both issues are addressed. The stability of switched observers is proved for a larger class of deterministic systems. Subsequently, a stochastic state and input observer is derived that handles measurements with additive Gaussian distributed noise. This result merges the concepts of switched observers and covariance matching. The new observer is applied to an example of target maneuver estimation in a planar intercept scenario. ISA

N94-24264 Technion - Israel Inst. of Tech., Haifa. Faculty of Aerospace Engineering.

DECENTRALIZED AUTONOMOUS ATTITUDE DETERMINATION USING AN INERTIALLY STABILIZED PAYLOAD **c13**

Yaakov Oshman and Michael Isakow *In* Israel Society of Aeronautics and Astronautics, The 33rd Israel Annual Conference on Aviation and Astronautics 25 Feb. 1993 p 263-274 (For primary document see N94-24241 06-01)

Copyright Avail: Issuing Activity (Israel Society of Aeronautics and Astronautics, c/o Faculty of Engineering, Tel-Aviv Univ., Ramat Aviv 69978, Israel)

A novel method is introduced for the autonomous determination of the attitude angles of a mini remotely piloted vehicle (RPV) with an inertially stabilized payload. The method is based on measurements of rate gyros used to inertially stabilize the payload, and other data which are normally available from conventional aircraft-mounted sensors. These measurements are used to drive a decentralized estimation algorithm, which uses the aircraft/payload mathematical models to bound the estimation errors. Exploiting modern multi-processor computer technology, the new estimation algorithm comprises two extended Kalman filters (EKF) working in parallel, and a data fusion algorithm. Real-time simulation tests, incorporating a payload model with real rate gyros mounted on a three-axis flight table, have validated the feasibility of the concept. The presented theoretical and experimental investigation demonstrates that the estimation algorithm is capable of estimating the attitude angles with an estimation error not exceeding one degree, at ouput rates of 13 Hz, thus constituting an efficient and reliable replacement for the conventional vertical gyroscope. ISA

N94-24265 Technion - Israel Inst. of Tech., Haifa. Faculty of Aerospace Engineering.

MAXIMUM LIKELIHOOD MODAL PARAMETER IDENTIFICATION AND REALIZATION OF STOCHASTIC SYSTEMS **c65**

Yaakov Oshman and Tal Mendelboim *In* Israel Society of Aeronautics and Astronautics, The 33rd Israel Annual Conference on Aviation and Astronautics 25 Feb. 1993 p 275-286 (For primary document see N94-24241 06-01)

Copyright Avail: Issuing Activity (Israel Society of Aeronautics and Astronautics, c/o Faculty of Engineering, Tel-Aviv Univ., Ramat Aviv 69978, Israel)

A new maximum likelihood (ML) realization/identification technique is presented. The method is based on using the recently introduced Eigensystem Realization Algorithm (ERA) in combination with a stochastic adaptive filter/fixed-interval smoother. The resulting algorithm, called ML/ERA, is thus capable of estimating a minimal, internally balanced realization for a stochastic system whose process and/or measurement noise covariances are not necessarily known. Belonging to the ML class of algorithms, the new method is consistent and asymptotically efficient under reasonable conditions. Moreover, by using standard statistical testing techniques, the user is able to assess the quality of the resulting estimates during the iterative estimation process. A numerical investigation of the performance of the new algorithm has shown a vast improvement over the performance of the original, unaugmented ERA. In cases where the ERA could not determine the system order because the data was completely masked by noise, the ML/ERA algorithm was able to identify the order and realize an accurate mathematical model of the system. Numerical examples, demonstrating the performance of the new algorithm, are included in the paper. ISA

N94-24266 Israel Aircraft Industries Ltd., Tashan.
PILOT EVALUATION SYSTEM **c53**
Y. Shub *In* Israel Society of Aeronautics and Astronautics, The 33rd Israel Annual Conference on Aviation and Astronautics 25 Feb. 1993 p 287-296 (For primary document see N94-24241 06-01)
Copyright Avail: Issuing Activity (Israel Society of Aeronautics and Astronautics, c/o Faculty of Engineering, Tel-Aviv Univ., Ramat Aviv 69978, Israel)

The Pilot Evaluation System (PES) is a fixed-based, self-contained and autonomous system, designed for the screening of candidates for pilot training and the evaluation of candidates' chances for success as operational pilots. The PES evaluates and analyzes the performance of the candidate in simulated flight-like conditions. The skills evaluated by the PES are correlated with those needed for the successful completion of flight training. The PES was designed and developed at Israel Aircraft Industries (IAI)-TASHAN by a group of experts consisting of senior fighter pilots, psychologists, physicians, engineers, and flight instructors. The measurement of performance under intense workload serves as a basis for the prediction of future pilots' abilities. In the PES, workload is defined as the combination of loads imposed on subjects by a combination of tasks in a given environment. Some air forces have acquired a PES version for their own use, and they are presently validating its performance. As the data are clients' property, they cannot be presented in this paper. ISA

N94-24267 Technion - Israel Inst. of Tech., Haifa. Faculty of Aerospace Engineering.
FAILURE-PROOF ESTIMATION UNDER CONDITIONS OF LACK OF INFORMATION **c38**
Alexander Vul *In* Israel Society of Aeronautics and Astronautics, The 33rd Israel Annual Conference on Aviation and Astronautics 25 Feb. 1993 p 297-302 (For primary document see N94-24241 06-01)
Copyright Avail: Issuing Activity (Israel Society of Aeronautics and Astronautics, c/o Faculty of Engineering, Tel-Aviv Univ., Ramat Aviv 69978, Israel)

This paper deals with some aspects of failure detection and isolation (FDI) theory and its implementation. Namely, the problems of failure distinction and compensation are investigated. The problem of failure-proof estimation under the criterion of fastest treatment of the occurred failure is solved. Some concrete algorithms of failure distinction and compensation are developed and results of their investigation by numerical simulations are shown. These algorithms can be useful in designing a failure-proof system. ISA

N94-24268 Israeli Air Force, Zahal.
COMPARISON OF C.T.S. BASED PREDICTION OF STORE TRAJECTORY WITH FLIGHT TEST DATA **c05**
E. Goldberg, A. Feldhuhn, Ts. Cohen, S. Fledel (Israel Aircraft Industries Ltd., Tashan.), M. Zilberman, M. Shay (Israel Aircraft Industries Ltd., Lod.), and I. Shruster (Israel Aircraft Industries Ltd., Lod.) *In* Israel Society of Aeronautics and Astronautics, The 33rd Israel Annual Conference on Aviation and Astronautics 25 Feb. 1993 p 303-309 (For primary document see N94-24241 06-01)
Copyright Avail: Issuing Activity (Israel Society of Aeronautics and Astronautics, c/o Faculty of Engineering, Tel-Aviv Univ., Ramat Aviv 69978, Israel)

The Captive Trajectory System (CTS) is used primarily for prediction of store separation trajectories in close proximity to the parent aircraft. The system serves as a main tool in store separation analysis. Thanks to the high level of correlation between CTS results and flight test results, it has been suggested that the use of the CTS be extended to predicting the interference of the aircraft with the store and the effect on its ballistic range. In a two year effort, several stores were analyzed by means of the CTS predictions. The article presents a comparison between the CTS based prediction and flight test results for store range and trajectory. This comparison proves the adequacy of the prediction of aircraft effects on the store, as well as providing a good numerical prediction of the impact point. In addition, the flight test results verify the simulation's prediction that Mach number and store initial location (aircraft station and position on multiple rack) have a significant effect on aircraft interference with the store and on the ground impact point. ISA

N94-24269 Israel Aircraft Industries Ltd., Tashan.
ATTACHMENT METHODS IN COMPOSITE JOINTS - ANALYSIS OF TEST RESULTS BY CONTROLLED EXPERIMENTS METHOD **c24**
T. Gottesman, D. Peled, N. Sela, and L. Solomon *In* Israel Society of Aeronautics and Astronautics, The 33rd Israel Annual Conference on Aviation and Astronautics 25 Feb. 1993 p 310-320 (For primary document see N94-24241 06-01)
Copyright Avail: Issuing Activity (Israel Society of Aeronautics and Astronautics, c/o Faculty of Engineering, Tel-Aviv Univ., Ramat Aviv 69978, Israel)

Tests of composite cold-bonded and wet lay-up joints were performed for various loadings. The test results were completed by linear extrapolation and analyzed statistically by the controlled experiments method. Principal parameters concerning mechanical performance were identified and, accordingly, design improvements were recommended. ISA

N94-24270 Israel Aircraft Industries Ltd., Lod. BEDEK Aviation Division.
S-2E TRACKER MARITIME PATROL AIRCRAFT RE-ENGINE AND SYSTEM UPGRADE PROGRAM **c07**
Ilan Berlowitz, Meir Zeierman, and Scott Martin (Marsh Aviation Co., Scottsdale, AZ.) *In* Israel Society of Aeronautics and Astronautics, The 33rd Israel Annual Conference on Aviation and Astronautics 25 Feb. 1993 p 321-332 (For primary document see N94-24241 06-01)
Copyright Avail: Issuing Activity (Israel Society of Aeronautics and Astronautics, c/o Faculty of Engineering, Tel-Aviv Univ., Ramat Aviv 69978, Israel)

Due to its strong construction, resistance to the marine environment, and projected service life, the S-2E Tracker aircraft was chosen for its operational performance to be extended through re-engining, systems upgrading, and integration of new avionics. The aircraft was originally designed for carrier based antisubmarine missions and is ideally suited for efficient and effective maritime patrol. With the installation of rapid-response, 1645 horsepower, Garrett TPE331-15AW turbo-propeller engines and five blade composite reversible propellers, the S-2E/turbine becomes a high performance aircraft with a greater climb rate and 50 percent reduction in fuel consumption over the original S-2E piston aircraft. Intensive flight tests have proven a dramatic increase in mission capability with increased area coverage and flight safety improvements. Israel Aircraft Industries (IAI) is conducting a program to retrofit S-2E Tracker aircraft with Federal Aviation Administration (FAA) and MIL-STD certified, state-of-the-art engines, avionics, and sub-systems. ISA

N94-24271 Israel Aircraft Industries Ltd., Yehud. MBT - Systems and Space Technology.
REACTIVE THRUST CRUISE FOR A GEOSYNCHRONOUS SATELLITE WITH MINIMUM FUEL CONSUMPTION **c18**
Marcel Sidi *In* Israel Society of Aeronautics and Astronautics, The 33rd Israel Annual Conference on Aviation and Astronautics 25 Feb. 1993 p 333-338 (For primary document see N94-24241 06-01)
Copyright Avail: Issuing Activity (Israel Society of Aeronautics and Astronautics, c/o Faculty of Engineering, Tel-Aviv Univ., Ramat Aviv 69978, Israel)

A simple control concept utilizing product of inertia is used to provide active nutation control of a reactive thrust control system of a geosynchronous momentum-based satellite. The reactive thrust control system itself is immune to sensor noise and thus prevents unnecessary thrust firings. Any nutation excitation is damped in a small number of nutational periods, with no fuel consumption. ISA

N94-24272 Israel Aircraft Industries Ltd., Yehud. System and Space Technology.
MOMENTUM MANAGEMENT AND TORQUE DISTRIBUTION c18
Ruth Azor *In* Israel Society of Aeronautics and Astronautics, The 33rd Israel Annual Conference on Aviation and Astronautics 25 Feb. 1993 p 339-347 (For primary document see N94-24241 06-01)
Copyright Avail: Issuing Activity (Israel Society of Aeronautics and Astronautics, c/o Faculty of Engineering, Tel-Aviv Univ., Ramat Aviv 69978, Israel)

In a satellite with four reaction wheels, it is necessary to find a momentum management law among the wheels. The method presented here is based on the minimal norm of the wheel rates, for any configuration of the wheels in the X-Y plane. ISA

N94-24273 Technion - Israel Inst. of Tech., Haifa. Faculty of Aerospace Engineering.
MODELLING THE IGNITION OF BORON/TITANIUM PARTICLES c25
Ilan Ibu and Alon Gany *In* Israel Society of Aeronautics and Astronautics, The 33rd Israel Annual Conference on Aviation and Astronautics 25 Feb. 1993 p 348-358 (For primary document see N94-24241 06-01)
Copyright Avail: Issuing Activity (Israel Society of Aeronautics and Astronautics, c/o Faculty of Engineering, Tel-Aviv Univ., Ramat Aviv 69978, Israel)

This paper addresses the ignition of porous composite boron-titanium particles. The model takes into account the exothermic reaction between boron and titanium particles within the composite particle. A possible reaction enhancement between boron and titanium sub-particles due to the sintering process has been considered. Calculations performed by using the present model showed a substantial shortening of the ignition process by adding some titanium to pure boron particles. Calculations using two models of boron oxidation reported in the literature were performed. A sintering model has been developed, taking into account the principal mechanisms of material transport, i.e., grain-boundary and volume dispersion. The theoretical results revealed a significant positive effect of internal condensed-phase reactions between B and Ti on boron particle ignition. ISA

N94-24274 Technion - Israel Inst. of Tech., Haifa. Faculty of Aerospace Engineering.
ON THE STABILITY OF THE PROCESS OF FORMATION OF COMBUSTION GENERATED PARTICLES BY COAGULATION AND SIMULTANEOUS SHRINKAGE DUE TO PARTICLE OXIDATION c25
Y. Tambour and S. Khosid *In* Israel Society of Aeronautics and Astronautics, The 33rd Israel Annual Conference on Aviation and Astronautics 25 Feb. 1993 p 359-368 Sponsored in part by Center for Absorption in Science, Ministry of Immigrant Absorption, State of Israel (For primary document see N94-24241 06-01)
Copyright Avail: Issuing Activity (Israel Society of Aeronautics and Astronautics, c/o Faculty of Engineering, Tel-Aviv Univ., Ramat Aviv 69978, Israel)

A mathematical stability analysis is conducted to define the domain of operating conditions under which a combustion generated particle will be formed by coagulation of incipient particles (or clusters). Two opposing concurrent mechanisms are considered, namely: (1) growth by coagulation, and (2) simultaneous shrinkage due to sublimation or oxidation of the particle. These two mechanisms are incorporated in the discrete coagulation equations. Then, summations are carried out over all discrete sizes, once for the total number of incipient particles and once for the total mass. A particle is formed under conditions of growth in mass and a decrease in total number of incipient particles. The stability analysis is based on Liapunov's theorem. Various mathematical forms of collisional kernels are analyzed. Our results indicate that only enhanced collision rates (e.g., kernels of the form of beta(sub ij) is approximately i.j) will lead to an unstable rapid growth of particles. This observation is in agreement with the conclusions drawn by Harris et al., who employed collisional enhancement factors to fit their theoretical soot size distribution calculations to the data on soot particles obtained in a premixed ethylene flame. ISA

N94-24275 Technion - Israel Inst. of Tech., Haifa. Faculty of Aerospace Engineering.
EXPERIMENTAL INVESTIGATION OF IGNITION OF BORON/TITANIUM COMPOSITE PARTICLES c25
V. Rosenband and A. Gany *In* Israel Society of Aeronautics and Astronautics, The 33rd Israel Annual Conference on Aviation and Astronautics 25 Feb. 1993 p 369-373 Sponsored by Wolfson Family Charitable Trust Program for the Absorption of Immigrant Scientists; Center for Absorption in Science, Ministry of Immigrant Absorption, State of Israel; and Ministry of Science and Technology, State of Israel (For primary document see N94-24241 06-01)
Copyright Avail: Issuing Activity (Israel Society of Aeronautics and Astronautics, c/o Faculty of Engineering, Tel-Aviv Univ., Ramat Aviv 69978, Israel)

The ignition and combustion of special composite titanium/boron particles were studied experimentally. It is assumed that a small addition of titanium may result in appreciable enhancement of the boron ignition and combustion due to exothermic chemical interactions of titanium with oxygen and boron. The experiments were carried out in a flat flame burner. Composite B/Ti particles, 100-150 microns in size containing 13 wt. percent of titanium were injected into the flat flame products of different oxygen content. Noticeable intensification of the ignition and combustion of composite boron/titanium particles in comparison with similar boron particles was detected. ISA

N94-24276 Technion - Israel Inst. of Tech., Haifa. Faculty of Aerospace Engineering.
MEAN STRESS MODELS FOR LOW CYCLE FATIGUE OF A NICKEL-BASE SUPERALLOY c39
Daining Fang and Avraham Berkovitz *In* Israel Society of Aeronautics and Astronautics, The 33rd Israel Annual Conference on Aviation and Astronautics 25 Feb. 1993 p 374-386 Supported in part by Rolls-Royce Ltd., Derby, England (For primary document see N94-24241 06-01)
Copyright Avail: Issuing Activity (Israel Society of Aeronautics and Astronautics, c/o Faculty of Engineering, Tel-Aviv Univ., Ramat Aviv 69978, Israel)

The aim of this study was to relate observed Low Cycle Fatigue responses under asymmetric loading to mean-stress effects on the cyclic behavior and fatigue life of nickel-base Incoloy 901 superalloy at room temperature. Based on experimental data, a mean-stress-relaxation of mean-stress on the total strain range and on cyclic plasticity. It was found that cyclic softening and mean-stress relaxation began when plastic strain started to develop, and increased in importance with increasing strain range. Both depended on the plastic strain range rather than on monotonic plastic deformation. For any given strain ratio, there was a value of strain range corresponding to peak mean stress sustained. Beyond this strain range, mean stress relaxation began. A mean-stress strength constant, representing the apex on the sigma(sub m) axis of the Goodman diagram, was introduced in order to modify the Goodman criterion, resulting in a modified strain-life relation. Both the mean-stress-relaxation model and the strain-life model were evaluated against LCF testing data. ISA

N94-24277 Ottawa Univ. (Ontario). Faculty of Engineering.
FRACTURE KINETICS ANALYSIS OF EMPIRICAL AND SEMI-EMPIRICAL CORROSION FATIGUE RELATIONS c39
K. Krausz and A. S. Krausz *In* Israel Society of Aeronautics and Astronautics, The 33rd Israel Annual Conference on Aviation and Astronautics 25 Feb. 1993 p 387-401 Sponsored by the Natural Sciences and Engineering Research Council of Canada (For primary document see N94-24241 06-01)
Copyright Avail: Issuing Activity (Israel Society of Aeronautics and Astronautics, c/o Faculty of Engineering, Tel-Aviv Univ., Ramat Aviv 69978, Israel)

The breakthrough provided by the recognition that the fracture mechanics quantity, delta K controls fatigue was of immense importance. The empirical Paris-type equations da/dn = C((delta K)/(delta K(sub 0)))(exp n) were used extensively for a long time and provide much information from experience. More than 70 of the Paris-type empirical relationships were developed. The empirical equations are more or less arbitrarily imposed on the experimental results to bring them into formal agreement with the measured data. Consequently, these are actual curve fitting equations - alternatives to the tabulated test data for which they were designed. In contrast to this, fracture kinetics descriptions are rigorously derived from basic principles of general validity. The fundamental processes of corrosion fatigue are a complex combination of corrosion and embrittlement chemical reactions, diffusion, and crack growth steps. It is of critical significance that the fracture kinetics description of crack growth includes the effects of the microstructure in quantitative expression. The validity of the fracture kinetics theory was demonstrated in extensive investigations; it was shown that for a large range of materials and imposed conditions, fatigue can be represented very well by the fracture kinetics constitutive law. To define the empirical and semi-empirical relations with microstructural and macroscopic quantities, three basic types are represented. ISA

N94-24278 Israel Aircraft Industries Ltd., Tashan.

EVALUATION OF THE FRACTURE RESISTANCE AND DURABILITY OF ADHESIVE BONDED JOINTS **c39**

H. Leibovich and V. Weissberg *In* Israel Society of Aeronautics and Astronautics, The 33rd Israel Annual Conference on Aviation and Astronautics 25 Feb. 1993 p 402-408 (For primary document see N94-24241 06-01)

Copyright Avail: Issuing Activity (Israel Society of Aeronautics and Astronautics, c/o Faculty of Engineering, Tel-Aviv Univ., Ramat Aviv 69978, Israel)

A methodology to evaluate the fracture resistance and durability of adhesive bonded joints is presented. This method fills the gap between simple comparative tests such as Lap Shear ASTM D1002, Wedge Crack or Floating Roller Peel (Bell Peel) ASTM D3167 and quantitative data for design calculations. The analytical basis of the method consists of recently developed relationships between the stress intensity factor (SIF) and the stress concentration factor (SCF) which is unique for adhesive bonded joints for any bonded attachment geometry. The Mixed Mode Flexure (MMF) test specimen was found to be appropriate to the analytical method. MMF is also sensitive to interface properties and easily fabricated and tested. Experimentally, four different surface treatments were evaluated using the MMF test specimens. Testing was conducted at room temperature and at 70 C after exposure to 60 C, 95 percent RH (relative humidity). Lap Shear and Bell Peel test specimens were also tested and compared with the new method. The MMF test results showed the following outstanding advantages: (1) quantitative design data are available in contrast with Lab Shear and Bell Peel test specimens; (2) both modes, shear and tension, could be evaluated at the same time; (3) the MMF testing provides realistic geometry and mode of loading as in actual structures; and (4) the newly developed methodology proved to be sensitive for evaluation of surface preparation and durability for bonding. ISA

N94-24279 Technion - Israel Inst. of Tech., Haifa. Department of Civil Engineering.

VIBRATIONS OF VARIABLE CROSS SECTION TIMOSHENKO BEAMS **c39**

Moshe Eisenberger *In* Israel Society of Aeronautics and Astronautics, The 33rd Israel Annual Conference on Aviation and Astronautics 25 Feb. 1993 p 409-412 (For primary document see N94-24241 06-01)

Copyright Avail: Issuing Activity (Israel Society of Aeronautics and Astronautics, c/o Faculty of Engineering, Tel-Aviv Univ., Ramat Aviv 69978, Israel)

The Timoshenko beam model incorporates the effect of shear deformations and rotary inertia in the vibration response of beams. For constant cross section beams it was shown that the effect is dependent on the aspect ratio of the beams, and for beams with large ratios, the effect is small. Exact vibration frequencies for variable cross section beams are found using the dynamic stiffness matrix approach. The stiffness matrix is frequency dependent, and the natural frequencies are those that cause the matrix to become singular. Examples are given and compared with known results of beams with various taper ratios. ISA

N94-24280 Technion - Israel Inst. of Tech., Haifa. Faculty of Aerospace Engineering.

GLOBAL DYNAMIC STABILITY OF A SHALLOW ARCH BY POINCARE-LIKE SIMPLE CELL MAPPING **c39**

J. Levitas, J. Singer, and T. Weller *In* Israel Society of Aeronautics and Astronautics, The 33rd Israel Annual Conference on Aviation and Astronautics 25 Feb. 1993 p 413-420 (For primary document see N94-24241 06-01)

Copyright Avail: Issuing Activity (Israel Society of Aeronautics and Astronautics, c/o Faculty of Engineering, Tel-Aviv Univ., Ramat Aviv 69978, Israel)

Global dynamic stability of a shallow elastic arch subject to a distributed constant load is studied by Poincare-like Simple Cell Mapping. The dynamic behavior due to displacement and velocity disturbances imposed on the arch is studied. The dynamic model has two modes, one symmetric and one antisymmetric. The global structure of the domains of attraction of the modes is determined and presented. ISA

N94-24281 Technion - Israel Inst. of Tech., Haifa. Faculty of Agricultural Engineering.

INVERSE DYNAMICS OF A RIGID ROD SYSTEM AS A SIMPLIFIED MODEL OF FLEXIBLE BEAM **c39**

D. Rubinstein, N. Galili, and A. Libai *In* Israel Society of Aeronautics and Astronautics, The 33rd Israel Annual Conference on Aviation and Astronautics 25 Feb. 1993 p 421-429 (For primary document see N94-24241 06-01)

Copyright Avail: Issuing Activity (Israel Society of Aeronautics and Astronautics, c/o Faculty of Engineering, Tel-Aviv Univ., Ramat Aviv 69978, Israel)

The problem of inverse dynamics of a system of rods and a flexible beam was discussed and analyzed. The role of boundary and initial conditions was examined by analysis of the linear problem of an Euler beam. It was demonstrated that the solution of an Euler beam for a fully inverse dynamics (where all six constraints were imposed on one end of the beam) depends solely on the boundary constraints and does not rely on any initial conditions. In addition, the boundary functions in this case should be analytic, with an infinite number of derivatives. ISA

N94-24282 Technion - Israel Inst. of Tech., Haifa. Faculty of Aerospace Engineering.

TRANSIENT PHENOMENA IN LAMINAR SPRAY COMBUSTION **c25**

J. B. Greenberg and I. Shpilberg *In* Israel Society of Aeronautics and Astronautics, The 33rd Israel Annual Conference on Aviation and Astronautics 25 Feb. 1993 p 430-438 (For primary document see N94-24241 06-01)

Copyright Avail: Issuing Activity (Israel Society of Aeronautics and Astronautics, c/o Faculty of Engineering, Tel-Aviv Univ., Ramat Aviv 69978, Israel)

The evolution of a Burke-Schumann type of spray diffusion flame is examined. Full representation of transport, spray and combustion is allowed through use of nonunity Lewis numbers for the gaseous components, local pointwise multisize droplet distribution for the spray, and a finite chemical Damkohler number based on a single global chemical reaction. It is found that under certain operating conditions the transient behavior of the spray flame exhibits the phenomenon of flame separation, even though a steady state is ultimately attained. The local polydispersity of the spray is shown to be one of the factors affecting the appearance of the separated flamelet. ISA

N94-24283 Technion - Israel Inst. of Tech., Haifa. Faculty of Applied Mathematics.

EFFECT OF INITIAL DROPLET-SIZE DISTRIBUTIONS ON FUEL-VAPOR PROFILES IN A SHEAR-LAYER FLOW **c34**

D. Katoshevski and Y. Tambour *In* Israel Society of Aeronautics and Astronautics, The 33rd Israel Annual Conference on Aviation and Astronautics 439-448 (SEE N94-24241 06-01) 25 Feb. 1993 (For primary document see N94-24241 06-01)

Copyright Avail: Issuing Activity (Israel Society of Aeronautics and Astronautics, c/o Faculty of Engineering, Tel-Aviv Univ., Ramat Aviv 69978, Israel)

The evaporation of a multisize (polydisperse) liquid fuel spray in a shear-layer between two parallel, unidirectional streams of unequal velocity was analyzed. The analysis is also applicable for a shear-layer between two radially spreading streams which share the same axis of symmetry. Similarity solutions are presented for the evolution in droplet size distributions across the shear-layer, and the effects of various initial droplet size distributions on the profiles of fuel-vapor concentrations are examined. A qualitative comparison between the present results for a typical computed total mass distribution of the liquid-phase and experimental results of the intensity of light scattering from droplets as reported by Lazaro and Lasheras shows similarity between the two profiles. This supports the assumptions and boundary-conditions employed in the present theoretical study. The general behavior of the theoretical SMD (Sauter Mean Diameter) distribution of the spray across the shear layer also compares well with the reported experimental results of Lazaro and Lasheras. ISA

N94-24284 Technion - Israel Inst. of Tech., Haifa. Faculty of Aerospace Engineering.

MULTIPLE FLAMES IN COUNTERFLOW SPRAY COMBUSTION **c25**

N. Sarig and J. B. Greenberg *In* Israel Society of Aeronautics and Astronautics, The 33rd Israel Annual Conference on Aviation and Astronautics 25 Feb. 1993 p 449-457 (For primary document see N94-24241 06-01)

Copyright Avail: Issuing Activity (Israel Society of Aeronautics and Astronautics, c/o Faculty of Engineering, Tel-Aviv Univ., Ramat Aviv 69978, Israel)

The formation of multiple flames in counterflow premixed spray combustion is studied in a new theoretical investigation. The fuel is introduced into the system in the form of a spray and vapor mixed homogeneously with oxygen and a diluent. Calculated results point to the possibility of the existence of three different modes of combustion depending on the ratio between fuel vapor to oxygen mass fractions in the injected stream and the vaporization Damkohler number of the spray. ISA

N94-24285 Aero-Design and Development Ltd., Rehovoth (Israel).

AERODYNAMIC MODELS FOR PERFORMANCE CALCULATIONS OF MODERN TECHNOLOGY PROPELLERS **c02**

I. Weissberg, G. Engel, and A. Rosen (Technion - Israel Inst. of Tech., Haifa.) *In* Israel Society of Aeronautics and Astronautics, The 33rd Israel Annual Conference on Aviation and Astronautics 25 Feb. 1993 p 458-468 (For primary document see N94-24241 06-01)

Copyright Avail: Issuing Activity (Israel Society of Aeronautics and Astronautics, c/o Faculty of Engineering, Tel-Aviv Univ., Ramat Aviv 69978, Israel)

Three numerical models for predicting the aerodynamic performance of Modern Technology Propellers (MTP) are described. The models include a Blade-Element/Momentum model, a Lifting Line model, and a VLM (Vortex Lattice Method) model. These three models are simple and characterized by numerical efficiency. The first two models use two dimensional tabulated airfoil data to account for the compressibility, viscosity, and nonlinear airfoil characteristics. The models also include corrections for various effects such as tip effect, sweep, and induced tangential velocity. The results of the three models are compared with experimental results for two MTP designs, one with straight blades and the other with swept ones. The results are explained and discussed. ISA

N94-24286 Technion - Israel Inst. of Tech., Haifa. Faculty of Aerospace Engineering.

THE INFLUENCE OF ELASTIC PITCH VARIATIONS ON HELICOPTER FLIGHT MECHANICS **c05**

Z. Beigleman and A. Rosen *In* Israel Society of Aeronautics and Astronautics, The 33rd Israel Annual Conference on Aviation and Astronautics 25 Feb. 1993 p 469-481 (For primary document see N94-24241 06-01)

Copyright Avail: Issuing Activity (Israel Society of Aeronautics and Astronautics, c/o Faculty of Engineering, Tel-Aviv Univ., Ramat Aviv 69978, Israel)

Due to the loads that act along a helicopter blade, it experiences elastic pitch variations. These elastic pitch variations are the result of elastic torsion along the blade and the flexibility of the pitch control system. The use of a simplified model, describing these elastic pitch variations, which is appropriate for flight mechanics analyses, is presented. Parameters which determine the elastic pitch variations include: the blade torsional stiffness, cross sectional locations of the center of mass and aerodynamic center, the airfoil aerodynamic moment coefficient, pitch control system flexibility, and damping along the blade and of the control system. The influence of such parameters on trim position, stability and control derivatives, stability roots, and time response is presented. ISA

N94-24287 Technion - Israel Inst. of Tech., Haifa. Faculty of Aerospace Engineering.

CONTINUOUS GUST RESPONSE AND SENSITIVITY DERIVATIVES USING STATE-SPACE MODELS **c08**

Arie Zole and Mordechay Karpel *In* Israel Society of Aeronautics and Astronautics, The 33rd Israel Annual Conference on Aviation and Astronautics 25 Feb. 1993 p 482-492 (For primary document see N94-24241 06-01)

Copyright Avail: Issuing Activity (Israel Society of Aeronautics and Astronautics, c/o Faculty of Engineering, Tel-Aviv Univ., Ramat Aviv 69978, Israel)

The dynamic response to atmospheric turbulence plays an important role in the design of flight vehicles. The presented work is an extension to the work on multidisciplinary optimization of aeroservoelastic systems using reduced-size models. The continuous-gust turbulence and the response parameters are represented in statistical terms by power spectral density (PSD) functions and root mean square (RMS) values. The time domain, state-space optimization model is extended to deal with gust excitation and to produce RMS response of section loads, structural velocities, and accelerations. Recommendations are given for the application of the physically weighted minimum-state aerodynamic approximation technique such that there is no need to increase the (relatively small) number of aerodynamic states beyond those required for stability analysis. The plant states are augmented by gust-filter states in a way that produces a dynamic system excited by white noise at the gust-filter inputs. This representation facilitates direct RMS computations by solving matrix Liapunov equations. Analytical expressions for the sensitivity derivatives of the dynamic matrix with respect to structural and control design variables yield another set of Liapunov equations which can be efficiently solved for many response derivatives. The suggested model is demonstrated to be considerably more efficient than classical frequency-domain models. ISA

N94-24288 Israel Aircraft Industries Ltd., Ben-Gurion Airport.

NONLINEAR ANALYSIS USING A MODAL BASED REDUCTION TECHNIQUE **c39**

D. Shalev and A. Unger *In* Israel Society of Aeronautics and Astronautics, The 33rd Israel Annual Conference on Aviation and Astronautics 25 Feb. 1993 p 493-501 (For primary document see N94-24241 06-01)

Copyright Avail: Issuing Activity (Israel Society of Aeronautics and Astronautics, c/o Faculty of Engineering, Tel-Aviv Univ., Ramat Aviv 69978, Israel)

A solution to nonlinear formulated problems using eigenfunctions computed by a linear free vibration solution is presented. The system of equations is extremely reduced compared with the finite element method. The solution is unique in its formulation as the governing equations represent the problem continuously and do not require an iterational solution over a tangent stiffness. Energy consideration is used and the Ritz method is applied to render the governing equations. The eigenfunctions are computed by a linear finite element code: MSC/NASTRAN. Several numerical examples are presented and compared with examples from the literature. ISA

N94-24289 Ottawa Univ. (Ontario). Faculty of Engineering.

ON THE DEFORMATION KINETICS CONSTITUTIVE LAW OF PLASTIC DEFORMATION: THE RATE EQUATION **c39**

A. S. Krausz and K. Krausz *In* Israel Society of Aeronautics and Astronautics, The 33rd Israel Annual Conference on Aviation and Astronautics 25 Feb. 1993 p 502-510 Sponsored by Natural Sciences and Engineering Research Council of Canada (For primary document see N94-24241 06-01)

Copyright Avail: Issuing Activity (Israel Society of Aeronautics and Astronautics, c/o Faculty of Engineering, Tel-Aviv Univ., Ramat Aviv 69978, Israel)

The extensively used empirical models of plastic deformation, the sinh and power function law relations, are valid only in a limited range and are not suitable for extrapolation. At low stresses, the sinh either overestimates or greatly underestimates the strain rate. The power function relation, being the tangent of the logarithm of strain rate vs. logarithm of stress plot, is a fair approximation near to the inflexion point only. The constitutive law of plastic deformation provides a rigorous expression that describes the behavior of solids under the effects of both the applied stress and the temperature, for the full range of the applied stress. ISA

N94-24923 Federal Aviation Administration, Washington, DC. Office of Aviation Policy and Plans.
GENERAL AVIATION ACTIVITY SURVEY Annual Summary Report, 1992
1992 217 p Limited Reproducibility: More than 20% of this document may be affected by microfiche quality
(Contract DTFA01-93-Y-1021)
(AD-A273284; FAA-APO-93-10) Avail: Issuing Activity (Defense Technical Information Center (DTIC))

The results of the annual General Aviation Activity Survey are presented. The survey is conducted by the FAA to obtain information on the flight activity of the United States registered general aviation aircraft fleet. Breakdowns of active aircraft, annual flight hours, average flight hours and other statistics by manufacturer/model group, aircraft type, state and region of based aircraft, and primary use are included. Also included are fuel consumption, lifetime airframe hours, engine hours, miles flown estimates, estimates of the number of landings, IFR hours flown, and grade of fuel consumed by the general aviation fleet. DTIC

N94-25096*# National Aeronautics and Space Administration. Langley Research Center, Hampton, VA.
NASA LARC WORKSHOP ON GUIDANCE, NAVIGATION, CONTROLS, AND DYNAMICS FOR ATMOSPHERIC FLIGHT, 1993
Carey S. Buttrill, ed. Dec. 1993 565 p Workshop held in Hampton, VA, 18-19 Mar. 1993
(RTOP 505-64-52-01)
(NASA-CP-10127; NAS 1.55:10127) Avail: CASI HC A24/MF A04

This publication is a collection of materials presented at a NASA workshop on guidance, navigation, controls, and dynamics (GNC&D) for atmospheric flight. The workshop was held at the NASA Langley Research Center on March 18-19, 1993. The workshop presentations describe the status of current research in the GNC&D area at Langley over a broad spectrum of research branches. The workshop was organized in eight sessions: overviews, general, controls, military aircraft, dynamics, guidance, systems, and a panel discussion. A highlight of the workshop was the panel discussion which addressed the following issue: 'Direction of guidance, navigation, and controls research to ensure U.S. competitiveness and leadership in aerospace technologies.' For individual titles, see N94-25097 through N94-25115.

N94-25097*# National Aeronautics and Space Administration. Langley Research Center, Hampton, VA.
US GENERAL AVIATION: THE INGREDIENTS FOR A RENAISSANCE. A VISION AND TECHNOLOGY STRATEGY FOR US INDUSTRY, NASA, FAA, UNIVERSITIES
Bruce Holmes *In its* NASA LaRC Workshop on Guidance, Navigation, Controls, and Dynamics for Atmospheric Flight, 1993 Dec. 1993 p 1-53 (For primary document see N94-25096 06-01)
Avail: CASI HC A04/MF A04

General aviation today is a vital component in the nation's air transportation system. It is threatened for survival but has enormous potential for expansion in utility and use. This potential for expansion is fueled by new satellite navigation and communication systems, small computers, flat panel displays, and advanced aerodynamics, materials and manufacturing methods, and propulsion technologies which create opportunities for new levels of environmental and economic acceptability. Expanded general aviation utility and use could have a large impact on the nation's jobs, commerce, industry, airspace capacity, trade balance, and quality of life. This paper presents, in viewgraph form, a general overview of U.S. general aviation. Topics covered include general aviation shipment and billings; airport and general aviation infrastructure; cockpit, airplane, and airspace technologies; market demand; air traffic operations and aviation accidents; fuel efficiency comparisons; and general aviation goals and strategy. CASI

N94-25098*# National Aeronautics and Space Administration. Langley Research Center, Hampton, VA.
FUTURE SPACE TRANSPORTATION SYSTEM ARCHITECTURE AVIONICS REQUIREMENTS **c16**
Howard Stone and Walt Engelund *In its* NASA LaRC Workshop on Guidance, Navigation, Controls, and Dynamics for Atmospheric Flight, 1993 Dec. 1993 p 55-83 (For primary document see N94-25096 06-01)
Avail: CASI HC A03/MF A04

NASA began a multi-center study in January 1993 to examine options for providing the most cost effective space transportation system in the future. The key advanced avionics requirements for these vehicle concepts are envisioned to provide significantly improved operational efficiency and effectiveness. It is very desirable to have adaptive guidance, navigation, and control approaches that will allow launch and return in almost any weather condition. The vehicles must be able to accommodate atmospheric density variations and winds without software changes. The flight operations must become much more autonomous in all flight regimes like an aircraft, and preflight checkout should make use of the onboard systems. When the vehicle returns to the launch site, subsystem health must be known and maintenance tasks scheduled accordingly. Ground testing of most subsystems must be eliminated. Also, the health monitoring system must be designed to enhance the ability to abort the mission significantly and save the crew and the vehicle. The displays and controls must be much less complex than current systems and must significantly reduce pilot work load. It is important to have low power, light weight displays and controls. Rendezvous and docking and all flight phases must have autopilot capability to reduce pilot work load for routine operations and in abort situations. The vehicles must have the demonstrated ability to return to the launch site. Abort from all mission phases can put additional demands on the communications system. Derived from text

N94-25099*# National Aeronautics and Space Administration. Langley Research Center, Hampton, VA.
HIGHLY-RELIABLE FLY-BY-LIGHT/POWER-BY-WIRE TECHNOLOGY **c08**
Felix L. Pitts *In its* NASA LaRC Workshop on Guidance, Navigation, Controls, and Dynamics for Atmospheric Flight, 1993 Dec. 1993 p 85-95 (For primary document see N94-25096 06-01)
Avail: CASI HC A03/MF A04

This paper presents in viewgraph format an overview of the program at NASA Langley Research Center to develop fly-by-light/power-by-wire (FBL/PBW) technology. Benefits of FBL/PBW include intrinsic electromagnetic interference (EMI) immunity and lifetime immunity to signal EMI of optics; simplified certification; the elimination of hydraulics, engine bleed air, and variable speed, constant frequency drive; and weight and volume reduction. The paper summarizes a study on the electromagnetic environmental effects on FBL/PBW systems. The paper concludes with FY 1993 plans. CASI

N94-25100*# National Aeronautics and Space Administration. Langley Research Center, Hampton, VA.
DIFFERENTIAL GPS FOR AIR TRANSPORT: STATUS **c04**
Richard M. Hueschen *In its* NASA LaRC Workshop on Guidance, Navigation, Controls, and Dynamics for Atmospheric Flight, 1993 Dec. 1993 p 97-114 (For primary document see N94-25096 06-01)
Avail: CASI HC A03/MF A04

The presentation presents background on what the Global Navigation Satellite System (GNSS) is, desired target dates for initial GNSS capabilities for aircraft operations, and a description of differential GPS (Global Positioning System). The presentation also presents an overview of joint flight tests conducted by LaRC and Honeywell on an integrated differential GPS/inertial reference unit (IRU) navigation system. The overview describes the system tested and the results of the flight tests. The last item presented is an overview of a current grant with Ohio University from LaRC which has the goal of developing a precision DGPS navigation system based on interferometry techniques. The fundamentals of GPS interferometry are presented and its application to determine attitude and heading and precision positioning are shown. The presentation concludes with the current status of the grant. Derived from text

N94-25101*# National Aeronautics and Space Administration. Langley Research Center, Hampton, VA.
FUTURE DIRECTIONS IN FLIGHT SIMULATION: A USER PERSPECTIVE **c09**
Bruce Jackson *In its* NASA LaRC Workshop on Guidance, Navigation, Controls, and Dynamics for Atmospheric Flight, 1993 Dec. 1993 p 115-135 (For primary document see N94-25096 06-01)
Avail: CASI HC A03/MF A04

Langley Research Center was an early leader in simulation technology, including a special emphasis in space vehicle simulations such as the rendezvous and docking simulator for the Gemini program and the lunar landing simulator used before Apollo. In more recent times, Langley operated the first synergistic six degree of freedom motion platform (the Visual Motion Simulator, or VMS) and developed the first dual-dome air combat simulator, the Differential Maneuvering Simulator (DMS). Each Langley simulator was developed more or less independently from one another with different programming support. At present time, the various simulation cockpits, while supported by the same host computer system, run dissimilar software. The majority of recent investments in Langley's simulation facilities have been hardware procurements: host processors, visual systems, and most recently, an improved motion system. Investments in software improvements, however, have not been of the same order. Author

N94-25102*# National Aeronautics and Space Administration. Langley Research Center, Hampton, VA.

A SIMULATION STUDY OF CONTROL AND DISPLAY REQUIREMENTS FOR ZERO-EXPERIENCE GENERAL AVIATION PILOTS **c54**

Eric C. Stewart *In its* NASA LaRC Workshop on Guidance, Navigation, Controls, and Dynamics for Atmospheric Flight, 1993 Dec. 1993 p 147-175 (For primary document see N94-25096 06-01)

Avail: CASI HC A03/MF A04

The purpose of this simulation study was to define the basic human factor requirements for operating an airplane in all weather conditions. The basic human factors requirements are defined as those for an operator who is a complete novice for airplane operations but who is assumed to have automobile driving experience. These operators thus have had no piloting experience or training of any kind. The human factor requirements are developed for a practical task which includes all of the basic maneuvers required to go from one airport to another airport in limited visibility conditions. The task was quite demanding including following a precise path with climbing and descending turns while simultaneously changing airspeed. The ultimate goal of this research is to increase the utility of general aviation airplanes - that is, to make them a practical mode of transportation for a much larger segment of the general population. This can be accomplished by reducing the training and proficiency requirements of pilots while improving the level of safety. It is believed that advanced technologies such as fly-by-wire (or light), and head-up pictorial displays can be of much greater benefit to the general aviation pilot than to the full-time, professional pilot. Author

N94-25103*# National Aeronautics and Space Administration. Langley Research Center, Hampton, VA.

PARAMETRIC UNCERTAINTY MODELING FOR APPLICATION TO ROBUST CONTROL **c08**

Christine M. Belcastro, B.-C. Chang (Drexel Univ., Philadelphia, PA.), and Robert Fischl (Drexel Univ., Philadelphia, PA.) *In its* NASA LaRC Workshop on Guidance, Navigation, Controls, and Dynamics for Atmospheric Flight, 1993 Dec. 1993 p 177-192 (For primary document see N94-25096 06-01)

Avail: CASI HC A03/MF A04

Viewgraphs and a paper on parametric uncertainty modeling for application to robust control are included. Advanced robust control system analysis and design is based on the availability of an uncertainty description which separates the uncertain system elements from the nominal system. Although this modeling structure is relatively straightforward to obtain for multiple unstructured uncertainties modeled throughout the system, it is difficult to formulate for many problems involving real parameter variations. Furthermore, it is difficult to ensure that the uncertainty model is formulated such that the dimension of the resulting model is minimal. A procedure for obtaining an uncertainty model for real uncertain parameter problems in which the uncertain parameters can be represented in a multilinear form is presented. Furthermore, the procedure is formulated such that the resulting uncertainty model is minimal (or near minimal) relative to a given state space realization of the system. The approach is demonstrated for a multivariable third-order example problem having four uncertain parameters. Author (revised)

N94-25104*# National Aeronautics and Space Administration. Langley Research Center, Hampton, VA.

HYPERSONIC VEHICLE CONTROL LAW DEVELOPMENT USING H(INFINITY) AND MICRON-SYNTHESIS **c08**

Irene M. Gregory, John D. McMinn, John D. Shaughnessy, and Rajiv S. Chowdhry (Lockheed Engineering and Sciences Co., Hampton, VA.) *In its* NASA LaRC Workshop on Guidance, Navigation, Controls, and Dynamics for Atmospheric Flight, 1993 Dec. 1993 p 193-208 (For primary document see N94-25096 06-01)

Avail: CASI HC A03/MF A04

Hypersonic vehicle control law development using H(infinity) and mu-synthesis is discussed. Airbreathing SSTO vehicles has a mutli-faceted mission that includes orbital operations, as well as re-entry and descent culminating in horizontal landing. However, the most challenging part of the operations is the ascent to orbit. The airbreathing propulsion requires lengthy atmospheric flight that may last as long as 30 minutes and take the vehicle half way around the globe. The vehicles's ascent is characterized by tight payload to orbit margins which translate into minimum fuel orbit as the performance criteria. Issues discussed include: SSTO airbreathing vehicle issues; control system performance requirements; robust control law framework; H(infinity) controller frequency analysis; and mu controller frequency analysis. Author (revised)

N94-25105*# National Aeronautics and Space Administration. Langley Research Center, Hampton, VA.

ON-LINE EVALUATION OF MULTILOOP DIGITAL CONTROLLER PERFORMANCE **c08**

Carol D. Wieseman *In its* NASA LaRC Workshop on Guidance, Navigation, Controls, and Dynamics for Atmospheric Flight, 1993 Dec. 1993 p 209-220 (For primary document see N94-25096 06-01)

Avail: CASI HC A03/MF A04

The purpose of this presentation is to inform the Guidance and Control community of capabilities which were developed by the Aeroservoelasticity Branch to evaluate the performance of multivariable control laws, on-line, during wind-tunnel testing. The capabilities are generic enough to be useful for all kinds of on-line analyses involving multivariable control in experimental testing. Consequently, it was decided to present this material at this workshop even though it has been presented elsewhere. Topics covered include: essential on-line analysis requirements; on-line analysis capabilities; on-line analysis software; frequency domain procedures; controller performance evaluation frequency-domain flutter suppression; and plant determination. Author (revised)

N94-25106*# Air Force Materials Lab., Wright-Patterson AFB, OH. Directorate of Engineering and Technical Management.

AIRCRAFT DIGITAL FLIGHT CONTROL TECHNICAL REVIEW **c08**

Otha B. Davenport and David B. Leggett (Wright Lab., Wright-Patterson AFB, OH.) *In* NASA. Langley Research Center, NASA LaRC Workshop on Guidance, Navigation, Controls, and Dynamics for Atmospheric Flight, 1993 Dec. 1993 p 243-250 (For primary document see N94-25096 06-01)

Avail: CASI HC A02/MF A04

The Aircraft Digital Flight Control Technical Review was initiated by two pilot induced oscillation (PIO) incidents in the spring and summer of 1992. Maj. Gen. Franklin (PEO) wondered why the Air Force development process for digital flight control systems was not preventing PIO problems. Consequently, a technical review team was formed to examine the development process and determine why PIO problems continued to occur. The team was also to identify the 'best practices' used in the various programs. The charter of the team was to focus on the PIO problem, assess the current development process, and document the 'best practices.' The team reviewed all major USAF aircraft programs with digital flight controls, specifically, the F-15E, F-16C/D, F-22, F-111, C-17, and B-2. The team interviewed contractor, System Program Office (SPO), and Combined Test Force (CTF) personnel on these programs. The team also went to NAS Patuxent River to interview USN personnel about the F/A-18 program. The team also reviewed experimental USAF and NASA systems with digital flight control systems: X-29, X-31, F-15 STOL and Maneuver Technology Demonstrator (SMTD), and the Variable In-Flight Stability Test Aircraft (VISTA). The team also discussed the problem with other experts in the field including Ralph Smith and personnel from Calspan. The major

conclusions and recommendations from the review are presented.
Author (revised)

N94-25107*# National Aeronautics and Space Administration. Langley Research Center, Hampton, VA.
DEVELOPMENT OF HIGH-ANGLE-OF-ATTACK NOSE-DOWN PITCH CONTROL MARGIN DESIGN GUIDELINES FOR COMBAT AIRCRAFT c08
Marilyn E. Ogburn and John V. Foster *In its* NASA LaRC Workshop on Guidance, Navigation, Controls, and Dynamics for Atmospheric Flight, 1993 Dec. 1993 p 293-322 (For primary document see N94-25096 06-01)
Avail: CASI HC A03/MF A04

A broad research program to identify maneuvering requirements for advanced fighters and the corresponding design criteria to aid in making critical design tradeoffs is being conducted under the NASA High-Angle-of-Attack Technology Program (HATP). As part of this activity, NASA and the U.S. Navy are conducting cooperative research to develop high-angle-of-attack control margin requirements. This paper will summarize the status of this program. Following some background information, the simulation study conducted to develop a set of preliminary guidelines for nose-down pitch control is reviewed, and the results of some very limited flight tests are described. Author (revised)

N94-25108*# Wright Lab., Wright-Patterson AFB, OH.
ROBUST, NONLINEAR, HIGH ANGLE-OF-ATTACK CONTROL DESIGN FOR A SUPERMANEUVERABLE VEHICLE c08
Richard J. Adams *In* NASA. Langley Research Center, NASA LaRC Workshop on Guidance, Navigation, Controls, and Dynamics for Atmospheric Flight, 1993 Dec. 1993 p 323-371 (For primary document see N94-25096 06-01)
Avail: CASI HC A03/MF A04

High angle-of-attack flight control laws are developed for a supermaneuverable fighter aircraft. The methods of dynamic inversion and structured singular value synthesis are combined into an approach which addresses both the nonlinearity and robustness problems of flight at extreme operating conditions. The primary purpose of the dynamic inversion control elements is to linearize the vehicle response across the flight envelope. Structured singular value synthesis is used to design a dynamic controller which provides robust tracking to pilot commands. The resulting control system achieves desired flying qualities and guarantees a large margin of robustness to uncertainties for high angle-of-attack flight conditions. The results of linear simulation and structured singular value stability analysis are presented to demonstrate satisfaction of the design criteria. High fidelity nonlinear simulation results show that the combined dynamics inversion/structured singular value synthesis control law achieves a high level of performance in a realistic environment. Author (revised)

N94-25109*# Joint Inst. for Advancement of Flight Sciences, Hampton, VA. Aircraft Guidance and Controls Branch.
X-31 AERODYNAMIC CHARACTERISTICS DETERMINED FROM FLIGHT DATA c05
Alex Kokolios *In* NASA. Langley Research Center, NASA LaRC Workshop on Guidance, Navigation, Controls, and Dynamics for Atmospheric Flight, 1993 Dec. 1993 p 373-387 (For primary document see N94-25096 06-01)
Avail: CASI HC A03/MF A04

The lateral aerodynamic characteristics of the X-31 were determined at angles of attack ranging from 20 to 45 deg. Estimates of the lateral stability and control parameters were obtained by applying two parameter estimation techniques, linear regression, and the extended Kalman filter to flight test data. An attempt to apply maximum likelihood to extract parameters from the flight data was also made but failed for the reasons presented. An overview of the System Identification process is given. The overview includes a listing of the more important properties of all three estimation techniques that were applied to the data. A comparison is given of results obtained from flight test data and wind tunnel data for four important lateral parameters. Finally, future research to be conducted in this area is discussed. Author (revised)

N94-25110*# Lockheed Engineering and Sciences Co., Hampton, VA. Aircraft Guidance and Control Branch.
NONLINEAR AERODYNAMIC MODELING USING MULTIVARIATE ORTHOGONAL FUNCTIONS c02
Eugene A. Morelli *In* NASA. Langley Research Center, NASA LaRC Workshop on Guidance, Navigation, Controls, and Dynamics for Atmospheric Flight, 1993 Dec. 1993 p 389-400 (For primary document see N94-25096 06-01)
Avail: CASI HC A03/MF A04

The problem to be addressed in this work is that of modeling nondimensional force and moment aerodynamic coefficients over the entire subsonic envelope. The particular application discussed here is the Z force coefficient for the F-18 High Angle of Attack Research Vehicle (HARV).
Author

N94-25111*# Vigyan Research Associates, Inc., Hampton, VA.
A STUDY OF ROLL ATTRACTOR AND WING ROCK OF DELTA WINGS AT HIGH ANGLES OF ATTACK c08
T. Niranjana, D. M. Rao, and Bandu N. Pamadi *In* NASA. Langley Research Center, NASA LaRC Workshop on Guidance, Navigation, Controls, and Dynamics for Atmospheric Flight, 1993 Dec. 1993 p 401-430 (For primary document see N94-25096 06-01)
Avail: CASI HC A03/MF A04

Wing rock is a high angle of attack dynamic phenomenon of limited cycle motion predominantly in roll. The wing rock is one of the limitations to combat effectiveness of the fighter aircraft. Roll Attractor is the steady state or equilibrium trim angle (phi(sub trim)) attained by the free-to-roll model, held at some angle of attack, and released form rest at a given initial roll (bank) angle (phi(sub O)). Multiple roll attractors are attained at different trim angles depending on initial roll angle. The test facility (Vigyan's low speed wind tunnel) and experimental work is presented here along with mathematical modelling of roll attractor phenomenon and analysis and comparison of predictions with experimental data. Derived from text

N94-25112*# National Aeronautics and Space Administration. Langley Research Center, Hampton, VA.
MODELING TRANSONIC AERODYNAMIC RESPONSE USING NONLINEAR SYSTEMS THEORY FOR USE WITH MODERN CONTROL THEORY c08
Walter A. Silva *In its* NASA LaRC Workshop on Guidance, Navigation, Controls, and Dynamics for Atmospheric Flight, 1993 Dec. 1993 p 431-457 (For primary document see N94-25096 06-01)
Avail: CASI HC A03/MF A04

The presentation begins with a brief description of the motivation and approach that has been taken for this research. This will be followed by a description of the Volterra Theory of Nonlinear Systems and the CAP-TSD code which is an aeroelastic, transonic CFD (Computational Fluid Dynamics) code. The application of the Volterra theory to a CFD model and, more specifically, to a CAP-TSD model of a rectangular wing with a NACA 0012 airfoil section will be presented. Author

N94-25113*# National Aeronautics and Space Administration. Langley Research Center, Hampton, VA.
EFFECT OF AEROELASTIC-PROPULSIVE INTERACTIONS ON FLIGHT DYNAMICS OF A HYPERSONIC VEHICLE c05
David L. Raney, John D. McMinn, Anthony S. Pototzky (Lockheed Engineering and Sciences Co., Hampton, VA.), and Christine L. Wooley (Cincinnati Univ., OH.) *In its* NASA LaRC Workshop on Guidance, Navigation, Controls, and Dynamics for Atmospheric Flight, 1993 Dec. 1993 p 459-472 (For primary document see N94-25096 06-01)
Avail: CASI HC A03/MF A04

The desire to achieve orbit-on-demand access to space with rapid turn-around capability and aircraft-like processing operations has given rise to numerous hypersonic aerospace plane design concepts which would take off horizontally from a conventional runway and employ air-breathing scramjet propulsion systems for acceleration to orbital speeds. Most of these air-breathing hypersonic vehicle concepts incorporate an elongated fuselage forebody to act as the aerodynamic compression surface for a scramjet combustor module. This type of airframe-integrated scramjet propulsion system tends to be highly sensitive to inlet conditions and angle-of-attack perturbations. Furthermore, the basic configuration of the fuselage, with its elongated and tapered forebody, produces relatively low frequency elastic modes which will cause perturbations in the combustor inlet conditions due to the oscillation of the forebody compression surface. The flexibility of the forebody compression surface, together with sensitivity of scramjet propulsion systems to inlet conditions, creates the potential for an unprecedented form of aeroelastic-propulsive interaction in which deflections of the vehicle fuselage give rise to propulsion transients, producing force and moment variations that may adversely impact the longitudinal flight dynamics and/or excite the elastic modes. These propulsive force and moment variations may have an appreciable impact on the performance, guidance, and control of a hypersonic aerospace plane. The objectives of this research are to quantify the magnitudes of propulsive force and moment perturbations resulting from elastic deformation of a representative hypersonic vehicle, and to assess the potential impact of these perturbations on the vehicle's longitudinal flight dynamics.

Derived from text

N94-25114*# National Aeronautics and Space Administration. Langley Research Center, Hampton, VA.

OPTIMAL RTLS ABORT TRAJECTORIES FOR AN HL-20 PERSONNEL LAUNCH VEHICLE c13

Kevin Dutton *In its* NASA LaRC Workshop on Guidance, Navigation, Controls, and Dynamics for Atmospheric Flight, 1993 Dec. 1993 p 481-496 (For primary document see N94-25096 06-01)
Avail: CASI HC A03/MF A04

The primary objective of this study was to determine whether Return To Launch Site (RTLS) abort at T seconds along the launch trajectory of the Personnel Launch System (PLS) is possible using optimal control theory. The secondary objective is to assess effects of bank angle constraint, lift coefficient constraint, free and fixed final boundary conditions, etc. of the vehicle. The PLS is a complementary system to the Space Shuttle.

Derived from text

N94-25115*# National Aeronautics and Space Administration. Langley Research Center, Hampton, VA.

ADVANCED INFORMATION PROCESSING SYSTEM (AIPS) c82

Felix L. Pitts *In its* NASA LaRC Workshop on Guidance, Navigation, Controls, and Dynamics for Atmospheric Flight, 1993 Dec. 1993 p 533-547 (For primary document see N94-25096 06-01)
Avail: CASI HC A03/MF A04

Advanced Information Processing System (AIPS) is a computer systems philosophy, a set of validated hardware building blocks, and a set of validated services as embodied in system software. The goal of AIPS is to provide the knowledgebase which will allow achievement of validated fault-tolerant distributed computer system architectures, suitable for a broad range of applications, having failure probability requirements of 10E-9 at 10 hours. A background and description is given followed by program accomplishments, the current focus, applications, technology transfer, FY92 accomplishments, and funding. Derived from text

N94-25169*# Eloret Corp., Palo Alto, CA.

ADVANCED BALLISTIC RANGE TECHNOLOGY Final Technical Report, 1 Jan. 1989 - 31 Jan. 1994

Leslie A. Yates 10 Mar. 1994 11 p
(Contract NCC2-583)
(NASA-CR-195198; NAS 1.26:195198) Avail: CASI HC A03/MF A01

The research conducted supported two facilities at NASA Ames Research Center: the Hypervelocity Free-Flight Aerodynamic Facility and the 16-Inch Shock Tunnel. During the grant period, a computerized film-reading system was developed, and five- and six-degree-of-freedom parameter-identification routines were written and successfully implemented. Studies of flow separation were conducted, and methods to extract phase shift information from finite-fringe interferograms were developed. Methods for constructing optical images from Computational Fluid Dynamics solutions were also developed, and these methods were used for one-to-one comparisons of experiment and computations. Author (revised)

N94-25068 General Electric Co., Cincinnati, OH. Aircraft Engines.

AVIATION: THE TIMELESS INDUSTRY

Brian H. Rowe *In* National Academy of Engineering, The Future of Aerospace: Proceedings of a Symposium Held in Honor of Alexander H. Flax 1993 p 29-36 (For primary document see N94-25065 06-99)
Copyright Avail: Issuing Activity

02 AERODYNAMICS

Includes aerodynamics of bodies, combinations, wings, rotors, and control surfaces; and internal flow in ducts and turbomachinery.

For related information see also *34 Fluid Mechanics and Heat Transfer.*

N94-22894*# California Polytechnic State Univ., San Luis Obispo. Aeronautical Engineering Dept.

AN EXPERIMENTAL INVESTIGATION OF THE EFFECT OF UPPER SURFACE BLOWING ON DYNAMIC STALL Semiannual Report, Jun. - Dec. 1993

Jin Tso 15 Dec. 1993 5 p
(Contract NCA2-811)
(NASA-CR-194863; NAS 1.26:194863) Avail: CASI HC A01/MF A01

An experimental investigation of the effect of upper surface blowing on dynamic stall was conducted. Progress made during the period from Jun. to Dec. 1993 is summarized. Topics covered include VR-7 wing model, pulse valve, and wing/load cell junction. CASI

N94-23116 Helsinki Univ. of Technology, Espoo (Finland). Lab. of Aerodynamics.

COMPUTATIONAL STUDY OF GA(W)-1: AIRFOIL NEAR STALL

J. Hoffren 1993 26 p Limited Reproducibility: More than 20% of this document may be affected by microfiche quality
(PB93-226249; SER-B-93-41) Avail: CASI HC A03

The testing of a new time-accurate thin-layer Navier-Stokes solver is continued with attempts to simulate the stall of the GA(W)-1 airfoil. Subsonic high Reynolds number flow at 7.0 - 19.5 degrees angle of attack is studied utilizing two different grids. Near the lower end of the angle of attack range, the results are reasonably good, but serious problems emerge as the stall proceeds. Unsteady solutions are obtained, although the time-averaged results agree poorly with measurements. The algebraic turbulence model applied is apparently inadequate for these types of time-dependent cases. The behavior of the solutions is also found to depend critically on the spatial resolution and the modeling of transition. The temporal accuracy may be an additional factor affecting the results. Since the calculations are very costly, it is not considered worthwhile to continue the effort with an improved resolution until a better, more physically sound turbulence model is available. NTIS

N94-23149# Institut Franco-Allemand de Recherches, Saint-Louis (France).

A NEW EXPERIMENTAL APPARATUS FOR THE STUDY OF THE UNSTEADY FLOWFIELD OVER AN AIRFOIL IN PITCHING AND HEAVING MOTIONS USING LASER DOPPLER ANEMOMETRY

P. Wernert, G. Koerber, and F. Wietrich 2 Oct. 1992 14 p Presented at the European Forum on Wind Tunnels and Wind Tunnel Test Techniques, Southampton, England, 14-17 Sep. 1992 See also A94-10438
(Contract DRET-86-156)
(ISL-CO-229/92; ETN-94-95126) Avail: CASI HC A03/MF A01

An experimental setup used for the study of the flowfield over an airfoil undergoing arbitrary pitching or heaving motions is described. This setup is basically composed of two parts: a novel driving mechanism, based on an automatic apparatus, two speed drives, two brushless motors and a support system, which allows the airfoil to be put into a wide range of periodic or transient motions and a classical two dimensional laser Doppler anemometry system which provides streamwise and transversal components of the velocity. Data acquisition, data reduction and synchronization problems are discussed. Results concerning dynamic stall features observed in the near wake of a pitching airfoil at a Reynolds number of 287,000 are given.

ESA

N94-23161# Institut Franco-Allemand de Recherches, Saint-Louis (France).

LDA MEASUREMENTS OF THE UNSTEADY NEAR WAKE BEHIND AN AIRFOIL UNDERGOING TRANSIENT AND PERIODIC PITCHING MOTIONS

P. Wernert, G. Koerber, and F. Wietrich 30 Jun. 1992 10 p Presented at the 6th International Symposium on Applications of Laser Techniques in Fluid Mechanics, Lisbon, Portugal, 20-23 Jul. 1992

(Contract DRET-86-156)
(ISL-CO-215/92; ETN-94-95124) Avail: CASI HC A02/MF A01

Results of two dimensional Laser Doppler Anemometry (LDA) measurements performed in the near wake of an airfoil undergoing stepwise motions and saw tooth periodic motions with incidence variations from -1 to 25 deg revealing dynamic stall features are presented. The driving mechanism used is based on an automatic apparatus which allows the airfoil to be put into a wide range of periodic or transient pitching and/or heaving motions. Time dependent velocity traces for the two components, streamwise velocity profiles, evolution of the semi-wake thickness, and vector velocity field are discussed. These results, obtained at a Reynolds number of 287,000, are compared to those corresponding to steady flow.
ESA

N94-23299*# National Aeronautics and Space Administration. Lewis Research Center, Cleveland, OH.
AN OVERVIEW OF A MODEL ROTOR ICING TEST IN THE NASA LEWIS ICING RESEARCH TUNNEL
Randall K. Britton (Sverdrup Technology, Inc., Brook Park, OH.), Thomas H. Bond, and Robert J. Flemming (Sikorsky Aircraft, Stratford, CT.) Jan. 1994 24 p Presented at the 32nd Aerospace Sciences Meeting, Reno, NV, 10-13 Jan. 1994; sponsored by AIAA
(Contract NAS3-25266; RTOP 505-68-11)
(NASA-TM-106471; E-8340; NAS 1.15:106471; AIAA Paper 94-0716)
Avail: CASI HC A03/MF A01

During two entries in late 1989, a heavily instrumented sub-scale model of a helicopter main rotor was tested in the NASA LeRC Icing Research Tunnel (IRT). The results of this series of tunnel tests were published previously. After studying the results from the 1989 test and comparing them to predictions, it became clear that certain test conditions still needed investigation. Therefore, a re-entry of the Sikorsky Aircraft Powered Force Model (PFM) in the IRT was instituted in order to expand upon the current rotor craft sub-scale model experimental database. The major areas of interest included expansion of the test matrix to include a larger number of points in the FAA AC 29-2 icing envelope, inclusion of a number of high power rotor performance points, close examination of warm temperature operations, operation of the model in constant lift mode, and testing for conditions for icing test points in the full scale helicopter database. The expanded database will allow further and more detailed examination and comparison with analytical models. Participants in the test were NASA LeRC, the U.S. Army Vehicle Propulsion Directorate based at LeRC, and Sikorsky Aircraft. The model rotor was exposed to a range of icing conditions (temperature, liquid water content, median droplet diameter) and was operated over ranges of shaft angle, rotor tip speed, advance ratio, and rotor lift. The data taken included blade strain gage and balance data, as well as still photography, video, ice profile tracings, and ice molds. A discussion of the details of the test is given herein. Also, a brief examination of a subset of the data taken is also given. Author (revised)

N94-23465*# National Aeronautics and Space Administration. Lewis Research Center, Cleveland, OH.
MEASUREMENTS AND MODELING OF FLOW STRUCTURE IN THE WAKE OF A LOW PROFILE WISHBONE VORTEX GENERATOR
B. J. Wendt and W. R. Hingst Jan. 1994 11 p Presented at the 32nd Aerospace Sciences Meeting and Exhibit, Reno, NV, 10-13 Jan. 1994; sponsored by AIAA
(RTOP 505-62-52)
(NASA-TM-106468; E-8334; NAS 1.15:106468; AIAA Paper 94-0620)
Avail: CASI HC A03/MF A01

The results of an experimental examination of the vortex structures shed from a low profile 'wishbone' generator are presented. The vortex generator height relative to the turbulent boundary layer was varied by testing two differently sized models. Measurements of the mean three-dimensional velocity field were conducted in cross-stream planes downstream of the vortex generators. In all cases, a counter-rotating vortex pair was observed. Individual vortices were characterized by three descriptors derived from the velocity data; circulation, peak vorticity, and cross-stream location of peak vorticity. Measurements in the cross plane at two axial locations behind the smaller wishbone characterize the downstream development of the vortex pairs. A single region of stream wise velocity deficit is shared by both vortex cores. This is in contrast to conventional generators, where each core coincides with a region of velocity deficit. The measured cross-stream velocities for each case are compared to an Oseen model with matching descriptors. The best comparison occurs with the data from the larger wishbone. Author (revised)

N94-23511*# Sverdrup Technology, Inc., Brook Park, OH.
SIMPLIFIED, INVERSE, EJECTOR DESIGN TOOL
Lawrence J. DeChant Dec. 1993 37 p
(Contract NAS3-25266; RTOP 505-69-50)
(NASA-CR-194438; E-8289; NAS 1.26:194438) Avail: CASI HC A03/MF A01

A simple lumped parameter based inverse design tool has been developed which provides flow path geometry and entrainment estimates subject to operational, acoustic, and design constraints. These constraints are manifested through specification of primary mass flow rate or ejector thrust, fully-mixed exit velocity, and static pressure matching. Fundamentally, integral forms of the conservation equations coupled with the specified design constraints are combined to yield an easily invertible linear system in terms of the flow path cross-sectional areas. Entrainment is computed by back substitution. Initial comparison with experimental and analogous one-dimensional methods show good agreement. Thus, this simple inverse design code provides an analytically based, preliminary design tool with direct application to High Speed Civil Transport (HSCT) design studies.
Author (revised)

N94-23512*# National Aeronautics and Space Administration. Langley Research Center, Hampton, VA.
LEADING-EDGE VOTEX-SYSTEM DETAILS OBTAINED ON F-106B AIRCRAFT USING A ROTATING VAPOR SCREEN AND SURFACE TECHNIQUES
John E. Lamar, Jay Brandon, Kathryn Stacy, Thomas D. Johnson, Jr. (Lockheed Engineering and Sciences Co., Hampton, VA.), Kurt Severance, and Brooks A. Childers Nov. 1993 159 p Original contains color illustrations
(RTOP 505-59-30-03)
(NASA-TP-3374; L-17150; NAS 1.60:3374) Avail: CASI HC A08/MF A02; 47 functional color pages

A flight research program to study the flow structure and separated-flow origins over an F-106B aircraft wing is described. The flight parameters presented include Mach numbers from 0.26 to 0.81, angles of attack from 8.5 deg to 22.5 deg, Reynolds numbers from 22.6 x 10(exp 6) to 57.3 x 10(exp 6) and load factors from 0.9 to 3.9 times the acceleration due to gravity. Techniques for vapor screens, image enhancement, photogrammetry, and computer graphics are integrated to analyze vortex-flow systems. Emphasis is placed on the development and application of the techniques. The spatial location of vortex cores and their tracks over the wing are derived from the analysis. Multiple vortices are observed and are likely attributed to small surface distortions in the wing leading-edge region. A major thrust is to correlate locations of reattachment lines obtained from the off-surface (vapor-screen) observations with those obtained from on-surface oil-flow patterns and pressure-port data. Applying vapor-screen image data to approximate reattachment lines is experimental, but depending on the angle of attack, the agreement with oil-flow results is generally good. Although surface pressure-port data are limited, the vapor-screen data indicate reattachment point occurrences consistent with the available data. Author (revised)

N94-23522*# National Aeronautics and Space Administration. Lewis Research Center, Cleveland, OH.
CHARACTERISTICS OF SURFACE ROUGHNESS ASSOCIATED WITH LEADING EDGE ICE ACCRETION
Jaiwon Shin Jan. 1994 18 p Presented at the AIAA 32nd Aerospace Sciences Meeting and Exhibit, Reno, NV, 10-13 Jan. 1994; sponsored by AIAA
(RTOP 505-68-10)
(NASA-TM-106459; E-8320; NAS 1.15:106459; AIAA Paper 94-0799)
Avail: CASI HC A03/MF A01

Detailed size measurements of surface roughness associated with leading edge ice accretions are presented to provide information on characteristics of roughness and trends of roughness development with various icing parameters. Data was obtained from icing tests conducted in the Icing Research Tunnel (IRT) at NASA Lewis Research Center (LeRC) using a NACA 0012 airfoil. Measurements include diameters, heights, and

spacing of roughness elements along with chordwise icing limits. Results confirm the existence of smooth and rough ice zones and that the boundary between the two zones (surface roughness transition region) moves upstream towards stagnation region with time. The height of roughness grows as the air temperature and the liquid water content increase, however, the airspeed has little effect on the roughness height. Results also show that the roughness in the surface roughness transition region grows during a very early stage of accretion but reaches a critical height and then remains fairly constant. Results also indicate that a uniformly distributed roughness model is only valid at a very initial stage of the ice accretion process.
Author (revised)

N94-23557*# National Aeronautics and Space Administration. Ames Research Center, Moffett Field, CA.

LinAir: A MULTI-ELEMENT DISCRETE VORTEX WEISSINGER AERODYNAMIC PREDICTION METHOD

Donald A. Durston Oct. 1993 76 p Original contains color illustrations
(RTOP 505-59-20)
(NASA-TM-108786; A-93111; NAS 1.15:108786) Avail: CASI HC A05/MF A01; 1 functional color page

LinAir is a vortex lattice aerodynamic prediction method similar to Weissinger's extended lifting-line theory, except that the circulation around a wing is represented by discrete horseshoe vortices, not a continuous distribution of vorticity. The program calculates subsonic longitudinal and lateral/directional aerodynamic forces and moments for arbitrary aircraft geometries. It was originally written by Dr. Ilan Kroo of Stanford University, and subsequently modified by the author to simplify modeling of complex configurations. The Polhamus leading-edge suction analogy was added by the author to extend the range of applicability of LinAir to low aspect ratio (i.e., fighter-type) configurations. A brief discussion of the theory of LinAir is presented, and details on how to run the program are given along with some comparisons with experimental data to validate the code. Example input and output files are given in the appendices to aid in understanding the program and its use. This version of LinAir runs in the VAX/VMS, Cray UNICOS, and Silicon Graphics Iris workstation environments at the time of this writing. Author (revised)

N94-23592*# National Aeronautics and Space Administration. Lewis Research Center, Cleveland, OH.

EFFECT OF DELTA TABS ON MIXING AND AXIS SWITCHING IN JETS FROM ASYMMETRIC NOZZLES

K. B. M. Q. Zaman Jan. 1994 20 p Presented at the 32nd Aerospace Sciences Meeting and Exhibit, Reno, NV, 10-13 Jan. 1994; sponsored by AIAA
(RTOP 537-02-22)
(NASA-TM-106450; E-8308; NAS 1.15:106450; AIAA Paper 94-0186)
Avail: CASI HC A03/MF A01

The effect of delta tabs on mixing and the phenomenon of axis switching in free air jets from various asymmetric nozzles was studied experimentally. Flow visualization and Pitot probe surveys were carried out with a set of small nozzles (D = 1.47 cm) at a jet Mach number, Mj = 1.63. Hot wire measurements for streamwise vorticity were carried out with larger nozzles (D = 6.35 cm) at Mj = 0.31. Jet mixing with the asymmetric nozzles, as indicated by the mass fluxes downstream, was found to be higher than that produced by a circular nozzle. The circular nozzle with four delta tabs, however, produced fluxes much higher than that produced by a asymmetric nozzles themselves or by most of the tab configurations tried with them. Even higher fluxes could be obtained with only a few cases, e.g., with 3:1 rectangular nozzle with two large delta tabs placed on the narrow edges. In this case, the jet 'fanned out' at a large angle after going through one axis switch. The axis switching could be either stopped or augmented with suitable choice of the tab configurations. Two mechanisms are identified governing the phenomenon. One, as described in Ref. 12 and referred to here as the omega(sub Theta)-induced dynamics, is due to differential induced velocities of different segments of a rolled up azimuthal vortical structure. The other is the omega(sub x)-induced dynamics due to the induced velocities of streamwise vortex pairs in the flow. While the former dynamics are responsible for rapid axis switching in periodically forced jets, the effect of the tabs is governed mainly by the latter. It is inferred that both dynamics are active in a natural asymmetric jet issuing from a nozzle having an upstream contraction. The tendency for axis switching caused by the omega(sub Theta)-induced dynamics is resisted by the omega(sub x)-induced dynamics, leading to a delayed or no switch over in that case. In jets from orifices and in screeching jets, the omega(sub Theta)-induced dynamics dominate causing a faster switch over. Author

N94-23625*# Purdue Univ., West Lafayette, IN. School of Aeronautics and Astronautics.

DEVELOPMENT OF A CODE FOR WALL CONTOUR DESIGN IN THE TRANSONIC REGION OF AXISYMMETRIC AND SQUARE NOZZLES Status Report, 1 Sep. 1992 - 1 Jan. 1994

Timothy Alcenius and Steven P. Schneider 1 Jan. 1994 46 p
(Grant NAG1-1133)
(NASA-CR-194857; NAS 1.26:194857) Avail: CASI HC A03/MF A01

Nozzle design codes developed earlier under NAG1-1133 were modified and used in order to design a supersonic wind tunnel nozzle with square cross sections. As part of the design process, a computer code was written to implement the Hopkins and Hill perturbation solution for the flow in the transonic region of axisymmetric nozzles. This technique is used to design the bleed slot of quiet-flow nozzles. This new design code is documented in this report. Author

N94-23975*# National Aeronautics and Space Administration. Ames Research Center, Moffett Field, CA.

COMPRESSIBILITY EFFECTS ON DYNAMIC STALL OF AIRFOILS UNDERGOING RAPID TRANSIENT PITCHING MOTION Final Report, 1 Oct. 1989 - 30 Sep. 1992

M. S. Chandrasekhara (Naval Postgraduate School, Monterey, CA.) and M. F. Platzer (Naval Postgraduate School, Monterey, CA.) Nov. 1992 28 p
Sponsored in part by Naval Air Systems Command
(Grants AF-AFOSR-0012-90; AF-AFOSR-0007-91; AF-AFOSR-0004-92; AF Proj. 2307)
(NASA-TM-109681; NAS 1.15:109681) Avail: CASI HC A03/MF A01

The research was carried out in the Compressible Dynamic Stall Facility, CDSF, at the Fluid Mechanics Laboratory (FML) of NASA Ames Research Center. The facility can produce realistic nondimensional pitch rates experienced by fighter aircraft, which on model scale could be as high as 3600/sec. Nonintrusive optical techniques were used for the measurements. The highlight of the effort was the development of a new real time interferometry method known as Point Diffraction Interferometry - PDI, for use in unsteady separated flows. This can yield instantaneous flow density information (and hence pressure distributions in isentropic flows) over the airfoil. A key finding is that the dynamic stall vortex forms just as the airfoil leading edge separation bubble opens-up. A major result is the observation and quantification of multiple shocks over the airfoil near the leading edge. A quantitative analysis of the PDI images shows that pitching airfoils produce larger suction peaks than steady airfoils at the same Mach number prior to stall. The peak suction level reached just before stall develops is the same at all unsteady rates and decreases with increase in Mach number. The suction is lost once the dynamic stall vortex or vortical structure begins to convect. Based on the knowledge gained from this preliminary analysis of the data, efforts to control dynamic stall were initiated. The focus of this work was to arrive at a dynamically changing leading edge shape that produces only 'acceptable' airfoil pressure distributions over a large angle of attack range. Author

N94-24052*# Virginia Polytechnic Inst. and State Univ., Blacksburg. Dept. of Aerospace Engineering.

ISSAC, JASON CHERIAN SES IN TRANSONIC FLOW

Jason Cherion Issac and Rakesh K. Kapania [1993] 80 p
(Grant NAG1-1411)
(NASA-CR-194837; NAS 1.26:194837; VPI-AOE-210) Avail: CASI HC A05/MF A01

Flutter analysis of a two degree of freedom airfoil in compressible flow is performed using a state-space representation of the unsteady aerodynamic behavior. Indicial response functions are used to represent the normal force and moment response of the airfoil. The structural equations of motion of the airfoil with bending and torsional degrees of freedom are coupled to the unsteady air loads and the aeroelastic system so modelled is solved as an eigenvalue problem to determine the stability. The aeroelastic equations are also directly integrated with respect to time and the time-domain results compared with the results from the eigenanalysis. A good agreement is obtained. The derivatives of the flutter speed obtained from the eigenanalysis are calculated with respect to the mass and stiffness parameters by both analytical and finite-difference methods for various transonic Mach numbers. The experience gained from the two degree of freedom model is applied to study the sensitivity of the flutter response of a wing with respect to various shape parameters. The parameters being considered are as follows: (1) aspect ratio; (2) surface area of the wing; (3) taper ratio; and (4) sweep. The wing deflections are represented by Chebyshev polynomials. The compressible aerodynamic state-space model used for the airfoil section is extended to represent the unsteady aerodynamic forces on a generally laminated tapered skewed wing. The aeroelastic equations are solved as an eigenvalue problem to determine the flutter speed of the wing. The derivatives of the flutter speed with respect to the shape parameters are calculated by both analytical and finite difference methods. Author (revised)

N94-24084*# National Aeronautics and Space Administration. Lewis Research Center, Cleveland, OH.

EVALUATION OF TURBULENCE MODELS IN THE PARC CODE FOR TRANSONIC DIFFUSER FLOWS

N. J. Georgiadis, J. E. Drummond (Akron Univ., OH.), and B. P. Leonard (Akron Univ., OH.) Jan. 1994 13 p Presented at the 32nd Aerospace Sciences Meeting and Exhibit, Reno, NV, 10-13 Jan. 1994; sponsored by AIAA

(RTOP 537-02-23)

(NASA-TM-106391; E-8216; NAS 1.15:106391; AIAA Paper 94-0582)

Avail: CASI HC A03/MF A01

Flows through a transonic diffuser were investigated with the PARC code using five turbulence models to determine the effects of turbulence model selection on flow prediction. Three of the turbulence models were algebraic models: Thomas (the standard algebraic turbulence model in PARC), Baldwin-Lomax, and Modified Mixing Length-Thomas (MMLT). The other two models were the low Reynolds number k-epsilon models of Chien and Speziale. Three diffuser flows, referred to as the no-shock, weak-shock, and strong-shock cases, were calculated with each model to conduct the evaluation. Pressure distributions, velocity profiles, locations of shocks, and maximum Mach numbers in the duct were the flow quantities compared. Overall, the Chien k-epsilon model was the most accurate of the five models when considering results obtained for all three cases. However, the MMLT model provided solutions as accurate as the Chien model for the no-shock and the weak-shock cases, at a substantially lower computational cost (measured in CPU time required to obtain converged solutions). The strong shock flow, which included a region of shock-induced flow separation, was only predicted well by the two k-epsilon models. Author (revised)

N94-24103*# California Polytechnic State Univ., San Luis Obispo. Dept. of Aeronautical Engineering.

LIFT AUGMENTATION ON A DELTA WING VIA LEADING EDGE FENCES AND THE GURNEY FLAP M.S. Thesis

Mark D. Buchholz Dec. 1992 71 p

(Contract NCC2-730)

(NASA-CR-194793; NAS 1.26:194793) Avail: CASI HC A04/MF A01

Wind tunnel tests were conducted on two devices for the purpose of lift augmentation on a 60 deg delta wing at low speed. Lift, drag, pitching moment, and surface pressures were measured. Detailed flow visualization was also obtained. Both the leading edge fence and the Gurney flap are shown to increase lift. The fences and flap shift the lift curve as much as 5 deg and 10 deg, respectively. The fences aid in trapping vortices on the upper surface, thereby increasing suction. The Gurney flap improves circulation at the trailing edge. The individual influences of both devices are roughly additive, creating high lift gain. However, the lower lift to drag ratio and the precipitation of vortex burst caused by the fences, and the nose down pitching moment created by the flap are also significant factors. Author

N94-24178 Montreal Univ. (Quebec). Dept. de Genie Mecanique.

THREE DIMENSIONAL STUDY OF AN AIRPLANE WING AND ITS WAKE IN THE SUBSONIC REGIME M.S. Thesis [ETUDE 3D D'UNE AILE D'AVION ET DE SON SILLAGE EN REGIME SUBSONIQUE]

Francis Normandin Aug. 1990 133 p In FRENCH

(ISBN-0-315-58963-9; CTN-94-60875) Copyright Avail: Micromedia Ltd., Technical Information Centre, 240 Catherine Street, Suite 305, Ottawa, Ontario, K2P 2G8, Canada HC/MF

A numerical method and a computer code were developed for the analysis of three dimensional (3D) airplane wing configurations in the subsonic regime. Comparisons with analytical solutions, experimental data, and commercial computer code validates the results. The overall approach is based on resolution of the Laplace equation. As is the case in any classical panel method, the linearity of the equation to be resolved allows limiting the problem to a surface integral. This linearity serves as a criterion of simplicity and will allow establishment of foundations for future developments in the 3D domain. The method is based directly on the full potential, which permits easy interpretation of the results. Using bi-linear doublet distributions only on triangular surface elements facilitates discretization of the configuration to be analyzed while limiting abrupt variations of the solution at the panel edges. To take into account the vorticity effects related to the lift developed on the wing, a wake relaxation is included which introduces a coupling approach into the calculation, since the shape of the wake is unknown at the start. A two dimensional semi-stationary development method is used to generate the wake behind the wing by convecting Treftz plans. Once the wake geometry is obtained, a new potential calculation is performed. Author (CISTI)

N94-24182 Pioneer Aerospace Corp., Melbourne, FL.

RADIALLY CONSTRUCTED CRUCIFORM PARACHUTE Patent

James D. Reuter, inventor (to Pioneer Aerospace Corp.) 12 Oct. 1993 18 p

(CA-Patent-1323021; Int-Patent-Class-B64D-017/02; CTN-94-60932)

Copyright Avail: Micromedia Ltd., Technical Information Centre, 240 Catherine Street, Suite 305, Ottawa, Ontario, K2P 2G8, Canada HC/MF

A radially constructed cruciform parachute is discussed. The parachute is adapted to support a load below it. The parachute itself includes a canopy having a hemispherically shaped member defining an apex in the uppermost portion. The canopy also defines a lower canopy edge that is generally circular around its lowermost portion. A plurality of panel members are each positioned extending vertically from a position adjacent the apex to the lower canopy edge. The panel members are attached with respect to one another along their vertically extending edges to form the hemispheric member of the canopy. Each panel includes upper and lower sections, and a plurality of the individual panels have lower panel sections which define open sections to form gores for facilitating stability of the overall parachute. These open sections extend from the lower canopy edge upwardly to the immediate edge of the upper panel and are defined laterally by the vertical edges of the adjacent panel sections. Each open section is positioned diametrically opposite another open section about the hemispheric member of the canopy to provide increased stability while inflating and after inflation. A plurality of support lines secured to the lower canopy edge extend downward to support the load. A preferred configuration of the parachute has 16 solid panels and eight panels with an open section. Author (CISTI)

N94-24295*# National Aeronautics and Space Administration. Hugh L. Dryden Flight Research Center, Edwards, CA.

REDUCTION OF STRUCTURAL LOADS USING MANEUVER LOAD CONTROL ON THE ADVANCED FIGHTER TECHNOLOGY INTEGRATION (AFTI)/F-111 MISSION ADAPTIVE WING

Stephen V. Thornton Washington Sep. 1993 31 p

(RTOP 505-63-50)

(NASA-TM-4526; H-1940; NAS 1.15:4526) Avail: CASI HC A03/MF A01

A transonic fighter-bomber aircraft, having a swept supercritical wing with smooth variable-camber flaps was fitted with a maneuver load control (MLC) system that implements a technique to reduce the inboard bending moments in the wing by shifting the spanwise load distribution inboard as load factor increases. The technique modifies the spanwise camber distribution by automatically commanding flap position as a function of flap position, true airspeed, Mach number, dynamic pressure, normal acceleration, and wing sweep position. Flight test structural loads data were obtained for loads in both the wing box and the wing root. Data from uniformly deflected flaps were compared with data from flaps in the MLC configuration where the outboard segment of three flap segments was deflected downward less than the two inboard segments. The changes in the shear loads in the forward wing spar and at the roots of the stabilators also are presented. The camber control system automatically reconfigures the flaps through varied flight conditions. Configurations having both moderate and full

trailing-edge flap deflection were tested. Flight test data were collected at Mach numbers of 0.6, 0.7, 0.8, and 0.9 and dynamic pressures of 300, 450, 600, and 800 lb/sq ft. The Reynolds numbers for these flight conditions ranged from 26 x 10(exp 6) to 54 x 10(exp 6) at the mean aerodynamic chord. Load factor increases of up to 1.0 g achieved with no increase in wing root bending moment with the MLC flap configuration.
Author (revised)

N94-24311*# National Aeronautics and Space Administration. Langley Research Center, Hampton, VA.
AN EXPERIMENTAL INVESTIGATION OF A MACH 3.0 HIGH-SPEED CIVIL TRANSPORT AT SUPERSONIC SPEEDS
Gloria Hernandez, Peter F. Covell, and Marvin E. McGraw, Jr. (Lockheed Engineering and Sciences Co., Hampton, VA.) Nov. 1993 94 p Microfiche as supplement
(RTOP 505-59-20-01)
(NASA-TP-3365; L-17171; NAS 1.60:3365) Avail: CASI HC A05/MF A01

An experimental study was conducted to determine the aerodynamic characteristics of a proposed high speed civil transport. This configuration was designed to cruise at Mach 3.0 and sized to carry 250 passengers for 6500 n.mi. The configuration consists of a highly blended wing body and features a blunt parabolic nose planform, a highly swept inboard wing panel, a moderately swept outboard wing panel, and a curved wingtip. Wind tunnel tests were conducted in the Langley Unitary Plan Wind Tunnel on a 0.0098-scale model. Force, moment, and pressure data were obtained for Mach numbers ranging from 1.6 to 3.6 and at angles of attack ranging from -4 to 10 deg. Extensive flow visualization studies (vapor screen and oil flow) were obtained in the experimental program. Both linear and advanced computational fluid dynamics (CFD) theoretical comparisons are shown to assess the ability to predict forces, moments, and pressures on configurations of this type. In addition, an extrapolation of the wind tunnel data, based on empirical principles, to full-scale conditions is compared with the theoretical aerodynamic predictions. Author (revised)

N94-24335*# National Aeronautics and Space Administration. Lewis Research Center, Cleveland, OH.
ETHYLENE TRACE-GAS TECHNIQUES FOR HIGH-SPEED FLOWS
David O. Davis and Bruce A. Reichert Feb. 1994 12 p Presented at the 32nd Aerospace Meeting and Exhibit, Reno, NV, 10-13 Jan. 1994; sponsored by AIAA
(RTOP 505-62-52)
(NASA-TM-106491; AIAA Paper 94-0733; E-8478; NAS 1.15:106491)
Avail: CASI HC A03/MF A01

Three applications of the ethylene trace-gas technique to high-speed flows are described: flow-field tracking, air-to-air mixing, and bleed mass-flow measurement. The technique involves injecting a non-reacting gas (ethylene) into the flow field and measuring the concentration distribution in a downstream plane. From the distributions, information about flow development, mixing, and mass-flow rates can be dtermined. The trace-gas apparatus and special considerations for use in high-speed flow are discussed. A description of each application, including uncertainty estimates is followed by a demonstrative example. Author

N94-24464*# National Aeronautics and Space Administration. Langley Research Center, Hampton, VA.
EXPERIMENTAL CAVITY PRESSURE MEASUREMENTS AT SUBSONIC AND TRANSONIC SPEEDS. STATIC-PRESSURE RESULTS
E. B. Plentovich, Robert L. Stallings, Jr. (Lockheed Engineering and Sciences Co., Hampton, VA.), and M. B. Tracy Dec. 1993 76 p
(RTOP 505-68-70-08)
(NASA-TP-3358; L-17157; NAS 1.60:3358) Avail: CASI HC A05/MF A01

An experimental investigation was conducted to determine cavity flow-characteristics at subsonic and transonic speeds. A rectangular box cavity was tested in the Langley 8-Foot Transonic Pressure Tunnel at Mach numbers from 0.20 to 0.95 at a unit Reynolds number of approximately 3 x 10(exp 6) per foot. The boundary layer approaching the cavity was turbulent. Cavities were tested over a range of length-to-depth ratios (l/h) of 1 to 17.5 for cavity width-to-depth ratios of 1, 4, 8, and 16. Fluctuating- and static-pressure data in the cavity were obtained; however, only static-pressure data is analyzed. The boundaries between the flow regimes based on cavity length-to-depth ratio were determined. The change to transitional flow from open flow occurs at l/h at approximately 6-8 however, the change from transitional- to closed-cavity flow occurred over a wide range of l/h and was dependent on Mach number and cavity configuration. The change from closed to open flow as found to occur gradually. The effect of changing cavity dimensions showed that if the vlaue of l/h was kept fixed but the cavity width was decreased or cavity height was increased, the cavity pressure distribution tended more toward a more closed flow distribution. Author (revised)

N94-24576*# National Aeronautics and Space Administration. Langley Research Center, Hampton, VA.
STRUCTURAL DYNAMICS DIVISION RESEARCH AND TECHNOLOGY ACCOMPLISHMENTS FOR FY 1993 AND PLANS FOR FY 1994
Eleanor C. Wynne Jan. 1994 84 p
(RTOP 505-63-50-13)
(NASA-TM-109036; NAS 1.15:109036) Avail: CASI HC A05/MF A01

The purpose is to present the Structural Dynamics Division's research accomplishments for F.Y. 1993 and research plans for F.Y. 1994. The work under each Branch (technical area) is described in terms of highlights of accomplishments during the past year and highlights of plans for the current year as they relate to 5-year plans for each technical area. This information will be useful in program coordination with other government organizations and industry in areas of mutual interest. Author (revised)

N94-24586*# National Aeronautics and Space Administration. Langley Research Center, Hampton, VA.
AERODYNAMIC CHARACTERISTICS AND PRESSURE DISTRIBUTIONS FOR AN EXECUTIVE-JET BASELINE AIRFOIL SECTION
Dennis O. Allison and Raymond E. Mineck Dec. 1993 103 p
(RTOP 505-59-10-30)
(NASA-TM-4529; L-17228; NAS 1.15:4529) Avail: CASI HC A06/MF A02

A wind tunnel test of an executive-jet baseline airfoil model was conducted in the adaptive-wall test section of the NASA Langley 0.3-Meter Transonic Cryogenic Tunnel. The primary goal of the test was to measure airfoil aerodynamic characteristics over a wide range of flow conditions that encompass two design points. The two design Mach numbers were 0.654 and 0.735 with corresponding Reynolds numbers of 4.5 x 10(exp 6) and 8.9 x 10(exp 6) based on chord, respectively, and normal-force coefficients of 0.98 and 0.51, respectively. The tests were conducted over a Mach number range from 0.250 to 0.780 and a chord Reynolds number range from 3 x 10(exp 6) to 18 x 10(exp 6). The angle of attack was varied from -2 deg to a maximum below 10 deg with one exception in which the maximum was 14 deg for a Mach number of 0.250 at a chord Reynolds number of 4.5 x 10(exp 6). Boundary-layer transition was fixed at 5 percent of chord on both the upper and lower surfaces of the model for most of the test. The adaptive-wall test section had flexible top and bottom walls and rigid sidewalls. Wall interference was minimized by the movement of the adaptive walls, and the airfoil aerodynamic characteristics were corrected for any residual top and bottom wall interference.
Author (revised)

N94-24606*# United Technologies Research Center, East Hartford, CT.
AN ANALYSIS FOR HIGH REYNOLDS NUMBER INVISCID/VISCID INTERACTIONS IN CASCADES Final Report
Mark Barnett, Joseph M. Verdon, and Timothy C. Ayer Washington May 1993 50 p
(Contract NAS3-25425; RTOP 584-03-11)
(NASA-CR-4519; E-7851; NAS 1.26:4519) Avail: CASI HC A03/MF A01

An efficient steady analysis for predicting strong inviscid/viscid interaction phenomena such as viscous-layer separation, shock/boundary-layer interaction, and trailing-edge/near-wake interaction in turbomachinery blade passages is needed as part of a comprehensive analytical blade design prediction system. Such an analysis is described. It uses an inviscid/viscid interaction approach, in which the flow in the outer inviscid region is assumed to be potential, and that in the inner or viscous-layer region is governed by Prandtl's equations. The inviscid solution is determined using an implicit, least-squares, finite-difference approximation, the viscous-layer solution using an inverse, finite-difference, space-marching method which is applied along the blade surfaces and wake streamlines. The inviscid and viscid solutions are coupled using a semi-inverse global iteration procedure, which permits the prediction of boundary-layer separation and other strong-interaction phenomena. Results are presented for three cascades, with a range of inlet flow conditions considered for one of them, including conditions leading to large-scale flow separations. Comparisons with Navier-Stokes solutions and experimental data are also given. Author (revised)

N94-24716*# National Aeronautics and Space Administration. Langley Research Center, Hampton, VA.

SUPERSONIC AERODYNAMIC CHARACTERISTICS OF A CIRCULAR BODY EARTH-TO-ORBIT VEHICLE

George M. Ware, Walter C. Engelund, and Ian O. MacConochie (Lockheed Engineering and Sciences Co., Hampton, VA.) Jan. 1994 69 p
(RTOP 506-40-61-01)
(NASA-TM-4533; L-17286; NAS 1.15:4533) Avail: CASI HC A04/MF A01

The circular body configuration is a generic single- or multi-stage reusable Earth-to-orbit transport. A thick clipped-delta wing is the major lifting surface. For directional control, three different vertical fin arrangements were investigated: a conventional aft-mounted center fin, wingtip fins, and a nose-mounted fin. The tests were conducted in the Langley Unitary Plan Wind Tunnel. The configuration is longitudinally stable about the estimated center of gravity of 0.72 body length up to a Mach number of about 3.0. Above Mach 3.0, the model is longitudinally unstable at low angles of attack but has a stable secondary trim point at angles of attack above 30 deg. The model has sufficient pitch control authority with elevator and body flap to produce stable trim over the test range. The model with the center fin is directionally stable at low angles of attack up to a Mach number of 3.90. The rudder-like surfaces on the tip fins and the all-movable nose fin are designed as active controls to produce artificial directional stability and are effective in producing yawing moment. The wing trailing-edge aileron surfaces are effective in producing rolling moment, but they also produce large adverse yawing moment. Author (revised)

N94-24773# Air Force Flight Dynamics Lab., Wright-Patterson AFB, OH.

NONLINEAR EQUATIONS OF MOTION FOR A PANEL SUBJECT TO EXTERNAL LOADS Interim Report, Jan. 1992 - Oct. 1993

Mark A. Hopkins Nov. 1993 45 p
(AF Proj. 2401)
(AD-A273142; WL-TM-93-308) Avail: CASI HC A03/MF A01

The equations of motion of a constant thickness, rectangular panel subject to external static loads and unsteady supersonic aerodynamic forces is derived. Both isotropic and orthotropic panels are examined. The static loads come from in-plane forces, a temperature differential, and a pressure differential. The equations allow for slight initial curvature due to manufacturing imperfections. The equations are derived using a nonlinear strain-displacement relationship which permits both linear and nonlinear panel response studies. First order piston theory predicts the unsteady aerodynamic forces due to the supersonic flow over the upper surface. DTIC

N94-24849 Mississippi State Univ., Mississippi State.

NUMERICAL FLOW SIMULATION FOR COMPLETE VEHICLE CONFIGURATIONS Final Report, 1 Apr. 1990 - 31 Mar. 1993

Bharat K. Soni 1 Sep. 1993 74 p Limited Reproducibility: More than 20% of this document may be affected by microfiche quality
(Contract F49620-90-C-0027)
(AD-A273588; AFOSR-93-0863TR) Avail: CASI HC A04

In the spirit of the Air Force Office of Scientific Research's (AFOSR) initiative to promote university/industry collaborative research, a collaborative project entitled, Numerical Flow Simulation for Complete Vehicle Configurations has been executed by the National Science Foundation Engineering Research Center for Computational Field Simulation (NSF ERC) at Mississippi State University. The industrial participants include McDonnell Aircraft Company, McDonnell Douglas Research and Development Company, and Teledyne Brown Engineering Company. The research and development activities of this effort are focused on the advancement of methodologies to increase the efficiency, quality, and productivity of an overall CFD simulation associated with geometrically complex configurations. The progress realized in the aforestated development is presented in this report. Progress concerning efforts designed to increase the efficiency and productivity of an overall CFD simulation process--from geometry definition to post processing of results as applied to complete aircraft configurations--is presented. This progress has been brought about through enhancements in geometry processing, surface grid generation, grid refinement, grid adaptation, and domain decomposition strategies. DTIC

N94-25051 Department of the Navy, Washington, DC.

REGULATED DRAG AREA PARACHUTE Patent

Elsa J. Hennings, inventor (to Navy) 28 Sep. 1993 11 p Filed 8 Apr. 1992
(AD-D015992; US-Patent-5,248,117; US-Patent-Appl-SN-866649; US-Patent-Class-244-152) Avail: US Patent and Trademark Office

The disclosed invention is a regulated drag area parachute for decelerating a manned ejection seat or an ejectable capsule at a low altitude from an aircraft or other air vehicle. This parachute comprises a canopy composed of two portions, suspension lines, and a means for controlling the inflation of the canopy so that the two portions of the canopy inflate independently from one another. This means for controlling the inflation of the canopy provides a manner to regulate the rate of infraction of the lower portion of the canopy. Thus, the invention allows the top, or apex portion of the canopy, to inflate rapidly while the remaining portion of the canopy can be inflated subsequently and in a controlled manner so that the effective drag area of the canopy can be regulated during the deployment of the parachute. DTIC

N94-25137# Defence Research Agency, Farnborough (England).

SUB-SONIC FLOW ABOUT A SLENDER PROFILE IN A TUNNEL HAVING PERFORATED WALLS [DOZVUKOVOE OBTEKANIE TONKOGO PROFILYA V KANALE S PERFORIROVANNYMI STENKAMI]

S. A. Glaskov 8 Feb. 1993 16 p Transl. into ENGLISH from Uchenye Zapiski Tsagi (Russia), v. 22, no. 2, 1991 p 3-12
(AD-A273184; DRA-Library-Trans-2202) Avail: CASI HC A03/MF A01

A solution has been found for the problem of flow about a profile by an ideal incompressible liquid in a tunnel, the upper and lower walls of which may have varying porosity, depending on whether gas flows in or out of the tunnel. Calculations have been made of the distributions of pressure on the walls of the tunnel and on the profile located at an angle of attack on the axis of symmetry of the tunnel. DTIC

N94-25173*# Sverdrup Technology, Inc., Brook Park, OH.

ANALYTICAL SKIN FRICTION AND HEAT TRANSFER FORMULA FOR COMPRESSIBLE INTERNAL FLOWS Final Report

Lawrence J. DeChant and Marc J. Tattar (Ohio Aerospace Inst., Brook Park.) Jan. 1994 20 p
(Contract NAS3-25266; RTOP 505-69-50)
(NASA-CR-191185; E-8096; NAS 1.26:191185) Avail: CASI HC A03/MF A01

An analytic, closed-form friction formula for turbulent, internal, compressible, fully developed flow was derived by extending the incompressible law-of-the-wall relation to compressible cases. The model is capable of analyzing heat transfer as a function of constant surface temperatures and surface roughness as well as analyzing adiabatic conditions. The formula reduces to Prandtl's law of friction for adiabatic, smooth, axisymmetric flow. In addition, the formula reduces to the Colebrook equation for incompressible, adiabatic, axisymmetric flow with various roughnesses. Comparisons with available experiments show that the model averages roughly 12.5 percent error for adiabatic flow and 18.5 percent error for flow involving heat transfer. Author (revised)

N94-25182*# National Aeronautics and Space Administration. Lewis Research Center, Cleveland, OH.

IMPROVING DIFFUSING S-DUCT PERFORMANCE BY SECONDARY FLOW CONTROL

Bruce A. Reichert and Bruce J. Wendt Feb. 1994 12 p Presented at the 32nd Aerospace Sciences Meeting and Exhibit, Reno, NV, 10-13 Jan. 1994; sponsored by AIAA
(RTOP 505-62-52)
(NASA-TM-106492; E-8479; NAS 1.15:106492; AIAA Paper 94-0365)
Avail: CASI HC A03/MF A01

The objective of this research was to study ways to reduce inlet flow distortion (i.e., total pressure nonuniformity) and improve total pressure recovery in a diffusing S-duct. This was accomplished by controlling the development of secondary flows within the duct through the use of tapered-fin type vortex generators. Reported are results for the bare duct and seven different configurations of vortex generators. Data presented for each configuration include surface static pressure, surface flow visualization, and exit plane total pressure and transverse velocity. The performance of each configuration was assessed by calculating total pressure recovery and inlet distortion descriptors from the data and comparing them to the values for the bare duct. The best configuration tested reduced distortion (as measured by the DC(45) and DC(90) descriptors) by more than 50 percent while improving total pressure recovery by 0.5 percent. These results should provide valuable guidance in designing vortex generator installations in ducts and for assessing the accuracy of computational fluid dynamics (CFD) methods to calculate duct flows with installed vortex generators. Author (revised)

N94-25187*# National Aeronautics and Space Administration. Ames Research Center, Moffett Field, CA.

EFFECT OF AN EXTENDABLE SLAT ON THE STALL BEHAVIOR OF A VR-12 AIRFOIL

P. Plantin DeHugues (Ministere des Affaires Etrangeres, Paris, France.), K. W. McAlister (Army Aviation Systems Command, Moffett Field, CA.), and C. Tung (Army Aviation Systems Command, Moffett Field, CA.) Sep. 1993 65 p

(RTOP 505-61-51)

(NASA-TP-3407; A-93056; NAS 1.60:3407; ATCOM-TR-93-A-002) Avail: CASI HC A04/MF A01

Experimental and computational tests were performed on a VR-12 airfoil to determine if the dynamic-stall behavior that normally accompanies high-angle pitch oscillations could be modified by segmenting the forward portion of the airfoil and extending it ahead of the main element. In the extended position the configuration would appear as an airfoil with a leading-edge slat, and in the retracted position it would appear as a conventional VR-12 airfoil. The calculations were obtained from a numerical code that models the vorticity transport equation for an incompressible fluid. These results were compared with test data from the water tunnel facility of the Aeroflightdynamics Directorate at Ames Research Center. Steady and unsteady flows around both airfoils were examined at angles of attack between 0 and 30 deg. The Reynolds number was fixed at 200,000 and the unsteady pitch oscillations followed a sinusoidal motion described by alpha = alpha(sub m) + 10 deg sin(omega t). The mean angle (alpha(sub m)) was varied from 10 to 20 deg and the reduced frequency from 0.05 to 0.20. The results from the experiment and the calculations show that the extended-slat VR-12 airfoil experiences a delay in both static and dynamic stall not experienced by the basic VR-12 airfoil. Author

N94-25411# Naval Surface Warfare Center, Dahlgren, VA.

STATE-OF-THE-ART ENGINEERING AEROPREDICTION METHODS WITH EMPHASIS ON NEW SEMIEMPIRICAL TECHNIQUES FOR PREDICTING NONLINEAR AERODYNAMICS ON COMPLETE MISSILE CONFIGURATIONS Final Report

Frank G. Moore Nov. 1993 165 p

(AD-A273680; NSWCDD/TR-93/551) Avail: CASI HC A08/MF A02

The pros and cons of numerical, semiempirical, and empirical aeroprediction codes are discussed and many state-of-the-art codes in use today are listed. It then summarizes many of the more popular approximate analytical methods used in State-of-the-Art (SOTA) semiempirical aeroprediction codes. It also summarizes some recent new nonlinear semiempirical methods that allow more accurate calculation of static aerodynamics on complete missile configurations to higher angles of attack. Results of static aerodynamic calculations on complete missile configurations compared to wind tunnel data are shown for several configurations at various flight conditions. Calculations show the new nonlinear methods being far superior to some of the former linear technology when used at angles of attack greater than about 15 degrees. DTIC

N94-25461# Institut Franco-Allemand de Recherches, Saint-Louis (France).

DETAILED DESCRIPTION OF TWO CALCULATION PROGRAMS FOR INCOMPRESSIBLE, STEADY STATE BOUNDARY LAYER FLOWS, APPLIED TO DETERMINE THE AERODYNAMIC CHARACTERISTICS OF NACA12 AND OA312 FOILS AT LOW REYNOLDS NUMBERS [DESCRIPTION DETAILLEE DE DEUX PROGRAMMES DE CALCUL DE COUCHE LIMITE STATIONNAIRE, INCOMPRESSIBLE, UTILISES POUR LA DETERMINATION DES CARACTERISTIQUES AERODYNAMIQUES DES PROFILS NACA12 ET OA312 A FAIBLE NOMBRE DE REYNOLDS]

P. Wernert 29 Apr. 1992 37 p In FRENCH

(ISL-N-604/92; ETN-94-95117) Avail: CASI HC A03/MF A01

In the scope of the study concerning unsteady flows due to oscillating foils, the steady pressure field was measured. Boundary layer computer programs were applied to calculate C(sub x), C(sub z), and C(sub m) coefficients. The two programs used for calculating boundary layer characteristics of oscillating foils in incompressible flows were CLTHA1 and THDIM. Both programs are based on the Thwaites integral method for laminar flows. The turbulent boundary layer is calculated with CLTHA1 by applying a Lazareff-Semezis modified integration method and with THDIM by the Head method. The block diagrams of both programs are included. ESA

N94-25517# Air Force Inst. of Tech., Wright-Patterson AFB, OH.

ANALYSIS AND CHARACTERISTICS OF COMPRESSOR STALL PRECURSOR SIGNALS IN FORWARD AND AFT SWEPT HIGH SPEED COMPRESSOR M.S. Thesis

Bernard J. Frank Dec. 1993 127 p

(AD-A273820; AFIT/GAE/ENY/93D-14) Avail: CASI HC A07/MF A02

The stall characteristics of four single-stage transonic compressor rotors were investigated as they were throttled to stall. Forward-swept, backward-swept, and straight leading edge rotors were examined. Three methods of analysis--windowed power spectrum densities of pressure and spatial Fourier coefficients, phase tracking analysis, and system identification--were used to identify the first appearance of modal waves and their accompanying frequencies in order to identify a stall warning time. A direct correlation between the amount of stall warning time and the shape of the compressor characteristic was found. Specifically, if the compressor characteristic had a significant period of flat or positive slope, more stall warning was noted. It was also found that the forward-swept rotor consistently provided more stall warning time than the backward-swept and straight leading edge rotors. DTIC

N94-23656*# Colorado Univ., Boulder. Dept. of Aerospace and Engineering Sciences.

SUPERSONIC MINIMUM LENGTH NOZZLE DESIGN FOR DENSE GASES

Andrew C. Aldo and Brian M. Argrow *In* NASA. Lewis Research Center, The Fifth Annual Thermal and Fluids Analysis Workshop Nov. 1993 p 329-341 (For primary document see N94-23634 06-34)

Avail: CASI HC A03/MF A04; 5 functional color pages

N94-23661*# Maine Univ., Orono. Div. of Mathematics.

AN ANALYTIC STUDY OF A TWO-PHASE LAMINAR AIRFOIL IN SIMULATED HEAVY RAIN

Yu-Kao Hsu *In* NASA. Lewis Research Center, The Fifth Annual Thermal and Fluids Analysis Workshop Nov. 1993 p 413-427 Sponsored by NASA. Langley Research Center (For primary document see N94-23634 06-34)

Avail: CASI HC A03/MF A04; 5 functional color pages

N94-24142*# Stanford Univ., CA. Center for Turbulence Research.

TOWARD MODELING WINGTIP VORTICES

O. Zeman *In its* Annual Research Briefs, 1993 Dec. 1993 p 31-40 (For primary document see N94-24138 06-34)

Avail: CASI HC A02/MF A04

N94-24143*# Stanford Univ., CA. Center for Turbulence Research.

NEW CONCEPTS FOR REYNOLDS STRESS TRANSPORT EQUATION MODELING OF INHOMOGENEOUS FLOWS

J. Blair Perot and Parviz Moin *In its* Annual Research Briefs, 1993

Dec. 1993 p 41-65 (For primary document see N94-24138 06-34)
Avail: CASI HC A03/MF A04

N94-24145*# Texas A&M Univ., College Station.
COMPUTATION OF TURBULENT FLOWS OVER BACKWARD AND FORWARD-FACING STEPS USING A NEAR-WALL REYNOLDS STRESS MODEL
Sung Ho Ko *In* Stanford Univ., Annual Research Briefs, 1993 Dec. 1993 p 75-90 (For primary document see N94-24138 06-34)
Avail: CASI HC A03/MF A04

N94-24150*# Stanford Univ., CA. Center for Turbulence Research.
TOWARD LARGE EDDY SIMULATION OF TURBULENT FLOW OVER AN AIRFOIL
Haecheon Choi *In its* Annual Research Briefs, 1993 Dec. 1993 p 145-149 (For primary document see N94-24138 06-34)
Avail: CASI HC A01/MF A04

N94-24164*# Stanford Univ., CA.
DIRECT SIMULATION OF ISOTHERMAL-WALL SUPERSONIC CHANNEL FLOW
Gary N. Coleman *In its* Annual Research Briefs, 1993 Dec. 1993 p 313-328 (For primary document see N94-24138 06-34)
Avail: CASI HC A03/MF A04

N94-24285 Aero-Design and Development Ltd., Rehovoth (Israel).
AERODYNAMIC MODELS FOR PERFORMANCE CALCULATIONS OF MODERN TECHNOLOGY PROPELLERS
I. Weissberg, G. Engel, and A. Rosen (Technion - Israel Inst. of Tech., Haifa.) *In* Israel Society of Aeronautics and Astronautics, The 33rd Israel Annual Conference on Aviation and Astronautics 25 Feb. 1993 p 458-468 (For primary document see N94-24241 06-01)
Copyright Avail: Issuing Activity (Israel Society of Aeronautics and Astronautics, c/o Faculty of Engineering, Tel-Aviv Univ., Ramat Aviv 69978, Israel)

N94-25110*# Lockheed Engineering and Sciences Co., Hampton, VA. Aircraft Guidance and Control Branch.
NONLINEAR AERODYNAMIC MODELING USING MULTIVARIATE ORTHOGONAL FUNCTIONS
Eugene A. Morelli *In* NASA. Langley Research Center, NASA LaRC Workshop on Guidance, Navigation, Controls, and Dynamics for Atmospheric Flight, 1993 Dec. 1993 p 389-400 (For primary document see N94-25096 06-01)
Avail: CASI HC A03/MF A04

03 AIR TRANSPORTATION AND SAFETY

Includes passenger and cargo air transport operations; and aircraft accidents.

For related information see also *16 Space Transportation* and *85 Urban Technology and Transportation.*

N94-23288*# Boeing Commercial Airplane Co., Seattle, WA. Avionics/Flight Systems.
AIRPORT SURFACE OPERATIONS REQUIREMENTS ANALYSIS Final Report
John L. Groce, Greg J. VonBokern, and Rick L. Wray Aug. 1993 101 p
(Contract NAS1-18027; RTOP 505-64-13-01)
(NASA-CR-191508; NAS 1.26:191508) Avail: CASI HC A06/MF A02

This report documents the results of the Airport Surface Operations Requirements Analysis (ASORA) study. This study was conducted in response to task 24 of NASA Contract NAS1-18027. This study is part of NASA LaRC's Low Visibility Surface Operations program, which is designed to eliminate the constraints on all-weather arrival/departure operations due to the airport/aircraft ground system. The goal of this program is to provide the capability for safe and efficient aircraft operations on the airport surface during low visibility conditions down to zero. The ASORA study objectives were to (1) develop requirements for operation on the airport surface in visibilities down to zero; (2) survey and evaluate likely technologies; (3) develop candidate concepts to meet the requirements; and (4) select the most suitable concept based on cost/benefit factors. Author

N94-23523*# National Aeronautics and Space Administration. Lewis Research Center, Cleveland, OH.
CLOSE-UP ANALYSIS OF INFLIGHT ICE ACCRETION
Andrew L. Reehorst, Thomas P. Ratvasky, and James Sims (Cortez 3 Services Corp., Brook Park, OH.) Jan. 1994 12 p Presented at the 32nd Aerospace Sciences Meeting and Exhibit, Reno, NV, 10-13 Jan. 1994; sponsored by AIAA
(Contract NAS3-24816; RTOP 505-68-10)
(NASA-TM-106457; E-8318; NAS 1.15:106457; AIAA Paper 94-0804)
Avail: CASI HC A03/MF A01

The objective of this effort was to validate in flight, data that has been gathered in the NASA Lewis Research Center's Icing Research Tunnel (IRT) over the past several years. All data was acquired in flight on the NASA Lewis Research Center's Twin Otter Icing Research Aircraft. A faired 3.5 in. diameter metal-clad cylinder exposed to the natural icing environment was observed by a close-up video camera. The grazing angle video footage was recorded to S-VHS video tape and after the icing encounter, the resultant ice shape was documented by 35 mm photography and pencil tracings. The feather growth area was of primary interest; however, all regions of the ice accretion, from the stagnation line to the aft edge of run back were observed and recorded. After analysis of the recorded data several interesting points became evident: (1) the measured flight feather growth rate is consistent with IRT values, (2) the feather growth rate appears to be influenced by droplet size, (3) the feathers were straighter in the lower, spottier LWC of flight in comparison to those observed in the IRT, (4) feather shedding and ice sublimation may be significant to the final ice shape, and (5) the snow encountered on these flights appeared to have little influence on ice growth. Author (revised)

N94-23579# National Transportation Safety Board, Washington, DC.
AIRCRAFT ACCIDENT REPORT: INADVERTENT IN-FLIGHT SLAT DEPLOYMENT, CHINA EASTERN AIRLINES FLIGHT 583, MCDONNELL DOUGLAS MD-11, B-2171, 950 NAUTICAL MILES SOUTH OF SHEMYA, ALASKA, 6 APRIL 1993
27 Oct. 1993 73 p
(PB93-910408; NTSB/AAR-93/07) Avail: CASI HC A04/MF A01

This report explains the inadvertent deployment of the MD-11 airplane's leading edge wing slats while the airplane was in cruise flight, about 950 nautical miles south of Shemya, Alaska, on April 6, 1993. Safety issues in the report focused on the inadequate design of the flap/slat actuation handle, the inadvertent extension of the leading edge wing slats, the longitudinal stability of the airplane during the pitch upset, the pilot-induced oscillations that can occur during recovery, the premature deterioration of the seat cushion fire-blocking material, and the inability of the material to provide the required seat cushion fire protection on transport-category airplanes. Safety recommendations on these issues were made to the Federal Aviation Administration. Author

N94-23810 National Inst. of Standards and Technology, Gaithersburg, MD. Building and Fire Research Lab.
DISPERSION OF FIRE SUPPRESSION AGENTS DISCHARGED FROM HIGH PRESSURE VESSELS: ESTABLISHING INITIAL/BOUNDARY CONDITIONS FOR THE FLOW OUTSIDE THE VESSEL
L. Y. Cooper Sep. 1993 38 p Sponsored by Department of the Air Force, Wright-Patterson AFB, OH Limited Reproducibility: More than 20% of this document may be affected by microfiche quality
(PB94-103660; NISTIR-5219) Avail: Issuing Activity (National Technical Information Service (NTIS))

The dispersion and extinguishment effectiveness of Halon and Halon-alternative fire extinguishment agents discharged from N2-pressurized vessels was studied. In the systems under consideration, as the agent exists from the vessel, thermodynamic and fluid-dynamic instabilities lead to flashing and break-up of the agent into a two-phase droplet/gaseous jet mixture. This occurs in a transition region relatively close to the vessel exit orifice/nozzle. Downstream of this region the two-phase agent jet then mixes with the ambient air environment and is dispersed in the protected space. A mathematical model was developed previously to simulate the time-dependent discharge of the agent from the pressure vessel. Using the output of this model and thermodynamic and fluid-dynamic considerations of the phenomena in the transition section, the present work develops a method for determining a set of initial/boundary conditions at an initial section of the jet, downstream of the transition region. These initial/boundary conditions are in a form that can be used to formulate and solve the problem of the development and dispersal of the ensuing mixed air/two-phase-agent jet. Example applications of the developed methodology are presented. These are for agent discharge from a half-liter cylindrical discharge vessel with a circular discharge nozzle/orifice of diameter 0.019m. Simulations involve discharge of the vessel when it is half-filled with either Freon 22 or Halon 1301 and then pressurized with N2 to 41.37 x 10(exp 5)Pa (600psi). NTIS

N94-24047*# National Aeronautics and Space Administration. Lewis Research Center, Cleveland, OH.

RIME-, MIXED- AND GLAZE-ICE EVALUATIONS OF THREE SCALING LAWS

David N. Anderson Jan. 1994 15 p Presented at the 32nd Aerospace Sciences Meeting and Exhibit, Reno, NV, 10-13 Jan. 1994; sponsored by AIAA
(RTOP 505-68-10)
(NASA-TM-106461; E-8323; NAS 1.15:106461; AIAA Paper 94-0718)
Avail: CASI HC A03/MF A01

This report presents the results of tests at NASA Lewis to evaluate three icing scaling relationships or 'laws' for an unheated model. The laws were LWC x time = constant, one proposed by a Swedish-Russian group and one used at ONERA in France. Icing tests were performed in the NASA Lewis Icing Research Tunnel (IRT) with cylinders ranging from 2.5- to 15.2-cm diameter. Reference conditions were chosen to provide rime, mixed and glaze ice. Scaled conditions were tested for several scenarios of size and velocity scaling, and the resulting ice shapes compared. For rime-ice conditions, all three of the scaling laws provided scaled ice shapes which closely matched reference ice shapes. For mixed ice and for glaze ice none of the scaling laws produced consistently good simulation of the reference ice shapes. Explanations for the observed results are proposed, and scaling issues requiring further study are identified. Author

N94-24062# National Transportation Safety Board, Washington, DC.

AIRCRAFT ACCIDENT REPORT: IN-FLIGHT ENGINE SEPARATION. JAPAN AIRLINES, INC., FLIGHT 46E, BOEING 747-121, N473EV, ANCHORAGE, ALASKA, 31 MARCH 1993

13 Oct. 1993 109 p
(PB93-410407; NTSB/AAR-93/06) Avail: CASI HC A06/MF A02

This report explains the in-flight separation of the No. 2 engine and engine pylon from a B-747-121 airplane shortly after its takeoff from Anchorage International Airport, Anchorage, Alaska, on March 31, 1993. The safety issues discussed in the report focused on the inspection of B-747 engine pylons, meteorological hazards to aircraft, the lateral load-carrying capability of engine pylon structures, and aircraft departure routes at Anchorage International Airport during turbulent weather conditions. Safety recommendations concerning these issues were addressed to the Federal Aviation Administration and the National Weather Service. Author

N94-24091# Advisory Group for Aerospace Research and Development, Neuilly-Sur-Seine (France).

AIRCRAFT FLIGHT SAFETY: A BIBLIOGRAPHY [LA SECURITE EN VOL: UNE BIBLIOGRAPHIE]

Dec. 1993 53 p
(AGARD-R-805; ISBN-92-835-0730-4) Copyright Avail: CASI HC A04/MF A01

A bibliography of publications held by NASA on aspects of aircraft flight safety is provided. The abstracts are listed by the following topics: human errors, injury reduction, engines, structures and materials, aircraft aging, fire, adverse weather, aircraft maintenance, future safety requirements, and miscellaneous items. The bibliography was compiled originally as a contribution to a conference on aircraft flight safety, sponsored jointly by AGARD and the Russian International Integration Association, which was held in Russia in August/September 1993. Author (revised)

N94-24718 Naval Postgraduate School, Monterey, CA.

A NUMERICAL STUDY OF AIRPLANES FLYING IN PROXIMITY M.S. Thesis

David B. Porter Sep. 1993 140 p Limited Reproducibility: More than 20% of this document may be affected by microfiche quality
(AD-A273373) Avail: Issuing Activity (Defense Technical Information Center (DTIC))

During an emergency such as an unsafe landing gear indication, a second aircraft is often used to perform an airborne visual inspection of the landing gear. The chase airplane may be quite dissimilar in size and wing loading and consequently experience unexpected aerodynamic forces and moments caused by the other airplane. A numerical study of the inherent danger involved with the aerodynamic interaction of aircraft flying in proximity was made using the low-order panel code PMARC (Panel Method Ames Research Center). PMARC validation was made by comparing wind tunnel and analytically derived stability data for T-34 and F-14 models with PMARC results. A T-34 was then placed at various distances underneath an F-14 to determine changes in lift and pitching moments on the T-34. Color illustrations of pressure coefficients were used to highlight the changes in aerodynamic forces and moments as vertical separation between the two aircraft was decreased. PMARC showed that 4.5 degrees of elevator trim change was required as a T-34 approached to within its semispan of an F-14. DTIC

N94-24750# Office of Technology Assessment, Washington, DC.

AIRCRAFT EVACUATION TESTING: RESEARCH AND TECHNOLOGY ISSUES

Sep. 1993 65 p
(PB94-107620) Avail: CASI HC A04/MF A01

The report explains and analyzes the current state of testing procedures used to certify aircraft in terms of emergency evacuation capability. A number of issues regarding the requirement for certification based on people evacuating an actual aircraft are reviewed, as are possible alternatives or supplements to the procedure. Technologies that might be considered for making survival times greater in a real emergency are identified. NTIS

N94-24781# Naval Postgraduate School, Monterey, CA.

INFORMATION SYSTEMS STRATEGY IN AIR TRANSPORT M.S. Thesis

Desmond P. McGlade Sep. 1993 135 p
(AD-A273125) Avail: CASI HC A07/MF A02

Seeking to improve the role of Information Technology (IT) and business practices in the Department of Defense, organizations were sought to serve as a model to aid in the improvement process. Southwest Airlines, a major U.S. carrier based in Dallas, Texas was chosen because of its record of profitability and its unique use of information technology. This case study describes Southwest's mission, goals, organization, business decisions, attitude, growth and information technology. The primary focus is the fact that Southwest does not participate in a major carrier's reservation system. Lessons learned for a military officer in terms of Information Technology are to avoid redundancy, improve functionality, avoid expensive enhancements that do not contribute to our requirements, and don't discount old technologies. DTIC

N94-24841# National Transportation Safety Board, Washington, DC. Office of Research and Engineering.

ANNUAL REVIEW OF AIRCRAFT ACCIDENT DATA. US GENERAL AVIATION CALENDAR YEAR 1990

17 Dec. 1993 83 p
(PB94-126869; NTSB/ARG-93/02) Avail: CASI HC A05/MF A01

This report presents a statistical compilation and review of general aviation accidents which occurred in 1990 in the United States, its territories and possessions, and in international waters. The accidents reported are all those involving U.S. registered aircraft not conducting operations under 14 CFR 121, 14 CFR 125, 14 CFR 127, or 14 CFR 135. This report is divided into five actions: all accidents, fatal accidents, serious injury accidents, property damage accidents, and midair collision accidents. Several tables present accident parameters for 1990 accidents only, and each section includes tabulations which present comparative statistics for 1990 and for the five-year period 1985-1989. Author (revised)

N94-24864# Anacapa Sciences, Inc., Fort Rucker, AL.

AVIATION SYSTEM SAFETY RISK MANAGEMENT TOOL ANALYSIS. VOLUME 2: APPENDICES Final Report

D. C. Thill and D. B. Hammilton Oct. 1993 372 p

(Contract MDA903-92-D-0025)
(AD-A273502; ARL-CR-120-Vol-2) Avail: CASI HC A16/MF A03

U.S. Army risk management is a process used to minimize loss of life, injuries, and property damage. One step in the risk management process is risk assessment. Currently, risk assessment assigns a probability value for an identified hazard, based on a subjective evaluation. The need exists to assign objective probability values when assessing the risks imposed by aircraft component and part failures. This research extracted UH-60 and UH-1 helicopter part failure data for a ten-year period from the Army Safety Management Information System (ASMIS) data base. Data inconsistencies were corrected, the corrected data were organized into groups, and failure rates were calculated. The results established that component and part failure analyses can be successfully conducted using available data bases and that these data can be used to quantify hazard probabilities for failed aircraft components and parts. Volume one of this report describes the methodology used to obtain the failure rates, presents the results of the analyses, discusses potential uses for the data, and provides recommendations for further research. Volume two provides a table of part failure rates and a list of records for the UH-60 (see Appendix A) and for the UH-1 (see Appendix B). DTIC

N94-24941# Federal Aviation Administration, Atlantic City, NJ.
FULL-SCALE FIRE TESTING OF SEAT COMPONENT MATERIALS
Patricia Gahill Oct. 1993 26 p
(AD-A273499; DOT/FAA/CT-TN93/13) Avail: CASI HC A03/MF A01

Full-scale fire testing was conducted in a furnished aircraft cabin to compare a currently used thermoplastic material and a new thermoplastic material with low heat and smoke release characteristics used in forming seat components. This testing was conducted due to questions concerning the exemption of seat components from the heat release and smoke requirement mandated for certain large surface area components in the aircraft fuselage. Results of the fullscale testing showed no significant difference in temperatures, smoke levels, or oxygen depletion between the two materials. While carbon monoxide and carbon dioxide emissions were slightly higher with the currently used material, it cannot be concluded that this material was the cause. Based on the overall data, it appears that the small amount of seat component material is not significantly contributing to increased fire hazards. DTIC

N94-25141# Army Aeromedical Research Lab., Fort Rucker, AL.
PROJECTED EFFECTIVENESS OF AIRBAG SUPPLEMENTAL RESTRAINT SYSTEMS IN US ARMY HELICOPTER COCKPITS Final Report
Dennis F. Shanahan, Samuel G. Shannon, and James E. Bruckart Sep. 1993 27 p
(DA Proj. 3M1-62787-A-878)
(AD-A273250) Avail: CASI HC A03/MF A01

Despite significant advances in accident prevention, crashworthiness, and individual protective equipment, head and torso injuries continue to cause death and disabling injuries in survivable Army helicopter accidents. Most of these injuries are caused by the occupant striking internal structures. The purpose of this study was to review Army helicopter accident records to determine the number of fatal and disabling injuries in pilots and copilots that could be prevented with the introduction of an airbag supplemental restraint system into U.S. Army helicopter cockpits. DTIC

N94-25153# General Accounting Office, Washington, DC. National Security and International Affairs Div.
C-17 LOT 3 PRODUCTION CONTRACT
24 Sep. 1993 6 p
(AD-A273180; GAO/NSIAD-93-301R) Avail: CASI HC A02/MF A01

This report responds to your request for information on the estimated cost at completion for the C-17 program's lot III production contract. Specifically, you requested that we (1) review the basis for the Defense Plant Representative Office's (DPRO) modification to its original cost estimate and (2) provide our assessment of whether costs are likely to exceed the C-17 lot III contract ceiling price. DTIC

N94-25175# National Transportation Safety Board, Washington, DC.
AIRCRAFT ACCIDENT REPORT: IN-FLIGHT LOSS OF PROPELLER BLADE AND UNCONTROLLED COLLISION WITH TERRAIN MITSUBISHI MU-2B-60, N86SD, ZWINGLE, IOWA, 19 APRIL 1993
16 Nov. 1993 130 p
(PB93-910409; NTSB/AAR-93/08) Avail: CASI HC A07/MF A02

The in-flight loss of propellar blade and subsequent crash of an Mu-2B-60 airplane, operated by the South Dakota Department of Transportation, while the flightcrew was attempting an approach to an emergency landing at Dubuque Regional Airport, Dubuque, Iowa, on 19 April 1993 is explained. The safety issues discussed include the propeller hub design, certification and continuing airworthiness, and air traffic control training. Recommendations concerning these issues were made to the Federal Aviation Administration. Author (revised)

N94-25272*# National Aeronautics and Space Administration. Ames Research Center, Moffett Field, CA.
CONFLICT-FREE TRAJECTORY PLANNING FOR AIR TRAFFIC CONTROL AUTOMATION
Rhonda Slattery and Steve Green Jan. 1994 19 p Original contains color illustrations
(RTOP 505-64-13)
(NASA-TM-108790; A-93132; NAS 1.15:108790) Avail: CASI HC A03/MF A01; 6 functional color pages

As the traffic demand continues to grow within the National Airspace System (NAS), the need for long-range planning (30 minutes plus) of arrival traffic increases greatly. Research into air traffic control (ATC) automation at ARC has led to the development of the Center-TRACON Automation System (CTAS). CTAS determines optimum landing schedules for arrival traffic and assists controllers in meeting those schedules safely and efficiently. One crucial element in the development of CTAS is the capability to perform long-range (20 minutes) and short-range (5 minutes) conflict prediction and resolution once landing schedules are determined. The determination of conflict-free trajectories within the Center airspace is particularly difficult because of large variations in speed and altitude. The paper describes the current design and implementation of the conflict prediction and resolution tools used to generate CTAS advisories in Center airspace. Conflict criteria (separation requirements) are defined and the process of separation prediction is described. The major portion of the paper will describe the current implementation of CTAS conflict resolution algorithms in terms of the degrees of freedom for resolutions as well as resolution search techniques. The tools described in this paper have been implemented in a research system designed to rapidly develop and evaluate prototype concepts and will form the basis for an operational ATC automation system. Author (revised)

N94-25273# National Transportation Safety Board, Washington, DC.
AIRCRAFT ACCIDENT/INCIDENT SUMMARY REPORT: CONTROLLED FLIGHT INTO TERRAIN GP EXPRESS AIRLINES, INC., N115GP BEECHCRAFT C-99, SHELTON, NEBRASKA, 28 APRIL 1993
19 Jan. 1994 67 p
(PB94-910401; NTSB/AAR-94/01/SUM) Avail: CASI HC A04/MF A01

The crash of N115GP into terrain at Shelton, Nebraska is explained. The safety issues discussed include attempted aerobatic maneuvers in commercial aircraft, check flights among peers, management responsibility to instill commitment of flight safety, and Federal Aviation Administration oversight of 14 CFR Part 135 operations. Author (revised)

04 AIRCRAFT COMMUNICATIONS AND NAVIGATION

Includes digital and voice communication with aircraft; air navigation systems (satellite and ground based); and air traffic control.

For related information see also *17 Space Communications, Spacecraft Communications, Command and Tracking* and *Communications and Radar.*

N94-24120 National Defence Headquarters, Ottawa (Ontario). Directorate of Research and Development Communications and Space.
AN OVERVIEW OF A GENERIC MULTI-SENSOR INTEGRATED NAVIGATION SYSTEM DESIGN
D. F. Liang Jun. 1993 22 p

(CTN-94-60916) Avail: Micromedia Ltd., Technical Information Centre, 165 Hotel de Ville, Place du Portage, Phase 2, Hull, Quebec J8X 3X2, Canada

The application of Kalman filtering technology to the design and development of a multi-sensor generic integrated navigation system (GINS) for aircraft is described. The primary system component is the integrated sensor unit which consists of all the selected navigation sensors. These sensors can be classified into two main categories: dead reckoning (DR) and radio navigation systems. To take advantage of the short-term stability of the DR system and the long-term stability of the radio navigation system, optimal estimation theory can be applied in the form of a Kalman filter (KF) to combine all the available measurements and provide a statistically optimal estimate of aircraft position and other parameters. To achieve the desired performance, the GINS processor must perform signal conditioning and sensor compensation functions and must contain efficient KF integration algorithms, error control, and performance monitoring routines. The system development approach is described, as well as system error modelling, and KF design. CISTI

N94-24127# Massachusetts Inst. of Tech., Lexington. Lincoln Lab.
ANALYSIS AND SURVEILLANCE PERFORMANCE AT CHICAGO O'HARE AIRPORT Project Report
Sylvia I. Altman, Douglas W. Burgess, Richard G. Potts, Ronald G. Sandholm, and M. Loren Wood 28 Jan. 1994 95 p
(Contracts DTFA-01-93-Z-02018; F19628-90-C-0002)
(DOT/FAA/RD-92/29; ATC-193) Avail: CASI HC A05/MF A01

The results of RF measurements of the 1030 and 1090 MHz environment in the Chicago terminal area conducted by Lincoln Laboratory in October 1991 are described. The measurements were made at the request of the FAA in response to reports by controllers in Chicago that TCAS interrogations are affecting the surveillance performance of the Chicago Secondary Surveillance Radar (SSR). The Airborne Measurements Facility (AM), developed at Lincoln Laboratory, was used to gather TCAS and SSR interrogation and reply data in the vicinity of O'Hare Airport during periods of active TCAS operation. Simultaneously, local aircraft track data were collected using the Automated Radar Terminal System (ARTS) data recording facility. Analysis of both the AMF data and the ARTS data show that TCAS interrogations do not cause a significant degradation in SSR surveillance performance and that the average Chicago ARTS track performance in the presence of TCAS-equipped aircraft is comparable to earlier measurements of track performance in Chicago as well as at a number of other high-density terminal areas. Specific regions within the Chicago surveillance area were observed to contain concentrations of poor ARTS track performance, and analysis of the data has shown the cause to be differential vertical lobing associated with the SSR antenna and faulty Mode S transponders on certain air carrier aircraft. Both of these problems were subsequently corrected. Author (revised)

N94-24176 New Brunswick Univ., Fredericton. Dept. of Surveying Engineering.
AN INVESTIGATION INTO ACCELERATION DETERMINATION FOR AIRBORNE GRAVIMETRY USING THE GLOBAL POSITIONING SYSTEM M.S. Thesis
Derrick R. Peyton Jun. 1990 155 p
(ISBN-0-315-59470-5; CTN-94-60873) Copyright Avail: Micromedia Ltd., Technical Information Centre, 240 Catherine Street, Suite 305 Ottawa, Ontario, K2P 2G8, Canada HC/MF

The determination of acceleration using the NAVSTAR Global Positioning System (GPS) is investigated for airborne gravimetric applications. The position and velocity requirements for airborne gravimetry were met using GPS observing and processing techniques. However, the separation of the aircraft acceleration from the observed gravity still remains to be resolved to the 1-2 milligal accuracy requirements. As a means to move toward achieving such accuracy, a model is developed in which the accelerations are obtained by utilizing the second time derivative of the GPS carrier phase. Carrier phase data were collected from pairs of GPS receivers located at fixed points. Spectral analysis techniques for determining acquired acceleration accuracy were applied to computed accelerations from these data sets. Low-pass filters were applied to the acceleration data to separate the high frequency receiver measurement noise from the low frequency acceleration data. The implications and handling of GPS data contaminated by selective availability are addressed. Results show that for carrier phase observations over a fixed baseline of under 100 m, differential techniques can give accelerations which meet the 1-2 milligal accuracy requirements. Author (CISTI)

N94-24472# Civil Aeromedical Inst., Oklahoma City, OK.
AN EXAMINATION OF THE OPERATIONAL ERROR DATABASE FOR AIR ROUTE TRAFFIC CONTROL CENTERS Final Report
Mark D. Rodgers, ed. Dec. 1993 29 p
(DOT/FAA/AM-93/22) Avail: CASI HC A03/MF A01

Monitoring the frequency and determining the causes of operational errors - defined as the loss of prescribed separation between aircraft - is one approach to assessing the operational safety of the air traffic control system. The Federal Aviation Administration (FAA) refers to the loss of separation standards between aircraft as an operational error (OE). The extent to which separation is lost determines the severity of the error. The first study examined the relationships between error occurrence, controller workload (number of aircraft and traffic complexity), and causal factors involved. The FAA's Final Operational Error/Deviation Reports for ARTCC facilities during calendar years 1985-88 comprised the data base. A majority of the errors occurred under conditions of below average (25 percent) or average (39 percent) complexity. Complexity and number of aircraft were highly correlated. However, there was a significant difference across facilities in average workload during an event. Improved guidelines for quality assurance personnel are needed to insure a more standardized determination and reporting of workload dimensions. Results suggest that the frequency of some of the causal factors varied in response to changes in number of aircraft worked and traffic complexity. The second study analyzed the workload and causal factors related to the severity of OE's at ARTCC's during 1988-91. Neither the number of aircraft being worked nor air traffic complexity were significantly associated with severity. In general, the causal factors that resulted in greater severity likely involved reduced situation awareness by the controller. The relationship of aircraft profiles and flight levels with OE severity is examined. Facility level differences are reviewed regarding controller workload and awareness of the developing error. More in depth information is needed to determine precisely the manner in which alterations in workload influence the nature of the error process. Both studies point to the need for increasing the level of objectivity in the operational error investigation process. Author (revised)

N94-24474 Synetics Corp., Wakefield, MA.
WORLDWIDE VESSEL LOCATING AND TRACKING SYSTEM, VOLUME 1 Final Report, Oct. 1991 - Dec. 1992
Kevin J. ODonnell and David A. Amos Dec. 1992 135 p Prepared in cooperation with Maritime Administration, Washington, DC Limited Reproducibility: More than 20% of this document may be affected by microfiche quality
(Contract DTMA91-91-C-10038)
(PB93-193217; MA-RD-840-93000-Vol-1) Avail: Issuing Activity (National Technical Information Service (NTIS))

The report contains an assessment of the possible design and implementation of an automated worldwide Vessel Locating and Tracking System (VESLOTS). During the Technology Assessment task, viable systems were identified for each technology class (i.e., navigation, communication, and display/interface) and each of three geographic operating regions (i.e., worldwide, coastal U.S./Great Lakes, and inland waterway). During the User Requirements analysis task, potential VESLOTS operators and users were surveyed to amass a set of operational requirements for a VESLOTS implementation based on five criteria: message data content, navigation system, communication system, display/interface, and land link. NTIS

N94-24826*# Massachusetts Inst. of Tech., Cambridge. Dept. of Earth, Atmospheric, and Planetary Sciences.
GPS SURVEY OF THE WESTERN TIEN SHAN Semiannual Report, 15 Mar. 1993 - 14 Mar. 1994
Peter H. Molnar 14 Mar. 1994 30 p
(Grants NAG5-1947; NAG5-1941; NSF EAR-91-15159; NSF EAR-91-17889)
(NASA-CR-195174; NAS 1.26:195174) Avail: CASI HC A03/MF A01

This report summarizes the background, field work, data collection and analysis, and future plans associated with a collaborative GPS experiment in the Tien Shan of the former Soviet Union. This project involves the amalgamation of two, separately funded projects, which were proposed separately by PIs Hamburger and Reilinger (NSF number EAR-9115159 and NASA number NAG5-1941) and Molnar and Hager (NSF number EAR9117889 and NASA number NAG5-1947). In addition, the work is being conducted under the auspices of the US-USSR Agreement on Cooperation in the Field of Environmental Protection, with support from the United States Geological Survey. Derived from text

N94-25444# Federal Aviation Agency, Oklahoma City, OK. Civil Aeromedical Inst.
AUTOMATION AND COGNITION IN AIR TRAFFIC CONTROL: AN EMPIRICAL INVESTIGATION Final Report
O. U. Vortac (Oklahoma Univ., Norman.), Mark B. Edwards (Oklahoma Univ., Norman.), Dana K. Fuller (Oklahoma Univ., Norman.), and Carol A. Manning Feb. 1994 20 p
(Contract DTFA02-91-C-91089)
(DOT/FAA/AM-94/3) Avail: CASI HC A03/MF A01

Several investigators have expressed concern that the imminent automation of air traffic control may have negative consequences on cognitive functioning, and ultimately on performance. These possibilities were investigated empirically by comparing normal, conventional air traffic control with an experimental condition designed to resemble an extreme version of automation. Overall, measures of performance were comparable between conditions. Most of the cognitive measures (attentional demands, visual search, recall of flights, and recall of flight data) were not impaired by the automation analog. Instead, two prospective measures (prospective memory, planning) showed improved performance. The prospective memory advantage is particularly surprising given that the automation-analog group was unable to manipulate external memory aids. Possible reasons for the prospective memory advantage include a reduced workload which allows the controller to get the necessary information in other ways, and a change in the nature of the task resulting from the 'automation' of the strip management module. Author (revised)

N94-25100*# National Aeronautics and Space Administration. Langley Research Center, Hampton, VA.
DIFFERENTIAL GPS FOR AIR TRANSPORT: STATUS
Richard M. Hueschen *In its* NASA LaRC Workshop on Guidance, Navigation, Controls, and Dynamics for Atmospheric Flight, 1993 Dec. 1993 p 97-114 (For primary document see N94-25096 06-01)
Avail: CASI HC A03/MF A04

N94-25495*# National Aeronautics and Space Administration. Ames Research Center, Moffett Field, CA.
APPLICATION OF AIRCRAFT NAVIGATION SENSORS TO ENHANCED VISION SYSTEMS
Barbara T. Sweet *In its* Proceedings of the Workshop on Augmented Visual Display (AVID) Research Dec. 1993 p 79-95 (For primary document see N94-25490 06-54)
Avail: CASI HC A03/MF A04

N94-25504*# National Aeronautics and Space Administration. Ames Research Center, Moffett Field, CA.
EXPANSION-BASED PASSIVE RANGING
Yair Barniv *In its* Proceedings of the Workshop on Augmented Visual Display (AVID) Research Dec. 1993 p 235-286 (For primary document see N94-25490 06-54)
Avail: CASI HC A04/MF A04

05 AIRCRAFT DESIGN, TESTING AND PERFORMANCE

Includes aircraft simulation technology.

For related information see also *18 Spacecraft Design, Testing and Performance* and *39 Structural Mechanics.*For land transportation vehicles see *85 Urban Technology and Transportation.*

N94-23146# Institut Franco-Allemand de Recherches, Saint-Louis (France).
COMPUTATION OF THE LOADS ON THE AH-1/OLS MODEL ROTOR IN FORWARD FLIGHT AND COMPARISON WITH WIND TUNNEL TESTS
M. Schaffar and J. Haertig 2 Oct. 1992 16 p Presented at the 18th European Rotorcraft Forum, Avignon, France, 15-18 Sep. 1992
(ISL-CO-230/92; ETN-94-95127; PB93-204303) Avail: CASI HC A03/MF A01

The vortex lattice method jointly used with a local conformal mapping (to transform the thin blade into a thick one) is described. In order to validate the aerodynamic code, the results are compared with wind tunnel tests for one flight case of the AH-1/OLS model rotor. The study of the wake shows 4 blade/wake interactions for blade 1 during one revolution but only two parallel interactions occur in the rotor plane; the comparison of the computed and measured blade pressures shows an overestimation on the advancing side and an acceptable agreement on the retreating side. ESA

N94-23254 Office National d'Etudes et de Recherches Aerospatiales, Paris (France).
BENT-TIP BLADE FOR AIRCRAFT ROTARY-WING Patent [PALE A EXTREMITE COURBE POUR VOILURE TOURNANTE D'AERONEF]
Alain E. Vuillet, inventor (to ONERA), Jean J. Philippe, inventor (to ONERA), and Andre Desopper, inventor (to ONERA) 30 Mar. 1993 29 p In FRENCH
(CA-Patent-1-315-259; Int-Patent-Class-B64C-27/46; CTN-94-60923)
Copyright Avail: Micromedia Ltd., Technical Information Centre, 240 Catherine Street, Suite 305, Ottawa, Ontario, K2P 2G8, Canada HC/MF

A bent-tip blade for a rotary wing aircraft comprises an attachment for fixing to a hub, a standard part having a leading and trailing edge whose profile has a chord of constant or evolutive length C, and a tip which extends the standard part outwardly, the leading edge of which prolongs the leading edge of the standard part directly rearward. The tip is furthermore inclined downward, and this inclination extends along the entire span of the tip and is continuous after the joint with the standard part up to the furthest edge of the tip such that it follows a curve whose extrados is convex and whose intrados is concave. The tip is not folded around a chord on a part of its span, but is curved progressively downward over all its span. Wind tunnel tests have shown that this continuous curvature is favorable in stationary and forward flight. Compared with a rotary wing blade having a rectilinear and rectangular tip, the curved tip of the invention permits a power gain of at least five percent for a given mass of aircraft. CISTI

N94-23489*# National Aeronautics and Space Administration. Ames Research Center, Moffett Field, CA.
SUMMARY OF LIFT AND LIFT/CRUISE FAN POWERED LIFT CONCEPT TECHNOLOGY
Woodrow L. Cook Aug. 1993 92 p
(NASA Order A-25364-D)
(NASA-CR-177619; A-93113; NAS 1.26:177619) Avail: CASI HC A05/MF A01

A summary is presented of some of the lift and lift/cruise fan technology including fan performance, fan stall, ground effects, ingestion and thrust loss, design tradeoffs and integration, control effectiveness and several other areas related to vertical short takeoff and landing (V/STOL) aircraft conceptual design. The various subjects addressed, while not necessarily pertinent to specific short takeoff/vertical landing (STOVL) supersonic designs being considered, are of interest to the general field of lift and lift/cruise fan aircraft designs and may be of importance in the future. The various wind tunnel and static tests reviewed are: (1) the Doak VZ-4 ducted fan, (2) the 0.57 scale model of the Bell X-22 ducted fan aircraft, (3) the Avrocar, (4) the General Electric lift/cruise fan, (5) the vertical short takeoff and landing (V/STOL) lift engine configurations related to ingestion and consequent thrust loss, (6) the XV-5 and other fan-in-wing stall consideration, (7) hybrid configurations such as lift fan and lift/cruise fan or engines, and (8) the various conceptual design studies by air-frame contractors. Other design integration problems related to small and large V/STOL transport aircraft are summarized including lessons learned during more recent conceptual design studies related to a small executive V/STOL transport aircraft. Author (revised)

N94-24181 Messier-Hispano-Bugatti S.A., Montrouge (France).
LANDING GEAR WITH SWIVELLING BEAM Patent [DISPOSITIF D'ATTERRISSAGE A POUTRE BASCULANTE]
Michel Derrien, inventor (to Messier-Hispano-Bugatti), Jacques Veaux,

inventor (to Messier-Hispano-Bugatti), and Jean-Pierre Hainaut, inventor (to Messier-Hispano-Bugatti) 12 Oct. 1993 14 p In FRENCH
(CA-Patent-1323020; Int-Patent-Class-B64C-025/34; CTN-94-60931)
Copyright Avail: Micromedia Ltd., Technical Information Centre, 240 Catherine Street, Suite 305, Ottawa, Ontario, K2P 2G8, Canada HC/MF

A landing gear apparatus is comprised of a pivoting casing in which a shock absorber rod is mounted projecting downward with respect to the casing and movable in an axial direction. A swivelling beam is mounted to pivot at a lower end from the shock absorber rod and supports a wheel train fore and aft. The upper branch of a linkage, comprising an upper and lower branch connected to each other in an articulated fashion, is connected to the casing in an articulated manner, and the lower branch is connected in an articulated manner to the swivelling beam. Blockage means are provided for limiting the downward pivoting movement of the upper branch of the linkage while the shock absorber rod is not completely extended. During all phases of pivoting of the swivelling beam, only the lower branch of the linkage pivots, such that the force transmitted by the linkage to the casing is directed following the longitudinal direction of the lower branch of the linkage. The blockage means can be either an abutment on the lower branch of the linkage or a telescoping connecting rod between the upper branch of the linkage and the casing. CISTI

N94-24304*# National Aeronautics and Space Administration. Langley Research Center, Hampton, VA.
STUDIES OF SHUTTLE ORBITER ARRESTMENT SYSTEM
Pamela A. Davis and Sandy M. Stubbs Dec. 1993 88 p Original contains color illustrations
(RTOP 505-63-10-02)
(NASA-TP-3370; L-17186; NAS 1.60:3370) Avail: CASI HC A05/MF A01; 5 functional color pages

Scale model studies of the Shuttle Orbiter Arrestment System (AS) were completed with a 1/27.5-scale model at the NASA Langley Research Center. The purpose of these studies was to determine the proper configuration for a net arrestment system to bring the orbiter to a safe stop with minimal damage in the event of a runway overrun. Tests were conducted for runway on-centerline and off-centerline engagements at simulated speeds up to approximately 100 knots (full scale). The results of these tests defined the interaction of the net and the orbiter, the dynamics of off-centerline engagements, and the maximum number of vertical net straps that may become entangled with the nose gear. In addition to these tests, a test program with a 1/8-scale model was conducted by the arrestment system contractor, and the results are presented in the appendix. Author (revised)

N94-24313# Advisory Group for Aerospace Research and Development, Neuilly-Sur-Seine (France). Structures and Materials Panel.
INTEGRATED AIRFRAME DESIGN TECHNOLOGY [LES TECHNOLOGIES POUR LA CONCEPTION INTEGREE DES CELLULES]
Dec. 1993 173 p In ENGLISH and FRENCH Workshop held in Antalya, Turkey, 19-20 Apr. 1993
(AGARD-R-794; ISBN-92-835-0729-0) Copyright Avail: CASI HC A08/MF A02

Integrated airframe design embraces the concept of bringing together all of the aspects of airframe design, including various disciplines such as structures, materials, aerodynamics, controls, and manufacturing, from conceptual design all the way through manufacturing. It also includes the sub-disciplines which are involved in each discipline and the interactions these have with one another. Moreover, an IAD process also affects the organizational structure of the personnel. In order to provide a broad-based approach to evaluating and identifying future research and development directions required to provide IAD technology, the First Integrated Airframe Design Technology Workshop, sponsored by AGARD, was held in Antalya, Turkey on 19-20 Apr. 1993. This document summarizes the output of that Workshop. For individual titles, see N94-24314 through N94-24327.

N94-24314*# National Aeronautics and Space Administration. Langley Research Center, Hampton, VA.
NEW COMPUTING SYSTEMS, FUTURE COMPUTING ENVIRONMENT, AND THEIR IMPLICATIONS ON STRUCTURAL ANALYSIS AND DESIGN
Ahmed K. Noor and Jerrold M. Housner *In* AGARD, Integrated Airframe Design Technology Dec. 1993 25 p (For primary document see N94-24313 06-05)
(Contract NCCw-11)
Copyright Avail: CASI HC A03/MF A02

Recent advances in computer technology that are likely to impact structural analysis and design of flight vehicles are reviewed. A brief summary is given of the advances in microelectronics, networking technologies, and in the user-interface hardware and software. The major features of new and projected computing systems, including high performance computers, parallel processing machines, and small systems, are described. Advances in programming environments, numerical algorithms, and computational strategies for new computing systems are reviewed. The impact of the advances in computer technology on structural analysis and the design of flight vehicles is described. A scenario for future computing paradigms is presented, and the near-term needs in the computational structures area are outlined. Author (revised)

N94-24315# Wright Lab., Wright-Patterson AFB, OH. Manufacturing Technology Directorate.
EARLY MANUFACTURING CONSIDERATIONS IN DESIGN
William C. Kessler, Gerald C. Shumaker, and Michael F. Hitchcock *In* AGARD, Integrated Airframe Design Technology Dec. 1993 7 p (For primary document see N94-24313 06-05)
Copyright Avail: CASI HC A02/MF A02

The successful and timely transition of new product technologies to weapon systems depends heavily on the technical maturity, flexibility, and cost effectiveness of the critical manufacturing processes and systems required to turn these technologies into tangible products. The whole concept of Integrated Product Process Development (a.k.a. Concurrent Engineering) encourages and facilitates the parallel design and development of these manufacturing processes and systems with the design and development of the product. As a result of new computer aided technologies and increased emphasis on manufacturing design, new tools and methodologies are emerging that will facilitate the early consideration of manufacturing in design. This paper will address the development of two such tools: Producibility Methodology; and Tools and Virtual Manufacturing. These tools will enhance the effectiveness of manufacturing engineers who are integrated product process development team members and enable design engineers to better understand the potential downstream implications of early design decisions. Author (revised)

N94-24316# Deutsche Aerospace A.G., Munich (Germany).
APPLICATIONS OF CFD CODES AND SUPERCOMPUTERS TO AIRCRAFT DESIGN ACTIVITIES
W. Schmidt and P. W. Sacher *In* AGARD, Integrated Airframe Design Technology Dec. 1993 9 p Sponsored in part by Aerospatiale; DLR; Aachen Univ.; Stuttgart Univ.; Dornier System G.m.b.H.; and Deutsche Airbus G.m.b.H. (For primary document see N94-24313 06-05)
Copyright Avail: CASI HC A02/MF A02

Integrated Design Technology has been pushed to a large extent by the tremendous progress achieved in the last two decades in the field of computational techniques with regard to flow simulation, engineering, and manufacturing. This paper concentrates on the impact of CFD on the overall design process reviewed from the view of aircraft industry in Germany. Selected examples will be given for applications of CFD during design and development of major products of European aerospace industry without claiming for completeness. General product categories and technology areas involved will be identified as having large potential for CFD and supercomputing efforts. In addition, present technology thrusts will be discussed, and examples for the impact of CFD and supercomputing demonstrated by applications in various programs will be given. Author (revised)

N94-24317*# National Aeronautics and Space Administration. Lewis Research Center, Cleveland, OH.
PROBABILISTIC SIMULATION OF CONCURRENT ENGINEERING OF PROPULSION SYSTEMS
C. C. Chamis and S. N. Singhal (Sverdrup Technology, Inc., Brook Park, OH.) *In* AGARD, Integrated Airframe Design Technology Dec. 1993 10 p (For primary document see N94-24313 06-05)
Copyright Avail: CASI HC A02/MF A02

Technology readiness and the available infrastructure is assessed for timely computational simulation of concurrent engineering for propulsion

systems. Results for initial coupled multidisciplinary, fabrication-process, and system simulators are presented including uncertainties inherent in various facets of engineering processes. An approach is outlined for computationally formalizing the concurrent engineering process from cradle-to-grave via discipline dedicated workstations linked with a common database.
Author (revised)

N94-24318# British Aerospace Defence Ltd., Preston (England). Military Aircraft Div.

FRAMEWORKS FOR INTEGRATED AIRFRAME DESIGN

A. L. Shaw *In* AGARD, Integrated Airframe Design Technology Dec. 1993 15 p (For primary document see N94-24313 06-05)

Copyright Avail: CASI HC A03/MF A02

British Aerospace is Britain's largest Manufacturing Group. Its products are divided into the following groups: Defense Systems, Commercial Aircraft, Cars, Civil Engineering, Property Development, Construction, and Project Management. BAe Defense is the largest defense company in Europe with a turnover of 4.2 billion British pounds. Its exports account for over 70 percent of the total sales. The Military Aircraft Division is an important part of the BAe Defense group. Its major projects are centered around the HAWK, HARRIER, TORNADO, and the European Fighter Aircraft EFA projects. Author (revised)

N94-24319# Deutsche Aerospace A.G., Munich (Germany). Military Aircraft Div.

THE PROCESS NETWORK IN THE DESIGN AND MANUFACTURING OF AIRCRAFT

J. Krammer and A. Ruettinger *In* AGARD, Integrated Airframe Design Technology Dec. 1993 10 p (For primary document see N94-24313 06-05)

Copyright Avail: CASI HC A02/MF A02

The first part of this paper presents some ideas for the investigation and improvement of developmental processes. Typical processes are shown using the Structured Analysis and Design Technique (SADT) and a process flow diagram. In the second part, a redesigned process chain for the design and manufacturing of complex composite parts is explained. Two examples show the functionality of the newly developed constructive design model for this process. Author (revised)

N94-24320# Deutsche Airbus G.m.b.H., Hamburg (Germany). Structural Mechanics Dept.

INTEGRATED STRESS AND STRENGTH ANALYSIS OF AIRPLANE STRUCTURES USING THE DATA PROCESSING TOOL ISSY

R. Werner, M. Wiedemann, and B. Evers *In* AGARD, Integrated Airframe Design Technology Dec. 1993 3 p (For primary document see N94-24313 06-05)

Copyright Avail: CASI HC A01/MF A02

The Integrated Structural Mechanics System (ISSY) is a modular structured tool used to perform a variety of different structural calculations on aircraft structures. ISSY integrates all model generation, analysis and evaluation programs used in structural mechanics under one user interface, and operates a common data base for all these programs. ISSY can be used to generate and analyze calculation models of structural assemblies (fuselage, wings, stabilizers, etc). This is performed by an interactive preprocessor implemented in ISSY. These calculations provide data for both the finite element analysis and for strength analysis, thereby avoiding redundancy of data. Model generation is supported by the use of parameterized standard models (and/or standard sub-models). In addition, model generation is made easier by comprehensive ISSY libraries which provide material data on aluminum, composites, in addition to geometric data on profile sections and rivet allowables. The geometry input data can be directly copied from the component loft data files. The model input data and calculation results are stored in relational data tables which can be analyzed by the postprocessor implemented in ISSY. In addition other modules convert conventionally generated calculation models into ISSY format and generate load case data. To aid partners work on international joint projects, ISSY is compatible with both standard NASTRAN and ISSY processed input and output data. A documentation of model and result data can be obtained in every phase of the justification report. Author

N94-24321# McDonnell-Douglas Corp., Saint Louis, MO.

APPLICATION OF CONCURRENT ENGINEERING PRINCIPLES TO AIRCRAFT STRUCTURAL DESIGN

M. Droegkamp, T. W. Hesterman, B. L. Matthews, T. M. Wilson, and John M. Coyle *In* AGARD, Integrated Airframe Design Technology Dec. 1993 9 p (For primary document see N94-24313 06-05)

Copyright Avail: CASI HC A02/MF A02

The process of designing aircraft structure requires many functional disciplines and associated interdisciplinary coupling. To achieve optimal performance, the various disciplines must work closely together and effectively exchange large amounts of pertinent data. In the past, this was accomplished either with independent analysis tools that were not tightly coupled or with a single analysis tool that lacked the required fidelity to truly support the needs of more than one discipline. In addition, the analyses were performed in series rather than concurrently. A major impediment to process improvement was the lack of a common geometry database that could be utilized by all disciplines required to support structural design. The rapid growth of computational capability and the gradual acceptance by engineers and management to the use of automated processes and common databases has allowed McDonnell Douglas Aerospace (MDA) to implement a concurrent engineering approach to structural design. Our present aircraft design process combines a common geometry approach and existing analysis tools with the power of engineering workstations to manipulate an integrated design database to arrive at an optimum design solution. Our modular approach divides the design process into smaller, more manageable tasks that can be performed concurrently. It achieves 'buy-in' from each engineering and manufacturing discipline by incorporating existing specialized design tools that have been developed by those groups and introduced into the process without taking away ownership. We use common geometry principles, neutral file structures, widely accepted third party and company proprietary applications coupled with consistent naming conventions and file management to achieve our integrated design methodology solution. The present system optimizes the vehicle structure for minimum weight against a given set of design requirements. It is currently used to evaluate advanced vehicles such as NASP and is also being applied to more conventional aircraft. In the future, capabilities will be added to this analysis system that allow it to be applied to detail design problems as well as increasing the fidelity of advanced design solutions. The major increase in capability will result from adding direct access to the computer aided design geometry and also in the incorporation of standard analysis checks into the system. We will design the architecture of the system such that new engineering and manufacturing applications can be easily added. This paper will discuss the evolution of the MDA integrated design methodology from the 80's to the present as well as our vision of the future. Author

N94-24322# Fokker B.V., Schipol-Oost (Netherlands).

SOME PRACTICAL PROBLEMS IN MULTIDISCIPLINARY DESIGN AND OPTIMISATION

D. J. Laan, H. Walgemoed, C. Schimmel, and R. Houwink *In* AGARD, Integrated Airframe Design Technology Dec. 1993 7 p (For primary document see N94-24313 06-05)

Copyright Avail: CASI HC A02/MF A02

Structural optimization software bears a great promise in multidisciplinary design as an effective way to find an optimal balance between the requirements from different disciplines. Due to the evolution of the airworthiness requirements and the increased complexity of aircraft systems it has become increasingly more difficult in the last few decades to establish the design loads. Thus, a clear need exists for quick and reliable load estimation procedures. The paper discusses some measures that can be taken to improve the load definition process. Finally, some examples of successful application of structural optimization software at Fokker Aircraft are given. The primary advantage of structural optimization software is that it aids a skilled designer in gaining a feel for the design space. It should aid the designer in his creative task instead of distracting his attention to using the software. This requires the software to be user friendly and to have built-in features for global and local sensitivity studies.
Derived from text

N94-24323# Deutsche Airbus G.m.b.H., Hamburg (Germany).

INFLUENCE OF ACTIVE CONTROLS ON THE DESIGN PROCESS OF A LARGE TRANSPORT AIRCRAFT

M. Molzow and H. Zimmermann (Deutsche Airbus G.m.b.H., Bremen, Germany.) *In* AGARD, Integrated Airframe Design Technology Dec. 1993 12 p (For primary document see N94-24313 06-05)
Copyright Avail: CASI HC A03/MF A02

The high complexity of an active controlled civil transport aircraft design with its multiple interactions between the different disciplines was presented. It was highlighted that in future design of this kind, different design procedures have to be established with the target to reduce the dominance of one discipline by a multidisciplinary optimization process to ensure an overall aircraft optimum. This has the consequence that the data availability in a certain quality (stiffnesses, aero data, systems data) must be better synchronized with the needs of the user of these data (handling quality, system, loads, flutter, structures) and that cost functions are introduced in the beginning of the design work to ensure a balanced design. It is the firm belief of the authors that already this would be an important step forward. Active Control systems are rather easily capable of being integrated by having in mind to use signals from additional sensors distributed over the A/C than are available from the ADIRU. There are some doubts that all these relations and interactions in real aircraft design can be replaced one day by a totally automated process but certainly more parts have to be put into a process chain to improve quality and safe design time. Author (revised)

N94-24324# McDonnell-Douglas Aerospace, Long Beach, CA.
CURRENT AND FUTURE DESIGN METHODS FOR LARGE TRANSPORT AIRCRAFT
J. P. Giesing, G. T. J. Tzong, and B. E. Schofield *In* AGARD, Integrated Airframe Design Technology Dec. 1993 15 p Prepared in cooperation with Douglas Aircraft Co., Inc., Long Beach, CA (For primary document see N94-24313 06-05)
Copyright Avail: CASI HC A03/MF A02

Current aircraft industry design practices produce high quality, safe, and affordable aircraft. However, future advanced and integrated methods offer the opportunity to significantly reduce the cost and development time of aircraft designs. This paper presents an overview of the current design process and an example for subsonic transport wing box design. It also describes a future process which is presently being implemented at the Douglas Aircraft Company, i.e. the Aeroelastic Design Optimization Program (ADOP), and its application to a similar subsonic transport wing. Specifically, stress and flutter are optimized and compression surface buckling and tension surface damage tolerance are integrated. Finally, the future direction of ADOP will be outlined which includes integration of aeroelastic loads, durability and damage tolerance, and concurrent structure and active controls optimization. Author

N94-24325# Alenia Aeronautica, Torino (Italy). Div. Velivoli Difesa.
THE INTEGRATION OF DESIGN AND MANUFACTURING PROCESSES AT ALENIA DVD
L. Chesta, M. Flaccavento, G. Pollano, and F. Staropoli *In* AGARD, Integrated Airframe Design Technology Dec. 1993 16 p (For primary document see N94-24313 06-05)
Copyright Avail: CASI HC A03/MF A02

In aeronautics, the age of high creativity, like the one in the fifties with the introduction of jet engines or the one in the thirties which started the age of monoplanes with metallic shell structures, is passed. Today, we are in a situation in which the final increment in basic performance (maximum speed, maneuver capability) is usually excessively expensive. It is now necessary to look to marginal areas to gain improvements in performance, to use new materials such as carbon fibers to tailor the structure to specific needs, and to simplify, with the help of electronics and servomechanisms, complicated mechanical systems to obtain aircraft architectures otherwise impossible to fly. But this is not enough; it is absolutely necessary to also improve the cost effectiveness by increasing the reliability, availability, and supportability of the weapon system, thereby reducing the usage cost and the production cost of the aircraft. This is not any more achievable using the single man capabilities on a single discipline, but it requires a new type of working organization which uses sophisticated means of calculation, integrated in order to optimize the overall design, and which compresses the time of the process by exploiting the synergism of the interdisciplinary couplings, overlapping as much as possible the design and manufacturing phases. Alenia Defense Aircraft Division, being involved in several programs, both by itself and in international cooperation, has followed this evolution and is actively pursuing the adequacy of its operative structure to the new requirements by adopting advanced technology processes. Derived from text

N94-24326*# National Aeronautics and Space Administration. Lewis Research Center, Cleveland, OH.
MULTI-DISCIPLINARY COUPLING FOR INTEGRATED DESIGN OF PROPULSION SYSTEMS c07
C. C. Chamis and S. N. Singhal (Sverdrup Technology, Inc., Brook Park, OH.) *In* AGARD, Integrated Airframe Design Technology Dec. 1993 12 p (For primary document see N94-24313 06-05)
Copyright Avail: CASI HC A03/MF A02

Effective computational simulation procedures are described for modeling the inherent multi-disciplinary interactions for determining the true response of propulsion systems. Results are presented for propulsion system responses including multi-discipline coupling effects via (1) coupled multi-discipline tailoring, (2) an integrated system of multidisciplinary simulators, (3) coupled material-behavior/fabrication-process tailoring, (4) sensitivities using a probabilistic simulator, and (5) coupled materials/structures/fracture/probabilistic behavior simulator. The results show that the best designs can be determined if the analysis/tailoring methods account for the multi-disciplinary coupling effects. The coupling across disciplines can be used to develop an integrated interactive multi-discipline numerical propulsion system simulator. Author

N94-24327# Dassault (E. M.) Co., Saint Cloud (France).
TRENDS OF DESIGN METHODOLOGY OF AIRFRAME [TENDANCES DANS LA METHODE DE CONCEPTION DES CELLULES D'AVION MILITAIRE]
C. Petiau *In* AGARD, Integrated Airframe Design Technology Dec. 1993 6 p In FRENCH (For primary document see N94-24313 06-05)
Copyright Avail: CASI HC A02/MF A02

First, it is reminded that organization of airframe design is directly linked to the performances of available tools. As a matter of fact, they condition the number and nature of project iterations. The organization which should nowadays be recommended in view of the means of CAD, computation and mathematical optimization at our disposal is presented and analyzed. This leads to a first design, followed by experimental verifications with a key role for flight tests. The final design is checked with the help of calculations models calibrated on tests. Then the new tools which are the factors of future evolution of design methodology are examined: to dispose of 'Design History' corresponding to the whole data of the process; parametric CAD and shape optimization; multidisciplinary optimization; 'Feature' Design; improvement of computation methods. As a conclusion we insist on the fact that aircraft manufacturers, CAD suppliers, and scientific searchers will be well advised to create a dialogue as to future design methodology. Author (revised)

N94-24332*# Embry-Riddle Aeronautical Univ., Daytona Beach, FL.
AIRCRAFT EMPENNAGE STRUCTURAL DETAIL DESIGN
Greg Meholic, Rhonda Brown, Melissa Hall, Robert Harvey, Michael Singer, and Gustavo Tella 19 Apr. 1993 73 p
(Contract NASw-4435)
(NASA-CR-195496; NAS 1.26:195496) Avail: CASI HC A04/MF A01

This project involved the detailed design of the aft fuselage and empennage structure, vertical stabilizer, rudder, horizontal stabilizer, and elevator for the Triton primary flight trainer. The main design goals under consideration were to illustrate the integration of the control systems devices used in the tail surfaces and their necessary structural supports as well as the elevator trim, navigational lighting system, electrical systems, tail-located ground tie, and fuselage/cabin interface structure. Accommodations for maintenance, lubrication, adjustment, and repairability were devised. Weight, fabrication, and (sub)assembly goals were addressed. All designs were in accordance with the FAR Part 23 stipulations for a normal category aircraft. Author

N94-24401*# California Polytechnic State Univ., San Luis Obispo. Aeronautical Engineering Dept.
JB-300: AN ADVANCED MEDIUM SIZE TRANSPORT FOR 2005
Giles deBrouwer, Katherine Graham, Jim Ison, Vince Juarez, Steve Moskalik, Jon Pankonin, and Arnold Weinstein May 1993 113 p Original contains color illustrations

(Contract NASw-4435)
(NASA-CR-195499; NAS 1.26:195499) Avail: CASI HC A06/MF A02; 2 functional color pages

In the fall of 1992, the TAC Team was presented with a Request for Proposal (PFP) for a mid-size (250-350 passenger) commercial transport. The aircraft was to be extremely competitive in the areas of passenger comfort, performance, and economic aspects. Through the use of supercritical airfoils, a technologically advanced Very High By-pass Ratio (VHBR) turbofan engine, a low overall drag configuration, a comparable interior layout, and mild use of composites, the JB-300 offers an economically viable choice to the airlines. The cents per passenger mile of the JB-300 is 1.76, which is considerably lower than current aircraft in the same range. Overall, the JB-300 is a technologically advanced aircraft, which will meet the demands of the 21st century. Author (revised)

N94-24462*# Notre Dame Univ., IN. Dept. of Aerospace and Mechanical Engineering.

NASA/USRA UNIVERSITY ADVANCED DESIGN PROGRAM, 1992-1993. THE DIAMONDBACK: A SIMULATED COMMERCIAL AIR TRANSPORTATION STUDY Final Report

Apr. 1993 151 p
(Contract NASw-4435)
(NASA-CR-195523; NAS 1.26:195523) Avail: CASI HC A08/MF A02

This document reports on the design of the Diamondback, an aircraft model of a 100-passenger aircraft designed to cruise at 28 ft/s and compete against the 40-passenger HB-40 in the fictional Aeroworld commercial transport market. Unlike conventional aircraft, the Diamondback utilizes an innovative configuration known as the joined wing. The topics addressed include: economic/cost analysis, aerodynamics, weight and structures, propulsion, stability and control, and performance. CASI

N94-24479*# Virginia Polytechnic Inst. and State Univ., Blacksburg. Dept. of Aerospace and Ocean Engineering.

DESIGN OF A VEHICLE BASED SYSTEM TO PREVENT OZONE LOSS

Sean R. Lynn, Deborah Bunker, Thomas D. Hesbach, Jr., Everett B. Howerton, G. Hreinsson, E. Kirk Mistr, Matthew E. Palmer, Claiborne Rogers, Dayna S. Tischler, and Daniel J. Wrona et al 28 Jul. 1993 70 p
(Contract NASw-4435)
(NASA-CR-195498; NAS 1.26:195498) Avail: CASI HC A04/MF A01

Reduced quantities of ozone in the atmosphere allow greater levels of ultraviolet light (UV) radiation to reach the earth's surface. This is known to cause skin cancer and mutations. Chlorine liberated from Chlorofluorocarbons (CFC's) and natural sources initiate the destruction of stratospheric ozone through a free radical chain reaction. The project goals are to understand the processes which contribute to stratospheric ozone loss, examine ways to prevent ozone loss, and design a vehicle-based system to carry out the prevention scheme. The 1992/1993 design objectives were to accomplish the first two goals and define the requirements for an implementation vehicle to be designed in detail starting next year. Many different ozone intervention schemes have been proposed though few have been researched and none have been tested. A scheme proposed by R.J. Cicerone, Scott Elliot and R.P.Turco late in 1991 was selected because of its research support and economic feasibility. This scheme uses hydrocarbon injected into the Antarctic ozone hole to form stable compounds with free chlorine, thus reducing ozone depletion. Because most polar ozone depletion takes place during a 3-4 week period each year, the hydrocarbon must be injected during this time window. A study of the hydrocarbon injection requirements determined that 100 aircraft traveling Mach 2.4 at a maximum altitude of 66,000 ft. would provide the most economic approach to preventing ozone loss. Each aircraft would require an 8,000 nm. range and be able to carry 35,000 lbs. of propane. The propane would be stored in a three-tank high pressure system. Missions would be based from airport regions located in South America and Australia. To best provide the requirements of mission analysis, an aircraft with L/D(sub cruise) = 10.5, SFC = 0.65 (the faculty advisor suggested that this number is too low) and a 250,000 lb TOGW was selected as a baseline. Modularity and multi-role functionality were selected to be key design features. Modularity provides ease of turnaround for the down-time critical mission. Multi-role functionality allows the aircraft to be used beyond its design mission, perhaps as an High Speed Civil Transport (HSCT) or for high altitude research. Author (revised)

N94-24492*# Ohio State Univ., Columbus.

NASA/USRA ADVANCED DESIGN PROGRAM

1992 79 p
(Contract NASw-4435)
(NASA-CR-195548; NAS 1.26:195548) Avail: CASI HC A05/MF A01

This report analyzes and presents a preliminary design for an experimental hypersonic vehicle. This plane will have a cruise speed of Mach 12 for one minute at an altitude of 120,000 feet. The major design areas of aerodynamics, propulsion, and weights are discussed in depth. An elementary analysis of thermal protection, trajectory, and cost is also presented. Finally, a discussion of future plans and recommendations is given, and overall conclusions are drawn. Author

N94-24498*# Embry-Riddle Aeronautical Univ., Daytona Beach, FL.

AIRCRAFT WING STRUCTURE DETAIL DESIGN

Garrett L. Sager, Ron Roberts, Bob Mallon, Mohamed Alameri, and Bill Steinbach 14 Apr. 1993 36 p
(Contract NASw-4435)
(NASA-CR-195485; NAS 1.26:195485) Avail: CASI HC A03/MF A01

The provisions of this project call for the design of the structure of the wing and carry-through structure for the Viper primary trainer, which is to be certified as a utility category trainer under FAR part 23. The specific items to be designed in this statement of work were Front Spar, Rear Spar, Aileron Structure, Wing Skin, and Fuselage Carry-through Structure. In the design of these parts, provisions for the fuel system, electrical system, and control routing were required. Also, the total weight of the entire wing planform could not exceed 216 lbs. Since this aircraft is to be used as a primary trainer, and the SOW requires a useful life of 107 cycles, it was decided that all of the principle stresses in the structural members would be kept below 10 ksi. The only drawback to this approach is a weight penalty. Derived from text

N94-24581*# Naval Postgraduate School, Monterey, CA.

DESIGN PROJECT: LONGBOW SUPERSONIC INTERCEPTOR

Robert Stoney, Matt Baker, Joseph G. Capstaff, Robert Dishman, Gregory Fick, Stephen N. Frick, and Mark Kelly Mar. 1993 129 p
(Contract NASw-4435)
(NASA-CR-195510; NAS 1.26:195510) Avail: CASI HC A07/MF A02

A recent white paper entitled 'From the Sea' has spotlighted the need for Naval Aviation to provide overland support to joint operations. The base for this support, the Aircraft Carrier (CVN), will frequently be unable to operate within close range of the battleground because of littoral land-based air and subsurface threats. A high speed, long range, carrier capable aircraft would allow the CVN to provide timely support to distant battleground operations. Such an aircraft, operating as a Deck-Launched Interceptor (DLI), would also be an excellent counter to Next Generation Russian Naval Aviation (NGRNA) threats consisting of supersonic bombers, such as the Backfire, equipped with the next generation of high-speed, long-range missiles. Additionally, it would serve as an excellent high speed Reconnaissance airplane, capable of providing Battle Force commanders with timely, accurate pre-mission targeting information and post-mission Bomb Damage Assessment (BDA). Recent advances in computational hypersonic airflow modeling has produced a method of defining aircraft shapes that fit a conical shock flow model to maximize the efficiency of the vehicle. This 'Waverider' concept provides one means of achieving long ranges at high speeds. A Request for Proposal (RFP) was issued by Professor Conrad Newberry that contained design requirements for an aircraft to accomplish the above stated missions, utilizing Waverider technology. Author

N94-24589*# Worcester Polytechnic Inst., Holden, MA.

NASA ADVANCED DESIGN PROGRAM. DESIGN AND ANALYSIS OF A RADIO-CONTROLLED FLYING WING AIRCRAFT

3 May 1993 100 p
(Contract NASw-4435)
(NASA-CR-195515; NAS 1.26:195515) Avail: CASI HC A05/MF A02

The main challenge of this project was to design an aircraft that will achieve stability while flying without a horizontal tail. The project focused on both the design, analysis and construction of a remotely piloted, elliptical shaped flying wing. The design team was composed of four sub-groups each of which dealt with the different aspects of the design, namely aerodynamics, stability and control, propulsion, and structures. Each member of the team initially researched the background information pertaining to specific facets of the project. Since previous work on this topic was limited, most of the focus of the project was directed towards developing an understanding of the natural instability of the aircraft. Once the design team entered the conceptual stage of the project, a series of compromises had to be made to satisfy the unique requirements of each sub-group. As a result of the numerous calculations and iterations necessary, computers were utilized extensively. In order to visualize the design and layout of the wing, engines and control surfaces, a solid modeling package was used to evaluate optimum design placements. When the design was finalized, construction began with the help of all the members of the project team. The nature of the carbon composite construction process demanded long hours of manual labor. The assembly of the engine systems also required precision hand work. The final product of this project is the Elang, a one-of-a-kind remotely piloted aircraft of composite construction powered by two ducted fan engines. Author (revised)

N94-24591*# Ohio State Univ., Columbus.
CONFIGURATION DEVELOPMENT STUDY OF THE OSU 1 HYPERSONIC RESEARCH VEHICLE
Matthew D. Stein, Chris Frankhauser, Warner Zee, Melvin Kosanchick, III, Nick Nelson, and William Hunt 31 May 1993 152 p
(Contract NASw-4435)
(NASA-CR-195522; NAS 1.26:195522) Avail: CASI HC A08/MF A02

In an effort to insure the future development of hypersonic cruise aircraft, the possible vehicle configurations were examined to develop a single-stage-to-orbit hypersonic research vehicle (HRV). Based on the needs of hypersonic research and development, the mission goals and requirements are determined. A body type is chosen. Three modes of propulsion and two liquid rocket fuels are compared, followed by the optimization of the body configuration through aerodynamic, weight, and trajectory studies. A cost analysis is included. Author (revised)

N94-24711*# California Polytechnic State Univ., San Luis Obispo. Aeronautical Engineering Dept.
THE CETACEOPTERYX: A GLOBAL RANGE MILITARY TRANSPORT AIRCRAFT
Chad Brivkalns, Nicole English, Tahmineh Kazemi, Kim Kopel, Seth Kroger, and Ed Ortega 14 May 1993 109 p
(Contract NASw-4435)
(NASA-CR-195519; NAS 1.26:195519) Avail: CASI HC A06/MF A02

This paper presents a design of a military transport aircraft capable of carrying 800,000 lbs of payload from any point in the United States to any other point in the world. Such massive airlift requires aggressive use of advanced technology and a unique configuration. The Cetaceopteyx features a joined wing, canard and six turbofan engines. The aircraft has a cost 1.07 billion (1993) dollars each. This paper presents in detail the mission description, preliminary sizing, aircraft configuration, wing design, fuselage design, empennage design, propulsion system, landing gear design, structures, drag, stability and control, systems layout, and cost analysis of the aircraft. Author

N94-24726*# Lockheed Engineering and Sciences Co., Hampton, VA.
A PARAMETRIC STUDY OF HARMONIC ROTOR HUB LOADS
Chengjian He Nov. 1993 60 p
(Contract NAS1-19000; RTOP 505-63-36)
(NASA-CR-4558; NAS 1.26:4558) Avail: CASI HC A04/MF A01

A parametric study of vibratory rotor hub loads in a nonrotating system is presented. The study is based on a CAMRAD/JA model constructed for the GBH (Growth Version of Blackhawk Helicopter) Mach-scaled wind tunnel rotor model with high blade twist (-16 deg). The theoretical hub load predictions are validated by correlation with available measured data. Effects of various blade aeroelastic design changes on the harmonic nonrotating frame hub loads at both low and high forward flight speeds are investigated. The study aims to illustrate some of the physical mechanisms for change in the harmonic rotor hub loads due to blade design variations. Author (revised)

N94-24787*# Naval Postgraduate School, Monterey, CA.
CONCEPTUAL DESIGN PROPOSAL: HUGO GLOBAL RANGE/MOBILITY TRANSPORT AIRCRAFT
Tom Johnston, Dave Perretta, Doug McBane, Greg Morin, Greg Thomas, Joe Woodward, and Steve Gulakowski Mar. 1993 116 p
(Contract NASw-4435)
(NASA-CR-195501; NAS 1.26:195501) Avail: CASI HC A06/MF A02

With the collapse of the former Soviet Union and the emergence of the United Nations actively pursuing a peace keeping role in world affairs, the United States has been forced into a position as the world's leading peace enforcer. It is still a very dangerous world with seemingly never ending ideological, territorial, and economic disputes requiring the U.S. to maintain a credible deterrent posture in this uncertain environment. This has created an urgent need to rapidly transport large numbers of troops and equipment from the continental United States (CONUS) to any potential world trouble spot by means of a global range/mobility transport aircraft. The most recent examples being Operation Desert Shield/Storm and Operation Restore Hope. To meet this challenge head-on, a request for proposal (RFP) was developed and incorporated into the 1992/1993 AIAA/McDonnell Douglas Corporation Graduate Team Aircraft Design Competition. The RFP calls for the conceptual design and justification of a large aircraft capable of power projecting a significant military force without surface transportation reliance. Derived from text

N94-24796*# United Technologies Corp., Stratford, CT. Aircraft Div.
WIND TUNNEL TEST OF A VARIABLE-DIAMETER TILTROTOR (VDTR) MODEL
David Matuska, Allen Dale, and Peter Lorber Jan. 1994 230 p
(Contract NAS2-13484)
(NASA-CR-177629; A-94018; NAS 1.26:177629) Avail: CASI HC A11/MF A03

This report documents the results from a wind tunnel test of a 1/6th scale Variable Diameter Tiltrotor (VDTR). This test was a joint effort of NASA Ames and Sikorsky Aircraft. The objective was to evaluate the aeroelastic and performance characteristics of the VDTR in conversion, hover, and cruise. The rotor diameter and nacelle angle of the model were remotely changed to represent tiltrotor operating conditions. Data is presented showing the propulsive force required in conversion, blade loads, angle of attack stability and simulated gust response, and hover and cruise performance. This test represents the first wind tunnel test of a variable diameter rotor applied to a tiltrotor concept. The results confirm some of the potential advantages of the VDTR and establish the variable diameter rotor a viable candidate for an advanced tiltrotor. This wind tunnel test successfully demonstrated the feasibility of the Variable Diameter rotor for tilt rotor aircraft. A wide range of test points were taken in hover, conversion, and cruise modes. The concept was shown to have a number of advantages over conventional tiltrotors such as reduced hover downwash with lower disk loading and significantly reduced longitudinal gust response in cruise. In the conversion regime, a high propulsive force was demonstrated for sustained flight with acceptable blade loads. The VDTR demonstrated excellent gust response capabilities. The horizontal gust response correlated well with predictions revealing only half the response to turbulence of the conventional civil tiltrotor. Author (revised)

N94-24803*# California Polytechnic State Univ., San Luis Obispo.
VLCT-13: A COMMERCIAL TRANSPORT FOR THE 21ST CENTURY
Pamela Beal, Terri Sowels, Hitoshi Takahashi, Matt Cotton, Will Balanon, and Manuel Parayo 14 May 1993 72 p
(Contract NASw-4435)
(NASA-CR-195492; NAS 1.26:195492) Avail: CASI HC A04/MF A01

The growth of the Pacific Rim market has spurred airframers to begin feasibility studies of a large commercial transport. By the year 2001, 30 million travelers are expected to travel the Transpacific. A transport capable of hauling 800 PAX and 30,000 pounds of cargo, 7,000 nm is of specific interest. Special problems associated with this design are configuration, landing gear, passenger safety, airport compatibility, and engine thrust. A group of students at the California Polytechnic State University at San Luis Obispo developed a very large commercial transport, VLCT-13, conventional looking design which is both comfortable and economical. Passenger comfort includes seat pitches of 34 in and 40 in, width's of 23 in and 25 in, respectfully, and a 27 ft diameter cross section. A direct operating cost of 2.3 cents per passenger per seat-mile is estimated for this airplane design. The airplane market price is estimated to be $195 million 1993 dollars based on an aircraft take off weight of 1.4 million pounds. The problems associated with the VLCT-13 are discussed and possible solutions are presented. Author (revised)

N94-24817*# Notre Dame Univ., IN. Dept. of Aerospace and Mechanical Engineering.
THE BLUE EMU Final Design Proposal
Doug Descalzi, John Gillett, Carlton Gordon, Ed Keener, Ken Novak, and Laura Puente Apr. 1993 125 p
(Contract NASw-4435)
(NASA-CR-195535; NAS 1.26:195535) Avail: CASI HC A06/MF A02

The primary goal in designing the Blue Emu was to provide an airline with a cost efficient and profitable means of transporting passengers between the major cities in Aeroworld. The design attacks the market where a demand for inexpensive transportation exists and for this reason the Blue Emu is an attractive investment for any airline. In order to provide a profitable aircraft, special attention was paid to cost and economics. For example, in manufacturing, simplicity was stressed in structural design to reduce construction time and cost. Aerodynamic design employed a tapered wing which reduced the induced drag coefficient while also reducing the weight of the wing. Even the propulsion system was selected with cost effectiveness in mind, yet also to maintain the marketability of the aircraft. Thus, in every aspect of the design, consideration was given to economics and marketability of the final product. Author (revised)

N94-24837*# Notre Dame Univ., IN. Dept. of Aerospace and Mechanical Engineering.
THE AIRPLANE: A SIMULATED COMMERCIAL AIR TRANSPORTATION STUDY Final Design Proposal
Mark DAuteuil, Pete Geniesse, Michael Hunniford, Kathleen Lawler, Elena Quirk, and Michael Tognarelli Apr. 1993 176 p
(Contract NASw-4435)
(NASA-CR-195525; NAS 1.26:195525) Avail: CASI HC A09/MF A02

The 'Airplane' is a moderate-range, 70 passenger aircraft. It is designed to serve demands for flights up to 10,000 feet and it cruises at 32 ft/s. The major drivers for the design of the Airplane are economic competitiveness, takeoff performance, and weight minimization. The Airplane is propelled by a single Astro 15 electric motor and a Zinger 12-8 propeller. The wing section is a Spica airfoil which, because of its flat bottom, provides simplicity in manufacturing and thus helps to cut costs. The wing is constructed of a single load bearing mainspar and shape-holding ribs coated with Monokote skin, lending to a light weight structural makeup. The fuselage houses the motor, flight deck and passenger compartments as well as the fuel and control actuating systems. The wing will be attached to the top of the fuselage as will the fuel and control actuator systems for easy disassembly and maintenance. The aircraft is maneuvered about its pitch axis by means of an aft elevator on the flat plate horizontal tail. The twin vertical tail surfaces are also flat plates and each features a rudder for both directional and roll control. Along with wing dihedral, the rudders will be used to roll the aircraft. The Airplane is less costly to operate at its own maximum range and capacity as well as at its maximum range and the HB-40's maximum capacity than the HB-40. Derived from text

N94-24915*# Naval Postgraduate School, Monterey, CA.
DUMBO HEAVY LIFTER AIRCRAFT
Peter Riester, Colleen Ellis, Michael Wagner, Scott Orren, Byron Smith, Michael Skelly, Craig Zgraggen, and Matt Webber Sep. 1992 102 p
(Contract NASw-4435)
(NASA-CR-195500; NAS 1.26:195500) Avail: CASI HC A06/MF A02

The world is rapidly changing from one with two military superpowers, with which most countries were aligned, to one with many smaller military powers. In this environment, the United States cannot depend on the availability of operating bases from which to respond to crises requiring military intervention. Several studies (e.g. the SAB Global Reach, Global Power Study) have indicated an increased need to be able to rapidly transport large numbers of troops and equipment from the continental United States to potential trouble spots throughout the world. To this end, a request for proposals (RFP) for the concept design of a large aircraft capable of 'projecting' a significant military force without reliance on surface transportation was developed. These design requirements are: minimum payload of 400,000 pounds at 2.5 g maneuver load factor; minimum unfueled range of 6,000 nautical miles; and aircraft must operate from existing domestic air bases and use existing airbases or sites of opportunity at the destination. Derived from text

N94-24953*# Maryland Univ., College Park.
AEROELASTIC RESPONSE AND STABILITY OF TILTROTORS WITH ELASTICALLY-COUPLED COMPOSITE ROTOR BLADES Ph.D. Thesis
Mark W. Nixon 1993 448 p
(NASA-TM-108758; NAS 1.15:108758) Avail: CASI HC A19/MF A04

There is a potential for improving the performance and aeroelastic stability of tiltrotors through the use of elastically-coupled composite rotor blades. To study the characteristics of tiltrotors with these types of rotor blades it is necessary to formulate a new analysis which has the capabilities of modeling both a tiltrotor configuration and an anisotropic rotor blade. Background for these formulations is established in two preliminary investigations. In the first, the influence of several system design parameters on tiltrotor aeroelastic stability is examined for the high-speed axial flight mode using a newly-developed rigid-blade analysis with an elastic wing finite element model. The second preliminary investigation addresses the accuracy of using a one-dimensional beam analysis to predict frequencies of elastically-coupled highly-twisted rotor blades. Important aspects of the new aeroelastic formulations are the inclusion of a large steady pylon angle which controls tilt of the rotor system with respect to the airflow, the inclusion of elastic pitch-lag coupling terms related to rotor precone, the inclusion of hub-related degrees of freedom which enable modeling of a gimballed rotor system and engine drive-train dynamics, and additional elastic coupling terms which enable modeling of the anisotropic features for both the rotor blades and the tiltrotor wing. Accuracy of the new tiltrotor analysis is demonstrated by a comparison of the results produced for a baseline case with analytical and experimental results reported in the open literature. Two investigations of elastically tailored blades on a baseline tiltrotor are then conducted. One investigation shows that elastic bending-twist coupling of the rotor blade is a very effective means for increasing the flutter velocity of a tiltrotor, and the magnitude of coupling required does not have an adverse effect on performance or blade loads. The second investigation shows that passive blade twist control via elastic extension-twist coupling of the rotor blade has the capability of significantly improving tiltrotor aerodynamic performance. This concept, however, is shown to have, in general, a negative impact on stability characteristics. Author

N94-24966*# California Polytechnic State Univ., San Luis Obispo. Aeronautical Engineering Dept.
THE AC-120: THE ADVANCED COMMERCIAL TRANSPORT
David Duran, Ernest Griffin, Saul Mendoza, Son Nguyen, Tim Pickett, and Clemm Noernberg 14 May 1993 89 p Original contains color illustrations
(Contract NASw-4435)
(NASA-CR-195491; NAS 1.26:195491) Avail: CASI HC A05/MF A01: 3 functional color pages

The main objective of this design was to fulfill a need for a new airplane to replace the aging 100 to 150 passenger, 1500 nautical mile range aircraft such as the Douglas DC9 and Boeing 737-100 airplanes. After researching the future aircraft market, conducting extensive trade studies, and analysis on different configurations, the AC-120 Advanced Commercial Transport final design was achieved. The AC-120's main design features include the incorporation of a three lifting surface configuration which is powered by two turboprop engines. The AC-120 is an economically sensitive aircraft which meets the new FM Stage Three noise requirements, and has lower NO(x) emissions than current turbofan powered airplanes. The AC-120 also improves on its contemporaries in passenger comfort, manufacturing, and operating cost. Author (revised)

N94-24968*# Georgia Inst. of Tech., Atlanta. School of Aerospace Engineering.
INTEGRATED DESIGN AND MANUFACTURING FOR THE HIGH SPEED CIVIL TRANSPORT Final Report
Jun. 1993 201 p
(Contract NASw-4435)
(NASA-CR-195511; NAS 1.26:195511) Avail: CASI HC A10/MF A03

In June 1992, Georgia Tech's School of Aerospace Engineering was awarded a NASA University Space Research Association (USRA) Advanced Design Program (ADP) to address 'Integrated Design and Manufacturing for the High Speed Civil Transport (HSCT)' in its graduate aerospace systems design courses. This report summarizes the results of the five courses incorporated into the Georgia Tech's USRA ADP program. It covers

AE8113: Introduction to Concurrent Engineering, AE4360: Introduction to CAE/CAD, AE4353: Design for Life Cycle Cost, AE6351: Aerospace Systems Design One, and AE6352: Aerospace Systems Design Two. AE8113: Introduction to Concurrent Engineering was an introductory course addressing the basic principles of concurrent engineering (CE) or integrated product development (IPD). The design of a total system was not the objective of this course. The goal was to understand and define the 'up-front' customer requirements, their decomposition, and determine the value objectives for a complex product, such as the high speed civil transport (HSCT). A generic CE methodology developed at Georgia Tech was used for this purpose. AE4353: Design for Life Cycle Cost addressed the basic economic issues for an HSCT using a robust design technique, Taguchi's parameter design optimization method (PDOM). An HSCT economic sensitivity assessment was conducted using a Taguchi PDOM approach to address the robustness of the basic HSCT design. AE4360: Introduction to CAE/CAD permitted students to develop and utilize CAE/CAD/CAM knowledge and skills using CATIA and CADAM as the basic geometric tools. AE6351: Aerospace Systems Design One focused on the conceptual design refinement of a baseline HSCT configuration as defined by Boeing, Douglas, and NASA in their system studies. It required the use of NASA's synthesis codes FLOPS and ACSYNT. A criterion called the productivity index (P.I.) was used to evaluate disciplinary sensitivities and provide refinements of the baseline HSCT configuration. AE6352: Aerospace Systems Design Two was a continuation of Aerospace Systems Design One in which wing concepts were researched and analyzed in more detail. FLOPS and ACSYNT were again used at the system level while other off-the-shelf computer codes were used for more detailed wing disciplinary analysis and optimization. The culmination of all efforts and submission of this report conclude the first year's efforts of Georgia Tech's NASA USRA ADP. It will hopefully provide the foundation for next year's efforts concerning continuous improvement of integrated design and manufacturing for the HSCT.
Author (revised)

N94-24969*# Embry-Riddle Aeronautical Univ., Daytona Beach, FL.
AIRCRAFT EMPENNAGE STRUCTURAL DETAIL DESIGN
David Lesnewski, Russ M. Snow, Lisa M. Combs, David Paufler, George Schnieder, and Roxanne Athousake 15 Apr. 1993 56 p
(Contract NASw-4435)
(NASA-CR-195486; NAS 1.26:195486) Avail: CASI HC A04/MF A01

The purpose of this project is to provide an empennage structural assembly that will withstand the operational loads defined in FAR Part 23, as well as those specified in the statement of work, i.e. snow, rain, humidity, tiedown forces, etc. The goal is to provide a simple yet durable lightweight structure that will transfer the aerodynamic forces produced by the tail surfaces through the most efficient load path to the airframe. The structure should be simple and cost-effective to manufacture and repair. All structures meet or exceed loading and fatigue criteria. The structure provides for necessary stiffness and ease of maintenance. Author (revised)

N94-24971*# Naval Postgraduate School, Monterey, CA.
SABOT HIGH SPEED INTERCEPTOR AE 4273 AIRCRAFT DESIGN
Dave Dober, Waleed Al-Hashel, Bob Baldocchi, Tim Berg, Curt Lindsay, Aaron McAtee, Dan Sergent, and Harry Dunbrack Sep. 1992 126 p
(Contract NASw-4435)
(NASA-CR-195495; NAS 1.26:195495) Avail: CASI HC A07/MF A02

Today's carrier based deck launched intercept (DLI) mission is a vital one that is aimed at protecting the carrier battle group and detering potential adversaries. The assets deployed on our carrier decks are able to complete this mission but with very limited range. The waverider concept has great potential to increase the range of this carrier based mission. As a result, a request for proposals (RFP) was developed which contains design requirements for an aircraft that can complete this mission through the utilization of waverider technology. Derived from text

N94-24972*# California Polytechnic State Univ., San Luis Obispo. Aeronautical Engineering Dept.
A GLOBAL RANGE MILITARY TRANSPORT: THE OSTRICH
John Aguiar, Cecilia Booker, Eric Hoffman, James Kramar, Orlando Manahan, Ray Serranzana, and Mike Taylor 14 May 1993 103 p
(Contract NASw-4435)
(NASA-CR-195494; NAS 1.26:195494) Avail: CASI HC A06/MF A02

Studies have shown that there is an increasing need for a global range transport capable of carrying large numbers of troops and equipment to potential trouble spots throughout the world. The Ostrich is a solution to this problem. The Ostrich is capable of carrying 800,000 pounds 6,500 n.m. and returning with 15 percent payload, without refueling. With a technology availability date in 2010 and an initial operating capability of 2015, the aircraft incorporates many advanced technologies including laminar flow control, composite primary structures, and a unique multibody design. By utilizing current technology, such as using McDonnell Douglas C-17 fuselage for the outer fuselages on the Ostrich, the cost for the aircraft was reduced. The cost of the Ostrich per aircraft is $1.2 billion with a direct operating cost of $56,000 per flight hour. The Ostrich will provide a valuable service as a logistical transport capable of rapidly projecting a significant military force or humanitarian aid anywhere in the world.
Author (revised)

N94-24974*# Embry-Riddle Aeronautical Univ., Daytona Beach, FL.
AIRCRAFT WING STRUCTURAL DETAIL DESIGN (WING, AILERON, FLAPS, AND SUBSYSTEMS)
Robert Downs, Mike Zable, James Hughes, Terry Heiser, and Kenneth Adrian 14 Apr. 1993 40 p
(Contract NASw-4435)
(NASA-CR-195487; NAS 1.26:195487) Avail: CASI HC A03/MF A01

The goal of this project was to design, in detail, the wing, flaps, and ailerons for a primary flight trainer. Integrated in this design are provisions for the fuel system, the electrical system, and the fuselage/cabin carry-through interface structure. This conceptual design displays the general arrangement of all major components in the wing structure, taking into consideration the requirements set forth by the appropriate sections of Federal Aviation Regulation Part 23 (FAR23) as well as those established in the statement of work. Derived from text

N94-24975*# California Polytechnic State Univ., San Luis Obispo. Aeronautical Engineering Dept.
WEASEL WORKS SA-150: DESIGN STUDY OF A 100 TO 150 PASSENGER TRANSPORT AIRCRAFT
Kevin Alkema, Michael Comeaux, Timothy Gilbert, Victor Para, and George Toepfer 14 May 1993 110 p
(Contract NASw-4435)
(NASA-CR-195489; NAS 1.26:195489) Avail: CASI HC A06/MF A02

As the year 2000 rapidly approaches, the airlines are faced with an extremely competitive and environmentally restrictive marketplace. In order to survive, commercial air carriers will need to find new ways to lower their direct operating costs, increase load factors and comply with tightening federal and international constraints. The SA-150 has been designed to meet these demands by focusing on the areas of aerodynamic efficiency, an improved level of passenger comfort, and a limited application of advanced technology. The SA-150 has been optimized for a 500 nmi. mission to help the airlines meet the challenges of the short haul, quick turnaround flight. With a maximum capacity of 124 passengers, and full baggage, the SA-150 is also capable of covering a range of 1500 nmi. This additional range capability will provide the airlines with flexibility when scheduling their routes. The aircraft features a 'V' tail, fly-by-wire system and is powered by two turbofans mounted under a twelve aspect ratio wing. The SA-150 will have an initial production run of 800 units and have a purchase price of $37.7 million in 1993 dollars. Author

N94-25001*# Notre Dame Univ., IN. Dept. of Aerospace and Mechanical Engineering.
THE BUNNY: A SIMULATED COMMERCIAL AIR TRANSPORTATION STUDY Final Design Proposal
David Fulton, Patrick Gallagher, William Grannan, Jennifer Martin, Nicole Mastej, and Brett Wujek Apr. 1993 123 p
(Contract NASw-4435)
(NASA-CR-195537; NAS 1.26:195537) Avail: CASI HC A06/MF A02

The Bunny is a single-engine, 100 passenger commercial transport designed to serve the high density short-to-medium range markets in AEROWORLD. The aircraft's design range is 10,000 feet at a cruise velocity of 30 ft/s. The aircraft features a low wing which incorporates polyhedral for roll control. Yaw and pitch control are accomplished by a rudder and elevator, respectively. Propulsion is provided by a nose-mounted Astro 15 electric motor powered by thirteen 1.2 V, 1000 mah batteries with a Zinger 12-6 propeller. The aircraft is structurally designed with a safety factor of

1.5 and is constructed primarily of balsa, bass, and birch wood. Passenger seating is arranged on two levels, with three-abreast on the lower level and two-abreast on the upper level. The factors which had the most significant influence on the final design were the direct operating cost and the take-off distance. The primary strength of The Bunny is its ability to compete economically with the HB-40. At full capacity and mid-range fuel costs, the cost per seat per thousand feet (CPSK) of this aircraft is 25% less than the HB-40. Another principal strength is its ability to operate in all airports in AEROWORLD. Also, The Bunny's two-piece removable wing is an advantage from a transportability standpoint. Derived from text

N94-25002*# Notre Dame Univ., IN. Dept. of Aerospace and Mechanical Engineering.

THE GOLD RUSH: A SIMULATED COMMERCIAL AIR TRANSPORTATION STUDY

Amanda Clarke, Chris Degiorgio, Edmund Galka, Albert Stumm, Lisa Valenta, and Tom Winter Apr. 1993 121 p
(Contract NASw-4435)
(NASA-CR-195528; NAS 1.26:195528) Avail: CASI HC A06/MF A02

The remotely piloted vehicle (RPV) GoldRush was designed to complete the mission of transporting passengers in AeroWorld at a lower cost per seat per thousand feet (CPSPK) than the competition, the HB-40. There were two major factors which were constant considerations in the design process. The cost of manufacturing was the most important. In light of this, the designs were kept as simple as possible while considering trade-offs in performance. For example, the wing was not tapered so that several ribs could be cut at one time. Also of major importance was the takeoff distance. In order to serve all the cities in AeroWorld it was necessary to maintain a takeoff distance requirement of 24 feet. The takeoff distance proved to be the number one force in driving the design process. The Astro 25 engine and 13 inch propellor, a large wing area, and the high lift Wortmann airfoil were all chosen in order to satisfy this objective. Derived from text

N94-25004*# Embry-Riddle Aeronautical Univ., Daytona Beach, FL.

THE TRITON: DESIGN CONCEPTS AND METHODS

Greg Meholic, Michael Singer, Percy vanRyn, Rhonda Brown, Gustavo Tella, and Bob Harvey 7 Dec. 1992 48 p
(Contract NASw-4435)
(NASA-CR-195542; NAS 1.26:195542) Avail: CASI HC A03/MF A01

During the design of the C & P Aerospace Triton, a few problems were encountered that necessitated changes in the configuration. After the initial concept phase, the aspect ratio was increased from 7 to 7.6 to produce a greater lift to drag ratio (L/D = 13) which satisfied the horsepower requirements (118 hp using the Lycoming O-235 engine). The initial concept had a wing planform area of 134 sq. ft. Detailed wing sizing analysis enlarged the planform area to 150 sq. ft., without changing its layout or location. The most significant changes, however, were made just prior to inboard profile design. The fuselage external diameter was reduced from 54 to 50 inches to reduce drag to meet the desired cruise speed of 120 knots. Also, the nose was extended 6 inches to accommodate landing gear placement. Without the extension, the nosewheel received an unacceptable percentage (25 percent) of the landing weight. The final change in the configuration was made in accordance with the stability and control analysis. In order to reduce the static margin from 20 to 13 percent, the horizontal tail area was reduced from 32.02 to 25.0 sq. ft. The Triton meets all the specifications set forth in the design criteria. If time permitted another iteration of the calculations, two significant changes would be made. The vertical stabilizer area would be reduced to decrease the aircraft lateral stability slope since the current value was too high in relation to the directional stability slope. Also, the aileron size would be decreased to reduce the roll rate below the current 106 deg/second. Doing so would allow greater flap area (increasing CL(sub max)) and thus reduce the overall wing area. C & P would also recalculate the horsepower and drag values to further validate the 120 knot cruising speed. Author (revised)

N94-25017*# Notre Dame Univ., IN. Dept. of Aerospace and Mechanical Engineering.

THE RTL-46: A SIMULATED COMMERCIAL AIR TRANSPORTATION STUDY Final Report

Christian Dunbar, John Prette, Gerald Andersen, Martin Sprunck, Christine Vogel, and Francisco Rivera Apr. 1993 128 p
(Contract NASw-4435)
(NASA-CR-195524; NAS 1.26:195524) Avail: CASI HC A07/MF A02

The RTL-46 provides an aircraft which utilizes advanced technology within the fictional Aeroworld market to better service the air travel customers and airlines of Aeroworld. The RTL-46 is designed to serve the portion of the travel market which flies less than 10,000 feet per flight. The design cruise velocity for the aircraft is 35 ft/sec, which rapidly expedites travel through Aeroworld. The major focus of the endeavor was to design an aircraft which would serve the Aeroworld market better than the existing aircraft, the HB-40. This could have been done through targeting another portion of the Aeroworld market or through serving the current HB-40 market more effectively. Due to the fact that approximately 70 percent of the potential Aeroworld passengers desired flights of 10,000 ft or less, this range became the target market for the RTL-46. Derived from text

N94-25021*# Embry-Riddle Aeronautical Univ., Daytona Beach, FL.

DESIGN PROJECT: VIPER

Stephen Haithcock, Kyle Koncak, Rich Neufang, David Paufler, Russ Snow, and Frank Wlad 1992 47 p
(Contract NASw-4435)
(NASA-CR-195484; NAS 1.26:195484) Avail: CASI HC A03/MF A01

The design specification of the primary flight trainer are: must conform to F.A.R. 23, including the crashworthiness standards; is limited to two to four occupants; engine must be FAA certified; must comply with FAA standards for VFR and allow for upgrade to IFR flights; must be at least utility category with good spin recovery characteristics; must have a structural lifetime of at least 10,000 flight hours; capable of either of two training missions: climb to 5,000 ft., cruise 500 Nm. plus reserve, land, or climb to 1,000 ft. and descend ten cycles for landing practice, climb to 3,000 ft., maneuver at two g's for 15 minutes, cruise 100 Nm. and land; must have a cruise speed of at least 120 knots; must take-off or land on a runway no longer than 3,000 ft; and has a cost goal of $50,000, not including avionics, for production of 1,000 airplanes over a five year period. Derived from text

N94-25052 Department of the Navy, Washington, DC.

GENERIC DRONE CONTROL SYSTEM Patent

David M. Elband, inventor (to Navy) and Lynn R. Kern, inventor (to Navy) 31 Aug. 1993 11 p Filed 3 Aug. 1992
(AD-D015993; US-Patent-5,240,207; US-Patent-Appl-SN-923867; US-Patent-Class-244-190) Avail: US Patent and Trademark Office

The disclosed invention is a generic Drone Control System or alternatively a method to remotely pilot an air vehicle. The present invention essentially comprises a converted aircraft or other air vehicle and a ground station from where the drone is remotely controlled. Also disclosed as part of the Drone Control System are a plurality of means to transfer information and data between the ground station and the drone. DTIC

N94-25152# General Accounting Office, Washington, DC. National Security and International Affairs Div.

B-2 BOMBER: ASSESSMENT OF DOD'S RESPONSE TO MANDATED CERTIFICATIONS AND REPORTS

3 Nov. 1993 6 p
(AD-A273179; GAO/NSIAD-94-75) Avail: CASI HC A02/MF A01

Department of Defense Authorization Acts for fiscal years 1990, 1992, and 1993 required the Secretary of Defense to deliver to the Congress, certain certifications and reports concerning the B-2 bomber program. The Congress restricted the Air Force's use of about $2.3 billion appropriated in fiscal years 1992 and 1993 for procurement of B-2 Aircraft until those certifications and reports are delivered and an act of the Congress is passed authorizing release of the funds. The authorization acts also call for our office to report to the Congress concerning the certifications and reports submitted by the Secretary. This is an interim report in response to that legislation. A detailed classified report will be issued shortly. DTIC

N94-25268*# Purdue Univ., West Lafayette, IN. School of Aeronautics and Astronautics.

HIGH LIFT AERODYNAMICS

John Sullivan, Steve Schneider, Bryan Campbell, Greg Bucci, Rod Boone (Shaw Univ., Raleigh, NC.), Shad Torgerson, Rick Erausquin, and Chad

Knauer 8 Mar. 1994 46 p
(Grant NAG2-854)
(NASA-CR-195183; NAS 1.26:195183) Avail: CASI HC A03/MF A01

The current program is aimed at providing a physical picture of the flow physics and quantitative turbulence data of the interaction of a high Reynolds number wake with a flap element. The impact of high lift on aircraft performance is studied for a 150 passenger transport aircraft with the goal of designing optimum high lift systems with minimum complexity.
Derived from text

N94-25301 Institut Franco-Allemand de Recherches, Saint-Louis (France).
THE ISL ROTOR BENCH [LE BANC ROTOR DE L'ISL]
C. Johe, J. Haertig, P. Gnemmi, and F. Vincent 18 May 1992 29 p
In FRENCH
(ISL-R-108/92; ETN-94-95120) Avail: Issuing Activity
(Fachinformationszentrum Karlsruhe, Eggenstein-Leopoldschafen 2, 7014 Karlsruhe, Germany)

The rotor test bench of the ISL (French acronym for Saint-Louis Institute) is described. The test facility was designed for aeroacoustic experiments of helicopter rotors. Special attention is given to noise at high speeds. The test bench mechanical systems and the operation procedures are described. The measurement and control electronic equipment and the applied software tools, developed for surveying tasks and data acquisition, are presented. The rotor acoustic signatures measured at low and at transonic speeds are discussed. ESA

N94-25440# McDonnell-Douglas Aerospace Information Services Co., Saint Louis, MO.
AIRCRAFT MANEUVERS FOR THE EVALUATION OF FLYING QUALITIES AND AGILITY. VOLUME 2: MANEUVER DESCRIPTIONS AND SECTION GUIDE Final Report, Sep. 1990 - Jun. 1993
David J. Wilson, David R. Riley, and Kevin D. Citurs Aug. 1993 92 p
(Contract F33615-90-C-3600)
(AD-A273685; WL-TR-93-3082-Vol-2) Avail: CASI HC A05/MF A01

A set of aircraft maneuvers was developed to augment evaluation maneuvers used currently by the flying qualities and flight test communities. These maneuvers extend evaluation to full aircraft dynamics throughout the aircraft flight envelope. As a result, a tie was established between operational use and design parameters without losing control of the aircraft evaluation process. Twenty maneuvers are described as an initial set to examine primarily high-angle-of-attack conditions. Perhaps as important as the maneuvers themselves is the method used to select them. These maneuvers will allow direct measurement of flying qualities throughout the flight envelope instead of merely comparing parameters to specification values. DTIC

N94-24245 Israel Aircraft Industries Ltd., Ben-Gurion Airport.
UAV CURRENT TECHNOLOGY AND FUTURE TRENDS
D. Harari *In* Israel Society of Aeronautics and Astronautics, The 33rd Israel Annual Conference on Aviation and Astronautics 25 Feb. 1993 p 83-88 (For primary document see N94-24241 06-01)
Copyright Avail: Issuing Activity (Israel Society of Aeronautics and Astronautics, c/o Faculty of Engineering, Tel-Aviv Univ., Ramat Aviv 69978, Israel)

N94-24250 Israel Aircraft Industries Ltd., Tashan. Wind Tunnels Center.
ON THE EFFECT OF THE DAMPING COEFFICIENTS ON THE TRAJECTORIES OF SYMMETRIC AND NON-SYMMETRIC STORES
Moshe Zilberman and Alex Cazes *In* Israel Society of Aeronautics and Astronautics, The 33rd Israel Annual Conference on Aviation and Astronautics 25 Feb. 1993 p 133-141 (For primary document see N94-24241 06-01)
Copyright Avail: Issuing Activity (Israel Society of Aeronautics and Astronautics, c/o Faculty of Engineering, Tel-Aviv Univ., Ramat Aviv 69978, Israel)

N94-24259 Israel Aircraft Industries Ltd., Ben-Gurion Airport. LAHAV Engineering Dept.
REPAIR OF CRACKED ALUMINUM AIRCRAFT STRUCTURE WITH COMPOSITE PATCHES
N. Sasson, A. Simon, H. Leibovich (Israel Aircraft Industries Ltd., Tashan.), and A. K. Green (Israel Aircraft Industries Ltd., Tashan.) *In* Israel Society of Aeronautics and Astronautics, The 33rd Israel Annual Conference on Aviation and Astronautics 25 Feb. 1993 p 213-224 (For primary document see N94-24241 06-01)
Copyright Avail: Issuing Activity (Israel Society of Aeronautics and Astronautics, c/o Faculty of Engineering, Tel-Aviv Univ., Ramat Aviv 69978, Israel)

N94-24261 Israel Aircraft Industries Ltd., Tashan.
DEVELOPMENT OF A DAMAGE TOLERANCE TOOL TO ANALYZE MULTIPLE-SITE DAMAGE IN AIRCRAFT STRUCTURE
A. Brot and A. Nathan *In* Israel Society of Aeronautics and Astronautics, The 33rd Israel Annual Conference on Aviation and Astronautics 25 Feb. 1993 p 237-245 (For primary document see N94-24241 06-01)
Copyright Avail: Issuing Activity (Israel Society of Aeronautics and Astronautics, c/o Faculty of Engineering, Tel-Aviv Univ., Ramat Aviv 69978, Israel)

N94-24268 Israeli Air Force, Zahal.
COMPARISON OF C.T.S. BASED PREDICTION OF STORE TRAJECTORY WITH FLIGHT TEST DATA
E. Goldberg, A. Feldhuhn, Ts. Cohen, S. Fledel (Israel Aircraft Industries Ltd., Tashan.), M. Zilberman, M. Shay (Israel Aircraft Industries Ltd., Lod.), and I. Shruster (Israel Aircraft Industries Ltd., Lod.) *In* Israel Society of Aeronautics and Astronautics, The 33rd Israel Annual Conference on Aviation and Astronautics 25 Feb. 1993 p 303-309 (For primary document see N94-24241 06-01)
Copyright Avail: Issuing Activity (Israel Society of Aeronautics and Astronautics, c/o Faculty of Engineering, Tel-Aviv Univ., Ramat Aviv 69978, Israel)

N94-24286 Technion - Israel Inst. of Tech., Haifa. Faculty of Aerospace Engineering.
THE INFLUENCE OF ELASTIC PITCH VARIATIONS ON HELICOPTER FLIGHT MECHANICS
Z. Beigleman and A. Rosen *In* Israel Society of Aeronautics and Astronautics, The 33rd Israel Annual Conference on Aviation and Astronautics 25 Feb. 1993 p 469-481 (For primary document see N94-24241 06-01)
Copyright Avail: Issuing Activity (Israel Society of Aeronautics and Astronautics, c/o Faculty of Engineering, Tel-Aviv Univ., Ramat Aviv 69978, Israel)

N94-25069 Boeing Co., Seattle, WA.
HIGH-ORDER TECHNOLOGY: APPLYING TECHNICAL EXCELLENCE TO NEW AIRPLANE DEVELOPMENT
Albertus D. Welliver *In* National Academy of Engineering, The Future of Aerospace: Proceedings of a Symposium Held in Honor of Alexander H. Flax 1993 p 37-44 (For primary document see N94-25065 06-99)
Copyright Avail: Issuing Activity

N94-25070 Army Aviation Systems Command, Moffett Field, CA. Advanced Systems Research and Analysis Office.
THE FUTURE OF ROTARY-WING AIRCRAFT
Richard M. Carlson *In* National Academy of Engineering, The Future of Aerospace: Proceedings of a Symposium Held in Honor of Alexander H. Flax 1993 p 45-63 (For primary document see N94-25065 06-99)
Copyright Avail: Issuing Activity

N94-25109*# Joint Inst. for Advancement of Flight Sciences, Hampton, VA. Aircraft Guidance and Controls Branch.
X-31 AERODYNAMIC CHARACTERISTICS DETERMINED FROM FLIGHT DATA
Alex Kokolios *In* NASA. Langley Research Center, NASA LaRC Workshop on Guidance, Navigation, Controls, and Dynamics for Atmospheric Flight, 1993 Dec. 1993 p 373-387 (For primary document see N94-25096 06-01)
Avail: CASI HC A03/MF A04

N94-25113*# National Aeronautics and Space Administration. Langley Research Center, Hampton, VA.
EFFECT OF AEROELASTIC-PROPULSIVE INTERACTIONS ON FLIGHT DYNAMICS OF A HYPERSONIC VEHICLE
David L. Raney, John D. McMinn, Anthony S. Pototzky (Lockheed Engineering and Sciences Co., Hampton, VA.), and Christine L. Wooley (Cincinnati Univ., OH.) *In its* NASA LaRC Workshop on Guidance, Navigation, Controls, and Dynamics for Atmospheric Flight, 1993 Dec. 1993 p 459-472 (For primary document see N94-25096 06-01)
Avail: CASI HC A03/MF A04

06 AIRCRAFT INSTRUMENTATION

Includes cockpit and cabin display devices; and flight instruments.

For related information see also *19 Spacecraft Instrumentation* and *35 Instrumentation and Photography.*

N94-24733 Naval Air Systems Command, Arlington, VA.
ADVANCED AVIONICS ARCHITECTURE AND TECHNOLOGY REVIEW. EXECUTIVE SUMMARY AND VOLUME 1: AVIONICS TECH NOLOGY. VOLUME 2: AVIONICS SYSTEMS ENGINEERING Final Report, Jul. 1992 - Aug. 1993
6 Aug. 1993 244 p Limited Reproducibility: More than 20% of this document may be affected by microfiche quality
(AD-A273630) Avail: Issuing Activity (Defense Technical Information Center (DTIC))

The purpose of this study was to review the current technology base, developing technologies, and the potential to apply them to meet military avionics requirements. The review also examined the technology integration methods used in the avionics community in order to develop a more efficient and more affordable avionics architectural strategy for the future. It provides a bold vision for the application of advanced technology to naval avionics. This study was accomplished as a cooperative venture by members of the Naval Aviation Systems team and over 50 leading firms from the electronics and aerospace industries. The study team also included representatives from the Air Force, Advanced Research Projects Agency, National Institute for Standards and Technology, and the Defense Systems Management College. Their goal was to review emerging technologies, investigate their potential for application to naval avionics, and identify potential cost savings. The Joint Aeronautical Commanders Group (JACG) will use this study as a basis for developing and implementing a better acquisition partnership between the military services and industry. This report is the only comprehensive compilation of today's avionics technology. It is a great reference book that contains easily understandable descriptions of today's technologies, including bus architectures, back planes, processors, software, and just about every aspect of avionics design and development. DTIC

N94-24774# Naval Postgraduate School, Monterey, CA.
EVALUATION OF THE UH-1N INSTRUMENT PANEL M.S. Thesis
Lawrence E. Miccolis Sep. 1993 72 p
(AD-A273145) Avail: CASI HC A04/MF A01

This study evaluates the current configuration of the U.S. Marine Corps LJH-IN helicopter instrument panel. Additionally, the alternatives for proposed multifunction display (MFD) symbologies associated with the COMM/NAV Block Upgrade for the UH-IN were evaluated. A survey was administered to 43 LJH-IN operational pilots from both east and west coast squadrons. Pilots were asked to rate instruments and devices currently included on the instrument panel on three factors: criticality, frequency of use, and satisfaction with display. The top ten and bottom ten instruments were identified for each of these three factors; 20 instruments rated high on all three factors while 10 rated low on all three. Several candidates for redesign were identified. Proposed multifunction display symbol sets from the Naval Air Warfare Center Aircraft Division, Warminster (NAWCADWAR), and MIL-STD-1295 (Proposed) were also assessed. Respondents rated symbols for (1) heading scale, present heading, and NAV steering bug (a pointer); (2) airspeed and present airspeed; (3) vertical velocity; (4) attitude, horizon, pitch angle, and aircraft reference; (5) altitude scale, present altitude, and high/low altitude warning; (6) torque; and (7) bank of roll scale, and slip. In general, the NAWCADWAR symbol set was referred. DTIC

07 AIRCRAFT PROPULSION AND POWER

Includes prime propulsion systems and systems components, e.g., gas turbine engines and compressors; and onboard auxilliary power plants for aircraft.

For related information see also *20 Spacecraft Propulsion and Power, 28 Propellants and Fuels,* and *44 Energy Production and Conversion.*

N94-23253 Pratt and Whitney Aircraft of Canada Ltd., Longueuil (Quebec).
TURBINE ENGINE WITH INDUCED PRE-SWIRL AT THE COMPRESSOR INLET Patent
Roger Lachance, inventor (to Pratt and Whitney Aircraft of Canad, Vasil Ozarapoglu, inventor (to Pratt and Whitney Aircraft of Canad, Jean Letourneau, inventor (to Pratt and Whitney Aircraft of Canad, and Svein Hubinette, inventor (to Pratt and Whitney Aircraft of Canad 11 May 1993 19 p
(CA-Patent-1-317-467; Int-Patent-Class-F01D-1/12; CTN-94-60922)
Copyright Avail: Micromedia Ltd., Technical Information Centre, 240 Catherine Street, Suite 305, Ottawa, Ontario, K2P 2G8, Canada HC/MF

An improved jet flap arrangement is provided for producing a pre-swirl at the compressor inlet of a gas turbine engine, in order to enhance engine stability and performance particularly at low-speed off-design conditions. According to the invention, an airflow path is defined between the shroud and hub of the engine for passing air to the compressor entry. A plurality of airfoils extends across the airflow path and upstream of the compressor entry. The airfoils are hollow and communicate with an air inlet in the shroud for communicating with a source of a pressurized gas flow. The airfoils have a leading and a trailing edge relative to the airflow path and a plurality of discrete openings which are closely spaced apart to define an axis extending across the airflow path from the shroud to the hub and spaced a short distance from the trailing edge. These openings form nozzles for discharge of the pressurized gas flow, thereby forming a jet flap across the airflow path for creating a pre-swirl in the airflow path. The airfoils may be struts extending between the shroud and hub in the airflow path. Author (CISTI)

N94-23255 General Electric Co., Fairfield, CT.
COUNTERROTATING AIRCRAFT PROPULSOR BLADES Patent
Joey L. Nelson, inventor (to General Electric Co.), Sidney B. Elston, inventor (to General Electric Co.), and Wu-Yang Tseng, inventor (to General Electric Co.) 22 Jun. 1993 42 p
(CA-Patent-1-319-357; Int-Patent-Class-B64C-11/20; Int-Patent-Class-B64C-11/48; CTN-94-60924) Copyright Avail: Micromedia Ltd., Technical Information Centre, 240 Catherine Street, Suite 305, Ottawa, Ontario, K2P 2G8, Canada HC/MF

A swept propeller blade is provided which is comprised of composite materials having the strength and airfoil configuration to provide an efficient blade for a counterrotating propeller system having highly swept, wide chord, thin blades for operating at transonic and supersonic speeds. A typical blade of the propulsor system includes an airfoil section having a tip end, a root end, and first and second surfaces between the ends intersecting in a convex leading edge and a concave trailing edge. Each surface is formed from a blade shell made of a plurality of angle plied composite laminates bonded together. A metallic blade spar is interposed between the first and second shells and is bonded to the shells for connecting the shell surfaces to the root end and for stiffening the blade. Foam filled airfoil cavities are created interposed between the first and second shells for decreasing the blade weight. A metallic plate sheath is bonded to the leading edge for preventing erosion and providing lightning protection. Counterweights in the blade spar fore and aft of the spar dovetail are adjustable to provide static balancing of the blade in radial and chord-wise directions. A polyurethane film is applied to the outer blade surface for protection. Author (CISTI)

N94-23466*# National Aeronautics and Space Administration. Lewis Research Center, Cleveland, OH.
TRANSIENT EJECTOR ANALYSIS (TEA) CODE USER'S GUIDE
Colin K. Drummond Dec. 1993 51 p
(RTOP 505-62-30)

(NASA-TM-106310; E-8050; NAS 1.15:106310) Avail: CASI HC A04/MF A01

A FORTRAN computer program for the semi analytic prediction of unsteady thrust augmenting ejector performance has been developed, based on a theoretical analysis for ejectors. That analysis blends classic self-similar turbulent jet descriptions with control-volume mixing region elements. Division of the ejector into an inlet, diffuser, and mixing region allowed flexibility in the modeling of the physics for each region. In particular, the inlet and diffuser analyses are simplified by a quasi-steady-analysis, justified by the assumption that pressure is the forcing function in those regions. Only the mixing region is assumed to be dominated by viscous effects. The present work provides an overview of the code structure, a description of the required input and output data file formats, and the results for a test case. Since there are limitations to the code for applications outside the bounds of the test case, the user should consider TEA as a research code (not as a production code), designed specifically as an implementation of the proposed ejector theory. Program error flags are discussed, and some diagnostic routines are presented. Author (revised)

N94-23519 Rolls-Royce Ltd., Derby (England).

ROLLS-ROYCE IN PERSPECTIVE: PAST, PRESENT AND FUTURE

Frank Turner 1991 37 p Presented at the 35th R. J. Mitchell Memorial Lecture to the Royal Aeronautical Society, Southampton, Hall of Aviation, United Kingdom, 6 Mar. 1991 Limited Reproducibility: More than 20% of this document may be affected by poor print

(PNR-90882; MISC-2514; ETN-93-93708) Copyright Avail: Issuing Activity (European Space Agency (ESA))

An historical account of the development of Rolls-Royce from the time their names first appeared together in 1904 on the classic radiator shape, which first adorned the little two cylinder ten horse power car, to the launch of the RB211 aircraft engine, is given. The historical account is presented under the following headings: the original Rolls-Royce cars, the Silver Ghost, subsequent car models, the entry of Rolls-Royce into aviation, the first aeroengine (the Eagle), second generation aeroengines, the Shneider Trophy, the Merlin, birth of the gas turbine, Barnoldswick and the jet engine, the jet engine postwar, establishing the gas turbine in commercial aviation, the commercial turbojet and turbofan, the launch of the RB211, the company today, civil engines today, and the future. ESA

N94-23545*# National Aeronautics and Space Administration. Lewis Research Center, Cleveland, OH.

HOLOGRAPHIC TESTING OF COMPOSITE PROPFANS FOR A CRUISE MISSILE WIND TUNNEL MODEL

Christopher J. Miller Jan. 1994 41 p

(RTOP 535-03-10)

(NASA-TM-105271; E-8203; NAS 1.15:105271) Avail: CASI HC A03/MF A01

Each of the approximately 90 composite propfan blades constructed for a 55 percent scale cruise missile wind tunnel model were holographically tested to obtain natural frequencies and mode shapes. These data were used not only for quality assurance, but also to select sets of similar blades for each blade row. Presented along with the natural frequency data is a description of a computer-based image processing system developed to supplement the photographic based system for holographic image analysis and storage. The new system is quicker and cheaper, the holograms are indexed better, and several engineers can access the data simultaneously. The only negative effect is a slight reduction in image resolution, which does not influence the end use. Author (revised)

N94-23552*# Rensselaer Polytechnic Inst., Troy, NY.

A RANDOM DISTRIBUTION REACTING MIXING LAYER MODEL Final Report

Richard A. Jones Jan. 1994 17 p

(Contract NCC3-213; RTOP 505-62-52)

(NASA-CR-194445; E-8315; NAS 1.26:194445) Avail: CASI HC A03/MF A01

A methodology for simulation of molecular mixing and the resulting velocity and temperature fields has been developed. The ideas are applied to the flow conditions present in the NASA Lewis Planar Reacting Shear Layer (PRSL) facility, and results compared to experimental data. A gaussian transverse turbulent velocity distribution is used in conjunction with a linearly increasing time scale to describe the mixing of different regions of the flow. Equilibrium reaction calculations are then performed on the mix to arrive at a new species composition and temperature. Velocities are determined through summation of momentum contributions. The analysis indicates a combustion efficiency of the order of 80 percent for the reacting mixing layer, and a turbulent Schmidt number of 2/3. The success of the model is attributed to the simulation of large-scale transport of fluid. The favorable comparison shows that a relatively quick and simple PC calculation is capable of simulating the basic flow structure in the reacting and non-reacting shear layer present in the facility given basic assumptions about turbulence properties. Author

N94-23570 Rolls-Royce Ltd., Derby (England).

THE RB211: THE FIRST 25 YEARS

Philip Ruffles 1992 33 p Presented at the 31st Short Brothers Commemorative Lecture to Royal Aeronautical Society, Queens University, Belfast, Ireland, 16 Jan. 1992 Limited Reproducibility: More than 20% of this document may be affected by poor print

(PNR-90977; MISC-2665; ETN-93-93707) Copyright Avail: Issuing Activity (European Space Agency (ESA))

The development of the RB211 high bypass turbofan engine is reviewed giving details on its early problems and inherent strengths, the dramatic evolution of the design and finally, how the engine family will address the future market. The RB211-22 first entered service in the L1011 Tristar with Eastern Airline in 1972. Now, twenty years later, the RB211 has been developed into an outstanding family of engines; the -524 for the Boeing 747 and 767, the smaller -535 on the Boeing 757 and the latest and most powerful Trent family, for the new Airbus A330, Boeing 777 and McDonnell Douglas MD-12 aircraft. The RN211 has now gained over 40 million hours experience with 64 customers and its evolutionary development has given rise to many unique innovations in design and manufacturing to meet the requirements of the customer. ESA

N94-23709 General Electric Co., Schenectady, NY. Corporate Research and Development.

EVALUATION OF REDUCING GAS TURBINE EMISSIONS THROUGH HYDROGEN-ENHANCED STEAM-INJECTED COMBUSTION Final Report, Nov. 1991 - Apr. 1993

J. R. Maughan, J. H. Bowen, S. G. Kimura, D. H. Cooke, and G. Joshi Apr. 1993 168 p Prepared in cooperation with Pullman Kellogg, Houston, TX. Sponsored by Gas Research Inst., Chicago, IL Limited Reproducibility: More than 20% of this document may be affected by microfiche quality

(Contract GRI-5091-293-2188)

(PB94-109873; GRI-93/0272) Avail: Issuing Activity (National Technical Information Service (NTIS))

The potential for reducing emissions from gas turbines by injecting steam for NO(x) control and hydrogen for CO control is evaluated through laboratory-scale combustion experiments. Results showed that hydrogen addition into a steam-injected diffusion combustor at hydrogen/fuel molar ratios of approximately 20% was associated with somewhat increased NO(x) production and reduced CO emissions. Both effects are attributed to an increase in the local stoichiometric flame temperature. However, the decrease in CO was greater than the increase in NO(x), resulting in a net emissions benefit, or a shifting of the NO(x)-CO curve toward the origin. Consequently, a greater range of NO(x)/CO emissions targets could be achieved when hydrogen was available. NTIS

N94-24082*# National Aeronautics and Space Administration. Lewis Research Center, Cleveland, OH.

CFD ASSESSMENT OF ORIFICE ASPECT RATIO AND MASS FLOW RATIO ON JET MIXING IN RECTANGULAR DUCTS

D. B. Bain (Computational Fluid Dynamics Research Corp., Huntsville, AL.), C. E. Smith (Computational Fluid Dynamics Research Corp., Huntsville, AL.), and J. D. Holdeman Jan. 1994 27 p Presented at the 32nd Aerospace Sciences Meeting and Exhibit, Reno, NV, 10-13 Jan. 1994; sponsored by AIAA Original contains color illustrations

(Contract NAS3-25967)

(NASA-TM-106434; E-8276; NAS 1.15:106434; AIAA Paper 94-0218)

Avail: CASI HC A03/MF A01; 8 functional color pages

Isothermal CFD analysis was performed on axially opposed rows of jets mixing with cross flow in a rectangular duct. Laterally, the jets' centerlines were aligned with each other on the top and bottom walls. The focus of this study was to characterize the effects of orifice aspect ratio and jet-to-mainstream mass flow ratio on jet penetration and mixing. Orifice aspect ratios (L/W) of 4-to-1, 2-to-1, and 1-to-1, along with circular holes, were parametrically analyzed. Likewise, jet-to-mainstream mass flow ratios (MR) of 2.0, 0.5, and 0.25 were systematically investigated. The jet-to-mainstream momentum-flux ratio (J) was maintained at 36 for all cases, and the orifice spacing-to-duct height (S/H) was varied until optimum mixing was attained for each configuration. The numerical results showed that orifice aspect ratio (and likewise orifice blockage) had little effect on jet penetration and mixing. Based on mixing characteristics alone, the 4-to-1 slot was comparable to the circular orifice. The 4-to-1 slot has a smaller jet wake which may be advantageous for reducing emissions. However, the axial length of a 4-to-1 slot may be prohibitively long for practical application, especially for MR of 2.0. The jet-to-mainstream mass flow ratio had a more significant effect on jet penetration and mixing. For a 4-to-1 aspect ratio orifice, the design correlating parameter for optimum mixing (C = (S/H)(sq. root J)) varied from 2.25 for a mass flow ratio of 2.0 to 1.5 for a mass flow ratio of 0.25. Author (revised)

N94-24106*# National Aeronautics and Space Administration. Hugh L. Dryden Flight Research Facility, Edwards, CA.

IDENTIFICATION OF INTEGRATED AIRFRAME: PROPULSION EFFECTS ON AN F-15 AIRCRAFT FOR APPLICATION TO DRAG MINIMIZATION

Gerard S. Schkolnik Nov. 1993 26 p Conference held in Monterey, CA, 9-11 Aug. 1993 See also A93-51359 Sponsored by NASA. Washington
(RTOP 533-02-39)
(NASA-TM-4532; H-1946; NAS 1.15:4532; AIAA Paper 93-3764)
Copyright Avail: CASI HC A03/MF A01

The application of an adaptive real-time measurement-based performance optimization technique is being explored for a future flight research program. The key technical challenge of the approach is parameter identification, which uses a perturbation-search technique to identify changes in performance caused by forced oscillations of the controls. The controls on the NASA F-15 highly integrated digital electronic control (HIDEC) aircraft were perturbed using inlet cowl rotation steps at various subsonic and supersonic flight conditions to determine the effect on aircraft performance. The feasibility of the perturbation-search technique for identifying integrated airframe-propulsion system performance effects was successfully shown through flight experiments and postflight data analysis. Aircraft response and control data were analyzed postflight to identify gradients and to determine the minimum drag point. Changes in longitudinal acceleration as small as 0.004 g were measured, and absolute resolution was estimated to be 0.002 g or approximately 50 lbf of drag. Two techniques for identifying performance gradients were compared: a least-squares estimation algorithm and a modified maximum likelihood estimator algorithm. A complementary filter algorithm was used with the least squares estimator. Author

N94-24180 General Electric Co., Fairfield, CT.

WING MOUNTED UNDUCTED FAN ENGINE Patent

A. P. Adamson, inventor (to General Electric Co.) and Wu-Yang Tseng, inventor (to General Electric Co.) 19 Oct. 1993 22 p
(CA-Patent-1323353; Int-Patent-Class-B64D-027/10; Int-Patent-Class-B64D-027/02; CTN-94-60930) Copyright Avail: Micromedia Ltd., Technical Information Centre, 240 Catherine Street, Suite 305, Ottawa, Ontario, K2P 2G8, Canada HC/MF

An aircraft propulsion system comprises a pusher type engine including propulsor blades and an engine mounting means which minimizes the two per revolution excitation of the blades due to a wake interaction with the blades. One embodiment of the system is an aircraft engine comprising a plurality of propulsor blades which define an engine disk and a wake interaction zone across the disk having a radial location on the disk, wherein the relative strength of the dynamic loads acting on the propulsor blades is a function of the radial location having at least one relative minimum along the blade length. The location is such that the value of the function is essentially a relative minimum. A more particular embodiment is a wing mounted pusher aircraft engine comprising a plurality of propulsor blades defining an engine disk and a wake interaction zone across the disk having a radial location on the disk wherein the wake is shed from the aircraft wing. The relative strength of the dynamic loads acting on the blades is a function of the radial location, which is such that the value of the function is essentially a relative minimum. Author (CISTI)

N94-24490 Mitsubishi Heavy Industries Ltd., Tokyo (Japan).

GAS TURBINE AND OPERATING METHOD OF THE SAME Patent Application

Susumu Morishita, inventor (to Micromedia Ltd.), Yoshiaki Miyake, inventor (to Micromedia Ltd.), and Seishi Uchida, inventor (to Micromedia Ltd.) 23 Nov. 1992 18 p
(CA-Patent-Appl-SN-2043039; Int-Patent-Class-F02C-007/042; CTN-94-60870) Copyright Avail: Micromedia Ltd., Technical Information Centre, 240 Catherine Street, Suite 305, Ottawa, Ontario, K2P 2G8, Canada HC/MF

A gas turbine is characterized by a centrifugal compressor driven by a high pressure turbine and a variable inlet guide vane (VIGV) located at the inlet of the compressor. An axial flow compressor is not provided between the centrifugal compressor and the VIGV. A thrust gas turbine is provided, equipped with a centrifugal compressor which compresses air, a combustor for combustion of fuel using the pressurized air, and a turbine driven to rotate with a part of the energy of the gas produced in the combustor and which drives the compressor; this turbine is characterized by a VIGV at the compressor inlet. A method for operating a gas turbine is also disclosed, characterized in that output is varied by driving the VIGV while keeping the rotation at a high level. According to this invention, it is possible to reduce the flow rate of air taken into an engine so as to reduce the brake horsepower of the engine even at high engine rotation by throttling the VIGV. When the VIGV is opened suddenly, the flow rate increases and the output also increases rapidly; thus the engine output response time is determined almost entirely by the VIGV response time. Thus, an engine with high responsiveness and reliability may be realized according to the invention. Embodiments of the invention include various aircraft engines. CISTI

N94-24594*# National Aeronautics and Space Administration. Lewis Research Center, Cleveland, OH.

MIXING CHARACTERISTICS OF DIRECTLY OPPOSED ROWS OF JETS INJECTED NORMAL TO A CROSSFLOW IN A RECTANGULAR DUCT

D. S. Liscinsky (United Technologies Research Center, East Hartford, CT.), B. True (United Technologies Research Center, East Hartford, CT.), and J. D. Holdeman Jan. 1994 12 p Presented at the 32nd Aerospace Sciences Meeting and Exhibit, Reno, NV, 10-13 Jan. 1994; sponsored by AIAA Original contains color illustrations
(Contract NAS3-25954; RTOP 537-02-21)
(NASA-TM-106477; E-8405; NAS 1.15:106477; AIAA Paper 94-0217)
Avail: CASI HC A03/MF A01; 5 functional color pages

An experimental investigation of the mixing of nonreacting opposed rows of inline jets injected perpendicular to a uniform crossflow has been conducted in a rectangular duct. Planar Mie-scattering was used to measure the time-average concentration distribution of the jet fluid in planes perpendicular to the duct axis. Orifice configurations with geometric blockages ranging from 0.59 to 0.89 had similar mixing performance when compared at one-half duct height downstream of injection. Blockage was varied by changing the orifice aspect ratio from 1-to-1 to 1-to-1.5 while maintaining orifice spacing-to-duct height (S/H) at 0.425, jet-to-mainstream mass flow ratio (MR) at 2.0, and jet-to-mainstream momentum-flux ratio (J) at 48. The result indicates that the design correlating expression (at MR = 2) for optimum in line mixing of 2.5 approximately equal to (S/H)(square root of J) is independent of the Webb between adjacent orifices and therefore independent of orifice width. Experimental and numerical results for an orifice aspect ratio 1-to-1 case were in good agreement. The results of a comparison of inline 45 degrees slanted slot and round orifice configuration indicate that in order to obtain equivalent mean concentration distributions at the same J it is necessary to use a smaller S/H for the round orifice configuration. Conclusions about the performance of various orifice shapes can only be obtained from comparison of optimized configurations. Inline jets with different momentum-flux ratios on opposite sides were compared at a constant mass flow ratio. The orifice spacing chosen was previously found to be an optimum configuration when opposing values of J were equal and also an optimum for single side injection. Experimental and empirical results were in good agreement. Author

N94-24776# Pratt and Whitney Aircraft, West Palm Beach, FL. Government Engines and Space Propulsion.
ADVANCED CAPABILITY EXHAUST SYSTEMS/INTEGRATED PRODUCT DEVELOPMENT FOR ADVANCED NOZZLES (ACES/IPD) Technical Report, Sep. 1991 - Sep. 1992
Austin L. Andrews and Alfredo Cires Dec. 1992 106 p
(Contract F33615-91-C-5733)
(AD-A273209; PW/GESP-FR-22402; WL-TR-93-8030) Avail: CASI HC A06/MF A02

The objective of the ACES/IPD program is to develop methodologies for incorporating integrated product development principles into the advanced exhaust nozzle development process to insure smooth transition to engineering development products, decreased development time, reduced life cycle costs, and increased system quality. This report documents the activities as part of tasks one and two of the ACES/IPD program. A comprehensive survey of Pratt and Whitney advanced nozzle programs was conducted and lessons learned were extracted to serve as a guide for future advanced technology exhaust system development. DTIC

N94-25085*# Ohio State Univ., Columbus.
[A CONCEPTUAL DESIGN OF AN UNMANNED TEST VEHICLE USING AN AIRBREATHING PROPULSION SYSTEM]
1992 60 p
(Contract NASw-4435)
(NASA-CR-195550; NAS 1.26:195550) Avail: CASI HC A04/MF A01

According to Aviation Week and Space Technology (Nov. 16, 1992), without a redefined approach to the problem of achieving single stage-to-orbit flight, the X-30 program is virtually assured of cancellation. One of the significant design goals of the X-30 program is to achieve single stage to low-earth orbit using airbreathing propulsion systems. In an attempt to avoid cancellation, the NASP Program has decided to design a test vehicle to achieve these goals. This report recommends a conceptual design of an unmanned test vehicle using an airbreathing propulsion system. Author (revised)

N94-25185*# National Aeronautics and Space Administration. Lewis Research Center, Cleveland, OH.
TWO-DIMENSIONAL CFD MODELING OF WAVE ROTOR FLOW DYNAMICS
Gerard E. Welch and Rodrick V. Chima Feb. 1994 16 p Presented at the 11th Computational Fluid Dynamics Conference, Orlando, FL, 6-9 Jul. 1993; sponsored by AIAA See also A93-45014
(RTOP 505-62-10)
(NASA-TM-106261; E-8404; NAS 1.15:106261) Avail: CASI HC A03/MF A01

A two-dimensional Navier-Stokes solver developed for detailed study of wave rotor flow dynamics is described. The CFD model is helping characterize important loss mechanisms within the wave rotor. The wave rotor stationary ports and the moving rotor passages are resolved on multiple computational grid blocks. The finite-volume form of the thin-layer Navier-Stokes equations with laminar viscosity are integrated in time using a four-stage Runge-Kutta scheme. Roe's approximate Riemann solution scheme or the computationally less expensive advection upstream splitting method (AUSM) flux-splitting scheme is used to effect upwind-differencing of the inviscid flux terms, using cell interface primitive variables set by MUSCL-type interpolation. The diffusion terms are central-differenced. The solver is validated using a steady shock/laminar boundary layer interaction problem and an unsteady, inviscid wave rotor passage gradual opening problem. A model inlet port/passage charging problem is simulated and key features of the unsteady wave rotor flow field are identified. Lastly, the medium pressure inlet port and high pressure outlet port portion of the NASA Lewis Research Center experimental divider cycle is simulated and computed results are compared with experimental measurements. The model accurately predicts the wave timing within the rotor passages and the distribution of flow variables in the stationary inlet port region. Author (revised)

N94-25200*# Sverdrup Technology, Inc., Brook Park, OH.
EFFECT OF POWER SYSTEM TECHNOLOGY AND MISSION REQUIREMENTS ON HIGH ALTITUDE LONG ENDURANCE AIRCRAFT Final Report
Anthony J. Colozza Feb. 1994 22 p
(Contract NAS3-25266; RTOP 537-10-20)
(NASA-CR-194455; E-8408; NAS 1.26:194455) Avail: CASI HC A03/MF A01

An analysis was performed to determine how various power system components and mission requirements affect the sizing of a solar powered long endurance aircraft. The aircraft power system consists of photovoltaic cells and a regenerative fuel cell. Various characteristics of these components, such as PV cell type, PV cell mass, PV cell efficiency, fuel cell efficiency, and fuel cell specific mass, were varied to determine what effect they had on the aircraft sizing for a given mission. Mission parameters, such as time of year, flight altitude, flight latitude, and payload mass and power, were also altered to determine how mission constraints affect the aircraft sizing. An aircraft analysis method which determines the aircraft configuration, aspect ratio, wing area, and total mass, for maximum endurance or minimum required power based on the stated power system and mission parameters is presented. The results indicate that, for the power system, the greatest benefit can be gained by increasing the fuel cell specific energy. Mission requirements also substantially affect the aircraft size. By limiting the time of year the aircraft is required to fly at high northern or southern latitudes, a significant reduction in aircraft size or increase in payload capacity can be achieved. Author (revised)

N94-23658*# Allied-Signal Aerospace Co., Phoenix, AZ.
THE 3-D CFD MODELING OF GAS TURBINE COMBUSTOR-INTEGRAL BLEED FLOW INTERACTION
D. Y. Chen and R. S. Reynolds *In* NASA. Lewis Research Center, The Fifth Annual Thermal and Fluids Analysis Workshop Nov. 1993 p 359-380 Original contains color illustrations (For primary document see N94-23634 06-34)
Avail: CASI HC A03/MF A04; 5 functional color pages

N94-24251 Technion - Israel Inst. of Tech., Haifa. Turbo and Jet Engine Laboratory.
THRUST VECTORING THEORY, LABORATORY AND FLIGHT TESTS
Benjamin Gal-Or and Valery Sherbaum *In* Israel Society of Aeronautics and Astronautics, The 33rd Israel Annual Conference on Aviation and Astronautics 25 Feb. 1993 p 142-153 (For primary document see N94-24241 06-01)
Copyright Avail: Issuing Activity (Israel Society of Aeronautics and Astronautics, c/o Faculty of Engineering, Tel-Aviv Univ., Ramat Aviv 69978, Israel)

N94-24253 Ben Gurion Univ. of the Negev, Beersheva (Israel). Dept. of Mechanical Engineering.
THE EFFECT OF HIGH ALTITUDE PRESSURE ON THE POWER AND EFFICIENCY OF AN AIRBORNE TWO-STROKE ENGINE
R. Harari and E. Sher *In* Israel Society of Aeronautics and Astronautics, The 33rd Israel Annual Conference on Aviation and Astronautics 25 Feb. 1993 p 159-165 (For primary document see N94-24241 06-01)
Copyright Avail: Issuing Activity (Israel Society of Aeronautics and Astronautics, c/o Faculty of Engineering, Tel-Aviv Univ., Ramat Aviv 69978, Israel)

N94-24270 Israel Aircraft Industries Ltd., Lod. BEDEK Aviation Division.
S-2E TRACKER MARITIME PATROL AIRCRAFT RE-ENGINE AND SYSTEM UPGRADE PROGRAM
Ilan Berlowitz, Meir Zeierman, and Scott Martin (Marsh Aviation Co., Scottsdale, AZ.) *In* Israel Society of Aeronautics and Astronautics, The 33rd Israel Annual Conference on Aviation and Astronautics 25 Feb. 1993 p 321-332 (For primary document see N94-24241 06-01)
Copyright Avail: Issuing Activity (Israel Society of Aeronautics and Astronautics, c/o Faculty of Engineering, Tel-Aviv Univ., Ramat Aviv 69978, Israel)

N94-24326*# National Aeronautics and Space Administration. Lewis Research Center, Cleveland, OH.
MULTI-DISCIPLINARY COUPLING FOR INTEGRATED DESIGN OF PROPULSION SYSTEMS
C. C. Chamis and S. N. Singhal (Sverdrup Technology, Inc., Brook Park, OH.) *In* AGARD, Integrated Airframe Design Technology Dec. 1993 12 p (For primary document see N94-24313 06-05)
Copyright Avail: CASI HC A03/MF A02

08 AIRCRAFT STABILITY AND CONTROL

Includes aircraft handling qualities; piloting; flight controls; and autopilots.

For related information see also *05 Aircraft Design, Testing and Performance.*

N94-23590*# Sverdrup Technology, Inc., Brook Park, OH.
A COMPARISON OF TWO MULTI-VARIABLE INTEGRATOR WINDUP PROTECTION SCHEMES Final Report
Duane Mattern Dec. 1993 11 p Presented at the 1993 AIAA Guidance, Navigation, and Control Conference, Monterey, CA, 9-11 Aug. 1993; sponsored by AIAA See also A93-51404
(Contract NAS3-25266; RTOP 505-62-50)
(NASA-CR-194436; E-8283; NAS 1.26:194436; AIAA Paper 93-3812)
Avail: CASI HC A03/MF A01

Two methods are examined for limit and integrator wind-up protection for multi-input, multi-output linear controllers subject to actuator constraints. The methods begin with an existing linear controller that satisfies the specifications for the nominal, small perturbation, linear model of the plant. The controllers are formulated to include an additional contribution to the state derivative calculations. The first method to be examined is the multi-variable version of the single-input, single-output, high gain, Conventional Anti-Windup (CAW) scheme. Except for the actuator limits, the CAW scheme is linear. The second scheme to be examined, denoted the Modified Anti-Windup (MAW) scheme, uses a scalar to modify the magnitude of the controller output vector while maintaining the vector direction. The calculation of the scalar modifier is a nonlinear function of the controller outputs and the actuator limits. In both cases the constrained actuator is tracked. These two integrator windup protection methods are demonstrated on a turbofan engine control system with five measurements, four control variables, and four actuators. The closed-loop responses of the two schemes are compared and contrasted during limit operation. The issue of maintaining the direction of the controller output vector using the Modified Anti-Windup scheme is discussed and the advantages and disadvantages of both of the IWP methods are presented. Author

N94-24551*# Embry-Riddle Aeronautical Univ., Daytona Beach, FL.
COCKPIT CONTROL SYSTEM CONCEPTUAL DESIGN
Greg Meholic, Rhonda Brown, Melissa Hall, Robert Harvey, Michael Singer, and Gustavo Tella 15 Mar. 1993 39 p
(Contract NASw-4435)
(NASA-CR-195543; NAS 1.26:195543) Avail: CASI HC A03/MF A01

The purpose of this project was to provide a means for operating the ailerons, elevator, elevator trim, rudder, nosewheel steering, and brakes in the Triton primary flight trainer. The main design goals under consideration were to illustrate system and subsystem integration, control function ability, and producibility. Weight and maintenance goals were addressed. Derived from text

N94-24804*# West Virginia Univ., Morgantown.
DETERMINATION OF THE STABILITY AND CONTROL DERIVATIVES OF THE NASA F/A-18 HARV USING FLIGHT DATA Contractor Report, 15 May - 15 Dec. 1993
Marcello R. Napolitano and Joelle M. Spagnuolo 15 Dec. 1993 123 p
(Contract NCC2-759)
(NASA-CR-194838; NAS 1.26:194838) Avail: CASI HC A06/MF A02

This report documents the research conducted for the NASA-Ames Cooperative Agreement No. NCC 2-759 with West Virginia University. A complete set of the stability and control derivatives for varying angles of attack from 10 deg to 60 deg were estimated from flight data of the NASA F/A-18 HARV. The data were analyzed with the use of the pEst software which implements the output-error method of parameter estimation. Discussions of the aircraft equations of motion, parameter estimation process, design of flight test maneuvers, and formulation of the mathematical model are presented. The added effects of the thrust vectoring and single surface excitation systems are also addressed. The results of the longitudinal and lateral directional derivative estimates at varying angles of attack are presented and compared to results from previous analyses. The results indicate a significant improvement due to the independent control surface deflections induced by the single surface excitation system, and at the same time, a need for additional flight data especially at higher angles of attack. Author (revised)

N94-24957*# Embry-Riddle Aeronautical Univ., Daytona Beach, FL.
COCKPIT CONTROL SYSTEM
David Lesnewski, Russ M. Snow, Dave Paufler, George Schnieder, Roxanne Athousake, and Lisa Combs 12 Mar. 1993 67 p
(Contract NASw-4435)
(NASA-CR-195488; NAS 1.26:195488) Avail: CASI HC A04/MF A01

The purpose of this project is to provide a detail design for the cockpit control system of the Viper PFT. The statement of work for this project requires provisions for control of the ailerons, elevator, rudder, and elevator trim. The system should provide adjustment for pilot stature, rigging, and maintenance. MIL-STD-1472 is used as a model for human factors criterion. The system is designed to the pilot limit loading outlined in FAR part 23.397. The general philosophy behind this design is to provide a simple, reliable control system which will withstand the daily abuse that is experienced in the training environment without excessive cost or weight penalties. Author (revised)

N94-25176*# Minnesota Univ., Minneapolis. Dept. of Aerospace Engineering and Mechanics.
FEEDBACK CONTROL LAWS FOR HIGHLY MANEUVERABLE AIRCRAFT Annual Report, 1 Feb. 1993 - 31 Jan. 1994
William L. Garrard and Gary J. Balas 10 Mar. 1994 7 p
(Grant NAG1-1380)
(NASA-CR-195195; NAS 1.26:195195) Avail: CASI HC A02/MF A01

During the first half of the year, the investigators concentrated their efforts on completing the design of control laws for the longitudinal axis of the HARV. During the second half of the year they concentrated on the synthesis of control laws for the lateral-directional axes. The longitudinal control law design efforts can be briefly summarized as follows. Longitudinal control laws were developed for the HARV using mu synthesis design techniques coupled with dynamic inversion. An inner loop dynamic inversion controller was used to simplify the system dynamics by eliminating the aerodynamic nonlinearities and inertial cross coupling. Models of the errors resulting from uncertainties in the principal longitudinal aerodynamic terms were developed and included in the model of the HARV with the inner loop dynamic inversion controller. This resulted in an inner loop transfer function model which was an integrator with the modeling errors characterized as uncertainties in gain and phase. Outer loop controllers were then designed using mu synthesis to provide robustness to these modeling errors and give desired response to pilot inputs. Both pitch rate and angle of attack command following systems were designed. The following tasks have been accomplished for the lateral-directional controllers: inner and outer loop dynamic inversion controllers have been designed; an error model based on a linearized perturbation model of the inner loop system was derived; controllers for the inner loop system have been designed, using classical techniques, that control roll rate and Dutch roll response; the inner loop dynamic inversion and classical controllers have been implemented on the six degree of freedom simulation; and lateral-directional control allocation scheme has been developed based on minimizing required control effort. Derived from text

N94-25516# Organization for Industrial Research, TNO, The Hague (Netherlands). Phyiscs and Electronics Lab.
REMOTE VIBRATION MEASUREMENTS AT A SUD AVIATION ALOUETTE 3 HELICOPTER WITH A CW CO2-LASER SYSTEM
H. E. Boetz 28 Sep. 1993 51 p
(AD-A273818; FEL-93-A183; TDCK-TD93-2777) Avail: CASI HC A04/MF A01

This report describes an experiment with a helicopter to quantify the performance of our experimental multifunctional CO2-laser heterodyne detection system as a vibration detection instrument. The laser system emitted a beam with a diameter of 35 mm with a divergence of 0.5 mrad and a continuous output of 0.4 Watt. The purpose of our measurements was to measure the vibration spectra of a helicopter from the Dutch Air Force at distances between 0.5 to 6 km at various aspect angles. Vibration detection with the help of lasers might prove important for classification of targets. Especially helicopters are of interest because of the typical constant rotor speeds and fixed speed-ratio's between the tail-and main rotor (T/R-ratio) and other characteristics of the spectra. The obtained spectral components are compared with maintenance (rotortuning) frequency measurements done at the airbase with accelerometers. The results are in accordance with each other. The rotor frequencies were determined at all positions of the helicopter. Depending on the place where the laser beam hits the target, the amplitudes of the spikes in the frequency spectrum may vary significantly. With an Advantest R9211C FFT spectrum analyzer, a measurement will take at least one second, yielding a recognizable spectrum at distances of the helicopter up to 4 km. DTIC

N94-25525 Air Force Inst. of Tech., Wright-Patterson AFB, OH.
FLIGHT CONTROLLER DESIGN USING MIXED H2/H INFINITY OPTIMIZATION WITH A SINGULAR H INFINITY CONSTRAINT M.S. Thesis
James P. Luke Dec. 1993 135 p Limited Reproducibility: More than 20% of this document may be affected by microfiche quality
(AD-A273831; AFIT/GAE/ENY/93D-21) Avail: CASI HC A07

This thesis explores the effectiveness of mixed H2/H Infinity optimal control design applied to a realistic flight control problem. The application used by this thesis is a single input single output problem dealing with a normal acceleration command following model of the AFTI F-16. The mixed H2/H Infinity control problem is broken into its component H2 and H Infinity parts; the H2 part is formulated as an LQG problem, and a weight is applied to system sensitivity in the H Infinity problem to obtain tracking performance. The sensitivity weight in the underlying H Infinity part results in a singular constraint on the mixed problem. A newly-developed numerical technique is applied and solutions are obtained for controllers of order equal to, first, the order of the underlying H2 problem and, second, the order of the underlying H Infinity problem. Performance characteristics of these controllers are compared to controllers designed using the more-conventional LQG/LTR design method. The results indicate the potential for controllers obtained through mixed H2/H Infinity optimization to provide excellent performance and robustness characteristics at orders less than those obtained through LQG/LTR. Since this conclusion grows in significance when applied to multiple input multiple output (MIMO) problems, a three input, five output example is introduced and the underlying H2 and H Infinity problems for two solution approaches are formulated. DTIC

N94-24244 California Univ., Los Angeles. Mechanical, Aerospace and Nuclear Engineering Dept.
AEROELASTIC, AEROMECHANICAL AND VIBRATION PROBLEMS IN HELICOPTERS
Peretz P. Friedmann *In* Israel Society of Aeronautics and Astronautics, The 33rd Israel Annual Conference on Aviation and Astronautics 25 Feb. 1993 p 37-81 (For primary document see N94-24241 06-01)
Copyright Avail: Issuing Activity (Israel Society of Aeronautics and Astronautics, c/o Faculty of Engineering, Tel-Aviv Univ., Ramat Aviv 69978, Israel)

N94-24287 Technion - Israel Inst. of Tech., Haifa. Faculty of Aerospace Engineering.
CONTINUOUS GUST RESPONSE AND SENSITIVITY DERIVATIVES USING STATE-SPACE MODELS
Arie Zole and Mordechay Karpel *In* Israel Society of Aeronautics and Astronautics, The 33rd Israel Annual Conference on Aviation and Astronautics 25 Feb. 1993 p 482-492 (For primary document see N94-24241 06-01)
Copyright Avail: Issuing Activity (Israel Society of Aeronautics and Astronautics, c/o Faculty of Engineering, Tel-Aviv Univ., Ramat Aviv 69978, Israel)

N94-25099*# National Aeronautics and Space Administration. Langley Research Center, Hampton, VA.
HIGHLY-RELIABLE FLY-BY-LIGHT/POWER-BY-WIRE TECHNOLOGY
Felix L. Pitts *In its* NASA LaRC Workshop on Guidance, Navigation, Controls, and Dynamics for Atmospheric Flight, 1993 Dec. 1993 p 85-95 (For primary document see N94-25096 06-01)
Avail: CASI HC A03/MF A04

N94-25103*# National Aeronautics and Space Administration. Langley Research Center, Hampton, VA.
PARAMETRIC UNCERTAINTY MODELING FOR APPLICATION TO ROBUST CONTROL
Christine M. Belcastro, B.-C. Chang (Drexel Univ., Philadelphia, PA.), and Robert Fischl (Drexel Univ., Philadelphia, PA.) *In its* NASA LaRC Workshop on Guidance, Navigation, Controls, and Dynamics for Atmospheric Flight, 1993 Dec. 1993 p 177-192 (For primary document see N94-25096 06-01)
Avail: CASI HC A03/MF A04

N94-25104*# National Aeronautics and Space Administration. Langley Research Center, Hampton, VA.
HYPERSONIC VEHICLE CONTROL LAW DEVELOPMENT USING H(INFINITY) AND MICRON-SYNTHESIS
Irene M. Gregory, John D. McMinn, John D. Shaughnessy, and Rajiv S. Chowdhry (Lockheed Engineering and Sciences Co., Hampton, VA.) *In its* NASA LaRC Workshop on Guidance, Navigation, Controls, and Dynamics for Atmospheric Flight, 1993 Dec. 1993 p 193-208 (For primary document see N94-25096 06-01)
Avail: CASI HC A03/MF A04

N94-25105*# National Aeronautics and Space Administration. Langley Research Center, Hampton, VA.
ON-LINE EVALUATION OF MULTILOOP DIGITAL CONTROLLER PERFORMANCE
Carol D. Wieseman *In its* NASA LaRC Workshop on Guidance, Navigation, Controls, and Dynamics for Atmospheric Flight, 1993 Dec. 1993 p 209-220 (For primary document see N94-25096 06-01)
Avail: CASI HC A03/MF A04

N94-25106*# Air Force Materials Lab., Wright-Patterson AFB, OH. Directorate of Engineering and Technical Management.
AIRCRAFT DIGITAL FLIGHT CONTROL TECHNICAL REVIEW
Otha B. Davenport and David B. Leggett (Wright Lab., Wright-Patterson AFB, OH.) *In* NASA. Langley Research Center, NASA LaRC Workshop on Guidance, Navigation, Controls, and Dynamics for Atmospheric Flight, 1993 Dec. 1993 p 243-250 (For primary document see N94-25096 06-01)
Avail: CASI HC A02/MF A04

N94-25107*# National Aeronautics and Space Administration. Langley Research Center, Hampton, VA.
DEVELOPMENT OF HIGH-ANGLE-OF-ATTACK NOSE-DOWN PITCH CONTROL MARGIN DESIGN GUIDELINES FOR COMBAT AIRCRAFT
Marilyn E. Ogburn and John V. Foster *In its* NASA LaRC Workshop on Guidance, Navigation, Controls, and Dynamics for Atmospheric Flight, 1993 Dec. 1993 p 293-322 (For primary document see N94-25096 06-01)
Avail: CASI HC A03/MF A04

N94-25108*# Wright Lab., Wright-Patterson AFB, OH.
ROBUST, NONLINEAR, HIGH ANGLE-OF-ATTACK CONTROL DESIGN FOR A SUPERMANEUVERABLE VEHICLE
Richard J. Adams *In* NASA. Langley Research Center, NASA LaRC Workshop on Guidance, Navigation, Controls, and Dynamics for Atmospheric Flight, 1993 Dec. 1993 p 323-371 (For primary document see N94-25096 06-01)
Avail: CASI HC A03/MF A04

N94-25111*# Vigyan Research Associates, Inc., Hampton, VA.
A STUDY OF ROLL ATTRACTOR AND WING ROCK OF DELTA WINGS AT HIGH ANGLES OF ATTACK
T. Niranjana, D. M. Rao, and Bandu N. Pamadi *In* NASA. Langley Research Center, NASA LaRC Workshop on Guidance, Navigation, Controls, and Dynamics for Atmospheric Flight, 1993 Dec. 1993 p 401-430 (For primary document see N94-25096 06-01)
Avail: CASI HC A03/MF A04

N94-25112*# National Aeronautics and Space Administration. Langley Research Center, Hampton, VA.

MODELING TRANSONIC AERODYNAMIC RESPONSE USING NONLINEAR SYSTEMS THEORY FOR USE WITH MODERN CONTROL THEORY

Walter A. Silva *In its* NASA LaRC Workshop on Guidance, Navigation, Controls, and Dynamics for Atmospheric Flight, 1993 Dec. 1993 p 431-457 (For primary document see N94-25096 06-01)
Avail: CASI HC A03/MF A04

09 RESEARCH AND SUPPORT FACILITIES (AIR)

Includes airports, hangars and runways; aircraft repair and overhaul facilities; wind tunnels; shock tubes; and aircraft engine test stands.

For related information see also *14 Ground Support Systems and Facilities (Space).*

N94-23091*# National Aeronautics and Space Administration. Lewis Research Center, Cleveland, OH.

FLOW QUALITY STUDIES OF THE NASA LEWIS RESEARCH CENTER ICING RESEARCH TUNNEL DIFFUSER

E. Allen Arrington (Sverdrup Technology, Inc., Brook Park, OH.), Mark T. Pickett, and David W. Sheldon Jan. 1994 18 p
(RTOP 505-62-84)
(NASA-TM-106311; E-8051; NAS 1.15:106311) Avail: CASI HC A03/MF A01

The purpose was to document the airflow characteristics in the diffuser of the NASA Lewis Research Center Icing Research Tunnel and to determine the effects of vortex generators on the flow quality in the diffuser. The results were used to determine how to improve the flow in this portion of the tunnel so that it can be more effectively used as an icing test section and such that overall tunnel efficiency can be improved. The demand for tunnel test time and the desire to test models that are too large for the test section were two of the drivers behind this diffuser study. For all vortex generator configurations tested, the flow quality was improved.
Author (revised)

N94-23303# Illinois Univ., Urbana. Dept. of Civil Engineering.

PERFORMANCE OF PREFABRICATED GEOCOMPOSITE SUBDRAINAGE SYSTEM IN AN AIRPORT RUNWAY Final Report

Barry J. Dempsey Oct. 1993 80 p
(Contract DTFAC1-87-Z-02015)
(DOT/FAA/RD-93/23) Avail: CASI HC A05/MF A01

A Prefabricated Geocomposite Subdrainage (PGS) system installed in Runway O9-27 at Kewanee Municipal Airport in 1985 was evaluated. The study demonstrated that a PGS system could be installed within the active runway area at a distance of 12.5 ft on either side of the centerline. There were no problems with settlement or distresses along the installation location. Subdrainage outflow measurements indicated that 25 percent to 45 percent of the rainfall water infiltrated the pavement and passed through the PGS system. Subdrainage outflows varied but a maximum outflow of over 1700 gal/hr was measured during the study. It was observed that water flow from the pavement joints and cracks ceased once the PGS system was installed. The FWD data indicated that the subgrade soil beneath Runway 09-27 ranged from less than 1 ksi to generally 3 ksi. Although there was some improvement in subgrade strength during the study period it was not possible to conclude that subdrainage was totally responsible for this improvement. There was an indication from the data analysis that there could be some raveling in the lower half of the full-depth asphalt concrete layer. The PCI study conducted on Runway 09-27 provided results from 1981 to 1990. The PCI ratings obtained after installation of the PGS system in 1985 indicated the possibility of some overall improvement in pavement performance. Visual observations indicated that surface seepage of water and frost heave problems did not occur again after installation of subdrainage. Visual inspection in January 1993 indicated there was no evidence of longitudinal reflective cracking in the 3 in. asphalt concrete overlay, that was placed during the summer 1990, in the area above the PCS system. It would appear that the PGS system is continuing to function properly and that Runway 09-27 at Kewanee Municipal Airport is performing very well.
Author

N94-23310* National Aeronautics and Space Administration. Ames Research Center, Moffett Field, CA.

DEPLOYABLE VIDEO CONFERENCE TABLE Patent

Marc M. Cohen, inventor (to NASA) and Peter Lissol, inventor (to NASA) 16 Nov. 1993 17 p Filed 3 Feb. 1992
(NASA-Case-ARC-11950-1; US-Patent-5,261,735; US-Patent-Appl-SN-829839; US-Patent-Class-312-282; US-Patent-Class-108-3; US-Patent-Class-108-59; Int-Patent-Class-A47B-77/10) Avail: US Patent and Trademark Office

A deployable table is presented. The table is stowed in and deployed from a storage compartment based upon a non-self rigidizing, 4-hinge, arch support structure that folds upon itself to stow and that expands to deploy. The work surfaces bypass each other above and below to allow the deployment mechanism to operate. This assembly includes the following: first and second primary pivot hinges placed at the opposite ends of the storage compartment; first and second lateral frame members with proximal ends connected to the first and second pivot hinges; a medial frame member offset from and pivotally connected to distal ends of the first and second members through third and fourth medial pivot hinges; and left-side, right-side, and middle trays connected respectively to the first, second, and third frame members and being foldable into and out of the storage compartment by articulation of the first, second, third, and fourth joints. At least one of the third and fourth joints are locked to set the first, second, and third frame members in a desired angular orientation with respect to each other. Official Gazette of the U.S. Patent and Trademark Office

N94-23539*# Old Dominion Univ., Norfolk, VA. Dept. of Aerospace Engineering.

PRELIMINARY EDDY CURRENT MODELLING FOR THE LARGE ANGLE MAGNETIC SUSPENSION TEST FIXTURE Progress Report, 1 May - 31 Oct. 1993

Colin Britcher Jan. 1994 20 p
(Grant NAG1-1056)
(NASA-CR-194772; NAS 1.26:194772) Avail: CASI HC A03/MF A01

This report presents some recent developments in the mathematical modeling of the Large Angle Magnetic Suspension Test Fixture (LAMSTF) at NASA Langley Research Center. It is shown that these effects are significant, but may be amenable to analysis, modeling and measurement. A theoretical framework is presented, together with a comparison of computed and experimental data.
Author

N94-23564*# General Applied Science Labs., Inc., Ronkonkoma, NY.

CALIBRATION OF HYPULSE FOR HYPERVELOCITY AIR FLOWS CORRESPONDING TO FLIGHT MACH NUMBERS 13.5, 15, AND 17

John Calleja and Jose Tamagno Dec. 1993 60 p
(Contract NAS1-18450; RTOP 505-70-62-09)
(NASA-CR-191578; TR-335; NAS 1.26:191578) Avail: CASI HC A04/MF A01

A series of air calibration tests were performed in GASL's HYPULSE facility in order to more accurately determine test section flow conditions for flows simulating total enthalpies in the Mach 13 to 17 range. Present calibration data supplements previous data and includes direct measurement of test section pitot and static pressure, acceleration tube wall pressure and heat transfer, and primary and secondary incident shock velocities. Useful test core diameters along with the corresponding free-stream conditions and usable testing times were determined. For the M13.5 condition, in-stream static pressure surveys showed the temporal and spacial uniformity of this quantity across the useful test core. In addition, finite fringe interferograms taken of the free-stream flow at the test section did not indicate the presence of any 'strong' wave system for any of the conditions investigated.
Author (revised)

N94-24072# Galaxy Scientific Corp., Pleasantville, NJ.

AIRPORT PAVEMENT TEST MACHINE DESIGN AND COST STUDY Final Report

Gordon F. Hayhoe, Roy D. McQueen, and Edward H. Guo Oct. 1993 126 p
(Contract DTFA03-89-C-00043)
(DOT/FAA/CT-93/51) Avail: CASI HC A07/MF A02

A design study was conducted to determine the feasibility of constructing and operating a test machine for performing accelerated airport pavement tests. The proposed design for the test machine satisfies the requirements of a comprehensive set of specifications formulated and developed by a government/industry working group. The primary purpose of the tests to be conducted with the test machine is to provide pavement response and performance data to be used in the development of new procedures for designing pavements for the next generation of large civil transport aircraft. The proposed test machine design allows for test pavements 60 feet wide by 900 feet long. Maximum load capacity is twelve wheels operating at 75,000 pounds each, for a maximum applied load of 900,000 pounds. Test speeds are 5 mph for normal testing and a maximum of 15 mph for special studies. Cost estimates were made for designing, constructing, and operating the test machine. The total initial cost required to design and construct the machine was estimated to be $15,000,000. Maximum annual operating costs after commissioning were estimated to be $2,300,000. Test pavement reconstruction accounts for $1,500,000 (65%) of the estimated annual operating cost. Author

N94-24117 Defence Research Establishment, Ottawa (Ontario). Radiation Effects Section.

SAFETY GUIDELINES FOR THE OPERATION OF THE DREO 10 m EMP SIMULATOR DREMPS

C. L. Gardner, J. S. Seregelyi, and P. Sevat Jan. 1993 38 p
(DREO-TN-93-5; CTN-94-60913) Avail: Micromedia Ltd., Technical Information Centre, 165 Hotel de Ville, Place du Portage, Phase 2, Hull, Quebec J8X 3X2, Canada

A large facility was recently completed which simulates the electromagnetic pulse (EMP) that would be produced by the explosion of a nuclear weapon outside the atmosphere. This EMP represents a threat to military electronic systems. To generate this EMP, a high voltage (600 kV) pulse generator is used. As with all high voltage equipment, the EMP simulator contains inherent hazards. Operators of the facility must follow strict safety precautions in its operation and maintenance. An outline is provided giving details of the hazards that may exist as well as procedures that must be followed to ensure safe operation and maintenance of the facility. Author (CISTI)

N94-24123 Defence Research Establishment, Ottawa (Ontario). Radiation Effects Section.

TEM CELL SAFETY REPORT

J. S. Seregelyi and C. Gardner Apr. 1993 17 p
(DREO-TN-93-9; CTN-94-60919) Avail: Micromedia Ltd., Technical Information Centre, 165 Hotel de Ville, Place du Portage, Phase 2, Hull, Quebec J8X 3X2, Canada

In order to test the susceptibility of a piece of equipment to an electromagnetic pulse (EMP), an accurate electric and magnetic field is required. One means of generating such fields is with a transverse electromagnetic (TEM) cell. This device is essentially a square coaxial line with known field properties. Although the design of the Defence Research Establishment Ottawa's EMP TEM cell includes devices for the protection of both operator and machine, safe use of the system depends upon the operator. The potential hazards of this TEM cell system are described and appropriate precautions are recommended to be followed during operation and maintenance. Safe and reliable operation can be expected if the machine is operated by personnel acquainted with its function and who follow the procedures outlined. Author (CISTI)

N94-24559# Federal Aviation Administration, Atlantic City, NJ.

COMBINED 1991 AND 1992 ROBINSON-22B (R-22) PARKING TEST RESULTS Technical Report, Sep. 1991 - Oct. 1992

Rosanne M. Weiss Sep. 1993 71 p
(AD-A273550; DOT/FAA/CT-TN93/6) Avail: CASI HC A04/MF A01

Tests were conducted in the fall of 1991 and 1992 at the Federal Aviation Administration (FAA) Technical Center to examine issues regarding rotor tip clearances for parking areas at heliports. These tests were initiated as a follow-on to previous parking tests documented in DOT/FAA/CT-TN88/30, 'Heliport Surface Maneuvering Test Results,' and DOT/FAA/CT-TN/92/1, 'Helicopter Nighttime Parking Test Results-UH-I.' Since those tests utilized a medium-size helicopter with a rotor diameter of 48 feet, similar tests were requested using a smaller helicopter with a rotor diameter of less than 30 feet. The results of these follow-on parking tests which used a Robinson-22B (R-22) helicopter are documented. Over 480 maneuvers were conducted at the FAA Technical Center's National Concepts Development and Demonstration Heliport/Vertiport, Atlantic City International Airport, NJ. All were conducted under head, tail, and crosswind conditions, both with and without an obstacle on the helipad. Pilot subjective data, in reference to these maneuvers, were collected via post-maneuver and post-flight questions. Data collection and analysis methodology and objective, as well as subjective issues, are discussed. Statistical and graphical analysis of pilot performance and perception data are provided. Conclusions are drawn about considerations that must be given to parking clearance criteria at heliports. DTIC

N94-24739 Technische Univ., Delft (Netherlands). Faculty of Aerospace Engineering.

PRE-DESIGN STUDY OF A GENERAL PURPOSE VEHICLE SIMULATOR PLATFORM

A. Winkens Jul. 1992 107 p See also PB92-199660 Prepared in cooperation with Technische Univ., Munich Limited Reproducibility: More than 20% of this document may be affected by microfiche quality
(PB93-215366; M-662) Avail: Issuing Activity (National Technical Information Service (NTIS))

In supporting fundamental flight simulation techniques as a part of academic research, the Delft University of Technology has recently launched the BARESIM program, the development of an advanced general-purpose vehicle simulator facility. The Structures and Materials Group of the faculty of Aerospace Engineering participates in the program by the design and construction of the simulator platform. The report describes the results of a pre-design study of the platform structure, which is performed as a semester project in the scope of the European student-exchange-program ERASMUS between the Munich University of Technology and the Delft University of Technology. NTIS

N94-24785 FMT International Trade A.B. (Sweden).

SYSTEM FOR AUTOMATIC TRANSPORTATION OF AIRCRAFT ON THE GROUND Patent

Nils-Eric Anderberg, inventor (to Micromedia Ltd.) 21 Sep. 1993 16 p
(CA-Patent-1-322-361; Int-Patent-Class-B64F-001/22; CTN-94-60933) Copyright Avail: Micromedia Ltd., Technical Information Centre, 240 Catherine Street, Suite 305, Ottawa, Ontario, K2P 2G8, Canada HC/MF

A system is provided for automatically transporting aircraft on the ground to a precise parking position. The system of the invention satisfies the requirements of environmental friendliness, reliability, flexibility, security, and accuracy of positioning, and can be adapted to all types of aircraft arriving at civil airports. The system is operated by remote means, such as by radio signals, with only minor assistance of ground personnel. The system can be preprogrammed so that it can park a heavy airliner with an accuracy down to one mm adjacent to, for example, a passenger loading device or in the position outside the gate from which the aircraft is to taxi by means of its own engines. The system of the invention consists of a carriage which catches and locks at least one wheel of the aircraft, preferably the nose wheel, and which is drivable back and forth along a guide means arranged on or in the ground. Each end of the guide means is provided with a capstan and a towing rope runs between both capstans. A computer control and monitoring system ensures that start and stop operations are performed properly and smoothly so as to put minimum strain on the landing gear of the aircraft. CISTI

N94-25184*# National Aeronautics and Space Administration. Lewis Research Center, Cleveland, OH.

TEMPERATURE MEASUREMENT USING INFRARED IMAGING SYSTEMS DURING TURBINE ENGINE ALTITUDE TESTING

Maureen E. Burns Feb. 1994 23 p
(RTOP 505-62-84)
(NASA-TM-105871; E-7336; NAS 1.15:105871) Avail: CASI HC A03/MF A01

This report details the use of infrared imaging for temperature measurement and thermal pattern determination during simulated altitude engine testing in the NASA Lewis Propulsion Systems Laboratory. Three identical argon-cooled imaging systems were installed in the facility exhaust collector behind sapphire windows to look at engine internal surfaces. The report describes the components of each system, presents the specifics of the complicated installation, and explains the operation of the systems during engine testing. During the program, several problems emerged, such as argon contamination system, component overheating, cracked sapphire windows, and other unexplained effects. This report includes a summary of the difficulties as well as the solutions developed. The systems performed well, considering they were in an unusually harsh exhaust environment. Both video and digital data were recorded, and the information provided valuable material for the engineers and designers to quickly make any necessary design changes to the engine hardware cooling system. The knowledge and experience gained during this program greatly simplified the installation and use of the systems during later test programs in the facility. The infrared imaging systems have significantly enhanced the measurement capabilities of the facility, and have become an outstanding and versatile testing resource in the Propulsion Systems Laboratory. Author (revised)

N94-25522 Air Force Inst. of Tech., Wright-Patterson AFB, OH.
AUTOMATIC PRESSURE CONTROL SYSTEM FOR THE WRIGHT LABORATORY COMPRESSOR RESEARCH FACILITY M.S. Thesis
Brian J. Hull Dec. 1993 96 p Limited Reproducibility: More than 20% of this document may be affected by microfiche quality
(AD-A273827; AFIT/GAE/ENY/93D-19) Avail: CASI HC A05

This thesis presents the design of a pressure control system for the Compressor Research Facility (CRF). Using a fluid dynamics model of the CRF, a controller was designed to track commanded test chamber pressure while the test compressor operated at varying speeds. This was accomplished by adjusting CRF inlet valves first with a coarse open-loop gain schedule, then closing the loop with a digital dynamic compensator for fine adjustments. The design was simulated on a digital computer and coded for incorporation into the CRF's current control algorithm. DTIC

N94-24247 Instituto de Estudos Avancados, Sao Jose dos Campos (Brazil).
AN INVESTIGATION ON A NEW TECHNIQUE TO IMPROVE THE PERFORMANCE OF THE SHOCK TUBE/TUNNEL TESTING IN THE EQUILIBRIUM INTERFACE CONDITION
Marco A. S. Minucci, Marco A. C. Nascimento, and Henry T. Nagamatsu (Rensselaer Polytechnic Inst., Troy, NY.) *In* Israel Society of Aeronautics and Astronautics, The 33rd Israel Annual Conference on Aviation and Astronautics 25 Feb. 1993 p 103-113 (For primary document see N94-24241 06-01)
Copyright Avail: Issuing Activity (Israel Society of Aeronautics and Astronautics, c/o Faculty of Engineering, Tel-Aviv Univ., Ramat Aviv 69978, Israel)

N94-25101*# National Aeronautics and Space Administration. Langley Research Center, Hampton, VA.
FUTURE DIRECTIONS IN FLIGHT SIMULATION: A USER PERSPECTIVE
Bruce Jackson *In its* NASA LaRC Workshop on Guidance, Navigation, Controls, and Dynamics for Atmospheric Flight, 1993 Dec. 1993 p 115-135 (For primary document see N94-25096 06-01)
Avail: CASI HC A03/MF A04

12 ASTRONAUTICS (GENERAL)

For extraterrestrial exploration see *91 Lunar and Planetary Exploration.*

N94-23015# Joint Publications Research Service, Arlington, VA.
JPRS REPORT: SCIENCE AND TECHNOLOGY. CENTRAL EURASIA: SPACE
31 Dec. 1993 43 p Transl. into ENGLISH from various Russian articles
(JPRS-USP-93-006) Avail: CASI HC A03/MF A01

Translations of articles covering the following topics are presented: space sciences, space engineering, space applications, and space policy/administration. Derived from text

N94-23292*# National Aeronautics and Space Administration. Lyndon B. Johnson Space Center, Houston, TX.
CATALOG OF APOLLO EXPERIMENT OPERATIONS
Thomas A. Sullivan Jan. 1994 161 p
(NASA-RP-1317; S-738; NAS 1.61:1317) Avail: CASI HC A08/MF A02

This catalog reviews Apollo mission reports, preliminary science reports, technical crew debriefings, lunar surface operations plans, and various relevant lunar experiment documents, collecting engineering- and operation-specific information by experiment. It is organized by discrete experimental and equipment items emplaced or operated on the lunar surface or at zero gravity during the Apollo missions. It also attempts to summarize some of the general problems encountered on the surface and provides guidelines for the design of future lunar surface experiments with an eye toward operations. Many of the problems dealt with on the lunar surface originated from just a few novel conditions that manifested themselves in various nasty ways. Low gravity caused cables to stick up and get caught on feet, and also made it easy for instruments to tip over. Dust was a problem and caused abrasion, visibility, and thermal control difficulties. Operating in a pressure suit limited a person's activity, especially in the hands. I hope to capture with this document some of the lessons learned from the Apollo era to make the jobs of future astronauts, principle investigators, engineers, and operators of lunar experiments more productive. Author

N94-23710*# National Aeronautics and Space Administration, Washington, DC.
SPACE TOURISM: A FLIGHT OF FANTASY OR THE NEXT MAJOR SPACE PRODUCT? PAPER SESSION 3: PRODUCTS
Barbara A. Stone 1994 8 p Presented at the Thirty-First Space Congress, Cocoa Beach, FL, 26-29 Apr. 1994
(NASA-TM-109385; NAS 1.15:109385) Avail: CASI HC A02/MF A01

In the euphoria of the early 1980's, a number of creative proposals for nontraditional uses of space were suggested. Taking tourists to space, possibly as early as the 1990's, was one such proposal. While it is now obvious that wherever explorers go, tourists (and hoteliers, restauranteurs, and tour guides) will someday follow. This paper discusses past and present efforts to promote space as a tourist destination. Author (revised)

N94-23770 National Inst. of Standards and Technology, Gaithersburg, MD. Building and Fire Research Lab.
PROCEEDINGS OF THE NIST CONFERENCE ON REDUCING THE COST OF SPACE INFRASTRUCTURE AND OPERATIONS: PART 1: ORAL PRESENTATIONS AND DISCUSSION
William C. Stone, ed. Aug. 1993 206 p Proceedings held in Gaithersburg, MD, 20-22 Nov. 1989 See Also PB94-109683 Limited Reproducibility: More than 20% of this document may be affected by microfiche quality
(PB94-111374; NISTIR-5255) Avail: Issuing Activity (National Technical Information Service (NTIS))

A conference was held from November 20-22, 1989 at the National Institute of Standards and Technology in Gaithersburg, Maryland for the purpose of discussing methods for reducing the cost of space infrastructure and operations. This was a multidisciplinary group that included invited speakers from both within and outside of the traditional aerospace community. Specific comparison was made in the case of habitats and extravehicular activity with commercially successful undersea operations on earth which operate daily under more severe environmental conditions and with operating budgets on the order of 1/1000 that of orbital analogs. NTIS

N94-23819 National Inst. of Standards and Technology, Gaithersburg, MD. Building and Fire Research Lab.
NATIONAL INSTITUTE OF STANDARDS AND TECHNOLOGY CONFERENCE ON REDUCING THE COST OF SPACE INFRASTRUCTURE AND OPERATIONS. PART 2: TOPICAL PAPERS
W. C. Stone Aug. 1993 238 p Conference held in Gaithersburg, MD, 20-22 Nov. 1989 See also PB94-111374 Limited Reproducibility: More than 20% of this document may be affected by microfiche quality
(PB94-113487; NISTIR-5256-Pt-2) Avail: Issuing Activity (National Technical Information Service (NTIS))

Table of Contents: The Industrial Space Facility; The SPACE PHOENIX Program; External Tank Habitat; A Numerical Procedure for the Evaluation of Drag and Aerodynamic Torque for Convex Shells of Revolution in Low Earth Orbit; EVA Life Cycle Cost Issues Summary; Flight Opportunity for Small Payloads; Commercial Launch Vehicles Using Hybrid Propulsion; Novel Integration Concepts; Payload Sensors; Cost Comparison Between the Space Flight and the Commercial Catalog Models of a Cesium Atomic Clock Module; Laser Propulsion Work at Lawrence Livermore National Laboratory; The Ram Accelerator as a Space Cargo Launcher; and Appendix A: List of Conference Participants. NTIS

N94-24497*# National Aeronautics and Space Administration. Goddard Space Flight Center, Greenbelt, MD.
AN EARTH ALBEDO MODEL: A MATHEMATICAL MODEL FOR THE RADIANT ENERGY INPUT TO AN ORBITING SPACECRAFT DUE TO THE DIFFUSE REFLECTANCE OF SOLAR RADIATION FROM THE EARTH BELOW
Thomas W. Flatley and Wendy A. Moore Washington Jan. 1994 33 p
(NASA-TM-104596; Rept-94B00034; NAS 1.15:104596) Avail: CASI HC A03/MF A01

Past missions have shown that the earth's albedo can have a significant effect on the sun sensors used for spacecraft attitude control information. In response to this concern, an algorithm was developed to simulate this phenomenon, consisting of two parts, the physical model of albedo and its effect on the sun sensors. This paper contains the theoretical development of this model, practical operational notes, and its implementation in a FORTRAN subroutine. Author

N94-24619*# Pennsylvania State Univ., University Park. Dept. of Aerospace Engineering.
A MISSION TO MERCURY AND A MISSION TO THE MOONS OF MARS Final Report
Jul. 1993 289 p
(Contract NASw-4435)
(NASA-CR-195530; NAS 1.26:195530) Avail: CASI HC A13/MF A03

Two Advanced Design Projects were completed this academic year at Penn State - a mission to the planet Mercury and a mission to the moons of Mars (Phobos and Deimos). At the beginning of the fall semester the students were organized into six groups and given their choice of missions. Once a mission was chosen, the students developed conceptual designs. These designs were then evaluated at the end of the fall semester and combined into two separate mission scenarios. To facilitate the work required for each mission, the class was reorganized in the spring semester by combining groups to form two mission teams. An integration team consisting of two members from each group was formed for each mission team so that communication and exchange of information would be easier among the groups. The types of projects designed by the students evolved from numerous discussions with Penn State faculty and mission planners at the Lewis Research Center Advanced Projects Office. Robotic planetary missions throughout the solar system can be considered valuable precursors to human visits and test beds for innovative technology. For example, by studying the composition of the Martian moons, scientists may be able to determine if their resources may be used or synthesized for consumption during a first human visit. Author

N94-24808*# Naval Postgraduate School, Monterey, CA.
NEAR EARTH ASTEROID RENDEZVOUS
15 Dec. 1992 146 p
(Contract NASw-4435)
(NASA-CR-195518; NAS 1.26:195518) Avail: CASI HC A07/MF A02

The Spacecraft Design Course is the capstone design class for the M.S. in astronautics at the Naval Postgraduate School. The Fall 92 class designed a spacecraft for the Near Earth Asteroid Rendezvous Mission (NEAR). The NEAR mission uses a robotic spacecraft to conduct up-close reconnaissance of a near-earth asteroid. Such a mission will provide information on Solar System formation and possible space resources. The spacecraft is intended to complete a NEAR mission as a relatively low-budget program while striving to gather as much information about the target asteroid as possible. A complete mission analysis and detailed spacecraft design were completed. Mission analysis includes orbit comparison and selection, payload and telemetry requirements, spacecraft configuration, and launch vehicle selection. Spacecraft design includes all major subsystems: structure, electrical power, attitude control, propulsion, payload integration, and thermal control. The resulting spacecraft demonstrates the possibility to meet the NEAR mission requirements using existing technology, 'off-the-shelf' components, and a relatively low-cost launch vehicle. Author (revised)

N94-24995*# Texas Univ., Austin. Ares Industries.
PERCIVAL MISSION TO MARS Preliminary Design Review
David W. Reed, Stewart Lilley, Melinda Sirman, Paul Bolton, Susan Elliott, Doug Hamilton, James Nickelson, and Artemus Shelton 10 Dec. 1992 88 p
(Contract NASw-4435)
(NASA-CR-195541; NAS 1.26:195541) Avail: CASI HC A05/MF A01

With the downturn of the world economy, the priority of unmanned exploration of the solar system has been lowered. Instead of foregoing all missions to our neighbors in the solar system, a new philosophy of exploration mission design has evolved to insure the continued exploration of the solar system. The 'Discovery-class' design philosophy uses a low cost, limited mission, available technology spacecraft instead of the previous 'Voyager-class' design philosophy that uses a 'do-everything at any cost' spacecraft. The Percival Mission to Mars was proposed by Ares Industries as one of the new 'Discovery-class' of exploration missions. The spacecraft will be christened Percival in honor of American astronomer Percival Lowell who proposed the existence of life on Mars in the early twentieth century. The main purpose of the Percival mission to Mars is to collect and relay scientific data to Earth suitable for designing future manned and unmanned missions to Mars. The measurements and observations made by Percival will help future mission designers to choose among landing sites based on the feasibility and scientific interest of the sites. The primary measurements conducted by the Percival mission include gravity field determination, surface and atmospheric composition, sub-surface soil composition, sub-surface seismic activity, surface weather patterns, and surface imaging. These measurements will be taken from the orbiting Percival spacecraft and from surface penetrators deployed from Mars orbit. The design work for the Percival Mission to Mars was divided among four technical areas: Orbits and Propulsion System, Surface Penetrators, Gravity and Science Instruments, and Spacecraft Structure and Systems. The results for each of the technical areas is summarized and followed by a design cost analysis and recommendations for future analyses. Author (revised)

N94-23924*# Centre National d'Etudes Spatiales, Toulouse (France).
MARS 1994/1996: THE FRENCH NAVIGATION TASKS
Frederic Bonneau, Jacques Bernard, and Damien Delobette (Societe d'Economie et de Mathematique Appliquees, Toulouse, France.) *In* JPL, SpaceOps 1992: Proceedings of the Second International Symposium on Ground Data Systems for Space Mission Operations 1 Mar. 1993 p 613-618 (For primary document see N94-23832 06-66)
Avail: CASI HC A02/MF A10

N94-24242 Jet Propulsion Lab., California Inst. of Tech., Pasadena.
THE JET PROPULSION LABORATORY SPACE EXPLORATION: PAST, PRESENT AND FUTURE
Josette Bellan *In* Israel Society of Aeronautics and Astronautics, The 33rd Israel Annual Conference on Aviation and Astronautics 25 Feb. 1993 p 1-26 (For primary document see N94-24241 06-01)
Copyright Avail: Issuing Activity (Israel Society of Aeronautics and Astronautics, c/o Faculty of Engineering, Tel-Aviv Univ., Ramat Aviv 69978, Israel)

N94-25067* National Aeronautics and Space Administration. Lyndon B. Johnson Space Center, Houston, TX.
THE FUTURE OF MANNED SPACEFLIGHT
Aaron Cohen *In* National Academy of Engineering, The Future of Aerospace: Proceedings of a Symposium Held in Honor of Alexander H. Flax 1993 p 15-27 (For primary document see N94-25065 06-99)
Copyright Avail: Issuing Activity

13 ASTRODYNAMICS

Includes powered and free-flight trajectories; and orbital and launching dynamics.

N94-24482*# National Aeronautics and Space Administration. Lewis Research Center, Cleveland, OH.
OPTIMAL SPACE STATION SOLAR ARRAY GIMBAL ANGLE DETERMINATION VIA RADIAL BASIS FUNCTION NEURAL NETWORKS
Daniel J. Clancy (Ohio State Univ., Columbus.), Uemit Oezguener (Ohio State Univ., Columbus.), and Ronald E. Graham Feb. 1994 21 p
(NASA-TM-106482; E-8412; NAS 1.15:106482) Avail: CASI HC A03/MF A01

The potential for excessive plume impingement loads on Space Station

Freedom solar arrays, caused by jet firings from an approaching Space Shuttle, is addressed. An artificial neural network is designed to determine commanded solar array beta gimbal angle for minimum plume loads. The commanded angle would be determined dynamically. The network design proposed involves radial basis functions as activation functions. Design, development, and simulation of this network design are discussed.
Author (revised)

N94-23257*# Jet Propulsion Lab., California Inst. of Tech., Pasadena. Tracking Systems and Applications Section.
A REVIEW OF GPS-BASED TRACKING TECHNIQUES FOR TDRS ORBIT DETERMINATION
B. J. Haines, S. M. Lichten, R. P. Malla, and S.-C. Wu *In its* The Telecommunications and Data Acquisition Report 15 Nov. 1993 p 1-16 (For primary document see N94-23256 06-32)
(RTOP 310-10-61-92-01)
Avail: CASI HC A03/MF A02

N94-23258*# Jet Propulsion Lab., California Inst. of Tech., Pasadena. Tracking Systems and Applications Section.
NEW APPROACHES FOR TRACKING EARTH ORBITERS USING MODIFIED GPS GROUND RECEIVERS
S. M. Lichten, L. E. Young, S. Nandi, B. J. Haines, C. E. Dunn, and C. D. Edwards *In its* The Telecommunications and Data Acquisition Report 15 Nov. 1993 p 17-31 (For primary document see N94-23256 06-32)
(RTOP 310-10-61-92-91)
Avail: CASI HC A03/MF A02

N94-23919*# Centre National d'Etudes Spatiales, Toulouse (France).
REAL-TIME ON-BOARD ORBIT DETERMINATION WITH DORIS
J.-P. Berthias, C. Jayles, and D. Pradines *In* JPL, SpaceOps 1992: Proceedings of the Second International Symposium on Ground Data Systems for Space Mission Operations 1 Mar. 1993 p 579-583 (For primary document see N94-23832 06-66)
Avail: CASI HC A01/MF A10

N94-23920*# National Aeronautics and Space Administration. Goddard Space Flight Center, Greenbelt, MD.
TOPEX/POSEIDON PRECISION ORBIT DETERMINATION PRODUCTION AND EXPERT SYSTEM
Barbara Putney, Nikita Zelensky (Hughes STX, Inc., Lanham, MD.), and Steven Klosko (Hughes STX, Inc., Lanham, MD.) *In* JPL, SpaceOps 1992: Proceedings of the Second International Symposium on Ground Data Systems for Space Mission Operations 1 Mar. 1993 p 585-590 (For primary document see N94-23832 06-66)
Avail: CASI HC A02/MF A10

N94-23923*# MATRA Marconi Space, Toulouse (France).
KALMAN FILTERING APPLIED TO REAL-TIME MONITORING OF APOGEE MANEUVERS
Frederic deBoer and Christian Barbier (Alcatel Espace, Toulouse, France.) *In* JPL, SpaceOps 1992: Proceedings of the Second International Symposium on Ground Data Systems for Space Mission Operations 1 Mar. 1993 p 607-612 (For primary document see N94-23832 06-66)
Avail: CASI HC A02/MF A10

N94-24258 Technion - Israel Inst. of Tech., Haifa. Faculty of Aerospace Engineering.
SATELLITE AUTONOMOUS NAVIGATION AND ORBIT DETERMINATION USING MAGNETOMETERS
G. Shorshi and Itzhack Y. Bar-Itzhack *In* Israel Society of Aeronautics and Astronautics, The 33rd Israel Annual Conference on Aviation and Astronautics 25 Feb. 1993 p 203-212 (For primary document see N94-24241 06-01)
Copyright Avail: Issuing Activity (Israel Society of Aeronautics and Astronautics, c/o Faculty of Engineering, Tel-Aviv Univ., Ramat Aviv 69978, Israel)

N94-24264 Technion - Israel Inst. of Tech., Haifa. Faculty of Aerospace Engineering.
DECENTRALIZED AUTONOMOUS ATTITUDE DETERMINATION USING AN INERTIALLY STABILIZED PAYLOAD
Yaakov Oshman and Michael Isakow *In* Israel Society of Aeronautics and Astronautics, The 33rd Israel Annual Conference on Aviation and Astronautics 25 Feb. 1993 p 263-274 (For primary document see N94-24241 06-01)
Copyright Avail: Issuing Activity (Israel Society of Aeronautics and Astronautics, c/o Faculty of Engineering, Tel-Aviv Univ., Ramat Aviv 69978, Israel)

N94-25114*# National Aeronautics and Space Administration. Langley Research Center, Hampton, VA.
OPTIMAL RTLS ABORT TRAJECTORIES FOR AN HL-20 PERSONNEL LAUNCH VEHICLE
Kevin Dutton *In its* NASA LaRC Workshop on Guidance, Navigation, Controls, and Dynamics for Atmospheric Flight, 1993 Dec. 1993 p 481-496 (For primary document see N94-25096 06-01)
Avail: CASI HC A03/MF A04

14 GROUND SUPPORT SYSTEMS AND FACILITIES (SPACE)

Includes launch complexes, research and production facilities; ground support equipment, e.g., mobile transporters; and simulators.

For related information see also *09 Research and Support Facilities (Air).*

N94-22889 Toronto Univ. (Ontario). Dept. of Aerospace Science and Engineering.
OPERATING THE DAISY FACILITY TO PERFORM CONTROL EXPERIMENTS M.S. Thesis
Louis Ian Cameron 1993 90 p
(ISBN-0-315-83554-0; CTN-94-60944) Copyright Avail: Micromedia Ltd., Technical Information Centre, 240 Catherine Street, Suite 305, Ottawa, Ontario, K2P 2G8, Canada HC/MF

The Daisy facility, a 23-degree of freedom large flexible space structure (LFSS) emulator, was made operational for the study of control of such structures. Software was written and tested which enables a researcher to implement control algorithms with a minimal understanding of Daisy's systems. The digital electro-optical position sensor system installed on Daisy was integrated with the control computer to track the position of all of Daisy's ribs. The Daisy structure was successfully brought under complete control in its fully flexible configuration. Two control methods, linear quadratic regulator (LQR) and position derivative, were compared on the basis of actual performance matching that were predicted by a mathematical simulation. For the cases attempted, LQR appeared to be the better method, avoiding an undesirable resonance that the other method could not handle. A tutorial for running Daisy and descriptions of the computer routines are included.
Author (CISTI)

N94-24309*# Logicon Control Dynamics Co., Huntsville, AL.
LSS SYSTEMS PLANNING AND PERFORMANCE PROGRAM Final Report, 2 Nov. 1987 - 15 Aug. 1993
Victoria Jones McKenna, Michael J. Dendy, Charles B. Naumann, Sally A. Rice, and John M. Weathers 11 Aug. 1993 131 p
(Contract NAS8-36670)
(NASA-CR-193882; NAS 1.26:193882) Avail: CASI HC A07/MF A02

This report describes, using viewgraphs, the Marshall Space Flight Center's Large Space Structures Ground Test Facilities located in building 4619. Major topics include the Active Control Evaluation of Systems (ACES) Laboratory; the Control-Structures Interaction/Controls, Astrophysics, and Structures Experiment in Space (CSI/CASES); Advanced Development Facility; and the ACES Guest Investigator Program.
Author (revised)

N94-24820*# Vanderbilt Univ., Nashville, TN. Dept. of Mechanical Engineering.
STIFFENING OF DEPLOYABLE SPACE BOOMS: AUTOMATED PROTEIN CRYSTAL GROWTH FACILITY
Thomas Cruse and Susan E. Ward Jun. 1993 109 p Original contains color illustrations

(Contract NASw-4435)
(NASA-CR-195547; NAS 1.26:195547) Avail: CASI HC A06/MF A02; 13 functional color pages

Part of the curriculum for the seniors at Vanderbilt University in the Mechanical Engineering Program is to take a design class. The purpose of the class is to expose the students to the open ended problems which working engineers are involved with every day. In the past, the students have been asked to work in a variety of projects developed by the professor. This year Vanderbilt was admitted into the Advanced Design Program (ADP) sponsored by the Universities Space Research Association (USRA) and the National Aeronautics and Space Association (NASA). The grant sponsored undergraduate design and research into new and innovative areas in which NASA is involved. The grant sponsors the Teaching Assistant as well as provides monies for travel and other expenses. The design and research of the seniors of the 1992-1993 school year in association with NASA and USRA is documented. Author (revised)

N94-25064# Range Commanders Council, White Sands Missile Range, NM. Telecommunications and Timing Group.
HORACE: PRESENTATION-LEVEL PROTOCOL STANDARD FOR DIGITAL TRANSMISSION OF MONOCHROME TELEVISION IMAGES
Nov. 1993 73 p See also N91-26428
(AD-A273395; IRIG-Standard-210-93; AD-A235276) Avail: CASI HC A04/MF A01

This document establishes a single digital television transmission standard with sufficient versatility to meet a large variety of instrumentation needs for DOD test ranges. Within the framework of the standard, the user can specify transmission rate, horizontal and temporal resolutions, and can determine what picture quality is required for any particular use. DTIC

N94-23843*# National Aeronautics and Space Administration. Goddard Space Flight Center, Greenbelt, MD.
SAMPEX PAYLOAD OPERATION CONTROL CENTER IMPLEMENTATION
Daniel Mandl, Jack Koslosky, Ron Mahmot, Michael Rackley, and Jack Lauderdale (Computer Sciences Corp., Laurel, MD.) *In* JPL, SpaceOps 1992: Proceedings of the Second International Symposium on Ground Data Systems for Space Mission Operations 1 Mar. 1993 p 63-68 (For primary document see N94-23832 06-66)
Avail: CASI HC A02/MF A10

N94-23849*# Logica Space and Communications Ltd., London (England).
ATOS-1: DESIGNING THE INFRASTRUCTURE FOR AN ADVANCED SPACECRAFT OPERATIONS SYSTEM
K. J. Poulter and H. N. Smith *In* JPL, SpaceOps 1992: Proceedings of the Second International Symposium on Ground Data Systems for Space Mission Operations 1 Mar. 1993 p 103-112 Prepared in cooperation with Logica Ltd., London, England (For primary document see N94-23832 06-66)
Avail: CASI HC A02/MF A10

N94-23851*# European Space Agency. European Space Operations Center, Darmstadt (Germany). Flight Control Systems Dept.
SCOS2: ESA'S NEW GENERATION OF MISSION CONTROL SYSTEMS
J. F. Kaufeler and N. C. Head *In* JPL, SpaceOps 1992: Proceedings of the Second International Symposium on Ground Data Systems for Space Mission Operations 1 Mar. 1993 p 119-124 (For primary document see N94-23832 06-66)
Avail: CASI HC A02/MF A10

N94-23855*# National Aeronautics and Space Administration. Goddard Space Flight Center, Greenbelt, MD.
NASA/GODDARD SPACE FLIGHT CENTER'S TESTBED FOR CCSDS COMPATIBLE SYSTEMS
Richard D. Carper *In* JPL, SpaceOps 1992: Proceedings of the Second International Symposium on Ground Data Systems for Space Mission Operations 1 Mar. 1993 p 143-148 (For primary document see N94-23832 06-66)
Avail: CASI HC A02/MF A10

N94-23856*# Centre National d'Etudes Spatiales, Toulouse (France).
SPOT4 OPERATIONAL CONTROL CENTER (CMP)
G. Zaouche *In* JPL, SpaceOps 1992: Proceedings of the Second International Symposium on Ground Data Systems for Space Mission Operations 1 Mar. 1993 p 149-154 (For primary document see N94-23832 06-66)
Avail: CASI HC A02/MF A10

N94-23888*# Jet Propulsion Lab., California Inst. of Tech., Pasadena.
MARS OBSERVER SCREEN DISPLAY DESIGN FOR A MULTIMISSION ENVIRONMENT
Roy L. Chafin *In its* SpaceOps 1992: Proceedings of the Second International Symposium on Ground Data Systems for Space Mission Operations 1 Mar. 1993 p 363-370 (For primary document see N94-23832 06-66)
Avail: CASI HC A02/MF A10

N94-23902*# Jet Propulsion Lab., California Inst. of Tech., Pasadena.
MAKING TOMORROW'S MISTAKES TODAY: EVOLUTIONARY PROTOTYPING FOR RISK REDUCTION AND SHORTER DEVELOPMENT TIME
Gary Friedman, Ursula M. Schwuttke, Scott Burliegh, Sanguan Chow, Randy Parlier, Lorrine Lee, Henry Castro, and Jim Gersbach *In its* SpaceOps 1992: Proceedings of the Second International Symposium on Ground Data Systems for Space Mission Operations 1 Mar. 1993 p 465-470 (For primary document see N94-23832 06-66)
Avail: CASI HC A02/MF A10

N94-23907*# Computer Technology Associates, Inc., Rockville, MD.
THE ADVANCED ORBITING SYSTEMS TESTBED PROGRAM: RESULTS TO DATE
Penny A. Newsome and John F. Otranto *In* JPL, SpaceOps 1992: Proceedings of the Second International Symposium on Ground Data Systems for Space Mission Operations 1 Mar. 1993 p 501-506 Sponsored by NASA, Washington (For primary document see N94-23832 06-66)
Avail: CASI HC A02/MF A10

N94-23913*# European Space Agency. European Space Operations Center, Darmstadt (Germany).
AUTOMATIC TOOLS FOR SYSTEM TESTING
N. M. Peccia *In* JPL, SpaceOps 1992: Proceedings of the Second International Symposium on Ground Data Systems for Space Mission Operations 1 Mar. 1993 p 537-540 (For primary document see N94-23832 06-66)
Avail: CASI HC A01/MF A10

N94-23940*# Cray Systems, Bristol (England). Space Div.
SIMSAT: AN OBJECT ORIENTED ARCHITECTURE FOR REAL-TIME SATELLITE SIMULATION
Adam P. Williams *In* JPL, SpaceOps 1992: Proceedings of the Second International Symposium on Ground Data Systems for Space Mission Operations 1 Mar. 1993 p 711-716 (For primary document see N94-23832 06-66)
Avail: CASI HC A02/MF A10

N94-24020# Fokker Space and Systems, Amsterdam (Netherlands).
THE DEVELOPMENT OF THE HERA TEST FACILITY (HTF)
Aad P. Eggers *In* ESA, The Fifth European Space Mechanisms and Tribology Symposium Apr. 1993 7 p (For primary document see N94-23985 06-37)
Copyright Avail: CASI HC A02/MF A04

N94-24255 Rafael Armament Development Authority, Haifa (Israel).
ALTITUDE SIMULATION FACILITY FOR TESTING LARGE SPACE MOTORS
U. Katz, J. Lustig, Y. Cohen, and I. Malkin *In* Israel Society of Aeronautics and Astronautics, The 33rd Israel Annual Conference on Aviation and Astronautics 25 Feb. 1993 p 175-184 (For primary document see N94-24241 06-01)
Copyright Avail: Issuing Activity (Israel Society of Aeronautics and

Astronautics, c/o Faculty of Engineering, Tel-Aviv Univ., Ramat Aviv 69978, Israel)

N94-24432*# East Carolina Univ., Greenville, NC. School of Human Environmental Sciences.
SPATIAL INTERPRETATION OF NASA'S MARSHALL SPACE FLIGHT CENTER PAYLOAD OPERATIONS CONTROL CENTER USING VIRTUAL REALITY TECHNOLOGY
Patricia F. Lindsey *In* Alabama Univ., The 1993 NASA/ASEE Summer Faculty Fellowship Program Nov. 1993 5 p (For primary document see N94-24405 06-80)
Avail: CASI HC A01/MF A03

N94-24436*# Auburn Univ., AL. Department of Computer Science and Engineering.
INTEGRATION AND EVALUATION OF A SIMULATOR DESIGNED TO BE USED WITHIN A DYNAMIC PROTOTYPING ENVIRONMENT
Loretta A. Moore *In* Alabama Univ., The 1993 NASA/ASEE Summer Faculty Fellowship Program Nov. 1993 5 p (For primary document see N94-24405 06-80)
Avail: CASI HC A01/MF A03

15 LAUNCH VEHICLES AND SPACE VEHICLES

Includes boosters; operating problems of launch/space vehicle systems; and reusable vehicles.

For related information see also *20 Spacecraft Propulsion and Power.*

N94-23208# NumerEx, Albuquerque, NM.
THE INTERNAL STRUCTURE AND DYNAMICS OF THE RAILGUN PLASMA ARMATURE BETWEEN INFINITELY WIDE ABLATING RAILS
M. H. Frese 1993 98 p Prepared for Los Alamos National Lab, NM
(Contract W-7405-eng-36)
(DE94-001473; LA-Sub-93-176) Avail: CASI HC A05/MF A02 (US Sales Only)

Conventional guns cannot achieve projectile velocities much greater than the sound speed in burned chemical propellants. Plasma armature railguns should not be subject to the same type of velocity limit. However, experiments indicate that there may be some other mechanism which can limit the velocity. A theory that accurately predicts the observed velocity limit could provide the insight necessary to raise or even lift that limit. As yet, there is no theoretical explanation drawn from physical first principles which predicts a limit to the achievable velocity. This report describes the first phase of an effort to use two-dimensional dynamic magnetohydrodynamic (MHD) simulation of the plasma motion in the bore to produce such an explanation. In this phase, MACH2, an Air Force two-dimensional MHD code has been quickly adapted to this problem. The principal goal of this effort was to demonstrate the feasibility and desirability of using MACH2 for railgun armature simulation. However, the simulations of plasma armatures described here are the most sophisticated models of the railgun arc presently available; they show the armature as a dynamic and developing plasma in a way never before seen. The goal could not have been more clearly achieved. DOE

N94-23210# Sandia National Labs., Albuquerque, NM.
PROJECTILE TRANSVERSE MOTION AND STABILITY IN ELECTROMAGNETIC INDUCTION LAUNCHERS
I. R. Shokair Aug. 1993 24 p
(Contract DE-AC04-94AL-85000)
(DE94-001557; SAND-93-1351) Avail: CASI HC A03/MF A01

The transverse motion of a projectile in an electromagnetic induction launcher is considered. The equations of motion for translation and rotation are derived assuming a rigid projectile and a flyway restoring force per unit length that is proportional to the local displacement. Transverse forces and torques due to energized coils are derived for displaced or tilted projectile elements based on a first order perturbation method. The resulting equations of motion for a rigid projectile composed of multiple elements in a multi-coil launcher are analyzed as a coupled oscillator system of equations and a simple stability condition is derived. The equations of motion are incorporated into the 2-D Slingshot code and numerical solutions for the transverse motion are obtained. For the 20 meter navy launcher parameters, we find that stability is achieved with a flyway spring constant of k is approximately equal to 1 x 10(exp 8) N/sq m. For k is approximately equal to 1.5 x 10(exp 8) N/sq m and sample coil misalignment modeled as a sine wave of 1 mm amplitude at wavelengths of one or two meters, the projectile displacement grows to a maximum of 4 mm. This growth is due to resonance between the natural frequency of the projectile transverse motion and the coil displacement wavelength. This resonance does not persist because of the changing axial velocity. Random coil displacement is also found to cause roughly the same projectile displacement. For the maximum displacement a rough estimate of the transverse pressure is 50 bars. DOE

N94-24690# Army Research Lab., Aberdeen Proving Ground, MD.
A COMPARISON OF IN-BORE PROJECTILE MOTION FROM AN ELECTROMAGNETIC RAILGUN VERSUS THAT OF A CONVENTIONAL CANNON BARREL Final Report, Aug. 1992 - May 1993
Lawrence W. Burton Oct. 1993 42 p
(DA Proj. 1L1-62618-AH-80)
(AD-A273473; ARL-TR-295) Avail: CASI HC A03/MF A01

An investigation was undertaken to examine electromagnetic (EM) gun-barrel/projectile interaction. The RASCAL code was used in this study because of its ability to easily manipulate relevant parameters such as gun tube centerline, projectile contact stiffness, and projectile design geometry. This work compares the projectile performance in the 9-MJ EM railgun at the University of Texas Center for Electromechanics (UTCEM) to that in a double-travel conventional gun. This comparison was made by varying the parameters listed above for two projectile designs: the M829 Link round; and a preliminary EM design. It was believed that adoption of this format would identify specific areas of the EM gun-projectile system that excite transverse loading. The results of the analysis are presented. DTIC

N94-24752*# California Univ., Los Angeles. Mechanical, Aerospace, and Nuclear Engineering Dept.
APPROXIMATE OPTIMAL GUIDANCE FOR THE ADVANCED LAUNCH SYSTEM
T. S. Feeley and J. L. Speyer Dec. 1993 163 p
(Grant NAG1-1090; RTOP 232-01-04-05)
(NASA-CR-4568; NAS 1.26:4568) Avail: CASI HC A08/MF A02

A real-time guidance scheme for the problem of maximizing the payload into orbit subject to the equations of motion for a rocket over a spherical, non-rotating earth is presented. An approximate optimal launch guidance law is developed based upon an asymptotic expansion of the Hamilton - Jacobi - Bellman or dynamic programming equation. The expansion is performed in terms of a small parameter, which is used to separate the dynamics of the problem into primary and perturbation dynamics. For the zeroth-order problem the small parameter is set to zero and a closed-form solution to the zeroth-order expansion term of Hamilton - Jacobi - Bellman equation is obtained. Higher-order terms of the expansion include the effects of the neglected perturbation dynamics. These higher-order terms are determined from the solution of first-order linear partial differential equations requiring only the evaluation of quadratures. This technique is preferred as a real-time, on-line guidance scheme to alternative numerical iterative optimization schemes because of the unreliable convergence properties of these iterative guidance schemes and because the quadratures needed for the approximate optimal guidance law can be performed rapidly and by parallel processing. Even if the approximate solution is not nearly optimal, when using this technique the zeroth-order solution always provides a path which satisfies the terminal constraints. Results for two-degree-of-freedom simulations are presented for the simplified problem of flight in the equatorial plane and compared to the guidance scheme generated by the shooting method which is an iterative second-order technique. Author (revised)

N94-24860*# Michigan Univ., Ann Arbor.
DESIGN OF AN AIRBORNE LAUNCH VEHICLE FOR AN AIR LAUNCHED SPACE BOOSTER
Chin Chao, Rich Choi, Scott Cohen, Brian Dumont, Mauricius Gibin, Rob Jorden, and Stefan Poth 1993 184 p
(Contract NASw-4435)
(NASA-CR-195534; NAS 1.26:195534) Avail: CASI HC A09/MF A02

A conceptual design is presented for a carrier vehicle for an air launched space booster. This airplane is capable of carrying a 500,000 pound satellite launch system to an altitude over 40,000 feet for launch. The airplane features a twin fuselage configuration for improved payload and landing gear integration, a high aspect ratio wing for maneuverability at altitude, and is powered by six General Electric GE-90 engines. The analysis methods used and the systems employed in the airplane are discussed. Launch costs are expected to be competitive with existing launch systems. Author

N94-25022*# Michigan Univ., Ann Arbor.
GRYPHON: AIR LAUNCHED SPACE BOOSTER
Jun. 1993 346 p
(Contract NASw-4435)
(NASA-CR-195497; NAS 1.26:195497) Avail: CASI HC A15/MF A03

The project chosen for the winter semester Aero 483 class was the design of a next generation Air Launched Space Booster. Based on Orbital Sciences Corporation's Pegasus concept, the goal of Aero 483 was to design a 500,000 pound air launched space booster capable of delivering 17,000 pounds of payload to Low Earth Orbit and 8,000 pounds of payload to Geosynchronous Earth Orbit. The resulting launch vehicle was named the Gryphon. The class of forty senior aerospace engineering students was broken down into eight interdependent groups. Each group was assigned a subsystem or responsibility which then became their field of specialization. Spacecraft Integration was responsible for ensuring compatibility between subsystems. This group kept up to date on subsystem redesigns and informed those parties affected by the changes, monitored the vehicle's overall weight and dimensions, and calculated the mass properties of the booster. This group also performed the cost/profitability analysis of the Gryphon and obtained cost data for competing launch systems. The Mission Analysis Group was assigned the task of determining proper orbits, calculating the vehicle's flight trajectory for those orbits, and determining the aerodynamic characteristics of the vehicle. The Propulsion Group chose the engines that were best suited to the mission. This group also set the staging configurations for those engines and designed the tanks and fuel feed system. The commercial satellite market, dimensions and weights of typical satellites, and method of deploying satellites was determined by the Payloads Group. In addition, Payloads identified possible resupply packages for Space Station Freedom and identified those packages that were compatible with the Gryphon. The guidance, navigation, and control subsystems were designed by the Mission Control Group. This group identified required tracking hardware, communications hardware telemetry systems, and ground sites for the location of the Gryphon's mission control center. The Structures group was responsible for ensuring the structural integrity of the vehicle. Their designs included the payload shroud, payload support structure, exterior hull and engine support struts. The Gryphon's power requirements were determined by the Power/Thermal/Attitude Control Group. This group then selected suitable batteries and other components to meet these requirements. The group also designed heat shielding and cooling systems to ensure subsystem performance. In addition to these responsibilities this group designed the attitude control methods and RCS components for the vehicle. The Aircraft Integration Group was responsible for all aspects of the booster aircraft connection. This included the design of the connection structure and the drop mechanism. This group also designed the vehicle assembly facility and identified possible ground bases for the plane. Author

N94-23249*# Purdue Univ., West Lafayette, IN. Engineering and Technology Dept.
FLAME TRENCH ANALYSIS OF NLS VEHICLES
Nuri Zeytinoglu *In* NASA. Kennedy Space Center, NASA/ASEE Summer Faculty Fellowship Program Oct. 1993 p 521-550 (For primary document see N94-23230 06-80)
Avail: CASI HC A03/MF A04

N94-24257 Centro Tecnico Aerospacial, San Jose dos Campos (Brazil). Instituto de Aeronautica e Espaco - IAE.
MODAL TEST OF THE BRAZILIAN SATELLITE LAUNCHER (VLS) CONFIGURATION BURN-OUT OF THE FIRST STAGE
R. L. R. Carmona, R. Pirk, D. D. daSilveira, D. J. Strafacci, and E. Barros *In* Israel Society of Aeronautics and Astronautics, The 33rd Israel Annual Conference on Aviation and Astronautics 25 Feb. 1993 p 196-202 (For primary document see N94-24241 06-01)
Copyright Avail: Issuing Activity (Israel Society of Aeronautics and Astronautics, c/o Faculty of Engineering, Tel-Aviv Univ., Ramat Aviv 69978, Israel)

N94-24434*# Alabama Univ., Tuscaloosa. Aerospace Engineering Dept.
ACCESS TO SPACE STUDIES
James A. Martin *In* Alabama Univ., The 1993 NASA/ASEE Summer Faculty Fellowship Program Nov. 1993 4 p (For primary document see N94-24405 06-80)
Avail: CASI HC A01/MF A03

16 SPACE TRANSPORTATION

Includes passenger and cargo space transportation, e.g., shuttle operations; and space rescue techniques.

For related information see also *03 Air Transportation and Safety* and *18 Spacecraft Design, Testing and Performance.* For space suits see *54 Man/System Technology and Life Support.*

N94-23571*# Lockheed Engineering and Sciences Co., Houston, TX.
IMPLEMENTING THE SPACE SHUTTLE DATA PROCESSING SYSTEM WITH THE SPACE GENERIC OPEN AVIONICS ARCHITECTURE
Richard B. Wray and John R. Stovall Jul. 1993 43 p
(Contract NAS9-17900)
(NASA-CR-188254; NAS 1.26:188254; LESC-30753) Avail: CASI HC A03/MF A01

This paper presents an overview of the application of the Space Generic Open Avionics Architecture (SGOAA) to the Space Shuttle Data Processing System (DPS) architecture design. This application has been performed to validate the SGOAA, and its potential use in flight critical systems. The paper summarizes key elements of the Space Shuttle avionics architecture, data processing system requirements and software architecture as currently implemented. It then summarizes the SGOAA architecture and describes a tailoring of the SGOAA to the Space Shuttle. The SGOAA consists of a generic system architecture for the entities in spacecraft avionics, a generic processing external and internal hardware architecture, a six class model of interfaces and functional subsystem architectures for data services and operations control capabilities. It has been proposed as an avionics architecture standard with the National Aeronautics and Space Administration (NASA), through its Strategic Avionics Technology Working Group, and is being considered by the Society of Aeronautic Engineers (SAE) as an SAE Avionics Standard. This architecture was developed for the Flight Data Systems Division of JSC by the Lockheed Engineering and Sciences Company, Houston, Texas. Author

N94-24057*# Thiokol Corp., Brigham City, UT. Space Operations.
POSTFLIGHT HARDWARE EVALUATION RSRM-29 (STS-54). APPENDIX D: NOZZLE POSTFIRE DATA Final Report
Sep. 1993 21 p
(Contract NAS8-38100)
(NASA-CR-193898; NAS 1.26:193898; TWR-64222) Avail: CASI HC A03/MF A01

Appendix D, Nozzle Postfire Data of the Final Postflight Hardware Evaluation Report RSRM-29 (STS-54) is provided. Data on the erosion and char of the following are included: forward exit cone assembly, throat assembly, nose inlet, cowl/OBR, fixed housing assembly and aft exit cone assembly. CASI

N94-24059*# National Aeronautics and Space Administration. John F. Kennedy Space Center, Cocoa Beach, FL.
DEBRIS/ICE/TPS ASSESSMENT AND INTEGRATED PHOTOGRAPHIC ANALYSIS FOR SHUTTLE MISSION STS-61
Gregory N. Katnik, Barry C. Bowen, and J. Bradley Davis Jan. 1994 111 p Original contains color illustrations
(NASA-TM-109195; NAS 1.15:109195) Avail: CASI HC A06/MF A02; 31 functional color pages

A debris/ice/thermal protection system (TPS) assessment and integrated photographic analysis was conducted for shuttle mission STS-61. Debris inspections of the flight elements and launch pad were performed before and after launch. Icing conditions on the external tank were assessed by the use of computer programs, nomographs, and infrared scanner data during cryogenic loading of the vehicle followed by on-pad visual inspection. High speed photography of the launch was analyzed to identify ice/debris sources and evaluate potential vehicle damage and/or in-flight anomalies. This report documents the ice/debris/TPS conditions and integrated photographic analysis of shuttle mission STS-61, and the resulting effect on the space shuttle program. Author (revised)

N94-24065*# Thiokol Corp., Brigham City, UT. Space Operations.
FINAL POSTFLIGHT HARDWARE EVALUATION REPORT RSRM-32 (STS-57) Final Report
Greg Nielson Nov. 1993 205 p
(Contract NAS8-38100)
(NASA-CR-193903; NAS 1.26:193903; TWR-64240) Avail: CASI HC A10/MF A03

This document is the final report for the postflight assessment of the RSRM-32 (STS-57) flight set. This report presents the disassembly evaluations performed at the Thiokol facilities in Utah and is a continuation of the evaluations performed at KSC (TWR-64239). The PEEP for this assessment is outlined in TWR-50051, Revision B. The PEEP defines the requirements for evaluating RSRM hardware. Special hardware issues pertaining to this flight set requiring additional or modified assessment are outlined in TWR-64237. All observed hardware conditions were documented on PFOR's which are included in Appendix A. Observations were compared against limits defined in the PEEP. Any observation that was categorized as reportable or had no defined limits was documented on a preliminary PFAR by the assessment engineers. Preliminary PFAR's were reviewed by the Thiokol SPAT Executive Board to determine if elevation to PFAR's was required. Derived from text

N94-24067*# Thiokol Corp., Brigham City, UT. Space Operations.
POSTFLIGHT HARDWARE EVALUATION RSRM-29 (STS-54). APPENDIX E: INSULATION POSTFIRE DATA Final Report
Sep. 1993 32 p
(Contract NAS8-38100)
(NASA-CR-193897; NAS 1.26:193897; TWR-64222) Avail: CASI HC A03/MF A01

Appendix E, Insulation Postfire Data for the Final Postflight Hardware Evaluation Report RSRM-29 (STS-54) is provided. Data on the following are included: nozzle-to-case joint performance; aft dome insulation performance; aft cylinder insulation performance; forward segment star tip insulation performance; and igniter chamber and adapter insulation performance. CASI

N94-24112*# Thiokol Corp., Brigham City, UT.
FINAL POSTFLIGHT HARDWARE EVALUATION REPORT RSRM-28 (STS-53) Final Report
William David Starrett, Jr. Nov. 1993 285 p
(Contract NAS8-38100)
(NASA-CR-193902; NAS 1.26:193902; TWR-64216) Avail: CASI HC A13/MF A03

The final report for the Clearfield disassembly evaluation and a continuation of the KSC postflight assessment for the RSRM-28 (STS-53) RSRM flight set is presented. All observed hardware conditions were documented on PFOR's and are included in Appendices A through C. Appendices D and E contain the measurements and safety factor data for the nozzle and insulation components. This report, along with the KSC Ten-Day Postflight Hardware Evaluation Report (TWR-64215), represents a summary of the RSRM-28 hardware evaluation. The as-flown hardware configuration is documented in TWR-63638. Disassembly evaluation photograph numbers are logged in TWA-1989. The RSRM-28 flight set disassembly evaluations described were performed at the RSRM Refurbishment Facility in Clearfield, Utah. The final factory joint demate occurred on July 15, 1993. Additional time was required to perform the evaluation of the stiffener rings per special issue 4.1.5.2 because of the washout schedule. The release of this report was after completion of all special issues per program management direction. Detailed evaluations were performed in accordance with the Clearfield PEEP, TWR-50051, Revision A. All observations were compared against limits that are also defined in the PEEP. These limits outline the criteria for categorizing the observations as acceptable, reportable, or critical. Hardware conditions that were unexpected and/or determined to be reportable or critical were evaluated by the applicable team and tracked through the PFAR system. Author (revised)

N94-24577*# National Aeronautics and Space Administration. John F. Kennedy Space Center, Cocoa Beach, FL.
DEBRIS/ICE/TPS ASSESSMENT AND INTEGRATED PHOTOGRAPHIC ANALYSIS FOR SHUTTLE MISSION STS-58 Final Report, 30 Oct. - 3 Nov. 1993
J. Bradley Davis, Jorge E. Rivera, Gregory N. Katnik, Barry C. Bowen, Robert F. Speece, and Pedro J. Rosado Jan. 1994 156 p Original contains color illustrations
(NASA-TM-109194; NAS 1.15:109194) Avail: CASI HC A08/MF A02; 67 functional color pages

A debris/ice/thermal protection system (TPS) assessment and integrated photographic analysis was conducted for Shuttle mission STS-58. Debris inspections of the flight elements and launch pad were performed before and after launch. Icing conditions on the External Tank were assessed by the use of computer programs, nomographs, and infrared scanner data during cryogenic loading of the vehicle followed by on-pad visual inspection. High speed photography of the launch was analyzed to identify ice/debris sources and evaluate potential vehicle damage and/or in-flight anomalies. The ice/debris/TPS conditions and integrated photographic analysis of Shuttle mission STS-58, and the resulting effect on the Space Shuttle Program are documented. Author (revised)

N94-24664*# Remtech, Inc., Huntsville, AL.
ANALYSIS AND EFFECTS OF THE ADVANCED SOLID ROCKET MOTOR ON THE SPACE SHUTTLE ELEMENTS Interim Final Report
15 Oct. 1993 44 p
(Contract NAS8-39235)
(NASA-CR-193879; NAS 1.26:193879; RTR-250-01) Avail: CASI HC A03/MF A01

This interim final report summarizes the activities and major accomplishments under NASA/MSFC Contract NAS8-39235 for the initial two year contractual effort beginning October 1, 1991, and ending September 30, 1993. It is not intended as an exhaustive treatment or review of any particular technical issue which was addressed during this two-year period, but does provide an overview of the many induced environment studies and test support activities undertaken by REMTECH and its subcontractors during this two-year period. The initial scope of work has been pursued vigorously through this two-year period by separating the effort into five functional areas. The five functional areas are ascent plume radiation, ascent plume convection, ascent aerodynamic heating, launch stand environments, and reentry heating. A work breakdown structure (WBS) for each functional area was devised to permit nearly autonomous activities within each functional responsibility while maintaining commonality in reporting procedures and cost accounting. The contract was modified 11 times to provide incremental funding and to expand the scope of work. Additional work breakdown structure was incorporated to meet the expanded scope. A contract chronology is provided in Section 2. The initial scope of work, expanded scope, and corresponding WBS designation are described in Section 3. A summary review of major accomplishments is also provided in Section 4 to show the breadth of activities and extent of reporting. Reports, meetings, test activities, and other accomplishments within each functional area are also summarized by WBS heading in the appendices. Derived from text

N94-24801*# United Technologies Corp., Huntsville, AL.
LIGHTNING TESTS AND ANALYSES OF TUNNEL BOND STRAPS AND SHIELDED CABLES ON THE SPACE SHUTTLE SOLID ROCKET BOOSTER Final Report
William M. Druen Nov. 1993 157 p
(Contract NAS8-36300)
(NASA-CR-193921; NAS 1.26:193921; SI-93-2679) Avail: CASI HC A08/MF A02

The purposes of the tests and analyses described in this report are as follows: (1) determine the lightning current survivability of five alternative changed designs of the bond straps which electrically bond the solid rocket booster (SRB) systems tunnel to the solid rocket motor (SRM) case; (2) determine the amount of reduction in induced voltages on operational flight (OF) tunnel cables obtained by a modified design of tunnel bond straps (both tunnel cover-to-cover and cover-to-motor case);

(3) determine the contribution of coupling to the OF tunnel cables by ground electrical and instrumentation (GEI) cables which enter the systems tunnel from unshielded areas on the surfaces of the motor case; and (4) develop a model (based on test data) and calculate the voltage levels at electronic 'black boxes' connected to the OF cables that run in the systems tunnel. Author (revised)

N94-24802*# Thiokol Corp., Brigham City, UT. Space Operations.
POSTFLIGHT HARDWARE EVALUATION (RSRM-29, STS-54) Final Report
Sep. 1993 37 p
(Contract NAS8-38100)
(NASA-CR-193895; NAS 1.26:193895; TWR-64222) Avail: CASI HC A03/MF A01

This document is the final report for the Clearfield disassembly evaluation and a continuation of the KSC postflight assessment for the RSRM-29 flight set. All observed hardware conditions were documented on PFOR's and are included in Appendices A, B, and C. Appendices D and E contain the measurements and safety factor data for the nozzle and insulation components. This report, along with the KSC Ten-Day Postflight Hardware Evaluation Report (TWR-64221), represents a summary of the RSRM-29 hardware evaluation. Disassembly evaluation photograph numbers are logged in TWA-1990. The RSRM-29 flight set disassembly evaluations described in this document were performed at the RSRM Refurbishment Facility in Clearfield, Utah. The final factory joint demate occurred on September 9, 1993. Detailed evaluations were performed in accordance with the Clearfield PEEP, TWR-50051, Revision A. All observations were compared against limits that are also defined in the PEEP. These limits outline the criteria for categorizing the observations as acceptable, reportable, or critical. Hardware conditions that were unexpected and/or determined to be reportable or critical were evaluated by the applicable CPT and tracked through the PFAR system. Derived from text

N94-24919*# University of Central Florida, Orlando. Dept. of Mechanical and Aerospace Engineering.
DEVELOPMENT OF A NONDESTRUCTIVE VIBRATION TECHNIQUE FOR BOND ASSESSMENT OF SPACE SHUTTLE TILES Final Report
Faissal A. Moslehy Feb. 1994 86 p Original contains color illustrations
(Grant NAG10-117)
(NASA-CR-195163; NAS 1.26:195163) Avail: CASI HC A05/MF A01; 14 functional color pages

This final report describes the achievements of the above titled project. The project is funded by NASA-KSC (Grant No. NAG 10-0117) for the period of 1 Jan. to 31 Dec. 1993. The purpose of this project was to develop a nondestructive, noncontact technique based on 'vibration signature' of tile systems to quantify the bond conditions of the thermal protection system) tiles of Space Shuttle orbiters. The technique uses a laser rapid scan system, modal measurements, and finite element modeling. Finite element models were developed for tiles bonded to both clamped and deformable integrated skin-stringer orbiter mid-fuselage. Results showed that the size and location of a disbonded tile can be determined from frequency and mode shape information. Moreover, a frequency response survey was used to quickly identify the disbonded tiles. The finite element results were compared with experimentally determined frequency responses of a 17-tile test panel, where a rapidscan laser system was employed. An excellent degree of correlation between the mathematical simulation and experimental results was realized. An inverse solution for single-tile assemblies was also derived and is being implemented into a computer program that can interact with the modal testing software. The output of the program displays the size and location of disbond. This program has been tested with simulated input (i.e., finite element data), and excellent agreement between predicted and simulated disbonds was shown. Finally, laser vibration imaging and acoustic emission techniques were shown to be well suited for detecting and monitoring the progressive damage in Graphite/Epoxy composite materials. Author (revised)

N94-24965*# Thiokol Corp., Brigham City, UT. Space Operations.
POSTFLIGHT HARDWARE EVALUATION 360T021 (RSRM-21, STS-45), REVISION A Final Report
Linda E. MacCauly Dec. 1992 322 p
(Contract NAS8-38100)
(NASA-CR-193904; NAS 1.26:193904; TWR-60695) Avail: CASI HC A14/MF A03

The Final Postflight Hardware Evaluation Report 360T021 (RSRM-21, STS-45) is included. All observed hardware conditions were documented on Postflight Observation Reports (PFOR's) and included in Appendices A through E. This report, along with the KSC Ten-Day Postflight Hardware Evaluation Report represents a summary of the 360T021 hardware evaluation. Derived from text

N94-24970*# Martin Marietta Corp., Denver, CO. Flight Systems.
SPACE TRANSFER VEHICLE CONCEPTS AND REQUIREMENTS. VOLUME 4: SUMMARY OF SPECIAL STUDIES
Sep. 1993 751 p
(Contract NAS8-37856)
(NASA-CR-193918; NAS 1.26:193918; MCR-93-1362-Vol-4) Avail: CASI HC A99/MF A06

Our final report for Phase 1 addressed the future space transportation needs and requirements based on the current assets, at the time, and their evolution through technology/advanced development using a path and schedule that supported the world leadership role of the United States in a responsible and realistic financial forecast. Always, and foremost, the recommendations placed high values on the safety and success of missions both manned and unmanned through a total quality management philosophy at Martin Marietta. The second phase of the STV contract involved the use of Technical Directives (TD) to provide short-term support for specialized tasks as required by the COTR. Three of these tasks were performed in parallel with Phase 1. These tasks were the Liquid Acquisition Experiment (LACE), Liquid Reorientation Experiment (LIRE), and Expert System for Design, Operation, and Technology Studies (ESDOTS). The results of these TD's were reported in conjunction with the Phase 1 Final Report. Cost analysis of existing launch systems has demonstrated a need for a new upper stage that will increase America's competitiveness in the global launch services market. To provide a growth path of future exploration class STV's, near-term low-cost upper stages featuring modularity, portability, scalability, and evolvability must be developed. These recommendations define a program that: leverages ongoing activities to establish a new development environment, develop technologies that benefit the entire life cycle of a system, and result in a scalable hardware platform that provides a growth path to future upper stages. Author (revised)

N94-25098*# National Aeronautics and Space Administration. Langley Research Center, Hampton, VA.
FUTURE SPACE TRANSPORTATION SYSTEM ARCHITECTURE AVIONICS REQUIREMENTS
Howard Stone and Walt Engelund *In its* NASA LaRC Workshop on Guidance, Navigation, Controls, and Dynamics for Atmospheric Flight, 1993 Dec. 1993 p 55-83 (For primary document see N94-25096 06-01)
Avail: CASI HC A03/MF A04

17 SPACE COMM., SPACECRAFT COMM., COMMAND & TRACKING

Includes telemetry; space communications networks; astronavigation and guidance; and radio blackout.

For related information see also *04 Aircraft Communications and Navigation* and *32 Communications and Radar.*

N94-23567*# National Aeronautics and Space Administration. Lewis Research Center, Cleveland, OH.
FAULT TOLERANT ONBOARD PACKET SWITCH ARCHITECTURE FOR COMMUNICATION SATELLITES: SHARED MEMORY PER BEAM APPROACH
Mary Jo Shalkhauser, Jorge A. Quintana, and Nitin J. Soni Jan. 1994 10 p Prepared for presentation at the 15th International Communications Satellite Systems Conference, San Diego, CA, 28 Feb. - 3 Mar. 1994; sponsored by AIAA
(RTOP 506-72-21)
(NASA-TM-106397; E-8224; NAS 1.15:106397; AIAA Paper 94-1101)
Avail: CASI HC A02/MF A01

The NASA Lewis Research Center is developing a multichannel communication signal processing satellite (MCSPS) system which will provide low data rate, direct to user, commercial communications services. The focus of current space segment developments is a flexible, high-throughput, fault tolerant onboard information switching processor. This information switching processor (ISP) is a destination-directed packet switch which performs both space and time switching to route user information among numerous user ground terminals. Through both industry study contracts and in-house investigations, several packet switching architectures were examined. A contention-free approach, the shared memory per beam architecture, was selected for implementation. The shared memory per beam architecture, fault tolerance insertion, implementation, and demonstration plans are described. Author (revised)

N94-23631*# Westinghouse Electric Corp., Baltimore, MD.
ADVANCED TECHNOLOGY FOR A SATELLITE MULTICHANNEL DEMULTIPLEXER/DEMODULATOR Final Report
Irwin J. Abramovitz, Drew E. Flechsig, and Richard M. Matteis, Jr. Jan. 1994 57 p
(Contract NAS3-25865; RTOP 235-01-04)
(NASA-CR-194435; E-8317; NAS 1.26:194435) Avail: CASI HC A04/MF A01

Satellite on-board processing is needed to efficiently service multiple users while at the same time minimizing earth station complexity. The processing satellite receives a wideband uplink at 30 GHz and down-converts it to a suitable intermediate frequency. A multichannel demultiplexer then separates the composite signal into discrete channels. Each channel is then demodulated by bulk demodulators, with the baseband signals routed to the downlink processor for retransmission to the receiving earth stations. This type of processing circumvents many of the difficulties associated with traditional bent-pipe repeater satellites. Uplink signal distortion and interference are not retransmitted on the downlink. Downlink power can be allocated in accordance with user needs, independent of uplink transmissions. This allows the uplink users to employ different data rates as well as different modulation and coding schemes. In addition, all downlink users have a common frequency standard and symbol clock on the satellite, which is useful for network synchronization in time division multiple access schemes. The purpose of this program is to demonstrate the concept of an optically implemented multichannel demultiplexer (MCD). A proof-of-concept (POC) model has been developed which has the ability to receive a 40 MHz wide composite signal consisting of up to 1000 40 kHz QPSK modulated channels and perform the demultiplexing process. In addition a set of special test equipment (STE) has been configured to evaluate the performance of the POC model. The optical MCD is realized as an acousto-optic spectrum analyzer utilizing the capability of Bragg cells to perform the required channelization. These Bragg cells receive an optical input from a laser source and an RF input (the signal). The Bragg interaction causes optical output diffractions at angles proportional to the RF input frequency. These discrete diffractions are optically detected and output to individual demodulators for baseband conversion. Optimization of the MCD design was conducted in order to achieve a compromise between two opposing sources of signal degradation: adjacent channel interference and intersymbol interference. The system was also optimized to allow simple, inexpensive ground stations communications with the MCD. These design goals led to the realization of a POC MCD which demonstrates the demultiplexing function with minimal signal degradation. Performance evaluation results using the STE equipment indicate that the dynamic range of the demultiplexer in the presence of adjacent and multiple channel loading is 40 - 50 dB. Measured bit error rate (BER) probabilities varied from the predicted theoretical results by one dB or less. The performance of the proof-of-concept model indicate that the development of a space qualified optically implemented MCD are feasible. The advantages to such an implementation include reduced size, weight and power and increased reliability when compared with electronic approaches. All of these factors are critical to on-board satellite processors. Further optimization can be conducted which trade ground station complexity and MCD performance to achieve desired system results. Author (revised)

N94-24121 Defence Research Establishment Atlantic, Dartmouth (Nova Scotia).
EXPERIMENTAL VERIFICATION OF AN ACOUSTIC TELEMETRY LINK BETWEEN AN AURORA AND CFAV QUEST
C. M. McIntyre, A. T. Ashley, J. W. MacDonald, and R. L. G. Whitehorne Feb. 1993 30 p
(DREA-TC-93-304; CTN-94-60917) Avail: Micromedia Ltd., Technical Information Centre, 165 Hotel de Ville, Place du Portage, Phase 2, Hull, Quebec J8X 3X2, Canada

To evaluate airborne sonar concepts operationally on a ship-based system, a mechanism must be developed for transmitting both acoustic and nonacoustic data from an aircraft to the ship. An initial evaluation of an acoustic telemetry link between an Aurora patrol aircraft and the research ship CFAV Quest is presented. The link was designed to transmit continuous, real-time acoustic data from sixteen DIFAR sonobuoys between the Aurora and the Quest. In two recent trials of the acoustic telemetry link system, reliable transmission was obtained out to ranges of 50 nautical miles with a tracking antenna receiving system and to ranges of seven nautical miles with an omnidirectional antenna. In each case, the aircraft was required to fly a dedicated pattern to maintain the link and there were short periods during each pattern that the link was poor due to transmission shadows cast by the aircraft or the ship. The acoustic telemetry link system is described in detail along with an initial evaluation of the operating envelopes currently imposed on the Aurora and the Quest in order to obtain reliable transmission. Recommendations are given for improving the quality and flexibility of the link. Author (CISTI)

N94-25095*# National Aeronautics and Space Administration. Lewis Research Center, Cleveland, OH.
BOUNDS AND SIMULATION RESULTS OF 32-ARY AND 64-ARY QUADRATURE AMPLITUDE MODULATION FOR BROADBAND-ISDN VIA SATELLITE
Muli Kifle and Mark Vanderaar (Sverdrup Technology, Inc., Brook Park, OH.) Feb. 1994 14 p
(Contracts NAS3-25266; NAS3-27186; RTOP 235-01-04)
(NASA-TM-106484; E-8470; NAS 1.15:106484) Avail: CASI HC A03/MF A01

Union bounds and Monte Carlo simulation Bit-Error-Rate (BER) performance results are presented for various 32-ary and 64-ary Quadrature Amplitude Modulation (QAM) schemes. Filtered and unfiltered modulation formats are compared for the best packing arrangement in peak power limited systems. It is verified that circular constellations which populate as many symbols as possible at the peak magnitude offer the best performance. For example: a 32-ary QAM scheme based on concentric circles offers about 1.05 dB better peak power improvement at a BER of 10(exp -6) over the scheme optimized for average power using triangular symbol packing. This peak power improvement increases to 1.25 dB for comparable 64-ary QAM schemes. This work serves as a precursor to determine the feasibility of a combined modem/codec that can accommodate Broadband Integrated Services Digital Network (B-ISDN) at a rate of 155.52 Mbps through typical transponder bandwidths of 36 MHz and 54 MHz. Author (revised)

N94-23921*# National Aeronautics and Space Administration. Lyndon B. Johnson Space Center, Houston, TX.
A REAL-TIME NAVIGATION MONITORING EXPERT SYSTEM FOR THE SPACE SHUTTLE MISSION CONTROL CENTER
Lui Wang and Malise Fletcher *In* JPL, SpaceOps 1992: Proceedings of the Second International Symposium on Ground Data Systems for Space Mission Operations 1 Mar. 1993 p 591-599 (For primary document see N94-23832 06-66)
Avail: CASI HC A02/MF A10

N94-23925*# Centre National d'Etudes Spatiales, Toulouse (France).
MERCATOR: METHODS AND REALIZATION FOR CONTROL OF THE ATTITUDE AND THE ORBIT OF SPACECRAFT
Gilles Tavernier and Genevieve Campan *In* JPL, SpaceOps 1992: Proceedings of the Second International Symposium on Ground Data Systems for Space Mission Operations 1 Mar. 1993 p 619-628 (For primary document see N94-23832 06-66)
Avail: CASI HC A02/MF A10

N94-23946*# Jet Propulsion Lab., California Inst. of Tech., Pasadena.
THE EVOLVING TREND IN SPACECRAFT HEALTH ANALYSIS
Russell L. Kirkpatrick *In its* SpaceOps 1992: Proceedings of the Second International Symposium on Ground Data Systems for Space Mission

Operations 1 Mar. 1993 p 751-755 (For primary document see N94-23832 06-66)
Avail: CASI HC A01/MF A10

N94-23947*# National Aeronautics and Space Administration. Goddard Space Flight Center, Greenbelt, MD.
ORBITAL SIGNATURE ANALYZER (OSA): A SPACECRAFT HEALTH/SAFETY MONITORING AND ANALYSIS TOOL
Steven Weaver (Computer Sciences Corp., Laurel, MD.), Charles DeGeorges (Computer Sciences Corp., Laurel, MD.), Joy Bush (Computer Sciences Corp., Laurel, MD.), Robert Shendock (TRW, Inc., Redondo Beach, CA.), and Daniel Mandl *In* JPL, SpaceOps 1992: Proceedings of the Second International Symposium on Ground Data Systems for Space Mission Operations 1 Mar. 1993 p 757-761 (For primary document see N94-23832 06-66)
Avail: CASI HC A01/MF A10

N94-23949*# National Aeronautics and Space Administration. Goddard Space Flight Center, Greenbelt, MD.
TELEMETRY GROUND SYSTEM DEVELOPMENT VIA THE COMPONENT APPROACH
Karen E. Thorn *In* JPL, SpaceOps 1992: Proceedings of the Second International Symposium on Ground Data Systems for Space Mission Operations 1 Mar. 1993 p 773-778 (For primary document see N94-23832 06-66)
Avail: CASI HC A02/MF A10

N94-23954*# European Space Agency. European Space Operations Center, Darmstadt (Germany).
THE EUROPEAN SPACE AGENCY STANDARD FOR SPACE PACKET UTILISATION
J.-F. Kaufeler, A. Parkes (NOVA Space Ltd., Bath, England.), and A. Pidgeon (VEGA Space Systems Engineering Ltd., Harpenden, England.) *In* JPL, SpaceOps 1992: Proceedings of the Second International Symposium on Ground Data Systems for Space Mission Operations 1 Mar. 1993 p 813-818 (For primary document see N94-23832 06-66)
Avail: CASI HC A02/MF A10

18 SPACECRAFT DESIGN, TESTING AND PERFORMANCE

Includes satellites; space platforms; space stations; spacecraft systems and components such as thermal and environmental controls; and attitude controls.

For life support systems see *54 Man/System Technology and Life Support.* For related information see also *05 Aircraft Design, Testing and Performance, 39 Structural Mechanics,* and *16 Space Transportation.*

N94-23329*# Dayton Univ., OH. Dept. of Engineering Management and Systems.
LIFE CYCLE COST MODELING OF CONCEPTUAL SPACE VEHICLES Interim Report, Jun. - Dec. 1993
Charles Ebeling 1993 67 p
(Grant NAG1-1327)
(NASA-CR-194813; NAS 1.26:194813) Avail: CASI HC A04/MF A01

This paper documents progress to date by the University of Dayton on the development of a life cycle cost model for use during the conceptual design of new launch vehicles and spacecraft. This research is being conducted under NASA Research Grant NAG-1-1327. This research effort changes the focus from that of the first two years in which a reliability and maintainability model was developed to the initial development of a life cycle cost model. Cost categories are initially patterned after NASA's three axis work breakdown structure consisting of a configuration axis (vehicle), a function axis, and a cost axis. The focus will be on operations and maintenance costs and other recurring costs. Secondary tasks performed concurrent with the development of the life cycle costing model include continual support and upgrade of the R&M model. The primary result of the completed research will be a methodology and a computer implementation of the methodology to provide for timely cost analysis in support of the conceptual design activities. The major objectives of this research are: to obtain and to develop improved methods for estimating manpower, spares, software and hardware costs, facilities costs, and other cost categories as identified by NASA personnel; to construct a life cycle cost model of a space transportation system for budget exercises and performance-cost trade-off analysis during the conceptual and development stages; to continue to support modifications and enhancements to the R&M model; and to continue to assist in the development of a simulation model to provide an integrated view of the operations and support of the proposed system. Derived from text

N94-23618*# Colorado Univ., Boulder. Center for Space Structures and Controls.
REAL-TIME DYNAMICS AND CONTROL STRATEGIES FOR SPACE OPERATIONS OF FLEXIBLE STRUCTURES Final Report, 15 Jan. 1992 - 14 Jul. 1993
K. C. Park, K. F. Alvin, and S. Alexander Jul. 1993 72 p
(Grant NAG9-574)
(NASA-CR-194794; NAS 1.26:194794; CU-CSSC-93-16) Avail: CASI HC A04/MF A01

This project (NAG9-574) was meant to be a three-year research project. However, due to NASA's reorganizations during 1992, the project was funded only for one year. Accordingly, every effort was made to make the present final report as if the project was meant to be for one-year duration. Originally, during the first year we were planning to accomplish the following: we were to start with a three dimensional flexible manipulator beam with articulated joints and with a linear control-based controller applied at the joints; using this simple example, we were to design the software systems requirements for real-time processing, introduce the streamlining of various computational algorithms, perform the necessary reorganization of the partitioned simulation procedures, and assess the potential speed-up realization of the solution process by parallel computations. The three reports included as part of the final report address: the streamlining of various computational algorithms; the necessary reorganization of the partitioned simulation procedures, in particular the observer models; and an initial attempt of reconfiguring the flexible space structures. Author (revised)

N94-23632*# Sverdrup Technology, Inc., Brook Park, OH.
A REVIEW OF WIRING SYSTEM SAFETY IN SPACE POWER SYSTEMS
Mark W. Stavnes and Ahmad N. Hammoud Dec. 1993 8 p Presented at the 28th Intersociety Energy Conversion Engineering Conference, 8-13 Aug. 1993; sponsored by ASC, AIAA, AIChE, ANS, ASME, IEEE, and SAE
(Contract NAS3-25266; RTOP 323-57-4A)
(NASA-CR-194439; E-8291; NAS 1.26:194439) Avail: CASI HC A02/MF A01

Wiring system failures have resulted from arc propagation in the wiring harnesses of current aerospace vehicles. These failures occur when the insulation becomes conductive upon the initiation of an arc. In some cases, the conductive path of the carbon arc track displays a high enough resistance such that the current is limited, and therefore may be difficult to detect using conventional circuit protection. Often, such wiring failures are not simply the result of insulation failure, but are due to a combination of wiring system factors. Inadequate circuit protection, unforgiving system designs, and careless maintenance procedures can contribute to a wiring system failure. This paper approaches the problem with respect to the overall wiring system, in order to determine what steps can be taken to improve the reliability, maintainability, and safety of space power systems. Power system technologies, system designs, and maintenance procedures which have led to past wiring system failures will be discussed. New technologies, design processes, and management techniques which may lead to improved wiring system safety will be introduced. Author

N94-23824* National Aeronautics and Space Administration. Marshall Space Flight Center, Huntsville, AL.
PRESSURE WALL PATCH Patent
Joel E. Williamsen, inventor (to NASA) and Bruce C. Weddendorf, inventor (to NASA) 18 Jan. 1994 7 p Filed 15 Oct. 1992 Supersedes N93-17061 (31 - 5, p 1088)
(NASA-Case-MFS-28724-1; US-Patent-5,279,092; US-Patent-Appl-SN-961293; US-Patent-Class-52-514;

US-Patent-Class-114-227; Int-Patent-Class-E02D-37/00) Avail: US Patent and Trademark Office

A rigid patch body for placing over a damaged portion (hole) of an external wall of a pressurized vessel, such as a space vehicle or a habitat, is discussed. The rigid patch body allows an astronaut to make temporary repairs to the pressurized vessel from the exterior of the vessel, which enables more permanent repairs to be made from the interior of the vessel. The pressure wall patch of the present invention includes a floor surrounded by four side members. Each side member includes a threaded screw for anchoring the patch body to the external wall of the pressurized vessel and a recess in its lower surface for supporting an inflatable bladder for surrounding the damaged portion (hole) of the external wall to seal the area surrounding the damaged portion. This allows the vessel to be repressurized. The floor of the rigid patch body supports a source of gas that is connected to the gas supply valve and a gas supply gauge in communication with the gas supply valve and the inflatable bladder. Official Gazette of the U.S. Patent and Trademark Office

N94-23828*# Triangle Research and Development Corp., Research Triangle Park, NC.

TELEROBOTIC RENDEZVOUS AND DOCKING VISION SYSTEM ARCHITECTURE Final Report, 11 Aug. 1989

Ben Gravely, Donald Myers, and David Moody 17 Jan. 1992 32 p
(Contract NAS5-30709; SBIR-05.01-2878)
(NASA-CR-191329; NAS 1.26:191329) Avail: CASI HC A03/MF A01

This research program has successfully demonstrated a new target label architecture that allows a microcomputer to determine the position, orientation, and identity of an object. It contains a CAD-like database with specific geometric information about the object for approach, grasping, and docking maneuvers. Successful demonstrations were performed selecting and docking an ORU box with either of two ORU receptacles. Small, but significant differences were seen in the two camera types used in the program, and camera sensitive program elements have been identified. The software has been formatted into a new co-autonomy system which provides various levels of operator interaction and promises to allow effective application of telerobotic systems while code improvements are continuing. Author (revised)

N94-24226*# Wisconsin Univ., Madison. Space Science and Engineering Center.

HUBBLE SPACE TELESCOPE HIGH SPEED PHOTOMETER ORBITAL VERIFICATION Test Report

Evan E. Richards Nov. 1991 160 p
(Contract NAS5-24487)
(NASA-CR-189333; NAS 1.26:189333) Avail: CASI HC A08/MF A02

The purpose of this report is to provide a summary of the results of the HSP (High Speed Photometer) Orbital Verification (OV) tests and to report conclusions and lessons learned from the initial operations of the HSP. The HSP OV plan covered the activities through fine (phase 3) alignment. This report covers all activities (OV, SV, and SAO) from launch to the completion of phase 3 alignment. Those activities in this period that are not OV tests are described to the extent that they relate to OV activities. Author (revised)

N94-24334*# Duke Univ., Durham, NC. Dept. of Mechanical Engineering and Materials Science.

MAGNETIC SHIELDING OF INTERPLANETARY SPACECRAFT AGAINST SOLAR FLARE RADIATION Final Report, 1992 - 1993

Franklin H. Cocks and Seth Watkins Jul. 1993 36 p
(Contract NASw-4435)
(NASA-CR-195539; NAS 1.26:195539) Avail: CASI HC A03/MF A01

The ultimate objective of this work is to design, build, and fly a dual-purpose, piggyback payload whose function is to produce a large volume, low intensity magnetic field and to test the concept of using such a magnetic field (1) to protect spacecraft against solar flare protons, (2) to produce a thrust of sufficient magnitude to stabilize low satellite orbits against orbital decay from atmospheric drag, and (3) to test the magsail concept. These all appear to be capable of being tested using the same deployed high temperature superconducting coil. In certain orbits, high temperature superconducting wire, which has now been developed to the point where silver-sheathed high T sub c wires one mm in diameter are commercially available, can be used to produce the magnetic moments required for shielding without requiring any mechanical cooling system. The potential benefits of this concept apply directly to both earth-orbital and interplanetary missions. The usefulness of a protective shield for manned missions needs scarcely to be emphasized. Similarly, the usefulness of increasing orbit perigee without expenditure of propellant is obvious. This payload would be a first step in assessing the true potential of large volume magnetic fields in the US space program. The objective of this design research is to develop an innovative, prototype deployed high temperature superconducting coil (DHTSC) system. Derived from text

N94-24590*# Naval Postgraduate School, Monterey, CA.

NPS ALTERNATE TECHSAT SATELLITE, DESIGN PROJECT FOR AE-4871

1993 110 p
(Contract NASw-4435)
(NASA-CR-195512; NAS 1.26:195512) Avail: CASI HC A06/MF A02

This project was completed as part of AE-4871, Advanced Spacecraft Design. The intent of the course is to provide experience in the design of all the major components in a spacecraft system. Team members were given responsibility for the design of one of the six primary subsystems: power, structures, propulsion, attitude control, telemetry, tracking and control (TT&C), and thermal control. In addition, a single member worked on configuration control, launch vehicle integration, and a spacecraft test plan. Given an eleven week time constraint, a preliminary design of each subsystem was completed. Where possible, possible component selections were also made. Assistance for this project came principally from the Naval Research Laboratory's Spacecraft Technology Branch. Specific information on components was solicited from representatives in industry. The design project centers on a general purpose satellite bus that is currently being sought by the Strategic Defense Initiative. Author (revised)

N94-24620*# Worcester Polytechnic Inst., MA.

CONCEPTUAL DESIGN OF A TWO STAGE TO ORBIT SPACECRAFT

Scott C. Armiger, Jennifer S. Kwarta, Kevin B. Horsley, Glenn A. Snow, Eric C. Koe, and Thomas G. Single 4 Mar. 1993 233 p
(Contract NASw-4435)
(NASA-CR-195536; NAS 1.26:195536; ME-ANA-TSTO) Avail: CASI HC A11/MF A03

This project, undertaken through the Advanced Space Design Program, developed a 'Conceptual Design of a Two Stage To Orbit Spacecraft (TSTO).' The design developed utilizes a combination of air breathing and rocket propulsion systems and is fully reusable, with horizontal takeoff and landing capability. The orbiter is carried in an aerodynamically designed bay in the aft section of the booster vehicle to the staging altitude. This TSTO Spacecraft design meets the requirements of replacing the aging Space Shuttle system with a more easily maintained vehicle with more flexible mission capability. Author (revised)

N94-24621*# Arizona Univ., Tucson. Aerospace and Mechanical Engineering Dept.

AUTONOMOUS SPACE PROCESSOR FOR ORBITAL DEBRIS (ASPOD)

Kumar Ramohalli, Dominique Mitchell, and Brett Taft 1992 330 p
(Contract NASw-4435)
(NASA-CR-195521; NAS 1.26:195521) Avail: CASI HC A15/MF A03

A project in the Advanced Design Program at the University of Arizona is described. The project is named the Autonomous Space Processor for Orbital Debris (ASPOD) and is a Universities Space Research Association (USRA) sponsored design project. The development of ASPOD and the students' abilities in designing and building a prototype spacecraft are the ultimate goals of this project. This year's focus entailed the development of a secondary robotic arm and end-effector to work in tandem with an existent arm in the removal of orbital debris. The new arm features the introduction of composite materials and a linear drive system, thus producing a light-weight and more accurate prototype. The main characteristic of the end-effector design is that it incorporates all of the motors and gearing internally, thus not subjecting them to the harsh space environment. Furthermore, the arm and the end-effector are automated by a control system with positional feedback. This system is composed of magnetic and optical encoders connected to a 486 PC via two servo-motor controller cards. Programming a series of basic routines and sub-routines allowed the ASPOD prototype to become more autonomous. The new system is

expected to perform specified tasks with a positional accuracy of 0.5 cm.
Author (revised)

N94-24625*# National Aeronautics and Space Administration. Lyndon B. Johnson Space Center, Houston, TX. Flight Crew Support System.
ORBITAL DOCKING SYSTEM CENTERLINE COLOR TELEVISION CAMERA SYSTEM TEST
Philip T. Mongan Dec. 1993 25 p
(NASA-TM-104783; S-743; NAS 1.15:104783) Avail: CASI HC A03/MF A01

A series of tests was run to verify that the design of the centerline color television camera (CTVC) system is adequate optically for the STS-71 Space Shuttle Orbiter docking mission with the Mir space station. In each test, a mockup of the Mir consisting of hatch, docking mechanism, and docking target was positioned above the Johnson Space Center's full fuselage trainer, which simulated the Orbiter with a mockup of the external airlock and docking adapter. Test subjects viewed the docking target through the CTVC under 30 different lighting conditions and evaluated target resolution, field of view, light levels, light placement, and methods of target alignment. Test results indicate that the proposed design will provide adequate visibility through the centerline camera for a successful docking, even with a reasonable number of light failures. It is recommended that the flight deck crew have individual switching capability for docking lights to provide maximum shadow management and that centerline lights be retained to deal with light failures and user preferences. Procedures for light management should be developed and target alignment aids should be selected during simulated docking runs. Author

N94-24702*# Texas Univ., Austin. Dept. of Aerospace Engineering and Mechanics.
A SMALL SATELLITE DESIGN FOR DEEP SPACE NETWORK TESTING AND TRAINING Final Design Report
Dennis McWilliams, Clint Slatton, Cassidy Norman, Joe Araiza, Jason Jones, Mark Tedesco, Michael Wortman, John Opiela, Pat Lett, and Michael Clavenna 8 May 1993 114 p Original contains color illustrations
(Contract NASw-4435)
(NASA-CR-195526; NAS 1.26:195526) Avail: CASI HC A06/MF A02; 2 functional color pages

With the continuing exploration of the Solar System and the reemphasis on Earth focused missions, the need for faster data transmission rates has grown. Ka-band could allow a higher data delivery rate over the current X-band, however the adverse effects of the Earth's atmosphere on Ka are as yet unknown. The Deep Space Network and Jet Propulsion Lab have proposed to launch a small satellite that would simultaneously transmit X and Ka signals to test the viability of switching to Ka-band. The Mockingbird Design Team at the University of Texas at Austin applied small satellite design principles to achieve this objective. The Mockingbird design, named BATSAT, incorporates simple, low-cost systems designed for university production and testing. The BATSAT satellite is a 0.64 m diameter, spherical panel led satellite, mounted with solar cells and omni-directional antennae. The antennae configuration negates the need for active attitude control or spin stabilization. The space-frame truss structure was designed for 11 g launch loads while allowing for easy construction and solar-panel mounting. The communication system transmits at 1 mW by carrying the required Ka and X-band transmitters, as well as an S band transmitter used for DSN training. The power system provides the 8.6 W maximum power requirements via silicon solar arrays and nickel-cadmium batteries. The BATSAT satellite will be lofted into an 1163 km, 70 deg orbit by the Pegasus launch system. This orbit fulfills DSN dish slew rate requirements while keeping the satellite out of the heaviest regions of the Van Allen radiation belts. Each of the three DSN stations capable of receiving Ka-band (Goldstone, Canberra, and Madrid) will have an average of 85 minutes of view-time per day over the satellites ten year design life. Mockingbird Designs hopes that its small satellite design will not only be applicable to this specific mission scenario, but that it could easily be modified for instrument capability for university, government, and/or commercial research. Author (revised)

N94-24710*# Wisconsin Univ., Madison. Space Science and Engineering Center.
HUBBLE SPACE TELESCOPE HIGH SPEED PHOTOMETER SCIENCE VERIFICATION TEST REPORT
Evan E. Richards Jul. 1992 157 p
(Contract NAS5-24487)
(NASA-CR-189322; NAS 1.26:189322) Avail: CASI HC A08/MF A02

The purpose of this report is to summarize the results of the HSP Science Verification (SV) tests, the status of the HSP at the end of the SV period, and the work remaining to be done. The HSP OV report (November 1991) covered all activities (OV, SV, and SAO) from launch to the completion of phase three alignment, OV 3233 performed in the 91154 SMS, on June 8, 1991. This report covers subsequent activities through May 1992. Author (revised)

N94-24824*# National Aeronautics and Space Administration. Goddard Space Flight Center, Greenbelt, MD.
SATELLITE SITUATION REPORT, VOLUME 33, NUMBER 4
31 Dec. 1993 403 p See N94-15712, vol. 33, no. 3
(NASA-TM-109677; NAS 1.15:109677) Avail: CASI HC A18/MF A04

The Satellite Situation Report is a listing of those satellites (objects) currently in orbit and those which have previously orbited the Earth. Some objects are too small or too far from the Earth's surface to be detected; therefore, the Satellite Situation Report does not include all manmade objects orbiting the Earth. Generally, satellites are classified as follows: (1) Payloads may contain one or more functioning or nonfunctioning experiments. Usually only the owners of the satellites know if the experiments are functioning, and there is no one source which indicates the operational status of all payloads and/or experiments. Payloads are normally the first listed in the Satellite Situation Report, i.e., 1982 087A, unless there are multiple payloads for the launch. In which case, the first objects cataloged are usually all payloads, unless a subsequent payload is later identified after objects other than payloads have been cataloged. (2) Platforms are used to support a payload while it is being placed into orbit. A platform may remain in orbit long after its purpose is served, usually longer than rocket bodies. It is usually the first object identified in the Satellite Situation Report listing after the payload(s), i.e., 1982 087B (when a platform is not used, the first object after the payload(s) is usually the rocket body). (3) Rocket bodies are used to place the payload and platform (if one is used) into orbit. Some launches may have more than one rocket body because of the payload weight or the type of orbit or experiment. Most rocket bodies decay within a short time after the payload (and platform) have achieved orbit. Rocket bodies are usually the third object listed in the Satellite Situation Report after the payload(s), i.e., 1982 087C. (4) Debris in orbit occurs when parts (nose cone shrouds, lens or hatch covers) are separated from the payload, when rocket bodies or payloads disintegrate or explode, or when objects are placed into free space from manned orbiting spacecraft during operations. Debris is detected by its size and distance from the Earth. Debris objects are the last objects after payload(s), platform, and rocket body(s) listed in the Satellite Situation Report, i.e., 1982 087D, 1982 087E, 1982 087F. Author (revised)

N94-24825*# National Aeronautics and Space Administration. Lewis Research Center, Cleveland, OH.
THERMAL CONTROL SYSTEM FOR SPACE STATION FREEDOM PHOTOVOLTAIC POWER MODULE
Thomas H. Hacha and Laura Howard (Rockwell International Corp., Canoga Park, CA.) Jan. 1994 13 p Presented at the 22nd International Conference on Environmental Systems, Seattle, WA, 13-16 Jul. 1992; sponsored by SAE See also A93-41305
(RTOP 474-46-10)
(NASA-TM-105650; E-7014; NAS 1.15:105650) Avail: CASI HC A03/MF A01

The electric power for Space Station Freedom (SSF) is generated by the solar arrays of the photovoltaic power modules (PVM's) and conditioned, controlled, and distributed by a power management and distribution system. The PVM's are located outboard of the alpha gimbals of SSF. A single-phase thermal control system is being developed to provide thermal control of PVM electrical equipment and energy storage batteries. This system uses ammonia as the coolant and a direct-flow deployable radiator. The description and development status of the PVM thermal control system is presented.
Author (revised)

N94-24828*# Texas Univ., Austin. Dept. of Mechanical Engineering.
DESIGN OF ORBITAL DEBRIS SHIELDS FOR OBLIQUE HYPERVELOCITY IMPACT Final Report

Eric P. Fahrenthold 14 Feb. 1994 111 p
(Grant NAG9-586)
(NASA-CR-195152; NAS 1.26:195152) Avail: CASI HC A06/MF A02

A new impact debris propagation code was written to link CTH simulations of space debris shield perforation to the Lagrangian finite element code DYNA3D, for space structure wall impact simulations. This software (DC3D) simulates debris cloud evolution using a nonlinear elastic-plastic deformable particle dynamics model, and renders computationally tractable the supercomputer simulation of oblique impacts on Whipple shield protected structures. Comparison of three dimensional, oblique impact simulations with experimental data shows good agreement over a range of velocities of interest in the design of orbital debris shielding. Source code developed during this research is provided on the enclosed floppy disk. An abstract based on the work described was submitted to the 1994 Hypervelocity Impact Symposium. Author (revised)

N94-24838*# Iowa State Univ. of Science and Technology, Ames.
IOWA SATELLITE PROJECT ISAT-1
25 Jul. 1993 298 p
(Contract NASw-4435)
(NASA-CR-195517; NAS 1.26:195517) Avail: CASI HC A13/MF A03

Satellite systems to date have been mainly scientific in nature. Only a few systems have been of direct use to the public such as for telephone or television transmission. Space enterprises have remained a mystery to the general public and beyond the reach of the small business community. The result is a less than supportive public when it comes to space activities. The purpose of the ISAT-1 program is to develop a small and relatively inexpensive satellite that will serve the State of Iowa, primarily for educational purposes. It will provide products, services, and activities that will be educational, practical, and useful for a large number for people. The emphasis is on public awareness, 'space literacy', and routine practical applications rather than high technology. The initial conceptual design phase was complete when the current team took over the project. Some areas of the conceptual design were taken a little farther, but for the most part this team started at the detailed design stage. Derived from text

N94-24916*# Texas Univ., Austin. Dept. of Aerospace Engineering.
EXTENDED DURATION LUNAR LANDER
Nikola Babic, Matt Carter, Donna Cosper, David Garza, Eloy Gonzalez, David Goodine, Edward Hirst, Ray Li, Martin Lindsey, and Tony Ng 15 May 1993 116 p Original contains color illustrations
(Contract NASw-4435)
(NASA-CR-195527; NAS 1.26:195527) Avail: CASI HC A06/MF A02; 2 functional color pages

Selenium Technologies has been conducting preliminary design work on a manned lunar lander for use in NASA's First Lunar Outpost (FLO) program. The resulting lander is designed to carry a crew of four astronauts to a prepositioned habitat on the lunar surface, remain on the lunar surface for up to 45 days while the crew is living in the habitat, then return the crew to earth via direct reentry and land recovery. Should the need arise, the crew can manually guide the lander to a safe lunar landing site, and live in the lander for up to ten days on the surface. Also, an abort to earth is available during any segment of the mission. The main propulsion system consists of a cluster of four modified Pratt and Whitney RL10 rocket engines that use liquid methane (LCH4) and liquid oxygen (LOX). Four engines are used to provide redundancy and a satisfactory engine out capability. Differences between the new propulsion system and the original system include slightly smaller engine size and lower thrust per engine, although specific impulse remains the same despite the smaller size. Concerns over nozzle ground clearance and engine reliability, as well as more information from Pratt and Whitney, brought about this change. The power system consists of a combination of regenerative fuel cells and solar arrays. While the lander is in flight to or from the moon, or during the lunar night, fuel cells provide all electrical power. During the lunar day, solar arrays are deployed to provide electrical power for the lander as well as electrolyzers, which separate some water back into hydrogen and oxygen for later use by the fuel cells. Total storage requirements for oxygen, hydrogen, and water are 61 kg, 551 kg, and 360 kg, respectively. The lander is a stage-and-a-half design with descent propellant, cargo, and landing gear contained in the descent stage, and the main propulsion system, ascent propellant, and crew module contained in the ascent stage. The primary structure for both stages is a truss, to which all tanks and components are attached. The crew module is a conical shape similar to that of the Apollo Command Module, but significantly larger with a height and maximum diameter of six meters. Author (revised)

N94-25007*# West Virginia Univ., Morgantown. Dept. of Mechanical and Aerospace Engineering.
PRELIMINARY DESIGN OF A UNIVERSAL MARTIAN LANDER
Timothy L. Norman, David E. Gaskin, Sean Adkins, Mary Gunawan, Raquel Johnson, David MacDonnell, Andrew Parlock, John Sarick, Charles Bodwell, and Kouichi Hashimoto et al 1993 147 p
(Contract NASw-4435)
(NASA-CR-195529; NAS 1.26:195529) Avail: CASI HC A07/MF A02

In the next 25 years, mankind will be undertaking yet another giant leap forward in the exploration of the solar system: a manned mission to Mars. This journey will provide important information on the composition and history of both Mars and the Solar System. A manned mission will also provide the opportunity to study how humans can adapt to long term space flight conditions and the Martian environment. As part of the NASA/USRA program, nineteen West Virginia University students conducted a preliminary design of a manned Universal Martian Lander (UML). The UML's design will provide a 'universal' platform, consisting of four modules for living and laboratory experiments and a liquid-fuel propelled Manned Ascent Return Vehicle (MARV). The distinguishing feature of the UML is the 'universal' design of the modules which can be connected to form a network of laboratories and living quarters for future missions thereby reducing development and production costs. The WVU design considers descent to Mars from polar orbit, a six month surface stay, and ascent for rendezvous. The design begins with an unmanned UML landing at Elysium Mons followed by the manned UML landing nearby. During the six month surface stay, the eight modules will be assembled to form a Martian base where scientific experiments will be performed. The mission will also incorporate hydroponic plant growth into a Controlled Ecological Life Support System (CELSS) for water recycling, food production, and to counteract psychological effects of living on Mars. In situ fuel production for the MARV will be produced from gases in the Martian atmosphere. Following surface operations, the eight member crew will use the MARV to return to the Martian Transfer Vehicle (MTV) for the journey home to Earth. Author

N94-25523 Air Force Inst. of Tech., Wright-Patterson AFB, OH.
MODELING OF A LARGE UNDAMPED SPACE STRUCTURE USING TIME DOMAIN TECHNIQUES M.S. Thesis
Anthony R. Nash Dec. 1993 118 p Limited Reproducibility: More than 20% of this document may be affected by microfiche quality
(AD-A273828; AFIT/GA/ENY/93D-7) Avail: CASI HC A06

The first phase of this project was the selection of accurate time domain state space modeling techniques by comparing the models generated by various methods against a known system. The techniques selected were the Eigensystem Realization Algorithm and the Backward Least Squares method. These modeling techniques were applied to the vibration data from the PACOSS dynamic test article. The resulting model transfer function was then compared to the frequency response function of the actual system, and was found to be an accurate match for the system poles, but not for the system zeros. DTIC

N94-25532# Air Force Inst. of Tech., Wright-Patterson AFB, OH. School of Engineering.
STEADY MOTIONS OF RIGID BODY SATELLITES IN A CENTRAL GRAVITATIONAL FIELD M.S. Thesis
Cynthia A. Provost Dec. 1993 89 p
(AD-A273742; AFIT/GA/ENY/93D-8) Avail: CASI HC A05/MF A01

Numerous studies have been conducted on equilibrium orientations of objects moving under the influence of a central gravitational field. The results of many of these studies conclude that equilibrium conditions exist only when one of the principal axes coincides with the radius vector. Furthermore, these results assume that the center of force is located within the orbit plane, thereby tracing a great circle orbit. While these previous works have approximated the gravitational potential, this study examines relative equilibria obtained by retaining an exact expression for the potential of a spherical primary body, as shown in a recent paper by Wang, Maddocks, and Krishnaprasad. The exact dynamic equations for the motion of a finite rigid body in an inverse square gravitational force field are investigated. Only circular orbits for a specific satellite model consisting of six masses connected by three massless rigid rods are considered. The system dynamics are comprised of seven nonlinear equations, which were numerically solved on a Cray computer. The existence of equilibrium orientations which establish non-great circle orbits was verified and other interesting results were noted. The operational significance of these results was also examined. DTIC

N94-25542# Boston Coll., Chestnut Hill, MA. Inst. for Space Research.
THE CRRES TIME HISTORY DATA BASE: ALL SENSORS
Dennis E. Delorey 28 Jun. 1993 133 p
(Contract F19628-90-K-0028)
(AD-A273737; BC-ISR-03; PL-TR-93-2146) Avail: CASI HC A07/MF A02

The Combined Release and Radiation Effects Satellite (CRRES) carried a complement of sensors designed for Radiation Belt studies. This document details the CRRES Time History Data Base (THDB) file structures as well as the telemetry data and analysis used in the generation of the THDB files. The complete set of CRRES sensors for which THDB files were required are included in this manuscript. DTIC

N94-22742*# Telesat Canada, Gloucester (Ontario).
THE MSAT SPACECRAFT OF TELESAT MOBILE INC. Abstract Only
E. Bertenyi *In* JPL, Proceedings of the Third International Mobile Satellite Conference (IMSC 1993) 1993 p 41 (For primary document see N94-22735 06-32)
Avail: CASI HC A01/MF A06

N94-23259*# Jet Propulsion Lab., California Inst. of Tech., Pasadena. Tracking Systems and Applications Section.
IMPROVED THERMAL FORCE MODELING FOR GPS SATELLITES
Y. Vigue, R. E. Schutz (Texas Univ., Austin.), and P. A. M. Abusali (Texas Univ., Austin.) *In its* The Telecommunications and Data Acquisition Report 15 Nov. 1993 p 32-41 (For primary document see N94-23256 06-32)
(RTOP 310-10-61-84-02)
Avail: CASI HC A02/MF A02

N94-23596*# Science Applications International Corp., Glendora, CA. Space Technology Div.
THE POSSIBLE EFFECTS OF THE NATURAL AND INDUCED SPACE ENVIRONMENT ON THE OPTICAL AND THERMAL PROPERTIES OF EOS SURFACES
Carl R. Maag and Richard A. Heppner (Perkin-Elmer Corp., Pomona, CA.) *In* NASA. Goddard Space Flight Center, The Fifth Calibration/Data Product Validation Panel Meeting 1992 11 p (For primary document see N94-23595 06-43)
Avail: CASI HC A03/MF A04

N94-23653*# National Aeronautics and Space Administration. Wallops Flight Facility, Wallops Island, VA.
DEVELOPMENT AND APPLICATION OF AN EMPIRICAL PROBABILITY DISTRIBUTION FOR THE PREDICTION ERROR OF RE-ENTRY BODY MAXIMUM DYNAMIC PRESSURE
R. James Lanzi and Brett T. Vincent (Computer Sciences Corp., Wallops Island, VA.) *In* NASA. Lewis Research Center, The Fifth Annual Thermal and Fluids Analysis Workshop Nov. 1993 p 269-280 (For primary document see N94-23634 06-34)
Avail: CASI HC A03/MF A04; 5 functional color pages

N94-23654*# General Dynamics Corp., San Diego, CA. Space Systems Div.
PREDICTION OF THREE SIGMA MAXIMUM DISPERSED DENSITY FOR AEROSPACE APPLICATIONS
Terri L. Charles and Michael D. Nitschke *In* NASA. Lewis Research Center, The Fifth Annual Thermal and Fluids Analysis Workshop Nov. 1993 p 281-305 (For primary document see N94-23634 06-34)
Avail: CASI HC A03/MF A04; 5 functional color pages

N94-23860*# Tokyo Univ., Sagamihara (Japan). Inst. of Space and Astronautical Science.
GROUND DATA SYSTEM FOR SPACE FLYER UNIT (SFU)
Takahiro Yamada, Susumu Sasaki, and Keiken Ninomiya *In* JPL, SpaceOps 1992: Proceedings of the Second International Symposium on Ground Data Systems for Space Mission Operations 1 Mar. 1993 p 179-184 (For primary document see N94-23832 06-66)
Avail: CASI HC A02/MF A10

N94-23864*# Jet Propulsion Lab., California Inst. of Tech., Pasadena.
GALILEO SPACECRAFT ANOMALY AND SAFING RECOVERY
Ralph R. Basilio and David M. Durham *In its* SpaceOps 1992: Proceedings of the Second International Symposium on Ground Data Systems for Space Mission Operations 1 Mar. 1993 p 203-208 (For primary document see N94-23832 06-66)
Avail: CASI HC A02/MF A10

N94-23865*# Martin Marietta Corp., Denver, CO. Astronautics Group.
MAGELLAN SPACECRAFT AND MEMORY STATE TRACKING: LESSONS LEARNED, FUTURE THOUGHTS
Allen W. Bucher *In* JPL, SpaceOps 1992: Proceedings of the Second International Symposium on Ground Data Systems for Space Mission Operations 1 Mar. 1993 p 209-214 (For primary document see N94-23832 06-66)
Avail: CASI HC A02/MF A10

N94-23869*# BSO/Aerospace and Systems B.V., Nieuwegein (Netherlands).
INTEGRATING PAYLOAD DESIGN, PLANNING, AND CONTROL IN THE DUTCH UTILISATION CENTRE
T. J. Grant *In* JPL, SpaceOps 1992: Proceedings of the Second International Symposium on Ground Data Systems for Space Mission Operations 1 Mar. 1993 p 237-242 (For primary document see N94-23832 06-66)
Avail: CASI HC A02/MF A10

N94-23910*# National Space Development Agency, Tokyo (Japan). Tracking and Data Acquisition Dept.
VERIFICATION OF TECHNICAL ELEMENTS OF THE ADVANCED SPACECRAFT BASED UPON THE CCSDS RECOMMENDATION
Hideo Hara, Sigeo Yamada, Yoshikatsu Yamamoto, Seiichi Fujii (Fujitsu Ltd., Tokyo, Japan.), Kaoru Tumura (Fujitsu Ltd., Tokyo, Japan.), Masato Yokomizo (Fujitsu Ltd., Tokyo, Japan.), and Hiroyuki Ogasawara (Fujitsu Ltd., Tokyo, Japan.) *In* JPL, SpaceOps 1992: Proceedings of the Second International Symposium on Ground Data Systems for Space Mission Operations 1 Mar. 1993 p 519-524 (For primary document see N94-23832 06-66)
Avail: CASI HC A02/MF A10

N94-23995# British Aerospace Public Ltd. Co., Bristol (England).
PRIMARY DEPLOYMENT MECHANISM FOR THE EUROPEAN POLAR PLATFORM
S. C. Burgess and M. E. Humphries *In* ESA, The Fifth European Space Mechanisms and Tribology Symposium Apr. 1993 6 p (For primary document see N94-23985 06-37)
Copyright Avail: CASI HC A02/MF A04

N94-24017# European Space Agency. European Space Research and Technology Center, ESTEC, Noordwijk (Netherlands).
NUMERICAL SIMULATION OF ULYSSES NUTATION
C. GarciaMarirrodriga, J. Zeischka (LMS International, Leuven, Belgium.), and E. C. Boslooper (Fokker Space and Systems, Amsterdam, Netherlands.) *In its* The Fifth European Space Mechanisms and Tribology Symposium Apr. 1993 8 p (For primary document see N94-23985 06-37)
Copyright Avail: CASI HC A02/MF A04

N94-24018# Southampton Univ. (England). Inst. of Sound and Vibration Research.
SPACECRAFT VIBRATIONS DUE TO MECHANISMS; MEASUREMENTS FROM OLYMPUS ON-STATION
N. S. Ferguson, J. N. Pinder, and D. E. L. Tunbridge (European Space Agency. European Space Research and Technology Center, ESTEC, Noordwijk, Netherlands.) *In* ESA, The Fifth European Space Mechanisms and Tribology Symposium Apr. 1993 7 p Sponsored by ESTEC

(For primary document see N94-23985 06-37)
Copyright Avail: CASI HC A02/MF A04

N94-24022# Ithaco, Inc., Ithaca, NY.
A COMBINED EARTH SCANNER AND MOMENTUM WHEEL FOR ATTITUDE DETERMINATION AND CONTROL OF SMALL SPACECRAFT
Bill Bialke *In* ESA, The Fifth European Space Mechanisms and Tribology Symposium Apr. 1993 6 p (For primary document see N94-23985 06-37)
Copyright Avail: CASI HC A02/MF A04

N94-24256 Academy of Sciences (USSR), Alma-Ata. Mechanical Engineering Research Institute.
NEARLY UNIFORM DEPLOYMENT/RETRIEVAL STRATEGY FOR SPACE TETHER SYSTEMS
E. M. Levin *In* Israel Society of Aeronautics and Astronautics, The 33rd Israel Annual Conference on Aviation and Astronautics 25 Feb. 1993 p 185-195 (For primary document see N94-24241 06-01)
Copyright Avail: Issuing Activity (Israel Society of Aeronautics and Astronautics, c/o Faculty of Engineering, Tel-Aviv Univ., Ramat Aviv 69978, Israel)

N94-24271 Israel Aircraft Industries Ltd., Yehud. MBT - Systems and Space Technology.
REACTIVE THRUST CRUISE FOR A GEOSYNCHRONOUS SATELLITE WITH MINIMUM FUEL CONSUMPTION
Marcel Sidi *In* Israel Society of Aeronautics and Astronautics, The 33rd Israel Annual Conference on Aviation and Astronautics 25 Feb. 1993 p 333-338 (For primary document see N94-24241 06-01)
Copyright Avail: Issuing Activity (Israel Society of Aeronautics and Astronautics, c/o Faculty of Engineering, Tel-Aviv Univ., Ramat Aviv 69978, Israel)

N94-24272 Israel Aircraft Industries Ltd., Yehud. System and Space Technology.
MOMENTUM MANAGEMENT AND TORQUE DISTRIBUTION
Ruth Azor *In* Israel Society of Aeronautics and Astronautics, The 33rd Israel Annual Conference on Aviation and Astronautics 25 Feb. 1993 p 339-347 (For primary document see N94-24241 06-01)
Copyright Avail: Issuing Activity (Israel Society of Aeronautics and Astronautics, c/o Faculty of Engineering, Tel-Aviv Univ., Ramat Aviv 69978, Israel)

N94-24449*# Pennsylvania State Univ., University Park. Dept. of Aerospace Engineering.
TORQUE EQUILIBRIUM ATTITUDES FOR THE SPACE STATION
Roger C. Thompson *In* Alabama Univ., The 1993 NASA/ASEE Summer Faculty Fellowship Program Nov. 1993 5 p (For primary document see N94-24405 06-80)
Avail: CASI HC A01/MF A03

N94-24873*# California Inst. of Tech., Pasadena.
OPTIMAL GAINS FOR A SINGLE POLAR ORBITING SATELLITE Abstract Only
Don Banfield, A. P. Ingersoll, and C. L. Keppenne (Jet Propulsion Lab., California Inst. of Tech., Pasadena.) *In* Lunar and Planetary Inst., Workshop on Atmospheric Transport on Mars 1993 p 5-6 (For primary document see N94-24871 06-91)
Avail: CASI HC A01/MF A01

N94-25383*# Cincinnati Univ., OH. Dept. of Aerospace Engineering.
SPACE STATION FLEXIBLE DYNAMICS UNDER PLUME IMPINGEMENT
Trevor Williams *In* NASA. Johnson Space Center, National Aeronautics and Space Administration (NASA)/American Society for Engineering Education (ASEE) Summer Faculty Fellowship Program, 1993, Volume 2 Dec. 1993 14 p (For primary document see N94-25367 06-99)
Avail: CASI HC A03/MF A03

19 SPACECRAFT INSTRUMENTATION

For related information see also *06 Aircraft Instrumentation* and *35 Instrumentation and Photography.*

N94-23478* National Aeronautics and Space Administration. Goddard Space Flight Center, Greenbelt, MD.
INSTRUMENT INTERFACE DESCRIPTION FOR NOAA 2000 INSTRUMENTS WITH EUROPEAN MORNING SPACECRAFT AND/OR NOAA-OPQ SPACECRAFT Interim Report
10 Aug. 1993 68 p Sponsored in part by NOAA and National Environmental Satellite Data and Information Service, Suitland, MD Limited Reproducibility: More than 20% of this document may be affected by microfiche quality
(NASA-TM-109406; GSFC-S-480-53-Rev-B; NAS 1.15:109406; PB93-227023) Avail: CASI HC A04

The purpose is to describe at a high level the common interface provisions and constraints placed on the NOAA-2000 instruments and the interfacing spacecraft elements in the following areas: electrical interface, mechanical interface, thermal interface, magnetic interface, electromagnetic compatibility, structural/mechanical environmental interface, contamination control, and the ionizing radiation environment. The requirements reflect the fact that these instruments must be compatible with a number of different polar orbiting satellite vehicles including the NOAA-OPQ satellites and the EUMETSAT METOP satellites. NTIS

N94-23479* National Aeronautics and Space Administration. Goddard Space Flight Center, Greenbelt, MD.
COMMAND/TELEMETRY BUS GENERAL SPECIFICATION FOR THE NOAA-OPQ POLAR ORBITING ENVIRONMENTAL SATELLITES AND EUMETSAT POLAR SATELLITE SYSTEMS
14 Jul. 1993 60 p See also PB93-227056 and PB93-227049 Sponsored in part by NOAA and National Environmental Satellite Data and Information Service, Suitland, MD Limited Reproducibility: More than 20% of this document may be affected by microfiche quality
(NASA-TM-109407; GSFC-S-480-72; NAS 1.15:109407; PB93-227031)
Avail: CASI HC A04

The document is a reference document in the Instrument Interface Description for NOAA-2000 Instruments (GSFC-S-480-53). The requirements reflect the fact that these instruments must be compatible with a number of different polar orbiting satellite vehicles including the NOAA-OPQ satellites and the EUMETSAT METOP satellites. The instrument payload will interface to the spacecraft via several standardized communication busses. The document defines the multiplex data bus conforming to the MIL-STD-1553B protocol for command and telemetry transfer between a spacecraft system and all instruments. NTIS

N94-23480* National Aeronautics and Space Administration. Goddard Space Flight Center, Greenbelt, MD.
LOW RATE DATA BUS GENERAL SPECIFICATION FOR THE NOAA-OPQ POLAR ORBITING ENVIRONMENTAL SATELLITES AND EUMETSAT POLAR SATELLITE SYSTEMS Interim Report
14 Jul. 1993 59 p See also PB93-227031 and PB93-227056 Sponsored in part by NOAA and National Environmental Satellite Data and Information Service, Suitland, MD Limited Reproducibility: More than 20% of this document may be affected by microfiche quality
(NASA-TM-109408; GSFC-S-480-73; NAS 1.15:109408; PB93-227049)
Avail: Issuing Activity (National Technical Information Service (NTIS))

The document is a reference document in the Instrument Interface Description for NOAA-2000 Instruments (GSFC-S-480-53). The requirements reflect the fact that these instruments must be compatible with a number of different polar orbiting satellite vehicles including the NOAA-OPQ satellites and the EUMETSAT METOP satellites. NTIS

N94-23481* National Aeronautics and Space Administration. Goddard Space Flight Center, Greenbelt, MD.
HIGH-RATE DATA LINK GENERAL SPECIFICATION FOR THE NOAA-OPQ POLAR ORBITING ENVIRONMENTAL SATELLITES AND EUMETSAT SATELLITE SYSTEMS Interim Report
14 Jul. 1993 60 p See also PB93-227031 and PB93-227049 Sponsored in part by NOAA and National Environmental Satellite Data Information Service, Suitland, MD Limited Reproducibility: More than 20% of this

document may be affected by microfiche quality
(NASA-TM-109384; GSFC-S-480-74; NAS 1.15:109384; PB93-227056)
Avail: Issuing Activity (National Technical Information Service (NTIS))

The document is a reference document in the Instrument Interface Description for NOAA-2000 Instruments (GSFC-S-480-53). The requirements reflect the fact that these instruments must be compatible with a number of different polar orbiting satellite vehicles including the NOAA-OPQ satellites and the EUMETSAT METOP satellites. The instrument payload will interface to the spacecraft via several standardized communication busses. The document defines a uni-directional point-to-point single-user interface for transfer of high rate data (greater than 100 kbs) between instruments and a spacecraft system. NTIS

N94-23484*# Southwest Research Inst., San Antonio, TX.
[PULSAUR 2] Interim Status Report
Jim Sharber and John Scherrer 1 Dec. 1993 11 p
(Grant NAG5-671; SwRI Proj. 15-3822)
(NASA-CR-194832; NAS 1.26:194832) Avail: CASI HC A03/MF A01

PULSAUR II is a sounding rocket experiment to investigate the pulsating aurora and related phenomena. The payload consists of a complementary set of instruments designed specifically to look at the pulsating aurora. The project will be managed by the Norwegian Space Center, with integration in Norway. The rocket is due for launch in January 1994 from the Andoya rocket range. Southwest Research Institute provided an electron sensor for this campaign. It is a 'top hat' electron spectrometer, referred to as AREA (Angle Resolving Energy Analyzer), and is based on the electron sensor developed for the CENTAUR mission. Author (revised)

N94-24767*# TRW, Inc., Redondo Beach, CA.
HIGH ENERGY COLLIMATING FINE GRIDS FOR HESP PROGRAM Final Report
Carol D. Eberhard and Edward Frazier Dec. 1993 36 p
(Contract NAS5-32529)
(NASA-CR-189317; NAS 1.26:189317) Avail: CASI HC A03/MF A01

There is a need to develop fine pitch x-ray collimator grids as an enabling technology for planned future missions. The grids consist of an array of thin parallel strips of x-ray absorbing material, such as tungsten, with pitches ranging from 34 microns to 2.036 millimeters. The grids are the key components of a new class of spaceborne instruments known as 'x-ray modulation collimators.' These instruments are the first to produce images of celestial sources in the hard x-ray and gamma-ray spectral regions. Author (revised)

N94-24840*# Texas Univ., Austin. Dept. of Aerospace Engineering and Engineering Mechanics.
PRELIMINARY DESIGN OF A SATELLITE OBSERVATION SYSTEM FOR SPACE STATION FREEDOM Final Report
Greg Cabe, ed., Chris Gallagher, Brian Wilson, James Rehfeld, Alexa Maurer, Dan Stern, Jaime Nualart, and Xuan-Trang Le 10 Dec. 1992 173 p
(Contract NASw-4435)
(NASA-CR-195514; NAS 1.26:195514) Avail: CASI HC A08/MF A02

Degobah Satellite Systems (DSS), in cooperation with the University Space Research Association (USRA), NASA - Johnson Space Center (JSC), and the University of Texas, has completed the preliminary design of a satellite system to provide inexpensive on-demand video images of all or any portion of Space Station Freedom (SSF). DSS has narrowed the scope of the project to complement the work done by Mr. Dennis Wells at Johnson Space Center. This three month project has resulted in completion of the preliminary design of AERCAM, the Autonomous Extravehicular Robotic Camera, detailed in this design report. This report begins by providing information on the project background, describing the mission objectives, constraints, and assumptions. Preliminary designs for the primary concept and satellite subsystems are then discussed in detail. Included in the technical portion of the report are detailed descriptions of an advanced imaging system and docking and safing systems that ensure compatibility with the SSF. The report concludes by describing management procedures and project costs. Derived from text

N94-24006# Technische Physische Dienst TNO-TH, Delft (Netherlands).
THE PRE-DEVELOPMENT OF THE ARISTOTELES CALIBRATION MECHANISM
B. C. Braam, M. P. Koster (Universiteit Twente, Enschede, Netherlands.), H. Bokhove, J. Hopman, W. M. G. Courage (Organisatie voor Toegepast Natuurwetenschappelijk Onderzoek, Delft, Netherlands.), G. Hijkoop (Organisatie voor Toegepast Natuurwetenschappelijk Onderzoek, Delft, Netherlands.), M. Aguirre (European Space Agency. European Space Research and Technology Center, ESTEC, Noordwijk, Netherlands.), and A. Robinson (European Space Agency. European Space Research and Technology Center, ESTEC, Noordwijk, Netherlands.) *In* ESA, The Fifth European Space Mechanisms and Tribology Symposium Apr. 1993 8 p (For primary document see N94-23985 06-37)
Copyright Avail: CASI HC A02/MF A04

N94-24038# BEI Motion Systems Co., Little Rock, AR. Precision Systems and Space Div.
HIGH RESOLUTION ENCODER-MOTOR USED IN THE ORBITAL SPIN SCAN RADIOMETER, GOES VAS SATELLITES
John M. Jumper *In* ESA, The Fifth European Space Mechanisms and Tribology Symposium Apr. 1993 6 p (For primary document see N94-23985 06-37)
Copyright Avail: CASI HC A02/MF A04

N94-24453*# Alabama Univ., Huntsville. Dept. of Physics and Center for Space Plasma and Aeronomic Research.
THE FAR ULTRAVIOLET (FUV) AURORAL IMAGER FOR THE INNER MAGNETOSPHERIC IMAGER (IMI) MISSION: OPTIONS
Gordon R. Wilson *In its* The 1993 NASA/ASEE Summer Faculty Fellowship Program Nov. 1993 5 p (For primary document see N94-24405 06-80)
Avail: CASI HC A01/MF A03

20 SPACECRAFT PROPULSION AND POWER

Includes main propulsion systems and components, e.g., rocket engines; and spacecraft auxilliary power sources.

For related information see also *07 Aircraft Propulsion and Power, 28 Propellants and Fuels, 44 Energy Production and Conversion,* and *15 Launch Vehicles and Space Vehicles.*

N94-23012 Lawrence Livermore National Lab., CA.
ANALYSIS AND EXPERIMENTS OF A WHISTLER-WAVE PLASMA THRUSTER
E. B. Hooper, S. W. Ferguson, M. A. Makowski, B. W. Stallard, and J. L. Power (National Aeronautics and Space Administration. Lewis Research Center, Cleveland, OH.) Aug. 1993 8 p Presented at the 23rd International Electric Propulsion Conference, Seattle, WA, 13-16 Sep. 1993 Limited Reproducibility: More than 20% of this document may be affected by microfiche quality
(Contract W-7405-eng-48)
(DE94-001533; UCRL-JC-114643; CONF-930948-1) Avail: CASI HC A02

A plasma thruster operating at high specific impulse (greater than or equal to 3500 s) has been proposed to be based on electron-cyclotron resonance heating of whistler waves propagating on a plasma column on a magnetic hill. Calculations using a particle-in-cell code demonstrate that the distortion of the electron velocity distribution by the heating significantly reduces the flow of plasma up the field, greatly improving efficiency and reducing material interactions relative to a thermal plasma. These and other calculations are presented together with initial experiments on the plasma generated in the proposed device. The experiments are conducted in a magnetic field (3.3 x 10(exp -2) T at resonance) and a magnetic mirror ratio of 5. Microwaves (0.915 GHz, less than 20 kW) are coupled to the plasma with a helical antenna. Vacuum field measurements are in good agreement with prediction. The desired plasma spatial distribution has not yet been achieved. DOE

N94-23028*# Pennsylvania State Univ., University Park.
NASA PROPULSION ENGINEERING RESEARCH CENTER, VOLUME 2 Annual Report
Nov. 1993 223 p Presented at the 5th Annual Propulsion Engineering Research Center Symposium, University Park, PA, 8-9 Sep. 1993
(Grant NAGw-1356)
(NASA-CR-194719-Vol-2; NAS 1.26:194719-Vol-2) Avail: CASI HC A10/MF A03

On 8-9 Sep. 1993, the Propulsion Engineering Research Center (PERC) at The Pennsylvania State University held its Fifth Annual Symposium. PERC was initiated in 1988 by a grant from the NASA Office of Aeronautics and Space Technology as a part of the University Space Engineering Research Center (USERC) program; the purpose of the USERC program is to replenish and enhance the capabilities of our Nation's engineering community to meet its future space technology needs. The Centers are designed to advance the state-of-the-art in key space-related engineering disciplines and to promote and support engineering education for the next generation of engineers for the national space program and related commercial space endeavors. Research on the following areas was initiated: liquid, solid, and hybrid chemical propulsion, nuclear propulsion, electrical propulsion, and advanced propulsion concepts. For individual titles, see N94-23029 through N94-23071.

N94-23029*# Pennsylvania State Univ., University Park. Propulsion Engineering Research Center and Dept. of Mechanical Engineering.

MEASUREMENT OF INTACT-CORE LENGTH OF ATOMIZING LIQUID JETS BY IMAGE DECONVOLUTION c34

Roger Woodward, Robert Burch, Kenneth Kuo, and Fan-Bill Cheung *In its* NASA Propulsion Engineering Research Center, Volume 2 Nov. 1993 p 1-4 (For primary document see N94-23028 06-20)
Avail: CASI HC A01/MF A03

The investigation of liquid jet breakup and spray development is critical to the understanding of combustion phenomena in liquid propellant rocket engines. Much work has been done to characterize low-speed liquid jet breakup and dilute sprays, but atomizing jets and dense sprays have yielded few quantitative measurements due to their high liquid load fractions and hence their optical opacity. Focus was on a characteristic of the primary breakup process of round liquid jets, namely the length of the intact-liquid core. The specific application considered is that of shear-coaxial-type rocket engine injectors in which liquid oxygen is injected through the center post while high velocity gaseous hydrogen is injected through a concentric annulus, providing a shear force to the liquid jet surface. Real-time x ray radiography, capable of imaging through the dense two-phase region surrounding the liquid core, is used to make the measurements. The intact-liquid-core length data were obtained and interpreted using two conceptually different methods to illustrate the effects of chamber pressure, gas-to-liquid momentum ratio, and cavitation. Author (revised)

N94-23030*# National Aeronautics and Space Administration. Lewis Research Center, Cleveland, OH.

SMALL ROCKET FLOWFIELD DIAGNOSTIC CHAMBERS

Sybil Morren and Brian Reed *In* Pennsylvania State Univ., NASA Propulsion Engineering Research Center, Volume 2 Nov. 1993 p 5-11 (For primary document see N94-23028 06-20)
Avail: CASI HC A02/MF A03

Instrumented and optically-accessible rocket chambers are being developed to be used for diagnostics of small rocket (less than 440 N thrust level) flowfields. These chambers are being tested to gather local fluid dynamic and thermodynamic flowfield data over a range of test conditions. This flowfield database is being used to better understand mixing and heat transfer phenomena in small rockets, influence the numerical modeling of small rocket flowfields, and characterize small rocket components. The diagnostic chamber designs include: a chamber design for gathering wall temperature profiles to be used as boundary conditions in a finite element heat flux model; a chamber design for gathering inner wall temperature and static pressure profiles; and optically-accessible chamber designs, to be used with a suite of laser-based diagnostics for gathering local species concentration, temperature, density, and velocity profiles. These chambers were run with gaseous hydrogen/gaseous oxygen (GH_2/GO_2) propellants, while subsequent versions will be run on liquid oxygen/hydrocarbon (LOX/HC) propellants. The purpose, design, and initial test results of these small rocket flowfield diagnostic chambers are summarized. Author (revised)

N94-23031*# Pennsylvania State Univ., University Park. Propulsion Engineering Research Center and Dept. of Mechanical Engineering.

A THEORETICAL EVALUATION OF ALUMINUM GEL PROPELLANT TWO-PHASE FLOW LOSSES ON VEHICLE PERFORMANCE

Donn C. Mueller and Stephen R. Turns *In its* NASA Propulsion Engineering Research Center, Volume 2 Nov. 1993 p 12-16 (For primary document see N94-23028 06-20)
Avail: CASI HC A01/MF A03

A one-dimensional model of a hydrocarbon/Al/O_2(gaseous) fueled rocket combustion chamber was developed to study secondary atomization effects on propellant combustion. This chamber model was coupled with a two dimensional, two-phase flow nozzle code to estimate the two-phase flow losses associated with solid combustion products. Results indicate that moderate secondary atomization significantly reduces propellant burnout distance and Al_2O_3 particle size; however, secondary atomization provides only moderate decreases in two-phase flow induced I(sub sp) losses. Despite these two-phase flow losses, a simple mission study indicates that aluminum gel propellants may permit a greater maximum payload than the hydrocarbon/O_2 bi-propellant combination for a vehicle of fixed propellant volume. Secondary atomization was also found to reduce radiation losses from the solid combustion products to the chamber walls, primarily through reductions in propellant burnout distance. Author (revised)

N94-23032*# National Aeronautics and Space Administration. Lewis Research Center, Cleveland, OH.

LASER DIAGNOSTICS FOR SMALL ROCKETS

Frank J. Zupanc and Wilhelmus A. deGroot (Sverdrup Technology, Inc., Cleveland, OH.) *In* Pennsylvania State Univ., NASA Propulsion Engineering Research Center, Volume 2 Nov. 1993 p 17-22 (For primary document see N94-23028 06-20)
Avail: CASI HC A02/MF A03

Two nonintrusive flowfield diagnostics based on spectrally-resolved elastic (Rayleigh) and inelastic (Raman) laser light scattering were developed for obtaining local flowfield measurements in low-thrust gaseous H_2/O_2 rocket engines. The objective is to provide an improved understanding of phenomena occurring in small chemical rockets in order to facilitate the development and validation of advanced computational fluid dynamics (CFD) models for analyzing engine performance. The laser Raman scattering diagnostic was developed to measure major polyatomic species number densities and rotational temperatures in the high-density flowfield region extending from the injector through the chamber throat. Initial application of the Raman scattering diagnostic provided O_2 number density and rotational temperature measurements in the exit plane of a low area-ratio nozzle and in the combustion chamber of a two-dimensional, optically-accessible rocket engine. In the low-density nozzle exit plane region where the Raman signal is too weak, a Doppler-resolved laser Rayleigh scattering diagnostic was developed to obtain axial and radial mean gas velocities, and in certain cases, H_2O translational temperature and number density. The results from these measurements were compared with theoretical predictions from the RPLUS CFD code for analyzing rocket engine performance. Initial conclusions indicate that a detailed and rigorous modeling of the injector is required in order to make direct comparisons between laser diagnostic measurements and CFD predictions at the local level. Author (revised)

N94-23033*# Pennsylvania State Univ., University Park. Propulsion Engineering Research Center and Dept. of Mechanical Engineering.

CFD ANALYSES OF COMBUSTOR AND NOZZLE FLOWFIELDS

Hsin-Hua Tsuei and Charles L. Merkle *In its* NASA Propulsion Engineering Research Center, Volume 2 Nov. 1993 p 23-27 (For primary document see N94-23028 06-20)
Avail: CASI HC A01/MF A03

The objectives of the research are to improve design capabilities for low thrust rocket engines through understanding of the detailed mixing and combustion processes. A Computational Fluid Dynamic (CFD) technique is employed to model the flowfields within the combustor, nozzle, and near plume field. The computational modeling of the rocket engine flowfields requires the application of the complete Navier-Stokes equations, coupled with species diffusion equations. Of particular interest is a small gaseous hydrogen-oxygen thruster which is considered as a coordinated part of an ongoing experimental program at NASA LeRC. The numerical procedure is performed on both time-marching and time-accurate algorithms, using an LU approximate factorization in time, flux split upwinding differencing in space. The integrity of fuel film cooling along the wall, its effectiveness in the mixing with the core flow including unsteady large scale effects, the resultant impact on performance and the assessment of the near plume

flow expansion to finite pressure altitude chamber are addressed.
Author (revised)

N94-23034*# Pennsylvania State Univ., University Park. Propulsion Engineering Research Center and Dept. of Mechanical Engineering.
LOX DROPLET VAPORIZATION IN A SUPERCRITICAL FORCED CONVECTIVE ENVIRONMENT **c34**
Chia-Chun Hsiao and Vigor Yang *In its* NASA Propulsion Engineering Research Center, Volume 2 Nov. 1993 p 28-32 (For primary document see N94-23028 06-20)
Avail: CASI HC A01/MF A03

Modern liquid rocket engines often use liquid oxygen (LOX) and liquid hydrogen (LH2) as propellants to achieve high performance, with the engine operational conditions in the supercritical regimes of the propellants. Once the propellant exceeds its critical state, it essentially becomes a puff of dense fluid. The entire field becomes a continuous medium, and no distinct interfacial boundary between the liquid and gas exists. Although several studies have been undertaken to investigate the supercritical droplet behavior at quiescent conditions, very little effort has been made to address the fundamental mechanisms associated with LOX droplet vaporization in a supercritical, forced convective environment. The purpose is to establish a theoretical framework within which supercritical droplet dynamics and vaporization can be studied systematically by means of an efficient and robust numerical algorithm. Author (revised)

N94-23035*# Pennsylvania State Univ., University Park. Propulsion Engineering Research Center and Dept. of Mechanical Engineering.
EVAPORATION AND COMBUSTION OF LOX UNDER SUPERCRITICAL AND SUBCRITICAL CONDITIONS **c25**
A. S. Yang, W. H. Hsieh, and K. K. Kuo *In its* NASA Propulsion Engineering Research Center, Volume 2 Nov. 1993 p 33-38 (For primary document see N94-23028 06-20)
Avail: CASI HC A02/MF A03

The objective is to study the evaporation and combustion of LOX under supercritical and subcritical conditions both experimentally and theoretically. In the evaporation studies, evaporation rate and surface temperature were measured when LOX vaporizing in helium environments at pressures ranging from 5 to 68 atm. A Varian 3700 gas chromatograph was employed to measure the oxygen concentration above the LOX surface. For the combustion tests, high-magnification video photography was used to record direct images of the flame shape of a LOX/H2/He laminar diffusion flame. The gas composition in the post-flame region is also being measured with the gas sampling and chromatography analysis. These data are being used to validate the theoretical model. A comprehensive theoretical model with the consideration of the solubility of ambient gases as well as variable thermophysical properties was formulated and solved numerically to study the gasification and burning of LOX at elevated pressures. The calculated flame shape agreed reasonably well with the edge of the observed luminous flame surface. The effect of gravity on the flame structure of laminar diffusion flames was found to be significant. In addition, the predicted results using the flame-sheet model were compared with those based upon full equilibrium calculations (which considered the formation of intermediate species) at supercritical pressures. Except at the flame front where temperature exceeded 2,800 K, the flame-sheet and equilibrium solutions in terms of temperature distributions were in very close agreement. The temperature deviation in the neighborhood of the flame front is caused by the effect of high-temperature dissociation. Author (revised)

N94-23036*# Pennsylvania State Univ., University Park.
DROPLET TURBULENCE INTERACTIONS UNDER SUBCRITICAL AND SUPERCRITICAL CONDITIONS **c34**
E. B. Coy, S. C. Greenfield, M. S. Ondas, Y.-H. Song, T. D. Spegar, and D. A. Santavicca *In its* NASA Propulsion Engineering Research Center, Volume 2 Nov. 1993 p 39-45 (For primary document see N94-23028 06-20)
Avail: CASI HC A02/MF A03

The goal of this research is to experimentally characterize the behavior of droplets in vaporizing liquid sprays under conditions typical of those encountered in high pressure combustion systems such as liquid fueled rocket engines. Of particular interest are measurements of droplet drag, droplet heating, droplet vaporization, droplet distortion, and secondary droplet breakup, under both subcritical and supercritical conditions. The paper presents a brief description of the specific accomplishments which have been made over the past year. Author (revised)

N94-23037*# National Aeronautics and Space Administration. Marshall Space Flight Center, Huntsville, AL.
SSME FUEL PREBURNER INJECTOR CHARACTERIZATION
John J. Hutt *In* Pennsylvania State Univ., NASA Propulsion Engineering Research Center, Volume 2 Nov. 1993 p 46-49 (For primary document see N94-23028 06-20)
Avail: CASI HC A01/MF A03

A project has been initiated at the Marshall Space Flight Center to determine if preburner inter- or intra-element mixture ratio maldistributions are the cause of temperature variations in the Space Shuttle Main Engine (SSME) High Pressure Fuel Turbopump (HPFTP) turbine inlet region. Temperature nonuniformity may contribute to the many problems experienced in this region. The project will involve high pressure cold-flow testing and Computational Fluid Dynamics (CFD) modeling. Author (revised)

N94-23038*# National Aeronautics and Space Administration. Lewis Research Center, Cleveland, OH.
SMALL ROCKET RESEARCH AND TECHNOLOGY
Steven Schneider and James Biaglow *In* Pennsylvania State Univ., NASA Propulsion Engineering Research Center, Volume 2 Nov. 1993 p 50-53 (For primary document see N94-23028 06-20)
Avail: CASI HC A01/MF A03

Small chemical rockets are used on nearly all space missions. The small rocket program provides propulsion technology for civil and government space systems. Small rocket concepts are developed for systems which encompass reaction control for launch and orbit transfer systems, as well as on-board propulsion for large space systems and earth orbit and planetary spacecraft. Major roles for on-board propulsion include apogee kick, delta-V, de-orbit, drag makeup, final insertions, north-south stationkeeping, orbit change/trim, perigee kick, and reboost. The program encompasses efforts on earth-storable, space storable, and cryogenic propellants. The earth-storable propellants include nitrogen tetroxide (NTO) as an oxidizer with monomethylhydrazine (MMH) or anhydrous hydrazine (AH) as fuels. The space storable propellants include liquid oxygen (LOX) as an oxidizer with hydrazine or hydrocarbons such as liquid methane, ethane, and ethanol as fuels. Cryogenic propellants are LOX or gaseous oxygen (GOX) as oxidizers and liquid or gaseous hydrogen as fuels. Improved performance and lifetime for small chemical rockets are sought through the development of new predictive tools to understand the combustion and flow physics, the introduction of high temperature materials to eliminate fuel film cooling and its associated combustion inefficiency, and improved component designs to optimize performance. Improved predictive technology is sought through the comparison of both local and global predictions with experimental data. Results indicate that modeling of the injector and combustion process in small rockets needs improvement. High temperature materials require the development of fabrication processes, a durability data base in both laboratory and rocket environments, and basic engineering property data such as strength, creep, fatigue, and work hardening properties at both room and elevated temperature. Promising materials under development include iridium-coated rhenium and a ceramic composite of mixed hafnium carbide and tantalum carbide reinforced with graphite fibers.
Author (revised)

N94-23039*# Phillips Lab., Edwards AFB, CA.
FUNDAMENTAL ROCKET INJECTOR/SPRAY PROGRAMS AT THE PHILLIPS LABORATORY
D. G. Talley *In* Pennsylvania State Univ., NASA Propulsion Engineering Research Center, Volume 2 Nov. 1993 p 54-57 (For primary document see N94-23028 06-20)
Avail: CASI HC A01/MF A03

The performance and stability of liquid rocket engines is determined to a large degree by atomization, mixing, and combustion processes. Control over these processes is exerted through the design of the injector. Injectors in liquid rocket engines are called upon to perform many functions. They must first of all mix the propellants to provide suitable performance in the shortest possible length. For main injectors, this is driven by the tradeoff between the combustion chamber performance, stability, efficiency, and its weight and cost. In gas generators and preburners, however, it is also driven by the possibility of damage to downstream components, for example piping and turbine blades. This can occur if unburned fuel and oxidant later react to create hot spots. Weight and cost considerations require that the injector design be simple and lightweight. For reusable engines, the injectors must also be durable and easily maintained. Suitable atomization and mixing must be produced with as small a pressure drop as possible, so that the size and weight of pressure vessels and turbomachinery can be minimized. However, the pressure drop must not be so small as to promote feed system coupled instabilities. Another important function of the injectors is to ensure that the injector face plate and the chamber and nozzle walls are not damaged. Typically this requires reducing the heat transfer to an acceptable level and also keeping unburned oxygen from chemically attacking the walls, particularly in reusable engines. Therefore the mixing distribution is often tailored to be fuel-rich near the walls. Wall heat transfer can become catastrophically damaging in the presence of acoustic instabilities, so the injector must prevent these from occurring at all costs. In addition to acoustic stability (but coupled with it), injectors must also be kinetically stable. That is, the flame itself must maintain ignition in the combustion chamber. This is not typically a problem with main injectors, but can be a consideration in preburners, where the desire to keep turbine inlet temperatures as cool as possible can make it advantageous for the preburners to operate as far from stoichiometry as can be tolerated. For some missions such as single stage to orbit, all of the above requirements must be maintained over a throttleable range, for example 5:1 to 10:1. Finally, the injectors must be ignitable during startup where pressures and temperatures are far from design conditions, and ignition transients must be minimized in order to avoid damage to engine components. In order to satisfy these various constraints, the injector designer must be able to perform design tradeoff studies, and it is important that this be done with minimal time and costs. In fact, it can easily be argued that reducing engine development time and costs is essential to maintaining U.S. competitiveness in space. The Propulsion Directorate of the Phillips Laboratory has invested in a number of programs to advance liquid rocket engine technology, and several of these are directed at improving design tools for liquid rocket injectors. The purpose of the presentation will be to describe some of these latter programs.

Derived from text

N94-23040*# Pennsylvania State Univ., University Park. Propulsion Engineering Research Center and Dept. of Mechanical Engineering.

AN EXPERIMENTAL STUDY OF CHARACTERISTIC COMBUSTION-DRIVEN FLOWS FOR CFD VALIDATION

S. Pal, J. J. Merenich, M. D. Moser, and R. J. Santoro *In its* NASA Propulsion Engineering Research Center, Volume 2 Nov. 1993 p 58-63
(For primary document see N94-23028 06-20)
Avail: CASI HC A02/MF A03

The application of laser-based diagnostic techniques has become commonplace to a wide variety of combustion problems. New insights into combustion phenomena at a level previously unattainable has been made possible by non-intrusive measurements of velocity, temperature, and species. However, due to the adverse conditions which exist inside rocket engines, relatively few studies have addressed these combustion environments. The high pressure, high speed, combusting environment in a rocket engine prohibits the application of several measurement techniques. However, in the rocket community, there is a critical need for rocket flow field data to validate computational fluid dynamic (CFD) codes. Currently at Penn State, there is an effort to obtain flowfield measurements inside a rocket engine. Velocity measurements have been made inside the combustion chamber of a uni-element (shear coaxial injector) optically accessible rocket chamber at several axial locations downstream of the injector. These measurements, combined with future measurements, will provide benchmark data for CFD code validation. Author (revised)

N94-23041*# Computational Fluid Dynamics Research Corp., Huntsville, AL.

NUMERICAL PARAMETRIC STUDIES OF SPRAY COMBUSTION INSTABILITY **c25**

M. Z. Pindera *In* Pennsylvania State Univ., NASA Propulsion Engineering Research Center, Volume 2 Nov. 1993 p 64-68 (For primary document see N94-23028 06-20)
Avail: CASI HC A01/MF A03

A coupled numerical algorithm has been developed for studies of combustion instabilities in spray-driven liquid rocket engines. The model couples gas and liquid phase physics using the method of fractional steps. Also introduced is a novel, efficient methodology for accounting for spray formation through direct solution of liquid phase equations. Preliminary parametric studies show marked sensitivity of spray penetration and geometry to droplet diameter, considerations of liquid core, and acoustic interactions. Less sensitivity was shown to the combustion model type although more rigorous (multi-step) formulations may be needed for the differences to become apparent. Derived from text

N94-23042*# Pennsylvania State Univ., University Park. Propulsion Engineering Research Center and Dept. of Mechanical Engineering.

SPRAY FORMATION PROCESSES OF IMPINGING JET INJECTORS **c34**

W. E. Anderson, H. M. Ryan, S. Pal, and R. J. Santoro *In its* NASA Propulsion Engineering Research Center, Volume 2 Nov. 1993 p 69-74
(For primary document see N94-23028 06-20)
(Grant AF-AFOSR-0336-91)
Avail: CASI HC A02/MF A03

A study examining impinging liquid jets has been underway to determine physical mechanisms responsible for combustion instabilities in liquid bi-propellant rocket engines. Primary atomization has been identified as an important process. Measurements of atomization length, wave structure, and drop size and velocity distribution were made under various ambient conditions. Test parameters included geometric effects and flow effects. It was observed that pre-impingement jet conditions, specifically whether they were laminar or turbulent, had the major effect on primary atomization. Comparison of the measurements with results from a two dimensional linear aerodynamic stability model of a thinning, viscous sheet were made. Measured turbulent impinging jet characteristics were contrary to model predictions; the structure of waves generated near the point of jet impingement were dependent primarily on jet diameter and independent of jet velocity. It has been postulated that these impact waves are related to pressure and momentum fluctuations near the impingement region and control the eventual disintegration of the liquid sheet into ligaments. Examination of the temporal characteristics of primary atomization (ligament shedding frequency) strongly suggests that the periodic nature of primary atomization is a key process in combustion instability. Author

N94-23043*# TRW Defense and Space Systems Group, Redondo Beach, CA. Applied Technology Div.

INHERENT STABILITY OF CENTRAL ELEMENT COAXIAL LIQUID-LIQUID INJECTORS **c34**

Frank J. Stoddard *In* Pennsylvania State Univ., NASA Propulsion Engineering Research Center, Volume 2 Nov. 1993 p 75-76 (For primary document see N94-23028 06-20)
Avail: CASI HC A01/MF A03

Most TRW liquid bi-propellant rocket engines built over the past thirty-plus years have employed a central element coaxial pintle injector and have operated with liquid/liquid propellant injection. This injector is a patented design exclusive to TRW and has unique features that make the rocket engine combustion characteristics different from those of other types of injector engine designs. Its many benefits include excellent combustion performance, efficient deep throttling, adaptability to low cost manufacturing, and high reliability. Approximately 200 pintle injector engines of various sizes and operating on a variety of propellants have been flown without a single inflight failure. An especially important feature of the pintle injector engine is its apparent inherent combustion stability. In over thirty years of development, testing, and production, TRW has never experienced combustion instability in any of its pintle injector engine designs. This has been true of engines operating over a range of thrust from 5 to 250,000 lbs. on earth-storable hypergolic propellants and a large number of smaller engines operating on a variety of propellants (21 combinations) in long duration-firing, pulsing (down to 2 msec), and deep throttling (as much as 19:1) modes. Operating chamber pressures have ranged from 10 to 3,500 psia. This record is particularly impressive given that typical TRW design practice does not consider combustion instability as an issue and no pintle engine has ever employed stability-enhancing features, such as baffles or acoustically resonant chambers. In spite of this, TRW engines have operated stably in regimes not possible with other types of injectors. Various physical explanations and combustion process models for this favorable stability characteristic have been postulated. However, a definitive study that unequivocally establishes the important stabilizing mechanisms still remains to be conducted. Derived from text

N94-23044*# National Aeronautics and Space Administration. Lewis Research Center, Cleveland, OH.
AXISYMMETRIC SINGLE SHEAR ELEMENT COMBUSTION INSTABILITY EXPERIMENT **c25**
Kevin J. Breisacher *In* Pennsylvania State Univ., NASA Propulsion Engineering Research Center, Volume 2 Nov. 1993 p 77-81 See also N94-10763 (For primary document see N94-23028 06-20)
Avail: CASI HC A01/MF A03

The combustion stability characteristics of a combustor consisting of a single shear element and a cylindrical chamber utilizing LOX and gaseous hydrogen as propellants are presented. The combustor geometry and the resulting longitudinal mode instability are axisymmetric. Hydrogen injection temperature and pyrotechnic pulsing were used to determine stability boundaries. Mixture ratio, fuel annulus gap, and LOX post configuration were varied. Performance and stability data were obtained for chamber pressures of 300 and 1000 psia. Author

N94-23045*# Pennsylvania State Univ., University Park. Propulsion Engineering Research Center and Dept. of Mechanical Engineering.
DEVELOPMENT OF A DROPLET BREAKUP MODEL CONSIDERING AERODYNAMIC AND DROPLET COLLISION EFFECTS **c34**
K. L. Wert and H. R. Jacobs *In its* NASA Propulsion Engineering Research Center, Volume 2 Nov. 1993 p 82-87 (For primary document see N94-23028 06-20)
Avail: CASI HC A02/MF A03

A model is currently under development to predict the occurrence and outcome of spray droplet breakup induced by aerodynamic forces and droplet collisions. It is speculated that these phenomena may be significant in determining the droplet size distribution in a spray subjected to acoustic velocity fluctuations. The goal is to integrate this breakup model into a larger spray model in order to examine the effects of combustion instabilities on liquid rocket motor fuel sprays. The model is composed of three fundamental components: a dynamic equation governing the deformation of the droplet, a criterion for breakage based on the amount of deformation energy stored in the droplet and an energy balance based equation to predict the Sauter mean diameter of the fragments resulting from breakup. Comparison with published data for aerodynamic breakup indicates good agreement in terms of predicting the occurrence of breakup. However, the model significantly over predicts the size of the resulting fragments. This portion of the model is still under development. Author

N94-23046*# Pennsylvania State Univ., University Park. Propulsion Engineering Research Center and Dept. of Mechanical Engineering.
DEVELOPMENT OF A COMPUTATIONAL TESTBED FOR NUMERICAL SIMULATION OF COMBUSTION INSTABILITY **c25**
Jeffrey Grenda, Sankaran Venkateswaran, and Charles L. Merkle *In its* NASA Propulsion Engineering Research Center, Volume 2 Nov. 1993 p 88-92 (For primary document see N94-23028 06-20)
Avail: CASI HC A01/MF A03

A synergistic hierarchy of analytical and computational fluid dynamic techniques is used to analyze three-dimensional combustion instabilities in liquid rocket engines. A mixed finite difference/spectral procedure is employed to study the effects of a distributed vaporization zone on standing and spinning instability modes within the chamber. Droplet atomization and vaporization are treated by a variety of classical models found in the literature. A multi-zone, linearized analytical solution is used to validate the accuracy of the numerical simulations at small amplitudes for a distributed vaporization region. This comparison indicates excellent amplitude and phase agreement under both stable and unstable operating conditions when amplitudes are small and proper grid resolution is used. As amplitudes get larger, expected nonlinearities are observed. The effect of liquid droplet temperature fluctuations was found to be of critical importance in driving the instabilities of the combustion chamber. Author

N94-23047*# Pennsylvania State Univ., University Park. Dept. of Aerospace Engineering and Propulsion Engineering Research Center.
SHEAR COAXIAL INJECTOR INSTABILITY MECHANISMS **c34**
T. Kaltz, M. Glogowski, and M. M. Micci *In its* NASA Propulsion Engineering Research Center, Volume 2 Nov. 1993 p 93-96 (For primary document see N94-23028 06-20)
Avail: CASI HC A01/MF A03

Although stable operating regimes for cryogenic coaxial injectors have been empirically determined, there is no knowledge of the spray characteristics corresponding to stable operation, or the physical processes which produce the atomization patterns that result in stable or unstable operation. The current engineering method for determining the stable operating regime of a cryogenic coaxial injector is the 'hydrogen temperature ramping' method, however there is no definitive knowledge of whether the hydrogen temperature influences the chamber stability by decreasing the injected gas velocity, by affecting a recirculation region at the base of the LOX Post, or by changing the pressure drop across the injector, allowing chamber pressure oscillations to couple to the fuel feed system. Results for the injector response from a linearized lumped-element model are presented as a function of temperature and frequency. LDV measurements in the recess region at the base of the LOX post show reverse flow indicative of a recirculation region. Finally, Phase Doppler Particle Analyzer (PDPA) measurements of droplet size and velocity distributions are discussed for a coaxial injector element similar to the SSME preburner element operating with water and air at atmospheric pressure and liquid and gaseous nitrogen at 20 bars. Author

N94-23048*# Pennsylvania State Univ., University Park. Propulsion Engineering Research Center and Dept. of Mechanical Engineering.
NUMERICAL INVESTIGATION OF TWO- AND THREE-DIMENSIONAL HEAT TRANSFER IN EXPANDER CYCLE ENGINES
Robert L. Burch and Fan-Bill Cheung *In its* NASA Propulsion Engineering Research Center, Volume 2 Nov. 1993 p 97-100 (For primary document see N94-23028 06-20)
Avail: CASI HC A01/MF A03

The concept of using tube canting for enhancing the hot-side convective heat transfer in a cross-stream tubular rocket combustion chamber is evaluated using a CFD technique in this study. The heat transfer at the combustor wall is determined from the flow field generated by a modified version of the PARC Navier-Stokes Code, using the actual dimensions, fluid properties, and design parameters of a split-expander demonstrator cycle engine. The effects of artificial dissipation on convergence and solution accuracy are investigated. Heat transfer results predicted by the code are presented. The use of CFD in heat transfer calculations is critically examined to demonstrate the care needed in the use of artificial dissipation for good convergence and accurate solutions. Author

N94-23049*# National Aeronautics and Space Administration. Lewis Research Center, Cleveland, OH.
FLOW VISUALIZATION STUDY IN HIGH ASPECT RATIO COOLING CHANNELS FOR ROCKET ENGINES
Michael L. Meyer and James E. Giuliani (Ohio Aerospace Inst., Brook Park.) *In* Pennsylvania State Univ., NASA Propulsion Engineering Research Center, Volume 2 Nov. 1993 p 101-105 (For primary document see N94-23028 06-20)
Avail: CASI HC A01/MF A03

The structural integrity of high pressure liquid propellant rocket engine thrust chambers is typically maintained through regenerative cooling. The coolant flows through passages formed either by constructing the chamber liner from tubes or by milling channels in a solid liner. Recently, Carlile and Quentmeyer showed life extending advantages (by lowering hot gas wall temperatures) of milling channels with larger height to width aspect ratios (AR is greater than 4) than the traditional, approximately square cross section, passages. Further, the total coolant pressure drop in the thrust chamber could also be reduced, resulting in lower turbomachinery power requirements. High aspect ratio cooling channels could offer many benefits to designers developing new high performance engines, such as the European Vulcain engine (which uses an aspect ratio up to 9). With platelet manufacturing technology, channel aspect ratios up to 15 could be formed offering potentially greater benefits. Some issues still exist with the high aspect ratio coolant channels. In a coolant passage of circular or square cross section, strong secondary vortices develop as the fluid passes through the curved throat region. These vortices mix the fluid and bring lower temperature coolant to the hot wall. Typically, the circulation enhances the heat transfer at the hot gas wall by about 40 percent over a straight channel. The effect that increasing channel aspect ratio has on the curvature heat transfer enhancement has not been sufficiently studied. If the increase in aspect ratio degrades the secondary flow, the fluid mixing will be reduced. Analysis has shown that reduced coolant mixing will result in significantly higher wall temperatures, due to thermal stratification in the coolant, thus decreasing the benefits of the high aspect ratio geometry. A better understanding of the fundamental flow phenomena in high aspect ratio channels with curvature is needed to fully evaluate the benefits of this geometry. The fluid dynamic and conjugate heat transfer problem of high aspect ratio rocket engine coolant channels are being investigated numerically, but these efforts have been hampered by a lack of validating data. Wall temperature data is available for the conjugate problem for channels without curvature and aspect ratio = 5.0, and unheated fluid dynamic data are available for square and circular cross section channels with curvature at Reynold's numbers up to 40,000. But the effects of aspect ratio on secondary flow development have not been experimentally studied. To provide some insight into the effects of channel aspect ratio on secondary flow and to qualitatively provide anchoring for the numerical codes, a flow visualization experiment was initiated at the NASA Lewis Research Center. Derived from text

N94-23050*# Pennsylvania State Univ., University Park. Propulsion Engineering Research Center and Dept. of Mechanical Engineering.

CFD ANALYSES OF COOLANT CHANNEL FLOWFIELDS

Jennifer A. Yagley, Jinzhang Feng, and Charles L. Merkle *In its* NASA Propulsion Engineering Research Center, Volume 2 Nov. 1993 p 106-110 See also A93-49715 (For primary document see N94-23028 06-20)
Avail: CASI HC A01/MF A03

The flowfield characteristics in rocket engine coolant channels are analyzed by means of a numerical model. The channels are characterized by large length to diameter ratios, high Reynolds numbers, and asymmetrical heating. At representative flow conditions, the channel length is approximately twice the hydraulic entrance length so that fully developed conditions would be reached for a constant property fluid. For the supercritical hydrogen that is used as the coolant, the strong property variations create significant secondary flows in the cross-plane which have a major influence on the flow and the resulting heat transfer. Comparison of constant and variable property solutions show substantial differences. In addition, the property variations prevent fully developed flow. The density variation accelerates the fluid in the channels increasing the pressure drop without an accompanying increase in heat flux. Analyses of the inlet configuration suggest that side entry from a manifold can affect the development of the velocity profile because of vortices generated as the flow enters the channel. Current work is focused on studying the effects of channel bifurcation on the flow field and the heat transfer characteristics. Author

N94-23051*# SECA, Inc., Huntsville, AL.

HEAT TRANSFER IN ROCKET COMBUSTION CHAMBERS

P. Anderson, G. Cheng, and R. Farmer *In* Pennsylvania State Univ., NASA Propulsion Engineering Research Center, Volume 2 Nov. 1993 p 111-114 (For primary document see N94-23028 06-20)
Avail: CASI HC A01/MF A03

Complexities of liquid rocket engine heat transfer which involve the injector faceplate and film cooled walls are being investigated by computational analysis. A conjugate heat transfer analysis was used to describe localized heating phenomena associated with particular injector configurations and film coolant flows. These components were analyzed, and the analyses verified when appropriate test data were available. The component analyses are being synthesized into an overall flowfield/heat transfer model. A Navier-Stokes flow solver, the FDNS code, was used to make the analyses. Particular attention was given to the representation of the thermodynamic properties of the fluid streams. Unit flow models of specific coaxial injector elements have been developed and are being used to describe the flame structure near the injector faceplate. Derived from text

N94-23052*# National Aeronautics and Space Administration. Lewis Research Center, Cleveland, OH.

ADVANCED MATERIALS FOR RADIATION-COOLED ROCKETS

Brian Reed, James Biaglow, and Steven Schneider *In* Pennsylvania State Univ., NASA Propulsion Engineering Research Center, Volume 2 Nov. 1993 p 115-118 (For primary document see N94-23028 06-20)
Avail: CASI HC A01/MF A03

The most common material system currently used for low thrust, radiation-cooled rockets is a niobium alloy (C-103) with a fused silica coating (R-512A or R-512E) for oxidation protection. However, significant amounts of fuel film cooling are usually required to keep the material below its maximum operating temperature of 1370 C, degrading engine performance. Also the R-512 coating is subject to cracking and eventual spalling after repeated thermal cycling. A new class of high-temperature, oxidation-resistant materials are being developed for radiation-cooled rockets, with the thermal margin to reduce or eliminate fuel film cooling, while still exceeding the life of silicide-coated niobium. Rhenium coated with iridium is the most developed of these high-temperature materials. Efforts are on-going to develop 22 N, 62 N, and 440 N engines composed of these materials for apogee insertion, attitude control, and other functions. There is also a complimentary NASA and industry effort to determine the life limiting mechanisms and characterize the thermomechanical properties of these materials. Other material systems are also being studied which may offer more thermal margin and/or oxidation resistance, such as hafnium carbide/tantalum carbide matrix composites and ceramic oxide-coated iridium/rhenium chambers. Author

N94-23053*# National Aeronautics and Space Administration. Lewis Research Center, Cleveland, OH.

MOLECULAR GAS DYNAMICS APPLIED TO LOW-THRUST PROPULSION

Donna Zelesnik (Ohio Aerospace Inst., Brook Park.), Paul F. Penko, and Iain D. Boyd (Cornell Univ., Ithaca, NY.) *In* Pennsylvania State Univ., NASA Propulsion Engineering Research Center, Volume 2 Nov. 1993 p 119-124 (For primary document see N94-23028 06-20)
Avail: CASI HC A02/MF A03

The Direct Simulation Monte Carlo method is currently being applied to study flowfields of small thrusters, including both the internal nozzle and the external plume flow. The DSMC method is employed because of its inherent ability to capture nonequilibrium effects and proper boundary physics in low-density flow that are not readily obtained by continuum methods. Accurate prediction of both the internal and external nozzle flow is important in determining plume expansion which, in turn, bears directly on impingement and contamination effects. Author

N94-23054*# National Aeronautics and Space Administration. Marshall Space Flight Center, Huntsville, AL.

COMPUTATIONAL FLUID DYNAMICS (CFD) APPLICATIONS IN ROCKET PROPULSION ANALYSIS AND DESIGN

P. K. McConnaughey, R. Garcia, L. W. Griffin, and J. H. Ruf *In* Pennsylvania State Univ., NASA Propulsion Engineering Research Center, Volume 2 Nov. 1993 p 125-129 (For primary document see N94-23028 06-20)
Avail: CASI HC A01/MF A03

Computational Fluid Dynamics (CFD) has been used in recent applications to affect subcomponent designs in liquid propulsion rocket engines. This paper elucidates three such applications for turbine stage, pump stage, and combustor chamber geometries. Details of these applications include the development of a high turning airfoil for a gas generator (GG) powered, liquid oxygen (LOX) turbopump, single-stage turbine using CFD as an integral part of the design process. CFD application to pump stage design has emphasized analysis of inducers, impellers, and diffuser/volute sections. Improvements in pump stage impeller discharge flow uniformity have been seen through CFD optimization on coarse grid models. In the area of combustor design, recent CFD analysis of a film cooled ablating combustion chamber has been used to quantify the interaction between film cooling rate, chamber wall contraction angle, and geometry and their effects of these quantities on local wall temperature. The results are currently guiding combustion chamber design and coolant flow rate for an upcoming subcomponent test. Critical aspects of successful integration of CFD into the design cycle includes a close-coupling of CFD and design organizations, quick turnaround of parametric analyses once a baseline CFD benchmark has been established, and the use of CFD methodology and approaches that address pertinent design issues. In this latter area, some problem details can be simplified while retaining key physical aspects to maintain analytical integrity. Author (revised)

N94-23055*# Pennsylvania State Univ., University Park. Propulsion Engineering Research Center and Dept. of Mechanical Engineering.

EFFICIENCY AND RELIABILITY ENHANCEMENTS IN PROPULSION FLOWFIELD MODELING c34

Philip E. O. Buelow, Sankaran Venkateswaran, and Charles L. Merkle *In its* NASA Propulsion Engineering Research Center, Volume 2 Nov. 1993 p 130-134 (For primary document see N94-23028 06-20)

Avail: CASI HC A01/MF A03

The implementation of traditional CFD algorithms in practical propulsion related flowfields often leads to dramatic reductions in efficiency and/or robustness. The present research is directed at understanding the reasons for this deterioration and finding methods to circumvent it. Work to date has focussed on low Mach number regions, viscous dominated regions, and high grid aspect ratios. Time derivative preconditioning, improved definition of the local time stepping, and appropriate application of boundary conditions are employed to decrease the required time to obtain a solution, while maintaining accuracy. A number of cases having features typical of rocket engine flowfields are computed to demonstrate the improvement over conventional methods. These cases include laminar and turbulent high Reynolds number flat plate boundary layers, flow over a backward-facing step, a diffusion flame, and wall heat-flux calculations in a turbulent converging-diverging nozzle. Results from these cases show convergence that is virtually independent of the local Mach number and the grid aspect ratio, which translates to a convergence speed-up of up to several orders of magnitude over conventional algorithms. Current emphasis is in extending these results to three-dimensional flows with highly stretched grids.

Author (revised)

N94-23056*# Fluent, Inc., Lebanon, NH.

COMPUTATION OF PROPULSION-RELATED FLOWFIELDS USING UNSTRUCTURED ADAPTIVE MESHES c34

Jonathan M. Weiss and Jayathi Y. Murthy *In* Pennsylvania State Univ., NASA Propulsion Engineering Research Center, Volume 2 Nov. 1993 p 135-139 (For primary document see N94-23028 06-20)

Avail: CASI HC A01/MF A03

In this paper, we describe a computational fluid dynamics (CFD) technique based on unstructured triangular/tetrahedral meshes. A finite-volume scheme is used in conjunction with a multi-stage Runge-Kutta algorithm. Convergence enhancements in the form of dual time-stepping and time-derivative preconditioning are used to overcome the limitations of conventional multi-stage schemes. The method is applied to propulsion-related flows and shown to perform satisfactorily. Author (revised)

N94-23057*# Rockwell International Corp., Canoga Park, CA. Rocketdyne Div.

DUAL-BELL ALTITUDE COMPENSATING NOZZLES

M. Horn and S. Fisher *In* Pennsylvania State Univ., NASA Propulsion Engineering Research Center, Volume 2 Nov. 1993 p 140-147 (For primary document see N94-23028 06-20)

Avail: CASI HC A02/MF A03

The primary objective of this cold flow test effort was to assess the performance characteristics of dual bell nozzles and to obtain preliminary design criteria by testing a number of configurations. Characteristics of interest included low altitude performance, high altitude performance, and the flow transition process. In combination with this performance data, other factors such as cost, weight, fabricability, and vehicle related issues could then be traded to establish the feasibility of the concept.

Author (revised)

N94-23058*# Pennsylvania State Univ., University Park. Dept. of Mechanical Engineering.

FOIL BEARING RESEARCH AT PENN STATE c37

Marc Carpino *In its* NASA Propulsion Engineering Research Center, Volume 2 Nov. 1993 p 148-151 (For primary document see N94-23028 06-20)

Avail: CASI HC A01/MF A03

Foil journal bearings consist of a compliant metal shell or foil which supports a rigid journal by means of a fluid film. Foil bearings are considered to be a potential alternative to rolling element or traditional rigid surface bearings in cryogenic turbomachinery applications. The prediction of foil bearing performance requires the coupled solution of the foil deflection and the fluid flow in the bearing clearance between the rotor and the foil. The investigations being conducted in the Department of Mechanical Engineering at Penn State are focused in three areas: theoretical prediction of steady state bearing performance, modeling of the dynamic bearing characteristics to determine performance in rotor systems, and experimental verification of analysis codes. The current status and results from these efforts will be discussed. Author

N94-23059*# National Aeronautics and Space Administration. Lewis Research Center, Cleveland, OH.

TWO STAGE TURBINE FOR ROCKETS c37

Joseph P. Veres *In* Pennsylvania State Univ., NASA Propulsion Engineering Research Center, Volume 2 Nov. 1993 p 152-158 (For primary document see N94-23028 06-20)

Avail: CASI HC A02/MF A03

The aerodynamic design and rig test evaluation of a small counter-rotating turbine system is described. The advanced turbine airfoils were designed and tested by Pratt & Whitney. The technology represented by this turbine is being developed for a turbopump to be used in an advanced upper stage rocket engine. The advanced engine will use a hydrogen expander cycle and achieve high performance through efficient combustion of hydrogen/oxygen propellants, high combustion pressure, and high area ratio exhaust nozzle expansion. Engine performance goals require that the turbopump drive turbines achieve high efficiency at low gas flow rates. The low mass flow rates and high operating pressures result in very small airfoil heights and diameters. The high efficiency and small size requirements present a challenging turbine design problem. The shrouded axial turbine blades are 50 percent reaction with a maximum thickness to chord ratio near 1. At 6 deg from the tangential direction, the nozzle and blade exit flow angles are well below the traditional design minimum limits. The blade turning angle of 160 deg also exceeds the maximum limits used in traditional turbine designs. Author (revised)

N94-23060*# Pennsylvania State Univ., University Park. Propulsion Engineering Research Center and Dept. of Mechanical Engineering.

COMPUTATIONAL FLUID DYNAMIC MODELLING OF CAVITATION c34

Manish Deshpande, Jinzhang Feng, and Charles L. Merkle *In its* NASA Propulsion Engineering Research Center, Volume 2 Nov. 1993 p 159-163 (For primary document see N94-23028 06-20)

Avail: CASI HC A01/MF A03

Models in sheet cavitation in cryogenic fluids are developed for use in Euler and Navier-Stokes codes. The models are based upon earlier potential-flow models but enable the cavity inception point, length, and shape to be determined as part of the computation. In the present paper, numerical solutions are compared with experimental measurements for both pressure distribution and cavity length. Comparisons between models are also presented. The CFD model provides a relatively simple modification to an existing code to enable cavitation performance predictions to be included. The analysis also has the added ability of incorporating thermodynamic effects of cryogenic fluids into the analysis. Extensions of the current two-dimensional steady state analysis to three-dimensions and/or time-dependent flows are, in principle, straightforward although geometrical issues become more complicated. Linearized models, however offer promise of providing effective cavitation modeling in three-dimensions. This analysis presents good potential for improved understanding of many phenomena associated with cavity flows. Author (revised)

N94-23061*# National Aeronautics and Space Administration. Lewis Research Center, Cleveland, OH.

A TECHNIQUE TO MEASURE ROTORDYNAMIC COEFFICIENTS IN HYDROSTATIC BEARINGS c37

Russell J. Capaldi *In* Pennsylvania State Univ., NASA Propulsion Engineering Research Center, Volume 2 Nov. 1993 p 164-169 (For primary document see N94-23028 06-20)

Avail: CASI HC A02/MF A03

An experimental technique is described for measuring the rotordynamic coefficients of fluid film journal bearings. The bearing tester incorporates a double-spool shaft assembly that permits independent control over the journal spin speed and the frequency of an adjustable-magnitude circular orbit. This configuration yields data that enables determination of the full linear anisotropic rotordynamic coefficient matrices. The dynamic force measurements were made simultaneously with two independent systems, one with piezoelectric load cells and the other with strain gage load cells. Some results are presented for a four-recess, oil-fed hydrostatic journal bearing. Author

N94-23062*# Pennsylvania State Univ., University Park. Dept. of Aerospace Engineering.
COMPUTATION OF FLOWS IN A TURN-AROUND DUCT AND A TURBINE CASCADE USING ADVANCED TURBULENCE MODELS c34
B. Lakshminarayana and J. Luo *In its* NASA Propulsion Engineering Research Center, Volume 2 Nov. 1993 p 170-175 (For primary document see N94-23028 06-20)
Avail: CASI HC A02/MF A03

Numerical investigation has been carried out to evaluate the capability of the Algebraic Reynolds Stress Model (ARSM) and the Nonlinear Stress Model (NLSM) to predict strongly curved turbulent flow in a turn-around duct (TAD). The ARSM includes the near-wall damping term of pressure-strain correlation phi(sub ij,w), which enables accurate prediction of individual Reynolds stress components in wall flows. The TAD mean flow quantities are reasonably well predicted by various turbulence models. The ARSM yields better predictions for both the mean flow and the turbulence quantities than the NLSM and the k-epsilon (k = turbulent kinetic energy, epsilon = dissipation rate of k) model. The NLSM also shows slight improvement over the k-epsilon model. However, all the models fail to capture the recovery of the flow from strong curvature effects. The formulation for phi(sub ij,w) appears to be incorrect near the concave surface. The hybrid k-epsilon/ARSM, Chien's k-epsilon model, and Coakley's q-omega (q = the square root of k, omega = epsilon/k) model have also been employed to compute the aerodynamics and heat transfer of a transonic turbine cascade. The surface pressure distributions and the wake profiles are predicted well by all the models. The k-epsilon model and the k-epsilon/ARSM model provide better predictions of heat transfer than the q-omega model. The k-epsilon/ARSM solutions show significant differences in the predicted skin friction coefficients, heat transfer rates and the cascade performance parameters, as compared to the k-epsilon model. The k-epsilon/ARSM model appears to capture, qualitatively, the anisotropy associated with by-pass transition. Author (revised)

N94-23063*# National Aeronautics and Space Administration. Lewis Research Center, Cleveland, OH.
BRUSH SEALS FOR CRYOGENIC APPLICATIONS c37
Margaret P. Proctor *In* Pennsylvania State Univ., NASA Propulsion Engineering Research Center, Volume 2 Nov. 1993 p 176-180 (For primary document see N94-23028 06-20)
Avail: CASI HC A01/MF A03

Brush seals are compliant, contacting seals and have significantly lower leakage than labyrinth seals in gas turbine applications. Their characteristics of long life and low leakage make them candidates for use in rocket engine turbopumps. Two-inch diameter brush seals with a nominal 0.005 inch radial interference were tested in liquid nitrogen at shaft speeds up to 35,000 rpm and pressure drops up to 175 psid per seal. A labyrinth seal was also tested to provide a baseline. Performance, staging effects, and wear results are presented. Author

N94-23064*# Pennsylvania State Univ., University Park. Dept. of Aerospace Engineering.
RELIABILITY ENHANCEMENT OF NAVIER-STOKES CODES THROUGH CONVERGENCE ENHANCEMENT c38
K.-Y. Choi and G. S. Dulikravich *In its* NASA Propulsion Engineering Research Center, Volume 2 Nov. 1993 p 181-186 (For primary document see N94-23028 06-20)
Avail: CASI HC A02/MF A03

Reduction of total computing time required by an iterative algorithm for solving Navier-Stokes equations is an important aspect of making the existing and future analysis codes more cost effective. Several attempts have been made to accelerate the convergence of an explicit Runge-Kutta time-stepping algorithm. These acceleration methods are based on local time stepping, implicit residual smoothing, enthalpy damping, and multigrid techniques. Also, an extrapolation procedure based on the power method and the Minimal Residual Method (MRM) were applied to the Jameson's multigrid algorithm. The MRM uses same values of optimal weights for the corrections to every equation in a system and has not been shown to accelerate the scheme without multigriding. Our Distributed Minimal Residual (DMR) method based on our General Nonlinear Minimal Residual (GNLMR) method allows each component of the solution vector in a system of equations to have its own convergence speed. The DMR method was found capable of reducing the computation time by 10-75 percent depending on the test case and grid used. Recently, we have developed and tested a new method termed Sensitivity Based DMR or SBMR method that is easier to implement in different codes and is even more robust and computationally efficient than our DMR method. Derived from text

N94-23065*# Pennsylvania State Univ., University Park. Propulsion Engineering Research Center and Dept. of Aerospace Engineering.
OPTIMIZATION OF ENERGY TRANSFER IN MICROWAVE ELECTROTHERMAL THRUSTERS
D. J. Sullivan and M. M. Micci *In its* NASA Propulsion Engineering Research Center, Volume 2 Nov. 1993 p 187-190 (For primary document see N94-23028 06-20)
Avail: CASI HC A01/MF A03

Results are presented from preliminary tests conducted to evaluate the performance of a prototype microwave electrothermal thruster. The primary component of the device is a microwave resonant cavity. The device produces stable axial plasmas within a pressurized section of the cavity with the plasma positioned in the inlet region of the nozzle. Plasma stability is enhanced by axial power coupling, an optimal distribution of electric power density within the cavity, and a propellant gas flow which has a large vortical velocity component. The thruster has been operated with a number of propellant gases: helium, nitrogen, ammonia, and hydrogen. Plasmas can be formed in a reliable manner at cavity pressures of 1 kPa and incident power levels ranging from 50 W to 350 W, depending on the gas used, and can be operated at pressures up to 300 kPa at power levels up to 2200 W. Ideal performance results of vacuum Isp and thermal efficiency vs. specific power are presented for each gas. Representative results of this preliminary work are: He - Isp = 625 s, eta-thermal = 90 percent; N2 - Isp = 270 s, eta-thermal = 41 percent; NH3 - Isp = 475 s, eta-thermal= 55 percent; H2 - Isp = 1040 s, eta-thermal = 53 percent. Derived from text

N94-23066*# Pennsylvania State Univ., University Park.
CFD MODELING OF MICROWAVE ELECTROTHERMAL THRUSTERS
Douglas A. Schwer, S. Venkateswaran, and Charles L. Merkle *In its* NASA Propulsion Engineering Research Center, Volume 2 Nov. 1993 p 191-194 (For primary document see N94-23028 06-20)
Avail: CASI HC A01/MF A03

Microwave-heated plasmas in convergent nozzles are analyzed using a coupled Maxwell and Navier-Stokes solver to examine relevant issues associated with microwave thermal propulsion. Parametric studies are conducted to understand the effect of power, pressure, and plasma location with respect to the nozzle throat. For nozzles in the 0.5 to 3 N range with helium flow, results show that specific impulses up to 550-650 seconds are possible, with further increases being limited by severe wall-heating. Coupling efficiencies of over 90 percent are consistently obtained, with overall efficiencies ranging from 40 percent to 80 percent. Size scale-up studies-done by scaling the frequency from 2.45 GHz to 0.91 GHz-indicate that plasma migration toward the walls occurs more frequently for the lower frequency. Increasing the cavity aspect ratio and detuning the cavity are found to be effective ways of keeping the plasma on axis. Derived from text

N94-23067*# Sverdrup Technology, Inc., Brook Park, OH.
ADVANCED SPACE PROPULSION CONCEPTS
Michael R. LaPointe *In* Pennsylvania State Univ., NASA Propulsion Engineering Research Center, Volume 2 Nov. 1993 p 195-198 (For primary document see N94-23028 06-20)
Avail: CASI HC A01/MF A03

The NASA Lewis Research Center has been actively involved in the evaluation and development of advanced spacecraft propulsion. Recent program elements have included high energy density propellants, electrode less plasma thruster concepts, and low power laser propulsion technology. A robust advanced technology program is necessary to develop new, cost-effective methods of spacecraft propulsion, and to continue to push the boundaries of human knowledge and technology. Derived from text

N94-23068*# Los Alamos National Lab., NM.
ADVANCED NUCLEAR THERMAL PROPULSION CONCEPTS
Steven D. Howe *In* Pennsylvania State Univ., NASA Propulsion Engineering Research Center, Volume 2 Nov. 1993 p 199-202 (For primary document see N94-23028 06-20)
Avail: CASI HC A01/MF A03

In 1989, a Presidential directive created the Space Exploration Initiative (SEI) which had a goal of placing mankind on Mars in the early 21st century. The SEI was effectively terminated in 1992 with the election of a new administration. Although the initiative did not exist long enough to allow substantial technology development, it did provide a venue, for the first time in 20 years, to comprehensively evaluate advanced propulsion concepts which could enable fast, manned transits to Mars. As part of the SEI based investigations, scientists from NASA, DoE National Laboratories, universities, and industry met regularly and proceeded to examine a variety of innovative ideas. Most of the effort was directed toward developing a solid-core, nuclear thermal rocket and examining a high-power nuclear electric propulsion system. In addition, however, an Innovative Concepts committee was formed and charged with evaluating concepts that offered a much higher performance but were less technologically mature. The committee considered several concepts and eventually recommended that further work be performed in the areas of gas core fission rockets, inertial confinement fusion systems, antimatter based rockets, and gas core fission electric systems. Following the committee's recommendations, some computational modeling work has been performed at Los Alamos in certain of these areas and critical issues have been identified. Derived from text

N94-23069*# Pennsylvania State Univ., University Park. Depts. of Physics, Nuclear Engineering and Aerospace Engineering.
AN ANTIPROTON DRIVER FOR ICF PROPULSION
Pi-Ren Chiang, R. A. Lewis, G. A. Smith, C. Gazze, K. Higman, R. Newton, M. Chiaverini, J. Dailey, M. Surratt, and W. Lance Werthman *In its* NASA Propulsion Engineering Research Center, Volume 2 Nov. 1993 p 203-206 (For primary document see N94-23028 06-20)
Avail: CASI HC A01/MF A03

Inertial confinement fusion (ICF) utilizing an anitprotoncatalyzed target is discussed as a possible source of propulsion for rapid interplanetary manned space missions. The relevant compression, ignition, and thrust mechanisms are presented. Progress on an experiment presently in progress at the Phillips Laboratory, Kirtland AFB, NM to demonstrate proof-of-principle is reviewed. Derived from text

N94-23070*# National Aeronautics and Space Administration. Marshall Space Flight Center, Huntsville, AL.
PERFORMANCE ASSESSMENT OF LOW PRESSURE NUCLEAR THERMAL PROPULSION
Harrold P. Gerrish, Jr. and Glen E. Doughty *In* Pennsylvania State Univ., NASA Propulsion Engineering Research Center, Volume 2 Nov. 1993 p 207-211 (For primary document see N94-23028 06-20)
Avail: CASI HC A01/MF A03

An increase in Isp for nuclear thermal propulsion systems is desirable for reducing the propellant requirements and cost of future applications, such as the Mars Transfer Vehicle. Several previous design studies have suggested that the Isp could be increased substantially with hydrogen dissociation/recombination. Hydrogen molecules (H2), at high temperatures and low pressures, will dissociate to monatomic hydrogen (H). The reverse process (i.e., formation of H2 from H) is exothermic. The exothermic energy in a nozzle increases the kinetic energy and therefore, increases the Isp. The low pressure nuclear thermal propulsion system (LPNTP) system is expected to maximize the hydrogen dissociation/recombination and Isp by operating at high chamber temperatures and low chamber pressures. The process involves hydrogen flow through a high temperature, low pressure fission reactor, and out a nozzle. The high temperature (approximately 3000 K) of the hydrogen in the reactor is limited by the temperature limits of the reactor material. The minimum chamber pressure is about 1 atm because lower pressures decrease the engines thrust to weight ratio below acceptable limits. This study assumes that hydrogen leaves the reactor and enters the nozzle at the 3000 K equilibrium dissociation level. Hydrogen dissociation in the reactor does not affect LPNTP performance like dissociation in traditional chemical propulsion systems, because energy from the reactor resupplies energy lost due to hydrogen dissociation. Recombination takes place in the nozzle due primarily to a drop in temperature as the Mach number increases. However, as the Mach number increases beyond the nozzle throat, the static pressure and density of the flow decreases and minimizes the recombination. The ideal LPNTP Isp at 3000 K and 10 psia is 1160 seconds due to the added energy from fast recombination rates. The actual Isp depends on the finite kinetic reaction rates which affect the amount of monatomic hydrogen recombination before the flow exits the nozzle. A LPNTP system has other technical issues (e.g. flow instability and two-phase flow) besides hydrogen dissociation/recombination which affect the systems practicality. In this study, only the effects of hydrogen dissociation/recombination are examined. Derived from text

N94-23071*# Pennsylvania State Univ., University Park. Dept. of Nuclear Engineering.
NUCLEAR PROPULSION CONTROL AND HEALTH MONITORING
P. B. Walter and R. M. Edwards *In its* NASA Propulsion Engineering Research Center, Volume 2 Nov. 1993 p 212-215 (For primary document see N94-23028 06-20)
Avail: CASI HC A01/MF A03

An integrated control and health monitoring architecture is being developed for the Pratt & Whitney XNR2000 nuclear rocket. Current work includes further development of the dynamic simulation modeling and the identification and configuration of low level controllers to give desirable performance for the various operating modes and faulted conditions. Artificial intelligence and knowledge processing technologies need to be investigated and applied in the development of an intelligent supervisory controller module for this control architecture. Derived from text

N94-23193# Science Applications International Corp., Albuquerque, NM.
AN F2D ANALYSIS OF THE FLOW INSTABILITY TEST (FIT) EXPERIMENT
A. Suo-Anttila 1993 12 p Presented at the 11th Symposium on Space Nuclear Power Systems, Albuquerque, NM, 9-13 Jan. 1994
(Contract DE-AC04-94AL-85000)
(DE94-001420; SAND-93-7080C; CONF-940101-6) Avail: CASI HC A03/MF A01

The F2D code was used to analyze the Flow-Instability-Test (FIT) experiments at Brookhaven National Laboratories. A one-dimensional analysis of the experiment indicated that at the higher temperature levels the element should be unstable. The experimental data corroborated this theory. The two-dimensional simulation behaved in a manner that was very similar to the experimentally measured behavior. In conclusion, the FIT experimental analysis yields partial code validation of F2D, and it also validates the methodology that is used in analyzing thermal flow stability. DOE

N94-23275*# Georgia Inst. of Tech., Atlanta. School of Aerospace Engineering.
THEORY AND COMPUTATION OF OPTIMAL LOW- AND MEDIUM-THRUST TRANSFERS Semiannual Status Report, 7 Jul. 1993 - 6 Jan. 1994
C.-H. Chuang 4 Jan. 1994 26 p
(Grant NAG8-921)
(NASA-CR-194812; NAS 1.26:194812) Avail: CASI HC A03/MF A01

This report presents two numerical methods considered for the computation of fuel-optimal, low-thrust orbit transfers in large numbers of burns. The origins of these methods are observations made with the extremal solutions of transfers in small numbers of burns; there seems to exist a trend such that the longer the time allowed to perform an optimal transfer the less fuel that is used. These longer transfers are obviously of interest since they require a motor of low thrust; however, we also find a trend that the longer the time allowed to perform the optimal transfer the more burns are required to satisfy optimality. Unfortunately, this usually increases the difficulty of computation. Both of the methods described use small-numbered burn solutions to determine solutions in large numbers of burns. One method is a homotopy method that corrects for problems that arise when a solution requires a new burn or coast arc for optimality. The other method is to simply patch together long transfers from smaller ones. An orbit correction problem is solved to develop this method. This method may also lead to a good guidance law for transfer orbits with long transfer times. Author

N94-23283# Los Alamos National Lab., NM.
REDUCTION OF THE ANODE FALL IN A COAXIAL PLASMA THRUSTER WITH AN APPLIED MAGNETIC NOZZLE
J. T. Scheuer, R. P. Hoyt, K. F. Schoenberg, R. A. Gerwin, R. W. Moses, I. Henins, R. M. Mayo (North Carolina State Univ., Raleigh.), and D. C. Black (North Carolina State Univ., Raleigh.) 1993 8 p Presented at the 11th Symposium on Space Nuclear Power Systems, Albuquerque, NM, 9-13 Jan. 1994
(Contract W-7405-eng-36)
(DE94-000670; LA-UR-93-3518; CONF-940101-8) Avail: CASI HC A02/MF A01 (US Sales Only)

The Coaxial Thruster Experiment at the Los Alamos National Laboratory has demonstrated 10 ms quasi-steady operation and ideal magnetohydrodynamic (MHD)-like performance. Previous experiments utilized an unoptimized applied magnetic configuration in which field lines intercepted both thruster electrodes. These experiments demonstrated the ability of magnetic connection between the plasma and the electrodes to control the anode fall. The effect of an evolved applied magnetic nozzle which provides magnetic connection of the electrodes to the bulk of the plasma without direct magnetic connection of the electrodes is reported. This magnetic nozzle configuration significantly reduces the anode fall fraction and thus may provide a promising means of improving magnetoplasmadynamic (MPD) thruster efficiency. DOE

N94-23343*# National Aeronautics and Space Administration. Goddard Space Flight Center, Greenbelt, MD.
CONTAMINATION CONTROL AND PLUME ASSESSMENT OF LOW-ENERGY THRUSTERS
John J. Scialdone May 1993 8 p
(NASA-TM-104585; 93E01024; NAS 1.15:104585) Avail: CASI HC A02/MF A01

Potential contamination of a spacecraft cryogenic surface by a xenon (Xe) ion generator was evaluated. The analysis involves the description of the plume exhausted from the generator with its relative component fluxes on the spacecraft surfaces, and verification of the conditions for condensation, adsorption, and sputtering at those locations. The data describing the plume fluxes and their effects on surfaces were obtained from two sources: the tests carried out with the Xe generator in a small vacuum chamber to indicate deposits and sputter on monitor slides; and the extensive tests with a mercury (Hg) ion thruster in a large vacuum chamber. The Hg thruster tests provided data on the neutrals, on low-energy ion fluxes, on high-energy ion fluxes, and on sputtered materials at several locations within the plume. Author (revised)

N94-23370*# National Aeronautics and Space Administration. Lewis Research Center, Cleveland, OH.
TRANSPARENT CONDUCTING THIN FILMS FOR SPACECRAFT APPLICATIONS
Marla E. Perez-Davis, Tania Malave-Sanabria (Ohio Aerospace Inst., Brook Park.), Paul Hambourger (Cleveland State Univ., OH.), Sharon K. Rutledge, David Roig (Cleveland State Univ., OH.), Kim K. deGroh, and Ching-Cheh Hung Jan. 1994 8 p Presented at the 32nd Aerospace Sciences Meeting and Exhibit, Reno, NV, 10-13 Jan. 1994; sponsored by AIAA
(Contract NCC3-19; RTOP 506-41-41)
(NASA-TM-106466; E-8332; NAS 1.15:106466; AIAA Paper 94-0375) Copyright Avail: CASI HC A02/MF A01

Transparent conductive thin films are required for a variety of optoelectronic applications: automotive and aircraft windows, and solar cells for space applications. Transparent conductive coatings of indium-tin-oxide (ITO)-magnesium fluoride (MgF2) and aluminum doped zinc oxide (AZO) at several dopant levels are investigated for electrical resistivity (sheet resistance), carrier concentration, optical properties, and atomic oxygen durability. The sheet resistance values of ITO-MgF2 range from 102 to 1011 ohms/square, with transmittance of 75 to 86 percent. The AZO films sheet resistances range from 107 to 1011 ohms/square with transmittances from 84 to 91 percent. It was found that in general, with respect to the optical properties, the zinc oxide (ZnO), AZO, and the high MgF2 content ITO-MgF2 samples, were all durable to atomic oxygen plasma, while the low MgF2 content of ITO-MgF2 samples were not durable to atomic oxygen plasma exposure. Author (revised)

N94-23372*# National Aeronautics and Space Administration. Lewis Research Center, Cleveland, OH.
POWER CONSOLE DEVELOPMENT FOR NASA'S ELECTRIC PROPULSION OUTREACH PROGRAM
Luis R. Pinero, Michael J. Patterson, and Vincent E. Satterwhite Dec. 1993 22 p Presented at the 23rd International Electric Propulsion Conference, Seattle, WA, 13-16 Sep. 1993; sponsored by AIAA, AIDAA, DGLR, and JSASS
(RTOP 506-42-31)
(NASA-TM-106428; E-8270; NAS 1.15:106428; IEPC-93-250) Avail: CASI HC A03/MF A01

NASA LeRC is developing a 30 cm diameter xenon ion thruster for auxiliary and primary propulsion applications. To maximize expectations for user-acceptance of ion propulsion technology, NASA LeRC, through their Electric Propulsion Outreach Program, is providing sectors of industry with portable power consoles for operation of 5 KW-class xenon ion thrusters. This power console provides all necessary functions to permit thruster operations over a 0.5-5 KW envelope under both manual and automated control. These functions include the following: discharge, cathode heater, neutralizer keeper, and neutralizer heater currents, screen and accelerator voltages, and a gas feed system to regulate and control propellant flow to the thruster. An electronic circuit monitors screen and accelerator currents and controls arcing events. The power console was successfully integrated with the NASA 30 cm thruster. Author (revised)

N94-23433# Los Alamos National Lab., NM.
ASSESSMENT OF AN SP-100 BI-MODAL PROPULSION AND POWER SYSTEM
J. J. Buksa, S. DeMuth, and T. Huber (Naval Academy, Annapolis, MD.) 1993 11 p Presented at the 11th Symposium on Space Nuclear Power Systems, Albuquerque, NM, 9-13 Jan. 1994
(Contract W-7405-eng-36)
(DE94-000889; LA-UR-93-3324; CONF-940101-4) Avail: CASI HC A03/MF A01 (US Sales Only)

The attractiveness of using the SP-100 space nuclear power system for both electric power production and direct thermal propulsion is discussed. A conceptual modification to the SP-100 generic flight system that uses its hot, primary coolant to directly heat hydrogen propellant is presented. An analytical model of the system and its orbital-mechanical behavior is presented and used to assess the benefits of a number of orbital transfer missions. Both a 500 kW and a 2.4 MW system are assessed. Preliminary results indicate that for LEO-to-GEO transfers, the SP-100 bimodal system offers a 100% increase in payload over conventional chemical-only propulsion systems with transfer times on the order of days. DOE

N94-23452# Los Alamos National Lab., NM.
SP-100 HEAT TRANSPORT TECHNOLOGY DEVELOPMENT
J. J. Buksa 1993 8 p Presented at the 11th Symposium on Space Nuclear Power Systems, Albuquerque, NM, 9-13 Jan. 1994
(Contract W-7405-eng-36)
(DE94-000769; LA-UR-93-3361; CONF-940101-11) Avail: CASI HC A02/MF A01 (US Sales Only)

SP-100 space nuclear power system heat transport technology is reviewed, and we discuss progress to date in several key areas. Technical challenges, achievements, and the current status of the thermoelectric-electromagnetic pump and gas separator/accumulator components are presented. Validation experiments, analytical models, and manufacturing processes developed for these components are summarized. Remaining components of the heat transport subsystems, including the auxiliary cooling and thaw subsystem are also discussed briefly. A concise bibliography is supplied, where further detailed information on specific technical issues can be found. DOE

N94-23459# Martin Marietta Astro Space, Philadelphia, PA.
GPHS-RTG'S IN SUPPORT OF THE CASSINI MISSION
24 Oct. 1993 93 p
(Contract DE-AC03-91SF-18852)
(DE94-001445; DOE/SF-18852/T31) Avail: CASI HC A05/MF A01

The following tasks were reported: Spacecraft integration and liaison; engineering support; safety; qualified unicouple fabrication; ETG fabrication/assembly/test; ground support equipment; RTG shipping and launch support; designs/reviews/mission applications; and project management/quality assurance/contract changes. DOE

N94-23531*# National Aeronautics and Space Administration. Lewis Research Center, Cleveland, OH.
INVESTIGATION OF A SUBSONIC-ARC-ATTACHMENT THRUSTER USING SEGMENTED ANODES
Darren H. Berns (Minnesota Univ., Minneapolis.), John M. Sankovic, and Charles J. Sarmiento Dec. 1993 25 p Presented at the 29th Joint Propulsion Conference and Exhibit, Monterey, CA, 28-30 Jun. 1993; sponsored by AIAA, SAE, ASME, and ASEE See also A93-49769
(RTOP 506-42-31)
(NASA-TM-106419; E-7790; NAS 1.15:106419; AIAA Paper 93-1899)
Avail: CASI HC A03/MF A01

To investigate high frequency arc instabilities observed in subsonic-arc-attachment thrusters, a 3 kW, segmented-anode arc jet was designed and tested using hydrogen as the propellant. The thruster nozzle geometry was scaled from a 30 kW design previously tested in the 1960's. By observing the current to each segment and the arc voltage, it was determined that the 75-200 kHz instabilities were results of axial movements of the arc anode attachment point. The arc attachment point was fully contained in the subsonic portion of the nozzle for nearly all flow rates. The effects of isolating selected segments were investigated. In some cases, forcing the arc downstream caused the restrike to cease. Finally, decreasing the background pressure from 18 to 0.05 Pa affected the pressure distribution in the nozzle including the pressure in the subsonic arc chamber. Author (revised)

N94-23555*# Sverdrup Technology, Inc., Brook Park, OH.
LOW POWER GROUND-BASED LASER ILLUMINATION FOR ELECTRIC PROPULSION APPLICATIONS Final Report
Michael R. LaPointe and Steven R. Oleson Jan. 1994 28 p Presented at the 23rd International Electric Propulsion Conference, Seattle, WA, 13-16 Sep. 1993; sponsored by AIAA, AIDAA, DGLR, and JSASS
(Contract NAS3-25266; RTOP 506-42-31)
(NASA-CR-194444; NAS 1.26:194444; IEPC-93-208) Avail: CASI HC A03/MF A01

A preliminary evaluation of low power, ground-based laser powered electric propulsion systems is presented. A review of available and near-term laser, photovoltaic, and adaptive optic systems indicates that approximately 5-kW of ground-based laser power can be delivered at an equivalent one-sun intensity to an orbit of approximately 2000 km. Laser illumination at the proper wavelength can double photovoltaic array conversion efficiencies compared to efficiencies obtained with solar illumination at the same intensity, allowing a reduction in array mass. The reduced array mass allows extra propellant to be carried with no penalty in total spacecraft mass. The extra propellant mass can extend the satellite life in orbit, allowing additional revenue to be generated. A trade study using realistic cost estimates and conservative ground station viewing capability was performed to estimate the number of communication satellites which must be illuminated to make a proliferated system of laser ground stations economically attractive. The required number of satellites is typically below that of proposed communication satellite constellations, indicating that low power ground-based laser beaming may be commercially viable. However, near-term advances in low specific mass solar arrays and high energy density batteries for LEO applications would render the ground-based laser system impracticable. Author (revised)

N94-23630*# National Aeronautics and Space Administration. Lewis Research Center, Cleveland, OH.
PERFORMANCE EVALUATION OF THE RUSSIAN SPT-100 THRUSTER AT NASA LeRC
John M. Sankovic, John A. Hamley, and Thomas W. Haag Jan. 1994 25 p Presented at the 23rd IEPC Conference, Seattle, WA, 13-16 Sep. 1993; sponsored by AIAA, AIDAA, DGLR, and JSASS
(RTOP 506-42-31)
(NASA-TM-106401; E-8235; NAS 1.15:106401; IEPC-93-094) Avail: CASI HC A03/MF A01

Performance measurements of a Russian flight-model SPT-100 thruster were obtained as part of a comprehensive program to evaluate engineering issues pertinent to integration with Western spacecraft. Power processing was provided by a US Government developed laboratory power conditioner. When received the thruster had been subjected to only a few hours of acceptance testing by the manufacturer. Accumulated operating time during this study totalled 148 h and included operation of both cathodes. Cathode flow fraction was controlled both manually and using the flow splitter contained within the supplied xenon flow controller. Data were obtained at current levels ranging from 3 A to 5 A and thruster voltages ranging from 200 V to 300 V. Testing centered on the design power of 1.35 kW with a discharge current of 4.5 A. The effects of facility pressure on thruster operation were examined by varying the pressure via injection of xenon into the vacuum chamber. The facility pressure had a significant effect on thruster performance and stability at the conditions tested. Periods of current instabilities were noted throughout the testing period and became more frequent as testing progressed. Performance during periods of stability agreed with previous data obtained in Russian laboratories. Author

N94-24061*# Rockwell International Corp., Canoga Park, CA. Rocketdyne Div.
HEAT PIPE COOLED HEAT REJECTION SUBSYSTEM MODELLING FOR NUCLEAR ELECTRIC PROPULSION Final Report
Michael P. Moriarty 16 Nov. 1993 174 p
(Contract NAS3-25808)
(NASA-CR-191132; NAS 1.26:191132) Avail: CASI HC A08/MF A02

NASA LeRC is currently developing a FORTRAN based computer model of a complete nuclear electric propulsion (NEP) vehicle that can be used for piloted and cargo missions to the Moon or Mars. Proposed designs feature either a Brayton or a K-Rankine power conversion cycle to drive a turbine coupled with rotary alternators. Both ion and magnetoplasmodynamic (MPD) thrusters will be considered in the model. In support of the NEP model, Rocketdyne is developing power conversion, heat rejection, and power management and distribution (PMAD) subroutines. The subroutines will be incorporated into the NEP vehicle model which will be written by NASA LeRC. The purpose is to document the heat pipe cooled heat rejection subsystem model and its supporting subroutines. The heat pipe cooled heat rejection subsystem model is designed to provide estimate of the mass and performance of the equipment used to reject heat from Brayton and Rankine cycle power conversion systems. The subroutine models the ductwork and heat pipe cooled manifold for a gas cooled Brayton; the heat sink heat exchanger, liquid loop piping, expansion compensator, pump and manifold for a liquid loop cooled Brayton; and a shear flow condenser for a K-Rankine system. In each case, the final heat rejection is made by way of a heat pipe radiator. The radiator is sized to reject the amount of heat necessary. Author (revised)

N94-24064*# Thiokol Corp., Brigham City, UT. Space Operations.
POSTFLIGHT HARDWARE EVALUATION RSRM-29 (STS-54). APPENDIX C: NOZZLE PFORs Final Report
Sep. 1993 86 p
(Contract NAS8-38100)
(NASA-CR-193894; NAS 1.26:193894; TWR-64222) Avail: CASI HC A05/MF A01

Appendix C, Nozzle Postflight Observation Records (PFOR's) for the Final Postflight Hardware Evaluation Report RSRM-29 (STS-54) is provided. PFOR data are included on: nozzle joint condition; nose inlet-to-throat joint condition; and nozzle subassembly phenolic bondline condition. CASI

N94-24361*# Sverdrup Technology, Inc., Brook Park, OH.
STATIONARY PLASMA THRUSTER PLUME CHARACTERISTICS Final Report
Roger M. Myers and David H. Manzella Feb. 1994 22 p Presented at the 23rd International Electric Propulsion Conference, Seattle, WA, 13-16 Sep. 1993; sponsored by AIAA
(Contract NAS3-25266; RTOP 506-42-31)
(NASA-CR-194454; E-840626; NAS 1.26:194454) Avail: CASI HC A03/MF A01

Stationary Plasma Thrusters (SPT's) are being investigated for application to a variety of near-term missions. This paper presents the results of a preliminary study of the thruster plume characteristics which are needed to assess spacecraft integration requirements. Langmuir probes, planar probes, Faraday cups, and a retarding potential analyzer were used to measure plume properties. For the design operating voltage of 300 V the centerline electron density was found to decrease from approximately 1.8 x 10 exp 17 cubic meters at a distance of 0.3 m to 1.8 X 10 exp 14 cubic meters at a distance of 4 m from the thruster. The electron temperature over the same region was between 1.7 and 3.5 eV. Ion current density measurements showed that the plume was sharply peaked, dropping by a factor of 2.6 within 22 degrees of centerline. The ion energy 4 m from the thruster and 15 degrees off-centerline was approximately 270 V. The thruster cathode flow rate and facility pressure were found to strongly affect the plume properties. In addition to the plume measurements, the data from the various probe types were used to assess the impact of probe design criteria Author (revised)

N94-24471*# SECA, Inc., Huntsville, AL.
HEAT TRANSFER IN ROCKET ENGINE COMBUSTION CHAMBERS AND REGENERATIVELY COOLED NOZZLES Final Report
16 Nov. 1993 169 p Original contains color illustrations
(Contract NAS8-38961)
(NASA-CR-195094; NAS 1.26:195094; SECA-FR-93-18) Avail: CASI HC A08/MF A02; 35 functional color pages

A conjugate heat transfer computational fluid dynamics (CFD) model to describe regenerative cooling in the main combustion chamber and nozzle and in the injector faceplate region for a launch vehicle class liquid rocket engine was developed. An injector model for sprays which treats the fluid as a variable density, single-phase media was formulated, incorporated into a version of the FDNS code, and used to simulate the injector flow typical of that in the Space Shuttle Main Engine (SSME). Various chamber related heat transfer analyses were made to verify the predictive capability of the conjugate heat transfer analysis provided by the FDNS code. The density based version of the FDNS code with the real fluid property models developed was successful in predicting the streamtube combustion of individual injector elements. Author (revised)

N94-24511# Westinghouse Idaho Nuclear Co., Inc., Idaho Falls.
IMPROVED GAS CORE PROPULSION MODEL
J. E. Tanner 1993 7 p Presented at the 11th Symposium on Space Nuclear Power Systems, Albuquerque, NM, 9-13 Jan. 1994.
(Contract DE-AC07-84ID-12435)
(DE94-000929; WINCO-11981; CONF-940101-13) Avail: CASI HC A02/MF A01 (US Sales Only)

A thermodynamic, radiation transport model of a gas core nuclear propulsion reactor has been developed in one-dimensional, spherical geometry, which satisfies local energy balance and allows for arbitrary variation of fuel/propellant ratio and flow rate as functions of radius. Initial cases calculated yield specific impulses of about 1150 sec, but very low thrusts ranging 5-10 kN. DOE

N94-24595*# Georgia Inst. of Tech., Atlanta. Electro-Optics, Environment and Materials Lab.
ASSESSMENT OF IMPACT DAMAGE OF COMPOSITE ROCKET MOTOR CASES Final Report, 1 Nov. 1993 - 28 Feb. 1994
Henry G. Paris 19 Feb. 1994 38 p
(Grant NAG8-1016)
(NASA-CR-195143; NAS 1.26:195143) Avail: CASI HC A03/MF A01

This contract reviewed the available literature on mechanisms of low velocity impact damage in filament wound rocket motor cases, NDE methods to quantify damage, critical coupon level test methods, manufacturing and material process variables and empirical and analytical modeling off impact damage. The critical design properties for rocket motor cases are biaxial hoop and axial tensile strength. Low velocity impact damage is insidious because it can create serious nonvisible damage at very low impact velocities. In thick rocket motor cases the prevalent low velocity impact damage is fiber fracture and matrix cracking adjacent to the front face. In contrast, low velocity loading of thin wall cylinders induces flexure, depending on span length and the flexure induces delamination and tensile cracking on the back face wall opposed to impact occurs due to flexural stresses imposed by impact loading. Important NDE methods for rocket motor cases are non-contacting methods that allow inspection from one side. Among these are vibrothermography, and pulse-echo methods based on acoustic-ultrasonic methods. High resolution techniques such as x-ray computed tomography appear to have merit for accurate geometrical characterization of local damage to support development of analytical models of micromechanics. The challenge of coupon level testing is to reproduce the biaxial stress state that the full scale article experiences, and to determine how to scale the composite structure to model full sized behavior. Biaxial tensile testing has been performed by uniaxially tensile loading internally pressurized cylinders. This is experimentally difficult due to gripping problems and pressure containment. Much prior work focused on uniaxial tensile testing of model filament wound cylinders. Interpretation of the results of some studies is complicated by the fact that the fabrication process did not duplicate full scale manufacturing. It is difficult to scale results from testing subscale cylinders since there are significant differences in out time of the resins relative to full scale cylinder fabrication, differences in hoop fiber tensioning and unsatisfactory coupon configurations. It appears that development of a new test method for subscale cylinders is merited. Damage tolerance may be improved by material optimization that uses fiber treatments and matrix modifications to control the fiber matrix interface bonding. It is difficult to develop process optimization in subscale cylinders without also modeling the longer out times resins experience in full scale testing. A major breakthrough in characterizing the effect of impact damage on residual strength, and understanding how to scale results of subscale evaluations, will be a sound micromechanical model that described progressive failure of the composite. Such models will utilize a three dimensional stress analysis due to the complex nature of low velocity impact stresses in thick composites. When these models are coupled with non-contact NDE methods that geometrically characterize the damage and acoustic methods that characterize the effective local elastic properties, accurate assessment of residual strength from impact damage may be possible. Directions for further development are suggested. Author

N94-24681*# National Aeronautics and Space Administration. Lewis Research Center, Cleveland, OH.
POWER GENERATION TECHNOLOGY OPTIONS FOR A MARS MISSION
John M. Bozek and Robert L. Cataldo Jan. 1994 8 p Presented at the Symposia on Space Nuclear Power Systems, Albuquerque, NM, 9-13 Jan. 1994; sponsored by University of New Mexico
(RTOP 233-02-0B)
(NASA-TM-106451; E-8310; NAS 1.15:106451) Avail: CASI HC A02/MF A01

The power requirements and resultant power system performances of an aggressive Mars mission are characterized. The power system technologies discussed will support both cargo and piloted space transport vehicles as well as a six-person crew on the Martian surface for 600 days. The mission uses materials transported by cargo vehicles and materials produced using in-situ planetary feed stock to establish a life-support cache and infrastructure for the follow-on piloted lander. Numerous power system technical options are sized to meet the mission power requirements using conventional and solar, nuclear, and wireless power transmission technologies for stationary, mobile surface, and space applications. Technology selections will depend on key criteria such as mass, volume, area, maturity, and application flexibility. Author

N94-24714*# Sverdrup Technology, Inc., Brook Park, OH.
NUMERICAL SIMULATION OF CYLINDRICAL, SELF-FIELD MPD THRUSTERS WITH MULTIPLE PROPELLANTS Final Report
Michael R. LaPointe Mar. 1994 21 p Presented at the 23rd International Electric Propulsion Conference, Seattle, WA, 13-16 1993; sponsored by ASC, AIAA, DGLR, AIDAA, and JSASS
(Contract NAS3-25266; RTOP 506-42-81)
(NASA-CR-194458; E-8481; NAS 1.26:194458) Avail: CASI HC A03/MF A01

A two-dimensional, two-temperature, single fluid MHD code was used to predict the performance of cylindrical, self-field magnetoplasmadynamic (MPD) thrusters operated with argon, lithium, and hydrogen propellants. A thruster stability equation was determined relating maximum stable J(sup 2)/m values to cylindrical thruster geometry and propellant species. The maximum value of J(sup 2)/m was found to scale as the inverse of the propellant molecular weight to the 0.57 power, in rough agreement with limited experimental data which scales as the inverse square root of the propellant molecular weight. A general equation which relates total thrust to electromagnetic thrust, propellant molecular weight, and J(sup 2)/m was determined using reported thrust values for argon and hydrogen and calculated thrust values for lithium. In addition to argon, lithium, and hydrogen, the equation accurately predicted thrust for ammonia at sufficiently high J(sup 2)/m values. A simple algorithm is suggested to aid in the preliminary design of cylindrical, self-field MPD thrusters. A brief example is presented to illustrate the use of the algorithm in the design of a low power MPD thruster. Author (revised)

N94-24766*# National Aeronautics and Space Administration. Lewis Research Center, Cleveland, OH.
PRELIMINARY FAR-FIELD PLUME SPUTTERING CHARACTERIZATION OF THE STATIONARY PLASMA THRUSTER (SPT-100)
Eric J. Pencil Jan. 1994 12 p Presented at the 23rd International Electric Propulsion Conference, Seattle, WA, 13-16 Sep. 1993; sponsored by AIAA, DGLR, AIDAA, and JSASS
(RTOP 506-42-31)
(NASA-TM-106464; E-8328; NAS 1.15:106464; IEPC-93-098) Avail: CASI HC A03/MF A01

For electric propulsion devices to be considered for use on communications satellites, integration impacts must be examined in detail. Two phenomena of concern associated with highly energetic plumes are contamination via sputtered material from the thruster and sputter erosion of downstream surfaces. In order to characterize the net effect of both phenomena, an array of witness plates were mounted in several types of holders and were exposed to the SPT-100 thruster plume for 50 hours. Surface analysis of the witness plates revealed that in the most energetic regions of the plume, there was a net removal of material from the samples facing the thruster. In the peripheral regions, net deposits were observed and characterized by the changes in optical properties of these samples. Changes in surface properties of samples located in collimators were within experimental uncertainty. Author

N94-24770*# National Aeronautics and Space Administration. Lewis Research Center, Cleveland, OH.
PERFORMANCE OF THE NASA cm ION THRUSTER
Michael J. Patterson, Thomas W. Haag, and Scot A. Hovan (Dayton Univ., OH.) Dec. 1993 27 p Presented at the 23rd International Electric Propulsion Conference, Seattle, WA, 13-16 Sep. 1993; sponsored by AIAA, AIDAA, DGLR, and JSASS
(RTOP 506-42-31)
(NASA-TM-106426; E-8268; NAS 1.15:106426; IEPC-93-108) Copyright Avail: CASI HC A03/MF A01

A 30 cm diameter xenon ion thruster is under development at NASA to provide an ion propulsion option for missions of national interest, and is being proposed for use on the USAF/TRW Space Surveillance, Tracking and Autonomous Repositioning (SSTAR) platform to validate ion propulsion. The thruster incorporates innovations in design, materials, and fabrication techniques compared to those employed in conventional ion thrusters. Specific development efforts include thruster design optimizations, component life testing and validation, vibration testing, and performance characterizations. Under this test program, the ion thruster will be brought to engineering model development status. This paper discusses the performance and power throttling test data for the NASA 30 cm diameter xenon ion thruster over an input power envelope of 0.7 to 4.9 kW, and corresponding thruster lifetime expectations. Author

N94-24834*# Texas Univ., Austin. Mechanical Engineering Dept.
EMBODIMENT DESIGN FOR A MULTIPROPELLANT RESISTOJET
Johnny Bao, Thierry Chilosi, Jason Goodwin, Jim Mocio, and Bruce Yeh 3 May 1993 59 p
(Contract NASw-4435)
(NASA-CR-195505; NAS 1.26:195505) Avail: CASI HC A04/MF A01

This document presents the design of a multipropellant resistojet to use as an auxiliary propulsion system on the Space Station. Such a system is necessary to counteract atmospheric drag effects encountered by the Station in its orbit. NASA specifications are strictly followed with emphasis on reliability, operating life, multipropellant capability, and exhaust emission control. Several design variants are considered, and the final solution is a resistojet with an electronic pressure regulator, variable control, an internal flow heater, and a conical nozzle. To construct the resistojet, the important components are resolved independently and then integrated with secondary units. The document also includes engineering drawings of the final design with assembly instructions. Before final utilization, a prototype testing is recommended to uncover possible problems. Author (revised)

N94-24979*# Texas Univ., Austin. Mechanical Engineering Dept.
DESIGN OF A RESISTOJET FOR SPACE STATION FREEDOM
Jose Garza, Jill Reisman, Jose Tapia, and Anthony Wright 3 May 1993 53 p
(Contract NASw-4435)
(NASA-CR-195506; NAS 1.26:195506) Avail: CASI HC A04/MF A01

In the mid 1990's, NASA will begin assembly of Space Station Freedom, a permanent outpost in a low-earth orbit. For the station to remain in that orbit, an altitude control system must be developed to resist the effects of atmospheric drag. One system being considered by NASA is called a resistojet, and it uses highly pressurized waste gases heated by electrical resistance to provide thrust on the order of 1 Newton. An additional function of the resistojet is to vent waste gases used by the station and its inhabitants. This report focuses on resolving the issues of system performance, flow and heater control, and materials selection and designing test procedures to resolve, by experimentation, any remaining issues. The conceptual model of the resistojet consists of a shell wrapped by a resistive coil with gases flowing internally through the tube with additional components such as regulators, transducers, and thermocouples. For system performance, the major parameters were calculated from the desired thrust range, the pressure within the resistojet and the cold flow mode of operation; waste gases were analyzed at 100 percent capacity and between 58.95 kPa and 552 kPa. The design team found that any ventilation under all conditions would produce thrust, and therefore, it was decided to limit the design of the ventilation function. The design team proceeded with a simplified model to determine the nozzle throat diameter and chamber diameter. Author (revised)

N94-25019*# United Technologies Corp., West Palm Beach, FL.
STE THRUST CHAMBER TECHNOLOGY: MAIN INJECTOR TECHNOLOGY PROGRAM AND NOZZLE ADVANCED DEVELOPMENT PROGRAM (ADP) Final Report
31 Oct. 1993 411 p
(Contract NAS8-37490)
(NASA-CR-193919; NAS 1.26:193919; FR-23116) Avail: CASI HC A18/MF A04

The purpose of the STME Main Injector Program was to enhance the technology base for the large-scale main injector-combustor system of oxygen-hydrogen booster engines in the areas of combustion efficiency, chamber heating rates, and combustion stability. The initial task of the Main Injector Program, focused on analysis and theoretical predictions using existing models, was complemented by the design, fabrication, and test at MSFC of a subscale calorimetric, 40,000-pound thrust class, axisymmetric thrust chamber operating at approximately 2,250 psi and a 7:1 expansion ratio. Test results were used to further define combustion stability bounds, combustion efficiency, and heating rates using a large injector scale similar to the Pratt & Whitney (P&W) STME main injector design configuration including the tangential entry swirl coaxial injection elements. The subscale combustion data was used to verify and refine analytical modeling simulation and extend the database range to guide the design of the large-scale system main injector. The subscale injector design incorporated fuel and oxidizer flow area control features which could be varied; this allowed testing of several design points so that the STME conditions could be bracketed. The subscale injector design also incorporated high-reliability and low-cost fabrication techniques such as a one-piece electrical discharged machined (EDMed) interpropellant plate. Both subscale and large-scale injectors incorporated outer row injector elements with scarfed tip features to allow evaluation of reduced heating rates to the combustion chamber. Author (revised)

N94-25189*# National Aeronautics and Space Administration. Lewis Research Center, Cleveland, OH.
POWER ELECTRONICS DEVELOPMENT FOR THE SPT-100 THRUSTER
John A. Hamley, Gerald M. Hill, and John M. Sankovic Feb. 1994 13 p Presented at the 23rd International Electric Propulsion Conference, Seattle, WA, 13-16 Sep. 1993; sponsored by AIAA, AIDAA, DGLA and JSASS
(RTOP 506-42-31)
(NASA-TM-106488; E-8475; NAS 1.15:106488; IEPEC-93-044) Avail: CASI HC A03/MF A01

Russian electric propulsion technologies have recently become available on the world market. Of significant interest is the Stationary Plasma Thruster

(SPT) which has a significant flight heritage in the former Soviet space program. The SPT has performance levels of up to 1600 seconds of specific impulse at a thrust efficiency of 0.50. Studies have shown that this level of performance is well suited for stationkeeping applications, and the SPT-100, with a 1.35 kW input power level, is presently being evaluated for use on Western commercial satellites. Under a program sponsored by the Innovative Science and Technology Division of the Ballistic Missile Defense Organization, a team of U.S. electric propulsion specialists observed the operation of the SPT-100 in Russia. Under this same program, power electronics were developed to operate the SPT-100 to characterize thruster performance and operation in the U.S. The power electronics consisted of a discharge, cathode heater, and pulse igniter power supplies to operate the thruster with manual flow control. A Russian designed matching network was incorporated in the discharge supply to ensure proper operation with the thruster. The cathode heater power supply and igniter were derived from ongoing development projects. No attempts were made to augment thruster electromagnet current in this effort. The power electronics successfully started and operated the SPT-100 thruster in performance tests at NASA Lewis, with minimal oscillations in the discharge current. The efficiency of the main discharge supply was measured at 0.92, and straightforward modifications were identified which could increase the efficiency to 0.94. Author (revised)

N94-25201*# National Aeronautics and Space Administration. Lewis Research Center, Cleveland, OH.

DEVELOPMENT OF A POWER ELECTRONICS UNIT FOR THE SPACE STATION PLASMA CONTACTOR

John A. Hamley, Gerald M. Hill, Michael J. Patterson, Joseph Saggio, Jr. (Analex Corp., Brook Park, OH.), Fred Terdan (Analex Corp., Brook Park, OH.), and Justin D. Mansell (Case Western Reserve Univ., Cleveland, OH.) Feb. 1994 14 p Presented at the 23rd International Electric Propulsion Conference, Seattle, WA, 13-16 Sep. 1993; sponsored by AIAA

(RTOP 506-42-31)

(NASA-TM-106486; E-8473; NAS 1.15:106486; IEPC-93-052) Avail: CASI HC A03/MF A01

A hollow cathode plasma contactor has been baselined as a charge control device for the Space Station (SS) to prevent deleterious interactions of coated structural components with the ambient plasma. NASA LeRC Work Package 4 initiated the development of a plasma contactor system comprised of a Power Electronics Unit (PEU), an Expellant Management Unit (EMU), a command and data interface, and a Plasma Contactor Unit (PCU). A breadboard PEU was designed and fabricated. The breadboard PEU contains a cathode heater and discharge power supply, which were required to operate the PCU, a control and auxiliary power converter, an EMU interface, a command and telemetry interface, and a controller. The cathode heater and discharge supplies utilized a push-pull topology with a switching frequency of 20 kHz and pulse-width-modulated (PWM) control. A pulse ignition circuit derived from that used in arcjet power processors was incorporated in the discharge supply for discharge ignition. An 8088 based microcontroller was utilized in the breadboard model to provide a flexible platform for controller development with a simple command/data interface incorporating a direct connection to SS Mulitplexer/Demultiplexer (MDM) analog and digital I/O cards. Incorporating this in the flight model would eliminate the hardware and software overhead associated with a 1553 serial interface. The PEU autonomously operated the plasma contactor based on command inputs and was successfully integrated with a prototype plasma contactor unit demonstrating reliable ignition of the discharge and steady-state operation. Author (revised)

N94-23641*# National Aeronautics and Space Administration. Lewis Research Center, Cleveland, OH.

UTILIZATION OF RECENTLY DEVELOPED CODES FOR HIGH POWER BRAYTON AND RANKINE CYCLE POWER SYSTEMS

Michael P. Doherty *In its* The Fifth Annual Thermal and Fluids Analysis Workshop Nov. 1993 p 83-94 Original contains color illustrations (For primary document see N94-23634 06-34)

Avail: CASI HC A02/MF A04; 5 functional color pages

N94-24243 In-Space Propulsion Ltd., Sacramento, CA.

LIQUID ROCKET PROPULSION: RETROSPECTIVE AND PROSPECTS

Sanders D. Rosenberg *In* Israel Society of Aeronautics and Astronautics, The 33rd Israel Annual Conference on Aviation and Astronautics 25 Feb. 1993 p 27-36 (For primary document see N94-24241 06-01)

Copyright Avail: Issuing Activity (Israel Society of Aeronautics and Astronautics, c/o Faculty of Engineering, Tel-Aviv Univ., Ramat Aviv 69978, Israel)

N94-24254 Technion - Israel Inst. of Tech., Haifa. Faculty of Aerospace Engineering.

DESIGN CONSIDERATIONS OF HYBRID ROCKETS

Adela Ben-Yakar *In* Israel Society of Aeronautics and Astronautics, The 33rd Israel Annual Conference on Aviation and Astronautics 25 Feb. 1993 p 166-174 (For primary document see N94-24241 06-01)

Copyright Avail: Issuing Activity (Israel Society of Aeronautics and Astronautics, c/o Faculty of Engineering, Tel-Aviv Univ., Ramat Aviv 69978, Israel)

N94-24419*# Ohio Univ., Athens. Dept. of Industrial and Systems Engineering.

A MINIMUM COST TOLERANCE ALLOCATION METHOD FOR ROCKET ENGINES AND ROBUST ROCKET ENGINE DESIGN

Richard J. Gerth *In* Alabama Univ., The 1993 NASA/ASEE Summer Faculty Fellowship Program Nov. 1993 5 p (For primary document see N94-24405 06-80)

Avail: CASI HC A01/MF A03

N94-24444*# Christian Brothers Coll., Memphis, TN. Mechanical Engineering Dept.

SPACE SHUTTLE MAIN ENGINE PERFORMANCE ANALYSIS

L. Michael Santi *In* Alabama Univ., The 1993 NASA/ASEE Summer Faculty Fellowship Program Nov. 1993 5 p (For primary document see N94-24405 06-80)

Avail: CASI HC A01/MF A03

N94-25352*# Louisiana Tech Univ., Ruston. Dept. of Electrical Engineering.

PARALLEL PROCESSING METHODS FOR SPACE BASED POWER SYSTEMS

F. C. Berry *In* NASA. Johnson Space Center, National Aeronautics and Space Administration (NASA)/American Society for Engineering Education (ASEE) Summer Faculty Fellowship Program, 1993, Volume 1 Dec. 1993 15 p (For primary document see N94-25348 06-99)

Avail: CASI HC A03/MF A03

23 CHEMISTRY AND MATERIALS (GENERAL)

N94-23500*# National Aeronautics and Space Administration. Lewis Research Center, Cleveland, OH.

THEORETICAL CONSIDERATIONS FOR REACTION-FORMED SILICON CARBIDE (RFSC) FORMATION BY MOLTEN SILICON INFILTRATION INTO SLURRY-DERIVED PREFORMS

D. R. Behrendt and M. Singh Dec. 1993 11 p

(RTOP 537-04-20)

(NASA-TM-106414; E-8250; NAS 1.15:106414) Avail: CASI HC A03/MF A01

For reaction-formed silicon carbide (RFSC) ceramics produced by silicon melt infiltration of porous carbon preforms, equations are developed to relate the amount of residual silicon to the initial carbon density. Also, for a slurry derived preform containing both carbon and silicon powder, equations are derived which relate the amount of residual silicon in the RFSC to the relative density of the carbon in the preform and to the amount of silicon powder added to the slurry. For a porous carbon preform that does not have enough porosity to prevent choking-off of the silicon infiltration, these results show that complete silicon infiltration can occur by adding silicon powder to the slurry mixture used to produce these preforms. Author (revised)

N94-23591*# National Aeronautics and Space Administration. Lewis Research Center, Cleveland, OH.

A METHOD TO REMOVE INTERCALATES FROM BROMINE AND IODINE INTERCALATED CARBON FIBERS

Ching-cheh Hung Dec. 1993 9 p Presented at the 21st Biennial Conference on Carbon, Buffalo, NY, 13-18 Jun. 1993; sponsored by the American Carbon Society
(RTOP 505-41-41)
(NASA-TM-106443; E-8287; NAS 1.15:16443) Avail: CASI HC A02/MF A01

Upon exposure to room-temperature fluorine, intercalated carbon fibers (containing either bromine alone or iodine and bromine together) become heavier and less stable. For Amoco P-100 graphitized carbon fibers which were intercalated with 18 percent bromine by weight, 1 hr of fluorine exposure results in a large weight increase, but causes only a small decrease in thermal stability. More than I hr of fluorine exposure time results in small additional increases in fiber weight, but significant further decreases in fiber thermal stability. Such phenomena do not occur if the fluorine exposure is at 250 C. These observations suggest the mechanism that at room temperature, fluorine is absorbed quickly by the intercalated fibers and intercalated slowly into the fibers. Most of the original intercalates are replaced by fluorine in the process of fluorine intercalation. Under an inert environment, the bromine intercalated fibers are much more thermally stable. After 800 C vacuum heating for two weeks, the brominated fibers lost about 45 percent of their bromine, and their resistivity increased from 64 omega-cm to a range of 95 to 170 micro omega-cm. This is still much lower than the 300 micro omega-cm value for pristine P-100. For practical purposes, in order to preserve their thermal stability, brominated fibers need to be protected from exposure to fluorine at room temperature, or to any intercalate at a temperature where, upon direct contact to graphite, an intercalation compound can easily be formed. Author

N94-24338*# National Aeronautics and Space Administration. Marshall Space Flight Center, Huntsville, AL.

MICROGRAVITY STUDIES OF ORGANIC AND POLYMERIC MATERIALS

D. O. Frazier, ed., C. E. Moore, ed., and B. H. Cardelino, ed. (Spelman Coll., Atlanta, GA.) Washington Dec. 1993 286 p Workshop held in Huntsville, AL, 27 Apr. 1993
(NASA-CP-3250; M-736; NAS 1.55:3250) Avail: CASI HC A13/MF A03

This document contains extended abstracts and presentation transcripts from a workshop on microgravity studies of organic and polymeric materials held in Huntsville, Alabama, April 27, 1993. For individual titles, see N94-24339 through N94-24354.

N94-24339*# Minnesota Mining and Mfg. Co., Saint Paul. Science Research Lab.

ORDERED ORGANIC THIN FILMS SELF-ASSEMBLED FROM THE VAPOR PHASE c27

M. K. Debe *In* NASA. Marshall Space Flight Center, Microgravity Studies of Organic and Polymeric Materials Dec. 1993 p 11-15 (For primary document see N94-24338 06-23)
Avail: CASI HC A01/MF A03

Organic films self-assembled from a liquid phase, as in Langmuir-Blodgett or adsorption from solution, have received much attention in the past decade as techniques to achieve highly oriented-ordered polymeric thin films. Many organic compounds including some of the same fatty acids have been vapor deposited as well. However, organic pigments and dyes comprise a major class of important materials which have very low solubilities yet excellent thermal stabilities, making them ideally suited for film deposition from the vapor phase. Surprisingly, such molecular systems exhibit a significant propensity to self order, a high sensitivity to deposition parameters, and a range of microstructural forms that cannot be duplicated by the less energetic mechanisms associated with solution adsorption processes. Molecular solids such as heterocyclic polynuclear aromatics are excellent candidates for film formation by vacuum deposition means. Over the past decade, our work and that of others investigating a wide variety of perylene and phthalocyanine derivatives identified five deposition parameters that can significantly affect film morphology, physical microstructure, and type and extent of ordering developed in vacuum and vapor transport grown films. These parameters are substrate temperature, deposition rate, substrate chemistry and epitaxy, ambient gas convective flows, and post deposition annealing. Examples of how each of these conditions manifest themselves in the film structure and ordering, most frequently revealed by scanning electron microscopy, reflection absorption infrared spectroscopy (RAIR), and grazing incidence x-ray diffraction (GIX), are presented. Author (revised)

N94-24340*# Auburn Univ., AL. Dept. of Mechanicial Engineering.

NUMERICAL MODELING OF PHYSICAL VAPOR TRANSPORT UNDER MICROGRAVITY CONDITIONS: EFFECT OF THERMAL CREEP AND STRESS c29

Daniel W. Mackowski and Roy W. Knight *In* NASA. Marshall Space Flight Center, Microgravity Studies of Organic and Polymeric Materials Dec. 1993 p 17-20 (For primary document see N94-24338 06-23)
Avail: CASI HC A01/MF A03

One of the most promising applications of microgravity (micro-g) environments is the manufacture of exotic and high-quality crystals in closed cylindrical ampoules using physical vapor transport (PVT) processes. The quality enhancements are believed to be due to the absence of buoyant convection in the weightless environment - resulting in diffusion-limited transport of the vapor. In a typical experiment, solid-phase sample material is initially contained at one end of the ampoule. The sample is made to sublime into the vapor phase and deposit onto the opposite end by maintaining the source at an elevated temperature with respect to the deposit. Identification of the physical factors governing both the rates and uniformity of crystal growth, and the optimization of the micro-g technology, will require an accurate modeling of the vapor transport within the ampoule. Previous micro-g modeling efforts have approached the problem from a 'classical' convective/diffusion formulation, in which convection is driven by the action of buoyancy on thermal and solutal density differences. The general conclusion of these works have been that in low gravity environments the effect of buoyancy on vapor transport is negligible, and vapor transport occurs in a diffusion-limited mode. However, it has been recently recognized than in the non-isothermal (and often low total pressure) conditions encountered in ampoules, the commonly-assumed no-slip boundary condition to the differential equations governing fluid motion can be grossly unrepresentative of the actual situation. Specifically, the temperature gradients can give rise to thermal creep flows at the ampoule side walls. In addition, temperature gradients in the vapor itself can, through the action of thermal stress, lead to bulk fluid convection. Author (revised)

N94-24341*# Rensselaer Polytechnic Inst., Troy, NY. Dept. of Chemistry.

ELECTRIC FIELD-MEDIATED PROCESSING OF POLYMER BLEND SOLUTIONS c27

G. E. Wnek and S. Krause *In* NASA. Marshall Space Flight Center, Microgravity Studies of Organic and Polymeric Materials Dec. 1993 p 21-23 (For primary document see N94-24338 06-23)
Avail: CASI HC A01/MF A03

Multiphase polymer blends in which the minor phases are oriented in a desired direction may demonstrate unique optical, electrical, and mechanical properties. While morphology development in shear fields was studied extensively, little work has focused on effects of electric fields on phase structure. The use of electric fields for blend morphology modulation with particular attention given to solvent casting of blends in d.c. fields was explored. Both homopolymer blends (average phase sizes of several microns) and diblock copolymer/homopolymer blends (average phase sizes of hundreds of Angstroms) were investigated. Summarized are important observations and conclusions. Author (revised)

N94-24342*# Michigan Univ., Ann Arbor. Materials Science and Engineering.

DEFECTS IN ELECTRO-OPTICALLY ACTIVE POLYMER SOLIDS c27

David C. Martin *In* NASA. Marshall Space Flight Center, Microgravity Studies of Organic and Polymeric Materials Dec. 1993 p 25-43 (For primary document see N94-24338 06-23)
Avail: CASI HC A03/MF A03

There is considerable current interest in the application of organic and polymeric materials for electronic and photonic devices. The rapid, non-linear optical (NLO) response of these materials makes them attractive candidates for waveguides, interferometers, and frequency doublers. In order to realize the full potential of these systems, it is necessary to develop processing schemes which can fabricate these molecules into ordered arrangements. There is enormous potential for introducing well-defined, local variations in microstructure to control the photonic properties of organic materials by rational 'defect engineering.' This effort may eventually become as technologically important as the manipulation of the electronic structure of solid-state silicon based devices is at present. The success of this endeavor will require complimentary efforts in the synthesis, processing, and characterization of new materials. Detailed information about local microstructure will be necessary to understand the influence of symmetry breaking of the solid phases near point, line, and planar defects. In metallic and inorganic polycrystalline materials, defects play an important role in modifying macroscopic properties. To understand the influence of particular defects on the properties of materials, it has proven useful to isolate the defect by creating bicrystals between two-component single crystals. In this way the geometry of a grain boundary defect and its effect on macroscopic properties can be determined unambiguously. In crystalline polymers it would be valuable to establish a similar depth of understanding about the relationship between defect structure and macroscopic properties. Conventionally processed crystalline polymers have small crystallites (10-20 nm), which implies a large defect density in the solid state. Although this means that defects may play an important or even dominant role in crystalline or liquid crystalline polymer systems, it also makes it difficult to isolate the effect of a particular boundary on a macroscopically observed property. However, the development of solid-state and thin-film polymerization mechanisms have facilitated the synthesis of highly organized and ordered polymers. These systems provide a unique opportunity to isolate and investigate in detail the structure of covalently bonded solids near defects and the effect of these defects on the properties of the material. The study of defects in solid polymers has been the subject of a recent review (Martin, 1993). Derived from text

N94-24343*# National Aeronautics and Space Administration. Marshall Space Flight Center, Huntsville, AL.

PREDICTION OF NONLINEAR OPTICAL PROPERTIES OF ORGANIC MATERIALS. GENERAL THEORETICAL CONSIDERATIONS Abstract Only c74

B. Cardelino (Atlanta Univ. Center, Inc., GA.), C. Moore, and S. Zutaut (Alabama Univ., Huntsville.) *In its* Microgravity Studies of Organic and Polymeric Materials Dec. 1993 p 45-46 (For primary document see N94-24338 06-23)

Avail: CASI HC A01/MF A03

The prediction of nonlinear optical properties of organic materials is geared to assist materials scientists in the selection of good candidate molecules. A brief summary of the quantum mechanical methods used for estimating hyperpolarizabilities will be presented. The advantages and limitations of each technique will be discussed. Particular attention will be given to the finite-field method for calculating first and second order hyperpolarizabilities, since this method is better suited for large molecules. Corrections for dynamic fields and bulk effects will be discussed in detail, focusing on solvent effects, conformational isomerization, core effects, dispersion, and hydrogen bonding. Several results will be compared with data obtained from third-harmonic-generation (THG) and dc-induced second harmonic generation (EFISH) measurements. These comparisons will demonstrate the qualitative ability of the method to predict the relative strengths of hyperpolarizabilities of a class of compounds. The future application of molecular mechanics, as well as other techniques, in the study of bulk properties and solid state defects will be addressed. The relationship between large values for nonlinear optical properties and large conjugation lengths is well known, and is particularly important for third-order processes. For this reason, the materials with the largest observed nonresonant third-order properties are conjugated polymers. An example of this type of polymer is polydiacetylene. One of the problems in dealing with polydiacetylene is that substituents which may enhance its nonlinear properties may ultimately prevent it from polymerizing. A model which attempts to predict the likelihood of solid-state polymerization is considered, along with the implications of the assumptions that are used. Calculations of the third-order optical properties and their relationship to first-order properties and energy gaps will be discussed. The relationship between monomeric and polymeric third-order optical properties will also be considered. Author

N94-24344*# Alabama Univ., Huntsville. Center for Microgravity and Materials Research.

TEMPERATURE DEPENDENCE OF PROTEIN SOLUBILITY-DETERMINATION, APPLICATION TO CRYSTALLIZATION, AND GROWTH KINETICS STUDIES Abstract Only c76

Franz Rosenberger *In* NASA. Marshall Space Flight Center, Microgravity Studies of Organic and Polymeric Materials Dec. 1993 p 47 (For primary document see N94-24338 06-23)

Avail: CASI HC A01/MF A03

A scintillation method was developed for determinations of the temperature dependence of the solubility, and of nucleation induction times of proteins, in 50-100 mu(l) volumes of solution. Solubility data for lysozyme and horse serum albumin were obtained for various combinations of pH and precipitant concentrations. These data and the nucleation induction information were used for dynamic crystallization control, that is, for the controlled separation of nucleation and growth stages. Individual lysozyme and horse serum albumin crystals were grown in 15-20 mu(l) solution volumes contained in x-ray capillaries. The morphology and kinetics of the growth and dissolution of lysozyme in aqueous solutions with 2.5 percent NaCl and at pH = 4.5 was studied in situ with a depth resolution of 300 A (4 unit cells) by high resolution optical microscopy and digital image processing. The bulk super- or under saturation, sigma, of the solution inside a closed growth cell was controlled by temperature. The growth habit was bound by (110) and (101) faces that grew through layer spreading, although with different growth rate dependencies on supersaturation/temperature. At sigma less than 10 (obtained at higher temperatures) growth was purely kinetic ally controlled, with impurity effects (macrostep formation and kinetic hindrance) becoming significant for sigma less than 2. At sigma greater than 10 (lower temperatures), anisotropies in the interfacial kinetics were more pronounced, with interfacial kinetics and bulk transport becoming equally important to the growth morphology. Growth rates were growth history dependent. The formation of striations (layers of irregularly incorporated solution) was unambiguously correlated with growth temperature variations. Etching exposed dislocations and various high-index faces whose growth morphologies were studied during return to the steady state growth form. Growth steps were observed to originate from two-dimensional nuclei or from outcrops of growth striations, and from dislocations that preferentially formed in growth sector boundaries. Author

N94-24345*# National Aeronautics and Space Administration. Marshall Space Flight Center, Huntsville, AL.

MODELING OF PCG FLUID DYNAMICS: SALIENT RESULTS c29

N. Ramachandran *In its* Microgravity Studies of Organic and Polymeric Materials Dec. 1993 p 49-60 (For primary document see N94-24338 06-23)

Avail: CASI HC A03/MF A03

Materials processing in space-based laboratories has already yielded higher quality crystals during previous space flights, and opportunities for several fluids experiments are anticipated during the extended duration missions planned for the future. Crystal growth in space benefits not only from its reduced gravity environment but also from the absence of the hydrostatic pressure which assists certain crystal growth and refinement methods. Gravity-driven phenomena are thus reduced in strength, and a purely diffusive fluid's behavior can be attained. In addition, past materials science experiments have shown that microgravity can also help produce larger crystals. While gravity-related effects are definitely curtailed in space, they are nevertheless present to some degree due to the acceleration environment onboard the spacecraft. This residual acceleration level is comprised of quasi-steady, oscillatory, and transient components, and is caused by a variety of mechanisms. For example, gravity gradient forces produce low frequency disturbances, and the operation of machinery, control thrusters, solar panels, human activity, etc. contribute to higher frequency accelerations. These disturbances are collectively referred to as g-jitter, and they can be deleterious to certain experiments where the minimization of the acceleration level is important. Advanced vibration isolation techniques can be utilized to actively filter out some of the detrimental frequencies and help in obtaining optimum results. However, the successful application of this technology requires the detailed analysis of candidate fluids experiments to gauge their response to g-jitter and to determine their acceleration sensitivities. Several crystal growth experiments in the Protein Crystal Growth (PCG) area, besides others, are expected to be carried out on future shuttle flights and on Space Station Freedom. The need for vibration isolation systems or components for microgravity science experiments can be expected to grow as experiments and available hardware becomes more complex. This technology will also find increased application as the science community develops an awareness of their specific needs relative to the environment available in manned space missions. Vibration isolation research strives to develop a microgravity environment requirement that defines tolerance limits on the allowable g-level, and provides the required technology to achieve it. This effort will assist in establishing the tolerable acceleration levels for specific fluids experiments. The primary effort is directed towards modeling PCG and the approach undertaken for this investigation is outlined. The objectives of this research are: (1) to computationally determine vibration sensitivity of protein crystal growth experiments; (2) determine if these experiments can benefit from vibration isolation techniques; and (3) provide realistic requirements for vibration isolation technology. Derived from text

N94-24346*# National Aeronautics and Space Administration. Marshall Space Flight Center, Huntsville, AL.

LOW-GRAVITY ELECTRODEPOSITION AND GROWTH OF POLYMER THIN FILMS WITH LARGE THIRD-ORDER OPTICAL NONLINEARITIES BY ELECTROCHEMICAL PROCESSES FOR DEVICES: THIOPHENE-BASED POLYMERS Abstract Only c29

Benjamin G. Penn and Clyde Riley (Alabama Univ., Huntsville.) *In its* Microgravity Studies of Organic and Polymeric Materials Dec. 1993 p 61-62 (For primary document see N94-24338 06-23)
Avail: CASI HC A01/MF A03

It has been proposed that NLO thin film properties may be improved by low-gravity processing. Strong candidates for NLO thin film applications are the polythiophenes. Polymeric thiophenes are attractive materials due to their ease of preparation, stability, and high X(exp 3). A simple and convenient method for preparation of polythiophenes is electrochemical oxidation. We will apply some of our experience and lessons learned in low-gravity metal, metal/cermet electrode position to improve the quality of polythiophene(s) thin films. In low gravity electrode position of Ni at a high rate on an Au substrate often results in the production of an x-ray non diffracting surface. Cobalt metal deposition does not give this result nor does Ni when deposited similarly on a glassy carbon substrate. Co/Ni alloy composition produced during electrode position is strongly dependent upon the amount of convection. Code position of neutral inert cermets with metals is influenced significantly by the presence of gravity and the size of the cermets. Tracks left in the 1-g surfaces by unsuccessful particle occlusion indicate suspension of the large particles is not the only reason for poor volume percentages of the larger particles in the deposits. All size particles are more homogeneously distributed in the deposits in low-gravity electrocodeposition than in 1-g. Low gravity gives larger volume percentages for the larger particles in the deposits, while 1-g gives larger volume percentages for the smaller particles. Intermediate size particles give mixed results. The experimental cells were constructed with flat electrode end plates such that 1-g bench reference electrode positions could be carried out at various orientations with respect to gravity. A series of bench studies using similar designed cells are suggested so that convection modification can be applied to electrochemical thin film preparation. Convection effects can then be coupled with other parameter variations in current, temperature, concentration, solvent, electrolyte, and anode substrates to optimize the properties of NLO thin films before resorting to low-gravity processing. Author

N94-24347*# National Aeronautics and Space Administration. Marshall Space Flight Center, Huntsville, AL.

POLYDIACETYLENE THIN FILMS FOR NONLINEAR OPTICAL APPLICATIONS Abstract Only c74

Mark S. Paley *In its* Microgravity Studies of Organic and Polymeric Materials Dec. 1993 p 63-64 (For primary document see N94-24338 06-23)
Avail: CASI HC A01/MF A03

One very promising class of organic compounds for nonlinear optical (NLO) applications are polydiacetylenes, which are novel in that they are highly conjugated polymers which can also be crystalline. Polydiacetylenes offer several advantages over other organic materials: because of their highly conjugated electronic structures, they are capable of possessing large optical nonlinearities with fast response times; because they are crystalline, they can be highly ordered, which is essential for optimizing their NLO properties; and, last, because they are polymeric, they can be formed as thin films, which are useful for device fabrication. We have actively been carrying out ground-based research on several compounds of interest. Derived from text

N94-24348*# Westinghouse Science and Technology Center, Pittsburgh, PA.

CRYSTAL GROWTH OF ORGANICS FOR NONLINEAR OPTICAL APPLICATIONS c74

N. B. Singh and R. Mazelsky *In* NASA. Marshall Space Flight Center, Microgravity Studies of Organic and Polymeric Materials Dec. 1993 p 65-66 (For primary document see N94-24338 06-23)
Avail: CASI HC A01/MF A03

The crystal growth and characterization of organic and inorganic nonlinear optical materials were extensively studied. For example, inorganic crystals such as thallium arsenic selenide were studied in our laboratory for several years and crystals in sizes over 2.5 cm in diameter are available. Organic crystals are suitable for the ultraviolet and near infrared region, but are relatively less developed than their inorganic counterparts. Very high values of the second harmonic conversion efficiency and the electro-optic coefficient were reported for organic compounds. Single crystals of a binary organic alloy based on m.NA and CNA were grown and higher second harmonic conversion efficiency than the values reported for m.NA were observed. Author (revised)

N94-24349*# Alabama Univ., Huntsville. Chemistry Dept.

NONLINEAR OPTICAL THIN FILMS c74

Thomas M. Leslie *In* NASA. Marshall Space Flight Center, Microgravity Studies of Organic and Polymeric Materials Dec. 1993 p 67-68 (For primary document see N94-24338 06-23)
Avail: CASI HC A01/MF A03

A focused approach to development and evaluation of organic polymer films for use in optoelectronics is presented. The issues and challenges that are addressed include: (1) material synthesis, purification, and the tailoring of the material properties; (2) deposition of uniform thin films by a variety of methods; (3) characterization of material physical properties (thermal, electrical, optical, and electro-optical); and (4) device fabrication and testing. Photonic materials, devices, and systems were identified as critical technology areas by the Department of Commerce and the Department of Defense. This approach offers strong integration of basic material issues through engineering applications by the development of materials that can be exploited as the active unit in a variety of polymeric thin film devices. Improved materials were developed with unprecedented purity and stability. The absorptive properties can be tailored and controlled to provide significant improvement in propagation losses and nonlinear performance. Furthermore, the materials were incorporated into polymers that are highly compatible with fabrication and patterning processes for integrated optical devices and circuits. By simultaneously addressing the issues of materials development and characterization, keeping device design and fabrication in mind, many obstacles were overcome for implementation of these polymeric materials and devices into systems. We intend to considerably improve the upper use temperature, poling stability, and compatibility with silicon based devices. The principal device application that was targeted is a linear electro-optic modulation etalon. Organic polymers need to be properly designed and coupled with existing integrated circuit technology to create new photonic devices for optical communication, image processing, other laser applications such as harmonic generation, and eventually optical computing. The progression from microscopic sample to a suitable film-forming material in a working device is a complex, multifaceted endeavor. It requires close attention to maintaining the optical properties of the electro-optic active portion of the polymer while manipulating the polymer structure to obtain the desired secondary polymer properties. Author (revised)

N94-24350*# Lehigh Univ., Bethlehem, PA. Emulsion Polymers Inst. and Dept. of Chemistry.

FEASIBILITY STUDY: MONODISPERSE POLYMER PARTICLES CONTAINING LASER-EXCITABLE DYES c27

John W. Vanderhoff and Jing-Hong Chen *In* NASA. Marshall Space Flight Center, Microgravity Studies of Organic and Polymeric Materials Dec. 1993 p 69-88 (For primary document see N94-24338 06-23)
Avail: CASI HC A03/MF A03

The objective was to determine the feasibility of the preparation of monodisperse spherical poly(methyl methacrylate) and polystyrene particles that contain laser-excitable dyes in the size range 0.1 microns to 1 cm. Poly(methyl methacrylate) and polystyrene were chosen because of their excellent optical properties. The sphericity was required for uniformity of spectral output of re-irradiated light from the dye-containing particles. The monodispersity was required to give each particle the same optical properties when exposed to laser light. Author (revised)

N94-24351*# Massachusetts Inst. of Tech., Cambridge. Dept. of Materials Science and Engineering.
PROCESSING OF SEMICRYSTALLINE POLYMERS c27
Peggy Cebe and Mark V. Brillhart *In* NASA. Marshall Space Flight Center, Microgravity Studies of Organic and Polymeric Materials Dec. 1993 p 89-91 (For primary document see N94-24338 06-23)
Avail: CASI HC A01/MF A03

Our research group has been interested in the processing-structure-property relationships in semicrystalline polymers and blends for many years. In situ real time x ray scattering at elevated temperatures is being used to monitor the development of structure. An ongoing collaboration with Dr. Malcolm Capel at the Brookhaven National Synchrotron Light Source allows the performance of real time wide and small angle x ray scattering to study the phase transformations in semicrystalline polymers. The first part of my presentation will be about our recent use of x ray scattering to study blends of poly(ethylene terephthalate) with polyarylates. The purpose of the next portion of the presentation is to show how we may study effects of self-deformation of polymers during processing in the gravity environment, using real time x ray scattering. In this way, how processing stresses alter the microstructure of semicrystalline polymers was learned, and ultimately microgravity processing strategies that will result in more uniform morphology in these polymers is hoped to be developed. Author (revised)

N94-24352*# University of Southern Mississippi, Hattiesburg. Dept. of Chemistry and Biochemistry.
CONVECTIVE INSTABILITIES IN TRAVELING FRONTS OF ADDITION POLYMERIZATION c27
John A. Pojman, Chris E. Jones, and Akhtar M. Khan *In* NASA. Marshall Space Flight Center, Microgravity Studies of Organic and Polymeric Materials Dec. 1993 p 93-97 (For primary document see N94-24338 06-23)
Avail: CASI HC A01/MF A03

An autocatalytic reaction in an unstirred vessel can support a constant velocity wavefront resulting from the coupling of diffusion to the chemical reaction. A flare front is a common example in which heat is the autocatalytic species that diffuses into unreacted regions stimulating a reaction that produces more heat. Traveling fronts were studied in synthetic polymerization reactions under high pressure by workers in the former USSR. More recently, propagating fronts of methacrylic acid polymerization were studied under ambient conditions, both with video techniques and by NMR. Author (revised)

N94-24353*# Tennessee Univ., Knoxville. Dept. of Chemistry.
POLYMER MORPHOLOGH c27
Bernhard Wunderlich *In* NASA. Marshall Space Flight Center, Microgravity Studies of Organic and Polymeric Materials Dec. 1993 p 99-104 (For primary document see N94-24338 06-23)
Avail: CASI HC A02/MF A03

All polymeric materials in their final application are aggregates of many molecules. For linear macromolecules, these aggregates are highly entangled and their macroscopic properties are affected in a little-known way by the interpenetration and entanglements of the molecules. Over the years, we have done occasional investigations of single molecule single crystals and found that there are many unsolved questions about their nucleation, growth, kinetically determined shape, and ultimate path to equilibrium morphology on annealing. This initial work could be extended by a study of the applicability of microgravity methods for the production and study of the formation of single molecule particles. The production of separated molecules of sufficient size to produce phase-like behavior would involve perhaps a spray of solutions containing single molecules, followed by evaporation of the volatiles, or precipitation out of dispersion droplets. Other methods may involve Langmuir films etc., as shown in our prior work. The microgravity environment should enhance the efficiency of any of these methods by avoiding the joining of growing particles by reduction of convection and settling due to density differences. Once produced, the single molecule droplets are to be quenched into the glassy state and analyzed morphologically and thermally. Their shape alone can be used for molecular mass determination (an old problem that suffered from the need to estimate the shape of collapsed (flat) droplets on a surface). Next would be the study of changes of properties as a function of time, temperature, and molecular mass (and distribution) on fusion to macroscopic single phases. Author (revised)

N94-24354*# Jet Propulsion Lab., California Inst. of Tech., Pasadena.
OPTIMIZATION OF MICROSCOPIC AND MACROSCOPIC SECOND ORDER OPTICAL NONLINEARITIES c74
Seth R. Marder and Joseph W. Perry (California Inst. of Tech., Pasadena.) *In* NASA. Marshall Space Flight Center, Microgravity Studies of Organic and Polymeric Materials Dec. 1993 p 107-117 (For primary document see N94-24338 06-23)
Avail: CASI HC A03/MF A03

Nonlinear optical materials (NLO) can be used to extend the useful frequency range of lasers. Frequency generation is important for laser-based remote sensing and optical data storage. Another NLO effect, the electro-optic effect, can be used to modulate the amplitude, phase, or polarization state of an optical beam. Applications of this effect in telecommunications and in integrated optics include the impression of information on an optical carrier signal or routing of optical signals between fiber optic channels. In order to utilize these effects most effectively, it is necessary to synthesize materials which respond to applied fields very efficiently. In this talk, it will be shown how the development of a fundamental understanding of the science of nonlinear optics can lead to a rational approach to organic molecules and materials with optimized properties. In some cases, figures of merit for newly developed materials are more than an order of magnitude higher than those of currently employed materials. Some of these materials are being examined for phased-array radar and other electro-optic switching applications. Author (revised)

N94-25238# Technische Univ., Eindhoven (Netherlands).
ON THE MECHANISM OF ACTION OF 3',5'-CYCLIC ADENOSINE MONOPHOSPHATE: A STUDY OF FOUR- AND FIVE-COORDINATED PHOSPHORUS COMPOUNDS, MODELLING THE ACTIVATED STATE OF cAMP Ph.D. Thesis
Nicolaas Lambertus H Broeders 1993 132 p
(ISBN-9-03-860222-7; ETN-94-95324) Avail: CASI HC A07/MF A02

A study to gain insight into the interaction of cyclic adenosine monophosphate (cAMP) with enzymes, like protein kinases and phosphodiesterases, is reported. The role of phosphorus in cAMP during its interaction with enzymes was concentrated upon. Five coordinated phosphorus model systems, with a Trigonal bipyramidal geometry (TBP), which are supposed to be intermediates formed during the interaction between cAMP and enzymes, like protein kinases and phosphodiesterases, were studied. During this process the coordination of phosphorus increases from four, P(sup 4), to five, P(sup 5). This phosphorus coordination enhancing process and the resulting structural properties of the intermediates are studied. A set of stable P(sup 5) model systems, simulating the interaction between cAMP and an enzyme (protein kinase, phosphodiesterase, or CAP-dimer), which are studied by H-1 NMR (nuclear magnetic resonance) spectroscopy, is dealt with. A P-31 NMR study on the alkaline hydrolysis of a set of O-18 labelled cis nucleotide 3',5' cyclic aryl monophosphates is presented. A cAMP model compound, that is 2'-O-methyl-cis adenosine 3',5' cyclic monophosphate, is dealt with. ESA

24 COMPOSITE MATERIALS

Includes physical, chemical, and mechanical properties of laminates and other composite materials.

For ceramic materials see *27 Nonmetallic Materials.*

N94-22890 Toronto Univ. (Ontario). Dept. of Chemical Engineering and Applied Chemistry.
THE USE OF EXPANDING MONOMERS IN CARBON FIBRE COMPOSITES M.S. Thesis
Zhang Xiaodong 1993 97 p
(ISBN-0-315-83550-8; CTN-94-60945) Copyright Avail: Micromedia Ltd., Technical Information Centre, 240 Catherine Street, Suite 305, Ottawa, Ontario, K2P 2G8, Canada HC/MF

It is considered that the toughness across the grain of carbon fiber composites can be improved by reducing the cure shrinkage of the matrix. In an experimental investigation, the expanding monomer dinorbornene spiro ortho carbonate (DNSOC) was added to the epoxy in an attempt to reduce shrinkage stress. In addition, a two stage curing process was used to ensure that the expanding monomer did not polymerize while the resin mixture was still liquid. A reduction in shrinkage stress was observed, accompanied by a reduction in the glass transition temperature. Bi-material strip tests and thermal expansion measurements showed that there was very little chemical shrinkage stress in the copolymer system. Stress relaxation measurements showed that the stress generated by the chemical expansion of the DNSOC disappeared quickly during the cure. It was thus concluded that the shrinkage pressure was not significantly affected by the expansion of the DNSOC. Rather, the reduction of the overall shrinkage was due entirely to the reduction of the glass transition temperature. The toughness of the composites remained unchanged. Author (CISTI)

N94-22892 Toronto Univ. (Ontario). Dept. of Aerospace Science and Engineering.

OPTIMIZATION OF LAMINATE ORIENTATION TO ENHANCE FAILURE PROPERTIES M.S. Thesis

Hui Hongwei 1993 94 p

(ISBN-0-315-83539-7; CTN-94-60947) Copyright Avail: Micromedia Ltd., Technical Information Centre, 240 Catherine Street, Suite 305, Ottawa, Ontario, K2P 2G8, Canada HC/MF

The APC-2 polyether ether ketone/carbon fiber composite laminate was studied in both static and fatigue tests. Laminate theory and static tests were employed to study the maximum failure stress. The load applied was uniaxial and its orientation started from 0 deg fiber direction. Laminate theory and experimental results show that as the load direction changes, the failure stress will change and reach a maximum at 22.5 deg and 67.5 deg. Theoretical maximum failure stress values at these angles are 20 percent higher than those at 0, 45, or 90 deg; static test results give values 10 percent higher, both in tension and compression. The finite element method was used to reveal the stress field in the laminate. As the load direction changed, both the stress pattern and failure modes changed. Fatigue results are consistent with static results. The quasi-isotropic laminate has the same in-plane mechanical properties when intact, but once first failure occurs, these properties change. This change manifests itself in both the maximum failure stress and fatigue properties. Current studies show that under uniaxial load, the best performance is at angles of 22.5 deg and 67.5 deg. Author (CISTI)

N94-22977# Ames Lab., IA.

EVALUATION OF A5SI3Z(x) INTERMETALLICS FOR USE AS HIGH TEMPERATURE STRUCTURAL MATERIALS

Y. Kim, A. J. Thom, M. K. Meyer, and M. Akinc 1993 33 p Presented at the Fall Meeting of the Minerals, Metals and Materials Society: Physical Metallurgy and Materials in Conjunction with Materials Week and the Materials Applications and Services Exposition, Pittsburgh, PA, 17-21 Oct. 1993

(Contract W-7405-eng-82)

(DE93-041127; IS-M-753; CONF-931009-3) Avail: CASI HC A03/MF A01

Refractory intermetallic silicides are receiving increasing consideration for use as high temperature structural materials. A5Si3 compositions are particularly interesting due to their ability to incorporate a variety of interstitial ternary additions. These ternary additions present a unique opportunity to potentially tailor physical properties. Previous experimental work has shown that these additions can decrease the inherent thermal expansion anisotropy of Ti5Si3. This paper reviews some of the literature with respect to binary and ternary silicides of the form A5Si3Z(x). Recent experimental work by the authors on two promising compositions, Ti5Si3 and Mo5Si3, is discussed. Interstitial additions substantially improve the isothermal oxidation resistance of both Ti5Si3 and Mo5Si3. The lattice parameter of Ti5Si3 is significantly changed by ternary interstitial additions, indicating the extensive solubility of Ti5Si3 for such additions. The level of similar additions affects the phase assemblage of Mo5Si3. Hardness and toughness values from indentation measurements for selected compositions are given. DOE

N94-23004 Ames Lab., IA.

NEW EXTENSIONS IN THE DEVELOPMENT OF DEFORMATION PROCESSED METAL-METAL MATRIX COMPOSITES

T. W. Ellis and E. D. Gibson 1993 4 p Presented at the Joint MMIJ/TMS International Conference on Processing Materials for Properties, Honolulu, HI, 7-10 Nov. 1993 Limited Reproducibility: More than 20% of this document may be affected by microfiche quality

(Contract W-7405-eng-82)

(DE94-000692; IS-M-763; CONF-931103-3) Avail: CASI HC A01

Copper-refractory metal composites have been under development for some time. The experience gained with these materials has been used as a starting point for investigations into other alloy systems. Deformation processing for the production of metal-metal matrix composites has been applied to titanium-yttrium, yttrium-niobium, copper-cobalt, aluminum-niobium, and magnesium-refractory metal alloys. This process has been used to produce elevated strength material and also for the production of electrical capacitors. DOE

N94-23005 Ames Lab., IA.

CREEP DEFORMATION CHARACTERISTICS OF DUCTILE DISCONTINUOUS FIBER REINFORCED COMPOSITES

S. B. Biner 1993 14 p Presented at the Fall Meeting of the Minerals, Metals and Materials Society: Physical Metallurgy and Materials in Conjunction With Materials Week and the Materials Applications and Services Exposition, Pittsburgh, PA, 17-21 Oct. 1993 Limited Reproducibility: More than 20% of this document may be affected by poor print

(Contract W-7405-eng-82)

(DE94-000697; IS-M-768; CONF-931009-4) Avail: Issuing Activity (Department of Energy (DOE))

Role of material parameters and geometric parameters of ductile reinforcing phase on the creep deformation behavior of 20% discontinuously reinforced composite was numerically investigated including debonding and pull-out mechanisms. Results indicate that for rigidly bonded interfaces, the creep rate of the composite is not significantly influenced by the material properties and geometric parameters of the ductile reinforcing phase due to development of large hydrostatic stress and constrained deformation in the reinforcement. For debonding interfaces, the geometric parameters of the reinforcing phase are important; however, even with very weak interfacial behavior low composite creep rates can be achieved by suitable selection of the geometric parameters of the ductile reinforcing phase. DOE

N94-23022# Oak Ridge National Lab., TN.

DEVELOPMENT OF SILICON NITRIDE COMPOSITES WITH CONTINUOUS FIBER REINFORCEMENT

T. L. Starr (Georgia Inst. of Tech., Atlanta.), D. L. Mohr (Georgia Inst. of Tech., Atlanta.), W. J. Lackey (Georgia Inst. of Tech., Atlanta.), and J. A. Hanigofsky (Georgia Inst. of Tech., Atlanta.) Oct. 1993 25 p

(Contract DE-AC05-84OR-21400)

(DE94-001996; ORNL/Sub-87-00184/04) Avail: CASI HC A03/MF A01

The composites were fabricated using ultrafine Si powders prepared by attritor milling; the powders exhibit full conversion to Si nitride in less than 3 h at less than 1200 C (these conditions reduce degradation of the fibers compared to conventional). Effects of processing conditions on fiber properties and the use of fiber coatings to improve stability during processing as well as change the fiber-matrix interfacial properties were investigated. A duplex carbon-silicon carbide coating, deposited by CVD, reduced fiber degradation in processing, and it modified the fiber-matrix adhesion. Si nitride matrix composites were fabricated using reaction sintering, forming laminates, filament-wound plates, and tubes. In each case, an attritor milled Si powder slurry is infiltrated into ceramic fiber preforms or tows, which are then assembled to form a 3-D structure for reaction sintering. The resulting composites have properties comparable to chemical vapor infiltration densified composites, with reasonable strengths and graceful composite fracture behavior. DOE

N94-23133# Institut National des Sciences Appliquees de Lyon, Villeurbanne (France).

CONTRIBUTION TO THE INTERFACE MICROMECHANICAL STUDY AND TO THE DAMAGE FUNDAMENTAL PHENOMENA IN GLASS FIBER EPOXY RESIN MODEL COMPOSITES Ph.D. Thesis [CONTRIBUTION A L'ETUDE MICROMECANIQUE DE L'INTERFACE ET DES PHENOMENES ELEMENTAIRES D'ENDOMMAGEMENT DANS DES COMPOSITES MODELES FIBRE DE VERRE/RESINE EPOXYDE]

Pascal Feillard 1993 139 p In FRENCH Sponsored by Saint-Gobain Recherche, France Original contains color illustrations
(ISAL-93-0027; ETN-94-95170) Avail: CASI HC A07/MF A02

The interfacial micromechanical study of glass/epoxy model composites was carried out by tearing, by fragmentation and by microindentation experiments. The purpose was to study the effect of the fiber's surface silane content on the fiber's charge transfer and test relationships. The interfacial characteristics are known to influence the mechanical behavior of a composite material. The fragmentation tests demonstrated that the fragmentation phenomena is not well known and that simplifying hypothesis induces wrong test evaluations. The matrix local behavior was highlighted. The effect of lubrication on the elementary damage and the effect of the indentator characteristics on the decoherence force were demonstrated. The complexity of the elementary damage was stressed. ESA

N94-23279*# National Aeronautics and Space Administration. Langley Research Center, Hampton, VA.

FATIGUE LIFE AND CRACK GROWTH PREDICTION METHODOLOGY

J. C. Newman, Jr., E. P. Phillips, and R. A. Everett, Jr. (Army Vehicle Structures Lab., Hampton, VA.) Oct. 1993 47 p Presented at the AGARD Structures and Materials Panel Workshop on an Assessment of Fatigue Damage and Crack Growth Prediction Techniques, Bordeaux, France, 29-30 Sep. 1993
(RTOP 538-02-10-01)
(NASA-TM-109044; NAS 1.15:109044) Avail: CASI HC A03/MF A01

The capabilities of a plasticity-induced crack-closure model and life-prediction code to predict fatigue crack growth and fatigue lives of metallic materials are reviewed. Crack-tip constraint factors, to account for three-dimensional effects, were selected to correlate large-crack growth rate data as a function of the effective-stress-intensity factor range (delta(K(sub eff))) under constant-amplitude loading. Some modifications to the delta(K(sub eff))-rate relations were needed in the near threshold regime to fit small-crack growth rate behavior and endurance limits. The model was then used to calculate small- and large-crack growth rates, and in some cases total fatigue lives, for several aluminum and titanium alloys under constant-amplitude, variable-amplitude, and spectrum loading. Fatigue lives were calculated using the crack growth relations and microstructural features like those that initiated cracks. Results from the tests and analyses agreed well. Author (revised)

N94-23280*# National Aeronautics and Space Administration. Langley Research Center, Hampton, VA.

TIME DEPENDENT BEHAVIOR OF A GRAPHITE/THERMOPLASTIC COMPOSITE AND THE EFFECTS OF STRESS AND PHYSICAL AGING

Thomas S. Gates and Mark Feldman (Old Dominion Univ., Norfolk, VA.) Nov. 1993 41 p Presented at the AIAA/ASME/ASCE/AHS/ASC 34th SDM Conference, La Jolla, CA, 19-21 Apr. 1993
(RTOP 505-63-50-04)
(NASA-TM-109047; NAS 1.15:109047) Avail: CASI HC A03/MF A01

Two complimentary studies were performed to determine the effects of stress and physical aging on the matrix dominated time dependent properties of IM7/8320 composite. The first of these studies, experimental in nature, used isothermal tensile creep/aging test techniques developed for polymers and adapted them for testing of the composite material. From these tests, the time dependent transverse (S22) and shear (S66) compliance's for an orthotropic plate were found from short term creep compliance measurements at constant, sub-T(sub g) temperatures. These compliance terms were shown to be affected by physical aging. Aging time shift factors and shift rates were found to be a function of temperature and applied stress. The second part of the study relied upon isothermal uniaxial tension tests of IM7/8320 to determine the effects of physical aging on the nonlinear material behavior at elevated temperature. An elastic/viscoplastic constitutive model was used to quantify the effects of aging on the rate-independent plastic and rate-dependent viscoplastic response. Sensitivity of the material constants required by the model to aging time were determined for aging times up to 65 hours. Verification of the analytical model indicated that the effects of prior aging on the nonlinear stress/strain/time data of matrix dominated laminates can be predicted. Author

N94-23493# Lawrence Livermore National Lab., CA.

MATERIALS SCIENCE AND ENGINEERING

D. R. Lesuer Mar. 1993 30 p
(Contract W-7405-eng-48)
(DE94-003018; UCRL-ID-112775) Avail: CASI HC A03/MF A01

Five papers are included: processing and characterization of laminated metal composites, casting process modeling, characterizing the failure of composite materials, fiber-optic Raman spectroscopy for cure monitoring of advanced polymer composites, and modeling superplastic materials. DOE

N94-23514*# National Aeronautics and Space Administration. Hugh L. Dryden Flight Research Center, Edwards, CA.

MECHANICAL AND THERMAL BUCKLING ANALYSIS OF SANDWICH PANELS UNDER DIFFERENT EDGE CONDITIONS

William L. Ko Washington Oct. 1993 14 p Presented at the Pacific International Conference on Aerospace Science and Technology PICAST'1, Taiwan, Republic of China, 6-9 Dec. 1993
(RTOP 505-63-40)
(NASA-TM-4535; H-1953; NAS 1.15:4535) Avail: CASI HC A03/MF A01

By using the Rayleigh-Ritz method of minimizing the total potential energy of a structural system, combined load (mechanical or thermal load) buckling equations are established for orthotropic rectangular sandwich panels supported under four different edge conditions. Two-dimensional buckling interaction curves and three dimensional buckling interaction surfaces are constructed for high-temperature honeycomb-core sandwich panels supported under four different edge conditions. The interaction surfaces provide easy comparison of the panel buckling strengths and the domains of symmetrical and antisymmetrical buckling associated with the different edge conditions. Thermal buckling curves of the sandwich panels also are presented. The thermal buckling conditions for the cases with and without thermal moments were found to be identical for the small deformation theory. In sandwich panels, the effect of transverse shear is quite large, and by neglecting the transverse shear effect, the buckling loads could be overpredicted considerably. Clamping of the edges could greatly increase buckling strength more in compression than in shear. Author (revised)

N94-23566*# Virginia Univ., Charlottesville. School of Engineering and Applied Science.

OUT OF PLANE GRADIENTS IN LAMINATED COMPOSITES Final Report, 17 Dec. 1987 - 31 Dec. 1993

Carl T. Herakovich 20 Jan. 1994 3 p
(Grant NAG1-841)
(NASA-CR-194875; NAS 1.26:194875) Avail: CASI HC A01/MF A01

The research under this grant focused on three different, but related, research projects. All three projects were concerned with predicting the interlaminar stresses that develop in laminated composites in the presence of free edges. The first project was dedicated to the development of a new semi-analytical approximate solution for predicting interlaminar stresses. The second project was devoted to a study of the influence of boundary conditions, geometric parameters, and material modelling on interlaminar stresses in stiffened composite panels. The third project was dedicated to the development of a new finite element for efficient analysis of interlaminar stresses in curved, stiffened panels. A summary of each of the projects is given. Author (revised)

N94-24083*# National Aeronautics and Space Administration. Langley Research Center, Hampton, VA.

ANALYSIS OF LOCAL DELAMINATIONS CAUSED BY ANGLE PLY MATRIX CRACKS

Satish A. Salpekar (Analytical Services and Materials, Inc., Hampton, VA.), T. Kevin OBrien (Army Vehicle Structures Lab., Hampton, VA.), and K. N. Shivakumar (North Carolina Agricultural and Technical State Univ., Greensboro.) Nov. 1993 67 p
(RTOP 538-02-10-01)
(NASA-TM-109052; NAS 1.15:109052) Avail: CASI HC A04/MF A01

Two different families of graphite/epoxy laminates with similar layups but different stacking sequences, (0,theta,-theta) sub s and (-theta/theta/0) sub s were analyzed using three-dimensional finite element analysis for theta = 15 and 30 degrees. Delaminations were modeled in the -theta/theta interface, bounded by a matrix crack and the stress free edge. The total strain energy release rate, G, along the delamination front was computed using three different techniques: the virtual crack closure technique (VCCT), the equivalent domain Integral (EDI) technique, and a global energy balance technique. The opening fracture mode component of the strain energy release rate, GI, along the delamination front was also computed for various delamination lengths using VCCT. The effect of residual thermal and moisture stresses on G was evaluated. Author (revised)

N94-24137 Institute for Aerospace Research, Ottawa (Ontario). Structures and Materials Lab.

A PREDICTION METHOD FOR THE COMPRESSIVE STRENGTH OF IMPACT DAMAGED COMPOSITE LAMINATES

Y. Xiong, C. Poon, P. V. Straznicky (Carleton Univ., Ottawa, Ontario.), and H. Vietinghoff (Carleton Univ., Ottawa, Ontario.) Sep. 1993 23 p
(CTN-94-60925) Avail: Micromedia Ltd., Technical Information Centre, 165 Hotel de Ville, Place du Portage, Phase 2, Hull, Quebec J8X 3X2, Canada

An analytical method for the prediction of the compressive strength of composite laminates containing impact damage has been developed. Using the characteristics of the impact damage detected by the ultrasonic time-of-flight C-scan technique, the state of the damage is modeled by an elliptical soft inclusion. The degradation of the elastic moduli of the material in the inclusion is determined by a sublaminate buckling analysis. The stress distribution in the laminate containing the inclusion with the reduced moduli is determined using a complex potential method and the stress results are used in conjunction with three failure criteria to predict the residual compressive strength. Compression after impact tests on flat laminates manufactured from the Toray T800H/3900-2 material have been conducted to produce experimental results for validating the analytical method. Good agreements between predicted residual compressive strengths and experimental results have been obtained. Author (CISTI)

N94-24224*# Fiber Materials, Inc., Biddeford, ME. Energy Materials Testing Lab.

HUMIDITY EFFECTS ON SOLUBLE CORE MECHANICAL AND THERMAL PROPERTIES (POLYVINYL ALCOHOL/MICROBALLOON COMPOSITE) TYPE CG EXTENDOSPHERES, VOLUME 2 Final Report

28 May 1993 314 p
(Contract NAS8-37800)
(NASA-CR-193893; NAS 1.26:193893; EMTL-Rept-1539; FMI-EMTL-W/A-3111) Avail: CASI HC A14/MF A03

This document constitutes the final report for the study of humidity effects and loading rate on soluble core (PVA/MB composite material) mechanical and thermal properties under Contract No. 100345. This report describes test results procedures employed, and any unusual occurrences or specific observations associated with this test program. The primary objective of this work was to determine if cured soluble core filler material regains its tensile and compressive strength after exposure to high humidity conditions and following a drying cycle. Secondary objectives include measurements of tensile and compressive modulus, and Poisson's ratio, and coefficient of thermal expansion (CTE) for various moisture exposure states. A third objective was to compare the mechanical and thermal properties of the composite using 'SG' and 'CG' type extendospheres. The proposed facility for the manufacture of soluble cores at the Yellow Creek site incorporates no capability for the control of humidity. Recent physical property tests performed with the soluble core filler material showed that prolonged exposure to high humidity significantly degradates in strength. The purpose of these tests is to determine if the product, process or facility designs require modification to avoid imparting a high risk condition to the ASRM. Derived from text

N94-24402*# Pennsylvania State Univ., University Park. Composites Manufacturing Technology Center.

STRUCTURAL DESIGN CRITERIA FOR FILAMENT-WOUND COMPOSITE SHELLS Final Report

H. T. Hahn, D. W. Jensen, S. J. Claus, S. P. Pai, and P. A. Hipp Jan. 1994 172 p
(Grant NAG1-982)
(NASA-CR-195125; NAS 1.26:195125) Avail: CASI HC A08/MF A02

Advanced composite cylinders, manufactured by filament winding, provide a cost effective solution to many present structural applications; however, the compressive performance of filament-wound cylinders is lower than comparable shells fabricated from unidirectional tape. The objective of this study was to determine the cause of this reduction in thin filament-wound cylinders by relating the manufacturing procedures to the quality of the cylinder and to its compressive performance. The experiments on cylinder buckling were complemented by eigenvalue buckling analysis using a detailed geometric model in a finite element analysis. The applicability of classical buckling analyses was also investigated as a design tool. Derived from text

N94-24547# Lawrence Livermore National Lab., CA.

HIGH STRAIN RATE SUPERPLASTICITY IN METALS AND COMPOSITES

T. G. Nieh, J. Wadsworth, and K. Higashi (Osaka Prefecture Univ., Sakai, Japan.) Jul. 1993 8 p Presented at the International Union of Materials Research Societies on Advanced Materials, Tokyo, Japan, 31 Aug. - 4 Sep. 1993
(Contract W-7405-eng-48)
(DE94-001521; UCRL-JC-114187; CONF-9308122-13) Avail: CASI HC A02/MF A01

Superplastic behavior at very high strain rates (at or above 1 s(exp -1)) in metallic-based materials is an area of increasing interest. The phenomenon has been observed quite extensively in metal alloys, metal-matrix composites (MMC), and mechanically-alloyed (MA) materials. In the present paper, experimental results on high strain rate behavior in 2124 Al-based materials, including Zr-modified 2124, SiC-reinforced 2124, MA 2124, and MA 2124 MMC, are presented. Except for the required fine grain size, details of the structural requirements of this phenomenon are not yet understood. Despite this, a systematic approach to produce high strain rate superplasticity (HSRS) in metallic materials is given in this paper. Evidences indicate that the presence of a liquid phase, or a low melting point region, at boundary interfaces is responsible for HSRS. DOE

N94-24579*# Massachusetts Inst. of Tech., Cambridge. Technology Lab. for Advanced Composites.

PREDICTION OF THERMAL CYCLING INDUCED CRACKING IN POLMER MATRIX COMPOSITES Semiannual Report, Aug. 1993 - Jan. 1994

Hugh L. McManus Feb. 1994 162 p
(Grant NAG1-1493)
(NASA-CR-195135; NAS 1.26:195135) Avail: CASI HC A08/MF A02

The work done in the period August 1993 through February 1994 on the 'Prediction of Thermal Cycling Induced Cracking In Polymer Matrix Composites' program is summarized. Most of the work performed in this period, as well as the previous one, is described in detail in the attached Master's thesis, 'Analysis of Thermally Induced Damage in Composite Space Structures,' by Cecelia Hyun Seon Park. Work on a small thermal cycling and aging chamber was concluded in this period. The chamber was extensively tested and calibrated. Temperatures can be controlled very precisely, and are very uniform in the test chamber. Based on results obtained in the previous period of this program, further experimental progressive cracking studies were carried out. The laminates tested were selected to clarify the differences between the behaviors of thick and thin ply layers, and to explore other variables such as stacking sequence and scaling effects. Most specimens tested were made available from existing stock at Langley Research Center. One laminate type had to be constructed from available prepreg material at Langley Research Center. Specimens from this laminate were cut and prepared at MIT. Thermal conditioning was carried out at Langley Research Center, and at the newly constructed MIT facility. Specimens were examined by edge inspection and by crack configuration studies, in which specimens were sanded down in order to examine the distribution of cracks within the specimens. A method for predicting matrix cracking due to decreasing temperatures and/or thermal cycling in all plies of an arbitrary laminate was implemented as a computer code. The code also predicts changes in properties due to the cracking. Extensive correlations between test results and code predictions were carried out. The computer code was documented and is ready for distribution. Author (revised)

N94-24632# Lawrence Livermore National Lab., CA.

CRASHWORTHINESS ANALYSIS USING ADVANCED MATERIAL MODELS IN DYNA3D

R. W. Logan, M. J. Burger, L. D. McMichael, and R. D. Parkinson (Kaiser Aluminum and Chemical Corp., Pleasanton, CA.) 22 Oct. 1993 12 p Presented at the Annual Winter Meeting of the American Society of

Mechanical Engineers, New Orleans, LA, 28 Nov. - 3 Dec. 1993
(Contract W-7405-eng-48)
(DE94-002988; UCRL-JC-114579; CONF-931121-30) Avail: CASI HC A03/MF A01

As part of an electric vehicle consortium, LLNL and Kaiser Aluminum are conducting experimental and numerical studies on crashworthy aluminum spaceframe designs. They have jointly explored the effect of heat treat on crush behavior and duplicated the experimental behavior with finite-element simulations. The major technical contributions to the state of the art in numerical simulation arise from the development and use of advanced material model descriptions for LLNL's DYNA3D code. Constitutive model enhancements in both flow and failure have been employed for conventional materials such as low-carbon steels, and also for lighter weight materials such as aluminum and fiber composites being considered for future vehicles. The constitutive model enhancements are developed as extensions from LLNL's work in anisotropic flow and multiaxial failure modeling. Analysis quality as a function of level of simplification of material behavior and mesh is explored, as well as the penalty in computation cost that must be paid for using more complex models and meshes. The lightweight material modeling technology is being used at the vehicle component level to explore the safety implications of small neighborhood electric vehicles manufactured almost exclusively from these materials. DOE

N94-24735 Department of the Navy, Washington, DC.
FIRE-RESISTANT BARRIERS FOR COMPOSITE MATERIALS Patent
Usman A. Sorathis, inventor (to Navy) and Vincent Castelli, inventor (to Navy) 17 Aug. 1993 3 p Filed 25 Oct. 1991
(AD-D016014; US-Patent-5,236,773; US-Patent-Appl-SN-783039; US-Patent-Class-428-213) Avail: US Patent and Trademark Office

Fiber-reinforced plastic composite materials are fire protected by the application thereon of a combination of coatings comprising a ceramic coating and an intumescent coating. The ceramic coating consists of zirconia stabilized with yttria. DTIC

N94-24779# Materials Sciences Corp., Blue Bell, PA.
TEST METHODS FOR COMPOSITES: A STATUS REPORT. VOLUME 2: COMPRESSION TEST METHODS Final Report, Sep. 1990 - May 1993
S. Chaterjee, D. F. Adams, and D. W. Oplinger Jun. 1993 183 p
(Contracts DTFA03-88-A-0029; DAAL04-89-C-0023)
(AD-A273522; DOT/FAA/CT-93/17-Vol-2) Avail: CASI HC A09/MF A02

This document embodies the results of an evaluation of current test methods for compression properties of composite materials consisting of high modules, high strength fibers in organic matrix materials. Mechanical testing is an important step in the 'building block' approach to design of composite aircraft structures. The document provides a source of information by which the current compression test methods for advanced composites can be evaluated and from which test methods which appear to give good-quality test data can be selected. Problems with the available compression test methods are also addressed as a means of providing recommendations for future research. DTIC

N94-24942# Materials Sciences Corp., Blue Bell, PA.
TEST METHODS FOR COMPOSITES: A STATUS REPORT. VOLUME 1: TENSION TEST METHODS Final Report, Sep. 1990 - May 1993
S. Chaterjee, D. Adams, and D. W. Oplinger Jun. 1993 93 p
(Contracts DTFA03-88-A-0029; DAAL04-89-C-0023)
(AD-A273501; DOT/FAA/CT-93/17-Vol-1) Avail: CASI HC A05/MF A01

This document provides an evaluation of current test methods for tension properties of composite materials consisting of high modules, high strength fibers in organic matrix materials. Mechanical testing is an important step in the 'building block' approach to design of composite aircraft structures. The document provides a source of information by which the current test methods can be evaluated and from which test methods which appear to give good-quality test data can be selected. Problems with current test methods are also addressed as a means of providing recommendations for future research. DTIC

N94-25158# New York Univ., New York. Inst. of Mathematical Sciences.
CENTER FOR ANALYSIS OF HETEROGENEOUS AND NONLINEAR MEDIA Final Report, 1 Jan. 1990 - 31 Aug. 1993
Robert Kohn 31 Aug. 1993 7 p
(Grant AF-AFOSR-0090-90)
(AD-A273515; AFOSR-93-0867TR) Avail: CASI HC A02/MF A01

The researcher had many publications and refereed journals under this grant. Kohn worked with G. Allaire on numerical shape optimization for minimum compliance in plane stress. This work makes use of a relaxed formulation, seeking an optimal design made from perforated composite materials. The latter surveys recent progress on optimal bounds. Topics addressed include the optimal energy bounds for elastic composites, proved using the Hashin-Shtrikman principle, and optimal bounds on the effective moduli of polycrystals, proven by means of the translation method. DTIC

N94-25163 Materials Sciences Corp., Blue Bell, PA.
TEST METHODS FOR COMPOSITES: A STATUS REPORT. VOLUME 3: SHEAR TEST METHODS Final Report, Sep. 1990 - May 1993
S. Chaterjee, D. Adams, and D. W. Oplinger Jun. 1993 188 p Limited Reproducibility: More than 20% of this document may be affected by microfiche quality
(Contracts DTFA03-88-A-0029; DAAL04-89-C-0023)
(AD-A273561; DOT/FAA/CT-93/17-Vol-3) Avail: CASI HC A09

This document provides an evaluation of current test methods for shear properties of composite materials consisting of high modulus, high strength fibers in organic matrix materials. Mechanical testing is an important step in the 'building block' approach to design of composite aircraft structures. This document provides a source of information by which the current shear test methods can be evaluated and from which test methods which appear to give good-quality test data can be selected. Problems with the available shear test methods are also addressed as a means of providing recommendations for future research. DTIC

N94-25186*# National Aeronautics and Space Administration. Lewis Research Center, Cleveland, OH.
MATRIX FATIGUE CRACKING MECHANISMS OF ALPHA(2) TMC FOR HYPERSONIC APPLICATIONS
Timothy P. Gabb and John Gayda Feb. 1994 29 p Proposed for presentation at the Life Prediction Methodology for Titanium Matrix Composites, Hilton Head, SC, 22-24 Mar. 1994; sponsored by the American Society for Testing and Materials
(RTOP 505-63-1A)
(NASA-TM-106506; E-8610; NAS 1.15:106506) Avail: CASI HC A03/MF A01

The objective of this work was to understand matrix cracking mechanisms in a unidirectional alpha(sub 2) TMC in possible hypersonic applications. A (0)(sub 8) SCS-6/Ti-24Al-11Nb (at. percent) TMC was first subjected to a variety of simple isothermal and nonisothermal fatigue cycles to evaluate the damage mechanisms in simple conditions. A modified ascent mission cycle test was then performed to evaluate the combined effects of loading modes. This cycle mixes mechanical cycling at 150 and 483 C, sustained loads, and a slow thermal cycle to 815 C. At low cyclic stresses and strains more common in hypersonic applications, environment-assisted surface cracking limited fatigue resistance. This damage mechanism was most acute for out-of-phase nonisothermal cycles having extended cycle periods and the ascent mission cycle. A simple linear fraction damage model was employed to help understand this damage mechanism. Time-dependent environmental damage was found to strongly influence out-of-phase and mission life, with mechanical cycling damage due to the combination of external loading and CTE mismatch stresses playing a smaller role. The mechanical cycling and sustained loads in the mission cycle also had a smaller role. Author (revised)

N94-25386# Technical Research Centre of Finland, Espoo. Structural Engineering Lab.
ALTERNATIVES FOR REINFORCEMENT: FIBER COMPOSITES [BETONITERAEKSEN VAIHTOEHTOJA: KUITUKOMPOSIITIT]
Matti Lanu Oct. 1992 60 p In FINNISH Sponsored by Technology Development Center, Finland
(VTT-TIED-1412; ISBN-951-38-4306-8; ETN-94-95253) Copyright Avail: CASI HC A04/MF A01

Research on the analysis of brittle tendons and fibers in a cement based matrix is presented. The aim is to find simple and reliable design assumptions when developing and studying structural ideas. Composite tendons are similar to the normal prestressing tendons, but they are soft and brittle. Ductility can be achieved by increasing the amount of tendons so that the tendons do not break, but rather that there are plastic deformations in the compression zone instead. The strength of fiber reinforced concrete can be estimated by the classical law of mixture method. Fiber concrete can be used as shear reinforcement and in thin structures without main reinforcement. A difficult task is to determine the bond strength between the matrix and fiber and the stress-strain relationship of a composite. The calculation methods presented give conservative results when compared to the test results. However, there is no additional benefit in strength or in material costs. The main interest concerns durability and ease of production. ESA

N94-25420# Technical Research Centre of Finland, Espoo. Textile Lab.
COMPOSITES AND TEXTILE REINFORCEMENT [KOMPOSIITIT JA TEKSTIILILUJITE]
Mikael Epstein, Esa Suokas, Salme Nurmi, and Mikko Karttunen Dec. 1992 176 p In FINNISH Sponsored by Technology Development Center, Finland, and Technical Research Centre of Finland, Espoo
(VTT-TIED-1424; ISBN-951-38-4318-1; ETN-94-95256) Copyright Avail: CASI HC A09/MF A02

The application of various textile processes to the reinforcement structures for composites and the properties given by the reinforcement structures to composites were investigated. The project concentrated on the development of formable, near-net-shape and pre-formed reinforcement structures as well as on the plastic composites reinforced by these reinforcements. An altered narrow fabric loom was used to fabricate T, H, and O profiles of glass yarn and roving. The critical yarn passages were investigated by yarn-tension measurements. Pultrusion products were the most interesting applications of the narrow reinforcement fabrics produced by this project. Knitting of different glass yarns into various basic main knit structures was part of the program of knitting investigation. Composites with matrices of thermoset resin were made with knitted reinforcement fabric using hand laminating and RTM (Resin Transfer Molding) techniques. The mechanical material tests with the composite materials as well as the formability tests with the knitted reinforcement fabrics indicate that knitted reinforcements apparently are suitable for easily formable reinforcements when using certain techniques with closed molds. Knitted fabrics with straight inlay yarns (glass roving) were produced in addition to the basic knitted fabrics. The laminates made with these reinforcements had properties corresponding to typical laminates made with reinforcement of unidirectional yarns. Multilayer braidings were made over mandrels to study braided reinforcement. Thereafter the braidings were impregnated with thermoset resin. Such pieces with near-set-shape braided reinforcement are probably usable, for example in the production of various pipe jointing elements. Sewing and grading techniques were used, for example in the research on the ballistic protection helmet and in the fabrication of various shaped products, for example ball valves. Textile technology can be used to produce reinforcements for composites in many different ways. By combining the possibilities offered by different methods at the product planning stage more flexible composite production methods can be developed. ESA

N94-24269 Israel Aircraft Industries Ltd., Tashan.
ATTACHMENT METHODS IN COMPOSITE JOINTS - ANALYSIS OF TEST RESULTS BY CONTROLLED EXPERIMENTS METHOD
T. Gottesman, D. Peled, N. Sela, and L. Solomon *In* Israel Society of Aeronautics and Astronautics, The 33rd Israel Annual Conference on Aviation and Astronautics 25 Feb. 1993 p 310-320 (For primary document see N94-24241 06-01)
Copyright Avail: Issuing Activity (Israel Society of Aeronautics and Astronautics, c/o Faculty of Engineering, Tel-Aviv Univ., Ramat Aviv 69978, Israel)

N94-24421*# Alabama Univ., Tuscaloosa. Dept. of Aerospace Engineering.
IMPACT DAMAGE IN FILAMENT WOUND COMPOSITE BOTTLES
Alton L. Highsmith *In* Alabama Univ., The 1993 NASA/ASEE Summer Faculty Fellowship Program Nov. 1993 5 p (For primary document see N94-24405 06-80)
Avail: CASI HC A01/MF A03

N94-24446*# Washington Univ., Saint Louis, MO. Dept. of Civil Engineering.
MICROMECHANICAL SIMULATION OF DAMAGE PROGRESSION IN CARBON PHENOLIC COMPOSITES
Kerry T. Slattery *In* Alabama Univ., The 1993 NASA/ASEE Summer Faculty Fellowship Program Nov. 1993 5 p (For primary document see N94-24405 06-80)
Avail: CASI HC A01/MF A03

N94-24450*# Tuskegee Inst., AL. Chemical Engineering Dept.
PROPERTIES AND PROCESSING CHARACTERISTICS OF LOW DENSITY CARBON CLOTH PHENOLIC COMPOSITES
C. Jeff Wang *In* Alabama Univ., The 1993 NASA/ASEE Summer Faculty Fellowship Program Nov. 1993 5 p (For primary document see N94-24405 06-80)
Avail: CASI HC A01/MF A03

25 INORGANIC AND PHYSICAL CHEMISTRY

Includes chemical analysis, e.g., chromatography; combustion theory; electrochemistry; and photochemistry.

For related information see also *77 Thermodynamics and Statistical Physics.*.

N94-22933# Los Alamos National Lab., NM.
DISCONTINUOUS PHASE FORMATION AND SELECTIVE ATTACK OF SiC MATERIALS EXPOSED TO LOW OXYGEN PARTIAL PRESSURE ENVIRONMENTS
D. P. Butt, R. E. Tressler (Pennsylvania State Univ., University Park.), and K. E. Spear (Pennsylvania State Univ., University Park.) 1993 13 p Presented at the North Atlantic Treaty Organization (NATO) Advanced Research Workshop on Corrosion of Advanced Ceramics, Tubingen, Germany, 30 Aug. - 3 Sep. 1993
(Contract W-7405-eng-36)
(DE93-040161; LA-UR-93-3189; CONF-9308163-2) Avail: CASI HC A03/MF A01

Three SiC materials were exposed to gas mixtures containing N2, H2, and CO at 1000-1300C, 1-740 torr for a few to 1000 h. Kinetic and thermodynamic studies indicate that CO is the predominant oxidizing species. A variety of corrosion processes were observed, including surface and internal pit formation, needle growth, grain boundary attack, and attack of impurities and surrounding material. In the case of a siliconized SiC, impurities such as Ca, Al, and Fe diffused rapidly through the Si matrix forming complex calcium aluminosilicates on the surface, leaving behind internal voids. Evaluation of the mechanical properties, including fractography, revealed a variety of degradative phenomena. Efforts to identify causes of pit formation suggested that the overall process was complex. Pits formed during attack of grain boundaries and regions containing transition metal impurities. Studies of single crystals showed preferential attack near impurities and crystalline defects, indicating that damaged crystals or certain crystal orientations in the polycrystalline materials are susceptible to attack. In addition, under some conditions where pit formation was observed, the strength of certain materials increased apparently due to flaw healing. It is suggested that flaws can heal in the absence of mechanical stress due to their high surface energy. However, second phases observed within partially healed surface cracks suggest impurities also contribute to the flaw healing processes. DOE

N94-22943# Los Alamos National Lab., NM.
THERMOCHEMISTRY OF THE ACTINIDES
P. D. Kleinschmidt 1993 15 p Presented at the Actinides 1993, Santa Fe, NM, 19--24 Sep. 1993
(Contract W-7405-eng-36)
(DE94-000895; LA-UR-93-3304; CONF-930905-10) Avail: CASI HC A03/MF A01

The measurement of equilibria by Knudsen effusion techniques and the enthalpy of formation of the actinide atoms is briefly discussed. Thermochemical data on the sublimation of the actinide fluorides is used to calculate the enthalpies of formation and entropies of the gaseous species. Estimates are made for enthalpies and entropies of the tetrafluorides and trifluorides for those systems where data is not available. The pressure of important species in the tetrafluoride sublimation processes is calculated based on this thermochemical data. DOE

N94-22983 Technische Univ., Delft (Netherlands). Faculteit der Werktuigbouwkunde en Maritieme Techniek.
INTEGRATED HYDROMETALLURGICAL JAROSITE TREATMENT Ph.D. Thesis
F. Elgersma 23 Jun. 1992 298 p Limited Reproducibility: More than 20% of this document may be affected by microfiche quality
(PB93-217990; ISBN-90-370-0073-8) Avail: CASI HC A13

Contents: Hydrometallurgical zinc refining; Acidic dissolution of zinc ferrite; Reductive dissolution of zinc ferrite; Simultaneous dissolution of zinc ferrite and precipitation of ammonium jarosite; Precipitation of jarosite (Chemical factors affecting production rate, incorporation of zinc in continuous experiments, incorporation of impurities in batch experiments); Incorporation of zinc in ferrous sulfate monohydrate; Integrating jarosite residue treatment processing in hydrometallurgical zinc winning--comparison of five potential processes; Emission factors for aqueous industrial cadmium emissions in the Rhine River basin; A historical reconstruction for the period 1977-1988. NTIS

N94-23023# Princeton Univ., NJ. Dept. of Mechanical and Aerospace Engineering.
MECHANISM AND ENHANCEMENT OF FLAME STABILIZATION
1993 4 p
(Contract DE-FG02-89ER-13988)
(DE94-002181; DOE/ER-13988/T2) Avail: CASI HC A01/MF A01

During this period, the following projects were completed: structural invariance of purely strained planar premixed flames, thermophoretic effects on seeding particles in LDV measurements, analysis of geometry of Bunsen flames, flame propagation in periodic flow fields, adiabatic flame stabilization, and chain-thermal theory of flame extinction. DOE

N94-23100 Technical Univ. of Denmark, Lyngby. Dept. of Chemical Engineering.
REBURNING RICH-LEAN KINETICS Annual Report, 1992
P. Glarborg, K. Dam-Johansen, and P. G. Kristensen 3 Feb. 1993 19 p See also PB92-205798 Sponsored by Gas Research Inst. Limited Reproducibility: More than 20% of this document may be affected by microfiche quality
(Contract GRI-5091-260-2126)
(PB93-220887; GRI-93/0206) Avail: CASI HC A03

The objective of the work, funded by the Physical Sciences Department of GRI and Nordic Gas Technology Center, is to improve the understanding of the nitrogen chemistry at the final air addition point in reburning and to identify optimum conditions for conversion of reactive nitrogen to N2 in the region. During the past year, a parametric study of the burnout zone nitrogen chemistry has been initiated. The effect of temperature, partitioning of HCN, NO and NH3 in the flue gas, and CO concentration on the conversion of reactive nitrogen has been investigated. Results show that a temperature window exists where both HCN and NH3 act as reducing agents for NO. At the optimum temperature, significant amounts of intermediate N2O is formed. Presence of CO and other combustibles moves the temperature window towards lower temperatures. A preliminary chemical kinetic model for the nitrogen chemistry has been established to analyze the results. NTIS

N94-23296# Lawrence Livermore National Lab., CA.
CONDENSED-PHASE THERMAL DECOMPOSITION OF TATB INVESTIGATED BY ATOMIC FORCE MICROSCOPY (AFM) AND SIMULTANEOUS THERMOGRAVIMETRIC MODULATED BEAM MASS SPECTROMETRY (STMBMS)
T. A. Land, W. J. Siekhaus, M. F. Foltz, and R. Behrens, Jr. (Sandia National Labs., Livermore, CA.) May 1993 10 p Presented at the 10th Detonation Symposium, Boston, MA, 12-16 Jul. 1993
(Contract W-7405-eng-48)
(DE94-000396; UCRL-JC-114109; CONF-930713-27) Avail: CASI HC A02/MF A01

A combination of techniques has been used to investigate the condensed-phase thermal decomposition of TATB. STMBMS has been used to identify the thermal decomposition products and their temporal correlations. These experiments have shown that the condensed-phase decomposition proceeds through several autocatalytic pathways. Both low and high molecular weight decomposition products have been identified. Mono-, di-, and tri-furazans products have been identified and their temporal behaviors are consistent with a stepwise loss of water. AFM has been used to correlate the decomposition chemistry with morphological changes occurring as a function of heating. Patches of small 25-140 nm round holes were observed throughout the lattice of TATB crystals that were heated briefly to 300 C. It is likely that these holes show where decomposition reactions have started. Evidence of decomposition products have been seen in TATB that has been held at 250 C for one hour. DOE

N94-23477 SRI International Corp., Menlo Park, CA.
DEVELOPMENT OF DURABLE HIGH-TEMPERATURE CATALYSTS FOR NATURAL GAS COMBUSTION Report, 1 Jul. 1991 - 31 Aug. 1992
Donald L. Hildenbrand, Kai-Hung Lau, and Jon G. McCarty Nov. 1992 70 p See also PB93-132736 Prepared for Gas Research Inst., Chicago, IL Limited Reproducibility: More than 20% of this document may be affected by microfiche quality
(Contract GRI-5091-260-2233; SRI Proj. PYH-2976)
(PB93-226447; GRI-92/0521) Avail: Issuing Activity (National Technical Information Service (NTIS))

As part of an effort to predict the chemical stability of metal oxide catalysts under methane combustion process conditions, a thermodynamic data base was developed for the relevant condensed and gaseous species of the single oxides of Al, Ba, Ca, Ce, Co, Cr, Cu, Fe, K, La, Mg, Mn, Na, Ni, Pd, Pt, Si, Sr, Ti, Zn, and Zr and for their corresponding gaseous metal hydroxide and oxyhydroxide species. The data base is used with the STANJAN computer code to calculate chemical equilibrium compositions for complex metal oxide mixtures under combustion conditions. These gaseous and solid phase compositions can predict catalyst component volatilities and chemical interactions that affect the operating lifetime of catalysts. NTIS

N94-23482 Leiden Univ. (Netherlands).
REDUCTION OF NITRIC OXIDE OVER PLATINUM, RHODIUM AND PLATINUM-RHODIUM SINGLE CRYSTAL SURFACES Ph.D. Thesis
J. Siera 11 Nov. 1992 149 p Limited Reproducibility: More than 20% of this document may be affected by microfiche quality
(PB93-230092) Avail: Issuing Activity (National Technical Information Service (NTIS))

Although platinum and rhodium are introduced separately in the three-way catalyst, it is established that Pt-Rh alloy particles are formed during its performance. Despite the widespread use of the three-way catalyst and the intensive research on the catalytic properties of the pure metals, relatively little is known about the alloy system. Results are described for the NO-H2, NO-NH3, CO-O2, and CO-NO reactions on the surfaces of Pt, Rh, and Pt-Rh alloy single crystals. NTIS

N94-23524*# SRI International Corp., Menlo Park, CA. Molecular Physics Lab.
SALI CHEMICAL ANALYSIS OF PROVIDED SAMPLES Final Report
Christopher H. Becker Aug. 1993 18 p
(Contract SRI-1-1EH-46755; SRI Proj. 3557)
(NASA-CR-194138; NAS 1.26:194138; MP-93-164) Avail: CASI HC A03/MF A01

SRI has completed the chemical analysis of all the samples supplied by NASA. The final batch of four samples consisted of: one inch diameter MgF2 mirror, control 1200-ID-FL3; one inch diameter neat resin, PMR-15, AO171-IV-55, half exposed and half unexposed; one inch diameter chromic acid anodized, EOIM-3 120-47 aluminum disc; and AO-exposed and unexposed samples of fullerene extract material in powdered form, pressed into In foil for analysis. Chemical analyses of the surfaces were performed by the surface analysis by laser ionization (SALI) method. The analyses emphasize surface contamination or general organic composition. SALI uses nonselective photoionization of sputtered or desorbed atoms and molecules above but close (approximately one mm) to the surface, followed by time-of-flight (TOF) mass spectrometry. In these studies, we used laser-induced desorption by 5-ns pulse-width 355-nm light (10-100 mJ/sq cm) and single-photon ionization (SPI) by coherent 118-nm radiation (at approximately 5 x 10(exp 5) W/sq cm). SPI was chosen primarily for its ability to obtain molecular information, whereas multiphoton ionization (not used in the present studies) is intended primarily for elemental and small molecule information. In addition to these four samples, the Au mirror (EOIM-3 200-11, sample four) was depth profiled again. Argon ion sputtering was used together with photoionization with intense 355-nm radiation (35-ps pulsewidths). Depth profiles are similar to those reported earlier, showing reproducibility. No chromium was found in the sample above noise level; its presence could at most be at the trace level. Somewhat more Ni appears to be present in the Au layer in the unexposed side, indicating thermal diffusion without chemical enhancement. The result of the presence of oxygen is apparently to tie-up/draw out the Ni as an oxide at the surface. The exposed region has a brownish tint appearance to the naked eye. Derived from text

N94-23716# Tennessee Univ., Knoxville. Dept. of Chemistry.
CAPILLARY ELECTROKINETIC SEPARATIONS WITH OPTICAL DETECTION
M. J. Sepaniak 1993 17 p
(Contract DE-FG05-86ER-13613)
(DE94-001639; DOE/ER-13613/45) Avail: CASI HC A03/MF A01

This program seeks the development of capillary electrokinetic separation techniques and associated optical methods of detection. Fundamental studies of pertinent separation and band broadening mechanisms are being conducted, with the emphasis on understanding systems that include highly-ordered assemblies as running buffer additives. The additives include cyclodextrins, affinity reagents, and soluble (entangled) polymers and are employed with capillary electrophoresis, CE and/or micellar electrokinetic capillary chromatography, MECC modes of separation. The utility of molecular modeling techniques for predicting the effects of highly ordered assemblies on the retention behavior of isomeric compounds is under investigation. The feasibility of performing separations using a non-aqueous solvent/fullerene electro- chromatographic system is being explored. The analytical methodologies associated with these capillary separation techniques are being advanced through the development of retention programming instumentation/techniques and new strategies for performing optical detection. The advantages of laser fluorimetry are extended through the inclusion of fluorogenic reagents in the running buffer. These reagents include oligonucleotide intercalation reagents for detecting DNA fragments. Chemiluminescence detection using post-capillary reactors/flow cells is also in progress. Successful development of these separation and detection systems will fill current voids in the capabilities of capillary separation techniques. DOE

N94-23736# Yale Univ., New Haven, CT. Dept. of Chemical Engineering.
FUNDAMENTAL AND EXPERIMENTAL STUDIES ON THE CATALYTIC COMBUSTION OF METHANE Annual Report, 1 Jul. 1991 - 30 Jun. 1992
L. D. Pfefferle and M. D. Smooke Nov. 1992 33 p
(Contract GRI-5091-260-2206)
(PB94-112661; GRI-92/0523) Avail: CASI HC A03/MF A01

The overall objective of the project is to obtain and use fundamental experimental data on surface reactivity to model real catalytic combustors. The objective is being approached by focusing on two experimental areas: the effect of surface reactivity on heat and mass transfer, and the surface reactivity of natural gas on supported metal catalysts. NTIS

N94-23780# Tennessee Univ., Knoxville. Dept. of Radiology.
SYNTHESIS AND IN-VIVO DETECTION OF BORONATED COMPOUNDS FOR USE IN BNCT
G. W. Kabalka Aug. 1993 18 p
(Contract DE-FG05-89ER-60892)
(DE94-001899; DOE/ER-60892/4) Avail: CASI HC A03/MF A01

Carboranes contain ten boron atoms in a three-dimensional space equivalent to a benzene ring; consequently, the carborane isomers can be utilized to prepare a variety of boron-rich agents for potential use in boron-neutron capture therapy. We developed synthetic methodology suitable for use with carboranes preparing amino acids and other physiologically active compounds of potential use in BNCT. The methodology involves the conversion of simple carboranes into more complex, reactive organometallic reagents which can then be utilized to prepare agents which will target the nuclei of tumor cells. Specific examples include the projected syntheses of boron analogs of known intercolators such as diazaquone (AZQ) which have been proven effective in chemotherapy. We have also synthesized and carried out biodistribution studies of gadolinium labeled liposomes (GLL) which were developed in our laboratory. Gadolinium, like boron-10, has an excellent neutron cross section and is considered to be of potential use in neutron capture therapy. GLL are constructed by adding gadolinium based amphiphiles. DOE

N94-23801 Oxford Univ. (England). Inorganic Chemistry Lab.
NEW METHANE CHEMISTRY SYNTHESIS OF MATERIALS FOR REVERSIBLE UPTAKE AND USEFUL FUNCTIONALIZATION OF METHANE Annual Report, Jan. - Dec. 1992
M. L. H. Green Jan. 1993 19 p See also PB91-136473 Limited Reproducibility: More than 20% of this document may be affected by microfiche quality
(Contract GRI-5086-260-1325)
(PB94-112786; GRI-93/0190) Avail: CASI HC A03

The objective of the report is to discover new methods and materials for the economic storage of methane and for the catalytic conversion of methane to useful chemicals. Methane is one of the most abundant fossil fuels but unlike oil it is expensive to transport as a gas or in a liquid form and it is difficult to convert methane to more useful organic materials. The transport of methane and the use of methane as a fuel, for example for automobile engines, would be greatly assisted if it were possible to find materials which would efficiently undergo reversible uptake of methane under mild conditions. The direct catalytic conversion of methane to dihydrogen and carbon monoxide, to methanol, formaldehyde, or by oxidative coupling to ethene are all examples of highly desirable economic processes. These reactions can in principle be achieved by using selective catalysts. The objectives of this proposal, therefore, are to seek new materials which will undergo efficient reversible uptake of methane or which will act as catalysts for the conversion of methane to useful chemicals. NTIS

N94-24073*# National Aeronautics and Space Administration. Marshall Space Flight Center, Huntsville, AL.
DEVELOPMENT OF INFRARED SENSORS USING ENERGY TRANSFER/ENERGY UPCONVERSION PROCESSES: STUDY OF LASER EXCITED FLUORESCENCE IN RARE EARTH ION DOPED CRYSTALS Final Report
S. K. Nash-Stevenson, B. R. Reddy (Alabama A & M Univ., Normal.), and P. Venkateswarlu (Alabama A & M Univ., Normal.) Feb. 1994 18 p
(NASA-TM-108437; NAS 1.15:108437) Avail: CASI HC A03/MF A01

A summary is presented of the spectroscopic study of three systems: LaF3:Ho(3+), LaF3:Er(3+) and CaF2:Nd(3+). When the D levels of Ho(3+) in LaF3 were resonantly excited with a laser beam of 640 nm, upconverted emissions were detected from J (416 nm), F (485 nm), and E (546 nm) levels. Energy upconverted emissions were also observed from F and E levels of Ho(3+) when the material was excited with an 800 nm near infrared laser. When the D levels of Er(3+) in LaF3 were resonantly excited with a laser beam of 637 nm, upconverted emissions were detected from the E (540 nm) and P (320, 400, and 468 nm) levels. Energy upconverted emissions were also observed from F, E, and D levels of Er(3+) when the material was resonantly excited with an 804 nm near infrared laser. When the D levels of Nd(3+) in CaF2 were resonantly excited with a laser beam of 577 nm, upconverted emissions were detected from the L (360 and 382 nm), K (418 nm), and I (432 nm) levels. Very weak upconverted emissions were detected when this system was irradiated with a near infrared laser. The numbers in parentheses are the wavelengths of the emissions. Author (revised)

N94-24113*# XSIRIUS Scientific, Inc., Camarillo, CA.
NEW CONCEPTS FOR HgI2 SCINTILLATOR GAMMA RAY SPECTROSCOPY Technical Status Report, 1 Sep. - 30 Nov. 1993
Jan S. Iwanczyk 14 Jan. 1994 15 p
(Contract NAS7-1204)
(NASA-CR-194819; NAS 1.26:194819) Avail: CASI HC A03/MF A01

The primary goals of this project are development of the technology for HgI2 photodetectors (PD's), development of a HgI2/scintillator gamma detector, development of electronics, and development of a prototype gamma spectrometer. Work on the HgI2 PD's involved HgI2 purification and crystal growth, detector surface and electrical contact studies, PD structure optimization, encapsulation and packaging, and testing. Work on the HgI2/scintillator gamma detector involved a study of the optical - mechanical coupling for the optimization of CsI(Tl)/HgI2 gamma ray detectors and determination of the relationship between resolution versus scintillator type and size. The development of the electronics focused on low noise amplification circuits using different preamp input FET's and the use of a coincidence technique to maximize the signal, minimize the noise contribution in the gamma spectra, and improve the overall system resolution. CASI

N94-24545# Brookhaven National Lab., Upton, NY.
IN SITU AND EX SITU SPECTROELECTROCHEMICAL AND X RAY ABSORPTION STUDIES ON RECHARGEABLE, CHEMICALLY-MODIFIED AND OTHER MnO2 MATERIALS
B. E. Conway (Ottawa Univ., Ontario.), D. Qu (Ottawa Univ., Ontario.), and J. McBreen (Ottawa Univ., Ontario.) 1992 24 p Presented at the NATO Advanced Research Workshop, Maderia, Portugal, 19 Dec. 1992
(Contract DE-AC02-76CH-00016)
(DE94-001387; BNL-49477; CONF-921277-3) Avail: CASI HC A03/MF A01

A combined series of in situ and ex situ UV spectroelectrochemical and X-ray absorption studies have been made on MnO2, chemically-modified by small amounts of Bi(3), and comparatively on other MnO2 materials such as a blank (Bi-free) and (gamma)-MnO2. These procedures are applied in order to follow the oxidation-states of Bi and of Mn during the course of discharge and recharge of MnO2 as a battery cathode material and the extents of rechargeability that can be achieved with such materials. The presence of Bi appears to provide a preferred 'heterogeneous' discharge/recharge pathway involving a soluble Mn(3) intermediate, over the alternative 'electron-proton' hopping, solid-state mechanism. From XAS results, it is concluded that presence of Bi, although not affecting the O-coordination, does influence the Mn-Mn coordination, determining the way the MnO2 coordination octahedra are connected. DOE

N94-24548# Oak Ridge National Lab., TN.
FIFTY YEARS OF CONTINUOUS IMPROVEMENT: WHAT HAS DOE DONE FOR ANALYTICAL CHEMISTRY?
W. D. Shults 1993 10 p Presented at the 34th ORNL/DOE Conference on Analytical Chemistry in Energy Technology, Gatlinburg, TN, 5-7 Oct. 1993
(Contract DE-AC05-84OR-21400)
(DE94-002539; CONF-931081-5) Avail: CASI HC A02/MF A01

Over the past fifty years, analytical scientists within the DOE complex have had a tremendous impact on the field of analytical chemistry. This paper suggests six 'high impact' research/development areas that either originated within or were brought to maturity within the DOE laboratories. 'High impact' means they lead to new subdisciplines or to new ways of doing business. DOE

N94-24549# Oak Ridge National Lab., TN.
TOTAL LIGHT LOSS OPTIC SPECTROSCOPY: PROGRESS TOWARDS A FIBER OPTIC RAMAN ORGANIC VAPOR SENSOR
K. R. Kyle, T. M. Vess, and S. M. Angel Sep. 1993 15 p Presented at the SPIE International Symposium on Optical Tools for Manufacturing and Advanced Automation, Boston, MA, 7-10 Sep. 1993
(Contract W-7405-eng-48)
(DE94-002545; UCRL-JC-115046; CONF-9309199-11) Avail: CASI HC A03/MF A01

A Raman probe has been developed utilizing a single optical fiber as both a light pipe and an active sensing element. By coating a small segment of the surface of an exposed glass fiber core with a thin polymer film, an inverted waveguide is formed where light transmitted down the fiber is stripped out of the core and into the polymer film. The polymer coating is used both as a waveguide and as a medium for concentrating small organic molecules to be interrogated by Raman spectroscopy. The ability of the fiber optic thin film waveguide probe to detect organic vapors is demonstrated. The utility of the probe in the detection of nonaqueous phase liquids (NAPL's) is also described. DOE

N94-24565*# United Technologies Research Center, East Hartford, CT.
STUDY OF STREAMWISE VORTICITY-STIRRED COMBUSTION
William T. Peschke and John B. McVey Dec. 1993 74 p Sponsored by NASA. Lewis Research Center Original contains color illustrations
(Contract DAAL03-89-C-0018)
(NASA-CR-194450; NAS 1.26:194450; UTRC-R93-958160-1; ARL-CR-141) Avail: CASI HC A04/MF A01; 10 functional color pages

Experiments were conducted to establish the effects of the introduction of streamwise vorticity in combusting flows modeling those developed within small gas turbine engines. The objective of the effort was to determine whether this combustion concept has the potential for improving the volumetric heat release rates that characterize these engines. Water flow-visualization tests were performed to evolve lobed mixer configurations that, while generating vortex arrays within both the primary and secondary streams, would also provide rapid intermixing between the streams. These experiments resulted in the definition of enhanced-mixing configurations that were characterized, according to air bubble and dye trajectories, by strong interactions between the two streams. These interactions induced a substantial vertical interchange of primary and secondary fluids. Intermingling of the two fluids occurred throughout a region covering 80 percent of the height of the duct within distances from the lobe mixer trailing edge ranging from approximately one-half to one duct height. Combustion experiments were carried out in a high-pressure (7 atm) combustion apparatus using lobe-mixer combinations that exhibited the ability to induce rapid interchange between the primary and secondary streams. Direct observation and gas sampling were employed to characterize the fuel-air ratio distribution effected by the mixers. Flame geometries were compared with those developed during shear-layer combustion occurring downstream from a conventional splitter plate. The results show that the lobed mixers induce a rapid relocation of the fuel-air mixture entering the combustion test section. As contrasted with the 5- to 7-degree flame front angles that occurred during shear layer combustion, the flame front angles developed during combustion using the lobed mixers were more than twice as great, attaining levels approaching 20 degrees. Author

N94-24673 Old Dominion Univ., Norfolk, VA. Dept. of Mathematical Sciences.
STABILITY OF PREMIXED LAMINAR FLAMES IN A STAGNATION POINT FLOW TO GENERAL DISTURBANCES Final Report, 1 May 1991 - 30 Apr. 1993
Thomas Jackson 30 Apr. 1993 8 p Limited Reproducibility: More than 20% of this document may be affected by microfiche quality
(Grant AF-AFOSR-0180-91)
(AD-A273429; AFOSR-93-0872TR) Avail: CASI HC A02

The researchers completed a stability analysis of the stagnation point flow for a general class of disturbances expressed an infinite series. They have shown that when truncated at some large N, a finite number of boundary value systems result for the determination of the growth rate and the flame shape that depends on N, on the cross stream wavenumber, and on all the relevant physiochemical parameters. The stability results thus obtained reduce to those of Kim and Matalon (1990) when N = O and extend them to include corrugations in the direction of stretch with wave number proportional to N. The results are discussed in terms of the Lewis number which is related to the mixture composition and the rate of strain experiences by the flame. This work was recently presented in the Fourth International Conference on Numerical Combustion held in St. Petersburg, FL and has recently been published in Combustion Science Technology. DTIC

N94-24772# New Mexico Univ., Albuquerque. Dept. of Chemistry.
CHEMICALLY SENSITIVE INTERFACIAL FORCE MICROSCOPY: CONTACT POTENTIAL MEASUREMENTS OF SELF-ASSEMBLING MONOLAYER FILMS Technical Report, 1 Aug. 1992 - 31 Jul. 1993
R. C. Thomas, P. Tangyunyong, J. E. Houston, T. A. Michalske, and R. M. Crooks 23 Nov. 1993 12 p
(Contract N00014-91-J-1991)
(AD-A273135) Avail: CASI HC A03/MF A01

We report contact potential difference (CPD) measurements of n-alkanethiol self-assembling monolayers (SAM's) adsorbed to Au substrates using an organomercaptan-modified Au probe. Our results demonstrate for the first time the feasibility and importance of controlling the chemical properties of force microscope probe surfaces. Moreover, control over the chemical characteristics of the probe provides a basis for distinguishing between chemically distinct surface features with nanometer resolution in force microscopy. We show that CPD values obtained using Au probes modified with methyl-terminated SAM's are stable and reproducible, whereas identical unmodified probes yield highly variable data. Our experimentally determined CPD values are in qualitative agreement with calculated CPD's for several Omega-terminated SAM's. DTIC

N94-24784 Army Construction Engineering Research Lab., Champaign, IL. Energy and Utilities Systems Div.
ELECTROCHEMICAL BEHAVIOR OF ION-PLATED TIN AND Cu-Cr COATINGS Final Report
Y. W. Lee, M. Metzger, and J. M. Rigsbee Sep. 1993 41 p Limited Reproducibility: More than 20% of this document may be affected by microfiche quality
(AD-A273411; USACERL-TR-FM-93/16) Avail: Issuing Activity (Defense Technical Information Center (DTIC))

The electrochemical (corrosion) behaviors of titanium nitride (TiN) and metastable copper-chromium (Cu-Cr) alloy coatings grown on glass, aluminum, and copper substrates using a plasma-assisted physical vapor deposition (ion-plating) technique were investigated. Various polarization techniques were used for corrosion tests in oxygen-saturated and deaerated 5 percent Na2SO4 and 3.5 percent NaCl solutions of two different acidities (pH--6 and 3). The structure, chemistry, and morphology of the coating surfaces before and after corrosion testing were analyzed with scanning electron microscope, x-ray diffraction, Auger, and x-ray photoelectron spectroscopic techniques. Titanium nitride coatings are chemically passive but do not provide effective protection for metallic substrates, under conditions involving pitting corrosion, due to the presence of pinholes in the as-deposited TiN coatings. The inherent properties of TiN do appear suitable for electromagnetic interference/electromagnetic pulse shield applications provided the problem of film defects (porosity, pinholes) can be solved or if the substrate type and corrosion conditions are such that passivation of the substrate surface occurs. Cu-Cr alloy coatings show a general corrosion behavior, with corrosion rates of a few mm per year at the free corrosion potential, which is unsatisfactory for a thin film coating application. DTIC

N94-24790# Rensselaer Polytechnic Inst., Troy, NY. Dept. of Chemistry.
ADSORPTION, DESORPTION, AND DECOMPOSITION OF HCl AND HBr ON Ge(100): COMPETITIVE PAIRINGAND NEAR-FIRST-ORDER DESORPTION KINETICS
Mark P. DEvelyn, Yuemei L. Yang, and Stephen M. Cohen Nov. 1993 38 p
(Contract N00014-91-J-1550)
(AD-A273504; TR-20-ONR) Avail: CASI HC A03/MF A01

We have investigated the surface chemistry of coadsorbed hydrogen and halogen atoms on Ge(100), produced by dissociative chemisorption of HCL and HBr, by temperature-programmed desorption. The initial sticking probability, S(sub 0), for HCL decreases from 0.6 at a substrate temperature of 270 K to 0.05 at 400 K, indicative of a precursor state to adsorption. For HBr S(sub 0) is constant at 0.7 over the same temperature range. A fraction, f, of adsorbed hydrogen atoms desorb associatively as H2 near 570 K, while the remaining (1-f) H atoms recombine with adsorbed halogen atoms and desorb as the hydrogen halide (HX) near 580 - 590 K. The activation energies for desorption of H2, HCL, and HBr are all approximately 40 kcal/mol. For both HCL and HBr, f is 0.7 at low initial coverage and decreases slightly to 0.6 at saturation. The fraction f of adsorbed halogen atoms left on the surface following the competitive desorption of H2 and HX desorb as the dihalides GeC12 and GeBr2 near 675 K and 710 K, respectively. Desorption of H2, HCL, and HBr occurs with near-first-order kinetics, similar to the behavior of hydrogen adsorbed alone, which we attribute to preferential pairing induced by the pi bond on unoccupied Ge dimers. We introduce and solve a generalized doubly-occupied dimer model incorporating competitive pairing of H+H, H+X, and X+X on Ge dimers to explain the near-first order kinetics. The model quantitatively accounts for both the desorption kinetics and the relative yields of H2 and HX with pairing energies of = approximatetely kcal/mol. DTIC

N94-24917 Emory Univ., Atlanta, GA. Dept. of Chemistry.
LPCVD OF InN ON GaAs(110) USING HN3 AND TMIn: COMPARISON WITH Si(100) RESULTS Technical Report
Y. Bu and M. C. Lin 7 Dec. 1993 7 p Limited Reproducibility: More than 20% of this document may be affected by microfiche quality
(Contract N00014-89-J-1235)
(AD-A273555; TR-22) Avail: CASI HC A02

Low-pressure chemical vapor deposition (LPCVD) of InN and laser-assisted LPCVD on GaAs(110) and Si(100) using HN3 and trimethyl indium (TMIn) has been studied with XPS, UPS, and SEM. Without 308-nm excimer laser irradiation, InN film was built on the GaAs but not on Si surface under the present low-pressure conditions. When the photon beam was introduced, InN films with In:N atomic ratio of 1.0 +/- 0.1 and a thickness of more than 20 A (the limit of the electron escaping depth for the In(3d) x ray photoelectrons) were formed on Si(100) surface. In both cases, the formation of surface nitrides at the initial film growth processes was clearly indicated in the XP spectra. The He(II) UP spectra taken from InN films on GaAs and Si are nearly identical and agree well with the result of a pseudo-potential calculation for the InN valence band. The corresponding SEM pictures showed smooth InN films on GaAs(110), while grains with diameter of approximately 100 nm were observed for InN on Si(100). DTIC

N94-24920# Liverpool Univ. (England). Dept. of Chemistry.
DESIGN OF NOVEL CATALYSTS FOR THE PARTIAL OXIDATION OF METHANE TO METHANOL Annual Report, Jan. - Dec. 1992
G. J. Hutchings, R. W. Joyner, and C. R. A. Catlow (Royal Institution of Great Britain, London.) Jan. 1993 82 p
(Contract GRI-5091-260-2141)
(PB94-114212; GRI-93/0267) Avail: CASI HC A05/MF A01

This work has three key objectives: to identify factors conducive to synergy in selective methane oxidation, by examination, using both experimental and theoretical methods, of the activation of methane, oxygen, methanol, and formaldehyde over a range of catalysts; to identify the role of surface defects and their interaction with surface structure in the catalytic activation of methane; and to apply the information obtained in the design of selective, active catalysts for the conversion of methane to methanol or formaldehyde at temperatures less than approximately 500 C. NTIS

N94-24925 South Carolina Univ., Columbia. Dept. of Chemistry.
POTENT SOLVENTS FOR C60 AND THEIR UTILITY FOR THE RAPID ACQUISITION OF 13CNMR DATA FOR FULLERENES Technical Report No. 27
Walter A. Scrivens and James M. Tour 22 Nov. 1993 10 p Limited Reproducibility: More than 20% of this document may be affected by microfiche quality
(Contract N00014-89-J-3062)
(AD-A273349; TR-27) Avail: Issuing Activity (Defense Technical Information Center (DTIC))

Described are several solvents for the dissolution of fullerenes. The two best solvents found were 1,2-dichlorobenzene and 1-methylnaphthalene which dissolve C60 up to 24.6 and 33.2 mg/mL, respectively. The solubility data was obtained gravimetrically. Precipitates were obtained when C60 was treated with 1,3,5-trimethylbenzene or 1,2,4-trichlorobenzene. Scanning electron micrographs and thermogravimetric analysis data were obtained on the precipitates and compared to the data obtained for pure C60. The efficacy of 1,2-dichlorobenzene and 1-methylnaphthalene as 13C NMR solvents for fullerene analysis was demonstrated as well as the utility of 1,2-dichlorobenzene for the extraction of higher fullerenes from soot. DTIC

N94-24984# Tokyo Inst. of Tech. (Japan). Dept. of Chemistry.
LABORATORY DETECTION OF C5S BY PULSED-DISCHARGE-NOZZLE FOURIER-TRANSFORM MICROWAVE SPECTROSCOPY
Yasuko Kasai, Kinichi Obi, Yasuhiro Oshima, Yasuhiro Hirahara, Yasuki Endo, Kentaro Kawaguchi, and Akinori Murakami 1993 15 p
(JTN-94-80519) Avail: CASI HC A03/MF A01

The rotational spectrum of C5S in the X(exp 1)sigma(+) (v = 0) ground state has been observed for the first time using a Fabry-Perot-type Fourier-transform microwave spectrometer combined with a pulsed discharge nozzle. C5S was generated by a discharge in a mixture of CS2 and C2H2 diluted in Ar, and subsequently cooled down to a few K in a supersonic jet. Eight rotational transitions of C5S-32 have been observed in the 5 - 20 GHz region. Three lines for the less abundant S-34 species have also been detected to confirm the carrier of the observed lines to be C5S. Determined spectroscopic constants will allow a deep radio astronomical search for C5S in interstellar clouds and circumstellar envelopes of late-type stars. Author (NASDA)

N94-25232 Technische Univ., Eindhoven (Netherlands).
ELECTROPHORESIS IN OPEN CAPILLARIES: SOME FUNDAMENTAL ASPECTS Ph.D. Thesis
Mariette Theodora Ackermans 1992 159 p Limited Reproducibility: More than 20% of this document may be affected by microfiche quality
(ETN-94-95290) Avail: CASI HC A08

Fundamental aspects of the separation process in capillary electrophoresis in open systems with UV detection are reported. The applicability of this technique is considered with the help of pharmaceuticals, which are used in veterinary practice. The principles of electrophoresis are explained and the qualitative and quantitative aspects are explored. The most important phenomena causing peak broadening in capillary electrophoresis, Joule heating, electroosmosis, diffusion, electrodispersion, injection and interactions of the solutes with the capillary wall are described and an estimation of the magnitude of these effects causing peak broadening in a Capillary Zone Electrophoresis (CZE) experiment is made. Characteristics of CZE are given. The determination of several pharmaceuticals with different modes of capillary electrophoresis is given. ESA

N94-25233# Technische Univ., Eindhoven (Netherlands).
CAPILLARY ELECTROPHORESIS OF BIOMOLECULES: THEORY, INSTRUMENTATION AND APPLICATIONS Ph.D. Thesis
Antonius Albertus A. vandeGoor 1992 136 p Sponsored by Netherlands Foundation for Scientific Research
(ETN-94-95297) Avail: CASI HC A07/MF A02

The principles of Capillary Electrophoresis (CE) are discussed. The instrumental aspects are discussed, by describing different set ups using UV and laser induced florescence detection. The characteristics of electroosmosis, which determines the resolution and reproducibility of CE, are described. Different application areas of biomolecules including the chemistry involved for detection, the columns involved for the separation, and systems used for the optimal resolution are described. The analysis of amino acids using CE is dealt with. The possibilities of CE for peptide analysis are discussed and a comparison to liquid chromatographic separation is made. The analysis of oligonucleotides and Deoxyribonucleic Acids (DNA) restriction fragments is considered. ESA

N94-25250 Technische Univ., Eindhoven (Netherlands).
THE STRUCTURE AND CATALYTIC PROPERTIES OF SUPPORTED PLATINUM CATALYSTS Ph.D. Thesis
Marinus Vaarkamp 1993 167 p Sponsored by Amoco Oil Research, Naperville, IL Limited Reproducibility: More than 20% of this document may be affected by microfiche quality
(ETN-94-95357) Avail: Issuing Activity (European Space Agency (ESA))

The relation between the structure of the metal particles and the metal-support interface, the electronic structure, and the catalytic properties of supported metal catalysts is studied. Attention is limited to platinum supported on two amorphous supports (silica and alumina) and zeolite L. To maximize the effect of the support on the structure of the metal particles, the structure of the metal-support interface, the electronic structure, and the catalytic properties, catalysts were prepared with very small particles. The main characterization method applied is X ray Absorption Spectroscopy (XAS). Improvements to the generally used methods of analysis of the Extended X ray Absorption Fine Structure (EXAFS) are discussed. Systematic errors arising from the used phase and backscattering amplitude are studied and theoretical methods to calculate the phase and backscattering amplitude are evaluated. The sulphur sensitivity of the highly active and selective dehydrocyclization catalyst Pt/BaK-LTL is studied. The structure and morphology of the platinum clusters and the structure of the metal-support interface of Pt/zeolite and Pt/gamma-Al_2O_3 catalysts are studied. The relation between electronic structure and catalytic properties of supported platinum catalysts is studied. The influence of support and reduction temperature on the activity and selectivity of supported platinum crystals in methylcyclopentane ring opening is reported. ESA

N94-25284# Technische Univ., Eindhoven (Netherlands).
MODELLING OF PREMIXED LAMINAR FLAMES Ph.D. Thesis
Rick deLange 1992 166 p
(ETN-94-95317) Avail: CASI HC A08/MF A02

A study whose aim is to model not only flames of pure, or low carbon, gases but also those of natural gas mixtures is presented. One dimensional flames and the determination of the reaction parameters are considered. An approach to describe freely propagating, or adiabatic, flames ruled by a one step reaction is presented. A numerical method suited to model laminar two dimensional flames in a Cartesian system is also presented. The stabilization of a flame on a parallel slit burner is described. This theory describes the influence of cooling, due to the burner rim, on the stand off distance, the distance between the cold burner rim and the flame sheet. The numerical results on stability limits, both near flashback and quenching limits, as well as global flame structure for premixed CH_4/air flame on a parallel plate burner are compared with experimental results. The results are used in a study of the combustion process in the tip of the flame. ESA

N94-25296# Technische Univ., Eindhoven (Netherlands).
THE ELECTROCHEMISTRY OF THE SOLVATED ELECTRON: A STUDY OF ITS PROPERTIES AND OF ITS APPLICATIONS Ph.D. Thesis
Pieterdina J. M. vanAndel-Scheffer 1992 98 p
(ETN-94-95313) Avail: CASI HC A05/MF A02

The electrochemistry of solvated electrons is discussed. The electrochemical generation of solvated electrons in hexamethyl phosphortriamide (HMPA) and in methylamine was investigated. Lithium chloride or lithium bromide was used as the elecrolyte. Because the rotating ring disk electrode (RRDE) technique was used in particular, this technique is described. Attention is paid to the merits of solvated electrons as a powerful reductant in electroorganic synthesis. In HMPA/Li salt solutions, solvated electrons can be cathodically generated at the disk of a RRDE and be oxidized when they reach the ring electrode. The use of this hydrodynamic technique to study several features of electrochemistry is described. It was shown that by means of transit time measurements, information can be obtained about the mobility of solvated electrons in HMPA/Li salt solutions. The reaction of solvated electrons with water and benzene is described. It is shown that various substituted benzylamines can be reduced in methylamine using lithium chloride as electrolyte. ESA

N94-25302# Technische Univ., Eindhoven (Netherlands).
DRYING DEFORMABLE MEDIA: KINETICS, SHRINKAGE AND STRESSES Ph.D. Thesis
Antonius Adrianus J. Ketelaars 1992 117 p Sponsored by Nederlandse Maatschappij voor Energie en Milieu B.V., Netherlands; Koninklijk Verbond van Nederlandse Baksteenfabrikanten, Netherlands; and Nederlandse Dakpannenfabrikanten Corp., Netherlands
(ETN-94-95314) Avail: CASI HC A06/MF A02

A model for drying of clays, which gives special attention to shrinkage and stresses, is developed. The drying kinetics model is developed based on the diffusion equation. Deformations due to shrinkage and stresses are taken into account. Essential in the use of a diffusion equation is a reliable experimental determination of the diffusion coefficient as a function of moisture content. An experimental method for the derivation of the diffusion coefficient, based on accurate measurements of transient moisture concentration profiles, is considered. Results for three clays are included. Results of the traditional method for the determination of the diffusion coefficient, which is based on the use of drying curves, are compared with these results. The influence of shrinkage on drying behavior is studied. Multidimensional simulations are performed in order to get a quantitative idea of the importance of shrinkage in drying of clays. ESA

N94-25427# Loughborough Univ. of Technology (England). Dept. of Mathematical Sciences.
LIAPUNOV STABILITY IN CHEMICAL ENGINEERING
C. Storey Jul. 1993 35 p Presented at the 2nd International Workshop on Mathematical Modelling in Chemical Engineering, Budapest, Hungary, 11-15 Jul. 1993
(MATHS-Rept-A-184; ETN-94-95227) Avail: CASI HC A03/MF A01

Liapunov stability theory and techniques in chemical engineering are reviewed. Attention is focused on the classical Liapunov methods. The main difficulty with Liapunov's direct method appear to lie in the fact that the stability theorems are sufficient only and in the difficulties involved in generating suitable Liapunov functions. The determination of domains of attraction via this method is also beset with numerical difficulties and gives conservative results. ESA

N94-23035*# Pennsylvania State Univ., University Park. Propulsion Engineering Research Center and Dept. of Mechanical Engineering.
EVAPORATION AND COMBUSTION OF LOX UNDER SUPERCRITICAL AND SUBCRITICAL CONDITIONS
A. S. Yang, W. H. Hsieh, and K. K. Kuo *In its* NASA Propulsion Engineering Research Center, Volume 2 Nov. 1993 p 33-38 (For primary document see N94-23028 06-20)
Avail: CASI HC A02/MF A03

N94-23041*# Computational Fluid Dynamics Research Corp., Huntsville, AL.
NUMERICAL PARAMETRIC STUDIES OF SPRAY COMBUSTION INSTABILITY
M. Z. Pindera *In* Pennsylvania State Univ., NASA Propulsion Engineering Research Center, Volume 2 Nov. 1993 p 64-68 (For primary document see N94-23028 06-20)
Avail: CASI HC A01/MF A03

N94-23044*# National Aeronautics and Space Administration. Lewis Research Center, Cleveland, OH.
AXISYMMETRIC SINGLE SHEAR ELEMENT COMBUSTION INSTABILITY EXPERIMENT
Kevin J. Breisacher *In* Pennsylvania State Univ., NASA Propulsion Engineering Research Center, Volume 2 Nov. 1993 p 77-81 See also N94-10763 (For primary document see N94-23028 06-20)
Avail: CASI HC A01/MF A03

N94-23046*# Pennsylvania State Univ., University Park. Propulsion Engineering Research Center and Dept. of Mechanical Engineering.
DEVELOPMENT OF A COMPUTATIONAL TESTBED FOR NUMERICAL SIMULATION OF COMBUSTION INSTABILITY
Jeffrey Grenda, Sankaran Venkateswaran, and Charles L. Merkle *In its* NASA Propulsion Engineering Research Center, Volume 2 Nov. 1993 p 88-92 (For primary document see N94-23028 06-20)
Avail: CASI HC A01/MF A03

N94-23233*# Randolph-Macon Coll., Ashland, VA. Dept. of Chemistry.
EVALUATION OF INORGANIC ZINC-RICH PRIMERS USING ELECTROCHEMICAL IMPEDANCE SPECTROSCOPY (EIS)
Luz M. Calle *In* NASA. Kennedy Space Center, NASA/ASEE Summer Faculty Fellowship Program Oct. 1993 p 47-76 (For primary document see N94-23230 06-80)
Avail: CASI HC A03/MF A04

N94-23245*# Florida Inst. of Tech., Melbourne. Dept. of Mechanical and Aerospace Engineering.
INTERPRETATION OF DISCREPANCIES IN MASS SPECTROSCOPY DATA OBTAINED FROM DIFFERENT EXPERIMENTAL CONFIGURATIONS
John M. Russell *In* NASA. Kennedy Space Center, NASA/ASEE Summer Faculty Fellowship Program Oct. 1993 p 403-432 (For primary document see N94-23230 06-80)
Avail: CASI HC A03/MF A04

N94-23683*# Yale Univ., New Haven, CT. Dept. of Computer Science and Mechanical Engineering.
NUMERICAL SOLUTION OF FLAME SHEET PROBLEMS WITH AND WITHOUT MULTIGRID METHODS
Craig C. Douglas and Alexandre Ern *In* NASA. Langley Research Center, The Sixth Copper Mountain Conference on Multigrid Methods, Part 1 Nov. 1993 p 143-157 Sponsored in part by CERMICS, ENPC, IBM, ONR and DOE (For primary document see N94-23673 06-64)
Avail: CASI HC A03/MF A03

N94-24155*# Centre Europeen Recherche et de Formation Advance en Calcul Scientific, Toulouse (France).
THE COMBUSTION PROGRAM AT CTR
Thierry J. Poinsot *In* Stanford Univ., Annual Research Briefs, 1993 Dec. 1993 p 195-203 (For primary document see N94-24138 06-34)
Avail: CASI HC A02/MF A04

N94-24156*# Ecole Centrale de Paris (France).
STRETCH-INDUCED QUENCHING IN FLAME-VORTEX INTERACTIONS
J.-M. Samaniego *In* Stanford Univ., Annual Research Briefs, 1993 Dec. 1993 p 205-218 (For primary document see N94-24138 06-34)
Avail: CASI HC A03/MF A04

N94-24158*# Ecole Centrale de Paris (France).
THE PRODUCTION OF PREMIXED FLAME SURFACE AREA IN TURBULENT SHEAR FLOW
A. Trouve *In* Stanford Univ., Annual Research Briefs, 1993 Dec. 1993 p 229-248 (For primary document see N94-24138 06-34)
Avail: CASI HC A03/MF A01

N94-24273 Technion - Israel Inst. of Tech., Haifa. Faculty of Aerospace Engineering.
MODELLING THE IGNITION OF BORON/TITANIUM PARTICLES
Ilan Ibu and Alon Gany *In* Israel Society of Aeronautics and Astronautics, The 33rd Israel Annual Conference on Aviation and Astronautics 25 Feb. 1993 p 348-358 (For primary document see N94-24241 06-01)
Copyright Avail: Issuing Activity (Israel Society of Aeronautics and Astronautics, c/o Faculty of Engineering, Tel-Aviv Univ., Ramat Aviv 69978, Israel)

N94-24274 Technion - Israel Inst. of Tech., Haifa. Faculty of Aerospace Engineering.
ON THE STABILITY OF THE PROCESS OF FORMATION OF COMBUSTION GENERATED PARTICLES BY COAGULATION AND SIMULTANEOUS SHRINKAGE DUE TO PARTICLE OXIDATION
Y. Tambour and S. Khosid *In* Israel Society of Aeronautics and Astronautics, The 33rd Israel Annual Conference on Aviation and Astronautics 25 Feb. 1993 p 359-368 Sponsored in part by Center for Absorption in Science, Ministry of Immigrant Absorption, State of Israel (For primary document see N94-24241 06-01)
Copyright Avail: Issuing Activity (Israel Society of Aeronautics and Astronautics, c/o Faculty of Engineering, Tel-Aviv Univ., Ramat Aviv 69978, Israel)

N94-24275 Technion - Israel Inst. of Tech., Haifa. Faculty of Aerospace Engineering.
EXPERIMENTAL INVESTIGATION OF IGNITION OF BORON/TITANIUM COMPOSITE PARTICLES
V. Rosenband and A. Gany *In* Israel Society of Aeronautics and Astronautics, The 33rd Israel Annual Conference on Aviation and Astronautics 25 Feb. 1993 p 369-373 Sponsored by Wolfson Family Charitable Trust Program for the Absorption of Immigrant Scientists; Center for Absorption in Science, Ministry of Immigrant Absorption, State of Israel; and Ministry of Science and Technology, State of Israel (For primary document see N94-24241 06-01)
Copyright Avail: Issuing Activity (Israel Society of Aeronautics and Astronautics, c/o Faculty of Engineering, Tel-Aviv Univ., Ramat Aviv 69978, Israel)

N94-24282 Technion - Israel Inst. of Tech., Haifa. Faculty of Aerospace Engineering.
TRANSIENT PHENOMENA IN LAMINAR SPRAY COMBUSTION
J. B. Greenberg and I. Shpilberg *In* Israel Society of Aeronautics and Astronautics, The 33rd Israel Annual Conference on Aviation and Astronautics 25 Feb. 1993 p 430-438 (For primary document see N94-24241 06-01)
Copyright Avail: Issuing Activity (Israel Society of Aeronautics and Astronautics, c/o Faculty of Engineering, Tel-Aviv Univ., Ramat Aviv 69978, Israel)

N94-24284 Technion - Israel Inst. of Tech., Haifa. Faculty of Aerospace Engineering.
MULTIPLE FLAMES IN COUNTERFLOW SPRAY COMBUSTION
N. Sarig and J. B. Greenberg *In* Israel Society of Aeronautics and Astronautics, The 33rd Israel Annual Conference on Aviation and Astronautics 25 Feb. 1993 p 449-457 (For primary document see N94-24241 06-01)
Copyright Avail: Issuing Activity (Israel Society of Aeronautics and

Astronautics, c/o Faculty of Engineering, Tel-Aviv Univ., Ramat Aviv 69978, Israel)

N94-25125*# Intersonics, Inc., Northbrook, IL.
CONTAINERLESS MEASUREMENTS ON LIQUIDS AT HIGH TEMPERATURES
Richard Weber *In* NASA. Lewis Research Center, Workshop on the Thermophysical Properties of Molten Materials Nov. 1993 p 87-98
(For primary document see N94-25120 06-26)
Avail: CASI HC A03/MF A03

N94-25132*# Auburn Univ., AL. Dept. of Mechanical Engineering.
AN EXTENDED LASER FLASH TECHNIQUE FOR THERMAL DIFFUSIVITY MEASUREMENT OF HIGH-TEMPERATURE MATERIALS
F. Shen and J. M. Khodadadi *In* NASA. Lewis Research Center, Workshop on the Thermophysical Properties of Molten Materials Nov. 1993 p 203-218 (For primary document see N94-25120 06-26)
(Grant NAGw-1192)
Avail: CASI HC A03/MF A03

N94-25134*# Jet Propulsion Lab., California Inst. of Tech., Pasadena.
MICROWAVE TECHNIQUES FOR PHYSICAL PROPERTY MEASUREMENTS
M. Barmatz *In* NASA. Lewis Research Center, Workshop on the Thermophysical Properties of Molten Materials Nov. 1993 p 231-234
(For primary document see N94-25120 06-26)
Avail: CASI HC A01/MF A03

N94-25135*# Jet Propulsion Lab., California Inst. of Tech., Pasadena.
ELECTROSTATIC LEVITATION TECHNOLOGY FOR THERMOPHYSICAL PROPERTIES OF MOLTEN MATERIALS
Won-Kyu Rhim *In* NASA. Lewis Research Center, Workshop on the Thermophysical Properties of Molten Materials Nov. 1993 p 235-245
(For primary document see N94-25120 06-26)
Avail: CASI HC A03/MF A03

N94-25365*# New Mexico State Univ., Las Cruces. Dept. of Mechanical Engineering.
INFLUENCE OF TEST CONFIGURATION ON THE COMBUSTION CHARACTERISTICS OF POLYMERS AS IGNITION SOURCES
Howard L. Julien *In* NASA. Johnson Space Center, National Aeronautics and Space Administration (NASA)/American Society for Engineering Education (ASEE) Summer Faculty Fellowship Program, 1993, Volume 1 Dec. 1993 13 p (For primary document see N94-25348 06-99)
Avail: CASI HC A03/MF A03

26 METALLIC MATERIALS

Includes physical, chemical, and mechanical properties of metals, e.g., corrosion; and metallurgy.

N94-22718# Argonne National Lab., IL.
RELATIONSHIP OF MICROSTRUCTURE AND MECHANICAL PROPERTIES FOR V-Cr-Ti ALLOYS
B. A. Loomis, J. Gazda, L. J. Nowicki, D. L. Smith, and S. Danyluk (Chicago Univ., IL.) Aug. 1993 14 p Presented at the 6th International Conference on Fusion Reactor Materials, Stresa, Italy, 27 Sep. - 1 Oct. 1993
(Contract W-31-109-eng-38)
(DE94-001431; ANL/ET/CP-80862; CONF-930928-9) Avail: CASI HC A03/MF A01

Relation of composition, number density, and diameter of precipitates in microstructures of unalloyed V and V-Cr-Ti alloys to the yield strength, hardness, creep stress, and ductile-brittle transition temperature (DBTT) for these materials was determined from analytical electron microscopy analyses of precipitates in these materials and from mechanical properties data. Unalloyed V and V-Cr-Ti alloys with less than or equal to 3 wt. % Ti contained VC and TI(CNO) precipitates that were coherent with the matrix. The most common precipitates in the alloys were Ti(C(1-x-y)N(x)O(y)) that were non-coherent with the matrix. The number density of non-coherent precipitates was maximum in V-3Ti and V-5Cr-3Ti alloys, and the average diameter of non-coherent precipitates was minimum in V-(1 - 3)Ti and V-5Cr-3Ti alloys. The increase of yield strength and hardness of V on alloying with Ti and Cr was shown to be primarily due to coherent precipitate, solute-atom misfit, and shear-modulus difference effects. The creep stress for rupture in 1000 hours was related to the number density of precipitates, whereas the DBTT was related to the volume fraction of precipitates. DOE

N94-22861# General Electric Co., Schenectady, NY. Knolls Atomic Power Lab.
FATIGUE CRACK GROWTH RATE STUDIES OF MEDIUM SULFUR LOW ALLOY STEELS TESTED IN HIGH TEMPERATURE WATER
T. A. Auten, S. Z. Hayden, and R. H. Emanuelson (Babcock and Wilcox Co., Alliance, OH.) May 1993 10 p Presented at the 6th International Symposium on Environmental Degradation of Materials in Nuclear Power Systems: Water Reactors, San Diego, CA, 3-5 Aug. 1993
(Contract DE-AC12-76SN-00052)
(DE93-040437; KAPL-4761; CONF-930825-6) Avail: CASI HC A02/MF A01

Fatigue crack propagation tests of medium sulfur (0.007 to 0.011 wt %) ASTM A508-Class 2 forgings were performed in deaerated high purity, high temperature water. In general, these forgings did not exhibit environmentally assisted cracking (EAC) in tests at 149C (300F) or at 260C (500F). Lowering the pH did not raise the crack growth rates significantly. However, adding a small amount of oxygenated water to the feedwater increased the fatigue crack growth rates (FCGR) by a factor of about 4. Automated analyses of the sulfide inclusions in polished sections of the forgings supported a previously proposed relationship for susceptibility to EAC. DOE

N94-22897# Wisconsin Univ., Madison.
ORGANOMETALLIC CHEMISTRY OF BIMETALLIC COMPOUNDS
C. P. Casey Jul. 1993 11 p
(Contract DE-FG02-85ER-13406)
(DE94-002313; DOE/ER-13406/8) Avail: CASI HC A03/MF A01

Research is reported under 5 headings: reactions of hetero-bimetallic dihydrides (hydrogenation of alkynes by Re, Pt complex), metal-metal double bonds (Re=Re), C5Me5Co=CoC5Me5 is actually (C5Me5)3Co3(mu)2-H3(mu)3-H), reactions of (C5Me5)3Co3-(mu)2-H3((mu)3-H), and wide bite angle phosphines in hydroformylation. DOE

N94-22932# Sandia National Labs., Albuquerque, NM.
CHROMATE-FREE TALC CHEMICAL CONVERSION COATINGS FOR ALUMINUM ALLOYS
R. G. Buchheit, C. A. Drewien, and G. E. Stoner (Virginia Univ., Charlottesville.) 1993 8 p Presented at the 183th Electrochemical Society Meeting, Honolulu, HI, 16-21 May 1993
(Contract DE-AC04-94AL-85000)
(DE94-001567; SAND-93-1648C; CONF-930571-28) Avail: CASI HC A02/MF A01

We have found that aluminum alloys exhibit unusual passivity when exposed to alkaline Li-salt solutions. Observed passivity is due to the formation of a polycrystalline Li2(Al2(OH)6)(sub 2)(center dot)CO3(center dot)3(H2O) film on the aluminum surface. This film is persistent in aggressive environments and provides a significant degree of corrosion protection. On this basis, we have developed a simple non-electrolytic method of forming corrosion resistant coatings in alkaline Li-salt solution. This process is procedurally similar to traditional conversion coating methods, offers desirable properties, and has a low toxic hazard. In this paper, coating methods, coating characterization, and coating properties are presented. Results from parallel test performed with a commercial chromate conversion coatings are presented for comparison. DOE

N94-22936# General Electric Co., Schenectady, NY. Atomic Power Lab.
ANALYSIS OF ALLOY 600 AND X-750 STRESS CORROSION CRACKS
C. D. Thompson, N. Lewis, and H. Krasodomski Jun. 1993 48 p Presented at the Alloy 600 Experts Meeting, Warrenton, VA, 5-9 Apr. 1993
(Contract DE-AC12-76SN-00052)
(DE94-001578; KAPL-4760; CONF-9304146-3) Avail: CASI HC A03/MF A01

A few months ago, KAPL evidence supported the view that Primary or

Pure Water Stress Corrosion Cracking (PWSCC) of Alloy 600 results from a hydrogen mechanism. An analytical Electron Microscope (AEM) analysis of a stress corrosion crack (SCC) crack in an A600 split tube U-bend specimen exposed to primary water at 338 C (640 F) for 462 days is shown. The features which appear to confirm a hydrogen mechanism are as follows: (1) a very narrow (less than 200 A) crack with a sharp tip, nearly free of deposits; (2) no evidence of severe plastic deformation in the region immediately ahead of the crack tip; and (3) a line of small voids preceding the main crack tip, of which the largest is about 5 x 10(exp -6) cm in length. Shen and Shewmon proposed that PWSCC of Alloy 600 occurs due to small microvoids ahead of a main crack tip. The hypothesis is that such voids result from pockets of methane gas formed by the reaction of atomic hydrogen with carbon in the base metal. The voids are about 10 x 10(exp -6) cm diameter, approximately a factor of 2 larger than the largest voids. DOE

N94-22939# Los Alamos National Lab., NM.
MAGNETIC PHASES IN UNiGe
V. Sechovsky (Karlova Univ., Prague, Czechoslovakia.), L. Havela (Karlova Univ., Prague, Czechoslovakia.), and A. Purwanto 1993 10 p Presented at the Actinides 1993, Santa Fe, NM, 19-24 Sep. 1993
(Contract W-7405-eng-36)
(DE94-000793; LA-UR-93-3350; CONF-930905-11) Avail: CASI HC A02/MF A01

Original measurements of 4.2 K magnetization curves and temperature dependence of magnetic susceptibility were completed by an extended study of magnetization, specific heat, and electric resistivity as a function of temperature and magnetic field. Neutron diffraction experiments were also performed on powder and single crystal. The specific heat shows a sharp peak at 41.5 K, corresponding to the first-order phase transition, and a broad anomaly around 50 K. The magnetic structures in UNiGe confirm that the strong bonding of 5f orbitals along the a axis leads to a huge magnetic anisotropy with U magnetic moments perpendicular to this direction. DOE

N94-22958# Lawrence Livermore National Lab., CA.
THE HISTORY OF DEVELOPMENT OF MOLYBDENUM ALLOYS FOR STRUCTURAL APPLICATIONS
J. Wadsworth and J. P. Wittenauer (Lockheed Missiles and Space Co., Palo Alto, CA.) Feb. 1993 26 p Presented at the 122nd Annual Meeting of the Minerals, Metals and Materials Society (TMS), Denver, CO, 21-25 Feb. 1993
(Contract W-7405-eng-48)
(DE94-000389; UCRL-JC-114114; CONF-9302103-5) Avail: CASI HC A03/MF A01

Molybdenum was first isolated as an element in 1893 and found initial commercial application as a filament support for incandescent lamps in 1910. The advent of arc melting practice in the 1940's led to an increase in availability of Mo sheet, bar, and plate products. Alloy development programs were heavily supported starting in the 1950's and several key alloys emerged over the next twenty years that remain in use to the present time such as Mo-TZM, unalloyed Mo, and Mo-Re. In recent years, improved understanding of the role of oxygen and carbide distributions at grain boundaries have led to increased reliability and use of Mo in aerospace products. Current developmental programs in areas of propulsion and energy conversion will ensure the prominent position of Mo as a high-temperature structural material. This paper highlights some of these key developments in the evolution of Mo alloys. DOE

N94-22965 Comision Nacional de Energia Atomica, Buenos Aires (Argentina). Dept. de Materiales.
INFLUENCE OF SINTERING ATMOSPHERES ON THE ALUMINUM SINTERING CHARACTERISTICS [INFLUENCIA DE LA ATMOSFERA DE SINTERIZACION EN LAS CARACTERISTICAS DE SINTERIZADO DEL ALUMINIO]
S. Mintzer and S. BermudezBelkys 1993 5 p In SPANISH Presented at the SAM 1993: 17th Metallurgical Sesssions of the Argentine Metals Association; 2nd Argentine Meeting on Ceramics and Refractories, San Carlos de Bariloche, Argentina, 13-16 Apr. 1993 Limited Reproducibility: More than 20% of this document may be affected by poor print
(DE93-632412; INIS-AR-013; CONF-9304174) Avail: Issuing Activity (Department of Energy (DOE)) (US Sales Only)

The aluminum powder (Al) cool compacted (at 95% from theoretical density) which was sintered at 903 K during 4 hours at different atmospheres, oxidizing (air), inert Argon (Ar), Nitrogen (N) and high vacuum is described. The results obtained show: (1) porosity measurements; greater porosity when sintering in Ar and air; (2) metallographic and scanning observations: many fine pores (less than 1 micron) and pore lines distributed at random, at air sintering and greater pores distributed preferentially near the surface, in Ar and N atmospheres; (3) dimensional changes: tendency to contraction of the samples at N and vacuum sintering and expansion in Ar or air; (d) mechanical properties: greater strength and fluence stresses at air and N sintering. The analysis of the results is performed considering sintering modes in presence of an oxide layer and dropped inert gases. DOE

N94-22966 Comision Nacional de Energia Atomica, Buenos Aires (Argentina). Dept. de Materiales.
DIFFUSION OF HYDROGEN IN IRON OXIDES [DIFUSION DE HIDROGENO EN OXIDOS DE HIERRO]
P. Bruzzoni and E. Riecke (Max-Planck-Inst. fuer Eisenforschung, Duesseldorf, Germany.) 1993 5 p In SPANISH Presented at the SAM 1993: 17th Metallurgical Sessions of the Argentine Metals Association; 2nd Argentine Meeting on Ceramics and Refractories, San Carlos de Bariloche, Argentina, 13-16 Apr. 1993 Limited Reproducibility: More than 20% of this document may be affected by poor print
(DE93-632430; INIS-AR-012; CONF-9304174) Avail: Issuing Activity (Department of Energy (DOE)) (US Sales Only)

The diffusion of hydrogen in transition metal oxides was recently studied at room temperature through the permeability electrochemical technique. This work studies thin oxide layers grown in air or in presence of oxidizing atmospheres at temperatures up to 200 C. The substrate was pure iron with different superficial treatments. It was observed that these oxides reduce up to three magnitude orders, the hydrogen stationary flux through membranes of usual thickness in comparison with iron membranes free of oxide. DOE

N94-22972# Institut National des Sciences Appliquees de Lyon, Villeurbanne (France). Groupe d'Etudes de Metallurgie Physique et de Physique des Materiaux.
DAMAGE UNDER MONOTONIC OR CYCLIC LOADS OF NEW AlSiFe ALLOYS PREPARED BY THE OSPREY (TM) PROCESS Ph.D. Thesis [ENDOMMAGEMENT SOUS SOLLICITATION MONOTONE OU CYCLIQUE DES NOUVEAUX ALLIAGES AL-SI-FE ELABORES PAR PROCEDE OSPREY (TM)]
Annick Mocellin 1993 259 p In FRENCH Sponsored by Societe Pechiney, France
(ISAL-93-0008; ETN-94-95169) Avail: CASI HC A12/MF A03

The mechanical behavior of AlSiFe alloys obtained by the Osprey (trademark) process is investigated. The microstructure of the AlSiFe is characterized by small grains containing silicon particles and intermetallic compounds. These alloys have a mechanical behavior similar to that of metal matrix composites reinforced with ceramic particles. The resistance to cyclic loads is found to be high. The fracture characteristics are investigated by tensile tests. The results show local plastic deformation between the matrix and the silicon particles, fracture of silicon particles in mode one, grain boundary shear stresses, and final intergranular decoherence of the fractured particles. The fatigue crack propagation behavior is discussed. The effect of the thermal stresses in the damage behavior is calculated by the iterative Eshelby method. A model to explain the phenomena observed is proposed. ESA

N94-22999# Bettis Atomic Power Lab., West Mifflin, PA.
IRRADIATION DAMAGE BEHAVIOR OF LOW ALLOY STEEL WROUGHT AND WELD MATERIALS
R. J. Stofanak, T. J. Poskie, Y. Y. Li, and G. L. Wire 1993 7 p Presented at the 6th International Symposium on Environmental Degradation of Materials in Nuclear Power Systems: Water Reactors, San Diego, CA, 3-5 Aug. 1993
(Contract DE-AC11-89PN-38014)
(DE94-000519; WAPD-T-2991; CONF-930825-7) Avail: CASI HC A02/MF A01

A study was undertaken to evaluate the irradiation damage response of several different types of low alloy steel: vintage type ASTM A302 Grade B (A302B) plates and welds containing different Ni and Cu concentrations, 3.5% Ni steels similar to ASTM A508 Class four, welds containing about 1% Ni (similar to type 105S), and 3.5% Ni steels with 'super-clean' composition. All materials were irradiated at several different irradiation damage levels ranging from 0.0003 to 0.06 dpa at 232 C (450 F). Complete Charpy V-notch impact energy transition temperature curves were generated for all materials before and after irradiation to determine transition temperature at 41 J (30 ft-lb) or 47 J (35 ft-lb) and the upper shelf energy. Irradiation damage behavior was measured by shift in Charpy 41 J or 47 J transition temperature (Delta TT(sub 41 J) or Delta TT(sub 47J)) and lowering of upper shelf Charpy energy at a given irradiation damage level. It was found that chemical composition greatly influenced irradiation damage behavior; highest irradiation damage (greatest Delta TT) was found in an A302B type weld containing 1.28% Ni and 0.20% Cu while the least damage was found in 3.5% Ni, 0.05% Cu, super-clean wrought materials. Combination of Ni and Cu was found to affect irradiation damage behavior at higher irradiation damage levels in the A302B welds where the 1.28% Ni, 0.20% Cu weld showed more damage than a 0.60% Ni, 0.31% Cu weld. For the 3.5% Ni steels, fabrication influenced irradiation behavior in that a silicon killed material showed greater irradiation damage than a low silicon material. In general, the 3.5% Ni materials with low copper showed less irradiation damage than the A302B materials. DOE

N94-23003# Los Alamos National Lab., NM.
INTERPLAY OF MAGNETIC AND SUPERCONDUCTING HEAVY FERMION GROUND STATES
R. H. Heffner 1993 7 p Presented at the 1993 International Workshop on Low Energy Muon Science, Santa Fe, NM, 4-8 Apr. 1993
(Contract W-7405-eng-36)
(DE94-000680; LA-UR-93-3473; CONF-9304145-3) Avail: CASI HC A02/MF A01

This talk will focus recent developments in the understanding of heavy fermion (HF) superconductors and the role that positive muon spin relaxation (mu SR) studies have played in helping to elucidate their properties. As illustrations, two systems will be discussed: UPd2Al13, one of the most recently discovered HF superconductors, which also displays coexisting magnetic order, and UBe13 doped with small quantities of Th substituted for U, which displays an interplay between its superconducting and magnetic ground states, leading to multiple superconducting states. DOE

N94-23009 Argonne National Lab., IL.
EFFECTS OF NEUTRON IRRADIATION AND HYDROGEN ON DUCTILE-BRITTLE TRANSITION TEMPERATURES OF V-Cr-Ti ALLOYS
B. A. Loomis, H. M. Chung, L. J. Nowicki, and D. L. Smith Aug. 1993 14 p Presented at the 6th International Conference on Fusion Reactor Materials, Stresa, Italy, 27 Sep. - 1 Oct. 1993 Limited Reproducibility: More than 20% of this document may be affected by poor print and microfiche quality
(Contract W-31-109-eng-38)
(DE94-001466; ANL/ET/CP-80889; CONF-930928-8) Avail: Issuing Activity (Department of Energy (DOE))

The effects of neutron irradiation and hydrogen on the ductile-brittle transition temperatures (DBTT's) of unalloyed vanadium and V-Cr-Ti alloys were determined from Charpy-impact tests on 1/3 ASTM standard size specimens and from impact tests on 3-mm diameter discs. The tests were conducted on specimens containing less than 30 appm hydrogen and 600-1200 appm hydrogen and on specimens after neutron irradiation to 28-46 dpa at 420, 520, and 600 C. The DBTT's were at a minimum (less than -220 C) for V-(105)Ti alloys under for V-4-Cr-4Ti alloy with less than 30 appm hydrogen. The effect of 600-1200 appm hydrogen in the specimens was to raise the DBTT's by 100-150 C. The DBTT's were minimum (less than -220 C) for V-(1-5)Ti alloys and V-4-Cr-4Ti alloys after neutron irradiation. DOE

N94-23017 Lawrence Livermore National Lab., CA.
TENSILE PROPERTIES OF 21-6-9 STAINLESS STEEL AT ELEVATED TEMPERATURES
S. G. Torres and G. A. Henshall Oct. 1993 17 p Limited Reproducibility: More than 20% of this document may be affected by microfiche quality
(Contract W-7405-eng-48)
(DE94-001852; UCRL-ID-114590) Avail: CASI HC A03

Tensile properties of Type 21-6-9 austenitic stainless steel were measured at temperatures ranging from ambient to 1200 C at a strain rate of 6.67 x 10(exp -4) /s. Data show that yield stress decreases rapidly from room temperature to about 300 C, followed by a nearly constant value in the 'plateau' region from 300 to 600 C. Beyond the plateau, there is a more rapid drop in yield stress as temperature increases. Ultimate tensile stress shows a plateau between 300 and 700 C, which may be caused by solutes. 21-6-9 stainless steel has excellent ductility, with the elongation to failure ranging from 55 to 95%. It appears that there is a local minimum in the ductility at approximately 700 C. Results are compared with earlier results of Kassner and co-workers. DOE

N94-23021 Los Alamos National Lab., NM.
TEXTURE GRADIENT EFFECTS IN TANTALUM
S. I. Wright, G. T. Gray, III, and A. J. Beaudoin (Reynolds Metals Co., Richmond, VA.) 1993 7 p Presented at the International Conference on Textures of Materials, Clausthal, Germany, 20-24 Sep. 1993 Limited Reproducibility: More than 20% of this document may be affected by microfiche quality
(Contract W-7405-eng-36)
(DE94-000689; LA-UR-93-3454; CONF-9309231-4) Avail: CASI HC A02

The effects of inhomogeneities in texture on the mechanical response of a tantalum plate were investigated. Through-thickness compression samples exhibited an hourglass shape after deformation. The compression tests were modeled using a finite-element approach. A polycrystal plasticity model is embedded at each element of the mesh enabling the simulation to account for the spatial distribution of texture and its evolution. The texture was characterized using spatially specific individual lattice orientation measurements. The orientations were measured using automatic analysis of electron backscatter Kikuchi diffraction patterns. The influence of the spatially nonuniform distribution of texture on the experimental and simulated results is discussed. This work demonstrates the capability of currently available tools for characterizing inhomogeneous microstructures and modeling the effects of variations in texture on mechanical behavior. DOE

N94-23119 Helsinki Univ. of Technology, Espoo (Finland). Lab. of Engineering Materials.
INTERNAL FRICTION ASSOCIATED WITH DISLOCATION RELAXATIONS IN VIRGIN MARTENSITE
L. Yong Apr. 1993 60 p Limited Reproducibility: More than 20% of this document may be affected by microfiche quality
(PB93-226280; ISBN-951-22-1523-3) Avail: CASI HC A04

Four internal friction peaks were observed during heating of virgin lenticular martensite from 82 to 350 K. Investigations on the effects of alloying contents and test conditions on the internal friction peaks have shown that there are three internal friction peaks exhibiting relation features, which can be attributed to the dislocation relaxation processes. Two of them can be attributed to the generation of kink-pairs along non-screw and screw dislocations, and one is due to the interaction between non-screw dislocations and carbon atoms. NTIS

N94-23194# Argonne National Lab., IL.
EFFECT OF NEUTRON IRRADIATION ON TENSILE PROPERTIES OF V-Cr-Ti ALLOYS
B. A. Loomis, L. J. Nowicki, and D. L. Smith Aug. 1993 15 p Presented at the 6th International Conference on Fusion Reactor Materials, Stresa, Italy, 27 Sep. - 1 Oct. 1993
(Contract W-31-109-eng-38)
(DE94-001433; ANL/ET/CP-80863; CONF-930928-7) Avail: CASI HC A03/MF A01

The tensile properties of V-4Cr-4Ti, V-9Cr-5Ti, V-14Cr-5Ti, V-3Ti-1Si, V-5Ti, and V-18Ti alloys were determined at 25, 420, 520, and 600 C after neutron irradiation to 28-46 dpa at 420, 520, and 600 C. The yield strength of the unirradiated alloys increased significantly (approximately 50%) on neutron irradiation. Irradiation hardening of the alloys at 25 C after irradiation at 420 C was on the order of V-18Ti less than V-3Ti-1Si less than V-5Ti less than V-4Cr-4Ti less than V-9Cr5Ti less than V-14Cr-5Ti. The total elongation of the irradiated alloys at 25 C after irradiation at 420 C ranged from 3% to 11% with total elongation of the alloys on the order of V-14Cr-5Ti less than V-9Cr-5Ti less than V-3Ti-1Si less than V-5Ti less than V-4Cr-4Ti less than V-18Ti. The total elongation of the alloys at 600 C after irradiation ranged from 11% to 23% with total elongation of the alloys on the order of V-14Cr-5Ti less than V-9Cr-5Ti less than V-4Cr-4Ti less than V-5Ti less than V-3Ti-1Si less than V-18Ti. DOE

N94-23219# Bettis Atomic Power Lab., West Mifflin, PA.

THERMALLY ACTIVATED LOW TEMPERATURE CREEP AND PRIMARY WATER STRESS CORROSION CRACKING OF NiCrFe ALLOYS

M. M. Hall, Jr. 1993 27 p Presented at the Alloy 600 Experts Meeting, Warrenton, VA, 5-9 Apr. 1993
(Contract DE-AC11-93PN-38195)
(DE94-001756; WAPD-T-3008; CONF-9304146-2) Avail: CASI HC A03/MF A01

A phenomenological stress corrosion cracking-crack growth rate (SCC-CGR) model is developed based on an a priori assumption that the SCC-CGR is controlled by low temperature creep (LTC). This mode of low temperature time dependent deformation occurs at stress levels above the athermal flow stress by a dislocation glide mechanism that is thermally activated and may be environmentally assisted. The SCC-CGR model equations developed contain thermal activation parameters descriptive of the dislocation creep mechanism. Thermal activation parameters are obtained by fitting the CGR model to SCC-CGR data obtained on Alloy 600 and Alloy X-750. These SCC-CGR activation parameters are compared to LTC activation parameters obtained from stress relaxation tests. When the high concentration of hydrogen at the tip of an SCC crack is considered, the SCC-CGR activation energies and rate sensitivities are shown to be quantitatively consistent with hydrogen reducing the activation energy and increasing the strain rate sensitivity in LTC stress relaxation tests. Stress dependence of SCC-CGR activation energy consistent with that found for the LTC activation energy. Comparisons between temperature dependence of the SCC-CGR stress sensitivity and LTC stress sensitivity provide a basis for speculation on effects of hydrogen and solute carbon on SCC crack growth rates. DOE

N94-23274*# National Aeronautics and Space Administration. Langley Research Center, Hampton, VA.

DETERMINATION OF FIBER-MATRIX INTERFACE FAILURE PARAMETERS FROM OFF-AXIS TESTS

Rajiv A. Naik (Analytical Services and Materials, Inc., Hampton, VA.) and John H. Crews, Jr. Oct. 1993 30 p
(RTOP 505-63-50-04)
(NASA-TM-109043; NAS 1.15:109043) Avail: CASI HC A03/MF A01

Critical fiber-matrix (FM) interface strength parameters were determined using a micromechanics-based approach together with failure data from off-axis tension (OAT) tests. The ply stresses at failure for a range of off-axis angles were used as input to a micromechanics analysis that was performed using the personal computer-based MICSTRAN code. FM interface stresses at the failure loads were calculated for both the square and the diamond array models. A simple procedure was developed to determine which array had the more severe FM interface stresses and the location of these critical stresses on the interface. For the cases analyzed, critical FM interface stresses were found to occur with the square array model and were located at a point where adjacent fibers were closest together. The critical FM interface stresses were used together with the Tsai-Wu failure theory to determine a failure criterion for the FM interface. This criterion was then used to predict the onset of ply cracking in angle-ply laminates for a range of laminate angles. Predictions for the onset of ply cracking in angle-ply laminates agreed with the test data trends. Author

N94-23297# Lawrence Livermore National Lab., CA.

PHASE TRANSFORMATIONS IN Cu-Zr MULTILAYERS

T. P. Weihs, T. W. Barbee, Jr., and M. A. Wall Apr. 1993 8 p Presented at the Spring Meeting of the Materials Research Society, San Francisco, CA, 12-16 Apr. 1993
(Contract W-7405-eng-48)
(DE94-000393; UCRL-JC-113810; CONF-930405-43) Avail: CASI HC A02/MF A01

A study of phase transformations is reported for Cu-rich, Cu-Zr multilayer foils synthesized using magnetron sputter deposition and annealed using a differential scanning calorimeter. The foils range in composition from 1.6 to 9.0 at% Zr and consist of alternate layers of polycrystalline Cu and Zr. Differential scanning calorimetry, X-ray analysis, and electron microscopy were used to examine three distinct reactions in the foils: a mixing and an amorphization of the Cu and the Zr, a crystallization of this amorphous phase to the metastable intermetallic Cu51Zr14, and a transformation of the Cu51Zr14 phase into the equilibrium phase Cu9Zr2. The as-deposited layering remained stable during the first two reactions and then broke down in the third reaction as large grains of Cu9Zr2 encompassed the smaller Cu grains. Heats of the reactions and activation energies of these reactions are measured and are compared to values reported for bulk samples. The measured heats provide evidence that amorphous Cu-Zr alloys phase separate and that mixing and short range ordering produce 3.5 times more heat than long range ordering produces when Cu and Zr react and form Cu51Zr14. DOE

N94-23434# Lawrence Livermore National Lab., CA.

DETERMINATION OF THE COMPATIBILITY BETWEEN STRUCTURAL ALLOYS AND MOLTEN METALS AT HIGH TEMPERATURES

G. A. Henshall, L. M. Wagner, B. A. Westfall, and R. P. Kershaw Aug. 1993 20 p
(Contract W-7405-eng-48)
(DE94-000954; UCRL-ID-114706) Avail: CASI HC A03/MF A01

The experimental methods for determining high-temperature compatibility between structural alloys and molten metals, particularly braze alloys, have been established. The structural alloys of interest are formed or machined into small crucibles into which the metal to be melted is placed. This system is placed in a furnace which typically will have a vacuum or inert gas environment; other atmospheres are possible as well. Multiple crucibles are exposed for various times and temperatures. Following cooling, a visual examination for loss of containment is performed. Each crucible is then sectioned and examined metallographically to document any loss in thickness of the crucible or any reactions between the materials. These procedures are fairly simple and require only common laboratory equipment; costs, therefore, are kept low. These experimental techniques were refined for use in determining the compatibility of both commercially pure vanadium and 21-6-9 stainless steel with a 92.5% Pb-5% In-2.5% Ag braze alloy. Both the vanadium and the stainless steel contained the molten Pb-In-Ag alloy for exposures ranging from 1000 C for 10 minutes up to 1200 C for 2 hours. DOE

N94-23446 Selskapet for Industriell og Teknisk Forskning, Trondheim (Norway). Div. of Applied Physics.

QUANTITATIVE ANALYSIS IN THE Al-Mg-Si SYSTEM WITH SMALL AMOUNTS OF Mg AND Si

Y. Tang (Norges Tekniske Hoegskole, Trondheim.), H. K. Nylund, R. Hoeier (Norges Tekniske Hoegskole, Trondheim.), and N. Ryum 28 Jan. 1993 5 p Limited Reproducibility: More than 20% of this document may be affected by microfiche quality
(PB93-201499; STF19-A92031) Avail: CASI HC A01

In the commercial Al-Mg-Si system, detailed knowledge of the precipitation rate of the Mg2Si needles and the dissolution rate of the original Mg2Si particles are of practical importance. However, due to low Mg and Si contents, experimental studies of the concentration gradients are difficult, especially if high spacial resolution is required. In these preliminary studies, the use of the energy dispersive x-ray (EDS) and electron energy loss spectroscopy (PEELS) methods have been investigated. The studies indicate that Mg may be quantified in the 0.6-1.0% regime with PEELS but not with EDS. The reverse is true for Si. NTIS

N94-23447 Selskapet for Industriell og Teknisk Forskning, Trondheim (Norway). Div. of Production Engineering.

THEORY OF EXTRUSION: ADVANCES AND CHALLENGES

S. Stoeren (Norges Tekniske Hoegskole, Trondheim.) 27 Nov. 1992 12 p Sponsored by Hydro Aluminum A/S Limited Reproducibility: More than 20% of this document may be affected by microfiche quality
(PB93-201572; STF20-A92187) Avail: Issuing Activity (National Technical Information Service (NTIS))

Plane-strain slip-line field theory, upper bound analysis and visioplasticity technique form the basis for the mechanics of extrusion. Bishop pointed out in 1957 that to make the theory useful in practice, one had to use the mechanics of extrusion to quantify phenomena that were primarily metallurgical, such as speed limit phenomena, flow resistance, the evolution of microstructure and properties of the extrudate. The practical part of the review focuses on unlubricated extrusion of aluminum alloys and on product and process development related to aluminum extrusions. NTIS

N94-23457# Argonne National Lab., Idaho Falls, ID.

GRAIN-BOUNDARY MICROCHEMISTRY AND INTERGRANULAR CRACKING OF IRRADIATED AUSTENITIC STAINLESS STEEL

H. M. Chung, W. E. Ruther, J. E. Sanecki, and T. F. Kassner Sep. 1993 10 p Presented at the 6th International Symposium on Environmental Degradation of Materials in Nuclear Power Systems: Water Reactors, San Diego, CA, 3-5 Aug. 1993
(Contract W-31-109-eng-38)
(DE94-000466; ANL/ET/CP-80756; CONF-930825-9) Avail: CASI HC A02/MF A01

Constant-extension-rate tensile tests and grain-boundary analysis by Auger electron spectroscopy were conducted on high- and commercial-purity (HP and CP) Type 304 stainless steel (SS) specimens from irradiated BWR components to identify mechanisms of irradiation-assisted stress corrosion cracking (IASCC). Susceptibility to intergranular fracture could not be correlated with radiation-induced segregation of impurities such as Si, P, C, or S, but a correlation was obtained with grain-boundary Cr concentration, indicating a role for Cr depletion. Grain-boundary chemistry was conducted on BWR neutron absorber tubes fabricated from two similar heats of HP Type 304 SS of virtually identical bulk chemical composition but exhibiting different susceptibility to IASCC after irradiation to approximately 2 x 10(exp 21) n/sq cm (E is greater than 1 MeV). Grain-boundary concentrations of Cr, Ni, Si, P, S, and C of the cracking-resistant and -susceptible HP heats were virtually identical. However, grain boundaries of the cracking-resistant material contained less N and more B and Li. This observation indicates that, besides the deleterious effect of grain-boundary Cr depletion, synergism between grain-boundary segregation of N and B and transmutation to H and Li plays an important role in IASCC. DOE

N94-23467*# National Aeronautics and Space Administration. Lewis Research Center, Cleveland, OH.

CHARACTERIZATION AND DURABILITY TESTING OF PLASMA-SPRAYED ZIRCONIA-YTTRIA AND HAFNIA-YTTRIA THERMAL BARRIER COATINGS. PART 2: EFFECT OF SPRAY PARAMETERS ON THE PERFORMANCE OF SEVERAL HAFNIA-YTTRIA AND ZIRCONIA-YTTRIA COATINGS

Robert A. Miller and George W. Leissler (Sverdrup Technology, Inc., Brook Park, OH.) Washington Mar. 1993 20 p
(Contract NAS3-25266; RTOP 505-63-5A)
(NASA-TP-3296; E-7152; NAS 1.60:3296) Avail: CASI HC A03/MF A01

This is the second of two reports which discuss initial experiments on thermal barrier coatings prepared and tested in newly upgraded plasma spray and burner rig test facilities at LeRC. The first report, part 1, describes experiments designed to establish the spray parameters for the baseline zirconia-yttria coating. Coating quality was judged primarily by the response to burner rig exposure, together with a variety of other characterization approaches including thermal diffusivity measurements. That portion of the study showed that the performance of the baseline NASA coating was not strongly sensitive to processing parameters. In this second part of the study, new hafnia-yttria coatings were evaluated with respect to both baseline and alternate zirconia-yttria coatings. The hafnia-yttria and the alternate zirconia-yttria coatings were very sensitive to plasma-spray parameters in that high-quality coatings were obtained only when specific parameters were used. The reasons for this important observation are not understood. Author (revised)

N94-23475 EG and G Rocky Flats, Inc., Golden, CO.

JBK-75 STAINLESS STEEL MACHINABILITY STUDY

A. P. McManigle and A. W. Simonis 2 Sep. 1993 38 p Limited Reproducibility: More than 20% of this document may be affected by microfiche quality
(Contract DE-AC34-90DP-62349)
(DE94-002268; RFP-4627) Avail: CASI HC A03

The study on forgings characterized machinability of the material by varying cutting speeds and feed-rates utilizing four tools for the roughing operation and four tools for the semi-finish operation. Tools tested were obtained from four manufacturers. Twelve parts were machined utilizing an experimental design to determine all possible interactions between cutting speeds and feed-rates. To evaluate the machinability of the material, quantitative measures in tool life, tool wear, surface finish, chip control, and material removal rates were analyzed. Benefits gained from this study are: higher material removal rates, longer tool life, minimal tool wear, improved chip control and reliability, increased productivity, and cost minimization. DOE

N94-23496 Rijksinstituut voor Volksgezondheid en Milieuhygieene, Bilthoven (Netherlands).

EXPLORATORY REPORT NICKEL AND NICKEL COMPOUNDS

W. Slooff, P. F. H. Bont (Resources Planning Consultants B.V., Delft, Netherlands.), J. A. Janus, and B. Loos Oct. 1992 53 p Limited Reproducibility: More than 20% of this document may be affected by microfiche quality
(PB93-223998; RIVM-710401017) Avail: CASI HC A04

The report contains general information on nickel and nickel compounds concerning the existing standards, emissions, exposure levels, and effect levels. The document is to be considered as a start for the national discussion during an exploratory meeting on integrated criteria documents. Pure nickel is not produced in the Netherlands, but nickel and nickel compounds are widely used. The most important sources of emissions to air are refineries and usage of diesel oil, whereas industry and agriculture contribute significantly to emissions to water and soil, respectively. By far the most important nickel-containing waste stream is domestic waste. In general the emissions are expected to decrease. NTIS

N94-23541# Los Alamos National Lab., NM.

THE EFFECTS OF TEXTURE AND STRAIN ON THE r-VA LUE OF HEAVY GAUGE TANTALUM PLATE

C. Michaluk (Cabot Corp., Boyertown, PA.), J. Bingert, and C. S. Choi (National Inst. of Standards and Technology, Gaithersburg, MD.) 1993 10 p Presented at the International Conference on Textures of Materials, Clausthal, Germany, 20-24 Sep. 1993
(Contract W-7405-eng-36)
(DE94-000690; LA-UR-93-3453; CONF-9309231-3) Avail: CASI HC A02/MF A01

Previous work by other researchers suggest that the r-values measured from thick-gauge tantalum plate do not correspond to the predicted r-values calculated from ODF coefficients. To understand this behavior, bulk texture analysis using neutron diffraction techniques was conducted on annealed samples of Ta and Ta-2.5W plate: the pure tantalum exhibited a primary (111) type texture, whereas the alloy contained a cube texture. For the pure tantalum, the r-values calculated from the texture of as-annealed and the deformed specimens were similar and correlated well with measured data. The r-value of the Ta-2.5W exhibited a greater degree of strain-sensitivity, such that the calculated r-values based on the initial texture did not represent those calculated or measured after tensile deformation. Strain sensitivity of r-values in Ta and Ta-2.5W plates is related to the generation of a ((bar 1)10) fiber texture during deformation. DOE

N94-23550*# National Aeronautics and Space Administration. Lewis Research Center, Cleveland, OH.

CHARACTERIZATION OF THE MICROSTRUCTURE OF Nb-1WT.%Zr-0.1WT.%C TUBES AS AFFECTED BY THERMOMECHANICAL PROCESSING

Mehmet Uz (Lafayette Coll., Easton, PA.) and Robert H. Titran Dec. 1993 12 p Presented at the 11th Symposium on Space Nuclear Power and Propulsion, Albuquerque, NM, 9-13 Jan. 1994 Sponsored by DOE
(Contract DE-2103-86SF-16310; RTOP 583-02-01)
(NASA-TM-106381; E-8194; NAS 1.15:106381; DOE/NASA/16310-21)
Avail: CASI HC A03/MF A01

Microstructure of Nb-1Zr-0.1C tubes were characterized as affected by extrusion temperature of the tube shell and its thermomechanical processing to tubing. Two tube shells of about 40-mm outside diameter (OD) and 25-mm inside diameter (ID) were extruded 8:1 from a vacuum arc-melted ingot at 1900 and 1550 K. Two different OD tubes of approximately 0.36-mm wall thickness were fabricated from each tube shell by a series of 26 cold drawing operations with two in process anneals. The microstructure of tube shells and the tubing before and after a 2-step heat treatment were characterized. Residue extracted chemically from each sample was also analyzed to identify the precipitates. The results concerning the effect of the initial extrusion temperature and subsequent processing on the microstructure of the tubes are presented together with a review of results from similar work on Nb-1Zr-0.1C sheet stock. Author (revised)

N94-23556*# National Aeronautics and Space Administration. Lewis Research Center, Cleveland, OH.

EFFECT OF HYDROGEN EXPOSURE ON A Cu-8 Cr-4 Nb ALLOY

David L. Ellis (Case Western Reserve Univ., Cleveland, OH.), Ajay K. Misra (Sverdrup Technology, Inc., Brook Park, OH.), and Robert L. Dreshfield Dec. 1993 8 p
(Contract NAS3-25266; RTOP 584-03-11)
(NASA-TM-106429; E-8271; NAS 1.15:106429) Avail: CASI HC A02/MF A01

The advanced regeneratively cooled rocket thrust chamber may require new materials to achieve long life and improved performance. Current materials such as NARloy-Z (Cu-3 wt. percent Ag-0.5 wt. percent Zr), while highly conductive, do not have sufficient high temperature strength and creep resistance to meet the projected needs of advanced rocket motors. A Cu-8 at. percent Cr-4 at. percent Nb (Cu-8 Cr-4 Nb) alloy has been identified as a promising material for this application. However, hydrogen embrittlement is a concern given the presence of high pressure, high temperature hydrogen in regeneratively cooled rocket motors. Thermodynamic analysis of the reaction between Cr-rich Cr2Nb and H2 showed that there is a possibility of reaction at temperatures up to 323 K in a 35 MPa H2 environment. Above 323 K the pressure necessary to achieve reaction rapidly increased beyond the range experienced in rocket motors. Tensile specimens exposed in 34.5 MPa H2 at room temperatures and during cycling to 705 C did not show any degradation of properties. No evidence of reaction was observed for Cr2Nb precipitate observed on the fracture surfaces. Based on these results the Cu-8 Cr-4 Nb alloy was judged to be sufficiently stable for use in rocket motors. Author (revised)

N94-23578*# National Aeronautics and Space Administration. Lewis Research Center, Cleveland, OH.

MULTILAYER RELAXATION AND SURFACE STRUCTURE OF ORDERED ALLOYS

Robert J. Kobistek (Victoreen, Inc., Solon, OH.), Guillermo Bozzolo (Analex Corp., Brook Park, OH.), John Ferrante, and Herbert Schlosser (Cleveland State Univ., OH.) Dec. 1993 16 p
(Contract NAS3-25776; RTOP 505-90-53)
(NASA-TM-106433; E-8275; NAS 1.15:106433) Avail: CASI HC A03/MF A01

Using BFS, a new semiempirical method for alloys, we study the surface structure of fcc ordered binary alloys in the Ll(sub 2) structure (Ni3Al and Cu3Au). We show that the surface energy is lowest for the mixed composition truncation of the low-index faces of such systems. Also, we present results for the interlayer relaxations for planes close to the surface, revealing different relaxations for atoms of different species producing a rippled surface layer. Author (revised)

N94-23714 Amsterdam Univ. (Netherlands).

MAGNETIC RESONANCE STUDIES OF 3D TRANSITION METAL IMPURITIES IN COMPOUND SEMICONDUCTORS Ph.D. Thesis

S. J. C. H. M. vanGisbergen 18 Feb. 1993 142 p See also DE89-609615 Sponsored by Stichting voor Fundamenteel Onderzoek der Materie, Amsterdam, Netherlands Limited Reproducibility: More than 20% of this document may be affected by microfiche quality
(PB93-232197) Avail: Issuing Activity (National Technical Information Service (NTIS))

In the thesis magnetic resonance is used to study transition element impurities with an electron configuration (Ar)3d(sup 5) (Mn(2+) and Fe(3+)) in compound semiconductors. The techniques employed are electron paramagnetic resonance (EPR); electron-nuclear double resonance (ENDOR), which combines EPR with nuclear magnetic resonance (NMR); and optically detected magnetic resonance (ODMR), in which detection of the EPR occurs via induced changes of a photoluminescence signal. The outline of the thesis is as follows: In chapter two an introduction is given to magnetic resonance and the experimental set-ups are described. In chapter three this is further specified for the case of 3d transition metal impurities in compound semiconductors. In chapter four the identification of interstitial Mn(2+) in GaAs and GaP by EPR is reported and in chapter five ENDOR measurements on substitutional Mn(2+) in GaAs are discussed. Chapter six deals with the observation of anomalous line intensities in the EPR spectrum of Fe(3+) in GaAs, for which electric quadrupole excitation effects are believed to be responsible. Finally, in chapter seven an ODMR study is performed on the diluted magnetic semiconductor Cd(0.905)Mn(0.095)Te. NTIS

N94-23715# Oak Ridge National Lab., TN.

THE STATISTICS OF SPUTTERING

M. T. Robinson 1993 14 p Presented at the ICACS 15th International Conference on Atomic Collision in Solids, London, Canada, 26-30 Jul. 1993
(Contract DE-AC05-84OR-21400)
(DE94-001128; CONF-930712-7) Avail: CASI HC A03/MF A01

The MARLOWE program was used to study the statistics of sputtering on the example of 1- to 100-keV Au atoms normally incident on static (001) and (111) Au crystals. The yield of sputtered atoms was examined as a function of the impact point of the incident particles ('ions') on the target surfaces. There were variations on two scales. The effects of the axial and planar channeling of the ions could be traced. The details depended upon the orientation of the target and the energies of the ions. Locally, the sputtering yield was very sensitive to the impact point, small changes in position often producing large changes yield. Results indicate strongly that the sputtering yield is a random ('chaotic') function of the impact point. DOE

N94-23717# Iowa State Univ. of Science and Technology, Ames. Dept. of Engineering.

STRENGTH, ACOUSTIC EVALUATION AND METALLURGY OF DIFFUSION BONDS

O. Buck and G. C. Ojard 1993 11 p Presented at the Fall Meeting of the Minerals, Metals and Materials Society: Physical Metallurgy and Materials, Pittsburgh, PA, 17-21 Oct. 1993
(Contract W-7405-eng-82)
(DE94-001804; IS-M-773; CONF-931009-6) Avail: CASI HC A03/MF A01

This paper discusses our efforts on two model systems to determine the bond strength, its correlation to acoustic NDE and the metallurgy involved in the process. Results indicate that the total acoustic energy, reflected from the original interface, can differentiate between the various bond strengths achieved. However, depending on types of materials to be joined, the atomistic processes, leading to a variety of microstructures in the bond planes, can become quite complex and strongly dominate the mechanical properties of such bonds. Origin of failure initiating defects is discussed. DOE

N94-23753# Ames Lab., IA.

LARGE-SCALE PRODUCTION OF Si(0.8)Ge(0.2) THERMOELECTRIC ALLOYS BY MECHANICAL ALLOYING

B. A. Cook, J. L. Harringa, S. Loughin (Martin Marietta Astro Space, Philadelphia, PA.), and D. X. Centurioni (Martin Marietta Astro Space, Philadelphia, PA.) 1993 4 p Presented at the 28th Intersociety Energy Conversion Engineering Conference, Atlanta, GA, 8-13 Aug. 1993
(Contract W-7405-eng-82)
(DE94-000695; IS-M-767; CONF-930804-20) Avail: CASI HC A01/MF A01

Advanced processing techniques were combined with refinements in composition to produce homogeneous, production-scale quantities of n- and p-type Si(0.8)Ge(0.2) alloys with improved thermoelectric properties. Two p-type compacts of Si(0.8)Ge(0.2) doped with 0.8 atom% boron and one n-type compact doped with 0.8 m/o GaP and a P/Ga ratio of 2.38 were prepared by mechanical alloying. Resulting powders were consolidated into 7.62 cm diameter compacts by vacuum hot pressing. Transport and thermoelectric properties were measured. As-pressed samples were found to have low carrier mobility. Metallographic analysis revealed a sub-micron grain size which would suggest a high density of grain boundary potential barriers. A heat treatment was applied and the measurements were repeated. The post-treatment p-type samples showed a 33% grain growth and an integrated average figure of merit of 0.6 x 10(exp -3) K(exp -1) over the 573-1273 K range. This paper presents the details of fabrication method and compares the thermoelectric properties with the properties of similar alloys manufactured by traditional vacuum casting and hot pressing. DOE

N94-23784# EG and G Mound Applied Technologies, Miamisburg, OH.

DEVELOPMENT TESTING OF THE TWO-WATT RTG HEAT SOURCE AND HASTELLOY-S/T-111 ALLOY COMPATIBILITY STUDIES

E. I. Howell and P. E. Teaney 29 Sep. 1993 29 p
(Contract DE-AC04-88DP-43495)
(DE94-002875; MLM-3786) Avail: CASI HC A03/MF A01

The two-watt radioisotope thermoelectric generator heat source capsules were tested to determine their survivability under extreme environmental conditions: high external pressure, high impact, and high internal pressure. Test results showed that the capsules could withstand external pressures of 1,000 bars and impacts at velocities near 150 meters per second. However, the results of the internal pressure tests (stress-rupture) were not so favorable, possibly because of copper contamination, leading to a recommendation for additional testing. A material compatibility study examined the use of Hastelloy-S as a material to clad the tantalum strength member of the two-watt radioisotopic heat source. Test capsules were subjected to high temperatures for various lengths of time, then cross sectioned and examined with a scanning electron microscope. Results of the study indicate that Hastelloy-S would be compatible with the underlying alloy, not only at the normal operating temperatures of the heat source, but also when exposed to the much higher temperatures of a credible accident scenario. DOE

N94-23792 Bettis Atomic Power Lab., West Mifflin, PA.
EFFECT OF IRRADIATION ON THE STRESS CORROSION CRACKING BEHAVIOR OF ALLOY X-750 AND ALLOY 625
W. J. Mills, M. R. Lebo, J. J. Kearns, R. C. Hoffman, J. J. Korinko, R. F. Luther, and G. B. Sykes 1993 10 p Presented at the 6th International Symposium on Environmental Degradation of Materials in Nuclear Power Systems: Water Reactors, San Diego, CA, 3-5 Aug. 1993 Limited Reproducibility: More than 20% of this document may be affected by microfiche quality
(Contracts DE-AC11-93PN38195; DE-AC11-89PN-38014)
(DE94-001759; WAPD-T-2990; CONF-930825-11) Avail: CASI HC A02

In-reactor testing of bolt-loaded precracked and as-notched compact tension specimens was performed in 360 C water to determine effect of irradiation on SCC of Condition HTH and Condition BH Alloy X-750 and age-hardened Alloy 625. Variables were stress intensity factor (K(sub I)) level, fluence, grade of HTH material, prestraining and material chemistry. Effects of irradiation on high temperature SCC and the rapid cracking that occurs during cooldown below 150 C were characterized. Significant degradation in the in-reactor SCC resistance of HTH material was observed at initial K(sub I) levels above 30 MPa(radical)m and fluences greater than 10(exp 19) n/sq cm (E greater than 1 MeV). A small degradation in SCC resistance of HTH material was observed at low fluences (less than 10(exp 16) n/sq cm). As-notched specimens displayed less degradation in SCC resistance than precracked specimens. Prestraining greatly improved in-flux and out-of-flux SCC resistance of HTH material, as little or no SCC was observed in precracked specimens prestrained 20 to 30%, whereas extensive cracking was observed in nonprestrained specimens. Condition HTH heats with low boron (10 ppM or less) had improved in-reactor SCC resistance compared to heats with high and intermediate boron (greater than 20 ppM). Age-hardened Alloy 625 exhibited superior in-reactor SCC behavior compared to HTH material as no crack extension occurred in any of the precracked Alloy 625 specimens tested at initial K(sub I) levels up to 80 MPa(radical)m. DOE

N94-23802 Environmental Protection Agency, Cincinnati, OH.
STATISTICAL PROCEDURES FOR CORROSION STUDIES
Barbara M. Wysock, Anne M. Sandvig (Economic and Engineering Services, Inc., Bellevue, WA.), Michael R. Schock, Christopher P. Frebie (Computer Sciences Corp., Cincinnati, OH.), and Boris Prokop (Economic and Engineering Services, Inc., Bellevue, WA.) 1993 23 p Limited Reproducibility: More than 20% of this document may be affected by microfiche quality
(PB93-199412; EPA/600/A-93/118) Avail: CASI HC A03

Many utilities will be conducting pipe loop and other experimental studies to optimize corrosion control under the Lead and Copper Rule. This paper presents a discussion of the background and justifications for the selection of different statistical techniques to evaluate experimental and pilot plant data. Tests covered include those for parametric and nonparametric comparisons among treatment or sampling sites; detection of trends in corrosion and inhibitor treatments; and selection of a proper number of samples and frequency of sampling. NTIS

N94-23811 Sandia National Labs., Albuquerque, NM. Advanced Materials Lab.
METAL-MULLITE REACTIONS
Ronald E. Loehman and Antoni P. Tomsia (Pask Research and Engineering, Inc., Berkeley, CA.) 1993 7 p Presented at the International Union of Materials Research Societies on Advanced Materials, Tokyo, Japan, 31 Aug. - 4 Sep. 1993 Limited Reproducibility: More than 20% of this document may be affected by poor print
(Contracts DE-AC04-94AL-85000; DE-AC04-76DP-00789)
(DE94-002038; SAND-93-0549C; CONF-9308122-11) Avail: Issuing Activity (Department of Energy (DOE))

Mullite was reacted with pure Al and with Ti or Zr dissolved in Ag-Cu eutectic alloys at 1100 C in Ar. Analysis of the Ti and Zr-containing specimens showed reaction zones with compositions of Ti(50)Cu(30)O(20) and ZrO2, respectively. The Al-mullite specimen showed much more extensive penetration into the ceramic and a more diffuse reaction zone than the other two systems. Al2O3 and Si were the main reaction products for Al-mullite reaction. DOE

N94-24066*# Auburn Univ., AL. Materials Engineering Program.
HOT HYDROGEN TESTING OF METALLIC TURBO PUMP MATERIALS Final Report, 13 May 1992 - 12 May 1993
Ralph Zee, Bryan Chin, and Rohit Inamdar 12 May 1993 80 p
(Contract NAS8-39131)
(NASA-CR-193880; NAS 1.26:193880) Avail: CASI HC A05/MF A01

The objectives of this investigation are to expose heat resistant alloys to hydrogen at elevated temperatures and to use various microstructural and analytical techniques to determine the chemical and rate process involved in degradation of these materials due to hydrogen environment. Inconel 718 and NASA-23 (wrought and cast) are candidate materials. The degradation of these materials in the presence of 1 to 5 atmospheric pressure of hydrogen from 450 C to 1100 C was examined. The hydrogen facility at Auburn University was used for this purpose. Control experiments were also conducted wherein the samples were exposed to vacuum so that a direct comparison of the results would separate the thermal contribution from the hydrogen effects. The samples were analyzed prior to and after exposure. A residual gas collection system was used to determine the gaseous species produced by any chemical reaction that may have occurred during the exposure. Analysis of this gas sample shows only the presence of H2 as expected. Analyses of the samples were conducted using optical microscopy, x-ray diffraction, scanning electron microscopy, and weight change. There appears to be no change in weight of the samples as a result of hydrogen exposure. In addition no visible change on the surface structure was detected. This indicates that the materials of interest do not have strong interaction with hot hydrogen. This is consistent with the microstructure results. Author (revised)

N94-24170 Toronto Univ. (Ontario). Dept. of Mechanical Engineering.
FEASIBILITY STUDY OF SHOT-PEENING MODELING
S. A. Meguid Mar. 1992 179 p
(CTN-94-60926) Avail: Micromedia Ltd., Technical Information Centre, 165 Hotel de Ville, Place du Portage, Phase 2, Hull, Quebec J8X 3X2, Canada

A review is presented of the state of the art in the field of shot peening to enhance fatigue life and inhibit stress corrosion cracking of aircraft structures, namely aluminum 2xxx and 7xxx series, high strength alloy steels 4xxx series and titanium alloys. The review examines the modeling of the process, the generation and relaxation of the resulting stress field, and their adequacy in interpreting the resulting fatigue life improvement of the treated parts. Attention is also devoted to the evaluation of peening residual stresses and their associated models. The fundamentals of shot peening are reviewed, the effect of residual stress on the fatigue fracture behavior of the above alloys is evaluated, and the effect of peening treatment on the stress corrosion cracking behavior of the materials of interest is assessed. The relaxation of the resulting residual stress field due to cyclic and thermal loadings is covered, and recommendations are made for future research. Author (CISTI)

N94-24469 University of Western Ontario, London. Dept. of Chemistry.
SEGREGATION AND OXIDATION STUDIES OF AL-LI AND AL-MG ALLOYS Ph.D. Thesis
Frank Joseph Esposto Jun. 1993 152 p

(ISBN-0-315-83993-7; CTN-94-60959) Copyright Avail: Micromedia Ltd., Technical Information Centre, 240 Catherine Street, Suite 305, Ottawa, Ontario, K2P 2G8, Canada HC/MF

Auger electron spectroscopy, work function measurements, low energy electron diffraction, nuclear reaction analysis, dynamic/static secondary ion mass spectrometry, thermal desorption spectroscopy, and synchrotron radiation photoemission spectroscopy were used to investigate the segregation and oxidation of (111) oriented Al-6.5 percent Li and (110) oriented Al-1.45 percent Mg single crystal binary alloys. The resulting Li and Mg equilibrium surface concentrations are found to be 0.16 and 0.47 respectively. For both alloys, the increase in surface concentration was associated with a decrease in the change in work function. Ordered surface alloy phases were observed accompanying surface segregation with Al-Li and Al-Mg single crystal alloys. Oxidation measurements clearly indicate that the reactivities of the two alloy surfaces are substantially increased at the equilibrium Li and Mg surface concentrations. Oxidation of the Li-segregated surface occurs immediately, forming a mixed oxide composed of Al, Li, and O. The oxidation of the Mg-segregated surface also occurs immediately and leads to formation of a combination oxide (Al2O3 + MgO) at higher exposures. Author (CISTI)

N94-24520# Los Alamos National Lab., NM.

PROCEDURES FOR DETERMINING MATMOD-4V MATERIAL CONSTANTS

T. C. Lowe 1993 17 p Presented at the Annual Winter Meeting of the American Society of Mechanical Engineers, New Orleans, LA, 28 Nov. - 3 Dec. 1993

(Contract W-7405-eng-36)

(DE94-002638; LA-UR-93-3584; CONF-931121-29) Avail: CASI HC A03/MF A01

The MATMOD-4V constitutive relations were developed from the original MATMOD model to extend the range of nonelastic deformation behaviors represented to include transient phenomena such as strain softening. Improvements in MATMOD-4V increased the number of independent material constants and the difficulty in determining their values. Though the constitutive relations are conceptually simple, their form and procedures for obtaining their constants can be complex. This paper reviews in detail the experiments, numerical procedures, and assumptions that have been used to determine a complete set of MATMOD-4V constants for high purity aluminum. DOE

N94-24612# Massachusetts Inst. of Tech., Cambridge. Dept. of Physics.

THERMAL PHASE BEHAVIOR OF METAL SURFACES: X-RAY SCATTERING STUDIES OF Pt(001)

D. L. Abernathy, S. G. J. Mochrie, M. Yoon, D. Gibbs (Brookhaven National Lab., Upton, NY.), G. Gruebel (Brookhaven National Lab., Upton, NY.), G. M. Watson (Brookhaven National Lab., Upton, NY.), and D. M. Zehner (Oak Ridge National Lab., TN.) 1993 9 p Presented at the 4th International Conference on the Structure of Surfaces, Shanghai, China, 16-19 Aug. 1993

(Contract DE-AC02-76CH-00016)

(DE94-002991; BNL-49483; CONF-9308154-2) Avail: CASI HC A02/MF A01

Recent highlights of the results of x-ray scattering studies of the structure and phase behavior of smooth and vicinal Pt(001) surfaces are reviewed. DOE

N94-24747# Los Alamos National Lab., NM.

A SURVEY OF METALLURGICAL RESEARCH ON SEVERAL ACTINIDES

J. D. Olivas and F. W. Schonfeld 1993 22 p Presented at the Actinides 1993 Conference, Santa Fe, NM, 19-24 Sep. 1993

(Contract W-7405-eng-36)

(DE94-002643; LA-UR-93-3628; CONF-930905-20) Avail: CASI HC A03/MF A01

A Los Alamos perspective on metallurgical research on neptunium, plutonium, americium, curium, and californium is presented. Alloying behaviors of these metals are discussed. Metal fabrication technologies, principally for plutonium, are emphasized. DOE

N94-24823 Virginia Univ., Charlottesville. Dept. of Materials Science and Engineering.

ENVIRONMENTALLY ASSISTED CRACKING OF HIGH STRENGTH BETA TITANIUM ALLOYS Annual Report, 15 Sep. 1992 - 15 Sep. 1993

Nov. 1993 118 p Limited Reproducibility: More than 20% of this document may be affected by microfiche quality

(Contract N00014-91-J-4164)

(AD-A273598) Avail: Issuing Activity (Defense Technical Information Center (DTIC))

The objective of this integrated research program is to define the conditions under which high strength Beta-titanium alloys resist environmentally assisted cracking (EAC) in marine environments. Specific goals are to: (1) characterize EAC for metallurgical, chemical, and mechanical conditions that could destabilize crack tip passive films to promote local dissolution and hydrogen (H) uptake, (2) test the hydrogen embrittlement mechanism for EAC, and (3) develop a mechanism-based model of EAC by integrating crack chemistry, surface dissolution and repassivation kinetics, hydrogen uptake to trap sites, and crack tip process zone micromechanics and damage. The following conclusions were established in FY 93 based on rising load fracture mechanics experiments with solution treated and peak aged Ti-15-3 (15V-3Cr-3A1-3Sn; wt%) and Beta 21S (Ti- 15Mo-3Nb-3Al; wt%) in aqueous NaCl. This work is detailed in the attached paper. DTIC

N94-25033 California Inst. of Tech., Pasadena. Lab of Engineering Materials.

SYMPOSIUM ON DIFFUSION IN ORDERED ALLOYS Final Report, 31 Mar. 1992 - 1 Jun. 1993

Brent Fulz 1 Jun. 1993 6 p Limited Reproducibility: More than 20% of this document may be affected by microfiche quality

(Contract N00014-92-J-1921)

(AD-A273643) Avail: Issuing Activity (Defense Technical Information Center (DTIC))

Diffusion in ordered alloys and intermetallic compounds has received little attention in recent years, even though it lies at the heart of many fundamental and practical problems. As opposed to diffusion in dilute alloys or solid solutions, atom movements in ordered alloys are affected by the state of order in the material. Conversely, atom movements change the state of order, either locally, leading to large diffusional correlation factors, or globally, leading to order-disorder transformations. Diffusion controls the sequence of compound formation during the intermixing of pure elements, and affects properties such as creep, hydrogen embrittlement, and stability against electromigration. DTIC

N94-25117*# National Aeronautics and Space Administration. Langley Research Center, Hampton, VA.

SURFACE COMPOSITIONAL VARIATIONS OF Mo-47Re ALLOY AS A FUNCTION OF TEMPERATURE

S. J. Hoekje (Analytical Services and Materials, Inc., Hampton, VA.), R. A. Outlaw, and S. N. Sankaran (Analytical Services and Materials, Inc., Hampton, VA.) Dec. 1993 31 p

(RTOP 763-23-45)

(NASA-TP-3402; L-17278; NAS 1.60:3402) Avail: CASI HC A03/MF A01

Molybdenum-rhenium alloys are candidate materials for the National Aero-Space Plane (NASP) as well as for other applications in generic hypersonics. These materials are expected to be subjected to high-temperature (above 1200 C) casual hydrogen (below 50 torr), which could potentially degrade the material strength. Since the uptake of hydrogen may be controlled by the contaminant surface barriers, a study of Mo-47Re was conducted to examine the variations in surface composition as a function of temperature from 25 C to 1000 C. Pure molybdenum and rhenium were also examined and the results compared with those for the alloy. The analytical techniques employed were Auger electron spectroscopy, electron energy loss spectroscopy, ion scattering spectroscopy, and x ray photoelectron spectroscopy. The native surface was rich in metallic oxides that disappeared at elevated temperatures. As the temperature increased, the carbon and oxygen disappeared by 800 C and the surface was subsequently populated by the segregation of silicon, presumably from the grain boundaries. The alloy readily chemisorbed oxygen, which disappeared with heating. The disappearance temperature progressively increased for successive dosings. When the alloy was exposed to 800 torr of hydrogen

at 900 C for 1 hour, no hydrogen interaction was observed.
Author (revised)

N94-25118*# Cornell Univ., Ithaca, NY.
FRANC2D: A TWO-DIMENSIONAL CRACK PROPAGATION SIMULATOR. VERSION 2.7: USER'S GUIDE Final Report
Paul Wawrzynek and Anthony Ingraffea Mar. 1994 66 p
(Grant NAG1-1184; RTOP 538-02-10-01)
(NASA-CR-4572; NAS 1.26:4572) Avail: CASI HC A04/MF A01

FRANC 2D (FRacture ANalysis Code, 2 Dimensions) is a menu driven, interactive finite element computer code that performs fracture mechanics analyses of 2-D structures. The code has an automatic mesh generator for triangular and quadrilateral elements. FRANC2D calculates the stress intensity factor using linear elastic fracture mechanics and evaluates crack extension using several methods that may be selected by the user. The code features a mesh refinement and adaptive mesh generation capability that is automatically developed according to the predicted crack extension direction and length. The code also has unique features that permit the analysis of layered structure with load transfer through simulated mechanical fasteners or bonded joints. The code was written for UNIX workstations with X-windows graphics and may be executed on the following computers: DEC DecStation 3000 and 5000 series, IBM RS/6000 series, Hewlitt-Packard 9000/700 series, SUN Sparc stations, and most Silicon Graphics models.
Author (revised)

N94-25120*# National Aeronautics and Space Administration. Lewis Research Center, Cleveland, OH.
WORKSHOP ON THE THERMOPHYSICAL PROPERTIES OF MOLTEN MATERIALS
Nov. 1993 247 p Workshop held in Cleveland, OH, 22-23 Oct. 1992
(RTOP 674-27-05)
(NASA-CP-10121; E-8069; NAS 1.55:10121) Avail: CASI HC A11/MF A03

The role of accurate thermophysical property data in the process design and modeling of solidification processes was the subject of a workshop held on 22-23 Oct. 1992 in Cleveland, Ohio. The workshop was divided into three sequential sessions dealing with (1) industrial needs and priorities for thermophysical data, (2) experimental capabilities for measuring the necessary data, and (3) theoretical capabilities for predicting the necessary data. In addition, a 2-hour panel discussion of the salient issues was featured as well as a 2-hour caucus that assessed priorities and identified action plans. For individual titles, see N94-25121 through N94-25135.

N94-25121*# United Technologies Research Center, East Hartford, CT.
THE IMPORTANCE OF PROPERTIES IN MODELING
A. F. Giamei *In* NASA. Lewis Research Center, Workshop on the Thermophysical Properties of Molten Materials Nov. 1993 p 15-29
(For primary document see N94-25120 06-26)
Avail: CASI HC A03/MF A03

Casting and welding of superalloys, stainless steel and titanium alloys are processes which can be improved through modeling of heat flow, fluid flow, residual stress development, and microstructural evolution. These simulations require inputs of thermophysical data, some of which involves the partially or totally liquid state. In particular, these processes involve melting, flow in the liquid, and solidification. Modeling of such processes can lead to an improved understanding of defects such as shrinkage, inclusions, cracks, incomplete filling (or penetration), macrosegregation, improper grain structure, and deviations from dimensional specifications. Effective modeling can shorten process development time and improve quality. An approach to these problems is to develop efficient models; validate through correlations with thermal, distortion, and microstructural data; run parametric studies; extract knowledge based rules; and apply to adaptive closed loop control systems. With the appropriate pre- and post-processing, such analyses can be made 'user friendly'. This would include graphical user interfaces as well as realistic images and color maps. In such form, these models can be used for sensitivity analyses, which are useful in defining appropriate sensors and in the development of control strategies. Such modeling can be done at several levels, e.g., the MARO level, modeling large scale phenomena such as heat and fluid flow or material deformation; the MICRO level, modeling the development of dendrites, grains or precipitates; or at the NANO level, modeling point defects, dislocations, stacking faults, etc. There are many computational issues associated with these simulations, e.g. computational efficiency and accuracy. In addition, there are many materials issues, not the least of which is the availability of accurate high temperature thermophysical data for complex alloys. This would include latent heat of fusion, temperature dependent heat capacity and thermal conductivity (for liquid and solid), viscosity, surface tension, thermal expansion, mechanical properties, etc. Preliminary data is frequently gathered from the literature; however, this is often not available for modern alloys. If additional data are required, measurements can be used; however, these are costly, time consuming and can be erroneous due to a lack of testing standards or impure materials. Microstructural predictors can be extracted from thermal information, e.g. cooling rate and thermal gradient; the prediction of microstructure is dependent on solidus and liquidus temperature, mushy zone permeability, the solidification curve, volume changes, phase transformations, alloying effects (such as surface tension or viscosity), mold/metal reactions, metal/environment reactions, etc. Defect maps may be needed to predict the onset of shrinkage, hot cracking or 'freckling'. Constants may be needed for stress relaxation, dendrite coarsening, vaporization, etc. Visualization was used as a tool to better comprehend complex data sets associated with the analysis of directional solidification (including crystal growth) and welding. Examples include not only isotherms, but also cooling rate, growth rate and thermal gradient. The latter two are not single valued scalars, but rather time and space dependent vector fields. Efficient models were developed for both casting and welding to predict heat flow and the relationship to dendrite and grain growth. These codes include many of the non-linear effects, e.g. radiation, which dominate these processes. The home-built FDM code(s) were designed to be useful not only to the scientist, but also to the process engineer. Special output can be requested to compare directly to experimental data. Visualization procedures were developed to visualize critical results, e.g. fusion zone width at the surface opposite that where the arc is applied ('penetration'). Both elaborate and simplified distortion analyses were carried out. It is clear that extensive mechanical property data are critical in order to accurately predict residual stress patterns. A scheme is currently being developed to integrate these modeling tools into a set of control algorithms; however, the success of this approach is critically dependent on the availability of accurate high temperature thermophysical data.
Author (revised)

N94-25122*# Auburn Univ., AL. Space Power Inst.
THERMOPHYSICAL PROPERTY SENSITIVITY EFFECTS IN STEEL SOLIDIFICATION
Tony Overfelt *In* NASA. Lewis Research Center, Workshop on the Thermophysical Properties of Molten Materials Nov. 1993 p 35-50
(For primary document see N94-25120 06-26)
Avail: CASI HC A03/MF A03

The simulation of advanced solidification processes via digital computer techniques has gained widespread acceptance during the last decade or so. Models today can predict transient temperature fields, fluid flow fields, important microstructural parameters, and potential defects in castings. However, the lack of accurate thermophysical property data on important industrial alloys threatens to limit the ability of manufacturers to fully capitalize on the technology's benefits. A study of the sensitivity of one such numerical model of a steel plate casting to imposed variations in the data utilized for the thermal conductivity, specific heat, density, and heat of fusion is described. The sensitivity of the data's variability is characterized by its effects on the net solidification time of various points along the centerline of the plate casting. Recommendations for property measurements are given and the implications of data uncertainty for modelers are discussed.
Author (revised)

N94-25123*# Purdue Univ., West Lafayette, IN. Center for Information and Numerical Data Analysis and Synthesis.
ESTABLISHMENT OF COMPUTERIZED NUMERICAL DATABASES ON THERMOPHYSICAL AND OTHER PROPERTIES OF MOLTEN AS WELL AS SOLID MATERIALS AND DATA EVALUATION AND VALIDATION FOR GENERATING RECOMMENDED RELIABLE REFERENCE DATA
c82
C. Y. Ho *In* NASA. Lewis Research Center, Workshop on the Thermophysical Properties of Molten Materials Nov. 1993 p 51-68
(For primary document see N94-25120 06-26)
Avail: CASI HC A03/MF A03

The Center for Information and Numerical Data Analysis and Synthesis, (CINDAS), measures and maintains databases on thermophysical, thermoradiative, mechanical, optical, electronic, ablation, and physical properties of materials. Emphasis is on aerospace structural materials especially composites and on infrared detector/sensor materials. Within CINDAS, the Department of Defense sponsors at Purdue several centers: the High Temperature Material Information Analysis Center (HTMIAC), the Ceramics Information Analysis Center (CIAC) and the Metals Information Analysis Center (MIAC). The responsibilities of CINDAS are extremely broad encompassing basic and applied research, measurement of the properties of thin wires and thin foils as well as bulk materials, acquisition and search of world-wide literature, critical evaluation of data, generation of estimated values to fill data voids, investigation of constitutive, structural, processing, environmental, and rapid heating and loading effects, and dissemination of data. Liquids, gases, molten materials and solids are all considered. The responsibility of maintaining widely used databases includes data evaluation, analysis, correlation, and synthesis. Material property data recorded on the literature are often conflicting, diverging, and subject to large uncertainties. It is admittedly difficult to accurately measure materials properties. Systematic and random errors both enter. Some errors result from lack of characterization of the material itself (impurity effects). In some cases assumed boundary conditions corresponding to a theoretical model are not obtained in the experiments. Stray heat flows and losses must be accounted for. Some experimental methods are inappropriate and in other cases appropriate methods are carried out with poor technique. Conflicts in data may be resolved by curve fitting of the data to theoretical or empirical models or correlation in terms of various affecting parameters. Reasons (e.g. phase transitions) must be found for unusual dependence or any anomaly. Such critical evaluation involves knowledge of theory, experience in measurement, familiarity with metallurgy (microstructural behavior) and not inconsiderable judgment. An examination of typical data compiled and analyzed by CINDAS shows that the thermal conductivity of a material reported in the literature may vary by a factor of two of more; the range of reported values increases as temperature increases reflecting the difficulty of high temperature measurements. Often only estimates of melt behavior are available, despite the importance of melt properties in modeling, welding, or other solidification processes. There may be only a few measurements available for properties such as kinematic viscosity, even for widely used materials such as stainless steel. In the face of such a paucity of existing data and in a national environment where too few new data are being generated it is nonetheless the responsibility of CINDAS to select and disseminate recommended values of a wide variety of thermophysical properties. Author

N94-25124*# National Inst. of Standards and Technology, Gaithersburg, MD.

DYNAMIC MEASUREMENTS OF THERMOPHYSICAL PROPERTIES OF METALS AND ALLOYS AT HIGH TEMPERATURES BY SUBSECOND PULSE HEATING TECHNIQUES

Ared Cezairliyan *In* NASA. Lewis Research Center, Workshop on the Thermophysical Properties of Molten Materials Nov. 1993 p 71-85
(For primary document see N94-25120 06-26)
Avail: CASI HC A03/MF A03

Rapid (subsecond) heating techniques developed at the National Institute of Standards and Technology for the measurements of selected thermophysical and related properties of metals and alloys at high temperatures (above 1000 C) are described. The techniques are based on rapid resistive self-heating of the specimen from room temperature to the desired high temperature in short times and measuring the relevant experimental quantities, such as electrical current through the specimen, voltage across the specimen, specimen temperature, length, etc., with appropriate time resolution. The first technique, referred to as the millisecond-resolution technique, is for measurements on solid metals and alloys in the temperature range 1000 C to the melting temperature of the specimen. It utilizes a heavy battery bank for the energy source, and the total heating time of the specimen is typically in the range of 100-1000 ms. Data are recorded digitally every 0.5 ms with a full-scale resolution of about one part in 8000. The properties that can be measured with this system are as follows: specific heat, enthalpy, thermal expansion, electrical resistivity, normal spectral emissivity, hemispherical total emissivity, temperature and energy of solid-solid phase transformations, and melting temperature (solidus). The second technique, referred to as the microsecond-resolution technique, is for measurements on liquid metals and alloys in the temperature range 1200 to 6000 C. It utilizes a capacitor bank for the energy source, and the total heating time of the specimen is typically in the range 50-500 micro-s. Data are recorded digitally every 0.5 micro-s with a full-scale resolution of about one part in 4000. The properties that can be measured with this system are: melting temperature (solidus and liquidus), heat of fusion, specific heat, enthalpy, and electrical resistivity. The third technique is for measurements of the surface tension of liquid metals and alloys at their melting temperature. It utilizes a modified millisecond-resolution heating system designed for use in a microgravity environment. Author (revised)

N94-25125*# Intersonics, Inc., Northbrook, IL.

CONTAINERLESS MEASUREMENTS ON LIQUIDS AT HIGH TEMPERATURES c25

Richard Weber *In* NASA. Lewis Research Center, Workshop on the Thermophysical Properties of Molten Materials Nov. 1993 p 87-98
(For primary document see N94-25120 06-26)
Avail: CASI HC A03/MF A03

The application of containerless techniques for measurements of the thermophysical properties of high temperature liquids is reviewed. Recent results obtained in the materials research laboratories at Intersonics are also presented. Work to measure high temperature liquid properties is motivated by both the need for reliable property data for modeling of industrial processes involving molten materials and generation of data form basic modeling of materials behavior. The motivation for this work and examples of variations in thermophysical property values from the literature are presented. The variations may be attributed to changes in the specimen properties caused by chemical changes in the specimen and/or to measurement errors. The two methods used to achieve containerless conditions were aeroacoustic levitation and electromagnetic levitation. Their qualities are presented. The accompanying slides show the layout of levitation equipment and present examples of levitated metallic and ceramic specimens. Containerless techniques provide a high degree of control over specimen chemistry, nucleation and allow precise control of liquid composition to be achieved. Effects of minor additions can thus be measured in a systematic way. Operation in reduced gravity enables enhanced control of liquid motion which can allow measurement of liquid transport properties. Examples of nucleation control, the thermodynamics of oxide contamination removal, and control of the chromium content of liquid aluminum oxide by high temperature containerless processes are presented. The feasibility of measuring temperature, emissivity, liquidus temperature, enthalpy, surface tension, density, viscosity, and thermal diffusivity are discussed in the final section of the paper. Author (revised)

N94-25126*# Intersonics, Inc., Northbrook, IL.

LIQUIDUS TEMPERATURE AND OPTICAL PROPERTIES MEASUREMENT BY CONTAINERLESS TECHNIQUES

Collin D. Anderson *In* NASA. Lewis Research Center, Workshop on the Thermophysical Properties of Molten Materials Nov. 1993 p 99-111
(For primary document see N94-25120 06-26)
Avail: CASI HC A03/MF A03

Reactive alloy liquidus temperatures measured by conventional, contained techniques are often in error due to reactions with containers and gaseous impurities. This paper describes a new liquidus temperature measurement technique that avoids these problems by employing containerless processing. This technique relies on precise and accurate noncontact temperature measurements (NCTM), which are made possible by spectral emissivity values. The spectral emissivities, epsilon(sub lambda), are measured along with the optical properties (real, n, and imaginary, k, components of the index of refraction) using polarimetric techniques on electromagnetically levitated specimens. Results from work done at Vanderbilt University and Intersonics on the Ti-Al system are presented to demonstrate the above techniques. Author (revised)

N94-25127*# Toronto Univ. (Ontario). Dept. of Metallurgy and Materials Science.

DETECTION OF VELOCITY IN HIGH TEMPERATURE LIQUID METALS

A. C. Mikrovas and S. A. Argyropoulos *In* NASA. Lewis Research Center, Workshop on the Thermophysical Properties of Molten Materials Nov. 1993 p 113-127 (For primary document see N94-25120 06-26)
Avail: CASI HC A03/MF A03

Various efforts have been made to measure velocity in liquid metals. All of these efforts, however, share the same inherent limitation, namely, not being operative at the high temperatures required by liquid metals and liquid slags in an industrial application. In this paper, the current methods used were reviewed, and a new technique was presented for the measurement of velocity in high temperature liquid metals. In using this technique there are two stages. Starting with the calibration stage and then moving to the actual measurement stage by making use of the data obtained from calibration stage. Calibration proceeds in the following manner. Metallic spheres moving with a specific velocity are immersed in liquid metal held under isothermal conditions and at specific temperature. Their melting times are determined very accurately with a novel technique. These measurements are repeated for different metal bath temperatures and for different velocities of metallic spheres. In this manner it is possible to calculate the correlation between velocity and melting times for each metal bath temperature. During the actual measurement stage, when the metal bath temperature is known and its velocity is unknown, the magnitude of the unknown liquid metal velocity can be derived as follows: metallic spheres are immersed into the moving liquid metal and their melting times are determined. Using the above mentioned correlations, it will be shown that the magnitude of the unknown velocity in liquid metal can be deduced. This new technique was applied to high temperature liquid aluminum and liquid steel and these results were presented. The potential applicability of this technique in other liquid metals and liquid slags will also be discussed. Author (revised)

N94-25128*# Purdue Univ., West Lafayette, IN.

AN OVERVIEW OF THE MEASUREMENTS OF THERMOPHYSICAL PROPERTIES AND SOME RESULTS ON MOLTEN SUPERALLOYS AND SEMICONDUCTORS

R. E. Taylor *In* NASA. Lewis Research Center, Workshop on the Thermophysical Properties of Molten Materials Nov. 1993 p 129-141 (For primary document see N94-25120 06-26)
Avail: CASI HC A03/MF A03

This presentation consists of two parts: comments on the results of measurements on thermophysical properties based on the paper, 'Things Mother Never Taught Me (About Thermophysical Properties of Solids)' and results of thermophysical property measurements on selected solid and molten semiconductors and a proprietary superalloy. The first part may be considered as a tutorial for those involved in using or procuring thermophysical property data. The second part is presented as illustrations of what has been accomplished on molten materials at the Thermophysical Properties Research Laboratory (TPRL). The materials include Ge, PbTe, PbSnTe, HgCdTe and a superalloy. Derived from text

---

N94-25129*# Intersonics, Inc., Northbrook, IL.

OPTICAL PROPERTIES AND EMISSIVITIES OF LIQUID METALS AND ALLOYS

Shankar Krishnan and Paul C. Nordine *In* NASA. Lewis Research Center, Workshop on the Thermophysical Properties of Molten Materials Nov. 1993 p 143-160 (For primary document see N94-25120 06-26)
Avail: CASI HC A03/MF A03

This paper presents the results from our on-going program to investigate the optical properties of liquid metals and alloys at elevated temperatures. Ellipsometric and polarimetric techniques have been used to investigate the optical properties of materials in the 1000 - 3000 K temperature range and in the 0.3 - 0.1 mu m wavelength range. The ellipsometric and polarimetric techniques are described and the characteristics of the instruments are presented. The measurements are conducted by reflecting a polarized laser beam from an electromagnetically levitated liquid metal or alloy specimen. A Rotating Analyzer Ellipsometer (RAE) or a four-detector Division-of-Amplitude Photopolarimeter (DOAP) is used to determine the polarimetric properties of the light reflected at an angle of incidence of approximately 68 deg. Optical properties of the specimen which are calculated from these measurements include the index of refraction, extinction coefficient, normal spectral emissivity, and spectral hemispherical emissivity. These properties have been determined at various wavelengths and temperatures for liquid Ag, Al, Au, Cu, Nb, Ni, Pd, Pt, Si, Ti, Ti-Al alloys, U, and Zr. We also describe new experiments using pulsed-dye laser spectroscopic ellipsometry for studies of the wavelength dependence of the emissivities and optical properties of materials at high temperature. Preliminary results are given for liquid Al. The application of four-detector polarimetry for rapid determination of surface emissivity and true temperature is also described. Characteristics of these devices are presented. An example of the accuracy of this instrument in measurements of the melting point of zirconium is illustrated. Author

---

N94-25130*# Ohio State Univ., Columbus. Dept. of Physics.

THERMOPHYSICAL PROPERTIES OF SIMPLE LIQUID METALS: A BRIEF REVIEW OF THEORY

David Stroud *In* NASA. Lewis Research Center, Workshop on the Thermophysical Properties of Molten Materials Nov. 1993 p 163-176 (For primary document see N94-25120 06-26)
Avail: CASI HC A03/MF A03

In this paper, we review the current theory of the thermophysical properties of simple liquid metals. The emphasis is on thermodynamic properties, but we also briefly discuss the nonequilibrium properties of liquid metals. We begin by defining a 'simple liquid metal' as one in which the valence electrons interact only weakly with the ionic cores, so that the interaction can be treated by perturbation theory. We then write down the equilibrium Hamiltonian of a liquid metal as a sum of five terms: the bare ion-ion interaction, the electron-electron interaction, the bare electron-ion interaction, and the kinetic energies of electrons and ions. Since the electron-ion interaction can be treated by perturbation, the electronic part contributes in two ways to the Helmholtz free energy: it gives a density-dependent term which is independent of the arrangement of ions, and it acts to screen the ion-ion interaction, giving rise to effective ion-ion pair potentials which are density-dependent, in general. After sketching the form of a typical pair potential, we briefly enumerate some methods for calculating the ionic distribution function and hence the Helmholtz free energy of the liquid: monte Carlo simulations, molecular dynamics simulations, and thermodynamic perturbation theory. The final result is a general expression for the Helmholtz free energy of the liquid metal. It can be used to calculate a wide range of thermodynamic properties of simple metal liquids, which we enumerate. They include not only a range of thermodynamic coefficients of both metals and alloys, but also many aspects of the phase diagram, including freezing curves of pure elements and phase diagrams of liquid alloys (including liquidus and solidus curves). We briefly mention some key discoveries resulting from previous applications of this method, and point out that the same methods work for other materials not normally considered to be liquid metals (such as colloidal suspensions, in which the suspended microspheres behave like ions screened by the salt solution in which they are suspended). We conclude with a brief discussion of some non-equilibrium (i.e., transport) properties which can be treated by an extension of these methods. These include electrical resistivity, thermal conductivity, viscosity, atomic self-diffusion coefficients, concentration diffusion coefficients in alloys, surface tension and thermal emissivity. Finally, we briefly mention two methods by which the theory might be extended to non-simple liquid metals: these are empirical techniques (i.e., empirical two- and three-body potentials), and numerical many-body approaches. Both may be potentially applicable to extremely complex systems, such as nonstoichiometric liquid semiconductor alloys. Author

---

N94-25131*# Wisconsin Univ., Madison. Dept. of Materials Science and Engineering.

A THERMODYNAMIC APPROACH TO OBTAIN MATERIALS PROPERTIES FOR ENGINEERING APPLICATIONS

Y. Austin Chang *In* NASA. Lewis Research Center, Workshop on the Thermophysical Properties of Molten Materials Nov. 1993 p 177-201 (For primary document see N94-25120 06-26)
Avail: CASI HC A03/MF A03

With the ever increases in the capabilities of computers for numerical computations, we are on the verge of using these tools to model manufacturing processes for improving the efficiency of these processes as well as the quality of the products. One such process is casting for the production of metals. However, in order to model metal casting processes in a meaningful way it is essential to have the basic properties of these materials in their molten state, solid state as well as in the mixed state of solid and liquid. Some of the properties needed may be considered as intrinsic such as the density, heat capacity or enthalpy of freezing of a pure metal, while others are not. For instance, the enthalpy of solidification of an alloy is not a defined thermodynamic quantity. Its value depends on the micro-segregation of the phases during the course of solidification.

The objective of the present study is to present a thermodynamic approach to obtain some of the intrinsic properties and combining thermodynamics with kinetic models to estimate such quantities as the enthalpy of solidification of an alloy. Derived from text

N94-25132*# Auburn Univ., AL. Dept. of Mechanical Engineering.
AN EXTENDED LASER FLASH TECHNIQUE FOR THERMAL DIFFUSIVITY MEASUREMENT OF HIGH-TEMPERATURE MATERIALS c25
F. Shen and J. M. Khodadadi *In* NASA. Lewis Research Center, Workshop on the Thermophysical Properties of Molten Materials Nov. 1993 p 203-218 (For primary document see N94-25120 06-26)
(Grant NAGw-1192)
Avail: CASI HC A03/MF A03

Knowledge of thermal diffusivity data for high-temperature materials (solids and liquids) is very important in analyzing a number of processes, among them solidification, crystal growth, and welding. However, reliable thermal diffusivity versus temperature data, particularly those for high-temperature liquids, are still far from complete. The main measurement difficulties are due to the presence of convection and the requirement for a container. Fortunately, the availability of levitation techniques has made it possible to solve the containment problem. Based on the feasibility of the levitation technology, a new laser flash technique which is applicable to both levitated liquid and solid samples is being developed. At this point, the analysis for solid samples is near completion and highlights of the technique are presented here. The levitated solid sample which is assumed to be a sphere is subjected to a very short burst of high power radiant energy. The temperature of the irradiated surface area is elevated and a transient heat transfer process takes place within the sample. This containerless process is a two-dimensional unsteady heat conduction problem. Due to the nonlinearity of the radiative plus convective boundary condition, an analytic solution cannot be obtained. Two options are available at this point. Firstly, the radiation boundary condition can be linearized, which then accommodates a closed-form analytic solution. Comparison of the analytic curves for the temperature rise at different points to the experimentally-measured values will then provide the thermal diffusivity values. Secondly, one may set up an inverse conduction problem whereby experimentally obtained surface temperature history is used as the boundary conditions. The thermal diffusivity can then be elevated by minimizing the difference between the real heat flux boundary condition (radiation plus convection) and the measurements. Status of an experimental study directed at measuring the thermal diffusivity of high-temperature solid samples of pure Nickel and Inconel 718 superalloys are presented. Preliminary measurements showing surface temperature histories are discussed. Author

N94-25133*# Case Western Reserve Univ., Cleveland, OH. Dept. of Chemical Engineering.
SURFACE CHEMISTRY OF LIQUID METALS
J. Adin Mann, Jr., Henry Peebles (Sandia National Labs., Albuquerque, NM.), Diamond Peebles (Sandia National Labs., Albuquerque, NM.), Robert Rye (Sandia National Labs., Albuquerque, NM.), and Fred Yost (Sandia National Labs., Albuquerque, NM.) *In* NASA. Lewis Research Center, Workshop on the Thermophysical Properties of Molten Materials Nov. 1993 p 221-229 (For primary document see N94-25120 06-26)
Avail: CASI HC A02/MF A03

The fundamental surface chemistry of the behavior of liquid metals spreading on a solid substrate is not at all well understood. Each of these questions involves knowing the details of the structure of interfaces and their dynamics. For example the structure of a monolayer of tin oxide on pure liquid tin is unknown. This is in contrast to the relatively large amount of data available on the structure of copper oxide monolayers on solid, pure copper. However, since liquid tin has a vapor pressure below 10(exp -10)torr for a reasonable temperature range above its melting point, it is possible to use the techniques of surface science to study the geometric, electronic and vibrational structures of these monolayers. In addition, certain techniques developed by surface chemists for the study of liquid systems can be applied to the ultra-high vacuum environment. In particular we have shown that light scattering spectroscopy can be used to study the surface tension tensor of these interfaces. The tin oxide layer in particular is very interesting in that the monolayer is rigid but admits of bending. Ellipsometric microscopy allows the visualization of monolayer thick films and show whether island formation occurs at various levels of dosing. Author

N94-25134*# Jet Propulsion Lab., California Inst. of Tech., Pasadena.
MICROWAVE TECHNIQUES FOR PHYSICAL PROPERTY MEASUREMENTS c25
M. Barmatz *In* NASA. Lewis Research Center, Workshop on the Thermophysical Properties of Molten Materials Nov. 1993 p 231-234 (For primary document see N94-25120 06-26)
Avail: CASI HC A01/MF A03

Industrial processing of metals and ceramics is now being streamlined by the development of theoretical models. High temperature thermophysical properties of these materials are required to successfully apply these theories. Unfortunately, there is insufficient experimental data available for many of these properties, particularly in the molten state. Microwave fields can be used to measure specific heat, thermal diffusivity, thermal conductivity and dielectric constants at high temperatures. We propose to (1) develop a microwave flash method (analogous to the laser flash technique) that can simultaneously measure the thermal diffusivity and specific heat of insulators and semiconductors at high temperatures, (2) an appropriate theory and experimental apparatus to demonstrate the measurement of the specific heat of a metal using a new microwave ac specific heat technique, and (3) experimental methods for noncontact measurement of the real and imaginary dielectric constants. Author

N94-25135*# Jet Propulsion Lab., California Inst. of Tech., Pasadena.
ELECTROSTATIC LEVITATION TECHNOLOGY FOR THERMOPHYSICAL PROPERTIES OF MOLTEN MATERIALS c25
Won-Kyu Rhim *In* NASA. Lewis Research Center, Workshop on the Thermophysical Properties of Molten Materials Nov. 1993 p 235-245 (For primary document see N94-25120 06-26)
Avail: CASI HC A03/MF A03

Measurements of thermophysical properties of undercooled liquids often require some kind of levitator which isolates samples from container walls. We introduce in this presentation a high temperature/high vacuum electrostatic levitator (HTHVESL) which promises some unique capabilities for the studies of thermophysical properties of molten materials. Although substantial progress has been made in the past several months, this technology is still in the development stage, therefore, in this presentation we only focus on the present state of the HTHVESL(1) and point out other capabilities which might be realized in the near future. Author

N94-25142# Army Armament Research, Development and Engineering Center, Watervliet, NY. Benet Lab.
X RAY DIFFRACTION ANALYSIS OF ELECTRODEPOSITED BETA-TANTALUM Final Report
John F. Thompson and Mark D. Miller Sep. 1993 21 p
(AD-A273254; ARCCB-TR-93031) Avail: CASI HC A03/MF A01

An adherent coating of beta-tantalum has been electrodeposited on copper from a FLINAK molten salt electrolyte. Electrolyte temperatures ranged from 700 to 800 C using pulse current electrolysis at current densities higher than 100 mA/sq cm. The beta-tantalum was deposited to a thickness of over 3 mils. The x ray diffraction pattern of the electrodeposited beta-tantalum was indexed using a Hull-Davey chart. The coatings were found to have a highly preferred orientation, and the tetragonal structure was found to have the lattice parameters of a = 6.419 A and c = 3.051 A. DTIC

N94-25171*# National Aeronautics and Space Administration. Lewis Research Center, Cleveland, OH.
STRUCTURE AND ENERGETICS OF HIGH INDEX Fe, Al, Cu AND Ni SURFACES USING EQUIVALENT CRYSTAL THEORY
Agustin M. Rodriguez (La Plata Univ., Argentina.), Guillermo Bozzolo (Analex Corp., Brook Park, OH.), and John Ferrante Dec. 1993 24 p
(RTOP 505-90-53)
(NASA-TM-106408; E-8245; NAS 1.15:106408) Avail: CASI HC A03/MF A01

Equivalent crystal theory (ECT) is applied to the study of multilayer relaxations and surface energies of high-index faces of Fe, Al, Ni, and Cu. Changes in interplanar spacing as well as registry of planes close to the surface and the ensuing surface energies changes are discussed in reference to available experimental data and other theoretical calculations. Since ECT is a semiempirical method, the dependence of the results on the variation of the input used was investigated. Author (revised)

N94-25242# Technische Univ., Eindhoven (Netherlands). Solid State Div.

METALLIC MULTILAYERS: EXPERIMENTAL INVESTIGATION OF MAGNETIC ANISOTROPY AND MAGNETIC INTERLAYER COUPLING
Ph.D. Thesis
Pascal Jean Henri Bloemen 1993 196 p Prepared in cooperation with Philips Gloeilampenfabrieken N.V., Eindhoven, Netherlands
(ETN-94-95364) Avail: CASI HC A09/MF A03

The preparation of multilayer samples (by sputtering and molecular beam epitaxy) and characterization (by X-ray diffraction, vibrating sample magnetometry, magnetooptical Kerr effect magnetometry, and ferromagnetic resonance) are discussed. The contributions to magnetic anisotropy important for thin films are discussed and studies on Co/Ni and Co/Ni/Co/Pt multilayers are reported. The physical mechanisms underlying magnetic interlayer coupling are considered together with recent developments in this field. ESA

N94-25316# Technical Research Centre of Finland, Espoo. Metals Lab.

SOLID STATE SYNTHESIS OF Fe-B-SI ALLOYS
Pekka Ruuskanen and Oleg Heczko Oct. 1992 34 p Sponsored by Technical Research Centre of Finland, Espoo; Stroemberg Industry/Automation, Vaasa, Finland; Rauma Oy High Speed Technology, Finland; and Trafotek Oy, Finland
(VTT-PUBS-118; ISBN-9-51-384236-5; ETN-94-95234) Copyright Avail: CASI HC A03/MF A01

Fe-B and Fe-B-Si elemental and intermetallic powders were synthesized by the mechanical alloying method. Vibratory and planetary type of ball mills were used. The alloying time and the alloying type in the results were investigated. The microstructure and the thermodymaic properties of the mechanically alloyed powders were characterized. X-ray diffractometry differential scanning calorimetry and a scanning electron microscopy were applied. The results show that it is possible to synthesize nanocrystalline and amorphous alloys from elemental and intermetallic Fe, B, and Si powders with the iron content of 80 percent. The crystallization temperature of the amorphous structure is 465 C. The measured magnetic properties suggest that in this way it is possible to produce new kinds of soft magnetic materials. The magnetic hysteresis properties of the compacted rings made from the mechanically alloyed Fe-B and Fe-B-Si powders were measured. ESA

N94-25346# Technical Research Centre of Finland, Espoo. Metallurgy Lab.

USE OF SCANNING TUNNELING MICROSCOPE IN CORROSION STUDIES [TUNNELOINTIMIKROSKOOPIN KAEYTTOE KORROOSIOTUTKIMUKSESSA]
Leena Carpen Nov. 1992 28 p In FINNISH
(VTT-TIED-1416; ISBN-9-51-384310-6; ETN-94-95255) Copyright Avail: CASI HC A03/MF A01

A study on the use of the Scanning Tunneling Microscope (STM) in corrosion research is reported. Using an STM it is possible to study the surfaces of metals in the circumstances where they are used. The measurements can be made in vacuum, gases--including air, and in liquids. When considering the simultaneous use of electrochemical measurements and STM, some development of designs and methods is still needed so that the tunneling current would not disturb the electrochemical current and vice versa. Some interesting issues to study with STM could be the dissolving of a metal on an atomistic scale, the location of anode areas during corrosion, and the time constants associated with them. Other practicable areas of applications in the field of corrosion could, among others, be the study of initiation and growth of pitting and the adsorption of aggressive anions and/or inhibitors on the metal surfaces. ESA

N94-25405# National Association of Corrosion Engineers, Houston, TX.

PROCEEDINGS OF THE 12TH INTERNATIONAL CONGRESS: CORROSION CONTROL FOR LOW-COST RELIABILITY. VOLUME 4: OIL/GAS PIPELINE
24 Sep. 1993 754 p Congress held in Houston, TX, 19-24 Sep. 1993
(AD-A273665; ISBN-1-877914-65-7) Avail: CASI HC A99/MF A06; NACE International, PO Box 218340, Houston, TX 77218-8340 HC

Proceedings from the 12th International Corrosion Congress, Volume 4 Oil/Gas/Pipeline are included. Topics covered in this volume include: Cathodic protection; Hydrogen effects; and Oil and gas production and refining workshop. DTIC

N94-25406# National Association of Corrosion Engineers, Houston, TX.

PROCEEDINGS OF THE 12TH INTERNATIONAL CONGRESS: CORROSION CONTROL FOR LOW-COST RELIABILITY. VOLUME 5A: CORROSION: GENERAL ISSUES
24 Sep. 1993 493 p Congress held in Houston, TX, 19-24 Sep. 1993
(AD-A273666; ISBN-1-877914-65-7) Avail: CASI HC A21/MF A04; NACE International, PO Box 218340, Houston, TX 77218-8340 HC

Proceedings from the 12th International corrosion Congress, Volume 5A Corrosion: General Issues are included. Topics covered include: (1) The role of corrosion in aging aircraft; (2) Hidden corrosion - needs and requirements; (3) Corrosion control as a necessary treatment; (4) Computer assisted aircraft paint stripping technology; (5) Reducing aircraft corrosion with desiccant dehumidifiers; (6) Corrosion contribution to environmental cracking failures of critical aircraft parts; (7) Designing metallic surface coatings for improved corrosion resistance; (8) Development of chromium based composite coatings; (9) In-situ analysis of corrosion in the crevice of automotive body by A.C. impedance measurement; (10) Designing a reinforced concrete against corrosion in chloride containing environments; (11) Carbonation of flyash-containing concrete electrochemical studies; (12) Evaluation of concrete corrosion inhibitors; (13) Cathodic protection of new steel reinforced concrete structure; (14) Reliability and corrosion testing of electronic components and assemblies; (15) Corrosion study of polymer-on-metal systems modified by processing conditions; (16) How to formulate corrosion knowledge for expert systems; and (17) Corrosion prediction from laboratory tests using artificial neural networks. DTIC

N94-25407# National Association of Corrosion Engineers, Houston, TX.

PROCEEDINGS OF THE 12TH INTERNATIONAL CONGRESS: CORROSION CONTROL FOR LOW-COST RELIABILITY. VOLUME 5B: CORROSION: GENERAL ISSUES
24 Sep. 1993 564 p Congress held in Houston, TX, 19-24 Sep. 1993
(AD-A273667; ISBN-1-877914-65-7) Avail: CASI HC A24/MF A04; NACE International, PO Box 218340, Houston, TX 77218-8340 HC

Proceedings of the 12th International Corrosion Congress, Volume 5B Corrosion: General Issues are included. Topics covered include: (1) Degradation by ripple-load effect - impact on life prediction; (2) Management of corrosion in the power industry; (3) Prediction of corrosion rate and probability on underground pipes; (4) The effects of complexing agents on the corrosion of copper/nickel alloys in sulfide polluted seawater under impingement attack; (5) Factors contributing to ennoblement of passive metals due to biofilms in seawater; (6) Microfouling induced corrosion of alloys; (7) Anaerobic corrosion of steel by phototrophic sulfur bacteria; (8) Effect of biofilms on crevice corrosion of stainless alloys in coastal seawater; (9) Electrochemical noise analysis as an indicator of microbiologically induced corrosion; (10) Results of electrochemical monitoring of microbiological activity; (11) SNMS studies on the oxidation behavior of titanium aluminides; (12) Passive film studies using neutron reflectivity; (13) XPS and electrochemical studies of the dissolution and passivation of molybdenum-implanted austenitic stainless steels; (14) Nuclear energy and waste storage; and (15) The impact of environmental consideration on corrosion control economics and technology. DTIC

N94-25408# National Association of Corrosion Engineers, Houston, TX.

PROCEEDINGS OF THE 12TH INTERNATIONAL CONGRESS: CORROSION CONTROL FOR LOW-COST RELIABILITY. VOLUME 6: ELECTRIC POWER INDUSTRY
24 Sep. 1993 259 p Congress held in Houston, TX, 19-24 Sep. 1993
(AD-A273668; ISBN-1-877914-65-7) Avail: CASI HC A12/MF A03; NACE International, PO Box 218340, Houston, TX 77218-8340 HC

Proceedings of the 12th International Corrosion Congress Volume 6 Electric Power Industry are included. Topics covered include: (1) Cutting the cost of corrosion and fouling by real-time performance monitoring; (2) Service water electrochemical monitoring development at Ontario hydro; (3) On line monitoring of fireside corrosion on power plants; (4) Experience with neutron activation for a real-time corrosion monitoring in a urea plant;

(5) Monitoring of microbiological activity in power plants; (6) Electrochemical monitoring of erosion-corrosion in multiphase flows; (7) Monitoring and prediction of environmentally assisted crack growth in stainless steel piping; (8) Corrosion monitoring using harmonic impedance spectroscopy; (9) An electrochemical sensor for oxygen and pH in Aqueous systems; (10) On line particulate iron and sulfur X-ray monitor; (11) On-line dissolution and analysis of corrosion products; (12) Remote monitoring of corrosion chemicals via fiber optic Raman spectroscopy; and (13) Surface enhanced Raman scattering as an in-reactor monitor of phenomena of interest to the nuclear power industry. DTIC

N94-25419# Technical Research Centre of Finland, Espoo. Production Engineering Lab.
WELDABILITY OF ACCELERATED-COOLED (AcC) HIGH STRENGTH TMCP STEEL X80
Pekka Nevasmaa, Mark Cederberg, and Martti Vilpas Oct. 1992 41 p
Sponsored by Nordic Industrial Fund; Technology Development Center, Finland; and Technical Research Centre of Finland, Espoo
(VTT-TIED-1413; ISBN-951-38-4307-6; ETN-94-95254) Copyright Avail: CASI HC A03/MF A01

The test results obtained in welding and weldability tests of an Accelerated Cooled (AcC) Thermochemically Processed (TMCP) X80 pipeline steel are discussed. The tests comprised mechanical testing of joints welded with arc energies ranging from 15 to 50 kJ/cm using Submerged Arc Welding (SAW) and Flux Cored Arc Welding (FCAW) processes. The results of weld thermal simulation and implant weldability tests for the steel are reported and discussed. The results demonstrate the improved weldability of the AcC X80 steel, as compared to normalized or quenched and tempered steels of a similar strength level. Welding without preheat was possible up to 15 to 25 mm plate thickness using arc energies of 10 and 22 kJ/cm, respectively. No weld metal cracking was observed in the heat input range studied in this X80 class, although welding was performed without preheat. The welded joints failed to meet the toughness requirements all through the arc energy range from 15 to 50 kJ/cm. Adequate hardness measurement of impact toughness was obtained only in one of the joints welded with a low arc energy of 15 kJ/cm. The Charpy 5 tests of simulated hardness measurements confirmed a deterioration in toughness at -40 C through the whole cooling time range t(sub 8/5) of 12 to 52 sec. Charpy 5 test data from real hardness measurements suggested that some improvement could be expected at temperatures of -20 C, when limiting the maximum allowable heat input below 15 kJ/cm. ESA

N94-25448# National Association of Corrosion Engineers, Houston, TX.
PROCEEDINGS OF THE 12TH INTERNATIONAL CONGRESS: CORROSION CONTROL FOR LOW-COST RELIABILITY. VOLUME 1: COATINGS
24 Sep. 1993 549 p Congress held in Houston, TX, 19-24 Sep. 1993
(AD-A273661; ISBN-1-877914-65-7) Avail: CASI HC A23/MF A04; NACE International, PO Box 218340, Houston, TX 77218-8340 HC

Topics presented include the following: (1) Coatings on steel; (2) Coatings; (3) Metallic coating and surface treatments; (4) and Non-metallic coatings on steel substrates. DTIC

N94-25449# National Association of Corrosion Engineers, Houston, TX.
PRECEEDINGS OF THE 12TH INTERNATIONAL CONGRESS: CORROSION CONTROL FOR LOW-COST RELIABILITY. VOLUME 2: PROCESS INDUSTRIES PLANT OPERATIONS
24 Sep. 1993 623 p Congress held in Houston, TX, 19-24 Sep. 1993
(AD-A273662; ISBN-1-877914-65-7) Avail: CASI HC A99/MF A06; NACE International, PO Box 218340, Houston, TX 77218-8340 HC

The principal topics covered include: (1) Atmospheric corrosion; (2) Chemical process industry workshop; and (3) High temperature corrosion. DTIC

N94-25450# National Association of Corrosion Engineers, Houston, TX.
PRECEEDINGS OF THE 12TH INTERNATIONAL CONGRESS: CORROSION CONTROL FOR LOW-COST RELIABILITY. VOLUME 3A: CORROSION: SPECIFIC ISSUES
24 Sep. 1993 648 p Congress held in Houston, TX, 19-24 Sep. 1993
(AD-A273663; ISBN-1-877914-65-7) Avail: CASI HC A99/MF A06; NACE International, PO Box 218340, Houston, TX 77218-8340 HC

This volume presents the following topics:, (1) Corrosion: materials performance; (2) Corrosion: modes and behavior; (3) Electrochemical techniques; and (4) Environmental cracking. DTIC

N94-25451# National Association of Corrosion Engineers, Houston, TX.
PROCEEDINGS OF THE 12TH INTERNATIONAL CONGRESS: CORROSION CONTROL FOR LOW-COST RELIABILITY. VOLUME 3B: CORROSION: SPECIFIC ISSUES
24 Sep. 1993 534 p Congress held in Houston, TX, 19-24 Sep. 1993
(AD-A273664; ISBN-1-877914-65-7) Avail: CASI HC A23/MF A04; NACE International, PO Box 218340, Houston, TX 77218-8340 HC

This volume presents the following principal topics: (1) Inhibitors; (2) Localized corrosion/crevices; (3) Localized corrosion/pitting; and (4) Passivity and breakdown. DTIC

N94-25531# Wright Lab., Wright-Patterson AFB, OH.
THE MECHANICAL PROPERTY DATA BASE FROM AN AIR FORCE/INDUSTRY COOPERATIVE TEST PROGRAM ON ADVANCED ALUMINUM ALLOYS (7064 AND CW67) Interim Report, 1 Dec. 1986 - 1 May 1990
Mary A. Phillips and Steven R. Thompson Aug. 1993 127 p
(AD-A273741; WL-TR-93-4090) Avail: CASI HC A07/MF A02

A mechanical property data base on Kaiser produced second generation P/M alloys 7064 forging and extrusion and Alcoa produced P/M alloys CW67 sheet, plate, forging, and extrusion was generated. Mechanical property data consisted of tension, compression, shear, bearing, and fracture toughness values. Fatigue, fatigue crack growth, and spectrum fatigue crack growth data were generated. DTIC

N94-23244*# Puerto Rico Univ., Mayaguez. Dept. of Mechanical Engineering.
STRESS CORROSION CRACKING PROPERTIES OF 15-5PH STEEL
Ferdinand Rosa *In* NASA. Kennedy Space Center, NASA/ASEE Summer Faculty Fellowship Program Oct. 1993 p 375-402 (For primary document see N94-23230 06-80)
Avail: CASI HC A03/MF A04

N94-24425*# Auburn Univ., AL. Materials Engineering.
WELD FRACTURE CRITERIA FOR COMPUTER SIMULATION
Wartan A. Jemian *In* Alabama Univ., The 1993 NASA/ASEE Summer Faculty Fellowship Program Nov. 1993 5 p (For primary document see N94-24405 06-80)
Avail: CASI HC A01/MF A03

N94-24428*# Indiana Univ. of Pennsylvania, Indiana, PA. Physics Dept.
DIFFUSION ON Cu SURFACES
Majid Karimi *In* Alabama Univ., The 1993 NASA/ASEE Summer Faculty Fellowship Program Nov. 1993 5 p (For primary document see N94-24405 06-80)
Avail: CASI HC A01/MF A03

N94-24448*# Wichita State Univ., KS. Dept. of Mechanical Engineering.
MICROSTRUCTURAL ANALYSIS OF THE 2195 ALUMINUM-LITHIUM ALLOY WELDS
George E. Talia *In* Alabama Univ., The 1993 NASA/ASEE Summer Faculty Fellowship Program Nov. 1993 5 p (For primary document see N94-24405 06-80)
Avail: CASI HC A01/MF A03

27 NONMETALLIC MATERIALS

Includes physical, chemical, and mechanical properties of plastics, elastomers, lubricants, polymers, textiles, adhesives, and ceramic materials.

For composite materials see *24 Composite Materials.*

N94-22910# Laboratoire d'Automatique et d'Analyse des Systemes, Toulouse (France). Groupe Microstructure Silicium et Microsystemes Integres.

DISILANE LPCVD DEPOSITED SILICON FILMS: DEPOSITION MECHANISMS, PROPERTIES AND CAPABILITY OF MAKING TRANSISTORS ON THIN FILMS Ph.D. Thesis - Inst. National des Sciences Appliquees de Lyon [FILMS DE SILICIUM DEPOSES PAR LPCVD A PARTIR DE DISILANE: MECANISMES DE DEPOT, PROPRIETES ET APTITUDE A LA REALISATION DE TRANSISTORS SUR FILMS MINCES]

Juan Jose PedroviejoPoyatos 1993 114 p In FRENCH
(LAAS-93156; ETN-94-95192) Avail: CASI HC A06/MF A02

The potentialities of Disilane in the production of Low Pressure Chemical Vapor Deposition (LPCVD) of polysilicon films are investigated. The purpose is to characterize the effects of deposition parameters on the film kinetics, homogeneity, crystallization, and oxidation at 600 C. The physicochemical phenomena occurring during deposition steps, which justify the homogeneity as well as the kinetic characteristics of the films obtained, are investigated. The 600 C neutral atmosphere annealing results show that Disilane allows the obtention of optimal crystallization and maximal oxidation films. The electric properties of thin film transistors are characterized. ESA

N94-22930# Lawrence Livermore National Lab., CA.

GAS-PRESSURE FORMING OF SUPERPLASTIC CERAMIC SHEET

T. G. Nieh and J. Wadsworth 24 Jun. 1993 4 p
(Contract W-7405-eng-48)
(DE94-001520; UCRL-CR-114189) Avail: CASI HC A01/MF A01

Superplasticity in ceramics has now advanced to the stage that technologically viable superplastic deformation processing can be performed. In this paper, examples of biaxial gas-pressure forming of several ceramics are given. These include yttria stabilized, tetragonal zirconia (YTZP), a 20% alumina/YTZP composite, and silicon. In addition, the concurrent superplastic forming and diffusion bonding of a hybrid YTZP/C103 (ceramic-metal) structure are presented. These forming processes offer technological advantages of greater dimensional control and increased variety and complexity of shapes than is possible with conventional ceramic shaping technology. DOE

N94-22931# Lawrence Livermore National Lab., CA.

CARBON AEROGELS: AN UPDATE ON STRUCTURE, PROPERTIES, AND APPLICATIONS

R. W. Pekala, S. T. Mayer, J. L. Kaschmitter, and F. M. Kong Jul. 1993 18 p Presented at the International Symposium on Advances in Sol-Gel Processing and Applications, Chicago, IL, 27-28 Aug. 1993
(Contract W-7405-eng-48)
(DE94-001528; UCRL-JC-114192; CONF-9308158-3) Avail: CASI HC A03/MF A01

Aerogels are unique porous materials whose composition, structure, and properties can be controlled at the nanometer scale. This paper examines the synthesis of organic aerogels and their carbonized derivatives. Carbon aerogels have low electrical resistivity, high surface area, and a tunable pore size. These materials are finding applications as electrodes in double layer capacitors. DOE

N94-22992 Argonne National Lab., IL.

THE STRUCTURE AND SPIN DYNAMICS OF LANTHANIDE-BEARING SILICATE GLASSES

A. J. G. Ellison, C. K. Loong, and J. Wagner 1993 13 p Presented at the 38th Annual Conference on Magnetism and Magnetic Materials, Minneapolis, MN, 15-18 Nov. 1993 Limited Reproducibility: More than 20% of this document may be affected by microfiche quality
(Contract W-31-109-eng-38)
(DE94-001320; ANL/IPNS/CP-79847; CONF-931133-4) Avail: CASI HC A03

Structures of 3Na2O(center dot)R2O3(center dot)6SiO2 (R = Nd, Yb and Lu) glasses were studied by time-of-flight neutron diffraction. Average Si-O and O-O nearest-neighbor coordination is found to be similar to SiO4 tetrahedral units in vitreous SiO2 and other silicate glasses. The RE ions coordinate with no more than 7 nearest-neighbor oxygen atoms. The dynamic and static response of these glasses and their isochemical crystalline analogs have been investigated by inelastic neutron scattering and magnetic susceptibility measurements. The magnetic excitation spectra were analyzed by a ligand-field model using a method of descending symmetry. Correlation between short-range atomic order in a network glass and magnetic interactions of the RE ions with the local environment is discussed. DOE

N94-23075* National Aeronautics and Space Administration. Langley Research Center, Hampton, VA.

DI(HYDROXYPHENYL)- 1,2,4-TRIAZOLE MONOMERS Patent

John W. Connell, inventor (to NASA), Paul M. Hergenrother, inventor (to NASA), and Peter Wolf, inventor (to NASA) 14 Sep. 1993 8 p Filed 29 Jun. 1992 Division of US-Patent-Appl-SN-650336, filed 24 Jan. 1991
(NASA-Case-LAR-14440-2; US-Patent-5,245,043;
US-Patent-Appl-SN-905708; US-Patent-Appl-SN-650336;
US-Patent-Class-548-269.4; US-Patent-Class-548-267.4;
US-Patent-Class-548-267.8; US-Patent-Class-548-268.6;
Int-Patent-Class-C07D-249/08) Avail: US Patent and Trademark Office

The di(hydroxyphenyl)- 1,2,4-triazole monomers were first synthesized by reacting bis (4-hydroxyphenyl) hydrazide with aniline hydrochloride at 250 C in the melt and also by reacting 1,3 or 1,4-bis- (4-hydroxyphenyl)-phenylene- dihydrazide with 2 moles of aniline hydrochloride in the melt. Purification of the di(hydroxyphenyl)- 1,2,4-triazole monomers was accomplished by recrystallization. Poly (1,2,4-triazoles) (PT) were prepared by the aromatic nucleophilic displacement reaction of di(hydroxyphenyl)-1,2,4-triazole monomers with activated aromatic dihalides or activated aromatic dinitro compounds. The reactions were carried out in polar aprotic solvents such as sulfolane or diphenylsulfone using alkali metal bases such as potassium carbonate at elevated temperatures under nitrogen. This synthetic route has provided high molecular weight PT of new chemical structure, is economically and synthetically more favorable than other routes, and allows for facile chemical structure variation due to the availability of a large variety of activated aromatic dihalides.

Official Gazette of the U.S. Patent and Trademark Office

N94-23076* National Aeronautics and Space Administration. Langley Research Center, Hampton, VA.

PREPARING POLYMERIC MATRIX COMPOSITES USING AN AQUEOUS SLURRY TECHNIQUE Patent

Norman J. Johnston, inventor (to NASA) and Timothy W. Towell, inventor (to NASA) 12 Oct. 1993 6 p Filed 6 Nov. 1991
(NASA-Case-LAR-14771-1; US-Patent-5,252,168;
US-Patent-Appl-SN-788403; US-Patent-Class-156-307.4;
US-Patent-Class-156-330.9; US-Patent-Class-428-367;
US-Patent-Class-428-408; US-Patent-Class-524-538;
US-Patent-Class-524-608; Int-Patent-Class-C09J-5/02) Avail: US Patent and Trademark Office

An aqueous process was developed to prepare a consolidated composite laminate from an aqueous slurry. An aqueous poly(amic acid) surfactant solution was prepared by dissolving a poly(amic acid) powder in an aqueous ammonia solution. A polymeric powder was added to this solution to form a slurry. The slurry was deposited on carbon fiber to form a prepreg which was dried and stacked to form a composite laminate. The composite laminate was consolidated using pressure and was heated to form the polymeric matrix. The resulting composite laminate exhibited high fracture toughness and excellent consolidation.

Official Gazette of the U.S. Patent and Trademark Office

N94-23079* National Aeronautics and Space Administration. Langley Research Center, Hampton, VA.

POLYIMIDE PROCESSING ADDITIVES Patent

J. Richard Pratt, inventor (to NASA), Terry L. St.Clair, inventor (to NASA), Diane M. Stoakley, inventor (to NASA), and Harold D. Burks, inventor (to NASA) 21 Dec. 1993 24 p Filed 22 May 1992 Continuation of US-Patent-Appl-SN-084064, filed 11 Aug. 1987
(NASA-Case-LAR-13669-2; US-Patent-5,272,248;
US-Patent-Appl-SN-892058; US-Patent-Appl-SN-084064;
US-Patent-Class-528-353; US-Patent-Class-528-170;

US-Patent-Class-528-171; US-Patent-Class-528-173;
US-Patent-Class-528-174; US-Patent-Class-528-176) Avail: US Patent and Trademark Office

A process for preparing polyimides having enhanced melt flow properties is described. The process consists of heating a mixture of a high molecular weight poly-(amic acid) or polyimide with a low molecular weight amic acid or imide additive in the range of 0.05 to 15 percent by weight of the additive. The polyimide powders so obtained show improved processability, as evidenced by lower melt viscosity by capillary rheometry. Likewise, films prepared from mixtures of polymers with additives show improved processability with earlier onset of stretching by TMA.

Official Gazette of the U.S. Patent and Trademark Office

N94-23183# Ames Lab., IA.

A NUMERICAL ANALYSIS OF CRACK PROPAGATION IN MICROCRACKING CERAMIC AND CERAMIC COMPOSITES

S. B. Biner 1993 24 p Presented at the 1st Meeting of the Pacific Rim Ceramic Societies, Honolulu, HI, 7-10 Nov. 1993
(Contract W-7405-eng-82)
(DE94-001192; IS-M-771; CONF-931142-1) Avail: CASI HC A03/MF A01

A set of numerical analyses of crack growth was performed to elucidate the mechanism of microcracking on the observed fracture behavior of ceramics and ceramic composites. The random nucleation, orientation and size effects of discrete microcracks and resulting interactions are fully accounted for in a hybrid finite element model. The results indicate that the energy expenditure due the microcrack nucleation seems not to contribute significantly to the resistance to crack growth. The main controlling parameter appears to be elastic interaction of the microcracks with the main crack in the absence of a reinforcing phase; therefore, the microcrack density plays an important role. In the case of the composites, the interaction of the main crack with the stress fields of the reinforcing phase, rather than interaction of microcracks, is the controlling parameter for the resistance to the crack growth even in the presence of a large population of microcracks. It will be also shown that the crack branching and crack kinking can readily develop as a result of microcracking. DOE

N94-23305* National Aeronautics and Space Administration. Langley Research Center, Hampton, VA.

DI(HYDROXYPHENYL)- BENZIMIDAZOLE MONOMERS Patent

John W. Connell, inventor (to NASA), Paul M. Hergenrother, inventor (to NASA), and Joseph G. Smith, inventor (to NASA) 14 Sep. 1993 10 p Filed 8 Sep. 1992 Division of US-Patent-Appl-SN-790730, filed 30 Oct. 1991
(NASA-Case-LAR-14643-2; US-Patent-5,245,044;
US-Patent-Appl-SN-941816; US-Patent-Appl-SN-790730;
US-Patent-Class-548-305.7; US-Patent-Class-548-305.4;
US-Patent-Class-548-145; Int-Patent-Class-C07D-235/18) Avail: US Patent and Trademark Office

Di(hydroxyphenyl)benzimidazole monomers were prepared from phenyl-hydroxybenzoate and aromatic bis(o-diamine)s. These monomers were used in the synthesis of soluble polybenzimidazoles. The reaction involved the aromatic nucleophilic displacement of various di(hydroxyphenyl)benzimidazole monomers with activated aromatic dihalides or activated aromatic dinitro compounds in the presence of an alkali metal base. These polymers exhibited lower glass transition temperatures, improved solubility, and better compression moldability over their commercial counterparts. Official Gazette of the U.S. Patent and Trademark Office

N94-23307* National Aeronautics and Space Administration. Langley Research Center, Hampton, VA.

PHENYLETHYNL-TERMINATED POLY(ARYLENE ETHERS) Patent

Brian J. Jensen, inventor (to NASA), Robert G. Bryant, inventor (to NASA), and Paul M. Hergenrother, inventor (to NASA) 7 Dec. 1993 9 p Filed 2 Apr. 1993
(NASA-Case-LAR-14797-1; US-Patent-5,268,444;
US-Patent-Appl-SN-045336; US-Patent-Class-528-125;
US-Patent-Class-528-126; US-Patent-Class-528-151;
US-Patent-Class-528-152; US-Patent-Class-528-153;
US-Patent-Class-528-155; US-Patent-Class-528-219) Avail: US Patent and Trademark Office

Phenylethynyl-terminated poly(arylene ethers) are prepared in a wide range of molecular weights by adjusting monomer ratio and adding an appropriate amount of 4-fluoro- 4'-phenylethynyl benzophenone during polymer synthesis. The resulting phenylethynyl-terminated poly(arylene ethers) react and crosslink upon curing for one hour at 350 C to provide materials with improved solvent resistance, higher modulus, and better high temperature properties than the linear, uncrosslinked polymers.

Official Gazette of the U.S. Patent and Trademark Office

N94-23311* National Aeronautics and Space Administration. Ames Research Center, Moffett Field, CA.

CERAMIC SILICON-BORON-CARBON FIBERS FROM ORGANIC SILICON-BORON-POLYMERS Patent

Salvatore R. Riccitiello, inventor (to NASA), Ming-Ta S. Hsu, inventor (to NASA), and Timothy S. Chen, inventor (to NASA) 29 Jun. 1993 12 p Filed 11 May 1992 Continuation-in-part of US-Patent-Appl-SN-643629, filed 18 Jan. 1991 which is a division of US-Patent-Appl-SN-361471, filed 5 Jun. 1989
(NASA-Case-ARC-11956-1-SB; US-Patent-5,223,461;
US-Patent-Appl-SN-880856; US-Patent-Appl-SN-643629;
US-Patent-Appl-SN-361471; US-Patent-Class-501-95;
US-Patent-Class-501-90; US-Patent-Class-501-92;
US-Patent-Class-264-DIG.19; Int-Patent-Class-C04B-35/52) Avail: US Patent and Trademark Office

Novel high strength ceramic fibers derived from boron, silicon, and carbon organic precursor polymers are discussed. The ceramic fibers are thermally stable up to and beyond 1200 C in air. The method of preparation of the boron-silicon-carbon fibers from a low oxygen content organosilicon boron precursor polymer of the general formula Si(R2)BR(sup 1) includes melt-spinning, crosslinking, and pyrolysis. Specifically, the crosslinked (or cured) precursor organic polymer fibers do not melt or deform during pyrolysis to form the silicon-boron-carbon ceramic fiber. These novel silicon-boron-carbon ceramic fibers are useful in high temperature applications because they retain tensile and other properties up to 1200 C, from 1200 to 1300 C, and in some cases higher than 1300 C.

Official Gazette of the U.S. Patent and Trademark Office

N94-23335# Federal Aviation Administration, Atlantic City, NJ.

INITIAL EVALUATION OF BURN CHARACTERISTICS OF PHENOLIC FOAM RUNWAY BRAKE ARRESTOR MATERIAL

Dung Do, Joseph Wright, and Lawrence Hampton Dec. 1993 46 p
(DOT/FAA/CT-TN93/7) Avail: CASI HC A03/MF A01

Tests of the burn characteristics of a phenolic foam, under evaluation as runway brake arrestor material, were conducted by the Fire Safety Branch of the Federal Aviation Administration (FAA) Technical Center. The purpose of these tests was to assess the fire propagation properties of phenolic foam when exposed to a free burning Jet A fuel fire and to determine the fire control time of phenolic foam immersed in a jet fuel fire when extinguished using three-percent aqueous film forming foam (AFFF). Three pool fire tests were conducted as follows: In the first and second tests, a 12-foot-square bed of phenolic foam material was placed adjacent to a 35-foot diameter jet fuel fire. This configuration resulted in ignition and flame propagation across to adjacent foam material, resulting in charring of over 30 percent of the exposed surface of the phenolic foam. In the third test, the phenolic foam material was immersed in the jet fuel fire to determine ease of extinguishment using conventional AFFF agent. The fire control time was three times longer than when the phenolic foam material was absent. The extinguishing time was an order of magnitude higher than that without the foam. In addition, the phenolic foam material was evaluated on the basis of FAA fire test requirements for cabin material. These small-scale tests measured burn length, weight loss, and heat release rate of the foam material in accordance with Federal Aviation Regulation (FAR) 25.853. These results showed the foam material passed the burn test requirements. Author (revised)

N94-23371*# National Aeronautics and Space Administration. Lewis Research Center, Cleveland, OH.

INFRARED ANALYSIS OF VAPOR PHASE DEPOSITED TRICRESYLPHOSPHATE (TCP)

Wilfredo Morales, Bengi Hanyaloglu (Cleveland State Univ., OH.), and Earl E. Graham (Cleveland State Univ., OH.) Jan. 1994 20 p
(RTOP 505-63-5A)

(NASA-TM-106423; E-8260; NAS 1.15:106423) Avail: CASI HC A03/MF A01

Infrared transmission was employed to study the formation of a lubricating film deposited on two different substrates at 700 C. The deposit was formed from tricresylphosphate vapors and collected onto a NaCl substrate and on an iron coated NaCl substrate. Analysis of the infrared data suggests that a metal phosphate is formed initially, followed by the formation of organophosphorus polymeric compounds. Author (revised)

N94-23431 Selskapet for Industriell og Teknisk Forskning, Trondheim (Norway).

SELECTIVE HYDROGEN SEPARATION BY PALLADIUM-BASED COMPOSITE MEMBRANES

E. Aksnes, I. Dahl, and A. Stori (Center for Industrial Research, Oslo, Norway.) 10 Feb. 1993 12 p Limited Reproducibility: More than 20% of this document may be affected by microfiche quality

(PB93-201671; STF28-A93013) Avail: Issuing Activity (National Technical Information Service (NTIS))

Composite Pd/Ag polymer membranes for selective hydrogen permeation have been made. Experiments show that there is good adhesion between plasma sputtered Pd/Ag films and polysulphone. With 30/70 (weight) Ag/Pd films room temperature stable metal films with thicknesses of less than 0.2 micrometers can be made. Even films with a thickness of 0.02 micrometers acted as an efficient barrier for an inert gas like N_2. The thinner films were the most stable towards mechanical and chemical stresses induced by cycling the hydrogen pressure. NTIS

N94-23486*# National Aeronautics and Space Administration. Langley Research Center, Hampton, VA.

COMPOSITE MATERIAL IMPREGNATION UNIT

S. P. Wilkinson (College of William and Mary, Williamsburg, VA.), J. M. Marchello (Old Dominion Univ., Norfolk, VA.), and N. J. Johnston Dec. 1993 74 p

(RTOP 233-01-01)

(NASA-TM-107751; NAS 1.15:107751) Avail: CASI HC A04/MF A01

This memorandum presents an introduction to the NASA multi-purpose prepregging unit which is now installed and fully operational at the Langley Research Center in the Polymeric Materials Branch. A description of the various impregnation methods that are available to the prepregger are presented. Machine operating details and protocol are provided for its various modes of operation. These include, where appropriate, the related equations for predicting the desired prepreg specifications. Also, as the prepregger is modular in its construction, each individual section is described and discussed. Safety concerns are an important factor and a chapter has been included that highlights the major safety features. Initial experiences and observations for fiber impregnation are described. These first observations have given great insight into the areas of future work that need to be addressed. Future memorandums will focus on these individual processes and their related problems. Author

N94-23561 Helsinki Univ. of Technology, Espoo (Finland).

SURFACE AND INTERFACIAL PROPERTIES OF POLYMER BLENDS. A LITERATURE SURVEY

M. Hiljanen, M. Heino, R. Holsti-Miettinen, J. Seppaelae, and J. Sjoeblom Mar. 1993 85 p Sponsored by Nordisk Industrifond Limited Reproducibility: More than 20% of this document may be affected by microfiche quality

(PB93-230191; ISBN-951-22-1449-0) Avail: Issuing Activity (National Technical Information Service (NTIS))

The commercial development of polymer alloys and blends has had a rapid growth in importance during the 1980's. For example, in 1987, it was estimated that 60 to 70% of polyolefins and 23% of other polymers were sold as blends. In the literature survey emphasis is put on the surface/interfacial properties of the blend components and of the final product. The reason for such a literature approach is that these properties are of extreme importance for final morphologies, and, hence they must be studied. The report gives a broad survey of different experimental techniques for determination of surface/interfacial energies. NTIS

N94-23720# State Univ. of New York, Alfred. College of Ceramics.

COMBUSTION SYNTHESIS AND ENGINEERING OF NANOPARTICLES FOR ELECTRONIC, STRUCTURAL AND SUPERCONDUCTOR APPLICATIONS

G. C. Stangle, V. R. W. Amarakoon, and W. A. Schulze 19 Aug. 1993 23 p

(Contract DE-FG02-93ER-12128)

(DE94-001865; DOE/ER-12128/2) Avail: CASI HC A03/MF A01

Fully dense, nanocrystalline ceramic articles were prepared by a new nanofabrication process. The process consists of two steps: synthesis of ceramic nanoparticles and fabrication of dense, nanocrystalline ceramic parts. The synthesis step produced 10-nanometer diameter crystallites, and is capable of being scaled up to kilogram/hour production rates. The fabrication step produced dense parts at significantly reduced sintering temperatures and times, representing a factor of 10-100 reduction in process energy requirements. Process was demonstrated by producing ultrafine-grained yttria-stabilized ZrO_2, an important material with a variety of energy-related applications (e.g., solid electrolytes, oxygen sensors, electrode materials, thermal barrier coatings, etc.). Results from this period illustrate capabilities of this energy-efficient and directly commercializable process for producing dense, nanocrystalline, multicomponent oxide ceramics. DOE

N94-23763# Technische Univ., Delft (Netherlands).

REACTION OF ISOCYANATES WITH CARBOXYLIC ACIDS AND ITS APPLICATION TO POLYMER SYNTHESIS Ph.D. Thesis

A. H. M. Schotman 28 Jun. 1993 137 p

(PB94-118858) Avail: CASI HC A07/MF A02

The thesis describes systematic examinations of the reaction of diisocyanates with dicarboxylic acids yielding various types of polyamides (PA) polymers and block copolymers. The investigations are split into two parts: (1) describes the chemistry of the carboxylic acid-isocyanate reaction using low molecular mass model compounds; (2) reports the synthesis of several new polymers, based on the reaction between diisocyanates and dicarboxylic acids. NTIS

N94-23783# Oak Ridge National Lab., TN.

DEVELOPMENT OF A THEORY OF THE WEAR OF CERAMICS

R. S. Cowan (Georgia Inst. of Tech., Atlanta.) and W. O. Winer (Georgia Inst. of Tech., Atlanta.) Oct. 1993 108 p

(Contract DE-AC05-84OR-21400)

(DE94-002773; ORNL/Sub-93-07802) Avail: CASI HC A06/MF A02

The objective of this program was to develop a theory to predict wear behavior of lubricated and unlubricated ceramics in sliding contact, and present it in a form useful for designers. It is assumed that the contact between bodies in sliding motion produces a stress field and frictional heat source that may induce severe wear from material yielding or fracture. A thermomechanical wear model is used to develop a wear transition equation for identifying the dominant factors that will reduce or control such wear by employing thermoelasticity analyses and contact mechanics. This equation is used to construct wear maps for ease of analysis. Studies are devoted to substantiating the thermomechanical wear model by using experimental results that emphasize the transition from mild to severe wear for dry and lubricated metallic and ceramic sliding contacts under load. DOE

N94-24129 Office National d'Etudes et de Recherches Aerospatiales, Paris (France).

GLASS-CERAMIC LI-AI-SI-O COMPOSITION AND PROCESS FOR ITS PRODUCTION Patent Application

Guy Larnac, inventor (to ONERA), Jean Phalippou, inventor (to ONERA), Michel Parlier, inventor (to ONERA), Marie-Helene Ritti, inventor (to ONERA), and Jean Jamet, inventor (to ONERA) 4 Dec. 1992 18 p

(CA-Patent-Appl-SN-2043757; Int-Patent-Class-C03B-014/00; Int-Patent-Class-C03B-003/085; CTN-94-60871) Copyright Avail: Micromedia Ltd., Technical Information Centre, 240 Catherine Street, Suite 305, Ottawa, Ontario, K2P 2G8, Canada HC/MF

A glass-ceramic composition is provided, comprising mainly SiO_2, Al_2O_3, and Li_2O and/or MgO. The composition is obtained by preparing a gel by hydrolysis and poly condensation of precursor metal compounds in solution in a solvent, removing the solvent, grinding the gel if required, and finally dehydrating and oxidizing the gel followed by compaction and ceramization by increasing the temperature. The precursors used are preferably silicon alcoholates and aluminum alcoholates, more particularly tetraethyl ortho silicate and aluminum sec butoxide, and inorganic compounds of Li and/or Mg. It has been found that the glass-ceramic composition is substantially in the form of solid ceramic solutions having a low expansion coefficient. This and other properties favor formation of fiber reinforced composites with good thermomechanical characteristics. To obtain a fiber reinforced composite with a refractory ceramic matrix, the fibers can be incorporated in the powder of the glass-ceramic composition before the compacting heat treatment. This procedure is particularly applied to SiC-based fibers. When these fibers contain an appreciable amount of oxygen and carbon on the surface, the composition preferably also contains at least one additional component such as Nb2O5 to limit adhesion of the composition to the fibers. CISTI

N94-24223*# Massachusetts Inst. of Tech., Cambridge. Materials Processing Center.

SELECTION OF POLYMER BINDERS AND FABRICATION OF SIC FIBER-REINFORCED REACTION-BONDED SILICON NITRIDE MATRIX COMPOSITES Final Report, 10 Dec. 1987 - 24 Feb. 1993

John S. Haggerty, A. Lightfoot, and J. Sigalovsky Nov. 1993 50 p
(Grant NAG3-845)
(NASA-CR-194874; NAS 1.26:194874; MIT-OSP-99857) Avail: CASI HC A03/MF A01

The topics discussed include the following: effects of solvent and polymer exposures on nitriding kinetics of high purity Si powders and on resulting phase distributions; effects of solvent and polymer exposures on Si Surface Chemistry; effects of solvent and polymeric exposures on nitriding kinetics; and fabrication of flexural test samples. CASI

N94-24228# Advisory Group for Aerospace Research and Development, Neuilly-Sur-Seine (France). Structures and Materials Panel.

INTRODUCTION OF CERAMICS INTO AEROSPACE STRUCTURAL COMPOSITES [L'INTRODUCTION DES CERAMIQUES DANS LES COMPOSITES UTILISES DANS LES STRUCTURES DES SYSTEMES AEROSPATIAUX]

Nov. 1993 160 p In ENGLISH and FRENCH Workshop held in Antalya, Turkey, 21-22 Apr. 1993
(AGARD-R-795; ISBN-92-835-0728-2) Copyright Avail: CASI HC A08/MF A02

Ceramics have been considered over the last two decades as a possible alternative to refractory metals and alloys to be used as structural materials for aeronautical use. The main disadvantage of these materials is their brittleness and the very low value of the critical size of defects leading to fracture. The concept of ceramic matrix composites has been recognized as one of the ways to escape this difficulty. Extensive work has been performed to identify the mechanisms of crack propagation and general fracture for unidirectional composites, laminates or other fabrics, including the understanding of their long term response: creep and fatigue effects or environmental degradation. The Workshop which has been held by AGARD SMP at Antalya (Turkey), April 1993, aimed at reviewing the present knowledge on all these aspects. For individual titles, see N94-24229 through N94-24240.

N94-24229# Office National d'Etudes et de Recherches Aerospatiales, Paris (France).

AN OVERVIEW ON THE MAIN AVAILABLE CERAMIC COMPOSITES AND THEIR PROCESSING ROUTES

J. F. Stohr *In* AGARD, Introduction of Ceramics into Aerospace Structural Composites Nov. 1993 16 p (For primary document see N94-24228 06-27)
Copyright Avail: CASI HC A03/MF A02

During the last decade, Ceramic Matrix Composites (CMC) have undergone a rapid development, and today, quite a number of composites are available. SiC/SiC and C/SiC, processed by Chemical Vapor Infiltration (CVI), are now produced on an industrial scale. C/SiC composites can currently operate at temperatures above 1600 C for propulsion applications on launchers and missiles. Other composites with oxide or silicon-nitride matrices are under development. The processing routes are moving from CVI to more cost-effective processes such as sol-gel and polymer precursor. These routes appear very promising since they currently use the technologies already developed for Organic Matrix Composites and carbon-carbon composites. The real challenge for these materials is in the areas of the working temperature, which must exceed 1600C, and the environmental behavior. To meet these requirements, new fibers with an increased thermal stability are under development. Author (revised)

N94-24230# California Univ., Santa Barbara. Dept. of Materials.

CERAMIC MATRIX COMPOSITES: CHALLENGES AND OPPORTUNITIES

A. G. Evans *In* AGARD, Introduction of Ceramics into Aerospace Structural Composites Nov. 1993 13 p (For primary document see N94-24228 06-27)
(Contract N00014-86-K-0753)
Copyright Avail: CASI HC A03/MF A02

A methodology for the straightforward and consistent evaluation of the constituent properties of CMC's is summarized. The methodology is based on an analyses of current literature. The results provide a constitutive law capable of simulating the stress/strain behavior of these materials. The approach is illustrated using data for two CMC's: SiC/CAS and SiC/SiC. The constituent properties are also used as input to mechanics procedures that characterize stress redistribution and predict the effect of strain concentrations on macroscopic performance. Author

N94-24231# Wright Research Development Center, Wright-Patterson AFB, OH.

INTERFACE EVALUATION IN CERAMIC COMPOSITES

Paul D. Jero, Triplicane A. Parthasarathy, and Ronald J. Kerans *In* AGARD, Introduction of Ceramics into Aerospace Structural Composites Nov. 1993 10 p (For primary document see N94-24228 06-27)
Copyright Avail: CASI HC A02/MF A02

The results of pushout tests on two ceramic matrix composites are presented and discussed. Emphasis is placed on the effect of interface roughness on the interfacial properties. Toward that end, techniques used to characterize fiber and interface topography are described and results presented. An advanced analysis, which takes account of the roughness contribution to the radial stress during debonding, is used to calculate interfacial properties. It is observed that the fiber fabrication technique has a profound effect on the nature of the interfacial topography. Author

N94-24232# Wright Research Development Center, Wright-Patterson AFB, OH.

MICROMECHANICAL FAILURE MODES IN BRITTLE MATRIX COMPOSITES

Nicholas J. Pagano *In* AGARD, Introduction of Ceramics into Aerospace Structural Composites Nov. 1993 18 p (For primary document see N94-24228 06-27)
Copyright Avail: CASI HC A03/MF A02

Ceramic-and glass ceramic matrix composites are being touted for application in high temperature structural components. Before their potential can be realized, however, understanding of the significance of the fracture modes that occur at very low stress levels well beneath those commonly assumed to initiate microcracking in the literature, will be essential. Unfortunately, at this point in the technology development, the precise definition of these mechanisms, i.e., the geography of the fracture plane(s), has been described rather incompletely in experimental research. In most cases, the experimental observations only provide views of these cracks at their intersection with a surface of the composite. Thus, in this presentation, we will provide some predictions of failure scenarios based upon a hypothetical idealized initial flaw in the matrix-an annular crack in a plane normal to the fibers of an unidirectional composite. Although many of the properties needed for the modeling study have not been realistically determined, especially the in-situ strength/ fracture properties, and the fracture criteria itself incorporates an undetermined parameter, i.e., initial flaw size, it is hoped that the modeling can serve to determine the nature of the parameters that require measurement and to help establish the sensitivity of the response to these parameters, as well as to guide experimental efforts to attempt validation of the failure processes hypothesized. The complexity of these processes seems to demand an iterative approach between the analyst and experimentalist. Derived from text

N94-24233# Office National d'Etudes et de Recherches Aerospatiales, Paris (France). Direction des Materiaux.

MICROMECHANICAL CHARACTERIZATION OF CERAMIC-MATRIX COMPOSITES USING THE INSTRUMENTED MICROINDENTATION TECHNIQUE [CARACTERISATION MICROMECANIQUE DES COMPOSITES A MATRICE CERAMIQUE A L'AIDE DE LA TECHNIQUE DE MICROINDENTATION INSTRUMENTEE]

M. Parlier, B. Passilly, and O. Sudre *In* AGARD, Introduction of Ceramics into Aerospace Structural Composites Nov. 1993 8 p In FRENCH See also A93-53607 (For primary document see N94-24228 06-27)

Copyright Avail: CASI HC A02/MF A02

The paper describes the potential of micromechanical studies using the instrumented Vickers indentation test in force and displacement. For ceramics reinforced by long fibers, it is possible to determine the hardness and the elastic modulus of the components as well as the mechanical characteristics of the fiber-matrix interface. Oxide and covalent (silicon carbide) matrix composites reinforced by SiC-Nicalon fibers are considered as examples. Author

N94-24234# Institut National des Sciences Appliquees, Lyon (France). Groupe d'Etudes de Metallurgie Physique et de Physique des Materiaux.

ROLE OF INTERFACES ON THE CYCLIC FATIGUE BEHAVIOUR OF CERAMIC MATRIX COMPOSITES

D. Rouby and P. Reynaud *In* AGARD, Introduction of Ceramics into Aerospace Structural Composites Nov. 1993 10 p Sponsored by CNRS; Ministere de la Recherche et de l'Espace; Direction des Recherches, Etudes et Techniques; and CNES (For primary document see N94-24228 06-27)

Copyright Avail: CASI HC A02/MF A02

Ceramics reinforced with continuous fibers exhibit delayed failure under pulsating load. A micromechanical model describing the fatigue effects is proposed. It is based on the decreasing of the shear stress at the fiber-matrix interfaces, resulting from interfacial wear due to the see-saw sliding. The main features of this model are the following: during first loading cycle, the material exhibits multiple matrix cracking and some fiber breaks. During subsequent cycles, the interfacial shear stress decreases, leading to increasing the failure probability of the bridging fibers. For a critical fraction of broken bridging fibers, instability occurs and the specimen fails, thus, defining the lifetime. For lower peak stresses, but higher still than the proportionality limit, the material also evolves but no failure occurs (up to one million cycles), indicating that the interfacial shear stress decreases to a non-zero lower bound. Fatigue induced changes of interfacial shear stress are also observed from fiber pull-out length analyses. Author

N94-24235# Caen Univ. (France).

MECHANICAL BEHAVIOR OF CMCs: CRACK GROWTH RESISTANCE AND CREEP ASPECTS

M. Gomina and J. L. Chermant *In* AGARD, Introduction of Ceramics into Aerospace Structural Composites Nov. 1993 18 p (For primary document see N94-24228 06-27)

Copyright Avail: CASI HC A03/MF A02

Rupture and creep behavior of ceramic matrix composites (CMC's) are discussed. The influence of the specimen geometry and size on the R-curve behavior for two types of SiC/C/SiC composite materials were investigated. The experimental results obtained using in-situ matrix crack lengths indicate that the shape of the resistance curve depends essentially on the predominant toughening mechanism (extensive matrix microcracking or fiber-matrix debonding) whereas the frontal process zone size is the same for both types of materials. K(sub R)-Delta(a) curves of SENB and small CT specimens rise as a consequence of the ligament which cannot contain the fully developed frontal process zone. Using large CT specimens, a minimum ligament size necessary to contain the frontal process zone and thus a K(sub R)-Delta(a) behavior free of structure size is observed. Creep results obtained using three point bending tests are also presented for these materials and for SiC-MLAS materials. Author (revised)

N94-24236# Warwick Univ., Coventry (England). Dept. of Physics.

MICROSTRUCTURE AND MICROMECHANICAL BEHAVIOUR OF CMCs

M. H. Lewis, A. Chamberlain, A. M. Daniel, M. W. Pharaoh, A. G. Razzell, and S. Sutherland *In* AGARD, Introduction of Ceramics into Aerospace Structural Composites Nov. 1993 13 p Sponsored by Science Research Council and Rolls Royce Ltd. (For primary document see N94-24228 06-27)

Copyright Avail: CASI HC A03/MF A02

A survey is presented of research aimed at an understanding of the relation between microstructure, interface properties, and macromechanical behavior of a range of silicate (glass ceramic) and nitride matrix composites. For silicate ceramic matrix composites (CMC's), hot-pressing cycle (P/T) in relation to matrix chemistry and fiber type is critical in avoiding mechanical and chemical damage of fibers with consequent reduction in ultimate CMC strength. Interfacial debond and shear stresses, measured via a fiber 'push-down' indentation technique exhibit a wide variation, dependent on CMC processing time, temperature and matrix chemistry and thermal expansion. 'Graceful' failure, typified by 3 stage stress-strain curves, may be obtained for debond energies Gamma and shear stresses tau up to approximately 20 Jm(sup -2) and approximately 50 MPa, respectively. Interface-oxidation-induced property degradation occurs at intermediate temperatures (400-800 C) but is suppressed at higher temperatures by passive oxidation of SiC fiber ends which prevents further carbon interface removal by channeled reaction. Higher temperature SiC (Textron CVD) monofilament based CMC's with Si3N4 (SRBSN) matrices were fabricated using tape-cast matrix preforms. Partially sacrificial C-coatings on the monofilaments provide low Gamma and tau interfaces and result in ideal composite response with separation between matrix cracking stress and ultimate stress, followed by filament pull-out. Although interface oxidation is a limiting problem for creep and stress rupture, these properties are superior to turbine superalloys. Author (revised)

N94-24237# Societe Europeenne de Propulsion, Saint-Medard-en-Jalles (France).

CERAMIC MATRIX COMPOSITE PARTS DESIGN

P. Lamicq and D. Boury *In* AGARD, Introduction of Ceramics into Aerospace Structural Composites Nov. 1993 12 p (For primary document see N94-24228 06-27)

Copyright Avail: CASI HC A03/MF A02

Ceramic matrix composites (CMC) are making up a new material family that presents a significant potential for thermostructure design. They show a good specific strength and stiffness up to high temperatures and these characteristics are associated to non-fragile behaviors which do correspond to the designer practical requirements. After a short description of the CMC most used by SEP designers, a thought on part design and dimensioning with these materials is presented. An approach of the currently used general methodology is presented, followed by various comments specific to the use of these materials. Finally, some examples of singular behaviors, which are currently poorly controlled by simple modeling and require advanced rupture criteria, are given. Derived from text

N94-24238# Deutsche Forschungs- und Versuchsanstalt fuer Luft- und Raumfahrt, Stuttgart (Germany). Inst. of Structures and Design.

CMC DESIGN CONSEQUENCES

W. Krenkel *In* AGARD, Introduction of Ceramics into Aerospace Structural Composites Nov. 1993 12 p (For primary document see N94-24228 06-27)

Copyright Avail: CASI HC A03/MF A02

Ceramic matrix composites (CMC) have widely demonstrated their feasibility and performance although no series production has been achieved. Today's status is characterized by long production times, high material qualities with high reproducibility and experience in the first structural components. Some unsolved problems are the joining and attachment of CMC parts, the lack of adequate nondestructive testing methods and the insufficient oxidative stability for long term applications. This paper deals with general valid design aspects as a consequence of the CMC materials characteristics and the demand for structural components of high reliability. Author

N94-24239# Maschinenfabrik Augsburg-Nuernberg A.G., Munich (Germany).

INTEGRATED APPROACH IN MODELLING, TESTING, AND DESIGN OF GRADIENT-CVI DERIVED CMC COMPONENTS

D. Sygulla, A. Muehlratzer, and P. Agatonovic *In* AGARD, Introduction of Ceramics into Aerospace Structural Composites Nov. 1993 13 p Sponsored by BMFT (For primary document see N94-24228 06-27)

Copyright Avail: CASI HC A03/MF A02

Ceramic composite materials with continuous fibers in a SIC matrix, manufactured by CVI, have shown benefits for structural applications due to high fracture toughness and damage tolerance under operational conditions. However, the production time associated with the hitherto applied CVI technique entails development cycles of hardly acceptable long duration. Therefore, there is growing interest for the CVI technique to manufacture reliable CMC parts, focusing special attention on a more efficient production technology. In this paper a current attempt to develop and qualify a new CVI process, the so-called gradient-CVI, is described and discussed. This process offers increased productivity appropriate for industrial production and excellent material properties. Author

N94-24240# Wright Lab., Wright-Patterson AFB, OH. Materials Directorate.

ULTRASONIC NONDESTRUCTIVE EVALUATION AS A TOOL FOR THE DEVELOPMENT OF AEROSPACE STRUCTURAL CERAMIC COMPOSITES

Theodore E. Matikas and Prasanna Karpur (Dayton Univ. Research Inst., OH.) *In* AGARD, Introduction of Ceramics into Aerospace Structural Composites Nov. 1993 7 p (For primary document see N94-24228 06-27)
(Contract F33615-89-C-5612)
Copyright Avail: CASI HC A02/MF A02

This paper outlines new concepts for the utilization of various ultrasonic techniques for the evaluation of different aspects of development and use of ceramic matrix composites. We introduce a novel mechanical parameter called the interfacial shear stiffness coefficient which can be measured using ultrasonic shear wave reflectivity technique to characterize and quantify the fiber-matrix interface. This newly proposed parameter is promising as a common basis of composite evaluation among the composites developing, composites mechanics modeling and composites testing groups. The paper will also discuss other ultrasonic NDE techniques such as ultrasonic microscopy which can provide comprehensive evaluation of the composite system during all phases of development and use. Derived from text

N94-24468 Toronto Univ. (Ontario). Dept. of Metallurgy and Materials Science.

STRUCTURAL CHARACTERIZATION AND THERMAL CYCLING BEHAVIOUR OF EB-PVD THERMAL BARRIER COATING SYSTEMS M.S. Thesis

Aline Faure-Geors 1993 85 p
(ISBN-0-315-83365-3; CTN-94-60958) Copyright Avail: Micromedia Ltd., Technical Information Centre, 240 Catherine Street, Suite 305, Ottawa, Ontario, K2P 2G8, Canada HC/MF

The behavior of thermal barrier coatings (TBC) produced by electron beam physical vapor deposition was investigated. Emphasis was placed on NiCoCrAlY type bond TBC. The effect of substrate temperature and ion beam assistance condition was first studied for top-coat free samples. Thermal cyclic tests of the samples were performed between 1,035 C and ambient temperature. Scanning electron microscopy and x-ray spectroscopic analyses conducted on the cross section showed the effect of ion beam assistance on modification of the composition profile of each element in as-deposited samples, which results in low Al content in the as-deposited bond coat and growth of a Cr-rich phase during thermal cycles. Samples with ceramic overlay were similarly studied. It was found that interdiffusion of alloying elements with the substrate and diffusion toward the oxide scale modified the bond coat composition and generated phase transformations or segregations, affecting the physical and/or mechanical properties of the bond coat and becoming involved in the degradation mechanism of the TBC. Raman spectroscopy showed that the predominant phase in ZrO2 having 7-10 weight percent of Y2O3 is tetragonal. This phase does not undergo the damaging transformation to monoclinic under the thermal cycling conditions studied. Preliminary work on compositionally graded TBC was also conducted. Author (CISTI)

N94-24558# South Carolina Univ., Columbia. Dept. of Chemistry and Biochemistry.

SYNTHESIS OF SOLUBLE HALOGENATED POLYPHENYLENES: MECHANISM FOR THE COUPLING HALOGENATED LITHIOBENZENES

Eric B. Stephens, Kenneth E. Kinsey, Joanna F. Davis, and James M. Tour 22 Nov. 1993 28 p
(Contract N00014-89-J-3062)
(AD-A273547; TR-23) Avail: CASI HC A03/MF A01

A method for the synthesis of soluble polyphenylenes that involves the polymerization of 1-halo-4-lithiobenzenes, 1-halo-3-lithiobenzenes, and 1,3- and 1,4-dilithiobenzenes in ethereal solvents is described. The lithiobenzenes are prepared from the corresponding dihalogenated benzenes using tert-butyllithium. By varying the monomers and conditions used, a variety of soluble halogenated polyphenylenes can be obtained with weight average molecular weights (Mw) as high as 6,000 with polydispersities (Mw/Mn) equal to approximately 2.8. The pre-quenched polymers can exist as multi-lithiated polymers if 2.0 equivalents of tert-butyllithium are used to form the aryllithium intermediates. The polymers are usually amorphous and contain significant amounts of phenylated polyphenylene units capped with halogens. The polymers are soluble in organic solvents such as THF, chloroform, and methylene chloride. Several of the polymers exhibited low melting and glass transition temperatures. The brominated polymers are easily dehalogenated upon treatment with tert-butyllithium in THF at -78 C followed by quenching with water. The molecular weights of several of the brominated polymers increased upon debromination with tert-butyllithium. When the polymerizations were carried out in the presence of 1,3-diphenylisobenzofuran, ortho-benzyne intermediates were trapped as their Diels-Alder adducts. LiH appears to be present in significant amounts upon completion of the polymerization. DTIC

N94-24562 Florida Univ., Gainesville. Dept. of Chemistry.

STM STUDIES OF LB DEPOSITED ALKYL SUBSTITUTED POLYANILINE AND ITS CORRESPONDING MONOMER

P. Quint, R. S. Duran, M. Hara, W. Knoll, and H. Sasabe 20 Oct. 1993 20 p Limited Reproducibility: More than 20% of this document may be affected by microfiche quality
(Contract N00014-91-J-1655)
(AD-A273553; TR-8) Avail: Issuing Activity (Defense Technical Information Center (DTIC))

STM investigations were carried out on monolayers of poly(o-pentadecyl aniline), o-pentadecyl aniline monomer, and p-hexadecyl aniline. The polymer was prepared by Langmuir polymerization on a 0.1 M H2SO4 sub phase, containing ammonium persulfate as the oxidizing agent. Monolayers of all the compounds were transferred by the LB technique from the air/liquid interface to a MoS2 substrate. After annealing, molecular resolution images were obtained for all three compounds. The o-pentadecyl aniline monomer showed a decreased mean molecular area on the MoS2 surface, compared to that at the liquid/air interface, while the polymer images showed similar packing at both interfaces. The p-hexadecyl aniline showed similar ordering on the substrate as the ortho substituted monomer. The polymer images showed evidence of backbone connectivity. After annealing all monolayers showed high positional and orientational order. DTIC

N94-24677 Princeton Univ., NJ. Dept. of Chemical Engineering.

NANODESIGNING OF HIERARCHICAL MULTIFUNCTIONAL CERAMICS Final Report, 1 Oct. 1990 - 31 Dec. 1992

Ilhan A. Aksay, M. Sarikaya, and D. M. Dabbs 28 Sep. 1993 36 p Limited Reproducibility: More than 20% of this document may be affected by microfiche quality
(Grant AF-AFOSR-0040-91)
(AD-A273466; AFOSR-93-0670TR) Avail: Issuing Activity (Defense Technical Information Center (DTIC))

Methods of processing nanometer scale ceramics for use in structural and optoelectronic applications have been developed. Colloidal processing of fine scale ceramic powders was used because such an approach represents the most feasible processing methodology for the production of large scale devices and components. The project consists of two primary task areas: (1) fundamental studies in synthesis and processing; and (2) the processing and properties of ceramic matrix composites. For task one, the emphasis has been on the basic science of the synthesis and use of nanometer size particles. Task two, on the other hand, has been on the application of colloidal methods to the production of ceramic matrix composites for use in engineering applications. This project began at the University of Washington and was continued at Princeton University. DTIC

N94-24682*# National Aeronautics and Space Administration. Lewis Research Center, Cleveland, OH.

DURABILITY EVALUATION OF CERAMIC COMPONENTS USING CARES/LIFE

Noel N. Nemeth, Lynn M. Powers (Cleveland State Univ., OH.), Lesley A. Janosik, and John P. Gyekenyesi Jan. 1994 15 p Proposed for presentation at the 39th International Gas Turbine and Aeroengine Congress, The Hague, The Netherlands, 13-16 Jun. 1994; sponsored by ASME
(NASA-TM-106475; E-8402; NAS 1.15:106475) Avail: CASI HC A03/MF A01

The computer program CARES/LIFE calculates the time-dependent reliability of monolithic ceramic components subjected to thermomechanical and/or proof test loading. This program is an extension of the CARES (Ceramics Analysis and Reliability Evaluation of Structures) computer program. CARES/LIFE accounts for the phenomenon of subcritical crack growth (SCG) by utilizing the power law, Paris law, or Walker equation. The two-parameter Weibull cumulative distribution function is used to characterize the variation in component strength. The effects of multiaxial stresses are modeled using either the principle of independent action (PIA), the Weibull normal stress averaging method (NSA), or the Batdorf theory. Inert strength and fatigue parameters are estimated from rupture strength data of naturally flawed specimens loaded in static, dynamic, or cyclic fatigue. Application of this design methodology is demonstrated using experimental data from alumina bar and disk flexure specimens which exhibit SCG when exposed to water. Author

N94-24720 Department of the Navy, Washington, DC.

MOLTEN SALT REACTOR FOR POTENTIOSTATIC ELECTROPLATING Patent

Kurt H. Stern, inventor (to Navy) and Ralph M. Hess, inventor (to Navy) 7 Sep. 1993 7 p Filed 12 Mar. 1992 Supersedes AD-D015358
(AD-D016020; US-Patent-5,242,563; US-Patent-Appl-SN-850107; US-Patent-Class-204-241) Avail: US Patent and Trademark Office

A molten salt reactor for potentiostatic electroplating that includes a reactor chamber defined by a peripheral wall, a bottom wall, and a top cover is described. The bottom wall of the reactor chamber has an opening, to which a first end of a gas inlet conduit is attached so as to be in fluid communication with the reactor chamber. A crucible support platform is positioned within the reactor chamber, and a crucible for holding a molten salt is mounted thereon. A furnace substantially surrounds the peripheral wall of the reactor chamber and the first end of the gas inlet conduit. The crucible support platform is electrically insulated from the reactor chamber. An inert gas flows from the gas inlet conduit, through a lower portion of the reactor chamber, past the crucible support platform, through an upper portion of the reactor chamber, and to a gas outlet in the upper portion of the reactor chamber. The inert gas is heated within the first end of the gas inlet conduit prior to flowing into the lower portion of the reaction chamber. DTIC

N94-24721 Department of the Navy, Washington, DC.

CURING PHTHALONITRILE RESINS WITH ACID AND AMINE Patent

Peter J. Burchill, inventor (to Navy) and Teddy M. Keller, inventor (to Navy) 17 Aug. 1993 6 p Filed 9 Jan. 1992
(AD-D016021; US-Patent-5,237,045; US-Patent-Appl-SN-818575; US-Patent-Class-528-362) Avail: US Patent and Trademark Office

Polymerization of cure of di-phthalonitrile monomers or prepolymers by a curing agent selected from (1) an acid and amine, (2) a salt of an acid and an amine, and (3) mixtures of (1) and (2). In a preferred embodiment, the curing agents are amine salts which are reaction products of an aromatic amine and an aromatic sulfonic acid. The use of the curing agents enhances curing rates and results in polymers which have high T(sub g). DTIC

N94-24732 Massachusetts Univ., Lowell. Dept. of Chemistry.

DIPOLAR RELAXATION IN A SECOND-ORDER NONLINEAR OPTICAL INTERPENETRATING POLYMER NETWORK Technical Report

J. I. Chen, S. Marturunkakul, L. Li, R. J. Jeng, and J. Kumar 29 Nov. 1993 17 p Limited Reproducibility: More than 20% of this document may be affected by microfiche quality
(Contract N00014-90-J-1148)
(AD-A273626; TR-94-02) Avail: Issuing Activity (Defense Technical Information Center (DTIC))

The nature of the relaxation process of the poled order in an inter-penetrating polymer network (IPN) system is found to be fundamentally different from that of a guest/host system. The IPN (Tg= 176 C) consists of a nonlinear optical (NLO) active epoxy-based polymer network and an NLO active phenoxy-silicon polymer network. The decay behavior of the second-order nonlinearity of this IPN was investigated in the range from 110 to 170 C. The stability of this IPN is superior to those of classic guest/host polymers as indicated by longer relaxation times at temperatures from 110 to 130 C. The relaxation process of the IPN system follows Arrhenius type behavior at temperatures ranging from 140 to 170 C. The IPN system provides a new approach to processing for stabilization of the second-order nonlinear optical properties. DTIC

N94-24737 Department of the Navy, Washington, DC.

HIGH TEMPERATURE ADHESIVE Patent

Teddy M. Keller, inventor (to Navy) and Charles M. Roland, inventor (to Navy) 7 Sep. 1993 7 p Filed 26 Feb. 1992 Supersedes AD-D015286
(AD-D016019; US-Patent-5,242,755; US-Patent-Appl-SN-841945; US-Patent-Class-428-457) Avail: US Patent and Trademark Office

A substrate assembly and method for its preparation, said substrate assembly comprising at least two substrates adhesively bonded with a cured thermosetting polymer being able to withstand a temperature of 200-400 C, is disclosed. The polymer is derived from a diphthalonitrile monomer and/or prepolymer with an aromatic moiety in the bridging group which monomer and/or prepolymer is solid at room temperature but which is rendered liquid by heating it to above its melting temperature. Said monomer in liquid state, and its prepolymer in liquid state, have tack with respect to said substrate. DTIC

N94-24749# Lehigh Univ., Bethlehem, PA. Energy Research Center.

ROBOTIC WELD OVERLAY COATINGS FOR EROSION CONTROL

B. F. Levin, J. N. Dupont, and A. R. Marder 20 Jul. 1993 28 p
(Contract DE-FG22-92PC-92542)
(DE94-002665; DOE/PC-92542/T3) Avail: CASI HC A03/MF A01

Twelve weld overlay hardfacing alloys have been selected for preliminary erosion testing based upon a literature review. Four of the selected coatings were deposited on a 1018 steel substrate using plasma arc welding process. During the past quarter, the remaining eight coatings were deposited in the same manner. Ten samples from each coating were prepared for erosion testing. Microstructural characterization of each coating is in progress. This progress report describes coating deposition and sample preparation procedures. Relation between coating hardness and formation of cracks in coatings is discussed. DOE

N94-24753*# Cummins Engine Co., Inc., Columbus, IN.

DEVELOPMENT OF HIGH TEMPERATURE LIQUID LUBRICANTS FOR LOW-HEAT REJECTION: HEAVY DUTY DIESEL ENGINES

P. D. Wiczynski and T. A. Marolewski Mar. 1993 77 p
(Contracts DEN3-373; DE-AI01-91CE-50306; RTOP 778-34-2A)
(NASA-CR-191197; NAS 1.26:191197; DOE/NASA/0373-1) Avail: CASI HC A05/MF A01

The objective of this DOE program was to develop a liquid lubricant that will allow advanced diesel engines to operate at top ring reversal temperatures approaching 500 C and sump temperatures approaching 250 C. The lubricants developed demonstrated at marginal increase in sump temperature capability, approximately 15 C, and an increase in top ring reversal temperature. A 15W-40 synthetic lubricant designated HTL-4 was the best lubricant developed in terms of stability, wear control, deposit control dispersancy, and particulate emissions. Author (revised)

N94-24782 Massachusetts Univ., Amherst. Dept. of Polymer Science and Engineering.

ULTRASTRUCTURE PROCESSING OF MACROMOLECULAR MATERIALS Final Report, 12 Feb. 1990 - 11 Feb. 1993

Frank E. Karasz 25 Jun. 1993 25 p Limited Reproducibility: More than 20% of this document may be affected by microfiche quality
(Contract F49620-90-C-0019)
(AD-A273413; AFOSR-93-0864TR) Avail: Issuing Activity (Defense Technical Information Center (DTIC))

The effect of microstructure on miscibility of polymer blends has been investigated in a number of model systems by thermal, mechanical, and novel spectroscopic techniques. An understanding of the fundamental basis of the metastable miscibility found in large number of high temperature systems, i.e. these typically involving polyimides or related materials with high Tg's has also been gained. In a complementary investigation, we have performed computer simulation studies of the equilibrium behavior of various blends, and under several types of constraint, to provide insights into behavior in binary systems at the segmental level. This study also investigated dynamic aspects, including phase separation. In another investigation, we have studied electro-optically active conjugated polymers, principally poly(p-phenylene vinylene) and its derivatives, modifications and blends. The emphasis has been on gaining a detailed understanding of the structural properties and concurrently exploiting the several electro-optical effects for which these polymer systems are noted. These include nonlinear optical phenomena and electroluminescence. Certain solution properties of polymer systems have also been studied. We have continued to use quasi-elastic light-scattering measurements to investigate translational diffusion of solvated polymers in porous media and other properties of polar and non-polar macromolecules. A synthetic effort in side-chain liquid crystal polymers has led to the systematic study of the thermal, mechanical and dielectric properties of several representation series and of their mixtures. DTIC

N94-24783 Massachusetts Univ., Amherst. Dept. of Polymer Science and Engineering.

CENTER FOR ADVANCED ELECTRICAL AND STRUCTURAL POLYMERS Final Report, 1 Mar. 1990 - 28 Feb. 1993

Frank E. Karasz 15 Oct. 1993 78 p Limited Reproducibility: More than 20% of this document may be affected by microfiche quality

(Grant AF-AFOSR-0150-90)

(AD-A273415; AFOSR-93-0866TR) Avail: Issuing Activity (Defense Technical Information Center (DTIC))

Research in the U.R.I. has been organized into five thrust areas each comprising collateral and coordinated investigations in three departments at the University of Mass. and at Wright State University, Foster Miller Inc. and MIT. Electrical properties of pi-conjugated polymers are the focus of one thrust and are defined in terms of their structure-property relationships as well as long term applications. A prototypical polymer has been poly-p-phenylene vinylene. A second thrust has concentrated on nonlinear optical effects in pi-conjugated and side chain liquid crystal polymers containing chromophoric mesogens which have been synthesized and characterized, as have low-molecular weight model compounds of systematically varying structure. The third thrust has focused on polymer blends and alloys including high temperature novel processible systems for application in extreme conditions. Miscibility studies in conventional model polymers has continued to yield insights into the fundamental principles underlying polymer-polymer interactions. A computer simulation project has complemented these studies. The thrust on novel macromolecular architecture and characterization has produced a range of new systems and techniques including measurements of polymer dynamics in constricted geometries, and detailed fine-structure investigations of block copolymers. A thrust on new processing technologies has largely centered on the FMI initiatives with respect to novel approaches for high temperature polymer blend melts. DTIC

N94-24788 Dayton Univ., OH. Research Inst.

ULTRASONIC PROCESS FOR CURING ADHESIVES Interim Report, Jun. 1992 - Feb. 1993

Naga Senapati and Ron Moulder Mar. 1993 40 p Limited Reproducibility: More than 20% of this document may be affected by microfiche quality

(Contract F33615-89-C-5643)

(AD-A273175; WL-TR-93-4037) Avail: Issuing Activity (Defense Technical Information Center (DTIC))

The objective of this program was to demonstrate in the laboratory the feasibility of using ultrasonic energy to cure a structural adhesive used to bond two pieces of 2024-T3 aluminum. A process was developed that demonstrated that American Cyanamid FM-73 adhesive could be cured using ultrasonic energy at a power level of less than 25 watts/sq. inch of adhesive area. The bonds produced using ultrasonic energy were just as strong as the bonds produced using a thermal process. A styrene butadiene rubber was found to be an excellent material to couple the ultrasonic energy to the adhesive through the aluminum substrate. The required coupling pressure ranged from 10 to 15 psi. Ultrasonic energy is absorbed by the adhesive and is converted to heat. Fine thermocouples embedded in the adhesive showed that the temperature of the adhesive increased from room temperature (70 F) to 250 F in less than 10 minutes. The method currently used to cure the epoxy adhesive bonding a composite repair patch to an aircraft structure employs a heating blanket over the patch and the surrounding aircraft structure. This method is inefficient and requires the area surrounding a patch to be heated to the same temperature required to cure the adhesive. Since ultrasonic energy is absorbed directly by the adhesive, very little energy is wasted heating up the area surrounding the patch. Thus, an ultrasonic heating process is more efficient than the heating blanket method. The ultrasonic process has the potential to be used for repairing aging aircraft structures with bonded composite patches. DTIC

N94-24789 South Carolina Univ., Columbia. Dept. of Chemistry.

METAL-CATALYZED ALKYNYLATION OF BROMINATED POLYPHENYLENES: THERMOSET PRECURSORS OF HIGH DENSITY MONOLITHIC GLASSY CARBON Technical Report

Eric B. Stephens and James M. Tour 22 Nov. 1993 14 p Limited Reproducibility: More than 20% of this document may be affected by microfiche quality

(Contract N00014-89-J-3062)

(AD-A273232; TR-21) Avail: Issuing Activity (Defense Technical Information Center (DTIC))

The functionalization of brominated polyphenylenes with several alkynes is described. The bromide groups on the polymer were replaced with terminal alkynes using a Pd/Cu catalyst system. Substitution of nearly all the original bromide locations was achieved. The functionalized polymers, freely soluble in THF, exhibited high char yields of up to 89% on thermolysis to 900 C under a nitrogen atmosphere. Several of the functionalized polymers, derived from brominated polyphenylenes with approximately equal amounts of meta- and para-linkages, flowed on heating. The polymer that was functionalized with phenylacetylene exhibited a well-defined melting point at approximately 200 C and flowed to produce a monolithic disk of glassy carbon. The amount of acetylenic crosslinking units in the polymers functionalized with phenylacetylene appears to be directly related to the char yields of the functionalized polymers. Predominantly meta-linked brominated polyphenylenes were also functionalized with a number of terminal alkynes and though high char yields of up to 86% were observed, these materials offered no improvements in flow properties. The structure/property relationships and material applications are discussed. DTIC

N94-24792# Florida Univ., Gainesville. Dept. of Chemistry.

ELECTROCHEMICALLY MEDIATED POLYMERIZATION OF 2-PENTADECYLANILINE CONFINED TO A PLANAR LIQUID-LIQUID INTERFACE

Wolfgang M. Sigmund, Andrew D. Child, John R. Reynolds, and Randolph S. Duran 20 Oct. 1993 30 p

(Contract N00014-91-J-1655)

(AD-A273541; TR-11) Avail: CASI HC A03/MF A01

Spreading, isotherms, and polymerization of 2-pentadecylaniline at a planar aqueous electrolyte-organic interface were examined by monitoring the interfacial pressure employing the Wilhelmy-plate method. These results indicate the presence of monomer confined to the interface. Application of a voltage across the interface using stainless steel electrodes results in polymerization to form an electroactive polymer. The interfacial polymerization appears to be affected by metal ions formed by oxidation of the anode that have diffused into the aqueous electrolyte. This phenomenon is dependent on the nature of the electrode material as successful polymerization was not observed with other electrode materials. The polymer formed was soluble in polar organic liquids, was green in its reduced state, and blue in its oxidized state when oxidized and reduced chemically or electrochemically as a thin film. Cyclic voltammetry of the polymer indicates one reversible redox process suggesting that there are only two different oxidation states available, i.e., the equivalent to leucoemeraldine cannot be formed with poly(2-pentadecylaniline) in a thin film. However, the fully reduced yellow leucoemeraldine can be formed in chloroform solution by hydrazine reduction. DTIC

N94-24813 Massachusetts Univ., Lowell. Dept. of Chemistry.
POLYTHIOPHENE DERIVATIVE WITH A SIDE CHAIN CHROMOPHORE AS PHOTOVOLTAIC AND PHOTOREFRACTIVE MATERIALS Technical Report
K. G. Chittibabu, L. Li, M. Kamath, J. Kumar, and S. K. Tripathy 17 Nov. 1993 38 p Limited Reproducibility: More than 20% of this document may be affected by microfiche quality
(Contract N00014-90-J-1148)
(AD-A273245; TR-94-01) Avail: Issuing Activity (Defense Technical Information Center (DTIC))

A new, solution processable, thiophene copolymer with a side chain nonlinear optical (NLO) chromophore namely Poly(3-octylthiophene co-N-(3-thenyl)-4-amino-2-nitro phenol) (POMDT) was chemically synthesized. The copolymer was further functionalized with a photocrosslinkable cinnamoyl group, and was doped with a photocrosslinkable NLO dye. The poled, photocrosslinked, dye doped copolymer exhibited relatively large second order NLO effects (d33 = 18.6 pm/V and 3.3 pm/V at 1.064 micrometers and 1.542 micrometers, respectively). The NLO properties of the photocrosslinked samples were stable at room temperature for 100 hours. The combination of reasonably good second order optical nonlinearity with established photoconducting behavior of the polythiophenes allows these type of polymers to be candidate materials in photovoltaic and photorefractive applications. DTIC

N94-24815 South Carolina Univ., Columbia.
ELECTROCHEMICAL AND ELECTRONIC PROPERTIES OF NEURAL AND OXIDIZED SOLUBLE ORTHOGONALLY-FUSED THIOPHENE OLIGOMERS Technical Report
J. Guay, A. Diaz, Ruilian Wu, and James M. Tour 22 Nov. 1993 22 p Limited Reproducibility: More than 20% of this document may be affected by microfiche quality
(Contract N00014-89-J-3062)
(AD-A273283) Avail: Issuing Activity (Defense Technical Information Center (DTIC))

The chemical and electrooxidation of spiro-fused thiophene trimers, SIII, and spiro-fused thiophene heptamers, SVII, with terminal alpha-Si(CH3)3 and Beta-CH3 groups were studied in Ch2Cl2 at room temperature. The heptamer segments in SVII oxidize stepwise to produce the mono radical cation, the bis(radical cation), the radical cation/dication, and the bis(dication), respectively. The existence of these intermediate ions was confirmed by vis/near-IR and ESR analyzed. The presence of anodic peaks at different potentials for the removal of the first and second electron from SIII and SVII suggests that some interaction exists between the radical cation and the neutral oligomers. However, once both oligomers are there appears to be no significant electronic interactions between tbe orthogonally positioned heptamer cations except possibly some weak magnetic coupling. With SIII, the trimer segments oxidize at fairly anodic potentials, and the four sequential intermediates are not observed because the less stable cations probably dimerize to form a bis(spire structure) containing a thiophene hexamer cation. DTIC

N94-24848# Army Construction Engineering Research Lab., Champaign, IL. Environmental Engineering Div.
AQUEOUS ALKALINE CLEANERS: AN ALTERNATIVE TO ORGANIC SOLVENTS Final Report
Robert W. Bird and Bernard A. Donahue Sep. 1993 87 p
(AD-A273510; USACERL-TR-EP-93/05) Avail: CASI HC A05/MF A01

Cleaning metal parts is a common task at U.S. Army installations. Because solvents are generally used for this service, large quantities of hazardous waste are generated daily at posts around the world. The environmental impacts and escalating cost of waste disposal have prompted the Department of Defense (DOD) to initiate programs seeking safe and efficient methods to reduce solvent waste generation. In response, the U.S. Army Construction Engineering Research Laboratories (USACERL) initiated a study to investigate the use of alkaline cleaners as an alternative to organic solvents now being used. Alkaline cleaning is an age-old technology used extensively throughout the industry. Recently, the use of alkaline cleaners has increased due to the growing awareness of environmental and personnel safety concerns associated with chlorinated and petroleum-based solvents (i.e., 1,1,1- trichloroethane and Stoddard solvent). Properties associated with alkaline cleaners (i.e., nontoxic, nonvolatile, noncombustible, and biodegradable) make them an environmentally acceptable alternative for use in metal parts cleaning. The USACERL analysis found that aqueous alkaline cleaning systems can be an alternative for degreasing operations at U.S. Army installations. Due to the unique operating conditions at every base, each system should be thoroughly tested. Preliminary testing will ensure a proper system design that will benefit both the installation and the environment. DTIC

N94-24863 South Carolina Univ., Columbia.
METAL-CATALYZED ALKYNYLATION OF (BROMOPHENYL)OLIGOPHENYLENES: A RAPID ROUTE TO THERMOSET PRECURSORS OF HIGH DENSITY MONOLITHIC GLASS-LIKE CARBON Technical Report
Eric B. Stephens and James M. Tour 22 Nov. 1993 10 p Limited Reproducibility: More than 20% of this document may be affected by microfiche quality
(Contract N00014-89-J-3062)
(AD-A273219; TR-15) Avail: Issuing Activity (Defense Technical Information Center (DTIC))

The functionalization of (bromophenyl) oligophenylene with several alkynes is described. The bromide groups on the oligomer were replaced with terminal alkynes using a Pd/Cu catalysts system. Substitution of nearly all the original bromide locations was achieved. The functionalized oligomers, freely soluble in THF, exhibited high char yields on thermolysis to 900 C under a nitrogen atmosphere. Several of the functionalized oligomers flowed on heating. The oligomer that was functionalized with phenylacetylene exhibited a well-defined melting point at 190 C and acetylenic coupling did not take place until 310 C. The hot oligomer flowed to form a monolith of glassy carbon. Depending on the alkyne used, a range of densities from 1.39-1.95 g/cc could be obtained in the final carbon glass. The structure/property relationships and the material applications are discussed. DTIC

N94-24922 South Carolina Univ., Columbia.
PLANAR POLY(p-PHENYLENE) DERIVATIVES: LADDER FORMATION FOR MAXIMIZATION OF EXTENDED CONJUGATION
James M. Tour and Jaydeep J. Lamba 22 Nov. 1993 8 p Limited Reproducibility: More than 20% of this document may be affected by microfiche quality
(Contract N00014-89-J-3062)
(AD-A273220) Avail: Issuing Activity (Defense Technical Information Center (DTIC))

Described is the synthesis of ladder polymers with a poly(p-phenylene) (PPP) backbone. The main PPP backbone was synthesized via palladium-catalyzed coupling of an arylbis(boronic ester) with an aryldibromide. Imine bridges, formed by exposure of the polymer to trifluoroacetic acid or HCl, are used to force the consecutive units into planarity. The bridging units are sp2 hybridized, thus, allowing for greater pi-electron flow between the consecutive phenyl units by lowering the band gap between the hydroquinoidal and the quinoidal forms of the phenylene backbone. Upon planarization, bathochromic shifts of 210-240 nm occur for the n-dodecyl substituted polymer. The optical spectra of the planar systems are compared to that of the parent nonplanarized polymers, oligo(p-phenylenes), PPP, and other near-planar PPP derivatives. When the bridges are n-dodecyl substituted, the fully planar structures can be made into flexible free standing films. DTIC

N94-24924 South Carolina Univ., Columbia. Dept. of Chemistry.
SYNTHESIS OF POLYPHENYLENES VIA BERGMAN CYCLIZATION OF ENEDIYNE MONOMERS
James M. Tour and Jens A. John 22 Nov. 1993 7 p Limited Reproducibility: More than 20% of this document may be affected by microfiche quality
(Contract N00014-89-J-3062)
(AD-A273298; TR-24) Avail: Issuing Activity (Defense Technical Information Center (DTIC))

Described is the synthesis of polyphenylenes via the Bergman cyclization of enediyne monomers. These monomers were synthesized via the Stephans-Castro/Sonogashira reaction and polymerized under varying conditions. DTIC

N94-24930# Florida Univ., Gainesville. Dept. of Chemistry.
THE 2-D POLYMERIZED LANGMUIR-BLODGETT FILMS STUDIED BY STM
T. S. Bailey, Wolfgang M. Sigmund, Randolph S. Duran, M. Hara, and H. Sasabe 20 Oct. 1993 17 p
(Contract N00014-91-J-1655)
(AD-A273542; TR-9) Avail: CASI HC A03/MF A01

The monomer 3-hexadecyl pyrrole was polymerized at the gas/liquid interface. Monomer and polymer were transferred from the interface to MoS2 for investigation by STM after annealing. Monolayers of monomer and polymer were highly ordered showing orientational and positional correlation of alkyl side chains. Polymer monolayers showed increased side chain packing density and side chain orientation more orthogonal to the surface. Polymer multilayers showed disorder, revealing connectivity and curvature of polymer chains. Conformations of polymer chains suggest growth in a parallel fashion at the gas/liquid interface. DTIC

N94-24937 Integrated Systems, Inc., Santa Clara, CA.
INTELLIGENT CONTROL OF CHEMICAL VAPOR DEPOSITION PROCESSES Final Report, 1 Sep. 1990 - 31 Aug. 1993
Sunil Shah 1 Sep. 1993 87 p Limited Reproducibility: More than 20% of this document may be affected by microfiche quality
(Contract F49620-90-C-0066)
(AD-A273356; AFOSR-93-0847TR) Avail: Issuing Activity (Defense Technical Information Center (DTIC))

Significant progress has been made in improving process control on the Technion TB reactor by using a model-based approach to control design. This approach has led to improvements in two areas. First, it has made the control design process more efficient by reducing the time required by a trial and error approach. This will lead to a cost saving in manpower. Second, it has led to design of effective controllers whose design is not evident in a trial and error approach. This has led to improved regulation of actuation and deposition conditions. Both these improvements are expected to lead to a quicker deployment to new deposition strategies and eventually to the cost-effective production of diamond. Progress made under this contract has set the stage for further refinement and implementation of these control strategies in a production environment. Work in this area is under progress on a related contract with Norton Diamond film entitled 'Integration of Intelligent Process Control and Monitoring.' DTIC

N94-25029 Army Belvoir Research and Development Center, Fort Belvoir, VA.
INVESTIGATION OF THE ULTRAFILTRATION TECHNIQUE USING MILITARY GREASES Final Report
In-Sik Rhee Oct. 1993 21 p Limited Reproducibility: More than 20% of this document may be affected by microfiche quality
(AD-A273633; BRDEC-TR/2544) Avail: CASI HC A03

Solid particle contamination in a grease intended for lubrication of instrument precision bearings can seriously degrade grease performance and bearing life. To produce clean grease, an ultrafiltration technique was recently introduced into the instrument bearing community. A major potential benefit of using this technique is that many instrument greases can be remanufactured from a variety of readily available lubricating greases. To assess this technique, an investigation was conducted to determine whether the physical and chemical properties of filtered greases are altered by the filtration process, and whether the filtered greases can improve instrument bearing life and their tribology properties. Results indicated that ultrafiltration can be performed on various types of greases with a substantial improvement in the resultant cleanliness level. However, some greases with rigid, discrete thickeners and solid additives are unlikely candidates for ultrafiltration due to their physical characteristic changes after filtering. DTIC

N94-25054 Department of the Navy, Washington, DC.
CURING PHTHALONITRILES WITH ACID Patent
Teddy M. Keller, inventor (to Navy) 21 Sep. 1993 7 p Filed 9 Jan. 1992
(AD-D015996; US-Patent-5,247,060; US-Patent-Appl-SN-818672; US-Patent-Class-525-362) Avail: US Patent and Trademark Office

Curing of phthalonitrile monomers and prepolymers is accelerated by inclusion of an acid curing agent. Cured phthalonitrile polymers have high thermal oxidative stability and are useful as resins in various compositions and as adhesives. DTIC

N94-25072# Naval Postgraduate School, Monterey, CA.
AN X RAY DIFFRACTION INVESTIGATION OF ALPHA-Al2O2 ADDITION TO YTTRIA STABILIZED ZIRCONIA (YSZ) THERMAL BARRIER COATINGS SUBJECT TO DESTABILIZING VANADIUM PENTOXIDE (V2O5) EXPOSURE M.S. Thesis
Dean M. Krestos Sep. 1993 79 p
(AD-A273403) Avail: CASI HC A05/MF A01

Since the mid 1970's the U.S. Navy has used yttria-stabilized zirconia (YSZ) as thermal barrier coatings for hot stage gas turbine components. Use of low cost, high contaminant, fuels has led to shortened component life from failure of YSZ coatings due to corrosive attack by vanadium and other combustion oxides. The object of this investigation was to determine the reactivity of adding alpha-Al2O3 to Current YSZ ceramics for creation of a ceramic composite which could improve mechanical properties and show improved durability to corrosive chemical attack. Ten powder samples of Zro2(8)Mol%YzO3, alpha-Al2O3, and V2Os5 of varying compositions were annealed at 900 C for 100 hours. X-ray diffraction analysis utilizing a standard 'search and match' method was used to determine the phases present in the reacted powder samples. Peak intensity comparisons between reacted and un-reacted samples allowed for a quantitative determination for the reactivity of a-A12O3 with the YSZ system exposed to V2O3. This investigation indicated that alpha-Al2O3 is non-reactive in all YSZ samples exposed to V2O5 at 900 C. DTIC

N94-25078# Technische Univ., Eindhoven (Netherlands).
THE MEASUREMENT OF THE FILM THICKNESS AND THE ROUGHNESS DEFORMATION OF LUBRICATED ELASTOMERS Ph.D. Thesis
Marnix Visscher 1992 263 p
(ETN-94-95293) Avail: CASI HC A12/MF A03

A method for film thickness measurements, which has sufficient resolving power to detect the (eventual deformed) roughness texture, which is applicable to elastomeric seals or similar contacts, and in which a rough elastomer is in sliding contact with a smooth rigid body, was developed. Different methods were investigated on their suitability for the proposed measurements and the focus error detection method was chosen as the most appropriate. Further analysis of this method and some preliminary measurements showed its ability for film thickness measurements and the conditions which must be fulfilled. The method can also be used to measure the deformed roughness texture in a statically loaded glass to elastomer contact. Two series of measurements are presented, one with and the other without liquid in the contact area. It is shown that a liquid in the contact area can influence the contact situation significantly. The measurements on the dry contact yields the conclusion that real contact areas can be found at different length scales. Further investigation and development is needed to obtain the required accuracy and frequency range for the film thickness measurements. ESA

N94-25084# Technische Univ., Eindhoven (Netherlands).
THE REACTION MECHANISM OF W-CVD IN Si Ph.D. Thesis
Paulus Adrianus Corn Groenen 1993 112 p Sponsored by Netherlands Foundation for Technical Sciences
(ETN-94-95329) Avail: CASI HC A06/MF A02

The Chemical Vapor Deposition of W (W-CVD) is investigated using WF6 as metal carrier. The study is performed in situ by a specially designed set up of a hot wall, continuous flow, full quartz reactor in combination with a mass spectrometer. The experimental apparatus is described. The reaction between WF6 and Si is studied. It results in a W layer of limited thickness. This reaction proceeds via a 'reaction layer' of about 80 atomic layers. This layer mainly consists of various fluorine containing species. The surface reaction between WF6 and SiH4 is investigated. This reaction is used to prevent Si consumption and to achieve thicker W layers. The study gives insights into the loss of selectivity. It is found that WF6 and SiH4 do react on a SiO2 surface. The result is a W containing species, that also acts as an independent reaction center and thus catalyzes the reaction. At approximately monolayer coverage, metallic W is formed. Based on the experimental observations, suggestions are made for the precursor state and the W containing species. ESA

N94-25136# Defence Research Establishment Atlantic, Dartmouth (Nova Scotia).
THE EFFECTS OF ZINC BORATE ADDITION ON THE FLAMMABILITY CHARACTERISTICS OF POLYESTER, VINYL ESTER, AND EPOXY GLASS REINFORCED PLASTICS
Richard M. Morchat Oct. 1993 24 p
(AD-A273164; DREA-TM-93/214) Avail: CASI HC A03/MF A01

The effects of an inorganic fire-retardant additive, zinc borate, on flammability characteristics and smoke generation of glass reinforced polyester, vinyl ester, and epoxy resin were evaluated. Information is presented on the flame spread index (ASTM E162), limiting oxygen index (ASTM D2863), density of smoke generated (ASTM E662), and toxic gases of combustion (Boeing BSS 7239). Results indicated that the addition of 10 phr of zinc borate to the polymeric materials significantly decreased the flame spread index and increased the limiting oxygen index; however, the amount of smoke generated during pyrolytic and flaming combustion was high and unacceptable. Finally, the toxic gas evolution data indicated that the threshold limit values for some gases were exceeded. DTIC

N94-25145# South Carolina Univ., Columbia. Dept. of Chemistry.
DISPERSION OF Rh/Cu IN A SOL-GEL MATRIX. HIGHLY CHEMO- AND STEREOSELECTIVE CATALYST FOR THE REDUCTION OF ALKYNES TO Z-ALKENES
James M. Tour, Shekhar L. Pendalwar, Cynthia M. Kafka, and Joel P. Cooper 22 Nov. 1993 11 p
(Contract N00014-89-J-3062)
(AD-A273306; TR-14) Avail: CASI HC A03/MF A01

Treatment of hydrated RhCl3 and Cu(NO3)2 in THF and H2O with triethoxysilane affords a highly chemo- and stereoselective catalyst system for the reduction of alkynes to Z-alkenes while alkyl-NO2, aryl-NO2, N-carbobenzyloxy, hydroxy, ester, enoate, benzyloxy, alkyl bromide, aryl bromide, and enone moieties remain unaffected. DTIC

N94-25159# Florida Univ., Gainesville. Dept. of Chemistry.
SURFACE-INDUCED STATIC UNDULATIONS IN MULTILAYER FILMS OF LIQUID-CRYSTALLINE POLYMERS
R. E. Geer, R. Shashidar, A. F. Thibodeaux, and R. S. Duran 20 Oct. 1993 27 p
(Contract N00014-91-J-1655)
(AD-A273517; TR-10) Avail: CASI HC A03/MF A01

The first detailed study of surface-induced undulations in a liquid-crystalline polymer is presented. By examining the non-specular diffuse scattering from a 30-layer film of ferroelectric liquid-crystal polymer, it is shown that the layer fluctuations are induced by the roughness of the film/substrate interface. This is in contrast to the case of free-standing films wherein thermal fluctuations play the major role. DTIC

N94-25222# Technische Univ., Eindhoven (Netherlands). Solid State Div.
THE NANOSTRUCTURE OF MULTILAYERED FILMS: A NMR STUDY Ph.D. Thesis
Honore Alphonsus Mar deGronckel 1993 131 p Sponsored in part by EEC
(ETN-94-95347) Avail: CASI HC A07/MF A02

Experimental results on the possibilities of Nuclear Magnetic Resonance (NMR) for the structural characterization of multilayered films are presented. The origin of the magnetic field at the nucleus (the magnetic hyperfine field) and its dependence on the structural parameters are discussed. The set up and the phenomena governing signal intensity are described. The experimental results and the application of NMR to the study of crystallographic structure, strain and interface roughness, and topology in Co based multilayers are presented. NMR is not only sensitive to static properties through the positions, splittings, widths of the NMR spectra, but also to the dynamic properties of the electron spin system through the nuclear spin-lattice relaxation time. In principle, by combination of a static and dynamic NMR study, this offers the opportunity to study locally the electronic structure within the multilayer. ESA

N94-25225# Technische Univ., Eindhoven (Netherlands).
MICROSTRUCTURE OF STYRENE METHYL METHACRYLATE COPOLYMERS GRAFTED ONTO POLYBUTADIENE SEEDS Ph.D. Thesis
Anna Maria Aerdts 1993 175 p Sponsored by General Electric Plastics
(ETN-94-95360) Avail: CASI HC A08/MF A02

An investigation aimed at a better understanding of the emulsion copolymerization of styrene and methyl methacrylate onto polybutadiene seed particles is described. Major relevant aspects of emulsion graft copolymerization are discussed. The determination of the intramolecular microstructure by proton Nuclear Magnetic Resonance (NMR) is described. The new peak assignment of the methoxy protons of styrene methyl methacrylate copolymers developed is confirmed by two dimensional NOESY (Nuclear Overhauser Effect Spectroscopy) NMR measurements. Due to the limited application of proton NMR to determine the intramolecular microstructure of styrene methyl methacrylate copolymers, the assignments of the carbon-13 NMR spectra are discussed. The free radical copolymerization models are critically examined and verified by measuring triad sequences by carbon-13 NMR. Experimental results and theoretical verification of the monomer partitioning experiments are discussed. The composition drift of grafted and free copolymer is studied in batch polymerizations. The copolymer composition, copolymer compositional distribution, the molecular weight, the degree of grafting, and grafting efficiency are obtained. The batch and semicontinuous graft polymerizations are investigated. The results comprise crucial information in terms of the degree of grafting, copolymer composition and compositional distribution and morphology, as a function of variation in the process conditions. ESA

N94-25230# Universiteit Twente, Enschede (Netherlands). Dept. of Mechanical Engineering.
LUBRICATION IN COLD ROLLING: NUMERICAL SIMULATION USING MULTIGRID TECHNIQUES Ph.D. Thesis
Pieter Martin Lugt 1992 194 p Sponsored by Aluminum Co. of America, PA, and Hoogovens, Ijmuiden, Netherlands
(ISBN-9-09-005313-1; ETN-94-95376) Copyright Avail: CASI HC A09/MF A03

A physical-mathematical model for predicting the quantity of lubricant between the rod and the strip is presented. The hydrodynamic approach is adopted. The running surfaces are assumed to be separated by a lubricant film and to deform elastically and/or plastically: the lubrication is called elasto-plasto-hydrodynamic. The elastic flattening of the rolls is described. Because of the complexity of the equations describing lubrication in cold rolling solution, several parameters can only be obtained if major simplifications are made. In order to avoid these simplifications a numerical approach is required. The equations are discretized on a grid covering the domain such that the solution of the resulting set of equations for all grid points approximates the solution of the continuous equation. The simulation model describing the smooth surface problem is presented. The numerical solution of the smooth surface problem is discussed. The equations are discretized and solved using these multigrid techniques. The results of the smooth surface problem are presented. Surface roughness effects are introduced. Two approaches are used: a simple friction multiplier, introduced to study the friction defect, and an empirical relation for the shear stresses on the surfaces. ESA

N94-25236# Technische Univ., Eindhoven (Netherlands). Polymer Chemistry Group.
PARTICLE NUCLEATION AND GROWTH IN BUTADIENE EMULSION POLYMERIZATION Ph.D. Thesis
Edwin Maria F. J. Verdurmen 1993 201 p Sponsored by DSM, Geleen, Netherlands
(ETN-94-95300) Avail: CASI HC A10/MF A03

Results of a kinetic and mechanistic investigation of the butadiene emulsion polymerization are presented. The following were considered in order to elucidate on the main drawback of this polymerization, its low rate of polymerization: the value of the propagation rate coefficient; reasons why the rate g polymerization per particle is virtually independent of the persulfate concentration; and the additional effects that would be caused by using Tertiary Dodecyl Mercaptan (TDM) as a chain transfer agent. In order to solve these problems, well defined seeded emulsion polymerizations were performed on monodisperse seed latexes prepared by emulsifier free emulsion polymerization. The process of emulsifier free emulsion polymerization is described. ESA

N94-25281# Technische Univ., Eindhoven (Netherlands). Solid State Chemistry and Materials Science Lab.

PREPARATION AND PROPERTIES OF TRANSLUCENT GAMMA-ALUMINIUM OXYNITRIDE Ph.D. Thesis

Henricus Xavier Willems 1992 191 p Sponsored by Philips Lighting B.V., Netherlands
(Grant IOP-TK-88A022)
(ETN-94-95305) Avail: CASI HC A09/MF A02

The preparation and properties of gamma aluminum oxynitride (also called gamma Alon), a ceramic material being investigated as a replacement to aluminum oxide, which has the disadvantage of being corroded by sodium vapor, are addressed. The thermodynamical stability of the Alon phase and the use of Ellingham and activity diagrams to get information on this kind of system are considered. The width of the Alon homogeneity region in the Al2O3AlN system is determined for various temperatures and the relation between the lattice parameter and the Alon composition is obtained. Also the phase diagram of the Al2O3AlNMgO system is determined to get some insight in the possibility of obtaining solid solutions with a spinel type crystal structure in this (quaternary) system. The crystal structure of the Alon phase and neutron diffraction experiments that were performed in order to get some insight into the occupation of the different lattice sites are described. Powder processing and sintering details for the production of translucent Alons, and the effect of sintering additives on the sintering process and the resulting microstructures are considered. The electron transport properties, mechanical properties and optical properties of Alon are presented. ESA

N94-25299 Technische Univ., Eindhoven (Netherlands).

EVALUATION OF MULTIAXIAL FRACTURE MODELS FOR TECHNICAL CERAMICS Ph.D. Thesis

Huibert Frank Scholten 1993 144 p Limited Reproducibility: More than 20% of this document may be affected by microfiche quality
(Grant IOP-TK-88B040)
(ISBN-9-03-860192-1; ETN-94-95362) Avail: CASI HC A07

The modeling of the strength of technical ceramics under various loading conditions is considered. The brittle fracture process which largely determines the applicability of this group of materials is described. From a single defect, the statistical behavior of the strength of brittle materials is derived. A number of theoretical strength models from literature are discussed, which consist of the weakest link concept in combination with a fracture criterion. By means of a proper fracture criterion, it should be possible to predict failure under multiaxial loading conditions. Technical ceramics contain a large variety of microstructure, and another objective was to examine whether there is a link between best applicable fracture criterion and the type of microstructure. ESA

N94-25404 Joint Inst. for Nuclear Research, Dubna (USSR). Lab. of Neutron Physics.

CRITICAL CURRENTS IN YBaCuO-CERAMICS

Yu. V. Obukhov 1991 11 p Limited Reproducibility: More than 20% of this document may be affected by microfiche quality
(DE93-617140; JINR-E-17-91-438) Avail: CASI HC A03 (US Sales Only)

The magnetization measurements on a ceramic YBaCuO sample were carried out. The M(H,T) dependence demonstrated some peculiarities which it was supposed to be connected with H(sub j1), H(sub j2), and H(sub c1) fields. By analyzing the magnetization in the field region between H(sub j1) and H(sub j2) within the frame of the critical state model one can find the dependence of the intergranular critical current density on field and temperature. DOE

N94-25409# Colorado State Univ., Fort Collins. Dept. of Chemistry.

TEMPLATE SYNTHESIS OF ELECTRONICALLY CONDUCTIVE POLYMERS

C. R. Martin, R. Parthasarathy, and V. Menon 1 Dec. 1993 17 p
(Contract N00014-82-K-0612)
(AD-A273673) Avail: CASI HC A03/MF A01

A method for synthesizing micro and nanoscopic fibers and tubules of electronically conductive polymers was developed. This method entails synthesis of the polymer within the pores of a microporous host membrane. Conductivities in the narrowest of these template-synthesized tubules and fibers can be significantly higher than in conventional forms (e.g. powders or thin films) of the analogous polymer. These previous conductivity data were based on a 2-point measurement of the resistance of the host membrane after synthesis of the conductive polymer fibers within this membrane. Results of conductivity measurements on thin films composed of the template-synthesized tubules and fibers are shown. A 4-point conductivity measurement was used on these thin films. These 4-point measurements corroborate the earlier 2-point conductivity data and, again, show that the template-synthesized materials are significantly more conductive. DTIC

N94-25410# Army Research Lab., Watertown, MA. Materials Directorate.

A PRELIMINARY EVALUATION OF THE PHOSPHAZENE RESIN PPZ Final Report

Adam J. Jaglowski, Karin M. Gabriel, and Marc S. Pepi Oct. 1993 24 p
(AD-A273674; ARL-TR-223) Avail: CASI HC A03/MF A01

A phosphazene material, PPZTM, is reported by Idemitsu Petrochemical Company (Tokyo, Japan) to have excellent chemical and abrasion resistance properties for hardcoating applications. An evaluation of the chemical resistance of this coating is presented. PPZ coated on poly(ethylene terephthalate) (PET) films were challenged with simulants (2-chloroethyl ethyl sulfide (CEES), 2-chloroethyl methyl sulfide (CEMS), diisopropyl methyphosphonate (DIMP)) and a decontaminant (DS-2) via a droplet test method. Preliminary results showed that the PPZ coating was affected by DIMP, CEES, and CEMS as observed by optical and scanning electron microscopy (SEM). Upon visual examination, the DS-2 treated specimen did show an effect; however, the coating's behavior to this corrosion liquid is inconclusive. In addition, PPZ(TM) resin was coated on polycarbon (PC) using a modified ASTM D823-87 method and cured by ultraviolet light. Curing time was determined by Fourier transform infrared spectroscopy (FTIR) using an attenuated total reflectance (ATR) technique. The Taber abrasion resistance of the PPZ-coated PC specimens were slightly lower than reported values. DTIC

N94-25413# Massachusetts Inst. of Tech., Cambridge. Dept. of Chemical Engineering.

MORPHOLOGY OF HIGHLY TEXTURED POLYETHYLENE/POLYETHYLENE- PROPYLENE SEMICRYSTALLINE DIBLOCK COPOLYMERS

P. Kofinas and R. E. Cohen 3 Dec. 1993 41 p
(Contract N00014-91-J-1045)
(AD-A273683; TR-11) Avail: CASI HC A03/MF A01

A series of semicrystalline diblock copolymers of poly(ethylene)/poly(ethylenepropylene) (E/EP) were subjected to high levels of plane strain compression using a channel die. Deformations were imposed both below and above the melting point of the E block. The crystallographic and morphological textures were examined using wide-angle x ray diffraction pole figure analysis and two dimensional small-angle x ray scattering. The lattice unit cell orientation of the crystallized E chains with respect to the lamellar superstructure was determined, as well as the lamellar orientation relative to the specimen boundaries. When the diblocks are textured above the E block melting point at various compression ratios, the lamellae orient perpendicular to the plane of shear, while texturing below T, causes the lamellae to orient parallel to the plane of shear. The orientation of the crystallized E chains was perpendicular to the lamellar normal, irrespective of the texturing temperature. DTIC

N94-25489# Ohio Univ., Athens. Dept. of Physics and Astronomy.

THE IN SITU OBSERVATION OF EPITAXIAL DIAMOND THIN FILM NUCLEATION AND GROWTH USING EMISSION ELECTRON MICROSCOPY Semiannual Report, 1 Jan. - 31 Jun. 1993

Martin E. Kordesch Dec. 1993 40 p
(Contract N00014-91-J-1596)
(AD-A273698) Avail: CASI HC A03/MF A01

In situ observation of CVD diamond dissolution and etching using photoemission electron microscopy (PEEM) suggests that nucleation of diamond occurs directly on molybdenum, with a Mo-carbide bulk diffusion barrier that facilitates surface carbon transport for growth. Low energy electron microscopy of doped homoepitaxial C(100) is hindered by surface roughness, which is visible in PEEM. Charging observed with type IIa diamond is no longer present, but the high secondary electron yield is still problematic for direct imaging. TEM studies of CVD diamond grown directly on Mo TEM grids show a 10 nm thick amorphous C layer after growth, which is easily removable with an isopropanol rinse. LEED studies of Si(310) substrates for diamond growth show a (2X1) Si(310) reconstructed surface, with some faceting with fourfold symmetry. Nucleation is sparse and random on the Si(310) surfaces examined to date. DTIC

N94-23243*# Puerto Rico Univ., Mayaguez. Dept. of Chemical Engineering.
FTIR QUANTIFICATION OF INDUSTRIAL HYDRAULIC FLUIDS IN PERCHLOROETHYLENE
Narinder K. Mehta *In* NASA. Kennedy Space Center, NASA/ASEE Summer Faculty Fellowship Program Oct. 1993 p 327-373 (For primary document see N94-23230 06-80)
Avail: CASI HC A03/MF A04

N94-24010# Centre National d'Etudes Spatiales, Toulouse (France).
TRIBOLOGICAL CHARACTERIZATION OF SPATIAL WET LUBRICANTS UNDER VACUUM
J. Sicre, Y. Berthier (Institut National des Sciences Appliquees, Lyon, France.), L. Flamand (Institut National des Sciences Appliquees, Lyon, France.), P. Reynaud (Institut National des Sciences Appliquees, Lyon, France.), P. Vergne (Institut National des Sciences Appliquees, Lyon, France.), and M. Godet (Institut National des Sciences Appliquees, Lyon, France.) *In* ESA, The Fifth European Space Mechanisms and Tribology Symposium Apr. 1993 7 p (For primary document see N94-23985 06-37)
Copyright Avail: CASI HC A02/MF A04

N94-24339*# Minnesota Mining and Mfg. Co., Saint Paul. Science Research Lab.
ORDERED ORGANIC THIN FILMS SELF-ASSEMBLED FROM THE VAPOR PHASE
M. K. Debe *In* NASA. Marshall Space Flight Center, Microgravity Studies of Organic and Polymeric Materials Dec. 1993 p 11-15 (For primary document see N94-24338 06-23)
Avail: CASI HC A01/MF A03

N94-24341*# Rensselaer Polytechnic Inst., Troy, NY. Dept. of Chemistry.
ELECTRIC FIELD-MEDIATED PROCESSING OF POLYMER BLEND SOLUTIONS
G. E. Wnek and S. Krause *In* NASA. Marshall Space Flight Center, Microgravity Studies of Organic and Polymeric Materials Dec. 1993 p 21-23 (For primary document see N94-24338 06-23)
Avail: CASI HC A01/MF A03

N94-24342*# Michigan Univ., Ann Arbor. Materials Science and Engineering.
DEFECTS IN ELECTRO-OPTICALLY ACTIVE POLYMER SOLIDS
David C. Martin *In* NASA. Marshall Space Flight Center, Microgravity Studies of Organic and Polymeric Materials Dec. 1993 p 25-43 (For primary document see N94-24338 06-23)
Avail: CASI HC A03/MF A03

N94-24350*# Lehigh Univ., Bethlehem, PA. Emulsion Polymers Inst. and Dept. of Chemistry.
FEASIBILITY STUDY: MONODISPERSE POLYMER PARTICLES CONTAINING LASER-EXCITABLE DYES
John W. Vanderhoff and Jing-Hong Chen *In* NASA. Marshall Space Flight Center, Microgravity Studies of Organic and Polymeric Materials Dec. 1993 p 69-88 (For primary document see N94-24338 06-23)
Avail: CASI HC A03/MF A03

N94-24351*# Massachusetts Inst. of Tech., Cambridge. Dept. of Materials Science and Engineering.
PROCESSING OF SEMICRYSTALLINE POLYMERS
Peggy Cebe and Mark V. Brillhart *In* NASA. Marshall Space Flight Center, Microgravity Studies of Organic and Polymeric Materials Dec. 1993 p 89-91 (For primary document see N94-24338 06-23)
Avail: CASI HC A01/MF A03

N94-24352*# University of Southern Mississippi, Hattiesburg. Dept. of Chemistry and Biochemistry.
CONVECTIVE INSTABILITIES IN TRAVELING FRONTS OF ADDITION POLYMERIZATION
John A. Pojman, Chris E. Jones, and Akhtar M. Khan *In* NASA. Marshall Space Flight Center, Microgravity Studies of Organic and Polymeric Materials Dec. 1993 p 93-97 (For primary document see N94-24338 06-23)
Avail: CASI HC A01/MF A03

N94-24353*# Tennessee Univ., Knoxville. Dept. of Chemistry.
POLYMER MORPHOLOGH
Bernhard Wunderlich *In* NASA. Marshall Space Flight Center, Microgravity Studies of Organic and Polymeric Materials Dec. 1993 p 99-104 (For primary document see N94-24338 06-23)
Avail: CASI HC A02/MF A03

N94-24412*# Marquette Univ., Milwaukee, WI. Dept. of Mechanical and Industrial Engineering.
CHARACTERISTICS OF PRODUCTS GENERATED BY SELECTIVE SINTERING AND STEREOLITHOGRAPHY RAPID PROTOTYPING PROCESSES
Vikram Cariapa *In* Alabama Univ., The 1993 NASA/ASEE Summer Faculty Fellowship Program Nov. 1993 5 p (For primary document see N94-24405 06-80)
Avail: CASI HC A01/MF A03

28 PROPELLANTS AND FUELS

Includes rocket propellants, igniters, and oxidizers; their storage and handling procedures; and aircraft fuels.

For related information see also *07 Aircraft Propulsion and Power, 20 Spacecraft Propulsion and Power,* and *44 Energy Production and Conversion.*

N94-22878# Department of Energy, Washington, DC. Office of Transportation Technologies.
FEDERAL ALTERNATIVE FUEL PROGRAM LIGHT DUTY VEHICLE OPERATIONS
Jul. 1993 56 p
(DE93-040663; DOE/EE-0004) Avail: CASI HC A04/MF A01

This annual report to Congress details the second year of the Federal light duty vehicle operations as required by Section 400AA(b)(1)(B) of the Energy Policy and Conservation Act as amended by the Alternative Motor Fuels Act of 1988, Public Law 100-494. In 1992, the Federal alternative fuel vehicle fleet expanded significantly, from the 65 M85 (85 percent methanol and 15 percent unleaded gasoline) vehicles acquired in 1991 to an anticipated total of 3,267 light duty vehicles. Operating data are being collected from slightly over 20 percent, or 666, of these vehicles. The 601 additional vehicles that were added to the data collection program in 1992 include 75 compressed natural gas Dodge full-size (8-passenger) vans, 25 E85 (85 percent denatured ethanol and 15 percent unleaded gasoline) Chevrolet Lumina sedans, 250 M85 Dodge Spirit sedans (planned to begin operation in fiscal year 1993), and 251 compressed natural gas Chevrolet C-20 pickup trucks. The locations where the Federal light duty alternative fuel vehicles that are participating in the data collection program are operating are illustrated. The primary criteria for placement of vehicles will continue to include air quality attainment status and the availability of an alternative fuel infrastructure to support the vehicles. The second year of the Federal light duty vehicle operations, from October 1991 through September 1992, is detailed. DOE

N94-23027# New Energy and Industrial Technology Development Organization, Tokyo (Japan).
PRELIMINARY STUDY CONCERNING DEVELOPMENT OF PETROLEUM-SUBSTITUTION ENERGY INTEGRATION TECHNOLOGY
Mar. 1993 172 p In JAPANESE
(DE94-714902; NEDO-P-9219) Avail: CASI HC A08/MF A02

With an objective to achieve compatibility among petroleum-substitution energy supply stability, energy efficiency, and energy demand, the energy utilization combining the conventional energy technologies is discussed.

First, the currently available individual technologies related to energy supply were sorted out focusing on substitution energies, and then the energy demand characteristics by fields were identified for the combined utilization. Using the results, evaluations were given on all of the combinations of individual technologies using as parameters the demand characteristics, environment preserving effect, novelty, and supply stability. Parallel use with conventional technologies was represented by hybrid use of photovoltaic power generation with solar heat collectors, paralleling heat supply using wind power with biomass utilization, and photovoltaic power generation with fuel cells. Selected series use with conventional technologies include a Stirling engine using heat collected by solar heat collectors, coal liquefaction and gasification using underground heat, a heat pump driven by solar energy generated power, regional heat supply using underground heat, and biomass fuel cells. Followability to regional demand characteristics and demand variation is important. DOE

N94-23436# Lawrence Livermore National Lab., CA.
THE IGNITION TEMPERATURE OF SOLID EXPLOSIVES EXPOSED TO A FIRE
J. R. Creighton Sep. 1993 8 p Presented at the PSAM Conference, San Diego, CA, 20-24 Mar. 1993
(Contract W-7405-eng-48)
(DE94-001047; UCRL-JC-114201; CONF-9303221-2) Avail: CASI HC A02/MF A01

When a system containing solid explosives is engulfed in a fire it receives a heat flux that causes the temperature of the system to rise monotonically. The temperature rise can often be approximated by a linear rise for extended periods of time. When some portion of the explosive, usually near the surface, reaches its ignition temperature, it will begin to burn. If the explosive is unconfined, or can breach its confinement at low pressure, it will burn, not explode. Typically the burn front will propagate through a slab or shell at speeds on the order of a centimeter a minute. If the explosive is confined, the gas resulting from its burning will generate pressures high enough to rupture the confinement, but the peak pressure will generally be only a fraction of the pressure from a true detonation. When a system is not engulfed in the fire, but is close enough to be heated slowly by the fire, the behavior will be different. If the explosive is heated slowly it will have a nearly uniform temperature and ignition will occur inside the explosive. This almost always causes an explosion, even when the explosive as a whole is unconfined. The reason for this behavior is not well understood but slow heating of an explosive generally results in a more violent explosion than fast heating. These two situations are recognized by fast and slow cookoff tests used with munitions. Many munitions pass the fast cookoff test with heating rates around 2 K/min. Slow cookoff tests with heating rates around 4 K/hr generally result in an explosion. (The equations in this paper assume absolute temperatures in Kelvins, equal to Celsius + 273.16.) Mathematical models predicting the time to explosion are usually based on the assumption that the explosive has a uniform initial temperature and that the outer surface is suddenly raised to some temperature and held there. The earliest such models where those of Semenov and Frank-Kamenetskii. DOE

N94-23778# Lawrence Livermore National Lab., CA.
ENERGY TRANSFER IN SOLID EXPLOSIVES
C. M. Tarver, L. E. Fried, A. J. Ruggiero, and D. F. Calef Jul. 1993 9 p Presented at the 10th Detonation Symposium, Boston, MA, 12-16 Jul. 1993
(Contract W-7405-eng-48)
(DE94-001523; UCRL-JC-111343; CONF-930713-32) Avail: CASI HC A02/MF A01

The nonequilibrium Zeldovich-von Neumann-Doring theory of detonation in solid explosives is extended to include recent nanosecond and picosecond experimental and theoretical results on each of the four main regions of the reaction zone. The first region is the three-dimensional, Mach stem dominated leading shock front which excites the phonon modes of the explosive molecules in less than a picosecond. The second region is the multiphonon up-pumping process in which the excited phonons anharmonically couple to the low frequency (doorway) vibrational modes which in turn equilibrate with the higher frequency modes by internal vibrational redistribution. This process may require on the order of tens of picoseconds. The third region is the chemical reconstitution region in which the vibrationally equilibrated transition state decomposes in a series of chain reaction steps into vibrationally excited diatomic and triatomic molecules in approximately one nanosecond. The fourth region is dominated by vibrational deexcitation and solid species formation as chemical and thermal equilibrium is approached. This is the region measured by current nanosecond resolution techniques and can last from nanoseconds to microseconds depending on the oxygen balance of the solid explosive. DOE

N94-23807 Lawrence Livermore National Lab., CA.
MULTIPLE SHOCK INITIATION OF LX-17
C. M. Tarver, T. M. Cook, P. A. Urtiew, and W. C. Tao Jul. 1993 10 p Presented at the 10th Detonation Symposium, Boston, MA, 12-16 Jul. 1993 Limited Reproducibility: More than 20% of this document may be affected by poor print
(Contract W-7405-eng-48)
(DE94-001524; UCRL-JC-111342; CONF-930713-30) Avail: Issuing Activity (Department of Energy (DOE))

The response of the insensitive TATB-based high explosive LX-17 to multiple shock impacts is studied experimentally in a four inch gas gun using embedded manganin gauges and numerically using the ignition and growth reactive flow model of shock initiation and detonation. Pressure histories are reported for LX-17 cylinders which are subjected to sustained shock pulses followed by secondary compressions from shocks reflected from metal discs attached to the backs of the explosive targets. These measured and calculated pressure histories show that the threshold for hot spot growth in LX-17 is 7 GPa, that LX-17 can be dead pressed at slightly lower pressures, and that the reaction rates behind reflected shocks increase greatly as the impedance of the metal increases. A study of the response of LX-17 to the collision of two reacting, diverging shocks forming a Mach stem wave inside the LX-17 charge demonstrated that this interaction can result in a high pressure region of sufficient size and strength to cause detonation under certain conditions. DOE

N94-24301*# National Aeronautics and Space Administration. Lewis Research Center, Cleveland, OH.
DISCRETE SENSITIVITY DERIVATIVES OF THE NAVIER-STOKES EQUATIONS WITH A PARALLEL KRYLOV SOLVER
Kumud Ajmani and Arthur C. Taylor, III (Old Dominion Univ., Norfolk, VA.) Jan. 1994 13 p Presented at the 32nd Aerospace Sciences Meeting and Exhibit, Reno, NV, 10-13 Jan. 1994; sponsored by AIAA
(Contract NCC3-233; RTOP 505-90-5K)
(NASA-TM-106481; ICOMP-94-2; E-8411; NAS 1.15:106481; AIAA Paper 94-0091) Avail: CASI HC A03/MF A01

This paper solves an 'incremental' form of the sensitivity equations derived by differentiating the discretized thin-layer Navier Stokes equations with respect to certain design variables of interest. The equations are solved with a parallel, preconditioned Generalized Minimal RESidual (GMRES) solver on a distributed-memory architecture. The 'serial' sensitivity analysis code is parallelized by using the Single Program Multiple Data (SPMD) programming model, domain decomposition techniques, and message-passing tools. Sensitivity derivatives are computed for low and high Reynolds number flows over a NACA 1406 airfoil on a 32-processor Intel Hypercube, and found to be identical to those computed on a single-processor Cray Y-MP. It is estimated that the parallel sensitivity analysis code has to be run on 40-50 processors of the Intel Hypercube in order to match the single-processor processing time of a Cray Y-MP. Author (revised)

N94-24578*# Arizona Univ., Tucson. Dept. of Aerospace and Mechanical Engineering.
SOLID ROCKET COMBUSTION SIMULATOR TECHNOLOGY USING THE HYBRID ROCKET FOR SIMULATION Final Report, 16 Jul. 1991 - 23 Jul. 1993
Kumar Ramohalli 22 Feb. 1994 56 p
(Grant NAG8-883)
(NASA-CR-195142; NAS 1.26:195142) Avail: CASI HC A04/MF A01

The hybrid rocket is reexamined in light of several important unanswered questions regarding its performance. The well-known heat transfer limited burning rate equation is quoted, and its limitations are pointed out. Several inconsistencies in the burning rate determination through fuel depolymerization are explicitly discussed. The resolution appears to be through the postulate of (surface) oxidative degradation of the fuel.

Experiments are initiated to study the fuel degradation in mixtures of nitrogen/oxygen in the 99.9 percent/0.1 percent to 98 percent/2 percent range. The overall hybrid combustion behavior is studied in a 2 in-diameter rocket motor, where a PMMA tube is used as the fuel. The results include detailed, real-time infrared video images of the combustion zone. Space- and time-averaged images give a broad indication of the temperature reached in the gases. A brief outline is shown of future work, which will specifically concentrate on the exploration of the role of the oxidizer transport to the fuel surface, and the role of the unburned fuel that is reported to escape below the classical time-averaged boundary layer flame. Author (revised)

N94-24618*# Cincinnati Univ., OH. Space Engineering Research Center.
DESIGN OF A LUNAR PROPELLANT PROCESSING FACILITY. NASA/USRA ADVANCED PROGRAM
Rajesh Batra, Jason Bell, J. Matt Campbell, Tom Cash, John Collins, Brian Dailey, Angelique France, Will Gareau, Mark Gleckler, and Charles Hamilton et al 28 Jul. 1993 312 p
(Contract NASw-4435)
(NASA-CR-195502; NAS 1.26:195502) Avail: CASI HC A14/MF A03

Mankind's exploration of space will eventually lead to the establishment of a permanent human presence on the Moon. Essential to the economic viability of such an undertaking will be prudent utilization of indigenous lunar resources. The design of a lunar propellant processing system is presented. The system elements include facilities for ore processing, ice transportation, water splitting, propellant storage, personnel and materials transportation, human habitation, power generation, and communications. The design scenario postulates that ice is present in the lunar polar regions, and that an initial lunar outpost was established. Mining, ore processing, and water transportation operations are located in the polar regions. Water processing and propellant storage facilities are positioned near the equator. A general description of design operations is outlined below. Regolith containing the ice is mined from permanently-shaded polar craters. Water is separated from the ore using a microwave processing technique, and refrozen into projectiles for launch to the equatorial site via railgun. A mass-catching device retrieves the ice. This ice is processed using fractional distillation to remove impurities, and the purified liquid water is fed to an electrolytic cell that splits the water into vaporous hydrogen and oxygen. The hydrogen and oxygen are condensed and stored separately in a tank farm. Electric power for all operations is supplied by SP-100 nuclear reactors. Transportation of materials and personnel is accomplished primarily using chemical rockets. Modular living habitats are used which provide flexibility for the placement and number of personnel. A communications system consisting of lunar surface terminals, a lunar relay satellite, and terrestrial surface stations provides capabilities for continuous Moon-Moon and Moon-Earth transmissions of voice, picture, and data. Author (revised)

N94-24700*# Pennsylvania State Univ., University Park. Dept. of Mechanical Engineering.
IGNITION AND COMBUSTION CHARACTERISTICS OF METALLIZED PROPELLANTS, PHASE 2 Annual Report, Jan. - Dec. 1993
D. C. Mueller and S. R. Turns Jan. 1994 27 p
(Grant NAG3-1044)
(NASA-CR-195107; NAS 1.26:195107) Avail: CASI HC A03/MF A01

Experimental and analytical investigations focusing on aluminum/hydrocarbon gel droplet secondary atomization and its effects on gel-fueled rocket engine performance are being conducted. A single laser sheet sizing/velocimetry diagnostic technique, which should eliminate sizing bias in the data collection process, has been designed and constructed to overcome limitations of the two-color forward-scatter technique used in previous work. Calibration of this system is in progress and the data acquisition/validation code is being written. Narrow-band measurements of radiant emission, discussed in previous reports, will be used to determine if aluminum ignition has occurred in a gel droplet. A one-dimensional model of a gel-fueled rocket combustion chamber, described in earlier reports, has been exercised in conjunction with a two-dimensional, two-phase nozzle code to predict the performance of an aluminum/hydrocarbon fueled engine. Estimated secondary atomization effects on propellant burnout distance, condensed particle radiation losses to the chamber walls, and nozzle two phase flow losses are also investigated. Calculations indicate that only modest secondary atomization is required to significantly reduce propellant burnout distances, aluminum oxide residual size, and radiation heat losses. Radiation losses equal to approximately 2-13 percent of the energy released during combustion were estimated, depending on secondary atomization intensity. A two-dimensional, two-phase nozzle code was employed to estimate radiation and nozzle two phase flow effects on overall engine performance. Radiation losses yielded a one percent decrease in engine Isp. Results also indicate that secondary atomization may have less effect on two-phase losses than it does on propellant burnout distance and no effect if oxide particle coagulation and shear induced droplet breakup govern oxide particle size. Engine Isp was found to decrease from 337.4 to 293.7 seconds as gel aluminum mass loading was varied from 0-70 wt percent. Engine Isp efficiencies, accounting for radiation and two phase flow effects, on the order of 0.946 were calculated for a 60 wt percent gel, assuming a fragmentation ratio of five. Author (revised)

N94-24728# Defence Research Establishment Atlantic, Dartmouth (Nova Scotia).
ISOTHIAZOLONE VOLATILITY STUDY OF A WATER BOTTOM FROM FUEL TREATED WITH KATHON (TM) FP1.5 BIOCIDE
R. D. Haggett and Richard M. Morchat Nov. 1993 23 p
(AD-A273165; DREA-TM-93/216) Avail: CASI HC A03/MF A01

An analytical method based on the gas chromatographic / mass spectrometry separation and detection of the two isothiazolones (5-chloro-2-methyl- 4-isothiazolin- 3-one and 2-methyl- 4-isothiazolin- 3-one), the active ingredients in one commercially available biocide used to treat fuel systems contaminated with microbiological growth, is described. A modification of this method, to allow static headspace detection of these isothiazolones, is also described. Results of experiments using the modified technique demonstrated that these two compounds do not volatilize from a sea water solution at temperatures up to 70 C. This suggests that un-depleted isothiazolone in the water bottom of fuel tanks treated with Kathon FP1.5 biocide would not volatilize into the habitable air space above the bilge to generate toxic components that could then be inhaled by the personnel working in the immediate vicinity. DTIC

N94-23657*# New Orleans Univ., LA. Dept. of Mechanical Engineering.
EXPERIMENTAL AND ANALYTICAL STUDY OF CRYOGENIC PROPELLANT BOILOFF TO DEVELOP AND VERIFY ALTERNATE PRESSURIZATION CONCEPTS FOR SPACE SHUTTLE EXTERNAL TANK USING A SCALED DOWN TANK
K. M. Akyuzlu, S. Jones (Martin Marietta Corp., New Orleans, LA.), and T. Meredith (Martin Marietta Corp., New Orleans, LA.) *In* NASA. Lewis Research Center, The Fifth Annual Thermal and Fluids Analysis Workshop Nov. 1993 p 343-358 Sponsored in part by Martin Marietta Corp. (For primary document see N94-23634 06-34)
Avail: CASI HC A03/MF A04; 5 functional color pages

N94-24252 Soreq Research Establishment, Israel Atomic Energy Commission, Yavneh.
BURNING RATE OF DOUBLE-BASE PROPELLANT IN THE PRESENCE OF PLASMA
S. Rozen, D. Saphier, and E. Sher (Ben Gurion Univ. of the Negev, Beersheva, Israel.) *In* Israel Society of Aeronautics and Astronautics, The 33rd Israel Annual Conference on Aviation and Astronautics 25 Feb. 1993 p 154-158 (For primary document see N94-24241 06-01)
Copyright Avail: Issuing Activity (Israel Society of Aeronautics and Astronautics, c/o Faculty of Engineering, Tel-Aviv Univ., Ramat Aviv 69978, Israel)

29 MATERIALS PROCESSING

Includes space-based development of products and processes for commercial applications.

For biological materials see *55 Space Biology.*

N94-23195# Universitaet der Bundeswehr Muenchen, Neubiberg (Germany). Inst. fuer Luft- und Raumfahrttechnik.
RESPONSE OF AN ANCHORED ANNULAR CYLINDRICAL LIQUID LAYER TO VARIOUS AXIAL EXCITATIONS IN ZERO-GRAVITY
Helmut F. Bauer 1992 22 p
(LRT-WE-9-FB-3-1992; ETN-94-95088) Avail: CASI HC A03/MF A01

An annular liquid layer is subjected in a zero gravity environment to different harmonic axial excitations. The liquid is treated as frictionless and is held together by free surface tension, which acts as the restoring force. The layer is placed between two parallel and concentric discs, at which rim it is, due to surface tension, anchored. The response of the system was determined for the free surface elevation and the velocity distribution. It was found, that the first resonance response is sharply tuned and could easily be missed in a sweeping experiment. The resonance peaks are at larger frequencies in comparison with those of an annular layer with freely slipping edges. ESA

N94-23287*# Universities Space Research Association, Huntsville, AL.
MICROGRAVITY SCIENCES APPLICATION VISITING SCIENTIST PROGRAM Quarterly Progress Report No. 8, 1 Oct. - 31 Dec. 1993
10 Jan. 1994 30 p
(Contract NAS8-38785)
(NASA-CR-194804; NAS 1.26:194804) Avail: CASI HC A03/MF A01

Contract NAS8-38785, Microgravity Experimental and Theoretical Research, is a project involving a large number of individual research programs related to: determination of the structure of human serum albumin and other biomedically important proteins; analysis of thermodynamic properties of various proteins and models of protein nucleation; development of experimental techniques for the growth of protein crystals in space; study of the physics of electrical double layers in the mechanics of liquid interfaces; computational analysis of vapor crystal growth processes in microgravity; analysis of the influence of magnetic fields in damping residual flows in directional solidification processes; crystal growth and characterization of II-VI semiconductor alloys; and production of thin films for nonlinear optics. It is not intended that the programs will be necessarily limited to this set at any one time. The visiting scientists accomplishing these programs shall serve on-site at MSFC to take advantage of existing laboratory facilities and the daily opportunities for technical communications with various senior scientists. Author

N94-23549*# Viable Systems, Inc., Medfield, MA.
THE STUDY OF DOPANT SEGREGATION BEHAVIOR DURING THE GROWTH OF GaAs IN MICROGRAVITY Final Report, 25 Jun. 1990 - 30 Sep. 1993
James A. Kafalas 29 Nov. 1993 3 p
(Contract NAS8-37858)
(NASA-CR-193905; NAS 1.26:193905) Avail: CASI HC A01/MF A01

A crystal growth experiment to be performed on USML-1 is presented. The objective is to determine the effect of microgravity growth on dopant segregation. Derived from text

N94-23594*# Houston Univ., TX. Dept. of Mechanical Engineering.
STUDIES OF TWO PHASE FLOW Final Report, Sep. 1991 - Nov. 1993
Larry C. Witte Feb. 1994 4 p
(Grant NAG9-546)
(NASA-CR-195099; NAS 1.26:195099; UH-BUDGET-1-5-54282) Avail: CASI HC A01/MF A01

The development of instrumentation for the support of research in two-phase flow in simulated microgravity conditions was performed. The funds were expended in the development of a technique for characterizing the motion and size distribution of small liquid droplets dispersed in a flowing gas. Phenomena like this occur in both microgravity and normal earth gravity situations inside of conduits that are carrying liquid-vapor mixtures at high flow rates. Some effort to develop a conductance probe for the measurement of liquid film thickness was also expended. Author (revised)

N94-25060# Technische Univ., Eindhoven (Netherlands).
THE INFLUENCE OF FLOW TYPE, PARTICLE TYPE AND GRAVITY ON ORTHOKINETIC COAGULATION Ph.D. Thesis
Lambertus Leonardus Krutzer 1993 111 p
(ETN-94-95333) Avail: CASI HC A06/MF A02

A study to obtain insight into some parameters determining the coagulation process is reported: the influence of the type of flow (laminar or turbulent), the influence of the kind of particles (size, density, and initial size distribution) and the influence of gravity are investigated. Theories describing the different forms of coagulation and the equations describing the interaction forces between the particles are summarized. Some methods to measure aggregation are described. The influence of the flow type on the coagulation rate of a polystyrene latex was studied. Experiments were performed in a Couette device, in laminar pipe flow and in an isotropic turbulent flow field. By studying the coagulation behavior of polystyrene, glass, quartz particles and silicaspheres, some insight into the influence of the initial size distribution, the influence of a density difference between the disperse and continuous phases, and the influence of the particle shape on the coagulation rate was obtained. Because coagulation experiments of particles having a density difference with the continuous phase cannot be performed at low shear rates, some microgravity coagulation experiments were performed. In these experiments quartz particles were coagulated at low stirring speeds. ESA

N94-24340*# Auburn Univ., AL. Dept. of Mechanicial Engineering.
NUMERICAL MODELING OF PHYSICAL VAPOR TRANSPORT UNDER MICROGRAVITY CONDITIONS: EFFECT OF THERMAL CREEP AND STRESS
Daniel W. Mackowski and Roy W. Knight *In* NASA. Marshall Space Flight Center, Microgravity Studies of Organic and Polymeric Materials Dec. 1993 p 17-20 (For primary document see N94-24338 06-23)
Avail: CASI HC A01/MF A03

N94-24345*# National Aeronautics and Space Administration. Marshall Space Flight Center, Huntsville, AL.
MODELING OF PCG FLUID DYNAMICS: SALIENT RESULTS
N. Ramachandran *In its* Microgravity Studies of Organic and Polymeric Materials Dec. 1993 p 49-60 (For primary document see N94-24338 06-23)
Avail: CASI HC A03/MF A03

N94-24346*# National Aeronautics and Space Administration. Marshall Space Flight Center, Huntsville, AL.
LOW-GRAVITY ELECTRODEPOSITION AND GROWTH OF POLYMER THIN FILMS WITH LARGE THIRD-ORDER OPTICAL NONLINEARITIES BY ELECTROCHEMICAL PROCESSES FOR DEVICES: THIOPHENE-BASED POLYMERS Abstract Only
Benjamin G. Penn and Clyde Riley (Alabama Univ., Huntsville.) *In its* Microgravity Studies of Organic and Polymeric Materials Dec. 1993 p 61-62 (For primary document see N94-24338 06-23)
Avail: CASI HC A01/MF A03

N94-24451*# Alabama A & M Univ., Huntsville. Dept. of Physics.
EFFECTS OF THERMAL-SOLUTAL CONVECTION ON TEMPERATURE AND SOLUTAL FIELDS UNDER VARIOUS GRAVITATIONAL ORIENTATIONS
Jai-Ching Wang *In* Alabama Univ., The 1993 NASA/ASEE Summer Faculty Fellowship Program Nov. 1993 5 p (For primary document see N94-24405 06-80)
Avail: CASI HC A01/MF A03

31 ENGINEERING (GENERAL)

Includes vacuum technology; control engineering; display engineering; cryogenics; and fire prevention.

N94-22981# Technische Univ., Delft (Netherlands). Faculteit der Werktuigbouwkunde en Maritieme Techniek.
PLAN GENERATION FOR FLEXIBLE ASSEMBLY SYSTEMS Thesis
N. Boneschanscher 1993 224 p Sponsored by Organisatie voor Toegepast Natuurwetenschappelijk Onderzoek, The Hague, Netherlands
(PB93-217974; ISBN-90-370-0081-9) Copyright Avail: CASI HC A10/MF A03

The work described in the thesis primarily concerns the generation of plans for flexible assembly systems. Aspects of the work are technical feasibility of a plan, optimization of a plan, and the roles that time and uncertainty play during plan generation. It should be stressed that the work in the thesis applies to a class of flexible assembly systems, and that the functional concept of DIAC, as introduced above, is one of the flexible assembly systems that falls into this class. NTIS

N94-23000# Sandia National Labs., Albuquerque, NM.

DEVELOPMENT AND EXPERIMENTAL VALIDATION OF COMPUTATIONAL METHODS TO SIMULATE ABNORMAL THERMAL AND STRUCTURAL ENVIRONMENTS

J. L. Moya, R. D. Skocypec, and R. K. Thomas 1993 13 p Presented at the Surety Technology Symposium, Chelyacinsk, Russia, 28 Sep. - 2 Oct. 1993
(Contract DE-AC04-76DP-00789)
(DE94-000554; SAND-93-2215C; CONF-9309215-3) Avail: CASI HC A03/MF A01

Over the past 40 years, Sandia National Laboratories (SNL) has been actively engaged in research to improve the ability to accurately predict the response of engineered systems to abnormal thermal and structural environments. These engineered systems contain very hazardous materials. Assessing the degree of safety/risk afforded the public and environment by these engineered systems, therefore, is of upmost importance. The ability to accurately predict the response of these systems to accidents (to abnormal environments) is required to assess the degree of safety. Before the effect of the abnormal environment on these systems can be determined, it is necessary to ascertain the nature of the environment. Ascertaining the nature of the environment, in turn, requires the ability to physically characterize and numerically simulate the abnormal environment. Historically, SNL has demonstrated the level of safety provided by these engineered systems by either of two approaches: a purely regulatory approach, or by a probabilistic risk assessment (PRA). This paper will address the latter of the two approaches. DOE

N94-23174# Technische Univ., Eindhoven (Netherlands). Electrical Energy Systems Div.

FLUE GAS CLEANING BY PULSE CORONA STREAMER

Yan Keping (Beijing Inst. of Tech., China.) and E. M. vanVeldhuizen Mar. 1993 81 p Sponsored by Netherlands Organization for Scientific Research
(EUT-93-E-272; ISBN-9-06-144272-9; ETN-94-94779) Avail: CASI HC A05/MF A01

Currents of up to 600 A are obtained on a corona wire of 1 m length by applying DC and pulse voltage. The energy input is upto 6 J/pulse. The current duration is between 100 and 600 ns, and depends strongly on the DC voltage, the stray inductance and resistance of the circuit. Breakdown can be avoided by choosing the appropriate values for the components in the pulse circuit. Average electron energies resolved in space and in time are obtained by means of optical spectroscopy for corona discharge streamers in a wire cylinder reactor in air and in flue gas. The electron energy for primary streamers in air is found to be in the order of 10 eV and increases slightly with the pulse voltage and is almost constant during the streamer propagation. The electron energy for the secondary streamer is about a factor two lower near the anode where its optical emission is strong. In the gap and near the cathode, its emission is much less and the electron energy is another three times lower. The secondary streamer is limited in length, because it must satisfy the stability field requirement. The larger attachment coefficient of flue gas in the low field region explains that in flue gas the secondary streamer is shorter than in air. The ratio of the electrical energy input into primary and secondary streamers is controlled by the length of the electrical pulse. Measurements of NO removal from flue gas indicate that a pulse duration equal to the time required by the primary streamer to cross the gap gives the highest cleaning efficiency. ESA

N94-23429 Selskapet for Industriell og Teknisk Forskning, Trondheim (Norway).

FIRE SAFETY ENGINEERING RESEARCH IN NORWAY

K. S. Pedersen (Norges Tekniske Hoegskole, Trondheim.) 2 Feb. 1993 13 p Presented at the International Fire Safety Engineering Conference, Sydney, Australia, 18-20 Oct. 1992 See also PB93-201622 Limited Reproducibility: More than 20% of this document may be affected by microfiche quality
(PB93-201630; STF25-A92042) Avail: CASI HC A03

Four different present projects or research areas will be described in the paper. These are as follows: (1) Integrated analysis of steel and aluminium structures exposed to fire; (2) Modelling of flame spread using cone calorimeter results; (3) Evacuation studies and simulation; and (4) FIREX--Program system for prediction of fire hazard. NTIS

N94-23430 Selskapet for Industriell og Teknisk Forskning, Trondheim (Norway).

EXTINGUISHMENT OF ENCLOSED GAS FIRES WITH WATER SPRAYS

R. Wighus (Norges Tekniske Hoegskole, Trondheim.) 23 Feb. 1993 14 p See also PB92-151273 Sponsored by Royal Norwegian Council for Scientific and Industrial Research and Norsk Hydro Limited Reproducibility: More than 20% of this document may be affected by microfiche quality
(PB93-201663; STF25-A92051) Avail: Issuing Activity (National Technical Information Service (NTIS))

Water sprays are widely used for fire fighting in industrial areas, and they are used for fire protection in the process industry and at offshore oil- and gas-production platforms. No real quantification of the effect of water sprays as a fire fighting medium exists. The water delivery is specified through standards and regulations which are based on industrial experience. In process areas, water spray is often used in deluge systems, intended to control the fire until the leakage of fuel has been shut down. For this purpose, there is a need for quantification of the ability a certain spray system has to remove heat from the fire and to reduce the fire load to the construction and process equipment. SINTEF NBL has studied extinguishment and control of enclosed hydrocarbon fires by means of water sprays. A scale model of a module of an offshore platform is used in studies of enclosed liquid hydrocarbon fire development. The model is instrumented to measure heat transfer, fire development, and production of soot and gases from combustion. NTIS

N94-23450 Selskapet for Industriell og Teknisk Forskning, Trondheim (Norway).

CALCULATION OF FLAME SPREAD ON LINING MATERIALS BY THE FIELD MODEL KAMELEON. PROJECT 5 OF THE EUREFIC FIRE RESEARCH PROGRAMME

K. Opstad (Norges Tekniske Hoegskole, Trondheim.) 22 Jan. 1993 37 p See also PB88-201330, PB91-188409, PB92-109875, PB92-142785 and PB92-151281 Sponsored by NORDTEST and Nordisk Industrifond Limited Reproducibility: More than 20% of this document may be affected by microfiche quality
(PB93-201614; STF25-A92016) Avail: Issuing Activity (National Technical Information Service (NTIS))

An advanced calculation tool for flame spread calculation is under development. The system is based on the cone calorimeter test results. The heat release properties as a function of the irradiation level and thermal properties for combustible materials are derived from the cone calorimeter results. These data are implemented into a field model, which already has the capabilities to handle reacting fluids (combustion). Soot radiation and blocking as well as soot production are considered. Several calculated scenarios in enclosed environment are given. The results are promising, especially in the way of predicting the main factors of fire development, heat release rate, area which is burning, unburnt fuel, ventilation rate and the internal flow field. The only input is the geometry, ventilation, lining product and ignition source. NTIS

N94-23476 Technische Univ., Eindhoven (Netherlands). Dept. of Mathematics and Computing Science.

SYSTEMS ENGINEERING: A FORMAL APPROACH. PART 1: SYSTEM CONCEPTS

K. M. vanHee 30 Mar. 1993 95 p Limited Reproducibility: More than 20% of this document may be affected by microfiche quality
(PB93-225308; CSN-93/09) Copyright Avail: CASI HC A05

Engineering is the scientific discipline focused on the creation of new artifacts that are supposed to be of some use to our society. Different types of artifacts require different engineering approaches. However, in all these disciplines the development of a new artifact is divided into stages. Three stages can always be recognized: Analysis, Design, and Realization. The book considers only the first two stages of the development process. It focuses on a specific type of artifacts, called discrete dynamic systems. These systems consist of active components of actors that consume and produce passive components or tokens. Three subtypes are studied in more detail: business systems (like a factory or restaurant), information systems (whether automated or not), and automated systems (systems that are controlled by an automated information system). The first subtype is studied by industrial engineers, the last by software engineers and electrical engineers, whereas the second is a battlefield for all three disciplines. The union of these disciplines is called systems engineering. NTIS

N94-23506 Selskapet for Industriell og Teknisk Forskning, Trondheim (Norway).

FIELD MODELS: THEIR PRESENT AND FUTURE APPLICATION IN FIRE SAFETY ENGINEERING

K. S. Pedersen and B. F. Magnussen (Norges Tekniske Hoegskole, Trondheim.) 29 Dec. 1992 15 p See also PB93-201630 and PB93-162659 Limited Reproducibility: More than 20% of this document may be affected by microfiche quality
(PB93-201622; STF25-A92041) Avail: Issuing Activity (National Technical Information Service (NTIS))

Different field models for calculating heat load, fire development, and smoke concentrations have been developed for use in fire safety engineering work. The field model versions of KAMELEON are based on a finite difference solution of the basic equations from fluid dynamics together with different mathematical models. The most important of these models are the kappa-epsilon model of turbulence, the eddy dissipation concept of combustion (EDC), the soot model by Magnussen, and the discrete transfer model for radiation by Shah and Lockwood. All the resulting equations are solved three dimensionally and in transient. A version under development is a calculation tool for flame spread on surface linings. The system uses input data from the cone calorimeter. The paper will mainly deal with the description of the numerical code and especially a version called KAMELEON FIRE E-3D, handling enclosed pool fires. NTIS

N94-23574*# National Aeronautics and Space Administration. Marshall Space Flight Center, Huntsville, AL.

RESULTS OF A LABORATORY EXPERIMENT THAT TESTS ROTATING UNBALANCED-MASS DEVICES FOR SCANNING GIMBALED PAYLOADS AND FREE-FLYING SPACECRAFT Final Report

D. C. Alhorn and M. E. Polites Washington Jan. 1994 35 p
(NASA-TP-3458; M-741; NAS 1.60:3458; CDDF-92-02) Avail: CASI HC A03/MF A01

Rotating unbalanced-mass (RUM) devices are a new way to scan space-based, balloon-borne, and ground-based gimbaled payloads, like x-ray and gamma-ray telescopes. They can also be used to scan free-flying spacecraft. Circular scans, linear scans, and raster scans can be generated. A pair of RUM devices generates the basic scan motion and an auxiliary control system using torque motors, control moment gyros, or reaction wheels keeps the scan centered on the target and produces some complementary motion for raster scanning. Previous analyses and simulation results show that this approach offers significant power savings compared to scanning only with the auxiliary control system, especially with large payloads and high scan frequencies. However, these claims have never been proven until now. This paper describes a laboratory experiment which tests the concept of scanning a gimbaled payload with RUM devices. A description of the experiment is given and test results that prove the concept are presented. The test results are compared with those from a computer simulation model of the experiment and the differences are discussed. Author

N94-23581# Technische Univ., Berlin (Germany). Inst. fuer Luft- und Raumfahrt.

RAIL CORRUGATIONS

Klaus Knothe, ed. 1992 126 p Papers presented at Symposium on Corrugation Problems, Berlin, Germany, 17 Apr. 1991
(ILR-BER-59; ISBN-3-7983-1505-1; ETN-93-94176) Avail: CASI HC A07/MF A02

The following topics were discussed: a rail corrugation theory, the possible initiator of corrugation in a rail joint, the limits of validity of a linear model for corrugation, lateral high frequency oscillations and stability of a wheel rolling on a flexible track, the wear characteristics of dry rolling/sliding systems, surface analysis of corrugated rail treads, the observation of stick slip oscillations in tightly conformal wheel/rail contacts, an contact analysis of rough rail surfaces. For individual titles, see N94-23582 through N94-23589.

N94-23582# British Railway Technical Centre, Derby (England).

A RAIL CORRUGATION THEORY WHICH ALLOWS FOR CONTACT PATCH SIZE

C. O. Frederick and J. C. Sinclair *In* Tech. Univ. Berlin, Rail Congurations 1992 p 1-27 (For primary document see N94-23581 06-31)
Avail: CASI HC A03/MF A02

A small creepage rail corrugation theory is presented. The formulation is based on infinitesimally small fluctuation approach, which was extended to allow a finite length contact patch between the wheel and the rail. The theory considers curvature interactions between the wheel, the rail's transverse profile and the potential corrugation wave. The corrugation behavior is influenced by the interaction between track and wheelset dynamics and other factors which control the wheel/rail contact conditions. Subtle changes in these conditions alter the corrugation behavior. The effect of wheel radius and transverse rail head shape on corrugation behavior, consistent with observations, are predicted. The effect of contact patch filtering suppressing short wavelength corrugations becomes significant for low vehicle speeds. An improved simulation of corrugated behavior may be obtained. ESA

N94-23583# Deutsche Bundesbahn, Munich (Germany). Bundesbahnzentralamt.

A RAIL JOINT: THE POSSIBLE INITIATOR OF CORRUGATION?

G. Hoelzl *In* Tech. Univ. Berlin, Rail Corrugations 1992 p 29-40 (For primary document see N94-23581 06-31)
Avail: CASI HC A03/MF A02

The corrugation found at a rail joint which seems to be the initiator of the formation of corrugation is investigated. The possibility that the development of corrugations depends on the magnitude of the traffic is discussed. Several corrugation profiles and roughness spectra were measured. The results indicate that the corrugation can be caused by the start of the locomotives motion at the rail road crossing. Such corrugations were also found in stations at places where locomotives usually start to move. ESA

N94-23584# Technische Univ., Berlin (Germany). Inst. fuer Luft- und Raumfahrt.

A LINEAR MODEL FOR CORRUGATION AND ITS LIMIT OF VALIDITY

Klaus Hempelmann, Arnold Gross-Thebing, and Klaus Knothe *In its* Rail Corrugations 1992 p 41-57 (For primary document see N94-23581 06-31)
Avail: CASI HC A03/MF A02

A model to predict corrugation patterns and wavelength distributions developing out of initial disturbances is presented. The purpose is to show how a modeling of the contact mechanics, especially the so called curvature excitation, will influence the results. The influence of structural dynamics of the wheelset and here especially of the crosscoupling of vertical and lateral dynamics is investigated. The model indicates that a feedback mechanism between structural dynamics and wear is responsible for the initiation of corrugations on the rail tread. ESA

N94-23585# Technische Univ., Brunswick (Germany). Inst. fuer Technische Mechanik.

LATERAL HIGH FREQUENCY OSCILLATIONS AND STABILITY OF A WHEEL ROLLING ON A FLEXIBLE TRACK

E. Brommundt *In* Tech. Univ. Berlin, Rail Corrugations 1992 p 59-74 (For primary document see N94-23581 06-31)
Avail: CASI HC A03/MF A02

A model for studying the stability and the lateral deformations of the wheel under high frequency oscillations is proposed. The model is based on linearized equations for a single laterally flexible wheel with a cylindrical surface, running on a viscoelastically founded Euler-Bernoulli beam. The point contact and Kalker's linearized theory for oscillatory contact behavior are assumed to hold for the rolling motion. The equations of motion and a solution procedure are presented. ESA

N94-23586# Technische Univ., Berlin (Germany). Inst. fuer Fahrzeugtechnik.

WEAR CHARACTERISTICS OF TECHNICAL DRY ROLLING/SLIDING SYSTEMS WITH RELATIONS TO CORRUGATION PROBLEMS

H. Lehna *In its* Rail Corrugations 1992 p 75-84 (For primary document see N94-23581 06-31)
Avail: CASI HC A02/MF A02

Corrugation problems induced by wear in rail/wheel system of railways are investigated. The purposes of the study are: optimizing the wear behavior, attaining knowledge about the considered wear process, finding out wear quantities and their relevant value range, and determining wear laws to make wear calculable. Experimental investigations were performed and wear characteristics were examined. A rolling/sliding test rig with cylindrical rollers measuring 50 mm in diameter and 6 mm in contact patch width were used. The rollers operating at different circumferential velocities were pressed against each other. The normal load was applied hydraulically. Carbon steel, Ck 60, was used for the driving and the driven rollers. The entire investigation program comprised 41 combinations of control values of the operational quantities normal force, creepage, and driving rotational speed. ESA

N94-23587# Technische Univ., Berlin (Germany). Inst. fuer Metallforschung.
SURFACE ANALYSIS OF CORRUGATED RAIL TREADS
H. G. Feller and K. Walf *In its* Rail Corrugations 1992 p 85-94
Sponsored by DFG (For primary document see N94-23581 06-31)
Avail: CASI HC A02/MF A02

Corrugated rail treads were examined by surface analysis. The aim was to obtain information on the friction and wear behavior of the system wheel/rail and on the formation of corrugation. Surface geometry, surface morphology, structure, hardness values, and chemical composition analyses were performed. The results lead to the conclusion that the vibration of the wheel/tread system leads to different amounts of loads at different areas at the surface. As a consequence, areas with higher loads, higher deformation, higher hardening and higher wear resistance, the 'hills' were found. Neighboring areas of lower deformation, the 'valleys' were observed. The valleys are deepened by wear, which is followed by corrosion attack. ESA

N94-23588# National Research Council of Canada, Vancouver (British Columbia). Tribology and Mechanics Lab.
SURFACE OBSERVATIONS OF STICK-SLIP OSCILLATIONS IN TIGHTLY CONFORMAL WHEEL/RAIL CONTACTS
J. Kalousek *In* Tech. Univ. Berlin, Rail Corrugations 1992 p 95-111
(For primary document see N94-23581 06-31)
Avail: CASI HC A03/MF A02

The reasons for the growth of corrugations on rails and wheels in the Vancouver (Canada) mass transit system are described. The measures taken to eliminate them are outlined. In the Vancouver transit system, by design, the longitudinal and lateral creepages in the wheel/rail interface were absent. The fastener subassembly contains a 25 mm thick layer of natural rubber to absorb vibrations and provide the desired resiliency. The track gauge is maintained to an accuracy of +/- 1 mm. According to the corrugation theories, the lack of longitudinal and lateral creepage in the rail wheel interface was expected to keep the system free from wheel rail vibrations, excessive noise, and corrugations. Yet, six months after opening, 85% of the track was corrugated and the noise levels were rather high. The corrugations on the rails and the wheels are eliminated by means of controlling the friction characteristic and the conformity of rail wheel profiles. ESA

N94-23589# Technische Univ., Berlin (Germany). Inst. fuer Luft- und Raumfahrt.
CONTACT ANALYSIS OF ROUGH RAIL SURFACES
G. Wang and K. Knothe *In its* Rail Corrugations 1992 p 113-120
(For primary document see N94-23581 06-31)
Avail: CASI HC A02/MF A02

A stress analysis in the contact region and in the thin layer below the rail surface was carried out. An experimentally measured profilogram of a well used rail surface was applied. The stress analysis is performed by a two dimensional contact mechanical calculation where Coulomb's friction is taken into account. Stress distributions in the contact area and the lines of equal von Mises yield Stress in the elastic body are given. A rough surface of rail track was simulated by overlapping a selected section from a profilogram into a plane. The calculation showed that the remaining profile roughness may be responsible for high von Mises stress in a thin layer of about 100 to 40 micrometers. ESA

N94-23735# National Inst. of Standards and Technology, Gaithersburg, MD. Building and Fire Research Lab.
ZONE FIRE MODELING WITH NATURAL BUILDING FLOWS AND A ZERO ORDER SHAFT MODEL
J. H. Klote and G. P. Forney Sep. 1993 43 p
(PB94-112166; NISTIR-5251) Avail: CASI HC A03/MF A01

The paper addresses applications of zone fire models to simulate smoke flow in multistory buildings. Natural flows in buildings are discussed. A zero order model for shaft smoke flow was developed which treated the shaft as one perfectly mixed zone. A two zone fire model was modified to simulate natural flows and the zero order shaft smoke flow. The extent to which the one zone model and the two zone model are appropriate to simulate smoke flow in shafts is discussed. NTIS

N94-23737# National Inst. of Standards and Technology, Gaithersburg, MD. Building and Fire Research Lab.
IMPACTS: NIST BUILDING AND FIRE RESEARCH LABORATORY (TECHNICAL AND SOCIETAL) Special Publication
N. J. Raufaste Aug. 1993 43 p See also PB94-110194
(PB94-113420; NIST/SP-838/4) Avail: CASI HC A03/MF A01

The Building and Fire Research Laboratory (BFRL) of the National Institute of Standards and Technology (NIST) is dedicated to the life cycle quality of constructed facilities. The report describes major effects of BFRL's program on building and fire research. Contents of the document include: structural reliability; nondestructive testing of concrete; structural failure investigations; seismic design and construction standards; rehabilitation codes and standards; alternative refrigerants research; HVAC simulation models; thermal insulation; residential equipment energy efficiency; residential plumbing standards; computer image evaluation of building materials; corrosion-protection for reinforcing steel; prediction of the service lives of building materials; quality of construction materials laboratory testing; roofing standards; simulating fires with computers; fire safety evaluation system; fire investigations; soot formation and evolution; cone calorimeter development; smoke detector standards; standard for the flammability of children's sleepwear; smoldering insulation fires; wood heating safety research; in-place testing of concrete; communication protocols for building automation and control systems; computer simulation of the properties of concrete and other porous materials; cigarette-induced furniture fires; carbon monoxide formation in enclosure fires; halon alternative fire extinguishing agents; turbulent mixing research; materials fire research; furniture flammability testing; standard for the cigarette ignition resistance of mattresses; support of navy firefighter trainer program; and using fire to clean up oil spills. NTIS

N94-23740# Michigan State Univ., East Lansing. Dept. of Mechanical Engineering.
EXTINGUISHMENT OF COMBUSTIBLE POROUS SOLIDS BY WATER DROPLETS Annual Progress Report, Sep. 1992
Arvind Atreya Apr. 1993 30 p Prepared in cooperation with National Inst. of Standards and Technology, Gaithersburg, MD
(Grant NANB8D0861)
(PB93-198893; NIST-GCR-93-621) Avail: CASI HC A03/MF A01

Two experimental configurations are chosen for the study. Stagnation-point flow apparatus allows the study of both the gas-phase and the condensed-phase suppression actions and enables transient chemical measurements in the exhaust gas. These measurements are used to study the suppression mechanisms and quantify the suppression effectiveness. Counterflow diffusion flame apparatus allows detailed flame structure measurements but is limited to studying gas-phase suppression mechanisms, chemical and/or physical. NTIS

N94-23790# Sandia National Labs., Albuquerque, NM.
LASER SOLDERING OF Sn PLATED BRASS INTEGRATOR ASSEMBLY HOUSINGS
D. M. Keicher, G. A. Poulter, and N. R. Sorensen Sep. 1993 9 p
Presented at the 1993 International Congress on Application of Lasers and Electro-Optics, Orlando, FL, 24-28 Oct. 1993
(Contract DE-AC04-76DP-00789)
(DE94-001149; SAND-93-1138; CONF-9310194-1) Avail: CASI HC A02/MF A01

The high conductivity provided by solder closure joints of component housings is sometimes required to ensure electrical shielding of the components contained within. However, using a soldering iron to produce the solder joints can lead to charring of the insulating materials within the housing. To overcome this problem, the localized heating characteristics of laser soldering can be exploited. The feasibility of laser soldering Sn plated brass housings with a CW Nd:YAG laser has been investigated. It has been determined that laser soldering of these housings using a low solids solder flux is a viable technique and will minimize the amount of heat input to the enclosed electronic components. Metallographic analysis has shown good wetting of the solder on the housing components. Accelerated aging experiments indicate that no significant corrosion potential due to solder flux residues exists. Although a low solids flux was used to make the joints, initial results indicate that a fluxless technique can be developed to eliminate fluxes completely. DOE

N94-23793# Oak Ridge National Lab., TN.
ENHANCED ABSORPTION CYCLE COMPUTER MODEL
G. Grossman (Technion - Israel Inst. of Tech., Haifa.) and M. Wilk (Technion - Israel Inst. of Tech., Haifa.) Sep. 1993 54 p Prepared in cooperation with Technion - Israel Inst. of Tech., Haifa
(Contract DE-AC05-84OR-21400)
(DE94-001997; ORNL/Sub-91-SH641/1) Avail: CASI HC A04/MF A01

Absorption heat pumps have received renewed and increasing attention in the past two decades. The rising cost of electricity has made the particular features of this heat-powered cycle attractive for both residential and industrial applications. Solar-powered absorption chillers, gas-fired domestic heat pumps, and waste-heat-powered industrial temperature boosters are a few of the applications recently subjected to intensive research and development. The absorption heat pump research community has begun to search for both advanced cycles in various multistage configurations and new working fluid combinations with potential for enhanced performance and reliability. The development of working absorption systems has created a need for reliable and effective system simulations. A computer code has been developed for simulation of absorption systems at steady state in a flexible and modular form, making it possible to investigate various cycle configurations with different working fluids. The code is based on unit subroutines containing the governing equations for the system's components and property subroutines containing thermodynamic properties of the working fluids. The user conveys to the computer an image of his cycle by specifying the different subunits and their interconnections. Based on this information, the program calculates the temperature, flow rate, concentration, pressure, and vapor fraction at each state point in the system, and the heat duty at each unit, from which the coefficient of performance (COP) may be determined. This report describes the code and its operation, including improvements introduced into the present version. Simulation results are described for LiBr-H2O triple-effect cycles, LiCl-H2O solar-powered open absorption cycles, and NH3-H2O single-effect and generator-absorber heat exchange cycles. An appendix contains the user's manual. DOE

N94-24459# National Inst. for Fusion Science, Nagoya (Japan).
REDUCTION OF HYDROCARBON IMPURITIES IN 200 l/h HELIUM LIQUEFIER-REFRIGERATOR SYSTEM
Shuichi Yamada, Toshiyuki Mito, Arata Nishimura, Kazuya Takahata, Sadao Satoh, Junya Yamamoto, Hidemasa Yamamura (Kobe Steel Ltd., Japan.), Kaoru Masuda (Kobe Steel Ltd., Japan.), Shinichirou Kashihara (Kobe Steel Ltd., Japan.), and Katsuaki Fukusada (Kobe Steel Ltd., Japan.) et al Nov. 1993 22 p
(NIFS-259) Avail: CASI HC A03/MF A01

A cryogenic system with the capacity of 200 l/h or 500 W at 4.4 K was developed in order to supply the superconducting conductors and coils of the LHD. As a by-product of operating the cryogenic system, the impurity densities of hydrocarbon gases in the circulating helium gas became much larger than the expected values for this cryogenic system. So much larger in fact, that it became necessary to carefully monitor the operational conditions of the circulating compressor by means of gas chromatography. Impurity gas densities of oxygen, nitrogen, and ethane increased significantly when the output capacity of the compressor was reduced. In a two-stage oil injected compression system, with a variable stroke mechanism for a first stage, a reduction in the capacity of the first stage leads to a larger compression ratio for the second stage, and the temperature of the injected oil becomes higher. The production of the impurities in the helium might be caused by decomposition of the injected oil in the compressor. The compressor, therefore, was reconstructed such that the injection oil is supplied sufficiently, and the compression ratio division becomes even for each stage. It was confirmed that the impurities were not produced after the modification. Author (revised)

N94-24473*# National Aeronautics and Space Administration. Langley Research Center, Hampton, VA.
ACTIVE CONTROL OF BUILDINGS DURING EARTHQUAKES
Vicki L. Vance (Stanford Univ., CA.) Dec. 1993 33 p
(RTOP 585-03-11-01)
(NASA-TM-109033; NAS 1.15:109033) Avail: CASI HC A03/MF A01

The objective of this report is to provide an overview of the different types of control systems used in buildings, to discuss the problems associated with current active control mechanisms, and to show the cost-effectiveness of applying active control to buildings. In addition, a small case study investigates the feasibility and benefits of using embedded actuators in buildings. Use of embedded actuators could solve many of the current problems associated with active control by providing a wider bandwidth of control, quicker speed of response, increased reliability and reduced power requirement. Though embedded actuators have not been developed for buildings, they have previously been used in space structures. Many similarities exist between large civil and aerospace structures indicating that direct transfer of concepts between the two disciplines may be possible. In particular, much of the Controls-Structures Interaction (CSI) technology currently being developed could be beneficially applied to civil structures. While several buildings with active control systems have been constructed in Japan, additional research and experimental verification are necessary before active control systems become widely accepted and implemented. Author

N94-24475 Technische Univ., Eindhoven (Netherlands). Dept. of Mathematics and Computing Science.
SYSTEMS ENGINEERING: A FORMAL APPROACH. PART 4: ANALYSIS METHODS
K. M. vanHee Apr. 1993 80 p See also PB94-101409 and PB93-225316 Limited Reproducibility: More than 20% of this document may be affected by microfiche quality
(PB94-101417; Computing Science Notes-93/12) Avail: CASI HC A05

There are several methods to analyze a model. To verify invariant properties there are two kinds of invariant methods: place invariants and transition invariants. Place invariants can be used to prove properties that hold in each reachable state. A transition invariant is a characterization of (finite) traces that bring an actor back to its initial state or an equivalent one. These methods are studied in the first section. The second section considers occurrence graph methods. They are used to check if a system can reach states with certain properties. These methods are specialized in section three to study the time behavior of systems, specifically to compute throughput or response times. NTIS

N94-24568# Oak Ridge National Lab., TN.
NORMAL ZONE PROPAGATION AND THERMAL HYDRAULIC QUENCHBACK IN A CABLE-IN-CONDUIT SUPERCONDUCTOR
J. W. Lue and L. Dresner 1993 8 p Presented at the International Cryogenic Engineering Conference and International Cryogenic Materials Conference, Albuquerque, NM, 12-16 Jul. 1993 16 Jul. 1993
(Contract DE-AC05-84OR-21400)
(DE94-002457; CONF-930703-37) Avail: CASI HC A02/MF A01

When a local normal zone appears in a cable-in-conduit superconductor, a slug of hot helium is produced. The pressure rises and the hot helium expands. Thus, the normal zone propagation in such a conductor can be governed by the hot helium expansion, rather than the heat conduction along the conductor. The expansion of the hot helium compresses the cold helium outside of the normal zone. This raises the temperature of the cold helium. When the temperature rise reaches the current sharing limit, the superconductor in contact goes normal. Thus a rapid increase in normal zone propagation occurs. This phenomenon is termed Thermal Hydraulic Quenchback (THQ). An experiment was performed to investigate this process. The existence of THQ was verified. Thresholds of THQ were also observed by varying the conductor current, the magnetic field, the temperature, and the initial normal zone length. When THQ occurred, normal zone propagation approaching the velocity of sound was observed. A better picture of THQ is obtained by a careful comparison of the data with analytical studies. DOE

N94-24648 Technische Univ., Twente (Netherlands). Tele-Informatics and Open Systems Group.
WHAT MAKES INDUSTRIES BELIEVE IN FORMAL METHODS
C. A. Vissers, M. vanSinderen, and L. F. Pires 1993 30 p Limited Reproducibility: More than 20% of this document may be affected by microfiche quality
(PB94-110848; Memo-INF-93-33) Copyright Avail: CASI HC A03

The paper revisits the requirements for formal description techniques and identifies some critical success and inhibiting factors associated with the introduction of formal methods in the industrial practice. One of the inhibiting factors is the often encountered lack of appropriateness of the formal model to express and manipulate the design concerns that determine the world of the engineer. This factor motivated research in the area of architectural and implementation design concepts. The last two sections of the paper report on some results of this research. NTIS

N94-24955 National Inst. of Standards and Technology, Gaithersburg, MD. Building and Fire Research Lab.
COLLABORATING WITH OUR CUSTOMERS: NIST BUILDING AND FIRE RESEARCH LABORATORY
Aug. 1993 28 p Limited Reproducibility: More than 20% of this document may be affected by poor print and microfiche quality
(PB94-110194; NIST/SP-838/3) Avail: Issuing Activity (National Technical Information Service (NTIS))

The 'Perspective' describes how BFRL's (Building and Fire Research Laboratory's) projects respond to needs of the principal classes of its customers in the construction and fire safety communities: owners, designers, and constructors; producers and suppliers; standards and codes interests; and the fire services. The authors' projects address major needs and opportunities for improving the life cycle performance of constructed facilities, including: high-performance concrete and steel; 'green' building technologies; integrated, automatic control systems for operation of constructed facilities; computer-integrated, effectively automated design and construction practices; and reduction of losses from unwanted fires, earthquakes, and extreme winds. NTIS

N94-25193*# Lockheed Sanders, Inc., Nashua, NH. Advanced Engineering and Technology Div.
NEW TECHNOLOGIES FOR SPACE AVIONICS, 1993 Final Report
David W. Aibel, David R. Harris, Dave Bartlett (New Hampshire Univ., Durham.), Steve Black (Lockheed Space Operations Co., Cocoa Beach, FL.), Dave Campagna, Nancy Fernald, and Ray Garbos Dec. 1993 77 p
(Contract NAS9-18873)
(NASA-CR-195157; NAS 1.26:195157) Avail: CASI HC A05/MF A01

The report reviews a 1993 effort that investigated issues associated with the development of requirements, with the practice of concurrent engineering and with rapid prototyping, in the development of a next-generation Reaction Jet Drive Controller. This report details lessons learned, the current status of the prototype, and suggestions for future work. The report concludes with a discussion of the vision of future avionics architectures based on the principles associated with open architectures and integrated vehicle health management. For individual titles, see N94-25194 through N94-25196.

N94-25194*# Lockheed Sanders, Inc., Nashua, NH.
APPENDIX A: PROPOSED STATEMENT OF WORK, 1994
In its New Technologies for Space Avionics, 1993 Dec. 1993 5 p
(For primary document see N94-25193 06-31)
Avail: CASI HC A01/MF A01

This NRA effort is devoted to developing new techniques and methodologies which utilize and/or provide support to Integrated Vehicle Health Management (IVHM) concepts and techniques, modern design processes, and open architectures to realize an avionics system architecture that relieves the flight control system (FCS) of the requirement of maintaining intimate knowledge and control of the vehicle subsystems (for instance, the reaction control system (RCS)). The benefit of this architecture is that future upgrades and enhancements to the system(s) or to individual components within the system(s) are greatly simplified. This approach also allows a much more straightforward treatment of failure analysis, system diagnosis, and the design of fault containment domains. This NRA effort is also devoted to realizing capabilities to provide an available avionics system (and subsystem(s)) at minimum operational cost. This thrust provides a direct benefit to NASA in that it seeks to accelerate the design cycle to allow state of the art components and designs to actually appear in the fielded system rather than merely in the initial design. To achieve this, this effort is intended to benefit from efforts already underway at Lockheed and other major contractors. For instance, Lockheed Sanders is currently engaged in a major DoD funded development program which has the goal of cutting design cycle time of high performance electronics by a factor of four while simultaneously improving quality also by a factor of four. The early work on this program was used to enable the rapid prototyping of the Reaction Jet Drive Controller which was accomplished in 1993. Similarly, maximum leverage will be derived from recent NASA and DoD efforts to increase the content of high quality commercial grade electronic components in systems for aerospace applications. Both of these goals result in a system with enhanced cost effectiveness, increased reliability, and greatly increased performance compared to a system developed using a more conventional approach. Derived from text

N94-25195*# Lockheed Sanders, Inc., Nashua, NH.
APPENDIX B: RAPID DEVELOPMENT APPROACHES FOR SYSTEM ENGINEERING AND DESIGN Interim Technical Report, Jul. 1993
In its New Technologies for Space Avionics, 1993 Dec. 1993 27 p
(For primary document see N94-25193 06-31)
Avail: CASI HC A03/MF A01

Conventional processes often produce systems which are obsolete before they are fielded. This paper explores some of the reasons for this, and provides a vision of how we can do better. This vision is based on our explorations in improved processes and system/software engineering tools. Author

N94-25196*# Lockheed Sanders, Inc., Nashua, NH.
APPENDIX C: RAPID DEVELOPMENT APPROACHES FOR SYSTEM ENGINEERING AND DESIGN Final Technical Report, Sep. 1993
In its New Technologies for Space Avionics, 1993 Dec. 1993 32 p
(For primary document see N94-25193 06-31)
Avail: CASI HC A03/MF A01

Conventional system architectures, development processes, and tool environments often produce systems which exceed cost expectations and are obsolete before they are fielded. This paper explores some of the reasons for this and provides recommendations for how we can do better. These recommendations are based on DoD and NASA system developments and on our exploration and development of system/software engineering tools. Author

N94-23892*# National Aeronautics and Space Administration. Lyndon B. Johnson Space Center, Houston, TX.
REAL-TIME AUTOMATED FAILURE IDENTIFICATION IN THE CONTROL CENTER COMPLEX (CCC)
Sarah Kirby, Janet Lauritsen, Ginger Pack, Anhhoang Ha (McDonnell-Douglas Space Systems Co., Houston, TX.), Steven Jowers (McDonnell-Douglas Space Systems Co., Houston, TX.), Robert McNenny (McDonnell-Douglas Space Systems Co., Houston, TX.), The Truong (McDonnell-Douglas Space Systems Co., Houston, TX.), and James Dell (Loral Space Information Systems, Houston, TX.) *In* JPL, SpaceOps 1992: Proceedings of the Second International Symposium on Ground Data Systems for Space Mission Operations 1 Mar. 1993 p 387-392 (For primary document see N94-23832 06-66)
Avail: CASI HC A02/MF A10

32 COMMUNICATIONS AND RADAR

Includes radar; land and global communications; communications theory; and optical communications.

For related information see also *04 Aircraft Communications and Navigation* and *17 Space Communications, Spacecraft Communications, Command and Tracking.* For search and rescue see *03 Air Transportation and Safety,* and *16 Space Transportation.*

N94-22729# Universiteit Twente, Enschede (Netherlands). Faculty of Applied Mathematics.
THE CHARACTERIZATION OF REACTION-CONVECTION-DIFFUSION PROCESSES BY TRAVELLING WAVES
B. H. Gilding and R. Kersner (Hungarian Academy of Sciences, Budapest.) Jan. 1993 68 p
(MEMO-1111; ETN-94-94747) Avail: CASI HC A04/MF A01

The necessary and sufficient criterion for finite speed of propagation for the general nonlinear reaction convection diffusion equation u(sub t) (a(u))(sub xx) + (b(u))(sub x) + c(u) is determined. The assumptions on the coefficients a, b and c are such that the classification unifies and generalizes previously known results. The technique employed is comparison of an arbitrary solution of the equation with suitably constructed traveling wave solutions and subsolutions. Basically the central conclusion is that the equation exhibits finite speed of propagation if and only if it admits a traveling wave solution with bounded support. Concurrently, the search for a traveling wave solution with bonded support can be reduced to the study of a singular nonlinear integral equation whose solution must satisfy a certain constraint. ESA

N94-22735*# Jet Propulsion Lab., California Inst. of Tech., Pasadena.
PROCEEDINGS OF THE THIRD INTERNATIONAL MOBILE SATELLITE CONFERENCE (IMSC 1993)
Robert Kwan, comp., Jack Rigley, comp. (Communications Research Centre, Ottawa, Ontario.), and Randy Cassingham, ed. 1993 593 p Conference held in Pasadena, CA, 16-18 Jun. 1993 Prepared in cooperation with Communications Research Centre, Ottawa, Ontario
(Contract NAS7-918)
(NASA-CR-194516; JPL-Publ-93-009; NAS 1.26:194516) Avail: CASI HC A25/MF A06

Satellite-based mobile communications systems provide voice and data communications to users over a vast geographic area. The users may communicate via mobile or hand-held terminals, which may also provide access to terrestrial cellular communications services. While the first and second International Mobile Satellite Conferences (IMSC) mostly concentrated on technical advances, this Third IMSC also focuses on the increasing worldwide commercial activities in Mobile Satellite Services. Because of the large service areas provided by such systems, it is important to consider political and regulatory issues in addition to technical and user requirements issues. Topics covered include: the direct broadcast of audio programming from satellites; spacecraft technology; regulatory and policy considerations; advanced system concepts and analysis; propagation; and user requirements and applications. For individual titles, see N94-22736 through N94-22836.

N94-22736*# United States Information Agency, Washington, DC. Voice of America.
WORLDWIDE SURVEY OF DIRECT-TO-LISTENER DIGITAL AUDIO DELIVERY SYSTEMS DEVELOPMENT SINCE WARC-1992
Dion D. Messer *In* JPL, Proceedings of the Third International Mobile Satellite Conference (IMSC 1993) 1993 p 3-8 (For primary document see N94-22735 06-32)
Avail: CASI HC A02/MF A06

Each country was allocated frequency band(s) for direct-to-listener digital audio broadcasting at WARC-92. These allocations were near 1500, 2300, and 2600 MHz. In addition, some countries are encouraging the development of digital audio broadcasting services for terrestrial delivery only in the VHF bands (at frequencies from roughly 50 to 300 MHz) and in the medium-wave broadcasting band (AM band) (from roughly 0.5 to 1.7 MHz). The development activity increase was explosive. Current development, as of February 1993, as it is known to the author is summarized. The information given includes the following characteristics, as appropriate, for each planned system: coverage areas, audio quality, number of audio channels, delivery via satellite/terrestrial or both, carrier frequency bands, modulation methods, source coding, and channel coding. Most proponents claim that they will be operational in 3 or 4 years. Author

N94-22737*# European Space Agency. European Space Research and Technology Center, ESTEC, Noordwijk (Netherlands).
ESA PERSONAL COMMUNICATIONS AND DIGITAL AUDIO BROADCASTING SYSTEMS BASED ON NON-GEOSTATIONARY SATELLITES
P. LoGalbo, J. Benedicto, and R. Viola *In* JPL, Proceedings of the Third International Mobile Satellite Conference (IMSC 1993) 1993 p 9-14 (For primary document see N94-22735 06-32)
Avail: CASI HC A02/MF A06

Personal Communications and Digital Audio Broadcasting are two new services that the European Space Agency (ESA) is investigating for future European and Global Mobile Satellite systems. ESA is active in promoting these services in their various mission options including non-geostationary and geostationary satellite systems. A Medium Altitude Global Satellite System (MAGSS) for global personal communications at L and S-band, and a Multiregional Highly inclined Elliptical Orbit (M-HEO) system for multiregional digital audio broadcasting at L-band are described. Both systems are being investigated by ESA in the context of future programs, such as Archimedes, which are intended to demonstrate the new services and to develop the technology for future non-geostationary mobile communication and broadcasting satellites. Author (revised)

N94-22738*# Jet Propulsion Lab., California Inst. of Tech., Pasadena.
DIRECT BROADCAST SATELLITE-RADIO, SPACE-SEGMENT/RECEIVER TRADEOFFS
Nasser Golshan *In its* Proceedings of the Third International Mobile Satellite Conference (IMSC 1993) 1993 p 15-20 Sponsored in part by United States Information Agency (For primary document see N94-22735 06-32)
Avail: CASI HC A02/MF A06

The balance between receiver complexity and the required satellite equivalent isotropically radiated power (EIRP) for Direct Broadcast Satellite-Radio (DBS-R) service is addressed. In general the required receiver complexity and cost can be reduced at the expense of higher space-segment cost by allowing a higher satellite EIRP. The tradeoff outcome is sensitive to the total number of anticipated receivers in a given service area, the number of audio programs, and the required audio quality. An understanding of optimum choice of satellite EIRP for DBS-R under various service requirements is a critical issue at this time when International Radio Consultative Committee (CCIR) is soliciting input in preparation for the International Telecommunications Union (ITU) planning conference for the service. Author (revised)

N94-22739*# Jet Propulsion Lab., California Inst. of Tech., Pasadena.
DIRECT BROADCAST SATELLITE-RADIO, RECEIVER DEVELOPMENT
A. Vaisnys, D. Bell, J. Gevargiz, and Nasser Golshan *In its* Proceedings of the Third International Mobile Satellite Conference (IMSC 1993) 1993 p 21-26 (For primary document see N94-22735 06-32)
Avail: CASI HC A02/MF A06

The status of the ongoing Direct Broadcast Satellite-Radio (DBS-R) Receiver Development Task being performed at the Jet Propulsion Laboratory, California Institute of Technology (JPL) is reported. This work is sponsored by the Voice of America/U.S. Information Agency through an agreement with NASA. The objective of this task is to develop, build, test, and demonstrate a prototype receiver that is compatible with reception of digital audio programs broadcast via satellites. The receiver is being designed to operate under a range of reception conditions, including fixed, portable, and mobile, as well as over a sufficiently wide range of bit rates to accommodate broadcasting systems with different cost/audio quality objectives. While the requirements on the receiver are complex, the eventual goal of the design effort is to make the design compatible with low cost production as a consumer product. One solution may be a basic low cost core design suitable for a majority of reception conditions, with optional enhancements for reception in especially difficult environments. Some of the receiver design parameters were established through analysis, laboratory tests, and a prototype satellite experiment accomplished in late 1991. Many of the necessary design trades will be made during the current

simulation effort, while a few of the key design options will be incorporated into the prototype for evaluation during the planned satellite field trials.
Author (revised)

N94-22740*# National Aeronautics and Space Administration. Lewis Research Center, Cleveland, OH.

UTILIZING A TDRS SATELLITE FOR DIRECT BROADCAST SATELLITE-RADIO PROPAGATION EXPERIMENTS AND DEMONSTRATIONS

James E. Hollansworth *In* JPL, Proceedings of the Third International Mobile Satellite Conference (IMSC 1993) 1993 p 27-32 (For primary document see N94-22735 06-32)
Avail: CASI HC A02/MF A06

The NASA/VOA Direct Broadcast Satellite - Radio (DBS-R) Program will be using a NASA Tracking Data Relay Satellite (TDRS) at 62 deg West longitude to conduct live satellite S-band propagation experiments and demonstrations of satellite sound broadcasting over the next two years (1993-1994). The NASA/VOA DBS-R program has applied intensive effort to garner domestic and international support for the DBS-R concept. An S-band DBS-R allocation was achieved for Region 2 at WARC-92 held in Spain. With this allocation, the DBS-R program now needs to conduct S-band propagation experiments and systems demonstrations that will assist in the development of planning approaches for the use of Broadcast Satellite Service (Sound) frequency bands prior to the planning conference called for by WARC-92. These activities will also support receiver concept development applied to qualities ranging from AM to Monophonic FM, Stereophonic FM, Monophonic CD, and Stereophonic CD quality. Author

N94-22741*# Communications Satellite Corp., Clarksburg, MD.

AERONAUTICAL AUDIO BROADCASTING VIA SATELLITE

Forrest F. Tzeng *In* JPL, Proceedings of the Third International Mobile Satellite Conference (IMSC 1993) 1993 p 33-38 (For primary document see N94-22735 06-32)
Avail: CASI HC A02/MF A06

A system design for aeronautical audio broadcasting, with C-band uplink and L-band downlink, via Inmarsat space segments is presented. Near-transparent-quality compression of 5-kHz bandwidth audio at 20.5 kbit/s is achieved based on a hybrid technique employing linear predictive modeling and transform-domain residual quantization. Concatenated Reed-Solomon/convolutional codes with quadrature phase shift keying are selected for bandwidth and power efficiency. RF bandwidth at 25 kHz per channel, and a decoded bit error rate at 10(exp -6) with E(sub b)/N(sub o) at 3.75 dB are obtained. An interleaver, scrambler, modem synchronization, and frame format were designed, and frequency-division multiple access was selected over code-division multiple access. A link budget computation based on a worst-case scenario indicates sufficient system power margins. Transponder occupancy analysis for 72 audio channels demonstrates ample remaining capacity to accommodate emerging aeronautical services. Author (revised)

N94-22742*# Telesat Canada, Gloucester (Ontario).

THE MSAT SPACECRAFT OF TELESAT MOBILE INC. Abstract Only
c18

E. Bertenyi *In* JPL, Proceedings of the Third International Mobile Satellite Conference (IMSC 1993) 1993 p 41 (For primary document see N94-22735 06-32)
Avail: CASI HC A01/MF A06

The MSAT spacecraft of the Canadian mobile satellite operator, Telesat Mobile Inc. (TMI) is described. When launched in 1994, the large geostationary MSAT spacecraft which is currently under construction by Hughes Aircraft Co. and Spar Aerospace Ltd. will enable TMI to provide mobile and transportable communications services to its customers even in the most remote parts of the North American continent. The main elements of TMI's mobile satellite system (described in a companion paper) are the space segment and the ground segment. TMI's space segment will employ one of two nearly identical satellites, one of which will be owned and operated by TMI, the other by the U.S. mobile satellite operator, American Mobile Satellite Corporation (AMSC). The two companies are participating in a joint spacecraft procurement in order to reduce the nonrecurring costs and to ensure system compatibility between the two systems; and they have also agreed to provide in-orbit backup to each other in the event of a catastrophic satellite failure. The program status, performance requirements, main parameters, and configuration of the MSAT spacecraft are reviewed. The major features of the communications subsystem are discussed in some detail, and a brief summary is presented of the spacecraft service module. Key technology items include the L-band RF power amplifier, which must operate with a high DC to RF power efficiency and generate low intermodulation when loaded with multi-carrier signals; and the large diameter deployable L-band antenna. The development status and expected performance of these spacecraft components is examined. Author (revised)

N94-22743*# European Space Agency. European Space Research and Technology Center, ESTEC, Noordwijk (Netherlands). Radio-Frequency Systems Div.

ADAPTIVE DIGITAL BEAMFORMING FOR A CDMA MOBILE COMMUNICATIONS PAYLOAD Abstract Only

Samuel G. Munoz-Garcia and Javier Benedicto Ruiz *In* JPL, Proceedings of the Third International Mobile Satellite Conference (IMSC 1993) 1993 p 43-44 (For primary document see N94-22735 06-32)
Avail: CASI HC A01/MF A06

In recent years, Spread-Spectrum Code Division Multiple Access (CDMA) has become a very popular access scheme for mobile communications due to a variety of reasons: excellent performance in multipath environments, high scope for frequency reuse, graceful degradation near saturation, etc. In this way, a CDMA system can support simultaneous digital communication among a large community of relatively uncoordinated users sharing a given frequency band. Nevertheless, there are also important problems associated with the use of CDMA. First, in a conventional CDMA scheme, the signature sequences of asynchronous users are not orthogonal and, as the number of active users increases, the self-noise generated by the mutual interference between users considerably degrades the performance, particularly in the return link. Furthermore, when there is a large disparity in received powers - due to differences in slant range or atmospheric attenuation - the non-zero cross-correlation between the signals gives rise to the so-called near-far problem. This leads to an inefficient utilization of the satellite resources and, consequently, to a drastic reduction in capacity. Several techniques were proposed to overcome this problem, such as Synchronized CDMA - in which the signature sequences of the different users are quasi-orthogonal - and power control. At the expense of increased network complexity and user coordination, these techniques enable the system capacity to be restored by equitably sharing the satellite resources among the users. An alternative solution is presented based upon the use of time-reference adaptive digital beamforming on board the satellite. This technique enables a high number of independently steered beams to be generated from a single phased array antenna, which automatically track the desired user signal and null the unwanted interference source. In order to use a time-reference adaptive antenna in a communications system, the main challenge is to obtain a reference signal highly correlated with the desired user signal and uncorrelated with the interferences. CDMA lends itself very easily to the generation of such a reference signal, thanks to the a priori knowledge of the user's signature sequence. First, the integration of an adaptive antenna in an asynchronous CDMA system is analyzed. The adaptive antenna system can provide increased interference rejection - much higher than that afforded by the code alone - and, since CDMA is mainly interference limited, any reduction in interference converts directly and linearly into an increase in capacity. Analyses and computer simulations are presented that show how an asynchronous CDMA system incorporating adaptive beamforming can provide at least as much capacity as a synchronous system. More importantly, the proposed concept allows the near-far effect to be mitigated without requiring a tight coordination of the users in terms of transmitted power control or network synchronization. The system is extremely robust to the near-far effect because the signals reaching the satellite from directions other than that of the desired user - which are likely to have different power levels - are adaptively canceled by the antenna. Finally, a payload architecture is presented that illustrates the practical implementation of this concept. This digital payload architecture demonstrates that with the advent of high performance CMOS digital processing, the on-board implementation of complex DSP techniques - in particular Digital Beamforming - has become possible, being most attractive for Mobile Satellite Communications. Author (revised)

N94-22744*# Harris Government Aerospace Systems Div., Melbourne, FL.

ELECTRICAL PERFORMANCE OF WIRE MESH FOR SPACECRAFT DEPLOYABLE REFLECTOR ANTENNAS Abstract Only

Greg Turner *In* JPL, Proceedings of the Third International Mobile Satellite Conference (IMSC 1993) 1993 p 45 (For primary document see N94-22735 06-32)

Avail: CASI HC A01/MF A06

Mobile satellite communications systems require large, high gain antennas at the spacecraft to minimize the antenna gain and power requirements for mobile user elements. The use of a deployable reflector antenna for these applications provides a lightweight system that can be compactly stowed prior to deployment on orbit. The mesh surface material is a critical component in the deployable reflector antenna design. The mesh is required to provide the desired electrical performance as well as the mechanical properties that are necessary to deploy and maintain the reflector surface on orbit. Of particular interest in multi-channel communications applications is the generation of Passive InterModulation (PIM) products at the reflector surface that can result in interference in the receive band. Wire mesh was specifically identified by some as having a high potential for PIM generation based solely on the existence of nonpermanent metal to metal contacts at the junctions that are inherent in the mesh design. There are a number of other factors, however, that reduce the likelihood of PIM occurring at the mesh reflector surface. Experimental data presented demonstrate that mesh PIM generation is not significant for typical applications. PIM and reflectivity performance of wire mesh composed of gold plated molybdenum wire in a tricot knit are described. This type of mesh was successfully used for the deployable Single Access Antennas of the Tracking and Data Relay Satellite System. Author (revised)

N94-22745*# Gorca Systems, Inc., Cherry Hill, NJ.

ADAPTIVE ARRAY ANTENNA FOR SATELLITE CELLULAR AND DIRECT BROADCAST COMMUNICATIONS

Charles R. Horton and Kenneth Abend *In* JPL, Proceedings of the Third International Mobile Satellite Conference (IMSC 1993) 1993 p 47-52 (For primary document see N94-22735 06-32)

Avail: CASI HC A02/MF A06

Adaptive phased-array antennas provide cost-effective implementation of large, light weight apertures with high directivity and precise beamshape control. Adaptive self-calibration allows for relaxation of all mechanical tolerances across the aperture and electrical component tolerances, providing high performance with a low-cost, lightweight array, even in the presence of large physical distortions. Beam-shape is programmable and adaptable to changes in technical and operational requirements. Adaptive digital beam-forming eliminates uplink contention by allowing a single electronically steerable antenna to service a large number of receivers with beams which adaptively focus on one source while eliminating interference from others. A large, adaptively calibrated and fully programmable aperture can also provide precise beam shape control for power-efficient direct broadcast from space. Advanced adaptive digital beamforming technologies are described for: (1) electronic compensation of aperture distortion, (2) multiple receiver adaptive space-time processing, and (3) downlink beam-shape control. Cost considerations for space-based array applications are also discussed. Author (revised)

N94-22746*# COM DEV Ltd., Cambridge (Ontario).

SAW BASED SYSTEMS FOR MOBILE COMMUNICATIONS SATELLITES

R. C. Peach, N. Miller, and M. Lee *In* JPL, Proceedings of the Third International Mobile Satellite Conference (IMSC 1993) 1993 p 53-58 (For primary document see N94-22735 06-32)

Avail: CASI HC A02/MF A06

Modern mobile communications satellites, such as INMARSAT 3, EMS, and ARTEMIS, use advanced onboard processing to make efficient use of the available L-band spectrum. In all of these cases, high performance surface acoustic wave (SAW) devices are used. SAW filters can provide high selectivity (100-200 kHz transition widths), combined with flat amplitude and linear phase characteristics; their simple construction and radiation hardness also makes them especially suitable for space applications. An overview of the architectures used in the above systems, describing the technologies employed, and the use of bandwidth switchable SAW filtering (BSSF) is given. The tradeoffs to be considered when specifying a SAW based system are analyzed, using both theoretical and experimental data. Empirical rules for estimating SAW filter performance are given. Achievable performance is illustrated using data from the INMARSAT 3 engineering model (EM) processors. Author (revised)

N94-22747*# Bristol Univ. (England). Centre for Communications Research.

BROADBAND LINEARISATION OF HIGH-EFFICIENCY POWER AMPLIFIERS c33

Peter B. Kenington, Kieran J. Parsons, and David W. Bennett *In* JPL, Proceedings of the Third International Mobile Satellite Conference (IMSC 1993) 1993 p 59-64 Sponsored in part by Northern Telecom Canada Ltd. (For primary document see N94-22735 06-32)

Avail: CASI HC A02/MF A06

A feedforward-based amplifier linearization technique is presented which is capable of yielding significant improvements in both linearity and power efficiency over conventional amplifier classes (e.g. class-A or class-AB). Theoretical and practical results are presented showing that class-C stages may be used for both the main and error amplifiers yielding practical efficiencies well in excess of 30 percent, with theoretical efficiencies of much greater than 40 percent being possible. The levels of linearity which may be achieved are required for most satellite systems, however if greater linearity is required, the technique may be used in addition to conventional pre-distortion techniques. Author (revised)

N94-22748*# American Mobile Satellite Corp., Washington, DC.

US DOMESTIC AND INTERNATIONAL REGULATORY ISSUES c84

Lon C. Levin and Dennis C. Nash *In* JPL, Proceedings of the Third International Mobile Satellite Conference (IMSC 1993) 1993 p 67-72 (For primary document see N94-22735 06-32)

Avail: CASI HC A02/MF A06

The U.S. domestic and international regulatory and policy milestones since 1982, when NASA filed its petition with the Federal Communications Commission (FCC) to establish the U.S. domestic Mobile Satellite Service (MSS), are described. In 1985, the FCC proposed to establish MSS services and allocate spectrum for such service. In 1986, the FCC allocated L-band spectrum for MSS. In 1987, at the Mobile World Administrative Radio Conference (MOB WARC-87), despite U.S., Canadian, and Mexican efforts, the WARC did not adopt a multi-service, generic MSS allocation. In 1989, the FCC licensed the first MSS system. After two decisions by the U.S. Court of Appeals, the FCC's licensing actions remain intact. The FCC also has permitted Comsat to provide international aeronautical and land MSS via the Inmarsat system. Inmarsat, however, may not serve the domestic U.S. market. In 1991, the FCC accepted applications for MSS systems, most of which were non-geostationary proposals, for operation in the Radiodetermination Satellite Service (RDSS) bands, and the VHF and UHF bands. In 1992, the FCC proposed rules for non-geostationary MSS systems and applied a negotiated rulemaking procedure to each. Also in 1992, the U.S. position for flexibility in existing MSS bands and for additional worldwide MSS allocations was adopted in large part at the 1992 World Administrative Radio Conference (WARC-92). Author (revised)

N94-22749*# Anglin and Giaccherini, Playa del Rey, CA.

INTERNATIONAL ORGANIZATIONS TO ENABLE WORLD-WIDE MOBILE SATELLITE SERVICES c84

Richard L. Anglin, Jr. *In* JPL, Proceedings of the Third International Mobile Satellite Conference (IMSC 1993) 1993 p 73-78 (For primary document see N94-22735 06-32)

Avail: CASI HC A02/MF A06

Numbers of systems exist or have been proposed to provide world-wide mobile satellite services (MSS). Developers of these systems have formulated institutional structures they consider most appropriate for profitable delivery of these services. MSS systems provide niche services and complement traditional telecommunications networks; they are not integrated into world-wide networks. To be successful, MSS system operators must be able to provide an integrated suite of services to support the increasing globalization, interconnectivity, and mobility of business. The critical issue to enabling 'universal roaming' is securing authority to provide MSS in all of the nations of the world. Such authority must be secured in the context of evolving trends in international telecommunications, and must specifically address issues of standardization, regulation and organization. Today, only one existing organization has such world-wide authority. The question is

how proponents of new MSS systems and services can gain similar authority. Securing the appropriate authorizations requires that these new organizations reflect the objectives of the nations in which services are to be delivered.
Author

N94-22750*# Taylor (Leslie A.) Associates, Bethesda, MD.
USE OF NEGOTIATED RULEMAKING IN DEVELOPING TECHNICAL RULES FOR LOW-EARTH ORBIT MOBILE SATELLITE SYSTEMS
Leslie A. Taylor *In* JPL, Proceedings of the Third International Mobile Satellite Conference (IMSC 1993) 1993 p 79-84 (For primary document see N94-22735 06-32)
Avail: CASI HC A02/MF A06

Technical innovations have converged with the exploding market demand for mobile telecommunications to create the impetus for low-earth orbit (LEO) communications satellite systems. The so-called 'Little LEO's' propose use of VHF and UHF spectrum to provide position - location and data messaging services. The so-called 'Big LEO's' propose to utilize the RDSS bands to provide voice and data services. In the United States, several applications were filed with the U.S. Federal Communications Commission (FCC) to construct and operate these mobile satellite systems. To enable the prompt introduction of such new technology services, the FCC is using innovative approaches to process the applications. Traditionally, when the FCC is faced with 'mutually exclusive' applications, e.g. a grant of one would preclude a grant of the others, it uses selection mechanisms such as comparative hearings or lotteries. In the case of the LEO systems, the FCC has sought to avoid these time-consuming approaches by using negotiated rulemakings. The FCC's objective is to enable the multiple applicants and other interested parties to agree on technical and service rules which will enable the grant of all qualified applications. With regard to the VHF/UHF systems, the Advisory Committee submitted a consensus report to the FCC. The process for the systems operating in the bands above 1 GHz involved more parties and more issues but still provided the FCC useful technical information to guide the adoption of rules for the new mobile satellite service. Author (revised)

N94-22751*# Department of Communications, Ottawa (Ontario).
THE PROVISION OF SPECTRUM FOR FEEDER LINKS OF NON-GEOSTATIONARY MOBILE SATELLITES
Robert R. Bowen *In* JPL, Proceedings of the Third International Mobile Satellite Conference (IMSC 1993) 1993 p 85-90 (For primary document see N94-22735 06-32)
Avail: CASI HC A02/MF A06

The possibility of sharing spectrum in the 30/20 GHz band between geostationary fixed-satellite systems and feeder-links of low-earth orbit (LEO) mobile-satellite systems is addressed, taking into account that International Telecommunications Union (ITU) Radio Regulation 2613 would be a factor in such sharing. Interference into each network in both the uplink at 30 GHz and the downlink at 20 GHz is considered. It is determined that if sharing were to take place the mobile-satellite may have to cease transmission often for intervals up to 10 seconds, may have to use high-gain tracking antennas on its spacecraft, and may find it an advantage to use code-division multiple access. An alternate solution suggested is to designate a band 50 to 100 MHz wide at 28 and 18 GHz to be used primarily for feeder links to LEO systems. Author (revised)

N94-22752*# European Space Agency. European Space Research and Technology Center, ESTEC, Noordwijk (Netherlands).
THE POSSIBILITIES FOR MOBILE AND FIXED SERVICES IN THE 20/30 GHz FREQUENCY BANDS Abstract Only
C. D. Hughes *In* JPL, Proceedings of the Third International Mobile Satellite Conference (IMSC 1993) 1993 p 91 (For primary document see N94-22735 06-32)
Avail: CASI HC A01/MF A06

With the wide range of services now offered by satellite communications and broadcasting and the increasing trend towards small terminal systems, the traditional distinctions between fixed and mobile services are becoming less important. In the future mobile, portable, and fixed services may well operate side by side in a hybrid manner. This trend is already apparent in Europe where extensive use is being made of the fixed service frequency allocations for broadcasting and for mobile services. Similarly many ostensibly mobile terminals are serving fixed installations. Although the immediate future of mobile satellite communications continues to lie in the L-band frequency allocations, in the longer term the 20/30 GHz frequency allocations, offer the possibility of a new beginning where the advantages of hybrid systems can be included in the overall system designs at the outset. The experience gained using 20/30 GHz within the Olympus Utilization program and the likely demands for future services to highlight the most promising avenues for future system development are addressed.
Author (revised)

N94-22753*# Department of Communications, Ottawa (Ontario).
USE OF THE 30/20 GHz BAND BY MULTIPURPOSE SATELLITE SYSTEMS
Stephen McNeil, Vassilios Mimis (Communications Research Centre, Ottawa, Ontario.), Vishnu Sahay, and Robert Bowen *In* JPL, Proceedings of the Third International Mobile Satellite Conference (IMSC 1993) 1993 p 93-98 (For primary document see N94-22735 06-32)
Avail: CASI HC A02/MF A06

The World Administrative Radio Conference (WARC) held in 1992 allocated the bands 19.7-20.2 GHz and 29.5-30.0 GHz to both the Mobile Satellite Service (MSS) and the Fixed Satellite Service (FSS) on a co-primary basis. An economic and flexible solution for the provision of both services is to place both payloads on one spacecraft. Some of the proposed applications of such a hybrid satellite network are described. It also examines the facility for spectrum sharing between the various applications and discusses the impact on coordination. It is concluded that the coordination process would not be more onerous than traditional FSS inter-satellite coordination. Author (revised)

N94-22754*# Department of Defense, Fort Meade, MD.
TRANSPARENT DATA SERVICE WITH MULTIPLE WIRELESS ACCESS
Richard A. Dean and Allen H. Levesque (GTE Government Systems Corp., Waltham, MA.) *In* JPL, Proceedings of the Third International Mobile Satellite Conference (IMSC 1993) 1993 p 101-106 (For primary document see N94-22735 06-32)
Avail: CASI HC A02/MF A06

The rapid introduction of digital wireless networks is an important part of the emerging digital communications scene. The introduction of Digital Cellular, LEO and GEO Satellites, and Personal Communications Services poses both a challenge and an opportunity for the data user. On the one hand wireless access will introduce significant new portable data services such as personal notebooks, paging, E-mail, and fax that will put the information age in the user's pocket. On the other hand the challenge of creating a seamless and transparent environment for the user in multiple access environments and across multiple network connections is formidable. A summary of the issues associated with developing techniques and standards that can support transparent and seamless data services is presented. The introduction of data services into the radio world represents a unique mix of RF channel problems, data protocol issues, and network issues. These problems require that experts from each of these disciplines fuse the individual technologies to support these services.
Author (revised)

N94-22755*# Jet Propulsion Lab., California Inst. of Tech., Pasadena.
INTERNETWORKING SATELLITE AND LOCAL EXCHANGE NETWORKS FOR PERSONAL COMMUNICATIONS APPLICATIONS
Richard S. Wolff (Bell Communications Research, Inc., Morristown, NJ.) and Deborah Pinck *In its* Proceedings of the Third International Mobile Satellite Conference (IMSC 1993) 1993 p 107-112 (For primary document see N94-22735 06-32)
Avail: CASI HC A02/MF A06

The demand for personal communications services has shown unprecedented growth, and the next decade and beyond promise an era in which the needs for ubiquitous, transparent and personalized access to information will continue to expand in both scale and scope. The exchange of personalized information is growing from two-way voice to include data communications, electronic messaging and information services, image transfer, video, and interactive multimedia. The emergence of new land-based and satellite-based wireless networks illustrates the expanding scale and trend toward globalization and the need to establish new local exchange and exchange access services to meet the communications needs of people on the move. An important issue is to identify the roles that satellite networking can play in meeting these new communications needs. The unique capabilities of satellites, in providing coverage to large geographic

areas, reaching widely dispersed users, for position location determination, and in offering broadcast and multicast services, can complement and extend the capabilities of terrestrial networks. As an initial step in exploring the opportunities afforded by the merger of satellite-based and land-based networks, several experiments utilizing the NASA ACTS satellite and the public switched local exchange network were undertaken to demonstrate the use of satellites in the delivery of personal communications services.
Author (revised)

N94-22756*# Ecole Polytechnique Federale de Lausanne (Switzerland). Telecommunications Lab.
POWER ATTENUATION CHARACTERISTICS AS SWITCH-OVER CRITERION IN PERSONAL SATELLITE MOBILE COMMUNICATIONS
c33
Jonathan P. Castro *In* JPL, Proceedings of the Third International Mobile Satellite Conference (IMSC 1993) 1993 p 113-118 (For primary document see N94-22735 06-32)
Avail: CASI HC A02/MF A06

A third generation mobile system intends to support communications in all environments (i.e., outdoors, indoors at home or office and when moving). This system will integrate services that are now available in architectures such as cellular, cordless, mobile data networks, paging, including satellite services to rural areas. One way through which service integration will be made possible is by supporting a hierarchical cellular structure based on umbrella cells, macro cells, micro and pico cells. In this type of structure, satellites are part of the giant umbrella cells allowing continuous global coverage, the other cells belong to cities, neighborhoods, and buildings respectively. This does not necessarily imply that network operation of terrestrial and satellite segments interconnect to enable roaming and spectrum sharing. However, the cell concept does imply hand-off between different cell types, which may involve change of frequency. Within this propsective, the present work uses power attenuation characteristics to determine a dynamic criterion that allows smooth transition from space to terrestrial networks. The analysis includes a hybrid channel that combines Rician, Raleigh and Log Normal fading characteristics. Author

N94-22757*# Jet Propulsion Lab., California Inst. of Tech., Pasadena.
INTEGRATION OF MOBILE SATELLITE AND CELLULAR SYSTEMS
Elliott H. Drucker (Drucker Associates, Kirkland, WA.), Polly Estabrook, Deborah Pinck, and Laura Ekroot *In its* Proceedings of the Third International Mobile Satellite Conference (IMSC 1993) 1993 p 119-124 (For primary document see N94-22735 06-32)
Avail: CASI HC A02/MF A06

By integrating the ground based infrastructure component of a mobile satellite system with the infrastructure systems of terrestrial 800 MHz cellular service providers, a seamless network of universal coverage can be established. Users equipped for both cellular and satellite service can take advantage of a number of features made possible by such integration, including seamless handoff and universal roaming. To provide maximum benefit at lowest posible cost, the means by which these systems are integrated must be carefully considered. Mobile satellite hub stations must be configured to efficiently interface with cellular Mobile Telephone Switching Offices (MTSO's), and cost effective mobile units that provide both cellular and satellite capability must be developed. Author

N94-22758*# MPR Teltech Ltd., Ottawa (Ontario).
INTERWORKING EVOLUTION OF MOBILE SATELLITE AND TERRESTRIAL NETWORKS
R. Matyas, P. Kelleher, P. Moller, and T. Jones (International Maritime Satellite Organization, London, England.) *In* JPL, Proceedings of the Third International Mobile Satellite Conference (IMSC 1993) 1993 p 125-130 (For primary document see N94-22735 06-32)
Avail: CASI HC A02/MF A06

There is considerable interest among mobile satellite service providers in interworking with terrestrial networks to provide a universal global network. With such interworking, subscribers may be provided a common set of services such as those planned for the Public Switched Telephone Network (PSTN), the Integrated Services Digital Network (ISDN), and future Intelligent Networks (IN's). This paper first reviews issues in satellite interworking. Next the status and interworking plans of terrestrial mobile communications service providers are examined with early examples of mobile satellite interworking including a discussion of the anticipated evolution towards full interworking between mobile satellite and both fixed and mobile terrestrial networks. Author

N94-22759*# Surrey Univ., Guildford (England). Centre for Satellite Engineering Research.
INTERWORKING AND INTEGRATION OF THE INMARSAT STANDARD-M WITH PAN-EUROPEAN GSM SYSTEM
R. Tafazolli and B. G. Evans *In* JPL, Proceedings of the Third International Mobile Satellite Conference (IMSC 1993) 1993 p 131-136 (For primary document see N94-22735 06-32)
Avail: CASI HC A02/MF A06

The market demand on mobile telephone communications has been increasing since the introduction of the cellular mobile telephone systems about twelve years ago. In Europe, projections indicate a demand of about 17 million subscribers for a fully deployed Pan European system. The Pan-European GSM system is to harmonize the growth of the terrestrial mobile system. Studies conducted by the European Space Agency (ESA) indicate that even with 60-70 percent of the area being covered by the GSM, a significant traffic demand (voice and data) will still exist for areas not covered by the terrestrial systems. This demand could be satisfied by a land mobile satellite system. The satellite system is therefore seen in a complementary role rather than in competition with the terrestrial system in an integrated telecommunications network. One possible scenario may be that initially the satellite system provides services to the rural areas together with areas still not covered by the GSM system. This service area is then gradually diminished as the terrestrial system expands until an optimum point is reached where the systems co-exist optimally. The objective of this paper is to investigate the possibility of integration of a space based system, in this case Inmarsat Standard-M, with the GSM (Global System for Mobile communications). One very important advantage of incorporating GSM services in Standard-M is that it will be feasible to extend the GSM services economically worldwide, not only to land mobiles but also to aeronautical and maritime mobiles. Author

N94-22760*# Florence Univ. (Italy). Dipt. di Ingegneria Elettronica.
ARCHITECTURES AND PROTOCOLS FOR AN INTEGRATED SATELLITE-TERRESTRIAL MOBILE SYSTEM
E. DelRe, F. DelliPriscoli (Rome Univ., Italy.), P. Iannucci, R. Menolascino (Centro Studi e Laboratori Telecomunicazioni, Turin, Italy.), and F. Settimo (Centro Studi e Laboratori Telecomunicazioni, Turin, Italy.) *In* JPL, Proceedings of the Third International Mobile Satellite Conference (IMSC 1993) 1993 p 137-142 (For primary document see N94-22735 06-32)
Avail: CASI HC A02/MF A06

This paper aims to depict some basic concepts related to the definition of an integrated system for mobile communications, consisting of a satellite network and a terrestrial cellular network. In particular three aspects are discussed: (1) architecture definition for the satellite network; (2) assignment strategy of the satellite channels; and (3) definition of 'internetworking procedures' between cellular and satellite network, according to the selected architecture and the satellite channel assignment strategy. Author

N94-22761*# Rome Univ. (Italy). Dipt. Ingegneria Elettronica.
HANDOVER PROCEDURES IN INTEGRATED SATELLITE AND TERRESTRIAL MOBILE SYSTEMS
G. E. Corazza, M. Ruggieri (Aquila Univ., Italy.), F. Santucci (Aquila Univ., Italy.), and F. Vatalaro *In* JPL, Proceedings of the Third International Mobile Satellite Conference (IMSC 1993) 1993 p 143-148 (For primary document see N94-22735 06-32)
Avail: CASI HC A02/MF A06

The integration of satellite and terrestrial mobile systems is investigated in terms of the strategies for handover across the integrated cellular coverage. The handover procedure is subdivided into an initialization phase, where the need for issuing a handover request must be identified, and an execution phase, where the request must be satisfied, if possible, according to a certain channel assignment strategy. A modeling approach that allows the design of the parameters that influence the performance of the overall handover procedure is presented, along with a few numerical results.
Author

N94-22762*# Westinghouse Electric Corp., Baltimore, MD.
MSAT AND CELLULAR HYBRID NETWORKING
Patrick W. Baranowsky, II *In* JPL, Proceedings of the Third International Mobile Satellite Conference (IMSC 1993) 1993 p 149-154 (For primary document see N94-22735 06-32)
Avail: CASI HC A02/MF A06

Westinghouse Electric Corporation is developing both the Communications Ground Segment and the Series 1000 Mobile Phone for American Mobile Satellite Corporation's (AMSC's) Mobile Satellite (MSAT) system. The success of the voice services portion of this system depends, to some extent, upon the interoperability of the cellular network and the satellite communication circuit switched communication channels. This paper will describe the set of user-selectable cellular interoperable modes (cellular first/satellite second, etc.) provided by the Mobile Phone and described how they are implemented with the ground segment. Topics including roaming registration and cellular-to-satellite 'seamless' call handoff will be discussed, along with the relevant Interim Standard IS-41 Revision B Cellular Radiotelecommunications Intersystem Operations and IOS-553 Mobile Station - Land Station Compatibility Specification. Author

N94-22763*# Hughes Aircraft Co., Los Angeles, CA.
TRENDS IN MOBILE SATELLITE COMMUNICATION
Klaus G. Johannsen, Mike W. Bowles, Samuel Milliken, Alan R. Cherrette, and Gregory C. Busche *In* JPL, Proceedings of the Third International Mobile Satellite Conference (IMSC 1993) 1993 p 157-162 (For primary document see N94-22735 06-32)
Avail: CASI HC A01/MF A06

Ever since the U.S. Federal Communication Commission opened the discussion on spectrum usage for personal handheld communication, the community of satellite manufacturers has been searching for an economically viable and technically feasible satellite mobile communication system. Hughes Aircraft Company and others have joined in providing proposals for such systems, ranging from low to medium to geosynchronous orbits. These proposals make it clear that the trend in mobile satellite communication is toward more sophisticated satellites with a large number of spot beams and onboard processing, providing worldwide interconnectivity. Recent Hughes studies indicate that from a cost standpoint the geosynchronous satellite (GEOS) is most economical, followed by the medium earth orbit satellite (MEOS) and then by the low earth orbit satellite (LEOS). From a system performance standpoint, this evaluation may be in reverse order, depending on how the public will react to speech delay and collision. This paper discusses the trends and various mobile satellite constellations in satellite communication under investigation. It considers the effect of orbital altitude and modulation/multiple access on the link and spacecraft design. Author

N94-22764*# France Telecom International, Issy-les-Moulineaux.
OPTIMIZING SPACE CONSTELLATIONS FOR MOBILE SATELLITE SYSTEMS
T. Roussel and J.-P. Taisant *In* JPL, Proceedings of the Third International Mobile Satellite Conference (IMSC 1993) 1993 p 163-168 (For primary document see N94-22735 06-32)
Avail: CASI HC A02/MF A06

Designing a mobile satellite system entails many complex trade-offs between a great number of parameters including: capacity, complexity of the payload, constellation geometry, number of satellites, quality of coverage, etc. This paper aims at defining a methodology which tries to split the variables to give rapidly some first results. The major input considered is the traffic assumption which would be offered by the system. A first key step is the choice of the best Rider or Walker constellation geometries - with different numbers of satellites - to insure a good quality of coverage over a selected service area. Another aspect to be addressed is the possible altitude location of the constellation, since it is limited by many constraints. The altitude ranges that seem appropriate considering the spatial environment, the launch and orbit keeping policy and the feasibility of the antenna allowing sufficient frequency reuse are briefly analyzed. To support these first considerations, some 'reference constellations' with similar coverage quality are chosen. The in-orbit capacity needed to support the assumed traffic is computed versus altitude. Finally, the exact number of satellite is determined. It comes as an optimum between a small number of satellites offering a high (and costly) power margin in bad propagation situation and a great number of less powerful satellites granting the same quality of service. Author

N94-22765*# European Space Agency. European Space Research and Technology Center, ESTEC, Noordwijk (Netherlands).
GEOSTATIONARY PAYLOAD CONCEPTS FOR PERSONAL SATELLITE COMMUNICATIONS
J. Benedicto, P. Rinous, I. Roberts, A. Roederer, and I. Stojkovic *In* JPL, Proceedings of the Third International Mobile Satellite Conference (IMSC 1993) 1993 p 169-174 Sponsored in part by British Aerospace Aircraft Group (For primary document see N94-22735 06-32)
Avail: CASI HC A02/MF A06

This paper reviews candidate satellite payload architectures for systems providing world-wide communication services to mobile users equipped with hand-held terminals based on large geostationary satellites. There are a number of problems related to the payload architecture, on-board routing and beamforming, and the design of the S-band Tx and L-band Rx antenna and front ends. A number of solutions are outlined, based on trade-offs with respect to the most significant performance parameters such as capacity, G/T, flexibility of routing traffic to beams and re-configuration of the spot-beam coverage, and payload mass and power. Candidate antenna and front-end configurations were studied, in particular direct radiating arrays, arrays magnified by a reflector and active focused reflectors with overlapping feed clusters for both transmit (multimax) and receive (beam synthesis). Regarding the on-board routing and beamforming sub-systems, analog techniques based on banks of SAW filters, FET or CMOS switches and cross-bar fixed and variable beamforming are compared with a hybrid analog/digital approach based on Chirp Fourier Transform (CFT) demultiplexer combined with digital beamforming or a fully digital processor implementation, also based on CFT demultiplexing. Author

N94-22766*# Spar Aerospace Ltd., Sainte-Anne-de-Bellevue (Quebec).
A SYSTEM ARCHITECTURE FOR AN ADVANCED CANADIAN WIDEBAND MOBILE SATELLITE SYSTEM
P. Takats, M. Keelty, and H. Moody *In* JPL, Proceedings of the Third International Mobile Satellite Conference (IMSC 1993) 1993 p 175-180 (For primary document see N94-22735 06-32)
Avail: CASI HC A02/MF A06

In this paper, the system architecture for an advanced Canadian ka-band geostationary mobile satellite system is described, utilizing hopping spot beams to support a 256 kbps wideband service for both N-ISDN and packet-switched interconnectivity to small briefcase-size portable and mobile terminals. An assessment is given of the technical feasibility of the satellite payload and terminal design in the post year 2000 timeframe. The satellite payload includes regeneration and on-board switching to permit single hop interconnectivity between mobile terminals. The mobile terminal requires antenna tracking and platform stabilization to ensure acquisition of the satellite signal. The potential user applications targeted for this wideband service includes: home-office, multimedia, desk-top (PC) videoconferencing, digital audio broadcasting, single and multi-user personal communications. Author

N94-22767*# British Aerospace Public Ltd. Co., Stevenage (England).
APPLICABILITY OF DIFFERENT ONBOARD ROUTING AND PROCESSING TECHNIQUES TO MOBILE SATELLITE SYSTEMS
A. D. Craig, P. C. Marston, P. M. Bakken (Frobe Radio A/S, Trondheim, Norway.), A. Vernucci (Space Engineering, Rome, Italy.), and J. Benedicto (European Space Agency. European Space Research and Technology Center, ESTEC, Noordwijk, Netherlands.) *In* JPL, Proceedings of the Third International Mobile Satellite Conference (IMSC 1993) 1993 p 181-186 (For primary document see N94-22735 06-32)
Avail: CASI HC A02/MF A06

The paper summarizes a study contract recently undertaken for ESA. The study compared the effectiveness of several processing architectures applied to multiple beam, geostationary global and European regional missions. The paper discusses architectures based on transparent SS-FDMA analog, transparent DSP and regenerative processing. Quantitative comparisons are presented and general conclusions are given with respect to suitability of the architectures to different mission requirements. Author

N94-22768*# Space Engineering, Rome (Italy).
A EUROPEAN MOBILE SATELLITE SYSTEM CONCEPT EXPLOITING CDMA AND OBP
A. Vernucci and A. D. Craig (British Aerospace Public Ltd. Co., Stevenage, England.) *In* JPL, Proceedings of the Third International Mobile Satellite Conference (IMSC 1993) 1993 p 187-192 (For primary document see N94-22735 06-32)
Avail: CASI HC A02/MF A06

This paper describes a novel Land Mobile Satellite System (LMSS) concept applicable to networks allowing access to a large number of gateway stations ('Hubs'), utilizing low-cost Very Small Aperture Terminals (VSAT's). Efficient operation of the Forward-Link (FL) repeater can be achieved by adopting a synchronous Code Division Multiple Access (CDMA) technique, whereby inter-code interference (self-noise) is virtually eliminated by synchronizing orthogonal codes. However, with a transparent FL repeater, the requirements imposed by the highly decentralized ground segment can lead to significant efficiency losses. The adoption of a FL On-Board Processing (OBP) repeater is proposed as a means of largely recovering this efficiency impairment. The paper describes the network architecture, the system design and performance, the OBP functions and impact on implementation. The proposed concept, applicable to a future generation of the European LMSS, was developed in the context of a European Space Agency (ESA) study contract. Author

N94-22769*# ATR Optical and Radio Communications Research Labs., Kyoto (Japan).
STUDY OF LEO-SAT MICROWAVE LINK FOR BROAD-BAND MOBILE SATELLITE COMMUNICATION SYSTEM
Masayuki Fujise, Wataru Chujo, Isamu Chiba, Yoji Furuhama, Kazuaki Kawabata (Toshiba Corp., Kawasaki, Japan.), and Yoshihiko Konishi (Mitsubishi Electric Corp., Tokyo, Japan.) *In* JPL, Proceedings of the Third International Mobile Satellite Conference (IMSC 1993) 1993 p 193-198 (For primary document see N94-22735 06-32)
Avail: CASI HC A02/MF A06

In the field of mobile satellite communications, a system based on low-earth-orbit satellites (LEO-SAT's) such as the Iridium system has been proposed. The LEO-SAT system is able to offer mobile telecommunication services in high-latitude areas. Rain degradation, fading and shadowing are also expected to be decreased when the system is operated at a high elevation angle. Furthermore, the propagation delay generated in the LEO-SAT system is less pronounced than that in the geostationary orbit satellite (GEO-SAT) system and, in voice services, the effect of the delay is almost negligible. We proposed a concept of a broad-band mobile satellite communication system with LEO-SAT's and Optical ISL. In that system, a fixed L-band (1.6/1.5 GHz) multibeam is used to offer narrow band service to the mobile terminals in the entire area covered by a LEO-SAT and steerable Ka-band (30/20 GHz) spot beams are used for the wide band service. In this paper, we present results of a study of LEO-SAT microwave link between a satellite and a mobile terminal for a broad-band mobile satellite communication system. First, the results of link budget calculations are presented and the antennas mounted on satellites are shown. For a future mobile antenna technology, we also show digital beamforming (DBF) techniques. DBF, together with modulation and/or demodulation, is becoming a key technique for mobile antennas with advanced functions such as antenna pattern calibration, correction, and radio interference suppression. In this paper, efficient DBF techniques for transmitting and receiving are presented. Furthermore, an adaptive array antenna system suitable for this LEO-SAT is presented. Author

N94-22770*# National Central Univ., Chung-Li (Taiwan).
ROCSAT-1 TELECOMMUNICATION EXPERIMENTS
J. F. Chang, R. R. Taur (Lockheed Missiles and Space Co., Calabasas, CA.), T. H. Chu (National Taiwan Univ., Taipei.), H. S. Li (National Taiwan Univ., Taipei.), Y. T. Su (National Cheng Kung Univ., Tainan, Taiwan.), Y. W. Kiang (National Taiwan Univ., Taipei.), S. L. Su (National Cheng Kung Univ., Tainan, Taiwan.), M. P. Shih (Telecommunication Lab. DGT, Chung-Li, Taiwan.), H. D. Lin (Telecommunication Lab. DGT, Chung-Li, Taiwan.), and C. D. Chung *In* JPL, Proceedings of the Third International Mobile Satellite Conference (IMSC 1993) 1993 p 199-204 (For primary document see N94-22735 06-32)
Avail: CASI HC A02/MF A06

This paper addresses a telecommunication payload project approved by the R.O.C. NSPO's ROCSAT-1 space program. This project will enable several innovative experiments via the low-earth-orbit satellite ROCSAT-1, including multipath fading channel characterization, ionospheric scintillation measurement, real-time voice communications, and CDMA data communications. A unified L/S-band transponder payload is proposed for conducting these experiments in an efficient way. The results of these experiments would provide the evolving mobile communication communities with fruitful information. Author

N94-22771*# Jet Propulsion Lab., California Inst. of Tech., Pasadena.
ACTS BROADBAND AERONAUTICAL EXPERIMENT
Brian S. Abbe, Thomas C. Jedrey, Polly Estabrook, and Martin J. Agan *In its* Proceedings of the Third International Mobile Satellite Conference (IMSC 1993) 1993 p 205-210 (For primary document see N94-22735 06-32)
Avail: CASI HC A02/MF A06

In the last decade, the demand for reliable data, voice, and video satellite communication links between aircraft and ground to improve air traffic control, airline management, and to meet the growing demand for passenger communications has increased significantly. It is expected that in the near future, the spectrum required for aeronautical communication services will grow significantly beyond that currently available at L-band. In anticipation of this, JPL is developing an experimental broadband aeronautical satellite communications system that will utilize NASA's Advanced Communications Technology Satellite (ACTS) as a satellite of opportunity and the technology developed under JPL's ACTS Mobile Terminal (AMT) Task to evaluate the feasibility of using K/Ka-band for these applications. The application of K/Ka-band for aeronautical satellite communications at cruise altitudes is particularly promising for several reasons: (1) the minimal amount of signal attenuation due to rain; (2) the reduced drag due to the smaller K/Ka-band antennas (as compared to the current L-band systems); and (3) the large amount of available bandwidth. The increased bandwidth available at these frequencies is expected to lead to significantly improved passenger communications - including full-duplex compressed video and multiple channel voice. A description of the proposed broadband experimental system will be presented including: (1) applications of K/Ka-band aeronautical satellite technology to U.S. industry; (2) the experiment objectives; (3) the experiment set-up; (4) experimental equipment description; and (5) industrial participation in the experiment and the benefits. Author

N94-22772*# Federal Aviation Administration, Washington, DC.
THE FAA SATELLITE COMMUNICATIONS PROGRAM
Karen L. Burcham *In* JPL, Proceedings of the Third International Mobile Satellite Conference (IMSC 1993) 1993 p 213-218 (For primary document see N94-22735 06-32)
Avail: CASI HC A02/MF A06

The Federal Aviation Administration is developing satellite communications capabilities to enhance air traffic services, first in oceanic and remote regions, and later for United States domestic services. The program includes four projects which develop technical standards, assure adequate system performance, support implementation, and provide for research and development for selected areas of U.S. domestic satellite communications. The continuing focus is the application of automated data communications, which is already permitting enhanced and regular position reporting. Voice developments, necessary for non-routine communications, are also included among the necessary activities to improve ATC communications. Author

N94-22773*# Communications Research Centre, Ottawa (Ontario).
CANADIAN AERONAUTICAL MOBILE DATA TRIALS
Allister Pedersen and Andrea Pearson (Telesat Mobile, Inc., Ottawa, Ontario.) *In* JPL, Proceedings of the Third International Mobile Satellite Conference (IMSC 1993) 1993 p 219-224 (For primary document see N94-22735 06-32)
Avail: CASI HC A02/MF A06

This paper describes a series of aeronautical mobile data trials conducted on small aircraft (helicopters and fixed wing) utilizing a low-speed store-and-forward mobile data service. The paper outlines the user requirements for aeronautical mobile satellite communications. 'Flight following' and improved wide-area dispatch communications were identified as high priority requirements. A 'proof-of-concept' trial in a Cessna Skymaster aircraft is described. This trial identified certain development work as essential to the introduction of commercial service including antenna development, power supply modifications and doppler software modifications. Other improvements were also proposed. The initial aeronautical mobile data service available for pre-operational (Beta) trials is outlined. Pre-operational field trials commenced in October 1992 and consisted of installations on a Gralen Communications Inc. Cessna 177 and an Aerospatiale Astar 350 series light single engine helicopter. The paper concludes with a discussion of desirable near term mobile data service developments, commercial benefits, current safety benefits and potential future applications for improved safety. Author

N94-22774*# Jet Propulsion Lab., California Inst. of Tech., Pasadena.
ACTS MOBILE SATCOM EXPERIMENTS
Brian S. Abbe, Robert E. Frye, and Thomas C. Jedrey *In its* Proceedings of the Third International Mobile Satellite Conference (IMSC 1993) 1993 p 225-230 (For primary document see N94-22735 06-32)
Avail: CASI HC A02/MF A06

Over the last decade, the demand for reliable mobile satellite communications (satcom) for voice, data, and video applications has increased dramatically. As consumer demand grows, the current spectrum allocation at L-band could become saturated. For this reason, NASA and the Jet Propulsion Laboratory are developing the Advanced Communications Technology Satellites (ACTS) mobile terminal (AMT) and are evaluating the feasibility of K/Ka-band (20/30 GHz) mobile satcom to meet these growing needs. U.S. industry and government, acting as co-partners, will evaluate K/Ka-band mobile satcom and develop new technologies by conducting a series of applications-oriented experiments. The ACTS and the AMT testbed will be used to conduct these mobile satcom experiments. The goals of the ACTS Mobile Experiments Program and the individual experiment configurations and objectives are further presented. Author

N94-22775*# Vigyan Research Associates, Inc., Hampton, VA.
COCKPIT WEATHER GRAPHICS USING MOBILE SATELLITE COMMUNICATIONS
Shashi Seth *In* JPL, Proceedings of the Third International Mobile Satellite Conference (IMSC 1993) 1993 p 231-233 (For primary document see N94-22735 06-32)
(Contract NAS1-19595)
Avail: CASI HC A01/MF A06

Many new companies are pushing state-of-the-art technology to bring a revolution in the cockpits of General Aviation (GA) aircraft. The vision, according to Dr. Bruce Holmes - the Assistant Director for Aeronautics at National Aeronautics and Space Administration's (NASA) Langley Research Center, is to provide such an advanced flight control system that the motor and cognitive skills you use to drive a car would be very similar to the ones you would use to fly an airplane. We at ViGYAN, Inc., are currently developing a system called the Pilot Weather Advisor (PWxA), which would be a part of such an advanced technology flight management system. The PWxA provides graphical depictions of weather information in the cockpit of aircraft in near real-time, through the use of broadcast satellite communications. The purpose of this system is to improve the safety and utility of GA aircraft operations. Considerable effort is being extended for research in the design of graphical weather systems, notably the works of Scanlon and Dash. The concept of providing pilots with graphical depictions of weather conditions, overlaid on geographical and navigational maps, is extremely powerful. Author

N94-22776*# EROS Data Center, Sioux Falls, SD.
THE AGRHYMET DATA COMMUNICATIONS PROJECT
G. R. Mah and D. P. Salpini (Information Resource Management Service, Arlington, VA.) *In* JPL, Proceedings of the Third International Mobile Satellite Conference (IMSC 1993) 1993 p 235-240 (For primary document see N94-22735 06-32)
(Contract USGS-AFR-0973-P-IC-9014)
Avail: CASI HC A02/MF A06

The U.S. Geological Survey (USGS) and the U.S. Agency for International Development (USAID) are providing technical assistance to the AGRHYMET program in West Africa. AGRHYMET staff use remote sensing technology to produce satellite image maps of the Sahel region of West Africa. These image maps may show vegetation greenness, sea surface temperatures, or processed weather satellite imagery. The image maps must be distributed from the AGRHYMET Regional Center in Niger to national AGRHYMET centers in the member countries of Burkina Faso, Cape Verde, Chad, Gambia, Guinea-Bissau, Mali, Mauritania, Niger, and Senegal. After consideration of a number of land- and space-based solutions for image map distribution, the best solution was determined to be use of International Maritime Satellite Organization (INMARSAT) land-based terminals. In April 1992, a field test and proof-of-concept demonstration using land-mobile terminals produced favorable results. The USGS and USAID are setting up a wide area network using INMARSAT terminals to link the AGRHYMET sites for image data transfer. The system is in the procurement and installation phase and initial opening capability may be operational for the 1993 growing season, starting in May 1993. Author

N94-22777*# Washington State Patrol, Bellevue.
USING SATELLITE COMMUNICATIONS FOR A MOBILE COMPUTER NETWORK
Douglas J. Wyman *In* JPL, Proceedings of the Third International Mobile Satellite Conference (IMSC 1993) 1993 p 241-244 (For primary document see N94-22735 06-32)
Avail: CASI HC A01/MF A06

The topics discussed include the following: patrol car automation, mobile computer network, network requirements, network design overview, MCN mobile network software, MCN hub operation, mobile satellite software, hub satellite software, the benefits of patrol car automation, the benefits of satellite mobile computing, and national law enforcement satellite. CASI

N94-22778*# Telesat Mobile, Inc., Ottawa (Ontario).
DESIGN AND IMPLEMENTATION CONSIDERATIONS OF A MSAT PACKET DATA NETWORK
Fouad G. Karam, Terry Hearn (Westinghouse Electric Corp., Baltimore, MD.), Doug Rohr (Westinghouse Canada, Inc., Hamilton, Ontario.), and Arthur F. Guibord *In* JPL, Proceedings of the Third International Mobile Satellite Conference (IMSC 1993) 1993 p 245-250 (For primary document see N94-22735 06-32)
Avail: CASI HC A02/MF A06

The Mobile Data System, which is intended to provide for packet switched data services is currently under development. The system is based on a star network topology consisting of a centralized Data Hub (DH) serving a large number of mobile terminals. Through the Data Hub, end-to-end connections can be established between terrestrial users on public or private data networks and mobile users. The MDS network will be capable of offering a variety of services some of which are based on the standard X.25 network interface protocol, and others optimized for short messages and broadcast messages. A description of these services and the trade-offs in the DH design are presented. Author

N94-22779*# International Maritime Satellite Organization, London (England).
EVOLUTION OF INMARSAT SYSTEMS AND APPLICATIONS: THE LAND MOBILE EXPERIENCE
Eugene Staffa and Ram Subramaniam *In* JPL, Proceedings of the Third International Mobile Satellite Conference (IMSC 1993) 1993 p 251-256 (For primary document see N94-22735 06-32)
Avail: CASI HC A02/MF A06

Inmarsat has provided mobile satellite communication services for land mobile applications for well over a decade. Having started with the Inmarsat-A voice and telex system, Inmarsat is committed to the evolution of services towards a global personal, handheld satellite communicator. Over the years, users have benefitted from the evolution of technologies, increased user friendliness and portability of terminals and ever decreasing cost of operations. This paper describes the various present systems, their characteristics and applications, and outlines their contributions in the evolution towards the personal global communicator. Author

N94-22780*# Jet Propulsion Lab., California Inst. of Tech., Pasadena.
ACTS ADVANCED SYSTEM CONCEPTS AND EXPERIMENTATION
Abstract Only
Brian S. Abbe and Noulie Theofylaktos (National Aeronautics and Space Administration. Lewis Research Center, Cleveland, OH.) *In its* Proceedings of the Third International Mobile Satellite Conference (IMSC 1993) 1993

p 257 (For primary document see N94-22735 06-32)
Avail: CASI HC A01/MF A06

Over the course of the first two years of experimentation with the Advanced Communications Technology Satellite (ACTS), many different K/Ka-band applications-oriented experiments will be conducted and evaluated for their commercial viability. In addition, the technological developments and advanced systems concepts associated with the various terminals and the satellite itself will also be examined. Beyond these existing experiments and the current terminal developments, many other new and exciting experiment ideas and advanced system concepts exist. With the additional use of ACTS for the last two years of its lifetime, many of these ideas could be explored. In the mobile satellite communications arena, a particular applications-oriented concept that has yet to be developed is a maritime-mobile experiment. Applications of K/Ka-band mobile satcom technologies to the pleasure cruise industry could provide similar communications services as those that are being developed for the broadband aeronautical experiments. A second applications-oriented experiment that could be of interest is the development of a hybrid satellite-cellular system experiment. In such an experimental system, a mobile K/Ka-band satellite service would extend the coverage of the already existing cellular network. Many new system concepts and terminal developments could also be accomplished. The initial characterization of the K/Ka-band mobile satellite communications propagation channel and evaluation of the currently existing rain compensation algorithms (RCA's) could lead to a second generation RCA development that would improve the overall ACTS Mobile Terminal (AMT) performance. In addition, the development of an enhanced modem to be used with the AMT that utilizes CDMA spread spectrum would also improve the overall terminal efficiency and provide a greater commercial potential for K/Ka-band applications. Other techniques worthy of further exploration and evaluation include the development of new Doppler estimation algorithms and demodulation techniques such as pseudo-coherent demodulation. The possibility of exploring these new and exciting experiment and conceptual ideas, as well as many others, with an extended ACTS satellite lifetime, are examined. Author

N94-22781*# Eutelsat, Paris (France).
EUTELTRACS: THE EUROPEAN EXPERIENCE ON MOBILE SATELLITE SERVICES
Jean-Noel Colcy and Rafael Steinhaeuser *In* JPL, Proceedings of the Third International Mobile Satellite Conference (IMSC 1993) 1993 p 261-266 (For primary document see N94-22735 06-32)
Avail: CASI HC A02/MF A06

EUTELTRACS is Europe's first commercially operated Mobile Satellite Service. Under the overall network operation of EUTELSAT, the European Telecommunications Satellite Organization, EUTELTRACS provides an integrated message exchange and position reporting service. This paper describes the EUTELTRACS system architecture, the message exchange and the position reporting services, including the result of recent analysis of message delivery time and positioning accuracy. It also provides an overview of the commercial deployment, the regulatory situation for its operation within Europe and new applications outside its target market, the international road transportation. Author

N94-22782*# Orbital Sciences Corp., Fairfax, VA.
THE ORBCOMM DATA COMMUNICATIONS SYSTEM
David C. Schoen and Paul A. Locke *In* JPL, Proceedings of the Third International Mobile Satellite Conference (IMSC 1993) 1993 p 267-272 (For primary document see N94-22735 06-32)
Avail: CASI HC A02/MF A06

The ORBCOMM system is designed to provide low-cost, two-way data communications for mobile and remote users. The communications system is ideally configured for low data rate applications where communicating devices are geographically dispersed and two-way communications through terrestrial means is cumbersome and not cost effective. The remote terminals use VHF frequencies which allow for the use of very small, low-cost terminals. ORBCOMM has entered into joint development agreements with several large manufacturers of both consumer and industrial electronics to design and build the remote terminals. Based on prototype work, the estimated retail cost of these units will range from $50 to $400 depending on the complexity of the design. Starting in the fall of 1993, ORBCOMM will begin service with a demonstration network consisting of two operating satellites. By the end of 1994, a full operating network of 26 satellites, four Gateway Earth Stations, and a Network Control Center will be in place. The full constellation will provide full coverage of the entire world with greater than 94 percent communications availability for the continental U.S. This paper describes the ORBCOMM system, the technology used in its implementation, and its applications. Author

N94-22783*# Optus Communications, Sydney (Australia). Mobile Services.
MOBILESAT (TM): A WORLD FIRST
Paul Cooper and Linda Crawley *In* JPL, Proceedings of the Third International Mobile Satellite Conference (IMSC 1993) 1993 p 273-277 (For primary document see N94-22735 06-32)
Avail: CASI HC A01/MF A06

Mobilesat will be the world's first truly mobile satellite telephony service to be offered in the land mobile market. Essentially a car phone which will be offered as a fixed service at a later date, mobilesat will bring circuit switched voice communications to remote and rural areas of Australia. This paper outlines where mobilesat fits as part of Optus, Australia's new telecommunications carrier, and briefly discuss the mobilesat system, its market, and the future of mobile communications in Australia. Author

N94-22784*# Westinghouse Electric Corp., Baltimore, MD.
IMPLEMENTATION OF A SYSTEM TO PROVIDE MOBILE SATELLITE SERVICES IN NORTH AMERICA
Gary A. Johanson, N. George Davies (Telesat Mobile, Inc., Ottawa, Ontario.), and William R. H. Tisdale (American Mobile Satellite Corp., Washington, DC.) *In* JPL, Proceedings of the Third International Mobile Satellite Conference (IMSC 1993) 1993 p 279-284 (For primary document see N94-22735 06-32)
Avail: CASI HC A02/MF A06

This paper describes the implementation of the ground network to support Mobile Satellite Services (MSS). The system is designed to take advantage of a powerful new satellite series and provides significant improvements in capacity and throughput over systems in service today. The system is described in terms of the services provided and the system architecture being implemented to deliver those services. The system operation is described including examples of a circuit switched and packet switched call placement. The physical architecture is presented showing the major hardware components and software functionality placement within the hardware. Author

N94-22785*# Motorola, Inc., McLean, VA.
THE IRIDIUM (TM) SYSTEM: PERSONAL COMMUNICATIONS ANYTIME, ANYPLACE
John E. Hatlelid and Larry Casey (Motorola, Inc., Chandler, AZ.) *In* JPL, Proceedings of the Third International Mobile Satellite Conference (IMSC 1993) 1993 p 285-290 (For primary document see N94-22735 06-32)
Avail: CASI HC A02/MF A06

The Iridium system is designed to provide handheld personal communications between diverse locations around the world at any time and without prior knowledge of the location of the personal units. This paper provides an overview of the system, the services it provides, its operation, and an overview of the commercial practices and relatively high volume satellite production techniques which will make the system cost effective. A constellation of 66 satellites will provide an orbiting, spherical-shell, infrastructure for this global calling capability. The satellites act as tall cellular towers and allow convenient operation for portable handheld telephones. The system will provide a full range of services including voice, paging, data, geolocation, and fax capabilities. Motorola is a world leader in the production of high volume, high quality, reliable telecommunications hardware. One of Iridium's goals is to apply these production techniques to high reliability space hardware. Concurrent engineering, high performance work teams, advanced manufacturing technologies, and improved assembly and test methods are some of the techniques that will keep the Iridium system cost effective. Mobile, global, flexible personal communications are coming that will allow anyone to call or receive a call from/to anyplace at anytime. The Iridium system will provide communications where none exist today. This connectivity will allow increased information transfer, open new markets for various business endeavors, and in general increase productivity and development. Author

N94-22786*# Loral Aerospace Corp., Palo Alto, CA.
THE GLOBALSTAR MOBILE SATELLITE SYSTEM FOR WORLDWIDE PERSONAL COMMUNICATIONS
Robert A. Wiedeman and Andrew J. Viterbi (Qualcomm, Inc., San Diego, CA.) *In* JPL, Proceedings of the Third International Mobile Satellite Conference (IMSC 1993) 1993 p 291-296 (For primary document see N94-22735 06-32)
Avail: CASI HC A02/MF A06

Loral Aerospace Corporation along with Qualcomm Inc. have developed a satellite system which offers global mobile voice and data services to and from handheld and mobile user terminals with omni-directional antennas. By combining the use of low-earth orbit (LEO) satellites with existing terrestrial communications systems and innovative, highly efficient spread spectrum techniques, the Globalstar system provides users with low-cost, reliable communications throughout the world. The Globalstar space segment consists of a constellation of 48 LEO satellites in circular orbits with 750 NM (1389 km) altitude. Each satellite communicates with the mobile users via the satellite-user links and with gateway stations. The gateway stations handle the interface between the Globalstar network and the OSTN/PLMN systems. Globalstar transceivers are similar to currently proposed digital cellular telephones in size and have a serial number that will allow the end user to make and receive calls from or to that device anywhere in the world. The Globalstar system is designed to operate as a complement to existing local, long-distance, public, private and specialized telecommunications networks. Service is primarily designed to serve the rural and thin route communications needs of consumers, government users, and private networks. Author

N94-22787*# TRW Space and Defense Sector, Redondo Beach, CA. Space and Electronics Group.
ODYSSEY PERSONAL COMMUNICATIONS SATELLITE SYSTEM
Christopher J. Spitzer *In* JPL, Proceedings of the Third International Mobile Satellite Conference (IMSC 1993) 1993 p 297-302 (For primary document see N94-22735 06-32)
Avail: CASI HC A02/MF A06

The spectacular growth of cellular telephone networks has proved the demand for personal communications. Large regions of the world are too sparsely populated to be economically served by terrestrial cellular communications. Since satellites are well suited to this application, TRW filed with the FCC on May 31, 1993 for the Odyssey construction permit. Odyssey will provide high quality wireless communication services worldwide from satellites. These services will include: voice, data, paging, and messaging. Odyssey will be an economical approach to providing communications. A constellation of 12 satellites will be orbited in three, 55 deg. inclined planes at an altitude of 10,354 km to provide continuous coverage of designated regions. Two satellites will be visible anywhere in the world at all times. This dual visibility leads to high line-of-sight elevation angles, minimizing obstructions by terrain, trees and buildings. Each satellite generates a multibeam antenna pattern that divides its coverage area into a set of contiguous cells. The communications system employs spread spectrum CDMA on both the uplinks and downlinks. This signaling method permits band sharing with other systems and applications. Signal processing is accomplished on the ground at the satellite's 'Gateway' stations. The 'bent pipe' transponders accommodates different regional standards, as well as signaling changes over time. The low power Odyssey handset will be cellular compatible. Multipath fade protection is provided in the handset. Author

N94-22788*# International Maritime Satellite Organization, London (England).
INMARSAT'S PERSONAL COMMUNICATOR SYSTEM Abstract Only
Nick Hart, Hans-C. Haugli, Peter Poskett, and K. Smith *In* JPL, Proceedings of the Third International Mobile Satellite Conference (IMSC 1993) 1993 p 303-304 (For primary document see N94-22735 06-32)
Avail: CASI HC A01/MF A06

Inmarsat has been providing near global mobile satellite communications since 1982 and Inmarsat terminals are currently being used in more than 130 countries. The terminals have been reduced in size and cost over the years and new technology has enabled the recent introduction of briefcase sized personal telephony terminals (Inmarsat-M). This trend continues and we are likely to see Inmarsat handheld terminals by the end of the decade. These terminals are called Inmarsat-P and this paper focuses on the various elements required to support a high quality service to handheld terminals. The main system elements are: the handheld terminals; the space segment with the associated orbits; and the gateways to terrestrial networks. It is both likely and desirable that personal handheld satellite communications will be offered by more than one system provider and this competition will ensure strong emphasis on service quality and cost of ownership. The handheld terminals also have to be attractive to a large number of potential users, and this means that the terminals must be small enough to fit in a pocket. Battery lifetime is another important consideration, and this coupled with radiation safety requirements limits the maximum radiated EIRP. The terminal G/T is mainly constrained by the gain of the omnidirectional antenna and the noise figure of the RF front end (including input losses). Inmarsat has examined, with the support of industry, a number of Geosynchronous (GSO), Medium Earth Orbit (MEO) and Low Earth Orbit (LEO) satellite options for the provision of a handheld mobile satellite service. This paper describes the key satellite and orbit parameters and tradeoffs which affect the overall quality of service and the space segment costing. The paper also stresses not only the importance of using and sharing the available mobile frequency band allocations efficiently, but also the key considerations affecting the choice of feeder link bands. The design of the gateways and the terrestrial network is critical to the overall viability of the service, and this paper also examines the key technical parameters associated with the Land Earth Stations (LES), which act as gateways into the Public Switched Telephone Network (PSTN). These not only include the design tradeoffs associated with the LES, but also the different terrestrial network interface options. The paper concludes with a brief description of the satellite propagation conditions associated with the use of handheld terminals. It describes how the handheld results in a number of propagation impairments which are not common to the previous measurements associated with vehicle mounted antennas. These measurements indicate that there is a complex tradeoff between link margin and the elevation angle to the satellite which has a significant impact on the space segment requirements and costing. Author

N94-22789*# European Space Agency. European Space Research and Technology Center, ESTEC, Noordwijk (Netherlands).
THE EUROPEAN MOBILE SYSTEM (EMS)
A. Jongejans, R. Rogard, I. Mistretta (Telespazio S.p.A., Rome, Italy.), and F. Ananasso (Telespazio S.p.A., Rome, Italy.) *In* JPL, Proceedings of the Third International Mobile Satellite Conference (IMSC 1993) 1993 p 305-310 (For primary document see N94-22735 06-32)
Avail: CASI HC A02/MF A06

The European Space Agency is presently procuring an L band payload in order to promote a regional European L band system coping with the specific needs of the European market. The payload, and the two communications systems to be supported, are described below. The potential market for EMS in Europe is discussed. Author

N94-22790*# Ministry of Posts and Telecommunications, Kashima (Japan). Space Research Center.
LAND MOBILE SATELLITE PROPAGATION MEASUREMENTS IN JAPAN USING ETS-V SATELLITE
Noriaki Obara, Kenji Tanaka, Shin-Ichi Yamamoto, and Hiromitsu Wakana *In* JPL, Proceedings of the Third International Mobile Satellite Conference (IMSC 1993) 1993 p 313-318 (For primary document see N94-22735 06-32)
Avail: CASI HC A02/MF A06

Propagation characteristics of land mobile satellite communications channels have been investigated actively in recent years. Information of propagation characteristics associated with multipath fading and shadowing is required to design commercial land mobile satellite communications systems, including protocol and error correction method. CRL (Communications Research Laboratory) has carried out propagation measurements using the Engineering Test Satellite-V (ETS-V) at L band (1.5 GHz) through main roads in Japan by a medium gain antenna with an autotracking capability. This paper presents the propagation statistics obtained in this campaign. Author

N94-22791*# Bradford Univ. (England). Dept. of Electronic and Electrical Engineering.
MEASUREMENTS ON THE SATELLITE-MOBILE CHANNEL AT L AND S BANDS

H. Smith, J. G. Gardiner, and S. K. Barton *In* JPL, Proceedings of the Third International Mobile Satellite Conference (IMSC 1993) 1993 p 319-324 Sponsored by United Kingdom Radiocommunications Agency and ESA (For primary document see N94-22735 06-32)
Avail: CASI HC A02/MF A06

An experiment is described in which measurements are made on the satellite-mobile channel at L and S bands. A light aircraft carrying a c.w. beacon is flown at elevation angles of 40, 60 and 80 degrees to a mobile receiver. The signal strength at the mobile is recorded in open, urban, suburban and tree shadowed environments. This data is then analyzed to produce statistics for the channel with respect to frequency, elevation angle, and environment. Results are presented together with a brief discussion, suggested interpretation, and conclusion. Author

N94-22792*# Johns Hopkins Univ., Laurel, MD. Applied Physics Lab.
K-BAND MOBILE PROPAGATION MEASUREMENTS USING ACTS
Julius Goldhirsh, Wolfhard J. Vogel (Texas Univ., Austin.), and Geoffrey W. Torrence (Texas Univ., Austin.) *In* JPL, Proceedings of the Third International Mobile Satellite Conference (IMSC 1993) 1993 p 325-330 (For primary document see N94-22735 06-32)
Avail: CASI HC A02/MF A06

An overview of two planned propagation campaigns employing land-mobile scenarios with ACTS is presented. The campaigns will be undertaken through a joint effort involving the Johns Hopkins University, Applied Physics Laboratory (APL), The University of Texas at Austin, Electrical Engineering Research Laboratory (EERL), and the NASA Lewis Research Center (NASA LeRC). Propagation campaigns are planned in Central Maryland in November 1993 (elevation angle approx. equals 40 deg.) and in Fairbanks, Alaska in June 1994 (elevation angle approx. equals 8 deg.) employing a computer controlled antenna tracking system located atop a van containing a receiver/data acquisition system. The antenna will track (in azimuth) downlink transmissions at 19.914 GHz from ACTS during the mobile propagation measurements. The major objectives of the campaigns are to measure the fade and multipath effects of trees and terrain at 20 GHz for rural and suburban scenarios and to extend existing models which were previously validated at UHF to S-Band. Author

N94-22793*# Ministry of Posts and Telecommunications, Kashima (Japan). Communications Research Lab.
MEASUREMENT OF MULTIPATH DELAY PROFILE IN LAND MOBILE SATELLITE CHANNELS
Tetsushi Ikegami, Yoshiya Arakaki, Hiromitsu Wakana, and Ryutaro Suzuki (Ministry of Education, Chiba, Japan.) *In* JPL, Proceedings of the Third International Mobile Satellite Conference (IMSC 1993) 1993 p 331-336 (For primary document see N94-22735 06-32)
Avail: CASI HC A02/MF A06

Mobile satellite communication channel has been evaluated mainly with fading statistics of signal. When bandwidth of transmitting signal becomes wider, frequency selectivity of fading becomes a significant factor of the channel. Channel characteristics, not only signal variation but multipath delay spread should be evaluated. A multipath measurement system is proposed and developed for mobile satellite applications. With this system and ETS-V satellite, multipath delay profiles are measured in various environments including Tokyo metropolis and Sapporo city at 1.5 GHz. Results show that the maximum excess delay is within 1 microsec and the maximum delay spread is 0.2 microsecs at elevation angles of 40 to 47 degrees. In wideband signal transmission of about 1 MHz and more, designers should consider the effect of selective fading due to the multipath of land mobile satellite channel. Author

N94-22794*# Communications Satellite Corp., Clarksburg, MD.
A STUDY OF SATELLITE MOTION-INDUCED MULTIPATH PHENOMENA
R. M. Allnutt, A. Dissanayake, C. Zaks, and K. T. Lin *In* JPL, Proceedings of the Third International Mobile Satellite Conference (IMSC 1993) 1993 p 337-342 (For primary document see N94-22735 06-32)
Avail: CASI HC A02/MF A06

Experiments have been undertaken at COMSAT Laboratories to determine some of the propagation effects likely to be encountered by handheld satellite communications devices. L-band pilot tones aboard geosynchronous satellites at 15 and 40 deg. elevations were used to examine diurnal signal variations measured by using a hemispherical antenna. It was found that the receiver with a hemispherical antenna suffered daily peak-to-peak signal level variations of up to 12 dB compared to only 2 to 3 dB for a receiver equipped with a directional antenna. These results were highly repeatable, and extensive tests were conducted to confirm the accuracy of the data. The results suggest that the diurnal variations were due to multipath effects caused by the motion of the satellite with respect to the receiver antenna. Noting that the orbit inclinations of the satellites used in the experiment were only on the order of 2 to 3 deg., the results also suggest a potentially serious signal variation problem for low-gain antenna-based communications systems using low earth orbit satellites, since the satellite elevation angles relative to earth change far more rapidly. Author

N94-22795*# Technische Univ., Eindhoven (Netherlands). Telecommunications Div.
ELECTROMAGNETIC FIELD STRENGTH PREDICTION IN AN URBAN ENVIRONMENT: A USEFUL TOOL FOR THE PLANNING OF LMSS
G. A. J. vanDooren, M. H. A. J. Herben, G. Brussaard, M. Sforza (European Space Agency. European Space Research and Technology Center, ESTEC, Noordwijk, Netherlands.), and J. P. V. PoiaresBaptista (European Space Agency. European Space Research and Technology Center, ESTEC, Noordwijk, Netherlands.) *In* JPL, Proceedings of the Third International Mobile Satellite Conference (IMSC 1993) 1993 p 343-348 (For primary document see N94-22735 06-32)
Avail: CASI HC A02/MF A06

A model for the prediction of the electromagnetic field strength in an urban environment is presented. The ray model, that is based on the Uniform Theory of Diffraction (UTD), includes effects of the non-perfect conductivity of the obstacles and their surface roughness. The urban environment is transformed into a list of standardized obstacles that have various shapes and material properties. The model is capable of accurately predicting the field strength in the urban environment by calculating different types of wave contributions such as reflected, edge and corner diffracted waves, and combinations thereof. Also, antenna weight functions are introduced to simulate the spatial filtering by the mobile antenna. Communication channel parameters such as signal fading, time delay profiles, Doppler shifts and delay-Doppler spectra can be derived from the ray-tracing procedure using post-processing routines. The model has been tested against results from scaled measurements at 50 GHz and proves to be accurate. Author

N94-22796*# European Space Agency. European Space Research and Technology Center, ESTEC, Noordwijk (Netherlands).
PROPAGATION MODEL FOR THE LAND MOBILE SATELLITE CHANNEL IN URBAN ENVIRONMENTS
M. Sforza, G. DiBernardo (Space Engineering, Rome, Italy.), and R. Cioni (IDS Ingegneria dei Sistemi S.p.A., Pisa, Italy.) *In* JPL, Proceedings of the Third International Mobile Satellite Conference (IMSC 1993) 1993 p 349-354 (For primary document see N94-22735 06-32)
Avail: CASI HC A02/MF A06

This paper presents the major characteristics of a simulation package capable of performing a complete narrow and wideband analysis of the mobile satellite communication channel in urban environments for any given orbital configuration. The wavelength-to-average urban geometrical dimension ratio has required the use of the Geometrical Theory of Diffraction (GTD). For the RF frequency range, the model has been designed to be (1 up to 60 GHz) extended to include effects of non-perfect conductivity and surface roughness. Taking advantage of the inherent capabilities of such a high frequency method, we are able to provide a complete description of the electromagnetic field at the mobile terminal. Using the information made available at the ray-tracer and GTD solver outputs, the Land Mobile Satellite (LMS) urban model can also give a detailed description of the communication channel in terms of power delay profiles, Doppler spectra, channel scattering functions, and so forth. Statistical data, e.g. cumulative distribution functions, level crossing rates or distributions of fades are also provided. The user can access the simulation tool through a Design-CAD user-friendly interface by means of which she can effectively design her own urban layout and run consequently all the envisaged routines. The software is optimized in its execution time so that numerous runs can be achieved in a considerably short time. Author (revised)

N94-22797*# Kokusai Denshin Denwa Co. Ltd., Saitama (Japan). Research and Development Labs.
A PREDICTION MODEL OF SIGNAL DEGRADATION IN LMSS FOR URBAN AREAS
Takashi Matsudo, Kenichi Minamisono, Yoshio Karasawa, and Takayasu Shiokawa *In* JPL, Proceedings of the Third International Mobile Satellite Conference (IMSC 1993) 1993 p 355-360 (For primary document see N94-22735 06-32)
(Contract INMARSAT-92-798/BK)
Avail: CASI HC A02/MF A06

A prediction model of signal degradation in a Land Mobile Satellite Service (LMSS) for urban areas is proposed. This model treats shadowing effects caused by buildings statistically and can predict a Cumulative Distribution Function (CDF) of signal diffraction losses in urban areas as a function of system parameters such as frequency and elevation angle and environmental parameters such as number of building stories and so on. In order to examine the validity of the model, we compared the percentage of locations where diffraction losses were smaller than 6 dB obtained by the CDF with satellite visibility measured by a radiometer. As a result, it was found that this proposed model is useful for estimating the feasibility of providing LMSS in urban areas. Author (revised)

N94-22798*# European Space Agency. European Space Research and Technology Center, ESTEC, Noordwijk (Netherlands).
GLOBAL COVERAGE MOBILE SATELLITE SYSTEMS: SYSTEM AVAILABILITY VERSUS CHANNEL PROPAGATION IMPAIRMENTS
M. Sforza, S. Buonomo, and J. P. V. PoiaresBaptista *In* JPL, Proceedings of the Third International Mobile Satellite Conference (IMSC 1993) 1993 p 361-366 (For primary document see N94-22735 06-32)
Avail: CASI HC A02/MF A06

Mobile Satellite Systems (MSS) in Highly Elliptical (HEO) and circular Earth orbits at Medium (MEO) and Low (LEO) altitudes have been intensively studied in the last few years as an effective means of providing global communication services. Such global coverage MSS networks are also expected to mitigate typical channel impairments usually encountered in geostationary Land Mobile Satellite (LMS) systems. In the design stages of these satellite networks, information regarding the mobile propagation channel is needed to assess the overall link availability versus elevation angle and environmental scenarios. For multisatellite LMS configurations, the mobile user on the Earth surface sees, at any given time, more than one satellite of the constellation. In our paper, it is shown that, under certain working assumptions regarding the statistics of the propagation channel, an improvement of the link availability may be achieved through the use of a multisatellite constellation. The analyses have been carried out using the European Space Agency (ESA) LMS propagation data base which presently covers a wide range of elevation angles and environmental scenarios. Author (revised)

N94-22799*# Motorola, Inc., Chandler, AZ. Satellite Communications.
SYSTEMS IMPLICATIONS OF L-BAND FADE DATA STATISTICS FOR LEO MOBILE SYSTEMS
Carrie L. Devieux *In* JPL, Proceedings of the Third International Mobile Satellite Conference (IMSC 1993) 1993 p 367-372 (For primary document see N94-22735 06-32)
Avail: CASI HC A02/MF A06

This paper examines and analyzes research data on the role of foliage attenuation in signal fading between a satellite transmitter and a terrestrial vehicle-mounted receiver. The frequency band of measurement, called L-Band, includes the region 1610.0 to 1626.5 MHz. Data from tests involving various combinations of foliage and vehicle movement conditions clearly show evidence of fast fading (in excess of 0.5 dB per millisecond) and fade depths as great or greater than 16 dB. As a result, the design of a communications link power control that provides the level of accuracy necessary for power sensitive systems could be significantly impacted. Specific examples of this include the communications links that employ Code Division Multiple Access (CDMA) as a modulation technique. Author (revised)

N94-22800*# Westinghouse Electric Corp., Baltimore, MD.
THE WESTINGHOUSE SERIES 1000 MOBILE PHONE: TECHNOLOGY AND APPLICATIONS
Brian Connelly *In* JPL, Proceedings of the Third International Mobile Satellite Conference (IMSC 1993) 1993 p 375-379 (For primary document see N94-22735 06-32)
Avail: CASI HC A01/MF A06

Mobile satellite communications will be popularized by the North American Mobile Satellite (MSAT) system. The success of the overall system is dependent upon the quality of the mobile units. Westinghouse is designing our unit, the Series 1000 Mobile Phone, with the user in mind. The architecture and technology aim at providing optimum performance at a low per unit cost. The features and functions of the Series 1000 Mobile Phone have been defined by potential MSAT users. The latter portion of this paper deals with who those users may be. Author (revised)

N94-22801*# European Space Agency. European Space Research and Technology Center, ESTEC, Noordwijk (Netherlands).
FIRST SATELLITE MOBILE COMMUNICATION TRIALS USING BLQS-CDMA
Maria LuzdeMateo, Simon Johns, Michel Dothey (Sait Electronics S.A., Brussels, Belgium.), Carl VanHimbeeck (Sait Electronics S.A., Brussels, Belgium.), Ivan Deman (Sait Electronics S.A., Brussels, Belgium.), and Bruno Wery (Sait Electronics S.A., Brussels, Belgium.) *In* JPL, Proceedings of the Third International Mobile Satellite Conference (IMSC 1993) 1993 p 381-386 (For primary document see N94-22735 06-32)
Avail: CASI HC A06

In this paper, technical results obtained in the first MSBN Land mobile technical trial are reported. MSBN (Mobile Satellite Business Network) is a new program undertaken by the European Space Agency (ESA) to promote mobile satellite communication in Europe, in particular voice capability. The first phase of the MSBN system implementation plan is an experimental phase. Its purpose is to evaluate through field experiments the performance of the MSBN system prior to finalization of its specifications. Particularly, the objective is to verify in the field and possibly improve the performance of the novel satellite access technique BLQS-CDMA (Band Limited Quasi-Synchronous-Code Division Multiple Access), which is proposed as baseline for the MSBN. Author (revised)

N94-22802*# Jet Propulsion Lab., California Inst. of Tech., Pasadena.
CHANNEL AND TERMINAL DESCRIPTION OF THE ACTS MOBILE TERMINAL
B. S. Abbe, M. J. Agan, C. C. Girardey (European Space Agency. European Space Operations Center, Darmstadt, Germany.), and T. C. Jedrey *In its* Proceedings of the Third International Mobile Satellite Conference (IMSC 1993) 1993 p 387-392 (For primary document see N94-22735 06-32)
Avail: CASI HC A02/MF A06

The Advanced Communications Technology Satellite (ACTS) Mobile Terminal (AMT) is a proof-of-concept K/Ka-band mobile satellite communications terminal under development by NASA at JPL. Currently the AMT is undergoing system integration and test in preparation for a July 1993 ACTS launch and the subsequent commencement of mobile experiments in the fall of 1993. The AMT objectives are presented followed by a discussion of the AMT communications channel and mobile terminal design and performance. Author (revised)

N94-22803*# Rockwell International Corp., Cedar Rapids, IA. Mobile Communications Satellite System.
LOW COST COHERENT DEMODULATION FOR MOBILE SATELLITE TERMINALS
Santanu Dutta and Steven J. Henely *In* JPL, Proceedings of the Third International Mobile Satellite Conference (IMSC 1993) 1993 p 393-398 (For primary document see N94-22735 06-32)
Avail: CASI HC A02/MF A06

This paper describes some low cost approaches to coherent BPSK demodulation for mobile satellite receivers. The specific application is an Inmarsat-C Land Mobile Earth Station (LMES), but the techniques are applicable to any PSK demodulator. The techniques discussed include combined sampling and quadrature downconversion with a single A/D and novel DSP algorithms for carrier acquisition offering both superior performance and economy of DSP resources. The DSP algorithms run at 5.7 MIPS, and the entire DSP subsystem, built with commercially available parts, costs under $60 at quantity-10,000. Author (revised)

N94-22804*# Communications Research Centre, Ottawa (Ontario).
DIRECT DIGITAL RF SYNTHESIS AND MODULATION FOR MSAT MOBILE APPLICATIONS
Stewart Crozier, Ravi Datta, and John Sydor *In* JPL, Proceedings of the Third International Mobile Satellite Conference (IMSC 1993) 1993 p 399-403 (For primary document see N94-22735 06-32)
Avail: CASI HC A01/MF A06

A practical method of performing direct digital RF synthesis using the Hilbert transform single sideband (SSB) technique is described. It is also shown that amplitude and phase modulation can be achieved directly at L-band with frequency stability and spurii performance exceeding stringent MSAT system requirements. Author

N94-22805*# Queens Univ., Kingston (Ontario). Dept. of Electrical Engineering.
ASYNCHRONOUS TIMING AND DOPPLER RECOVERY IN DSP BASED DPSK MODEMS FOR FIXED AND MOBILE SATELLITE APPLICATIONS
B. Koblents, M. Belanger, D. Woods, and P. J. McLane *In* JPL, Proceedings of the Third International Mobile Satellite Conference (IMSC 1993) 1993 p 405-410 Sponsored by Telecommunications Research Inst. of Ontario and Natural Sciences and Engineering Research Council (For primary document see N94-22735 06-32)
Avail: CASI HC A02/MF A06

While conventional analog modems employ some kind of clock wave regenerator circuit for synchronous timing recovery, in sampled modem receivers the timing is recovered asynchronously to the incoming data stream, with no adjustment being made to the input sampling rate. All timing corrections are accomplished by digital operations on the sampled data stream, and timing recovery is asynchronous with the uncontrolled, input A/D system. A good timing error measurement algorithm is a zero crossing tracker proposed by Gardner. Digital, speech rate (2400 - 4800 bps) M-PSK modem receivers employing Gardner's zero crossing tracker were implemented and tested and found to achieve BER performance very close to theoretical values on the AWGN channel. Nyguist pulse shaped modem systems with excess bandwidth factors ranging from 100 to 60 percent were considered. We can show that for any symmetric M-PSK signal set Gardner's NDA algorithm is free of pattern jitter for any carrier phase offset for rectangular pulses and for Nyquist pulses having 100 percent excess bandwidth. Also, the Nyquist pulse shaped system is studied on the mobile satellite channel, where Doppler shifts and multipath fading degrade the pi/4-DQPSK signal. Two simple modifications to Gardner's zero crossing tracker enable it to remain useful in the presence of multipath fading. Author (revised)

N94-22806*# SED Systems, Inc., Saskatoon (Saskatchewan).
IMPROVED FRAME SYNCHRONIZATION SCHEMES FOR INMARSAT-B/M SCPC AND TDM CHANNELS
Si-Ming Pan, Randy L. Hanson, Donald H. Madill, and Paul C. Chapman *In* JPL, Proceedings of the Third International Mobile Satellite Conference (IMSC 1993) 1993 p 411-416 (For primary document see N94-22735 06-32)
Avail: CASI HC A02/MF A06

This paper proposes faster, more robust, frame synchronization schemes for various Inmarsat-B and Inmarsat-M communication and signalling channels. Equations are developed which permit frame synchronization strategies of the type specified by Inmarsat to be evaluated in terms of average true lock time, average false maintenance time, and average search time. Evaluation o. the currently specified framing schemes shows that a significant performance improvement is obtained by optimizing the threshold parameters of the scheme. The optimization seeks a compromise between the conflicting requirements of maximizing true lock time and minimizing search time. Author (revised)

N94-22807*# University of South Australia, Pooraka. Digital Communications Group.
ESTIMATION OF FREQUENCY OFFSET IN MOBILE SATELLITE MODEMS
W. G. Cowley, M. Rice, and A. N. McLean *In* JPL, Proceedings of the Third International Mobile Satellite Conference (IMSC 1993) 1993 p 417-422 Sponsored by Australian Space Office and Optus Communications (For primary document see N94-22735 06-32)
Avail: CASI HC A02/MF A06

In mobilesat applications, frequency offset on the received signal must be estimated and removed prior to further modem processing. A straightforward method of estimating the carrier frequency offset is to raise the received MPSK signal to the M-th power, and then estimate the location of the peak spectral component. An analysis of the lower signal to noise threshold of this method is carried out for BPSK signals. Predicted thresholds are compared to simulation results. It is shown how the method can be extended to pi/M MPSK signals. A real-time implementation of frequency offset estimation for the Australian mobile satellite system is described. Author

N94-22808*# Communications Research Centre, Ottawa (Ontario).
THEORETICAL AND SIMULATED PERFORMANCE FOR A NOVEL FREQUENCY ESTIMATION TECHNIQUE
Stewart N. Crozier *In* JPL, Proceedings of the Third International Mobile Satellite Conference (IMSC 1993) 1993 p 423-428 (For primary document see N94-22735 06-32)
Avail: CASI HC A02/MF A06

A low complexity, open-loop, discrete-time, delay-multiply-average (DMA) technique for estimating the frequency offset for digitally modulated MPSK signals is investigated. A nonlinearity is used to remove the MPSK modulation and generate the carrier component to be extracted. Theoretical and simulated performance results are presented and compared to the Cramer-Rao lower bound (CRLB) for the variance of the frequency estimation error. For all signal-to-noise ratios (SNR's) above threshold, it is shown that the CRLB can essentially be achieved with linear complexity. Author (revised)

N94-22809*# Nippon Electric Co. Ltd., Kawasaki (Japan). C and C Systems Research Labs.
A PATTERN JITTER FREE AFC SCHEME FOR MOBILE SATELLITE SYSTEMS
Shousei Yoshida *In* JPL, Proceedings of the Third International Mobile Satellite Conference (IMSC 1993) 1993 p 429-434 (For primary document see N94-22735 06-32)
Avail: CASI HC A02/MF A06

This paper describes a scheme for pattern jitter free automatic frequency control (AFC) with a wide frequency acquisition range. In this scheme, equalizing signals fed to the frequency discriminator allow pattern jitter free performance to be achieved for all roll-off factors. In order to define the acquisition range, frequency discrimination characateristics are analyzed on a newly derived frequency domain model. As a result, it is shown that a sufficiently wide acquisition range over a given system symbol rate can be achieved independent of symbol timing errors. Additionally, computer simulation demonstrates that frequency jitter performance improves in proportion to E(sub b)/N(sub 0) because pattern-dependent jitter is suppressed in the discriminator output. These results show significant promise for applciation to mobile satellite systems, which feature relatively low symbol rate transmission with an approximately 0.4-0.7 roll-off factor. Author

N94-22810*# European Space Agency. European Space Research and Technology Center, ESTEC, Noordwijk (Netherlands). Directorate of Telecommunication Programmes.
A CDMA SYNCHRONISATION SCHEME
C. Soprano *In* JPL, Proceedings of the Third International Mobile Satellite Conference (IMSC 1993) 1993 p 437-442 (For primary document see N94-22735 06-32)
Avail: CASI HC A02/MF A06

CDMA (Code Division Multiple Access) is known to decrease inter-service interference in Satellite Communication Systems. Its performance is increased by chip quasi-synchronous operation which virtually eliminates the self-noise; however, the theory shows that the time error on the synchronization has to be kept at less than one tenth of a chip which, for 1 Mchip/sec. spreading rate, corresponds to 10(exp -7) sec. This, on the return-link, may only be achieved by means of a closed loop control system which, for mobile communication systems, has to be capable of autonomous operation. Until now some results have been reported on the feasibility of chip quasi-synchronous operation for mobile communication systems only including satellites on GEO (Geostationary Earth Orbit). In what follows, the basic principles are exposed, and results are presented showing how low chip synchronism error may be achieved by means of an autonomous control loop operating through satellites on any Earth orbit. Author (revised)

N94-22811*# Maryland Univ., College Park. Center for Satellite and Hybrid Communication Networks.
A PROTOCOL FOR SATELLITE ACCESS VIA USE OF SPOT-BEAMS
Stefan Ramseier and Anthony Ephremides *In* JPL, Proceedings of the Third International Mobile Satellite Conference (IMSC 1993) 1993 p 443-448 (For primary document see N94-22735 06-32)
Avail: CASI HC A02/MF A06

In this paper, we develop a new protocol for multiple access to a GEO-satellite that utilizes an electronically-switched spot-beam. The emphasis is on an integrated voice/data protocol which takes advantage of the propagation latency and which offers centralized control with excellent delay and throughput characteristics. The protocol also allows full exploitation of the advantages of a hopping beam satellite, such as smaller earth stations and frequency re-use. Author (revised)

N94-22812*# Surrey Univ., Guildford (England). Centre for Satellite Engineering Research.
A HIGH QUALITY VOICE CODER WITH INTEGRATED ECHO CANCELLER AND VOICE ACTIVITY DETECTOR FOR MOBILE SATELLITE APPLICATIONS
A. M. Kondoz and B. G. Evans *In* JPL, Proceedings of the Third International Mobile Satellite Conference (IMSC 1993) 1993 p 449-454 (For primary document see N94-22735 06-32)
Avail: CASI HC A02/MF A06

In the last decade, low bit rate speech coding research has received much attention resulting in newly developed, good quality, speech coders operating at as low as 4.8 Kb/s. Although speech quality at around 8 Kb/s is acceptable for a wide variety of applications, at 4.8 Kb/s more improvements in quality are necessary to make it acceptable to the majority of applications and users. In addition to the required low bit rate with acceptable speech quality, other facilities such as integrated digital echo cancellation and voice activity detection are now becoming necessary to provide a cost effective and compact solution. In this paper we describe a CELP speech coder with integrated echo canceller and a voice activity detector all of which have been implemented on a single DSP32C with 32 KBytes of SRAM. The quality of CELP coded speech has been improved significantly by a new codebook implementation which also simplifies the encoder/decoder complexity making room for the integration of a 64-tap echo canceller together with a voice activity detector. Author (revised)

N94-22813*# Nippon Telegraph and Telephone Public Corp., Yokosuka (Japan).
PERFORMANCE OF THE UNIQUE-WORD-REVERSE-MODULATION TYPE DEMODULATOR FOR MOBILE SATELLITE COMMUNICATIONS
Tomohiro Dohi, Kazumasa Nitta, and Takashi Ueda *In* JPL, Proceedings of the Third International Mobile Satellite Conference (IMSC 1993) 1993 p 455-460 (For primary document see N94-22735 06-32)
Avail: CASI HC A02/MF A06

This paper proposes a new type of coherent demodulator, the unique-word (UW)-reverse-modulation type demodulator, for burst signal controlled by voice operated transmitter (VOX) in mobile satellite communication channels. The demodulator has three individual circuits: a pre-detection signal combiner, a pre-detection UW detector, and a UW-reverse-modulation type demodulator. The pre-detection signal combiner combines signal sequences received by two antennas and improves bit energy-to-noise power density ratio (E(sub b)/N(sub 0)) 2.5 dB to yield 10(exp -3) average bit error rate (BER) when carrier power-to-multipath power ratio (CMR) is 15 dB. The pre-detection UW detector improves UW detection probability when the frequency offset is large. The UW-reverse-modulation type demodulator realizes a maximum pull-in frequency of 3.9 kHz, the pull-in time is 2.4 seconds and frequency error is less than 20 Hz. The performances of this demodulator are confirmed through computer simulations and its effect is clarified in real-time experiments at a bit rate of 16.8 kbps using a digital signal processor (DSP). Author (revised)

N94-22814*# Politecnico di Torino (Italy). Dipt. di Elettronica.
DS-SSMA CAPACITY FOR A MOBILE SATELLITE SYSTEM
Francesco Bartucca and Ezio Biglieri *In* JPL, Proceedings of the Third International Mobile Satellite Conference (IMSC 1993) 1993 p 461-466 Prepared for Italian Space Agency, Rome (For primary document see N94-22735 06-32)
Avail: CASI HC A02/MF A06

We consider a cellular satellite system conceived to enhance the capabilities of the pan-European terrestrial system (GSM). The system adopts EHF band and highly-inclined orbits. We present a preliminary assessment of system capacity based on asynchronous direct-sequence spread-spectrum multiple access (DS-SSMA). Performance is measured in terms of error probability achieved by K users simultaneously accessing the system with a given signal-to-noise ratio. Author (revised)

N94-22815*# Communications Research Centre, Ottawa (Ontario).
SEPARABLE CONCATENATED CODES WITH ITERATIVE MAP DECODING FOR RICIAN FADING CHANNELS
J. H. Lodge and R. J. Young *In* JPL, Proceedings of the Third International Mobile Satellite Conference (IMSC 1993) 1993 p 467-472 (For primary document see N94-22735 06-32)
Avail: CASI HC A02/MF A06

Very efficient signalling in radio channels requires the design of very powerful codes having special structure suitable for practical decoding schemes. In this paper, powerful codes are obtained by combining comparatively simple convolutional codes to form multi-tiered 'separable' convolutional codes. The decoding of these codes, using separable symbol-by-symbol maximum a posteriori (MAP) 'filters', is described. It is known that this approach yields impressive results in non-fading additive white Gaussian noise channels. Interleaving is an inherent part of the code construction, and consequently, these codes are well suited for fading channel communications. Here, simulation results for communications over Rician fading channels are presented to support this claim.
Author (revised)

N94-22816*# European Space Agency. European Space Research and Technology Center, ESTEC, Noordwijk (Netherlands). RF System Div.
DIVERSITY RECEPTION FOR ADVANCED MULTI-SATELLITE NETWORKS: A CDMA APPROACH
E. Colzi, R. DeGaudenzi, C. Elia, F. Giannetti (Pisa Univ., Italy.), and R. Viola *In* JPL, Proceedings of the Third International Mobile Satellite Conference (IMSC 1993) 1993 p 473-478 (For primary document see N94-22735 06-32)
Avail: CASI HC A02/MF A06

Diversity reception for Synchronous CDMA (S-CDMA) is introduced and analyzed. A Gaussian co-channel synchronous and asynchronous interference approximation is derived to evaluate the effects on the system bit error rate. Numerical results are provided for a simple mobile communication system where the signals transmitted by two distinct satellites in visibility are coherently combined by a three fingers Rake receiver. A second example showing performance of an integrated ground/satellite single frequency network for digital audio broadcasting is presented. Results show the capacity advantage of utilizing S-CDMA in combination with diversity reception. Author

N94-22817*# Communications Satellite Corp., Clarksburg, MD.
SYSTEM SERVICES AND ARCHITECTURE OF THE TMI SATELLITE MOBILE DATA SYSTEM
D. Gokhale, A. Agarwal, and A. Guibord (Telesat Mobile, Inc., Ottawa, Ontario.) *In* JPL, Proceedings of the Third International Mobile Satellite Conference (IMSC 1993) 1993 p 479-484 (For primary document see N94-22735 06-32)
Avail: CASI HC A02/MF A06

The North American Mobile Satellite Service (MSS) system being developed by AMSC/TMI and scheduled to go into service in early 1995 will include the provision for real time packet switched services (mobile data service - MDS) and circuit switched services (mobile telephony service - MTS). These services will utilize geostationary satellites which provide access to mobile terminals (MT's) through L-band beams. The MDS system utilizes a star topology with a centralized data hub (DH) and will support a large number of mobile terminals. The DH, which accesses the satellite via a single Ku band beam, is responsible for satellite resource management, for providing mobile users with access to public and private data networks, and for comprehensive network management of the system. This paper describes the various MDS services available for the users, the ground segment elements involved in the provisioning of these services, and a summary description of the channel types, protocol architecture, and network management capabilities provided within the system. Author (revised)

N94-22818*# California Univ., Davis.

A COMPARISON BETWEEN COHERENT AND NONCOHERENT MOBILE SYSTEMS IN LARGE DOPPLER SHIFT, DELAY SPREAD, AND C/I ENVIRONMENT

Kamilo Feher *In* JPL, Proceedings of the Third International Mobile Satellite Conference (IMSC 1993) 1993 p 485-490 (For primary document see N94-22735 06-32)

Avail: CASI HC A02/MF A06

The performance and implementation complexity of coherent and of noncoherent QPSK and GMSK modulation/demodulation techniques in a complex mobile satellite systems environment, including large Doppler shift, delay spread, and low C/I, are compared. We demonstrate that for large f(sub d)T(sub b) products, where f(sub d) is the Doppler shift and T(sub b) is the bit duration, noncoherent (discriminator detector or differential demodulation) systems have a lower BER floor than their coherent counterparts. For significant delay spreads, e.g., tau(sub rms) greater than 0.4 T(sub b), and low C/I, coherent systems outperform noncoherent systems. However, the synchronization time of coherent systems is longer than that of noncoherent systems. Spectral efficiency, overall capacity, and related hardware complexity issues of these systems are also analyzed. We demonstrate that coherent systems have a simpler overall architecture (IF filter implementation-cost versus carrier recovery) and are more robust in an RF frequency drift environment. Additionally, the prediction tools, computer simulations, and analysis of coherent systems is simpler. The threshold or capture effect in low C/I interference environment is critical for noncoherent discriminator based systems. We conclude with a comparison of hardware architectures of coherent and of noncoherent systems, including recent trends in commercial VLSI technology and direct baseband to RF transmit, RF to baseband (0-IF) receiver implementation strategies. Author (revised)

N94-22819*# Jet Propulsion Lab., California Inst. of Tech., Pasadena.

PSEUDO-COHERENT DEMODULATION FOR MOBILE SATELLITE SYSTEMS

Dariush Divsalar and Marvin K. Simon *In its* Proceedings of the Third International Mobile Satellite Conference (IMSC 1993) 1993 p 491-496 (For primary document see N94-22735 06-32)

Avail: CASI HC A02/MF A06

This paper proposes three so-called pseudo-coherent demodulation schemes for use in land mobile satellite channels. The schemes are derived based on maximum likelihood (ML) estimation and detection of an N-symbol observation of the received signal. Simulation results for all three demodulators are presented to allow comparison with the performance of differential PSK (DPSK) and ideal coherent demodulation for various system parameter sets of practical interest. Author (revised)

N94-22820*# Ottawa Univ. (Ontario). Dept. of Electrical Engineering.

TRANSMISSION OVER EHF MOBILE SATELLITE CHANNELS

W. Zhuang, J.-Y. Chouinard, and A. Yongacoglu *In* JPL, Proceedings of the Third International Mobile Satellite Conference (IMSC 1993) 1993 p 499-504 (For primary document see N94-22735 06-32) (Grant NSERC-STR-0100720)

Avail: CASI HC A02/MF A06

Land mobile satellite communications at Ka-band (30/20 GHz) are attracting an increasing interest among researchers because of the frequency band availability and the possibility of small earth station designs. However, communications at the Ka-band pose significant challenges in the system designs due to severe channel impairments. Because only very limited experimental data for mobile applications at Ka-band is available, this paper studies the channel characteristics based on experimental data at L-band (1.6/1.5 GHz) and the use of frequency scaling. The land mobile satellite communication channel at Ka-band is modelled as log-normal Rayleigh fading channel. The first and second-order statistics of the fading channel are studied. The performance of a coherent BPSK system over the fading channel at L-band and K-band is evaluated theoretically and validated by computer simulations. Conclusions on the communication channel characteristics and system performance at L-band and Ka-band are presented. Author (revised)

N94-22821*# Ministry of Posts and Telecommunications, Ibaraki (Japan). Communications Research Lab.

ADAPTIVE DATA RATE CONTROL TDMA SYSTEMS AS A RAIN ATTENUATION COMPENSATION TECHNIQUE

Masaki Sato, Hiromitsu Wakana, Takashi Takahashi, Makoto Takeuchi, and Minoru Yamamoto *In* JPL, Proceedings of the Third International Mobile Satellite Conference (IMSC 1993) 1993 p 505-510 (For primary document see N94-22735 06-32)

Avail: CASI HC A02/MF A06

Rainfall attenuation has a severe effect on signal strength and impairs communication links for future mobile and personal satellite communications using Ka-band and millimeter wave frequencies. As rain attenuation compensation techniques, several methods such as uplink power control, site diversity, and adaptive control of data rate or forward error correction have been proposed. In this paper, we propose a TDMA system that can compensate rain attenuation by adaptive control of transmission rates. To evaluate the performance of this TDMA terminal, we carried out three types of experiments: experiments using a Japanese CS-3 satellite with Ka-band transponders, in house IF loop-back experiments, and computer simulations. Experimental results show that this TDMA system has advantages over the conventional constant-rate TDMA systems, as resource sharing technique, in both bit error rate and total TDMA burst lengths required for transmitting given information. Author

N94-22822*# Hewlett-Packard Co., Palo Alto, CA.

SATCOM SIMULATOR SPEEDS MSS DEPLOYMENT AND LOWERS COSTS

Tim Carey, Roland Hassun, and Dave Koberstein *In* JPL, Proceedings of the Third International Mobile Satellite Conference (IMSC 1993) 1993 p 511-516 (For primary document see N94-22735 06-32)

Avail: CASI HC A02/MF A06

Mobile satellite systems (MSS) are being proposed and licensed at an accelerating rate. How can the design, manufacture, and performance of these systems be optimized at costs that allow a reasonable return on investment? The answer is the use of system simulation techniques beginning early in the system design and continuing through integration, pre- and post-launch monitoring, and in-orbit monitoring. This paper focuses on using commercially available, validated simulation instruments to deliver accurate, repeatable, and cost effective measurements throughout the life of a typical mobile satellite system. A satellite communications test set is discussed that provides complete parametric test capability with a significant improvement in measurement speed for manufacturing, integration, and pre-launch and in-orbit testing. The test set can simulate actual up and down link traffic conditions to evaluate the effects of system impairments, propagation and multipath on bit error rate (BER), channel capacity and transponder and system load balancing. Using a standard set of commercial instruments to deliver accurate, verifiable measurements anywhere in the world speeds deployment, generates measurement confidence, and lowers total system cost. Author

N94-22823*# Loral Aerospace Corp., Palo Alto, CA.

DEVELOPMENT OF A MULTILAYER INTERFERENCE SIMULATION PROGRAM FOR MSS SYSTEMS

Jamal S. Izadian *In* JPL, Proceedings of the Third International Mobile Satellite Conference (IMSC 1993) 1993 p 517-522 (For primary document see N94-22735 06-32)

Avail: CASI HC A02/MF A06

This paper discusses the development of a multilayer interference analysis and simulation program which is used to evaluate interference between non-geostationary and geostationary satellites. In addition to evaluating interference, this program can be used in the development of sharing criteria and coordination among various Mobile Satellite Services (MSS) systems. A C++/Windows implementation of this program, called Globalstar Interference Simulation Program (GISP), has been developed. Author (revised)

N94-22824*# Bristol Univ. (England). Centre for Communications Research.
HANDOVER ASPECTS FOR A LOW EARTH ORBIT (LEO) CDMA LAND MOBILE SATELLITE (LMS) SYSTEM
P. Carter and M. A. Beach *In* JPL, Proceedings of the Third International Mobile Satellite Conference (IMSC 1993) 1993 p 523-528 Sponsored by Science Research Council and Roke Manor Research Ltd. (For primary document see N94-22735 06-32)
Avail: CASI HC A02/MF A06

This paper addresses the problem of handoff in a land mobile satellite (LMS) system between adjacent satellites in a low earth orbit (LEO) constellation. In particular, emphasis is placed on the application of soft handoff in a direct sequence code division multiple access (DS-CDMA) LMS system. Soft handoff is explained in terms of terrestrial macroscopic diversity, in which signals transmitted via several independent fading paths are combined to enhance the link quality. This concept is then reconsidered in the context of a LEO LMS system. A two-state Markov channel model is used to simulate the effects of shadowing on the communications path from the mobile to each satellite during handoff. The results of the channel simulation form a platform for discussion regarding soft handoff, highlighting the potential merits of the scheme when applied in a LEO LMS environment. Author

N94-22825*# Kokusai Denshin Denwa Co. Ltd., Saitama (Japan). Research and Development Labs.
STUDY ON NETWORKING ISSUES OF MEDIUM EARTH ORBIT SATELLITE COMMUNICATIONS SYSTEMS
Noriyuki Araki, Hideyuki Shinonaga, and Yasuhiko Ito *In* JPL, Proceedings of the Third International Mobile Satellite Conference (IMSC 1993) 1993 p 529-534 (For primary document see N94-22735 06-32)
Avail: CASI HC A02/MF A06

Two networking issues of communications systems with medium earth orbit (MEO) satellites, namely network architectures and location determination and registration methods for hand-held terminals, are investigated in this paper. For network architecture, five candidate architectures are considered and evaluated in terms of signaling traffic. For location determination and registration, two methods are discussed and evaluated. Author (revised)

N94-22826*# European Space Agency. European Space Research and Technology Center, ESTEC, Noordwijk (Netherlands).
THE DESIGN AND NETWORKING OF DYNAMIC SATELLITE CONSTELLATIONS FOR GLOBAL MOBILE COMMUNICATION SYSTEMS
Cionaith J. Cullen, Xavier Benedicto, Rahim Tafazolli (Surrey Univ., Guildford, England.), and Barry Evans (Surrey Univ., Guildford, England.) *In* JPL, Proceedings of the Third International Mobile Satellite Conference (IMSC 1993) 1993 p 535-540 (For primary document see N94-22735 06-32)
Avail: CASI HC A02/MF A06

Various design factors for mobile satellite systems, whose aim is to provide worldwide voice and data communications to users with hand-held terminals, are examined. Two network segments are identified - the ground segment (GS) and the space segment (SS) - and are seen to be highly dependent on each other. The overall architecture must therefore be adapted to both of these segments, rather than each being optimized according to its own criteria. Terrestrial networks are grouped and called the terrestrial segment (TS). In the SS, of fundamental importance is the constellation altitude. The effect of the altitude on decisions such as constellation design choice and on network aspects like call handover statistics are fundamental. Orbit resonance is introduced and referred to throughout. It is specifically examined for its useful properties relating to GS/SS connectivities. Author (revised)

N94-22827*# Bradford Univ. (England). Dept. of Electrical Engineering.
LOW EARTH ORBIT SATELLITE/TERRESTRIAL MOBILE SERVICE COMPATIBILITY Abstract Only
R. E. Sheriff and J. G. Gardiner *In* JPL, Proceedings of the Third International Mobile Satellite Conference (IMSC 1993) 1993 p 541 (For primary document see N94-22735 06-32)
Avail: CASI HC A01/MF A06

Digital cellular mobile 'second generation' systems are now gradually being introduced into service; one such example is GSM, which will provide a digital voice and data service throughout Europe. Total coverage is not expected to be achieved until the mid '90's, which has resulted in several proposals for the integration of GSM with a geostationary satellite service. Unfortunately, because terrestrial and space systems have been designed to optimize their performance for their particular environment, integration between a satellite and terrestrial system is unlikely to develop further than the satellite providing a back-up service. This lack of system compatibility is now being addressed by system designers of third generation systems. The next generation of mobile systems, referred to as FPLMTS (future public land mobile telecommunication systems) by CCIR and UMTS (universal mobile telecommunication system) in European research programs, are intended to provide inexpensive, hand-held terminals that can operate in either satellite, cellular, or cordless environments. This poses several challenges for system designers, not least in terms of the choice of multiple access technique and power requirements. Satellite mobile services have been dominated by the geostationary orbital type. Recently, however, a number of low earth orbit configurations have been proposed, for example Iridium. These systems are likely to be fully operational by the turn of the century, in time for the implementation of FPLMTS. The developments in LEO mobile satellite service technology were recognized at WARC-92 with the allocation of specific frequency bands for 'big' LEO's, as well as a frequency allocation for FPLMTS which included a specific satellite allocation. When considering integrating a space service into the terrestrial network, LEO's certainly appear to have their attractions: they can provide global coverage, the round trip delay is of the order of tens of milliseconds, and good visibility to the satellite is usually possible. This has resulted in their detailed investigation in the European COST 227 program and in the work program of the European Telecommunications Standards Institute (ETSI). This paper will consider the system implications of integrating a LEO mobile service with a terrestrial service. Results will be presented from simulation software to show how a particular orbital configuration affects the performance of the system in terms of area coverage and visibility to a terminal for various locations and minimum elevation angle. Possible network topologies are then proposed for an integrated satellite/terrestrial network. Author (revised)

N94-22828*# Hughes Aircraft Co., Los Angeles, CA.
A PRACTICAL SYSTEM FOR REGIONAL MOBILE SATELLITE SERVICES
Randall Glein, Dennis Leverson, and Dean Olmstead *In* JPL, Proceedings of the Third International Mobile Satellite Conference (IMSC 1993) 1993 p 543-548 (For primary document see N94-22735 06-32)
Avail: CASI HC A02/MF A06

The Regional Mobile Satellite (MSAT) concept proposes a worldwide, interconnected mobile satellite service (MSS) network in which MSAT-type satellites provide the space segment services to separate regions (i.e., one or a few countries). Using this concept, mobile communications users across entire continents can now be served by a handful of regionally controlled satellites in geostationary earth orbit (GEO). All requirements, including hand-held telephone capabilities, can be cost-effectively provided using proven technologies. While other concepts of regional or global mobile communications continue to be explored, the Hughes Regional MSAT system demonstrates the near-term viability of the GEO approach. Author (revised)

N94-22829*# Ministry of Posts and Telecommunications, Tokyo (Japan). Communications Research Lab.
ADVANCED MOBILE SATELLITE COMMUNICATIONS USING COMETS SATELLITE IN MM-WAVE AND Ka-BAND
Shingo Ohmori, Shunkichi Isobe, Makoto Takeuchi, and Hideyuki Naito *In* JPL, Proceedings of the Third International Mobile Satellite Conference (IMSC 1993) 1993 p 549-553 (For primary document see N94-22735 06-32)
Avail: CASI HC A01/MF A06

Early in the 21st century, the demand for personal communications using mobile, hand-held, and VSAT terminals will rapidly increase. In a future system, many different types of services should be provided with one-hop connection. The Communications Research Laboratory (CRL) has studied a future advanced mobile satellite communications system using millimeter wave and Ka band. In 1990, CRL started the Communications and Broadcasting Engineering Test Satellite (COMETS) project. The satellite

has been developed in conjunction with NASDA and will be launched in 1997. This paper describes the COMETS payload configuration and the experimental system for the advanced mobile communications mission.
Author (revised)

N94-22830*# Manitoba Univ., Winnipeg. Dept. of Electrical and Computer Engineering.
LOW COST ANTENNAS FOR MSAT VEHICULAR APPLICATIONS
L. Shafai and M. Barakat (InfoMagnetics Technologies Corp., Winnipeg, Manitoba.) *In* JPL, Proceedings of the Third International Mobile Satellite Conference (IMSC 1993) 1993 p 557-562 (For primary document see N94-22735 06-32)
Avail: CASI HC A02/MF A06

For Mobile MSAT applications a number of vehicular antennas have been developed that meet the program requirements. They are, however, costly to manufacture. Two antenna candidates are described here that provide adequate gain in the coverage zone and are also lower cost. One is the mast antenna that uses three or four element arrays of aquadrifilar helices. It generates omnidirectional pattern in azimuth and its beam is scanned in elevation. The second unit is a planar spiral antenna; it generates directional beams by a summation of the azimuthal modes. A variation of this antenna uses conical spirals to fulfill the same task. In both cases beam scanning is achieved by means of electronic switches rather than phase shifters, thus resulting in simpler configurations. Author (revised)

N94-22831*# Jet Propulsion Lab., California Inst. of Tech., Pasadena.
K- AND Ka-BAND MOBILE-VEHICULAR SATELLITE-TRACKING REFLECTOR ANTENNA SYSTEM FOR THE NASA ACTS MOBILE TERMINAL
Art Densmore, Vahraz Jamnejad, T. K. Wu, and Ken Woo *In its* Proceedings of the Third International Mobile Satellite Conference (IMSC 1993) 1993 p 563-568 (For primary document see N94-22735 06-32)
Avail: CASI HC A02/MF A06

This paper describes the development of the K- and Ka-band mobile-vehicular satellite-tracking reflector antenna system for NASA's ACTS Mobile Terminal (AMT) project. ACTS is NASA's Advanced Communications Technology Satellites. The AMT project will make the first experimental use of ACTS soon after the satellite is operational, to demonstrate mobile communications via the satellite from a van on the road. The AMT antenna system consists of a mechanically steered small reflector antenna, using a shared aperture for both frequency bands and fitting under a radome of 23 cm diameter and 10 cm height, and a microprocessor controlled antenna controller that tracks the satellite as the vehicle moves about. The RF and mechanical characteristics of the antenna and the antenna tracking control system are discussed. Measurements of the antenna performance are presented. Author

N94-22832*# Jet Propulsion Lab., California Inst. of Tech., Pasadena.
AN ACTIVE K/Ka-BAND ANTENNA ARRAY FOR THE NASA ACTS MOBILE TERMINAL
A. Tulintseff, R. Crist, Art Densmore, and L. Sukamto *In its* Proceedings of the Third International Mobile Satellite Conference (IMSC 1993) 1993 p 569-574 (For primary document see N94-22735 06-32)
Avail: CASI HC A02/MF A06

An active K/Ka-band antenna array is currently under development for NASA's ACTS Mobile Terminal (AMT). The AMT task will demonstrate voice, data, and video communications to and from the AMT vehicle in Los Angeles, California, and a base station in Cleveland, Ohio, via the ACTS satellite at 30 and 20 GHz. Satellite tracking for the land-mobile vehicular antenna system involves 'mechanical dithering' of the antenna, where the antenna radiates a fixed beam 46 deg. above the horizon. The antenna is to transmit horizontal polarization and receive vertical polarization at 29.634 plus or minus 0.15 GHz and 19.914 plus or minus 0.15 GHz, respectively. The active array will provide a minimum of 22 dBW EIRP transmit power density and a -8 dB/K deg. receive sensitivity.
Author (revised)

N94-22833*# Consejo Superior de Investigaciones Cientificas, Madrid (Spain).
MICROSTRIP MONOPULSE ANTENNA FOR LAND MOBILE COMMUNICATIONS
Q. Garcia, C. Martin, J. C. delValle (DCG Ingenieros, Madrid, Spain.), A. Jongejans (European Space Agency. European Space Research and Technology Center, ESTEC, Noordwijk, Netherlands.), P. Rinous (European Space Agency. European Space Research and Technology Center, ESTEC, Noordwijk, Netherlands.), and M. N. Travers (European Space Agency. European Space Research and Technology Center, ESTEC, Noordwijk, Netherlands.) *In* JPL, Proceedings of the Third International Mobile Satellite Conference (IMSC 1993) 1993 p 575-580 (For primary document see N94-22735 06-32)
Avail: CASI HC A02/MF A06

Low cost is one of the main requirements in a communication system suitable for mass production, as it is the case for satellite land mobile communications. Microstrip technology fulfills this requirement which must be supported by a low cost tracking system design. The tradeoff led us to a prototype antenna composed of microstrip patches based on electromechanical closed-loop principle; the design and the results obtained are described. Author

N94-22834*# California Univ., Los Angeles. Dept. of Electrical Engineering.
ISOLATED AND COUPLED SUPERQUADRIC LOOP ANTENNAS FOR MOBILE COMMUNICATIONS APPLICATIONS
Michael A. Jensen and Yahya Rahmat-Samii *In* JPL, Proceedings of the Third International Mobile Satellite Conference (IMSC 1993) 1993 p 581-586 Sponsored in part by NSF (For primary document see N94-22735 06-32)
(Contract DAAB07-92-R-C977)
Avail: CASI HC A02/MF A06

This work provides an investigation of the performance of loop antennas for use in mobile communications applications. The analysis tools developed allow for high flexibility by representing the loop antenna as a superquadric curve, which includes the case of circular, elliptical, and rectangular loops. The antenna may be in an isolated environment, located above an infinite ground plane, or placed near a finite conducting plate or box. In cases where coupled loops are used, the two loops may have arbitrary relative positions and orientations. Several design examples are included to illustrate the versatility of the analysis capabilities. The performance of coupled loops arranged in a diversity scheme is also evaluated, and it is found that high diversity gain can be achieved even when the antennas are closely spaced. Author

N94-22835*# Jet Propulsion Lab., California Inst. of Tech., Pasadena.
L-BAND MOBILE TERMINAL ANTENNAS FOR HELICOPTERS
T. K. Wu, K. Farazian, N. Golshan, D. Divsalar, and S. Hinedi *In its* Proceedings of the Third International Mobile Satellite Conference (IMSC 1993) 1993 p 587-592 (For primary document see N94-22735 06-32)
Avail: CASI HC A02/MF A06

The feasibility of using a low gain antenna (LGA) as a mobile terminal antenna for a helicopter is described in this paper. The objectives are to select the lowest cost antenna system which can be easily mounted on a helicopter and capable of communicating with a satellite, and to determine the best antenna position on the helicopter to mitigate the signal blockage due to rotor blades and the multipath effect from the helicopter's body. The omnidirectional LGA is selected because it is simple, reliable, and low cost. The helix antenna is selected among the many LGA's because it is the most economical one and has the widest elevation beamwidth. Both 2-arm and 4-arm helices are studied experimentally to determine the antenna's performance and the scattering effects from the helicopter's body. It is found that the LGA should be located near the tail section and at least eight inches above the helicopter. Author (revised)

N94-22836*# Communications Research Centre, Ottawa (Ontario). Dept. of Communications.
AERONAUTICAL SATELLITE ANTENNA STEERING USING MAGNETIC FIELD SENSORS
John Sydor and Martial Dufour *In* JPL, Proceedings of the Third International Mobile Satellite Conference (IMSC 1993) 1993 p 593-598 (For primary document see N94-22735 06-32)
Avail: CASI HC A02/MF A06

Designers of aeronautical satellite terminals are often faced with the problem of steering a directive antenna from an airplane or helicopter. This problem is usually solved by using aircraft orientation information derived from inertial sensors on-board the aircraft in combination with satellite ephemeris information calculated from geographic coordinates. This procedure works well but relies heavily on avionics that are external to the terminal. For the majority of small aircraft and helicopters which will form the bulk of future aeronautical satcom users, such avionics either do not exist or are difficult for the satellite terminal to interface with. At the Communications Research Center (CRC), work has been undertaken to develop techniques that use the geomagnetic field and satellite antenna pointing vectors (both of which are stationary in a local geographical area) to track the position of a satellite relative to a moving platform such as an aircraft. The performance of this technique is examined and a mathematical steering transformation is developed within this paper. Details are given regarding the experimental program that will be undertaken to test the concepts proposed herein. Author

N94-22876# Technische Univ., Eindhoven (Netherlands). Electromagnetics Div.

RIGOROUS ANALYSIS OF THICK MICROSTRIP ANTENNAS AND WIRE ANTENNAS EMBEDDED IN A SUBSTRATE

A. B. Smolders Jul. 1992 73 p
(EUT-92-E-263; ISBN-9-06-144263-X; ETN-94-94770) Avail: CASI HC A04/MF A01

An efficient and rigorous method for the analysis of electrically thick rectangular microstrip antennas and wire antennas with a dielectric cover is presented. The method of moments is used in combination with the exact spectral domain Green's function in order to find the unknown currents on the antenna. The microstrip antenna is fed by a coaxial cable. A proper model of the feeding coaxial structure is used. In addition, a special attachment mode was applied to ensure continuity of current at the patch-coax transition. The efficiency of the method of moments is improved by using the so called source term extraction technique, where a great part of the infinite integrals involved with the method of moment formulation is calculated analytically. Computation time can be saved by selecting a set of basis functions that describes the current distribution on the patch and probe in an accurate way using only a few terms of this set. Thick microstrip antennas have broadband characteristics. However, a proper match to 50 Ohms is often difficult. This matching problem can be avoided by using a slightly different excitation structure. The patch is now electromagnetically coupled to the feeding probe. A bandwidth of more than 40 can easily be obtained for this type of microstrip antenna. The price to be paid is a degradation of the radiation characteristics. ESA

N94-23081# Office of Technology Assessment, Washington, DC.

MAKING GOVERNMENT WORK: ELECTRONIC DELIVERY OF FEDERAL SERVICES

Sep. 1993 185 p
(OTA-TCT-578; ISBN-0-16-042080-6) Avail: CASI HC A09/MF A02; SOD HC

Federal, State, and local governments face the challenge of delivering better services faster and at less cost at a time when demand is growing and budgets are tighter. Computer and telecommunication technologies offer a number of near-term opportunities for delivering Federal services electronically in partnership with State/local agencies and the private sector. To assure that these technologies benefit all citizens - not just the affluent and highly educated - will require Congress to pay special attention to policy and oversight. It will also require agencies to be innovative and skillful in introducing new electronic delivery systems. The Office of Technology Assessment's (OTA's) assessment of electronic service delivery was requested by Senator John Glenn, Chairman, Senate Committee on Governmental Affairs. This report provides Congress with alternative strategies for improving the performance of government by using modern information technologies. The report offers new perspectives to Congress as it considers reauthorizing the Paperwork Reduction Act and responds to the Administration's 'National Performance Review' and 'National Information Infrastructure' initiatives. More broadly, the report will contribute to the public debate over the role of information technology in reinventing government. Author (revised)

N94-23087*# Analex Corp., Brook Park, OH.

PHASE LINEARITY OF THE 914H COUPLED-CAVITY TRAVELING WAVE TUBE Final Report

Frank E. Kavanagh Jan. 1994 52 p
(Contract NAS3-25776; RTOP 506-72-00)
(NASA-CR-191056; E-7830; NAS 1.26:191056) Avail: CASI HC A04/MF A01

Tests of phase deviation from linearity were made on two 914H coupled-cavity traveling wave tubes (TWT). One tube had a voltage standing wave ratio (VSWR) of 2.4 and the other 1.4. The data showed that phase deviation is primarily a function of the amplitude and shape of the output VSWR. It was predicted that the low-VSWR tube would give a better system performance than the tube with a high VSWR. This prediction was confirmed by the Advanced Communications Technology Satellite (ACTS) system tests performed at the NASA Lewis Research Center. A possible improvement in the construction and stability of coupled-cavity TWT's is discussed. Author (revised)

N94-23225# Helsinki Univ. of Technology, Espoo (Finland). Electromagnetics Lab.

PROCEEDINGS OF THE 1993 BI-ISOTROPICS WORKSHOP ON NOVEL MICROWAVE MATERIALS

A. Sihvola Feb. 1993 92 p Workshop held in Helsinki, Finland, Feb. 1993
(PB93-224772; ISBN-951-22-1442-3) Avail: CASI HC A05/MF A01

During the first week of February 1993, the Workshop Bi-isotropics'93 was held at the Helsinki University of Technology in Finland. The topic of the meeting was the electromagnetics and microwave engineering aspects of novel materials, such as chiral, nonreciprocal, and even bianisotropic media. The Proceedings contains abstracts, summaries, and other written material relevant to the talks given at the Workshop. NTIS

N94-23256*# Jet Propulsion Lab., California Inst. of Tech., Pasadena.

THE TELECOMMUNICATIONS AND DATA ACQUISITION REPORT Progress Report, Jul. - Sep. 1993

Joseph H. Yuen, ed. 15 Nov. 1993 188 p
(NASA-CR-194766; TDA-PR-42-115; NAS 1.26:194766) Avail: CASI HC A09/MF A02

This quarterly publication provides archival reports on developments in programs managed by JPL's Office of Telecommunications and Data Acquisition (TDA). In space communications, radio navigation, radio science, and ground-based radio and radar astronomy, it reports on activities of the Deep Space Network (DSN) in planning, supporting research and technology, implementation, and operations. Also included are standards activity at JPL for space data and information systems and reimbursable DSN work performed for other space agencies through NASA. The papers included in this document cover satellite tracking and ground-based navigation, spacecraft-ground communications, and optical communication systems for the Deep Space Network. For individual titles, see N94-23257 through N94-23269.

N94-23257*# Jet Propulsion Lab., California Inst. of Tech., Pasadena. Tracking Systems and Applications Section.

A REVIEW OF GPS-BASED TRACKING TECHNIQUES FOR TDRS ORBIT DETERMINATION c13

B. J. Haines, S. M. Lichten, R. P. Malla, and S.-C. Wu *In its* The Telecommunications and Data Acquisition Report 15 Nov. 1993 p 1-16
(For primary document see N94-23256 06-32)
(RTOP 310-10-61-92-01)
Avail: CASI HC A03/MF A02

This article evaluates two fundamentally different approaches to the Tracking and Data Relay Satellite (TDRS) orbit determination utilizing Global Positioning System (GPS) technology and GPS-related techniques. In the first, a GPS flight receiver is deployed on the TDRS. The TDRS ephemerides are determined using direct ranging to the GPS spacecraft, and no ground network is required. In the second approach, the TDRS's broadcast a suitable beacon signal, permitting the simultaneous tracking of GPS and Tracking and Data Relay Satellite System satellites by ground receivers. Both strategies can be designed to meet future operational requirements for TDRS-II orbit determination. Author

N94-23258*# Jet Propulsion Lab., California Inst. of Tech., Pasadena. Tracking Systems and Applications Section.

NEW APPROACHES FOR TRACKING EARTH ORBITERS USING MODIFIED GPS GROUND RECEIVERS c13

S. M. Lichten, L. E. Young, S. Nandi, B. J. Haines, C. E. Dunn, and C. D.

Edwards *In its* The Telecommunications and Data Acquisition Report 15 Nov. 1993 p 17-31 (For primary document see N94-23256 06-32)
(RTOP 310-10-61-92-91)
Avail: CASI HC A03/MF A02

A Global Positioning System (GPS) flight receiver provides a means to precisely determine orbits for satellites in low to moderate altitude orbits. Above a 5000-km altitude, however, relatively few GPS satellites are visible. New approaches to orbit determination for satellites at higher altitudes could reduce DSN antenna time needed to provide navigation and orbit determination support to future missions. Modification of GPS ground receivers enables a beacon from the orbiter to be tracked simultaneously with GPS data. The orbit accuracy expected from this GPS-like tracking (GLT) technique is expected to be in the range of a few meters or better for altitudes up to 100,000 km with a global ground network. For geosynchronous satellites, however, there are unique challenges due to geometrical limitations and to the lack of strong dynamical signature in tracking data. We examine two approaches for tracking the Tracking and Data Relay Satellite System (TDRSS) geostationary orbiters. One uses GLT with a global network; the other relies on a small 'connected element' ground network with a distributed clock for short-baseline differential carrier phase (SB Delta Phi). We describe an experiment planned for late 1993, which will combine aspects of both GLT and SB Delta Phi, to demonstrate a new approach for tracking the Tracking and Data Relay Satellites (TDRSs) that offers a number of operationally convenient and attractive features. The TDRS demonstration will be in effect a proof-of-concept experiment for a new approach to tracking spacecraft which could be applied more generally to deep-space as well as near-Earth regimes. Author (revised)

N94-23259*# Jet Propulsion Lab., California Inst. of Tech., Pasadena. Tracking Systems and Applications Section.
IMPROVED THERMAL FORCE MODELING FOR GPS SATELLITES c18
Y. Vigue, R. E. Schutz (Texas Univ., Austin.), and P. A. M. Abusali (Texas Univ., Austin.) *In its* The Telecommunications and Data Acquisition Report 15 Nov. 1993 p 32-41 (For primary document see N94-23256 06-32)
(RTOP 310-10-61-84-02)
Avail: CASI HC A02/MF A02

Geophysical applications of the Global Positioning System (GPS) require the capability to estimate and propagate satellite orbits with high precision. An accurate model of all the forces acting on a satellite is an essential part of achieving high orbit accuracy. Methods of analyzing the perturbation due to thermal radiation and determining its effects on the long-term orbital behavior of GPS satellites are presented. The thermal imbalance force, a nongravitational orbit perturbation previously considered negligible, is the focus of this article. The earth's shadowing of a satellite in orbit causes periodic changes in the satellite's thermal environment. Simulations show that neglecting thermal imbalance in the satellite force model gives orbit error larger than ten meters over several days for eclipsing satellites. This orbit mismodeling can limit accuracy in orbit determination and in estimation of baselines used for geophysical applications. Author (revised)

N94-23260*# Jet Propulsion Lab., California Inst. of Tech., Pasadena. Ground Antennas and Facilities Engineering Section.
EXPERIMENTAL MODIFICATION AND IDENTIFICATION OF THE DSS-13 ANTENNA CONTROL SYSTEM MODEL c37
C. S. Racho and W. K. Gawronski *In its* The Telecommunications and Data Acquisition Report 15 Nov. 1993 p 42-53 (For primary document see N94-23256 06-32)
(RTOP 310-20-65-63-00)
Avail: CASI HC A03/MF A02

This work is the first step toward increasing the bandwidth of the DSS-13 antenna position loop controller. A wider bandwidth of the controller allows for faster tracking rates and better pointing performance under windy conditions. To achieve this goal, the antenna control system model has to be improved, such that it will accurately reflect the dynamic properties of the antenna. The existing analytical model, due to its many uncertainties, could not be used in the design of the controller. However, by using experimental data, the analytical model is modified and improved, and a new model is obtained through system identification techniques. Author

N94-23261*# Jet Propulsion Lab., California Inst. of Tech., Pasadena. Ground Antennas and Facilities Engineering Section.
PERFORMANCE OF THE X-/Ka/KABLE-BAND DICHROIC PLATE IN THE DSS-13 BEAM WAVEGUIDE ANTENNA
J. C. Chen, P. H. Stanton, and H. F. Reilly *In its* The Telecommunications and Data Acquisition Report 15 Nov. 1993 p 54-64 (For primary document see N94-23256 06-32)
(RTOP 310-20-64-83-02)
Avail: CASI HC A03/MF A02

The first Ka-band downlink demonstration was recently carried out by the Ka-Band Link Experiment (KABLE) in association with the Mars Observer spacecraft. In order to support the mission, a dichroic plate was required in the DSS-13 beam waveguide antenna to allow simultaneous X- and Ka-band operation. An X-/ Ka-/ KABLE-band dichroic plate was designed to transmit Ka-band downlink (31.8-32.3 GHz), Ka-band uplink (34.2-34.7 GHz), and KABLE (33.6-33.8 GHz) frequencies, while reflecting X-band (8.4-8.5 GHz). A computer program was developed for the analysis of a dichroic plate with rectangular apertures by using the mode-matching method. The plate was then fabricated and tested. The reflection, group delay, and noise temperature in the antenna system due to the dichroic plate were measured. The experimental results show good agreement with theoretical prediction. Author

N94-23262*# Jet Propulsion Lab., California Inst. of Tech., Pasadena. Radio Frequency and Microwave Subsystems Section.
CRYOGENIC, LOW-NOISE HIGH ELECTRON MOBILITY TRANSISTOR AMPLIFIERS FOR THE DEEP SPACE NETWORK c33
J. J. Bautista *In its* The Telecommunications and Data Acquisition Report 15 Nov. 1993 p 65-80 (For primary document see N94-23256 06-32)
(RTOP 310-20-66-09-01)
Avail: CASI HC A03/MF A02

The rapid advances recently achieved by cryogenically cooled high electron mobility transistor (HEMT) low-noise amplifiers (LNA's) in the 1- to 10-GHz range are making them extremely competitive with maser amplifiers. In order to address future spacecraft navigation, telemetry, radar, and radio science needs, the Deep Space Network is investing both maser and HEMT amplifiers for its Ka-band (32-GHz) downlink capability. This article describes the current state cryogenic HEMT LNA development at Ka-band for the DSN. Noise performance results at S-band (2.3 GHz) and X-band (8.5 GHz) for HEMT's and masers are included for completeness. Author

N94-23263*# Jet Propulsion Lab., California Inst. of Tech., Pasadena. Ground Antennas and Facilities Engineering Section.
ANALYSIS OF OPEN-LOOP CONICAL SCAN POINTING ERROR AND VARIANCE ESTIMATORS
L. S. Alvarez *In its* The Telecommunications and Data Acquisition Report 15 Nov. 1993 p 81-90 (For primary document see N94-23256 06-32)
(RTOP 310-20-65-63-00)
Avail: CASI HC A02/MF A02

General pointing error and variance estimators for an open-loop conical scan (conscan) system are derived and analyzed. The conscan algorithm is modeled as a weighted least-squares estimator whose inputs are samples of receiver carrier power and its associated measurement uncertainty. When the assumptions of constant measurement noise and zero pointing error estimation are applied, the variance equation is then strictly a function of the carrier power to uncertainty ratio and the operator selectable radius and period input to the algorithm. The performance equation is applied to a 34-m mirror-based beam-waveguide conscan system interfaced with the Block V Receiver Subsystem tracking a Ka-band (32-GHz) downlink. It is shown that for a carrier-to-noise power ratio greater than or equal to 30 dB-Hz, the conscan period for Ka-band operation may be chosen well below the current DSN minimum of 32 sec. The analysis presented forms the basis of future conscan work in both research and development as well as for the upcoming DSN antenna controller upgrade for the new DSS-24 34-m beam-waveguide antenna. Author (revised)

N94-23264*# Jet Propulsion Lab., California Inst. of Tech., Pasadena. Communications Systems Research Section.
SPUR-REDUCED DIGITAL SINUSOID SYNTHESIS

M. J. Flanagan and G. A. Zimmerman *In its* The Telecommunications and Data Acquisition Report 15 Nov. 1993 p 91-104 (For primary document see N94-23256 06-32)
(RTOP 310-30-70-87-02)
Avail: CASI HC A03/MF A02

This article presents and analyzes a technique for reducing the spurious signal content in digital sinusoid synthesis. Spurious-harmonic (spur) reduction is accomplished through dithering both amplitude and phase values prior to word-length reduction. The analytical approach developed for analog quantization is used to produce new bounds on spur performance in these dithered systems. Amplitude dithering allows output word-length reduction without introducing additional spurs. Effects of periodic dither similar to those produced by a pseudonoise (PN) generator are analyzed. This phase-dithering method provides a spur reduction of 6(M plus one) dB per phase bit when the dither consists of M uniform variates. While the spur reduction is at the expense of an increase in system noise, the noise power can be made white, making the power spectral density small. This technique permits the use of a smaller number of phase bits addressing sinusoid lookup tables, resulting in an exponential decrease in system complexity. Amplitude dithering allows the use of less complicated multipliers and narrower data paths in purely digital applications, as well as the use of coarse resolution, highly linear digital to analog converters (DAC's) to obtain spur performance limited by the DAC linearity rather than its resolution. Author (revised)

N94-23265*# Jet Propulsion Lab., California Inst. of Tech., Pasadena.
BOX CODES OF LENGTHS 48 AND 72
G. Solomon and Y. Jin (California Inst. of Tech., Pasadena.) *In its* The Telecommunications and Data Acquisition Report 15 Nov. 1993 p 105-109 (For primary document see N94-23256 06-32)
(RTOP 310-30-71-83-02)
Avail: CASI HC A01/MF A02

A self-dual code length 48, dimension 24, with Hamming distance essentially equal to 12 is constructed here. There are only six code words of weight eight. All the other code words have weights that are multiples of four and have a minimum weight equal to 12. This code may be encoded systematically and arises from a strict binary representation of the (8,4;5) Reed-Solomon (RS) code over GF (64). The code may be considered as six interrelated (8,7;2) codes. The Mattson-Solomon representation of the cyclic decomposition of these codes and their parity sums are used to detect an odd number of errors in any of the six codes. These may then be used in a correction algorithm for hard or soft decision decoding. A (72,36;15) box code was constructed from a (63,35;8) cyclic code. The theoretical justification is presented herein. A second (72,36;15) code is constructed from an inner (63,27;16) Bose Chaudhuri Hocquenghem (BCH) code and expanded to length 72 using box code algorithms for extension. This code was simulated and verified to have a minimum distance of 15 with even weight words congruent to zero modulo four. The decoding for hard and soft decision is still more complex than the first code constructed above. Finally, an (8,4;5) RS code over GF (512) in the binary representation of the (72,36;15) box code gives rise to a (72,36;16*) code with nine words of weight eight, and all the rest have weights greater than or equal to 16. Author (revised)

N94-23266*# Jet Propulsion Lab., California Inst. of Tech., Pasadena. Communications Systems Research Section.
INTEGER COSINE TRANSFORM COMPRESSION FOR GALILEO AT JUPITER: A PRELIMINARY LOOK
L. Ekroot, S. Dolinar, and K.-M. Cheung *In its* The Telecommunications and Data Acquisition Report 15 Nov. 1993 p 110-123 (For primary document see N94-23256 06-32)
(RTOP 310-30-71-83-02)
Avail: CASI HC A03/MF A02

The Galileo low-gain antenna mission has a severely rate-constrained channel over which we wish to send large amounts of information. Because of this link pressure, compression techniques for image and other data are being selected. The compression technique that will be used for images is the integer cosine transform (ICT). This article investigates the compression performance of Galileo's ICT algorithm as applied to Galileo images taken during the early portion of the mission and to images that simulate those expected from the encounter at Jupiter. Author

N94-23267*# Jet Propulsion Lab., California Inst. of Tech., Pasadena. Advanced Information Systems Section.
LINK MONITOR AND CONTROL OPERATOR ASSISTANT: A PROTOTYPE DEMONSTRATING SEMIAUTOMATED MONITOR AND CONTROL **c63**
L. F. Lee and L. P. Cooper *In its* The Telecommunications and Data Acquisition Report 15 Nov. 1993 p 124-134 (For primary document see N94-23256 06-32)
(RTOP 310-40-73-90-01)
Avail: CASI HC A03/MF A02

This article describes the approach, results, and lessons learned from an applied research project demonstrating how artificial intelligence (AI) technology can be used to improve Deep Space Network operations. Configuring antenna and associated equipment necessary to support a communications link is a time-consuming process. The time spent configuring the equipment is essentially overhead and results in reduced time for actual mission support operations. The NASA Office of Space Communications (Code O) and the NASA Office of Advanced Concepts and Technology (Code C) jointly funded an applied research project to investigate technologies which can be used to reduce configuration time. This resulted in the development and application of AI-based automated operations technology in a prototype system, the Link Monitor and Control Operator Assistant (LMC OA). The LMC OA was tested over the course of three months in a parallel experimental mode on very long baseline interferometry (VLBI) operations at the Goldstone Deep Space Communications Center. The tests demonstrated a 44 percent reduction in pre-calibration time for a VLBI pass on the 70-m antenna. Currently, this technology is being developed further under Research and Technology Operating Plan (RTOP)-72 to demonstrate the applicability of the technology to operations in the entire Deep Space Network. Author (revised)

N94-23268*# Jet Propulsion Lab., California Inst. of Tech., Pasadena. Ground Antennas and Facilities Engineering Section.
BEAM-WAVEGUIDE ANTENNA SERVO DESIGN ISSUES FOR TRACKING LOW EARTH-ORBITING SATELLITES **c37**
W. K. Gawronski and J. A. Mellstrom *In its* The Telecommunications and Data Acquisition Report 15 Nov. 1993 p 135-152 (For primary document see N94-23256 06-32)
(RTOP 314-30-50-12-80)
Avail: CASI HC A03/MF A02

Upcoming NASA missions will require tracking of low-orbit satellites. As a consequence, NASA antennas will be required to track satellites at higher rates than for the current deep space missions. This article investigates servo design issues for the 34-m beam-waveguide antennas that track low-orbit satellites. This includes upgrading the servo with a feedforward loop, using a monopulse controller design, and reducing tracking errors through either proper choice of elevation pinion location, application of a notch filter, or adjustment of the elevation drive amplifier gain. Finally, improvement of the signal-to-noise ratio through averaging of the over-sampled monopulse signal is described. Author

N94-23269*# Jet Propulsion Lab., California Inst. of Tech., Pasadena. Communications Systems Research and Telecommunications Systems Sections.
OPTICAL SUBNET CONCEPTS FOR THE DEEP SPACE NETWORK
K. Shaik, D. Wonica, and M. Wilhelm *In its* The Telecommunications and Data Acquisition Report 15 Nov. 1993 p 153-181 (For primary document see N94-23256 06-32)
(Contracts JPL-958733; JPL-958734; RTOP 315-91-30-20-03)
Avail: CASI HC A03/MF A02

This article describes potential enhancements to the Deep Space Network, based on a subnet of receiving stations that will utilize optical communications technology in the post-2010 era. Two optical subnet concepts are presented that provide full line-of-sight coverage of the ecliptic, 24 hours a day, with high weather availability. The technical characteristics of the optical station and the user terminal are presented, as well as the effects of cloud cover, transmittance through the atmosphere, and background noise during daytime or nighttime operation on the communications link. In addition, this article identifies candidate geographic sites for the two network concepts and includes a link design for a hypothetical Pluto mission in 2015. Author

N94-23473# Oak Ridge National Lab., TN.
SYSTEM IDENTIFICATION USING A WAVELET-BASED APPROACH
D. A. Schoenwald 1993 3 p Presented at the 32nd Institute of Electrical and Electronic Engineers (IEEE) Conference on Decision and Control, San Antonio, TX, Dec. 1993
(Contract DE-AC05-84OR-21400)
(DE94-002191; CONF-931233-2) Avail: CASI HC A01/MF A01

In this paper, an approach to system identification using the wavelet transform is outlined. The method is based on system identification algorithms that belong to the class of modulating function methods. In particular, the Pearson-Lee method is modified to make use of wavelet basis functions which provide a more precise time window to process the plant input-output data. It is proposed here that replacing these modulating functions with wavelet basis functions will provide data filtering which is less sensitive to noise and initial conditions. DOE

N94-23508# Selskapet for Industriell og Teknisk Forskning, Trondheim (Norway).
SOURCE SPACING IN B-ISDN
Finn Arve Aagesen 22 Dec. 1992 34 p See also PB93-162618 and PB93-162634
(PB93-201747; STF40-A92145) Avail: CASI HC A03/MF A01

A vital part of the future high capacity networks seems to be B-ISDN based on ATM. Flow management is the set of functions related to the control of the traffic flow from the applications during information transfer. Flow management is considered within the context of the user - user flow, the user - transport system flow, the transport system internal flow, the transport - ATM system flow and the ATM system internal flow. Flow management must be related to specific time resolution regions. The extreme, burst, frame, average, packet, message, and stretching interval time resolution regions are defined. The report proposes a total flow management scheme. The basic principle has been to adapt the flow management to the pattern of the applications. Such an adaption is possible by using transport system flow management mechanisms that reflect the application flow parameters and a formally defined ATM system service that makes important flow parameters visible for the ATM system. The ATM system internal flow management comprises three mechanisms: spacing, rate-control-based policing and stop-and-wait flow control. Spacing schemes based on stretching are proposed for the various transport system service classes. NTIS

N94-23622*# Loyola Coll., Baltimore, MD. International Technology Research Inst.
SATELLITE COMMUNICATIONS SYSTEMS AND TECHNOLOGY. EXECUTIVE SUMMARY
Burton I. Edelson (George Washington Univ., Washington, DC.), Joseph N. Pelton (Colorado Univ., Boulder.), Charles W. Bostian (Virginia Polytechnic Inst., Blacksburg.), William T. Brandon (Mitre Corp., McLean, VA.), Vincent W. S. Chan (Massachusetts Inst. of Tech., Cambridge.), E. Paul Hager (George Mason Univ., Fairfax, VA.), Neil R. Helm (George Washington Univ., Washington, DC.), Raymond D. Jennings (National Telecommunications and Information Administration, Washington, DC.), Robert Kwan (Jet Propulsion Lab., California Inst. of Tech., Pasadena.), and Christoph E. Mahle (Communications Satellite Corp., Washington, DC.) et al Jul. 1993 11 p Sponsored by NASA, Washington
(NASA-TM-109388; NAS 1.15:109388; PB93-231116) Avail: CASI HC A03/MF A01

NASA and the National Science Foundation (NSF) commissioned a panel of US experts to study the international status of satellite communications systems and technology. The study covers emerging systems concepts, applications, services, and the attendant technologies. The panel members travelled to Europe, Japan, and Russia to gather information first-hand. They visited 17 sites in Europe, 20 sites in Japan, and four in Russia. These included major manufacturers, government organizations, service providers, and associated R&D facilities. The panel's report was reviewed by the sites visited, by the panel, and by representatives of US industry. The report details the information collected and compares it to US activities. Author (revised)

N94-23627*# Loyola Coll., Baltimore, MD. International Technology Research Inst.
SATELLITE COMMUNICATIONS SYSTEMS AND TECHNOLOGY. VOLUME 1: ANALYTICAL CHAPTERS
Burton I. Edelson, ed. (George Washington Univ., Washington, DC.), Joseph N. Pelton, ed. (Colorado Univ., Boulder.), Charles W. Bostian (Virginia Polytechnic Inst., Blacksburg.), William T. Brandon (Mitre Corp., McLean, VA.), Vincent W. S. Chan (Massachusetts Inst. of Tech., Cambridge.), E. Paul Hager (George Mason Univ., Fairfax, VA.), Neil R. Helm (George Washington Univ., Washington, DC.), Raymond D. Jennings (National Telecommunications and Information Administration, Washington, DC.), Robert K. Kwan (Jet Propulsion Lab., California Inst. of Tech., Pasadena.), and Christoph E. Mahle (Communications Satellite Corp., Washington, DC.) et al Jul. 1993 340 p Sponsored by NASA, Washington
(Grant NSF ENG-91-11333)
(NASA-TM-109398; NAS 1.15:109398; PB93-209815; ISBN-1-883712-26-2)
Copyright Avail: CASI HC A15/MF A03

This is Volume 1 (Analytical Chapters) of the final report of the NASA/NSF Panel Satellite Communications Systems and Technology. The panel surveyed advanced technology being developed for commercial use in the satellite communications field in Europe, Japan, and Russia. All aspects of satellite communications were considered, including fixed, broadcast, mobile, personal communications, navigation, low earth orbit, and small satellites. The focus was on experimental and advanced technology being developed in R&D and demonstration programs rather than on today's production capabilities. Focus was on commercial satellite technology, and does not review defense-related or other confidential satellite communications capabilities. The NASA/NSF panel concluded that the United States has lost its leading position in many critical satellite communications technologies. Although U.S. industry retains a leading position in today's marketplace for satellite communications systems and services, this position is largely founded on technologies and capabilities developed in the 1960's and 1970's. Because the United States is losing ground with respect to a wide range of technologies and systems that will be key to future communications markets, the market share of the U.S. satellite communications industry is at risk. Author (revised)

N94-23628*# Loyola Coll., Baltimore, MD. International Technology Research Inst.
SATELLITE COMMUNICATIONS SYSTEMS AND TECHNOLOGY. VOLUME 2: SITE REPORTS
Burton I. Edelson, ed. (George Washington Univ., Washington, DC.), Joseph N. Pelton, ed. (Colorado Univ., Boulder.), Charles W. Bostian (Virginia Polytechnic Inst., Blacksburg.), William T. Brandon (Mitre Corp., McLean, VA.), Vincent W. S. Chan (Massachusetts Inst. of Tech., Cambridge.), E. Paul Hager (George Mason Univ., Fairfax, VA.), Neil R. Helm (George Washington Univ., Washington, DC.), Raymond D. Jennings (National Telecommunications and Information Administration, Washington, DC.), Robert K. Kwan (Jet Propulsion Lab., California Inst. of Tech., Pasadena.), and Christoph E. Mahle (Communications Satellite Corp., Washington, DC.) et al Jul. 1993 193 p Sponsored in part by NASA, Washington and NSF
(NASA-TM-109399; NAS 1.15:109399; PB94-100187; ISBN-1-883712-27-0)
Copyright Avail: CASI HC A09/MF A03

This is volume 2 of the final report of the NASA/NSF Panel on Satellite Communications Systems and Technology. It consists of the site reports from the panel's visits to satellite communications facilities and laboratories in Europe, Japan, and Russia. The Executive Summary of the panel's final report is published separately. Volume 1, also published separately, consists of the panel's analytical chapters. Information on ordering the Executive Summary and Volume 1 from the National Technical Information Service is included. Author (revised)

N94-23719# National Inst. of Standards and Technology, Gaithersburg, MD. Electricity Div.
RESEARCH FOR ELECTRIC ENERGY SYSTEMS Annual Report
W. E. Anderson, ed. Oct. 1993 38 p
(DE94-001839; NISTIR-5268) Avail: CASI HC A03/MF A01

This report documents the technical progress in the two investigations which make up the project 'Support of Research Projects for Electrical Energy Systems,' Department of Energy Task Order Number 137, funded by the US Department of Energy and performed by the Electricity Division of the National Institute of Standards and Technology (NIST). The first investigation is concerned with the measurement of magnetic fields in support of epidemiogical and in vitro studies of biological field effects. During 1992, the derivation of equations which predict differences between the average magnetic flux density using circular coil probes and the flux density at the center of the probe, assuming a dipole magnetic field, were completed. The information gained using these equations allows the determination of measurement uncertainty due to probe size when magnetic fields from many electrical appliances are characterized. Consultations with various state and federal organizations and the development of standards related to electric and magnetic field measurements continued. The second investigation is concerned with two different activities related to compressed-gas insulated high voltage systems: the measurement of dissociative electron attachment cross sections and negative ion production in S2F10, S2OF10, and S2O2F10, and Monte-Carlo simulations of ac-generated partial-discharge pulses that can occur in SF6-insulated power systems and can be sources of gas decomposition. DOE

N94-23727# Technische Univ., Delft (Netherlands). Lab. of Electromagnetic Research.

COMPATIBILITY RELATIONS AND THE FINITE-ELEMENT FORMULATION OF ELECTROMAGNETIC FIELD PROBLEMS

G. Mur 1993 5 p

(PB94-110996; ET/EM-1993-01) Copyright Avail: CASI HC A01/MF A01

When computing an electromagnetic field using the finite element method, it is possible that, although Maxwell's equations are discretized accurately, highly inaccurate computational results are obtained. In those cases it can easily be shown that (some of) the electromagnetic compatibility relations (field properties that follow from Maxwell's equations) are not satisfied. The divergence condition on the fluxes, for instance, follows directly from the field equations but not necessarily from their discretized counterparts. This necessitates inclusion of the compatibility relations in the finite-element formulation of the field problem. A survey is given of all electromagnetic compatibility relations. NTIS

N94-23728# Technische Univ., Delft (Netherlands). Lab. of Electromagnetic Research.

STUDY OF A LOCAL ABSORBING BOUNDARY CONDITION FOR THE MODELING OF AN INFINITE EXTERNAL DOMAIN IN THE TIME-DOMAIN FINITE-ELEMENT PACKAGE FEMAXT

K. Pinardi 1993 31 p

(PB94-111002; ET/EM-1993-03) Copyright Avail: CASI HC A03/MF A01

Absorbing boundary conditions are used for modeling the infinite surroundings of a finite domain of computation. A simple local absorbing boundary condition that is used in a time-domain finite-element package is investigated. Numerical results are given for the fluctuation at the error as a function of time, as a function of the angle of incidence, and as a function of the frequency of the field to be computed. NTIS

N94-23729# Technische Univ., Delft (Netherlands). Lab. of Electromagnetic Research.

ELECTROMAGNETIC SCATTERING BY INHOMOGENEOUS OBJECTS. SOLUTION METHODS BASED UPON RECIPROCITY THEOREMS OF TIME-CONVOLUTION AND TIME-CORRELATION TYPE

R. Remis 1993 64 p

(PB94-111010; ET/EM-1993-02) Copyright Avail: CASI HC A04/MF A01

The standard method for the solution of the problem of scattering of an electromagnetic wave by an inhomogeneous object is the domain-integral equation formulation. This domain-integral equation is obtained from an appropriate application of Lorentz' reciprocity theorem of the convolution type. A domain-integral equation based upon Lorentz' reciprocity theorem of the correlation type was obtained. Both types of Lorentz' reciprocity theorem were applied to a one-dimensional slab with dielectric contrast only. It is shown that it is possible to recover the domain-integral equation of the convolution type from the domain-integral equation of the correlation type. Further, the domain-integral equation of the correlation type can be manipulated into a form which is interesting to investigate numerically in the future. NTIS

N94-23733# Technische Univ., Delft (Netherlands). Lab. of Electromagnetic Research.

FEMAX FINITE-ELEMENT PACKAGE FOR COMPUTING THREE-DIMENSIONAL TIME-DOMAIN ELECTROMAGNETIC FIELDS IN INHOMOGENEOUS MEDIA

G. Mur 1993 12 p

(PB94-111093; ET/EM-1993-11) Copyright Avail: CASI HC A03/MF A01

An efficient and accurate finite-element package is described for computing transient as well as time-harmonic three-dimensional electromagnetic fields in inhomogeneous media. For the expansion of the field in an inhomogeneous configuration, edge elements are used along the interfaces between media with different medium properties to allow for the continuity conditions of the field across these interfaces, nodal elements are used in the remaining homogeneous subdomains. In the domain of computation the package decides locally what type of element has to be used for obtaining the user-specified accuracy of modeling the field. In this way optimum results are obtained both in regard to computational efficiency and in regard to desired accuracy. The electromagnetic compatibility relations are implemented for avoiding spurious solutions. NTIS

N94-23742 National Defence Research Establishment, Linkoeping (Sweden). Huvudavdelning foer Informationsteknologi.

RADAR SIGNATURE RELATED RADOME TECHNIQUES FOR FLUSH-MOUNTED HF-, VHF- AND, UHF COMMUNICATION ANTENNAS [RADARSIGNATURANPASSAD RADOMTEKNIK FOER PLATTFORMSINTEGRERADE KOMMUNIKATIONSANTENNER FOER HF, VHF OCH UHF]

Goeran Svennerus, Leif Pettersson, and Ake Bergquist Feb. 1993 41 p In SWEDISH; Text in Swedish; summary in English. See also PB89-145858 and PB91-207746 Limited Reproducibility: More than 20% of this document may be affected by microfiche quality

(PB93-204618; FOA-C-30703-3.2) Avail: Issuing Activity (National Technical Information Service (NTIS))

Different radome concepts and their potential use for covering flush-mounted HF, VHF, and UHF communication antennas are discussed. Antenna properties as well as radar signature aspects are taken into account. The structure and design of three types of frequency selective radome materials are given. When applied in typical antenna cases, these radome structures are evaluated on the basis of a simple analysis of expected antenna and radar cross section properties. NTIS

N94-23773 National Defence Research Establishment, Linkoeping (Sweden). Huvudadelning foer Informationsteknologi.

CALIBRATION BLOCK FOR DIGITAL BEAM FORMING ANTENNA [KALIBRERINGSENHET FOER ANTENNER MED DIGITAL LOBFORMNING]

J. Piotr Starski Feb. 1993 37 p See also PB92-122670, PB92-195429 and AD-A200030 Limited Reproducibility: More than 20% of this document may be affected by microfiche quality

(PB93-204550; FOA-C-30700-8.4; FOA-C-30700-3.2) Avail: CASI HC A03

Future communication and radar systems will require antennas with capabilities to steer the beam by electronic means. In the older antenna systems the beamforming function was performed by shaping a reflector into a desired form. The result was a good electrical performance, but the system was slow, clumsy, and could follow only one target at the same time. The present systems use computer controlled digital phase shifters (i.e. the phase shift is controlled in steps, by smallest increment, corresponding to the smallest phase shifter bit). By using an all digital beam former for a phased array antenna, the problems with phase and amplitude accuracy in the beam forming network can be virtually eliminated. This is achieved by maintaining the phase and amplitude information in each antenna element channel separately. It is very important to know the transmission data for each channel separately. This is done by including in the system a calibration network. A calibration circuit for a digital beam forming antenna is described. The circuit is designed in stripline technology and consists of a combination of couplers and power dividers. NTIS

N94-23827* National Aeronautics and Space Administration. Goddard Space Flight Center, Greenbelt, MD.

MICRO PULSE LASER RADAR Patent

James D. Spinhirne, inventor (to NASA) 31 Aug. 1993 12 p Filed 13 Aug. 1992 Supersedes N94-17322 (32 - 3, p 1004)
(NASA-Case-GSC-13493-1; US-Patent-5,241,315;
US-Patent-Appl-SN-929216; US-Patent-Class-342-54;
US-Patent-Class-342-26; US-Patent-Class-356-5; US-Patent-Class-356-28.5;
US-Patent-Class-356-342; Int-Patent-Class-G01C-3/08;
Int-Patent-Class-G01S-13/95) Avail: US Patent and Trademark Office

An eye safe, compact, solid state lidar for profiling atmospheric cloud and aerosol scattering is disclosed. The transmitter of the micro pulse lidar is a diode pumped micro-J pulse energy, high repetition rate Nd:YLF laser. Eye safety is obtained through beam expansion. The receiver employs a photon counting solid state Geiger mode avalanche photodiode detector. Data acquisition is by a single card multichannel scaler. Daytime background induced quantum noise is controlled by a narrow receiver field-of-view and a narrow bandwidth temperature controlled interference filter. Dynamic range of the signal is limited to optical geometric signal compression. Signal simulations and initial atmospheric measurements indicate that micropulse lider systems are capable of detecting and profiling all significant cloud and aerosol scattering through the troposphere and into the stratosphere. The intended applications are scientific studies and environmental monitoring which require full time, unattended measurements of the cloud and aerosol height structure. Official Gazette of the U.S. Patent and Trademark Office

N94-23830*# Laser Data Technology, Inc., Saint Louis, MO.
MULTI-ACCESS LASER COMMUNICATIONS TERMINAL Final Report
3 Nov. 1992 305 p Original contains color illustrations
(Contract NAS5-31170; SBIR-14.02-2250)
(NASA-CR-191251; NAS 1.26:191251) Avail: CASI HC A14/MF A03; 3 functional color pages

The Optical Multi-Access (OMA) Terminal is capable of establishing up to six simultaneous high-data-rate communication links between low-Earth-orbit satellites and a host satellite at synchronous orbit with only one 16-inch-diameter antenna on the synchronous satellite. The advantage over equivalent RF systems in space weight, power, and swept volume is great when applied to NASA satellite communications networks. A photograph of the 3-channel prototype constructed under the present contract to demonstrate the feasibility of the concept is presented. The telescope has a 10-inch clear aperture and a 22 deg full field of view. It consists of 4 refractive elements to achieve a telecentric focus, i.e., the focused beam is normal to the focal plane at all field angles. This feature permits image pick-up optics in the focal plane to track satellite images without tilting their optic axes to accommodate field angle. The geometry of the imager-pick-up concept and the coordinate system of the swinging arm and disk mechanism for image pick-up are shown. Optics in the arm relay the telescope focus to a communications and tracking receiver and introduce the transmitted beacon beam on a path collinear with the receive path. The electronic circuits for the communications and tracking receivers are contained on the arm and disk assemblies and relay signals to an associated PC-based operator's console for control of the arm and disk motor drive through a flexible cable which permits +/- 240 deg travel for each arm and disk assembly. Power supplies and laser transmitters are mounted in the cradle for the telescope. A single-mode fiber in the cable is used to carry the laser transmitter signal to the arm optics. The promise of the optical multi-access terminal towards which the prototype effort worked is shown. The emphasis in the prototype development was the demonstration of the unique aspect of the concept, and where possible, cost avoidance compromises were implemented in areas already proven on other programs. The design details are described in section 2, the prototype test results in section 3, additional development required in section 4, and conclusions in section 5. Author

N94-24085 British Broadcasting Corp., Kingswood (England). Engineering Div.
THE HDTV DIGITAL AUDIO MATRIX
A. J. Mason 1993 12 p
(BBC-RD-1993/9) Copyright Avail: Issuing Activity

Multichannel sound systems are being studied as part of the Eureka 95 and Radio-communication Bureau TG10-1 investigations into high definition television. One emerging sound system has five channels; three at the front and two at the back. This raises some compatibility issues. The listener might have only, say, two loudspeakers or the material to be broadcast may have fewer than five channels. The problem is how best to produce a set of signals to be broadcast, which is suitable for all listeners, from those that are available. To investigate this area, a device has been designed and built which has six input channels and six output channels. Each output signal is a linear combination of the input signals. The inputs and outputs are in AES/EBU digital audio format using BBC-designed AESIC chips. The matrix operation, to produce the six outputs from the six inputs, is performed by a Motorola DSP56001. The user interface and 'housekeeping' is managed by a T222 transputer. The operator of the matrix uses a VDU to enter sets of coefficients and a rotary switch to select which set to use. A set of analog controls is also available and is used to control operations other than the simple compatibility matrixing. The matrix has been very useful for simple tasks: mixing a stereo signal into mono, creating a stereo signal from a mono signal, applying a fixed gain or attenuation to a signal, exchanging the A and B channels of an AES/EBU bitstream, and so on. These are readily achieved using simple sets of coefficients. Additions to the user interface software have led to several more sophisticated applications which still consist of a matrix operation. Different multichannel panning laws have been evaluated. The analog controls adjust the panning; the audio signals are processed digitally using a matrix operation. A digital SoundField microphone decoder has also been implemented. The signal processing is a matrix operation, the analog controls being used to adjust the characteristics of the decoded microphone. DSP software for specific tasks not requiring operator control has also been used. Adaptive filtering and signal restoration are two examples. The transputer in this case can be left to perform the housekeeping. The design of the HDTV digital audio matrix is such that it can be applied to a wide variety of signal processing tasks. The combination of a dedicated DSP chip programmed in assembly language for speed of operation and a general purpose processor for user interface tasks programmed in a high level language has been found to be extremely useful. Author (revised)

N94-24086 British Broadcasting Corp., Kingswood (England). Engineering Div.
AN INTRODUCTION TO DIGITAL MODULATION AND OFDM TECHNIQUES
M. C. D. Maddocks 1993 13 p
(BBC-RD-1993/10) Copyright Avail: Issuing Activity

This report differs from most BBC Research Department reports in that it does not contain details of a specific project undertaken at Kingswood Warren. While there has been a continuing development of aspects of digital modulation systems by BBC research engineers over many years, the purpose of this report is to be tutorial. That is, digital transmission techniques need to be explained in a general way if full advantage is to be obtained from other reports concerning digital broadcasting transmission systems. There are, however, references to other specialized publications if particular details are required. The text of this report is based on a paper which was prepared for an Institution of Electrical Engineers' vacation school on new broadcast standards and systems. It discusses, at a general level, the various issues and trade-offs that must be considered in the design of a digital modulation system for broadcast use. It particularly concentrates on giving a simple description of the use and benefits of OFDM systems. The particular issues can be applied to various future broadcast systems which are under development at the BBC and as part of collaborative work in international projects. Author (revised)

N94-24101*# National Aeronautics and Space Administration. Lewis Research Center, Cleveland, OH.
INTEGRATION AND TEST OF HIGH-SPEED TRANSMITTER ELECTRONICS FOR FREE-SPACE LASER COMMUNICATIONS
Nitin J. Soni and Paul J. Lizanich (Analex Corp., Brook Park, OH.) Feb. 1994 15 p Prepared for presentation at the 15th International Communications Satellite Systems Conference, San Diego, CA, 28 Feb. - 3 Mar. 1994; sponsored by AIAA
(RTOP 506-72-21)
(NASA-TM-106295; E-8033; NAS 1.15:106295; AIAA Paper 94-1158)
Avail: CASI HC A03/MF A01

The NASA Lewis Research Center in Cleveland, Ohio, has developed the electronics for a free-space, direct-detection laser communications system demonstration. Under the High-Speed Laser Integrated Terminal Electronics (Hi-LITE) Project, NASA Lewis has built a prototype full-duplex, dual-channel electronics transmitter and receiver operating at 325 megabit

S per second (Mbps) per channel and using quaternary pulse-position modulation (QPPM). This paper describes the integration and testing of the transmitter portion for future application in free-space, direct-detection laser communications. A companion paper reviews the receiver portion of the prototype electronics. Minor modifications to the transmitter were made since the initial report on the entire system, and this paper addresses them. The digital electronics are implemented in gallium arsenide integrated circuits mounted on prototype boards. The fabrication and implementation issues related to these high-speed devices are discussed. The transmitter's test results are documented, and its functionality is verified by exercising all modes of operation. Various testing issues pertaining to high-speed circuits are addressed. A description of the transmitter electronics packaging concludes the paper. Author (revised)

N94-24105*# California Inst. of Tech., Pasadena. Sublimiter Observatory.

A LOW NOISE 665 GHz SIS QUASI-PARTICLE WAVEGUIDE RECEIVER

J. W. Kooi, C. K. Walker (Arizona Univ., Tucson.), H. G. LeDuc (Jet Propulsion Lab., California Inst. of Tech., Pasadena.), T. R. Hunter, D. J. Benford, and T. G. Phillips [1993] 16 p

(Grants NAGw-107; NSF AST-90-15755)

(NASA-CR-194735; NAS 1.26:194735) Avail: CASI HC A03/MF A01

Recent results on a 565-690 GHz SIS heterodyne receiver employing a 0.36 micron(sup 2) Nb/AlOx/Nb SIS tunnel junction with high quality circular non-contacting back short and E-plane tuners in a full height wave guide mount are reported. No resonant tuning structures were incorporated in the junction design at this time, even though such structures are expected to help the performance of the receiver. The receiver operates to at least the gap frequency of Niobium, approximately 680 GHz. Typical receiver noise temperatures from 565-690 GHz range from 160K to 230K with a best value of 185K DSB at 648 GHz. With the mixer cooled from 4.3K to 2K the measured receiver noise temperatures decreased by approximately 15 percent, giving roughly 180K DSB from 660 to 680 GHz. The receiver has a full 1 GHz IF pass band and was successfully installed at the Caltech Submillimeter Observatory in Hawaii. Author (revised)

N94-24115 McMaster Univ., Hamilton (Ontario). Communications Research Lab.

AUTOMATIC MODULATION RECOGNITION BASED ON SPATIAL PATTERN CLASSIFICATION USING ARTIFICIAL NEURAL NETWORKS Final Report

Nasir Ghani Jul. 1992 195 p

(CTN-94-60897) Copyright Avail: Micromedia Ltd., Technical Information Centre, 165 Hotel de Ville, Place du Portage, Phase 2, Hull, Quebec J8X 3X2, Canada

In an electronic countermeasures project, an automatic modulation recognition system has been designed and tested based on backpropagation neural networks. The system successfully distinguishes between the specified 10 signal classes to a very high degree and uses a Welch periodogram processor. Experimental results show that the neural networks match and even outdo the performance of the conventional K-nearest neighbor classifier for the same preprocessor, upper 90's percentages. Significant optimization of the neural networks is also shown using the optimal brain damage pruning algorithm. The design issues, preprocessing techniques, backpropagation algorithms, implementation details, and results of the project are fully discussed. A user manual of the software developed during the project, complete with program listings in the C language, is included. Author (CISTI)

N94-24118 Defence Research Establishment, Ottawa (Ontario). Radar Countermeasures Section.

CF-18 AN/ALQ-126B-MG 13 IIP INTERFACE TO THE DREO ELECTRONIC WARFARE ENGAGEMENT SIMULATION FACILITY

James Loo and Serge Labeaume Nov. 1992 25 p

(DREO-TN-93-4; CTN-94-60914) Avail: Micromedia Ltd., Technical Information Centre, 165 Hotel de Ville, Place du Portage, Phase 2, Hull, Quebec J8X 3X2, Canada

The AN/ALQ-126B is the radar jammer carried aboard CF-18 fighter aircraft to jam non-coherent pulsed radars. The jammer is software programmable and capable of generating a variety of radar countermeasures signals. To evaluate the effectiveness of radar jammers and jamming techniques, the Defence Research Establishment Ottawa has developed the Electronic Warfare Engagement Simulation Facility (EWESF). The fundamental concepts of electronic countermeasures effectiveness evaluation are described along with the EWESF layout, the AN/ALQ-126B radar jammer, and the jammer interface to the EWESF to jam the MG-13 IIP air intercept radar. Some of the advantages and drawbacks of the configuration are discussed. The EWESF serves as a test bed for operating the jammer and testing its responses on different types of experimental radars. The test configuration is also useful for the CF-18 Integrated Support Station (ISS) project where open-loop jamming tests using new countermeasures techniques may be performed as they are developed. Some limitations of the present test configuration are discussed as well as several modifications to improve the performance and user friendliness of the EWESF. These options include upgrading the scenario control computers and software, upgrading the tracking radar, and adding a continuous target angle motion capability. Author (CISTI)

N94-24131 Calian Communications, Kanata (Ontario).

DETECTION AND ANALYSIS OF UNBALANCED QPSK IN GAUSSIAN NOISE, VERSION 1.0

J. Bodie 1 May 1992 164 p

(DREO-12-020.1; CTN-94-60896) Copyright Avail: Micromedia Ltd., Technical Information Centre, 165 Hotel de Ville, Place du Portage, Phase 2, Hull, Quebec J8X 3X2, Canada

The problem of detecting and analyzing a variety of phase shift keying (PSK) signal formats in the presence of noise is addressed. The signal to noise ratios of the discrete tones appearing at the outputs of second- and fourth-order nonlinearities are derived and are used to determine the measurement bandwidth required to achieve given detection statistics. The processor performance requirements are analyzed for fast Fourier transform-based signal detection. Approaches are proposed for the determination of the modulation characteristics of the input signal from the levels of the discrete tones. The performance of phase locked loop carrier and data clock recovery circuits is also analyzed. Author (CISTI)

N94-24132 Victoria Univ. (British Columbia). Dept. of Electrical and Computer Engineering.

CODING FOR FREQUENCY HOPPED SPREAD SPECTRUM SATELLITE COMMUNICATIONS Annual Report, 1 Apr. 1990 - 31 Mar. 1991

Q. Wang, G. Li, I. F. Blake (Waterloo Univ., Ontario.), V. K. Bhargava, Q. Chen, and T. A. Gulliver 31 May 1991 166 p

(ECE-91-1; CTN-94-60903) Avail: Micromedia Ltd., Technical Information Centre, 165 Hotel de Ville, Place du Portage, Phase 2, Hull, Quebec J8X 3X2, Canada

A nonlinear diversity combining scheme using the Viterbi ratio threshold (RT) technique is discussed. Performances of the RT diversity combiner in fast frequency hop spread spectrum systems with M-ary frequency shift keying with and without additive white Gaussian noise (AWGN) are analyzed. Exact bit error probabilities are computed and relationships between system performance and parameters such as RT, diversity order, and thermal noise level are illustrated. Performances under band multitone jamming and partial band noise jamming are compared. Performance of M-ary differential phase shift keying (MDPSK) signalling in the presence of both tone jamming and AWGN is described. Larger signal sets than in a previous report are considered along with skewed differential phases with unequal decision regions. The error performance when a frequency offset exists between a jamming tone and a MDPSK carrier is also considered. Error correlation in DPSK demodulation is examined in terms of its effects on the block and decoded error probabilities, which are derived and computed for AWG and worst-case partial band noise. Comparisons are made with the approximate block and decoded error probabilities based on a memoryless model which ignores the error correlation. The effectiveness of interleaving in improving the error performance under various conditions is addressed. Author (CISTI)

N94-24133 Applied Silicon, Inc., Ottawa (Ontario).

ASPT SOFTWARE SOURCE CODE: ASPT SIGNAL EXCISION SOFTWARE PACKAGE

Hugh Parliament 17 Aug. 1992 207 p

(CTN-94-60904) Avail: Micromedia Ltd., Technical Information Centre, 165 Hotel de Ville, Place du Portage, Phase 2, Hull, Quebec J8X 3X2, Canada

The source code for the ASPT Signal Excision Software Package which is part of the Adaptive Signal Processing Testbed (ASPT) is presented. The source code covers the programs 'excision', 'ab.out', 'd0.out', 'bd1.out', 'develop', 'despread', 'sorting', and 'convert'. These programs are concerned with collecting data, filtering out interference from a spread spectrum signal, analyzing the results, and developing and testing new filtering algorithms. Author (CISTI)

N94-24179 New Brunswick Univ., Fredericton. Dept. of Electrical Engineering.
A CONSTRAINED OPTIMIZATION TECHNIQUE FOR ARBITRARY ANTENNA ARRAYS AND VARIOUS PERFORMANCE INDICES M.S. Thesis
Li Xiaodan Jun. 1990 112 p
(ISBN-0-315-59455-1; CTN-94-60876) Copyright Avail: Micromedia Ltd., Technical Information Centre, 240 Catherine Street, Suite 305, Ottawa, Ontario, K2P 2G8, Canada HC/MF

Some optimization techniques used for optimization of array antenna performance indices are reviewed and evaluated. A new constrained optimization algorithm is presented which uses the Lagrange multiplier and the property of the Hermitian matrix to obtain the optimum solution for the minimum average sidelobe problem in the radiation pattern for arbitrarily configured antenna arrays with constrained conditions, such as steerable pencil beam, multi-beam, and null steering. The algorithm is presented for different array configurations and element patterns, with emphasis on the microstrip circular patch antenna array. The modelling of mutual coupling between microstrip elements is also discussed. The utilization of Bessel functions and the symmetry property of Hermitian matrices are presented in this algorithm, which greatly improves the computational efficiency. Another important complement is to include other array performance indices into the objectives of the algorithm, such as radiation efficiency. The developed algorithm is useful for optimized antenna array design and provides an approach to test and simulate radiation performance for arrays of different configuration and element type. Numerical results are illustrated in the form of printed tables or two- and three-dimensional plots. Author (CISTI)

N94-24183 Motorola, Inc., Phoenix, AZ.
SATELLITE COMMUNICATIONS SYSTEM Patent Application
Robert J. Schwendeman, inventor (to Motorola) 17 Apr. 1993 14 p
(CA-Patent-Appl-SN-2053597; CTN-94-60934) Copyright Avail: Micromedia Ltd., Technical Information Centre, 240 Catherine Street, Suite 305, Ottawa, Ontario, K2P 2G8, Canada HC/MF

A satellite communication system is disclosed which provides an increased probability of reception by selective call receivers. In carrying out the invention in one form, there is provided a method comprising the step of relaying, from two or more locations via at least one satellite, a transmission to a receiver. By relaying the information being transmitted from two different locations (angles) at different points in time, the probability of reception is increased. Programming means are provided for determining the first and second locations and times of transmitting the information. Author (CISTI)

N94-24296 Toronto Univ. (Ontario).
EVALUATION OF EHF MULTI-BEAM ADAPTIVE ARRAYS Final Report
J. L. Yen and P. Kremer 30 Apr. 1992 27 p
(CTN-94-60898) Avail: Micromedia Ltd., Technical Information Centre, 165 Hotel de Ville, Place du Portage, Phase 2, Hull, Quebec J8X 3X2, Canada

An experimental three-beam 44-GHz adaptive antenna for frequency hopped communication systems is described. A software package called AJSIM for the simulation of multi-beam antennas and multi-element arrays for anti-jamming in frequency hopping systems is presented. The software makes use of a graphics user interface and allows visualization of many pertinent operational performances of the array under simulation. The simplifying assumptions, the method of analysis, and some results and deductions are included. The evaluation of the experimental three-beam anti-jamming antenna confirms that such an array performs as predicted. Optimization of element weights in such a small array can be achieved without a sophisticated controller. Simulation studies using AJSIM indicate that arrays are superior to a single multi-beam antenna for anti-jamming because of the grating lobes and the ability to produce deep holes in the pattern. AJSIM can be used to perform a systematic search for user-jammer scenarios which are vulnerable to a particular array-beam configuration. A user manual for AJSIM is appended. Author (CISTI)

N94-24298 Defence Research Establishment Atlantic, Dartmouth (Nova Scotia).
PROPWR: A VERSATILE TOOL FOR 1/3 OCTAVE PROCESSING AND NARROWBAND LINE TRACKING
Joseph B. Farrell Feb. 1993 47 p
(DREA-TC-93-303; CTN-94-60911) Avail: Micromedia Ltd., Technical Information Centre, 165 Hotel de Ville, Place du Portage, Phase 2, Hull, Quebec J8X 3X2, Canada

PROPWR is a versatile power spectrum processing program designed to process both real and complex format power spectrum files. The program runs on Concurrent Computer Corporation 5000-6000 series and Digital Equipment VAX computers. PROPWR has a powerful user interface which allows wide latitude in setting up parameters for calibration of power spectra, 1/3 octave calculations, and narrowband line tracking. Some of the main features of the program include: 1/3 octave processing of Defense Research Establishment Atlantic format power spectrum files, with selectable parameters including frames and channels to process, center frequency of first 1/3 octave band, and output file format; time series of power levels in 1/3 octave bands; fully configurable tracking (frequency, signal level, and noise level) of up to 20 narrowband lines; and calibration of power spectrum data. A sample terminal session is included along with a description of the user interface. Author (CISTI)

N94-24530 National Defence Research Establishment, Linkoeping (Sweden). Huvudadelning foer Informationsteknologi.
CALIBRATION NETWORK INTENDED FOR PHASE-ARRAY ANTENNAS AT 3 GHz [KALIBRERINGSNAET FOER DIGITALA GRUPPANTENNER VID 3 GHZ]
Lars-David Wernlund Feb. 1993 19 p In SWEDISH See also PB92-195429 Limited Reproducibility: More than 20% of this document may be affected by microfiche quality
(PB93-204352; FOA-C-30699-8.4; FOA-C-30699-3.2) Avail: CASI HC A03

Couplers have been developed for a calibration network intended for phased-array antennas in a multistatic radar project. Capacitive couplers have been studied and realized in two different types of transmission lines. NTIS

N94-24531 National Defence Research Establishment, Linkoeping (Sweden). Huvudavdelning foer Informationsteknologi.
RADIO COMMUNICATION AND WAVE PROPAGATION. A VISIT TO THE NETHERLANDS IN DECEMBER 1992 [RADIOKOMMUNIKATION OCH VAGUTBREDNING. EN STUDIERESA TILL NEDERLAENDERNA DECEMBER 1992]
Lars Ahlin, Gunnar Hedby, and Jens Zander Feb. 1993 19 p In SWEDISH See also N91-30366 Limited Reproducibility: More than 20% of this document may be affected by microfiche quality
(PB93-204360; FOA-C-30701-8.3) Avail: Issuing Activity (National Technical Information Service (NTIS))

A study travel to the Netherlands with a visit to TNO Defence Research has been carried out during 13-16 December 1992. Besides the Physics and Electronics Laboratory at TNO, the authors also visited Delft University of Technology and NCR in Utrecht. The main purpose of the visit was to identify research areas of common interest. The report gives an overview of some research projects at the different organizations. NTIS

N94-24554# Naval Postgraduate School, Monterey, CA.
A SIMULATION AND EVALUATION OF NATO STANDARDIZATION AGREEMENT (STANAG) 4214 M.S. Thesis
Michael A. Dorko and Robert G. Schultz Sep. 1993 124 p
(AD-A273195) Avail: CASI HC A06/MF A02

An object-oriented simulation model is developed to evaluate the effectiveness of NATO Standardization Agreement (STANAG) 4214, which promulgates the protocol for international telephone call routing and directories for tactical communications. The model simulates communication systems using the STANAG 4214 protocol to isolate discrepancies which could lead to the inability to successfully complete calls within the system. The model also simulates protocol modifications created to correct existing discrepancies and verifies their effectiveness in making the protocol more robust. Results show that these modifications improve STANAG call completion rate from a potential low of under 70 percent to 100 percent, while simultaneously easing the restrictions on lateral communication connections. The model is menu-driven with both graphical and hard copy output, making it useful to network planners, protocol designers, and tactical communications officers. DTIC

N94-24582*# Virginia Polytechnic Inst. and State Univ., Blacksburg. Dept. of Aerospace and Ocean Engineering.
LOLA: LUNAR OPTICAL LONG-BASELINE ARRAY. 1992-1993 SPACE DESIGN
Daniel Bronte, Joanne Chaney, Christine Curran, Keith Ferguson, Eric Flint, Tony Giunta, Duane Knill, Daniel Levesque, Donald Lyon, and Sean Murphy et al Jun. 1993 206 p Original contains color illustrations
(Contract NASw-4435)
(NASA-CR-195533; NAS 1.26:195533) Avail: CASI HC A10/MF A03: 5 functional color pages

In the fall of 1992, the design and analysis of a lunar-based optical interferometer telescope array was initiated by a group of students in the Department of Aerospace Engineering at Virginia Tech. This project was undertaken at the suggestion of the Space Exploration Initiative Office at the NASA Langley Research Center. The original array design requirements, listed below, centered on the primary objective of resolving earth-type planets about stars out to a distance of ten parsecs: spectrum coverage spanning wavelengths from five nm to five mm, with a primary operating mode in the visible spectrum; a total collecting area providing a signal-to-noise ratio (SNR) of no less than 10.0 for a median wavelength of 500 nm; the individual array elements must be identical and have a maximum optical diameter of 2.0 m; and lunar site selection is limited to ten degrees north and south of the lunar equator on the lunar far side while not closer than 15 degrees to either near-side limb. Following construction by astronaut crews, array operation will be conducted from earth and astronomical observations will not be conducted during the lunar day. The entire system is designed for minimum achievable mass. The majority of the original design requirements for the telescope array were met. Derived from text

N94-24593 Technische Univ., Delft (Netherlands). Lab. of Electromagnetic Research.
EDGE ELEMENTS, THEIR ADVANTAGES AND DISADVANTAGES
Territ Mur 1993 5 p Limited Reproducibility: More than 20% of this document may be affected by microfiche quality
(PB94-111069; ET/EM-1993-09) Copyright Avail: CASI HC A01

In finite element methods for solving electromagnetic field problems, the use of edge elements has become very popular. In fact, edge elements are often believed to be a cure for many difficulties that are encountered, and they are claimed to yield accurate results. In the present paper, we shall analyze these claims for tetrahedral elements. In particular, we shall compare two different types of 'linear' edge elements and the classical linear nodal element, comparisons for higher order elements and elements defined on other shapes, for instance on cubes, run along the same lines and yield similar conclusions. NTIS

N94-24597 Technische Univ., Delft (Netherlands). Lab. of Electromagnetic Research.
FINITE-ELEMENT MODELLING OF THREE-DIMENSIONAL ELECTROMAGNETIC FIELDS USING EDGE AND NODAL ELEMENTS
Gerrit Mur 1993 23 p Limited Reproducibility: More than 20% of this document may be affected by microfiche quality
(PB94-111077; ET/EM-1993-10) Copyright Avail: CASI HC A03

An efficient and accurate finite-element method is presented for computing transient as well as time-harmonic electromagnetic fields in three-dimensional configurations containing arbitrarily inhomogeneous media that may be anisotropic. To obtain accurate results with an optimum computational efficiency, both consistently linear edge and consistently linear nodal elements are used for approximating the spatial distribution of the field. As compared with earlier work, our formulation is generalized by adding a method for explicitly modeling the normal continuity along interfaces that are free of surface charge. In addition to this, the conditions for efficiently solving time-harmonic problems using a code designed for solving transient problems are discussed. Finally, a general and simple method for implementing arbitrary inhomogeneous absorbing boundary conditions for modeling arbitrary incident fields is introduced. NTIS

N94-24616*# Arizona State Univ., Tempe. Telecommunications Research Center.
HIGH-FREQUENCY TECHNIQUES FOR RCS PREDICTION OF PLATE GEOMETRIES AND A PHYSICAL OPTICS/EQUIVALENT CURRENTS MODEL FOR THE RCS OF TRIHEDRAL CORNER REFLECTORS, PARTS 1 AND 2 Semiannual Progress Report, 1 Aug. 1993 - 31 Jan. 1994
Constantine A. Balanis, Lesley A. Polka, and Anastasis C. Polycarpou 1994 30 p
(Grant NAG1-562)
(NASA-CR-195140; NAS 1.26:195140; TRC-EM-CAB-9402) Avail: CASI HC A01/MF A01

Formulations for scattering from the coated plate and the coated dihedral corner reflector are included. A coated plate model based upon the Uniform Theory of Diffraction (UTD) for impedance wedges was presented in the last report. In order to resolve inaccuracies and discontinuities in the predicted patterns using the UTD-based model, an improved model that uses more accurate diffraction coefficients is presented. A Physical Optics (PO) model for the coated dihedral corner reflector is presented as an intermediary step in developing a high-frequency model for this structure. The PO model is based upon the reflection coefficients for a metal-backed lossy material. Preliminary PO results for the dihedral corner reflector suggest that, in addition to being much faster computationally, this model may be more accurate than existing moment method (MM) models. An improved Physical Optics (PO)/Equivalent Currents model for modeling the Radar Cross Section (RCS) of both square and triangular, perfectly conducting, trihedral corner reflectors is presented. The new model uses the PO approximation at each reflection for the first- and second-order reflection terms. For the third-order reflection terms, a Geometrical Optics (GO) approximation is used for the first reflection; and PO approximations are used for the remaining reflections. The previously reported model used GO for all reflections except the terminating reflection. Using PO for most of the reflections results in a computationally slower model because many integrations must be performed numerically, but the advantage is that the predicted RCS using the new model is much more accurate. Comparisons between the two PO models, Finite-Difference Time-Domain (FDTD) and experimental data are presented for validation of the new model. Author (revised)

N94-24630 Grenoble-1 Univ. (France). Lab. d'Astrophysique.
OPTIMIZATION OF TECHNIQUES TO RECONSTRUCT IMAGES DISTURBED BY ATMOSPHERIC TURBULENCE IN THE NEAR INFRA-RED Final Report [OPTIMISATION DE TECHNIQUES DE RECONSTRUCTION D'IMAGES PERTURBEES PAR LA TURBULENCE ATMOSPHERIQUE DANS LE PROCHE INFRA-ROUGE]
P. Ghez 1993 14 p In FRENCH Sponsored by Direction des Recherches, Etudes et Techniques Limited Reproducibility: More than 20% of this document may be affected by microfiche quality
(PB93-199784) Avail: Issuing Activity (National Technical Information Service (NTIS))

The author optimized an instrument for reconstructing images at the diffraction limit. The work involved optimizing signal processing for an interferometry experiment in the aperture diaphragm plane, establishing processing and image-correction algorithms, and reconstructing images from two-dimensional astronomical sources using interferometric data. The main advantage of the device is that it provides a self-calibrated measurement of the visibility module. Measurements are independent of atmospheric turbulence provided that turbulence is correctly established and sampled. The major drawback is that it does not provide an image directly, supplying only its Fourier transform. NTIS

N94-24637 Technische Univ., Delft (Netherlands). Lab. of Electromagnetic Research.
FINITE-ELEMENT METHOD FOR COMPUTING THREE-DIMENSIONAL ELECTROMAGNETIC FIELDS IN INHOMOGENEOUS MEDIA (1993)
Gerrit Mur and Ioan Lager (Transilvania Univ., Brasov, Romania.) 1993 14 p See also PB86-147022 Limited Reproducibility: More than 20% of this document may be affected by microfiche quality

(PB94-111101; ET/EM-1993-13) Copyright Avail: Issuing Activity (National Technical Information Service (NTIS))

An efficient and accurate finite-element method is described for computing three-dimensional time-harmonic electromagnetic fields in strongly inhomogeneous, (an)isotropic media, such as are encountered in the human body, subsurface structures of the earth, and in many engineering applications. For the expansion of the field in an inhomogeneous configuration, Cartesian (nodal) elements are used in its homogeneous subdomains and edge elements are used to account for the continuity relations of the field across the interfaces between those subdomains. In the domain of computation the FEMAX package in which this approach has been implemented decides locally what type of element has to be used for obtaining the user-specified accuracy of modeling the field. In this way, optimum results are obtained both in regard to computational efficiency and in regard to desired accuracy. The electromagnetic compatibility relations are used for elimination of spurious solutions. Numerical results are presented that demonstrate the package to be efficient as well as accurate. NTIS

N94-24650 Technische Univ., Twente (Netherlands). Tele-Informatics and Open Systems Group.

SERVICE DESCRIPTION OF COMMUNICATION SYSTEMS SUPPORTING MULTI-MEDIA MULTI-USER APPLICATIONS

G. J. Heijenk, X. Hou, and I. G. Niemegeers 1993 26 p Limited Reproducibility: More than 20% of this document may be affected by microfiche quality

(PB94-110855; TIOS-93/20) Copyright Avail: CASI HC A03

The paper presents a service description of communication systems supporting multi-media multi-user applications. In particular, it focuses on service elements related to the call control. The service description specifies the functional behavior of the communication system as a whole. It can be used as a common reference in the next design stages, e.g., in the protocol design and implementation of both Customer Premises Networks and public telecommunication networks. After discussing the requirements of multi-media multi-user applications, a call model is presented. This model creates an abstract view of those aspects of the call relevant for the design and helps us in structuring the service. Only those service elements of a communication system that are related to the call establishment, modification and termination are fully specified by describing service primitives, their parameters and temporal ordering constraints. NTIS

N94-24656# California Univ., Berkeley. Lawrence Berkeley Lab.

THE USE OF HARMONICS IN 3-D MAGNETIC FIELDS

S. Caspi, M. Helm, and L. J. Laslett Sep. 1993 4 p Presented at the 13th International Conference on Magnet Technology, Victoria, Canada, 20-24 Sep. 1993

(Contract DE-AC03-76SF-00098)

(DE94-002274; LBL-33432; CONF-930926-18) Avail: CASI HC A01/MF A01

Motivated by the need for new means for specification and determination of 3-D fields that are produced by electromagnetic lens elements in the region interior to coil windings and seeking to obtain techniques that will be convenient for accurate conductor placement and dynamical study of particle motion, the authors have generalized the representation of a 2-D magnetic field to 3-D. They have shown that the 3-D magnetic field components of a multipole magnet in the curl-free divergence-free region near the axis $r = 0$ can be derived from one dimensional functions A(sub n)(z) and their derivatives. In this report they apply both methods to the 'end' region of a 40 mm bore SSC quadrupole, calculating first the field harmonics and then reconstructing the field comparing both results with direct Biot-Savart calculation. DOE

N94-24668# Naval Postgraduate School, Monterey, CA.

COMPARISON OF HF GROUNDWAVE PROPAGATION MODELS M.S. Thesis

Celso V. Davila Jun. 1993 70 p

(AD-A273146) Avail: CASI HC A04/MF A01

The groundwave component of high frequency (HF) radio propagation is utilized in both civilian and military applications. A variety of groundwave propagation models exist to predict field strength loss over the transmission path. In this thesis, groundwave field strength predictions were compared for programs which employ such models: GRWAVE, MIXPATH, and ADVANCED PROPHET. A range of parameter values was used to generate predictions for comparison. HF groundwave field strength predictions by PROPHET were 3 to 10 dB stronger than those of the other programs. GRWAVE and MIXPATH field strength predictions were in close agreement, the difference generally being less than 1 or 2 dB. Field measurements of path loss for two AM broadcast frequencies were evaluated by comparison with estimates provided by ADVANCED PROPHET. The measured groundwave field strengths were found to be from 8 dB weaker at short distances to 18 dB stronger at large distances it is recommended that future efforts be directed toward improving and validating the accuracy of the groundwave propagation models used in these programs. It is also recommended that more extensive documentation be developed for GRWAVE. DTIC

N94-24669# Naval Postgraduate School, Monterey, CA.

SIMULATION OF ADJACENT CHANNEL INTERFERENCE IN A UHF SATELLITE SYSTEM M.S. Thesis

Juan C. Minuto Sep. 1993 71 p

(AD-A273147) Avail: CASI HC A04/MF A01

In this thesis, the adjacent channel interference in a ultra high frequency (UHF) satellite channel is evaluated by simulation differential binary phase-shift keying (DBPSK) and is compared with continuous phase frequency-shift keying (CPFSK). First, a measure of the interfering power is obtained and a method to compute carrier-to-interference ratios in a non-linear channel is developed. Next a DBPSK receiver is simulated when two interfering channels separated in frequency are present, and bit errors are detected and counted. Then, coherent reception of minimum-shift keying (MSK) and CPFSK with modulation index $h = 0.4$ are simulated in the same conditions as DBPSK. Finally, noncoherent MSK is analyzed in the same way, and a comparative behavior it obtained. It is found that the best performance in the presence of adjacent channel interference is given by coherent reception of MSK. DTIC

N94-24670# Naval Postgraduate School, Monterey, CA.

MITIGATION OF EMI/RFI PRODUCED BY A 1.2 kW UNINTERRUPTIBLE POWER SUPPLY M.S. Thesis

Efthimios Mikros Sep. 1993 129 p

(AD-A273149) Avail: CASI HC A07/MF A02

Recently installed equipment in naval receiving sites, such as Uninterruptible Power Supplies (UPS), digital telephone switching systems, and personal computers, inject noise into receiver systems via power conductors, cable shields, and grounds, thus reducing the probability of intercept of a signal of interest in the 2-100 NMHz range. In this thesis a survey of EMI/RFI sources at receiving sites is performed. The effectiveness of a Barrier-Filter-Ground architecture in containing/eliminating EMI/RFI from a 1.2 kW UPS is tested. The spectral and temporal properties of the EMI/RFI from the UPS are recorded. Estimates for the EMI/RFI power are obtained from 60Hz to 100kHz, and a possible solution is proposed for obtaining noise power estimates for higher frequencies. DTIC

N94-24676 IIT Research Inst., Chicago, IL.

ELF COMMUNICATIONS SYSTEM ECOLOGICAL MONITORING PROGRAM Summary Report, 1982-1992

J. E. Zapotosky and J. R. Gauger Oct. 1993 107 p Limited Reproducibility: More than 20% of this document may be affected by microfiche quality

(Contract N00039-93-C-0001)

(AD-A273456; IITRI-D06205-3) Avail: Issuing Activity (Defense Technical Information Center (DTIC))

The U.S. Navy has been conducting a long-term monitoring program to examine flora, fauna, and their ecological relationships for possible effects from electromagnetic fields produced by its Extremely Low Frequency (ELF) Communications System. Physiological, developmental, behavioral, and ecological variables for dominant biota in upland, wetland, and riverine habitats near the ELF System have been examined since 1982. Monitoring studies use a split-plot or blocked design to examine differences in space and time. Observations have been made during preoperational, intermittent-use, and full-operational use periods near ELF transmitters located-in Michigan and Wisconsin. Data collection for studies located near the Naval Radio Transmitting Facility (NRTF)-Clam Lake, Wisconsin, was completed, as scheduled, during 1989. Investigators concluded that there were no effects from intermittent or full operations of the transmitter in Wisconsin. Data collection for studies located near the NRTF-Republic, Michigan, progressed during 1992 and are to continue during 1993. Final results and conclusions for Michigan studies are expected after all data have been analyzed in 1994. DTIC

N94-24678*# Illinois Univ., Urbana. Dept. of Electrical and Computer Engineering.
INTEGRATED REFLECTOR ANTENNA DESIGN AND ANALYSIS Final Report
M. L. Zimmerman, S. W. Lee, S. Ni, M. Christensen, and Y. M. Wang Oct. 1993 188 p
(Contract NCC3-156)
(NASA-CR-195164; NAS 1.26:195164; TR-94-4) Avail: CASI HC A09/MF A02

Reflector antenna design is a mature field and most aspects were studied. However, of that most previous work is distinguished by the fact that it is narrow in scope, analyzing only a particular problem under certain conditions. Methods of analysis of this type are not useful for working on real-life problems since they can not handle the many and various types of perturbations of basic antenna design. The idea of an integrated design and analysis is proposed. By broadening the scope of the analysis, it becomes possible to deal with the intricacies attendant with modem reflector antenna design problems. The concept of integrated reflector antenna design is put forward. A number of electromagnetic problems related to reflector antenna design are investigated. Some of these show how tools for reflector antenna design are created. In particular, a method for estimating spillover loss for open-ended waveguide feeds is examined. The problem of calculating and optimizing beam efficiency (an important figure of merit in radiometry applications) is also solved. Other chapters deal with applications of this general analysis. The wide angle scan abilities of reflector antennas is examined and a design is proposed for the ATDRSS triband reflector antenna. The development of a general phased-array pattern computation program is discussed and how the concept of integrated design can be extended to other types of antennas is shown. The conclusions are contained in the final chapter. Author (revised)

N94-24687# Army Electronic Proving Ground, Fort Huachuca, AZ.
ANALOG COMMUNICATION TRANSMITTER AND RECEIVER TEST PROCEDURES Final Report
13 Oct. 1993 105 p
(AD-A273423; ITOP-6-2-242) Avail: CASI HC A06/MF A02

This ITOP defines and describes the necessary test procedures to be conducted for evaluating the performance of analog modulated (AM and FM) communication transmitters and receivers. Although this document provides a full test suite, the amount of testing conducted for a specific test item should be in accordance with its anticipated conditions of use and quality level. In order to provide a broad scope of application, this document does not impose any specification limits. Therefore, those limits may be derived from the equipment specifications or any established sources such as MIL-STD's or other national and European standards. Some test parameters are specified, however, to produce test data allowing performance comparisons between different equipment. The scope of these procedures is comprehensive enough to model complete systems (made of several transmitters and receivers) and to derive system performance or inter-system compatibility data. DTIC

N94-24694 Carleton Univ., Ottawa (Ontario). Dept. of Electronics.
ANALYSIS OF TIME-DIVERSITY COMBINING METHODS FOR FREQUENCY-HOPPED SIGNALS
Rolands Ezers and J. S. Wight Apr. 1992 71 p
(CU-DOE-92-09; CTN-94-60899) Avail: Micromedia Ltd., Technical Information Centre, 165 Hotel de Ville, Place du Portage, Phase 2, Hull, Quebec J8X 3X2, Canada

Fast frequency hopped (FFH) noncoherent frequency shift keyed (NCFSK) communication systems with time diversity (TD) and diversity combining are discussed. A literature review of diversity combining techniques is provided. An analytical method was developed for one of the techniques, linear diversity combining (LDC). With this method, the bit error probability for demodulation of FFH NCFSK systems with TD and LDC and the probability of detection and probability of false alarm for uplink coarse-time synchronization of a FFH NCFSK satellite communication system with TD and LDC combining have been computed in broadband noise and multiple-tone jamming. A novel analytical result was derived for computing the bit error probability for the demodulation of FFH NCFSK systems with TD and 4-2- or 2-1-moment method diversity combining in independent Rayleigh fading. For demodulation, LDC is an excellent method in broadband noise and good in severe multiple tone jamming. In weak multiple tone jamming, LDC is not a good method because of its susceptibility to Houston-sense multiple tone jamming with a small jamming fraction. In independent Rayleigh fading, square-law combining was best for the particular situation considered. TD and LDC could be used to improve performance in uplink coarse-time synchronization. Author (CISTI)

N94-24696 Carleton Univ., Ottawa (Ontario).
COMPOSITE SEQUENCES FOR RAPID ACQUISITION OF DIRECT-SEQUENCE SPREAD SPECTRUM SIGNALS Ph.D. Thesis
Sean Faulkner Sep. 1992 173 p
(Contract W7714-9-9213/01-SS)
(CTN-94-60901) Copyright Avail: Micromedia Ltd., Technical Information Centre, 165 Hotel de Ville, Place du Portage, Phase 2, Hull, Quebec J8X 3X2, Canada

The composite sequences, a class of spreading sequences for direct-sequence spread spectrum communication (DS-SS), is investigated for the case of components which are binary maximal length sequences. The relevant properties of the composite sequences are derived and the acquisition time performance is determined for a noisy environment. It is demonstrated that the composite sequences are a large, balanced class of spreading sequences with a high linear span, reasonable autocorrelation performance, an essentially featureless power spectrum, improved security, and rapid acquisition capability. A novel subclass of composite sequences, termed the sliding composite sequences (SCS), is also presented, and their properties and performance are investigated and derived. It is shown that SCS are a large, nearly balanced class of spreading sequences with high linear span, an essentially featureless power spectrum, and improved security. Most importantly, through exploitation of the inherent rapid acquisition structure of SCS construction, a novel acquisition algorithm is developed which gives orders of magnitude reduction in acquisition time for DS-SS communications. In addition, a novel algorithm for generating primitive polynomials is presented and the aperiodic autocorrelation magnitude of m-sequences is bounded empirically. Author (CISTI)

N94-24697 Victoria Univ. (British Columbia). Dept. of Electrical and Computer Engineering.
CODING FOR FREQUENCY HOPPED SPREAD SPECTRUM SATELLITE COMMUNICATIONS Final Report, April 1 1991 to March 31 1992
Q. Wang, G. Li, I. F. Blake (Waterloo Univ., Ontario.), V. K. Bhargava, and Q. Chen 1 Apr. 1992 118 p
(Contract 36001-0-3503/01-SS)
(ECE-92-1; CTN-94-60902) Avail: Micromedia Ltd., Technical Information Centre, 165 Hotel de Ville, Place du Portage, Phase 2, Hull, Quebec J8X 3X2, Canada

The performance of fast frequency hopped spread spectrum systems with M-ary frequency shift keying and error correction coding under jamming conditions are analyzed. Ratio threshold diversity combining is used. The decoding scheme is error erasure decoding with metrics generated by the diversity combiner. The bit error probability of the system is computed and improvements offered by error correction coding are shown. The performance of several error correction codes is compared under different channel conditions. The notion of an arbitrarily varying channel (AVC) is discussed, including capacities of AVC's and a discrete memoryless channel, and two Gaussian AVC models are described. Coded performance of a slow frequency hopped differential phase shift keying (DPSK) system in presence of both additive white Gaussian noise and tone jamming is studied. The error correlation due to DPSK demodulation and the effect of tone jamming are considered in evaluating the block and decoded error probabilities. The effect of interleaving on system performance is addressed. A nearly optimum code rate for a length 255 Reed-Solomon code is derived for systems employing interleaving. Finally, a parallel approach to the design of universal receivers for unknown and time-varying channels is applied to DPSK systems in the presence of noise and tone interference.
Author (CISTI)

N94-24707*# Nebraska Univ., Lincoln. Dept. of Electrical Engineering.
[A CONSTRAINED JOINT SOURCE/CHANNEL CODER DESIGN AND VECTOR QUANTIZATION OF NONSTATIONARY SOURCES]
Semiannual Status Report, 15 Jun. - 15 Dec. 1993
Khalid Sayood, Y. C. Chen, S. Nori, and A. Araj 15 Dec. 1993 42 p
(Grant NAG5-1612)
(NASA-CR-195145; NAS 1.26:195145) Avail: CASI HC A03/MF A01

The emergence of broadband ISDN as the network for the future brings with it the promise of integration of all proposed services in a flexible environment. In order to achieve this flexibility, asynchronous transfer mode (ATM) has been proposed as the transfer technique. During this period a study was conducted on the bridging of network transmission performance and video coding. The successful transmission of variable bit rate video over ATM networks relies on the interaction between the video coding algorithm and the ATM networks. Two aspects of networks that determine the efficiency of video transmission are the resource allocation algorithm and the congestion control algorithm. These are explained in this report. Vector quantization (VQ) is one of the more popular compression techniques to appear in the last twenty years. Numerous compression techniques, which incorporate VQ, have been proposed. While the LBG VQ provides excellent compression, there are also several drawbacks to the use of the LBG quantizers including search complexity and memory requirements, and a mismatch between the codebook and the inputs. The latter mainly stems from the fact that the VQ is generally designed for a specific rate and a specific class of inputs. In this work, an adaptive technique is proposed for vector quantization of images and video sequences. This technique is an extension of the recursively indexed scalar quantization (RISQ) algorithm. Derived from text

N94-24926 Mitre Corp., Bedford, MA.
ELECTROMAGNETIC INTERFERENCE IMPACT OF THE PROPOSED EMITTERS FOR THE HIGH FREQUENCY ACTIVE AURORAL RESEARCH PROGRAM (HAARP) Interim Report
G. A. Robertshaw, A. L. Snyder, and M. M. Weiner 14 May 1993 134 p Limited Reproducibility: More than 20% of this document may be affected by microfiche quality
(Contract F19628-89-C-0001)
(AD-A273401; M93B0000044RI; PL-TR-93-2114) Avail: Issuing Activity (Defense Technical Information Center (DTIC))

The proposed HAARP emitters at the Gakona (Alaska) preferred site and at the Clear AFS (Alaska) alternative site are the Ionospheric Research Instrument (IRI), the Incoherent Scatter Radar (ISR), and the Vertical Incidence Sounder (VIS). The electromagnetic interference (EMI) impact of those emitters on receiving systems in the vicinity of the sites is estimated in this study. The results are intended for use as an input to the Air Force Environmental Impact Statement as part of the Environmental Impact Analysis Process. DTIC

N94-25005*# Virginia Polytechnic Inst. and State Univ., Blacksburg. Satellite Communications Group.
FEASIBILITY STUDY OF A SYNTHESIS PROCEDURE FOR ARRAY FEEDS TO IMPROVE RADIATION PERFORMANCE OF LARGE DISTORTED REFLECTOR ANTENNAS Final Report
W. L. Stutzman, K. Takamizawa, and J. LaPean Dec. 1993 17 p
(Grant NAG1-859)
(NASA-CR-195167; NAS 1.26:195167; SATCOM-93-20) Avail: CASI HC A03/MF A01

There were several tangible products that resulted from the reflector antenna research program. The initial technical effort was to develop techniques to compensate for distortions over the surface of the main reflector of a large reflector antenna system. An in-depth investigation of this problem resulted in a new technique for the electronic correction of surface errors. A journal article on the findings describe the use of the iterative sampling method. Shortly after the 'Mission to Planet Earth' program started, we began investigating the use of large reflector antennas in geostationary orbit for passive earth remote sensing. A study panel was coordinated by Virginia Tech to set technical goals for the effort. These were used to guide the design of several antennas. The original interest stemmed from an industrial (Reynolds Metals) need and currently involves work with industry (Prodelin Corporation) on high technology, low cost reflectors. The intervening years (1987 - 1993) is the period of this report and Virginia Tech's reflector antenna activity then was exclusively with NASA LaRC. Derived from text

N94-25038 Department of the Navy, Washington, DC.
CONVEYING DIGITAL DATA IN NOISY, UNSTABLE, MULTIPATH ENVIRONMENTS Patent
Richard A. Daniel, inventor (to Navy) 24 Aug. 1993 12 p Filed 24 Jun. 1991
(AD-D015980; US-Patent-5,239,560; US-Patent-Appl-SN-720129; US-Patent-Class-375-38) Avail: US Patent and Trademark Office

This patent discloses a decoding system for transmitting a signal through a noisy, unstable multipath environment. In this system, the signal consisting of eight possible symbols is encoded using four of eight possible frequencies in an orthogonal Hadamard matrix, transmitted through the environment, and decoded using the same orthogonal Hadamard matrix. This provides a correlation result which can compensate for at least one error in the received signal for each symbol. DTIC

N94-25040 Department of the Navy, Washington, DC.
RADAR TARGET DISCRIMINATION BY SPECTRUM ANALYSIS Patent
Duane Ruth, inventor (to Navy) and Larry M. Morrison, inventor (to Navy) 3 Aug. 1993 24 p Filed 13 Nov. 1992
(AD-D015982; US-Patent-5,233,354; US-Patent-Appl-SN-976048; US-Patent-Class-342-160) Avail: US Patent and Trademark Office

A method for distinguishing between a target and clutter analyzes frequency components of returned wave energy to detect target energy characterized by being present in a narrow range of frequencies, by increasing in the range over time, or by remaining substantially in the range over time. The method utilizes time sequential spectra of the returned energy. The spectra may be signals from a plurality of band pass filters or may be a spectrogram. The energy in adjacent band pass signals and spectra frequencies are correlated to detect energy in a narrow range of frequencies. Differences in successive spectra are integrated to detect increasing energy in a range of frequencies. An energy peak detected in a narrow range by correlation is integrated to detect that the peak remains in the range. The method is adapted for use with a network having inputs receiving successive samples of the returned energy and having outputs individually connected to the inputs through multiplier elements providing selectable factors, a summing element, and a selectable and generally sigmoidal activation function. DTIC

N94-25041 Department of the Navy, Washington, DC.
RADAR TARGET DISCRIMINATION SYSTEMS USING ARTIFICIAL NEURAL NETWORK TOPOLOGY Patent
Larry M. Morrison, inventor (to Navy) and Duane Roth, inventor (to Navy) 10 Aug. 1993 25 p Filed 13 Nov. 1992
(AD-D015984; US-Patent-5,235,339; US-Patent-Appl-SN-977301; US-Patent-Class-342-159) Avail: US Patent and Trademark Office

A system for distinguishing between a target and clutter is presented. The system analyzes the frequency components of returned wave energy by one or more networks each having inputs receiving successive samples of the returned energy and having outputs individually connected to the inputs through multiplier clements providing selectable factors. The multipliers corresponding to each output are connected to the output through a summing element and a selectable and generally sigmoidal activation function. The factors may be bandpass filter coefficients or discrete Fourier transform coefficients so as to generate frequency components of the energy. Predetermined frequency characteristics of the returned energy may be detected by providing the outputs of a network to a network in which the factors are selected as correlation or convolution coefficients, are selected to integrate feedback outputs, or are selected to sum several outputs within a predetermined range. The activation functions may be selected for thresholding, linearity, limiting, or generation of logarithms. DTIC

N94-25045 Department of the Navy, Washington, DC.
LAYERED PARALLEL INTERFACE FOR AN ACTIVE ANTENNA ARRAY Patent
William M. Waters, inventor (to Navy) 21 Sep. 1993 13 p Filed 24 Jun. 1992
(AD-D016002; US-Patent-5,247,310; US-Patent-Appl-SN-903316; US-Patent-Class-342-368) Avail: US Patent and Trademark Office

A transmit/receive layer is provided adjacent to an array of antenna elements. The transmit/receive layer has an array of transmit receive modules, each module associated with one of the antenna elements. An analog to digital converter and a digital to optical converter of one of the modules couple an RF signal from the associated antenna element to optical fibers. An optical to RF converter in each of the modules converts an amplitude modulated optical transmit signal from an optical fiber to an RF transmit signal for transmission by the associated antenna element. Frequency down and up converters can be added to perform super heterodyne frequency conversion based on a reference frequency control signal transmitted over the optical fibers. At the ends of the optical fibers opposite to the transmit/receive layer, a receive layer, a transmit layer, transmit and receive beamforming layers, dedicated signal synthesizer, control signals, and amplitude modulated optical diode lasers and photodiodes are provided. DTIC

N94-25048 Department of the Navy, Washington, DC.
PREPROCESSOR AND ADAPTIVE BEAMFORMER FOR LINEAR-FREQUENCY MODULATION ACTIVE SIGNALS Patent
James C. Lockwood, inventor (to Navy) 5 Oct. 1993 25 p Filed 6 Oct. 1992
(AD-D016008; US-Patent-5,251,186; US-Patent-Appl-SN-957544; US-Patent-Class-367-103) Avail: US Patent and Trademark Office

A device is provided for processing an echo received by an array of N receiving elements from a target at range R ensonified by a linear-frequency modulation (LFM) signal of bandwidth B transmitted for a duration T. The device receives each elements output f(sub n(t)) over the elements total receiving time and selects time window element outputs f(sub n(t)), which are discrete portions of f(sub n(t)), each time window extending from an arbitrary initial time T(sub o) to time T(sub f) and is spaced from. T(sub o) no more than T and, if there is a target within the window, an echo is received at time T(sub n). Further the device produces element frequency difference outputs g(sub n(t)) from the frequency difference between a replica of at least a portion of the transmitted LFM signal and the time window, element outputs f(sub n(t)), the outputs g(sub n(t)) being tones with frequencies directly proportional to the time T(sub n) of the target from the time To so that the target range R=(c/2)(T(sub o) + T(sub n)) + delta(R(sub n)), where cis the speed of sound, and delta R, is the distance by which R exceeds each element's range to the target. DTIC

N94-25049 Department of the Navy, Washington, DC.
VERY LOW FREQUENCY AND LOW FREQUENCY TRANSMITTING ANTENNA PARAMETER MONITORING SYSTEM Patent
Steven C. Tietsworth, inventor (to Navy) 3 Aug. 1993 40 p Filed 11 Jun. 1991
(AD-D015989; US-Patent-5,233,537; US-Patent-Appl-SN-713658; US-Patent-Class-364-481) Avail: US Patent and Trademark Office

A very low frequency and low frequency transmitting antenna parameter monitoring system is used to measure the electric circuit parameters in near real time of very low frequency and low frequency transmitting antenna systems transmitting frequency shift keyed modulation. The primary parameters measured by the system are the antenna feed-point voltage, antenna current, gross resistance, gross reactance, and steady-state phase angle between the voltage and current. Four primary sections provide for antenna system sensing by sensors, triggering, analog-to-digital conversion of the sensor outputs, and computer processing of the digital data to arrive at the desired antenna parameters. These parameters are essential in evaluating antenna performance and in diagnosing problems with the antenna system. DTIC

N94-25056 Department of the Navy, Washington, DC.
METHOD AND APPARATUS OF GENERATING SUM OR DIFFERENCE SIGNALS CORRESPONDING TO AN APPARENT BEAM IN A MONOPULSE RADAR SYSTEM Patent
Dean D. Howard, inventor (to Navy) 31 Aug. 1993 16 p Filed 29 May 1992
(AD-D015998; US-Patent-5,241,318; US-Patent-Appl-SN-889920; US-Patent-Class-342-149) Avail: US Patent and Trademark Office

The invention relates to an apparatus and method for generating target range, azimuth angle, or elevation angle output signals corresponding to an apparent beam in a multiple-feed monopulse radar system. The multiple-feed monopulse radar system according to the present invention includes a transmitter/receiver unit, an adder/subtracter unit and a video comparator/adder unit. The transmitter/receiver unit is used to generate first and second actual antenna beams. Echoes caused by such actual beams are received and processed to provide first sum and first difference signals and second sum and second difference signals corresponding to the first and second actual beams, respectively. These signals are then supplied to the adder/subtracter unit which adds the first sum and first difference signals to provide a result sigma(sub 1) + K delta(sub 1), subtracts the first sum and first difference signals to provide a result sigma(sub 1) - K delta, adds the second sum and second difference signals to provide a result sigma(sub 2) + K delta (sub 1), and subtracts the second sum and second difference signals to provide a result sigma(sub 2) - K delta(sub 2). DTIC

N94-25057 Department of the Navy, Washington, DC.
SYSTEM FOR PRODUCING SYNCHRONIZED SIGNALS Patent
Louis M. Pecora, inventor (to Navy) 14 Sep. 1993 13 p Filed 19 Feb. 1991
(AD-D016003; US-Patent-Appl-SN-656330; US-Patent-Class-380-48) Avail: US Patent and Trademark Office

A system for producing two synchronized signals comprises a nonlinear dynamical primary system and a nonlinear dynamical secondary response subsystem. The primary system comprises a nonlinear dynamical drive subsystem for producing at least one drive signal, and a nonlinear dynamical primary response subsystem responsive to said at least one drive signal for producing a primary signal, wherein said primary response subsystem has a complete set of at least one primary sub-Lyapunov exponents, all of said at least one primary sub-Lyapunov exponents being negative. The second response subsystem is responsive to said at least one drive signal for producing a secondary signal in synchronization with said primary signal, said secondary response subsystem being substantially a duplicate of said primary response subsystem, wherein said secondary response subsystem has a complete set of at least one secondary sub-Lyapunov exponents, all of said at least one secondary sub-Lyapunov exponents being negative. DTIC

N94-25058 Department of the Navy, Washington, DC.
METHOD AND APPARATUS FOR DETERMINING TARGET ELEVATION ANGLE, ALTITUDE AND RANGE, AND THE LIKE IN A MONOPULSE RADAR SYSTEM WITH REDUCED MULTIPATH ERRORS Patent
Dean D. Howard, inventor (to Navy) 31 Aug. 1993 18 p Filed 29 May 1992
(AD-D016005; US-Patent-5,241,317; US-Patent-Appl-SN-889806; US-Patent-Class-342-149) Avail: US Patent and Trademark Office

The present invention relates to a method and system for determining target elevation angle, altitude, range, and the like in a monopulse radar system with reduced multipath errors. A transmitter/receiver unit receives monopulse sum and difference signals caused by echoes from targets. The sum and difference signals are then logarithmically amplified in a logarithmic amplifier unit. A selector selects one of the sum and difference signals having the largest amplitude, and generates a selection signal indicating which of the sum and difference signals has the largest amplitude. The selection signal is provided to search radar target tracking unit which determines whether a target at a given range interval and azimuth interval, for example, has been selected for tracking by an operator. The search radar target tracking unit then controls a gate unit to selectively provide either the logarithmically amplified sum signal or the logarithmically amplified difference signal to a peak detection unit based on the selection signal, and based on whether a particular target has been selected for tracking. DTIC

N94-25077# Technische Univ., Eindhoven (Netherlands).
PSYCHOPHYSICAL AND SIGNAL-PROCESSING ASPECTS OF SPEECH REPRESENTATION Ph.D. Thesis
Changxue Ma 1992 140 p
(ETN-94-95292) Avail: CASI HC A07/MF A02

The ways to improve the Linear Prediction Code (LPC) analysis and synthesis techniques are studied. An improved way to estimate the LPC parameters, in particular for high pitched voices and to estimate the time instants of glottal closure, is presented. A new weighted LPC analysis of speech is investigated. In this approach, a weighting function is derived from the short time energy function of the speech signal. The estimates of the LPC coefficients by this novel LPC analysis are therefore more accurate than those obtained from the conventional LPC analysis. The relation between the Covariance Linear Prediction (CLP) analysis of a frame of a speech signal and the CLP analysis of its subframes is established. A Singular Value Decomposition (SVD) approach is developed to detect the glottal closure instant in the speech signal. A new approach for ascertaining whether a signal is uniquely determined by the phase of its Fourier transform is discussed. It is shown that uniqueness corresponds to the nonsingularity of a matrix which can be formed from the finite length real sequence. The perceptual study of speech sounds, mainly concerned with auditory masking, is carried out. ESA

N94-25089# Naval Research Lab., Washington, DC.
NORTHERN EXPOSURE 1992: AN INVESTIGATION OF TRANSAURORAL HF RADIO SKYWAVE PROPAGATION Interim Report
Leonard S. Wagner, Joseph A. Goldstein, Michael A. Rupar, and Edward J. Kennedy 29 Sep. 1993 52 p
(NR Proj. LR0-330244)
(AD-A273363; NRL/FR/5554-93-9575) Avail: CASI HC A04/MF A01

The primary objective of the Northern Exposure 92 campaign was to assist in the evaluation of the performance capabilities of a wideband, high frequency, Rake radio receiver on a transauroral skywave channel. A review of the data collected on the transauroral channel during the Northern Exposure 92 exercises indicates that one is likely to encounter three types of signals on the channel: (1) a strong, specularly reflected signal characterized by the usual ionospheric dispersive delay spread and negligible Doppler spread, (2) strong specular multipath signals, exhibiting extensive delay and Doppler spread, and (3) weak scatter signals, exhibiting the widest delay and Doppler spreads. The nonspread reflected signals are encountered during magnetically quiet, daytime conditions where the ionosphere may be described as laminar. The strong, specular-multipath signals occur mostly at night and are associated with reflections from large scale irregularities of electron density characterized by strong horizontal gradients capable of reflecting signals whose frequencies lie below some equivalent maximum usable frequency (MUF) defined by the path, the background ionosphere, and the maximum electron density in the irregularity region. The weak scattered signals occur at night and are associated with volume scatter from the irregular medium. The scattered signals present the greatest challenge to communication systems with amplitudes approx. 30 dB less than those of reflected signals and with 2 sigma Doppler spreads as large as 30 Hz. DTIC

N94-25150 Department of the Navy, Washington, DC.
FIELD EMITTER ARRAY Patent
Richard F. Greene, inventor (to Navy) and Henry F. Gray, inventor (to Navy) 22 Sep. 1992 11 p Filed 20 Jun. 1991
(AD-D016023; US-Patent-5,150,192; US-Patent-Appl-SN-718034; US-Patent-Class-357-68) Avail: US Patent and Trademark Office

A field emitter structure is disclosed which comprises: a substrate selected from the group consisting of a semi-insulating substrate and an insulating substrate, the substrate having first and second surfaces and at least one hole therethrough; a first conducting layer disposed on the first surface of the substrate and having at least one aperture aligned with an associated at least one hole in the substrate, the at least one aperture of the first conducting layer comprising an extraction electrode, and a second conducting layer disposed on the second surface and projecting into the at least one hole in the substrate and into the at least one associated aperture of the first conducting layer and forming at least one associated apex inside the at least one hole, the at least one associated apex comprising an associated electron field emitter. In a second embodiment of the invention, a conducting substrate is substituted for the insulating or semi-insulating substrate, a first insulating layer is disposed between the first surface of the conducting substrate and the first conducting layer, and the second conducting layer disposed on the second surface also projects through at least one associated aperture of the first insulating layer. DTIC

N94-25155 Range Commanders Council, White Sands Missile Range, NM. Electronic Trajectory Measurements Group.
IRIG RADAR CALIBRATION CATALOG. VERSION 2: THE IRIG ERROR MODEL REFERENCE FOR RADAR CALIBRATIONS
Oct. 1993 81 p Limited Reproducibility: More than 20% of this document may be affected by microfiche quality
(AD-A273344; RCC-256-93) Avail: Issuing Activity (Defense Technical Information Center (DTIC))

This document does not provide discussion of all radar error sources identified by other IRIG documents but rather addresses those major error sources for which mathematical models exist and calibration procedures have been developed. DTIC

N94-25191*# West Virginia State Coll., Charleston. Community Coll. Div.
MAGNETIC EARTH IONOSPHERE RESONANT FREQUENCIES Semiannual Progress Report
Craig Spaniol 15 Jan. 1994 42 p
(Grant NAG5-1267)
(NASA-CR-195131; NAS 1.26:195131) Avail: CASI HC A03/MF A01

The Community College Division is pleased to report progress of NASA funded research at West Virginia State College. During this reporting period, the project research group has continued with activities to develop instrumentation capability designed to monitor resonant cavity frequencies in the atmospheric region between the Earth's surface and the ionosphere. In addition, the project's principal investigator, Dr. Craig Spaniol, and NASA technical officer, Dr. John Sutton, have written and published technical papers intended to expand the scientific and technical framework needed for project research. This research continues to provide an excellent example of government and education working together to provide significant research in the college environment. This cooperative effort has provided many students with technical project work which compliments their education. For individual titles, see N94-25192 through N94-25192.

N94-25192*# National Aeronautics and Space Administration. Goddard Space Flight Center, Greenbelt, MD.
AN ACTIVE ANTENNA FOR ELF MAGNETIC FIELDS
John F. Sutton and Craig Spaniol (West Virginia State Coll., Charleston.) *In* West Virginia State Coll., Magnetic Earth Ionosphere Resonant Frequencies 15 Jan. 1994 21 p (For primary document see N94-25191 06-32)
Avail: CASI HC A03/MF A01

The work of Nikola Tesla, especially that directed toward world-wide electrical energy distribution via excitation of the earth-ionosphere cavity resonances, has stimulated interest in the study of these resonances. Not only are they important for their potential use in the transmission of intelligence and electrical power, they are important because they are an integral part of our natural environment. This paper describes the design of a sensitive, untuned, low noise active antenna which is uniquely suited to modern earth-ionosphere cavity resonance measurements employing fast-Fourier transform techniques for near-real-time data analysis. It capitalizes on a little known field-antenna interaction mechanism. Recently, the authors made preliminary measurements of the magnetic fields in the earth-ionosphere cavity. During the course of this study, the problem of designing an optimized ELF magnetic field sensor presented itself. The sensor would have to be small, light weight (for portable use), and capable of detecting the 5-50 Hz picoTesla-level signals generated by the natural excitations of the earth-ionosphere cavity resonances. A review of the literature revealed that past researchers had employed very large search coils, both tuned and untuned. Hill and Bostick, for example, used coils of 30,000 turns wound on high permeability cores of 1.83 m length, weighing 40 kg. Tuned coils are unsuitable for modern fast-Fourier transform data analysis techniques which require a broad spectrum input. 'Untuned' coils connected to high input impedance voltage amplifiers exhibit resonant responses at the resonant frequency determined by the coil inductance and the coil distributed winding capacitance. Also, considered as antennas, they have effective areas equal only to their geometrical areas. Author (revised)

N94-25217 Department of the Navy, Washington, DC.
WIDE BANDWIDTH DIFFERENTIAL AMPLIFIER Patent
Mark H. Berry, inventor (to Navy) and Debra J. Gookin, inventor (to Navy) 10 Aug. 1993 8 p Filed 21 Feb. 1991
(AD-D015985; US-Patent-5,235,455; US-Patent-Appl-SN-666125; US-Patent-Class-359-276) Avail: US Patent and Trademark Office

A differential amplifier for gigahertz bandwidth electrical signals using fiber optics and integrated optical devices has a differential gain which is

a function of the electrical to optical and optical to electrical conversion factors. The common mode rejection ratio of the differential amplifier at 1 GHz was greater than 30 dB and the common mode rejection ratio depended on the time difference between the differential amplifier inputs. A differential amplifier fabricated in accordance with this inventive concept could be used as an integrated module in radar and communications systems.
DTIC

N94-25234# Technische Univ., Eindhoven (Netherlands).
ON THE QUALITY OF SYNTHETIC SPEECH EVALUATION AND IMPROVEMENTS Ph.D. Thesis
Josephus Hubertus Eggen 1992 139 p Prepared in cooperation with Philips Gloeilampenfabrieken N.V., Eindhoven, Netherlands
(ETN-94-95298) Avail: CASI HC A07/MF A02

The human letter to sound conversion is modeled in a text to speech system. The purpose of the study is the assessment of some limitations of Linear Predictive Coding (LPC) as a scheme for speech analysis, manipulation and synthesis, and the exploration of ways to remove some of the drawbacks of LPC. The intelligibility of synthetic speech, which is an important attribute of speech quality, is studied. A perception experiment, in which an articulated test without noise and a Monosyllabic Adaptive Speech Interference Test (MASIT) were used to evaluate the intelligibility of nine different speech coding schemes, was conducted. The naturalness of synthetic speech is studied. The preservation of the identity of a speaker, as a feature of a high quality speech coding scheme, is studied. The relative importance of coded vocal tract and voice source information for perceived speaker identity is investigated. ESA

N94-25266*# Communications Satellite Corp., Clarksburg, MD.
MODULATION AND SYNCHRONIZATION TECHNIQUE FOR MF-TDMA SYSTEM Final Report
Faris Faris, Thomas Inukai, and Soheil Sayegh 28 Jan. 1994 81 p
(Contract NAS3-25933; RTOP 506-72-21)
(NASA-CR-194448; E-8324; NAS 1.26:194448) Avail: CASI HC A05/MF A01

This report addresses modulation and synchronization techniques for a multi-frequency time division multiple access (MF-TDMA) system with onboard baseband processing. The types of synchronization techniques analyzed are asynchronous (conventional) TDMA, preambleless asynchronous TDMA, bit synchronous timing with a preamble, and preambleless bit synchronous timing. Among these alternatives, preambleless bit synchronous timing simplifies onboard multicarrier demultiplexer/demodulator designs (about 2:1 reduction in mass and power), requires smaller onboard buffers (10:1 to approximately 3:1 reduction in size), and provides better frame efficiency as well as lower onboard processing delay. Analysis and computer simulation illustrate that this technique can support a bit rate of up to 10 Mbit/s (or higher) with proper selection of design parameters. High bit rate transmission may require Doppler compensation and multiple phase error measurements. The recommended modulation technique for bit synchronous timing is coherent QPSK with differential encoding for the uplink and coherent QPSK for the downlink. Author (revised)

N94-25292# Technische Univ., Eindhoven (Netherlands). Circuit and System Design Group.
LINEAR AND NONLINEAR ADAPTIVE FILTERING AND THEIR APPLICATION TO SPEECH INTELLIGIBILITY ENHANCEMENT Ph.D. Thesis
Yu Hua Gu 1992 220 p
(ISBN-9-09-005342-5; ETN-94-95309) Copyright Avail: CASI HC A10/MF A03

The speech separation problem, where one speaker has to be selected from a signal being the sum of two speakers, is investigated: the situation where the noise itself is interference speech. Algorithms for an adaptive speech separation system were developed. The stochastic model theory to pitch contour estimation, with a specific application to the adaptive cochannel speech separation, is discussed. Linear and nonlinear adaptive filters for nonstationary signal processing are investigated. This includes the investigation of time-transform domain least mean square adaptive filters, as well as recursive least square types of algorithms with an adaptive size of the data window. General applications and simulations are described. A robust algorithm for simultaneous multipitch contour estimation is developed. After reviewing the human auditory pitch perception models and the previous research on this field, a general structure is proposed by using a pitch candidate estimator plus a pitch contour estimator based on a stochastic model. Algorithms associated with an adaptive speech separation system are described. ESA

N94-25303# Technische Univ., Eindhoven (Netherlands).
DELAY-INSENSITIVE COMMUNICATION Ph.D. Thesis
Hubert Marie Jean-Lo Schols 1992 300 p
(ETN-94-95315) Copyright Avail: CASI HC A13/MF A03

Communication is called delay insensitive if it is delay safe and it has absence of transmission interference hazard. The communication model proposed is introduced. The communication model provides a clear separation between the interpretation of physical issues and the formalism. The communication behavior of a module and the communication of an interconnection are distinguished. The concept of computation interference hazard and a technique to transform other correctness concerns into absence of computation interference hazard are presented. The delay safe communication and the absence of computation interference hazard are discussed. The attention is focused on the communication behavior of mechanisms that communicate in a delay safe way. Within the context of delay safe communication, the absence of transmission interference hazard is introduced. The necessary and sufficient conditions for composition under some given correctness concerns and a method to calculate the composition under these conditions are given. ESA

N94-25521 Air Force Inst. of Tech., Wright-Patterson AFB, OH.
DIFFUSION IN ELECTRONEGATIVE DISCHARGES WITH MAGNETIC FIELDS Ph.D. Thesis
David E. Bell 3 Dec. 1993 207 p Limited Reproducibility: More than 20% of this document may be affected by microfiche quality
(AD-A273826; AFIT/DS/ENP/93-08) Avail: CASI HC A10

Electronegative plasmas are important in a variety of electric discharge applications, such as plasma reactors, negative ion sources, and even electropositive discharges when contaminated with an electronegative impurity. The need for an understanding of the processes and phenomena associated with these electronegative discharges has spurred the development of numerical simulations and models. While many of the devices incorporate various configurations of external magnetic fields, specific attention to the influence of the magnetic field on the discharge operating point, structure, and stability is lacking. To address this deficiency, a collisional model for diffusion in three-component plasmas with an applied magnetic field is developed; it is an extension of Schottky theory allowing for negative ions and a magnetic field. This study analyzes the effect of magnetic fields on diffusion in three-component plasmas; provides an analytic solution for the collisional model in a magnetic field; evaluates the validity of effective diffusion coefficients through an analysis of the afterglow; and provides a regime of validity for the model in terms of magnetic field strength by looking at the onset of anomalous diffusion. DTIC

N94-23231*# Towson State Univ., MD. Dept. of Physics.
WIDE BAND FIBER-OPTIC COMMUNICATIONS
Harry E. Bates *In* NASA. Kennedy Space Center, NASA/ASEE Summer Faculty Fellowship Program Oct. 1993 p 1-25 (For primary document see N94-23230 06-80)
Avail: CASI HC A03/MF A04

N94-23676*# Oxford Univ. (England). Computing Lab.
MULTIGRID AND CYCLIC REDUCTION APPLIED TO THE HELMHOLTZ EQUATION
Kenneth Brackenridge *In* NASA. Langley Research Center, The Sixth Copper Mountain Conference on Multigrid Methods, Part 1 Nov. 1993 p 31-41 (For primary document see N94-23673 06-64)
Avail: CASI HC A03/MF A03

N94-23834*# European Space Agency. European Space Operations Center, Darmstadt (Germany). Mission Operations Dept.
COMMONALITY OF FLIGHT CONTROL SYSTEMS FOR SUPPORT OF EUROPEAN TELECOMMUNICATIONS MISSIONS
Kurt Debatin *In* JPL, SpaceOps 1992: Proceedings of the Second International Symposium on Ground Data Systems for Space Mission

Operations 1 Mar. 1993 p 7-14 (For primary document see N94-23832 06-66)
Avail: CASI HC A02/MF A10

N94-23835*# National Space Development Agency, Tokyo (Japan).
NASDA'S VIEW OF GROUND CONTROL IN MISSION OPERATIONS
Satoshi Tateno *In* JPL, SpaceOps 1992: Proceedings of the Second International Symposium on Ground Data Systems for Space Mission Operations 1 Mar. 1993 p 15-20 (For primary document see N94-23832 06-66)
Avail: CASI HC A02/MF A10

N94-23838*# National Aeronautics and Space Administration. Lyndon B. Johnson Space Center, Houston, TX.
COMMON FRONT END SYSTEMS FOR SPACE SHUTTLE AND SPACE STATION CONTROL CENTERS AT JOHNSON SPACE CENTER
Linda Uljon and John Muratore *In* JPL, SpaceOps 1992: Proceedings of the Second International Symposium on Ground Data Systems for Space Mission Operations 1 Mar. 1993 p 33-38 (For primary document see N94-23832 06-66)
Avail: CASI HC A02/MF A10

N94-23842*# Jet Propulsion Lab., California Inst. of Tech., Pasadena.
MISSION PLANNING FOR SHUTTLE IMAGING RADAR-C (SIR-C) WITH A REAL-TIME INTERACTIVE PLANNING SOFTWARE
Su K. Potts *In its* SpaceOps 1992: Proceedings of the Second International Symposium on Ground Data Systems for Space Mission Operations 1 Mar. 1993 p 57-62 (For primary document see N94-23832 06-66)
Avail: CASI HC A02/MF A10

N94-23847*# Mitre Corp., Greenbelt, MD.
A REFERENCE MODEL FOR SPACE DATA SYSTEM INTERCONNECTION SERVICES
John Pietras and Gerhard Theis (European Space Agency. European Space Operations Center, Darmstadt, Germany.) *In* JPL, SpaceOps 1992: Proceedings of the Second International Symposium on Ground Data Systems for Space Mission Operations 1 Mar. 1993 p 91-96 (For primary document see N94-23832 06-66)
Avail: CASI HC A02/MF A10

N94-23848*# Jet Propulsion Lab., California Inst. of Tech., Pasadena.
AN OSI ARCHITECTURE FOR THE DEEP SPACE NETWORK
W. Randy Heuser and Lynne P. Cooper *In its* SpaceOps 1992: Proceedings of the Second International Symposium on Ground Data Systems for Space Mission Operations 1 Mar. 1993 p 97-101 (For primary document see N94-23832 06-66)
Avail: CASI HC A01/MF A10

N94-23859*# National Aeronautics and Space Administration. Goddard Space Flight Center, Greenbelt, MD.
A QUICK UPLINK, EXPANDABLE EXECUTABLE FOR THE NSSC-1 OF THE HUBBLE SPACE TELESCOPE
Glenn T. Foley and Elizabeth A. Citrin *In* JPL, SpaceOps 1992: Proceedings of the Second International Symposium on Ground Data Systems for Space Mission Operations 1 Mar. 1993 p 173-178 (For primary document see N94-23832 06-66)
Avail: CASI HC A02/MF A10

N94-23870*# Jet Propulsion Lab., California Inst. of Tech., Pasadena.
VOYAGER UPLINK PLANNING IN THE INTERSTELLAR MISSION ERA
Susan H. Linick and Kathryn R. Weld *In its* SpaceOps 1992: Proceedings of the Second International Symposium on Ground Data Systems for Space Mission Operations 1 Mar. 1993 p 243-248 (For primary document see N94-23832 06-66)
Avail: CASI HC A02/MF A10

N94-23908*# Computer Technology Associates, Inc., Rockville, MD.
RELIABLE TRANSFER OF DATA FROM GROUND TO SPACE
Fred Brosi *In* JPL, SpaceOps 1992: Proceedings of the Second International Symposium on Ground Data Systems for Space Mission Operations 1 Mar. 1993 p 507-512 (For primary document see N94-23832 06-66)
Avail: CASI HC A02/MF A10

N94-23909*# Logica Space and Communications Ltd., London (England).
THE EURECA TELECOMMANDING CHAIN: EXPERIENCE WITH PACKET TELECOMMAND AND TELEMETRY SYSTEMS
C. Mueller, R. Bater, and E. M. Sorensen (European Space Agency. European Space Operations Center, Darmstadt, Germany.) *In* JPL, SpaceOps 1992: Proceedings of the Second International Symposium on Ground Data Systems for Space Mission Operations 1 Mar. 1993 p 513-518 (For primary document see N94-23832 06-66)
Avail: CASI HC A02/MF A10

N94-23912*# Jet Propulsion Lab., California Inst. of Tech., Pasadena.
DIGITAL TEST SIGNAL GENERATION: AN ACCURATE SNR CALIBRATION APPROACH FOR THE DSN
Benito O. Gutierrez-Luaces *In its* SpaceOps 1992: Proceedings of the Second International Symposium on Ground Data Systems for Space Mission Operations 1 Mar. 1993 p 531-536 (For primary document see N94-23832 06-66)
Avail: CASI HC A02/MF A10

N94-23914*# Jet Propulsion Lab., California Inst. of Tech., Pasadena.
REPRESENTING OPERATIONS PROCEDURES USING TEMPORAL DEPENDENCY NETWORKS
Kristina E. Fayyad and Lynne P. Cooper *In its* SpaceOps 1992: Proceedings of the Second International Symposium on Ground Data Systems for Space Mission Operations 1 Mar. 1993 p 541-546 (For primary document see N94-23832 06-66)
Avail: CASI HC A02/MF A10

N94-23915*# Jet Propulsion Lab., California Inst. of Tech., Pasadena.
SITUATION MANAGEMENT IN THE LINK MONITOR AND CONTROL OPERATOR ASSISTANT (LMCOA)
Randall W. Hill, Jr. and Lorrine F. Lee *In its* SpaceOps 1992: Proceedings of the Second International Symposium on Ground Data Systems for Space Mission Operations 1 Mar. 1993 p 547-552 (For primary document see N94-23832 06-66)
Avail: CASI HC A02/MF A10

N94-23918*# National Aeronautics and Space Administration. Goddard Space Flight Center, Greenbelt, MD.
A METHOD FOR INTERFERENCE MITIGATION IN SPACE COMMUNICATIONS SCHEDULING
Yen F. Wong and James L. Rash *In* JPL, SpaceOps 1992: Proceedings of the Second International Symposium on Ground Data Systems for Space Mission Operations 1 Mar. 1993 p 565-571 (For primary document see N94-23832 06-66)
Avail: CASI HC A02/MF A10

N94-23922*# Jet Propulsion Lab., California Inst. of Tech., Pasadena.
XRTD: AN X-WINDOWS BASED, REAL-TIME RADIOMETRIC DISPLAY AND ANALYSIS SYSTEM
Vincent M. Pollmeier *In its* SpaceOps 1992: Proceedings of the Second International Symposium on Ground Data Systems for Space Mission Operations 1 Mar. 1993 p 601-606 (For primary document see N94-23832 06-66)
Avail: CASI HC A02/MF A10

N94-23986# Spar Aerospace Ltd., Sainte-Anne-de-Bellevue (Quebec).
THE DOWN, RELEASE, AND DEPLOYMENT OF THE RADARSAT SAR ANTENNA
G. S. Bush *In* ESA, The Fifth European Space Mechanisms and Tribology Symposium Apr. 1993 7 p Sponsored by Canadian Space Agency (For primary document see N94-23985 06-37)
Copyright Avail: CASI HC A02/MF A04

N94-23996# Dornier System G.m.b.H., Friedrichshafen (Germany).
INVESTIGATIONS INTO DEPLOYMENT COMPLICATIONS OF THE ERS-1 SAR ANTENNA
R. Barho *In* ESA, The Fifth European Space Mechanisms and Tribology

Symposium Apr. 1993 4 p (For primary document see N94-23985 06-37)
Copyright Avail: CASI HC A01/MF A04

N94-24194*# Lockheed Engineering and Sciences Co., Houston, TX.
PERFORMING SPEECH RECOGNITION RESEARCH WITH HYPERCARD
Chip Shepherd *In* NASA. Johnson Space Center, Crew Interface Analysis: Selected Articles on Space Human Factors Research, 1987 - 1991 Jul. 1993 p 64-67 (For primary document see N94-24185 06-54)
Avail: CASI HC A01/MF A02; 5 functional color pages

N94-24423*# Puerto Rico Univ., Mayaguez. Electrical and Computer Engineering Dept.
ON THE ANALYSIS OF CLEAR AIR RADAR ECHOES SEVERELY CONTAMINATED BY CLUTTER
H. Mario Ierkic *In* Alabama Univ., The 1993 NASA/ASEE Summer Faculty Fellowship Program Nov. 1993 6 p (For primary document see N94-24405 06-80)
Avail: CASI HC A02/MF A03

N94-24439*# Tuskegee Inst., AL.
ERROR CODING SIMULATIONS
Viveca K. Noble *In* Alabama Univ., The 1993 NASA/ASEE Summer Faculty Fellowship Program Nov. 1993 5 p (For primary document see N94-24405 06-80)
Avail: CASI HC A01/MF A03

N94-25353*# Southern Vital Records Center, Inc., Flora, MS. Dept. of Computer Science.
A PROTOTYPE TO AUTOMATE THE VIDEO SUBSYSTEM ROUTING FOR THE VIDEO DISTRIBUTION SUBSYSTEM OF SPACE STATION FREEDOM
Jessie M. Bethly Betz *In* NASA. Johnson Space Center, National Aeronautics and Space Administration (NASA)/American Society for Engineering Education (ASEE) Summer Faculty Fellowship Program, 1993, Volume 1 Dec. 1993 10 p (For primary document see N94-25348 06-99)
Avail: CASI HC A02/MF A03

N94-25360*# Wyoming Univ., Laramie. Dept. of Computer Science.
FAILURE DETECTION AND RECOVERY IN THE ASSEMBLY/CONTINGENCY SUBSYSTEM
Rex E. Gantenbein *In* NASA. Johnson Space Center, National Aeronautics and Space Administration (NASA)/American Society for Engineering Education (ASEE) Summer Faculty Fellowship Program, 1993, Volume 1 Dec. 1993 15 p (For primary document see N94-25348 06-99)
Avail: CASI HC A03/MF A03

N94-25374*# Tarrant County Junior Coll., Fort Worth, TX. Computer Science Dept.
MODELING AND ANALYSIS OF SELECTED SPACE STATION COMMUNICATIONS AND TRACKING SUBSYSTEMS
Elmer Raydean Richmond *In* NASA. Johnson Space Center, National Aeronautics and Space Administration (NASA)/American Society for Engineering Education (ASEE) Summer Faculty Fellowship Program, 1993, Volume 2 Dec. 1993 15 p (For primary document see N94-25367 06-99)
Avail: CASI HC A03/MF A03

N94-25379*# Colorado Univ., Colorado Springs. Dept. of Electrical Engineering.
CONCEPTUAL COMMUNICATIONS SYSTEM DESIGN IN THE 25.25-27.5 AND 37.0-40.5 GHz FREQUENCY BANDS
Michael W. Thompson *In* NASA. Johnson Space Center, National Aeronautics and Space Administration (NASA)/American Society for Engineering Education (ASEE) Summer Faculty Fellowship Program, 1993, Volume 2 Dec. 1993 15 p (For primary document see N94-25367 06-99)
Avail: CASI HC A03/MF A03

N94-25381*# Amarillo Coll., TX. Electronics Technology Dept.
MODELING OF THE GROUND-TO-SSFMB LINK NETWORKING FEATURES USING SPW
John C. Watson *In* NASA. Johnson Space Center, National Aeronautics and Space Administration (NASA)/American Society for Engineering Education (ASEE) Summer Faculty Fellowship Program, 1993, Volume 2 Dec. 1993 15 p (For primary document see N94-25367 06-99)
Avail: CASI HC A03/MF A03

N94-25493*# Lear Astronics Corp., Santa Monica, CA.
THE 94 GHz MMW IMAGING RADAR SYSTEM
Yair Alon and Lon Ulmer *In* NASA. Ames Research Center, Proceedings of the Workshop on Augmented Visual Display (AVID) Research Dec. 1993 p 47-60 (For primary document see N94-25490 06-54)
Avail: CASI HC A03/MF A04

N94-25494*# TRW, Inc., Redondo Beach, CA. Applied Technology Div.
PASSIVE MILLIMETER-WAVE IMAGING
Stephen K. Young, Roger A. Davidheiser, Bruce Hauss, Paul S. C. Lee, Michael Mussetto, Merit M. Shoucri, and Larry Yujiri *In* NASA. Ames Research Center, Proceedings of the Workshop on Augmented Visual Display (AVID) Research Dec. 1993 p 61-78 (For primary document see N94-25490 06-54)
Avail: CASI HC A03/MF A04

N94-25497*# Technology Service Corp., Santa Monica, CA.
THE RADAR IMAGE GENERATION (RIG) MODEL
Anthony J. Stenger *In* NASA. Ames Research Center, Proceedings of the Workshop on Augmented Visual Display (AVID) Research Dec. 1993 p 121-131 (For primary document see N94-25490 06-54)
Avail: CASI HC A03/MF A04

N94-25498*# TRW, Inc., Redondo Beach, CA. Space and Electronics Group.
ADVANCED RADIOMETRIC AND INTERFEROMETRIC MILIMETER-WAVE SCENE SIMULATIONS
B. I. Hauss, P. J. Moffa, W. G. Steele, H. Agravante, R. Davidheiser, T. Samec, and S. K. Young *In* NASA. Ames Research Center, Proceedings of the Workshop on Augmented Visual Display (AVID) Research Dec. 1993 p 133-162 (For primary document see N94-25490 06-54)
Avail: CASI HC A03/MF A04

N94-25503*# Westinghouse Electric Corp., Sunnyvale, CA.
RADAR E-O IMAGE FUSION
William F. ONeil *In* NASA. Ames Research Center, Proceedings of the Workshop on Augmented Visual Display (AVID) Research Dec. 1993 p 225-232 (For primary document see N94-25490 06-54)
Avail: CASI HC A02/MF A04

33 ELECTRONICS AND ELECTRICAL ENGINEERING

Includes test equipment and maintainability; components, e.g., tunnel diodes and transistors; microminiaturization; and integrated circuitry.

For related information see also *60 Computer Operations and Hardware* and *76 Solid-State Physics.*

N94-22883# Grenoble-1 Univ. (France). Lab. ARTEMIS.
FORMAL VERIFICATION OF DIGITAL CIRCUITS DESCRIBED IN VHDL Ph.D. Thesis [VERIFICATION FORMELLE DES CIRCUITS DIGITAUX DECRITS EN VHDL]
Ashraf Mohammed El-F Salem 1992 132 p In FRENCH
(ETN-94-95165) Avail: CASI HC A07/MF A02

The formal verification of digital circuits described in VHSIC (very high speed integrated circuit) hardware description language (VHDL) is presented. VHDL is made processable by proof tools. A subset, called P-VHDL, dedicated to the description of combinatorial and synchronous sequential circuits is defined. The semantics of this subset is much simpler than the complete VHDL. The delta delay is replaced by a serialization function, and the time scale is chosen equal to the clock period. The use of the finite state machine as a formal model for the subset became possible. The finite state machine semantics is shown to represent the P-VHDL semantics. Based on this formal model, a proof oriented compiler for P-VHDL is written. A complete denotational semantic for P-VHDL is defined. Three different domains for the three values holders in the language are proposed: the variables, the signals, and the registers. Formal semantics for the VHDL timing constructs are given. The equivalence between these semantics and the VHDL informal operational semantics is proven. It is shown that semantics can form a basis for building a formal timing verifier. ESA

N94-22909# Laboratoire d'Automatique et d'Analyse des Systemes, Toulouse (France). Groupe Composants et Circuits Micro-Ondes.
MICROWAVE ANALOG FREQUENCY DIVIDERS: DESIGN, MODELING AND REALIZATION Ph.D. Thesis - Toulouse Univ. [LES DIVISEURS ANALOGIQUES DE FREQUENCE MICRO-ONDES: MODELISATION, CONCEPTION ET REALISATION]
Hicham Amine 1993 137 p In FRENCH
(LAAS-93139; ETN-94-95191) Avail: CASI HC A07/MF A02

The design and modeling of microwave analog frequency dividers are investigated. Frequency domain and harmonic balance simulations of the transistor behavior, to permit self-biasing to be understood, are carried out. An approach to analog frequency dividers, based on the nonlinear feedback control of metal semiconductor field effect transistor in the forced oscillation mode, is proposed. The input signal is employed to control transistor gain. An optimal modeling of analog frequency dividers is proposed and tested by the use of time domain simulation. To validate this model, a 1/2 analog frequency divider is designed. Its measured performances were compared to the theoretical ones. A nonlinear model of analog frequency dividers noise conversion characteristics is accomplished. This model based on the conversion matrix method is used to evaluate the phase noise limit of our circuit. ESA

N94-22950# Lawrence Livermore National Lab., CA.
PICOSECOND HIGH PRESSURE GAS SWITCH EXPERIMENT
W. R. Cravey, E. K. Freytag, D. A. Goerz, P. Poulsen, and P. A. Pincosy Aug. 1993 6 p Presented at the 9th IEEE Pulsed Power Conference, Albuquerque, NM, 21-23 Jun. 1993
(Contract W-7405-eng-48)
(DE93-040853; UCRL-JC-112339; CONF-930616-39) Avail: CASI HC A02/MF A01

A High Pressure Gas Switch has been developed and tested at LLNL. Risetimes on the order of 200 picoseconds have been observed at 1 kHz prf and 1 atmosphere pressures. Calculations show that switching closure times on the order of tens of picoseconds can be achieved at higher pressures and electric fields. A voltage hold-off of 1 MV/cm has been measured at 10 atmospheres and several MV/cm appears possible with the HPGS. With such high electric field levels, energy storage of tens of Joules in a reasonably sized package is achievable. Initial HPGS performance has been characterized using the WASP pulse generator at LLNL. A detailed description of the switch used for initial testing is given. Switch recovery times of 1-ms have been measured at 1 atmosphere. Data on the switching uniformity, voltage hold-off recovery, and pulse repeatability, is presented. In addition, a physics switch model is described and results are compared with experimental data. Modifications made to the WASP HV pulser in order to drive the HPGS will also be discussed. Recovery times of less than 1 ms were recorded without gas flow in the switch chambers. Low pressure synthetic air was used as the switch dielectric. Longer recovery times were required when it was necessary to over-voltage the switch. DOE

N94-22955# Stanford Linear Accelerator Center, CA.
PROGRESS ON THE DESIGN OF A DATA PUSH ARCHITECTURE FOR AN ARRAY OF OPTIMIZED TIME TAGGING PIXELS
S. Shapiro, D. Cords, S. Mani (California Univ., Davis.), B. Holbrook (California Univ., Davis.), and E. Atlas (Adept IC Design, Oceanside, CA.) Jun. 1993 4 p Presented at the Workshop on Charged-Coupled Devices and Advanced Image Sensors, Waterloo, Ontario, 9-11 Jun. 1993
(Contracts DE-AC03-76SF-00515; DE-FG03-91ER-40674)
(DE93-041011; SLAC-PUB-6249; CONF-9306256-1) Avail: CASI HC A01/MF A01

A pixel array has been proposed which features a completely data driven architecture. A pixel cell has been designed that has been optimized for this readout. It retains the features of preceding designs which allow low noise operation, time stamping, analog signal processing, XY address recording, ghost elimination and sparse data transmission. The pixel design eliminates a number of problems inherent in previous designs, by the use of sampled data techniques, destructive readout, and current mode output drivers. This architecture and pixel design is directed at applications such as a forward spectrometer at the SSC, an e(sup +)e(sup -) B factory at SLAC, and fixed target experiments at FNAL. DOE

N94-22987 Los Alamos National Lab., NM.
DEVELOPMENTS IN MATERIALS FOR HIGH-FIELD MAGNETS
J. R. Sims, M. A. Hill, and R. P. Walsh (National Inst. of Standards and Technology, Boulder, CO.) 1993 4 p Presented at the 13th International Conference on Magnet Technology, Victoria, Ontario, 20-24 Sep. 1993 Limited Reproducibility: More than 20% of this document may be affected by microfiche quality
(Contract W-7405-eng-36)
(DE94-000761; LA-UR-93-3391; CONF-930926-13) Avail: CASI HC A01

Results of the National High Magnetic Field Laboratory's program of characterization of materials and fabrication techniques used in the construction of high-field pulsed magnets are reported. High-field pulsed magnets require conductors with high mechanical strength (750 MPa or greater YS at 77K) and high electrical conductivity (70% IACS or greater at RT). Electrical insulation and resin systems for vacuum impregnation with high compressive strength (500 MPa at 77K) and moderate thermal conductivity (1kW/mK at 77K) are also required. Developments and future plans for the characterization of new magnet material systems are discussed. Testing result are reported: mechanical and fatigue testing, electrical conductivity testing and thermal expansion measurements of high strength, high conductivity conductors at cryogenic and room temperature, mechanical testing of a coil support material at cryogenic and room temperature, and thermal expansion and thermal conductivity tests of an electrical insulating system at cryogenic temperatures. DOE

N94-23008# Lawrence Livermore National Lab., CA.
CUSTOMIZABLE VLSI ARTIFICIAL NEURAL NETWORK CHIPS BASED ON A NOVEL TECHNOLOGY
C. Y. Fu, B. Law, G. Chapline, and D. Swenson (Naval Air Warfare Center, China Lake, CA.) 14 Sep. 1993 2 p Presented at the Government Microcircuit Applications Conference: Microelectronics in the New World Order, Las Vegas, NV, 9-12 Nov. 1992
(Contract W-7405-eng-48)
(DE94-001418; UCRL-JC-110366; CONF-921188-3) Avail: CASI HC A01/MF A01

The human cerebral cortex contains approximately 10(exp 11) neurons and 10(exp 14) synapses. It thus seems logical that any technology intended to mimic human capabilities should have the ability to fabricate a very large number of neurons and even larger numbers of synapses. This paper describes an implementation of hardware neural networks using highly linear thin-film resistor technology and an 8-bit binary weight circuit to produce customizable artificial neural network chips and systems. DOE

N94-23019# Oak Ridge National Lab., TN.
SIMPLE ESTIMATE OF STORED ENERGY AND CONDUCTOR INSULATION VOLTAGE-WITHSTAND REQUIREMENTS FOR ADVANCED SOLENOID MAGNET DESIGNS
S. W. Schwenterly and L. Dresner 1993 6 p Presented at the International Cryogenic Engineering Conference and International Cryogenic Materials Conference, Albuquerque, NM, 12-16 Jul. 1993
(Contract DE-AC05-84OR-21400)
(DE93-041048; CONF-930703-34) Avail: CASI HC A02/MF A01

Compact, lightweight, high-current-density superconducting magnets are of interest for many applications. Minimizing the area taken up by conductor stabilizer material and insulation can lead to high dump voltages if the magnet is protected by discharging it through an external resistor. The dump voltages per turn for circular solenoids are estimated for this situation, in terms of the well-known 'hotspot integral' H(Delta(T)), the maximum on-axis magnetic field B(sub z), and the stored energy E. The field and stored energy are calculated in terms of the coil geometry parameters alpha and beta. The results depend only on B(sub z), H(Delta(T)), and certain scaling factors, and are independent of the coil size. The relations give simple estimates of the average turn dump voltages for a coil of a given field and geometry which are useful for preliminary scoping studies during conceptual design of the magnet. DOE

N94-23104 Helsinki Univ. of Technology, Espoo (Finland). Lab. of Electromechanics.

LECTURES ON MAGNETOHYDRODYNAMICAL DRIVES

Villem Loigom 1993 69 p Prepared in cooperation with Tallinn Polytechnic Inst. Limited Reproducibility: More than 20% of this document may be affected by microfiche quality

(PB93-224962; Rept-1993/39) Avail: CASI HC A04

The paper deals with nonconventional types of electrical machines and drives - magnetohydrodynamical (MHD) machines and drives. In cardinal it is based on the research conducted with participation of the author in Tallinn Technical University at the Institute of Electrical Drives and Power Electronics, where the use of magnetohydrodynamical motors and drives in the metallurgical and casting industries have been studied for a long time. Major research interests include the qualities and applications of the induction MHD-drives for set in the motion (pumping, turning, dosing, mixing, etc.) non-ferrous molten metals like Al, Mg, Sn, Pb, Na, K, and their alloys. The first part of the paper describes induction MHD motors and their electrohydraulical qualities. In the second part energy conversion problems are described. Also, on the basis of the analogy between electromechanical and electrohydraulical phenomenas, static and dynamic qualities of MHD drives with induction MHD machines are discussed. NTIS

N94-23105# Helsinki Univ. of Technology, Espoo (Finland). Electromagnetics Lab.

STATIC IMAGE METHOD FOR COMPUTING THE ELECTRIC POTENTIAL DUE TO SOURCES IN A LAYERED SPHERE

J. C. E. Sten and R. J. Ilmoniemi Mar. 1993 24 p

(PB93-224970; ISBN-951-22-1455-5) Avail: CASI HC A03/MF A01

Following the approach of Neumann and Lindell, the authors derive an equivalent image line source that produces in a homogeneous medium the same electric field as a point source in a layered sphere. The image charge density function for the sphere with two interfaces of arbitrary radii and permittivities is solved analytically. Approximations are derived for the case when the two layers have nearly the same permittivities and for the case of thin outer layer. An image expression for the thin-layered sphere with three interfaces is developed. The authors suggest that a replacement of the image line by discrete point charges may be used to speed up computations of the electric potential on the scalp due to sources in the brain. In the lowest-order approximation, a single point source is placed at the center of gravity of the image line distribution. NTIS

N94-23130 Helsinki Univ. of Technology, Espoo (Finland). Circuit Theory Lab.

TRANSIENT ANALYSIS OF CIRCUITS INCLUDING FREQUENCY-DEPENDENT COMPONENTS USING TRANSGYRATOR AND CONVOLUTION

P. Stenius, P. Heikkilae, and M. Valtonen Feb. 1993 22 p Limited Reproducibility: More than 20% of this document may be affected by microfiche quality

(PB93-225001; ISBN-951-22-1494-6) Avail: Issuing Activity (National Technical Information Service (NTIS))

A practical method for the transient analysis of circuits including frequency-dependent components, as well as the implementation of the method in a circuit-simulation software package called APLAC, has been presented. The main differences between the method and those previously presented are that the authors introduced the transgyrator and that the authors carefully minimized the number of mathematical operations needed in the analysis. These improvements finally make the method practical for usage in a circuit simulation software package intended for engineers. The implementation of the method in APLAC, using the NPort component model, consists of two separate C programming language source code files, together amounting to only 16 kB. Due to the object-oriented nature of all components written for APLAC, the coding time of the implementation was reduced considerably. NTIS

N94-23136# Technische Univ., Eindhoven (Netherlands). Digital Informations Systems Section.

MULTIDISCIPLINARY SPECIFICATION AND DESIGN OF MICROELECTRONICS IN PRODUCTS [MULTIDISCIPLINAR SPECIFICEREN EN ONTWERPEN VAN MICROELEKTRONICA IN PRODUKTEN]

P. H. A. vanderPutten Jan. 1993 116 p In DUTCH

(EUT-93-E-269; ISBN-9-06-144269-9; ETN-94-94776) Avail: CASI HC A06/MF A02

The specification of products, incorporating information technology, requires the interaction with various disciplines. Complete specification may seem to be expensive, but it can reduce the number of iterations in the product development process. From the point of view of digital electronic design, interacting disciplines are shown, illustrated with examples. The report can be used as a source of ideas to improve the specification and design process. ESA

N94-23154# Institut National Polytechnique, Grenoble (France). Techniques de l'Informatique, des Mathematiques, de la Microelectronique et de la Microscopie.

AMICAL: AN AID FOR ARCHITECTURAL SYNTHESIS AND EXPLORATION OF CONTROL CIRCUITS Ph.D. Thesis [AMICAL: UN ASSISTANT POUR LA SYNTHESE ET L'EXPLORATION ARCHITECTURALE DES CIRCUITS DE COMMANDE]

Inhag Park 1992 197 p In FRENCH

(ETN-94-95177) Avail: CASI HC A09/MF A03

AMICAL is an architectural synthesis system for control flow dominated circuits. A behavioral finite state machine specification, where the scheduling and register allocation were performed, is presented. An abstract architecture specification that may feed existing silicon compilers acting at the logic and register transfer levels is described. AMICAL consists of five main functions allowing automatic, interactive and manual synthesis, as well as the combination of these methods. These functions are a synthesizer, a graphics editor, a verifier, an evaluator, and a documentor. Automatic synthesis is achieved by algorithms that allocate both functional units, stored in an expandable user defined library, and connections. AMICAL also allows the designer to interrupt the synthesis process at any stage and make interactive modifications via a specially designed graphics editor. The user's modifications are verified and evaluated to ensure that no design rules are broken and that any imposed constraints are still met. A documentor provides the designer with status and feedback reports from the synthesis process. ESA

N94-23165# Institut National Polytechnique, Grenoble (France). Lab. de Genie Informatique.

GENERATION OF MODULES FOR CONTROL COMMUNICATION CIRCUITS: A DESIGN STUDY USED IN THE FRAMEWORK OF THE SAFE VEHICLE PROMETHEUS Ph.D. Thesis [GENERATION DE MODULES DEDIES AUX CIRCUITS DE COMMUNICATION DE CONTROLE-COMMANDE: UNE ETUDE DE CONCEPTION APPLIQUEE DANS LE CADRE DE LA VOITURE SURE PROMETHEUS]

Imad Sabouni 1992 375 p In FRENCH

(ETN-94-95171) Avail: CASI HC A16/MF A03

The implementation of communication protocols on silicon integrated circuits for access control is considered. The field of application is the European PROMETHEUS (Program for European Traffic with Highest Efficiency and Unprecedented Safety) project. The design of communication circuits for network access control is discussed. The control type local network and the related protocols are analyzed. Market available communication controllers are presented. The functions and the architecture of network control systems are described and the interfaces with the host system are considered. A method based on the generation of modules for communication circuit's design is proposed. Examples of circuits generated for vehicle application networks are given. The feasibility of obstacle detection distributed system is investigated. ESA

N94-23281*# National Aeronautics and Space Administration. Goddard Space Flight Center, Greenbelt, MD.

MODULATION CHARACTERISTICS OF A HIGH-POWER SEMICONDUCTOR MASTER OSCILLATOR POWER AMPLIFIER (MOPA)

Donald Mitchell Cornwell, Jr. Washington Nov. 1992 115 p

(NASA-TM-104577; NAS 1.15:104577; Rept-93B00016) Avail: CASI HC A06/MF A02

A semiconductor master oscillator-power amplifier was demonstrated using an anti-reflection (AR) coated broad area laser as the amplifier. Under CW operation, diffraction-limited single-longitudinal-mode powers up to 340 mW were demonstrated. The characteristics of the far-field pattern were measured and compared to a two-dimensional reflective Fabry-Perot amplifier model of the device. The MOPA configuration was modulated by the master oscillator. Prior to injection into the amplifier, the amplitude and frequency modulation properties of the master oscillator were characterized. The frequency response of the MOPA configuration was characterized for an AM/FM modulated injection beam, and was found to be a function of the frequency detuning between the master oscillator and the resonant amplifier. A shift in the phase was also observed as a function of frequency detuning; this phase shift is attributed to the optical phase shift imparted to a wave reflected from a Fabry-Perot cavity. Square-wave optical pulses were generated at 10 MHz and 250 MHz with diffraction-limited peak powers of 200 mW and 250 mW. The peak power for a given modulation frequency is found to be limited by the injected power and the FM modulation at that frequency. The modulation results make the MOPA attractive for use as a transmitter source in applications such as free-space communications and ranging/altimetry. Author

N94-23304*# Clemson Univ., SC. Radar Systems Lab.
ON THE ESTIMATION OF THE CORRELATION DIMENSION AND ITS APPLICATION TO RADAR REFLECTOR DISCRIMINATION Final Report
Kevin D. Barnett Dec. 1993 72 p
(Grant NAG1-928; RTOP 505-64-12-02)
(NASA-CR-4564; NAS 1.26:4564; DOT/FAA/RD-93/41; TR-073093-357OP; RSL-TR-17) Avail: CASI HC A04/MF A01

Recently, system theorists have recognized that low order systems of nonlinear differential equations can give rise to solutions which are neither periodic, constant, nor predictable in steady state, but which are nonetheless bounded and deterministic. This behavior, which was first described in the study of weather systems, has been termed 'chaotic.' Much study of chaotic systems has concentrated on analysis of the systems' phase space attractors. It has been recognized that invariant measures of the attractor possess inherent information about the system. One such measure is the dimension of the attractors. The dimension of a chaotic attractor has been shown to be noninteger, leading to the term 'strange attractor;' the attractor is said to have a fractal structure. The correlation dimension has become one of the most popular measures of dimension. However, many problems have been identified in correlation dimension estimation from time sequences. The most common methods for obtaining the correlation dimension have been least squares curves fitting to find the slope of the correlation integral and the Takens Estimator. However, these estimates show unacceptable sensitivity to the upper limit on the distance chosen. Here, a new method is proposed which is shown to be rather insensitive to the upper limit and to perform in a very stable manner, at least in the absence of noise. The correlation dimension is also shown to be an effective discriminant in distinguishing between radar returns resulting from weather and those from the ground. The weather returns are shown to have a correlation dimension generally between 2.0 and 3.0, while ground returns have a correlation dimension exceeding 3.0. Author (revised)

N94-23520# Lawrence Livermore National Lab., CA.
FABRICATION OF SUB-40-nm p-n JUNCTIONS FOR 0.18 MICRON MOS DEVICE APPLICATIONS USING A CLUSTER-TOOL-COMPATIBLE, NANOSECOND THERMAL DOPING TECHNIQUE
K. H. Weiner and A. M. McCarthy 20 Sep. 1993 8 p Presented at the Society of Photo-Optical Instrumentation Engineers (SPIE) Symposium on Microelectronics Processing, Monterey, CA, 27-29 Sep. 1993
(Contract W-7405-eng-48)
(DE94-001608; UCRL-JC-114003; CONF-9309264-1) Avail: CASI HC A02/MF A01

In this paper, we introduced an alternative deep-submicrometer doping technology, Projection Gas Immersion Laser Doping (P-GILD). Representing the marriage of lithography and diffusion, P-GILD is a resistless, step-and-repeat doping process that utilizes excimer laser light patterned by a dielectric reticle to selectively heat and, thereby, dope regions of an integrated circuit. Results of physical and electrical characterization are presented for ultra-shallow p(sup +) (minus)n and n(sup +) (minus)p junctions produced by gas immersion laser doping (GILD), a phenomenologically identical technique that utilizes an aluminum contact mask rather than a dielectric reticle to pattern the beam. Junctions produced using GILD exhibit uniformly-doped, abrupt impurity profiles with no apparent defect formation in the silicon. Electrically, sheet and contact resistivities of the ultra-shallow junctions are less than 100(Omega)/sheet and 1 x 10(exp -6) (Omega)*sq cm, respectively, while n(sup +) (minus)p and p(sup +) (minus)n diodes exhibit nearly ideal forward bias behavior and reverse leakage current densities less than 5 nA/sq cm at -5V. Uniformity of both diode characteristics and sheet resistance for junctions produced by the step-and-repeat process is also shown to be better than (plus minus)5% across a 4-inch wafer. DOE

N94-23777# Sandia National Labs., Albuquerque, NM.
THE ELECTRONICS QUALITY/RELIABILITY CENTER: LESSONS LEARNED FROM PARTNERING WITH INDUSTRY
Theodore A. Dellin 1993 4 p Presented at the 1993 Government Microcircuit Application Conference, New Orleans, LA, 1-4 Nov. 1993
(Contract DE-AC04-94AL-85000)
(DE94-001501; SAND-93-2100C; CONF-9311101-4) Avail: CASI HC A01/MF A01

The government electronics community faces the exciting challenge of entering into new types of partnerships with the commercial electronics industry. Past interactions were based primarily on the needs of government. Future interactions will be based more on the needs of industry, particularly its need to be competitive in commercial products. The most successful groups will be those most adept at forming this new type of 'win-win' partner. Fortunately, both government and industry want to make these new partnerships successful. The government is driven by the necessity of establishing a common government/commercial manufacturing base and the desire to support U.S. competitiveness. Industry is driven by the need to partner with government to remain competitive. Unfortunately, there are no detailed guides available to help government electronics groups and their sponsors in the Administration and Congress cross this uncharted terrain. The purpose of this paper is to share some 'lessons learned' from the experiences of a government electronics group that has been active in establishing these new types of partnerships with industry. It is our hope that by sharing these lessons we will make it easier for other government groups to work with the commercial industry. DOE

N94-23820* National Aeronautics and Space Administration. Pasadena Office, CA.
NON-VOLATILE, SOLID STATE BISTABLE ELECTRICAL SWITCH Patent
Roger M. Williams, inventor (to NASA) (Jet Propulsion Lab., California Inst. of Tech., Pasadena.) 11 Jan. 1994 9 p Filed 28 Jan. 1991
Supersedes N90-17010 (28 - 9, p 1209) Continuation of abandoned US-Patent-Appl-SN-414820, filed 29 Sep. 1989
(NASA-Case-NPO-17621-1-CU; US-Patent-5,278,636;
US-Patent-Appl-SN-654439; US-Patent-Appl-SN-414820;
US-Patent-Class-257-2; US-Patent-Class-307-201; US-Patent-Class-338-13;
US-Patent-Class-338-38; US-Patent-Class-361-500;
US-Patent-Class-257-528) Avail: US Patent and Trademark Office

A bistable switching element is made of a material whose electrical resistance reversibly decreases in response to intercalation by positive ions. Flow of positive ions between the bistable switching element and a positive ion source is controlled by means of an electrical potential applied across a thermal switching element. The material of the thermal switching element generates heat in response to electrical current flow therethrough, which in turn causes the material to undergo a thermal phase transition from a high electrical resistance state to a low electrical resistance state as the temperature increases above a predetermined value. Application of the electrical potential in one direction renders the thermal switching element conductive to pass electron current out of the ion source. This causes positive ions to flow from the source into the bistable switching element and intercalate the same to produce a non-volatile, low resistance logic state. Application of the electrical potential in the opposite direction causes reverse current flow which de-intercalates the bistable logic switching element and produces a high resistance logic state.

Official Gazette of the U.S. Patent and Trademark Office

N94-23821*# National Aeronautics and Space Administration. Pasadena Office, CA.

PLANAR VARACTOR FREQUENCY MULTIPLIER DEVICES WITH BLOCKING BARRIER Patent

Udo Lieneweg, inventor (to NASA) (Jet Propulsion Lab., California Inst. of Tech., Pasadena.), Margaret A. Frerking, inventor (to NASA) (Jet Propulsion Lab., California Inst. of Tech., Pasadena.), and Joseph Maserjian, inventor (to NASA) (Jet Propulsion Lab., California Inst. of Tech., Pasadena.) 11 Jan. 1994 13 p Filed 26 Feb. 1992 Supersedes N92-23464 (30- 14, p 2369)
(NASA-Case-NPO-18428-1-CU; US-Patent-5,278,444;
US-Patent-Appl-SN-842297; US-Patent-Class-257-476;
US-Patent-Class-257-15; US-Patent-Class-257-199;
US-Patent-Class-257-480; US-Patent-Class-257-482;
US-Patent-Class-257-486; US-Patent-Class-257-506) Avail: US Patent and Trademark Office

The invention relates to planar varactor frequency multiplier devices with a heterojunction blocking barrier for near millimeter wave radiation of moderate power from a fundamental input wave. The space charge limitation of the submillimeter frequency multiplier devices of the BIN(sup +) type is overcome by a diode structure comprising an n(sup +) doped layer of semiconductor material functioning as a low resistance back contact, a layer of semiconductor material with n-type doping functioning as a drift region grown on the back contact layer, a delta doping sheet forming a positive charge at the interface of the drift region layer with a barrier layer, and a surface metal contact. The layers thus formed on an n(sup +) doped layer may be divided into two isolated back-to-back BNN(sup +) diodes by separately depositing two surface metal contacts. By repeating the sequence of the drift region layer and the barrier layer with the delta doping sheet at the interfaces between the drift and barrier layers, a plurality of stacked diodes is formed. The novelty of the invention resides in providing n-type semiconductor material for the drift region in a GaAs/AlGaAs structure, and in stacking a plurality of such BNN(sup +) diodes stacked for greater output power with and connected back-to-back with the n(sup +) GaAs layer as an internal back contact and separate metal contact over an AlGaAs barrier layer on top of each stack.
Official Gazette of the U.S. Patent and Trademark Office

N94-23823* National Aeronautics and Space Administration. Pasadena Office, CA.

OVERCHARGE AND OVERDISCHARGE PROTECTION OF AMBIENT TEMPERATURE SECONDARY LITHIUM CELLS Patent

Chen-Kuo Huang, inventor (to NASA) (Jet Propulsion Lab., California Inst. of Tech., Pasadena.), Subbarao Surampudi, inventor (to NASA) (Jet Propulsion Lab., California Inst. of Tech., Pasadena.), Alan I. Attia, inventor (to NASA) (Jet Propulsion Lab., California Inst. of Tech., Pasadena.), and Gerald Halpert, inventor (to NASA) (Jet Propulsion Lab., California Inst. of Tech., Pasadena.) 11 Jan. 1994 8 p Filed 2 Sep. 1992 Supersedes N93-11456 (31 - 2, p 290)
(NASA-Case-NPO-18343-1-CU; US-Patent-5,278,000;
US-Patent-Appl-SN-942491; US-Patent-Class-429-91;
US-Patent-Class-426-191; US-Patent-Class-429-194;
US-Patent-Class-429-218; Int-Patent-Class-H01M-10/48) Avail: US Patent and Trademark Office

A cathode additive is provided for protecting an ambient temperature secondary lithium cell from overcharging or overdischarging. The cathode additive is chosen to create an upper voltage plateau which is slightly higher than a characteristic charge cutoff voltage of the cathode of the cell. The cathode additive additionally creates a lower voltage plateau which is slightly lower than the characteristic discharge cutoff voltage of the cell. Preferably, the cathode additive is a transition metal oxide or a sulfide and may, for example, include a mixture of Li2Mn2O4 and Li(0.1)MoO2. Official Gazette of the U.S. Patent and Trademark Office

N94-24056*# National Aeronautics and Space Administration. Lewis Research Center, Cleveland, OH.

GENERALIZED THREE-DIMENSIONAL SIMULATION OF FERRULED COUPLED-CAVITY TRAVELING-WAVE-TUBE DISPERSION AND IMPEDANCE CHARACTERISTICS

Joseph W. Maruschek (Ohio Aerospace Inst., Brook Park.), Carol L. Kory (Analex Corp., Brook Park, OH.), and Jeffrey D. Wilson Washington Nov. 1993 15 p
(RTOP 506-72-00)
(NASA-TP-3389; E-7977; NAS 1.60:3389) Avail: CASI HC A03/MF A01

The frequency-phase dispersion and Pierce on-axis interaction impedance of a ferruled, coupled-cavity, traveling-wave tube (TWT), slow-wave circuit were calculated using the three-dimensional simulation code Micro-SOS. The utilization of the code to reduce costly and time-consuming experimental cold tests is demonstrated by the accuracy achieved in calculating these parameters. A generalized input file was developed so that ferruled coupled-cavity TWT slow-wave circuits of arbitrary dimensions could be easily modeled. The practicality of the generalized input file was tested by applying it to the ferruled coupled-cavity slow-wave circuit of the Hughes Aircraft Company model 961HA TWT and by comparing the results with experimental results. Author (revised)

N94-24070*# Minnesota Univ., Minneapolis. Dept. of Mechanical Engineering.

ARC ELECTRODE INTERACTION STUDY Final Report

X. Zhou, D. Berns, and J. Heberlein 31 Jan. 1994 26 p Original contains color illustrations
(Grant NAG3-1332)
(NASA-CR-195096; NAS 1.26:195096) Avail: CASI HC A03/MF A01; 7 functional color pages

The project consisted of two parts: (1) the cathode interaction studies which were a continuation of previous work and had the objective of increasing our understanding of the microscopic phenomena controlling cathode erosion in arc jet thrusters, and (2) the studies of the anode attachment in arc jet thrusters. The cathode interaction studies consisted of (1) a continuation of some modeling work in which the previously derived model for the cathode heating was applied to some specific gases and electrode materials, and (2) experimental work in which various diagnostics was applied to the cathode. The specific diagnostics used were observation of the cathode tip during arcing using a Laser Strobe Video system in conjunction with a tele-microscope, a monochromator with an optical multichannel analyzer for the determination of the cathode temperature distribution, and various ex situ materials analysis methods. The emphasis of our effort was shifted to the cathode materials analysis because a parallel project was in place during the second half of 1993 with a visiting scientist pursuing arc electrode materials studies. As a consequence, the diagnostic investigations of the arc in front of the cathode had to be postponed to the first half of 1994, and we are presently preparing these measurements. The results of last year's study showed some unexpected effects influencing the cathode erosion behavior, such as increased erosion away from the cathode tip, and our understanding of these effects should improve our ability to control cathode erosion. The arc jet anode attachment studies concentrated on diagnostics of the instabilities in subsonic anode attachment arc jet thrusters, and were supplemental measurements to work which was performed by one of the authors who spent the summer as an intern at NASA Lewis Research Center. A summary of the results obtained during the internship are included because they formed an integral part of the study. Two tasks for 1994, the diagnostics of the anode closure phenomenon, and the use of arc jet thrusters for the deposition of c-BN, are being prepared. Author (revised)

N94-24308*# National Aeronautics and Space Administration. Lewis Research Center, Cleveland, OH.

SPATIAL FREQUENCY MULTIPLIER WITH ACTIVE LINEARLY TAPERED SLOT ANTENNA ARRAY

Rainee N. Simons (Sverdrup Technology, Inc., Brook Park, OH.) and Richard Q. Lee Feb. 1994 6 p Prepared for presentation at the IEEE MTT-S International Microwave Symposium, San Diego, CA, 23-28 May 1994; sponsored by IEEE
(Contract NAS3-25266; RTOP 506-44-2C)
(NASA-TM-106494; E-8060; NAS 1.15:106494) Avail: CASI HC A02/MF A01

A frequency multiplier with active linearly tapered slot antennas (LTSA's) has been demonstrated at the second harmonic frequency. In each antenna element, a GaAs monolithic microwave integrated circuit (MMIC) distributed amplifier is integrated with two LTSA's. The multiplier has a very wide bandwidth and large dynamic range. The fundamental-to-second harmonic conversion efficiency is 8.1 percent. The spatially combined second harmonic signal is 50 dB above the noise level. The design is suitable for constructing a large array using monolithic integration techniques. Author

N94-24457# National Inst. for Fusion Science, Nagoya (Japan).
A STUDY OF NON-IDEAL FOCUS PROPERTIES OF 30 DEG PARALLEL PLATE ENERGY ANALYZERS
A. Fujisawa, H. Iguchi, and Y. Hamada Dec. 1993 24 p
(NIFS-263) Avail: CASI HC A03/MF A01

A succinct model is proposed to describe non-ideal characteristics owing to electric field penetration into the drift region in actual parallel plate energy analyzers. A good agreement has been obtained between the theoretically expected and experimentally observed focus properties of the 30 degree parallel plate analyzer. Author

N94-24500# Los Alamos National Lab., NM.
COMPUTER MODELING OF PLASMA FLOW SWITCHES-HIGH CURRENT SWITCHING ON PROCYON
R. L. Bowers, A. E. Greene, D. L. Peterson, and N. F. Roderick (New Mexico Univ., Albuquerque.) 1993 13 p Presented at the 9th IEEE Pulsed Power Conference, Albuquerque, NM, 21-23 Jun. 1993
(Contract W-7405-eng-36)
(DE93-040189; LA-UR-93-3070; CONF-930616-38) Avail: CASI HC A03/MF A01

Procyon is a high explosive driven pulsed power system designed to drive plasma z-pinch experiments to the 1-MJ level. Details of this system are provided elsewhere in these proceedings. The final switching stage of the Procyon system is a plasma flow switch (PFS). Our most recent experiment (April 29, 1993) included a full power test of the PFS designed for the Procyon system. In this test the Mark IX explosively driven generator delivered 22 MA of current to the storage inductor. The slight flux compression that occurs in the explosively formed fuse (EFF) opening switch increased this current to 24.5 MA. The EFF then opened and switched 16.5 MA to the PFS. The PFS switched 15.5 MA to the load region (the slot that will contain an imploding foil liner in future experiments) with a 10-90 rise time of 500 ns. In this present paper we discuss the computer modeling we have done on this Procyon plasma flow switch. In the next section we discuss the design of the Procyon switch and preshot calculations. Although the April 1993 experiment was quite successful there were significant surprises in the performance of the PFS. In the last sections of this paper we discuss the work we have done in understanding the results of this experiment and the conclusions that we have reached to date. DOE

N94-24685# Naval Postgraduate School, Monterey, CA.
CROSSTALK ANALYSIS OF SYNCHRONOUS AND ASYNCHRONOUS OPTICAL CHIP INTERCONNECTS WITH DIRECT DETECTION M.S. Thesis
Rena M. Loesch Sep. 1993 96 p
(AD-A273261) Avail: CASI HC A05/MF A01

This thesis provides a crosstalk analysis of optical chip interconnects via single-mode waveguides with synchronous transmission and asynchronous transmission. This crosstalk model is general and can be used for any type of waveguide network. Three cases of laser sources will be considered: (1) each channel operates with an independent laser sources, (2) all laser sources have the same mean wavelength but with different phase noise processes, and (3) all laser sources are identical with the exception of the initial phases. The analysis takes into account the coupling-induced crosstalks between adjacent waveguides, the laser linewidth, the shot noise, the dark current generated by the photodiode, and the post-detection thermal noise. Bit error probabilities versus received peak powers are presented together with power penalties. DTIC

N94-24736 Department of the Navy, Washington, DC.
FIELD EMITTER ARRAY MEMORY DEVICE Patent
Henry F. Gray, inventor (to Navy) 27 Jul. 1993 7 p Filed 2 Jul. 1990
(AD-D016015; US-Patent-5,231,606; US-Patent-Appl-SN-546817; US-Patent-Class-365-225.6) Avail: US Patent and Trademark Office

A field emitter array memory device having two or more collector electrodes, an extraction electrode, at least one deflector electrode, and at least one electron field emitter is disclosed. The field emitter array memory circuit has bias voltages for collector electrodes, for at least one deflector electrode and for the extraction electrode. In a preferred embodiment of the invention, first and second input signal voltages selectively applied to first and second deflector electrodes selectively switch the flow of electrons emitted from an electron field emitter from a first collector electrode to a second collector electrode and vice versa. A latched memory output is also included. Electron flow from the electron field emitter to one of the first and second collector electrodes is maintained until a signal voltage is applied to a deflector electrode to cause the electron flow to deflect from one collector electrode to the other collector electrode. DTIC

N94-24748# Sandia National Labs., Albuquerque, NM.
CARBON SUPERCAPACITORS
F. M. Delnick 1993 14 p Presented at the Symposium on Science of Advanced Batteries, Cleveland, OH, 8-9 Nov. 1993
(Contract DE-AC04-94AL-85000)
(DE94-002652; SAND-93-2421C; CONF-9311115-1) Avail: CASI HC A03/MF A01

Carbon supercapacitors are represented as distributed RC networks with transmission line equivalent circuits. At low charge/discharge rates and low frequencies these networks approximate a simple series R(sub ESR)C circuit. The energy efficiency of the supercapacitor is limited by the voltage drop across the ESR. The pore structure of the carbon electrode defines the electrochemically active surface area which in turn establishes the volume specific capacitance of the carbon material. To date, the highest volume specific capacitance reported for a supercapacitor electrode is 220 F/cm(exp 3) in aqueous H2SO4 and approximately 60 F/cm(exp 3) in nonaqueous electrolyte. DOE

N94-24754*# Barnes Engineering Co., Shelton, CT.
WORST CASE ANALYSIS: EARTH SENSOR ASSEMBLY FOR THE TROPICAL RAINFALL MEASURING MISSION OBSERVATORY
Michael P. Conley Nov. 1993 132 p
(Contract NAS5-32463)
(NASA-CR-189320; NAS 1.26:189320; CDRL-12B) Avail: CASI HC A07/MF A02

This worst case analysis verifies that the TRMMESA electronic design is capable of maintaining performance requirements when subjected to worst case circuit conditions. The TRMMESA design is a proven heritage design and capable of withstanding the most worst case and adverse of circuit conditions. Changes made to the baseline DMSP design are relatively minor and do not adversely effect the worst case analysis of the TRMMESA electrical design. Author (revised)

N94-24818 Mission Research Corp., Newington, VA.
DESIGN AND TESTING OF UBITRON AMPLIFIER TUBES Final Technical Report
Dean Pershing Oct. 1993 199 p Limited Reproducibility: More than 20% of this document may be affected by microfiche quality
(Contract N00014-85-C-2141)
(AD-A273297; MRC/WDC-R-316) Avail: Issuing Activity (Defense Technical Information Center (DTIC))

The components for a single-stage/single-pass Ku band ubitron amplifier were designed, constructed, and tested. Notable features of this device include a high quality electron beam and circularly polarized microwave and wiggler fields. Stable operation of the assembled amplifier was achieved during initial testing using a modified SLAC klystron electron gun. In addition, amplifier and oscillator operation was measured using an unusual rippled beam parameter regime. The ubitron was only operated in the small signal regime; no large signal measurements (e.g. saturation) were attempted. In this regime, peak gains of 19 dB were measured with greater than 25% bandwidth. The general performance characteristics are in reasonable agreement with theoretical predictions, although there are discrepancies between the measured and theoretical gain vs. frequency profiles. More work is needed to determine whether this is a deficiency in the model or if operational characteristics are not adequately well known, e.g. details of the wiggler field profile. An investigation of ubitron amplifier performance limits, including performance enhancement through system parameter tapering, should be possible with operation at the design voltage using the advanced electron gun. DTIC

N94-24819# Engineering Societies Library, New York.
THE 5TH ENGINEERING FOUNDATION CONFERENCE: ADVANCED HETEROSTRUCTURE TRANSISTORS Final Report
Dec. 1992 22 p Conference held in Kona, HI, 29 Nov. - 4 Dec. 1992
(Contract N00014-93-1-0125)
(AD-A273508) Avail: CASI HC A03/MF A01

The session on Heterostructure FET's concentrated on power devices. L. Eastman of Cornell University reported 5 W at 4 GHz with 70% efficiency and 15 dB of gain from a GE device, and 1 W at 4 GHz with 80% efficiency from Raytheon. J. Wolter described avalanche breakdown via DX centers in AlGaAs, and theoretical optimization of deep submicron HFET's for power handling was reported by M. Das. Silicon-germanium HBT's have made several improvements. K. Ismail of Cairo University and IBM showed how the Si/SiGe band lineup can be changed by strain relief, producing barriers to electrons as well as holes. Very high mobilities were reported, and the claim was made that SiGe devices at 77 K may be operationally equivalent to III-V devices at room temperature. This would clearly be important given the fabrication advantages of silicon-based technologies. Silicon-germanium HBT technology seemed to be too complex to insert into digital processes, but SiGe FET's may not be. Resonant-tunneling diodes (RTD's) have been combined into potentially multigigahertz shift-register circuits by G. Sollner at MIT Lincoln Laboratory. R. Behringer of AT&T reported experiments in optically controlled patterned growth of Na gratings using a technique that may be applicable to imaging In or Ga atoms during MBE growth. The consequences of optical phonon propagation in AlGaAs structures were discussed experimentally by G. Maracas of Motorola and L. Eastman of Cornell, and theoretically by K. W. Kim of the University of North Carolina. Interesting effects occur because optical phonons in GaAs cannot propagate in AlAs and conversely. HBT papers from III-V materials dwelt on materials issues nad centered on carbon doping and its associated strain and activation. Derived from text

N94-24870*# Sverdrup Technology, Inc., Brook Park, OH.
COMPARATIVE M-H CHARACTERISTICS OF 1-5 AND 2-17 TYPE SAMARIUM-COBALT PERMANENT MAGNETS TO 300 C
Janis M. Niedra Mar. 1994 8 p
(Contract NAS3-25266; RTOP 583-02-21)
(NASA-CR-194440; E-8481; NAS 1.26:194440) Avail: CASI HC A02/MF A01

Recent consideration of the use of permanent magnets in space power converters at heat rejection temperatures exceeding 250 C and in miniature high temperature actuators is supporting a search for permanent magnets resistant to demagnetizing forces at high temperature. The present paper investigates the short-term demagnetization resistance to applied bucking fields and at temperatures up to 300 C of SmCo5 type magnets, in the form of 1-cm cubes, from several commercial sources. Quasistatic, 2nd quadrant M-H data taken at selected temperatures are the source of derived plots which are then compared to similar data for previously tested Sm2Co17 type magnets. The 1-5 magnet remanence tends to be about 1.5 kG below that of the 2-17 magnets throughout the temperature range. However, the intrinsic coercivities and M-H curve 'knee-fields' seen in particular 1-5 magnets were considerably above those seen previously in the 2-17 magnets. This superior resistance to demagnetizing fields attainable in 1-5 magnets is also illustrated by safe operating area plots based on the knee-field, the magnetic induction swing and temperature. Comments are made on the possibility that a remanence versus knee-field tradeoff can make 1-5 material competitive with 2-17 in applications where a magnet has to withstand large bucking fields at high temperature. Author (revised)

N94-25035 Department of the Navy, Washington, DC.
METHOD FOR FABRICATING SELF-ALIGNED GATE DIFFUSED JUNCTION FIELD EFFECT TRANSISTOR Patent
Richard Nguyen, inventor (to Navy) and Charles A. Hewett, inventor (to Navy) 28 Sep. 1993 7 p Filed 28 Aug. 1992
(AD-D015975; US-Patent-5,248,626; US-Patent-Appl-SN-937916) Avail: US Patent and Trademark Office

A method for fabricating a self-aligned, gate diffused junction field effect transistor is provided which includes the steps of forming an n-type layer on an indium phosphide, semi-insulating substrate; forming spaced apart source/drain metal contacts on the n-type layer; forming a metal gate on the n-type layer between the spaced apart source/drain contacts, where the metal gate is insulated from the source/drain contacts and includes a metallic p-type dopant material; and forming a p-type region in the n-type layer beneath the metal gate so that the gate contact and the p-type region have coincident boundaries with respect to each other at the surface of the n-type layer. The method may also be employed to manufacture a bipolar transistor by allowing the self-aligned and diffused p-type region to extend through the n-type layer to the semi-insulating substrate. DTIC

N94-25036 Department of the Navy, Washington, DC.
LASER ENERGIZED HIGH VOLTAGE DIRECT CURRENT POWER SUPPLY Patent
Larry D. Flesner, inventor (to Navy) and Wadad B. Dubbelday, inventor (to Navy) 28 Sep. 1993 14 p Filed 31 Jul. 1991
(AD-D015977; US-Patent-5,248,931; US-Patent-Appl-SN-745045; US-Patent-Class-322-2R) Avail: US Patent and Trademark Office

A light energized high voltage direct current power supply comprises a light source including solid-state laser diodes powered by electrical current at a voltage level, V(sub 1), for generating light; a photocell array positioned to receive the light and fabricated with silicon-on-sapphire for providing electrical power having an output voltage V(sub 2), where V(sub 2) is greater than V(sub 1), where the photocell array includes serially connected photovoltaic cells; and a voltage regulator operably coupled to the light source and the photocell array for controlling the output of the power supply to a predetermined voltage level. DTIC

N94-25039 Department of the Navy, Washington, DC.
SOLID STATE TIME BASE CORRECTOR (TBC) Patent
John L. Piri, inventor (to Navy) and Marc L. Moulton, inventor (to Navy) 3 Aug. 1993 18 p Filed 10 Apr. 1985
(AD-D015981; US-Patent-5,233,420; US-Patent-Appl-SN-721821; US-Patent-Class-358-149) Avail: US Patent and Trademark Office

Synchronization of remotely originating video signals to a standardized frequency is assured on a field-by-field basis. The video signals are digitized, multiplexed, and stored in fields in accordance with their horizontal and vertical sync signals. A reading out of storage, demultiplexing, and reconversion to video signals at the standardized frequency on a field-by-field basis allows a real time presentation to standard equipments at a standardize rates. DTIC

N94-25042 Department of the Navy, Washington, DC.
BRIDGE TYPE OPTOELECTRONIC SAMPLE AND HOLD CIRCUIT Patent
Chen-Kuo Sun, inventor (to Navy), Chao-C. Wu, inventor (to Navy), Ching-T. Chang, inventor (to Navy), Lai Paul K. Yu, inventor (to Navy), and William H. McKnight, inventor (to Navy) 24 Aug. 1993 10 p Filed 31 Dec. 1990
(AD-D015986; US-Patent-5,239,181; US-Patent-Appl-SN-636808; US-Patent-Class-250-551) Avail: US Patent and Trademark Office

A novel bridge type optoelectronic (OE) sample and hold circuit based upon current steering demonstrates a clear superiority in performance with respect to a direct OE sample and hold circuit. The bridge type OE sample and hold circuit permits a high-speed signal to be sampled with high accuracy to offer high charging capability, commanding signal isolation, reduced time jitter and reduced holding charge leakage which are distinct advantages over conventional electronic sample and hold circuits. DTIC

N94-25050 Department of the Navy, Washington, DC.
MOS ANALOG MEMORY WITH INJECTION CAPACITORS Patent
Randy L. Shimabukuro, inventor (to Navy), Michael E. Steward, inventor (to Navy), Patrick A. Shoemaker, inventor (to Navy), and Graham A. Garcia, inventor (to Navy) 12 Oct. 1993 15 p Filed 9 Jan. 1991
(AD-D015990; US-Patent-5,253,196; US-Patent-Appl-SN-639500; US-Patent-Class-365-45) Avail: US Patent and Trademark Office

An integrated circuit memory element is capable of storing analog information. The memory value can be increased and decreased incrementally with no knowledge of the current state and may be stored for a long period of time. Analog memory information is stored as an electrical charge on a floating gate structure and modification of this information is accomplished by the use of hot-carrier injection to transport electrons off of as well as onto the floating gate (to erase as well as to program electrically). Charge is written onto and off of the gate by injection capacitors in deep depletion and is accomplished by having the floating gate contiguous with a piece of crystalline p-type silicon, in which a deep-depletion region may be formed so that hot electrons may be ejected from (ejected off of) the floating gate structure through the surrounding insulating oxide, and having the floating gate structure capacitively coupled to a second piece of crystalline silicon from which electrons may be injected onto the floating gate structure. The novelty of the invention resides in the utilization of avalanche injection of electrons onto and off of the floating gate using injection capacitors. This requires far less current and is more symmetric than the original dual polarity MOS analog memory devices of the prior art. DTIC

N94-25083# Technische Univ., Eindhoven (Netherlands). Electronic Design Group.
PLANET: A HIERARCHICAL NETWORK SIMULATOR Ph.D. Thesis
Thomas Andreas Maria Kevenaar 1993 143 p
(Contract IC-EEL-88.036)
(ISBN-9-09-005693-9; ETN-94-95328) Copyright Avail: CASI HC A07/MF A02

A Piecewise Linear (PL) network simulator called PLANET that can be used in a hierarchical design environment is presented. The most important descriptions of PL functions are compared. A method for generating a PL model automatically for an arbitrary combinatorial logic function is developed. Almost every aspect of the simulator is treated. A numerical integration method that fits in with the hierarchical structure of the simulation tree is given. The simulator is extended by a network description compiler to furnish it with a flexible interface which is almost mandatory if the simulator must be interfaced with an automatic synthesis unit. This is explained by describing a coupling with the synthesis tool. Some simulation examples are given. ESA

N94-25170*# National Aeronautics and Space Administration. Lewis Research Center, Cleveland, OH.
TEMPERATURE DEPENDENT PERFORMANCE OF COPLANAR WAVEGUIDE (CPW) ON SUBSTRATES OF VARIOUS MATERIALS
Susan R. Taub and Paul Young (Toledo Univ., OH.) Feb. 1994 5 p
Proposed for presentation at the MTT-S International Microwave Symposium, San Diego, CA, 23-28 May 1994; sponsored by IEEE
(RTOP 235-01-08)
(NASA-TM-106505; E-8583; NAS 1.15:106505) Avail: CASI HC A01/MF A01

The attenuation (a) and effective dielectric constant (E(sub eff)) of Coplanar Waveguide (CPW) transmission lines on high-resistivity silicon and diamond substrates as a function of both temperature and frequency are presented. The technique used to obtain the values for a and E(sub eff) involves the use of a unique cryogenic probe station designed and built by NASA. Attenuation of gold CPW lines on diamond substrates is compared with that of superconducting CPW lines. Author (revised)

N94-25253 Technische Univ., Delft (Netherlands).
ON THE CHARACTERIZATION AND OPTIMIZATION OF HIGH-SPEED SILICON BIPOLAR TRANSISTORS Ph.D. Thesis
Paul Jacques vanWijnen 1992 272 p Prepared in cooperation with Philips Research Labs.-Signetics, Sunnyvale, CA, and Philips Gloeilampenfabrieken N.V., Eindhoven, Netherlands Limited Reproducibility: More than 20% of this document may be affected by microfiche quality
(ETN-94-95367) Copyright Avail: CASI HC A12

An on wafer high frequency measurement technique and its application to accurate small signal characterization and optimization of high speed bipolar transistors is presented. The evolution of high speed bipolar transistors and the need for accurate tools for device characterization, device modeling and parameter extraction, and device optimization are discussed. An introduction of small signal analysis and two port parameters is given. The scattering or s parameters and their relationships to the more conventional z, y, h, g, a and b Kirchhoff based two port parameter sets are derived. The custom high frequency small signal measurement setup, assembled from commercially available components, is described. The basic measurement methodology developed in order to account for these errors in a consistent manner is discussed. In particular, how this general methodology can be specialized to apply to on wafer measurements, is also discussed. High frequency characterization of small geometry bipolar transistors up to 18 GHz at various bias conditions is discussed. The device optimization is studied in the context of improving the high frequency performance. The use of a localized collector implant to improve the performance of polysilicon transistors is considered. ESA

N94-25276# ETREMA Products, Inc., Ames, IA.
IMPROVED MAGNETOSTRICTIVE TRANSDUCER DRIVE ELEMENTS ACHIEVED BY REDUCTION OF CRYSTALLINE DEFECTS AND IMPROVED CRYSTALLINE ORIENTATION Final Report
Dale McMasters 29 Oct. 1993 25 p
(Contract N00014-92-C-0210)
(AD-A273391) Avail: CASI HC A03/MF A01

The discovery of the 'giant' magnetostrictive rare earth-iron alloys in the 1970's was a direct result of the efforts initiated at DOD's Naval Surface Warfare Center (NSWC), Silver Spring, MD in conjunction with DOE's Ames Laboratory (AL), Ames, IA. This research into these new materials was specifically targeted for the development of low frequency, high power transducers for underwater sonar systems. The most technologically advanced of these materials is TERFENOL-D, Tb(3)Dy(7)Fe(1.9-1.95) an intermetallic compound consisting of iron (Fe) and the rare earth metals terbium (Tb), and dysprosium (Dy). Because of the advantages over existing transducer materials, the use of TERFENOL-D as a transducer drive element is expanding into a broad range of commercial applications and advanced defense systems. One of the disadvantages is the cost of these drivers, primarily due to the terbium and dysprosium raw materials. DTIC

N94-25286# Technische Univ., Delft (Netherlands). Delft Inst. of Microelectronics and Submicron Technology.
MESOSCOPIC PHENOMENA IN METALLIC POINT CONTACTS Ph.D. Thesis
Philippus Antonius M Holweg 1992 143 p Sponsored by Stichting voor Fundamenteel Onderzoek der Materie, Netherlands
(ETN-94-95371) Avail: CASI HC A07/MF A02

Electron transport studies on microfabricated metallic point contacts, ultrasmall devices with a typical size of 10 nm, are described. Point contacts, consisting of a very small bridge between two metal films, were fabricated with a typical diameter of 10 nm. By varying the purity of the metal applied in these point contacts, the constriction diameter is much smaller than the elastic and inelastic electron mean free path (ballistic transport) or comparable to the elastic mean free path (quasi ballistic transport). Two new phenomena were observed in the ballistic point contacts. These are two level fluctuations of the conductance as a function of time, and time independent aperiodic fluctuations of the conductance as a function of voltage and magnetic field. These are both sample specific, mesoscopic phenomena, because they are very sensitive to the precise location of defects around the constriction. ESA

N94-25319# Sheffield Univ. (England). Dept. of Automatic Control and Systems Engineering.
ADAPTIVE NOISE CANCELLATION USING RECURRENT RADIAL BASIS FUNCTION NETWORKS
S. A. Billings and C. F. Fung Mar. 1993 35 p
(RR-472; ETN-94-95139) Avail: CASI HC A03/MF A01

The design of nonlinear Far Infrared (FIR) and Imaging Infrared (IIR) noise cancellation filters is discussed. Radial basis function neural network architectures are introduced. It is shown that by exploiting the duality with system identification that the nonlinear IIR filter can be configured as a recurrent radial basis function network. The network training, the inclusion of linear dynamic network links, and the metrics for performance monitoring are discussed. Examples to demonstrate the degree of noise suppression that can be achieved based on the new design are included. ESA

N94-25421# Ecole Centrale de Lyon (France). Lab. d'Electrotechnique.
CONTRIBUTION TO THE STUDY OF HF CONVERTERS RADIATED DISTURBANCES Ph.D. Thesis [CONTRIBUTION A L'ETUDE DES PERTURBATIONS RAYONNEES PAR LES CONVERTISSEURS H.F.]
Antoine Puzo 1992 213 p In FRENCH
(ECL-92-34; ETN-94-95200) Avail: CASI HC A10/MF A03

The perturbations originated from switching on or off circuits which make up converters are investigated. In order to study and quantify the phenomena resulting from the ways radiated interferences are generated, the study centered on the switching circuits which represent the main switching modes: the forced switching, the zero current switching and the zero voltage switching. The evolution of the radiated electric and magnetic fields were determined. These fields were calculated from the voltage and the current produced in the different loops of the converter device. The importance of the parasitic components which constitute the active and the passive elements, as well as the wiring, on creating and transmitting the radiated interferences was stressed. This analysis was made from a theoretical study and was validated by a numerical simulation. The bases for the simulation of conducted and radiated perturbations were established. The study of the mechanics used for the transmission of radiated interference was performed by modifying the electric and topological quantities of the static converters used. ESA

N94-25457 Max-Planck-Inst. fuer Physik und Astrophysik, Garching (Germany). Werner-Heisenberg-Inst.

CsI(Tl)-PHOTODIODE DETECTORS FOR SPECTROSCOPY AT LOW RADIATION LEVELS

Rainer Kotthaus Oct. 1992 21 p Submitted for publication Limited Reproducibility: More than 20% of this document may be affected by microfiche quality

(MPI-PhE/92-22; ETN-94-95113) Copyright Avail: CASI HC A03

Some aspects of CsI(Tl) photodiode detectors relevant for applications in low level radiation spectroscopy in the MeV energy range are studied. The attention is focused on a search for the lepton number violating neutrinoless double beta decay of Mo-100. Energy resolutions of slightly less than 100 keV, limited by electronic noise, were obtained for crystal masses up to more than 3 kg. The improved energy resolution facilitates a sensitive investigation of crystal contaminations with nuclides of the Th and U chains by spectroscopic analysis of alpha decays. The cleanest crystal was free of U and Th contaminations at the detection limit of 0.27 alpha decays per kg and per hour, a radiopurity satisfactory for applications in low level spectroscopy. ESA

N94-25460 Institut Franco-Allemand de Recherches, Saint-Louis (France).

STUDY OF A SYSTEM FOR PRODUCING A PULSED MAGNETIC FIELD (B 2T) WITH A FREQUENCY OF 50 Hz [ETUDE D'UN SYSTEME PRODUISANT UN CHAMP MAGNETIQUE PULSE (B 2T) AVEC UNE FREQUENCE DE 50 HZ]

P. Lehmann and G. Buderer 7 Feb. 1992 24 p In FRENCH Limited Reproducibility: More than 20% of this document may be affected by microfiche quality

(ISL-N-601/92; ETN-94-95116) Avail: CASI HC A03

An electromagnetic circuit and a synchronized switch designed to generate a 2 T magnetic field are described. The aim was to produce the 2 T magnetic field with a frequency of 50 Hz in 25 microseconds. The equations characterizing several axially symmetric magnetic coils are given. The electric circuit of a magnet of eleven spirals and containing two silver coils is described. It is shown that a 2 T magnetic field can be obtained at the coil's axis by using a 1382 micro-F capacitor, a 36 milli-ohms resistance, and applying 220 V. The proposed system requires a 10 cu cm/s water flow for cooling the coil during the time gap between two pulses. ESA

N94-25488# Martin Marietta Labs., Baltimore, MD.

COLLOCATED TUNABLE WAVENUMBER SENSOR/ACTUATORS FOR SMART STRUCTURES Report, 1-30 Nov. 1993

K. Bridger and L. Jones 6 Dec. 1993 5 p

(Contract N00014-92-C-0214)

(AD-A273697; MML-TM-93-25) Avail: CASI HC A01/MF A01

The third actuator module is currently in burnout. The volume fraction of binder/plasticizer in the tape was reduced from 43% to 41% and the tape still laminated well. Decreasing the binder content decreases the chance of flaws appearing during burnout. The burnout schedule has also been extended. It is felt that with these modifications and planned changes in the sintering schedule this actuator module should be acceptable. DTIC

N94-25539# Air Force Inst. of Tech., Wright-Patterson AFB, OH.

SHIELDED COIL ELECTRODYNAMIC PROPULSION (SCEP). A FEASIBILITY STUDY M.S. Thesis

Richard J. Ladouceur Dec. 1993 112 p

(AD-A273824; AFIT/GSO/ENY/93D-6) Avail: CASI HC A06/MF A02

This study investigated Shielded Coil Electrodynamic Propulsion (SCEP). The use of the earth's magnetic field as a propulsion source has been previously investigated. It was found that a significant amount of power and long conductors were required. A more compact propulsion concept which requires significantly less power is proposed. This concept relies on the feasibility of significantly reducing the magnetic force induced by the earth's magnetic field on selected segments of a coil. An experiment design to support the theoretical findings was conducted. The experiment results support the theoretical model. DTIC

N94-22747*# Bristol Univ. (England). Centre for Communications Research.

BROADBAND LINEARISATION OF HIGH-EFFICIENCY POWER AMPLIFIERS

Peter B. Kenington, Kieran J. Parsons, and David W. Bennett *In* JPL, Proceedings of the Third International Mobile Satellite Conference (IMSC 1993) 1993 p 59-64 Sponsored in part by Northern Telecom Canada Ltd. (For primary document see N94-22735 06-32)

Avail: CASI HC A02/MF A06

N94-22756*# Ecole Polytechnique Federale de Lausanne (Switzerland). Telecommunications Lab.

POWER ATTENUATION CHARACTERISTICS AS SWITCH-OVER CRITERION IN PERSONAL SATELLITE MOBILE COMMUNICATIONS

Jonathan P. Castro *In* JPL, Proceedings of the Third International Mobile Satellite Conference (IMSC 1993) 1993 p 113-118 (For primary document see N94-22735 06-32)

Avail: CASI HC A02/MF A06

N94-23239*# Michigan Univ., Ann Arbor. Dept. of Electrical Engineering.

REDUCED COST ALTERNATIVES TO PREMISE WIRING USING ATM AND MICROCELLULAR TECHNOLOGIES

Raghvendra R. Gejji *In* NASA. Kennedy Space Center, NASA/ASEE Summer Faculty Fellowship Program Oct. 1993 p 195-227 (For primary document see N94-23230 06-80)

Avail: CASI HC A03/MF A04

N94-23262*# Jet Propulsion Lab., California Inst. of Tech., Pasadena. Radio Frequency and Microwave Subsystems Section.

CRYOGENIC, LOW-NOISE HIGH ELECTRON MOBILITY TRANSISTOR AMPLIFIERS FOR THE DEEP SPACE NETWORK

J. J. Bautista *In its* The Telecommunications and Data Acquisition Report 15 Nov. 1993 p 65-80 (For primary document see N94-23256 06-32)

(RTOP 310-20-66-09-01)

Avail: CASI HC A03/MF A02

N94-23401* National Aeronautics and Space Administration. Lewis Research Center, Cleveland, OH.

ELECTRICAL POWER TECHNOLOGY FOR ROBOTIC PLANETARY ROVERS

C. P. Bankston (Jet Propulsion Lab., California Inst. of Tech., Pasadena.), M. Shirbacheh (Jet Propulsion Lab., California Inst. of Tech., Pasadena.), D. J. Bents, and J. M. Bozek *In* CNES, Missions, Technologies, and Design of Planetary Mobile Vehicles Jan. 1993 p 327-336 (For primary document see N94-23373 06-91)

Copyright Avail: Issuing Activity (CEPADUES-Editions, 111, rue Nicolas-Vaquelin, 31100 Toulouse, France)

N94-23409 Air Force Test Pilot School, Edwards AFB, CA.

CARBON MONOXIDE FUEL CELLS AS A SOURCE FOR MARS ROVER ELECTRIC POWER

Mitchell Burnside Clapp *In* CNES, Missions, Technologies, and Design of Planetary Mobile Vehicles Jan. 1993 p 405-409 (For primary document see N94-23373 06-91)

Copyright Avail: Issuing Activity (CEPADUES-Editions, 111, rue Nicolas-Vaquelin, 31100 Toulouse, France)

N94-23989# ETEL S.A., Motiers (Switzerland).
LOW NOISE ELECTRIC MOTOR
E. Favre, M. Correvon, and M. A. P. Verain (European Space Agency. European Space Research and Technology Center, ESTEC, Noordwijk, Netherlands.) *In* ESA, The Fifth European Space Mechanisms and Tribology Symposium Apr. 1993 7 p (For primary document see N94-23985 06-37)
(Contract ESTEC-9239/90/NL/PP)
Copyright Avail: CASI HC A02/MF A04

N94-24036# ETEL S.A., Motiers (Switzerland).
SENSORLESS, BRUSHLESS MOTOR TO DRIVE A SEALED FREON-AMMONIA PUMP
N. Wavre *In* ESA, The Fifth European Space Mechanisms and Tribology Symposium Apr. 1993 5 p (For primary document see N94-23985 06-37)
Copyright Avail: CASI HC A01/MF A04

N94-24037# ETEL S.A., Motiers (Switzerland).
DESIGN AND PERFORMANCES OF ELECTROMAGNETIC INITIATORS FOR SPACE MECHANISMS: AN ALTERNATIVE TO PYROTECHNIC SYSTEM
N. Wavre *In* ESA, The Fifth European Space Mechanisms and Tribology Symposium Apr. 1993 4 p (For primary document see N94-23985 06-37)
Copyright Avail: CASI HC A01/MF A04

N94-24411*# Alabama Univ., Huntsville. Dept. of Civil and Environmental Engineering.
FINITE ELEMENT BASED ELECTRIC MOTOR DESIGN OPTIMIZATION
C. Warren Campbell *In its* The 1993 NASA/ASEE Summer Faculty Fellowship Program Nov. 1993 5 p (For primary document see N94-24405 06-80)
Avail: CASI HC A01/MF A03

34 FLUID MECHANICS AND HEAT TRANSFER

Includes boundary layers; hydrodynamics; fluidics; mass transfer; and ablation cooling.

For related information see also *02 Aerodynamics* and *77 Thermodynamics and Statistical Physics.*

N94-22713# Universiteit Twente, Enschede (Netherlands). Faculty of Applied Mathematics.
A MULTIGRID MULTIBLOCK SOLVER FOR COMPRESSIBLE TURBULENT FLOW
Hans G. M. Kuerten and Bernard J. Geurts Mar. 1993 16 p
(MEMO-1125; ETN-94-94761) Avail: CASI HC A03/MF A01

A multigrid multiblock method for compressible turbulent flow simulations is described and results obtained from calculations on a two element airfoil are presented. A vertex based spatial discretization method and explicit multistage Runge-Kutta time stepping are used. The slow convergence of a single grid method makes the multigrid method, which yields a speed up with a factor of about 12.5, indispensable. The numerical predictions are in good agreement with experimental results. The convergence of the multigrid process is shown to depend considerably on the ordering of the various loops. If the block loop is put inside the stage loop, the process converges more rapidly than if the block loop is situated outside the stage loop in the case where a three stage Runge-Kutta method is used. If a five stage scheme is used, the process does not converge in the latter block ordering. The process based on the five stage method is about 60% more efficient than with the three stage method.
ESA

N94-22852# Technische Univ., Berlin (Germany). Inst. fuer Luft- und Raumfahrt.
EXPERIMENTAL METHODS IN SEPARATED FLOWS [EXPERIMENTELLE METHODEN IN ABGELOESTEN STROEMUNGEN]
W. Nitsche, ed. 1991 87 p In ENGLISH and GERMAN Presented at 4th Workshop DFG-Schwerpunkt: Physik Abgeloester Stroemungen, Berlin, Germany, 1 Mar. 1991
(ILR-Mitt-260(1991); ETN-94-95077) Avail: CASI HC A05/MF A01

In the framework of the physics of separated flows, some strategies of experimental methodologies are presented. The following topics are included: turbulence meters for separated flows; current capabilities and future requirements; measurement of kinematically unsteady separated flows; pressure oscillation measurements in turbulent flows; SFOLDA (Semiconductor Fiber Optic Laser Doppler Anemometer) anemometry for measurements in complex flows; use of near wall hot wire probes for time resolved skin friction measurements; image processing for acquisition of fluid rest time in the running of an artificial heart valve; turbulent separated flow above an obstacle in an open channel and a method for recognition of frequency cells in a flow around a cylinder, taking into account wall effects. For individual titles, see N94-22853 through N94-22860.

N94-22853# Siegen Univ., (Germany). Inst. fuer Fluid- und Thermodynamik.
TURBULENCE SENSORS FOR SEPARATED FLOWS: CURRENT CAPABILITIES, FUTURE REQUIREMENTS [TURBULENZSENSORIK FUER ABGELOESTE STROEMUNGEN: GEGENWAERTIGER LEISTUNGSSTAND - KUENFTIGE ANFORDERUNGEN]
A. Leder and D. Geropp *In* Tech. Univ. Berlin, Experimental Methods in Separated Flows 1991 p 1-14 In GERMAN (For primary document see N94-22852 06-34)
Avail: CASI HC A03/MF A01

Turbulent flow fields are studied with emphasis on calculation of oscillation terms. Two methods of computation of Reynolds stresses, based on the Boussinesq approximation or the transport equations, are presented. The model of Launder-Spalding was used for calculation of turbulent energy and dissipation rate. Experimental procedures, based on laser Doppler measurements, are proposed for both methods. An experimental facility for estimation of turbulent energy is described. A two channel argon laser Doppler system was used with two photomultipliers for converting optical signals into electrical ones. After an electronic frequency shift of both photomultiplier signals, an amplification and a band pass filtration, the Doppler bursts were processed by two counters and a coincidence filtering was carried out in a buffer interface with both signals. The coupling of the laser Doppler anemometer facility to the oscillating flow process was achieved using a phase detector made of a hot wire anemometer and a filter for the analog signal.
ESA

N94-22854# Technische Hochschule, Aachen (Germany). Inst. fuer Strahlantriebe und Turboarbeitsmaschinen.
MEASUREMENT OF KINEMATICALLY UNSTATIONARY SEPARATED FLOWS [VERMESSUNG DER KINEMATIK INSTATIONAER ABGELOESTER STROEMUNGEN]
C. A. Poensgen and H. E. Gallus *In* Tech. Univ. Berlin, Experimental Methods in Separated Flows 1991 p 15-29 In GERMAN (For primary document see N94-22852 06-34)
Avail: CASI HC A03/MF A01

The development of flow separation between the hub wall and the blade suction side in an axial compressor annular cascade is examined with several measurement techniques. The flow was first assumed to be stationary; separation could be estimated with flow visualization and pneumatic pressure measurements on lateral walls and blade surfaces were carried out for evaluating flow losses in the cascade. Measurements at airfoil surfaces with hot wire probes and hot film sensors gave information about the development of the blade boundary layer. The influence of the unstationary flow on the development of airfoil boundary layers and the separation at the hub with dependence of the aerodynamic loading is studied. Cylindrical bars were used instead of a real blading in order to obtain typical wakes without potential interactions between rotor and stator. Experimental examinations similar to the one described for the steady flow were carried out. It is found that flow losses increase in the airfoil boundary layer while they drop to the hub separation. By and large, the total losses are found to be lower with unsteady flow.
ESA

N94-22855# Technische Univ., Berlin (Germany). Inst. fuer Luft- und Raumfahrt.

PRESSURE OSCILLATION MEASUREMENTS IN TURBULENT FLOWS [DRUCKSCHWANKUNGSMESSUNGEN IN TURBULENTEN STROEMUNGEN]

M. Nasseri and W. Nitsche *In its* Experimental Methods in Separated Flows 1991 p 30-43 In GERMAN (For primary document see N94-22852 06-34)

Avail: CASI HC A03/MF A01

Rotation symmetric internal flows with and without separation, which occur by variation of the aperture angle of a diffusor, are investigated. A probe for time and spatial measurements in turbulent flows was developed for estimating the pressure diffusion term in the equation of the k-epsilon turbulence model and for testing a gradient diffusion model for the transport of kinetic turbulent energy. For velocity measurement, a hot wire technique was chosen; for measuring the total pressure a sensor was mounted behind the hot wire. The conversion of the pressure signal into an electrical one was based on an electrical variometer and pressure proportional sensors, which allow the total pressure to be converted in a velocity and to be measured with a miniaturized hot wire; this process was chosen for simultaneous measurements of pressure and velocity oscillations. A miniaturized pressure chamber, in which a microphone and the pressure probe were parallel mounted, was used for estimating the frequency behavior of the pressure probe. An examination in the relaxation area of a 6 deg diffusor shows that the measuring instrumentation allows static pressure oscillations to be obtained and correlated with the velocity. ESA

N94-22856# Erlangen-Nuremberg Univ. (Germany). Lehrstuhl fuer Stroemungsmechanik.

SFOLDA: A SEMICONDUCTOR LDA FOR MEASUREMENTS IN COMPLEX FLOWS [SFOLDA: EIN HALBLEITER-LDA FUER MESSUNGEN IN KOMPLEXEN STROEMUNGEN]

M. Stieglmeier and C. Tropea *In* Tech. Univ. Berlin, Experimental Methods in Separated Flows 1991 p 44-51 In GERMAN (For primary document see N94-22852 06-34)

Avail: CASI HC A02/MF A01

The SFOLDA (Semiconductor Fiber Optic Laser Doppler Anemometer) is described and some application examples are presented. The system uses a temperature controlled diode laser head, a collimator lens system for beam diameter reduction, and an optical isolator based on the Faraday principle for suppression of optical feedback on the laser diode. A first system in which a Bragg cell simultaneously plays the role of beam separator and frequency shift unit allows weakly or strongly turbulent flows to be examined. In a second system with variable frequency shift, an optimal adaption of signal frequency to the signal processor is possible. In both systems, both beams are decoupled and focused in measure volume after beam amplification; the diffused light is detected above the emission lens and focused on a receptive fiber which drives the optical signal to an avalanche photodiode. The following examinations were carried out: boundary layer investigation in running trains; velocity measurements in fired combustion engine; and flow examination in a T shaped tube branch. The flexible, compact, and robust system is found to be particularly fitted to the study of flows with special boundary conditions. ESA

N94-22857# Technische Univ., Berlin (Germany). Hermann-Foettinger-Inst. fuer Thermo- und Fluiddynamik.

THE USE OF NEAR-WALL HOT-WIRE PROBES FOR TIME-RESOLVED SKIN-FRICTION MEASUREMENTS

Peter M. Wagner *In its* Experimental Methods in Separated Flows 1991 p 52-58 Submitted for publication (For primary document see N94-22852 06-34)

Avail: CASI HC A02/MF A01

The mean and fluctuating wall shear stress in turbulent air flows were measured. Hot wires were mounted at a fixed small distance from the wall and connected to a constant temperature anemometer and were operated at an overheat ratio of 35%. The mean skin friction was measured by a Preston tube. The pressure was determined using a digital micromanometer, directly read by a microcomputer. A calibration procedure was developed and the distortion of the probability density distribution due to the calibration curve nonlinearity was corrected. Experimental results in a flat plate boundary layer were obtained and compared to pulsed wire measurements. ESA

N94-22858# Technische Univ., Berlin (Germany).

IMAGE PROCESSING FOR ACQUISITION OF FLUID REST TIME IN THE RUNNING OF AN ARTIFICIAL HEART VALVE [BILDVERARBEITUNG ZUR ERFASSUNG DER VERWEILZEITEN DES FLUIDS IM NACHLAUF EINER KUENSTLICHEN HERZKLAPPE]

K. Affeld, K. Schichl, A. Ziemann, and M. Freydefont (Ecole Polytechnique, Paris, France.) *In* Tech. Univ. Berlin, Experimental Methods in Separated Flows 1991 p 59-66 (For primary document see N94-22852 06-34)

Avail: CASI HC A02/MF A01

The blood flow separation which plays an important role in thrombosis formation is examined. A fluorescent coloring was homogeneously mixed with the water volume behind the valve in the aorta root for modeling blood platelets; a longitudinal circulating coloring cloud corresponds to a beginning of thrombosis while the water depicts the fresh blood. Coloring concentration was varied and these lightness changes were examined with a video system so that the gray values were quantified and their time dependence evaluated. The mean value was calculated and the concentration was established as an exponential function of time. The results show the thrombosis risk due to artificial heart valves. ESA

N94-22859# Karlsruhe Univ. (Germany).

TURBULENT SEPARATED FLOWS ABOVE AN OBSTACLE IN AN OPEN CHANNEL [TURBULENTE ABGELOSTE STROMUNG UBER GRUNDSCHWELLEN IN EINEM OFFENEN GERINNE]

T. Loy, R. Friedrich, and U. Kertzscher *In* Tech. Univ. Berlin, Experimental Methods in Separated Flows 1991 p 67-76 (For primary document see N94-22852 06-34)

Avail: CASI HC A02/MF A01

The two dimensional, subcritical flow above several obstacles placed in an open rectangular channel is investigated. A resistance thermometer was used for temperature measurement and a laser Doppler anemometer for velocity measurement in the viscous sublayer. The separation and spreading behavior of the turbulence produced in the shear layer was experimentally estimated with dependence on obstacle geometry, cross flow, and water depth. Some comparative measurements in a two layer flow were carried out. Turbulence isolines which show that the turbulent transverse exchange increases with flatness of obstacles were obtained. The normed streamline function was deduced from measured profiles of mean velocity, through integration on the water depth; the calculations show that separation area length and height increase with obstacle flatness. ESA

N94-22860# Goettingen Univ. (Germany). Inst. fuer Angewandte Mechanik und Stroemungsphysik.

A METHOD FOR RECOGNITION OF FREQUENCY CELLS IN A CYLINDER FLOW INFLUENCED BY WALL EFFECTS [EINE METHODE ZUR ERKENNUNG VON FREQUENZZELLEN IM VON RANDEFFEKTEN BEEINFLUSSTEN ZYLINDERNACHLAUF]

H. Eisenlohr, M. Koenig, and H. Eckelmann *In* Tech. Univ. Berlin, Experimental Methods in Separated Flows 1991 p 77-84 (For primary document see N94-22852 06-34)

Avail: CASI HC A02/MF A01

The flow around a cylinder too short to be considered as an infinite body is investigated with particular emphasis on the frequency of vortex separation from the cylinder. The time signal of a hot wire anemometer was evaluated in order to know the frequency as a function of time, in some areas where vortex branchings are observed and the spectrum shows two maxima at a node. A system with a voltage controlled oscillator, frequency modulation demodulators mounted on a chip and some phase comparators was used in order to obtain a phase locked loop. The Tritton spring, which is a discontinuity in the representation of Strouhal number as a function of Reynolds number and is considered as a boundary effect, is ascertained with the measurements. ESA

N94-22870# Los Alamos National Lab., NM.

NONLOCAL MODELS IN CONTINUUM MECHANICS

N. L. Johnson and N. Phan-Thien (Sydney Univ., Australia.) 1993 15 p Presented at the Annual Winter Meeting of the American Society of Mechanical Engineers, New Orleans, LA, 28 Nov. - 3 Dec. 1993

(Contract W-7405-eng-36)

(DE93-040146; LA-UR-93-3124; CONF-931121-21) Avail: CASI HC A03/MF A01

The recent appearance of nonlocal methods is examined in the light of traditional continuum mechanics. A comparison of nonlocal approaches in the fields of solid and fluid mechanics reveals that no consistent definition of a nonlocal theory has been used. A definition based on the violation of the principle of local action in continuum mechanics was suggested. From the consideration of the implications of a nonlocal theory based on this definition, it was concluded that constitutive relations with nonlocal terms can confuse the traditional separation of the roles between conservation laws and constitutive relations. The diversity of motivations for the nonlocal approaches are presented, resulting primarily from deficiencies in numerical solutions to practical problems. To illustrate these concepts, the history of nonlocal terms in the field of viscoelastic fluids is reviewed. A specific example of a viscoelastic constitutive relation that contains a stress diffusion term is applied to a simple shear flow and found not to be a physical description of any known fluid. Questions that should be asked of nonlocal approaches are listed. DOE

N94-22971# Ecole Centrale de Lyon (France). Lab. de Mecanique des Fluides et d'Acoustique.

IMAGE ANALYSIS APPLICATIONS TO MIXING PHENOMENA AND TURBULENT DISPERSIONS Ph.D. Thesis [APPLICATIONS DE L'ANALYSE D'IMAGES A DES PHENOMENES DE MELANGE ET DE DISPERSION TURBULENTS]

Serge Simoens 1992 184 p In FRENCH Sponsored by Metraflu, Ecully, France Original contains color illustrations
(ECL-92-29; ETN-94-95168) Avail: CASI HC A09/MF A02

The purpose of the study is to demonstrate the importance of image analysis for flow visualization methods. Several classical flow visualization methods and image processing techniques are reviewed. Two image processing techniques are proposed. The first one is a qualitative analysis method applying a three dimensional reconstruction algorithm for complex shapes and laser tomography. The main difficulty is the nonreproducibility of three dimensional complex shapes. The solution adopted consists of harmonic analysis of two dimensional boundary layers. The following cases are used to test the method: coherent structures observed at the boundary layer transition zone and the reconstruction of gas plumes ejected into the atmosphere. A method developed for simultaneously measuring flow velocity and concentration fields is described. The results obtained by applying this technique to a nearly isotropic turbulent jet flow are discussed. ESA

N94-22985# Amsterdam Univ. (Netherlands).

LOCAL GRID REFINEMENT METHOD FOR THE EULER EQUATIONS Ph.D. Thesis

H. T. M. VanderMaarel 23 Feb. 1993 149 p See also PB92-202274
(PB93-223329) Avail: CASI HC A07/MF A02

The thesis considers the Euler equations of fluid dynamics for a perfect gas. Our main interest is the numerical approximation of solutions of the steady, two-dimensional Euler equations, by a solution-adaptive method, which uses local grid refinement (enrichment) and a multigrid method to solve the system of discrete equations. The Euler equations model the flow of a compressible, inviscid fluid, without taking into account the conduction of heat. Aerospace aerodynamics is an area of application interested in a physical model that neglects viscosity and heat conduction effects in the flow of a perfect gas. For an object moving through a gas, viscosity and heat conduction tend to play an important role only in the close vicinity of that object. Hence, in the 'outer' region (away from the object), a realistic description can often be made with the Euler equations. NTIS

N94-23072*# California Polytechnic State Univ., San Luis Obispo.

AN EXPERIMENTAL STUDY OF THE FLOW FIELD SURROUNDING A SUBSONIC JET IN A CROSS FLOW M.S. Thesis

Robert Foster Dennis Jun. 1993 162 p
(Contract NCC2-731)
(NASA-CR-194770; NAS 1.26:194770) Avail: CASI HC A08/MF A02

An experimental investigation of the flow interaction of a 5.08 cm (2.00 in.) diameter round subsonic jet exhausting perpendicularly to a flat plate in a subsonic cross flow was conducted in the NASA Ames 7x1O ft. Wind Tunnel Number One. Flat plate surface pressures were measured at 400 locations in a 30.48 cm (12.0 in.) concentric circular array surrounding the jet exit. Results from these measurements are provided in tabular and graphical form for jet-to-crossflow velocity ratios ranging from 4 to 12, and for jet exit Mach numbers ranging from 0.50 to 0.93. Laser doppler velocimeter (LDV) three component velocity measurements were made in selected regions in the developed jet plume and near the flat plate surface, at a jet Mach number of 0.50 and jet-to-crossflow velocity ratios of 6 and 8. The results of both pressure and LDV measurements are compared with the results of previous experiments. In addition, pictures of the jet plume shape at jet velocity ratios ranging from 4 to 12 were obtained using schleiren photography. The LDV measurements are consistent with previous work, but more extensive measurements will be necessary to provide a detailed picture of the flow field. The surface pressure results compare closely with previous work and provide a useful characterization of jet induced surface pressures. The results demonstrate the primary influence of jet velocity ratio and the secondary influence of jet Mach number in determining such surface pressures. Author (revised)

N94-23077* National Aeronautics and Space Administration. Ames Research Center, Moffett Field, CA.

PROBE SHAPES THAT MEASURE TIME-AVERAGED STREAMWISE MOMENTUM AND CROSS-STREAM TURBULENCE INTENSITY Patent

Vernon J. Rossow, inventor (to NASA) 7 Sep. 1993 21 p Filed 21 Feb. 1991
(NASA-Case-ARC-11934-1; US-Patent-5,241,866;
US-Patent-Appl-SN-660473; US-Patent-Class-73-861.66;
US-Patent-Class-73-170.14; US-Patent-Class-73-147;
US-Patent-Class-73-180; Int-Patent-Class-G01F-1/46) Avail: US Patent and Trademark Office

A method and apparatus for directly measuring the time-averaged streamwise momentum in a turbulent stream use a probe which has total head response which varies as the cosine-squared of the angle of incidence. The probe has a nose with a slight indentation on its front face for providing the desired response. The method of making the probe incorporates unique design features. Another probe may be positioned in a side-by-side relationship to the first probe to provide a direct measurement of the total pressure. The difference between the two pressures yields the sum of the squares of the cross-stream components of the turbulence level. Official Gazette of the U.S. Patent and Trademark Office

N94-23089*# Institute for Computer Applications in Science and Engineering, Hampton, VA.

FLAMES IN DUSTY MIXTURES: THEIR STRUCTURE AND STABILITY Final Report

J. Buckmaster (Illinois Univ., Urbana.) and T. Jackson Nov. 1993 24 p Submitted for publication
(Contract NAS1-19480; RTOP 505-90-52-01)
(NASA-CR-191567; NAS 1.26:191567; ICASE-93-86) Avail: CASI HC A03/MF A01

The structure and stability of flames in dusty mixtures is investigated. The presence of the dust leads to significant transport of energy by radiation and the fundamental goal of the analysis is to explore to what extent this displaces the classical non-hydrodynamical stability boundaries of the plane degradation. An approximate description of the radiative transport permits analysis for arbitrary values of both the planck length and the Boltzman number. It is shown that the pulsating/traveling-wave instability usually associated with values of Lewis number (L(sub e)) bigger than 1 is stongly enhanced by the presence of radiation and can be present even if L(sub e) is less than 1. On the other hand radiation tends to supress the cellular instability normally associated with values of L(sub e) less than 1. The latter is consisitent with preliminary experimental observations of Abbud-Madrid and Ronney. Author (revised)

N94-23114# Helsinki Univ. of Technology, Espoo (Finland). Lab. of Aerodynamics.

TWO-DIMENSIONAL NAVIER-STOKES COMPUTATIONS OF SUBSONIC AND SUPERSONIC FLOWS THROUGH TURBINE CASCADES

H. Pan 1993 38 p
(PB93-226223; ISBN-951-22-1482-2) Avail: CASI HC A03/MF A01

The report describes the computation of 2-D viscous flows in turbine cascades. The program is a 2-D FINFLO code developed at the Laboratory of Aerodynamics, Helsinki University of Technology. The original code was developed for external flows and dimensionless variables are employed in the computation. The external version of the code was modified to be suitable for internal flows and dimensional input-output quantities was used.

A subsonic 2-D axial turbine cascade flow case and a supersonic 2-D radial turbine cascade flow case was calculated. The results from the first case are compared with the results of the experiment conducted by NASA. NTIS

N94-23115 Helsinki Univ. of Technology, Espoo (Finland). Lab. of Aerodynamics.

POISs3: A 3D POISSON SMOOTHER OF STRUCTURED GRIDS

R. Lehtimaeki 1993 50 p Limited Reproducibility: More than 20% of this document may be affected by microfiche quality
(PB93-226231; SER-B-93-42) Avail: CASI HC A03

Flow solvers based on solving Navier-Stokes or Euler equations generally need a computational grid to represent the domain of the flow. A structured computational grid can be efficiently produced by algebraic methods like transfinite interpolation. Unfortunately, algebraic methods propagate all kinds of unsmoothness of the boundary into the field. Unsmoothness of the grid, in turn, can result in inaccuracy in the flow solver. In the present work a 3D elliptic grid smoother was developed. The smoother is based on solving three Poisson equations, one for each curvilinear direction. The Poisson equations formed in the physical region are first transformed to the computational (rectilinear) region. The resulting equations form a system of three coupled elliptic quasi-linear partial differential equations in the computational domain. A short review of the Poisson method is presented. The regularity of a grid cell is studied and a skewness value is developed. NTIS

N94-23160# Institut Franco-Allemand de Recherches, Saint-Louis (France). Gasdynamics Dept.

INTERFEROMETRY IN RAREFIED GAS FLOWS

G. Smeets 10 Apr. 1992 14 p Presented at the Advance Research Workshop on New Trends in Instrumentation for Hypersonic Research, Le Fauga, France, 27 Apr. - 1 May 1992
(ISL-CO-207/92; ETN-94-95123) Avail: CASI HC A03/MF A01

A survey of optical interferometry using a Wollaston prism differential interferometer is given. With a number of selected examples, its potential, especially in the field of low density flow diagnostics, is demonstrated. Differential interferometry with spark light sources is treated and is shown to be a very effective means for high sensitive flow visualization. The laser differential interferometer originating from a combination of the differential interferometer with collimated light beams from a continuous wave laser is described. Of special interest for applications to rarefied flows is its capability of resolving optical path changes down to 0.00001 of the light wavelength. This is three orders of magnitude beyond the resolution limit of classical interferometry based on fringe shift analysis. ESA

N94-23197# Universitaet der Bundeswehr Muenchen, Neubiberg (Germany). Inst. fuer Luft- und Raumfahrttechnik.

LIQUID OSCILLATIONS IN A SPHERICAL SYSTEM WITH SLIDING EDGES BOUNDARY BY TWO CONICAL SOLID SURFACES IN ZERO-GRAVITY

Helmut F. Bauer 1992 30 p
(LRT-WE-9-FB-5-1992; ETN-94-95090) Avail: CASI HC A03/MF A01

The natural frequencies and damped natural frequencies of an annular spherical liquid system bounded by two conical solid surfaces were determined by considering three cases for the contact line motion. These were the freely slipping contact line, the 'sliding', and the anchored contact line. The analytical results are applied to a semispherical drop, where it was found that the natural frequencies range from those for free slipping to those for anchored edges. The system of viscous liquid also exhibits a domain where only aperiodic motion is possible. ESA

N94-23198# Max-Planck-Inst. fuer Stroemungsforschung, Goettingen (Germany).

FORCED VIBRATIONS OF A NON-VISCOUS DROP

W. Moehring and R. Ravindran (Indian Inst. of Science, Bangalore.) Oct. 1992 66 p Sponsored by Alexander von Humboldt Stiftung
(MPIS-24/1992; ETN-94-95104) Avail: CASI HC A04/MF A01

Using a variational principle with the Lagrangian dictated by the pressure, the nonlinear axisymmetric oscillations of a drop in an incompressible inviscid fluid are studied. The drop shape and periodicity of oscillation of the unperturbed drop are investigated. The variational principle is modified to account for an external enforced oscillation. The motion of the drop under the effect of external oscillations with various periods is studied using Poincare maps, Melnikov method, and winding numbers. Of special interest are 'mode locked' states, where the drop oscillates with the external frequency. ESA

N94-23213# Argonne National Lab., IL.

ASYMPTOTIC ANALYSIS: WORKING NOTE NO. 3, BOUNDARY LAYERS

M. Garbey (Lyon-1 Univ., Villeurbanne, France.) and H. G. Kaper Sep. 1993 20 p
(Contract W-31-109-eng-38)
(DE94-002299; ANL/MCS-TM-181) Avail: CASI HC A03/MF A01

In this chapter the authors discuss the asymptotic approximation of functions that display boundary layer behavior. The purpose here is to introduce the basic concepts underlying the phenomenon, to illustrate its importance, and to describe some of the fundamental tools available for its analysis. To achieve their purpose in the clearest way possible, the authors will work with functions that are assumed to be given explicitly - that is, functions f : (0,epsilon(sub 0)) yields X whose expressions are known, at least in principle. Only in the following chapter will they begin the study of functions that are given implicitly as solutions of boundary value problems - the real stuff of which singular perturbation theory is made. Boundary-layer behavior is associated with asymptotic expansions that are regular 'almost everywhere' - that is, expansions that are regular on every compact subset of the domain of definition, but not near the boundary. These regular asymptotic expansions can be continued in a certain sense all the way up to the boundary, but a separate analysis is still necessary in the boundary layer. The boundary layer analysis is purely local and aims at constructing local approximations in the neighborhood of each point of the singular part of the boundary. The problem of finding an asymptotic approximation is thus reduced to matching the various local approximations to the existing regular expansion valid in the interior of the domain. The authors are thinking, for example, of fluid flow (viscosity), combustion (Lewis number), and superconductivity (Ginzburg-Landau parameter) problems. Their solution may remain smooth over a wide range of parameter values, but as the parameters approach critical values, complicated patterns may emerge. DOE

N94-23220# Sandia National Labs., Albuquerque, NM.

A METHOD TO SIMULATE VISCOUS DIFFUSION OF VORTICITY BY CONVECTIVE TRANSPORT OF VORTICES AT A NON-SOLENOIDAL VELOCITY

S. N. Kempka and J. H. Strickland Aug. 1993 30 p
(Contract DE-AC04-94AL-85000)
(DE94-001777; SAND-93-1763) Avail: CASI HC A03/MF A01

A numerical method to simulate viscous diffusion of vorticity using vortex blobs (i.e., without a grid) is presented. The method consists of casting the effects of viscous diffusion into an effective 'diffusion velocity' at which vortex blobs convect. The diffusion velocity was proposed previously by Ogami and Akamatsu, but they did not consider the effects of the divergence of the diffusion velocity. In fact, the diffusion velocity is highly non-solenoidal, which significantly affects the area over which a vortex blob diffuses. A formulation is presented that relates the area expansion to the diffusion velocity divergence. By taking into account the area expansion, more accurate simulations of diffusion are obtained, as demonstrated by a comparison of numerical and analytical diffusion solutions. Results from simulations show that vortex areas expand significantly in regions of large vorticity gradients. As a result of the area expansion, adjacent vortices remain overlapped, thereby maintaining smooth solution fields. The non-solenoidal diffusion velocity method is easily implemented in vortex blob algorithms, thus facilitating the development of vortex methods to simulate flows with finite Reynolds numbers. DOE

N94-23227# Von Karman Inst. for Fluid Dynamics, Rhode-Saint-Genese (Belgium).

ACTIVITIES REPORT TO NATO Annual Report No. 33, Oct. 1991 - Sep. 1992

30 Sep. 1992 78 p
(ETN-94-95047) Avail: CASI HC A05/MF A01

Academic, research and financial developments at the von Karman Institute for Fluid Dynamics during the period from 1 Oct. 1991 - 30 Sep. 1992 are reported. The Institute is incorporated as an international scientific association with the following aims: to promote the training of scientists and engineers from NATO (North Atlantic Treaty Organization) countries in the field of fluid dynamics; to contribute to the dissemination of knowledge in the field of fluid dynamics; to undertake, to investigate, and to promote studies and research in the field of theoretical and experimental fluid dynamics, including numerical methods. Education and research are conducted within three broad areas of fluid dynamics, each of which is reflected in the name of a department: aeronautics/aerospace; environmental and applied fluid dynamics; and turbomachinery. ESA

N94-23302*# Institute for Computer Applications in Science and Engineering, Hampton, VA.
A REPRESENTATION FOR THE TURBULENT MASS FLUX CONTRIBUTION TO REYNOLDS-STRESS AND TWO-EQUATION CLOSURES FOR COMPRESSIBLE TURBULENCE Final Report
J. R. Ristorcelli Nov. 1993 24 p Submitted for publication
(Contract NAS1-19480; RTOP 505-90-52-01)
(NASA-CR-191569; NAS 1.26:191569; ICASE-93-88) Avail: CASI HC A03/MF A01

The turbulent mass flux, or equivalently the fluctuating Favre velocity mean, appears in the first and second moment equations of compressible kappa-epsilon and Reynolds stress closures. Mathematically it is the difference between the unweighted and density-weighted averages of the velocity field and is therefore a measure of the effects of compressibility through variations in density. It appears to be fundamental to an inhomogeneous compressible turbulence, in which it characterizes the effects of the mean density gradients, in the same way the anisotropy tensor characterizes the effects of the mean velocity gradients. An evolution equation for the turbulent mass flux is derived. A truncation of this equation produces an algebraic expression for the mass flux. The mass flux is found to be proportional to the mean density gradients with a tensor eddy-viscosity that depends on both the mean deformation and the Reynolds stresses. The model is tested in a wall bounded DNS at Mach 4.5 with notable results. Author (revised)

N94-23306* National Aeronautics and Space Administration. Ames Research Center, Moffett Field, CA.
PROBE SYSTEMS FOR MEASURING STATIC PRESSURE AND TURBULENCE INTENSITY IN FLUID STREAMS Patent
Vernon J. Rossow, inventor (to NASA) 10 Aug. 1993 19 p Filed 24 Apr. 1991
(NASA-Case-ARC-11935-1; US-Patent-5,233,865; US-Patent-Appl-SN-690440; US-Patent-Class-73-147; US-Patent-Class-73-861.65; Int-Patent-Class-G01F-1/46; Int-Patent-Class-G01P-5/165) Avail: US Patent and Trademark Office

A method and an apparatus for measuring time-averaged static or ambient pressure and turbulence intensity in a turbulent stream are discussed. The procedure involves placing a plurality of probes in the stream. Each probe responds in a different manner to characteristics of the fluid stream, preferably as a result of having varying cross sections. The responses from the probes are used to eliminate unwanted components in the measured quantities for accurate determination of selected characteristics.
Official Gazette of the U.S. Patent and Trademark Office

N94-23339*# National Aeronautics and Space Administration. Langley Research Center, Hampton, VA.
EXPERIMENTAL INVESTIGATION OF GENERIC THREE-DIMENSIONAL SIDEWALL-COMPRESSION SCRAMJET INLETS AT MACH 6 IN TETRAFLUOROMETHANE
Scott D. Holland Dec. 1993 47 p
(RTOP 506-40-41-02)
(NASA-TM-4497; L-17133; NAS 1.15:4497) Avail: CASI HC A03/MF A01

Three-dimensional sidewall-compression scramjet inlets with leading-edge sweeps of 30 deg and 70 deg were tested in the Langley Hypersonic CF4 Tunnel at Mach 6 and with a ratio of specific heats of 1.2. The parametric effects of leading-edge sweep, cowl position, contraction ratio, and Reynolds number were investigated. The models were instrumented with 42 static pressure orifices that were distributed on the sidewalls, base plate, and cowl. Schlieren movies were made of each test for flow visualization of the effects of the internal flow spillage on the external flow field. To obtain an approximate characterization of the flow field, a modification to two-dimensional, inviscid, oblique shock theory was derived to accommodate the three-dimensional effects of leading-edge sweep. This theory qualitatively predicted the reflected shock structure (i.e., sidewall impingement locations) and the observed increase in spillage with increasing leading-edge sweep. The primary effect of moving the cowl forward was capturing the flow that would have otherwise spilled out ahead of the cowl. Increasing the contraction ratio increases the number of internal shock reflections and hence incrementally increases the sidewall pressure distribution. Significant Reynolds number effects were noted over a small range of Reynolds number. Author (revised)

N94-23460# National Inst. for Fusion Science, Nagoya (Japan).
TRACKING SHARP INTERFACE OF TWO FLUIDS BY THE CIP (CUBIC-INTERPOLATED PROPAGATION) SCHEME
T. Yabe (Gunma Univ., Kiryu, Japan.) and F. Xiao (Gunma Univ., Kiryu, Japan.) Jan. 1993 19 p
(DE93-508322; NIFS-206) Avail: CASI HC A03/MF A01

A method to treat a sharp discontinuity by the density function is proposed. The surface of the density function is described by one grid throughout the calculation even when the surface is largely distorted. This description is made possible by the CIP method combined with variable transformation. This scheme is applied to the linear wave propagation in one- and two-dimensions. In the nonlinear case, the injection of heavier fluid into lighter fluid his calculated and the winding of mushroom structure is successfully treated by the density function. DOE

N94-23470# Lawrence Livermore National Lab., CA.
SHOCK-INDUCED TURBULENT FLOW IN BAFFLE SYSTEMS
A. L. Kuhl and H. Reichenbach (Fraunhofer Inst. fuer Kurzzeitdynamik, Freiburg im Breisgau, Germany.) Jul. 1993 13 p Presented at the 19th International Symposium on Shock Waves, Marseille, France, 26-30 Jul. 1993
(Contract W-7405-eng-48)
(DE94-001532; UCRL-JC-113309; CONF-930788-6) Avail: CASI HC A03/MF A01

Experiments are described on shock propagation through 2-D aligned and staggered baffle systems. Flow visualization was provided by shadow and schlieren photography, which was recorded by the Cranz-Schardin camera. Also, single-frame, infinite-fringe, color interferograms were used. Intuition suggests that this is a rather simple 2-D shock diffraction problem. However, flow visualization reveals that the flow rapidly evolved into a complex 3-D turbulent mixing problem. Mushroom-shaped mixing regions blocked the flow into the next baffle orifice. Thus energy was transferred from the directed kinetic energy (induced by the shock) to the rotational energy of turbulent mixing and then dissipated by molecular effects. These processes dramatically dissipate the strength of the shock wave. The experiments provide an excellent test case that could be used to assess the accuracy of computer code calculations of such problems. DOE

N94-23513*# Queensland Univ., Saint Lucia (Australia). Dept. of Mechanical Engineering.
SHOCK TUNNEL STUDIES OF SCRAMJET PHENOMENA, SUPPLEMENT 7
R. J. Bakos, R. G. Morgan, S. L. Tuttle, G. M. Kelly, A. Paull, J. M. Simmons, R. J. Stalker, M. V. Pulsonetti, D. Buttsworth, and G. A. Allen, Jr. et al Dec. 1993 143 p
(Grant NAGw-674; RTOP 505-70-62-02)
(NASA-CR-191572; NAS 1.26:191572) Avail: CASI HC A07/MF A02

Reports by the staff of the University of Queensland on various research studies related to the advancement of scramjet technology are presented. These reports document the tests conducted in the reflected shock tunnel T4 and supporting research facilities that have been used to study the injection, mixing, and combustion of hydrogen fuel in generic scramjets at flow conditions typical of hypersonic flight. In addition, topics include the development of instrumentation and measurement technology, such as combustor wall shear and stream composition in pulse facilities, and numerical studies and analyses of the scramjet combustor process and the test facility operation. This research activity is Supplement 7 under NASA Grant NAGW-674. Author

N94-23525*# National Aeronautics and Space Administration. Lewis Research Center, Cleveland, OH.
THE USE OF TRANSITION REGION CHARACTERISTICS TO IMPROVE THE NUMERICAL SIMULATION OF HEAT TRANSFER IN BYPASS TRANSITIONAL FLOWS
Frederick F. Simon Dec. 1993 19 p Prepared for presentation at the 5th International Symposium on Transport Phenomena and Dynamics of Rotating Machinery, Kaanapali, Maui, HI, 8-11 May 1994; sponsored by the Pacific Center of Thermal-Fluids Engineering
(RTOP 505-62-52)
(NASA-TM-106445; E-8290; NAS 1.15:106445) Avail: CASI HC A03/MF A01

A method is presented for improving the numerical prediction of bypass transition heat transfer on a flat plate in a high-disturbance environment with zero or favorable pressure gradient. The method utilizes low Reynolds number k-epsilon turbulence models in combination with the characteristic parameters of the transition region. The parameters representing the characteristics of the transition region used are the intermittency, transition length and turbulent spot properties. An analysis is made of the transition length in terms of turbulent spot variables. The nondimensional spot formation rate, required for the prediction of the transition length, is shown by the analysis to be a function of the spot spreading angle, the dimensionless spot velocity ratio and the dimensionless spot area ratio. The intermittency form of the k-epsilon equations were derived from conditionally averaged equations which have been shown to be an improvement over global-time-averaged equations for the numerical calculation of the transition region. The numerical predictions are in general good agreement with the experimental data and indicate the potential use of the method in accelerating flows. Turbulence models of the k-epsilon type are known to underpredict the transition length. The present work demonstrates how incorporating transition region characteristics improves the ability of two-equation turbulence models to simulate bypass transition for flat plates with potential application to turbine vanes and blades. Author (revised)

N94-23532*# Queensland Univ., Saint Lucia (Australia). Dept. of Mechanical Engineering.
SHOCK TUNNEL STUDIES OF SCRAMJET PHENOMENA, SUPPLEMENT 8
R. J. Stalker, P. Hollis, G. A. Allen, G. T. Roberts, S. Tuttle, R. J. Bakos, R. G. Morgan, M. V. Pulsonetti, C. Brescianini, and D. R. Buttsworth et al Dec. 1993 131 p
(Grant NAGw-674; RTOP 505-70-62-16)
(NASA-CR-191573; NAS 1.26:191573) Avail: CASI HC A07/MF A02

Reports by the staff of the University of Oueensland on various research studies related to the advancement of scramjet technology are presented. These reports document the tests conducted in the reflected shock tunnel T4 and supporting research facilities that have been used to study the injection, mixing, and combustion of hydrogen fuel in generic scramjets at flow conditions typical of hypersonic flight. In addition, topics include the development of instrumentation and measurement technology, such as combustor wall shear and stream composition in pulse facilities, and numerical studies and analyses of the scramjet combustor process and the test facility operation. This research activity is Supplement 8 under NASA Grant NAGW-674. Author

N94-23634*# National Aeronautics and Space Administration. Lewis Research Center, Cleveland, OH.
THE FIFTH ANNUAL THERMAL AND FLUIDS ANALYSIS WORKSHOP
Nov. 1993 533 p Workshop held in Brook Park, OH, 16-20 Aug. 1993; cosponsored by Ohio Aerospace Inst. Original contains color illustrations
(NASA-CP-10122; E-8094; NAS 1.55:10122) Avail: CASI HC A23/MF A04; 5 functional color pages

The Fifth Annual Thermal and Fluids Analysis Workshop was held at the Ohio Aerospace Institute, Brook Park, Ohio, cosponsored by NASA Lewis Research Center and the Ohio Aerospace Institute, 16-20 Aug. 1993. The workshop consisted of classes, vendor demonstrations, and paper sessions. The classes and vendor demonstrations provided participants with the information on widely used tools for thermal and fluid analysis. The paper sessions provided a forum for the exchange of information and ideas among thermal and fluids analysts. Paper topics included advances and uses of established thermal and fluids computer codes (such as SINDA and TRASYS) as well as unique modeling techniques and applications. For individual titles, see N94-23635 through N94-23672.

N94-23635*# National Aeronautics and Space Administration. Marshall Space Flight Center, Huntsville, AL.
ADVANCED X RAY ASTROPHYSICS FACILITY-IMAGING (AXAF-I) THERMAL ANALYSES USING INTEGRATED THERMAL ANALYSIS SYSTEM (ITAS) PROGRAM
Benny Ghaffarian (Sverdrup Technology, Inc., Huntsville, AL.) and Ramona Cummings *In* NASA. Lewis Research Center, The Fifth Annual Thermal and Fluids Analysis Workshop Nov. 1993 p 3-12 (For primary document see N94-23634 06-34)
Avail: CASI HC A02/MF A04; 5 functional color pages

The complex geometry and stringent thermal requirements associated with the Advanced X-ray Astrophysics Facility - Imaging (AXAF-I) necessitate a detailed and accurate thermal analysis of the proposed system. A brief description of said geometry and thermal requirements is included. Among the tools considered for the aforementioned analysis is a PC-compatible version of the Integrated Thermal Analysis System (ITAS). Several bench-mark studies were performed to evaluate the capabilities of ITAS and to compare the corresponding results with those obtained using TRASYS and SINDA. Comparative studies were conducted for a typical Space Station module. Four models were developed using various combinations of the available software packages (i.e. ITAS, SINDA, and TRASYS). Orbital heating and heat transfer calculations were performed to determine the temperature distributions along the surfaces of this module. A comparison of the temperature distributions obtained for each of the four cases is presented. Results of this investigation were used to verify the different ITAS modules including those used for model generation, steady state and transient orbital heating analyses, radiative and convective heat flow analyses, and SINDA/TRASYS model translation. The results suggest that ITAS is well suited to subsequent analyses of the AXAF-I. Author (revised)

N94-23636*# Wright Lab., Wright-Patterson AFB, OH.
AN ENGINEERING CODE TO ANALYZE HYPERSONIC THERMAL MANAGEMENT SYSTEMS
Valerie J. VanGriethuysen and Clark E. Wallace (Science Applications International Corp., Torrance, CA.) *In* NASA. Lewis Research Center, The Fifth Annual Thermal and Fluids Analysis Workshop Nov. 1993 p 13-26 (For primary document see N94-23634 06-34)
Avail: CASI HC A03/MF A04; 5 functional color pages

Thermal loads on current and future aircraft are increasing and as a result are stressing the energy collection, control, and dissipation capabilities of current thermal management systems and technology. The thermal loads for hypersonic vehicles will be no exception. In fact, with their projected high heat loads and fluxes, hypersonic vehicles are a prime example of systems that will require thermal management systems (TMS) that have been optimized and integrated with the entire vehicle to the maximum extent possible during the initial design stages. This will not only be to meet operational requirements, but also to fulfill weight and performance constraints in order for the vehicle to takeoff and complete its mission successfully. To meet this challenge, the TMS can no longer be two or more entirely independent systems, nor can thermal management be an after thought in the design process, the typical pervasive approach in the past. Instead, a TMS that was integrated throughout the entire vehicle and subsequently optimized will be required. To accomplish this, a method that iteratively optimizes the TMS throughout the vehicle will not only be highly desirable, but advantageous in order to reduce the manhours normally required to conduct the necessary tradeoff studies and comparisons. A thermal management engineering computer code that is under development and being managed at Wright Laboratory, Wright-Patterson AFB, is discussed. The primary goal of the code is to aid in the development of a hypersonic vehicle TMS that has been optimized and integrated on a total vehicle basis. Author (revised)

N94-23637*# Mississippi State Univ., Mississippi State. Thermal and Fluid Dynamics Lab.
UNCERTAINTY ANALYSIS OF DIFFUSE-GRAY RADIATION ENCLOSURE PROBLEMS: A HYPERSENSITIVE CASE STUDY
Robert P. Taylor, Rogelio Luck, B. K. Hodge, and W. Glenn Steele *In* NASA. Lewis Research Center, The Fifth Annual Thermal and Fluids Analysis

Workshop Nov. 1993 p 27-40 (For primary document see N94-23634 06-34)
Avail: CASI HC A03/MF A04; 5 functional color pages

An uncertainty analysis of diffuse-gray enclosure problems is presented. The genesis was a diffuse-gray enclosure problem which proved to be hypersensitive to the specification of view factors. This genesis is discussed in some detail. The uncertainty analysis is presented for the general diffuse-gray enclosure problem and applied to the hypersensitive case study. It was found that the hypersensitivity could be greatly reduced by enforcing both closure and reciprocity for the view factors. The effects of uncertainties in the surface emissivities and temperatures are also investigated. Author

N94-23638*# National Aeronautics and Space Administration. Lewis Research Center, Cleveland, OH.
A COMPARISON OF TSS AND TRASYS IN FORM FACTOR CALCULATION
Eric Golliher *In its* The Fifth Annual Thermal and Fluids Analysis Workshop Nov. 1993 p 41-46 (For primary document see N94-23634 06-34)
Avail: CASI HC A02/MF A04; 5 functional color pages

As the workstation and personal computer become more popular than a centralized mainframe to perform thermal analysis, the methods for space vehicle thermal analysis will change. Already, many thermal analysis codes are now available for workstations, which were not in existence just five years ago. As these changes occur, some organizations will adopt the new codes and analysis techniques, while others will not. This might lead to misunderstandings between thermal shops in different organizations. If thermal analysts make an effort to understand the major differences between the new and old methods, a smoother transition to a more efficient and more versatile thermal analysis environment will be realized. Author (revised)

N94-23639*# European Space Agency. European Space Research and Technology Center, ESTEC, Noordwijk (Netherlands). Thermal Control and Life Support Div.
ACCURACY CONTROL IN MONTE CARLO RADIATIVE CALCULATIONS
P. Planas Almazan *In* NASA. Lewis Research Center, The Fifth Annual Thermal and Fluids Analysis Workshop Nov. 1993 p 47-62 (For primary document see N94-23634 06-34)
Avail: CASI HC A03/MF A04; 5 functional color pages

The general accuracy law that rules the Monte Carlo, ray-tracing algorithms used commonly for the calculation of the radiative entities in the thermal analysis of spacecraft are presented. These entities involve transfer of radiative energy either from a single source to a target (e.g., the configuration factors). or from several sources to a target (e.g., the absorbed heat fluxes). In fact, the former is just a particular case of the latter. The accuracy model is later applied to the calculation of some specific radiative entities. Furthermore, some issues related to the implementation of such a model in a software tool are discussed. Although only the relative error is considered through the discussion, similar results can be derived for the absolute error. Author (revised)

N94-23640*# Sandia National Labs., Albuquerque, NM. Thermal and Fluid Engineering Dept.
THERMAL CONTROL SYSTEM FOR SSF SENSOR/ELECTRONICS
R. L. Akau and D. E. Lee *In* NASA. Lewis Research Center, The Fifth Annual Thermal and Fluids Analysis Workshop Nov. 1993 p 63-79 (For primary document see N94-23634 06-34)
(Contract DE-AC04-76DP-00789)
(SAND-92-0652C) Avail: CASI HC A03/MF A04; 5 functional color pages

A thermal control system was designed for the Space Station Freedom (SSF) sensor/electronics box (SSTACK). Multi-layer insulation and heaters are used to maintain the temperatures of the critical components within their operating and survival temperature limits. Detailed and simplified SSTACK thermal models were developed and temperatures were calculated for worst-case orbital conditions. A comparison between the two models showed very good agreement. Temperature predictions were also compared to measured temperatures from a thermal-vacuum test. Author (revised)

N94-23641*# National Aeronautics and Space Administration. Lewis Research Center, Cleveland, OH.
UTILIZATION OF RECENTLY DEVELOPED CODES FOR HIGH POWER BRAYTON AND RANKINE CYCLE POWER SYSTEMS c20
Michael P. Doherty *In its* The Fifth Annual Thermal and Fluids Analysis Workshop Nov. 1993 p 83-94 Original contains color illustrations (For primary document see N94-23634 06-34)
Avail: CASI HC A02/MF A04; 5 functional color pages

Two recently developed FORTRAN computer codes for high power Brayton and Rankine thermodynamic cycle analysis for space power applications are presented. The codes were written in support of an effort to develop a series of subsystem models for multimegawatt Nuclear Electric Propulsion, but their use is not limited just to nuclear heat sources or to electric propulsion. Code development background, a description of the codes, some sample input/output from one of the codes, and state future plans/implications for the use of these codes by NASA's Lewis Research Center are provided. Author (revised)

N94-23642*# Akron Univ., OH. Dept. of Mechanical Engineering.
STUDY OF TRANSIENT BEHAVIOR OF FINNED COIL HEAT EXCHANGERS
S. P. Rooke and M. G. Elissa *In* NASA. Lewis Research Center, The Fifth Annual Thermal and Fluids Analysis Workshop Nov. 1993 p 95-109 (For primary document see N94-23634 06-34)
(Grants ORSSP-R2444; FRG-1244)
Avail: CASI HC A03/MF A04; 5 functional color pages

The status of research on the transient behavior of finned coil cross-flow heat exchangers using single phase fluids is reviewed. Applications with available analytical or numerical solutions are discussed. Investigation of water-to-air type cross-flow finned tube heat exchangers is examined through the use of simplified governing equations and an up-wind finite difference scheme. The degenerate case of zero air-side capacitance rate is compared with available exact solution. Generalization of the numerical model is discussed for application to multi-row multi-circuit heat exchangers. Author (revised)

N94-23643*# Pennsylvania State Univ., Erie. School of Engineering and Engineering Technology.
PREDICTION OF PRESSURE DROP IN FLUID TUNED MOUNTS USING ANALYTICAL AND COMPUTATIONAL TECHNIQUES
William C. Lasher, Amir Khalilollahi, John Mischler, and Tom Uhric *In* NASA. Lewis Research Center, The Fifth Annual Thermal and Fluids Analysis Workshop Nov. 1993 p 111-125 Sponsored by Lord Corp. and Ben Franklin Partnership of Pennsylvania (For primary document see N94-23634 06-34)
Avail: CASI HC A03/MF A04; 5 functional color pages

A simplified model for predicting pressure drop in fluid tuned isolator mounts was developed. The model is based on an exact solution to the Navier-Stokes equations and was made more general through the use of empirical coefficients. The values of these coefficients were determined by numerical simulation of the flow using the commercial computational fluid dynamics (CFD) package FIDAP. Author (revised)

N94-23644*# Pennsylvania State Univ., Erie. School of Engineering and Engineering Technology.
SOLUTION OF MIXED CONVECTION HEAT TRANSFER FROM ISOTHERMAL IN-LINE FINS
Amir Khalilollahi *In* NASA. Lewis Research Center, The Fifth Annual Thermal and Fluids Analysis Workshop Nov. 1993 p 127-136 (For primary document see N94-23634 06-34)
Avail: CASI HC A02/MF A04; 5 functional color pages

Transient and steady state combined natural and forced convective flows over two in-line finite thickness fins (louvers) in a vertical channel are numerically solved using two methods. The first method of solution is based on the 'Simple Arbitrary Lagrangian Eulerian' (SALE) technique which incorporates mainly two computational phases: (1) a Lagrangian phase in which the velocity field is updated by the effects of all forces, and (2) an Eulerian phase that executes all advective fluxes of mass, momentum and energy. The second method of solution uses the finite element code entitled FIDAP. In the first part, comparison of the results by FIDAP, SALE, and available experimental work were done and discussed for steady state forced convection over louvered fins. Good agreements were deduced between the three sets of results especially for the flow over a single fin. In the second part and in the absence of experimental literature, the numerical predictions were extended to the transient transports and to the opposing flow where pressure drop is reversed. Results are presented and discussed for heat transfer and pressure drop in assisting and opposing mixed convection flows. Author (revised)

N94-23645*# Pennsylvania State Univ., University Park. Dept. of Aerospace Engineering.
A DIRECT APPROACH TO FINDING UNKNOWN BOUNDARY CONDITIONS IN STEADY HEAT CONDUCTION
Thomas J. Martin and George S. Dulikravich *In* NASA. Lewis Research Center, The Fifth Annual Thermal and Fluids Analysis Workshop Nov. 1993 p 137-149 (For primary document see N94-23634 06-34)
Avail: CASI HC A03/MF A04; 5 functional color pages

The capability of the boundary element method (BEM) in determining thermal boundary conditions on surfaces of a conducting solid where such quantities are unknown was demonstrated. The method uses a non-iterative direct approach in solving what is usually called the inverse heat conduction problem (IHCP). Given any over-specified thermal boundary conditions such as a combination of temperature and heat flux on a surface where such data is readily available, the algorithm computes the temperature field within the object and any unknown thermal boundary conditions on surfaces where thermal boundary values are unavailable. A two-dimensional, steady-state BEM program was developed and was tested on several simple geometries where the analytic solution was known. Results obtained with the BEM were in excellent agreement with the analytic values. The algorithm is highly flexible in treating complex geometries, mixed thermal boundary conditions, and temperature-dependent material properties and is presently being extended to three-dimensional and unsteady heat conduction problems. The accuracy and reliability of this technique was very good but tended to deteriorate when the known surface conditions were only slightly over-specified and far from the inaccessible surface. Author (revised)

N94-23646*# Nevada Univ., Reno. Dept. of Mechanical Engineering.
SECOND LAW ANALYSIS OF A CONVENTIONAL STEAM POWER PLANT c77
Geng Liu, Robert H. Turner, and Yunus A. Cengel *In* NASA. Lewis Research Center, The Fifth Annual Thermal and Fluids Analysis Workshop Nov. 1993 p 151-166 (For primary document see N94-23634 06-34)
Avail: CASI HC A03/MF A04; 5 functional color pages

A numerical investigation of exergy destroyed by operation of a conventional steam power plant is computed via an exergy cascade. An order of magnitude analysis shows that exergy destruction is dominated by combustion and heat transfer across temperature differences inside the boiler, and conversion of energy entering the turbine/generator sets from thermal to electrical. Combustion and heat transfer inside the boiler accounts for 53.83 percent of the total exergy destruction. Converting thermal energy into electrical energy is responsible for 41.34 percent of the total exergy destruction. Heat transfer across the condenser accounts for 2.89 percent of the total exergy destruction. Fluid flow with friction is responsible for 0.50 percent of the total exergy destruction. The boiler feed pump turbine accounts for 0.25 percent of the total exergy destruction. Fluid flow mixing is responsible for 0.23 percent of the total exergy destruction. Other equipment including gland steam condenser, drain cooler, deaerator and heat exchangers are, in the aggregate, responsible for less than one percent of the total exergy destruction. An energy analysis is also given for comparison of exergy cascade to energy cascade. Efficiencies based on both the first law and second law of thermodynamics are calculated for a number of components and for the plant. The results show that high first law efficiency does not mean high second law efficiency. Therefore, the second law analysis has been proven to be a more powerful tool in pinpointing real losses. The procedure used to determine total exergy destruction and second law efficiency can be used in a conceptual design and parametric study to evaluate the performance of other steam power plants and other thermal systems. Author (revised)

N94-23647*# National Aeronautics and Space Administration. Langley Research Center, Hampton, VA.
SOME USEFUL INNOVATIONS WITH TRASYS AND SINDA-85 c61
Ruth M. Amundsen *In* NASA. Lewis Research Center, The Fifth Annual Thermal and Fluids Analysis Workshop Nov. 1993 p 169-184 Original contains color illustrations (For primary document see N94-23634 06-34)
Avail: CASI HC A03/MF A04; 5 functional color pages

Several innovative methods were used to allow more efficient and accurate thermal analysis using SINDA-85 and TRASYS, including model integration and reduction, planetary surface calculations, and model animation. Integration with other modeling and analysis codes allows an analyst to import a geometry from a solid modeling or computer-aided design (CAD) software package, rather than building the geometry 'by hand.' This is more efficient as well as potentially more accurate. However, the use of solid modeling software often generates large analytical models. The problem of reducing large models was elegantly solved using the response of the transient derivative to a forcing step function. The thermal analysis of a lunar rover implemented two unusual features of the TRASYS/SINDA system. A little-known TRASYS routine SURFP calculates the solar heating of a rover on the lunar surface for several different rover positions and orientations. This is used not only to determine the rover temperatures, but also to automatically determine the power generated by the solar arrays. The animation of transient thermal results is an effective tool, especially in a vivid case such as the 14-day progress of the sun over the lunar rover. An animated color map on the solid model displays the progression of temperatures. Author (revised)

N94-23648*# Teledyne Brown Engineering, Huntsville, AL.
ANALYSIS OF HIGH VACUUM SYSTEMS USING SINDA'85 c61
R. A. Spivey, S. E. Clanton, and J. D. Moore *In* NASA. Lewis Research Center, The Fifth Annual Thermal and Fluids Analysis Workshop Nov. 1993 p 185-204 (For primary document see N94-23634 06-34)
Avail: CASI HC A03/MF A04; 5 functional color pages

The theory, algorithms, and test data correlation analysis of a math model developed to predict performance of the Space Station Freedom Vacuum Exhaust System are presented. The theory used to predict the flow characteristics of viscous, transition, and molecular flow is presented in detail. Development of user subroutines which predict the flow characteristics in conjunction with the SINDA'85/FLUINT analysis software are discussed. The resistance-capacitance network approach with application to vacuum system analysis is demonstrated and results from the model are correlated with test data. The model was developed to predict the performance of the Space Station Freedom Vacuum Exhaust System. However, the unique use of the user subroutines developed in this model and written into the SINDA'85/FLUINT thermal analysis model provides a powerful tool that can be used to predict the transient performance of vacuum systems and gas flow in tubes of virtually any geometry. This can be accomplished using a resistance-capacitance (R-C) method very similar to the methods used to perform thermal analyses. Author (revised)

N94-23649*# Sverdrup Technology, Inc., Huntsville, AL.
FEATURES OF A SINDA/FLUINT MODEL OF A LIQUID OXYGEN SUPPLY LINE
Boris G. Simmonds *In* NASA. Lewis Research Center, The Fifth Annual Thermal and Fluids Analysis Workshop Nov. 1993 p 205-222 (For primary document see N94-23634 06-34)
Avail: CASI HC A03/MF A04; 5 functional color pages

The modeling features used in a steady-state heat transfer problem using SINDA/FLUINT are described. The problem modeled is a 125 feet long, 3 inch diameter pipe, filled with liquid oxygen flow driven by a given pressure gradient. The pipe is fully insulated in five sections. Three sections of 1 inch thick spray-on foam and two sections of vacuum jacket. The model evaluates friction, turns losses and convection heat transfer between the fluid and the pipe wall. There is conduction through the foam insulation with temperature dependent thermal conductivity. The vacuum space is modeled with radiation and gas molecular conduction, if present, in the annular gap. Heat is transferred between the outer surface and surrounding ambient by natural convection and radiation; and, by axial conduction along the pipe and through the vacuum jacket spacers and welded seal flanges. The model makes extensive use of SINDA/FLUINT basic capabilities such as the GEN option for nodes and conductors (to generate groups of nodes or conductors), the SIV option (to generate single, temperature varying conductors), the SIM option (for multiple, temperature varying conductors) and the M HX macros for fluids (to generate strings of lumps, paths, and ties representing a diabatic duct). It calls subroutine CONTRN (returns the relative location in the G-array of a network conductor, given

an actual conductor number) enabling an extensive manipulation of conductor (calculates an assignment of their values) with DO loops. Models like this illustrate to the new and even to the old SINDA/FLUINT user, features of the program that are not so obvious or known, and that are extremely handy when trying to take advantage of both, the automation of the DATA headers and make surgical modifications to specific parameters of the thermal or fluid elements in the OPERATIONS portion of the model.
Author (revised)

N94-23650*# Phillips Lab., Kirtland AFB, NM.
THERMAL ANALYSIS OF COMBINATORIAL SOLID GEOMETRY MODELS USING SINDA c61
Diane Gerencser, George Radke, Rob Introne, John Klosterman (Battelle Columbus Labs., OH.), and Dave Miklosovic (Battelle Columbus Labs., OH.) *In* NASA. Lewis Research Center, The Fifth Annual Thermal and Fluids Analysis Workshop Nov. 1993 p 223-235 (For primary document see N94-23634 06-34)
Avail: CASI HC A03/MF A04; 5 functional color pages

Algorithms have been developed using Monte Carlo techniques to determine the thermal network parameters necessary to perform a finite difference analysis on Combinatorial Solid Geometry (CSG) models. Orbital and laser fluxes as well as internal heat generation are modeled to facilitate satellite modeling. The results of the thermal calculations are used to model the infrared (IR) images of targets and assess target vulnerability. Sample analyses and validation are presented which demonstrate code products. Author

N94-23651*# Sverdrup Technology, Inc., Brook Park, OH.
CONVECTION EQUATION MODELING: A NON-ITERATIVE DIRECT MATRIX SOLUTION ALGORITHM FOR USE WITH SINDA c61
Dean S. Schrage *In* NASA. Lewis Research Center, The Fifth Annual Thermal and Fluids Analysis Workshop Nov. 1993 p 237-251 (For primary document see N94-23634 06-34)
Avail: CASI HC A03/MF A04; 5 functional color pages

The determination of the boundary conditions for a component-level analysis, applying discrete finite element and finite difference modeling techniques often requires an analysis of complex coupled phenomenon that cannot be described algebraically. For example, an analysis of the temperature field of a coldplate surface with an integral fluid loop requires a solution to the parabolic heat equation and also requires the boundary conditions that describe the local fluid temperature. However, the local fluid temperature is described by a convection equation that can only be solved with the knowledge of the locally-coupled coldplate temperatures. Generally speaking, it is not computationally efficient, and sometimes, not even possible to perform a direct, coupled phenomenon analysis of the component-level and boundary condition models within a single analysis code. An alternative is to perform a disjoint analysis, but transmit the necessary information between models during the simulation to provide an indirect coupling. For this approach to be effective, the component-level model retains full detail while the boundary condition model is simplified to provide a fast, first-order prediction of the phenomenon in question. Specifically for the present study, the coldplate structure is analyzed with a discrete, numerical model (SINDA) while the fluid loop convection equation is analyzed with a discrete, analytical model (direct matrix solution). This indirect coupling allows a satisfactory prediction of the boundary condition, while not subjugating the overall computational efficiency of the component-level analysis. In the present study a discussion of the complete analysis of the derivation and direct matrix solution algorithm of the convection equation is presented. Discretization is analyzed and discussed to extend of solution accuracy, stability and computation speed. Case studies considering a pulsed and harmonic inlet disturbance to the fluid loop are analyzed to assist in the discussion of numerical dissipation and accuracy. In addition, the issues of code melding or integration with standard class solvers such as SINDA are discussed to advise the user of the potential problems to be encountered. Author

N94-23652*# Ohio State Univ., Columbus. Dept. of Aeronautical and Astronautical Engineering.
SIMULATION OF UNSTEADY FLOWS THROUGH STATOR AND ROTOR BLADES OF A GAS TURBINE USING THE CHIMERA METHOD
S. Nakamura and J. N. Scott *In* NASA. Lewis Research Center, The Fifth Annual Thermal and Fluids Analysis Workshop Nov. 1993 p 255-267 Sponsored in part by Ohio Aerospace Inst. (For primary document see N94-23634 06-34)
Avail: CASI HC A03/MF A04; 5 functional color pages

A two-dimensional model to solve compressible Navier-Stokes equations for the flow through stator and rotor blades of a turbine is developed. The flow domains for the stator and rotor blades are coupled by the Chimera method that makes grid generation easy and enhances accuracy because the area of the grid that have high turning of grid lines or high skewness can be eliminated from the computational domain after the grids are generated. The results of flow computations show various important features of unsteady flows including the acoustic waves interacting with boundary layers, Karman vortex shedding from the trailing edge of the stator blades, pulsating incoming flow to a rotor blade from passing stator blades, and flow separation from both suction and pressure sides of the rotor blades.
Author

N94-23653*# National Aeronautics and Space Administration. Wallops Flight Facility, Wallops Island, VA.
DEVELOPMENT AND APPLICATION OF AN EMPIRICAL PROBABILITY DISTRIBUTION FOR THE PREDICTION ERROR OF RE-ENTRY BODY MAXIMUM DYNAMIC PRESSURE c18
R. James Lanzi and Brett T. Vincent (Computer Sciences Corp., Wallops Island, VA.) *In* NASA. Lewis Research Center, The Fifth Annual Thermal and Fluids Analysis Workshop Nov. 1993 p 269-280 (For primary document see N94-23634 06-34)
Avail: CASI HC A03/MF A04; 5 functional color pages

The relationship between actual and predicted re-entry maximum dynamic pressure is characterized using a probability density function and a cumulative distribution function derived from sounding rocket flight data. This paper explores the properties of this distribution and demonstrates applications of this data with observed sounding rocket re-entry body damage characteristics to assess probabilities of sustaining various levels of heating damage. The results from this paper effectively bridge the gap existing in sounding rocket reentry analysis between the known damage level/flight environment relationships and the predicted flight environment. Author

N94-23654*# General Dynamics Corp., San Diego, CA. Space Systems Div.
PREDICTION OF THREE SIGMA MAXIMUM DISPERSED DENSITY FOR AEROSPACE APPLICATIONS c18
Terri L. Charles and Michael D. Nitschke *In* NASA. Lewis Research Center, The Fifth Annual Thermal and Fluids Analysis Workshop Nov. 1993 p 281-305 (For primary document see N94-23634 06-34)
Avail: CASI HC A03/MF A04; 5 functional color pages

Free molecular heating (FMH) is caused by the transfer of energy during collisions between the upper atmosphere molecules and a space vehicle. The dispersed free molecular heating on a surface is an important constraint for space vehicle thermal analyses since it can be a significant source of heating. To reduce FMH to a spacecraft, the parking orbit is often designed to a higher altitude at the expense of payload capability. Dispersed FMH is a function of both space vehicle velocity and atmospheric density, however, the space vehicle velocity variations are insignificant when compared to the atmospheric density variations. The density of the upper atmosphere molecules is a function of altitude, but also varies with other environmental factors, such as solar activity, geomagnetic activity, location, and time. A method has been developed to predict three sigma maximum dispersed density for up to 15 years into the future. This method uses a state-of-the-art atmospheric density code, MSIS 86, along with 50 years of solar data, NASA and NOAA solar activity predictions for the next 15 years, and an Aerospace Corporation correlation to account for density code inaccuracies to generate dispersed maximum density ratios denoted as 'K-factors'. The calculated K-factors can be used on a mission unique basis to calculate dispersed density, and hence dispersed free molecular heating rates. These more accurate K-factors can allow lower parking orbit altitudes, resulting in increased payload capability. Author

N94-23655*# Northeastern Univ., Boston, MA. Dept. of Mechanical Engineering.
MIXING AND UNMIXEDNESS IN PLASMA JETS 1: NEAR-FIELD ANALYSIS c75
Olusegun J. Ilegbusi *In* NASA. Lewis Research Center, The Fifth Annual

Thermal and Fluids Analysis Workshop Nov. 1993 p 307-328 (For primary document see N94-23634 06-34)
Avail: CASI HC A03/MF A04; 5 functional color pages

The flow characteristics in the near-field of a plasma jet are simulated with a two-fluid model. This model accounts for both gradient-diffusion mixing and uni-directional sifting motion resulting from pressure-gradient-body-force imbalance. This latter mechanism is believed to be responsible for the umixedness observed in plasma jets. The unmixedness is considered to be essentially a Rayleigh-Taylor kind instability. Transport equations are solved for the individual plasma and ambient gas velocities, temperatures and volume fractions. Empirical relations are employed for the interface transfers of mass, momentum and heat. The empirical coefficients are first established by comparison of predictions with available experimental data for shear flows. The model is then applied to an Argon plasma jet ejecting into stagnant air. The predicted results show the significant build-up of unmixed air within the plasma gas, even relatively far downstream of the torch. By adjusting the inlet condition, the model adequately reproduces the experimental data. Author

N94-23656*# Colorado Univ., Boulder. Dept. of Aerospace and Engineering Sciences.
SUPERSONIC MINIMUM LENGTH NOZZLE DESIGN FOR DENSE GASES **c02**
Andrew C. Aldo and Brian M. Argrow *In* NASA. Lewis Research Center, The Fifth Annual Thermal and Fluids Analysis Workshop Nov. 1993 p 329-341 (For primary document see N94-23634 06-34)
Avail: CASI HC A03/MF A04; 5 functional color pages

Recently, dense gases have been investigated for many engineering applications such as for turbomachinery and wind tunnels. Supersonic nozzle design for these gases is complicated by their nonclassical behavior in the transonic flow regime. In this paper a method of characteristics (MOC) is developed for two-dimensional (planar) and, primarily, axisymmetric flow of a van der Waals gas. Using a straight aortic line assumption, a centered expansion is used to generate an inviscid wall contour of minimum length. The van der Waals results are compared to previous perfect gas results to show the real gas effects on the flow properties and inviscid wall contours. Author

N94-23657*# New Orleans Univ., LA. Dept. of Mechanical Engineering.
EXPERIMENTAL AND ANALYTICAL STUDY OF CRYOGENIC PROPELLANT BOILOFF TO DEVELOP AND VERIFY ALTERNATE PRESSURIZATION CONCEPTS FOR SPACE SHUTTLE EXTERNAL TANK USING A SCALED DOWN TANK **c28**
K. M. Akyuzlu, S. Jones (Martin Marietta Corp., New Orleans, LA.), and T. Meredith (Martin Marietta Corp., New Orleans, LA.) *In* NASA. Lewis Research Center, The Fifth Annual Thermal and Fluids Analysis Workshop Nov. 1993 p 343-358 Sponsored in part by Martin Marietta Corp. (For primary document see N94-23634 06-34)
Avail: CASI HC A03/MF A04; 5 functional color pages

Self pressurization by propellant boiloff is experimentally studied as an alternate pressurization concept for the Space Shuttle external tank (ET). The experimental setup used in the study is an open flow system which is composed of a variable area test tank and a recovery tank. The vacuum jacketed test tank is geometrically similar to the external LOx tank for the Space Shuttle. It is equipped with instrumentation to measure the temperature and pressure histories within the liquid and vapor, and viewports to accommodate visual observations and Laser-Doppler Anemometry measurements of fluid velocities. A set of experiments were conducted using liquid Nitrogen to determine the temperature stratification in the liquid and vapor, and pressure histories of the vapor during sudden and continuous depressurization for various different boundary and initial conditions. The study also includes the development and calibration of a computer model to simulate the experiments. This model is a one-dimensional, multi-node type which assumes the liquid and the vapor to be under non-equilibrium conditions during the depressurization. It has been tested for a limited number of cases. The preliminary results indicate that the accuracy of the simulations is determined by the accuracy of the heat transfer coefficients for the vapor and the liquid at the interface which are taken to be the calibration parameters in the present model. Author

N94-23658*# Allied-Signal Aerospace Co., Phoenix, AZ.
THE 3-D CFD MODELING OF GAS TURBINE COMBUSTOR-INTEGRAL BLEED FLOW INTERACTION **c07**
D. Y. Chen and R. S. Reynolds *In* NASA. Lewis Research Center, The Fifth Annual Thermal and Fluids Analysis Workshop Nov. 1993 p 359-380 Original contains color illustrations (For primary document see N94-23634 06-34)
Avail: CASI HC A03/MF A04; 5 functional color pages

An advanced 3-D Computational Fluid Dynamics (CFD) model was developed to analyze the flow interaction between a gas turbine combustor and an integral bleed plenum. In this model, the elliptic governing equations of continuity, momentum and the k-e turbulence model were solved on a boundary-fitted, curvilinear, orthogonal grid system. The model was first validated against test data from public literature and then applied to a gas turbine combustor with integral bleed. The model predictions agreed well with data from combustor rig testing. The model predictions also indicated strong flow interaction between the combustor and the integral bleed. Integral bleed flow distribution was found to have a great effect on the pressure distribution around the gas turbine combustor. Author

N94-23659*# University of South Alabama, Mobile. Dept. of Mechanical Engineering.
NUMERICAL ANALYSIS OF A VORTEX CONTROLLED DIFFUSER
Robert E. Spall *In* NASA. Lewis Research Center, The Fifth Annual Thermal and Fluids Analysis Workshop Nov. 1993 p 381-393 (For primary document see N94-23634 06-34)
Avail: CASI HC A03/MF A04; 5 functional color pages

A numerical study of a prototypical vortex controlled diffuser is performed. The basic diffuser geometry consists of a step expansion in a pipe of area ratio 2.25:1. The incompressible Reynolds averaged Navier-Stokes equations, employing the K-epsilon turbulence model, are solved. Results are presented for bleed rates ranging from 1 to 7 percent. Diffuser efficiencies in excess of 80 percent are obtained. Reattachment lengths are reduced by a factor of up to 3. These results are in qualitative agreement with previous experimental work. However, differences in some basic details of experimentally observed and the present numerically generated flowfields exist. The effect of swirl is also investigated. Author

N94-23660*# Clemson Univ., SC. Dept. of Mechanical Engineering.
THE 3-D NUMERICAL STUDY OF AIRFLOW IN THE COMPRESSOR/COMBUSTOR PREDIFFUSER AND DUMP DIFFUSER OF AN INDUSTRIAL GAS TURBINE **c37**
Ajay K. Agrawal and Tah-Teh Yang *In* NASA. Lewis Research Center, The Fifth Annual Thermal and Fluids Analysis Workshop Nov. 1993 p 395-409 (For primary document see N94-23634 06-34)
Avail: CASI HC A03/MF A04; 5 functional color pages

This paper describes the 3D computations of a flow field in the compressor/combustor diffusers of an industrial gas turbine. The geometry considered includes components such as the combustor support strut, the transition piece and the impingement sleeve with discrete cooling air holes on its surface. Because the geometry was complex and 3D, the airflow path was divided into two computational domains sharing an interface region. The body-fitted grid was generated independently in each of the two domains. The governing equations for incompressible Navier-Stokes equations were solved using the finite volume approach. The results show that the flow in the prediffuser is strongly coupled with the flow in the dump diffuser and vice versa. The computations also revealed that the flow in the dump diffuser is highly nonuniform. Author

N94-23661*# Maine Univ., Orono. Div. of Mathematics.
AN ANALYTIC STUDY OF A TWO-PHASE LAMINAR AIRFOIL IN SIMULATED HEAVY RAIN **c02**
Yu-Kao Hsu *In* NASA. Lewis Research Center, The Fifth Annual Thermal and Fluids Analysis Workshop Nov. 1993 p 413-427 Sponsored by NASA. Langley Research Center (For primary document see N94-23634 06-34)
Avail: CASI HC A03/MF A04; 5 functional color pages

A mathematical model for a two-phase flow laminar airfoil in simulated heavy rain has been established. The set of non-linear partial differential equations has been converted into a set of finite difference equations; appropriate initial and boundary conditions are provided. The numerical results are compared with the experimental measurements. They show good agreement in quality. Author

N94-23662*# Air Force Inst. of Tech., Wright-Patterson AFB, OH. Dept. of Aerospace Engineering.

TRANSIENT STUDIES OF CAPILLARY-INDUCED FLOW

M. K. Reagan and W. J. Bowman *In* NASA. Lewis Research Center, The Fifth Annual Thermal and Fluids Analysis Workshop Nov. 1993 p 429-438 (For primary document see N94-23634 06-34)
Avail: CASI HC A02/MF A04; 5 functional color pages

This paper presents the numerical and experimental results of a study performed on the transient rise of fluid in a capillary tube. The capillary tube problem provides an excellent mechanism from which to launch an investigation into the transient flow of a fluid in a porous wick structure where capillary forces must balance both adverse gravitational effects and frictional losses. For the study, a capillary tube, initially charged with a small volume of water, was lowered into a pool of water. The behavior of the column of fluid during the transient that followed as more water entered the tube from the pool was both numerically and experimentally studied. Author

N94-23663*# Illinois Univ., Urbana-Champaign. Dept. of Mechanical and Industrial Engineering.

ON THE DETERMINATION OF LOCAL INSTANTANEOUS AVERAGES IN PARTICULATE FLOW MEASUREMENTS

R. E. VandeWall and S. L. Soo *In* NASA. Lewis Research Center, The Fifth Annual Thermal and Fluids Analysis Workshop Nov. 1993 p 439-448 (For primary document see N94-23634 06-34)
(Grant NSF CTS-90-14914)
Avail: CASI HC A02/MF A04; 5 functional color pages

Determination of instantaneous local average particle density of a gas-particle suspension requires satisfying both the time scale relation and the volume scale relation or its continuum counter part of time averaging. This procedure was validated by comparing simultaneous velocity and mass flux measurements and the laser phase Doppler measurements. Author

N94-23664*# Pennsylvania State Univ., University Park. Dept. of Aerospace Engineering.

THREE-DIMENSIONAL SOLIDIFICATION AND MELTING USING MAGNETIC FIELD CONTROL c76

George S. Dulikravich and Vineet Ahuja *In* NASA. Lewis Research Center, The Fifth Annual Thermal and Fluids Analysis Workshop Nov. 1993 p 449-464 (For primary document see N94-23634 06-34)
Avail: CASI HC A03/MF A04; 5 functional color pages

A new two-fluid mathematical model for fully three dimensional steady solidification under the influence of an arbitrary acceleration vector and with or without an arbitrary externally applied steady magnetic field have been formulated and integrated numerically. The model includes Joule heating and allows for separate temperature dependent physical properties within the melt and the solid. Latent heat of phase change during melting/solidification was incorporated using an enthalpy method. Mushy region was automatically captured by varying viscosity orders of magnitude between liquidus and solidus temperature. Computational results were obtained for silicon melt solidification in a parallelepiped container cooled from above and from a side. The results confirm that the magnetic field has a profound influence on the solidifying melt flow field thus changing convective heat transfer through the boundaries and the amount and shape of the solid accrued. This suggests that development of a quick-response algorithm for active control of three dimensional solidification is feasible since it would require low strength magnetic fields. Author (revised)

N94-23665*# Pennsylvania State Univ., University Park. Dept. of Aerospace Engineering.

UNSTEADY THREE-DIMENSIONAL THERMAL FIELD PREDICTION IN TURBINE BLADES USING NONLINEAR BEM

Thomas J. Martin and George S. Dulikravich *In* NASA. Lewis Research Center, The Fifth Annual Thermal and Fluids Analysis Workshop Nov. 1993 p 467-476 (For primary document see N94-23634 06-34)
Avail: CASI HC A02/MF A04; 5 functional color pages

A time-and-space accurate and computationally efficient fully three dimensional unsteady temperature field analysis computer code has been developed for truly arbitrary configurations. It uses boundary element method (BEM) formulation based on an unsteady Green's function approach, multi-point Gaussian quadrature spatial integration on each panel, and a highly clustered time-step integration. The code accepts either temperatures or heat fluxes as boundary conditions that can vary in time on a point-by-point basis. Comparisons of the BEM numerical results and known analytical unsteady results for simple shapes demonstrate very high accuracy and reliability of the algorithm. An example of computed three dimensional temperature and heat flux fields in a realistically shaped internally cooled turbine blade is also discussed. Author (revised)

N94-23666*# OLTech Corp., Chesterland, OH.

A DUAL RECIPROCAL BOUNDARY ELEMENT FORMULATION FOR VISCOUS FLOWS

Olu Lafe *In* NASA. Lewis Research Center, The Fifth Annual Thermal and Fluids Analysis Workshop Nov. 1993 p 477-487 (For primary document see N94-23634 06-34)
Avail: CASI HC A03/MF A04; 5 functional color pages

The advantages inherent in the boundary element method (BEM) for potential flows are exploited to solve viscous flow problems. The trick is the introduction of a so-called dual reciprocal technique in which the convective terms are represented by a global function whose unknown coefficients are determined by collocation. The approach, which is necessarily iterative, converts the governing partial differential equations into integral equations via the distribution of fictitious sources or dipoles of unknown strength on the boundary. These integral equations consist of two parts. The first is a boundary integral term, whose kernel is the unknown strength of the fictitious sources and the fundamental solution of a convection-free flow problem. The second part is a domain integral term whose kernel is the convective portion of the governing PDEs. The domain integration can be transformed to the boundary by using the dual reciprocal (DR) concept. The resulting formulation is a pure boundary integral computational process. Author (revised)

N94-23667*# University of Southern Illinois, Carbondale. Dept. of Mechanical Engineering and Energy Processes.

A THEOREM REGARDING ROOTS OF THE ZERO-ORDER BESSEL FUNCTION OF THE FIRST KIND

X.-A. Lin and O. P. Agrawal *In* NASA. Lewis Research Center, The Fifth Annual Thermal and Fluids Analysis Workshop Nov. 1993 p 489-498 (For primary document see N94-23634 06-34)
Avail: CASI HC A02/MF A04; 5 functional color pages

This paper investigates a problem on the steady-state, conduction-convection heat transfer process in cylindrical porous heat exchangers. The governing partial differential equations for the system are obtained using the energy conservation law. Solution of these equations and the concept of enthalpy lead to a new approach to prove a theorem that the sum of inverse squares of all the positive roots of the zero order Bessel function of the first kind equals to one-forth. As a corollary, it is shown that the sum of one over pth power (p greater than or equal to 2) of the roots converges to some constant. Author (revised)

N94-23668*# Arizona Univ., Tucson. Dept. of Aerospace and Mechanical Engineering.

AN APPLICATION OF SMALL-GAP EQUATIONS IN SEALING DEVICES

Carlos A. Vionnet and Juan C. Heinrich *In* NASA. Lewis Research Center, The Fifth Annual Thermal and Fluids Analysis Workshop Nov. 1993 p 499-512 (For primary document see N94-23634 06-34)
Avail: CASI HC A03/MF A04; 5 functional color pages

The study of a thin, incompressible Newtonian fluid layer trapped between two almost parallel, sliding surfaces has been actively pursued in the last decades. This subject includes lubrication applications such as slider bearings or the sealing of non-pressurized fluids with rubber rotary shaft seals. In the present work we analyze numerically the flow of lubricant fluid through a micro-gap of sealing devices. The first stage of this study is carried out assuming that a 'small-gap' parameter delta attains an extreme value in the Navier-Stokes equations. The precise meaning of small-gap is achieved by the particular limit delta = 0 which, within the bounds of the hypotheses, predicts transport of lubricant through the sealed area by centrifugal instabilities. Numerical results obtained with the penalty function approximation in the finite element method are presented. In particular, the influence of inflow and outflow boundary conditions, and their impact in the simulated flow, are discussed. Author (revised)

N94-23669*# Pennsylvania State Univ., Erie.

COMPARISON OF NUMERICAL SIMULATION AND EXPERIMENTAL DATA FOR STEAM-IN-PLACE STERILIZATION

Jack H. Young and William C. Lasher *In* NASA. Lewis Research Center, The Fifth Annual Thermal and Fluids Analysis Workshop Nov. 1993 p 513-522 (For primary document see N94-23634 06-34)
Avail: CASI HC A02/MF A04; 5 functional color pages

A complex problem involving convective flow of a binary mixture containing a condensable vapor and noncondensable gas in a partially enclosed chamber was modelled and results compared to transient experimental values. The finite element model successfully predicted transport processes in dead-ended tubes with inside diameters of 0.4 to 1.0 cm. When buoyancy driven convective flow was dominant, temperature and mixture compositions agreed with experimental data. Data from 0.4 cm tubes indicate diffusion to be the primary air removal method in small diameter tubes and the diffusivity value in the model to be too large. Author

N94-23670*# National Aeronautics and Space Administration. Lewis Research Center, Cleveland, OH.

A COMPARATIVE STUDY OF COMPUTATIONAL SOLUTIONS TO FLOW OVER A BACKWARD-FACING STEP

M. Mizukami, N. J. Georgiadis, and M. R. Cannon *In its* The Fifth Annual Thermal and Fluids Analysis Workshop Nov. 1993 p 523-530 (For primary document see N94-23634 06-34)
Avail: CASI HC A02/MF A04; 5 functional color pages

A comparative study was conducted for computational fluid dynamic solutions to flow over a backward-facing step. This flow is a benchmark problem, with a simple geometry, but involves complicated flow physics such as free shear layers, reattaching flow, recirculation, and high turbulence intensities. Three Reynolds-averaged Navier-Stokes flow solvers with k-epsilon turbulence models were used, each using a different solution algorithm: finite difference, finite element, and hybrid finite element - finite difference. Comparisons were made with existing experimental data. Results showed that velocity profiles and reattachment lengths were predicted reasonably well by all three methods, while the skin friction coefficients were more difficult to predict accurately. It was noted that, in general, selecting an appropriate solver for each problem to be considered is important. Author

N94-23671*# Wisconsin Univ., Platteville. Dept. of Mechanical Engineering.

RESPONSE-COEFFICIENT METHOD FOR HEAT-CONDUCTION TRANSIENTS WITH TIME-DEPENDENT INPUTS

Tamer Ceylan *In* NASA. Lewis Research Center, The Fifth Annual Thermal and Fluids Analysis Workshop Nov. 1993 p 531-537 (For primary document see N94-23634 06-34)
Avail: CASI HC A02/MF A04; 5 functional color pages

A theoretical overview of the response coefficient method for heat conduction transients with time-dependent input forcing functions is presented with a number of illustrative applications. The method may be the most convenient and economical if the same problem is to be solved many times with different input-time histories or if the solution time is relatively long. The method is applicable to a wide variety of problems, including irregular geometries, position-dependent boundary conditions, position-dependent physical properties, and nonperiodic irregular input histories. Nonuniform internal energy generation rates within the structure can also be handled by the method. The area of interest is long-time solutions, in which initial condition is unimportant, and not the early transient period. The method can be applied to one dimensional problems in cartesian, cylindrical, and spherical coordinates as well as to two dimensional problems in cartesian and cylindrical coordinates. Author (revised)

N94-23672*# Ohio State Univ., Columbus. Dept. of Aeronautical and Astronautical Engineering.

UPWIND MACCORMACK EULER SOLVER WITH NON-EQUILIBRIUM CHEMISTRY c61

Scott E. Sherer and James N. Scott *In* NASA. Lewis Research Center, The Fifth Annual Thermal and Fluids Analysis Workshop Nov. 1993 p 539-552 (For primary document see N94-23634 06-34)
Avail: CASI HC A03/MF A04; 5 functional color pages

A computer code, designated UMPIRE, is currently under development to solve the Euler equations in two dimensions with non-equilibrium chemistry. UMPIRE employs an explicit MacCormack algorithm with dissipation introduced via Roe's flux-difference split upwind method. The code also has the capability to employ a point-implicit methodology for flows where stiffness is introduced through the chemical source term. A technique consisting of diagonal sweeps across the computational domain from each corner is presented, which is used to reduce storage and execution requirements. Results depicting one dimensional shock tube flow for both calorically perfect gas and thermally perfect, dissociating nitrogen are presented to verify current capabilities of the program. Also, computational results from a chemical reactor vessel with no fluid dynamic effects are presented to check the chemistry capability and to verify the point implicit strategy. Author

N94-23809# Los Alamos National Lab., NM.

INVESTIGATIONS ON DETONATION SHOCK DYNAMICS AND RELATED TOPICS

D. S. Stewart 1993 308 p Prepared in cooperation with Illinois Univ., Urbana
(Contract W-7405-eng-36)
(DE94-002570; LA-SUB-93-299) Avail: CASI HC A14/MF A03

A final report that summarizes the research findings and research activities between the University of Illinois and the University of California is presented. The main focus of the work was on investigations of Detonation Shock Dynamics. A second emphasis was on modeling compaction of energetic materials and deflagration to detonation in those materials. The work has led to a number of extensions of the theory of Detonation Shock Dynamics (DSD) and its application as an engineering design method for high explosive systems. The work also enhanced the hydrocode capabilities of researchers in M-Division by modifications to CAVEAT, an existing Los Alamos hydrocode. Linear stability studies of detonation flows were carried out for the purpose of code verification. This work also broadened the existing theory for detonation. The work in this contract led to the development of one-phase models for dynamic compaction of porous energetic materials and laid the groundwork for subsequent studies. Some work that modeled the discrete heterogeneous behavior of propellant beds was also performed. DOE

N94-24063*# National Aeronautics and Space Administration. Lewis Research Center, Cleveland, OH.

RELIABILITY IN SECOND MOMENT TURBULENCE CLOSURES REVISITED

Tsan-Hsing Shih, Aamir Shabbir, and John L. Lumley (Cornell Univ., Ithaca, NY.) Jan. 1994 68 p
(Contract NCC3-233; RTOP 505-90-5K)
(NASA-TM-106469; E-8336; NAS 1.15:106469; ICOMP-93-51; CMOTT-93-18) Avail: CASI HC A04/MF A01

Realizability in turbulence modeling, i.e., the non-negativity of the normal Reynolds stresses and scalar variances and the Schwarz' inequality between any two fluctuating quantities, has been accepted as an important concept in the study of turbulence closures. Properly developed model equations based on realizability can prevent non-physical results and also reduce numerical stiffness. However, much confusion about the realizability concept has been created recently by Speziale et al. In order to provide a better understanding of realizability and its application in turbulence modeling, the following important subjects are discussed: the properties of general turbulent correlation matrices and the related realizability concept, the general realizability conditions and the method of their implementation. The detailed realizability constraints for various model terms in the second moment equations (including Reynolds stresses and scalar fluxes) that, we believe, are useful for developing more general turbulence models are presented. As an example, the realizable behavior of such realizably constrained second moment closures based on the work of Shih and Lumley for turbulent flows under various critical situations is demonstrated. For the purpose of comparisons, a recently proposed model by Speziale et al. that makes no attempt to satisfy realizability and the IP model of Launder, Reece and Rodi are also included. Comparisons clearly show the superior realizable behavior of the models based on realizability over that of the models not considering realizability. Author (revised)

N94-24096*# California Univ., Los Angeles. Mechanical, Aerospace and Nuclear Engineering Dept.
HEAT PIPE VAPOR DYNAMICS Ph.D. Thesis
Farrokh Issacci 1990 172 p
(Grant NAG3-899)
(NASA-CR-194217; NAS 1.26:194217) Avail: CASI HC A08/MF A02

The dynamic behavior of the vapor flow in heat pipes is investigated at startup and during operational transients. The vapor is modeled as two-dimensional, compressible viscous flow in an enclosure with inflow and outflow boundary conditions. For steady-state and operating transients, the SIMPLER method is used. In this method a control volume approach is employed on a staggered grid which makes the scheme very stable. It is shown that for relatively low input heat fluxes the compressibility of the vapor flow is low and the SIMPLER scheme is suitable for the study of transient vapor dynamics. When the input heat flux is high or the process under a startup operation starts at very low pressures and temperatures, the vapor is highly compressible and a shock wave is created in the evaporator. It is shown that for a wide range of input heat fluxes, the standard methods, including the SIMPLER scheme, are not suitable. A nonlinear filtering technique, along with the centered difference scheme, are then used for shock capturing as well as for the solution of the cell Reynolds-number problem. For high heat flux, the startup transient phase involves multiple shock reflections in the evaporator region. Each shock reflection causes a significant increase in the local pressure and a large pressure drop along the heat pipe. Furthermore, shock reflections cause flow reversal in the evaporation region and flow circulations in the adiabatic region. The maximum and maximum-averaged pressure drops in different sections of the heat pipe oscillate periodically with time because of multiple shock reflections. The pressure drop converges to a constant value at steady state. However, it is significantly higher than its steady-state value at the initiation of the startup transient. The time for the vapor core to reach steady-state condition depends on the input heat flux, the heat pipe geometry, the working fluid, and the condenser conditions. However, the vapor transient time, for an Na-filled heat pipe is on the order of seconds. Depending on the time constant for the overall system, the vapor transient time may be very short. Therefore, the vapor core may be assumed to be quasi-steady in the transient analysis of a heat pipe operation. Author

N94-24098*# California Inst. of Tech., Pasadena. Graduate Aeronautical Labs.
SKIN FRICTION MEASUREMENT IN COMPLEX FLOWS USING THIN OIL FILM TECHNIQUES Final Report, 1 Oct. 1989 - 31 Oct. 1993
31 Jan. 1994 7 p
(Grant NAG2-261)
(NASA-CR-194872; NAS 1.26:194872) Avail: CASI HC A02/MF A01

The NASA Grant NAG2-261 was initiated to support a program of research to study complex flows that occur in flight and laboratory experiments by building, testing and optimizing an on-board technique for direct measurement of surface shear stress using thin oil film techniques. The program of research has proceeded under the supervision of the NASA Ames Research Center and with further cooperation from the NASA Ames-Dryden and NASA Langley Research Centers. In accordance with the original statement of work, the following research milestones were accomplished: (1) design and testing of an internally mounted one-directional skin friction meter to demonstrate the feasibility of the concept; (2) design and construction of a compact instrument capable of measuring skin friction in two directions; (3) study of transitional and fully turbulent boundary layers over a flat plate with and without longitudinal pressure gradients utilizing the compact two-directional skin friction meter; (4) study of the interaction between a turbulent boundary layer and a shock wave generated by a compression corner using the two-directional meter; and (5) flight qualification of the compact meter and accompanying electronic and pneumatic systems, preliminary installation into flight test fixture.
Derived from text

N94-24138*# Stanford Univ., CA. Center for Turbulence Research.
ANNUAL RESEARCH BRIEFS, 1993
Dec. 1993 390 p Sponsored by NASA. Ames Research Center
(NASA-CR-194755; NAS 1.26:194755) Avail: CASI HC A17/MF A04

The 1993 annual progress reports of the Research Fellow and students of the Center for Turbulence Research are included. The first group of reports are directed towards the theory and application of active control in turbulent flows including the development of a systematic mathematical procedure based on the Navier Stokes equations for flow control. The second group of reports are concerned with the prediction of turbulent flows. The remaining articles are devoted to turbulent reacting flows, turbulence physics, experiments, and simulations. For individual titles, see N94-24139 through N94-24169.

N94-24139*# Stanford Univ., CA. Center for Turbulence Research.
OPTIMAL FEEDBACK CONTROL OF TURBULENT CHANNEL FLOW
Thomas Bewley, Haecheon Choi, Roger Temam (Paris-Sud Univ., Orsay, France.), and Parviz Moin *In its* Annual Research Briefs, 1993 Dec. 1993 p 3-14 (For primary document see N94-24138 06-34)
(Contract F49620-93-1-0078)
Avail: CASI HC A03/MF A04

Feedback control equations were developed and tested for computing wall normal control velocities to control turbulent flow in a channel with the objective of reducing drag. The technique used is the minimization of a 'cost functional' which is constructed to represent some balance of the drag integrated over the wall and the net control effort. A distribution of wall velocities is found which minimizes this cost functional some time shortly in the future based on current observations of the flow near the wall. Preliminary direct numerical simulations of the scheme applied to turbulent channel flow indicates it provides approximately 17 percent drag reduction. The mechanism apparent when the scheme is applied to a simplified flow situation is also discussed. Author (revised)

N94-24140*# Stanford Univ., CA. Center for Turbulence Research.
DRAG REDUCTION AT A PLANE WALL
D. C. Hill *In its* Annual Research Briefs, 1993 Dec. 1993 p 15-19
(For primary document see N94-24138 06-34)
Avail: CASI HC A01/MF A04

The objective is to determine by analytical means how drag on a plane wall may be modified favorably using a minimal amount of flow information - preferably only information at the wall. What quantities should be measured? How should that information be assimilated in order to arrive at effective control? As a prototypical problem, incompressible, viscous flow, governed by the Navier-Stokes equations, past a plane wall at which the no-slip condition was modified was considered. The streamwise and spanwise velocity components are required to be zero, but the normal component is to be specified according to some control law. The challenge is to choose the wall-normal velocity component based on flow conditions at the wall so that the mean drag is as small as possible. There can be no net mass flux through the wall, and the total available control energy is constrained. A turbulent flow is highly unsteady and has detailed spatial structure. The mean drag on the wall is the integral over the wall of the local shear forces exerted by the fluid, which is then averaged in time; it is a 'macroscopic' property of the flow. It is not obvious how unsteady boundary control is to be applied in order to modify the mean flow most effectively, especially in view of the non- self-adjoint nature of the governing equations. An approximate analytical solution to the suboptimal scheme is pursued. Author (revised)

N94-24141*# Stanford Univ., CA. Center for Turbulence Research.
BOUNDARY LAYER RECEPTIVITY AND CONTROL
D. C. Hill *In its* Annual Research Briefs, 1993 Dec. 1993 p 21-29
(For primary document see N94-24138 06-34)
Avail: CASI HC A02/MF A04

Receptivity processes initiate natural instabilities in a boundary layer. The instabilities grow and eventually break down to turbulence. Consequently, receptivity questions are a critical element of the analysis of the transition process. Success in modeling the physics of receptivity processes thus has a direct bearing on technological issues of drag reduction. The means by which transitional flows can be controlled is also a major concern: questions of control are tied inevitably to those of receptivity. Adjoint systems provide a highly effective mathematical method for approaching many of the questions associated with both receptivity and control. The long term objective is to develop adjoint methods to handle increasingly complex receptivity questions, and to find systematic procedures for deducing effective control strategies. The most elementary receptivity problem is that in which a parallel boundary layer is forced by time-harmonic sources of various types. The characteristics of the response to such forcing form the building blocks for more complex receptivity mechanisms. The first objective of this year's research effort was to investigate how a parallel Blasius boundary layer responds to general direct forcing. Acoustic disturbances in the freestream can be scattered by flow non-uniformities to produce Tollmien-Schlichting waves. For example, scattering by surface roughness is known to provide an efficient receptivity path. The present effort is directed towards finding a solution by a simple adjoint analysis, because adjoint methods can be extended to more complex problems. In practice, flows are non-parallel and often three-dimensional. Compressibility may also be significant in some cases. Recent developments in the use of Parabolized Stability Equations (PSE) offer a promising possibility. By formulating and solving a set of adjoint parabolized equations, a method for mapping the efficiency with which external forcing excites the three-dimensional motions of a non-parallel boundary layer was developed. The method makes use of the same computationally efficient formulation that makes the PSE currently so appealing. In the area of flow control, adjoint systems offer a powerful insight into the effect of control forces. One of the simplest control strategies for boundary layers involves the application of localized mean wall suction. Author (revised)

N94-24142*# Stanford Univ., CA. Center for Turbulence Research.
TOWARD MODELING WINGTIP VORTICES c02
O. Zeman *In its* Annual Research Briefs, 1993 Dec. 1993 p 31-40 (For primary document see N94-24138 06-34)
Avail: CASI HC A02/MF A04

Wingtip vortices are generated by lifting airfoils; their salient features are compactness and relatively slow rate of decay. The principal motivation for studying the far field evolution of wingtip vortices is the need to understand and predict the extent of the vortex influence during aircraft take-off or landing. On submarines a wingtip vortex ingested into a propeller can be a source of undesirable noise. The main objectives of this research are (1) to establish theoretical understanding of the principal mechanisms that govern the later (diffusive) stages of a turbulent vortex, (2) to develop a turbulence closure model representing the basic physical mechanisms that control the vortex diffusive stage, and further (3) to investigate coupling between the near and far field evolutions; in other words, to study the effect of initial conditions on the vortex lifetime and the ultimate state. Author (revised)

N94-24143*# Stanford Univ., CA. Center for Turbulence Research.
NEW CONCEPTS FOR REYNOLDS STRESS TRANSPORT EQUATION MODELING OF INHOMOGENEOUS FLOWS c02
J. Blair Perot and Parviz Moin *In its* Annual Research Briefs, 1993 Dec. 1993 p 41-65 (For primary document see N94-24138 06-34)
Avail: CASI HC A03/MF A04

The ability to model turbulence near solid walls and other types of boundaries is important in predicting complex engineering flows. Most turbulence modeling has concentrated either on flows which are nearly homogeneous or isotropic, or on turbulent boundary layers. Boundary layer models usually rely very heavily on the presence of mean shear and the production of turbulence due to that mean shear. Most other turbulence models are based on the assumption of quasi-homogeneity. However, there are many situations of engineering interest which do not involve large shear rates and which are not quasi-homogeneous or isotropic. Shear-free turbulent boundary layers are the prototypical example of such flows, with practical situations being separation and reattachment, bluff body flow, high free-stream turbulence, and free surface flows. Although these situations are not as common as the variants of the flat plate turbulent boundary layer, they tend to be critical factors in complex engineering situations. The models developed are intended to extend classical quasi-homogeneous models into regions of large inhomogeneity. These models do not rely on the presence of mean shear or production, but are still applicable when those additional effects are included. Although the focus is on shear-free boundary layers as tests for these models, results for standard shearing boundary layers are also shown. Author (revised)

N94-24144*# Cambridge Univ. (England).
TURBULENCE MODELING FOR NON-EQUILIBRIUM FLOWS
Paul A. Durbin *In* Stanford Univ., Annual Research Briefs, 1993 Dec. 1993 p 67-74 (For primary document see N94-24138 06-34)
Avail: CASI HC A02/MF A04

Two projects are reported. The first is the development and testing of an eddy viscosity transport model. This project also is a starting point for our work on developing computational tools for solving turbulence models in complex geometries. The second project is a stochastic analysis of the realizability of Reynolds stress transport models. Author (revised)

N94-24145*# Texas A&M Univ., College Station.
COMPUTATION OF TURBULENT FLOWS OVER BACKWARD AND FORWARD-FACING STEPS USING A NEAR-WALL REYNOLDS STRESS MODEL c02
Sung Ho Ko *In* Stanford Univ., Annual Research Briefs, 1993 Dec. 1993 p 75-90 (For primary document see N94-24138 06-34)
Avail: CASI HC A03/MF A04

Separation and reattachment of turbulent shear layers is observed in many important engineering applications, yet it is poorly understood. This has motivated many studies on understanding and predicting the processes of separation and reattachment of turbulent shear layers. Both of the situations in which separation is induced by adverse pressure gradient, or by discontinuities of geometry, have attracted attention of turbulence model developers. Formulation of turbulence closure models to describe the essential features of separated turbulent flows accurately is still a formidable task. Computations of separated flows associated with sharp-edged bluff bodies are described. For the past two decades, the backward-facing step flow, the simplest separated flow, has been a popular test case for turbulence models. Detailed studies on the performance of many turbulence models, including two equation turbulence models and Reynolds stress models, for flows over steps can be found in the papers by Thangam & Speziale and Lasher & Taulbee). These studies indicate that almost all the existing turbulence models fail to accurately predict many important features of back step flow such as reattachment length, recovery rate of the redeveloping boundary layers downstream of the reattachment point, streamlines near the reattachment point, and the skin friction coefficient. The main objectives are to calculate flows over backward and forward-facing steps using the NRSM and to make use of the newest DNS data for detailed comparison. This will give insights for possible improvements of the turbulence model. Author (revised)

N94-24146*# Stanford Univ., CA. Center for Turbulence Research.
LARGE EDDY SIMULATION OF A BOUNDARY LAYER WITH CONCAVE STREAMWISE CURVATURE
Thomas S. Lund *In its* Annual Research Briefs, 1993 Dec. 1993 p 91-99 (For primary document see N94-24138 06-34)
Avail: CASI HC A02/MF A04

One of the most exciting recent developments in the field of large eddy simulation (LES) is the dynamic subgrid-scale model. The dynamic model concept is a general procedure for evaluating model constants by sampling a band of the smallest scales actually resolved in the simulation. To date, the procedure has been used primarily in conjunction with the Smagorinsky model. The dynamic procedure has the advantage that the value of the model constant need not be specified a priori, but rather is calculated as a function of space and time as the simulation progresses. This feature makes the dynamic model especially attractive for flows in complex geometries where it is difficult or impossible to calibrate model constants. The dynamic model was highly successful in benchmark tests involving homogeneous and channel flows. Having demonstrated the potential of the dynamic model in these simple flows, the overall direction of the LES effort at CTR shifted toward an evaluation of the model in more complex situations. The current test cases are basic engineering-type flows for which Reynolds averaged approaches were unable to model the turbulence to within engineering accuracy. Flows currently under investigation include a backward-facing step, wake behind a circular cylinder, airfoil at high angles of attack, separated flow in a diffuser, and boundary layer over a concave surface. Preliminary results from the backward-facing step and cylinder wake simulations are encouraging. Progress on the LES of a boundary layer on a concave surface is discussed. Although the geometry of a concave wall is not very complex, the boundary layer that develops on its surface is difficult to model due to the presence of streamwise Taylor-Gortler vortices. These vortices arise as a result of a centrifugal instability associated with the convex curvature. Author (revised)

N94-24147*# Deutsche Forschungsanstalt fuer Luft- und Raumfahrt, Oberpfaffenhofen (Germany).
LARGE-EDDY SIMULATION OF FLOW IN A PLANE, ASYMMETRIC DIFFUSER

Hans-Jakob Kaltenbach *In* Stanford Univ., Annual Research Briefs, 1993 Dec. 1993 p 101-109 (For primary document see N94-24138 06-34)
Avail: CASI HC A02/MF A04

Recent improvements in subgrid-scale modeling as well as increases in computer power make it feasible to investigate flows using large-eddy simulation (LES) which have been traditionally studied with techniques based on Reynolds averaging. However, LES has not yet been applied to many flows of immediate technical interest. Preliminary results from LES of a plane diffuser flow are described. The long term goal of this work is to investigate flow separation as well as separation control in ducts and ramp-like geometries. Author (revised)

N94-24148*# Columbia Univ., New York, NY.
ON THE LARGE EDDY SIMULATION OF TURBULENT FLOWS IN COMPLEX GEOMETRY
Sandip Ghosal *In* Stanford Univ., Annual Research Briefs, 1993 Dec. 1993 p 111-128 (For primary document see N94-24138 06-34)
Avail: CASI HC A03/MF A04

Application of the method of Large Eddy Simulation (LES) to a turbulent flow consists of three separate steps. First, a filtering operation is performed on the Navier-Stokes equations to remove the small spatial scales. The resulting equations that describe the space time evolution of the 'large eddies' contain the subgrid-scale (sgs) stress tensor that describes the effect of the unresolved small scales on the resolved scales. The second step is the replacement of the sgs stress tensor by some expression involving the large scales - this is the problem of 'subgrid-scale modeling'. The final step is the numerical simulation of the resulting 'closed' equations for the large scale fields on a grid small enough to resolve the smallest of the large eddies, but still much larger than the fine scale structures at the Kolmogorov length. In dividing a turbulent flow field into 'large' and 'small' eddies, one presumes that a cut-off length delta can be sensibly chosen such that all fluctuations on a scale larger than delta are 'large eddies' and the remainder constitute the 'small scale' fluctuations. Typically, delta would be a length scale characterizing the smallest structures of interest in the flow. In an inhomogeneous flow, the 'sensible choice' for delta may vary significantly over the flow domain. For example, in a wall bounded turbulent flow, most statistical averages of interest vary much more rapidly with position near the wall than far away from it. Further, there are dynamically important organized structures near the wall on a scale much smaller than the boundary layer thickness. Therefore, the minimum size of eddies that need to be resolved is smaller near the wall. In general, for the LES of inhomogeneous flows, the width of the filtering kernel delta must be considered to be a function of position. If a filtering operation with a nonuniform filter width is performed on the Navier-Stokes equations, one does not in general get the standard large eddy equations. The complication is caused by the fact that a filtering operation with a nonuniform filter width in general does not commute with the operation of differentiation. This is one of the issues that we have looked at in detail as it is basic to any attempt at applying LES to complex geometry flows. Our principal findings are summarized. Author (revised)

N94-24149*# Rochester Univ., NY.
DYNAMIC LOCALIZATION AND SECOND-ORDER SUBGRID-SCALE MODELS IN LARGE EDDY SIMULATIONS OF CHANNEL FLOW
William H. Cabot *In* Stanford Univ., Annual Research Briefs, 1993 Dec. 1993 p 129-144 (For primary document see N94-24138 06-34)
Avail: CASI HC A03/MF A04

The objective here is to test the Dynamic Localization (DL) model in a wall-bounded channel flow for numerical stability and accuracy of results. Algebraic stress models suggest that the model for the residual subgrid-scale (SGS) Reynolds stress and scalar flux should generally have terms comprising most of the unique products of the resolved strain (S) and rotation (R) tensors with S and the resolved scalar gradient. The standard dynamic SGS model uses a simple (Smagorinsky) base model for the residual Reynolds stress, which is made proportional to S, and down-gradient base models for residual scalar fluxes; these correspond to the lowest, 'first-order' terms in algebraic stress models. Temporal scaling terms in these base models are formed from the magnitude of the resolved strain rate. While this is appropriate for simple shear flows, it may not be appropriate for more complicated flows (relevant to geophysical and astrophysical problems) that include any combination of shear, rotation, buoyancy, etc. On the other hand, the coefficient in the dynamic SGS model readily adjusts itself to different flow conditions and may adequately take account of these effects without the need for more complicated base models. Cabot (1993) has begun to test the dynamic SGS model in buoyant flows (Rayleigh-Benard and internally heated convection) with and without buoyancy terms explicitly included in the scaling terms of the base model; no great differences were found in large eddy simulation (LES) results for the different base model scalings. The second objective in this work is to test base models with additional, 'second-order' terms (e.g., S(sup 2) and RS for the residual Reynolds stress). These terms have been found to improve large-scale flow predictions by kappa-epsilon models in the presence of rotation and shear. Second-order base models will be tested here in the LES of channel flow with and without solid-body rotation and compared with results from the standard first-order base models to determine if there are significant differences or improvements in results that would warrant the added complexity of the second-order base models. Derived from text

N94-24150*# Stanford Univ., CA. Center for Turbulence Research.
TOWARD LARGE EDDY SIMULATION OF TURBULENT FLOW OVER AN AIRFOIL c02
Haecheon Choi *In its* Annual Research Briefs, 1993 Dec. 1993 p 145-149 (For primary document see N94-24138 06-34)
Avail: CASI HC A01/MF A04

The flow field over an airfoil contains several distinct flow characteristics, e.g. laminar, transitional, turbulent boundary layer flow, flow separation, unstable free shear layers, and a wake. This diversity of flow regimes taxes the presently available Reynolds averaged turbulence models. Such models are generally tuned to predict a particular flow regime, and adjustments are necessary for the prediction of a different flow regime. Similar difficulties are likely to emerge when the large eddy simulation technique is applied with the widely used Smagorinsky model. This model has not been successful in correctly representing different turbulent flow fields with a single universal constant and has an incorrect near-wall behavior. Germano et al. (1991) and Ghosal, Lund & Moin have developed a new subgrid-scale model, the dynamic model, which is very promising in alleviating many of the persistent inadequacies of the Smagorinsky model: the model coefficient is computed dynamically as the calculation progresses rather than input a priori. The model has been remarkably successful in prediction of several turbulent and transitional flows. We plan to simulate turbulent flow over a '2D' airfoil using the large eddy simulation technique. Our primary objective is to assess the performance of the newly developed dynamic subgrid-scale model for computation of complex flows about aircraft components and to compare the results with those obtained using the Reynolds average approach and experiments. The present computation represents the first application of large eddy simulation to a flow of aeronautical interest and a key demonstration of the capabilities of the large eddy simulation technique. Derived from text

N94-24151*# Stanford Univ., CA. Center for Turbulence Research.
UNSTRUCTURED GRID LARGE EDDY SIMULATION OF WALL BOUNDED TURBULENT FLOWS
Kenneth Jansen *In its* Annual Research Briefs, 1993 Dec. 1993 p 151-156 (For primary document see N94-24138 06-34)
Avail: CASI HC A02/MF A04

Historically, large eddy simulations (LES) have been restricted to simple geometries where spectral or finite difference methods have dominated due to their efficient use of structured grids. Structured grids, however, not only have difficulty representing complex domains and adapting to complicated flow features, but also are rather inefficient for simulating flows at high Reynolds numbers. The lack of efficiency stems from the need to resolve the viscous sub layer which requires very fine resolution in all three directions near the wall. Structured grids make use of a stretching to reduce the normal grid spacing but must carry the fine resolution in the streamwise and spanwise directions throughout the domain. The unnecessarily fine grid for much of the domain leads to disturbingly high grid estimates. Chapman (1979), and later Moin & Jimenez (1993), pointed out that, in order to advance the technology to airfoils at flight Reynolds numbers, structured grids must be abandoned in lieu of what are known as nested or unstructured grids. We illustrate the ability of an unstructured mesh to refine only the near wall region. Note the large number of points near the wall (where the fine vortical features need better resolution) and the coarseness in all directions away from the wall (where the scales are much larger). The important difference between this approach and the usual structured grid stretching is that the number of elements used to discretize the spanwise and streamwise features of the flow is reduced in each successive layer coming off the wall. This is due to the fact that the elements not only grow in the normal direction, but in the other directions as well. This greatly reduces the total number of points or elements required for a given Reynolds number flow. Derived from text

N94-24152*# National Aeronautics and Space Administration. Ames Research Center, Moffett Field, CA.

INVESTIGATION OF THE ASYMPTOTIC STATE OF ROTATING TURBULENCE USING LARGE-EDDY SIMULATION

Kyle D. Squires (Vermont Univ., Burlington.), Jeffrey R. Chasnov (Columbia Univ., New York, NY.), Nagi N. Mansour, and Claude Cambon (Ecole Centrale de Lyon, France.) *In* Stanford Univ., Annual Research Briefs, 1993 Dec. 1993 p 157-170 (For primary document see N94-24138 06-34)

Avail: CASI HC A03/MF A04

Study of turbulent flows in rotating reference frames has long been an area of considerable scientific and engineering interest. Because of its importance, the subject of turbulence in rotating reference frames has motivated over the years a large number of theoretical, experimental, and computational studies. The bulk of these previous works has served to demonstrate that the effect of system rotation on turbulence is subtle and remains exceedingly difficult to predict. A rotating flow of particular interest in many studies, including the present work, is examination of the effect of solid-body rotation on an initially isotropic turbulent flow. One of the principal reasons for the interest in this flow is that it represents the most basic turbulent flow whose structure is altered by system rotation but without the complicating effects introduced by mean strains or flow inhomogeneities. The assumption of statistical homogeneity considerably simplifies analysis and computation. The principal objective of the present study has been to examine the asymptotic state of solid-body rotation applied to an initially isotropic, high Reynolds number turbulent flow. Of particular interest has been to determine the degree of two-dimensionalization and the existence of asymptotic self-similar states in homogeneous rotating turbulence. Derived from text

N94-24153*# Madrid Univ. (Spain).

ENERGY TRANSFER AND CONSTRAINED SIMULATIONS IN ISOTROPIC TURBULENCE

Javier Jimenez *In* Stanford Univ., Annual Research Briefs, 1993 Dec. 1993 p 171-186 (For primary document see N94-24138 06-34)

Avail: CASI HC A03/MF A04

The defining characteristic of turbulent flows is their ability to dissipate energy, even in the limit of zero viscosity. The Euler equations, if constrained in such a way that the velocity derivatives remain bounded, conserve energy. But when they arise as the limit of the Navier-Stokes (NS) equations, when the Reynolds number goes to infinity, there is persuasive empirical evidence that the gradients become singular as just the right function of Re for the dissipation to remain non-zero and to approach a well defined limit. It is generally believed that this limiting value of the dissipation is a property of the Euler equations themselves, independent of the particular dissipative mechanism involved, and that it can be normalized with the large scale properties of the turbulent flow (e.g. the kinetic energy per unit volume u'(exp 2)/2, and the integral scale L) without reference to the Reynolds number or to other dissipative quantities. This is usually taken to imply that the low wave number end of the energy spectrum, far from the dissipative range, is also independent of the particular mechanism chosen to dispose of the energy transfer. In the following sections, we present some numerical experiments on the effect of substituting different dissipation models into the truncated Euler equations. We will see that the effect is mainly felt in the 'near dissipation' range of the energy spectrum, but that this range can be quite wide in some cases, contaminating a substantial range of wave numbers. In the process, we will develop a 'practical' approximation to the subgrid energy transfer in isotropic turbulence, and we will gain insight into the structure of the nonlinear interactions among turbulent scales of comparable size, and into the nature of energy backscatter. Some considerations on future research directions are offered at the end. Derived from text

N94-24154*# State Univ. of New York, Stony Brook.

A LARGE EDDY SIMULATION SCHEME FOR TURBULENT REACTING FLOWS

Feng Gao *In* Stanford Univ., Annual Research Briefs, 1993 Dec. 1993 p 187-194 (For primary document see N94-24138 06-34)

Avail: CASI HC A02/MF A04

The recent development of the dynamic subgrid-scale (SGS) model has provided a consistent method for generating localized turbulent mixing models and has opened up great possibilities for applying the large eddy simulation (LES) technique to real world problems. Given the fact that the direct numerical simulation (DNS) can not solve for engineering flow problems in the foreseeable future (Reynolds 1989), the LES is certainly an attractive alternative. It seems only natural to bring this new development in SGS modeling to bear on the reacting flows. The major stumbling block for introducing LES to reacting flow problems has been the proper modeling of the reaction source terms. Various models have been proposed, but none of them has a wide range of applicability. For example, some of the models in combustion have been based on the flamelet assumption which is only valid for relatively fast reactions. Some other models have neglected the effects of chemical reactions on the turbulent mixing time scale, which is certainly not valid for fast and non-isothermal reactions. The probability density function (PDF) method can be usefully employed to deal with the modeling of the reaction source terms. In order to fit into the framework of LES, a new PDF, the large eddy PDF (LEPDF), is introduced. This PDF provides an accurate representation for the filtered chemical source terms and can be readily calculated in the simulations. The details of this scheme are described. Derived from text

N94-24155*# Centre Europeen Recherche et de Formation Advance en Calcul Scientific, Toulouse (France).

THE COMBUSTION PROGRAM AT CTR c25

Thierry J. Poinsot *In* Stanford Univ., Annual Research Briefs, 1993 Dec. 1993 p 195-203 (For primary document see N94-24138 06-34)

Avail: CASI HC A02/MF A04

Understanding and modeling of turbulent combustion are key problems in the computation of numerous practical systems. Because of the lack of analytical theories in this field and of the difficulty of performing precise experiments, direct numerical simulation (DNS) appears to be one of the most attractive tools to use in addressing this problem. The general objective of DNS of reacting flows is to improve our knowledge of turbulent combustion but also to use this information for turbulent combustion models. For the foreseeable future, numerical simulation of the full three-dimensional governing partial differential equations with variable density and transport properties as well as complex chemistry will remain intractable; thus, various levels of simplification will remain necessary. On one hand, the requirement to simplify is not necessarily a handicap: numerical simulations allow the researcher a degree of control in isolating specific physical phenomena that is inaccessible in experiments. CTR has pursued an intensive research program in the field of DNS for turbulent reacting flows since 1987. DNS of reacting flows is quite different from DNS of non-reacting flows: without reaction, the equations to solve are clearly the five conservation equations of the Navier Stokes system for compressible situations (four for incompressible cases), and the limitation of the approach is the Reynolds number (or in other words the number of points in the computation). For reacting flows, the choice of the equations, the species (each species will require one additional conservation equation), the chemical scheme, and the configuration itself is more complex. Author

N94-24156*# Ecole Centrale de Paris (France).

STRETCH-INDUCED QUENCHING IN FLAME-VORTEX INTERACTIONS c25

J.-M. Samaniego *In* Stanford Univ., Annual Research Briefs, 1993 Dec. 1993 p 205-218 (For primary document see N94-24138 06-34)

Avail: CASI HC A03/MF A04

The flame-vortex interaction problem is a natural configuration in which several issues relevant to turbulent combustion can be addressed: effect of strain-rate and curvature, effect of the Lewis number, effect of heat losses, effect of complex chemistry, and flame-generated turbulence. In such an approach, the interaction of an isolated vortex with a laminar premixed flame is viewed as a unit process of a turbulent premixed flame in which the reaction zone keeps a laminar like structure locally; this is precisely the case of the wrinkled flame or flamelet regime in turbulent combustion. The present work complements previous studies and involves the study of the interaction of a vortex pair and a laminar premixed flame in a planar two-dimensional geometry, together with numerical simulations. This geometry is quite unique since most studies have considered axisymmetric vortex rings. Such a geometry offers several advantages over previous studies. Derived from text

N94-24157*# Rouen Univ. (France).

A TRANSPORT EQUATION FOR THE SCALAR DISSIPATION IN REACTING FLOWS WITH VARIABLE DENSITY: FIRST RESULTS

T. Mantel *In* Stanford Univ., Annual Research Briefs, 1993 Dec. 1993 p 219-228 (For primary document see N94-24138 06-34)
Avail: CASI HC A02/MF A04

Although the different regimes of premixed combustion are not well defined, most of the recent developments in turbulent combustion modeling are led in the so-called flamelet regime. The goal of these models is to give a realistic expression to the mean reaction rate (w). Several methods can be used to estimate (w). Bray and coworkers (Libby & Bray 1980, Bray 1985, Bray & Libby 1986) express the instantaneous reaction rate by means of a flamelet library and a frequency which describes the local interaction between the laminar flamelets and the turbulent flowfield. In another way, the mean reaction rate can be directly connected to the flame surface density (Sigma). This quantity can be given by the transport equation of the coherent flame model initially proposed by Marble & Broadwell 1977 and developed elsewhere. The mean reaction rate, (w), can also be estimated thanks to the evolution of an arbitrary scalar field G(x, t) = G(sub O) which represents the flame sheet. G(x, t) is obtained from the G-equation proposed by Williams 1985, Kerstein et al. 1988 and Peters 1993. Another possibility proposed in a recent study by Mantel & Borghi 1991, where a transport equation for the mean dissipation rate (epsilon(sub c)) of the progress variable c is used to determine (w). In their model, Mantel & Borghi 1991 considered a medium with constant density and constant diffusivity in the determination of the transport equation for (epsilon(sub c)). A comparison of different flamelet models made by Duclos et al. 1993 shows the realistic behavior of this model even in the case of constant density. Our objective in this present report is to present preliminary results on the study of this equation in the case of variable density and variable diffusivity. Assumptions of constant pressure and a Lewis number equal to unity allow us to significantly simplify the equation. A systematic order of magnitude analysis based on adequate scale relations is performed on each term of the equation. As in the case of constant density and constant diffusivity, the effects of stretching of the scalar field by the turbulent strain field, of local curvature, and of chemical reactions are predominant. In this preliminary work, we suggest closure models for certain terms, which will be validated after comparisons with DNS data. Derived from text

N94-24158*# Ecole Centrale de Paris (France).

THE PRODUCTION OF PREMIXED FLAME SURFACE AREA IN TURBULENT SHEAR FLOW c25

A. Trouve *In* Stanford Univ., Annual Research Briefs, 1993 Dec. 1993 p 229-248 (For primary document see N94-24138 06-34)
Avail: CASI HC A03/MF A01

In the present work, we use three-dimensional Direct Numerical Simulation (DNS) of premixed flames in turbulent shear flow to characterize the effect of a mean shear motion on flame surface production. The shear is uniform in the unburnt gas, and simulations are performed for different values of the mean shear rate, S. The data base is then used to estimate and compare the different terms appearing in the Sigma-equation as a function of S. The analysis gives in particular the relative weights f the turbulent flow and mean flow components, a(sub T) and A(sub T), of the flame surface production term. This comparison indicates whether the dominant effects of a mean flow velocity gradient on flame surface area are implicit and scale with the modified turbulent flow parameters, kappa and epsilon, or explicit and scale directly with the rate of deformation. Derived from text

N94-24159*# National Aeronautics and Space Administration. Ames Research Center, Moffett Field, CA.

ON STREAK SPACING IN WALL-BOUNDED TURBULENT FLOWS

James M. Hamilton (Harvard Univ., Cambridge, MA.) and John J. Kim *In* Stanford Univ., Annual Research Briefs, 1993 Dec. 1993 p 249-257 (For primary document see N94-24138 06-34)
Avail: CASI HC A02/MF A04

The present study is a continuation of the examination by Hamilton et al. of the regeneration mechanisms of near-wall turbulence and an attempt to investigate the conjecture of Waleffe et al. The basis of this study is an extension of the 'minimal channel' approach of Jimenez and Moin that emphasizes the near-wall region and reduces the complexity of the turbulent flow by considering a plane Couette flow of near minimum Reynolds number and stream-wise and span-wise extent. Reduction of the flow Reynolds number to the minimum value which will allow turbulence to be sustained has the effect of reducing the ratio of the largest scales to the smallest scales or, equivalently, of causing the near-wall region to fill more of the area between the channel walls. A plane Couette flow was chosen for study since this type of flow has a mean shear of a single sign, and at low Reynolds numbers, the two wall regions are found to share a single set of structures. Derived from text

N94-24160*# Stanford Univ., CA.

NUMERICAL SIMULATION OF NON-NEWTONIAN FREE SHEAR FLOWS

G. M. Homsy and J. Azaiez *In its* Annual Research Briefs, 1993 Dec. 1993 p 259-268 (For primary document see N94-24138 06-34)
Avail: CASI HC A02/MF A04

Free shear flows, like those of mixing layers, are encountered in aerodynamics, in the atmosphere, and in the ocean as well as in many industrial applications such as flow reactors or combustion chambers. It is, therefore, crucial to understand the mechanisms governing the process of transition to turbulence in order to predict and control the evolution of the flow. Delaying transition to turbulence as far downstream as possible allows a gain in energy expenditure while accelerating the transition can be of interest in processes where high mixing is desired. Various methods, including the use of polymer additives, can be effective in controlling fluid flows. The drag reduction obtained by the addition of small amounts of high polymers has been an active area of research for the last three decades. It is now widely believed that polymer additives can affect the stability of a large variety of flows and that dilute solutions of these polymers have been shown to produce drag reductions of over 80 percent in internal flows and over 60 percent in external flows under a wide range of conditions. The major thrust of this work is to study the effects of polymer additives on the stability of the incompressible mixing layer through large scale numerical simulations. In particular, we focus on the two dimensional flow and examine how the presence of viscoelasticity may affect the typical structures of the flow, namely roll-up and pairing of vortices. Derived from text

N94-24161*# National Aeronautics and Space Administration. Ames Research Center, Moffett Field, CA.

TRANSITION TO TURBULENCE IN AN ELLIPTIC VORTEX

Thomas S. Lundgren (Minnesota Univ., Minneapolis.) and N. N. Mansour *In* Stanford Univ., Annual Research Briefs, 1993 Dec. 1993 p 269-284 (For primary document see N94-24138 06-34)
Avail: CASI HC A03/MF A04

We study the three dimensional instability and nonlinear growth of the two dimensional flow described by the stream function Psi = (A sin b1 x sin b2 y)/(b1(exp 2) + b2(exp 2)) where b1 = pi/L1, b2 = pi/L2. This is a swirling flow in a box which is bounded by 0 less than x less than L1, 0 less than y less than L2 and is infinite in the z direction. This flow is a solution of the Navier-Stokes equation with A = exp(-v(b1(exp 2) + b2(exp 2))t) which slowly decays. We seek a viscous solution which starts near this one and slips along but does not penetrate the bounding walls. The vorticity of the basic flow is w(sub z) = A sin b1 x sin b2 y which has maximum value A at the center of the box and drops to zero at the boundaries. We can think of the resulting flow as that of a captive vortex. Derived from text

N94-24162*# State Univ. of New York, Buffalo.

VORTICAL STRUCTURE IN A FORCED PLANE MIXING LAYER

Richard L. LeBoeuf *In* Stanford Univ., Annual Research Briefs, 1993 Dec. 1993 p 285-298 (For primary document see N94-24138 06-34)
Avail: CASI HC A03/MF A04

The objective of this phase of an ongoing study is to obtain detailed three dimensional phase-averaged measurements of forced mixing layer vorticity development and evolution. Acoustic forcing is being used to phase-lock the initial development and subsequent pairing of the span wise vortical structures. Phase averaged measurements of the three velocity components will permit the study of three dimensional vorticity distributions without invoking Taylor's hypothesis which is known to introduce uncertainty. Currently two sine waves, one at the fundamental roll-up frequency and the second, its subharmonic, are being used to force the initial roll-up and first pairing of the span wise rollers. The two dimensional measurements described in this report were obtained in order to determine the best operating conditions for the detailed three dimensional study of the mixing layer undergoing pairing via various pairing mechanisms. Author (revised)

N94-24163*# Colorado Univ., Boulder.
SOUND RADIATION DUE TO BOUNDARY LAYER TRANSITION c71
Meng Wang *In* Stanford Univ., Annual Research Briefs, 1993 Dec. 1993 p 299-312 (For primary document see N94-24138 06-34)
Avail: CASI HC A03/MF A04

This report describes progress made to date towards calculations of noise produced by the laminar-turbulence transition process in a low Mach number boundary layer formed on a rigid wall. The primary objectives of the study are to elucidate the physical mechanisms by which acoustic waves are generated, to clarify the roles of the fluctuating Reynolds stress and the viscous stress in the presence of a solid surface, and to determine the relative efficiency as a noise source of the various transition stages. In particular, we will examine the acoustic characteristics and directivity associated with three-dimensional instability waves, the detached high-shear layer, and turbulent spots following a laminar breakdown. Additionally, attention will be paid to the unsteady surface pressures during the transition, which provide a source of flow noise as well as a forcing function for wall vibration in both aeronautical and marine applications. Derived from text

N94-24164*# Stanford Univ., CA.
DIRECT SIMULATION OF ISOTHERMAL-WALL SUPERSONIC CHANNEL FLOW c02
Gary N. Coleman *In its* Annual Research Briefs, 1993 Dec. 1993 p 313-328 (For primary document see N94-24138 06-34)
Avail: CASI HC A03/MF A04

The motivation for this work is the fact that in turbulent flows where compressibility effects are important, they are often poorly understood. A few examples of such flows are those associated with astrophysical phenomena and those found in combustion chambers, supersonic diffusers and nozzles, and over high-speed airfoils. For this project, we are primarily interested in compressibility effects near solid surfaces. Our main objective is an improved understanding of the fundamentals of compressible wall-bounded turbulence, which can in turn be used to cast light upon modeling concepts such as the Morkovin hypothesis and the Van Driest transformation. To this end, we have performed a direct numerical simulation (DNS) study of supersonic turbulent flow in a plane channel with constant-temperature walls. All of the relevant spatial and temporal scales are resolved so that no sub grid scale or turbulence model is necessary. The channel geometry was chosen so that finite Mach number effects can be isolated by comparing the present results to well established incompressible channel data. Here the fluid is assumed to be an ideal gas with constant specific heats, constant Prandtl number, and power-law temperature-dependent viscosity. Isothermal-wall boundary conditions are imposed so that a statistically stationary state may be obtained. The flow is driven by a uniform (in space) body force (rather than a mean pressure gradient) to preserve stream wise homogeneity, with the body force defined so that the total mass flux is constant. Derived from text

N94-24165*# Stanford Univ., CA.
EFFECTS OF SHOCK STRENGTH ON SHOCK TURBULENCE INTERACTION
Sangsan Lee *In its* Annual Research Briefs, 1993 Dec. 1993 p 329-345 (For primary document see N94-24138 06-34)
Avail: CASI HC A03/MF A04

Direct numerical simulation (DNS) and linear analysis (LIA) of isotropic turbulence interacting with a shock wave are performed for several upstream shock normal Mach numbers (M(sub 1)). Turbulence kinetic energy (TKE) is amplified across the shock wave, but this amplification tends to saturate beyond M(sub 1) = 3.0. TKE amplification and Reynolds stress anisotropy obtained in DNS are consistent with LIA predictions. Rapid evolution of TKE immediate downstream of the shock wave persists for all shock strengths and is attributed to the transfer between kinetic and potential modes of turbulence energy through acoustic fluctuations. Changes in energy spectra and various length scales across the shock wave are predicted by LIA, which is consistent with DNS results. Most turbulence length scales decrease across the shock. Dissipation length scale (rho-bar q(exp 3) / epsilon), however, increases slightly for shock waves with M(sub 1) less than 1.65. Fluctuations in thermodynamic variables behind the shock wave stay nearly isentropic for M(sub 1) less than 1.2 and deviate significantly from isentropy for the stronger shock waves due to large entropy fluctuation generated through the interaction. Author (revised)

N94-24166*# Melbourne Univ., Parkville (Australia).
LOCAL ISOTROPY IN DISTORTED TURBULENT BOUNDARY LAYERS AT HIGH REYNOLDS NUMBER
Seyed G. Saddoughi *In* Stanford Univ., Annual Research Briefs, 1993 Dec. 1993 p 347-363 (For primary document see N94-24138 06-34)
Avail: CASI HC A03/MF A04

This is a report on the continuation of our experimental investigations of the hypothesis of local isotropy in shear flows. This hypothesis, which states that at sufficiently high Reynolds numbers the small-scale structures of turbulent motions are independent of large-scale structures and mean deformations, has been used in theoretical studies of turbulence and computational methods such as large-eddy simulation. Since Kolmogorov proposed his theory, there have been many experiments, conducted in wakes, jets, mixing layers, a tidal channel, and atmospheric and laboratory boundary layers, in which attempts have been made to verify - or refute - the local-isotropy hypothesis. However, a review of the literature over the last five decades indicated that, despite all these experiments in shear flows, there was no consensus in the scientific community regarding this hypothesis, and, therefore, it seemed worthwhile to undertake a fresh experimental investigation into this question. Derived from text

N94-24167*# Columbia Univ., New York, NY.
COMPUTATION OF LARGE-SCALE STATISTICS IN DECAYING ISOTROPIC TURBULENCE
Jeffrey R. Chasnov *In* Stanford Univ., Annual Research Briefs, 1993 Dec. 1993 p 365-371 (For primary document see N94-24138 06-34)
Avail: CASI HC A02/MF A04

We have performed large-eddy simulations of decaying isotropic turbulence to test the prediction of self-similar decay of the energy spectrum and to compute the decay exponents of the kinetic energy. In general, good agreement between the simulation results and the assumption of self-similarity were obtained. However, the statistics of the simulations were insufficient to compute the value of gamma which corrects the decay exponent when the spectrum follows a k(exp 4) wave number behavior near k = 0. To obtain good statistics, it was found necessary to average over a large ensemble of turbulent flows. Derived from text

N94-24168*# California Univ., Irvine.
ON THE DYNAMICS OF APPROXIMATING SCHEMES FOR DISSIPATIVE NONLINEAR EQUATIONS
Donald A. Jones *In* Stanford Univ., Annual Research Briefs, 1993 Dec. 1993 p 373-386 (For primary document see N94-24138 06-34)
Avail: CASI HC A03/MF A04

Since one can rarely write down the analytical solutions to nonlinear dissipative partial differential equations (PDE's), it is important to understand whether, and in what sense, the behavior of approximating schemes to these equations reflects the true dynamics of the original equations. Further, because standard error estimates between approximations of the true solutions coming from spectral methods - finite difference or finite element schemes, for example - and the exact solutions grow exponentially in time, this analysis provides little value in understanding the infinite time behavior of a given approximating scheme. The notion of the global attractor has been useful in quantifying the infinite time behavior of dissipative PDEs, such as the Navier-Stokes equations. Loosely speaking, the global attractor is all that remains of a sufficiently large bounded set in phase space mapped infinitely forward in time under the evolution of the PDE. Though the attractor has been shown to have some nice properties - it is compact, connected, and finite dimensional, for example - it is in general quite complicated. Nevertheless, the global attractor gives a way to understand how the infinite time behavior of approximating schemes such as the ones coming from a finite difference, finite element, or spectral method relates to that of the original PDE. Indeed, one can often show that such approximations also have a global attractor. We therefore only need to understand how the structure of the attractor for the PDE behaves under approximation. This is by no means a trivial task. Several interesting results have been obtained in this direction. However, we will not go into the details. We mention here that approximations generally lose information about the system no matter how accurate they are. There are examples that show certain parts of the attractor may be lost by arbitrary small perturbations of the original equations. Derived from text

N94-24169*# Columbia Univ., New York, NY.
TENSORAL FOR POST-PROCESSING USERS AND SIMULATION AUTHORS **c61**
Eliot Dresselhaus *In* Stanford Univ., Annual Research Briefs, 1993 Dec. 1993 p 387-394 (For primary document see N94-24138 06-34)
Avail: CASI HC A02/MF A04

The CTR post-processing effort aims to make turbulence simulations and data more readily and usefully available to the research and industrial communities. The Tensoral language, which provides the foundation for this effort, is introduced here in the form of a user's guide. The Tensoral user's guide is presented in two main sections. Section one acts as a general introduction and guides database users who wish to post-process simulation databases. Section two gives a brief description of how database authors and other advanced users can make simulation codes and/or the databases they generate available to the user community via Tensoral database back ends. The two-part structure of this document conforms to the two-level design structure of the Tensoral language. Tensoral has been designed to be a general computer language for performing tensor calculus and statistics on numerical data. Tensoral's generality allows it to be used for stand-alone native coding of high-level post-processing tasks (as described in section one of this guide). At the same time, Tensoral's specialization to a minute task (namely, to numerical tensor calculus and statistics) allows it to be easily embedded into applications written partly in Tensoral and partly in other computer languages (here, C and Vectoral). Embedded Tensoral, aimed at advanced users for more general coding (e.g. of efficient simulations, for interfacing with pre-existing software, for visualization, etc.), is described in section two of this guide. Author (revised)

N94-24177 Laval Univ. (Quebec). Ecole des Gradues.
EXPERIMENTAL STUDY OF A TURBULENT BOUNDARY LAYER IN PRESENCE OF EXTERNAL MANIPULATORS OF NACA 0009 PROFILE IN THE TRANSONIC REGIME M.S. Thesis [ETUDE EXPERIMENTALE D'UNE COUCHE LIMITE TURBULENTE EN PRESENCE DE MANIPULATEURS EXTERNES DE PROFIL NACA 0009 EN REGIME TRANSSONIQUE]
Diane Poirier May 1990 293 p In FRENCH
(ISBN-0-315-57633-2; CTN-94-60874) Copyright Avail: Micromedia Ltd., Technical Information Centre, 240 Catherine Street, Suite 305, Ottawa, Ontario, K2P 2G8, Canada HC/MF

An experimental study was conducted to determine the effectiveness of manipulators of external-type turbulence on the reduction of wall drag in a turbulent boundary layer in the transonic regime. The manipulators used, NACA 0009 thin profile type, have an aerodynamic behavior inappropriate for this type of application. Flow visualizations show that the flow on the manipulator is complex, with regions of separation, as well as recirculation, and that the wake of the manipulator is sometimes very unstable. Some of such behavior may be the origin of the high levels of drag encountered and adversely affects the effectiveness of this method in the sense of net balance. The analysis of the average velocity profiles, downstream of the single manipulator, does not permit reaching definitive quantitative conclusions since it leads to abnormally high reductions of the coefficient of wall drag, due apparently to the presence of a longitudinal pressure gradient which was not considered in the equation of motion. CISTI

N94-24336*# National Aeronautics and Space Administration. Lewis Research Center, Cleveland, OH.
CENTER FOR MODELING OF TURBULENCE AND TRANSITION: RESEARCH BRIEFS, 1993 Annual Report, Jun. 1992 - Jul. 1993
William W. Liou, ed. Jan. 1994 249 p
(Contract NCC3-233; RTOP 505-90-5K)
(NASA-TM-106383; ICOMP-93-44; E-8202; NAS 1.15:106383; CMOTT-93-16) Avail: CASI HC A11/MF A03

This research brief contains the progress reports of the research staff of the Center for Modeling of Turbulence and Transition (CMOTT) from June 1992 to July 1993. It is also an annual report to the Institute for Computational Mechanics in Propulsion located at Ohio Aerospace Institute and NASA Lewis Research Center. The main objectives of the research activities at CMOTT are to develop, validate, and implement turbulence and transition models for flows of interest in propulsion systems. Currently, our research covers eddy viscosity one- and two-equation models, Reynolds-stress algebraic equation models, Reynolds-stress transport equation models, nonequilibrium multiple-scale models, bypass transition models, joint scalar probability density function models, and Renormalization Group Theory and Direct Interaction Approximation methods. Some numerical simulations (LES and DNS) have also been carried out to support the development of turbulence modeling. Last year was CMOTT's third year in operation. During this period, in addition to the above mentioned research, CMOTT has also hosted the following programs: an eighteen-hour short course on 'Turbulence--Fundamentals and Computational Modeling (Part I)' given by CMOTT at the NASA Lewis Research Center; a productive summer visitor research program that has generated many encouraging results; collaborative programs with industry customers to help improve their turbulent flow calculations for propulsion system designs; a biweekly CMOTT seminar series with speakers from within and without the NASA Lewis Research Center including foreign speakers. In addition, CMOTT members have been actively involved in the national and international turbulence research activities. The current CMOTT roster and organization are listed in Appendix A. Listed in Appendix B are the abstracts of the biweekly CMOTT seminar. Appendix C lists the papers contributed by CMOTT members. Author (revised)

N94-24356*# National Aeronautics and Space Administration. Langley Research Center, Hampton, VA.
THE RADIATED NOISE FROM ISOTROPIC TURBULENCE REVISITED Final Report
Geoffrey M. Lilley Dec. 1993 56 p Submitted for publication
(Contract NAS1-19480; RTOP 505-90-52-01)
(NASA-CR-191547; ICASE-93-75; NAS 1.26:191547) Avail: CASI HC A04/MF A01

The noise radiated from isotropic turbulence at low Mach numbers and high Reynolds numbers, as derived by Proudman (1952), was the first application of Lighthill's Theory of Aerodynamic Noise to a complete flow field. The theory presented by Proudman involves the assumption of the neglect of retarded time differences and so replaces the second-order retarded-time and space covariance of Lighthill's stress tensor, Tij, and in particular its second time derivative, by the equivalent simultaneous covariance. This assumption is a valid approximation in the derivation of the second partial derivative of Tij/derivative of t exp 2 covariance at low Mach numbers, but is not justified when that covariance is reduced to the sum of products of the time derivatives of equivalent second-order velocity covariances as required when Gaussian statistics are assumed. The present paper removes these assumptions and finds that although the changes in the analysis are substantial, the change in the numerical result for the total acoustic power is small. The present paper also considers an alternative analysis which does not neglect retarded times. It makes use of the Lighthill relationship, whereby the fourth-order Tij retarded-time covariance is evaluated from the square of similar second order covariance, which is assumed known. In this derivation, no statistical assumptions are involved. This result, using distributions for the second-order space-time velocity squared covariance based on the Direct Numerical Simulation (DNS) results of both Sarkar and Hussaini(1993) and Dubois(1993), is compared with the re-evaluation of Proudman's original model. These results are then compared with the sound power derived from a phenomenological model based on simple approximations to the retarded-time/space covariance of Txx. Finally, the recent numerical solutions of Sarkar and Hussaini(1993) for the acoustic power are compared with the results obtained from the analytic solutions. Author (revised)

N94-24460*# National Aeronautics and Space Administration. Lewis Research Center, Cleveland, OH.
WORKSHOP ON COMPUTATIONAL TURBULENCE MODELING

A. Shabbir, comp., T.-H. Shih, comp., and L. A. Povinelli, comp. Jan. 1994 419 p Workshop held in Cleveland, OH, 15-16 Sep. 1993; sponsored by Institute for Computational Mechanics in Propulsion and Center for Modeling of Turbulence and Transition
(Contract NCC3-233; RTOP 505-90-5K)
(NASA-CP-10130; ICOMP-93-46; E-8201; NAS 1.55:10130; CMOTT-93-17)
Avail: CASI HC A18/MF A04

The purpose of this meeting was to discuss the current status and future development of turbulence modeling in computational fluid dynamics for aerospace propulsion systems. Various turbulence models have been developed and applied to different turbulent flows over the past several decades and it is becoming more and more urgent to assess their performance in various complex situations. In order to help users in selecting and implementing appropriate models in their engineering calculations, it is important to identify the capabilities as well as the deficiencies of these models. This also benefits turbulence modelers by permitting them to further improve upon the existing models. This workshop was designed for exchanging ideas and enhancing collaboration between different groups in the Lewis community who are using turbulence models in propulsion related CFD. In this respect this workshop will help the Lewis goal of excelling in propulsion related research. This meeting had seven sessions for presentations and one panel discussion over a period of two days. Each presentation session was assigned to one or two branches (or groups) to present their turbulence related research work. Each group was asked to address at least the following points: current status of turbulence model applications and developments in the research; progress and existing problems; and requests about turbulence modeling. The panel discussion session was designed for organizing committee members to answer management and technical questions from the audience and to make concluding remarks. Author (revised)

N94-24481*# National Aeronautics and Space Administration. Lewis Research Center, Cleveland, OH.
STAGNATION REGION HEAT TRANSFER: THE INFLUENCE OF TURBULENCE PARAMETERS, REYNOLDS NUMBER AND BODY SHAPE
G. James VanFossen and Robert J. Simoneau Feb. 1994 17 p Prepared for presentation at the 6th AIAA/ASME Thermophysics and Heat Transfer Conference, Colorado Springs, CO, 20-23 Jun. 1994; sponsored by AIAA, and ASME
(RTOP 505-62-52)
(NASA-TM-106504; E-8534; NAS 1.15:106504) Avail: CASI HC A03/MF A01

The effect of velocity gradient on stagnation region heat transfer augmentation by free stream turbulence was investigated. Heat transfer was measured in the stagnation region of four models with elliptical leading edges with ratios of major to minor axes of 1:1, 1.5:1, 2.25:1, and 3:1. Four geometrically similar, square bar, square mesh, biplane grids were used to generate free stream turbulence with different intensities and length. Heat transfer measurements were made for the following ranges of parameters: Reynolds number, based on leading edge diameter, 37,000 to 228,000; dimensionless leading edge velocity gradient, 1.20 to 1.80; turbulence intensity, 1.1 to 15.9%; and length scale to leading edge diameter ratio, 0.05 to 0.30. Stagnation point heat transfer augmentation by free stream turbulence can be predicted using a modified version of a previously developed correlation for a circular leading edge. Heat transfer augmentation was independent of body shape at the stagnation point. The heat transfer distribution down-stream from the stagnation point can be predicted using the normalized laminar heat transfer distribution. Author

N94-24495*# National Aeronautics and Space Administration. Hugh L. Dryden Flight Research Facility, Edwards, CA.
THERMAL-FLUID ANALYSIS OF THE FILL AND DRAIN OPERATIONS OF A CRYROGENIC FUEL TANK
Craig A. Stephens (Planning Research Corp., Edwards, CA.), Gregory J. Hanna (Hanna Technology Resources, Boulder, CO.), and Leslie Gong Washington Dec. 1993 20 p Presented at the SEM Structural Testing Technology at High Temperature 2 Conference, Ojai, CA, 8-10 Nov. 1993
(RTOP 505-70-63)
(NASA-TM-104273; H-1961; NAS 1.15:104273) Avail: CASI HC A03/MF A01

The Generic Research Cryogenic Tank was designed to establish techniques for testing and analyzing the behavior of reusable fuel tank structures subjected to cryogenic fuels and aerodynamic heating. The Generic Research Cryogenic Tank tests will consist of filling a pressure vessel to a prescribed fill level, waiting for steady-state conditions, then draining the liquid while heating the external surface to simulate the thermal environment associated with hypersonic flight. Initial tests of the Generic Research Cryogenic Tank will use liquid nitrogen with future tests requiring liquid hydrogen. Two-dimensional finite-difference thermal-fluid models were developed for analyzing the behavior of the Generic Research Cryogenic Tank during fill and drain operations. The development and results of the two-dimensional fill and drain models, using liquid nitrogen, are provided, along with results and discussion on extrapolating the model results to the operation of the full-size Generic Research Cryogenic Tank. These numerical models provided a means to predict the behavior of the Generic Research Cryogenic Tank during testing and to define the requirements for the Generic Research Cryogenic Tank support systems such as vent, drain, pressurization, and instrumentation systems. In addition, the fill model provided insight into the unexpected role of circumferential conduction in cooling the Generic Research Cryogenic Tank pressure vessel during fill operations. Author

N94-24574 Technische Univ., Eindhoven (Netherlands). Dept. of Mathematics and Computing Science.
CONSERVATION EQUATIONS FOR REACTING GAS FLOW
J. H. M. tenThijeBoonkkamp Jun. 1993 21 p Limited Reproducibility: More than 20% of this document may be affected by microfiche quality
(PB94-111168; EUT-93-WSK-01) Avail: Issuing Activity (National Technical Information Service (NTIS))

The conservation equations for reacting gas flow are derived from continuum mechanics. Models for the transport properties, which are relevant to combustion problems, are presented. Finally, the Shvab-Zeldovich formulation of the conservation equations, in case of a single chemical reaction, is discussed. NTIS

N94-24602*# Institute for Computer Applications in Science and Engineering, Hampton, VA.
THE ACOUSTIC AND INSTABILITY WAVES OF JETS CONFINED INSIDE AN ACOUSTICALLY LINED RECTANGULAR DUCT Final Report
Fang Q. Hu (Old Dominion Univ., Norfolk, VA.) Dec. 1993 30 p Submitted for publication
(Contract NAS1-19480; RTOP 505-90-52-01)
(NASA-CR-191586; NAS 1.26:191586; ICASE-93-98) Avail: CASI HC A03/MF A01

An analysis of linear wave modes associated with supersonic jets confined inside an acoustically lined rectangular duct is presented. Mathematical formulations are given for the vortex-sheet model and continuous mean flow model of the jet flow profiles. Detailed dispersion relations of these waves in a two-dimensional confined jet as well as an unconfined free jet are computed. Effects of the confining duct and the liners on the jet instability and acoustic waves are studied numerically. It is found that the effect of the liners is to attenuate waves that have supersonic phase velocities relative to the ambient flow. Numerical results also show that the growth rates of the instability waves could be reduced significantly by the use of liners. In addition, it is found that the upstream propagating neutral waves of an unconfined jet could become attenuated when the jet is confined. Author

N94-24605*# Institute for Computer Applications in Science and Engineering, Hampton, VA.
RESPONSES OF A FINITE BAFFLED PLATE SUBJECT TO TURBULENT AND MEAN FLOW EXCITATIONS Final Report
Sean F. Wu (Wayne State Univ., Detroit, MI.) and Lucio Maestrello Dec. 1993 28 p Submitted for publication
(Contract NAS1-19480; RTOP 505-90-52-01)
(NASA-CR-191570; NAS 1.26:191570; ICASE-93-89) Avail: CASI HC A03/MF A01

Formulations for predicting dynamic and acoustic responses of a finite plate flush-mounted on an infinite baffle subject to turbulent and mean flow excitations are presented. In deriving these formulations, the effects of stretching due to in-plane force and coupling between structural vibration and acoustic radiation are taken into account. The resulting equation governing plate vibration contains cubic nonlinearities. To obtain an approximate solution, the plate flexural displacement is expanded into orthogonal base functions. The unknown coefficients associated with base functions are determined by solving a set of coupled nonlinear integral equations using Galerkin's method. A stability analysis is given using the basic existence-uniqueness theorem. In particular, stable conditions for a linearized system are obtained using the Routh algorithm. It is shown that structural instabilities can be induced by fluid loading and mean flow. Two unstable mechanisms are found to be attributable to added damping and stiffness due to acoustic radiation. The effect of added damping increases linearly, while that of added stiffness increases quadratically with the Mach number of mean flow. Finally, the cross-power spectral density functions of plate flexural vibration and radiated acoustic pressure are derived and expressed in terms of the cross-power spectral density function of turbulent flow. Author

N94-24640*# California Polytechnic State Univ., San Luis Obispo.
IMPLEMENTATION OF THE BALDWIN-BARTH TURBULENCE MODEL INTO THE ZETA CODE AND ITS DIAGNOSIS M.S. Thesis
Scott L. Low 16 Jun. 1993 112 p Original contains color illustrations
(Contract NCA2-722)
(NASA-CR-194795; NAS 1.26:194795) Copyright Avail: CASI HC A06/MF A02; 14 functional color pages

The Baldwin-Barth turbulence model was implemented into Zeta, a time-accurate, zonal, integro-differential code for incompressible laminar and turbulent flows. The implementation procedure is patterned after the model subroutine in ARC2D. The results of ZETA with the Baldwin-Barth turbulence model were compared with experimental data, with ZETA using Baldwin-Lomax model, and with ARC2D using the Baldwin-Barth model. The Baldwin-Barth model subroutine was tested by inputting an ARC2D velocity solution of an NACA-0012 airfoil at R(sub e) = 3.9 x 10(exp 6) and alpha = 5 deg. The resultant turbulent viscosity and Reynolds stresses compared favorably with the original data. For the same grid having grid points inside the laminar sublayer, which is necessary due to the one-equation nature of the model, ZETA however predicts early separation. It was found that the current ZETA has problem with such a fine grid. Further work is in progress to solve this problem. Author

N94-24641# Technische Univ., Delft (Netherlands). Faculty of Technical Mathematics and Informatics.
SOLUTION OF THE DISCRETIZED INCOMPRESSIBLE NAVIER-STOKES EQUATIONS WITH ITERATIVE METHODS
C. Vuik 1993 14 p Conference on the 26th ISATA, Supercomputing Applications in the Automative Industries held in Aachen, Germany, Sep. 1993 See also PB91-217687
(PB94-118635; Rept-93-54) Copyright Avail: CASI HC A03/MF A01

We describe a numerical solution method for the incompressible Navier-Stokes equations in complex geometries. We use a finite volume technique in combination with boundary-fitted coordinates. The physical domain is mapped onto a computational domain consisting of a number of regular blocks. We restrict ourselves to the one block case. In these problems it is important to obtain fast iterative methods to solve the discretized equations. This is easier using a finite volume technique instead of a finite element technique. Finally, the structured grid enables us to develop a fast implementation of the methods on vector computers. NTIS

N94-24655# California Univ., Berkeley. Lawrence Berkeley Lab.
A TWO-DIMENSIONAL DISPERSION MODULE FOR THE TOUGH2 SIMULATOR
C. M. Oldenburg and K. Pruess Sep. 1993 64 p
(Contract DE-AC03-76SF-00098)
(DE94-002262; LBL-32505) Avail: CASI HC A04/MF A01

A standard model for hydrodynamic dispersion has been added to TOUGH2--the dispersion model, intended for use with the EOS7 fluid properties module, accounts for the effects of hydrodynamic dispersion and molecular diffusion in two-dimensional rectangular domains. Because the model requires Darcy velocity and species concentration gradient vectors at all connections, known vector components (perpendicular to the grid block interfaces) from neighboring connections are interpolated to form the unknown components (parallel to the grid block interfaces) at each connection. Thus, the dispersive fluxes depend not only on the primary variables of the two connected grid blocks but on all p variables of the six neighbor grid blocks of each interface. This gives rise to added terms in the Jacobian matrix relative to standard TOUGH2 where fluxes depend only on primary variables in the two connected grid blocks. For flexibility in implementing boundary conditions, the model allows the user to define a flow domain that is a subset of the calculation domain. The PARAM and SELEC blocks of the TOUGH2 input file are used to specify parameters and boundary condition options for the dispersion module. The dispersion module has been verified by comparing computed results to analytical solutions. As an introduction to applications, we demonstrate the solution of a difficult two dimensional flow problem with variable salinity and strong coupling between dispersive and advective flow. DOE

N94-24686# Naval Postgraduate School, Monterey, CA.
FREE-SURFACE/VORTICITY INTERACTION M.S. Thesis
John B. Carroll Sep. 1993 57 p
(AD-A273263) Avail: CASI HC A04/MF A01

The unsteady flow phenomena resulting from the interaction of wakes and vortices with the free surface are of particular importance in naval hydrodynamics. Ship and submarine wakes produce a three-dimensional complex signature, comprised of a narrow dark band bordered by two bright lines in synthetic-aperture-radar (SAR) images. The dark band signifies the suppression of waves at the Bragg frequency as a consequence of the interaction between the free surface and the imposed vorticity. In the present investigation, the vorticity field is provided by a single tip vortex generated by an airfoil. The results, obtained with an LDV, have shown that the free surface redistributes part or all of the normal turbulent kinetic energy into streamwise and spanwise components. The turbulent kinetic energy first decreases sharply with increasing vertical distance from the vortex and then remains nearly constant within a thin layer below the 'roughened' free surface. The results explain the longevity of the structures and lend further credence to the simulation of near-surface structures via vortex- or contour-dynamics. DTIC

N94-24689 Lehigh Univ., Bethlehem, PA. Dept. of Mechanical Engineering and Mechanics.
HEAT TRANSFER AND FLOW STRUCTURE IN END-WALL BOUNDARY LAYERS Final Report, 15 Mar. 1991 - 15 Mar. 1993
C. R. Smith and J. D. Walker 11 Aug. 1993 27 p Limited Reproducibility: More than 20% of this document may be affected by microfiche quality
(Grant AF-AFOSR-0218-91)
(AD-A273470; AFOSR-93-0875TR) Avail: Issuing Activity (Defense Technical Information Center (DTIC))

Research progress is described for a combined analytical/experimental program examining the flow structure and resultant surface heat transfer in end-wall boundary layers (e.g. wing-body. type junctures). Emphasis is placed on flow structure development and correlation of vortex-induced surface interactions with transient, local surface heat transfer. Analytically, numerical studies using an impulsively-started approach flow have documented the flow development and surface heat transfer on the symmetry plane for several end-wall flows; highly unsteady vortex formation and ejection are observed, with concomitant sharp, transient variations in surface heat transfer. Analysis of the complete three-dimensional behavior indicates the presence of strong interactions between the end-wall (surface) and the side-wall (bluff-body) boundary layers. Experimentally, a constant heat flux test system has been developed and instrumented for surface temperature detection using temperature-sensitive liquid crystals and color computer-image analysis; tests indicate dramatic effects of transient end-wall vortices on surface heat transfer, confirming the analytical results. A systematic visualization study indicates a very strong influence of the junction-induced pressure gradient on the approach boundary layer in promoting the unsteady vortex formation processes in the end-wall region. DTIC

N94-24712*# Institute for Computer Applications in Science and Engineering, Hampton, VA.
CARRYING THE MASS FLUX TERMS EXACTLY IN THE FIRST AND SECOND MOMENT EQUATIONS OF COMPRESSIBLE TURBULENCE Final Report
J. R. Ristorcelli Nov. 1993 10 p Submitted for publication
(Contract NAS1-19480; RTOP 505-90-52-01)
(NASA-CR-191568; NAS 1.26:191568; ICASE-93-87) Avail: CASI HC A02/MF A01

In compressible turbulence models, it is assumed that the Favre-mean velocities are suitable approximations to the Reynolds-mean velocities in order to close unknown terms. This neglects, in the mean momentum and energy equations, the contribution to the stress and work terms by the mean of the fluctuating Favre velocity, a quantity proportional to the turbulent mass flux. As the stress and work terms do not introduce any new unknown correlations requiring closure in either k-epsilon or Reynolds stress closures and because the exact form of the terms can, with little additional work, be carried there is no need to make any modeling assumptions. In the Reynolds stress equations the viscous terms appear naturally in Reynolds variables while the problem is posed in Favre variables. In the process of splitting the viscous terms into the viscous transport terms, carried in Favre variables, and the dissipation terms, carried in Reynolds variables, important contributions from the mass flux appear. The accurate accounting of these terms is important for any consistent near wall modeling and the retention of the mass flux terms is important in complex compressible turbulent flows. Author (revised)

N94-24713*# National Aeronautics and Space Administration. Lewis Research Center, Cleveland, OH.
A VORTICITY DYNAMICS BASED MODEL FOR THE TURBULENT DISSIPATION: MODEL DEVELOPMENT AND VALIDATION
Tsan-Hsing Shih, William W. Liou, Aamir Shabbir, Zhigang Yang, and Jian Zhu Jan. 1994 31 p
(Contract NCC3-233; RTOP 505-90-5K)
(NASA-TM-106177; ICOMP-93-20; CMOTT-93-08; E-7877; NAS 1.15:106177) Avail: CASI HC A03/MF A01

A new model dissipation rate equation is proposed based on the dynamic equation of the mean-square vorticity fluctuation for large Reynolds number turbulence. The advantage of working with the vorticity fluctuation equation is that the physical meanings of the terms in this equation are more clear than those in the dissipation rate equation. Hence, the model development based on the vorticity fluctuation equation is more straightforward. The resulting form of the model equation is consistent with the spectral energy cascade analysis introduced by Lumley. The proposed model dissipation rate equation is numerically well behaved and can be applied to any level of turbulence modeling. It is applied to a realizable eddy viscosity model. Flows that are examined include: rotating homogeneous shear flows; free shear flows; a channel flow and flat plate boundary layers with and without pressure gradients; and backward facing step separated flows. In most cases, the present model predictions show considerable improvement over the standard kappa-epsilon model. Author (revised)

N94-24725*# High Technology Corp., Hampton, VA.
RELATIONSHIP BETWEEN TRANSITION AND MODES OF INSTABILITY IN SUPERSONIC BOUNDARY LAYERS
Jamal A. Masad Dec. 1993 26 p
(Contract NAS1-19299; RTOP 537-03-23-03)
(NASA-CR-4562; NAS 1.26:4562) Avail: CASI HC A03/MF A01

The relationship between the predicted transition location and the first and second modes of instability in two-dimensional supersonic boundary-layer flow on a flat plate is examined. Linear stability theory and the N-factor criterion are used to predict transition location. The effect of heat transfer is also studied; the results demonstrate that the transition reversal phenomenon can be explained by the opposite effect of cooling on the first and second modes of instability. Compressibility of destabilizing at free-stream Mach numbers of 2 to 3.5. The predicted transition location is due to the oblique first modes of instability, up to free-stream Mach numbers between 6 and 6.5. At higher Mach numbers, the predicted transition location is due to a combination of two-dimensional first and second modes of instability. Author

N94-24761 Technische Univ., Eindhoven (Netherlands). Dept. of Mathematics and Computing Science.
BEM SOLUTION FOR THE SIMULATION OF AXISYMMETRIC VISCOUS SINTERING
G. A. L. vandeVorst Nov. 1992 14 p Limited Reproducibility: More than 20% of this document may be affected by microfiche quality
(PB93-237717; RANA-92-16) Avail: CASI HC A03

A numerical method to simulate particular axisymmetric viscous sintering problems is presented. In these problems the material transport is modeled as a viscous incompressible Newtonian volume flow driven solely by surface tension. The numerical simulation is carried out by solving the governing Stokes equations for a fixed domain through a Boundary Element Method (BEM). The resulting velocity field then determines an approximate geometry at a next time level by employing a variable step, variable order Backward Differences Formulas (BDF) method. This numerical algorithm is demonstrated for the sintering of two equal spheres. NTIS

N94-24771*# General Applied Science Labs., Inc., Ronkonkoma, NY.
HYPULSE COMBUSTOR ANALYSIS
O. F. Rizkalla Dec. 1993 47 p
(Contract NAS1-18450; RTOP 763-23-21)
(NASA-CR-191579; TR-352; NAS 1.26:191579) Avail: CASI HC A03/MF A01

The analysis of selected data from tests of unit fuel injectors in a generic scramjet combustor model is presented. The tests were conducted in the NASA HYPULSE expansion tube at conditions typical of flight at Mach 13.5 and 17. The analysis used a three-stream tube method, with finite-rate chemistry, in which the fuel, test gas, and mixing/combustive streams were treated independently but with the same static pressure. Performance of three candidate fuel injectors is examined based on deduced mixing and combustion efficiencies. Author

N94-24793# Illinois Inst. of Tech., Chicago. Fluid Dynamics Research Center.
INTERACTIVE CONTROL IN TURBULENT SHEAR LAYERS Final Report, Feb. 1990 - Jan. 1993
Candace E. Wark and Hassan M. Nagib 11 Oct. 1993 30 p
(Grant AF-AFOSR-0171-90)
(AD-A273544; AFOSR-93-0876TR) Avail: CASI HC A03/MF A01

Investigations of wall-bounded shear flow at IIT have been primarily focused on the following issues: (1) inner- and outer-layer effects on the dynamics of a turbulent boundary layer (TBL), (2) a PIV study of fully developed turbulent pipe flow, (3) the effects of intermittency on the wall-layer dynamics, and (4) the visualization of active events near the wall. The motivations behind these investigations are to understand the Reynolds number sensitivity and relative importance of the different scales of motion, with regard to the dynamics of turbulent wall-bounded flow and to document and study the instantaneous structure of the flow vis-a-vis the numerous coherent structure studies of the last two decades. A temporal filtering scheme was devised to separate the contribution of the different scales of motion to the u' signal and the Reynolds stress in the buffer and logarithmic region. Also, using PIV, instantaneous large-scale structures were observed, which are not seen in low Reynolds number direct numerical simulations of bounded turbulent shear flows. The analysis of flow visualization records of active events in a TBL was performed in the frame of a conjectured model that is based on Theodorsen's original hairpin vortex flow module. Information on the character, size, location, intensity and duration of the events was documented and tabulated. DTIC

N94-24821# Army Construction Engineering Research Lab., Champaign, IL. Energy and Utilities Systems Div.
FLOW AND TEMPERATURE DISTRIBUTION IN A NATURALLY STRATIFIED THERMAL STORAGE TANK Final Report
Maurice W. Wildin and Chang W. Sohn Oct. 1993 34 p
(AD-A273511; USACERL-TR-FE-94/01) Avail: CASI HC A03/MF A01

Thermal energy storage for building and process cooling is employed in two principal forms: sensible and latent. Each form has its advantages and disadvantages. Currently, water is the most frequently used storage medium for cooling, with the solid/liquid phase change being used for latent storage and chilled liquid water used for sensible storage. This report deals exclusively with sensible storage in water. Researchers studied the effects of mixing on the creation and maintenance of a thermocline during the charging of a thermal storage tank for cooling and the effects of momentum of inlet fluid and buoyancy due to temperature differences on the creation and maintenance of thermoclines. From the design point of view, the inlet parameters and their ranges for optimal performance of a stratified thermal storage tank have been more clearly delineated. The upper limit of the range of the Reynolds number for optimal stratified chilled water storage tank performance appears to be between 400 and 600. The upper limit of the densimetric Froude number range was determined in a previous study, and is about 2. DTIC

N94-24858*# North Carolina State Univ., Raleigh. Dept. of Mechanical and Aerospace Engineering.

NUMERICAL SOLUTIONS OF THE COMPLETE NAVIER-STOKES EQUATIONS Progress Report No. 24, 1 Jul. - 31 Dec. 1993

H. A. Hassan 31 Dec. 1993 10 p
(Grant NAG1-244)
(NASA-CR-194780; NAS 1.26:194780) Avail: CASI HC A02/MF A01

The objective of this study is to compare the use of assumed pdf (probability density function) approaches for modeling supersonic turbulent reacting flowfields with the more elaborate approach where the pdf evolution equation is solved. Assumed pdf approaches for averaging the chemical source terms require modest increases in CPU time typically of the order of 20 percent above treating the source terms as 'laminar.' However, it is difficult to assume a form for these pdf's a priori that correctly mimics the behavior of the actual pdf governing the flow. Solving the evolution equation for the pdf is a theoretically sound approach, but because of the large dimensionality of this function, its solution requires a Monte Carlo method which is computationally expensive and slow to coverage. Preliminary results show both pdf approaches to yield similar solutions for the mean flow variables. Author (revised)

N94-24859*# North Carolina State Univ., Raleigh. Dept. of Mechanical and Aerospace Engineering.

COMPUTATIONAL FLUID MECHANICS Progress Report No. 29, 15 Jun. - 14 Dec. 1993

H. A. Hassan 14 Dec. 1993 43 p
(Contract NCC1-22)
(NASA-CR-194765; NAS 1.26:194765) Avail: CASI HC A03/MF A01

Two papers are included in this progress report. In the first, the compressible Navier-Stokes equations have been used to compute leading edge receptivity of boundary layers over parabolic cylinders. Natural receptivity at the leading edge was simulated and Tollmien-Schlichting waves were observed to develop in response to an acoustic disturbance, applied through the farfield boundary conditions. To facilitate comparison with previous work, all computations were carried out at a free stream Mach number of 0.3. The spatial and temporal behavior of the flowfields are calculated through the use of finite volume algorithms and Runge-Kutta integration. The results are dominated by strong decay of the Tollmien-Schlichting wave due to the presence of the mean flow favorable pressure gradient. The effects of numerical dissipation, forcing frequency, and nose radius are studied. The Strouhal number is shown to have the greatest effect on the unsteady results. In the second paper, a transition model for low-speed flows, previously developed by Young et al., which incorporates first-mode (Tollmien-Schlichting) disturbance information from linear stability theory has been extended to high-speed flow by incorporating the effects of second mode disturbances. The transition model is incorporated into a Reynolds-averaged Navier-Stokes solver with a one-equation turbulence model. Results using a variable turbulent Prandtl number approach demonstrate that the current model accurately reproduces available experimental data for first and second-mode dominated transitional flows. The performance of the present model shows significant improvement over previous transition modeling attempts. Author (revised)

N94-24869*# Institute for Computer Applications in Science and Engineering, Hampton, VA.

VORTEX GENERATION AND WAVE-VORTEX INTERACTION OVER A CONCAVE PLATE WITH ROUGHNESS AND SUCTION Final Report

Fabio Bertolotti Dec. 1993 42 p Submitted for publication
(Contract NAS1-19480; RTOP 505-90-52-01)
(NASA-CR-191589; ICASE-93-101; NAS 1.26:191589) Avail: CASI HC A03/MF A01

The generation and amplification of vortices by surface homogeneities, both in the form of surface waviness and of wall-normal velocity, is investigated using the nonlinear parabolic stability equations. Transients and issues of algebraic growth are avoided through the use of a similarity solution as initial condition for the vortex. In the absence of curvature, the vortex decays as the square root of 1/x when flowing over streamwise aligned riblets of constant height, and grows as the square root of x when flowing over a corresponding streamwise aligned variation of blowing/suction transpiration velocity. However, in the presence of wall inhomogeneities having both streamwise and spanwise periodicity, the growth of the vortex can be much larger. In the presence of curvature, the vortex develops into a Gortler vortex. The 'direct' and 'indirect' interaction mechanisms possible in wave-vortex interaction are presented. The 'direct' interaction does not lead to strong resonance with the flow conditions investigated. The 'indirect' interaction leads to K-type transition. Author (revised)

N94-24929 Princeton Univ., NJ. Dept. of Aerospace and Mechanical Sciences.

DEVELOPMENT AND VALIDATION OF RNG METHODOLOGY FOR COMPRESSIBLE TURBULENCE Final Report, 1 Apr. 1989 - 31 Mar. 1993

G. E. Karniadakis and A. Smits Oct. 1993 5 p Limited Reproducibility: More than 20% of this document may be affected by microfiche quality
(Grant AF-AFOSR-0261-90)
(AD-A273469; AFOSR-93-0868TR) Avail: Issuing Activity (Defense Technical Information Center (DTIC))

All three different categories of tasks described in our AFOSR proposal (Grant 90-0261) were completed successfully: (1) Development of Renormalization Group theory (RNG) for compressible turbulence; (2) Design and measurements of a compressible boundary layer experiment, and (3) Development of spectral element algorithms for compressible flows. A brief summary follows. On the theoretical side first, the new results obtained for compressible turbulence are: (1) At the large scales the effective sound velocity in compressible turbulence is scale-dependent and obeys a universal equation of state; (2) The effective, scale-dependent Mach number based on the rms value of velocity approaches a fixed point corresponding to effectively subsonic flow; (3) The potential component of the velocity field (sound waves) does not alter the scaling of the energy spectrum of incompressible (rotational) component. This decoupling of events in rotational and compressibility effects suggests that most of the RNG modeling for incompressible flows is also valid for compressible flows as long as compressibility is taken into account. DTIC

N94-25032# University of Southern Illinois, Carbondale. Dept. of Physics.

ELECTRO-RHEOLOGY FLUIDS AND LIQUID FUEL FLOW Final Report, 1 Jul. 1991 - 1 Oct. 1993

Rongjia Tao 1 Oct. 1993 22 p
(Contract N00014-90-J-4041)
(AD-A273640) Avail: CASI HC A03/MF A01

The goals of this research are to: understand and clarify the physical mechanism underlying the electro-rheological (ER) phenomenon, such as viscosity, the structure of ER fluids, phase transitions, and properties; apply the ER phenomenon to fuels to control viscosity; and study cryogenic ER fluids and investigate applications of the ER effect to slurry rocket fuels. DTIC

N94-25094*# State Univ. of New York, Buffalo. Dept. of Mechanical and Aerospace Engineering.

LES, DNS AND RANS FOR THE ANALYSIS OF HIGH-SPEED TURBULENT REACTING FLOWS Semiannual Report, 1 Aug. 1993 - 31 Jan. 1994

Peyman Givi 1994 6 p
(Grant NAG1-1122)
(NASA-CR-195196; NAS 1.26:195196) Avail: CASI HC A02/MF A01

The objective of this research is to continue our efforts in advancing the state of knowledge in Large Eddy Simulation (LES), Direct Numerical Simulation (DNS), and Reynolds Averaged Navier Stokes (RANS) methods for the analysis of high-speed reacting turbulent flows. In the first phase of this research, conducted within the past six months, focus was in three directions: RANS of turbulent reacting flows by Probability Density Function (PDF) methods, RANS of non-reacting turbulent flows by advanced turbulence closures, and LES of mixing dominated reacting flows by a dynamics subgrid closure. A summary of our efforts within the past six months of this research is provided in this semi-annual progress report. Author (revised)

N94-25119*# National Aeronautics and Space Administration. Lewis Research Center, Cleveland, OH.

TURBULENCE MODELS AND REYNOLDS ANALOGY FOR TWO-DIMENSIONAL SUPERSONIC COMPRESSION RAMP FLOW

Chi R. Wang and Maleina C. Bidek (Cornell Univ., Ithaca, NY.) Jan. 1994 15 p Proposed for presentation at the 1994 Thermophysics and Heat

Transfer Conference, Colorado Springs, CO, 20-23 Jun. 1994; sponsored by ASME
(RTOP 505-62-52)
(NASA-TM-106474; E-8349; NAS 1.15:106474) Avail: CASI HC A03/MF A01

Results of the application of turbulence models and the Reynolds analogy to the Navier-Stokes computations of Mach 2.9 two-dimensional compression ramp flows are presented. The Baldwin-Lomax eddy viscosity model and the kappa-epsilon turbulence transport equations for the turbulent momentum flux modeling in the Navier-Stokes equations are studied. The Reynolds analogy for the turbulent heat flux modeling in the energy equation was also studied. The Navier-Stokes equations and the energy equation were numerically solved for the flow properties. The Reynolds shear stress, the skin friction factor, and the surface heat transfer rate were calculated and compared with their measurements. It was concluded that with a hybrid kappa-epsilon turbulence model for turbulence modeling, the present computations predicted the skin friction factors of the 8 deg and 16 deg compression ramp flows and with the turbulent Prandtl number Pr(sub t) = 0.93 and the ratio of the turbulent thermal and momentum transport coefficients mu(sub q)/mu(sub t) = 2/Prt, the present computations also predicted the surface heat transfer rates beneath the boundary layer flow of the 16 compression ramp. Author (revised)

N94-25140# Naval Command, Control and Ocean Surveillance Center, San Diego, CA. Research, Development, Technology and Evaluation Div.

ACTIVE CONTROL OF OSCILLATORY LIFT FORCES ON A CIRCULAR CYLINDER Professional Paper

D. M. Ladd, D. S. Park, E. W. Hendricks, and N. S. Nosseir Aug. 1993 8 p
(AD-A273243) Avail: CASI HC A02/MF A01

The results of a computational and experimental study of feedback control of Karman vortex shedding behind a circular cylinder are presented. The experiments were performed in a nominally two dimensional flow around a 12.7 mm cylinder at Reynolds numbers up to 10,000. The computations utilized the two-dimensional Navier-Stokes equations at Reynolds numbers up to 100. In both experimental and numerical studies blowing and suction slots were used to control the vortex shedding. In the numerical study complete suppression of vortex shedding is achieved up to a Reynolds number Re = 80 (about 70% above the onset Reynolds number for vortex shedding). In the experimental study using the fluctuating lift force as feedback, about 50% suppression of the rms fluctuations has been achieved at a Reynolds number of approximately 10,000. DTIC

N94-25157# George Washington Univ., Washington, DC. Office of Sponsored Research.

DEVELOPMENT AND APPLICATION OF NEW ALGORITHMS FOR THE SIMULATION OF VISCOUS COMPRESSIBLE FLOWS WITH MOVING BODIES IN THREE DIMENSIONS Final Report, 15 Sep. 1991 - 31 Oct. 1993

Rainold Lohner and Jean Cabello 22 Sep. 1993 50 p
(Contract F49620-92-J-0058)
(AD-A273514; AFOSR-93-0861TR) Avail: CASI HC A03/MF A01

The work carried out under this contract may be sub-divided according to the following topics: development of implicit ALE Navier-Stokes solvers; implementation of turbulence models; development of gridding techniques for three dimensional viscous flows; and demonstration calculation and results. DTIC

N94-25180*# National Aeronautics and Space Administration. Lewis Research Center, Cleveland, OH.

A CONTINUING SEARCH FOR A NEAR-PERFECT NUMERICAL FLUX SCHEME. PART 1: AUSM+

Meng-Sing Liou Mar. 1994 47 p Presented at the 5th International Symposium on Computational Fluid Dynamics, Sendai, Japan, 31 Aug. - 3 Sep. 1993
(RTOP 505-62-52)
(NASA-TM-106524; NAS 1.15:106524) Avail: CASI HC A03/MF A01

While enjoying demonstrated improvement in accuracy, efficiency, and robustness over existing schemes, the Advection Upstream Splitting Scheme (AUSM) was found to have some deficiencies in extreme cases. This recent progress towards improving the AUSM while retaining its advantageous features is described. The new scheme, termed AUSM+, features: unification of velocity and Mach number splitting; exact capture of a single stationary shock; and improvement in accuracy. A general construction of the AUSM+ scheme is layed out and then focus is on the analysis of the a scheme and its mathematical properties, heretofore unreported. Monotonicity and positivity are proved, and a CFL-like condition is given for first and second order schemes and for generalized curvilinear co-ordinates. Finally, results of numerical tests on many problems are given to confirm the capability and improvements on a variety of problems including those failed by prominent schemes. Author (revised)

N94-25183*# National Aeronautics and Space Administration. Lewis Research Center, Cleveland, OH.

MEASUREMENTS OF THE INFLUENCE OF INTEGRAL LENGTH SCALE ON STAGNATION REGION HEAT TRANSFER

G. James VanFossen and Chang Y. Ching (Syracuse Univ., NY.) Feb. 1994 22 p Proposed for presentation at the 5th Symposium on Transport Phenomena and Dynamics of Rotating Machinery, Kaanapali, HI, 8-11 May 1994; sponsored by the Pacific Center of Thermal Fluids Engineers
(RTOP 505-62-52)
(NASA-TM-106503; E-8532; NAS 1.15:106503) Avail: CASI HC A03/MF A01

The purpose was twofold: first, to determine if a length scale existed that would cause the greatest augmentation in stagnation region heat transfer for a given turbulence intensity and second, to develop a prediction tool for stagnation heat transfer in the presence of free stream turbulence. Toward this end, a model with a circular leading edge was fabricated with heat transfer gages in the stagnation region. The model was qualified in a low turbulence wind tunnel by comparing measurements with Frossling's solution for stagnation region heat transfer in a laminar free stream. Five turbulence generating grids were fabricated; four were square mesh, biplane grids made from square bars. Each had identical mesh to bar width ratio but different bar widths. The fifth grid was an array of fine parallel wires that were perpendicular to the axis of the cylindrical leading edge. Turbulence intensity and integral length scale were measured as a function of distance from the grids. Stagnation region heat transfer was measured at various distances downstream of each grid. Data were taken at cylinder Reynolds numbers ranging from 42,000 to 193,000. Turbulence intensities were in the range 1.1 to 15.9 percent while the ratio of integral length scale to cylinder diameter ranged from 0.05 to 0.30. Stagnation region heat transfer augmentation increased with decreasing length scale. An optimum scale was not found. A correlation was developed that fit heat transfer data for the square bar grids to within +4 percent. The data from the array of wires were not predicted by the correlation; augmentation was higher for this case indicating that the degree of isotropy in the turbulent flow field has a large effect on stagnation heat transfer. The data of other researchers are also compared with the correlation. Author (revised)

N94-25227# Technische Univ., Delft (Netherlands).

MECHANISMS OF DROPLET FORMATION Ph.D. Thesis

Gabriel Marinus Henr Meesters 1992 156 p
(ISBN-9-06-275765-0; ETN-94-95369) Avail: CASI HC A08/MF A02

The production of droplets in the micrometer range (1 to 5 micrometers) and the production of droplets a few decades larger (70 micrometer to 2 mm) is considered. In the production of droplets in the micrometer range, the liquids are dispersed with the help of a strong electric field. A phenomenon known as the Taylor cone is used for dispersion of the liquid. A Taylor cone is a conically shaped liquid droplet from whose apex small droplets are emitted. The phenomena of these liquid cones were also investigated. In producing droplets of diameter 70 micrometers to 2 mm, the liquid jet is forced to break up by applying a vibration onto the jet causing it to break up with the imposed frequency. Two different pieces of equipment were set up to investigate the break up behavior of liquids of low and high viscosity. Using this apparatus it was possible to define a particle size distribution over a wide range of diameters and to tailor it. ESA

N94-25243 Universiteit Twente, Enschede (Netherlands). Faculty of Mechanical Engineering.

FORCES ON AN OSCILLATING CYLINDER AND RELATED FLUID FLOW PHENOMENA Ph.D. Thesis

Andries Otter 1992 141 p Sponsored by Shell Research B.V.,

Netherlands Prepared in cooperation with Koninklijke/Shell Exploratie en Produktie Lab., Rijswijk, Netherlands nds Limited Reproducibility: More than 20% of this document may be affected by microfiche quality
(ISBN-9-09-005589-4; ETN-94-95377) Avail: Issuing Activity (European Space Agency (ESA))

The interaction between a circular cylinder oscillating along a diameter and the fluid surrounding it is studied. Attention is focused on the forces on the cylinder and the related fluid flow. The information will be applied to the design of certain offshore structures in deep waters. The flow phenomena associated with changes in the fluid induced forces, the transition and separation of the boundary layers, are reviewed. Laboratory experiments were carried out in which the in line and transverse forces on an oscillating cylinder were measured. Flow visualization experiments were performed to investigate the boundary layer stability and the boundary layer separation. In the review of the transition from laminar flow around a transversely oscillating cylinder, two different mechanisms are identified. It is explained that the same mechanisms are feasible in the case of a circular cylinder oscillating in rotation around its axis. It appears that an experiment on this configuration can be used in answering questions whether an interaction between the two mechanisms takes place and which are the consequences regarding the energy dissipation. The results of flow visualization experiments suggest that an interaction might occur. However, at the transition from laminar flow, no significant increase in the moment acting on the cylinder was found. ESA

N94-25247# Technische Univ., Eindhoven (Netherlands).
THE HYDRODYNAMICS OF A MOVING FLUID-LIQUID CONTACT LINE Ph.D. Thesis
Antonius Johannus J. vanderZanden 1993 105 p
(ETN-94-95352) Avail: CASI HC A06/MF A02

The hydrodynamics associated with an advancing contact line, where a viscous liquid displaces a fluid with a negligible viscosity, is examined. A model is proposed which approximates the shape of an advancing meniscus in a tube or between parallel plates. Comparison of the predictions of the model with available numerical and experimental results provides an indication of its reliability. This model is applied to receding contact lines, where a viscous liquid is displaced by a fluid of negligible viscosity. The model is extended to examine moving liquid-liquid contact lines where the viscosity of neither fluid can be neglected. Experiments concerning the macroscopic shape of a meniscus in a tube and experiments which lay claim to be able to peep into the microscopic region close to the contact line not accessible with the naked eye are presented. ESA

N94-25248# Technische Univ., Eindhoven (Netherlands).
DECAY OF SWIRL IN TURBULENT PIPE FLOWS Ph.D. Thesis
Rene Raymond Parchen 1993 149 p Sponsored by N.V. Dutch Gasunie, Netherlands
(ETN-94-95353) Avail: CASI HC A07/MF A02

An overview of the most widely used models of turbulence is given. The assumptions on which the models are based, starting from the most general closure scheme, the Reynolds stress model of turbulence, are described. To reveal some of the conceptual differences, the lower order schemes are derived from the more general schemes. Focus is on the modeling of flows with swirl. The prediction of axisymmetric swirling pipe flows is discussed. Employing existing turbulence closure schemes, simplified expressions for the turbulent stresses are derived. These simplified expressions allow the predicted effects of swirl on the turbulence as predicted by the various methods to be assessed. A detailed description of the consequences of the various assumptions on the prediction of the decay of swirl in turbulent pipe flows is given. The question of whether the assumption of axisymmetry in swirling pipe flows is valid is addressed. Numerical experiments are used to investigate the stability of the flow against nonaxisymmetric disturbances. The feasibility of numerical predictions of installation effects is discussed. ESA

N94-25254 Technische Univ., Delft (Netherlands). Kramers Lab. voor Fysische Technologie.
HYDRODYNAMICS OF STIRRED GAS-LIQUID DISPERSIONS Ph.D. Thesis
Andries Bakker 1992 129 p Limited Reproducibility: More than 20% of this document may be affected by microfiche quality
(Contract STW-DTN-40.0566)
(ETN-94-95368) Copyright Avail: CASI HC A07

Results of an investigation of the gas-liquid hydrodynamics of stirred tanks equipped with (profiled) axial flow impellers are reported. Three different flow regimes are distinguished. Only at low gas flow rates, when the gas-liquid flow is dominated by the liquid flow pattern as induced by the impeller, the flow pattern is steady state and the gas well dispersed. The mass transfer performance of these axial flow impellers was compared with that of disc turbines. Results of a computational study on the single phase flow with both radial pumping and axial pumping impellers are described. All computations were carried out with the fluid flow code FLUENT and the results were validated with experimental LDV (Laser Doppler Velocimetry) data. These single phase flow patterns serve as a basis for further study of the gas dispersion process in those hydrodynamic regimes where the flow is stable. The development of a predictive model for the gas-liquid flow in stirred vessels is considered. This model is incorporated in a code named GHOST (Gas Holdup Simulation Tool) which calculates local values of gas holdup, bubble size, and mass transfer rate on the basis of conservation equations and the single phase flow patterns computed earlier. The computational results are validated against experimental data gathered with optical fiber probes. A qualitative description of the spatial distribution of the gas holdup, the bubble size, and the mass transfer rate in stirred mixing vessels is given. This description results from using a combination of experimental data and GHOST results. Conclusions about further possible optimization of gassed stirred tanks are drawn. ESA

N94-25291# Technische Univ., Eindhoven (Netherlands).
COHERENT STRUCTURES OVER GROOVED SURFACES Ph.D. Thesis
Adriana Dymphena Schwarz-vanManen 1992 153 p Sponsored by Netherlands Foundation for Technical Sciences, and Stichting voor Fundamenteel Onderzoek der Materie Prepared in cooperation with Tech. Univ. Delft, Netherlands Original contains color illustrations
(ETN-94-95308) Avail: CASI HC A08/MF A02

The effectiveness of riblet surfaces on the coherent motions in the near wall turbulent boundary layer was investigated. The effectiveness of drag reducing flat riblet surfaces during adverse pressure gradient flows was then examined. Some problems which are relevant for applications, like the angle between the flow and the riblets, the partial covering of a flat plate by riblets, and a ship model covered with riblets, were studied. ESA

N94-25446# Air Force Flight Test Center, Edwards AFB, CA.
ANALYSIS OF THE EFFECTS OF WAKE PASSAGE ON HEAT TRANSFER IN A LINEAR TURBINE CASCADE M.S. Thesis
Kevin S. Allen Dec. 1993 104 p
(AD-A273729; AFIT/GAE/ENY/93D-2) Avail: CASI HC A06/MF A02

The effect of wake passage on the heat transfer in a linear turbine cascade was investigated. The apparatus used was the Air-Force Institute of Technology Linear Turbine Cascade Test Facility (TCTF). The TCTF was fitted with a belt and pulley system to facilitate a series of translating bars. The bars, when passed upstream of the cascade, created a series of wakes. The parameters varied were freestream model Reynolds number and bar conditions, i.e., bars in, bars out, and bar passing frequency. One blade in the TCTF was instrumented to allow pressure and temperature measurements at discrete points on the blade's surface. From the pressure and temperature data the convective heat transfer coefficient at these discrete locations was calculated. Results were compared to previous TCTF heat transfer data, empirical solutions, and other wake passage experiments. For all tests with closely spaced bars, the effect of wake passing on the heat transfer of the blade was similar to the effect of grid-generated 10% freestream turbulence on the cascade. DTIC

N94-25462 Institut Franco-Allemand de Recherches, Saint-Louis (France).
MEASUREMENT OF THE VOLUME MASS BY SPONTANEOUS RAMAN SCATTERING. STUDY OF TURBULENT FLUCTUATIONS OF MIXING IN A SUBSONIC FREE JET. MEASUREMENTS IN SUPERSONIC WIND TUNNELS [MESURE DE LA MASSE VOLUMIQUE PAR DIFFUSION RAMAN SPONTANEE. ETUDE DES FLUCTUATIONS TURBULENTES DE MELANGE DANS UN JET LIBRE SUBSONIQUE. MESURES EN SOUFFLERIE SUPERSONIQUE]
L. Bobin and G. Brom 12 Feb. 1992 38 p In FRENCH Limited

Reproducibility: More than 20% of this document may be affected by microfiche quality
(Contract DRET-88-201)
(ISL-R-102/92; ETN-94-95118) Avail: CASI HC A03

The turbulent variations of the mass flow occurring in the mixing zone of a CO2 free jet in the air are calculated by Raman scattering. The calculation method consists in correlating photons given by the mass autocorrelation function. The mass of each component is obtained. The relationship between the amplitude of the mass flow turbulent variations and the measuring device pass band is shown. For a 64 channel photon correlator the analyzed band width was 2/3 octaves. The mean local mass around a cylindric-conic shape model tested in a supersonic wind tunnel was calculated. The wind tunnel flow was disturbed by a transversal methane flow. The calculated and the measured pressure fields at the wall are compared. It is shown that the resulting pressure forces can be calculated by the method. ESA

N94-25463# Institut Franco-Allemand de Recherches, Saint-Louis (France).
STUDY OF THE BLADE/VORTEX INTERACTION: ACOUSTICS, AERODYNAMICS AND MODELS Final Report [ETUDE DE L'INTERACTION PALE/TOURBILLON: ACOUSTIQUE, AERODYNAMIQUE, MODELISATIONS]
P. Gnemmi, J. Haertig, C. Johe, and M. Schaffar 7 Apr. 1992 76 p
In FRENCH Original contains color illustrations
(Contract DRET-88-214)
(ISL-R-104/92; ETN-94-95119) Avail: CASI HC A05/MF A01

A program for calculating the load noise of a helicopter rotor was developed. The method, which requires the knowledge of the local blade load values, was extended to calculate the two dimensional flow around a foil in a field of vortices. A three dimensional method based on the lifting surface theory was developed to simulate the turbulent field developed by a pitch oscillating foil and interacting with another foil placed downstream. The calculated and the measured lift evolution values were compared. The flow velocity was measured by laser velocimetry and the configuration of the rotational flow field was obtained. ESA

N94-25466 Heidelberg Univ. (Germany). Sonderforschungsbereich 123.
AN ADAPTIVE STREAMLINE DIFFUSION FINITE ELEMENT METHOD FOR HYPERBOLIC SYSTEMS IN GAS DYNAMICS
Guohui Zhou Sep. 1992 141 p Sponsored by DFG Limited Reproducibility: More than 20% of this document may be affected by microfiche quality
(Preprint-688; ETN-94-95084) Avail: CASI HC A07

The paintwise error analysis of the streamline diffusion method for two dimensional stationary problem with constant coefficients is extended to the time dependent problem. The purpose of the study is to justify a local mesh refinement strategy. The one dimensional Euler equations coming from the shock tube and Riemann's problem in gas dynamics are used. The gas is assumed to be at rest on both sides of the membrane, with pressure and density different on each side. The case where the problem is scalar and linear is discussed. Linear systems of hyperbolic type in one space variable and nonlinear scalar problems are studied. ESA

N94-25467# Universitaet der Bundeswehr Muenchen, Neubiberg (Germany). Inst. fuer Mathematik.
APPLICATIONS OF THE HOMOGENIZATION METHOD TO FLOW AND TRANSPORT IN POROUS MEDIA
Ulrich Hornung Sep. 1991 57 p
(Ber-9110; RB-5459; ETN-94-95086) Avail: CASI HC A04/MF A01

A survey of the homogenization method applied to porous media is presented. From a theoretical point of view the method studies partial differential equations with oscillatory coefficients, either periodically or stochastically. The homogenization of elliptic problems with periodic coefficients is discussed. Media with a spatially periodic array of obstacles are considered. It is shown that for time dependent problems the method of homogenization may lead to non-local equations. A formal derivation of Darcy's law is given. Two new problems are introduced: the problem of heterogeneous catalysis and the problem of reactive transport through an array of cells with semipermeable membranes. ESA

N94-25484# Technische Univ., Eindhoven (Netherlands).
APPLICATION OF BODY FITTED-COORDINATES IN HEAT CONDUCTION PROBLEMS Ph.D. Thesis
Petrus Johannes Mari Sonnemans 1992 156 p
(ETN-94-95338) Avail: CASI HC A08/MF A02

A method to determine the 'effective' conductivity of a repetitive complex structure of a composite material is developed. The principles of heat transfer and some related numerical aspects are reviewed. The Taylor series method is presented as discretization technique to solve differential equations numerically. The discretization technique is generalized to solve two dimensional heat transport problems. The transport equation to be solved, is discretized on the simple rectangular structure in the new body fitted coordinate system. The influence of geometrical variations on relevant transport properties is studied. It is shown that the influence of the element size as well as of the order of the discretization scheme on the achieved accuracy and on the required computing time is in agreement with the results. This influence is not affected by the coordinate transformation. The concept of body fitted coordinate systems is applied to model the heat transport in a realistic complex structure. The effective conductivity of a perforated brass plate is modeled by averaging detailed information about the heat flux and about the temperature distribution. The averaging procedure is generalized to determine the possible anisotropic behavior due to the geometric complexity. ESA

N94-25486# Cranfield Inst. of Tech., Bedford (England). Dept. of Aerospace Science.
A NUMERICAL INVESTIGATION OF THE ARTIFICIAL COMPRESSIBILITY METHOD FOR THE SOLUTION OF THE NAVIER-STOKES EQUATIONS
D. T. Elsworth and E. F. Toro Nov. 1992 17 p
(Cranfield-Aero-9213; ISBN-1-87-156455-7; ETN-94-95220) Avail: CASI HC A03/MF A01

Aspects of the numerical solution of the incompressible Navier-Stokes equations are examined. The artificial compressibility approach is a numerical method for solving the incompressible Navier-Stokes equations. The use of five different Riemann solvers for the equations of the artificial compressibility method is addressed. The performance of the Riemann solvers is examined. Four of these are approximate Riemann solvers and one is an exact solver. Three ways in which the boundary conditions can be treated are studied. The choice of c, the artificial compressibility coefficient, is investigated. ESA

N94-25530# Wright Lab., Wright-Patterson AFB, OH.
DIRECT MEASUREMENT OF TURBULENT DISSIPATION RATE USING DUAL LASER DOPPLER VELOCIMETERS Interim Report, Jun. - Dec. 1992
Richard D. Gould and Abdollah S. Nejad Jan. 1993 19 p
(AD-A273740; WL-TR-93-2053) Avail: CASI HC A03/MF A01

The analysis of two-point velocity correlation measurement, made in the anisotropic flowfield of axisymmetric sudden expansion using two-single component LDV systems, has been performed. Estimations of the Taylor microscale were made and the one dimensional energy spectrum was determined using the spatial and autocorrelation functions from these measurements. Difficulties in estimating the Taylor microscale from spatial and autocorrelations are discussed and methods to overcome these difficulties are suggested. Calculations of the one dimensional energy spectrum from curve fits to the correlation functions are explored and some hazards of the process are highlighted. DTIC

N94-25534# Air Force Inst. of Tech., Wright-Patterson AFB, OH. School of Engineering.
OFF-DESIGN PERFORMANCE OF CRENULATED BLADES IN A LINEAR COMPRESSOR CASCADE M.S. Thesis
Michael J. Costello 1 Dec. 1993 133 p
(AD-A273744; AFIT/GAE/ENY/93D-9) Avail: CASI HC A07/MF A02

The effects of using compressor blades with a crenulated (notched) trailing edge in a low aspect ratio (AR = 1) linear compressor cascade at four incidence angles (-1.08 deg, +4.49 deg, +9.32 deg and +12.44 deg) were investigated. Blade performance and wake mixing characteristics for crenulated blades were compared with similar data for blades with a straight trailing edge. A seven-bladed cascade was operated with a flow Mach number of 0.4 and a blade chord Reynolds number of 4.1 x 10(exp

5). The diffusion factor ranged from 0.22 to 0.42 and strong three-dimensional flow effects were present. Total pressure losses were measured with a total pressure rake. Velocities and flow angles were measured using hot-film anemometry. Crenulated blades were found to enhance wake mixing from 20 to 50 percent depending on blade loading and downstream location. Crenulated blades were also found to reduce flow deflection by 1.9 deg at the lowest incidence and by 3.7 deg at the highest incidence. At the highest blade loading, crenulations were found to reduce total pressure losses by 20 percent and inhibit large scale flow degradation and vortex breakdown. At mild blade loadings, negligible differences in losses were observed. DTIC

N94-23029*# Pennsylvania State Univ., University Park. Propulsion Engineering Research Center and Dept. of Mechanical Engineering.
MEASUREMENT OF INTACT-CORE LENGTH OF ATOMIZING LIQUID JETS BY IMAGE DECONVOLUTION
Roger Woodward, Robert Burch, Kenneth Kuo, and Fan-Bill Cheung *In its* NASA Propulsion Engineering Research Center, Volume 2 Nov. 1993 p 1-4 (For primary document see N94-23028 06-20)
Avail: CASI HC A01/MF A03

N94-23034*# Pennsylvania State Univ., University Park. Propulsion Engineering Research Center and Dept. of Mechanical Engineering.
LOX DROPLET VAPORIZATION IN A SUPERCRITICAL FORCED CONVECTIVE ENVIRONMENT
Chia-Chun Hsiao and Vigor Yang *In its* NASA Propulsion Engineering Research Center, Volume 2 Nov. 1993 p 28-32 (For primary document see N94-23028 06-20)
Avail: CASI HC A01/MF A03

N94-23036*# Pennsylvania State Univ., University Park.
DROPLET TURBULENCE INTERACTIONS UNDER SUBCRITICAL AND SUPERCRITICAL CONDITIONS
E. B. Coy, S. C. Greenfield, M. S. Ondas, Y.-H. Song, T. D. Spegar, and D. A. Santavicca *In its* NASA Propulsion Engineering Research Center, Volume 2 Nov. 1993 p 39-45 (For primary document see N94-23028 06-20)
Avail: CASI HC A02/MF A03

N94-23042*# Pennsylvania State Univ., University Park. Propulsion Engineering Research Center and Dept. of Mechanical Engineering.
SPRAY FORMATION PROCESSES OF IMPINGING JET INJECTORS
W. E. Anderson, H. M. Ryan, S. Pal, and R. J. Santoro *In its* NASA Propulsion Engineering Research Center, Volume 2 Nov. 1993 p 69-74 (For primary document see N94-23028 06-20)
(Grant AF-AFOSR-0336-91)
Avail: CASI HC A02/MF A03

N94-23043*# TRW Defense and Space Systems Group, Redondo Beach, CA. Applied Technology Div.
INHERENT STABILITY OF CENTRAL ELEMENT COAXIAL LIQUID-LIQUID INJECTORS
Frank J. Stoddard *In* Pennsylvania State Univ., NASA Propulsion Engineering Research Center, Volume 2 Nov. 1993 p 75-76 (For primary document see N94-23028 06-20)
Avail: CASI HC A01/MF A03

N94-23045*# Pennsylvania State Univ., University Park. Propulsion Engineering Research Center and Dept. of Mechanical Engineering.
DEVELOPMENT OF A DROPLET BREAKUP MODEL CONSIDERING AERODYNAMIC AND DROPLET COLLISION EFFECTS
K. L. Wert and H. R. Jacobs *In its* NASA Propulsion Engineering Research Center, Volume 2 Nov. 1993 p 82-87 (For primary document see N94-23028 06-20)
Avail: CASI HC A02/MF A03

N94-23047*# Pennsylvania State Univ., University Park. Dept. of Aerospace Engineering and Propulsion Engineering Research Center.
SHEAR COAXIAL INJECTOR INSTABILITY MECHANISMS
T. Kaltz, M. Glogowski, and M. M. Micci *In its* NASA Propulsion Engineering Research Center, Volume 2 Nov. 1993 p 93-96 (For primary document see N94-23028 06-20)
Avail: CASI HC A01/MF A03

N94-23055*# Pennsylvania State Univ., University Park. Propulsion Engineering Research Center and Dept. of Mechanical Engineering.
EFFICIENCY AND RELIABILITY ENHANCEMENTS IN PROPULSION FLOWFIELD MODELING
Philip E. O. Buelow, Sankaran Venkateswaran, and Charles L. Merkle *In its* NASA Propulsion Engineering Research Center, Volume 2 Nov. 1993 p 130-134 (For primary document see N94-23028 06-20)
Avail: CASI HC A01/MF A03

N94-23056*# Fluent, Inc., Lebanon, NH.
COMPUTATION OF PROPULSION-RELATED FLOWFIELDS USING UNSTRUCTURED ADAPTIVE MESHES
Jonathan M. Weiss and Jayathi Y. Murthy *In* Pennsylvania State Univ., NASA Propulsion Engineering Research Center, Volume 2 Nov. 1993 p 135-139 (For primary document see N94-23028 06-20)
Avail: CASI HC A01/MF A03

N94-23060*# Pennsylvania State Univ., University Park. Propulsion Engineering Research Center and Dept. of Mechanical Engineering.
COMPUTATIONAL FLUID DYNAMIC MODELLING OF CAVITATION
Manish Deshpande, Jinzhang Feng, and Charles L. Merkle *In its* NASA Propulsion Engineering Research Center, Volume 2 Nov. 1993 p 159-163 (For primary document see N94-23028 06-20)
Avail: CASI HC A01/MF A03

N94-23062*# Pennsylvania State Univ., University Park. Dept. of Aerospace Engineering.
COMPUTATION OF FLOWS IN A TURN-AROUND DUCT AND A TURBINE CASCADE USING ADVANCED TURBULENCE MODELS
B. Lakshminarayana and J. Luo *In its* NASA Propulsion Engineering Research Center, Volume 2 Nov. 1993 p 170-175 (For primary document see N94-23028 06-20)
Avail: CASI HC A02/MF A03

N94-23675*# Queens Univ., Kingston (Ontario). Dept. of Mechanical and Chemical Engineering.
FAS MULTIGRID CALCULATIONS OF THREE DIMENSIONAL FLOW USING NON-STAGGERED GRIDS
D. Matovic, A. Pollard, H. A. Becker, and E. W. Grandmaison *In* NASA. Langley Research Center, The Sixth Copper Mountain Conference on Multigrid Methods, Part 1 Nov. 1993 p 17-29 (For primary document see N94-23673 06-64)
Avail: CASI HC A03/MF A03

N94-23689*# Naval Postgraduate School, Monterey, CA. Dept. of Mathematics.
MULTIGRID METHODS FOR A SEMILINEAR PDE IN THE THEORY OF PSEUDOPLASTIC FLUIDS
Van Emden Henson and A. W. Shaker *In* NASA. Langley Research Center, The Sixth Copper Mountain Conference on Multigrid Methods, Part 1 Nov. 1993 p 231-242 (For primary document see N94-23673 06-64)
(Grant ZZ867-ZZ899/5986)
Avail: CASI HC A03/MF A03

N94-23690*# Lawrence Livermore National Lab., CA.
A MULTILEVEL ADAPTIVE PROJECTION METHOD FOR UNSTEADY INCOMPRESSIBLE FLOW
Louis H. Howell *In* NASA. Langley Research Center, The Sixth Copper Mountain Conference on Multigrid Methods, Part 1 Nov. 1993 p 243-257 (For primary document see N94-23673 06-64)
(Contracts W-7405-eng-48; IACRO-93-817)
Avail: CASI HC A03/MF A03

N94-23693*# Johns Hopkins Univ., Laurel, MD. Applied Physics Lab.
MULTI-GRID DOMAIN DECOMPOSITION APPROACH FOR SOLUTION OF NAVIER-STOKES EQUATIONS IN PRIMITIVE VARIABLE FORM
Hwar-Ching Ku and Bala Ramaswamy (Rice Univ., Houston, TX.) *In* NASA. Langley Research Center, The Sixth Copper Mountain Conference

on Multigrid Methods, Part 1 Nov. 1993 p 293-304 (For primary document see N94-23673 06-64)
(Contract N00039-91-C-0001)
Avail: CASI HC A03/MF A03

N94-23694*# Technische Hogeschool, Twente (Netherlands). Dept. of Applied Mathematics.
COMPRESSIBLE TURBULENT FLOW SIMULATION WITH A MULTIGRID MULTIBLOCK METHOD
Hans Kuerten and Bernard Geurts *In* NASA. Langley Research Center, The Sixth Copper Mountain Conference on Multigrid Methods, Part 1 Nov. 1993 p 305-315 (For primary document see N94-23673 06-64)
Avail: CASI HC A03/MF A03

N94-24248 Technion - Israel Inst. of Tech., Haifa. Faculty of Aerospace Engineering.
STABILITY OF HYPERSONIC FLOW OF A DETONABLE GAS MIXTURE IN THE STAGNATION REGION OF A BLUNT BODY AND A FORWARD FACING STEP
Genadi Tivanov and Joseph Rom *In* Israel Society of Aeronautics and Astronautics, The 33rd Israel Annual Conference on Aviation and Astronautics 25 Feb. 1993 p 114-124 (For primary document see N94-24241 06-01)
Copyright Avail: Issuing Activity (Israel Society of Aeronautics and Astronautics, c/o Faculty of Engineering, Tel-Aviv Univ., Ramat Aviv 69978, Israel)

N94-24249 Israel Aircraft Industries Ltd., Tashan. Aerodynamics Dept.
NEW FEATURES IN COMPUTATIONAL FLUID DYNAMICS (CFD) TECHNOLOGY AT THE TASHAN ENGINEERING CENTER AT IAI
B. Epstein *In* Israel Society of Aeronautics and Astronautics, The 33rd Israel Annual Conference on Aviation and Astronautics 25 Feb. 1993 p 125-132 (For primary document see N94-24241 06-01)
Copyright Avail: Issuing Activity (Israel Society of Aeronautics and Astronautics, c/o Faculty of Engineering, Tel-Aviv Univ., Ramat Aviv 69978, Israel)

N94-24283 Technion - Israel Inst. of Tech., Haifa. Faculty of Applied Mathematics.
EFFECT OF INITIAL DROPLET-SIZE DISTRIBUTIONS ON FUEL-VAPOR PROFILES IN A SHEAR-LAYER FLOW
D. Katoshevski and Y. Tambour *In* Israel Society of Aeronautics and Astronautics, The 33rd Israel Annual Conference on Aviation and Astronautics 439-448 (SEE N94-24241 06-01) 25 Feb. 1993 (For primary document see N94-24241 06-01)
Copyright Avail: Issuing Activity (Israel Society of Aeronautics and Astronautics, c/o Faculty of Engineering, Tel-Aviv Univ., Ramat Aviv 69978, Israel)

N94-24430*# Alabama Univ., Huntsville. Dept. of Mechanical and Aerospace Engineering.
CFD SIMULATION OF COAXIAL INJECTORS
D. Brian Landrum *In its* The 1993 NASA/ASEE Summer Faculty Fellowship Program Nov. 1993 6 p (For primary document see N94-24405 06-80)
Avail: CASI HC A02/MF A03

N94-25356*# Texas A&M Univ., Galveston. Maritime System Engineering.
UNIFIED APPROACH FOR INCOMPRESSIBLE FLOWS
Tyne-Hsien Chang *In* NASA. Johnson Space Center, National Aeronautics and Space Administration (NASA)/American Society for Engineering Education (ASEE) Summer Faculty Fellowship Program, 1993, Volume 1 Dec. 1993 6 p (For primary document see N94-25348 06-99)
Avail: CASI HC A02/MF A03

35 INSTRUMENTATION AND PHOTOGRAPHY

Includes remote sensors; measuring instruments and gages; detectors; cameras and photographic supplies; and holography.

For aerial photography see *43 Earth Resources and Remote Sensing*. For related information see also *06 Aircraft Instrumentation*, and *19 Spacecraft Instrumentation*.

N94-22902# Laboratoire d'Automatique et d'Analyse des Systemes, Toulouse (France).
PYROELECTRIC SENSORS IN COPOLYMER INTEGRATED ON SILICON Ph.D. Thesis - Toulouse Univ. [DETECTEURS PYROELECTRIQUES EN COPOLYMERE INTEGRES SUR SILICIUM]
Jean-Paul Beconne 1993 142 p In FRENCH
(LAAS-93044; ETN-94-95184) Avail: CASI HC A07/MF A02

The advantage of pyroelectric over semiconductor sensors for industrial applications is their low cost and their ability to work at room temperature. This advantage provided a context in which to study new materials such as polar polymers. Polyvinylidene fluoride and, one of its copolymers, polyvinylidene trifluro ethylene, were selected among polar polymers and applied to the problem of passive obstacle detection in a moving automobile. Copolymer sensors integrated on silicon are investigated. Successive processing steps are detailed: copolymer deposition in the liquid phase, characterization by electrooptical sensors, and modelization of the results from the characterization. The two deposition methods for the copolymer are compared, and the balance between their advantages and drawbacks is detailed. The main parameters involved in sensor technology are specified. ESA

N94-22954# Sandia National Labs., Albuquerque, NM.
ROBUST, WIDE-RANGE HYDROGEN SENSOR FOR USE IN COMMERCIAL, SPACE, AND GOVERNMENT APPLICATIONS
P. McWhorter and J. Rodriguez 1993 2 p Presented at the 10th World Hydrogen Energy Conference, Cocoa Beach, FL, 20-24 Jun. 1993
(Contract DE-AC04-76DP-00789)
(DE93-040902; SAND-93-2155C; CONF-9306254-1) Avail: CASI HC A01/MF A01

Hydrogen leaks pose a constant fire and explosion threat, and existing techniques for detecting hydrogen suffer from a number of limitations. Existing hydrogen sensors have limited dynamic range, poor reproducibility and reversibility, are subject to false alarms, and tend to be slow, unreliable and difficult to use. In order to address this need, Sandia has designed, fabricated, tested, and demonstrated a new generation of hydrogen sensor which overcomes the limitations of existing technology. This new technology, known as the Robust, Wide-Range Hydrogen Sensor Technology, was created by integrating special catalytic alloy films into Sandia's existing CMOS micro-electronic based hydrogen sensor technology. The Sensor contains PdNi transistor sensors for detecting low concentrations of hydrogen, PdNi resistor sensors for detecting higher concentrations of hydrogen, and on-chip micro-thermometers and micro-heaters for maintaining constant chip temperature. Derived from text

N94-22989# Stanford Univ., CA. High Temperature Gasdynamics Lab.
A PRESSURIZED THERMOGRAVIMETRIC ANALYZER FOR USE IN STUDIES OF GAS/SOLID SYSTEMS
R. E. Mitchell 22 Sep. 1993 6 p
(Contract DE-FG05-92ER-79119)
(DE94-001224; DOE/ER-79119/1) Avail: CASI HC A02/MF A01

A TG-151 Thermogravimetric Experimental Station, which measures and records weight changes of a solid material over a wide dynamic temperature range at a wide range of pressures in controlled environments, was purchased from Cahn Instruments, Inc. The TG-151 permits temperature to be programmed to follow a precise temperature profile of ramp and/or isothermal segments while monitoring the changes in weight of solid samples exposed to a gaseous environment of specified composition at a preset pressure. Weight and temperature measurements are made at user-specified time intervals and total time (up to 48 hours). Data are stored on the disk of a dedicated computer. The data can be processed by a data analysis program or exported to spreadsheet programs. The pressure vessel is designed to operate in vacuum to 10(exp -5) torr and over a wide range of pressures. At normal room temperature, the TG-151 can operate up to 100 atm and at 1273 K, it can operate up to 70 atm. The null balance has a sensitivity of 10 micrograms, capacity up to 100 grams, and a dynamic range of 10(exp 6):1. Both reducing and oxidizing environments can be established in the reaction chamber. For our specific needs the instrument had to be slightly modified to allow for two reactant gas streams to enter the pressure vessel at prescribed times. This required the purchase and installation of a gas blending system. The gas blending system permits coal and char samples to be heated at a specified rate to a desired temperature in an inert environment before the sample is exposed to an oxidizing environment. DOE

N94-23162# Oxford Univ. (England). Robotics Research Group.
STEREO FOR GAZING AND CONVERGING CAMERAS. PART 1: BASIC GEOMETRY
David W. Murray 1992 15 p
(OUEL-1915/92; ETN-94-95144) Avail: CASI HC A03/MF A01

Geometrical descriptions of the imaging system of the common elevation configuration when fixating on an arbitrary point in space are developed, and the use of cyclotorsion to convert from one gazing system to another is indicated. The development of approximations for the disparity under small angle conditions is shown to be easier by referring points to the gazing cyclopean frame, rather than the primary or resting cyclopean frame, at least one piece of evidence in support of Ballard's assertion that this is the 'natural' reference frame. The approximations made are shown to be correct to first order even for points with large displacements from the optic axis in the cyclopean frame, and an approximation correct to second order when this displacement is small is obtained. ESA

N94-23200# Sandia National Labs., Albuquerque, NM.
GENERIC MICROELECTRONIC SMART SENSOR PLATFORM FOR DETECTION OF TOXIC, HAZARDOUS, AND FLAMMABLE GASES
J. Rodriguez, W. Corbett, S. Montague, M. Knoll, and P. McWhorter 1993 3 p Presented at the International Electron Devices Meeting, Washington, DC, 5-8 Dec. 1993
(Contract DE-AC04-76DP-00789)
(DE93-017626; SAND-93-1617C; CONF-931215-1) Avail: CASI HC A01/MF A01

Extensive work has been performed in the past which demonstrates that various metal alloys can be used to detect different toxic, hazardous, and flammable gases. Work has been performed using Pd, Pt, Ir, PdNi, PdAg and Pt/Pd for detecting things such as Hydrogen, Hydrazine, Hydrogen Sulfide, Deuterium, Tritium, Ethanol and Hexane. Perhaps the most familiar is the use of Pd and PdNi for the detection of Hydrogen. These devices work by examining the effect of the gases on the material properties of the metal alloys. Two of the most common material properties examined in these sensors are the resistance of thin film resistors, and the flatband or threshold voltage shifts of MOS structures fabricated with a particular alloy as the gate material. While research into these sensing techniques has shown much promise, few manufacturable, fieldable devices have resulted. These sensing techniques are prone to drift problems due to temperature variations, and typically have large sample to sample variations in performance due to process control issues. Typically, these sensors require significant external instrumentation for measurement and control, making the systems large and expensive. Sandia National Laboratories has designed, fabricated and demonstrated complete functionality of a generic microelectronic based smart sensor platform intended to effectively exploit the research mentioned above into high performance, manufacturable, fieldable devices. This smart sensor platform technology fabricates 2 (mu)m CMOS digital and analog control electronics, sensing elements, and temperature control elements on the same silicon integrated circuit. Our initial demonstration of this technology incorporates PdNi as the sensing alloy for the detection of hydrogen. DOE

N94-23285*# Rose-Hulman Inst. of Tech., Terre Haute, IN.
DESIGN OF A SURFACE DEFORMATION MEASURING INSTRUMENT FOR THE SURFACE TENSION DRIVEN CONVECTION EXPERIMENT (STDCE-2) Final Technical Report
H. Philip Stahl 23 Dec. 1993 209 p
(Grant NAG3-1300)
(NASA-CR-194758; NAS 1.26:194758) Avail: CASI HC A10/MF A03

This final technical report covers the work accomplished (under NAG3-1300) from 1 October 1991 to 1 October 1993. The grant is a direct result of Dr. H. Philip Stahl's (of Rose-Hulman Institute of Technology) participation in the NASA/ASEE Summer Faculty Fellowship Program at NASA Lewis Research Center sponsored by Case Western Reserve University and the Ohio Aerospace Institute. The Surface Tension Driven Convection Experiment (STDCE) is a fundamental fluid physics experiment designed to provide quantitative data on the thermocapillary flow of fluid under the influence of an increased localized surface temperature. STDCE flew on the Space Shuttle Columbia in the First United States Microgravity Laboratory (USML-1) in June 1992. The second flight of this experiment (STDCE-2) is scheduled for 1995. The specific science objectives of STDCE-2 are to determine the extent and nature of thermocapillary flows, the effect of heating mode and level, the effect of the liquid free-surface shape, and the onset conditions for and nature of oscillatory flows. In order to satisfy one of these objectives, an instrument for measuring the shape of an air/oil free surface must be developed. Author (revised)

N94-23498*# Old Dominion Univ., Norfolk, VA. Dept. of Engineering Technology.
FEASIBILITY OF DETECTING AIRCRAFT WAKE VORTICES USING PASSIVE MICROWAVE RADIOMETERS Final Report
Richard F. Harrington Dec. 1993 47 p
(Contract NAS1-19858; RTOP 505-64-12-04)
(NASA-CR-191553; NAS 1.26:191553) Avail: CASI HC A03/MF A01

The feasibility of detecting the cold core of the wake vortex from the wingtips of an aircraft using a passive microwave radiometer was investigated. It was determined that there is a possibility that a cold core whose physical temperature drop is 10 C or greater and which has a diameter of 5 m or greater can be detected by a microwave radiometer. The radiometer would be a noise injection balanced Dicke radiometer operating at a center frequency of 60 GHz. It would require a noise figure of 5 dB, a predetection bandwidth of 6 GHz, and an integration time of 2 seconds resulting in a radiometric sensitivity of 0.018 K. However, three additional studies are required. The first would determine what are the fluctuations in the radiometric antenna temperature due to short-term fluctuations in atmospheric pressure, temperature, and relative humidity. Second, what is the effect of the pressure and temperature drop within the cold core of the wake vortex on its opacity. The third area concerns the possibility of developing a 60 GHz radiometer with a radio metric sensitivity an order of magnitude improvement over the existing state of the art. Author (revised)

N94-23826* National Aeronautics and Space Administration. Lewis Research Center, Cleveland, OH.
HIGH TEMPERATURE, OXIDATION RESISTANT NOBLE METAL-Al ALLOY THERMOCOUPLE Patent
James L. Smialek, inventor (to NASA) and Michael G. Gedwill, inventor (to NASA) 4 Jan. 1994 7 p Filed 6 Jul. 1993 Supersedes N93-31298 (31 - 12, p 3729)
(NASA-Case-LEW-15515-1; US-Patent-5,275,670;
US-Patent-Appl-SN-086584; US-Patent-Class-136-236.1;
US-Patent-Class-136-241; Int-Patent-Class-H01L-35/12) Avail: US Patent and Trademark Office

A thermocouple is disclosed. The thermocouple is comprised of an electropositive leg formed of a noble metal-Al alloy and an electronegative leg electrically joined to form a thermocouple junction. The thermocouple provides for accurate and reproducible measurement of high temperatures (600 - 1300 C) in inert, oxidizing or reducing environments, gases, or vacuum. Furthermore, the thermocouple circumvents the need for expensive, strategic precious metals such as rhodium as a constituent component. Selective oxidation of rhodium is also thereby precluded.
Official Gazette of the U.S. Patent and Trademark Office

N94-24054# Institut Franco-Allemand de Recherches, Saint-Louis (France).
REAL-TIME HOLOGRAPHIC ENDOSCOPY
P. Smigielski, F. Albe, and B. Dischli 27 Jan. 1992 11 p Presented at the SPIE Biomedical Optic 1992 International Symposium, Los Angeles, CA, 19-24 Jan. 1992
(ISL-CO-203/92; ETN-94-95122) Avail: CASI HC A03/MF A01

Experiments concerning holographic endoscopy are presented. The quantitative measurements of deformations of objects are obtained by the double exposure and double reference beam method using either a continuous wave laser or a pulsed laser. Qualitative experiments using an argon laser with time average holographic endoscopy are also presented. A video film on real time endoscopic holographic interferometry was recorded with the help of a frequency doubled YAG laser working at 25 Hz for the first time. ESA

N94-24069*# National Aeronautics and Space Administration. Lewis Research Center, Cleveland, OH.
MINIATURE CONVECTION COOLED PLUG-TYPE HEAT FLUX GAUGES
Curt H. Liebert Feb. 1994 16 p Proposed for presentation at the 40th International Instrumentation Symposium, Baltimore, MD, 1-5 May 1994; sponsored by the Instrument Society of America
(RTOP 505-62-50)
(NASA-TM-106483; E-8420; NAS 1.15:106483) Avail: CASI HC A03/MF A01

Tests and analysis of a new miniature plug-type heat flux gauge configuration are described. This gauge can simultaneously measure heat flux on two opposed active surfaces when heat flux levels are equal to or greater than about 0.2 MW/m(sup 2). The performance of this dual active surface gauge was investigated over a wide transient and steady heat flux and temperature range. The tests were performed by radiatively heating the front surface with an argon arc lamp while the back surface was convection cooled with air. Accuracy is about +20 percent. The gauge is responsive to fast heat flux transients and is designed to withstand the high temperature (1300 K), high pressure (15 MPa), erosive and corrosive environments in modern engines. This gauge can be used to measure heat flux on the surfaces of internally cooled apparatus such as turbine blades and combustors used in jet propulsion systems and on the surfaces of hypersonic vehicles. Heat flux measurement accuracy is not compromised when design considerations call for various size gauges to be fabricated into alloys of various shapes and properties. Significant gauge temperature reductions (120 K), which can lead to potential gauge durability improvement, were obtained when the gauges were air-cooled by forced convection. Author (revised)

N94-24184 Litton Systems, Inc., Minneapolis, MN.
INTEGRATED ACCELEROMETER ASSEMBLY Patent
Henry C. Abbink, inventor (to Litton Systems, Inc.) and Nicholas F. Pier, inventor (to Litton Systems, Inc.) 14 Sep. 1993 22 p
(CA-Patent-1322107; Int-Patent-Class-G01P-015/02; Int-Patent-Class-G01P-015/08; CTN-94-60935) Copyright Avail: Micromedia Ltd., Technical Information Centre, 240 Catherine Street, Suite 305, Ottawa, Ontario, K2P 2G8, Canada HC/MF

An integrated assembly is provided for a dry accelerometer of the pendulous mass type. The assembly includes a planar support base having an aperture in the center and a pendulous member including two arms. A pair of spaced flexible hinges having a first end of each attached to the support base and a second end of each attached to one of the arms pivotally support the pendulous member within the aperture. A pair of limit stops welded to opposed sides of the support base limit the movement of the pendulous member. The support base includes a plurality of apertures for anchoring the hinge welds and limit stop welds and the pendulous member includes a plurality of copper filled apertures for anchoring the hinge welds. Procedures for fabrication of the integrated assembly are also disclosed. The invention provides a means for relatively inexpensive and easy fabrication of dry accelerometer assemblies having less loss of accuracy over time compared to assemblies of the prior art. Author (CISTI)

N94-24360*# Northrop Corp., Hawthorne, CA. Electronics Systems Div.
DOPPLER GLOBAL VELOCIMETRY: DEVELOPMENT OF A FLIGHT RESEARCH INSTRUMENTATION SYSTEM FOR APPLICATION TO NON-INTRUSIVE MEASUREMENTS OF THE FLOW FIELD Final Report
Hiroshi Komine, Stephen J. Brosnan, William H. Long, and Eddy A. Stappaerts 26 Jan. 1994 54 p Original contains color illustrations
(Contract NAS1-19440; RTOP 505-59-10-09)
(NASA-CR-191490; NAS 1.26:191490) Avail: CASI HC A04/MF A01; 4 functional color pages

Doppler Global Velocimetry (DGV) is a new diagnostic tool that offers potential for flow field measurements in flight by acquiring three-component velocity data in near real-time during flight maneuvers. The feasibility of implementation of a flight DGV system aboard NASA's High-Angle-of-Attack Research Vehicle (HARV) was addressed in this work by identifying the essential characteristics of a flight measurement system and by performing calibration and error tests. Results from this work were: an outline that establishes a preliminary basis for system configurations by analyzing measurement errors, installation issues, and operating requirements; measurement of the accuracy of the DGV technique using a laboratory breadboard DGV system based on a frequency-doubled Nd: YAG laser and iodine Absorption Line Filter (ALF), which showed excellent agreement between the DGV data and pilot measurements on a laminar flow jet with velocities of up to 150 m/sec; a survey of DGV system components and technologies that are relevant to the design of a flight measurement system, including a survey of cameras for the next generation DGV receivers; an assessment of the candidate lasers and absorption line filters for the flight system, resulting in a near-term recommendation of Nd: host lasers and an iodine ALF for both flight and wind tunnel applications. Author (revised)

N94-24362*# National Aeronautics and Space Administration. Lewis Research Center, Cleveland, OH.
IMPROVED PRESSURE MEASUREMENT SYSTEM FOR CALIBRATION OF THE NASA LeRC 10X10 SUPERSONIC WIND TUNNEL
Philip Z. Blumenthal (Sverdrup Technology, Inc., Brook Park, OH.) and Stephen M. Helland Jan. 1994 16 p Proposed for presentation at the 40th International Instrumentation Symposium, Baltimore, MD, 1-5 May 1994; sponsored by the Instrument Society of America
(Contract NAS3-25266; RTOP 505-62-84)
(NASA-TM-106470; E-8338; NAS 1.15:106470) Avail: CASI HC A03/MF A01

This paper discusses a method used to provide a significant improvement in the accuracy of the Electronically Scanned Pressure (ESP) Measurement System by means of a fully automatic floating pressure generating system for the ESP calibration and reference pressures. This system was used to obtain test section Mach number and flow angularity measurements over the full envelope of test conditions for the 10 x 10 Supersonic Wind Tunnel. The uncertainty analysis and actual test data demonstrated that, for most test conditions, this method could reduce errors to about one-third to one-half that obtained with the standard system. Author (revised)

N94-24723 Department of the Navy, Washington, DC.
METHOD OF FABRICATING A RECEPTOR-BASED SENSOR Patent
Thomas L. Fare, inventor (to Navy) and Frances S. Ligler, inventor (to Navy) 6 Jul. 1993 8 p Filed 14 Jan. 1992
(AD-D016026; US-Patent-5,225,374; US-Patent-Appl-SN-820123; US-Patent-Class-437-225) Avail: US Patent and Trademark Office

This invention relates to a semiconductor substrate having a porous surface and to the amperometric receptor-based sensors formed with the substrate. More specifically, this invention pertains to the substrate in the form of a bipolar junction transistor having a porous hydrophilic surface directly on its base wherein the surface forms a support for an amperometric sensor. The invention also pertains to the methods of making and using the substrate and sensor. DTIC

N94-24734 Department of the Navy, Washington, DC.
METHOD AND APPARATUS FOR THE NON-INVASIVE MEASUREMENT OF PRESSURE INSIDE PIPES USING A FIBER OPTIC INTERFEROMETER SENSOR Patent
Gerard P. Carroll, inventor (to Navy) 8 Jun. 1993 6 p Filed 20 May 1991
(AD-D016013; US-Patent-5,218,197; US-Patent-Appl-SN-702540; US-Patent-Class-250-227.19) Avail: US Patent and Trademark Office

A method and apparatus for the non-invasive sensing of the pressure within a pipe (or other vessel) is disclosed. An optical source produces a first light beam. This first light beam is split between a first (reference) and a second (measurement) optical fiber. The second optical fiber is associated with the pipe such that circumferential displacements in the pipe, due to changes in internal pressure, result in corresponding displacements in the length of the second optical fiber. Length changes in the optical fibers result in variations in the phase of the light emerging therefrom. The phase difference between the light beams emitted from the first and second optical fibers is then determined and related to changes in the internal pressure of the pipe. DTIC

N94-24831# Edgerton, Germeshausen and Grier, Inc., Idaho Falls, ID.

MEASUREMENT OF INTERFACIAL TENSION BY USE OF PENDANT DROP VIDEO TECHNIQUES

Melvin D. Herd, Charles P. Thomas, Gregory A. Bala, and Gordon D. Lassahn Sep. 1993 68 p
(Contract DE-AC07-76ID-01570)
(DE93-000168; DOE/ID-01570/T170) Avail: CASI HC A04/MF A01

This report describes an instrument to measure the interfacial tension (IFT) of aqueous surfactant solutions and crude oil. The method involves injection of a drop of fluid (such as crude oil) into a second immiscible phase to determine the IFT between the two phases. The instrument is composed of an AT-class computer, optical cell, illumination, video camera and lens, video frame digitizer board, monitor, and software. The camera displays an image of the pendant drop on the monitor, which is then processed by the frame digitizer board and non-proprietary software to determine the IFT. Several binary and ternary phase systems were taken from the literature and used to measure the precision and accuracy of the instrument in determining IFT's. A copy of the software program is included in the report. A copy of the program on diskette can be obtained from the Energy Science and Technology Software Center, P.O. Box 1020, Oak Ridge, TN 37831-1020. The accuracy and precision of the technique and apparatus presented is very good for measurement of IFT's in the range from 72 to 10(exp -2) mN/m, which is adequate for many EOR applications. With modifications to the equipment and the numerical techniques, measurements of ultralow IFT's (less than 10(exp -3) mN/m) should be possible as well as measurements at reservoir temperature and pressure conditions. The instrument has been used at the Idaho National Engineering Laboratory to support the research program on microbial enhanced oil recovery. Measurements of IFT's for several bacterial supernatants and unfractionated acid precipitates of microbial cultures containing biosurfactants against medium to heavy crude oils are reported. These experiments demonstrate that the use of automated video imaging of pendant drops is a simple and fast method to reliably determine interfacial tension between two immiscible liquid phases, or between a gas and a liquid phase. DOE

N94-24852*# Alabama Univ., Huntsville. Physics Dept.

POLARIZATION ANALYSIS OF A BALLOON-BORNE SOLAR MAGNETOGRAPH Final Report

Daniel J. Reiley and Russell A. Chipman 14 Dec. 1993 58 p
(Contract NAS8-38609)
(NASA-CR-193908; NAS 1.26:193908) Avail: CASI HC A04/MF A01

The 10(exp -5) polarization specification for the Balloon-borne Vector Magnetograph (BVM) can be met. The 10(exp -5) specification is shown to be a limitation on the diattenuation and retardance along the chief ray path through the optical system, such that the magnitude of the polarization aberration piston term is constrained to be less than .5(10)(exp -5). Coating specification sheets are provided which will ensure that the polarization sensitivity of the BVM will be less than 10(exp -5). An optical design is provided for a vector magnetograph. Finally, to provide a concrete mathematical meaning for polarization sensitivity, the polarization aberration matrix is averaged of the exit pupil. This shows that the coupling between circular and linear states depends only on the magnitude of the polarization aberration piston term. Author (revised)

N94-24977# Tokuyama Coll. of Technology (Japan).

PERFORMANCE OF INVERSE PHOTOEMISSION SPECTROMETER WITH A NEW BANDPASS PHOTON DETECTOR OF NARROW BANDWIDTH AND HIGH SENSITIVITY

Yoshifumi Ueda, Katsuhiro Nishihara, Kojiro Mimura, Yasuko Hari, Masaki Taniguchi, and Masami Fujisawa Mar. 1993 18 p Sponsored by Ministry of Education, Science and Culture, Tokyo, Japan and Ogasawara Science and Technology Foundation, Japan
(Rept-A-2659; JTN-94-80530) Avail: CASI HC A03/MF A01

A combination of a SrF2 entrance window and a photomultiplier with the Cu-BeO first dynode coated with KCl film realizes the bandpass photon detector with the FWHM (Full Width at Half Maximum) of 0.47 eV centered at .43 eV and the sensitivity improved by about one order of magnitude in comparison with the detector without the KCl film. The overall energy resolution of the inverse photoemission spectrometer, consisting of an electron gun with a BeO cathode and the new detector, has been estimated to be 0.56 eV using polycrystalline Au. Typical counting rate is 10(exp 2) -10(exp 3) counts /(mu A sec) for unoccupied states near the Fermi level of the Au at an acceptance angle of about 0.8 pi steradians with an Al collecting mirror. Author (NASDA)

N94-25000*# Alabama Univ., Huntsville. Dept. of Chemistry.

ANALYSIS OF SOFCAL CALIBRATION DATA Final Report

John C. Gregory Dec. 1993 20 p
(Contract NAS8-38609)
(NASA-CR-193910; NAS 1.26:193910) Avail: CASI HC A03/MF A01

Ionization calorimeters determine the total energy of a particle by absorbing, within the mass of the calorimeter, the entire energy of the particle or a significant (and determinable) fraction of it. The JACEE group has used passive ionization calorimetery, which employs photographic emulsions as the detector medium, to measure the charge composition and energy spectrum of cosmic rays up to, and exceeding, 10(exp 14)eV. The SOFIC approach depends similarly on the use of three-dimensional nuclear-electromagnetic shower theory to relate the ionization deposits obtained during a shower to the energy of the particle causing the shower. Bundles of thousands of scintillating optical fibers are read out using image-intensified CCD's. Such an event may be triggered by a fast shower detector placed under the instrument or if only heavy particles are of interest, from a fast primary Cerention detector placed above the calorimeter. In the first study, fast Hammatsu photomultiplier tubes were purchased and tested for possible application for a triggering purpose. In the second study, some refinements have been made to the theoretical treatment of hadronic interactions in the central collision region. These will be helpful in improving the simulations necessary for observations of high energy cosmic ray nuclei with a SOFIC. Author (revised)

N94-25037 Department of the Navy, Washington, DC.

THERMISTOR CONTROLLED CURRENT SOURCE VERSATILE TEMPERATURE SENSOR Patent

Thomas E. Stixrud, inventor (to Navy) 19 Oct. 1993 6 p Filed 7 Oct. 1992
(AD-D015979; US-Patent-5,253,938; US-Patent-Appl-SN-957563; US-Patent-Class-374-173) Avail: US Patent and Trademark Office

An uncomplicated and reliable temperature sensor is presented. The sensor has a pair of thermistors coupled in parallel with a current source that is connected in series with a load resistor. Temperature variations cause a robust current output change that generates a corresponding robust output voltage determined by a proper selection of the load resistor. Increased sensitivity is provided by the robust current to avoid many of the problems otherwise associated with D.C. amplifiers (e.g., drift). DTIC

N94-25053 Department of the Navy, Washington, DC.

SYSTEM FOR CANCELLING PHASE NOISE IN AN INTERFEROMETRIC FIBER OPTIC SENSOR ARRANGEMENT Patent

Alan D. Kersey, inventor (to Navy) 13 Jul. 1993 11 p Filed 24 Apr. 1991
(AD-D015994; US-Patent-5,227,857; US-Patent-Appl-SN-690437; US-Patent-Class-356-345) Avail: US Patent and Trademark Office

A fiber optic sensor system for cancelling phase noise while it senses a measurand field is disclosed. The system includes circuitry for developing a light beam that is frequency modulated at a fundamental frequency. First and second unbalanced interferometers, having equal path imbalances, are responsive to the frequency modulated light beam for producing respective first and second optical outputs. Detection circuitry is responsive to the fundamental frequency, the second harmonic of the fundamental frequency, and the first and second optical outputs for producing a plurality of sine and cosine signals containing phase difference and phase noise components. A signal processor is responsive to the plurality of sine and cosine signals for cancelling the phase noise components and only producing output sine and cosine components of the difference in the phase shift between the first and second unbalanced interferometers. The system can further include a demodulator for demodulating the sine and cosine components to produce an output signal proportional to the phase shift difference between the first and second unbalanced interferometers. DTIC

N94-25116*# National Aeronautics and Space Administration. Lewis Research Center, Cleveland, OH.

VLSI-BASED VIDEO EVENT TRIGGERING FOR IMAGE DATA COMPRESSION

Glenn L. Williams Feb. 1994 11 p Proposed for presentation at the 40th ISA International Instrumentation Symposium, Baltimore, MD, 1-5 May 1994; sponsored by the Instrument Society of America
(RTOP 694-03-OC)
(NASA-TM-106500; E-8512; NAS 1.15:106500) Avail: CASI HC A03/MF A01

Long-duration, on-orbit microgravity experiments require a combination of high resolution and high frame rate video data acquisition. The digitized high-rate video stream presents a difficult data storage problem. Data produced at rates of several hundred million bytes per second may require a total mission video data storage requirement exceeding one terabyte. A NASA-designed, VLSI-based, highly parallel digital state machine generates a digital trigger signal at the onset of a video event. High capacity random access memory storage coupled with newly available fuzzy logic devices permits the monitoring of a video image stream for long term (DC-like) or short term (AC-like) changes caused by spatial translation, dilation, appearance, disappearance, or color change in a video object. Pre-trigger and post-trigger storage techniques are then adaptable to archiving only the significant video images. Author (revised)

N94-25151# New Mexico Univ., Albuquerque. Dept. of Chemistry.
SCANNING PROBE SURFACE MODIFICATION Technical Report, 1 Aug. 1992 - 31 Jul. 1993
R. M. Crooks, T. S. Corbitt, C. B. Ross, M. J. Hampden-Smith, and J. K. Schoer 23 Nov. 1993 17 p
(Contract N00014-91-J-1991)
(AD-A273178) Avail: CASI HC A03/MF A01

Nanometer-scale manipulation of surfaces is important because subtle changes in surface structure often result in new electronic, magnetic, photonic, and mechanical materials properties. In this brief article we address one aspect of nanometer-scale surface manipulation that is of both technological and fundamental interest: scanning probe microscope (SPM)-induced patterning of surfaces. We begin by discussing traditional methods for submicron patterning, then we address some general aspects of SPM surface manipulation, and finally we present some specific results from our own laboratory. DTIC

N94-25154# Stanford Univ., CA. Solid-State Electronics Lab.
HIGH PRECISION X RAY LITHOGRAPHIC MASKS Final Report
R. F. Pease and R. Browning 1992 79 p
(Contract N00014-90-K-2000)
(AD-A273342) Avail: CASI HC A05/MF A01

This contract period was first concerned with winding up the projects on the embedded X-ray Mask structure and on the 'quantum lithography' idea. As a result of developments elsewhere it became clear that among the most critical issues in achieving high precision X-ray masks were those associated with achieving high precision in both feature size and feature placement in electron beam lithography. Most of the effort in this reporting period was aimed at achieving precision in feature size; notably an attack on the problem of proximity effects. There were two approaches: (1) A short term approach aimed at correcting effects in existing electron beam pattern generators (notably the ETEC MEBES 3 and 4) for feature sizes down 500 nm; and (2) A long term approach aimed at avoiding proximity effects by employing low energy electron exposure for feature size below 500 nm. DTIC

N94-25202*# National Aeronautics and Space Administration. Lewis Research Center, Cleveland, OH.
THERMODYNAMIC MODELS FOR BOUNDING PRESSURANT MASS REQUIREMENTS OF CRYOGENIC TANKS
Neil T. VanDresar and Mark S. Haberbusch (Ohio Aerospace Inst., Brook Park.) Jan. 1994 11 p Presented at the 1993 Cryogenic Engineering Conference, Albuquerque, NM, 12-16 Jul. 1993; sponsored by Los Alamos National Laboratory
(RTOP 506-42-73)
(NASA-TM-106476; E-8403; NAS 1.15:106476) Avail: CASI HC A03/MF A01

Thermodynamic models have been formulated to predict lower and upper bounds for the mass of pressurant gas required to pressurize a cryogenic tank and then expel liquid from the tank. Limiting conditions are based on either thermal equilibrium or zero energy exchange between the pressurant gas and initial tank contents. The models are independent of gravity level and allow specification of autogenous or non-condensible pressurants. Partial liquid fill levels may be specified for initial and final conditions. Model predictions are shown to successfully bound results from limited normal-gravity tests with condensable and non-condensable pressurant gases. Representative maximum collapse factor maps are presented for liquid hydrogen to show the effects of initial and final fill level on the range of pressurant gas requirements. Maximum collapse factors occur for partial expulsions with large final liquid fill fractions. Author

N94-25415# Max-Planck-Inst. fuer Physik und Astrophysik, Garching (Germany).
EXAMINATION OF THE RESPONSE CAPACITY OF A SILICON PIXEL DETECTOR FOR IONS AND MOLECULES IN THE ENERGY AREA 100 TO 300 keV Thesis - Tech. Univ. Munich [UNTERSUCHUNG DES ANSPRECHVERMOEGENS EINES SILIZIUM-PIXELDETEKTORS FUER IONEN UND MOLEKUELE IM ENERGIEBEREICH VON 100 BIS 300 KEV]
Robert Hartmann Sep. 1992 83 p In GERMAN
(MPE-241; ETN-94-95208) Copyright Avail: CASI HC A05/MF A01

An element of an extensive silicon pixel detector, developed for a suprathermal time of flight sensor and implemented in the satellite experiment Soho (Solar and Heliospheric Observatory) for energy estimation of low and high energy particles, is examined. Two dimensional computerized simulations were carried out in order to solve Poisson, transport, and continuity equations, so that electrical properties were obtained and functioning parameters were optimized. Energy resolution of the detector at room temperature was obtained with measurements with alpha particles and is shown to be limited by detector window thickness. The functioning principle of the asynchronously triggered readout electronics was established with measurements in the particle beam of an accelerator. The dependence of the measured detector signal on particle energy and species was estimated; the results were successfully compared to Monte Carlo calculations. The identification of molecule ions after passing through thin carbon foils is shown to be possible due to the pixel structure. ESA

N94-25472# Oxford Univ. (England). Robotics Research Group.
ACTIVE CAMERA CALIBRATION FOR A HEAD-EYE PLATFORM USING A VARIABLE STATE DIMENSION FILTER
Philip F. McLauchlan and David W. Murray 1993 29 p Sponsored in part by EEC
(Grant SERC-GR/G-30003)
(OUEL-1975/93; ETN-94-95159) Avail: CASI HC A03/MF A01

A technique for calibrating a camera mounted on a controllable head/eye platform is presented. It uses the trajectories of an arbitrary number of tracked corner features to improve the calibration parameter estimates over time, utilizing a novel variable state dimension form of the Kalman filter. No special visual stimuli are required and no assumptions are made about the structure of the scene, other than that it is stationary relative to the head. The algorithm runs at 4 frames per second on a single transputer, and is fully integrated into an active vision system for object detection and tracking. Updated calibration parameters are regularly passed to the vision modules that require them. Although the algorithm requires an initial estimate of camera focal length, results are presented from real experiments demonstrating that convergence is achieved for initial errors up to fifty percent. ESA

N94-25499*# Lockheed Engineering and Sciences Co., Moffett Field, CA.
SIMULATION OF A PASSIVE MILLIMETER WAVE SENSOR
William W. Kahlbaum *In* NASA. Ames Research Center, Proceedings of the Workshop on Augmented Visual Display (AVID) Research Dec. 1993 p 163-180 (For primary document see N94-25490 06-54)
Avail: CASI HC A03/MF A04

N94-25502*# David Sarnoff Research Center, Princeton, NJ.
ENHANCED IMAGE CAPTURE THROUGH FUSION
Peter J. Burt, Keith Hanna, and Raymond J. Kolczynski *In* NASA. Ames Research Center, Proceedings of the Workshop on Augmented Visual Display (AVID) Research Dec. 1993 p 207-224 (For primary document see N94-25490 06-54)
Avail: CASI HC A03/MF A04

36 LASERS AND MASERS

Includes parametric amplifiers.
For related information see also *76 Solid-State Physics.*

N94-22867# Lawrence Livermore National Lab., CA.
CHARACTERIZATION OF GERMANIUM STRIPE X RAY LASERS
A. S. Wan, J. C. Moreno, and B. J. MacGowan Jul. 1993 10 p Presented at the Annual Meeting of the Society of Photo-Optical Instrumentation Engineers (SPIE), San Diego, CA, 11-16 Jul. 1993
(Contract W-7405-eng-48)
(DE93-019629; UCRL-JC-112553; CONF-930722-32) Avail: CASI HC A02/MF A01

One method of improving the transverse spatial coherence of x-ray lasers (XRL's) is by adaptive spatial filtering of XRL apertures using geometric shaping in the form of bowtie or wedge XRLS. However, we must maintain the desired geometric shapes in exploding foil or slab configurations during the lasing period. As a first step toward understanding lasing in such geometries, the behavior of simple stripe XRL's was studied. Past experience with stripe XRL's deposited on thick plastic substrates resulted in significantly weaker laser intensities as compared to line-focused slab XRL's. Possible reasons for this intensity reduction of stripe XRL's could include mixing at the laser boundary, and changes in plasma, kinetics, and hydrodynamic properties which affect laser gains and propagation. Experimental and theoretical characterizations of germanium line-focused and stripe XRL's are presented. Key experimental parameters we will study include images of emission profiles of the laser blow-off, angular divergences, XRL output intensities, and ionization balances as we vary XRL designs. The experimental results are compared with two-dimensional (2-D) laser deposition and hydrodynamics simulations using LASNEX, and the changes in ionization balances and level populations from post-processing LASNEX results are studied. DOE

N94-22874# Technische Univ., Eindhoven (Netherlands). Telecommunications Div.
LASER LINEWIDTH MEASUREMENT IN THE PRESENCE OF RIN AND USING THE RECIRCULATING SELF HETERODYNE METHOD
M. Groten and W. vanEtten Jul. 1992 27 p
(EUT-92-E-262; ISBN-9-06-144262-1; ETN-94-94769) Avail: CASI HC A03/MF A01

Laser linewidth measurements using the recirculating self heterodyne method are analyzed. Both the relative intensity noise (RIN) and the phase noise are considered. The delay time of the optical feedback loop is assumed to be considerably larger than the laser's coherence time, a condition to be met for unperturbed reconstruction of the laser spectrum. The superposition of the laser's phase noise spectrum on its RIN spectrum is shown. ESA

N94-22914# Aeronautical Research Labs., Melbourne (Australia).
PROCEEDINGS OF WORKSHOP ON LASER DIAGNOSTICS IN FLUID MECHANICS AND COMBUSTION
1 Oct. 1993 183 p Workshop held in Fishermans Bend, Victoria, 30 Sep. - 1 Oct. 1993
(AD-A272808; DODA-AR-008-393) Avail: CASI HC A09/MF A02

Proceedings of the Workshop on Laser Diagnostics in Fluid Mechanics and Combustion are presented. Topics included are: Accuracy of Laser Doppler Anemometry; Applications of Raman-Rayleigh-LIF Diagnostics in Combustion Research; Phase Doppler Anemometer Technique Concepts and Applications; CARS; Particle Image Velocimetry; Practical Consideration in the Use and Design of Laser Velocimetry Systems in Turbomachinery Applications; Phase Doppler Measurements of Gas-Particle Flow Through a Tube Bank; Degenerate Four Wave Mixing for Shock Tunnel Studies of Supersonic Combustion; Laser Induced Photodissociation and Fluorescence (LIPF) of Sodium Species Present in Coal Combustion; 3D Holographic Measurements Inside a Spark Ignition Engine; Laser Doppler Velocimeter Measurements in Compressible Flow; Bursting in a Tornado Vortex; Quantitative Imaging of OH and Temperature Using a Single Laser Source and Single Intensified Camera; and Laser Doppler Measurements Inside an Artificial Heart Valve. DTIC

N94-22922# Japan Atomic Energy Research Inst., Tokyo.
PROPERTIES OF THE TRANSFER MATRICES OF DEFLECTING MAGNET SYSTEMS FOR FREE ELECTRON LASER
Masaru Takao Jan. 1993 17 p In JAPANESE
(DE93-508257; JAERI-M-92-211) Avail: CASI HC A03/MF A01

The oscillation of the free electron laser (FEL) requires the high current and low emittance electron beam. The beam transport system should be achromatic and isochronous to preserve the brightness and the emittance of the electron beam. In this paper we clarify the algebraic properties of the transfer matrices of the magnetic deflection system, which is a key component in the beam transport line. DOE

N94-22967 Bhabha Atomic Research Centre, Bombay (India).
A NEW AUTOMATIC DESIGN METHOD TO DEVELOP MULTILAYER THIN FILM DEVICES FOR HIGH POWER LASER APPLICATIONS
N. K. Sahoo and K. V. S. R. Apparao 1992 60 p Limited Reproducibility: More than 20% of this document may be affected by microfiche quality
(DE93-632490; BARC-1992/E/047) Avail: CASI HC A04 (US Sales Only)

Optical thin film devices play a major role in many areas of frontier technology like development of various laser systems to the designing of complex and precision optical systems. Design and development of these devices are really challenging when they are meant for high power laser applications. In these cases besides desired optical characteristics, the devices are expected to satisfy a whole range of different needs like high damage threshold, durability etc. In the present work a completely automatic design method based on Modified Complex Method was developed for designing of high power thin film devices. Unlike most of the other methods it does not need any suitable starting design. A quarterwave design is sufficient to start with. If required, it is capable of generating its own starting design. The computer code of the method is very simple to implement. This automatic design method is discussed and various practicable output designs generated by it are presented. The relative efficiency of the method along with other powerful methods was presented while designing a broadband IR antireflection coating. The method is also incorporated with 2D and 3D electric field analysis programs to produce high damage threshold designs. Some experimental devices developed using such designs are also presented. DOE

N94-22974# Pacific Northwest Lab., Richland, WA.
EVALUATION OF URANIUM TRANSITIONS FOR ISOTOPICALLY-SELECTIVE LASER INDUCED FLUORESCENCE WITH DIODE LASERS (TECHNICAL REPORT FOR ST064)
B. D. Cannon Oct. 1993 40 p
(Contract DE-AC06-76RL-01830)
(DE94-002000; PNL-8864) Avail: CASI HC A03/MF A01

Isotopically-selective excitation of uranium atoms by diode lasers can be the basis for a portable instrument to perform uranium isotopic assays in the field. Such an instrument would improve the ability of on-site inspections to detect and deter nuclear proliferation. Published and unpublished spectroscopic data on atomic uranium were examined to identify candidate transitions for isotopically-selective laser excitation with diode lasers. Eleven candidate transitions were identified and evaluated for their potential usefulness for a portable uranium assay instrument. Eight of these transitions are suitable for laser induced fluorescence using different excitation and detection wavelengths, which will improve sensitivity and elemental selectivity. Data sheets on the 25 uranium transitions in the wavelength range 629 nm to 1,000 nm that originate in the ground or first excited states of neutral atomic uranium are included. Each data sheet provides the wavelength, upper and lower energy levels, angular momentum quantum numbers, U-235 isotope shift (relative to U-238, and high-resolution spectra of weapons-grade uranium (93% U-235 and 7% U-238). DOE

N94-22982 Technische Univ., Delft (Netherlands). Ministerie van Economische Zaken.
PARTICLE FORMATION IN A LASER-HEATED AEROSOL REACTOR. APPLICATION TO SILICON AND SILICON NITRIDE SYNTHESIS Ph.D. Thesis
F. E. Kruis 1993 133 p Sponsored by Ministerie van Economische Zaken, The Hague, Netherlands Limited Reproducibility: More than 20% of this document may be affected by microfiche quality

(PB93-217982; ISBN-90-9006115-0) Copyright Avail: CASI HC A07/MF A02

Highly homogeneous and stable industrial materials which do not occur naturally are produced commercially by use of artificially synthesized starting materials, inorganic nonmetallic solids with ionic and covalent bonding. These technical ceramic materials are produced by sintering a powder, often at high-temperature and high-pressure. In the past 10 years, interest in high temperature structural ceramics has led to a search for starting materials with ideal properties for the production of high quality ceramic components. One of the most promising structural materials is silicon nitride. Powder control is very important in controlling the quality of the ceramics. The scope of the work is to reach a more fundamental insight into the processes taking place in the reactor. The knowledge should be used to optimize the process. Since the reactor is essentially an aerosol reactor, the different stages in particle formation are first investigated theoretically. NTIS

N94-23123# Optical Concepts, Inc., Lompoc, CA.

InGaAsP/InP BASED 1.3/1.55 MICRON VERTICAL CAVITY SURFACE EMITTING LASERS FOR WAVELENGTH DIVISION MULTIPLEXED HIGH SPEED DISTRIBUTED COMPUTING, PHASE 1 Final Technical Report, 26 Feb. - 26 Sep. 1993

M. K. Kilcoyne and Jeff W. Scott 11 Oct. 1993 49 p
(Contract DASG60-93-C-0048)
(AD-A271081) Avail: CASI HC A03/MF A01

Wavelength division multiplexed communication systems are becoming increasingly attractive for maximizing the data capacity of long range fiber optic links. Currently, distributed feedback (DFB) semiconductor lasers must be used due to the system requirements of precise single frequency lasers. The high cost of DFB lasers and associated control circuitry has made these systems too expensive for wide acceptance. In this research, the possibility of using wavelength division multiplexed arrays of single 1.55 micron InGaAsP vertical cavity surface emitting lasers has been analyzed. The laser arrays have the potential to dramatically reduce the costs of sources compared with distributed feedback laser arrays. This research has focused on the technologies of wafer fusion, step etching and current constriction to develop designs that meet wavelength division multiplexed system requirements. Experiments and modeling has shown that 4x4 arrays of vertical cavity lasers spaced 2 nm apart in wavelength are a realistic goal. The sixteen lasers would each be capable of launching single mode powers above 1 mw into a fiber at drive currents below 8 mA. DTIC

N94-23168# Technische Univ., Eindhoven (Netherlands). Electronic Devices Group.

MANUFACTURING AND CHARACTERIZATION OF GaAs/AlGaAs MULTIPLE QUANTUMWELL RIDGE WAVEGUIDE LASERS

J. S. Wellen, F. Karouta, M. E. C. Schemmann, E. Smalbrugge, and L. M. F. Kaufmann Nov. 1992 88 p
(EUT-92-E-265; ISBN-9-06-144265-6; ETN-94-94772) Avail: CASI HC A05/MF A01

The manufacturing process for GaAs/AlGaAs ridge waveguide lasers made with quantum well structures was investigated. Broad area and narrow ridge lasers were produced and characterized. Laser arrays and flared waveguide lasers were manufactured and their performance was measured. A good technique for the inspection of layer structures was found to be the oxidation of cleaved facets. The manufacturing process produces well functioning devices. However, improvements to the etching of small ridges is desirable for deeper structures and the metallization of the back contact needs to be improved for better bonding. Laser chips can in this way be mounted on heatsinks. Further problems arise mainly with the breaking procedure resulting in poor mirror quality of quite a number of lasers. With broad area lasers, the quantum well structures give good results. Measurements show low internal absorption and transparency current densities. Narrow ridge lasers perform very well with continuous operation. Threshold currents as low as 10.8 mA were measured. Laser arrays show promising results. Problems due to geometrical inaccuracy can probably be solved by using a special light field mask and better cleaving of the laser chips. Of the flared waveguide lasers, the tapered versions in particular seem to function well. With improvement of the cavity shape, better results could be obtained. ESA

N94-23181# Lawrence Livermore National Lab., CA.

HIGH-ORDER SUM AND DIFFERENCE-FREQUENCY GENERATION IN HELIUM

J. K. Crane and M. D. Perry 12 May 1993 17 p Presented at the NATO Workshop, Han-Sur-Lesse, Belgium, 8-14 Jan. 1993
(Contract W-7405-eng-48)
(DE94-001064; UCRL-JC-114025; CONF-9301119-3) Avail: CASI HC A03/MF A01

High-order harmonic generation provides a new method for generating coherent, XUV radiation. These harmonics are characterized by a rapid, perturbative drop at low orders, followed by a broad plateau extending to photon energies of 150 eV in the lighter, rare gas atoms. An experimentally observed limit coincides with the theoretical limit for harmonic generation in neutral atoms given by the expression E(sub c)(eV)=IP(0)+3U(sub p)(I), where E(sub c) is the energy cutoff of the harmonic plateau, IP(O) is the field-free ionization potential and U(sub p) is the electron quiver energy at the maximum intensity, I, seen by the atom. As part of an effort to develop this technique into a general purpose XUV source, extensive work to understand the phase-matching between the harmonic and driving fields, and the resulting effect on the conversion efficiency, angular distribution and spectral brightness has been undertaken at several. Though, certain aspects of the harmonically generated radiation such as the polarization, relative strength of a given harmonic, and the plateau extent, are defined by the single atom-field interaction. Specifically, the single-atom harmonic spectrum is determined primarily by the interaction of a driven, quasi-free electron with the atomic potential. Using two independent fields, one can affect the electron motion by controlling the relative strength, polarization, and phase of the fields and alter the harmonic spectrum. In this paper, we discuss initial, two-color experiments where we drive the atom with two fields of different frequencies: 1053 nm (1(omega)) and 526 nm (2(omega)). In addition to the higher, odd harmonics, we observe sets of three additional peaks that we attribute to sum and difference-frequency generation between the two fields. By controlling the relative polarization between the two fields we can control the relative strength of the harmonic and mixing components, as well as the polarization of the output XUV photon. DOE

N94-23185# Sandia National Labs., Albuquerque, NM.

POWER BEAMING TO SPACE USING A NUCLEAR REACTOR-PUMPED LASER

R. J. Lipinski, D. K. Monroe, and P. S. Pickard 1993 8 p Presented at the 11th Symposium on Space Nuclear Power Systems, Albuquerque, NM, 9-13 Jan. 1994
(Contract DE-AC04-76DP-00789)
(DE94-001208; SAND-93-2244C; CONF-940101-5) Avail: CASI HC A02/MF A01

The present political and environmental climate may slow the inevitable direct utilization of nuclear power in space. In the meantime, there is another approach for using nuclear energy for space power. That approach is to let nuclear energy generate a laser beam in a ground-based nuclear reactor-pumped laser (RPL), and then beam the optical energy into space. Potential space applications for a ground-based RPL include (1) illuminating geosynchronous communication satellites in the earth's shadow to extend their lives, (2) beaming power to orbital transfer vehicles, (3) providing power (from earth) to a lunar base during the long lunar night, and (4) removing space debris. FALCON is a high-power, steady-state, nuclear reactor-pumped laser (RPL) concept that is being developed by the Department of Energy with Sandia National Laboratories as the lead laboratory. The FALCON program has experimentally demonstrated reactor-pumped lasing in various mixtures of xenon, argon, neon, and helium at wavelengths of 0.585, 0.703, 0.725, 1.271, 1.733, 1.792, 2.032, 2.63, 2.65, and 3.37 microns with intrinsic efficiency as high as 2.5%. Frequency-doubling the 1.733-micron line would yield a good match for photovoltaic arrays at 0.867 microns. Preliminary designs of an RPL suitable for power beaming have been completed. The MW-class laser is fairly simple in construction, self-powered, closed-cycle (no exhaust gases), and modular. This paper describes the FALCON program accomplishments and power-beaming applications. DOE

N94-23203 Los Alamos National Lab., NM.

VAPORIZATION BEHAVIOR OF NON-STOICHIOMETRIC REFRACTORY CARBIDE MATERIALS AND DIRECT OBSERVATIONS OF THE VAPOR PHASE USING LASER DIAGNOSTICS

D. P. Butt, P. J. Wantuck, S. J. Rehse, and T. C. Wallace, Sr. 1993 13 p Presented at the NATO Advanced Research Workshop on Corrosion of Advanced Ceramics, Tubingen, Germany, 30 Aug. - 3 Sep. 1993 Limited Reproducibility: More than 20% of this document may be affected by microfiche quality
(Contract W-7405-eng-36)
(DE93-040094; LA-UR-93-2942; CONF-9308163-1) Avail: CASI HC A03

Transition metal and actinide carbides, such as ZrC or NbC and UC or ThC, exhibit a wide range of stoichiometry, and therefore vaporize incongruently. At long times, steady state vaporization can be achieved where relative concentrations of atomic species on solid surface equals that in the gas phase. The surface composition under these steady state conditions is termed the congruently vaporizing composition, (CVC). Modeling the vaporization or corrosion behavior of this dynamic process is complex and requires an understanding of how the surface composition changes with time and a knowledge of CVC, which is both temperature and atmosphere dependent. This paper describes vaporization and corrosion behavior of non-stoichiometric refractory carbide materials and, as an example, describes a thermokinetic model that characterizes the vaporization behavior of the complex carbide U(x)Zr(1-x)C(y) in hydrogen at 2500 to 3200 K. This model demonstrates that steady state corrosion of U(x)Zr(1-x)C(y) is rate limited by gaseous transport of Zr where partial pressure of Zr is determined by CVC. This paper also briefly describes efforts to image and characterize the vapor phase above the surface of ZrC in static and flowing gas environments using planar laser induced fluorescence. We have developed the method for monitoring and controlling the corrosion behavior of nuclear fuels in nuclear thermal rockets. However, the techniques described can be used, to image boundary layers, and could be used verifying corrosion models. DOE

N94-23209# Sandia National Labs., Albuquerque, NM.
CHARACTERIZATION OF HEAT TRANSPORT AND RADIATION HYDRODYNAMICS IN COLLISIONAL LASER PLASMAS USING COLLECTIVE THOMSON SCATTERING
S. M. Cameron 1993 7 p Presented at the 6th International Symposium on Laser-Aided Plasma Diagnostics, Bar Harbor, ME, 25-28 Oct. 1993
(Contracts DE-AC04-94AL-85000; W-7405-eng-48)
(DE94-001502; SAND-93-2182C; CONF-9310195-1) Avail: CASI HC A02/MF A01

The author proposes using the collective Thomson scattering lineshape from ion acoustic waves to measure the spatial structure of local heat transport parameters and collisionality. Ion acoustic peak height asymmetry is used in conjunction with a recently developed model describing the effects of collisional and Landau damping contributions on the low-frequency electron density fluctuation spectrum to extract the relative electron drift. The local heat flux q(sub e) (proportional to drift) and the electron thermal conductivity (kappa)(sub e(approximately)) - q(sub e)/(gradient)T(sub e) would be inferred from experimentally determined temperature gradients (gradient)T(sub e). Damping of the entropy wave component at zero mode frequency is shown to be an estimate of the ion thermal conductivity (kappa)(sub i), and its visibility is a direct measure of the ion-ion mean free path (lambda)(sub ii). DOE

N94-23286*# Case Western Reserve Univ., Cleveland, OH. Dept. of Materials Science and Engineering.
LASER LIGHT SCATTERING INSTRUMENT ADVANCED TECHNOLOGY DEVELOPMENT Final Report
J. F. Wallace Sep. 1993 10 p
(Contract NCC3-74)
(NASA-CR-194803; NAS 1.26:194803; CWRU-342-7658) Avail: CASI HC A02/MF A01

The objective of this advanced technology development (ATD) project has been to provide sturdy, miniaturized laser light scattering (LLS) instrumentation for use in microgravity experiments. To do this, we assessed user requirements, explored the capabilities of existing and prospective laser light scattering hardware, and both coordinated and participated in the hardware and software advances needed for a flight hardware instrument. We have successfully breadboarded and evaluated an engineering version of a single-angle glove-box instrument which uses solid state detectors and lasers, along with fiber optics, for beam delivery and detection. Additionally, we have provided the specifications and written verification procedures necessary for procuring a miniature multi-angle LLS instrument which will be used by the flight hardware project which resulted from this work and from this project's interaction with the laser light scattering community. Author (revised)

N94-23490# Lawrence Livermore National Lab., CA.
SODIUM-LAYER LASER GUIDE STARS
H. W. Friedman 3 Aug. 1993 11 p Presented at the NATO/ASI Conference on Adaptive Optics for Astronomy, Cargese, France, 29 Jun. - 9 Aug. 1993
(Contract W-7405-eng-48)
(DE93-019621; UCRL-JC-114438; CONF-9306245-1) Avail: CASI HC A03/MF A01

The requirements and design of a laser system to generate a sodium-layer beacon is presented. Early results of photometry and wavefront sensing are given. DOE

N94-23702# Columbia Univ., New York, NY. Dept. of Physics.
INVERSE FREE ELECTRON LASER BEAT-WAVE ACCELERATOR RESEARCH
T. C. Marshall and A. Bhattacharjee Sep. 1993 5 p
(Contract DE-FG02-91ER-40669)
(DE94-002597; DOE/ER-40669/3) Avail: CASI HC A01/MF A01

A calculation on the stabilization of the sideband instability in the free electron laser (FEL) and inverse FEL (IFEL) was completed. The issue arises in connection with the use of a tapered ('variable-parameter') undulator of extended length, such as might be used in an 'enhanced efficiency' traveling-wave FEL or an IFEL accelerator. In addition, the FEL facility at Columbia was configured as a traveling wave amplifier for a 10-kW signal from a 24-GHz magnetron. The space charge field in the bunches of the FEL was measured. Completed work has been published. DOE

N94-24488*# National Aeronautics and Space Administration. Langley Research Center, Hampton, VA.
PROGRESS TOWARD ULTRA-STABLE LASERS FOR USE IN SPACE
A. M. Buoncristiani, S. P. Sandford, and R. M. Amundsen 1992 20 p
(NASA-TM-109678; NAS 1.15:109678) Avail: CASI HC A03/MF A01

This is a summary of a research project that has come to be known as SUNLITE, initially standing for Stanford University - NASA laser in space technology experiment. It involves scientists from the NASA Langley Research Center (LaRC), Stanford University, the National Institute of Standards and Technology (NIST), and the Joint Institute for Laboratory Astrophysics (JILA), and a growing number of other institutions. The long range objective of the SUNLITE effort is to examine the fundamental linewidth and frequency stability limits of an actively stabilized laser oscillator in the microgravity and vibration-free environment of space. The ground-based SUNLITE activities supporting that objective will develop a space-qualified, self-contained and completely automated terahertz oscillator stabilized to a linewidth of less than 3 Hz, along with a measurement system capable of determining laser linewidth to one part in 10(exp 16). The purpose of this paper is to discuss the critical technologies needed to place stabilized lasers in space and to describe the progress made by the SUNLITE project to develop these technologies. Derived from text

N94-24629 Direction des Recherches, Etudes et Techniques, Paris (France). Centre de Documentation de l'Armement.
EXCIPLEX LASER STUDY: DISCHARGE AND MAGNETIC SWITCHING SYSTEMS Final Report [ETUDE DES LASERS EXCIPLEXES: SYSTEMES A DOUBLE DECHARGE ET COMMUTATION MAGNETIQUE]
P. Delaporte Nov. 1992 42 p In FRENCH Limited Reproducibility: More than 20% of this document may be affected by microfiche quality
(PB93-199768) Avail: Issuing Activity (National Technical Information Service (NTIS))

The goal of the study was to make a repetitive excimer laser with a double discharge and magnetic switching circuit that is capable of firing impulses lasting 500 nanoseconds. The authors compared different types of electrical circuits based on double discharge and magnetic switching, as well as switch, diode, and overshoot modes to see which would produce the best results in repetitive mode. Their study showed that the laser performance of switch and overshoot modes are very close, but overshoot requires less magnetic material, which can lead to faster energy injection if the inductance of the laser head is low enough. NTIS

N94-24659# Sandia National Labs., Albuquerque, NM.
ELECTROCHEMICAL SULFUR PASSIVATION OF VISIBLE (APPROXIMATELY 670nm) AlGaInP LASERS
A. J. Howard, C. I. H. Ashby, J. A. Lott, R. P. Schneider, and R. F. Corless 1993 15 p Presented at the 40th National Symposium of the American Vacuum Society (AVS), Orlando, FL, 15-19 Nov. 1993
(Contract DE-AC04-94AL-85000)
(DE94-002293; SAND-93-1127C; CONF-9311104-6) Avail: CASI HC A03/MF A01

The 3-5 based devices such as FET's, HBT's, and lasers often have surface leakage and thermal degradation problems due to surface states which pin the Fermi level to the mid-gap. Sulfur based passivation processes are known to improve device performance by altering surface-state densities. The authors have developed a voltage-controlled anodic sulfur passivation scheme using Na2S dissolved in ethylene glycol. Their process has repeatedly produced a approximately 25% improvement in peak output power near the catastrophic damage limit in visible (lambda = 670 nm) AlGaInP edge-emitting lasers. The threshold current density and electrical characteristics were unchanged after catastrophic failure indicating that passivation raises the threshold for facet damage. DOE

N94-24851*# National Aeronautics and Space Administration. Langley Research Center, Hampton, VA.
TEMPORAL MODEL OF AN OPTICALLY PUMPED CO-DOPED SOLID STATE LASER
T. G. Wangler (Illinois Benedictine Coll., Lisle.), J. J. Swetits (Old Dominion Univ., Norfolk, VA.), and A. M. Buoncristiani 1993 16 p Repr. from Mathl. Comput. Modelling (Pergamon Press Ltd., England), v. 17, no. 6, 1993 p 67-82
(Grant NGT-50346)
(NASA-TM-109680; NAS 1.15:109680) Copyright Avail: CASI HC A03/MF A01

Currently, research is being conducted on the optical properties of materials associated with the development of solid state lasers in the two micron region. In support of this effort, a mathematical model describing the energy transfer in a holmium laser sensitized with thulium is developed. In this paper, we establish some qualitative properties of the solution of the model, such as non-negativity, boundedness, and integrability. A local stability analysis is then performed from which conditions for asymptotic stability are attained. Finally, we report on our numerical analysis of the system and how it compares with experimental results. Author (revised)

N94-24934 Massachusetts Inst. of Tech., Cambridge. Research Lab of Electronics.
COMPACT FREE ELECTRON LASERS FOR MEDICAL APPLICATIONS Final Report, 30 Sep. 1990 - 30 Nov. 1993
George Bekefi 2 Dec. 1993 12 p Limited Reproducibility: More than 20% of this document may be affected by microfiche quality
(Contract N00014-90-J-4130)
(AD-A273609) Avail: Issuing Activity (Defense Technical Information Center (DTIC))

We have designed, built, tested, and operated a 70-period electromagnet planar microwiggler for use in free electron lasers (FEL's), constructed of current conductors wound on ferromagnetic cores. The device has an 8.8 mm period and a 4.2 mm gap and produces 0.5-msec magnetic field pulses of greater than 4.0 kG at a rate of 1/2 Hz. The field of each half-period of the wiggler is independently adjustable; we have developed a novel tuning regimen and employed it to reduce the RMS spread in peak amplitude of a uniform field profile to 0.12%, the best of any sub-cm period wiggler of which we are aware. In addition, the field at the ends of the wiggler have been tapered for reduced electron-beam steering and deflection. DTIC

N94-24938 Schwartz Electro-Optics, Inc., Orlando, FL.
NONLINEAR DYNAMICAL CONTROL OF LASERS Final Report
30 Oct. 1993 57 p Limited Reproducibility: More than 20% of this document may be affected by microfiche quality
(Contract N00014-93-C-0053)
(AD-A273359) Avail: Issuing Activity (Defense Technical Information Center (DTIC))

Schwartz Electro-Optics, Inc. (SEO) was awarded this Small Business Innovation Research (SBIR) Phase I program entitled, Nonlinear Dynamical Control of Laser under Contract No. N0001 4-93-C-0053 from the Office of Naval Research (ONR), Arlington, VA. SEO successfully demonstrated stable blue-green output via second harmonic generation (SHG) from a solid state laser using a KNbO3 crystal in an external resonant cavity. The experiments were conducted at SEO, Orlando, Florida while the computer modelling was subcontracted to Dr. Donna Bandy's group at Oklahoma State University (OSU). The physics of lasers and SHG devices and their combination, naturally involves random chaotic fluctuations that can be attributed to the system nonlinearities. Controlling this behavior is demonstrated and a fundamental understanding of the role of the nonlinearities is exploited. DTIC

N94-24952 Department of the Navy, Washington, DC.
LASER-DEPOSITED BIOCOMPATIBLE FILMS AND METHODS AND APPARATUSES FOR PRODUCING SAME Patent
Catherine M. Cotell, inventor (to Navy), Douglas H. Chrisey, inventor (to Navy), Kenneth S. Grabowski, inventor (to Navy), and James A. Sprague, inventor (to Navy) 7 Sep. 1993 11 p Filed 31 Jul. 1991 Supersedes AD-D015181
(AD-D016017; US-Patent-5,242,706; US-Patent-Appl-SN-738362; US-Patent-Class-427-2) Avail: US Patent and Trademark Office

Biocompatible material can be deposited onto a substrate by laser deposition, such as pulsed laser beam deposition and ion-assisted pulsed laser beam deposition. The deposition can be done at room temperature, in a variety of different atmospheres, with control over the stoichiometry, adhesion, and porosity of the deposited film. The apparatus for carrying out the deposition, and articles formed by such deposition, are also described. The articles so formed are particularly useful as medical prosthesis such as implants. DTIC

N94-25044 Department of the Navy, Washington, DC.
TUNABLE LASERS PUMPED BY VISIBLE LASER DIODES Patent
Richard Scheps, inventor (to Navy) 28 Sep. 1993 12 p Filed 28 May 1992
(AD-D016000; US-Patent-5,249,189; US-Patent-Appl-SN-894508; US-Patent-Class-372-20) Avail: US Patent and Trademark Office

A laser having a Cr(3+) doped Colquiriite mineral host gain element, such as Cr:LiCAF, Cr:LiSAF or Cr:LiSGAF, is pumped by the pumping beam from at least one visible laser diode to provide tunable laser emission. The Cr(3+) doped Colquiriite mineral host gain element has an exterior face provided with a dichroic coating highly transmissive to the pumping beam and highly reflective to the tunable laser emission and has an interior face provided with an AR coating antireflective to the tunable laser emission. An output coupler mirror, provided with a coating that is partially reflective to the tunable laser emission, has an appropriate radius of curvature and is appropriately located to concentrate reflected tunable laser emission in a waist in a resonator mode on an exterior face of the Cr(3+) doped Colquiriite gain element to assure the visible light diode pumping thereof. A lens is disposed to receive the pumping beam to focus it at or near the waist on the exterior face of the Cr(3+) doped Colquiriite gain element. DTIC

N94-25216 Department of the Navy, Washington, DC.
INTERNALLY FOLDED SCALABLE LASER Patent
Richard Scheps, inventor (to Navy) 28 Sep. 1993 16 p Filed 21 May 1992
(AD-D015978; US-Patent-5,249,196; US-Patent-Appl-SN-887202; US-Patent-Class-372-93) Avail: US Patent and Trademark Office

An internally folded scalable laser is presented. The laser has a gain medium with an internal face and an external face and at least one internal fold face subtending an angle which may be about 90 deg. An output coupler that is partially reflective of the resonator mode is oriented to receive and reflect the resonator mode in a direction normal to the internal face to avoid resonator mode astigmatism and to define a folded hemispherically-shaped resonator cavity extending from the output coupler and through an active volume in the gain medium to the external face. A pumping mode source disposed adjacent to the external face is oriented to focus a first pumping mode in a direction normal to the external face in a boom waist at or inside the external face in the folded resonator cavity to define an active volume in the gain medium and to avoid pumping mode astigmatism. Other pumping mode sources direct more pumping mode through the internal-fold faces into a portion of the active volume to partially or completely overlap the pumping and resonator modes. Simultaneously pumping the gain medium along more than one axis for each fold surface assures scaling and physical separation of the pumped regions reduces thermal lensing problems. Other angles between the external and internal faces could be formed in multifaceted configurations of the gain medium so long as the pumping mode beam is normal to the external face and the resonator mode beam is normal to the internal face. DTIC

N94-25218# Technische Univ., Eindhoven (Netherlands).
THE EVOLUTION OF THE LASER: A SYSTEMS PERSPECTIVE ON SCIENCE, TECHNOLOGY AND SOCIETY Ph.D. Thesis [DE EVOLUTIE VAN DE LASER: EEN SYSTEEMPERSPECTIEF OP WETENSCHAP, TECHNOLOGIE EN SAMENLEVING]
Willem deRuiter 1992 362 p In DUTCH
(ETN-94-95319) Avail: CASI HC A16/MF A03

The evolution of laser technology is addressed, and an attempt is made to correlate this evolution to the macrosociological theory of Juergen Habermas. The economic and social consequences of innovations are evaluated. Different laser applications are described. The evolution of the semiconductor laser is discussed. The evolution of optical telecommunication systems is outlined. The Habermas theory of communicative action, focussing on the theoretical distinction between 'system' and 'lifeworld,' is treated. The modified theory of Habermas is applied to the evolution of the laser. The embedding of a number of laser applications in the social context is discussed: laser isotope separation, compact disc players, and the Strategic Defense Initiative. ESA

N94-25294# Technische Univ., Eindhoven (Netherlands).
LASER ABLATION AND DEPOSITION OF METALS Ph.D. Thesis
Jacques Constant Ste Kools 1992 163 p Prepared in cooperation with Philips Gloeilampenfabrieken N.V., Eindhoven, Netherlands
(ETN-94-95311) Avail: CASI HC A08/MF A02

The processes and applications of laser ablation deposition (LAD), also known as pulsed laser deposition (PLD), which is the deposition of a physical thin film, are introduced. The main advantages of this technique, when compared to other thin film deposition techniques, are enumerated. The time of flight (TOF) system which is used to perform angular resolved TOF measurements on the deposition flux (atoms, ions, and molecules) generated by the ablation process, and which consequently provides means to characterize this flux, is described. A UHV deposition system for LAD of metals and nitrides is also discussed. The excimer lasers and UV optics used in LAD, and the methods of calibration of the fluence, are described. The following are also considered: kinetic energies of ablated neutrals, ionized species in the ablation plume, light emission by ablation plumes, deposition of metallic multilayers, and deposition of TiN films. ESA

N94-25304# Deutsche Forschungsanstalt fuer Luft- und Raumfahrt, Stuttgart (Germany). Inst. fuer Technische Physik.
MICROWAVE EXCITATION OF PULSED HIGH PRESSURE GAS DISCHARGE LASERS Ph.D. Thesis - Ruhr Univ. [MIKROWELLENANREGUNG VON GEPULSTEN HOCHDRUCK-GASENTLADUNGSLASERN]
Frank Gekat Feb. 1993 145 p In GERMAN
(Contract BMFT-13-N-55-45)
(DLR-FB-93-12; ETN-94-95201) Avail: CASI HC A07/MF A02

The microwave discharge as alternative means to the TEA and electron beam discharges is investigated. Experiments were performed with the XeCl excimer laser and the Xe laser. The theory of high pressure discharges was reviewed with special emphasis on microwave discharges. For experimental purposes a transversely propagative coupling structure was developed and numerically analyzed. The discharges were operated in two ways: directly with the discharge matched to the transmitter during the laser emission and indirectly by storing the microwave energy in a resonator comprising also the discharge vessel. By igniting the gas discharge the microwave resonator was discharged rapidly producing microwave pulses with power levels exceeding the transmitter power. This pulse compression technique facilitated the realization of a microwave excited XeCl laser with pulse energies exceeding 4 mJ. ESA

N94-25445# Air Force Inst. of Tech., Wright-Patterson AFB, OH. School of Engineering.
THE EFFECTS OF OPTICAL FEEDBACK ON POLARIZATION OF VERTICAL CAVITY SURFACE EMITTING LASERS M.S. Thesis
Gregory J. Vansuch Dec. 1993 61 p
(AD-A273728; AFIT/GAP/ENP/93D-09) Avail: CASI HC A04/MF A01

Vertical Cavity Surface Emitting Lasers (VCSEL's) are a type of semiconductor laser with a cavity oriented orthogonally to the planes of material growth. These lasers differ from conventional edge emitting lasers in several important ways. They have symmetric output beams and they are easily built into two dimensional arrays, making them very attractive as photonic components. The characteristic of interest is polarization. While the asymmetric cavities of edge emitters exhibit a clear preference for light polarized in a particular direction, the cylindrically symmetric cavity of a VCSEL has no clear preference. Therefore, it should be relatively easy to change the polarization of a VCSEL. The polarization switching effects of optical feedback from an external reflector are examined. By feeding back various amounts of cross-polarized light, the switching susceptibility of the VCSEL can be determined. Measurements confirmed that the polarization of a VCSEL can be switched through polarized optical feedback, with the degree of switching depending on the strength of feedback. This switching was a relatively rare behavior, indicating that most VCSEL's had some type of preferential polarization. This preference could be due to the VCSEL structure itself or the manner in which it was excited. DTIC

N94-25482# International Centre for Theoretical Physics, Trieste (Italy).
EXCITATION MECHANISMS FOR XUV AND X RAY LASERS
T. M. El-Sherbini and M. M. Arrubban (Qatar Univ., Doha.) Nov. 1992 9 p
(DE93-617006; LAMP-92/4) Avail: CASI HC A02/MF A01 (US Sales Only)

Two excitation mechanisms leading to lasing action in the extreme ultraviolet and soft X-ray spectral regions are proposed. Boron- like ions of Mg VIII, Al IX and Si X plasmas are used as the active laser material. The upper laser level is the metastable 1s2 2s2 4p(2p) state while the lower level is the short lived 1s2 2s2 3d(2D) state. DOE

37 MECHANICAL ENGINEERING

Includes auxiliary systems (nonpower); machine elements and processes; and mechanical equipment.

N94-22865 Lawrence Livermore National Lab., CA.
ECONOMICS OF ELECTRON BEAM AND ELECTRICAL DISCHARGE PROCESSING FOR POST-COMBUSTION NO(x) CONTROL IN INTERNAL COMBUSTION ENGINES
B. M. Penetrante 2 Aug. 1993 8 p Presented at the 6th Strategic Defense Initiative Organization/Office of Naval Research (SDIO/ONR) Pulse Power Meeting, Chicago, IL, 9-11 Aug. 1993 Limited Reproducibility: More than 20% of this document may be affected by microfiche quality
(Contract W-7405-eng-48)
(DE93-019574; UCRL-JC-114927; CONF-9308145-1) Avail: CASI HC A02

The physics and chemistry of non-thermal plasma processing for post-combustion NO(x) control in internal combustion engines are discussed. A comparison of electron beam and electrical discharge processing is made regarding their power consumption, radical production, NO(x) removal mechanisms, and by-product formation. Pollution control applications present a good opportunity for transferring pulsed power techniques to the commercial sector. However, unless advances are made to drastically reduce the price and power consumption of electron beam sources and pulsed power systems, these plasma techniques will not become commercially competitive with conventional thermal or surface-catalytic methods. DOE

N94-22866 Lawrence Livermore National Lab., CA.
FUNDAMENTAL LIMITATIONS OF NON-THERMAL PLASMA PROCESSING FOR INTERNAL COMBUSTION ENGINE NO(x) CONTROL
B. M. Penetrante 19 Aug. 1993 8 p Presented at the 4th International Symposium on High Pressure Low Temperature Plasma Chemistry, Bratislava, Slovakia, 29 Aug. - 1 Sep. 1993 Limited Reproducibility: More than 20% of this document may be affected by microfiche quality

(Contract W-7405-eng-48)
(DE93-019622; UCRL-JC-114852; CONF-9308149-1) Avail: CASI HC A02

The physics and chemistry of non-thermal plasma processing for post-combustion NO(x) control in internal combustion engines are discussed. A comparison of electron beam and electrical discharge processing is made regarding their power consumption, radical production, NO(x) removal mechanisms, and by-product formation. Can non-thermal deNO(x) operate efficiently without additives or catalysts? How much electrical power does it cost to operate? What are the by-products of the process? These fundamental issues are addressed based on an analysis of the electron-molecule processes and chemical kinetics. DOE

N94-22881# Department of Energy, Washington, DC. Office of Transportation Technologies.
ELECTRIC AND HYBRID VEHICLES PROGRAM
Aug. 1993 61 p
(DE93-040664; DOE/EE-0003) Avail: CASI HC A04/MF A01

The progress achieved in developing electric and hybrid vehicle technologies, beginning with highlights of recent accomplishments in FY 1992 is described. Detailed descriptions are provided of program activities during FY 1992 in the areas of battery, fuel cell, and propulsion system development, and testing and evaluation of new technology in fleet site operations and in laboratories. This Annual Report also contains a status report on incentives and use of foreign components, as well as a list of publications resulting from the DOE program. DOE

N94-22885# Ecole Centrale de Lyon (France).
METHOD FOR SIMULATING A VEHICLE SHOCK TEST: DESIGN AND REALIZATION OF THE REQUIRED IMPLEMENTATION TOOLS Ph.D. Thesis [METHODOLOGIE DE SIMULATION D'UN ESSAI DE CHOC DE VEHICULE: CONCEPTION ET REALISATION DES OUTILS NECESSAIRES A SA MISE EN OEUVRE]
Jean-Paul Mizzi 1992 498 p In FRENCH
(ECL-92-14; ETN-94-95167) Avail: CASI HC A21/MF A04

A mathematical multibody model which simulates the behavior of a passenger car during various frontal crash configurations is presented. A formulation of the motion equations based on the Lie group of displacements is considered. The main difficulty is to know the laws of behavior of the springs. An identification method from the configuration of the experimental results was envisaged. In order to know the vehicle real behavior during a crash trial, it is necessary to have experimental devices which make it possible to rebuild the space kinematics of the components. In each case, the acquisition and processing suitable software was designed. Different nonparametric and parametric identification methods were tested on simple and complex models. The results highlight the model most adapted to solve the problem. ESA

N94-22991# Argonne National Lab., IL.
VEHICLE/GUIDEWAY INTERACTION AND RIDE COMFORT IN MAGLEV SYSTEMS
Y. Cai, S. S. Chen, D. M. Rote, and H. T. Coffey 1993 7 p Presented at the International Conference on Speed Technology for Railway and Maglev Vehicles, Yokohama, Japan, 22-25 Nov. 1993
(Contract W-31-109-eng-38)
(DE94-001319; ANL/ET/CP-80643; CONF-931102-2) Avail: CASI HC A02/MF A01

The importance of vehicle/guideway dynamics in maglev systems is discussed. The particular interest associated with modeling vehicle guide-way interactions and explaining response characteristics of maglev systems for a multicar, multiload vehicle traversing on a single- or double-span flexible guideway are considered, with an emphasis on vehicle/guideway coupling effects, comparison of concentrated and distributed loads, and ride comfort. Coupled effects of vehicle/guideway interactions over a wide range of vehicle speeds with various vehicle and guideway parameters are investigated, and appropriate critical vehicle speeds or crossing frequencies are identified. DOE

N94-22996 Argonne National Lab., IL.
PERFORMANCE ANALYSIS OF THE COMBINED EDS MAGLEV PROPULSION, LEVITATION, AND GUIDANCE SYSTEM
J. L. He, H. T. Coffey, and D. M. Rote 1993 7 p Presented at the International Conference on Speed Technology for Railway and Maglev Vehicles, Yokohama, Japan, 22-25 Nov. 1993 Limited Reproducibility: More than 20% of this document may be affected by poor print and microfiche quality
(Contract W-31-109-eng-38)
(DE94-001346; ANL/ES/CP-80771; CONF-931102-1) Avail: Issuing Activity (Department of Energy (DOE))

An analysis of the Japanese maglev system which uses only one set of coils in the guideway for combined levitation, propulsion, and guidance functions is presented in this paper. This preliminary study, using the dynamic circuit approach, indicates that the system is very promising. DOE

N94-23025 Skoda Works, Pilsen (Czechoslovakia).
NEW WELDING AND FINISHING PROCEDURES
1992 200 p Presented at the New Welding and Finishing Procedures, Plzen, Czechoslovakia, 21-22 Oct. 1992 Limited Reproducibility: More than 20% of this document may be affected by microfiche quality
(DE94-602022; INIS-mf-13703; CONF-9210401) Avail: CASI HC A09 (US Sales Only)

The proceedings contain texts of the 31 contributions presented at the conference. One of them, dealing with the reheat crackability in the heat affected zone of steels for WWER-440 and WWER-1000 reactor vessels, was inputted in INIS. The behavior of the steels was determined by the simulation technique. DOE

N94-23078* National Aeronautics and Space Administration. Goddard Space Flight Center, Greenbelt, MD.
SPLINE SCREW MULTIPLE ROTATIONS MECHANISM Patent
John M. Vranish, inventor (to NASA) 21 Dec. 1993 10 p Filed 17 Sep. 1992
(NASA-Case-GSC-13452-1; US-Patent-5,271,286;
US-Patent-Appl-SN-946111; US-Patent-Class-74-89.15;
US-Patent-Class-244-161; US-Patent-Class-403-13; US-Patent-Class-403-24;
US-Patent-Class-439-362; Int-Patent-Class-F16H-25/20;
Int-Patent-Class-F16D-1/00) Avail: US Patent and Trademark Office

A system for coupling two bodies together and for transmitting torque from one body to another with mechanical timing and sequencing is reported. The mechanical timing and sequencing is handled so that the following criteria are met: (1) the bodies are handled in a safe manner and nothing floats loose in space, (2) electrical connectors are engaged as long as possible so that the internal processes can be monitored throughout by sensors, and (3) electrical and mechanical power and signals are coupled. The first body has a splined driver for providing the input torque. The second body has a threaded drive member capable of rotation and limited translation. The embedded drive member will mate with and fasten to the splined driver. The second body has an embedded bevel gear member capable of rotation and limited translation. This bevel gear member is coaxial with the threaded drive member. A compression spring provides a preload on the rotating threaded member, and a thrust bearing is used for limiting the translation of the bevel gear member so that when the bevel gear member reaches the upward limit of its translation the two bodies are fully coupled and the bevel gear member then rotates due to the input torque transmitted from the splined driver through the threaded drive member to the bevel gear member. An output bevel gear with an attached output drive shaft is embedded in the second body and meshes with the threaded rotating bevel gear member to transmit the input torque to the output drive shaft. Official Gazette of the U.S. Patent and Trademark Office

N94-23082* National Aeronautics and Space Administration. Goddard Space Flight Center, Greenbelt, MD.
SPLIT SPLINE SCREW Patent
John M. Vranish, inventor (to NASA) 16 Nov. 1993 8 p Filed 27 Jul. 1992
(NASA-Case-GSC-13434-1; US-Patent-5,261,758;
US-Patent-Appl-SN-918747; US-Patent-Class-403-348;
US-Patent-Class-403-359; US-Patent-Class-901-30;
Int-Patent-Class-F16B-3/00; Int-Patent-Class-B25J-11/00) Avail: US Patent and Trademark Office

A split spline screw type payload fastener assembly, including three identical male and female type split spline sections, is discussed. The male spline sections are formed on the head of a male type spline driver. Each of the split male type spline sections has an outwardly projecting

load baring segment including a convex upper surface which is adapted to engage a complementary concave surface of a female spline receptor in the form of a hollow bolt head. Additionally, the male spline section also includes a horizontal spline releasing segment and a spline tightening segment below each load bearing segment. The spline tightening segment consists of a vertical web of constant thickness. The web has at least one flat vertical wall surface which is designed to contact a generally flat vertically extending wall surface tab of the bolt head. Mutual interlocking and unlocking of the male and female splines results upon clockwise and counter clockwise turning of the driver element.
Official Gazette of the U.S. Patent and Trademark Office

N94-23164# Oxford Univ. (England). Dept. of Engineering Science.
THE DESIGN OF A TURBINE VANE COOLING SYSTEM USED IN THE TOPPING CYCLE
P. T. Ireland and T. V. Jones Nov. 1992 43 p
(OUEL-1963/92; ETN-94-95150) Avail: CASI HC A03/MF A01

The design of a cooling system for a cascade of two dimensional blades tested in the side stream is described. The measured discharge through the three blade, accurately manufactured model agrees well with predictions from the design analytic model. A water flow rig was built and used to investigate the effect of reducing the trailing edge feed tube pressure on the flow distribution. Analysis of the coolant flow rates during the commissioning tests indicated that coolant was being lost from the leading edge tube delivery system. The measured coolant flow rate to the trailing edge tubes during commissioning was very close to the predicted value. The predicted blade temperatures are all within approximately 20% of the measured temperatures. The temperature differences are explainable in terms of uncertainty in the analytic model. ESA

N94-23178# Oxford Univ. (England). Dept. of Engineering Science.
TIME-FREQUENCY DOMAIN ANALYSIS OF VIBRATION SIGNALS FOR MACHINERY DIAGNOSTICS.(4): INTERPRETATION USING IMAGE PROCESSING TECHNIQUES
W. J. Wang and P. D. McFadden 1992 27 p Sponsored by United Kingdom Science and Engineering Research Council
(OUEL-1953/92; ETN-94-95148) Avail: CASI HC A03/MF A01

A system which uses image processing techniques to assist in the automatic interpretation of gear vibration signatures for early failure detection and fault diagnosis is described. The time signature of an individual gear in a gearbox is extracted by the time domain synchronous averaging technique from the total vibration signal measured in the gearbox casing. The time frequency distribution of the gear vibration signature, determined from the local power spectral density, is treated as an image, and the early failure detection and fault diagnosis are performed by interpreting the patterns in the image by the procedures of segmentation, connectivity analysis, and feature extraction. The implementation of the technique, the criteria for analysis of the image, and experimental examples are described. ESA

N94-23191# Kansas State Univ., Manhattan.
PUSHING TECHNOLOGY TO SATISFY WORLD APPLICATIONS
J. R. Hague 1993 15 p
(Contract DE-FC07-91ID-13074)
(DE94-001365; DOE/ID-13074/T9) Avail: CASI HC A03/MF A01

K-State has concluded the first quarter of the third year, demonstrating and evaluating electric vehicle technology. The G-Van has failed to operate during this period. Although plans are being made to install new batteries in the G-Van, the vehicle has little to prove or demonstrate in the way of advanced technologies. As such, there was an agreement by the Site Operator Users Task Force that no additional federal funding would be spent to maintain or operate the G-Vans. The DSEP van, received from DOE during the latter part of January remains idle. The DSEP vehicle may never be refurbished and used in the Site Operator Program as an operational vehicle. It may be used as a lab vehicle or in a special projects capacity. The cost of operating or maintaining this one-of-a-kind vehicle is high and the value of the vehicle to the program is questionable. Kansas State University is using and is pleased with its first Soleq's EVcort. The vehicle has been used on a routine basis around campus, at the Nebraska State Fair, the Kansas State Fair, and other specific functions. The vehicle continues to operate in an efficient manner, is well received by the public, and clearly demonstrates what is possible in EV technology. Professor Hague continued to serve as the Chairman of the Site Operator Users Task Force. As such, K-State is involved at all levels in promoting electric vehicle legislation and technology. The electric vehicle technology continues to be debated and discussed at all levels of government. The next year should bring incremental improvements for funding. The SOUTF has established an effort to 'push' the EV technology forward with the development of a common specification to be used in the purchase of electric vehicles during the next year. DOE

N94-23215 General Electric Co., Fairfield, CT.
VIBRATION ISOLATING ENGINE MOUNT Patent
Stanley I. Bender, inventor (to General Electric Co.), Peter W. Dawes, inventor (to General Electric Co.), and Lawrence Butler, inventor (to General Electric Co.) 27 Jul. 1993 24 p
(CA-Patent-1-320-710; Int-Patent-Class-B64D-27/26;
Int-Patent-Class-F16F-15/04; Int-Patent-Class-F02C-7/20; CTN-94-60929)
Copyright Avail: Micromedia Ltd., Technical Information Centre, 240 Catherine Street, Suite 305, Ottawa, Ontario, K2P 2G8, Canada HC/MF

An improved engine suspension system is provided for attenuating vibration in a gas turbine engine. In one embodiment, the invention is directed to an aircraft engine suspension system for mounting a gas turbine engine to a supporting frame by mounts arranged in first and second parallel, spaced axial mounting planes of the engine. First and second vibration isolation mounts are aligned in the first mounting plane and couple the engine to the supporting frame. Each of the first and second mounts provides both radial and axial vibration damping to the engine as well as radial and axial stiffness. A third vibration isolation mount is aligned in the second mounting plane and couples the engine and support frame together to provide radial and tangential vibration damping to the engine as well as radial and tangential stiffness. The mounts are arranged axially and radially such that the suspension system is statically and dynamically determinate.
Author (CISTI)

N94-23448 Selskapet for Industriell og Teknisk Forskning, Trondheim (Norway). Welding Center.
WELD CLADDING OF HARD SURFACES
T. Habrekke 1 Feb. 1993 15 p Limited Reproducibility: More than 20% of this document may be affected by microfiche quality
(PB93-201598; STF20-A93022) Avail: Issuing Activity (National Technical Information Service (NTIS))

A literature study about clad welding of hard surfaces on steel is performed. The purpose was to see what kind of methods are mainly used, and particular attention is paid to clad welding of rolls. The main impression from this study is that several methods are in use. Some of these must be considered as 'too exotic' for the aim of the program, such as laser build-up welding. However, clad welding of hard surfaces to rolls is widely used around the world, and there is no need for particularly advanced welding methods to perform the work. The welding consumables and the way the welding is carried out is of more important character. The report will give some comments to this, and hopefully will give a short review of the current technology in this field. NTIS

N94-23449 Selskapet for Industriell og Teknisk Forskning, Trondheim (Norway).
PLASMA ARC KEYHOLE WELDING OF ALUMINUM
H. Fostervoll 8 Feb. 1993 49 p Sponsored by Nordisk Industrifond Limited Reproducibility: More than 20% of this document may be affected by microfiche quality
(PB93-201606; STF20-A93032) Avail: Issuing Activity (National Technical Information Service (NTIS))

An increasing and more advanced use of aluminum as a construction material make higher demands to the effectiveness and quality in aluminum joining. Furthermore, if the advantages of aluminum shall be exploited in the best possible way, it is necessary to use the best processes available for the certain application. Today, the most widely used processes of aluminum welding are gas metal arc welding (GMAW) and gas tungsten arc welding (GTAW). Plasma arc welding (PAW) is another interesting process, which is rather newly adopted for aluminum welding. However, up to now the use is limited and most of the users are within the space industry in USA (NASA); also the new space industry in Europe has adopted the process. The reason for the great interest for PAW in the space industry is, according to NASA, higher weld quality and less repair costs, less heat distortion, and less groove preparations costs. Of these reasons, PAW should also be of interest for the aluminum industry in Scandinavia. The aim of the project is to focus on the possibilities and to some extent testing the PAW process. NTIS

N94-23533# Tracer Technologies, Inc., Somerville, MA.
NEW METHOD FOR INCREASING MACHINE SERVICE-LIFE, PHASE 2 Final Report
Alfred M. Ajami Oct. 1992 19 p Sponsored by NSF, Washington, DC
(Grant NSF MSM-85-00195)
(PB93-200707; NSF/ISI-92005) Avail: CASI HC A03/MF A01

The service life of lubricants used in high-speed small bearings can limit the use life of the mechanical system; such service life is dependent upon the oxidation resistance of the lubricant. Lubricant additives are used to protect the lubricant from oxidation and additive service life becomes the system limiting factor. A method of increasing the service life of lubricant additives is to alter their rate of chemical oxidation through deuteration at primary sites of reaction. Researchers previously demonstrated the feasibility of increasing the service life of a class of lubricant additives, the zinc dialkyldithiophosphates, by deuteration to prevent nucleophilic substitution at the alpha-carbon in the alkyl chain. In the Phase II program, attempts were made to scale up the synthesis procedures used to prepare four deuterated zinc dialkyldithiophosphates. The products, provided to a commercial formulator of bearing lubricants, were observed to increase the acidity of the additive and cause the lubricant to have a noxious odor. Considerable efforts to purify the additives did not solve the problems.
NTIS

N94-23797# General Atomics Technologies Corp., San Diego, CA.
PERFORMANCE CHARACTERISTICS OF THE DIII-D ADVANCED DIVERTOR CRYOPUMP
M. M. Menon (Oak Ridge National Lab., TN.), R. Maingi (Oak Ridge National Lab., TN.), M. R. Wade (Oak Ridge National Lab., TN.), C. B. Baxi, G. L. Campbell, K. L. Holtrop, A. W. Hyatt, G. J. Laughon, C. C. Makariou, and M. A. Mahdavi et al Oct. 1993 4 p Presented at the Symposium on Fusion Engineering, Hyannis, MA, 11-15 Oct. 1993
(Contracts DE-AC03-89ER-51114; DE-AC05-84OR-21400)
(DE94-002745; GA-A-21412; CONF-931018-55) Avail: CASI HC A01/MF A01

A cryocondensation pump, cooled by forced flow of two-phase helium, has been installed for particle exhaust from the divertor region of the DIII-D tokamak. The Inconel pumping surface is of coaxial geometry, 25.4 mm in outer diameter and 11.65 m in length. Because of the tokamak environment, the pump is designed to perform under relatively high pulsed heat loads (300 Wm(exp -2)). Results of measurements made on the pumping characteristics for D2, H2, and Ar are discussed. DOE

N94-23822* National Aeronautics and Space Administration. Lyndon B. Johnson Space Center, Houston, TX.
FINGERED BOLA BODY, BOLA WITH SAME, AND METHODS OF USE Patent
John M. Dzenitis, inventor (to NASA) and Linda W. Billica, inventor (to NASA) 18 Jan. 1994 7 p Filed 5 Jun. 1992 Supersedes N92-30026 (30 - 20, p 3479)
(NASA-Case-MSC-21967-1; US-Patent-5,279,482;
US-Patent-Appl-SN-892053; US-Patent-Class-244-161;
US-Patent-Class-294-86.1; US-Patent-Class-294-66.1;
US-Patent-Class-273-84R; US-Patent-Class-102-504;
Int-Patent-Class-B64G-1/64) Avail: US Patent and Trademark Office

The present invention discloses bola bodies, bolas, and a snaring method which makes use such devices. A bola body, according to the present invention, is nonspherical or irregular in shape rather than a smooth sphere or ovoid body. One or more fingers extends from the bola body. These fingers may be relatively straight or they may have crooked or bent portions to enhance entanglement with a bola line or lines or with each other. Two or more of such fingers may be used and may be regularly or irregularly spaced apart on a bola body. A bola with such bodies includes lines which are connected to the other bodies. In one particular embodiment of a bola body, according to the present invention, the body has an irregular shape with a bottom rectangular portion and a top pyramid portion forming a nose. A plurality of fingers is extended from the pyramidal top portion with one finger extended up and away from each of four corners of the top portion. Such a bola body tends to be initially oriented with its nose and fingers against an object being snared since the body is pulled nose first when a bola line is secured at the tip of the pyramidal portion of the bola body. With such a bola, an unwrapping bola body can slip around a target member so that two of the rod-shaped fingers catch a bola line and guide it into an area or crook between the fingers and a side of the top pyramidal portion of the bola body. Tension on the bola line maintains the line in the crook and tends to press the fingers against the unwrapped target member to stabilize the wrapping of the line about the target member. With such a bola, it is difficult for two or more lines unwrapping in different directions to move past one another without being forced together by line tension. Also, the fingers of such bola bodies may hook and hold each other. The fingers may also hook or entangle some object on or portion of the target member. A probable known target member has known dimensions and shapes so that the bola may be sized and configured to reliably snare such a known target. The bolas can be optimally sized, fashioned, and configured to contact and hold a probable target of known size, dimension, and shape.
Official Gazette of the U.S. Patent and Trademark Office

N94-23831* National Aeronautics and Space Administration. Goddard Space Flight Center, Greenbelt, MD.
MAGNETIC POWER PISTON FLUID COMPRESSOR Patent
Max G. Gasser, inventor (to NASA) 4 Jan. 1994 9 p Filed 2 Mar. 1993
(NASA-Case-GSC-13565-1; US-Patent-5,275,537;
US-Patent-Appl-SN-024971; US-Patent-Class-417-48;
US-Patent-Class-417-50; Int-Patent-Class-F04B-37/00) Avail: US Patent and Trademark Office

A compressor with no moving parts in the traditional sense having a housing having an inlet end allowing a low pressure fluid to enter and an outlet end allowing a high pressure fluid to exit is described. Within the compressor housing is at least one compression stage to increase the pressure of the fluid within the housing. The compression stage has a quantity of magnetic powder within the housing, is supported by a screen that allows passage of the fluid, and a coil for selectively providing a magnetic field across the magnetic powder such that when the magnetic field is not present the individual particles of the powder are separated allowing the fluid to flow through the powder and when the magnetic field is present the individual particles of the powder pack together causing the powder mass to expand preventing the fluid from flowing through the powder and causing a pressure pulse to compress the fluid.
Official Gazette of the U.S. Patent and Trademark Office

N94-23969* National Aeronautics and Space Administration. Goddard Space Flight Center, Greenbelt, MD.
ELECTROMAGNETIC BRAKE/CLUTCH DEVICE Patent
John M. Vranish, inventor (to NASA) 4 Jan. 1994 11 p Filed 3 Dec. 1992
(NASA-Case-GSC-13502-1; US-Patent-5,275,261;
US-Patent-Appl-SN-986632; US-Patent-Appl-Class-188-82.2;
US-Patent-Class-188-82.3; US-Patent-Class-188-82.84;
US-Patent-Class-188-163; US-Patent-Class-188-171;
US-Patent-Class-192-44; US-Patent-Class-192-45.1) Avail: US Patent and Trademark Office

An electromagnetic brake/clutch device includes a drive shaft supported by at least one bearing for transmitting torque, a housing, affixed to prevent its rotation, surrounding the drive shaft, and an electromagnetically activated device within the housing to selectively prevent and allow rotation of the drive shaft. The electromagnetically activated device includes a plurality of cammed rollers to prevent counter-clockwise rotation of the drive shaft. The drive shaft includes a circumferential disk and the housing includes a reaction ring for engagement with the plurality of cammed rollers. The plurality of cammed rollers are released from engagement with the circumferential disk and the reaction ring by a plurality of tripping mechanisms within the housing. The tripping action uses the locking force to act as a release force merely by changing the boundary conditions of the roller interface angles. The tripping mechanisms include trippers for disengaging the plurality of cammed rollers and an anvil shaped portion for providing lateral movement of the trippers. The plurality of cammed rollers is preloaded to engagement with the circumferential disk and reaction ring by a spring, and is located with respect to an adjacent tripping mechanism with another spring. Official Gazette of the U.S. Patent and Trademark Office

N94-23985# European Space Agency, Paris (France).
THE FIFTH EUROPEAN SPACE MECHANISMS AND TRIBOLOGY SYMPOSIUM
W. R. Burke, comp. Noordwijk, Netherlands Apr. 1993 399 p Symposium held in Noordwijk, Netherlands, 28-30 Oct. 1992; sponsored by Netherlands Agency for Aerospace Programs and CNES
(ESA-SP-334; ISBN-9-29-092178-1; ETN-94-94862) Copyright Avail: CASI HC A17/MF A04

The main subjects presented at the Fifth European Space Mechanisms and Tribology Symposium were: satellite antennas, actuators, drives, tribology, deployment mechanisms, scientific instrument mechanisms, special function mechanisms, pointing and scanning mechanisms, analytical methods and performance testing. For individual titles, see N94-23986 through N94-24046.

N94-23986# Spar Aerospace Ltd., Sainte-Anne-de-Bellevue (Quebec).
THE DOWN, RELEASE, AND DEPLOYMENT OF THE RADARSAT SAR ANTENNA c32
G. S. Bush *In* ESA, The Fifth European Space Mechanisms and Tribology Symposium Apr. 1993 7 p Sponsored by Canadian Space Agency (For primary document see N94-23985 06-37)
Copyright Avail: CASI HC A02/MF A04

The Canadian RADARSAT remote sensing satellite is described. RADARSAT employs a Synthetic Aperture Radar (SAR) instrument with a very flexible set of operating capabilities that include selectable swath widths, ground incidence angle and resolution. The SAR antenna is a 15 by 1.5 m slotted waveguide planar array with a mass of 730 kg. This SAR antenna is able to alter its beam pointing angle to anywhere within a 500 km Earth ground track with either a wide or narrow swath, at ground incidence angles from 20 to 49 degrees. The antenna and spacecraft requirements associated with the tie down and deployment activities for RADARSAT are described. System tradeoffs involved with the selection of the design approach adopted for the tie down assemblies and extendible support structure are discussed. The selected mechanisms and their important components are provided. ESA

N94-23987# Starsys Research Corp., Boulder, CO.
METAL BAND DRIVES IN SPACECRAFT MECHANISMS
Daryl Maus *In* ESA, The Fifth European Space Mechanisms and Tribology Symposium Apr. 1993 6 p (For primary document see N94-23985 06-37)
Copyright Avail: CASI HC A02/MF A04

Band drives, rack and pinion gears, and bell cranks are compared for effectiveness. Band drive issues are discussed including materials, bend radius, fabrication, attachment and reliability. Mechanisms illustrating practical applications of band drives are shown. Metal band drives offer several advantages including: small size, high efficiency, low contamination and long life. They provide solutions of problems involving variable output from a constant input. Several properties of a cobalt-chromium-nickel alloy, named Elgiloy are presented. Elgiloy is found to be an excellent choice for the drive band. ESA

N94-23988# Erno Raumfahrttechnik G.m.b.H., Bremen (Germany). Structure Mech.
MICRO-GRAVITY COMPATIBLE DRIVE (MGCD)
Bhoj Nagwaney, T. K. Lien (Norges Tekniske Hoegskole, Trondheim.), N. Wavre (ETEL S.A., Motiers, Switzerland.), and A. Robinson (European Space Agency. European Space Research and Technology Center, ESTEC, Noordwijk, Netherlands.) *In* ESA, The Fifth European Space Mechanisms and Tribology Symposium Apr. 1993 6 p (For primary document see N94-23985 06-37)
Copyright Avail: CASI HC A02/MF A04

The Microgravity Compatible Drive (MGCD) is one of the most demanding subsystems of the future manipulator systems on orbit such as Equipment Manipulator And Transportation System (EMATS). It is developed to provide a linear motion of EMATS in the z-axis of the Columbus attached module and/or the pressurized module of the FreeFlyer. A breadboard model of a MGCD was designed, manufactured and tested. The MGCD consists of the components which are typical for any joint/limb of a manipulator or other drive systems. The approach followed was to make a selection of appropriate technologies and try to reduce the disturbances right away at their sources of generation. The test results in the time domain were found to be within the micro-g requirements, however, the target levels were exceeded in the frequency domain. The main source of disturbances was found to be the harmonic reduction gear which also excited different modes of the structure. ESA

N94-23989# ETEL S.A., Motiers (Switzerland).
LOW NOISE ELECTRIC MOTOR c33
E. Favre, M. Correvon, and M. A. P. Verain (European Space Agency. European Space Research and Technology Center, ESTEC, Noordwijk, Netherlands.) *In* ESA, The Fifth European Space Mechanisms and Tribology Symposium Apr. 1993 7 p (For primary document see N94-23985 06-37)
(Contract ESTEC-9239/90/NL/PP)
Copyright Avail: CASI HC A02/MF A04

The purpose is to point out a motor/driver assembly which has a so called 'low noise' behavior, minimizing the noise and vibrations generated to the external environment. Vibrations created by an electric motor may be harmful to the experiments made in the vicinity. For the motor, noise and vibrations are involved either by magnetic parasitic forces or by non-controlled mechanical tolerances. The importance of the perturbations depends on the amplitude of the parasitic forces and on the natural frequencies of the mechanical parts subject to these pulsating constraints. The study is focussed on the available motor/driver design opportunities leading to a reduction of the amplitude of these forces. The cost in weight and volume involved by a low noise design is pointed out for a given 0.5 Nm/2500 rpm application. ESA

N94-23990# Swiss Center for Electronics and Microtechnology, Inc., Neuchatel.
NEW TRIBOCOATING COMBINATION FOR VACUUM OPERATION
M. Maillat and H. E. Hintermann *In* ESA, The Fifth European Space Mechanisms and Tribology Symposium Apr. 1993 5 p (For primary document see N94-23985 06-37)
Copyright Avail: CASI HC A01/MF A04

A new coating combination to obtain low wear, a low and stable friction coefficient in a vacuum and dry air, as well as in humid air is proposed. The main properties of MoS_2, TiC, amorphous carbon a-C:H, and diamond like carbon coatings are summarized. Examples of tribological behavior of a-C:H coatings from different suppliers are presented. The effect of humidity on friction of a-C:H is discussed. These differences show that a-C:H coatings, which are potentially very interesting, should be investigated in order to be space qualified for future tribological problems. Diamond like carbon can be an excellent sliding coating for space applications. ESA

N94-23991# Liege Univ. (Belgium). Service d'Elements de Machines et de Tribologie.
TRIBOLOGICAL BEHAVIOUR OF FLUORINATED RESINS AND POLYIMIDE RESINS SLIDING OVER A METALLIC SURFACE IN LIQUID NITROGEN
Jean-Luc Bozet and Rene Gras (Institut Superieur des Materiaux et de la Construction Mecanique, Saint-Ouen, France.) *In* ESA, The Fifth European Space Mechanisms and Tribology Symposium Apr. 1993 5 p (For primary document see N94-23985 06-37)
Copyright Avail: CASI HC A01/MF A04

In a cryogenic fluid, the sliding of polymers over a metallic surface is governed by adhesion more than by deformation phenomena. Polyimide resins and fluorinated resins submerged into a cryogenic fluid exhibit a noticeable increase of hardness which induces a decrease of the friction coefficient and of the wear rate compared to a sliding process performed in ambient air. The decrease of wear and friction coefficient is linked to adhesive and deformation phenomena. For fluorinated resins a cold flow is observed. This behavior is illustrated and quantified from test results. Polychlorotrifluorethylene and polyimide resins are characterized. ESA

N94-23992# National Aerospace Lab., Tokyo (Japan).
TRIBOLOGICAL CHARACTERISTICS OF BALL BEARINGS LUBRICATED WITH A SPUTTERED MOLYBDENUM DISULPHIDE FILM IN A VACUUM UNDER A HIGH THRUST LOAD
M. Suzuki and M. Nishimura *In* ESA, The Fifth European Space

Mechanisms and Tribology Symposium Apr. 1993 6 p (For primary document see N94-23985 06-37)
Copyright Avail: CASI HC A02/MF A04

Ball bearing tests performed in vacumm under a contact stress of 2.3 GPa are reported. The bearings were lubricated with an MoS2 sputtered film and contained in a polytetrafluoroethylene cage. After the MoS2 film failure, frictional torque increased drastically, however, no seizure occurred. In a test using a bearing without the MoS2 coating, transfer film formed from the cage proved to be an effective lubricant under a contact stress of 2.1 GPa. An X-ray photoelectron spectroscopy analysis of the balls revealed the presence of Mo and metal fluoride on the ball surfaces.
ESA

N94-23993# European Space Tribology Lab., Risley (England).
THE TRIBOLOGY OF SOME MoS2-LUBRICATED ENGINEERING CERAMICS
J. M. Cunningham, M. J. Anderson, S. G. Gould, and E. W. Roberts *In* ESA, The Fifth European Space Mechanisms and Tribology Symposium Apr. 1993 6 p (For primary document see N94-23985 06-37)
Copyright Avail: CASI HC A02/MF A04

The tribological properties of ceramics involving friction and wear slide tests in both air and vacuum were investigated. Tests with and without lubrication were performed. The ceramics tested were silicon nitride, silicon carbide, titanium carbide, titanium nitride and zirconia. The study demonstrated that, in general, unlubricated ceramics yield high friction in both air and vacuum. MoS2 lubricated ceramics give low friction in vacuum, their friction and wear properties are compared with that of MoS2 coated bearing steels. The results indicate that MoS2 lubricated ceramic bearings should prove superior to similarly coated steel bearings in terms of reduced torque and prolonged low friction lifetime. This is particularly attractive to the space industry.
ESA

N94-23994# Fokker Space and Systems, Amsterdam (Netherlands).
THE COLUMBUS SOLAR ARRAY MECHANISMS **c44**
R. Zwanenburg *In* ESA, The Fifth European Space Mechanisms and Tribology Symposium Apr. 1993 6 p (For primary document see N94-23985 06-37)
Copyright Avail: CASI HC A02/MF A04

The concepts and the development efforts of the new and very large rigid panel solar array for the ESA Polar Platform are summarized. The large array size required the development of new mechanical systems to support and deploy the array panels. The solar array is fixed to the spacecraft with 16 hold down points. Flexibility in the hold down connections is incorporated for load distribution. A continuous Kevlar cable loop was developed to cope with the increased preloads. The panels are deployed by a mechanism of supporting beams and a motorized cable system. An engineering model of this panel deployment mechanism was built and tested.
ESA

N94-23995# British Aerospace Public Ltd. Co., Bristol (England).
PRIMARY DEPLOYMENT MECHANISM FOR THE EUROPEAN POLAR PLATFORM **c18**
S. C. Burgess and M. E. Humphries *In* ESA, The Fifth European Space Mechanisms and Tribology Symposium Apr. 1993 6 p (For primary document see N94-23985 06-37)
Copyright Avail: CASI HC A02/MF A04

The principal mechanism design requirements of the Primary Deployment Mechanism (PDM) are summarized. The solution developed to meet these requirements is presented. The PDM is responsible for deploying the solar array and for maintaining its alignment and power transfer for a minimum of four years. The PDM contains a 3.8 m arm structure with three deployable powered hinges. The powered hinges contain a patented actuation and locking system that is reliable and simple to test. The PDM also contains two passive hinges that are aligned by spring compression forces. The passive hinges have a torsional stiffness that enables the PDM to withstand enforced displacements during launch and they also reduce shock loads at the end of deployment of each hinge.
ESA

N94-23996# Dornier System G.m.b.H., Friedrichshafen (Germany).
INVESTIGATIONS INTO DEPLOYMENT COMPLICATIONS OF THE ERS-1 SAR ANTENNA **c32**
R. Barho *In* ESA, The Fifth European Space Mechanisms and Tribology Symposium Apr. 1993 4 p (For primary document see N94-23985 06-37)
Copyright Avail: CASI HC A01/MF A04

The Synthetic Aperture Radar (SAR) antenna is an important part of the first European Remote Sensing Satellite (ERS-1). In deployed configuration it consists of a 10 by 1 m planar array, divided into a 5 single panel arrangement. The results of the investigations and tests on antenna and component level to find out the reason of this deployment hindrance of the ERS-1 SAR antenna are presented. Test results and corrective actions for the ERS-1 flight model resulted in a successful deployment in space and with the metal oxide semiconductor powder treatment of the rubber surfaces as small hardware modification for ERS-2. 'Sticking' or 'sucking' phenomena were detected on a rubber material. To avoid similar problems in other projects it is recommended to close the gap of knowledge concerning this phenomena by a respective test program, or at least to verify a long time storage effect by respective component tests.
ESA

N94-23997# Hughes Aircraft Co., Los Angeles, CA. Space and Communications Group.
LOW MELTING TEMPERATURE ALLOY DEPLOYMENT MECHANISM
M. J. Madden *In* ESA, The Fifth European Space Mechanisms and Tribology Symposium Apr. 1993 5 p (For primary document see N94-23985 06-37)
Copyright Avail: CASI HC A01/MF A04

A concept of a low melting temperature alloy deployment mechanism is presented. Conventional dimethyl-silicone fluid damped mechanisms are reviewed. Design fundamentals of the melting alloy mechanism are introduced. Benefits of the new over the old are compared. This mechanism is promising, and its use may soon be recommended. A demonstration unit is powered-up to visually illustrate the deployment. This technology is proposed in the following applications: a light payload retention latch and release device; a method to relieve large misalignments between shuttle and payload; and zero backlash latch mechanisms.
ESA

N94-23998# Dornier System G.m.b.H., Friedrichshafen (Germany).
DEVELOPMENT STEPS ON THE BASIS OF TEST WITH THE LOCSTAR REFLECTOR DEPLOYMENT MECHANISM
I. Koeker and C.-C. Etzler *In* ESA, The Fifth European Space Mechanisms and Tribology Symposium Apr. 1993 5 p (For primary document see N94-23985 06-37)
Copyright Avail: CASI HC A01/MF A04

The development phase of the deployment mechanisms through various tests on various test devices is presented. The test results and the step by step process to recognize the reasons for the unexpected behavior and their elimination are summarized. The deployment mechanisms for two 3 by 3 m parabolic reflectors, to be mounted on the LOCSTAR satellite, allow a deployment of the reflectors from storage for launch and their arresting with high accuracy and high stiffness in operating configuration in orbit. The results of the tests showed that the temperature drift of the deployment angle was out of the specification. In order to achieve thermal stability, the materials of the latching equipment components have to be chosen carefully. Thermostability components like Carbon Fiber Reinforced Plastics (CFRP) do not prevent a change of length of the surrounding components. For thermoelastic analysis CFRP components as well as the materials of the surrounding construction have to be taken into account. The mechanical coupling restraints of connected parts have an influence on the thermal stability of the deployment mechanism. To prevent the angular movement, the thermal extension and elastic deformation due to the coupling restraint has to be avoided. A single degree of freedom in lateral direction has to be available.
ESA

N94-23999# Max-Planck-Inst. fuer Aeronomie, Katlenburg-Lindau (Germany).
ULTRA-CLEAN HIGH-PRECISION MECHANISMS FOR THE SUMER EUV SPECTROMETER ON SOHO
W. Engelhardt and H. Hartwig *In* ESA, The Fifth European Space Mechanisms and Tribology Symposium Apr. 1993 4 p (For primary document see N94-23985 06-37)
Copyright Avail: CASI HC A01/MF A04

The Solar Ultraviolet Measurements of Emitted Radiation in the Extreme Ultraviolet (SUMER EUV) spectrometer on Solar and Heliospheric

Observatory (Soho) contains a total of eight mechanisms; two of them with redundant drives. The design and lubrication concepts, the performance data and some test results for the following mechanisms are presented: the pointing mechanism that rotates the off axis paraboloid telescope mirror about its focal point 1300 mm away with a resolution of less than 0.5 arcsec; the aperture cover with a hinge drive of varying reduction ratio able to combine a short closing time with a high final closing force, where a redundant release mechanism based on a sealed paraffin actuator was implemented; the focussing platform mechanism with redundant ball lead screw drives and both static and dynamic balancing. The major design drivers for these mechansims are: the stringent cleanliness requirements mandatory for this class of EUV instruments; the nominal design lifetime of two years of operation in the interplanetary space environment. ESA

N94-24000# Technical Research Centre of Finland, Espoo. Instrument Lab.
PERISCOPE MECHANISM FOR SWAN INSTRUMENT
Heikki Huomo, Heikki Hannula, and Kai Viherkanto *In* ESA, The Fifth European Space Mechanisms and Tribology Symposium Apr. 1993 5 p Sponsored by Technology Development Center and Technical Research Centre of Finland Prepared incooperation with CNRS, Verrieres le Buisson, France and Finnish Meteorological Inst., Helsinki, Finland (For primary document see N94-23985 06-37)
Copyright Avail: CASI HC A01/MF A04

The Solar Wind Anisotropies (SWAN) instrument is a Lyman-a imaging spectrometer on board the Solar and Heliospheric Observatory (Soho) spacecraft. The SWAN instrument comprises two identical sensor units and an electronics unit. The total weight of the instrument is about 14 kg. Both sensor units have a two axis periscope mechanism. This allows the SWAN instrument to make a full sky map of the Lyman-a intensity at any given time. The SWAN instrument mechanism and the components critical to the mechanism performance are described. The scientific and budgetary requirements for the mechanism are summarized. Actual construction and the component level performance testing is discussed. The tests performed for the mechanism subsystem are discussed. Concluding remarks are given. ESA

N94-24001# Saab-Space A.B., Linkoeping (Sweden).
OPENING MECHANISM FOR ISO/CVV COVER RELEASE
Torbjoern Andersson *In* ESA, The Fifth European Space Mechanisms and Tribology Symposium Apr. 1993 6 p (For primary document see N94-23985 06-37)
Copyright Avail: CASI HC A02/MF A04

The cover to the Infrared Space Observatory/Cryostatic Vacuum Vessel (ISO/CVV) will be released and ejected after several days in orbit. The specific need for a clean and reliable low temperature operation and the possibility of using a partly recurrent design from clamp bands used for spacecraft release were identified. A new developed opening mechanism is used instead of the conventional connecting bolt and pyrotechnic bolt cutter. The design is a mechanism which connects the two clamp band halves together. The mechanism provides an opening moment also for the worst case friction expected in operation. The tensioning forces from the two clamp band halves are reduced in several steps so that they could be handled by a small shaft which prevents the mechanism from opening in locked position. The initiation of the opening is made by an electromagnet which pulls the shaft. The surface treatment used for the mechanism is titanium nitride and the limited lubrication is made by molybdenum disulfide which is burnished into the contact surface. The mechanism functioning was verified. ESA

N94-24002# Officine Galileo S.p.A., Florence (Italy).
WIDTH MODULATOR MECHANISM FOR SPECTROMETER ENTRANCE SLITS
G. Mondello, G. Basile, G. Cherubini, and N. Tonetti *In* ESA, The Fifth European Space Mechanisms and Tribology Symposium Apr. 1993 7 p (For primary document see N94-23985 06-37)
Copyright Avail: CASI HC A02/MF A04

The development for the mechanisms of the Ultraviolet Coronograph Spectrometer (UVCS) to study the ultraviolet and visible light spectrums of the solar corona is reported. The UVCS was designed to be integrated on the Solar and Heliospheric Observatory (Soho). The modulation mechanism has the purpose of changing the field of view of the spectrometers entrance beam by adjusting its width through the translation of one edge defining the entrance slit. The mechanism is required to maintain a stable configuration during observations, to smoothly modulate the edge position in the range between 10 to 355 micrometers, and to ensure repeatability and stability in slit edge positioning. The investigated solution is presented with spotlights on several design aspects like flexural element, bearings, lubrication system, and motion laws under the specific constraints. A development model is under evaluation and a comparison between required accuracies in a space environment and measured accuracies in 1 g environment before and after environmental testing is given. ESA

N94-24003# Construcciones Aeronauticas S.A., Madrid (Spain). Space Div.
GOLF MECHANISMS
M. Lancho, J. Escobar, A. Martinez, and J. Marczyk *In* ESA, The Fifth European Space Mechanisms and Tribology Symposium Apr. 1993 11 p (For primary document see N94-23985 06-37)
Copyright Avail: CASI HC A03/MF A04

One of the payloads of the Solar and Heliospheric Observatory (Soho) is the experiment on Global Oscillations at Low Frequencies (GOLF). The design, functional simulation, and preliminary test results of the three mechanisms of GOLF are summarized. These mechanisms are of two types: a shutter and two polarizers. The experiment has two main scientific objectives: to measure the global solar line of sight oscillations; and to measure the global solar line of sight magnetic field component. To meet these objectives, the GOLF instrument was designed to achieve the highest sensitivity of the above measurements. From the operational point of view, the objectives of the experiment are: long time and continuity observations; and high sensitivity and stability. ESA

N94-24004# Sener S.A., Las Arenas (Spain).
DOCKING MECHANISMS: AN OVERVIEW OF DIFFERENT SYSTEMS
J. J. GonzalezVallejo and V. S. Syromiatnikov (Nauchno-Proizvodstvennoe Obedinenie Energija, Kaliningrad, USSR.) *In* ESA, The Fifth European Space Mechanisms and Tribology Symposium Apr. 1993 6 p (For primary document see N94-23985 06-37)
Copyright Avail: CASI HC A02/MF A04

The main characteristics of two different types of docking systems derived from different requirements and experiences are described. One is used in the Mir orbital Space Station, while the other one is planned to be used as a docking system for the European manned spacecraft. The docking system allows the joining of two spacecraft in order to establish a temporary or permanent new composite spacecraft. The main functions of a docking system for manned spacecraft are the capture of one vehicle by the other one with dissipation of the kinetic energy, and then the structural and functional connections providing a safe pressurized passageway between both spacecraft for transfer of crewmen and goods. ESA

N94-24005# Fokker Space and Systems, Amsterdam (Netherlands).
HERA (HERMES ROBOT ARM) OVERVIEW
J. F. M. vandenBosch and H. Alai *In* ESA, The Fifth European Space Mechanisms and Tribology Symposium Apr. 1993 6 p (For primary document see N94-23985 06-37)
Copyright Avail: CASI HC A02/MF A04

An overview of the specific Hermes Robot Arm (HERA) design driving requirements and parameters is given. The mechanisms, tribology aspects, and the current HERA development status are underlined. HERA is operated from the Hermes Spaceplane to service the Columbus Free Flyer (FF) and is stored on the FF in the absence of Hermes. HERA is designed for an operational lifetime of 10 years in a low Earth orbit. The key requirements imposed on the mechanisms are provided. The HERA design is described. For each mechanism, a functional description is provided and the current design is presented. The tribology aspects and test results are discussed. ESA

N94-24006# Technische Physische Dienst TNO-TH, Delft (Netherlands).
THE PRE-DEVELOPMENT OF THE ARISTOTELES CALIBRATION MECHANISM c19
B. C. Braam, M. P. Koster (Universiteit Twente, Enschede, Netherlands.), H. Bokhove, J. Hopman, W. M. G. Courage (Organisatie voor Toegepast Natuurwetenschappelijk Onderzoek, Delft, Netherlands.), G. Hijkoop

(Organisatie voor Toegepast Natuurwetenschappelijk Onderzoek, Delft, Netherlands.), M. Aguirre (European Space Agency. European Space Research and Technology Center, ESTEC, Noordwijk, Netherlands.), and A. Robinson (European Space Agency. European Space Research and Technology Center, ESTEC, Noordwijk, Netherlands.) *In* ESA, The Fifth European Space Mechanisms and Tribology Symposium Apr. 1993 8 p (For primary document see N94-23985 06-37)
Copyright Avail: CASI HC A02/MF A04

The GRADIO instrument is designed to measure the Earth gravity field, using accelerometers, onboard the Aristoteles (Applications and Research Involving Space Techniques for the Observation of the Earth's fields from Low Earth orbit Spacecraft) satellite. An overview of different concepts that were generated during predevelopment activities for the Aristoteles calibration device is given. The final concept, which is a rectilinear movement system based on elastic elements, is described. The generation of the concept was based on fundamentals of mechanical design, such as degrees of freedom, and knowledge on the behavior of elastic elements. The concept can be adapted to other applications. Larger amplitudes are possible and better results on decenter are feasible. More specific applications are precision linear guides for optical components and sensitive accelerometers. The high lateral stiffness facilitates clamping of the system and makes it useful for space applications. ESA

N94-24007# Tecnospazio S.p.A., Milan (Italy).
A SYSTEM FOR THE CHALLENGING TASK OF COLLECTING SAMPLES FROM A COMET SURFACE
M. Fenzi, E. Pozzi, and P. A. Coste (European Space Agency. European Space Research and Technology Center, ESTEC, Noordwijk, Netherlands.) *In* ESA, The Fifth European Space Mechanisms and Tribology Symposium Apr. 1993 6 p (For primary document see N94-23985 06-37)
Copyright Avail: CASI HC A02/MF A04

In the reference scenario of the Rosetta comet nucleus sample return mission, the sample acquisition system is to be mounted on the comet lander, together with the anchoring subsystem. Its tasks are to anchor the lander to the comet, acquire three kinds of cometary samples and transfer them to the Earth return capsule. The sample acquisition system comprises mainly: a coring tool, a shovelling tool, an external sample cutting device, a handling arm, the associated three anchoring systems, and the control electronics. The design of the prototype corer, surface sampling tool, and anchor for testing at cryogenic temperatures, in various materials representing cometary soil, are presented. Preliminary test results are discussed. ESA

N94-24008# Sener S.A., Las Arenas (Spain).
PRELOADED LAUNCH LOCKING DEVICES FOR SILEX
J. J. Echevarria, F. Quintana, J. Rivacoba, and A. Bizkarguenaga *In* ESA, The Fifth European Space Mechanisms and Tribology Symposium Apr. 1993 6 p (For primary document see N94-23985 06-37)
Copyright Avail: CASI HC A02/MF A04

SILEX, an experimental inter orbit communication system, is described. It makes use of a laser beam as transmission support between a so called Low Earth Orbit (LEO) terminal, to be installed on SPOT 4, and a so called Geostationary Orbit (GEO) terminal, to be installed on Artemis. For laser beam stability reasons, the laser source, the receiver, the collecting telescope, and other equipment must be monolithically grouped in a carrier structure which, in turn, is mounted on a coarse pointing mechanism making up the whole aerial. The total mass of this assembly can reach 70 to 90 kg and must be firmly held down during launch in order to withstand the quasistatic and dynamic loads. The stiffness requirement for the launch locking devices is up to 130 Hz in the case of the SILEX program. The mechanical configuration and the design requirements of the launch locking devices are discussed. ESA

N94-24009# European Space Tribology Lab., Risley (England).
THERMAL VACUUM PERFORMANCE OF CYCLOID AND HARMONIC GEARBOXES WITH SOLID (MoS2) AND LIQUID (BRAYCOTE 601) LUBRICATION
S. Gill, D. J. Forster, and R. A. Rowntree *In* ESA, The Fifth European Space Mechanisms and Tribology Symposium Apr. 1993 6 p (For primary document see N94-23985 06-37)
Copyright Avail: CASI HC A02/MF A04

The tribological performance of cycloid and harmonic gearboxes for spacecraft applications is investigated. The tests performed on high torque capacity gearboxes, in an in-vacuo test facility, are reported and the test facility is described. The purpose of the tests was to research the efficiency of dry and grease lubricated gearboxes in vacuo. Although the harmonic drive was superior in terms of efficiency over the cycloid gearbox, the wear of the gear teeth was evident after only a short test duration, whether grease or dry lubrication was used. A full scale life test of any design incorporating a novel gearbox is recommended to prove the long term durability with space lubricants in the space environment. ESA

N94-24010# Centre National d'Etudes Spatiales, Toulouse (France).
TRIBOLOGICAL CHARACTERIZATION OF SPATIAL WET LUBRICANTS UNDER VACUUM **c27**
J. Sicre, Y. Berthier (Institut National des Sciences Appliquees, Lyon, France.), L. Flamand (Institut National des Sciences Appliquees, Lyon, France.), P. Reynaud (Institut National des Sciences Appliquees, Lyon, France.), P. Vergne (Institut National des Sciences Appliquees, Lyon, France.), and M. Godet (Institut National des Sciences Appliquees, Lyon, France.) *In* ESA, The Fifth European Space Mechanisms and Tribology Symposium Apr. 1993 7 p (For primary document see N94-23985 06-37)
Copyright Avail: CASI HC A02/MF A04

The tribological tests performed on three (two oil-based and one grease) selected wet lubricants are reported. The tests were carried out on a vacuum friction test bench which allows the control of the main contact parameters: speed, load, kinematics, atmosphere. Variations of physical properties versus temperature and pressure are taken into account in the test results analysis through a rheological characterization performed on the lubricants tested. The tribological tests under vacuum show that the supply conditions depend on the properties of the liquid and on imposed conditions. When the lubricant supply is insufficient, the liquid film is broken and risks of direct interaction between the first bodies appear. In vacuum conditions, this is a redhibitory defect. The study is directed towards the identification of phenomena that cause a protective third body to form in space conditions. ESA

N94-24011# European Space Tribology Lab., Risley (England).
IN-VACUUM PERFORMANCE OF FOMBLIN Z25-LUBRICATED, 52100 STEEL BEARINGS WITH TIC-COATED BALLS
S. Gill, W. B. Price, R. A. Rowntree, H. J. Boving (Swiss Center for Electronics and Microtechnology, Inc., Neuchatel.), and H.-E. Hintermann (Swiss Center for Electronics and Microtechnology, Inc., Neuchatel.) *In* ESA, The Fifth European Space Mechanisms and Tribology Symposium Apr. 1993 6 p (For primary document see N94-23985 06-37)
Copyright Avail: CASI HC A02/MF A04

The effectiveness of TiC coated AISI 440C stainless steel balls in preventing the in vacuo degradation of Fomblin Z25 oil was evaluated. The balls were incorporated into SAE 52100 steel 20 mm bore angular contact ball bearings, and run in a vacuum bearing test facility. One pair of bearings was run at 200 rpm for 1.4 x 10(exp 8) revolutions, whilst the second pair performed 9 x 10(exp 8) revolutions at 1400 rpm. At 200 rpm, there was also a significant increase brought by the TiC coating to the life expectancy of Fomblin Z25 oil, with no evidence of lubricant degradation after 1.4 x 10(exp 8) revolutions. The balls remained in pristine condition at the end of the test, with no evidence of damage to the TiC coating. ESA

N94-24012# Centre National d'Etudes Spatiales, Toulouse (France).
INTERFEROMETER SCAN UNIT MECHANISM DEFINITION
M. Privat *In* ESA, The Fifth European Space Mechanisms and Tribology Symposium Apr. 1993 5 p (For primary document see N94-23985 06-37)
Copyright Avail: CASI HC A01/MF A04

A design study of the mechanism of an infrared atmospheric sounder is presented. The instrument is designed to measure the emission spectrum of the atmosphere in the 3.4 to 15.5 micrometers range. This sounder, based on the interferometric principle, is composed of a scan unit, an interferometer, and detectors. The mission requirements and the resulting specifications of the mechanism are expressed. A ball bearings and flexural pins solution and a magnetic bearings solution are compared. The selection is based on the dynamic performance, the overall dimensions, the reliability, and the lifetime of the two solutions. The selected design of the scan system is described. Future work for the development and the qualification of this mechanism is suggested. ESA

N94-24013# Officine Galileo S.p.A., Florence (Italy).
HIGH PRECISION DOUBLE FOUR BAR LINKAGE MECHANISM FOR INTERFEROMETRIC LINEAR SCANNING
M. Brotini, A. Barbis, B. Carli (Consiglio Nazionale delle Ricerche, Florence, Italy.), F. Fabbrizzi, and V. Spicci *In* ESA, The Fifth European Space Mechanisms and Tribology Symposium Apr. 1993 6 p (For primary document see N94-23985 06-37)
Copyright Avail: CASI HC A02/MF A04

A model of the mechanical linear scanner for the Spectroscopy of the Atmosphere by Far InfraRed Emission (SAFIRE) was developed. The mechanism has the function of continuously varying the optical path difference between two optical paths in a Fourier transform interferometer for infrared emissions. The model requirements, hardware configuration, servo analysis and simulations, structure dynamic analysis under launch conditions, and motion accuracy measured are presented. The purpose of the SAFIRE experiment is to improve the understanding of the middle atmosphere ozone distribution for conducting global scale measurements of the important chemical, radiative, and dynamical processes which influence ozone changes. ESA

N94-24014# Societe d'Applications Generales d'Electricite et de Mecanique, Cergy-Pontoise (France).
AN EARTH OBSERVATION TELESCOPE REFOCUSING MECHANISM
M. Lavadoux and J. F. Patin (Aerospatiale, Cannes, France.) *In* ESA, The Fifth European Space Mechanisms and Tribology Symposium Apr. 1993 5 p (For primary document see N94-23985 06-37)
Copyright Avail: CASI HC A01/MF A04

The refocusing mechanism developed for an observation satellite is described. The mechanism fulfills the following functions: it holds the focus lens in the nominal flight position throughout the launch phase; and it acquires and maintains the focus lens position during observation to compensate for dimensional variations in the telescope in orbit. When the telescope is in orbit, the mechanism is capable of moving the lens in steps of approximately 20 microns and positioning it accurately both in tilt and lateral offset of its center. The main difficulties encountered in developing the product are presented. The mechanism was validated by several tests. ESA

N94-24015# Aerospatiale, Cannes (France).
DATA RELAY SYSTEM SATELLITE: THE DEVELOPMENT OF AN ANTENNA POINTING MECHANISM FOR THE INTER-ORBIT LINK ANTENNA
Laurent Curbillon and Gilles Labruyere (European Space Agency. European Space Research and Technology Center, ESTEC, Noordwijk, Netherlands.) *In* ESA, The Fifth European Space Mechanisms and Tribology Symposium Apr. 1993 7 p (For primary document see N94-23985 06-37)
Copyright Avail: CASI HC A02/MF A04

The feasibility of an Antenna Pointing Mechanism (APM) suited to the interorbit link antenna of a Data Relay System (DRS) spacecraft was investigated. The APM mission, requirements, design of the mechanism, breadboard model development, and available test results are summarized. The APM concept selected is based on a large motorized gimbal, which is built around the antenna feed. The main components of the mechanism are dry lubricated, solid preloaded, angular contact ball bearings, stepper motors, and low backlash speed reducers. The gimbal mechanism holds a 1 m long carbon fiber reinforced plastic arm at the tip of which arm the reflector is attached. ESA

N94-24016# MATRA Marconi Space, Toulouse (France).
INTER ORBIT LINK ANTENNA POINTING MECHANISMS DESIGN USING STANDARD ACTUATORS
D. Buvat, M. Souliac, B. Bruneau, and G. Muller *In* ESA, The Fifth European Space Mechanisms and Tribology Symposium Apr. 1993 12 p (For primary document see N94-23985 06-37)
Copyright Avail: CASI HC A03/MF A04

The interorbit link Antenna Pointing Mechanism (APM) is discussed. The steps leading to the choice of superimposed actuators with their rotation axis crossing at focus are summarized. The APM actuators are space qualified stepper motors using harmonic drive reducers with large reduction ratios without backlash. These actuators are open loop current controlled in microstep mode and equipped with redundant windings. Large annular ball bearings were selected for the gimbal first articulation, to ensure enough stiffness and to withstand the launch loads within the small clearance allowed around the antenna feed volume. The gimbal second articulation is achieved by two opposite gimbal pairs. Wet lubrication was selected for both actuators and gimbal ball bearings. Required antenna reflector motion is achieved without singularity, using quasi-linear and high reduction ratios, within allowed APM volume. ESA

N94-24017# European Space Agency. European Space Research and Technology Center, ESTEC, Noordwijk (Netherlands).
NUMERICAL SIMULATION OF ULYSSES NUTATION c18
C. GarciaMarirrodriga, J. Zeischka (LMS International, Leuven, Belgium.), and E. C. Boslooper (Fokker Space and Systems, Amsterdam, Netherlands.) *In its* The Fifth European Space Mechanisms and Tribology Symposium Apr. 1993 8 p (For primary document see N94-23985 06-37)
Copyright Avail: CASI HC A02/MF A04

The in-orbit instability of the Ulysses spacecraft was numerically simulated. The thermal excitation from the solar flux, the flexible axial boom, and the deployment mechanism were modeled and analyzed. In order to model a non-isolated mechanical system, the link between thermal, structural, and multibody dynamics packages is considered. The simulation shows that the nutation build-up was originated by the solar input on the axial boom coupled with the nutational frequency of the spacecraft. The results agree with the observed behavior. ESA

N94-24018# Southampton Univ. (England). Inst. of Sound and Vibration Research.
SPACECRAFT VIBRATIONS DUE TO MECHANISMS; MEASUREMENTS FROM OLYMPUS ON-STATION c18
N. S. Ferguson, J. N. Pinder, and D. E. L. Tunbridge (European Space Agency. European Space Research and Technology Center, ESTEC, Noordwijk, Netherlands.) *In* ESA, The Fifth European Space Mechanisms and Tribology Symposium Apr. 1993 7 p Sponsored by ESTEC (For primary document see N94-23985 06-37)
Copyright Avail: CASI HC A02/MF A04

The results of the Olympus satellite vibration monitoring experiment are analyzed. The in-orbit responses arising from various sources were identified and ranked. Methods of automatic identification and classification were taken into account. The following sources were considered: thrusters, reaction wheels and momentum wheels, waveguide switches, solar array drive mechanisms, and the antenna pointing mechanisms. The primary aim was to quantify the vibration environment and establish a database of the vibration characteristics of the onboard equipment. A secondary purpose was to enable the long term condition monitoring of the equipment. The structural modeling applied to estimate the signal characteristics at the mechanism location is described. ESA

N94-24019# Bertin et Cie., Plaisir (France).
MICROWELDING DUE TO RANDOM VIBRATION
D. Coquelet and G. Gallay *In* ESA, The Fifth European Space Mechanisms and Tribology Symposium Apr. 1993 6 p (For primary document see N94-23985 06-37)
Copyright Avail: CASI HC A02/MF A04

The non-actuation of the latching of the direct broadcast satellite antenna and the boom deployment mechanisms are discussed. The aim is to show the logic that took place to solve the problem of the microwelding of contact areas due to random vibration which is the cause of the jamming of the device and to propose a feedback solution. The on site statements and the visual inspection which took place during the test campaign lead to the following conclusions: the blocking of the latch was probably initiated by microwelding or surface bonding evidenced by metal transfer; the system recovers its nominal performance once the system is manually activated due to shearing of the microwelding spots; and the failure occurs only during dynamic vibration once a threshold level is passed over giving sufficient energy to initiate the surface bonding. ESA

N94-24020# Fokker Space and Systems, Amsterdam (Netherlands).
THE DEVELOPMENT OF THE HERA TEST FACILITY (HTF) c14

Aad P. Eggers *In* ESA, The Fifth European Space Mechanisms and Tribology Symposium Apr. 1993 7 p (For primary document see N94-23985 06-37)
Copyright Avail: CASI HC A02/MF A04

The Hermes Robot Arm (HERA) Test Facility (HTP) is a two axis zero gravity facility used for HERA integration and testing. The current facility concept is the result of system level trade studies which showed its potential advantages over the standard flat floor concept. The advantage is that the test results can be used to verify computer models. The servosupports introduce disturbance forces into the arm movement. The servosupports simulate a zero gravity environment by eliminating the effects of gravity on the arm with air bearings and minimizing the dynamic variables introduced by the drive and leveling subsystems. The weight components of the arm are counteracted by constant support forces. A facility to demonstrate the practical application of the servosupport concept and minimize the technical risk of implementing a new complex system is presented. ESA

N94-24021# Toshiba Corp., Kawasaki (Japan).
DEVELOPMENT OF GEARS FOR SPACE USE
Y. Nodomi, T. Honda, A. Sasaki, N. Kawashima (Toshiba Research and Development Center, Kawasaki, Japan.), K. Seki (National Aerospace Lab., Tokyo, Japan.), M. Nishimura (National Aerospace Lab., Tokyo, Japan.), and Y. Miyakawa (Hosei Univ., Tokyo, Japan.) *In* ESA, The Fifth European Space Mechanisms and Tribology Symposium Apr. 1993 6 p (For primary document see N94-23985 06-37)
Copyright Avail: CASI HC A02/MF A04

The development of gears for high load use in space applications is presented. The work was carried out for selecting the best material/lubricant combinations for gears. The lubricant that presented the best tribological performance was chosen. A lubricant screening test was carried out on lubricated 440C alloy. Organic resin bonded MoS2 film showed good tribological performance. Three kinds of lubricants were applied for three kinds of material combinations of gears which were selected from the rolling-sliding test results and nine cases of gear tests were carried out.
ESA

N94-24022# Ithaco, Inc., Ithaca, NY.
A COMBINED EARTH SCANNER AND MOMENTUM WHEEL FOR ATTITUDE DETERMINATION AND CONTROL OF SMALL SPACECRAFT
c18
Bill Bialke *In* ESA, The Fifth European Space Mechanisms and Tribology Symposium Apr. 1993 6 p (For primary document see N94-23985 06-37)
Copyright Avail: CASI HC A02/MF A04

The design ground rules, the tradeoff analyses, and the performance results of a modular momentum/reaction wheel with an integral conical earth scanner are reported. The aim of the project was to satisfy the stringent cost and power requirements of small satellites. The momentum wheel provides momentum bias and control torques about the pitch axis of a spacecraft. An angled scan mirror coupled to the rotating shaft of the momentum wheel provides a conical scan of the field of view of an infrared sensor to provide pitch and roll attitude information. By using the same motor and bearings for the momentum wheel and earth scanner, the overall power consumption is reduced and the system reliability is enhanced. ESA

N94-24023# Swiss Center for Electronics and Microtechnology, Inc., Neuchatel.
NEW PIN-ON-DISK EQUIPMENT FOR VACUUM TRIBOMETRY
M. Maillat, H. R. Kocher, and H. E. Hintermann *In* ESA, The Fifth European Space Mechanisms and Tribology Symposium Apr. 1993 5 p (For primary document see N94-23985 06-37)
Copyright Avail: CASI HC A01/MF A04

A compact vacuum tribometer developed for precise friction and wear measurements with different accessories is described. Based on a pin on disk configuration, the friction coefficient can be measured while rotating the disk. Wear is measured after the test. The sliding is performed either in dry lubricated conditions or immersed in a vacuum compatible fluid. All these tests can be performed with a geometry of flat against flat. In the case of a fixed ball or pin, the supporting arm is lifted from outside of the vacuum chamber, so that adhesion and the impact force are measured when reloading the pin on the disk. ESA

N94-24024# Teldix Luftfahrt-Ausruestungs G.m.b.H., Heidelberg (Germany).
THE LOW NOISE MOMENTUM WHEEL MW-X: EM DESIGN AND PREDICTED PROPERTIES
T. Eckardt *In* ESA, The Fifth European Space Mechanisms and Tribology Symposium Apr. 1993 6 p (For primary document see N94-23985 06-37)
Copyright Avail: CASI HC A02/MF A04

A new class of magnetic bearing momentum wheels was developed. This wheel, called MW-X, has an overall diameter of 34 cm and offers an angular momentum capability of more than 60 Nms, joined with a vernier gimballing angle of +/- 1.7 degrees and a gimbal torque of up to 3 Nm. The wheel noise is orders of magnitude lower than the noise of a ball bearing wheel of comparable size. It provides an inertial actuator for low noise microgravity missions. The wheel is expandable to more than 100 Nms and +/- 3 degrees gimballing angle. ESA

N94-24025# Souriau, Paray (France). Space Div.
CONNECTOR MECHANISMS IN COMPLIANCE WITH EXTREME SPACE CONDITIONS
Y. Dohan *In* ESA, The Fifth European Space Mechanisms and Tribology Symposium Apr. 1993 2 p (For primary document see N94-23985 06-37)
Copyright Avail: CASI HC A01/MF A04

New concept technology connectors were developed for the Space Station Freedom. These concepts allow full telerobotic operation of electronic and optical connections in extreme vacuum and temperature conditions, high density of signals, extensive number of operations and the highest reliability. For each program, the connectors that are developed are specific and take advantage of previous experience and techniques. The space connectors are assembled in a facility which conforms to 10,000 PPM class cleanliness standard and is qualified to MIL STD 790 E. The stringent objectives are achieved and demonstrated in an active space thermal vacuum chamber. ESA

N94-24026# Sener S.A., Las Arenas (Spain).
PRECISION DISPLACEMENT MECHANISM (PDM)
J. I. Bueno, F. delCampo, and P. Coste (European Space Agency. European Space Research and Technology Center, ESTEC, Noordwijk, Netherlands.) *In* ESA, The Fifth European Space Mechanisms and Tribology Symposium Apr. 1993 6 p (For primary document see N94-23985 06-37)
Copyright Avail: CASI HC A02/MF A04

A mechanism designed to fulfill the requirements of the Precision Displacement Mechanism (PDM) for the Far Infrared and Submillimeter Space Telescope (FIRST) antenna is described. The PDM function is to perform the fine adjustment of the position of the main reflector folding panels. The main requirement for such a mechanism was to achieve small displacements without backlash, while having a high stiffness, in a cryogenic environment and being thermally stable. The PDM design is based on a structure deformed by a linear actuator and is capable of generating submicron steps. The structure deformation provides the necessary reduction to the output of the linear actuator. A breadboard model of this mechanism was built and tested. The results show that the PDM meets the expected performance. ESA

N94-24027# Sener S.A., Las Arenas (Spain).
AN OPENING MECHANISM FOR THE SCIENTIFIC AIRLOCK OUTER HATCH
C. Compostizo and I. deOlazabal *In* ESA, The Fifth European Space Mechanisms and Tribology Symposium Apr. 1993 6 p (For primary document see N94-23985 06-37)
Copyright Avail: CASI HC A02/MF A04

The hatch mechanisms of the scientific airlock, one of the Attached Pressurized Module (APM) subsystems, are described. The scientific airlock consists of an enclosed cylindrical volume that may be opened alternatively to the environments of space and module atmosphere. Closure of the volume is obtained by an inner and outer hatch. Between all the airlock mechanisms, the hinge and opening mechanism of the outer hatch can be highlighted. The hatch is closed from the inside and sealed under pressure loading, but opening in opposite direction. This approach was made feasible by defining an elliptical shape for the outer opening and the outer hatch.

Such a geometry allows the minor axis of the hatch to pass through the major axis of the opening. ESA

N94-24028# Max-Planck-Inst. fuer Aeronomie, Katlenburg-Lindau (Germany).

THE DEVELOPMENT OF THE SOHO SUMER MECHANISMS

W. Engelhardt, H. Hartwig, and K. Poser *In* ESA, The Fifth European Space Mechanisms and Tribology Symposium Apr. 1993 2 p (For primary document see N94-23985 06-37)

Copyright Avail: CASI HC A01/MF A04

The reliability of the Solar Ultraviolet Measurements of Emitted Radiation (SUMER) mechanisms, for the Extreme Ultraviolet (EUV) spectrometer, are discussed. These mechanisms are designed to adjust the optical elements of the SUMER EUV spectrometer to the needs of the varying observational modes. These mechanisms were designed to keep the development and qualification effort for their components under control: all of them make use of drive trains where stepper motors are directly coupled to ball lead screws and translations are supported by ball bushings. One of the main problems of SUMER is its sensitivity to contamination, especially to organic outgassing products which are rapidly polymerized on the optical surfaces under UV illumination. Efforts to develop custom versions of critical components were made. ESA

N94-24029*# National Aeronautics and Space Administration. Goddard Space Flight Center, Greenbelt, MD.

THE SUBMILLIMETER WAVE ASTRONOMY SATELLITE (SWAS) SOLAR ARRAY SYSTEM

Gary Sneiderman *In* ESA, The Fifth European Space Mechanisms and Tribology Symposium Apr. 1993 5 p (For primary document see N94-23985 06-37)

Copyright Avail: CASI HC A01/MF A04

The SWAS (Submillimeter Wave Astronomy Satellite) solar array system is described. It is an innovative approach to meet the missions requirements. The SWAS satellite provides a three axis stabilized platform to survey a variety of galactic cloud structures. This system includes highly reliable, lightweight launch latch, deployment, and lock mechanisms, and solar array panels that provide the maximum solar cell area. The design of the solar arrays are the result of system trades that included instrument and spacecraft thermal constraints, attitude control system maneuvering rates and pointing accuracies, the power system, and the spacecraft structure. ESA

N94-24030# Erno Raumfahrttechnik G.m.b.H., Bremen (Germany).

RELIABLE REDUNDANT DEVICE FOR MECHANISMS

R. Felkai *In* ESA, The Fifth European Space Mechanisms and Tribology Symposium Apr. 1993 15 p (For primary document see N94-23985 06-37)

Copyright Avail: CASI HC A03/MF A04

A drive mechanism with a redundant feature for driving subsystems in a spacecraft was investigated. The purpose of the study was to build a breadboard model to be able to demonstrate the function of the proposed design. Subsystems that can be driven by such a mechanism include hinge booms, telescoping axial booms, extendable and retractable antennas, solar arrays, radiators, or the like, as well as locking and unlocking mechanisms. It is necessary to design the drive for such subsystems with redundant features for components which are subject to failure. The results show that the model of the redundant device operates successfully. ESA

N94-24031# Oesterreichische Raumfahrt- und Systemtechnik, Vienna (Austria).

VISCOUS ROTARY DAMPER

F. Koller, T. Nitschko, and G. Labruyere (European Space Agency. European Space Research and Technology Center, ESTEC, Noordwijk, Netherlands.) *In* ESA, The Fifth European Space Mechanisms and Tribology Symposium Apr. 1993 6 p (For primary document see N94-23985 06-37)

Copyright Avail: CASI HC A02/MF A04

Directly driven viscous rotary dampers, for limiting deployment rates of spring driven mechanisms, are presented. They provide sufficient resistive torque without mass and reliability penalties associated with high ratio gears as required for equivalent devices such as centrifugal brakes or eddy current dampers. This type of damper necessitates application of highly viscous silicone oil as the working fluid. Contamination associated with leakage of the damper is the key problem with respect to the viscous rotary damper application. The device presented is designed for temperature ranges for survival and for operation of -150 to +150 C as well as -30 to +50 C, respectively. Sample tests of the shaft seals proved leak tightness in case of loads and environmental conditions to be expected in course of the damper life cycle. This damper concept seems promising for future application. ESA

N94-24032# Dornier System G.m.b.H., Friedrichshafen (Germany).

DEVELOPMENT OF A LOW-TEMPERATURE GEAR MOTOR (LOG)

M. Schmid *In* ESA, The Fifth European Space Mechanisms and Tribology Symposium Apr. 1993 4 p (For primary document see N94-23985 06-37)

Copyright Avail: CASI HC A01/MF A04

A precision actuator designed to exceed the common temperature range for space actuators, down to values in the range of minus 160 C, is described. The actuator covers a wide range of potential space applications such as antenna pointing, solar array rotation, mirror adjustment or deployment. One of the main features of the actuator, consisting of a rotary disc stepper motor combined with a harmonic drive gear stage, is its good low temperature performance required in infrared satellites or experiments with long nonoperating times in cold space. The low temperature gear motor provides a peak output torque in the 10 Nm range and microstepping is possible. ESA

N94-24033# Ecole Centrale de Lyon (France). Lab. de Tribologie et Dynamique des Systemes.

AN ANALYTICAL ULTRA-HIGH VACUUM TRIBOMETER FOR SOLID LUBRICANT STUDIES

T. LeMogne, Y. Chevallier, C. Donnet, and J. M. Martin *In* ESA, The Fifth European Space Mechanisms and Tribology Symposium Apr. 1993 5 p Sponsored by Region of Rhone-Alpes (For primary document see N94-23985 06-37)

Copyright Avail: CASI HC A01/MF A04

An analytical ultrahigh vacuum tribometer, allowing complete tribochemistry studies of various kinds of materials, was developed in view of ultrahigh vacuum or a controlled partial pressure of O2, H2, or H2O. The main advantage of this device is the direct coupling of tribological/analytical characterization with the possibility to carry out surface treatments. This apparatus is suitable for studying fundamentals in friction, correlated with a fine description of the friction induced chemical modifications of the tested materials. MoS2 coatings were sputter deposited onto silicon substrates. An in situ x ray photoelectron spectroscopy characterization of the first growth stage of the interface indicates a chemical reaction between sulphur and silicon, whereas the growing film is constituted of pure, nearly stoichiometric MoS2. The tribological behavior of a 60 nm thick MoS2 coating in situ prepared is characterized by a low value of the friction coefficient during the first 90 cycles. ESA

N94-24034# Able Engineering Co., Inc., Santa Barbara, CA.

A NOVEL ROTARY ACTUATOR FOR SPACECRAFT

P. Alan Jones, T. Jeffrey Harvey, and Scott F. Tibbitts (Starsys Research Corp., Boulder, CO.) *In* ESA, The Fifth European Space Mechanisms and Tribology Symposium Apr. 1993 5 p (For primary document see N94-23985 06-37)

Copyright Avail: CASI HC A01/MF A04

The design, development and testing of a new rotary actuator model, the AEC Able Engineering (ABLE) Repeatable Rotary Actuator (ARRA) are presented. The ARRA operates under a wide range of both torque and rotation angle. The ARRA system allows the torque and rotation of an individual actuator to be tailored to the specific mission requirements by modification of a single feature on just one part. The ARRA employs a high output parraffin linear actuator to supply linear motion that is converted to rotary motion by means of a tailorable helix cam. The use of a tailorable helix cam allows for the inclusion of multiple hingeline functions into a single mechanism. These functions include variable torque and stowed and deployed latching. This reliable device is one of the least costly controllable bidirectional units available. ESA

N94-24035# MECON B.V., Doetinchem (Netherlands).

MULTIPURPOSE CLAMPING DEVICE WITH ELECTRICAL CONNECTOR FOR IN ORBIT ATTACHMENT OF PAYLOADS

W. C. Hemink, H. W. T. Braakman (Technische Physische Dienst TNO-TH,

Delft, Netherlands.), B. C. Braam (Technische Physische Dienst TNO-TH, Delft, Netherlands.), W. Teerink, G. B. Mersch (European Space Agency. European Space Research and Technology Center, ESTEC, Noordwijk, Netherlands.), J. Gavira (European Space Agency. European Space Research and Technology Center, ESTEC, Noordwijk, Netherlands.), and C. P. W. Leurs (Leuveco, Bergambacht, Netherlands.) *In* ESA, The Fifth European Space Mechanisms and Tribology Symposium Apr. 1993 4 p (For primary document see N94-23985 06-37)
Copyright Avail: CASI HC A01/MF A04

The Multipurpose Clamping Device (MCD), designed for in orbit positioning of payloads on the Space Station, is presented. The MCD provides a mechanical connection between the payload and a support structure. A redundant electrical connector can be integrated. The current design is dedicated to the need of one candidate payload for Space Station. The MCD can be scaled to any payload size and configuration and applied in any environment. The MCD design meets the given performance requirements and design criteria. The handling of MCD is simple and in addition MCD assists the robotics in positioning of payloads. The MCD guarantees a firm mechanical fixation and is backlash free. ESA

N94-24036# ETEL S.A., Motiers (Switzerland).
SENSORLESS, BRUSHLESS MOTOR TO DRIVE A SEALED FREON-AMMONIA PUMP c33
N. Wavre *In* ESA, The Fifth European Space Mechanisms and Tribology Symposium Apr. 1993 5 p (For primary document see N94-23985 06-37)
Copyright Avail: CASI HC A01/MF A04

The performances of a brushless motor, including sleeve losses and electronic performances, specially designed to drive a sealed pump wheel are presented. Low flow rate pumps with high efficiency are expected for both Columbus and Hermes. The challenge was to design a motor as short as a magnetic coupling and to assemble the rotor directly on the pump wheel subassembly. The use of a new sensorless driver technique was proposed. The electronic driver, the motor and the pump are remarkably efficient for a low power system (30W). The pump assembly is extremely compact. ESA

N94-24037# ETEL S.A., Motiers (Switzerland).
DESIGN AND PERFORMANCES OF ELECTROMAGNETIC INITIATORS FOR SPACE MECHANISMS: AN ALTERNATIVE TO PYROTECHNIC SYSTEM c33
N. Wavre *In* ESA, The Fifth European Space Mechanisms and Tribology Symposium Apr. 1993 4 p (For primary document see N94-23985 06-37)
Copyright Avail: CASI HC A01/MF A04

The design of different actuators used for the Infrared Space Observatory (ISO) and Cassini mission Huygens titan space probe is presented. The electromagnetic actuator creates no particle debris and is reusable many times during system calibration and qualification. An electromagnetic initiator uses the reluctant principle with a preload spring and without magnets. The electromagnetic initiators were tested down to minus 168 C under vacuum conditions. An increase in release time can certainly be recognized between the test step at minus 140 C and minus 168 C, under the maximum radial load. Under this condition the release time was below 20 ms with the nominal current. Non-firing current of 1 amp is verified over the temperature range from ambient down to minus 168 C. ESA

N94-24038# BEI Motion Systems Co., Little Rock, AR. Precision Systems and Space Div.
HIGH RESOLUTION ENCODER-MOTOR USED IN THE ORBITAL SPIN SCAN RADIOMETER, GOES VAS SATELLITES c19
John M. Jumper *In* ESA, The Fifth European Space Mechanisms and Tribology Symposium Apr. 1993 6 p (For primary document see N94-23985 06-37)
Copyright Avail: CASI HC A02/MF A04

The techniques employed to produce the high resolution, high accuracy encoder motor assembly are presented. The encoder motor assembly positions the primary mirror, which enables the radiometer to produce detailed images of the Earth from geosynchronous orbit by Geostationary Operational Environmental Satellite (GOES) VISSR Atmospheric Sounder (VAS). The major requirements, a description of the GOES VAS encoder motor assembly, and basic encoder motor construction are summarized. The optical, electronic, and mechanical techniques used to achieve the required resolution and accuracy, as well as the tests conducted on the flight qualification unit are presented. In orbit performance indicates no degradation in accuracy or performance of the GOES VAS encoder motors. ESA

N94-24039# Contraves Italiana, Rome.
RECHARGE MECHANISM BASED ON SHAPE MEMORY ALLOY
M. Grattarola, G. Pedrazzoli, and G. Secci *In* ESA, The Fifth European Space Mechanisms and Tribology Symposium Apr. 1993 3 p (For primary document see N94-23985 06-37)
Copyright Avail: CASI HC A01/MF A04

The Deployment And Retraction Mechanism (DARM) is described. The mechanism was designed for the deployment and subsequent retraction of payloads. The DARM is a spring actuated mechanism. For its maneuvers, the DARM draws entirely on the elastic energy stored in a spiral spring. It carries out a limited number of sequences in accordance with the maximum energy stored in the spring. The recharge mechanism eliminates the problem of the limited range of sequences by recharging the spiral spring during idle times of the mechanism. The main characteristic of the recharge mechanism consists of the use of shape memory alloys, which enable thermal energy to be changed to mechanical energy. ESA

N94-24040# Societe Anonyme d'Etudes et Realisations Nucleaires, Limeil-Brevannes (France).
A FIFTEEN YEARS LIFETIME MECHANISM FOR AN INFRARED EARTH SENSOR
Marc Pochard *In* ESA, The Fifth European Space Mechanisms and Tribology Symposium Apr. 1993 6 p (For primary document see N94-23985 06-37)
Copyright Avail: CASI HC A02/MF A04

The design, development, life tests, and in flight performance of the scanning mechanism of infrared Earth sensors are presented. The lubrication of ball bearings by transfer film technology and the difficulties involving noise, stress corrosion and reproducible torques, which were encountered during the development phase, are analyzed. Design rules, life time modeling and remedies to overcome the difficulties are discussed. Developments in infrared sensor mechanisms and in lubrication technologies are summarized. ESA

N94-24041# European Space Agency. European Space Research and Technology Center, ESTEC, Noordwijk (Netherlands). Communications Satellites Dept.
THE OLYMPUS PAX, MEASUREMENT OF MECHANISM INDUCED VIBRATION
D. Tunbridge *In its* The Fifth European Space Mechanisms and Tribology Symposium Apr. 1993 6 p (For primary document see N94-23985 06-37)
Copyright Avail: CASI HC A02/MF A04

The ultrasensitive accelerometer package known as the PSDE (Payload and Spacecraft Demonstration and Experimentation program) Accelerometer Experiment, or 'PAX', is described. This package, which is onboard the Olympus telecommunication satellite, was designed to measure the minute disturbances caused by the operation of onboard equipment. This data was used to study the operating environment to be experienced by a highly sensitive laser based communications package called SILEX to be flown on the next generation of ESA telecommunications spacecraft, Artemis and DRS (Data Relay Satellite). A secondary purpose of PAX is to monitor the different mechanisms on board Olympus at intervals throughout their lifetime, in order to detect trends in performance. ESA

N94-24042# European Space Tribology Lab., Risley (England).
BLAST, A NEW LUBRICANT SCREENING TESTER FOR SPACE OILS AND GREASES
S. Gill, M. K. Vine, and R. A. Rowntree *In* ESA, The Fifth European Space Mechanisms and Tribology Symposium Apr. 1993 7 p (For primary document see N94-23985 06-37)
Copyright Avail: CASI HC A02/MF A04

The design, development, commissioning, and evaluation of a Boundary Lubrication Accelerated Screening Tester (BLAST) are presented. BLAST was designed to provide a valid means of rapidly evaluating and ranking the boundary lubrication performance and degradation resistance of spacecraft liquid lubricants. BLAST is commissioned and capable of running accelerated tests on oils and greases in vacuum, and assessing the effects of differing coatings and substrates. Results to date gave a ranking directly comparable with that of real life tests. To date, more than 60 tests of differing space lubricants, bearing materials and surface treatments/coatings were performed. The benefits (or not) of new space lubricants and novel surface treatments/coatings are described. ESA

N94-24043# European Space Tribology Lab., Risley (England).
STATIC ADHESION IN PRELOADED CONTACTS SUBJECTED TO LONG-TERM VACUUM EXPOSURE
S. Gill and R. A. Rowntree *In* ESA, The Fifth European Space Mechanisms and Tribology Symposium Apr. 1993 6 p (For primary document see N94-23985 06-37)
Copyright Avail: CASI HC A02/MF A04

A facility, developed to support ESA missions and designed to investigate the sensitivity of material combinations to differing contact stress levels during long term exposure to vacuum conditions is described. The facility allows measurement of the static adhesion forces in vacuum. The materials investigated are of relevance to the mechanism designer, and the time periods under consideration are up to ten years. The results show that the possibility of static adhesion occurring in an interface which is not disturbed seems remote. ESA

N94-24044# European Space Tribology Lab., Risley (England).
AN ASSESSMENT OF SOLID LUBRICANT FILMS FOR USE IN HIGH TEMPERATURE SPACE APPLICATIONS
M. J. Anderson and E. W. Roberts *In* ESA, The Fifth European Space Mechanisms and Tribology Symposium Apr. 1993 6 p (For primary document see N94-23985 06-37)
Copyright Avail: CASI HC A02/MF A04

Solid lubricant coatings were applied to Inconel 600 substrates and evaluated under reciprocating sliding motion against unlubricated Inconel 600 pins. MoS2, Ag, WS2 and PS212 lubricants were applied. Tests were carried out in a nitrogen atmosphere at room temperature, 400C and 800C. It was found that materials which provided effective room temperature lubrication were less effective at high temperatures. The exception was a PS212 film (a composite of CaF2, BaF2, Ag, and Cr3C2 in a nickel cobalt matrix) which gave rise to lower friction as the temperature was increased above room temperature. Unlubricated Inconel versus unlubricated Inconel gave rise to high friction. The overall trend in the values of the peak friction coefficients is towards increased values with increasing temperature. ESA

N94-24045# European Space Tribology Lab., Risley (England).
THE DEVELOPMENT OF DRY-LUBRICATED CERAMIC CAGES
W. B. Price and E. W. Roberts *In* ESA, The Fifth European Space Mechanisms and Tribology Symposium Apr. 1993 5 p (For primary document see N94-23985 06-37)
Copyright Avail: CASI HC A01/MF A04

Ceramic ball bearing cages lubricated with molybdenum disulphide (MoS2) were fabricated and tested. The materials tested were reaction bonded silicon carbide, reaction bonded silicon nitride, and sintered silicon nitride. The silicon carbide cages performed best in bearing tests. Reaction bonded silicon carbide, coated with sputter deposited MoS2 was also tested in sliding motion using a tribometer. Alkali etching the surface of the ceramic, to increase its porosity, led to a reduction in durability of the MoS2 lubricant film. Vacuum impregnation of the porous ceramic with powdered MoS2 prevented the subsequent layer of sputter deposited MoS2 from bonding to the ceramic substrate, and led to a catastrophic reduction in lubricant life. ESA

N94-24046# Codechamp S.A., Champagnat (France).
ENCODERS FOR SPACE APPLICATIONS c74
Daniel Gaumet, Alain Grass, and L. Bongrand *In* ESA, The Fifth European Space Mechanisms and Tribology Symposium Apr. 1993 2 p (For primary document see N94-23985 06-37)
Copyright Avail: CASI HC A01/MF A04

Advanced optical encoders for space applications are presented. In the field of angular position control, optical encoders show significant advantages in high resolution, and low weight and consumption. The reliability of the technology was demonstrated during a qualification program of a 21 bits encoder carried out especially for optoelectronical and ASIC (Application Specific Integrated Circuits) components. Designs and manufactures for spatializable encoders with resolutions up to 22 bits in a 127 mm diameter are under development. Their angular accuracy can reach +/- 2 arc sec. These encoders, both absolute and incremental, function in a range of temperature going from approximately -40C to +100C. An integrated cold redundancy is available from a diameter of 36 mm as well as an integrated partial control of functions. ESA

N94-24055 Societe Nationale Industrielle Aerospatiale, Paris (France).
INTERNAL COMBUSTION ENGINE WITH A CENTRAL CRANKSHAFT AND INTEGRAL TANDEM ANNULAR PISTONS Patent [MOTEUR A COMBUSTION INTERNE A PISTONS ANNULAIRES, EN OPPOSITION ET SOLIDAIRES, ET A ARBRE CENTRAL]
Bernard Esparbes, inventor (to Micromedia Ltd.) 3 Aug. 1993 41 p In FRENCH
(CA-Patent-1-320-878; Int-Patent-Class-F02B-75/26; CTN-94-60928)
Copyright Avail: Micromedia Ltd., Technical Information Centre, 240 Catherine Street, Suite 305, Ottawa, Ontario, K2P 2G8, Canada HC/MF

An internal combustion engine with tandem annular pistons and a central crankshaft is disclosed, based on that found in British patent 11027 of 11 May 1914. The piston block formed by the two pistons presents, at each axial extremity, a double axial skirt fitted with an outer crown forming the head of the piston as such, and an inner crown forming an inlet pump with a holding chamber radially located at the inside of the corresponding annular cylinder, in which the piston head delimits a combustion chamber. Radial fingers, crossing axial openings of the crankcase and radial holes of the piston block, have their inner radial ends engaged within wavy sinusoidal peripheral slots arranged in a bulging central portion of the central crankshaft set into rotation by alternating axial movements of the piston block. The admission of fuel or combustion sustaining gas is ensured axially by the extremities, valves, and openings in the end plates closing the holding chambers in which the inner crowns slide, fitted with valves to act as an inlet pump. The invention is particularly applicable to aircraft engines in view of the ease in which the shaft rotation can be adapted to such a use. CISTI

N94-24076 Southampton Univ. (England). Inst. of Sound and Vibration Research.
VIBRATIONAL POWER TRANSMISSION ANALYSIS OF MACHINERY INSTALLATIONS IN SHIPS WITH THE OBJECTIVE OF NOISE REDUCTION
B. J. Dobson, R. J. Pinnington, and R. G. White Jan. 1993 74 p
(ISVR-TR-216) Copyright Avail: Issuing Activity

Vibrational power transmission or 'power flow' analysis is a unifying concept which is used to study the many paths between machines and remote, noise radiating surfaces. The method may be employed analytically or experimentally to rank the many transmission paths from a machine in order to develop vibration control procedures. This may be done either at the design stage or to examine existing installations in order to reduce the vibrational power which ultimately reaches externally radiating surfaces. Theoretical methods are given here for studying power transmission from machinery sources through isolators, seating structures, pipes, structural elements and air-borne paths. Complementary experimental techniques for measuring vibrational power transmission through isolators, pipe work and structures are also described. The principal field of application described here is large machinery installations, and examples of laboratory scale studies are presented. Author

N94-24081*# Texas A&M Univ., College Station. Dept. of Mechanical Engineering.
THERMOHYDRODYNAMIC ANALYSIS OF CRYOGENIC LIQUID TURBULENT FLOW FLUID FILM BEARINGS Annual Progress Report, 1 Jan. - 31 Dec. 1993
Luis San Andres Dec. 1993 137 p
(Grant NAG3-1434)
(NASA-CR-194869; NAS 1.26:194869) Avail: CASI HC A07/MF A02

A thermohydrodynamic analysis is presented and a computer code developed for prediction of the static and dynamic force response of hydrostatic journal bearings (HJB's), annular seals or damper bearing seals, and fixed arc pad bearings for cryogenic liquid applications. The study includes the most important flow characteristics found in cryogenic fluid

film bearings such as flow turbulence, fluid inertia, liquid compressibility and thermal effects. The analysis and computational model devised allow the determination of the flow field in cryogenic fluid film bearings along with the dynamic force coefficients for rotor-bearing stability analysis.
Author (revised)

__N94-24088*#__ Alabama Univ., Huntsville. Electrical and Computer Engineering Dept.
DESIGN OF A NEW HIGH-PERFORMANCE POINTING CONTROLLER FOR THE HUBBLE SPACE TELESCOPE Final Report, 3 Aug. 1992 - 3 Oct. 1993
C. D. Johnson Oct. 1993 99 p
(Contract NAS8-38609)
(NASA-CR-193891; NAS 1.26:193891; UAH-5-33020) Avail: CASI HC A05/MF A02

A new form of high-performance, disturbance-adaptive pointing controller for the Hubble Space Telescope (HST) is proposed. This new controller is all linear (constant gains) and can maintain accurate 'pointing' of the HST in the face of persistent randomly triggered uncertain, unmeasurable 'flapping' motions of the large attached solar array panels. Similar disturbances associated with antennas and other flexible appendages can also be accommodated. The effectiveness and practicality of the proposed new controller is demonstrated by a detailed design and simulation testing of one such controller for a planar-motion, fully nonlinear model of HST. The simulation results show a high degree of disturbance isolation and pointing stability.
Author (revised)

__N94-24090*#__ Rensselaer Polytechnic Inst., Troy, NY.
WEAR REDUCTION IN CERAMIC BEARINGS BY SURFACE GENERATED PYROLYTIC CARBON CONTINUOUSLY REPLENISHED BY ETHYLENE GAS Final Report
J. L. Lauer and L. C. Davis 13 Dec. 1993 46 p Prepared in cooperation with General Motors Corp., Indianapolis, IN
(Contract NAS3-25950)
(NASA-CR-189214; NAS 1.26:189214; EDR-16732; AVSCOM-TR-92-C-032) Avail: CASI HC A03/MF A01

Sliding tests with a pin-on-disc tribometer and both sliding and rolling tests with a modified four-ball tester at bulk temperatures of about 500 C and contact pressures of about 2.2 GPa have demonstrated up to 80% reductions of friction and wear with silicon nitride surfaces when a stream of ethylene is directed into the conjunction region. The effects are even more pronounced when the ethylene is prenucleated by a flow over a coil of nichrome wire electrically heated to about 800 C and located about 30 cm upstream of the exit nozzle. Steel and Ni-plated steel are lubricated by this method even more efficiently at lower temperatures. Author (revised)

N94-24128 General Electric Co., Fairfield, CT.
SEAL ASSEMBLY Patent
Jonathan G. Salt, inventor (to General Electric Co.), Ronald W. Korzun, inventor (to General Electric Co.), and David R. Abbott, inventor (to General Electric Co.) 19 Jan. 1993 25 p
(CA-Patent-163126888; Int-Patent-Class-F16J-15/44; Int-Patent-Class-F012C-7/28; CTN-94-60869) Copyright Avail: Micromedia Ltd., Technical Information Centre, 240 Catherine Street, Suite 305, Ottawa, Ontario, K2P 2G8, Canada HC/MF

A unitary annular seal structure is provided for attachment to a turbine nozzle in a gas turbine engine. The nozzle includes an annular platform disposed about a longitudinal axis of the engine. An annular array of vanes is secured to the platform. The seal structure includes an abradable annular seal member, a seal backing member, and a seal attachment ring. The ring includes an annular, radially extending, axially acting spring member positioned to cooperate with a plurality of radially extending tabs on the backing member. In use, the seal structure is positioned within a circular opening within the turbine nozzle. The nozzle includes a radially depending appendage formed as part of the nozzle platform. The spring member abuts one side of the appendage and the tabs are positioned to abut another side of the appendage for holding the annular spring member in gas sealing engagement with the appendage to thus provide a seal against gas leakage and to restrain the seal structure axially. The spring member and tabs comprise a radially slideable joint for the seal structure. To restrict circumferential motion of the structure, slots are formed in the appendage for receiving the tabs. The seal is easily replaced by bending the tabs and sliding the seal structure axially out of the nozzle. Differential thermal expansion is accommodated by the slideable seal arrangement.
CISTI

N94-24175# Lockheed Corp., Burbank, CA.
FLUSH HEAD FASTENER Patent
Charles R. Smith, inventor (to Lockheed), Anthony E. Brindisi, inventor (to Lockheed), and Gerald W. Tyree, inventor (to Lockheed) 13 Oct. 1992 25 p
(CA-Patent-1308581; Int-Patent-Class-F16B-19/00; Int-Patent-Class-F16B-31/00; CTN-94-60872) Copyright Avail: Micromedia Ltd., Technical Information Centre, 240 Catherine Street, Suite 305, Ottawa, Ontario, K2P 2G8, Canada HC/MF

A flush head fastener is provided for joining two or more structural elements together, each element having a fastener hole with a recess for receiving the fastener head in communication with one surface of the structural elements. The fastener comprises a shank, a head joined to the shank, and a layer of non-resilient material permanently joined to and generally covering the entire top surface of the fastener. This layer is readily reconfigurable relative to the fastener head and the structural elements such that upon installation of the fastener in the hole, the layer can be reshaped by deformation, filling any gap between the head, the layer of material of the fastener, and the recessed end of the hole. Excess material above that needed to blend the layer of material into substantial conformity with the one surface of the structural elements can be easily removed. The fastener of the invention is capable of producing an aerodynamically smooth external surface, even when the surface is curved, and can be used with both metal and composite materials. The fastener produces no electrical discontinuities on the surface after installation. The fastener of the invention is especially intended for use in fastening aerodynamic surfaces of aircraft onto the underlying structural elements.
CISTI

__N94-24483*#__ National Aeronautics and Space Administration. Lewis Research Center, Cleveland, OH.
APPLICATION OF FAULT DETECTION TECHNIQUES TO SPIRAL BEVEL GEAR FATIGUE DATA
James J. Zakrajsek, Robert F. Handschuh (Army Research Lab., Cleveland, OH.), and Harry J. Decker (Army Research Lab., Cleveland, OH.) Jan. 1994 14 p Proposed for presentation at the 48th Mechanical Failures Prevention Group Meeting, Wakefield, MA, 19-21 Apr. 1994; sponsored by ONR
(RTOP 505-62-10; DA Proj. 1L1-62211-A-47-A)
(NASA-TM-106467; E-8333; NAS 1.15:106467; ARL-TR-345) Avail: CASI HC A03/MF A01

Results of applying a variety of gear fault detection techniques to experimental data is presented. A spiral bevel gear fatigue rig was used to initiate a naturally occurring fault and propagate the fault to a near catastrophic condition of the test gear pair. The spiral bevel gear fatigue test lasted a total of eighteen hours. At approximately five and a half hours into the test, the rig was stopped to inspect the gears for damage, at which time a small pit was identified on a tooth of the pinion. The test was then stopped an additional seven times throughout the rest of the test in order to observe and document the growth and propagation of the fault. The test was ended when a major portion of a pinion tooth broke off. A personal computer based diagnostic system was developed to obtain vibration data from the test rig, and to perform the on-line gear condition monitoring. A number of gear fault detection techniques, which use the signal average in both the time and frequency domain, were applied to the experimental data. Among the techniques investigated, two of the recently developed methods appeared to be the first to react to the start of tooth damage. These methods continued to react to the damage as the pitted area grew in size to cover approximately 75% of the face width of the pinion tooth. In addition, information gathered from one of the newer methods was found to be a good accumulative damage indicator. An unexpected result of the test showed that although the speed of the rig was held to within a band of six percent of the nominal speed, and the load within eighteen percent of nominal, the resulting speed and load variations substantially affected the performance of all of the gear fault detection techniques investigated.
Author

N94-24588*# Thiokol Corp., Brigham City, UT. Space Operations.
FLEX BEARING UUEC, VOLUME 2 Final Report
M. L. Clapper 14 Sep. 1993 78 p
(Contract NAS8-38100)
(NASA-CR-193901; NAS 1.26:193901; TWR-64983-Vol-2) Avail: CASI HC A05/MF A01

This volume, Volume 2, of this Flex Bearing UUEC Final Report documents findings and data pertaining to Team B's tasks. Team B was organized as one of two sub-teams of the Unplanned/Unintended Event or Condition (UUEC) board established per InterOffice Memorandum (IOM) A100-FY93-072. Team A determined the cause of the unacceptable unbonds (referred to as 'heat-affect' unbonds), including the initial, light rust film, in the FSM #3 flex bearing was overheating of the Forward End Ring (FER) during cure, specifically in zone 8 of the mold. Team A's findings are documented in Volume 1 of this report. Team B developed flight rationale for existing bearings, based on absence or presence of an unpropitious unbond condition like that in FSM #3's flex bearing. Author (revised)

N94-24614# Fermi National Accelerator Lab., Batavia, IL.
WELDING OF NIOBIUM TO STAINLESS
M. Kuchnir and R. E. Hiller 2 Nov. 1993 4 p
(Contract DE-AC02-76CH-03000)
(DE94-003365; FNAL-TM-1831) Avail: CASI HC A01/MF A01

Experiences are reported of welding niobium to stainless steel for the TESLA accelerator superconducting cavities. DOE

N94-24699*# Arizona State Univ., Tempe. Telecommunications Research Center.
ADVANCED ELECTROMAGNETIC METHODS FOR AEROSPACE VEHICLES Semiannual Progress Report, 1 Jul. - 31 Dec. 1993
Constantine A. Balanis, Weimin Sun, El-Budawy El-Sharawy, James T. Aberle, Craig R. Birtcher, Jian Peng, Panayiotis A. Tirkas, William V. Andrew, David Kokotoff, and Frank Zavosh 1993 97 p
(Grant NAG1-1082)
(NASA-CR-195111; NAS 1.26:195111; TRC-EM-CAB-9401) Avail: CASI HC A05/MF A02

The Advanced Helicopter Electromagnetics (AHE) Industrial Associates Program has fruitfully completed its fourth year. Under the support of the AHE members and the joint effort of the research team, new and significant progress has been achieved in the year. Following the recommendations by the Advisory Task Force, the research effort is placed on more practical helicopter electromagnetic problems, such as HF antennas, composite materials, and antenna efficiencies. In this annual report, the main topics to be addressed include composite materials and antenna technology. The research work on each topic has been driven by the AHE consortium members' interests and needs. The remarkable achievements and progresses in each subject is reported respectively in individual sections of the report. The work in the area of composite materials includes: modeling of low conductivity composite materials by using Green's function approach; guidelines for composite material modeling by using the Green's function approach in the NEC code; development of 3-D volume mesh generator for modeling thick and volumetric dielectrics by using FD-TD method; modeling antenna elements mounted on a composite Comanche tail stabilizer; and antenna pattern control and efficiency estimate for a horn antenna loaded with composite dielectric materials. Derived from text

N94-24703*# National Aeronautics and Space Administration, Washington, DC.
HUMAN-LIKE ROBOTS FOR SPACE AND HAZARDOUS ENVIRONMENTS
Allen Cogley, David Gustafson, Warren White, Ruth Dyer, Tom Hampton, ed., and Jon Freise, ed. 1990 82 p
(Contract NASw-4435)
(NASA-CR-195549; NAS 1.26:195549) Avail: CASI HC A05/MF A01

The three year goal for this NASA Senior Design team is to design and build a walking autonomous robotic rover. The rover should be capable of rough terrain crossing, traversing human made obstacles (such as stairs and doors), and moving through human and robot occupied spaces without collision. The rover is also to evidence considerable decision making ability, navigation and path planning skills. These goals came from the concept that the robot should have the abilities of both a planetary rover and a hazardous waste site scout. Derived from text

N94-24751*# Auburn Univ., AL. Dept. of Mechanical Engineering.
INFLUENCE OF BACKUP BEARINGS AND SUPPORT STRUCTURE DYNAMICS ON THE BEHAVIOR OF ROTORS WITH ACTIVE SUPPORTS Semiannual Status Report
George T. Flowers Feb. 1994 9 p
(Grant NAG3-1507)
(NASA-CR-195106; NAS 1.26:195106) Avail: CASI HC A02/MF A01

Substantial progress has been made toward the goals of this research effort in the past six months. A simplified rotor model with a flexible shaft and backup bearings has been developed. The model is based upon the work of Ishii and Kirk. Parameter studies of the behavior of this model are currently being conducted. A simple rotor model which includes a flexible disk and bearings with clearance has been developed and the dynamics of the model investigated. The study consists of simulation work coupled with experimental verification. The work is documented in the attached paper. A rotor model based upon the T-501 engine has been developed which includes backup bearing effects. The dynamics of this model are currently being studied with the objective of verifying the conclusions obtained from the simpler models. Parallel simulation runs are being conducted using an ANSYS based finite element model of the T-501. Derived from text

N94-24805*# Minnesota Univ., Minneapolis.
LUNAR TRANSPORTATION SYSTEM Final Report
21 Jul. 1993 106 p
(Contract NASw-4435)
(NASA-CR-195540; NAS 1.26:195540) Avail: CASI HC A06/MF A02

The University Space Research Association (USRA) requested the University of Minnesota Spacecraft Design Team to design a lunar transportation infrastructure. This task was a year long design effort culminating in a complete conceptual design and presentation at Johnson Space Center. The mission objective of the design group was to design a system of vehicles to bring a habitation module, cargo, and crew to the lunar surface from LEO and return either or both crew and cargo safely to LEO while emphasizing component commonality, reusability, and cost effectiveness. During the course of the design, the lunar transportation system (LTS) has taken on many forms. The final design of the system is composed of two vehicles, a lunar transfer vehicle (LTV) and a lunar excursion vehicle (LEV). The LTV serves as an efficient orbital transfer vehicle between the earth and the moon while the LEV carries crew and cargo to the lunar surface. Presented in the report are the mission analysis, systems layout, orbital mechanics, propulsion systems, structural and thermal analysis, and crew systems, avionics, and power systems for this lunar transportation concept. CASI

N94-24806*# Idaho Univ., Moscow. Dept. of Mechanical Engineering.
DESIGN OF A WHEELED ARTICULATING LAND ROVER
Larry Stauffer, Mathew Dilorenzo, and Barbara Yandle [1994] 103 p
(Contract NASw-4435)
(NASA-CR-195520; NAS 1.26:195520) Avail: CASI HC A06/MF A02

The WALRUS is a wheeled articulating land rover that will provide Ames Research Center with a reliable, autonomous vehicle for demonstrating and evaluating advanced technologies. The vehicle is one component of the Ames Research Center's on-going Human Exploration Demonstration Project. Ames Research Center requested a system capable of traversing a broad spectrum of surface types and obstacles. In addition, this vehicle must have an autonomous navigation and control system on board and its own source of power. The resulting design is a rover that articulates in two planes of motion to allow for increased mobility and stability. The rover is driven by six conical shaped aluminum wheels, each with an independent, internally coupled motor. Mounted on the rover are two housings and a removable remote control system. In the housings, the motor controller board, tilt sensor, navigation circuitry, and QED board are mounted. Finally, the rover's motors and electronics are powered by thirty C-cell rechargeable batteries, which are located in the rover wheels and recharged by a specially designed battery charger. Author

N94-24842*# Alabama Univ., Tuscaloosa. College of Engineering.
DESIGN AND APPLICATION OF ELECTROMECHANICAL ACTUATORS FOR DEEP SPACE MISSIONS Semiannual Progress Report No. 2, 16 Aug. 1993 - 15 Feb. 1994
Tim A. Haskew and John Wander Feb. 1994 72 p

(Grant NAG8-240)
(NASA-CR-195134; NAS 1.26:195134; BER-605-163) Avail: CASI HC A04/MF A01

This progress report documents research and development efforts performed from August 16, 1993 through February 15, 1994 on NASA Grant NAG8-240, 'Design and Application of Electromechanical Actuators for Deep Space Missions.' Following the executive summary are four report sections: Motor Selection, Tests Stand Development, Health Monitoring and Fault Management, and Experiment Planning. Three specific motor types have been considered as prime movers for TVC EMA applications: the brushless dc motor, the permanent magnet synchronous motor, and the induction motor. The fundamental finding was that, in general, the primary performance issues were energy efficiency and thermal dissipation (rotor heating). In terms of all other issues, the three motor types were found to compare quite equally. Among the design changes made to the test stand since the last progress report is the addition of more mounting holes in the side beams. These additional holes allow the movable end beam to be attached in a greater number of positions than previously. With this change the movable end beam can move from full forward to full back in three inch increments. Specific mathematical details on the approach that have been employed for health monitoring and fault management (HMFM) have been reported previously. This approach is based on and adaptive Kalman filter strategy. In general, a bank of filters can be implemented for each primary fault type. Presently under consideration for the brushless dc machine are the following faults: armature winding open-circuits, armature winding short-circuits (phase-to-phase and phase-to-ground), bearing degradation, and rotor flux weakening. The mechanically oriented experiments include transient loading experiments, transverse loading experiment, friction experiment, motor performance experiment, and HMFM experiment. Derived from text

N94-24846*# Texas Univ., Brownsville. Dept. of Mathematics.

THE H(SUB INFINITY) OPTIMAL CONTROLLER DESIGN AND REDUCTION FOR THE INERTIAL HOLD MODE OF THE ATTITUDE CONTROL SYSTEM OF THE XTE SPACECRAFT

Zhong Ling Xu and Gui An Zhou 5 Feb. 1994 27 p
(Grant NAG5-2210)
(NASA-CR-195137; NAS 1.26:195137) Avail: CASI HC A03/MF A01

The Inertial Hold Mode (IHM) is one mode of the attitude control system of the X-ray Timing Explorer spacecraft that is disturbed by both parametric uncertainties and external torque disturbance. The IHM model is modified into a typical H-infinity mixed-sensitivity problem through choosing suitable weighting functions W(sub 1)(s) and W(sub 3)(s). The controller is designed by the H-infinity optimization technique with the transformation of shifting the imaginary axis. It can stabilize the plant with uncertainties from the natural frequencies of the flexible body. The gain margin and phase margin of the system are 24.03 db and 55.04 deg, respectively. The step response attenuates to zero within 150 seconds. These show that the controller satisfies the specified requirements. Since the order of the controller appears high, it is reduced to fourth order one. The results show that the stability and the performance of the system with the reduced controller are retained perfectly. Author (revised)

N94-24998*# Texas A&M Univ., College Station. Dept. of Mechanical Engineering.

A FINITE-ELEMENT-BASED PERTURBATION MODEL FOR THE ROTORDYNAMIC ANALYSIS OF SHROUDED PUMP IMPELLERS: PART 1: MODEL DEVELOPMENT AND APPLICATIONS Final Report

Erian A. Baskharone Sep. 1993 174 p
(Contract NAS8-37821)
(NASA-CR-193916; NAS 1.26:193916) Avail: CASI HC A08/MF A02

This study concerns the rotor dynamic characteristics of fluid-encompassed rotors, with special emphasis on shrouded pump impellers. The core of the study is a versatile and categorically new finite-element-based perturbation model, which is based on a rigorous flow analysis and what we have generically termed the 'virtually' deformable finite-element approach. The model is first applied to the case of a smooth annular seal for verification purposes. The rotor excitation components, in this sample problem, give rise to a purely cylindrical, purely conical, and a simultaneous cylindrical/conical rotor whirl around the housing centerline. In all cases, the computed results are compared to existing experimental and analytical data involving the same seal geometry and operating conditions. Next, two labyrinth-seal configurations, which share the same tooth-to-tooth chamber geometry but differ in the total number of chambers, were investigated. The results, in this case, are compared to experimental measurements for both seal configurations. The focus is finally shifted to the shrouded-impeller problem, where the stability effects of the leakage flow in the shroud-to-housing secondary passage are investigated. To this end, the computational model is applied to a typical shrouded-impeller pump stage, fabricated and rotor dynamically tested by Sulzer Bros., and the results compared to those of a simplified 'bulk-flow' analysis and Sulzer Bros.' test data. In addition to assessing the computed rotor dynamic coefficients, the shrouded-impeller study also covers a controversial topic, namely that of the leakage-passage inlet swirl, which was previously cited as the origin of highly unconventional (resonance-like) trends of the fluid-exerted forces. In order to validate this claim, a 'microscopic' study of the fluid/shroud interaction mechanism is conducted, with the focus being on the structure of the perturbed flow field associated with the impeller whirl. The conclusions of this study were solidified by the outcome of a numerical-certainty exercise, where the grid dependency of the numerical results is objectively examined. The final phase of the shrouded-impeller investigation involves the validation of a built-in assumption, in all other perturbation models, whereby single-harmonic tangential distributions of all the flow thermophysical properties are imposed. The last phase of the investigation course is aimed at verifying the fine details of the perturbed flow field in light of recent set of detailed LDA measurements in a smooth annular seal. Grid dependency of the fluid-induced forces is also investigated, and specific recommendations are made. Author (revised)

N94-24999*# Texas A&M Univ., College Station. Dept. of Mechanical Engineering.

A FINITE-ELEMENT-BASED PERTURBATION MODEL FOR THE ROTORDYNAMIC ANALYSIS OF SHROUDED PUMP IMPELLERS: PART 2: USER'S GUIDE

Erian A. Baskharone Sep. 1993 75 p
(Contract NAS8-37821)
(NASA-CR-193917; NAS 1.26:193917) Avail: CASI HC A04/MF A01

This report describes the computational steps involved in executing a finite-element-based perturbation model for computing the rotor dynamic coefficients of a shrouded pump impeller or a simple seal. These arise from the fluid/rotor interaction in the clearance gap. In addition to the sample cases, the computational procedure also applies to a separate category of problems referred to as the 'seal-like' category. The problem, in this case, concerns a shrouded impeller, with the exception that the secondary, or leakage, passage is totally isolated from the primary-flow passage. The difference between this and the pump problem is that the former is analytically of the simple 'seal-like' configuration, with two (inlet and exit) flow-permeable stations, while the latter constitutes a double-entry / double-discharge flow problem. In all cases, the problem is that of a rotor clearance gap. The problem here is that of a rotor excitation in the form of a cylindrical whirl around the housing centerline for a smooth annular seal. In its centered operation mode, the rotor is assumed to give rise to an axisymmetric flow field in the clearance gap. As a result, problems involving longitudinal or helical grooves, in the rotor or housing surfaces, go beyond the code capabilities. Discarding, for the moment, the pre- and post-processing phases, the bulk of the computational procedure consists of two main steps. The first is aimed at producing the axisymmetric 'zeroth-order' flow solution in the given flow domain. Detailed description of this problem, including the flow-governing equations, turbulence closure, boundary conditions, and the finite-element formulation, was covered by Baskharone and Hensel. The second main step is where the perturbation model is implemented, with the input being the centered-rotor 'zeroth-order' flow solution and a prescribed whirl frequency ratio (whirl frequency divided by the impeller speed). The computational domain, in the latter case, is treated as three dimensional, with the number of computational planes in the circumferential direction being specified a priori. The reader is reminded that the deformations in the finite elements are all infinitesimally small because the rotor eccentricity itself is a virtual displacement. This explains why we have generically termed the perturbation model the 'virtually' deformable finite-element category. The primary outcome of implementing the perturbation model is the tangential and radial components, F(sub theta)(sup *) and F(sub r)(sup *) of the fluid-exerted force on the rotor surface due to the whirling motion. Repetitive execution of the perturbation

model subprogram over a sufficient range of whirl frequency ratios, and subsequent interpolation of these fluid forces, using the least-square method, finally enable the user to compute the impeller rotor dynamic coefficients of the fluid/rotor interaction. These are the direct and cross-coupled stiffness, damping, and inertia effects of the fluid/rotor interaction.
Derived from text

N94-25020*# Thiokol Corp., Brigham City, UT. Space Operations.
POSTFLIGHT HARDWARE EVALUATION RSRM-29 (STS-54). CASE, SEALS, AND JOINTS PFORs, APPENDIX B Final Report
Sep. 1993 85 p
(Contract NAS8-38100)
(NASA-CR-193899; NAS 1.26:193899; TWR-64222) Avail: CASI HC A05/MF A01

Appendix B, Case, Seals, and Joints Postflight Observation Records (PFOR's) for the Final Postflight Hardware Evaluation Report for RSRM-29 (STS-54) is included. CASI

N94-25046 Department of the Navy, Washington, DC.
PRECISION DRIVE AND SPEED REDUCTION DEVICE Patent
Kenneth W. Stark, inventor (to Navy) 3 Aug. 1993 7 p Filed 16 Jul. 1991
(AD-D016004; US-Patent-Appl-SN-730620; US-Patent-Class-310-83) Avail: US Patent and Trademark Office

A method and device for precisely driving a rotary object are described. The device includes a motor mounted in a housing and a reduction device comprising first and second harmonic drives, which connect the motor to the object to be driven via an output shaft. The output shaft is connected to the object to be driven via an adapter cup and a bellows which is stiff in torsion but which tolerates misalignments between the drive device and the object. All elements are designed to maximize stiffness and precision and to minimize backlash while maintaining maximum concentricity between the elements. DTIC

N94-25055 Department of the Navy, Washington, DC.
ELECTRO-RHEOLOGICAL CONTROL VALVE Patent
Vincent M. Iorio, inventor (to Navy) and Joseph H. Morris, inventor (to Navy) 7 Sep. 1993 5 p Filed 21 Sep. 1992
(AD-D015997; US-Patent-5,241,991; US-Patent-Appl-SN-947591; US-Patent-Class-137-807) Avail: US Patent and Trademark Office

An E-R hydraulic control valve that has two or more surfaces that can be moved relatively to one another to adjust a flow orifice size while maintaining a control voltage gradient across the E-R fluid and to seat one surface against the other to shut off fluid flow. Combining movable mechanical fluid flow elements with E-R fluid control allows initial tuning of the valve to a particular application by mechanical restriction of an orifice, and E-R operating control of the fluid. Seating the mechanical surfaces provides a fail-safe shut-down mode. DTIC

N94-25174*# Pratt and Whitney Aircraft, West Palm Beach, FL. Government Engines and Space Propulsion.
ADVANCED LAUNCH SYSTEM. ADVANCED DEVELOPMENT OXIDIZER TURBOPUMP PROGRAM Final Report
29 Oct. 1993 294 p
(Contract NAS8-37595)
(NASA-CR-193920; NAS 1.26:193920; FR-23115) Avail: CASI HC A13/MF A03

On May 19, 1989, Pratt & Whitney was awarded contract NAS8-37595 by the National Aeronautics and Space Administration, Marshall Space Flight Center, Huntsville Alabama for an Advanced Development Program (ADP) to design, develop and demonstrate a highly reliable low cost, liquid oxygen turbopump for the Advanced Launch System (ALS). The ALS had an overall goal of reducing the cost of placing payloads in orbit by an order of magnitude. This goal would require a substantial reduction in life cycle costs, with emphasis on recurring costs, compared to current launch vehicles. Engine studies supporting these efforts were made for the Space Transportation Main Engine (STME). The emphasis on low cost required design simplification of components and subsystems such that the ground maintenance and test operations was minimized. The results of the Oxygen Turbopump ADP technology effort would provide data to be used in the STME. Initially the STME baseline was a gas generator cycle engine with a vacuum thrust level of 580,000 lbf. This was later increased to 650,000 lbf and the oxygen turbopump design approach was changed to reflect the new thrust level. It was intended that this ADP program be conducted in two phases. Phase 1, a basic phase, would encompass the preliminary design effort, and Phase II, an optional contract phase to cover design, fabrication and test evaluation of an oxygen turbopump at a component test facility at the NASA John C. Stennis Space Center in Mississippi. The basic phase included preliminary design and analysis, evaluation of low cost concepts, and evaluation of fabrication techniques. The option phase included design of the pump and support hardware, analysis of the final configuration to ensure design integrity, fabrication of hardware to demonstrate low cost, DVS Testing of hardware to verify the design, assembly of the turbopump and full scale turbopump testing. In December 1990, the intent of this ADP to support the design and development was changed. The design effort for the oxygen turbopump became part of the STME Phase B contract. The status of the pump design funded through this ADP was presented at the Preliminary Design Review (PDR) at the MSFC on October 24, 1990. Advancements in the design of the pump were subsequently continued under the Phase B Contract. The emphasis of this ADP became the demonstration of individual technologies that would have the greatest potential for reducing the recurring cost and increasing reliability. In October of 1992, overall program funding was reduced and work on this ADP was terminated. Derived from text

N94-25181*# National Aeronautics and Space Administration. Lewis Research Center, Cleveland, OH.
NASA/ARMY ROTORCRAFT TRANSMISSION RESEARCH, A REVIEW OF RECENT SIGNIFICANT ACCOMPLISHMENTS
Timothy L. Krantz (Army Research Lab., Cleveland, OH.) Mar. 1994 16 p Proposed for presentation at the American Helicopter Society 50th Annual Forum and Technology Display, Washington, DC, 11-13 May 1994; sponsored by the American Helicopter Society
(RTOP 505-62-36; DA Proj. 1L1-62211-A-47-A)
(NASA-TM-106508; E-8616; NAS 1.15:106508; ARL-MR-138) Copyright Avail: CASI HC A03/MF A01

A joint helicopter transmission research program between NASA Lewis Research Center and the U.S. Army Research Lab has existed since 1970. Research goals are to reduce weight and noise while increasing life, reliability, and safety. These research goals are achieved by the NASA/Army Mechanical Systems Technology Branch through both in-house research and cooperative research projects with university and industry partners. Some recent significant technical accomplishments produced by this cooperative research are reviewed. The following research projects are reviewed: oil-off survivability of tapered roller bearings, design and evaluation of high contact ratio gearing, finite element analysis of spiral bevel gears, computer numerical control grinding of spiral bevel gears, gear dynamics code validation, computer program for life and reliability of helicopter transmissions, planetary gear train efficiency study, and the Advanced Rotorcraft Transmission (ART) program. Author (revised)

N94-25249 Technische Univ., Eindhoven (Netherlands).
DESIGN OF GAS BEARING SYSTEMS FOR PRECISION APPLICATIONS Ph.D. Thesis
Junming Wang 1993 151 p Sponsored by Botech, Helmond, Netherlands, and Mitutoyo Nederland, Netherlands Limited Reproducibility: More than 20% of this document may be affected by microfiche quality
(ISBN-9-03-860112-3; ETN-94-95355) Avail: CASI HC A08

Research to provide the up to date knowledge and efficient tools to design better Externally Pressurized Gas (EPG) bearing systems, including the design of individual bearings, and to arrange all the bearings used in an optimal way is reported. Both circular and rectangular EPG pads with rigid bearing surfaces and rigid inlet restrictors were used. The following topics closely related to the applications in precision engineering are discussed: influences of gap shape on the bearing performance; effects of bearing body tilt on the bearing performance; influences of bearing surface imperfections on bearing performance; temperature drops in EPG bearings in quasistationary conditions; the optimal use of multiple bearings in a mechanical system; the use of EPG bearing damping characteristics in the design; and the effects of motion velocity. ESA

N94-25274*# Carnegie-Mellon Univ., Pittsburgh, PA. Robotics Inst.
[DESIGN OF A WALKING ROBOT] Final Report
William Whittaker and Kevin Dowling 4 Mar. 1994 132 p

(Contract NCC3-297)
(NASA-CR-195200; NAS 1.26:195200) Copyright Avail: CASI HC A07/MF A02

Carnegie Mellon University's Autonomous Planetary Exploration Program (APEX) is currently building the Daedalus robot; a system capable of performing extended autonomous planetary exploration missions. Extended autonomy is an important capability because the continued exploration of the Moon, Mars and other solid bodies within the solar system will probably be carried out by autonomous robotic systems. There are a number of reasons for this - the most important of which are the high cost of placing a man in space, the high risk associated with human exploration and communication delays that make teleoperation infeasible. The Daedalus robot represents an evolutionary approach to robot mechanism design and software system architecture. Daedalus incorporates key features from a number of predecessor systems. Using previously proven technologies, the Apex project endeavors to encompass all of the capabilities necessary for robust planetary exploration. The Ambler, a six-legged walking machine was developed by CMU for demonstration of technologies required for planetary exploration. In its five years of life, the Ambler project brought major breakthroughs in various areas of robotic technology. Significant progress was made in: mechanism and control, by introducing a novel gait pattern (circulating gait) and use of orthogonal legs; perception, by developing sophisticated algorithms for map building; and planning, by developing and implementing the Task Control Architecture to coordinate tasks and control complex system functions. The APEX project is the successor of the Ambler project. Author (revised)

N94-25322# Sheffield Univ. (England). Robotics Research Group.
GENETIC-BASED MOTION PLANNING FOR ARTICULATED ROBOTIC MANIPULATORS
Kwong K. Chan and Ali M. S. Zalzala May 1993 6 p
(Grant RSG/323)
(RR-476; ETN-94-95142) Avail: CASI HC A02/MF A01

A genetic based algorithm for the minimum time trajectory planning of articulated robotic manipulators is proposed. The planning procedure is performed in the configuration space and respects all physical constraints imposed on the manipulator design, including the limits on the torque values applied to the motor of each joint of the arm. The complete nonlinear dynamic robot model is incorporated in the formulation. The purpose of the algorithm is to tessellate joint space into a grid of possible motion nodes, where at each option node, given the position and velocity at the previous node, possible velocity values are constrained by the time optimality together with the dynamics of the arm. The algorithm is proven to be more efficient than conventional heuristic search technique with a reduction of the execution time. ESA

N94-25436# Florida International Univ., Miami. Dept. of Mechanical Engineering.
RESEARCH EXPERIENCE FOR UNDERGRADUATES IN ROBOTICS AND MATERIALS Final Report, Sep. 1991 - Dec. 1992
T. C. Yih, I. N. Tansel, and K. H. Wu Mar. 1993 41 p
(Contract F33615-91-C-5737)
(AD-A273659; WL-TR-93-8021) Avail: CASI HC A03/MF A01

Florida International University successfully completed the proposed project entitled, 'Research Experience for Undergraduates in Robotics and Materials.' Nineteen students designed and manufactured a 'user-friendly' industrial robot with three functional axes and an IBM-PC-based C-based controller. The accuracy of the robot is 0.0005 inch when two axes are used. An operator can control the motions of the robot with a few hours of training by using the PC-based controller mouse. The controller also provides graphical simulation of the robot motions. DTIC

N94-23058*# Pennsylvania State Univ., University Park. Dept. of Mechanical Engineering.
FOIL BEARING RESEARCH AT PENN STATE
Marc Carpino *In its* NASA Propulsion Engineering Research Center, Volume 2 Nov. 1993 p 148-151 (For primary document see N94-23028 06-20)
Avail: CASI HC A01/MF A03

N94-23059*# National Aeronautics and Space Administration. Lewis Research Center, Cleveland, OH.
TWO STAGE TURBINE FOR ROCKETS
Joseph P. Veres *In* Pennsylvania State Univ., NASA Propulsion Engineering Research Center, Volume 2 Nov. 1993 p 152-158 (For primary document see N94-23028 06-20)
Avail: CASI HC A02/MF A03

N94-23061*# National Aeronautics and Space Administration. Lewis Research Center, Cleveland, OH.
A TECHNIQUE TO MEASURE ROTORDYNAMIC COEFFICIENTS IN HYDROSTATIC BEARINGS
Russell J. Capaldi *In* Pennsylvania State Univ., NASA Propulsion Engineering Research Center, Volume 2 Nov. 1993 p 164-169 (For primary document see N94-23028 06-20)
Avail: CASI HC A02/MF A03

N94-23063*# National Aeronautics and Space Administration. Lewis Research Center, Cleveland, OH.
BRUSH SEALS FOR CRYOGENIC APPLICATIONS
Margaret P. Proctor *In* Pennsylvania State Univ., NASA Propulsion Engineering Research Center, Volume 2 Nov. 1993 p 176-180 (For primary document see N94-23028 06-20)
Avail: CASI HC A01/MF A03

N94-23232*# University of Central Florida, Orlando. Dept. of Mechanical and Aerospace Engineering.
CONTROL OF A SERPENTINE MANIPULATOR WITH COLLISION AVOIDANCE
Robert M. Byers *In* NASA. Kennedy Space Center, NASA/ASEE Summer Faculty Fellowship Program Oct. 1993 p 27-46 (For primary document see N94-23230 06-80)
Avail: CASI HC A03/MF A04

N94-23235*# Florida Univ., Gainesville. Dept. of Electrical Engineering.
MASS PROPERTIES MEASUREMENT SYSTEM DYNAMICS
Keith L. Doty *In* NASA. Kennedy Space Center, NASA/ASEE Summer Faculty Fellowship Program Oct. 1993 p 91-110 (For primary document see N94-23230 06-80)
Avail: CASI HC A03/MF A04

N94-23236*# Florida Univ., Gainesville. Dept. of Electrical Engineering.
MASS PROPERTIES MEASUREMENT SYSTEM: DYNAMICS AND STATICS MEASUREMENTS
Keith L. Doty *In* NASA. Kennedy Space Center, NASA/ASEE Summer Faculty Fellowship Program Oct. 1993 p 111-134 (For primary document see N94-23230 06-80)
Avail: CASI HC A03/MF A04

N94-23242*# Tuskegee Inst., AL. Dept. of Mechanical Engineering.
RACK INSERTION END EFFECTOR (RIEE) AUTOMATION
Narasimha Malladi *In* NASA. Kennedy Space Center, NASA/ASEE Summer Faculty Fellowship Program Oct. 1993 p 301-326 (For primary document see N94-23230 06-80)
Avail: CASI HC A03/MF A04

N94-23260*# Jet Propulsion Lab., California Inst. of Tech., Pasadena. Ground Antennas and Facilities Engineering Section.
EXPERIMENTAL MODIFICATION AND IDENTIFICATION OF THE DSS-13 ANTENNA CONTROL SYSTEM MODEL
C. S. Racho and W. K. Gawronski *In its* The Telecommunications and Data Acquisition Report 15 Nov. 1993 p 42-53 (For primary document see N94-23256 06-32)
(RTOP 310-20-65-63-00)
Avail: CASI HC A03/MF A02

N94-23268*# Jet Propulsion Lab., California Inst. of Tech., Pasadena. Ground Antennas and Facilities Engineering Section.
BEAM-WAVEGUIDE ANTENNA SERVO DESIGN ISSUES FOR TRACKING LOW EARTH-ORBITING SATELLITES
W. K. Gawronski and J. A. Mellstrom *In its* The Telecommunications and Data Acquisition Report 15 Nov. 1993 p 135-152 (For primary

document see N94-23256 06-32)
(RTOP 314-30-50-12-80)
Avail: CASI HC A03/MF A02

N94-23374 Academy of Sciences (USSR), Saint Petersburg.
SOVIET DEVELOPMENTS OF PLANET ROVERS IN PERIOD OF 1964 - 1990
A. L. Kemurdjian, V. V. Gromov, I. F. Kazhukalo, G. V. Kozlov, V. I. Komissarov, G. N. Korepanov, B. N. Martinov, V. I. Malenkov, A. V. Mitskevich, and V. K. Mishkinyuk et al *In* CNES, Missions, Technologies, and Design of Planetary Mobile Vehicles Jan. 1993 p 25-43 (For primary document see N94-23373 06-91)
Copyright Avail: Issuing Activity (CEPADUES-Editions, 111, rue Nicolas-Vaquelin, 31100 Toulouse, France)

N94-23375* Jet Propulsion Lab., California Inst. of Tech., Pasadena.
PAST US STUDIES AND DEVELOPMENTS FOR PLANETARY ROVERS
James D. Burke (Planetary Society, Pasadena, CA.) *In* CNES, Missions, Technologies, and Design of Planetary Mobile Vehicles Jan. 1993 p 45-60 (For primary document see N94-23373 06-91)
Copyright Avail: Issuing Activity (CEPADUES-Editions, 111, rue Nicolas-Vaquelin, 31100 Toulouse, France)

N94-23377* National Aeronautics and Space Administration. Lyndon B. Johnson Space Center, Houston, TX.
ROVER REQUIREMENTS FOR THE PLANET SURFACE SEGMENT OF THE SPACE EXPLORATION INITIATIVE
Barney B. Roberts and John F. Connolly *In* CNES, Missions, Technologies, and Design of Planetary Mobile Vehicles Jan. 1993 p 97-106 (For primary document see N94-23373 06-91)
Copyright Avail: Issuing Activity (CEPADUES-Editions, 111, rue Nicolas-Vaquelin, 31100 Toulouse, France)

N94-23395 Academy of Sciences (USSR), Moscow. Inst. of Space Research.
MARS 96 ROVER: SCIENCE, INSTRUMENTATION, AND CONTROL Abstract Only
V. M. Linkin and V. V. Kerzhanovich *In* CNES, Missions, Technologies, and Design of Planetary Mobile Vehicles Jan. 1993 p 273 (For primary document see N94-23373 06-91)
Copyright Avail: Issuing Activity (CEPADUES-Editions, 111, rue Nicolas-Vaquelin, 31100 Toulouse, France)

N94-23398* Jet Propulsion Lab., California Inst. of Tech., Pasadena.
THE NEW FAMILY OF JPL PLANETARY SURFACE VEHICLES
Donald B. Bickler *In* CNES, Missions, Technologies, and Design of Planetary Mobile Vehicles Jan. 1993 p 301-306 Sponsored by NASA, Washington (For primary document see N94-23373 06-91)
Copyright Avail: Issuing Activity (CEPADUES-Editions, 111, rue Nicolas-Vaquelin, 31100 Toulouse, France)

N94-23399 Fiat Spazio, Rome (Italy).
FEASIBILITY STUDY OF AN AUTOMATIC VEHICLE FOR PLANETARY EXPLORATION
C. Gerli, A. Murolo, R. Mugnuolo (Italian Space Agency, Matera.), E. Gallo (Telerobot, Genoa, Italy.), F. Cantatore (Telerobot, Genoa, Italy.), and L. Giardino (Tecnospazio S.p.A., Milan, Italy.) *In* CNES, Missions, Technologies, and Design of Planetary Mobile Vehicles Jan. 1993 p 307-312 (For primary document see N94-23373 06-91)
Copyright Avail: Issuing Activity (CEPADUES-Editions, 111, rue Nicolas-Vaquelin, 31100 Toulouse, France)

N94-23400 Centre National d'Etudes Spatiales, Toulouse (France).
ROVER: AUTONOMOUS CONCEPTS FOR MARS EXPLORATION
A. Baiget, B. Castets, H. Chochon, M. Hayard, H. Lamarre, and A. Lamothe *In its* Missions, Technologies, and Design of Planetary Mobile Vehicles Jan. 1993 p 313-326 Prepared in cooperation with Aerospatiale, Cannes, France; Alcatel Espace, Toulouse, France; Societe Generale de Constructions Electriques et Mecaniques Alsthon, Massy, France; and Societe d'Applications Generales d'Electricite et de Mecanique, Paris, France (For primary document see N94-23373 06-91)
Copyright Avail: Issuing Activity (CEPADUES-Editions, 111, rue Nicolas-Vaquelin, 31100 Toulouse, France)

N94-23402 Tokyo Univ., Sagamihara (Japan). Inst. of Space and Astronautical Science.
DEVELOPMENT/DRILLING TEST OF AUGER BORING MACHINE ON BOARD MARS ROVER FOR MARS EXPLORATION
N. Kawashima, I. Nakatani, J. Kawaguchi, K. Saito (Nishimatsu Construction Co. Ltd., Tokyo, Japan.), M. Kojima (Nishimatsu Construction Co. Ltd., Tokyo, Japan.), and N. Fujii (Nagoya Univ., Japan.) *In* CNES, Missions, Technologies, and Design of Planetary Mobile Vehicles Jan. 1993 p 337-343 (For primary document see N94-23373 06-91)
Copyright Avail: Issuing Activity (CEPADUES-Editions, 111, rue Nicolas-Vaquelin, 31100 Toulouse, France)

N94-23403 Commissariat a l'Energie Atomique, Fontenay-aux-Roses (France). Robotics Unit.
MECHANICAL DESIGN OF A PLANETARY ROVER
F. Littmann, E. Villedieu, and J. M. Idasiak *In* CNES, Missions, Technologies, and Design of Planetary Mobile Vehicles Jan. 1993 p 345-359 (For primary document see N94-23373 06-91)
Copyright Avail: Issuing Activity (CEPADUES-Editions, 111, rue Nicolas-Vaquelin, 31100 Toulouse, France)

N94-23404 Centre National d'Etudes Spatiales, Toulouse (France).
PLANETARY ROVER LOCOMOTION MECHANISMS
J. B. Mondier *In its* Missions, Technologies, and Design of Planetary Mobile Vehicles Jan. 1993 p 361-368 (For primary document see N94-23373 06-91)
Copyright Avail: Issuing Activity (CEPADUES-Editions, 111, rue Nicolas-Vaquelin, 31100 Toulouse, France)

N94-23405 Paris VII Univ. (France). Lab. de Robotique et Intelligence Artificielle.
CONCEPTUAL DESIGN AND ARCHITECTURE OF HEXAPOD ROBOTIC VEHICLES FOR THE (L)OVLA PROJECT
Jean-Jacques Kessis, Jean-Pierre Rambaut, and Antoine Labeyrie (College de France, Paris.) *In* CNES, Missions, Technologies, and Design of Planetary Mobile Vehicles Jan. 1993 p 369-375 (For primary document see N94-23373 06-91)
Copyright Avail: Issuing Activity (CEPADUES-Editions, 111, rue Nicolas-Vaquelin, 31100 Toulouse, France)

N94-23406 Technische Univ., Munich (Germany). Lehrstuhl B fuer Mechanik.
WALKING MACHINES FOR SPACE
J. Eltze, H.-J. Weidemann, and F. Pfeiffer *In* CNES, Missions, Technologies, and Design of Planetary Mobile Vehicles Jan. 1993 p 377-384 (For primary document see N94-23373 06-91)
Copyright Avail: Issuing Activity (CEPADUES-Editions, 111, rue Nicolas-Vaquelin, 31100 Toulouse, France)

N94-23407 European Space Agency. European Space Research and Technology Center, ESTEC, Noordwijk (Netherlands). Robotics Section.
AUTOMATION TECHNOLOGY FOR REMOTE SAMPLE ACQUISITION
Anders Elfving *In* CNES, Missions, Technologies, and Design of Planetary Mobile Vehicles Jan. 1993 p 385-394 (For primary document see N94-23373 06-91)
Copyright Avail: Issuing Activity (CEPADUES-Editions, 111, rue Nicolas-Vaquelin, 31100 Toulouse, France)

N94-23411 Academy of Sciences (USSR), Saint Petersburg.
MACHINES FOR MOVING IN SOIL Abstract Only
V. V. Gromov and P. N. Brodsky *In* CNES, Missions, Technologies, and Design of Planetary Mobile Vehicles Jan. 1993 p 415 (For primary document see N94-23373 06-91)
Copyright Avail: Issuing Activity (CEPADUES-Editions, 111, rue Nicolas-Vaquelin, 31100 Toulouse, France)

N94-23412 Centre National d'Etudes Spatiales, Toulouse (France).
THE MARS 96 BALLOON GUIDEROPE: AN AUTONOMOUS SYSTEM IN EXTREME ENVIRONMENT CONDITIONS

H. Laplace, M. Moreliere, and C. Gorse *In its* Missions, Technologies, and Design of Planetary Mobile Vehicles Jan. 1993 p 417-421 Prepared in cooperation with THARSYS, France (For primary document see N94-23373 06-91)
Copyright Avail: Issuing Activity (CEPADUES-Editions, 111, rue Nicolas-Vaquelin, 31100 Toulouse, France)

N94-23413 Laboratoire d'Automatique et d'Analyse des Systemes, Toulouse (France).
THE REMOTE-OPERATED AUTONOMOUS-ROBOT CONCEPT: FROM DEEP SEA TO OUTER SPACE APPLICATIONS
Georges Giralt, Raja Chatila, and Rachid Alami *In* CNES, Missions, Technologies, and Design of Planetary Mobile Vehicles Jan. 1993 p 425-441 (For primary document see N94-23373 06-91)
Copyright Avail: Issuing Activity (CEPADUES-Editions, 111, rue Nicolas-Vaquelin, 31100 Toulouse, France)

N94-23414* National Aeronautics and Space Administration, Washington, DC.
EVOLVING DIRECTIONS IN NASA'S PLANETARY ROVER REQUIREMENTS AND TECHNOLOGY
C. R. Weisbin (Jet Propulsion Lab., California Inst. of Tech., Pasadena.), Mel Montemerlo, and W. Whittaker (Carnegie-Mellon Univ., Pittsburgh, PA.) *In* CNES, Missions, Technologies, and Design of Planetary Mobile Vehicles Jan. 1993 p 443-454 (For primary document see N94-23373 06-91)
Copyright Avail: Issuing Activity (CEPADUES-Editions, 111, rue Nicolas-Vaquelin, 31100 Toulouse, France)

N94-23415 Tokyo Inst. of Tech. (Japan).
DUAL ROVER CONCEPT FOR MARS EXPLORATION
Y. Ohkami, K. Matsumoto (National Aerospace Lab., Tokyo, Japan.), and T. Yoshida (Shimizu Corp., Japan.) *In* CNES, Missions, Technologies, and Design of Planetary Mobile Vehicles Jan. 1993 p 455-464 (For primary document see N94-23373 06-91)
Copyright Avail: Issuing Activity (CEPADUES-Editions, 111, rue Nicolas-Vaquelin, 31100 Toulouse, France)

N94-23416 Academy of Sciences (USSR), Moscow. Inst. of Space Research.
RESULTS OF THE MOJAVE TESTS OF THE MARS 96 ROVER Abstract Only
V. M. Linkin, V. V. Kerzhanovich, A. I. Kemurdjian (Academy of Sciences, USSR, Saint Petersburg.), V. V. Gromov (Academy of Sciences, USSR, Saint Petersburg.), K. Pichkhaze (Babakin Engineering and Research Center, Moscow, Russia.), G. Rogovsky (Babakin Engineering and Research Center, Moscow, Russia.), L. Friedman (Planetary Society, Pasadena, CA.), and H. Schurmeier (Planetary Society, Pasadena, CA.) *In* CNES, Missions, Technologies, and Design of Planetary Mobile Vehicles Jan. 1993 p 465 (For primary document see N94-23373 06-91)
Copyright Avail: Issuing Activity (CEPADUES-Editions, 111, rue Nicolas-Vaquelin, 31100 Toulouse, France)

N94-23417 Academy of Sciences (USSR), Moscow. Inst. of Space Research.
MARS 96 ROVER: TECHNICAL VISION AND NAVIGATION Abstract Only
V. M. Linkin, V. V. Kerzhanovich, I. Sitenko, and S. Szalai (Hungarian Academy of Sciences, Budapest.) *In* CNES, Missions, Technologies, and Design of Planetary Mobile Vehicles Jan. 1993 p 466 (For primary document see N94-23373 06-91)
Copyright Avail: Issuing Activity (CEPADUES-Editions, 111, rue Nicolas-Vaquelin, 31100 Toulouse, France)

N94-23418 Academy of Sciences (USSR), Saint Petersburg.
MARSOHKOD MOVEMENT CONTROL Abstract Only
P. S. Sologub, S. V. Fedoseev, V. V. Gromov, and G. V. Kozlov *In* CNES, Missions, Technologies, and Design of Planetary Mobile Vehicles Jan. 1993 p 467 (For primary document see N94-23373 06-91)
Copyright Avail: Issuing Activity (CEPADUES-Editions, 111, rue Nicolas-Vaquelin, 31100 Toulouse, France)

N94-23419 Massachusetts Inst. of Tech., Cambridge. Artificial Intelligence Lab.
WALKING, JUMPING, AND TUMBLING: MORE THAN ONE WAY TO GET AROUND MARS Abstract Only
R. Brooks *In* CNES, Missions, Technologies, and Design of Planetary Mobile Vehicles Jan. 1993 p 469 (For primary document see N94-23373 06-91)
Copyright Avail: Issuing Activity (CEPADUES-Editions, 111, rue Nicolas-Vaquelin, 31100 Toulouse, France)

N94-23420 Academy of Sciences (USSR), Saint Petersburg.
PERSPECTIVE OF CREATION OF MEANS FOR COLLECTING INFORMATION CONCERNING TRANSPORT SITUATION Abstract Only
V. Mishkinyuk, I. Bolhovitinov, I. Kalyaev, V. Kuznetsov, and V. Noskov *In* CNES, Missions, Technologies, and Design of Planetary Mobile Vehicles Jan. 1993 p 471 (For primary document see N94-23373 06-91)
Copyright Avail: Issuing Activity (CEPADUES-Editions, 111, rue Nicolas-Vaquelin, 31100 Toulouse, France)

N94-23421 Canadian Space Agency, Ottawa (Ontario).
SENSING AND MODELLING CONCEPTS FOR AUTONOMOUS AND REMOTE MOBILE ROBOT CONTROL
S. K. Yeung, W. S. McMath, D. Necsulescu (Ottawa Univ., Ontario.), and E. M. Petriu (Ottawa Univ., Ontario.) *In* CNES, Missions, Technologies, and Design of Planetary Mobile Vehicles Jan. 1993 p 473-482 (For primary document see N94-23373 06-91)
(Contracts DSS-9F011-2-0923; DSS-9F011-2-0976)
Copyright Avail: Issuing Activity (CEPADUES-Editions, 111, rue Nicolas-Vaquelin, 31100 Toulouse, France)

N94-23422 British Aerospace Public Ltd. Co., Bristol (England).
TOWARDS REAL-TIME STEREOVISION SYSTEMS FOR PLANETARY MISSIONS
Stephen Maxwell Parkes *In* CNES, Missions, Technologies, and Design of Planetary Mobile Vehicles Jan. 1993 p 483-498 (For primary document see N94-23373 06-91)
(Contract ESTEC-8741/90/NL/JG(SC))
Copyright Avail: Issuing Activity (CEPADUES-Editions, 111, rue Nicolas-Vaquelin, 31100 Toulouse, France)

N94-23423 Dassault-Breguet Aviation, Saint Cloud (France).
A DTM-BASED PATH PLANNING METHOD FOR PLANETARY ROVERS
R. Morlans and A. Liegeois (Montpellier Univ., France.) *In* CNES, Missions, Technologies, and Design of Planetary Mobile Vehicles Jan. 1993 p 499-507 (For primary document see N94-23373 06-91)
Copyright Avail: Issuing Activity (CEPADUES-Editions, 111, rue Nicolas-Vaquelin, 31100 Toulouse, France)

N94-23424 M2A Engineering, Paris (France).
BOND GRAPH MODELING, SIMULATION, AND REFLEX CONTROL OF THE MARS PLANETARY AUTOMATIC VEHICLE
Maher Amara, Jean Pierre Friconneau (Nutech, Saint-Quetin-en-Yvelines, France.), and Alain Micaelli (Commissariat a l'Energie Atomique, Fontenay-aux-Roses, France.) *In* CNES, Missions, Technologies, and Design of Planetary Mobile Vehicles Jan. 1993 p 509-529 (For primary document see N94-23373 06-91)
Copyright Avail: Issuing Activity (CEPADUES-Editions, 111, rue Nicolas-Vaquelin, 31100 Toulouse, France)

N94-23425* Jet Propulsion Lab., California Inst. of Tech., Pasadena.
MOBILITY ANALYSIS, SIMULATION, AND SCALE MODEL TESTING FOR THE DESIGN OF WHEELED PLANETARY ROVERS
Randel A. Lindemann and Howard J. Eisen *In* CNES, Missions, Technologies, and Design of Planetary Mobile Vehicles Jan. 1993 p 531-536 Sponsored by NASA, Washington (For primary document see N94-23373 06-91)
Copyright Avail: Issuing Activity (CEPADUES-Editions, 111, rue Nicolas-Vaquelin, 31100 Toulouse, France)

N94-23426 Grenoble-1 Univ. (France). Inst. IMAG.
PHYSICAL MODELING AND DYNAMIC SIMULATION OF PLANET VEHICLES: APPLICATION TO THE MOTION PREDICTION
Annie Luciani, Stephane Jimenez, and Christian Laugier *In* CNES, Missions, Technologies, and Design of Planetary Mobile Vehicles Jan. 1993 p 537-544 Sponsored in part by CNES and Rhone-Alps Region SHARP Project (For primary document see N94-23373 06-91)
Copyright Avail: Issuing Activity (CEPADUES-Editions, 111, rue Nicolas-Vaquelin, 31100 Toulouse, France)

N94-23427* Jet Propulsion Lab., California Inst. of Tech., Pasadena.
EXPERIMENTS WITH A SMALL BEHAVIOUR CONTROLLED PLANETARY ROVER
David P. Miller, Rajiv S. Desai, Erann Gat, Robert Ivlev, and John Loch *In* CNES, Missions, Technologies, and Design of Planetary Mobile Vehicles Jan. 1993 p 545-551 Sponsored by NASA, Washington (For primary document see N94-23373 06-91)
Copyright Avail: Issuing Activity (CEPADUES-Editions, 111, rue Nicolas-Vaquelin, 31100 Toulouse, France)

N94-23660*# Clemson Univ., SC. Dept. of Mechanical Engineering.
THE 3-D NUMERICAL STUDY OF AIRFLOW IN THE COMPRESSOR/COMBUSTOR PREDIFFUSER AND DUMP DIFFUSER OF AN INDUSTRIAL GAS TURBINE
Ajay K. Agrawal and Tah-Teh Yang *In* NASA. Lewis Research Center, The Fifth Annual Thermal and Fluids Analysis Workshop Nov. 1993 p 395-409 (For primary document see N94-23634 06-34)
Avail: CASI HC A03/MF A04; 5 functional color pages

N94-23841*# Canadian Space Agency, Vanier (Ontario). Mobile Servicing System Space Operations.
GROUND OPERATION OF ROBOTICS ON SPACE STATION FREEDOM
Z. Alex Wojcik, David G. Hunter, and Marc R. Cantin (KEOPS Informatique, Montreal, Quebec.) *In* JPL, SpaceOps 1992: Proceedings of the Second International Symposium on Ground Data Systems for Space Mission Operations 1 Mar. 1993 p 51-55 (For primary document see N94-23832 06-66)
Avail: CASI HC A01/MF A10

N94-24408*# Alabama Univ., Huntsville. Dept. of Mechanical and Aerospace Engineering.
VISCOELASTIC ANALYSIS OF SEALS FOR EXTENDED SERVICE LIFE
Mark V. Bower *In its* The 1993 NASA/ASEE Summer Faculty Fellowship Program Nov. 1993 5 p (For primary document see N94-24405 06-80)
Avail: CASI HC A01/MF A03

N94-24415*# Alabama Univ., Huntsville. Mechanical and Aerospace Engineering Dept.
FOIL BEARINGS
David A. Elrod *In its* The 1993 NASA/ASEE Summer Faculty Fellowship Program Nov. 1993 5 p (For primary document see N94-24405 06-80)
Avail: CASI HC A01/MF A03

N94-24427*# Colorado Univ., Boulder. Dept. of Aerospace Engineering Sciences.
WELD JOINT CONCEPTS FOR ON-ORBIT REPAIR OF SPACE STATION FREEDOM FLUID SYSTEM TUBE ASSEMBLIES
Steven D. Jolly *In* Alabama Univ., The 1993 NASA/ASEE Summer Faculty Fellowship Program Nov. 1993 5 p (For primary document see N94-24405 06-80)
Avail: CASI HC A01/MF A03

N94-24440*# Texas A&M Univ., College Station. Mechanical Engineering Dept.
SIMULATION OF CRYOGENIC TURBOPUMP ANNULAR SEALS
Alan B. Palazzolo *In* Alabama Univ., The 1993 NASA/ASEE Summer Faculty Fellowship Program Nov. 1993 5 p (For primary document see N94-24405 06-80)
Avail: CASI HC A01/MF A03

N94-24441*# Alabama Univ., Huntsville. Dept. of Mechanical Engineering.
CONTROLLER MODELING AND EVALUATION FOR PCV ELECTRO-MECHANICAL ACTUATOR
Joey K. Parker *In its* The 1993 NASA/ASEE Summer Faculty Fellowship Program Nov. 1993 5 p (For primary document see N94-24405 06-80)
Avail: CASI HC A01/MF A03

N94-25350*# Texas Technological Univ., Lubbock. Dept. of Mechanical Engineering.
MODELLING THE SHUTTLE REMOTE MANIPULATOR SYSTEM: ANOTHER FLEXIBLE MODEL
Alan A. Barhorst *In* NASA. Johnson Space Center, National Aeronautics and Space Administration (NASA)/American Society for Engineering Education (ASEE) Summer Faculty Fellowship Program, 1993, Volume 1 Dec. 1993 17 p (For primary document see N94-25348 06-99)
Avail: CASI HC A03/MF A03

38 QUALITY ASSURANCE AND RELIABILITY

Includes product sampling procedures and techniques; and quality control.

N94-22872 Argonne National Lab., IL.
THEORETICAL STUDIES OF WAVE PROPAGATION IN MULTILAYERED PIEZOELECTRIC MEDIA
Hual-Te Chien, Shuh-Haw Sheen, and A. C. Raptis Aug. 1993 13 p Presented at the 20th Annual Review of Progress in Quantitative Nondestructive Evaluation (NDE), Brunswick, ME, 1-6 Aug. 1993 Limited Reproducibility: More than 20% of this document may be affected by poor print and microfiche quality
(Contract W-31-109-eng-38)
(DE93-040273; ANL/ET/CP-79670; CONF-9308167-1) Avail: Issuing Activity (Department of Energy (DOE))

The purpose is to extend the analysis of a single plate or substrate to the case of a multilayered medium. Due to the requiring of higher operating frequency, lower attenuation, and stronger piezoelectricity, layered structure becomes necessary. This technique is rapidly applied in the field of nondestructive evaluation and testing (NDE/T). Recently, a new feature of applying the piezoelectric effect for remote sensing, actuating, and vibration controlling came under study and development in aerospace and automative industries. DOE

N94-22918# Sandia National Labs., Albuquerque, NM.
PROBABILISTIC ANALYSIS OF MECHANICAL SYSTEMS
T. G. Priddy, T. L. Paez, and P. S. Veers 1993 11 p Presented at the 64th Shock and Vibration Symposium, Ft. Walton Beach, FL, 25-28 Oct. 1993
(Contract DE-AC04-76DP-00789)
(DE93-041145; SAND-93-2081C; CONF-9310167-2) Avail: CASI HC A03/MF A01

This paper proposes a framework for the comprehensive analysis of complex problems in probabilistic structural mechanics. Tools that can be used to accurately estimate the probabilistic behavior of mechanical systems are discussed, and some of the techniques proposed in the paper are developed and used in the solution of a problem in nonlinear structural dynamics. DOE

N94-22935# Lawrence Livermore National Lab., CA.
ANALYSIS OF A PROPOSED COMPTON BACKSCATTER IMAGING TECHNIQUE
J. Hall and B. Jacoby Dec. 1992 14 p Presented at the International Symposium on Substance Identification Technologies, Innsbruck, Austria, 4-8 Oct. 1993
(Contract W-7405-eng-36)
(DE93-040537; UCRL-JC-113254; CONF-9310164-3) Avail: CASI HC A03/MF A01

Imaging techniques which require access to only one side of the object being viewed are potentially useful in situations where conventional projection radiography and tomography cannot be applied, such as looking for voids in a large container where access to the back of the object is inconvenient or even impossible. One-sided imaging techniques are currently being used in nondestructive evaluation of surfaces and shallow subsurface structures. In this work we present both analytical calculations and detailed Monte Carlo simulations aimed at assessing the capability of a proposed Compton backscatter imaging technique designed to detect and characterize voids located several centimeters below the surface of a solid. The proposed technique, based on a scheme suggested by Farmer and Collins, encodes the spatial position and structure of voids in a solid in the energy spectrum of the Compton-scattered photons as recorded by a high resolution detector. Our calculations model a Cs-137 source projecting a 1 sq mm pencil beam of 662 keV gammas into a target slab at an incident angle of 45 degrees and a collimated detector (also oriented at 45 degrees with respect to the surface) which views the beam path at a central angle of 90 degrees. The detector collimator is modeled here as a triangular slit viewing a 2.54 cm (1.000 inch) segment of the beam path at a depth of 2 cm below the surface of the slab. Our results suggest that the proposed technique should be capable of an absolute position resolution of approximately 0.25 mm (approximately equal to 0.010 inches) for isolated voids and an overall object resolution of approximately 1 lp/mm (approximately 0.040 inches). The predicted signal contrast for voids packed with various contraband materials will be discussed as well as multiple scattering contributions to the predicted yields. DOE

N94-24074*# National Aeronautics and Space Administration. Lewis Research Center, Cleveland, OH.

ENGINE MATERIALS CHARACTERIZATION AND DAMAGE MONITORING BY USING X RAY TECHNOLOGIES

George Y. Baaklini Washington Oct. 1993 103 p Original contains color illustrations
(RTOP 510-01-50)
(NASA-TP-3328; E-7549; NAS 1.60:3328) Avail: CASI HC A06/MF A02; 29 functional color pages

X ray attenuation measurement systems that are capable of characterizing density variations in monolithic ceramics and damage due to processing and/or mechanical testing in ceramic and intermetallic matrix composites are developed and applied. Noninvasive monitoring of damage accumulation and failure sequences in ceramic matrix composites is used during room-temperature tensile testing. This work resulted in the development of a point-scan digital radiography system and an in situ x ray material testing system. The former is used to characterize silicon carbide and silicon nitride specimens, and the latter is used to image the failure behavior of silicon-carbide-fiber-reinforced, reaction-bonded silicon nitride matrix composites. State-of-the-art x ray computed tomography is investigated to determine its capabilities and limitations in characterizing density variations of subscale engine components (e.g., a silicon carbide rotor, a silicon nitride blade, and a silicon-carbide-fiber-reinforced beta titanium matrix rod, rotor, and ring). Microfocus radiography, conventional radiography, scanning acoustic microscopy, and metallography are used to substantiate the x ray computed tomography findings. Point-scan digital radiography is a viable technique for characterizing density variations in monolithic ceramic specimens. But it is very limited and time consuming in characterizing ceramic matrix composites. Precise x ray attenuation measurements, reflecting minute density variations, are achieved by photon counting and by using microcollimators at the source and the detector. X ray computed tomography is found to be a unique x ray attenuation measurement technique capable of providing cross-sectional spatial density information in monolithic ceramics and metal matrix composites. X ray computed tomography is proven to accelerate generic composite component development. Radiographic evaluation before, during, and after loading shows the effect of preexisting volume flaws on the fracture behavior of composites. Results from one-, three-, five-, and eight-ply ceramic composite specimens show that x ray film radiography can monitor damage accumulation during tensile loading. Matrix cracking, fiber-matrix debonding, fiber bridging, and fiber pullout are imaged throughout the tensile loading of the specimens. In situ film radiography is found to be a practical technique for estimating interfacial shear strength between the silicon carbide fibers and the reaction-bonded silicon nitride matrix. It is concluded that pretest, in situ, and post-test x ray imaging can provide greater understanding of ceramic matrix composite mechanical behavior. Author (revised)

N94-24136 Defence Research Establishment Pacific, Victoria (British Columbia).

AN EVALUATION OF COMPTON SCATTER IMAGING USING COMSCAN

R. D. Finlayson, W. Ramsbottom, and W. R. Sturrock May 1993 44 p
(DREP-TM-93-38; CTN-94-60921) Avail: Micromedia Ltd., Technical Information Centre, 165 Hotel de Ville, Place du Portage, Phase 2, Hull, Quebec J8X 3X2, Canada

A number of test samples, representative of aircraft materials and structures, were evaluated using a commercial x-ray backscatter radiation device called COMSCAN, developed by Philips. COMSCAN produces 22 simultaneous radiographic slices of a test object with only one-sided access. The slices, stored in computer memory, can then be paged through one at a time for viewing. The system has been integrated with a six-axis gantry robot system. During the COMSCAN evaluation, a number of test samples of graphite/epoxy, honeycomb, aluminum, and other low atomic number materials found on today's aircraft were scanned to determine the detectability of a variety of manufactured discontinuities including water in honeycomb, disbonds, delaminations, and corrosion. COMSCAN's ability to image a volume of 100 mm by 50 mm by 10 mm depth was very useful and allowed image display and analysis in both two and three dimensions. The collected images clearly show COMSCAN is well suited for detection of voids and defects where loss of material has occurred, such as corrosion pitting. COMSCAN, however, cannot detect delaminations. Author (CISTI)

N94-24174*# Rockwell International Corp., Canoga Park, CA. Rocketdyne Div.

SYSTEM FOR ANOMALY AND FAILURE DETECTION (SAFD) SYSTEM DEVELOPMENT Final Report

D. OReilly 30 Sep. 1993 220 p
(Contract NAS8-40000)
(NASA-CR-193907; NAS 1.26:193907) Avail: CASI HC A10/MF A03

The System for Anomaly and Failure Detection (SAFD) algorithm was developed as an improvement over the current redline system used in the Space Shuttle Main Engine Controller (SSMEC). Simulation tests and execution against previous hot fire tests demonstrated that the SAFD algorithm can detect engine failures as much as tens of seconds before the redline system recognized the failure. Although the current algorithm only operates during steady state conditions (engine not throttling), work is underway to expand the algorithm to work during transient conditions. This task assignment originally specified developing a platform for executing the algorithm during hot fire tests at Technology Test Bed (TTB) and installing the SAFD algorithm on that platform. Two units were built and installed in the Hardware Simulation Lab and at the TTB in December 1991. Since that time, the task primarily entailed improvement and maintenance of the systems, additional testing to prove the feasibility of the algorithm, and support of hot fire testing. This document addresses the work done since the last report of June 1992. The work on the System for Anomaly and Failure Detection during this period included improving the platform and the algorithm, testing the algorithm against previous test data and in the Hardware Simulation Lab, installing other algorithms on the system, providing support for operations at the Technology Test Bed, and providing routine maintenance. Author (revised)

N94-24553# Naval Postgraduate School, Monterey, CA.

AN ANALYSIS OF TRADITIONAL OPERATIONAL TESTING TO PROJECT HOW TESTING WILL BE CONDUCTED IN THE FUTURE M.S. Thesis

Lawrence L. Turner, Jr. Sep. 1993 140 p
(AD-A273189) Avail: CASI HC A07/MF A02

The purpose is to analyze current operational testing and to alert the reader to how testing will be conducted in the future. This analysis is conducted from a tester's point of view and is targeted at program offices so that Program Managers will be able to ensure that beneficial operational testing is conducted on their programs. A detailed description of current and future systems used to instrument development systems, analyze the test data, and produce a final test report is provided. It also provides a detailed analysis of a testing tool called Model-Test-Model (M-T-M). The goal of M-T-M is to save the Army time and money by using a validated model to provide operational test data. Finally, an analysis of the changes that will need to be made in the T&E community as a result of a new defense environment is provided. These areas include the need for minimizing duplication between development and operational testing, using modeling and simulation, and taking advantage of other areas where testing costs can be reduced. DTIC

N94-24613# Lawrence Livermore National Lab., CA.
NONDESTRUCTIVE EVALUATIONS
S. Kulkarni Mar. 1993 26 p
(Contract W-7405-eng-48)
(DE94-003020; UCRL-ID-112777) Avail: CASI HC A03/MF A01

This report discusses Nondestructive Evaluation (NDE) thrust area which supports initiatives that advance inspection science and technology. The goal of the NDE thrust area is to provide cutting-edge technologies that have promise of inspection tools three to five years in the future. In selecting projects, the thrust area anticipates the needs of existing and future Lawrence Livermore National Laboratory (LLNL) programs. NDE provides materials characterization inspections, finished parts, and complex objects to find flaws and fabrication defects and to determine their physical and chemical characteristics. NDE also encompasses process monitoring and control sensors and the monitoring of in-service damage. For concurrent engineering, NDE becomes a frontline technology and strongly impacts issues of certification and of life prediction and extension. In FY-92, in addition to supporting LLNL programs and the activities of nuclear weapons contractors, NDE has initiated several projects with government agencies and private industries to study aging infrastructures and to advance manufacturing processes. Examples of these projects are (1) the Aging Airplanes Inspection Program for the Federal Aviation Administration, (2) Signal Processing of Acoustic Signatures of Heart Valves for Shiley, Inc., and (3) Turbine Blade Inspection for the Air Force, jointly with Southwest Research Institute and Garrett. In FY-92, the primary contributions of the NDE thrust area, described in this report, were in fieldable chemical sensor systems, computed tomography, and laser generation and detection of ultrasonic energy. DOE

N94-24769*# Ohio State Univ., Cleveland. Dept. of Mechanical Engineering.
INVESTIGATION OF THE EFFECTS OF MANUFACTURING VARIATIONS AND MATERIALS ON FATIGUE CRACK DETECTION METHODS IN GEAR TEETH
Jeffrey A. Wheitner and Donald R. Houser Jan. 1994 114 p
(Grant NAG3-1147)
(NASA-CR-195093; NAS 1.26:195093) Avail: CASI HC A06/MF A02

The fatigue life of a gear tooth can be thought of as the sum of the number of cycles required to initiate a crack, N(sub i), plus the number of cycles required to propagate the crack to such a length that fracture occurs, N(sub p). The factors that govern crack initiation are thought to be related to localized stress or strain at a point, while propagation of a fatigue crack is a function of the crack tip parameters such as crack shape, stress state, and stress intensity factor. During a test there is no clear transition between initiation and propagation. The mechanisms of initiation and propagation are quite different and modeling them separately produces a higher degree of accuracy, but then the question that continually arises is 'what is a crack?' The total life prediction in a fracture mechanics model presently hinges on the assumption of an initial crack length, and this length can significantly affect the total life prediction. The size of the initial crack is generally taken to be in the range of 0.01 in. to 0.2 in. Several researchers have used various techniques to determine the beginning of the crack propagation stage. Barhorst showed the relationship between dynamic stiffness changes and crack propagation. Acoustic emissions, which are stress waves produced by the sudden movement of stressed materials, have also been successfully used to monitor the growth of cracks in tensile and fatigue specimens. The purpose of this research is to determine whether acoustic emissions can be used to define the beginning of crack propagation in a gear using a single-tooth bending fatigue test.
Derived from text

N94-24814 Army Construction Engineering Research Lab., Champaign, IL.
DEMONSTRATION OF POLYSCANN ULTRASONIC BUTT-FUSION INSPECTION SYSTEM FOR POLYETHYLENE PIPES Final Report
Orange S. Marshall, Jr. and James B. Hunt Jul. 1993 56 p Limited Reproducibility: More than 20% of this document may be affected by microfiche quality
(AD-A273279; CERL-FEAP-TR-FM-93/06) Avail: Issuing Activity (Defense Technical Information Center (DTIC))

The demonstration of the Polyscann Ultrasonic Butt-Fusion Inspection System and laboratory research into its effectiveness as a quality control tool for installation of polyethylene pipe are described. In the demonstration, conducted at North Fort Hood, TX, 13 sections of 8 in. diameter polyethylene pipe were assembled and tied into a previously installed 8 in. gas pipeline. The system was successfully used to inspect each new butt-fusion joint in its entirety, and provided a computerized record of joint cross-sections and status. Laboratory tests indicated that the equipment results were mostly reliable, but it could not detect a low-density weld contaminant such as dried grass. Benefits of the Polyscann system include its nondestructive evaluation technology, capability of evaluating all joints without interrupting pipeline productivity, data-logging capabilities, ease of use, and ability to identify necessary repairs before the pipe is buried. After this demonstration was concluded, the manufacturer discontinued the system that was tested, and is redesigning it to be portable by one person and capable of detecting low-density contaminants such as grass. Price and release date for the updated system are pending. DTIC

N94-25295# Technische Univ., Eindhoven (Netherlands).
RELIABILITY ANALYSIS OF A REPAIRABLE DEPENDENT PARALLEL SYSTEM Ph.D. Thesis
Marcus Johannes Petr Pijnenburg 1992 211 p
(ETN-94-95312) Avail: CASI HC A10/MF A03

A study to develop a stochastic model to describe a system's failure behavior is reported. The systems analyzed are thought of as industrial machinery, equipment, or products. Basic stochastic models in reliability theory are introduced. Systems with bivariate exponentially distributed life times, phase type distributed life and repair times, and bivariate phase type distributed life times are studied. An opportunistic replacement policy for the two unit dependent parallel system, in continuous time and at component level, is described. The gradual deterioration of the parallel system is considered. ESA

N94-25475# Oxford Univ. (England). Dept. of Engineering Science.
FAULT DETECTION IN HVAC SYSTEMS USING FUZZY MODELS
A. L. Dexter and B. K. K. Mok 1993 28 p
(OUEL-1977/93; AN25/UK/151092/1.1; ETN-94-95160) Avail: CASI HC A03/MF A01

A fault detection scheme which uses qualitative models, consisting of sets of fuzzy rules, to describe the generic behavior of both fault free and faulty operation of plant is described. It is applied to Heating, Ventilating and Air Conditioning (HVAC) systems. These fuzzy reference models are generated off line from training data produced by computer simulation of a typical plant, with and without the faults, using a fuzzy identification scheme. A computationally efficient, fuzzy identification algorithm, that is suitable for implementation in packaged controls, is used to estimate the credibility of each of the rules. Faults are detected by comparing the behavior of the plant with the behavior predicted by the fuzzy reference models. Two methods of comparing the actual and predicted behavior are examined: a prediction based method in which faults are detected by comparing measurements, available from the building energy management system connected to the plant, with the predictions of the fuzzy reference models; and a rule similarity method in which data collected on line from the real plant are used to identify a partial fuzzy model. The degree to which faulty or correct operation is present, is determined by comparing the rules of the partial fuzzy model with the rules of the fuzzy reference models, using a fuzzy measure of similarity. Results which demonstrate the ability of both schemes to detect faults in the mixing box of the air handling unit of an air conditioning system are presented. ESA

N94-23064*# Pennsylvania State Univ., University Park. Dept. of Aerospace Engineering.
RELIABILITY ENHANCEMENT OF NAVIER-STOKES CODES THROUGH CONVERGENCE ENHANCEMENT
K.-Y. Choi and G. S. Dulikravich *In its* NASA Propulsion Engineering Research Center, Volume 2 Nov. 1993 p 181-186 (For primary document see N94-23028 06-20)
Avail: CASI HC A02/MF A03

N94-23931*# OAO Corp., Altadena, CA.
THE APPLICATION OF TOTAL QUALITY MANAGEMENT PRINCIPLES TO SPACECRAFT MISSION OPERATIONS
Maury Sweetin *In* JPL, SpaceOps 1992: Proceedings of the Second International Symposium on Ground Data Systems for Space Mission Operations 1 Mar. 1993 p 655-659 (For primary document see N94-23832 06-66)
Avail: CASI HC A01/MF A10

N94-23932*# Jet Propulsion Lab., California Inst. of Tech., Pasadena.
MISSION OPERATIONS AND COMMAND ASSURANCE: INSTILLING QUALITY INTO FLIGHT OPERATIONS
Linda L. Welz, Mona M. Witkowski, Kristin J. Bruno, and Sherrill S. Potts *In its* SpaceOps 1992: Proceedings of the Second International Symposium on Ground Data Systems for Space Mission Operations 1 Mar. 1993 p 661-666 (For primary document see N94-23832 06-66)
Avail: CASI HC A02/MF A10

N94-23939*# Jet Propulsion Lab., California Inst. of Tech., Pasadena.
SPECIFYING DESIGN CONSERVATISM: WORST CASE VERSUS PROBABILISTIC ANALYSIS
Ralph F. Miles, Jr. *In its* SpaceOps 1992: Proceedings of the Second International Symposium on Ground Data Systems for Space Mission Operations 1 Mar. 1993 p 703-709 (For primary document see N94-23832 06-66)
Avail: CASI HC A02/MF A10

N94-24267 Technion - Israel Inst. of Tech., Haifa. Faculty of Aerospace Engineering.
FAILURE-PROOF ESTIMATION UNDER CONDITIONS OF LACK OF INFORMATION
Alexander Vul *In* Israel Society of Aeronautics and Astronautics, The 33rd Israel Annual Conference on Aviation and Astronautics 25 Feb. 1993 p 297-302 (For primary document see N94-24241 06-01)
Copyright Avail: Issuing Activity (Israel Society of Aeronautics and Astronautics, c/o Faculty of Engineering, Tel-Aviv Univ., Ramat Aviv 69978, Israel)

N94-24454*# Tuskegee Inst., AL. Aerospace Science Engineering Dept.
EVALUATION OF ADVANCED MATERIALS THROUGH EXPERIMENTAL MECHANICS AND MODELLING
Yii-Ching Yang *In* Alabama Univ., The 1993 NASA/ASEE Summer Faculty Fellowship Program Nov. 1993 5 p (For primary document see N94-24405 06-80)
Avail: CASI HC A01/MF A03

N94-25372*# Virginia Commonwealth Univ., Richmond. Dept. of Mathematical Sciences.
MODELLING EARLY FAILURES IN SPACE STATION FREEDOM
Sharon E. Navard *In* NASA. Johnson Space Center, National Aeronautics and Space Administration (NASA)/American Society for Engineering Education (ASEE) Summer Faculty Fellowship Program, 1993, Volume 2 Dec. 1993 13 p (For primary document see N94-25367 06-99)
Avail: CASI HC A03/MF A03

39 STRUCTURAL MECHANICS

Includes structural element design and weight analysis; fatigue; and thermal stress.

For applications see *05 Aircraft Design, Testing and Performance* and *18 Spacecraft Design, Testing and Performance.*

N94-22871# Los Alamos National Lab., NM.
FRACTURE SIMULATIONS VIA MASSIVELY PARALLEL MOLECULAR DYNAMICS
B. L. Holian, F. F. Abraham (International Business Machines Corp., San Jose, CA.), and R. Ravelo (Texas Univ., El Paso.) 1993 11 p Presented at the Annual Winter Meeting of the American Society of Mechanical Engineers, New Orleans, LA, 28 Nov. - 3 Dec. 1993
(Contract W-7405-eng-36)
(DE93-040159; LA-UR-93-3184; CONF-931121-22) Avail: CASI HC A03/MF A01

Fracture simulations at the atomistic level have been carried out for relatively small systems of particles, typically 10,000 or less. In order to study anything approaching a macroscopic system, massively parallel molecular dynamics (MD) must be employed. In two spatial dimensions (2D), it is feasible to simulate a sample that is 0.1 microns on a side. Recent MD simulations of mode 1 crack extension under tensile loading at high strain rates are reported. The method of uniaxial, homogeneously expanding periodic boundary conditions was employed to represent tensile stress conditions near the crack tip. The effects of strain rate, temperature, material properties (equation of state and defect energies), and system size were examined. It was found that, in order to mimic a bulk sample, several tricks (in addition to expansion boundary conditions) need to be employed: (1) the sample must be pre-strained to nearly the condition at which the crack will spontaneously open; (2) to relieve the stresses at free surfaces, such as the initial notch, annealing by kinetic-energy quenching must be carried out to prevent unwanted rarefactions; (3) sound waves emitted as the crack tip opens and dislocations emitted from the crack tip during blunting must be absorbed by special reservoir regions. The tricks described briefly will be especially important to carrying out feasible massively parallel 3D simulations via MD. DOE

N94-22960*# National Aeronautics and Space Administration. Lyndon B. Johnson Space Center, Houston, TX.
PROOF TEST OF THE COMPUTER PROGRAM BUCKY FOR PLASTICITY PROBLEMS
James P. Smith Jan. 1994 10 p
(NASA-TP-3444; S-753; NAS 1.60:3444) Avail: CASI HC A02/MF A01

A theoretical equation describing the elastic-plastic deformation of a cantilever beam subject to a constant pressure is developed. The theoretical result is compared numerically to the computer program BUCKY for the case of an elastic-perfectly plastic specimen. It is shown that the theoretical and numerical results compare favorably in the plastic range. Comparisons are made to another research code to further validate the BUCKY results. This paper serves as a quality test for the computer program BUCKY developed at NASA Johnson Space Center. Author

N94-23112 Centro Nazionale Univ. per il Calcolo Elettronico, Pisa (Italy).
CONTROL OF THE INTERNAL STRESSES IN PLANE ELASTICITY
S. Bennati (Pisa Univ., Italy.), S. DegIInnocenti, and C. Padovani 1993 26 p Limited Reproducibility: More than 20% of this document may be affected by microfiche quality
(PB93-225514) Avail: Issuing Activity (National Technical Information Service (NTIS))

A circular domain is subjected to radial surface forces varying according to a sinusoidal law. The existence of a tensile region included in a purely compressive one is proven and its asymptotic behavior studied when the surface forces converge to two concentrated loads acting along a same diameter. The results show that any maximum principle for the principal stress components would require conditions stronger than the simple negativity of both on the boundary of the domain. NTIS

N94-23113 Helsinki Univ. of Technology, Espoo (Finland). Inst. of Technology.
ENERGY ESTIMATES AND ASYMPTOTIC ANALYSIS IN THE THEORY OF SHELLS
J. Piila May 1993 139 p Limited Reproducibility: More than 20% of this document may be affected by microfiche quality
(PB93-225738; ISBN-951-22-1564-0) Avail: Issuing Activity (National Technical Information Service (NTIS))

In the plate bending problem, the energy methods were used successfully to derive error estimates between the two-dimensional model and the actual three-dimensional model. The report extends these ideas into certain model problems for shells. The asymptotic behavior of a thin shell which is loaded by a smooth surface traction and is rigidly supported throughout its rim is also studied. NTIS

N94-23118# Helsinki Univ. of Technology, Espoo (Finland). Lab. of Machine Design.
FUNDAMENTALS OF FATIGUE ANALYSIS

J. Saeaeski 1993 31 p
(PB93-226264; ISBN-951-22-1499-7) Avail: CASI HC A03/MF A01

The paper reviews the three primary methods available for a fatigue analysis - the stress-life approach, the strain-life approach and the fracture mechanics approach. The understanding of a single method provides a technique which may be used to perform a fatigue analysis. However, it is the insights gained from the understanding of all three methods which allow the engineer to correctly choose the method or methods that are most appropriate for the given problem. NTIS

N94-23120# Helsinki Univ. of Technology, Espoo (Finland). Lab. of Engineering Materials.
THERMAL FATIGUE: A LITERATURE REVIEW
Knut Bartsch, Hannu Haenninen, and Markku Nieminen Mar. 1993 98 p
(PB93-226306; ISBN-951-22-1478-4) Avail: CASI HC A05/MF A02

In the literature review, theories and testing methods concerning thermal fatigue are presented. Of the wide variety of different material groups special attention is paid on the hot work tool steels. NTIS

N94-23184# Iowa State Univ. of Science and Technology, Ames.
DEVELOPMENT OF SMALL PUNCH TESTING TECHNIQUE AND ITS APPLICATION TO EVALUATION OF MECHANICAL PROPERTIES DEGRADATION
J. Kameda 1993 18 p Presented at the Fall Meeting of the Minerals, Metals and Materials Society: Physical Metallurgy and Materials, Pittsburgh, PA, 17-21 Oct. 1993
(Contract W-7405-eng-82)
(DE94-001193; IS-M-772; CONF-931009-5) Avail: CASI HC A03/MF A01

The present paper summarizes a small punch (SP) testing technique developed and its application to mechanical properties characterization. It has been clearly shown on ferritic alloys that the SP test was evaluate the intergranular embrittling potency of segregated solute, such as P, Sn and Sb causing temper embrittlement, and the effects of neutron irradiation and post-irradiation annealing, giving rise to changes in the hardness and intergranular solute segregation, on the fracture properties in terms of the ductile-brittle transition temperature (DBTT). A linear relation of the DBTT determined by the SP test to that by Charpy V-notched tests has been theoretically and experimentally established. In Al alloy substrates coated with amorphous and overlaying ceramics, moreover, the global and local fracture properties were well characterized by the SP test together with acoustic emission techniques. DOE

N94-23196# Universitaet der Bundeswehr Muenchen, Neubiberg (Germany). Inst. fuer Luft- und Raumfahrttechnik.
COUPLED FREQUENCIES OF A HYDROELASTIC RECTANGULAR SYSTEM
Helmut F. Bauer 1992 60 p
(LRT-WE-9-FB-4-1992; ETN-94-95089) Avail: CASI HC A04/MF A01

The coupled hydroelastic frequencies of a liquid in a rectangular channel covered by a membrane or plate (beam in the treated two dimensional case) were obtained for various boundary conditions. The coupled eigenvalues were obtained and show a decrease for increasing length of the beam to liquid height ratio, while for increasing mass ratio of the beam mass per unit length to the liquid mass per unit length exhibit an increase of the coupled eigenvalue. ESA

N94-23217# Sandia National Labs., Albuquerque, NM.
CONTINUUM REPRESENTATIONS OF CELLULAR SOLIDS
M. K. Neilsen Sep. 1993 116 p
(Contract DE-AC04-94AL-85000)
(DE94-001706; SAND-93-1287) Avail: CASI HC A06/MF A02

Cellular materials consist of interconnected struts or plates which form cells. The struts or plates are constructed from a variety of metals, polymers, ceramics, and wood products. Cellular materials are often used in impact limiters for shipping containers to protect the contents from accidental impact events. These materials exhibit a variety of complex behavior when subjected to crushing loads. This research focuses on the development of continuum representations of cellular solids that can be used in the finite element analysis of shipping container accidents. A significant portion of this work is the development of a new methodology to relate localized deformations to appropriate constitutive descriptions. This methodology provides the insight needed to select constitutive descriptions for cellular solids that capture the localized deformations that are observed experimentally. Constitutive relations are developed for two different cellular materials, aluminum honeycomb and polyurethane foam. These constitutive relations are based on plasticity and continuum damage theories. Plasticity is used to describe the permanent deformation exhibited by both aluminum honeycomb and polyurethane foam. Continuum damage is needed to capture the change in elastic parameters due to cracking of the polyurethane cell wall materials. The new constitutive description of polyurethane foam is implemented in both static and dynamic finite element codes, and analytical and numerical predictions are compared with available experimental data. DOE

N94-23221 Technische Univ., Delft (Netherlands). Faculty of Aerospace Engineering.
SHELL BUCKLING RESEARCH AT DELFT, 1976 - 1992
J. Arbocz 1993 26 p Limited Reproducibility: More than 20% of this document may be affected by microfiche quality
(PB93-224442; M-614) Avail: CASI HC A03

The dilemma of the stability analysis of axially compressed cylindrical shells is well known. Trying to explain the discrepancy between the theoretical predictions based on the linearized small deflection theory and the experimental results has occupied some of the most eminent scientists of this century. The central goal of the shell research being carried out at the Aerospace Engineering Faculty of the TU-Delft is the development of an 'Improved Shell Design Criteria', which incorporates all the theoretical knowledge accumulated in the last, say, 25 years through intensive research in the Aerospace, the Nuclear, and the Offshore fields and which makes efficient use of the currently available interactive and (super) computing facilities. NTIS

N94-23294*# National Aeronautics and Space Administration. Marshall Space Flight Center, Huntsville, AL.
ANALYSIS AND TEST OF LOW PROFILE ALUMINUM AEROSPACE TANK DOME
R. Ahmed and J. M. Wilhelm Washington Dec. 1993 37 p
(NASA-TP-3442; M-737; NAS 1.60:3442) Avail: CASI HC A03/MF A01

In order to increase the structural performance of cryogenic tanks, the aerospace industry is beginning to employ low-profile bulkheads in new generation launch vehicle designs. This report details the analysis and test of one such dome made from 2219 aluminum. Such domes have two potential failure modes under internal pressure, general tensile failure and hoop compression buckling (in regions near the equator). The test determined the buckling load and ultimate tensile load of the hardware and showed that both compared well with the analysis predictions. This effort was conducted under the auspices of NASA and the General Dynamics Cryogenic Tank Technology Program (CTTP). Author (revised)

N94-23308* National Aeronautics and Space Administration. Langley Research Center, Hampton, VA.
METHOD OF DETERMINING SHEAR STRESS EMPLOYING A MONOMER-POLYMER LAMINATE STRUCTURE Patent
Jag J. Singh, inventor (to NASA), Abe Eftekhari, inventor (to NASA), and Devendra S. Parmar, inventor (to NASA) 14 Dec. 1993 12 p Filed 8 Feb. 1993 Division of US-Patent-Appl-SN-849612, filed 2 Mar. 1992
(NASA-Case-LAR-14654-2; US-Patent-5,270,781; US-Patent-Appl-SN-014960; US-Patent-Appl-SN-849612; US-Patent-Class-356-32; US-Patent-Class-428-1; US-Patent-Class-428-409; US-Patent-Class-428-480; US-Patent-Class-428-913; US-Patent-Class-359-67) Avail: US Patent and Trademark Office

A laminate structure attached to the test surface of an article is presented. The laminate structure is comprised of a liquid crystal polymer substrate. A light absorbing coating is applied to the substrate and is thin enough to permit bonding steric interaction between the liquid crystal polymer substrate and an overlying liquid crystal monomer thin film. Light is directed through and reflected by the liquid crystal monomer thin film and unreflected light is absorbed by the underlying coating. The wavelength of the reflected light is indicative of the shear stress experienced by the test surface.
Official Gazette of the U.S. Patent and Trademark Office

N94-23342*# National Aeronautics and Space Administration. Marshall Space Flight Center, Huntsville, AL.

REVIEW OF THE PROBABILISTIC FAILURE ANALYSIS METHODOLOGY AND OTHER PROBABILISTIC APPROACHES FOR APPLICATION IN AEROSPACE STRUCTURAL DESIGN

J. Townsend, C. Meyers, R. Ortega, J. Peck, M. Rheinfurth, and B. Weinstock (Vitro Corp., Washington, DC.) Washington Nov. 1993 72 p
(NASA-TP-3434; M-734; NAS 1.60:3434) Avail: CASI HC A04/MF A01

Probabilistic structural analyses and design methods are steadily gaining acceptance within the aerospace industry. The safety factor approach to design has long been the industry standard, and it is believed by many to be overly conservative and thus, costly. A probabilistic approach to design may offer substantial cost savings. This report summarizes several probabilistic approaches: the probabilistic failure analysis (PFA) methodology developed by Jet Propulsion Laboratory, fast probability integration (FPI) methods, the NESSUS finite element code, and response surface methods. Example problems are provided to help identify the advantages and disadvantages of each method. Author (revised)

N94-23368*# National Aeronautics and Space Administration. Langley Research Center, Hampton, VA.

A STRUCTURAL DESIGN DECOMPOSITION METHOD UTILIZING SUBSTRUCTURING

Stephen J. Scotti Jan. 1994 16 p
(RTOP 505-63-50-08)
(NASA-TM-107750; NAS 1.15:107750) Avail: CASI HC A03/MF A01

A new method of design decomposition for structural analysis and optimization is described. For this method, the structure is divided into substructures where each substructure has its structural response described by a structural-response subproblem, and its structural sizing determined from a structural-sizing subproblem. The structural responses of substructures that have rigid body modes when separated from the remainder of the structure are further decomposed into displacements that have no rigid body components, and a set of rigid body modes. The structural-response subproblems are linked together through forces determined within a structural-sizing coordination subproblem which also determines the magnitude of any rigid body displacements. Structural-sizing subproblems having constraints local to the substructures are linked together through penalty terms that are determined by a structural-sizing coordination subproblem. All the substructure structural-response subproblems are totally decoupled from each other, as are all the substructure structural-sizing subproblems, thus there is significant potential for use of parallel solution methods for these subproblems. Author (revised)

N94-23487*# National Aeronautics and Space Administration. Hugh L. Dryden Flight Research Center, Edwards, CA.

STRAIN GAGE MEASUREMENT ERRORS IN THE TRANSIENT HEATING OF STRUCTURAL COMPONENTS

W. Lance Richards Washington Dec. 1993 15 p Presented at the SEM Fall Connference and Exhibit: Structural Testing at High Temperature 2, Ojai, CA, 8-10 Nov. 1993
(RTOP 505-70-63)
(NASA-TM-104274; H-1960; NAS 1.15:104274) Avail: CASI HC A03/MF A01

Significant strain-gage errors may exist in measurements acquired in transient thermal environments if conventional correction methods are applied. Conventional correction theory was modified and a new experimental method was developed to correct indicated strain data for errors created in radiant heating environments ranging from 0.6 C/sec (1 F/sec) to over 56 C/sec (100 F/sec). In some cases the new and conventional methods differed by as much as 30 percent. Experimental and analytical results were compared to demonstrate the new technique. For heating conditions greater than 6 C/sec (10 F/sec), the indicated strain data corrected with the developed technique compared much better to analysis than the same data corrected with the conventional technique. Author (revised)

N94-23551*# National Aeronautics and Space Administration. Lewis Research Center, Cleveland, OH.

MATERIAL DATA REPRESENTATION OF HYSTERESIS LOOPS FOR HASTELLOY X USING ARTIFICIAL NEURAL NETWORKS

Javed Alam (Youngstown State Univ., OH.), Laszlo Berke, and Pappu L. N. Murthy Dec. 1993 11 p
(RTOP 505-63-5B)
(NASA-TM-105990; E-7301; NAS 1.15:105990) Avail: CASI HC A03/MF A01

The artificial neural network (ANN) model proposed by Rumelhart, Hinton, and Williams is applied to develop a functional approximation of material data in the form of hysteresis loops from a nickel-base superalloy, Hastelloy X. Several different ANN configurations are used to model hysteresis loops at different cycles for this alloy. The ANN models were successful in reproducing the hysteresis loops used for its training. However, because of sharp bends at the two ends of hysteresis loops, a drift occurs at the corners of the loops where loading changes to unloading and vice versa (the sharp bends occurred when the stress-strain curves were reproduced by adding stress increments to the preceding values of the stresses). Therefore, it is possible only to reproduce half of the loading path. The generalization capability of the network was tested by using additional data for two other hysteresis loops at different cycles. The results were in good agreement. Also, the use of ANN led to a data compression ratio of approximately 22:1. Author

N94-23560# Colorado Univ., Boulder. Dept. of Aerospace Engineering.

A STRUCTURAL DESIGN METHODOLOGY FOR LARGE ANGLE ARTICULATED TRUSSES CONSIDERING REALISTIC JOINT MODELING

Gregory Thorwald and Martin M. Mikulas, Jr. 31 Jan. 1994 226 p
Avail: CASI HC A11/MF A03

A structural design methodology is developed by quantifying the magnitude that large angle articulations and realistic modeling considerations adversely affect a truss's structural stiffness. Batten actuators provide the ability for the truss both to deploy and articulate. Such an articulated truss can be used in space crane applications. With geometry and modeling considerations identified and examined, strategies to alleviate the truss's stiffness reduction are developed and evaluated. Using these strategies, an improved articulated truss is then demonstrated. Observing that the design strategies are effective for the planar truss models similar 3-D truss models are then analyzed. The results show that the improvement strategies benefit both the 2-D and 3-D truss models. Author

N94-23789# Acoustical Society of America, New York, NY.

US TAG FOR ISO/TC 108 MECHANICAL VIBRATION AND SHOCK: MINUTES OF THE ACCREDITED STANDARDS COMMITTEE ON MECHANICAL VIBRATION AND SHOCK, S2

19 May 1993 45 p Meeting held in Ottawa, Canada, 19 May 1993
(AD-A273015; S2/251) Avail: CASI HC A03/MF A01

The minutes of the May 19, 1993 meeting of Standards Committee on Mechanical Shock and Vibration are presented. In addition, a list of current working groups and a summary of activities is provided. CASI

N94-24359*# Rockwell International Corp., Huntsville, AL. Space Systems Div.

MODELING DYNAMICALLY COUPLED FLUID-DUCT SYSTEMS WITH FINITE LINE ELEMENTS Final Report

J. B. Saxon Feb. 1994 17 p
(Contract NAS8-38550)
(NASA-CR-193909; NAS 1.26:193909) Avail: CASI HC A03/MF A01

Structural analysis of piping systems, especially dynamic analysis, typically considers the duct structure and the contained fluid column separately. Coupling of these two systems, however, forms a new dynamic system with characteristics not necessarily described by the superposition of the two component system's characteristics. Methods for modeling the two coupled components simultaneously using finite line elements are presented. Techniques for general duct intersections, area or direction changes, long radius bends, hydraulic losses, and hydraulic impedances are discussed. An example problem and results involving time transients are presented. Additionally, a program to enhance post-processing of line element models is discussed. Author

N94-24478# Instituut TNO voor Bouwmaterialen en Bouwconstructies, Delft (Netherlands).

HYDRO-ELASTIC ANALYSIS USING A SELECTION OF COMMERCIAL ANALYSIS PROGRAMS Final Report No. 2

1993 70 p Sponsored by Stichting Coordinatie Maritiem Onderzoek, Rotterdam, The Netherlands

(PB94-118734; TNO-93-CMC-R0210-2) Copyright Avail: CASI HC A04/MF A01

It has been investigated whether and how a number of commercial finite element software systems can be used for predicting the response of a ship hull to excitation by a cavitating propeller. In this typical fluid-structure interaction problem, the cavitating propeller is represented as a monopole source. The software systems considered in this study are DIANA, MSC/NASTRAN, SYSNOISE, ABAQUS, and USA-CODE. For calculating the response for the frequency range of interest, it is sufficient to model the surrounding water by an incompressible fluid without free surface waves and radiation damping. It is shown how to model a monopole in a finite element response analysis if the system does not allow for a direct input of a monopole. It is found that software which uses boundary elements for describing the fluid domain is strongly preferable in this type of analysis. This saves the laborious work required for 3D meshing of the fluid domain and hence makes 3D response analyses of ship hulls feasible. For a two dimensional test case, results obtained with different software systems showed large deviations compared to each other and to an analytical solution. NTIS

N94-24587*# Massachusetts Inst. of Tech., Cambridge. Technology Lab. for Advanced Composites.

DAMAGE TOLERANCE OF PRESSURIZED GRAPHITE/EPOXY TAPE CYLINDERS UNDER UNIAXIAL AND BIAXIAL LOADING M.S. Thesis

Stacy Marie Priest Dec. 1993 318 p

(Grant NAG1-991)

(NASA-CR-195101; NAS 1.26:195101; TELAC-93-19) Avail: CASI HC A14/MF A03

The damage tolerance behavior of internally pressurized, axially slit, graphite/epoxy tape cylinders was investigated. Specifically, the effects of axial stress, structural anisotropy, and subcritical damage were considered. In addition, the limitations of a methodology which uses coupon fracture data to predict cylinder failure were explored. This predictive methodology was previously shown to be valid for quasi-isotropic fabric and tape cylinders but invalid for structurally anisotropic (+/-45/90)(sub s) and (+/-45/0)(sub s) cylinders. The effects of axial stress and structural anisotropy were assessed by testing tape cylinders with (90/0/+/-45)(sub s), (+/-45/90)(sub s), and (+/-45/0)(sub s) layups in a uniaxial test apparatus, specially designed and built for this work, and comparing the results to previous tests conducted in biaxial loading. Structural anisotropy effects were also investigated by testing cylinders with the quasi-isotropic (0/+/-45/90)(sub s) layup which is a stacking sequence variation of the previously tested (90/0/+/-45)(sub s) layup with higher D(sub 16) and D(sub 26) terms but comparable D(sub 16) and D(sub 26) to D(sub 11) ratios. All cylinders tested and used for comparison are made from AS4/3501-6 graphite/epoxy tape and have a diameter of 305 mm. Cylinder slit lengths range from 12.7 to 50.8 mm. Failure pressures are lower for the uniaxially loaded cylinders in all cases. The smallest percent failure pressure decreases are observed for the (+/-45/90)(sub s) cylinders, while the greatest such decreases are observed for the (+/-45/0)(sub s) cylinders. The relative effects of the axial stress on the cylinder failure pressures do not correlate with the degree of structural coupling. The predictive methodology is not applicable for uniaxially loaded (+/-45/90)(sub s) and (+/-45/0)(sub s) cylinders, may be applicable for uniaxially loaded (90/0/+/-45)(sub s) cylinders, and is applicable for the biaxially loaded (90/0/+/-45)(sub s) and (0/+/-45/90)(sub s) cylinders. This indicates that the ratios of D(sub 16) and D(sub 26) to D(sub 11), as opposed to the absolute magnitudes of D(sub 16) and D(sub 26), may be important in the failure of these cylinders and in the applicability of the methodology. Discontinuities observed in the slit tip hoop strains for all the cylinders tested indicate that subcritical damage can play an important role in the failure of tape cylinders. This role varies with layup and loading condition and is likely coupled to the effects of structural anisotropy. Biaxial failure pressures may exceed the uniaxial values because the axial stress contributes to the formation of 0 deg ply splitting (accompanied by delamination) or similar stress-mitigating subcritical damage. The failure behavior of similar cylinders can also vary as a result of differences in the role of subcritical damage as observed for the case of a biaxially loaded (90/0/+/-45)(sub s) cylinder with a 12.7 mm slit. For this case, the methodology is valid when the initial coupon and cylinder fracture modes agree. However, the methodology underpredicts the failure pressure of the cylinder when a circumferential fracture path, suggestive of a 0 deg ply split, occurs at one slit tip. Thus, the failure behavior of some tape cylinders may be highly sensitive to the initial subcritical damage mechanism. Finite element analyses are recommended to determine how structural anisotropy and axial stress modify the slit tip stress states in cylinders from those found in flat plates since similarity of these stress states is a fundamental assumption of the current predictive methodology. Author

N94-24604*# Case Western Reserve Univ., Cleveland, OH.

THE EFFECTS OF ANISOTROPY ON THE NONLINEAR BEHAVIOR OF BRIDGED CRACKS IN LONG STRIPS Final Report

R. Ballarini and H. A. Luo (Xian Jiaotong Univ., China.) Feb. 1994 39 p

(Grant NAG3-856; RTOP 505-63-5B)

(NASA-CR-194453; E-8388; NAS 1.26:194453) Avail: CASI HC A03/MF A01

A model which can be used to predict the two-dimensional nonlinear behavior of bridged cracks in orthotropic strips is presented. The results obtained using a singular integral equation formulation which incorporates the anisotropy rigorously show that, although the effects of anisotropy are significant, the nondimensional quantities employed by Cox and Marshall can generate nearly universal results (R-curves, for example) for different levels of relative anisotropy. The role of composite constituent properties in the behavior of bridged cracks is clarified. Author (revised)

N94-24645 Technische Univ., Delft (Netherlands).

STABILITY ANALYSIS OF ANISOTROPIC CONICAL SHELLS Ph.D. Thesis

Guo-Qi Zhang 1993 295 p Limited Reproducibility: More than 20% of this document may be affected by microfiche quality

(PB94-119054; ISBN-90-6275-876-2/CIP) Copyright Avail: CASI HC A13

In this investigation, a rigorous treatment of the bifurcation buckling and initial postbuckling behavior of perfect and imperfect anisotropic conical shells is presented, which includes the effects of boundary conditions and nonlinear prebuckling deformations. This analysis is based on nonlinear Donnell-type strain-displacement relations and uses an extension of Koiter's initial postbuckling theory. To carry out the above analysis, the nonlinear Donnell-type anisotropic shell equations in terms of the radial displacement W and the Airy stress function F are derived via the stationary potential energy criterion. A complete set of boundary conditions, which partially or completely satisfies Seide's geometric constraint, is also formulated in terms of W and F. By using the perturbation technique proposed by Koiter, three sets of differential equations governing the prebuckling, buckling, and postbuckling problems, and the corresponding boundary conditions are obtained. To solve the resulting boundary value problems, the nonlinear prebuckling solution is assumed to be axisymmetric, while the circumferential dependence of the buckling and postbuckling equations is eliminated by Fourier decomposition. NTIS

N94-24715*# National Aeronautics and Space Administration. Lewis Research Center, Cleveland, OH.

ELEVATED TEMPERATURE CRACK PROPAGATION

Thomas W. Orange Feb. 1994 17 p Presented at the Symposium on Fatigue and Fracture, 114th Winter Annual Meeting, New Orleans, LA, 29 Nov. - 3 Dec. 1993; sponsored by ASME

(RTOP 505-63-5B)

(NASA-TM-106490; E-8477; NAS 1.15:106490) Avail: CASI HC A03/MF A01

This paper is a summary of two NASA contracts on high temperature fatigue crack propagation in metals. The first evaluated the ability of fairly simple nonlinear fracture parameters to correlate crack propagation. Hastelloy-X specimens were tested under isothermal and thermomechanical cycling at temperatures up to 980 degrees C (1800 degrees F). The most successful correlating parameter was the crack tip opening displacement derived from the J-integral. The second evaluated the ability of several path-independent integrals to correlate crack propagation behavior. Inconel 718 specimens were tested under isothermal, thermomechanical, temperature gradient, and creep conditions at temperatures up to 650 degrees C (1200 degrees F). The integrals formulated by Blackburn and by Kishimoto correlated the data reasonably well under all test conditions. Author (revised)

N94-24742 Swedish Inst. for Materials Testing, Boras.
VARIABLE AMPLITUDE FATIGUE, MODELLING AND TESTING
T. Svensson 1993 63 p Limited Reproducibility: More than 20% of this document may be affected by microfiche quality
(PB93-204469; SP-RAPP-1993:13) Avail: CASI HC A04

Problems related to metal fatigue modelling and testing are here treated in four different papers. In the first paper different views of the subject are summarized in a literature survey. In the second paper a new model for fatigue life is investigated. Experimental results are established which are promising for further development of the model. In the third paper a method is presented that generates a stochastic process, suitable to fatigue testing. The process is designed in order to resemble certain fatigue related features in service life processes. In the fourth paper fatigue problems in transport vibrations are treated. NTIS

N94-24745 Technische Univ., Delft (Netherlands). Faculty of Aerospace Engineering.
BUCKLING OF CIRCULAR CYLINDRICAL SHELLS SUBJECTED TO COMBINED LOADS (AXIAL COMPRESSION, NORMAL PRESSURE, BENDING AND TRANSVERSE SHEAR LOADING)
E. Karyadi Sep. 1992 19 p See also PB91-114637 and PB92-199611 Limited Reproducibility: More than 20% of this document may be affected by microfiche quality
(PB93-215358; M-663) Avail: Issuing Activity (National Technical Information Service (NTIS))

The paper deals with the buckling behavior of anisotropic or isotropic stiffened cylindrical shells subjected to combined loading defined in the title. A rigorous satisfaction of the boundary conditions at the ends of the cylinder was included. The analysis is started with the formulation of the buckling equations for anisotropic stiffened cylinders under the specified loading condition. In this stage of analysis, membrane condition of prebuckling stresses in the cylinder is assumed. Further, to solve the buckling equations, solution functions in terms of the independent displacement variables u, v and w are introduced. In order to satisfy the homogeneous boundary conditions, the axial dependence of the displacement variables is assumed to be an unknown function of the axial coordinate. In the circumferential direction, Fourier series expansions will be applied. By using the Galerkin process and a finite difference approximation, the buckling equations will be reduced to a standard eigenvalue problem. For calculating the eigenvalues and the corresponding mode shapes, the requisite software is developed. NTIS

N94-24839*# National Aeronautics and Space Administration. Langley Research Center, Hampton, VA.
DYNAMIC ANALYSIS OF PRETWISTED ELASTICALLY-COUPLED ROTOR BLADES
Mark W. Nixon and Howard E. Hinnant Jan. 1994 19 p Presented at the 1992 ASME Winter Annual Meeting, Anaheim, CA, 8-13 Nov. 1992 See also A93-21125
(RTOP 505-63-50-15)
(NASA-TM-109070; NAS 1.15:109070) Avail: CASI HC A03/MF A01

The accuracy of using a one-dimensional analysis to predict frequencies of elastically-coupled highly-twisted rotor blades is addressed. Degrees of freedom associated with shear deformation are statically condensed from the formulation, so the analysis uses only those degrees of freedom associated with classical beam theory. The effects of cross section deformation (warping) are considered, and are shown to become significant for some types of elastic coupling. Improved results are demonstrated for highly-coupled blade structures through account of warping in a local cross section analysis, without explicit inclusion of these effects in the beam analysis. A convergence study is also provided which investigates the potential for improving efficiency of elastically-coupled beam analysis through implementation of a p-version beam finite element. Author (revised)

N94-24845*# National Aeronautics and Space Administration. Lewis Research Center, Cleveland, OH.
MERITS AND LIMITATIONS OF OPTIMALITY CRITERIA METHOD FOR STRUCTURAL OPTIMIZATION
Surya N. Patnaik (Ohio Aerospace Inst., Brook Park.), James D. Guptill, and Laszlo Berke Washington Nov. 1993 49 p
(RTOP 505-63-1C)
(NASA-TP-3373; E-7325; NAS 1.60:3373) Avail: CASI HC A03/MF A01

The merits and limitations of the optimality criteria (OC) method for the minimum weight design of structures subjected to multiple load conditions under stress, displacement, and frequency constraints were investigated by examining several numerical examples. The examples were solved utilizing the Optimality Criteria Design Code that was developed for this purpose at NASA Lewis Research Center. This OC code incorporates OC methods available in the literature with generalizations for stress constraints, fully utilized design concepts, and hybrid methods that combine both techniques. Salient features of the code include multiple choices for Lagrange multiplier and design variable update methods, design strategies for several constraint types, variable linking, displacement and integrated force method analyzers, and analytical and numerical sensitivities. The performance of the OC method, on the basis of the examples solved, was found to be satisfactory for problems with few active constraints or with small numbers of design variables. For problems with large numbers of behavior constraints and design variables, the OC method appears to follow a subset of active constraints that can result in a heavier design. The computational efficiency of OC methods appears to be similar to some mathematical programming techniques. Author

N94-25143 Illinois Univ., Urbana. Dept. of Civil Engineering.
THREE-DIMENSIONAL, INELASTIC RESPONSE OF SINGLE-EDGE NOTCH BEND SPECIMENS SUBJECTED TO IMPACT LOADING Final Report, Oct. 1988 - Sep. 1992
Pedro M. Vargas and Robert H. Dodds, Jr. Aug. 1993 206 p Limited Reproducibility: More than 20% of this document may be affected by microfiche quality
(Contract N61533-88-C-0035)
(AD-A273302; UILU-ENG-93/2006; CARDIVNSWC-TR-61-CR-93-02)
Avail: Issuing Activity (Defense Technical Information Center (DTIC))

Three-dimensional dynamic analyses are performed for three different specimen configurations (a/W equivalent 0.5, 0.15, 0.0725) of single edge bend, SE(B), fracture specimens subjected to impact loading. DTIC

N94-25188*# National Aeronautics and Space Administration. Lewis Research Center, Cleveland, OH.
PROBABILISTIC ASSESSMENT OF SMART COMPOSITE STRUCTURES
Christos C. Chamis and Michael C. Shiao (Sverdrup Technology, Inc., Brook Park, OH.) Jan. 1994 21 p Presented at the 38th International SAMPE Symposium and Exhibit, Anaheim, CA, 10-13 May 1993; sponsored by the Society for the Advancement of Materials and Process Engineering
(RTOP 510-02-12)
(NASA-TM-106358; E-8145; NAS 1.15:106358) Avail: CASI HC A03/MF A01

A composite wing with spars and bulkheads is used to demonstrate the effectiveness of probabilistic assessment of smart composite structures to control uncertainties in distortions and stresses. Results show that a smart composite wing can be controlled to minimize distortions and to have specified stress levels in the presence of defects. Structural responses such as changes in angle of attack, vertical displacements, and stress in the control and controlled plies are probabilistically assessed to quantify their respective uncertainties. Sensitivity factors are evaluated to identify those parameters that have the greatest influence on a specific structural response. Results show that smart composite structures can be configured to control both distortions and ply stresses to satisfy specified design requirements. Author

N94-25267*# Alabama Univ., Tuscaloosa. Dept. of Engineering Mechanics.
USE OF PHOTOSTRESS TO CHARACTERIZE THE MECHANICAL BEHAVIOR OF WELDMENTS Final Report
S. C. Gambrell, Jr. Sep. 1992 143 p Original contains color illustrations
(Grant NAG8-212)
(NASA-CR-195201; NAS 1.26:195201; BER-570-97) Avail: CASI HC A07/MF A02; 19 functional color pages

Welded aluminum is an important part of many space structures. Knowledge of the properties and behavior of weld material and the material surrounding the weld is important for modeling and design of the structures. Photoelastic coatings (Photostress) and strain gages were used to determine behavior of heat treated and as welded joints made from 2219T87 parent material and 2319 weld material subjected to tensile loads. TIG welds of

1/8, 1/2, and 1.4 inches thickness were investigated. Discontinuous yielding was observed in all tests and highly non-uniform behavior through the weld thickness was observed in joints having welds 1.4 inches thick. Joints having welds 1/8 and 1/2 inches thick had only small differences in behavior through the thickness of the weld. Joints in the 1/2 inch thick material contained distinct zones of constant strain within the normal strain gradient extending outward from the weld centerline. These zones had different thickness and locations. Points at the weld centerline, and for a distance of nearly one inch from the centerline, exhibited very nonlinear behavior during the first loading but exhibited near perfect strain hardening during the second loading. Author

N94-25325# Oxford Univ. (England). Dept. of Engineering Science.
RING NUCLEI OF STRAIN FOR BONDED DISSIMILAR ELASTIC HALF SPACES WITH PARTICULAR APPLICATION TO AXISYMMETRIC CRACK PROBLEMS
Alexander M. Korsunsky 1992 29 p
(OUEL-1966/92; ETN-94-95152) Avail: CASI HC A03/MF A01

A class of fundamental solutions for axisymmetric elastic problems for two perfectly bonded dissimilar elastic half spaces is developed. The nuclei of strain corresponding to infinitesimal dislocation loops (finite displacement discontinuities prescribed over infinitesimal area) are chosen as the starting point. These are integrated along a circular contour to produce the solutions for normal axial, normal radial, and tangential displacement discontinuities along a ring. Formulae for stresses in the material containing the nuclei of strain are given in terms of the Lipschitz-Hankel type integrals, which in their turn are expressed using elliptic functions. ESA

N94-25385# Technical Research Centre of Finland, Espoo. Structural Engineering Lab.
CONSTITUTIVE MODELLING OF FIBER-REINFORCED CONCRETE UNDER UNIAXIAL TENSILE LOADING [VEDONALAISEN KUITULUJITETUN BETONIN KONSTITUTIIVINEN MALLINTAMINEN]
Jyrki Kullaa Jan. 1993 115 p In FINNISH
(VTT-JULK-774; ISBN-951-38-4122-7; ETN-94-95248) Copyright Avail: CASI HC A06/MF A02

The mechanics of fiber reinforced concrete under uniaxial loading is studied. The focus is on the behavior after cracking. The interaction between the fiber and the matrix is the shear stress transfer. The stress can be elastic or frictional in nature. The bond parameters can be obtained by a simple pull-out test and theory. The load displacement curves for fibers of different lengths can be created by means of the calculated parameters. In a simple constitutive model, the main assumption is that the fibers are continuous and there exists multiple cracking in the matrix. After cracking, the fibers only carry the loading. The model uses efficiency factors in taking into account the short and randomly distributed fibers. Only the strengthening portion of the stress strain curve is analyzed. In the statistical model created, it is assumed that only one crack will develop. The theory ignores the strain of the matrix in fiber pull-out. The strain softening behavior is taken into consideration. A constitutive model which takes into account the strain softening part of the stress strain curve is developed. The crack distance and crack width are also calculated. The model takes into account one crack or multiple cracking states and different fracture mechanisms: fiber fracture or pull-out. The fibers are smooth and straight. They can be short or continuous, aligned or randomly distributed, brittle or ductile, and stiff or flexible. Different types of fibers may lie in the same matrix. The results of the model are consistent with the other two models referred. The effects of different parameters can be studied and even new formulas can be found. The model can be used in the design of composite materials and is valid for other brittle matrix composites, such as fiber reinforced ceramics. ESA

N94-25418# Technical Research Centre of Finland, Espoo. Metals Lab.
STRENGTH AND LIFE OF PRESSURE VESSELS SUBJECTED TO IMPACTS AND THERMOMECHANICAL GFRP LOADING [LAEMPOE-JA ISKURASITETTUJEN LUJITEMUOVIPAINEASTIOIDEN JAEAENNOESLUJUUS JA ELINIKAE]
Pekka H. Pankakoski, Tero Uuttu, Pentti Kauppinen, Matti Sarkimo, and Pertti Auerkari Oct. 1992 66 p In FINNISH Sponsored by Technology Development Center, Finland; Technical Research Centre of Finland, Espoo; Oy Muokkaus AB, Finland; Neste Oy, Finland; and Hollming Oy, Finland Original contains color illustrations
(VTT-JULK-771; ISBN-951-38-4119-7; ETN-94-95243) Copyright Avail: CASI HC A04/MF A01

Non-insulated GRFP (Glass Fiber Reinforced Plastics) pipes were experimentally investigated. Particular consideration was given to the effects of short term thermal overloads and impact damage. It was shown that for a matrix with a long term specified service temperature of less than 140 C and starting from 140 C at 10 bar pressure up to 200 C and 30 bar pressure up to 170 C such thermalcycling up to some 100 cycles is acceptable when the hold time at the peak temperature is less than one hour. A prerequisite for this is the outer surface of the pipes remaining non-insulated and cooler (by about 30 C) than the content. No significant creep strain under static 10 bar pressure at 140 C was measured up to 350 hours of testing time. At 200 C and 30 bar, creep was fast enough to produce failure in a few hours. Clearly, the matrix material is not well suited to these high temperatures. Nevertheless, temporary surges in inside temperature to 170 C or even relatively long periods peaking at 140 C should not cause significant problems at normal service pressures near 10 bar, at least up to some 100 cycles. Impact testing and subsequent static pressure testing showed that for a given type of material, the leakage pressure of the vessel can be relatively easily predicted from the incident impact energy or from the ultrasonically determined size of the impact defect. ESA

N94-25478# Oxford Univ. (England). Dept. of Engineering Science.
THE COMPLETE STRESS FIELD DUE TO A DISLOCATION LOCATED ANYWHERE IN TWO BONDED QUARTER PLANES
P. Kelly, D. A. Hills, and D. Nowell 1993 31 p
(OUEL-1990/93; ETN-94-95161) Avail: CASI HC A03/MF A01

A method to deal with the state of stress arising anywhere within the two quarter planes induced by a dislocation situated anywhere within the quarter planes is developed. It provides the means of solving the problem of a crack lying anywhere within the quarter planes. This problem is of some practical importance as the fracture resistance of interfaces between ceramics and metals is often greater than that of the ceramic component. Thus crack propagation often occurs within the ceramic component rather than on the interface itself. ESA

N94-25520 Air Force Inst. of Tech., Wright-Patterson AFB, OH.
NUMERICAL ANALYSIS OF THE MOTION OF A RIGID BODY WITH AN ATTACHED SPRING-MASS-DAMPER M.S. Thesis
Anne E. Chinnery Dec. 1993 62 p Limited Reproducibility: More than 20% of this document may be affected by microfiche quality
(AD-A273825; AFIT/GAE/ENY/93D-8) Avail: CASI HC A04

This study analyzed the stability characteristics and the unstable motion of a rigid body with a spring-mass-damper unit (nutation damper) attached parallel to one of the system's principal axes. The equations of motion are presented and non-dimensionalized. Then, they are numerically integrated over time. An analysis using a Liaponuv function develops the critical values of the moments of inertia for stability of the system, as well as the critical values of a dimensionless parameter k related to the spring constant. A discussion of the effects of the various parameters on the motion of the system is provided and some representative plots are included. The parameter b related to the distance of the nutation damper from the principal axis is found to determine whether unstable motion approaches an apparent limit cycle or a new principal axis. Parameter k affects the final position of the mass and can also influence the system toward limit cycle or equilibrium point motion. Parameter c representing the damping coefficient affects how quickly the system reaches its steady state motion. A summary of the unstable motions of the system and recommendations for further work are included. DTIC

N94-25529# Technical Research Centre of Finland, Espoo. Building Materials Lab.
FROST EFFECTS ON THE MICROSTRUCTURE OF HIGH STRENGTH CONCRETE, AND METHODS FOR THEIR ANALYSIS Ph.D. Thesis - Helsinki Univ. of Technology, Espoo, Finland
Heikki Kukko Dec. 1992 179 p Sponsored by Technical Research Centre of Finland, Espoo, and Alpo and Kyllikki Lippa Fund, Finland Original contains color illustrations
(VTT-PUBS-126; ISBN-9-51-384244-4; ETN-94-95236) Copyright Avail: CASI HC A09/MF A02

The aims of the study are to identify and analyze the applicability of experimental methods through studies of the freeze thaw durability of high strength concretes with different binder compositions and to elucidate the microstructural changes that occur during freeze thaw degradation. The main features of concrete microstructure, existing analysis methods, and main theories of concrete frost resistance are surveyed. Pore and crack properties of concrete were measured by automatic analysis method. Five high strength concrete mixes with various binder compositions and one medium strength concrete were prepared. They were subjected to as many as 1000 freeze thaw cycles, and the defects were studied. Strength loss was used as the basic measure of degradation. Image analysis results can be used in mathematical modeling of strength changes of concrete. Visual optical analysis of thin sections was proved to be a reliable method. Mercury porosimetry results did not give a reliable basis for the estimation of frost crack increase due to ettringite formations in the cracks. Scanning electron microscopy is a valuable tool for detecting the causes of changes found in porosimetric analysis. The principle of critical degree of saturation applies to high strength concrete. The mathematical modeling of strength loss during frost tests can be based on a combined model including changes in total porosity and maximum crack length. ESA

N94-24246 MacNeal-Schwendler Corp., Gouda (Netherlands).
THE PLASTIC RESPONSE OF A CYLINDRICAL SHELL SUBJECTED TO AN INTERNAL BLAST WAVE WITH A FINITE WIDTH SHOCK FRONT
Y. Kivity, C. Florie, and H. Lenselink *In* Israel Society of Aeronautics and Astronautics, The 33rd Israel Annual Conference on Aviation and Astronautics 25 Feb. 1993 p 89-102 (For primary document see N94-24241 06-01)
Copyright Avail: Issuing Activity (Israel Society of Aeronautics and Astronautics, c/o Faculty of Engineering, Tel-Aviv Univ., Ramat Aviv 69978, Israel)

N94-24260 Israel Aircraft Industries Ltd., Ben-Gurion Airport.
POST BUCKLING BEHAVIOUR OF STIFFENED COMPOSITE PANELS LOADED IN CYCLIC COMPRESSION AND SHEAR
A. Segal, Y. Frostig, D. Shalev, T. Weller (Technion - Israel Inst. of Tech., Haifa.), and Y. Sheinman (Technion - Israel Inst. of Tech., Haifa.) *In* Israel Society of Aeronautics and Astronautics, The 33rd Israel Annual Conference on Aviation and Astronautics 25 Feb. 1993 p 225-236 (For primary document see N94-24241 06-01)
Copyright Avail: Issuing Activity (Israel Society of Aeronautics and Astronautics, c/o Faculty of Engineering, Tel-Aviv Univ., Ramat Aviv 69978, Israel)

N94-24276 Technion - Israel Inst. of Tech., Haifa. Faculty of Aerospace Engineering.
MEAN STRESS MODELS FOR LOW CYCLE FATIGUE OF A NICKEL-BASE SUPERALLOY
Daining Fang and Avraham Berkovitz *In* Israel Society of Aeronautics and Astronautics, The 33rd Israel Annual Conference on Aviation and Astronautics 25 Feb. 1993 p 374-386 Supported in part by Rolls-Royce Ltd., Derby, England (For primary document see N94-24241 06-01)
Copyright Avail: Issuing Activity (Israel Society of Aeronautics and Astronautics, c/o Faculty of Engineering, Tel-Aviv Univ., Ramat Aviv 69978, Israel)

N94-24277 Ottawa Univ. (Ontario). Faculty of Engineering.
FRACTURE KINETICS ANALYSIS OF EMPIRICAL AND SEMI-EMPIRICAL CORROSION FATIGUE RELATIONS
K. Krausz and A. S. Krausz *In* Israel Society of Aeronautics and Astronautics, The 33rd Israel Annual Conference on Aviation and Astronautics 25 Feb. 1993 p 387-401 Sponsored by the Natural Sciences and Engineering Research Council of Canada (For primary document see N94-24241 06-01)
Copyright Avail: Issuing Activity (Israel Society of Aeronautics and Astronautics, c/o Faculty of Engineering, Tel-Aviv Univ., Ramat Aviv 69978, Israel)

N94-24278 Israel Aircraft Industries Ltd., Tashan.
EVALUATION OF THE FRACTURE RESISTANCE AND DURABILITY OF ADHESIVE BONDED JOINTS
H. Leibovich and V. Weissberg *In* Israel Society of Aeronautics and Astronautics, The 33rd Israel Annual Conference on Aviation and Astronautics 25 Feb. 1993 p 402-408 (For primary document see N94-24241 06-01)
Copyright Avail: Issuing Activity (Israel Society of Aeronautics and Astronautics, c/o Faculty of Engineering, Tel-Aviv Univ., Ramat Aviv 69978, Israel)

N94-24279 Technion - Israel Inst. of Tech., Haifa. Department of Civil Engineering.
VIBRATIONS OF VARIABLE CROSS SECTION TIMOSHENKO BEAMS
Moshe Eisenberger *In* Israel Society of Aeronautics and Astronautics, The 33rd Israel Annual Conference on Aviation and Astronautics 25 Feb. 1993 p 409-412 (For primary document see N94-24241 06-01)
Copyright Avail: Issuing Activity (Israel Society of Aeronautics and Astronautics, c/o Faculty of Engineering, Tel-Aviv Univ., Ramat Aviv 69978, Israel)

N94-24280 Technion - Israel Inst. of Tech., Haifa. Faculty of Aerospace Engineering.
GLOBAL DYNAMIC STABILITY OF A SHALLOW ARCH BY POINCARE-LIKE SIMPLE CELL MAPPING
J. Levitas, J. Singer, and T. Weller *In* Israel Society of Aeronautics and Astronautics, The 33rd Israel Annual Conference on Aviation and Astronautics 25 Feb. 1993 p 413-420 (For primary document see N94-24241 06-01)
Copyright Avail: Issuing Activity (Israel Society of Aeronautics and Astronautics, c/o Faculty of Engineering, Tel-Aviv Univ., Ramat Aviv 69978, Israel)

N94-24281 Technion - Israel Inst. of Tech., Haifa. Faculty of Agricultural Engineering.
INVERSE DYNAMICS OF A RIGID ROD SYSTEM AS A SIMPLIFIED MODEL OF FLEXIBLE BEAM
D. Rubinstein, N. Galili, and A. Libai *In* Israel Society of Aeronautics and Astronautics, The 33rd Israel Annual Conference on Aviation and Astronautics 25 Feb. 1993 p 421-429 (For primary document see N94-24241 06-01)
Copyright Avail: Issuing Activity (Israel Society of Aeronautics and Astronautics, c/o Faculty of Engineering, Tel-Aviv Univ., Ramat Aviv 69978, Israel)

N94-24288 Israel Aircraft Industries Ltd., Ben-Gurion Airport.
NONLINEAR ANALYSIS USING A MODAL BASED REDUCTION TECHNIQUE
D. Shalev and A. Unger *In* Israel Society of Aeronautics and Astronautics, The 33rd Israel Annual Conference on Aviation and Astronautics 25 Feb. 1993 p 493-501 (For primary document see N94-24241 06-01)
Copyright Avail: Issuing Activity (Israel Society of Aeronautics and Astronautics, c/o Faculty of Engineering, Tel-Aviv Univ., Ramat Aviv 69978, Israel)

N94-24289 Ottawa Univ. (Ontario). Faculty of Engineering.
ON THE DEFORMATION KINETICS CONSTITUTIVE LAW OF PLASTIC DEFORMATION: THE RATE EQUATION
A. S. Krausz and K. Krausz *In* Israel Society of Aeronautics and Astronautics, The 33rd Israel Annual Conference on Aviation and Astronautics 25 Feb. 1993 p 502-510 Sponsored by Natural Sciences and Engineering Research Council of Canada (For primary document see N94-24241 06-01)
Copyright Avail: Issuing Activity (Israel Society of Aeronautics and Astronautics, c/o Faculty of Engineering, Tel-Aviv Univ., Ramat Aviv 69978, Israel)

N94-24418*# Alabama A & M Univ., Huntsville. Dept. of Civil Engineering.
A STUDY OF THE CORE MODULE SIMULATOR FLOOR CAPABILITY
James W. Foreman *In* Alabama Univ., The 1993 NASA/ASEE Summer Faculty Fellowship Program Nov. 1993 4 p (For primary document see N94-24405 06-80)
Avail: CASI HC A01/MF A03

N94-24429*# Alabama Univ., Huntsville. Dept. of Mathematical Sciences.

J-INTEGRAL PATCH FOR FINITE ELEMENT ANALYSIS OF DYNAMIC FRACTURE DUE TO IMPACT OF PRESSURE VESSELS

Boris I. Kunin *In its* The 1993 NASA/ASEE Summer Faculty Fellowship Program Nov. 1993 5 p (For primary document see N94-24405 06-80)
Avail: CASI HC A01/MF A03

42 GEOSCIENCES (GENERAL)

N94-24800*# National Aeronautics and Space Administration. Goddard Inst. for Space Studies, New York, NY.

RICE CULTIVATION AND METHANE EMISSION: DOCUMENTATION OF DISTRIBUTED GEOGRAPHIC DATA SETS

Elaine Matthews (Hughes STX, Inc., Greenbelt, MD.), Jasmin John (Columbia Univ., New York, NY.), and Inez Fung Jan. 1994 26 p
(NASA-TM-104595; Rept-94B00030; NAS 1.15:104595) Avail: CASI HC A03/MF A01

High-resolution global data bases on the geographic and seasonal distribution of rice cultivation and associated methane emission, compiled by Matthews et al., were archived for public use. In addition to the primary data sets identifying location, seasonality, and methane emission from rice cultivation, a series of supporting data sets is included, allowing users not only to replicate the work of Matthews et al. but to investigate alternative cultivation and emission scenarios. The suite of databases provided, at 1 latitude by 1 longitude resolution for the globe, includes (1) locations of rice cultivation, (2) monthly arrays of actively growing rice areas, (3) countries and political subdivisions, and (4) monthly arrays of methane emission from rice cultivation. Ancillary data include (1) a listing, by country, of harvested rice areas and seasonal distribution of crop cycles and (2) country names and codes. Summary tables of zonal/monthly distributions of actively growing rice areas and of methane emissions are presented. Users should consult original publications for complete discussion of the data bases. This short paper is designed only to document formats of the distributed information and briefly describe the contents of the data sets and their initial application to evaluating the role of rice cultivation in the methane budget. Author (revised)

43 EARTH RESOURCES AND REMOTE SENSING

Includes remote sensing of earth resources by aircraft and spacecraft; photogrammetry; and aerial photography.
For instrumentation see *35 Instrumentation and Photography.*

N94-22896 Physics and Electronics Lab. TNO, The Hague (Netherlands).

EXPERIMENTAL EVALUATION OF CAMOUFLAGE EFFECTIVENESS IN THE THERMAL INFRARED

P. A. M. Jacobs Mar. 1993 29 p Original contains color illustrations
(Contract A90/KL/656)
(FEL-93-A043; TD93-0749; ETN-94-94953) Copyright Avail: TNO Physics and Electronics Laboratory, P.O. Box 96864, 2509 JG The Hague, Netherlands

The experimental quantification of the behavior of the apparent temperature of background elements and potential camouflage measures are discussed. The detectability of a target in the infrared spectral region is determined by differences between the radiative signatures of the target and the local background. This implies that both the temperature difference and the emissivity difference and the distribution of these differences over the target area and the background are of importance. Camouflage measures have to address both issues in order to achieve maximum signature adaptation to the background. Statistical analyses for various camouflage materials in relation to a number of background elements are given. Camouflage effectiveness is expressed in the percentage of time for which the apparent temperature contrast between the camouflage material and a background element is 1 C, 2 C, and 5 C. Analyses are performed for five consecutive weeks of measurements in the spring, the summer, and the winter, using data which were taken during a measurement campaign in 1990. ESA

N94-22961*# National Aeronautics and Space Administration. Hugh L. Dryden Flight Research Facility, Edwards, CA.

A PHOTOGRAMMETRIC SOLUTION TO A PARTICULAR PROBLEM

David R. Hedgley, Jr. and Fanny A. Zuniga Washington Dec. 1993 13 p
(RTOP 505-68-71)
(NASA-TP-3415; H-1888; NAS 1.60:3415) Avail: CASI HC A03/MF A01

A closed-form mathematical solution to the classical photogrammetric problem is presented. Although quite general, the solution is more applicable to problems in which the image-space conjugates are very difficult to match but one of the elements of the pair is not. Additionally, observations are made that should make the solution to the general problem of automatic matching less computationally intensive. This approach was used to analyze flow visualization data for the F-18 High Alpha Research Vehicle. The conditions for this analysis were less than ideal for image-to-object-space transformation. Author

N94-23001# National Oceanic and Atmospheric Administration, Boulder, CO. Wave Propagation Lab.

A FIELD EVALUATION OF REMOTE SENSOR MEASUREMENTS OF WIND, TEMPERATURE, AND MOISTURE FOR ARM INTEGRATED SOUNDING SYSTEM RESEARCH

B. E. Martner, E. R. Westwater, and R. G. Strauch et al 1993 110 p
(Contracts DE-AI06-91RL-12089; DE-AI06-91RL-12090; DE-AI06-91RL-12092)
(DE94-000565; DOE/RL-12089/T2) Avail: CASI HC A06/MF A02

Remote sensing systems were operated in Colorado in February and March 1991 to obtain detailed profiles of the kinematic and thermodynamic structure of the atmosphere for the US Department of Energy's Atmospheric Radiation Measurement (ARM) research program. The instruments included wind profilers, radio acoustic sounding systems (RASS), microwave and infrared radiometers, an infrared spectrometer, ceilometers, radiosondes, surface meteorological stations, and other equipment. A mesoscale data assimilation model will be used to combine the data into dynamically consistent four-dimensional fields as part of an integrated data assimilation sounding system. This report evaluates the performance of the NOAA remote sensors used in the 1991 field data collection. These included five different wind profilers, each equipped with RASS capability for temperature profiling, and microwave radiometers for measurements of path-integrated water vapor and liquid water content. The design and initial testing of a Fourier-transform infrared sounder (FIRS) for humidity profiling is also described. The ranges of height coverage and measurement accuracies for each wind profiler/RASS are examined. Specific recommendations for optimizing the design and configuration of similar instruments are made for the ARM cloud and radiation testbed (CART) sites, based on results of the 1991 field work and earlier tests. Examples of routine processed data products are presented for three intensive operating period studies to further illustrate the remote sensors' capabilities. DOE

N94-23145# Beleidscommissie Remote Sensing, Delft (Netherlands).

VIERS-1, PHASE 3 Final Report

P. Snoeij (Technische Univ., Delft, Netherlands.), E. vanHalsema (Physics and Electronics Lab. TNO, The Hague, Netherlands.), J. Vogelzang (Rijkswaterstaat, Rijswijk, Netherlands.), S. Waas (Heidelberg Univ., Germany.), S. Zecchetto (Consiglio Nazionale delle Ricerche, Venice, Italy.), H. Janssen (Royal Netherlands Meteorological Inst., De Bilt.), W. Oost, B. Jaehne (Scripps Institution of Oceanography, San Diego, CA.), and C. Calkoen (Delft Hydraulics Lab., Netherlands.) Jun. 1993 166 p Sponsored by Beleidscommissie Remote Sensing, Delft, Netherlands and State Baden Wurttemburg, Germany
(Contract ST2J-0451-C(GDF))
(BCRS-92-24; ISBN-9-05-411068-6; ETN-94-95037) Avail: CASI HC A08/MF A02

The third phase of the VIERS (Dutch acronym for preparation and interpretation of ERS-1 data) project, which was aimed at the improvement of wind extraction algorithms by development of a model, based on physics, which describes the end to end process of wind scatterometry, is reported. In order to develop such a model it was essential to gain knowledge on the scattering processes at the water surface. The experiment was carried out in wind/wave tanks (where conditions could be controlled and precisely reproduced) and on an ocean based platform. ESA

N94-23148# Winand Staring Centre, Wageningen (Netherlands). Agricultural Research Dept.
INTEGRATED USE OF HYDROLOGICAL MODELLING AND REMOTE SENSING IN THE PROVINCE OF DRENTHE (THE NETHERLANDS): POSSIBILITIES AND RESTRICTIONS
Sandra M. L. Verheijden 1992 67 p Original contains color illustrations
(Rept-61; ETN-94-95041) Copyright Avail: CASI HC A04/MF A01

For the eastern part of the Province of Drenthe (The Netherlands) an investigation of the possibilities of an integrated use of hydrological modeling and remote sensing was performed. A comparison was made between relative crop transpiration values according to the remote sensing approach and as simulated with the model SWACROP. Great deviations occurred between the relative crop transpiration values calculated with both methods. In contradiction with the expectations a more detailed SWACROP input did not improve the correspondence of SWACROP and remote sensing results. It is expected that the deviations are mainly caused by differences in temporal and spatial scale. Moreover the importance of visual interpretation of remote sensing images has proven to be a valuable tool in the validation of a seepage/infiltration map. ESA

N94-23158# Max-Planck-Inst. fuer Meteorologie, Hamburg (Germany).
MODES OF OCEAN VARIABILITY IN THE TROPICAL PACIFIC AS DERIVED FROM GEOSAT ALTIMETRY
Jiansheng Zou (Hamburg Univ., Germany.) and Mojib Latif Apr. 1993 40 p
(Grant EV5V-CT92-0121)
(MPIM-103; ETN-94-95110) Avail: CASI HC A03/MF A01

Satellite derived (Geosat) sea surface height anomalies for the period Nov. 1986 - Aug. 1989 were investigated in order to extract the dominant modes of climate variability in the tropical Pacific. Four modes are identified by applying the principle oscillation patterns (POP) technique. The first mode has a time scale of about three months and can be identified with the first baroclinic equatorial Kelvin wave mode. The second mode has a time scale of about six months and describes the semi-annual cycle in tropical Pacific sea level. Equatorial wave propagation is also crucial for this mode. The third mode is the annual cycle which is dominated by Ekman dynamics. Wave propagation or reflection are found to be unimportant. The fourth mode is associated with the El Nino/southern oscillation (ENSO) phenomenon. The ENSO mode is found to be consistent with the 'delayed action oscillator' scenario. The results are substantiated by a companion analysis of the sea surface height variability simulated with an oceanic general circulation model (OGCM) forced by observed wind stresses for the period 1961-1989. The modal decomposition of the sea level variability is found to be similar to that derived from the Geosat data. The high consistency between the satellite and the model data indicates the high potential value of satellite altimetry for climate modeling and forecasting. ESA

N94-23177# Beleidscommissie Remote Sensing, Delft (Netherlands).
OPTICAL COMPONENT MAC EUROPE GROUND TRUTH REPORT: FLEVOLAND 1991 (NETHERLANDS)
C. Bueker (Wageningen Agricultural Univ., Netherlands.), J. G. P. W. Clevers (Wageningen Agricultural Univ., Netherlands.), H. J. C. vanLeeuwen (Wageningen Agricultural Univ., Netherlands.), B. A. M. Bouman (Centre for Agrobiological Research, Wageningen, Netherlands.), and D. Uenk (Centre for Agrobiological Research, Wageningen, Netherlands.) Jun. 1993 62 p
(BCRS-92-27; ISBN-9-05-411072-4; ETN-94-95039) Avail: CASI HC A04/MF A01

Part of a European remote sensing campaign which took place in Flevoland (Netherlands) is addressed. Within the framework of this campaign (MAC Europe), a DC8 aircraft carrying the three frequency (C, L and P band), full polarimetric Synthetic Aperture Radar (SAR), and an ER 2 aircraft carrying the Airborne Visible Infrared Imaging Spectrometer (AVIRIS) and the thematic mapper simulator were deployed. In addition, three CCD (Charge Coupled Device) Airborne Experimental Scanner for Application in Remote sensing (CAESAR) flights were performed in dual look mode. Also, three missions with multispectral aerial photography were performed. A detailed description of the ground truth on agricultural crops collected during the growing season of 1991 is given. A description of the test site and the farming practice of the main crops is given and the growth of selected crops, field reflectance spectra, single leaf reflectance and transmittance spectra, are described. Stereo photographs of single plants were taken. Meteorological data of the test site were provided. The leaf area index of the selected crops was ascertained from reflectance measurements. A preliminary analysis of the radiometric ground truth data is presented. ESA

N94-23224# Helsinki Univ. of Technology, Espoo (Finland). Lab. of Space Technology.
APPLICATION OF ERS-1 ACTIVE MICROWAVE INSTRUMENTATION DATA TO REMOTE SENSING OF SNOW
M. Hallikainen, V. Jaeaeskelaeinen, T. Haeme (Technical Research Centre of Finland, Espoo.), and J. Peraelae (National Board of Waters and the Environment, Helsinki, Finland.) Aug. 1992 35 p
(PB93-224756; Rept-6) Avail: CASI HC A03/MF A01

Two test sites will be used to study the feasibility of the ERS-1 SAR and Wind Scatterometer for remote sensing of snow. Especially, the effect of vegetation to snow mapping is investigated. The test site in northern Finland consists of both sparsely forested areas and open areas (bogs, lakes, and clear-cut areas). The test site in North America consists mainly of agricultural prairies with lakes and some forested areas. The research plan of Finnish national ERS-1 snow program is presented. The first part includes the development of measurement and data processing techniques and preparations for the airborne measurement campaigns. In the second part satellite data, airborne data and surface data on the test site will be acquired. In the last part the capability of ERS-1 to map snow-covered ground and melting snow will be analyzed. Also, the usefulness of complementing SAR data with other types of satellite data will be examined. NTIS

N94-23492# Edgerton, Germeshausen and Grier, Inc., Idaho Falls, ID.
IMAGING SYSTEM (INEL) T805 PROTOTYPE Status Report
J. K. Partin, G. D. Lassahn, and J. R. Davidson Mar. 1993 83 p
(Contract DE-AC07-76ID-01570)
(DE94-002807; EGG-EE-10723) Avail: CASI HC A05/MF A01 (US Sales Only)

This report describes an automatic target recognition (ATR) system developed for use with the airborne multisensor pod system. This ATR system is useful for finding pre-selected objects in a scene, given several different types of images of the scene. This ATR system includes image data fusion and uncertainty estimation. DOE

N94-23494# Lawrence Livermore National Lab., CA.
REMOTE SENSING, IMAGING, AND SIGNAL ENGINEERING
J. M. Brase Mar. 1993 33 p
(Contract W-7405-eng-48)
(DE94-003021; UCID-ID-112778) Avail: CASI HC A03/MF A01

This report discusses the remote sensing, imaging, and signal engineering (RISE) thrust area which has been very active in working to define new directions. Signal and image processing have always been important support for existing programs at Lawrence Livermore National Laboratory (LLNL), but now these technologies are becoming central to the formation of new programs. Exciting new applications such as high resolution telescopes, radar remote sensing, and advanced medical imaging are allowing us to participate in the development of new programs. DOE

N94-23573*# Kansas Univ., Lawrence. Radar Systems and Remote Sensing Lab.
SYNTHESIS OF PASSIVE MICROWAVE AND RADAR ALTIMETER DATA FOR ESTIMATING ACCUMULATION RATES OF POLAR SNOW
Curt H. Davis [1993] 6 p
(Grant NAGw-3346)
(NASA-CR-194864; NAS 1.26:194864) Avail: CASI HC A02/MF A01

In this paper, we compare dry-snow extinction coefficients derived from radar altimeter data with brightness temperature data from passive microwave measurements over a portion of the East Antarctic plateau. The comparison between the extinction coefficients and the brightness temperatures shows a strong negative correlation, where the correlation coefficients ranged from -0.87 to -0.95. The extinction coefficient of the dry polar snow decreases with increasing surface elevation, while the average brightness temperature increases with surface elevation. Our analysis shows that the observed trends are related to geographic variations in scattering coefficient of snow, which in turn are controlled by variations in surface temperature and snow accumulation rate. By combining information present in the extinction coefficient and brightness temperature data sets, we develop a model that can be used to obtain quantitative estimates of the accumulation rate of dry polar snow. Author

N94-23595*# National Aeronautics and Space Administration. Goddard Space Flight Center, Greenbelt, MD.

THE FIFTH CALIBRATION/DATA PRODUCT VALIDATION PANEL MEETING

1992 485 p Meeting held in Boulder, CO, 7-10 Apr. 1992
(NASA-TM-108270; NAS 1.15:108270) Avail: CASI HC A21/MF A04

The minutes and associated documents prepared from presentations and meetings at the Fifth Calibration/Data Product Validation Panel meeting in Boulder, Colorado, April 8 - 10, 1992, are presented. Key issues include (1) statistical characterization of data sets: finding statistics that characterize key attributes of the data sets, and defining ways to characterize the comparisons among data sets; (2) selection of specific intercomparison exercises: selecting characteristic spatial and temporal regions for intercomparisons, and impact of validation exercises on the logistics of current and planned field campaigns and model runs; and (3) preparation of data sets for intercomparisons: characterization of assumptions, transportable data formats, labeling data files, content of data sets, and data storage and distribution (EOSDIS interface). For individual titles, see N94-23596 through N94-23617.

N94-23596*# Science Applications International Corp., Glendora, CA. Space Technology Div.

THE POSSIBLE EFFECTS OF THE NATURAL AND INDUCED SPACE ENVIRONMENT ON THE OPTICAL AND THERMAL PROPERTIES OF EOS SURFACES c18

Carl R. Maag and Richard A. Heppner (Perkin-Elmer Corp., Pomona, CA.) *In* NASA. Goddard Space Flight Center, The Fifth Calibration/Data Product Validation Panel Meeting 1992 11 p (For primary document see N94-23595 06-43)
Avail: CASI HC A03/MF A04

Space missions, including that of EOS (Earth Observing System), will continue to be subjected to both the natural and induced space environment. The concerns associated with this fact will not go away. The NASA and DoD have recognized the need for long-life stability of materials and structures to the space environment. The major areas of interest include: thermal cycling, UV degradation, space radiation exposure, orbital debris, atomic oxygen erosion, and contamination control. Having flown a number of space environmental effects monitors, SAIC has developed both a data base to understand the magnitude of this problem and mitigation techniques to reduce the impact. Derived from text

N94-23597*# National Aeronautics and Space Administration. Goddard Space Flight Center, Greenbelt, MD.

SPDB (SCIENCE PROCESSING DATABASE): QUICK REFERENCE GUIDE c82

In its The Fifth Calibration/Data Product Validation Panel Meeting 1992 2 p (For primary document see N94-23595 06-43)
Avail: CASI HC A01/MF A04

This contents of this draft copy include: how to log into the SPDB (Science Processing DataBase); how to navigate through menus; how to use ESC keys; how to get help; and how to quit the program. The Science Processing Database is an interactive, on-line system that provides updated information about Earth Observing System Project, including instruments, investigators, output data products, input requirements, retrieval algorithms, and VO datasets archived at DAAC's. Derived from text

N94-23598*# Jet Propulsion Lab., California Inst. of Tech., Pasadena.

DEFINITIONS IN USE BY THE VISIBLE AND NEAR-INFRARED, AND THERMAL WORKING GROUPS

Carol J. Bruegge, Ed Miller, Bob Martin, Hugh H. Kieffer (Geological Survey, Flagstaff, AZ.), and James M. Palmer (Arizona Univ., Tucson.) *In* NASA. Goddard Space Flight Center, The Fifth Calibration/Data Product Validation Panel Meeting 1992 14 p (For primary document see N94-23595 06-43)
Avail: CASI HC A03/MF A04

The Calibration Advisory Panel (CAP) is composed of calibration experts from each of the Earth Observing System (EOS) instruments, science investigation, and cross-calibration teams. These members come from a variety of institutions and backgrounds. In order to facilitate an exchange of ideas, and assure a common basis for communication, it was desirable to assemble this list of definitions. These definitions were developed for use by the visible and near-infrared working group, and the thermal infrared working group. Where necessary or appropriate, deviations from these for specific instruments or other sensor types are given in the individual calibration plans. The definitions contained in this document are derived, wherever possible, from definitions accepted by international and national metrological commissions including the United States National Institute of Standards and Technology (NIST), the International Bureau of Weights and Measures (BIPM), the International Electrotechnical Commission (IEC), the International Organization for Standardization (ISO), and the International Organization of Legal Metrology (OIML). Derived from text

N94-23599*# Jet Propulsion Lab., California Inst. of Tech., Pasadena.

CROSS-CALIBRATION SURVEY (VISNIR)

Carol J. Bruegge *In* NASA. Goddard Space Flight Center, The Fifth Calibration/Data Product Validation Panel Meeting 1992 10 p (For primary document see N94-23595 06-43)
Avail: CASI HC A02/MF A04

Included in the summary of the VISNIR survey is (1) a statement of the preferred cross-calibration approach, as endorsed by select members of the VISNIR group, (2) two viewgraphs which summarize the wavelength and fields-of-view of the various instruments, and (3) a listing of these same data, as given by the respective calibration representatives in the survey responses. The Earth Observing System (EOS) Project is fundamentally committed to the acquisition of data which can be reduced to geophysical data products of high and known accuracy. One possible method of insuring the primary data products are of known accuracy is to use the instruments themselves against the same sources to provide an independent check that a common understanding of accuracy exists. The goal then of the radiometric 'Cross-Calibration' at the integrator facility (GE) would be to convincingly establish as late as feasible in the Integration and Test (I&T) cycle that, when stimulated with common sources, the appropriate EOS instrument measurements agree within their previously established accuracy estimates across a useful radiance range, accounting for the additional uncertainty associated with the unique properties of the test set-up itself. Derived from text

N94-23600*# National Aeronautics and Space Administration. Goddard Space Flight Center, Greenbelt, MD.

MODIS CALIBRATION Status Report

John L. Barker *In its* The Fifth Calibration/Data Product Validation Panel Meeting 1992 32 p (For primary document see N94-23595 06-43)
Avail: CASI HC A03/MF A04

The MODIS/MCST (MODIS Characterization Support Team) Status Report contains an outline of the calibration strategy, handbook, and plan. It also contains an outline of the MODIS/MCST action item from the 4th EOS Cal/Val Meeting, for which the objective was to locate potential MODIS calibration targets on the Earth's surface that are radiometrically homogeneous on a scale of 3 by 3 Km. As appendices, draft copies of the handbook table of contents, calibration plan table of contents, and detailed agenda for MODIS calibration working group are included. Derived from text

N94-23601*# Arizona Univ., Tucson. Remote Sensing Group.

EOS CROSS-CALIBRATION RADIOMETERS

Stuart F. Biggar *In* NASA. Goddard Space Flight Center, The Fifth Calibration/Data Product Validation Panel Meeting 1992 27 p (For primary document see N94-23595 06-43)
Avail: CASI HC A03/MF A04

Viewgraphs are presented on the philosophy, spectral coverage and specific design of EOS radiometers. Derived from text

N94-23602*# National Aeronautics and Space Administration. Langley Research Center, Hampton, VA.

FLIGHT SOLAR CALIBRATIONS USING THE MIRROR ATTENUATOR MOSAIC (MAM): LOW SCATTERING MIRROR

Robert B. Lee, III *In* NASA. Goddard Space Flight Center, The Fifth Calibration/Data Product Validation Panel Meeting 1992 15 p Repr. from Calibration of Passive Remote Observing Optical and Microwave Instrumentation (Bellingham, WA, SPIE), v. 1943, 1991 p 267-280 (For primary document see N94-23595 06-43)

Avail: CASI HC A03/MF A04

Measurements of solar radiances reflected from the mirror attenuator mosaic (MAM) were used to calibrate the shortwave portions of the Earth Radiation Budget Experiment (ERBE) thermistor bolometer scanning radiometers. The MAM is basically a low scattering mirror which has been used to attenuate and reflect solar radiation into the fields of view for the broadband shortwave (0.2 to 5 micrometers) and total (0.2 to 50.0+ micrometers) ERBE scanning radiometers. The MAM assembly consists of a tightly packed array of aluminum, 0.3175-cm diameter concave spherical mirrors and field of view limiting baffles. The spherical mirrors are masked by a copper plate, electro-plated with black chrome. Perforations (0.14 centimeter in diameter) in the copper plate serve as apertures for the mirrors. Black anodized aluminum baffles limit the MAM clear field of view to 7.1 degrees. The MAM assemblies are located on the Earth Radiation Budget Satellite (ERBS) and on the National Oceanic and Atmospheric Administration NOAA-9 and NOAA-10 spacecraft. The 1984-1985 ERBS and 1985-1986 NOAA-9 solar calibration datasets are presented. Analyses of the calibrations indicate that the MAM exhibited no detectable degradation in its reflectance properties and that the gains of the shortwave scanners did not change. The stability of the shortwave radiometers indicates that the transmission of the Suprasil W1 filters did not degrade detectably when exposed to Earth/atmosphere-reflected solar radiation. Author

N94-23603*# TOVS Pathfinder Scientific Working Group.

TOVS PATHFINDER PRODUCT VALIDATION AND INTERCOMPARISON Final Report

In NASA. Goddard Space Flight Center, The Fifth Calibration/Data Product Validation Panel Meeting 1992 6 p (For primary document see N94-23595 06-43)

Avail: CASI HC A02/MF A04

Validation and intercomparison is an essential part of the Pathfinder program. Since its organization within the International TOVS Working Group, the TOVS community has continuously emphasized this aspect of the product retrieval problem. In the previous sections of this report, the TOVS Pathfinder SWG has recommended a careful and coherent reorganization and archiving of TOVS radiance data, and three distinct pathways for deriving product variables from this TOVS radiance archive. The importance in taking this multiple path approach to creating climate datasets rests in our firm belief that there is now global 'absolute truth' data for any of the derived physical parameters. Each of the selected methods is based upon a different set of assumptions. The challenge in interpreting Pathfinder data is to determine what alterations in the physical attributes of the environment contribute to evidence of global change extracted from observed or derived Pathfinder datasets. The Pathfinder validation and intercomparison activity must include validation of the forward problem, by which one calculates an estimate of upwelling radiance information from given earth and atmospheric data, and validation of the inverse problem, by which one calculates estimates of earth and atmospheric information from given upwelling satellite spectral radiance data. Derived from text

N94-23604*# National Oceanic and Atmospheric Administration, Boulder, CO. Climate Monitoring and Diagnostics Lab.

EVALUATING NOAA SATELLITE PRODUCTS FOR GLOBAL CLIMATE MONITORING

John J. Bates *In* NASA. Goddard Space Flight Center, The Fifth Calibration/Data Product Validation Panel Meeting 1992 38 p (For primary document see N94-23595 06-43)

Avail: CASI HC A03/MF A04

The topics covered include validation criteria for satellite products, long-term global validation examples, and lessons of history -- applications to the EOS era. Derived from text

N94-23605*# National Inst. of Standards and Technology, Gaithersburg, MD.

[ACTIVITIES OF NIST (NATIONAL INST. OF STANDARDS AND TECHNOLOGY)]

In NASA. Goddard Space Flight Center, The Fifth Calibration/Data Product Validation Panel Meeting 1992 14 p (For primary document see N94-23595 06-43)

Avail: CASI HC A03/MF A04

The Radiometric Physics Division of the NIST is responsible for the national standards in radiation thermometry, spectroradiometry, photometry, and spectrophotometry; dissemination of these standards by providing measurement services to customers requiring calibrations of the highest accuracy; and conducting fundamental and applied research to develop the scientific basis for future measurement services. Its relevance to EOS/TIR calibration includes calibrating unknown blackbody for radiance using a well-characterized NIST blackbody source by matching the radiant fluxes with an IR radiometer. The TIR Round Robin is used to verify the calibration of the sources that are used for the absolute radiometric calibration of the individual EOS sensors. Derived from text

N94-23606*# Jet Propulsion Lab., California Inst. of Tech., Pasadena.

DIFFUSE PANEL STUDIES: CONCLUSIONS Quarterly Report

In NASA. Goddard Space Flight Center, The Fifth Calibration/Data Product Validation Panel Meeting 1992 12 p (For primary document see N94-23595 06-43)

Avail: CASI HC A03/MF A04

In the evaluation of new candidate materials for flight applications, considerations are given to: optical performance (lambertian, spatially and spectrally uniform, high reflectance); static charge build-up; environmental stability (ruggedness, UV exposure, particle bambardment, etc.); and fabricability. ITO coated Spectralon appears to have produced a conductive material. Many other design issues remain. Author

N94-23607*# Utah State Univ., Logan. Space Dynamics Lab.

CALIBRATION OF A HELIUM-COOLED INFRARED SPATIAL RADIOMETER AND GRATING SPECTROMETER

Larry Jacobsen, Steve Sargent, Clair L. Wyatt, and Allan J. Steed *In* NASA. Goddard Space Flight Center, The Fifth Calibration/Data Product Validation Panel Meeting 1992 11 p Repr. from Cryogenic Optical Systems and Instruments 4 (SPIE), v. 1340, 1990 p 217-227 Previously announced in IAA as A92-22870 (For primary document see N94-23595 06-43)

Avail: CASI HC A03/MF A04

Methods used by the Space Dynamics Laboratory of Utah State University (SDL/USU) to calibrate infrared sensors are described, using the Infrared Background Signature Survey (IBSS) spatial radiometer and grating spectrometer as examples. A calibration equation and a radiometric model are given for each sensor to describe their responsivity in terms of individual radiometric parameters. The calibration equation terms include dark offset, linearity, absolute responsivity, and measurement uncertainty, and the radiometric model domains include spatial, spectral, and temporal domains. A portable calibration facility, designed and fabricated by SDL/USU, provided collimated, extended, diffuse scatter, and Jones sources in a single cryogenic dewar. This multi-function calibrator allowed calibration personnel to complete a full calibration of the IBSS infrared radiometer and spectrometer in two 15-day periods. A calibration data system was developed to control and monitor the calibration facility, and to record and analyze sensor data. Author

N94-23608*# Utah State Univ., Logan. Space Dynamics Lab.

INFRARED CALIBRATION

Larry Jacobsen *In* NASA. Goddard Space Flight Center, The Fifth Calibration/Data Product Validation Panel Meeting 1992 18 p (For primary document see N94-23595 06-43)

Avail: CASI HC A03/MF A04

Recent calibration efforts at the Space Dynamics Laboratory/Utah State University (SDL/USU) are outlined. CASI

N94-23609*# National Research Lab. of Metrology, Tokyo (Japan).

CONCEPT OF ASTER CALIBRATION REQUIREMENT

A. Ono *In* NASA. Goddard Space Flight Center, The Fifth Calibration/Data

Product Validation Panel Meeting 1992 18 p (For primary document see N94-23595 06-43)
Avail: CASI HC A03/MF A04

The document of ASTER Calibration Requirement specifies the following items related to spectral and radiometric characteristics of the ASTER instrument: (1) characteristics whose knowledge is specified, (2) requirement for knowledge of the characteristics, (3) methodology for characteristics evaluation, and (4) supplementary information and data related with characteristics evaluation. This document is applicable to the document of the ASTER Instrument Specification on Observational Performances, and will be a part of the ASTER Calibration Plan. ASTER Calibration Requirement is scheduled to establish the concept and framework by March 1992 when the 5th Calibration and Data Validation Panel Meeting is held, and to determine details including requirement values and evaluation methodologies by October 1992 around which the Calibration Peer Review may be held. The ASTER Calibration Plan is planned to finish by the same time.
Author

N94-23610*# National Research Lab. of Metrology, Tokyo (Japan).
VNIR AND SWIR TRANSFER RADIOMETERS DEVELOPED AT NRLM FOR PREFLIGHT LABORATORY CROSS-CALIBRATION
A. Ono *In* NASA. Goddard Space Flight Center, The Fifth Calibration/Data Product Validation Panel Meeting 1992 28 p (For primary document see N94-23595 06-43)
Avail: CASI HC A03/MF A04

One purpose of preflight laboratory cross-calibration is to avoid the incorrect setting of instrument dynamic range due to calibration mistakes at individual instrument manufacturers. A second purpose is to make corrections of instrument responsivities to have consistent radiance scales among instruments. A third reason is to clarify the state of the art in the absolute responsivity determination of VIS/NIR and SWIF instruments in the EOS era. And fourth is the purpose of improving the preflight calibration accuracy if necessary to meet the EOS requirement. Derived from text

N94-23611*# Geological Survey of Japan, Ibaraki. Advanced Spaceborne Thermal Emission and Reflection Radiometer Team.
IN-FLIGHT CROSS-CALIBRATION OF ASTER/TIR AND MODIS-N
Yasushi Yamaguchi *In* NASA. Goddard Space Flight Center, The Fifth Calibration/Data Product Validation Panel Meeting 1992 8 p (For primary document see N94-23595 06-43)
Avail: CASI HC A02/MF A04

The purpose of the in-flight cross-calibration of ASTER/TIR and MODIS-N is to improve absolute radiometric (temperature) accuracy of ASTER/TIR (particularly in the low temperature region). Derived from text

N94-23612*# Fujitsu Ltd., Kawasaki (Japan).
ASTER TIR SUBSYSTEM AND CALIBRATION
Hirokazu Ohmae *In* NASA. Goddard Space Flight Center, The Fifth Calibration/Data Product Validation Panel Meeting 1992 24 p (For primary document see N94-23595 06-43)
Avail: CASI HC A03/MF A04

Viewgraphs are given on the purpose of TIR, major functions, characteristics and design of various components, and calibration. The major functions are to acquire image data on the earth's surface in thermal infrared wavelength band, using mercury cadmium telluride (HgCdTe) detectors; to convert the obtained image data into the digital data to meet the Common Signal Processor (CSP) interface, and output the signals; pointing function in cross-track direction to get the wide swath of 232 km; and to calibrate the whole TIR with the blackbody on orbit, then the amplifier and subsequent transmission units are calibrated electrically.
Derived from text

N94-23613*# Colorado Univ., Boulder. Operations and Information Systems Group.
OASIS-CC PRESENTATION
In NASA. Goddard Space Flight Center, The Fifth Calibration/Data Product Validation Panel Meeting 1992 15 p (For primary document see N94-23595 06-43)
Avail: CASI HC A03/MF A04

The Operations and Science Instrument Support (OASIS) project is a long-term effort to help produce operations capabilities that can support space science missions of the next century. Portions of the OASIS concept in software have been implemented under the general name OASIS-R/T. OASIS-CC is the OASIS Command and Control, for monitoring and controlling science instruments and spacecraft during test, integration, launch and on-orbit operations. Viewgraphs are presented on the OASIS-CC functionality description, OASIS-CC support, and OASIS-CC as a tool.
Derived from text

N94-23614*# Jet Propulsion Lab., California Inst. of Tech., Pasadena.
GEWEX
In NASA. Goddard Space Flight Center, The Fifth Calibration/Data Product Validation Panel Meeting 1992 18 p (For primary document see N94-23595 06-43)
Avail: CASI HC A03/MF A04

The GEWEX (Global Energy and Water cycle EXperiment) objectives are as follows: to determine the hydrologic cycle and energy fluxes by means of global measurements of observable atmospheric and surface properties; to model the global hydrologic cycle and its effects on the atmosphere and oceans; to foster the development of observing techniques and data management and assimilation systems; and to develop the ability to predict the variations of global and regional hydrologic processes and water resources, and their response to environmental change.
Derived from text

N94-23615*# Jet Propulsion Lab., California Inst. of Tech., Pasadena.
VALIDATING A LARGE GEOPHYSICAL DATA SET: EXPERIENCES WITH SATELLITE-DERIVED CLOUD PARAMETERS
Ralph Kahn, Robert D. Haskins, James E. Knighton, Andrew Pursch, and Stephanie Granger-Gallegos *In* NASA. Goddard Space Flight Center, The Fifth Calibration/Data Product Validation Panel Meeting 1992 8 p Sponsored by NASA, Washington (For primary document see N94-23595 06-43)
Avail: CASI HC A02/MF A04

We are validating the global cloud parameters derived from the satellite-borne HIRS2 and MSU atmospheric sounding instrument measurements, and are using the analysis of these data as one prototype for studying large geophysical data sets in general. The HIRS2/MSU data set contains a total of 40 physical parameters, filling 25 MB/day; raw HIRS2/MSU data are available for a period exceeding 10 years. Validation involves developing a quantitative sense for the physical meaning of the derived parameters over the range of environmental conditions sampled. This is accomplished by comparing the spatial and temporal distributions of the derived quantities with similar measurements made using other techniques, and with model results. The data handling needed for this work is possible only with the help of a suite of interactive graphical and numerical analysis tools. Level 3 (gridded) data is the common form in which large data sets of this type are distributed for scientific analysis. We find that Level 3 data is inadequate for the data comparisons required for validation. Level 2 data (individual measurements in geophysical units) is needed. A sampling problem arises when individual measurements, which are not uniformly distributed in space or time, are used for the comparisons. Standard 'interpolation' methods involve fitting the measurements for each data set to surfaces, which are then compared. We are experimenting with formal criteria for selecting geographical regions, based upon the spatial frequency and variability of measurements, that allow us to quantify the uncertainty due to sampling. As part of this project, we are also dealing with ways to keep track of constraints placed on the output by assumptions made in the computer code. The need to work with Level 2 data introduces a number of other data handling issues, such as accessing data files across machine types, meeting large data storage requirements, accessing other validated data sets, processing speed and throughput for interactive graphical work, and problems relating to graphical interfaces. Author

N94-23616*# National Aeronautics and Space Administration. Goddard Space Flight Center, Greenbelt, MD.
EXPERIENCE OF THE JPL EXPLORATORY DATA ANALYSIS TEAM AT VALIDATING HIRS2/MSU CLOUD PARAMETERS
Ralph Kahn (Jet Propulsion Lab., California Inst. of Tech., Pasadena.), Robert D. Haskins (Jet Propulsion Lab., California Inst. of Tech., Pasadena.), Stephanie Granger-Gallegos (Jet Propulsion Lab., California Inst. of Tech., Pasadena.), Andrew Pursch (Jet Propulsion Lab., California Inst. of Tech., Pasadena.), and Anthony DelGenio *In its* The Fifth Calibration/Data

Product Validation Panel Meeting 1992 28 p (For primary document see N94-23595 06-43)
Avail: CASI HC A03/MF A04

Validation of the HIRS2/MSU cloud parameters began with the cloud/climate feedback problem. The derived effective cloud amount is less sensitive to surface temperature for higher clouds. This occurs because as the cloud elevation increases, the difference between surface temperature and cloud temperature increases, so only a small change in cloud amount is needed to effect a large change in radiance at the detector. By validating the cloud parameters it is meant 'developing a quantitative sense for the physical meaning of the measured parameters', by: (1) identifying the assumptions involved in deriving parameters from the measured radiances, (2) testing the input data and derived parameters for statistical error, sensitivity, and internal consistency, and (3) comparing with similar parameters obtained from other sources using other techniques.
Derived from text

N94-23617*# National Aeronautics and Space Administration. Goddard Space Flight Center, Greenbelt, MD.

AN OVERVIEW OF THE UARS DATA VALIDATION EFFORT

In its The Fifth Calibration/Data Product Validation Panel Meeting 1992 22 p (For primary document see N94-23595 06-43)
Avail: CASI HC A03/MF A04

An overview is given of the Upper Atmosphere Research Satellite (UARS) data validation effort. An introduction to UARS is outlined as is the UARS validation chronology.
CASI

N94-23734# Wageningen Agricultural Univ. (Netherlands). Dept. of Water Resources.

METHODOLOGY FOR THE ASSESSMENT OF SURFACE RESISTANCE AND SOIL WATER STORAGE VARIABILITY AT MESOSCALE BASED ON REMOTE SENSING MEASUREMENTS. A CASE STUDY WITH HAPEX-EFEDA DATA. UNESCO-INTERNATIONAL HYDROLOGICAL PROGRAM 4

W. G. M. Bastiaanssen (Winand Staring Centre, Wageningen, Netherlands.), D. H. Hoekman, and R. A. Roebeling (Winand Staring Centre, Wageningen, Netherlands.) Jul. 1993 78 p
(PB94-111721; Rept-38) Avail: CASI HC A05/MF A01

A new remote sensing algorithm has been tested with normalized difference vegetation index, surface albedo, and surface temperature data obtained during the Thematic Mapper simulator flight in the HAPEX-EFEDA field experiment (Hydrological and Atmospheric Pilot Experiment-Echival Field Experiment in a Desertification Threatened Area). Its high spatial resolution allowed for a comparison of its results with soil moisture obtained from the moisture monitoring network. The microwave backscatter coefficient derived from AIRSAR data provided a possibility to compare the evaporation and topsoil moisture content. Having the surface energy balance instantaneously quantified in a distributed manner, it was finally possible to inversely derive the surface resistance to evaporation from the latent heat flux and to study the non-linear relationship between surface resistance and soil water content at mesoscale for the Mediterranean climate present in Spain.
NTIS

N94-23755 Wageningen Agricultural Univ. (Netherlands). Dept. of Water Resources.

GROUNDTRUTH COLLECTION FOR THE JPL-SAR AND ERS-1 CAMPAIGN IN FLEVOLAND AND VELUWE, NETHERLANDS, 1991

M. A. M. Vissers and J. J. vanderSanden 1992 72 p Limited Reproducibility: More than 20% of this document may be affected by microfiche quality
(PB93-230654; Rept-31) Copyright Avail: CASI HC A04

Ground data was collected for soil and vegetation in agricultural areas comprising crops (Flevoland) and grasslands (Veluwe). Forest data was collected in selected study stands in the Horsterwold and Speulderbos. A database will be established suitable for the study of land use and soil moisture mapping.
NTIS

N94-23779# Brookhaven National Lab., Upton, NY.

CLOUD-FREE AEROSOL OPTICAL DEPTH DETERMINATION OVER OCEANS FROM SATELLITE RADIOMETRY

R. Wagener, S. Nemesure, C. M. Benkovitz, S. E. Schwartz, C. M. Berkowitz (Battelle Pacific Northwest Labs., Richland, WA.), and S. J. Ghan (Battelle Pacific Northwest Labs., Richland, WA.) Jun. 1993 8 p Presented at the 74th American Meteorological Society Annual Meeting, Nashville, TN, 23-28 Jan. 1994
(Contracts DE-AC02-76CH-00016; DE-AC06-76RL-01830)
(DE94-001897; BNL-49530; CONF-940115-7) Avail: CASI HC A02/MF A01

Shortwave radiative forcing of climate by anthropogenic sulfate aerosol has been estimated to be of comparable global-average magnitude, but opposite sign, to longwave forcing by greenhouse gases. It is therefore important that this forcing be accurately represented in climate models. Sulfate concentrations calculated by a global chemistry model driven by operational meteorological data exhibit high spatial and temporal variations that closely reproduce observations at continental sites. However, because of the sparsity of sulfate concentration measurements over oceans, aerosol optical depth determinations from satellite data are needed to evaluate the performance of the model over oceans. Previous studies of aerosol optical depths over oceans have employed advanced very high resolution radiometer global area coverage (AVHRR GAC) data that should yield the required information, but the emphasis in these studies has been to produce wide spatial coverage by time averaging for periods of a week to a month, thereby masking the high spatial and temporal variability associated with the data and required for model evaluation. The Rao et al. method is employed in the production of the weekly composite aerosol maps by NOAA since June 1987. The authors report results obtained with a modified Durkee algorithm that provides instantaneous optical depths averaged over individual GChM model grid cells (1.125 degrees x 1.125 degrees) for comparison with optical depths predicted by the chemistry model at the same times and places. The optical depth retrieval is improved by a more accurate removal of sun-glint contamination, using the formulation of Cox and Munk for sun-glint probability as a function of wind speed, together with the wind speeds available from the operational meteorological data used to drive the chemistry model.
DOE

N94-24060*# Kansas Univ., Lawrence. Radar and Remote Sensing Lab.

THE EFFECT OF SUB-SURFACE VOLUME SCATTERING ON THE ACCURACY OF ICE-SHEET ALTIMETER RETRACKING ALGORITHMS

Curt H. Davis [1993] 5 p
(Grant NAGw-3346)
(NASA-CR-194825; NAS 1.26:194825) Avail: CASI HC A01/MF A01

The NASA and ESA retracking algorithms are compared with an algorithm based upon a combined surface and volume (S/V) scattering model. First, the S/V, NASA, and ESA algorithms were used to retrack over 400,000 altimeter return waveforms from the Greenland and Antarctic ice sheets. The surface elevations from the S/V algorithm were compared with the elevations produced by the NASA and ESA algorithms to determine the relative accuracy of these algorithms when subsurface volume-scattering occurs. The results show that the NASA algorithm produced surface elevations within 35 to 50 cm of the S/V algorithm, while the performance of the ESA algorithm was slightly worse. Next, by analyzing several thousand satellite crossover points from the Antarctic data set, we determined the retracking algorithm that produced the most repeatable surface elevations. The elevations derived from the S/V algorithm had the smallest RMS error for the region of the East Antarctic plateau examined here. The ESA algorithm produced erroneous estimates of elevation change when seasonal variations were present; it measured 0.7 to 1.6-m change in elevation over a 6-month period on the East Antarctic plateau where accumulation rates are only 10 cm/year.
Derived from text

N94-24095*# National Aeronautics and Space Administration. Lyndon B. Johnson Space Center, Houston, TX.

ANALYSIS OF IMPACTOR RESIDUES IN TRAY CLAMPS FROM THE LONG DURATION EXPOSURE FACILITY. PART 2: CLAMPS FROM BAY B OF THE SATELLITE

Ronald P. Bernhard (Lockheed Engineering and Sciences Co., Houston, TX.) and Michael E. Zolensky Feb. 1994 275 p
(NASA-TM-104784; S-748; NAS 1.15:104784) Avail: CASI HC A12/MF A03

The Long Duration Exposure Facility (LDEF) was placed in low-Earth orbit (LEO) in 1984 and recovered 5.7 years later. The LDEF was host to several individual experiments specifically designed to characterize critical aspects of meteoroid and debris environment in LEO. However, it was realized from the beginning that the most efficient use of the satellite would be to examine the entire surface for impact features. In this regard, particular interest centered on common exposed materials that faced in all LDEF pointing directions. Among the most important of these materials was the tray clamps. Therefore, in an effort to better understand the nature of particulates in LEO and their effects on spacecraft hardware, residues found in impact features on LDEF tray clamp surfaces are being analyzed. This catalog presents all data from clamps from Bay B of the LDEF. NASA Technical Memorandum 104759 has cataloged impacts that occurred on Bay B (published March 1993). Subsequent catalogs will include clamps from succeeding bays of the satellite. Author (revised)

N94-24303*# National Academy of Sciences - National Research Council, Washington, DC. Commission on Physical Sciences, Mathematics, and Applications.
PANEL TO REVIEW EOSDIS PLANS Final Report
1994 94 p
(Contract NASw-4627)
(NASA-CR-195088; NAS 1.26:195088) Copyright Avail: CASI HC A05/MF A01

Formed in Jan. 1992, the Panel to Review EOSDIS Plans was charged with advising NASA on its plans for developing the Earth Observing System (EOS) Data and Information System (EOSDIS). Specifically, the panel was asked to do the following: assess the validity of the engineering and technical underpinnings of the EOSDIS; assess its potential value to scientific users; suggest how technical risk can be minimized; and assess whether current plans are sufficiently resilient to be adaptable to changing technology and requirements such as budget environments, data volumes, new users, and new databases. The panel completed an interim report (Addendum A) and transmitted it to NASA and other interested parties in the government on 9 Apr. 1992. Because of a delay in NASA's plans to select the contractor for EOSDIS, the panel was not able to complete its review of the program according to the original government request. With the issuance of a letter report (Addendum B) on 28 Sep. 1992, the panel became inactive until such time as NASA could release the details of the contractor's proposed architecture, schedule, and costs for developing EOSDIS. In early 1993, NASA awarded the contract for the EOSDIS Core System (ECS). On 20 Apr. 1993, NASA asked the panel to reconvene to do the following: (1) complete its review of NASA's approach to the EOSDIS architecture and implementation; (2) appraise NASA's responses to the panel's previous recommendations; and (3) review the planning for EOSDIS in the context of NASA's role in the Global Change Data and Information System (GCDIS) implementation plan. To respond to the NASA charge, the panel met three times in 1993 including sessions with NASA officials and the EOSDIS contractor. In addition, several of the panel members visited individual Distributed Active Archive Centers (DAAC's) to obtain additional views of EOSDIS. The panel has now obtained substantial information on the EOSDIS budget, contractor work program, and current baseline architecture that was not previously available, due to procurement restrictions. This report presents the panel's findings and recommendations based on this additional information. Author (revised)

N94-24357 Utah State Univ., Logan. Coll. of Natural Resources.
MAPPING TOMORROW'S RESOURCES: A SYMPOSIUM ON THE USES OF REMOTE SENSING, GEOGRAPHIC INFORMATION SYSTEMS (GIS), AND GLOBAL POSITIONING SYSTEMS (GPS) FOR NATURAL RESOURCES MANAGEMENT
Allan Falconer, ed. 1993 93 p Symposium held in Logan, UT, 23-24 Apr. 1992; sponsored by Utah State Univ., S. J. and Jesse E. Quinney Foundation, the Soil Conservation Service, the Fish and Wildlife Service, Forest Service, and Utah Geographic Alliance *Its* Natural Resources and Environmental Issues, Volume 2
Copyright Avail: Issuing Activity (Quinney Library, Coll. of Natural Resources, Utah State Univ., Logan, UT 84322-5260)

The College of Natural Resources recognizes the important role it has in educating natural resources managers and leaders who can provide the guidance and knowledge needed to increase the production of the earth's renewable resources while sustaining and enhancing the global environment and the natural resource base. The College's teaching, research, extension, and service efforts focus on the many aspects of sustained multiple-natural-resources management and their relationship to man. Through its many programs, the College of Natural Resources focuses on solving local, state, national, and global problems to enhance a more efficient and contemporary use of the world's natural resources. Natural Resources and Environmental Issues (NREI) which began publication in 1993, is a technical series that addresses current topics relevant to natural resources and to the environment. The journal is published as a series of volumes, with at least one being issued each year as the proceedings of the Natural Resources Week Symposium. In the issue on Mapping Tommorrow's Resources, the following topics are discussed: Natural Resource Information from Monopoly to Competition; Global Resources and Mission to Planet Earth; Geographic Information Systems (GIS) Systems and Data Management for Global Data Sets in Natural Resources; the Global Resource Information Database; Overview of GIS Technology in Utah State Government; Politically Correct Global Mapping and Monitoring; Integrating Satellite Imagery and GIS into Natural Resources Management; Forest Service Applications of Remote Sensing and the National Training Program; the Position of the Global Positioning System (GPS) in Wildlife and Habitat Mapping; and the Bureau of Land Management's (BLM's) Remote Sensing Program in Utah. Derived from text

N94-24403*# National Aeronautics and Space Administration. Ames Research Center, Moffett Field, CA.
FACTORS AFFECTING THE IDENTIFICATION OF PHYTOPLANKTON GROUPS BY MEANS OF REMOTE SENSING
Ellen C. Weaver (San Jose State Univ., CA.) and Robert Wrigley Jan. 1994 121 p
(RTOP 199-30-92-14)
(NASA-TM-108799; A-94022; NAS 1.15:108799) Avail: CASI HC A06/MF A02

A literature review was conducted on the state of the art as to whether or not information about communities and populations of phytoplankton in aquatic environments can be derived by remote sensing. In order to arrive at this goal, the spectral characteristics of various types of phytoplankton were compared to determine first, whether there are characteristic differences in pigmentation among the types and second, whether such differences can be detected remotely. In addition to the literature review, an extensive, but not exhaustive, annotated bibliography of the literature that bears on these questions is included as an appendix, since it constitutes a convenient resource for anyone wishing an overview of the field of ocean color. The review found some progress has already been made in remote sensing of assemblages such as coccolithophorid blooms, mats of cyanobacteria, and red tides. Much more information about the composition of algal groups is potentially available by remote sensing particularly in water bodies having higher phytoplankton concentrations, but it will be necessary to develop the remote sensing techniques required for working in so-called Case 2 waters. It is also clear that none of the satellite sensors presently available or soon to be launched is ideal from the point of view of what we might wish to know; it would seem wise to pursue instruments with the planned characteristics of the Moderate Resolution Imaging Spectrometer-Tilt (MODIS-T) or Medium Resolution Imaging Spectrometer (MERIS). Author (revised)

N94-24596*# Wisconsin Univ., Madison. Space Science and Engineering Center.
AN INVESTIGATION OF CURRENT AND FUTURE SATELLITE AND IN-SITU DATA FOR THE REMOTE SENSING OF THE LAND SURFACE ENERGY BALANCE Final Report, Nov. 1989 - Jan. 1994
George R. Diak Feb. 1994 24 p
(Grant NAGw-1858)
(NASA-CR-195138; NAS 1.26:195138) Avail: CASI HC A03/MF A01

This final report from the University of Wisconsin-Madison Cooperative Institute for Meteorological Satellite Studies (CIMSS) summarizes a research program designed to improve our knowledge of the water and energy balance of the land surface through the application of remote sensing and in-situ data sources. The remote sensing data source investigations to be detailed involve surface radiometric ('skin') temperatures and also high-spectral-resolution infrared radiance data from atmospheric sounding instruments projected to be available at the end of the decade, which have shown promising results for evaluating the land-surface water and energy budget. The in-situ data types to be discussed are measurements of the temporal changes of the height of the planetary boundary layer and measurements of air temperature within the planetary boundary layer. Physical models of the land surface, planetary boundary layer and free atmosphere have been used as important tools to interpret the in-situ and remote sensing signals of the surface energy balance. A prototype 'optimal' system for combining multiple data sources into a three-dimensional estimate of the surface energy balance was developed and first results from this system will be detailed. Potential new sources of data for this system and suggested continuation research will also be discussed. Author

N94-24636 Technische Univ., Delft (Netherlands). Faculty of Civil Engineering.

HYDRAULICS AND MORPHOLOGY OF MOUNTAIN RIVERS: A LITERATURE SURVEY. COMMUNICATIONS ON HYDRAULIC AND GEOTECHNICAL ENGINEERING

A. Sieben Jan. 1993 148 p Limited Reproducibility: More than 20% of this document may be affected by microfiche quality
(PB94-110772; Rept-93-4) Avail: CASI HC A07

The report is a literature survey of recent research on mountain rivers. The study aims to describe or refer to research on fluvial processes of mountain rivers from a hydraulic and morphological point of view. With this survey, an attempt was made to describe the state of the art on the subject and to distinguish priorities in research. In Chapter Two, attention is paid to the general characteristics of mountain rivers compared to low-land rivers. Chapter Three describes general hydraulic processes and includes a review of the formulation of resistance to flow. In Chapter Four, the morphological features of mountain rivers are described. Movements of sediment are described in Chapter Five, which concentrates on the rate, composition, and mode of sediment transport. Effects of a changing rheology of flow due to high rates of sediment transport are described briefly in Chapter Six. Here, also remarks can be found on discharge measurements and prediction of solute transport in mountain rivers. Conclusions are presented in Chapter Seven, where recommendations are made on topics of further research. NTIS

N94-24741 Research Inst. of National Defence, Linkoeping (Sweden).

METHOD FOR SELECTION OF WAVELENGTH BANDS FOR MULTISPECTRAL CLASSIFICATION [METOD FOER VAL AV VAGLAENGDSBAND VID MULTISPEKTRAL KLASSIFICERING]

M. Ulvklo Nov. 1992 85 p In SWAHILI Limited Reproducibility: More than 20% of this document may be affected by microfiche quality
(PB93-204378; FOA-C-30688-3.1) Avail: Issuing Activity (National Technical Information Service (NTIS))

Multispectral technics are normally used for civil and military satellite remote sensing. Multispectral images from six wavelength bands in the visual range already exist at FOA Linkoping. The images are recorded in ground level and contain a vehicle in outdoor scenes. The main objective in the final project is to investigate if the result of object detection in the images is good enough if only three wavelength bands are used instead of all six. In the final project a maximum likelihood multispectral classifier is used for segmentation of areas which can be vehicles. For these areas a number of statistical features are computed. The features are extracted from the first principal component which is calculated with Hotelling transform. Evidential reasoning is used to determine if the areas are vehicle or not. A method of selection of the optimal subset of wavelength bands has also been worked out in the final project. The idea of the method is to use the covariance matrix to achieve the subset of wavelength bands that is most uncorrelated. A comparing study shows that the number of false targets increases with a factor of four when only three wavelength bands are used instead of six. The result is therefore not satisfying when only three wavelength bands are used. NTIS

N94-24757# Oak Ridge National Lab., TN.

TOOLS FOR VISUALIZING LANDSCAPE PATTERN FOR LARGE GEOGRAPHIC AREAS

S. P. Timmins (Analysas Corp., Oak Ridge, TN.) and C. T. Hunsaker 1993 10 p Presented at the 2nd International Workshop in Integrating Geographic Information Systems and Environmental Modeling, Breckenridge, CO, 27-29 Sep. 1993
(Contract DE-AC05-84OR-21400)
(DE94-001121; CONF-9309230-2) Avail: CASI HC A02/MF A01

Landscape pattern can be modelled on a grid with polygons constructed from cells that share edges. Although this model only allows connections in four directions, the programming is convenient because both coordinates and attributes take discrete integer values. A typical raster land-cover data set is a multimegabyte matrix of byte values derived by classification of images or gridding of maps. Each matrix may have thousands of raster polygons (patches), many of them islands inside other larger patches. These data sets have complex topology that can overwhelm vector geographic information systems. The goal is to develop tools to quantify change in the landscape structure in terms of the shape and spatial distribution of patches. Three milestones toward this goal are as follows: (1) creating polygon topology on a grid, (2) visualizing patches, and (3) analyzing shape and pattern. An efficient algorithm has been developed to locate patches, measure area and perimeter, and establish patch topology. A powerful visualization system with an extensible programming language is used to write procedures to display images and perform analysis. DOE

N94-24809# Edwards Underground Water District, San Antonio, TX.

EVALUATION OF THE USE OF REMOTE-SENSING DATA TO IDENTIFY CROP TYPES AND ESTIMATE IRRIGATED ACREAGE, UVALDE AND MEDINA COUNTIES, TEXAS, 1989

Lee H. Raymond, Gregory M. Nalley, and Paul L. Rettman 1992 58 p
(PB93-193159; USGS/WRI-92-4117) Avail: CASI HC A04/MF A01

Remote-sensing data were used to estimate that 190,000 acre-feet of water was pumped from the Edwards aquifer in 1989 to irrigate crops in Uvalde and Medina Counties. Landsat digital satellite images for March and July 1989 were combined and classified to identify the areas of crops irrigated with water from the Edwards aquifer in the two counties. Normalized difference, the difference between the infrared and red reflectance values divided by the total of those values, was used to discriminate vegetative from nonvegetative ground cover. The images subsequently were classified using maximum likelihood, an unsupervised classification procedure. Detailed vegetation distribution maps of two calibration sites in the study area, and boundaries of the areas probably irrigated in 1989, helped to interpret the results and to separate probable irrigated areas from the rest of the image. Results were verified using crop acreages reported by the U.S. Department of Agriculture. Irrigated-crop areas subsequently were multiplied by the respective duties of water to calculate the total quantity of water pumped from the aquifer for irrigation. NTIS

N94-24827*# AI Signal Research, Inc., Huntsville, AL.

DEVELOP ADVANCED NONLINEAR SIGNAL ANALYSIS TOPOGRAPHICAL MAPPING SYSTEM Technical Progress Report

Jan. 1994 25 p
(Contract NAS8-39393)
(NASA-CR-195128; NAS 1.26:195128; TR-4002-94-01) Avail: CASI HC A03/MF A01

The Space Shuttle Main Engine (SSME) has been undergoing extensive flight certification and developmental testing, which involves some 250 health monitoring measurements. Under the severe temperature, pressure, and dynamic environments sustained during operation, numerous major component failures have occurred, resulting in extensive engine hardware damage and scheduling losses. To enhance SSME safety and reliability, detailed analysis and evaluation of the measurements signal are mandatory to assess its dynamic characteristics and operational condition. Efficient and reliable signal detection techniques will reduce catastrophic system failure risks and expedite the evaluation of both flight and ground test data, and thereby reduce launch turn-around time. The basic objective of this contract are threefold: (1) develop and validate a hierarchy of innovative signal analysis techniques for nonlinear and nonstationary time-frequency analysis. Performance evaluation will be carried out through detailed analysis of extensive SSME static firing and flight data. These techniques will be incorporated into a fully automated system; (2) develop an advanced nonlinear signal analysis topographical mapping system (ATMS) to generate a Compressed SSME TOPO Data Base (CSTDB). This ATMS system will convert tremendous amount of complex vibration signals from the entire SSME test history into a bank of succinct image-like patterns while retaining all respective phase information. High compression ratio can be achieved to allow minimal storage requirement, while providing fast signature retrieval, pattern comparison, and identification capabilities; and (3) integrate the nonlinear correlation techniques into the CSTDB data base with compatible TOPO input data format. Such integrated ATMS system will provide the large test archives necessary for quick signature comparison. This study will provide timely assessment of SSME component operational status, identify probable causes of malfunction, and indicate feasible engineering solutions. The final result of this program will yield an ATMS system of nonlinear and nonstationary spectral analysis software package integrated with the Compressed SSME TOPO Data Base (CSTDB) on the same platform. This system will allow NASA engineers to retrieve any unique defect signatures and trends associated with different failure modes and anomalous phenomena over the entire SSME test history across turbo pump families. Author (revised)

N94-24856*# AI Signal Research, Inc., Huntsville, AL.
DEVELOP ADVANCED NONLINEAR SIGNAL ANALYSIS TOPOGRAPHICAL MAPPING SYSTEM Technical Progress Report
Jen-Yi Jong Dec. 1993 16 p
(Contract NAS8-39393)
(NASA-CR-194785; NAS 1.26:194785; TR-4002-93-12) Avail: CASI HC A03/MF A01

As reported in the monthly technical progress report for July 1993, a new signal analysis technique called instantaneous frequency correlation (IFC) for time delay estimation was developed which will be incorporated into the ATMS system. In this report, a different technique for time delay estimation called phase difference time derivative estimator (FDTDE) will be discussed. The FDTDE technique does not replace the IFC method since their application conditions are different. The IFC technique can estimate the time delay between two spectral components of two measurement signals when the center frequency of the components is constant, while the FDTDE method can provide accurate time delay estimation when the frequency of the subject component changes linearly such as during engine startup or shut-down. Author (revised)

N94-23840*# Jet Propulsion Lab., California Inst. of Tech., Pasadena.
ASTER, A MULTINATIONAL EARTH OBSERVING CONCEPT
Graham W. Bothwell, Gary N. Geller, Steven A. Larson, Andrew D. Morrison, and David A. Nichols *In its* SpaceOps 1992: Proceedings of the Second International Symposium on Ground Data Systems for Space Mission Operations 1 Mar. 1993 p 45-50 (For primary document see N94-23832 06-66)
Avail: CASI HC A02/MF A10

N94-24442*# Oakwood Coll., Huntsville, AL. Biology Dept.
THE MEASUREMENT AND ANALYSIS OF LEAF SPECTRAL REFLECTANCE OF TWO STANDS OF LOBLOLLY PINE POPULATIONS
Anthony D. Paul *In* Alabama Univ., The 1993 NASA/ASEE Summer Faculty Fellowship Program Nov. 1993 2 p (For primary document see N94-24405 06-80)
Avail: CASI HC A01/MF A03

44 ENERGY PRODUCTION AND CONVERSION

Includes specific energy conversion systems, e.g., fuel cells; global sources of energy; geophysical conversion; and windpower.

For related information see also *07 Aircraft Propulsion and Power, 20 Spacecraft Propulsion and Power,* and *28 Propellants and Fuels.*

N94-22723# M-C Power Corp., Burr Ridge, IL.
ADVANCED RESEARCH AND TECHNOLOGY DEVELOPMENT OF MCFCs
T. G. Benjamin, R. J. Remick, and R. A. Donado 1993 9 p Presented at the Joint Contractors Meeting on Advanced Turbine Systems, Fuel Cells and Coal-Fired Heat, Morgantown, WV, 3-5 Aug. 1993
(Contract DE-AC21-90MC-27394)
(DE94-001918; DOE/MC-27394/94/C0263; CONF-930893-6) Avail: CASI HC A02/MF A01

The objective is to lower contact resistance losses associated with protective oxide layer that forms on the surface of stainless steel in the MCFC (molten carbonate fuel cell) cathode environment. The approach being taken is to coat the top surface of the stainless steel with a thin film of iron oxide. A 316L stainless steel sheet metal was coated with 3-micron thick layer of Fe2O3 using jet vapor deposition. The films were examined by SEM/EDX and the conductivity measured. Resistance of cell with only a 316L separator was 0.116 ohm, while that of the cell with the iron oxide coated separator was 0.124 ohm. DOE

N94-22862# Delaware Univ., Newark. Inst. of Energy Conversion.
POLYCRYSTALLINE THIN FILM MATERIALS AND DEVICES
R. W. Birkmire, J. E. Phillips, W. N. Shafarman, S. S. Hegedus, B. E. McCandless, and T. A. Yokimcus Aug. 1993 135 p Prepared for Midwest Research Inst., Golden, CO
(Contract DE-AC02-83CH-10093)
(DE93-018213; NREL/TP-451-5755) Avail: CASI HC A07/MF A02

Results and conclusions of the final phase (3) of a three-year research program on polycrystalline thin-film heterojunction solar cells is described. The research consisted of the investigation of the relationships between processing, materials properties, and device performance. This relationship was quantified by device modeling and analysis. The analysis of thin-film polycrystalline heterojunction solar cells explains how minority-carrier recombination at the metallurgical interface and at grain boundaries can be greatly reduced by the proper doping of the window and absorber layers. Additional analysis and measurements show that the present solar cells are limited by the magnitude of the diode current, which appears to be caused by recombination in the space charge region. Developing an efficient commercial-scale process for fabricating large-area polycrystalline, thin-film solar cells from a research process requires a detailed understanding of the individual steps in making the solar cell, and their relationship to device performance and reliability. The complexities involved in characterizing a process are demonstrated with results from our research program on CuInSe2 and CdTe processes. DOE

N94-22888# Midwest Research Inst., Golden, CO. National Renewable Energy Lab.
PROGRESS IN PHASES 2 AND 3 OF THE PHOTOVOLTAIC MANUFACTURING TECHNOLOGY PROJECT (PVMaT)
C. E. Witt, R. L. Mitchell, G. D. Mooney, L. O. Herwig (Department of Energy, Washington, DC.), D. Hasti (Sandia National Labs., Albuquerque, NM.), and R. Sellers (Solar Energy Industries Association, Washington, DC.) Oct. 1993 6 p Presented at the 23rd Institute of Electrical and Electronic Engineers (IEEE) Photovoltaic Specialists Conference, Louisville, KY, 10-14 May 1993
(Contract DE-AC02-83CH-10093)
(DE94-000206; NREL/TP-411-5501; CONF-930540-11) Avail: CASI HC A02/MF A01

This first year of the process-specific activities of the Photovoltaic Manufacturing Technology (PVMaT) project was completed, and the first subcontracts for teamed efforts on R&D of a general nature were awarded. A second solicitation for process-specific research and development (R&D) is in the evaluation stage for award of subcontracts. The technical accomplishments of the first process-specific subcontracts (Phase 2A), the status of the teamed research (Phase 3A), and the status of the solicitation for the second process-specific solicitation (Phases 2B) are described. DOE

N94-22962# Brookhaven National Lab., Upton, NY.
A NOVEL METHOD FOR DETERMINATION OF TRANSPORT PARAMETERS OF H2 AND O2 IN PEMFCs
Masanobu Wakizoe, J. Kim, S. Srinivasan (Texas A&M Univ., College Station.), and J. McBreen 1993 14 p Presented at the 183rd Electrochemical Society Meeting, Honolulu, HI, 16-21 May 1993
(Contract DE-AC02-76CH-00016)
(DE94-001492; BNL-49537; CONF-930571-27) Avail: CASI HC A03/MF A01

A knowledge of the transport parameters of hydrogen and oxygen in proton exchange membrane fuel cells (PEMFC's) is of vital importance for the following: (1) an elucidation of the kinetics of the half-cell reactions; (2) analyzing mass transport phenomena in the electrodes and membranes; (3) estimating the cross-over currents during fuel cell operation; and (4) evaluating membranes from different manufacturers and selecting the most promising candidate. Previous studies to determine diffusion coefficients and solubilities of H2 and O2 in proton conducting membranes have rarely been made under fuel cell operating conditions.This paper deals with novel approaches to determine the transport parameters in PEMFC's using steady state and transient techniques. The transient technique proved to be the most desirable for this purpose. Experiments were conducted in PEMFC's with Asahi Chemical Aciplex(TM)-S Membranes and DuPont's Nafion(TM)-117 membranes. The diffusion coefficients (D) of H2 and of O2 are higher in the Nafion(TM) membranes, while their solubilities (C0)

are higher in the Aciplex(TM) membranes. The D values are higher for O2 than for H2 in both membranes while the opposite behavior is the case in respect to C0 values. The values of activation energies for diffusion of H2 or O2 in the membrane are of the same order as in aqueous electrolytes. There is an anomalous temperature dependence of the solubilities of H2 and O2 in the two membranes. This is not the case with the product DC0. The diffusion rate of H2 through the membranes is higher than that of O2.
DOE

N94-23102 Helsinki Univ. of Technology, Espoo (Finland). Dept. of Technical Physics.

MODELLING OF SOLID POLYMER AND DIRECT METHANOL FUEL CELLS: PHENOMENOLOGICAL EQUATIONS AND ANALYTICAL SOLUTIONS

P. S. Kauranen 7 Apr. 1993 53 p Limited Reproducibility: More than 20% of this document may be affected by microfiche quality
(PB93-224897; TKK-F-C149) Avail: CASI HC A04

In the solid state concept of a direct methanol fuel cell (DMFC), methanol is directly oxidized at the anode of a solid polymer electrolyte fuel cell (SPEFC). Mathematical modelling of the transport and reaction phenomena within the electrodes and the electrolyte membrane is needed in order to get a closer insight into the operation of the fuel cell. In the work, macro-homogenous porous electrode and dilute solution theories are used to derive the phenomenological equations describing the transport and reaction mechanisms in a SPEFC single cell. The equations are first derived for a conventional H2/air SPEFC, and then extended for a DMFC. The basic model is derived in a one dimensional form in which it is assumed that species transport take place only in the direction crossing the cell sandwich. In addition, two dimensional descriptions of the catalyst layer are reviewed.
NTIS

N94-23212 Department of Energy, Morgantown, WV.

MATHEMATICAL MODELING OF MCFC CELLS/STACKS AND NETWORKS

M. C. Williams, J. Wimer, F. Sudhoff, and D. Archer (Carnegie-Mellon Univ., Pittsburgh, PA.) 1993 8 p Presented at the 206th American Chemical Society (ACS) National Meeting, Chicago, IL, 22-27 Aug. 1993 Limited Reproducibility: More than 20% of this document may be affected by poor print
(DE94-001914; DOE/METC-C/94/7109; CONF-930802-15) Avail: Issuing Activity (Department of Energy (DOE))

In this paper, various molten carbonate fuel cell (MCFC) cell/stack, network, and system models available in the public domain are discussed. Parametric and phenomenological fuel cell mathematical models are being used to simulate individual MCFC cell/stack performance. With initial demonstration of full-area, full-height 250-kW to 2-MW MCFC power plants, the spatial configuration of the MCFC stacks into networks in the fuel cell power plant takes on new importance. MCFC network and power plant system flowsheet performance is being modeled using the ASPEN system model. ASPEN is a tear and iterate flowsheet simulator in the public domain. ASPEN is suitable for MCFC network simulation since it has strong systems and property database capabilities. With emergence of larger MCFC power plant system demonstrations, system modeling of MCFC power plants is now essential. DOE routinely uses MCFC models in making performance comparisons and in decision making.
DOE

N94-23295# Utility Power Group, Chatsworth, CA.

AMORPHOUS SILICON PVMaT, PHASE 2A

G. Duran, K. Mackamul, D. Metcalf, M. Stern, H. Volltrauer (Advanced Photovoltaic Systems, Inc., Princeton, NJ.), T. Varar (Advanced Photovoltaic Systems, Inc., Princeton, NJ.), E. Urbanski (Advanced Photovoltaic Systems, Inc., Princeton, NJ.), T. DiBiaso (Advanced Photovoltaic Systems, Inc., Princeton, NJ.), and D. Skinner (Advanced Photovoltaic Systems, Inc., Princeton, NJ.) Sep. 1993 42 p
(Contract DE-AC02-83CH-10093)
(DE93-018221; NREL/TP-411-5739-Phase-2A) Avail: CASI HC A03/MF A01

This report describes work done under a subcontract to significantly advance the photovoltaic manufacturing technologies, reduce module production costs, increase average module performance, and increase the production capacity existing at Utility Power Group (UPG) and Advanced Photovoltaic Systems, Inc. (APS). Areas of focus include the following: (1) encapsulation and termination, (2) product design, (3) process and quality control, and (4) automation. UPG will improve its encapsulation system through the development of advanced encapsulation materials and processes that result in a module that does not require backing glass. In addition, UPG will work to develop advanced termination materials and processes. APS will perform development activities centered on the EUREKA manufacturing line. Developments in the APS EUREKA encapsulation system will be in addition to the UPG activity on encapsulation and will offer an alternative approach to the problems of encapsulating large-area thin-film modules.
DOE

N94-23296 International Solar Electric Technology, Inglewood, CA.

NOVEL TWO-STAGE SELENIZATION METHODS FOR FABRICATION OF THIN-FILM CIS CELLS AND SUBMODULES

B. M. Basol, V. K. Kapur, A. Halani, and C. Leidholm Oct. 1993 20 p Prepared for Midwest Research Inst., Golden, CO Limited Reproducibility: More than 20% of this document may be affected by microfiche quality
(Contract DE-AC02-83CH-10093)
(DE94-000220; NREL/TP-413-5844) Avail: CASI HC A03

This is the Phase 1 Annual Technical Progress Report of a subcontract enitled Novel Two-Stage Selenization Methods for Fabrication of Thin-Film CIS Cells and Submodules. The objectives of the program are the development of a cost effective process for CIS film deposition, optimization of various layers forming the CIS solar cell, and fabrication of submodules using these processes and devices. During this first phase of the program, the authors have completed their 1 sq ft size processing capabilities and added to their facilities an in-line sputtering system that can handle up to 1 sq ft size substrates. They have optimized the sputtering conditions for the Mo contact as well as the Cu and In films. Thickness uniformity of the Cu and In layers have also been optimized by masking the magnetron cathodes to obtain a variation of 3% throughout a sq ft substrate. Using the resulting films, they have demonstrated their first large area CIS submodules with outputs of about 3W/sq ft. Addition of a computer controlled mechanical scriber to the fabrication facilities, and optimization of the large-area ZnO layers are expected to improve the power output of these submodules to over 5W/sq ft shortly. In addition to the large-area submodule work, the authors have also carried out research aimed at the development of a non-vacuum processing approach for the growth of CIS layers. They have deposited films using this technique, and small-area cells with over 10% conversion efficiency have been demonstrated on such CIS layers.
DOE

N94-23345*# National Aeronautics and Space Administration. Lewis Research Center, Cleveland, OH.

SPACE ELECTROCHEMICAL RESEARCH AND TECHNOLOGY

Nov. 1993 249 p Conference held in Cleveland, OH, 14-15 Apr. 1993
(RTOP 506-41-21)
(NASA-CP-3228; E-8075; NAS 1.55:3228) Avail: CASI HC A11/MF A03

This document contains the proceedings of NASA's fourth Space Electrochemical Research and Technology (SERT) Conference, held at the NASA Lewis Research Center on April 14-15, 1993. The objective of the conference was to assess the present status and general thrust of research and development in those areas of electrochemical technology required to enable NASA missions into the next century. The conference provided a forum for the exchange of ideas and opinions of those actively involved in the field, in order to define new opportunities for the application of electrochemical processes in future NASA missions. Papers were presented in three technical areas: advanced secondary batteries, fuel cells, and advanced concepts for space power. This document contains the papers presented. For individual titles, see N94-23346 through N94-23367.

N94-23346*# National Aeronautics and Space Administration, Washington, DC.

AEROSPACE APPLICATIONS OF BATTERIES

Shahid Habib *In* NASA. Lewis Research Center, Space Electrochemical Research and Technology Nov. 1993 p 3-12 (For primary document see N94-23345 06-44)
Avail: CASI HC A02/MF A03

NASA has developed battery technology to meet the demanding requirements for aerospace applications; specifically, the space vacuum, launch loads, and high duty cycles. Because of unique requirements and operating environments associated with space applications, NASA has written its own standards and specifications for batteries. Author

N94-23347*# Case Western Reserve Univ., Cleveland, OH. Dept. of Chemistry.

APPLICATIONS OF X RAY ABSORPTION FINE STRUCTURE TO THE IN SITU STUDY OF THE EFFECT OF COBALT IN NICKEL HYDROUS OXIDE ELECTRODES FOR FUEL CELLS AND RECHARGEABLE BATTERIES

Sunghyun Kim, Donald A. Tryk, Daniel A. Scherson, and Mark R. Antonio (Argonne National Lab., IL.) *In* NASA. Lewis Research Center, Space Electrochemical Research and Technology Nov. 1993 p 13-19 Sponsored in part by DOE (For primary document see N94-23345 06-44)

Avail: CASI HC A02/MF A03

Electronic and structural aspects of composite nickel-cobalt hydrous oxides have been examined in alkaline solutions using in situ X-ray absorption fine structure (XAFS). The results obtained have indicated that cobalt in this material is present as cobaltic ions regardless of the oxidation state of nickel in the lattice. Furthermore, careful analysis of the Co K-edge Extended X-ray absorption fine structure data reveals that the co-electrodeposition procedure generates a single phase, mixed metal hydrous oxide, in which cobaltic ions occupy nickel sites in the NiO2 sheet-like layers and not two intermixed phases each consisting of a single metal hydrous oxide. Author

N94-23348*# Eagle-Picher Industries, Inc., Colorado Springs, CO.

REVIEW OF SUPER Ni/Cd CELL DESIGNS AND PERFORMANCE

Bruce Abrams-Blakemore *In* NASA. Lewis Research Center, Space Electrochemical Research and Technology Nov. 1993 p 21-25 (For primary document see N94-23345 06-44)

Avail: CASI HC A01/MF A03

Eagle-Picher Industries, Inc., in cooperation with Hughes Aircraft Company, began production of the Super Nickel-Cadmium cell in 1989. Since that time the Super Nickel-Cadmium cell has been deployed in a wide variety of satellites. This paper will review one of those programs and provide a performance update. We will discuss storage requirements and capacity histories for the various Super NiCad Cell designs. Author

N94-23349*# Pennsylvania State Univ., University Park. Center for Advanced Materials.

THERMODYNAMICS OF NICKEL-CADMIUM AND NICKEL-HYDROGEN BATTERIES

Digby D. Macdonald and Mark L. Challingsworth *In* NASA. Lewis Research Center, Space Electrochemical Research and Technology Nov. 1993 p 27-39 (For primary document see N94-23345 06-44)

Avail: CASI HC A03/MF A03

Thermodynamic parameters for Nickel-Cadmium (NiCad) and Nickel-Hydrogen (NiH2) batteries are calculated for temperatures ranging from 273.15K (0 C) to 373.15K (100 C). For both systems, we list equilibrium and thermoneutral voltages for the cells, and in the case of the NiH2 battery, these data are provide for hydrogen fugacities ranging from 0.01 to 100 (atm) to simulate the full discharged and charged states. The quality of the input thermodynamic data are assessed and the effect of assuming different cell reactions is analyzed. Author

N94-23350*# Eagle-Picher Industries, Inc., Joplin, MO.

HIGH SPECIFIC ENERGY, HIGH CAPACITY NICKEL-HYDROGEN CELL DESIGN

James R. Wheeler *In* NASA. Lewis Research Center, Space Electrochemical Research and Technology Nov. 1993 p 41-47 (For primary document see N94-23345 06-44)

Avail: CASI HC A02/MF A03

A 3.5 inch rabbit-ear-terminal nickel-hydrogen cell was designed and tested to deliver high capacity at steady discharge rates up to and including a C rate. Its specific energy yield of 60.6 wh/kg is believed to be the highest yet achieved in a slurry-process nickel-hydrogen cell, and its 10 C capacity of 113.9 AH the highest capacity yet of any type in a 3.5 inch diameter size. The cell also demonstrated a pulse capability of 180 amps for 20 seconds. Specific cell parameters and performance are described. Also covered is an episode of capacity fading due to electrode swelling and its successful recovery by means of additional activation procedures. Author (revised)

N94-23351*# Auburn Univ., AL. Dept. of Chemical Engineering and Space Power Inst.

HIGH SURFACE AREA, LOW WEIGHT COMPOSITE NICKEL FIBER ELECTRODES

Bradley A. Johnson, Richard E. Ferro, Greg M. Swain, and Bruce J. Tatarchuk *In* NASA. Lewis Research Center, Space Electrochemical Research and Technology Nov. 1993 p 49-60 (For primary document see N94-23345 06-44)

(Grant NAG3-II54)

Avail: CASI HC A03/MF A03

The energy density and power density of light weight aerospace batteries utilizing the nickel oxide electrode are often limited by the microstructures of both the collector and the resulting active deposit in/on the collector. Heretofore, these two microstructures were intimately linked to one another by the materials used to prepare the collector grid as well as the methods and conditions used to deposit the active material. Significant weight and performance advantages were demonstrated by Britton and Reid at NASA-LeRC using FIBREX nickel mats of ca. 28-32 microns diameter. Work in our laboratory investigated the potential performance advantages offered by nickel fiber composite electrodes containing a mixture of fibers as small as 2 microns diameter (Available from Memtec America Corporation). These electrode collectors possess in excess of an order of magnitude more surface area per gram of collector than FIBREX nickel. The increase in surface area of the collector roughly translates into an order of magnitude thinner layer of active material. Performance data and advantages of these thin layer structures are presented. Attributes and limitations of their electrode microstructure to independently control void volume, pore structure of the Ni(OH)2 deposition, and resulting electrical properties are discussed. Author (revised)

N94-23352*# Ovonic Battery Co., Troy, MI.

OVONIC NICKEL METAL HYDRIDE BATTERIES FOR SPACE APPLICATIONS

S. Venkatesan, D. A. Corrigan, M. A. Fetcenko, P. R. Gifford, S. K. Dhar, and S. R. Ovshinsky *In* NASA. Lewis Research Center, Space Electrochemical Research and Technology Nov. 1993 p 61-66 (For primary document see N94-23345 06-44)

Avail: CASI HC A02/MF A01

Ovonic nickel-metal hydride (NiMH) rechargeable batteries are easily adaptable to a variety of applications. Small consumer NiMH cells were developed and are now being manufactured by licensees throughout the world. This technology was successfully scaled up in larger prismatic cells aimed at electric vehicle applications. Sealed cells aimed at satellite power applications were also built and cycle tested by OBC and other outside agencies. Prototype batteries with high specific energy (over 80 Wh/kg), high energy density (245 Wh/L), and excellent power capability (400 W/kg) were produced. Ovonic NiMH batteries demonstrated an excellent cycle life of over 10,000 cycles at 30 percent DOD. Presently, Ovonic Battery Company is working on an advanced version of this battery for space applications as part of an SBIR contract from NASA. Author (revised)

N94-23353*# Texas A&M Univ., College Station. Engineering Experiment Station.

ALLOYS FOR HYDROGEN STORAGE IN NICKEL/HYDROGEN AND NICKEL/METAL HYDRIDE BATTERIES

Anaba Anani, Arnaldo Visintin, Konstantin Petrov, Supramaniam Srinivasan, James J. Reilly (Brookhaven National Lab., Upton, NY.), John R. Johnson (Brookhaven National Lab., Upton, NY.), Ricardo B. Schwarz (Los Alamos National Lab., NM.), and Paul B. Desch (Los Alamos National Lab., NM.) *In* NASA. Lewis Research Center, Space Electrochemical Research and Technology Nov. 1993 p 67-84 (For primary document see N94-23345 06-44)

Avail: CASI HC A03/MF A03

Since 1990, there has been an ongoing collaboration among the authors in the three laboratories to (1) prepare alloys of the AB(sub 5) and AB(sub 2) types, using arc-melting/annealing and mechanical alloying/annealing techniques; (2) examine their physico-chemical characteristics (morphology, composition); (3) determine the hydrogen absorption/desorption behavior (pressure-composition isotherms as a function of temperature); and (4) evaluate their performance characteristics as hydride electrodes (charge/discharge, capacity retention, cycle life, high rate capability). The work carried out on representative AB(sub 5) and AB(sub 2) type modified alloys (by partial substitution or with small additives of other elements) is presented. The purpose of the modification was to optimize the thermodynamics and kinetics of the hydriding/dehydriding reactions and enhance the stabilities of the alloys for the desired battery applications. The results of our collaboration, to date, demonstrate that (1) alloys prepared by arc melting/annealing and mechanical alloying/annealing techniques exhibit similar morphology, composition and hydriding/dehydriding characteristics; (2) alloys with the appropriate small amounts of substituent or additive elements: (1) retain the single phase structure, (2) improve the hydriding/dehydriding reactions for the battery applications, and (3) enhance the stability in the battery environment; and (3) the AB(sub 2) type alloys exhibit higher energy densities than the AB(sub 5) type alloys but the state-of-the-art, commercialized batteries are predominantly manufactured using Ab(sub 5) type alloys. Author (revised)

N94-23354*# Jet Propulsion Lab., California Inst. of Tech., Pasadena.
STATUS OF THE DEVELOPMENT OF RECHARGEABLE LITHIUM CELLS
G. Halpert, S. Surampudi, D. Shen, C-K. Huang, S. Narayanan, E. Vamos, and D. Perrone *In* NASA. Lewis Research Center, Space Electrochemical Research and Technology Nov. 1993 p 85-95 (For primary document see N94-23345 06-44)
Avail: CASI HC A03/MF A03

The progress in the development of the ambient temperature lithium - titanium disulfide rechargeable cell under development at the Jet Propulsion Laboratory is described in this paper. Originally aimed at achieving a specific energy of 100 Wh/kg, 'AA' cells have demonstrated 125 Wh/kg at the C/3 discharge rate. The results of evaluating cell design parameters are discussed and cycling test data are also included in the paper. Safety tests results at various over-charge and over discharge conditions and rates proved to be uneventful. The test results of cell with built-in overcharge mechanism proved the concept was feasible. Replacing the lithium foil electrode with a Li(x)C resulted in a capacity at 1mA/cm(exp 2) of 200 mAh/gm and 235 mAh/gm at 0.167 mA. Author (revised)

N94-23355*# National Aeronautics and Space Administration. Lewis Research Center, Cleveland, OH.
IMPEDANCE MEASUREMENTS ON A SPIRAL-WOUND NICKEL/METAL HYDRIDE CELL CYCLED IN A SIMULATED LEO ORBIT
Margaret A. Reid *In its* Space Electrochemical Research and Technology Nov. 1993 p 97-108 (For primary document see N94-23345 06-44)
Avail: CASI HC A03/MF A03

A spiral-wound size C cell was cycled at 25 C in a low earth orbit (LEO) regime at 50 percent depth of discharge (DOD) with approximately five percent over-charge. The nominal capacity was 3.5 AH. The cell was cycled for 2000 cycles. Capacity checks and impedance measurements over the complete range of state of charge were made upon receipt and after 500, 1000, and 2000 cycles. The capacity of the cell was essentially unchanged until after the impedance measurements at 2000 cycles. Only small changes in the impedance parameters were observed, but there was somewhat more scatter in the data after 2000 cycles. When the cell was returned to LEO cycling after 2000 cycles, only 38 percent of the capacity could be obtained. It is believed that the cell failed because of an equipment failure at the end of the final impedance measurements which allowed an over-discharge. Author (revised)

N94-23356*# National Aeronautics and Space Administration. Lewis Research Center, Cleveland, OH.
NASA LEWIS ADVANCED IPV NICKEL-HYDROGEN TECHNOLOGY
John J. Smithrick and Doris L. Britton *In its* Space Electrochemical Research and Technology Nov. 1993 p 109-125 (For primary document see N94-23345 06-44)
Avail: CASI HC A03/MF A03

Individual pressure vessel (IPV) nickel-hydrogen technology was advanced at NASA Lewis and under Lewis contracts. Some of the advancements are as follows: to use 26 percent potassium hydroxide electrolyte to improve cycle life and performance, to modify the state of the art cell design to eliminate identified failure modes and further improve cycle life, and to develop a lightweight nickel electrode to reduce battery mass, hence reduce launch and/or increase satellite payload. A breakthrough in the LEO cycle life of individual pressure vessel nickel-hydrogen battery cells was reported. The cycle life of boiler plate cells containing 26 percent KOH electrolyte was about 40,000 accelerated LEO cycles at 80 percent DOD compared to 3,500 cycles for cells containing 31 percent KOH. Results of the boiler plate cell tests have been validated at NWSC, Crane, Indiana. Forty-eight ampere-hour flight cells containing 26 and 31 percent KOH have undergone real time LEO cycle life testing at an 80 percent DOD, 10 C. The three cells containing 26 percent KOH failed on the average at cycle 19,500. The three cells containing 31 percent KOH failed on the average at cycle 6,400. Validation testing of NASA Lewis 125 Ah advanced design IPV nickel-hydrogen flight cells is also being conducted at NWSC, Crane, Indiana under a NASA Lewis contract. This consists of characterization, storage, and cycle life testing. There was no capacity degradation after 52 days of storage with the cells in the discharged state, on open circuit, 0 C, and a hydrogen pressure of 14.5 psia. The catalyzed wall wick cells have been cycled for over 22,694 cycles with no cell failures in the continuing test. All three of the non-catalyzed wall wick cells failed (cycles 9,588; 13,900; and 20,575). Cycle life test results of the Fibrex nickel electrode has demonstrated the feasibility of an improved nickel electrode giving a higher specific energy nickel-hydrogen cell. A nickel-hydrogen boiler plate cell using an 80 mil thick, 90 percent porous Fibrex nickel electrode has been cycled for 10,000 cycles at 40 percent DOD. Derived from text

N94-23357*# Los Alamos National Lab., NM. Advanced Engineering Technology Group.
PRIMARY AND SECONDARY ELECTRICAL SPACE POWER BASED ON ADVANCED PEM SYSTEMS
N. E. Vanderborgh, J. C. Hedstrom, K. R. Stroh, and J. R. Huff (Ballard Power Corp., Albuquerque, NM.) *In* NASA. Lewis Research Center, Space Electrochemical Research and Technology Nov. 1993 p 129-137 See also N94-14689 (For primary document see N94-23345 06-44)
Avail: CASI HC A02/MF A03

For new space ventures, power continues to be a pacing function for mission planning and experiment endurance. Although electrochemical power is a well demonstrated space power technology, current hardware limitations impact future mission viability. In order to document and augment electrochemical technology, a series of experiments for the National Aeronautics and Space Administration Lewis Research Center (NASA LeRC) are underway at the Los Alamos National Laboratory that define operational parameters on contemporary proton exchange membrane (PEM) hardware operating with hydrogen and oxygen reactants. Because of the high efficiency possible for water electrolysis, this hardware is also thought part of a secondary battery design built around stored reactants - the so-called regenerative fuel cell. An overview of stack testing at Los Alamos and of analyses related to regenerative fuel cell systems are provided in this paper. Finally, this paper describes work looking at innovative concepts that remove complexity from stack hardware with the specific intent of higher system reliability. This new concept offers the potential for unprecedented electrochemical power system energy densities.
Derived from text

N94-23358*# Giner, Inc., Waltham, MA.
PEM REGENERATIVE FUEL CELLS
Larry L. Swette, Anthony B. LaConti, and Stephen A. McCatty *In* NASA. Lewis Research Center, Space Electrochemical Research and Technology Nov. 1993 p 139-148 (For primary document see N94-23345 06-44) (Contract NAS3-24635)
Avail: CASI HC A02/MF A03

This paper will update the progress in developing electrocatalyst systems and electrode structures primarily for the positive electrode of single-unit solid polymer proton exchange membrane (PEM) regenerative fuel cells. The work was done with DuPont Nafion 117 in complete fuel cells (40 sq cm electrodes). The cells were operated alternately in fuel cell mode and electrolysis mode at 80 C. In fuel cell mode, humidified hydrogen and oxygen were supplied at 207 kPa (30 psi); in electrolysis mode, water was pumped over the positive electrode and the gases were evolved at ambient pressure. Cycling data will be presented for Pt-Ir catalysts and limited bifunctional data will be presented for Pt, Ir, Ru, Rh, and Na(x)Pt3O4 catalysts as well as for electrode structure variations. Author (revised)

N94-23359*# Lynntech, Inc., College Station, TX.
HIGH POWER DENSITY PROTON EXCHANGE MEMBRANE FUEL CELLS
Oliver J. Murphy, G. Duncan Hitchens, and David J. Manko *In* NASA. Lewis Research Center, Space Electrochemical Research and Technology Nov. 1993 p 149-166 (For primary document see N94-23345 06-44)
(Contracts F04611-90-C-0095; N00024-91-C-4067)
Avail: CASI HC A03/MF A03

Proton exchange membrane (PEM) fuel cells use a perfluorosulfonic acid solid polymer film as an electrolyte which simplifies water and electrolyte management. Their thin electrolyte layers give efficient systems of low weight, and their materials of construction show extremely long laboratory lifetimes. Their high reliability and their suitability for use in a microgravity environment makes them particularly attractive as a substitute for batteries in satellites utilizing high-power, high energy-density electrochemical energy storage systems. In this investigation, the Dow experimental PEM (XUS-13204.10) and unsupported high platinum loading electrodes yielded very high power densities, of the order of 2.5 W cm(exp -2). A platinum black loading of 5 mg per cm(exp 2) was found to be optimum. On extending the three-dimensional reaction zone of fuel cell electrodes by impregnating solid polymer electrolyte into the electrode structures, Nafion was found to give better performance than the Dow experimental PEM. The depth of penetration of the solid polymer electrolyte into electrode structures was 50-70 percent of the thickness of the platinum-catalyzed active layer. However, the degree of platinum utilization was only 16.6 percent and the roughness factor of a typical electrode was 274. Author (revised)

N94-23360*# Case Western Reserve Univ., Cleveland, OH. Center for Electrochemical Sciences.
THE ELECTROLYTE CHALLENGE FOR A DIRECT METHANOL-AIR POLYMER ELECTROLYTE FUEL CELL OPERATING AT TEMPERATURES UP TO 200 C
Robert Savinell, Ernest Yeager, Donald Tryk, Uziel Landau, Jesse Wainright, Dominic Gervasio, Boris Cahan, Morton Litt, Charles Rogers, and Daniel Scherson *In* NASA. Lewis Research Center, Space Electrochemical Reseearch and Technology Nov. 1993 p 167-179 (For primary document see N94-23345 06-44)
(Contract N00014-92-J-1848)
Avail: CASI HC A03/MF A03

Novel polymer electrolytes are being evaluated for use in a direct methanol-air fuel cell operating at temperatures in excess of 100 C. The evaluation includes tests of thermal stability, ionic conductivity, and vapor transport characteristics. The preliminary results obtained to date indicate that a high temperature polymer electrolyte fuel cell is feasible. For example, Nafion 117 when equilibrated with phosphoric acid has a conductivity of at least 0.4 Omega(exp -1)cm(exp -1) at temperatures up to 200 C in the presence of 400 torr of water vapor and methanol vapor cross over equivalent to 1 mA/cm(exp 2) under a one atmosphere methanol pressure differential at 135 C. Novel polymers are also showing similar encouraging results. The flexibility to modify and optimize the properties by custom synthesis of these novel polymers presents an exciting opportunity to develop an efficient and compact methanol fuel cell. Author (revised)

N94-23361*# Jet Propulsion Lab., California Inst. of Tech., Pasadena.
ADVANCES IN DIRECT OXIDATION METHANOL FUEL CELLS
S. Surampudi, S. R. Narayanan, E. Vamos, H. Frank, G. Halpert, Anthony B. LaConti (Giner, Inc., Waltham, MA.), J. Kosek (Giner, Inc., Waltham, MA.), G. K. Surya Prakash (University of Southern California, Los Angeles.), and G. A. Olah (University of Southern California, Los Angeles.) *In* NASA. Lewis Research Center, Space Electrochemical Research and Technology Nov. 1993 p 181-191 Sponsored in part by ARPA (For primary document see N94-23345 06-44)
Avail: CASI HC A03/MF A03

Fuel cells that can operate directly on fuels such as methanol are attractive for low to medium power applications in view of their low weight and volume relative to other power sources. A liquid feed direct methanol fuel cell has been developed based on a proton exchange membrane electrolyte and Pt/Ru and Pt catalyzed fuel and air/O2 electrodes, respectively. The cell has been shown to deliver significant power outputs at temperatures of 60 to 90 C. The cell voltage is near 0.5 V at 300 mA/cm(exp 2) current density and an operating temperature of 90 C. A deterrent to performance appears to be methanol crossover through the membrane to the oxygen electrode. Further improvements in performance appear possible by minimizing the methanol crossover rate. Author (revised)

N94-23362*# United Technologies Corp., Windsor Locks, CT. Standard Div.
RECENT ADVANCES IN SPE (TM) WATER ELECTROLYZER
James F. McElroy *In* NASA. Lewis Research Center, Space Electrochemical Research and Technology Nov. 1993 p 193-201 (For primary document see N94-23345 06-44)
Avail: CASI HC A02/MF A03

A new cell structure has been introduced into the SPE Water Electrolyzer which has improved overall characteristics significantly. Weight, reliability, and efficiency are the characteristics that are improved the most, with volume having a second order improvement. This paper discusses the capabilities of the new cell structure and the impact it would have in various space applications. Author

N94-23363*# Eltech Systems, Inc., Fairport Harbor, OH.
HIGH ENERGY DENSITY ALUMINUM-OXYGEN CELL
E. J. Rudd and D. W. Gibbons *In* NASA. Lewis Research Center, Space Electrochemical Research and Technology Nov. 1993 p 205-218 (For primary document see N94-23345 06-44)
(Contract MDA972-91-C-0040)
Avail: CASI HC A03/MF A03

An alternative to a secondary battery as the power source for vehicle propulsion is a fuel cell. An example of this is the metal-air fuel cell using metals such as aluminum, zinc, or iron. Aluminum is a particularly attractive candidate, having high energy and power densities, being environmentally acceptable, and having a large, established industrial base for production and distribution. An aluminum-oxygen system is currently under development for a UUV test vehicle, and recent work has focussed upon low corrosion aluminum alloys and an electrolyte management system for processing the by-products of the energy-producing reactions. This paper summarizes the progress made in both areas. Anode materials capable of providing high utilization factors over current densities ranging from S to 150 mA/sq cm have been identified. These materials are essential to realizing an acceptable mission life for the UUV. With respect to the electrolyte management system, a filter/precipitator unit has been successfully operated for over 250 hours in a large scale, half-cell system. Author (revised)

N94-23364*# Auburn Univ., AL. Dept. of Chemical Engineering and the Space Power Inst.
COMPOSITE FIBER STRUCTURES FOR CATALYSTS AND ELECTRODES
Christopher J. Marrion, Donald R. Cahela, Soonho Ahn, and Bruce J. Tatarchuk *In* NASA. Lewis Research Center, Space Electrochemical Research and Technology Nov. 1993 p 219-230 Sponsored in part by the Exxon Foundation (For primary document see N94-23345 06-44)
(Contracts DNA001-85-C-0183; DNA001-90-C-0127; DAAL03-92-2-60205)
Avail: CASI HC A03/MF A03

We have recently envisioned a process wherein fibers of various metals in the 0.5 to 15 micron diameter range are slurried in concert with cellulose fibers and various other materials in the form of particulates and/or fibers. The resulting slurry is cast via a wet-lay process into a sheet and dried to produce a free-standing sheet of 'composite paper.' When the 'preform' sheet is sintered in hydrogen, the bulk of the cellulose is removed with the secondary fibers and/or particulates being entrapped by the sinter-locked network provided by the metal fibers. The resulting material is unique, in that it allows the intimate contacting and combination of heretofore mutually exclusive materials and properties. Moreover, due to the ease of paper manufacture and processing, the resulting materials are relatively inexpensive and can be fabricated into a wide range of three-dimensional structures. Also, because cellulose is both a binder and a pore-former, structures combining high levels of active surface area and high void volume (i.e., low pressure drop) can be prepared as freestanding flow through monoliths. Author (revised)

N94-23365*# Auburn Univ., AL. Space Power Inst.

LIMITING FACTORS FOR CARBON BASED CHEMICAL DOUBLE LAYER CAPACITORS

M. Frank Rose, C. Johnson, T. Owens, and B. Stevens *In* NASA. Lewis Research Center, Space Electrochemical Research and Technology Nov. 1993 p 231-241 (For primary document see N94-23345 06-44)
(Contract DNA001-91-C-0127)
Avail: CASI HC A03/MF A03

The Chemical Double Layer (CDL) capacitor improves energy storage density dramatically when compared with conventional electrolytic capacitors. When compared to batteries, the CDL Capacitor is much less energy dense; however, the power density is orders of magnitude better. As a result, CDL-battery combinations present an interesting pulse power system with many potential applications. Due to the nature of the CDL it is inherently a low voltage device. The applications of the CDL can be tailored to auxiliary energy and burst mode storages which require fast charge/discharge cycles. Typical of the applications envisioned are power system backup, directed energy weapons concepts, electric automobiles, and electric actuators. In this paper, we will discuss some of the general characteristics of carbon-based CDL technology describing the structure, performance parameters, and methods of construction. Further, analytical and experimental results which define the state of the art are presented and described in terms of impact on applications. Author (revised)

N94-23366*# PSI Technology Co., Andover, MA.

A HIGH PERFORMANCE H2-Cl2 FUEL CELL FOR SPACE POWER APPLICATIONS

Everett B. Anderson, E. Jennings Taylor, Gerald Wilemski, and Alan Gelb *In* NASA. Lewis Research Center, Space Electrochemical Research and Technology Nov. 1993 p 243-250 (For primary document see N94-23345 06-44)
Avail: CASI HC A02/MF A03

NASA has numerous airborne/spaceborne applications for which high power and energy density power sources are needed. The proton exchange membrane fuel cell (PEMFC) is an attractive candidate for such a power source. PEMFC's offer many advantages for airborne/spaceborne applications. They have high power and energy densities, convert fuel to electrical power with high efficiency at both part and full load, and can rapidly startup and shutdown. In addition, PEMFC's are lightweight and operate silently. A significant impediment to the attainment of very high power and energy densities by PEMFC's is their current exclusive reliance on oxygen as the oxidant. Conventional PEMFC's oxidize hydrogen at the anode and reduce oxygen at the cathode. The electrode kinetics of oxygen reduction are known to be highly irreversible, incurring large overpotential losses. In addition, the modest open circuit potential of 1.2V for the H2-O2 fuel cell is unattainable due to mixed potential effects at the oxygen electrode. Because of the high overpotential losses, cells using H2 and O2 are capable of achieving high current densities only at very low cell voltages, greatly curtailing their power output. Based on experimental work on chlorine reduction in a gas diffusion electrode, we believe significant increases in both the energy and power densities of PEMFC systems can be achieved by employing chlorine as an alternative oxidant.
Author (revised)

N94-23367*# State Univ. of New York, Buffalo. Composite Materials Research Lab.

HAIRY CARBON ELECTRODES STUDIED BY CYCLIC VOLTAMMETRY AND BATTERY DISCHARGE TESTING

Deborah D. L. Chung, Xiaoping Shui, and Christine A. Frysz (Wilson Greatbatch Ltd., Clarence, NY.) *In* NASA. Lewis Research Center, Space Electrochemical Research and Technology Nov. 1993 p 251-257 (For primary document see N94-23345 06-44)
Avail: CASI HC A02/MF A03

Hairy carbon is a new material developed by growing submicron carbon filaments on conventional carbon substrates. Typical substrate materials include carbon black, graphite powder, carbon fibers, and glassy carbon. A catalyst is used to initiate hair growth with carbonaceous gases serving as the carbon source. To study the electrochemical behavior of hairy carbons, cyclic voltammetry (CV) and discharge testing were conducted. In both cases, hairy carbon results surpassed those of the substrate material alone. Author

N94-23472# Sandia National Labs., Albuquerque, NM.

A REVIEW OF THE WORKSHOP ON FATIGUE LIFE METHODOLOGIES FOR WIND TURBINES

H. J. Sutherland and C. P. Butterfield 1993 8 p Presented at the 13th Energy-Sources Technology Conference and Exhibition (ETCE) on Wind Energy, New Orleans, LA, 23-26 Jan. 1994
(Contracts DE-AC04-94AL-85000; DE-AC04-76DP-00789; DE-FC02-86CH-10311)
(DE94-002039; SAND-93-1375C; CONF-940113-2) Avail: CASI HC A02/MF A01

From March 31 - April 1, 1993, Sandia National Laboratories (SNL) and the National Renewable Energy Laboratory (NREL) hosted a workshop entitled 'Fatigue Life Methodologies.' The purpose of this workshop was to bring together a representative panel of experts to discuss the prediction and measurement of infrequent events that contribute significantly to the damage of wind turbine components. The diverse backgrounds of the participants yielded discussions that covered a wide range of research and design activities from many varying viewpoints. Consensus was not reached on most of the questions raised at the workshop; however, the workshop laid the foundation for a program that now knows what questions must be answered. DOE

N94-23704# Sandia National Labs., Albuquerque, NM.

CONTROL ALGORITHMS FOR EFFECTIVE OPERATION OF VARIABLE-SPEED WIND TURBINES

Oct. 1993 45 p
(Contract DE-AC04-94AL-85000)
(DE94-002607; SAND-90-7112) Avail: CASI HC A03/MF A01

This report describes a computer code, called ASYM, and provides results from its application in simulating the control of the 34-m Test Bed vertical-axis wind turbine (VAWT) in Bushland, Texas. The code synthesizes dynamic wind speeds on a second-by-second basis in the time domain. The wind speeds conform to a predetermined spectral content governed by the hourly average wind speed that prevails at each hour of the simulation. The hourly average values are selected in a probabilistic sense through the application of Markov chains, but their cumulative frequency of occurrence conforms to a Rayleigh distribution that is governed by the mean annual wind speed of the site selected. The simulated wind speeds then drive a series of control algorithms that enable the code to predict key operational parameters such as number of annual starts and stops, annual energy production, and annual fatigue damage at a critically stressed joint on the wind turbine. This report also presents results from the application of ASYM that pertain to low wind speed cut-in and cut-out conditions and controlled operation near critical speed ranges that excite structural vibrations that can lead to accelerated fatigue damage. DOE

N94-23781# Department of Energy, Morgantown, WV. Energy Technology Center.

OVERVIEW OF MOLTEN CARBONATE FUEL CELL TECHNOLOGY DEVELOPMENT

M. C. Williams, E. L. Parsons, Jr., and M. J. Mayfield 1993 9 p Presented at the 28th Intersociety Energy Conversion Engineering Conference, Atlanta, GA, 8-13 Aug. 1993
(DE94-001911; DOE/METC-C/94/7110; CONF-930804-21) Avail: CASI HC A02/MF A01

The molten carbonate fuel cell (MCFC) has been identified as a promising energy conversion product for development and commercialization. Overall DOE MCFC program goal is to develop and commercialize low-cost, simple fuel cell systems. Objective of the MCFC program is to develop and demonstrate MCFC power plant systems. Significant progress has already been made in developing the MCFC technology in the U.S. Manufacturing and test facility development and testing by the MCFC developers has also been significant. Product improvement issues need to be resolved to vector the MCFC technology from its current status to a multi-fuel, integrated, simple, low-cost, modular, market-responsive power plant product. MCFC's must undergo continuing product refinement to ensure that durability and cost reduction through modularization and stack manufacturing scale-up occurs. MCFC developers need to continue to be responsive to end-users in potential markets. MCFC's appear to have a place in a decentralized power industry future. Natural gas availability appears to play a key role in MCFC commercialization. DOE

N94-23785# Westinghouse Electric Corp., Pittsburgh, PA. Science and Technology Center.

CONTAMINANT EFFECTS IN SOLID OXIDE FUEL CELLS

E. R. Ray and N. J. Maskalick 1993 12 p Presented at the Joint Contractors Meeting on Advanced Turbine Systems, Fuel Cells and Coal-Fired Heat, Morgantown, WV, 3-5 Aug. 1993
(Contract DE-AC21-89MC-26355)
(DE94-002963; DOE/MC-26355/94/C0254; CONF-930893-16) Avail: CASI HC A03/MF A01

Ammonia impurity up to 5000 ppM in simulated coal gas does not contribute much to SOFC voltage degradation (1000 C, 350 mA/sq cm) over 6500 h (as testing time increases, this effect is expected to be nil). HCl impurity in coal gas at 1 ppM does not have a detectable effect on SOFC performance up to 6500 h. H_2S impurity at 0.1 ppM in coal gas can be tolerated by state of the art SOFC's, along with 5000 ppM ammonia and 1 ppM HCl, over at least 5000 h. Silica impurity in coal gas can be carried over to the SOFC and deposited; this carryover is not enhanced by 56% H_2O in the fuel; silica is not expected to have a major effect on SOFC performance. Zinc vapor impurity in coal gas, as generated over heated ZnO, may be carried over to SOFC but not deposit; the carryover may be enhanced by HCl. DOE

N94-24071*# National Aeronautics and Space Administration. Lewis Research Center, Cleveland, OH.

A SOLAR PHOTOVOLTAIC POWER SYSTEM FOR USE IN ANTARCTICA

Lisa L. Kohout, Anthony Merolla (Sverdrup Technology, Inc., Brook Park, OH.), and Anthony Colozza (Sverdrup Technology, Inc., Brook Park, OH.) Dec. 1993 15 p
(Contract NAS3-25266; RTOP 199-52-82)
(NASA-TM-106417; E-8254; NAS 1.15:106417) Avail: CASI HC A03/MF A01

A solar photovoltaic power system was designed and built at the NASA Lewis Research Center as part of the NASA/NSF Antarctic Space Analog Program. The system was installed at a remote field camp at Lake Hoare in the Dry Valleys, and provided a six-person field team with electrical power for personal computers and printers, lab equipment, lighting, and a small microwave oven. The system consists of three silicon photovoltaic sub-arrays delivering a total of 1.5 kWe peak power, three lead-acid gel battery modules supplying 2.4 kWh, and an electrical distribution system which delivers 120 Vac and 12 Vdc to the user. The system was modularized for ease of deployment and operation. Previously the camp has been powered by diesel generators, which have proven to be both noisy and polluting. The NSF, in an effort to reduce their dependence on diesel fuel from both an environmental and cost standpoint, is interested in the use of alternate forms of energy, such as solar power. Such a power system also will provide NASA with important data on system level deployment and operation in a remote location by a minimally trained crew, as well as validate initial integration concepts. Author (revised)

N94-24499# Oak Ridge National Lab., TN.

CONSIDERATIONS IN IMPLEMENTING INTEGRATED BIOMASS ENERGY SYSTEMS IN DEVELOPING COUNTRIES

R. D. Perlack and J. W. Ranney 1993 6 p Presented at the 1st Biomass Conference of the Americas: Energy, Environment, Agriculture, and Industry, Burlington, VT, 30 Aug. - 2 Sep. 1993
(Contract DE-AC05-84OR-21400)
(DE93-018720; CONF-9308106-1) Avail: CASI HC A02/MF A01

In this paper, we discuss the issues and barriers associated with implementing integrated biomass energy systems in developing countries. An integrated biomass energy system is dependent on sustainably grown and managed energy crops, is supportive of rural development, is environmentally beneficial (locally and globally), is adapted to local conditions, takes advantage of by- and co-products, and uses conversion technologies that have been optimized for biomass. A preliminary evaluation of a biomass to electricity project relying on plantation grown feedstocks in rural Yunnan Province in Southwest China provided some financial/economic results, general conclusions, and an initial framework for conducting such assessments. Our assessment indicates that social and environmental benefits are substantial and that investment in the facility is well-justified. However, there are so many considerations to take into account when assessing biomass energy systems that their evaluation is exceedingly complex. These considerations are grouped into biomass production, biomass logistics and transport, and biomass conversion. Implementing such systems requires another grouping of considerations into energy and economics, institutional and social issues, and environmental issues. These are further defined in an effort to establish a framework of evaluation and assessment for other such projects. The conclusions that such a project would be viable in rural China is shadowed by many site-specific circumstances and highlights the need for systematic and integrated appraisal. DOE

N94-24509# Midwest Research Inst., Golden, CO.

THIN FILM CADMIUM TELLURIDE PHOTOVOLTAIC CELLS

C. D. Compaan (Toledo Univ., OH.) and R. G. Bohn (Toledo Univ., OH.) Oct. 1993 28 p
(Contract DE-AC02-83CH-10093)
(DE94-000201; NREL/TP-451-5813) Avail: CASI HC A03/MF A01

This report describes work to develop and optimize radio-frequency (RF) sputtering and laser-driven physical vapor deposition (LDPVD) for CdTe-based thin-film solar cells. Both of these techniques are vacuum-based and share several other common physical principles. However, they differ somewhat in the typical kinetic energies of Cd, Te, and S that impact on the growth surface. The values of several processing parameters-optimized with the LDPVD technique-were taken as starting values for the RF sputtering method. We completed an initial optimization of the sputtering parameters for the CdTe growth and also successfully sputtered CdS for the first time. In addition, we successfully fabricated what we believe are the first CdS/CdTe cells in which RF sputtering was used for both CdS and CdTe layers. We achieved an all-LDPVD cell with an air mass (AM) 1.5 efficiency of 10.5% and an all-RF-sputtered cell with AM 1.5 efficiency of 10.4%, as tested by NREL. DOE

N94-24512# Midwest Research Inst., Golden, CO.

OVERVIEW OF THE STATUS AND PROGRESS IN PHOTOVOLTAICS RESEARCH IN THE UNITED STATES

T. Surek 1993 7 p Presented at the International Solar Energy Society World Congress, Budapest, Hungary, 23-27 Aug. 1993
(Contract DE-AC02-83CH-10093)
(DE94-000981; CONF-930838-2) Avail: CASI HC A02/MF A01

Photovoltaics (PV) is a semiconductor technology that directly converts sunlight to electricity. Research over the past 20 years has resulted in the discovery of new PV materials, devices, and fabrication approaches: continuing improvements in the efficiency and reliability of solar cells and modules: and lower PV module and system costs. Along with improvements in the technology and manufacturing have come a large number of new, cost-effective uses, including international applications in mostly off-grid, remote locations, and various grid-connected and off-grid applications in the United States. This paper reviews the rapid progress from the laboratory to the marketplace in PV technology in the United States. DOE

N94-24563*# Jet Propulsion Lab., California Inst. of Tech., Pasadena.

RESULTS OF THE 1993 NASA/JPL BALLOON FLIGHT SOLAR CELL CALIBRATION PROGRAM

B. E. Anspaugh and R. S. Weiss 1 Oct. 1993 23 p
(NASA-CR-195158; JPL-PUBL-93-30; NAS 1.26:195158) Avail: CASI HC A03/MF A01

The 1993 solar cell calibration balloon flight was completed on July 29, 1993. All objectives of the flight program were met. Forty modules were carried to an altitude of 120,000 ft (36.6 km). Data telemetered from the modules was corrected to 28 C and to 1 AU. The calibrated cells have been returned to 8 participants and can now be used as reference standards in simulator testing of cells and arrays. Derived from text

N94-24654# Argonne National Lab., IL.

SUPERCONDUCTING ENERGY STORAGE

R. F. Giese 1 Oct. 1993 82 p
(Contract W-31-109-eng-38)
(DE94-002248; ANL/ES/RP-81001) Avail: CASI HC A05/MF A01

This report describes the status of energy storage involving superconductors and assesses what impact the recently discovered ceramic superconductors may have on the design of these devices. Our description is intended for R&D managers in government, electric utilities, firms, and national laboratories who wish an overview of what has been done and what remains to be done. It is assumed that the reader is acquainted with superconductivity, but not an expert on the topics discussed here. Indeed, it is the author's aim to enable the reader to better understand the experts who may ask for the reader's attention, support, or funding. This report may also inform scientists and engineers who, though expert in related areas, wish to have an introduction to our topic. DOE

N94-24701*# Alaska Univ., Fairbanks. Dept. of Electrical and Mechanical Engineering.
WISPER: WIRELESS SPACE POWER EXPERIMENT Final Report
Joseph Hawkins Jun. 1993 211 p
(Contract NASw-4435)
(NASA-CR-195538; NAS 1.26:195538) Avail: CASI HC A10/MF A03

The 1993 Advanced Design Project at the University of Alaska Fairbanks was to design a spacecraft as a technology demonstration of wireless power transmission (WPT). With cost effectiveness as a design constraint, a micro-satellite in low earth orbit (LEO) was chosen for the mission. Existing and near term technologies were analyzed and selected for the project. In addition to the conceptual design of the payload, support systems, and structure, the analysis included attention to safety, environmental impact, cost, and schedule for construction and operation. Wireless power beaming is not a new concept. Experimental demonstrations and study efforts have continued since the early 1960's. With the latest progress in transmitter and receiver technology, the next natural step is to beam power from earth to space. This proposed flight demonstration will advance the science of power beaming and prove the viability of various applications of WPT in space. Two methods of power beaming will be examined during the two separate phases of the spacecraft life. The first phase will demonstrate the technology and examine the theory of microwave power transmission at a high frequency. Special aspects of the first phase will include a highly accurate attitude control system and a 14 m inflatable parabolic antenna. The second phase will investigate the utilization of high intensity laser power using modified photovoltaic arrays. Special instrumentation on the spacecraft will measure the conversion efficiency from the received microwave or laser power to direct current power. Author

N94-25417# Technical Research Centre of Finland, Espoo. Metals Lab.
METAL HYDRIDE STORAGE [HYDRIDIVETYVARASTO]
Seppo Taehtinen Oct. 1992 33 p In FINNISH Sponsored by Ministry of Trade and Industry, Finland, and Technical Research Centre of Finland, Espoo
(VTT-JULK-769; ISBN-951-38-4117-0; ETN-94-95242) Copyright Avail: CASI HC A03/MF A01

The worldwide use of wind and solar energy as sources for heat and electricity is not a viable energy choice due to unavailability of an environmentally benign energy carrier which is also storable, transportable, and convertible. Hydrogen is an almost ideal energy carrier, and it is compatible with existing energy systems. In the long term, hydrogen is capable of replacing fossil energy sources. Metal hydrides react reversibly with hydrogen and are a compact and safe method to store hydrogen gas at ambient temperatures and pressures. The construction and testing of a metal hydride hydrogen storage vessel is reported. The storage capacity of the vessel was 1.6 cu m of hydrogen gas. Filling pressure was 5 bar at the temperature of 20 C. Release pressure depended on the temperature and varied between 2 to 40 bar as the storage temperature varied between 20 to 75 C. Reversibility of the storage vessel was 93 percent at a temperature of 20 C. ESA

N94-25464# Deutsche Forschungsanstalt fuer Luft- und Raumfahrt, Stuttgart (Germany). Abt. Bauteilgestaltung.
THE HEXAGONAL COMPOUND PARABOLIC CONCENTRATOR DESIGN AND CONSTRUCTION
Walter E. C. Pritzkow Dec. 1990 32 p
(DLR-Mitt-93-03; ETN-94-95205) Avail: CASI HC A03/MF A01

The hexagonal compound parabolic concentrator, a secondary concentrator with a concentration ratio of three, is presented. This concentrator is designed for the Small Solar Power System Central Receiver System (SSPS-CRS) solar tower power plant to concentrate in a second stage the solar radiation gathered by the heliostat field. The flux distribution at the exit will be higher and more homogeneous. This concentrator is designed with a hexagonally shaped inlet contour to allow a modular design of secondary concentrators and windowed volumetric receivers. The modular design is needed because the receiver window size is limited due to manufacturing restrictions. ESA

N94-25479# Deutsche Forschungsanstalt fuer Luft- und Raumfahrt, Stuttgart (Germany). Abt. Bauteilgestaltung.
THE PRESSURE LOADED VOLUMETRIC CERAMIC RECEIVER 500 kW VERSION DESIGN AND CONSTRUCTION
Walter E. C. Pritzkow Dec. 1990 35 p
(DLR-Mitt-93-02; ETN-94-95204) Avail: CASI HC A03/MF A01

The design of a Pressure Loaded Volumetric Ceramic Receiver (PLVCR), a solar receiver to convert concentrated solar radiation into process heat, is presented. The PLVCR has a domed quartz glass window, a segmented domed ceramic foam absorber, and was designed for a power level of 500 kW to heat up air from ambient to 1000C at pressures up to 10 bar. With a secondary concentrator located in front of the receiver the whole system was installed on the Small Solar Power System Central Receiver System (SSPS-CRS) tower. During first tests, air was heated up to 700C at pressures up to 3.6 bar, showing the function of a modular design of receiver and secondary concentrator. ESA

N94-23994# Fokker Space and Systems, Amsterdam (Netherlands).
THE COLUMBUS SOLAR ARRAY MECHANISMS
R. Zwanenburg *In* ESA, The Fifth European Space Mechanisms and Tribology Symposium Apr. 1993 6 p (For primary document see N94-23985 06-37)
Copyright Avail: CASI HC A02/MF A04

45 ENVIRONMENT POLLUTION

Includes atmospheric, noise, thermal, and water pollution.

N94-22887# Argonne National Lab., IL.
OVERVIEW OF GLOBAL GREENHOUSE EFFECTS
R. A. Reck 1993 12 p Presented at the 5th International Energy Conference, Seoul, Republic of Korea, 18-22 Oct. 1993
(Contract W-31-109-eng-38)
(DE93-041165; ANL/ER/CP-80457; CONF-9310173-1) Avail: CASI HC A03/MF A01

The factors that influence the evolution of climate and climate change are reviewed. Recent studies have confirmed that CO2, O3, N2O, CH4, and chlorofluorocarbons are increasing in abundance in the atmosphere and can alter the radiation balance by means of the so-called greenhouse effect. The greenhouse effect is a well-accepted phenomenon, but the prediction of its consequences is much less certain. Attempts to detect a human-caused temperature change are still inconclusive. A discussion of the scientific basis for the greenhouse effect, its relationship to the abundances of greenhouse gases, and the evidence confirming the increases in the abundances are presented. The basis for climate modeling is presented together with an example of the model outputs from one of the most sophisticated modeling efforts. Uncertainties in the present understanding of climate are outlined. DOE

N94-22913# National Oceanic and Atmospheric Administration, Boulder, CO. Wave Propagation Lab.
NOAA FEDERAL/STATE COOPERATIVE PROGRAM IN ATMOSPHERIC MODIFICATION RESEARCH. COLLECTED PUBLICATION TITLES AND ABSTRACTS
R. F. Reinking Apr. 1993 92 p
(PB93-198125; NOAA-TM-ERL-WPL-231) Avail: CASI HC A05/MF A01

The volume contains the titles and abstracts of technical publications through fiscal year 1992 that are the products of the NOAA Federal/State Cooperative Program in Atmospheric Modification Research. The program is focused on the very interdisciplinary science of purposeful cloud modification for precipitation enhancement and hail suppression, and unintentional modification of clouds and precipitation. The audience includes, for example, water managers, policy makers, scientists, practitioners in the field, and the interested public. Listed are publications on topics including but not limited to: cloud and precipitation processes, numerical cloud and atmospheric mesoscale modeling, atmospheric and storm monitoring instrumentation and technologies, aerosol transport and dispersion in clouds and over complex terrain, cloud seeding technologies and effects, agricultural responses to cloud modification, weather economics and societal aspects of cloud modification, unintentional weather and climate modification, and precipitation and hydrological assessment and forecasting. NTIS

N94-23016 Pacific Northwest Lab., Richland, WA.
US DEPARTMENT OF ENERGY PHASEOUT OF CFC-REFRIGERANTS
K. B. Miller, C. W. Purcell, M. H. Turner, and D. R. Conover Sep. 1993 13 p Presented at the International Specialty Conference on Control of Ozone Depleting Substances: Delivering the Montreal Protocol, Whistler, Ontario, 22-24 Sep. 1993 Limited Reproducibility: More than 20% of this document may be affected by poor print
(Contract DE-AC06-76RL-01830)
(DE94-001668; PNL-SA-23021; CONF-9309137-1) Avail: Issuing Activity (Department of Energy (DOE))

DOE's goal is to phase out the use of Ozone Depleting Substances (ODS's) by implementing environmentally safe alternative substances and processes within a timeframe that is consistent with the requirements and spirit of Executive Order 12843 and Title 6 of the Clean Air Act. Refrigeration and air conditioning uses of CFC's present a challenge to DOE, as well as other industrial users of these applications, because of the limited number of approved CFC alternatives currently available. The estimated costs associated with retrofitting or replacing refrigerant equipment are high, and there is some concern over whether sufficient production capacity exists to meet the demand for equipment and retrofits from all consumers. On the other hand, there is also concern that DOE facilities and other users of CFC refrigerants may have difficulty obtaining sufficient quantities of these chemicals to service existing needs. To assist DOE facilities in planning for CFC phaseout, DOE Headquarters contracted with PNL to develop a Refrigerant Management Plan that uses a life-cycle cost analysis based on the equipment's remaining useful life. DOE

N94-23026# New Energy and Industrial Technology Development Organization, Tokyo (Japan).
FEASIBILITY STUDY ON A CO2 GLOBAL RECYCLING SYSTEM USING NATURAL ENERGY
Mar. 1993 226 p In JAPANESE
(DE94-714889; NEDO-GET-9210-2) Avail: CASI HC A11/MF A03

A proposal was made to solve global environmental problems and energy problems simultaneously by combining treatment of a great amount of CO2 with transportation of new energies difficult of large-scale, long-distance transportation. This system uses solar cells to produce hydrogen, which is synthesized with recovered CO2 to produce CH3OH and transported to users by tankers. Solar energy is available several thousand times as much as the currently mineable fossil fuels (=10 TW), and can handle the worldwide demand even with solar cells of 10% efficiency that are installed covering 2% to 3% of the desert area. A problem is that the production site is located very far away from demand areas, for example, 10,000 km on average from Japan, and moreover across oceans. The CO2 recycling system has problems on energy balance and material balance. The energy balance is from -60% to -75%. Accordingly, the energy base was selected at 'window of the desert' (desert adjoining the seashore), and a new type CO2 tanker was proposed. CO2 causes a carbon deficiency because the CO2 purity is less than 90%. DOE

N94-23277*# Pennsylvania State Univ., University Park. Dept. of Meteorology.
IN SITU DETECTION OF TROPOSPHERIC OH, HO2, NO2, AND NO BY LASER-INDUCED FLUORESCENCE IN DETECTION CHAMBERS AT REDUCED PRESSURES Semiannual Progress Report, 1 Apr. - 30 Sep. 1993
William H. Brune 26 Dec. 1993 36 p Submitted for publication
(Grant NAG1-1057)
(NASA-CR-194810; NAS 1.26:194810) Avail: CASI HC A03/MF A01

This report is a brief summary of the status of work on the grant entitled 'In situ detection of tropospheric OH, HO2, NO2, and NO by laser induced fluorescence in detection chambers at low pressures.' The basic instrument characteristics have been established, and have been reported in a manuscript, included as an appendix to this report, that has been accepted by the Journal of Geophysical Research. Currently, two efforts are under way. First, instrument tests and calibrations are continuing. These efforts include field measurements and an informal inter comparison in Colorado last August and September. Second, new technologies in lasers and detectors are being implemented to make the instrument smaller, lighter, and more energy efficient. Such instrument modifications are essential for measurements from aircraft, high scaffolding in forests, and ships. Derived from text

N94-23497# Rijksinstituut voor Volksgezondheid en Milieuhygieene, Bilthoven (Netherlands).
EXPLORATORY REPORT ANTIMONY AND ANTIMONY COMPOUNDS
W. Slooff, P. F. H. Bont (Resources Planning Consultants B.V., Delft, Netherlands.), J. M. Hesse, and B. Loos Oct. 1992 47 p
(PB93-224004; RIVM-710401020) Avail: CASI HC A03/MF A01

The report contains general information on antimony and antimony compounds concerning the existing standards, emissions, exposure levels, and effect levels. The document is to be considered as a start for the national discussion during an exploratory meeting on integrated criteria documents. Antimony is not produced in the Netherlands, but is found in various ores processed in the Netherlands. Antimony is applied as a fire retardant, in alloys and pigments, as a catalyst, and in light bulbs. Many antimony-emitting sources are known but the emission figures are often lacking. The most important known sources of emissions to air are light bulb production and pigment industry, and possibly the burning of fire retardants, whereas hunting, shooting, and sport fishing contribute significantly to emissions to soil and water. NTIS

N94-23700# Lawrence Livermore National Lab., CA.
RADIATIVE FORCING CALCULATIONS FOR SF6 AND CH4 USING A CORRELATED k-DISTRIBUTION TRANSMISSION MODEL
A. S. Grossman, K. E. Grant, and D. J. Wuebbles 11 Aug. 1993 23 p
(Contract W-7405-eng-48)
(DE94-001855; UCRL-ID-115042) Avail: CASI HC A03/MF A01

A correlated k-distribution model for the atmospheric transmission of major molecular species has been used to calculate the tropospheric radiative forcing for the ground state, v(sub 3) band of SF6 and CH4. A mid-latitude summer, clear sky approximation, temperature-pressure distribution was used in the radiative transfer calculations. For the SF6 calculations a value of 0.26 W/m(exp 2) was obtained for the v(sub 3) band forcing using a new value of the measured integrated band absorption for SF6. The abundance used was 1 ppbv of SF6. Hot band contributions to the forcing are estimated to be on the order of three times the value of the v(sub 3) value giving a total radiative forcing of about 0.73 W/m(exp 2). For the CH4 calculation a value of 1.71 W/m(exp 2) was obtained and this number agrees with previously published CH4 radiative forcing values to within four percent. The radiative forcing calculation for SF6 is used to estimate the global warming potential (GWP) of SF6 using an approximate model developed to provide reasonably accurate GWP's. The results give GWP's for SF6 of the order of 12000-25000 (CO2 = 1). We estimate the likely range of the radiative forcing and GWP values based on two recent measurements of the total integrated band strength of SF6. Comparison of the GWP's of SF6 to those of CF4 (3600-8500) and CFC-11 (4500-1400) indicates that SF6 has the potential to be a major greenhouse gas if large amounts are introduced into the atmosphere. DOE

N94-23794# Oak Ridge National Lab., TN.
PERFORMANCE OF THE CARBON DIOXIDE INFORMATION ANALYSIS CENTER (CDIAC)
F. W. Stoss and S. B. Jones 1993 13 p Presented at the INFOTECH 1993 Conference, Oak Ridge, TN, 20-23 Oct. 1993
(Contract DE-AC05-84OR-21400)
(DE94-002190; CONF-9310145-2) Avail: CASI HC A03/MF A01

The Carbon Dioxide Information Analysis Center (CDIAC) provides information and data resources in support of the US Department of Energy's Global Change Research Program. CDIAC also serves as a resource of global change information for a broader international community of researchers, policymakers, managers, educators, and students. The number of requests for CDIAC's data products, information services, and publications has grown over the years and represents multidisciplinary interests in the physical, life, and social sciences and from diverse work settings in government, business, and academia. CDIAC's staff addresses thousands of requests yearly for data and information resources. In response to these requests, CDIAC has distributed tens of thousands of data products, technical reports, newsletters, and other information resources worldwide since 1982. This paper describes CDIAC, examines CDIAC's user community, and describes CDIAC's response to requests for information. The CDIAC Information System, which serves as a comprehensive PC-based inventory and information management tracking system, is also described. DOE

N94-23813 National Swedish Road and Traffic Research Inst., Linkoeping.

ESTIMATION OF DELAYS AND EMISSIONS AT FOUR-WAY JUNCTIONS WITH DIFFERENT FORMS OF REGULATION, PRINCIPALLY FOUR-WAY MANDATORY STOP [UPPSKATTNING AV FOERDROEJNING OCH AVGASUTSLAEPP IFYRVAEGSKORSNINGAR MED OLIKA REGLERINGSFORMER, SPECIELLT FYRVAEGSSTOPP]

P. Henriksson 1992 48 p In SWAHILI Limited Reproducibility: More than 20% of this document may be affected by microfiche quality
(PB94-105236; VTI/Meddelande-700) Avail: Issuing Activity (National Technical Information Service (NTIS))

The bulletin reports an estimation of emissions and delays at four-way junctions with different types of regulation: mandatory stop on two approaches, mandatory stop on four approaches, and traffic signals. Variables such as incoming traffic flow, traffic distribution on the primary and secondary road, and the proportion of turning vehicles have been varied. The delay at a junction with mandatory stop on all approaches has been estimated to be of the same order of size as the delay at a junction regulated by signals, i.e. up to twice as long as in the case of a mandatory stop on two approaches. Emissions are lowest at a junction with mandatory stop on two approaches. With traffic signals, emissions increase by 5-10% and with mandatory stop on all approaches the increase is 10-20%. The difference in emissions increases when either the proportion of turning vehicles decreases or the distribution of the traffic on the intersecting roads is uneven. NTIS

N94-23818 Research Triangle Inst., Research Triangle Park, NC.

FUNDAMENTAL STUDY OF NO(x) CONTROL IN CATALYTIC COMBUSTION Annual Report, Jan. - Dec. 1992

S. K. Agarwal, B. W. Jang, M. Oecal (Pittsburgh Univ., PA.), A. Riley (Pittsburgh Univ., PA.), and G. Marcelin (Pittsburgh Univ., PA.) Jan. 1993 61 p Limited Reproducibility: More than 20% of this document may be affected by microfiche quality
(Contract GRI-5092-260-2333)
(PB94-112323; GRI-93/0076) Avail: CASI HC A04

A series of La(1-x)Sr(x)CoO3 perovskite catalysts have been used to study the catalytic combustion of methane and the formation/destruction of NO(x). Addition of Sr to LaCoO3 increased the catalytic activity for methane combustion and NO(x) reduction. While the methane combustion activity exhibited an optimum with the Sr content in the catalyst, the NO(x) reduction activity increased linearly with the Sr amount. Catalyst characterization using TPR, TPOE, and SSITKA showed an increase in oxygen exchange and oxygen mobility with the Sr content. The results suggest that the NO(x) destruction activity is related to the catalyst oxygen mobility. Under catalytic combustion conditions, emissions of NO(x) are less than 3 ppm at temperatures up to 1100 C. NTIS

N94-24078*# National Aeronautics and Space Administration. Goddard Space Flight Center, Greenbelt, MD.

PARTICIPATION IN TOMS MISSIONS

Robert D. Hudson 8 Feb. 1994 17 p
(Grant NAG5-1696)
(NASA-CR-195110; NAS 1.26:195110) Avail: CASI HC A03/MF A01

In the past year we have been investigating a new algorithm for the derivation of column sulfur dioxide, column ozone, and aerosol optical depth from the Total Ozone Mapping Spectrometer (TOMS) High Density TOMS (HDT) archived albedos. Simulations of the measured albedos were made using a radiative transfer model, and a technique developed to separate the effects of the aerosol optical depth from the absorption optical depth. The retrieval adopted obtained values from the three parameters with high accuracy. This retrieval was then applied to the TOMS data. Derived from text

N94-24104*# National Aeronautics and Space Administration. Goddard Space Flight Center, Greenbelt, MD.

THE ATMOSPHERIC EFFECTS OF STRATOSPHERIC AIRCRAFT: A THIRD PROGRAM REPORT

Richard S. Stolarski, ed. and Howard L. Wesoky, ed. (National Aeronautics and Space Administration, Washington, DC.) Washington NASA Nov. 1993 405 p
(NASA-RP-1313; NAS 1.61:1313) Avail: CASI HC A18/MF A04

A third report from the Atmospheric Effects of Stratospheric Aircraft (AESA) component of NASA's High-Speed Research Program (HSRP) is presented. Market and technology considerations continue to provide an impetus for high-speed civil transport research. A recent United Nations Environment Program scientific assessment showed that considerable uncertainty still exists about the possible impact of aircraft on the atmosphere. The AESA was designed to develop the body of scientific knowledge necessary for the evaluation of the impact of stratospheric aircraft on the atmosphere. The first Program report presented the basic objectives and plans for AESA. This third report marks the midpoint of the program and presents the status of the ongoing research on the impact of stratospheric aircraft on the atmosphere as reported at the third annual AESA Program meeting in June 1993. The focus of the program is on predicted atmospheric changes resulting from projected HSCT emissions. Topics reported on cover how high-speed civil transports (HSCT) might affect stratospheric ozone, emissions scenarios and databases to assess potential atmospheric effects from HSCT's, calculated results from 2-D zonal mean models using emissions data, engine trace constituent measurements, and exhaust plume/aircraft wake vortex interactions.
Author (revised)

N94-24476 Environmental Protection Agency, Research Triangle Park, NC. Office of Air Quality Planning and Standards.

ALTERNATIVE CONTROL TECHNIQUES DOCUMENT: NOx EMISSIONS FROM STATIONARY RECIPROCATING INTERNAL COMBUSTION ENGINES

Jul. 1993 317 p Limited Reproducibility: More than 20% of this document may be affected by microfiche quality
(PB94-104494; EPA/453/R-93/032) Avail: Issuing Activity (National Technical Information Service (NTIS))

The alternative control techniques (ACT) document describes available control techniques for reducing NOx emission levels from rich-burn and lean-burn natural gas-fired, diesel, and dual-fuel stationary reciprocating internal combustion engines. A discussion of the formation of NOx and uncontrolled emission levels is included. Control techniques include parameter adjustments, prestratified charge, selective and nonselective catalytic reduction, and low-emission combustion. Achievable controlled NOx emission levels, costs and cost effectiveness, and environmental impacts are presented, and the applicability of these control techniques to new equipment and retrofit applications is discussed. NTIS

N94-24506# Sandia National Labs., Albuquerque, NM.

OZONE DEPLETION, PARADIGMS, AND POLITICS

Ronald L. Iman 1993 8 p Presented at the 1993 American Society for Quality Control/American Statistics Association Fall Meeting, Rochester, NY, 14-15 Oct. 1993
(Contract DE-AC04-94AL-85000)
(DE94-001600; SAND-93-1296C; CONF-9310203-1) Avail: CASI HC A02/MF A01

The destruction of the Earth's protective ozone layer is a prime environmental concern. Industry has responded to this environmental problem in the following ways: implementing conservation techniques to reduce the emission of ozone-depleting chemicals (ODC's); using alternative cleaning solvents that have lower ozone depletion potentials (ODP's); developing new, non-ozone-depleting solvents, such as terpenes; and developing low-residue soldering processes. This paper presents an overview of a joint testing program at Sandia and Motorola to evaluate a low-residue (no-clean) soldering process for printed wiring boards (PWB's). Such processes are in widespread use in commercial applications because they eliminate the cleaning operation. The goal of this testing program was to develop a database that could be used to support changes in the mil-specs. In addition, a joint task force involving industry and the military has been formed to conduct a follow-up evaluation of low-residue processes that encompass the concerns of the tri-services. The goal of the task force is to gain final approval of the low-residue technology for use in military applications. DOE

N94-24525 Environmental Protection Agency, Ann Arbor, MI. Office of Mobile Sources.
EPA'S SURVEY OF IN-USE DRIVING PATTERNS: IMPLICATIONS FOR MOBILE SOURCE EMISSION INVENTORIES
Phil Enns, John German, and Jim Markey 1993 20 p See also PB93-197903 Limited Reproducibility: More than 20% of this document may be affected by microfiche quality
(PB94-118502) Avail: CASI HC A03

The paper presents EPA's preliminary findings on in-use driving behavior and vehicle emissions. EPA contracted for several large-scale studies of in-use driving patterns in order to assess the adequacy of the driving cycle used in the current FTP. The driving behavior characteristics covered here are: soak time, start driving, and speed and acceleration not represented in the current FTP. Two additional factors, air conditioning and road grade, are examined for their potential emission impact. Following this introduction, the paper is divided into five sections. This is followed by a discussion of EPA's cycle development efforts. The third section discusses the vehicle emission testing program and the fourth section presents an emission assessment based on the results of the test program. The last section summarizes the preliminary implications for current emission inventories.
NTIS

N94-24573 Rijkswaterstaat, The Hague (Netherlands). Tidal Waters Div.
ANALYSIS OF VULNERABILITY TO THE IMPACTS OF SEA LEVEL RISE: A CASE STUDY FOR THE NETHERLANDS
Aug. 1992 95 p Limited Reproducibility: More than 20% of this document may be affected by microfiche quality
(PB94-111150; DGW-93.034) Avail: Issuing Activity (National Technical Information Service (NTIS))

The Netherlands' case study on the vulnerability to the impacts of sea level rise is one of a series of case studies according to the common methodology for the execution of Vulnerability Analysis (VA). The Netherlands case study aimed to provide: a contribution to the development of the common methodology for the execution of VA case studies; an automated procedure for the generation and presentation of vulnerability profiles; an assessment of the Netherlands' vulnerability to sea level rise for different scenarios and response strategies.
NTIS

N94-24633 Selskapet for Industriell og Teknisk Forskning, Trondheim (Norway).
SNOW MODELING, WATER RESOURCES, CLIMATE CHANGE
Sten Bergstroem (Swedish Meteorological and Hydrological Inst., Norkoeping.), Carl Egede Boeggild (Alfred-Wegener-Inst. for Polar Research, Bremerhaven, Germany.), Kristinn Einarsson (National Energy Authority, Iceland.), Yngvar Gjessing (Bergen Univ., Norway.), and Nils Roar Saelthun (Norwegian Water Resources and Electricity Board, Oslo.) 30 Sep. 1992 16 p Limited Reproducibility: More than 20% of this document may be affected by microfiche quality
(PB93-201770; STF60-A92023) Avail: CASI HC A03

Effects of climate change have during the last few years been addressed between hydrologists. In 1991 a research project: 'Climate Change and Energy Production' was started as a joint project between the Nordic countries. The scope of the project is to assess the impacts of a climate change on water resources. As the energy production in the Nordic countries heavily relies on hydropower, climate change impacts on water resources will also affect energy production systems as well as energy consumption. Therefore, the impacts on energy production are focused on in the project.
NTIS

N94-24853*# California Univ., Irvine. Dept. of Earth System Science.
EFFECT OF LAND USE CHANGE ON THE CARBON CYCLE IN AMAZON SOILS Final Technical Report, 20 Feb. 1994
Susan E. Trumbore and Eric A. Davidson (Woods Hole Research Center, MA.) 1994 27 p
(Grant NAGw-2748)
(NASA-CR-195168; NAS 1.26:195168) Avail: CASI HC A03/MF A01

The overall goal of this study was to provide a quantitative understanding of the cycling of carbon in the soils associated with deep-rooting Amazon forests. In particular, we wished to apply the understanding gained by answering two questions: (1) what changes will accompany the major land use change in this region, the conversion of forest to pasture? and (2) what is the role of carbon stored deeper than one meter in depth in these soils? To construct carbon budgets for pasture and forest soils we combined the following: measurements of carbon stocks in above-ground vegetation, root biomass, detritus, and soil organic matter; rates of carbon inputs to soil and detrital layers using litterfall collection and sequential coring to estimate fine root turnover; C-14 analyses of fractionated SOM and soil CO2 to estimate residence times; C-13 analyses to estimate C inputs to pasture soils from C-4 grasses; soil pCO2, volumetric water content, and radon gradients to estimate CO2 production as a function of soil depth; soil respiration to estimate total C outputs; and a model of soil C dynamics that defines SOM fractions cycling on annual, decadal, and millennial time scales.
Author (revised)

N94-24861*# Woods Hole Research Center, MA.
HUMAN IMPACTS ON SOIL CARBON DYNAMICS OF DEEP-ROOTED AMAZONIAN FORESTS Final Technical Report
Daniel C. Nepstad, Thomas A. Stone, and Eric A. Davidson 16 Feb. 1994 31 p
(Grant NAGw-2750)
(NASA-CR-195127; NAS 1.26:195127) Avail: CASI HC A03/MF A01

Deforestation and logging degrade more forest in eastern and southern Amazonia than in any other region of the world. This forest alteration affects regional hydrology and the global carbon cycle, but our current understanding of these effects is limited by incomplete knowledge of tropical forest ecosystems. It is widely agreed that roots are concentrated near the soil surface in moist tropical forests, but this generalization incorrectly implies that deep roots are unimportant in water and C budgets. Our results indicate that half of the closed-canopy forests of Brazilian Amazonic occur where rainfall is highly seasonal, and these forests rely on deeply penetrating roots to extract soil water. Pasture vegetation extracts less water from deep soil than the forest it replaces, thus increasing rates of drainage and decreasing rates of evapotranspiration. Deep roots are also a source of modern carbon deep in the soil. The soils of the eastern Amazon contain more carbon below 1 m depth than is present in above-ground biomass. As much as 25 percent of this deep soil C could have annual to decadal turnover times and may be lost to the atmosphere following deforestation. We compared the importance of deep roots in a mature, evergreen forest with an adjacent man-made pasture, the most common type of vegetation on deforested land in Amazonia. The study site is near the town of Paragominas, in the Brazilian state of Para, with a seasonal rainfall pattern and deeply-weathered, kaolinitic soils that are typical for large portions of Amazonia. Root distribution, soil water extraction, and soil carbon dynamics were studied using deep auger holes and shafts in each ecosystem, and the phenology and water status of the leaf canopies were measured. We estimated the geographical distribution of deeply-rooting forests using satellite imagery, rainfall data, and field measurements.
Author (revised)

N94-25092*# California Univ., San Diego, La Jolla. Inst. of Oceanography.
CARBON AND HYDROGEN ISOTOPE COMPOSITION AND C-14 CONCENTRATION IN METHANE FROM SOURCES AND FROM THE ATMOSPHERE: IMPLICATIONS FOR A GLOBAL METHANE BUDGET Final Report, 1 Jan. - 30 Jun. 1991
Martin Wahlen 1 Mar. 1994 25 p
(Grants NAGw-843; NAGw-2542; NAGw-2729)
(NASA-CR-195166; NAS 1.26:195166) Avail: CASI HC A03/MF A01

The topics covered include the following: biogenic methane studies; forest soil methane uptake; rice field methane sources; atmospheric measurements; stratospheric samples; Antarctica; California; and Germany.
CASI

N94-25167 Food and Agriculture Organization of the United Nations, Rome (Italy).
MANUAL ON MEASUREMENT OF METHANE AND NITROUS OXIDE EMISSIONS FROM AGRICULTURE
Nov. 1992 91 p Prepared in cooperation with International Atomic Energy Agency, Vienna (Austria) Limited Reproducibility: More than 20% of this document may be affected by microfiche quality
(DE93-616429; IAEA-TECDOC-674) Avail: CASI HC A05 (US Sales Only)

Nitrous oxide and methane are two of the gases primarily responsible for atmospheric warming, or the 'greenhouse effect'. Agricultural activities are an important source of methane and nitrous oxide emissions, but quantitation of these sources is generally lacking. This manual describes techniques to evaluate current emissions from diverse animal and crop production practices and suggests methods for decreasing these emissions. DOE

N94-25223# Technische Univ., Eindhoven (Netherlands).
SOIL POLLUTION AT FORMER INDUSTRIAL SITES, THE HERITAGE OF 150 YEARS OF INDUSTRIAL DEVELOPMENT IN NOORD-BRABANT, THE NETHERLANDS Ph.D. Thesis [BODEMVERONTREINIGING OP VOORMALIGE BEDRIJFSTERREINEN, DE ERFENIS VAN ANDERHALVE EEUW INDUSTRIELE ONTWIKKELING IN NOORD-BRABANT]
Jurgen Adam Willem Nieuwkoop 1993 556 p In DUTCH Sponsored by Ministerie van Volkshuisvesting, Ruimtelijk Ordening en Milieubeheer, Netherlands
(ISBN-9-09-005756-7; ETN-94-95348) Copyright Avail: CASI HC A24/MF A04

A method for a systematic approach to establishing priorities and formulating a clean up policy for potentially polluted former industrial sites is applied to the province of Noord-Brabant. The development of soil clean up policy in the Netherlands, and specifically in Noord-Brabant, between 1980 and 1990, is described. The selection of potentially polluting industrial activities from all economic activities in the Netherlands is discussed. The origin of industrial soil pollution is outlined. The development of environmental consciousness and environmental legislation in the Netherlands between 1800 and 1950 is discussed. The behavior of contaminants in the soil is described. A model with six variables to calculate the degree of soil pollution was developed. The main soil pollution on former industrial sites in Noord-Brabant are surveyed. ESA

N94-25414# Deutsche Forschungsanstalt fuer Luft- und Raumfahrt, Oberpfaffenhofen (Germany). Abt. Globale Atmosphaerendynamik.
COLLECTION AND EVALUATION OF NUMERICAL MODELS WITH THE AIM TO INVESTIGATE THE IMPACT OF AIRCRAFT EMISSIONS [ZUSAMMENSTELLUNG UND BEWERTUNG VON NUMERISCHEN MODELLEN IM HINBLICK AUF UNTERSUCHUNGEN ZU DEM THEMA SCHADSTOFFE IN DER LUFTFAHRT]
Martin Dameris Feb. 1993 43 p In GERMAN
(DLR-Mitt-93-06; ETN-94-95207) Avail: CASI HC A03/MF A01

Models which are used for examination and analysis of aircraft emissions and their effects on Earth climate are presented. Several classifications of models are depicted: radiation and transport models for atmospheric trace gases distributions, two dimensional models for annual variations of phenomena, and tropospherical and stratospherical models. One dimensional chemistry models are fitted to the estimation of vertical distributions of trace gases in the atmosphere and allow sensitivity studies to be realized. Two dimensional chemistry models are divided into Euler models, for describing the transport of a continuum at fixed points in a spatial grid, and Lagrange models, which consider air circulation. With global three dimensional models, partial differential equations can be solved for estimation of wind, temperature, mass, and pressure. With a coupling of dynamical and chemical processes, a parametrization for photochemical reactions regarding ozone can be developed. Some deficiencies of existing models are investigated with emphasis on the lack of global climate middle atmosphere models, for description of mutual troposphere/stratosphere interactions. The problem of computation time and computer capacity was addressed. ESA

N94-23237*# Purdue Univ., West Lafayette, IN. Dept. of Agricultural Engineering.
A PROTOTYPE EXPERT/INFORMATION SYSTEM FOR EXAMINING ENVIRONMENTAL RISKS OF KSC ACTIVITIES
Bernard A. Engel *In* NASA. Kennedy Space Center, NASA/ASEE Summer Faculty Fellowship Program Oct. 1993 p 135-163 (For primary document see N94-23230 06-80)
Avail: CASI HC A03/MF A04

46 GEOPHYSICS

Includes aeronomy; upper and lower atmosphere studies; ionospheric and magnetospheric physics; and geomagnetism.
For space radiation see *93 Space Radiation.*

N94-23084*# Stanford Univ., CA. STAR Lab.
COMPUTER ASSISTED ANALYSIS OF AURORAL IMAGES OBTAINED FROM HIGH ALTITUDE POLAR SATELLITES Final Report, Jul. 1988 - Jan. 1993
Ramin Samadani and Michael Flynn 7 Sep. 1993 18 p
(Contract NAS5-30428)
(NASA-CR-194873; NAS 1.26:194873) Avail: CASI HC A03/MF A01

Automatic techniques that allow the extraction of physically significant parameters from auroral images were developed. This allows the processing of a much larger number of images than is currently possible with manual techniques. Our techniques were applied to diverse auroral image datasets. These results were made available to geophysicists at NASA and at universities in the form of a software system that performs the analysis. After some feedback from users, an upgraded system was transferred to NASA and to two universities. The feasibility of user-trained search and retrieval of large amounts of data using our automatically derived parameter indices was demonstrated. Techniques based on classification and regression trees (CART) were developed and applied to broaden the types of images to which the automated search and retrieval may be applied. Our techniques were tested with DE-1 auroral images. Author (revised)

N94-23124*# Universities Space Research Association, Huntsville, AL.
ATMOSPHERIC NUMERICAL MODELING RESOURCE ENHANCEMENT AND MODEL CONVECTIVE PARAMETERIZATION/SCALE INTERACTION STUDIES Final Progress Report No. 25, 6 Oct. 1987 - 31 Dec. 1993
Paula P. Cushman 31 Dec. 1993 9 p
(Contract NAS8-37141)
(NASA-CR-194769; NAS 1.26:194769) Avail: CASI HC A02/MF A01

Research will be undertaken in this contract in the area of Modeling Resource and Facilities Enhancement to include computer, technical and educational support to NASA investigators to facilitate model implementation, execution and analysis of output; to provide facilities linking USRA and the NASA/EADS Computer System as well as resident work stations in ESAD; and to provide a centralized location for documentation, archival and dissemination of modeling information pertaining to NASA's program. Additional research will be undertaken in the area of Numerical Model Scale Interaction/Convective Parameterization Studies to include implementation of the comparison of cloud and rain systems and convective-scale processes between the model simulations and what was observed; and to incorporate the findings of these and related research findings in at least two refereed journal articles. Author (revised)

N94-23157# Max-Planck-Inst. fuer Meteorologie, Hamburg (Germany).
LOCALLY MODIFIED BOTT-SCHEME FOR HIGHLY CONVECTIVE FLOWS
Andreas Chlond Jan. 1993 40 p
(MPIM-99; ETN-94-95108) Avail: CASI HC A03/MF A01

A simple and effective self adjusting hybrid technique was introduced to develop a new conservative and monotonic advection scheme that exhibits very low numerical diffusion of resolvable scales. The proposed scheme combines Bott's area preserving flux form algorithm with an area preserving exponential interpolating scheme, the use of either at any particular location being automatically controlled by the local ratio of the nodal values involved in the approximation process. The performance of the combined scheme is illuminated in a series of one and two dimensional linear advection experiments. The comparative test calculations presented demonstrate that the combined scheme provides highly accurate solutions both in regions where the transported flow variable is smooth and in the vicinity of sharp gradients. The self adjusting hybrid technique is highly effective in removing numerical artefacts such as dispersive ripples and simultaneously requires only an admissible additional computational effort relative to Bott's scheme. It is thus concluded that the combined scheme is well suited for many atmospheric modeling applications where advection plays a significant role. ESA

N94-23159# Max-Planck-Inst. fuer Meteorologie, Hamburg (Germany).
CLIMATE VARIABILITY IN A COUPLED GCM. PART 2: THE INDIAN OCEAN AND MONSOON
Mojib Latif, Andreas Sterl (Royal Netherlands Meteorological Inst., De Bilt.), Michel Assenbaum, Martina M. Junge, and Ernst Maier-Reimer Apr. 1993 35 p Sponsored in part by Koerber Project
(Contract EV5V-CT92-0121)
(MPIM-104; ETN-94-95111) Avail: CASI HC A03/MF A01

The seasonal cycle and the interannual variability of the tropical Indian Ocean circulation and the Indian summer monsoon simulated by a coupled ocean atmosphere general circulation model (GCM) in a 26 year integration were investigated. Although the model exhibits significant climate drift, it simulates realistically the seasonal changes in the tropical Indian Ocean and the onset and evolution of the Indian summer monsoon. The amplitudes of the seasonal changes, however, are somewhat underestimated. The coupled GCM also simulates considerable interannual variability in the tropical Indian Ocean circulation which is partly related to the El Nino/southern oscillation (ENSO) phenomenon and the associated changes in the Walker circulation. Changes in the surface wind stress appear to be crucial in forcing interannual variations in the Indian Ocean sea surface temperature (SST). As in the Pacific Ocean, the net surface heat flux acts as a negative feedback on anomalies. The interannual variability in monsoon rainfall is simulated by the coupled GCM only about half as strongly as observed. This is related to the fact that the simulated interannual variability in the Indian monsoon is caused by internal processes within the atmosphere only. In contrast, observations show a clear lead-lag relationship between interannual variations in the monsoon rainfall and tropical Pacific SST anomalies. The atmospheric GCM also fails to reproduce this lead-lag relationship, when run in a stand alone integration with observed SSTs prescribed. These results indicate that important physical processes relating tropical Pacific SST to Indian monsoon rainfall are not adequately modeled in this atmospheric GCM. ESA

N94-23175# Groningen Rijksuniv. (Netherlands).
ATMOSPHERIC FLOW IN HETEROGENEOUS VEGETATED REGIONS M.S. Thesis
R. Luppes Feb. 1993 53 p
(W-9303; ETN-94-94788) Avail: CASI HC A04/MF A01

The simulation of atmospheric flow and fluxes during or after changes in surface properties is addressed. Wind velocity, temperature and specific humidity and the corresponding atmospheric fluxes of momentum, sensible heat and latent heat of an airflow which moves along different vegetated areas, are described. For example, a flow can be simulated during a heath-forest transition or the reverse, a forest-heath transition. In the model, the pressure terms are added in the atmospheric flow equations, following viscous boundary layer theory, which should give more realistic calculations. An upper boundary condition on the horizontal wind velocity in aerodynamics and boundary layer theory, the so called interaction law, is used, instead of the matched load condition on the upper friction velocity as used by Klaassen. The equations are solved by means of habitual methods of numerical mathematics. The structure of the computer program SAFFACS, which solves the model is described, making use of the program easier as the solution of the model by means of iterative processes is explained. ESA

N94-23271*# Universities Space Research Association, Huntsville, AL.
SCIENTIFIC INVESTIGATIONS OF ATMOSPHERIC PROCESSES Quarterly Progress Report No. 24, 1 Oct. - 31 Dec. 1993
10 Jan. 1994 6 p
(Contract NAS8-37140)
(NASA-CR-194805; NAS 1.26:194805) Avail: CASI HC A02/MF A01

Research was performed in atmospheric, dynamical, and thermodynamical processes and in other disciplines necessary to accomplish the following tasks: develop procedures for combining generalized radiative transfer codes with dynamic atmospheric model codes; perform diagnostic analysis of atmospheric processes to gain a better understanding of the evolution and development of mesoscale circulation systems and their precipitation structures; and to develop algorithms and software necessary to graphically display diagnostic sets on the MSFC McIDAS and EADS to facilitate scientific study and sensor capability evaluation. Research activities during this reporting period are detailed. Author (revised)

N94-23282*# National Aeronautics and Space Administration. Goddard Space Flight Center, Greenbelt, MD.
AN IMPROVED GRAVITY MODEL FOR MARS: GODDARD MARS MODEL-1 (GMM-1)
D. E. Smith, F. J. Lerch, R. S. Nerem, M. T. Zuber, G. B. Patel (Hughes STX, Inc., Lanham, MD.), S. K. Fricke (RMS Technologies, Inc., Landover, MD.), and F. G. Lemoine (Colorado Univ., Boulder.) Washington May 1993 51 p Original contains color illustrations
(NASA-TM-104584; NAS 1.15:104584; Rept-93B00077) Avail: CASI HC A04/MF A01; 3 functional color pages

Doppler tracking data of three orbiting spacecraft have been reanalyzed to develop a new gravitational field model for the planet Mars, GMM-1 (Goddard Mars Model-1). This model employs nearly all available data, consisting of approximately 1100 days of S-bank tracking data collected by NASA's Deep Space Network from the Mariner 9, and Viking 1 and Viking 2 spacecraft, in seven different orbits, between 1971 and 1979. GMM-1 is complete to spherical harmonic degree and order 50, which corresponds to a half-wavelength spatial resolution of 200-300 km where the data permit. GMM-1 represents satellite orbits with considerably better accuracy than previous Mars gravity models and shows greater resolution of identifiable geological structures. The notable improvement in GMM-1 over previous models is a consequence of several factors: improved computational capabilities, the use of optimum weighting and least-squares collocation solution techniques which stabilized the behavior of the solution at high degree and order, and the use of longer satellite arcs than employed in previous solutions that were made possible by improved force and measurement models. The inclusion of X-band tracking data from the 379-km altitude, near-polar orbiting Mars Observer spacecraft should provide a significant improvement over GMM-1, particularly at high latitudes where current data poorly resolves the gravitational signature of the planet. Author

N[illegible]3337*# Auburn Univ., AL. Dept. of Agronomy and Soils
SPATIAL AND TEMPORAL VARIABILITY OF SOIL TEMPERATURE, MOISTURE AND SURFACE SOIL PROPERTIES Final Report
B. F. Hajek and J. H. Dane 25 Aug. 1993 58 p Original contains color illustrations
(Grant NAGw-0758)
(NASA-CR-194109; NAS 1.26:194109; AU-5-34046) Avail: CASI HC A04/MF A01; 4 functional color pages

The overall objectives of this research were to: (l) Relate in-situ measured soil-water content and temperature profiles to remotely sensed surface soil-water and temperature conditions; to model simultaneous heat and water movement for spatially and temporally changing soil conditions; (2) Determine the spatial and temporal variability of surface soil properties affecting emissivity, reflectance, and material and energy flux across the soil surface. This will include physical, chemical, and mineralogical characteristics of primary soil components and aggregate systems; and (3) Develop surface soil classes of naturally occurring and distributed soil property assemblages and group classes to be tested with respect to water content, emissivity and reflectivity. This document is a report of studies conducted during the period funded by NASA grants. The project was designed to be conducted over a five year period. Since funding was discontinued after three years, some of the research started was not completed. Additional publications are planned whenever funding can be obtained to finalize data analysis for both the arid and humid locations. Derived from text

N94-23344*# National Academy of Sciences - National Research Council, Washington, DC. Commission on Geosciences, Environment, and Resources.
THE NATIONAL GEOMAGNETIC INITIATIVE
1993 260 p Sponsored in part by NOAA, NSF, USAF, DOE, and US Geological Survey
(Grant NAGw-2667)
(LC-93-85739; ISBN-0-309-04977-6) Copyright Avail: CASI HC A12/MF A03

The Earth's magnetic field, through its variability over a spectrum of spatial and temporal scales, contains fundamental information on the solid Earth and geospace environment (the latter comprising the atmosphere, ionosphere, and magnetosphere). Integrated studies of the geomagnetic field have the potential to address a wide range of important processes in the deep mantle and core, asthenosphere, lithosphere, oceans, and the solar-terrestrial environment. These studies have direct applications to important societal problems, including resource assessment and exploration, natural hazard mitigation, safe navigation, and the maintenance and survivability of communications and power systems on the ground and in space. Studies of the Earth's magnetic field are supported by a variety of federal and state agencies as well as by private industry. Both basic and applied research is presently supported by several federal agencies, including the National Science Foundation (NSF), U.S. Geological Survey (USGS), U.S. Department of Energy (DOE), National Oceanic and Atmospheric Administration (NOAA), National Aeronautics and Space Administration (NASA), and U.S. Department of Defense (DOD) (through the Navy, Air Force, and Defense Mapping Agency). Although each agency has a unique, well-defined mission in geomagnetic studies, many areas of interest overlap. For example, NASA, the Navy, and USGS collaborate closely in the development of main field reference models. NASA, NSF, and the Air Force collaborate in space physics. These interagency linkages need to be strengthened. Over the past decade, new opportunities for fundamental advances in geomagnetic research have emerged as a result of three factors: well-posed, first-order scientific questions; increased interrelation of research activities dealing with geomagnetic phenomena; and recent developments in technology. These new opportunities can be exploited through a national geomagnetic initiative to define objectives and encourage coordination of efforts among federal and state agencies, academic institutions, and industry to systematically characterize the spatial and temporal behavior of the Earth's magnetic field on local, regional, and global scales in order to understand the physical processes in the solid earth and geospace environment, and to apply this understanding to a variety of scientific problems and to technical and societal needs.

Derived from text

N94-23516# Colorado School of Mines, Golden. Center for Wave Phenomena.

DYNAMIC RAY TRACING AND ITS APPLICATION IN TRIANGULATED MEDIA Ph.D. Thesis

A. Rueger Jul. 1993 76 p
(Contract DE-FG02-89ER-14079)
(DE94-000875; DOE/ER-14079/27; CWP-139) Avail: CASI HC A05/MF A01

Hale and Cohen developed software to generate two-dimensional computer models of complex geology. Their method uses a triangulation technique designed to support efficient and accurate computation of seismic wavefields for models of the earth's interior. Subsequently, Hale used this triangulation approach to perform dynamic ray tracing and create synthetic seismograms based on the method of Gaussian beams. Here, I extend this methodology to allow an increased variety of ray-theoretical experiments. Specifically, the developed program GBmod (Gaussian Beam MODeling) can produce arbitrary multiple sequences and incorporate attenuation and density variations. In addition, I have added an option to perform Fresnel-volume ray tracing. Corrections for reflection and transmission losses at interfaces, and for two-and-one-half-dimensional (2.5-D) spreading are included. However, despite these enhancements, difficulties remain in attempts to compute accurate synthetic seismograms if strong lateral velocity inhomogeneities are present. Here, these problems are discussed and, to a certain extent, reduced. I provide example computations of high-frequency seismograms based on the method of Gaussian beams to exhibit the advantages and disadvantages of the proposed modeling method and illustrate new features for both surface and vertical seismic profiling (VSP) acquisition geometries. DOE

N94-23721# Lawrence Livermore National Lab., CA.

PHYSICS OF IRON

O. Anderson Oct. 1993 86 p Presented at the 14th International Conference of the International Association for the Advancement of High Pressure Science and Technology, Colorado Springs, CO, 27 Jun. - 2 Jul. 1993
(Contract W-7405-eng-48)
(DE94-002002; CONF-930676-Suppl) Avail: CASI HC A05/MF A01

This volume comprises papers presented at the AIRAPT Conference, 28 June - 2 July 1993. The iron sessions at the meeting were identified as the Second Ironworkers Convention. The renewal of interest stems from advances in technologies in both diamond-anvil cell (DAC) and shock wave studies as well as from controversies arising from a lack of consensus among both experimentalists and theoreticians. These advances have produced new data on iron in the pressure-temperature regime of interest for phase diagrams and for temperatures of the core/mantle and inner-core/outer-core boundaries. Particularly interesting is the iron phase diagram inferred from DAC studies. A new phase, (beta), with a (gamma)-(beta)-(epsilon) triple point at about 30 GPa and 1190 K, and possible sixth phase, (omega), with an (epsilon)-(Theta)-melt triple point at about 190 GPa and 4000 K are deemed possible. The importance of the equation of state of iron in consideration of Earth's heat budget and the origin of its magnetic field invoke the interest of theoreticians who argue on the basis of molecular dynamics and other first principles methods. While the major thrust of both meetings was on the physics of pure iron, there were notable contributions on iron alloys. Hydrogen-iron alloys, iron-sulfur liquids, and the comparability to rhenium in phase diagram studies are discussed. The knowledge of the physical properties of iron were increased by several contributions. DOE

N94-24089*# Michigan Univ., Ann Arbor. Dept. of Atmospheric, Oceanic and Space Science.

DATA ANALYSIS AND THEORETICAL STUDIES OF THE UPPER MESOSPHERE AND LOWER THERMOSPHERE Annual Report, Apr. 1993 - Apr. 1994

Alan Burns and Timothy L. Killeen 4 Feb. 1994 42 p
(Grant NAGw-3457)
(NASA-CR-195108; NAS 1.26:195108) Avail: CASI HC A03/MF A01

The work proposed under this grant came in three parts. The first involved extending our continuing study of electrodynamical feedback between the thermosphere/ionosphere and the magnetosphere. The second was a model-experiment comparison study of global dynamics and the third was a 'spectral energetics' analysis of tidal dissipation and energy exchange mechanisms. In the past year, progress has been made on all three topics. A paper is in press about electrodynamic feedback, and another is also in press on an element of the 'spectral energetics' analysis. Furthermore, a paper is being prepared on global dynamics variations in response to geomagnetic storms. In addition, much of the data needed for further studies on global dynamics is being prepared for inclusion in a relational database. This report is organized into several separate sections. In the next section, we present an introduction to the work that we are doing in this proposal. We discuss the progress made in our work and some results in section 3. In the last section, we summarize the work.

Derived from text

N94-24108# Max-Planck-Inst. fuer Meteorologie, Hamburg (Germany).

TROPOSPHERIC OZONE LIDAR INTERCOMPARISON EXPERIMENT, TROLIX 1991 Field Phase Report

Jens Boesenberg, Gerard Ancellet (Centre National de la Recherche Scientifique, Verrieres-Le Buisson, France.), Arnoud Apituley (Rijksinstituut voor Volksgezondheid en Milieuhygieene, Bilthoven, Netherlands.), Hans Bergwerff (Rijksinstituut voor Volksgezondheid en Milieuhygieene, Bilthoven, Netherlands.), Goetz v.Cossart (Academy of Sciences, Kuhlungsborn, German D.R..), Hans Edner (Lund Inst. of Tech., Sweden.), Jens Fiedler (Academy of Sciences, Kuhlungsborn, German D.R..), Bo Galle (Institutet foer Vatten-Och Luftvaardsforskning, Goeteborg, Sweden.), Cora deJonge (Rijksinstituut voor Volksgezondheid en Milieuhygieene, Bilthoven, Netherlands.), and Johan Mellqvist (Institutet foer Vatten-Och Luftvaardsforskning, Goeteborg, Sweden.) et al Apr. 1993 244 p
(MPIM-102; ETN-94-95109) Avail: CASI HC A11/MF A03

The TROLIX '91 experiment, which was based on the simultaneous operation of different types of Differential Absorption Lidars (DIAL), a special version of a Differential Optical Absorption Spectroscopy (DOAS) instrument, helicopter borne in situ instruments, and many other supporting measurements, is addressed. The major objectives of the experiment were: to determine, which and how many wavelengths are required for a sufficiently accurate ozone retrieval in the lower troposphere, in the presence of aerosol, water vapor, oxygen, sulfur dioxide, and possibly other pollutants; to assess the accuracy which can be achieved under realistic conditions; to compare the performance of different types of systems already developed; to compare lidar to in situ measurements; to study ozone vertical distribution with high temporal resolution and coverage (including diurnal cycle); and to study the relation between ground level ozone concentrations and vertical distribution for several meteorological conditions. The general methodology is introduced, the instruments are described, the experimental operations are explained, and a selection of data are presented. Examples for the results of the intercomparison are given, as far as they were available at the present stage of evaluation. An overview of the material collected during the experiment is provided in order to facilitate further detailed studies in cooperation between the different groups which have participated. ESA

N94-24465*# National Aeronautics and Space Administration. Goddard Space Flight Center, Greenbelt, MD.
STEADY INDUCTION EFFECTS IN GEOMAGNETISM. PART 1C: GEOMAGNETIC ESTIMATION OF STEADY SURFICIAL CORE MOTIONS: APPLICATION TO THE DEFINITIVE GEOMAGNETIC REFERENCE FIELD MODELS
Coerte V. Voorhies NASA. Washington Oct. 1993 28 p
(NASA-TP-3272-Pt-1C; NAS 1.60-3272-Pt-1C; Rept-94B00008-Pt-1C)
Avail: CASI HC A03/MF A01

In the source-free mantle/frozen-flux core magnetic earth model, the non-linear inverse steady motional induction problem was solved using the method presented in Part 1B. How that method was applied to estimate steady, broad-scale fluid velocity fields near the top of Earth's core that induce the secular change indicated by the Definitive Geomagnetic Reference Field (DGRF) models from 1945 to 1980 are described. Special attention is given to the derivation of weight matrices for the DGRF models because the weights determine the apparent significance of the residual secular change. The derived weight matrices also enable estimation of the secular change signal-to-noise ratio characterizing the DGRF models. Two types of weights were derived in 1987-88: radial field weights for fitting the evolution of the broad-scale portion of the radial geomagnetic field component at Earth's surface implied by the DGRF's, and general weights for fitting the evolution of the broad-scale portion of the scalar potential specified by these models. The difference is non-trivial because not all the geomagnetic data represented by the DGRF's constrain the radial field component. For radial field weights (or general weights), a quantitatively acceptable explication of broad-scale secular change relative to the 1980 Magsat epoch must account for 99.94271 percent (or 99.98784 percent) of the total weighted variance accumulated therein. Tolerable normalized root-mean-square weighted residuals of 2.394 percent (or 1.103 percent) are less than the 7 percent errors expected in the source-free mantle/frozen-flux core approximation. Author (revised)

N94-24486*# Michigan Univ., Ann Arbor. Space Physics Research Lab.
MESOSPHERIC AND LOWER THERMOSPHERIC WINDS, TEMPERATURES DENSITIES, AND VOLUME EMISSION RATES Annual Report
Timothy L. Killeen 1994 23 p
(Grant NAG1-1315)
(NASA-CR-195147; NAS 1.26:195147) Avail: CASI HC A03/MF A01

This memo has been written to report on the progress made under grant NAG1-1315 and to request a continuation of funding for this work. Our proposal involved a plan to utilize an existing ground-based chain of optical and radar facilities to assemble a comprehensive, long-term, multi-station base of upper-mesospheric and lower thermospheric measurements of neutral winds, temperatures, and volume emission rates that can be used to make comparisons with data from the HRDI and WINDII instruments that are flying aboard the UARS spacecraft. The ground-based, optical data were to be obtained on a routine basis from five geographically separated observatories at: Thule, Greenland; Sondrestrom, Greenland; Watson Lake, Yukon (replacing Calgary, Alberta); Ann Arbor, Michigan; and Maynooth, Eire. Several different optical instruments are present at these sites: the total array of instruments is comprised of five Fabry-Perot interferometers, two half meter Ebert-Fastie spectrometers, one all-sky CCD imager, and a near infra-red Michelson Fourier transform spectrometer. In addition to these optical instruments, data were to be obtained from the incoherent scatter radar at Sondrestrom, Greenland. These radar measurements are comprised of neutral winds, temperatures, and densities from altitudes between approximately 70 - 120 km. The optical measurements are obtained locally from specific altitudes depending on the emission line studied. For example, red line optical data come from about 220 km. In this report we summarize the progress made in obtaining these data and relate it to the specific tasks outlined in the original grant application. These tasks are discussed in the next section. Progress towards their completion is discussed in section three, while future plans and summary are described in section four. Derived from text

N94-24491# Max-Planck-Inst. fuer Meteorologie, Hamburg (Germany).
NORTHERN HEMISPHERE TROPOSPHERIC MID-LATITUDE CIRCULATION AFTER VIOLENT VOLCANIC ERUPTIONS
Hans-F. Graf, Judith Perlwitz (Zentralinstitut fuer Kernforschung, Berlin, Germany.), and Ingo Kirchner May 1993 24 p
(Contract BMFT-07-KFT-86/2)
(MPIM-107; ETN-94-95112) Avail: CASI HC A03/MF A01

The strengths of the polar stratospheric vortex and geopotential height anomalies of the 500 hPa layer were studied shortly after violent volcanic eruptions. After all tropical eruptions, the polar stratospheric vortex was intensified. The tropospheric anomaly patterns after tropical eruptions are very similar to those of Winter months with a very strong stratospheric vortex, irrespective of whether volcanically forced or not. Hence, if they have any effect on the wintertime tropospheric circulation, tropical eruptions seem to force a natural mode of the stratospheric Winter circulation which is associated with a specific response of the tropospheric circulation with maximum amplitude over the North Atlantic and adjacent continental regions. Therefore, it remains difficult to give statistical evidence of volcanic impact on climate on the basis of the few observations after these rare events. A combination of observational studies and model experiments may help to overcome these difficulties in the future. ESA

N94-24580*# Princeton Univ., NJ. Dept. of Geological and Geophysical Sciences.
THE TRANSITION FROM DIAPIRISM TO DIKE INTRUSION: IMPLICATIONS FOR PLANETARY VOLCANISM Status Report, 1 Apr. 1993 - 31 Mar. 1994
Allan M. Rubin 1994 4 p
(Grant NAGw-3589)
(NASA-CR-195133; NAS 1.26:195133) Avail: CASI HC A01/MF A01

Magma transport processes influence the rate of magma transport and how far the magma travels before it freezes, the degree to which the magma communicates chemically with the host rock, the morphology of volcanic landforms on planetary surfaces, the interplay between magmatism and regional tectonics, and even the direction the magma moves. The primary question motivating this research is: How does magma rheology influence the mechanisms by which it is transported through planetary lithospheres? It is widely recognized that on Earth basaltic intrusions typically take the form of narrow dikes, while granites are typically found in more equidimensional plutons. Several explanations for this observation were offered over the last 50 years. While basalts and rhyolites vary somewhat in temperature and density, the major difference is the 2 to 8 orders of magnitude contrast in viscosity. The significant ductile strains associated with many granitic plutons has led to the statement that the occurrence of granites in diapirs rather than dikes results from the fact that there is insufficient viscosity contrast between the magma and wall rock for the granite to intrude narrow cracks. A second explanation states that granites are so viscous that they cannot propagate far before freezing. Despite the length of time these explanations have been around, there has been relatively little effort to investigate them quantitatively. My goal has been to evaluate these explanations through a series of well-posed numerical models. These models can be tested by the decades of field data collected by structural geologists that have yet to be integrated into any coherent theory, and the results should have important implications for volcanism on the terrestrial planets. Author

N94-24592 Technische Univ., Delft (Netherlands). Lab. of Electromagnetic Research.
TIME-DOMAIN ANALYSIS OF CONDUCTION AND DISPLACEMENT CURRENT DISTRIBUTIONS IN INHOMOGENEOUS AND ANISOTROPIC LAYERED MEDIA
Umesh C. Das and Adrianus T. deHoop 1993 8 p Limited Reproducibility: More than 20% of this document may be affected by microfiche quality
(PB94-111036; ET/EM-1993-04) Copyright Avail: CASI HC A02

Anisotropy in the electrical properties of the earth's material is a widespread phenomenon and its effect in the transient electromagnetic measurements of geophysical prospecting must be quantified. The authors consider the calculation of the quasi-static electrical field quantities, electrical potential and the vertical component of total volume density of electric current, in a horizontally layered, piecewise homogeneous and arbitrarily anisotropic earth due to a system of current-carrying electrodes. Using a one-sided time Laplace transformation with real positive parameter, and a Fourier transformation with respect to the horizontal space coordinates, the authors obtain, from (Maxwell's) quasi-static equations, the system of transform-domain differential equations in the vertical (depth) coordinate. At each interface of the layered earth the scattering-matrix formalism relates the outward flow constituents to the inward ones. The general formalism that has been developed is applied to the specific cases of both an anisotropic infinite medium and some two-layer problems. NTIS

N94-24598 Groningen Rijksuniv. (Netherlands). Dept. of Mathematics.
HAMILTONIAN APPROACH TO FAIRLY LOW AND LONG GRAVITY WAVES
W. A. vanDerVeen and F. W. Wubs 1993 31 p Limited Reproducibility: More than 20% of this document may be affected by microfiche quality
(PB94-111119; W-9314) Avail: Issuing Activity (National Technical Information Service (NTIS))

The study relates to irrotational nonlinear dispersive gravity waves in an inviscid incompressible fluid. In Chapter 2 we derive an alternative positive-definite first-order approximation to the Hamiltonian. In the implementation of this alternative only two Helmholtz-type equations need to be solved and the matrix is symmetric. Numerical aspects are considered in Chapter 3. For the time-integration of our Boussinesq equations the classical fourth-order Runge-Kutta method was used and for spatial discretization we used fourth-order accurate discretization schemes. The conjugate gradient method was employed in conjunction with a preconditioning for solving the Helmholtz-type equations. Two preconditioning techniques were used: polynomial preconditioning and preconditioners based on incomplete Cholesky decomposition. Some first results are presented in Chapter 4. The results obtained by the two models differ only by a few percents, which is quite acceptable. The speed improvement is about 2.5. NTIS

N94-24647 Technische Univ., Delft (Netherlands).
NEAR-SURFACE SEISMIC IMAGING Ph.D. Thesis
Bernardus Cornelis Scheffers 1993 219 p Limited Reproducibility: More than 20% of this document may be affected by microfiche quality
(PB94-119096; ISBN-90-9006108-8) Copyright Avail: Issuing Activity (National Technical Information Service (NTIS))

Processing of seismic data requires more and more sophisticated techniques as hydrocarbon plays get smaller and smaller. Depth migration, for example, depends on accurate velocity models of the subsurface to obtain correctly imaged depth sections or depth cubes of small hydrocarbon reservoirs. Much research is carried out on new techniques for the estimation of such macro-velocity models. Currently, research is concentrated in two directions: techniques for estimating the velocity of the weather layer (the ultra shallow zone), and techniques for estimating the macro model of the total overburden (of the deep zone). The objective of this thesis is to present an improved and cost-effective data acquisition and inversion technique that provides a velocity macro model of ultra shallow and the shallow zone, using an algorithm that incorporates all available information. NTIS

N94-24674 Florida State Univ., Tallahassee. Geophysical Fluid Dynamics Inst.
NONLINEAR DYNAMICS APPLIED TO ATMOSPHERIC PREDICTION Annual Report, 15 Sep. 1993 - 14 Oct. 1993
Richard L. Pfeffer 14 Oct. 1993 26 p Limited Reproducibility: More than 20% of this document may be affected by microfiche quality
(Contract F49620-92-J-0498)
(AD-A273437; AFOSR-93-0857TR) Avail: Issuing Activity (Defense Technical Information Center (DTIC))

Under AFOSR grant F49620-92-J-0498, Barcilon and Nathan are studying the impact of steady, zonally varying vorticity forcing on topographic instability and finite amplitude, low frequency oscillations. The model consists of a viscous, barotropic fluid on a zonally periodic, midlatitude B-plane channel, bounded above by a flat, rigid boundary, below by a bottom topography, and laterally by sidewalls at y = o,TT Topographically induced low frequency oscillations in the presence of a steady, zonally varying vorticity source have been studied. The source has been shown to interact with the perturbation field to produce zonally rectified wave fluxes that change the zonal momentum balance of the system. This change provides a mechanism for coupling the topographic and vorticity forcings leading to a dramatic alteration in the Hopf bifurcation from stationary to low frequency, finite amplitude oscillation. DTIC

N94-24738*# Smithsonian Astrophysical Observatory, Cambridge, MA.
MEASUREMENT OF HO2 AND OTHER TRACE GASES IN THE STRATOSPHERE USING A HIGH RESOLUTION FAR-INFRARED SPECTROMETER Semiannual Status Report No. 33, 1 Jul. - 31 Dec. 1993
Wesley A. Traub, Kelley V. Chance, David G. Johnson, Kenneth W. Jucks, Steven C. Wofsy, Changqin Xue, and Paola Ciarpallini Jan. 1994 86 p
(Grant NsG-5175)
(NASA-CR-195173; NAS 1.26:195173) Avail: CASI HC A05/MF A01

This report covers the time period 1 Jul. to 31 Dec. 1993. There were no balloon or airplane flights during this reporting period, instead we concentrated on analyzing our existing data. This was facilitated by a recently completed program of enhancements made in our data reduction software. We are using our data sets to examine the changes in stratospheric chemistry over a variety of time scales. Ongoing projects include investigating the diurnal variation of OH, HO2, and H2O2 and exploring their relationships with other simultaneously measured species; measuring long term trends in HF and HCl; and looking for changes caused by the June 1991 Pinatubo eruption. We are also continuing to analyze the large set of data collected during the AASE 2. Author (revised)

N94-24794# State Univ. of New York, Albany. Research Foundation.
OBSERVATIONAL CASE STUDIES AND DIAGNOSTIC ANALYSES OF LONG-LIVED LARGE-AMPLITUDE INERTIA-GRAVITY WAVES Technical Report, 15 Oct. 1992 - 14 Oct. 1993
Lance F. Bosart and Daniel Keyser 18 Oct. 1993 5 p
(Contract F49620-93-1-0002)
(AD-A273545; AFOSR-93-0853TR) Avail: CASI HC A01/MF A01

Effort for the first year has concentrated on: (1) preparing a gravity wave climatology; (2) documenting a long-lived large-amplitude wake low trough event on 16-17 November 1987; and (3) analyzing the large-amplitude gravity wave present in the notable Midwest cyclone of 15 December 1987. The gravity wave climatology is based on hourly surface observations spanning a 10 - 15 year period at approximately 100 stations distributed fairly evenly across the United States. Preliminary results (7 stations) suggest that large-amplitude gravity wave events occur at a frequency of one or two times per year at a given station. It is hypothesized that the more complete wave-event climatology to be derived in the second year will show regional variations understandable in terms of characteristic synoptic-scale signatures conducive to wave genesis. In the 16-17 November 1987 wake low event, the wake trough remains confined to the back edge of the precipitation shield associated with a major mesoscale convective system over the lower Mississippi Valley. The approach of the wake trough is marked by the cessation of precipitation and the onset of gusty easterly winds, consistent with simple gravity wave theory. Finally, in the 15 December 1987 Midwest gravity wave event, present research is focused on the initiation of the wave event; preliminary results suggest that frontogenetical forcing may be contributing to wave generation. DTIC

N94-24843*# Georgia Inst. of Tech., Atlanta. School of Electrical Engineering.
INVESTIGATION OF PASSIVE ATMOSPHERIC SOUNDING USING MILLIMETER AND SUBMILLIMETER WAVELENGTH CHANNELS Semiannual Status Report No. 6, 1 Jul. - 31 Dec. 1993
Albin J. Gasiewski 1993 115 p
(Grant NAG5-1490)
(NASA-CR-194858; NAS 1.26:194858) Avail: CASI HC A06/MF A02

Presented in this study are the results of controlled partially polarimetric measurements of thermal emission at 91.65 GHz from a striated water surface as corroborated by a geometrical optics radiative model. The measurements were obtained outdoors using a precision polarimetric radiometer which directly measured the first three modified Stokes' parameters. Significant variations in these parameters as a function of azimuthal water wave angle were found, with peak-to-peak variations in T(sub u) of up to approximately 10 K. The measurements are well corroborated by the GO model over a range of observations angles from near nadir up to approximately 65 degrees from nadir. The model incorporates both multiple scattering and a realistic downwelling background brightness field. Derived from text

N94-24854*# California Univ., San Diego. Inst. for Geophysics and Planetary Physics.
GEOMAGNETIC FIELD MODELS INCORPORATING PHYSICAL CONSTRAINTS ON THE SECULAR VARIATION Final Report, 1 Jan. 1992 - 31 Dec. 1993
Catherine Constable and Robert L. Parker 1993 3 p
(Grant NAGw-2966)
(NASA-CR-195165; NAS 1.26:195165) Avail: CASI HC A01/MF A01

This proposal has been concerned with methods for constructing geomagnetic field models that incorporate physical constraints on the secular variation. The principle goal that has been accomplished is the development of flexible algorithms designed to test whether the frozen flux approximation is adequate to describe the available geomagnetic data and their secular variation throughout this century. These have been applied to geomagnetic data from both the early and middle part of this century and convincingly demonstrate that there is no need to invoke violations of the frozen flux hypothesis in order to satisfy the available geomagnetic data. Author

N94-24980# Tokyo Inst. of Tech., Yokahama (Japan). Dept. of Earth and Planetary Sciences.
ELECTROMAGNETIC FIELD CHANGES AS A PRECURSORY PHENOMENA OF EARTHQUAKES AND VOLCANIC ERUPTIONS Interim Report [CHIKAKU HAKAI NO ZENCHO GENSHO TO SHITENO DENJI HOSHA NO TOKUSEI NI KANSURU KENKYU]
Yoshimori Honkura, Yuri Kuwata, Osamu Nishizawa, Tsuneo Ishido, Xinglin Lei, Kinichiro Kusunose, Yuji Enomoto, Hiroshi Hashimoto, Shigeyuki Mori, and Yoshiyuki Asabe et al 29 Mar. 1993 401 p In ENGLISH and JAPANESE
(Rept-157; JTN-94-80510) Avail: CASI HC A18/MF A04

The systematic approach to the prediction of earthquakes and volcanic eruptions is expected to provide a more reliable information for issuing alarms to mitigate the disasters. There is a growing interest in the electromagnetic radiation phenomena of low frequency as a candidate of imminent precursory phenomena. The principal objective of this research project is to evaluate the phenomena to know whether and how they are useful for the prediction. The approaches were directed the following categories: (1) analytical estimation of decay of the electromagnetic signals originated from source regions in heterogeneous media in conductivity; (2) laboratory experiments of rock fracture to infer the dominant mechanism of the electromagnetic phenomena preceding the crustal ruptures; and (3) field experiments by various measurement instruments to find the most efficient physical equations to be observed, locate source region, and to find probabilistic relations of anomarous phenomena with earthquake and with volcanic eruptions. Author (NASDA)

N94-25203*# Smithsonian Astrophysical Observatory, Cambridge, MA.
MEASUREMENT AND INTERPRETATION OF CRUSTAL DEFORMATION RATES ASSOCIATED WITH POSTGLACIAL REBOUND Semiannual Status Report No. 3, 15 Mar. - 14 Sep. 1993
James L. Davis Dec. 1993 19 p
(Grant NAG5-1930)
(NASA-CR-195193; NAS 1.26:195193) Avail: CASI HC A03/MF A01

This project involves obtaining GPS measurements in Scandinavia, and using the measurements to estimate the viscosity profile of the Earth's mantle and to correct tide-gauge measurements for the rebound effect. Below, we report on several aspects of this project. The DSGS was occupied in August 1993. This campaign also inaugurated SWEPOS, the Swedish permanent GPS network. Initial results are presented in Johansson et al., a copy of which is contained in Appendix A. An important technical advance we intend for this project is to use the full three dimensional site velocity information for inferring geophysical parameters. To this end, we have investigated using VLBI determined baseline length rates in North America to constraining proposed combinations of ice history and earth rheology, and presented this work in Mitrovica et al., a copy of which is contained in Appendix B. For individual titles, see N94-25204 through N94-25205.

N94-25204*# Onsala Space Observatory (Sweden).
FIRST RESULTS FROM THE FENNOSCANDIAN GPS NETWORKS
J. M. Johansson and R. T. K. Jaldehag *In* Smithsonian Astrophysical Observatory, Measurement and Interpretation of Crustal Deformation Rates Associated with Postglacial Rebound Dec. 1993 12 p Presented at the AGU Fall Meeting, 1993 (For primary document see N94-25203 06-46)
Avail: CASI HC A03/MF A01

Temporal correlations were measured of data obtained by the Swedish Permanent GPS Network for Positioning (SWEPOS). The model for correlations, r(Delta t) = exp(-(absolute value of (Delta t))/tau), can be used to predict precision of averaged values for different values of tau. Results indicate that tau is approximately equal to 1 day (r less than 1% after 5 days). The results show that the network can be used in geophysical applications such as the DOSE investigation on postglacial rebound. Derived from text

N94-25205*# Toronto Univ. (Ontario). Dept. of Physics.
CONSTRAINING PROPOSED COMBINATIONS OF ICE HISTORY AND EARTH RHEOLOGY USING VLBI DETERMINED BASELINE LENGTH RATES IN NORTH AMERICA
J. X. Mitrovica, J. L. Davis (Smithsonian Astrophysical Observatory, Cambridge, MA.), and I. I. Shapiro (Smithsonian Astrophysical Observatory, Cambridge, MA.) *In* Smithsonian Astrophysical Observatory, Measurement and Interpretation of Crustal Deformation Rates Associated with Postglacial Rebound Dec. 1993 4 p Sponsored in part by NSERC and Smithsonian Institute (For primary document see N94-25203 06-46)
Avail: CASI HC A01/MF A01

We predict the present-day rates of change of the lengths of 19 North American baselines due to the glacial isostatic adjustment process. Contrary to previously published research, we find that the three dimensional motion of each of the sites defining a baseline, rather than only the radial motions of these sites, needs to be considered to obtain an accurate estimate of the rate of change of the baseline length. Predictions are generated using a suite of Earth models and late Pleistocene ice histories, these include specific combinations of the two which have been proposed in the literature as satisfying a variety of rebound related geophysical observations from the North American region. A number of these published models are shown to predict rates which differ significantly from the VLBI observations. Author

N94-25229# Technische Univ., Delft (Netherlands). Faculty of Applied Physics.
DOWNWARD EXTRAPOLATION OF MULTI-COMPONENT SEISMIC DATA Ph.D. Thesis
Gregory Carlo Haime 1992 170 p Sponsored by DELPHI Consortium
(ISBN-9-09-005213-5; ETN-94-95373) Copyright Avail: CASI HC A08/MF A02

An evaluation of the problems involved in elastic seismic migration is presented. Elastic wave field extrapolated operators are presented that are applicable to a general three dimensional elastic and anisotropic medium. Although the elastic operators derived are stand alone elements and can be used in any migration scheme, they are developed to take part in the stepwise elastic inversion scheme proposed by Berkhout and Wapenaar. The advantages of multicomponent seismic acquisition are discussed. The necessity of multicomponent data in elastic processing is demonstrated by an example, and a global description of all modules in the stepwise elastic inversion scheme is given. Elastic P and S extrapolation operators are derived starting from the full elastic Kirchhoff-Helmholtz integral. An analysis of the contribution of the different elastic terms in the extrapolation process is presented. It is made clear that there are many different ways to generate extrapolation operators for a so called macro model. (Such a macro model represents a global description of the subsurface in terms of velocities and densities and must be estimated before the actual extrapolation step can be performed.) A quantitative error analysis of the extrapolation operators proposed is performed. The influence of macro model errors on the amplitudes of the extrapolated P and S wave fields is examined. The use of the elastic P and S extrapolation operators in redatuming and migration schemes is considered. ESA

N94-25251 Technische Univ., Delft (Netherlands). Faculty of Applied Physics.
DECOMPOSITION OF MULTI-COMPONENT MEASUREMENTS INTO P AND S WAVES Ph.D. Thesis

Philippe Charles Herrmann 1992 178 p Limited Reproducibility: More than 20% of this document may be affected by microfiche quality
(ISBN-9-09-005197-X; ETN-94-95365) Copyright Avail: CASI HC A09

Elastic wavefield decomposition is defined as a transformation of a two way vector wavefield representation into a one way scalar wavefield representation. Starting from this definition and using the relations between the two way and normal one way wavefield components, a general formalism for the wavefield decomposition of elastic waves was developed. For surface seismic data the following topics were addressed: two Dimensional (2D) and 3D seismic wavefields; isotropic and anisotropic media; lateral variant media; wave decomposition at the detector and source side; extra wavefield information; and sensitivity analysis. It was concluded that proper preprocessing (statics, coupling) prior to decomposition is a prerequisite with surface land data. In the case of a low velocity near surface medium, the wavetype separation is largely made by the horizontal and vertical component source/receivers. The same topics were addressed for data acquisition along a borehole, the so called VSP technique. Due to the strong vertical velocity variations that may occur along the VSP well, the wavefield decomposition has to be done in the space-frequency domain. If the data can be well fitted by few plane waves (by for example, two downgoing, two upgoing) it is preferable to do a parametric wavefield decomposition. If the data is complex, it is preferrable to do the wavefield decomposition by means of convolutional products. As the convolution operators play an important part in wavefield decomposition, it is interesting to continue their development. For instance, the weighting function, as introduced for the computation of the operators in the space-frequency domain, is defined in a very simple manner. An improvement will be obtained by updating the weighting function in an iterative way (one or two iterations). ESA

N94-25430# Loughborough Univ. of Technology (England). Dept. of Mathematical Sciences.
THE SCATTERING AND COLLISION OF GRAVITATIONAL WAVES IN FRIEDMANN-ROBERTSON-WALKER OPEN UNIVERSES
Jiri Bicak (Karlova Univ., Prague, Czechoslovakia.) and Jerry B. Griffiths Aug. 1993 17 p Sponsored by Loughborough Univ. of Technol., England; Royal Society, London, England; and Cambridge Univ., England
(MATHS-Rept-A-193; ETN-94-95230) Avail: CASI HC A03/MF A01

An exact solution which describes the scattering of a gravitational wave in an open expanding universe is described. The background region ahead of the wave is taken to be a Friedmann-Robertson-Walker (k = 1) space-time containing a perfect fluid with an extreme relativistic equation of state p = rho. Plane surfaces are determined in this background. Solutions describing the scattering of a single wave with a wave front given by such a surface and the collision of two such waves can be obtained. ESA

N94-25535# Phillips Lab., Hanscom AFB, MA.
REPORT ON OPERATIONS OF THE AIR FORCE GEOPHYSICS LABORATORY INFRARED ARRAY SPECTROMETER Final Report
G. C. Sloan, P. D. LeVan, and P. C. Tandy 25 Jan. 1993 120 p
(AD-A273800; AD-E201725; PL-TR-93-2012; IP-345; XC-PL/HANSCOM)
Avail: CASI HC A06/MF A02

We describe the Geophysics Laboratory Infrared Array Spectrometer, a long-slit spectrometer configured for astronomical observations at wavelengths of 7 to 14 microns. We present the history of the instrument's development and use at the Wyoming Infrared Observatory, discuss some of the problems faced, and describe the resultant scientific publications. The appendices to this report contain several of the more important scientific publications. DTIC

N94-25536# Danish Meteorological Inst., Copenhagen.
HIGH LATITUDE CUSP SIGNATURE OBSERVATIONS FOR SOUTHWARD IMF B SUB Z Final Report, 15 May 1989 - 14 May 1992
Per Hoeg Mar. 1993 24 p
(Grant AF-AFOSR-0459-89)
(AD-A273801; AD-E201703; PL-TR-93-2068) Avail: CASI HC A03/MF A01

High latitude coherent and incoherent radar systems have given much new information about the physical processes at auroral latitudes. This report presents observational features of the Cusp, situated close to magnetic noon at 70-75 degrees inv. latitude, when the Interplanetary Magnetic Field of the Solar Wind is southward and staying southward for more than half a day. For this condition, the observations of the convectional flow pattern comply with the two-cell model of the global convectional flow at auroral and polar cap latitudes. During moderate disturbed magnetic conditions, the temporal extent of the Cusp can be defined by an increased F-region electron density, while the E-region density decreases or stays constant for mostly northward convectional flow in the magnetic noon sector. The temporal extent of this condition is observed to be up to two hours. When the Cusp is overhead of the radars in Sondre Stromfjord, Greenland, the ionograms show enhanced spread-F condition, a phenomenon associated to electron density enhancements in a turbulent plasma, which flows into the polar cap. Ionogram oblique F-region traces are observed in conjunction with drifting patches. Patches drift through the Cusp region, but they are also observed before and after the defined Cusp and seem not to be confined by the latter. Spectral analysis of F-region electron density variations in the noon sector has been performed. Periods down to the Pc5 range are observed more frequently in the northward convectional flow regime near noon than in the adjacent time sectors. The same analysis of the magnetic pulsations from the Greenland Magnetometer Chain give periods of 10 minutes in the whole dawn sector until the time when the Cusp is observed by the radars. DTIC

N94-25537# Phillips Lab., Hanscom AFB, MA.
A NIGHTTIME STRUCTURE MODEL OF ATMOSPHERIC OPTICAL TURBULENCE, c2(n), DERIVED FROM THERMOSONDE AND HIGH RESOLUTION RAWINSONDE MEASUREMENTS Interim Report, Jan. 1991 - Jan. 1993
James H. Brown 26 Jan. 1993 70 p
(AD-A273803; ADXC-E201701; PL-TR-93-2016; ERP-1119; XC-PL/HANSCOM) Avail: CASI HC A04/MF A01

Data from fifteen thermosonde flights was used to develop a simple nighttime structure model of C2 sub n. High resolution rawinsondes provide fine scale estimates of atmospheric temperature gradients and variances of wind speed. Nonlinear regression applied between the thermosonde and rawinsonde measurements provides the model C2 sub n estimator. This quasi-empirical model is based upon the theoretical description given by Tatarski and upon an exponentially scaled estimate of a theoretical model of the eddy dissipation rate given by Weinstock. A discussion of previous models and a comparison with the Dewan et al. microshear model is presented. Model profiles computed for other sites and seasons are compared favorably to related thermosonde profiles. DTIC

N94-25538# California Univ., Davis. Intercollege Div. of Statistics.
PARAMETRIC AND NONPARAMETRIC DISCRIMINANTS FOR REGIONAL EARTHQUAKES AND EXPLOSIONS
Joseph E. Cavanaugh, Allan D. McQuarrie, and Robert H. Shumway 31 Jul. 1993 54 p
(Contract F19628-91-K-0033)
(AD-A273807; AD-E201709; PL-TR-93-2164; SR-2) Avail: CASI HC A04/MF A01

Conventional methods for discriminating between earthquakes and explosions at regional distances have concentrated on extracting specific features such as amplitude and spectral ratios from the waveforms of the P and S phases. We consider here an optimum nonparametric classification procedure derived from the classical approach to discriminating between two Gaussian processes with unequal spectra. Two robust variations based on the minimum discrimination information statistic and Renyi's entropy are also considered. We compare the optimum classification procedure with various amplitude and spectral ratio discriminants and show that its performance is superior when applied to a small population of 8 land-based earthquakes and 8 mining explosions recorded in Scandinavia. Several parametric characterizations of the notion of complexity based on modeling earthquakes and explosions as autoregressive or modulated autoregressive processes are also proposed and their performance compared with the nonparametric and feature extraction approaches. DTIC

N94-25540# Organisatie voor Toegepast Natuurwetenschappelijk Onderzoek, The Hague (Netherlands). Physics and Electronics Lab.
RESULTS FROM THE VISA PROJECT
G. J. Kunz 1 Sep. 1993 79 p
(AD-A273752; FEL-93-A058; TDCK-TD-93-0756) Avail: CASI HC A05/MF A01

The small lidar system has been used to measure the vertical structure of the atmospheric extinction in a dune area bordering The Hague (The Netherlands), at about 2.6 km from the North Sea. The atmospheric optical properties at this location are determined by a mixture of industrial, urban, rural and marine aerosols, which composition depends on the air mass history. The measurements were made unattended, around the clock, five days a week. About 250 extinction profiles were recorded every day. This report reviews the data base obtained and presents some selected results. The lidar system is described briefly. Factors influencing the accuracy of the inversion of lidar signals are discussed. DTIC

N94-25364*# Houston Univ., TX. Dept. of Mathematics.
NEAR SURFACE ANALYSIS
Gordon G. Johnson *In* NASA. Johnson Space Center, National Aeronautics and Space Administration (NASA)/American Society for Engineering Education (ASEE) Summer Faculty Fellowship Program, 1993, Volume 1 Dec. 1993 11 p (For primary document see N94-25348 06-99)
Avail: CASI HC A03/MF A03

47 METEOROLOGY AND CLIMATOLOGY

Includes weather forecasting and modification.

N94-23129 State Agricultural Univ., Wageningen (Netherlands).
URBAN/RURAL APPLICATION OF WEATHER RADAR FOR FLOW FORECASTING. PROCEEDINGS OF THE INFORMAL CEc -WORKSHOP
J. N. M. Stricker, ed. Jul. 1992 98 p Limited Reproducibility: More than 20% of this document may be affected by microfiche quality
(PB93-220135; Rept-26) Avail: CASI HC A05/MF A02

Contents: A calibration study of Ingham Radar; The radar site at Delft University of Technology; Use of x-band over urban areas - what resolution in time and space is required; Use of Doppler Radar in Veneto Region and improvement of precipitation measurement; Adjustment of Radar-Rainfall totals over Alenquer Basin using a telemetering raingauge; Hydrological use of the 'Cevennes 86-88' data. Limitations and ongoing studies; Radar rainfall and ground data--What is the truth; Grid-square rainfall-runoff modeling for the Wyre catchment in North-West England; Radar rainfall forecasting over London for flash-flood warning; A rainfall-discharge model for a regional sewer system and a first application of radar generated input; Semi-distributed modeling for real-time flood forecasting--The case of mountainous regions; Recent applications of weather radar to urban drainage systems; On the use of distrometers for quantification of rainfall; Application of rainfall-runoff model HEC-1 to the Alenguer's watershed; A real-time flow forecasting system for region-wide application; A brief presentation of the software Hydrorad. NTIS

N94-23132*# National Aeronautics and Space Administration. Goddard Space Flight Center, Greenbelt, MD.
ESTIMATES OF MONTHLY MEAN SOIL MOISTURE FOR 1979-1989
J. Schemm (General Sciences Corp., Laurel, MD.), S. Schubert, J. Terry (General Sciences Corp., Laurel, MD.), and S. Bloom (Universities Space Research Association, Columbia, MD.) Oct. 1992 240 p
(NASA-TM-104571; NAS 1.15:104571; Rept-93B00006) Avail: CASI HC A11/MF A03

This technical report presents estimated monthly mean global soil moisture distributions for 1979-1989. The soil moisture datasets were prepared as part of the boundary conditions for an atmospheric general circulation model (GEOS-1). Also included are the 11-year averages of monthly mean soil moisture, surface air temperature, monthly total precipitation, evapotranspiration, and potential evapotranspiration. The standard deviation of the monthly mean soil moisture is provided as a measure of year-to-year variability. Author (revised)

N94-23156# Max-Planck-Inst. fuer Meteorologie, Hamburg (Germany).
MONTE CARLO CLIMATE CHANGE FORECASTS WITH A GLOBAL COUPLED OCEAN-ATMOSPHERE MODEL
U. Cubasch (Deutsches Klimarechenzentrum G.m.b.H., Hamburg, Germany.), B. D. Santer (Lawrence Livermore National Lab., CA.), A. Hellbach (Deutsches Klimarechenzentrum G.m.b.H., Hamburg, Germany.), G. Hegerl, H. Hoeck, E. Maier-Reimer, U. Mikolajewicz, A. Stoessel, and R. Voss (Hamburg Univ., Germany.) Dec. 1992 47 p Sponsored by BMFT; Max-Planck-Gesellschaft; Freie und Hansestadt Hamburg; and EEC
(MPIM-97; ETN-94-95107) Avail: CASI HC A03/MF A01

The Monte Carlo approach, which has increasingly been used during the last decade in the field of extended range weather forecasting, was applied for climate change experiments. Four integrations with a global coupled ocean-atmosphere model were started from different initial conditions, but with the same greenhouse gas forcing according to the IPCC scenario A. All experiments were run for a period of 50 years. The results indicate that the time evolution of the global mean warming depends strongly on the initial state of the climate system. It can vary between 6 and 31 years. The Monte Carlo approach delivers information about both the mean response and the statistical significance of the response. While the individual members of the ensemble show a considerable variation in the climate change pattern of temperature after 50 years, the ensemble mean climate change pattern closely resembles the pattern obtained in a 100 year integration and is, at least over most of the land areas, statistically significant. The ensemble averaged sea level change due to thermal expansion is significant in the global mean and locally over wide regions of the Pacific. The hydrological cycle is also significantly enhanced in the global mean, but locally the changes in precipitation and soil moisture are masked by the variability of the experiments. ESA

N94-23199# Max-Planck-Inst. fuer Meteorologie, Hamburg (Germany).
MODAL STRUCTURE OF VARIATIONS IN THE TROPICAL CLIMATE SYSTEM. PART 2: ORIGINS OF THE LOW-FREQUENCY MODE
Timothy P. Barnett (Scripps Institution of Oceanography, La Jolla, CA.), Mojib Latif, Nicholas E. Graham (Scripps Institution of Oceanography, La Jolla, CA.), and Moritz Fluegel 17 Dec. 1992 31 p Sponsored in cooperation with Scripps Institution of Oceanography, CA
(Grant NSF ATM-88-14571)
(MPIM-96; ETN-94-95106) Avail: CASI HC A03/MF A01

A series of model simulations were used to try to understand the origins of Low Frequency (LF) variations and the role of the seasonal cycle, if any, in its generation. This modeling work is complementary to the observed data analysis of part one in which it was found that simulations with ocean and atmospheric general circulation models and a hybrid coupled model reproduce well the observed features of variability in the LF mode. The model results show the origins of the LF to be in the ocean and suggest this phenomenon is a natural mode of the tropical Pacific Basin. Air-sea interactions amplify the ocean mode by a factor of 5 to 6 so it obtains climatological importance. These same interactions introduce the LF to the atmosphere. The physical processes responsible for these results are presented. The LF mode of interannual variability is not directly driven by the annual cycle. But it does depend importantly on the fact that the ocean-atmosphere coupling strength varies with respect to the annual cycle. The LF mode appears to be rather sharply peaked in wave number space but broadbanded in frequency space. ESA

N94-23284# Los Alamos National Lab., NM.
ON TESTING TWO MAJOR CUMULUS PARAMETERIZATION SCHEMES USING THE CSU REGIONAL ATMOSPHERIC MODELING SYSTEM
C. Y. J. Kao, J. E. Bossert, J. Winterkamp, and C. C. Lai 1993 8 p Presented at the 74th American Meteorological Society Annual Meeting, Nashville, TN, 23-28 Jan. 1994
(Contract W-7405-eng-36)
(DE94-000703; LA-UR-93-3439; CONF-940115-3) Avail: CASI HC A02/MF A01

One of the objectives of the DOE ARM Program is to improve the parameterization of clouds in general circulation models (GCM's). The approach taken in this research is two fold. The behavior of cumulus parameterization schemes are examined by comparing their performance against the results from explicit cloud simulations with state-of-the-art microphysics. This is conducted in a two-dimensional (2-D) configuration of an idealized convective system. The cumulus parameterization schemes are then applied to realistic three-dimensional (3-D) simulations over the western US for a case with an enormous amount of convection in an extended period of five days. In the 2-D idealized tests, cloud effects are parameterized in the 'parameterization cases' with a coarse resolution, whereas each cloud is explicitly resolved by the 'microphysics cases' with a much finer resolution. Thus, the capability of the parameterization schemes in reproducing the growth and life cycle of a convective system can then be evaluated. These 2-D tests will form the basis for further 3-D realistic simulations which have the model resolution equivalent to that of the next generation of GCM's. Two cumulus parameterizations are used in this research: the Arakawa-Schubert (A-S) scheme used in Kao and Ogura and the Kuo scheme used in Tremback. The numerical model used in this research is the Regional Atmospheric Modeling System (RAMS) developed at Colorado State University (CSU). DOE

N94-23471# Lawrence Livermore National Lab., CA.
LIGHTNING, ATMOSPHERIC ELECTRICITY, AND CLIMATE CHANGE
C. Price Oct. 1993 8 p Presented at the 74th Annual Meeting Symposium on Global Electrical Circuit, Global Change and the Meteorological Applications of Lightning Information, Boston, MA, 23-28 Jan. 1994
(Contract W-7405-eng-48)
(DE94-002003; UCRL-JC-115035; CONF-940139-1) Avail: CASI HC A02/MF A01

Temperature records indicate that a global warming of 0.5 to 0.7 C has occurred over the past century. Whether this trend is a result of increased trace gas concentrations in the atmosphere or simply a result of natural variability is still not known. These temperature trends are derived from thousands of observations worldwide. However, these observations are concentrated largely over continental areas, and then mainly in the northern hemisphere's populated regions. This northern hemisphere continental bias results in large uncertainties in estimates of global temperature trends. Due to the increasing evidence that the present buildup of greenhouse gases in the atmosphere may result in an additional global warming of 1-5 C by the year 2050, it is increasingly important to find alternative methods to monitor fluctuations in global surface temperatures. As shown by two recent studies, the global atmospheric electric circuit may provide a promising alternative for monitoring future climate change. DOE

N94-23542*# Wisconsin Univ., Madison.
ATMOSPHERIC MOISTURE FIELDS DERIVED BY SATELLITE OBSERVATIONS OVER THE TROPICAL PACIFIC OCEAN Abstract Only
Hyosang Chung (Yonsei Univ., Seoul, Republic of Korea.) May 1993 2 p
(Grant NAG8-845)
(NASA-CR-194852; NAS 1.26:194852) Avail: CASI HC A01/MF A01

Values of precipitable water are retrieved over the tropical and subtropical Pacific Ocean from TOVS infrared and microwave channel brightness temperature and OLR observations by means of stepwise linear regression. The most useful temperature and moisture sensing channels are pre-selected from sensitivity tests of a radiative transfer model. Numerous models are developed and tested against collocated radiosonde observations and Nimbus-7 SMMR precipitable water estimates. For RAOB comparisons, the best estimator used 15 TOVS predictors and captured 71.1 deg percent of the variance (+0.62 g/sq cm standard error) for column precipitable water; for precipitable water of 700-500 mb bulk layer, these values were 71.7 percent and +/- 0.17 g/sq cm. Little skill of estimated precipitable water was obtained for moisture above 500 mb. Regressions were less skillful against SMMR, unless collocation parameters were tightly controlled; SMMR was less acceptable than RAOB's because of observational drift and errors. Generally, the most skillful predictors were boundary layer brightness temperatures of TOVS channels and satellite estimated stability indices. 'Moisture channels' were hardly useful except for estimating middle and upper tropospheric moisture. Additional regression models were constructed testing the sensitivity to different observational and meteorological characteristics. Models which used some in situ observations surface observations or stabilities calculated from RAOB, were the most successful. The best of these explained 87.5 percent of the variance but the regression selected almost no TOVS channels, relying instead on conventional RAOB and surface observations. A set of four regression models were developed, stratifying atmospheric characteristics on the basis of collocated OLR values. These models improved the variance explained by 5.0 percent; the model associated with the highest OLR values (275 W/sq m less than or equal to OLR; that is, no cloud) showed only marginal skill. Precipitable water fields were generated from the best TOVS-only model for seven days in January 1983 and compared with SMMR-estimated fields. OLR fields and ECMWF precipitable water analysis. The TOVS regression model compared favorably to the SMMR analysis in amplitudes and features. It revealed more evolving synoptic signal than the ECMWF analysis. In synoptically active regions, it differed with respect to the OLR analysis, primarily because of actual differences in the vertical distribution of water vapor. Author (revised)

N94-23576*# Ensco, Inc., Melbourne, FL. Applied Meteorology Unit.
IMPLEMENTATION AND EVALUATION OF THE NEW WIND ALGORITHM IN NASA'S 50 MHz DOPPLER RADAR WIND PROFILER Final Report
Gregory E. Taylor, John T. Manobianco, Robin S. Schumann, Mark M. Wheeler, and Ann M. Yersavich 1993 118 p Original contains color illustrations
(Contract NAS10-11844)
(NASA-CR-194880; NAS 1.26:194880) Avail: CASI HC A06/MF A02; 3 functional color pages

The purpose of this report is to document the Applied Meteorology Unit's implementation and evaluation of the wind algorithm developed by Marshall Space Flight Center (MSFC) on the data analysis processor (DAP) of NASA's 50 MHz doppler radar wind profiler (DRWP). The report also includes a summary of the 50 MHz DRWP characteristics and performance and a proposed concept of operations for the DRWP. Derived from text

N94-23577*# Texas A&M Univ., College Station. Dept. of Meteorology.
UNCERTAINTIES IN CLIMATE DATA SETS
James P. McGuirk 1992 6 p Presented at the 17th NOAA Diagnostic Workshop, Norman, OK, Oct. 1992
(Grant NAG8-845)
(NASA-CR-194848; NAS 1.26:194848) Avail: CASI HC A02/MF A01

Climate diagnostics are constructed from either analyzed fields or from observational data sets. Those that have been commonly used are normally considered ground truth. However, in most of these collections, errors and uncertainties exist which are generally ignored due to the consistency of usage over time. Examples of uncertainties and errors are described in NMC and ECMWF analyses and in satellite observational sets-OLR, TOVS, and SMMR. It is suggested that these errors can be large, systematic, and not negligible in climate analysis. Author

N94-23619*# Texas A&M Univ., College Station.
CONVECTIVE ORGANIZATION IN THE PACIFIC ITCZ: MERGING OLR, TOVS, AND SSM/I INFORMATION
Patrick M. Hayes and James P. McGuirk 1993 2 p Presented at the 20th AMS Conference on Hurricanes and Tropical Meteorology, San Antonio, TX, May 1993
(Grant NAG8-845)
(NASA-CR-194850; NAS 1.26:194850) Avail: CASI HC A01/MF A01

One of the most striking features of the planet's long-time average cloudiness is the zonal band of concentrated convection lying near the equator. Large-scale variability of the Intertropical Convergence Zone (ITCZ) has been well documented in studies of the planetary spatial scales and seasonal/annual/interannual temporal cycles of convection. Smaller-scale variability is difficult to study over the tropical oceans for several reasons. Conventional surface and upper-air data are virtually non-existent in some regions; diurnal and annual signals overwhelm fluctuations on other time scales; and analyses of variables such as geopotential and moisture are generally less reliable in the tropics. These problems make the use of satellite data an attractive alternative and the preferred means to study variability of tropical weather systems. Derived from text

N94-23620*# Iowa State Univ. of Science and Technology, Ames.
MODELLING TOVS RADIANCES OF SYNOPTIC SYSTEMS Abstract Only
Thomas Eddy Coe Dec. 1992 2 p
(Grant NAG8-845)
(NASA-CR-194847; NAS 1.26:194847) Avail: CASI HC A01/MF A01

Two operational analysis models, produced by ECMWF and NMC, are compared against observed satellite radiances by converting the analyzed variables into synthetic radiances using a radiative transfer model (RTM). Observed TOVS satellite radiances are used as a ground truth, since they are the only source of continuous, synoptic-scale resolution observations available over the data-sparse tropical Pacific Ocean. It is assumed that if the analysis models correctly simulate atmospheric conditions, the observed and modelled radiance fields will have similar patterns and magnitudes. In each of seven TOVS channels examined, the mean temperature difference between the models was small, but the differences between the models and the observations were large. The mean temperature difference within each channel was larger than the standard deviation in most cases. The moisture channels of the RTM were sensitive to changes in moisture content, but none of the channels were significantly affected by changes in temperature. Single-day modelled radiance analyses contain synoptic information similar to the satellite observations. ECMWF is often too noisy, producing features not verified by the satellite; NMC is often too smooth. NMC more closely resembles the TOVS contours. Modelled water vapor channel analyses resemble observed monthly and composited observations well, but do not accurately reproduce the highly-variable single-day fields. ECMWF generally has more accurate gradients. Neither model simulates the tropics well. The water vapor channels, especially channel eleven (weighted at 700 mb), most closely resembled the tropical plume composite described by McGuirk and Ulsh. The only plume evidence found in the thermal or microwave channels, in either the observations or the models, was a composite trough situated in the correct location, extending from the mid-latitudes into the subtropics. This feature was not readily discernable until the definition and mature stages. Additional information besides the modelled temperatures would be required to produce an accurate forecast for the tropics. Model patterns more closely resembled the observations in the quiescent atmosphere, though the magnitudes were not any closer. ECMWF simulates the TOVS quiescent state better than NMC. The moisture channels continue to present the most realistic patterns. The models contained more detail in the tropics than was verified by the satellite observations, apparently trying to force an active ITCZ. Lag correlations showed TOVS to be more persistent than the models. TOVS also showed a smoother lag trend, but all products appeared to have adequate ability to react to changes in the atmosphere over time. Author (revised)

N94-23621*# Texas A&M Univ., College Station.
DIAGNOSTIC BUDGETS OF ANALYZED AND MODELLED TROPICAL PLUMES
James P. McGuirk and Gerry W. Vest May 1993 2 p Presented at the 20th Conference on Hurricanes and Tropical Meteorology, San Antonio, TX, May 1993
(Grant NAG8-845)
(NASA-CR-194853; NAS 1.26:194853) Avail: CASI HC A01/MF A01

Blackwell et al. successfully simulated tropical plumes in a global barotropic model valid at 200 mb. The plume evolved in response to strong equatorial convergence which simulated a surge in the Walker Circulation. The defining characteristics of simulated plumes are: a subtropical jet with southerlies emanating from the deep tropics; a tropical/mid-latitude trough to the west; a convergence/divergence dipole straddling the trough; and strong cross contour flow at the tropical base of the jet. Diagnostic budgets of vorticity, divergence, and kinetic energy are calculated to explain the evolution of the modelled plumes. Budgets describe the unforced (basic) state, forced plumes, forced cases with no plumes, and ECMWF analyzed plumes. Derived from text

N94-24048*# Kansas Univ., Lawrence. Radar Systems and Remote Sensing Lab.
PRECIPITATION MEASUREMENT USING SIR-C: A FEASIBILITY STUDY
Atiq Ahamad and Richard K. Moore Nov. 1993 36 p
(Contract NAS7-918)
(NASA-CR-195104; NAS 1.26:195104; RSL-TR-8370-1) Avail: CASI HC A03/MF A01

A precipitation detection and measurement experiment is planned for the SIR-C/X-SAR mission. This study was conducted to determine under what conditions an off-nadir experiment is feasible. The signal-to-clutter ratio, the signal-to-noise ratio, and the minimum detectable rain rate were investigated. Available models, used in previous studies, were used for the surface clutter and the rain echo. The study also considers the attenuation of the returns at X band. It was concluded that an off-nadir rain-measurement experiment is feasible only for rain rates greater than 10 mm/hr for look angles greater than 60 deg. For the range of look angles 5 less than theta(sub 1) less than 50, the rain rate required is very high for adequate signal-to-clutter ratio, and hence the feasibility of the experiment. Author (revised)

N94-24049*# Purdue Univ., West Lafayette, IN.
A REGIONAL ANALYSIS OF CLOUDY MEAN SPHERICAL ALBEDO OVER THE MARINE STRATOCUMULUS REGION AND THE TROPICAL ATLANTIC OCEAN M.S. Thesis
Kathryn M. Ginger Dec. 1993 133 p
(Grant NAGw-3150)
(NASA-CR-194771; NAS 1.26:194771) Avail: CASI HC A07/MF A02

Since clouds are the largest variable in Earth's radiation budget, it is critical to determine both the spatial and temporal characteristics of their radiative properties. The relationships between cloud properties and cloud fraction are studied in order to supplement grid scale parameterizations. The satellite data used is from three hourly ISCCP (International Satellite Cloud Climatology Project) and monthly ERBE (Earth Radiation Budget Experiment) data on a 2.5 deg x 2.5 deg latitude-longitude grid. Mean cloud spherical albedo, the mean optical depth distribution, and cloud fraction are examined and compared off the coast of California and the mid-tropical Atlantic for July 1987 and 1988. Individual grid boxes and spatial averages over several grid boxes are correlated to Coakley's theory of reflection for uniform and broken layered cloud and to Kedem, et al.'s findings that rainfall volume and fractional area of rain in convective systems is linear. Kedem's hypothesis can be expressed in terms of cloud properties. That is, the total volume of liquid in a box is a linear function of cloud fraction. Results for the marine stratocumulus regime indicate that albedo is often invariant for cloud fractions of 20% to 80%. Coakley's satellite model of small and large clouds with cores (1 km) and edges (100 m) is consistent with this observation. The cores maintain high liquid water concentrations and large droplets while the edges contain low liquid water concentrations and small droplets. Large clouds are just a collection of cores. The mean optical depth (TAU) distributions support the above observation with TAU values of 3.55 to 9.38 favored across all cloud fractions. From these results, a method based upon Kedem, et al's theory is proposed to separate the cloud fraction and liquid water path (LWP) calculations in a general circulation model (GCM). In terms of spatial averaging, a linear relationship between albedo and cloud fraction is observed. For tropical locations outside the Intertropical Convergence Zone (ITCZ), results of cloud fraction and albedo spatial averaging followed that of the stratus boxes containing few overcast scenes. Both the ideas of Coakley and Kedem, et al. apply. Within the ITCZ, the grid boxes tended to have the same statistical properties as stratus boxes containing many overcast scenes. Because different dynamical forcing mechanisms are present, it is difficult to devise a method for determining subgrid scale variations. Neither of the theories proposed by Kedem, et al. or Coakley works well for the boxes with numerous overcast scenes. Author (revised)

N94-24080*# National Aeronautics and Space Administration. Marshall Space Flight Center, Huntsville, AL.
MAMS DATA FOR THE CONVECTION AND MOISTURE EXPERIMENT (CAMEX)
A. R. Guillory, G. J. Jedlovec, and R. J. Atkinson (Martin Marietta Corp., Huntsville, AL.) Jan. 1994 29 p
(NASA-TM-108435; NAS 1.15:108435) Avail: CASI HC A03/MF A01

During the fall of 1993, NASA sponsored a field program called the Convection And Moisture Experiment (CAMEX). The field effort focused on: convective storms in order to investigate their associated electrical properties, precipitation, and predictability, and atmospheric moisture studies. The data collected from the Multispectral Atmospheric Mapping Sensor (MAMS) onboard a NASA ER-2 aircraft which was deployed out of NASA/Wallops Flight Facility, Wallops Island, Virginia, from 11 Sep. through 7 Oct., 1993, is described. Author (revised)

N94-24087*# Kansas Univ., Lawrence. Radar Systems and Remote Sensing Lab.
ESTIMATION OF THE RAIN SIGNAL IN THE PRESENCE OF LARGE SURFACE CLUTTER
Atiq Ahamad and Richard K. Moore Jan. 1994 16 p
(Contract NAS7-918)
(NASA-CR-195105; NAS 1.26:195105; RSL-TR-8730-3) Avail: CASI HC A03/MF A01

The principal limitation for the use of a spaceborne imaging SAR as a rain radar is the surface-clutter problem. Signals may be estimated in the presence of noise by averaging large numbers of independent samples.

This method was applied to obtain an estimate of the rain echo by averaging a set of N(sub c) samples of the clutter in a separate measurement and subtracting the clutter estimate from the combined estimate. The number of samples required for successful estimation (within 10-20%) for off-vertical angles of incidence appears to be prohibitively large. However, by appropriately degrading the resolution in both range and azimuth, the required number of samples can be obtained. For vertical incidence, the number of samples required for successful estimation is reasonable. In estimating the clutter it was assumed that the surface echo is the same outside the rain volume as it is within the rain volume. This may be true for the forest echo, but for convective storms over the ocean the surface echo outside the rain volume is very different from that within. It is suggested that the experiment be performed with vertical incidence over forest to overcome this limitation. Author (revised)

N94-24097*# Swarthmore Coll., PA. Dept. of Physics and Astronomy.

THE THREE-DIMENSIONAL STRUCTURE OF THE INFRARED CIRRUS Final Technical Report

John E. Gaustad 10 Jan. 1994 3 p
(Grant NAG5-1152)
(NASA-CR-194870; NAS 1.26:194870) Avail: CASI HC A01/MF A01

This project was carried out over a period of four years, beginning 6/15/89 and continuing through 9/15/93. Intermediate results have been reported as poster papers at several meetings of the American Astronomical Society. A brief summary was presented in April 1993 at a symposium on the infrared cirrus. The final results were published in late 1993. The measurements have been deposited in NASA's Astronomical Data Center. Briefly, the results are as follows: Using the IRAS data base, we surveyed the 1808 06-B9.5 stars in the Bright Star Catalog for extended excess emission at 60 micrometers, indicating the presence of heated dust (cirrus hotspots) at the location of the star. Measurements of the angular size and infrared flux at 12, 25, 60 and 100 micrometers were obtained for 302 objects. From these basic data we calculated the radius, absorption, optical depth, color temperature, and dust density for each object. Arguing that the stars are randomly distributed point probes of the ISM, we showed that the filling factor of the dust-bearing component of the ISM is 14.6 + 2.4 percent within 400 pc of the sun for clouds with an equivalent hydrogen density greater than 0.5 cm(exp -3). Above a density of 1.0 cm(exp -3) the density distribution function appears to follow a power law of index -1.25. Further, we showed that the dust is distributed more sparsely in a region near the sun about 60 pc wide and extending several hundred parsecs in the direction of longitudes 80-260 deg. The distances to the dust clouds were determined from the spectroscopic parallaxes of the embedded stars; when the HIPPARCOS parallaxes become available, we will be able to produce a more accurate three-dimensional view of the local ISM. Derived from text

N94-24125*# Wisconsin Univ., Madison. Space Science and Engineering Center.

IMPLEMENTATION OF A STATE OF THE ART AUTOMATED SYSTEM FOR THE PRODUCTION OF CLOUD/WATER VAPOR MOTION WINDS FROM GEOSTATIONARY SATELLITES Progress Report, 1 Jul. - 31 Dec. 1993

Christopher S. Velden Feb. 1994 12 p
(Grant NAG8-974)
(NASA-CR-195087; NAS 1.26:195087) Avail: CASI HC A03/MF A01

The thrust of the proposed effort under this contract is aimed at improving techniques to track water vapor data in sequences of imagery from geostationary satellites. In regards to this task, significant testing, evaluation, and progress was accomplished during this period. Sets of winds derived from Meteosat data were routinely produced during Atlantic hurricane events in the 1993 season. These wind sets were delivered via Internet in real time to the Hurricane Research Division in Miami for their evaluation in a track forecast model. For eighteen cases in which 72-hour forecasts were produced, thirteen resulted in track forecast improvements (some quite significant). In addition, quality-controlled Meteosat water vapor winds produced by NESDIS were validated against rawinsondes, yielding an 8 m/s RMS. This figure is comparable to upper-level cloud drift wind accuracies. Given the complementary horizontal coverage in cloud-free areas, we believe that water vapor vectors can supplement cloud-drift wind information to provide good full-disk coverage of the upper tropospheric flow. The impact of these winds on numerical analysis and forecasts will be tested in the next reporting period. Derived from text

N94-24126*# Kansas Univ., Lawrence. Radar Systems and Remote Sensing Lab.

PRECIPITATION MEASUREMENT USING SIR-C: A FEASIBILITY STUDY. INVESTIGATION AT NADIR

Atiq Ahamad and Richard K. Moore Dec. 1993 24 p
(Contract NAS7-918)
(NASA-CR-195103; NAS 1.26:195103; RSL-TR-8370-2) Avail: CASI HC A03/MF A01

The most significant limitation of the imaging SAR in rain measurements is the ground return coupled to the rain cell. Here we report a study of the possibility of using the X-SAR and the C-band channel of SIR-C for rain measurement. Earlier signal-to-clutter calculations rule out the use of X-SAR at steeper off-vertical angles of incidence (i.e., 20 less than theta less than 50). Only rain rates greater than 30 mm/hr at angles of incidence greater than 60 degrees showed good signal-to-clutter ratio (SCR). This study involved calculations at vertical incidence. There is adequate signal-to-noise ratio (SNR) at vertical incidence, but the presence of high-range side-lobe levels leads to small SCR for measurement over oceans at both X and C bands. For larger rain thickness (greater than two km), the SCR gets better and smaller rain rates (greater than 10 mm/hr) can be measured. However, rain measurements over forests seem to be feasible at nadir even for smaller rain thickness (less than two km). We conclude that X band may be usable over the forest at vertical incidence to measure rain rates greater than five mm/hr even for shallow rain thickness and over ocean for large rain thickness. Author (revised)

N94-24355*# National Aeronautics and Space Administration. Goddard Space Flight Center, Greenbelt, MD.

NIMBUS-7 TOTAL OZONE MAPPING SPECTROMETER (TOMS) DATA PRODUCTS USER'S GUIDE

Richard D. McPeters, Arlin J. Krueger, P. K. Bhartia, Jay R. Herman, Arnold Oaks, Ziuddin Ahmad (Hughes STX, Inc., Lanham, MD.), Richard P. Cebula (Hughes STX, Inc., Lanham, MD.), Barry M. Schlesinger (Hughes STX, Inc., Lanham, MD.), Tom Swissler (Hughes STX, Inc., Lanham, MD.), and Steven L. Taylor (Hughes STX, Inc., Lanham, MD.) et al Washington Nov. 1993 93 p
(Contract NAS5-29386; RTOP 916-00-00)
(NASA-RP-1323; Rept-94B00013; NAS 1.61:1323) Avail: CASI HC A05/MF A01

Two tape products from the Total Ozone Mapping Spectrometer (TOMS) aboard the Nimbus-7 have been archived at the National Space Science Data Center. The instrument measures backscattered Earth radiance and incoming solar irradiance; their ratio -- the albedo -- is used in ozone retrievals. In-flight measurements are used to monitor changes in the instrument sensitivity. The algorithm to retrieve total column ozone compares the observed ratios of albedos at pairs of wavelengths with pair ratios calculated for different ozone values, solar zenith angles, and optical paths. The initial error in the absolute scale for TOMS total ozone is 3 percent, the one standard-deviation random error is 2 percent, and the drift is +/- 1.5 percent over 14.5 years. The High Density TOMS (HDTOMS) tape contains the measured albedos, the derived total ozone amount, reflectivity, and cloud-height information for each scan position. It also contains an index of SO2 contamination for each position. The Gridded TOMS (GRIDTOMS) tape contains daily total ozone and reflectivity in roughly equal area grids (110 km in latitude by about 100-150 km in longitude). Detailed descriptions of the tape structure and record formats are provided. Author

N94-24374*# National Aeronautics and Space Administration. Goddard Space Flight Center, Greenbelt, MD.

REPORT OF THE PROCEEDINGS OF THE COLLOQUIUM AND WORKSHOP ON MULTISCALE COUPLED MODELING

Steven E. Koch, ed. Washington Jun. 1993 131 p Workshop held in Calverton, MD, 22-25 Feb. 1993
(NASA-CP-3217; Rept-93B00083; NAS 1.55:3217) Avail: CASI HC A07/MF A02

The Colloquium and Workshop on Multiscale Coupled Modeling was held for the purpose of addressing modeling issues of importance to planning for the Cooperative Multiscale Experiment (CME). The colloquium presentations attempted to assess the current ability of numerical models to accurately simulate the development and evolution of mesoscale cloud and precipitation systems and their cycling of water substance, energy, and trace species. The primary purpose of the workshop was to make specific recommendations for the improvement of mesoscale models prior to the CME, their coupling with cloud, cumulus ensemble, hydrology, air chemistry models, and the observational requirements to initialize and verify these models. For individual titles, see N94-24375 through N94-24400.

N94-24375*# National Oceanic and Atmospheric Administration, Silver Spring, MD.

UNITED STATES WEATHER RESEARCH PROGRAM (USWRP)

Chandrakant Bhumralkar *In* NASA. Goddard Space Flight Center, Report of the Proceedings of the Colloquium and Workshop on Multiscale Coupled Modeling Jun. 1993 p 3-4 (For primary document see N94-24374 06-47)

Avail: CASI HC A01/MF A02

After more than a decade of development by a broad cross-section of the U.S. atmospheric research community involved in planning for the National STORM Program, the Subcommittee on Atmospheric Research (SAR) of the Committee on Earth and Environmental Science (CEES) led the development of a strategic plan to realize the objectives of STORM so as to improve our nation's capability to provide accurate short-term forecasts of weather. This strategic plan will guide the planning and implementation of what is now called the United States Weather Research Program (USWRP). The USWRP is charged with achieving operational atmospheric prediction based on mesoscale observations and model results and establishing the scientific and technological basis for global atmospheric mesoscale prediction by the year 2000. The key scientific questions that are addressed under USWRP are discussed. Author (revised)

N94-24376*# Science and Technology Corp., Washington, DC.

GEWEX CONTINENTAL-SCALE INTERNATIONAL PROJECT (GCIP)

Paul Try *In* NASA. Goddard Space Flight Center, Report of the Proceedings of the Colloquium and Workshop on Multiscale Coupled Modeling Jun. 1993 p 4-6 (For primary document see N94-24374 06-47)

Avail: CASI HC A01/MF A02

The Global Energy and Water Cycle Experiment (GEWEX) represents the World Climate Research Program activities on clouds, radiation, and land-surface processes. The goal of the program is to reproduce and predict, by means of suitable models, the variations of the global hydrological regime and its impact on atmospheric and oceanic dynamics. However, GEWEX is also concerned with variations in regional hydrological processes and water resources and their response to changes in the environment such as increasing greenhouse gases. In fact, GEWEX contains a major new international project called the GEWEX Continental-scale International Project (GCIP), which is designed to bridge the gap between the small scales represented by hydrological models and those scales that are practical for predicting the regional impacts of climate change. The development and use of coupled mesoscale-hydrological models for this purpose is a high priority in GCIP. The objectives of GCIP are presented. Author (revised)

N94-24377*# National Center for Atmospheric Research, Boulder, CO.

GEWEX CLOUD SYSTEMS STUDY (GCSS)

Mitch Moncrieff *In* NASA. Goddard Space Flight Center, Report of the Proceedings of the Colloquium and Workshop on Multiscale Coupled Modeling Jun. 1993 p 6-8 (For primary document see N94-24374 06-47)

Avail: CASI HC A01/MF A02

The Global Energy and Water Cycle Experiment (GEWEX) Cloud Systems Study (GCSS) program seeks to improve the physical understanding of sub-grid scale cloud processes and their representation in parameterization schemes. By improving the description and understanding of key cloud system processes, GCSS aims to develop the necessary parameterizations in climate and numerical weather prediction (NWP) models. GCSS will address these issues mainly through the development and use of cloud-resolving or cumulus ensemble models to generate realizations of a set of archetypal cloud systems. The focus of GCSS is on mesoscale cloud systems, including precipitating convectively-driven cloud systems like MCS's and boundary layer clouds, rather than individual clouds, and on their large-scale effects. Some of the key scientific issues confronting GCSS that particularly relate to research activities in the central U.S. are presented. Author (revised)

N94-24378*# National Aeronautics and Space Administration. Goddard Space Flight Center, Greenbelt, MD.

GEWEX WATER VAPOR PROJECT (GVaP)

David Starr *In its* Report of the Proceedings of the Colloquium and Workshop on Multiscale Coupled Modeling Jun. 1993 p 8- (For primary document see N94-24374 06-47)

Avail: CASI HC A01/MF A02

The goal of the Global Energy and Water Cycle Experiment (GEWEX) Water Vapor Project (GVaP) is to improve the understanding of water vapor in meteorological, hydrological, and climatological processes through improving knowledge of water vapor and its variability on all scales. This goal clearly requires a multiscale observing strategy. A pilot project was deemed the most appropriate first step toward achieving this goal. An implementation plan was developed for this pilot phase. The four research components of the pilot phase are presented here. Author (revised)

N94-24379*# Battelle Northwest Labs., Richland, WA.

ATMOSPHERIC RADIATION MEASUREMENT (ARM)/CART SITE

Bill Pennell *In* NASA. Goddard Space Flight Center, Report of the Proceedings of the Colloquium and Workshop on Multiscale Coupled Modeling Jun. 1993 p 9-11 (For primary document see N94-24374 06-47)

Avail: CASI HC A01/MF A02

The DOE's Atmospheric Radiation Measurement (ARM) goals are as follows: (1) to provide an experimental test bed for improving the treatment of radiative transfer in global climate models (GCM's) under all kinds of cloud cover; and (2) to improve the parameterization and modeling of cloud formation, maintenance, dissipation, and related processes in GCM's. The scientific requirements which are most critical to the objectives of ARM are discussed. Author (revised)

N94-24380*# National Center for Atmospheric Research, Boulder, CO.

AVIATION WEATHER PROGRAM (AWP)

Brant Foote *In* NASA. Goddard Space Flight Center, Report of the Proceedings of the Colloquium and Workshop on Multiscale Coupled Modeling Jun. 1993 p 11 (For primary document see N94-24374 06-47)

Avail: CASI HC A01/MF A02

The Aviation Weather Program (AWP) combines additional weather observations, improved forecast technology, and more efficient distribution of information to pilots, controllers, and automated systems to improve the weather information provided to the air traffic control system, pilots, and other users of aviation weather information. Specific objectives include the needs to: improve airport and en-route capacity by accurate, high resolution, timely forecasts of changing weather conditions affecting airport and en-route operations; improve analyses and forecasts of upper-level winds for efficient flight planning and traffic management; and increase flight safety through improved aviation weather hazard forecasting (e.g. icing, turbulence, severe storms, microbursts, or strong winds). The AWP would benefit from participation in a cooperative multiscale experiment by obtaining data for: evaluation of aviation weather forecast products, analysis of four dimensional data assimilation schemes, and experimental techniques for retrieving aerosol and other visibility parameters. A multiscale experiment would also be helpful to AWP by making it possible to evaluate the added benefit of enhanced data sets collected during the experiment on those forecast and analysis products. The goals of the Coperative Multiscale Experiment (CME) are an essential step in attaining the long-term AWP objective of providing two-to-four hour location-specific forecasts of significant weather. Although the possibility of a funding role for the AWP in the CME is presently unclear, modest involvement of Federal Aviation Administration (FAA)/AWP personnel could be expected. Derived from text

N94-24381*# Colorado State Univ., Fort Collins. Dept. of Atmospheric Science.

SCIENTIFIC GOALS OF THE COOPERATIVE MULTISCALE EXPERIMENT (CME)

William Cotton *In* NASA. Goddard Space Flight Center, Report of the Proceedings of the Colloquium and Workshop on Multiscale Coupled

Modeling Jun. 1993 p 12-15 (For primary document see N94-24374 06-47)
Avail: CASI HC A01/MF A02

Mesoscale Convective Systems (MCS) form the focus of CME. Recent developments in global climate models, the urgent need to improve the representation of the physics of convection, radiation, the boundary layer, and orography, and the surge of interest in coupling hydrologic, chemistry, and atmospheric models of various scales, have emphasized the need for a broad interdisciplinary and multi-scale approach to understanding and predicting MCS's and their interactions with processes at other scales. The role of mesoscale systems in the large-scale atmospheric circulation, the representation of organized convection and other mesoscale flux sources in terms of bulk properties, and the mutually consistent treatment of water vapor, clouds, radiation, and precipitation, are all key scientific issues concerning which CME will seek to increase understanding. The manner in which convective, mesoscale, and larger scale processes interact to produce and organize MCS's, the moisture cycling properties of MCS's, and the use of coupled cloud/mesoscale models to better understand these processes, are also major objectives of CME. Particular emphasis will be placed on the multi-scale role of MCS's in the hydrological cycle and in the production and transport of chemical trace constituents. The scientific goals of the CME consist of the following: understand how the large and small scales of motion influence the location, structure, intensity, and life cycles of MCS's; understand processes and conditions that determine the relative roles of balanced (slow manifold) and unbalanced (fast manifold) circulations in the dynamics of MCS's throughout their life cycles; assess the predictability of MCS's and improve the quantitative forecasting of precipitation and severe weather events; quantify the upscale feedback of MCS's to the large-scale environment and determine interrelationships between MCS occurrence and variations in the large-scale flow and surface forcing; provide a data base for initialization and verification of coupled regional, mesoscale/hydrologic, mesoscale/chemistry, and prototype mesoscale/cloud-resolving models for prediction of severe weather, ceilings, and visibility; provide a data base for initialization and validation of cloud-resolving models, and for assisting in the fabrication, calibration, and testing of cloud and MCS parameterization schemes; and provide a data base for validation of four dimensional data assimilation schemes and algorithms for retrieving cloud and state parameters from remote sensing instrumentation. Derived from text

---

N94-24382*# National Aeronautics and Space Administration. Goddard Space Flight Center, Greenbelt, MD.

GRAND CHALLENGE SCIENTIFIC QUESTIONS IN COUPLED MODELING

Steven Koch *In its* Report of the Proceedings of the Colloquium and Workshop on Multiscale Coupled Modeling Jun. 1993 p 15-17 (For primary document see N94-24374 06-47)
Avail: CASI HC A01/MF A02

Most convective field experiments in the past (e.g., SESAME, CCOPE, CINDE) have attempted to resolve only the immediate scales of moist convection using network arrays that spanned two or three atmospheric scales at most. Furthermore, these scales have been defined more on practical considerations (cost, manpower, etc.) than on a clear understanding of their theoretical significance. Unfortunately, this has precluded a description of the entire life cycle of MCS's and their interaction with larger scale systems, the land surface, and trace species. Fortunately, the following factors now make it possible to attempt to simulate scale contraction processes from the synoptic scale down to the cloud scale, as well as interactions between complex meteorological, land surface, precipitation, chemical, and hydrologic processes with coupled, multiscale models: the availability of new technology to sample meteorological fields at high temporal and spatial resolution over a broad region made possible by the weather observing modernization program; increased computer power and improved numerical approaches to run limited area models with nonhydrostatic precipitation physics so as to explicitly resolve MCS (Mesoscale Convective System) processes; and four dimensional assimilation of non-conventional data to provide dynamically consistent datasets for diagnostic analysis of nonlinear scale-interactive dynamics. Several examples of scale-interactive processes which present grand challenges for coupled, multiscale modeling were presented. Derived from text

---

N94-24383*# National Aeronautics and Space Administration. Goddard Space Flight Center, Greenbelt, MD.

NEXT GENERATION INITIATION TECHNIQUES

Tom Warner (Pennsylvania State Univ., University Park.), John Derber (National Meteorological Center, Camp Springs, MD.), Milija Zupanski (National Meteorological Center, Camp Springs, MD.), Steve Cohn, and Hans Verlinde (Colorado State Univ., Fort Collins.) *In its* Report of the Proceedings of the Colloquium and Workshop on Multiscale Coupled Modeling Jun. 1993 p 17-19 (For primary document see N94-24374 06-47)
Avail: CASI HC A01/MF A02

Four-dimensional data assimilation strategies can generally be classified as either current or next generation, depending upon whether they are used operationally or not. Current-generation data-assimilation techniques are those that are presently used routinely in operational-forecasting or research applications. They can be classified into the following categories: intermittent assimilation, Newtonian relaxation, and physical initialization. It should be noted that these techniques are the subject of continued research, and their improvement will parallel the development of next generation techniques described by the other speakers. Next generation assimilation techniques are those that are under development but are not yet used operationally. Most of these procedures are derived from control theory or variational methods and primarily represent continuous assimilation approaches, in which the data and model dynamics are 'fitted' to each other in an optimal way. Another 'next generation' category is the initialization of convective-scale models. Intermittent assimilation systems use an objective analysis to combine all observations within a time window that is centered on the analysis time. Continuous first-generation assimilation systems are usually based on the Newtonian-relaxation or 'nudging' techniques. Physical initialization procedures generally involve the use of standard or nonstandard data to force some physical process in the model during an assimilation period. Under the topic of next-generation assimilation techniques, variational approaches are currently being actively developed. Variational approaches seek to minimize a cost or penalty function which measures a model's fit to observations, background fields and other imposed constraints. Alternatively, the Kalman filter technique, which is also under investigation as a data assimilation procedure for numerical weather prediction, can yield acceptable initial conditions for mesoscale models. The third kind of next-generation technique involves strategies to initialize convective scale (non-hydrostatic) models. Derived from text

---

N94-24384*# Oklahoma Univ., Norman.

EXAMPLES OF DATA ASSIMILATION IN MESOSCALE MODELS

Fred Carr, John Zack (Mesoscale Environmental Simulations and Operations, Inc., Troy, NY.), Jerry Schmidt (National Oceanic and Atmospheric Administration, Boulder, CO.), John Snook (National Oceanic and Atmospheric Administration, Boulder, CO.), Stan Benjamin (National Oceanic and Atmospheric Administration, Boulder, CO.), and David Stauffer (Pennsylvania State Univ., University Park.) *In* NASA. Goddard Space Flight Center, Report of the Proceedings of the Colloquium and Workshop on Multiscale Coupled Modeling Jun. 1993 p 19-23 (For primary document see N94-24374 06-47)
Avail: CASI HC A01/MF A02

The keynote address was the problem of physical initialization of mesoscale models. The classic purpose of physical or diabatic initialization is to reduce or eliminate the spin-up error caused by the lack, at the initial time, of the fully developed vertical circulations required to support regions of large rainfall rates. However, even if a model has no spin-up problem, imposition of observed moisture and heating rate information during assimilation can improve quantitative precipitation forecasts, especially early in the forecast. The two key issues in physical initialization are the choice of assimilating technique and sources of hydrologic/hydrometeor data. Another example of data assimilation in mesoscale models was presented in a series of meso-beta scale model experiments with and 11 km version of the MASS model designed to investigate the sensitivity of convective initiation forced by thermally direct circulations resulting from differential surface heating to four dimensional assimilation of surface and radar data. The results of these simulations underscore the need to accurately initialize and simulate grid and sub-grid scale clouds in meso- beta scale models. The status of the application of the CSU-RAMS mesoscale model by the NOAA Forecast Systems Lab for producing real-time forecasts with 10-60 km mesh resolutions over (4000 km)(exp 2) domains for use by the aviation community was reported. Either MAPS or LAPS model data are used to initialize the RAMS model on a 12-h cycle. The use of MAPS (Mesoscale Analysis and Prediction System) model was discussed. Also discussed was the mesobeta-scale data assimilation using a triply-nested nonhydrostatic version of the MM5 model. Derived from text

N94-24385*# National Aeronautics and Space Administration. Goddard Space Flight Center, Greenbelt, MD.
MEASUREMENT AND MODELING OF MOIST PROCESSES
William Cotton (Colorado State Univ., Fort Collins.), David Starr, Kenneth Mitchell (National Oceanic and Atmospheric Administration, Washington, DC.), Rex Fleming (National Center for Atmospheric Research, Boulder, CO.), Steve Koch, Steve Smith (National Oceanic and Atmospheric Administraion, Fort Collins, CO.), Jocelyn Mailhot (Recherche en Prevision Numerique, Dorval, Quebec.), Don Perkey (Drexel Univ., Philadelphia, PA.), and Greg Tripoli (Wisconsin Univ., Madison.) *In its* Report of the Proceedings of the Colloquium and Workshop on Multiscale Coupled Modeling Jun. 1993 p 23-26 (For primary document see N94-24374 06-47)
Avail: CASI HC A01/MF A02

The keynote talk summarized five years of work simulating observed mesoscale convective systems with the RAMS (Regional Atmospheric Modeling System) model. Excellent results are obtained when simulating squall line or other convective systems that are strongly forced by fronts or other lifting mechanisms. Less highly forced systems are difficult to model. The next topic in this colloquium was measurement of water vapor and other constituents of the hydrologic cycle. Impressive accuracy was shown measuring water vapor with both the airborne DIAL (Differential Absorption Lidar) system and the the ground-based Raman Lidar. NMC's plans for initializing land water hydrology in mesoscale models was presented before water vapor measurement concepts for GCIP were discussed. The subject of using satellite data to provide mesoscale moisture and wind analyses was next. Recent activities in modeling of moist processes in mesoscale systems was reported on. These modeling activities at the Canadian Atmospheric Environment Service (AES) used a hydrostatic, variable-resolution grid model. Next the spatial resolution effects of moisture budgets was discussed; in particular, the effects of temporal resolution on heat and moisture budgets for cumulus parameterization. The conclusion of this colloquium was on modeling scale interaction processes.
Derived from text

N94-24386*# National Aeronautics and Space Administration. Goddard Space Flight Center, Greenbelt, MD.
PARAMETERIZATION OF SUB-GRID SCALE CONVECTION
William Frank (Pennsylvania State Univ., University Park.), John Molinari (State Univ. of New York, Albany.), Jack Kain (Pennsylvania State Univ., University Park.), Mitch Moncrieff (National Center for Atmospheric Research, Boulder, CO.), Mohan Karyampudi, and Georg Grell (National Oceanic and Atmospheric Administration, Boulder, CO.) *In its* Report of the Proceedings of the Colloquium and Workshop on Multiscale Coupled Modeling Jun. 1993 p 26-29 (For primary document see N94-24374 06-47)
Avail: CASI HC A01/MF A02

The following topics are discussed: an overview of the cumulus parameterization problem; interactions between explicit and implicit processes in mesoscale models; effects of model grid size on the cumulus parameterization problem; parameterizing convective effects on momentum fields in mesoscale models; differences between slantwise and vertical cumulus parameterization; experiments with different closure hypotheses; and coupling cumulus parameterizations to boundary layer, stable cloud, and radiation schemes. CASI

N94-24387*# National Aeronautics and Space Administration. Goddard Space Flight Center, Greenbelt, MD.
COUPLED LAND SURFACE/HYDROLOGIC/ATMOSPHERIC MODELS
Roger Pielke (Colorado State Univ., Fort Collins.), Lou Steyaert (Geological Survey, Reston, VA.), Ray Arritt (Kansas Univ., Lawrence.), Mercedes Lahtakia (Pennsylvania State Univ., University Park.), Chris Smith (Pennsylvania State Univ., University Park.), Conrad Ziegler (National Oceanic and Atmospheric Administration, Boulder, CO.), Su Tzai Soong (California Univ., Davis.), Roni Avissar (Rutgers Univ., New Brunswick, NJ.), Peter Wetzel, and Piers Sellers *In its* Report of the Proceedings of the Colloquium and Workshop on Multiscale Coupled Modeling Jun. 1993 p 31-36 (For primary document see N94-24374 06-47)
Avail: CASI HC A02/MF A02

The topics covered include the following: prototype land cover characteristics data base for the conterminous United States; surface evapotranspiration effects on cumulus convection and implications for mesoscale models; the use of complex treatment of surface hydrology and thermodynamics within a mesoscale model and some related issues; initialization of soil-water content for regional-scale atmospheric prediction models; impact of surface properties on dryline and MCS evolution; a numerical simulation of heavy precipitation over the complex topography of California; representing mesoscale fluxes induced by landscape discontinuities in global climate models; emphasizing the role of subgrid-scale heterogeneity in surface-air interaction; and problems with modeling and measuring biosphere-atmosphere exchanges of energy, water, and carbon on large scales. Derived from text

N94-24388*# National Center for Atmospheric Research, Boulder, CO.
INCORPORATION OF THE PLANETARY BOUNDARY LAYER IN ATMOSPHERIC MODELS
Chin-Hoh Moeng, John Wyngaard (Pennsylvania State Univ., University Park.), Roger Pielke (Colorado State Univ., Fort Collins.), and Steve Krueger (Utah Univ., Salt Lake City.) *In* NASA. Goddard Space Flight Center, Report of the Proceedings of the Colloquium and Workshop on Multiscale Coupled Modeling Jun. 1993 p 37-41 (For primary document see N94-24374 06-47)
Avail: CASI HC A01/MF A02

The topics discussed include the following: perspectives on planetary boundary layer (PBL) measurements; current problems of PBL parameterization in mesoscale models; and convective cloud-PBL interactions. Derived from text

N94-24389*# California Univ., San Diego, La Jolla.
THE ROLE OF RADIATION IN MESOSCALE FLOWS: PHYSICS, PARAMETERIZATIONS, CODES
P. J. Flatau, Dean Churchill (Miami Univ., FL.), and Robert D. Cess (State Univ. of New York, Stony Brook.) *In* NASA. Goddard Space Flight Center, Report of the Proceedings of the Colloquium and Workshop on Multiscale Coupled Modeling Jun. 1993 p 42-43 (For primary document see N94-24374 06-47)
Avail: CASI HC A01/MF A02

The topics discussed include the following: an overview of radiation and mesoscale flows and lessons learned from the intercomparison of GCM radiative codes. Derived from text

N94-24390*# National Aeronautics and Space Administration. Goddard Space Flight Center, Greenbelt, MD.
CHEMISTRY ON THE MESOSCALE: MODELING AND MEASUREMENT ISSUES
Anne Thompson, John Pleim (Environmental Protection Agency, Research Triangle Park, NC.), Christopher Walcek (State Univ. of New York, Albany.), Jason Ching (Environmental Protection Agency, Research Triangle Park, NC.), Frank Binkowski (Environmental Protection Agency, Research Triangle Park, NC.), Wei-Kuo Tao, Russell Dickerson (Maryland Univ., College Park.), and Kenneth Pickering *In its* Report of the Proceedings of the Colloquium and Workshop on Multiscale Coupled Modeling Jun. 1993 p 43-48 (For primary document see N94-24374 06-47)
Avail: CASI HC A02/MF A02

The topics covered include the following: Regional Acid Deposition Model (RADM) -- a coupled chemistry/mesoscale model; convection in RADM; unresolved issues for mesoscale modeling with chemistry -- nonprecipitating clouds; unresolved issues for mesoscale modeling with chemistry -- aerosols; tracer studies with Goddard Cumulus Ensemble Model (GCEM); field observations of trace gas transport in convection; and photochemical consequences of convection. Derived from text

N94-24391*# National Aeronautics and Space Administration. Goddard Space Flight Center, Greenbelt, MD.
VALIDATION OF MESOSCALE MODELS
Bill Kuo (National Center for Atmospheric Research, Boulder, CO.), Tom Warner (Pennsylvania State Univ., University Park.), Stan Benjamin (National Oceanic and Atmospheric Administration, Boulder, CO.), Steve Koch, and

Andrew Staniforth (Recherche en Prevision Numerique, Dorval, Quebec.) *In its* Report of the Proceedings of the Colloquium and Workshop on Multiscale Coupled Modeling Jun. 1993 p 48-50 (For primary document see N94-24374 06-47)
Avail: CASI HC A01/MF A02

The topics discussed include the following: verification of cloud prediction from the PSU/NCAR mesoscale model; results form MAPS/NGM verification comparisons and MAPS observation sensitivity tests to ACARS and profiler data; systematic errors and mesoscale verification for a mesoscale model; and the COMPARE Project and the CME. Derived from text

N94-24392*# Oklahoma Univ., Norman.
TECHNIQUES AND RESOURCES FOR STORM-SCALE NUMERICAL WEATHER PREDICTION
Kelvin Droegemeier, Georg Grell (National Oceanic and Atmospheric Administration, Boulder, CO.), James Doyle (Naval Research Lab., Monterey, CA.), Su-Tzai Soong (California Univ., Davis.), William Skamarock (National Center for Atmospheric Research, Boulder, CO.), David Bacon (Science Applications International Corp., McLean, VA.), Andrew Staniforth (Recherche en Prevision Numerique, Dorval, Quebec.), Andrew Crook (National Center for Atmospheric Research, Boulder, CO.), and Robert Wilhelmson (Illinois Univ., Urbana.) *In* NASA. Goddard Space Flight Center, Report of the Proceedings of the Colloquium and Workshop on Multiscale Coupled Modeling Jun. 1993 p 50-61 (For primary document see N94-24374 06-47)
Avail: CASI HC A03/MF A02

The topics discussed include the following: multiscale application of the 5th-generation PSU/NCAR mesoscale model, the coupling of nonhydrostatic atmospheric and hydrostatic ocean models for air-sea interaction studies; a numerical simulation of cloud formation over complex topography; adaptive grid simulations of convection; an unstructured grid, nonhydrostatic meso/cloud scale model; efficient mesoscale modeling for multiple scales using variable resolution; initialization of cloud-scale models with Doppler radar data; and making effective use of future computing architectures, networks, and visualization software. Derived from text

N94-24393*# Colorado State Univ., Fort Collins. Dept. of Atmospheric Science.
JOINT SESSIONS ON MOISTURE PROCESSES AND CUMULUS PARAMETERIZATION
William Cotton *In* NASA. Goddard Space Flight Center, Report of the Proceedings of the Colloquium and Workshop on Multiscale Coupled Modeling Jun. 1993 p 62 (For primary document see N94-24374 06-47)
Avail: CASI HC A01/MF A02

The session on measurement/modeling of moisture processes from the proceedings of the Colloquium and Workshop on Multiscale Coupled Modeling is covered. The specific recommendations of the workshop session on the measurement and modeling of moist processes are presented. Derived from text

N94-24394*# Pennsylvania State Univ., University Park.
SESSION ON CUMULUS PARAMETERIZATION
Bill Frank *In* NASA. Goddard Space Flight Center, Report of the Proceedings of the Colloquium and Workshop on Multiscale Coupled Modeling Jun. 1993 p 63-64 (For primary document see N94-24374 06-47)
Avail: CASI HC A01/MF A02

The session on cumulus parameterization from the Colloquium and Workshop on Multiscale Coupled Modeling is covered. The ten major issues raised that were suggested to be critical unknowns requiring immediate attention are presented. Derived from text

N94-24395*# Colorado State Univ., Fort Collins. Dept. of Atmospheric Science.
SESSION ON COUPLED LAND SURFACE/HYDROLOGICAL/ATMOSPHERIC MODELS
Roger Pielke *In* NASA. Goddard Space Flight Center, Report of the Proceedings of the Colloquium and Workshop on Multiscale Coupled Modeling Jun. 1993 p 65-68 (For primary document see N94-24374 06-47)
Avail: CASI HC A01/MF A02

The current model capabilities in the context of land surface interactions with the atmosphere include only one-dimensional characteristics of vegetation and soil surface heat, moisture, momentum, and selected other trace gas fluxes (e.g., CO2). The influence of spatially coherent fluxes that result from landscape heterogeneity were not included. Valuable representations of several aspects of the landscape pattern currently exist. These include digital elevation data and measures of the leaf area index (i.e., Normalized Difference Vegetation Index (NDVI) from Advanced Very High Resolution Radiometer (AVHRR) data). A major deficiency, however, is the lack of an ability to sample spatially representative shallow and (especially) deep soil moisture. Numerous mesoscale modeling and observed studies demonstrated the sensitivity of planetary boundary layer structure and deep convection to the magnitude of the surface moisture flux. Author (revised)

N94-24396*# National Center for Atmospheric Research, Boulder, CO.
JOINT SESSIONS ON MODELING OF BOUNDARY LAYER AND RADIATIVE TRANSFER PROCESSES
Chin-Hoh Moeng *In* NASA. Goddard Space Flight Center, Report of the Proceedings of the Colloquium and Workshop on Multiscale Coupled Modeling Jun. 1993 p 68-70 (For primary document see N94-24374 06-47)
Avail: CASI HC A01/MF A02

During the session on modeling of the planetary boundary layer (PBL) processes the following topics were addressed: current PBL parameterizations used in mesoscale models; critical issues in improving PBL parameterizations for mesoscale models; suggestions for future modeling efforts; and suggestions for observing system strategies. Author (revised)

N94-24397*# California Univ., San Diego, La Jolla.
SESSION ON MODELING OF RADIATIVE TRANSFER PROCESSES
Piotr Flatau *In* NASA. Goddard Space Flight Center, Report of the Proceedings of the Colloquium and Workshop on Multiscale Coupled Modeling Jun. 1993 p 71-72 (For primary document see N94-24374 06-47)
Avail: CASI HC A01/MF A02

The session on modeling of radiative transfer processes is reviewed. Six critical issues surfaced in the discussion concerning scale-interactive radiative processes relevent to the mesoscale convective systems (MCS's). These issues are the need to expand basic knowledge of how MCS's influence climate through extensive cloud shields and increased humidity in the upper troposphere; to improve radiation parameterizations used in mesoscale and General Circulation Model (GCM) models; to improve our basic understanding of the influence of radiation on MCS dynamics due to diabatic heating, production of condensate, and vertical and horizontal heat fluxes; to quantify our understanding of radiative impacts of MCS's on the surface and free atmosphere energy budgets; to quantify and identify radiative and microphysical processes important in the evolution of MCS's; and to improve the capability to remotely sense MCS radiative properties from space and ground-based systems. Derived from text

N94-24398*# National Aeronautics and Space Administration. Goddard Space Flight Center, Greenbelt, MD.
SESSION ON COUPLED ATMOSPHERIC/CHEMISTRY COUPLED MODELS
Anne Thompson *In its* Report of the Proceedings of the Colloquium and Workshop on Multiscale Coupled Modeling Jun. 1993 p 72-77 (For primary document see N94-24374 06-47)
Avail: CASI HC A02/MF A02

The session on coupled atmospheric/chemistry coupled models is reviewed. Current model limitations, current issues and critical unknowns, and modeling activity are addressed. Specific recommendations and experimental strategies on the following are given: multiscale surface layer - planetary boundary layer - chemical flux measurements; Eulerian budget study; and Langrangian experiment. Nonprecipitating cloud studies, organized convective systems, and aerosols - heterogenous chemistry are also discussed. CASI

N94-24399*# National Center for Atmospheric Research, Boulder, CO.
SESSION ON VALIDATION OF COUPLED MODELS
Bill Kuo *In* NASA. Goddard Space Flight Center, Report of the Proceedings

of the Colloquium and Workshop on Multiscale Coupled Modeling Jun. 1993 p 77-79 (For primary document see N94-24374 06-47)
Avail: CASI HC A01/MF A02

The session on validation of coupled models is reviewed. The current use of a mesoscale model with a grid size of 20-km during STORM-FEST in 1992 has proven to be extremely valuable. The availability of forecast products at a much higher temporal and spatial resolution was very helpful for mesoscale forecasting, mission planning, and the guidance of research aircraft. Recent numerical simulation of ocean cyclones and mesoscsle convective systems using nonhydrostatic cloud/mesoscale models with a grid size as small as 2-km have demonstrated the potential of these models for predicting mesoscale convective systems, squall lines, hurricane rainbands, mesoscale gravity waves, and mesoscale frontal structures embedded within an extratropical cyclone. Although mesoscale/cloud scale models have demonstrated strong potential for use in operational forecasting, very limited quantitative evaluation (and verification) of these models were performed. As a result, the accuracy, the systematic biases, and the useful forecasts limits were not properly defined for these models. Also, no serious attempts were made to use these models for operational prediction of mesoscale convective systems. Author (revised)

N94-24400*# Oklahoma Univ., Norman.
SESSION ON TECHNIQUES AND RESOURCES FOR STORM-SCALE NUMERICAL WEATHER PREDICTION
Kelvin Droegemeier *In* NASA. Goddard Space Flight Center, Report of the Proceedings of the Colloquium and Workshop on Multiscale Coupled Modeling Jun. 1993 p 79-112 (For primary document see N94-24374 06-47)
Avail: CASI HC A03/MF A02

The session on techniques and resources for storm-scale numerical weather prediction are reviewed. The recommendations of this group are broken down into three area: modeling and prediction, data requirements in support of modeling and prediction, and data management. The current status, modeling and technological recommendations, data requirements in support of modeling and prediction, and data management are addressed. Derived from text

N94-24485*# Purdue Univ., West Lafayette, IN. Dept. of Earth and Atmospheric Sciences.
OBSERVATIONAL AND MODELING STUDIES OF HEAT, MOISTURE, PRECIPITATION AND GLOBAL-SCALE CIRCULATION PATTERNS Final Technical Report, 20 Jul. 1990 - 19 Jan. 1994
Dayton G. Vincent 19 Jan. 1994 8 p
(Grant NAG8-836)
(NASA-CR-195148; NAS 1.26:195148) Avail: CASI HC A02/MF A01

This research grant was a revised version of an original proposal. The period of the grant was for three years with a six-month no-cost extension; thus, it was from 20 July 1990 to 19 January 1994. The objectives of the grant were to identify periods and locations of active convection centers, primarily over the Southern Hemisphere tropical Indian and Pacific Oceans; determine reasons for any periodic behavior found in the first objective; identify cases where subtropical jets over the South Pacific persisted for several days and examine the influences of tropical versus extra-tropical mechanisms in maintaining them; obtain estimates of precipitation by Q(sub 1) and Q(sub 2) budgets, including the importance of terms in each of the respective budgets, and compare these estimates to those obtained by other methods; and diagnose the distributions of moisture and precipitable water over the North Atlantic Ocean using routine analyses and satellite microwave data. To accomplish these objectives, we used grant funds to purchase several data sets, including the Global Precipitation Climate Project (GPCP) observations of station precipitation, ECMWF WCRP/TOGA archive two analyses for January 1985 - December 1990, ECMWF WMO analyses for January 1980 - December 1987, and OLR data for July 1974 - December 1991. We already had some SSM/I data and GLA analyses from a previous grant. In addition, to improve our computing power, we also used grant funds to purchase an IBM PS/2 with accessories, a NEC laser jet printer, and a microcomputer system for word processing. This report is organized as follows. Our research team is listed first. Section two contains a summary of our significant accomplishments; however, a detailed discussion of research results is not included since this information can be found in the accompanying reprints and preprints. Section three offers some concluding remarks, and a complete bibliographic summary is given in Section four. Derived from text

N94-24705*# South Dakota School of Mines and Technology, Rapid City. Inst. of Atmospheric Sciences.
FURTHER STUDIES TO EXTEND AND TEST THE AREA-TIME-INTEGRAL TECHNIQUE APPLIED TO SATELLITE DATA Semiannual Status Report, 1 Jul. - 31 Dec. 1993
Paul L. Smith and Thomas H. VonderHaar (ASTeR, Inc., Fort Collins, CO.) 1993 10 p
(Grant NAG5-386)
(NASA-CR-195132; NAS 1.26:195132) Avail: CASI HC A02/MF A01

The principal goal of this project is to establish relationships that would allow application of area-time integral (ATI) calculations based upon satellite data to estimate rainfall volumes. The research has been pursued using two different approaches, which for convenience can be designated as the 'fixed-threshold approach' and the 'variable-threshold approach'. In the former approach, an attempt is made to determine a single temperature threshold in the satellite infrared data that would yield ATI values for identifiable cloud clusters which are most closely related to the corresponding rainfall amounts. Results thus far have indicated that a strong correlation exists between the rain volumes and the satellite ATI values, but the optimum threshold for this relationship seems to differ from one geographic location to another. The difference is probably related to differences in the basic precipitation mechanisms that dominate in the different regions. The average rainfall rate associated with each cloudy pixel is also found to vary across the spectrum of ATI values. Work on the second, or 'variable-threshold', approach for determining the satellite ATI values was essentially suspended during this period due to exhaustion of project funds. Most of the ATI work thus far has dealt with cloud clusters from the Lagrangian or 'floating-target' point of view. For many purposes, however, the Eulerian or 'fixed-target' perspective is more appropriate. For a very large target area encompassing entire cluster life histories, the rain volume-ATI relationship would obviously be the same in either case. The important question for the Eulerian perspective is how small the fixed area can be made while maintaining consistency in that relationship. Derived from text

N94-24850 Massachusetts Inst. of Tech., Lexington. Lincoln Lab.
ASR-9 MICROBURST DETECTION ALGORITHM Project Report
O. J. Newell and J. A. Cullen 22 Oct. 1993 68 p Limited Reproducibility: More than 20% of this document may be affected by microfiche quality
(Contract DTFA01-89-Z-0203)
(AD-A273591; ATC-197; DOT/FAA/NR-93/2) Avail: Issuing Activity (Defense Technical Information Center (DTIC))

The ASR-9 Wind Shear Processor (WSP) is intended as an economical alternative for those airports that have not been slated to receive a Terminal Doppler Weather Radar(TDWR) but have, or will be receiving, an ASR-9 radar. Lincoln Laboratory has developed a prototype ASR-9 WSP system which was demonstrated during the summer months of the past three years in Orlando, Florida. During the operational test period, microburst and gust front warnings, as well as storm motion indications, were provided to the Air Traffic Control in real time. The ASR-9 Microburst Detection Algorithm (AMDA) is based on the earlier TDWR Microburst Detection Algorithm, but has been substantially modified to better match the particular strengths and weaknesses of the ASR-9 rapid-scanning fan-beam radar. The most significant additions included a capability to detect overhead microbursts, a reflectivity processing step used to help detect velocity signatures that have been biased by overhanging precipitation, and a modification to some of the shear segment grouping and thresholding parameters to accommodate better the typical on-air siting of the ASR-9. In addition, the AMDA has been designed to be as efficient as possible to allow it to run at the radar's 4.8 seconds/scan antennas rotation rate on a single-board computer. A detailed description of AMDA, as well as the performance evaluation strategy and results, are presented in this report. DTIC

N94-25071# Naval Postgraduate School, Monterey, CA. Dept. of Meteorology.

OBSERVED AND NAVY OPERATIONAL GLOBAL MODEL CLIMATOLOGIES OF SYNOPTIC DISTURBANCES OVER THE TROPICAL WESTERN PACIFIC DURING WINTER 1991-1992 Final Report, Oct. 1992 - Oct. 1993

C.-P. Chang and Liana Zambresky Oct. 1993 111 p
(AD-A273400; NPS-MR-93-003) Avail: CASI HC A06/MF A02

This study compares the structure and characteristics of tropical synoptic timescale wave disturbances over the western Pacific, particularly around the Caroline Islands where six upper air stations are present, as contained in radiosonde observations and the initial analysis (tau00) and 48-h forecast (tau48) of the Navy Operational Global Atmospheric Prediction System (NOGAPS) during northern winter of 1991-1992. The observed, analyzed and forecast disturbance climatologies are all determined from power spectral and cross-spectral analyses focusing on the synoptic frequency band encompassing three adjacent period points: 4.6-, 5.3-, and 6.4-day. The meridional wind at 850 hPa is used as the principal parameter for defining the disturbances. The power spectra of the NOGAPS tau00 analysis agree reasonably closely with the radiosonde observations, but the tau48 forecast shows larger differences. Nevertheless, the observed horizontal structure of the disturbances are all well represented in both the analysis and the forecast at all levels. These include the westward propagation, a 850 hPa wavelength near 33 deg along 10 deg N and near 38 deg along the equator, a 200 hPa wavelength near 50-60 deg, and a northeast-southwest meridional tilt. In general, the analysis and the forecast produce a higher spatial coherency than that shown from the radiosonde observations.
DTIC

N94-25162 Naval Research Lab., Washington, DC.

AN AVHRR CLOUD CLASSIFICATION DATABASE TYPED BY EXPERTS Final Report

C. L. Crosiar Oct. 1993 31 p Limited Reproducibility: More than 20% of this document may be affected by microfiche quality
(DA Proj. X15-96)
(AD-A273560; NRL/MR/7531-93-7207) Avail: Issuing Activity (Defense Technical Information Center (DTIC))

The primary objective of this project was to utilize satellite-data from the NOAA Advanced Very High Resolution Radiometer (AVHRR) sensor and the satellite data interpretation knowledge of experts to develop environmental algorithms for the Navy. This objective was met by the design and implementation of software to extract information from the experts and the satellite sensor images, e.g., cloud type, five channels of spectral data, and three textural parameters. The experts classified clouds over seven regions in the Northern Hemisphere covering a one year period. Although these data will be used to develop a tactical algorithm to automatically classify clouds by type, the agreement among experts will help to form a baseline for the developed objective technique. DTIC

N94-25261# Technische Univ., Eindhoven (Netherlands).

WIND CLIMATE AND URBAN GEOMETRY Ph.D. Thesis

Marcel Bottema 1993 223 p
(ISBN-9-03-860132-8; ETN-94-95350) Copyright Avail: CASI HC A10/MF A03

A study to analyze and supplement existing knowledge of prediction of wind comfort, and to communicate the results to architects and town planners by means of either verbal or graphical design rules, is presented. This aim can be summarized with the words 'technology transfer'. Outdoor climate and its incorporation into the design process is discussed. Theories of boundary layer meteorology and obstacle aerodynamics are presented. Measuring and numerical simulation techniques are discussed. Wind climate at the considered site is mainly dependent on the wind amplification factor, with contribution on three different scale levels: surrounding terrain; building and building group; details of site. Each of these contributions are discussed. Distributions of discomfort probability around buildings are presented. An example of wind comfort evaluation is given. Development of a town plan at a windy location in Amsterdam (Netherlands) is described, as well as cooperation between the architect and the wind expert. Rules of thumb for design are presented. ESA

N94-25271*# Ensco, Inc., Melbourne, FL. Applied Meteorology Unit.

THE EVALUATION OF ASOS FOR THE KENNEDY SPACE CENTER'S SHUTTLE LANDING FACILITY Final Report

Ann Yersavich, Mark Wheeler, Gregory Taylor, Robin Schumann, and John Manobianco Mar. 1994 66 p
(Contract NAS10-11844)
(NASA-CR-195685; NAS 1.26:195685; Rept-94-001) Avail: CASI HC A04/MF A01

This report documents the Applied Meteorology Unit's (AMU) evaluation of the effectiveness and utility of the Automated Surface Observing System (ASOS) in terms of spaceflight operations and user requirements. In particular, the evaluation determines which of the Shuttle Landing Facility (SLF) observation requirements can be satisfied by ASOS. This report also includes a summary of ASOS' background, current configuration and specifications, system performance, and the possible concepts of operations for use of ASOS at the SLF. This evaluation stems from a desire by the Air Force to determine if ASOS units could be used to reduce the cost of SLF meteorological observations. Derived from text

N94-23238*# Pennsylvania State Univ., University Park. Dept. of Meteorology.

LIGHTNING STUDIES USING LDAR AND LLP DATA

Gregory S. Forbes *In* NASA. Kennedy Space Center, NASA/ASEE Summer Faculty Fellowship Program Oct. 1993 p 165-194 (For primary document see N94-23230 06-80)
Avail: CASI HC A03/MF A04

N94-23248*# University of Western Carolina, Cullowhee, NC. Dept. of Mathematics and Computer Science.

HURRICANE RISK ASSESSMENT: ROLLBACK OR RIDE OUT

Richard A. Wohlman *In* NASA. Kennedy Space Center, NASA/ASEE Summer Faculty Fellowship Program Oct. 1993 p 487-519 (For primary document see N94-23230 06-80)
Avail: CASI HC A03/MF A04

N94-23687*# Clarkson Univ., Potsdam, NY. Dept. of Mathematics and Computer Science.

AN ADAPTIVE MULTIGRID MODEL FOR HURRICANE TRACK PREDICTION

Scott R. Fulton *In* NASA. Langley Research Center, The Sixth Copper Mountain Conference on Multigrid Methods, Part 1 Nov. 1993 p 207-214 (For primary document see N94-23673 06-64)
(Grant NSF ATM-91-18966)
Avail: CASI HC A02/MF A03

N94-24409*# Columbia State Community Coll., TN. Computer Information Systems.

CAPE FOR CaPE

Joni Brooks *In* Alabama Univ., The 1993 NASA/ASEE Summer Faculty Fellowship Program Nov. 1993 5 p (For primary document see N94-24405 06-80)
Avail: CASI HC A01/MF A03

N94-24414*# Oklahoma Univ., Norman. School of Meteorology.

WATER CYCLE RESEARCH ASSOCIATED WITH THE CaPE HYDROMETEOROLOGY PROJECT (CHymP

Claude E. Duchon *In* Alabama Univ., The 1993 NASA/ASEE Summer Faculty Fellowship Program Nov. 1993 5 p (For primary document see N94-24405 06-80)
Avail: CASI HC A01/MF A03

N94-24443*# Alabama Univ., Huntsville. Dept. of Mathematical Sciences.

LRAT: LIGHTNING RADIATIVE TRANSFER

Dieudonne D. Phanord *In its* The 1993 NASA/ASEE Summer Faculty Fellowship Program Nov. 1993 5 p (For primary document see N94-24405 06-80)
Avail: CASI HC A01/MF A03

48 OCEANOGRAPHY

Includes biological, dynamic, and physical oceanography; and marine resources.

For related information see also *43 Earth Resources and Remote Sensing.*

N94-23176# Beleidscommissie Remote Sensing, Delft (Netherlands).

LITERATURE STUDY ON: REMOTE FRAUNHOFER LUMINESCENCE DETECTION OF ALGAL BLOOM IN MARINE ENVIRONMENTS

W. M. terKuile (Organisatie voor Toegepast Natuurwetenschappelijk Onderzoek, Delft, Netherlands.) Jun. 1993 56 p In ENGLISH and DUTCH Sponsored by Beleidscommissie Remote Sensing, Delft, Netherlands

(BCRS-92-25; TNO-IMW-R-92/396; ISBN-9-05-411070-8; ETN-94-95038) Avail: CASI HC A04/MF A01

Results of literature survey on passive remote sensing of fluorescence of algae on the dark (Fraunhofer) absorption lines in the spectrum of the Sun are reported. The Fraunhofer Line Detector (FLD) and the second generation instrument FLD 2 which was provided with a linear scanner and used as a remote sensing imager, are described. The use of the FLD for remote sensing of environmental pollutants is described. Fluorescence spectra of two known noxious algae types were measured in a fluorescence spectrometer. One of the maxima of each of these spectra appears to coincide with a Fraunhofer line very well. It is demonstrated that the fluorescence of algae containing phycocyane can be detected with high sensitivity. The investigation of the measurement of the phycocyane and chlorophyll ratio by means of the FLD technique is recommended. For water quality management this ratio is a relevant parameter. The FLD technique might provide a highly suitable method for this purpose. ESA

N94-23291*# National Aeronautics and Space Administration. Goddard Space Flight Center, Greenbelt, MD.

SeaWIFS TECHNICAL REPORT SERIES. VOLUME 9: THE SIMULATED SeaWIFS DATA SET, VERSION 1

Watson W. Gregg, Frank C. Chen (General Sciences Corp., Laurel, MD.), Ahmed L. Mezaache (General Sciences Corp., Laurel, MD.), Judy D. Chen (General Sciences Corp., Laurel, MD.), Jeffrey A. Whiting (General Sciences Corp., Laurel, MD.), Stanford B. Hooker, ed., Elaine R. Firestone, ed. (General Sciences Corp., Laurel, MD.), and A. W. Indest, ed. (General Sciences Corp., Laurel, MD.) Washington May 1993 19 p

(NASA-TM-104566-Vol-9; NAS 1.15:104566-Vol-9; Rept-93B00086-Vol-9) Avail: CASI HC A03/MF A01

Data system development activities for the Sea-viewing Wide Field-of-view Sensor (SeaWiFS) must begin well before the scheduled 1994 launch. To assist in these activities, it is essential to develop a simulated SeaWiFS data set as soon as possible. Realism is of paramount importance in this data set, including SeaWiFS spectral bands, orbital and scanning characteristics, and known data structures. Development of the simulated data set can assist in identification of problem areas that can be addressed and solved before the actual data are received. This paper describes the creation of the first version of the simulated SeaWiFS data set. The data set includes the spectral band, orbital, and scanning characteristics of the SeaWiFS sensor and SeaStar spacecraft. The information is output in the data structure as it is stored onboard. Thus, it is a level-0 data set which can be taken from start to finish through a prototype data system. The data set is complete and correct at the time of printing, although the values in the telemetry fields are left blank. The structure of the telemetry fields, however, is incorporated. Also, no account for clouds has been included. However, this version facilitates early prototyping activities by the SeaWiFS data system, providing a realistic data set to assess performance. Author

N94-23338*# National Aeronautics and Space Administration. Goddard Space Flight Center, Greenbelt, MD.

SeaWIFS TECHNICAL REPORT SERIES. VOLUME 11: ANALYSIS OF SELECTED ORBIT PROPAGATION MODELS FOR THE SeaWIFS MISSION

Frederick S. Patt (General Sciences Corp., Laurel, MD.), Charles M. Hoisington (Science Systems and Applications, Inc., Lanham, MD.), Watson W. Gregg, Patrick L. Coronado, Stanford B. Hooker, ed., Elaine R. Firestone, ed. (General Sciences Corp., Laurel, MD.), and A. W. Indest, ed. (General Sciences Corp., Laurel, MD.) Jun. 1993 18 p

(NASA-TM-104566-Vol-11; NAS 1.15:104566-Vol-11; Rept-93B00097-Vol-11) Avail: CASI HC A03/MF A01

An analysis of orbit propagation models was performed by the Mission Operations element of the Sea-viewing Wide Field-of-View Sensor (SeaWiFS) Project, which has overall responsibility for the instrument scheduling. The orbit propagators selected for this analysis are widely available general perturbations models. The analysis includes both absolute accuracy determination and comparisons of different versions of the models. The results show that all of the models tested meet accuracy requirements for scheduling and data acquisition purposes. For internal Project use the SGP4 propagator, developed by the North American Air Defense (NORAD) Command, has been selected. This model includes atmospheric drag effects and, therefore, provides better accuracy. For High Resolution Picture Transmission (HRPT) ground stations, which have less stringent accuracy requirements, the publicly available Brouwer-Lyddane models are recommended. The SeaWiFS Project will make available portable source code for a version of this model developed by the Data Capture Facility (DCF). Author

N94-23517# Los Alamos National Lab., NM.

GLOBAL OCEAN MODELING ON THE CONNECTION MACHINE

R. D. Smith, J. K. Dukowicz, and R. C. Malone 1993 4 p Presented at the 5th Annual Symposium on Global Change Studies, Nashville, TN, 24-28 Jan. 1994

(Contract W-7405-eng-36)

(DE94-000888; LA-UR-93-3327; CONF-940131-1) Avail: CASI HC A01/MF A01

The authors have developed a version of the Bryan-Cox-Semtner ocean model for massively parallel computers. Such models are three-dimensional Eulerian models that use latitude and longitude as the horizontal spherical coordinates and fixed depth levels as the vertical coordinate. The incompressible Navier-Stokes equations, with a turbulent eddy viscosity, and mass continuity equation are solved, subject to the hydrostatic and Boussinesq approximations. The traditional model formulation uses a rigid-lid approximation (vertical velocity = 0 at the ocean surface) to eliminate fast surface waves. These waves would otherwise require that a very short time step be used in numerical simulations, which would greatly increase the computational cost. To solve the equations with the rigid-lid assumption, the equations of motion are split into two parts: a set of two-dimensional 'barotropic' equations describing the vertically-averaged flow, and a set of three-dimensional 'baroclinic' equations describing temperature, salinity and deviations of the horizontal velocities from the vertically-averaged flow. DOE

N94-24107# Beleidscommissie Remote Sensing, Delft (Netherlands).

HERACLITUS, PHASE 1. HARBOUR ENTRANCE OF ROTTERDAM RADAR BASED CURRENT RELATED INFORMATION FOR TRAFFIC GUIDANCE OF SHIPS: FEASIBILITY OF DERIVING CURRENT PROFILE DATA FROM SEA SURFACE OBSERVATIONS IN THE ROTTERDAM (NETHERLANDS) PORT ENTRANCE

C. Deelen (Rotterdam Municiple Port Management, Netherlands.), H. C. Peters (Rijkswaterstaat, Rijswijk, Netherlands.), J. Starke (Rijkswaterstaat, The Hague, Netherlands.), A. C. Noordijk (Rotterdam Municiple Port Management, Netherlands.), A. Gerretsen (Internationale Navigatie Apparaten B.V., Netherlands.), G. J. Wensink (Delft Hydraulics Lab., Netherlands.), and C. F. deValk (Delft Hydraulics Lab., Netherlands.) Jun. 1993 74 p

(BCRS-93-04; ISBN-9-05-411079-1; ETN-94-95040) Avail: CASI HC A04/MF A01

The feasibility of deriving current profile data surface current observations in stratified flow conditions was investigated. Based on historical in situ current measurements, attempts were made to describe the current profile by mathematical modeling. It was concluded that it is possible to reconstruct current profiles in the test area by using a relatively simple hydrodynamic model and surface current field data. This reconstruction can be improved by using online data from the scheduled fixed Acoustic Doppler Current Profiler (ADCP) in the Maasmond area. Due to the firm physical basis of the proposed approach it can be expected that the model can be applied under a wide range of hydrodynamic conditions without excessive efforts in calibration and empirical modeling. As certain components of the model still need to be calibrated on a suitable data set it is recommended that we proceed with a validation campaign. This should involve VHF/HF radar measurements combined with inverse current modeling, together with simultaneous reference measurements to verify the overall feasibility of such a current information system. It is also recommended that we use this campaign to demonstrate the current information system to the future users in a quasi operational environment. ESA

N94-24600 Rijkswaterstaat, The Hague (Netherlands). Tidal Waters Div.
RECENT DEVELOPMENTS IN THE MATHEMATICAL MODELLING AND PHYSICAL UNDERSTANDING OF TRANSPORT AND DISPERSION IN AQUATIC SYSTEMS, WITH SPECIAL REFERENCE TO TIDAL WATERS
G. C. vanDam 9 Mar. 1993 146 p Limited Reproducibility: More than 20% of this document may be affected by microfiche quality
(PB94-111135) Avail: Issuing Activity (National Technical Information Service (NTIS))

In the discussion of mathematical modeling and computer simulation, the main subject will be the application of model particles (tracers) directly corresponding with dissolved, suspended and deposited particles in nature. Emphasis will be on modeling in three spatial dimensions so as to be able to account for the main physical mechanisms explicitly. Attention will be paid to the interaction between model simulations and insight in mechanisms and, in this connection, to the role of field observations. Results will be shown relating to the North Sea and Dutch estuaries, with reference to practical applications, plans and perspectives. NTIS

N94-24601 Rijkswaterstaat, The Hague (Netherlands). Tidal Waters Div.
NUTRIENTS AND LIGHT AS FACTORS CONTROLLING PHYTOPLANKTON BIOMASS ON THE DUTCH CONTINENTAL SHELF (NORTH SEA), 1988-1990
J. C. H. Peeters, H. A. Haas, L. Peperzak, and I. deVries Jan. 1993 67 p Limited Reproducibility: More than 20% of this document may be affected by microfiche quality
(PB94-111143; DGW-93.004; ISBN-90-369-0272-X) Avail: Issuing Activity (National Technical Information Service (NTIS))

In the last fifty years the riverine phosphorus and nitrogen loads discharged into the North Sea have increased considerably. Extensive oxygen deficiencies in the German Bight and the increase in phytoplankton and shifts in its species composition have been attributed to eutrophication. From 1988-1990 the effects of eutrophication on the oxygen economy, primary production, phytoplankton species composition, biomass and the principal limiting factors throughout the North Sea were studied in the EUZOUT project. The data generated in this project were used for the report. The report describes the results of methods for the detection of nutrient stress to samples taken from the coastal and central North Sea in 1988, 1989 and 1990 during the EUZOUT project. NTIS

N94-24671# University of Southern Mississippi, Bay Saint Louis. Center for Ocean and Atmospheric Modeling.
AN EFFICIENT DATA ASSIMILATION ALGORITHM WITH A GAUSSIAN COVARIANCE STRUCTURE
Ranjit M. Passi, Kent Goodrich, John C. Derber, and Mark Limber Oct. 1993 44 p
(Contract N00014-92-J-4112)
(AD-A273152; COAM-TR-2/94) Avail: CASI HC A03/MF A01

Details are provided of our attempts to develop computationally efficient and widely acceptable data assimilation algorithms. Our initial data assimilation work was done with a scheme which was developed by Derber and Rosati (1989) for their global data assimilation application. The scheme is quite efficient; however, when it was combined with a primitive equation, numerical model of the Gulf of Mexico, the nowcasting step took too much computer time for it to be useful in real-time applications. So, after an initial implementation and test of the scheme, our obvious thrust was to enhance and make it more efficient. Most of the computation resources while using the Derber-Rosati scheme are required in approximating a matrix product Sigma-mg, where Sigma-m is the covariance matrix of the model output error having a Gaussian spatial covariance structure that stays fixed, and g is a varying vector. They approximate this product by repeated application of a Laplacian operator. A new algorithm is developed that, while maintaining the accuracy, approximates Sigma-mg far more efficiently than the Laplacian algorithm. It also admits a wider class of covariance structures with equal ease and efficiency. The new algorithm approximates Sigma-mg by applying a product of two operators that are polynomials in simple averaging operators. The algorithm is efficient and general with the only restriction that Sigma-m be based on a covariance function that is a product of factors, which are even functions in a single dimension. DTIC

N94-24719 Woods Hole Oceanographic Inst., MA.
GLOBAL ACOUSTIC MAPPING OF OCEAN TEMPERATURES (GAMOT) Quarterly Progress Report No. 2, 1 Jul. - 30 Sep. 1993
John L. Spiesberger 15 Oct. 1993 66 p Limited Reproducibility: More than 20% of this document may be affected by microfiche quality
(Contract MDA972-93-1-0004)
(AD-A273387) Avail: Issuing Activity (Defense Technical Information Center (DTIC))

Work continues on all GAMOT tasks as described in ARPA Grant No: MDA972-93-1-0004 and remains on schedule with the exception of tasks C and D. Task C work is behind schedule and there will be a delay in the initial deployment of the operational SSARs of approximately six weeks. Task D, the autonomous mooring, is behind schedule and the total delay cannot be calculated until the impact of the increased scope of Task D, which now includes procurement of a 70 Hz source, can be determined. Task A involves the success of ray theory in identifying multipaths arrivals at basin scales. Task B tasks and deliverables are on schedule. Remote forced NE Pacific (NEP) model runs have been completed for 1961-1991 driven by equatorial Kelvin waves. Rossby waves propagating off the coast are shown to significantly alter acoustic travel times. All elements of the SSAR development are underway and on schedule. The initial SSAR prototype test deployment was conducted. Guidelines for the scope of task D include: trequency of the source will be 70 Hz; the schedule could be extended to accommodate the additional engineering and source procurement lead time; and consider both m-sequence and FM coding sources. DTIC

N94-24795 Rhode Island Univ., Narragansett. Graduate School of Oceanography.
VERTICAL MOTION IN THE SYNOP CENTRAL ARRAY Report, May 1988 - Aug. 1990
Scott S. Lindstrom and D. R. Watts Oct. 1993 93 p Limited Reproducibility: More than 20% of this document may be affected by microfiche quality
(Contract N00014-92-J-4013)
(AD-A273593; GSO-TR-93-2) Avail: Issuing Activity (Defense Technical Information Center (DTIC))

As part of the SYNOP (Synoptic Ocean Prediction experiment) field program, twelve tall moorings measured the Gulf Stream's temperature and velocity fields with current meters (CM) at nominal depths of 400 m, 700 m, 1000 m, and 3500 m for two years, from May 1988 through August 1990. Simultaneously, 24 inverted echo sounders (IES) monitored the thermocline topography. A third observational component of the experiment was the release of isopycnal RAFOS floats; 70 such floats traversed the area monitored by the CM and the IES. This report documents the methods used to compute vertical motion for each data source, and the differences and similarities between the three methods. Typical velocities during 'strong' events, as observed by or inferred from all three instruments, was 1-2 mm/s in regions near the center of the Gulf Stream. The comparison of RAFOS vertical motions and vertical motions diagnosed from CM data showed excellent agreement; furthermore, CM vertical motions and IES vertical motions are statistically coherent for periods longer than 12 days. We conclude that we may map mesoscale fields of w(x,y,t); the fields mapped are consistent with quasi-geostrophic dynamics. DTIC

N94-24918 Environmental Research Inst. of Michigan, Ann Arbor.
EXAMINATION OF THE PHYSICAL, ELECTRICAL, AND MICROWAVE EVOLUTION OF WATER INTO YOUNG SEA ICE Final Report, 1 Sep. - 28 Feb. 1993
Robert G. Onstott Nov. 1993 59 p Limited Reproducibility: More than 20% of this document may be affected by microfiche quality
(Contract N00014-92-C-0140)
(AD-A273559; ERIM-248500-1-F) Avail: Issuing Activity (Defense Technical Information Center (DTIC))

Knowledge of the interrelationships between ice thickness, its temperature profile, the distribution of salinity, the dielectric property profile, and the roughness of the air-ice interface is important to the understanding of the backscatter response of new and young sea ice. Backscatter, physical, and electrical property measurements were made during the first 120 hours of growth for a saline ice sheet grown in an outdoor laboratory tank. The purpose of this work is to describe the evolution of open water to ice 15 cm thick. Ambient air temperatures were -15 C during the critical growth period to 10 cm and then warmed to 10 C during the final 5 cm of growth. Radar backscatter data were obtained at 5.3, 9.6, 13.6, and 16.6 GHz to correlate with the changes in the microwave signatures with ice thickness, ice surface temperature, the salinity profile, the dielectric profile, and modifications which occur naturally to the air-ice interface of the ice sheet. Linear antenna transmit-receive polarizations were used and include vertical-vertical and horizontal-horizontal. Angle of incidence scans were made from vertical to 50 deg. The change in the backscatter response with changing ice thickness is documented and discussed in terms of the physical-chemical-electrical property changes. DTIC

N94-24944# Massachusetts Univ., Amherst. Dept. of Electrical and Computer Engineering.
USE OF MICROWAVE POLARIMETRY TO ENHANCE SAR IMAGES OF THE OCEAN SURFACE Final Report
Robert E. McIntosh Sep. 1993 51 p
(Contract N00014-89-J-3230)
(AD-A273568) Avail: CASI HC A04/MF A01

The goal of this study is the investigation of coherent backscatter of microwave signals from the ocean surface to better understand the effects of surface motion on synthetic aperture radar images. The objective is to analyze the behavior of coherent electromagnetic backscatter from the ocean surface for a dual frequency, dual polarization radar. Frequency and polarization diversity provides a picture of the mechanisms involved in the microwave backscatter. In this study, data was obtained from various University of Massachusetts radar systems to obtain extensive radar observations of the ocean surface at the FPN research tower in the North Sea, Germany. DTIC

N94-24948# Hawaii Univ., Honolulu. Dept. of Oceanography.
STATISTICAL METHODS IN PHYSICAL OCEANOGRAPHY
Peter Mueller, ed. and Diane Henderson, ed. Nov. 1993 534 p Presented at the Aha Huliko'a Hawaiian Winter Workshop, Manoa, HI, 12-15 Jan. 1993
(Contract N00014-93-1-0156)
(AD-A273612) Avail: CASI HC A23/MF A04

These proceedings contain the lectures given at the seventh Aha Huliko'a Hawaiian Winter Workshop on 'Statistical Methods in Physical Oceanography' and a meeting report. The lectures and the meeting report cover special probabilistic, statistical, and stochastic methods employed by physical oceanographers to analyze ocean data and formulate ocean models. DTIC

N94-25088# Alaska Univ., Fairbanks. Geophysical Inst.
NATIONAL ACADEMY OF SCIENCES-ACADEMY OF SCIENCES OF THE USSR WORKSHOP ON THE MECHANICS OF ICE AND ITS APPLICATIONS
Wilford F. Weeks 1993 91 p Workshop held in Moscow and Leningrad, Russia, 6-21 Jun. 1991
(Contract N00014-91-J-4134)
(AD-A273338) Avail: CASI HC A05/MF A01

The United States and the former Soviet Union have strong common interests in obtaining a better understanding of the behavior of ice at all scales. In particular, Russia and the United States have vast resources in the North, notably off the shelves of Alaska and Siberia. In order to safely and economically exploit these resources, both countries require an in-depth understanding of the movement of the ice cover, the forces which moving ice can exert against bottom founded structures, and the ice resistance on vessels used to transport these resources to market. The goal of the Ice Mechanics Workshop was to facilitate the exchange of technical information between the United States and the Soviet Union. Although specialists in both countries had made great efforts to keep abreast of each other's achievements, the exchange of ice technology between the two countries could be characterized as poor. This was primarily due to language barriers and constraints on communication and distribution of literature. DTIC

N94-25164 Hawaii Univ., Manoa.
REACTIVE TRACE METALS AS INDICATORS OF SUBDUCTION AND VENTILATION PROCESSES IN THE OCEAN Final Report
Chris Measures 24 Nov. 1993 2 p Limited Reproducibility: More than 20% of this document may be affected by microfiche quality
(Contract N00014-90-J-1681)
(AD-A273585) Avail: Issuing Activity (Defense Technical Information Center (DTIC))

The continuation of the work of this proposal, which was originally proposed to the ONR in 1990, had to be curtailed after the cancellation of the Barents Sea cruise in 1990 and after the P.I. was denied space on the trans-Polar expedition during the summer of 1991. Instead, after consultation with the ONR program manager, the P.I. participated in a cruise designed to use trace elements to survey the hydrothermal plumes generated by sea-floor hydrothermal activity between 9 deg and 11 deg N on the East Pacific Rise. The P.I.'s participation in this cruise was designed to determine the magnitude and variability of dissolved Al enrichment in the hydrothermal plumes which result from the mixing of hydrothermal vent fluids with the overlying sea water. DTIC

N94-25165 Woods Hole Oceanographic Inst., MA. Dept. of Geology and Geophysics.
SEAFLOOR CHARACTERIZATION/GALAPAGOS PROPAGATING RIFT Final Report
Martin C. Kleinrock, Peter R. Shaw, and Deborah K. Smith 18 Oct. 1993 4 p Limited Reproducibility: More than 20% of this document may be affected by microfiche quality
(Contract N00014-89-J-1021)
(AD-A273586) Avail: Issuing Activity (Defense Technical Information Center (DTIC))

Our goal is to better understand the system that produces the oceanic crust. Because the seafloor is a product of this system, we believe that fundamental insight can be gained through the study of seafloor topography and the spatial variation in its characteristics. Our project has focused on applying and further developing our techniques for analyzing seafloor topography and combining our techniques for seafloor characterization with other data sources (e.g., seismicity) and models. DTIC

N94-25435# Woods Hole Oceanographic Inst., MA.
ANALYSIS OF MODAL EVOLUTION CAUSED BY A WEAKLY RANGE-DEPENDENT SEABED IN SHALLOW WATER AND ITS APPLICATION TO INVERSION FOR GEOACOUSTIC PROPERTIES Ph.D. Thesis
Kazuhiko Ohta Sep. 1993 266 p
(Contract N00014-91-J-1379)
(AD-A273656; WHOI-93-35) Avail: CASI HC A12/MF A03

In a shallow water ocean environment, the range-dependent variation of the geoacoustic properties of the seabed is one of the crucial factors affecting sound propagation. Since the local modes of propagation depend on the spatial changes in the bottom sediments, the local eigenvalues of these modes are useful as tools for examining the range dependence of the sediment properties. In order to extract the local eigenvalues from measurements of the pressure field in a laterally inhomogeneous waveguide, the zero-order asymptotic Hankel transform with a short sliding window is utilized. The local peak positions in the output spectra differ from the local eigenvalues due to both the range variation of the local modes and the interference of adjacent modes. The departure due to the former factor is evaluated analytically by using the stationary phase method. In order to reduce the error induced by the latter factor, mode filtering is utilized by incorporating data from a fixed vertical array of receivers. The use of the above zero-order Hankel transform in a three-dimensionally varying waveguide results in an underestimate of the local eigenvalues due to the effect of horizontal refraction. Thus a general asymptotic Hankel transform with a two dimensional sliding window is used to correct for the underestimated amount. By expanding the latter transform with respect to the azimuthal angle, it can also be shown that the first term in the Taylor series corresponds to the former transform; the rest of the terms account for the value difference between the underestimated and actual local eigenvalues. DTIC

51 LIFE SCIENCES (GENERAL)

N94-23088*# National Aeronautics and Space Administration. Ames Research Center, Moffett Field, CA.

INCREASING ACCURACY IN THE ASSESSMENT OF MOTION SICKNESS: A CONSTRUCT METHODOLOGY

Cynthia S. Stout and Patricia S. Cowings Dec. 1993 17 p
(RTOP 199-70-12-14)
(NASA-TM-108797; A-94014; NAS 1.15:108797) Avail: CASI HC A03/MF A01

The purpose is to introduce a new methodology that should improve the accuracy of the assessment of motion sickness. This construct methodology utilizes both subjective reports of motion sickness and objective measures of physiological correlates to assess motion sickness. Current techniques and methods used in the framework of a construct methodology are inadequate. Current assessment techniques for diagnosing motion sickness and space motion sickness are reviewed, and attention is called to the problems with the current methods. Further, principles of psychophysiology that when applied will probably resolve some of these problems are described in detail. Author (revised)

N94-23454# Amsterdam Univ. (Netherlands). Dept. of Experimental Zoology.

ELECTROPHYSIOLOGY OF THE RAT NUCLEUS ACCUMBENS: LOCAL CIRCUITRY, NEUROMODULATION AND SYNAPTIC PLASTICITY Ph.D. Thesis

C. Pennartz 1992 222 p
(PB93-232254) Copyright Avail: CASI HC A10/MF A03

The general aim of the thesis is to elucidate neurotransmitter and neuromodulator functions in a limbic-innervated part of the basal ganglia--the nucleus accumbens. This basal forebrain nucleus is presumed to have a variety of functions, including regulation of reward-dependent behavior, modulation of neuroendocrine function and feedback to limbic cortico-thalamic circuits. All experiments were done in an in vitro slice preparation that comprised the nucleus accumbens and closely adjacent brain structures. NTIS

N94-23468 Argonne National Lab., IL.

APPLICATIONS OF THE AURORA PARALLEL PROLOG SYSTEM TO COMPUTATIONAL MOLECULAR BIOLOGY

E. L. Lusk, R. Overbeek, S. Mudambi (Knox Coll., Galesburg, IL.), and P. Szeredi (IQSOFT, Budapest, Hungary.) 1993 15 p Presented at the International Logic Programming Symposium, Vancouver, British Columbia, 26-29 Oct. 1993 Limited Reproducibility: More than 20% of this document may be affected by microfiche quality
(Contract W-31-109-eng-38)
(DE93-041166; ANL/MCS/CP-80305; CONF-9310172-1) Avail: CASI HC A03

We describe an investigation into the use of the Aurora parallel Prolog system in two applications within the area of computational molecular biology. The computational requirements were large, due to the nature of the applications, and were carried out on a scalable parallel computer, the BBN 'Butterfly' TC-2000. Results include both a demonstration that logic programming can be effective in the context of demanding applications on large-scale parallel machines and some insights into parallel programming in Prolog. DOE

N94-23501*# California Univ., Irvine.

[INVESTIGATION OF EVOLUTION-RELATED ASPECTS OF BACTERIAL RHODOPSINS] Final Report

19 Jan. 1994 4 p
(Grant NAGw-212)
(NASA-CR-194826; NAS 1.26:194826) Avail: CASI HC A01/MF A01

We have investigated evolution-related aspects of bacterial rhodopsins, the unique retinal-based energy transducing systems of halophilic archae. The approach was to describe both structural and functional aspects: the structure by sequencing genes to explore which regions are conserved, and the function by comparing proton and chloride transport in the closely related systems, bacteriorhodopsin and halorhodopsin, respectively. In the latter, we have made a good start toward the ultimate goal of separating the attributes of the general principles of retinal-based ionic pumps from those of the specific ion specificities, by determining the thermodynamics of the internal steps of the protein-mediated active transport process, as well as some of the intraprotein ion-transfer steps. Our present emphasis is on continuing to acquire the tools for studying what distinguishes proton transport from chloride transport. We consider it important, therefore, that we have been able to provide firm mathematical grounds for the kinetics analyses which underlies these studies. Our molecular biological studies have received a great boost from the expression vector for the bop gene based on a halobacterial plasmid, that we recently developed. Derived from text

N94-23521# Center for Mathematics and Computer Science, Amsterdam (Netherlands). Dept. of Analysis, Algebra and Geometry.

THE COMPUTATION OF R(SUB 0) FOR DISCRETE-TIME EPIDEMIC MODELS WITH DYNAMIC HETEROGENEITY

M. C. M. DeJong (CDI, Lelystad, Netherlands.), O. Diekmann (Leiden Univ., Netherlands.), and J. A. P. Heesterbeek Jan. 1993 20 p
(CWI-AM-R9301; ETN-94-94712) Copyright Avail: CASI HC A03/MF A01

An explicit algorithm for the computation of the basic reproduction ratio R(sub 0) for a class of discrete time epidemic models is given. These models allow for a finite number of different individual types, type changes at fixed time dependent intervals, arbitrary contact intensity between individuals of the various types and variable infectivity. The models reflect the situation where an infectious disease spreads in a population of animals that are reared in different stables on farms. It is shown analytically that R(sub 0) depends, for any given type, on the product of the susceptibility and the total infectivity of that type and not on these factors separately. This product is called the transmission weight of the type. The maximum overall transmission weights gives an upper bound for R(sub 0), irrespective of the particular submodels for type change and contact structure. Therefore, reduction of all transmission weights below one, by vaccination or some other control measure, will result in R(sub 0) less than 1 and will hence lead to eradication of the disease. ESA

N94-23538*# University of South Florida, Saint Petersburg.

[ALGORITHM-DEVELOPMENT ACTIVITIES] Quarterly Report, Jul. - Dec. 1993

Kendall L. Carder 15 Jan. 1994 26 p
(Contract NAS5-31716)
(NASA-CR-193225; NAS 1.26:193225) Avail: CASI HC A03/MF A01

The task of algorithm-development activities at USF continues. The algorithm for determining chlorophyll alpha concentration, (Chl alpha) and gelbstoff absorption coefficient for SeaWiFS and MODIS-N radiance data is our current priority. Derived from text

N94-23633*# Texas Univ., San Antonio.

MONOCLONAL ANTIBODIES DIRECTED AGAINST SURFACE MOLECULES OF MULTICELL SPHEROIDS Semiannual Status Report, 1 Jul. - 31 Dec. 1993

Andrew O. Martinez 31 Dec. 1993 33 p
(Grant NAG2-819)
(NASA-CR-195102; NAS 1.26:195102) Avail: CASI HC A03/MF A01

The objective of this project is to generate a library of monoclonal antibodies (MAbs) to surface molecules of mammalian tumor and transformed cells grown as multicell spheroids (MCS). These MCS are highly organized, three dimensional multicellular structures which exhibit many characteristics of in vivo organized tissues not found in conventional monolayer or suspension culture; therefore, MCS make better in vitro model systems to study the interactions of mammalian cells. Additionally, they provide a functional assay for surface adhesion molecules. Derived from text

N94-24124*# Arizona Univ., Tucson. Dept. of Biochemistry.

SKELETAL MUSCLE METABOLISM IN HYPOKINETIC RATS Final Technical Report, Jul. 1981 - Dec. 1993

Marc E. Tischler 1993 10 p
(Grants NAGw-227; NAG2-384)
(NASA-CR-195082; NAS 1.26:195082) Avail: CASI HC A02/MF A01

This grant focused on the mechanisms of metabolic changes associated with unweighting atrophy and reduced growth of hind limb muscles of juvenile rats. Metabolic studies included a number of different areas. Amino acid metabolic studies placed particular emphasis on glutamine and branched-chain amino acid metabolism. These studies were an outgrowth of understanding stress effects and the role of glucocorticoids in these animals. Investigations on protein metabolism were largely concerned with selective loss of myofibrillar proteins and the role of muscle proteolysis. These investigations lead to finding important differences from denervation and atrophy and to define the roles of cytosolic versus lysosomal proteolysis in these atrophy models. A major outgrowth of these studies was demonstrating an ability to prevent atrophy of the unweighted muscle for at least 24 hours. A large amount of work concentrated on carbohydrate metabolism and its regulation by insulin and catecholamines. Measurements focused on glucose transport, glycogen metabolism, and glucose oxidation. The grant was used to develop an important new in situ approach for studying protein metabolism, glucose transport, and hormonal effects which involves intramuscular injection of various agents for up to 24 hours. Another important consequence of this project was the development and flight of Physiological-Anatomical Rodent Experiment-1 (PARE-1), which was launched aboard Space Shuttle Discovery in September 1991. Detailed descriptions of these studies can be found in the 30 peer-reviewed publications, 15 non-reviewed publications, 4 reviews and 33 abstracts (total 82 publications) which were or are scheduled to be published as a result of this project. A listing of these publications grouped by area (i.e. amino acid metabolism, protein metabolism, carbohydrate metabolism, and space flight studies) are included. Author

N94-24290# National Defence Research Establishment, Umea (Sweden). Microbiology Div.
MICROINJECTION OF THE YERSINIA YopE CYTOTOXIN IN MAMMALIAN CELLS INDUCES ACTIN MICROFILAMENT DISRUPTION
Roland Rosqvist, Aake Forsberg, and Hans Wolf-Watz (Umea Univ., Sweden.) 1991 2 p Repr. from Biochemical Society Transactions, v. 19, 1991 p 113-114
(Grants SMRC-07-490-5A; BU-4426-301; STuF-90-005-770)
(FOA-B-40418-4.4; ETN-93-93763) Avail: CASI HC A01

Pathogenic Yersinia possess a common virulence plasmid of about 70 kb in size. Upon incubation at 37 C in the absence of Ca(2+) ions, strains harboring the plasmid stop growing and start producing a number of proteins denoted Yops (Yersinia outer membrane proteins). Results and discussions of an experiment which showed that secreted Yops can induce cytotoxicity in cultured cells if the proteins are delivered inside the cell by microinjection are given. Furthermore, the intracellular target of this cytotoxic effect is essential for maintenance of normal actin microfilament structure. It is concluded that YopE is a cytotoxin which mediates disruption of actin microfilaments, and YopD is involved in the translocation of YopE though the host membrane. ESA

N94-24294 Materials Research Labs., Ascot Vale (Australia). Defence Science and Technology Organisation.
INTERACTION OF TACRINE AT M(1) AND M(2) CHOLINOCEPTORS IN GUINEA PIG BRAIN
Maria Szilagyi and Wai-Man Lau Switzerland S. Karger AG, Basel, Switzerland 1993 7 p Repr. from Pharmacology 1993, v. 47, p 223-229
Copyright Avail: Issuing Activity

Tacrine (THA) actively modulates binding of M(sub 1) ligands in an allosteric fashion causing positive cooperativity. The binding affinity of THA to M(sub 1) and M(sub 2) cholinoceptors is similar. It is therefore proposed that the allosteric selectivity of THA is a function of the binding site and not of THA itself. Its interaction of M(sub 1) and M(sub 2) cholinoceptors was examined in guinea pig brain homogenates using the selective M(sub 1) and M(sub 2) antagonists (3H)-pirenzepine ((3H)PZ) and (3H)AF-DX 384. The dissociation constants were 0.36 nmol/l for the M(sub 1) receptor and 0.23 nmol/l for the M(sub 2) receptor. The binding of THA and methoctramine (MTA) at M2 receptors were also compared. Tacrine displayed similar binding affinity for both M(sub 1) and M(sub 2) receptor subtypes. MTA was 100 times more potent an inhibitor of (3H)AF-DX 384 binding at M(sub 2) receptors than THA. In addition, THA was found to slow the dissociation of (3H)PZ from the M(sub 1) receptor. In contrast, the dissociation of (3H)AF-DX 384 from M(sub 2) receptor subtypes was unaffected. It was concluded that THA acts as an agonist at M(sub 1) cholinoceptors because it slowed the dissociation of (3H)PZ. At M(sub 2) cholinoceptors its nature is that of an antagonist because it had no effect on (3H)AF-DX 384 dissociation. Author (revised)

N94-24310*# Sverdrup Technology, Inc., Huntsville, AL.
MICROBIOLOGICAL ANALYSIS OF DEBRIS FROM SPACE TRANSPORTATION SYSTEM (STS)-55 SPACELAB D-2 Final Report
T. L. Huff Jan. 1994 10 p
(Contract NAS8-37814)
(NASA-CR-193883; NAS 1.26:193883) Avail: CASI HC A02/MF A01

Filter debris from the Spacelab module D-2 of STS-55 was analyzed for microbial contamination. Debris from cabin and avionics filters was collected by Kennedy Space Center personnel on May 8, 1993, 2 days postflight. Debris weights were similar to those of previous Spacelab missions. Approximately 5.1E+5 colony forming units per gram of debris were enumerated from the cabin and avionics filter debris, respectively. these numbers were similar in previous missions for which the entire contents were analyzed without sorting of the material. Bacterial diversity was small compared to previous missions, with no gram negative bacteria isolated. Only one bacterial species, Corynebacterium pseudodiphtheriticum, was not isolated previously by the laboratory from Spacelab debris. This organism is a normal inhabitant of the pharynx. A table listing all species of bacteria isolated by the laboratory from previous Spacelab air filters debris collection is provided. Author

N94-24688 SRI International Corp., Menlo Park, CA.
IN VITRO SYSTEM FOR STUDYING METABOLISM OF ENVIRONMENTAL CHEMICALS IN HUMAN CELLS Annual Report, 30 Apr. 1992 - 29 Apr. 1993
Carol E. Green 5 Nov. 1993 32 p Limited Reproducibility: More than 20% of this document may be affected by microfiche quality
(Contract F49620-91-C-0050)
(AD-A273427; AFOSR-93-0854TR) Avail: CASI HC A03

The objective of the project is to establish and use an in vitro system of intact hepatocytes from rodent and human tissues to develop quantitative data on the metabolism of toxic chemicals that can be used in risk assessments. Currently, two different in vitro models are most frequently used for comparative metabolism studies-isolated hepatocytes and precision-cut liver slices. In the second year of the project, hepatocytes and liver slices from rat and human livers were compared to determine their capability to metabolize chloroform and a model substrate, 7-ethoxycoumarin. The 7-ethoxycoumarin O-deethylation activity of hepatocytes was consistently higher than the activity measured with liver slices, when standardized by protein content of the two preparations. The metabolism of chloroform by hepatocytes isolated from male F344 rats was characterized by analyzing headspace and medium concentrations. The kinetic constants, estimated from the headspace data generated in these experiments, are K. = 34 nmol/flask and V max. = 24 pmol/min/106 cells. Headspace analysis was also useful for determining chloroform metabolism by liver slices. After addition of 3.6 nmol/flask, the rate of chloroform loss was 2.5 pmol/min/mg tissue. DTIC

N94-24704 National Academy of Sciences - National Research Council, Washington, DC.
A BIOLOGICAL SURVEY FOR THE NATION
1993 211 p
(LC-93-85920; ISBN-0-309-04984-0) Copyright Avail: Issuing Activity

The idea of a national biological survey has a long history in the United States. In recent years, increasing concerns about the nation's biological resources have led to calls for a new biological survey. Recently, the process of forming a National Biological Survey (NBS) within the Department of the Interior (DOI) was initiated. A research agenda for the NBS is proposed that is far broader than the existing research effort in DOI but that is also focused according to likely immediate and long-term user needs. A National Biotic Resources Information System is envisioned to make reliable biological information more accessible to diverse users. Also described is how the many public and private entities involved in current research on biological resources can work together in a new entity, which the committee has called the National Partnership for Biological Survey, to provide comprehensive information that will be useful for decision-makers at all levels of government and outside government. Derived from text

N94-24791# University of Southern California, Los Angeles. Dept. of Biological Sciences.
SYMBIOSIS IN MARINE LUMINOUS BACTERIA Final Report
Edward G. Ruby 1993 3 p
(Contract N00014-92-J-1716)
(AD-A273540) Avail: CASI HC A01/MF A01

This work indicates that the distribution and abundance of a class of marine microorganisms, the symbiotic luminous bacteria, are controlled by the dynamics of their relationship with their host. Such a conclusion constitutes the first time that the ecology of any marine bacterium could be related to a predictive biological factor. This-study also points to the presence of a significant population of typically culturable V. fischeri cells in seawater that have entered a non-culturable state from which they can be recovered only through an association with a specific animal tissue. Such a phenomenon changes the way we view the initiation of the light organ symbiosis. However, of even broader interest, it suggests that at least a portion of the 99.9% of bacteria in seawater that can not be cultured may not be unknown or new species, but in fact are well-known, typically culturable bacteria that are awaiting a specific environmental cue that signals these cells to re-enter a proliferative stage in their cell cycle.
DTIC

N94-24807*# National Aeronautics and Space Administration. Ames Research Center, Moffett Field, CA.
THE EVOLUTION OF ENERGY-TRANSDUCING SYSTEMS. STUDIES WITH AN EXTREMELY HALOPHILIC ARCHAEBACTERIUM Final Report, Feb. 1989 - Aug. 1992
Helga Stan-Lotter Aug. 1992 11 p
(Contract NCC2-578)
(NASA-CR-193803; NAS 1.26:193803) Avail: CASI HC A03/MF A01

The F-type ATPases are found in remarkably similar versions in the energy-transducing membranes of eubacteria, chloroplasts, and mitochondria. Thus, it is likely that they have originated early in the evolution of life, which is consistent with their function as key enzymes of cellular metabolism. The archaebacteria are a group of microorganisms which, as shown by molecular sequencing and biochemical data, have diverged early from the main line of prokaryotic evolution. From studies of members of all three major groups of archaebacteria - the halophiles, methanogens, and thermoacidophiles - it emerged that they possess a membrane ATPase which differs from the F-ATPases. The goal of this project was a comparison of the ATPase from the halophilic archaebacterium Halobacterium saccharovorum with the well-characterized F-type ATPases on the molecular level. Amino acid sequences of critical regions of the enzyme were to be determined, as well as immunoreactions of single subunits in the search for common epitopes. The results were expected to allow a decision about the nature of archaebacterial ATPases, their classification as one of the known or, alternatively, novel enzyme complexes, and possibly deduction of events during the early evolution of energy-transducing systems.
Derived from text

N94-24810*# Florida Univ., Gainesville. Dept. of Aerospace Engineering, Mechanics and Engineering Science.
BIOREGENERATIVE LIFE SUPPORT SYSTEMS FOR MICROGRAVITY
Gail E. Nevill, Jr., Michael I. Hessel, Jr., Jose Rodriguez, and Steve Morgan, ed. Apr. 1993 72 p
(Contract NASw-4435)
(NASA-CR-195516; NAS 1.26:195516) Avail: CASI HC A04/MF A01

NASA's Controlled Ecological Life Support System (CELSS) project centers on growing plants and recycling wastes in space. The current version of the biomass production chamber (BPC) uses a hydroponic system for nutrient delivery. To optimize plant growth and conserve system resources, the content of the nutrient solution which feeds the plants must be constantly monitored. The macro-nutrients (greater than ten ppm) in the solution include nitrogen, phosphorous, potassium, calcium, magnesium, and sulphur; the micro-nutrients (less than ten ppm) include iron, copper, manganese, zinc, and boron. The goal of this project is to construct a computer-controlled system of ion detectors that will accurately measure the concentrations of several necessary ions in solution. The project focuses on the use of a sensor array to eliminate problems of interference and temperature dependence.
Derived from text

N94-24811*# National Aeronautics and Space Administration. Ames Research Center, Moffett Field, CA.
THE EVOLUTION OF ENERGY-TRANSDUCING SYSTEMS. STUDIES WITH ARCHAEBACTERIA Semiannual Progress Report, Sep. 1993 - Feb. 1994
Helga Stan-Lotter Feb. 1994 5 p
(Contract NCC2-578)
(NASA-CR-195129; NAS 1.26:195129) Avail: CASI HC A01/MF A01

N-ethylmaleimide (NEM) inhibits the ATPase of H. saccharovorum in a nucleotide protectable manner. The bulk of C-14 NEM is incorporated into subunit one. Cyanogen bromide cleavage of labeled subunit one indicated that NEM bound to a peptide of a Mr of about 8,900. Thus, Cys 262 (H. salinarium numbering) may be the NEM binding site. Cyanogen bromide fragments have been submitted for sequencing. To prove the presence of three Cys residues in subunit one, alkaline cleavage following treatment with NTCB was carried out. Thiol reagents such as p-chloro mercuri phenyl sulfonate also inhibited the ATPase. However, this inhibition was not nucleotide-protectable, suggesting a different location and role for the PCMS-sensitive Cys. The proteolipid which was extracted with chloroform/methanol from the membranes of H. saccharovorum cross-reacted with an antiserum against subunit c (the DCCD-binding protein) of Escherichia coli. Following labeling of membranes from H. saccharovorum with C-14 DCCD under conditions, which inhibited ATP synthesis, the isotope was incorporated into one protein of Mr of about 6,500. Thus, the proteolipid of H. saccharovorum and the DCCD-labeled peptide may be identical. If so, these results suggest that the proteolipid is a component of the membrane sector of an archaeal F-type ATP synthase. Author (revised)

N94-25146# Naval Postgraduate School, Monterey, CA. Dept. of Operations Research.
AN EXPLORATORY STOCHASTIC MODEL FOR TOXIC EFFECTS ON CELLS
R. L. Carpenter, D. P. Gaver, and P. A. Jacobs Sep. 1993 81 p
(AD-A273438; NPS-OR-93-104) Avail: CASI HC A05/MF A01

A multivariate dynamic Markov model is formulated to describe the possible effect of a generic chemical toxin on a generic cell population in an organ. Asymptotic methods (large cell population) are used to show that numbers and toxin may be jointly Gaussian/normally distributed; the joint stochastic process is approximately Ornstein-Uhlenbeck. Application to dose-response, and hence risk analysis, is briefly discussed. DTIC

N94-23241*# University of Central Florida, Orlando. Dept. of Chemistry.
CHEMICAL CHARACTERIZATION OF SOME AEROBIC LIQUIDS IN CELSS
Brooks C. Madsen *In* NASA. Kennedy Space Center, NASA/ASEE Summer Faculty Fellowship Program Oct. 1993 p 269-299 (For primary document see N94-23230 06-80)
Avail: CASI HC A03/MF A04

N94-24426*# Alabama Univ., Huntsville. Dept. of Biological Sciences.
MEASURING THE DYNAMICS OF STRUCTURAL CHANGES IN BIOLOGICAL MACROMOLECULES FROM LIGHT SCATTERING DATA
Adriel D. Johnson *In its* The 1993 NASA/ASEE Summer Faculty Fellowship Program Nov. 1993 3 p (For primary document see N94-24405 06-80)
Avail: CASI HC A01/MF A03

N94-24437*# Alabama Univ., Huntsville. Dept. of Biological Sciences.
EVALUATION OF OVOSTATIN AND OVOSTATIN ASSAY
Debra M. Moriarity *In its* The 1993 NASA/ASEE Summer Faculty Fellowship Program Nov. 1993 5 p (For primary document see N94-24405 06-80)
Avail: CASI HC A01/MF A03

N94-25357*# Texas A&M Univ., College Station. Bioengineering Program.
NON-INVASIVE OPTICAL DETECTION OF GLUCOSE IN CELL CULTURE NUTRIENT MEDIUM
Gerald L. Cote *In* NASA. Johnson Space Center, National Aeronautics and Space Administration (NASA)/American Society for Engineering Education (ASEE) Summer Faculty Fellowship Program, 1993, Volume 1

Dec. 1993 11 p (For primary document see N94-25348 06-99)
Avail: CASI HC A03/MF A03

N94-25368*# Houston Univ., Clear Lake, TX. Div. of Biology.
DESIGN AND TESTING OF A UNIQUE RANDOMIZED GRAVITY, CONTINUOUS FLOW BIOREACTOR
Carroll B. Lassiter *In* NASA. Johnson Space Center, National Aeronautics and Space Administration (NASA)/American Society for Engineering Education (ASEE) Summer Faculty Fellowship Program, 1993, Volume 2 Dec. 1993 15 p (For primary document see N94-25367 06-99)
Avail: CASI HC A03/MF A03

52 AEROSPACE MEDICINE

Includes physiological factors; biological effects of radiation; and effects of weightlessness on man and animals.

N94-22732# CryoLife, Inc., Marietta, GA.
CELLULAR AND TISSUE INJURY DURING NONFREEZING COLD INJURY AND FROSTBITE Report No. 8, May - Aug. 1993
Patrick Curran 30 Sep. 1993 76 p
(Contract N00014-91-C-0044)
(AD-A270883) Avail: CASI HC A05/MF A01

We have continued our investigations in the following five major areas: (1) the effects of cold-induced membrane phase changes on the function of transmembrane ion pumps; (2) the mechanism of metabolic inhibition under cold, acidotic conditions; (3) the influence of these conditions on the function of skeletal and smooth muscle; (4) the role of free radicals in reperfusion injury in human cells; and (5) developing methods for amelioration of cell and tissue damage during non-freezing injury and frostbite, based on the results of the aforementioned studies. Abstracts and publications presented since Apr. 1993 are listed in Appendix 1. The text of the abstracts and publications described in this report may be found in Appendix 2. DTIC

N94-23313# Advisory Group for Aerospace Research and Development, Neuilly-Sur-Seine (France).
CARDIOPULMONARY ASPECTS IN AEROSPACE MEDICINE [LES ASPECTS CARDIOPULMONAIRES EN MEDECINE AEROSPATIALE]
Oct. 1993 74 p Lectures held in Lisbon, Portugal, 25-26 Oct. 1993, in Athens, Greece, 1-2 Nov. 1993, in Ankara, Turkey, 4-5 Nov. 1993, and in Brussels, Belgium, 8-9 Nov. 1993
(AGARD-LS-189; ISBN-92-835-0722-3) Copyright Avail: CASI HC A04/MF A01

This Lecture Series will update the information presented in the 1987 AGARD Short course on the Cardiopulmonary Aspects of Aerospace Medicine, and will be of primary relevance to military internists and cardiologists with an interest in aviation medicine, and to military Flight Surgeons. Topics to be discussed will include the following: screening to asymptomatic coronary artery disease in an aircrew population; the aeromedical disposition of aviators with coronary disease; the utility of screening aircrew candidates with echocardiography and echocardiographic findings in trained aircrew; etc. The Lecture Series is designed to be interactive rather than strictly didactic to encourage discussion of problems particular to participating NATO countries. For individual titles, see N94-23314 through N94-23328.

N94-23314# Defence and Civil Inst. of Environmental Medicine, Toronto (Ontario). Medical Assessment Section.
CARDIOVASCULAR AND PULMONARY DISEASE IN NATO AIRCREW: AN OVERVIEW
Gary W. Gray *In* AGARD, Cardiopulmonary Aspects in Aerospace Medicine Oct. 1993 6 p (For primary document see N94-23313 06-52)
Copyright Avail: CASI HC A02/MF A01

In 1987, the AGARD Aeromedical Panel (AMP) sponsored a Short Course on the Cardiopulmonary Aspects of Aerospace Medicine. The aim of the course was to disseminate current information about the aeromedical implications of cardiac and pulmonary conditions to NATO Flight Surgeons. At the time of the first course, it was proposed that an update course be run every five to six years to keep NATO Flight Surgeons abreast of current developments in aviation cardiology and pulmonology. Since the 1987 Lecture Series, there have been a number of new developments in aviation cardiology. The purpose of this Lecture Series is to disseminate this information. Author (revised)

N94-23315# Air Force Systems Command, Brooks AFB, TX. Clinical Sciences Div.
SCREENING FOR ASYMPTOMATIC CORONARY HEART DISEASE
William B. Kruyer *In* AGARD, Cardiopulmonary Aspects in Aerospace Medicine Oct. 1993 5 p (For primary document see N94-23313 06-52)
Copyright Avail: CASI HC A01/MF A01

Predicting the presence of coronary heart disease in an asymptomatic population is a very difficult task. Because of the possible sudden and incapacitating presentation of coronary heart disease and its common occurrence in industrialized nations, screening for this disorder is an important aeromedical concern. Nonsignificant disease can lead to coronary events and is also likely to progress to significant disease. Also, lifestyle changes and other interventions may affect the progress of insignificant disease. Screening efforts in the military aviator population should therefore be aimed at detecting any measurable degree of disease. This review will discuss problems inherent to screening an asymptomatic population, different screening tests, and risk stratified approaches to screening for coronary heart disease. Author (revised)

N94-23316# Air Force Systems Command, Brooks AFB, TX. Clinical Sciences Div.
AEROMEDICAL DISPOSITION FOR CORONARY ARTERY DISEASE
P. V. Celio *In* AGARD, Cardiopulmonary Aspects in Aerospace Medicine Oct. 1993 6 p (For primary document see N94-23313 06-52)
Copyright Avail: CASI HC A02/MF A01

Coronary artery disease continues to be a significant concern in aerospace medicine. Coronary disease is a major cause of deaths and sudden incapacitation for males in the flying age population. When coronary disease is found in an aviator, the benefits of his remaining on flying duties must be weighed against his risk of an incapacitating event. The following chapter reviews the probability of a cardiac event in populations of varying degrees of coronary disease including patients following myocardial infarction, angioplasty, and coronary artery bypass surgery. The U.S. Air Force (USAF) experience and recommendation for flying waivers will also be discussed. Author

N94-23317# Air Force Systems Command, Brooks AFB, TX. Clinical Sciences Div.
PRIMARY PREVENTION OF CORONARY HEART DISEASE
William B. Kruyer *In* AGARD, Cardiopulmonary Aspects in Aerospace Medicine Oct. 1993 6 p (For primary document see N94-23313 06-52)
Copyright Avail: CASI HC A02/MF A01

The primary prevention of coronary heart disease is a very prominent and vigorously discussed topic in the medical literature, especially in the area of appropriate lipid profile management. Secondary preventive efforts in patients with known disease seem to be clearly beneficial, but the literature and opinions vary considerably regarding primary preventive efforts and how the existing data should be applied to other patient population subgroups. Studies demonstrating regression of coronary artery atherosclerotic lesions seem to lend support to the validity of primary prevention. This topic is of major interest to the military aerospace medicine practitioner. Classic risk factors which are most applicable to the military aviator include lipid profile, smoking, and regular exercise. These factors will be discussed with pertinent information from the literature with the intent of providing a better understanding of the issues and a reasonable approach to this problem. Author (revised)

N94-23318# Air Force Systems Command, Brooks AFB, TX. Clinical Sciences Div.
AEROMEDICAL DISPOSITION OF ARRHYTHMIAS AND ELECTROCARDIOGRAPHIC FINDINGS IN AIRCREW
P. V. Celio *In* AGARD, Cardiopulmonary Aspects in Aerospace Medicine Oct. 1993 9 p (For primary document see N94-23313 06-52)
Copyright Avail: CASI HC A02/MF A01

Screening asymptomatic individuals for occult cardiac disease continues to be a difficult task. One of the standard screening procedures continues to be electrocardiography. Electrocardiography is neither a sensitive nor specific tool in identifying heart disease but continues to offer useful information. Interpretation of these studies for aeromedical purposes requires an appreciation for certain differences between a standard clinical population from which the significance of most ECG findings were obtained and the asymptomatic, generally healthy aviator population. The United States Air Force Central Electrocardiographic Library is the repository for all electrocardiograms obtained on Air Force aviators. This facility was established in 1957 in order to review electrocardiograms performed on Air Force aviators to determine the significance of electrocardiographic findings in asymptomatic individuals and to provide consultative services to local flight surgeons as well as the Surgeon General. The following sections discuss the major classes of electrocardiographic findings, their significance, and additional evaluations required by the USAF. Author (revised)

N94-23319# Defence and Civil Inst. of Environmental Medicine, Toronto (Ontario). Medical Assessment Section.

ECHOCARDIOGRAPHIC SCREENING OF AIRCREW CANDIDATES

Gary Gray *In* AGARD, Cardiopulmonary Aspects in Aerospace Medicine Oct. 1993 2 p (For primary document see N94-23313 06-52)
Copyright Avail: CASI HC A01/MF A01

Military pilot training is expensive for all NATO countries, and screening techniques which detect medical conditions at selection which might later result in grounding or operational restriction of trained pilots are generally cost-effective. Although a careful physical examination and electrocardiogram will detect most disqualifying conditions, there are a number of structural cardiac abnormalities which may be missed by these standard screening measures. These include the following: mitral valve prolapse; bicuspid aortic valve; hypertrophic cardiomyopathy; left ventricular hypertrophy; diastolic dysfunction; regurgitant valves--aortic, mitral, tricuspid, and pulmonic; significant stenosis--aortic, pulmonic, and mitral; and congenital lesions, e.g Ebstein's anomaly. Only four of thirteen NATO aeromedical agencies polled by questionnaire reported that an echo cardiogram is included in the routine initial screening of air crew candidates. The detection of disqualifying or limiting cardiac abnormalities in trained air crew is a clear argument in favor of screening, but it is really the incidence of such abnormalities detected in air crew candidates which determines the cost effectiveness of the procedure. Author (revised)

N94-23320# Air Force Systems Command, Brooks AFB, TX. Clinical Sciences Div.

ECHOCARDIOGRAPHIC FINDINGS IN TRAINED AIRCREW: THE EFFECT OF +Gz ON CARDIAC STRUCTURE (WORKING GROUP 18)

P. V. Celio *In* AGARD, Cardiopulmonary Aspects in Aerospace Medicine Oct. 1993 2 p (For primary document see N94-23313 06-52)
Copyright Avail: CASI HC A01/MF A01

During the AGARD conference 'Medical Selection and Physiologic Training of Future Fighter Aircrew' in Apr. 1985, a paper was presented on echocardiography in Mirage 2000 pilots. In this study, 32 Mirage 2000 pilots and 34 transport pilots underwent echocardiography in order to evaluate the possibility of cardiac changes occurring because of high performance flying. The authors found a statistically significant increase in left atrial size and left ventricular septal thickness. They also felt that there was a very significant difference in right ventricular dimensions. The mean right ventricular size for the transport pilots and the Mirage pilots was 13.265 mm and 16.750 mm, respectively. They felt that 8 of the Mirage 2000 pilots had dilated right ventricles whereas only one of the transport pilots had an enlarged right ventricle. Although the cause of this apparent difference could not be determined by the study, the presence of right ventricular dilatation in high performance pilots raised a significant occupational concern among the NATO countries. Although this may simply be an artifact of the small sample size or a result of the inherent difficulty in obtaining right ventricular dimensions, the possibility that this represented a true occupational hazard was seriously considered. In order to determine the significance of this finding, a larger study was undertaken. The intention of this study is to perform a large cross-sectional study comparing the echocardiographic findings obtained on pilots flying high sustained G aircraft with non high sustained G pilots (tanker, bomber, transport, helicopter pilots, etc.). Author (revised)

N94-23321# Royal Air Force, London (England). Central Medical Establishment.

LEFT VENTRICULAR HYPERTROPHY AND ATHLETE'S HEART

David H. Hull *In* AGARD, Cardiopulmonary Aspects in Aerospace Medicine Oct. 1993 4 p (For primary document see N94-23313 06-52)
Copyright Avail: CASI HC A01/MF A01

Left ventricular hypertrophy (LVH) means literally, overgrowth of the left side of the heart. However the term is generally limited to an abnormal increase in the mass of the left ventricular heart muscle. In pathological terms, this means an increase in the size of the cardiac myocytes as opposed to hyperplasia, an increase in their number. In common parlance, any thickening of the left ventricular wall tends to be described as LVH; this is incorrect where the thickening is due to increase in the size or number of cells other than myocytes, such as fibroblasts, or to abnormal deposits, e.g., amyloid. LVH may be present with normal wall thickness in an enlarged ventricle, for example in volume overload. In health, left ventricular mass is directly related to stature and to body weight, and it increases steadily with age so a single standard (maximum) left ventricular wall thickness for all ages, both sexes, and all bodily configurations must be inappropriate. However, normative standards incorporating these sources of variability are rarely employed. Author (revised)

N94-23322# Royal Air Force, London (England). Central Medical Establishment.

AORTIC VALVE DISEASE

David H. Hull *In* AGARD, Cardiopulmonary Aspects in Aerospace Medicine Oct. 1993 2 p (For primary document see N94-23313 06-52)
Copyright Avail: CASI HC A01/MF A01

The aortic valve, like the pulmonary valve, forms early in foetal cardiac development soon after the fusion of the 2 bulbar ridges which thus become a septum dividing the primitive bulbus cordis into the aortic and pulmonary trunks. Two cusps of each valve arise from the fused ridges, whilst a third cusp is formed from accessory ridges in each outflow tract. The normal arrangement is of symmetrical semilunar 3-cusped valves in the aorta and the pulmonary trunk, but variations are common. A bicuspid aortic valve is present in 1-2 percent of adults; a unicuspid or quadricuspid valve is much rarer. Bicuspid valves are 4 times commoner in men than in women. Lesser degrees of asymmetry are so common as to be the rule; in one series, only 16 percent of normal aortic valves were perfectly symmetrical in the sense that all 3 cusps were within 5 percent of each others dimensions; in 33 percent of valves, all 3 cusps differed from each other by more than this amount. The significance of these minor degrees of asymmetry, particularly with regard to the later development of aortic valve disease, is unknown. Congenital aortic valve abnormalities are common associations of other types of congenital heart disease, notably of coarctation of the aorta and ventricular septal defect. Aortic valve lesions are asymptomatic in most young people; because of this, and of male preponderance, congenital aortic valve disease is quite common in applicants for flying training; as abnormal physical signs are often trivial or absent, acceptance into air crew training is probably the rule, and the abnormality is recognized only later. Author (revised)

N94-23323# Air Force Systems Command, Brooks AFB, TX. Clinical Sciences Div.

AEROMEDICAL IMPLICATIONS OF MITRAL VALVE PROLAPSE

P. V. Celio *In* AGARD, Cardiopulmonary Aspects in Aerospace Medicine Oct. 1993 3 p (For primary document see N94-23313 06-52)
Copyright Avail: CASI HC A01/MF A01

Mitral valve prolapse (MVP) is the most common cardiac valve disorder in the general adult population. Although the prevalence has been estimated at between 4 percent and 21 percent, the true prevalence is dependent upon the specific population evaluated and the diagnostic criteria applied. For the adult male population of aircrew age, the prevalence is probably between 4 to 7 percent. Although the prognosis of individuals with MVP is generally good, rare complications do occur which include sudden death, infective endocarditis, stroke, transient ischemic attacks, and progressive mitral regurgitation. The following discussion will review the diagnostic criteria as well as the probable risk of each reported complication. Author (revised)

N94-23324# Royal Air Force, London (England). Central Medical Establishment.
CHRONIC OBSTRUCTIVE PULMONARY DISEASE
David H. Hull *In* AGARD, Cardiopulmonary Aspects in Aerospace Medicine Oct. 1993 4 p (For primary document see N94-23313 06-52)
Copyright Avail: CASI HC A01/MF A01

Chronic Obstructive Pulmonary Disease (COPD) remains a common cause of illness and death in many Western countries and is an increasing problem in developing nations. Although COPD is declining slowly in the UK, it still causes 15,000 deaths annually and is responsible for 10 percent of all working days lost through illness. This is despite improved working conditions, reduced atmospheric pollution, and decreased tobacco consumption. In the USA, COPD is the fifth most common cause of death, causing 57,000 deaths per year. It is estimated that 81.5 percent of this toll is due to cigarette smoking. Clinically apparent disease is largely confined to middle-aged and elderly people, but many young cigarette smokers can be shown to have early evidence of airways disease if adequately investigated. Two main types of COPD are seen, chronic bronchitis and emphysema, though patients may show features of both disorders. Chronic bronchitis is defined as the production of mucoid sputum on most days for at least 3 months during 2 consecutive years. Recurrent respiratory infection is increasingly common as the disease progresses. Stopping smoking may, especially early in the disease, arrest or slow its progression. Otherwise deterioration is relentless. Apart from variable rhonchi, physical signs are often slight till the onset of cor pulmonale, that is failure secondary to the broncho-pulmonary disease. Finger-clubbing, raised venous pressure, fluid retention, evidence of right ventricular hypertrophy, hypercarbia with respiratory acidosis and raised intracranial pressure, and eventually hypoxaemia are the main features; despite remissions cor pulmonale is usually fatal within a few years. Author (revised)

N94-23325# Royal Air Force, London (England). Central Medicine Establishment.
SARCOIDOSIS AND THE AVIATOR
David H. Hull *In* AGARD, Cardiopulmonary Aspects in Aerospace Medicine Oct. 1993 3 p (For primary document see N94-23313 06-52)
Copyright Avail: CASI HC A01/MF A01

Sarcoidosis is a chronic granulomatous disease of unknown aetiology. It is of particular importance in clinical aviation practice, for a number of reasons. Although it is a world-wide disease, it appears to be much more prevalent in the populations of developed countries. It is common in young adults; in Europe, more men than women being affected, but possibly the reverse in the USA. The onset may be acute and incapacitating, for example with florid erythema nodosum and acute arthropathy. Other cases are a symptomatic and may be detected only by special tests, e.g., screening chest x-ray, ECG, or blood biochemistry. Though often apparently confined to the thorax, sarcoidosis is typically a multi-system disease with involvement, often silent, of many organs: the skin, eyes, liver, spleen, lymphnodes, bone, central nervous, and cardiovascular systems. Hypercalcaemia is quite a common feature but causes symptoms only when potentially dangerous blood calcium levels are attained. No curative treatment is known, but moderate, severe or progressive disease usually leads to steroid treatment which may have to be prolonged and given in high doses. Cardiac involvement is often inapparent, but can be present with incapacitating arrhythmias, complete heart block with Stokes-Adams attacks, or sudden death. A table summarizes the aspects of main aeromedical concern. Author (revised)

N94-23326# Royal Air Force, London (England). Central Medical Establishment.
SPONTANEOUS PNEUMOTHORAX, CYSTS AND BULLAE
David H. Hull *In* AGARD, Cardiopulmonary Aspects in Aerospace Medicine Oct. 1993 2 p (For primary document see N94-23313 06-52)
Copyright Avail: CASI HC A01/MF A01

Spontaneous pneumothorax is defined as the presence of air in the pleural cavity without apparent cause. Pulmonary conditions such as tuberculosis or cancer may cause spontaneous pneumothorax, but are excessively rare in aeromedical practice. The usual victims are apparently healthy young men, often in the third decade of life, very often tall and of lean, asthenic build. The chest x-ray may be normal before or after the illness, but may show sub-pleural blebs or small cysts, usually at the lung apex; the rupture of a bleb creates a broncho-pleural communication and the natural elastic lung recoil plus negative pleural pressure draws air into the pleural space. Consequent pulmonary collapse and contraction will narrow and perhaps seal the defect, which usually closes spontaneously in a few days. However the air may take several weeks to reabsorb fully, especially if the pneumothorax is large, so that some form of evacuation of the air, e.g., by underwater seal or flutter valve, is usually desirable for any but the smallest pneumothoraces. The disease is disproportionately important in aeromedical practice, for various reasons. Author (revised)

N94-23327# Defence and Civil Inst. of Environmental Medicine, Toronto (Ontario). Medical Assessment Section.
ASTHMA IN AIRCREW
Gary Gray *In* AGARD, Cardiopulmonary Aspects in Aerospace Medicine Oct. 1993 3 p (For primary document see N94-23313 06-52)
Copyright Avail: CASI HC A01/MF A01

Asthma is a disease characterized by airway inflammation and increased bronchial reactivity. Symptoms, which characteristically are variable, include wheezing, shortness of breath, chest tightness, and cough with sputum. In the past, attention was focused on the airway hyper-reactivity with bronchospasm and wheezing, and treatment was directed towards bronchodilation as first line therapy. In recent years the central role of airway inflammation in the pathogenesis of asthma has gained increasing recognition. Airway inflammation is present in even mild asthmatics, and the treatment of asthma has evolved towards more aggressive management of the underlying inflammatory response as a key element in control. Author (revised)

N94-23328# Royal Air Force, London (England). Central Medical Establishment.
ARTERIAL HYPERTENSION AND THE AVIATOR
David H. Hull *In* AGARD, Cardiopulmonary Aspects in Aerospace Medicine Oct. 1993 7 p (For primary document see N94-23313 06-52)
Copyright Avail: CASI HC A02/MF A01

Arterial hypertension is of great importance in the practice of clinical aviation medicine, mainly because of its prominence as a major risk factor for coronary artery disease and other disabling cardiovascular diseases and because it is so common. Timely recognition of early or mild hypertension should facilitate appropriate intervention which will prevent complications and enable the air crewman to continue his career, hopefully, to normal retirement age. The consequent health benefits and fiscal advantages, both to the individual and to the air forces and airlines of the world, are obvious and substantial Author (revised)

N94-23331*# Louisville Univ., KY. Dept. of Microbiology and Immunology.
CYTOKINES AND IMMUNE SURVEILLANCE IN HUMANS Final Report
Gerald Sonnenfeld 7 Jan. 1994 5 p
(Grant NAG9-485)
(NASA-CR-194801; NAS 1.26:194801) Avail: CASI HC A01/MF A01

Evidence from both human and rodent studies has indicated that alterations in immunological parameters occur after space flight. Among the parameters shown, by us and others, to be affected is the production of interferons. Interferons are a family of cytokines that are antiviral and play a major role in regulating immune responses that control resistance to infection. Alterations in interferon and other cytokine production and activity could result in changes in immunity and a possible compromise of host defenses against both opportunistic and external infections. The purpose of the present study is to explore further the effects of space flight on cytokines and cytokine-directed immunological function. Among the tests carried out are interferon-alpha production, interferon-gamma production, interleukin-1 and -2 production, signal transduction in neutrophils, signal transduction in monocytes, and monocyte phagocytic activity. The experiments will be performed using peripheral blood obtained from human subjects. It is our intent to eventually carry out these experiments using astronauts as subjects to determine the effects of space flight on cytokine production and activity. However, these subjects are not currently available. Until they become available, we will carry out these experiments using subjects maintained in the bed-rest model for microgravity. Derived from text

N94-23530*# National Aeronautics and Space Administration. John F. Kennedy Space Center, Cocoa Beach, FL.

RESPONSES TO LBNP IN MEN WITH VARYING PROFILES OF STRENGTH AND AEROBIC CAPACITY: IMPLICATIONS FOR FLIGHT CREWS Technical Paper, Jul. 1985 - Apr. 1986

Victor A. Convertino, Karen L. Mathes (Krug International, Houston, TX.), Mary L. Lasley (Bionetics Corp., Cocoa Beach, FL.), Clare Marie Tomaselli (John B. Pierce Foundation of Connecticut, New Haven.), Mary Anne Bassett Frey (Lockheed Engineering and Sciences Co., Washington, DC.), and G. Wyckliffe Hoffler Mar. 1993 36 p

(NASA-TP-3346; NAS 1.60:3346) Avail: CASI HC A03/MF A01

Hemodynamic and hormonal responses to lower-body negative pressure (LBNP) were examined in 24 healthy men to test the hypothesis that responsiveness of reflex control of blood pressure during orthostatic stress is associated with strength and/or aerobic capacity. Subjects underwent treadmill tests to determine peak oxygen uptake (peak VO2) and isokinetic dynamo meter tests to determine leg strength. Based on predetermined criteria, the subjects were classified into one of four fitness profiles of six subjects each matched for age, height, and weight: (1) low strength/low aerobic fitness; (2) low strength/high aerobic fitness; (3) high strength/low aerobic fitness; and (4) high strength/high aerobic fitness. Following 90 min of 6 degree head-down tilt (HDT), each subject underwent graded LBNP through -50 mmHg or presyncope, with maximal duration 15 min. All groups exhibited typical hemodynamic, hormonal, and fluid shift responses during LBNP, with no intergroup differences except for catecholamines. Seven subjects, distributed among the four fitness profiles, became presyncopal. Subjects who showed greatest reduction in mean arterial pressure (MAP) during LBNP had greater elevations in vasopressin and lesser increases in heart rate and peripheral resistance. Peak VO2 nor leg strength were correlated with fall in MAP or with syncopal episodes. We conclude that neither aerobic nor strength fitness characteristics are good predictors of responses to LBNP stress. Author

N94-23544*# National Aeronautics and Space Administration. Lyndon B. Johnson Space Center, Houston, TX.

FLUID-LOADING SOLUTIONS AND PLASMA VOLUME: ASTRO-ADE AND SALT TABLETS WITH WATER

Suzanne M. Fortney, Laura Seinmann (Krug Life Sciences, Inc., Houston, TX.), Joan A. Young (Krug Life Sciences, Inc., Houston, TX.), Cherylynn N. Hoskin (Krug Life Sciences, Inc., Houston, TX.), and Linda H. Barrows (Krug Life Sciences, Inc., Houston, TX.) Jan. 1994 24 p

(NASA-TP-3456; S-756; NAS 1.60:3456) Avail: CASI HC A03/MF A01

Fluid loading with salt and water is a countermeasure used after space flight to restore body fluids. However, gastrointestinal side effects have been frequently reported in persons taking similar quantities of salt and water in ground-based studies. The effectiveness of the Shuttle fluid-loading countermeasure (8 gms salt, 0.97 liters of water) was compared to Astro-ade (an isotonic electrolyte solution), to maintain plasma volume (PV) during 4.5 hrs of resting fluid restriction. Three groups of healthy men (n=6) were studied: a Control Group (no drinking), an Astro-ade Group, and a Salt Tablet Group. Changes in PV after drinking were calculated from hematocrit and hemoglobin values. Both the Salt Tablet and Astro-ade Groups maintained PV at 2-3 hours after ingestion compared to the Control Group, which had a 6 percent decline. Side effects (thirst, stomach cramping, and diarrhea) were noted in at least one subject in both the Astro-ade and Salt Tablet Groups. Nausea and vomiting were reported in one subject in the Salt Tablet Group. It was concluded that Astro-ade may be offered as an alternate fluid-loading countermeasure but further work is needed to develop a solution that is more palatable and has fewer side effects. Author (revised)

N94-23575*# National Aeronautics and Space Administration. Ames Research Center, Moffett Field, CA.

EXERCISE, EXERCISE TRAINING, AND THE IMMUNE SYSTEM. A COMPENDIUM OF RESEARCH (1902-1991)

A. J. Hardesty, J. E. Greenleaf, S. Simonson (University of Northern Colorado, Greeley.), A. Hu (University of Northern Colorado, Greeley.), and C. G. R. Jackson (University of Northern Colorado, Greeley.) Nov. 1993 167 p

(RTOP 199-18-12-07)

(NASA-TM-108778; A-93091; NAS 1.15:108778) Avail: CASI HC A08/MF A02

This compendium includes abstracts and synopses of clinical observations and of more basic studies involving physiological mechanisms concerning interaction of physical exercise and the human immune system. If the author's abstract or summary was appropriate, it was included. In other cases, a more detailed synopsis of the paper was prepared under the subheadings 'Purpose,' 'Methods,' 'Results,' and 'Conclusions.' Author and subject indices are provided, plus a selected bibliography of related work or those papers received after the volume was being prepared for publication. This volume includes material published from 1902 through 1991. Author (revised)

N94-23623# Civil Aeromedical Inst., Oklahoma City, OK.

VISION IMPAIRMENT AND CORRECTIVE CONSIDERATIONS OF CIVIL AIRMEN

Van B. Nakagawara, Kathryn J. Wood, and Ronald W. Montgomery Dec. 1993 8 p

(DOT/FAA/AM-93/21) Avail: CASI HC A02/MF A01

Civil aviation is a major commercial and technological industry in the United States. The Federal Aviation Administration (FAA) is responsible for the regulation and promotion of aviation safety in the National Airspace System. The Office of Aviation Medicine oversees investigations on visual disorders and vision corrective devices of airmen and air traffic controllers. A review of the demographics of the civil airman population was performed using FAA publications and databases. Approximately 48 percent of the civil airman population is greater than or equal to 40 years of age (average age = 39.8 years). Many of these aviators are becoming presbyopic and will need corrective devices for near and intermediate vision. In fact, there has been an approximate 12 percent increase in the number of aviators with near vision restrictions in the last decade. Ophthalmic considerations for eye care practitioners prescribing and dispensing for civil aviators are discussed. This data is useful for the Office of Aviation Medicine to guide policy changes and educational programs for airmen with vision impairment and who use corrective ophthalmic lenses in the aviation environment, particularly the increasing number of presbyopic airmen. Author (revised)

N94-24093# Civil Aeromedical Inst., Oklahoma City, OK.

INDEX TO FAA OFFICE OF AVIATION MEDICINE REPORTS: 1961 THROUGH 1993 Final Report

William E. Collins and Michael E. Wayda Jan. 1994 72 p

(DOT/FAA/AM-94/1) Avail: CASI HC A04/MF A01

An index to FAA Office of Aviation Medicine Reports (1964-1993) and Civil Aeromedical Institute Reports is presented as for those engaged in aviation medicine and related activities. The index lists all FAA aviation medicine reports published from 1961 through 1993: chronologically, alphabetically by author, and alphabetically by subject. Author (revised)

N94-24102*# National Aeronautics and Space Administration. Ames Research Center, Moffett Field, CA.

AUTOGENIC-FEEDBACK TRAINING: A POTENTIAL TREATMENT FOR POST-FLIGHT ORTHOSTATIC INTOLERANCE IN AEROSPACE CREWS

Patricia S. Cowings, William B. Toscano (California Univ., Los Angeles.), Neil E. Miller (Yale Univ., New Haven, CT.), Thomas G. Pickering (Cornell Univ., New York, NY.), and David Shapiro (California Univ., Los Angeles.) Sep. 1993 15 p

(RTOP 199-14-12-06)

(NASA-TM-108785; A-93109; NAS 1.15:108785) Avail: CASI HC A03/MF A01

Postflight orthostatic intolerance was identified as a serious biomedical problem associated with long duration exposure to microgravity in space. High priority was given to the development of countermeasures for this disorder which are both effective and practical. A considerable body of clinical research demonstrated that people can be taught to increase their own blood pressure voluntarily and that this is an effective treatment for chronic orthostatic intolerance in paralyzed patients. The present pilot study was designed to examine the feasibility of adding training in control of blood pressure to an existing preflight training program designed to facilitate astronaut adaptation to microgravity. Using an operant conditioning procedure, Autogenic-Feedback Training (AFT), three men and two women participated in four to nine (15-30 training sessions). At the end of training, the average increase in systolic and diastolic pressure, as well as mean arterial pressures that the subjects made, ranged between 20 and 50 mmHg under both supine and 45 deg head-up tilt conditions. These findings suggest that AFT may be a useful alternative treatment or supplement to existing approaches for preventing postflight orthostatic intolerance. Further, the use of operant conditioning methods for training cardiovascular responses may contribute to the general understanding of the mechanisms of orthostatic intolerance. Author (revised)

N94-24227*# Essex Corp., Orlando, FL.
TRANSFER OF PERCEPTUAL ADAPTATION TO SPACE SICKNESS: WHAT ENHANCES AN INDIVIDUAL'S ABILITY TO ADAPT? Final Report
9 Aug. 1993 15 p
(Contract NAS9-18035)
(NASA-CR-188256; NAS 1.26:188256) Avail: CASI HC A03/MF A01

The objectives of this project were to explore systematically the determiners of transfer of perceptual adaptation as these principles might apply to the space adaptation syndrome. The perceptual experience of an astronaut exposed to the altered gravitational forces involved in spaceflight shares much with that of the subject exposed in laboratory experiments to optically induced visual rearrangement with tilt and dynamic motion illusions such as vection; and experiences and symptoms reported by the trainee who is exposed to the compellingly realistic visual imagery of flight simulators and virtual reality systems. In both of these cases the observer is confronted with a variety of inter- and intrasensory conflicts that initially disrupt perception, as well as behavior, and also produce symptoms of motion sickness. Derived from text

N94-24865 North Carolina Univ., Chapel Hill. Div. of Otolaryngology.
AUDITORY SPECTRO-TEMPORAL PATTERN ANALYSIS Annual Report, 1 Jan. - 31 Dec. 1993
Joseph W. Hall 31 Dec. 1993 4 p Limited Reproducibility: More than 20% of this document may be affected by microfiche quality
(Contract F40620-93-1-0045)
(AD-A273554; AFOSR-93-0856TR) Avail: Issuing Activity (Defense Technical Information Center (DTIC))

The present research is a continuation of an AFOSR-sponsored program that has supported our research on CMR essentially since the discovery of the phenomenon. Over the past six years, the research program has revealed several important findings related to CMR: the phenomenon is based primarily upon an across-frequency analysis of amplitude envelope; all portions of the envelope do not appear to contribute equally to CMR - envelope dips carry the critical information; CMR increases with the number of comodulated noise bands present, with diminishing returns after three bands are present; the presence of non-comodulated bands within a set of comodulated bands can substantially decrease CMR; when auditory grouping principles are applied to segregate the noncomodulated bands from the comodulated bands, CMR can be restored to a significant extent; CMR occurs for FM, but a much smaller magnitude than for AM; and part of the MLD appears to be based upon a process that is essentially identical to CMR. DTIC

N94-24928 Aerospace Medical Research Labs., Brooks AFB, TX. Crew Systems Directorate.
ARTIFICIAL GRAVITY IN SPACE FLIGHT Interim Report
Russell R. Burton 1994 5 p Limited Reproducibility: More than 20% of this document may be affected by microfiche quality
(AF Proj. 7930)
(AD-A273420; AL/CF-PC-1993-0040) Avail: Issuing Activity (Defense Technical Information Center (DTIC))

The role of G in space using a short-radius centrifuge has operation implications in preventing physiologic deconditioning from weightlessness. The relationship between periodic gravity exposures on simulated weightless effects, once determined systematically, will provide crucial information on the role of gravity as a regulator of physiologic functions. DTIC

N94-24945# Brooke Army Medical Center, Fort Sam Houston, TX.
ANNUAL RESEARCH PROGRESS REPORT, FISCAL YEAR 1992. VOLUME 2: DEPARTMENT OF CLINICAL INVESTIGATION
1992 321 p
(AD-A273584) Avail: CASI HC A14/MF A03

Presented are research progress reports of clinical investigations sponsored by Brooke Army Medical Center. Progress reports are grouped by the following categories: animal studies, southwest oncology group, pediatric oncology group, and gynecology oncology group. Progress reports list the investigators, the objectives of the research, the technical approach taken, and progress to date. CASI

N94-24950# Naval Medical Research Inst., Bethesda, MD.
A STATISTICAL ANALYSIS OF RECENT NAVAL EXPERIMENTAL DIVING UNIT (NEDU) SINGLE-DEPTH HUMAN EXPOSURES TO 100 PERCENT OXYGEN AT PRESSURE Technical Report, 1987 - 1991
A. L. Harabin and S. S. Survanshi Oct. 1993 28 p
(NMRI Proj. M00-99)
(AD-A273488; NMRI-93-59) Avail: CASI HC A03/MF A01

Using the data from 688 human, single-depth, hyperbaric oxygen (O2) exposures conducted at the Naval Experimental Diving Unit and reported on from 1979-1986, we developed a mathematical model that can predict the risk of developing symptoms of central nervous system O2 toxicity as a function of time and depth of exposure. Maximum likelihood analysis with models relating depth and time of exposure to risk accumulation was used to estimate probability of symptom development and confidence intervals. U.S. Navy single depth-time O2 diving limits were evaluated for safety as a function of actual PO2 achieved in the breathing apparatus. These results suggest that current limits are not of equal risk. Long shallow exposures might present unacceptably high risk if an F1O2 = 1.0 were achieved in the breathing rig. Adherence to current recommended purging procedures results in acceptably low (less than 1%) risk predictions for all depths. DTIC

N94-25359*# Tulane Univ., New Orleans, LA. Dept. of Mechanical Engineering.
LOADING, ELECTROMYOGRAPH, AND MOTION DURING EXERCISE
Fernando Figueroa *In* NASA. Johnson Space Center, National Aeronautics and Space Administration (NASA)/American Society for Engineering Education (ASEE) Summer Faculty Fellowship Program, 1993, Volume 1 Dec. 1993 11 p (For primary document see N94-25348 06-99)
Avail: CASI HC A03/MF A03

N94-25376*# Saint Louis Univ., MO. School of Nursing.
DEVELOPMENT OF A MODEL TO ASSESS ORTHOSTATIC RESPONSES
Marilyn Rubin *In* NASA. Johnson Space Center, National Aeronautics and Space Administration (NASA)/American Society for Engineering Education (ASEE) Summer Faculty Fellowship Program, 1993, Volume 2 Dec. 1993 15 p (For primary document see N94-25367 06-99)
Avail: CASI HC A03/MF A03

N94-25378*# Akron Univ., OH. Biomedical Engineering.
EVALUATION OF BIOIMPEDANCE FOR THE MEASUREMENT OF PHYSIOLOGIC VARIABLES AS RELATED TO HEMODYNAMIC STUDIES IN SPACE FLIGHT
Bruce C. Taylor *In* NASA. Johnson Space Center, National Aeronautics and Space Administration (NASA)/American Society for Engineering Education (ASEE) Summer Faculty Fellowship Program, 1993, Volume 2 Dec. 1993 15 p (For primary document see N94-25367 06-99)
Avail: CASI HC A03/MF A03

N94-25380*# Alabama Univ., Huntsville. Dept. of Engineering Science and Mechanics.
LOADING, ELECTROMYOGRAPH, AND MOTION DURING EXERCISE
Beth A. Todd *In* NASA. Johnson Space Center, National Aeronautics and Space Administration (NASA)/American Society for Engineering Education (ASEE) Summer Faculty Fellowship Program, 1993, Volume 2 Dec. 1993 11 p (For primary document see N94-25367 06-99)
Avail: CASI HC A03/MF A03

53 BEHAVIORAL SCIENCES

Includes psychological factors; individual and group behavior; crew training and evaluation; and psychiatric research.

N94-24467 Toronto Univ. (Ontario). Dept. of Electrical Engineering.
PREDICTIVE HEAD MOVEMENT TRACKING USING INNOVATIONS GENERATED BY KALMAN FILTERS M.S. Thesis

Andrew Muwanga Kiruluta 1993 124 p
(ISBN-0-315-83371-8; CTN-94-60957) Copyright Avail: Micromedia Ltd., Technical Information Centre, 240 Catherine Street, Suite 305, Ottawa, Ontario, K2P 2G8, Canada HC/MF

The use of head movements for control leaves hands free for other tasks and utilizes the mobility of the head to acquire and track targets over a wide field of view. Kalman filtering was applied to generate prediction estimates for tracking head positions. For relatively slow smooth head movements, a constant velocity model (CVM) sufficiently represents head dynamics. However, when the head undergoes significant maneuvers, a constant acceleration model (CAM) is preferred. To take advantage of the prediction performance of the CVM under relatively slow smooth dynamics and those of the CAM under fast dynamics, a simple adaptive algorithm is proposed. Using the adaptive model yields a compromise performance for both relatively slow and fast smooth head movements. For abrupt head movements, all the above models were inadequate. An input estimation algorithm was implemented but its prediction performance degrades significantly for head accelerations in excess of 5,000 deg/sec. To provide for a baseline comparison for tracking performance, a simple parabolic polynomial fit generated prediction estimates. The resulting fit yielded prediction root mean square errors of over 2 and 23 deg for smooth and abrupt head movements respectively. Hence, the Kalman filter does indeed yield better estimates of head positions than a simple polynomial predictor.
Author (CISTI)

N94-24799*# Pennsylvania State Univ., University Park. Behavioral Psychophysiology Lab.

EEG AND CHAOS: DESCRIPTION OF UNDERLYING DYNAMICS AND ITS RELATION TO DISSOCIATIVE STATES Final Progress Report

William J. Ray 23 Feb. 1994 10 p
(Grant NAG1-1441)
(NASA-CR-195171; NAS 1.26:195171) Avail: CASI HC A02/MF A01

The goal of this work is the identification of states especially as related to the process of error production and lapses of awareness as might be experienced during aviation. Given the need for further articulation of the characteristics of 'error prone state' or 'hazardous state of awareness,' this NASA grant focused on basic ground work for the study of the psychophysiology of these states. In specific, the purpose of this grant was to establish the necessary methodology for addressing three broad questions. The first is how the error prone state should be conceptualized, and whether it is similar to a dissociative state, a hypnotic state, or absent mindedness. Over 1200 subjects completed a variety of psychometric measures reflecting internal states and proneness to mental lapses and absent mindedness; the study suggests that there exists a consistency of patterns displayed by individuals who self-report dissociative experiences such that those individuals who score high on measures of dissociation also score high on measures of absent mindedness, errors, and absorption, but not on scales of hypnotizability. The second broad question is whether some individuals are more prone to enter these states than others. A study of 14 young adults who scored either high or low on the dissociation experiences scale performed a series of six tasks. This study suggests that high and low dissociative individuals arrive at the experiment in similar electrocortical states and perform cognitive tasks (e.g., mental math) in a similar manner; it is in the processing of internal emotional states that differences begin to emerge. The third question to be answered is whether recent research in nonlinear dynamics, i.e., chaos, offer an addition and/or alternative to traditional signal processing methods, i.e., fast Fourier transforms, and whether chaos procedures can be modified to offer additional information useful in identifying brain states. A preliminary review suggests that current nonlinear dynamical techniques such as dimensional analysis can be successfully applied to electrocortical activity. Using the data set developed in the study of the young adults, chaos analyses using the Farmer algorithm were performed; it is concluded that dimensionality measures reflect information not contained in traditional EEG Fourier analysis.
CASI

N94-24855*# National Aeronautics and Space Administration, Washington, DC.

A WHITE PAPER: NASA VIRTUAL ENVIRONMENT RESEARCH, APPLICATIONS, AND TECHNOLOGY

Cynthia H. Null, ed. (National Aeronautics and Space Administration. Ames Research Center, Moffett Field, CA.) and James P. Jenkins, ed. 1 Oct. 1993 127 p
(NASA-TM-109682; NAS 1.15:109682) Avail: CASI HC A07/MF A02

Research support for Virtual Environment technology development has been a part of NASA's human factors research program since 1985. Under the auspices of the Office of Aeronautics and Space Technology (OAST), initial funding was provided to the Aerospace Human Factors Research Division, Ames Research Center, which resulted in the origination of this technology. Since 1985, other Centers have begun using and developing this technology. At each research and space flight center, NASA missions have been major drivers of the technology. This White Paper was the joint effort of all the Centers which have been involved in the development of technology and its applications to their unique missions. Appendix A is the list of those who have worked to prepare the document, directed by Dr. Cynthia H. Null, Ames Research Center, and Dr. James P. Jenkins, NASA Headquarters. This White Paper describes the technology and its applications in NASA Centers (Chapters 1, 2 and 3), the potential roles it can take in NASA (Chapters 4 and 5), and a roadmap of the next 5 years (FY 1994-1998). The audience for this White Paper consists of managers, engineers, scientists and the general public with an interest in Virtual Environment technology. Those who read the paper will determine whether this roadmap, or others, are to be followed.
Author

N94-25298 Technische Univ., Eindhoven (Netherlands).

LUMINANCE-BRIGHTNESS MAPPING: THE MISSING DECADES Ph.D. Thesis

Gerard Schouten 1993 129 p Limited Reproducibility: More than 20% of this document may be affected by microfiche quality
(ETN-94-95351) Avail: CASI HC A07

A study directed at the understanding of brightness perception in relation to the information reduction involved is reported. Concentration is on brightness representations of images that can be considered as single, nonrelated entities. Particularly, it is investigated whether differences between the luminance map and the brightness map may be interpreted as appearances of compression mechanisms. First of all psychophysical experiments were conducted. Some general comments concerned with the experiments can be made. Stimuli consisting of a Ganzfeld, a homogeneous field of view, on which a number of disks were superimposed, were used. The whole visual field was thus stimulated in a controllable manner. The method employed was brightness matching. More specifically, to investigate the luminance-brightness compression, the large luminance range was traversed in two different ways. In a first experiment exploring brightness constancy, scene luminances were varied with certain multipliers. In the second series of experiments, luminance ratios within a scene were altered. Subsequently, the compression mechanisms revealed by the experimental results are integrated into a novel brightness algorithm which is presented. This algorithm is applied to a set of brightness illusions including brightness induction and brightness assimilation phenomena, Mach bands, and Craik-O'Brien-Cornsweet effects.
ESA

N94-25437# Minnesota Univ., Minneapolis. Dept. of Physiology.

MECHANISMS OF EYE-HAND COORDINATION Final Report, 1 Jul. 1992 - 30 Jun. 1993

Apostolos P. Georgopoulos 29 Nov. 1993 8 p
(Contract N00014-92-J-1905)
(AD-A273687) Avail: CASI HC A02/MF A01

We studied the capacities of human subjects to localize tactile stimuli in three dimensional space. For that purpose, five subjects (three women and two men) were asked to make a pointing movement to a visual stimulus in otherwise complete darkness. At some random time before, during or after this initial movement, a tactile probe was presented to the tip of the subject's index finger. The probe (1-mm diameter, 0.75-mm extent, 5-ms duration) was applied by a lightweight (80 g) tactile stimulator worn on the subject's hand. To complete the task, the subject was required to point to the three dimensional spatial location at which the probe was applied. Hand position was monitored (200 Hz) by a video-based motion analysis system. In each subject, probes presented just before or during the initial movement were systematically mislocalized in the direction of that movement so that subjects perceived the probe to be at the location occupied by the hand 50 to 100 ms after probe onset. This mislocalization is likely to be important in dealing with objects in the dark, especially with obstacles encountered along a movement's path.
DTIC

N94-25442# Federal Aviation Administration, Oklahoma City, OK. Civil Aeromedical Inst.
PERCEPTIONS OF ORGANIZATIONAL SUPPORT AND AFFECTIVITY AS PREDICTORS OF JOB SATISFACTION Final Report
L. Alan Witt Feb. 1994 13 p
(DOT/FAA/AM-94/2) Avail: CASI HC A03/MF A01

Staw, Bell, and Clausen have suggested that employees 'bring a positive or negative disposition to the work setting, process information about the job in a way that is consistent with that disposition, and then experience job satisfaction or dissatisfaction as a result.' Although this is not a universally held viewpoint, given such endeavors as the FAA Job Satisfaction Survey and managerial efforts to improve overall job satisfaction, the issue of employee disposition is important. Agency attempts to alter the work situation for the purposes of increasing job satisfaction could have limited potential for success to the extent that job satisfaction is a function of disposition. Several hypotheses examining both the main and interactive effects on job satisfaction of variables assessing the person (disposition) and situation (organizational climate) across several organizations were tested. Disposition refers to employee descriptions of how they generally feel in response to the PANAS Affectivity scale developed by Watson and Clark. The PANAS is comprised of 20 adjectives that describe both positive (PA) and negative (NA) affect. Data were accumulated by meta-analysis from 1,491 employees in 35 different organizational systems. This included survey data from employees at the FAA Aeronautical Center (N=1,029) in Oklahoma City, Air Traffic Control Specialist trainees from the FAA Academy Nonradar Screen Program (N=397) in Oklahoma City, and teachers from a rural public school system (N=65) in Illinois. Employees in each of those groups were participants in larger surveys of job satisfaction and other attitudinal factors that influence job satisfaction. Results indicated that perceptions of organizational support were more strongly related to job satisfaction than was disposition (positive affectivity (PA) or negative affectivity (NA)). NA had a larger moderating effect than PA on the perceived support-job satisfaction relationship. These results suggest that NA may have influenced the extent to which perceptions of organizational support impact employee job satisfaction. Considered together with longitudinal studies in this area, these findings suggest that dispositional differences in affectivity should be considered in interventions designed to have an impact on the attitudes of agency employees. Organizational development specialists and managers should give some consideration to how individual differences in affectivity can influence responses to the existing organizational climate and culture as attempts are made to promote organizational change and improve overall job satisfaction.

Author (revised)

N94-23933*# Instituto de Pesquisas Espaciais, Sao Jose dos Campos (Brazil).
OPERATIONAL TRAINING FOR THE MISSION OPERATIONS AT THE BRAZILIAN NATIONAL INSTITUTE FOR SPACE RESEARCH (INPE)
Pawel Rozenfeld *In* JPL, SpaceOps 1992: Proceedings of the Second International Symposium on Ground Data Systems for Space Mission Operations 1 Mar. 1993 p 667-671 (For primary document see N94-23832 06-66)
Avail: CASI HC A01/MF A10

N94-23934*# Jet Propulsion Lab., California Inst. of Tech., Pasadena.
TRAINING: PLUGGING THE INFORMATION GAPS
Carol J. Scott *In its* SpaceOps 1992: Proceedings of the Second International Symposium on Ground Data Systems for Space Mission Operations 1 Mar. 1993 p 673-677 (For primary document see N94-23832 06-66)
Avail: CASI HC A01/MF A10

N94-23979# Pennsylvania State Univ., University Park. Dept. of Psychology.
PERCEPTION IN FLIGHT: SHAPE AND MOTION PERCEPTION, SPACE PERCEPTION, SPATIAL ORIENTATION, AND VISUAL VESTIBULAR INTERACTION
Herschel W. Leibowitz *In* AGARD, Visual Problems in Night Operations May 1992 9 p (For primary document see N94-23976 06-54)
Copyright Avail: CASI HC A02/MF A01

N94-23980# Centre d'Enseignement et de Recherches de Medecine Aeronautique, Paris (France). Dept. Ergonomie Aerospatiale.
MENTAL IMAGES [LES IMAGES MENTALES]
Rene Amalberti *In* AGARD, Visual Problems in Night Operations 10 p(SEE N94-23976 06-54) May 1992 In FRENCH (For primary document see N94-23976 06-54)
Copyright Avail: CASI HC A02/MF A01

N94-24266 Israel Aircraft Industries Ltd., Tashan.
PILOT EVALUATION SYSTEM
Y. Shub *In* Israel Society of Aeronautics and Astronautics, The 33rd Israel Annual Conference on Aviation and Astronautics 25 Feb. 1993 p 287-296 (For primary document see N94-24241 06-01)
Copyright Avail: Issuing Activity (Israel Society of Aeronautics and Astronautics, c/o Faculty of Engineering, Tel-Aviv Univ., Ramat Aviv 69978, Israel)

N94-24438*# Alabama Univ., Huntsville. Dept. of Industrial Engineering.
EVALUATION OF COMPUTER-AIDED INSTRUCTION TECHNIQUES FOR THE CREW INTERFACE COORDINATION POSITION
Gary P. Moynihan *In its* The 1993 NASA/ASEE Summer Faculty Fellowship Program Nov. 1993 5 p (For primary document see N94-24405 06-80)
Avail: CASI HC A01/MF A03

N94-25351*# Mount Holyoke Coll., South Hadley, MA. Dept. of Biological Sciences.
THE ROLE OF VISUAL CONTEXT IN MANUAL TARGET LOCALIZATION
Susan R. Barry *In* NASA. Johnson Space Center, National Aeronautics and Space Administration (NASA)/American Society for Engineering Education (ASEE) Summer Faculty Fellowship Program, 1993, Volume 1 Dec. 1993 14 p (For primary document see N94-25348 06-99)
Avail: CASI HC A03/MF A03

N94-25492*# Honeywell, Inc., Minneapolis, MN. Systems and Research Center.
SYNTHETIC VISION SYSTEM FLIGHT TEST RESULTS AND LESSONS LEARNED
Jeffrey Radke *In* NASA. Ames Research Center, Proceedings of the Workshop on Augmented Visual Display (AVID) Research Dec. 1993 p 29-45 (For primary document see N94-25490 06-54)
Avail: CASI HC A03/MF A04

54 MAN/SYSTEM TECHNOLOGY AND LIFE SUPPORT

Includes human engineering; biotechnology; and space suits and protective clothing.

For related information see also *16 Space Transportation.*

N94-22997# Oak Ridge National Lab., TN.
EYE-GAZE CONTROL OF THE COMPUTER INTERFACE: DISCRIMINATION OF ZOOM INTENT
J. H. Goldberg (Pennsylvania State Univ., University Park.) and J. C. Schryver 1993 6 p Presented at the Human Factors and Ergonomics Society Meeting, Seattle, WA, 11-15 Oct. 1993
(Contracts DE-AC05-84OR-21400; DE-AC05-76OR-00033)
(DE94-000480; CONF-9310100-3) Avail: CASI HC A02/MF A01

An analysis methodology and associated experiment were developed to assess whether definable and repeatable signatures of eye-gaze characteristics are evident, preceding a decision to zoom-in, zoom-out, or not to zoom at a computer interface. This user intent discrimination procedure can have broad application in disability aids and telerobotic control. Eye-gaze was collected from ten subjects in a controlled experiment, requiring zoom decisions. The eye-gaze data were clustered, then fed into a multiple discriminant analysis (MDA) for optimal definition of heuristics separating the zoom-in, zoom-out, and no-zoom conditions. Confusion matrix analyses showed that a number of variable combinations classified at a statistically significant level, but practical significance was more difficult to establish.

Composite contour plots demonstrated the regions in parameter space consistently assigned by the MDA to unique zoom conditions. Peak classification occurred at about 1200-1600 msec. Improvements in the methodology to achieve practical real-time zoom control are considered.
DOE

N94-23080*# Fairchild Space Co., Germantown, MD.
MANNED MARS MISSION ON-ORBIT OPERATIONS FTS CAPABILITIES ASSESSMENT Final Report
Frank G. Gallo and Stewart W. Jackson 30 Jun. 1989 54 p
(Contract NAS5-30189)
(NASA-CR-189328; NAS 1.26:189318) Avail: CASI HC A04/MF A01

This document presents an overview of the characteristics and capabilities of the flight telerobotic servicer (FTS), under development at GSFC at the time the report was prepared; the project has since been cancelled. The assessment was directed toward developing the FTS to enable assembly and servicing of the Mars vehicle at the space station; facilitate rendezvous, docking, and fluid transfer operations involving the Mars vehicle fuel tank; to perform strip-mining operations on the lunar/martian surfaces; and to construct a three-story shelter on the martian surface. The report considers the FTS' mechanical, electrical, thermal, and operational subsystems, as well as its proposed manipulator capabilities. Author (revised)

N94-23083# Galaxy Scientific Corp., Pleasantville, NJ.
PILOT-VEHICLE INTERFACE Final Report
L. Harrison, J. Janowitz, and M. Castronuovo Nov. 1993 182 p
(Contract DTFA03-89-C-00043)
(DOT/FAA/CT-92/21) Avail: CASI HC A09/MF A02

The cockpits of the early transport aircraft were quite different from those produced today. Older cockpits contained numerous 'steam gauge' style indicators. As technology advanced, these older electromechanical indicators were gradually replaced by newer, more reliable digital systems. Digital flight control and avionic systems are being used increasingly in modern aircraft. This trend yields cockpits of greater complexity and has swelled the amount of information with which the crew must deal. The way the pilot controls and monitors the state of the aircraft has also been greatly influenced by the increased use of digital systems. Additionally, new methods of aircraft system monitoring and control are being researched and implemented. These systems use new display technology, programmable display formats, voice input and output, and other new input and control devices. Systems and their cockpit interfaces were added as technological advances were made and new requirements generated. The human interface was given little consideration in the layout of the cockpit. Human qualities and failure modes were not taken into account in the cockpit design process. As the number of systems, components, indicators, and switches multiplied, the potential for error also grew. The emphasis of this report is on civil transport aircraft. This includes technologies such as displays, controls, and design methodologies, along with human factors concerns. The report consists of four sections: civil transport cockpit, cockpit standards, cockpit technology, and cockpit human factors. This report is to serve as a guide to Certification Engineers who are faced with the task of certification of new cockpit technologies. Author

N94-23290*# Martin Marietta Corp., Denver, CO. Advanced Launch Systems.
TASK 1: HEALTH MANAGEMENT DEMONSTRATION. TASK 2: PROCESS MANAGEMENT ENVIRONMENT AND SUPPORT OF ENTERPRISE INTEGRATION. TASK 3: NEW ALGORITHM DEVELOPMENT IN THE PME Final Report
W. A. Clark and D. Wilks 30 Sep. 1993 138 p
(Contract NAS9-18879)
(NASA-CR-188268; NAS 1.26:188268; MCR-93-5013) Avail: CASI HC A07/MF A02

Integrated Vehicle Health Management (IVHM) consists of instrumenting measurable parameters to collect information on an existing system that then aids decision making which leads to reduced life-cycle costs. The information must be extracted from data measured and reduced to a point where people can make good, logical decisions. IVHM requires sensors coupled to data reduction systems that allow patterns to be detected, operating environments characterized, and system performance verified in order to optimize the overall system to reduce costs. A key component in building an IVHM system is the communications capability between the actual parameter being measured and the final user of the information extracted. This information flow must be sufficiently flexible to allow the sensors and parameters measured to change as the needs and requirements of the overall system changes. The first step in creating an IVHM is to make the sensor interface more intelligent and thereby more flexible. This is a Final Report for the NASA Research Announcement (NRA) Strategic Avionics Technology Definition Studies Martin Marietta Task entitled 'Health Management and Process Demonstration for Aerospace Systems'. This report covers Task 1: Health Management Demonstration and is submitted to Johnson Space Center (JSC) in fulfillment of the reports of work specified in the contract (NAS9-18879). Task 2: Process Management Environment and Support of Enterprise Integration, and Task 3: New Algorithm Development in the PME, are also presented. Derived from text

N94-23527*# Western Aerospace Labs., Inc., Monte Sereno, CA.
ACTIVITY CATALOG TOOL (ACT) USER MANUAL, VERSION 2.0
Leon D. Segal and Anthony D. Andre Jan. 1994 25 p
(Contract NCC2-486)
(NASA-CR-177634; A-94046; NAS 1.26:177634) Avail: CASI HC A03/MF A01

This report comprises the user manual for version 2.0 of the Activity Catalog Tool (ACT) software program, developed by Leon D. Segal and Anthony D. Andre in cooperation with NASA Ames Aerospace Human Factors Research Division, FLR branch. ACT is a software tool for recording and analyzing sequences of activity over time that runs on the Macintosh platform. It was designed as an aid for professionals who are interested in observing and understanding human behavior in field settings, or from video or audio recordings of the same. Specifically, the program is aimed at two primary areas of interest: human-machine interactions and interactions between humans. The program provides a means by which an observer can record an observed sequence of events, logging such parameters as frequency and duration of particular events. The program goes further by providing the user with a quantified description of the observed sequence, through application of a basic set of statistical routines, and enables merging and appending of several files and more extensive analysis of the resultant data. Author (revised)

N94-23743 National Defence Research Establishment, Linkoeping (Sweden). Huvudadelning foer Maensklig Prestation och Funktion.
SURVIVAL SUIT FOR SUBMARINE PERSONNEL: SUMMARY OF EVALUATION STUDIES [RAEDDNINGSDRAEKT FOER UBATSPERSONAL: SLUTRAPPORT]
Mikael Gennser, Ake Larsson, and Hans Oernhagen Mar. 1993 33 p
In SWEDISH See also PB90-201021 Limited Reproducibility: More than 20% of this document may be affected by microfiche quality
(PB93-204634; FOA-A-50014-5.1) Avail: CASI HC A03

Survival suits for submarine personnel should be able to protect against drowning and hypothermia for long periods of severe weather conditions. The Division of Naval Medicine of the Swedish Defense Research Establishment has carried out a series of tests of survival suits with and without a one-man life-raft in cold water during simulated winter conditions. Tests were also carried out with a modified suit to evaluate suggested modifications. The tests were completed with a study of the buoyancy and floating position of the suits in heavy sea. An investigation of different materials for diapers to improve the urine collection system and an experimental study regarding the possibility of reducing the urine output during stays in cold water using a synthetic antidiuretic hormone were also carried out. In the report the main results of the tests are summarized, the problems with the various suits are discussed, and improvements are suggested. In conclusion three suit concepts that are thought to be able to fulfill the requirements are described and ranked: (1) a double-layered suit with life-raft, (2) a single-layered suit with extra buoyancy and life-raft, and (3) a modified double-layered suit with extra buoyancy. NTIS

N94-23744 Eurocontrol Experimental Centre, Bretigny (France).
HARMONISATION OF MAN-MACHINE INTERFACE EXPERIMENTS IN THE CONTEXT OF THE DEVELOPMENT OF PHARE ADVANCED TOOLS Report, Jan. - Aug. 1992
S. Broadbent 1993 130 p Limited Reproducibility: More than 20% of this document may be affected by microfiche quality
(PB93-204725; EEC-256) Copyright Avail: Issuing Activity (National Technical Information Service (NTIS))

The objective of the document is to provide PHARE researchers concerned with Human-Machine Interfaces (HMI) evaluation studies with a series of indications as to the experimental methods that can be employed to evaluate interface prototypes. The document does not require the reader to have specific expertise in human factors experimental methods, but attempts to provide the background for some fundamental principles of experimental design. The proposed evaluation methodology consists of a controlled experimental methodology which will involve part-task investigations, i.e., a small sub-component of the control activity will be examined in each study. The experimenter isolates the function or functions of the interface that require close scrutiny and design specific experimental environments to assess users' interactions with that particular feature of the interface. Ten steps of experimentation are detailed in the document including the selection of assessment measures, the selection of experimental subjects, and decisions about design and results analysis. For each step a number of indications is be provided on the rationale behind one or another design option. NTIS

N94-23970*# National Aeronautics and Space Administration. Ames Research Center, Moffett Field, CA.

REDUCING VIDEO FRAME RATE INCREASES REMOTE OPTIMAL FOCUS TIME

Richard F. Haines (RECOM Technologies, Inc., Moffett Field, CA.) Jun. 1993 8 p
(RTOP 476-14-03)
(NASA-TM-104018; A-93075; NAS 1.15:104018) Avail: CASI HC A02/MF A01

Twelve observers made best optical focus adjustments to a microscope whose high-resolution pattern was video monitored and displayed first on a National Television System Committee (NTSC) analog color monitor and second on a digitally compressed computer monitor screen at frame rates ranging (in six steps) from 1.5 to 30 frames per second (fps). This was done to determine whether reducing the frame rate affects the image focus. Reducing frame rate has been shown to be an effective and acceptable means of reducing transmission bandwidth of dynamic video imagery sent from Space Station Freedom (SSF) to ground scientists. Three responses were recorded per trial: time to complete the focus adjustment, number of changes of focus direction, and subjective rating of final image quality. It was found that: the average time to complete the focus setting increases from 4.5 sec at 30 fps to 7.9 sec at 1.5 fps (statistical probability = 1.2 x 10(exp -7)); there is no significant difference in the number of changes in the direction of focus adjustment across these frame rates; and there is no significant change in subjectively determined final image quality across these frame rates. These data can be used to help pre-plan future remote optical-focus operations on SSF. Author (revised)

N94-23974*# National Aeronautics and Space Administration. Ames Research Center, Moffett Field, CA.

EVALUATION OF VISUAL ACUITY WITH GEN 3 NIGHT VISION GOGGLES

Arthur Bradley (Indiana Univ., Indianapolis.) and Mary K. Kaiser Jan. 1994 40 p
(NASA-TM-108792; A-93134; NAS 1.15:108792) Avail: CASI HC A03/MF A01

Using laboratory simulations, visual performance was measured at luminance and night vision imaging system (NVIS) radiance levels typically encountered in the natural nocturnal environment. Comparisons were made between visual performance with unaided vision and that observed with subjects using image intensification. An Amplified Night Vision Imaging System (ANVIS6) binocular image intensifier was used. Light levels available in the experiments (using video display technology and filters) were matched to those of reflecting objects illuminated by representative night-sky conditions (e.g., full moon, starlight). Results show that as expected, the precipitous decline in foveal acuity experienced with decreasing mesopic luminance levels is effectively shifted to much lower light levels by use of an image intensification system. The benefits of intensification are most pronounced foveally, but still observable at 20 deg eccentricity. Binocularity provides a small improvement in visual acuity under both intensified and unintensified conditions. Author (revised)

N94-23976# Advisory Group for Aerospace Research and Development, Neuilly-Sur-Seine (France). Aerospace Medical Panel.

VISUAL PROBLEMS IN NIGHT OPERATIONS [PROBLEMES DE VISION DANS LES OPERATIONS DE NUIT]

May 1992 96 p In ENGLISH and FRENCH Lecture series held in Madrid, Spain, 1-2 Jun. 1992, in Soesterberg, Netherlands, 4-5 Jun. 1992, and in Brooks AFB, TX, 15-16 Jun. 1992
(AGARD-LS-187; ISBN-92-835-0676-6) Copyright Avail: CASI HC A05/MF A01

The aim of this Lecture Series is to provide the aeromedical specialist with a thorough understanding of the physiology of the visual system with particular concentration on the impact of the environment presented during night tactical air operations. Methods to preserve, protect, or enhance unaided night vision will be discussed. Information concerning visual performances with electro-optic devices derived from aeromedical research and field experiences will be detailed to provide the medical specialists, the engineers, and operational pilots with appropriate understanding of these increasingly common operational tools. This Lecture Series, sponsored by the Aerospace Medical Panel of AGARD, was implemented by the Consultant and Exchange Programme of AGARD. For individual titles, see N94-23977 through N94-23984.

N94-23977# Aerospace Medical Research Labs., Williams AFB, AZ. Aircrew Training Research Div.

NIGHT OPERATIONS

William E. Berkley *In* AGARD, Visual Problems in Night Operations May 1992 4 p (For primary document see N94-23976 06-54)
Copyright Avail: CASI HC A01/MF A01

Strategists have long sought to exploit the night in military operations, not only to avoid detection and as a means to defeat visually or optically aimed weapons, but also to deny the enemy an opportunity to rest or resupply his troops. With the advent of practical and effective imaging devices, true night war fighting capability has at last become a reality (as demonstrated in the recent Gulf War). It is safe to assume that night military operations will receive even more emphasis in the future. Current aviation activities range from basic single pilot helicopter operations with night vision goggles (NVG's) to complex missions utilizing a mix of highly sophisticated aircraft with multiple sensors, precise navigational capabilities, and advanced weapons delivery systems. Author (revised)

N94-23978# Centre d'Enseignement et de Recherches de Medecine Aeronautique, Paris (France). Dept. Ergonomie Aerospatiale.

PHYSICAL ASPECTS OF THE VISUAL STIMULUS [ASPECTS PHYSIQUES DU STIMULUS VISUEL]

Jean-Pierre Menu *In* AGARD, Visual Problems in Night Operations May 1992 8 p In FRENCH (For primary document see N94-23976 06-54)
Copyright Avail: CASI HC A02/MF A01

The various physical and psychophysical aspects of the visual stimulus are considered. It is a question of defining as precisely as possible the physical stimulation of input to the visual systems (nature of radiation, light intensities, colors, and organization in space and time). It is often difficult to dissociate the physical aspect from the psychophysical aspect. This last aspect translates the impact of the physical aspect on the socket and the treatment of information through the visual channel. It is consequently important to define as precisely as possible the operation of the retinal sensor. Mechanisms of the integration of information are described. The physical structure of the images of several systems of substitution to night vision are analyzed. Transl. by FLS

N94-23979# Pennsylvania State Univ., University Park. Dept. of Psychology.

PERCEPTION IN FLIGHT: SHAPE AND MOTION PERCEPTION, SPACE PERCEPTION, SPATIAL ORIENTATION, AND VISUAL VESTIBULAR INTERACTION c53

Herschel W. Leibowitz *In* AGARD, Visual Problems in Night Operations May 1992 9 p (For primary document see N94-23976 06-54)
Copyright Avail: CASI HC A02/MF A01

Differences between the normal terrestrial and the flight environment are described which may lead to perceptual errors in flight. Specific examples involving the perception of shape and height are discussed as they may relate to nighttime landing accidents. The possible role of misperceived

risk is suggested as a contributing factor. The mechanisms subserving motion perception and gaze stability are outlined briefly as the basis for understanding false sensations, illusory motion, spatial disorientation, and motion sickness. It is suggested that an appropriate countermeasure to perceptual errors in the nighttime flight environment is to inform flight crews of the mechanisms and mode of operation of the perceptual systems involved as the basis for understanding how they might misfunction.
Derived from text

N94-23980# Centre d'Enseignement et de Recherches de Medecine Aeronautique, Paris (France). Dept. Ergonomie Aerospatiale.
MENTAL IMAGES [LES IMAGES MENTALES] c53
Rene Amalberti *In* AGARD, Visual Problems in Night Operations 10 p(SEE N94-23976 06-54) May 1992 In FRENCH (For primary document see N94-23976 06-54)
Copyright Avail: CASI HC A02/MF A01

The concept of mental images is paradoxically poorly linked to visual perception. It is related to the domain of mental representation, and thus is explained with reference to the field of cognitive psychology. This domain being relatively new for most of the listeners of this short course, basic concepts are didactically introduced. A framework model of cognitive activities is set up, introducing first the various memories, then focusing on mental representation processes. The specificites of mental representation are detailed (laconism, distorsion, parcimony, and task-oriented). Special emphasis is given to the mental representation theory of double coding: verbal and image coding and its relationship with activity. A last section describes how mental representation, especially mental image, could serve or impair night-flight activities. Author (revised)

N94-23981# Centre d'Enseignement et de Recherches de Medecine Aeronautique, Paris (France). Dept. Ergonomie Aerospatiale.
MULTI-SENSORAL APPROACH TO NIGHT FLIGHT: PERCEPTIVE AND COGNITIVE LIMITATIONS [APPROCHE MULTI-SENSEURS POUR LE VOL DE NUIT: LIMITATIONS PERCEPTIVES ET COGNITIVES]
Rene Amalberti *In* AGARD, Visual Problems in Night Operations May 1992 9 p In FRENCH (For primary document see N94-23976 06-54)
Copyright Avail: CASI HC A02/MF A01

Night-flight activities have significantly grown to allow Forces being permanently operational. The level of performance for these activities is expected to be the same as it is in day time. Thus, visual support systems have been designed to mitigate the consequences of night-vision limitations, e.g. Electro-optical systems (radar), NVG, FLIR, and Real-time terrain image. Some of these support-systems are mixed, using several sources although they provide the pilot with only one resulting integrated image. Moreover, when the pilot continues to have a direct vision of the external world (vision through the optical system), the human vision has to be considered as another point of view to be integrated with this type of visual support system. This is typically what is termed the integrated multi-sensor and sensory approach. Humans have a special position in such conditions: first, from a perceptive point of view, although they are impaired by night-conditions, their eyes complement machine vision. Second, from a reasoning and decision making point of view, they must adapt their mental processes to this complex visual input made of a mixture of natural and artificial vision. The resulting effects of this position for perception and reasoning activities are described. The framework model of cognitive activities described in the previous course on mental images serves as a departure point. Then the following are discussed: (1) how humans solve the possible distorsions between sensors and human vision; (2) how these perceptive input are integrated into mental representations; (3) the central question of confidence into visual support-systems; and (4) the related consequences for workload. Author (revised)

N94-23982# Aerospace Medical Research Labs., Wright-Patterson AFB, OH.
NIGHT VISION DEVICES AND CHARACTERISTICS
H. Lee Task *In* AGARD, Visual Problems in Night Operations May 1992 8 p (For primary document see N94-23976 06-54)
Copyright Avail: CASI HC A02/MF A01

Night vision goggles (NVG's) are widely used to enhance visual capability during night operations. NVG's are basically composed of an objective lens which focuses an image onto the photo-cathode of an image intensifier tube which in turn produces an amplified image that is viewed through an eyepiece lens. There are several versions of NVG's in use and in development. These include the AN/PVS-Five, AN/AVS-Six, PVS-Seven, Cat's Eyes, Nite-Op, Eagle Eyes, Merlin, and others. The first section of this paper provides a brief description and characterization of each of these NVG's. There are several parameters that are used to characterize the image quality and capability of NVG's. These parameters include field-of-view (FOV), resolution, spectral sensitivity, brightness gain, distortion, magnification, optical axes alignment, image rotation, overlap, beamsplitter ratio, exit pupil diameter, eye relief, and others. Each of these is discussed in the second section of this paper. Author (revised)

N94-23983# Aerospace Medical Research Labs., Wright-Patterson AFB, OH.
COCKPIT/NVG VISUAL INTEGRATION ISSUES
H. Lee Task *In* AGARD, Visual Problems in Night Operations May 1992 6 p (For primary document see N94-23976 06-54)
Copyright Avail: CASI HC A02/MF A01

This paper is divided into two main sections: visual significance of night vision goggles (NVG) characteristics and cockpit/NVG integration issues. The first section deals with the relationship between the NVG characteristics discussed in the previous paper and visual capability. The second section explores several issues associated with successfully integrating the NVG with the aircraft cockpit for optimum system performance.
Author (revised)

N94-23984# Aerospace Medical Research Labs., Williams AFB, AZ. Aircrew Training Research Div.
NIGHT VISION GOGGLE ILLUSIONS AND VISUAL TRAINING
William E. Berkley *In* AGARD, Visual Problems in Night Operations May 1992 6 p (For primary document see N94-23976 06-54)
Copyright Avail: CASI HC A02/MF A01

Night vision goggles (NVG's) possess certain specific visual characteristics related to their limited resolution, field of view and automatic gain control. In addition, the near infrared energy to which NVG's are most sensitive has somewhat different properties as compared to visible light. These factors combine to produce certain effects, limitations and illusions not ordinarily encountered with unaided vision. NVG visual training for aircrew members is conducted with didactic presentations, terrain board simulation, video tape presentations of intensified imagery, flight simulators utilizing computer generated imagery, and actual flight with NVG's. Computer based training and an interactive videodisc are under development.
Derived from text

N94-24114 Defence and Civil Inst. of Environmental Medicine, Downsview (Ontario).
PHYSIOLOGICAL PROTECTION FOR AIRCREW AT HIGH ALTITUDES: A REVIEW OF THE LITERATURE
L. S. Goodman Apr. 1993 48 p
(DCIEM-93-13; CTN-94-60895) Copyright Avail: Micromedia Ltd., Technical Information Centre, 165 Hotel de Ville, Place du Portage, Phase 2, Hull, Quebec J8X 3X2, Canada

The greater performance characteristics of modern tactical aircraft allow flight at extreme altitudes. If oxygen breathing systems should fail or the canopy seal be broken, exposure to low levels of oxygen pressure will lead to hypoxia. Unconsciousness will occur within seconds at altitudes of 60,000 ft and up. The technology of hypoxia protection for aircrew during emergency cabin decompression is beginning to address this issue; in fact, the altitude performance of modern aircraft is limited by their 1950's generation oxygen systems. The basic physiology of hypoxia is first reviewed. The use of positive pressure breathing (PPB) for emergency hypoxia protection, sufficient to allow the pilot to maintain useful consciousness until the aircraft rapidly descends to safe altitudes, is then discussed in a historical perspective. The gas-exchange physiology and mechanisms whereby the correction or reduction of hypoxia is achieved are explained. This is followed by detailed discussion of the pulmonary and cardiovascular disruptions caused by PPB. The means for preventing these disruptions are reviewed, including G-suit inflation and thoracic counterpressure garments. More recently developed PPB garment technologies are highlighted and trends in PPB garment research and development are predicted. Author (CISTI)

N94-24119 Defence and Civil Inst. of Environmental Medicine, Downsview (Ontario).

OPERATION FRICTION: DEVELOPMENT AND INTRODUCTION OF PERSONAL COOLING FOR CH124 SEA KING AIRCREW

L. L. M. Bossi, K. C. Glass, J. Frim, and M. J. Ballantyne Jan. 1993 61 p

(DCIEM-93-06; CTN-94-60915) Copyright Avail: Micromedia Ltd., Technical Information Centre, 165 Hotel de Ville, Place du Portage, Phase 2, Hull, Quebec J8X 3X2, Canada

Sea King helicopters and aircrew were deployed to the Persian Gulf as part of Canadian support to the United Nations actions against Iraq in 1990. Due to the expected high temperatures and the requirement to operate in the aircrew chemical defense (CD) ensemble, personal cooling was required to maintain operational effectiveness. A system developed for cooling bomb disposal personnel was adapted for this purpose. This included not only manufacture and delivery within one week, but also design and implementation of CD ensemble and aircraft modifications. The cooling system included a shirt made of Nomex stretch fabric with plasticized tubing stitched throughout the inside; the tubing was connected to a pump and a bottle containing water and ice. Modifications included adapting the pump to run on aircraft power instead of battery supply. The development of doctrine, operational use of the cooling ensembles, and training of aircrew and support staff were accomplished on ship enroute to the Gulf. Physiological and operational evaluations of the cooling system show that the operational capability of the aircrews was significantly enhanced by the personal cooling system. Dressed in the full CD ensemble, the aircrews could function without being limited by heat stress. Author (CISTI)

N94-24171 Toronto Univ. (Ontario). Dept. of Industrial Engineering.

INVESTIGATION OF TIME AND INTENSITY EFFECTS IN OPERATOR WORKLOAD AND PERFORMANCE

Jianqiao Liao and Paul Milgram Jun. 1993 181 p

(CTN-94-60927) Copyright Avail: Micromedia Ltd., Technical Information Centre, 165 Hotel de Ville, Place du Portage, Phase 2, Hull, Quebec J8X 3X2, Canada

The concept of mental workload is examined and various factors affecting mental workload are discussed. Methods of mental workload measurement methods are evaluated and models of human information processing are reviewed. In a review of modeling of time and intensity domain aspects of mental workload, it is concluded that it is useful to model the human information processor as a capacity limited information channel. To test the proposed model, the performance of a simulated air traffic control (ATC) task was experimentally investigated, using NASA TLX scores to assess the subjects' mental workload. Ratings of overall mental workload were found to be sensitive to changes in the number of aircraft and the simulation update interval. High correlations were found among the six dimensions of NASA TLX. From the experimental data, a model of human performance was derived based on the concept of limited capacity. A preliminary network simulation was also developed independently, based on the assumption that the human operator could do only one task at a time. The simulation was found to predict subjects' performance well under low task demand conditions but not under high task demand conditions. It is believed that this simulation model can be greatly improved. Substantial bibliographies on mental workload are included. Author (CISTI)

N94-24185*# National Aeronautics and Space Administration. Lyndon B. Johnson Space Center, Houston, TX.

CREW INTERFACE ANALYSIS: SELECTED ARTICLES ON SPACE HUMAN FACTORS RESEARCH, 1987 - 1991

Tandi Bagian, comp. Jul. 1993 137 p Sponsored by NASA. Washington Original contains color illustrations

(NASA-TM-104756; S-697; NAS 1.15:104756) Avail: CASI HC A07/MF A02; 5 functional color pages

As part of the Flight Crew Support Division at NASA, the Crew Interface Analysis Section is dedicated to the study of human factors in the manned space program. It assumes a specialized role that focuses on answering operational questions pertaining to NASA's Space Shuttle and Space Station Freedom Programs. One of the section's key contributions is to provide knowledge and information about human capabilities and limitations that promote optimal spacecraft and habitat design and use to enhance crew safety and productivity. The section provides human factors engineering for the ongoing missions as well as proposed missions that aim to put human settlements on the Moon and Mars. Research providing solutions to operational issues is the primary objective of the Crew Interface Analysis Section. The studies represent such subdisciplines as ergonomics, space habitability, man-computer interaction, and remote operator interaction. For individual titles, see N94-24186 through N94-24206.

N94-24186*# Lockheed Engineering and Sciences Co., Houston, TX.

SPACECRAFT CREW PROCEDURES FROM PAPER TO COMPUTERS

Michael ONeal and Meera Manahan *In* NASA. Johnson Space Center, Crew Interface Analysis: Selected Articles on Space Human Factors Research, 1987 - 1991 Jul. 1993 p 5-9 (For primary document see N94-24185 06-54)

(Contract NAS9-17900)

Avail: CASI HC A01/MF A02; 5 functional color pages

Large volumes of paper are launched with each Space Shuttle Mission that contain step-by-step instructions for various activities that are to be performed by the crew during the mission. These instructions include normal operational procedures and malfunction or contingency procedures and are collectively known as the Flight Data File (FDF). An example of nominal procedures would be those used in the deployment of a satellite from the Space Shuttle; a malfunction procedure would describe actions to be taken if a specific problem developed during the deployment. A new FDF and associated system is being created for Space Station Freedom. The system will be called the Space Station Flight Data File (SFDF). NASA has determined that the SFDF will be computer-based rather than paper-based. Various aspects of the SFDF are discussed. Derived from text

N94-24187*# National Aeronautics and Space Administration. Lyndon B. Johnson Space Center, Houston, TX.

PROCESS AND REPRESENTATION IN GRAPHICAL DISPLAYS

Douglas J. Gillan (Lockheed Engineering and Sciences Co., Houston, TX.), Robert Lewis (Rice Univ., Houston, TX.), and Marianne Rudisill *In its* Crew Interface Analysis: Selected Articles on Space Human Factors Research, 1987 - 1991 Jul. 1993 p 10-16 (For primary document see N94-24185 06-54)

Avail: CASI HC A02/MF A02; 5 functional color pages

Our initial model of graphic comprehension has focused on statistical graphs. Like other models of human-computer interaction, models of graphical comprehension can be used by human-computer interface designers and developers to create interfaces that present information in an efficient and usable manner. Our investigation of graph comprehension addresses two primary questions: how do people represent the information contained in a data graph?; and how do they process information from the graph? The topics of focus for graphic representation concern the features into which people decompose a graph and the representations of the graph in memory. The issue of processing can be further analyzed as two questions: what overall processing strategies do people use?; and what are the specific processing skills required? Derived from text

N94-24188*# Rice Univ., Houston, TX.

DESIGNERS' MODELS OF THE HUMAN-COMPUTER INTERFACE

Douglas J. Gillan and Sarah D. Breedin (Lockheed Engineering and Sciences Co., Houston, TX.) *In* NASA. Johnson Space Center, Crew Interface Analysis: Selected Articles on Space Human Factors Research, 1987 - 1991 Jul. 1993 p 17-26 (For primary document see N94-24185 06-54)

(Contract NAS9-17900)

Avail: CASI HC A02/MF A02; 5 functional color pages

Understanding design models of the human-computer interface (HCI) may produce two types of benefits. First, interface development often requires input from two different types of experts: human factors specialists and software developers. Given the differences in their backgrounds and roles, human factors specialists and software developers may have different cognitive models of the HCI. Yet, they have to communicate about the interface as part of the design process. If they have different models, their interactions are likely to involve a certain amount of miscommunication. Second, the design process in general is likely to be guided by designers' cognitive models of the HCI, as well as by their knowledge of the user, tasks, and system. Designers do not start with a blank slate; rather they begin with a general model of the object they are designing. The author's approach to a design model of the HCI was to have three groups make judgments of categorical similarity about the components of an interface:

human factors specialists with HCI design experience, software developers with HCI design experience, and a baseline group of computer users with no experience in HCI design. The components of the user interface included both display components such as windows, text, and graphics, and user interaction concepts, such as command language, editing, and help. The judgments of the three groups were analyzed using hierarchical cluster analysis and Pathfinder. These methods indicated, respectively, how the groups categorized the concepts, and network representations of the concepts for each group. The Pathfinder analysis provides greater information about local, pairwise relations among concepts, whereas the cluster analysis shows global, categorical relations to a greater extent. Derived from text

N94-24189*# Lockheed Engineering and Sciences Co., Houston, TX.
AUTOMATED SYSTEM FUNCTION ALLOCATION AND DISPLAY FORMAT: TASK INFORMATION PROCESSING REQUIREMENTS
Mary P. Czerwinski *In* NASA. Johnson Space Center, Crew Interface Analysis: Selected Articles on Space Human Factors Research, 1987 - 1991 Jul. 1993 p 27-35 Sponsored by NASA. Washington (For primary document see N94-24185 06-54)
Avail: CASI HC A02/MF A02; 5 functional color pages

An important consideration when designing the interface to an intelligent system concerns function allocation between the system and the user. The display of information could be held constant, or 'fixed', leaving the user with the task of searching through all of the available information, integrating it, and classifying the data into a known system state. On the other hand, the system, based on its own intelligent diagnosis, could display only relevant information in order to reduce the user's search set. The user would still be left the task of perceiving and integrating the data and classifying it into the appropriate system state. Finally, the system could display the patterns of data. In this scenario, the task of integrating the data is carried out by the system, and the user's information processing load is reduced, leaving only the tasks of perception and classification of the patterns of data. Humans are especially adept at this form of display processing. Although others have examined the relative effectiveness of alphanumeric and graphical display formats, it is interesting to reexamine this issue together with the function allocation problem. Currently, Johnson Space Center is the test site for an intelligent Thermal Control System (TCS), TEXSYS, being tested for use with Space Station Freedom. Expert TCS engineers, as well as novices, were asked to classify several displays of TEXSYS data into various system states (including nominal and anomalous states). Three different display formats were used: fixed, subset, and graphical. The hypothesis tested was that the graphical displays would provide for fewer errors and faster classification times by both experts and novices, regardless of the kind of system state represented within the display. The subset displays were hypothesized to be the second most effective display format/function allocation condition, based on the fact that the search set is reduced in these displays. Both the subset and the graphic display conditions were hypothesized to be processed more efficiently than the fixed display conditions. Author (revised)

N94-24190*# Lockheed Engineering and Sciences Co., Houston, TX.
THE USE OF ANALYTICAL MODELS IN HUMAN-COMPUTER INTERFACE DESIGN
Leo Gugerty *In* NASA. Johnson Space Center, Crew Interface Analysis: Selected Articles on Space Human Factors Research, 1987 - 1991 Jul. 1993 p 36-44 (For primary document see N94-24185 06-54)
Avail: CASI HC A02/MF A02; 5 functional color pages

Recently, a large number of human-computer interface (HCI) researchers have investigated building analytical models of the user, which are often implemented as computer models. These models simulate the cognitive processes and task knowledge of the user in ways that allow a researcher or designer to estimate various aspects of an interface's usability, such as when user errors are likely to occur. This information can lead to design improvements. Analytical models can supplement design guidelines by providing designers rigorous ways of analyzing the information-processing requirements of specific tasks (i.e., task analysis). These models offer the potential of improving early designs and replacing some of the early phases of usability testing, thus reducing the cost of interface design. This paper describes some of the many analytical models that are currently being developed and evaluates the usefulness of analytical models for human-computer interface design. This paper will focus on computational, analytical models, such as the GOMS model, rather than less formal, verbal models, because the more exact predictions and task descriptions of computational models may be useful to designers. The paper also discusses some of the practical requirements for using analytical models in complex design organizations such as NASA. Derived from text

N94-24191*# National Aeronautics and Space Administration. Lyndon B. Johnson Space Center, Houston, TX.
USING COMPUTER GRAPHICS TO DESIGN SPACE STATION FREEDOM VIEWING
Betty S. Goldsberry (Lockheed Engineering and Sciences Co., Houston, TX.), Buddy O. Lippert (Lockheed Engineering and Sciences Co., Houston, TX.), Sandra D. McKee (Lockheed Engineering and Sciences Co., Houston, TX.), James L. Lewis, Jr., and Francis E. Mount *In its* Crew Interface Analysis: Selected Articles on Space Human Factors Research, 1987 - 1991 Jul. 1993 p 47-51 (For primary document see N94-24185 06-54)
Avail: CASI HC A01/MF A02; 5 functional color pages

Viewing requirements were identified early in the Space Station Freedom program for both direct viewing via windows and indirect viewing via cameras and closed-circuit television (CCTV). These requirements reside in NASA Program Definition and Requirements Document (PDRD), Section 3: Space Station Systems Requirements. Currently, analyses are addressing the feasibility of direct and indirect viewing. The goal of these analyses is to determine the optimum locations for the windows, cameras, and CCTV's in order to meet established requirements, to adequately support space station assembly, and to operate on-board equipment. PLAID, a three-dimensional computer graphics program developed at NASA JSC, was selected for use as the major tool in these analyses. PLAID provides the capability to simulate the assembly of the station as well as to examine operations as the station evolves. This program has been used successfully as a tool to analyze general viewing conditions for many Space Shuttle elements and can be used for virtually all Space Station components. Additionally, PLAID provides the ability to integrate an anthropometric scale-modeled human (representing a crew member) with interior and exterior architecture. Author (revised)

N94-24192*# National Aeronautics and Space Administration. Lyndon B. Johnson Space Center, Houston, TX.
A SIMULATION SYSTEM FOR SPACE STATION EXTRAVEHICULAR ACTIVITY
Jose A. Marmolejo and Chip Shepherd (Lockheed Engineering and Sciences Co., Houston, TX.) *In its* Crew Interface Analysis: Selected Articles on Space Human Factors Research, 1987 - 1991 Jul. 1993 p 52-58 (For primary document see N94-24185 06-54)
Avail: CASI HC A02/MF A02; 5 functional color pages

America's next major step into space will be the construction of a permanently manned Space Station which is currently under development and scheduled for full operation in the mid-1990's. Most of the construction of the Space Station will be performed over several flights by suited crew members during an extravehicular activity (EVA) from the Space Shuttle. Once fully operational, EVA's will be performed from the Space Station on a routine basis to provide, among other services, maintenance and repair operations of satellites currently in Earth orbit. Both voice recognition and helmet-mounted display technologies can improve the productivity of workers in space by potentially reducing the time, risk, and cost involved in performing EVA. NASA has recognized this potential and is currently developing a voice-controlled information system for Space Station EVA. Two bench-model helmet-mounted displays and an EVA simulation program have been developed to demonstrate the functionality and practicality of the system. Author (revised)

N94-24193*# Lockheed Engineering and Sciences Co., Houston, TX.
USE OF INFRARED TELEMETRY AS PART OF A NONINTRUSIVE INFLIGHT DATA COLLECTION SYSTEM TO COLLECT HUMAN FACTORS DATA
Angelo Micocci *In* NASA. Johnson Space Center, Crew Interface Analysis: Selected Articles on Space Human Factors Research, 1987 - 1991 Jul. 1993 p 59-63 (For primary document see N94-24185 06-54)
Avail: CASI HC A01/MF A02; 5 functional color pages

The objective of this paper is to present a methodology and rationale for development of a Nonintrusive Inflight Data Collection System (NIDCS) to collect Human Factors (HF) data during a space mission. These data will enable the research team to identify and resolve issues. This paper will present the background and history of the NIDCS, the methodology and techniques employed versus those in current use on Earth, initial results of the effort--including a brief description of the equipment, and, finally, a discussion of the scientific importance and possible future applications of this system elsewhere. The schema for the NIDCS includes a collection of three types of data: behavioral, physiological, and biomechanical. These will be collected using videotape of crew members' activities, bioelectric signal measurement, and measurement of kinematics and kinetics, respectively. This paper will focus on the second type of data, physiological activity as determined by changes in bioelectric potentials as crew members perform daily assignments. Author (revised)

N94-24194*# Lockheed Engineering and Sciences Co., Houston, TX.
PERFORMING SPEECH RECOGNITION RESEARCH WITH HYPERCARD
c32
Chip Shepherd *In* NASA. Johnson Space Center, Crew Interface Analysis: Selected Articles on Space Human Factors Research, 1987 - 1991 Jul. 1993 p 64-67 (For primary document see N94-24185 06-54)
Avail: CASI HC A01/MF A02; 5 functional color pages

The purpose of this paper is to describe a HyperCard-based system for performing speech recognition research and to instruct Human Factors professionals on how to use the system to obtain detailed data about the user interface of a prototype speech recognition application. Author

N94-24195*# National Aeronautics and Space Administration. Lyndon B. Johnson Space Center, Houston, TX.
ILLUMINATION REQUIREMENTS FOR OPERATING A SPACE REMOTE MANIPULATOR
George O. Chandlee (Lockheed Engineering and Sciences Co., Houston, TX.), Randy L. Smith (Lockheed Engineering and Sciences Co., Houston, TX.), and Charles D. Wheelwright *In its* Crew Interface Analysis: Selected Articles on Space Human Factors Research, 1987 - 1991 Jul. 1993 p 68-72 (For primary document see N94-24185 06-54)
(Contract NAS9-17900)
Avail: CASI HC A01/MF A02; 5 functional color pages

Critical issues and requirements involved in illuminating remote manipulator operations in space help establish engineering designs for these manipulators. A remote manipulator is defined as any mechanical device that is controlled indirectly or from a distance by a human operator for the purpose of performing potentially dangerous or hazardous tasks to increase safety, reliability, and efficiency. Future space flights will rely on remote manipulators for a variety of tasks including satellite repair and servicing, structural assembly, data collection and analysis, and performance of contingency tasks. Carefully designed illumination of these manipulators will assure that these tasks will be completed efficiently and successfully. Studies concerning the influence of illumination on operation of a remote manipulator are few. Available results show that illumination can influence how successfully a human operates a remote manipulator. The intent of this study was to more fully examine this topic. Author (revised)

N94-24196*# National Aeronautics and Space Administration. Lyndon B. Johnson Space Center, Houston, TX.
PREVIOUS EXPERIENCE IN MANNED SPACE FLIGHT: A SURVEY OF HUMAN FACTORS LESSONS LEARNED
George O. Chandlee (Lockheed Engineering and Sciences Co., Houston, TX.) and Barbara Woolford *In its* Crew Interface Analysis: Selected Articles on Space Human Factors Research, 1987 - 1991 Jul. 1993 p 73-77 (For primary document see N94-24185 06-54)
(Contract NAS9-17900)
Avail: CASI HC A01/MF A02; 5 functional color pages

Previous experience in manned space flight programs can be used to compile a data base of human factors lessons learned for the purpose of developing aids in the future design of inhabited spacecraft. The objectives are to gather information available from relevant sources, to develop a taxonomy of human factors data, and to produce a data base that can be used in the future for those people involved in the design of manned spacecraft operations. A study is currently underway at the Johnson Space Center with the objective of compiling, classifying, and summarizing relevant human factors data bearing on the lessons learned from previous manned space flights. The research reported defines sources of data, methods for collection, and proposes a classification for human factors data that may be a model for other human factors disciplines. Author (revised)

N94-24197*# National Aeronautics and Space Administration. Lyndon B. Johnson Space Center, Houston, TX.
HAND CONTROLLER COMMONALITY EVALUATION PROCESS
Mark A. Stuart (Lockheed Engineering and Sciences Co., Houston, TX.), John M. Bierschwale (Lockheed Engineering and Sciences Co., Houston, TX.), Robert P. Wilmington (Lockheed Engineering and Sciences Co., Houston, TX.), Susan C. Adam (Lockheed Engineering and Sciences Co., Houston, TX.), Manuel F. Diaz (Lockheed Engineering and Sciences Co., Houston, TX.), and Dean G. Jensen *In its* Crew Interface Analysis: Selected Articles on Space Human Factors Research, 1987 - 1991 Jul. 1993 p 79-84 (For primary document see N94-24185 06-54)
Avail: CASI HC A02/MF A02; 5 functional color pages

Hand controller selection for NASA's Orbiter and Space Station Freedom is an important area of human-telerobot interface design and evaluation. These input devices will control remotely operated systems that include large crane-like manipulators (e.g., Remote Manipulator System or RMS), smaller, more dexterous manipulators (e.g., Flight Telerobotic Servicer or FTS), and free flyers (e.g., Orbital Maneuvering Vehicle or OMV). Candidate hand controller configurations for these systems vary in many ways: shape, size, number of degrees-of-freedom (DOF), operating modes, provision of force reflection, range of movement, and 'naturalness' of use. Unresolved design implementation issues remain, including such topics as how the current Orbiter RMS rotational and translational rate hand controllers compare with the proposed Space Station Freedom hand controllers, the advantages that position hand controllers offer for these applications, and whether separate hand controller configurations are required for each application. Since previous studies contain little empirical hand controller task performance data, a controlled study is needed that tests Space Station Freedom candidate hand controllers during representative tasks. This study also needs to include anthropometric and biomechanical considerations. Author (revised)

N94-24198*# Lockheed Engineering and Sciences Co., Houston, TX.
PROGRAMMABLE DISPLAY PUSHBUTTONS ON THE SPACE STATION'S TELEROBOT CONTROL PANEL
Mark A. Stuart, Randy L. Smith, and Ervette P. Moore *In* NASA. Johnson Space Center, Crew Interface Analysis: Selected Articles on Space Human Factors Research, 1987 - 1991 Jul. 1993 p 85-90 (For primary document see N94-24185 06-54)
(Contract NAS9-17900)
Avail: CASI HC A02/MF A02; 5 functional color pages

The Man-Systems Telerobotics Laboratory at NASA's Johnson Space Center and supported by Lockheed, is working to ensure that the Flight Telerobotic Servicer (FTS) to be used on the Space Shuttle (Orbiter) and the Space Station has a well designed user interface from a Human Factors perspective. The FTS, which is a project led by NASA's Goddard Space Flight Center, will be a telerobot used for Space Station construction, maintenance, and satellite repair. It will be directly controlled from workstations on the Orbiter and the Space Station and monitored from a ground workstation. The FTS will eventually evolve into a more autonomous system, but in the short-term the system will be manually operated (teleoperated) for many tasks. This emphasizes the importance of the human/telerobot interface on this system. This phase of the FTS workstation evaluation covers a preliminary study of programmable display pushbuttons (PDP's). The PDP is constructed of a matrix of directly addressable electroluminescent (EL) pixels which can be used to form dot-matrix characters. PDP's can be used to display more than one message and to control more than one function. Since the PDP's have these features, then a single PDP may possibly replace the use of many single-function pushbuttons, rotary switches, and toggle switches, thus using less panel space. It is of interest to determine if PDP's can be used to adequately perform complex hierarchically structured task sequences. The objective of this investigation was to compare the performance of experienced and inexperienced Remote Manipulator System (RMS) operators while performing an RMS like task on simulated PDP and non-PDP computer prototypes so that guidelines governing the use of programmable display pushbuttons on the FTS workstation could be created. The functionality of the RMS on the Orbiter was used as a model for this evaluation since the functionality

of the FTS at the time of this writing has not been solidified.
Author (revised)

N94-24199*# Lockheed Engineering and Sciences Co., Houston, TX.
SPEECH VERSUS MANUAL CONTROL OF CAMERA FUNCTIONS DURING A TELEROBOTIC TASK
John M. Bierschwale, Carlos E. Sampaio, Mark A. Stuart, and Randy L. Smith *In* NASA. Johnson Space Center, Crew Interface Analysis: Selected Articles on Space Human Factors Research, 1987 - 1991 Jul. 1993 p 91-97 (For primary document see N94-24185 06-54)
(Contract NAS9-17900)
Avail: CASI HC A02/MF A02; 5 functional color pages

This investigation has evaluated the voice-commanded camera control concept. For this particular task, total voice control of continuous and discrete camera functions was significantly slower than manual control. There was no significant difference between voice and manual input for several types of errors. There was not a clear trend in subjective preference of camera command input modality. Task performance, in terms of both accuracy and speed, was very similar across both levels of experience.
Derived from text

N94-24200*# Lockheed Engineering and Sciences Co., Houston, TX.
SPACE STATION FREEDOM COUPLING TASKS: AN EVALUATION OF THEIR TELEROBOTIC AND EVA COMPATIBILITY
Carlos E. Sampaio, John M. Bierschwale, Terence F. Fleming, and Mark A. Stuart *In* NASA. Johnson Space Center, Crew Interface Analysis: Selected Articles on Space Human Factors Research, 1987 - 1991 Jul. 1993 p 98-103 (For primary document see N94-24185 06-54)
(Contract NAS9-17900)
Avail: CASI HC A02/MF A02; 5 functional color pages

Of the couplings included in this study, several design components were found to be of interest. With respect to the operation of the couplings, the various concepts resulted in differing reactions from the four subjects who participated in this study. The purpose of this study was not to conceive the final coupling design. Rather, it was intended as a step along an interactive process. The newly modified coupling will be included in a series of further controlled, as well as subjective, evaluations. This part of the ongoing work in the Remote Operator Interaction Laboratory (ROIL) designed to enhance the overall interface by improving design at both the teleoperator and telerobot ends of the system.
Derived from text

N94-24201*# Lockheed Engineering and Sciences Co., Houston, TX.
THE EFFECTS OF SPATIALLY DISPLACED VISUAL FEEDBACK ON REMOTE MANIPULATOR PERFORMANCE
Randy L. Smith and Mark A. Stuart *In* NASA. Johnson Space Center, Crew Interface Analysis: Selected Articles on Space Human Factors Research, 1987 - 1991 Jul. 1993 p 104-110 (For primary document see N94-24185 06-54)
(Contract NAS9-17900)
Avail: CASI HC A02/MF A02; 5 functional color pages

The results of this evaluation have important implications for the arrangement of remote manipulation worksites and the design of workstations for telerobot operations. This study clearly illustrates the deleterious effects that can accompany the performance of remote manipulator tasks when viewing conditions are less than optimal. Future evaluations should emphasize telerobot camera locations and the use of image/graphical enhancement techniques in an attempt to lessen the adverse effects of displaced visual feedback. An important finding in this evaluation is the extent to which results from previously performed direct manipulation studies can be generalized to remote manipulation studies. Even though the results obtained were very similar to those of the direct manipulation evaluations, there were differences as well. This evaluation has demonstrated that generalizations to remote manipulation applications based upon the results of direct manipulation studies are quite useful, but they should be made cautiously.
Derived from text

N94-24202*# Lockheed Engineering and Sciences Co., Houston, TX.
SIMULATION OF THE HUMAN-TELEROBOT INTERFACE ON THE SPACE STATION
Mark A. Stuart and Randy L. Smith *In* NASA. Johnson Space Center, Crew Interface Analysis: Selected Articles on Space Human Factors Research, 1987 - 1991 Jul. 1993 p 111-115 (For primary document see N94-24185 06-54)
(Contract NAS9-17900)
Avail: CASI HC A02/MF A02; 5 functional color pages

Many issues remain unresolved concerning the components of the human-telerobot interface presented in this work. It is critical that these components be optimally designed and arranged to ensure, not only that the overall system's goals are met, but but that the intended end-user has been optimally accommodated. With sufficient testing and evaluation throughout the development cycle, the selection of the components to use in the final telerobotic system can promote efficient, error-free performance. It is recommended that whole-system simulation with full-scale mockups be used to help design the human-telerobot interface. It is contended that the use of simulation can facilitate this design and evaluation process.
Derived from text

N94-24203*# Lockheed Engineering and Sciences Co., Houston, TX.
QUANTITATIVE ASSESSMENT OF HUMAN MOTION USING VIDEO MOTION ANALYSIS
John D. Probe *In* NASA. Johnson Space Center, Crew Interface Analysis: Selected Articles on Space Human Factors Research, 1987 - 1991 Jul. 1993 p 119-121 (For primary document see N94-24185 06-54)
Avail: CASI HC A01/MF A02; 5 functional color pages

In the study of the dynamics and kinematics of the human body a wide variety of technologies has been developed. Photogrammetric techniques are well documented and are known to provide reliable positional data from recorded images. Often these techniques are used in conjunction with cinematography and videography for analysis of planar motion, and to a lesser degree three-dimensional motion. Cinematography has been the most widely used medium for movement analysis. Excessive operating costs and the lag time required for film development, coupled with recent advances in video technology, have allowed video based motion analysis systems to emerge as a cost effective method of collecting and analyzing human movement. The Anthropometric and Biomechanics Lab at Johnson Space Center utilizes the video based Ariel Performance Analysis System (APAS) to develop data on shirtsleeved and space-suited human performance in order to plan efficient on-orbit intravehicular and extravehicular activities. APAS is a fully integrated system of hardware and software for biomechanics and the analysis of human performance and generalized motion measurement. Major components of the complete system include the video system, the AT compatible computer, and the proprietary software.
Derived from text

N94-24204*# National Aeronautics and Space Administration. Lyndon B. Johnson Space Center, Houston, TX.
REACH PERFORMANCE WHILE WEARING THE SPACE SHUTTLE LAUNCH AND ENTRY SUIT DURING EXPOSURE TO LAUNCH ACCELERATIONS
James P. Bagian, Michael C. Greenisen, Lauren E. Schafer (Lockheed Engineering and Sciences Co., Houston, TX.), John D. Probe (Lockheed Engineering and Sciences Co., Houston, TX.), and Robert W. Krutz, Jr. (Krug International, Houston, TX.) *In its* Crew Interface Analysis: Selected Articles on Space Human Factors Research, 1987 - 1991 Jul. 1993 p 122-125 (For primary document see N94-24185 06-54)
Avail: CASI HC A01/MF A02; 5 functional color pages

Crewmen aboard the Space Shuttle are subjected to accelerations during ascent (the powered flight phase of launch) which range up to +3 G(sub x). Despite having 33 missions and nine years experience, not to mention all the time spent in development prior to the first flight, no truly quantitative reach study wearing actual crew equipment, using actual Shuttle seats and restraints has ever been done. What little information exists on reach performance while under acceleration has been derived primarily from subjective comments gathered retrospectively from Shuttle flight crews during their post mission debrief. This lack of reach performance data has resulted in uncertainty regarding emergency procedures that can realistically be performed during and actual Shuttle ascent versus what is practiced in the ground-fixed and motion-based Shuttle Simulators. With the introduction on STS-26 of the current Shuttle escape system, the question of reach performance under launch accelerations was once again raised. The escape system's requirement that each crewman wear a Launch/Entry Suit (LES), parachute harness, and parachute were all anticipated to contribute to a further degradation of reach performance during Shuttle ascent accelerations.

In order to answer the reach performance question in a quantitative way, a photogrammetric method was chosen so that the actual reach values and associated envelopes could be captured. This would allow quantitative assessment of potential task performance impact and identify areas where changes to our Shuttle ascent emergency procedures might be required. Also, such a set of reach values would be valid for any similar acceleration profile using the same crew equipment. Potential Space Station applications of this data include predicting reach performance during Assured Crew Return Vehicle (ACRV) operations. Derived from text

N94-24205*# National Aeronautics and Space Administration. Lyndon B. Johnson Space Center, Houston, TX.

DEVELOPMENT OF BIOMECHANICAL MODELS FOR HUMAN FACTORS EVALUATIONS

Barbara Woolford, Abhilash Pandya (Lockheed Engineering and Sciences Co., Houston, TX.), and James Maida (Lockheed Engineering and Sciences Co., Houston, TX.) *In its* Crew Interface Analysis: Selected Articles on Space Human Factors Research, 1987 - 1991 Jul. 1993 p 126-131
(For primary document see N94-24185 06-54)
Avail: CASI HC A02/MF A02; 5 functional color pages

Computer aided design (CAD) techniques are now well established and have become the norm in many aspects of aerospace engineering. They enable analytical studies, such as finite element analysis, to be performed to measure performance characteristics of the aircraft or spacecraft long before a physical model is built. However, because of the complexity of human performance, CAD systems for human factors are not in widespread use. The purpose of such a program would be to analyze the performance capability of a crew member given a particular environment and task. This requires the design capabilities to describe the environment's geometry and to describe the task's requirements, which may involve motion and strength. This in turn requires extensive data on human physical performance which can be generalized to many different physical configurations. PLAID is developing into such a program. Begun at Johnson Space Center in 1977, it was started to model only the geometry of the environment. The physical appearance of a human body was generated, and the tool took on a new meaning as fit, access, and reach could be checked. Specification of fields-of-view soon followed. This allowed PLAID to be used to predict what the Space Shuttle cameras or crew could see from a given point. Derived from text

N94-24206*# National Aeronautics and Space Administration. Lyndon B. Johnson Space Center, Houston, TX.

ESTABLISHING A RELATIONSHIP BETWEEN MAXIMUM TORQUE PRODUCTION OF ISOLATED JOINTS TO SIMULATE EVA RATCHET PUSH-PULL MANEUVER: A CASE STUDY

Abhilash Pandya (Lockheed Engineering and Sciences Co., Houston, TX.), James Maida (Lockheed Engineering and Sciences Co., Houston, TX.), Scott Hasson (Texas Univ., Houston.), Michael Greenisen, and Barbara Woolford *In its* Crew Interface Analysis: Selected Articles on Space Human Factors Research, 1987 - 1991 Jul. 1993 p 132-135 (For primary document see N94-24185 06-54)
Avail: CASI HC A01/MF A02; 5 functional color pages

As manned exploration of space continues, analytical evaluation of human strength characteristics is critical. These extraterrestrial environments will spawn issues of human performance which will impact the designs of tools, work spaces, and space vehicles. Computer modeling is an effective method of correlating human biomechanical and anthropometric data with models of space structures and human work spaces. The aim of this study is to provide biomechanical data from isolated joints to be utilized in a computer modeling system for calculating torque resulting from any upper extremity motions: in this study, the ratchet wrench push-pull operation (a typical extravehicular activity task). Established here are mathematical relationships used to calculate maximum torque production of isolated upper extremity joints. These relationships are a function of joint angle and joint velocity. Derived from text

N94-24292# National Defence Research Establishment, Umea (Sweden). NBC Defence Dept.

TOWARDS A NEW RADIATION PROTECTION ORGANIZATION [PAA VAEG MOT EN NY RADIAKSKYDDSORGANISATION]

Tor Larsson, Gunnar Persson, Thomas Ulvsand, Kay Edvarson (Statens Straalskyddinst., Stockholm, Sweden.), Rolf Hellman (Statens Straalskyddinst., Stockholm, Sweden.), Aake Persson (Statens Straalskyddinst., Stockholm, Sweden.), Ingela Flink (National Rescue Services Board, Sweden.), Enrico Lundin (National Rescue Services Board, Sweden.), and Lena Tistad (National Rescue Services Board, Sweden.) Jan. 1993 34 p In SWEDISH
(FOA-C-40304-4.3; ETN-93-94490) Avail: CASI HC A03/MF A01; National Defence Research Establishment, S-901 82 Umea, Sweden, HC

Work has been initiated to create a new protection organization for warning and mapping in radioactive fallout situations in Sweden. This organization should be the same in peace, crises and war and be able to deal with fallout, both from accidents in nuclear power stations and nuclear weapons explosions. The two present organizations, one for peace and one for war, will be substituted by the common organization. The first steps in this work are described. A description of the two present organizations is made and they are compared for two different fallout levels. This comparison is evaluated and some proposals are made for the local and regional organizations level. ESA

N94-24299 Defence and Civil Inst. of Environmental Medicine, Downsview (Ontario).

COMPUTER CONTROL OF AN ELECTRO-MECHANCIAL REGULATOR FOR PROVIDING POSITIVE PRESSURE BREATHING AND AN ELECTRONIC G-VALVE FOR HUMAN +Gz RESEARCH

M. Pecaric, F. Buick, and J. Maloan Jan. 1993 48 p
(DCIEM-93-05; CTN-94-60912) Copyright Avail: Micromedia Ltd., Technical Information Centre, 165 Hotel de Ville, Place du Portage, Phase 2, Hull, Quebec J8X 3X2, Canada

Electronic G-valves and breathing regulators are being incorporated into some life support systems designed for aircrew protection. An electronically controlled G-valve and electromechanical breathing regulator were obtained and a prototype, computer controlled, life support system interface was developed and evaluated in the centrifuge. The interface was used to provide different schedules for G-suit inflation and positive pressure breathing during +Gz (PBG). Output pressures from both a G-valve and breathing regulator were driven by a voltage proportional to the centrifuge +Gz level. The required voltages were calculated from the pressure schedule. The schedules and performance of the G-valve and breathing regulator were also evaluated at different +Gz onset rates. G-suit pressure and PBG level accurately tracked the +Gz level. Outputs of both G-valve and breathing regulator reached maximum pressure within 0.2 seconds of reaching the peak +Gz level. The greatest tracking errors occurred during onset to peak +Gz with 3.0 +Gz/second profiles, most of the error being attributed to the slow response of the controller software. Author (CISTI)

N94-24329*# EXOS, Inc., Woburn, MA.

DEVELOPMENT OF A FORCE FEEDBACK ANTHROPOMORPHIC TELEOPERATION INPUT DEVICE FOR CONTROL OF ROBOT HANDS

Progress Report, 1 Oct - 31 Dec. 1993

4 Feb. 1994 11 p
(Contract NAS8-39364)
(NASA-CR-195109; NAS 1.26:195109) Avail: CASI HC A03/MF A01

During the last period, the objectives specified in our last quarterly report were completed: integrated the thumb mechanism/actuator package simulation and VK software; tested the thumb mechanism/actuator package performance; designed the index finger and thumb actuation package; and developed concepts for the wrist mechanism. Author (revised)

N94-24330*# Texas Univ., Austin.

CONCEPTUAL DESIGN OF A DEVICE TO MEASURE HAND SWELLING IN A MICRO-GRAVITY ENVIRONMENT

Christopher L. Hysinger 12 Mar. 1993 19 p
(Contract NASw-4435)
(NASA-CR-195509; NAS 1.26:195509) Avail: CASI HC A03/MF A01

In the design of pressurized suits for use by astronauts in space, proper fit is an important consideration. One particularly difficult aspect of the suit design is the design of the gloves. If the gloves of the suit do not fit properly, the grip strength of the astronaut can be decreased by as much as fifty percent. These gloves are designed using an iterative process and can cost over 1.5 million dollars. Glove design is further complicated by the way the body behaves in a micro-gravity environment. In a micro-gravity setting, fluid from the lower body tends to move into the upper body. Some of this fluid collects in the hands and causes the hands to swell. Therefore, a pair of gloves that fit well on earth may not fit well when they are used in space. The conceptual design process for a device which can measure the swelling that occurs in the hands in a micro-gravity environment is described. This process involves developing a specifications list and function structure for the device and generating solution variants for each of the sub functions. The solution variants are then filtered, with the variants that violate any of the specifications being discarded. After acceptable solution variants are obtained, they are combined to form design concepts. These design concepts are evaluated against a set of criteria and the design concepts are ranked in order of preference. Through this process, the two most plausible design concepts were an ultrasonic imaging technique and a laser mapping technique. Both of these methods create a three dimensional model of the hand, from which the amount of swelling can be determined. In order to determine which of the two solutions will actually work best, a further analysis will need to be performed. Author (revised)

N94-24331*# Texas Univ., Austin.
NASA PROJECT 1: FULL-BODY DYNAMOMETER
Li-Dai Lu 2 Jun. 1993 11 p
(Contract NASw-4435)
(NASA-CR-195507; NAS 1.26:195507) Avail: CASI HC A03/MF A01

In space, where the body does only a fraction of work it does on earth, muscle atrophy is a major concern. The bones and the muscles will begin to deteriorate after a short stay in weightlessness. Bone decalcification appears to be a major problem with extensive living in microgravity. Resistance exercise is not only essential to prevent muscle atrophy in space, it also helps to keep bone decalcification in check. For a space station, where the astronauts are expected to live for months at a time, exercise is especially important. Experts recommend about an hour and a half to two hours of exercise per day to keep the muscles in good condition in microgravity. The exercises will not only keep the astronauts in excellent physical condition, it will also make it easier for them to readjust to earth's gravity on return. The stationary bicycle and the treadmill have been the astronauts' primary sources of exercise since the 1970's. The major problem with both the stationary bicycle and the treadmill is that while they may keep the leg muscles from deteriorating in microgravity, they do little for muscles in the upper body. The National Aeronautics and Space Administration (NASA) is currently developing a full-body dynamometer (FBD), which will provide the astronauts with a full-body workout. It will also test the astronauts for muscle atrophy and rehabilitate the weakened muscle. The specification and the function structure for the FBD is presented. Author (revised)

N94-24667*# Texas Univ., Austin. Mechanical Engineering Dept.
CONCEPTS AND EMBODIMENT DESIGN OF A REENTRY RECUMBENT SEATING SYSTEM FOR THE NASA SPACE SHUTTLE
Scott McMillan, Brent Looby, Chris Devany, Chris Chudej, and Barry Brooks 3 May 1993 53 p
(Contract NASw-4435)
(NASA-CR-195504; NAS 1.26:195504) Avail: CASI HC A04/MF A01

This report deals with the generation of a recumbent seating system which will be used by NASA to shuttle astronauts from the Russian space station Mir. We begin by examining the necessity for designing a special couch for the returning astronauts. Next, we discuss the operating conditions and constraints of the recumbent seating system and provide a detailed function structure. After working through the conceptual design process, we came up with ten alternative designs which are presented in the appendices. These designs were evaluated and weighted to systematically determine the best choice for embodiment design. A detailed discussion of all components of the selected system follows with design calculations for the seat presented in the appendices. The report concludes with an evaluation of the resulting design and recommendations for further development. Author

N94-24706*# Harvard Univ., Cambridge, MA. Div. of Applied Sciences.
MICROBIAL BIOFILM FORMATION AND ITS CONSEQUENCES FOR THE CELSS PROGRAM Final Report
R. Mitchell 31 Jan. 1994 4 p
(Contract NCC2-628)
(NASA-CR-195146; NAS 1.26:195146) Avail: CASI HC A01/MF A01

A major goal of the Controlled Ecology Life Support System (CELSS) program is to provide reliable and efficient life support systems for long-duration space flights. A principal focus of the program is on the growth of higher plants in growth chambers. These crops should be grown without the risk of damage from microbial contamination. While it is unlikely that plant pathogens will pose a risk, there are serious hazards associated with microorganisms carried in the nutrient delivery systems and in the atmosphere of the growth chamber. Our experience in surface microbiology showed that colonization of surfaces with microorganisms is extremely rapid even when the inoculum is small. After initial colonization extensive biofilms accumulate on moist surfaces. These microbial films metabolize actively and slough off continuously to the air and water. During plant growth in the CELSS program, microbial biofilms have the potential to foul sensors and to plug nutrient delivery systems. In addition both metabolic products of microbial growth and degradation products of materials being considered for use as nutrient reservoirs and for delivery are likely sources of chemicals known to adversely affect plant growth. Author (revised)

N94-24786*# Texas Univ., Austin. Mechanical Engineering Dept.
DESIGN OF A RECUMBENT SEATING SYSTEM
Scott Croyle, Jose DeLaRosa, Daren George, Cathy Hinkle, and Stephen Karas 3 May 1993 61 p
(Contract NASw-4435)
(NASA-CR-195503; NAS 1.26:195503) Avail: CASI HC A04/MF A01

Future space shuttle missions presented by NASA might require the shuttle to rendezvous with the Russian space station Mir for the purpose of transporting astronauts back to earth. Due to the atrophied state of these astronauts, a special seating system must be designed for their transportation. The main functions of this seating system are to support and restrain the astronauts during normal reentry flight and to dampen some of the loading that might occur in a crash situation. Through research, the design team developed many concept variants for these functional requirements. By evaluating each variant, the concepts were eliminated until the four most attractive designs remained. The team used a decision matrix to determine the best concept to carry through embodiment. This concept involved using struts for support during reentry flight and a spring damper/shock absorber system to dampen crash landing loads. The embodiment design process consisted of defining the layout of each of the main functional components, specifically, the seat structure and the strut structure. Through the use of MCS/pal two, the design was refined until it could handle all required loads and dampen to the forces specified. The auxiliary function carriers were then considered. Following the design of these components, the complete final layout could be determined. It is concluded that the final design meets all specifications outlined in the conceptual design. The main advantages of this design are its low weight, simplicity, and large amount of function sharing between different components. The disassembly of this design could potentially present a problem because of time and size constraints involved. Overall, this design meets or exceeds all functional requirements. Author (revised)

N94-24830# Galaxy Scientific Corp., Pleasantville, NJ.
PILOT-VEHICLE INTERFACE HANDBOOK, CHAPTER 19. VOLUME 2: DIGITAL SYSTEMS VALIDATION
L. Harrison, J. Janowitz, and M. Castronuovo Nov. 1993 118 p
(Contract DTFA03-89-C-0043)
(DOT/FAA/CT-88/10-Vol-2) Avail: CASI HC A06/MF A02

The cockpits of the early transport aircraft were quite different from those produced today. Older cockpits contained numerous 'steam gauge' style indicators. As technology advanced, these older electromechanical indicators were gradually replaced by newer, more reliable digital systems. Digital flight control and avionic systems are being used increasingly in modern aircraft. This trend yields cockpits of greater complexity and has swelled the amount of information with which the crew must deal. The way the pilot controls and monitors the state of the aircraft has also been greatly influenced by the increased use of digital systems. Additionally, new methods of aircraft system monitoring and control are being researched and implemented. These systems use new display technology, programmable display formats, voice input and output, and other new input and control devices. Systems and their cockpit interfaces were added as technological advances were made and new requirements generated. The human interface was given little consideration in the layout of the cockpit. Human qualities and failure modes were not taken into account in the cockpit design process. As the number of systems, components, indicators, and switches multiplied, the potential for error also grew. The emphasis of this report is on civil transport aircraft. This includes technologies such as display, control, and design methodologies, along with human factors concerns. The report consists of four sections: civil transport cockpit, cockpit standards, cockpit technology, and cockpit human factors. This report is to serve as a guide to Certification Engineers who are faced with the task of certification of new cockpit technologies. Author (revised)

N94-24835*# Texas Univ., Austin.
SPECIFICATION LIST AND FUNCTION STRUCTURE FOR A FULL-BODY DYNAMOMETER TO BE USED ABOARD SPACE STATION FREEDOM
Robert McMahan 19 Feb. 1993 11 p
(Contract NASw-4435)
(NASA-CR-195508; NAS 1.26:195508) Avail: CASI HC A03/MF A01

NASA has a need for a machine which can be used as an exercise device and as an instrument to measure an astronaut's muscle performance. The purpose of the exercise device is to work various muscle groups of the astronaut to prevent muscle atrophy, the loss of muscle strength and mass from prolonged exposure to a microgravity environment. The measurement part of the machine will be used to collect data on the strength and power of the astronaut's muscle groups to be used in studies examining the effects of prolonged space inhabitation. The principle device used in this machine to both exercise and measure muscle performance is the dynamometer. The dynamometer converts electrical energy to mechanical energy and mechanical energy to electrical energy or signals. The task of the designer will be to incorporate a dynamometer into a device which can meet all of the needs discussed above. This memorandum has two sections which clarify the design task of producing a full-body dynamometer. The first section is a specification list. The specification list provides the requirements that the designer must meet in his/her design. The second part is a function structure. The function structure shows graphically the flow of material, energy, and information through the machine. These two items will be used by the designer in the design process for the full-body dynamometer. Derived from text

N94-24857*# North Carolina Univ., Charlotte. Dept. of Mechanical Engineering and Engineering Science.
DESIGN AND SIMULATION OF EVA TOOLS FOR FIRST SERVICING MISSION OF HST Semiannual Report, 15 Jan. - 14 Jul. 1993
Dipak Naik and P. H. DeHoff 14 Jul. 1993 12 p
(Grant NAG5-2038)
(NASA-CR-194784; NAS 1.26:194784; TR-ME/ES-93-2) Avail: CASI HC A03/MF A01

The Hubble Space Telescope (HST) was launched into near-earth orbit by the space shuttle Discovery on April 24, 1990. The payload of two cameras, two spectrographs, and a high-speed photometer is supplemented by three fine-guidance sensors that can be used for astronomy as well as for star tracking. A widely reported spherical aberration in the primary mirror causes HST to produce images of much lower quality than intended. A space shuttle repair mission in late 1993 will install small corrective mirrors that will restore the full intended optical capability of the HST. The first servicing mission (FSM) will involve considerable extravehicular activity (EVA). It is proposed to design special EVA tools for the FSM. This report includes details of the data acquisition system being developed to test the performance of the various EVA tools in ambient as well as simulated space environment. Author (revised)

N94-24956*# Texas Univ., Austin. Dept. of Mechanical Engineering.
CONCEPTUAL DESIGN OF AN ASTRONAUT HAND ANTHROPOMETRY DEVICE
Robert McMahan 12 Mar. 1993 18 p
(Contract NASw-4435)
(NASA-CR-195490; NAS 1.26:195490) Avail: CASI HC A03/MF A01

In a microgravity environment, fluid equalizes throughout the body, causing the upper body to swell. This causes the hands to swell which can cause problems for astronauts trying to do work in pressurized EVA (extravehicular activity) gloves. To better design these gloves, accurate measurements of the astronauts swollen hands are needed. Five concepts were developed in this report from an original field of 972 possible concepts. These five concepts were based on mold impression, ultrasound, laser topography, white light photography, and video imaging. From a decision matrix based on nine weighted criteria, the video imaging technique was found to be the best design to pursue. Author (revised)

N94-25490*# National Aeronautics and Space Administration. Ames Research Center, Moffett Field, CA.
PROCEEDINGS OF THE WORKSHOP ON AUGMENTED VISUAL DISPLAY (AVID) RESEARCH
Mary K. Kaiser, ed. and Barbara T. Sweet, ed. Dec. 1993 428 p
Workshop held in Moffett Field, CA, 10-12 Mar. 1993
(RTOP 505-64-36)
(NASA-CP-10128; A-93123; NAS 1.55:10128) Avail: CASI HC A19/MF A04

The papers, abstracts, and presentations were presented at a three day workshop focused on sensor modeling and simulation, and image enhancement, processing, and fusion. The technical sessions emphasized how sensor technology can be used to create visual imagery adequate for aircraft control and operations. Participants from industry, government, and academic laboratories contributed to panels on Sensor Systems, Sensor Modeling, Sensor Fusion, Image Processing (Computer and Human Vision), and Image Evaluation and Metrics. For individual titles, see N94-25491 through N94-25514.

N94-25491*# FLIR Systems, Inc., Portland, OR.
INFRARED SENSORS AND SYSTEMS FOR ENHANCED VISION/AUTONOMOUS LANDING APPLICATIONS c74
J. Richard Kerr *In* NASA. Ames Research Center, Proceedings of the Workshop on Augmented Visual Display (AVID) Research Dec. 1993 p 5-27 (For primary document see N94-25490 06-54)
Avail: CASI HC A03/MF A04

There exists a large body of data spanning more than two decades, regarding the ability of infrared imagers to 'see' through fog, i.e., in Category III weather conditions. Much of this data is anecdotal, highly specialized, and/or proprietary. In order to determine the efficacy and cost effectiveness of these sensors under a variety of climatic/weather conditions, there is a need for systematic data spanning a significant range of slant-path scenarios. These data should include simultaneous video recordings at visible, midwave (3-5 microns), and longwave (8-12 microns) wavelengths, with airborne weather pods that include the capability of determining the fog droplet size distributions. Existing data tend to show that infrared is more effective than would be expected from analysis and modeling. It is particularly more effective for inland (radiation) fog as compared to coastal (advection) fog, although both of these archetypes are oversimplifications. In addition, as would be expected from droplet size vs wavelength considerations, longwave outperforms midwave, in many cases by very substantial margins. Longwave also benefits from the higher level of available thermal energy at ambient temperatures. The principal attraction of midwave sensors is that staring focal plane technology is available at attractive cost-performance levels. However, longwave technology such as that developed at FLIR Systems, Inc. (FSI), has achieved high performance in small, economical, reliable imagers utilizing serial-parallel scanning techniques. In addition, FSI has developed dual-waveband systems particularly suited for enhanced vision flight testing. These systems include a substantial, embedded processing capability which can perform video-rate image enhancement and multisensor fusion. This is achieved with proprietary algorithms and includes such operations as real-time histograms, convolutions, and fast Fourier transforms. Author (revised)

N94-25492*# Honeywell, Inc., Minneapolis, MN. Systems and Research Center.
SYNTHETIC VISION SYSTEM FLIGHT TEST RESULTS AND LESSONS LEARNED c53
Jeffrey Radke *In* NASA. Ames Research Center, Proceedings of the Workshop on Augmented Visual Display (AVID) Research Dec. 1993 p 29-45 (For primary document see N94-25490 06-54)
Avail: CASI HC A03/MF A04

Honeywell Systems and Research Center developed and demonstrated an active 35 GHz Radar Imaging system as part of the FAA/USAF/Industry sponsored Synthetic Vision System Technology Demonstration (SVSTD) Program. The objectives of this presentation are to provide a general overview of flight test results, a system level perspective that encompasses the efforts of the SVSTD and Augmented Visual Display (AVID) programs, and more importantly, provide the AVID workshop participants with Honeywell's perspective on the lessons that were learned from the SVS flight tests. One objective of the SVSTD program was to explore several known system issues concerning radar imaging technology. The program ultimately resolved some of these issues, left others open, and in fact created several new concerns. In some instances, the interested community has drawn improper conclusions from the program by globally attributing implementation specific issues to radar imaging technology in general. The motivation for this presentation is therefore to provide AVID researchers with a better understanding of the issues that truly remain open, and to identify the perceived issues that are either resolved or were specific to Honeywell's implementation. Author

N94-25493*# Lear Astronics Corp., Santa Monica, CA.
THE 94 GHz MMW IMAGING RADAR SYSTEM c32
Yair Alon and Lon Ulmer *In* NASA. Ames Research Center, Proceedings of the Workshop on Augmented Visual Display (AVID) Research Dec. 1993 p 47-60 (For primary document see N94-25490 06-54)
Avail: CASI HC A03/MF A04

The 94 GHz MMW airborne radar system that provides a runway image in adverse weather conditions is now undergoing tests at Wright-Patterson Air Force Base (WPAFB). This system, which consists of a solid state FMCW transceiver, antenna, and digital signal processor, has an update rate of 10 times per second, 0.35x azimuth resolution and up to 3.5 meter range resolution. The radar B scope (range versus azimuth) image, once converted to C scope (elevation versus azimuth), is compatible with the standard TV presentation and can be displayed on the Head Up Display (HUD) or Head Down Display (HDD) to aid the pilot during landing and takeoff in limited visibility conditions. Author (revised)

N94-25494*# TRW, Inc., Redondo Beach, CA. Applied Technology Div.
PASSIVE MILLIMETER-WAVE IMAGING c32
Stephen K. Young, Roger A. Davidheiser, Bruce Hauss, Paul S. C. Lee, Michael Mussetto, Merit M. Shoucri, and Larry Yujiri *In* NASA. Ames Research Center, Proceedings of the Workshop on Augmented Visual Display (AVID) Research Dec. 1993 p 61-78 (For primary document see N94-25490 06-54)
Avail: CASI HC A03/MF A04

Millimeter-wave hardware systems are being developed. Our approach begins with identifying and defining the applications. System requirements are then specified based on mission needs using our end-to-end performance model. The model was benchmarked against existing data bases and, where data is deficient, it is acquired via field measurements. The derived system requirements are then validated with the appropriate field measurements using our imaging testbeds and hardware breadboards. The result is a final system that satisfies all the requirements of the target mission. Author (revised)

N94-25495*# National Aeronautics and Space Administration. Ames Research Center, Moffett Field, CA.
APPLICATION OF AIRCRAFT NAVIGATION SENSORS TO ENHANCED VISION SYSTEMS c04
Barbara T. Sweet *In its* Proceedings of the Workshop on Augmented Visual Display (AVID) Research Dec. 1993 p 79-95 (For primary document see N94-25490 06-54)
Avail: CASI HC A03/MF A04

In this presentation, the applicability of various aircraft navigation sensors to enhanced vision system design is discussed. First, the accuracy requirements of the FAA for precision landing systems are presented, followed by the current navigation systems and their characteristics. These systems include Instrument Landing System (ILS), Microwave Landing System (MLS), Inertial Navigation, Altimetry, and Global Positioning System (GPS). Finally, the use of navigation system data to improve enhanced vision systems is discussed. These applications include radar image rectification, motion compensation, and image registration. Author

N94-25496*# Technology Service Corp., Santa Monica, CA.
THE IRGen INFRARED DATA BASE MODELER c82
Uri Bernstein *In* NASA. Ames Research Center, Proceedings of the Workshop on Augmented Visual Display (AVID) Research Dec. 1993 p 99-120 (For primary document see N94-25490 06-54)
Avail: CASI HC A03/MF A04

IRGen is a modeling system which creates three-dimensional IR data bases for real-time simulation of thermal IR sensors. Starting from a visual data base, IRGen computes the temperature and radiance of every data base surface with a user-specified thermal environment. The predicted gray shade of each surface is then computed from the user specified sensor characteristics. IRGen is based on first-principles models of heat transport and heat flux sources, and it accurately simulates the variations of IR imagery with time of day and with changing environmental conditions. The starting point for creating an IRGen data base is a visual faceted data base, in which every facet has been labeled with a material code. This code is an index into a material data base which contains surface and bulk thermal properties for the material. IRGen uses the material properties to compute the surface temperature at the specified time of day. IRGen also supports image generator features such as texturing and smooth shading, which greatly enhance image realism. Author

N94-25497*# Technology Service Corp., Santa Monica, CA.
THE RADAR IMAGE GENERATION (RIG) MODEL c32
Anthony J. Stenger *In* NASA. Ames Research Center, Proceedings of the Workshop on Augmented Visual Display (AVID) Research Dec. 1993 p 121-131 (For primary document see N94-25490 06-54)
Avail: CASI HC A03/MF A04

RIG is a modeling system which creates synthetic aperture radar (SAR) and inverse SAR images from 3-D faceted data bases. RIG is based on a physical optics model and includes the effects of multiple reflections. Both conducting and dielectric surfaces can be modeled; each surface is labeled with a material code which is an index into a data base of electromagnetic properties. The inputs to the program include the radar processing parameters, the target orientation, the sensor velocity, and (for inverse SAR) the target angle rates. The current version of RIG can be run on any workstation, however, it is not a real-time model. We are considering several approaches to enable the program to generate realtime radar imagery. In addition to its image generation function, RIG can also generate radar cross-section (RCS) plots as well as range and doppler radar return profiles. Author

N94-25498*# TRW, Inc., Redondo Beach, CA. Space and Electronics Group.
ADVANCED RADIOMETRIC AND INTERFEROMETRIC MILIMETER-WAVE SCENE SIMULATIONS c32
B. I. Hauss, P. J. Moffa, W. G. Steele, H. Agravante, R. Davidheiser, T. Samec, and S. K. Young *In* NASA. Ames Research Center, Proceedings of the Workshop on Augmented Visual Display (AVID) Research Dec. 1993 p 133-162 (For primary document see N94-25490 06-54)
Avail: CASI HC A03/MF A04

Smart munitions and weapons utilize various imaging sensors (including passive IR, active and passive millimeter-wave, and visible wavebands) to detect/identify targets at short standoff ranges and in varied terrain backgrounds. In order to design and evaluate these sensors under a variety of conditions, a high-fidelity scene simulation capability is necessary. Such a capability for passive millimeter-wave scene simulation exists at TRW. TRW's Advanced Radiometric Millimeter-Wave Scene Simulation (ARMSS) code is a rigorous, benchmarked, end-to-end passive millimeter-wave scene simulation code for interpreting millimeter-wave data, establishing scene signatures and evaluating sensor performance. In passive millimeter-wave imaging, resolution is limited due to wavelength and aperture size. Where high resolution is required, the utility of passive millimeter-wave imaging is confined to short ranges. Recent developments in interferometry have made possible high resolution applications on military platforms. Interferometry or synthetic aperture radiometry allows the creation of a high resolution image with a sparsely filled aperture. Borrowing from research work in radio astronomy, we have developed and tested at TRW scene reconstruction algorithms that allow the recovery of the scene from a relatively small number of spatial frequency components. In this paper, the TRW modeling capability is described and numerical results are presented. Derived from text

N94-25499*# Lockheed Engineering and Sciences Co., Moffett Field, CA.
SIMULATION OF A PASSIVE MILLIMETER WAVE SENSOR c35
William W. Kahlbaum *In* NASA. Ames Research Center, Proceedings of

the Workshop on Augmented Visual Display (AVID) Research Dec. 1993 p 163-180 (For primary document see N94-25490 06-54)
Avail: CASI HC A03/MF A04

The visual display expected to be generated by a Passive Millimeter Wave (PMMW) camera and sensor system has been simulated on a Silicon Graphics IRIS workstation at the NASA Langley Research Center (LaRC). The low resolution of the sensor has been simulated by graphically manipulating the scene as it is being drawn by the IRIS in real time. Camera field of view, sensor resolution, and sensor update rate are the controllable parameters. Physical effects such as lens model, radome effects, and noise have not been included at this time. An approximate dynamic model of the atmospheric phenomenology has been included which generates the gray-scale intensity values in real time for the simulated image. The gray-scale values are proportional to temperature. A snapshot capability which captures individual image frames during real-time operation has been included. These images were used to validate the approximate phenomenology model against a more rigorous physical model. Author

N94-25500*# National Aeronautics and Space Administration. Ames Research Center, Moffett Field, CA.
ENGINEERING WORKSTATION: SENSOR MODELING
M Pavel and B. Sweet *In its* Proceedings of the Workshop on Augmented Visual Display (AVID) Research Dec. 1993 p 181-190 (For primary document see N94-25490 06-54)
Avail: CASI HC A02/MF A04

The purpose of the engineering workstation is to provide an environment for rapid prototyping and evaluation of fusion and image processing algorithms. Ideally, the algorithms are designed to optimize the extraction of information that is useful to a pilot for all phases of flight operations. Successful design of effective fusion algorithms depends on the ability to characterize both the information available from the sensors and the information useful to a pilot. The workstation is comprised of subsystems for simulation of sensor-generated images, image processing, image enhancement, and fusion algorithms. As such, the workstation can be used to implement and evaluate both short-term solutions and long-term solutions. The short-term solutions are being developed to enhance a pilot's situational awareness by providing information in addition to his direct vision. The long term solutions are aimed at the development of complete synthetic vision systems. One of the important functions of the engineering workstation is to simulate the images that would be generated by the sensors. The simulation system is designed to use the graphics modeling and rendering capabilities of various workstations manufactured by Silicon Graphics Inc. The workstation simulates various aspects of the sensor-generated images arising from phenomenology of the sensors. In addition, the workstation can be used to simulate a variety of impairments due to mechanical limitations of the sensor placement and due to the motion of the airplane. Although the simulation is currently not performed in real-time, sequences of individual frames can be processed, stored, and recorded in a video format. In that way, it is possible to examine the appearance of different dynamic sensor-generated and fused images. Author (revised)

N94-25501*# National Aeronautics and Space Administration. Ames Research Center, Moffett Field, CA.
IMAGE FUSION
M. Pavel (Western Aerospace Labs., Inc., Moffett Field, CA.) *In its* Proceedings of the Workshop on Augmented Visual Display (AVID) Research Dec. 1993 p 193-205 (For primary document see N94-25490 06-54)
(Contract NCC2-486)
Avail: CASI HC A03/MF A04

The topics covered include the following: a system overview of the basic components of a system designed to improve the ability of a pilot to fly through low-visibility conditions such as fog; the role of visual sciences; fusion issues; sensor characterization; sources of information; image processing; and image fusion. CASI

N94-25502*# David Sarnoff Research Center, Princeton, NJ.
ENHANCED IMAGE CAPTURE THROUGH FUSION c35
Peter J. Burt, Keith Hanna, and Raymond J. Kolczynski *In* NASA. Ames Research Center, Proceedings of the Workshop on Augmented Visual Display (AVID) Research Dec. 1993 p 207-224 (For primary document see N94-25490 06-54)
Avail: CASI HC A03/MF A04

Image fusion may be used to combine images from different sensors, such as IR and visible cameras, to obtain a single composite with extended information content. Fusion may also be used to combine multiple images from a given sensor to form a composite image in which information of interest is enhanced. We present a general method for performing image fusion and show that this method is effective for diverse fusion applications. We suggest that fusion may provide a powerful tool for enhanced image capture with broad utility in image processing and computer vision. Author

N94-25503*# Westinghouse Electric Corp., Sunnyvale, CA.
RADAR E-O IMAGE FUSION c32
William F. ONeil *In* NASA. Ames Research Center, Proceedings of the Workshop on Augmented Visual Display (AVID) Research Dec. 1993 p 225-232 (For primary document see N94-25490 06-54)
Avail: CASI HC A02/MF A04

The fusion of radar and electro-optic (E-O) sensor images presents unique challenges. The two sensors measure different properties of the real three-dimensional (3-D) world. Forming the sensor outputs into a common format does not mask these differences. In this paper, the conditions under which fusion of the two sensor signals is possible are explored. The program currently planned to investigate this problem is briefly discussed. Author

N94-25504*# National Aeronautics and Space Administration. Ames Research Center, Moffett Field, CA.
EXPANSION-BASED PASSIVE RANGING c04
Yair Barniv *In its* Proceedings of the Workshop on Augmented Visual Display (AVID) Research Dec. 1993 p 235-286 (For primary document see N94-25490 06-54)
Avail: CASI HC A04/MF A04

This paper describes a new technique of passive ranging which is based on utilizing the image-plane expansion experienced by every object as its distance from the sensor decreases. This technique belongs in the feature/object-based family. The motion and shape of a small window, assumed to be fully contained inside the boundaries of some object, is approximated by an affine transformation. The parameters of the transformation matrix are derived by initially comparing successive images, and progressively increasing the image time separation so as to achieve much larger triangulation baseline than currently possible. Depth is directly derived from the expansion part of the transformation. To a first approximation, image-plane expansion is independent of image-plane location with respect to the focus of expansion (FOE) and of platform maneuvers. Thus, an expansion-based method has the potential of providing a reliable range in the difficult image area around the FOE. In areas far from the FOE the shift parameters of the affine transformation can provide more accurate depth information than the expansion alone, and can thus be used similarly to the way they have been used in conjunction with the Inertial Navigation Unit (INU) and Kalman filtering. However, the performance of a shift-based algorithm, when the shifts are derived from the affine transformation, would be much improved compared to current algorithms because the shifts--as well as the other parameters--can be obtained between widely separated images. Thus, the main advantage of this new approach is that, allowing the tracked window to expand and rotate, in addition to moving laterally, enables one to correlate images over a very long time span which, in turn, translates into a large spatial baseline resulting in a proportionately higher depth accuracy. Derived from text

N94-25505*# National Aeronautics and Space Administration. Ames Research Center, Moffett Field, CA.
MULTIPLE-CAMERA/MOTION STEREOSCOPY FOR RANGE ESTIMATION IN HELICOPTER FLIGHT
Phillip N. Smith, Banavar Sridhar, and Raymond E. Suorsa *In its* Proceedings of the Workshop on Augmented Visual Display (AVID) Research Dec. 1993 p 287-291 (For primary document see N94-25490 06-54)
Avail: CASI HC A01/MF A04

Aiding the pilot to improve safety and reduce pilot workload by detecting obstacles and planning obstacle-free flight paths during low-altitude helicopter flight is desirable. Computer vision techniques provide an attractive method of obstacle detection and range estimation for objects within a large field of view ahead of the helicopter. Previous research has had considerable success by using an image sequence from a single moving camera to solving this problem. The major limitations of single camera approaches are that no range information can be obtained near the instantaneous direction of motion or in the absence of motion. These limitations can be overcome through the use of multiple cameras. This paper presents a hybrid motion/stereo algorithm which allows range refinement through recursive range estimation while avoiding loss of range information in the direction of travel. A feature-based approach is used to track objects between image frames. An extended Kalman filter combines knowledge of the camera motion and measurements of a feature's image location to recursively estimate the feature's range and to predict its location in future images. Performance of the algorithm will be illustrated using an image sequence, motion information, and independent range measurements from a low-altitude helicopter flight experiment. Author (revised)

N94-25506*# National Aeronautics and Space Administration. Ames Research Center, Moffett Field, CA.

VALIDATION OF VISION-BASED RANGE ESTIMATION ALGORITHMS USING HELICOPTER FLIGHT DATA **c74**

Phillip N. Smith *In its* Proceedings of the Workshop on Augmented Visual Display (AVID) Research Dec. 1993 p 293-311 (For primary document see N94-25490 06-54)

Avail: CASI HC A03/MF A04

The objective of this research was to demonstrate the effectiveness of an optic flow method for passive range estimation using a Kalman-filter implementation with helicopter flight data. This paper is divided into the following areas: (1) ranging algorithm; (2) flight experiment; (3) analysis methodology; (4) results; and (5) concluding remarks. The discussion is presented in viewgraph format. Author (revised)

N94-25507*# National Aeronautics and Space Administration. Langley Research Center, Hampton, VA.

A MODEL-BASED APPROACH FOR DETECTION OF OBJECTS IN LOW RESOLUTION PASSIVE-MILLIMETER WAVE IMAGES

Yuan-Liang Tang (Pennsylvania State Univ., University Park.), Sadashiva Devadiga (Pennsylvania State Univ., University Park.), Rangachar Kasturi (Pennsylvania State Univ., University Park.), and Randall L. Harris, Sr. *In* NASA. Ames Research Center, Proceedings of the Workshop on Augmented Visual Display (AVID) Research Dec. 1993 p 313-328 (For primary document see N94-25490 06-54)

(Grant NAG1-1371)

Avail: CASI HC A03/MF A04

We describe a model-based vision system to assist pilots in landing maneuvers under restricted visibility conditions. The system was designed to analyze image sequences obtained from a Passive Millimeter Wave (PMMW) imaging system mounted on the aircraft to delineate runways/taxiways, buildings, and other objects on or near runways. PMMW sensors have good response in a foggy atmosphere; but, their spatial resolution is very low. However, additional data such as airport model and approximate position and orientation of aircraft are available. We exploit these data to guide our model-based system to locate objects in the low resolution image and generate warning signals to alert the pilots. We also derive analytical expressions for the accuracy of the camera position estimate obtained by detecting the position of known objects in the image. Author (revised)

N94-25508*# Honeywell, Inc., Minneapolis, MN. Systems and Research Center.

IMAGE PROCESSING FOR FLIGHT CREW ENHANCED SITUATION AWARENESS

Barry Roberts *In* NASA. Ames Research Center, Proceedings of the Workshop on Augmented Visual Display (AVID) Research Dec. 1993 p 329-360 (For primary document see N94-25490 06-54)

Avail: CASI HC A03/MF A04

This presentation describes the image processing work that is being performed for the Enhanced Situational Awareness System (ESAS) application. Specifically, the presented work supports the Enhanced Vision System (EVS) component of ESAS. Author (revised)

N94-25509*# National Aeronautics and Space Administration. Ames Research Center, Moffett Field, CA.

DCT QUANTIZATION MATRICES VISUALLY OPTIMIZED FOR INDIVIDUAL IMAGES **c74**

Andrew B. Watson *In its* Proceedings of the Workshop on Augmented Visual Display (AVID) Research Dec. 1993 p 363-377 (For primary document see N94-25490 06-54)

Avail: CASI HC A03/MF A04

This presentation describes how a vision model incorporating contrast sensitivity, contrast masking, and light adaptation is used to design visually optimal quantization matrices for Discrete Cosine Transform image compression. The Discrete Cosine Transform (DCT) underlies several image compression standards (JPEG, MPEG, H.261). The DCT is applied to 8x8 pixel blocks, and the resulting coefficients are quantized by division and rounding. The 8x8 'quantization matrix' of divisors determines the visual quality of the reconstructed image; the design of this matrix is left to the user. Since each DCT coefficient corresponds to a particular spatial frequency in a particular image region, each quantization error consists of a local increment or decrement in a particular frequency. After adjustments for contrast sensitivity, local light adaptation, and local contrast masking, this coefficient error can be converted to a just-noticeable-difference (jnd). The jnd's for different frequencies and image blocks can be pooled to yield a global perceptual error metric. With this metric, we can compute for each image the quantization matrix that minimizes the bit-rate for a given perceptual error, or perceptual error for a given bit-rate. Implementation of this system demonstrates its advantages over existing techniques. A unique feature of this scheme is that the quantization matrix is optimized for each individual image. This is compatible with the JPEG standard, which requires transmission of the quantization matrix. Author (revised)

N94-25510*# National Aeronautics and Space Administration. Ames Research Center, Moffett Field, CA.

EXTRACTING HEADING AND TEMPORAL RANGE FROM OPTIC FLOW: HUMAN PERFORMANCE ISSUES

Mary K. Kaiser, John A. Perrone, Leland Stone, Martin S. Banks (California Univ., Berkeley.), and James A. Crowell (California Univ., Berkeley.) *In its* Proceedings of the Workshop on Augmented Visual Display (AVID) Research Dec. 1993 p 379-396 (For primary document see N94-25490 06-54)

Avail: CASI HC A03/MF A04

Pilots are able to extract information about their vehicle motion and environmental structure from dynamic transformations in the out-the-window scene. In this presentation, we focus on the information in the optic flow which specifies vehicle heading and distance to objects in the environment, scaled to a temporal metric. In particular, we are concerned with modeling how the human operators extract the necessary information, and what factors impact their ability to utilize the critical information. In general, the psychophysical data suggest that the human visual system is fairly robust to degradations in the visual display, e.g., reduced contrast and resolution or restricted field of view. However, extraneous motion flow, i.e., introduced by sensor rotation, greatly compromises human performance. The implications of these models and data for enhanced/synthetic vision systems are discussed. Author (revised)

N94-25511*# National Aeronautics and Space Administration. Ames Research Center, Moffett Field, CA.

OPTICAL INFORMATION IN LANDING SCENES

Walter W. Johnson *In its* Proceedings of the Workshop on Augmented Visual Display (AVID) Research Dec. 1993 p 397-406 (For primary document see N94-25490 06-54)

Avail: CASI HC A02/MF A04

During landing, the visual scene contains optical information about speed, altitude, glide slope, and track that is useful for the maintenance of spatial orientation and awareness. This information, embedded in the structure and transformations of the optical patterns, may be globally, regionally, or locally available. Global changes occur everywhere in the visual field during landing and include such information as flow rate acceleration due to changing speed and/or altitude. Regional changes occur within a more restricted area and include such information as horizon line motion due to aircraft pitching and rolling. Locally available changes are the most restricted and include such information as changes in runway form ratios due to changing glide slopes. Thus, within partially or fully synthetic displays, or within sensor-driven displays, preservation of flow rate and horizon motion information requires a minimum of knowledge about the details of the airport layout, while runway outlines do require much more knowledge of the layout. All may be important, however, and these, as well as other sources of optical information, can provide a pilot with his most natural framework for maintaining orientation.

Author (revised)

N94-25512*# National Aeronautics and Space Administration. Ames Research Center, Moffett Field, CA.

SENSOR FUSION DISPLAY EVALUATION USING INFORMATION INTEGRATION MODELS IN ENHANCED/SYNTHETIC VISION APPLICATIONS

David C. Foyle *In its* Proceedings of the Workshop on Augmented Visual Display (AVID) Research Dec. 1993 p 409-419 (For primary document see N94-25490 06-54)

Avail: CASI HC A03/MF A04

Based on existing integration models in the psychological literature, an evaluation framework is developed to assess sensor fusion displays as might be implemented in an enhanced/synthetic vision system. The proposed evaluation framework for evaluating the operator's ability to use such systems is a normative approach: The pilot's performance with the sensor fusion image is compared to models' predictions based on the pilot's performance when viewing the original component sensor images prior to fusion. This allows for the determination as to when a sensor fusion system leads to: poorer performance than one of the original sensor displays, clearly an undesirable system in which the fused sensor system causes some distortion or interference; better performance than with either single sensor system alone, but at a sub-optimal level compared to model predictions; optimal performance compared to model predictions; or, super-optimal performance, which may occur if the operator were able to use some highly diagnostic 'emergent features' in the sensor fusion display, which were unavailable in the original sensor displays.

Author (revised)

N94-25513*# National Aeronautics and Space Administration. Ames Research Center, Moffett Field, CA.

QUALITY METRICS FOR SENSOR IMAGES

Al Ahumada *In its* Proceedings of the Workshop on Augmented Visual Display (AVID) Research Dec. 1993 p 421-422 (For primary document see N94-25490 06-54)

Avail: CASI HC A01/MF A04

Methods are needed for evaluating the quality of augmented visual displays (AVID). Computational quality metrics will help summarize, interpolate, and extrapolate the results of human performance tests with displays. The FLM Vision group at NASA Ames has been developing computational models of visual processing and using them to develop computational metrics for similar problems. For example, display modeling systems use metrics for comparing proposed displays, halftoning optimizing methods use metrics to evaluate the difference between the halftone and the original, and image compression methods minimize the predicted visibility of compression artifacts. The visual discrimination models take as input two arbitrary images A and B and compute an estimate of the probability that a human observer will report that A is different from B. If A is an image that one desires to display and B is the actual displayed image, such an estimate can be regarded as an image quality metric reflecting how well B approximates A. There are additional complexities associated with the problem of evaluating the quality of radar and IR enhanced displays for AVID tasks. One important problem is the question of whether intruding obstacles are detectable in such displays. Although the discrimination model can handle detection situations by making B the original image A plus the intrusion, this detection model makes the inappropriate assumption that the observer knows where the intrusion will be. Effects of signal uncertainty need to be added to our models. A pilot needs to make decisions rapidly. The models need to predict not just the probability of a correct decision, but the probability of a correct decision by the time the decision needs to be made. That is, the models need to predict latency as well as accuracy. Luce and Green have generated models for auditory detection latencies. Similar models are needed for visual detection. Most image quality models are designed for static imagery. Watson has been developing a general spatial-temporal vision model to optimize video compression techniques. These models need to be adapted and calibrated for AVID applications.

Derived from text

N94-25514*# National Aeronautics and Space Administration. Ames Research Center, Moffett Field, CA.

EVALUATION OF IMAGE QUALITY

M. Pavel (Western Aerospace Labs., Inc., Moffett Field, CA.) *In its* Proceedings of the Workshop on Augmented Visual Display (AVID) Research Dec. 1993 p 423-431 (For primary document see N94-25490 06-54)

Avail: CASI HC A02/MF A04

This presentation outlines in viewgraph format a general approach to the evaluation of display system quality for aviation applications. This approach is based on the assumption that it is possible to develop a model of the display which captures most of the significant properties of the display. The display characteristics should include spatial and temporal resolution, intensity quantizing effects, spatial sampling, delays, etc. The model must be sufficiently well specified to permit generation of stimuli that simulate the output of the display system. The first step in the evaluation of display quality is an analysis of the tasks to be performed using the display. Thus, for example, if a display is used by a pilot during a final approach, the aesthetic aspects of the display may be less relevant than its dynamic characteristics. The opposite task requirements may apply to imaging systems used for displaying navigation charts. Thus, display quality is defined with regard to one or more tasks. Given a set of relevant tasks, there are many ways to approach display evaluation. The range of evaluation approaches includes visual inspection, rapid evaluation, part-task simulation, and full mission simulation. The work described is focused on two complementary approaches to rapid evaluation. The first approach is based on a model of the human visual system. A model of the human visual system is used to predict the performance of the selected tasks. The model-based evaluation approach permits very rapid and inexpensive evaluation of various design decisions. The second rapid evaluation approach employs specifically designed critical tests that embody many important characteristics of actual tasks. These are used in situations where a validated model is not available. These rapid evaluation tests are being implemented in a workstation environment.

Author (revised)

N94-23929*# Honeywell, Inc., Minneapolis, MN. Sensor and Systems Development Center.

INTELLIGENT TUTORING AND AIDING IN SATELLITE GROUND CONTROL Ph.D. Thesis - Georgia Inst. of Tech., 1991

Rose W. Chu and Christine M. Mitchell (Georgia Inst. of Tech., Atlanta.) *In* JPL, SpaceOps 1992: Proceedings of the Second International Symposium on Ground Data Systems for Space Mission Operations 1 Mar. 1993 p 645-650 (For primary document see N94-23832 06-66)
(Contract NAS5-28575)

Avail: CASI HC A02/MF A10

N94-23936*# National Aeronautics and Space Administration. Goddard Space Flight Center, Greenbelt, MD.

AUTOMATING A HUMAN FACTORS EVALUATION OF GRAPHICAL USER INTERFACES FOR NASA APPLICATIONS: AN UPDATE ON CHIMES

Jian-Ping Jiang (Computer Technology Associates, Inc., Rockville, MD.), Elizabeth D. Murphy (Computer Technology Associates, Inc., Rockville, MD.), Sidney C. Bailin (Computer Technology Associates, Inc., Rockville, MD.), and Walter F. Truszkowski *In* JPL, SpaceOps 1992: Proceedings of the Second International Symposium on Ground Data Systems for Space Mission Operations 1 Mar. 1993 p 685-690 Sponsored in part by NASA, Washington (For primary document see N94-23832 06-66)
(Contract NAS5-30680)

Avail: CASI HC A02/MF A10

N94-24447*# Saint John Fisher Coll., Rochester, NY. Chemistry Dept.

A CHEMICAL SENSOR AND BIOSENSOR BASED TOTALLY AUTOMATED WATER QUALITY MONITOR FOR EXTENDED SPACE FLIGHT: STEP 1

Robert S. Smith *In* Alabama Univ., The 1993 NASA/ASEE Summer Faculty Fellowship Program Nov. 1993 5 p (For primary document see N94-24405 06-80)

Avail: CASI HC A01/MF A03

N94-25102*# National Aeronautics and Space Administration. Langley Research Center, Hampton, VA.
A SIMULATION STUDY OF CONTROL AND DISPLAY REQUIREMENTS FOR ZERO-EXPERIENCE GENERAL AVIATION PILOTS
Eric C. Stewart *In its* NASA LaRC Workshop on Guidance, Navigation, Controls, and Dynamics for Atmospheric Flight, 1993 Dec. 1993 p 147-175 (For primary document see N94-25096 06-01)
Avail: CASI HC A03/MF A04

N94-25354*# Nebraska Univ., Omaha. Dept. of Industrial and Management Systems Engineering.
INVESTIGATION OF HAND CAPABILITIES UNDER A VARIETY OF PERFORMANCE CONDITIONS AND AN ATTEMPT TO EXPLAIN PERFORMANCE DIFFERENCES
Ram R. Bishu and Lisa Bronkema *In* NASA. Johnson Space Center, National Aeronautics and Space Administration (NASA)/American Society for Engineering Education (ASEE) Summer Faculty Fellowship Program, 1993, Volume 1 Dec. 1993 14 p (For primary document see N94-25348 06-99)
Avail: CASI HC A03/MF A03

N94-25363*# Houston Univ., TX. College of Technology.
IMAGE REMAPPING STRATEGIES APPLIED AS PROTHESES FOR THE VISUALLY IMPAIRED
Curtis D. Johnson *In* NASA. Johnson Space Center, National Aeronautics and Space Administration (NASA)/American Society for Engineering Education (ASEE) Summer Faculty Fellowship Program, 1993, Volume 1 Dec. 1993 11 p (For primary document see N94-25348 06-99)
Avail: CASI HC A03/MF A03

N94-25369*# Wyoming Univ., Laramie. Dept. of Computer Science.
AN EVALUATION OF THREE-DIMENSIONAL SENSORS FOR THE EXTRAVEHICULAR ACTIVITY HELPER/RETREIVER
Michael Magee *In* NASA. Johnson Space Center, National Aeronautics and Space Administration (NASA)/American Society for Engineering Education (ASEE) Summer Faculty Fellowship Program, 1993, Volume 2 Dec. 1993 8 p (For primary document see N94-25367 06-99)
Avail: CASI HC A02/MF A03

N94-25371*# Purdue Univ., West Lafayette, IN. Dept. of Agricultural Engineering.
ROBOTICS IN A CONTROLLED, ECOLOGICAL LIFE SUPPORT SYSTEM
Gaines E. Miles and Kimberly J. Krom *In* NASA. Johnson Space Center, National Aeronautics and Space Administration (NASA)/American Society for Engineering Education (ASEE) Summer Faculty Fellowship Program, 1993, Volume 2 Dec. 1993 27 p (For primary document see N94-25367 06-99)
Avail: CASI HC A03/MF A03

N94-25375*# Bevill State Community Coll., Fayette, AL. Chemistry Dept.
INVESTIGATING PYROLYSIS/INCINERATION AS A METHOD OF RESOURCE RECOVERY FROM SOLID WASTE
Bobby J. Robertson and Christopher S. LeMay *In* NASA. Johnson Space Center, National Aeronautics and Space Administration (NASA)/American Society for Engineering Education (ASEE) Summer Faculty Fellowship Program, 1993, Volume 2 Dec. 1993 11 p (For primary document see N94-25367 06-99)
Avail: CASI HC A03/MF A03

55 SPACE BIOLOGY

Includes exobiology; planetary biology; and extraterrestrial life.

N94-23754 Finnish Artificial Intelligence Society, Helsinki.
SETI: SEARCH FOR EXTRATERRESTRIAL INTELLIGENCE. AN INTERNATIONAL INTERDISCIPLINARY SEMINAR, STAR DAYS
S. Linnaluoto and J. Seppaenen 1992 237 p Conference held in Heureka, Vantaa, Finland, 6-7 Mar. 1993 See also PB93-161206 Prepared in cooperation with Helsinki Univ. of Technology, Espoo, Finland Limited Reproducibility: More than 20% of this document may be affected by microfiche quality
(PB93-230597; ISBN-951-96735-0-4) Avail: Issuing Activity (National Technical Information Service (NTIS))

The volume contains papers read at the International Interdisciplinary Seminar on SETI - Search for Extraterrestrial Intelligence held on 6-7 March 1993 at Heureka, The Finnish Science Center, Vantaa, Finland. The aim of the seminar was to bring together specialists on SETI from abroad as well as Finnish scientists from nearby disciplines to present their views and to discuss the question of life and especially of intelligent life and technological civilizations elsewhere in our universe. NTIS

59 MATHEMATICAL AND COMPUTER SCIENCES (GENERAL)

N94-25090*# Institute for Computer Applications in Science and Engineering, Hampton, VA.
[RESEARCH IN PROGRESS AND OTHER ACTIVITIES OF THE INSTITUTE FOR COMPUTER APPLICATIONS IN SCIENCE AND ENGINEERING] Final Semiannual Report, 1 Apr. - 30 Sep. 1993
Dec. 1993 113 p
(Contract NAS1-19480; RTOP 505-90-52-01)
(NASA-CR-191576; NAS 1.26:191576) Avail: CASI HC A06/MF A02

This report summarizes research conducted at the Institute for Computer Applications in Science and Engineering in applied mathematics and computer science during the period April 1, 1993 through September 30, 1993. The major categories of the current ICASE research program are: (1) applied and numerical mathematics, including numerical analysis and algorithm development; (2) theoretical and computational research in fluid mechanics in selected areas of interest to LaRC, including acoustic and combustion; (3) experimental research in transition and turbulence and aerodynamics involving LaRC facilities and scientists; and (4) computer science. Author

60 COMPUTER OPERATIONS AND HARDWARE

Includes hardware for computer graphics, firmware, and data processing.
For components see *33 Electronics and Electrical Engineering.*

N94-22900 Institut National Polytechnique, Grenoble (France). Lab. de Genie Informatique.
RESOLUTION OF MARKOV MODELS ON DISTRIBUTED MEMORY MACHINES Ph.D. Thesis [RESOLUTION DES MODELES MARKOVIENS SUR MACHINES A MEMOIRES DISTRIBUEES]
Abderezak Touzene 1992 233 p In FRENCH Limited Reproducibility: More than 20% of this document may be affected by microfiche quality
(ETN-94-95182) Avail: CASI HC A11

Parallel computing is used to overcome problems in computer systems performance evaluation. Performance evaluation is an important step in the conception and development of computer systems. These systems are complex and their models are too large. To solve these models on a computer, two problems are found: memory and speed requirements. In the area of parallel computing, the communication cost on a distributed memory machine and the aspect of parallel computing related to data mapping, is studied. This aspect is assumed to perform a parallel vector matrix product which is the basic component of numerical iterative methods for solving models. Some iterative schemes to solve Markovian models are proposed. A parallelization of a Stochastic Automata Networks (SAN) solver which is specific to SAN modeling is developed. This parallelization leads to solved task allocation and reduced communication cost. The result of this parallelization is the ability to treat large models, many millions of states, in a reasonable time. ESA

N94-22901# Institut National Polytechnique, Grenoble (France). Lab. Conception de Systemes Integres.

DESIGN OF INTEGRATED ARCHITECTURES FOR LOW LEVEL IMAGE PROCESSING Ph.D. Thesis [CONCEPTION D'ARCHITECTURES INTEGREES DE TRAITEMENT D'IMAGE DE BAS NIVEAU]

Ahmed Boubekeur 1992 177 p In FRENCH

(ETN-94-95183) Avail: CASI HC A09/MF A02

Methods and tools for the design of massively parallel low level image processing integrated systems are presented. The design of a programmable two dimensional array of 6720 single bit Processors (PE's) implemented on a wafer is addressed. Two level defect tolerance techniques were used. At a subsystem level, a spare column is provided to replace defective PE's. At the wafer level, an original switching network (externally controlled) is used to bypass defective subarrays. A high level synthesis tool is used to synthesize automatically from a behavioral specifications a dedicated array from a specific application. Resources in terms of registers, connections (multiplexers), and memory points are minimized. ESA

N94-22903 Laboratoire d'Automatique et d'Analyse des Systemes, Toulouse (France). Groupe Outils et Logiciels pour la Communication.

REPRESENTATION AND SPECIFICATION OF ARCHITECTURES FOR HETEROGENEOUS INTERNETWORKING: USING A KNOWLEDGE BASED APPROACH Ph.D. Thesis - Toulouse Univ. [REPRESENTATION ET SPECIFICATION D'ARCHITECTURES D'INTERCONNEXION DE RESEAUX HETEROGENES: VERS LA DEFINITION D'UNE BASE DE CONNAISSANCES]

Stella Zwecker 1993 193 p In FRENCH Limited Reproducibility: More than 20% of this document may be affected by microfiche quality

(LAAS-93088; ETN-94-95185) Avail: CASI HC A09

A method for specifying architectures for heterogeneous internetworking is presented. This method was integrated in a system based on artificial intelligence techniques. The method is defined at a high level of abstraction. It evaluates the degree of incompatibility between interconnected networks, described as multilayer architectures, and determines a level of the architecture, called the incompatibility frontier, from which techniques to control the incompatibilities can be applied. The evaluation of incompatibilities is founded on the comparison of the network's addresses and of their service-protocol pairs; for communicating, distant entities must be able to identify themselves and exchange messages with a same service quality. Based on reliability criteria, the resulting internetworking architecture is specified. The specification relies on two types of interconnecting techniques: conversion and encapsulation. To integrate the method in a knowledge based system, the different types of domain concepts are modeled: a model, defined for the representation of addresses in a multilayer architecture, is formalized. An implemented prototype combines two knowledge representation formalisms: an object oriented formalism that structures complex knowledge, and a logic based formalism that implements inferences on the structure of knowledge. This system is interactive, providing a pedagogical tool for a user to conceptually study cases of internetworking: long haul networks with a connection oriented or a connectionless network layer and local area networks without a network layer. ESA

N94-23125*# California Polytechnic State Univ., San Luis Obispo.

TOOLS REFERENCE MANUAL FOR A REQUIREMENTS SPECIFICATION LANGUAGE (RSL), VERSION 2.0

Gene L. Fisher and Gerald C. Cohen (Boeing Defense and Space Group, Seattle, WA.) Nov. 1993 69 p

(Contract NAS1-18586; RTOP 505-64-10-07)

(NASA-CR-191461; NAS 1.26:191461) Avail: CASI HC A04/MF A01

This report describes a general-purpose Requirements Specification Language, RSL. The purpose of RSL is to specify precisely the external structure of a mechanized system and to define requirements that the system must meet. A system can be comprised of a mixture of hardware, software, and human processing elements. RSL is a hybrid of features found in several popular requirements specification languages, such as SADT (Structured Analysis and Design Technique), PSL (Problem Statement Language), and RMF (Requirements Modeling Framework). While languages such as these have useful features for structuring a specification, they generally lack formality. To overcome the deficiencies of informal requirements languages, RSL has constructs for formal mathematical specification. These constructs are similar to those found in formal specification languages such as EHDM (Enhanced Hierarchical Development Methodology), Larch, and OBJ3. Author (revised)

N94-23153# Institut National Polytechnique, Grenoble (France). Lab. de Genie Informatique.

CONTRIBUTION TO THE EVALUATION OF EFFICIENCY OF A MICROPROCESSOR FUNCTIONAL TEST Ph.D. Thesis [CONTRIBUTION A L'EVALUATION DE L'EFFICACITE DU TEST FONCTIONNEL DE MICROPROCESSEURS]

Bernard Martinet 1992 186 p In FRENCH

(ETN-94-95176) Avail: CASI HC A09/MF A02

A method for studying the efficiency of a microprocessor functional test is presented. The efficacity of a test consists in its capability of distinguishing perfect circuits from defective ones. The purpose of the functional test is to assist validation design and diagnosis of complex circuits. The method comprises the introduction of defects, by a laser device, into perfect circuits. Several experiments were performed on 8 bits and 16 bits commercially available microprocessors. The efficacity of the proposed test method and that of the manufacturer's structural test are compared. The principles of the parametric test, the dynamic test and the logical test, are summarized. The most common physical defects occurring in integrated circuits are reviewed. ESA

N94-23170# Technische Univ., Eindhoven (Netherlands). Digital Information Systems Section.

A METHOD FOR THE GENERAL SIMULTANEOUS FULL DECOMPOSITION OF SEQUENTIAL MACHINES: ALGORITHMS AND IMPLEMENTATION Thesis

Lech Jozwiak and Albert P. H. vanDijk Dec. 1992 107 p

(EUT-92-E-267; ISBN-9-06-144267-2; ETN-94-94774) Avail: CASI HC A06/MF A02

Research to develop, implement and test an efficient heuristic method for the general simultaneous full decomposition of Moore machines with encoded inputs and outputs and symbolic states is reported. The method was required to be able to discover the natural decompositional structure of the sequential machine. The method constructs the limited set of near optimal decompositions using a beam search bottom up hierarchical clustering algorithm, with decision making based on correlations between the information flows in the sequential machine. In order to get an impression about the performance of the method, a number of experiments were performed. In these experiments some machines were used with a known optimal decompositional structure and other machines were taken from the international benchmark set. The preliminary results are promising: in all the checked cases, the method was able to discover the natural decompositional structure by a very limited search; however, checking the method on larger samples of machines is still necessary in order to obtain more complete and more reliable information on the performance of the method. ESA

N94-23788 Canon Information Systems, Inc., Palo Alto, CA.

SOME BACKGROUND INFORMATION ON PERCEPTUAL COLOR MATCHING PERTINENT TO COMPUTER APPLICATIONS Final Report

G. B. Beretta 1993 48 p See also PB89-195309 Limited Reproducibility: More than 20% of this document may be affected by microfiche quality

(PB93-200327; CIS-N-93-742) Copyright Avail: Issuing Activity (National Technical Information Service (NTIS))

In closed color reproduction systems, color can be controlled with densitometric methods. With the advent of distributed document management systems-which entail device independence-these methods fail, and the use of colorimetry is necessary. However, even with colorimetry, a number of problems remain hard to solve, especially across media. It is often believed that such problems can be solved using more general models, like those developed in the study of color appearance. The report is an attempt to provide some background information about the modeling of color appearance. To guide the exposition, the author asks the question: 'Why are computer users willing to spend hundreds of dollars more for their equipment to add color.' After defining color appearance, he presents some published models from the literature. Finally, he relates it to colorimetry and reviews the possible benefits for desktop document preparation.

NTIS

N94-24538# Oak Ridge National Lab., TN.
THE DESIGN OF A STANDARD MESSAGE PASSING INTERFACE FOR DISTRIBUTED MEMORY CONCURRENT COMPUTERS
D. W. Walker Oct. 1993 29 p
(Contract DE-AC05-84OR-21400)
(DE94-002536; ORNL/TM-12512) Avail: CASI HC A03/MF A01

This paper presents an overview of MPI, a proposed standard message passing interface for MIMD distributed memory concurrent computers. The design of MPI has been a collective effort involving researchers in the United States and Europe from many organizations and institutions. MPI includes point-to-point and collective communication routines, as well as support for process groups, communication contexts, and application topologies. While making use of new ideas where appropriate, the MPI standard is based largely on current practice. DOE

N94-24540 Technische Univ., Eindhoven (Netherlands).
REAL-TIME PROCESS LOGIC
J. C. M. Baeten, J. A. Bergstra (Amsterdam Univ., Netherlands.), and R. N. Bol 1993 42 p Prepared in cooperation with Utrecht State Univ. (Netherlands), and Amsterdam Univ. (Netherlands) Limited Reproducibility: More than 20% of this document may be affected by microfiche quality
(PB94-101441; COMPUTING SCIENCE NOTES-93/15) Copyright Avail: CASI HC A03

Systems can be described at various levels of abstraction: automata, processes and behavior. The authors take the ready trace set as a description of the behavior of a process, and they present a ready trace model of symbolic (untimed) and real time process algebra. They argue that, especially in the real time case, properties of ready trace sets are best formulated in a dedicated logic. They present the syntax and semantics of a logic that could serve this purpose, and they apply it on two examples: expressing the correctness of a concurrent alternating bit protocol, and demonstrating the (well-known) non-existence of so-called coordinated attack protocols. A connection is made with the metric temporal logic of Koymans. NTIS

N94-24724 Department of the Navy, Washington, DC.
CROSSTIE RANDOM ACCESS MEMORY ELEMENT HAVING ASSOCIATED READ/WRITE CIRCUITRY Patent
Leonard J. Schwee, inventor (to Navy) 20 Jul. 1993 10 p Filed 19 Nov. 1990
(AD-D016027; US-Patent-,5,229,961; US-Patent-Appl-SN-615832; US-Patent-Class-365-87) Avail: US Patent and Trademark Office

A nonvolatile random access memory array is formed by permalloy thin films patterned into 'wiggle' shapes. Address lines for reading and/or writing into the memory cells are operatively connected to associated circuitry such that writing at a selected location in the array is accomplished using coincident currents. Each memory cell in the array is arranged for passage of column conducted current to effect magnetoresistance readout in conjunction with row address lines and the aforementioned associated circuitry. DTIC

N94-24981# Electrotechnical Lab., Tsukuba (Japan).
STUDY ON FINE GRAIN DYNAMIC DATAFLOW COMPUTER [SAIRYUDO DAINAMIKKU DETA FURO KEISANKI NO KENKYU]
Toshio Shimada 26 Mar. 1993 116 p In JAPANESE
(Rept-946; JTN-94-80515) Avail: CASI HC A06/MF A02

A study was conducted to solve problems for building a practical data flow computer, to build it, and to verify that its performance is comparable with von Neuman computers. The following subjects are outlined: (1) description of a data flow computation model and discussion on the necessary features of data flow programming languages; (2) an execution model which incorporates a concept of finite resources into a data flow computation model; (3) the architecture of the data flow computer SIGMA-1, including the system configuration, addressing of the definitions of instructions and packets, data representation, the processing element, the structure element, and the network; (4) the design of the data flow programming language DFC (Data-Flow C); (5) various optimization techniques, including a clean graph generation method, an efficient execution mechanism of a loop structure, and a concurrency control mechanism; and (6) evaluation of the SIGMA-1 performance. The results of the study verified the feasibility of a data flow computer by showing that an effective performance of the data flow computer SIGMA-1 is 118 Million Floating Point Operations Per Second (MFLOPS). Author (NASDA)

N94-25034 Department of the Navy, Washington, DC.
HIGH SPEED ELECTRONIC ANALOG COMPUTERS USING LOW-GAIN AMPLIFIERS Patent
Arthur D. Delagrange, inventor (to Navy) 17 Aug. 1993 10 p Filed 29 Aug. 1991
(AD-D015974; US-Patent-5,237,526; US-Patent-Appl-SN-751479; US-Patent-Class-364-807) Avail: US Patent and Trademark Office

The operational amplifiers conventionally used in electronic analog computers can be replaced with fixed gain differential amplifiers having no external negative feedback to control their gain. This allows a large increase in the bandwidth of the computers, with a resulting faster response time. Circuits for summing, integration, and differentiations are specifically disclosed using fixed-gain amplifiers. DTIC

N94-25081# Technische Univ., Eindhoven (Netherlands).
SPECIAL SIGNATURE SCHEMES Ph.D. Thesis
Eugene Josephus L. J vanHeijst 1992 137 p
(ETN-94-95296) Avail: CASI HC A07/MF A02

Different aspects of digital signatures are discussed. An overview of the public key cryptography, the message confidentiality and authentication, the cryptosystems based on discrete logarithm and RSA (Rivest-Shamir-Adleman), blobs, and zero knowledge is given. Theoretical results for the security oflarge classes of RSA based signatures are presented. Three new kinds of signature schemes and constructions for them are given: group signatures, undeniable signatures unconditionally secure for the signer, and convertible signatures unconditionally secure for the signer. An efficient construction for fail-stop signatures is included. Two applications of signature methods, a payment system and a new kind of blob, are discussed. ESA

N94-25312# Sheffield Univ. (England). Dept. of Automatic Control and Systems Engineering.
TRANSPUTER BENCHMARKS AND PERFORMANCE COMPARISONS WITH OTHER COMPUTING MACHINES
Ian J. Cornish and Ali M. S. Zalzala Feb. 1993 7 p
(RR-467; ETN-94-95134) Avail: CASI HC A02/MF A01

A performance index for several hardware/software combinations, to ease the decision making process, is presented. The aim is to provide a tool to enable engineering researchers to assess their needs and choices before starting a job. The actual implementation of a computer based control application can be expensive and time consuming. The performance of a single transputer, and of a network of transputers, is compared with that of a variety of Von Neumann type processors. The effect of the choice of language on a system performance is assessed. ESA

N94-25313# Sheffield Univ. (England). Robotics Research Group.
ADVANCED CONTROL STRUCTURES: A TRANSPUTER-BASED MULTI-ROBOT SYSTEM
Ali M. S. Zalzala, Gordon I. Dodds (Queens Univ., Belfast, Northern Ireland.), and George W. Irwin (Queens Univ., Belfast, Northern Ireland.) Feb. 1993 7 p
(RR-468; ETN-94-95135) Avail: CASI HC A02/MF A01

An efficient motion planner for a two robot system operating in a unified environment is implemented. The distributed formulation of the planner is mapped on a network of T800 transputers and caters to the needs of minimum time and collision free robot motion in real time. Practical implementation of the planner for two coordinated RTX robots is reported. Performance results of an execution run are given. The total system hardware comprises a network of 10 transputers hosted by a UNIX based workstation, where in addition to the planning algorithm reported, 4 transputers are used to interface the robots. The planning and interface networks are activated simultaneously by downloading the appropriate booting codes. The system is seen as a development tool for further phases of advanced robotics research. ESA

N94-25438# Edgewood Arsenal, Aberdeen Proving Ground, MD. Research, Development and Engineering Center.
THE TRANSPUTER Final Report, Feb. - Jun. 1993

L. R. Williams Oct. 1993 19 p
(DA Proj. 101-62622-A-553)
(AD-A273688; ERDEC-TR-123) Avail: CASI HC A03/MF A01

In 1984, Inmos introduced the transputer. The transputer is a microprocessor that is designed to operate in parallel with other transputers in the same system. Most aspects of the transputer were designed with this fact in mind. As a result, inter-processor and inter-process communication is a very important part of the design of the transputer. These parallel processing communications abilities can be very valuable to the Army in the area of chemical detection and its subsequent signal processing needs. DTIC

N94-23250*# Missouri Univ., Rolla. Dept. of Computer Science.
SWITCH CONFIGURATION FOR MIGRATION TO OPTICAL FIBER NETWORK
George W. Zobrist *In* NASA. Kennedy Space Center, NASA/ASEE Summer Faculty Fellowship Program Oct. 1993 p 551-579 (For primary document see N94-23230 06-80)
Avail: CASI HC A03/MF A04

N94-23917*# Jet Propulsion Lab., California Inst. of Tech., Pasadena.
DEEP SPACE NETWORK (DSN), NETWORK OPERATIONS CONTROL CENTER (NOCC) COMPUTER-HUMAN INTERFACES
Alvin Ellman and Magdi Carlton *In its* SpaceOps 1992: Proceedings of the Second International Symposium on Ground Data Systems for Space Mission Operations 1 Mar. 1993 p 561-564 (For primary document see N94-23832 06-66)
Avail: CASI HC A01/MF A10

N94-25377*# Memphis State Univ., TN. Dept. of Electrical Engineering.
DIGITAL DATA, COMPOSITE VIDEO MULTIPLEXER AND DEMULTIPLEXER BOARDS FOR AN IBM PC/AT COMPATIBLE COMPUTER
Dean Lance Smith *In* NASA. Johnson Space Center, National Aeronautics and Space Administration (NASA)/American Society for Engineering Education (ASEE) Summer Faculty Fellowship Program, 1993, Volume 2 Dec. 1993 5 p (For primary document see N94-25367 06-99)
Avail: CASI HC A01/MF A03

61 COMPUTER PROGRAMMING AND SOFTWARE

Includes computer programs, routines, alogorithms, and specific applications, e.g., CAD/CAM.

N94-22711# Universiteit Twente, Enschede (Netherlands). Faculty of Applied Mathematics.
ON DYNAMIC INPUT-OUTPUT LINEARIZATION OF DISCRETE-TIME NONLINEAR SYSTEMS
U. Kotta and H. Nijmeijer (Academy of Sciences of the Estonian SSR, Tallinn.) Mar. 1993 41 p Sponsored in part by Dutch Network in Systems and Control
(MEMO-1123; ETN-94-94759) Avail: CASI HC A03/MF A01

The problem of linearizing the input output map of an analytic discrete time nonlinear system locally around a given trajectory is studied. Necessary and sufficient conditions are given for the existence of a regular dynamic state feedback control law under which the input dependent part of the response of a nonlinear system becomes linear in the input and independent of the initial state. The proposed conditions are less restrictive than those obtained by Lee and Marcus for linearizing the input output map via a static state feedback. Instrumental in the problem solution is the inversion (structure) algorithm for discrete time nonlinear system. The solvability conditions are expressed in terms of the inversion algorithm. The proof of the existence and construction of the dynamic state feedback compensator relies on this algorithm. ESA

N94-22731# Technische Univ., Eindhoven (Netherlands). Information and Communication Theory Group.
ALGORITHMS FOR SPEECH CODING SYSTEMS BASED ON LINEAR PREDICTION
J. E. Rooijackers May 1992 95 p
(EUT-92-E-260; ISBN-9-06-144260-5; ETN-94-94767) Avail: CASI HC A05/MF A01

An introduction to speech coding systems based on a signal model and linear prediction is presented with the object of systems comprehension and recognition and comprehension of their kinship. A set of algorithms for speech coding systems is presented. The mathematical background of the algorithms and their source text are given. The software package is written in TURBOPASCAL. Attention is given to the interrelations between the methods and to the computational efficiency. ESA

N94-22882# Grenoble-1 Univ. (France). Lab. de Genie Informatique.
DEFINITION AND REALIZATION OF A FORMAL VERIFICATION TOOL OF LUSTRE PROGRAMS: THE LESAR SYSTEM Ph.D. Thesis [DEFINITION ET REALISATION D'UN OUTIL DE VERIFICATION FORMELLE DE PROGRAMMES LUSTRE: LE SYSTEME LESAR]
Christophe Ratel 1992 189 p In FRENCH
(ETN-94-95164) Avail: CASI HC A09/MF A02

The formal verification methods of LUSTRE programs is defined and implemented. LUSTRE is a programming language dedicated to the design of reactive systems. The verification of a system consists of ensuring that all its behaviors are correct when compared to specifications. The behaviors of a LUSTRE program can be represented by a finite state machine. The standard approach implementing the method is bounded by the explosion problem of the generated machine. A new approach avoiding this problem is presented. Two original implementations of a standard and a new approach using a symbolic technique are presented. Diagnosis aspects corresponding to the case of programs that do not agree with their specifications are considered. ESA

N94-22899 Institut National Polytechnique, Grenoble (France). Lab. de Genie Informatique.
VERIFICATION OF SYNCHRONOUS SEQUENTIAL NUMERICAL MATERIAL SYSTEMS: APPLICATION OF THE LUSTRE LANGUAGE AND OF THE LESAR VERIFICATION TOOL Ph.D. Thesis [VERIFICATION DES SYSTEMES MATERIALS NUMERIQUES SEQUENTIELS SYNCHRONES: APPLICATION DU LANGUAGE LUSTRE ET DE L'OUTIL DE VERIFICATION LESAR]
Bachir Berkane 1992 157 p In FRENCH Limited Reproducibility: More than 20% of this document may be affected by microfiche quality
(ETN-94-95181) Avail: CASI HC A08

The functional verification of hardware design consists of checking that a given system operates as specified. Two kinds of high level specifications are used in hardware design: a complete specification given by a high abstraction level; and a partial high level specification made up of a set of properties that the system must satisfy. These two different kinds of hardware specifications give rise to two different verification problems. A unified framework to handle the two verification problems on synchronous sequential digital hardware systems is presented. Each verification problem comes down to defining a verification machine with a single output flag and to verifying that that flag is always true. The application of the langage LUSTRE and the verification tool LESAR are studied. Verification problems can be handled by defining a LUSTRE program with a single output flow. The verification is automatically performed by the verification tool LESAR. ESA

N94-22911# Laboratoire d'Automatique et d'Analyse des Systemes, Toulouse (France).
CAUSAL LABELED TRANSITION SYSTEMS: A NEW APPROACH FOR DESCRIBING THE BEHAVIOR OF CONCURRENT SYSTEMS Ph.D. Thesis - Toulouse Univ. [SYSTEMES DE TRANSITIONS ETIQUETES CAUSAUX: UNE NOVVELLE APPROCHE POUR LA DESCRIPTION DU COMPORTEMENT EVENEMENTIEL DE SYSTEMES CONCURRENTS]
Rosvelter Joao CoelhodaCosta 1993 138 p In FRENCH Sponsored by Coordenacao de Aperfeicoamento de Pesoal de Nivel Superior, Brazil, and Santa Catarina Univ., Fioriaopolis, Brazil
(LAAS-93179; ETN-94-95193) Avail: CASI HC A07/MF A02

Causal labeled transition systems are proposed. This consists of a model of concurrent systems which has the same degree of simplicity as conventional labeled transition systems but permits concurrency among events to be expressed by causal independency. A concurrent system's behavior is modeled by a transition system, and the causality among events is expressed by a transition labeling mechanism similar to the variable abstraction of Lambda-notation. This approach describes the behavior of concurrent systems. Many concepts and results developed for conventional labeled transition systems are extended to causal labeled transition systems. The concept of bisimilarity is characterized in terms of causal labeled transition systems. A causality based operational semantics of the Calculus of Communicating Systems (CCS), based on causal labeled transition systems, is presented. ESA

N94-22980 Lawrence Livermore National Lab., CA.

A GEOMETRIC WEIGHTED ELLIPTIC GRID REGENERATION METHOD FOR 3D UNSTRUCTURED ALE HYDRODYNAMICS

E. Dube and G. Rodrigue 20 Aug. 1993 6 p Presented at the 5th International Symposium on Computational Fluid Dynamics, Sendai, Japan, 31 Aug. - 3 Sep. 1993 Limited Reproducibility: More than 20% of this document may be affected by microfiche quality
(Contract W-7405-eng-48)
(DE94-000309; UCRL-JC-114363; CONF-9308172-1) Avail: Issuing Activity (Department of Energy (DOE))

The theory for an elliptic mesh generator is developed for use in the advection step of a 3D ALE algorithm. This mesh generator is derived by a variational principle for an unstructured 3D grid using finite elements. An arbitrary weight function is introduced which is based on the geometric properties of the existing mesh. These geometric weights should allow for a smooth grid that retains the general shape of the original mesh. DOE

N94-23024 Algiers Univ. (Algeria). Laboratoire des Techniques Nucleaires.

VTGRAPH:COMPUTER GRAPHICS PROGRAM USING ReGIS MODE

M. A. Benamar, N. Benouali, A. Tchantchane, A. Azbouche, and S. Tobbeche Feb. 1993 9 p Limited Reproducibility: More than 20% of this document may be affected by microfiche quality
(DE94-600342; INIS-mf-13691) Avail: CASI HC A02 (US Sales Only)

A computer graphics program was developed for plotting spectra generated from different nuclear analysis techniques and discrete data for the VT240 graphics and compatible IBM PC using ST240 configuration. The Remote Graphics Instruction Set (ReGIS) commands were used. DOE

N94-23073*# Arizona State Univ., Tempe. Center for Systems Science and Engineering.

ON THE NUMERIC INTEGRATION OF DYNAMIC ATTITUDE EQUATIONS Abstract Only

P. E. Crouch, Y. Yan, and Robert Grossman (Illinois Univ., Chicago.) Feb. 1992 1 p
(Grants NAG2-513; NSF DMS-91-01089)
(NASA-CR-194788; NAS 1.26:194788) Avail: CASI HC A01/MF A01

We describe new types of numerical integration algorithms developed by the authors. The main aim of the algorithms is to numerically integrate differential equations which evolve on geometric objects, such as the rotation group. The algorithms provide iterates which lie on the prescribed geometric object, either exactly, or to some prescribed accuracy, independent of the order of the algorithm. This paper describes applications of these algorithms to the evolution of the attitude of a rigid body. Author

N94-23074*# Arizona State Univ., Tempe. Center for Systems Science and Engineering.

THE EXPLICIT COMPUTATION OF INTEGRATION ALGORITHMS AND FIRST INTEGRALS FOR ORDINARY DIFFERENTIAL EQUATIONS WITH POLYNOMIALS COEFFICIENTS USING TREES Abstract Only

P. E. Crouch and Robert Grossman (Illinois Univ., Chicago.) Mar. 1992 2 p
(Grant NAG2-513)
(NASA-CR-194787; NAS 1.26:194787) Avail: CASI HC A01/MF A01

This note is concerned with the explicit symbolic computation of expressions involving differential operators and their actions on functions. The derivation of specialized numerical algorithms, the explicit symbolic computation of integrals of motion, and the explicit computation of normal forms for nonlinear systems all require such computations. More precisely, if R = k(x(sub 1),...,x(sub N)), where k = R or C, F denotes a differential operator with coefficients from R, and g member of R, we describe data structures and algorithms for efficiently computing g. The basic idea is to impose a multiplicative structure on the vector space with basis the set of finite rooted trees and whose nodes are labeled with the coefficients of the differential operators. Cancellations of two trees with r + 1 nodes translates into cancellation of O(N(exp r)) expressions involving the coefficient functions and their derivatives. Author (revised)

N94-23086*# National Aeronautics and Space Administration. Langley Research Center, Hampton, VA.

A DATAFLOW ANALYSIS TOOL FOR PARALLEL PROCESSING OF ALGORITHMS

Robert L. Jones, III Nov. 1993 21 p
(RTOP 233-01-03)
(NASA-TM-109054; NAS 1.15:109054) Avail: CASI HC A03/MF A01

A graph-theoretic design process and software tool is presented for selecting a multiprocessing scheduling solution for a class of computational problems. The problems of interest are those that can be described using a dataflow graph and are intended to be executed repetitively on a set of identical parallel processors. Typical applications include signal processing and control law problems. Graph analysis techniques are introduced and shown to effectively determine performance bounds, scheduling constraints, and resource requirements. The software tool is shown to facilitate the application of the design process to a given problem. Author

N94-23092*# Institute for Computer Applications in Science and Engineering, Hampton, VA.

DYNAMIC DATA DISTRIBUTIONS IN VIENNA FORTRAN Final Report

Barbara Chapman (Wien Univ., Austria.), Piyush Mehrotra, Hans Moritsch (Wien Univ., Austria.), and Hans Zima (Wien Univ., Austria.) Dec. 1993 21 p Submitted for publication
(Contract NAS1-19480; RTOP 505-90-52-01)
(NASA-CR-191575; NAS 1.26:191575; ICASE-93-92) Avail: CASI HC A03/MF A01

Vienna Fortran is a machine-independent language extension of Fortran, which is based upon the Single-Program-Multiple-Data (SPMD) paradigm and allows the user to write programs for distributed-memory systems using global addresses. The language features focus mainly on the issue of distributing data across virtual processor structures. Those features of Vienna Fortran that allow the data distributions of arrays to change dynamically, depending on runtime conditions are discussed. The relevant language features are discussed, their implementation is outlined, and how they may be used in applications is described. Author (revised)

N94-23096# Vrije Univ., Amsterdam (Netherlands). Faculteit der Wiskunde en Informatica.

ASYNCHRONOUS RENDEZVOUS IN DISTRIBUTED LOGIC PROGRAMMING

A. Elieens and E. P. deVink Sep. 1992 33 p See also PB92-108646 and AD-A171 902
(PB93-220614; IR-304) Avail: CASI HC A03/MF A01

The semantics of the communication mechanism of the distributed logic programming language DLP is studied. DLP combines logic programming with object oriented features and parallelism. For an abstract subset of DLP, both an operational and denotational semantics is given. The language DLP supports active objects, method call by rendezvous and moreover distributed backtracking over the results of such a rendezvous. To enable further exploitation of parallelism, the rendezvous provided is asynchronous. A distinction is made between the creation of a process for evaluating the method call on the one hand, and the request for an answer on the other hand. To model this communication mechanism, syntactic resumptions are employed. The notion of a resumption explains the backtracking taking place in the asynchronous rendezvous. In addition, resumptions facilitate the systematic comparison of the operational and denotational semantics presented. NTIS

N94-23097 Vrije Univ., Amsterdam (Netherlands). Faculteit der Wiskunde en Informatica.

LINEAR ALGORITHM FOR FLATTENING LIST GRAPHS

P. Boncz Sep. 1992 33 p Limited Reproducibility: More than 20% of

this document may be affected by microfiche quality
(PB93-220648; IR-300) Avail: Issuing Activity (National Technical Information Service (NTIS))

List Graphs are directed graphs in which the vertices correspond to the elements of a number of N lists. The edges of the graph are formed by the links between the elements in the N lists. When trying to flatten a List Graph, the occurrence of cycles rules out an optimal solution, in which all N original lists are sublist of the combined list. The linear flattening algorithm described in this paper produces a sorted list in which the number of elements that contradict the order of an original list is minimized. Also, the mu lists with the highest priority are sublist of it (1 = or less than mu = or less than N). It can be proven that a solution with more than the mu highest lists being sublist does not exist. NTIS

N94-23103 Helsinki Univ. of Technology, Espoo (Finland). Dept. of Computer Science.
DISTRIBUTED OPERATING SYSTEMS AND MACH. PROCEEDINGS OF THE SPRING 1992 GRADUATE SEMINAR ON DISTRIBUTED SYSTEMS
Johannes Helander, ed. and Heikki Saikkonen, ed. 1993 172 p Seminar held in Helsinki, Finland, 1992 Limited Reproducibility: More than 20% of this document may be affected by microfiche quality
(PB93-224905; TKO-C61) Avail: CASI HC A08

Contents of the document include the following: unstructured mesh generation - a server for the Mach operating system; porting a debugger to the Mach 3 operating system; red zone memory allocator under Mach 3.0; Mach 3 scheduler improvements for memory usage; how to detect faulty network time servers; Mach 3.0 OS emulation considerations; distributed shared memory algorithms; running multiple UNIX servers under Mach; the design and implementation of a replicating file system under Mach; fault-tolerant computing with Mach; authentication in distributed systems; floppy disk device driver for Mach; process migration and Mach 3.0; a multi-user shadow paging transaction manager on Mach 3.0; the consideration of multiprocessor systems and OS for photogrammetry and remote sensing; attempt to solve memory access conflict problem in multiprocessor environment multifunction distributed shared memory architecture; and operating system support for dynamic typing and garbage collection. NTIS

N94-23111 Centro Nazionale Univ. per il Calcolo Elettronico, Pisa (Italy).
SOFTWARE FOR SCIENTIFIC VISUALIZATION: STATE OF THE ART AND EXPERIENCES
P. Palamidese and A. Crise (Osservatorio Geofisico Sperimentale, Trieste, Italy.) 1993 37 p Limited Reproducibility: More than 20% of this document may be affected by microfiche quality
(PB93-225183) Avail: CASI HC A03

The contents of this document include the following: Which Types of Users are Emerging; Which Requirements Do Scientists Have; Which Software Do Scientists Need for Scientific Visualizations; Concrete Visualization Experiences; and Some Conclusions. NTIS

N94-23117 Helsinki Univ. of Technology, Espoo (Finland). Lab. of Machine Design.
HYPERMEDIA SUPPORT FOR ENGINEERING DESIGN SYSTEM
J. Saeaeski Mar. 1993 29 p See also PB93-165587 Limited Reproducibility: More than 20% of this document may be affected by microfiche quality
(PB93-226256; ISBN-951-22-1500-4) Avail: CASI HC A03

The report is a literature study about the possibilities of using hypermedia for supporting engineering design systems. Hypermedia is an electronic document in which information is stored in a network of nodes connected by links. Nodes can contain text, graphics, photos, music, speech, animation and video. References between nodes are possible through links. Links need not to be in sequential order so nodes can be accessed in a non-linear fashion. Hypermedia's underlying notion of linking nodes of information and its capability to handle these information entities stored in various forms appear to be well suited for engineering design support systems. NTIS

N94-23151 Institut National Polytechnique, Grenoble (France). Lab. de Conception de Systemes Integres.
LOGIC SYNTHESIS ON PROGRAMMABLE NETWORKS Ph.D. Thesis [SYNTHESE LOGIQUE SUR RESEAUX PROGRAMMABLES]
Laurent Bouchet 1992 180 p In FRENCH Limited Reproducibility: More than 20% of this document may be affected by microfiche quality
(ETN-94-95174) Avail: CASI HC A09

The logic synthesis problems on two types of programmable devices, the programmable gate array and the programmable array logic, are studied. The programmable gate array is organized as a network of elementary cells, in which each elementary cell can implement any boolean function or couple of boolean functions of k variables. In the programmable array logic, the basic block implements k boolean functions expressed as a sum of k prime product terms of k double prime variables. In both cases the lexicographical factorization method is proposed. It consists of writing in an optimized way a set of boolean functions while respecting an input order, called the lexicographical order, in the parenthesis of the expression. A decomposition into subfunctions mappable on the basic blocks relies on this lexicographical order, and looks for subfunctions depending on successive subsequences or slices of the input sequence. Two types of decompositions are proposed, one oriented towards area optimization and one oriented towards speed optimization. Practical results on a set of international benchmarks are shown. ESA

N94-23155 Institut National Polytechnique, Grenoble (France). Lab. de Genie Informatique.
A TYPE DECLARATIVE SYSTEM FOR PROLOG Ph.D. Thesis [UN SYSTEME DECLARATIF DE TYPES POUR PROLOG]
Lan NguyenPhuong 1992 124 p In FRENCH Limited Reproducibility: More than 20% of this document may be affected by microfiche quality
(ETN-94-95178) Avail: CASI HC A06

A polymorphic type declarative system for PROLOG language is developed. The principles of a type system for PROLOG and examples of solutions are given. Several typing approaches and real system examples are studied. The role of the mode concept for the language and for type systems is justified. Concerning the user, the following topics are discussed: type languages, predicate statements, and main order relationship between types. The theorem which states type corrections for characteristic typed programs is proven. The inner statements, the algorithms, and the techniques applied to implement a prototype on the system are presented. A type language allowing the parametric polymorphic concept and the type inclusion relationship to be described is developed. The sufficient condition for a satisfactory typing result is presented and validated. ESA

N94-23169# Technische Univ., Eindhoven (Netherlands). Design Automation Section.
USING GENETIC ALGORITHMS FOR SCHEDULING DATA FLOW GRAPHS
L. J. M. Cluitmans Dec. 1992 85 p
(EUT-92-E-266; ISBN-9-06-144266-4; ETN-94-94773) Avail: CASI HC A05/MF A01

A scheduling problem in High Level Synthesis, a section in a silicon compiler for the automatic design of integrated circuits, is addressed. In the High Level Synthesis section, the functional specification is transformed into a description for a network of modules (like adders or multipliers) and a controller for that network. A scheduler that uses a 'genetic algorithm' to perform the optimization is described. Internally it uses a (resource constrained) 'list scheduler' in the process of representing schedules. The genetic scheduler is fast and produces good results. Several features that would be nice for a scheduler (chaining, pipelining, taking into account register costs, etc.) are not yet implemented. The genetic part of the scheduler could not be tested very well because for many problems the initialization of the algorithm already gave the optimal solution. Larger benchmarks are necessary to test the genetic part more thoroughly. ESA

N94-23172# Technische Univ., Eindhoven (Netherlands). Faculty of Electrical Engineering.
PROGRIL: A LANGUAGE FOR THE DEFINITION OF PROTOCOL GRAMMARS
R. H. J. Bloks Mar. 1993 42 p
(EUT-93-E-270; ISBN-9-06-144270-2; ETN-94-94777) Avail: CASI HC A03/MF A01

One of the results of the protocol engine research project, which is targeted towards the automatic generation of hardware implementations for modern complex data communication protocols, is reported. The word 'automatic' implies the use of computers to accomplish the task which in turn requires a formal language that can be used to describe these protocols. Such a language and a compiler for it have now been created. The language is based on an extension of context free grammars and is called PROGRIL (Protocol Grammar Interface Language). The syntax and semantics of the protocol grammar interface language are informally described. In addition to defining a protocol grammar, PROGRIL contains some constructs that are necessary to link multiple grammars together in order to obtain a larger cooperating system. All sections of a PROGRIL description are explained, the exact syntax is given and for all possible constructs a textual explanation is given with some examples to clarify its use. Operator priorities and tables with all keywords with their use and meaning are given and the concept of time is introduced. Since there may be no ambiguities or inconsistencies in the protocol description language, its syntax must follow some strict rules, defined in a meta grammar. In principle, this meta description defines the exact syntax of the grammar, but it is not easily readable. The syntax is therefore explained in an easier to read and understand form. Context conditions are explained separately where necessary. The protocol grammar is used as a formal language to describe complex protocols in such a way, that they can be directly implemented in hardware, but also that formal verification methods are still applicable and interfacing to other high level languages remains possible. ESA

N94-23173# Technische Univ., Eindhoven (Netherlands). Faculty of Electrical Engineering.
CODE GENERATION FOR THE ATTRIBUTE EVALUATOR OF THE PROTOCOL ENGINE GRAMMAR PROCESSOR UNIT
R. H. J. Bloks Mar. 1993 40 p
(EUT-93-E-271; ISBN-9-06-144271-0; ETN-94-94778) Avail: CASI HC A03/MF A01

One of the results of the protocol engine research project, which is targeted towards the automatic generation of hardware implementations for modern complex data communication protocols, is reported. The word 'automatic' implies the use of computers to accomplish the task which in turn requires a formal language that can be used to describe these protocols. Such a language and a compiler for it have now been created. The language is based on an extension of context free grammars and is called PROGRIL (Protocol Grammar Interface Language). The process of code generation for the attribute expression evaluation is explained. A protocol grammar consists of a set of attributes or variables, a set of symbols, a set of production rules and attribute relations between the attributes of symbols appearing in the rules. Whenever a certain symbol is parsed, the expressions for its attributes must be evaluated. These protocol grammars can be implemented on protocol pushdown automata, which are extensions of the standard pushdown automaton. One of the extensions to this basic automaton is the attribute evaluator, which is in fact a custom designed processor capable of performing all operations required for the manipulation of attributes of the protocol grammar. All expressions given in the grammar are assignment expressions, using constants, declared attributes, and system variables or functions. These expressions must be translated directly into machine language code for the attribute evaluator by the PROGRIL compiler. This code will be referred to as explicit code. In contrast to the explicit code, there is also implicit code, which is necessary for correct operation of the system, but is not directly 'programmed' by the writer of the grammar. Instead, this code is implicitly defined by and extracted from the grammar. It is used to do attribute memory management, passing attribute values, and other system functions. ESA

N94-23180# Grenoble-1 Univ. (France). Lab. ARTEMIS.
MIXED ANALOG-DIGITAL DESCRIPTION AND SIMULATION: PROPOSITION FOR VHDL-ANALOGUE [DESCRIPTION ET SIMULATION MIXTES ANALOGIQUE-NUMERIQUE: PROPOSITIONS POUR VHDL-ANALOGIQUE]
Dominique Rodriguez (Anacad Computer Systems, Meylan, France.) Jan. 1992 49 p In FRENCH
(RR-908-I; ETN-93-94997) Avail: CASI HC A03/MF A01

Simulation is most widely used for the verification of Very Large Scale Integration (VLSI) circuits design. The importance of mixed mode digital analog simulation is highlighted and its basic principles are described. Several mixed mode simulators are presented. Hardware description languages that cover both the digital and the electric levels are considered. The generalities are presented together with the current standardization effort for analog Very Hardware Description Language (VHDL). The main requirements are analyzed, and examples are given to compare alternative solutions. ESA

N94-23207 Argonne National Lab., IL.
PROGRAMMING IN FORTRAN M
I. Foster, R. Olson, and S. Tuecke Aug. 1993 53 p Limited Reproducibility: More than 20% of this document may be affected by poor print
(Contract W-31-109-eng-38)
(DE94-000541; ANL-93/26) Avail: Issuing Activity (Department of Energy (DOE))

Fortran M is a small set of extensions to Fortran that supports a modular approach to the construction of sequential and parallel programs. Fortran M programs use channels to plug together processes which may be written in Fortran M or Fortran 77. Processes communicate by sending and receiving messages on channels. Channels and processes can be created dynamically, but programs remain deterministic unless specialized nondeterministic constructs are used. Fortran M programs can execute on a range of sequential, parallel, and networked computers. This report incorporates both a tutorial introduction to Fortran M and a users guide for the Fortran M compiler developed at Argonne National Laboratory. The Fortran M compiler, supporting software, and documentation are made available free of charge by Argonne National Laboratory, but are protected by a copyright which places certain restrictions on how they may be redistributed. See the software for details. The latest version of both the compiler and this manual can be obtained by anonymous ftp from Argonne National Laboratory in the directory pub/fortran-m at info.mcs.anl.gov. DOE

N94-23226# Helsinki Univ. of Technology, Espoo (Finland). Circuit Theory Lab.
APLAC: AN OBJECT-ORIENTED ANALOG CIRCUIT SIMULATOR AND DESIGN TOOL. 6.1 SYSTEM SIMULATIONS MANUAL
S. Rosnell and J. Liukkonen 1992 456 p See also PB93-187193 and PB93-187201 Prepared in cooperation with Nokia Research Center, Espoo, Finland
(PB93-224871; ISBN-951-22-1601-9) Copyright Avail: CASI HC A20/MF A04

The system simulations manual for the Analysis Program for Linear Active Circuits (APLAC), version 6.1 is presented. The main goal of APLAC is to give the user full freedom in solving his/her problems without the restrictions of conventional simulators. The sixth generation of APLAC was created having improved convergence algorithms for DC, transient, and harmonic analyses and improved menu-driven actions. In addition, convolution technique was implemented enabling the use of frequency-dependent components in the transient analysis of nonlinear circuits. NTIS

N94-23228# European Space Agency, Paris (France).
THE TOPSIM 4 GRAPHIC USER INTERFACE
G. Taricco (Politecnico di Torino, Italy.) and W. R. Burke, ed. Jul. 1993 31 p
(ESA-STM-247; ISBN-9-29-092212-5; ETN-94-95195) Copyright Avail: CASI HC A03/MF A01

A user interface for the telecommunication system simulation program TOPSIM 4 is described. Some key aspects for the development of user interfaces in this area are introduced and the available command set of the TOPSIM graphic user interface is described. The design of a sample system and the analysis of simulation results are presented. ESA

N94-23229# European Space Agency. European Space Research and Technology Center, ESTEC, Noordwijk (Netherlands). Software Standardization and Control Board.
GUIDE TO SOFTWARE CONFIGURATION MANAGEMENT
Nov. 1992 72 p
(ESA-PSS-05-09-Issue-1; ETN-94-95196) Copyright Avail: CASI HC A04/MF A01

The software engineering standards to be applied for all deliverable software implemented for the European Space Agency (ESA), either in house or by industry, are described. ESA Procedures, Specifications, Standards PSS-05-0 requires that the configuration of the code and documentation be managed throughout the software development life cycle. This activity is called Software Configuration Management (SCM). Each project must define its SCM activities in a SCM Plan (SCMP). Software configuration management is explained, guidelines on how to do it are provided, and the contents of a SCMP are detailed. This guide should be read by everyone concerned with developing, installing, and changing software, that is software project managers, software librarians, and software engineers. Some sections describing procedures for handling software problems and changing documents are of interest to users. ESA

N94-23301*# Illinois Univ., Chicago.
PATH PLANNING BY QUERYING PERSISTENT STORES OF TRAJECTORY SEGMENTS Abstract Only
Robert L. Grossman, S. Mehta, and Xiao Qin Sep. 1993 1 p Submitted for publication
(Grants NAG2-513; NSF DMS-91-01089)
(NASA-CR-194789; NAS 1.26:194789) Avail: CASI HC A01/MF A01

We introduce an algorithm for path planning (long duration) paths of dynamical systems, given a persistent object store containing suitable collections of short duration trajectory segments. We also describe experimental results from a proof-of-concept implementation of the algorithm. The basic idea is to interpret a path planning algorithm as a suitable query on a persistent object store consisting of short duration trajectory segments. The query returns a concatenation of short duration trajectory segments which is close to the desired path. The needed short duration segments are computed by using a divide and conquer algorithm to break up the original path into shorter paths; each shorter path is then matched to a nearby trajectory segment which is part of the persistent object store by using a suitable index function. Author

N94-23340*# Institute for Computer Applications in Science and Engineering, Hampton, VA.
PHASED-MISSION SYSTEM ANALYSIS USING BOOLEAN ALGEBRAIC METHODS
Arun K. Somani (Washington Univ., Seattle.) and Kishor S. Trivedi (Duke Univ., Durham, NC.) Nov. 1993 21 p
(Contract NAS1-19480; RTOP 505-90-52-01)
(NASA-CR-191564; ICASE-93-84; NAS 1.26:191564) Avail: CASI HC A03/MF A01

Most reliability analysis techniques and tools assume that a system is used for a mission consisting of a single phase. However, multiple phases are natural in many missions. The failure rates of components, system configuration, and success criteria may vary from phase to phase. In addition, the duration of a phase may be deterministic or random. Recently, several researchers have addressed the problem of reliability analysis of such systems using a variety of methods. A new technique for phased-mission system reliability analysis based on Boolean algebraic methods is described. Our technique is computationally efficient and is applicable to a large class of systems for which the failure criterion in each phase can be expressed as a fault tree (or an equivalent representation). Our technique avoids state space explosion that commonly plague Markov chain-based analysis. A phase algebra to account for the effects of variable configurations and success criteria from phase to phase was developed. Our technique yields exact (as opposed to approximate) results. The use of our technique was demonstrated by means of an example and present numerical results to show the effects of mission phases on the system reliability. Author (revised)

N94-23341*# Institute for Computer Applications in Science and Engineering, Hampton, VA.
AUTOMATED PARALLELIZATION OF TIMED PETRI-NET SIMULATIONS Final Report
David M. Nicol (College of William and Mary, Williamsburg, VA.) and Weizhen Mao (College of William and Mary, Williamsburg, VA.) Dec. 1993 30 p Submitted for publication
(Contracts NAS1-19480; NAS1-18605; NAG1-060; NAG1-787; NAG1-1132; NSF ASC-88-19373; NSF CCR-92-01195; NSF CCR-92-10372; RTOP 505-90-52-01)
(NASA-CR-191574; NAS 1.26:191574; ICASE-93-91) Avail: CASI HC A03/MF A01

Timed Petri-nets are used to model numerous types of large complex systems, especially computer architectures and communication networks. While formal analysis of such models is sometimes possible, discrete-event simulation remains the most general technique available for assessing the model's behavior. However, simulation's computational requirements can be massive, especially on the large complex models that defeat analytic methods. One way of meeting these requirements is by executing the simulation on a parallel machine. Simple techniques for the automated parallelization of timed Petri-net simulations are described. Both the issue of processor synchronization, as well as the automated mapping, static and dynamic, of the Petri-net to the parallel architecture are addressed. As part of this effort, a new mapping algorithm, one that also applies to more general parallel computations, is described. Analytic properties of the solution produced by the algorithm, including optimality on some regular topologies, are established. The viability of our integrated approach is demonstrated empirically on the Intel iPSC/860 and Delta architectures using many processors. Excellent performance is observed on models of parallel architectures. Author (revised)

N94-23369*# North Carolina Univ., Chapel Hill. Dept. of Computer Science.
IMAGE PATTERN RECOGNITION SUPPORTING INTERACTIVE ANALYSIS AND GRAPHICAL VISUALIZATION Final Report
James M. Coggins Jan. 1992 31 p
(Contract NAS5-30428; RTOP 506-59-11)
(NASA-CR-194878; NAS 1.26:194878) Avail: CASI HC A03/MF A01

Image Pattern Recognition attempts to infer properties of the world from image data. Such capabilities are crucial for making measurements from satellite or telescope images related to Earth and space science problems. Such measurements can be the required product itself, or the measurements can be used as input to a computer graphics system for visualization purposes. At present, the field of image pattern recognition lacks a unified scientific structure for developing and evaluating image pattern recognition applications. The overall goal of this project is to begin developing such a structure. This report summarizes results of a 3-year research effort in image pattern recognition addressing the following three principal aims: (1) to create a software foundation for the research and identify image pattern recognition problems in Earth and space science; (2) to develop image measurement operations based on Artificial Visual Systems; and (3) to develop multiscale image descriptions for use in interactive image analysis. Author (revised)

N94-23441# Technische Univ., Eindhoven (Netherlands). Dept. of Mathematics and Computing Science.
LINEAR TIME ALGORITHM TO SCHEDULE TREES WITH COMMUNICATION DELAYS OPTIMALLY ON TWO MACHINES
M. Veldhorst Mar. 1993 22 p
(PB93-237782; MEMO-COSOR-93-07) Avail: CASI HC A03/MF A01

For the implementation of a parallel program, considered as a collection of processes, on a parallel computer, one of the major problems is to determine which processor should execute which process and at what time; the purpose is that the moment of time that all processes have been executed (i.e., the execution of the parallel program has finished), occurs as early as possible. Besides the possibility that processes may have different execution lengths (possibly not exactly known in advance), processes might use (intermediate) results computed by other processes. Making these results available may require an additional (to the execution length) amount of time, the communication delay. During this communication, delay processors may execute processes that have already obtained all necessary data. The paper uses the general approach of list scheduling that yields feasible schedules, and proves that under certain conditions the algorithm runs in linear time. Then it concentrates on the creation of the list, such that the list-scheduling algorithm yields an optimal schedule and runs in linear time. NTIS

N94-23443 Selskapet for Industriell og Teknisk Forskning, Trondheim (Norway). Div. of Industrial Mathematics.
VISUALIZATION OF RESULTS FROM METEOROLOGICAL SIMULATIONS ON CRAY
S. Groenas and Ketil Aamnes Dec. 1992 34 p See also PB93-201366 Limited Reproducibility: More than 20% of this document may be affected by microfiche quality
(PB93-201358; STF10-A92019) Avail: Issuing Activity (National Technical Information Service (NTIS))

The report considers the problem of graphical display of the results from Numerical Weather Prediction (NWP) simulations based on the model used by the Norwegian Meteorological Institute (DNMI). First a brief description of this Norwegian NWP model and its use in Norway is given. Then the presentation aspects are introduced, the activity concerning visualization of meteorological information. Animation of 3D presentations, an activity called 4D visualization, has been tried in NWP research using high-end workstations as platforms. A main objective of the report is to investigate the present status of available software and HW-platforms for 4D visualization, and see if 4D presentations now can be done on low-end workstations. Some available software for 4D visualization of model output has been tried on a case describing the New Years Day Storm 1992, one of the strongest storms hitting Norway in modern time. A video has been made containing animated sequences from two of these systems. NTIS

N94-23444 Selskapet for Industriell og Teknisk Forskning, Trondheim (Norway). Div. of Industrial Mathematics.
GLview USER'S GUIDE
Ketil Aamnes Feb. 1993 35 p See also PB93-201341 Limited Reproducibility: More than 20% of this document may be affected by microfiche quality
(PB93-201366; STF10-A93002) Avail: Issuing Activity (National Technical Information Service (NTIS))

The report describes the scientific visualization program GLview. The program is written in C, and utilizes the Graphics Library (GL) for high performance 3D graphics. A Motif user interface enables easy interaction with the program. GLview is meant to be an effective tool for visualization of scientific data. This includes animation of models or results, and a variety of display options. The program is well suited for realtime animation on a screen or video tape. GLview is compatible with the MOVIE.BYU file format. This format includes a description of geometry, scalar and vector files. Since GLview does not make any assumptions concerning the physical significance of the scalar and vector files, they can be from any discipline. NTIS

N94-23451 Selskapet for Industriell og Teknisk Forskning, Trondheim (Norway). Reguleringsteknikk.
MITS ARCHITECTURE V1.0
O. J. Roedseth 8 Jan. 1993 34 p Limited Reproducibility: More than 20% of this document may be affected by microfiche quality
(PB93-201762; STF48-A93001) Avail: Issuing Activity (National Technical Information Service (NTIS))

The document gives a short overview of the Maritime Information Technology Standard (MITS) network. It looks at the programmer's model which is characterized by connection-oriented simple interface by point-to-point communication to a distributed database. The physical implementation is characterized by using established standards, as far as possible. The communication layers on top of TCP/IP are particular to MITS, but still open. It makes the application interface as simple as possible. Most complexity is hidden in application-independent and, hence, reusable modules. The MITS concept is useful for many different network architectures. NTIS

N94-23488# Sandia National Labs., Albuquerque, NM.
OBJECT ORIENTED SIMULATION IMPLEMENTATION IN SUPPORT OF ROBUST SYSTEM DESIGN
1993 8 p Presented at the Winter Simulation Conference, Los Angeles, CA, 12-15 Dec. 1993
(Contract DE-AC04-76DP-00789)
(DE93-011687; SAND-93-0922C; CONF-931208-1) Avail: CASI HC A02/MF A01

A very brief description of two 'classes' developed for use in design optimization and sensitivity analyses are given. These classes are used in simulations of systems in early design phases as well as system response assessments. The instantiated classes were coupled to system models to demonstrate the practicality and efficiency of using these objects in complex robust design processes. DOE

N94-23507*# George Washington Univ., Washington, DC. Dept. of Electrical Engineering and Computer Science.
A KNOWLEDGE BASED SYSTEM FOR SCIENTIFIC DATA VISUALIZATION Final Report
Hikmet Senay and Eve Ignatius Jan. 1992 23 p Original contains color illustrations
(Contract NAS5-30428; RTOP 506-59-11)
(NASA-CR-194879; NAS 1.26:194879) Avail: CASI HC A03/MF A01; 4 functional color pages

A knowledge-based system, called visualization tool assistant (VISTA), which was developed to assist scientists in the design of scientific data visualization techniques, is described. The system derives its knowledge from several sources which provide information about data characteristics, visualization primitives, and effective visual perception. The design methodology employed by the system is based on a sequence of transformations which decomposes a data set into a set of data partitions, maps this set of partitions to visualization primitives, and combines these primitives into a composite visualization technique design. Although the primary function of the system is to generate an effective visualization technique design for a given data set by using principles of visual perception the system also allows users to interactively modify the design, and renders the resulting image using a variety of rendering algorithms. The current version of the system primarily supports visualization techniques having applicability in earth and space sciences, although it may easily be extended to include other techniques useful in other disciplines such as computational fluid dynamics, finite-element analysis and medical imaging. Author (revised)

N94-23510*# National Aeronautics and Space Administration. Ames Research Center, Moffett Field, CA.
THE AUTOMATED INSTRUMENTATION AND MONITORING SYSTEM (AIMS) REFERENCE MANUAL
Jerry Yan (RECOM Software, Inc., San Jose, CA.), Philip Hontalas, and Sherry Listgarten (RECOM Software, Inc., San Jose, CA.) et al Nov. 1993 61 p
(RTOP 509-10-33)
(NASA-TM-108795; A-94012; NAS 1.15:108795) Avail: CASI HC A04/MF A01

Whether a researcher is designing the 'next parallel programming paradigm,' another 'scalable multiprocessor' or investigating resource allocation algorithms for multiprocessors, a facility that enables parallel program execution to be captured and displayed is invaluable. Careful analysis of execution traces can help computer designers and software architects to uncover system behavior and to take advantage of specific application characteristics and hardware features. A software tool kit that facilitates performance evaluation of parallel applications on multiprocessors is described. The Automated Instrumentation and Monitoring System (AIMS) has four major software components: a source code instrumentor which automatically inserts active event recorders into the program's source code before compilation; a run time performance-monitoring library, which collects performance data; a trace file animation and analysis tool kit which reconstructs program execution from the trace file; and a trace post-processor which compensate for data collection overhead. Besides being used as prototype for developing new techniques for instrumenting, monitoring, and visualizing parallel program execution, AIMS is also being incorporated into the run-time environments of various hardware test beds to evaluate their impact on user productivity. Currently, AIMS instrumentors accept FORTRAN and C parallel programs written for Intel's NX operating system on the iPSC family of multi computers. A run-time performance-monitoring library for the iPSC/860 is included in this release. We plan to release monitors for other platforms (such as PVM and TMC's CM-5) in the near future. Performance data collected can be graphically displayed on workstations (e.g. Sun Sparc and SGI) supporting X-Windows (in particular, XI IR5, Motif 1.1.3). Author (revised)

N94-23518 Rome Univ. (Italy). Dipt. di Fisica.
A WORKING ALGORITHM TO ISOLATE INTEGRABLE SURFACES IN E CUBED
D. Levi (Istituto Nazionale di Fisica Nucleare, Rome, Italy.), A. Sym (Warsaw Univ., Poland.), and Tu Gui-Zhang (Academia Sinica, Beijing, China.) 10 Oct. 1990 5 p Sponsored in part by Ministry of Public Education, Italy, and Ist. Nazionale di Fisica Nucleare, Rome, Italy Limited Reproducibility: More than 20% of this document may be affected by poor print
(SSCL-Preprint-761; ETN-93-93653) Avail: Issuing Activity (European Space Agency (ESA))

A working algorithm to isolate integrable parametric surfaces in E(cubed) is presented. It constitutes another application of the technique of Lie point symmetries of a system of partial differential equations. The standard tensorial notation and the standard surface-geometric terminology are applied. ESA

N94-23534 Selskapet for Industriell og Teknisk Forskning, Trondheim (Norway). Div. of Industrial Mathematics.
SIMULTANEOUS SIMULATION AND VISUALIZATION USING DGL
Ketil Aamnes, Vegard Vesterheim, and Terje Roelvag 31 Dec. 1992 30 p See also PB93-201358 Limited Reproducibility: More than 20% of this document may be affected by microfiche quality
(PB93-201341; STF10-A92018) Avail: Issuing Activity (National Technical Information Service (NTIS))

The main objective of the project was to develop knowledge about distributed graphics using the network transparent feature of the Graphics Library (GL) called the Distributed GL (DGL), which is part of the Cray Visual Tools (CVT). A program called GL view has been implemented on the CRAY utilizing DGL. The goal was to use this knowledge to develop a system for simultaneous simulation and visualization. It would allow the user to interrupt and communicate with the simulation as it proceeds. This gives the user a better understanding of the progress of a simulation. Part of the work has been concentrated on the development of a socket communication between a simulation program and the visualization program allowing these two processes to communicate even though they are executed on different machines. As a case to implement these ideas, a simulation program called FEDEM was chosen. FEDEM (Finite Element Dynamics of Elastic Mechanisms) is a program for simulating the dynamics of complex 2- and 3-dimensional mechanisms, including the elasticities of links. A socket communication between FEDEM and GL view has been implemented. NTIS

N94-23559*# Columbia Univ., New York, NY. Astrophysics Lab.
A COMPLETE PUBLIC ARCHIVE FOR THE EINSTEIN IPC Annual Status Report, 24 Sep. 1992 - 23 Sep. 1993
David J. Helfand Nov. 1993 7 p
(Contract NAS5-32063)
(NASA-CR-189316; NAS 1.26:189316; CAL-2145) Avail: CASI HC A02/MF A01

This report documents progress made in the period 29 September 1992 and 28 September 1993, on the project described in our proposal 'A Complete Public Archive for the Einstein IPC,' which was approved under the Astrophysics Data Program last year. All of the principal first-year objectives were achieved and we expect to continue our efforts over the next two years toward the goal of transferring the entire activity to the HEASARC. Author (revised)

N94-23568*# National Aeronautics and Space Administration. Ames Research Center, Moffett Field, CA.
A REVIEW OF EUROPEAN APPLICATIONS OF ARTIFICIAL INTELLIGENCE TO SPACE
Mark Drummond, ed. and Helen Stewart, ed. Oct. 1993 62 p
(RTOP 586-02-21)
(NASA-TM-108789; A-93127; NAS 1.15:108789) Avail: CASI HC A04/MF A01

The purpose is to describe the applications of Artificial Intelligence (AI) to the European Space program that are being developed or have been developed. The results of a study sponsored by the Artificial Intelligence Research and Development program of NASA's Office of Advanced Concepts and Technology (OACT) are described. The report is divided into two sections. The first consists of site reports, which are descriptions of the AI applications seen at each place visited. The second section consists of two summaries which synthesize the information in the site reports by organizing this information in two different ways. The first organizes the material in terms of the type of application, e.g., data analysis, planning and scheduling, and procedure management. The second organizes the material in terms of the component technologies of Artificial Intelligence which the applications used, e.g., knowledge based systems, model based reasoning, procedural reasoning, etc. Author (revised)

N94-23624*# Wallace (T. L.), Nashville, TN.
[DEVELOPMENT OF AN ANALYTICAL-NUMERICAL MODEL TO PREDICT RADIANT EMISSION OR ABSORPTION] Final Report, Dec. 1993
Tim L. Wallace 17 Jan. 1994 2 p
(NASA Order H-18070-D)
(NASA-CR-194860; NAS 1.26:194860; FPR8-TLW-01794; DCN-1-3-EB-29681) Avail: CASI HC A01/MF A01

The development of an analytical-numerical model to predict radiant emission or absorption is discussed. A voigt profile is assumed to predict the spectral qualities of a singlet atomic transition line for atomic species of interest to the OPAD program. The present state of this model is described in each progress report required under contract. Model and code development is guided by experimental data where available. When completed, the model will be used to provide estimates of specie erosion rates from spectral data collected from rocket exhaust plumes or other sources. Author (revised)

N94-23701# Mission Research Corp., Los Alamos, NM.
RADAR STIMULATOR INTERFACE PROTOCOL, PRELIMINARY INTERFACE DESIGN AND DOPPLER BEAM SHARPENING IMPLEMENTATION
C. H. Aldrich 30 Jun. 1993 23 p Prepared in cooperation with Los Alamos National Lab., NM
(Contract W-7405-eng-36)
(DE94-002567; LA-SUB-93-236) Avail: CASI HC A03/MF A01

This is the final report for a subcontract to supply a Doppler Beam Sharpening model to interface with the radar stimulation package running on the Cray supercomputers. The article describes the beam sharpening model, and the way beam sharpening is implemented by the model. Changes from previous work are emphasized in this report. DOE

N94-23707# Vrije Univ., Amsterdam (Netherlands). Dept. of Mathematics and Computer Science.
TRANSITION SYSTEM SPECIFICATIONS IN STALK FORMAT WITH BISIMULATION AS A CONGRUENCE
V. vanOostrom and E. P. deVink Jul. 1993 22 p
(PB94-110608; IR-332) Avail: CASI HC A03/MF A01

A many-sorted variant, called stalk format, of the single sorted tyft-format for transition system specifications is proposed. The stalk format is shown to be a convenient formalism to express continuation-style transition systems for languages incorporating concepts such as, e.g., process creation or backtracking, for which the existing formats seem less adequate. It is proved, extending a similar result for the single sorted case, that for an appropriate generalization of (strong) bisimilarity for the present many-sorted setting, bisimulation with respect to a transition system specification in stalk format is a congruence. It is argued that the several conditions, required for the type of transition system specification put forward in the paper, can not be relaxed without loosing this congruence. Finally, the present format is compared with several existing ones in the literature, viz. De Simone-, GSOS- and pure tyft-format. NTIS

N94-23745 Vrije Univ., Amsterdam (Netherlands). Faculteit der Wiskunds en Informatica.
OBJECT DISTRIBUTION IN ORCA USING COMPILE-TIME AND RUN-TIME TECHNIQUES
Hans E. Bal and M. Frans Kaashoek Jul. 1993 19 p See also PB94-110590 and PB93-142594 Sponsored by Netherlands Organization for Applied Scientific Research TNO Limited Reproducibility: More than 20% of this document may be affected by microfiche quality
(PB94-110574; IR-328) Avail: CASI HC A03

Orca is a language for parallel programming on distributed systems. Communication in Orca is based on shared data-objects, which is a form of distributed shared memory. The performance of Orca programs depends strongly on how shared data-objects are distributed among the local physical memories of the processors. The paper studies a new and efficient solution to this problem, based on an integration of compile-time and run-time techniques. The Orca compiler has been extended to determine the access patterns of processes to shared objects. The compiler passes a summary of this information to the run-time system, which uses it to make good decisions about which objects to replicate and where to store nonreplicated objects. Measurements show that the new system gives better overall performance than any previous implementation of Orca. NTIS

N94-23750# Technische Hogeschool Twente, Enschede (Netherlands). Faculteit der Informatica.
MICRO SIL-1 SIMULATOR
E. Molenkamp 1993 40 p
(PB94-110889; Memo-INF-93-38) Copyright Avail: CASI HC A03/MF A01

In the design flow of a digital system an intermediate is often used to come from a specification language to a realization. In the paper, the intermediate used is SIL-1, the SPRITE Input Language. As specification language the author uses VHDL. This specification is translated into a SIL-1 description, a number of transformations are performed on the generated signal flow graph, and finally is synthesized. During the developing phase of the VHDL to SIL translator, it is necessary to check if the generated SIL-1 graph has the same behavior as the original VHDL description, e.g. to detect programming errors in the translator. Since there is no SIL-1 simulator, the paper describes a simulator for a subset of a SIL-1 graph (structured types and sets are not supported). In many cases a one to one translation from a SIL-1 description to a VHDL description is performed. The generated VHDL description is simulated against the original VHDL description. NTIS

N94-23751# Technische Hogeschool Twente, Enschede (Netherlands). Tele-Informatics and Open Systems Group.
ADVANCED DESIGN CONCEPTS FOR OPEN DISTRIBUTED SYSTEMS DEVELOPMENT
L. F. Pires, M. vanSinderen, and C. A. Vissers 1993 13 p
(PB94-110897; TIOS-93/23) Copyright Avail: CASI HC A03/MF A01

Experience with the engineering of large scale open distributed systems has shown that their design should be specified at several well defined levels of abstractions, where each level aims at satisfying specific user, architectural and implementation purposes. Therefore, designers should dispose of a comprehensive design methodology, which allows them to conceive a specification at a certain abstraction level and transform this specification into a conforming specification at a lower abstraction level. The collection of these transformations should abridge the total design trajectory from initial user requirements to final implementation. The paper presents and discusses some advanced design concepts that provide a basis for such a design methodology. NTIS

N94-23759# Tilburg Univ. (Netherlands). Dept. of Economics.
ALGORITHM ON ADDITION CHAINS WITH RESTRICTED MEMORY Research Memo
M. J. Coster 1 Jun. 1993 23 p
(PB94-118692; FEW-603) Avail: CASI HC A03/MF A01

This paper considers addition chains, addition sequences and vector addition chains, introducing a new constraint--namely restricted memory--which is important in all of the applications on computers. We consider an algorithm for calculating addition chains, addition sequences, and vector addition chains--namely, a Generalized Continued Fraction Algorithm--which uses just a restricted number of memory locations on the computer. The average length of addition chains/sequences constructed by this algorithm will be calculated using a number of theoretical tools (from Ergodic Theory and Special Function Theory). Finally, this algorithm will be compared to some other known algorithms. NTIS

N94-23768 Technische Univ., Eindhoven (Netherlands). Dept. of Mathematics and Computing Science.
EXERCISES IN MULTIPROGRAMMING
P. D. Moerland 1993 109 p Limited Reproducibility: More than 20% of this document may be affected by microfiche quality
(PB94-101458; COMPUTING SCIENCE NOTES-93/07) Copyright Avail: Issuing Activity (National Technical Information Service (NTIS))

The topic of the report is the construction of multiprograms, i.e. cooperating sequential programs operating on shared variables. Three different approaches to the construction of multiprograms can be distinguished. The main part of the report consists of a series of derivations; e.g. a derivation of Peterson's (general) mutual exclusion algorithm and of Lamport's Bakery Algorithm. The first four chapters present the theory of Owicki and Gries, develop a small body of useful theorems and introduce the format of the derivations. The last chapter contains a small set of exercises. NTIS

N94-23796# Lawrence Livermore National Lab., CA.
A MATRIX ANALYSIS OF CONJUGATE GRADIENT ALGORITHMS
S. F. Ashby and M. H. Gutknecht (Eidgenoessische Technische Hochschule, Zurich, Switzerland.) Apr. 1993 16 p Presented at the 9th Symposium on Precondition Conjugate Gradients, Yokohama, Japan, 2 Mar. 1993
(Contract W-7405-eng-48)
(DE94-002546; UCRL-JC-113560; CONF-9303237-1) Avail: CASI HC A03/MF A01

This paper explores the relationships between the conjugate gradient algorithms Orthodir, Orthomin, and Orthores. To facilitate this exploration, a matrix formulation for each algorithm is given. It is shown that Orthodir directly computes a Hessenberg matrix H(sub k) at step k. Orthores also computes a Hessenberg matrix, G(sub k), which is similar to a Hessenberg matrix obtained from H(sub k) by perturbing its last column. (This perturbation vanishes at convergence.) Orthomin, on the other hand, computes a UL and LU factorization of the perturbed H(sub k) and G(sub k), respectively. The breakdown of Orthomin and Orthores are interpreted in terms of these underlying matrix factorizations. A connection with Lanczos algorithms is also examined, as is the special case of B-normal(1) matrices (for which efficient three-term CG algorithms exist). DOE

N94-23817# Technische Univ., Eindhoven (Netherlands). Dept. of Mathematics and Computing Science.
TYPECHECKER FOR BIJECTIVE PURE TYPE SYSTEMS
E. Poll 1993 39 p Sponsored by Netherlands Organization for Applied Scientific Research TNO
(PB94-110814; Computing Science Notes-93/22) Copyright Avail: CASI HC A03/MF A01

A type inference algorithm is given, which closely follows to the type derivation rules for Pure Type Systems. Soundness and completeness of the algorithm are proved for a large class of Pure Type Systems, which includes all systems in Barendregt's lambda-cube. NTIS

N94-24050*# Smithsonian Astrophysical Observatory, Cambridge, MA.
SAO MISSION SUPPORT SOFTWARE AND DATA STANDARDS, VERSION 1.0 Final Report
P. Hsieh Nov. 1993 16 p
(Contract NAS8-36123)
(NASA-CR-193906; NAS 1.26:193906; SAO-AXAF-DR-93-059) Avail: CASI HC A03/MF A01

This document defines the software developed by the SAO AXAF Mission Support (MS) Program and defines standards for the software development process and control of data products generated by the software. The SAO MS is tasked to develop and use software to perform a variety of functions in support of the AXAF mission. Software is developed by software engineers and scientists, and commercial off-the-shelf (COTS) software is used either directly or customized through the use of scripts to implement analysis procedures. Software controls real-time laboratory instruments, performs data archiving, displays data, and generates model predictions. Much software is used in the analysis of data to generate data products that are required by the AXAF project, for example, on-orbit mirror performance predictions or detailed characterization of the mirror reflection performance with energy. Derived from text

N94-24110*# Research Inst. for Advanced Computer Science, Moffett Field, CA.
ON THE DYNAMICS OF SOME GRID ADAPTION SCHEMES
Peter K. Sweby (Reading Univ., England.) and Helen C. Yee (National Aeronautics and Space Administration. Ames Research Center, Moffett Field, CA.) Feb. 1994 14 p Proceedings of the 4th International Conference on Numerical Grid Generation in Computational Fluid Dynamics and Related Fields held in Swansea, England, 6-8 Apr. 1994 Submitted for publication
(Contract NAS2-13721)
(NASA-CR-195092; NAS 1.26:195092; RIACS-TR-94-02) Avail: CASI HC A03/MF A01

The dynamics of a one-parameter family of mesh equidistribution schemes coupled with finite difference discretisations of linear and nonlinear

convection-diffusion model equations is studied numerically. It is shown that, when time marched to steady state, the grid adaption not only influences the stability and convergence rate of the overall scheme, but can also introduce spurious dynamics to the numerical solution procedure.
Author (revised)

N94-24111*# Auburn Univ., AL. Dept. of Computer Science and Engineering.
UPDATE OF GRASP/Ada REVERSE ENGINEERING TOOLS FOR Ada
James H. Cross, II 14 Dec. 1993 65 p
(Contract NAS8-39131)
(NASA-CR-193890; NAS 1.26:193890) Avail: CASI HC A04/MF A01

The GRASP/Ada project (Graphical Representations of Algorithms, Structures, and Processes for Ada) successfully created and prototyped a new algorithmic level graphical representation for Ada software, the Control Structure Diagram (CSD). The primary impetus for creation of the CSD was to improve the comprehension efficiency of Ada software and, as a result, improve reliability and reduce costs. The emphasis was on the automatic generation of the CSD from Ada PDL or source code to support reverse engineering and maintenance. The CSD has the potential to replace traditional pretty printed Ada source code. In Phase 1 of the GRASP/Ada project, the CSD graphical constructs were created and applied manually to several small Ada programs. A prototype CSD generator (Version 1) was designed and implemented using FLEX and BISON running under VMS on a VAX 11-780. In Phase 2, the prototype was improved and ported to the Sun 4 platform under UNIX. A user interface was designed and partially implemented using the HP widget toolkit and the X Windows System. In Phase 3, the user interface was extensively reworked using the Athena widget toolkit and X Windows. The prototype was applied successfully to numerous Ada programs ranging in size from several hundred to several thousand lines of source code. Following Phase 3,e two update phases were completed. Update'92 focused on the initial analysis of evaluation data collected from software engineering students at Auburn University and the addition of significant enhancements to the user interface. Update'93 (the current update) focused on the statistical analysis of the data collected in the previous update and preparation of Version 3.4 of the prototype for limited distribution to facilitate further evaluation. The current prototype provides the capability for the user to generate CSD's from Ada PDL or source code in a reverse engineering as well as forward engineering mode with a level of flexibility suitable for practical application. An overview of the GRASP/Ada project with an emphasis on the current update is provided.
Author (revised)

N94-24116 Applied Silicon, Inc., Ottawa (Ontario).
ASPT SOFTWARE SOURCE CODE: ASPT APPLICATION SOFTWARE PACKAGE, HOST COMPONENT
Hugh Parliament 17 Aug. 1992 171 p
(CTN-94-60907) Avail: Micromedia Ltd., Technical Information Centre, 165 Hotel de Ville, Place du Portage, Phase 2, Hull, Quebec J8X 3X2, Canada

The source code for the Adaptive Signal Processing Testbed application software package, host component, is presented. The source code covers the programs 'acqtool', 'aspt acq', 'acq convert', 'evaltool', 'ewacq server', 'aspt convert', and 'plot'. These programs are mainly concerned with data acquisition and data display. The files listed comprise the user interface program and the acquisition server for the testbed's data acquisition software. All of the configuration options for the acquisition and processing are set by the programs, along with the control options for starting and stopping the acquisition via the acquisition server.
Author (CISTI)

N94-24122 Defence Research Establishment Pacific, Victoria (British Columbia).
A COLOUR IMAGE PROCESSING ALGORITHM TO IDENTIFY COPPER-BASED PARTICLES IN FILTER DEBRIS SAMPLES
K. K. Yeung, G. A. Luoma, and A. J. Mckenzie Mar. 1993 27 p
(DREP-TM-93-19; CTN-94-60918) Avail: Micromedia Ltd., Technical Information Centre, 165 Hotel de Ville, Place du Portage, Phase 2, Hull, Quebec J8X 3X2, Canada

In oil-wetted aircraft machinery fitted with coarse filtration systems, sufficient fine particulate wear debris passes through the filter to enable meaningful spectrometric oil analysis (SOA) of the oil sample debris for off-line condition monitoring. The use of fine filters in F404 engines has severely limited the usefulness of oil analysis techniques because the filters remove almost all the debris of significance. Filter debris analysis (FDA) has been developed as an alternative off-line monitoring procedure for those engines. FDA can also supplement conventional oil analysis for condition monitoring of machinery with coarse filtration by evaluating the accumulated wear debris generated between filter changes. The method has been very successful at predicting wear anomalies and is being adopted into the routine maintenance procedures for selected machinery. The main drawbacks of FDA are that it is time consuming, manpower intensive, and prone to subjective interpretation. The use of computer-aided image analysis to interpret filter debris is being investigated with the goal of incorporating FDA results into an expert system for condition monitoring. Results of image capture and interpretation of FDA are presented, and implications of these developments on condition monitoring of oil-wetted machinery are discussed.
Author (CISTI)

N94-24130 Defence Research Establishment Pacific, Victoria (British Columbia).
THE DETECTION PERFORMANCE OF A LONG-TERM SPECTRAL INTEGRATOR USING NORMALIZED AND QUANTIZED DATA
B. H. Maranda Feb. 1993 35 p
(DREP-TM-93-11; CTN-94-60893) Avail: Micromedia Ltd., Technical Information Centre, 165 Hotel de Ville, Place du Portage, Phase 2, Hull, Quebec J8X 3X2, Canada

The standard method for detection of narrowband signals is to use an energy detector implemented by a fast Fourier transform (FFT) followed by a squarer. For display and storage purposes, the FFT spectra are normalized and then quantized, and a long-term noncoherent integration is then attained visually by stacking the quantized spectra in a frequency time intensity (FTI) display, or lofargram. The effect of both normalization and quantization on the narrowband detection performance of a long-term spectral integrator is examined in order to determine whether heavily quantized spectra give adequate performance. The performance is described by the receiver operating characteristic, which is computed numerically from the probability density function of the detection statistic. It is found that the loss in performance due to normalization is small, less than 0.2 dB for an example case. The loss due to quantization depends on the number of bits used. When the quantizer uses only one bit, the loss is about 1 dB. This loss can be decreased to under 0.1 dB by the use of three bits in the quantizer.
Author (CISTI)

N94-24134 Applied Silicon, Inc., Ottawa (Ontario).
ASPT SOFTWARE SOURCE CODE: DEVELOPMENT SYSTEM PACKAGE, LIBRARY COMPONENT
Hugh Parliament 17 Aug. 1992 227 p
(CTN-94-60905) Avail: Micromedia Ltd., Technical Information Centre, 165 Hotel de Ville, Place du Portage, Phase 2, Hull, Quebec J8X 3X2, Canada

The source code for the library component of the development system package, part of the Adaptive Signal Processing Testbed, is presented. The source code is in a combination of C and assembler language, and covers the library routines for the testbed's VMEC30 signal processor board executive functions, various digital signal processing functions, and functions for interfacing the VMEC30 to the host.
Author (CISTI)

N94-24135 Applied Silicon, Inc., Ottawa (Ontario).
ASPT SOFTWARE SOURCE CODE: ASPT APPLICATION SOFTWARE PACKAGE, VME-C30 COMPONENT
Hugh Parliament 17 Aug. 1992 100 p
(CTN-94-60906) Avail: Micromedia Ltd., Technical Information Centre, 165 Hotel de Ville, Place du Portage, Phase 2, Hull, Quebec J8X 3X2, Canada

The source code for the Adaptive Signal Processing Testbed application software package is presented. The source code covers the programs 'dacq.out' and 'eval.out' which are TM320C30 signal processor programs for the testbed's VMEC30 board. They interact with the programs in the host component and collect and process data before passing it to the host.
Author (CISTI)

N94-24297 Software Kinetics Ltd., Stittsville (Ontario).
ACES SPECTRAL DISPLAY SOFTWARE: SOFTWARE DESCRIPTION
30 Apr. 1992 23 p

(SK-1600-99-003; CTN-94-60908) Avail: Micromedia Ltd., Technical Information Centre, 165 Hotel de Ville, Place du Portage, Phase 2, Hull, Quebec J8X 3X2, Canada

The Advanced Communications Electronic Support Measures System (ACES) is a testbed to be used in the development of technologies for an electronic support measures (ESM) system. The system is to be capable of real-time detection and identification of low probability of intercept high and very high frequency communication signals. The user interface subsystem provides the user with a real-time display of the frequency spectrum of received signals. It consists of a personal computer with a high resolution graphics display and an integral digital signal processor card. The ACES Spectral Display software is the software portion of this subsystem. The individual components of this software that support the user interface are described. These include the main routine that calls the upper level routines, initialization and termination routines, user input and output routines, the axis-drawing routine, the color pallet routine, and routines for executing the real-time processing loop. CISTI

N94-24470*# Harris Corp., Melbourne, FL. Government Aerospace Systems Div.

A HOMOTOPY ALGORITHM FOR DIGITAL OPTIMAL PROJECTION CONTROL GASD-HADOC Final Report

Emmanuel G. Collins, Jr., Stephen Richter, and Lawrence D. Davis Oct. 1993 163 p

(Contract NAS8-38575)

(NASA-CR-193881; NAS 1.26:193881) Avail: CASI HC A08/MF A02

The linear-quadratic-gaussian (LQG) compensator was developed to facilitate the design of control laws for multi-input, multi-output (MIMO) systems. The compensator is computed by solving two algebraic equations for which standard closed-loop solutions exist. Unfortunately, the minimal dimension of an LQG compensator is almost always equal to the dimension of the plant and can thus often violate practical implementation constraints on controller order. This deficiency is especially highlighted when considering control-design for high-order systems such as flexible space structures. This deficiency motivated the development of techniques that enable the design of optimal controllers whose dimension is less than that of the design plant. A homotopy approach based on the optimal projection equations that characterize the necessary conditions for optimal reduced-order control. Homotopy algorithms have global convergence properties and hence do not require that the initializing reduced-order controller be close to the optimal reduced-order controller to guarantee convergence. However, the homotopy algorithm previously developed for solving the optimal projection equations has sublinear convergence properties and the convergence slows at higher authority levels and may fail. A new homotopy algorithm for synthesizing optimal reduced-order controllers for discrete-time systems is described. Unlike the previous homotopy approach, the new algorithm is a gradient-based, parameter optimization formulation and was implemented in MATLAB. The results reported may offer the foundation for a reliable approach to optimal, reduced-order controller design. Author (revised)

N94-24480*# Richmond Univ., VA. Dept. of Mathematics and Computer Science.

THE ADAM LANGUAGE: Ada EXTENDED WITH SUPPORT FOR MULTIWAY ACTIVITIES Final Report

Arthur Charlesworth Dec. 1993 65 p

(Grant NAG1-774; RTOP 505-64-10)

(NASA-CR-4565; NAS 1.26:4565) Avail: CASI HC A04/MF A01

The Adam language is an extension of Ada that supports multiway activities, which are cooperative activities involving two or more processes. This support is provided by three new constructs: diva procedures, meet statements, and multiway accept statements. Diva procedures are recursive generic procedures having a particular restrictive syntax that facilitates translation for parallel computers. Meet statements and multiway accept statements provide two ways to express a multiway rendezvous, which is an n-way rendezvous generalizing Ada's 2-way rendezvous. While meet statements tend to have simpler rules than multiway accept statements, the latter approach is a more straightforward extension of Ada. The only nonnull statements permitted within meet statements and multiway accept statements are calls on instantiated diva procedures. A call on an instantiated diva procedure is also permitted outside a multiway rendezvous; thus sequential Adam programs using diva procedures can be written. Adam programs are translated into Ada programs appropriate for use on parallel computers. Author

N94-24507 Tilburg Univ. (Netherlands). Dept. of Economics.

VERIFICATION AND VALIDATION OF MODELS

Jack P. C. Kleijnen 1993 38 p Limited Reproducibility: More than 20% of this document may be affected by microfiche quality

(PB94-110566; FEW-571) Avail: Issuing Activity (National Technical Information Service (NTIS))

The paper surveys verification and validation of models, especially simulation models in operations research. For verification it discusses the followi ng topics: (1) general good programming practice (such as modular programming), (2) checking intermediate simulation outputs through tracing and statistical testing per module, (3) statistical testing of final simulation outputs against analytical results, and (4) animation. For validation it discusses the following topics: (1) obtaining real-world data; (2) comparing simulated and real data through simple tests such as graphical, Schruben-Turing, and t tests; (3) testing whether simulated and real responses are positively correlated and moreover have the same mean using two new statistical procedures based on regression analysis; (4) sensitivity analysis based on design of experiments and regression analysis, and risk or uncertainty analysis based on Monte Carlo sampling; and (5) white versus black box simulation models. Both verification and validation require good documentation, and are crucial parts of assessment, credibility, and accreditation. A bibliography with 53 references is included. NTIS

N94-24513 Technische Univ., Eindhoven (Netherlands). Dept. of Mathematics and Computing Science.

SYSTEMS ENGINEERING: A FORMAL APPROACH. PART 3: MODELING METHODS

K. M. vanHee 30 Mar. 1993 113 p See also PB94-101417 and PB94-101391 Limited Reproducibility: More than 20% of this document may be affected by microfiche quality

(PB94-101409; Computing Science Notes-93/11) Avail: Issuing Activity (National Technical Information Service (NTIS))

In the book a method is a set of guidelines and techniques that can be used for the following tasks: (1) Construction of a model for a system. Two cases are distinguished: Making a model after reality; and transforming a given model into another one. (2) Analysis of a model. Again, two cases are distinguished: Verifying properties of a model by means of a formal proof; and validating a model by means of simulation of the behavior of the model. NTIS

N94-24534 Rutherford Appleton Lab., Chilton (England). Software Engineering Group.

MERILL: AN EQUATIONAL REASONING SYSTEM IN STANDARD ML: A USER GUIDE (PRERELEASE VERSION 0.4)

Brian Matthews Apr. 1993 58 p See also PB86-173812 and PB91-121749 Limited Reproducibility: More than 20% of this document may be affected by microfiche quality

(PB93-204501; RAL-93-026) Avail: Issuing Activity (National Technical Information Service (NTIS))

The document is intended to be a guide to the features available in the MERILL equational reasoning system. The author gives an overview and then walks through an example session. A more detailed description of all the commands and features of the MERILL system is then given. It gives some pointers to the underlying theory involved and examples of the system's use. MERILL is a general purpose order-sorted equational reasoning system. It is written in Standard ML. NTIS

N94-24535# Yale Univ., New Haven, CT. Dept. of Computer Science.

FAST FOURIER TRANSFORMS OF PIECEWISE CONSTANT FUNCTIONS

Eugene Sorets Sep. 1993 21 p

(Grant NSF DMS-90-12135)

(AD-A272648; YALEU/DCS/RR-986) Avail: CASI HC A03/MF A01

We present an algorithm for the evaluation of the Fourier transform of piecewise constant functions of two variables. The algorithm overcomes the accuracy problems associated with computing the Fourier transform of discontinuous functions; in fact, its time complexity is O(log(3)(1/epsilon)N(2) + log(2)(1/epsilon)(N(2)log N)), where epsilon is the accuracy and N is the size of the problem. The algorithm is based on the Lagrange interpolation formula and the Green's theorem, which are used to preprocess the data before applying the fast Fourier transform. It admits natural generalizations to higher dimensions and to piecewise smooth functions. DTIC

N94-24556# Naval Postgraduate School, Monterey, CA.
AN AUTOMATED TOOL TO FACILITATE CODE TRANSLATION FOR SOFTWARE FAULT TREE ANALYSIS M.S. Thesis
Robert R. Ordonio Sep. 1993 211 p
(AD-A273205) Avail: CASI HC A10/MF A03

A safe system is defined as a system that prevents unsafe states from producing safety failures, where an unsafe state is defined as a state that may lead to safety failure unless some specific action is taken to avert it. The problem addressed is how to find places in Ada programs where faults are likely to occur during program execution. The approach is to build an automated translation tool that translates Ada programs into a software fault tree. The tool works as follows: (1) The Ada parser and lexical analyzer calls the Automated Code Translation Tool (ACTT) upon recognition of an Ada statement; (2) The ACTT produces a template representing the statement; (3) The templates are linked together as a software fault tree. The result is a program that takes Ada source code as input and produces a software fault tree as output. DTIC

N94-24566# Argonne National Lab., IL.
HIGH-PERFORMANCE COMPUTING AND COMMUNICATIONS
R. Stevens 1993 10 p Presented at the International Symposium on Highly-Advanced Computing, Sendai, Japan, 9 Nov. 1993
(Contract W-31-109-eng-38)
(DE94-002215; ANL/MCS/CP-81094; CONF-9311117-1) Avail: CASI HC A02/MF A01

This presentation has two parts. The first part discusses the US High-Performance Computing and Communications program -- its goals, funding, process, revisions, and research in high-performance computing systems, advanced software technology, and basic research and human resources. The second part of the presentation covers specific work conducted under this program at Argonne National Laboratory. Argonne's efforts focus on computational science research, software tool development, and evaluation of experimental computer architectures. In addition, the author describes collaborative activities at Argonne in high-performance computing, including an Argonne/IBM project to evaluate and test IBM's newest parallel computers and the Scalable I/O Initiative being spearheaded by the Concurrent Supercomputing Consortium. DOE

N94-24570 Vrije Univ., Amsterdam (Netherlands).
COMBINATORY REDUCTION SYSTEMS: INTRODUCTION AND SURVEY
J. W. Klop, V. vanOostrom, and F. vanRaamsdonk 1993 30 p Prepared in cooperation with Centrum voor Wiskunde en Informatica, Amsterdam (Netherlands) Limited Reproducibility: More than 20% of this document may be affected by microfiche quality
(PB94-110582) Avail: CASI HC A03

Combinatory Reduction Systems (CRS's) were designed to combine the usual first-order format of term rewriting with the presence of bound variables as in pure lambda-calculus and various typed lambda-calculi. The paper introduces the class of orthogonal CRS's, illustrated with many examples, discusses its expressive power, and gives an outline of a short proof of confluence. There is a well-known connection between the parallel reduction and the concept of 'developments', and a classical lemma in the theory of lambda-calculus is that of 'Finite Developments', a strong normalization result. It turns out that the notion of 'parallel reduction' gives rise to a generalized form of developments, called 'superdevelopments' and on which it briefly comments. It concludes by mentioning the results of a comparison of CRS's with the recently proposed and strongly related format of higher-order rewriting: Nipkow's HRS's (Higher-order Rewrite Systems). NTIS

N94-24599 Groningen Rijksuniv. (Netherlands). Dept. of Mathematics.
SIGNATURES OF SELFADJOINT PENCILS
Aad Dijksma and Aurelian Gheondea 1993 34 p Limited Reproducibility: More than 20% of this document may be affected by microfiche quality
(PB94-111127; W-9313) Avail: CASI HC A03

For bounded selfadjoint operators F and G on a Hilbert space with F(R(G)bar) included in R(G), we give formulae and estimates of the positive/negative signatures kappa(+-)((lambda)G - F) of the pencil (lambda)G - F. For example, we prove that for all real lambda, kappa(+-) ((lambda)G - F) = or less than min (kappa(+-) ((lambda - 0)G - F), kappa(+-) ((lambda + 0)G - F)). These results are reformulated in terms of the pencil (lambda)I - A where A is a selfadjoint operator in a Krein space and then proved by means of the spectral theory of definitizable operators. NTIS

N94-24603*# National Aeronautics and Space Administration. Langley Research Center, Hampton, VA.
A PROGRAMMING ENVIRONMENT FOR DISTRIBUTED COMPLEX COMPUTING. AN OVERVIEW OF THE FRAMEWORK FOR INTERDISCIPLINARY DESIGN OPTIMIZATION (FIDO) PROJECT. NASA LANGLEY TOPS EXHIBIT H120B
James C. Townsend, Robert P. Weston, and Thomas M. Eidson (High Technology Corp., Hampton, VA.) Dec. 1993 15 p
(RTOP 505-59-53-08)
(NASA-TM-109058; NAS 1.15:109058) Avail: CASI HC A03/MF A01

The Framework for Interdisciplinary Design Optimization (FIDO) is a general programming environment for automating the distribution of complex computing tasks over a networked system of heterogeneous computers. For example, instead of manually passing a complex design problem between its diverse specialty disciplines, the FIDO system provides for automatic interactions between the discipline tasks and facilitates their communications. The FIDO system networks all the computers involved into a distributed heterogeneous computing system, so they have access to centralized data and can work on their parts of the total computation simultaneously in parallel whenever possible. Thus, each computational task can be done by the most appropriate computer. Results can be viewed as they are produced and variables changed manually for steering the process. The software is modular in order to ease migration to new problems: different codes can be substituted for each of the current code modules with little or no effect on the others. The potential for commercial use of FIDO rests in the capability it provides for automatically coordinating diverse computations on a networked system of workstations and computers. For example, FIDO could provide the coordination required for the design of vehicles or electronics or for modeling complex systems. Author

N94-24626# Los Alamos National Lab., NM.
THE EXPERIMENTAL PHYSICS AND INDUSTRIAL CONTROL SYSTEM ARCHITECTURE: PAST, PRESENT, AND FUTURE
Leo R. Dalesio, Jeffrey O. Hill, Martin Kraimer (Argonne National Lab., IL.), Steven Lewis (California Univ., Berkeley. Lawrence Berkeley Lab.), Douglas Murray (Superconducting Super Collider Lab., Dallas, TX.), Stephan Hunt (Superconducting Super Collider Lab., Dallas, TX.), Matthias Claussen (Deutsches Elektronen-Synchrotron, Hamburg, Germany.), William Watson (Continuous Electron Beam Accelerator Facility, Newport New, VA.), and John Dalesio (Tate Integrated Systems.) 1993 8 p Presented at the International Conference on Accelerator and Large Experimental Control Systems, Berlin, Germany, 18-22 Oct. 1993
(Contracts W-7405-eng-36; DE-AC35-89ER-40486; W-31-109-eng-38)
(DE94-002639; LA-UR-93-3640; CONF-931023-6) Avail: CASI HC A02/MF A01

The Experimental Physics and Industrial Control System (EPICS), has been used at a number of sites for performing data acquisition, supervisory control, closed-loop control, sequential control, and operational optimization. The EPICS architecture was originally developed by a group with diverse backgrounds in physics and industrial control. The current architecture represents one instance of the 'standard model.' It provides distributed processing and communication from any LAN device to the front end controllers. This paper will present the genealogy, current architecture, performance envelope, current installations, and planned extensions for requirements not met by the current architecture. DOE

N94-24638*# Institute for Computer Applications in Science and Engineering, Hampton, VA.
FAST SIMULATION OF PACKET LOSS RATES IN A SHARED BUFFER COMMUNICATIONS SWITCH Final Report
Cheng-Shang Chang (National Tsing Hua Univ., Hsinchu, Taiwan.), Philip Heidelberger, and Perwez Shahabuddin (International Business Machines Corp., Yorktown Heights, NY.) Nov. 1993 23 p Submitted for publication

(Contract NAS1-19480; RTOP 505-90-52-01)
(NASA-CR-191556; NAS 1.26:191556; ICASE-93-79) Avail: CASI HC A03/MF A01

This paper describes an efficient technique for estimating, via simulation, the probability of buffer overflows in a queueing model that arises in the analysis of ATM (Asynchronous Transfer Mode) communication switches. There are multiple streams of (autocorrelated) traffic feeding the switch that has a buffer of finite capacity. Each stream is designated as either being of high or low priority. When the queue length reaches a certain threshold, only high priority packets are admitted to the switch's buffer. The problem is to estimate the loss rate of high priority packets. An asymptotically optimal importance sampling approach is developed for this rare event simulation problem. In this approach, the importance sampling is done in two distinct phases. In the first phase, an importance sampling change of measure is used to bring the queue length up to the threshold at which low priority packets get rejected. In the second phase, a different importance sampling change of measure is used to move the queue length from the threshold to the buffer capacity. Author

N94-24661# Christopher Newport Coll., Newport News, VA.
COMPUTER MODELING OF NONLINEARITIES
A. M. Buoncristiani, G. Armagan (College of William and Mary, Williamsburg, VA.), and A. A. Kaminskii (Academy of Sciences, USSR, Moscow.) [1991] 10 p
Avail: CASI HC A02/MF A01

Efforts to improve the performance of lasers used as spectroscopic probes or as measurement tools have resulted in significant refinements of the properties of the laser light: higher power, higher spectral brightness, longer coherence length and coherence time, and shorter pulses. These efforts have also uncovered novel nonlinear responses in the laser itself and in its interaction with matter; these new phenomena challenge our understanding of laser dynamics and of the interaction of laser radiation with matter. This paper will describe some anomalous behavior arising from nonlinearities in laser processes and in material response. It will examine the nonlinearities that arise from inter-ionic processes and from stimulated emission and discuss the difficulties introduced by these nonlinearities in computations required to predict laser performance and the response of a nonlinear medium to laser excitation. Examples of these phenomena will be drawn from the YAG:Tm,Ho solid state laser system. Author (revised)

N94-24679*# Institute for Computer Applications in Science and Engineering, Hampton, VA.
RUNTIME SUPPORT AND COMPILATION METHODS FOR USER-SPECIFIED DATA DISTRIBUTIONS Final Report
Ravi Ponnusamy (Maryland Univ., College Park.), Joel Saltz (Maryland Univ., College Park.), Alok Choudhury (Syracuse Univ., NY.), Yuan-Shin Hwang (Maryland Univ., College Park.), and Geoffrey Fox (Syracuse Univ., NY.) Dec. 1993 36 p Submitted for publication
(Contracts NAS1-19480; NAG1-1485; ONR-SC-292-1-22913; NSF ASC-92-13821; NSF CCR-93-57840; RTOP 505-90-52-01)
(NASA-CR-191587; NAS 1.26:191587; ICASE-93-99) Avail: CASI HC A03/MF A01

This paper describes two new ideas by which an HPF compiler can deal with irregular computations effectively. The first mechanism invokes a user specified mapping procedure via a set of compiler directives. The directives allow use of program arrays to describe graph connectivity, spatial location of array elements, and computational load. The second mechanism is a simple conservative method that in many cases enables a compiler to recognize that it is possible to reuse previously computed information from inspectors (e.g. communication schedules, loop iteration partitions, information that associates off-processor data copies with on-processor buffer locations). We present performance results for these mechanisms from a Fortran 90D compiler implementation. Author

N94-24680*# Institute for Computer Applications in Science and Engineering, Hampton, VA.
A COMPARISON OF APPROXIMATE INTERVAL ESTIMATORS FOR THE BERNOULLI PARAMETER Final Report
Lawrence Leemis (College of William and Mary, Williamsburg, VA.) and Kishor S. Trivedi (Duke Univ., Durham, NC.) Dec. 1993 17 p Submitted for publication
(Contract NAS1-19480; RTOP 505-90-52-01)
(NASA-CR-191585; NAS 1.26:191585; ICASE-93-97) Avail: CASI HC A03/MF A01

The goal of this paper is to compare the accuracy of two approximate confidence interval estimators for the Bernoulli parameter p. The approximate confidence intervals are based on the normal and Poisson approximations to the binomial distribution. Charts are given to indicate which approximation is appropriate for certain sample sizes and point estimators. Author

N94-24684# Naval Postgraduate School, Monterey, CA.
AN INVESTIGATION OF REQUIREMENTS TRACEABILITY TO SUPPORT SYSTEMS DEVELOPMENT M.S. Thesis
Gale A. Harrington and Kathleen M. Rondeau Sep. 1993 94 p
(AD-A273167) Avail: CASI HC A05/MF A01

Department of Defense Standard 2167A mandates that requirements traceability be conducted during the development of government systems. This and other standards, as well as current literature, however, do not provide a comprehensive model of what information should be captured as a part of a traceability scheme. The primary goal of this research is to develop a model of requirements traceability at the level of systems design which relates requirements to all system components. An empirical study using focus groups was conducted with various stakeholders involved with the development of large, complex systems. Based on an analysis of the information obtained by the focus group sessions, a model for traceability was developed. This model describes the various relationships or linkages between requirements and system components that must be captured and maintained to support various system development activities. Finally, several issues which must be addressed in successfully implementing a comprehensive scheme for traceability are discussed. DTIC

N94-24693# Carnegie-Mellon Univ., Pittsburgh, PA. Dept. of Computer Science.
A TYPE-THEORETIC APPROACH TO HIGHER-ORDER MODULES WITH SHARING
Robert Harper and Mark Lillibridge Oct. 1993 23 p
(Contract F19628-91-C-0168; ARPA Order 8313)
(AD-A273566; CMU-CS-93-197) Avail: CASI HC A03/MF A01

The design of a module system for constructing and maintaining large programs is a difficult task that raises a number of theoretical and practical issues. A fundamental issue is the management of the flow of information between program units at compile time via the notion of an interface. Experience has shown that fully opaque interfaces are awkward to use in practice since too much information is hidden, and that fully transparent interfaces lead to excessive interdependencies, creating problems for maintenance and separate compilation. The 'sharing' specifications of Standard ML address this issue by allowing the programmer to specify equational relationships between types in separate modules, but are not expressive enough to allow the programmer complete control over the propagation of type information between modules. These problems are addressed from a type-theoretic viewpoint by considering a calculus based on Girard's system F(sub omega). The calculus differs from those considered in previous studies by relying exclusively on a new form of weak sum type to propagate information at compile-time, in contrast to approaches based on strong sums which rely on substitution. The new form of sum type allows for the specification of equational, as well as type and kind, information in interfaces. This provides complete control over the propagation of compile-time information between program units and is sufficient to encode in a straightforward way most uses of type sharing specifications in Standard ML. DTIC

N94-24740*# Institute for Computer Applications in Science and Engineering, Hampton, VA.
AN INTEGRATED RUNTIME AND COMPILE-TIME APPROACH FOR PARALLELIZING STRUCTURED AND BLOCK STRUCTURED APPLICATIONS Final Report
Gagan Agrawal (Maryland Univ., College Park.), Alan Sussman (Maryland Univ., College Park.), and Joel Saltz (Maryland Univ., College Park.) Oct. 1993 33 p Submitted for publication
(Contracts NAS1-19480; NAG1-1485; ONR-SC-292-1-22913; NSF ASC-92-13821; RTOP 505-90-52-01)
(NASA-CR-191554; NAS 1.26:191554; ICASE-93-77) Avail: CASI HC A03/MF A01

Scientific and engineering applications often involve structured meshes. These meshes may be nested (for multigrid codes) and/or irregularly coupled (called multiblock or irregularly coupled regular mesh problems). A combined runtime and compile-time approach for parallelizing these applications on distributed memory parallel machines in an efficient and machine-independent fashion was described. A runtime library which can be used to port these applications on distributed memory machines was designed and implemented. The library is currently implemented on several different systems. To further ease the task of application programmers, methods were developed for integrating this runtime library with compilers for HPK-like parallel programming languages. How this runtime library was integrated with the Fortran 90D compiler being developed at Syracuse University is discussed. Experimental results to demonstrate the efficacy of our approach are presented. A multiblock Navier-Stokes solver template and a multigrid code were experimented with. Our experimental results show that our primitives have low runtime communication overheads. Further, the compiler parallelized codes perform within 20 percent of the code parallelized by manually inserting calls to the runtime library.
Author (revised)

N94-24758 Technische Univ., Twente (Netherlands). Dept. of Computer Science and Electrical Engineering.
VALIDATION ACTIVITIES FOR LOTOS BASED ON STATIC DATA FLOW ANALYSIS M.S. Thesis
H. vanderSchoot 1993 122 p Limited Reproducibility: More than 20% of this document may be affected by microfiche quality
(PB94-110863; TIOS-93/21,) Copyright Avail: CASI HC A06

The thesis discusses data flow based validation of Full LOTOS specifications and their implementations. By performing static data flow analysis, the flow of data expressed in a given LOTOS specification is explicitly exposed. This explicit exposure facilitates two validation activities, namely, data flow anomaly detection and data flow oriented test selection. Data flow anomalies may indicate possible errors in the specification. A new criterion for data flow oriented test selection, called the maximal IO-df-chains criterion, is proposed for selecting a finite set of paths from the specification. The selected paths are subsequently used to guide the generation of executable test sequences. NTIS

N94-24765 Technische Univ., Eindhoven (Netherlands). Dept. of Mathematics and Computing Science.
CLASS OF STRONG VALID INEQUALITIES FOR THE DISCRETE LOT-SIZING AND SCHEDULING PROBLEM
Stan VanHoesel and Antoon Kolen Mar. 1993 24 p Limited Reproducibility: More than 20% of this document may be affected by microfiche quality
(PB93-237774; MEMO-COSOR-93-08) Avail: CASI HC A03

A class of strong valid inequalities for the discrete lot-sizing and scheduling problem is presented. Necessary and sufficient conditions are derived for valid inequalities in this class to be facet-defining. The separation problem for these inequalities is shown to be solvable in polynomial time by dynamic programming. NTIS

N94-24775# Naval Postgraduate School, Monterey, CA.
A METHODOLOGY FOR SOFTWARE COST ESTIMATION USING MACHINE LEARNING TECHNIQUES M.S. Thesis
Michael A. Kelly 3 Sep. 1993 143 p
(AD-A273158) Avail: CASI HC A07/MF A02

The Department of Defense expends billions of dollars on software development and maintenance annually. Many Department of Defense projects fail to be completed, at large monetary cost to the government, due to the inability of current software cost-estimation techniques to estimate, at an early project stage, the level of effort required for a project to be completed. One reason is that current software cost-estimation models tend to perform poorly when applied outside of narrowly-defined domains. Machine learning offers an alternative approach to the current models. In machine learning, the domain specific data and the computer can be coupled to create an engine for knowledge discovery. Using neural networks, genetic algorithms, and genetic programming along with a published software project data set, several cost estimation models were developed. Testing was conducted using a separate data set. All three techniques showed levels of performance that indicate that each of these techniques can provide software project managers with capabilities that can be used to obtain better software cost estimates. DTIC

N94-24797*# National Aeronautics and Space Administration. Goddard Space Flight Center, Greenbelt, MD.
INTELLIGENT SYSTEMS AND ADVANCED USER INTERFACES FOR DESIGN, OPERATION, AND MAINTENANCE OF COMMAND MANAGEMENT SYSTEMS Semiannual Status Report, 1 Apr. - 30 Dec. 1993
William J. Potter and Christine M. Mitchell (Georgia Inst. of Tech., Atlanta.) Dec. 1993 17 p
(Grant NAG5-2226)
(NASA-CR-195172; NAS 1.26:195172) Avail: CASI HC A03/MF A01

Historically, command management systems (CMS) have been large and expensive spacecraft-specific software systems that were costly to build, operate, and maintain. Current and emerging hardware, software, and user interface technologies may offer an opportunity to facilitate the initial formulation and design of a spacecraft-specific CMS as well as to develop a more generic CMS system. New technologies, in addition to a core CMS common to a range of spacecraft, may facilitate the training and enhance the efficiency of CMS operations. Current mission operations center (MOC) hardware and software include Unix workstations, the C/C++ programming languages, and an X window interface. This configuration provides the power and flexibility to support sophisticated and intelligent user interfaces that exploit state-of-the-art technologies in human-machine interaction, artificial intelligence, and software engineering. One of the goals of this research is to explore the extent to which technologies developed in the research laboratory can be productively applied in a complex system such as spacecraft command management. Initial examination of some of these issues in CMS design and operation suggests that application of technologies such as intelligent planning, case-based reasoning, human-machine systems design and analysis tools (e.g., operator and designer models), and human-computer interaction tools (e.g., graphics, visualization, and animation) may provide significant savings in the design, operation, and maintenance of the CMS for a specific spacecraft as well as continuity for CMS design and development across spacecraft. The first six months of this research saw a broad investigation by Georgia Tech researchers into the function, design, and operation of current and planned command management systems at Goddard Space Flight Center. As the first step, the researchers attempted to understand the current and anticipated horizons of command management systems at Goddard. Preliminary results are given on CMS commonalities and causes of low re-use, and methods are proposed to facilitate increased re-use. CASI

N94-24812# Army Construction Engineering Research Lab., Champaign, IL.
THE USE OF DESIGN AUTOMATION SOFTWARE BY GOVERNMENT-CONTRACTED ARCHITECT/ENGINEER FIRMS: A STATUS REPORT Interim Report
Michael L. Golish, Carrie J. McCunn, and Beth A. Symonds Sep. 1993 46 p
(AD-A273181; CERL-IR-FF-93/06) Avail: CASI HC A03/MF A01

Most Architecture and Engineering (A/E) design firms and Corps of Engineers District offices have found that computer-aided design and drafting (CADD) has a great potential for improving productivity, profitability, communication, and design quality. Yet, clients' demand for design and construction information created with CADD and delivered in a variety of specified computer formats can hinder scheduling, quality control, and profitability of A/E firms. This phase of research collected information on the status and use of CADD by A/E firms to identify trends in hardware, software, CADD staffing and compensation, and trends in how design firms that use CADD have accepted this form of automation. Secondary objectives were to determine how CADD has improved design firm productivity, design quality, documentation, and profitability, and to note any outstanding problems associated with the use of CADD in the design process. The second phase will review and analyze reports from the Army's Automated Review Management System (ARMS) and the Construction Evaluation Retrieval System (CERS) to determine how automation has affected Corps review procedures, and to locate and classify repetitive data that may be streamlined in future design and construction projects.
DTIC

N94-24822# Hydrologic Engineering Center, Davis, CA.
THE HEC NexGen SOFTWARE DEVELOPMENT PROJECT
Darryl W. Davis Jan. 1993 15 p
(AD-A273512; HEC-TP-138) Avail: CASI HC A03/MF A01

The NexGen project, a five year project begun in 1990, is developing successor software packages to the existing family of HEC hydrologic engineering computer programs. The project is being accomplished through a management process that employs teams comprised of technical specialists, computer scientists, and consultants. Modern software engineer methods of requirements analysis, prototype development, field testing, and feedback, are employed. Object-oriented program architecture implemented with C++ and advanced data features of FORTRAN 90 are being used. Prototype models of NexGen software packages in catchment and river analysis are now operational and beta-test versions will be completed at the end of this next year. Final packages are expected to be completed on schedule. The packages will be functional for RISC-chip and Intel-chip based desktop computers. DTIC

N94-24927 Naval Postgraduate School, Monterey, CA.
PARAMETRIC UNCERTAINTY REDUCTION IN ROBUST MULTIVARIABLE CONTROL Ph.D. Thesis
David L. Krueger Sep. 1993 105 p Limited Reproducibility: More than 20% of this document may be affected by microfiche quality
(AD-A273412) Avail: Issuing Activity (Defense Technical Information Center (DTIC))

This dissertation presents a method for reducing the number of parametric uncertainties used in the design of a robust H-infinity controller. The resulting controller is shown to meet robust stability and performance requirements in the presence of all the modeled uncertainties. The approach used involves grouping parametric variations affecting the same open loop eigenvalue, then scaling one or more of these variations to accommodate the eigenvalue change caused by all the parametric uncertainties. This method is effective in those cases where a large number of parametric uncertainties cause current computer aided design software to fail to find a robust controller for the plant. DTIC

N94-24932 Carnegie-Mellon Univ., Pittsburgh, PA. School of Computer Science.
PERFORMANCE MEASUREMENTS OF THE MULTIMEDIA TESTBED ON MACH 3.0: EXPERIENCE WRITING REAL-TIME DEVICE DRIVERS, SERVERS, AND APPLICATIONS
Roger B. Dannenberg, David B. Anderson, Tom Neuendorffer, Dean Rubine, and Jim Zelenka 21 Jul. 1993 25 p Limited Reproducibility: More than 20% of this document may be affected by microfiche quality
(AD-A273600; CMU-CS-93-205) Avail: CASI HC A03

Multimedia has generated a widespread interest in real-time support within general purpose operating systems. In addition to real-time support, multimedia often requires large amounts of data to be moved between devices and processes. The Multimedia Testbed is a set of applications that stress consistent low-latency response and efficient interprocess communication for large blocks of data. The Multimedia Testbed was ported to the Mach 3.0 Operating System where performance was measured. Experiments were conducted to compare various techniques for IPC and disk reads. Experience with fixed priority scheduling, user-level device drivers, and a high-resolution timer are also reported. DTIC

N94-24933 Carnegie-Mellon Univ., Pittsburgh, PA. School of Computer Science.
ANALYZING THE PROPERTIES OF USER INTERFACE SOFTWARE
Rick Kazman, Len Bass, Gregory Abowd, and Mike Webb Oct. 1993 26 p Limited Reproducibility: More than 20% of this document may be affected by microfiche quality
(Contract F19628-90-L-0003)
(AD-A273601; CMU-CS-93-201) Avail: Issuing Activity (Defense Technical Information Center (DTIC))

Software architecture is an increasingly important research topic and in this report we investigate the potential role of architecture in evaluating the properties of a system built to a particular architecture. Currently such architectural analysis is complicated for two main reasons: authors of new architectures describe their creations in idiosyncratic terms; and there is no clear way of understanding an architecture with respect to an organization's life cycle concerns--efficiency, maintainability, modifiability, and so forth. This report addresses these shortcomings by proposing a domain-based method for analyzing software architectures called SAAM (Software Architecture Analysis Method). DTIC

N94-24935 Army Construction Engineering Research Lab., Champaign, IL.
DECLARATIVE OBJECT MANIPULATION ENVIRONMENT (DOME): ALPHA VERSION Final Report
R. A. Whitehurst and John Pietrzak Sep. 1993 56 p Limited Reproducibility: More than 20% of this document may be affected by microfiche quality
(DA Proj. 4A1-62784-AT-41)
(AD-A273233; CERL-TR-FF-93/12) Avail: Issuing Activity (Defense Technical Information Center (DTIC))

The Declarative Object Manipulation Environment (DOME) is a programming language developed as part of the Integrated Systems Language Environment (ISLE) that combines elements of object-oriented programming with knowledge-based and declarative programming facilities. The alpha version of this system, named ModLog (for 'Modular Logic') was built as a declarative extension to the Army's ModSim language. This report traces the evolution of declarative programming extensions from their beginnings in the Prolog programming language, through ModLog, to the first implementation of the DOME system. The integration of process-based simulation with DOME's declarative rule-based capabilities creates a powerful modeling paradigm that is superior to conventional imperative approaches. DTIC

N94-25023*# Computer Software Management and Information Center, Athens, GA.
COSMIC MONTHLY PROGRESS REPORT
Jan. 1994 17 p
(Contract NASw-4670)
(NASA-CR-195153; NAS 1.26:195153) Avail: CASI HC A03/MF A01

Activities of the Computer Software Management and Information Center (COSMIC) are summarized for the month of January 1994. Tables showing the current inventory of programs available from COSMIC are presented and program processing and evaluation activities are discussed. Marketing and customer service activities in this period are presented as is the progress report of NASTRAN maintenance and support. Tables of disseminations and budget summary conclude the report. CASI

N94-25061# Technische Univ., Eindhoven (Netherlands).
GENERALIZED LINEAR MIXED MODELS AND THEIR APPLICATION IN PLANT BREEDING RESEARCH Ph.D. Thesis
Johannes Jansen 1993 143 p
(ETN-94-95335) Avail: CASI HC A07/MF A02

Variance components play a prominent role in applications of plant breeding research involving discrete data. The study shows that the class of Generalized Linear Mixed Models (GLMM's) provides a powerful and unified way of modeling discrete data involving variance components. The generalized linear mixed model is described. The Gaussian-Hermite quadrature, used for approximating integrals in the likelihood function of a GLMM is presented. It is shown, for a simple GLMM, that maximum likelihood estimation of the fixed effects and the variance component representing between-unit variation can be carried out by iterative weighted least squares. The use of a parametric family of link functions is considered. It is shown that the maximum likelihood estimates of the variance component of a GLMM are based downwards. A threshold model for ordinal data, which contains a GLMM for binary/binomial data as a special case, is summarized. It is argued that for ordinal data a distinction between lack of fit and between-unit variation should be made. It is shown that the methods for ordinal data can be extended to copy with more than one variance component. For Poisson counts involving two variance components, the simplification is approximated by a quadratic function. ESA

N94-25063# Technische Univ., Eindhoven (Netherlands). Dept. of Mathematics and Computing Systems Science.
BINARY BLOCK CODES FOR CORRECTING ASYMMETRIC OR UNIDIRECTIONAL ERRORS Ph.D. Thesis
Gang Fang 1993 104 p
(ETN-94-95337) Avail: CASI HC A06/MF A02

Bounds and constructions of Asymmetric or Unidirectional Error Correcting

(AsEC or UEC) codes are studied. The properties of codes for correcting asymmetric errors are investigated. The uniqueness of optimal block codes and the properties of uniformly weakly perfect codes are considered. Basic results for obtaining bounds on the maximum sizes of codes for correcting asymmetric errors are given. Most of these results can be applied to codes for correcting unidirectional errors. Bounds on the maximum size of binary block, t-AsEC and t-UEC of length less than or equal to 27 with t greater than or equal to 5 and t less than or equal to 8 are considered. The uniqueness of optimal 1-AsEC codes of length less than 9 is discussed. ESA

N94-25074# Naval Postgraduate School, Monterey, CA.
REENGINEERING REAL-TIME SOFTWARE SYSTEMS M.S. Thesis
Randall C. Scott 9 Sep. 1993 72 p
(AD-A273408) Avail: CASI HC A04/MF A01

The problem this thesis solves is how to reengineer existing real-time applications implemented without software engineering (SE) attributes, with poor modularity and robustness, and that are difficult to read and maintain. The real-time system chosen for this study was the Model-based Mobile robot Language (MML) used on the Yamabico-11 mobile robot, which was implemented without SE attributes. The approach taken was reengineering MML with a focus on improving modifiability while preserving functionality. First we developed a systematic plan using manual static analysis, then we incrementally reengineered the application with thorough system-level testing. Code review was used to locate and remove dead code, and synonymous and redundant variables and functions (improving modifiability, readability and robustness). Call-hierarchy tracing was used to gain explicit module restructuring insight for tighter cohesion (improving modifiability, modularity, and readability). Global-variable tracing was used to improve module coupling by localizing and minimizing global variables (improving modularity, readability, and robustness). The results were as follows: a method for applying SE to existing real-time applications after-the-fact called 'Reengineering Real-Time Software Systems' was developed, which improves modifiability, modularity, robustness and readability. MML now has improved modularity and robustness, and is easier to read and maintain. DTIC

N94-25080# Technische Univ., Eindhoven (Netherlands).
AREA-POWER-DELAY TRADE-OFF IN LOGIC SYNTHESIS Ph.D. Thesis
Michel R. C. M. Berkelaar 1992 128 p
(ISBN-9-09-005332-8; ETN-94-95295) Copyright Avail: CASI HC A07/MF A02

New concepts to perform area-power-delay tradeoffs in a logic synthesis system are discussed. To achieve this, a delay model which gives accurate delay estimations for arbitrary sets of Boolean expressions is presented. Algorithms for a number of different optimization tasks within logic synthesis are presented. There are algorithms to create prime irredundant Boolean expressions, to perform technology mapping for use with standard cell generators, and to perform gate sizing. A view of computer aided very large scale integration design and the synthesis of a system named EUCLID (Eindhoven University Combinatorial Logic Implementation system with Decomposition) are given. Basic problems of logic synthesis are discussed. The issue of prime irredundant expressions, which is important for testability of the design, is analyzed. A new algorithm based on Shannon expansion is presented. A basic delay model is derived, and extended to be used in all stages of the logic synthesis process. The technology mapping problem for generated basic cells and the gate sizing problem are discussed. ESA

N94-25138# Naval Postgraduate School, Monterey, CA.
AN IMPLEMENTATION OF THE REPRESENTATION AND MAINTENANCE OF PROCESS KNOWLEDGE (REMAP) MODEL IN THE KNOWLEDGE-BASED SOFTWARE ASSISTANT CONCEPT DEMONSTRATION SYSTEM M.S. Thesis
Frank J. Hughes and Steven C. Kendall Sep. 1993 82 p
(AD-A273207) Avail: CASI HC A05/MF A01

The REpresentation and MAintenance of Process knowledge (REMAP) model supports the various stakeholders involved in software design during development and maintenance by capturing the rationale behind design decisions. This process knowledge is invaluable with changing requirements and assumptions. In the context of formal software development, process knowledge about the development of formal specifications from informal requirements will facilitate the understanding and maintenance of such specifications. We have implemented the REMAP model in the United States Air Force Rome Laboratory's KBSA Concept Demonstration system (a formal software development environment) to capture this process knowledge. We provide a graphical browser to facilitate the instantiation, browsing and modification of REMAP model primitives and a mechanism to reason with the knowledge in the Concept Demonstration system. DTIC

N94-25148# Software Productivity Consortium, Herndon, VA.
REUSE-DRIVEN SOFTWARE PROCESSES GUIDEBOOK, VERSION 02.00.03
Nov. 1993 400 p Supersedes AD-A259404. See also AD-A259405
(Contract MDA972-92-J-1018)
(AD-A273644; SPC-92019-CMC) Avail: CASI HC A17/MF A04

The Reuse-Driven Software Processes Guidebook describes the Synthesis family of reuse-driven software development processes. In particular, it prescribes the practice for two example members of this family, illustrating the different stages of reuse capability that can be addressed by this family. Development organizations choose the process that matches their reuse goals. Synthesis is a comprehensive, business-area-level solution to problems of software productivity and quality in the building of systems to meet diverse and changing needs. Synthesis is most appropriate for development organizations that produce many similar systems or single unique systems with highly-volatile requirements during system development and maintenance. Synthesis is a systematic approach to software development founded on the belief that the resources of a business-area organization should be managed not only to meet the immediate needs of customers, but also as an investment in future capability. This guidebook serves as a detailed guide to the practice of Synthesis, addressing all activities and work products related to the production of software, in support of the needs and objectives of a business-area organization and its customers. DTIC

N94-25149# Software Productivity Consortium, Herndon, VA.
REUSE ADOPTION GUIDEBOOK, VERSION 02.00.05
Nov. 1993 280 p
(Contract MDA972-92-J-1018)
(AD-A273652; SPC-92051-CMC) Avail: CASI HC A13/MF A03

The Reuse Adoption Guidebook was produced for use by organizations to assist them in improving their competitiveness through the adoption and institutionalization of software reuse technology. Reuse refers to the use of a software asset in the solution of different problems or different versions of a problem. While many forms of reuse technology are currently available and the technology can address many different organizational objectives, crafting the opportunities into an implementable program that meets a particular organization's objectives is a difficult task. This guidebook prescribes a reuse adoption process to help perform that task. A key component in the reuse adoption process is a Reuse Capability Model, which is a tool that can aid an organization in understanding its current capabilities and in establishing goals for its reuse adoption process. DTIC

N94-25156 Raytheon Co., Tewksbury, MA. Missile Systems Lab.
DARPA DICE MANUFACTURING OPTIMIZATION Quarterly Technical Report No. 7, 1 Jul. - 30 Sep. 1993
Linda J. Lapointe and Robert F. Bryant 1993 25 p Limited Reproducibility: More than 20% of this document may be affected by microfiche quality
(Contract MDA972-92-C-0020; ARPA Order 8363)
(AD-A273345) Avail: Issuing Activity (Defense Technical Information Center (DTIC))

This is the Quarterly Technical Report for the DARPA DICE Manufacturing Optimization. The goal of the Manufacturing Optimization (MO) system is to facilitate a two tiered team approach to the product/process development cycle where a product design is analyzed by multiple manufacturing engineers, and product/process changes are traded concurrently in the product and process domains. The system will support Design for Manufacturing and Assembly (DFMA) with a set of tools to model manufacturing processes, and manage tradeoffs across multiple processes. The subject of this report is the technical work accomplished during the seventh quarter of the contract. The main thrust of the seventh quarter was integration and test of the MO software and the development of the MO user manual. Highlighted in this report is the tutorial section of the user manual. DTIC

N94-25179*# Ohio State Univ., Columbus. Dept. of Electrical Engineering.
DESIGN AND IMPLEMENTATION OF A DISTRIBUTED VERSION OF THE NASA ENGINE PERFORMANCE PROGRAM Final Report
Jeffrey T. Cours Mar. 1994 62 p
(Grant NAG3-1369; RTOP 505-69-50)
(NASA-CR-194475; E-8619; NAS 1.26:194475) Avail: CASI HC A04/MF A01

Distributed NEPP is a new version of the NASA Engine Performance Program that runs in parallel on a collection of Unix workstations connected through a network. The program is fault-tolerant, efficient, and shows significant speed-up in a multi-user, heterogeneous environment. This report describes the issues involved in designing distributed NEPP, the algorithms the program uses, and the performance distributed NEPP achieves. It develops an analytical model to predict and measure the performance of the simple distribution, multiple distribution, and fault-tolerant distribution algorithms that distributed NEPP incorporates. Finally, the appendices explain how to use distributed NEPP and document the organization of the program's source code. Author (revised)

N94-25219# Technische Univ., Eindhoven (Netherlands).
UNDERSTANDING AND FACILITATING DISCOVERY LEARNING IN COMPUTER-BASED SIMULATION ENVIRONMENT Ph.D. Thesis
Wouter Reinder vanJoolingen 1993 210 p
(ISBN-9-03-860242-1; ETN-94-95320) Avail: CASI HC A10/MF A03

Computer simulations are presented as a mean for creating exploratory learning environments. The global instructional characteristics are discussed. The notions of constructivism and exploratory learning are given. Based on the structure of exploratory learning environment, both from the simulationist and from qualitative reasoning research and the theory on exploratory and inductive learning, a theoretical framework for describing the most important exploratory learning processes is presented. The domain and the simulation environment used are described. An instrument for supporting hypothesis formation, which can be used for starting hypothesis, a hypothesis scratchpad, is presented. The effect of supplying the learner with such an instrument under different conditions is investigated. The conditions under which the learners apply specific subprocesses of hypothesis formation are discussed. A computer program for making automatic analysis of hypotheses stated by the learner is presented. ESA

N94-25237# Technische Univ., Eindhoven (Netherlands).
DESIGNS WITH A SMALL NUMBER OF RUNS FOR FACTORIAL EXPERIMENTS Ph.D. Thesis
Pieter Martinus Upperman 1993 268 p
(ISBN-9-03-860162-X; ETN-94-95323) Avail: CASI HC A12/MF A03

Nearly 40 designs for quantitative factors are developed. Aspects of linear regression theory and experimental design such as the linear regression model, D and G efficiency, and the techniques of replacement and collapsing are overviewed. Methods to find D optimal experimental designs for the incomplete quadratic model in which d variables have linear and quadratic terms, but the other (k - d) variables have only linear terms, are presented. These D optimal designs were constructed to be able to calculate the D efficiencies of a large number of designs. A measure of orthogonality, the variance inflation factor, is introduced. Two applications of the designs developed and two methods to construct designs with 16 experimental units are given. New designs with two and three level factors are developed using orthogonal columns of some main effect designs. The 39 new and six existing designs are discussed and compared using various design characteristics. ESA

N94-25252 Technische Univ., Delft (Netherlands). Telecommunications and Traffic-Control Systems Group.
ON CHAIN CODING OF LINE DRAWINGS Ph.D. Thesis
Kun Liu 1992 181 p Limited Reproducibility: More than 20% of this document may be affected by microfiche quality
(ISBN-9-06-275778-2; ETN-94-95366) Copyright Avail: CASI HC A09

The digital encoding of (handwritten) line drawings is addressed. Focus is on real time image coding of handwriting by adopting space sampling. Design and the performance of chain codes depend on the characteristics of the line drawing source being dealt with. Statistical modeling of line drawings is, thus, an important issue. For chain coding of handwriting, probabilistic spatial distributions of sampled line segments are empirically studied and analytically modeled. Based on this, the performance in terms of distortion and coding efficiency is analyzed and compared for a class of standard chain codes. In particular, the relationship between the distortion and the rate of a chain code is established, which provides a quantitative means for the design of practical chain coding systems with desired performance. For given chain codes of line drawings, the problem of generating efficient binary representation for real time transmission is considered. The problem is studied with considerations of possible bit errors caused by the physical limitations of real transmission channels. The performance of a class of chain encoding schemes is determined and compared within this framework. By exploiting the correlation between adjacent spatially quantized line segments, these encoding schemes permit more reduction of encoded data rate than the standard chain coding. The chain coding technique for real time handwriting is also applied to facsimile coding of line graphic blocks often found in mixed mode documents in multimedia applications. The performance of standard chain coding, in terms of data compression, is compared with that of run length coding. It is quantitatively shown that chain coding permits higher coding efficiency, provided that the total length of curves within a block is not excessive. The critical value of the total curve length is derived for which chain coding becomes less efficient. ESA

N94-25263# Technische Univ., Eindhoven (Netherlands). Design Automation Section.
FROM CIRCUIT TO SIGNAL: DEVELOPMENT OF A PIECEWISE LINEAR SIMULATOR Ph.D. Thesis
Hendrik Willem Buurman 1993 129 p
(Grant EEL66.1206)
(ISBN-9-09-005713-7; ETN-94-95356) Copyright Avail: CASI HC A07/MF A02

The development of the electronic circuit simulator called PLATO (Piecewise Linear Analysis Tool) is described. An insight in the choices of the algorithms used in the creation of an efficient simulator is given. The basics of the piecewise modeling technique are introduced. Several of its basic properties are derived and a theorem on the existence of solutions is proved. Examples show the capabilities of the modeling. The models have three different types of variables and equations: linear, dynamic, and piecewise linear. The basic data structures are introduced and the solution algorithm for the linear equations is discussed. The Van de Panne algorithm is presented. A method to find a DC solution is given. The solution of the dynamic equations is discussed and the multirate integration method is investigated. The combination of the Van de Panne algorithm and the integration method is also discussed. Several aspects of the implementation, to improve the efficiency and accuracy of the simulator, are considered. Examples of systems simulated with PLATO are shown. Conclusions are formulated and future extensions are discussed. A 'small' model for certain functions is derived and non-standard notations are explained. ESA

N94-25287# STATCOM, Inc., McLean, VA.
COMPUTERIZED TESTING SYSTEM SOFTWARE CONVERSION AND DEVELOPMENT: IDENTIFYING SOFTWARE AND HARDWARE PORTABILITY ISSUES AND SOLUTIONS Interim Report, Jul. 1991 - Dec. 1992
Rodney Rosse (American Inst. for Research, Washington, DC.), David Dodd, and Jay M. Silva (Army Research Office, Washington, DC.) Oct. 1993 63 p
(Contract MDA903-91-D-0024; DA Proj. 2Q1-62785-A-791)
(AD-A273489; ARI-TR-990) Avail: CASI HC A04/MF A01

This report identifies hardware and software issues associated with the transition of computerized tests from old hardware and software configurations to currently available hardware and software. Hardware issues addressed include the following: real-time clock performance, storage devices, video adapter, central processing unit (CPU), and CPU processing speed. Software issues addressed include conversion from PASCAL to C code and hardware-dependent routines. DTIC

N94-25311# Sheffield Univ. (England). Dept. of Automatic Control and Systems Engineering.
UNWRAPPING THE PHASE RESPONSE FUNCTIONS FOR NONLINEAR SYSTEMS
H. Zhang and S. A. Billings 7 Dec. 1992 29 p

(Grant SERC-GR/F-8564.2)
(RR-465; ETN-94-95133) Avail: CASI HC A03/MF A01

The phase unwrapping problem for nonlinear systems was studied. Two algorithms were developed to unwrap the higher order generalized phase response functions. The higher order phase response functions contain important information about the behavior of nonlinear systems. Algorithms based on integrating the partial derivatives of the phase and using multiples of 2pi to amend the principle value were derived and implemented. The use of unwrapped phase allows the entire phase response to be calculated by superposing the phase of the various factors. The parametric estimation approach for the generalized frequency response functions provides a powerful tool for the analysis of nonlinear systems in the frequency domain. ESA

N94-25315# Sheffield Univ. (England). Dept. of Automatic Control and Systems Engineering.
GENETIC ALGORITHMS IN CONTROL SYSTEMS ENGINEERING
P. J. Fleming and C. M. Fonseca 15 Mar. 1993 9 p Sponsored by Junta Nacional de Investigacao Cientifica e Tecnologia, Portugal
(RR-470; ETN-94-95137) Avail: CASI HC A02/MF A01

Recent control applications of genetic algorithms are discussed. Genetic algorithms are adaptive search techniques, based on the principles of natural genetics and natural selection, which, in control systems engineering, can be used as an optimization tool or as the basis of general adaptive systems. The versatile and robust qualities of these algorithms are reviewed and their relevance for control systems is highlighted. Applications and implementation issues including parallelization are addressed. Prospective future directions are identified. ESA

N94-25321# Sheffield Univ. (England). Dept. of Automatic Control and Systems Engineering.
TWO-DIMENSIONAL PATTERN ANALYSIS AND CLASSIFICATION USING A COMPLEX ORTHOGONAL ESTIMATION ALGORITHM
K. M. Tsang (Hong Kong Polytechnic, Kowloon.) and S. A. Billings 1993 31 p
(RR-475; ETN-94-95141) Avail: CASI HC A03/MF A01

An orthogonal estimation algorithm is derived. The algorithm is developed to evaluate parameters associated with the complex autoregressive boundary model of two dimensional shapes. It is shown that the coefficients of the orthogonal model and the original system parameters are invariant to rotation around the origin, to the choice of starting point in tracing the boundary, and to scale and translation. The error reduction ratios derived can be used to detect which terms should be included in the system model. The classification based on the orthogonal parameters is shown to be less susceptible to incorrect model order specification. The classification based on orthogonal data sets is also derived. It is demonstrated that this approach can avoid some problems associated with classification based on the model parameters alone. ESA

N94-25432 Joint Inst. for Nuclear Research, Dubna (USSR).
NEW ALGORITHM FOR MINIMIZING (CHI)(SUP 2) FUNCTIONALS WITH CONSTRAINTS
A. Zh. Ketikyan, E. V. Komissarov, V. S. Kurbatov, and I. N. Silin 1991 10 p In RUSSIAN Limited Reproducibility: More than 20% of this document may be affected by microfiche quality
(DE93-616800; JINR-R-10-91-482) Avail: CASI HC A02 (US Sales Only)

The problem of minimization of the functional is considered. A new algorithm is proposed for the solution of these problems. It is based on simultaneous linearization of the experimental constraint functions followed by expression of some variables in terms of others. Expressions for covariance matrix are provided, and an algorithm for the minimum search is presented. In comparison with the Lagrange multipliers method, this algorithm requires less computation and is applicable to a wider class of problems. DOE

N94-25453# Dayton Univ., OH. Research Inst.
BIRDSTRIKE RESISTANT CREW ENCLOSURE PROGRAM Final Report, 1 Aug. 1984 - 1 Mar. 1992
Gregory J. Stenger Aug. 1993 11 p
(Contract F33615-84-C-3404)
(AD-A273700; UDR-TR-92-87; WL-TR-93-3088) Avail: CASI HC A03/MF A01

This final report defines the program objectives, presents an abstract for each technical report generated, and lists the major papers and presentations resulting from the technical effort. Major program accomplishments, both generic and specific, are also enumerated. DTIC

N94-25455# Hughes Aircraft Co., San Diego, CA.
CADBIT 2: COMPUTER-AIDED DESIGN FOR BUILT-IN TEST, VOLUME 1 Final Report
Michael Davis, Sonny Kwan, and Tony Holzer Jun. 1993 79 p
(Contract F30602-90-C-0116)
(AD-A273702; HMSC-CADBIT-FR-93-1; RL-TR-93-117-Vol-1) Avail: CASI HC A05/MF A01

The objective of CADBIT 2 was to develop a CAD workstation-based system with software to help designers incorporate Built-In Test (BIT) in their CAD-based circuit board designs. The CADBIT 2 system consists of a Unix-based workstation, electronic CAD software, and the contractor-developed CADBIT 2 software module. CADBIT II benefits printed circuit board designers through four major functions. The Tutorial function increases awareness and understanding of Built-In Test techniques. This function offers on-line access to an extensive database of information on current techniques used to implement built-in test in digital, analog, and hybrid (mixed digital and analog) circuit boards. The Selection function helps designers choose the best technique for their design. The selection log compares characteristics and attributes of each BIT technique in the CADBIT database to information about the user's specific 'Circuit Under Test'. The CAD Insertion function helps designers implement a selected BIT technique in a CAD schematic. This function provides a Default Design: with a consistent set of components to implement the selected BIT technique. The Evaluation function analyzes the design impact of adding Built-In-Test circuitry based on total board area, weight, and power 'penalties' for each BIT. DTIC

N94-25456# Hughes Aircraft Co., San Diego, CA.
CADBIT 2: COMPUTER-AIDED DESIGN FOR BUILT-IN TEST, VOLUME 2 Final Report
Michael Davis, Sonny Kwan, and Tony Holzer Jun. 1993 260 p
(Contract F30602-90-C-0116)
(AD-A273703; HMSC-CADBIT-FR-93-2; RL-TR-93-117-Vol-2) Avail: CASI HC A12/MF A03

The objective of CADBIT 2 was to develop a CAD workstation-based system with software to help designers incorporate Built-In Test (BIT) in their CAD-based circuit board designs. The CADBIT 2 system consists of a Unix-based workstation, electronic CAD software, and the contractor-developed CADBIT 2 software module. CADBIT 2 benefits printed circuit board designers through four major functions. The Tutorial function increases awareness and understanding of Built-In Test techniques. This function offers on-line access to an extensive database of information on current techniques used to implement built-in test in digital, analog, and hybrid (mixed digital and analog) circuit boards. The Selection function helps designers choose the best technique for their design. The selection log compares characteristics and attributes of each BIT technique in the CADBIT database to information about the user's specific 'Circuit Under Test'. The CAD Insertion function helps designers implement a selected BIT technique in a CAD schematic. This function provides a Default Design: with a consistent set of components to implement the selected BIT technique. The Evaluation function analyzes the design impact of adding Built-In-Test circuitry based on total board area, weight, and power 'penalties' for each BIT. DTIC

N94-25468# Oxford Univ. (England). Robotics Research Group.
A SOFT ROBOT INTERFACE
Y. K. H. Lau 1992 25 p Sponsored in part by Croucher Foundation
(OUEL-1948/92; ETN-94-95155) Avail: CASI HC A03/MF A01

A hardware design and production mechanism in which special purpose hardware is generated mainly by a software engineering process is described. By specifying the essential requirements of a device in Communicating Sequential Processes (CSP), mapping the CSP specification into a subset of OCCAM, compiling the OCCAM program into netlist descriptions of parallel hardware which can be implemented using field programmable gate arrays, a cost effective and time saving way of hardware production is described. The resultant hardware has the advantage of being dynamically reconfigurable through the alteration of software. Furthermore, as the overall design mechanism is based on formal mathematics, the hardware specification and the compiler are provably correct, meaning that the developed devices will have a high degree of correctness. Such a product is suitable for applications in safety critical systems. The application of this hardware generating mechanism in the design and development of an intelligent multi axis encoder interface can be obtained. The device interfaces to a real world robot and a transputer based control system. As it is implemented using a field programmable gata array, its embedded intelligence may be enhanced at any stage of the development. The described hardware generation mechanism is evaluated and its practicality in solving real world problems is demonstrated. ESA

N94-25471# Oxford Univ. (England). Robotics Research Group.
EXTRACTING PROJECTIVE INFORMATION FROM SINGLE VIEWS OF 3D POINT SETS
C. A. Rothwell, D. A. Forsyth, A. Zisserman, and J. L. Mundy Feb. 1993 22 p Sponsored by General Electric; Oxford Univ., England; Iowa Univ.; and EEC
(OUEL-1973/93; ETN-94-95158) Avail: CASI HC A03/MF A01

Projectively invariant indexing functions, given some structural assumptions, are constructed for three dimensional point sets. Projective invariants are derived for two classes of object: the first is for points that lie on the vertices of polyhedra, and the second for objects that are projectively equivalent to ones possessing a bilateral symmetry. The first approach extends to structures whose features can be embedded within conceptual polyhedra and is called caging. The recovery of the projective structure of polyhedra and the application to caging point sets are described. The recovery of projective structure for objects with bilateral symmetry is discussed. The motivations for computing such invariants are: they can be used for recognition; they can be used to compute projective structure. Examples of invariants computed from real images are given. ESA

N94-23240*# La Salle Univ., Philadelphia, PA. Management Dept.
COST BENEFITS OF ADVANCED SOFTWARE: A REVIEW OF METHODOLOGY USED AT KENNEDY SPACE CENTER
Prafulla N. Joglekar *In* NASA. Kennedy Space Center, NASA/ASEE Summer Faculty Fellowship Program Oct. 1993 p 229-268 (For primary document see N94-23230 06-80)
Avail: CASI HC A03/MF A04

N94-23410 Massachusetts Inst. of Tech., Cambridge. Artificial Intelligence Lab.
THE MASS OF MASSIVE ROVER SOFTWARE
David P. Miller *In* CNES, Missions, Technologies, and Design of Planetary Mobile Vehicles Jan. 1993 p 411-414 Prepared in cooperation with Jet Propulsion Lab., California Inst. of Tech., Pasadena (For primary document see N94-23373 06-91)
Copyright Avail: Issuing Activity (CEPADUES-Editions, 111, rue Nicolas-Vaquelin, 31100 Toulouse, France)

N94-23647*# National Aeronautics and Space Administration. Langley Research Center, Hampton, VA.
SOME USEFUL INNOVATIONS WITH TRASYS AND SINDA-85
Ruth M. Amundsen *In* NASA. Lewis Research Center, The Fifth Annual Thermal and Fluids Analysis Workshop Nov. 1993 p 169-184 Original contains color illustrations (For primary document see N94-23634 06-34)
Avail: CASI HC A03/MF A04; 5 functional color pages

N94-23648*# Teledyne Brown Engineering, Huntsville, AL.
ANALYSIS OF HIGH VACUUM SYSTEMS USING SINDA'85
R. A. Spivey, S. E. Clanton, and J. D. Moore *In* NASA. Lewis Research Center, The Fifth Annual Thermal and Fluids Analysis Workshop Nov. 1993 p 185-204 (For primary document see N94-23634 06-34)
Avail: CASI HC A03/MF A04; 5 functional color pages

N94-23650*# Phillips Lab., Kirtland AFB, NM.
THERMAL ANALYSIS OF COMBINATORIAL SOLID GEOMETRY MODELS USING SINDA
Diane Gerencser, George Radke, Rob Introne, John Klosterman (Battelle Columbus Labs., OH.), and Dave Miklosovic (Battelle Columbus Labs., OH.) *In* NASA. Lewis Research Center, The Fifth Annual Thermal and Fluids Analysis Workshop Nov. 1993 p 223-235 (For primary document see N94-23634 06-34)
Avail: CASI HC A03/MF A04; 5 functional color pages

N94-23651*# Sverdrup Technology, Inc., Brook Park, OH.
CONVECTION EQUATION MODELING: A NON-ITERATIVE DIRECT MATRIX SOLUTION ALGORITHM FOR USE WITH SINDA
Dean S. Schrage *In* NASA. Lewis Research Center, The Fifth Annual Thermal and Fluids Analysis Workshop Nov. 1993 p 237-251 (For primary document see N94-23634 06-34)
Avail: CASI HC A03/MF A04; 5 functional color pages

N94-23672*# Ohio State Univ., Columbus. Dept. of Aeronautical and Astronautical Engineering.
UPWIND MACCORMACK EULER SOLVER WITH NON-EQUILIBRIUM CHEMISTRY
Scott E. Sherer and James N. Scott *In* NASA. Lewis Research Center, The Fifth Annual Thermal and Fluids Analysis Workshop Nov. 1993 p 539-552 (For primary document see N94-23634 06-34)
Avail: CASI HC A03/MF A04; 5 functional color pages

N94-23696*# Murray State Univ., KY. Dept. of Mathematics.
MULTIGRID METHOD FOR INTEGRAL EQUATIONS AND AUTOMATIC PROGRAMS
Hosae Lee *In* NASA. Langley Research Center, The Sixth Copper Mountain Conference on Multigrid Methods, Part 1 Nov. 1993 p 331-343 (For primary document see N94-23673 06-64)
Avail: CASI HC A03/MF A03

N94-23893*# National Aeronautics and Space Administration. Goddard Space Flight Center, Greenbelt, MD.
THE MISSION EVENTS GRAPHIC GENERATOR SOFTWARE: A SMALL TOOL WITH BIG RESULTS
Mark Lupisella, Jack Leibee, and Charles Scaffidi *In* JPL, SpaceOps 1992: Proceedings of the Second International Symposium on Ground Data Systems for Space Mission Operations 1 Mar. 1993 p 393-397 (For primary document see N94-23832 06-66)
Avail: CASI HC A01/MF A10

N94-23911*# Centre National d'Etudes Spatiales, Toulouse (France).
DISTRIBUTED COMPUTING ENVIRONMENTS FOR FUTURE SPACE CONTROL SYSTEMS
Pierre Viallefont *In* JPL, SpaceOps 1992: Proceedings of the Second International Symposium on Ground Data Systems for Space Mission Operations 1 Mar. 1993 p 525-529 (For primary document see N94-23832 06-66)
Avail: CASI HC A01/MF A10

N94-23927*# Deutsche Forschungsanstalt fuer Luft- und Raumfahrt, Oberpfaffenhofen (Germany). Space Operations Center.
THE GEO-CONTROL SYSTEM FOR STATION KEEPING AND COLOCATION OF GEOSTATIONARY SATELLITES
O. Montenbruck, M. C. Eckstein, and J. Gonner (Societe Europeenne des Satellites, Betzdorf, Luxembourg.) *In* JPL, SpaceOps 1992: Proceedings of the Second International Symposium on Ground Data Systems for Space Mission Operations 1 Mar. 1993 p 629-634 (For primary document see N94-23832 06-66)
Avail: CASI HC A02/MF A10

N94-23962*# Centre National d'Etudes Spatiales, Toulouse (France).
FROM REQUIREMENTS TO ACCEPTANCE TESTS
Lionel Baize and Helene Pasquier *In* JPL, SpaceOps 1992: Proceedings of the Second International Symposium on Ground Data Systems for Space Mission Operations 1 Mar. 1993 p 863-866 (For primary document see N94-23832 06-66)
Avail: CASI HC A01/MF A10

N94-24169*# Columbia Univ., New York, NY.
TENSORAL FOR POST-PROCESSING USERS AND SIMULATION AUTHORS
Eliot Dresselhaus *In* Stanford Univ., Annual Research Briefs, 1993

Dec. 1993 p 387-394 (For primary document see N94-24138 06-34)
Avail: CASI HC A02/MF A04

N94-24262 Israel Aircraft Industries Ltd., Tashan.
COMPUTER BASED EXPERT SYSTEM FOR BATTLE DAMAGE REPAIR OF COMPOSITE STRUCTURES
S. Gali, Z. Karuchro, D. Naor, I. Kressel, H. Lebovitz, J. Baron (Israeli Air Force, Zahal.), and J. Gerrassy (Israeli Air Force, Zahal.) *In* Israel Society of Aeronautics and Astronautics, The 33rd Israel Annual Conference on Aviation and Astronautics 25 Feb. 1993 p 246-250 (For primary document see N94-24241 06-01)
Copyright Avail: Issuing Activity (Israel Society of Aeronautics and Astronautics, c/o Faculty of Engineering, Tel-Aviv Univ., Ramat Aviv 69978, Israel)

N94-24410*# Armstrong State Coll., Savannah, GA. Dept. of Mathematics and Computer Science.
A REVIEW OF ISEAS DESIGN
Alex Bykat *In* Alabama Univ., The 1993 NASA/ASEE Summer Faculty Fellowship Program Nov. 1993 6 p (For primary document see N94-24405 06-80)
Avail: CASI HC A02/MF A03

N94-24422*# Auburn Univ., AL. Dept. of Electrical Engineering.
OCTAVE: A MARSYAS POST-PROCESSOR FOR COMPUTER-AIDEED CONTROL SYSTEM DESIGN
A. Scottedward Hodel *In* Alabama Univ., The 1993 NASA/ASEE Summer Faculty Fellowship Program Nov. 1993 5 p (For primary document see N94-24405 06-80)
Avail: CASI HC A01/MF A03

N94-24445*# Texas A&I Univ., Kingsville. Dept. of Electrical Engineering and Computer Science.
EVALUATION OF THE EFFICIENCY AND FAULT DENSITY OF SOFTWARE GENERATED BY CODE GENERATORS
Barbara Schreur *In* Alabama Univ., The 1993 NASA/ASEE Summer Faculty Fellowship Program Nov. 1993 4 p (For primary document see N94-24405 06-80)
Avail: CASI HC A01/MF A03

N94-25382*# Southeastern Oklahoma State Univ., Durant. Computer Science/Information Systems Dept.
SOFTWARE ENGINEERING METHODOLOGIES AND TOOLS
Lawrence M. Wilcox *In* NASA. Johnson Space Center, National Aeronautics and Space Administration (NASA)/American Society for Engineering Education (ASEE) Summer Faculty Fellowship Program, 1993, Volume 2 Dec. 1993 15 p (For primary document see N94-25367 06-99)
Avail: CASI HC A03/MF A03

62 COMPUTER SYSTEMS

Includes computer networks and special application computer systems.

N94-22973# Argonne National Lab., IL.
USERS MANUAL FOR THE CHAMELEON PARALLEL PROGRAMMING TOOLS
William Gropp and Barry Smith (California Univ., Los Angeles.) Jun. 1993 71 p
(Contracts W-31-109-eng-38; N00014-90-J-1695)
(DE94-001934; ANL-93/23) Avail: CASI HC A04/MF A01

Message passing is a common method for writing programs for distributed-memory parallel computers. Unfortunately, the lack of a standard for message passing has hampered the construction of portable and efficient parallel programs. In an attempt to remedy this problem, a number of groups have developed their own message-passing systems, each with its own strengths and weaknesses. Chameleon is a second-generation system of this type. Rather than replacing these existing systems, Chameleon is meant to supplement them by providing a uniform way to access many of these systems. Chameleon's goals are to (1) be very lightweight (low over-head), (2) be highly portable, and (3) help standardize program startup and the use of emerging message-passing operations such as collective operations on subsets of processors. Chameleon also provides a way to port programs written using PICL or Intel NX message passing to other systems, including collections of workstations. Chameleon is tracking the Message-Passing Interface (MPI) draft standard and will provide both an MPI implementation and an MPI transport layer. Chameleon provides support for heterogeneous computing by using p4 and PVM. Chameleon's support for homogeneous computing includes the portable libraries p4, PICL, and PVM and vendor-specific implementation for Intel NX, IBM EUI (SP-1), and Thinking Machines CMMD (CM-5). Support for Ncube and PVM 3.x is also under development. DOE

N94-22986# Technische Univ., Twente (Netherlands). Faculteit der Informatica.
ACOS: THE PERFORMANCE BASED APPROACH TO BUILD A PARALLEL COMPLEX OBJECT SERVER
W. B. Teeuw, M. Klein, and H. M. Blanken 1993 31 p See also N90-24770, PB90-173410 and N91-15766
(PB93-223816; Memo-INF-93-11) Copyright Avail: CASI HC A03/MF A01

The paper describes the design and implementation of a complex object server for the distributed operating system Amoeba. The server is called ACOS (Amoeba Complex Object Server). In order to meet the requirements of non-standard database environments, a complex object server has to provide a high performance. The authors show how they want to control the expected performance of ACOS during its design. By using a top-down design/implementation method, in which a simulation model is evolved into a real system by gradual addition of detail, they want to detect performance bottlenecks in as early a stage as possible. In this way, they expect to obtain an optimal physical design for ACOS. NTIS

N94-23085*# George Washington Univ., Washington, DC. Inst. for Applied Space Research.
SUPERCOMPUTER NETWORKING FOR SPACE SCIENCE APPLICATIONS Final Report, 29 Jan. - 31 Dec. 1991
B. I. Edelson 15 May 1992 42 p
(Contract NAS5-30428; RTOP 506-59-11)
(NASA-CR-194876; NAS 1.26:194876) Avail: CASI HC A03/MF A01

The initial design of a supercomputer network topology including the design of the communications nodes along with the communications interface hardware and software is covered. Several space science applications that are proposed experiments by GSFC and JPL for a supercomputer network using the NASA ACTS satellite are also reported. Author (revised)

N94-23134# Institut National Polytechnique, Grenoble (France). Lab. de Genie Informatique.
MODELING PARALLELISM AND SYNCHRONIZATION Ph.D. Thesis [MODELISATION DU PARALLELISME ET DE LA SYNCHRONISATION]
Karim Atif 1992 264 p In FRENCH
(ETN-94-95179) Avail: CASI HC A12/MF A03

The purpose is to investigate a modeling concept named Stochastic Automata Network (SAN). Many modeling tools were realized in order to analyze systems' dynamic behavior. The performance of these tools depends on the expression power, large systems analysis and numerical or analytical resolution. The work into these axes motivated the conception of an efficient methodology which permits the modeling of parallel activities and synchronization points systems. This methodology is expressed by SAN. SAN modeling is studied under Markovian assumptions. ESA

N94-23167# Institut National Polytechnique, Grenoble (France). Lab. de Genie Informatique.
A PARALLEL PROLOG SYSTEM FOR DISTRIBUTED MEMORY MULTIPROCESSOR Ph.D. Thesis [UN SYSTEME PROLOG PARALLELE POUR MACHINES A MEMOIRE DISTRIBUEE]
Michel Favre 1992 200 p In FRENCH
(ETN-94-95173) Avail: CASI HC A09/MF A03

The implementation of PROLOG on distributed memory architectures is investigated. The OPERA model is presented. It uses OR parallelism to distribute dynamical program evaluation on several nodes of a network of processing elements. The OPERA system is multisequential: parallelization occurs only when a processor become idle. The system is composed of an operative part which computes PROLOG program and a control part which allocates jobs to workers. The choice of a memory representation for the OR tree, the management of multiple binding and control on branch allocation to abstract machines are difficult tasks. The load balancing strategy is based on heuristics. The scheduler works on an approximate global state obtained by sampling worker's local states. An OPERA prototype was implemented on Supernode, a dynamically reconfigurable transputer network. Dynamic configuration is used to reduce communication overhead. Communications are performed in parallel with computation. The prototype provides good speedups and OPERA is one of the most efficient existing parallel PROLOG systems. ESA

N94-23252*# Boeing Defense and Space Group, Seattle, WA.
TOWARDS THE FORMAL SPECIFICATION OF THE REQUIREMENTS AND DESIGN OF A PROCESSOR INTERFACE UNIT: HOL LISTINGS
David A. Fura, Phillip J. Windley (Idaho Univ., Moscow.), and Gerald C. Cohen Nov. 1993 247 p
(Contract NAS1-18586; RTOP 505-64-10-07)
(NASA-CR-191465; NAS 1.26:191465) Avail: CASI HC A11/MF A03

This technical report contains the HOL listings of the specification of the design and major portions of the requirements for a commercially developed processor interface unit (or PIU). The PIU is an interface chip performing memory interface, bus interface, and additional support services for a commercial microprocessor within a fault-tolerant computer system. This system, the Fault-Tolerant Embedded Processor (FTEP), is targeted towards applications in avionics and space requiring extremely high levels of mission reliability, extended maintenance-free operation, or both. This report contains the actual HOL listings of the PIU specification as it currently exists. Section two of this report contains general-purpose HOL theories that support the PIU specification. These theories include definitions for the hardware components used in the PIU, our implementation of bit words, and our implementation of temporal logic. Section three contains the HOL listings for the PIU design specification. Aside from the PIU internal bus (I-Bus), this specification is complete. Section four contains the HOL listings for a major portion of the PIU requirements specification. Specifically, it contains most of the definition for the PIU behavior associated with memory accesses initiated by the local processor. Derived from text

N94-23293*# SRI International Corp., Menlo Park, CA. Computer Science Lab.
FORMAL METHODS AND DIGITAL SYSTEMS VALIDATION FOR AIRBORNE SYSTEMS Final Report, 1 Oct. 1991 - 18 Nov. 1993
John Rushby Washington Dec. 1993 305 p Sponsored in part by FAA, Atlantic City, NJ
(Contract NAS1-18969; RTOP 505-64-10-13)
(NASA-CR-4551; NAS 1.26:4551; ECU-8200-150) Avail: CASI HC A14/MF A03

This report has been prepared to supplement a forthcoming chapter on formal methods in the FAA Digital Systems Validation Handbook. Its purpose is as follows: to outline the technical basis for formal methods in computer science; to explain the use of formal methods in the specification and verification of software and hardware requirements, designs, and implementations; to identify the benefits, weaknesses, and difficulties in applying these methods to digital systems used on board aircraft; and to suggest factors for consideration when formal methods are offered in support of certification. These latter factors assume the context for software development and assurance described in RTCA document DO-178B, 'Software Considerations in Airborne Systems and Equipment Certification,' Dec. 1992. Author (revised)

N94-23483*# Rensselaer Polytechnic Inst., Troy, NY. Scientific Computation Research Center.
PARALLEL UNSTRUCTURED GRID GENERATION FOR COMPUTATIONAL AEROSCIENCES Status Report, 1 Apr. - 30 Sep. 1993
Mark S. Shephard 30 Sep. 1993 14 p
(Grant NAG2-832)
(NASA-CR-192244; NAS 1.26:192244) Avail: CASI HC A03/MF A01

The objective of this research project is to develop efficient parallel automatic grid generation procedures for use in computational aerosciences. This effort is focused on a parallel version of the Finite Octree grid generator. Progress made during the first six months is reported. Author (revised)

N94-23491# Sandia National Labs., Albuquerque, NM.
A LOWER BOUND FOR ROUTING ON A COMPLETELY CONNECTED OPTICAL COMMUNICATION PARALLEL COMPUTER
L. A. Goldberg, M. Jerrum (Edinburgh Univ., Scotland.), and P. D. MacKenzie (Texas Univ., Austin.) 3 Aug. 1993 19 p Presented at the Symposium on Discrete Algorithms, Arlington, VA, 23-26 Jan. 1994
(Contract DE-AC04-76DP-00789)
(DE93-040752; SAND-93-1866C; CONF-940130-1) Avail: CASI HC A03/MF A01

The task of routing a 2-relation on an n-processor completely connected optical communication parallel computer (OCPC) is considered. A lower bound is presented that applies to any randomized distributed algorithm for this task: specifically, it is shown that the expected number of steps required to route a 2-relation is (Omega)((radical) log log n) in the worst case. For comparison, the best upper bound known is O(log log n). DOE

N94-23504*# Colorado Univ., Boulder. Center for Space Structures and Controls.
EXTENDING SUBSTRUCTURE BASED ITERATIVE SOLVERS TO MULTIPLE LOAD AND REPEATED ANALYSES Progress Report No. 3
Charbel Farhat Aug. 1993 25 p
(Grants NAG2-827; NSF ASC-92-17394)
(NASA-CR-194822; NAS 1.26:194822) Avail: CASI HC A03/MF A01

Direct solvers currently dominate commercial finite element structural software, but do not scale well in the fine granularity regime targeted by emerging parallel processors. Substructure based iterative solvers--often called also domain decomposition algorithms--lend themselves better to parallel processing, but must overcome several obstacles before earning their place in general purpose structural analysis programs. One such obstacle is the solution of systems with many or repeated right hand sides. Such systems arise, for example, in multiple load static analyses and in implicit linear dynamics computations. Direct solvers are well-suited for these problems because after the system matrix has been factored, the multiple or repeated solutions can be obtained through relatively inexpensive forward and backward substitutions. On the other hand, iterative solvers in general are ill-suited for these problems because they often must restart from scratch for every different right hand side. In this paper, we present a methodology for extending the range of applications of domain decomposition methods to problems with multiple or repeated right hand sides. Basically, we formulate the overall problem as a series of minimization problems over K-orthogonal and supplementary subspaces, and tailor the preconditioned conjugate gradient algorithm to solve them efficiently. The resulting solution method is scalable, whereas direct factorization schemes and forward and backward substitution algorithms are not. We illustrate the proposed methodology with the solution of static and dynamic structural problems, and highlight its potential to outperform forward and backward substitutions on parallel computers. As an example, we show that for a linear structural dynamics problem with 11640 degrees of freedom, every time-step beyond time-step 15 is solved in a single iteration and consumes 1.0 second on a 32 processor iPSC-860 system; for the same problem and the same parallel processor, a pair of forward/backward substitutions at each step consumes 15.0 seconds. Author

N94-23706# Vrije Univ., Brussels (Belgium). Dept. of Mathematics and Computer Science.
ARC CONSISTENCY PROBLEM: AN EXERCISE IN PARALLEL PROGRAMMING WITH SHARED OBJECTS
I. Athanasiu (Bucharest Polytechnic Inst., Romania.) and H. E. Bal Jul. 1993 19 p See also PB94-110574 Prepared in cooperation with Bucharest Polytechnic Inst., Romania
(PB94-110590; IR-331) Avail: CASI HC A03/MF A01

The authors consider a new model for parallel programming of distributed computing systems. This model allows processes on different machines of a network to communicate through shared objects. The paper describes their experiences in using this model for implementing the Arc Consistency Problem (ACP). ACP algorithms can be used as an initial step in solving the Constraint Satisfaction Problem, a fundamental artificial intelligence (AI) problem. They have used this application as a case study for distributed programming with shared data-objects. The shared data-object model provides logically shared data to the programmer, rather than message passing. The model is the basis of the Orca programming language. NTIS

N94-23752# Technische Hogeschool Twente, Enschede (Netherlands). Tele-Informatics and Open Systems Group.
DESIGN AND IMPLEMENTATION ISSUES OF END-TO-END PROTOCOLS IN HIGH-SPEED NETWORKS
A. L. Olah and S. M. HeemstradeGroot 1993 25 p
(PB94-110905; TIOS-93/24) Copyright Avail: CASI HC A03/MF A01

Optical transmission technology opens the way to design computer networks which offer bandwidth in the order of Gigabits/s to individual computers. Backed by the improvements of microprocessor technology, there are numerous applications that are ready to exploit the advantages of high-speed networks. The effects of this new networking environment on the design and implementation of communication protocols has become the subject of extensive research. The paper focuses on issues related to the design and implementation of end-to-end protocols because the upper layer protocols are identified by many researchers as a possible bottleneck in high-speed communication. A survey of the literature concerning the problem is given. NTIS

N94-23756 Technische Univ., Eindhoven (Netherlands). Dept. of Mathematics and Computing Science.
PREEMPTIVE SCHEDULING IN A TWO-STAGE MULTIPROCESSOR FLOW SHOP IS Np-HARD
J. A. Hoogeveen, J. K. Lenstra, and B. Veltman Jul. 1993 10 p Limited Reproducibility: More than 20% of this document may be affected by microfiche quality
(PB94-111648; MEMO-COSOR-93-20) Avail: Issuing Activity (National Technical Information Service (NTIS))

An efficient algorithm for minimizing makespan in a two-machine flow shop was previously given; there is no advantage to preemption in this case. A wrap-around rule finds a shortest preemptive schedule on identical parallel machines in linear time. A similarly efficient algorithm is unlikely to exist for the simplest common generalization of these problems. The authors show that preemptive scheduling in a two-stage flow shop, with at leasttwo identical parallel machines in one of the stages so as to minimize makespan, is NP-hard in the strong sense. NTIS

N94-23767 Technische Univ., Eindhoven (Netherlands). Dept. of Mathematics and Computing Science.
THREE, FOUR, FIVE, SIX OR THE COMPLEXITY OF SCHEDULING WITH COMMUNICATION DELAYS
J. A. Hoogeveen, J. K. Lenstra, and B. Veltman Jul. 1993 15 p See also N91-18684, N92-21291 and PB93-237626 Limited Reproducibility: More than 20% of this document may be affected by microfiche quality
(PB94-111630; MEMO-COSOR-93-19) Avail: Issuing Activity (National Technical Information Service (NTIS))

A set of unit-time tasks has to be processed on identical parallel processors subject to precedence constraints and unit-time communication delays; does there exist a schedule of maximum length, d? The problem has two variants, depending on whether the number of processors is restrictively small or not. For the first variant, the question can be answered in polynomial time for $d = 3$ and is NP-complete for $d = 4$. The second variant is solvable in polynomial time for $d = 5$ and NP-complete for $d = 6$. As a consequence, neither of the corresponding optimization problems has a polynomial approximation scheme, unless $P = NP$. NTIS

N94-24075*# Boeing Defense and Space Group, Seattle, WA.
TOWARDS THE FORMAL VERIFICATION OF THE REQUIREMENTS AND DESIGN OF A PROCESSOR INTERFACE UNIT
David A. Fura, Phillip J. Windley (Idaho Univ., Moscow.), and Gerald C. Cohen Dec. 1993 57 p
(Contract NAS1-18586; RTOP 505-64-10-07)
(NASA-CR-4522; NAS 1.26:4522) Avail: CASI HC A04/MF A01

The formal verification of the design and partial requirements for a Processor Interface Unit (PIU) using the Higher Order Logic (HOL) theorem-proving system is described. The processor interface unit is a single-chip subsystem within a fault-tolerant embedded system under development within the Boeing Defense and Space Group. It provides the opportunity to investigate the specification and verification of a real-world subsystem within a commercially-developed fault-tolerant computer. An overview of the PIU verification effort is given. The actual HOL listing from the verification effort are documented in a companion NASA contractor report entitled 'Towards the Formal Verification of the Requirements and Design of a Processor Interface Unit - HOL Listings' including the general-purpose HOL theories and definitions that support the PIU verification as well as tactics used in the proofs. Author (revised)

N94-24463*# Boeing Defense and Space Group, Seattle, WA.
TOWARDS THE FORMAL SPECIFICATION OF THE REQUIREMENTS AND DESIGN OF A PROCESSOR INTERFACE UNIT
David A. Fura, Phillip J. Windley (Idaho Univ., Moscow.), and Gerald C. Cohen Dec. 1993 90 p
(Contract NAS1-18586; RTOP 505-64-10-07)
(NASA-CR-4521; NAS 1.26:4521) Avail: CASI HC A05/MF A01

Work to formally specify the requirements and design of a Processor Interface Unit (PIU), a single-chip subsystem providing memory interface, bus interface, and additional support services for a commercial microprocessor within a fault-tolerant computer system, is described. This system, the Fault-Tolerant Embedded Processor (FTEP), is targeted towards applications in avionics and space requiring extremely high levels of mission reliability, extended maintenance free operation, or both. The approaches that were developed for modeling the PIU requirements and for composition of the PIU subcomponents at high levels of abstraction are described. These approaches were used to specify and verify a nontrivial subset of the PIU behavior. The PIU specification in Higher Order Logic (HOL) is documented in a companion NASA contractor report entitled 'Towards the Formal Specification of the Requirements and Design of a Processor Interfacs Unit - HOL Listings.' The subsequent verification approach and HOL listings are documented in NASA contractor report entitled 'Towards the Formal Verification of the Requirements and Design of a Processor Interface Unit' and NASA contractor report entitled 'Towards the Formal Verification of the Requirements and Design of a Processor Interface Unit - HOL Listings.' Author (revised)

N94-24524 Technische Univ., Twente (Netherlands). Faculty of Applied Mathematics.
TOOL SHARING, PART 3
W. M. Nawijn May 1993 19 p Limited Reproducibility: More than 20% of this document may be affected by microfiche quality
(PB94-111697; MEMO-1134) Avail: CASI HC A03

Given are two identical machines each of which performs the same N operations O(sub i), one less than or equal to i less than or equal to N, cyclically and indefinitely, i.e. a production run on a machine looks like O(sub 1), O(sub 2), ..., O(sub N), O(sub 1), O(sub 2), ..., O(sub N), etc. For each of the operations O(sub i), i a member of (1,2, ... ,N) (j,k), a single tool is available. Operations O(sub j) and O(sub k), however, are processed by the same tool. The tools, which are shared by both machines, are transported between the machines by means of an infinitely fast transport device. We analyze several transport strategies, including cyclic behavior, and determine the corresponding cycle times. NTIS

N94-24692# Carnegie-Mellon Univ., Pittsburgh, PA. Dept. of Computer Science.
OPTIMIZING PARALLELIZATION
Greg Morrisett and Maurice Herlihy Oct. 1993 15 p Sponsored by NSF
(AD-A273565; CMU-CS-93-171) Avail: CASI HC A03/MF A01

To transform a sequential program into a concurrent program, a compiler typically divides the sequential program into a partially-ordered set of basic blocks, allowing unrelated blocks to execute concurrently. Blocks may execute concurrently only if there are no dependencies among them, and therefore a compiler can introduce concurrency only to the extent that it can guarantee the absence of dependencies. A limitation of this technique is that it is necessarily conservative: it may be difficult or impossible to prove the absence of dependencies even when no dependencies exist. This paper investigates optimistic parallelization, a complementary technique for parallelizing sequential code. Blocks with potential conflicts are allowed to execute in parallel, and conflicts are detected at run-time. When a conflict is detected, the conflicting blocks are rolled back and re-executed in sequential order. Optimistic parallelization can enhance concurrency when the compiler cannot prove the absence of dependence among independent blocks, and when dependencies occur, but are sufficiently rare. We show how conflict detection and roll-back can be accomplished efficiently through relatively simple changes to the caches and the cache-coherence protocol of a shared-memory multiprocessor. DTIC

N94-24764 Technische Univ., Eindhoven (Netherlands). Dept. of Mathematics and Computing Science.
SENSITIVITY ANALYSIS OF LIST SCHEDULING HEURISTICS
A. W. J. Kolen, A. H. G. RinnooyKan, C. P. M. VanHoesel, and A. P. M. Wagelmans Mar. 1993 27 p Prepared in cooperation with Erasmus Univ., Rotterdam, Netherlands and Limburg Univ. Maastricht, Netherlands Limited Reproducibility: More than 20% of this document may be affected by microfiche quality
(PB93-237766; MEMO-COSOR-93-10) Avail: Issuing Activity (National Technical Information Service (NTIS))

When jobs have to be processed on a set of identical parallel machines so as to minimize the makespan of the schedule, list scheduling rules form a popular class of heuristics. When all processing times are exactly known, a given list scheduling rule will generate a unique assignment of jobs to machines. However, when there exists a priori uncertainty with respect to one of the processing times, then there will be, in general, several possibilities for the assignment that will be generated once that processing time is known. That number of possible assignments may be viewed as a measure of the sensitivity of the list scheduling rule that is applied. Bounds on the maximum number of possible assignments for several list scheduling heuristics are derived, and the makespan associated with these assignments was also studied. In this way it obtains analytical support for the intuitively plausible notion that the sensitivity of a list scheduling rule increases with the quality of the schedule produced. NTIS

N94-24939 Massachusetts Inst. of Tech., Cambridge.
NEW DIRECTIONS IN NETWORK FLOWS Final Report, 1 Feb. 1992 - 31 Jan. 1993
James Orlin 31 Jan. 1993 3 p Limited Reproducibility: More than 20% of this document may be affected by microfiche quality
(Contract F49620-92-J-0116)
(AD-A273467; AFOSR-93-0862TR) Avail: Issuing Activity (Defense Technical Information Center (DTIC))

Progress has been made on a number of problems including improved algorithms for the minimum cut problem and the arrangement problem and new data compression techniques for the shortest path problem. DTIC

N94-25030 Ohio State Univ., Columbus. Research Foundation.
HIGH-LEVEL CONNECTIONIST MODELS Final Report
Jordan B. Pollack Oct. 1993 45 p Limited Reproducibility: More than 20% of this document may be affected by microfiche quality
(Contract N00014-93-1-0059)
(AD-A273638; OSURF-760388; OSURF-726944) Avail: Issuing Activity (Defense Technical Information Center (DTIC))

Our goals this year involved learning in connectionist networks while automatically decomposing behaviors in order to support those behaviors with modular architectures. While there has been some work in this area, we desired to have the modules fully evolve in response to the demands of the task. To accomplish this, we needed a training mechanism more robust than backpropagation, so we turned towards genetic algorithms (GAs). These algorithms, based on principles adopted from natural selection, allow solutions to be evolved which fit the requirements of an environment. There is an extensive body of work applying GAs to evolving neural networks, but most simply use GAs to set the weights for a fixed-structure network. DTIC

N94-25062# Technische Univ., Eindhoven (Netherlands).
THE DESIGN OF THE EMPS MULTIPROCESSOR EXECUTIVE FOR DISTRIBUTED COMPUTING Ph.D. Thesis
Gerardus Johannes W. vanDijk 1993 164 p
(ETN-94-95336) Avail: CASI HC A08/MF A02

The design of the Eindhoven Multi Processor System (EMPS) executive for distributed computing is described. Research is concentrated on the hardware architecture, the software architecture, interprocess communication, and process migration. The motivations that led to certain choices in the design of the hardware architecture for the EMPS multiprocessor executive are given. The different modules that can be used to construct an EMPS hardware configuration are summarized. The design of the software architecture of the EMPS multiprocessor executive is presented. The implementation of interprocess communication via mailboxes is described using the object oriented paradigm. The EMPS kernel supports location transparent communication between application processes, which is required for process migration. The design and implementation of the process migration facility in the EMPS system is described. The performance of the process migration facility is compared to process migration facilities in other distributed systems. ESA

N94-25221# Technische Univ., Eindhoven (Netherlands).
MULTIPROCESSOR SCHEDULING WITH COMMUNICATION DELAYS Ph.D. Thesis
Bart Veltman 1993 127 p Prepared in cooperation with Center for Mathematics and Computer Science, Amsterdam, Netherlands
(ETN-94-95346) Avail: CASI HC A07/MF A02

It is important, when programming a parallel computer, to assign the tasks to processors while respecting the information dependencies inbetween the tasks. The purpose of the work is to investigate the allocation of program modules or tasks to parallel processors in the context of deterministic machine scheduling theory. An extension of an already applied scheduling model is proposed. A model allowing for communication delays is discussed. The tradeoff between the optimal makespan of schedules with and without duplicated tasks is investigated. The computational complexity of scheduling multiprocessor tasks with prespecified processor allocations is studied. The hybrid invariant, in which some tasks are to be allocated to either of two processors and others have a prespecified allocation to a single processor, is considered. A detailed description of Tosca's method and its implementation are given. ESA

N94-25226 Technische Univ., Eindhoven (Netherlands).
MODELS OF TRACE THEORY SYSTEMS Ph.D. Thesis
Joanna Maria vandeMortel-Fronczak 1993 211 p Limited Reproducibility: More than 20% of this document may be affected by microfiche quality
(ETN-94-95361) Avail: CASI HC A10

A formalism for reasoning about parallel system using the partial order approach is presented. The systems considered are described in terms of trace theory. The part of trace theory that forms the background for the study is presented. This includes basic concepts and notions, followed by several useful results. Properties of processes and systems concerned with disabling and divergence are discussed. The failures model of systems is defined. An operational view of systems is given. In this approach, concurrency is not modeled by interleaving. Concepts used for defining the testing relations are introduced. Some properties of the testing relations are proved. Specifically, parallel composition and projection are monotonic with respect to the implementation relation (sat), and the equivalence relation induced by sat is a congruence with respect to parallel composition and to projection. Comparing systems in this setting involves calculations on a large domain of tests. An abstract model for comparing systems is proposed. This model is compositional with respect to the parallel composition operator and to the projection operator. The abstract model is used to define a semantics of a subset of Tangram programs. Incorporating fairness assumptions into the abstract model of systems is considered. The Alternating Bit Protocol is discussed. ESA

N94-25278# Technische Univ., Eindhoven (Netherlands).
DESIGNING PARALLEL PROGRAMS OF PARAMETERIZED GRANULARITY Ph.D. Thesis
Pieter Struik 1992 96 p Sponsored by Philips Gloeilampenfabrieken N.V., Eindhoven, Netherlands
(ETN-94-95302) Avail: CASI HC A05/MF A01

A method for designing fine grained programs is discussed. The design method is explained by identifying five phases in the design of a parallel program. Each phase is addressed separately. A design decision made in one phase usually has impact on some next design phases. Two programs that serve as running examples throughout are derived. The implementation of parallel programs on processor networks is considered. A model to analyze an implementation's speedup is presented. A technique for transforming fine grained programs into programs of a coarser grain is discussed. This technique yields programs of parameterized granularity. The proposed technique is applied to two types of programs. The running examples are transformed into parallel programs of parameterized grain size. It is shown that the transformation technique is generally applicable to any fine grained program. Experimental results for both very large scale integration and processor network implementations of the running examples are presented. ESA

N94-25282# Technische Univ., Eindhoven (Netherlands). Dept. of Mathematics and Computing Science.

A DESIGN METHOD FOR PARALLEL PROGRAMS Ph.D. Thesis

Ludovicus Daniel Jos Loyens 1992 125 p Prepared in cooperation with Philips Gloeilampenfabrieken N.V., Eindhoven, Netherlands
(ETN-94-95331) Avail: CASI HC A06/MF A02

The purpose of the work is to give basic guidelines to master the complexity of parallel programs. A parallel programming method is built. Several aspects of parallel programs are discussed. The skeleton of the design method, based on the use of parameterized invariants and on the knowledge of sequential programming, is presented. A derivation of a parallel program and examples are given. Simple distributions of arrays and matrices together with two examples of making new distributions are studied. The properties of distributions are discussed in order to obtain a better understanding of their role in parallel programs. The proposed parallel programming techniques are applied to a class of segment problems. A parallel program for the solution of a special class of symmetric system is derived. A space parallel Cholesky factorization program is obtained. The resulting algorithms can be used as building blocks for many algorithms that need the solution of a sparse symmetric positive definite system. Timing results for the parallel programs are also given. ESA

N94-25454# Wright Lab., Wright-Patterson AFB, OH.

EXPERT SYSTEM RULE-BASE EVALUATION USING REAL-TIME PARALLEL PROCESSING Final Report, 1 Jun. - 1 Aug. 1993

James L. Noyes Sep. 1993 35 p
(AD-A273701; WL-TR-93-3098) Avail: CASI HC A03/MF A01

A large rule-based expert system with each rule involving perhaps 10 out of 100,000 possible Boolean criteria, can require a significant amount of processing time to evaluate. This time can be reduced if all rules have a single consequent and have antecedents that contain only conjunctions of the Boolean criteria or their complements. If the consequences do not insert new facts into the rule-base, then parallel processing can be used with great efficiency. The value of a rule-based expert system to help solve a variety of diagnostic and advisory needs has been well-demonstrated over the last 2 decades. Parallel processing has become increasingly important for embedded systems in order to accelerate a variety of computations. This report discusses research connected to the development of a data structure and algorithm to perform parallel inferencing in rule-based systems. It also discusses a simulation technique for estimating the number of processors needed to evaluate a given number of rules and criteria within the required time. DTIC

N94-23697*# Duesseldorf Univ. (Germany). Mathematisches Inst.

AN OBJECT-ORIENTED APPROACH FOR PARALLEL SELF ADAPTIVE MESH REFINEMENT ON BLOCK STRUCTURED GRIDS

Max Lemke, Kristian Witsch, and Daniel Quinlan (Colorado Univ., Denver.) *In* NASA. Langley Research Center, The Sixth Copper Mountain Conference on Multigrid Methods, Part 1 Nov. 1993 p 345-359 (For primary document see N94-23673 06-64)
(Contract NAS1-18606; BMFT-ITR-900689)
Avail: CASI HC A03/MF A03

63 CYBERNETICS

Includes feedback and control theory, artificial intelligence, robotics and expert systems.

For related information see also *54 Man/System Technology and Life Support.*

N94-22703# Universiteit Twente, Enschede (Netherlands). Faculty of Applied Mathematics.

DECOUPLING PROBLEMS AROUND A TRAJECTORY: FROM LINEARITY TO NONLINEARITY

A. C. Ruiz and H. Nijmeijer Feb. 1993 26 p Sponsored by CONACyT, Mexico
(MEMO-1115; ETN-94-94751) Avail: CASI HC A03/MF A01

Given a nonlinear control system for which an admissible state trajectory is specified, the input output decoupling problem around this nominal trajectory is solved approximately. An approximate solution for this problem is obtained by dealing with the linearized system along this trajectory. An exact solution to the input output decoupling problem for the linearization is shown to be an approximate solution to the input output decoupling problem around the nominal trajectory for the original nonlinear system. In a similar way, an approximate solution to the disturbance decoupling problem around a specified trajectory of the nonlinear system is provided. The nonlinear model of a two link robot manipulator is used to illustrate the results on input output decoupling. ESA

N94-22705# Universiteit Twente, Enschede (Netherlands). Faculty of Applied Mathematics.

BALANCING FOR UNSTABLE NONLINEAR SYSTEMS

J. M. A. Scherpen 23 Feb. 1993 22 p Sponsored by Dutch Systems and Control Theory Network
(MEMO-1118; ETN-94-94753) Avail: CASI HC A03/MF A01

A previously obtained method of balancing for stable nonlinear systems is extended to unstable nonlinear systems. The similarity invariants obtained by the concept of LQG balancing for an unstable linear system can also be obtained by considering a past and future energy function of the system. By considering a past and future energy function for an unstable nonlinear system, the concept of these similarity invariants for linear systems is extended to nonlinear systems. Furthermore the relation of this balancing method with the previously obtained method of balancing the coprime factorization of an unstable nonlinear system is considered. Both methods are introduced with the aim of using them as a tool for model reduction. ESA

N94-22706# Universiteit Twente, Enschede (Netherlands). Faculty of Applied Mathematics.

NONLINEAR STATE SPACE H(SUB INFINITY) CONTROL THEORY

A. J. vanderSchaft Feb. 1993 41 p
(MEMO-1119; ETN-94-94754) Avail: CASI HC A03/MF A01

A concise treatment of L(sub 2) gain analysis of nonlinear systems is presented and the state feedback H-infinity suboptimal control problem is addressed. A result concerning robustness of H-infinity suboptimal state feedbacks is derived. The necessary conditions for the full (dynamic output feedback) H-infinity control problem are surveyed, including the derivation of a generalized version of a separation principle. The main novelty is in the derivation of the nonlinear central controller, which in general is an infinite dimensional system. An explicit solution to the H-infinity optimal control problem for nonlinear lossless systems is discussed. ESA

N94-22707# Universiteit Twente, Enschede (Netherlands). Systems and Control Group.

NONLINEAR SYSTEMS WHICH HAVE FINITE-DIMENSIONAL H(SUB INFINITY) SUBOPTIMAL CENTRAL CONTROLLERS

A. J. vanderSchaft Feb. 1993 8 p
(MEMO-1120; ETN-94-94755) Avail: CASI HC A02/MF A01

Following up the work of Basar and Bernhard, the nonlinear central controller solving the nonlinear (standard) H-infinity suboptimal control problem was recently derived. This nonlinear central controller is an infinite dimensional system, and the situation is very much like in nonlinear stochastic filtering or nonlinear deterministic filtering. In the linear case the nonlinear central controller is shown to reduce to the finite dimensional central controller of Doyle, Glover, Khargonekar and Francis, and consideration is given to whether there are truly nonlinear systems having finite dimensional central controllers. Guided by similar considerations in nonlinear stochastic and deterministic filtering, a specific class of nonlinear systems having finite dimensional central controllers is characterized. This class can be regarded as the deterministic H-infinity analog of the class of nonlinear systems admitting finite dimensional filters as identified by Benes. ESA

N94-22712# Universiteit Twente, Enschede (Netherlands). Systems and Control Group.

NORMAL FORMS OF KINEMATIC SINGULARITIES OF 3R ROBOT MANIPULATORS

Krzysztof Tchon (Technical Univ. of Wroclaw, Poland.) Mar. 1993 23 p
(MEMO-1124; ETN-94-94760) Avail: CASI HC A03/MF A01

Using the singularity theory approach, kinematic singularities of 3R robot manipulators satisfying certain geometric conditions are studied. A classification of singular configurations is given and three mathematical models (normal forms) of the kinematics around singular configurations are derived. ESA

N94-22714# Universiteit Twente, Enschede (Netherlands). Faculty of Applied Mathematics.
FEEDBACK LINEARIZATION OF PARAMETRIZED NONLINEAR TIME-VARYING SYSTEMS
H. Nijmeijer and G. Campion (Universite Catholique de Louvain, Belgium.) Mar. 1993 10 p
(MEMO-1126; ETN-94-94762) Avail: CASI HC A02/MF A01

The feedback linearization of a parametrized nonlinear system, which is not necessarily linear in the parameters, is studied. This in particular includes a result on linearization of a time varying nonlinear system, in the case where the parameters are time varying. A necessary and sufficient condition for feedback linearization, depending on the time evolution of the parameters, and a structural sufficient condition independent of the parameters evolution, are derived. For the case of a linearly parametrized system, this sufficient condition is shown to be equivalent to one of the matching conditions. ESA

N94-22873# Technische Univ., Eindhoven (Netherlands). Measurement and Control Div.
IDENTIFICATION FOR ROBUST CONTROL USING AN H(SUB INFINITY) NORM
T. J. J. vandenBoom, A. A. H. Damen, and Martin Klompstra Jul. 1992 44 p
(EUT-92-E-261; ISBN-9-06-144261-3; ETN-94-94768) Avail: CASI HC A03/MF A01

An identification method using H(sub infinity) norm which yields a nominal model and information about the model uncertainties applicable to H(sub infinity) robust control design is presented. Disturbances and noise signals at the input and output of the system are characterized as norm-bounded. The first step in the identification method is to compute uncertainty regions for the process dynamics on the complex plane. The a priori knowledge about the norm bounds on the disturbances and properties of conformal mappings are used to compute these regions. The second step is to find a model in a model set that minimizes the H(sub infinity) norm of the model errors, given the uncertainty regions. An elementary implementation of the method is presented with two simulation studies. ESA

N94-22877# Technische Univ., Eindhoven (Netherlands). Medical Electrical Engineering Div.
THE ADAPTIVE RESONANCE THEORY NETWORK: (CLUSTERING-) BEHAVIOUR IN RELATION WITH BRAINSTEM AUDITORY EVOKED POTENTIAL PATTERNS M.S. Thesis
L. W. Freriks, P. J. M. Cluitmans, and M. J. vanGils Nov. 1992 105 p
(EUT-92-E-264; ISBN-9-06-144264-8; ETN-94-94771) Avail: CASI HC A06/MF A02

A discussion on neural networks and pattern recognition is presented and a study of the adaptive resonance theory (ART) network in relation with a pattern recognition problem, extraction of features from auditory evoked potential (AEP) patterns, is described. The automatic extraction of features from AEP is desired in a medical engineering servo anesthesia project, because there is possible correlation between AEP patterns and variations in 'anesthetic depth.' From a literature search, three networks were concluded to be possible tools for solving the AEP problem: the multilayer perceptron, the counter propagation network, and the ART network. ART one, which handles binary valued input patterns, and ART two, which handles analog input patterns, are addressed. The last network was used to solve the pattern recognition problem. Investigations to find an algorithm for this network are described. The AEP problem was not solved but the criterion to which ART two clusters AEP patterns is shown to be very clear. Due to this criterion it is expected that it will not be easy to solve the AEP pattern recognition problem with an ART two network. ESA

N94-22884# Grenoble-1 Univ. (France). Equipe Reconnaissance de Formes et Microscopie Quantitative.
ARTIFICIAL NEURAL NETWORKS: APPLICATION TO THE OPTICAL RECOGNITION OF MUSIC PARTITIONS Ph.D. Thesis [RESEAUX DE NEURONES ARTIFICIELS: APPLICATION A LA RECONNAISSANCE OPTIQUE DE PARTITIONS MUSICALES]
Philippe Martin 1992 184 p In FRENCH
(ETN-94-95166) Avail: CASI HC A09/MF A02

The development and use of artificial neural networks to solve an unusual pattern recognition problem, those of optical musical score recognition, are discussed. A bibliographical study of the main connectionist models, the most frequently used in the pattern recognition field, is presented. Different techniques which are useful to design a multilayer architecture and train it with the known gradient backpropagation learning algorithm are reviewed. The special case of threshold automata networks is studied. Their properties and links with conventional classification techniques are enhanced. A new hierarchical learning scheme for these networks is proposed. A low level image analysis system for engraved musical scores is described. Several solutions for preprocessing, segmentation, and classification are proposed. These solutions involve both classical image analysis techniques and connectionist methods. Experimental results are presented. ESA

N94-22898# Institut National Polytechnique, Grenoble (France). Lab. d'Informatique Fondamentale et d'Intelligence Artificielle.
MOTION PLANNING FOR A NON-HOLONOMIC MOBILE IN A DYNAMIC WORKSPACE Ph.D. Thesis [PLANIFICATION DE MOUVEMENT POUR MOBILE NON-HOLONOME EN ESPACE DE TRAVAIL DYNAMIQUE]
Thierry Fraichard 1992 91 p In FRENCH
(ETN-94-95180) Avail: CASI HC A05/MF A01

Motion planning for a mobile A which is subject to kinematic and dynamic constraints and moves within a dynamic workspace W is investigated. This problem can be solved efficiently if W is naturally structured for A, that is, if it is possible to define a set of free regions within which A is able to move. In this case the problem considered can be tackled along two complementary directions: path planning which takes into account the fixed obstacles of W and the kinematic constraints of A; and trajectory planning which takes into account the moving obstacles of W and the dynamic constraints of A. A car-like mobile in the road network is considered. The free regions are defined by the lanes of the roadway. A is subject to a non holonomic kinematic constraint which compels it to move in a direction which is perpendicular to the axle of its wheels. The gyration radius and the acceleration and the velocity of A are bounded. Two techniques to solve the planning problems are presented. How to integrate these two techniques within a motion planner which is able to efficiently solve the problem considered is shown. ESA

N94-22904# Laboratoire d'Automatique et d'Analyse des Systemes, Toulouse (France). Groupe Robotique et Intelligence Artificielle.
CONTRIBUTION TO GEOMETRIC AND DYNAMIC MODELING OF PARALLEL ROBOTS Ph.D. Thesis - Toulouse Univ. [CONTRIBUTION A LA MODELISATION GEOMETRIQUE ET DYNAMIQUE DES ROBOTS PARALLELES]
Mourad Ait-Ahmed 1993 132 p In FRENCH
(LAAS-93089; ETN-94-95186) Avail: CASI HC A07/MF A02

The geometric and dynamic modeling of parallel robots are investigated. The kinematic chains are considered from a topologic and geometric viewpoint so as to ascertain their degree of mobility. The geometric description of these chains is discussed. In all cases, the method proposed allows use of one frame only per link and a maximum of five parameters to define the situation of a link relative to its neighbor. In fact this number reduces to four in the case of a simple kinematic chain structure. The parallel robots most often used in the literature are presented together with methods of modeling involved. The direct geometric modeling of a parallel robot is analyzed by two methods: iterative, based on the computation of a jacobian; and analytical, reducing to the computation of the roots of a polynomial equation. A method for the computation of the dynamic model of mechanisms with a closed chain structure is proposed. This dynamic model is computed as a function of its minimum equivalent tree mechanism. The constraint equations due to the closing of mechanical loops are taken into account. ESA

N94-22906# Laboratoire d'Automatique et d'Analyse des Systemes, Toulouse (France).
AN ARCHITECTURE FOR TELEPROGRAMMING AUTONOMOUS MOBILE ROBOTS AT TASK LEVEL Ph.D. Thesis - Toulouse Univ. [UNE ARCHITECTURE POUR LA TELEPROGRAMMATION AU NIVEAU TACHE D'UN ROBOT MOBILE AUTONOME]
Bernard Degallaix 1993 173 p In FRENCH Sponsored by IFREMER, France
(LAAS-93107; ETN-94-95188) Avail: CASI HC A08/MF A02

The class of intervention mobile robots that have to perform tasks in unknown environments, which are often remote or involve difficult or dangerous access, are investigated. Underwater robotics projects, a Mars rover for planet exploration, or intervention robots for public safety applications are usual examples. Efficient task programming and constant adaptation to the environment by the robot are required for remote applications when limited bandwith and substantial communication delays make it impossible to perform tasks via classical teleoperation. This class of problems demands a specific decisional architecture which couples 'intelligence' at the programming level with 'intelligence' at the level of the physical machine. This second requirement implies that the machine exhibits the attributes of an autonomous intelligent robot. A generic architecture to achieve task control of a remote intervention robot is developed. It is composed of an operator station and the onboard robot control system. Given a set of goals to be achieved, the operator station plans and refines the mission, taking into account temporal constraints. The robot control system is autonomous at the task level. The task assignments are transformed into sequences of actions using its own interpretation and planning capacities. These actions are processed while the system remains reactive to events and environment. ESA

N94-22907# Laboratoire d'Automatique et d'Analyse des Systemes, Toulouse (France). Groupe Robotique et Intelligence Artificielle.

INTERPRETATION OF EVOLUTIVE ENVIRONMENT BY A MULTISENSORY PERCEPTION MACHINE Ph.D. Thesis - Toulouse Univ. [INTERPRETATION D'ENVIRONNEMENT EVOLUTIF PAR UNE MACHINE DE PERCEPTION MULTI-SENSORIELLE]

Jean-Philippe Thibault 1993 173 p In FRENCH
(LAAS-93111; ETN-94-95189) Avail: CASI HC A08/MF A02

A multisensory perception machine is a system that continuously receives and actively gathers information on its environment. A consistent interpretation of the environment evolution is kept. The work is focused on a perception machine in a structured environment with knowledge about its features and models of its objects. Interpretations rest on data fusion both at the level of numerical information and at the level of hypotheses on partial interpretations. The perception is active in the sense that the perception machine has means to move and to adjust functioning modalities of the sensors in order to gather missing information. The management of sensory hypotheses, with the hypothetical reasoning from these hypotheses to constitute an interpretation, and with the execution control of the interpretation process and the resources devoted to it, is investigated. The state of the art of reason maintenance systems is surveyed. A system implemented and used in the multisensory perception machine is presented. The interpretation of the environment in the perception machine is analyzed. How the reliable interpretations are built from perceived sensory data is shown. The control system and the control results from compiling specifications of perceptual tasks are presented. ESA

N94-22908# Laboratoire d'Automatique et d'Analyse des Systemes, Toulouse (France). Groupe Robotique et Intelligence Artificielle.

PERCEPTION AND 3D ENVIRONMENT MODELING FOR MOBILE ROBOT AUTONOMOUS NAVIGATION Ph.D. Thesis - Toulouse Univ. [PERCEPTION ET MODELISATION D'UN ENVIRONNEMENT TRIDIMENSIONNEL POUR LA NAVIGATION AUTONOME D'UN ROBOT MOBILE]

Fawzi Nashashibi 1993 181 p In FRENCH
(LAAS-93117; ETN-94-95190) Avail: CASI HC A09/MF A02

Autonomous mobile robots are designed to perform intelligent modeling of the world and to build internally descriptive representations of encountered terrain. The choice of the representation depends on the sensor, the terrain's topography, and on the nature of the required mission. Range sensory data is considered. The study of the laser range finders used, the modeling of their performances, and the problem of their intrinsic and extrinsic calibrations are discussed. Two different approaches to deal with terrain modeling are proposed. The first model is called the digital terrain model. The second model is called the three dimensional polyhedral model. The approach to build digital navigation maps is described. Incremental modeling, terrain maps fusion, and robot position estimation are considered. The relocation/fusion paradigm is reviewed when handling the modeling of indoor scene structured environments. The perception subsystem and low level modeling procedures are described. The robot localization is studied. The fusion of snapshot models into a global three dimensional polyhedral model is performed. A terrain analysis and an interpretation phase are studied. Three dimensional feature extraction from the global model and the problem of maintaining its global coherence are described. The approach to build a hybrid three dimensional model combining the digital terrain model and the three dimensional polyhedral model is summarized. ESA

N94-23011 Lawrence Livermore National Lab., CA.

A NOVEL PROCESS MONITORING AND CONTROL SYSTEM BASED ON A NEURAL MANUFACTURING CONCEPT

Chi Yung Fu, L. Petrich, and B. Law 14 Sep. 1993 5 p Presented at the Government Microcircuit Applications Conference: Microelectronics in the New World Order, Las Vegas, NV, 9-12 Nov. 1992 Limited Reproducibility: More than 20% of this document may be affected by microfiche quality
(Contract W-7405-eng-48)
(DE94-001516; UCRL-JC-110367; CONF-921188-2) Avail: CASI HC A01

This paper describes our work to produce 'smart' equipment using a neural network to provide intelligence for process monitoring, adaptive control, metrology, and equipment diagnostics. This novel system will improve both quality and yield for critical thin films used in semiconductors, superconductors, high-density magnetic and optical storage, and advanced displays, all of which are critical to maintaining our leadership in the multibillion-dollar electronic and computer industries. The equipment will have on-line, real-time diagnostics capabilities to detect component problems early in order to minimize maintenance and downtime. DOE

N94-23137 National Aerospace Lab., Amsterdam (Netherlands). Informatics Div.

GLOSSARY KNOWLEDGE ENGINEERING [KENNISTECHNOLOGIE BEGRIPPENLIJST]

J. C. Donker and J. M. Nibourg 18 Nov. 1991 70 p In DUTCH Submitted for publication Limited Reproducibility: More than 20% of this document may be affected by microfiche quality
(NLR-TP-91435-U; ETN-94-94784) Avail: CASI HC A04

A glossary of terms used in knowledge engineering is presented. To establish this glossary several sources were consulted. For a number of terms there exists no Dutch equivalent; for clarity the corresponding English term for most of the terms is also given. ESA

N94-23147 Oxford Univ. (England). Dept. of Engineering Science.

HOW MUCH INTEGRAL ACTION CAN A CONTROL SYSTEM TOLERATE?

Denis Mustafa 3 Apr. 1992 6 p Submitted for publication Limited Reproducibility: More than 20% of this document may be affected by microfiche quality
(OUEL-1923/92; ETN-94-95147) Avail: CASI HC A02

A closed formula for the largest amount of integral action that an integral controllable system can tolerate without losing closed loop stability is derived. A block structured guardian map approach is used. A connection is obtained with the calculation of the maximal stability range of a singularly perturbed system. ESA

N94-23152 Institut National Polytechnique, Grenoble (France). Lab. de Modelisation et Calcul.

INSTALLATION OF AN ARTIFICIAL NEURAL NETWORK ON DISTRIBUTED MEMORY MICROPROCESSORS Ph.D. Thesis [IMPLANTATION DE RESEAUX DE NEURONES ARTIFICIELS SUR MULTI-PROCESSEURS A MEMOIRE DISTRIBUEE]

Herve Frydlender 1992 144 p In FRENCH Limited Reproducibility: More than 20% of this document may be affected by microfiche quality
(ETN-94-95175) Avail: CASI HC A07

Techniques for accelerating computation times are investigated. The neural network data processing acceleration can be performed by applying either parallel machines, dedicated processors, or parallelism and coprocessors. Several neuro-computing algorithms are reviewed. A partitioning method is developed and applied to the vector matrix iterated product in order to reduce the whole communication volume. The parallelization of neurocomputing model on a distributed multiprocessor machine is discussed. Algorithms and neuro-computing processors related to coprocessor implantations are studied. Application examples on L-neuro coprocessors are given. A European project involving the development of a general purpose neuro-computer and a silicon compiler is summarized. The implantation of parallel and pipeline modes of low level virtual machine language is included. ESA

N94-23163# Oxford Univ. (England). Dept. of Engineering Science.
REDUCED-ORDER MODELLING AND CONTROL OF A CLASS OF SYSTEMS FOR WHICH BALANCED TRUNCATION IS HANKEL-NORM OPTIMAL
Denis Mustafa and Munther A. Dahleh (Massachusetts Inst. of Tech., Cambridge.) 1992 19 p Sponsored in part by Commonwealth Fund Harkness Fellowship, NY
(Contract AF-AFOSR-0276B-89; F33615-90-C-3608; DL-H-418511)
(OUEL-1922/92; ETN-94-95146) Avail: CASI HC A03/MF A01

Various aspects of model and controller reduction are studied for members of a certain class of linear multivariable systems. Such systems can arise as finite difference models of partial differential equations. A number of properties of the balanced approximants are derived explicitly in terms of the original plant poles. For example, it is shown that each balanced approximant is Hankel norm optimal. When the plant is not stable, the closed loop technique of H(sub infinity) balanced truncation is studied as a way of obtaining reduced order controllers. The focus is on the effect of removing unstable poles, which can happen inadvertently. Although the small gain theorem can pre-test for the ability of the reduced order controller to stabilize the full order plant, it is shown that if any unstable poles are truncated then the small gain condition is always violated. In fact, if an unstable pole is removed the resulting reduced order controller is actually destabilizing. ESA

N94-23179# Oxford Univ. (England). Robotics Research Group.
A TRACKING SONAR SENSOR FOR VEHICLE GUIDANCE
James M. Manyika and Hugh F. Durrant-Whyte 1992 29 p
(OUEL-1956/92; ETN-94-95149) Avail: CASI HC A03/MF A01

A sonar sensor capable of fixating on and tracking environment features moving with relative angular velocities up to 0.6 rad/s and linear speeds up to 2.4 m/s is described. The sensor exploits the predominately specular nature of sonar to model target features as Regions of Constant Depth (RCD) characterized by a single range and bearing measurement. To extract these characteristics at high data rates, the sonar uses a monopulse arrangement of single transmitter and spaced receiver pair to provide both range and differential target bearing information. The monopulse arrangement is mounted on a high speed servo which is used to null the monopulse signal and thereby continuously aim the sonar at the center of an RCD. The design, construction, and modeling of this RCD monopulse sonar sensor are described. It is shown that the sensor can provide accurate and reliable relative location information for a platform moving at speed through typical indoor environments. The implementation of an algorithm which uses this information to enable the device to act as a stand alone guidance sensor is described. ESA

N94-23201# Sandia National Labs., Albuquerque, NM.
GRAPHICAL PROGRAMMING: A SYSTEMS APPROACH FOR TELEROBOTIC SERVICING OF SPACE ASSETS
J. T. Pinkerton (New Mexico Univ., Albuquerque.), M. J. McDonald, R. D. Palmquist, and R. Patten (Oceaneering Space Systems, Webster, TX.) 1993 12 p Presented at the SOAR 1993 Conference, Houston, TX, 3-5 Aug. 1993
(Contract DE-AC04-76DP-00789)
(DE93-019016; SAND-93-1835C; CONF-9308159-1) Avail: CASI HC A03/MF A01

Satellite servicing is in many ways analogous to subsea robotic servicing in the late 1970's. A cost effective, reliable, telerobotic capability had to be demonstrated before the oil companies invested money in deep water robot serviceable production facilities. In the same sense, aeronautic engineers will not design satellites for telerobotic servicing until such a quantifiable capability has been demonstrated. New space servicing systems will be markedly different than existing space robot systems. Past space manipulator systems, including the Space Shuttle's robot arm, have used master/slave technologies with poor fidelity, slow operating speeds and most importantly, in-orbit human operators. In contrast, new systems will be capable of precision operations, conducted at higher rates of speed, and be commanded via ground-control communication links. Challenges presented by this environment include achieving a mandated level of robustness and dependability, radiation hardening, minimum weight and power consumption, and a system which accommodates the inherent communication delay between the ground station and the satellite. There is also a need for a user interface which is easy to use, ensures collision free motions, and is capable of adjusting to an unknown workcell (for repair operations the condition of the satellite may not be known in advance). This paper describes the novel technologies required to deliver such a capability. DOE

N94-23300*# Illinois Univ., Chicago.
VIEWING HYBRID SYSTEMS AS PRODUCTS OF CONTROL SYSTEMS AND AUTOMATA Abstract Only
R. L. Grossman and R. G. Larson Feb. 1992 2 p
(Grants NAG2-513; NSF DMS-91-01089)
(NASA-CR-194792; NAS 1.26:194792) Avail: CASI HC A01/MF A01

The purpose of this note is to show how hybrid systems may be modeled as products of nonlinear control systems and finite state automata. By a hybrid system, we mean a network of consisting of continuous, nonlinear control system connected to discrete, finite state automata. Our point of view is that the automata switches between the control systems, and that this switching is a function of the discrete input symbols or letters that it receives. We show how a nonlinear control system may be viewed as a pair consisting of a bialgebra of operators coding the dynamics, and an algebra of observations coding the state space. We also show that a finite automata has a similar representation. A hybrid system is then modeled by taking suitable products of the bialgebras coding the dynamics and the observation algebras coding the state spaces. Author (revised)

N94-23332*# Washington Univ., Seattle. Dept. of Aeronautics and Astronautics.
A RELIABLE ALGORITHM FOR OPTIMAL CONTROL SYNTHESIS Final Technical Report, Jan. 1991 - Dec. 1992
Brett VanSteenwyk and Uy-Loi Ly 1992 178 p
(Grant NAG2-691)
(NASA-CR-194809; NAS 1.26:194809) Avail: CASI HC A09/MF A02

In recent years, powerful design tools for linear time-invariant multivariable control systems have been developed based on direct parameter optimization. In this report, an algorithm for reliable optimal control synthesis using parameter optimization is presented. Specifically, a robust numerical algorithm is developed for the evaluation of the H(sup 2)-like cost functional and its gradients with respect to the controller design parameters. The method is specifically designed to handle defective degenerate systems and is based on the well-known Pade series approximation of the matrix exponential. Numerical test problems in control synthesis for simple mechanical systems and for a flexible structure with densely packed modes illustrate positively the reliability of this method when compared to a method based on diagonalization. Several types of cost functions have been considered: a cost function for robust control consisting of a linear combination of quadratic objectives for deterministic and random disturbances, and one representing an upper bound on the quadratic objective for worst case initial conditions. Finally, a framework for multivariable control synthesis has been developed combining the concept of closed-loop transfer recovery with numerical parameter optimization. The procedure enables designers to synthesize not only observer-based controllers but also controllers of arbitrary order and structure. Numerical design solutions rely heavily on the robust algorithm due to the high order of the synthesis model and the presence of near-overlapping modes. The design approach is successfully applied to the design of a high-bandwidth control system for a rotorcraft. Author

N94-23463 Finnish Artificial Intelligence Society, Helsinki.
NEURAL NETWORK RESEARCH IN FINLAND. SYMPOSIUM
A. Bulsari and B. Saxen 1993 113 p Symposium held in Turku, Finland, 21 Jan. 1993 Limited Reproducibility: More than 20% of this document may be affected by microfiche quality
(PB93-224822; ISBN-951-650-188-5) Avail: CASI HC A06

The symposium covered the following: Unsupervised Formation of Feature Detectors Through Residual Data Clustering; Image Compression by Neural Networks: A Comparison Study; Basic Requirements for Cognitive and Conscious Machines; Some Results on Feed-forward Neural Networks with a Continuum of Nodes; Modelling Non-linear Time Series by Neural Networks: An Example; Fast Organization of the Self-Organizing Map; Self-Organizing

Maps for Navigation and Collision Free Movement; SOM in Statistical Analysis: Supermarket Customer Profiling; Dynamic Fault Diagnosis Using Radial Basis Function Networks; Recursive Identification Method for Neural Networks; Cognitive Grammar and Map Digitization. NTIS

N94-23558*# Institute for Computer Applications in Science and Engineering, Hampton, VA.

EXPERIENCE WITH PARAMETRIC BINARY DISSECTION Final Report

Shahid H. Bokhari (University of Engineering and Technology, Lahore, Pakistan.) Oct. 1993 14 p

(Contract NAS1-19480; RTOP 505-90-52-01)

(NASA-CR-191552; ICASE-IR-25; NAS 1.26:191552) Avail: CASI HC A03/MF A01

Parametric Binary Dissection (PBD) is a new algorithm that can be used for partitioning graphs embedded in 2- or 3-dimensional space. It partitions explicitly on the basis of nodes + (lambda)x(edges cut), where lambda is the ratio of time to communicate over an edge to the time to compute at a node. The new algorithm is faster than the original binary dissection algorithm and attempts to obtain better partitions than the older algorithm, which only takes nodes into account. The performance of parametric dissection with plain binary dissection on 3 large unstructured 3-d meshes obtained from computational fluid dynamics and on 2 random graphs were compared. It was showm that the new algorithm can usually yield partitions that are substantially superior, but that its performance is heavily dependent on the input data. Author (revised)

N94-23747# Vrije Univ., Amsterdam (Netherlands). Faculteit der Wiskunde en Informatica.

LOGIC OF CAPABILITIES

W. vanderHoek, B. vanLinder, and J. J. C. Meyer Jul. 1993 50 p

(PB94-110715; IR-330) Avail: CASI HC A03/MF A01

A logic of capabilities is introduced. We start by defining a language L in which not only knowledge and actions of a set of agents can be expressed but also their abilities. To formalize the planning of the agents, a Can-predicate and a Cannot-predicate are used. The former indicates that an agent knows that he can achieve a given goal by performing a given action, the latter indicates that the agent knows that he cannot achieve the given goal by performing the given action. We will define two classes of models, of which one is a restricted version of the other. Using these classes, a semantics for the language L is defined. For the second class of models, a sound and complete axiomatization is given. We define the notion of action transformation, a function that transforms actions into other actions. The semantics that we define is such that two actions that can be transformed into one another have equivalent results and that the abilities of an agent are closed under the action transformations. It turns out that the possibility to express the abilities of an agent provides for a flexible and intuitively appealing framework. NTIS

N94-23748# Vrije Univ., Amsterdam (Netherlands). Aculteit der Wiskunde en Informatica.

EPISTEMIC LOGIC FOR DEFEASIBLE REASONING USING A META-LEVEL ARCHITECTURE METAPHOR

J. J. C. Meyer and W. vanderHoek Jul. 1993 29 p See also PB92-198720

(PB94-110723; IR-329) Avail: CASI HC A03/MF A01

The chapter is concerned with default reasoning, or reasoning by default. In particular, we indicate how default logic can be based on epistemic logic, and particularly, how we may employ Halpern and Moses' minimal epistemic states and the entailment relation based on these for this purpose. In this way, we obtain a simple and natural S5-based logic for default reasoning. We discuss these issues in terms of reflective architectures: Halpern and Moses' entailment corresponds to an 'upward reflection', deriving some kind of meta-knowledge that is important for the application of defaults. We discuss some possibilities to deal with the default beliefs that are the outcome of default reasoning, in terms of 'downward reflection', deriving object knowledge from meta-knowledge. This is of particular importance in case the default beliefs contain conflicting information. We also provide one way to resolve possible inconsistencies in the special case of defaults with specificity, even before reflecting down. NTIS

N94-23760# Tilburg Univ. (Netherlands). Dept. of Economics.

COORDINATE-FREE INTERPRETATIONS OF THE OPTIMAL COSTS FOR Lq PROBLEMS SUBJECT TO IMPLICIT SYSTEMS Research Memo

T. Geerts 1993 54 p Sponsored by Nederlandse Organisatie voor Wetenschappelijk Onderzoek, The Hague

(PB94-118700; FEW-604) Avail: CASI HC A04/MF A01

We consider linear-quadratic control problems with and without stability, subject to an arbitrary implicit continuous-time system, in a simple distributional framework, and it will be shown that the associated optimal costs, if existent, are solutions of our Dissipation Inequality for implicit systems. This concept is related to the Linear Matrix Inequality, which is expressed in original system coefficients only, and the above-mentioned optimal costs turn out to be characterizable uniquely by certain solutions of this inequality. However, these solutions need not be rank minimizing if the underlying system is not standard, and we will specify why this is the case. Our statements are valid for regular as well as for singular problems, and the possible significance of the algebraic Riccati equation will be illustrated for both regular and singular problems. Furthermore, we will present necessary and sufficient conditions for solvability of our problems and for existence of optimal controls and associated optimal state trajectories. Finally, we will elaborate on the uniqueness of these controls and state trajectories. NTIS

N94-24068*# National Aeronautics and Space Administration. Lyndon B. Johnson Space Center, Houston, TX.

MAKING INTELLIGENT SYSTEMS TEAM PLAYERS: ADDITIONAL CASE STUDIES

Jane T. Malin, Debra L. Schreckenghost (Mitre Corp., Houston, TX.), and Ron W. Rhoads (Mitre Corp., Houston, TX.) Dec. 1993 65 p

(NASA-TM-104786; S-752; NAS 1.15:104786) Avail: CASI HC A04/MF A01

Observations from a case study of intelligent systems are reported as part of a multi-year interdisciplinary effort to provide guidance and assistance for designers of intelligent systems and their user interfaces. A series of studies were conducted to investigate issues in designing intelligent fault management systems in aerospace applications for effective human-computer interaction. The results of the initial study are documented in two NASA technical memoranda: TM 104738 Making Intelligent Systems Team Players: Case Studies and Design Issues, Volumes 1 and 2; and TM 104751, Making Intelligent Systems Team Players: Overview for Designers. The objective of this additional study was to broaden the investigation of human-computer interaction design issues beyond the focus on monitoring and fault detection in the initial study. The results of this second study are documented which is intended as a supplement to the original design guidance documents. These results should be of interest to designers of intelligent systems for use in real-time operations, and to researchers in the areas of human-computer interaction and artificial intelligence. Author (revised)

N94-24518# Los Alamos National Lab., NM.

DIAGNOSING PROCESS FAULTS USING NEURAL NETWORK MODELS

K. L. Buescher, R. D. Jones, and M. J. Messina 1993 10 p Presented at the Allerton Conference on Communication, Control, and Computing, Urbana, IL, 29 Sep. - 1 Oct. 1993

(Contract W-7405-eng-36)

(DE94-002633; LA-UR-93-3598; CONF-9309272-1) Avail: CASI HC A02/MF A01

In order to be of use for realistic problems, a fault diagnosis method should have the following three features. First, it should apply to nonlinear processes. Second, it should not rely on extensive amounts of data regarding previous faults. Lastly, it should detect faults promptly. The authors present such a scheme for static (i.e., non-dynamic) systems. It involves using a neural network to create an associative memory whose fixed points represent the normal behavior of the system. DOE

N94-24542* Technische Univ., Eindhoven (Netherlands). Dept. of Mathematics and Computing Science.

DISCRETE-TIME H(INFINITY) CONTROL PROBLEM WITH STRICTLY PROPER MEASUREMENT FEEDBACK Final Report

Anton A. Stoorvogel, Ali Saberi (Washington State Univ., Pullman.), and Ben M. Chen (State Univ. of New York, Stony Brook.) Jun. 1993 16 p

See also PB93-197523 Sponsored by NASA, Washington Limited Reproducibility: More than 20% of this document may be affected by microfiche quality
(Grant NAG1-1210)
(NASA-CR-195089; NAS 1.26:195089; PB94-111200;
MEMO-COSOR-93-16) Avail: Issuing Activity (National Technical Information Service (NTIS))

The paper is concerned with the discrete-time H(sub infinity) control problem with strictly proper measurement feedback. The authors derive necessary and sufficient conditions for the existence of a strictly proper compensator which achieves a given H(sub infinity) norm bound. Note that contrary to the continuous time, in discrete time there might exist a suitable proper compensator but no suitable strictly proper compensator. Finally, they give an explicit formula for one controller which achieves this bound. NTIS

N94-24543 Vrije Univ., Amsterdam (Netherlands). Faculteit der Wiskunde en Informatica.

COMPOSITIONAL ARCHITECTURE FOR SIMPLE DESIGN FORMALLY SPECIFIED IN DESIRE

Izak VanLangevelde, Albert Philipsen, and Jan Treur Dec. 1992 66 p Limited Reproducibility: More than 20% of this document may be affected by microfiche quality
(PB94-119013; IR-318) Avail: Issuing Activity (National Technical Information Service (NTIS))

A simple generic design task is described whereafter a simple scheduling task is described as a specific instance of it. A concise description of DESIRE, a framework for specification of compositional architectures, is presented. It is demonstrated how a generic compositional architecture for simple design can be formally specified by means of DESIRE and how an architecture for simple scheduling can be specified as an instantiation of the generic specification. The reasoning behavior of the resulting architecture is elucidated by reasoning trace. The full specification of the scheduling architecture is included as the appendix. NTIS

N94-24544 Newcastle-upon-Tyne Univ. (England). Dept. of Computing Science.

SYSTEMATIC CONSTRUCTION OF TRIGONOMETRIC NEURAL NETWORKS

G. M. Megson 1993 26 p Limited Reproducibility: More than 20% of this document may be affected by microfiche quality
(PB93-200228; TRS-416) Copyright Avail: Issuing Activity (National Technical Information Service (NTIS))

A new type of multi-layer neural network based on sets of trigonometric polynomials is introduced. It is shown that the weights of the network can be derived directly from the coefficients of the discrete analog form of the Fourier least squares polynomial for the set generated from the output patterns, and a so-called separator function produced from input patterns of the 'training' set. As a consequence the need for a protracted training period is removed and replaced by a more systematic analysis of output functions. The method is illustrated on a collection of examples. Some general properties and design principles regarding network size and generalization abilities are also considered. NTIS

N94-24609 Technische Univ., Eindhoven (Netherlands). Dept. of Mathematics and Computing Science.

DISCRETE TIME MINIMUM ENTROPY H(INFINITY) CONTROL PROBLEM

A. A. Stoorvogel and J. H. A. Ludlage (IPCOS B.V., Best, Netherlands.) Mar. 1993 19 p Limited Reproducibility: More than 20% of this document may be affected by microfiche quality
(PB93-237808; MEMO-COSOR-93-05) Avail: CASI HC A03

The paper completely solves the discrete time minimum entropy control problem. It is shown that in discrete time, the central controller has the additional interpretation as the controller which minimizes a minimum entropy criterion. This is completely analogous to the continuous time. However, although the H(infinity) control problems for discrete and continuous time can be connected via the bilinear transform, it is shown that this is not the case for the corresponding minimum entropy control problems, and hence, the bilinear transform does not connect the central controllers in continuous and discrete time. NTIS

N94-24622 University of Southern California, Los Angeles. Dept. of Electrical Engineering and Electrophysics.

PHOTONIC TECHNOLOGY FOR IMPLEMENTATION OF GENERALIZABLE NEURAL NETWORKS: A SYNTHETIC APPROACH Final Report, 30 Sep. 1989 - 15 Sep. 1993

B. K. Jenkins, Anupam Madhukar, and Armand R. Tanguay 28 Oct. 1993 70 p Limited Reproducibility: More than 20% of this document may be affected by microfiche quality
(Grant AF-AFOSR-0466-89)
(AD-A273497; AFOSR-93-0878TR) Avail: Issuing Activity (Defense Technical Information Center (DTIC))

This report describes progress and results on the grant, 'Photonic Technology for Implementation of Generalizable Neural Networks: A Synthetic Approach,' DARPA/AFOSR Grant No. AFOSR-89-0466, for the annual reporting period 30 Sep. 1991 - 29 Sep. 1992, and for the final reporting period 30 Sep. 1989 - 15 Sep. 1993. Substantial progress and results have been achieved in the areas of neural network models for optoelectronic systems, photonic neural network architectures, incoherent/coherent holographic interconnections, optical disk spatial light modulators with parallel readout (as input devices), and high bandwidth spatial light modulators (for neuron unit arrays) including mutually compatible silicon detectors, silicon electronics, and high contrast ratio InGaAs/GaAs modulators. DTIC

N94-24627 Centre d'Etudes et de Recherches, Toulouse (France). Dept. d'Etudes et de Recherches en Automatique.

ASYMPTOTIC CORRECTORS: THE LTR Final Report [CORRECTEURS ASYMPTOTIQUES: LE LTR]

J. F. Magni and P. Mouyon Jan. 1992 55 p In FRENCH See also PB91-199489 Sponsored by Direction des Recherches, Etudes et Techniques Limited Reproducibility: More than 20% of this document may be affected by microfiche quality
(PB93-199701; CERT-2/7766-DERA) Avail: Issuing Activity (National Technical Information Service (NTIS))

The report proposes a modal approach for reconstructing a recovery transfer using a loop. It is the 'Loop Transfer Recovery' problem. The authors pay particular attention to non-minimal phase shift systems. Their ultimate goal is to improve H sub infinity techniques by mastering the pole/zero simplifications that are so troublesome for applications. NTIS

N94-24635*# National Aeronautics and Space Administration. Langley Research Center, Hampton, VA.

ADMITTANCE MODEL FOR THE SHUTTLE REMOTE MANIPULATOR SYSTEM IN FOUR CONFIGURATIONS M.S. Thesis

Loukas Papadopoulos (George Washington Univ., Hampton, VA.) and Robert H. Tolson (George Washington Univ., Hampton, VA.) Nov. 1993 213 p
(Contract NCC1-104; RTOP 586-02-11)
(NASA-CR-4555; NAS 1.26:4555) Avail: CASI HC A10/MF A03

A possible scenario for robot task performance in space is to mount two small, dexterous arms to the end of the Shuttle Remote Manipulator System (SRMS). As these small robots perform tasks, the flexibility of the SRMS may cause unsuccessful task executions. In order to simulate the dynamic coupling between the SRMS and the arms, admittance models of the SRMS in four brakes locked configurations were developed. The admittance model permits calculation of the SRMS end-effector response due to end-effector disturbing forces. The model will then be used in conjunction with a Stewart Platform, a vehicle emulation system. An application of the admittance model was shown by simulating the disturbing forces using two SRMS payloads, the Dextrous Orbital Servicing System (DOSS) manipulator and DOSS carrying a 1000 lb. cylinder. Mode by mode comparisons were conducted to determine the minimum number of modes required in the admittance model while retaining dynamic fidelity. It was determined that for all four SRMS configurations studied, between 4 and 6 modes of the SRMS structure (depending on the excitation loads) were sufficient to retain tolerance of 0.01 inches and 0.01 deg. These tolerances correspond to the DOSS manipulator carrying no object. When the DOSS carries the 1000 lb. cylinder, between 15 and 20 modes were sufficient, approximately three or four times as many modes as for the unloaded case. Author

N94-24755 Technische Univ., Eindhoven (Netherlands). Dept. of Mathematics and Computing Science.
CONTROLLED INVARIANCE OF NONLINEAR SYSTEMS: NONEXACT FORMS SPEAK LOUDER THAN EXACT FORMS
H. J. C. Huijberts and C. H. Moog Mar. 1993 20 p Limited Reproducibility: More than 20% of this document may be affected by microfiche quality
(PB93-237790; MEMO-COSOR-93-06) Avail: CASI HC A03/MF A01

A general setting is developed which describes controlled invariance for nonlinear control systems and which incorporates the previous approaches dealing with controlled invariant distributions. The main feature of the theory developed is that it is able to clarify the controlled invariance of distributions which are not necessarily integrable. The latter are of major importance for the geometric description of e.g. dynamic feedback problems. NTIS

N94-24760*# Massachusetts Inst. of Tech., Cambridge. Dept. of Aeronautics and Astronautics.
CONTROL OF NONLINEAR SYSTEMS REPRESENTED IN QUASILINEAR FORM Ph.D. Thesis, 1994 Final Report
Josef A. Coetsee Dec. 1993 204 p
(Grant NAG1-126)
(NASA-CR-194840; NAS 1.26:194840) Copyright Avail: CASI HC A10/MF A03

Methods to synthesize controllers for nonlinear systems are developed by exploiting the fact that under mild differentiability conditions, systems of the form: x-dot = f(x) + G(x)u can be represented in quasilinear form, viz: x-dot = A(x)x + B(x)u. Two classes of control methods are investigated. The first is zero-look-ahead control, where the control input depends only on the current values of A(x) and B(x). For this case the control input is computed by continuously solving a matrix Riccati equation as the system progresses along a trajectory. The second is controllers with look-ahead, where the control input depends on the future behavior of A(x) and B(x). These controllers use the similarity between quasilinear systems and linear time varying systems to find approximate solutions to optimal control type problems. The methods that are developed are not guaranteed to be globally stable. However in simulation studies they were found to be useful alternatives for synthesizing control laws for a general class of nonlinear systems. Author (revised)

N94-24762 Technische Univ., Eindhoven (Netherlands). Dept. of Mathematics and Computing Science.
GENERICITY OF STABILIZABILITY FOR TIME-DELAY SYSTEMS
L. C. G. J. M. Habets May 1993 40 p Limited Reproducibility: More than 20% of this document may be affected by microfiche quality
(PB93-237725; MEMO-COSOR-93-14) Avail: Issuing Activity (National Technical Information Service (NTIS))

Conditions for the stabilizability of time-delay systems with non-commensurate point delays by dynamic state feedback are known in the literature. It is shown that these conditions are satisfied generically. Although an algebraic approach is used to describe the class of all time-delay systems with point delays, the concept of genericity is formulated in a topological framework. In the metric space consisting of all parametrizations of time-delay systems, the subset of all stabilizable systems is an open and dense subset. The proof is given for the commensurate delay case first. At the end it is pointed out that the non-commensurate delay case is not significantly more difficult, and that the same arguments prove also that systems with non-commensurate time-delays are generically stabilizable. NTIS

N94-24862# Naval Postgraduate School, Monterey, CA.
OBJECT RECOGNITION THROUGH IMAGE UNDERSTANDING FOR AN AUTONOMOUS MOBILE ROBOT M.S. Thesis
Mark J. DeClue Sep. 1993 195 p
(AD-A273206) Avail: CASI HC A09/MF A03

The problem addressed in this research was to provide a capability for sensing previously unknown rectilinear, polyhedral-shaped objects in the operating environment of the autonomous mobile robot Yamabico-11. The approach to the system design was based on the application of edge extraction and least squares line fitting algorithms of PET92 to real-time camera images with subsequent filtering based on the environmental model of STE92. The output of this processing was employed in the recognition of obstacles and the determination of object range and dimensions. These measurements were then used in path tracking commands, supported by Yamabico's Model-based Mobile Robot Language (MML), for performing smooth, safe obstacle avoidance maneuvers. This work resulted in a system able to localize objects in images taken from the robot, provide location and size data, and cause proper path adjustments. Accuracies on the order of one to ten centimeters in range and one-half to two centimeters in dimensions were achieved. DTIC

N94-24943# Stanford Univ., CA.
CHANGE-POINT DETECTION AND ADAPTIVE CONTROL OF TIME-VARYING SYSTEMS Final Report, 1 Jun. 1992 - 31 May 1993
David Siegmund 8 Sep. 1993 3 p
(Contract F49620-92-J-0411)
(AD-A273509; AFOSR-93-0860TR) Avail: CASI HC A01/MF A01

Fundamental progress was made in the sequential and fixed sample detection and estimation of abrupt changes in stochastic systems and in the related problem of adaptive control of dynamical systems with time varying parameters. Advances were also made in recursive estimation and adaptive control of linear stochastic systems, optimal sequential testing of composite hypotheses, and regression analysis of censored failure time data. DTIC

N94-24963 Institut National de Recherche d'Informatique et d'Automatique, Valbonne (France). Programme 4: Robotique, Image et Vision.
PRELIMINARY RESULTS ON TIME-VARYING FEEDBACK STABILIZATION OF A NONHOLONOMIC CAR-LIKE MOBILE ROBOT
Claude Samson Sep. 1991 16 p Presented at the 30th IEEE Conference on Decision and Control Submitted for publication Limited Reproducibility: More than 20% of this document may be affected by poor print
(INRIA-RR-1512; ETN-93-93710) Avail: Issuing Activity (European Space Agency (ESA))

Time varying smooth feedbacks, that is feedbacks which depend explicitly on the time index, are applied to a front wheel driven cart for which a set of globally stabilizing time varying smooth feedback controls is derived. The control inputs are assumed to be the two motorized wheels' angular velocities: advancement velocity and steering angular velocity. ESA

N94-25139# Naval Command, Control and Ocean Surveillance Center, San Diego, CA. Research, Development, Technology and Evaluation Div.
DETERMINING NEURAL NETWORK HIDDEN LAYER SIZE USING EVOLUTIONARY PROGRAMMING Professional Paper
John R. McDonnell and Don Waagen Oct. 1993 6 p
(AD-A273242) Avail: CASI HC A02/MF A01

This work investigates the application of evolutionary programming, a stochastic search technique, for simultaneously determining the weights and the number of hidden units in a fully-connected, multi-layer neural network. The simulated evolution search paradigm provides a means for optimizing both network structure and weight coefficients. Orthogonal learning is implemented by independently modifying network structure and weight parameters. Different structural level search strategies are investigated by comparing the training processes for the 3-bit parity problem. The results indicate that evolutionary programming provides a robust framework for evolving neural networks. DTIC

N94-25224 Technische Univ., Eindhoven (Netherlands).
PRACTICAL EVALUATION OF ROBUST CONTROL FOR A CLASS OF NONLINEAR MECHANICAL DYNAMIC SYSTEMS Ph.D. Thesis
Abraham Gilles deJager 1992 193 p Limited Reproducibility: More than 20% of this document may be affected by microfiche quality
(ISBN-9-03-860092-5; ETN-94-95359) Copyright Avail: CASI HC A09

A study to assess the robustness potential of controllers for a class of nonlinear mechanical systems, to get insight into the achievable performance of these control systems, and to grade several controller design methods according to the two aspects mentioned above is reported. This was achieved by using a multistage evaluation strategy, with a literature search, numerical experiments, and laboratory experiments. The control schemes studied are mostly based on the use of a nominal model of a more complicated nonlinear system. The model is used by the controller to linearize the nominal model, or to generate control inputs that achieve almost the same goal. This part of the controller can be combined with a stabilizing component, a robustifying component, and a parameter adaptation component. The use of acceleration signals to improve the estimation of state variables and to enhance the robustness is studied. Control concepts that adapt the structure of the controller, instead of only the parameters, are not studied. The development of an appreciation strategy, using observation, manipulation, and experimentation techniques, to find and qualify robust controllers is discussed. ESA

N94-25262# Technische Univ., Eindhoven (Netherlands).
MIMO SYSTEM IDENTIFICATION FOR H(INFINITY) ROBUST CONTROL: A FREQUENCY DOMAIN APPROACH WITH MINIMUM ERROR BOUNDS Ph.D. Thesis
Antonius Josephus J. vandenBoom 1993 223 p
(ETN-94-95354) Avail: CASI HC A10/MF A03

A frequency domain system identification procedure for MIMO systems that yields a model with a bounded unstructured model error is presented. The disturbances on the input and output of the process are assumed to be bounded in the frequency domain, which implies that there exist bounding functions for the absolute value of the discrete Fourier transform of the noise signals. The identification of a SISO process is considered. Uncertainty regions for the process dynamics are derived and an optimal model by H(sub infinity) fitting is found. The identification method is extended to MIMO systems and various model error structures are considered. It is shown that for a fixed model the true model error can be expressed as a function of a known matrix G(z) and an unknown diagonal matrix Q(sub t)(z). An upper bound for the largest singular value of the model error is derived. The theory of structured singular values and of the so called Redheffer star products are used. The upper bounds for the model error are minimized in some norm sense. The choice of a linear parametrization leads to a convex optimization problem and the algorithms are robustly convergent. A case study, where a laboratory process with 2 inputs and 2 outputs is identified and a model with a bound on the model error, is derived. ESA

N94-25290# Technische Univ., Eindhoven (Netherlands).
DATA STRUCTURES AND AMORTIZED COMPLEXITY IN A FUNCTIONAL SETTING Ph.D. Thesis
Lambertus Adrianus M Schoenmakers 1992 208 p
(ETN-94-95307) Avail: CASI HC A10/MF A03

The purpose of the work is to increase the understanding of amortized complexity, particularly in the nature of potential functions. Potentials for a number of data structures were derived as systematically as possible. The necessary tools needed to specify and design several data structures are given. The notion of algebra refinement is defined for monoalgebras only. It is shown that any amortized analysis can be done in terms of a potential function. It is also shown that: the fact that the number of deckey operations on each node is bounded by a constant K gives rise to more efficient implementations; and that, depending on the ratio of the number of unions and the number of delmins, different bounds for the amortized costs of these operations are obtained. The conjecture that the log phi bound for top down melding is tight is made. ESA

N94-25307# Sheffield Univ. (England). Dept. of Automatic Control and Systems Engineering.
ON-LINE CONTROL OF DYNAMIC SYSTEMS USING FEEDFORWARD NEURAL NETWORKS
Eliezer Colina-Morles and Niel Mort Aug. 1992 23 p
(RR-457; ETN-94-95129) Avail: CASI HC A03/MF A01

An adaptive neural network based control scheme is proposed. Its performance was digitally simulated using an unknown plant which belongs to a certain class of nonlinear systems. The role of the multilayer neural network considered was to make an online estimation of the unknown input/output behavior of the plant. The purpose is to drive the system's behavior according to the specifications given by a reference model. The learning algorithm used to update the weights of the network allows dynamic adjustment of their values to cope with varying signals coming from the unknown plant. The best results were obtained using a three layer neural network to estimate the unknown input/output behavior of the plant and by assuming that the teaching signal was not a constant one. In this case, the inputs to the neural network were three unitary step functions. ESA

N94-25308# Sheffield Univ. (England). Dept. of Automatic Control and Systems Engineering.
THE PHASE RESPONSE OF NONLINEAR SYSTEMS
S. A. Billings and H. Zhang 11 Aug. 1992 34 p
(Grant SERC-GR/F-8564.2)
(RR-458; ETN-94-95130) Avail: CASI HC A03/MF A01

The phase response function is analyzed and interpreted to provide a clear understanding of nonlinear systems. Systems which include delay elements are also discussed. Simulations of both continuous and discrete time nonlinear systems are included. Results for linear systems are reviewed. An expression for the phase response for a wide class of nonlinear systems is derived. The phase response to a multifrequency input is derived to illustrate how the phase shift of both the input excitation and the phase response of the nonlinear system influence the overall system response. The effects of delay elements on the system are considered. The importance of phase in the interpretation of nonlinear frequency response functions is demonstrated. Frequency mixing, which plays a prominent part in nonlinear frequency response analysis, is overviewed. ESA

N94-25345# Deutsche Forschungsanstalt fuer Luft- und Raumfahrt, Oberpfaffenhofen (Germany). Abt. Raumflugdynamik.
ROSAT MISSION PLANNING USING ARTIFICIAL INTELLIGENCE METHODS [ROSAT-MISSIONSPLANUNG MIT METHODEN DER KUENSTLICHEN INTELLIGENZ]
Yukio Oku 21 Apr. 1993 39 p In GERMAN
(DLR-FB-93-14; ETN-94-95202) Avail: CASI HC A03/MF A01

The artificial intelligence scheduler, SPIKE (Science Planning Interactive Knowledge Environment) was successfully applied to the planning task of ROSAT. SPIKE supports two modes: an automatic mode for offline scheduling and a graphical interactive mode for users, which can make problem diagnostics. The SPIKE architecture contains two levels: a low constraint representation and reasoning level and a high strategic scheduling level, which allows multistart stochastic repair mechanisms, which come from a discrete stochastic neural network. The ROSAT mission planning through SPIKE is depicted: parameter value estimation and initialization, calculation of suitability functions and interactive planning. SPIKE advantages, such as software readability, high performance, user friendly interface, effective preprocessing and possibility of handling preferences and uncertain factors, are assessed. ESA

N94-25428# Loughborough Univ. of Technology (England). Dept. of Mathematical Sciences.
KERNELS OF ANTI-CAUSAL OPERATORS AND THE MULTIVARIABLE GENERALIZED PREDICTIVE CONTROL PROBLEM
B. Kouvaritakis (Oxford Univ., England.), J. A. Rossiter, and A. O. T. Chang (Oxford Univ., England.) Aug. 1993 25 p Sponsored by United Kingdom Science and Engineering Research Council, and Croucher Foundation
(MATHS-Rept-A-191; ETN-94-95228) Avail: CASI HC A03/MF A01

Eigenvector or principal direction projections provide a convenient means of decomposing the multivariable problem into a set of scalar control problem. They can be solved using single input single output generalized predictive control. The bicausal nature of eigenvector or principal direction representations leads to anticausality difficulties. The use 'kernels' of bicausal operators is proposed as an effective remedy for the scalar case. The relationship between these kernels and scaling of the bicausal representations is studied. Algorithms which overcome the pseudodelay problems in the multivariable case are proposed. An algorithm for the characterization of all the available degrees of freedom is given. They are introduced into the scalar predictive control cost and the control law is computed by a process of back projection. The algorithms proposed match the set point following behavior and remove the problem of pseudo delays. ESA

N94-25429# Loughborough Univ. of Technology (England). Dept. of Mathematical Sciences.
ADVANCES IN GENERALIZED AND CONSTRAINED GENERALIZED PREDICTIVE CONTROL WITH APPLICATION TO A DYNAMOMETER MODEL
J. A. Rossiter and B. Kouvaritakis (Oxford Univ., England.) Aug. 1993 14 p
(MATHS-Rept-A-192; ETN-94-95229) Avail: CASI HC A03/MF A01

The Stable Generalized Predictive Control (SGPC) and Constrained Stable Generalized Predictive Control (CSGPC) algorithms are described. The advantages of these algorithms over existing ones are presented. The efficacy of CSGPC was illustrated by means of a design study on a model of a dynamometer feedback control system. The simulation results show that an approach to constraints could be disastrously wrong and that constraint inequality during the optimization stage must be taken into account. CSGPC does that and produces stable and optimal results, and overcomes problems of short term infeasibility. ESA

N94-25431# Technische Univ., Eindhoven (Netherlands).
THE USE OF KNOWLEDGE SYSTEMS Ph.D. Thesis [HET NUT VAN KENNISSYSTEMEN]
Robert Victor Schuwer 1993 194 p In DUTCH
(ETN-94-95318) Avail: CASI HC A09/MF A03

An investigation as to the situations for which a knowledge base system is a proper solution, and what is the added value that a knowledge base system can provide compared to alternative solving methods is presented. A formal model that unambiguously describes the architecture of a knowledge base system was developed. This model is mainly used for the identification of situations in which knowledge base systems have an added value. A knowledge base system can serve as a solution when a demand exists to clarify the way of reasoning of a system to the user, and in those situations where an explicit need for knowledge management exists. To be accepted and used in an operational environment, knowledge base systems have to be integrated within a total systems architecture. ESA

N94-25469# Oxford Univ. (England). Dept. of Engineering Science.
STABILITY QUESTIONS IN PREDICTIVE CONTROL
Pierre O. M. Scokaert and David W. Clarke 26 Jan. 1993 24 p
(OUEL-1970/93; ETN-94-95156) Avail: CASI HC A03/MF A01

Stability results are derived for well known predictive controllers. The conditions known to give rise to a stable closed loop with a Constrained Receding Horizon Predictive Controller (CRHPC) are extended and a Generalized Predictive Controller (GPC) which stabilizes open loop stable systems is proposed. Closed loop studies are performed using the proved monotonicity property of the receding horizon cost. ESA

N94-25470# Oxford Univ. (England). Dept. of Engineering Science.
ADAPTIVE PREDICTIVE CONTROL OF THE BENCHMARK PLANT
Tae-Woong Yoon and David W. Clarke 1993 7 p
(OUEL-1972/93; ETN-94-95157) Avail: CASI HC A02/MF A01

An adaptive Constrained Receding Horizon Predictive Control (CRHPC) scheme coupled with a least squares based estimator was employed to control the benchmark plant, which features large time variations. The adaptive control algorithm used is described and the design procedure is discussed. Simulation results and conclusions are given. It was shown that an adaptive CRHPC controller can cope well with time variations. ESA

N94-25526# Technische Univ., Eindhoven (Netherlands). Dept. of Mathematics and Computing Science.
PRODUCT FORMS AS A SOLUTION BASE FOR QUEUEING SYSTEMS
Ivo J. B. F. Adan and Jaap Wessels Sep. 1992 14 p
(MEMO-COSOR-92-37; ETN-94-94798; PB94-126596) Avail: CASI HC A03/MF A01

Queueing systems which have solutions in the form of linear combinations of product forms are investigated. The case when the equilibrium distribution of one or two dimensional Markovian queueing systems can be written as linear combination of products of powers is discussed. Cases with extra supplementary variables are investigated. Product form networks as the solution of a set of partial difference equations with boundary conditions are studied. The queueing system E(sub K)/E(sub r)/c is presented. The general theory for two dimensional systems is given. The results show that the concept of constructing solutions in the form of linear combinations of product forms is useful for several queueing problems. ESA

N94-23247*# Wake Forest Univ., Winston-Salem, NC. Dept. of Mathematics and Computer Science.
EXPANDING THE KATE TOOLBOX
Stan J. Thomas *In* NASA. Kennedy Space Center, NASA/ASEE Summer Faculty Fellowship Program Oct. 1993 p 467-486 (For primary document see N94-23230 06-80)
Avail: CASI HC A03/MF A04

N94-23267*# Jet Propulsion Lab., California Inst. of Tech., Pasadena. Advanced Information Systems Section.
LINK MONITOR AND CONTROL OPERATOR ASSISTANT: A PROTOTYPE DEMONSTRATING SEMIAUTOMATED MONITOR AND CONTROL
L. F. Lee and L. P. Cooper *In its* The Telecommunications and Data Acquisition Report 15 Nov. 1993 p 124-134 (For primary document see N94-23256 06-32)
(RTOP 310-40-73-90-01)
Avail: CASI HC A03/MF A02

N94-23900*# Jet Propulsion Lab., California Inst. of Tech., Pasadena.
COMBINING REAL-TIME MONITORING AND KNOWLEDGE-BASED ANALYSIS IN MARVEL
Ursula M. Schwuttke, A. G. Quan, R. Angelino, and J. R. Veregge *In its* SpaceOps 1992: Proceedings of the Second International Symposium on Ground Data Systems for Space Mission Operations 1 Mar. 1993 p 453-458 (For primary document see N94-23832 06-66)
Avail: CASI HC A02/MF A10

N94-23916*# Jet Propulsion Lab., California Inst. of Tech., Pasadena.
USING MACH THREADS TO CONTROL DSN OPERATIONAL SEQUENCES
Juan Urista *In its* SpaceOps 1992: Proceedings of the Second International Symposium on Ground Data Systems for Space Mission Operations 1 Mar. 1993 p 553-559 (For primary document see N94-23832 06-66)
Avail: CASI HC A02/MF A10

N94-24263 Eidgenoessische Technische Hochschule, Zurich (Switzerland). Measurement and Control Laboratory.
A MIXED MAP/VARIABLE STRUCTURE OBSERVER FOR TARGET TRACKING
S. A. R. Hepner, Luca L. Bagnaschi, and H. P. Geering *In* Israel Society of Aeronautics and Astronautics, The 33rd Israel Annual Conference on Aviation and Astronautics 25 Feb. 1993 p 251-262 (For primary document see N94-24241 06-01)
Copyright Avail: Issuing Activity (Israel Society of Aeronautics and Astronautics, c/o Faculty of Engineering, Tel-Aviv Univ., Ramat Aviv 69978, Israel)

N94-24433*# Texas A&M Univ., College Station. Marine Engineering Dept.
NEURAL NETWORK-BASED CONTROL USING LYAPUNOV FUNCTIONS
Leon A. Luxemburg *In* Alabama Univ., The 1993 NASA/ASEE Summer Faculty Fellowship Program Nov. 1993 5 p (For primary document see N94-24405 06-80)
Avail: CASI HC A01/MF A03

N94-24452*# Alabama Univ., Tuscaloosa. Dept. of Aerospace Engineering.
USING NEURAL NETWORKS TO ASSIST IN OPAD DATA ANALYSIS
Kevin W. Whitaker *In* Alabama Univ., The 1993 NASA/ASEE Summer Faculty Fellowship Program Nov. 1993 5 p (For primary document see N94-24405 06-80)
Avail: CASI HC A01/MF A03

N94-25370*# Rice Univ., Houston, TX. Dept. of Mechanical Engineering and Materials Science.
DEVELOPMENT OF PROGRAMMABLE ARTIFICIAL NEURAL NETWORKS
Andrew J. Meade *In* NASA. Johnson Space Center, National Aeronautics and Space Administration (NASA)/American Society for Engineering Education (ASEE) Summer Faculty Fellowship Program, 1993, Volume 2 Dec. 1993 14 p (For primary document see N94-25367 06-99)
Avail: CASI HC A03/MF A03

64 NUMERICAL ANALYSIS

Includes iteration, difference equations, and numerical approximation.

N94-22710# Universiteit Twente, Enschede (Netherlands). Faculty of Applied Mathematics.
TOOL SHARING: AN APPLICATION OF MAX-ALGEBRA, PART 2
W. M. Nawijn Mar. 1993 12 p
(MEMO-1122; ETN-94-94758) Avail: CASI HC A03/MF A01

The second part of a study on the long run behavior of a system of recurrent equations to be studied in max-algebra is presented. Given are m identical machines each of which performs the same N operations 0(sub i), i less than or equal to N and greater than or equal to 1, cyclically and indefinitely, that is, a production run looks like 0(sub 1), 0(sub 2),..., 0(sub N), 0(sub 1), 0(sub 2),..., 0(sub N), 0(sub 1)... There are n(sub i) less than or equal to m tools available to perform operation i. The tools are transported between the machines by means of an infinitely fast transport device. The existence of stationary cyclic behavior is proved and the corresponding cycle time is derived. As a particular case, the system in which the tools can be partitioned into two subsets W and W(bar), such that W = (j : n(sub j) = m) and W(bar) = (j : n(sub j) = 1) is discussed. ESA

N94-22715# Universiteit Twente, Enschede (Netherlands). Faculty of Applied Mathematics.
TOUGHNESS AND TRIANGLE-FREE GRAPHS
D. Bauer (Stevens Inst. of Tech., Hoboken, NJ.), J. P. vandenHeuvel, and E. Schmeichel (San Jose State Univ., CA.) Mar. 1993 20 p Sponsored in part by Netherlands Organization for Scientific Research
(Grants NATO-CRG-921251; NSF DMS-92-06991)
(MEMO-1127; ETN-94-94763) Avail: CASI HC A03/MF A01

A study which proves that there exist triangle free graphs with arbitrarily large toughness is given, thereby settling a longstanding open question. The problem of whether there exists a t-tough, n/(t + 1) regular, triangle free graph on n vertices for various values of t is explored, and a relatively complete answer for small values of t is provided. ESA

N94-22725# Universiteit Twente, Enschede (Netherlands). Faculty of Applied Mathematics.
SETTING TEST LIMITS UNDER PRESCRIBED CONSUMER LOSS
W. Albers, W. C. M. Kallenberg, and G. D. Otten Jan. 1993 25 p
(MEMO-1107; ETN-94-94743) Avail: CASI HC A03/MF A01

In inspection of manufactured parts inaccuracies of the measurement process compel use of test limits which are more strict than the given specification limits. To avoid violation of the prescribed bound gamma on the consumer loss, in practice overly conservative informal approaches are used leading to a loss of yield. Approximations are derived for which gamma is realized with high precision. The expressions involved are sufficiently simple and explicit to allow extension to the more realistic case where the parameters of the underlying distributions need to be estimated. Various criteria are presented to measure the closeness of the resulting stochastic consumer losses to gamma. Some attention is devoted to the sampling schemes involved. ESA

N94-22726# Universiteit Twente, Enschede (Netherlands). Faculty of Applied Mathematics.
TOOL SHARING: AN APPLICATION OF MAX-ALGEBRA, PART 1
W. M. Nawijn Jan. 1993 26 p
(MEMO-1108; ETN-94-94744) Avail: CASI HC A03/MF A01

The first part of a study on long run behavior of a system of recurrent equations to be studied in max-algebra is presented. There are m identical machines each of which perform the same N operations, with processing times a(sub 1), a(sub 2),..., a(sub N) cyclically and indefinitely. There is only one tool per operation. The tools are transported between the machines by means of an infinitely fast transport device. The behavior of the system in the long run is investigated. In particular, the existence of stationary cyclic behavior is proved and the corresponding cycle time is determined. The time to reach the stationary cycle is also determined. The problem is analyzed by means of max-algebra. ESA

N94-22727# Universiteit Twente, Enschede (Netherlands). Faculty of Applied Mathematics.
LONG CYCLES IN GRAPHS WITH PRESCRIBED TOUGHNESS AND MINIMUM DEGREE
D. Bauer (Stevens Inst. of Tech., Hoboken, NJ.), H. J. Broersma, J. P. M. vandenHeuvel, and H. J. Veldman Jan. 1993 14 p
(Contract NATO-CRG-921251; MDA904-84-H-2008)
(MEMO-1109; ETN-94-94745) Avail: CASI HC A03/MF A01

A cycle C of a graph G is a D(sub lambda) cycle if every component of G - V(C) has order less than lambda. Using the notion of D(sub lambda) cycles, results concerning long cycles in graphs with prescribed toughness and minimum degree are established. Let G be a t-tough graph on n greater than or equal to 3 vertices. If delta is greater than (n/(t + lambda)) + delta - 2 for some lambda less than or equal to t + 1, then G contains a D(sub lambda) cycle. In particular, if delta is greater than (n/(t + 1)) - 1, then G is hamiltonian, improving a classical result of Dirac for t greater than 1. If G is nonhamiltonian and delta is greater than (n/(t + lambda)) + lambda - 2 for some lambda less than or equal to t + 1, then G contains a cycle of length at least (t + 1)(delta - lambda + 2) + t, partially improving another classical result of Dirac for t greater than 1. ESA

N94-22969 Instituto de Fisica Teorica, Sao Paulo (Brazil).
OFF-CRITICAL W(INFINITY) AND VIRASORO ALGEBRAS AS DYNAMICAL SYMMETRIES OF THE INTEGRABLE MODELS
G. Sotkov and M. Stanishkov (Sao Paulo Univ., Brazil.) 1993 22 p Presented at the NATO Workshop on Integrable Quantum Field Theories, Como, Italy, Sep. 1992 Limited Reproducibility: More than 20% of this document may be affected by microfiche quality
(DE93-633215; IFT-P-001/93) Avail: CASI HC A03 (US Sales Only)

An infinite set of new non-commuting conserved charges in a specific class of perturbed CFT's is founded and a criterion for their existence is presented. They appear to be higher momenta of the already known commuting conserved currents. The algebra they close consists of two non-commuting W(infinity) algebras. Various Virasoro subalgebras of the full symmetry algebra are founded. It is shown on the examples of the perturbed Ising and Potts models that one of them plays an essential role in the computation of the correlation functions of the fields of the theory. DOE

N94-22975# Oak Ridge National Lab., TN.
IMPLEMENTATION AND PARALLELIZATION OF FAST MATRIX MULTIPLICATION FOR A FAST LEGENDRE TRANSFORM
Wentao Chen (Denison Univ., Granville, OH.) Sep. 1993 30 p
(Contract DE-AC05-84OR-21400)
(DE94-002184; ORNL/TM-12285) Avail: CASI HC A03/MF A01

An algorithm was presented by Alpert and Rokhlin for the rapid evaluation of Legendre transforms. The fast algorithm can be expressed as a matrix-vector product followed by a fast cosine transform. Using the Chebyshev expansion to approximate the entries of the matrix and exchanging the order of summations reduces the time complexity of computation from O(n(exp 2)) to O(n log n), where n is the size of the input vector. Our work has been focused on the implementation and the parallelization of the fast algorithm of matrix-vector product. Results have shown the expected performance of the algorithm. Precision problems which arise as n becomes large can be resolved by doubling the precision of the calculation. DOE

N94-22984# Vrije Univ., Amsterdam (Netherlands). Faculteit der Wiskunde en Informatica.
MAKING SOME ISSUES OF IMPLICIT KNOWLEDGE EXPLICIT
W. VanDerHoek and J. J. C. Meyer May 1992 34 p
(PB93-220606; IR-290) Avail: CASI HC A03/MF A01

The authors discuss issues of expressibility and completeness of the logic of implicit knowledge (I) and 'everybody's knowledge' (E), as introduced in a system with a number m of epistemic agents by Halpern and Moses. The operator E is defined as a conjunction and corresponds semantically to the union of the m accessibility relations. Dually, the operator I is semantically associated with an intersection, but it is, surprisingly, not equivalent with a disjunction. From the view of Kripke structures, there is a related asymmetry: although union can be modally defined, intersection cannot. The authors discuss consequences (in terms of (in)expressibility, correspondence and completeness) of this property for the epistemic logic under consideration and also present an extension of modal logic in which intersection is expressible. NTIS

N94-23090*# Institute for Computer Applications in Science and Engineering, Hampton, VA.
ON THE DAUBECHIES-BASED WAVELET DIFFERENTIATION MATRIX Final Report
Leland Jameson Dec. 1993 54 p Submitted for publication
(Contract NAS1-19480; RTOP 505-90-52-01)
(NASA-CR-191583; NAS 1.26:191583; ICASE-93-95) Avail: CASI HC A04/MF A01

The differentiation matrix for a Daubechies-based wavelet basis is constructed and superconvergence is proven. That is, it will be proven that under the assumption of periodic boundary conditions that the differentiation matrix is accurate of order 2M, even though the approximation subspace can represent exactly only polynomials up to degree M-1, where M is the number of vanishing moments of the associated wavelet. It is illustrated that Daubechies-based wavelet methods are equivalent to finite difference methods with grid refinement in regions of the domain where small-scale structure is present. Author

N94-23093 Vrije Univ., Amsterdam (Netherlands). Faculteit der Wiskunde en Informatica.
MEDIAN STABILIZATION DEGREE OF A MEDIAN ALGEBRA
H. J. Bandelt and M. VandeVel (Hamburg Univ., Germany.) Nov. 1992 15 p See also PB88-127774 Limited Reproducibility: More than 20% of this document may be affected by microfiche quality
(PB93-220010; WS-405) Avail: CASI HC A03

The median stabilization degree (msd) of a median algebra measures the largest possible number of steps needed to generate a sub-algebra with an arbitrary set of generators. The authors determine the value of msd of a graphic n-cube Q(sub n) and they derive an estimation of msd for the natural median operator of R(sup n) which is sharp up to one or two units. Interestingly, msd of Q(sub n) and of R(sup n) grows like log to the base 1.5 of n. Finally, the authors characterize median algebras and median graphs of msd less than or equal to one in terms of forbidden subspaces and in terms of the exchange number. NTIS

N94-23098 Vrije Univ., Amsterdam (Netherlands). Faculteit der Wiskunde en Informatica.
CHARACTERIZATION OF MEASURES WITH A CONVEX MATRIX-k-RANGE
J. Gouweleeuw May 1992 23 p Limited Reproducibility: More than 20% of this document may be affected by microfiche quality
(PB93-220655; WS-396) Avail: CASI HC A03

Let mu vector = (mu (sub i),...,mu (sub n)) be a vector measure on a measurable space (Omega, F) such that each mu(sub i) is finite. Necessary and sufficient conditions on mu vector are given such that the matrix-k-range is convex. This will lead to conditions on mu vector such that the partition-range is convex. The results are generalizations of those of Dvoretzky, Wald and Wolfowitz, and Dubins and Spanier. NTIS

N94-23106 Helsinki Univ. of Technology, Espoo (Finland). Inst. of Mathematics.
INCOMPLETE CORRECTIONS IN NONLINEAR PROBLEMS
T. Eirola, A. M. Krasnoselskii, M. A. Krasnoselskii, N. A. Kuznetsov, and O. Nevanlinna Feb. 1993 18 p Limited Reproducibility: More than 20% of this document may be affected by microfiche quality
(PB93-225746; ISBN-951-22-1428-8) Avail: CASI HC A03

A general setting of incomplete iterations--u(sub n+1)(x) = u(sub n)(x) + lambda(sub n)(x)(Fu(sub n)(x) - u(sub n)(x))--is considered. Using methods from the theory of positive operators, general results about convergence of this setting are given. These results relate the convergence of the iterations to the series summation over n, of lambda(x) and its divergence. As an application, the authors consider asynchronous iteration with parallel processors. NTIS

N94-23107 Tilburg Univ. (Netherlands). Dept. of Economics.
THE p-RANKS OF LATIN SQUARE GRAPHS
R. Peeters 1993 25 p Limited Reproducibility: More than 20% of this document may be affected by microfiche quality
(PB93-230498; FEW-600) Avail: Issuing Activity (National Technical Information Service (NTIS))

After a general introduction of Latin square graphs, the author determines the relevant p-ranks of their adjacency matrices, that is, the rank of A + 3I over the field F(sub p), the finite field with p elements, where A is the adjacency matrix and p a prime dividing the order of the Latin square. Furthermore, he derives some results for the relevant p-ranks of net graphs. NTIS

N94-23121 Katholieke Univ., Nijmegen (Netherlands).
NUMBER OF MODULI OF FAMILIES OF CURVES ON TORIC SURFACES Thesis
R. J. Koelman 1993 122 p Limited Reproducibility: More than 20% of this document may be affected by microfiche quality
(PB93-230381; ISBN-90-9004155-9) Avail: CASI HC A06

An algebraic torus T of dimension n is an algebraic group isomorphic to (C*)(sup n), where n is equal to or greater than 1. A toric variety is a variety which contains a n-dimensional algebraic torus T as an open subvariety and such that the action of T on itself extends to an action on the whole variety. The easiest examples are C(sup n) and P(sup n). Topics discussed in the thesis include: Toric varieties--definitions and invariants; Families of curves on a toric surface; Properties of curves on a toric surface; Classification of polygons; and The ideal of a projective embedded toric variety. NTIS

N94-23122 Tilburg Univ. (Netherlands). Dept. of Economics.
TEMPORAL AGGREGATION IN A PERIODICALLY INTEGRATED AUTOREGRESSIVE PROCESS
P. H. Franses and H. P. Boswijk 1993 19 p Limited Reproducibility: More than 20% of this document may be affected by microfiche quality
(PB93-230480; FEW-599) Avail: Issuing Activity (National Technical Information Service (NTIS))

A periodically integrated autoregressive process for a time series which is observed s times per year is a process for which there exist s-1 co-integration relations between the annual series containing the s seasonal observations. This means that there is a single unit root in the vector autoregression for these annual series. In the paper it is shown that temporally aggregating such a process does not effect the presence of this unit root, i.e. the aggregated series is also periodically integrated. NTIS

N94-23138# Groningen Rijksuniv. (Netherlands). Dept. of Mathematics.
THE HAMILTONIAN DOUBLE-ZERO EIGENVALUE
Henk W. Broer, Shui-Nee Chow (Georgia Inst. of Tech., Atlanta.), Yong-In Kim (Ulsan Univ., Republic of Korea.), and Gert Vegter 1993 20 p
(W-9304; ETN-94-94789) Avail: CASI HC A03/MF A01

A universal local bifurcation analysis of an autonomous Hamiltonian system around a certain equilibrium point is presented. This central equilibrium has a double zero eigenvalue, the other eigenvalues being in general position. Emphasis is given to the two degrees of freedom case where these other eigenvalues are purely imaginary. By normal form techniques and catastrophe theory unfoldings are obtained, having 'integrable' approximations related to the fold and to the elliptic and hyperbolic umbilic catastrophes. ESA

N94-23139# Groningen Rijksuniv. (Netherlands). Vakgruep Wiskunde RuG.
A RATIONAL ELLIPTIC SURFACE RELATED TO THE QUESTION OF EXPRESSING SQUARES AS SUM OF CONSECUTIVE SQUARES
Jaap Top and Masato Kuwata (McGill Univ., Montreal, Quebec.) Mar. 1993 13 p
(W-9305; ETN-94-94790) Avail: CASI HC A03/MF A01

The theory of Mordell-Weil lattices is applied to a specific example of a rational elliptic surface. This provides a complete description of the sections of this surface, and of the sections which are defined over Q. The surface is related to the diophantine problem of expressing squares as a sum of consecutive squares. Some consequences which the description has to this problem are discussed. ESA

N94-23140# Groningen Rijksuniv. (Netherlands). Dept. of Mathematics and Computer Science.
ON THE NUMERICAL COMPUTATION OF INVARIANT MANIFOLDS
A. J. Homburg, H. M. Osinga, and G. Vegter 1 Apr. 1993 18 p
(Grants NWO-611-307-018; NWO-611-306-523)
(W-9306; ETN-94-94791; PB94-111663) Avail: CASI HC A03/MF A01

A method for the numerical computation of invariant manifolds of hyperbolic fixed points of diffeomorphisms is presented. The derivation of this algorithm is based on well known features of (almost) invariant foliations. Numerical results illustrate the performance of the method. ESA

N94-23141# Groningen Rijksuniv. (Netherlands). Dept. of Mathematics.
THE CUSP HORSESHOE AND ITS BIFURCATIONS IN THE UNFOLDING OF AN INCLINATION-FLIP HOMOCLINIC ORBIT
Ale Jan Homburg, Hiroshi Kokubu (Kyoto Univ., Japan.), and Martin Krupa 8 Apr. 1993 40 p
(W-9307; ETN-94-94792) Avail: CASI HC A03/MF A01

A referenced study demonstrates a mechanism through which a perturbation of a vector field having an inclination-flip homoclinic orbit would have a Smale horseshoe. A study which proves that if the eigenvalues of the saddle to which the homoclinic orbit is asymptotic satisfy the condition 2 lambda(sup u) is less than min(-lambda(sup s), lambda(sup uu)), then there are arbitrarily small perturbations of the vector field which possess a Smale horseshoe, is presented. A sequence of bifurcations leading to the annihilation of the horseshoe is analyzed. This sequence contains, in particular, the points of existence of n homoclinic orbits with arbitrary n. ESA

N94-23144# Technische Univ., Eindhoven (Netherlands). Dept. of Mathematics and Computing Science.
A MIXED H2/H(INFINITY) FUNCTION FOR A DISCRETE TIME SYSTEM
Marc A. Peters Sep. 1992 21 p
(MEMO-COSOR-92-36; ETN-94-94797) Avail: CASI HC A03/MF A01

A mixed H2/H(infinity) function defined for a discrete time system is addressed. There are two inputs and one output. One input signal is a white noise stochastic process, and represents errors for example resulting from measurement noise. The other input has a more deterministic character. If there is a reference signal (for example a step) as input, this cannot be modeled as white noise, but it fits nicely into this new class of inputs. The objective is to minimize the effect of these exogenuous signals on the output of the system. The analysis of this function leads to a very useful expression in terms of a discrete algebraic Riccati equation. ESA

N94-23166 Institut National Polytechnique, Grenoble (France). Lab. ARTEMIS.
STRUCTURES OF TETRAHEDRIZATION: A MATHEMATICAL AND ALGORITHMICAL POINT OF VIEW Ph.D. Thesis [STRUCTURES DE TETRAEDRISATION: APPROCHES MATHEMATIQUE ET ALGORITHMIQUE]
Agnes Darmet 1992 114 p In FRENCH Limited Reproducibility: More than 20% of this document may be affected by microfiche quality
(ETN-94-95172) Avail: CASI HC A06

The generalization of a graph concept is studied. The new object, named surgraph, is defined as the union of a graph and of a set of faces defined by three vertices. The extension is similar to the one existing between triangulations and tetrahedrizations. The aim of the work is to compare the properties satisfied by triangulations and by tetrahedrizations. The interest and significance of Euler's formula, the preservation of planarity in minors, the characterization of planarity with a list of forbidden minors are discussed. These properties can be generalized in dimension three with some restrictions. A rectilinear representation of complexes is obtained. It is shown that the properties satisfied by triangulations cannot be extended to tetrahedrizations. Representations of graphs with a family of circles are considered. The proof of a part of a theorem due to Andreev and a conjecture of Lovasz on four regular planar graphs are presented. ESA

N94-23272*# Institute for Computer Applications in Science and Engineering, Hampton, VA.
THE THEORETICAL ACCURACY OF RUNGE-KUTTA TIME DISCRETIZATIONS FOR THE INITIAL BOUNDARY VALUE PROBLEM: A CAREFUL STUDY OF THE BOUNDARY ERROR Final Report
Mark H. Carpenter (National Aeronautics and Space Administration. Langley Research Center, Hampton, VA.), David Gottlieb (Brown Univ., Providence, RI.), Saul Abarbanel (Tel-Aviv Univ., Israel.), and Wai-Sun Don (Brown Univ., Providence, RI.) NASA Nov. 1993 16 p Submitted for publication
(Contract NAS1-19480; RTOP 505-90-52-01)
(NASA-CR-191561; NAS 1.26:191561; ICASE-93-83) Avail: CASI HC A03/MF A01

The conventional method of imposing time dependent boundary conditions for Runge-Kutta (RK) time advancement reduces the formal accuracy of the space-time method to first order locally, and second order globally, independently of the spatial operator. This counter intuitive result is analyzed in this paper. Two methods of eliminating this problem are proposed for the linear constant coefficient case: (1) impose the exact boundary condition only at the end of the complete RK cycle, (2) impose consistent intermediate boundary conditions derived from the physical boundary condition and its derivatives. The first method, while retaining the RK accuracy in all cases, results in a scheme with much reduced CFL condition, rendering the RK scheme less attractive. The second method retains the same allowable time step as the periodic problem. However it is a general remedy only for the linear case. For non-linear hyperbolic equations the second method is effective only for for RK schemes of third order accuracy or less. Numerical studies are presented to verify the efficacy of each approach. Author

N94-23278*# Institute for Computer Applications in Science and Engineering, Hampton, VA.
ON THE GIBBS PHENOMENON 3: RECOVERING EXPONENTIAL ACCURACY IN A SUB-INTERVAL FROM A SPECTRAL PARTIAL SUM OF A PIECEWISE ANALYTIC FUNCTION Final Report
David Gottlieb (Brown Univ., Providence, RI.) and Chi-Wang Shu (Brown Univ., Providence, RI.) Nov. 1993 20 p
(Contracts NAS1-19480; NAG1-1145; N00014-91-J-4016; DAAL03-91-G-0123; AF-AFOSR-0090-93; NSF DMS-92-11820; RTOP 505-90-52-01)
(NASA-CR-191560; NAS 1.26:191560) Avail: CASI HC A03/MF A01

The investigation of overcoming Gibbs phenomenon was continued, i.e., obtaining exponential accuracy at all points including at the discontinuities themselves, from the knowledge of a spectral partial sum of a discontinuous but piecewise analytic function. It was shown that if we are given the first N expansion coefficients of an L(sub 2) function f(x) in terms of either the trigonometrical polynomials or the Chebyshev or Legendre polynomials, an exponentially convergent approximation to the point values of f(x) in any sub-interval in which it is analytic can be constructed. Author (revised)

N94-23437# Technische Univ., Eindhoven (Netherlands). Dept. of Mathematics and Computing Science.
NOTE ON THE USE OF SPHERICAL VECTORFIELDS IN CLIFFORD ANALYSIS
J. deGraaf Apr. 1993 16 p
(PB93-237667; RANA-93-06) Avail: CASI HC A03/MF A01

The author discusses some properties and (anti)-commutation relations of Clifford differentiation operators on R(sup n) which are geometrical invariants. The results are a happy and accidental combination of earlier work on spherical vector fields and inspiration drawn from Van Acker's PhD-Thesis on Clifford differential operators. NTIS

N94-23438# Technische Univ., Eindhoven (Netherlands). Dept. of Mathematics and Computing Science.
MATHEMATICAL ADDENDA TO HOPPER'S MODEL OF PLANE STOKES FLOW DRIVEN BY CAPILLARITY ON A FREE SURFACE
J. deGraaf Jan. 1993 24 p
(PB93-237691; RANA-93-03) Avail: CASI HC A03/MF A01

In a series of papers, Hopper presents some special exact solutions of the shape evolution of a piece of viscous matter driven by surface tension on the free boundary. In Chapter 2 of this paper, the author studies several mathematical aspects of Hopper's equation. On the 'state space', which is a part of an ellipsoid in Hilbert space, Hopper's evolution equation can be considered as an infinite system of ordinary differential equations. For this system there are 3 'exhausting' series of finite dimensional sub systems leading to solutions which are: (1) complex polynomials with real coefficients, (2) complex polynomials with complex coefficients, (3) rational functions. Some local results on these finite dimensional sub systems are presented. NTIS

N94-23439# Technische Univ., Eindhoven (Netherlands). Dept. of Mathematics and Computing Science.
STABILITY BEHAVIOR OF SYSTEMS OBTAINED BY INDEX-REDUCTION
R. Lamour, R. Maerz, and R. M. M. Mattheij Jan. 1993 26 p
(PB93-237709; RANA-93-01) Avail: CASI HC A03/MF A01

Index reduction may drain the asymptotic stability of stationary solutions. It is analyzed in some detail how index reduction via artificial Lagrangian multiplier as well as the Baumgarte method behave. NTIS

N94-23442# Technische Univ., Eindhoven (Netherlands). Dept. of Mathematics and Computing Science.
CHARACTERIZATIONS OF SHIFT-INVARIANT DISTRIBUTIONS BASED ON SUMMATION MODULO ONE
R. J. G. Wilms and J. G. F. Thiemann Jun. 1993 18 p
(PB93-237824; MEMO-COSOR-93-02) Avail: CASI HC A03/MF A01

For n a member of N, let X,Y(1),...,Y(n) be independent random variables, and suppose that X is distributed in ((bracket) 0,1), but not uniformly. The authors characterize the distributions of X and Y(s) (s=1,...,n) satisfying the equation (brace)X+Y(1)+...+Y(n)(brace) (equality in distribution) X, where (in braces: Z) denotes the fractional part of a random variable Z. In the case of full generality, Y(s) is lattice, and X is shift-invariant with respect to a discrete uniform distribution on ((bracket) 0,1). The authors also give a characterization of such shift invariant distributions. The authors consider some special cases of this equation: If X (equality in distribution) Y(1), then X has a shifted discrete uniform distribution on ((bracket) 0,1); further the case that Y(1),...,Y(n) are identically distributed, and a generalization of the equation with X,Y(1),...,Y(n) identically distributed is considered. These results generalize results of Goldman (1968) and of Arnold and Meeden (1976). NTIS

N94-23455# Technische Univ., Eindhoven (Netherlands). Dept. of Mathematics and Computing Science.
DIFFERENTIAL ALGEBRAIC EQUATIONS
P. M. E. J. Wijckmans Jan. 1993 34 p See also DE89-009584
(PB93-237618; RANA-93-02) Avail: CASI HC A03/MF A01

Differential Algebraic Equations (DAE's) arise in many applications, such as mechanical systems with constraints, the modeling of electrical networks, and flow of incompressible fluids. This class of problems presents numerical and analytical difficulties which are quite different from Ordinary Differential Equations (ODE's). In the paper, the theory and the numerical solution of DAE's are examined. NTIS

N94-23456# Technische Univ., Eindhoven (Netherlands). Dept. of Mathematics and Computing Science.
BAYESIAN DECISION THEORY WITH IMPRECISE PRIOR PROBABILITIES APPLIED TO REPLACEMENT PROBLEMS
F. P. A. Coolen Mar. 1993 16 p See also PB93-197507
(PB93-237634; MEMO-COSOR-93-09) Avail: CASI HC A03/MF A01

The Bayesian framework for statistical inference offers the possibility of taking expert opinions into account, and is, therefore, attractive for practical problems concerning inspection and replacement of technical systems. However, the use of a single prior distribution fails to indicate the amount of information on which subjective probabilities are based, and leads to problems when combining the opinions of several experts. The introduction of imprecise prior probabilities solves these problems, and leads to simpler and clearer elicitation of prior information. Problems concerning elicitation of lifetime distributions, combination of opinions, introduction of statistical models and calculation of bounds on expected loss within Bayesian decision theory have been analyzed and solutions proposed. In the paper, application of the concept to an age replacement problem is described. The entire process, from elicitation and model assumptions to reaching a final decision, is discussed. NTIS

N94-23547# Institut des Hautes Etudes Scientifiques, Bures-sur-Yvette (France).
LACUNARY SERIES AS QUADRATIC DIFFERENTIALS IN CONFORMAL DYNAMICS
Frederick P. Gardiner and Dennis Sullivan Jun. 1993 30 p Sponsored by NSF, Washington, DC
(PB93-238061; IHES/M/93/37) Avail: CASI HC A03/MF A01

Given a polynomial-like mapping P acting on a plane domain, one denotes the forward iterates of P under composition by P(sup n). These iterates determine a dynamical system acting on a neighborhood of the Julia set. If one assumes the Julia set is connected, one may uniformize the complement of the Julia set by a Riemann mapping r, mapping the complement to the exterior of the unit disk. The forward iterates P(sup n) are conjugated to iterates r (circle) P(sup n) (circle) 1/r, which forms a dynamical system acting on the exterior of the unit disk and which extends to an action on the unit circle. This conjugated dynamical system is expanding along the unit circle, which is a repeller. The chief result of this paper is that such dynamical systems, for a given degree, form part of a Teichmuller space. It is an infinite dimensional complex manifold modeled on a Banach space and it has a Teichmuller's metric which is complete. The Banach space is a space of quadratic differentials and, for a special case, this space is identifiable with certain lacunary series. NTIS

N94-23548# Institut des Hautes Etudes Scientifiques, Bures-sur-Yvette (France).
WHEN AN INFINITELY-RENORMALIZABLE ENDOMORPHISM OF THE INTERVAL CAN BE SMOOTHED
Charles Tresser (International Business Machines Corp., Yorktown Heights, NY.) and Amie Wilkinson (California Univ., Berkeley.) Jul. 1993 27 p
(PB93-238087; IHES/M/93/39) Avail: CASI HC A03/MF A01

Let K be a closed subset of a smooth manifold M, and let f:K approaches K be a continuous self-map of K. It is shown that f is smoothable if it is conjugate to the restriction of a smooth map by a homeomorphism of the ambient space M. A necessary condition is given for the smoothability of the infinitely interval-renormalizable homeomorphisms of Cantor sets in the unit interval. This class contains, in particular, all minimal homeomorphisms of Cantor sets in the line which extend to continuous maps of an interval with zero topological entropy. NTIS

N94-23554*# National Aeronautics and Space Administration. Lewis Research Center, Cleveland, OH.
AN IMPLICIT NUMERICAL SCHEME FOR THE SIMULATION OF INTERNAL VISCOUS FLOWS ON UNSTRUCTURED GRIDS
Philip C. E. Jorgenson and Richard H. Pletcher (Iowa State Univ. of Science and Technology, Ames.) Jan. 1994 18 p Presnted at the 32nd Aerospace Sciences Meeting and Exhibit, Reno, NV, 10-13 Jan. 1994; sponsored by AIAA
(RTOP 505-62-52)
(NASA-TM-106437; E-8279; NAS 1.15:106437; AIAA Paper 94-0306; ICOMP-93-48) Avail: CASI HC A03/MF A01

The Navier-Stokes equations are solved numerically for two-dimensional steady viscous laminar flows. The grids are generated based on the method of Delaunay triangulation. A finite-volume approach is used to discretize the conservation law form of the compressible flow equations written in terms of primitive variables. A preconditioning matrix is added to the equations so that low Mach number flows can be solved economically. The equations are time marched using either an implicit Gauss-Seidel iterative procedure or a solver based on a conjugate gradient like method. A four color scheme is employed to vectorize the block Gauss-Seidel relaxation procedure. This increases the memory requirements minimally and decreases the computer time spent solving the resulting system of equations substantially. A factor of 7.6 speed up in the matrix solver is typical for the viscous equations. Numerical results are obtained for inviscid flow over a bump in a channel at subsonic and transonic conditions for validation with structured solvers. Viscous results are computed for developing flow in a channel, a symmetric sudden expansion, periodic tandem cylinders in a cross-flow, and a four-port valve. Comparisons are made with available results obtained by other investigators. Author (revised)

N94-23593*# National Aeronautics and Space Administration. Lewis Research Center, Cleveland, OH.
OPTIMIZATION OF ORIFICE GEOMETRY FOR CROSS-FLOW MIXING IN A CYLINDRICAL DUCT
W. A. Sowa (California Univ., Irvine.), J. T. Kroll (California Univ., Irvine.), G. S. Samuelsen (California Univ., Irvine.), and J. D. Holdeman Jan.

1994 25 p Presented at the 32nd Aerospace Sciences Meeting and Exhibit, Reno, NV, 10-13 Jan. 1994; sponsored by AIAA Original contains color illustrations
(RTOP 537-02-20)
(NASA-TM-106436; E-8278; NAS 1.15:106436; AIAA Paper 94-0219)
Avail: CASI HC A03/MF A01; 8 functional color pages

Mixing of gaseous jets in a cross-flow has significant applications in engineering, one example of which is the dilution zone of a gas turbine combustor. Despite years of study, the design of jet injection in combustors is largely based on practical experience. A series of experiments was undertaken to delineate the optimal mixer orifice geometry. A cross-flow to core-flow momentum-flux ratio of 40 and a mass flow ratio of 2.5 were selected as representative of an advanced design. An experimental test matrix was designed around three variables: the number of orifices, the orifice aspect ratio (long-to-short dimension), and the orifice angle. A regression analysis was performed on the data to arrive at an interpolating equation that predicted the mixing performance of orifice geometry combinations within the range of the test matrix parameters. Results indicate that mixture uniformity is a non-linear function of the number of orifices, the orifice aspect ratio, and the orifice angle. Optimum mixing occurs when the asymptotic mean jet trajectories are in the range of 0.35 less than r/R less than 0.5 (where $r = 0$ is at the mixer wall) at $z/R = 1.0$. At the optimum number of orifices, the difference between shallow-angled slots with large aspect ratios and round holes is minimal and either approach will lead to good mixing performance. At the optimum number of orifices, it appears possible to have two local optimums where one corresponds to an aspect ratio of 1.0 and the other to a high aspect ratio. Author

N94-23673*# National Aeronautics and Space Administration. Langley Research Center, Hampton, VA.
THE SIXTH COPPER MOUNTAIN CONFERENCE ON MULTIGRID METHODS, PART 1
N. Duane Melson, ed., T. A. Manteuffel, ed. (Colorado Univ., Denver.), and S. F. McCormick, ed. (Colorado Univ., Denver.) Nov. 1993 351 p Workshop held in Copper Mountain, CO, 4-9 Apr. 1993 Sponsored in part by AFOSR, Bolling AFB, Washington, DC, DOE, and NSF
(RTOP 505-59-53-01)
(NASA-CP-3224-Pt-1; L-17275-Pt-1; NAS 1.55:3224-Pt-1) Avail: CASI HC A16/MF A03

The Sixth Copper Mountain Conference on Multigrid Methods was held on 4-9 Apr. 1993, at Copper Mountain, CO. This book is a collection of many of the papers presented at the conference and as such represents the conference proceedings. NASA LaRC graciously provided printing of this document so that all of the papers could be presented in a single forum. Each paper was reviewed by a member of the conference organizing committee under the coordination of the editors. The multigrid discipline continues to expand and mature, as is evident from these proceedings. The vibrancy in this field is amply expressed in these important papers, and the collection clearly shows its rapid trend to further diversity and depth. For individual titles, see N94-23674 through N94-23697.

N94-23674*# Zurich Univ. (Switzerland). Institut fuer Angewandte Mathematik.
A MULTIGRID SOLVER FOR THE SEMICONDUCTOR EQUATIONS
Bernhard Bachmann (Allmanna Svenska Elektriska A.B. Brown Boveri, Baden, Switzerland.) *In* NASA. Langley Research Center, The Sixth Copper Mountain Conference on Multigrid Methods, Part 1 Nov. 1993 p 1-15 (For primary document see N94-23673 06-64)
Avail: CASI HC A03/MF A03

We present a multigrid solver for the exponential fitting method. The solver is applied to the current continuity equations of semiconductor device simulation in two dimensions. The exponential fitting method is based on a mixed finite element discretization using the lowest-order Raviart-Thomas triangular element. This discretization method yields a good approximation of front layers and guarantees current conservation. The corresponding stiffness matrix is an M-matrix. 'Standard' multigrid solvers, however, cannot be applied to the resulting system, as this is dominated by an unsymmetric part, which is due to the presence of strong convection in part of the domain. To overcome this difficulty, we explore the connection between Raviart-Thomas mixed methods and the nonconforming Crouzeix-Raviart finite element discretization. In this way we can construct nonstandard prolongation and restriction operators using easily computable weighted L(exp 2)-projections based on suitable quadrature rules and the upwind effects of the discretization. The resulting multigrid algorithm shows very good results, even for real-world problems and for locally refined grids. Author (revised)

N94-23675*# Queens Univ., Kingston (Ontario). Dept. of Mechanical and Chemical Engineering.
FAS MULTIGRID CALCULATIONS OF THREE DIMENSIONAL FLOW USING NON-STAGGERED GRIDS **c34**
D. Matovic, A. Pollard, H. A. Becker, and E. W. Grandmaison *In* NASA. Langley Research Center, The Sixth Copper Mountain Conference on Multigrid Methods, Part 1 Nov. 1993 p 17-29 (For primary document see N94-23673 06-64)
Avail: CASI HC A03/MF A03

Grid staggering is a well known remedy for the problem of velocity/pressure coupling in incompressible flow calculations. Numerous inconveniences occur, however, when staggered grids are implemented, particularly when a general-purpose code, capable of handling irregular three-dimensional domains, is sought. In several non-staggered grid numerical procedures proposed in the literature, the velocity/pressure coupling is achieved by either pressure or velocity (momentum) averaging. This approach is not convenient for simultaneous (block) solvers that are preferred when using multigrid methods. A new method is introduced in this paper that is based upon non-staggered grid formulation with a set of virtual cell face velocities used for pressure/velocity coupling. Instead of pressure or velocity averaging, a momentum balance at the cell face is used as a link between the momentum and mass balance constraints. The numerical stencil is limited to 9 nodes (in 2D) or 27 nodes (in 3D), both during the smoothing and inter-grid transfer, which is a convenient feature when a block point solver is applied. The results for a lid-driven cavity and a cube in a lid-driven cavity are presented and compared to staggered grid calculations using the same multigrid algorithm. The method is shown to be stable and produce a smooth (wiggle-free) pressure field. Author (revised)

N94-23676*# Oxford Univ. (England). Computing Lab.
MULTIGRID AND CYCLIC REDUCTION APPLIED TO THE HELMHOLTZ EQUATION **c32**
Kenneth Brackenridge *In* NASA. Langley Research Center, The Sixth Copper Mountain Conference on Multigrid Methods, Part 1 Nov. 1993 p 31-41 (For primary document see N94-23673 06-64)
Avail: CASI HC A03/MF A03

We consider the Helmholtz equation with a discontinuous complex parameter and inhomogeneous Dirichlet boundary conditions in a rectangular domain. A variant of the direct method of cyclic reduction (CR) is employed to facilitate the design of improved multigrid (MG) components, resulting in the method of CR-MG. We demonstrate the improved convergence properties of this method. Author (revised)

N94-23677*# Cornell Univ., Ithaca, NY.
UNIFORM CONVERGENCE OF MULTIGRID V-CYCLE ITERATIONS FOR INDEFINITE AND NONSYMMETRIC PROBLEMS
James H. Bramble, Do Y. Kwak (Korea Advanced Inst. of Science and Technology, Taejon, Republic of Korea.), and Joseph E. Pasciak (Brookhaven National Lab., Upton, NY.) *In* NASA. Langley Research Center, The Sixth Copper Mountain Conference on Multigrid Methods, Part 1 Nov. 1993 p 43-59 (For primary document see N94-23673 06-64)
(Contract DE-AC02-76CH-00016; NSF DMS-90-07185)
Avail: CASI HC A03/MF A03

In this paper, we present an analysis of a multigrid method for nonsymmetric and/or indefinite elliptic problems. In this multigrid method various types of smoothers may be used. One type of smoother which we consider is defined in terms of an associated symmetric problem and includes point and line, Jacobi, and Gauss-Seidel iterations. We also study smoothers based entirely on the original operator. One is based on the normal form, that is, the product of the operator and its transpose. Other smoothers studied include point and line, Jacobi, and Gauss-Seidel. We show that the uniform estimates for symmetric positive definite problems carry over to these algorithms. More precisely, the multigrid iteration for the nonsymmetric and/or indefinite problem is shown to converge at a uniform rate provided that the coarsest grid in the multilevel iteration is sufficiently fine (but not depending on the number of multigrid levels). Author (revised)

N94-23678*# Coast Guard, Groton, CT. Research and Development Center.
A MULTILEVEL COST-SPACE APPROACH TO SOLVING THE BALANCED LONG TRANSPORTATION PROBLEM
Kevin J. Cavanaugh and Van Emden Henson (Naval Postgraduate School, Monterey, CA.) *In* NASA. Langley Research Center, The Sixth Copper Mountain Conference on Multigrid Methods, Part 1 Nov. 1993 p 61-75 (For primary document see N94-23673 06-64)
(Grant MA000-MA999/4476-4479)
Avail: CASI HC A03/MF A03

We develop a multilevel scheme for solving the balanced long transportation problem, that is, given a set (c(sub kj)) of shipping costs from a set of M supply nodes S(sub k) to a set of N demand nodes D(sub j), we seek to find a set of flows, (x(sub kj)), that minimizes the total cost Sigma(sub k=1)(exp M) Sigma(sub j=1)(exp N) x(sub kj)c(sub kj). We require that the problem be balanced, that is, the total demand must equal the total supply. Solution techniques for this problem are well known from optimization and linear programming. We examine this problem, however, in order to develop principles that can then be applied to more intractible problems of optimization. We develop a multigrid scheme for solving the problem, defining the grids, relaxation, and intergrid operators. Numerical experimentation shows that this line of research may prove fruitful. Further research directions are suggested. Author (revised)

N94-23679*# University of Southwestern Louisiana, Lafayette. Center for Advanced Computer Studies.
VECTORIZATION AND PARALLELIZATION OF THE FINITE STRIP METHOD FOR DYNAMIC MINDLIN PLATE PROBLEMS
Hsin-Chu Chen and Ai-Fang He (Illinois Wesleyan Univ., Bloomington.) *In* NASA. Langley Research Center, The Sixth Copper Mountain Conference on Multigrid Methods, Part 1 Nov. 1993 p 77-91 (For primary document see N94-23673 06-64)
(Grant DE-FG02-85ER-25001)
Avail: CASI HC A03/MF A03

The finite strip method is a semi-analytical finite element process which allows for a discrete analysis of certain types of physical problems by discretizing the domain of the problem into finite strips. This method decomposes a single large problem into m smaller independent subproblems when m harmonic functions are employed, thus yielding natural parallelism at a very high level. In this paper we address vectorization and parallelization strategies for the dynamic analysis of simply-supported Mindlin plate bending problems and show how to prevent potential conflicts in memory access during the assemblage process. The vector and parallel implementations of this method and the performance results of a test problem under scalar, vector, and vector-concurrent execution modes on the Alliant FX/80 are also presented. Author

N94-23680*# Rice Univ., Houston, TX. Dept. of Computational and Applied Mathematics.
DOMAIN DECOMPOSITION METHODS FOR NONCONFORMING FINITE ELEMENT SPACES OF LAGRANGE-TYPE
Lawrence C. Cowsar *In* NASA. Langley Research Center, The Sixth Copper Mountain Conference on Multigrid Methods, Part 1 Nov. 1993 p 93-109 (For primary document see N94-23673 06-64)
(Grant NSF DMS-91-12847)
Avail: CASI HC A03/MF A03

In this article, we consider the application of three popular domain decomposition methods to Lagrange-type nonconforming finite element discretizations of scalar, self-adjoint, second order elliptic equations. The additive Schwarz method of Dryja and Widlund, the vertex space method of Smith, and the balancing method of Mandel applied to nonconforming elements are shown to converge at a rate no worse than their applications to the standard conforming piecewise linear Galerkin discretization. Essentially, the theory for the nonconforming elements is inherited from the existing theory for the conforming elements with only modest modification by constructing an isomorphism between the nonconforming finite element space and a space of continuous piecewise linear functions. Author

N94-23681*# Technische Hogeschool, Delft (Netherlands).
NESTED KRYLOV METHODS AND PRESERVING THE ORTHOGONALITY
Eric DeSturler and Diederik R. Fokkema (Utrecht State Univ., Netherlands.) *In* NASA. Langley Research Center, The Sixth Copper Mountain Conference on Multigrid Methods, Part 1 Nov. 1993 p 111-125 (For primary document see N94-23673 06-64)
Avail: CASI HC A03/MF A03

Recently the GMRESR inner-outer iteraction scheme for the solution of linear systems of equations was proposed by Van der Vorst and Vuik. Similar methods have been proposed by Axelsson and Vassilevski and Saad (FGMRES). The outer iteration is GCR, which minimizes the residual over a given set of direction vectors. The inner iteration is GMRES, which at each step computes a new direction vector by approximately solving the residual equation. However, the optimality of the approximation over the space of outer search directions is ignored in the inner GMRES iteration. This leads to suboptimal corrections to the solution in the outer iteration, as components of the outer iteration directions may reenter in the inner iteration process. Therefore we propose to preserve the orthogonality relations of GCR in the inner GMRES iteration. This gives optimal corrections; however, it involves working with a singular, non-symmetric operator. We will discuss some important properties, and we will show by experiments that, in terms of matrix vector products, this modification (almost) always leads to better convergence. However, because we do more orthogonalizations, it does not always give an improved performance in CPU-time. Furthermore, we will discuss efficient implementations as well as the truncation possibilities of the outer GCR process. The experimental results indicate that for such methods it is advantageous to preserve the orthogonality in the inner iteration. Of course we can also use iteration schemes other than GMRES as the inner method; methods with short recurrences like GICGSTAB are of interest. Author (revised)

N94-23682*# Yale Univ., New Haven, CT. Dept. of Computer Science.
IMPLEMENTING ABSTRACT MULTIGRID OR MULTILEVEL METHODS
Craig C. Douglas *In* NASA. Langley Research Center, The Sixth Copper Mountain Conference on Multigrid Methods, Part 1 Nov. 1993 p 127-141 Sponsored in part by IBM and ONR (For primary document see N94-23673 06-64)
Avail: CASI HC A03/MF A03

Multigrid methods can be formulated as an algorithm for an abstract problem that is independent of the partial differential equation, domain, and discretization method. In such an abstract setting, problems not arising from partial differential equations can be treated. A general theory exists for linear problems. The general theory was motivated by a series of abstract solvers (Madpack). The latest version was motivated by the theory. Madpack now allows for a wide variety of iterative and direct solvers, preconditioners, and interpolation and projection schemes, including user callback ones. It allows for sparse, dense, and stencil matrices. Mildly nonlinear problems can be handled. Also, there is a fast, multigrid Poisson solver (two and three dimensions). The type of solvers and design decisions (including language, data structures, external library support, and callbacks) are discussed. Based on the author's experiences with two versions of Madpack, a better approach is proposed. This is based on a mixed language formulation (C and FORTRAN + preprocessor). Reasons for not using FORTRAN, C, or C++ (individually) are given. Implementing the proposed strategy is not difficult. Author (revised)

N94-23683*# Yale Univ., New Haven, CT. Dept. of Computer Science and Mechanical Engineering.
NUMERICAL SOLUTION OF FLAME SHEET PROBLEMS WITH AND WITHOUT MULTIGRID METHODS c25
Craig C. Douglas and Alexandre Ern *In* NASA. Langley Research Center, The Sixth Copper Mountain Conference on Multigrid Methods, Part 1 Nov. 1993 p 143-157 Sponsored in part by CERMICS, ENPC, IBM, ONR and DOE (For primary document see N94-23673 06-64)
Avail: CASI HC A03/MF A03

Flame sheet problems are on the natural route to the numerical solution of multidimensional flames, which, in turn, are important in many engineering applications. In order to model the structure of flames more accurately, we use the vorticity-velocity formulation of the fluid flow equations, as opposed to the streamfunction-vorticity approach. The numerical solution of the resulting nonlinear coupled elliptic partial differential equations involves a pseudo transient process and a steady state Newton iteration. Rather than working with dimensionless variables, we introduce scale factors that can yield significant savings in the execution time. In this context, we also investigate the applicability and performance of several multigrid methods, focusing on nonlinear damped Newton multigrid, using either one way or correction schemes. Author

N94-23684*# Bowling Green State Univ., OH. Dept. of Physics and Astronomy.
A MIXED METHOD POISSON SOLVER FOR THREE-DIMENSIONAL SELF-GRAVITATING ASTROPHYSICAL FLUID DYNAMICAL SYSTEMS **c90**
Comer Duncan and Jim Jones (Colorado Univ., Denver.) *In* NASA. Langley Research Center, The Sixth Copper Mountain Conference on Multigrid Methods, Part 1 Nov. 1993 p 159-173 (For primary document see N94-23673 06-64)
Avail: CASI HC A03/MF A03

A key ingredient in the simulation of self-gravitating astrophysical fluid dynamical systems is the gravitational potential and its gradient. This paper focuses on the development of a mixed method multigrid solver of the Poisson equation formulated so that both the potential and the Cartesian components of its gradient are self-consistently and accurately generated. The method achieves this goal by formulating the problem as a system of four equations for the gravitational potential and the three Cartesian components of the gradient and solves them using a distributed relaxation technique combined with conventional full multigrid V-cycles. The method is described, some tests are presented, and the accuracy of the method is assessed. We also describe how the method has been incorporated into our three-dimensional hydrodynamics code and give an example of an application to the collision of two stars. We end with some remarks about the future developments of the method and some of the applications in which it will be used in astrophysics. Author

N94-23685*# California Univ., Los Angeles. Dept. of Mathematics.
MULTIGRID METHODS FOR DIFFERENTIAL EQUATIONS WITH HIGHLY OSCILLATORY COEFFICIENTS
Bjorn Engquist and Erding Luo *In* NASA. Langley Research Center, The Sixth Copper Mountain Conference on Multigrid Methods, Part 1 Nov. 1993 p 175-189 (For primary document see N94-23673 06-64)
(Contracts N00014-92-J-1890; DAAL03-91-G-0162; NSF DMS-91-03104)
Avail: CASI HC A03/MF A03

New coarse grid multigrid operators for problems with highly oscillatory coefficients are developed. These types of operators are necessary when the characters of the differential equations on coarser grids or longer wavelengths are different from that on the fine grid. Elliptic problems for composite materials and different classes of hyperbolic problems are practical examples. The new coarse grid operators can be constructed directly based on the homogenized differential operators or hierarchically computed from the finest grid. Convergence analysis based on the homogenization theory is given for elliptic problems with periodic coefficients and some hyperbolic problems. These are classes of equations for which there exists a fairly complete theory for the interaction between shorter and longer wavelengths in the problems. Numerical examples are presented. Author

N94-23686*# Kent State Univ., OH. Dept. of Mathematics and Computer Science.
APPLICATION OF MULTIGRID METHODS TO THE SOLUTION OF LIQUID CRYSTAL EQUATIONS ON A SIMD COMPUTER **c76**
Paul A. Farrell, Arden Ruttan, and Reinhardt R. Zeller *In* NASA. Langley Research Center, The Sixth Copper Mountain Conference on Multigrid Methods, Part 1 Nov. 1993 p 191-206 (For primary document see N94-23673 06-64)
(Grant DMR89-20147)
Avail: CASI HC A03/MF A03

We will describe a finite difference code for computing the equilibrium configurations of the order-parameter tensor field for nematic liquid crystals in rectangular regions by minimization of the Landau-de Gennes Free Energy functional. The implementation of the free energy functional described here includes magnetic fields, quadratic gradient terms, and scalar bulk terms through the fourth order. Boundary conditions include the effects of strong surface anchoring. The target architectures for our implementation are SIMD machines, with interconnection networks which can be configured as 2 or 3 dimensional grids, such as the Wavetracer DTC. We also discuss the relative efficiency of a number of iterative methods for the solution of the linear systems arising from this discretization on such architectures. Author (revised)

N94-23687*# Clarkson Univ., Potsdam, NY. Dept. of Mathematics and Computer Science.
AN ADAPTIVE MULTIGRID MODEL FOR HURRICANE TRACK PREDICTION **c47**
Scott R. Fulton *In* NASA. Langley Research Center, The Sixth Copper Mountain Conference on Multigrid Methods, Part 1 Nov. 1993 p 207-214 (For primary document see N94-23673 06-64)
(Grant NSF ATM-91-18966)
Avail: CASI HC A02/MF A03

This paper describes a simple numerical model for hurricane track prediction which uses a multigrid method to adapt the model resolution as the vortex moves. The model is based on the modified barotropic vorticity equation, discretized in space by conservative finite differences and in time by a Runge-Kutta scheme. A multigrid method is used to solve an elliptic problem for the streamfunction at each time step. Nonuniform resolution is obtained by superimposing uniform grids of different spatial extent; these grids move with the vortex as it moves. Preliminary numerical results indicate that the local mesh refinement allows accurate prediction of the hurricane track with substantially less computer time than required on a single uniform grid. Author

N94-23688*# Clarkson Univ., Potsdam, NY. Dept. of Mathematics and Computer Science.
RELAXATION SCHEMES FOR CHEBYSHEV SPECTRAL MULTIGRID METHODS
Yimin Kang and Scott R. Fulton *In* NASA. Langley Research Center, The Sixth Copper Mountain Conference on Multigrid Methods, Part 1 Nov. 1993 p 215-229 (For primary document see N94-23673 06-64)
(Grant NSF ATM-91-18966)
Avail: CASI HC A03/MF A03

Two relaxation schemes for Chebyshev spectral multigrid methods are presented for elliptic equations with Dirichlet boundary conditions. The first scheme is a pointwise-preconditioned Richardson relaxation scheme and the second is a line relaxation scheme. The line relaxation scheme provides an efficient and relatively simple approach for solving two-dimensional spectral equations. Numerical examples and comparisons with other methods are given. Author

N94-23689*# Naval Postgraduate School, Monterey, CA. Dept. of Mathematics.
MULTIGRID METHODS FOR A SEMILINEAR PDE IN THE THEORY OF PSEUDOPLASTIC FLUIDS **c34**
Van Emden Henson and A. W. Shaker *In* NASA. Langley Research Center, The Sixth Copper Mountain Conference on Multigrid Methods, Part 1 Nov. 1993 p 231-242 (For primary document see N94-23673 06-64)
(Grant ZZ867-ZZ899/5986)
Avail: CASI HC A03/MF A03

We show that by certain transformations the boundary layer equations for the class of non-Newtonian fluids named pseudoplastic can be generalized in the form the vector differential operator(u) + p(x)u(exp -lambda) = 0, where x is a member of the set Omega and Omega is a subset of R(exp n), n is greater than or equal to 1 under the classical conditions for steady flow over a semi-infinite flat plate. We provide a survey of the existence, uniqueness, and analyticity of the solutions for this problem. We also establish numerical solutions in one- and two-dimensional regions using multigrid methods. Author

N94-23690*# Lawrence Livermore National Lab., CA.
A MULTILEVEL ADAPTIVE PROJECTION METHOD FOR UNSTEADY INCOMPRESSIBLE FLOW **c34**
Louis H. Howell *In* NASA. Langley Research Center, The Sixth Copper Mountain Conference on Multigrid Methods, Part 1 Nov. 1993 p 243-257 (For primary document see N94-23673 06-64)
(Contracts W-7405-eng-48; IACRO-93-817)
Avail: CASI HC A03/MF A03

There are two main requirements for practical simulation of unsteady flow at high Reynolds number: the algorithm must accurately propagate discontinuous flow fields without excessive artificial viscosity, and it must have some adaptive capability to concentrate computational effort where it is most needed. We satisfy the first of these requirements with a second-order Godunov method similar to those used for high-speed flows with shocks, and the second with a grid-based refinement scheme which avoids some of the drawbacks associated with unstructured meshes. These two features of our algorithm place certain constraints on the projection method used to enforce incompressibility. Velocities are cell-based, leading to a Laplacian stencil for the projection which decouples adjacent grid points. We discuss features of the multigrid and multilevel iteration schemes required for solution of the resulting decoupled problem. Variable-density flows require use of a modified projection operator--we have found a multigrid method for this modified projection that successfully handles density jumps of thousands to one. Numerical results are shown for the 2D adaptive and 3D variable-density algorithms. Author (revised)

N94-23691*# South Carolina Univ., Columbia.
WAVELET MULTIRESOLUTION ANALYSES ADAPTED FOR THE FAST SOLUTION OF BOUNDARY VALUE ORDINARY DIFFERENTIAL EQUATIONS
Bjoern Jawerth and Wim Sweldens (Katholieke Univ. te Leuven, Belgium.) *In* NASA. Langley Research Center, The Sixth Copper Mountain Conference on Multigrid Methods, Part 1 Nov. 1993 p 259-273 (For primary document see N94-23673 06-64)
(Contract N00014-90-J-1343; AF-AFOSR-0455-89)
Avail: CASI HC A03/MF A03

We present ideas on how to use wavelets in the solution of boundary value ordinary differential equations. Rather than using classical wavelets, we adapt their construction so that they become (bi)orthogonal with respect to the inner product defined by the operator. The stiffness matrix in a Galerkin method then becomes diagonal and can thus be trivially inverted. We show how one can construct an O(N) algorithm for various constant and variable coefficient operators. Author

N94-23692*# Bordeaux 1 Univ., Talence (France).
A COMPARISON OF LOCALLY ADAPTIVE MULTIGRID METHODS: LDC, FAC AND FIC
Khodor Khadra, Philippe Angot (Aix-Marseilles Univ., France.), and Jean-Paul Caltagirone *In* NASA. Langley Research Center, The Sixth Copper Mountain Conference on Multigrid Methods, Part 1 Nov. 1993 p 275-292 (For primary document see N94-23673 06-64)
Avail: CASI HC A03/MF A03

This study is devoted to a comparative analysis of three 'Adaptive ZOOM' (ZOom Overlapping Multi-level) methods based on similar concepts of hierarchical multigrid local refinement: LDC (Local Defect Correction), FAC (Fast Adaptive Composite), and FIC (Flux Interface Correction)--which we proposed recently. These methods are tested on two examples of a bidimensional elliptic problem. We compare, for V-cycle procedures, the asymptotic evolution of the global error evaluated by discrete norms, the corresponding local errors, and the convergence rates of these algorithms. Author (revised)

N94-23693*# Johns Hopkins Univ., Laurel, MD. Applied Physics Lab.
MULTI-GRID DOMAIN DECOMPOSITION APPROACH FOR SOLUTION OF NAVIER-STOKES EQUATIONS IN PRIMITIVE VARIABLE FORM **c34**
Hwar-Ching Ku and Bala Ramaswamy (Rice Univ., Houston, TX.) *In* NASA. Langley Research Center, The Sixth Copper Mountain Conference on Multigrid Methods, Part 1 Nov. 1993 p 293-304 (For primary document see N94-23673 06-64)
(Contract N00039-91-C-0001)
Avail: CASI HC A03/MF A03

The new multigrid (or adaptive) pseudospectral element method was carried out for the solution of incompressible flow in terms of primitive variable formulation. The desired features of the proposed method include the following: (1) the ability to treat complex geometry; (2) high resolution adapted in the interesting areas; (3) requires minimal working space; and (4) effective in a multiprocessing environment. The approach for flow problems, complex geometry or not, is to first divide the computational domain into a number of fine-grid and coarse-grid subdomains with the inter-overlapping area. Next, it is necessary to implement the Schwarz alternating procedure (SAP) to exchange the data among subdomains, where the coarse-grid correction is used to remove the high frequency error that occurs when the data interpolation from the fine-grid subdomain to the coarse-grid subdomain is conducted. The strategy behind the coarse-grid correction is to adopt the operator of the divergence of the velocity field, which intrinsically links the pressure equation, into this process. The solution of each subdomain can be efficiently solved by the direct (or iterative) eigenfunction expansion technique with the least storage requirement, i.e. O(N(exp 3)) in 3-D and O(N(exp 2)) in 2-D. Numerical results of both driven cavity and jet flow will be presented in the paper to account for the versatility of the proposed method. Author (revised)

N94-23694*# Technische Hogeschool, Twente (Netherlands). Dept. of Applied Mathematics.
COMPRESSIBLE TURBULENT FLOW SIMULATION WITH A MULTIGRID MULTIBLOCK METHOD **c34**
Hans Kuerten and Bernard Geurts *In* NASA. Langley Research Center, The Sixth Copper Mountain Conference on Multigrid Methods, Part 1 Nov. 1993 p 305-315 (For primary document see N94-23673 06-64)
Avail: CASI HC A03/MF A03

We describe a multigrid multiblock method for compressible turbulent flow simulations and present results obtained from calculations on a two-element airfoil. A vertex-based spatial discretization method and explicit multistage Runge-Kutta time-stepping are used. The slow convergence of a single grid method makes the multigrid method, which yields a speed factor of about 20, indispensable. The numerical predictions are in good agreement with experimental results. It is shown that the convergence of the multigrid process depends considerably on the ordering of the various loops. If the block loop is put inside the stage loop, the process converges more rapidly than if the block loop is situated outside the stage loop when a three-stage Runge-Kutta method is used. If a five-stage scheme is used, the process does not converge in the latter block ordering. Finally, the process based on the five-stage method is about 60 percent more efficient than with the three-stage method, if the block loop is inside the stage loop. Author (revised)

N94-23695*# Wisconsin Univ., Madison. Dept. of Mathematics.
A NONCONFORMING MULTIGRID METHOD USING CONFORMING SUBSPACES
Chang Ock Lee *In* NASA. Langley Research Center, The Sixth Copper Mountain Conference on Multigrid Methods, Part 1 Nov. 1993 p 317-330 (For primary document see N94-23673 06-64)
(Grants NSF CDA-90-24618; NSF DMS-92-03502)
Avail: CASI HC A03/MF A03

For second-order elliptic boundary value problems, we develop a nonconforming multigrid method using the coarser-grid correction on the conforming finite element subspaces. The convergence proof with an arbitrary number of smoothing steps for nu-cycle is presented. Author (revised)

N94-23696*# Murray State Univ., KY. Dept. of Mathematics.
MULTIGRID METHOD FOR INTEGRAL EQUATIONS AND AUTOMATIC PROGRAMS **c61**
Hosae Lee *In* NASA. Langley Research Center, The Sixth Copper Mountain Conference on Multigrid Methods, Part 1 Nov. 1993 p 331-343 (For primary document see N94-23673 06-64)
Avail: CASI HC A03/MF A03

Several iterative algorithms based on multigrid methods are introduced for solving linear Fredholm integral equations of the second kind. Automatic programs based on these algorithms are introduced using Simpson's rule and the piecewise Gaussian rule for numerical integration. Author (revised)

N94-23697*# Duesseldorf Univ. (Germany). Mathematisches Inst.
AN OBJECT-ORIENTED APPROACH FOR PARALLEL SELF ADAPTIVE MESH REFINEMENT ON BLOCK STRUCTURED GRIDS **c62**
Max Lemke, Kristian Witsch, and Daniel Quinlan (Colorado Univ., Denver.) *In* NASA. Langley Research Center, The Sixth Copper Mountain Conference on Multigrid Methods, Part 1 Nov. 1993 p 345-359 (For primary document see N94-23673 06-64)
(Contract NAS1-18606; BMFT-ITR-900689)
Avail: CASI HC A03/MF A03

Self-adaptive mesh refinement dynamically matches the computational demands of a solver for partial differential equations to the activity in the application's domain. In this paper we present two C++ class libraries, P++ and AMR++, which significantly simplify the development of sophisticated adaptive mesh refinement codes on (massively) parallel distributed memory architectures. The development is based on our previous research in this area. The C++ class libraries provide abstractions to separate the issues of developing parallel adaptive mesh refinement applications into those of parallelism, abstracted by P++, and adaptive mesh refinement, abstracted by AMR++. P++ is a parallel array class library to permit efficient development of architecture independent codes for structured grid applications, and AMR++ provides support for self-adaptive mesh refinement on block-structured grids of rectangular non-overlapping blocks. Using these libraries, the application programmers' work is greatly simplified to primarily specifying the serial single grid application and obtaining the parallel and self-adaptive mesh refinement code with minimal effort. Initial results for simple singular perturbation problems solved by self-adaptive multilevel techniques (FAC, AFAC), being implemented on the basis of prototypes of the P++/AMR++ environment, are presented. Singular perturbation problems frequently arise in large applications, e.g. in the area of computational fluid dynamics. They usually have solutions with layers which require adaptive mesh refinement and fast basic solvers in order to be resolved efficiently. Author (revised)

N94-23708# Amsterdam Univ. (Netherlands).

MEDIANS AND STEINER TREES

M. vandeVel and E. Verheul Jul. 1993 12 p See also PB93-221075
(PB94-110616; WS-412) Avail: CASI HC A03/MF A01

The theory of Steiner trees deals with the problem of designing a network connecting a set of points and minimizing the total connection length. We consider this problem in median metric spaces. It is shown that Steiner trees exist and can be found in a finite number of steps. This generalizes and strengthens a result of M. Hanan for the plane. The method employed by Hanan is rather technical and ad-hoc as it involves highly specific constructions in the plane. In contrast, we have based our methods on a fairly well-developed geometry of median metric spaces. In particular, there is no need to restrict to two dimensions. NTIS

N94-23722 Technische Univ., Twente (Netherlands). Faculty of Applied Mathematics.

THE THIRD TWENTE WORKSHOP ON GRAPHS AND COMBINATORIAL OPTIMIZATION

U. Faigle and C. Hoede May 1993 242 p Workshop of the Scientific Program was held in Enschede, 2-4 Jun. 1993 See also PB94-110954, N92-24905 and PB93-195568 Limited Reproducibility: More than 20% of this document may be affected by microfiche quality
(PB94-110947; MEMO-1132) Avail: Issuing Activity (National Technical Information Service (NTIS))

Contents of the document include: almost distance-hereditary graphs; toughness and triangle-free graphs; applications of an algebraic Monge property; on special antimagic labelings; a linear time algorithm for finding tree-decompositions of small treewidth; cycle lengths in non-bipartite graphs; Steiner trees and packing constants in graph-metric spaces; ordered matroids and regular independence systems; generalized strongly chordal graphs; Nordhaus-Gaddum type inequalities for the average distance of a graph; determination of the rank of Lefschetz matrices of products of posets; linear programming in random polynomial time; polymatroids of the cone of boolean submodular functions; and bipartite regular graphs with large diameters. NTIS

N94-23724# Technische Hogeschool Twente, Enschede (Netherlands). Dept. of Mathematics and Computing Science.

RELATIONAL ALGEBRA AND EQUATIONAL PROOFS

E. deKogel 1993 34 p
(PB94-110822; Computing Science Notes-93/23) Copyright Avail: CASI HC A03/MF A01

We show that two concepts involving equational probability can be elegantly formalized in terms of a relational algebra, equipped with two special-purpose mappings. We derive some calculus in order to prove that these concepts are equivalent, and that they are sound and complete. We illustrate the use of the relational framework by a few examples. We show the decidability of probability of an equation from a finite set of variable-free equations, where all equations are variable-free. Then we discuss a method by Reeves to deal with equations in semantic tableaux, that we can now prove to be complete in a very simple way. Finally, we discuss an equational proof format that is naturally induced by the relational formulation, and serves as a guideline in finding proofs. The relation between Reeves' rules and the construction of such proofs is made explicit. NTIS

N94-23725# Technische Hogeschool Twente, Enschede (Netherlands). Dept. of Computer Science.

MULTI-SET EXTENDED RELATIONAL ALGEBRA: A FORMAL APPROACH TO A PRACTICAL ISSUE

P. W. P. J. Grefen and R. A. deBy 1993 20 p
(PB94-110830; Memo-INF-93-31) Copyright Avail: CASI HC A03/MF A01

The report proposes a complete extended relational algebra with multi-set semantics. The algebra has both a clear formal background and a close connection to the standard relational algebra. The usual relational expression equivalences hold in this algebra. It further includes constructs that extend the algebra to a complete sequential database manipulation language. The complete range of topics from elementary database structures to multi-statement transactions is covered. The language can either be used as a formal background to other multi-set languages like SQL, or as a database manipulation language on its own. The practical usability of the latter option has been demonstrated in the PRISMA/DB database project, where a variant of the language, called XRA, has been used as the primary database language. NTIS

N94-23757# Technische Univ., Delft (Netherlands). Faculty of Technical Mathematics and Informatics.

EFFICIENT INTERPOLATION OF VELOCITY AND FLUX COMPONENTS DEFINED ON 2- AND 3-DIMENSIONAL NON-CARTESIAN GRIDS

P. vanBeek 1993 23 p
(PB94-118619; REPT-93-52) Copyright Avail: CASI HC A03/MF A01

The purpose of this work is to compare the computational efficiency of some interpolation procedures that accompany the discretization of the Navier-Stokes equations on non-Cartesian staggered grids. The conclusion is reached that, as far as the computational efficiency of the involved interpolation procedures is concerned, the covariant velocity formulation is the best choice in 3D while in 2D the formulation with contravariant fluxes is optimal. NTIS

N94-23758# Technische Univ., Delft (Netherlands). Faculty of Technical Mathematics and Informatics.

LOGARITHM OF PROBABILITY MEASURES AND INFINITE DIVISIBILITY OF SUB-STABLE RANDOM VECTORS

J. K. Misiewicz 1993 16 p
(PB94-118627; REPT-93-53) Copyright Avail: CASI HC A03/MF A01

We discuss infinite divisibility of sub-stable finite dimensional random vectors. Usually one must guess the corresponding Levy measure, nu, for given a infinitely divisible measure, mu, which is rather hard. In some cases, however, it seems to be possible to get the measure, nu, as a limit of a sequence of signed measures derived from the measure, mu. Obviously the convergence cannot be weak or normed, as is usually done in functional analysis, because a probability measure has variation 1 and this lies on the boundary of the corresponding ball of convergence. We give some partial results in this area applied to sub-stable random vectors. In view of these results, it seems possible that every finite dimensional sub-stable distribution is of the form of generalized Poisson measure for some signed sigma-finite measure on R(sup n). NTIS

N94-23762# Vrije Univ., Brussels (Belgium).

DESIGN AND SPECIFICATION OF A GENERIC TASK MODEL FOR SOLVING BOOLEAN CONSTRAINT SATISFACTION PROBLEMS

P. Geelen, W. Kowalczyk, Z. Ruttkay, and J. Treur Dec. 1992 92 p
(PB94-118841; IR-314) Avail: CASI HC A05/MF A01

We introduce the Boolean constraint satisfaction problem (Boolean CSP), as a natural generalization of the traditional CSP. We give motivations for this generalization, and formulate a small design example as a Boolean CSP. The language of many-sorted predicate logic serves as the basis for defining syntax and semantics of Boolean constraints. We also discuss the issue of representing such constraints in the Design and Specification of Interacting Reasoning modules (DESIRE) framework. We propose a generic task model for solving Boolean CSP's. We fully specify the resulting model, describe the separate modules in detail, and discuss two refinements. NTIS

N94-23765# Vrije Univ., Brussels (Belgium).
TWO APPLICATIONS OF A GENERIC TASK MODEL FOR SOLVING BOOLEAN CONSTRAINT SATISFACTION PROBLEMS
P. Geelen, W. Kowalczyk, Z. Ruttkay, and J. Treur Dec. 1992 64 p See also PB94-119039
(PB94-119047; IR-315) Avail: CASI HC A04/MF A01

This report presents two applications of the generic task model for solving Boolean Constraint Satisfaction Problems (BCSP's) to two problems: routing international money payments and the office assignment problem. The two problems are formulated as BCSP's. Relevant expert's knowledge is identified and specified in the Design and Specification of Interacting Reasoning modules (DESIRE) framework. The resulting systems have confirmed the correctness of the chosen task model and provided some feedback for its improvement. NTIS

N94-23775 Institut des Hautes Etudes Scientifiques, Bures-sur-Yvette (France).
PERIODIC NONLINEAR SCHROEDINGER EQUATION AND INVARIANT MEASURES
Jean Bourgain Jun. 1993 26 p Limited Reproducibility: More than 20% of this document may be affected by microfiche quality
(PB93-238012; IHES/M/93/28) Avail: CASI HC A03

Investigations of a nonlinear Schroedinger equation in the periodic case originate from the work of Lebowitz-Rose-Speer on the statistical mechanics aspects of the flow. Some of their investigations are completed here by proving the invariance of the measure they introduced on a certain (natural) statistical ensemble. Derived from text

N94-23776 Institut des Hautes Etudes Scientifiques, Bures-sur-Yvette (France).
CAUCHY PROBLEM FOR PERIODIC KDV-TYPE EQUATIONS
Jean Bourgain Jun. 1993 53 p Limited Reproducibility: More than 20% of this document may be affected by microfiche quality
(PB93-238020; IHES/M/93/29) Avail: CASI HC A04

The paper continues an investigation started in a 1993 paper by the author on questions of wellposedness for space-periodic evolution equations, mainly modified KdV equations. In general, these equations are not integrable and there is a lack of conserved quantities to apply approximate solution techniques. In the nonperiodic case there has been recently progress on such questions. The main point is applying a fixpoint theorem to get a local solution is a smoothness gain for which the solution operator to the linear equation is responsible. In periodic problems, there is no exact analogue to such phenomenon and the argument for regularity gain is based on an interplay between linear and nonlinear part of the equation, the exact structure of the nonlinear term being of importance. NTIS

N94-23786 Leiden Univ. (Netherlands). Div. of Applied Mathematics.
ERROR DUE TO THE STOPPING OF THE NEWTON ITERATION IN IMPLICIT LINEAR MULTISTEP METHODS
J. Groeneweg and N. M. Spijker Mar. 1993 15 p Limited Reproducibility: More than 20% of this document may be affected by microfiche quality
(PB94-101425; TW-93-05) Avail: Issuing Activity (National Technical Information Service (NTIS))

The paper concerns the numerical solution of initial value problems for nonlinear ordinary differential equations by implicit linear multistep methods. For non-stiff problems, fixed point iteration (Picard iteration), is a classical approach to the solution of the system of algebraic equations occurring in each time step of these methods. The order of the error due to the stopping of this process after a fixed number of iterations is well understood. For stiff problems, Picard iteration is not appropriate and some variant of the Newton method is usually used instead. The paper addresses the problem of estimating the stopping error of Newton-like iterations. One aims for an understanding of this error comparable to what is known about Picard iterations. Because of stiffness, the theory is more delicate than for Picard iterations. NTIS

N94-23787 Technische Hogeschool Twente, Enschede (Netherlands). Faculty of Applied Mathematics.
NON-TRIVIAL EXAMPLES OF REAL ISOLATED SINGULARITY AT THE ORIGIN Memorandum Report
A. AlDhahir Apr. 1993 24 p Limited Reproducibility: More than 20% of this document may be affected by microfiche quality
(PB94-110939; Memo-1129) Avail: CASI HC A03

The existence of nontrivial examples of real polynomial (or differentiable) maps with isolated singularity at the origin has been shown in most dimensions. Church and Lamotke used a result by Looijenga to prove the existence of such examples. Church and Timourian have shown when such examples exist. However, such examples are rare. Milnor, in his book 'Singularities of Complex Hypersurfaces', has cited an example by Kuiper of an isolated singularity at the origin which does not come from a complex one. A'Campo has presented another example in one of his papers. The objective is to survey all these results and examples and bring them together in one article. In Section One, we introduce basic definitions and properties. Section Two is reserved for the results by Church and Lamotke, Church and Timourian, Looijenga and Milnor; while in Section Three, the only known explicit examples are stated. NTIS

N94-23799 Technische Univ., Eindhoven (Netherlands). Dept. of Mathematics and Computing Science.
SOME GENERALIZED SUBSET SELECTION PROCEDURES
Paul vanderLaan and Constance vanEeden (British Columbia Univ., Vancouver.) Jul. 1993 10 p See also PB93-237857 Limited Reproducibility: More than 20% of this document may be affected by poor print and microfiche quality
(PB94-111655; MEMO-COSOR-93-21) Avail: Issuing Activity (National Technical Information Service (NTIS))

In this paper, some generalizations of Gupta's subset selection procedure are discussed. Assume k (greater than or equal to 2) populations are given and assume that the associated random variables have distributions with unknown location parameters theta(sub i), i = 1,...,k. The ordered parameters are denoted by theta(sub 1) less than or equal to ... less than or equal to theta(sub k). On the basis of independent samples from these populations, Gupta selects a subset, as small as possible, which contains, with probability at least P*, the best population. Two generalizations are discussed. Each one is designed to give a smaller expected subset size, Epsilon S, than Gupta's procedure. The first procedure selects, with probability at least P*, an epsilon-best population whose location parameter is at least theta(sub k) - epsilon (with epsilon greater than or equal to 0). Some efficiency results for normal populations are presented. The second procedure uses a loss function and it upperbounds either the expected loss or the expected subset size, or both. The loss is taken as zero when the subset contains an epsilon-best population. Some properties of the procedure, for the case of two normal populations, are presented. NTIS

N94-24053# Universiteit Twente, Enschede (Netherlands). Faculty of Applied Mathematics.
TOUGHNESS IN HAMILTONICITY IN ALMOST CLAW-FREE GRAPHS
H. J. Broersma, Z. Ryjacek (College of Mechanical and Electrical Engineering, Plzen, Czechoslovakia.), and I. Schiermeyer (Technische Hochschule, Aachen, Germany.) Feb. 1993 11 p
(MEMO-1114; ETN-94-94749) Avail: CASI HC A03/MF A01

Results on claw free (K(sub 1,3-free) graphs are generalized to the larger class of almost claw free graphs which were introduced by Ryjacek. In particular, a 2-connected almost claw free graph is shown to be 1-tough, and a 2-connected almost claw free graph on n vertices is shown to be hamiltonian if delta is greater than or equal to (1/3)(n - 2), thereby (partly) generalizing results of Matthews and Sumner. A result of Bauer et al. is used to show that a 2-connected almost claw free graph on n vertices is hamiltonian if d(u) + d(v) + d(w) is greater than or equal to n for all independent sets of vertices u, v and w. ESA

N94-24291*# Institute for Computer Applications in Science and Engineering, Hampton, VA.
ON THE DIFFERENTIATION MATRIX FOR DAUBECHIES-BASED WAVELETS ON AN INTERVAL Final Report
Leland Jameson Dec. 1993 34 p Submitted for publication
(Contracts NAS1-19480; AF-AFOSR-0090-93; N00014-91-J-4016; NSF

DMS-92-11820; RTOP 505-90-52-01)
(NASA-CR-191582; NAS 1.26:191582; ICASE-93-94) Avail: CASI HC A03/MF A01

The differentiation matrix for a Daubechies-based wavlet basis defined on an interval will be constructed. It will be shown that the differentiation matrix based on the currently available boundary constructions does not maintain the superconvergence encountered under periodic boundary conditions. Author

N94-24503# Lawrence Livermore National Lab., CA.
STUDIES ON THE IMPLEMENTATION OF NORMALS AND CURVATURES. PART 1: THE FIRST OR MEAN CURVATURE
Carl Rosenkilde 2 Jul. 1993 21 p
(Contract W-7405-eng-48)
(DE94-001546; UCRL-ID-115168-Pt-1) Avail: CASI HC A03/MF A01

We are interested in the construction of the unit normal and the curvatures on some surface which is represented by finite elements. We shall start with the usual definitions for the unit normal and the first and second curvatures on a continuous surface. The unit normal on some surface defined by (var phi)(x) = 0 is given by (cflx n) = (del) (phi)/the absolute value of (del) (phi), where (del) signifies the familiar three-dimensional gradient operator in space, rather than the two-dimensional gradient on the a surface, which is commonly utilized in differential geometry. The first and second curvatures, J and K, which involve invariant functions of this normal, may be expressed in the form: 2J = (del)(center dot)(cflx n) and 2K = (del)(center dot)((cflx n)((del)(center dot)(cflx n)) + (cflx n) x ((del) x (cflx n)). The expression for J has the same formal appearance regardless of which gradient operator is used, but the expression for K differs from the two-dimensional version because of the expansion for the Laplacian of a vector. DOE

N94-24526 Tilburg Univ. (Netherlands). Dept. of Econometrics.
UNIFORM LIMIT THEOREMS FOR MARKED POINT PROCESSES
Gert Niewenhuis 1993 40 p Limited Reproducibility: More than 20% of this document may be affected by microfiche quality
(PB94-118726; FEW-606) Avail: CASI HC A03

Let P be the distribution of a stationary marked point process on R and let P(sup 0, sub L) be its Palm distribution with respect to a set L of marks. Starting from P, the probability measures P(sub i,L), i is an element of Z, arise by shifting the origin to the i'th occurrence with mark in L. Q(sup 0, sub L) is a probability measure which equals P(sup 0, sub L) under a weak ergodicity condition. In the present research this uniform limit theorem is generalized by replacing 1(sub B) by functions f with the absolute value of f uniformly bounded by a fixed function g. It is also proved that similar results hold if the starting point P is replaced by P(sup 0, sub L'), where L' is another set of marks with L intersection L' = 0. As a preliminary, a theorem is proved which implies an easy way to express P(sup 0, sub L')-expectations in terms of P(sup 0, sub L)-expectations. In a 'dual' theorem roles of P and P(sup 0, sub L) are interchanged. Starting from P(sup 0, sub L) similar uniform limit theorems are derived for Cesaro averaged functionals. The limits can be expressed as expectations under a probability measure Q(sub L) which equals P under weak ergodicity condition. In a final section it is shown that uniform approximation of P(sup 0, sub L) and P is still possible without ergodicity restraints. NTIS

N94-24527 Vrije Univ., Amsterdam (Netherlands). Faculteit der Wiskunde en Informatica.
EXTENSION OF THE CRITICAL PATH METHOD
F. J. Juengen Dec. 1992 44 p See also PB92-219559 Limited Reproducibility: More than 20% of this document may be affected by microfiche quality
(PB94-118817; IR-311) Avail: Issuing Activity (National Technical Information Service (NTIS))

In this report, the Extended Critical Path Method (ECPM) is presented. The ECPM is an extension of the Critical Path Method (CPM), a methodology for project management based on network planning, that has its roots in the late fifties. This methodology has a number of drawbacks which make it of limited use in interactive computer systems. These drawbacks of the CPM are identified and an extension of the CPM is presented which is suitable to be used in interactive computer systems. This claim is supported by an interactive computer system prototype for project management that has actually been built: Interactive Project Scheduler (IPS). NTIS

N94-24536 Institut des Hautes Etudes Scientifiques, Bures-sur-Yvette (France).
QUASICONFORMAL MAPPINGS, OPERATORS ON HILBERT SPACE, AND LOCAL FORMULAE FOR CHARACTERISTIC CLASSES
Alain Connes, Dennis Sullivan, and Nicolas Teleman Jul. 1993 28 p Limited Reproducibility: More than 20% of this document may be affected by microfiche quality
(PB93-238079; IHES/M/93/38) Avail: CASI HC A03

Local formulae are given for the characteristic classes of a quasiconformal manifold using the subspace of exact forms in the Hilbert space of middle dimensional forms. The method applies to combinatorial manifolds and all topological manifolds except certain ones in dimension four. NTIS

N94-24539 Technische Univ., Eindhoven (Netherlands).
SEQUENTIAL COMPOSITION, ACTION PREFIXES AND PROCESS PREFIX
J. C. M. Baeten and J. A. Bergstra (Amsterdam Univ., Netherlands.) 1993 30 p Prepared in cooperation with Utrecht Rijksuniversiteit (Netherlands), Dept. of Philosophy, and Amsterdam Univ. (Netherlands), Programming Research Group Limited Reproducibility: More than 20% of this document may be affected by microfiche quality
(PB94-101433; COMPUTING SCIENCE NOTES-93/14) Copyright Avail: CASI HC A03

The authors illustrate the difference between sequential composition in process algebra axiomatizations like ACP and action prefixing in process calculi like CCS. They define both early and late input in a general framework extending ACP, and consider various subalgebras, some very close to value passing CCS, another one close to CSP. NTIS

N94-24541 Technische Univ., Twente (Netherlands). Faculty of Applied Mathematics.
INVESTIGATION ON INTERVAL EDGE-COLORING OF GRAPHS
A. S. Asratian and R. R. Kamalian Mar. 1993 8 p Limited Reproducibility: More than 20% of this document may be affected by microfiche quality
(PB94-110913; MEMO-1130) Avail: CASI HC A02

An edge-coloring of a simple graph G with colors 1, 2, ..., t is called an interval t-coloring if at least one edge of G is colored by color i, i = 1, ..., t and the edges incident with each vertex x are colored by d(sub G)(x) consecutive colors, where d(sub G)(x) is the degree of the vertex x. In this paper, we investigate some properties of interval colorings and their variations. It is proved, in particular, that if a simple graph G = (V,E) without triangles has an interval t-coloring, then t = or less than (absolute value of V) -1. NTIS

N94-24561# Rutgers - The State Univ., Piscataway, NJ.
DISCRETE APPLIED MATHEMATICS Final Report, 1 Sep. 1989 - 31 May 1993
Peter L. Hammer 31 May 1993 49 p
(Grant AF-AFOSR-0512-89)
(AD-A273552; AFOSR-93-0877TR) Avail: CASI HC A03/MF A01

Significant progress was made with solution of location problems and in preprocessing and decomposition for discrete optimization. There was also research on the application of techniques from combinational optimization to nonlinear problems. DTIC

N94-24564*# Georgia Inst. of Tech., Atlanta. School of Aerospace Engineering.
ROBUST STABILITY OF SECOND-ORDER SYSTEMS Semiannual Status Report, 24 Aug. 1993 - 23 Feb. 1994
C.-H. Chuang 23 Feb. 1994 22 p
(Grant NAG1-1397)
(NASA-CR-195175; NAS 1.26:195175) Avail: CASI HC A03/MF A01

Nonlinear control using feedback linearization or inverse dynamics for robotic manipulators yields good results in the absence of modeling uncertainty. However, modeling uncertainties due to unknown joint friction coefficients and payload variations can give rise to undesirable characteristics when these control systems are implemented. It is shown how passivity concepts can be used to supplement the feedback linearization control design technique, in order to make it robust with respect to the uncertain effects mentioned above. Results are obtained for space manipulators with freely floating base; however, they are applicable to fixed base manipulators as well. The controller guarantees asymptotic tracking of the joint variables.

Closed-loop simulation results are illustrated for planar space manipulators for cases where uncertainty exists in friction modeling and payload inertial parameters. Author

N94-24572# Technische Univ., Delft (Netherlands). Faculty of Technical Mathematics and Informatics.
POLYNOMIALS ORTHOGONAL WITH RESPECT TO AN INNER PRODUCT INVOLVING DIFFERENCES
H. Bavinck 1992 18 p
(PB94-110731; Rept-92-81) Copyright Avail: CASI HC A03/MF A01

In this paper we consider the inner product (f,g) = integral over R of f g d(phi)(x) + lambda (delta)f(c) (delta)g(c), where c is a member of R and phi is a distribution function with infinite spectrum such that the interval (c,c+1) does not contain points of the spectrum of phi. Furthermore lambda less than or equal to 0, f and g are functions on R and (delta)f(c) = f(c+1) - f(c). Let (Q(sub n, sup lambda)(x)) be the sequence of monic orthogonal polynomials with respect to this inner product and (P(sub n)(x)), (P(sub n, sup c)(x)) the sequences of monic standard orthogonal polynomials (lambda = 0) with respect to d(phi)(x) and (x-c)(x-c-1)d(phi)(x) respectively. We derive an explicit representation for Q(sub n, sup lambda)(x) in terms of P(sub n)(x) and P(sub n, sup c)(x) and we present some results on the distribution of the zeros of Q(sub n, sup lambda)(x) in relation to the zeros of P(sub n)(x). Finally we treat the special case where P(sub n)(x) are Charlier polynomials and c = 0. NTIS

N94-24608 Technische Univ., Eindhoven (Netherlands). Dept. of Mathematics and Computing Science.
SQUARING-DOWN AND THE PROBLEMS OF ALMOST-ZEROS FOR CONTINUOUS-TIME SYSTEMS
A. A. Stoorvogel and J. H. A. Ludlage (IPCOS B.V., Best, Netherlands.) Mar. 1993 16 p Limited Reproducibility: More than 20% of this document may be affected by microfiche quality
(PB93-237758; MEMO-COSOR-93-11) Avail: CASI HC A03

The authors construct precompensators which square-down a system such that the resulting square system has the same unstable zeros and system gains. We derive the minimal gain of the precompensator to achieve such a square system. If the gain of this precompensator is too large, then we derive an explicit trade-off between the gain of the precompensator and the number of unstable zeros that we will allow the precompensator to introduce in the system. NTIS

N94-24610 Institut des Hautes Etudes Scientifiques, Bures-sur-Yvette (France).
STABLE NON-GAUSSIAN DIFFUSIVE PROFILES
J. Bricmont (Universite Catholique de Louvain, Belgium.) and A. Kupiainen (Helsinki Univ., Finland.) Jun. 1993 15 p Limited Reproducibility: More than 20% of this document may be affected by microfiche quality
(Grants NSF DMS-89-03041; EEC-SCI-CT91-0695)
(PB93-238053; IHES/P/93/36) Avail: CASI HC A03

The authors prove two stability results for the scale invariant solutions of the nonlinear heat equation partial differential of u with respect to t = (Delta)u - (absolute value of u)(sup p-1)u with 1 greater than p greater than 1 + 2n, n being the spatial dimension. The first result is that a small perturbation of a scale invariant solution vanishes as t yields infinity. The second result is a global, with a positivity condition on the initial data. NTIS

N94-24615 Technische Univ., Eindhoven (Netherlands). Dept. of Mathematics and Computing Science.
SYSTEMS ENGINEERING: A FORMAL APPROACH. PART 2: FRAMEWORKS
K. M. vanHee 30 Mar. 1993 145 p See also PB93-225308 and PB94-101409 Limited Reproducibility: More than 20% of this document may be affected by microfiche quality
(PB94-101391; Computing Science Notes-93/10) Avail: CASI HC A07

Part 2 defines the formalisms used to model and analyze systems. The first framework presented is called the transition systems framework. It formalizes the concept of discrete dynamic systems and their properties. The second framework is called the object framework. It formalizes the concepts of simplexes and complexes. These are static concepts used for modeling state spaces (or data bases). The third framework is called the actor framework, because it formalizes the concepts of actors and networks of actors. It generalizes the framework of Petri nets. NTIS

N94-24643 Vrije Univ., Amsterdam (Netherlands). Artificial Intelligence Group.
NON-BRITTLENESS OF A DESIRE-MODEL FOR AN OFFICE ASSIGNMENT TASK
Pieter Geelen, Sofia Ruttkay, and Jan Treur Dec. 1992 43 p Limited Reproducibility: More than 20% of this document may be affected by microfiche quality
(PB94-119021; IR-317) Avail: Issuing Activity (National Technical Information Service (NTIS))

The first challenge was to build a model for solving a given office assignment problem. Then the brittleness of the built model had to be explored, by testing it against a slightly modified version of the initially given problem. We briefly discuss our original model and analyze the trace of solving the first problem. Then, after having clarified possible reasons for brittleness, we analyze the behavior of our model with respect to the modified problem. We show that by some minor changes, we could improve our model in such a way that it could cope with the modified problem as well. The modification could be carried out easily due to the clear, modular architecture of our model. The modifications correspond to alternative interpretations of pieces of the problem solving protocol of the first problem. Moreover, it is shown that our initial model can always be turned into a non-brittle one without introducing any additional module, such as one for backtracking. NTIS

N94-24651 Technische Univ., Twente (Netherlands). Faculty of Applied Mathematics.
CRITERION FOR SOME HAMILTONIAN GRAPHS TO BE HAMILTON-CONNECTED Memorandum Report
A. S. Asratian May 1993 13 p Limited Reproducibility: More than 20% of this document may be affected by microfiche quality
(PB94-110921; MEMO-1131) Avail: Issuing Activity (National Technical Information Service (NTIS))

Let M = (G/K(sub n,n) included in G included in K(sub n) V (K bar)(sub n) for some n = or greater than 3) where V is the join operation. The author and N. K. Khachatrian proved that a connected graph G of order at least 3 is hamiltonian if d(u) + d(v) = or greater than the absolute value of (N(u) joined to N(v) joined to N(w)) for each triple of vertices u, v, w with d(u,v) = 2 and w is a member of N(u) (intersection) N(v) where N(x) is the neighborhood of a vertex x. We prove here that a graph G satisfying the above conditions is Hamilton-connected if and only if G is 3-connected and G is not a member of M. NTIS

N94-24652 Technische Univ., Twente (Netherlands). Faculty of Applied Mathematics.
THE THIRD TWENTE WORKSHOP ON GRAPHS AND COMBINATORIAL OPTIMIZATION: ABSTRACTS AND LATE EXTENDED ABSTRACTS
U. Faigle and C. Hoede May 1993 24 p Workshop held in Enschede, 2-4 Jun. 1993 See also PB94-110947 Limited Reproducibility: More than 20% of this document may be affected by microfiche quality
(PB94-110954; MEMO-1132A) Avail: Issuing Activity (National Technical Information Service (NTIS))

Contents: On the complexity of poset properties; Cube subgraphs without squares; Score vectors of multi-tournaments; Extremal functions for sequences; Providing lower bounds on integer programs for global routing problems with integrated placements; Diameters and cardinalities of two-distance sets; Chip firing on digraphs; Monotone decreasing property of the jump number for some N-free posets; The Bondage number of a graph doesn't depend only on Delta(G); The Monge-Property and efficient algorithms for the Traveling Salesman Problem; Packing bipartite graphs; A simple approach to communication in parallel branch and bound. NTIS

N94-24653 Technische Univ., Twente (Netherlands). Faculty of Applied Mathematics.
IRREDUCIBLE CORE OF A MINIMUM COST SPANNING TREE GAME
Harry F. M. Aarts and Theodore S. H. Driessen May 1993 15 p See also PB93-194728 Limited Reproducibility: More than 20% of this document may be affected by microfiche quality
(PB94-110962; MEMO-1133) Avail: Issuing Activity (National Technical Information Service (NTIS))

It is a known result that for a minimum cost spanning tree (mcst) game a Core allocation can be deduced directly from a mcst in the underlying network. To determine this Core allocation one only needs to determine a mcst in the network and it is not necessary to calculate the coalition values of the corresponding mcst game. The paper deduces other Core allocations directly from the network, without determining the corresponding mcst game itself: it presents two procedures that determine a part of the Core (called the Irreducible Core) from the network. NTIS

N94-24727*# National Aeronautics and Space Administration. Marshall Space Flight Center, Huntsville, AL.
CORSS: CYLINDER OPTIMIZATION OF RINGS, SKIN, AND STRINGERS
J. Finckenor, P. Rogers, and N. Otte Washington Jan. 1994 91 p
(NASA-TP-3457; M-740; NAS 1.60:3457) Avail: CASI HC A05/MF A01

Launch vehicle designs typically make extensive use of cylindrical skin stringer construction. Structural analysis methods are well developed for preliminary design of this type of construction. This report describes an automated, iterative method to obtain a minimum weight preliminary design. Structural optimization has been researched extensively, and various programs have been written for this purpose. Their complexity and ease of use depends on their generality, the failure modes considered, the methodology used, and the rigor of the analysis performed. This computer program employs closed-form solutions from a variety of well-known structural analysis references and joins them with a commercially available numerical optimizer called the 'Design Optimization Tool' (DOT). Any ring and stringer stiffened shell structure of isotropic materials that has beam type loading can be analyzed. Plasticity effects are not included. It performs a more limited analysis than programs such as PANDA, but it provides an easy and useful preliminary design tool for a large class of structures. This report briefly describes the optimization theory, outlines the development and use of the program, and describes the analysis techniques that are used. Examples of program input and output, as well as the listing of the analysis routines, are included. Author (revised)

N94-24763 Technische Univ., Eindhoven (Netherlands). Dept. of Mathematics and Computing Science.
EFFICIENCY OF SUBSET SELECTION OF AN EPSILON-BEST UNIFORM POPULATION RELATIVE TO SELECTION OF THE BEST ONE
Paul vanderLaan Apr. 1993 13 p Limited Reproducibility: More than 20% of this document may be affected by microfiche quality
(PB93-237741; MEMO-COSOR-93-12) Avail: CASI HC A03

Assume k(= or greater than 2) uniform populations are given on (mu(i) - 1/2, mu(i) + 1/2) with location parameter mu(i) a member of R(sup 1), i = 1,...,k. The best population is defined as the population with the largest value of the location parameter. In epsilon-best population (with epsilon = or greater than 0) is a population with location parameter on a distance not larger than epsilon from the largest value of mu. It is possible to consider subset selection for an epsilon-best population relative to subset selection for the best one. The relative efficiency is defined and computed in dependence of k and epsilon for some values of the confidence level P* of selection. NTIS

N94-24768# Polish Academy of Sciences, Warsaw. Inst. Fundamental Technological Research.
TWO-POINT PADE APPROXIMANTS FOR STIELTJES SERIES
Stanislaw Tokarzewski, Jerzy Blawzdziewicz, and Igor Andrianov 1993 18 p
Avail: CASI HC A03/MF A01

We have proved that certain two-point Pade approximants to Stieltjes series occupying the diagonal of the Pade table form sequences of lower and upper bounds uniformly converging to the Stieltjes function. The results can be applied in the theory of inhomogeneous media to calculate the bounds on the effective transport coefficients of heterogeneous materials. Author

N94-24836*# Institute for Computer Applications in Science and Engineering, Hampton, VA.
PROJECTION TECHNIQUES FOR ITERATIVE SOLUTION OF A(BAR x) EQUALS (BAR b) WITH SUCCESSIVE RIGHT-HAND SIDES Final Report
Paul F. Fischer (Brown Univ., Providence, RI.) Dec. 1993 14 p Submitted for publication
(Contract NAS1-19480; NSF ASC-91-07674; RTOP 505-90-52-01)
(NASA-CR-191571; NAS 1.26:191571; ICASE-93-90) Avail: CASI HC A03/MF A01

Two projection techniques for computing approximate solutions to linear systems of the form A(bar x)(sup n) = (bar b)(sup n), for a sequence n = 1, 2, ..., e.g., such as arises from time discretization of a partial differential equation, are presented. The inexpensive approximate solutions can be used as initial guesses for iterative solution of the system, resulting in significantly reduced computational expense. Examples of two- and three-dimensional incompressible Navier-Stokes calculations are presented in which x represents the pressure, and A is a discrete Poisson operator. In flows containing significant dynamic activity, these projection techniques lead to as much as a two-fold reduction in solution time. Author (revised)

N94-24847*# Texas Univ., Brownsville. Dept. of Mathematics.
EXPLOITING STRUCTURE: INTRODUCTION AND MOTIVATION Annual Status Report, 1 Mar. 1993 - 28 Feb. 1994
Zhong Ling Xu Feb. 1994 10 p
(Grant NAG5-2210)
(NASA-CR-195136; NAS 1.26:195136) Avail: CASI HC A02/MF A01

This annual report summarizes the research activities that were performed from 26 Jun. 1993 to 28 Feb. 1994. We continued to investigate the Robust Stability of Systems where transfer functions or characteristic polynomials are affine multilinear functions of parameters. An approach that differs from 'Stability by Linear Process' and that reduces the computational burden of checking the robust stability of the system with multilinear uncertainty was found for low order, 2-order, and 3-order cases. We proved a crucial theorem, the so-called Face Theorem. Previously, we have proven Kharitonov's Vertex Theorem and the Edge Theorem by Bartlett. The detail of this proof is contained in the Appendix. This Theorem provides a tool to describe the boundary of the image of the affine multilinear function. For SPR design, we have developed some new results. The third objective for this period is to design a controller for IHM by the H-infinity optimization technique. The details are presented in the Appendix. Author (revised)

N94-24914*# Institute for Computer Applications in Science and Engineering, Hampton, VA.
TRIANGULAR SPECTRAL ELEMENTS FOR INCOMPRESSIBLE FLUID FLOW Final Report
C. Mavriplis (George Washington Univ., Washington, DC.) and John VanRosendale Dec. 1993 19 p Presented at the AIAA 11th CFD Conference, Orlando, FL, 6-9 Jul. 1993
(Contract NAS1-19480; NSF ECS-92-09347; RTOP 505-90-52-01)
(NASA-CR-191588; ICASE-93-100; NAS 1.26:191588) Avail: CASI HC A03/MF A01

We discuss the use of triangular elements in the spectral element method for direct simulation of incompressible flow. Triangles provide much greater geometric flexibility than quadrilateral elements and are better conditioned and more accurate when small angles arise. We employ a family of tensor product algorithms for triangles, allowing triangular elements to be handled with comparable arithmetic complexity to quadrilateral elements. The triangular discretizations are applied and validated on the Poisson equation. These discretizations are then applied to the incompressible Navier-Stokes equations and a laminar channel flow solution is given. These new triangular spectral elements can be combined with standard quadrilateral elements, yielding a general and flexible high order method for complex geometries in two dimensions. Author (revised)

N94-24921# Naval Command, Control and Ocean Surveillance Center, San Diego, CA. Research, Development, Technology and Evaluation Div.
EVOLVING NEURAL NETWORK CONNECTIVITY Professional Paper
J. R. McDonnell and D. Waagen Oct. 1993 8 p
(AD-A273134) Avail: CASI HC A02/MF A01

This work investigates the application of evolutionary programming, a stochastic search technique, for determining connectivity in feedforward neural networks. The method is capable of simultaneously evolving both the connection scheme and the network weights. The number of connections are incorporated into an objective function so that network parameter optimization is done with respect to network complexity as well as mean pattern error. Experimental results are shown for simple binary mapping problems. DTIC

N94-24947 Yale Univ., New Haven, CT. Dept. of Computer Science.
GENERALIZED GAUSSIAN QUADRATURE RULES FOR SYSTEMS OF ARBITRARY FUNCTIONS
J. Ma, V. Rokhlin, and S. Wandzura Oct. 1993 59 p Limited Reproducibility: More than 20% of this document may be affected by microfiche quality
(Contracts F49620-91-C-0084; N00014-89-J-1527)
(AD-A273610; YALEU/DCS/RR-990) Avail: Issuing Activity (Defense Technical Information Center (DTIC))

In an earlier work, a far-reaching generalization of the classical Gaussian quadrature rules is introduced, replacing the polynomials with a wide class of functions. While the rules of that report possess most of the desirable properties of the classical Gaussian integration formulae (positivity of the weights, etc.), it is not clear from said research how such quadrature rules can be obtained numerically. In this paper, we present a numerical scheme for the generation of such generalized Gaussian quadratures. The algorithm is applicable to a variety of functions, including smooth functions as well as functions with end-point singularities. The performance of the algorithm is demonstrated with several numerical examples. DTIC

N94-24954 Technische Univ., Eindhoven (Netherlands). Dept. of Mathematics and Computing Science.
CHARACTERISTIC METHOD FOR ONE-DIMENSIONAL SCALAR HYPERBOLIC CONSERVATION LAWS WITH STIFF SOURCE TERMS
A. C. Berkenbosch, E. F. Kaasschieter, and J. H. M. tenThijeBoonkamp Mar. 1993 21 p Limited Reproducibility: More than 20% of this document may be affected by microfiche quality
(PB93-237675; RANA-93-05) Avail: CASI HC A03

The initial value problem for scalar hyperbolic conservation laws in one space dimension, with (stiff) source terms was considered. The source term admits two equilibrium states as solutions of the underlying characteristic equation, one unstable and one stable. An essential numerical difficulty for this initial value problem is that numerical reaction waves are propagating at non-physical wave speeds. An implicit numerical method is introduced which produces discontinuities propagating at the correct speed. It is proved that this method preserves monotone profiles and an estimate for the global discretization error is given. The numerical results illustrate the correct behavior of this method. NTIS

N94-25079# Technische Univ., Eindhoven (Netherlands). Discrete Mathematics Group.
ALGEBRAIC-GEOMETRIC CODES AND THEIR DECODING ALGORITHMS Ph.D. Thesis
Ba-Zhong Shen 1992 118 p
(ETN-94-95294) Avail: CASI HC A06/MF A02

Several problems involving algebraic-geometric codes and Goppa codes are discussed: how to handle all linear codes using algebraic geometry; is it possible to give an explicit construction with less complexity of asymptotically good binary codes meeting a good bound; and how to give an efficient encoding and decoding algorithm for algebraic-geometric codes. It is shown that all linear codes can be described as algebraic-geometric codes. A sequence of asymptotically good binary concatenated codes using curves is given. A class of algebraic-geometric codes which have similar properties as maximal distance separable codes is considered. A correct account of the results found by another author concerning a decoding algorithm for Goppa codes is given. The gamma-graded algebra, the gamma basis and a minimal solution of a congruence are provided. Codes constructed from Hermitian curves and the way to compute the residues explicitly by a given data base are presented. ESA

N94-25166 International Centre for Theoretical Physics, Trieste (Italy).
SUPER BELTRAMI DIFFERENTIALS AND N EQUAL TO 4 SUPERCONFORMAL ANOMALIES
T. Lhallabi Aug. 1992 22 p Limited Reproducibility: More than 20% of this document may be affected by microfiche quality
(DE93-613047; IC-92/183) Avail: CASI HC A03 (US Sales Only)

The N = 4 super Beltrami parametrization is formulated in the two-dimensional harmonic superspace. The N = 4 superconformal anomaly and its compensating action are constructed. Then the anomalous Ward-identities are derived and the operator product expansions of the N = 4 superstress energy tensors are obtained. DOE

N94-25213 International Centre for Theoretical Physics, Trieste (Italy).
THE RENORMALIZATION GROUP FOR FLAG MANIFOLDS
S. Randjbar-Daemi and J. Strathdee Oct. 1992 23 p Limited Reproducibility: More than 20% of this document may be affected by microfiche quality
(DE93-616846; IC-92/354) Avail: CASI HC A03 (US Sales Only)

The renormalization group equations for a class of non-relativistic quantum sigma-models targeted on flag manifolds are given. These models emerge in a continuum limit of generalized Heisenberg antiferromagnets. The case of the SU(3)/U(1)xU(1) manifold is studied in greater detail. It was shown that at zero temperature there is a fixed point of the RG transformations in (2 + epsilon)-dimensions where the theory becomes relativistic. The linearized RG transformations in the vicinity of this fixed point are studied and it was shown that half of the couplings are irrelevant. It was also shown that at this fixed point there is an enlargement of the global isometries of the target manifold. A discrete non-abelian enlargement of this kind was constructed. DOE

N94-25214 International Centre for Theoretical Physics, Trieste (Italy).
THE FUNDAMENTAL GROUP OF THE COMPLEMENT OF COMPLEXIFIED REAL ARRANGEMENTS
Viet Dung Nguyen Oct. 1992 11 p Limited Reproducibility: More than 20% of this document may be affected by microfiche quality
(DE93-616847; IC-92/355) Avail: CASI HC A03 (US Sales Only)

Let V be a finite dimensional vector space over the real or complex numbers. An arrangement in V is a finite collection of affine hyperplanes of V. Given a real arrangement A in a real vector space V, then its complexification, A(sub C), is a complex arrangement in the complex vector space V(sub C), and will be called a complexified real arrangement. A presentation for the fundamental group of the complement of a complexified real arrangement was proved. DOE

N94-25244 Amsterdam Univ. (Netherlands).
THE STATE SPACE METHOD FOR INTEGRO-DIFFERENTIAL EQUATIONS OF CONVOLUTION TYPE WITH RATIONAL MATRIX SYMBOLS Ph.D. Thesis
Andre Bauke Kuijper 1992 179 p Sponsored by Netherlands Organization for Scientific Research
(ETN-94-95379) Copyright Avail: CASI HC A09/MF A02

The state space method, developed to deal with problems in mathematical analysis involving rational matrix valued functions, is used to study systems of integro-differential equations. The spectral properties of matrix pencils and realizations are studied. A number of auxiliary results that play an important role later are presented. Singular differential equations are reviewed. The general solutions are described in terms of the data for the decomposition of the pencil. Equations where differentiations occur under the integral sign are reduced by a linearization method to equations of type (H). Equations with distributional right hand sides are presented. The connection between the inversion properties of the operator T(sub W) and a factorization of its symbol W is discussed. The analogs of some theorems for the finite interval are given. Results concerning the projection method for some of the equations are summarized. ESA

N94-25245# Amsterdam Univ. (Netherlands). Dept. of Mathematics and Computer Science.
WIENER-HOPF FACTORIZATION OF RATIONAL MATRIX FUNCTIONS IN TERMS OF REALIZATIONS: AN ALTERNATIVE VERSION Ph.D. Thesis
Gilbert Joseph Groenewald 1993 142 p Sponsored by Vrije Univ., Amsterdam, Netherlands
(ETN-94-95380) Avail: CASI HC A07/MF A02

An alternative version of the construction of a noncanonical Wiener-Hopf factorization is presented. The canonical factorization theorem for rational matrix functions and an inversion theorem for a block Toeplitz are summarized. The advantages of the chosen representaion of the function W are explained. The explicit formulas for a Wiener-Hopf factorization for W are presented. The main Wiener-Hopf factorization theorem derived is shown. Preliminaries about null pole triples association are shown. Certain standard null pole triples are presented in a canonical way. The notion of a minimal supplement and standard null pole triples associated with minimal realizations defined by admissible Sylvester data sets and minimal supplements are developed. Particular minimal supplements are constructed.

It is shown that the associated rational matrix functions are column reduced up to the basis transformation. An auxiliary factorization result which is used to give the proof of the Wiener-Hopf factorization theorem is presented. An alternative proof of the main result is given. Auxiliary material about full range and null kernel pairs which is of independent interest and will be needed to obtain the parametrization of the set of all solutions of the problem is included. The results are specified and developed for matrix polynomials. ESA

N94-25277# Technische Univ., Eindhoven (Netherlands).
INTRODUCTION TO A BEHAVIORAL APPROACH FOR CONTINUOUS TIME SYSTEMS Ph.D. Thesis
Johannes Maria Soethoudt 1993 173 p
(ETN-94-95301) Avail: CASI HC A08/MF A02

An approach to find necessary and sufficient conditions for a continuous time dynamical system to satisfy an AR-relation is presented. Frechet spaces and their duals are introduced. Some properties of Fourier transform, defined in several spaces, are presented. The translation-invariant operators are characterized. The statement that all intrinsic properties of a behavior B are present in its restriction B(sup infinity) to C(sup infinity) (R, (R sup g)) is made. The AR-descriptions for systems consisting of C(R)-signals are discussed. The case of C(sup(-k)) spaces is analyzed. A new chain of Frechet spaces that can be used to interpret differential equations in case the signals are not differentiable is presented. The way the results can be generalized to other Frechet spaces is indicated. ESA

N94-25306# Sheffield Univ. (England). Dept. of Automatic Control and Systems Engineering.
APPROXIMATION TO NONLINEAR EQUATIONS USING NONLINEAR RATIONAL MODELS
Q. M. Zhu and S. A. Billings Aug. 1992 24 p
(Grant SERC-GR/F-2417.7)
(RR-448; ETN-94-95128) Avail: CASI HC A03/MF A01

The feasibility of approximating several nonlinear dynamic equations which dominate several engineering disciplines is investigated. A nonlinear rational model formulation is used. The purpose is to describe typical nonlinear stochastic dynamics in engineering systems. The studies are based on identification from input and output data rather than analytical transformation from a nonlinear equation to a nonlinear rational model. The results show that the rational model can be used to approximate discontinuous nonlinear elements. ESA

N94-25309 Sheffield Univ. (England). Dept. of Automatic Control and Systems Engineering.
FIXED POINTS AND SHIFT CYCLES IN CELLULAR AUTOMATA
S. P. Banks and S. Djirar Sep. 1992 20 p Limited Reproducibility: More than 20% of this document may be affected by microfiche quality
(RR-459; ETN-94-95131) Avail: CASI HC A03

A technique for determining fixed points and shift cycles in one and two dimensional cellular automata based on graph theory is given. The technique uses the theory of graphs and applies to both one and two dimensional systems. The method produces an easily computable result to be implemented on a computer. Graphs as finite state machines were used in the computation theory of cellular automata, but not for detecting fixed points. One dimensional problems for a rule of any length and the case of a 5 bit two dimensional rule with periodic boundary conditions are considered. ESA

N94-25310# Sheffield Univ. (England). Dept. of Automatic Control and Systems Engineering.
ON THE INVERSION OF THE n-DIMENSIONAL LAPLACE TRANSFORM
S. P. Banks and A. Moser Sep. 1992 26 p
(RR-461; ETN-94-95132) Avail: CASI HC A03/MF A01

The inversion of the multidimensional Laplace transform by a combination of a general partial fraction expansion formula and the theory of residues is studied. The ideas may be applied to nonlinear systems defined by the Volterra series. The main objective is to develop a generalization of the ordinary one dimensional Laplace transform theory to the n dimensional case. This involves a generalized partial fraction expansion theory using the techniques of ideal theory. The theory of residues is applied to compute the inverse transforms of the resulting quotient forms in which the denominators are irreducible polynomials in C(sup n)(X) to emphasize the connection with the Laplace variables. ESA

N94-25318# Sheffield Univ. (England). Dept. of Automatic Control and Systems Engineering.
FREQUENCY RESPONSE FUNCTIONS FOR NONLINEAR RATIONAL MODELS
H. Zhang, S. A. Billings, and Q. M. Zhu 16 Mar. 1993 32 p
(Grant SERC-GR/F-8564.2)
(RR-471; ETN-94-95138) Avail: CASI HC A03/MF A01

A recursive algorithm defined as the ratio of two polynomial functions is derived using the harmonic expansion method. The algorithm maps a general class of nonlinear rational model into the frequency domain. The algebric expression enables the frequency response behavior to be related to the structure and parameters of the corresponding time domain model. The new algorithm provides a direct analytic map from the time domain rational model parameters to the higher order frequency response functions. Complex nonlinear time domain behaviors can be analyzed and interpreted in the frequency domain. Examples to illustrate the concepts involved are included. ESA

N94-25320# Sheffield Univ. (England). Dept. of Automatic Control and Systems Engineering.
RELATIONSHIP BETWEEN THE STRUCTURE AND PERFORMANCE OF IDENTIFIED NONLINEAR POLYNOMIAL MODELS
L. A. Aguirre and S. A. Billings May 1993 60 p
(Grants CNPq-200597/90-6; SERC-GR/H-35286)
(RR-474; ETN-94-95140) Avail: CASI HC A04/MF A01

The effect of the structure of identified nonlinear polynomial models on the dynamical behavior of such models is investigated. The effects of the sampling rate, the number of process terms and the order of the models are studied and input design is considered. Bifurcation diagrams and Poincare sections are used. The identified models were estimated from data generated by the Duffing-Ueda equation. The identified models are compared to the original system over a wide range of parameter values for which the Duffing-Ueda equation exhibits regular oscillations, period doubling cascades, pitchfork bifurcations, and chaos. ESA

N94-25324# Oxford Univ. (England). Dept. of Engineering Science.
BALANCED TRUNCATION IS HANKEL-NORM OPTIMAL WHEN USED TO APPROXIMATE A FINITE-DIFFERENCE MODEL OF A PARABOLIC PDE
Denis Mustafa 3 Apr. 1992 6 p Presented at the 31st IEEE Conference on Decision and Control
(OUEL-1921/92; ETN-94-95145) Avail: CASI HC A02/MF A01

A standard finite difference model for a parabolic Partial Differential Equation (PDE) is developed. The model is shown to belong to a class of state space systems whose balanced approximants are optimal with respect to the Hankel norm. ESA

N94-25334# International Centre for Theoretical Physics, Trieste (Italy).
ON A NEW FUNCTIONAL INTEGRAL FORMALISM FOR HUBBARD MODEL
Hoang Anh Tuan (Institute of Theoretical Physics, Hanoi, Viet Nam.), Nguyen Toan Thang (Institute of Theoretical Physics, Hanoi, Viet Nam.), and Nguyen Ngoc Thuan Sep. 1992 7 p
(DE93-614017; IC-92/276) Avail: CASI HC A02/MF A01 (US Sales Only)

By using the functional integral perturbative theory proposed by Sarker, we have derived the system of self-consistent equations for renormalized Green function of electron in strongly correlated electron system. DOE

N94-25338# Joint Inst. for Nuclear Research, Dubna (USSR). Lab. of Theoretical Physics.
THE CASIMIR ENERGY OF THE RIGID STRING WITH MASSIVE ENDS
V. V. Nesterenko and N. R. Shvets 1991 16 p Submitted for publication
(DE93-616851; JINR-E-2-91-566) Avail: CASI HC A03/MF A01 (US Sales Only)

The Casimir energy in the rigid string with massive ends is investigated. This system models the flux tube of finite thickness that connects the massive quarks. The string and quark mass give additive contributions to the Casimir energy, the second contribution being the same as in the Nambu-Goto string with massive ends. The string hardness results in an additional positive contribution to the Casimir energy, however, it alone does not compensate the negative Casimir energy in the Nambu-Goto string. Only common consideration of the string thickness and the quark mass enables one to get the positive Casimir energy, i.e. to remove the tachyon from the string spectrum. DOE

N94-25433 International Centre for Theoretical Physics, Trieste (Italy).
EXTENSION PROBLEM FOR GENERALIZED MULTI-MONOGENIC FUNCTIONS IN CLIFFORD ANALYSIS
Tran Quyet Thang Oct. 1992 10 p Limited Reproducibility: More than 20% of this document may be affected by microfiche quality
(DE93-616818; IC-92/343) Avail: CASI HC A02 (US Sales Only)

The main purpose of this paper is to extend some properties of multi-monogenic functions, which are a generalization of monogenic functions in higher dimensions, for a class of functions satisfying Vekua-type generalized Cauchy-Riemann equations in Clifford analysis. It is proved that the Hartogs theorem is valid for these functions. DOE

N94-25434 International Centre for Theoretical Physics, Trieste (Italy).
THE LEAST ENERGY CRITICAL SET
Le Dung Oct. 1992 24 p Limited Reproducibility: More than 20% of this document may be affected by microfiche quality
(DE93-616820; IC-92/363) Avail: CASI HC A03 (US Sales Only)

We present a procedure for finding the least energy critical set of functional and then study the existence and boundedness of the solutions of strongly degenerate quasilinear elliptic equations. DOE

N94-25452# Army Topographic Engineering Center, Fort Belvoir, VA.
EDGE DETECTION USING A COMPLEX WAVELET
Richard A. Hevenor and Eugene A. Margerum Dec. 1993 10 p
(AD-A273699; TEC-R-200) Avail: CASI HC A02/MF A01

A complex wavelet of the form Psi(x, y) = C(x jy)exp(-p(x-sq + y-sq)) wavelet transform to obtain edges from a digital image in two orthogonal directions. In the above equation Psi(x, y) is a two dimensional complex wavelet, C and p are constants, j is the square root of -1, and x and y are position variables. The square root of the sum of the squares of the real and imaginary parts of the wavelet transform are used to find the edges in an arbitrary direction. Theoretical models are derived for the cases of a step edge and a ramp edge. The computer implementation of the wavelet edge detector involves the creation of two masks; one for the real part and one for the imaginary part. An expression is derived for the size of the edge masks using the inflection points of a curve derived from the wavelet. Finally, the edge detector is applied to two synthetic aperture radar images and the resulting images are shown. DTIC

N94-25473 International Centre for Theoretical Physics, Trieste (Italy).
ORBIT SPACES OVER COMMUTATIVE RINGS AND PROJECTIVES AS SEMI-ISOMORPHISMS
H. N. Bhattarai Nov. 1992 9 p Limited Reproducibility: More than 20% of this document may be affected by microfiche quality
(DE93-616822; IC-92/400) Avail: CASI HC A02 (US Sales Only)

For a free module of finite rank over a commutative (local) ring, the group of projectivities of the associated projective space is shown to be isomorphic to the group of geometric semi-isomorphisms of the associated geometric space of orbits. DOE

N94-25527# Technische Univ., Eindhoven (Netherlands). Dept. of Mathematics and Computing Science.
A REACHABILITY TEST FOR SYSTEMS OVER POLYNOMIAL RINGS USING GROEBNER BASES
L. C. G. J. M. Habets 8 Sep. 1992 23 p Submitted for publication Sponsored by Netherlands Organization for Scientific Research
(MEMO-COSOR-92-38; ETN-94-94799; PB94-126588) Avail: CASI HC A03/MF A01

The conditions for the reachability of a system over a polynomial ring are verified. It is shown how the Groebner bases method makes it possible to carry out the test. The algorithm presented has the advantage of a good performance of both reachable and non-reachable systems. The method can be used to obtain a right or left inverse of a general non-square polynomial matrix. Such inverse matrices are often required for the design of feedback compensators. A modification of the reachability test is given to speed up the computations in the non-reachable case. The concept of reachability and the conditions under which a system over a polynomial ring is reachable are reviewed. It is shown how the reachability test can be speeded up by applying the algorithm recursively. The effectiveness of the proposed methods is illustrated. ESA

65 STATISTICS AND PROBABILITY

Includes data sampling and smoothing; Monte Carlo method; and stochastic processes.

N94-22702# Universiteit Twente, Enschede (Netherlands). Faculty of Applied Mathematics.
ON SOME APPROXIMATELY BALANCED COMBINATORIAL COOPERATIVE GAMES
U. Faigle and W. Kern Feb. 1993 16 p
(MEMO-1113; ETN-94-94750) Avail: CASI HC A03/MF A01

A model of taxation for cooperative n person games is introduced where proper coalitions are taxed proportionally to their value. Games with non empty core under taxation at rate epsilon are epsilon balanced. Sharp bounds on epsilon in matching games on (not necessarily bipartite) graphs are established. Upper and lower bounds on the best epsilon in bin packing games are derived and euclidean random traveling salesman problem games are seen to be, with high probability, epsilon balanced for epsilon approximately equal to 0.06. ESA

N94-22724# Universiteit Twente, Enschede (Netherlands). Faculty of Applied Mathematics.
LOSS PROBABILITIES IN BATCH-ARRIVAL BULK-SERVICE QUEUES WITH FINITE CAPACITY
J. C. W. vanOmmeren Dec. 1992 11 p
(MEMO-1106; ETN-94-94742) Avail: CASI HC A03/MF A01

Buffer overflow is an important problem in communication and production systems. For the case where batches arrive according to a Poisson process and the service is in geometrically distributed batches, a method to find the exact loss probability is derived. An asymptotic approximation for the loss probability is also derived. Numerical experiments indicate that the buffer sizes needed to achieve a specified loss probability increase when the expected service batch size increases and the offered load is kept constant. ESA

N94-22728# Universiteit Twente, Enschede (Netherlands). Faculty of Applied Mathematics.
NONLINEAR SMOOTHING FOR RANDOM FIELDS
Shin Ichi Aihara (Science Univ. of Tokyo, Japan.) and Arunabha Bagchi Jan. 1993 22 p
(MEMO-1110; ETN-94-94746) Avail: CASI HC A03/MF A01

Stochastic nonlinear elliptic partial differential equations with white noise disturbances are studied in the countably additive measure set up. Introducing the Onsager-Machlup function to the system model, the smoothing problem for maximizing the modified likelihood functional is solved and the explicit form of nonlinear smoother is presented in the finitely additive observation noise set up. ESA

N94-23108# Technische Univ., Twente (Netherlands). Tele-Informatics and Open Systems Group.
SIMPLE CALCULUS OF FINITE PROBABILISTIC PROCESSES
D. Latella 1993 20 p
(PB93-223782; TIOS-93/08) Copyright Avail: CASI HC A03/MF A01

A simple language of finite probabilistic processes is presented. Its formal syntax and interleaving semantics are provided. The relation between the language and a subset of LOTOS is discussed, and it is proven to be testing equivalence. Finally, some examples are given. NTIS

N94-23142# Technische Univ., Eindhoven (Netherlands). Dept. of Mathematics and Computing Science.
ON THE ASYMPTOTICALLY UNIFORM DISTRIBUTION MODULO 1 OF EXTREME ORDER STATISTICS
R. J. G. Wilms and J. J. A. M. Brands Jan. 1993 19 p Revised

(MEMO-COSOR-91-38-Rev; ETN-94-94793) Avail: CASI HC A03/MF A01

Let (x(sub m))(sub 1)(sup infinity) be a sequence of independent and identically distributed random variables. Sufficient conditions are given for the fractional part of max(x(sub 1),..., x(sub n)) to converge in distribution, as n approaches infinity, to a random variable with a uniform distribution on the interval (0, 1) closed to the left. ESA

N94-23143# Technische Univ., Eindhoven (Netherlands). Dept. of Mathematics and Computing Science.

ON NON-INFORMATIVENESS IN A CLASSICAL BAYESIAN INFERENCE PROBLEM

F. P. A. Coolen Sep. 1992 16 p

(MEMO-COSOR-92-35; ETN-94-94796) Avail: CASI HC A03/MF A01

Not only between frequentists and Bayesians, but also among Bayesians, there is discrepancy on the answer of the essential question: given s successes in n previous trials, what is the probability of success at the next trial (all trials identical and independent). The Bayesian answer to this problem is discussed considering noninformative prior subjective data. Paradoxes related to this problem are discussed. The actual paradox seems to be that the feeling about using subjective information additional to real data that have become available depends on these data, which is not allowed in the Bayesian framework. ESA

N94-23440# Technische Univ., Eindhoven (Netherlands). Dept. of Mathematics and Computing Science.

LIMITING DISTRIBUTION OF FRACTIONAL PARTS OF EXTREME ORDER STATISTICS

R. J. G. Wilms Apr. 1993 21 p

(PB93-237733; MEMO-COSOR-93-13) Avail: CASI HC A03/MF A01

Let X sub 1, X sub 2, ... be a sequence of independent and identically distributed random variables with distribution function F, and suppose that F belongs to the domain of attraction of an extreme value distribution. The author gives (additional) sufficient conditions on F for the fractional part of max (X sub 1, ..., X sub n) to converge in distribution to a random variable with a uniform distribution on (0, 1), or to diverge in distribution as n approaches infinity. NTIS

N94-23546# Technische Univ., Eindhoven (Netherlands). Dept. of Mathematics and Computing Science.

SUBSET SELECTION FOR THE BEST OF TWO POPULATIONS: TABLES OF THE EXPECTED SUBSET SIZE

Paul vanderLaan and Constance vanEeden (British Columbia Univ., Vancouver.) Jan. 1993 19 p

(PB93-237857; MEMO-COSOR-93-01) Avail: CASI HC A03/MF A01

Assume two independent populations are given. The associated independent random variables have Normal distributions with unknown expectations theta (1) and theta (2), respectively, and known common variance sigma(squared). The selection goal of Gupta's subset selection for two populations is to select a non-empty subset which contains the best, in the sense of largest expectation, population with confidence level P*(1/2 less than P* less than 1). In Van der Laan and Van Eeden, a generalized selection goal has been introduced and investigated. In the report, extended tables with values of the expected subset size are given. NTIS

N94-23749# Technische Hogeschool Twente, Enschede (Netherlands). Tele-Informatics and Open Systems Group.

MEAN-VALUE OF PRODUCT-FORM STOCHASTIC PETRI NET MODELS OF SLOTTED-RING SYSTEMS

A. J. Coyle (Adelaide Univ., Australia.), B. R. Haverkort, W. Henderson (Adelaide Univ., Australia.), and C. E. M. Pearce (Adelaide Univ., Australia.) 1993 27 p

(PB94-110871; TIOS-93/22) Copyright Avail: CASI HC A03/MF A01

The paper offers a mean-value analysis (MVA) approach for the solution of product-form stochastic Petri net models of slotted-ring systems. It presents the exact product form solution, and from that, develops the MVA recursion scheme. The presented MVA allows for the movement of batches of customers rather than just individual customers, as is the case in the traditional MVA schemes. Furthermore, the MVA allows for non-disjoint place invariants whereas previous MVA schemes always addressed only disjoint ones. Apart from the MVA recursive relations, it gives details on the implementation of these relations. The advantage of an MVA approach is that it usually allows for much larger models to be solved than the usual numerical solution based on the global balance equations would. The MVA is demonstrated by the analysis of a number of fairly large models for slotted-ring systems. NTIS

N94-23771 Technische Univ., Eindhoven (Netherlands). Dept. of Mathematics and Computing Science.

MAXIMAL TYPE TEST STATISTICS BASED ON CONDITIONAL PROCESSES

Jan Beirlant (Katholieke Univ. te Leuven, Belgium.) and John H. J. Einmahl Jun. 1993 27 p Limited Reproducibility: More than 20% of this document may be affected by poor print and microfiche quality

(PB94-111614; MEMO-COSOR-93-17) Avail: Issuing Activity (National Technical Information Service (NTIS))

A general methodology is presented for non-parametric testing of independence, location, and dispersion in multiple regression. The proposed testing procedures are based on the concepts of conditional distribution function, conditional quantile, and conditional shortest t-fraction. Techniques involved come from empirical process and extreme-value theory. The asymptotic distributions are standard Gumbel. NTIS

N94-23772 Technische Univ., Eindhoven (Netherlands). Dept. of Mathematics and Computing Science.

DECISION MAKING WITH IMPRECISE PROBABILITIES

F. P. A. Coolen Jul. 1993 17 p Limited Reproducibility: More than 20% of this document may be affected by poor print and microfiche quality

(PB94-111622; MEMO-COSOR-93-18) Avail: Issuing Activity (National Technical Information Service (NTIS))

In many decision problems the only information available about a random event is expert opinion. The theory of imprecise probabilities, a generalization of standard subjective probability, allows one to deal with such information. The use of imprecise probabilities is discussed, with emphasis on elicitation and combination of opinions and decision making, and some recent results are briefly mentioned. NTIS

N94-23774 Technische Univ., Eindhoven (Netherlands). Dept. of Mathematics and Computing Science.

ASYMPTOTIC CONFIDENCE INTERVALS FOR THE LENGTH OF THE SHORTT UNDER RANDOM CENSORING

Jan Beirlant and John H. J. Einmahl Feb. 1993 14 p Limited Reproducibility: More than 20% of this document may be affected by microfiche quality

(PB93-237816; MEMO-COSOR-93-03) Avail: Issuing Activity (National Technical Information Service (NTIS))

A shortt of a one dimensional probability distribution is defined to be an interval which has at least probability t and minimal length. The length of a shortt and its obvious estimator are significant measures of scale of a distribution and the corresponding random sample, respectively. In this note, a non-parametric asymptotic confidence interval for the length of the (uniqueness is assumed) shortt is established in the random censorship from the right model. The estimator of the length of the shortt is based on the product-limit (PL) estimator of the unknown distribution function. The proof of the result mainly follows from an appropriate combination of the Glivenko-Cantelli theorem and the functional central limit theorem for the PL estimator. NTIS

N94-23798 Technische Univ., Eindhoven (Netherlands). Dept. of Mathematics and Computing Science.

SUBSET SELECTION WITH A GENERALIZED SELECTION GOAL BASED ON A LOSS FUNCTION

Paul vanDerLaan and Constance vanEeden (British Columbia Univ., Vancouver.) Jun. 1993 27 p Limited Reproducibility: More than 20% of this document may be affected by poor print and microfiche quality

(PB94-111192; MEMO-COSOR-93-15) Avail: Issuing Activity (National Technical Information Service (NTIS))

Assume k (integer k greater than or equal to 2) populations are given. The associated independent random variables have continuous distribution functions with an unknown location parameter. The selection goal is to select a non-empty subset which contains the best, in the sense of largest location parameter, population with confidence level P* (k(exp -1) less than P* less than 1). In this paper a generalized selection goal based on a general loss function is presented. This new loss function takes into account the difference, in parameter value, between the best population in the selected subset and the best of all k populations minus epsilon (epsilon greater than or equal to 0); it is zero if an epsilon-best population is an element of the subset. An epsilon-best population is any population with a parameter value within epsilon of the value of the largest parameter. The generalized selection goal is thought to be of great value from an application point of view. The subset selection goal of Gupta is a special case of the introduced generalized selection goal. The special case of two normal populations is studied in detail. NTIS

N94-23814 Tilburg Univ. (Netherlands). Dept. of Economics.

FIRST ORDER CONDITIONS FOR THE MAXIMUM LIKELIHOOD ESTIMATION OF AN EXACT ARMA MODEL

J. vanderLeeuw 1993 31 p See also PB93-138014 Limited Reproducibility: More than 20% of this document may be affected by microfiche quality

(PB94-110533; FEW-611) Avail: Issuing Activity (National Technical Information Service (NTIS))

Using the exact covariance matrix of ARMA(p,q) errors, first order conditions for the parameters are derived and solved. This is done for the pure MA case, the pure AR case and the general ARMA model. The approach applies both to maximum likelihood and minimum distance estimation. The exact covariance is written in the form of lag matrices, which can simply be differentiated. The resulting first order conditions have at least one solution. The difference between maximum likelihood and minimum distance estimation amounts to a function of the elements of the covariance matrix. This function is simple in case of the pure MA or AR case, but more complicated in the general ARMA case. Of course, the solution for the AR and MA parameters are in general conditional. Only in the pure MA and AR case of a time series model without explanatory variables direct solutions are found. NTIS

N94-23815# Technische Univ., Eindhoven (Netherlands). Dept. of Mathematics and Computing Science.

INFINITE DIVISIBLE AND STABLE DISTRIBUTIONS MODULO 1

R. J. G. Wilms Jul. 1993 26 p See also N92-20184 and PB93-237824

(PB94-110640; MEMO-COSOR-93-22) Avail: CASI HC A03/MF A01

In his 1983 paper, Schatte studied infinite divisibility modulo 2pi (mod 2pi). He gave a representation theorem for infinite divisible (infdiv) (mod 2pi) Fourier-Stieltjes Sequences (FSS's) and a limit theorem for sequences of infdiv (mod 2pi) FSS's. Furthermore, under an infinite smallness (mod 2pi) condition he considered convergence of sums to infdiv (mod 2pi) distributions. We consider distributions modulo 1 (mod 1). In Section 2, we give some notations, definitions, and properties of FSS's, and in Section 3 we reformulate Schatte's results for infdiv (mod 1) distributions. From Schatte's representation, we deduce in Section 4 two other representations: one similar to the Levy-Khinchine canonical form, and the other to the Kilmogorov canonical form. In addition, we give a new characterization of infdiv (mod 1) distributions and characterize these distributions in two theorems. Finally, in Section 6, we generalize a limit theorem proved by Schatte. NTIS

N94-24508 Technische Univ., Eindhoven (Netherlands). Dept. of Mathematics and Computing Science.

TAIL PROCESSES UNDER HEAVY RANDOM CENSORSHIP WITH APPLICATIONS

John H. J. Einmahl and Fritz H. Ruymgaart (Texas Technological Univ., Lubbock.) Jul. 1993 18 p Limited Reproducibility: More than 20% of this document may be affected by microfiche quality

(Grant NATO-CRG-910397)

(PB94-110632; Memo-COSOR-93-23) Avail: Issuing Activity (National Technical Information Service (NTIS))

The authors consider a type of heavy random censoring where the number of uncensored observations still tends to infinity. Under natural conditions the life distribution can be locally analyzed by generalizing tail empirical processes to the heavily censored case. A uniform central limit theorem for the tail product-limit process and the tail empirical cumulative hazard process is established. Statistical applications include a local confidence band for the cumulative life distribution and a test concerning the value of its density at the origin. NTIS

N94-24560# Harvard Univ., Cambridge, MA. Dept. of Statistics.

BOUNDS AND ASYMPTOTIC EXPANSIONS FOR SOLUTIONS OF THE FREE BOUNDARY PROBLEMS RELATED TO SEQUENTIAL DECISION VERSIONS OF A BIOEQUIVALENCE PROBLEM

John Bather and Herman Chernoff 23 Nov. 1993 58 p

(Contract N00014-91-J-1005)

(AD-A273551; TR-ONR-C-15) Avail: CASI HC A04/MF A01

The numerical solutions of two related variations of a sequential version of a form of the bioequivalence problem was presented in a report by Hwang. In that report he referred to our unpublished results bounding the solutions and providing asymptotic expansions. The present report has two major functions. One is to derive and amplify these results, and incidentally to correct an error. The second is to gather together in one place, and with relatively little of the abbreviation characteristics of previous publications, many of the details that are useful in deriving the asymptotic expansions. In Hwang's report he presented the Bayesian decision theoretic approach in which the problem is related to a stopping problem involving Brownian motion, a stopping cost represented by a single cost parameter c, and an initial point (y,s) depending on the prior normal distribution of an unknown parameter and other known parameters of the problem. The solution of the problem is represented by dividing up the set ((y,s):s greater than 0) into a continuation set C and a stopping set S. DTIC

N94-24571 Technische Univ., Eindhoven (Netherlands). Dept. of Mathematics and Computing Science.

PROBABILISTIC METHODS IN PROBLEMS OF APPLIED ANALYSIS

F. W. Steutel Aug. 1993 18 p Limited Reproducibility: More than 20% of this document may be affected by microfiche quality

(PB94-110681; MEMO-COSOR-93-24) Avail: CASI HC A03

This paper presents some, mostly rather recent, situations where methods from probability theory have been used to prove results in non-stochastic problems of (applied) analysis. Applications are given from three areas of probability including brief applications of the law of large numbers and of infinite divisibility, a more extensive application involving Poisson processes, and the central limit theorem. The three areas of application are approximation theory, deconvolution of positive functions, and a description and solution of a problem concerning of the breakdown of insulator gases by ionization. Section 2 contains a review of some probability concepts, and Sections 3, 4, and 5 discuss the three applications mentioned previously. NTIS

N94-24634 Tilburg Univ. (Netherlands). Dept. of Information Systems and Auditing.

TWO-STAGE VERSUS SEQUENTIAL SAMPLE-SIZE DETERMINATION IN REGRESSION ANALYSIS OF SIMULATION EXPERIMENTS

Jack P. C. Kleijnen and Willem vanGroenendaal 1993 38 p Limited Reproducibility: More than 20% of this document may be affected by microfiche quality

(PB94-110558; FEW-572) Avail: Issuing Activity (National Technical Information Service (NTIS))

In practice, simulation models usually have responses with variances that vary with the inputs. Then the number of observations (also called simulation runs or replications) per combination of simulation inputs can be selected such that the variances of the average simulation responses become (approximately) equal; in other words, combinations with high variability are replicated more often. These average responses can be analyzed through a regression metamodel. To estimate the regression parameters (or simulation input effects), Weighted Least Squares (WLS) can be applied. WLS becomes identical to Ordinary Least Squares (OLS) applied to the average simulation responses. Because the response variances are unknown, they are estimated by repeating the simulation runs with different random numbers. The estimated response variances yield the number of runs required to obtain approximately equal variances per average simulation response. Two rules for selecting the required number of simulation runs are presented, namely a two-stage and a sequential rule. The rules are first formalized and analyzed, and then evaluated through a Monte Carlo experiment. Both procedures turn out to yield confidence intervals for the estimated regression parameters that have acceptable coverage probabilities. NTIS

N94-24639 Leiden Univ. (Netherlands). Div. of Applied Mathematics.
RAO-BLACKWELL THEOREM IN STEREOLOGY AND SOME COUNTEREXAMPLES
A. J. Baddeley (Center for Mathematics and Computer Science, Amsterdam, Netherlands.) and L. M. Cruz-Orive (Bern Univ., Switzerland.) 1993 21 p Sponsored by Schweizerischer Nationalfonds zur Foerderung der Wissenschaftlichen Forschung Limited Reproducibility: More than 20% of this document may be affected by poor print and microfiche quality
(PB94-111713; TW-93-07) Avail: Issuing Activity (National Technical Information Service (NTIS))

A version of the Rao-Blackwell theorem is shown to apply to most, but not all, stereological sampling designs. Estimators based on random test grids typically have larger variance than quadrat estimators; random s-dimensional samples are worse than random r-dimensional samples for s less than r. Furthermore, the standard stereological ratio estimators of different dimensions are canonically related to each other by the Rao-Blackwell process. However, there are realistic cases where sampling with a lower-dimensional probe increases efficiency. For example, estimators based on (conditionally) non-randomized test point grids may have smaller variance than quadrat estimators. Relative efficiency is related to issues in geostatistics and the theory of wide-sense stationary random fields. NTIS

N94-24744 Vrije Univ., Amsterdam (Netherlands). Dept. of Mathematics and Computer Science.
GENERAL OPTIMAL STOPPING THEOREMS FOR SEMI-MARKOV PROCESSES
Jose M. Gouweleeuw and Frans A. Boshuizen (Erasmus Univ., Rotterdam, Netherlands.) Dec. 1992 33 p Prepared in cooperation with Erasmus Univ. Limited Reproducibility: More than 20% of this document may be affected by microfiche quality
(PB93-214989; WS-406) Avail: Issuing Activity (National Technical Information Service (NTIS))

Optimal stopping problems for semi-Markov processes are studied in a fairly general setting. In such a process, transitions are made from state to state in accordance with a Markov chain, but the amount of time spent in each state is random. The times spent in each state follow a general renewal process. They may depend on the present state as well as on the state into which the next transition is made. The goal is to maximize the net return, which is given as a function of the state at time t minus some cost function. Discounting may or may not be considered. The main theorems (Theorem 3.3 and 3.10) are expressions for the optimal stopping time in the undiscounted and discounted case. These theorems generalize results of Zuckerman, and Boshuizen and Gouweleeuw. Applications are given in various special cases. The results developed in this paper can also be applied to semi-Markov shock models, as considered in papers by Taylor, Feldman, and Zuckerman. NTIS

N94-24778# Naval Command, Control and Ocean Surveillance Center, San Diego, CA. Research, Development, Technology and Evaluation Div.
EVOLVING RECURRENT PERCEPTRONS Professional Paper
John R. McDonnell and Don Waagen Oct. 1993 14 p
(AD-A273241) Avail: CASI HC A03/MF A01

This work investigates the application of evolutionary programming, a multi-agent stochastic search technique, to the generation of recurrent perceptrons (nonlinear IIR filters) for time-series prediction tasks. The evolutionary programming paradigm is discussed and analogies are made to classical stochastic optimization methods. A hybrid optimization scheme is proposed based on multi-agent and single-agent random optimization techniques. This method is then used to determine both the model order and weight coefficients of linear, nonlinear, and parallel linear-nonlinear next-step predictors. The AIC is used as the cost function to score each candidate solution. DTIC

N94-24931# Oregon State Univ., Corvallis. Dept. of Mathematics.
TOPICS IN PROBABILITY AND DYNAMICS Final Report, 1 Apr. 1990 - 31 Mar. 1993
Robert Burton, Jr. 31 Mar. 1993 6 p
(Grant AF-AFOSR-0251-90)
(AD-A273543; AFOSR-93-0873TR) Avail: CASI HC A02/MF A01

Progress on problems on multivariate aging of systems and components and the modeling of conjunction, separation and magnetization of reliability systems was significant, as judged by acceptance and publication of over 15 papers on these areas. A specific result was that the statistical malfunction content of a positively dependent random variable is larger than the information content of independent random variables. DTIC

N94-24951# Rome Lab., Griffiss AFB, NY.
CORRELATION FUNCTION ESTIMATOR PERFORMANCE IN NON-GAUSSIAN SPHERICALLY INVARIANT RANDOM PROCESSES
James H. Michels Oct. 1993 32 p
(AF Proj. 2304)
(AD-A273498; RL-TR-93-179) Avail: CASI HC A03/MF A01

In this report, analytic expressions are developed for the variance, error variance, and bias of the time-averaged correlation function estimator for stationary, discrete, non-Gaussian complex processes. The expressions derived here pertain to the general class of non-Gaussian processes known as Spherically Invariant Random Processes (SIRP's). Specific results are shown for K-distributed processes which form a special case of the SIRP's. Furthermore, these equations are derived for the general case of processes with unconstrained quadrature components; i.e., for processes exhibiting elliptical symmetry. For the special case of complex processes with constrained correlation between the quadrature components (i.e., circular symmetry), the resulting analytic expressions attain a simplified form. Validity of the analytic expressions is presented using Monte-Carlo simulations. DTIC

N94-25147 Tennessee Univ., Knoxville. Dept. of Mathematics.
INFINITELY DIVISIBLE PROCESSES AND THEIR NONLINEAR FUNCTIONALS; A STUDY OF THEIR STRUCTURAL, STATISTICAL AND SAMPLE PATH PROPERTIES AND THEIR PREDICTION PROBLEMS Final Report, 1 Mar. 1990 - 28 Feb. 1993
Balram Rajput 28 Feb. 1993 8 p Limited Reproducibility: More than 20% of this document may be affected by microfiche quality
(Grant AF-AFOSR-0168-90)
(AD-A273468; AFOSR-93-0871TR) Avail: Issuing Activity (Defense Technical Information Center (DTIC))

During the period of research for this grant, accomplishments were made in the following areas: (1) tail behavior of certain probability laws, and the behavior of Gaussian laws of translated balls; (2) supports and densities of certain infinitely divisible (i.d.) laws and the zero-one dichotomy for certain non-linear functionals of i.d. random vectors; and (3) the best linear predictors for certain i.d. processes. DTIC

N94-25518# Air Force Inst. of Tech., Wright-Patterson AFB, OH.
SOLVING THE RANKING AND SELECTION INDIFFERENCE-ZONE FORMULATION FOR NORMAL DISTRIBUTIONS USING COMPUTER SOFTWARE M.S. Thesis
Catherine A. Poston Dec. 1993 135 p
(AD-A273821; AFIT/GSO/ENS/ENC/93D-12) Avail: CASI HC A07/MF A02

Ranking and selection procedures are statistical methods used to compare and choose the best among a group of similar statistically distributed populations. The two predominant approaches to solving ranking and selection problems are Gupta's subset selection formulation and Bechhofer's indifference-zone formulation. For the indifference-zone formulation where the populations have equal sample sizes, Barr and Rizvi developed an integral expression of the probability of correct selection (PCS). Given appropriate parameters, the integral expression can be solved to determine the common sample size required to attain a desired PCS. Tables with selected solutions to the integral expression are available for a variety of population distributions. These tables, however, are not included in any single reference, sometimes require interpolation, and only provide approximate results for the case of unequal sample sizes. Using a computer software program to solve the integral expression for the unknown parameters can eliminate these burdens. This paper describes the computer software developed to solve the integral expression of the indifference-zone formulation for normally distributed populations having either equal or unequal sample sizes, The software was written in QuickBASIC and Mathematica. The QuickBASIC code is a menu-driven interface that develops input files for Mathematica. Mathematica is the mathematical software package which performs the computationally intensive calculations required to solve the integral expressions. DTIC

N94-25528 Leiden Univ. (Netherlands). Dept. of Mathematics and Computer Science.
ON FINDING OPTIMAL POLICIES FOR MARKOV DECISION CHAINS: A UNIFYING FRAMEWORK FOR MEAN-VARIANCE-TRADEOFFS
Ying Huang and L. C. M. Kallenberg 1992 23 p Revised Limited Reproducibility: More than 20% of this document may be affected by microfiche quality
(TW-92-13; TW-90-10; ETN-94-94831) Avail: CASI HC A03

The existence of optimal policies for maximum one period mean to standard deviation ratio, negative variance with bounded mean and mean penalized by variance Markov decision chains is proven. The chains are reduced to a related mathematical program. This program entails maximizing (xB/D(xb)) + C(xb) over x in a polytope and with given bounds on xb where C and D are convex and either D is constant or D is positive and nondecreasing, C is nondecreasing and xB is nonpositive. This program is reduced to maximizing x(B + theta(b)) over x in the polytope parametrically in theta. Under the nonnegative initial distribution assumption, the rule of constructing a stationary maximum average reward policy from an extreme optimal solution of the associated linear program is generalized. Formulations and existence results for problems discussed by other authors are unified and extended. A computational procedure to solve them, related to another method, is given. ESA

N94-24265 Technion - Israel Inst. of Tech., Haifa. Faculty of Aerospace Engineering.
MAXIMUM LIKELIHOOD MODAL PARAMETER IDENTIFICATION AND REALIZATION OF STOCHASTIC SYSTEMS
Yaakov Oshman and Tal Mendelboim *In* Israel Society of Aeronautics and Astronautics, The 33rd Israel Annual Conference on Aviation and Astronautics 25 Feb. 1993 p 275-286 (For primary document see N94-24241 06-01)
Copyright Avail: Issuing Activity (Israel Society of Aeronautics and Astronautics, c/o Faculty of Engineering, Tel-Aviv Univ., Ramat Aviv 69978, Israel)

N94-24407*# Alabama Univ., Huntsville. Dept. of Industrial Engineering.
RISK IDENTIFICATION AND REDUCTION IN INTEGRATED PRODUCT TEAMS
Robert G. Batson *In its* The 1993 NASA/ASEE Summer Faculty Fellowship Program Nov. 1993 4 p (For primary document see N94-24405 06-80)
Avail: CASI HC A01/MF A03

66 SYSTEMS ANALYSIS

Includes mathematical modeling; network analysis; and operations research.

N94-22708# Universiteit Twente, Enschede (Netherlands). Faculty of Applied Mathematics.
GENERALIZED CONCAVITY IN COOPERATIVE GAME THEORY: CHARACTERIZATIONS IN TERMS OF THE CORE
Theo S. H. Driessen Mar. 1993 20 p Presented at the 4th International Workshop on Generalized Convexity, Pecs, Hungary, 31 Aug. - 2 Sep. 1992
(MEMO-1121; ETN-94-94756) Avail: CASI HC A03/MF A01

A notion of generalized concavity, called k concavity, for cooperative n person cost games is introduced. The k concavity of a cost game is shown to fully characterize the structure of the core of the game and vice versa. The first characterization states that for the k concavity of an n person cost game it is both necessary and sufficient that all the (((n - k) factorial) to the minus 1st power)n factorial so called marginal cost allocations belong to the core of the game. The second characterization states that a cost game is k concave if and only if the core of the game coincides with the specific core catcher, that is the convex hull of the set of all marginal cost allocations in the game. The notion of k concave n person games is illustrated by three examples: the airport game, the location game, and the carpooling game. ESA

N94-22716# Universiteit Twente, Enschede (Netherlands). Faculty of Applied Mathematics.
ON THE REDUCED GAME PROPERTY FOR AND THE AXIOMATIZATION OF THE TAU-VALUE
Theo S. H. Driessen Mar. 1993 16 p
(MEMO-1128; ETN-94-94764) Avail: CASI HC A03/MF A01

The tau value is a one point solution concept for cooperative games in characteristic function form. A particular type of reduced games is introduced. It is established that the tau value possesses the reduced game property with respect to the reduced game presented. That is, there is no inconsistency in what the players of the reduced game receive, either in the original game or in the reduced game, according to the tau value concept. An axiomatic characterization of the tau value is provided by means of the relevant reduced game property. ESA

N94-23764# Vrije Univ., Brussels (Belgium).
STRUCTURED CONSTRAINT SATISFACTION
Z. Ruttkay Dec. 1992 52 p See also PB94-119047
(PB94-119039; IR-316) Avail: CASI HC A04/MF A01

In this report, generalization of the traditional constraint satisfaction problem, the so-called structured constraint satisfaction problem (SCSP) is dealt with: we consider a set of CSPs at the same time, and are aiming at finding a solution for any of the given problems. The set CSPs to be considered are gained by structuring an initially given set of constraints. Boolean, hierarchical, and partial constraint satisfaction problems can be formulated as SCSPs with an appropriate structuring. From the point of view of modeling real problems, an SCSP model is more expressive than a traditional CSP. In addition, by allowing SCSPs some pragmatic drawbacks due to the difficulty of CSP solving may be avoided. For solving a SCSP, the generic scheme of alternating search is proposed, containing alternating steps to generate a traditional CSP and to find a solution of it. We identify the generic tasks of solving SCSPs; we outline different strategies to co-ordinate the alternating search, and discuss measures which can be used to guide the search in the two individual search spaces. NTIS

N94-23800 Technische Univ., Twente (Netherlands). Faculty of Applied Mathematics.
EGALITARIAN NON-AVERAGE CONTRIBUTION METHOD FOR COOPERATIVE GAMES
T. S. H. Driessen and Y. Funaki Jun. 1993 19 p See also N89-23266 Limited Reproducibility: More than 20% of this document may be affected by poor print and microfiche quality
(PB94-111705; MEMO-1135) Avail: Issuing Activity (National Technical Information Service (NTIS))

The first topic is the introduction of a new solution concept for cooperative games, called egalitarian non-average contribution (ENAC) method. The method is based on the egalitarian allocation of the amount that is left of the total profits after each player has already been paid his average contribution. The average contribution of a player represents an average of his part of the joint contribution of any two-person coalition including himself. In addition, the average contribution of any player can be interpreted as an upper core bound derived from the (n - 2)-person coalitions in an n-person game. The second topic is the study of several conditions which are sufficient for the coincidence of the ENAC-solution and the prenucleolus. The main sufficient condition requires that the maximal excesses at the ENAC-solution of an n-person game are determined by the (n - 2)-person coalitions. NTIS

N94-23832*# Jet Propulsion Lab., California Inst. of Tech., Pasadena.
SPACEOPS 1992: PROCEEDINGS OF THE SECOND INTERNATIONAL SYMPOSIUM ON GROUND DATA SYSTEMS FOR SPACE MISSION OPERATIONS
1 Mar. 1993 869 p Symposium held in Pasadena, CA, 16-20 Nov. 1992
(Contract NAS7-918)
(NASA-CR-194486; JPL-Publ-93-5; NAS 1.26:194486) Avail: CASI HC A99/MF A10

The Second International Symposium featured 135 oral presentations in these 12 categories: Future Missions and Operations; System-Level Architectures; Mission-Specific Systems; Mission and Science Planning and Sequencing; Mission Control; Operations Automation and Emerging Technologies; Data Acquisition; Navigation; Operations Support Services;

Engineering Data Analysis of Space Vehicle and Ground Systems; Telemetry Processing, Mission Data Management, and Data Archiving; and Operations Management. Topics focused on improvements in the productivity, effectiveness, efficiency, and quality of mission operations, ground systems, and data acquisition. Also emphasized were accomplishments in management of human factors; use of information systems to improve data retrieval, reporting, and archiving; design and implementation of logistics support for mission operations; and the use of telescience and teleoperations. For individual titles, see N94-23833 through N94-23968.

N94-23833*# National Aeronautics and Space Administration, Washington, DC.
STRATEGIES IN TRANSITION
Alphonso V. Diaz *In* JPL, SpaceOps 1992: Proceedings of the Second International Symposium on Ground Data Systems for Space Mission Operations 1 Mar. 1993 p 1-6 (For primary document see N94-23832 06-66)
Avail: CASI HC A02/MF A10

A new vision has emerged within the Office of Space Science and Applications (OSSA), and within the agency as a whole, for how to design missions to be responsive to the changing budget environment of the 1990s. The overall space science and applications program had to be looked at, restructuring the most expensive and complex projects to bring down costs and ensure their place in the mission queue of the future. The recent restructuring of some of OSSA's largest programs in development and the work to improve efficiency for those in operation is part of OSSA's effort to free funds for more frequent space science missions in the future. Instead of more great observatories, we are looking toward a new vision encompassing a level of great activity through small, frequent missions. The strategy developed for attaining this vision was to lower costs by reducing size and complexity through new technology, while at the same time making progress in space science. The strategy comprises two interwoven parts: the flight program strategy of each of the science disciplines and OSSA's new-technology strategy. The overall purpose of all OSSA's efforts to date has been to free resources for maximizing the space science program in a tough fiscal environment. Derived from text

N94-23834*# European Space Agency. European Space Operations Center, Darmstadt (Germany). Mission Operations Dept.
COMMONALITY OF FLIGHT CONTROL SYSTEMS FOR SUPPORT OF EUROPEAN TELECOMMUNICATIONS MISSIONS c32
Kurt Debatin *In* JPL, SpaceOps 1992: Proceedings of the Second International Symposium on Ground Data Systems for Space Mission Operations 1 Mar. 1993 p 7-14 (For primary document see N94-23832 06-66)
Avail: CASI HC A02/MF A10

This paper is concerned with the presentation of mission-independent software systems that provide a common software platform to ground data systems for mission operations. The objectives of such common software platforms are to reduce the cost of the development of mission-dedicated software systems and to increase the level of reliability of the ground data systems for mission operations. In accordance with this objective, the Multi-Satellite Support System (MSSS) was developed at the European Space Operations Center (ESOC). Between 1975 and 1992, the MSSS provided support to 16 European Space Agency (ESA) missions, among them very demanding science missions such as GEOS, EXOSAT, and Giotto. The successful support of these missions proved the validity of the MSSS concept with its extended mission-independent platform. This paper describes the MSSS concept and focuses on the wide use of MSSS as a flight control system for geosynchronous telecommunications satellites. Reference is made to more than 15 telecommunications missions that are operated from Western Europe using flight control systems with an underlying MSSS concept, demonstrating the benefits of a commonly used software platform. Finally, the paper outlines the design of the new generation of flight control systems, which is being developed at ESOC for this decade, following a period of more than 15 years of MSSS support.
Author (revised)

N94-23835*# National Space Development Agency, Tokyo (Japan).
NASDA'S VIEW OF GROUND CONTROL IN MISSION OPERATIONS c32
Satoshi Tateno *In* JPL, SpaceOps 1992: Proceedings of the Second International Symposium on Ground Data Systems for Space Mission Operations 1 Mar. 1993 p 15-20 (For primary document see N94-23832 06-66)
Avail: CASI HC A02/MF A10

This paper presents an overview of the present status and future plans of the National Space Development Agency of Japan 's (NASDA's) ground segment and related space missions. The described ground segment consists of the tracking and data acquisition (T&DA) system and the Earth Observation Center (EOC) system. In addition to these systems, the current plan of the Engineering Support Center (ESC) for the Japanese Experiment Module (JEM) attached to Space Station Freedom is introduced. Then, NASDA's fundamental point of view on the future trend of operations and technologies in the coming new space era is discussed. Within the discussion, the increasing importance of international cooperation is also mentioned.
Author (revised)

N94-23836*# National Aeronautics and Space Administration, Washington, DC.
FUTURE TRENDS IN NASA SPACE OPERATIONS
Charles F. Fuechsel *In* JPL, SpaceOps 1992: Proceedings of the Second International Symposium on Ground Data Systems for Space Mission Operations 1 Mar. 1993 p 21-23 (For primary document see N94-23832 06-66)
Avail: CASI HC A01/MF A10

It is a great privilege for me to address my colleagues at SpaceOps 92. Today, I would like to share with you some current directions we are pursuing in NASA's Office of Space Communications (OSC). The space agencies of the world have produced some remarkable achievements in conducting our missions. It is also true that we consume significant resources in controlling and operating our spacecraft. In these challenging economic times, the degree to which our agencies can develop new missions will depend on our ability to reduce operating costs. I believe that there are many opportunities for doing this, and I will explore some of our plans in this regard. First, I will review the business of space operations.
Author (revised)

N94-23837*# Centre National d'Etudes Spatiales, Toulouse (France). Div. for Geostationary Satellites.
THE SPACE OPERATIONS AT CNES
Roland Ivarnez *In* JPL, SpaceOps 1992: Proceedings of the Second International Symposium on Ground Data Systems for Space Mission Operations 1 Mar. 1993 p 25-28 (For primary document see N94-23832 06-66)
Avail: CASI HC A01/MF A10

This paper presents an overview of current space operations performed by the French space agency at the Toulouse Space Center. The missions are briefly presented and a description of the architecture of the ground facilities involved in the space operations is provided. The improvements subject to current activity are presented and the associated methods and tools are listed.
Author

N94-23838*# National Aeronautics and Space Administration. Lyndon B. Johnson Space Center, Houston, TX.
COMMON FRONT END SYSTEMS FOR SPACE SHUTTLE AND SPACE STATION CONTROL CENTERS AT JOHNSON SPACE CENTER c32
Linda Uljon and John Muratore *In* JPL, SpaceOps 1992: Proceedings of the Second International Symposium on Ground Data Systems for Space Mission Operations 1 Mar. 1993 p 33-38 (For primary document see N94-23832 06-66)
Avail: CASI HC A02/MF A10

In the beginning of the fiscal year 1992, the development organizations of Johnson Space Center (JSC) were poised to begin two major projects: the Space Station Control Center and the refurbishment of the telemetry processing area of the Space Shuttle Mission Control Center. A study team established that a common front end concept could be used and could reduce development costs for both projects. A standard processor was defined to support most of the front end functions of both control centers and supports a consolidation of control positions which effectively reduces operations cost. This paper defines that common concept and describes the progress that has been made in development of the Consolidated Communications Facility (CCF) during the past year.
Author (revised)

N94-23839*# National Aeronautics and Space Administration. Goddard Space Flight Center, Greenbelt, MD.

MISSION OPERATIONS UPDATE FOR THE RESTRUCTURED EARTH OBSERVING SYSTEM (EOS) MISSION

Angelita Castro Kelly and Edward S. Chang *In* JPL, SpaceOps 1992: Proceedings of the Second International Symposium on Ground Data Systems for Space Mission Operations 1 Mar. 1993 p 39-44 (For primary document see N94-23832 06-66)

Avail: CASI HC A02/MF A10

The National Aeronautics and Space Administration's (NASA) Earth Observing System (EOS) will provide a comprehensive long term set of observations of the Earth to the Earth science research community. The data will aid in determining global changes caused both naturally and through human interaction. Understanding man's impact on the global environment will allow sound policy decisions to be made to protect our future. EOS is a major component of the Mission to Planet Earth program, which is NASA's contribution to the U.S. Global Change Research Program. EOS consists of numerous instruments on multiple spacecraft and a distributed ground system. The EOS Data and Information System (EOSDIS) is the major ground system developed to support EOS. The EOSDIS will provide EOS spacecraft command and control, data processing, product generation, and data archival and distribution services for EOS spacecraft. Data from EOS instruments on other Earth science missions (e.g., Tropical Rainfall Measuring Mission (TRMM)) will also be processed, distributed, and archived in EOSDIS. The U.S. and various International Partners (IP) (e.g., the European Space Agency (ESA), the Ministry of International Trade and Industry (MITI) of Japan, and the Canadian Space Agency (CSA)) participate in and contribute to the international EOS program. The EOSDIS will also archive processed data from other designated NASA Earth science missions (e.g., UARS) that are under the broad umbrella of Mission to Planet Earth. Derived from text

N94-23840*# Jet Propulsion Lab., California Inst. of Tech., Pasadena.

ASTER, A MULTINATIONAL EARTH OBSERVING CONCEPT c43

Graham W. Bothwell, Gary N. Geller, Steven A. Larson, Andrew D. Morrison, and David A. Nichols *In its* SpaceOps 1992: Proceedings of the Second International Symposium on Ground Data Systems for Space Mission Operations 1 Mar. 1993 p 45-50 (For primary document see N94-23832 06-66)

Avail: CASI HC A02/MF A10

The Advanced Spaceborne Thermal Emission and Reflection Radiometer (ASTER) is a facility instrument selected for launch in 1998 on the first in a series of spacecraft for NASA's Earth Observing System (EOS). The ASTER instrument is being sponsored and built in Japan. It is a three telescope, high spatial resolution imaging instrument with 15 spectral bands covering the visible through to the thermal infrared. It will play a significant role within EOS providing geological, biological, land hydrological information necessary for intense study of the Earth. The operational capabilities for ASTER, including the necessary interfaces and operational collaborations between the US and Japanese participants, are under development. EOS operations are the responsibility of the EOS Project at NASA's Goddard Space Flight Center (GSFC). Although the primary EOS control center is at GSFC, the ASTER control facility will be in Japan. Other aspects of ASTER are discussed. Author (revised)

N94-23841*# Canadian Space Agency, Vanier (Ontario). Mobile Servicing System Space Operations.

GROUND OPERATION OF ROBOTICS ON SPACE STATION FREEDOM c37

Z. Alex Wojcik, David G. Hunter, and Marc R. Cantin (KEOPS Informatique, Montreal, Quebec.) *In* JPL, SpaceOps 1992: Proceedings of the Second International Symposium on Ground Data Systems for Space Mission Operations 1 Mar. 1993 p 51-55 (For primary document see N94-23832 06-66)

Avail: CASI HC A01/MF A10

This paper reflects work carried out on Ground Operated Telerobotics (GOT) in 1992 to refine further the ideas, procedures, and technologies needed to test the procedures in a high latency environment, and to integrate GOT into Space Station Freedom operations. Space Station Freedom (SSF) will be in operation for 30 years, and will depend on robots to carry out a significant part of the assembly, maintenance, and utilization workload. Current plans call for on-orbit robotics to be operated by on-board crew members. This approach implies that on-orbit robotics operations use up considerable crew time, and that these operations cannot be carried out when SSF is unmanned. GOT will allow robotic operations to be operated from the ground, with on-orbit crew interventions only when absolutely required. The paper reviews how GOT would be implemented, how GOT operations would be planned and supported, and reviews GOT issues, critical success factors, and benefits. Author (revised)

N94-23842*# Jet Propulsion Lab., California Inst. of Tech., Pasadena.

MISSION PLANNING FOR SHUTTLE IMAGING RADAR-C (SIR-C) WITH A REAL-TIME INTERACTIVE PLANNING SOFTWARE c32

Su K. Potts *In its* SpaceOps 1992: Proceedings of the Second International Symposium on Ground Data Systems for Space Mission Operations 1 Mar. 1993 p 57-62 (For primary document see N94-23832 06-66)

Avail: CASI HC A02/MF A10

The Shuttle Imaging Radar-C (SIR-C) mission will operate from the payload bay of the space shuttle for 8 days, gathering Synthetic Aperture Radar (SAR) data over specific sites on the Earth. The short duration of the mission and the requirement for realtime planning offer challenges in mission planning and in the design of the Planning and Analysis Subsystem (PAS). The PAS generates shuttle ephemerides and mission planning data and provides an interactive real-time tool for quick mission replanning. It offers a multi-user and multiprocessing environment, and it is able to keep multiple versions of the mission timeline data while maintaining data integrity and security. Its flexible design allows one software to provide different menu options based on the user's operational function, and makes it easy to tailor the software for other Earth orbiting missions. Author (revised)

N94-23843*# National Aeronautics and Space Administration. Goddard Space Flight Center, Greenbelt, MD.

SAMPEX PAYLOAD OPERATION CONTROL CENTER IMPLEMENTATION c14

Daniel Mandl, Jack Koslosky, Ron Mahmot, Michael Rackley, and Jack Lauderdale (Computer Sciences Corp., Laurel, MD.) *In* JPL, SpaceOps 1992: Proceedings of the Second International Symposium on Ground Data Systems for Space Mission Operations 1 Mar. 1993 p 63-68 (For primary document see N94-23832 06-66)

Avail: CASI HC A02/MF A10

The Solar Anomolous and Magnetospheric Explorer (SAMPEX) satellite was launched in July 1992. It was the first in the NASA Small Explorer (SMEX) series. In building the real-time control center facility, several new mission support challenges had to be met: CCSDS telemetry and command format, 900 Kbps telemetry data, and shorter turn-around time for control center development than previous missions. The SAMPEX Payload Operations Control Center (POCC) was also the first control center for a new satellite to be based on the Transportable Payload Operations Control Center (TPOCC) system architecture and methodology. This approach has both guided the implementation of the SAMPEX control center and provided some of the building blocks. By using the TPOCC architecture to build the SAMPEX POCC, the real-time operations area was miniaturized into one room, whereas previous missions needed multiple large rooms. The development cost of the SAMPEX POCC was reduced from previous missions and will provide for further cost savings in the future SMEX satellites. This paper describes the system as built and some of the enhancements in progress to create this teleoperations environment. Author (revised)

N94-23844*# European Space Agency. European Space Operations Center, Darmstadt (Germany).

A USER VIEW OF THE EURECA GROUND SEGMENT

Paolo Ferri and Steve J. Kellock *In* JPL, SpaceOps 1992: Proceedings of the Second International Symposium on Ground Data Systems for Space Mission Operations 1 Mar. 1993 p 69-74 (For primary document see N94-23832 06-66)

Avail: CASI HC A02/MF A10

The European Retrievable Carrier (EURECA) was launched on 31 Jul. 1992. It is the largest ESA spacecraft ever launched, and the first one to be launched and retrieved by the NASA Space Shuttle. This paper describes the lessons learned during the first months of utilization of the EURECA ground segment from the point of view of the flight control team. Author (revised)

N94-23845*# Jet Propulsion Lab., California Inst. of Tech., Pasadena.
DEVELOPMENT OF THE CASSINI GROUND DATA SYSTEM IN A MULTIMISSION ENVIRONMENT
G. Madrid and G. Wanczuk *In its* SpaceOps 1992: Proceedings of the Second International Symposium on Ground Data Systems for Space Mission Operations 1 Mar. 1993 p 75-80 (For primary document see N94-23832 06-66)
Avail: CASI HC A02/MF A10

As baselined, the Cassini Ground Data System (GDS) will be composed of Project specific and multimission elements. The former will be developed by the Cassini Project and the latter by two JPL institutional organizations, the Telecommunications and Data Acquisition Office (TDA) and the Multimission Operations Systems Office (MOSO). The GDS will be developed in three principal phases: Spacecraft Test, Launch-cruise, and Science Tour, with a significant part of the development deferred until the post-launch period. New capabilities are being introduced that are key to the achievement of more cost effective operations. Successful development of the system will require careful planning and will involve participation of diverse disciplines. This paper introduces the Cassini Project from the Ground Data System perspective and discusses development approaches expected to produce systems which meet functional and performance requirements and which will be delivered on schedule and within budget. Author (revised)

N94-23846*# Centre National d'Etudes Spatiales, Toulouse (France).
SPOT SATELLITE FAMILY: PAST, PRESENT, AND FUTURE OF THE OPERATIONS IN THE MISSION AND CONTROL CENTER
Pacholczyk Philippe *In* JPL, SpaceOps 1992: Proceedings of the Second International Symposium on Ground Data Systems for Space Mission Operations 1 Mar. 1993 p 81-86 (For primary document see N94-23832 06-66)
Avail: CASI HC A02/MF A10

SPOT sun-synchronous remote sensing satellites are operated by CNES since February 1986. Today, the SPOT mission and control center (CCM) operates SPOT1, SPOT2, and is ready to operate SPOT3. During these seven years, the way to operate changed and the CCM, initially designed for the control of one satellite, has been modified and upgraded to support these new operating modes. All these events have shown the performances and the limits of the system. A new generation of satellite (SPOT4) will continue the remote sensing mission during the second half of the 90's. Its design takes into account the experience of the first generation and supports several improvements. A new generation of control center (CMP) has been developed and improves the efficiency, quality, and reliability of the operations. The CMP is designed for operating two satellites at the same time during launching, in-orbit testing, and operating phases. It supports several automatic procedures and improves data retrieval and reporting. Derived from text

N94-23847*# Mitre Corp., Greenbelt, MD.
A REFERENCE MODEL FOR SPACE DATA SYSTEM INTERCONNECTION SERVICES c32
John Pietras and Gerhard Theis (European Space Agency. European Space Operations Center, Darmstadt, Germany.) *In* JPL, SpaceOps 1992: Proceedings of the Second International Symposium on Ground Data Systems for Space Mission Operations 1 Mar. 1993 p 91-96 (For primary document see N94-23832 06-66)
Avail: CASI HC A02/MF A10

The widespread adoption of standard packet-based data communication protocols and services for spaceflight missions provides the foundation for other standard space data handling services. These space data handling services can be defined as increasingly sophisticated processing of data or information received from lower-level services, using a layering approach made famous in the International Organization for Standardization (ISO) Open System Interconnection Reference Model (OSI-RM). The Space Data System Interconnection Reference Model (SDSI-RM) incorporates the conventions of the OSIRM to provide a framework within which a complete set of space data handling services can be defined. The use of the SDSI-RM is illustrated through its application to data handling services and protocols that have been defined by, or are under consideration by, the Consultative Committee for Space Data Systems (CCSDS). Author (revised)

N94-23848*# Jet Propulsion Lab., California Inst. of Tech., Pasadena.
AN OSI ARCHITECTURE FOR THE DEEP SPACE NETWORK c32
W. Randy Heuser and Lynne P. Cooper *In its* SpaceOps 1992: Proceedings of the Second International Symposium on Ground Data Systems for Space Mission Operations 1 Mar. 1993 p 97-101 (For primary document see N94-23832 06-66)
Avail: CASI HC A01/MF A10

The flexibility and robustness of a monitor and control system are a direct result of the underlying inter-processor communications architecture. A new architecture for monitor & Control at the Deep Space Network Communications Complexes has been developed based on the Open System Interconnection (OSI) standards. The suitability of OSI standards for DSN M&C has been proven in the laboratory. The laboratory success has resulted in choosing an OSI-based architecture for DSS-13 M&C. DSS-13 is the DSN experimental station and is not part of the 'operational' DSN; it's role is to provide an environment to test new communications concepts can be tested and conduct unique science experiments. Therefore, DSS-13 must be robust enough to support operational activities, while also being flexible enough to enable experimentation. This paper describes the M&C architecture developed for DSS-13 and the results from system and operational testing. Author (revised)

N94-23849*# Logica Space and Communications Ltd., London (England).
ATOS-1: DESIGNING THE INFRASTRUCTURE FOR AN ADVANCED SPACECRAFT OPERATIONS SYSTEM c14
K. J. Poulter and H. N. Smith *In* JPL, SpaceOps 1992: Proceedings of the Second International Symposium on Ground Data Systems for Space Mission Operations 1 Mar. 1993 p 103-112 Prepared in cooperation with Logica Ltd., London, England (For primary document see N94-23832 06-66)
Avail: CASI HC A02/MF A10

The space industry has identified the need to use artificial intelligence and knowledge based system techniques as integrated, central, symbolic processing components of future mission design, support and operations systems. Various practical and commercial constraints require that off-the-shelf applications, and their knowledge bases, are reused where appropriate and that different mission contractors, potentially using different KBS technologies, can provide application and knowledge sub-modules of an overall integrated system. In order to achieve this integration, which we call knowledge sharing and distributed reasoning, there needs to be agreement on knowledge representations, knowledge interchange-formats, knowledge level communications protocols, and ontology. Research indicates that the latter is most important, providing the applications with a common conceptualization of the domain, in our case spacecraft operations, mission design, and planning. Agreement on ontology permits applications that employ different knowledge representations to interwork through mediators which we refer to as knowledge agents. This creates the illusion of a shared model without the constraints, both technical and commercial, that occur in centralized or uniform architectures. This paper explains how these matters are being addressed within the ATOS program at ESOC, using techniques which draw upon ideas and standards emerging from the DARPA Knowledge Sharing Effort. In particular, we explain how the project is developing an electronic Ontology of Spacecraft Operations and how this can be used as an enabling component within space support systems that employ advanced software engineering. We indicate our hope and expectation that the core ontology developed in ATOS, will permit the full development of standards for such systems throughout the space industry. Author (revised)

N94-23850*# Jet Propulsion Lab., California Inst. of Tech., Pasadena.
DISTRIBUTED SCIENCE OPERATIONS FOR JPL PLANETARY MISSIONS
Richard D. Benson and Peter B. Kahn *In its* SpaceOps 1992: Proceedings of the Second International Symposium on Ground Data Systems for Space Mission Operations 1 Mar. 1993 p 113-118 (For primary document see N94-23832 06-66)
Avail: CASI HC A02/MF A10

Advances in spacecraft, flight instruments, and ground systems provide an impetus and an opportunity for scientific investigation teams to take direct control of their instruments' operations and data collection while at the same time, providing a cost effective and flexible approach in support of increasingly complex science missions. Operations of science instruments have generally been integrated into planetary flight and ground systems at a very detailed level. That approach has been successful, but the cost of incorporating instrument expertise into the central mission operations system has been high. This paper discusses an approach to simplify planetary science operations by distributing instrument computing and data management tasks from the central mission operations system to each investigator's home center of observational expertise. Some early results of this operations concept will be presented based on the Mars Observer (MO) Project experience and Cassini Project plans. Author (revised)

N94-23851*# European Space Agency. European Space Operations Center, Darmstadt (Germany). Flight Control Systems Dept.
SCOS2: ESA'S NEW GENERATION OF MISSION CONTROL SYSTEMS **c14**
J. F. Kaufeler and N. C. Head *In* JPL, SpaceOps 1992: Proceedings of the Second International Symposium on Ground Data Systems for Space Mission Operations 1 Mar. 1993 p 119-124 (For primary document see N94-23832 06-66)
Avail: CASI HC A02/MF A10

The paper describes the next generation Spacecraft Control System infrastructure (SCOSII) which is being developed at the Operations Centre (ESOC) of the European Space Agency (ESA). The objectives of the new system and selected areas of the proposed hardware and software approach are described. Author

N94-23852*# Jet Propulsion Lab., California Inst. of Tech., Pasadena.
OPERATIONS CONCEPTS FOR MARS MISSIONS WITH MULTIPLE MOBILE SPACECRAFT
William C. Dias *In its* SpaceOps 1992: Proceedings of the Second International Symposium on Ground Data Systems for Space Mission Operations 1 Mar. 1993 p 125-130 (For primary document see N94-23832 06-66)
Avail: CASI HC A02/MF A10

Missions are being proposed which involve landing a varying number (anywhere from one to 24) of small mobile spacecraft on Mars. Mission proposals include sample returns, in situ geochemistry and geology, and instrument deployment functions. This paper discusses changes needed in traditional space operations methods for support of rover operations. Relevant differences include more frequent commanding, higher risk acceptance, streamlined procedures, and reliance on additional spacecraft autonomy, advanced fault protection, and prenegotiated decisions. New methods are especially important for missions with several Mars rovers operating concurrently against time limits. This paper also discusses likely mission design limits imposed by operations constraints . Author

N94-23853*# Jet Propulsion Lab., California Inst. of Tech., Pasadena.
PREPARING THE DSN OPERATIONS CONCEPTS
A. J. Salazar, M. D. Bailey, N. R. Kuo, and B. M. Wilkinson *In its* SpaceOps 1992: Proceedings of the Second International Symposium on Ground Data Systems for Space Mission Operations 1 Mar. 1993 p 131-135 (For primary document see N94-23832 06-66)
Avail: CASI HC A01/MF A10

Operations concepts are prepared to support a specific application and can, therefore, be classified accordingly. Studies of NASA and military operations concepts suggest three major types: data services, customer services, and systems oriented. Data services concepts concentrate on data types (e.g., telemetry and command) and how these data are processed and delivered to the user. Such concepts are normally used by data-processing centers to describe data-coding schemes and data formats. Customer services concepts concentrate on the customers' requirements and describe how these requirements are met using the systems available to the operation. Project centers use such concepts to describe the various types of data as they flow from the source (e.g., a spacecraft) to the end user (i.e., the customer). Systems oriented concepts concentrate on the use of systems for processing and delivering customer data. This paper examines the latter type and the 'concepts' that are inherent within them. Author (revised)

N94-23854*# National Space Development Agency, Tsukuba (Japan).
NASDA SATELLITE MISSION OPERATION SYSTEM AND OPERATIONS
Kousaku Yamaya, Fumiyoshi Yoshida, Harushige Noguchi, Tetsuo Takahashi, and Kazuhiro Tanaka *In* JPL, SpaceOps 1992: Proceedings of the Second International Symposium on Ground Data Systems for Space Mission Operations 1 Mar. 1993 p 137-142 (For primary document see N94-23832 06-66)
Avail: CASI HC A02/MF A10

NASDA has recently developed a new tracking and control system as a basis for future satellite mission operation. It is named type-I Space Operations and Data Systems (type-I SODS). The software of this system is separated into three parts: operation and control system, network system, and support and information system. The operation control system treats telemetry and command operations. The network system controls the communication line and ground station equipments to connect the satellite and the operation control system. The support and information system provides to other systems necessary information. JERS-1 which was launched in February of this year is the first satellite operated by type-I SODS. We explain the architecture and operation methods of this system using JERS-1 mission operations. Author (revised)

N94-23855*# National Aeronautics and Space Administration. Goddard Space Flight Center, Greenbelt, MD.
NASA/GODDARD SPACE FLIGHT CENTER'S TESTBED FOR CCSDS COMPATIBLE SYSTEMS **c14**
Richard D. Carper *In* JPL, SpaceOps 1992: Proceedings of the Second International Symposium on Ground Data Systems for Space Mission Operations 1 Mar. 1993 p 143-148 (For primary document see N94-23832 06-66)
Avail: CASI HC A02/MF A10

A testbed for flight and ground systems compatible with the Consultative Committee for Space Data Systems (CCSDS) Recommendations has been developed at NASA's Goddard Space Flight Center. The subsystems of an end-to-end CCSDS based data system are being developed. All return link CCSDS telemetry services (except Internet) and both versions of the CCSDS frame formats are being implemented. In key areas of uncertainty, multiple design approaches are being performed. In addition, key flight-qualifiable hardware components, such as Reed-Solomon encoders, are being developed to complement the testbed element development. The testbed and its capabilities are described. The method of dissemination of the testbed results are given, as are plans to make the testbed capabilities available to outside users. Plans for the development of standardized conformance and compatibility tests are provided. Author (revised)

N94-23856*# Centre National d'Etudes Spatiales, Toulouse (France).
SPOT4 OPERATIONAL CONTROL CENTER (CMP) **c14**
G. Zaouche *In* JPL, SpaceOps 1992: Proceedings of the Second International Symposium on Ground Data Systems for Space Mission Operations 1 Mar. 1993 p 149-154 (For primary document see N94-23832 06-66)
Avail: CASI HC A02/MF A10

CNES(F) is responsible for the development of a new generation of Operational Control Center (CMP) which will operate the new heliosynchronous remote sensing satellite (SPOT4). This Operational Control Center takes large benefit from the experience of the first generation of control center and from the recent advances in computer technology and standards. The CMP is designed for operating two satellites all the same time with a reduced pool of controllers. The architecture of this CMP is simple, robust, and flexible, since it is based on powerful distributed workstations interconnected through an Ethernet LAN. The application software uses modern and formal software engineering methods, in order to improve quality and reliability, and facilitate maintenance. This software is table driven so it can be easily adapted to other operational needs. Operation tasks are automated to the maximum extent, so that it could be possible to operate the CMP automatically with very limited human interference for supervision and decision making. This paper provides an overview of the SPOTS mission and associated ground segment. It also details the CMP, its functions, and its software and hardware architecture. Author (revised)

N94-23857*# Centre National d'Etudes Spatiales, Toulouse (France).
CNES ORGANIZATION FOR STATION POSITIONING OF GEOSTATIONARY SATELLITES
Jean Dulac *In* JPL, SpaceOps 1992: Proceedings of the Second International Symposium on Ground Data Systems for Space Mission

Operations 1 Mar. 1993 p 159-163 (For primary document see N94-23832 06-66)
Avail: CASI HC A01/MF A10

Since 1975, the Toulouse Space Centre (a technical establishment of the French Space Agency, CNES) has successfully brought 15 geostationary satellites on to station. During these 17 years of experience, an organization of human and material resources has been built up that ensures a very high level of reliability in the execution of these station positioning operations. The main characteristics of this organization are a rigourous definition of the roles and responsibilities of each person involved, very detailed operations documentation, and methodical preparation of the operations. Author (revised)

N94-23858*# Erno Raumfahrttechnik G.m.b.H., Bremen (Germany).
MISSION ACTIVITIES PLANNING FOR A HERMES MISSION BY MEANS OF AI-TECHNOLOGY
U. Pape, G. Hajen, N. Schielow, P. Mitschdoerfer, and F. Allard (European Space Agency. European Space Research and Technology Center, ESTEC, Noordwijk, Netherlands.) *In* JPL, SpaceOps 1992: Proceedings of the Second International Symposium on Ground Data Systems for Space Mission Operations 1 Mar. 1993 p 165-172 (For primary document see N94-23832 06-66)
Avail: CASI HC A02/MF A10

Mission Activities Planning is a complex task to be performed by mission control centers. AI technology can offer attractive solutions to the planning problem. This paper presents the use of a new AI-based Mission Planning System for crew activity planning. Based on a HERMES servicing mission to the COLUMBUS Man Tended Free Flyer (MTFF) with complex time and resource constraints, approximately 2000 activities with 50 different resources have been generated, processed, and planned with parametric variation of operationally sensitive parameters. The architecture, as well as the performance of the mission planning system, is discussed. An outlook to future planning scenarios, the requirements, and how a system like MARS can fulfill those requirements is given. Author (revised)

N94-23859*# National Aeronautics and Space Administration. Goddard Space Flight Center, Greenbelt, MD.
A QUICK UPLINK, EXPANDABLE EXECUTABLE FOR THE NSSC-1 OF THE HUBBLE SPACE TELESCOPE **c32**
Glenn T. Foley and Elizabeth A. Citrin *In* JPL, SpaceOps 1992: Proceedings of the Second International Symposium on Ground Data Systems for Space Mission Operations 1 Mar. 1993 p 173-178 (For primary document see N94-23832 06-66)
Avail: CASI HC A02/MF A10

The Hubble Space Telescope, launched in April 1990, contains two primary on-board computers. In the past, modifications to the flight software have been accomplished via patches to the on-board executable image (performed while software is executing) or via halt and reload of the computer memory with a new flight software version. This paper describes a method of reloading flight software with a new software version while continuing the onboard execution of a reduced set of spacecraft payload functions. Author (revised)

N94-23860*# Tokyo Univ., Sagamihara (Japan). Inst. of Space and Astronautical Science.
GROUND DATA SYSTEM FOR SPACE FLYER UNIT (SFU) **c18**
Takahiro Yamada, Susumu Sasaki, and Keiken Ninomiya *In* JPL, SpaceOps 1992: Proceedings of the Second International Symposium on Ground Data Systems for Space Mission Operations 1 Mar. 1993 p 179-184 (For primary document see N94-23832 06-66)
Avail: CASI HC A02/MF A10

The Space Flyer Unit (SFU) is an unmanned, multi-purpose, retrievable and reusable space platform. The first mission of SFU (SFU-1) will be launched by NASDA's H-2 launch vehicle in early 1995 and retrieved by NASA's Space Shuttle after several months in orbit. Two Japanese ground stations, several ground stations belonging to NASA, and a ground station in Chile will be used for tracking of SFU-1. The control center of SFU-1 is the Sagamihara Operations Center (SOC) of ISAS located in Sagamihara, Japan. This paper describes the tracking and data acquisition network for SFU-1, the configuration and design policy of the SFU operations control system, and data processing schemes used for mission operations of SFU. Author (revised)

N94-23861*# Jet Propulsion Lab., California Inst. of Tech., Pasadena.
RADIOASTRON FLIGHT OPERATIONS
V. I. Altunin (Academy of Sciences, USSR, Moscow.), K. G. Sukhanov (Babakin Engineering and Research Center, Moscow, Russia.), and K. R. Altunin *In its* SpaceOps 1992: Proceedings of the Second International Symposium on Ground Data Systems for Space Mission Operations 1 Mar. 1993 p 185-190 (For primary document see N94-23832 06-66)
Avail: CASI HC A02/MF A10

Radioastron is a space-based very-long-baseline interferometry (VLBI) mission to be operational in the mid-90's. The spacecraft and space radio telescope (SRT) will be designed, manufactured, and launched by the Russians. The United States is constructing a DSN subnet to be used in conjunction with a Russian subnet for Radioastron SRT science data acquisition, phase link, and spacecraft and science payload health monitoring. Command and control will be performed from a Russian tracking facility. In addition to the flight element, the network of ground radio telescopes which will be performing co-observations with the space telescope are essential to the mission. Observatories in 39 locations around the world are expected to participate in the mission. Some aspects of the mission that have helped shaped the flight operations concept are: separate radio channels will be provided for spacecraft operations and for phase link and science data acquisition; 80-90 percent of the spacecraft operational time will be spent in an autonomous mode; and, mission scheduling must take into account not only spacecraft and science payload constraints, but tracking station and ground observatory availability as well. This paper will describe the flight operations system design for translating the Radioastron science program into spacecraft executed events. Planning for in-orbit checkout and contingency response will also be discussed. Author (revised)

N94-23862*# Cray Systems, Bristol (England).
THE ULYSSES SPACECRAFT CONTROL AND MONITORING CONCEPTS AND REALITIES
Paul Hamer and Nigel Angold (European Space Agency. European Space Operations Center, Darmstadt, Germany.) *In* JPL, SpaceOps 1992: Proceedings of the Second International Symposium on Ground Data Systems for Space Mission Operations 1 Mar. 1993 p 191-196 (For primary document see N94-23832 06-66)
Avail: CASI HC A02/MF A10

Ulysses is a joint ESA-NASA mission, the primary purpose of the mission is to make scientific measurements of the Sun outside the plane of the ecliptic. The delay in launching Ulysses, due to the Challenger disaster, meant that the hardware on which the Spacecraft Control and Monitoring System (SCMS) resides was becoming obsolete, and it was decided to convert SCMS to run on a DEC/VAX machine under VMS. The paper will cover the spacecraft, the conversion, the converted SCMS, problems found, and the upgrades implemented for solutions. It will also discuss the future for and enhancements already made to the converted SCMS. Author (revised)

N94-23863*# European Space Agency. European Space Operations Center, Darmstadt (Germany).
ULYSSES LOG 1992
Raul Garcia Perez *In* JPL, SpaceOps 1992: Proceedings of the Second International Symposium on Ground Data Systems for Space Mission Operations 1 Mar. 1993 p 197-202 (For primary document see N94-23832 06-66)
Avail: CASI HC A02/MF A10

The Ulysses Log tells the story of some intriguing problems that we (=The Spacecraft Team) have encountered. Ulysses was launched on 6 Oct. 1990, and it made the fastest trip to Jupiter (8 Feb. 1992). It is presently going out of the ecliptic. This paper presents log entries from the following areas: (1) ingenious maneuvers; (2) telecommunication problems; and (3) surprises. Author (revised)

N94-23864*# Jet Propulsion Lab., California Inst. of Tech., Pasadena.
GALILEO SPACECRAFT ANOMALY AND SAFING RECOVERY **c18**
Ralph R. Basilio and David M. Durham *In its* SpaceOps 1992: Proceedings of the Second International Symposium on Ground Data Systems for Space Mission Operations 1 Mar. 1993 p 203-208 (For primary document see N94-23832 06-66)
Avail: CASI HC A02/MF A10

A high-level anomaly recovery plan which identifies the steps necessary to recover from a spacecraft 'Safing' incident was developed for the Galileo spacecraft prior to launch. Since launch, a total of four in-flight anomalies have lead to entry into a system fault protection 'Safing' routine which has required the Galileo flight team to refine and execute the recovery plan. These failures have allowed the flight team to develop an efficient recovery process when permanent spacecraft capability degradation is minimal and the cause of the anomaly is quickly diagnosed. With this previous recovery experience and the very focused boundary conditions of a specific potential failure, a Gaspra asteroid recovery plan was designed to be implemented in as quickly as forty hours (desired goal). This paper documents the work performed above, however, the Galileo project remains challenged to develop a generic detailed recovery plan which can be implemented in a relatively short time to configure the spacecraft to a nominal state prior to future high priority mission objectives. Author (revised)

N94-23865*# Martin Marietta Corp., Denver, CO. Astronautics Group.
MAGELLAN SPACECRAFT AND MEMORY STATE TRACKING: LESSONS LEARNED, FUTURE THOUGHTS **c18**
Allen W. Bucher *In* JPL, SpaceOps 1992: Proceedings of the Second International Symposium on Ground Data Systems for Space Mission Operations 1 Mar. 1993 p 209-214 (For primary document see N94-23832 06-66)
Avail: CASI HC A02/MF A10

Numerous studies have been dedicated to improving the two main elements of Spacecraft Mission Operations: Command and Telemetry. As a result, not much attention has been given to other tasks that can become tedious, repetitive, and error prone. One such task is Spacecraft and Memory State Tracking, the process by which the status of critical spacecraft components, parameters, and the contents of on-board memory are managed on the ground to maintain knowledge of spacecraft and memory states for future testing, anomaly investigation, and on-board memory reconstruction. The task of Spacecraft and Memory State Tracking has traditionally been a manual task allocated to Mission Operations Procedures. During nominal Mission Operations this job is tedious and error prone. Because the task is not complex and can be accomplished manually, the worth of a sophisticated software tool is often questioned. However, in the event of an anomaly which alters spacecraft components autonomously or a memory anomaly such as a corrupt memory or flight software error, an accurate ground image that can be reconstructed quickly is a priceless commodity. This study explores the process of Spacecraft and Memory State Tracking used by the Magellan Spacecraft Team highlighting its strengths as well as identifying lessons learned during the primary and extended missions, two memory anomalies, and other hardships encountered due to incomplete knowledge of spacecraft states. Ideas for future state tracking tools that require minimal user interaction and are integrated into the Ground Data System will also be discussed.
Author (revised)

N94-23866*# European Space Agency. European Space Operations Center, Darmstadt (Germany).
A REVIEW OF MISSION PLANNING SYSTEMS
M. Jones, E. M. Sorensen, T. Wolff, and C. R. Haddow (Logica Space and Communications Ltd., London, England.) *In* JPL, SpaceOps 1992: Proceedings of the Second International Symposium on Ground Data Systems for Space Mission Operations 1 Mar. 1993 p 219-224 (For primary document see N94-23832 06-66)
Avail: CASI HC A02/MF A10

A general definition of Mission Planning is given. The definition covers the full scope of an end-to-end mission planning system. Noting the mission-specific nature of most mission planning systems, a classification of autonomous spacecraft missions is made into Observatory, Survey, multi-instrument science, and Telecommunications missions. The mission planning approach for one mission in each category is examined critically. The following missions were chosen: ISO (Infrared Space Observatory); ERS-1 (European Remote Sensing Satellite); and Eureca (European Retrievable Carrier). The paper gives a summary of lessons learned from these missions suggesting improvements in areas such as requirements analysis, testing, user interfacing, rules, and constraints handling. The paper will also examine commonalities in functions, which could constitute a basis for identification of generic mission planning support tools.
Author (revised)

N94-23867*# Jet Propulsion Lab., California Inst. of Tech., Pasadena.
THE MARS MAPPER SCIENCE AND MISSION PLANNING TOOL
Martin W. Lo *In its* SpaceOps 1992: Proceedings of the Second International Symposium on Ground Data Systems for Space Mission Operations 1 Mar. 1993 p 225-229 (For primary document see N94-23832 06-66)
Avail: CASI HC A01/MF A10

The Mars Mapper Program (MOm) is an interactive tool for science and mission design developed for the Mars Observer Mission (MO). MOm is a function of the Planning and Sequencing Element of the MO Ground Data System. The primary users of MOm are members of the science and mission planning teams. Using MOm, the user can display digital maps of Mars in various projections and resolutions ranging from 1 to 256 pixels per degree squared. The user can overlay the maps with ground tracks of the MO spacecraft (S/C) and footprints and swaths of the various instruments on-board the S/C. Orbital and instrument geometric parameters can be computed on demand and displayed on the digital map or plotted in XY-plots. The parameter data can also be saved into files for other uses. MOm is divided into 3 major processes: Generator, Mapper, Plotter. The Generator Process is the main control which spawns all other processes. The processes communicate via sockets. At any one time, only 1 copy of MOm may operate on the system. However, up to 5 copies of each of the major processes may be invoked from the Generator. MOm is developed on the Sun SPARCStation 2GX with menu driven graphical user interface (GUI). The map window and its overlays are mouse-sensitized to permit on-demand calculations of various parameters along an orbit. The program is currently under testing and will be delivered to the MO Mission System Configuration Management for distribution to the MO community in 3/93.
Author (revised)

N94-23868*# Cray Systems, Bristol (England).
MISSION PLANNING FOR AN EARTH OBSERVATION LOW EARTH ORBITER: ERS-1
Paul Lockyer *In* JPL, SpaceOps 1992: Proceedings of the Second International Symposium on Ground Data Systems for Space Mission Operations 1 Mar. 1993 p 231-236 (For primary document see N94-23832 06-66)
Avail: CASI HC A02/MF A10

ERS-1, the first European Remote Sensing satellite, has a payload which consists primarily of microwave instruments and is in a polar sun-synchronous orbit. All ground and on-board activities from user requests to delivery of data products are combined into one integrated system. In view of the high number of products which can be generated by ERS-1, the Mission Planning System (MPS), which plans the on-board activities of ERS-1, is an essential tool for operations since manual planning of the large number of daily operations is out of the question. In addition the MPS, in line with the integrated nature of the ERS-1 system, also plans activities at the prime ground station, including among others, the operation of the payload data processing systems there. This paper outlines the operations concepts for ERS-1 mission planning, and describes the Mission Planning System used at the ERS-1 Control Center. Novel functionalities, such as automatic resource clash resolution, are described. A critical discussion gives lessons learned for future mission planning systems.
Author (revised)

N94-23869*# BSO/Aerospace and Systems B.V., Nieuwegein (Netherlands).
INTEGRATING PAYLOAD DESIGN, PLANNING, AND CONTROL IN THE DUTCH UTILISATION CENTRE **c18**
T. J. Grant *In* JPL, SpaceOps 1992: Proceedings of the Second International Symposium on Ground Data Systems for Space Mission Operations 1 Mar. 1993 p 237-242 (For primary document see N94-23832 06-66)
Avail: CASI HC A02/MF A10

Spacecraft payload design, experiment planning and scheduling, and payload control are traditionally separate areas of activity. This paper describes the development of a prototype software tool--the Activity Scheduling System (ASS)--which integrates these activity areas. ASS is part of a larger project to build a Dutch Utilisation Centre (DUC), intended eventually to support all space utilization activities in The Netherlands. ASS has been tested on the High Performance Capillary Electrophoresis payload. The paper outlines the integrated preparation and operations concept embodied in ASS. It describes the ASS prototype, including a typical session. The results of testing are summarized. Possible enhancement of ASS, including integration into DUC, is sketched. Author (revised)

N94-23870*# Jet Propulsion Lab., California Inst. of Tech., Pasadena.
VOYAGER UPLINK PLANNING IN THE INTERSTELLAR MISSION ERA
c32
Susan H. Linick and Kathryn R. Weld *In its* SpaceOps 1992: Proceedings of the Second International Symposium on Ground Data Systems for Space Mission Operations 1 Mar. 1993 p 243-248 (For primary document see N94-23832 06-66)
Avail: CASI HC A02/MF A10

The Voyager Project has entered its last phase of discovery--the Voyager Interstellar Mission (VIM). Because of the reduced scope of the project and a lower budget, new ways had to be developed to program two spacecraft with fewer people and to allow for some sequence development flexibility without additional risk. In the previous cruise era, it took a seven-person sequence team 12 weeks to develop a nominal eight week cruise sequence. Today it takes a three-person team six weeks to develop a 13 week sequence load. This paper will describe in detail the sequencing strategy which reduces the volume and frequency of sequence loads, and the new tools and processes developed which reduce the manual effort required to generate these sequences without adding risk.
Author (revised)

N94-23871*# Jet Propulsion Lab., California Inst. of Tech., Pasadena.
SCIENCE PLANNING AND SEQUENCING FOR CASSINI
Randii R. Wessen and Daniel F. Finnerty *In its* SpaceOps 1992: Proceedings of the Second International Symposium on Ground Data Systems for Space Mission Operations 1 Mar. 1993 p 249-254 (For primary document see N94-23832 06-66)
Avail: CASI HC A02/MF A10

This paper will address the science planning and sequencing aspects of the command generation process for the scientifically diverse Cassini Mission. The mission's prime objectives are to study the Saturnian system and deliver the Huygens Probe to the moon Titan. Together, the spacecraft and probe will be the largest and most complicated craft ever launched to another planet. The presentation will begin with an overview of the Cassini spacecraft and its scientific instrumentation. This will be followed with a description of the Oct. 1997 mission. Next, the structure of the science planning and sequencing process, with special emphasis on science's role, will be outlined. Finally, this presentation will conclude with a discussion of some of the unique challenges faced by the Ground System during Cassini's four-year orbital tour. Author (revised)

N94-23872*# Jet Propulsion Lab., California Inst. of Tech., Pasadena.
TECHNIQUES AND SOFTWARE FOR OPTIMUM AND EFFICIENT MISSION SCIENCE SEQUENCE DEVELOPMENT
David A. Bliss *In its* SpaceOps 1992: Proceedings of the Second International Symposium on Ground Data Systems for Space Mission Operations 1 Mar. 1993 p 255-260 (For primary document see N94-23832 06-66)
Avail: CASI HC A02/MF A10

Highly successful mission operations require efficient and cost-effective science sequence development. Of key importance is the Science Planning and Operations Team's (SPOT's) ability to complete science observation design and integration early in the sequence development process (i.e., before the sequence enters into a formal change control process). Once under formal change control, careful change paper documentation, Flight Team checks, and mission software checks make sequence changes more labor-intensive. This paper discusses team organization, strategies, scheduling, and software employed by the Voyager and Galileo SPOT's to complete science observation design and integration early in the sequence development process. Author (revised)

N94-23873*# Johns Hopkins Univ., Laurel, MD. Applied Physics Lab.
A PACKET-BASED CONCEPT FOR SPACECRAFT COMMAND PLANNING
Valerie B. Barnes *In* JPL, SpaceOps 1992: Proceedings of the Second International Symposium on Ground Data Systems for Space Mission Operations 1 Mar. 1993 p 261-266 (For primary document see N94-23832 06-66)
(Contract N00039-91-C-0001)
Avail: CASI HC A02/MF A10

The current generation of spacecraft being developed and operated by the Applied Physics Laboratory provides users with access to a broad spectrum of scientific instruments on maneuverable platforms that can be oriented for observation of both moving and stationary targets of interest. The capability of these increasingly complex spacecraft to perform data collection operations is approaching one observation per orbit. To enable both rapid configuration and generation of complex spacecraft command sequences, as well as reusability of command sequences among data collection operations, a packet-based concept for spacecraft command planning has been developed. The configuration of the spacecraft for any operation is designed using 'packets' where a packet represents a set of commands that is reusable. The packets can be combined in varying levels of functionality, and in varying time relationships, to create an observation timeline. At the lowest packet level are primitives. Primitives relate the details of command generation for a particular spacecraft to a 'message template.' Thus the packet concept itself is reusable from one spacecraft to the next. Author (revised)

N94-23874*# Johns Hopkins Univ., Laurel, MD. Applied Physics Lab.
CONNECTING SCIENCE AND OPERATIONS: THE OPERATIONS COORDINATOR
Madeleine H. Marshall and John A. Landshof *In* JPL, SpaceOps 1992: Proceedings of the Second International Symposium on Ground Data Systems for Space Mission Operations 1 Mar. 1993 p 267-271 (For primary document see N94-23832 06-66)
Avail: CASI HC A01/MF A10

For a current space mission under development at the Applied Physics Laboratory, the Mission Operations staff includes a team of 'Operations Coordinators' who have been working with the Mission Science and Spacecraft Development teams since completion of mission conceptual design. The Operations Coordinators are responsible for bringing knowledge of the spacecraft to the Mission Science team and bringing knowledge of the experiment requirements to the Spacecraft Development and Mission Operations teams. Once on-orbit operations begin, the Operations Coordinators will be responsible for implementation of specific science experiments from analysis through scheduling, generation of spacecraft command sequences, delivery of science data to the end user, and operations assessment. The Operations Coordinator concept is proving very effective during the development phase of the current mission.
Author (revised)

N94-23875*# Jet Propulsion Lab., California Inst. of Tech., Pasadena.
THE INSTANT SEQUENCING TASK: TOWARD CONSTRAINT-CHECKING A COMPLEX SPACECRAFT COMMAND SEQUENCE INTERACTIVELY
Joan C. Horvath, Leon J. Alkalaj, Karl M. Schneider, Arthur V. Amador, and Joseph N. Spitale (California Inst. of Tech., Pasadena.) *In its* SpaceOps 1992: Proceedings of the Second International Symposium on Ground Data Systems for Space Mission Operations 1 Mar. 1993 p 273-278 (For primary document see N94-23832 06-66)
Avail: CASI HC A02/MF A10

Robotic spacecraft are controlled by sets of commands called 'sequences.' These sequences must be checked against mission constraints. Making our existing constraint checking program faster would enable new capabilities in our uplink process. Therefore, we are rewriting this program to run on a parallel computer. To do so, we had to determine how to run constraint-checking algorithms in parallel and create a new method of specifying spacecraft models and constraints. This new specification gives us a means of representing flight systems and their predicted response to commands which could be used in a variety of applications throughout the command process, particularly during anomaly or high-activity operations. This commonality could reduce operations cost and risk for future complex missions. Lessons learned in applying some parts of this system to the TOPEX/Poseidon mission will be described. Author (revised)

N94-23876*# Centre National d'Etudes Spatiales, Toulouse (France).
AGENDA: A TASK ORGANIZER AND SCHEDULER
Isabelle Fratter *In* JPL, SpaceOps 1992: Proceedings of the Second International Symposium on Ground Data Systems for Space Mission

Operations 1 Mar. 1993 p 279-284 (For primary document see N94-23832 06-66)
Avail: CASI HC A02/MF A10

AGENDA will be the main tool used in running the SPOT 4 Earth Observation Satellite's Operational Control Center. It will reduce the operator's work load and make the task easier. AGENDA sets up the work plan for a day of operations, automatically puts the day's tasks into sequence and monitors their progress in real time. Monitoring is centralized, and the tasks are run on different computers in the Center. Once informed of any problems, the operator can intervene at any time while an activity is taking place. To carry out the various functions, the operator has an advanced, efficient, ergonomic graphic interface based on X11 and OSF/MOTIF. Since AGENDA is the heart of the Center, it has to satisfy several constraints that have been taken into account during the various development phases. AGENDA is currently in its final development stages. Author (revised)

N94-23877*# Space Applications Services, Brussels (Belgium).
COLUMBUS SYSTEM SUPPORT FOR TELESCIENCE OPERATIONS
David W. Lytton and Rolf Schulze (European Space Agency. European Space Research and Technology Center, ESTEC, Noordwijk, Netherlands.) *In* JPL, SpaceOps 1992: Proceedings of the Second International Symposium on Ground Data Systems for Space Mission Operations 1 Mar. 1993 p 285-290 (For primary document see N94-23832 06-66)
Avail: CASI HC A02/MF A10

With the given constraints of the space environment, the telescience concept aims at providing a space mission user with optimum flexibility and responsiveness for spaceborne investigations. The concept includes automated system management functions, which allocate and monitor planned resources and time windows, within which the investigator can perform his science interactively responding 'on-line' to experimental data. During the telescience operation, the user is given the capability to send telecommands to the payload from the User Home Base with transparency to the rest of the system. Any violation of the 'booked' time and resources will be detected by the system and reported back to the user for appropriate action. Ultimately, the system will react to maintain the integrity of the system and its payload. Upon completion of the telescience session, the system management function reverses the system configuration and deallocates resources automatically. Author (revised)

N94-23878*# National Aeronautics and Space Administration. Marshall Space Flight Center, Huntsville, AL.
GENERIC MISSION PLANNING CONCEPTS FOR SPACE ASTRONOMY MISSIONS
O. T. Guffin and J. F. Onken *In* JPL, SpaceOps 1992: Proceedings of the Second International Symposium on Ground Data Systems for Space Mission Operations 1 Mar. 1993 p 291-296 (For primary document see N94-23832 06-66)
Avail: CASI HC A02/MF A10

The past two decades have seen the rapid development of space astronomy, both manned and unmanned, and the concurrent proliferation of the operational concepts and software that have been produced to support each individual project. Having been involved in four of these missions since the '70's and three yet to fly in the present decade, the authors believe it is time to step back and evaluate this body of experience from a macro-systems point of view to determine the potential for generic mission planning concepts that could be applied to future missions. This paper presents an organized evaluation of astronomy mission planning functions, functional flows, iteration cycles, replanning activities, and the requirements that drive individual concepts to specific solutions. The conclusions drawn from this exercise are then used to propose a generic concept that could support multiple missions. Author (revised)

N94-23879*# Jet Propulsion Lab., California Inst. of Tech., Pasadena.
A MOS FOR ALL SEASONS
Larry Bryant *In its* SpaceOps 1992: Proceedings of the Second International Symposium on Ground Data Systems for Space Mission Operations 1 Mar. 1993 p 301-306 (For primary document see N94-23832 06-66)
Avail: CASI HC A02/MF A10

From a systems perspective, this paper examines the challenges of a single system to support multiple JPL space exploration missions and the need for unitary responsibility for the system. The focus is a Mission Operations System (MOS), which is effectively a mission management organization with direct authority over data system operations, command sequencing, flight operations control, data management, trajectory determination, telemetry and data acquisition, and spacecraft analysis. Stratagems for training and the approach to processes, procedures, and interfaces to facilitate the transition from the present situation to a truly multimission operational environment are developed. The outcome is a paradigm for a MOS that is achievable, that can effectively support multiple projects, and that can take advantage of technological changes without perturbing the entire system. Author (revised)

N94-23880*# National Aeronautics and Space Administration, Washington, DC.
AN OPERATIONS CONCEPT METHODOLOGY TO ACHIEVE LOW-COST MISSION OPERATIONS
Kenneth W. Ledbetter and Stephen D. Wall (Jet Propulsion Lab., California Inst. of Tech., Pasadena.) *In* JPL, SpaceOps 1992: Proceedings of the Second International Symposium on Ground Data Systems for Space Mission Operations 1 Mar. 1993 p 307-312 (For primary document see N94-23832 06-66)
Avail: CASI HC A02/MF A10

Historically, the Mission Operations System (MOS) for a space mission has been designed last because it is needed last. This has usually meant that the ground system must adjust to the flight vehicle design, sometimes at a significant cost. As newer missions have increasingly longer flight operations lifetimes, the MOS becomes proportionally more difficult and more resource-consuming. We can no longer afford to design the MOS last. The MOS concept may well drive the spacecraft, instrument, and mission designs, as well as the ground system. A method to help avoid these difficulties, responding to the changing nature of mission operations is presented. Proper development and use of an Operations Concept document results in a combined flight and ground system design yielding enhanced operability and producing increased flexibility for less cost. Author

N94-23881*# National Aeronautics and Space Administration. Goddard Space Flight Center, Greenbelt, MD.
MISSION ENGINEERING
Paul Ondrus and Michael Fatig (Bendix Field Engineering Corp., Seabrook, MD.) *In* JPL, SpaceOps 1992: Proceedings of the Second International Symposium on Ground Data Systems for Space Mission Operations 1 Mar. 1993 p 313-318 (For primary document see N94-23832 06-66)
Avail: CASI HC A02/MF A10

Goddard Space Flight Center's projects are facing new challenges with respect to the cost effective development and operation of spaceflight missions. Challenges, such as cost limits, compression of schedules, rapidly changing technology, and increasing mission complexity are making the mission development process more dynamic. A concept of 'Mission Engineering' as a means of addressing these challenges is proposed. It is an end-to-end, multimission development methodology that seeks to integrate the development processes between the space, ground, science, and operations segments of a mission. It thereby promotes more mission-oriented system solutions, within and across missions. Author (revised)

N94-23882*# Deutsche Forschungsanstalt fuer Luft- und Raumfahrt, Oberpfaffenhofen (Germany).
MANNED SPACE-LABORATORIES CONTROL CENTER (MSCC) OPERATIONS CONCEPT
Joachim Kehr *In* JPL, SpaceOps 1992: Proceedings of the Second International Symposium on Ground Data Systems for Space Mission Operations 1 Mar. 1993 p 319-325 (For primary document see N94-23832 06-66)
Avail: CASI HC A02/MF A10

The initiation of the (German-) nationally funded control center for manned spaceflight operations triggered by the invitation of President Reagan to ESA, Japan, and Canada in 1984 to join the International Space Station Freedom Program is recalled. The requirements for a Manned Space-Laboratories Control Center (MSCC) as defined at the beginning of the planning and construction process in 1987 and the resulting modifications during the various programmatic scenario changes on NASA and ESA side between 1987 and now are presented. The validity of the original requirements with respect to the current scenario, which asks for a logical evolution from the execution of the D-2 mission in January 1993 via the European Columbus Precursor flights (in particular the E-1 mission) towards Columbus Attached Laboratory (APM)-operations by the end of this century are discussed. The resulting tasks of the MSCC for the various missions, the current configuration, and the ensuing operations concept leading from a more centralized concept for D-2 towards a decentralized payload operations concept for the APM and the implications with respect to European and International interfaces are presented. The planned Columbus MSCC facility architecture and its expected modifications introduced by the ESA Ministerial Conference in Munich (Nov. 1991) and follow-on discussions are briefly addressed. The last chapter outlines the planned services to be provided by the MSCC to the decentralized User (experimenter) community. Issues like decentralized mission planning on executional level, command validation, data flow coordination, archiving services, and telescience capabilities are highlighted from a MSCC point of view. Author (revised)

N94-23883*# Jet Propulsion Lab., California Inst. of Tech., Pasadena.
MAKING ADAPTABLE SYSTEMS WORK FOR MISSION OPERATIONS: A CASE STUDY
Barbara E. Holder and Michael E. Levesque *In its* SpaceOps 1992: Proceedings of the Second International Symposium on Ground Data Systems for Space Mission Operations 1 Mar. 1993 p 327-331 (For primary document see N94-23832 06-66)
Avail: CASI HC A01/MF A10

The Advanced Multimission Operations System (AMMOS) at NASA's Jet Propulsion Laboratory is based on a highly adaptable multimission ground data system (MGDS) for mission operations. The goal for MGDS is to support current flight project science and engineering personnel and to meet the demands of future missions while reducing associated operations and software development costs. MGDS has become a powerful and flexible mission operations system by using a network of heterogeneous workstations, emerging open system standards, and selecting an adaptable tools-based architecture. Challenges in developing adaptable systems for mission operations and the benefits of this approach are described. Author (revised)

N94-23884*# Jet Propulsion Lab., California Inst. of Tech., Pasadena.
AN APPROACH TO THE DESIGN OF OPERATIONS SYSTEMS
Roy L. Chafin and Patrick S. Curran *In its* SpaceOps 1992: Proceedings of the Second International Symposium on Ground Data Systems for Space Mission Operations 1 Mar. 1993 p 333-341 (For primary document see N94-23832 06-66)
Avail: CASI HC A02/MF A10

The MultiMission Control Team (MMCT) consists of mission controllers which provides Real-Time operations support for the Mars Observer project. The Real-Time Operations task is to insure the integrity of the ground data system, to insure that the configuration is correct to support the mission, and to monitor the spacecraft for the Spacecraft Team. Operations systems are typically developed by adapting operations systems from previous projects. Problems tend to be solved empirically when they are either anticipated or observed in testing. This development method has worked in the past when time was available for extensive Ops testing. In the present NASA budget environment, a more cost conscious design approach has become necessary. Cost is a concern because operations is an ongoing, continuous activity. Reducing costs entails reducing staff. Reducing staffing levels potentially increases the risk of mission failure. Therefore, keeping track of the risk level is necessary. Author

N94-23885*# Jet Propulsion Lab., California Inst. of Tech., Pasadena.
OBJECT-ORIENTED TECHNOLOGIES IN A MULTI-MISSION DATA SYSTEM
Susan C. Murphy, Kevin J. Miller, and John J. Louie *In its* SpaceOps 1992: Proceedings of the Second International Symposium on Ground Data Systems for Space Mission Operations 1 Mar. 1993 p 343-348 (For primary document see N94-23832 06-66)
Avail: CASI HC A02/MF A10

The Operations Engineering Laboratory (OEL) at JPL is developing new technologies that can provide more efficient and productive ways of doing business in flight operations. Over the past three years, we have worked closely with the Multi-Mission Control Team to develop automation tools, providing technology transfer into operations and resulting in substantial cost savings and error reduction. The OEL development philosophy is characterized by object-oriented design, extensive reusability of code, and an iterative development model with active participation of the end users. Through our work, the benefits of object-oriented design became apparent for use in mission control data systems. Object-oriented technologies and how they can be used in a mission control center to improve efficiency and productivity are explained. The current research and development efforts in the JPL Operations Engineering Laboratory are also discussed to architect and prototype a new paradigm for mission control operations based on object-oriented concepts. Author (revised)

N94-23886*# Jet Propulsion Lab., California Inst. of Tech., Pasadena.
MANAGEMENT OF INFORMATION FOR MISSION OPERATIONS USING AUTOMATED KEYWORD REFERENCING c82
Roger A. Davidson and Patrick S. Curran *In its* SpaceOps 1992: Proceedings of the Second International Symposium on Ground Data Systems for Space Mission Operations 1 Mar. 1993 p 349-354 (For primary document see N94-23832 06-66)
Avail: CASI HC A02/MF A10

Although millions of dollars have helped to improve the operability and technology of ground data systems for mission operations, almost all mission documentation remains bound in printed volumes. This form of documentation is difficult and timeconsuming to use, may be out-of-date, and is usually not cross-referenced with other related volumes of mission documentation. A more effective, automated method of mission information access is needed. A new method of information management for mission operations using automated keyword referencing is proposed. We expound on the justification for and the objectives of this concept. The results of a prototype tool for mission information access that uses a hypertextlike user interface and existing mission documentation are shared. Finally, the future directions and benefits of our proposed work are described. Author (revised)

N94-23887*# European Space Agency. European Space Operations Center, Darmstadt (Germany).
AMFESYS: MODELLING AND DIAGNOSIS FUNCTIONS FOR OPERATIONS SUPPORT
J. Wheadon *In* JPL, SpaceOps 1992: Proceedings of the Second International Symposium on Ground Data Systems for Space Mission Operations 1 Mar. 1993 p 355-360 Sponsored in part by Siemens A.G. (For primary document see N94-23832 06-66)
Avail: CASI HC A02/MF A10

Packetized telemetry, combined with low station coverage for close-earth satellites, may introduce new problems in presenting to the operator a clear picture of what the spacecraft is doing. A recent ESOC study has gone some way to show, by means of a practical demonstration, how the use of subsystem models combined with artificial intelligence techniques, within a real-time spacecraft control system (SCS), can help to overcome these problems. A spin-off from using these techniques can be an improvement in the reliability of the telemetry (TM) limit-checking function, as well as the telecommand verification function, of the Spacecraft Control systems (SCS). The problem and how it was addressed, including an overview of the 'AMF Expert System' prototype are described, and proposes further work which needs to be done to prove the concept. The Automatic Mirror Furnace is part of the payload of the European Retrievable Carrier (EURECA) spacecraft, which was launched in July 1992. Author (revised)

N94-23888*# Jet Propulsion Lab., California Inst. of Tech., Pasadena.
MARS OBSERVER SCREEN DISPLAY DESIGN FOR A MULTIMISSION ENVIRONMENT c14
Roy L. Chafin *In its* SpaceOps 1992: Proceedings of the Second International Symposium on Ground Data Systems for Space Mission Operations 1 Mar. 1993 p 363-370 (For primary document see N94-23832 06-66)
Avail: CASI HC A02/MF A10

The Multi Mission Control Team (MMCT) is responsible for support to real time operations of the Mars Observer Mission. The team has the responsibility for monitoring the ground data system for the integrity of the telemetry and command data links. It also supports the Mars Observers Spacecraft Team in monitoring spacecraft events. The Data Monitor and Display subsystem (DMD) workstation provides the data interface with the ground data system. DMD workstation displays were developed to support the Mission Controllers in accomplishing their assigned tasks for supporting

the Mars Observer mission. The display design concepts that were used in the Mar Observer MMCT displays to minimize the cognitive demands on the controllers and enhance the MMCT operations were presented. The Data Monitor and Display subsystem (DMD) is the controllers window into the spacecraft and the ground data system. The DMD is a workstation that provides a variety of formatted data displays to the controller. The displays present both spacecraft telemetry data and ground system monitor data. Some displays are preplanned and developed prior to the operations in which they are used. These are called fixed displays and are quite versatile in format and content. Other displays and plots can be created in real time. These displays have limited formats but flexibility in content. These are called list or message displays. They can be rapidly generated by the controller as needed. The MMCT display repertoire provides a mix of displays appropriate to the needs of the MMCT controllers.
Author (revised)

N94-23889*# Bendix Field Engineering Corp., Seabrook, MD.

THE FOT TOOL KIT CONCEPT

Michael Fatig *In* JPL, SpaceOps 1992: Proceedings of the Second International Symposium on Ground Data Systems for Space Mission Operations 1 Mar. 1993 p 371-374 (For primary document see N94-23832 06-66)
Avail: CASI HC A01/MF A10

Flight operations and the preparation for it has become increasingly complex as mission complexities increase. Further, the mission model dictates that a significant increase in flight operations activities is upon us. Finally, there is a need for process improvement and economy in the operations arena. It is therefore time that we recognize flight operations as a complex process requiring a defined, structured, and life cycle approach vitally linked to space segment, ground segment, and science operations processes. With this recognition, an FOT Tool Kit consisting of six major components designed to provide tools to guide flight operations activities throughout the mission life cycle was developed. The major components of the FOT Tool Kit and the concepts behind the flight operations life cycle process as developed at NASA's GSFC for GSFC-based missions are addressed. The Tool Kit is therefore intended to increase productivity, quality, cost, and schedule performance of the flight operations tasks through the use of documented, structured methodologies; knowledge of past lessons learned and upcoming new technology; and through reuse and sharing of key products and special application programs made possible through the development of standardized key products and special program directories.
Author (revised)

N94-23890*# National Aeronautics and Space Administration. Goddard Space Flight Center, Greenbelt, MD.

GSMS AND SPACE VIEWS: ADVANCED SPACECRAFT MONITORING TOOLS

Douglas Carlton (Computer Sciences Corp., Greenbelt, MD.), David Vaules, Jr. (Computer Sciences Corp., Greenbelt, MD.), and Daniel Mandl *In* JPL, SpaceOps 1992: Proceedings of the Second International Symposium on Ground Data Systems for Space Mission Operations 1 Mar. 1993 p 375-380 (For primary document see N94-23832 06-66)
Avail: CASI HC A02/MF A10

The Graphical Spacecraft Monitoring System (GSMS) processes and translates real-time telemetry data from the Gamma Ray Observatory (GRO) spacecraft into high resolution 2-D and 3-D color displays showing the spacecraft's position relative to the Sun, Earth, Moon, and stars, its predicted orbit path, its attitude, instrument field of views, and other items of interest to the GRO Flight Operations Team (FOT). The GSMS development project is described and the approach being undertaken for implementing Space Views, the next version of GSMS, is presented. Space Views is an object-oriented graphical spacecraft monitoring system that will become a standard component of Goddard Space Flight Center's Transportable Payload Operations Control Center (TPOCC). Author

N94-23891*# Martin Marietta Corp., Denver, CO. Astronautics Group.

VMPLOT: A VERSATILE ANALYSIS TOOL FOR MISSION OPERATIONS

Allen W. Bucher *In* JPL, SpaceOps 1992: Proceedings of the Second International Symposium on Ground Data Systems for Space Mission Operations 1 Mar. 1993 p 381-386 (For primary document see N94-23832 06-66)
Avail: CASI HC A02/MF A10

VMPLOT is a versatile analysis tool designed by the Magellan Spacecraft Team to graphically display engineering data used to support mission operations. While there is nothing revolutionary or innovative about graphical data analysis tools, VMPLOT has some distinguishing features that set it apart from other custom or commercially available software packages. These features include the ability to utilize time in a Universal Time Coordinated (UTC) or Spacecraft Clock (SCLK) format as an enumerated data type, the ability to automatically scale both axes based on the data to be displayed (including time), the ability to combine data from different files, and the ability to utilize the program either interactively or in batch mode, thereby enhancing automation. Another important feature of VMPLOT not visible to the user is the software engineering philosophies utilized. A layered approach was used to isolate program functionality to different layers. This was done to increase program portability to different platforms and to ease maintenance and enhancements due to changing requirements. The functionality of the unique features of VMPLOT as well as highlighting the algorithms that make these features possible are described. The software engineering philosophies used in the creation of the software tool are also summarized. Author (revised)

N94-23892*# National Aeronautics and Space Administration. Lyndon B. Johnson Space Center, Houston, TX.

REAL-TIME AUTOMATED FAILURE IDENTIFICATION IN THE CONTROL CENTER COMPLEX (CCC) c31

Sarah Kirby, Janet Lauritsen, Ginger Pack, Anhhoang Ha (McDonnell-Douglas Space Systems Co., Houston, TX.), Steven Jowers (McDonnell-Douglas Space Systems Co., Houston, TX.), Robert McNenny (McDonnell-Douglas Space Systems Co., Houston, TX.), The Truong (McDonnell-Douglas Space Systems Co., Houston, TX.), and James Dell (Loral Space Information Systems, Houston, TX.) *In* JPL, SpaceOps 1992: Proceedings of the Second International Symposium on Ground Data Systems for Space Mission Operations 1 Mar. 1993 p 387-392 (For primary document see N94-23832 06-66)
Avail: CASI HC A02/MF A10

A system which will provide real-time failure management support to the Space Station Freedom program is described. The system's use of a simplified form of model based reasoning qualifies it as an advanced automation system. However, it differs from most such systems in that it was designed from the outset to meet two sets of requirements. First, it must provide a useful increment to the fault management capabilities of the Johnson Space Center (JSC) Control Center Complex (CCC) Fault Detection Management system. Second, it must satisfy CCC operational environment constraints such as cost, computer resource requirements, verification, and validation, etc. The need to meet both requirement sets presents a much greater design challenge than would have been the case had functionality been the sole design consideration. The choice of technology, discussing aspects of that choice and the process for migrating it into the control center is overviewed. Author (revised)

N94-23893*# National Aeronautics and Space Administration. Goddard Space Flight Center, Greenbelt, MD.

THE MISSION EVENTS GRAPHIC GENERATOR SOFTWARE: A SMALL TOOL WITH BIG RESULTS c61

Mark Lupisella, Jack Leibee, and Charles Scaffidi *In* JPL, SpaceOps 1992: Proceedings of the Second International Symposium on Ground Data Systems for Space Mission Operations 1 Mar. 1993 p 393-397 (For primary document see N94-23832 06-66)
Avail: CASI HC A01/MF A10

Utilization of graphics has long been a useful methodology for many aspects of spacecraft operations. A personal computer based software tool that implements straight-forward graphics and greatly enhances spacecraft operations is presented. This unique software tool is the Mission Events Graphic Generator (MEGG) software which is used in support of the Hubble Space Telescope (HST) Project. MEGG reads the HST mission schedule and generates a graphical timeline. Author (revised)

N94-23894*# MATRA Marconi Space, Toulouse (France).

INFLUENCE OF A NEW GENERATION OF OPERATIONS SUPPORT SYSTEMS ON CURRENT SPACECRAFT OPERATIONS PHILOSOPHY: THE USERS FEEDBACK

Jean Michel Darroy *In* JPL, SpaceOps 1992: Proceedings of the Second International Symposium on Ground Data Systems for Space Mission

Operations 1 Mar. 1993 p 403-409 (For primary document see N94-23832 06-66)
Avail: CASI HC A02/MF A10

Current trends in the spacecraft mission operations area (spacecraft & mission complexity, project duration, required flexibility are requiring a breakthrough for what concerns philosophy, organization, and support tools. A major evolution is related to space operations 'informationalization', i.e adding to existing operations support & data processing systems a new generation of tools based on advanced information technologies (object-oriented programming, artificial intelligence, data bases, hypertext) that automate, at least partially, operations tasks that used be performed manually (mission & project planning/scheduling, operations procedures elaboration & execution, data analysis & failure diagnosis). All the major facets of this 'informationalization' are addressed at MATRA MARCONI SPACE, operational applications were fielded and generic products are becoming available. These various applications have generated a significant feedback from the users (at ESA, CNES, ARIANESPACE, MATRA MARCONI SPACE), which is now allowing us to precisely measure how the deployment of this new generation of tools, that we called OPSWARE, can 'reengineer' current spacecraft mission operations philosophy, how it can make space operations faster, better, and cheaper. This paper can be considered as an update of the keynote address 'Knowledge-Based Systems for Spacecraft Control' presented during the first 'Ground Data Systems for Spacecraft Control' conference in Darmstadt, June 1990, with a special emphasis on these last two years users feedback. Author (revised)

N94-23895*# Mitre Corp., Houston, TX.
PILOT: AN INTELLIGENT DISTRIBUTED OPERATIONS SUPPORT SYSTEM
Arthur N. Rasmussen *In* JPL, SpaceOps 1992: Proceedings of the Second International Symposium on Ground Data Systems for Space Mission Operations 1 Mar. 1993 p 411-416 (For primary document see N94-23832 06-66)
Avail: CASI HC A02/MF A10

The Real-Time Data System (RTDS) project is exploring the application of advanced technologies to the real-time flight operations environment of the Mission Control Centers at NASA's Johnson Space Center. The system, based on a network of engineering workstations, provides services such as delivery of real time telemetry data to flight control applications. To automate the operation of this complex distributed environment, a facility called PILOT (Process Integrity Level and Operation Tracker) is being developed. PILOT comprises a set of distributed agents cooperating with a rule-based expert system; together they monitor process operation and data flows throughout the RTDS network. The goal of PILOT is to provide unattended management and automated operation under user control. Author

N94-23896*# European Space Agency. European Space Operations Center, Darmstadt (Germany).
ESSOPE: TOWARDS S/C OPERATIONS WITH REACTIVE SCHEDULE PLANNING
J. Wheadon *In* JPL, SpaceOps 1992: Proceedings of the Second International Symposium on Ground Data Systems for Space Mission Operations 1 Mar. 1993 p 417-422 (For primary document see N94-23832 06-66)
Avail: CASI HC A02/MF A10

The ESSOPE is a prototype front-end tool running on a Sun workstation and interfacing to ESOC's MSSS spacecraft control system for the exchange of telecommand requests (to MSSS) and telemetry reports (from MSSS). ESSOPE combines an operations Planner-Scheduler, with a Schedule Execution Control function. Using an internal 'model' of the spacecraft, the Planner generates a schedule based on utilization requests for a variety of payload services by a community of Olympus users, and incorporating certain housekeeping operations. Conflicts based on operational constraints are automatically resolved, by employing one of several available strategies. The schedule is passed to the execution function which drives MSSS to perform it. When the schedule can no longer be met, either because the operator interferes (by delays or changes of requirements), or because ESSOPE has recognized some spacecraft anomalies, the Planner produces a modified schedule maintaining the on-going procedures as far as consistent with the new constraints or requirements. Author

N94-23897*# European Space Agency. European Space Operations Center, Darmstadt (Germany).
THE ADVANCED TECHNOLOGY OPERATIONS SYSTEM: ATOS
J.-F. Kaufeler, H. A. Laue, K. Poulter (Logica Ltd., London, England.), and H. Smith (Logica Space and Communications Ltd., London, England.) *In* JPL, SpaceOps 1992: Proceedings of the Second International Symposium on Ground Data Systems for Space Mission Operations 1 Mar. 1993 p 425-434 (For primary document see N94-23832 06-66)
Avail: CASI HC A02/MF A10

Mission control systems supporting new space missions face ever-increasing requirements in terms of functionality, performance, reliability and efficiency. Modern data processing technology is providing the means to meet these requirements in new systems under development. During the past few years the European Space Operations Centre (ESOC) of the European Space Agency (ESA) has carried out a number of projects to demonstrate the feasibility of using advanced software technology, in particular, knowledge based systems, to support mission operations. A number of advances must be achieved before these techniques can be moved towards operational use in future missions, namely, integration of the applications into a single system framework and generalization of the applications so that they are mission independent. In order to achieve this goal, ESA initiated the Advanced Technology Operations System (ATOS) program, which will develop the infrastructure to support advanced software technology in mission operations, and provide applications modules to initially support: Mission Preparation, Mission Planning, Computer Assisted Operations, and Advanced Training. The first phase of the ATOS program is tasked with the goal of designing and prototyping the necessary system infrastructure to support the rest of the program. The major components of the ATOS architecture is presented. This architecture relies on the concept of a Mission Information Base (MIB) as the repository for all information and knowledge which will be used by the advanced application modules in future mission control systems. The MIB is being designed to exploit the latest in database and knowledge representation technology in an open and distributed system. In conclusion the technological and implementation challenges expected to be encountered, as well as the future plans and time scale of the project, are presented. Author (revised)

N94-23898*# National Space Development Agency, Tokyo (Japan). Tracking and Control Center.
NASDA KNOWLEDGE-BASED NETWORK PLANNING SYSTEM
K. Yamaya, M. Fujiwara, S. Kosugi, M. Yambe (Fujitsu Ltd., Tokyo, Japan.), and M. Ohmori (Fujitsu Social Systems Engineering Ltd., Tokyo, Japan.) *In* JPL, SpaceOps 1992: Proceedings of the Second International Symposium on Ground Data Systems for Space Mission Operations 1 Mar. 1993 p 435-440 (For primary document see N94-23832 06-66)
Avail: CASI HC A02/MF A10

One of the SODS (space operation and data system) sub-systems, NP (network planning) was the first expert system used by NASDA (national space development agency of Japan) for tracking and control of satellite. The major responsibilities of the NP system are: first, the allocation of network and satellite control resources and, second, the generation of the network operation plan data (NOP) used in automated control of the stations and control center facilities. Up to now, the first task of network resource scheduling was done by network operators. NP system automatically generates schedules using its knowledge base, which contains information on satellite orbits, station availability, which computer is dedicated to which satellite, and how many stations must be available for a particular satellite pass or a certain time period. The NP system is introduced. Author (revised)

N94-23899*# MATRA Marconi Space, Toulouse (France). Action de Recherche et Application MATRA IRIT en Interaction Homme Systeme.
A CROSS-DISCIPLINARY RESPONSE TO IMPROVE TEST ACTIVITIES: THE CORPORATE MEMORY CAPITALIZATION IN ARIANE4 TEST DOMAIN **c82**
Dinh Phuoc Vo, Christian Soler, N. Aussenac (Centre National de la Recherche Scientifique, Toulouse, France.), and D. Macchion (Centre National de la Recherche Scientifique, Toulouse, France.) *In* JPL, SpaceOps 1992: Proceedings of the Second International Symposium on Ground Data Systems for Space Mission Operations 1 Mar. 1993

p 441-450 (For primary document see N94-23832 06-66)
Avail: CASI HC A03/MF A10

The Assembly, Integration, Test, and Validation (AIT/AIV) of the Ariane4 Vehicle Equipment Bay was held at Matra Marconi Space (MMS) site of Toulouse for several years. For this activity, incident interpretation necessitates a great deal of different knowledge. When complex faults occur, particularly those appearing during overall control tests, experts of various domains (EGSE, software, on-board equipment) have to join for investigation sessions. Thus, an assistance tool for the identification of faulty equipment will improve the efficiency of diagnosis and the overall productivity of test activities. As a solution, the Aramiihs laboratory proposed considering the opportunity of a knowledge based system intended to assist the tester in diagnosis. This knowledge based system is, in fact, a short-term achievement of a long-term goal which is the capitalization of corporate memory in the Ariane4 test domain. Aramiihs is a research unit where engineers from MMS and researchers from the IRIT-CNRS cooperate on problems concerning new types of man-system interaction.
Author (revised)

N94-23900*# Jet Propulsion Lab., California Inst. of Tech., Pasadena.

COMBINING REAL-TIME MONITORING AND KNOWLEDGE-BASED ANALYSIS IN MARVEL c63

Ursula M. Schwuttke, A. G. Quan, R. Angelino, and J. R. Veregge *In its* SpaceOps 1992: Proceedings of the Second International Symposium on Ground Data Systems for Space Mission Operations 1 Mar. 1993 p 453-458 (For primary document see N94-23832 06-66)
Avail: CASI HC A02/MF A10

Real-time artificial intelligence is gaining increasing attention for applications in which conventional software methods are unable to meet technology needs. One such application area is the monitoring and analysis of complex systems. MARVEL, a distributed monitoring and analysis tool with multiple expert systems, was developed and successfully applied to the automation of interplanetary spacecraft operations at NASA's Jet Propulsion Laboratory. MARVEL implementation and verification approaches, the MARVEL architecture, and the specific benefits that were realized by using MARVEL in operations are described. Author (revised)

N94-23901*# OAO Corp., Altadena, CA.

THE APPLICATION OF AUTOMATED OPERATIONS AT THE INSTITUTIONAL PROCESSING CENTER

Thomas H. Barr *In* JPL, SpaceOps 1992: Proceedings of the Second International Symposium on Ground Data Systems for Space Mission Operations 1 Mar. 1993 p 459-464 (For primary document see N94-23832 06-66)
Avail: CASI HC A02/MF A10

The JPL Institutional and Mission Computing Division, Communications, Computing and Network Services Section, with its mission contractor, OAO Corporation, have for some time been applying automation to the operation of JPL's Information Processing Center (IPC). Automation does not come in one easy to use package. Automation for a data processing center is made up of many different software and hardware products supported by trained personnel. The IPC automation effort formally began with console automation, and has since spiraled out to include production scheduling, data entry, report distribution, online reporting, failure reporting and resolution, documentation, library storage, and operator and user education, while requiring the interaction of multi-vendor and locally developed software. To begin the process, automation goals are determined. Then a team including operations personnel is formed to research and evaluate available options. By acquiring knowledge of current products and those in development, taking an active role in industry organizations, and learning of other data center's experiences, a forecast can be developed as to what direction technology is moving. With IPC management's approval, an implementation plan is developed and resources identified to test or implement new systems. As an example, IPC's new automated data entry system was researched by Data Entry, Production Control, and Advance Planning personnel. A proposal was then submitted to management for review. A determination to implement the new system was made and elements/personnel involved with the initial planning performed the implementation. The final steps of the implementation were educating data entry personnel in the areas effected and procedural changes necessary to the successful operation of the new system. Author (revised)

N94-23902*# Jet Propulsion Lab., California Inst. of Tech., Pasadena.

MAKING TOMORROW'S MISTAKES TODAY: EVOLUTIONARY PROTOTYPING FOR RISK REDUCTION AND SHORTER DEVELOPMENT TIME c14

Gary Friedman, Ursula M. Schwuttke, Scott Burliegh, Sanguan Chow, Randy Parlier, Lorrine Lee, Henry Castro, and Jim Gersbach *In its* SpaceOps 1992: Proceedings of the Second International Symposium on Ground Data Systems for Space Mission Operations 1 Mar. 1993 p 465-470 (For primary document see N94-23832 06-66)
Avail: CASI HC A02/MF A10

In the early days of JPL's solar system exploration, each spacecraft mission required its own dedicated data system with all software applications written in the mainframe's native assembly language. Although these early telemetry processing systems were a triumph of engineering in their day, since that time the computer industry has advanced to the point where it is now advantageous to replace these systems with more modern technology. The Space Flight Operations Center (SFOC) Prototype group was established in 1985 as a workstation and software laboratory. The charter of the lab was to determine if it was possible to construct a multimission telemetry processing system using commercial, off-the-shelf computers that communicated via networks. The staff of the lab mirrored that of a typical skunk works operation -- a small, multi-disciplinary team with a great deal of autonomy that could get complex tasks done quickly. In an effort to determine which approaches would be useful, the prototype group experimented with all types of operating systems, inter-process communication mechanisms, network protocols, packet size parameters. Out of that pioneering work came the confidence that a multi-mission telemetry processing system could be built using high-level languages running in a heterogeneous, networked workstation environment. Experience revealed that the operating systems on all nodes should be similar (i.e., all VMS or all PC-DOS or all UNIX), and that a unique Data Transport Subsystem tool needed to be built to address the incompatibilities of network standards, byte ordering, and socket buffering. The advantages of building a telemetry processing system based on emerging industry standards were numerous: by employing these standards, we would no longer be locked into a single vendor. When new technology came to market which offered ten times the performance at one eighth the cost, it would be possible to attach the new machine to the network, re-compile the application code, and run. In addition, we would no longer be plagued with lack of manufacturer support when we encountered obscure bugs. And maybe, hopefully, the eternal elusive goal of software portability across different vendors' platforms would finally be available. Some highlights of our prototyping efforts are described. Derived from text

N94-23903*# National Space Development Agency, Tokyo (Japan). Tracking and Data Acquisition Dept.

NASDA'S ADVANCED ON-LINE SYSTEM (ADOLIS)

Yoshikatsu Yamamoto, Hideo Hara, Shigeo Yamada, Nobuyuki Hirata (Nippon Electric Co. Ltd., Yokohama, Japan.), Shigenori Komatsu (Nippon Electric Co. Ltd., Yokohama, Japan.), Seiji Nishihata (Nippon Electric Co. Ltd., Yokohama, Japan.), and Akio Oniyama (Nippon Electric Co. Ltd., Yokohama, Japan.) *In* JPL, SpaceOps 1992: Proceedings of the Second International Symposium on Ground Data Systems for Space Mission Operations 1 Mar. 1993 p 471-476 (For primary document see N94-23832 06-66)
Avail: CASI HC A02/MF A10

Spacecraft operations including ground system operations are generally realized by various large or small scale group work which is done by operators, engineers, managers, users and so on, and their positions are geographically distributed in many cases. In face-to-face work environments, it is easy for them to understand each other. However, in distributed work environments which need communication media, if only using audio, they become estranged from each other and lose interest in and continuity of work. It is an obstacle to smooth operation of spacecraft. NASDA has developed an experimental model of a new real-time operation control system called 'ADOLIS' (ADvanced On-Line System) adopted to such a distributed environment using a multi-media system dealing with character, figure, image, handwriting, video and audio information which is accommodated to operation systems of a wide range including spacecraft and ground systems. This papor describes the results of the development of the experimental model. Author (revised)

N94-23904*# National Aeronautics and Space Administration. Ames Research Center, Moffett Field, CA.
CONSTRAINT-BASED SCHEDULING **c81**
Monte Zweben *In* JPL, SpaceOps 1992: Proceedings of the Second International Symposium on Ground Data Systems for Space Mission Operations 1 Mar. 1993 p 477-484 (For primary document see N94-23832 06-66)
Avail: CASI HC A02/MF A10

The GERRY scheduling system developed by NASA Ames with assistance from the Lockheed Space Operations Company, and the Lockheed Artificial Intelligence Center, uses a method called constraint-based iterative repair. Using this technique, one encodes both hard rules and preference criteria into data structures called constraints. GERRY repeatedly attempts to improve schedules by seeking repairs for violated constraints. The system provides a general scheduling framework which is being tested on two NASA applications. The larger of the two is the Space Shuttle Ground Processing problem which entails the scheduling of all the inspection, repair, and maintenance tasks required to prepare the orbiter for flight. The other application involves power allocation for the NASA Ames wind tunnels. Here the system will be used to schedule wind tunnel tests with the goal of minimizing power costs. In this paper, we describe the GERRY system and its application to the Space Shuttle problem. We also speculate as to how the system would be used for manufacturing, transportation, and military problems. Author

N94-23905*# National Aeronautics and Space Administration. Goddard Space Flight Center, Greenbelt, MD.
CUSTOMIZING GRAPHICAL USER INTERFACE TECHNOLOGY FOR SPACECRAFT CONTROL CENTERS
Edward Beach (Computer Sciences Corp., Laurel, MD.), Peter Giancola (Computer Sciences Corp., Laurel, MD.), Steven Gibson (Integral Systems, Inc., Lanham, MD.), and Ronald Mahmot *In* JPL, SpaceOps 1992: Proceedings of the Second International Symposium on Ground Data Systems for Space Mission Operations 1 Mar. 1993 p 485-490 (For primary document see N94-23832 06-66)
Avail: CASI HC A02/MF A10

The Transportable Payload Operations Control Center (TPOCC) project is applying the latest in graphical user interface technology to the spacecraft control center environment. This project of the Mission Operations Division's (MOD) Control Center Systems Branch (CCSB) at NASA Goddard Space Flight Center (GSFC) has developed an architecture for control centers which makes use of a distributed processing approach and the latest in Unix workstation technology. The TPOCC project is committed to following industry standards and using commercial off-the-shelf (COTS) hardware and software components wherever possible to reduce development costs and to improve operational support. TPOCC's most successful use of commercial software products and standards has been in the development of its graphical user interface. This paper describes TPOCC's successful use and customization of four separate layers of commercial software products to create a flexible and powerful user interface that is uniquely suited to spacecraft monitoring and control. Author

N94-23906*# National Space Development Agency, Tokyo (Japan).
APPLICATIONS OF CCSDS RECOMMENDATIONS TO INTEGRATED GROUND DATA SYSTEMS (IGDS)
Hiroshi Mizuta, Daniel Martin (Hitachi Ltd., Yokohama, Japan.), Hatsuhiko Kato (Hitachi Ltd., Yokohama, Japan.), and Hirokazu Ihara (Hitachi Ltd., Yokohama, Japan.) *In* JPL, SpaceOps 1992: Proceedings of the Second International Symposium on Ground Data Systems for Space Mission Operations 1 Mar. 1993 p 495-500 (For primary document see N94-23832 06-66)
Avail: CASI HC A02/MF A10

This paper describes an application of the CCSDS Principle Network (CPH) service model to communications network elements of a postulated Integrated Ground Data System (IGDS). Functions are drawn principally from COSMICS (Cosmic Information and Control System), an integrated space control infrastructure, and the Earth Observing System Data and Information System (EOSDIS) Core System (ECS). From functional requirements, this paper derives a set of five communications network partitions which, taken together, support proposed space control infrastructures and data distribution systems. Our functional analysis indicates that the five network partitions derived in this paper should effectively interconnect the users, centers, processors, and other architectural elements of an IGDS. This paper illustrates a useful application of the CCSDS (Consultive Committee for Space Data Systems) Recommendations to ground data system development. Author (revised)

N94-23907*# Computer Technology Associates, Inc., Rockville, MD.
THE ADVANCED ORBITING SYSTEMS TESTBED PROGRAM: RESULTS TO DATE **c14**
Penny A. Newsome and John F. Otranto *In* JPL, SpaceOps 1992: Proceedings of the Second International Symposium on Ground Data Systems for Space Mission Operations 1 Mar. 1993 p 501-506 Sponsored by NASA, Washington (For primary document see N94-23832 06-66)
Avail: CASI HC A02/MF A10

The Consultative Committee for Space Data Systems Recommendations for Packet Telemetry and Advanced Orbiting Systems (AOS) propose standard solutions to data handling problems common to many types of space missions. The Recommendations address only space/ground and space/space data handling systems. Goddard Space Flight Center's AOS Testbed (AOST) Program was initiated to better understand the Recommendations and their impact on real-world systems, and to examine the extended domain of ground/ground data handling systems. Central to the AOST Program are the development of an end-to-end Testbed and its use in a comprehensive testing program. Other Program activities include flight-qualifiable component development, supporting studies, and knowledge dissemination. The results and products of the Program will reduce the uncertainties associated with the development of operational space and ground systems that implement the Recommendations. The results presented in this paper include architectural issues, a draft proposed standardized test suite and flight-qualifiable components. Author

N94-23908*# Computer Technology Associates, Inc., Rockville, MD.
RELIABLE TRANSFER OF DATA FROM GROUND TO SPACE **c32**
Fred Brosi *In* JPL, SpaceOps 1992: Proceedings of the Second International Symposium on Ground Data Systems for Space Mission Operations 1 Mar. 1993 p 507-512 (For primary document see N94-23832 06-66)
Avail: CASI HC A02/MF A10

This paper describes the problems involved in uplink of data from control centers on the ground to spacecraft, and explores the solutions to those problems, past. present. and future. The evolution of this process, from simple commanding to transfer of large volumes of data and commands is traced. The need for reliable end-to-end protocols for commanding and file transfer is demonstrated, and the shortcomings of both existing telecommand protocols and commercial products to meet this need are discussed. Recent developments in commercial protocols that may be adaptable to the mentioned operations environment are surveyed, and current efforts to develop a suite of protocols for reliable transfer in this environment are presented. Author

N94-23909*# Logica Space and Communications Ltd., London (England).
THE EURECA TELECOMMANDING CHAIN: EXPERIENCE WITH PACKET TELECOMMAND AND TELEMETRY SYSTEMS **c32**
C. Mueller, R. Bater, and E. M. Sorensen (European Space Agency. European Space Operations Center, Darmstadt, Germany.) *In* JPL, SpaceOps 1992: Proceedings of the Second International Symposium on Ground Data Systems for Space Mission Operations 1 Mar. 1993 p 513-518 (For primary document see N94-23832 06-66)
Avail: CASI HC A02/MF A10

The European Retrieval Carrier (EURECA) was launched on its first flight on the 31st July 1992 by the Space Shuttle Atlantis. EURECA is characterized by several new on-board features, most notable Packet Telemetry and a partial implementation of Packet Telecommanding using an early version of the Command Operation Procedure (COP-1) protocol. EURECA has also very low contact time with its Ground Station, with a consequent high number of out-of-visibility onboard operations. This paper concentrates on the implementation and operational experience with the COP-1 Protocol and the effect the short ground contact time has on the design of the Commanding System. Another interesting feature is that the COP-1 is implemented at the control center rather than at the ground

station. The COP-1 protocol also successfully supported the mission during the launch where commands were sent via NASCOM and the Shuttle.
Author

N94-23910*# National Space Development Agency, Tokyo (Japan). Tracking and Data Acquisition Dept.
VERIFICATION OF TECHNICAL ELEMENTS OF THE ADVANCED SPACECRAFT BASED UPON THE CCSDS RECOMMENDATION c18
Hideo Hara, Sigeo Yamada, Yoshikatsu Yamamoto, Seiichi Fujii (Fujitsu Ltd., Tokyo, Japan.), Kaoru Tumura (Fujitsu Ltd., Tokyo, Japan.), Masato Yokomizo (Fujitsu Ltd., Tokyo, Japan.), and Hiroyuki Ogasawara (Fujitsu Ltd., Tokyo, Japan.) *In* JPL, SpaceOps 1992: Proceedings of the Second International Symposium on Ground Data Systems for Space Mission Operations 1 Mar. 1993 p 519-524 (For primary document see N94-23832 06-66)
Avail: CASI HC A02/MF A10

We are going to meet the era when advanced spacecraft such as space stations are developed and operated. The current system of the satellite operations control will need to undergo many changes. We consider that the future system will require the following functions: the function for interchanging data between international agencies, processing the various kinds of space data, and distributing data as many unspecified users require. However, we have to solve the following problems in order to satisfy these requirements: the problem of standardization of space data communication protocol, establishment of multimedia data management method, and standardization of the user interface. This paper describes three techniques to solve the above mentioned problems. That is, standardization of the data communication protocol between space and ground by AOS (Advanced Orbiting System) protocol of CCSDS (Consultative Committee for Space Data Systems) Recommendation, management of multimedia data by catalog reference, standardization of user interface by SFDU(Standard Formatted Data Unit) of CCSDS Recommendation.
Author (revised)

N94-23911*# Centre National d'Etudes Spatiales, Toulouse (France).
DISTRIBUTED COMPUTING ENVIRONMENTS FOR FUTURE SPACE CONTROL SYSTEMS c61
Pierre Viallefont *In* JPL, SpaceOps 1992: Proceedings of the Second International Symposium on Ground Data Systems for Space Mission Operations 1 Mar. 1993 p 525-529 (For primary document see N94-23832 06-66)
Avail: CASI HC A01/MF A10

The aim of this paper is to present the results of a CNES research project on distributed computing systems. The purpose of this research was to study the impact of the use of new computer technologies in the design and development of future space applications. The first part of this study was a state-of-the-art review of distributed computing systems. One of the interesting ideas arising from this review is the concept of a 'virtual computer' allowing the distributed hardware architecture to be hidden from a software application. The 'virtual computer' can improve system performance by adapting the best architecture (addition of computers) to the software application without having to modify its source code. This concept can also decrease the cost and obsolescence of the hardware architecture. In order to verify the feasibility of the 'virtual computer' concept, a prototype representative of a distributed space application is being developed independently of the hardware architecture. Author (revised)

N94-23912*# Jet Propulsion Lab., California Inst. of Tech., Pasadena.
DIGITAL TEST SIGNAL GENERATION: AN ACCURATE SNR CALIBRATION APPROACH FOR THE DSN c32
Benito O. Gutierrez-Luaces *In its* SpaceOps 1992: Proceedings of the Second International Symposium on Ground Data Systems for Space Mission Operations 1 Mar. 1993 p 531-536 (For primary document see N94-23832 06-66)
Avail: CASI HC A02/MF A10

In support of the on-going automation of the Deep Space Network (DSN) a new method of generating analog test signals with accurate signal-to-noise ratio (SNR) is described. High accuracy is obtained by simultaneous generation of digital noise and signal spectra at the desired bandwidth (base-band or bandpass). The digital synthesis provides a test signal embedded in noise with the statistical properties of a stationary random process. Accuracy is dependent on test integration time and limited only by the system quantization noise (0.02 dB). The monitor and control as well as signal-processing programs reside in a personal computer (PC). Commands are transmitted to properly configure the specially designed high-speed digital hardware. The prototype can generate either two data channels modulated or not on a subcarrier, or one QPSK channel, or a residual carrier with one biphase data channel. The analog spectrum generated is on the DC to 10 MHz frequency range. These spectra may be up-converted to any desired frequency without loss on the characteristics of the SNR provided. Test results are presented. Author

N94-23913*# European Space Agency. European Space Operations Center, Darmstadt (Germany).
AUTOMATIC TOOLS FOR SYSTEM TESTING c14
N. M. Peccia *In* JPL, SpaceOps 1992: Proceedings of the Second International Symposium on Ground Data Systems for Space Mission Operations 1 Mar. 1993 p 537-540 (For primary document see N94-23832 06-66)
Avail: CASI HC A01/MF A10

As spacecraft control and other space-related ground systems become increasingly complex, the effort required in testing and validation also increases. Implementation of a spacecraft control system normally involves a number of incremental deliveries. In addition kernel or general purpose software may also be involved, which must itself be considered in the integration and testing program. Tools can be used to assist this testing. These can reduce the effort required or alternatively they can ensure that for a given level of effort, a better job is done. Great benefit could be derived by automating certain types of testing (interactive software) which up to now has been performed manually at a terminal. This paper reports on an on-going study. The study examines means of automating spacecraft control system testing, evaluates relevant commercial tools and aims to prototype basic automatic testing functions. Author

N94-23914*# Jet Propulsion Lab., California Inst. of Tech., Pasadena.
REPRESENTING OPERATIONS PROCEDURES USING TEMPORAL DEPENDENCY NETWORKS c32
Kristina E. Fayyad and Lynne P. Cooper *In its* SpaceOps 1992: Proceedings of the Second International Symposium on Ground Data Systems for Space Mission Operations 1 Mar. 1993 p 541-546 (For primary document see N94-23832 06-66)
Avail: CASI HC A02/MF A10

DSN Link Monitor & Control (LMC) operations consist primarily of executing procedures to configure, calibrate, test, and operate a communications link between an interplanetary spacecraft and its mission control center. Currently the LMC operators are responsible for integrating procedures into an end-to-end series of steps. The research presented in this paper is investigating new ways of specifying operations procedures that incorporate the insight of operations, engineering, and science personnel to improve mission operations. The paper describes the rationale for using Temporal Dependency Networks (TDN's) to represent the procedures, a description of how the data is acquired, and the knowledge engineering effort required to represent operations procedures. Results of operational tests of this concept, as implemented in the LMC Operator Assistant Prototype (LMCOA), are also presented. Author

N94-23915*# Jet Propulsion Lab., California Inst. of Tech., Pasadena.
SITUATION MANAGEMENT IN THE LINK MONITOR AND CONTROL OPERATOR ASSISTANT (LMCOA) c32
Randall W. Hill, Jr. and Lorrine F. Lee *In its* SpaceOps 1992: Proceedings of the Second International Symposium on Ground Data Systems for Space Mission Operations 1 Mar. 1993 p 547-552 (For primary document see N94-23832 06-66)
Avail: CASI HC A02/MF A10

This paper describes a knowledge-based system called the Situation Manager that was developed for the Link Monitor and Control Operator Assistant (LMCOA) at the Jet Propulsion Laboratory. This system was developed in response to a number of deficiencies that were identified in an earlier version of the LMCOA: the need to close the control loop between sending a directive and knowing when its execution is complete (versus just closing the communications loop), the need to recognize an anomaly and alert the operator when a directive is rejected or a link device fails, and the need to suggest ways to work around an anomaly, provided that it is recognizable. In response to these needs, the Situation

Manager has been designed to provide the LMCOA with three basic capabilities: situation assessment, anomaly diagnosis, and recovery from commonly occurring problems. Author

N94-23916*# Jet Propulsion Lab., California Inst. of Tech., Pasadena.
USING MACH THREADS TO CONTROL DSN OPERATIONAL SEQUENCES **c63**
Juan Urista *In its* SpaceOps 1992: Proceedings of the Second International Symposium on Ground Data Systems for Space Mission Operations 1 Mar. 1993 p 553-559 (For primary document see N94-23832 06-66)
Avail: CASI HC A02/MF A10

The Link Monitor and Control Operator Assistant prototype (LMCOA) is a state-of-the-art, semiautomated monitor and control system based on an object-oriented design. The purpose of the LMCOA prototyping effort is to both investigate new technology (such as artificial intelligence) to support automation and to evaluate advances in information systems toward developing systems that take advantage of the technology. The emergence of object-oriented design methodology has enabled a major change in how software is designed and developed. This paper describes how the object-oriented approach was used to design and implement the LMCOA and the results of operational testing. The LMCOA is implemented on a NeXT workstation using the Mach operating system and the Objective-C programming language. Author

N94-23917*# Jet Propulsion Lab., California Inst. of Tech., Pasadena.
DEEP SPACE NETWORK (DSN), NETWORK OPERATIONS CONTROL CENTER (NOCC) COMPUTER-HUMAN INTERFACES **c60**
Alvin Ellman and Magdi Carlton *In its* SpaceOps 1992: Proceedings of the Second International Symposium on Ground Data Systems for Space Mission Operations 1 Mar. 1993 p 561-564 (For primary document see N94-23832 06-66)
Avail: CASI HC A01/MF A10

The Network Operations Control Center (NOCC) of the DSN is responsible for scheduling the resources of DSN, and monitoring all multi-mission spacecraft tracking activities in real-time. Operations performs this job with computer systems at JPL connected to over 100 computers at Goldstone, Australia and Spain. The old computer system became obsolete, and the first version of the new system was installed in 1991. Significant improvements for the computer-human interfaces became the dominant theme for the replacement project. Major issues required innovating problem solving. Among these issues were: How to present several thousand data elements on displays without overloading the operator? What is the best graphical representation of DSN end-to-end data flow? How to operate the system without memorizing mnemonics of hundreds of operator directives? Which computing environment will meet the competing performance requirements? This paper presents the technical challenges, engineering solutions, and results of the NOCC computer-human interface design. Author

N94-23918*# National Aeronautics and Space Administration. Goddard Space Flight Center, Greenbelt, MD.
A METHOD FOR INTERFERENCE MITIGATION IN SPACE COMMUNICATIONS SCHEDULING **c32**
Yen F. Wong and James L. Rash *In* JPL, SpaceOps 1992: Proceedings of the Second International Symposium on Ground Data Systems for Space Mission Operations 1 Mar. 1993 p 565-571 (For primary document see N94-23832 06-66)
Avail: CASI HC A02/MF A10

Increases in the number of user spacecraft and data rates supported by NASA's Tracking and Data Relay Satellite System (TDRSS) in the S and Ku bands could result in communications conflicts due to mutual interference. More attention must be paid to this problem in terms of communications scheduling. A method based on consideration of all relevant communications parameters has been developed to mitigate interference while minimizing unnecessary scheduling restrictions on both the TDRSS network and user resources. This method calculates required separation angles at TDRS and produces potential interference intervals, which can be used in the production of schedules free of unacceptable interference. The method also can be used as the basis for analysis, evaluation, and optimization of user schedules with respect to communications performance. This paper describes the method and its proposed application to scheduling in space communications. Test cases relative to missions operating at Ku-band, including Space Shuttle, are discussed. Author

N94-23919*# Centre National d'Etudes Spatiales, Toulouse (France).
REAL-TIME ON-BOARD ORBIT DETERMINATION WITH DORIS **c13**
J.-P. Berthias, C. Jayles, and D. Pradines *In* JPL, SpaceOps 1992: Proceedings of the Second International Symposium on Ground Data Systems for Space Mission Operations 1 Mar. 1993 p 579-583 (For primary document see N94-23832 06-66)
Avail: CASI HC A01/MF A10

A spaceborne orbit determination system is being developed by the French Space Agency (CNES) for the SPOT 4 satellite. It processes DORIS measurements to produce an orbit with an accuracy of about 500 meters rms. In order to evaluate the reliability of the software, it was combined with the MERCATOR man/machine interface and used to process the TOPEX/Poseidon DORIS data in near real time during the validation phase of the instrument, at JPL and at CNES. This paper gives an overview of the orbit determination system and presents the results of the TOPEX/Poseidon experiment. Author (revised)

N94-23920*# National Aeronautics and Space Administration. Goddard Space Flight Center, Greenbelt, MD.
TOPEX/POSEIDON PRECISION ORBIT DETERMINATION PRODUCTION AND EXPERT SYSTEM **c13**
Barbara Putney, Nikita Zelensky (Hughes STX, Inc., Lanham, MD.), and Steven Klosko (Hughes STX, Inc., Lanham, MD.) *In* JPL, SpaceOps 1992: Proceedings of the Second International Symposium on Ground Data Systems for Space Mission Operations 1 Mar. 1993 p 585-590 (For primary document see N94-23832 06-66)
Avail: CASI HC A02/MF A10

TOPEX/Poseidon (T/P) is a joint mission between NASA and the Centre National d'Etudes Spatiales (CNES), the French Space Agency. The TOPEX/Poseidon Precision Orbit Determination Production System (PODPS) was developed at Goddard Space Flight Center (NASA/GSFC) to produce the absolute orbital reference required to support the fundamental ocean science goals of this satellite altimeter mission within NASA. The orbital trajectory for T/P is required to have a RMS accuracy of 13 centimeters in its radial component. This requirement is based on the effective use of the satellite altimetry for the isolation of absolute long-wavelength ocean topography important for monitoring global changes in the ocean circulation system. This orbit modeling requirement is at an unprecedented accuracy level for this type of satellite. In order to routinely produce and evaluate these orbits, GSFC has developed a production and supporting expert system. The PODPS is a menu driven system allowing routine importation and processing of tracking data for orbit determination, and an evaluation of the quality of the orbit so produced through a progressive series of tests. Phase 1 of the expert system grades the orbit and displays test results. Later phases undergoing implementation, will prescribe corrective actions when unsatisfactory results are seen. This paper describes the design and implementation of this orbit determination production system and the basis for its orbit accuracy assessment within the expert system. Author

N94-23921*# National Aeronautics and Space Administration. Lyndon B. Johnson Space Center, Houston, TX.
A REAL-TIME NAVIGATION MONITORING EXPERT SYSTEM FOR THE SPACE SHUTTLE MISSION CONTROL CENTER **c17**
Lui Wang and Malise Fletcher *In* JPL, SpaceOps 1992: Proceedings of the Second International Symposium on Ground Data Systems for Space Mission Operations 1 Mar. 1993 p 591-599 (For primary document see N94-23832 06-66)
Avail: CASI HC A02/MF A10

The ONAV (Onboard Navigation) Expert System has been developed as a real time console assistant for use by ONAV flight controllers in the Mission Control Center at the Johnson Space Center. This expert knowledge based system is used to monitor the Space Shuttle onboard navigation system, detect faults, and advise flight operations personnel. This application is the first knowledge-based system to use both telemetry and trajectory data from the Mission Operations Computer (MOC). To arrive at this stage, from a prototype to real world application, the ONAV project has had to deal with not only AI issues but operating environment issues. The AI issues included the maturity of AI languages and the debugging tools, verification, and availability, stability and size of the expert pool. The environmental issues included real time data acquisition, hardware suitability, and how to achieve acceptance by users and management. Author

N94-23922*# Jet Propulsion Lab., California Inst. of Tech., Pasadena.
XRTD: AN X-WINDOWS BASED, REAL-TIME RADIOMETRIC DISPLAY AND ANALYSIS SYSTEM c32
Vincent M. Pollmeier *In its* SpaceOps 1992: Proceedings of the Second International Symposium on Ground Data Systems for Space Mission Operations 1 Mar. 1993 p 601-606 (For primary document see N94-23832 06-66)
Avail: CASI HC A02/MF A10

XRTD is a graphical user interface (GUI) based tool for monitoring real time radiometric spacecraft data. The tool is designed to allow the navigation analyst to both view and analyze the characteristics of Doppler and ranging data. This capability is critical if ground personnel wish to verify the correct performance of ongoing maneuvers. The raw tracking data is transferred from Deep Space Network (DSN) computers to a local workstation, where the predicted value for the observable is subtracted from the actual observed value to create a residual. The tool then allows the navigation analyst to rescale and replot the data using simple GUI techniques. The navigator may then perform a number of data analysis and modeling techniques on the resulting residuals to allow for the real time characterization of spacecraft events. These techniques include the modeling of maneuvers, the compression and differencing of data, and Fast Fourier transforms of the data. This tool has shortened the amount of time required for initial characterization of spacecraft maneuvers from several hours to a few minutes. Author (revised)

N94-23923*# MATRA Marconi Space, Toulouse (France).
KALMAN FILTERING APPLIED TO REAL-TIME MONITORING OF APOGEE MANEUVERS c13
Frederic deBoer and Christian Barbier (Alcatel Espace, Toulouse, France.) *In* JPL, SpaceOps 1992: Proceedings of the Second International Symposium on Ground Data Systems for Space Mission Operations 1 Mar. 1993 p 607-612 (For primary document see N94-23832 06-66)
Avail: CASI HC A02/MF A10

Part of the Space Mathematics Division in CNES, the Flight Dynamics Center provides attitude and orbit determinations and maneuvers during the Launch and Early Operation Phase (LEOP) of geostationary satellites. Orbit determination is based on a Kalman filter method; when the 2 GHz CNES/NASA network is used, Doppler measurements are available and allow orbit determination during the apogee maneuvers. This method was used for TELE-X and TDF 2 LEOP (3-axis controlled satellites) and also for TELECOM 2 and HISPASAT (spun satellites): it enables us to follow the evolution of the maneuver and gives out a quite accurate estimation of the reached orbit. In this paper, we briefly describe the dynamic models of the orbit evolution in both cases, '3-axis' and 'inertial' thrust. Then, we present the results obtained for each case. Afterwards, we present some cases to show the robustness of the filter. Author

N94-23924*# Centre National d'Etudes Spatiales, Toulouse (France).
MARS 1994/1996: THE FRENCH NAVIGATION TASKS c12
Frederic Bonneau, Jacques Bernard, and Damien Delobette (Societe d'Economie et de Mathematique Appliquees, Toulouse, France.) *In* JPL, SpaceOps 1992: Proceedings of the Second International Symposium on Ground Data Systems for Space Mission Operations 1 Mar. 1993 p 613-618 (For primary document see N94-23832 06-66)
Avail: CASI HC A02/MF A10

In the fall of 1994, Russia will launch a spacecraft to Mars. France is involved in many scientific experiments which are onboard the spacecraft, as PI or CI. Some days before the Mars orbit insertion maneuver, two small stations and two penetrators will be injected into an entry trajectory. They will carry out for at least six months in situ analysis on the Martian surface. Two years later, a second spacecraft will be launched. It will carry the French balloon and a small rover. The scientific data of these landers will be relayed to earth via the spacecraft. However, during the first 20 days of their mission, Mars Observer will be used. To this end, a Mars balloon relay will be used, which will receive the data from the landers and store them into the memory of the Mars Observer camera. The spacecraft will also be used to localize the landers with the help of relative one-way Doppler measurements. An international cooperative is set up for this process, including JPS, Russian ballistic centers (Babakine, Institute of Applied Mathematics, Moscow Flight Control Center), and CNES Toulouse. Another task dedicated to the space mathematics division of CNES is to support the French scientists to prepare their telecommands and to analyze their telemetry. This second part is integrated into the French ground segment created for the Mars 94/96 mission. This paper describes the method used in CNES for the localization process, the support provided to the scientists, and the links for the data exchange. Author (revised)

N94-23925*# Centre National d'Etudes Spatiales, Toulouse (France).
MERCATOR: METHODS AND REALIZATION FOR CONTROL OF THE ATTITUDE AND THE ORBIT OF SPACECRAFT c17
Gilles Tavernier and Genevieve Campan *In* JPL, SpaceOps 1992: Proceedings of the Second International Symposium on Ground Data Systems for Space Mission Operations 1 Mar. 1993 p 619-628 (For primary document see N94-23832 06-66)
Avail: CASI HC A02/MF A10

Since 1974, CNES has been involved in geostationary positioning. Among different entities participating in operations and their preparation, the Flight Dynamics Center (FDC) is in charge of performing the following tasks: orbit determination; attitude determination; computation, monitoring, and calibration of orbit maneuvers; computation, monitoring, and calibration of attitude maneuvers; and operational predictions. In order to fulfill this mission, the FDC receives telemetry from the satellite and localization measurements from ground stations (e.g., CNES, NASA, INTELSAT). These data are processed by space dynamics programs integrated in the MERCATOR system which is run on SUN workstations (UNIX O.S.). The main features of MERCATOR are redundancy, modularity, and flexibility: efficient, flexible, and user friendly man-machine interface; and four identical SUN stations redundantly linked in an Ethernet network. Each workstation can perform all the tasks from data acquisition to computation results dissemination through a video network. A team of four engineers can handle the space mechanics aspects of a complete geostationary positioning from the injection into a transfer orbit to the final maneuvers in the station-keeping window. MERCATOR has been or is to be used for operations related to more than ten geostationary positionings. Initially developed for geostationary satellites, MERCATOR's methodology was also used for satellite control centers and can be applied to a wide range of satellites and to future manned missions. Author (revised)

N94-23926*# Jet Propulsion Lab., California Inst. of Tech., Pasadena.
NAVIGATION OF SPACE VLBI MISSIONS: RADIOASTRON AND VSOP
Jordan Ellis *In its* SpaceOps 1992: Proceedings of the Second International Symposium on Ground Data Systems for Space Mission Operations 1 Mar. 1993 p 625-628 (For primary document see N94-23832 06-66)
Avail: CASI HC A01/MF A10

In the mid-1990s, Russian and Japanese space agencies will each place into highly elliptic earth orbit a radio telescope consisting of a large antenna and radio astronomy receivers. Very long baseline interferometry (VLBI) techniques will be used to obtain high resolution images of radio sources observed by the space and ground based antennas. Stringent navigation accuracy requirements are imposed on the space VLBI missions by the need to transfer an ultra-stable ground reference frequency standard to the spacecraft and by the demands of the VLBI correlation process. Orbit determination for the mission will be the joint responsibility of navigation centers in the U.S., Russia, and Japan with orbit estimates based on combining tracking data from NASA, Russian, and Japanese sites. This paper describes the operational plans, the inter-agency coordination, and data exchange between the navigation centers required for space VLBI navigation. Author (revised)

N94-23927*# Deutsche Forschungsanstalt fuer Luft- und Raumfahrt, Oberpfaffenhofen (Germany). Space Operations Center.
THE GEO-CONTROL SYSTEM FOR STATION KEEPING AND COLOCATION OF GEOSTATIONARY SATELLITES c61
O. Montenbruck, M. C. Eckstein, and J. Gonner (Societe Europeenne des Satellites, Betzdorf, Luxembourg.) *In* JPL, SpaceOps 1992: Proceedings of the Second International Symposium on Ground Data Systems for Space Mission Operations 1 Mar. 1993 p 629-634 (For primary document see N94-23832 06-66)
Avail: CASI HC A02/MF A10

GeoControl is a compact but powerful and accurate software system for station keeping of single and colocated satellites, which has been developed at the German Space Operations Center. It includes four core modules for orbit determination (including maneuver estimation), maneuver planning, monitoring of proximities between colocated satellites, and interference and event prediction. A simple database containing state vector and maneuver information at selected epochs is maintained as a central interface between the modules. A menu driven shell utilizing form screens for data input serves as the central user interface. The software is written in Ada and FORTRAN and may be used on VAX workstations or mainframes under the VMS operating system. Author (revised)

N94-23928*# Centre National d'Etudes Spatiales, Toulouse (France).

HISPASAT LAUNCH AND EARLY OPERATIONS PHASES: COMPUTATION AND MONITORING OF GEOSTATIONARY SATELLITE POSITIONING

Pascal Brousse and Arnaud Desprairies (MATRA Marconi Space, Toulouse, France.) *In* JPL, SpaceOps 1992: Proceedings of the Second International Symposium on Ground Data Systems for Space Mission Operations 1 Mar. 1993 p 635-640 (For primary document see N94-23832 06-66)
Avail: CASI HC A02/MF A10

Since 1974, CNES, the French National Space Agency, has been involved in the geostationary launch and early operations phases (LEOP) of moving satellites from a transfer orbit delivered by a launcher to a geostationary point. During the operations and their preparation, the Flight Dynamics Center (FDC), part of CNES LEOP facilities, is in charge of the space mechanics aspects. What is noteworthy about the Spanish HISPASAT satellite positioning is that all the operations were performed on the customer's premises, and consequently the FDC was duplicated in Madrid, Spain. The first part of this paper is the FDC presentation: its role, its hardware configuration, and its space dynamics ground control system called MERCATOR. The second part of this paper details the preparation used by the FDC for the HISPASAT mission: hardware and software installation in Madrid, integration with the other entities, and technical and operational qualifications. The third part gives results concerning flight dynamics aspects and operational activities. Author (revised)

N94-23929*# Honeywell, Inc., Minneapolis, MN. Sensor and Systems Development Center.

INTELLIGENT TUTORING AND AIDING IN SATELLITE GROUND CONTROL Ph.D. Thesis - Georgia Inst. of Tech., 1991 **c54**

Rose W. Chu and Christine M. Mitchell (Georgia Inst. of Tech., Atlanta.) *In* JPL, SpaceOps 1992: Proceedings of the Second International Symposium on Ground Data Systems for Space Mission Operations 1 Mar. 1993 p 645-650 (For primary document see N94-23832 06-66) (Contract NAS5-28575)
Avail: CASI HC A02/MF A10

In supervisory control systems such as satellite ground control, there is a need for human-centered automation where the focus is to understand and enhance the human-system interaction experience in the complex task environment. Operator support in the form of off-line intelligent tutoring and on-line intelligent aiding is one approach towards this effort. The tutor/aid paradigm is proposed here as a design approach that integrates the two aspects of operator support in one system for technically oriented adults in complex domains. This paper also presents GT-VITA, a proof-of-concept graphical, interactive, intelligent tutoring system that is a first attempt to illustrate the tutoring aspect of the tutor/aid paradigm in the domain of satellite ground control. Evaluation on GT-VITA is conducted with NASA personnel with very positive results. GT-VITA is presented being fielded as it is at Goddard Space Flight Center. Author (revised)

N94-23930*# Jet Propulsion Lab., California Inst. of Tech., Pasadena.

OPERABILITY ENGINEERING IN THE DEEP SPACE NETWORK

Belinda Wilkinson *In its* SpaceOps 1992: Proceedings of the Second International Symposium on Ground Data Systems for Space Mission Operations 1 Mar. 1993 p 651-654 (For primary document see N94-23832 06-66)
Avail: CASI HC A01/MF A10

Many operability problems exist at the three Deep Space Communications Complexes (DSCC's) of the Deep Space Network (DSN). Four years ago, the position of DSN Operability Engineer was created to provide the opportunity for someone to take a system-level approach to solving these problems. Since that time, a process has been developed for personnel and development engineers and for enforcing user interface standards in software designed for the DSCC's. Plans are for the participation of operations personnel in the product life-cycle to expand in the future. Author (revised)

N94-23931*# OAO Corp., Altadena, CA.

THE APPLICATION OF TOTAL QUALITY MANAGEMENT PRINCIPLES TO SPACECRAFT MISSION OPERATIONS **c38**

Maury Sweetin *In* JPL, SpaceOps 1992: Proceedings of the Second International Symposium on Ground Data Systems for Space Mission Operations 1 Mar. 1993 p 655-659 (For primary document see N94-23832 06-66)
Avail: CASI HC A01/MF A10

By now, the philosophies of Total Quality Management have had an impact on every aspect of American industrial life. The trail-blazing work of Deming, Juran, and Crosby, first implemented in Japan, has 're-migrated' across the Pacific and now plays a growing role in America's management culture. While initially considered suited only for a manufacturing environment, TQM has moved rapidly into the 'service' areas of offices, sales forces, and even fast-food restaurants. The next logical step has also been taken - TQM has found its way into virtually all departments of the Federal Government, including NASA. Because of this widespread success, it seems fair to ask whether this new discipline is directly applicable to the profession of spacecraft operations. The results of quality emphasis on OAO Corporation's contract at JPL provide strong support for Total Quality Management as a useful tool in spacecraft operations. Author (revised)

N94-23932*# Jet Propulsion Lab., California Inst. of Tech., Pasadena.

MISSION OPERATIONS AND COMMAND ASSURANCE: INSTILLING QUALITY INTO FLIGHT OPERATIONS **c38**

Linda L. Welz, Mona M. Witkowski, Kristin J. Bruno, and Sherrill S. Potts *In its* SpaceOps 1992: Proceedings of the Second International Symposium on Ground Data Systems for Space Mission Operations 1 Mar. 1993 p 661-666 (For primary document see N94-23832 06-66)
Avail: CASI HC A02/MF A10

Mission Operations and Command Assurance (MO&CA) is a Total Quality Management (TQM) task on JPL projects to instill quality in flight mission operations. From a system engineering view, MO&CA facilitates communication and problem-solving among flight teams and provides continuous process improvement to reduce the probability of radiating incorrect commands to a spacecraft. The MO&CA task has evolved from participating as a member of the spacecraft team to an independent team reporting directly to flight project management and providing system level assurance. JPL flight projects have benefited significantly from MO&CA's effort to contain risk and prevent rather than rework errors. MO&CA's ability to provide direct transfer of knowledge allows new projects to benefit from previous and ongoing flight experience. Author

N94-23933*# Instituto de Pesquisas Espaciais, Sao Jose dos Campos (Brazil).

OPERATIONAL TRAINING FOR THE MISSION OPERATIONS AT THE BRAZILIAN NATIONAL INSTITUTE FOR SPACE RESEARCH (INPE) **c53**

Pawel Rozenfeld *In* JPL, SpaceOps 1992: Proceedings of the Second International Symposium on Ground Data Systems for Space Mission Operations 1 Mar. 1993 p 667-671 (For primary document see N94-23832 06-66)
Avail: CASI HC A01/MF A10

This paper describes the selection and training process of satellite controllers and data network operators performed at INPE's Satellite Tracking and Control Center in order to prepare them for the mission operations of the INPE's first (SCD1) satellite. An overview of the ground control system and SCD1 architecture and mission is given. Different training phases are described, taking into account that the applicants had no previous knowledge of space operations requiring, therefore, a training which started from the basics. Author (revised)

N94-23934*# Jet Propulsion Lab., California Inst. of Tech., Pasadena.

TRAINING: PLUGGING THE INFORMATION GAPS **c53**

Carol J. Scott *In its* SpaceOps 1992: Proceedings of the Second International Symposium on Ground Data Systems for Space Mission

Operations 1 Mar. 1993 p 673-677 (For primary document see N94-23832 06-66)
Avail: CASI HC A01/MF A10

Training is commonly viewed as an add-on function to the development cycle. It is imperative that this view be changed. The training developer needs to be a colleague in the system development process, contributing and learning along with the other development participants. Training developers can make contributions to design concepts that favor end-users. Early involvement will enhance the likelihood of training availability concurrent with software delivery. End-users will benefit and cost-savings will be realized. Author (revised)

N94-23935*# Italian Space Agency, Rome.
THE COLUMBUS LOGISTICS SUPPORT AT THE APMC: REQUIREMENTS AND IMPLEMENTATION ASPECTS
C. Canu, L. Battocchio (Alenia Spazio S.p.A., Turin, Italy.), and S. Masullo (Compagnia Italiana Servizi Tecnici, Rome.) *In* JPL, SpaceOps 1992: Proceedings of the Second International Symposium on Ground Data Systems for Space Mission Operations 1 Mar. 1993 p 679-684 (For primary document see N94-23832 06-66)
Avail: CASI HC A02/MF A10

This paper focuses on the logistics support to be provided by the APM Center (APMC). Among the Columbus ground infrastructures, this center is tasked to provide logistics, sustaining engineering and P/L integration support to the ongoing missions of the APM, i.e. the Columbus Laboratory attached to the Freedom Space Station. The following is illustrated: an analysis of the requirements that are levied on the logistics support of the APM; how such requirements are reflected in the corresponding support to be available on-ground and at APMC; the functional components of the APMC logistics support and how such components interact each other; how the logistics support function interfaces with the other functions of the ground support; and how the logistics support is being designed in terms of resources (such as hardware, data bases, etc.). Emphasis is given to the data handling aspects and to the related data bases that will constitute for the logistics activities the fundamental source of information during the APM planned lifetime. Functional and physical architectures, together with trades for possible implementation, are addressed. Commonalities with other centers are taken into account and recommendations are made for possible reuse of tools already developed in the C/D phase. Finally, programmatic considerations are discussed for the actual implementation of the center. Author (revised)

N94-23936*# National Aeronautics and Space Administration. Goddard Space Flight Center, Greenbelt, MD.
AUTOMATING A HUMAN FACTORS EVALUATION OF GRAPHICAL USER INTERFACES FOR NASA APPLICATIONS: AN UPDATE ON CHIMES **c54**
Jian-Ping Jiang (Computer Technology Associates, Inc., Rockville, MD.), Elizabeth D. Murphy (Computer Technology Associates, Inc., Rockville, MD.), Sidney C. Bailin (Computer Technology Associates, Inc., Rockville, MD.), and Walter F. Truszkowski *In* JPL, SpaceOps 1992: Proceedings of the Second International Symposium on Ground Data Systems for Space Mission Operations 1 Mar. 1993 p 685-690 Sponsored in part by NASA, Washington (For primary document see N94-23832 06-66)
(Contract NAS5-30680)
Avail: CASI HC A02/MF A10

Capturing human factors knowledge about the design of graphical user interfaces (GUI's) and applying this knowledge on-line are the primary objectives of the Computer-Human Interaction Models (CHIMES) project. The current CHIMES prototype is designed to check a GUI's compliance with industry-standard guidelines, general human factors guidelines, and human factors recommendations on color usage. Following the evaluation, CHIMES presents human factors feedback and advice to the GUI designer. The paper describes the approach to modeling human factors guidelines, the system architecture, a new method developed to convert quantitative RGB primaries into qualitative color representations, and the potential for integrating CHIMES with user interface management systems (UIMS). Both the conceptual approach and its implementation are discussed. This paper updates the presentation on CHIMES at the first International Symposium on Ground Data Systems for Spacecraft Control. Author (revised)

N94-23937*# Technischer Uerberwachungs-Verein Rheinland e.V., Cologne (Germany).
SECURITY ASPECTS OF SPACE OPERATIONS DATA **c82**
Stefan Schmitz *In* JPL, SpaceOps 1992: Proceedings of the Second International Symposium on Ground Data Systems for Space Mission Operations 1 Mar. 1993 p 691-696 (For primary document see N94-23832 06-66)
Avail: CASI HC A02/MF A10

This paper deals with data security. It identifies security threats to European Space Agency's (ESA) In Orbit Infrastructure Ground Segment (IOI GS) and proposes a method of dealing with its complex data structures from the security point of view. It is part of the 'Analysis of Failure Modes, Effects Hazards and Risks of the IOI GS for Operations, including Backup Facilities and Functions' carried out on behalf of the European Space Operations Center (ESOC). The security part of this analysis has been prepared with the following aspects in mind: ESA's large decentralized ground facilities for operations, the multiple organizations/users involved in the operations and the developments of ground data systems, and the large heterogeneous network structure enabling access to (sensitive) data which does involve crossing organizational boundaries. An IOI GS data objects classification is introduced to determine the extent of the necessary protection mechanisms. The proposal of security countermeasures is oriented towards the European 'Information Technology Security Evaluation Criteria (ITSEC)' whose hierarchically organized requirements can be directly mapped to the security sensitivity classification. Author (revised)

N94-23938*# National Aeronautics and Space Administration. Goddard Space Flight Center, Greenbelt, MD.
MISSION AND SCIENCE ACTIVITY SCHEDULING LANGUAGE **c81**
Larry G. Hull *In* JPL, SpaceOps 1992: Proceedings of the Second International Symposium on Ground Data Systems for Space Mission Operations 1 Mar. 1993 p 697-702 (For primary document see N94-23832 06-66)
Avail: CASI HC A02/MF A10

To support the distributed and complex operational scheduling required for future National Aeronautics and Space Administration (NASA) missions, a formal, textual language, the Scheduling Applications Interface Language (SAIL), has been developed. Increased geographic dispersion of investigators is leading to distributed mission and science activity planning, scheduling, and operations. SAIL is an innovation which supports the effective and efficient communication of scheduling information among physically dispersed applications in distributed scheduling environments. SAIL offers a clear, concise, unambiguous expression of scheduling information in a readable, hardware independent format. The language concept, syntax, and semantics incorporate language features found useful during five years of research and prototyping with scheduling languages in physically distributed environments. SAIL allows concise specification of mission and science activity plans in a format which promotes repetition and reuse. Author (revised)

N94-23939*# Jet Propulsion Lab., California Inst. of Tech., Pasadena.
SPECIFYING DESIGN CONSERVATISM: WORST CASE VERSUS PROBABILISTIC ANALYSIS **c38**
Ralph F. Miles, Jr. *In its* SpaceOps 1992: Proceedings of the Second International Symposium on Ground Data Systems for Space Mission Operations 1 Mar. 1993 p 703-709 (For primary document see N94-23832 06-66)
Avail: CASI HC A02/MF A10

Design conservatism is the difference between specified and required performance, and is introduced when uncertainty is present. The classical approach of worst-case analysis for specifying design conservatism is presented, along with the modern approach of probabilistic analysis. The appropriate degree of design conservatism is a tradeoff between the required resources and the probability and consequences of a failure. A probabilistic analysis properly models this tradeoff, while a worst-case analysis reveals nothing about the probability of failure, and can significantly overstate the consequences of failure. Two aerospace examples will be presented that illustrate problems that can arise with a worst-case analysis. Author

N94-23940*# Cray Systems, Bristol (England). Space Div.
SIMSAT: AN OBJECT ORIENTED ARCHITECTURE FOR REAL-TIME SATELLITE SIMULATION **c14**

Adam P. Williams *In* JPL, SpaceOps 1992: Proceedings of the Second International Symposium on Ground Data Systems for Space Mission Operations 1 Mar. 1993 p 711-716 (For primary document see N94-23832 06-66)
Avail: CASI HC A02/MF A10

Real-time satellite simulators are vital tools in the support of satellite missions. They are used in the testing of ground control systems, the training of operators, the validation of operational procedures, and the development of contingency plans. The simulators must provide high-fidelity modeling of the satellite, which requires detailed system information, much of which is not available until relatively near launch. The short time-scales and resulting high productivity required of such simulator developments culminates in the need for a reusable infrastructure which can be used as a basis for each simulator. This paper describes a major new simulation infrastructure package, the Software Infrastructure for Modelling Satellites (SIMSAT). It outlines the object oriented design methodology used, describes the resulting design, and discusses the advantages and disadvantages experienced in applying the methodology. Author (revised)

N94-23941*# Martin Marietta Corp., Denver, CO. Astronautics Group.
USING SFOC TO FLY THE MAGELLAN VENUS MAPPING MISSION
Allen W. Bucher, Robert E. Leonard, Jr., and Owen G. Short *In* JPL, SpaceOps 1992: Proceedings of the Second International Symposium on Ground Data Systems for Space Mission Operations 1 Mar. 1993 p 721-726 (For primary document see N94-23832 06-66)
Avail: CASI HC A02/MF A10

Traditionally, spacecraft flight operations at the Jet Propulsion Laboratory (JPL) have been performed by teams of spacecraft experts utilizing ground software designed specifically for the current mission. The Jet Propulsion Laboratory set out to reduce the cost of spacecraft mission operations by designing ground data processing software that could be used by multiple spacecraft missions, either sequentially or concurrently. The Space Flight Operations Center (SFOC) System was developed to provide the ground data system capabilities needed to monitor several spacecraft simultaneously and provide enough flexibility to meet the specific needs of individual projects. The Magellan Spacecraft Team utilizes the SFOC hardware and software designed for engineering telemetry analysis, both real-time and non-real-time. The flexibility of the SFOC System has allowed the spacecraft team to integrate their own tools with SFOC tools to perform the tasks required to operate a spacecraft mission. This paper describes how the Magellan Spacecraft Team is utilizing the SFOC System in conjunction with their own software tools to perform the required tasks of spacecraft event monitoring as well as engineering data analysis and trending.
Author (revised)

N94-23942*# Computer Sciences Corp., Lanham, MD.
LONG TERM TRENDING OF ENGINEERING DATA FOR THE HUBBLE SPACE TELESCOPE **c89**
Ross M. Cox *In* JPL, SpaceOps 1992: Proceedings of the Second International Symposium on Ground Data Systems for Space Mission Operations 1 Mar. 1993 p 727-732 (For primary document see N94-23832 06-66)
Avail: CASI HC A02/MF A10

A major goal in spacecraft engineering analysis is the detection of component failures before the fact. Trending is the process of monitoring subsystem states to discern unusual behaviors. This involves reducing vast amounts of data about a component or subsystem into a form that helps humans discern underlying patterns and correlations. A long term trending system has been developed for the Hubble Space Telescope. Besides processing the data for 988 distinct telemetry measurements each day, it produces plots of 477 important parameters for the entire 24 hours. Daily updates to the trend files also produce 339 thirty day trend plots each month. The total system combines command procedures to control the execution of the C-based data processing program, user-written FORTRAN routines, and commercial off-the-shelf plotting software. This paper includes a discussion the performance of the trending system and of its limitations.
Author

N94-23943*# National Aeronautics and Space Administration. Goddard Space Flight Center, Greenbelt, MD.
HIGH PERFORMANCE, LOW COST, SELF-CONTAINED, MULTIPURPOSE PC BASED GROUND SYSTEMS
Michael Forman, William Nickum (General Electric Co., Greenbelt, MD.), and Gregory Troendly (General Electric Co., Greenbelt, MD.) *In* JPL, SpaceOps 1992: Proceedings of the Second International Symposium on Ground Data Systems for Space Mission Operations 1 Mar. 1993 p 733-737 (For primary document see N94-23832 06-66)
Avail: CASI HC A01/MF A10

The use of embedded processors greatly enhances the capabilities of personal computers when used for telemetry processing and command control center functions. Parallel architectures based on the use of transputers are shown to be very versatile and reusable, and the synergism between the PC and the embedded processor with transputers results in single unit, low cost workstations of 20 less than MIPS less than or equal to 1000. Author (revised)

N94-23944*# Jet Propulsion Lab., California Inst. of Tech., Pasadena.
EXPERT DIAGNOSTICS SYSTEM AS A PART OF ANALYSIS SOFTWARE FOR POWER MISSION OPERATIONS
Jennifer A. Harris and Khosrow A. Bahrami *In its* SpaceOps 1992: Proceedings of the Second International Symposium on Ground Data Systems for Space Mission Operations 1 Mar. 1993 p 739-744 (For primary document see N94-23832 06-66)
Avail: CASI HC A02/MF A10

The operation of interplanetary spacecraft at JPL has become an increasingly complex activity. This complexity is due to advanced spacecraft designs and ambitious mission objectives which lead to operations requirements that are more demanding than those of any previous mission. For this reason, several productivity enhancement measures are underway at JPL within mission operations, particularly in the spacecraft analysis area. These measures aimed at spacecraft analysis include: the development of a multi-mission, multi-subsystem operations environment; the introduction of automated tools into this environment; and the development of an expert diagnostics system. This paper discusses an effort to integrate the above mentioned productivity enhancement measures. A prototype was developed that integrates an expert diagnostics system into a multi-mission, multi-subsystem operations environment using the Galileo Power / Pyro Subsystem as a testbed. This prototype will be discussed in addition to background information associated with it. Author (revised)

N94-23945*# National Aeronautics and Space Administration. Goddard Space Flight Center, Greenbelt, MD.
GENSAA: A TOOL FOR ADVANCING SATELLITE MONITORING WITH GRAPHICAL EXPERT SYSTEMS
Peter M. Hughes and Edward C. Luczak (Computer Sciences Corp., Beltsville, MD.) *In* JPL, SpaceOps 1992: Proceedings of the Second International Symposium on Ground Data Systems for Space Mission Operations 1 Mar. 1993 p 745-750 (For primary document see N94-23832 06-66)
Avail: CASI HC A02/MF A10

During numerous contacts with a satellite each day, spacecraft analysts must closely monitor real time data for combinations of telemetry parameter values, trends, and other indications that may signify a problem or failure. As satellites become more complex and the number of data items increases, this task is becoming increasingly difficult for humans to perform at acceptable performance levels. At the NASA Goddard Space Flight Center, fault-isolation expert systems have been developed to support data monitoring and fault detection tasks in satellite control centers. Based on the lessons learned during these initial efforts in expert system automation, a new domain-specific expert system development tool named the Generic Spacecraft Analyst Assistant (GenSAA) is being developed to facilitate the rapid development and reuse of real-time expert systems to serve as fault-isolation assistants for spacecraft analysts. Although initially domain-specific in nature, this powerful tool will support the development of highly graphical expert systems for data monitoring purposes throughout the space and commercial industry. Author (revised)

N94-23946*# Jet Propulsion Lab., California Inst. of Tech., Pasadena.
THE EVOLVING TREND IN SPACECRAFT HEALTH ANALYSIS **c17**
Russell L. Kirkpatrick *In its* SpaceOps 1992: Proceedings of the Second International Symposium on Ground Data Systems for Space Mission Operations 1 Mar. 1993 p 751-755 (For primary document see N94-23832 06-66)
Avail: CASI HC A01/MF A10

The Space Flight Operations Center inaugurated the concept of a central data repository for spacecraft data and the distribution of computing power to the end users for that data's analysis at the Jet Propulsion Laboratory. The Advanced Multimission Operations System is continuing the evolution of this concept as new technologies emerge. Constant improvements in data management tools, data visualization, and hardware lead to ever expanding ideas for improving the analysis of spacecraft health in an era of budget constrained mission operations systems. The foundation of this evolution, its history, and its current plans will be discussed. Author

N94-23947*# National Aeronautics and Space Administration. Goddard Space Flight Center, Greenbelt, MD.

ORBITAL SIGNATURE ANALYZER (OSA): A SPACECRAFT HEALTH/SAFETY MONITORING AND ANALYSIS TOOL c17

Steven Weaver (Computer Sciences Corp., Laurel, MD.), Charles DeGeorges (Computer Sciences Corp., Laurel, MD.), Joy Bush (Computer Sciences Corp., Laurel, MD.), Robert Shendock (TRW, Inc., Redondo Beach, CA.), and Daniel Mandl *In* JPL, SpaceOps 1992: Proceedings of the Second International Symposium on Ground Data Systems for Space Mission Operations 1 Mar. 1993 p 757-761 (For primary document see N94-23832 06-66)

Avail: CASI HC A01/MF A10

Fixed or static limit sensing is employed in control centers to ensure that spacecraft parameters remain within a nominal range. However, many critical parameters, such as power system telemetry, are time-varying and, as such, their 'nominal' range is necessarily time-varying as well. Predicted data, manual limits checking, and widened limit-checking ranges are often employed in an attempt to monitor these parameters without generating excessive limits violations. Generating predicted data and manual limits checking are both resource intensive, while broadening limit ranges for time-varying parameters is clearly inadequate to detect all but catastrophic problems. OSA provides a low-cost solution by using analytically selected data as a reference upon which to base its limits. These limits are always defined relative to the time-varying reference data, rather than as fixed upper and lower limits. In effect, OSA provides individual limits tailored to each value throughout all the data. A side benefit of using relative limits is that they automatically adjust to new reference data. In addition, OSA provides a wealth of analytical by-products in its execution. Author

N94-23948*# National Aeronautics and Space Administration. Goddard Space Flight Center, Greenbelt, MD.

EOS GROUND DATA SYSTEMS: A DESCRIPTION AND INTERFACE OVERVIEW

Gene Smith *In* JPL, SpaceOps 1992: Proceedings of the Second International Symposium on Ground Data Systems for Space Mission Operations 1 Mar. 1993 p 767-772 (For primary document see N94-23832 06-66)

Avail: CASI HC A02/MF A10

The Earth Observing System (EOS) is planned as a space-based measurement system, earth-science research program, and data and information system (EOSDIS). It will consist of several high data rate spacecraft with multiple earth sensing instruments which provide investigators with a thorough, longterm view of the earth's environment. Up to seven spacecraft may be supported at once, either in operational, checkout, or testing phases; and the average data rate from the EOS satellites in orbit at any one time is expected to be from 18 to 60 Mbps. Providing the data processing and flight operations support for EOS will be the EOSDIS Core System (ECS). The ECS will command and control the spacecraft; process and store the EOS data; provide access to the data for years; and support researchers. The data processing aspects of the ECS consist of a collection of Distributed Active Archive Centers (DAAC's) which perform the product generation, data archive and distribution, and information management services. Flight operations aspects will be provided by the EOS Operations Center, by instrument control centers, and by widely distributed instrument support terminals. The communications and system management aspects will be provided by the EOSDIS Science Network and the System Management Center. In addition to the EOS satellite data, other data sets from earlier earth science missions are also to be added to designated DAAC's. Other ground data systems which will provide support to EOS for acquiring, transporting, processing, and distributing the transformed spacecraft data are currently being defined or are being upgraded for the EOS era. These systems include the Space Network consisting of the Tracking and Data Relay Satellite System (TDRSS), the TDRSS Ground Terminals, and the Network Control Center as well as the night Dynamics Facility, the EOS Data and Operations System, and EOS Communications. This paper briefly describes data handling by the ECS, the support data systems, their interfaces, and their roles. Author

N94-23949*# National Aeronautics and Space Administration. Goddard Space Flight Center, Greenbelt, MD.

TELEMETRY GROUND SYSTEM DEVELOPMENT VIA THE COMPONENT APPROACH c17

Karen E. Thorn *In* JPL, SpaceOps 1992: Proceedings of the Second International Symposium on Ground Data Systems for Space Mission Operations 1 Mar. 1993 p 773-778 (For primary document see N94-23832 06-66)

Avail: CASI HC A02/MF A10

NASA's deployment of major space projects such as the Earth Observing System (EOS) will demand increased functionality and ground-based telemetry processing performance well above current capabilities. At the NASA/Goddard Space Flight Center, custom hardware and software components have been developed and combined into a unique architecture to address this problem. The hardware components utilize Application Specific Integrated Circuits (ASIC's) developed specifically to support NASA's telemetry data systems needs and designed to handle data rates up to 300 Mbps. A generalized set of software components, called the Telemetry Processing Control Environment facilitate the rapid construction of control and monitoring functions for the ground-based telemetry processing systems. This combination of hardware and software elements enables rapid construction of flexible, cost-effective telemetry processing systems capable of meeting the performance requirements facing NASA in the coming decade. Author

N94-23950*# Jet Propulsion Lab., California Inst. of Tech., Pasadena.

USING THE SPICE SYSTEM TO HELP PLAN AND INTERPRET SPACE SCIENCE OBSERVATIONS c82

Charles H. Acton, Jr. *In its* SpaceOps 1992: Proceedings of the Second International Symposium on Ground Data Systems for Space Mission Operations 1 Mar. 1993 p 781-786 (For primary document see N94-23832 06-66)

Avail: CASI HC A02/MF A10

A portable multimission information system named SPICE is used to assemble, archive, and provide easy user access to viewing geometry and other ancillary information needed by space scientists to interpret observations of bodies within our solar system. The modular nature of this system lends it to use in planning such observations as well. With a successful proof of concept on Voyager, the SPICE system has been adapted to the Magellan, Galileo and Mars Observer missions, and to a variety of ground based operations. Adaptation of SPICE for Cassini and the Russian Mars 94/96 projects is underway, and work on Cassini will follow, SPICE has been used to support observation planning for moving targets on the Hubble Space Telescope Project. Applications for SPICE on earth science, space physics and other astrophysics missions are under consideration. Author

N94-23951*# European Space Agency. European Space Operations Center, Darmstadt (Germany). Missions Operations Dept.

AN ENGINEERING DATABASE MANAGEMENT SYSTEM FOR SPACECRAFT OPERATIONS c82

Gregorio Cipollone, Michael H. McKay, and Joseph Paris (BIM SA/NV, Everberg, Belgium.) *In* JPL, SpaceOps 1992: Proceedings of the Second International Symposium on Ground Data Systems for Space Mission Operations 1 Mar. 1993 p 787-790 (For primary document see N94-23832 06-66)

Avail: CASI HC A01/MF A10

Studies at ESOC have demonstrated the feasibility of a flexible and powerful Engineering Database Management System in support for spacecraft operations documentation. The objectives set out were three-fold: first an analysis of the problems encountered by the Operations team in obtaining and managing operations documents; secondly, the definition of a concept for operations documentation and the implementation of prototype to prove the feasibility of the concept; and thirdly, definition of standards and protocols required for the exchange of data between the top-level partners in a satellite project. The EDMS prototype was populated with ERS-I satellite design data and has been used by the operations team at

ESOC to gather operational experience. An operational EDMS would be implemented at the satellite prime contractor's site as a common database for all technical information surrounding a project and would be accessible by the cocontractor's and ESA teams. Author

N94-23952*# Computer Resources International A/S (Denmark).
THE ESIS QUERY ENVIRONMENT PILOT PROJECT c82
Jens J. Fuchs, Alessandro Ciarlo (European Space Agency. ESRIN, Frascati, Italy.), and Stefano Benso (Compagnia Italiana Servizi Tecnici, Rome.) *In* JPL, SpaceOps 1992: Proceedings of the Second International Symposium on Ground Data Systems for Space Mission Operations 1 Mar. 1993 p 791-801 (For primary document see N94-23832 06-66)
Avail: CASI HC A03/MF A10

The European Space Information System (ESIS) was originally conceived to provide the European space science community with simple and efficient access to space data archives, facilities with which to examine and analyze the retrieved data, and general information services. To achieve that ESIS will provide the scientists with a discipline specific environment for querying in a uniform and transparent manner data stored in geographically dispersed archives. Furthermore it will provide discipline specific tools for displaying and analyzing the retrieved data. The central concept of ESIS is to achieve a more efficient and wider usage of space scientific data, while maintaining the physical archives at the institutions which created them, and has the best background for ensuring and maintaining the scientific validity and interest of the data. In addition to coping with the physical distribution of data, ESIS is to manage also the heterogenity of the individual archives' data models, formats and data base management systems. Thus the ESIS system shall appear to the user as a single database, while it does in fact consist of a collection of dispersed and locally managed databases and data archives. The work reported in this paper is one of the results of the ESIS Pilot Project which is to be completed in 1993. More specifically it presents the pilot ESIS Query Environment (ESIS QE) system which forms the data retrieval and data dissemination axis of the ESIS system. The others are formed by the ESIS Correlation Environment (ESIS CE) and the ESIS Information Services. The ESIS QE Pilot Project is carried out for the European Space Agency's Research and Information center, ESRIN, by a Consortium consisting of Computer Resources International, Denmark, CISET S.p.a, Italy, the University of Strasbourg, France and the Rutherford Appleton Laboratories in the U.K. Furthermore numerous scientists both within ESA and space science community in Europe have been involved in defining the core concepts of the ESIS system. Derived from text

N94-23953*# Jet Propulsion Lab., California Inst. of Tech., Pasadena.
MARS OBSERVER DATA PRODUCTION, TRANSFER, AND ARCHIVAL: THE DATA PRODUCTION ASSEMBLY LINE c82
David B. Childs *In its* SpaceOps 1992: Proceedings of the Second International Symposium on Ground Data Systems for Space Mission Operations 1 Mar. 1993 p 803-811 (For primary document see N94-23832 06-66)
Avail: CASI HC A02/MF A10

This paper describes the data production, transfer, and archival process designed for the Mars Observer Flight Project. It addresses the developmental and operational aspects of the archive collection production process. The developmental aspects cover the design and packaging of data products for archival and distribution to the planetary community. Also discussed is the design and development of a data transfer and volume production process capable of handling the large throughput and complexity of the Mars Observer data products. The operational aspects cover the main functions of the process: creating data and engineering products, collecting the data products and ancillary products in a central repository, producing archive volumes, validating volumes, archiving, and distributing the data to the planetary community. Author

N94-23954*# European Space Agency. European Space Operations Center, Darmstadt (Germany).
THE EUROPEAN SPACE AGENCY STANDARD FOR SPACE PACKET UTILISATION c17
J.-F. Kaufeler, A. Parkes (NOVA Space Ltd., Bath, England.), and A. Pidgeon (VEGA Space Systems Engineering Ltd., Harpenden, England.) *In* JPL, SpaceOps 1992: Proceedings of the Second International Symposium on Ground Data Systems for Space Mission Operations 1 Mar. 1993 p 813-818 (For primary document see N94-23832 06-66)
Avail: CASI HC A02/MF A10

This paper presents the ESA concept for the use of CCSDS defined Telemetry and Telecommand Packets at the application level. These Packets are used to monitor and control remotely a space born application. This concept is defined in a Packet Utilisation Standard (PUS) which should become applicable for all ESA missions using Packets. The production of this standard is under the responsibility of an ESA standardization group called 'COES'. Author

N94-23955*# Jet Propulsion Lab., California Inst. of Tech., Pasadena.
MULTIMISSION IMAGE PROCESSING AND SCIENCE DATA VISUALIZATION c82
William B. Green *In its* SpaceOps 1992: Proceedings of the Second International Symposium on Ground Data Systems for Space Mission Operations 1 Mar. 1993 p 819-821 (For primary document see N94-23832 06-66)
Avail: CASI HC A01/MF A10

The Operational Science Analysis (OSA) Functional area supports science instrument data display, analysis, visualization and photo processing in support of flight operations of planetary spacecraft managed by the Jet Propulsion Laboratory (JPL). This paper describes the data products generated by the OSA functional area, and the current computer system used to generate these data products. The objectives on a system upgrade now in process are described. The design approach to development of the new system are reviewed, including use of the Unix operating system and X-Window display standards to provide platform independence, portability, and modularity within the new system, is reviewed. The new system should provide a modular and scaleable capability supporting a variety of future missions at JPL. Author

N94-23956*# Centre National de la Recherche Scientifique, Toulouse (France). Inst. de Recherche en Informatique.
COMPRESSION FOR AN EFFECTIVE MANAGEMENT OF TELEMETRY DATA c82
J.-P. Arcangeli, M. Crochemore (Centre National de la Recherche Scientifique, Paris, France.), J.-N. Hourcastagnou (Centre National d'Etudes Spatiales, Toulouse, France.), and J.-E. Pin (Centre National de la Recherche Scientifique, Paris, France.) *In* JPL, SpaceOps 1992: Proceedings of the Second International Symposium on Ground Data Systems for Space Mission Operations 1 Mar. 1993 p 823-830 Sponsored in part by CNES (For primary document see N94-23832 06-66)
Avail: CASI HC A02/MF A10

A Technological DataBase (T.D.B.) records all the values taken by the physical on-board parameters of a satellite since launch time. The amount of temporal data is very large (about 15 Gbytes for the satellite TDF1) and an efficient system must allow users to have a fast access to any value. This paper presents a new solution for T.D.B. management. The main feature of our new approach is the use of lossless data compression methods. Several parametrizable data compression algorithms based on substitution, relative difference and run-length encoding are available. Each of them is dedicated to a specific type of variation of the parameters' values. For each parameter, an analysis of stability is performed at decommutation time, and then the best method is chosen and run. A prototype intended to process different sorts of satellites has been developed. Its performances are well beyond the requirements and prove that data compression is both time and space efficient. For instance, the amount of data for TDF1 has been reduced to 1.05 Gbytes (compression ratio is 1/13) and access time for a typical query has been reduced from 975 seconds to 14 seconds. Author

N94-23957*# National Aeronautics and Space Administration, Washington, DC.
SPACE STATION FREEDOM GROUND DATA SYSTEM: DESIGN AND OPERATIONS c82
Richard A. Dunning, Jr. (Booz-Allen and Hamilton, Inc., Washington, DC.), Frederick W. Knops, III (Booz-Allen and Hamilton, Inc., Seabrook, MD.), Stanley A. Fishkind, and Michael P. Pasciuto *In* JPL, SpaceOps 1992: Proceedings of the Second International Symposium on Ground Data Systems for Space Mission Operations 1 Mar. 1993 p 831-836 (For primary document see N94-23832 06-66)
Avail: CASI HC A02/MF A10

Over the previous year the Space Station Freedom (SSF) Program (SSFP) ground data distribution system has become independent of a number of data systems that were to have been provided by other National Aeronautics and Space Administration (NASA) programs. Consequently, the SSFP has outlined the basic architecture of a new data system dedicated to supporting SSF requirements. This has been accomplished through a complete redesign of the ground network and a reallocation of selected functions. There are a number of aspects of the new ground data distribution system that are unique among NASA programs. These considerations make SSF ground data distribution one of the most extensive and complex data management challenges encountered in the arena of Space Operations. A description of this system comprises the main focus of the paper. Author

N94-23958*# Defence Research Agency, Farnborough (England). Data Technology Section.

EARTH OBSERVATION ARCHIVE ACTIVITIES AT DRA FARNBOROUGH **c82**

M. D. Palmer and J. M. Williams (Serco Space Ltd., Southall, England.) *In* JPL, SpaceOps 1992: Proceedings of the Second International Symposium on Ground Data Systems for Space Mission Operations 1 Mar. 1993 p 837-840 (For primary document see N94-23832 06-66)
Avail: CASI HC A01/MF A10

Space Sector, Defence Research Agency (DRA), Farnborough have been actively involved in the acquisition and processing of Earth Observation data for over 15 years. During that time an archive of over 20,000 items has been built up. This paper describes the major archive activities, including: operation and maintenance of the main DRA Archive, the development of a prototype Optical Disc Archive System (ODAS), the catalog systems in use at DRA, the UK Processing and Archive Facility for ERS-1 data, and future plans for archiving activities. Author

N94-23959*# Compagnia Italiana Servizi Tecnici, Rome.

OPERATIONAL CHARACTERISATION OF REQUIREMENTS AND EARLY VALIDATION ENVIRONMENT FOR HIGH DEMANDING SPACE SYSTEMS **c82**

E. Barro, A. DelBufalo, and F. Rossi *In* JPL, SpaceOps 1992: Proceedings of the Second International Symposium on Ground Data Systems for Space Mission Operations 1 Mar. 1993 p 845-850 (For primary document see N94-23832 06-66)
Avail: CASI HC A02/MF A10

The definition of some modern high demanding space systems requires a different approach to system definition and design from that adopted for traditional missions. System functionality is strongly coupled to the operational analysis, aimed at characterizing the dynamic interactions of the flight element with its surrounding environment and its ground control segment. Unambiguous functional, operational and performance requirements are to be defined for the system, thus improving also the successive development stages. This paper proposes a Petri Nets based methodology and two related prototype applications (to ARISTOTELES orbit control and to Hermes telemetry generation) for the operational analysis of space systems through the dynamic modeling of their functions and a related computer aided environment (ISIDE) able to make the dynamic model work, thus enabling an early validation of the system functional representation, and to provide a structured system requirements data base, which is the shared knowledge base interconnecting static and dynamic applications, fully traceable with the models and interfaceable with the external world. Author

N94-23960*# National Aeronautics and Space Administration, Washington, DC.

TOWARD LOWERING THE COST OF MISSION OPERATIONS

S. D. Wall (Jet Propulsion Lab., California Inst. of Tech., Pasadena.) and K. W. Ledbetter *In* JPL, SpaceOps 1992: Proceedings of the Second International Symposium on Ground Data Systems for Space Mission Operations 1 Mar. 1993 p 851-855 (For primary document see N94-23832 06-66)
Avail: CASI HC A01/MF A10

The mission operations system is one of the more significant drivers of the cost of the mission operations and data analysis segment of missions. In large or long-lived projects, the MOS can also be a driver in total mission cost. Larger numbers of missions, together with an increasingly cost-conscious environment, dictate that future missions must more strictly control costs as they perform to their requirements. It is therefore prudent to examine the conduct of past missions for ways to conserve resources. In this paper we review inputs made to past projects' 'lessons-learned' activities, in which personnel from past projects (among other things) identified major cost drivers of MOS's and considered how economies were or might have been realized in both design and performance of their MOS. Common themes among four such reviews are summarized in an attempt to provide suggestions for cost reduction in future missions. Author

N94-23961*# National Aeronautics and Space Administration. Goddard Space Flight Center, Greenbelt, MD.

NEW MISSION REQUIREMENTS METHODOLOGIES FOR SERVICES PROVIDED BY THE OFFICE OF SPACE COMMUNICATIONS

Dwight P. Holmes (Jet Propulsion Lab., California Inst. of Tech., Pasadena.), J. R. Hall (Jet Propulsion Lab., California Inst. of Tech., Pasadena.), William Macoughtry, and Robert Spearing (Telos Corp., Chantilly, VA.) *In* JPL, SpaceOps 1992: Proceedings of the Second International Symposium on Ground Data Systems for Space Mission Operations 1 Mar. 1993 p 857-862 (For primary document see N94-23832 06-66)
Avail: CASI HC A02/MF A10

The Office of Space Communications, NASA Headquarters, has recently revised its methodology for receiving, accepting and responding to customer requests for use of that office's tracking and communications capabilities. This revision is the result of a process which has become over-burdened by the size of the currently active and proposed missions set, requirements reviews that focus on single missions rather than on mission sets, and negotiations most often not completed early enough to effect needed additions to capacity or capability prior to launch. The requirements-coverage methodology described is more responsive to project/program needs and provides integrated input into the NASA budget process early enough to effect change, and describes the mechanisms and tools in place to insure a value-added process which will benefit both NASA and its customers. Key features of the requirements methodology include the establishment of a mechanism for early identification of and systems trades with new customers, and delegates the review and approval of requirements documents to NASA centers in lieu of Headquarters, thus empowering the system design teams to establish and negotiate the detailed requirements with the user. A Mission Requirements Request (MRR) is introduced to facilitate early customer interaction. The expected result is that the time to achieve an approved set of implementation requirements which meet the customer's needs can be greatly reduced. Finally, by increasing the discipline in requirements management, through the use of base lining procedures, a tighter coupling between customer requirements and the budget is provided. A twice-yearly projection of customer requirements accommodation, designated as the Capacity Projection Plan (CPP), provides customer feedback allowing the entire mission set to be serviced. Author

N94-23962*# Centre National d'Etudes Spatiales, Toulouse (France).

FROM REQUIREMENTS TO ACCEPTANCE TESTS **c61**

Lionel Baize and Helene Pasquier *In* JPL, SpaceOps 1992: Proceedings of the Second International Symposium on Ground Data Systems for Space Mission Operations 1 Mar. 1993 p 863-866 (For primary document see N94-23832 06-66)
Avail: CASI HC A01/MF A10

From user requirements definition to accepted software system, the software project management wants to be sure that the system will meet the requirements. For the development of a telecommunication satellites Control Centre, C.N.E.S. has used new rules to make the use of tracing matrix easier. From Requirements to Acceptance Tests, each item of a document must have an identifier. A unique matrix traces the system and allows the tracking of the consequences of a change in the requirements. A tool has been developed, to import documents into a relational data base. Each record of the data base corresponds to an item of a document, the access key is the item identifier. Tracing matrix is also processed, providing automatically links between the different documents. It enables the reading on the same screen of traced items. For example one can read simultaneously the User Requirements items, the corresponding Software Requirements items and the Acceptance Tests. Author

N94-23963*# Jet Propulsion Lab., California Inst. of Tech., Pasadena.
RESOURCE ALLOCATION PLANNING WITH INTERNATIONAL COMPONENTS **c81**
Gene Burke, Ralph Durham, Frank Leppla, and David Porter (California Inst. of Tech., Pasadena.) *In its* SpaceOps 1992: Proceedings of the Second International Symposium on Ground Data Systems for Space Mission Operations 1 Mar. 1993 p 867-874 (For primary document see N94-23832 06-66)
Avail: CASI HC A02/MF A10

Dumas, Briggs, Reid and Smith (1989) describe the need for identifying mutually acceptable methodologies for developing standard agreements for the exchange of tracking time or facility use among international components. One possible starting point is the current process used at the Jet Propulsion Laboratory (JPL) in planning the use of tracking resources. While there is a significant promise of better resource utilization by international cooperative agreements, there is a serious challenge to provide convenient user participation given the separate project and network locations. Coordination among users and facility providers will require a more decentralized communication process and a wider variety of automated planning tools to help users find potential exchanges. This paper provides a framework in which international cooperation in the utilization of ground based space communication systems can be facilitated. Author

N94-23964*# National Aeronautics and Space Administration. Goddard Space Flight Center, Greenbelt, MD.
AN INTELLIGENT PLANNING AND SCHEDULING SYSTEM FOR THE HST SERVICING MISSIONS **c81**
Jay Johnson (Bendix Field Engineering Corp., Seabrook, MD.), Lynn Bogovich (Bendix Field Engineering Corp., Seabrook, MD.), Alan Tuchman (Bendix Field Engineering Corp., Seabrook, MD.), Andrew Kispert (Bendix Field Engineering Corp., Seabrook, MD.), Brenda Page (Bendix Field Engineering Corp., Seabrook, MD.), Christian Burkhardt (Bendix Field Engineering Corp., Seabrook, MD.), Ronald Littlefield (Bendix Field Engineering Corp., Seabrook, MD.), David McLean (Bendix Field Engineering Corp., Seabrook, MD.), William Potter, and William Ochs et al *In* JPL, SpaceOps 1992: Proceedings of the Second International Symposium on Ground Data Systems for Space Mission Operations 1 Mar. 1993 p 875-880 (For primary document see N94-23832 06-66)
(Contract NAS5-27772)
Avail: CASI HC A02/MF A10

A new, intelligent planning and scheduling system has been delivered to NASA-Goddard Space Flight Center (GSFC) to provide support for the up-coming Hubble Space Telescope (HST) Servicing Missions. This new system is the Servicing Mission Planning and Replanning Tool (SM/PART). SM/PART is written in C and runs on a UNIX-based workstation (IBM RS/6000) under Motif. SM/PART effectively automates the complex task of building or rebuilding integrated timelines and command plans which are required by HST Servicing Mission personnel at their consoles during the missions. SM/PART is able to quickly build or rebuild timelines based on information stored in a Knowledge Base (KB) by using an Artificial Intelligence (AI) tool called the Planning And Resource Reasoning (PARR) shell. After a timeline has been built in the batch mode, it can be displayed and edited in an interactive mode with help from the PARR shell. Finally a detailed command plan is generated. The capability to quickly build or rebuild timelines and command plans provides an additional safety factor for the HST, Shuttle and Crew. Author

N94-23965*# National Aeronautics and Space Administration. Goddard Space Flight Center, Greenbelt, MD.
SCHEDULING THE FUTURE NASA SPACE NETWORK: EXPERIENCES WITH A FLEXIBLE SCHEDULING PROTOTYPE **c81**
Nadine Happell (Stanford Telecommunications, Inc., Reston, VA.), Karen L. Moe, and Jay Minnix (Stanford Telecommunications, Inc., Reston, VA.) *In* JPL, SpaceOps 1992: Proceedings of the Second International Symposium on Ground Data Systems for Space Mission Operations 1 Mar. 1993 p 881-886 (For primary document see N94-23832 06-66)
Avail: CASI HC A02/MF A10

NASA's Space Network (SN) provides telecommunications and tracking services to low earth orbiting spacecraft. One proposal for improving resource allocation and automating conflict resolution for the SN is the concept of flexible scheduling. In this concept, each Payload Operations Control Center (POCC) will possess a Space Network User POCC Interface (SNUPI) to support the development and management of flexible requests. Flexible requests express the flexibility, constraints, and repetitious nature of the user's communications requirements. Flexible scheduling is expected to improve SN resource utilization and user satisfaction, as well as reduce the effort to produce and maintain a schedule. A prototype testbed has been developed to better understand flexible scheduling as it applies to the SN. This testbed consists of a SNUPI workstation, an SN scheduler, and a flexible request language that conveys information between the two systems. All three are being evaluated by operations personnel. Benchmark testing is being conducted on the scheduler to quantify the productivity improvements achieved with flexible requests. Author

N94-23966*# National Aeronautics and Space Administration. Goddard Space Flight Center, Greenbelt, MD.
SOFTWARE REUSE IN SPACECRAFT PLANNING AND SCHEDULING SYSTEMS **c81**
David McLean (Bendix Field Engineering Corp., Seabrook, MD.), Alan Tuchman (Bendix Field Engineering Corp., Seabrook, MD.), Todd Broseghini (Bendix Field Engineering Corp., Seabrook, MD.), Wen Yen (Bendix Field Engineering Corp., Seabrook, MD.), Brenda Page (Bendix Field Engineering Corp., Seabrook, MD.), Jay Johnson (Bendix Field Engineering Corp., Seabrook, MD.), Lynn Bogovich (Bendix Field Engineering Corp., Seabrook, MD.), Chris Burkhardt (Bendix Field Engineering Corp., Seabrook, MD.), James McIntyre (Bendix Field Engineering Corp., Seabrook, MD.), and Scott Klein (Bendix Field Engineering Corp., Seabrook, MD.) et al *In* JPL, SpaceOps 1992: Proceedings of the Second International Symposium on Ground Data Systems for Space Mission Operations 1 Mar. 1993 p 887-892 (For primary document see N94-23832 06-66)
(Contract NAS5-27772)
Avail: CASI HC A02/MF A10

The use of a software toolkit and development methodology that supports software reuse is described. The toolkit includes source-code-level library modules and stand-alone tools which support such tasks as data reformatting and report generation, simple relational database applications, user interfaces, tactical planning, strategic planning and documentation. The current toolkit is written in C and supports applications that run on IBM-PC's under DOS and UNIX-based workstations under OpenLook and Motif. The toolkit is fully integrated for building scheduling systems that reuse AI knowledge base technology. A typical scheduling scenario and three examples of applications that utilize the reuse toolkit will be briefly described. In addition to the tools themselves, a description of the software evolution and reuse methodology that was used is presented. Author

N94-23967*# Centre National d'Etudes Spatiales, Toulouse (France).
PLANNING: MANAGEMENT OF PREDICTABILITY AND UNCERTAINTY AND KEEPING ABREAST OF DEVELOPMENTS **c81**
Christophe Bastien-Thiry and Gerard Verfaillie *In* JPL, SpaceOps 1992: Proceedings of the Second International Symposium on Ground Data Systems for Space Mission Operations 1 Mar. 1993 p 893-898 (For primary document see N94-23832 06-66)
Avail: CASI HC A02/MF A10

The purpose of this study is to propose method to set up and control of a space mission plan such as that of the HERMES spaceplane. The interest of this subject, other than its complexity, is due to the need to manage imprecision and uncertainty during a mission, as well as changes in between missions. Under these conditions, the set up and control of a flight plan require certain special attention and this has led us to define a certain number of qualities: mastery of complexity in order to resolve conflicts between activities: configuration, resource and time management; consideration of various criteria such as risk minimization or the attainment of mission objectives; robustness and flexibility to allow for hazards and deviations from the norm during operation without having to draw up new plans; aptness for replanning by making changes to the plan without having to set up the whole plan again; and memorization and explanation facility in order to manage developments between missions. Author

N94-23968*# Jet Propulsion Lab., California Inst. of Tech., Pasadena.
ESTIMATING THE DEEP SPACE NETWORK MODIFICATION COSTS TO PREPARE FOR FUTURE SPACE MISSIONS BY USING MAJOR COST DRIVERS **c83**
Donald S. Remer, Josef Sherif, and Harry R. Buchanan *In its* SpaceOps 1992: Proceedings of the Second International Symposium on Ground Data

Systems for Space Mission Operations 1 Mar. 1993 p 899-904 (For primary document see N94-23832 06-66)
Avail: CASI HC A02/MF A10

This paper develops a cost model to do long range planning cost estimates for Deep Space Network (DSN) support of future space missions. The paper focuses on the costs required to modify and/or enhance the DSN to prepare for future space missions. The model is a function of eight major mission cost drivers and estimates both the total cost and the annual costs of a similar future space mission. The model is derived from actual cost data from three space missions: Voyager (Uranus), Voyager (Neptune), and Magellan. Estimates derived from the model are tested against actual cost data for two independent missions, Viking and Mariner Jupiter/Saturn (MJS). Author

N94-24302*# National Aeronautics and Space Administration. Lewis Research Center, Cleveland, OH.
CONTROLLABILITY OF FREE-PISTON STIRLING ENGINE/LINEAR ALTERNATOR DRIVING A DYNAMIC LOAD
M. David Kankam and Jeffrey S. Rauch (Sverdrup Technology, Inc., Brook Park, OH.) Feb. 1994 9 p Presented at the 28th Intersociety Energy Conversion Engineering Conference, Atlanta, GA, 8-13 Aug. 1993; sponsored by ANS, SAE, ACS, IEEE, ASME, AIAA, and AIChE
(Contract NAS3-25266; RTOP 590-13-11)
(NASA-TM-106497; E-8488; NAS 1.15:106497) Avail: CASI HC A02/MF A01

This paper presents the dynamic behavior of a Free-Piston Stirling Engine/linear alternator (FPSE/LA) driving a single-phase fractional horse-power induction motor. The controllability and dynamic stability of the system are discussed by means of sensitivity effects of variations in system parameters, engine controller, operating conditions, and mechanical loading on the induction motor. The approach used expands on a combined mechanical and thermodynamic formulation employed in a previous paper. The application of state-space technique and frequency domain analysis enhances understanding of the dynamic interactions. Engine-alternator parametric sensitivity studies, similar to those of the previous paper, are summarized. Detailed discussions are provided for parametric variations which relate to the engine controller and system operating conditions. The results suggest that the controllability of a FPSE-based power system is enhanced by proper operating conditions and built-in controls. Author

N94-24523 Technische Univ., Twente (Netherlands). Dept. of Applied Mathematics.
REDUCED GAME PROPERTIES OF EGALITARIAN DIVISION RULES FOR COOPERATIVE GAMES
T. S. H. Driessen and Y. Funaki Jun. 1993 32 p Limited Reproducibility: More than 20% of this document may be affected by microfiche quality
(PB94-111689; MEMO-1136) Avail: Issuing Activity (National Technical Information Service (NTIS))

The egalitarian non-individual contribution (ENIC) value represents the equal division of the surplus of the total profits, given that each player is already allocated some kind of a yet unspecified individual contribution. Four particular versions of the ENIC-value are also considered by specifying the notion of individual contribution. An axiomatic characterization of the ENIC-value is provided on the class of cooperative games with a fixed player set as well as a variable player set. The latter axiomatization involves a consistency axiom in terms of reduced games. NTIS

N94-25008# Advisory Group for Aerospace Research and Development, Neuilly-Sur-Seine (France).
NEW ADVANCES IN MISSION PLANNING AND REHEARSAL SYSTEMS [LES NOUVELLES APPROCHES POUR LES SYSTEMES DE PLANIFICATION ET DE SIMULATION DES MISSIONS]
Oct. 1993 125 p Lectures held in Kjeller, Norway, 11-12 Oct. 1993, in Madrid, Spain, 14-15 Oct. 1993, and in Hanscom AFB, MA, 28-29 Oct. 1993
(AGARD-LS-192; ISBN-92-835-0723-1) Copyright Avail: CASI HC A06/MF A02

Modern data processing technology with greatly enhanced capabilities is being used in both the airborne and ground-based segments of the NATO Air Forces. A key element in the interface between these segments is provided by the mission planning systems which are used to analyze, fuse, and refine the information at air bases. The synergy of modern avionics systems and ground-based data networks cannot be fully realized unless mission data are provided effectively and rapidly to aircraft before the mission is commenced. Aircrew workloads must be minimized by the development of user-friendly planning systems which incorporate rehearsal facilities. To present some of the design and engineering aspects of mission planning systems, with particular emphasis on human factors considerations, examples of modern mission planning and rehearsal systems will be described. For individual titles, see N94-25009 through N94-25016.

N94-25009# Draper (Charles Stark) Lab., Inc., Cambridge, MA.
OVERALL SYSTEM CONCEPTS IN MISSION PLANNING
Stephan E. Kolitz and Robert M. Beaton *In* AGARD, New Advances in Mission Planning and Rehearsal Systems, Oct. 1993 17 p (For primary document see N94-25008 06-66)
Copyright Avail: CASI HC A03/MF A02

This paper describes the fundamental system concepts that are useful in addressing future growth areas of mission planning systems as reported in Section 2.1 of the AGARD Advisory Report 313 'Mission Planning Systems for Tactical Aircraft' (Pre-Flight and In-Flight). A significant requirement for mission planning systems, especially for autonomous vehicles, is the ability to quickly plan and/or replan a complex task or mission. Fast, efficient replanning is especially important because the state of the world can change abruptly and radically during the course of a mission. Mission planning systems must embody the capabilities necessary to swiftly replan actions in order to accommodate a vehicle's changing health or environment while continuing to pursue mission objectives. The complexity of mission planning problems has led to the use of hierarchical decompositions to make those problems manageable. The hierarchical approach to decision-making decomposes a large problem into a number of separate levels or sub-problems, thereby reducing the overall complexity, ideally without compromising overall system performance. In this lecture paper, an architecture for a mission planning system is presented with descriptions of the associated planning algorithms and planning management functions. Author (revised)

N94-25010# Royal Air Force, Farnborough (England). Inst. of Aviation Medicine.
HUMAN FACTORS OF MISSION PLANNING SYSTEMS: THEORY AND CONCEPTS
R. M. Taylor *In* AGARD, New Advances in Mission Planning and Rehearsal Systems Oct. 1993 22 p (For primary document see N94-25008 06-66)
Copyright Avail: CASI HC A03/MF A02

Human factors of advanced Mission Planning Systems (MPS) are considered from a theoretical and conceptual point of view. MPS's are treated as a class of human-machine systems concerned with the functions of planning and rehearsal of mission tasks. The functions of planning and rehearsal are considered in relation to decision-making and actions in dynamic situations. Planning and rehearsal are essential for the identification and clarification of mission goals. Planning and rehearsal are cognitive tasks involving the skills of reasoning, decision-making, visualization, and mental simulation, with associated human capabilities and limitations. Performance of these preparatory cognitive skills reduces in-flight workload and affects the availability, quality, and structure of mission-relevant knowledge. Knowledge and understanding gained during planning influences the performance of in-flight mission tasks. Perceptions of mission problems and situations are initially formulated during planning and rehearsal. Inappropriate perceptions result in inappropriate plans, reduced in-flight situational awareness, erroneous decisions, and degraded mission performance. The psychology of systems design is reviewed with reference to MPS requirements. Particular attention is given to the role of automation and aiding technology in the performance of planning and rehearsal tasks. The nature of air crew involvement in MPS decision making is a key system design issue determining mission effectiveness. Relevant human capabilities and limitations, and the level of air crew active involvement and machine autonomy, need to be carefully considered in initial systems design. A human-systems design paradigm based on principles of adaptive aiding and co-operative functioning is proposed for advanced MPS design. The cognitive compatibility of the air crew task and system interface is a key requirement for effective air crew involvement in MPS processes and for successful MPS functioning. Author (revised)

N94-25011# British Aerospace Defense Ltd., Farnborough (England).
HUMAN FACTORS OF MISSION PLANNING SYSTEMS: APPLICATIONS AND IMPLEMENTATION
I. Ross *In* AGARD, New Advances in Mission Planning and Rehearsal Systems Oct. 1993 7 p (For primary document see N94-25008 06-66)
Copyright Avail: CASI HC A02/MF A02

It was apparent from the beginning of the work carried out by the Joint Working Group in Phase One, that the successful application and implementation of human factors considerations were an essential part of the design of Mission Planning Systems (MPS). Although these considerations were discussed in Phase One, in Phase Two human factors were investigated in greater detail. It was considered essential that, as with all systems design, a full understanding of the information requirements and information flow of MPS's in Pre-flight, In-flight, and Post-flight situations was understood, as well as the dependencies under which the system must operate. Ideally, each component should be complimentary and be designed in accordance with requirements of each component as well as the 'mission' system as a whole. The Phase One report included descriptions of the emerging MPS including the ergonomics and the interface of each system. There was a high degree of similarity apparent in both approach and implementation. The Phase Two report explored many of the issues raised in greater detail, particularly that of trust that aircrew must have in the systems and the subsequently planned mission and the interface through which the user must communicate with the system. Author (revised)

N94-25012# Draper (Charles Stark) Lab., Inc., Cambridge, MA.
COMPUTING TECHNIQUES IN MISSION PLANNING
Stephan E. Kolitz *In* AGARD, New Advances in Mission Planning and Rehearsal Systems Oct. 1993 20 p (For primary document see N94-25008 06-66)
Copyright Avail: CASI HC A03/MF A02

This lecture paper addresses issues related to the major concern stated in Section 5.1 of the AGARD Advisory Report 313 'Mission Planning Systems for Tactical Aircraft (Pre-Flight and In-Flight).' A major concern involving all aspects of mission planning systems is the tremendous computational burden that is required for a wide variety of mission planning functions. The approaches for solving the Mission Planning Problem can generally be grouped into two categories: approaches that guarantee optimality; and heuristic approaches that do not guarantee optimality. Useful solution methodologies can be characterized by polynomial running time complexity. This paper concentrates on computational issues that arise when using hierarchical decomposition to solve the Mission Planning Problem. An analytic methodology and sample analyses are presented for an abstract planning system. Author (revised)

N94-25013# Defence Research Agency, Farnborough (England).
MISSION PLANNING AND MISSION REHEARSAL SYSTEMS: DISPLAYS AND OTHER INTERACTIVE TECHNIQUES
Geoffrey H. Hunt *In* AGARD, New Advances in Mission Planning and Rehearsal Systems Oct. 1993 12 p (For primary document see N94-25008 06-66)
Copyright Avail: CASI HC A03/MF A02

Recent years have witnessed a very rapid growth in the power of computer-based systems of all types. This rapid growth has been based on faster devices, better interfaces, and the use of parallel processing. Mission planning systems have shared in this evolution and there is every reason to believe that, for the medium term at least, this increase in power will continue. The effective use of this power by the user implies that a proper collaboration is established between the user (man) and the system (machine) which can utilize to the maximum the particular capabilities of each. This requires that the greatest attention is given to the design of the interface between machine and user since the interface can significantly constrain the overall performance of the man-machine system. This lecture describes the man-machine interface technologies which are currently available to the developer of mission planning systems and provides descriptions of some of the advances in these technologies which are expected to become available in the short to medium term. Author (revised)

N94-25014# GEC Avionics Ltd., Rochester (England). Display Systems Group.
GROUND BASED MISSION PLANNING SYSTEMS
J. Milligan and B. H. Camp *In* AGARD, New Advances in Mission Planning and Rehearsal Systems Oct. 1993 12 p (For primary document see N94-25008 06-66)
Copyright Avail: CASI HC A03/MF A02

For complex combined missions, it has been necessary for Ground Based Mission Planning to be performed as close to the individual mission as possible. With the advent of intelligent Automated Mission Planning Systems (AMPS) and reliable, secure communications, the speed of data exchange and completion of the subsequent mission planning has greatly increased. This paper outlines the mission cycle and briefly examines a range of mission tasking activity. This framework is used to describe a possible operating base tasking and planning system architecture, within which the AMPS architecture is explained. Typical AMPS databases and functions are examined before a description of the actual task definition and mission planning processes. Mission validation and rehearsal capabilities are outlined, and the range of data outputs is examined. The paper concludes by briefly explaining the archiving of the resulting data. Author (revised)

N94-25015# Dassault-Breguet Aviation, Saint Cloud (France).
IN FLIGHT MISSION PLANNING IN THE COPILOTE ELECTRONIQUE
G. Champigneux *In* AGARD, New Advances in Mission Planning and Rehearsal Systems Oct. 1993 12 p (For primary document see N94-25008 06-66)
Copyright Avail: CASI HC A03/MF A02

This paper describes the functional aspects and the engineering guidelines of an in-flight mission planning system. The system is being developed as a part of the French project known as 'Electronic Copilot.' This project is lead by Dassault Aviation with the support of French official services (DRET STTE) and involves many industrial and scientific partners. Emphasis is put on the in-flight Pilot-System relationship and dynamic task allocation. A few words are said about knowledge acquisition methodologies and tools that are suitable for the development of a cognitive planning assistant. Author (revised)

N94-25016# Evans and Sutherland Computer Corp., Salt Lake City, UT. Simulation Div.
MISSION REHEARSAL IN THE SOF-ATS PROGRAM
John Ellis *In* AGARD, New Advances in Mission Planning and Rehearsal Systems Oct. 1993 8 p (For primary document see N94-25008 06-66)
Copyright Avail: CASI HC A02/MF A02

The USAF SOF-ATS program includes both aircrew training and mission rehearsal elements. Recent advances in computer image generation and database generation have made possible the rapid database construction and scene realism necessary for mission rehearsal. This paper describes the development of computer image generator technology from that used in military flight simulation to meet the needs of the SOF-ATS mission rehearsal system. Author

N94-25293# Technische Univ., Eindhoven (Netherlands).
TIMED COLOURED PETRI NETS AND THEIR APPLICATION TO LOGISTICS Ph.D. Thesis
Willibrordus M. P. vanderAalst 1992 277 p
(ETN-94-95310) Avail: CASI HC A13/MF A03

The modeling and analysis of complex logistic systems are studied. An approach based on a timed colored Petri net model is presented. The Petri net concept meets the requirements set out by the distributed nature of a logistic system. The addition of color and time enables the modeling of data structures and a complex temporal behavior. A major advantage compared to other methods is the availability of various kinds of analysis. The interval timed colored Petri nets model is described. The semantics of this model is given in terms of a transition system. To do this, some basic notations and concepts are introduced. Three of the four analysis methods, developed to analyze interval timed colored Petri nets, are presented. These methods are compared with existing analysis methods. It is shown how these methods can be used to analyze interval timed colored Petri nets with large color sets. The language ExSpect and the tools developed to support this language are described. The field of logistics and the application of Petri nets to logistic problems are presented. A library containing logistic building blocks is included. The usefulness of the approach is discussed. ESA

N94-23234*# Florida Agricultural and Mechanical Univ., Tallahassee. Dept. of Industrial Engineering.
A FRAMEWORK FOR SFC/DC SYSTEM DATA ANALYSIS
Martha A. Centeno *In* NASA. Kennedy Space Center, NASA/ASEE Summer Faculty Fellowship Program Oct. 1993 p 77-90 (For primary document see N94-23230 06-80)
Avail: CASI HC A03/MF A04

67 THEORETICAL MATHEMATICS

Includes topology and number theory.

N94-23094 Vrije Univ., Amsterdam (Netherlands). Faculteit der Wiskunde en Informatica.
CHARACTERIZATION OF MEASURES WITH A CONVEX RANGE: A GENERALIZATION OF LYAPOUNOV'S THEOREM
J. Gouweleeuw Mar. 1992 20 p See also PB92-198696 Limited Reproducibility: More than 20% of this document may be affected by microfiche quality
(PB93-220523; WS-394) Avail: CASI HC A03

Let mu vector = (mu(sub 1),...,mu(sub n)) be a vector measure on a measurable space (Omega, F prime), such that each mu(sub i) is nonnegative and finite. In the paper, necessary and sufficient conditions on mu vector are stated such that R(mu vector) := ((mu(sub 1)(F),...,mu(sub n)(F)): F is a member of F prime) is convex. The result is a generalization of Lyapounov's theorem. NTIS

N94-24658# California Univ., Berkeley. Lawrence Berkeley Lab.
COADJOINT ORBITS AND CONFORMAL FIELD THEORY Ph.D. Thesis
W. Taylor, IV Aug. 1993 151 p
(Contract DE-AC03-76SF-00098)
(DE94-002285; LBL-34507; UCB-PTH-93/26) Avail: CASI HC A08/MF A02

This thesis is primarily a study of certain aspects of the geometric and algebraic structure of coadjoint orbit representations of infinite-dimensional Lie groups. The goal of this work is to use coadjoint orbit representations to construct conformal field theories, in a fashion analogous to the free-field constructions of conformal field theories. The new results which are presented in this thesis are as follows: first, an explicit set of formulae are derived giving an algebraic realization of coadjoint orbit representations in terms of differential operators acting on a polynomial Fock space. These representations are equivalent to dual Verma module representations. Next, intertwiners are explicitly constructed which allow the construction of resolutions for irreducible representations using these Fock space realizations. Finally, vertex operators between these irreducible representations are explicitly constructed as chain maps between the resolutions; these vertex operators allow the construction of rational conformal field theories according to an algebraic prescription. DOE

N94-24936 Yale Univ., New Haven, CT.
FRACTAL GEOMETRY IN PHYSICS Technical Report, 1 Oct. 1992 - 30 Sep. 1993
Benoit B. Mandelbrot 30 Sep. 1993 3 p Limited Reproducibility: More than 20% of this document may be affected by microfiche quality
(Contract N00014-90-J-1026)
(AD-A273271) Avail: Issuing Activity (Defense Technical Information Center (DTIC))

Fractal geometry in physics is discussed. Simulation studies of diffraction-limited aggregation (DLA)-coexistence of self similar features and of features that clearly depart from self similarity are addressed. Development of the concept of numerical lacunarities is also discussed. DTIC

N94-25314# Sheffield Univ. (England). Dept. of Automatic Control and Systems Engineering.
VALIDATING IDENTIFIED NONLINEAR MODELS WITH CHAOTIC DYNAMICS
Luis A. Aguirre and S. A. Billings Mar. 1993 32 p
(Grants CNPq-200597/90-6; SERC-GR/H-35286)
(RR-469; ETN-94-95136) Avail: CASI HC A03/MF A01

The effectiveness of several criteria for validating models which exhibit chaotic dynamics is investigated. Trajectories in the pseudo phase plane, Poincare sections, bifurcation diagrams, the largest Lyapunov exponent, and the correlation dimension are considered. The Duffing-Ueda equation and four identified models are used. The purpose was to assess the real benefit of using such criteria as measures of the quality of the identified model. The results show that models with similar invariants may have very different bifurcation behaviors. The requirement that an identified model should reproduce the bifurcation pattern of the original system is a well suited criterion for validation purposes. ESA

N94-25323# Sheffield Univ. (England). Dept. of Automatic Control and Systems Engineering.
CONTROLLING REGULAR AND CHAOTIC DYNAMICS IN THE DUFFING-UEDA OSCILLATOR
Luis A. Aguirre and S. A. Billings May 1993 34 p
(Grants CNPq-200597/90-6; SERC-GR/H-35286)
(RR-477; ETN-94-95143) Avail: CASI HC A03/MF A01

The control of the electrical oscillator which is modeled by the Duffing-Ueda equation is investigated. Two control schemes are suggested: the addition of an external weak force operating in a closed loop, and a model based control scheme. The first is concerned with suppressing chaos by means of adding an external weak force to the input driving oscillator. The second procedure uses a reference model to produce appropriate signals for the oscillator. It is shown that this control scheme is effective in regulating and in track problems. A procedure for determining the model of the system is discussed. A discrete model of the oscillator is used. A procedure for identifying models based on nonlinear autoregressive moving average model with exogenous inputs is indicated. ESA

N94-25328# International Centre for Theoretical Physics, Trieste (Italy).
ON THE CONTINUITY OF LIMIT CAPACITY OF CENTRAL CANTOR SETS
M. E. Munoz and V. J. Vera Sep. 1992 8 p
(DE93-613022; IC-92/264) Avail: CASI HC A02/MF A01 (US Sales Only)

A metric topology is defined on the family of central Cantor sets. In this topology, the Hausdorff dimension and the limit capacity depend continuously on the central Cantor set. DOE

N94-25480# Cranfield Inst. of Tech., Bedford (England). Dept. of Aerospace Science.
ARBITRARY-ORDER NUMERICAL SCHEMES FOR LINEAR HYPERBOLIC SYSTEMS
Jian Shi Sep. 1992 21 p
(Cranfield-Aero-9211; ISBN-1-87-156449-2; ETN-94-95218) Avail: CASI HC A03/MF A01

An extension of the work carried out on arbitrary order numerical methods for model scalar hyperbolic equation is presented. These methods are extended to linear hyperbolic systems where waves can propagate in both directions. A generalized numerical formula which can accommodate arbitrary wave speeds for scalar advection equation is defined. In order to illustrate its application, three, four, and five point generalized numerical schemes are derived. According to the theory of linear systems, the generalized schemes are extended to linear hyperbolic systems in a straight forward manner. ESA

70 PHYSICS (GENERAL)

For precision time and time interval (PTTI) see *35 Instrumentation and Photography;* for geophysics, astrophysics or solar physics see *46 Geophysics, 90 Astrophysics,* or *92 Solar Physics.*

N94-23101 Helsinki Univ. of Technology, Espoo (Finland). Low Temperature Lab.
ACOUSTIC AND OPTICAL INVESTIGATIONS OF SUPERFLUID He-3 Ph.D. Thesis
A. Manninen 15 Jun. 1993 199 p See also PB89-221584 and

PB93-161222 Limited Reproducibility: More than 20% of this document may be affected by microfiche quality
(PB93-224889) Avail: CASI HC A09

The thesis is an experimental survey of properties of rotating and stationary superfluid He-3. Two techniques, acoustics and optics, were used. Ultrasound, together with NMR, has provided most of the present experimental knowledge about the superfluid phases of He-3. The author applied acoustics for the first time to study rotating He-3. The main result was the discovery of a new vortex in (3)He-A when the magnetic field is low. New phenomena were observed in stationary He-3 as well. Most importantly, one of the collective modes, the real squashing (rsq) mode, of (3)He-B could be excited by means of two-phonon absorption. Superfluid He-3 was studied optically for the first time. No one has previously seen He-3 in the superfluid state. The principal achievement was developing techniques which facilitate optical experiments at temperatures below 1 mK, required to study superfluid He-3. Optical fibers were used to transmit light between room temperature and the cold parts of the cryostat. Before these investigations, photography had not been done below 10 mK. The usefulness of optics as a probe of the superfluid phases of He-3 was demonstrated by studying the macroscopic shape of the free surface of rotating (3)He-B. The classical parabolic meniscus was observed, which is indicative of the equilibrium density of vortices. NTIS

N94-23110 Helsinki Univ. of Technology, Espoo (Finland). Electromagnetics Lab.
TRANSIENT ANALYSIS OF CONDUCTING HALF-PLANE PROBLEM WITH NONCAUSAL SCATTERING IMAGE
K. I. Nikoskinen, I. V. Lindell, and M. E. Ermutlu Apr. 1993 12 p See also PB92-190990 Limited Reproducibility: More than 20% of this document may be affected by microfiche quality
(PB93-225027; ISBN-951-22-1524-1) Avail: Issuing Activity (National Technical Information Service (NTIS))

Two-dimensional transient scattering from a perfectly conducting half plane is studied. The excitation is an infinite impulsive line current parallel to edge of the conductor. Due to the symmetry of the problem, the electromagnetic field everywhere is TM along the direction defined by the edge. The analysis presented in the paper is based on new time-harmonic image solution found for the scattered field. The frequency-domain image current giving the reflected and diffracted fields is an exact function that can be expressed in terms of simple trigonometric functions. It is dependent only on the coordinates and the amplitude of the source, but interestingly, it is independent of frequency. Thus, the corresponding time-domain image is independent of time, which makes it noncausal. However, when integrating this image to compute the actual field, physical, and causal results are obtained. NTIS

N94-23131 Helsinki Univ. of Technology, Espoo (Finland).
POLARIZABILITY OF GYROTROPIC SPHERE
A. Sihvola and I. Lindell Apr. 1993 8 p See also PB90-189143 Limited Reproducibility: More than 20% of this document may be affected by microfiche quality
(PB93-225019; ISBN-951-22-1501-2) Avail: CASI HC A02

The polarizability of gyrotropic spheres is derived in the letter. Gyrotropic media are anisotropic in two respects: the symmetric part of the permittivity dyadic is uniaxial; and there is an antisymmetric component to the permittivity. The analysis shows how the dyadic polarizability components depend on the permittivity components of the material. NTIS

N94-23730# Technische Univ., Delft (Netherlands). Lab. of Electromagnetic Research.
SIMILARITY IN WAVE PROPAGATION UNDER A GLOBAL RELAXATION LAW
A. T. deHoop 1993 10 p Presented at the 2nd Conference on Mathematical and Numerical Aspects of Wave Propagation, Newark, DE, 7-10 Jun. 1993
(PB94-111028; ET/EM-1993-05) Copyright Avail: CASI HC A02/MF A01

The propagation of acoustic, electromagnetic, and elastodynamic waves in inhomogeneous media is usually, in the first instance, mathematically modeled under the assumption of negligible medium losses. In practice, however, often attenuation and dispersion in the wave phenomena are observed. These must be attributed to some unknown relaxation phenomenon. As a first try to model these phenomena, the use of a global relaxation law is suggested by which the time derivatives in the first-order coupled wave equations are replaced by a relaxation operator with a constant coefficient. Via the Schouten - Van der Pol theorem of the one-sided Laplace transformation with respect to time, the wave motion in such a medium can directly be expressed in terms of the one present in the medium's lossless counterpart (for which the relaxation coefficients have the value zero). The example for acoustic waves in a fluid is worked out in detail. NTIS

N94-23731# Technische Univ., Delft (Netherlands). Lab. of Electromagnetic Research.
ANALYSIS OF TIME-DOMAIN ACOUSTIC WAVEFIELDS IN HORIZONTALLY CONTINUOUSLY LAYERED CONFIGURATIONS BASED ON THE MODIFIED CAGNIARD METHOD
M. D. Verweij and A. T. deHoop 1993 18 p
(PB94-111044; ET/EM-1993-06) Copyright Avail: CASI HC A03/MF A01

A combination of the Neumann series and the modified Cagniard method is used to derive a theoretically exact space-time domain solution for the 3-D acoustic wave propagation problem in horizontally continuously layered fluids. Firstly, integral transformations (among which a one-sided temporal Laplace transformation) are applied to the space-time domain basic acoustic equations. Secondly, a system of transform domain integral equations is derived, which is solved using a convergent Neumann series. Finally, the individual terms of this series are transformed back to the space-time domain using the modified Cagniard method. The space-time domain series turns out to be convergent for every continuously layered configuration and at any time instant. In contrast to the standard angular wave number-frequency domain analysis, in the present analysis difficulties due to turning points, etc., are avoided. It is noted that the method can be extended to deal with other kinds (elastodynamic or electromagnetic) of waves. NTIS

N94-24533 Rutherford Appleton Lab., Chilton (England).
SPIN FLUCTUATIONS IN AN ORDERED HEISENBERG FERROMAGNET WITH DIPOLAR INTERACTIONS
Stephen W. Lovesey Apr. 1993 17 p See also PB93-164721 Limited Reproducibility: More than 20% of this document may be affected by microfiche quality
(PB93-204493; RAL-93-013) Avail: Issuing Activity (National Technical Information Service (NTIS))

Results from a theoretical analysis of the Heisenberg model of a ferromagnet, including dipolar interactions, are successfully used to interpret recent measurements performed on EuS, just below the critical temperature, that probe the dynamics of long wavelength spin fluctuations parallel (longitudinal) and perpendicular (transverse) to the spontaneous magnetization. Attention is given in the paper to longitudinal fluctuations following this and other related experimental investigations on the topic. With a view to future experiments, properties of the spin dynamics in the critical region are discussed within the framework of the coupled mode approximation. NTIS

N94-24583# Michigan State Univ., East Lansing.
THE 7TH ANNUAL NATIONAL CONFERENCE OF BLACK PHYSICS STUDENTS
1993 44 p Conference held in East Lansing, MI, 12-13 Feb. 1993
Avail: CASI HC A03/MF A01

The goals of the conference were: develop a network within the Black physics community; make Black students in physics, particularly at the graduate level, aware of academic and professional opportunities; and bring important issues and developments in the field to the attention of these students. Statistical evaluations of sociocultural information are presented here along with expenditures, suggestions for 1994, and an executive summary. Derived from text

N94-25208 International Centre for Theoretical Physics, Trieste (Italy).
DERIVATION OF THE MACROSCOPIC RATE EQUATIONS FOR THE DRIVEN DIFFUSIVE ISING MODEL AT PAIR LEVEL OF APPROXIMATION
N. C. Pesheva Oct. 1992 16 p Limited Reproducibility: More than

20% of this document may be affected by microfiche quality
(DE93-616839; IC-92/350) Avail: CASI HC A03 (US Sales Only)

The driven diffusive Ising model (DDIM), i.e. the kinetic Ising model with Kawasaki or spin-exchange dynamics in nonequilibrium steady state, was considered. It was shown how to modify the coarse graining procedure of the master equation suggested by van Baal in order to account for the anisotropy induced by the driving force. Applying van Kampen's Omega-expansion one arrives at the macroscopic rate equations of the homogeneous short range ordering which has two components and the equation governing the fluctuations around the macroscopic part (Fokker-Planck equation). DOE

N94-25389 International Centre for Theoretical Physics, Trieste (Italy).
A VIBRATING WIRE PARALLEL TO A TYPE 2 SUPERCONDUCTING SLAB OF ARBITRARY THICKNESS
A. G. Saif Oct. 1992 12 p Limited Reproducibility: More than 20% of this document may be affected by microfiche quality
(DE93-617134; IC-92/358) Avail: CASI HC A03 (US Sales Only)

The distribution of the internal and external magnetic fields of the systems of a type II superconducting infinite slab of arbitrary thickness subjected to a vibrating wire (between two vibrating wires) carrying a direct current are developed. The power losses on the surface of the slab is calculated and the role of the London penetration depth on the power losses is studied. In the limiting case, a satisfactory agreement with previous results are achieved. The exact analytical solutions are obtained in compact form which can serve the technological development. DOE

71 ACOUSTICS

Includes sound generation, transmission and attenuation.
For noise pollution see *45 Environmental Pollution.*

N94-22959 Southampton Univ. (England). Inst. of Sound and Vibration Research.
A MODELLING OF THE NOISE FROM SIMPLE CO-AXIAL JETS. PART 2: IN A SIMULATED FLIGHTSTREAM
M. J. Fisher and G. A. Preston Nov. 1993 41 p
(ISVR-TR-226) Copyright Avail: Issuing Activity

This report forms part of a continuing study of co-axial jet noise, and describes the work undertaken to predict the noise emitted by a cold, co-axial, co-planar jet within a flow to simulate flight. Three sound producing regions, identified in a previous report, appear to behave in flight exactly as a single jet does, with sound levels reduced over the whole spectrum by an amount proportional to the relative velocity ratio; the sum of the three corrected spectra predicts the co-axial jet spectrum to a useful degree of accuracy. Author

N94-23206# Oak Ridge National Lab., TN.
CLASSICAL SCATTERING THEORY OF WAVES FROM THE VIEW POINT OF AN EIGENVALUE PROBLEM AND APPLICATION TO TARGET IDENTIFICATION
C. Bottcher, M. R. Strayer, and M. F. Werby (Naval Research Lab., Bay Saint Louis, MS.) 1993 9 p Presented at the SPIE OE/Aerospace Science and Sensing Meeting, Orlando, FL, 11-16 Apr. 1993
(Contract DE-AC05-84OR-21400)
(DE94-000472; CONF-930445-26) Avail: CASI HC A02/MF A01

The Helmholtz-Poincare Wave Equation (H-PWE) arises in many areas of classical wave scattering theory. In particular it can be found for the cases of acoustical scattering from submerged bounded objects and electromagnetic scattering from objects. The extended boundary integral equations (EBIE) method is derived from considering both the exterior and interior solutions of the H-PWE's. This coupled set of expressions has the advantage of not only offering a prescription for obtaining a solution for the exterior scattering problem, but it also obviates the problem of irregular values corresponding to fictitious interior eigenvalues. Once the coupled equations are derived, they can by obtained in matrix form by expanding all relevant terms in partial wave expansions, including a biorthogonal expansion of the Green function. However some freedom of choice in the choice of the surface expansion is available since the unknown surface quantities may be expanded in a variety of ways as long as closure is obtained. Out of many possible choices, we develop an optimal method to obtain such expansions which is based on the optimum eigenfunctions related to the surface of the object. In effect, we convert part of the problem (that associated with the Fredholms integral equation of the first kind) an eigenvalue problem of a related Hermition operator. The methodology will be explained in detail and examples will be presented. DOE

N94-23312* National Aeronautics and Space Administration. Ames Research Center, Moffett Field, CA.
HEAD RELATED TRANSFER FUNCTION PSEUDO-STEREOPHONY Patent
Durand R. Begault, inventor (to NASA) 22 Dec. 1992 10 p Filed 29 Jan. 1992
(NASA-Case-ARC-11919-1-NP; US-Patent-5,173,944;
US-Patent-Appl-SN-826749; US-Patent-Class-381-17;
US-Patent-Class-381-24; US-Patent-Class-381-26;
Int-Patent-Class-H04R-5/00) Avail: US Patent and Trademark Office

An apparatus for producing pseudo-stereophonic sound from a monaural signal is discussed. The apparatus includes a monaural source that has a speaker placed in an anechoic room and has a sound output generated by the monaural signal. The second, third, fourth, and fifth speakers are placed in the anechoic room symmetrically about a listener. The monaural signal from the source is processed to output processed signals to each of the second, third, fourth, and fifth speakers, each speaker producing a sound output corresponding to the received processed signal. A pair of microphones is placed in the ears of the listener for receiving the sound outputs of the first, second, third, fourth, and fifth speakers and producing two differentiated audio channels.
Official Gazette of the U.S. Patent and Trademark Office

N94-23464*# National Aeronautics and Space Administration. Lewis Research Center, Cleveland, OH.
REFRACTION OF HIGH FREQUENCY NOISE IN AN ARBITRARY JET FLOW
Abbas Khavaran (Sverdrup Technology, Inc., Brook Park, OH.) and Eugene A. Krejsa Jan. 1994 19 p Presented at the 32nd Aerospace Sciences Meeting and Exhibit, Reno, NV, 10-13 Jan. 1994; sponsored by AIAA
(Contract NAS3-25266; RTOP 537-02-23)
(NASA-TM-106465; E-8330; NAS 1.15:106465; AIAA Paper 94-0139)
Avail: CASI HC A03/MF A01

Refraction of high frequency noise by mean flow gradients in a jet is studied using the ray-tracing methods of geometrical acoustics. Both the two-dimensional (2D) and three-dimensional (3D) formulations are considered. In the former case, the mean flow is assumed parallel and the governing propagation equations are described by a system of four first order ordinary differential equations. The 3D formulation, on the other hand, accounts for the jet spreading as well as the axial flow development. In this case, a system of six first order differential equations are solved to trace a ray from its source location to an observer in the far field. For subsonic jets with a small spreading angle both methods lead to similar results outside the zone of silence. However, with increasing jet speed the two prediction models diverge to the point where the parallel flow assumption is no longer justified. The Doppler factor of supersonic jets as influenced by the refraction effects is discussed and compared with the conventional modified Doppler factor. Author (revised)

N94-23698*# Barron Associates, Inc., Standardsville, VA.
ADAPTIVE NONLINEAR POLYNOMIAL NEURAL NETWORKS FOR CONTROL OF BOUNDARY LAYER/STRUCTURAL INTERACTION Final Report, 16 Jan. - 15 Aug. 1991
B. Eugene Parker, Jr., Richard L. Cellucci, Dean W. Abbott, Roger L. Barron, Paul R. Jordan, III, and H. Vincent Poor (Princeton Univ., NJ.) Dec. 1993 70 p
(Contract NAS1-19271; RTOP 324-01-00; SBIR-02.10-4400)
(NASA-CR-189645; NAS 1.26:189645) Avail: CASI HC A04/MF A01

The acoustic pressures developed in a boundary layer can interact with an aircraft panel to induce significant vibration in the panel. Such vibration is undesirable due to the aerodynamic drag and structure-borne cabin noises that result. The overall objective of this work is to develop effective and practical feedback control strategies for actively reducing this flow-induced structural vibration. This report describes the results of initial evaluations using polynomial, neural network-based, feedback control to reduce flow induced vibration in aircraft panels due to turbulent boundary layer/structural interaction. Computer simulations are used to develop and analyze feedback control strategies to reduce vibration in a beam as a first step. The key differences between this work and that going on elsewhere are as follows: that turbulent and transitional boundary layers represent broadband excitation and thus present a more complex stochastic control scenario than that of narrow band (e.g., laminar boundary layer) excitation; and secondly, that the proposed controller structures are adaptive nonlinear infinite impulse response (IIR) polynomial neural network, as opposed to the traditional adaptive linear finite impulse response (FIR) filters used in most studies to date. The controllers implemented in this study achieved vibration attenuation of 27 to 60 dB depending on the type of boundary layer established by laminar, turbulent, and intermittent laminar-to-turbulent transitional flows. Application of multi-input, multi-output, adaptive, nonlinear feedback control of vibration in aircraft panels based on polynomial neural networks appears to be feasible today. Plans are outlined for Phase 2 of this study, which will include extending the theoretical investigation conducted in Phase 2 and verifying the results in a series of laboratory experiments involving both bum and plate models. Author (revised)

N94-23718# Sandia National Labs., Albuquerque, NM.

CHEMICALLY SENSITIVE INTERFACES ON SAW DEVICES

A. J. Ricco, S. J. Martin, R. M. Crooks (Texas A&M Univ., College Station.), Chuanjing Xu (Texas A&M Univ., College Station.), and R. E. Allred (Adherent Technologies, Albuquerque, NM.) 1993 17 p Presented at the 206th American Chemical Society (ACS) National Meeting, Chicago, IL, 22-27 Aug. 1993

(Contract DE-AC04-94AL-85000)

(DE94-001832; SAND-93-2265C; CONF-930802-16) Avail: CASI HC A03/MF A01

Using surface acoustic wave (SAW) devices, three approaches to the effective use of chemically sensitive interfaces that are not highly chemically selective have been examined: molecular identification from time-resolved permeation transients; using multifrequency SAW devices to determine the frequency dependence of analyte/film interactions; and use of an array of SAW devices bearing diverse chemically sensitive interfaces to produce a distinct response pattern for each analyte. In addition to their well-known sensitivity to mass changes (0.0035 monolayer of N2 can be measured), SAW devices respond to the mechanical and electronic properties of thin films, enhancing response information content but making a thorough understanding of the perturbation critical. Simultaneous measurement of changes in frequency and attenuation, which can provide the information necessary to determine the type of perturbation, are used as part of the above discrimination schemes. DOE

N94-23726# Technische Univ., Delft (Netherlands). Lab. of Electromagnetic Research.

DIFFRACTION ANALYSIS OF TRANSIENT ACOUSTIC WAVES: HALF-PLANE IN A LAYERED MEDIUM

K. F. I. Haak 1993 185 p

(PB94-110988; ET/EM-1993-15) Copyright Avail: CASI HC A09/MF A02

In marine seismics, acoustic waves serve as standard diagnostic tools to probe the earth geology below the sea bottom. Some processing methods in marine seismics result from a proper application of the theorem of reciprocity. In this theorem, the actual field quantities to be probed interact with the computational quantities of a probing state in such a processing method. The configuration consists of a fluid layer with a semi-infinite pressure-free screen in it. A homogeneous half-space models the subsurface of the sea floor. The transient wave problem is then solved by means of an iterative scheme in which successive application of the Wiener-Hopf technique and the Cagniard-De Hoop method is used. From the numerical results it turns out that only the first and second order diffracted wave field give a significant contribution to the geometrical wave field. Application of these results in the iterative scheme yields a very effective solution scheme in which the transient wave field in the configuration at hand can be calculated within any finite time window. NTIS

N94-24172*# McDonnell-Douglas Aerospace, Long Beach, CA. Transport Aircraft.

VARIABILITY OF MEASURED SONIC BOOM SIGNATURES. VOLUME 1: TECHNICAL REPORT Final Report

K. R. Elmer and M. C. Joshi Jan. 1994 43 p

(Contract NAS1-19060; RTOP 537-03-21-03)

(NASA-CR-191483-Vol-1; NAS 1.26:191483-Vol-1) Avail: CASI HC A03/MF A01

Sonic boom signatures from two databases, the BOOMFILE and the XB-70, were analyzed in terms of C-weighted sound exposure level (CSEL), A-weighted sound exposure level (ASEL), and Stevens Mark VII perceived level (PLdB), as well as the more traditional peak positive overpressure and rise time. The variability of these parameters due to propagation through atmosphere was analyzed for different aircraft Mach number and altitude groups. The low Mach number/low altitude group had significantly greater variation in rise time, overpressure, and loudness level than the high Mach number/high altitude group. The loudness of measured booms were found to have a variation of up to 25 dB relative to the loudness of boom predicted for a non-turbulent atmosphere. This is due primarily to the steeper ray paths of the high Mach number/high altitude group and the corresponding shorter distances traveled by these rays through the lower atmosphere resulting in reduced refraction effects. The general trend of decreased overpressure and loudness level with increasing lateral distance was also seen. Sonic boom signatures from early morning flights had less variation in rise time and overpressure than afternoon flights because of reduced turbulence. Measures of asymmetry (difference between compression and expansion portion of the signature) showed that the variability in Delta loudness level was greater than the variability in Delta overpressure due to the large influence of turbulence on rise time. Lastly, analysis of data within 50 percent of lateral cutoff showed that the mean value for overpressure and loudness level was independent of time of day but that the frequency with which it occurred was greater in the morning. This is a clear indicator of increased turbulence in the afternoon. Author (revised)

N94-24173*# McDonnell-Douglas Aerospace, Long Beach, CA. Transport Aircraft.

VARIABILITY OF MEASURED SONIC BOOM SIGNATURES. VOLUME 2: DATA REPORT Final Report

K. R. Elmer and M. C. Joshi Jan. 1994 148 p

(Contract NAS1-19060; RTOP 537-03-21-03)

(NASA-CR-191483-Vol-2; NAS 1.26:191483-Vol-2) Avail: CASI HC A07/MF A02

Sonic boom signatures from two databases, the BOOMFILE and the XB-70, were analyzed in terms of C-weighted sound exposure level (CSEL), A-weighted sound exposure level (ASEL), and Stevens Mark VII perceived level (PLdB), as well as the more traditional peak positive overpressure and rise time. The variability of these parameters due to propagation through atmosphere was analyzed for different aircraft Mach number and altitude groups. The low Mach number/low altitude group had significantly greater variation in rise time, overpressure, and loudness level than the high Mach number/high altitude group. The loudness of measured booms were found to have a variation of up to 25 dB relative to the loudness of boom predicted for a non-turbulent atmosphere. This is due primarily to the steeper ray paths of the high Mach number/high altitude group and the corresponding shorter distances traveled by these rays through the lower atmosphere resulting in reduced refraction effects. The general trend of decreased overpressure and loudness level with increasing lateral distance was also seen. Sonic boom signatures from early morning flights had less variation in rise time and overpressure than afternoon flights because of reduced turbulence. Measures of asymmetry (difference between compression and expansion portion of the signature) showed that the variability in Delta loudness level was greater than the variability in Delta overpressure due to the large influence of turbulence on rise time. Lastly, analysis of data within 50 percent of lateral cutoff showed that the mean value for overpressure and loudness level was independent of time of day but that the frequency with which it occurred was greater in the morning. This is a clear indicator of increased turbulence in the afternoon. Author (revised)

N94-24207*# National Aeronautics and Space Administration. Langley Research Center, Hampton, VA.

JOINT ACOUSTIC PROPAGATION EXPERIMENT (JAPE-91) WORKSHOP

William L. Willshire, Jr., comp. and David Chestnutt, comp. Dec. 1993 190 p Workshop held in Hampton, VA, 28 Apr. 1993 Sponsored in

part by Univ. of Mississippi, Oxford
(RTOP 505-63-70-02)
(NASA-CP-3231; L-17331; NAS 1.55:3231) Avail: CASI HC A09/MF A02

The Joint Acoustic Propagation Experiment (JAPE), was conducted at the White Sands Missile Range, New Mexico, USA, during the period 11-28 Jul. 1991. JAPE consisted of various short and long range propagation experiments using various acoustic sources including speakers, propane cannons, helicopters, a 155 mm howitzer, and static high explosives. Of primary importance to the performance of theses tests was the extensive characterization of the atmosphere during these tests. This atmospheric characterization included turbulence measurements. A workshop to disseminate the results of JAPE-91 was held in Hampton, VA, on 28 Apr. 1993. This report is a compilation of the presentations made at the workshop along with a list of attendees and the agenda. For individual titles, see N94-24208 through N94-24222.

N94-24208*# Army Engineer Waterways Experiment Station, Vicksburg, MS. Structures Lab.

JOINT ACOUSTIC PROPAGATION EXPERIMENT (JAPE)

Benny L. Carnes, Robert O. Olsen (Army Research Lab., White Sands Missle Range, NM.), and Bruce W. Kennedy (New Mexico State Univ., Las Cruces.) *In* NASA. Langley Research Center, Joint Acoustic Propagation Experiment (JAPE-91) Workshop Dec. 1993 p 1-17 (For primary document see N94-24207 06-71)
Avail: CASI HC A03/MF A02

The Joint Acoustic Propagation Experiment (JAPE), performed under the auspices of NATO and the Acoustics Working Group, was conducted at White Sands Missile Range, New Mexico, USA, during the period 11-28 Jul. 1991. JAPE consisted of 220 trials using various acoustic sources including speakers, propane cannon, various types of military vehicles, helicopters, a 155mm howitzer, and static high explosives. Of primary importance to the performance of these tests was the intensive characterization of the atmosphere before and during the trials. Because of the wide range of interests on the part of the participants, JAPE was organized in such a manner to provide a broad cross section of test configurations. These included short and long range propagation from fixed and moving vehicles, terrain masking, and vehicle detection. A number of independent trials were also performed by individual participating agencies using the assets available during JAPE. These tests, while not documented in this report, provided substantial and important data to those groups. Perhaps the most significant feature of JAPE is the establishment of a permanent data base which can be used by not only the participants but by others interested in acoustics. A follow-on test was performed by NASA LaRC during the period 19-29 Aug. 1991 at the same location. These trials consisted of 59 overflights of supersonic aircraft in order to establish the relationship between atmospheric turbulence and the received sonic boom energy at the surface. Author (revised)

N94-24209*# Atlas Elektronik G.m.b.H., Bremen (Germany).

SOME RESULTS GAINED FROM JAPE: AN OVERVIEW

Gunnar R. Becker *In* NASA. Langley Research Center, Joint Acoustic Propagation Experiment (JAPE-91) Workshop Dec. 1993 p 19-30 (For primary document see N94-24207 06-71)
Avail: CASI HC A03/MF A02

During JAPE, a variety of sound propagation experiments were conducted including long range measurements and investigations of the masking of sound by natural barriers. An overview of the measurements is given. A comparison between measured SPL's and theoretical estimates is presented. Author (revised)

N94-24210*# New Mexico State Univ., Las Cruces. Physical Science Lab.

INTERCOMPARISON OF REMOTE AND BALLOON-BORNE SENSORS OPERATED AT JAPE-91

Richard J. Okrasinski, Greg J. Cook, and Robert O. Olsen (Army Research Lab., White Sands Missle Range, NM.) *In* NASA. Langley Research Center, Joint Acoustic Propagation Experiment (JAPE-91) Workshop Dec. 1993 p 31-39 (For primary document see N94-24207 06-71)
Avail: CASI HC A02/MF A02

In recent years, there has been an increased availability of different types of remote sensors for measuring atmospheric parameters. With the introduction of remote sensors into field operation, questions have arisen as to their accuracy and precision. An attempt was made to address this issue by analyzing and intercomparing sets of wind and temperature data obtained during the Joint Acoustic Propagation Experiment (JAPE-9l) conducted at White Sands Missile Range, New Mexico, in Jul. and Aug. 1991. The remote sensing systems that were deployed included a 924 MHz wind profiler, two Doppler acoustic sodars, and a Radio Acoustic Sounding System (RASS). In situ measurements of wind, temperature, and humidity were also obtained from radiosondes. Individual system characteristics and the results of intercomparing the derived wind and temperature data from each of the systems are presented. Author (revised)

N94-24211*# Lockheed Sanders, Inc., Nashua, NH.

EFFECTS OF ATMOSPHERIC VARIATIONS ON ACOUSTIC SYSTEM PERFORMANCE

Robert Nation, Stephen Lang, Robert Olsen (Army Research Lab., White Sands Missle Range, NM.), and Prasan Chintawongvanich (New Mexico State Univ., Las Cruces.) *In* NASA. Langley Research Center, Joint Acoustic Propagation Experiment (JAPE-91) Workshop Dec. 1993 p 41-53 (For primary document see N94-24207 06-71)
Avail: CASI HC A03/MF A02

Acoustic propagation over medium to long ranges in the atmosphere is subject to many complex, interacting effects. Of particular interest at this point is modeling low frequency (less than 500 Hz) propagation for the purpose of predicting ranges and bearing accuracies at which acoustic sources can be detected. A simple means of estimating how much of the received signal power propagated directly from the source to the receiver and how much was received by turbulent scattering was developed. The correlations between the propagation mechanism and detection thresholds, beamformer bearing estimation accuracies, and beamformer processing gain of passive acoustic signal detection systems were explored. Author (revised)

N94-24212*# Mississippi Univ., University. Physical Acoustics Research Group.

COMPARISON OF MEASURED AND PREDICTED PURE TONE PROPAGATION LEVELS FROM JAPE-1: AN EVALUATION OF THE PERFORMANCE OF ASOPRAT

Carl K. Frederickson, Henry E. Bass, Richard Raspet, and John Messer *In* NASA. Langley Research Center, Joint Acoustic Propagation Experiment (JAPE-91) Workshop Dec. 1993 p 55-64 (For primary document see N94-24207 06-71)
Avail: CASI HC A02/MF A02

Joint Acoustic Propagation Experiment Phase One (JAPE-1) short range propagation data has been used to evaluate the performance of the Advanced Sound Propagation in the Atmosphere (ASOPRAT) prediction code. The pure tone short range data was Fourier analyzed giving the propagated pressure levels as a function of frequency. Meteorological profiles measured at the experimental site were used as input for the acoustic prediction routine ASOPRAT. Predicted and measured propagation levels are compared in decibels (dB) relative to one of the measurement positions for receivers on the line passing between the two thirty meter towers. Agreement between predicted and measured levels is very good. Source strength data was not available, hence the comparisons show good agreement as to the shape of the propagation loss curve not necessarily the propagation levels. Author (revised)

N94-24213*# Open Univ., Milton (England). Engineering Mechanics Discipline.

GROUND CHARACTERIZATION FOR JAPE

Keith Attenborough and Shahram Taherzadeh *In* NASA. Langley Research Center, Joint Acoustic Propagation Experiment (JAPE-91) Workshop Dec. 1993 p 65-78 Sponsored in part by U.S. Army, Eoropean Research Office (For primary document see N94-24207 06-71)
Avail: CASI HC A03/MF A02

Above-ground propagation modelling at the JAPE (Joint Acoustic Propagation Experiment) site requires a reasonably accurate model for the acoustical properties of the ground. Various models for the JAPE site are offered based on theoretical fits to short range data and to longer range data obtained with random noise and pure tones respectively from a loudspeaker under approximately quiescent isothermal conditions. Author

N94-24214*# Institut Franco-Allemand de Recherches, Saint-Louis (France).

JAPE 91: INFLUENCE OF TERRAIN MASKING OF THE ACOUSTIC PROPAGATION OF HELICOPTER NOISE

P. Naz *In* NASA. Langley Research Center, Joint Acoustic Propagation Experiment (JAPE-91) Workshop Dec. 1993 p 79-85 Sponsored in part by Direction de Reserches Etudes et Techniques, Paris, France (For primary document see N94-24207 06-71)

Avail: CASI HC A02/MF A02

The acoustic propagation in the case of a noise source masked by a small element of terrain has been investigated experimentally. These data have been measured during the 'terrain masking' experiment of the NATO JAPE 91 experimental campaign. The main objective of that experiment was to study the acoustic detection of a helicopter masked by a small hill. Microphones have been placed at different locations on the shadow zone of the hill to study the effect of the terrain obstruction on sound propagation. The results presented come from data measured by Atlas Elektronik and by ISL, and have been processed together. The terrain obstruction causes an excess attenuation of the SPL (Sound Pressure Level) for all the frequencies, but this attenuation is more effective for the high frequencies than for the low frequencies. Results typical of diffraction phenomena have been observed; the SPL is minimal at the foot of the hill and is relatively constant beyond it. Author

N94-24215*# Mississippi Univ., University. National Center for Physical Acoustics.

COMPARISONS OF CALCULATED AND MEASURED HELICOPTER NOISE NEAR INSTRUMENT HILL

Henry E. Bass and Chulsoo You *In* NASA. Langley Research Center, Joint Acoustic Propagation Experiment (JAPE-91) Workshop Dec. 1993 p 87-92 (For primary document see N94-24207 06-71)

Avail: CASI HC A02/MF A02

The polar parabolic equation (POPE) method solves for the diffraction of sound by a curved surface including a realistic sound speed profile. POPE is outlined briefly to describe diffraction which propagates the field over a hill. Experimental data are compared with POPE predictions using the measured sound speed profile and ground impedance. Two trial cases are considered for the comparisons: the helicopter located at the base of the hill and far away from the base of the hill, respectively. The physical mechanisms for sound propagation over a hill are examined with and of POPE calculations and experimental data. The shedding of rays from the hillside gives an interference effect with a wave along the flat surface beyond the base of a hill. Author

N94-24216*# Michigan Technological Univ., Houghton.

PRELIMINARY ANALYSIS OF AMPLITUDE AND PHASE FLUCTUATIONS IN THE JAPE MULTIPLE TONE DATA TO DISTANCES OF 500 METERS

James Rogers, Radomir Sokolov, Daniel Hicks (Army Tank-Automotive Research and Development Command, Warren, MI.), and Lloyd Cartwright (Army Tank-Automotive Research and Development Command, Warren, MI.) *In* NASA. Langley Research Center, Joint Acoustic Propagation Experiment (JAPE-91) Workshop Dec. 1993 p 93-106 (For primary document see N94-24207 06-71)

Avail: CASI HC A03/MF A02

The JAPE short range data provide a good opportunity for studying phase and amplitude fluctuations of acoustic signals in the atmosphere over distances of several hundred meters. Several factors contribute to the usefulness of these data: extensive meteorological measurements were made, controlled sources were used, the data were recorded with a high dynamic range digital system that preserved phase information and a significant number of measurement points were obtained allowing both longitudinal and transverse studies. Further, Michigan Tech, in cooperation with the U.S. Army TARDEC, has developed phase tracking algorithms for studying vehicle acoustic signals. These techniques provide an excellent tool for analyzing the amplitude and phase fluctuations of the JAPE data. The results of studies such as those reported here have application at several levels: the mechanisms of signal amplitude and phase fluctuations in propagating acoustic signals are not well understood nor are the mathematical models highly developed, acoustic arrays depend strongly on signal coherence and signal amplitude stability in order to perform to their design specifications and active noise control implementation in regions considerably removed from the primary and secondary sources depends upon signal amplitude and phase stability. Work reported here is preliminary in nature but it does indicate the utility of the phase tracking and amplitude detection algorithms. The results obtained indicate that the phase fluctuations of the JAPE continuous multiple tone data (simultaneous transmission of 80, 200 and 500 Hz) are in general agreement with existing theories but the amplitude fluctuations are seen to be less well behaved and show less consistency. Author

N94-24217*# Pennsylvania State Univ., University Park. Graduate Program in Acoustics and Dept. of Meteorology.

DIMENSIONAL ANALYSIS OF ACOUSTICALLY PROPAGATED SIGNALS

Scott D. Hansen and Dennis W. Thomson *In* NASA. Langley Research Center, Joint Acoustic Propagation Experiment (JAPE-91) Workshop Dec. 1993 p 107-11 (For primary document see N94-24207 06-71)

Avail: CASI HC A03/MF A02

Traditionally, long term measurements of atmospherically propagated sound signals have consisted of time series of multiminute averages. Only recently have continuous measurements with temporal resolution corresponding to turbulent time scales been available. With modern digital data acquisition systems we now have the capability to simultaneously record both acoustical and meteorological parameters with sufficient temporal resolution to allow us to examine in detail relationships between fluctuating sound and the meteorological variables, particularly wind and temperature, which locally determine the acoustic refractive index. The atmospheric acoustic propagation medium can be treated as a nonlinear dynamical system, a kind of signal processor whose innards depend on thermodynamic and turbulent processes in the atmosphere. The atmosphere is an inherently nonlinear dynamical system. In fact one simple model of atmospheric convection, the Lorenz system, may well be the most widely studied of all dynamical systems. In this paper we report some results of our having applied methods used to characterize nonlinear dynamical systems to study the characteristics of acoustical signals propagated through the atmosphere. For example, we investigate whether or not it is possible to parameterize signal fluctuations in terms of fractal dimensions. For time series one such parameter is the limit capacity dimension. Nicolis and Nicolis were among the first to use the kind of methods we have to study the properties of low dimension global attractors. Derived from text

N94-24218*# Army Research Lab., White Sands Missle Range, NM. Battlefield Environment Directorate.

COMPARISON BETWEEN 1-MINUTE AND 15-MINUTE AVERAGES OF TURBULENCE PARAMETERS

John M. Noble *In* NASA. Langley Research Center, Joint Acoustic Propagation Experiment (JAPE-91) Workshop Dec. 1993 p 119-12 (For primary document see N94-24207 06-71)

Avail: CASI HC A02/MF A02

Sonic anemometers are good instruments for measuring temperature and wind speed and are fast enough to calculate the temperature and wind structure parameters used to calculate the variance in the acoustic index of refraction. However, the turbulence parameters are typically 15-minute averaged point measurements. There are several problems associated with making point measurements and using them to represent a turbulence field. Some of the sonic anemometer data analyzed from the Joint Acoustic Propagation Experiment (JAPE) conducted during July 1991 at DIRT Site located at White Sands Missile Range, New Mexico, are examined. Author (revised)

N94-24219*# National Research Council of Canada, Ottawa (Ontario).

BEAMFORMING IN AN ACOUSTIC SHADOW Abstract Only

David Havelock, Michael Stinson, and Gilles Daigle *In* NASA. Langley Research Center, Joint Acoustic Propagation Experiment (JAPE-91) Workshop Dec. 1993 p 129 (For primary document see N94-24207 06-71)

Avail: CASI HC A01/MF A02

The sound field deep within an acoustic shadow region is less well understood than that outside the shadow region. Signal levels are substantially lower within the shadow, but beamforming difficulties arise for other reasons such as loss of spatial coherence. Based on analysis of JAPE-91 data, and other data, three types of characteristic signals within acoustic shadow regions are identified. These signal types may correspond to different, intermittent signal propagation conditions. Detection and classification algorithms might take advantage of the signal characteristics. Frequency coherence is also discussed. The extent of coherence across frequencies is shown to be limited, causing difficulties for source classification based on harmonic amplitude relationships. Discussions emphasize short-term characteristics on the order of one second. A video presentation on frequency coherence shows the similarity, in the presence of atmospheric turbulence, between the received signal from a stable set of harmonics generated by a loudspeaker and that received from a helicopter hovering behind a hill. Author

N94-24220*# Army Engineer Waterways Experiment Station, Vicksburg, MS.

ANALYSIS OF PASSIVE ACOUSTIC RANGING OF HELICOPTERS FROM THE JOINT ACOUSTIC PROPAGATION EXPERIMENT

Benny L. Carnes and John C. Morgan *In* NASA. Langley Research Center, Joint Acoustic Propagation Experiment (JAPE-91) Workshop Dec. 1993 p 131-17 (For primary document see N94-24207 06-71)
Avail: CASI HC A03/MF A02

For more than twenty years, personnel of the U.S.A.E. Waterways Experiment Station (WES) have been performing research dealing with the application of sensors for detection of military targets. The WES research has included the use of seismic, acoustic, magnetic, and other sensors to detect, track, and classify military ground targets. Most of the WES research has been oriented toward the employment of such sensors in a passive mode. Techniques for passive detection are of particular interest in the Army because of the advantages over active detection. Passive detection methods are not susceptible to interception, detection, jamming, or location of the source by the threat. A decided advantage for using acoustic and seismic sensors for detection in tactical situations is the non-line-of-sight capability; i.e., detection of low flying helicopters at long distances without visual contact. This study was conducted to analyze the passive acoustic ranging (PAR) concept using a more extensive data set from the Joint Acoustic Propagation Experiment (JAPE). Author (revised)

N94-24221*# IIT Research Inst., Dayton, OH.

ACOUSTIC TARGET DETECTION AND CLASSIFICATION USING NEURAL NETWORKS

James A. Robertson and Mark Conlon (IIT Research Inst., Las Cruces, NM.) *In* NASA. Langley Research Center, Joint Acoustic Propagation Experiment (JAPE-91) Workshop Dec. 1993 p 171-18 (For primary document see N94-24207 06-71)
(Contract DLA900-86-C-0022)
Avail: CASI HC A02/MF A02

A neural network approach to the classification of acoustic emissions of ground vehicles and helicopters is demonstrated. Data collected during the Joint Acoustic Propagation Experiment conducted in July of l991 at White Sands Missile Range, New Mexico was used to train a classifier to distinguish between the spectrums of a UH-1, M60, M1 and M114. An output node was also included that would recognize background (i.e. no target) data. Analysis revealed specific hidden nodes responding to the features input into the classifier. Initial results using the neural network were encouraging with high correct identification rates accompanied by high levels of confidence. Author (revised)

N94-24222*# Army Engineer Waterways Experiment Station, Vicksburg, MS.

PRELIMINARY ANALYSIS OF THE JAPE GROUND VEHICLE TEST DATA WITH AN ARTIFICIAL NEURAL NETWORK CLASSIFIER

Nathan F. Larsen and Ben L. Carnes *In* NASA. Langley Research Center, Joint Acoustic Propagation Experiment (JAPE-91) Workshop Dec. 1993 p 181-18 (For primary document see N94-24207 06-71)
Avail: CASI HC A02/MF A02

Remotely sensing and classifying military vehicles in a battlefield environment have been the source of much research over the past 20 years. The ability to know where threat vehicles are located is an obvious advantage to military personnel. In the past active methods of ground vehicle detection such as radar have been used, but with the advancement of technology to locate these active sensors, passive sensors are preferred. Passive sensors detect acoustic emissions, seismic movement, electromagnetic radiation, etc., produced by the target and use this information to describe it. Deriving the mathematical models to classify vehicles in this manner has been, and is, quite complex and not always reliable. However, with the resurgence of artificial neural network (ANN) research in the past few years, developing models for this work may be a thing of the past. Preliminary results from an ANN analysis to the tank signatures recorded at the Joint Acoustic Propagation Experiment (JAPE) at the US Army White Sands Missile Range, NM, in July 1991, are presented. Author (revised)

N94-24307*# Research Inst. for Advanced Computer Science, Moffett Field, CA.

UNSTRUCTURED ADAPTIVE MESH COMPUTATIONS OF ROTORCRAFT HIGH-SPEED IMPULSIVE NOISE

Roger Strawn (Army Aviation Systems Command, Moffett Field, CA.), Michael Garceau (Stanford Univ., CA.), and Rupak Biswas Oct. 1993 13 p Presented at the AIAA 15th Aeroacoustics Conference, Long Beach, CA, 25-27 Oct. 1993
(Contract NAS2-13721)
(NASA-CR-195090; NAS 1.26:195090; RIACS-TR-93-10; AIAA Paper 93-4359) Avail: CASI HC A03/MF A01

A new method is developed for modeling helicopter high-speed impulsive (HSI) noise. The aerodynamics and acoustics near the rotor blade tip are computed by solving the Euler equations on an unstructured grid. A stationary Kirchhoff surface integral is then used to propagate these acoustic signals to the far field. The near-field Euler solver uses a solution-adaptive grid scheme to improve the resolution of the acoustic signal. Grid points are locally added and/or deleted from the mesh at each adaptive step. An important part of this procedure is the choice of an appropriate error indicator. The error indicator is computed from the flow field solution and determines the regions for mesh coarsening and refinement. Computed results for HSI noise compare favorably with experimental data for three different hovering rotor cases. Author (revised)

N94-24514 Institut Franco-Allemand de Recherches, Saint-Louis (France).

VALIDATION OF THE ROTAC CODE FOR THE ROTOR NOISE PREDICTION

P. Gnemmi, J. Haertig, and C. Johe 1992 18 p See also PB93-204303 Sponsored by Direction des Recherches, Etudes et Techniques and Centre de Documentation de l'Armement Limited Reproducibility: More than 20% of this document may be affected by microfiche quality
(PB93-204311; ISL-CO-228/92) Avail: CASI HC A03

The blade/vortex interaction noise and the thickness noise are the impulsive noises radiated by a helicopter rotor flying at low speed. A prediction code of the thickness and loading noises applied to a helicopter rotor has been developed at ISL. This code, named ROTAC, is very briefly described here. In order to validate this acoustic code, calculations are compared with measurements obtained by ISL and by a DLR US-ARMY collaboration. The thickness noise of a rotor in hover and forward flight is correctly predicted up to a tip Mach number near 0.88. For a flight configuration with occurrence of blade/vortex interaction, the small number of blade pressure measurements does not allow the determination of the amplitude of the loading noise but these entry data make it possible to examine qualitatively the agreement between calculations and measurements. NTIS

N94-25026 National Physical Lab., Teddington (England).

EXERCISE KEEVIL: NOISE LEVELS OF SIX MILITARY HELICOPTERS

B. F. Berry, A. L. Harris, R. J. Weston (Royal Air Force, Halton, England.), and D. Steele (Royal Air Force, Halton, England.) 1993 38 p Limited Reproducibility: More than 20% of this document may be affected by microfiche quality
(PB93-210722; NPL-RSA(EXT)0042) Copyright Avail: Issuing Activity (National Technical Information Service (NTIS))

For a number of years the National Physical Laboratory, supported by the Ministry of Defense, has been developing AIRNOISE, a mathematical model for computing aircraft noise contours. The model is now being extended to include helicopter operations. In order to provide basic source noise data for the model, a special noise trial - Exercise Keevil - has been conducted at RAF Keevil in Wiltshire. One helicopter of each of six types performed a variety of flight operations over an array of microphones. Information on aircraft position and speed were obtained by video tracking techniques. The report describes the trial and presents the results obtained. NTIS

N94-25073 Naval Research Lab., Washington, DC.
MEASUREMENTS AND MODELING OF MULTITONE, LOW-FREQUENCY ACOUSTIC DATA FROM THE ARRAIAL DO CABO RANGE Final Report
William Soares-Filho, Jose R. MottadaSilva, and Stephen N. Wolf 15 Oct. 1993 36 p Limited Reproducibility: More than 20% of this document may be affected by microfiche quality
(AD-A273406; NRL/FR/7127-93-9580) Avail: Issuing Activity (Defense Technical Information Center (DTIC))

A study was performed to characterize short-range, low-frequency acoustic propagation at the Arraial do Cabo acoustic range, which is located in shallow water on the Southeast coast of Brazil. Acoustic transmission data, obtained by using multitone continuous-wave (CW) transmissions from uncalibrated sound sources and omnidirectional receivers were compared with predictions of normal-mode acoustic transmission models. The measurements, which were made along the 17- and 47-m isobaths, extended over the frequency range from 12 to 375 Hz. It was found that, for most of the data, short-range multipath interference patterns were in agreement with results calculated by modeling the ocean bottom as a fluid. At frequencies below 80 Hz, the influence of shear waves in the ocean bottom was found to be important for the data taken in water depth 17 m. Recommendations are made to help guide follow-on modeling and experimental acoustic propagation studies. DTIC

N94-25172*# National Aeronautics and Space Administration. Lewis Research Center, Cleveland, OH.
FAN NOISE RESEARCH AT NASA
John F. Groeneweg Feb. 1994 12 p Proposed for presentation at the 1994 National Conference on Noise Control Engineering, Fort Lauderdale, FL, 1-4 May 1994; sponsored by the Institute of Noise Control Engineering
(RTOP 538-03-11)
(NASA-TM-106512; E-8623; NAS 1.15:106512) Avail: CASI HC A03/MF A01

Results of recent NASA research to reduce aircraft turbofan noise are described. As the bypass ratio of a turbofan engine increases from five to as much as 20, the dominant source of engine noise is the fan. A primary mechanism of tone noise generation is the rotor blade wakes interacting with downstream stator vanes. Methods of analyzing rotor stator tone noise generation are described and sample results are given. The role of an acoustic modal description is emphasized. Wind tunnel tests of model fans and nacelles are described including a novel rotating microphone technique for modal measurement. Sample far field results are given showing the effects of inlet length, and modal measurements are shown which point to a new generation mechanism. Concepts for active fan noise control at the source are addressed. Implications of the research which have general relevance to fan noise generation and control are discussed. Author (revised)

N94-25177*# Old Dominion Univ., Norfolk, VA. Dept. of Mechanical Engineering.
THE EFFECTS OF PROFILES ON SUPERSONIC JET NOISE Progress Report, period ending 31 Jan. 1994
S. N. Tiwari and T. R. S. Bhat Feb. 1994 39 p
(Grant NAG1-1581)
(NASA-CR-195184; NAS 1.26:195184) Avail: CASI HC A03/MF A01

The effect of velocity profiles on supersonic jet noise are studied by using stability calculations made for a shock-free coannular jet, with both the inner and outer flows supersonic. The Mach wave emission process is modeled as the noise generated by the large scale turbulent structures or the instability waves in the mixing region. Both the vortex-sheet and the realistic finite thickness shear layer models are considered. The stability calculations were performed for both inverted and normal velocity profiles. Comparisons are made with the results for an equivalent single jet, based on equal thrust, mass flow rate and exit area to that of the coannular jet. The advantages and disadvantages of these velocity profiles as far as noise radiation is concerned are discussed. It is shown that the Rayleigh's model prediction of the merits and demerits of different velocity profiles are in good agreement with the experimental data. Author (revised)

N94-25220# Technische Univ., Eindhoven (Netherlands).
SOME SUBJECTS IN DIGITAL AUDIO, NOISE SHAPING, SAMPLE RATE CONVERSION, DYNAMIC RANGE COMPRESSION AND TESTING Ph.D. Thesis
Eduard Ferdinand Stikvoort 1992 247 p Prepared in cooperation with Philips Gloeilampenfabrieken N.V., Eindhoven, Netherlands
(ISBN-9-09-005162-7; ETN-94-95321) Copyright Avail: CASI HC A11/MF A03

The following subjects in the field of digital audio are presented: digital sample rate conversion between nonrelated rates, digital noise shaping code conversion, distortion analysis, and dynamic range compression. The sample rate conversion of digital audio signals between nonrelated frequencies concerns the conversion between, for example, 48 kHz and 44.1 kHz and conversion between nominally equal sample frequencies which are derived from different master clocks. The one bit coding of a digital signal is used. The results of quantization and quantizing noise taken from the literature are discussed. The digital distortion analyzer which is used for testing of A/D converters or the signal processing is presented. The tuning mechanism of the notch filter and the corresponding frequency detection which was found is described. The implementation and performance of the distortion analyzer are given. The dynamic range compression is realized by multiplying the left and right hand audio signals with a gain control signal. The realized compression aims at minimizing artifacts and distortion and the compression ratio is made constant over the entire input range of the compressor. The hardware, based on modular set up and used for implementation of real time digital audio processing, is described. ESA

N94-25289# Technische Univ., Eindhoven (Netherlands).
ON THE AUDITORY DISCRIMINATION OF SPECTRAL SHAPE Ph.D. Thesis
Nicolaus Jacobus Versfeld 1992 149 p Sponsored by Netherlands Organization for the Advancement of Scientific Research
(ETN-94-95306) Avail: CASI HC A07/MF A02

The ability of the human auditory system to discriminate between very simple sounds is investigated. The simplest sounds that still may comprise a change in the spectral shape are considered. The experiments are not restricted to signals with bandwidths that exceed the critical bandwidth. Both within channel and across channel comparison is studied. Experiments with multitone complexes are performed. By variation of the number of components and the component spacing, an attempt to gain some insight into the important factors influencing spectral shape discrimination is made. The results show that two tone complexes of which the amplitudes are changed in opposite direction are interesting signals in the light of profile analysis. Thresholds for changes in the amplitudes are measured systematically as a function of signal parameters such as frequency separation, center frequency, and overall intensity. The results are used to evaluate some models on spectral shape discrimination. The discriminability of a change in the sign of the spectral slope of a noise band is examined. The results give some insight into the discrimination processes with noise-like signals. They are used to relate discrimination of signals with continuous spectra to those with discrete spectra. ESA

N94-24163*# Colorado Univ., Boulder.
SOUND RADIATION DUE TO BOUNDARY LAYER TRANSITION
Meng Wang *In* Stanford Univ., Annual Research Briefs, 1993 Dec. 1993 p 299-312 (For primary document see N94-24138 06-34)
Avail: CASI HC A03/MF A04

72 ATOMIC AND MOLECULAR PHYSICS

Includes atomic structure, electron properties, and molecular spectra.

N94-22720# Washington Univ., Seattle. Dept. of Chemistry.
ATOMIC PROBES OF SURFACE STRUCTURE AND DYNAMICS
E. J. Heller and H. Jonsson 1992 7 p
(Contract DE-FG06-91ER-14224)
(DE94-001651; DOE/ER-14224/T1) Avail: CASI HC A02/MF A01

The following were studied: a new semiclassical method for scattering calculations, He atom scattering from defective Pt surfaces, He atom scattering from Xe overlayers, thermal dissociation of H2 on Cu(110), spin flip scattering of atoms from surfaces, and Car-Parrinello simulations of surface processes. DOE

N94-22733# Wisconsin Univ., Milwaukee.
INELASTIC ELECTRON SCATTERING FROM SURFACES
1993 26 p
(Contract DE-FG02-84ER-45076)
(DE94-001368; DOE/ER-45076/T2) Avail: CASI HC A03/MF A01

This program uses ab-initio and multiple scattering to study surface dynamical processes; high-resolution electron-energy loss spectroscopy is used in particular. Off-specular excitation cross sections are much larger if electron energies are in the LEED range (50-300 eV). The analyses have been extended to surfaces of ordered alloys. Phonon eigenvectors and eigenfrequencies were used as inputs to electron-energy-loss multiple scattering cross section calculations. Work on low-energy electron and positron holography is mentioned. DOE

N94-22869# Lawrence Livermore National Lab., CA.
LIMITS ON HIGH-ORDER HARMONIC GENERATION FROM SINGLE-ATOM CALCULATIONS
K. C. Kulander and K. J. Schafer 18 Aug. 1993 7 p Presented at the 6th International Conference on Multiphoton Processes, Quebec City, Quebec, 25-30 Jun. 1993
(Contract W-7405-eng-48)
(DE93-019950; UCRL-JC-114857; CONF-9306125-4) Avail: CASI HC A02/MF A01

In the quantum mechanical calculations of electron and photon emission from atoms in strong laser fields, a single-active-electron (SAE) model was employed. The effect of the time varying electric field of the laser on each of the valence electrons separately was determined. The active electron in each calculation moves in the time-independent mean field of the remaining, unexcited electrons and the nucleus. This approach works well for the rare gas atoms, at least partially because the neglected double or higher excitations involve states well above the ionization threshold. The photoelectron and photon emission spectra calculated using this technique agree quantitatively with observed emission rates. A simple semiclassical model for high intensity ionization which reproduces the observed harmonic emission spectra obtained in this regime and which provides considerable insight into the dynamics of this process is presented. The basic models was used in the past to predict electron energy distributions in the tunneling regime and it will be used for harmonics. DOE

N94-22923# Brookhaven National Lab., Upton, NY.
THE STATUS OF GLUEBALLS
S. J. Lindenbaum 14 Apr. 1993 7 p Presented at the Future Directions in Particle and Nuclear Physics at Multi-GeV Hadron Beam Facilities, Upton, NY, 4-6 Mar. 1993 Prepared in cooperation with City Coll. of the City Univ. of New York, NY
(Contract DE-AC02-76CH-00016)
(DE93-040040; BNL-49416; CONF-930389-22) Avail: CASI HC A02/MF A01

The Status of Glueballs is presented considering them the most popular candidates from among the isoscalars in the J(sup PC) = 0(exp ++), 0(exp -+) and 2(exp ++) channels. It is shown that in the 0(exp ++) channel the f(sub 0)(1720) which was discovered earlier (the S*(prime)(1720)) at BNL is highly likely the same state as the SLAC (theta)(1720) now that its spin has been found to be 0 instead of the 2 claimed for a long period. In the 0(exp ++) channel there is likely a complex of 2-3 states zeta/eta(1280), lambda/eta(1420) and iota/eta(1520) involving at least one extra isoscalar. In the 2(exp ++), the g(sub T)(2010), g(sub T)(prime)(2300) and g(sub T)(double prime)(2340) (phi)(phi) states found in pi(exp (minus)) p yields (phi)(phi)n (OZI forbidden glueball filter channel) strikingly, approximately, completely break the OZI suppression and comprise within the errors all the (phi)(phi) cross-section. The only viable explanation of these states in the context of QCD is that they are produced by 1-3 primary 2(exp ++) glueballs. All alternate explanations in the past 15 years have failed. DOE

N94-22928# Los Alamos National Lab., NM.
PIONS AND NEUTRINOS AS PROBES OF THE NUCLEON AND NUCLEAR FEW-BODY SYSTEM
C. M. Hoffman 1993 9 p Presented at the 14th European Conference on Few-Body Problems in Physics, Amsterdam, Netherlands, 22-27 Aug. 1993
(Contract W-7405-eng-36)
(DE93-040127; LA-UR-93-3006; CONF-9308164-1) Avail: CASI HC A02/MF A01

A number of studies of few-body nucleon and nuclear systems are being pursued at LAMPF using pions and neutrinos as probes. These include: a high-statistics measurement of the cross section for the reaction pi(exp +)p yields pi(exp +)pi(exp 0)p to determine the 1 = 2 (pi)(pi) scattering length; precision measurements of the pi(exp -)p charge exchange cross section in the region of the Delta; measurements of the cross section for the (pi(exp +)p yields pi(exp +)pi(exp +)p), from D, He-3 and He-4 as tests of charge symmetry and reaction mechanisms; measurements of the pi(exp +)p cross section below the Delta; and studies of vp elastic scattering at low Q(exp 2) to determine the quark content of the proton spin. Some of these experiments acquired data last year, while others are presently running. LAMPF, the highest power proton accelerator in the world, is presently in the midst of its 1993 production run. DOE

N94-22937# Toledo Univ., OH. Dept. of Physics and Astronomy.
SEMIEMPIRICAL STUDIES OF ATOMIC STRUCTURE
L. J. Curtis 1993 46 p
(Contract DE-FG05-88ER-13958)
(DE94-001588; DOE/ER-13958/43) Avail: CASI HC A03/MF A01

Atomic structure/properties of highly ionized many-electron systems are studied using semiempirical data systematization, experiment, and theory. Measurements are made using fast ion beams, combined with data from laser- and tokamak-produced plasmas, astrophysical sources, and light sources. Results during this 3-yr period are discussed under the following headings: Invited review article (decay rates in systems of negative ions to very heavy one-electron ions), fast ion beam lifetime measurements (Pt sequence, neutral carbon, Na sequence), multiplexed decay curve measurements (lifetimes of alkali-like resonance transitions, spin-forbidden intercombination lines), lifetimes in Ne sequence, lifetimes for H and He sequences, data-based semiempirical formulations, calculations, and accelerator studies. DOE

N94-22948# Argonne National Lab., IL.
PROCEEDINGS OF THE FIFTH USERS MEETING FOR THE ADVANCED PHOTON SOURCE
Dec. 1992 335 p Meeting held in Argonne, IL, 14-15 Oct. 1992
(Contract W-31-109-eng-38)
(DE93-040692; ANL/APS/CP-5; CONF-9210290) Avail: CASI HC A15/MF A03

The Fifth Users Meeting for the Advanced Photon Source (APS) was held on October 14-15, 1992, at Argonne National Laboratory. Scientists and engineers from universities, industry, and national laboratories came to review the status of the facility and to look ahead to the types of forefront science that will be possible when the APS is completed. The presentations at the meeting included an overview of the project, funding opportunities, advances in synchrotron radiation applications, and technical developments at the APS. In addition, the 15 Collaborative Access Teams that have been approved to date participated in a poster session, and several vendors displayed their wares. The actions taken at the 1992 Business Meeting of the Advanced Photon Source Users Organization are also documented. DOE

N94-22951# New Mexico State Univ., Las Cruces. Dept. of Physics.
MOMENTUM AND COORDINATE SPACE THREE-NUCLEON POTENTIALS
S. A. Coon and M. T. Pena (Continuous Electron Beam Accelerator Facility, Newport New, VA.) 10 Jun. 1993 32 p
(Contract DE-AC05-84ER-40150)
(DE93-040868; CEBAF-TH-93-09; DOE/ER-40150/236) Avail: CASI HC A03/MF A01

In this paper we give explicit formulae in momentum and coordinate space for the three-nucleon potentials due to rho and pi meson exchange, derived from off-mass-shell meson-nucleon scattering amplitudes which are constrained by the symmetries of QCD and by the experimental data. Those potentials have already been applied to nuclear matter calculations. Here we display additional terms which appear to be the most important for nuclear structure. The potentials are decomposed in a way that separates the contributions of different physical mechanisms involved in the meson-nucleon amplitudes. The same type of decomposition is presented for the pi minus pi TM force: The Delta isobar, the chiral symmetry breaking and the nucleon pair terms are isolated. DOE

N94-22952 Continuous Electron Beam Accelerator Facility, Newport New, VA.
GAUGE INVARIANCE AND THE ELECTROMAGNETIC CURRENT OF COMPOSITE PIONS
M. R. Frank (Hampton Univ., VA.) and P. C. Tandy (Kent State Univ., OH.) 1993 13 p Limited Reproducibility: More than 20% of this document may be affected by microfiche quality
(Contract DE-AC05-84ER-40150)
(DE93-040869; CEBAF-TH-93-05; HUPhy-01-93; DOE/ER-40150/240)
Avail: Issuing Activity (Department of Energy (DOE))

The Global Color-symmetry Model of QCD is extended to deal with a background electromagnetic field and the associated conserved current is identified for composite (bar q)q pion modes of the model. Although the analysis is limited to tree level in the bilocal fields that bosonize the model, the identified photon-pion vertex produces the charge form factor associated with ladder Bethe-Salpeter pion amplitudes. A Ward-Takahashi identity for this vertex is derived in terms of the effective inverse propagator for the equivalent local pion field and the intrinsic ladder Bethe-Salpeter amplitudes. This identity is then used to illustrate gauge invariance by showing that identical vertex information is produced from the gauge change of the free action once proper account is taken of the gauge transformation properties of the bilocal pion fields. Comments are made on the location of the vector dominance mechanism in this treatment. DOE

N94-22956# Oak Ridge National Lab., TN.
ELECTRON SPECTROSCOPIC STUDIES OF THE NEUTRALIZATION OF SLOW MULTICHARGED IONS DURING INTERACTIONS WITH A METAL SURFACE
F. W. Meyer, L. Folkerts, C. C. Havener, I. G. Hughes, S. H. Overbury, D. M. Zehner, and P. A. ZeijlmansvanEmmichoven 1993 11 p Presented at the 18th International Conference on the Physics of Electronic and Atomic Collisions, Aarhus, Denmark, 21-27 Jul. 1993
(Contract DE-AC05-84OR-21400)
(DE93-041046; CONF-930711-1) Avail: CASI HC A03/MF A01

Recent experimental results of electron spectroscopic studies of the neutralization and relaxation of slow multicharged ions interacting with metal surfaces are summarized. Discussed are measurements of projectile K-Auger electron emission during interactions of N(sup 6+) ions with clean and cesiated Au, as well as clean Cu single crystal targets. While the dominant component in the measured K-Auger spectra is shown to be due to sub-surface electron emission, at incident perpendicular velocities below about 10(exp -2) au, small features become evident in the measured K-Auger spectra that are consistent with above surface projectile electron emission. Experimental results are compared with results of modelling studies of above- and sub-surface electron emission. Also presented are measurements of low energy electron emission during multicharged ion-surface interactions, together with a discussion and analysis of the various contributing low energy emission mechanisms. DOE

N94-22970 International Centre for Theoretical Physics, Trieste (Italy).
FLAVOR CHANGING STRINGS AND DOMAIN WALLS
G. Dvali and G. Senjanovic Apr. 1993 12 p Limited Reproducibility: More than 20% of this document may be affected by microfiche quality
(DE93-633217; IC-93/77) Avail: Issuing Activity (Department of Energy (DOE)) (US Sales Only)

The cosmological consequences of a spontaneous breaking of non-abelian discrete symmetries, which may appear as a natural remnant of a continuous symmetry, such as a family symmetry, is considered. The result may be a stable domain wall across which an electron would turn into a muon (or nu(sub e) into nu(sub mu)) or a flavor analog of an Alice string-domain wall structure with the same property. DOE

N94-22988 Lawrence Livermore National Lab., CA.
RELATIVISTIC CONFIGURATION INTERACTION CALCULATION OF THE CORRELATION ENERGIES OF HIGHLY-CHARGED IONS
M. H. Chen, K. T. Cheng, and W. R. Johnson (Notre Dame Univ., IN.) Jul. 1993 2 p Limited Reproducibility: More than 20% of this document may be affected by microfiche quality
(Contract W-7405-eng-48)
(DE94-001055; UCRL-JC-114367) Avail: CASI HC A01

We are developing a new relativistic configuration interacion (CI) method for calculating the atomic structure of many-electron ions using complete finite basis sets constructed from B spline functions of piecewise polynomials. This method is based on the relativistic no-pair Hamiltonian from quantum electrodynamics (QED). Eigenfunctions of the Hamiltonican are expanded in a basis of configuration state functions constructed from products of one-electron orbitals. Eigenvaluses and eigenfunctions of the low-lying states of the ions are then determined by diagonalizing the Hamiltonian matrix which incudes the contributions both from the Coulomb and retarded Breit interactions. Derived from text

N94-23002# California Univ., Berkeley. Lawrence Berkeley Lab.
HIGH-RESOLUTION SOFT X RAY PHOTOIONIZATION STUDIES OF SELECTED MOLECULES Ph.D. Thesis
E. A. Hudson Aug. 1993 195 p
(Contract DE-AC03-76SF-00098)
(DE94-000568; LBL-34481) Avail: CASI HC A09/MF A03

Near-edge soft x ray photoionization spectra were measured for CO, SF6, H2S, and D2S in the gas phase, using the Free University of Berlin plane-grating SX-700-II monochromator at the synchrotron radiation source BESSY. Photoionization spectra of carbon monoxide were measured near the carbon and oxygen K edges. Vibrational spacings and bond lengths are derived for several resonances. Results are consistent with equivalent-core model and indicate the different influences of the carbon and oxygen 1s core holes. Corresponding spectra of H2CO and D2CO were also measured. Assignment of complex vibrational structure in valence-shell and Rydberg resonances is facilitated by comparison of spectra for the two isotopic species. Geometric and vibrational parameters are derived for several carbon 1s core-excited states. Isotopic shifts are observed in the energies and linewidths of some core-excited states. Sulfur hexafluoride photoionization spectra, measured near the sulfur L(sub 2,3) edges, show several series of weak, narrow Rydberg resonances. High resolution and good counting statistics allow a complete assignment of these states. Lineshapes of the broad inner-well resonances are analyzed to establish the magnitudes of vibrational and lifetime broadening in these states. Spectra of the H2S and D2S molecules were also measured near the sulfur L(sub 2,3) edges. Besides lower-energy transitions to inner-well states, a complex manifold of overlapping Rydberg resonances is observed. The rich fine structure of these states arises mainly from removal of orbital degeneracies in molecular field. Additional structure due to vibrational excitations in the final state is identified by comparison of the spectra for the two isotopic species. DOE

N94-23007# Brookhaven National Lab., Upton, NY.
LOW P(SUB T) PHOTON PRODUCTION IN PROTON-NUCLEUS COLLISIONS AT 18 GeV/c
D. Lissauer, H. Takai, and C. Woody 1993 6 p Presented at the 10th International Conference on Ultra-Relativistic Nucleus-Nucleus Collisions, Borlaenge, Sweden, 20-24 Jun. 1993
(Contract DE-AC02-76CH-00016)
(DE94-001380; BNL-49453; CONF-930636-6) Avail: CASI HC A02/MF A01

The inclusive single photon spectrum has been measured in the p(sub T) range from a few MeV/c up to approximately 1 GeV/c at several rapidities in the interval from -2.1 less than y(sub cm) less than +0.5 in 18 GeV/c proton-beryllium and proton-tungsten collisions at the Brookhaven AGS. The measured photon distributions are compared with the expected distribution of photons from (pi)(sup 0) decays and hadronic bremsstrahlung in a search for new sources of 'soft' photons at low transverse momentum. DOE

N94-23018# Wisconsin Univ., Madison.
A MEASUREMENT OF THE FORWARD-BACKWARD ASYMMETRY AND SIN(SUP 2)(THETA)(SUB W) FROM THE PROCESS Z(SUP 0) (YIELDS) (MU)(SUP +)(MU)(SUP (MINUS)) AT (RADICAL)S = 1.8 TeV Ph.D. Thesis
L. A. Markosky 1992 224 p

(Contract DE-AC02-76ER-00881)
(DE94-001908; DOE/ER-00881/T4) Avail: CASI HC A10/MF A03

A measurement of the forward-backward charge asymmetry in the decay of Z(sup 0) bosons produced from (bar p)p collisions at (radical)s = 1.8 TeV at the Fermilab Tevatron collider, and decaying to (mu)(+) (mu)(-) pairs is presented. From this asymmetry, a value for the Weinburg angle, sin(exp 2) (theta)(sub W), is extracted and compared to values from other experiments. DOE

N94-23218 California Univ., Berkeley. Lawrence Berkeley Lab.
TOWARDS A THEORY OF QUARK AND LEPTON MASSES
L. J. Hall 23 Feb. 1993 10 p Presented at the 3rd Symposium on Particles, Strings and Cosmology and the 16th Texas Symposium on Relativistic Astrophysics Conference, Berkeley, CA, 13-18 Dec. 1992 Limited Reproducibility: More than 20% of this document may be affected by poor print
(Contracts DE-AC03-76SF-00098; DE-AC02-76ER-01545)
(DE94-001726; LBL-33677; UCB-PTH-93/04; CONF-921261-4) Avail: Issuing Activity (Department of Energy (DOE))

The question of whether or not any progress has been made on understanding and predicting the 13 parameters which describe the observed masses and mixing angles of the quarks and leptons is discussed. Arguments are given in favor of pursuing schemes in which grand unified and family symmetries provide many relations among these 13 parameters. A sequence of simple assumptions leads to a supersymmetric SO(10) theory with 8 predictions: tan (beta), m(sub t), V(sub cb), m(sub s), m(sub s)/m(sub d), m(sub u)/m(sub d), V(sub ub) and the amount of CP violation J. These predictions are presented together with experiments which will test them. DOE

N94-23435# Wisconsin Univ., Madison. Center for Plasma Theory and Computation.
NONLINEAR ION-MIXING-MODE PARTICLE TRANSPORT IN THE DISSIPATIVE TRAPPED ELECTRON REGIME
A. S. Ware and P. W. Terry Sep. 1993 37 p
(Contract DE-FG02-86ER-53218)
(DE94-000989; UW-CPTC-93-5) Avail: CASI HC A03/MF A01

The nonlinear particle transport arising from the convection of nonadiabatic electron density by ion temperature gradient driven turbulence is examined for trapped electron collisionality regimes. The renormalized dissipative nonadiabatic trapped electron phase space density response is derived and used to calculate the nonlinear particle flux along with an ansatz for the turbulently broadened frequency spectrum. In the lower temperature end of this regime, trapped electrons are collisional and all components of the quasilinear particle flux are outward (i.e., in the direction of the gradients). Nonlinear effects can alter the phase between the nonadiabatic trapped electron phase space density and the electrostatic potential, producing inward components in the particle flux. Specifically, both turbulent shifting of the peak of the frequency spectrum and nonlinear source terms in the trapped electron response can give rise to inward components. However, in the dissipative regime these terms are small, and the trapped electron response remains dominantly laminar. When the trapped electrons are collisionless, there is a temperature threshold above which the electron temperature gradient driven component of the quasilinear particle flux changes sign and becomes inward. For finite amplitude turbulence, however, turbulent broadening of both the electron collisional resonance and the frequency spectrum removes this threshold, and the temperature gradient driven component remains outward. DOE

N94-23505 Selskapet for Industriell og Teknisk Forskning, Trondheim (Norway). Div. of Applied Physics.
PERTURBATION THEORY IN ELECTRON DIFFRACTION
L. N. Bakken, K. Marthinsen (Norges Tekniske Hoegskole, Trondheim.), and R. Hoeier (Norges Tekniske Hoegskole, Trondheim.) 8 Dec. 1992 6 p Limited Reproducibility: More than 20% of this document may be affected by microfiche quality
(PB93-201424; STF19-A92019) Avail: CASI HC A02

The Bloch-wave approach is used for discussing multiple inelastic electron scattering and higher-order perturbation theory in inelastic high-energy electron diffraction. In contrast to previous work, the present work describes three-dimensional diffraction so that higher-order Laue zone (HOLZ) effects are incorporated. Absorption is included and eigenvalues and eigenvectors are calculated from a structure matrix with the inclusion of an absorptive potential. Centrosymmetric as well as non-centrosymmetric crystal structures are allowed. An iteration method with a defined generalized propagation function for solving the inelastic coupling equations is described. It is shown that a similar iteration method with the same propagation function can be used for obtaining higher-order perturbation terms for the wave-function when a perturbation is added to the crystal potential. Finally, perturbation theory by matrix calculations when a general perturbation is added to the structure matrix is considered. NTIS

N94-23543 Auburn Univ., AL. Dept. of Physics.
THEORETICAL ATOMIC PHYSICS FOR FUSION
M. S. Pindzola 1993 15 p Limited Reproducibility: More than 20% of this document may be affected by poor print
(Contract DE-FG05-86ER-53217)
(DE94-000712; DOE/ER-53217/T2) Avail: Issuing Activity (Department of Energy (DOE))

The understanding of electron-ion collision processes in plasmas remains a key factor in the ultimate development of nuclear fusion as a viable energy source for the nation. Our 1993-1995 research proposal delineated several areas of research in electron-ion scattering theory. Efforts in 1993 are summarized. DOE

N94-23699# California Univ., San Diego.
PROGRESS REPORT FOR THE UCSD EXPERIMENTAL HEP GROUP
1993 9 p
(Contract DE-FG03-90ER-40546)
(DE94-001357; DOE/ER-40546/T3) Avail: CASI HC A02/MF A01

This progress report concerns the second year of the five-year proposal of the UCSD experimental high energy physics group. The main activity continues to be the L3 experiment at LEP. Recent activities are reviewed and the current status of the group is described. The research plan to continue participation in L3 physics and upgrades and to work on the design and construction of the GEM detector is outlined. DOE

N94-23713 Amsterdam Univ. (Netherlands). Inst. of Mass Spectrometry.
REACTIVITY OF AMBIDENT ANIONS IN THE GAS PHASE Ph.D. Thesis
Ivo. L. Freriks 15 Dec. 1992 126 p Sponsored by Netherlands Foundation for Chemical Research, and Nederlandse Organisatie voor Wetenschappelijk Onderzoek, The Hague Limited Reproducibility: More than 20% of this document may be affected by microfiche quality
(PB93-232189) Avail: CASI HC A07

Ambident anions are negative ions in which several reactive centra are coupled via resonance. When these ions react, there is a competition possible between the reaction channels via each of these reactive centra. A systematic study on the reactivity of several ambident anions in a Fourier transform ion cyclotron resonance mass spectrometer is described in the thesis. Via probe reactions it is shown that a gas-phase ion/molecule reaction between an ambident anion and an unsaturated polyfluorocarbon compound enables a distinction between the competing reaction channels mentioned. The obtained product distributions can be interpreted using simple perturbation theory. In chapter one of the thesis several models and concepts (such as hard and soft acids and bases, HSAB, perturbation theory and the Allopolarisierungs-Prinzip) are described which have been used previously to explain the reactivity of ambident ions in solution. NTIS

N94-23746# Amsterdam Univ. (Netherlands).
LOW MASS MUON PAIR PRODUCTION IN 450 GeV p-Be COLLISIONS Ph.D. Thesis
R. J. Veenhof 12 May 1993 132 p Sponsored by Stichting voor Fundamenteel Onderzoek der Materie and European Organization for Nuclear Research Prepared in cooperation with Natio naal Inst. voor Kernfysica en Hoge Energiefysica, Amsterdam, Netherlands
(PB94-110699) Avail: CASI HC A07/MF A02

The Helios experiment was proposed in 1983 to investigate in detail the origin of low mass lepton pairs. The Helios setup combines an electron spectrometer, a muon spectrometer, a photon detector, almost hermetic calorimetry and a device to measure the multiplicity. The Helios detector is described in Chapter 2.0 with particular emphasis on the performance of the drift chamber system. The event selection and the reconstruction of the muons is described in Chapter 3.0. Chapter 4.0 summarizes the current knowledge of the decays of mesons into low mass muon pairs. The author's own measurements of meson properties are presented in Chapter 5.0. The question whether one needs anomalous pairs to explain the data, is answered in Chapter 6.0. Helios reaches the conclusion that there is no evidence for the production of anomalous pairs at central rapidity and low p(sub T) in pBe collisions. This result complements the recent finding of the RISK experiment, which is also able to observe Dalitz decays, that low mass lepton pair production in the forward region in pi(-)C interactions is compatible with meson decays. NTIS

N94-23803 Stanford Linear Accelerator Center, CA.
PHOTON-PHOTON COLLISIONS AT THE NEXT LINEAR COLLIDER: THEORY
S. J. Brodsky Aug. 1993 15 p Presented at the International Workshop on Physics and Instrumentation at Future Linear Colliders, Kona, HI, 26-30 Apr. 1993 Limited Reproducibility: More than 20% of this document may be affected by microfiche quality
(Contract DE-AC03-76SF-00515)
(DE93-041025; SU-SLAC-Pub-6314; CONF-930449-5) Avail: CASI HC A03/MF A01

The collisions of photons at a high energy electron-positron collider provide a comprehensive laboratory for testing QCD, electroweak interactions, and extensions of the standard model. It is expected that by using back-scattered laser beams that the effective luminosity and energy of photon-photon collisions will be comparable to that of the primary e(+)e(-) collisions. In this talk, I will focus on tests of electroweak theory in photon-photon annihilation such as (gamma)(gamma) yields W(+)W(-), (gamma)(gamma) yields Higgs boson, and higher-order loop processes, such as (gamma)(gamma) yields (gamma)(gamma), Z(gamma) and ZZ. Since each photon can be resolved into a W(+)W(-) pair, high energy photon-photon collisions can also provide a remarkable background-free laboratory for studying WW collisions and annihilation. I also review high energy (gamma)(gamma) tests of quantum chromodynamics, such as the scaling of the photon structure function, t(bar t) production, mini-jet processes, and diffractive reactions. DOE

N94-23804# Sandia National Labs., Albuquerque, NM.
DISORDER EFFECTS ON SMALL-POLARON FORMATION AND HOPPING
D. Emin 1993 10 p Presented at the 5th International Conference on Hopping and Related Phenomena, Glasgow (United Kingdom), 31 Aug. - 3 Sep. 1993
(Contract DE-AC04-76DP-00789)
(DE94-001205; SAND-93-2046C; CONF-930879-1) Avail: CASI HC A02/MF A01

Small-polarons will only form in covalent crystals whose electronic halfbandwidths are sufficiently narrow, E(sub b) greater than W. The absence of small polaronic carriers in most covalent crystals presumably indicates that E(sub b) less than W in these instances. However, evidence of small polarons is commonly found in disordered materials despite the estimates of E(sub b) and W not being significantly different from those of crystals. This result is rationed by stating that disorder has slowed carrier motion enough to permit small-polaron formation. Recently the question of how disorder affects the stability of quasifree carriers with respect to small-polaron formation was addressed. It is found that only modest energetic disorder is required to induce small-polaron formation. I first succinctly describe essential elements of this work. Second, I address the role of disorder on the adiabatic hopping motion of small polarons. Energy bands in most materials in which small-polarons are found are thought to be sufficiently wide (greater than a phonon energy) that the small-polaronic hopping is 'adiabatic.' That is, the electronic carriers move between sites sufficiently rapidly to follow the atomic motions. In this situation the small-polaron jump rates are independent of intersite separations. The magnitudes of the preexponential factors of the measured hopping mobilities typically support this view. Further support for this picture is found from experiments that determine weak dependences of the mobility on hydrostatic pressure. DOE

N94-23806 Argonne National Lab., IL.
B-QUARK PRODUCTION AT HADRON COLLIDERS
Ruibin Meng and S. Riemersma (Southern Methodist Univ., Dallas, TX.) Aug. 1993 10 p Presented at the Workshop on B Physics at Hadron Colliders, Snowmass, CO, Jun. 1993 Limited Reproducibility: More than 20% of this document may be affected by poor print
(Contract W-31-109-eng-38)
(DE94-001459; ANL-HEP-CP-93-66; CONF-9306258-3) Avail: Issuing Activity (Department of Energy (DOE))

Studying B-physics at hadron accelerators requires a good understanding of the total and differential cross sections for b-quark production. This knowledge gives those involved in B(bar B) mixing, rare B decays, and those trying to determine the CKM angles (alpha), (beta), and (gamma) an idea of how many events they can expect, given the luminosity and the branching ratios. It is particularly important for those studying rare B decays as they set limits on where we can hope to see new physics. For these reasons and others, the complete (Omicron)((alpha)(sub s)(sup 3)) corrections to heavy-quark production at hadron accelerators were calculated in. Also three groups have attempted to calculate heavy-quark production using resummation techniques in the small-x kinematic region. These resummation techniques are necessary since the b-quark mass m(sub b) is small relative to the center-of-mass energies (radical)S of the TeVatron and the SSC. While these techniques offer some hope of obtaining reasonable predictions for b-production at these machines, the current results can best be considered as preliminary. Thus we must turn to fixed-order perturbative QCD for guidance, as we have no other real choice at this point. However, let us submit a caveat here: fixed-order perturbative QCD works best when all the scales are roughly comparable, i.e. (radical)s is approximately equal to m(sub b) approximately equal to p(sub t), (radical)s being the partonic center-of-mass energy. When we are not in this regime, for example at the TeVatron and the SSC, our predictions will then be less reliable. Bearing this in mind, let us continue to the results section. DOE

N94-23825* National Aeronautics and Space Administration. Lewis Research Center, Cleveland, OH.
METHOD AND APPARATUS FOR PRODUCING A THERMAL ATOMIC OXYGEN BEAM Patent
Bruce A. Banks, inventor (to NASA) and Sharon K. Rutledge, inventor (to NASA) 18 Jan. 1994 6 p Filed 25 Jan. 1993 Supersedes N93-19026 (31 - 6, p 1656)
(NASA-Case-LEW-15614-1; US-Patent-5,280,174;
US-Patent-Appl-SN-008026; US-Patent-Class-250-251;
Int-Patent-Class-H05H-3/00) Avail: US Patent and Trademark Office

Atomic oxygen atoms are routed to a material through a sufficiently tortuous path so that vacuum ultraviolet radiation is obstructed from arriving at the surface of the material. However, the material surface continues to be exposed to the atomic oxygen.
Official Gazette of the U.S. Patent and Trademark Office

N94-24077 Aerospace Corp., El Segundo, CA. Engineering and Technology Group.
OPTICAL SPIN POLARIZATION AND STATE-SENSITIVE DETECTION OF A CESIUM ATOMIC BEAM
B. Jaduszliwer and Y. C. Chan 15 Jan. 1994 9 p Repr. from Physical Review A (American Physical Soceity), v. 48, no. 3, Sep. 1993 p 1050-2947
(ATR-92(8436)-1) Copyright Avail: Issuing Activity

A cesium atomic beam having a high degree of polarization is prepared by optical pumping with two circularly polarized diode lasers, and a technique for state-sensitive atomic detection involving laser induced fluorescence in a magnetic field (LIFB) is introduced. An atomic-beam polarization of 93 percent is measured using the LIFB technique, and the combined use of optical-state preparation and LIFB detection in an atomic-recoil experiment to study spin-changing electron-atom collisions is demonstrated.
Author (revised)

N94-24487*# Norfolk State Univ., VA. Materials Research Lab.
RADIATIVE PROPERTIES OF MOLECULAR NITROGEN IONS PRODUCED BY HELIUM PENNING IONIZATION AND ARGON EFFECTS Interim Report, 1 Sep. 1993 - 4 Feb. 1994
George Miller, III and Kyo-Dong Song 4 Feb. 1994 67 p
(Grant NAG1-1513)
(NASA-CR-195126; NAS 1.26:195126) Avail: CASI HC A04/MF A01

The development of hypersonic aerospace vehicles requires a better understanding on the thermal and chemical nonequilibrium kinetics of participating species in shock layers. The computational fluid dynamic (CFD) codes developed for such flowfields overestimate the radiation in the spectral region of 300 - 600 nm. A speculation for this overestimation is that inclusion of Ar, CO2, and H2O at the upper atmosphere flight region makes a significant impact on radiative kinetics of molecular nitrogen ions. To define the effects of minority species on the radiative kinetics of N2(+), an experimental setup was made by using the helium Penning ionization. The vibrational and rotational temperature were measured by mapping the vibrational and rotational distributions of N2(+) emission with high spectroscopic resolution and absolute intensity measurements. Measured vibrational temperatures were in the range from 18,000 to 36,000 K, and rotational temperatures were in the range from 300 to 370 K. The irradiance of 391.44 nm line and rotational and vibrational temperatures were analyzed to define argon and CO2 effects on the N2(+) emission. When Ar or CO2 is injected with N2, the rotational temperature did not change. The irradiances were reduced by 34 percent and 78 percent for the 50 percent of mixture of Ar and CO2, respectively. The vibrational temperatures were increased by 24.1 percent and 82.9 percent for the 50 percent of mixture of Ar and CO2, respectively. It appears that there are no significant effects from small concentrations of Ar and CO2 at the upper atmosphere flight region. Author (revised)

N94-24505# Los Alamos National Lab., NM.
EFFECTS OF IONIZING RADIATION ON MODERN ION EXCHANGE MATERIALS
S. Fredric Marsh and K. K. S. Pillay Oct. 1993 25 p
(Contract W-7405-eng-36)
(DE94-001569; LA-12655-MS) Avail: CASI HC A03/MF A01

We review published studies of the effects of ionizing radiation on ion exchange materials emphasizing those published in recent years. A brief overview is followed by a more detailed examination of recent developments. Our review includes styrene/divinylbenzene copolymers with cation-exchange or anion-exchange functional groups, polyvinylpyridine anion exchangers, chelating resins, multifunctional resins, and inorganic exchangers. In general, strong-acid cation exchange resins are more resistant to radiation than are strong-base anion exchange resins, and polyvinylpyridine resins are more resistant than polystyrene resins. Cross-linkage, salt form, moisture content, and the surrounding medium all affect the radiation stability of a specific exchanger. Inorganic exchangers usually, but not always, exhibit high radiation resistance. Liquid ion exchangers, which have been used so extensively in nuclear processing applications, also are included. DOE

N94-24510# Oak Ridge National Lab., TN.
EXPERIMENTAL AND THEORETICAL FEATURES OF STRONG SUPPRESSION AND SHIFTING PHENOMENA IN ODD-PHOTON RESONANT EXCITATIONS AND STIMULATED EMISSIONS
W. R. Garrett 1993 5 p Presented at the 11th International Conference on Laser Spectroscopy, Hot Springs, VA, Jun. 1993
(Contract DE-AC05-84OR-21400)
(DE94-000341; CONF-9306200-1) Avail: CASI HC A01/MF A01

Descriptions are given of recent theoretical and experimental results of dramatic effects, during the interval of the excitation pulse, in optically pumped stimulated emissions (OPSE). Forward-directed OPSE from a two-photon resonantly excited state to a lower state which is also coupled to the ground state is strongly suppressed and backward emissions are frequency shifted. Surprisingly, the effects are caused by an interference from a wave-mixing field. Several other implications of this effect are given and, on the basis of this phenomenon, several puzzling ASE observations mentioned in other published work are noted and clarified. DOE

N94-24515# Fermi National Accelerator Lab., Batavia, IL.
SEARCH FOR THE TOP QUARK AND OTHER NEW PARTICLES AT D0
P. C. Bhat Sep. 1993 7 p Presented at the 19th International Conference on Elastic and Diffractive Scattering (5th Blois Workshop), Providence, RI, 8-12 Jun. 1993
(Contract DE-AC02-76CH-03000)
(DE94-001220; FNAL/C-93/279-E; CONF-9306221-5) Avail: CASI HC A02/MF A01

Preliminary results from the search for the top quark and other new particles in p(bar-p) collisions at the square root of s = 1.8 TeV are reported. In a data sample corresponding to an integrated luminosity of about 7.5 pb(exp -1), one candidate event for the top quark is found in the di-lepton channel. A lower limit for the mass of the top quark of 103 GeV/sq c (99 Gev/sq c) is obtained at 95% confidence level with (without) background subtraction. Status of searches for other new particles that may arise from new phenomena beyond the standard model is summarized. DOE

N94-24555# New Mexico Univ., Albuquerque. Dept. of Chemistry.
INTERACTIONS BETWEEN ORGANIZED, SURFACE-CONFINED MONOLAYERS AND VAPOR-PHASE PROBE MOLECULES. 7: COMPARISON OF SELF-ASSEMBLYING ORGANOMERCAPTAN MONOLAYERS DEPOSITED ON GOLD FROM LIQUID AND VAPOR PHASES Report, 1 Aug. 1992 - 31 Jul. 1993
O. Chailapakul, L. Sun, C. Xu, and R. M. Crooks 23 Nov. 1993 11 p
(Contract N00014-91-J-1991)
(AD-A273196) Avail: CASI HC A03/MF A01

A comparative study of the structure and chemistry of methyl-terminated n-alkanethiol self-assembling monolayers (SAM's) formed from liquid and vapor phases is reported. Three different SAM's are considered: Au/HS(CH2)(sub n)CH3, n = 5, 11, and 15. Liquid-phase-deposited films were prepared by exposure of Au substrates to dilute ethanol solutions of the n-alkanethiols followed by ethanol rinsing, and vapor-phase-deposited SAM's were prepared by exposure of the Au surface to 10%-of-saturation n-alkanethiol vapors followed by N2 purging, which removes loosely bound n-alkanethiol molecules from the surface. The matrix of 6 organic surfaces were studied by FTIR external reflectance spectroscopy (FTIR-ERS), ellipsometry, and cyclic voltammetry, which provide information about the average structure of the SAM's, and a newly developed scanned tunneling microscope (STM)-based method, which provides information about individual SAM defect structures. FTIR-ERS and ellipsometry indicate no detectable differences between liquid- and vapor-phase-deposited SAM's. Data obtained using cyclic voltammetry and STM show that the barrier properties of SAM's depend on the ambient phase from which the SAM assemblies, the length of the n-alkanethiol, and the chemical nature of the molecular probe used to evaluate the monolayer structure. DTIC

N94-24569# Oak Ridge National Lab., TN.
INTEGRAL EQUATIONS FOR THE MICROSTRUCTURES OF SUPERCRITICAL FLUIDS
L. L. Lee and H. D. Cochran 1993 67 p Presented at the NATO Advanced Study Institute on Composition, Geochemistry and Conversion of Oil Shales and Supercritical Fluids, Akcay, Turkey, 18-31 Jul. 1993
(Contract DE-AC05-84OR-21400)
(DE94-002460; CONF-930776-3) Avail: CASI HC A04/MF A01

Molecular interactions and molecular distributions are at the heart of the supercritical behavior of fluid mixtures. The distributions, i.e. structure, can be obtained through any of the three routes: (1) scattering experiments, (2) Monte Carlo or molecular dynamics simulation, and (3) integral equations that govern the relation between the molecular interactions u(r) and the probability distributions g(sub ij)(r). Most integral equations are based on the Ornstein-Zernike relation connecting the total correlation to the direct correlation. The OZ relation requires a 'closure' equation to be solvable. Thus the Percus-Yevick, hypernetted chain, and mean spherical approximations have been proposed. The authors outline the numerical methods of solution for these integral equations including the Picard, Labik-Gillan, and Baxter methods. Solution of these equations yields the solvent-solute, solvent-solvent, and solute-solute pair correlation functions (pcf's). Interestingly, these pcf's exhibit characteristical signatures for supercritical mixtures that are classified as 'attractive' or 'repulsive' in nature. Close to the critical locus, the pcf shows enhanced first neighbor peaks with concomitant long-range build-ups (sic attractive behavior) or reduced first peaks plus long-range depletion (sic repulsive behavior) of neighbors. For ternary mixtures with entrainers, there are synergistic effects between solvent and cosolvent, or solute and cosolute. These are also detectable on the distribution function level. The thermodynamic consequences are deciphered through the Kirkwood-Buff fluctuation integrals (G(sub ij)) and their matrix inverses--the direct correlation function integrals (DCFI's). These quantities connect the correlation functions to the chemical potential derivatives (macroscopic variables) thus acting as 'bridges' between the two world views. DOE

N94-24611# Fermi National Accelerator Lab., Batavia, IL.
ELECTRO-WEAK, QCD AND TOP PHYSICS AT THE TEVATRON

H. T. Diehl Sep. 1993 16 p Presented at the Workshop on Physics at Current Accelerators and the Supercollider, Argonne, IL, 2-5 Jun. 1993
(Contract DE-AC02-76CH-03000)
(DE94-002304; FNAL/C-93/286; CONF-9306176-12) Avail: CASI HC A03/MF A01

The 1992-1993 Tevatron collider run ended yesterday. Approximately 21 (16)pb(exp -1) of p(bar-p) collisions at the square root of S = 1800 GeV were collected at CDF (D0). New measurements of the W and Z cross section x branching ratios indicate that Gamma(W) is 2.033 +/- 0.069 +/- 0.057 GeV. The upper limit for the top quark mass, if it is produced in W decays, is 62 GeV/cu c. Gauge boson pair production studies are beginning to constrain electro-weak parameters. No neutral gauge bosons with mass greater than M(sub z) have appeared. Inclusive jet production and angular distribution studies are compared to NLO perturbative QCD predictions. A new topological jet analysis from CDF is sensitive to the low x gluon distribution. The direct photon cross section shows a steeper fall-off with E(sub t) than does the theory prediction. D0 has one candidate t(bar-t) event in the dilepton mode. The lower limit on M(sub T(sub op)) has been raised to 99 GeV/sq c. DOE

N94-24675 North Carolina Univ., Chapel Hill. Dept. of Chemistry.
FREE ENERGY PROFILES FOR Li(+) AND I(-) IONS APPROACHING Pt(100) SURFACE: A MOLECULAR DYNAMICS STUDY Technical Report
L. Perera and Max L. Berkowitz Nov. 1993 25 p Limited Reproducibility: More than 20% of this document may be affected by microfiche quality
(Contract N00014-89-J-1169)
(AD-A273455; TR-14) Avail: Issuing Activity (Defense Technical Information Center (DTIC))

We calculated the potential of mean force profiles for Li(+) and I(-) ions approaching a non-charged Pt(100) surface and solvated in water. These profiles show that while for I(-) the traditional picture placing the anion in contact with the metal surface is justified, for Li(+) the traditional picture presenting the cation separated from the metal surface by layers of water is not correct. DTIC

N94-24717# Oregon State Univ., Corvallis. Dept. of Physics.
MATTER-WAVE INTERFEROMETRY WITH LASER COOLED ATOMS Final Report
David McIntyre Nov. 1993 13 p
(Contract N00014-91-J-1198)
(AD-A273249) Avail: CASI HC A03/MF A01

This research program is concerned with matter-wave interferometry of laser cooled atoms. A slow beam of laser cooled rubidium atoms will be used as the matter-wave source. The atom optical elements are microfabricated amplitude transmission gratings which will be used in a three-grating interferometer to split and recombine the rubidium beam. The atomic interferometer will be a useful new tool with which to perform precision experiments in atomic physics, quantum optics, and gravitation. The research program takes advantage of three new technologies, the combination of which provides a unique opportunity to construct a compact and stable interferometer. The techniques of laser cooling and trapping are used to produce cold rubidium atoms in a well-collimated beam. Commercially available diode lasers with optical feedback frequency stabilization are used for the laser cooling and trapping beams and for atomic beam diagnostics. Finally, submicron transmission gratings made with high-resolution electron-beam lithography are used as the coherent beam splitters of the atomic interferometer. DTIC

N94-24729# New Mexico Univ., Albuquerque. Dept. of Chemistry.
SYNTHESIS AND CHARACTERIZATION OF TWO-DIMENSIONAL MOLECULAR RECOGNITION INTERFACES Technical Report, 1 Aug. 1992 - 31 Jul. 1993
R. M. Crooks, O. Chailapakul, C. B. Ross, L. Sun, and J. K. Schoer 23 Nov. 1993 23 p
(Contract N00014-91-J-1991)
(AD-A273177) Avail: CASI HC A03/MF A01

We have used self-assembly chemistry to synthesize monolayer assemblies that function as molecular recognition interfaces. In the first part of this paper, we show that one-component self-assembled n-alkanethiol monolayers with carboxylic acid functionalized endgroups specifically adsorb vapor-phase acid-terminated molecules via hydrogen bonding or vapor-phase amine-terminate molecules via proton-transfer interactions. In the second part, we demonstrate that two-component monolayers, which consist of inert n-alkanethiol framework molecules and defect-inducing template molecules, can discriminate between solution-phase probe molecules based on their physical and chemical characteristics. By electrochemically etching the defects and then imaging the resulting surface by scanning tunneling microscopy, the defect sites can be indirectly visualized. DTIC

N94-24798*# Florida Agricultural and Mechanical Univ., Tallahassee. Dept. of Physics.
APPLICATION AND DEVELOPMENT OF THE SCHWINGER MULTICHANNEL SCATTERING THEORY AND THE PARTIAL DIFFERENTIAL EQUATION THEORY OF ELECTRON-MOLECULE SCATTERING Final Report
Charles A. Weatherford 17 Dec. 1993 83 p
(Contract NCC2-492)
(NASA-CR-194774; NAS 1.26:194774) Avail: CASI HC A05/MF A01

One version of the multichannel theory for electron-target scattering based on the Schwinger variational principle, the SMC method, requires the introduction of a projection parameter. The role of the projection parameter a is investigated and it is shown that the principal-value operator in the SMC equation is Hermitian regardless of the value of a as long as it is real and nonzero. In a basis that is properly orthonormalizable, the matrix representation of this operator is also Hermitian. The use of such basis is consistent with the Schwinger variational principle because the Lippmann-Schwinger equation automatically builds in the correct boundary conditions. Otherwise, an auxiliary condition needs to be introduced, and Takatsuka and McKoy's original value of a is one of the three possible ways to achieve Hermiticity. In all cases but one, a can be uncoupled from the Hermiticity condition and becomes a free parameter. An equation for a based on the variational stability of the scattering amplitude is derived; its solution has an interesting property that the scattering amplitude from a converged SMC calculation is independent of the choice of a even though the SMC operator itself is a-dependent. This property provides a sensitive test of the convergence of the calculation. For a static-exchange calculation, the convergence requirement only depends on the completeness of the one-electron basis, but for a general multichannel case, the a-invariance in the scattering amplitude requires both the one-electron basis and the N plus 1-electron basis to be complete. The role of a in the SMC equation and the convergence property are illustrated using two examples: e-CO elastic scattering in the static-exchange approximation, and a two-state treatment of the e-H2 Chi(sup 1)Sigma(sub g)(+) yields b(sup 3)Sigma(sub u)(+) excitation. Author (revised)

N94-24844# Joint Inst. for Nuclear Research, Dubna (USSR).
NEW EVALUATION OF HADRONIC CONTRIBUTIONS TO THE ANOMALOUS MAGNETIC MOMENT OF CHARGED LEPTONS
A. Z. Dubnickova, S. Dubnicka, and P. Strizenec 1992 14 p
(DE93-634394; JINR-E-2-92-281) Avail: CASI HC A03/MF A01 (US Sales Only)

A re-evaluation of the lowest-order hadronic vacuum-polarization contribution to the anomalous magnetic moment of the electron, muon, and tau-lepton with a higher precision in comparison with previous estimates is carried out. The latter is achieved because new data on some exclusive processes have appeared recently, more accomplished models for a description of the pion and kaon electromagnetic structure were developed and the revised (due to a new value of the coefficient of the third power of alpha(sub s)) QCD formula for R = sigma(sub tot) (e(sup +)e(sup -) yields (had)/sigma(sub tot) (e(sup +)e(sup -) yields mu(sup +)mu(sup -)) with electroweak corrections was applied to analyze all existing data in a proper way. The final results are a(sub e)(sup (2)had) = (1.810 (+-) 0.011 (+-) 0.002) x 10(sup -12) a(sub mu)(sup (2)had) = (6.986 (+-) 0.042 (+-) 0.016) x 10(sup -8) and a(sub tau)(sup (2)had) = (3.436 (+-) 0.024 (+-) 0.024) x 10(sup -6). DOE

N94-24868# National Inst. for Fusion Science, Nagoya (Japan).
A RESEARCH OF POSSIBILITY FOR NEGATIVE MUON PRODUCTION BY A LOW ENERGY ELECTRON BEAM ACCOMPANYING ION BEAM
Joshin Uramoto Dec. 1993 39 p
(NIFS-266) Avail: CASI HC A03/MF A01

A low energy electron beam (less than or equal to 2000 eV) is injected perpendicularly into a uniform magnetic field, together with a low energy positive ion beam. On this magnetic mass analysis (using the uniform magnetic field), a peak of secondary electron current to the beam collector (arranged as a mass analyzer of 90 deg type), appears at an analyzing magnetic field which corresponds exactly to a relation of negative muon, mu- (the mass m = 207 m(sub e) and the charge q = e, where m(sub e) and e are mass and charge of electron). The ion beam is essential for the peak appearance, which is produced by decelerating electrically the electron beam in front of the entrance slit of the mass analyzer, and by introducing a neutral gas into the electron beam region and producing a plasma through the ionization. We consider that a very small amount of negative muons may be produced through local cyclotron motions of the injected beam electrons in the ion beam or by an interaction between the bunched beam electrons and beam ions. Author (revised)

N94-24940 North Carolina Univ., Chapel Hill. Dept. of Chemistry.
STRUCTURES OF Cl(-)(H2O)(n) AND F(-)(H2O)(n) (n EQUAL TO 2,3...15) CLUSTERS: MOLECULAR DYNAMICS COMPUTER SIMULATIONS Technical Report, 1 Jul. 1993 - 30 Jun. 1994
L. Perera and M. Berkowitz Nov. 1993 43 p Limited Reproducibility: More than 20% of this document may be affected by microfiche quality
(Contract N00014-89-J-1169)
(AD-A273474) Avail: Issuing Activity (Defense Technical Information Center (DTIC))

We have performed molecular dynamics calculations on Cl(-)(H2O)n and F(-)(H2O)n (n=2,3,...15) clusters. The calculations show that the F(-) ion is solvated in these clusters, while Cl(-) remains attached to the water in the clusters. We also obtained the minimum energy structures for the Cl(-)(H2O)n and F(-)(H2O)n (n=6,7,8) clusters. From the comparison of these structures with the dynamical structures we conclude that the solvation of F(-) ion is due to the entropy effect. DTIC

N94-25047 Department of the Navy, Washington, DC.
NUCLEAR MAGNETIC RESONANCE IMAGING WITH SHORT GRADIENT PULSES Patent
David G. Cory, inventor (to Navy), Joel B. Miller, inventor (to Navy), and Allen N. Garroway, inventor (to Navy) 13 Jul. 1993 11 p Filed 29 Nov. 1990
(AD-D016006; US-Patent-5,227,725; US-Patent-Appl-SN-619567; US-Patent-Class-324-309) Avail: US Patent and Trademark Office

An improved method and apparatus for nuclear magnetic resonance (NMR) imaging are provided by intercalating a magnetic field gradient in the form of short pulses into an NMR line-narrowing sequence. By inserting the short pulses into predetermined windows in the line-narrowing pulse sequence, the resolution of NMR images obtained thereby is increased and image artifacts from homogenous contributions to the natural linewidth are reduced. Furthermore, the short gradient pulses may be intercalated into known multiple pulse sequences or new multiple pulse sequences for specific imaging purposes which allows far more freedom in designing efficient and improved pulse cycles for NMR imaging. DTIC

N94-25082# Technische Univ., Eindhoven (Netherlands).
COMPUTER SIMULATION OF LOW ENERGY SCATTERING Ph.D. Thesis
Camillus Adrianus Severijns 1992 110 p
(ETN-94-95326) Avail: CASI HC A06/MF A02

Two relevant aspects for the interpretation of data obtained with the surface analysis technique Low Energy Ion Scattering (LEIS) are studied: neutralization and the tail at the low energy side of the surface peak in energy spectra. A simulation code called SISS-92 (Simulation of Ion Surface Scattering 1992) was developed. With LEIS both the chemical composition and the structure of a surface can be determined. The differences that can appear between the surface and the bulk, are pointed out. An overview of the computer models in the literature is given. The structure of the SISS-92 code is described. When selecting a numerical technique, its accuracy is a major consideration. An efficient and accurate numerical approximation of the classical collision integrals is based on rational functions. An algorithm for calculating such an approximation is described. The searching for a target atom is also an often performed and time consuming task in a simulation. A fast method for searching and for calculating the data needed in the searching is given. The results of simulations with the SISS-92 code are compared to experimental data. Analytical results for the neutralization integral that generalize the results of Godfrey-Woodruff and Richard-Eschenbacher are presented. The influence of the approximating ion trajectory is studied. Several charge exchange models are used to study the neutralization of Ne(+) ions scattering from the Ni(100) surface. Both localized and non localized models are used. The shape of the tails extending from the surface peaks in energy spectra are studied. ESA

N94-25087# South Carolina Univ., Columbia.
SYNTHESIS OF MOLECULAR WIRES BY A NOVEL DIVERGENT/CONVERGENT APPROACH
James M. Tour and Jeffry S. Schumm 22 Nov. 1993 9 p
(Contract N00014-89-J-3062)
(AD-A273332; TR-26; ONR-TR-26) Avail: CASI HC A02/MF A01

Described is the synthesis of oligo(2-ethylphenyl -ethynylene)s and oligo(2-(3'ethylheptyl) phenyl-ethynylene)s via an iterative divergent convergent approach. Synthesized were the monomer, dimer, tetramer, and octamer of the ethyl derivative and the monomer, dimer, tetramer, octamer, and 16-mer of the ethylheptyl derivative. The 16-mer is 128 A long. At each stage in the iteration, the length of the framework doubles. Only three sets of reaction conditions are needed for the entire iterative synthetic sequence; an iodination, a protodesilation, and a Pd/Cu-catalyzed cross coupling. The oligomers were characterized spectroscopically and by mass spectrometry. DTIC

N94-25228# Technische Univ., Delft (Netherlands). Dept. of Radiation Physics.
MICROSCOPIC DYNAMICS IN DENSE HELIUM-NEON MIXTURES: NEUTRON SCATTERING, KINETIC THEORY AND COMPUTER SIMULATIONS Ph.D. Thesis
Peter Westerhuijs 1992 139 p
(ISBN-9-07-386105-5; ETN-94-95370) Avail: CASI HC A07/MF A02

The microscopic dynamics in eleven dense helium-neon gas mixtures is investigated by means of neutron scattering, kinetic theory and computer simulations. The concentration ratio of helium in the mixture is varied from 0 to 1 at temperatures of 39 and 47 K and pressures between 114 bar and 285 bar. The study is made by considering the partial and total dynamic structure factors of the mixture. The question is addressed how the behavior of two fundamental quantities in simple dense noble gas fluids, that is, the decay frequency of microscopic density fluctuations and the sound dispersion of small scale sound oscillations extend to the simplest of all binary mixtures: He-Ne. ESA

N94-25231# Amsterdam Univ. (Netherlands).
THE L3 VISUALIZATION SYSTEM AND ITS USE IN THE Z(ZERO) LINE SHAPE ANALYSIS Ph.D. Thesis
Rene Wilhelm 1992 115 p Sponsored by Stichting voor Fundamenteel Onderzoek der Materie, Netherlands Original contains color illustrations
(ETN-94-95382) Avail: CASI HC A06/MF A02

The design and implementation of an interactive graphics system that can visualize the events registered by the L3 detector, which is located at the Large Electron Positron (LEP) collider, are presented. The different components of the detector and the online system of data acquisition and monitoring are described. The following components of the offline software base are presented: reconstruction, simulation, data base and graphics. The graphics software is discussed showing design principles and the implementation on Apollo computers. The analysis of the Z neutral line shape, from which several parameters of the Standard Model are extracted with great precision, is performed. ESA

N94-25239# Technische Univ., Eindhoven (Netherlands). Dept. of Physics.
ULTRACOLD ATOMS IN TRAPS AND FOUNTAINS Ph.D. Thesis
Eite Tiesinga 1993 109 p Sponsored by Netherlands Organization for the Advancement of Scientific Research
(ETN-94-95325) Avail: CASI HC A06/MF A02

Six papers or manuscripts of papers, each addressing a different aspect of ultracold atoms, are presented. Collisions of cesium (Cs-133) atoms in a magnetic trap with a special emphasis on resonances and centrifugal barrier phenomena are described. Possibilities to realize the Bose-Einstein condensed state in such a trap are considered. Hyperfine changing collisions of magnetically trapped sodium (Na-23) atoms, of importance for estimating the decay of the atomic density in a magnetic trap, are described. The collisional frequency shift is the only frequency shift in a cesium atomic fountain clock which cannot be reduced by reducing atomic velocities and as such constitutes an essential limitation for cold cesium clocks. This shift and its consequences for the accuracy are described. Measurements of the hyperfine induced spin exchange parameter for the hydrogen maser show a discrepancy in sign with the predicted value calculated a few years ago by another group. This discrepancy is one of the motivations for the theoretical study of the atomic deuterium maser. A comparison with experiment may contribute to an explanation for the discrepancy. The reflection of a hydrogen atom against a superfluid helium surface is studied with special attention for the role of the long wavelength ripplons. ESA

N94-25240# Technische Univ., Eindhoven (Netherlands).

INTRAMULTIPLET MIXING FOR Ne(**)(3p)+He AT SUPERTHERMAL ENERGIES Ph.D. Thesis

Willem Boom 1993 160 p

(ETN-94-95327) Avail: CASI HC A08/MF A02

The mechanisms of fine structure changing transitions within the multiplet of short lived, laser excited neon atoms due to collisions with ground state helium atoms are investigated. These transitions are commonly referred to as intramultiplet mixing. Electronically excited states play an important role in gas lasers, plasma physics, and gas discharges. The orientation of the outer 3p valence electron with respect to the collision partner can strongly influence the collision dynamics. The use of a hollow cathode arc Ne source enables study of intramultiplet mixing at superthermal collision energies between 200 and 1200 meV. From a theoretical point of view, the experimental cross sections can be directly compared with fully quantum mechanical coupled channels calculations. Large discrepancies on the order of a factor of two between experimental and quantum mechanically calculated cross section magnitudes are found. A semiclassical model, strongly enhancing insight into the transition dynamics of intramultiplet mixing, was developed. ESA

N94-25246 Amsterdam Univ. (Netherlands).

THE DETERMINATION OF THE BRANCHING RATIOS OF THE Z(ZERO) BOSON INTO HEAVY QUARKS USING NEURAL NETWORKS Ph.D. Thesis

Nicolo deGroot 1993 97 p Sponsored by Stichting voor Fundamenteel Onderzoek der Materie, Netherlands Limited Reproducibility: More than 20% of this document may be affected by microfiche quality

(ETN-94-95381) Avail: CASI HC A05

The measurement of the branching ratios of the Z neutral boson into heavy quarks is discussed. The purpose is twofold: measuring the branching ratios and studying the feasibility of the use of neural networks. It is demonstrated that it is possible to identify events with heavy flavored quarks in a reliable way. The results obtained for the branching ratios are stable under a large variety of systematic effects and the method is competitive with others. The physics at the Large Electron-Positron (LEP) accelerator is reviewed and neural networks are introduced. A description of the LEP accelerator, the DELPHI (Detector with Lepton, Proton and Hadron Identification) detector, the analysis chain and the inner detector is given. The analysis of the branching ratio of the Z neutral into heavy quarks is presented. ESA

N94-25255# Amsterdam Univ. (Netherlands).

BOTTOM QUARK PRODUCTION AT THE Z RESONANCE Ph.D. Thesis

Tim Foreman 1993 154 p Sponsored by Stichting voor Fundamenteel Onderzoek der Materie, Netherlands

(ISBN-9-09-006217-3; ETN-94-95383) Avail: CASI HC A08/MF A02

Study of heavy flavor production, in particular the production of the bottom quark, and its implications on the Standard Model parameters is presented. The attention is focused on the part of the analysis that is done by muon tagging only. The phenomenological models invented to describe this process are explained. B neutral-anti B neutral mixing, a second order process in which a B meson oscillates between two mass eigenstates, is modeled and the decay of B hadrons is described. A detailed description of the L3 muon detector is given together with the other subdetectors. The L3 muon detector consists of two Ferris wheels each containing eight independent units called octants. Each octant is made out of five precision drift chambers. The L3 muon simulation and reconstruction and the selection of heavy flavors are discussed. The mixing parameter and the branching ratio are determined and the observed forward backward asymmetry is measured. ESA

N94-25259 Amsterdam Univ. (Netherlands).

RELATIVISTIC HADRONS IN AN EXTERNAL FIELD Ph.D. Thesis

Robert Peter Oderkerk 1992 224 p Sponsored by Stichting voor Fundamenteel Onderzoek der Materie Prepared in cooperation with Nationaal Inst. voor Kernfysica en hoge Energiefysica, Amsterdam, Netherlands, and Erlangen-Nuernberg Univ., Germany Limited Reproducibility: More than 20% of this document may be affected by microfiche quality

(ETN-94-95387) Avail: CASI HC A10

The model dependence of the impulse approximation for proton-nucleus elastic scattering stemming from off-shell and non local effects is investigated. A perturbative treatment allows a direct comparison between off-shell and relativistic effects. Off-shell effects are found to be significantly smaller and unable to account in a natural way for the needed repulsive central potential in the nuclear interior region at proton energies between 300 and 880 MeV. A further problem connected to Dirac phenomenology is also studied: the extent to which it is possible to describe a composite particle with an equation which is valid for relativistic point particles. The issue is investigated within the framework of a solvable field theoretic model: quantum chromodynamics in one space and one time dimension in the limit of a large number of colors. ESA

N94-25317 International Centre for Theoretical Physics, Trieste (Italy).

A SCALAR-VECTOR MODEL OF QUARK-ANTIQUARK INTERACTION UNDER LINEAR CONFINEMENT

S. Chakrabarty Aug. 1992 16 p Limited Reproducibility: More than 20% of this document may be affected by microfiche quality

(DE93-616871; IC-92/200) Avail: CASI HC A03 (US Sales Only)

Considering the idea that the constituent quark mass is the dressed sum of current quark mass and dynamical quark mass, and using the standard values of current quark masses, we obtain approximate values of constituent quark masses, which are then used in our extensively studied Bethe-Salpeter-reduced potential model. We find that the mass formulas become much simpler for linear potential ar with zero anomalous magnetic moment lambda, the values of scalar-vector fraction ((eta)) and 'a' in the linear potential being (1/4) and (1/5), respectively. Also, some of the quantities can be related to each other and the match with experimental data is good. DOE

N94-25341 Gosudarstvennyi Komitet po Ispolzovaniyu Atomnoi Energii, Serpukhov (USSR).

PROTON SPIN: THE ROLE OF QUARK-GLUON AND HADRON DEGREES OF FREEDOM

A. V. Kiselev and V. A. Petrov 1991 48 p Limited Reproducibility: More than 20% of this document may be affected by microfiche quality

(DE93-616867; IFVE-OTF-91-171) Avail: CASI HC A03 (US Sales Only)

A theoretical analysis of the proton spin structure is conducted both in terms of parton and hadron fields. Diagonal matrix element (ME) of the axial singlet quark current appears to be the object of consideration of the given review. This ME describes the total quark contribution to the spin part of the proton angular momentum, and its component values are directly linked with the experimentally measured values. DOE

N94-25388 International Centre for Theoretical Physics, Trieste (Italy).

LOCALIZED EXCITATIONS IN COMPETING BOND-ORDER-WAVE, CHARGE-DENSITY-WAVE AND SPIN-DENSITY-WAVE SYSTEMS. 2: COMPETING CHARGE-DENSITY-WAVE AND SPIN-DENSITY-WAVE

Wen-Zheng Wang, Chui-Lin Wang (China Center for Advanced Science and Technology, Beijing.), Zhao-Bin Su, and Lu Yu Nov. 1992 38 p Limited Reproducibility: More than 20% of this document may be affected by microfiche quality

(DE93-617131; IC-92/380) Avail: CASI HC A03 (US Sales Only)

The extended Peierls-Hubbard model is used to study the competition of the spin-density-wave (SDW) and charge-density-wave (CDW) states as well as the attendant localized excitations in quasi-one-dimensional systems like MX-chains. The ground state properties are first studied as a function of the Coulomb interaction U and the on-site electron-phonon coupling lambda(sub 2). The SDW state dominates in the region of large U and small lambda(sub 2), while the CDW state prevails in the opposite limit. In the intermediate region these two states compete with each other, one being stable, whereas the other being metastable. The localized excitations (polarons and excitons) are studied in detail in each region using the Bogoliubov-de Gennes formalism. The self-trapped excitons (STE) in the CDW dominating regime contain locally non-vanishing SDW distortions and vice versa. As lambda(sub 2) increases, the number of bound states changes from two to four for the exciton case and from two to three for the polaron case. Upon its further increase, one type of STE with a certain pattern of SDW distortion and charge transfer is transforming into another type of STE with a different pattern. The possibilities of verifying the ground state properties in optical and transport experiments and identifying these local excitations in Raman and ENDOR measurements are discussed. DOE

N94-25443# Air Force Inst. of Tech., Wright-Patterson AFB, OH. School of Engineering.

INFRARED FLUORESCENCE STUDIES OF ELECTRONIC-TO-VIBRATIONAL ENERGY TRANSFER IN A Br2:NO SYSTEM M.S. Thesis

Michael R. Hawks Dec. 1993 70 p

(AD-A273727; AFIT/GAP/ENP/93D-03) Avail: CASI HC A04/MF A01

Steady-state photolysis techniques were used to study electronic-to-vibrational energy transfer mechanisms from atomic bromine to nitric oxide. Molecular bromine was photodissociated by 488nm radiation to produce equal parts Br(P-2)(sub 1/2) and Br(P-2(sub 3/2). Side fluorescence intensity from Br(P-2)(sub 1 /2) at 2.7 microns and from No (v = 1 and 2) around 5.3 microns measured as a function of bromine pressure and nitric oxide pressure. The branching ratio collisional transfer into the first and second states of NO was determined, and previously reported rates for quenching of No by molecular bromine were verified. DTIC

N94-25465# Nationaal Inst. voor Kernfysica en Hoge Energiefysica, Amsterdam (Netherlands).

HEAVY FLAVOUR PHYSICS AT LEP

Peter M. Kluit 1992 23 p Presented at 20th SLAC Summer Institute on Particle Physics Topical Conference, Jul. 1992

(NIKHEF-H/92-19; ETN-94-95046) Avail: CASI HC A03/MF A01

The European Large Electron Positron (LEP) storage ring results on heavy flavor physics are summarized. The topics covered are: the B physics at the Z neutral resonance, the beauty signals, and B lifetime measurements. The width gamma(sub b anti-b) and the asymmetry A(sub b anti-b)(sup fb) for the decay process Z neutral to b anti-b are calculated. The average mixing parameter chi of the b quark is determined. Evidence for B(sub s), lambda(sub b), and J/psi production in Z neutral decays is shown. Measurements of the average b lifetime and the lifetimes for charged and neutral B hadrons are presented. ESA

N94-25474 International Centre for Theoretical Physics, Trieste (Italy).

A QUARK STRUCTURE OF HADRONS AND NUCLEI

S. Chakrabarty and S. Deoghuria Aug. 1992 107 p Limited Reproducibility: More than 20% of this document may be affected by microfiche quality

(DE93-616872; IC-92/201) Avail: CASI HC A06 (US Sales Only)

In this review we look into the recent understanding of mesons, baryons, and nuclei as a few quark bound states within the framework of quantum chromodynamics (QCD). In particular, we have reviewed our understanding of the nature of confining interaction, the spin-dependence of color forces, and the role of non-perturbative effects in the study of quark forces in the potential model approach. We also give a comparative study of results obtained by several potential models with reference to the experimental data. We find that although the Lorentz nature of confinement and the nature of spin-dependent color forces have been better understood now, only a partial understanding of these problems are obtained so far. Our study reveals that properties of baryons could be explained by the same potential model which successfully describe the mesons. However, the nuclei require chiral symmetry and non-perturbative methods for their description. We also discuss the relation between constituent, current and dynamical quark masses. We conclude that QCD motivated approaches have shown much success in explaining many results on hadronic and nuclear data. DOE

N94-25476 Moscow State Univ. (Russia). Inst. for Nuclear Physics.

ON THE HADRON FORMATION TIME IN PION-NUCLEUS INTERACTION

L. V. Bravina, V. L. Korotkikh, L. I. Sarycheva, and S. Yu. Sivoklokov 1992 20 p Limited Reproducibility: More than 20% of this document may be affected by microfiche quality

(DE93-616879; INP-MSU-91-45-249) Avail: CASI HC A03 (US Sales Only)

Differences in the observable characteristics of pion-nucleus interactions at high energy are investigated for two definitions of the hadron formation time. The Monte Carlo simulation of hadron-nucleus interactions and quark-gluon string model for hadron-hadron collisions are used. It is shown that the momentum spectrum of the protons in the target fragmentation region is most sensitive to the definition of the formation time. The inclusive meson and meson resonance spectra are similar in the both versions. DOE

N94-25477 Joint Inst. for Nuclear Research, Dubna (USSR). Lab. of Theoretical Physics.

WEAK INTERACTIONS IN A BILOCAL CHIRAL THEORY

Yu. L. Kalinovskij, W. Kallies, L. Muenchow, and V. N. Pervushin 1992 15 p Limited Reproducibility: More than 20% of this document may be affected by microfiche quality

(DE93-616887; JINR-E-4-92-9) Avail: CASI HC A03 (US Sales Only)

The calculus to describe meson-decay constants and the nonleptonic transitions for D and B mesons in a bilocal meson field theory are formulated. DOE

N94-25481 Joint Inst. for Nuclear Research, Dubna (USSR). Lab. of High Energy.

ON THE TRANSVERSE SIZE OF A FAST MOVING NUCLEON

V. A. Belyakov and V. N. Streltsov 1991 8 p Limited Reproducibility: More than 20% of this document may be affected by microfiche quality

(DE93-616891; JINR-E-2-91-531) Avail: CASI HC A02 (US Sales Only)

On the basis of the relativistic Yukawa potential , it is shown that the nucleon 'transverse size' corresponding to equipotential values grows with increasing its energy as (ln(gamma))(exp 0.8)-ln(gamma) ((gamma) is the Lorentz-factor) due to the field of virtual spin mesons. The opinion is expressed that the known growth of the interaction cross section is probably just due to the indicated reason. DOE

N94-25519# Air Force Inst. of Tech., Wright-Patterson AFB, OH.

EXPERIMENTAL CHARACTERIZATION OF THE AFIT NEUTRON FACILITY M.S. Thesis

Oscar J. Lessard Sep. 1993 114 p

(AD-A273822; AFIT/GAP/ENP/93D-06) Avail: CASI HC A06/MF A02

AFIT's Neutron Facility was characterized for room-return neutrons using a Cf-252 source and a Bonner sphere spectrometer with three experimental models: the shadow shield; the Eisenhauer, Schwartz, and Johnson (ESJ); and the polynomial models. The free-field fluences at one meter from the ESJ and polynomial models were compared to the equivalent value from the accepted experimental shadow shield model to determine the suitability of the models in the AFIT facility. The polynomial model behaved erratically, as expected, while the ESJ model compared to within 4.8% of the shadow shield model results for the four Bonner sphere calibration. The ratio of total fluence to free-field fluence at one meter for the ESJ model was then compared to the equivalent ratio obtained by a Monte Carlo Neutron-Photon transport code (MCNP), an accepted computational model. The ESJ model compared to within 6.2% of the MCNP results. AFIT's fluence ratios were compared to equivalent ratios reported by three other neutron facilities which verified that AFIT's results fit previously published trends based on room volumes. The ESJ model appeared adequate for health physics applications and was chosen for calibration of the AFIT facility. DTIC

73 NUCLEAR AND HIGH-ENERGY PHYSICS

Includes elementary and nuclear particles; and reactor theory.
For space radiation see *93 Space Radiation.*

N94-23273*# National Aeronautics and Space Administration. Goddard Space Flight Center, Greenbelt, MD.
CRRES MICROELECTRONICS PACKAGE FLIGHT DATA ANALYSIS
E. G. Stassinopoulos, G. J. Brucker (Radiation Effects Consultants, West Long Branch, NJ.), and C. A. Stauffer (Systems Engineering and Security, Inc., Greenbelt, MD.) Washington Jun. 1993 72 p Sponsored in part by DNA
(RTOP 900-00-00)
(NASA-TP-3423; Rept-94B00007; NAS 1.60:3423) Avail: CASI HC A04/MF A01

A detailed in-depth analysis was performed on the data from some of the CRRES MEP (Microelectronics Package) devices. These space flight measurements covered a period of about fourteen months of mission lifetime. Several types of invalid data were identified and corrections were made. Other problems were noted and adjustments applied, as necessary. Particularly important and surprising were observations of abnormal device behavior in many parts that could neither be explained nor correlated to causative events. Also, contrary to prevailing theory, proton effects appeared to be far more significant and numerous than cosmic ray effects. Another unexpected result was the realization that only nine out of thirty-two p-MOS dosimeters on the MEP indicated a valid operation. Comments, conclusions, and recommendations are given. Author

N94-23485*# Old Dominion Univ., Norfolk, VA. Dept. of Mathematics and Statistics.
THEORETICAL STUDIES OF A MOLECULAR BEAM GENERATOR Progress Report, 1 Jul. - 31 Dec. 1993
John Heinbockel Jan. 1994 15 p
(Grant NAG1-1424)
(NASA-CR-194779; NAS 1.26:194779) Avail: CASI HC A03/MF A01

At present no adequate computer code exists for predicting the effects of thermal nonequilibrium on the flow quality of a converging-diverging N2 nozzle. It is the purpose of this research to develop such a code and then perform parametric studies to determine the effects of intermolecular forces (high gas pressure) and thermal nonequilibrium (the splitting of temperature into a vibrational and rotational-translational excitation) upon the flow quality. The two models to be compared are given. Appendix A contains nomenclature and additional relationships. Author (revised)

N94-23495*# Iowa Univ., Iowa City. Dept. of Physics and Astronomy.
MULTI-ION, MULTI-EVENT TEST OF ION CYCLOTRON RESONANCE HEATING Semiannual Status Report, 1 Sep. - 30 Dec. 1993
Ann M. Persoon 30 Dec. 1993 20 p
(Grant NAGw-3576)
(NASA-CR-194859; NAS 1.26:194859) Avail: CASI HC A03/MF A01

The multi-ion, multi-event study of ion cyclotron resonance heating has been funded to study ion energization through ion cyclotron resonance with low frequency broadband electromagnetic turbulence. The modeling algorithm for the ion cyclotron resonance heating (ICRH) of oxygen ions was presented in Crew et al. (1990). Crew and his co-authors developed a two-parameter representation of selected oxygen conic distributions and modelled the conic formation in terms of resonance heating. The first year of this study seeks to extend the work of Crew and his co-authors by testing the applicability of the ICRH mechanism to helium ion conic distributions, using data obtained from the Energetic Ion Composition Spectrometer and the Plasma Wave Instrument on Dynamics Explorer 1. Author (revised)

N94-23509*# National Aeronautics and Space Administration. Langley Research Center, Hampton, VA.
OPTICAL MODEL ANALYSES OF GALACTIC COSMIC RAY FRAGMENTATION IN HYDROGEN TARGETS
Lawrence W. Townsend Dec. 1993 13 p
(RTOP 199-45-16-11)
(NASA-TP-3404; L-17306; NAS 1.60:3404) Avail: CASI HC A03/MF A01

Quantum-mechanical optical model methods for calculating cross sections for the fragmentation of galactic cosmic ray nuclei by hydrogen targets are presented. The fragmentation cross sections are calculated with an abrasion-ablation collision formalism. Elemental and isotopic cross sections are estimated and compared with measured values for neon, sulfur, and calcium ions at incident energies between 400A MeV and 910A MeV. Good agreement between theory and experiment is obtained. Author

N94-23791# Northwestern Univ., Evanston, IL.
STRONG INTERACTIONS STUDIES WITH MEDIUM ENERGY PROBES Progress Report, 1 Dec. 1992 - 30 Nov. 1993
Kamal K. Seth Oct. 1993 19 p
(Contract DE-FG02-87ER-40344)
(DE94-001446; DOE/ER-40344/7) Avail: CASI HC A03/MF A01

This progress report refers to the period Aug. 1992 to Aug. 1993, which includes the first year of the three-year period 1 Dec. 1992 - 30 Nov. 1995 of the existing research contract. As anticipated in the 1992-1995 proposal, the major preoccupation during 1992-1993 was with Fermilab experiment E760. This experiment, whose primary objective is to make very high-resolution study of Charmonium Spectroscopy via proton-antiproton annihilations, has turned out to be a veritable gold-mine of exciting hadronic physics in other areas as well. These include the proton form factor in the time-life region, proton-antiproton forward scattering, QCD scaling laws, and light quark spectroscopy. A large fraction of the data from E760 was analyzed during this year, and several papers were published. In addition to the E760 experiment at Fermilab, continued progress was made in nuclear physics-related experiments at LAMPF, MIT, and NIKHEF, and their results were prepared for publication. Topics include high-resolution electron scattering, quasi-free electron scattering, and low-energy pion double charge exchange. DOE

N94-24305*# National Aeronautics and Space Administration. Langley Research Center, Hampton, VA.
MOMENTUM LOSS IN PROTON-NUCLEUS AND NUCLEUS-NUCLEUS COLLISIONS
Ferdous Khan (Old Dominion Univ., Norfolk, VA.) and Lawrence W. Townsend Dec. 1993 12 p
(RTOP 199-45-16-11)
(NASA-TP-3405; L-17304; NAS 1.60:3405) Avail: CASI HC A03/MF A01

An optical model description, based on multiple scattering theory, of longitudinal momentum loss in proton-nucleus and nucleus-nucleus collisions is presented. The crucial role of the imaginary component of the nucleon-nucleon transition matrix in accounting for longitudinal momentum transfer is demonstrated. Results obtained with this model are compared with Intranuclear Cascade (INC) calculations, as well as with predictions from Vlasov-Uehling-Uhlenbeck (VUU) and quantum molecular dynamics (QMD) simulations. Comparisons are also made with experimental data where available. These indicate that the present model is adequate to account for longitudinal momentum transfer in both proton-nucleus and nucleus-nucleus collisions over a wide range of energies. Author (revised)

N94-24662# Continuous Electron Beam Accelerator Facility, Newport New, VA.
THE CEBAF BEAM LOSS SENSORS
J. Perry, E. Woodworth, L. Merminga, S. Simrock, R. May, and G. Stapleton Jul. 1993 4 p
(Contract DE-AC05-84ER-40150)
(CEBAF-PR-93-032) Avail: CASI HC A01/MF A01

The CEBAF beam can burn through the vacuum wall in approximately 100 microseconds. The authors have developed an inexpensive beam loss sensor that will unambiguously detect a true beam loss and shut off the beam within this time without tripping on moderate interference from other sources. They have incorporated a full system test into the system, with provision for direct replacement of faulty sensors without adjustment. This paper describes the sensors, the signal processing design, system test results, and characterization procedures. Author (revised)

N94-24663# Continuous Electron Beam Accelerator Facility, Newport New, VA.
POLARIZED STRUCTURE FUNCTIONS OF THE NUCLEON IN THE RESONANCE REGION
Volker D. Burkert 1994 14 p Presented at the Symposium on

Polarized Structure Functions, New Haven, CT, 5-6 Jan. 1994
(Contract DE-AC05-84ER-40150)
(CEBAF-PR-94-001) Avail: CASI HC A03/MF A01

Aspects of the spin structure functions of protons and neutrons at low momentum transfer Q(sup 2) and energy transfer nu, i.e. in the region of the nucleon resonance, are discussed. Experiments to measure (A(sub 1))(sup p), (A(sub 2))(sup p), and (A(sub 1))(sup n) structure functions at CEBAF in a Q(sup 2) range from 0.15 to 2.0 GeV(sup 2) and a W range from threshold to 2.2 GeV are presented. Author (revised)

N94-25256 Amsterdam Univ. (Netherlands).
THE DATA-ACQUISITION AND SECOND LEVEL TRIGGER SYSTEM FOR ZEUS CALORIMETER Ph.D. Thesis
Hermen Jasper vanderLugt 1993 159 p Sponsored by Stichting voor Fundamenteel Onderzoek der Materie, Netherlands Limited Reproducibility: More than 20% of this document may be affected by microfiche quality
(ETN-94-95384) Avail: Issuing Activity (European Space Agency (ESA))

The electron-proton collider HERA (German acronym for hadron electron storage ring) at DESY (German electron synchrotron) has successfully produced the first collisions between 26.6 GeV electrons and 820 GeV protons. The electron-proton collisions are studied by two experiments located at two of the four possible interaction points. These detectors are called H1 and ZEUS. The main contribution to the ZEUS experiment, the data acquisition of the ZEUS calorimeter, and the way in which the calorimeter information is used by the second level of the ZEUS trigger system are described. Details of the calorimeter data acquisition and the calorimeter second level trigger are given. The general performance of the calorimeter data acquisition system is presented. ESA

N94-25335# Academia Sinica, Beijing (China). Inst. of High Physics.
[ACTIVITIES OF ACADEMIA SINICA] Annual Report, 1989
Aug. 1990 94 p
(DE93-614529; INIS-MF-13429) Avail: CASI HC A05/MF A01 (US Sales Only)

The research activities of Institute of High Energy Physics (IHEP) Academia Sinica of China during the year of 1989 were summarized. Within this year, Beijing positron electron collider, Beijing Spectrometer, and the Synchrotron Radiation Experimental Facilities have one after another passed technical appraisal. The 35 MeV proton Linac was formally accepted by the State after technical appraisal was obeyed. Scientific research has been developing healthily with all the research programs being performed according to plan. Several international conferences which achieved good results were managed to be hosted under difficult conditions. DOE

N94-25342 Moscow State Univ. (Russia). Inst. for Nuclear Physics.
BEHAVIOR OF THE INTERMITTENCY EXPONENTS AND A QUARK-GLUON PLASMA FORMATION IN THE HEAVY ION COLLISIONS
B. B. Levchenko 1991 12 p Limited Reproducibility: More than 20% of this document may be affected by microfiche quality
(DE93-616869; INP-MSU-91-42-236) Avail: CASI HC A03 (US Sales Only)

Within the framework of the multiple scattering model of nucleus-nucleus collision, the normalized factorial moments of q particle are calculated and the behavior of the anomalous fractal dimensions d(sub q) are analyzed. If any collective effects are absent for central collisions of heavy nuclei, all d(sub q) vanish and no possibility to discriminate the effects of multiple scattering in nuclei, the first order phase transition and self-similar cascade mechanism of particle production in intranuclei subprocesses. Existence of a q dependence of d(sub q) for central collisions of heavy nuclei can be a signature of particle production processes like the second order phase transition. DOE

74 OPTICS

Includes light phenomena; and optical devices.
For lasers see *36 Lasers and Masers.*

N94-22722# Lawrence Livermore National Lab., CA.
THERMOELECTRIC COOLED, PURGE-AND-TRAP DEVICE FOR ENHANCING THE UTILITY OF FIBER OPTIC VOC SENSORS
E. A. Mizusawa, P. F. Daley, K. R. Kyle, K. C. Langry, and S. M. Angel Aug. 1993 11 p Presented at the Society of Photo-Optical Instrumentation Engineer's (SPIE) International Symposium on Optical Tools for Manufacturing and Advanced Automation, Boston, MA, 7-10 Sep. 1993
(Contract W-7405-eng-48)
(DE94-001772; UCRL-JC-115005; CONF-9309199-10) Avail: CASI HC A03/MF A01

A thermoelectric cooled, purge-and trap device (TEC) has been developed to enhance the utility of fiber optic VOC sensors. This simple device consists of a thin copper radiator which is sandwiched between two thermoelectric coolers. Two water-cooled, copper heat sinks are used to maintain the hot side surfaces of the thermoelectric coolers at 5 C, allowing internal surface temperatures of the radiator to be controlled between 5 C to -43 C. This paper describes the use of the TEC with a reversible, fiber optic, carbon tetrachloride sensor. The sensor by itself has a detection limit of around 1,000 ppmv carbon tetrachloride in nitrogen. When the sensor is used with the TEC, vapor phase concentrations down to 100 ppmv can be measured. DOE

N94-22868# Lawrence Livermore National Lab., CA.
RAY AND WAVE OPTICS MODELING OF LABORATORY X RAY LASERS
R. P. Ratowsky, R. A. London, M. D. Feit, R. W. Walling, G. M. Shimkaveg, and R. S. Craxton (Rochester Univ., NY.) Jun. 1993 11 p Presented at the Annual Meeting of the Society of Photo-Optical Instrumentation Engineers (SPIE), San Diego, CA, 11-16 Jul. 1993
(Contract W-7405-eng-48)
(DE93-019940; UCRL-JC-114493; CONF-930722-34) Avail: CASI HC A03/MF A01

Much progress has been made recently in characterizing the emission from neon-like Yttrium exploding foil x ray lasers at Lawrence Livermore National Laboratory. Concomitant with that effort, detailed modeling to enhance our understanding of the experiments and improve their design was carried out. Our modeling includes target hydrodynamics, calculation of gain, and both ray and wave optics propagation. Our modeling of Yt x ray lasers, including first simulations using a two transverse dimensional gain calculation, are described. Our calculations indicate that the time-integrated signal is very sensitive to the time history of the gain, because of the rapid sweep of the beam in angle measured with respect to the plane of the foil. It was found that better agreement with experiment is achieved if the falloff of the gain with time is made slightly faster than our codes predict. In the vertical direction (normal to exploding foil direction), the experimental beam pattern is typically broader than calculated. It was found that ray and wave optics calculations are in good agreement. The coherence length obtained by a wave optics calculation is larger than seen in experiments; this is probably due to fluctuations and/or the smooth variation of the pump laser line focus. Possible improvements to our modeling which would include such nonideal effects are discussed. DOE

N94-22891 Toronto Univ. (Ontario).
FIBER OPTIC DETECTION OF LASER GENERATED ULTRASOUND FOR MATERIALS CHARACTERIZATION M.S. Thesis
Andrew Michael Davis 1993 185 p
(ISBN-0-315-83541-9; CTN-94-60946) Copyright Avail: Micromedia Ltd., Technical Information Centre, 240 Catherine Street, Suite 305, Ottawa, Ontario, K2P 2G8, Canada HC/MF

A fiber optic Michelson interferometer with an active homodyne demodulation system was used to detect ultrasound generated by a Q-switched Nd-YAG laser. The sensing arm of the interferometer was adhered to or embedded in the materials under investigation. Insonification occurred at either the surface or inside the test specimen. In-situ generation was accomplished using an embedded fiber optic delivery system. The ultrasonic transients so generated and detected were used to determine the velocity of certain bulk wave modes propagating in specimens of aluminum, epoxy, and graphite epoxy laminates. The experimentally determined velocities are reported and compared to those in the literature. Ultrasonic velocity is related to or is an indicator of a number of material properties and hence is a very useful parameter for materials characterization. Author (CISTI)

N94-22895 Institute for Perception RVO-TNO, Soesterberg (Netherlands). Afd. Waarneming.
VALIDATION OF A SECOND GENERATION CONSPICUITY METER Final Report [VALIDATIESTUDIES MET DE TWEEDE GENERATIE OPVALLENDHEIDSMETER]
A. H. Wertheim 16 Mar. 1993 44 p In DUTCH
(Contract A92/KLu/325)
(IZF-1993-A-11; TD93-0373; ETN-94-94928) Copyright Avail: TNO Institute for Perception, Kampweg 5, Postbus 23, 3769 DE Soesterberg, Netherlands

The development and empirical validation of an optical instrument for the operational measurement of visual conspicuity of objects are discussed. The instrument measures visual conspicuity by assessing two parameters in combination. The first is eccentricity: how far aside the object can we look before we reach the point where it cannot any more be discriminated from the other details in the visual field. The second is sector contrast reduction: how much should we reduce sector contrast (defined as the ratio of object luminance and average luminance across the whole sector of the visual field of the instrument) to reach the point where the object cannot be discriminated any more. Experiments show that the meter yields a valid visual conspicuity index, at least in principle. It is suggested how the detected deficiencies of the instrument could be remedied, and how it could be made simpler and more user friendly. ESA

N94-22915# Wright Lab., Wright-Patterson AFB, OH.
A FULLY AUTOMATED STAGE FOR OPTICAL WAVEGUIDE MEASUREMENTS Final Report, 9 Sep. 1992 - 1993
E. T. Kensky Sep. 1993 121 p
(AF Proj. 2305)
(AD-A273042; WL-TR-93-4092) Avail: CASI HC A06/MF A02

Nonlinear optical (NLO) materials are becoming increasingly important to the Air Force, and their expanding use in future systems is inevitable. Applications ranging from communications and optical computing to lasers and laser hardening will all be affected by the development of these materials. Because of this need, basic research and development of these materials are extremely important. Within the Materials Directorate of Wright Laboratory, the Electronic and Optical Materials Branch is performing basic R&D in various areas of nonlinear optical materials. Central to this research is the measurement of the optical properties of these materials. In order to apply these materials to device and systems, it is important to understand how they behave under the influence of various forces and conditions. These include applied voltages and currents, incident electromagnetic radiation and temperature changes. How they behave under these various conditions can be either useful or detrimental depending on the application. In the case of optical transmission, changes in material properties due to applied voltage are useful for applications where modulation is important. DTIC

N94-22917# Edgerton, Germeshausen and Grier, Inc., Idaho Falls, ID.
NOVEL FRINGE SCANNING/FOURIER TRANSFORM METHOD OF SYNTHETIC IMAGING
T. M. Crawford and R. K. Albano 1993 8 p Presented at the Annual Meeting of the Society of Photo-Optical Instrumentation Engineers (SPIE), San Diego, CA, 11-16 Jul. 1993
(Contract DE-AC07-76ID-01570)
(DE93-018936; EGG-M-93041; CONF-930722-43) Avail: CASI HC A02/MF A01

We have developed a one-dimensional theory and a computer model for synthetically imaging scenes using a novel fringe scanning/Fourier transform technique. Our method probes a scene using two interfering beams of slightly different frequency. These beams form a moving fringe pattern which scans the scene and resonates with any spatial frequency components having the same spatial frequency as the scanning fringe pattern. A simple, non-imaging detector above the scene observes any scattered radiation from the scene falling onto it. If a resonance occurs between the scanning fringe pattern and the scene, then the scattered radiation will be modulated at the difference frequency between the two probing beams. By changing the spatial period of the fringe pattern and then measuring the amplitude and phase of the modulated radiation that is scattered from the scene, the Fourier amplitudes and phases of the different spatial frequency components making up the scene can be measured. A synthetic image of the scene being probed can be generated from this Fourier amplitude and phase data by taking the inverse Fourier transform of this information. This technique could be used to image objects using light, ultrasonic, or other electromagnetic or acoustic waves. DOE

N94-22979# Bhabha Atomic Research Centre, Bombay (India).
DESIGN REFINEMENT OF MULTILAYER OPTICAL THIN FILM DEVICES WITH TWO OPTIMIZATION TECHNIQUES
K. V. S. R. Apparao (Bhabha Atomic Research Centre, Bombay, India.) 1992 29 p
(DE93-634228; BARC-1992/E/042) Avail: CASI HC A03/MF A01 (US Sales Only)

The design efficiency of two different optimization techniques for designing multilayer optical thin film devices is compared. Ten different devices of varying complexities are chosen as design examples for the comparison. The design refinement efficiency and the design parameter characteristics of all the sample designs obtained with the two techniques are compared. The results of the comparison demonstrate that the new method of design developed using damped least squares technique with indirect derivatives give superior and efficient designs compared to the method developed with direct derivatives. DOE

N94-23171# Technische Univ., Eindhoven (Netherlands). Telecommunications Div.
AN OPTICAL ASK AND FSK PHASE DIVERSITY TRANSMISSION SYSTEM
H. vandenBoom, W. vanEtten, W. H. C. deKrom, P. vanBennekom, F. Huijskens, L. Niessen, and F. deLeijer Dec. 1992 101 p
(EUT-92-E-268; ISBN-9-06-144268-0; ETN-94-94775) Avail: CASI HC A06/MF A02

The results of a contribution to an electrooptical project for a 'phase diversity system', covering ASK and FSK (Amplitude and Frequency Shift Keying), are described. Specifications of subsystems, and tolerances and consequences of these tolerances for the final system performance, were derived. For the optical network of the phase diversity receiver, a manufacturing set up for three by three fused biconical taper fiber couplers was developed. In order to characterize planar optical networks, a set up was constructed to measure the phase relations at 1523 nm. The optical frequency of the local oscillator laser has to be locked on to the frequency of the received optical signal. This locking circuit is described. A complete optical three by three phase diversity transmission system was developed that can be used as a testbed for subsystems. The sensitivity of the receiver at a bit error rate of 10 to the minus 9th power is -47.2 dBm, which is 4.2 dB better than the value of the specifications. ESA

N94-23202 Sandia National Labs., Albuquerque, NM.
PHOTO-INDUCED AND ELECTROOPTIC PROPERTIES OF (Pb,La)(Zr,Ti)O3 FILMS FOR OPTICAL MEMORIES
D. Dimos, B. G. Potter, M. B. Sinclair, B. A. Tuttle, and W. L. Warren 1993 12 p Presented at the International Symposium on Integrated Ferroelectrics, Colorado Springs, CO, 19-21 Apr. 1993 Limited Reproducibility: More than 20% of this document may be affected by microfiche quality
(Contract DE-AC04-76DP-00789)
(DE93-019820; SAND-93-0547C; CONF-9304197-2) Avail: CASI HC A03

Photo-induced hysteresis changes and electro-optic effects in sol-gel Pb(Zr,Ti)03 (PZT) and PLZT films have been studied in an effort to evaluate these materials for optical memory applications. The films exhibit two types of photo-induced changes in their hysteresis behavior which are suitable for optical storage. Both types of photo-induced hysteresis changes are due to trapping of photo-generated charge carriers at sites which minimize internal depolarizing fields. The photo-induced changes are reproducible and stable, which indicates that the charge traps are stable. However, improvements in photosensitivity will be required to develop a competitive technology for optical memories. In addition, polarization-dependent changes in the refractive indices can be the basis of a nondestructive optical readout technique. The index changes of films have been determined using a waveguide refractometry technique, which allows the extraordinary and ordinary index changes to be obtained independently. DOE

N94-23270* National Aeronautics and Space Administration. Pasadena Office, CA.

DUAL FREQUENCY OPTICAL CARRIER TECHNIQUE FOR TRANSMISSION OF REFERENCE FREQUENCIES IN DISPERSIVE MEDIA Patent

Lutfollah Maleki, inventor (to NASA) (Jet Propulsion Lab., California Inst. of Tech., Pasadena.) 30 Nov. 1993 7 p Filed 7 Jan. 1993 Continuation of abandoned US-Patent-Appl-SN-703238, filed 20 May 1991
(NASA-Case-NPO-18007-2-CU; US-Patent-5,267,072; US-Patent-Appl-SN-000902; US-Patent-Appl-SN-703238; US-Patent-Class-359-158; US-Patent-Class-359-154; US-Patent-Class-359-173; US-Patent-Class-359-183; US-Patent-Class-359-189; Int-Patent-Class-H04B-10/00) Avail: US Patent and Trademark Office

Two different carrier frequencies modulated by a reference frequency are transmitted to each receiver to be synchronized therewith. Each receiver responds to local phase differences between the two received signals to correct the phase of one of them so as to maintain the corrected signal as a reliable synchronization reference.
Official Gazette of the U.S. Patent and Trademark Office

N94-23309* National Aeronautics and Space Administration. Ames Research Center, Moffett Field, CA.

OUTPUT OPTICS FOR LASER VELOCIMETERS Patent

Dana H. Lynch, inventor (to NASA), William D. Gunter, inventor (to NASA), and Kenneth W. McAlister, inventor (to NASA) 23 Nov. 1993 5 p Filed 17 Apr. 1991
(NASA-Case-ARC-11889-1-SB; US-Patent-5,264,907; US-Patent-Appl-SN-691602; US-Patent-Class-356-28.5; US-Patent-Class-359-362; Int-Patent-Class-G01P-3/36) Avail: US Patent and Trademark Office

Space savings are effected in the optical output system of a laser velocimeter. The output system is comprised of pairs of optical fibers having output ends from which a beam of laser light emerges, a transfer lens for each light beam, and at least one final (LV) lens for receiving the light passing through the transfer lenses and for focussing that light at a common crossing point or area. In order to closely couple the transfer lenses to the final lens, each transfer lens is positioned relative to the final lens receiving light therefrom such that the output waist of the corresponding beam received by the final lens from the transfer lens is a virtual waist located before the transfer lens.
Official Gazette of the U.S. Patent and Trademark Office

N94-23458# Oak Ridge National Lab., TN.

SURFACE MODIFICATION OF SAPPHIRE FOR ENHANCED INFRARED WINDOW PERFORMANCE

C. J. McHargue (Tennessee Univ., Knoxville.), D. L. Joslin (Tennessee Univ., Knoxville.), J. M. Williams, and M. E. OHern (Nano Instruments, Inc., Knoxville, TN.) 1993 4 p Presented at the International Union of Materials Research Societies on Advanced Materials, Tokyo, Japan, 31 Aug. - 4 Sep. 1993
(Contract DE-AC05-84OR-21400)
(DE94-000333; CONF-9308122-7) Avail: CASI HC A01/MF A01

Two ion implantation conditions were evaluated for improving the mechanical performance of sapphire IR window material. Both increased the average strength as measured by 4-point bend tests and were effective in preventing the propagation of surface flaws. Ion implantation that produced a damaged crystalline surface improved the reliability at lower stresses more than the implantation that produced an amorphous surface. Neither process significantly affected the IR transmission. DOE

N94-23461# Oak Ridge National Lab., TN.

FIBER OPTIC TEMPERATURE SENSOR USING A Y2O2S:Eu THERMOGRAPHIC PHOSPHOR

Todd V. Smith (Bethel Coll., Saint Paul, MN.) and D. Barton Smith 1993 8 p Presented at the Society of Photo-Optical Instrumentation Engineer's International Symposium on Optical Tools for Manufacturing and Advanced Automation, Boston, MA, 7-10 Sep. 1993
(Contract DE-AC05-84OR-21400)
(DE94-000331; CONF-9309199-5) Avail: CASI HC A02/MF A01

This report details the development and testing of a thermographic-phosphor-based fiber-optic temperature sensor. The sensor is constructed by removing a region of the fiber jacket and cladding, then coating the exposed core with yttrium oxysulfide doped with a europium activator (Y2O2S:Eu). When photoexcited, the europium in the host lattice emits a sharp-line fluorescence spectrum that is characteristic of the temperature of the host crystal lattice. By measuring fluorescence lifetimes, we can deduce the temperature of an optical fiber that is in thermal contact with the fiber. Two different distributions of Y2O2S:Eu in the cladding region were evaluated with regard to light coupling efficiency. Theoretical waveguide calculations indicate that a thin core/cladding boundary distribution of Y2O2S:Eu couples light more efficiently into the cores guided modes than does a bulk distribution of phosphor in the cladding. The sensor tests showed reproducible response from 20 to 180 Celsius. This technique has several advantages over other fiber optic temperature sensing techniques: the temperature measurement is independent of the strain applied to the fiber; the measurements are potentially accurate to within half a degree centigrade; the sensor allows temperature to be measured at precise locations; and the method does not preclude the use of the fiber for the simultaneous measurement of other parameters. DOE

N94-23502*# Louisiana State Univ., Baton Rouge. Dept. of Electrical and Computer Engineering.

THEORETICAL INVESTIGATION OF VARIABLE PERIODICITY (GRADED) MULTILAYERS FOR HARD X RAY APPLICATIONS Final Report

Ralph A. Kinney 20 Jan. 1994 66 p
(NASA Order H-13034-D)
(NASA-CR-194824; NAS 1.26:194824) Avail: CASI HC A04/MF A01

The objective of this research was to investigate the possibility of increasing the useful bandwidth of multilayer mirrors. Mirrors 'constructed' with non-periodically spaced reflecting surfaces were considered. These structures included depth-graded and laterally-graded mirrors as well as those with reflectors located via a log-periodic spacing rule. No enhancement of bandwidth resulted from simulations of simple versions of any of the three non-periodic mirrors. However, certain depth-graded structures did exhibit reflectances essentially the same as from uniform mirrors. Moreover, it was found that some control was possible regarding the location (with respect to energy) of the maximum reflectance peak. Effective bandwidth was increased when composite models were simulated. In two of the cases studied, bandwidth was enhanced by a factor of approximately 3. One model consisted of a depth-graded mirror constructed with three separately defined structures, or blocks. Each block consisted of two layer-pairs repeated three times. Then, the entire 18 layer-pair group was repeated several times. Simulation of this 3 block depth-graded configuration yielded three reflectance peaks, one representative of each depth-graded block. The other configurations resulting in enhanced bandwidth assumed independently constructed mirrors immediately adjacent to each other and sharing the same substrate. Reflectance peaks from each mirror appeared in the response. Both basic models show greatly enhanced effective bandwidths even though the reflectance curves appear as non-overlapping for these specific models. Additionally, these configurations are realizable. Details are contained in the section, DESIGN SIMULATIONS. Author

N94-23529*# Virginia Polytechnic Inst. and State Univ., Blacksburg. Physics Dept.

SPATIOTEMPORAL BEHAVIOR AND NONLINEAR DYNAMICS IN A PHASE CONJUGATE RESONATOR

Siuying Raymond Liu Dec. 1993 225 p
(Grant NAG1-1363; RTOP 233-03-01-01)
(NASA-CR-4567; NAS 1.26:4567) Avail: CASI HC A10/MF A03

The work described can be divided into two parts. The first part is an investigation of the transient behavior and stability property of a phase conjugate resonator (PCR) below threshold. The second part is an experimental and theoretical study of the PCR's spatiotemporal dynamics above threshold. The time-dependent coupled wave equations for four-wave mixing (FWM) in a photorefractive crystal, with two distinct interaction regions caused by feedback from an ordinary mirror, was used to model the transient dynamics of a PCR below threshold. The conditions for self-oscillation were determined and the solutions were used to define the PCR's transfer function and analyze its stability. Experimental results for the buildup and decay times confirmed qualitatively the predicted behavior. Experiments were carried out above threshold to study the spatiotemporal dynamics of the PCR as a function of Pragg detuning and the resonator's

Fresnel number. The existence of optical vortices in the wavefront were identified by optical interferometry. It was possible to describe the transverse dynamics and the spatiotemporal instabilities by modeling the three-dimensional-coupled wave equations in photorefractive FWM using a truncated modal expansion approach. Author (revised)

N94-23629 Selskapet for Industriell og Teknisk Forskning, Trondheim (Norway). Div. of Applied Physics.
MUELLER MATRIX ANALYSIS OF INFRARED ELLIPSOMETRY
E. Wold and J. Bremer (Norges Tekniske Hoegskole, Trondheim.) 2 Feb. 1993 31 p See also PB92-102896 Limited Reproducibility: More than 20% of this document may be affected by microfiche quality
(PB93-201549; STF19-A93003) Avail: Issuing Activity (National Technical Information Service (NTIS))

A Mueller analysis has been made of IR ellipsometry performed with imperfect optical components. Equations linking together experimental and calculated Fourier coefficients have been derived and consistently solved. Correction routines for permittivity measurements are demonstrated and discussed with Au and SrTiO3 as examples. It is shown that such effects as interferometer polarization, detector dichroism, transmission and phase-changes in polarizers can be effectively removed from the spectra. The problems of calibration and multiple reflections between IR polarizers are discussed and error propagation in permittivity measurements is analyzed. NTIS

N94-23723 National Defence Research Establishment, Linkoeping (Sweden). Huvudavdelning foer Informationsteknologi.
INTELLIGENT MATERIAL SYSTEMS AND STRUCTURES (IMSS). PART 5: FIBER OPTIC REGISTRATION OF DEFORMATION IN CARBON LAMINATES 91/92 [INTELLIGENTA MATERIALSYSTEM OCH STRUKTURER, IMSS, DEL 5: FIBEROPTISKA MAETNINGAR PA KOLFIBERLAMINAT 91/92]
Svante Oedman, Jan-Peter Bengtsson, Markus Danilsons, Ola Dickman, Stig Gruffman, Kjell Lindersson, and Timor Tanriverdi Feb. 1993 25 p In SWEDISH See also PB92-219195 Limited Reproducibility: More than 20% of this document may be affected by microfiche quality
(PB93-204600; FOA-C-306960-8.4-Pt-5; FOA-C-306960-3.1-Pt-5) Avail: CASI HC A03

Mechanical deformations induced by stretching optical fibers and epoxy-carbon laminates with embedded optical fibers were studied with fiber optic measurement technology: intensity measurements, reflectometry, and interferometry. The results from the measurements were compared in order to judge which method could be further developed for strain measurement in a laboratory. The conclusion is that the interferometry can be developed into a laboratory method for measuring deformations in carbon laminates. NTIS

N94-23732# Technische Univ., Delft (Netherlands). Faculteit der Elektrotechniek.
ANALYSIS FOR THE COMPUTATIONAL MODELING OF FINITE CLADDING AND LOSSY COATING EFFECTS IN FIBERS
R. M. Bertrand 1993 40 p
(PB94-111085; ET/EM-1993-12) Copyright Avail: CASI HC A03/MF A01

In recent papers, an unknown phenomenon is reported concerning fibers operating near the cutoff frequency. This phenomenon is the existence of anomalous oscillations, appearing when fibers are optimized in order to enlarge the transmission capacity, and was not predicted by theory. A possible explanation takes the influence of the cladding into account, and predicts interactions between fundamental modes and cladding modes which may occur when the field in the fiber - operating near cutoff - extends into the cladding. As 'classical' programs (made with the assumption of the infinite cladding) can not calculate the cladding modes, a new program had to be developed for use at PTT Research Neher Laboratory, taking not only the finite cladding, but also the lossy coating into account. A method that uses the numerical stable scattering-matrix formalism is presented. With this method, two recursive scattering relations are arrived at for implementation in the new program. The two above mentioned relations were used for the implementation, but the resulting program did not work well because of numerical problems. Some recommendations to solve the problems are given in the last chapter, the most important one being the possibility to use another set of Bessel functions for the implementation of the two derived recursive relations. NTIS

N94-23829*# OPTRA, Inc., Beverly, MA.
[MEASURING ELECTRICALLY CHARGED PARTICLE FLUXES IN SPACE USING A FIBER OPTIC LOOP SENSOR] Final Report
Jul. 1992 23 p
(Contract NAS5-30883; SBIR-08.13-7670)
(NASA-CR-191328; NAS 1.26:191328) Avail: CASI HC A03/MF A01

The purpose of this program was to demonstrate the potential of a fiber optic loop sensor for the measurement of electrically charged particle fluxes in space. The key elements of the sensor are a multiple turn loop of low birefringence, single mode fiber, with a laser diode light source, and a low noise optical receiver. The optical receiver is designed to be shot noise limited, with this being the limiting sensitivity factor for the sensor. The sensing element is the fiber optic loop. Under a magnetic field from an electric current flowing along the axis of the loop, there is a non-vanishing line integral along the fiber optic loop. This causes a net birefringence producing two states of polarization whose phase difference is correlated to magnetic field strength and thus, current in the optical receiver electronic processing. The objectives in this program were to develop a prototype laser diode powered fiber optic sensor. The performance specification of a minimum detectable current density of 1 (mu)amp/sq m-(radical)Hz, should be at the shot noise limit of the detection electronics. OPTRA has successfully built and tested a 3.2 m diameter loop with 137 turns of low birefringence optical fiber and achieved a minimum detectable current density of 5.4 x 10(exp-5) amps/(radical)Hz. If laboratory space considerations were not an issue, with the length of optical fiber available to us, we would have achieved a minimum detectable current density of 4 x 10(exp -7) amps/(radical)Hz. Derived from text

N94-24466 Toronto Univ. (Ontario).
FIBER OPTIC DETECTION OF ULTRASOUND AND ITS APPLICATION TO CURE MONITORING M.S. Thesis
Myo Myint Ohn 1992 152 p
(ISBN-0-315-83424-2; CTN-94-60956) Copyright Avail: Micromedia Ltd., Technical Information Centre, 240 Catherine Street, Suite 305, Ottawa, Ontario, K2P 2G8, Canada HC/MF

A fiber optic Michelson sensor with an active homodyne demodulation scheme used for detection of high frequency elastic waves is presented. A comparative analysis was attempted by quantitatively studying the fiber sensor response and open beam interferometer response to ultrasonic pulses. This technique of embedded and surface bonded fiber optic detection was extended for the purpose of materials characterization. By combining the interrogative nature of ultrasound and the in-situ sensing capabilities of optical fibers, a hybrid technique of monitoring the cure of epoxies and epoxy matrix composites (graphite epoxy) is reported. Using this fiber optic and ultrasonic approach to cure monitoring, a parameter exhibiting a similar inverse trend to the viscosity of the epoxy is proposed. Author (CISTI)

N94-24489 Saab Missles A.B., Linkoeping (Sweden).
DEVICE FOR THE SELECTIVE DETECTION OF OBJECTS Patent
Jan-Erik Lundin, inventor (to Micromedia Ltd.) 29 Sep. 1992 31 p
(CA-Patent-1-308-179; Int-Patent-Class-G01S-3/78; Int-Patent-Class-G01C-3/08; CTN-94-60868) Copyright Avail: Micromedia Ltd., Technical Information Centre, 240 Catherine Street, Suite 305, Ottawa, Ontario, K2P 2G8, Canada HC/MF

Conventional infrared scanners used to detect targets cannot distinguish between insignificant objects, such as birds, at a relatively close distance and significant objects such as aircraft at a greater distance, which leads to false alarms. A scanner is disclosed which makes it possible to distinguish between relatively close objects from which radiation is emitted and objects at a greater distance which subtend a similar solid angle. The scanner of the invention does this by suppressing signals whose amplitude is a function of the scanned azimuth or elevation shows a relatively great extension compared with signals that show a relatively small extension. The invention comprises at least one sensor unit, including at least one focusing means arranged to focus rays from the objects to be detected to at least one corresponding focal plane. At least one radiation sensitive detector is positioned in the focal plane and arranged to emit signals corresponding to the incoming radiation. The device is arranged to scan an angular field in azimuth and/or elevation, and has a signal evaluation unit which selects targets and suppresses certain signals as indicated above. CISTI

N94-24529 National Defence Research Establishment, Linkoeping (Sweden). Huvudavdening foer Informationsteknologi.
FIBER OPTICAL ANGULAR SENSOR: LITERATURE STUDY AND EXPERIMENTAL RESULTS [FIBEROPTISK VINKELGIVARE: LITTERATURSTUDIE OCH MAETRESULTAT]
Curt Larsson Nov. 1992 31 p In SWEDISH See also PB86-184165 Limited Reproducibility: More than 20% of this document may be affected by microfiche quality
(PB93-204345; FOA-C-30689-3.1) Avail: CASI HC A03

Effects of bending in an optical fiber are treated and formulas for calculation of attenuation are given. Theoretical and experimental results show that it is possible to use these effects of bending for sensors. This is shown especially for a sensor that measures angles. The fiber sensor properties make them very suitable for instance in 'inconvenient' environments. NTIS

N94-24550 Argonne National Lab., IL.
GERMANIUM X RAY PHASE PLATES FOR THE PRODUCTION OF CIRCULARLY POLARIZED X RAYS
C. J. Yahnke, G. Srajer, D. R. Haeffner, D. M. Mills, and L. Assoufid Oct. 1993 15 p Presented at the Synchrotron Radiation Instrumentation, Gaithersburg, MD, 23-26 Aug. 1993 Limited Reproducibility: More than 20% of this document may be affected by poor print
(Contract W-31-109-eng-38)
(DE94-002908; ANL/XFD/CP-81131; CONF-930824-20) Avail: Issuing Activity (Department of Energy (DOE))

The authors have constructed an x-ray phase plate to produce both linearly and circularly polarized x-rays at discrete energies between 20 keV and 88 keV. The plate is a monolithic two-crystal design, constructed from germanium, which increases the resultant degree of circular polarization of the output beam. They have measured the degree of circular polarization at 65 keV to be 90% +/- 4%, significantly better than that produced by silicon phase plates. This radiation was used to measure the magnetic Compton profile for Fe, which was found to be in good agreement with theory and previous work. The underlying x-ray optics and the characterization of the device between 62 keV and 93 keV at the Cornell High Energy Synchrotron Source are presented. DOE

N94-24631 Bordeaux 1 Univ., Talence (France). Centre de Physique Moleculaire Optique et Hertzienne.
WHITE-LIGHT, PRESSURE, AND TEMPERATURE INTERFEROPOLARIMETRIC SENSOR FEATURING OPTICAL FIBERS [CAPTEUR INTERFEROPOLARIMETRIQUE DE PRESSION ET DE TEMPERATURE EN LUMIERE BLANCHE, A FIBRES OPTIQUES]
F. Picherit 1993 18 p In FRENCH Sponsored by Direction des Recherches, Etudes et Techniques and Centre de Documentation de l'Armement Limited Reproducibility: More than 20% of this document may be affected by microfiche quality
(PB93-199792) Avail: Issuing Activity (National Technical Information Service (NTIS))

The feasibility of a white-light, pressure and temperature interferopolarimetric sensor using optical fibers was established through doctoral research and granted a CNRS (National Center for Scientific Research) patent. The proposed study involved eliminating the discrete optical components (polarizers, analyzers, coupling optics) initially used. The author also miniaturized the sensor, analyzed the propagation of waves in the device's different birefringent fibers, and studied the behavior of those optical fibers under varying temperatures and pressures. The results are presented in the report. NTIS

N94-24665*# Alabama Univ., Huntsville. Center for Applied Physics.
INVESTIGATE ZERO-STRESS REPLICATED OPTICS Final Report, Nov. 1992 - Aug. 1993
Darell Engelhaupt and Robert Rood 1993 45 p
(Contract NAS8-38609)
(NASA-CR-193889; NAS 1.26:193889; UAH-5-33127) Avail: CASI HC A03/MF A01

The contracted activities for the procurement of 'Investigate Zero-Stress Replicated Optics' to support the AXAF-S x-ray spectrometer mirrors has been completed. To date four large Wolter I grazing incidence x-ray optical shells have been electroformed from nickel. The mirrors were fabricated utilizing each of two nickel alloy plated aluminum substrates twice. A wide variety of testing has been completed by NASA MSFC and UAH. This testing includes heat treatment control tests, subscale plating and fixture testing, alloy control of the electroless nickel, adhesion and release testing of the gold to electroless nickel, electroforming instrumentation and software and fabrication of subscale models. The full scale shells are one millimeter thick nickel electrodeposited over a thin gold layer which in turn has the optical surface on the inside. The optical surface is the replicate of the surface prepared on the substrate. Appendix I briefly outlines the fabrication process. Major objectives which were shared by UAH and MSFC include the design of facilities, equipment and tooling and procurement of materials and equipment. Process development followed with the fabrication of small scale pilot units. Procurement commenced immediately and equipment and materials were ordered to implement the fabrication of first surface full scale substrates (mandrels) and the second surface electroformed optical components. All principal objectives have been achieved. Inspection of the mirrors in visible and x-ray modes validates that the required performance and the quality can be achieved by an electroforming replication process. A very distinct progressive improvement has been achieved with each of the four mirrors produced. The final mirror exceeded the original goals and set an improved standard for flight hardware. The future goal of a 30 arc second resolution at 8 KEV x-ray appears to be achievable by this process when proper cleanliness and process control is utilized. Derived from text

N94-24672# JAYCOR, Vienna, VA.
INVESTIGATION OF RAMAN BEAM CLEANUP AND PHASE CONJUGATION Final Report, 1 May 1989 - 16 Apr. 1993
Rita Mahon 5 Nov. 1993 42 p
(Contract N00014-89-C-2146)
(AD-A273157) Avail: CASI HC A03/MF A01

There are seven main topics which will be discussed in detail in this report: (1) multiple pulse effects on raman gain; (2) higher order Stokes generation; (3) quantum limited imaging; (4) competition between signal and noise in narrowband Raman amplifiers; (5) imaging through turbid media; (6) application to tissue imaging; and (7) real-time imaging of debris in oil. DTIC

N94-24722 Department of the Navy, Washington, DC.
HETERODYNE ARRAY FOR MEASUREMENT OF TARGET VELOCITY Patent
Marc D. Mermelstein, inventor (to Navy) 3 Aug. 1993 15 p Filed 30 Jun. 1992
(AD-D016025; US-Patent-5,233,403; US-Patent-Appl-SN-906649; US-Patent-Class-356-28.5) Avail: US Patent and Trademark Office

A system for determining the angular velocity of a mobile target relative to a station is described. The system develops first and second reference beams and a beam to the target to enable the target to generate first and second signals. Optical devices preferably fiber-optical devices, responsive to the first and second reference beams and to the first and second signals respectively received from the target at discrete first and second positions on the station, respectively produce first and second interference pattern signals. Each of said received signals has a Doppler shift as a function of the movement of the target. An electrical processing circuit then processes the interference pattern signals to develop a signal indicative of the target's angular velocity. DTIC

N94-24730 Army Topographic Engineering Center, Fort Belvoir, VA.
HYPERSPECTRAL IMAGERY CLASSIFICATION USING A BACKPROPAGATION NEURAL NETWORK Scientific Paper
Pi-Fuay Chen and Tho C. Tran Dec. 1993 7 p Limited Reproducibility: More than 20% of this document may be affected by microfiche quality
(AD-A273615; TEC-R-199) Avail: Issuing Activity (Defense Technical Information Center (DTIC))

A backpropagation neural network was developed and implemented for classifying AVIRIS (Airborne Visible/Infrared Imaging Spectrometer) hyperspectral imagery. It is a fully interconnected linkage of three layers of neural network. Fifty input layer neurons take in signals from bands 41 to 90 of the AVIRIS spectral data in parallel. Test images are classified into four terrain categories of water, grassland, golf courses, and built-up areas using four output neurons. A hidden layer consisting of 12 neurons is

used. A training set containing 1,700 pixels for each of the four desired terrain categories is extracted and created from the first test image. Good classification accuracies of 81.8 percent to 95.5 percent are achieved despite the moderate AVIRIS pixel resolution of 20 meters by 20 meters.
DTIC

N94-24731 Environmental Research Inst. of Michigan, Ann Arbor.
OPTICAL WAVELET TRANSFORM PROCESSOR Interim Report, 1 Jun. - 20 Sep. 1993
Nikola S. Subotic and Carl C. Aleksoff 22 Nov. 1993 31 p Limited Reproducibility: More than 20% of this document may be affected by microfiche quality
(Contract N00014-93-C-0108)
(AD-A273625; ERIM-254400-1-P) Avail: Issuing Activity (Defense Technical Information Center (DTIC))

In this report we outline a time-integrating hybrid-optical processor to perform the wavelet transform of two dimensional spatial or spectral data. This architecture partitions the optical/electronic workload for most general and efficient operation. This processor architecture is very general in that it allows a large class of analyzing wavelet kernels, does not require special encoding methods to accommodate the bipolar nature of the wavelet kernel, naturally accommodates the serial nature of sensor data readout, has the ability to be easily reprogrammed for different wavelet kernels, and makes most efficient use of wavelength, spatial, and temporal multiplexing for fast operation. The processor is based on a triple product processor architecture which uses acousto-optic modulators and laser diodes as a means of high throughput data insertion into the system. The architecture is not limited by requiring the use of two dimensional spatial light modulators and fixed masks which are the basis for many current wavelet processor concepts. We provide the result of a simulation of the optical processor to show its potential performance. DTIC

N94-24816*# Virginia Polytechnic Inst. and State Univ., Blacksburg. Dept. of Aerospace and Ocean Engineering.
LOITA: LUNAR OPTICAL/INFRARED TELESCOPE ARRAY
Jun. 1993 166 p
(Contract NASw-4435)
(NASA-CR-195532; NAS 1.26:195532) Avail: CASI HC A08/MF A02

LOITA (Lunar Optical/Infrared Telescope Array) is a lunar-based interferometer composed of 18 alt-azimuth telescopes arranged in a circular geometry. This geometry results in excellent uv coverage and allows baselines up to 5 km long. The angular resolution will be 25 micro-arcsec at 500 nm and the main spectral range of the array will be 200 to 1100 nm. For infrared planet detection, the spectral range may be extended to nearly 10 mu m. The telescope mirrors have a Cassegrain configuration using a 1.75 m diameter primary mirror and a 0.24 m diameter secondary mirror. A three-stage (coarse, intermediate, and fine) optical delay system, controlled by laser metrology, is used to equalize path lengths from different telescopes to within a few wavelengths. All instruments and the fine delay system are located within the instrument room. Upon exiting the fine delay system, all beams enter the beam combiner and are then directed to the various scientific instruments and detectors. The array instrumentation will consist of CCD detectors optimized for both the visible and infrared as well as specially designed cameras and spectrographs. For direct planet detection, a beam combiner employing achromatic nulling interferometry will be used to reduce star light (by several orders of magnitude) while passing the planet light. A single telescope will be capable of autonomous operation. This telescope will be equipped with four instruments: wide field and planetary camera, faint object camera, high resolution spectrograph, and faint object spectrograph. These instruments will be housed beneath the telescope. The array pointing and control system is designed to meet the fine pointing requirement of one micro-arcsec stability and to allow precise tracking of celestial objects for up to 12 days. During the lunar night, the optics and the detectors will be passively cooled to 70-80 K temperature. To maintain a continuous communication with the earth a relay satellite placed at the L4 libration point will be used in conjunction with the Advanced Tracking and Data Relay Satellite System (ATDRSS). Electrical power of about 10 kW will be supplied by a nuclear reactor based on the SP-100 technology. LOITA will be constructed in three phases of six telescopes each. The total mass of the first operational phase is estimated at 58,820 kg. The cost of the fully operational first phase of the observatory is estimated at $8.9 billion. LOITA's primary objectives will be to detect and characterize planets around nearby stars (up to ten parsec away), study physics of collapsed stellar objects, solar/stellar surface features and the processes in nuclear regions of galaxies and quasars. An interferometric array such as LOITA will be capable of achieving resolutions three orders of magnitude greater than Hubble's design goal. LOITA will also be able to maintain higher signal to noise ratios than are currently attainable due to long observation times available on the moon.
Author (revised)

N94-24967*# Puerto Rico Univ., Mayaguez. Dept. of Physics.
SOFT X RAY OPTICS BY PULSED LASER DEPOSITION Status Report, 15 Aug. 1993 - 15 Feb. 1994
Felix E. Fernandez 1994 4 p
(Grant NAG5-2188)
(NASA-CR-195139; NAS 1.26:195139) Avail: CASI HC A01/MF A01

A series of molybdenum thin film depositions by PLD (Pulsed Laser Deposition) have been carried out, seeking appropriate conditions for multilayer fabrication. Green (532 nm) and UV (355 nm) light pulses, in a wide range of fluences, were used. Relatively large fluences (in comparison with Si) are required to cause evaporation of molybdenum. The optical penetration depths and reflectivities for Mo at these two wavelengths are comparable, which means that results should be, and do appear to be similar for equal fluences. For all fluences above threshold used, a large number of incandescent particles is ejected by the target (either a standard Mo sputtering target or a Mo sheet were tried), together with the plasma plume. Most of these particles are clearly seen to bounce off the substrate. The films were observed with light microscopy using Nomarski and darkfield techniques. There is no evidence of large debris. Smooth films plus micron-sized droplets are usually seen. The concentration of these droplets embedded in the film appears not to vary strongly with the laser fluence employed. Additional characterization with SEM and XRD is under way.
Derived from text

N94-24982# Electrotechnical Lab., Tsukuba (Japan).
A STUDY ON ELECTROSTATIC QUADRUPOLE LENSES AND THEIR APPLICATION TECHNOLOGIES [YONKYOKUSHI RENZU TO SONO RIYO GIJUTSU NI KANSURU KENKYU]
Shigeo Okayama 26 Mar. 1993 166 p In JAPANESE
(Rept-948; JTN-94-80516) Avail: CASI HC A08/MF A02

A study was conducted to provide solutions to the problems which hinders the utilization of the quadrupole lens systems in place of the conventional round lenses. A new simplified lens capable of correcting third order aperture aberration is proposed. The results of the study are outlined as follows: (1) potential distribution and electron optical properties of electrostatic quadrupole lenses are accurately obtained, and focal properties of the quadrupole lenses for various electrode length are calculated using the modified bell shaped model; (2) focal properties of the electrostatic quadrupole lens are accurately obtained from accurate measurements of the shadow image of fine grids and the experimental results agree with those calculated; (3) a Quadrupole Electron-Beam Lithography System (QEBS) is proposed and high precision electrostatic quadrupole triplet has been developed for the system; and (4) the corrections of aperture aberration of quadrupole systems are presented, and a new simplified lens possessing the function of correction of the aperture aberration is proposed. A complete lens system consisting of four stage quadrupoles and five aperture electrodes is proposed as a 1:1 probe forming lens and as a corrector for rotationally symmetrical objective lens. Author (NASDA)

N94-25043 Department of the Navy, Washington, DC.
CONFORMAL METHOD OF FABRICATING AND OPTICAL WAVEGUIDE ON A SEMICONDUCTOR SUBSTRATE Patent
Stephen D. Russell, inventor (to Navy) 24 Aug. 1993 7 p Filed 30 Apr. 1992
(AD-D015988; US-Patent-5,238,877; US-Patent-Appl-SN-876615; US-Patent-Class-437-231) Avail: US Patent and Trademark Office

A method for fabricating a conformal optical waveguide on a semiconductor substrate which results in an improved conformal processing method of producing ferroelectric ceramic waveguides that is integratable with conventional electronic and optoelectronic devices is described. First, a patterning of a desired waveguide configuration is made on desired semiconductor substrate. A conformal confinement layer is fabricated in the pattern of the desired waveguide configuration on the semiconductor substrate. The conformal confinement layer has an index of refraction. Next, the method calls for a placing of a sol-gel waveguide precursor in the conformal confinement layer. Next the spin casting of a sol-gel waveguide precursor shapes a sol-gel conformal waveguide layer in the conformal confinement layer on the semiconductor substrate. The annealing of the spin cast sol-gel conformal waveguide layer forms the conformal optical waveguide which has an index of refraction that is greater than the refractive index of the conformal confinement layer. DTIC

N94-25144# New Mexico Univ., Albuquerque. Dept. of Chemistry.
SCANNING PROBE LITHOGRAPHY. 2: SELECTIVE CHEMICAL VAPOR DEPOSITION OF COPPER INTO SCANNING TUNNELING MICROSCOPE-DEFINED PATTERNS
Jonathan K. Schoer, Claudia B. Ross, Richard M. Crooks, Thomas S. Corbitt, and Mark J. Hampden-Smith 23 Nov. 1993 22 p
(Contract N00014-91-J-1991)
(AD-A273304; TR-12) Avail: CASI HC A03/MF A01

A scanning tunneling microscope (STM) has been used to define features having critical dimensions ranging from 0.05 to 5.0 micrometer within a self-assembled monolayer resist of octadecylmercaptan, HS(CH2)17CH3, confined to a Au (111) surface. Low temperature chemical vapor deposition (CVD) methods were used to metalize the STM-patterned surface with Cu. At substrate temperatures near 120 C, the Cu CVD precursor, hexafluoroacetyl acetonatocopper(I) - (1,5-cyclooctadiene), disproportionates to deposit Cu on the STM-etched portion of the substrate, but not on the unetched methyl-terminated monolayer resist surface. At substrate temperatures significantly above 120 C the degree of selectivity is reduced, probably as a result of thermal desorption of the organomercaptan monolayer. DTIC

N94-25161 Wright Lab., Wright-Patterson AFB, OH.
A COMPARISON OF FREE-SPACE AND FIBER MIXER PERFORMANCES Final Report, 1 Jan. 1991 - 31 Mar. 1992
Martin B. Mark Aug. 1993 30 p Limited Reproducibility: More than 20% of this document may be affected by microfiche quality
(AD-A273558; WL-TR-93-1136) Avail: Issuing Activity (Defense Technical Information Center (DTIC))

This report compares the heterodyne reception mixing efficiency of a laser radar employing a conventional free-space mixer to one employing a fiber mixer. A rigorous derivation for speckle targets shows the two mixing schemes will have approximately the same mixing efficiency. The fiber mixing efficiency is optimized by choosing the optics numerical aperture (NA) equal to the fiber NA. DTIC

N94-25209# International Centre for Theoretical Physics, Trieste (Italy).
SOLUTIONS OF THE 2-D HELMHOLTZ EQUATION FOR OPTICAL WAVEGUIDES
A. Sharma and P. Bindal (Indian Inst. of Tech., New Delhi.) Nov. 1992 30 p
(DE93-616840; LAMP-92/2) Avail: CASI HC A03/MF A01 (US Sales Only)

In both optical fibers and integrated optical devices, the basic phenomenon is that of waveguidance, and in order to effectively analyze and design these waveguides, it is necessary to understand the phenomenon of guidance through them. In the most basic form, this requires the solutions of Maxwell's equations for the boundary conditions represented by the waveguiding structure. Fortunately, for optical waveguides, in most cases of practical importance, it suffices to solve the much simpler Helmholtz equation. However, it is still difficult to solve this equation for those integrated optical structures which provide two-dimensional confinement to optical waves. In this case the Helmholtz equation is a partial differential equation and one has to use approximate and/or numerical techniques to obtain its solutions. The present report is concerned with some of such techniques developed recently. DOE

N94-25305# Deutsche Forschungsanstalt fuer Luft- und Raumfahrt, Oberpfaffenhofen (Germany). Abt. Lasertechnik.
IMPROVEMENT OF SYSTEM PROPERTIES OF A PULSED LASER DOPPLER ANEMOMETER WITH RESPECT TO AN OPTICAL AMPLIFIER Ph.D. Thesis - Tech. Univ. Munich [VERBESSERUNG DER SYSTEMEIGENSCHAFTEN EINES GEPULSTEN LASER-DOPPLER-ANEMOMETERS UNTER BERUECKSICHTIGUNG EINES OPTISCHEN VERSTAERKERS]
Stephan Rahm May 1993 103 p In GERMAN
(DLR-FB-93-19; ETN-94-95203) Avail: CASI HC A06/MF A02

The use of an optical detector preamplifier in a pulsed laser Doppler system operating at the wavelength 10.6 micrometers is investigated. Especially the possibility of improvement of the SNR (Signal to Noise Ratio) from the whole lidar system was examined. Theoretically developed models were compared with experimental data. For this task an optical amplifier was developed from a pulsed CO2 laser. This amplifier was integrated in a Doppler lidar system. With this system, measurements at a hard target and in the atmosphere were done. An improvement of the SNR of a factor 70 (hard target) or 23 (atmosphere) and an improvement in the range of factor 13 were obtained in agreement with the theoretic results. ESA

N94-25533# Air Force Inst. of Tech., Wright-Patterson AFB, OH. School of Engineering.
A THEORETICAL INVESTIGATION OF ELECTRICALLY TUNABLE BIREFRINGENT OPTICAL FILTERS AS THE SPECIAL DISCRIMINATOR IN HYPERSPECTRAL IMAGING SYSTEMS M.S. Thesis
Duane A. Sauve Dec. 1993 67 p
(AD-A273743; AFIT/GEO/ENP/93D-02) Avail: CASI HC A04/MF A01

This study investigated electrically tunable birefringent optical filters for use as the spectral discriminator in hyperspectral imaging systems. Spectral discrimination requirements for hyperspectral systems were defined using specification from two state-of-the-art hyperspectral imaging systems. The spectral discrimination requirements led to the definition of the ideal tunable optical filter for spectral discrimination purposes. Analytical and computer analysis was performed for known birefringent filters which showed promise of electrical tunability, excluding acousto-optic filters. No perfect match was found to the ideal tunable optical filter for hyperspectral imaging defined in this thesis. Both Lyot and Solc based filters exhibited two drawbacks for hyperspectral imaging application: narrow tuning range with linear bandwidth dependence on center wavelength, or wide tuning range and quadratic bandwidth dependence on center wavelength. The Delta-n-tuned Solc filter provided the best compromise between tuning range and bandwidth control; however, it is not practical due to the excessive number of elements required. This thesis provides the needed background for further research in this area and identifies a number of areas for further worthwhile research. DTIC

N94-24046# Codechamp S.A., Champagnat (France).
ENCODERS FOR SPACE APPLICATIONS
Daniel Gaumet, Alain Grass, and L. Bongrand *In* ESA, The Fifth European Space Mechanisms and Tribology Symposium Apr. 1993 2 p (For primary document see N94-23985 06-37)
Copyright Avail: CASI HC A01/MF A04

N94-24343*# National Aeronautics and Space Administration. Marshall Space Flight Center, Huntsville, AL.
PREDICTION OF NONLINEAR OPTICAL PROPERTIES OF ORGANIC MATERIALS. GENERAL THEORETICAL CONSIDERATIONS Abstract Only
B. Cardelino (Atlanta Univ. Center, Inc., GA.), C. Moore, and S. Zutaut (Alabama Univ., Huntsville.) *In its* Microgravity Studies of Organic and Polymeric Materials Dec. 1993 p 45-46 (For primary document see N94-24338 06-23)
Avail: CASI HC A01/MF A03

N94-24347*# National Aeronautics and Space Administration. Marshall Space Flight Center, Huntsville, AL.
POLYDIACETYLENE THIN FILMS FOR NONLINEAR OPTICAL APPLICATIONS Abstract Only
Mark S. Paley *In its* Microgravity Studies of Organic and Polymeric

Materials Dec. 1993 p 63-64 (For primary document see N94-24338 06-23)
Avail: CASI HC A01/MF A03

N94-24348*# Westinghouse Science and Technology Center, Pittsburgh, PA.
CRYSTAL GROWTH OF ORGANICS FOR NONLINEAR OPTICAL APPLICATIONS
N. B. Singh and R. Mazelsky *In* NASA. Marshall Space Flight Center, Microgravity Studies of Organic and Polymeric Materials Dec. 1993 p 65-66 (For primary document see N94-24338 06-23)
Avail: CASI HC A01/MF A03

N94-24349*# Alabama Univ., Huntsville. Chemistry Dept.
NONLINEAR OPTICAL THIN FILMS
Thomas M. Leslie *In* NASA. Marshall Space Flight Center, Microgravity Studies of Organic and Polymeric Materials Dec. 1993 p 67-68 (For primary document see N94-24338 06-23)
Avail: CASI HC A01/MF A03

N94-24354*# Jet Propulsion Lab., California Inst. of Tech., Pasadena.
OPTIMIZATION OF MICROSCOPIC AND MACROSCOPIC SECOND ORDER OPTICAL NONLINEARITIES
Seth R. Marder and Joseph W. Perry (California Inst. of Tech., Pasadena.) *In* NASA. Marshall Space Flight Center, Microgravity Studies of Organic and Polymeric Materials Dec. 1993 p 107-117 (For primary document see N94-24338 06-23)
Avail: CASI HC A03/MF A03

N94-24420*# Auburn Univ., AL. Aerospace Engineering.
VALIDATION OF A NONINTRUSIVE OPTICAL TECHNIQUE FOR THE MEASUREMENT OF LIQUID MASS DISTRIBUTION IN A TWO-PHASE SPRAY
Roy Hartfield, Jr. *In* Alabama Univ., The 1993 NASA/ASEE Summer Faculty Fellowship Program Nov. 1993 5 p (For primary document see N94-24405 06-80)
Avail: CASI HC A01/MF A03

N94-25491*# FLIR Systems, Inc., Portland, OR.
INFRARED SENSORS AND SYSTEMS FOR ENHANCED VISION/AUTONOMOUS LANDING APPLICATIONS
J. Richard Kerr *In* NASA. Ames Research Center, Proceedings of the Workshop on Augmented Visual Display (AVID) Research Dec. 1993 p 5-27 (For primary document see N94-25490 06-54)
Avail: CASI HC A03/MF A04

N94-25506*# National Aeronautics and Space Administration. Ames Research Center, Moffett Field, CA.
VALIDATION OF VISION-BASED RANGE ESTIMATION ALGORITHMS USING HELICOPTER FLIGHT DATA
Phillip N. Smith *In its* Proceedings of the Workshop on Augmented Visual Display (AVID) Research Dec. 1993 p 293-311 (For primary document see N94-25490 06-54)
Avail: CASI HC A03/MF A04

N94-25509*# National Aeronautics and Space Administration. Ames Research Center, Moffett Field, CA.
DCT QUANTIZATION MATRICES VISUALLY OPTIMIZED FOR INDIVIDUAL IMAGES
Andrew B. Watson *In its* Proceedings of the Workshop on Augmented Visual Display (AVID) Research Dec. 1993 p 363-377 (For primary document see N94-25490 06-54)
Avail: CASI HC A03/MF A04

75 PLASMA PHYSICS

Includes magnetohydrodynamics and plasma fusion.

For ionospheric plasmas see *46 Geophysics*. For space plasmas see *90 Astrophysics*.

N94-22721# Massachusetts Inst. of Tech., Cambridge. Plasma Fusion Center.
MASSACHUSETTS INSTITUTE OF TECHNOLOGY PLASMA FUSION CENTER 1992-1993 REPORT TO THE PRESIDENT
Jul. 1993 30 p
(Contract DE-AC02-78ET-51013)
(DE94-001725; PFC/IR-93-1; DOE/ET-51013/302) Avail: CASI HC A03/MF A01

This report discusses research being conducted at MIT's plasma fusion center. Some of the areas covered are: plasma diagnostics, RF plasma heating, gyrotron research, treatment of solid waste by arc plasma, divertor experiments, tokamak studies, and plasma and fusion theory. DOE

N94-22916# Oak Ridge National Lab., TN.
ASSESSMENT OF STELLARATORS AS REACTORS
J. F. Lyon 1993 26 p Presented at the 9th International Atomic Energy Agency (IAEA) Workshop on Stellarators, Garching, Germany, 10-14 May 1993
(Contract DE-AC05-84OR-21400)
(DE93-017775; CONF-9305210-2) Avail: CASI HC A03/MF A01

Stellarators have significant operational advantages over tokamaks as ignited steady-state reactors: no dangerous disruptions, no need for continuous current drive and power recirculated to the plasma, less severe constraints on the plasma parameters and profiles, and access from the inboard side for easier maintenance. The U.S. is starting a multi-year multi-institutional stellarator reactor study whose purpose is to 'identify and assess the feasibility of critical issues and their consequences for development of the stellarator concept as a steady-state fusion reactor.' The activities during the first year are focusing on physics optimization and selection of one or more stellarator coil configurations for more detailed engineering design evaluation. The physics team is focusing on torsatron modularization, modular stellarators with lower aspect ratio, the divertor geometry, development of transport models, and overall system studies. The engineering team is studying design issues relating to minimizing the inboard thickness of the blanket and shields, the feasibility of the superconducting magnets, and maintenance schemes. DOE

N94-22924# Japan Atomic Energy Research Inst., Tokyo.
REPORT OF THE JOINT SEMINAR ON SOLID STATE PHYSICS, ATOMIC AND MOLECULAR PHYSICS, AND MATERIALS SCIENCE IN THE ENERGY REGION OF TANDEM ACCELERATORS
Yukio Kazumata, ed. Jan. 1993 103 p In ENGLISH and JAPANESE Seminar held in Tokai, Japan, 22-23 Jan. 1991
(DE93-508268; JAERI-M-92-202; CONF-9101168) Avail: CASI HC A06/MF A02

The Joint Seminar on Solid State Physics, Atomic and Molecular Physics, and Materials Science in the Energy Region of Tandem Acceleration was held at Tokai Research Establishment of JAERI for two days from January 22 to 23, 1991. About 60 physicists and material scientists participated and 18 papers were presented in this seminar. The topics presented in this seminar included lattice defects in semiconductors, ion-solid collisions, atomic collisions by high energy particles, radiation effects on high T(sub c) superconducting materials and FCC metals, radiation effects on materials of space and fusion reactors, uranium compounds and superlattice. DOE

N94-22945# Oak Ridge National Lab., TN.
ACTIVE PROBING OF PLASMA EDGE TURBULENCE AND FEEDBACK STUDIES ON THE TEXAS EXPERIMENTAL TOKAMAK (TEXT)
T. Uckan, B. Richards (Texas Univ., Austin.), and R. D. Bengtson (Texas Univ., Austin.) Aug. 1993 13 p
(Contract DE-AC05-84OR-21400)
(DE94-001017; ORNL/TM-12424) Avail: CASI HC A03/MF A01

A novel experiment is under way on the Texas Experimental Tokamak (TEXT) to actively modify the turbulence at the plasma edge by launching waves using electrostatic probes in the shadow of the limiter. The experiments are carried out with a wave launching system consisting of two Langmuir probes, which are about 1.8 cm apart in the poloidal direction, with respect to the magnetic field. These probes are operated in the electron side of the (I,V) characteristic. The probe tips are fed separately by independent ac power supplies. Measurements indicate that the wave, launched with a typical frequency image of 15-50 kHz from the edge of the machine top, is received by sensing probes located halfway around the torus. The detected signal strength depends on the frequency of the wave, the plasma current, and the phasing of the applied ac signal between the launching probes. Modifications to the spectra of the density and potential fluctuations are observed. These experiments have been extended to control of the edge plasma fluctuation level using feedback to explore its effects on confinement. When the launcher is driven by the floating potential of the fluctuating plasma at the location of the launching probes, then the fluctuations are suppressed or excited, depending on the phasing between the probe tips, both locally and at the downstream sensing probes. The fluctuation-induced particle flux also varies with the feedback phasing. DOE

N94-22949# Lawrence Livermore National Lab., CA.

IMAGING XUV SPECTROSCOPY OF A Z-PINCH PLASMA IN THE FORMER SOVIET UNION

H. C. Bruns, P. T. Springer, J. A. Emig, N. E. Lanier, and J. A. Hernandez 11 Aug. 1993 9 p Presented at the Annual Meeting of the Society of Photo-Optical Instrumentation Engineers (SPIE), San Diego, CA, 11-16 Jul. 1993
(Contract W-7405-eng-48)
(DE93-040849; UCRL-JC-114803; CONF-930722-38) Avail: CASI HC A02/MF A01

In 1991 a group of scientists from the Angara 5 pulsed power facility at the Kurchatov Institute in Troitsk, Russia had determined the thermal emission from an implosion of xenon gas onto an annular, molybdenum doped foam liner to be 30 TW/sq cm. This represents an extremely efficient conversion of energy into a high fluence radiation field. In order to verify this claim and better understand the process of producing radiation by means of a Z-pinch plasma device, a series of experiments were proposed through a collaboration from Sandia National Laboratory, Albuquerque, Los Alamos National Laboratory, and Lawrence Livermore National Laboratory. Due to previous experience with x-ray spectroscopic measurements in the XUV region, the team from Lawrence Livermore Lab took on the task of designing, constructing, and fielding the necessary diagnostic equipment to spatially and temporally resolve plasma temperatures throughout the implosion of the high Z foam target. DOE

N94-22963# Wisconsin Univ., Madison. Plasma Physics Research.

CHAOS IN PLASMA SIMULATION AND EXPERIMENT

C. Watts (Texas Univ., Austin.), D. E. Newman (Oak Ridge National Lab., TN.), and J. C. Sprott Sep. 1993 39 p
(Contract DE-FG02-85ER-53198)
(DE94-001574; DOE/ER-53198/223) Avail: CASI HC A03/MF A01

We investigate the possibility that chaos and simple determinism are governing the dynamics of reversed field pinch (RFP) plasmas using data from both numerical simulations and experiment. A large repertoire of nonlinear analysis techniques is used to identify low dimensional chaos. These tools include phase portraits and Poincare sections, correlation dimension, the spectrum of Lyapunov exponents, and short term predictability. In addition, nonlinear noise reduction techniques are applied to the experimental data in an attempt to extract any underlying deterministic dynamics. Two model systems are used to simulate the plasma dynamics. These are the DEBS code, which models global RFP dynamics, and the dissipative trapped electron mode (DTEM) model, which models drift wave turbulence. Data from both simulations show strong indications of low dimensional chaos and simple determinism. Experimental data were obtained from the Madison Symmetric Torus RFP and consist of a wide array of both global and local diagnostic signals. None of the signals shows any indication of low dimensional chaos or other simple determinism. Moreover, most of the analysis tools indicate the experimental system is very high dimensional with properties similar to noise. Nonlinear noise reduction is unsuccessful at extracting an underlying deterministic system. DOE

N94-22964# National Inst. for Fusion Science, Nagoya (Japan).

CHAOTIC PHENOMENA IN PLASMA, 2

Y. Kawai, ed. Nov. 1992 62 p
(DE93-508286; NIFS-MEMO-7) Avail: CASI HC A04/MF A01

To review the present status of the research on plasma chaos, a working group was organized in 1990. The second meeting of the working group was held on December 1991 at National Institute for Fusion Science. This is the report of the second meeting, which contains both experimental and theoretical works. DOE

N94-22976# Wisconsin Univ., Madison. Dept. of Physics.

PLASMA RESEARCH IN THE MADISON SYMMETRIC TORUS (MST)

S. C. Prager 1993 14 p
(Contract DE-FG02-85ER-53198)
(DE94-002318; DOE/ER-53198/226) Avail: CASI HC A03/MF A01

We present physics results divided into the four categories (confinement optimization, transport measurements, fluctuations and fluctuation-induced transport, and fluctuation suppression). For simplicity, we highlight a subset of original MST results which are presented as 13 specific conclusions (not listed in order of importance), each followed by a brief elaboration. Within each of the four categories, we also present other progress. DOE

N94-22998# Oak Ridge National Lab., TN.

FLUCTUATIONS AND CONFINEMENT IN ATF

R. C. Isler, J. H. Harris, and M. Murakami 1993 6 p Presented at the 9th IAEA Workshop on Stellarators, Garching, Germany, 10-14 May 1993
(Contract DE-AC05-84OR-21400)
(DE94-000485; CONF-9305210-5) Avail: CASI HC A02/MF A01

In the period immediately prior to the suspension of ATF operation in November, 1991, a great deal of emphasis was placed on investigations of the fundamental mechanisms controlling confinement in this device. At that time, measurements of the density fluctuations throughout the plasma volume indicated the existence of theoretically predicted dissipative trapped electron and resistive interchange instabilities. These identifications were supported by results of dynamic configuration scans of the magnetic fields during which the extent of the magnetic well, shear, and fraction of confined trapped particles were changed continuously. Interpretation of the data from these experiments has been an ongoing exercise. Most recently, analysis of discharges employing strong gas puffing to change density gradients and fluctuation levels have strengthened the view that dissipative trapped electron modes may be present but do not play a significant direct role in energy transport. The present paper summarizes the current understanding concerning the identification of instabilities and their relationship to confinement in ATF. DOE

N94-23013 Lawrence Livermore National Lab., CA.

SUPERCONDUCTING MAGNET SYSTEM FOR THE TPX TOKAMAK

W. V. Hassenzahl, M. R. Chaplin, J. R. Heim, D. D. Lang, T. G. OConnor, D. S. Slack, R. L. Wong, J. P. Zbasnik, T. G. Brown (Princeton Univ., NJ.), and J. C. Citrolo (Princeton Univ., NJ.) 15 Sep. 1993 4 p Presented at the 13th International Conference on Magnet Technology, Victoria, Ontario, 20-24 Sep. 1993 Limited Reproducibility: More than 20% of this document may be affected by microfiche quality
(Contract W-7405-eng-48)
(DE94-001535; UCRL-JC-114679; CONF-930926-15) Avail: CASI HC A01

The Tokamak Physics Experiment (TPX) will be the first Tokamak using superconducting magnets for both the poloidal and toroidal field. It is designed for advanced Tokamak physics experiments in steady-state and long-pulse operation. The TPX superconducting magnets use an advanced cable-in-conduit conductor (CICC) design similar to that developed in support of the International Thermonuclear Experimental Reactor (ITER). The toroidal field magnets provide 4.0 T at 2.25 m with a stored energy of 1.05 GJ. The poloidal field magnets provide 18.0 V-s to ohmically start and control long burns of a 2.0 MA plasma. DOE

N94-23014 Lawrence Livermore National Lab., CA.

STRUCTURAL ANALYSIS OF A SUPERCONDUCTING CENTRAL SOLENOID FOR THE TOKAMAK PHYSICS EXPERIMENT

T. G. OConnor and J. R. Heim 15 Sep. 1993 4 p Presented at the 13th International Conference on Magnet Technology, Victoria, Ontario, 20-24 Sep. 1993 Limited Reproducibility: More than 20% of this document may be affected by poor print

(Contract W-7405-eng-48)
(DE94-001536; UCRL-JC-112765; CONF-930926-17) Avail: Issuing Activity (Department of Energy (DOE))

The Tokamak Physics Experiment (TPX) concept design uses superconducting coils to accomplish magnetic confinement. The central solenoid (CS) magnet is divided vertically into 8 equal segments which are powered independently. The eddy current heating from the pulsed operation is too high for a case type construction; therefore, a 'no case' design has been chosen. This no case design uses the conductor conduit as the primary structure and the electrical insulation as a structural adhesive. This electrical insulation is the 'weak link' in the coil winding pack structure and needs to be modeled in detail. A global finite element model with smeared winding pack properties was used to study the CS magnet structural behavior. The structural analysis results and peak stresses will be presented. DOE

N94-23182# General Atomics Technologies Corp., San Diego, CA.
CAMAC THROUGHPUT OF A NEW RISC-BASED DATA ACQUISITION COMPUTER AT THE DIII-D TOKAMAK
J. F. VanderLaan and J. W. Cummings Oct. 1993 5 p Presented at the Symposium on Fusion Engineering, Hyannis, MA, 11-15 Oct. 1993
(Contract DE-AC03-89ER-51114)
(DE94-001113; GA-A-21416; CONF-931018-11) Avail: CASI HC A01/MF A01

The amount of experimental data acquired per plasma discharge at DIII-D has continued to grow. The largest shot size in May 1991 was 49 Mbyte; in May 1992, 66 Mbyte; and in April 1993, 80 Mbyte. The increasing load has prompted the installation of a new Motorola 88100-based MODCOMP computer to supplement the existing core of three older MODCOMP data acquisition CPU's. New Kinetic Systems CAMAC serial highway driver hardware runs on the 88100 VME bus. The new operating system is MODCOMP REAL/IX version of AT&T System V UNIX with real-time extensions and networking capabilities; future plans call for installation of additional computers of this type for tokamak and neutral beam control functions. Experiences with the CAMAC hardware and software will be chronicled, including observation of data throughput. The Enhanced Serial Highway crate controller is advertised as twice as fast as the previous crate controller, and computer I/O speeds are expected to also increase data rates. DOE

N94-23192 Wisconsin Univ., Madison.
1993 ANNUAL REPORT FOR THE PHAEDRUS-T RF CURRENT DRIVE EXPERIMENTS
N. Hershkowitz 1993 7 p Limited Reproducibility: More than 20% of this document may be affected by poor print
(Contract DE-FG02-88ER-53264)
(DE94-001369; DOE/ER-53264/4) Avail: Issuing Activity (Department of Energy (DOE))

After a series of antenna modifications and a program of optimizing our Boronization procedures, we have succeeded in coupling 300 kill of RF power to the plasma. Thomson Scattering shows a 20-60% increase in core T(sub e), and constitutes experimental evidence that the waves are interacting with the electron population. Beam Emission Spectroscopy (BES) data show that the power is deposited in the core and at the edge as predicted by theoretical modeling. Ninety degree phasing of the antenna caused loop voltage drops of 15-25%, which can be interpreted as an increase 5 kA of toroidal plasma current for co-injection phasing versus counter injection phasing. Biased H-modes have been created with a biased electrode. These plasmas have a steeper edge density gradient and reduced edge fluctuations than our normal limiter plasmas and a D(sub alpha) emission drop at the limiter. Radial profiles of soft x-ray line emission have been measured by the Johns Hopkins group and significantly aided in our understanding of impurity generation with RF and in the biased H-mode. Initial reflectometry data shows the presence of RF density fluctuations in the plasma. Different boronization techniques have been tried leading to a higher boron content in the deposited layer and reduced wall recycling. In this report, we outline the series of experiments that we have performed in the last year that led us to our present encouraging results. DOE

N94-23211# Wisconsin Univ., Madison. Plasma Physics Research.
CHAOS AND SIMPLE DETERMINISM IN REVERSED FIELD PINCH PLASMAS: NONLINEAR ANALYSIS OF NUMERICAL SIMULATION AND EXPERIMENTAL DATA Ph.D. Thesis
C. A. Watts Sep. 1993 114 p
(Contract DE-FG02-85ER-53198)
(DE94-001575; DOE/ER-53198/224) Avail: CASI HC A06/MF A02

In this dissertation the possibility that chaos and simple determinism are governing the dynamics of reversed field pinch (RFP) plasmas is investigated. To properly assess this possibility, data from both numerical simulations and experiment are analyzed. A large repertoire of nonlinear analysis techniques is used to identify low dimensional chaos in the data. These tools include phase portraits and Poincare sections, correlation dimension, the spectrum of Lyapunov exponents and short term predictability. In addition, nonlinear noise reduction techniques are applied to the experimental data in an attempt to extract any underlying deterministic dynamics. Two model systems are used to simulate the plasma dynamics. These are the DEBS code, which models global RFP dynamics, and the dissipative trapped electron mode (DTEM) model, which models drift wave turbulence. Data from both simulations show strong indications of low dimensional chaos and simple determinism. Experimental data were obtained from the Madison Symmetric Torus RFP and consist of a wide array of both global and local diagnostic signals. None of the signals shows any indication of low dimensional chaos or low simple determinism. Moreover, most of the analysis tools indicate the experimental system is very high dimensional with properties similar to noise. Nonlinear noise reduction is unsuccessful at extracting an underlying deterministic system. DOE

N94-23462# Oak Ridge National Lab., TN.
OVERVIEW OF THE ATF STELLARATOR PROGRAM
J. F. Lyon 1993 5 p Presented at the 9th International Atomic Energy Agency (IAEA) Workshop on Stellarators, Garching, Germany, 10-14 May 1993
(Contract DE-AC05-84OR-21400)
(DE94-000371; CONF-9305210-4) Avail: CASI HC A01/MF A01

ATF, the world's largest stellarator, has major radius R(sub 0) = 2.1 m, average plasma radius alpha(sub p) = 0.27 m, and on-axis field B(sub 0) = 2 T. In May 1991, an electrical arc occurred in one of the joints in a helical field (HF) winding, causing severe damage to two of the HF winding segments. A temporary repair was made and ATF resumed operation in September 1991, but operation was limited to B(sub 0) = 1 T. A set of experiments on microwave scattering, confinement scaling, and ion cyclotron heating was completed before ATF was shut down for a permanent repair in November 1991. The microwave scattering measurements of electron density fluctuations in the core of low-collisionality electron cyclotron heated (ECH) plasmas showed features that might be evidence of trapped electron instabilities. DOE

N94-23474# Argonne National Lab., IL.
COMPUTATIONAL MODEL OF SURFACE ABLATION FROM TOKAMAK DISRUPTIONS
D. Ehst and A. Hassanein Oct. 1993 4 p Presented at the Symposium on Fusion Engineering, Hyannis, MA, 11-15 Oct. 1993
(Contract W-31-109-eng-38)
(DE94-002204; ANL/EP/CP-79902; CONF-931018-36) Avail: CASI HC A01/MF A01

Energy transfer to material surfaces is dominated by photon radiation through low temperature plasma vapors if tokamak disruptions are due to low kinetic energy particles (less than 100 eV). Simple models of radiation transport are derived and incorporated into a fast-running computer routine to model this process. The results of simulations are in fair agreement with plasma gun erosion tests on several metal targets. DOE

N94-23565*# Lockheed Missiles and Space Co., Palo Alto, CA. Research and Development Div.
ARTIFICIAL PLASMA EXPERIMENTS. CHEMICAL RELEASE OBSERVATIONS ASSOCIATED WITH THE CRRES PROGRAM Final Report, 12 Apr. 1985 - 23 Dec. 1993
Stephen B. Mende 21 Jan. 1994 87 p
(Contract NAS8-36630)
(NASA-CR-194871; NAS 1.26:194871) Avail: CASI HC A05/MF A01

This report submitted is the final report and covers work performed

under the contract for the period Apr. 12, 1985 - Dec. 23, 1993. The CRRES program investigated earth plasma environment by active experiments in which metal vapors were injected into the upper atmosphere and magnetosphere. The vapor clouds perturb the ambient ionospheric / magnetospheric environment and the effects could be monitored by passive observing instruments. Our part of the CRRES program, the Artificial Plasma Experiment program, was a ground based and aircraft based investigation to observe artificial chemical releases by optical techniques.
Derived from text

N94-23703# Lawrence Livermore National Lab., CA.
INERTIAL CONFINEMENT FUSION Quarterly Report, Apr. - Jun. 1993
B. J. MacGowan, ed., M. Kotowski, ed., and D. Schleich, ed. 1993 53 p
(Contract W-7405-eng-48)
(DE94-002602; UCRL-LR-105821-93-3) Avail: CASI HC A04/MF A01

This issue of the ICF Quarterly contains six articles describing recent advances in Lawrence Livermore National Laboratory's inertial confinement fusion (ICF) program. The current emphasis of the ICF program is in support of DOE's National Ignition Facility (NIF) initiative for demonstrating ignition and gain with a 1-2 MJ glass laser. The articles describe recent Nova experiments and investigations tailored towards enhancing understanding of the key physics and technological issues for the NIF. Titles of the articles are: development of large-aperture KDP crystals; inner-shell photo-ionized x-ray lasers; x-ray radiographic measurements of radiation-driven shock and interface motion in solid density materials; the role of nodule defects in laser-induced damage of multilayer optical coatings; techniques for Mbar to near-Gbar equation-of-state measurements with the Nova laser; and parametric instabilities and laser-beam smoothing. DOE

N94-23782# General Atomics Technologies Corp., San Diego, CA.
THE ROLE OF THE RADIAL ELECTRIC FIELD IN CONFINEMENT AND TRANSPORT IN H-MODE AND VH-MODE DISCHARGES IN THE DIII-D TOKAMAK
P. Gohil, K. H. Burrell, R. J. Groebner, T. H. Osborne, E. J. Doyle (California Univ., Los Angeles.), and C. L. Rettig (California Univ., Los Angeles.) Aug. 1993 6 p Presented at the Workshop on Local Transport Studies in Fusion Plasmas, Varenna, Italy, 30 Aug. - 3 Sep. 1993
(Contract DE-AC03-89ER-51114)
(DE94-002746; GA-A-21415; CONF-9308183-3) Avail: CASI HC A02/MF A01

Measurements of the radial electric field, E(sub r), with high spatial and high time resolution in H-mode and VH-mode discharges in the DIII-D tokamak have revealed the significant influence of the shear in E(sub r) on confinement and transport in these discharges. These measurements are made using the DIII-D Charge Exchange Recombination (CER) System. At the L-H transition in DIII-D plasmas, a negative well-like E(sub r) profile develops just within the magnetic separatrix. A region of shear in E(sub r) results, which extends 1 to 2 cm into the plasma from the separatrix. At the transition, this region of sheared E(sub r) exhibits the greatest increase in impurity ion poloidal rotation velocity and the greatest reduction in plasma fluctuations. A transport barrier is formed in this same region of E times B velocity shear as is signified by large increases in the observed gradients of the ion temperature, the carbon density, the electron temperature and electron density. The development of the region of sheared E(sub r), the increase in impurity ion poloidal rotation, the reduction in plasma turbulence, and the transport barrier all occur simultaneously at the L-H transition. Measurements of the radial electric field, plasma turbulence, thermal transport, and energy confinement have been performed for a wide range of plasma conditions and configurations. The results support the supposition that the progression of improving confinement at the L-H transition, into the H-mode and then into the VH-mode can be explained by the hypothesis of the suppression of plasma turbulence by the increasing penetration of the region of sheared E times B velocity into the plasma interior. DOE

N94-23808 Department of Energy, Washington, DC. Advanced Physics and Technology Div.
FUSION PLASMA THEORY PROJECT SUMMARIES
Oct. 1993 107 p Limited Reproducibility: More than 20% of this document may be affected by poor print
(DE94-001712; DOE/ER-0603T) Avail: Issuing Activity (Department of Energy (DOE))

This Project Summary book is a published compilation consisting of short descriptions of each project supported by the Fusion Plasma Theory and Computing Group of the Advanced Physics and Technology Division of the Department of Energy, Office of Fusion Energy. The summaries contained in this volume were written by the individual contractors with minimal editing by the Office of Fusion Energy. Previous summaries were published in February of 1982 and December of 1987. The Plasma Theory program is responsible for the development of concepts and models that describe and predict the behavior of a magnetically confined plasma. Emphasis is given to the modelling and understanding of the processes controlling transport of energy and particles in a toroidal plasma and supporting the design of the International Thermonuclear Experimental Reactor (ITER). A tokamak transport initiative was begun in 1989 to improve understanding of how energy and particles are lost from the plasma by mechanisms that transport them across field lines. The Plasma Theory program has actively participated in this initiative. Recently, increased attention has been given to issues of importance to the proposed Tokamak Physics Experiment (TPX). Particular attention has been paid to containment and thermalization of fast alpha particles produced in a burning fusion plasma as well as control of sawteeth, current drive, impurity control, and design of improved auxiliary heating. In addition, general models of plasma behavior are developed from physics features common to different confinement geometries. This work uses both analytical and numerical techniques. The Fusion Theory program supports research projects at U.S. government laboratories, universities and industrial contractors. Its support of theoretical work at universities contributes to the office of Fusion Energy mission of training scientific manpower for the U.S. Fusion Energy Program. DOE

N94-24293# Institute of Plasma Physics, Prague (Czechoslovakia).
IPP PRAGUE CONTRIBUTIONS TO THE IAEA TECHNICAL COMMITTEE MEETING ON RESEARCH USING SMALL TOKAMAKS
Jan. 1993 31 p Meeting held in Wurzburg, Germany, 28-29 Sep. 1992
(IPPCZ-329) Avail: CASI HC A03/MF A01

Reports include the following: 'Correlation and Dimensional Analysis of Density Fluctuations on CASTOR Tokamak'; 'Regimes with Improved Particle Confinement on CASTOR Tokamak'; 'Hard X-ray Intensity Reduction during Lower Hybrid Current Drive Experiments'; and 'Diagnostic Arc Source of Neutral Lithium Beam.' CASI

N94-24306# National Inst. for Fusion Science, Nagoya (Japan).
SOME THEORETICAL PROBLEMS OF MAGNETIC DIAGNOSTICS IN TOKAMAKS AND STELLARATORS
V. D. Pustovitov (Kurchatov, I. V. Inst. of Atomic Energy, Moscow, USSR.) Dec. 1993 22 p Submitted for publication
(NIFS-262) Avail: CASI HC A03/MF A01

The main problem of magnetic diagnostics is discussed: which plasma characteristics can be determined from magnetic measurements in tokamaks and stellarators? The reasons are elucidated as to why diamagnetic measurements are reliable and easily interpreted. We also discuss the capabilities of diagnostics based on the measurements of poloidal fields outside the plasma. Author

N94-24358# National Inst. for Fusion Science, Nagoya (Japan).
PELLET ABLATION IN THE LARGE HELICAL DEVICE
Boris V. Kuteev (Kalinin, M. I. Polytechnical Inst., Leningrad, USSR.) Nov. 1993 60 p Original contains color illustrations
(NIFS-260) Avail: CASI HC A04/MF A01

In the program of physical studies on the Large Helical Device (LHD) injection of several hydrogen and deuterium pellets is foreseen. Injection of impurity pellets also may be useful for the plasma diagnostics. The pellet penetration into the LHD plasma is analyzed. In part 1, the present status of the ablation theory and experiment is discussed and an ablation model is formulated. It takes into account the energy distribution of the particles (both electrons and ions) participating in the ablation process, electrostatic effects of the cloud charging and changes of the pellet form during ablation. Plasma shielding effects are not significant in the ablation. The ablation model is compared with the experiments on T-10, JET, TFTR, Heliotron-E, and Tore Supra in part 2. Finally, in part 3, several regimes of the pellet injection into the LHD plasma are simulated including multiple-pellet sequence injection. Optimization of the injection regime is discussed.
Author (revised)

N94-24456# National Inst. for Fusion Science, Nagoya (Japan).
TEMPORAL BEHAVIOR OF THE ELECTRON DENSITY PROFILE DURING LIMITER BIASING IN THE HYBTOK-2 TOKAMAK
S. Sasaki (Nagoya Univ., Japan.), Y. Uesugi (Nagoya Univ., Japan.), S. Takamura (Nagoya Univ., Japan.), H. Sanuki, and K. Kadota (Nagoya Univ., Japan.) Nov. 1993 16 p Sponsored by Ministry of Education, Science and Culture
(NIFS-257) Avail: CASI HC A03/MF A01

A rapid change in the detailed edge electron density profile during positively biased limiter experiment is obtained with high temporal resolution of approximately 20 microns using a laser blow-off lithium beam probe technique in HYBTOK-II tokamak. The transient change in the electron density profile and the movement of the position where a steep gradient is formed are experimentally observed. The temporal behavior of the electron density profile correlates well with reductions in the biasing current and the H-alpha emission in the scrape-off layer, and the suppression of electrostatic fluctuations near the edge of the core region.
Author (revised)

N94-24458# National Inst. for Fusion Science, Nagoya (Japan).
PROPOSAL OF MODULAR HELIOTRON: ADVANCED MODULAR HELICAL SYSTEM COMPATIBLE WITH CLOSED HELICAL DIVERTOR
Kozo Yamazaki Nov. 1993 30 p
(NIFS-261) Avail: CASI HC A03/MF A01

A new modular helical configuration named 'Modular Heliotron' with clean and efficient helical magnetic divertor is proposed as an extension of the present conventional design of the continuous helical coil system. The sectored helical coils on one plane of the torus and the sectored returning vertical field coils on the other plane are combined. This coil system produces magnetic surfaces nearly equivalent to those of the $l=2$ helical system with one-pair of poloidal coils, and overcomes the defects of construction and maintenance difficulties of the continuous coil systems. This concept satisfies the compatibility between the coil modularity and the sufficient divertor-space utilization, different from previous modular coil designs. The allowable length of the gap between each modular coil is clarified to keep good magnetic surfaces. Typical examples of the reactor coil configuration are described as an extension of the LHD (Large Helical Device) configuration.
Author (revised)

N94-24502# Lawrence Livermore National Lab., CA.
STABILIZATION OF THE EXTERNAL KINK AND OTHER MHD ISSUES
J. P. Freidberg (Massachusetts Inst. of Tech., Cambridge.), R. J. Goldston, S. C. Jardin (Princeton Univ., NJ.), G. H. Neilson (Oak Ridge National Lab., TN.), and M Rosenbluth 13 Aug. 1993 28 p Presented at the General Atomics Workshop, San Diego, CA, 23-25 Jun. 1993
(Contract W-7405-eng-48)
(DE94-001541; UCRL-JC-114754; CONF-9306267-1) Avail: CASI HC A03/MF A01

An MHD workshop entitled 'Stabilization of the External Kink and Other MHD Issues' was held 23-25 June 1993. This is a summary report of activities at that workshop, structured to respond to the three questions in the charge. The experimental and theoretical status of these issues, and the R&D needs in each area, are addressed. We discuss the potential impact on the TPX and ITER programs of these issues. The workshop participants came from a broad and diverse range of institutions in the fusion program, including international participants. As a result, we believe the summary here reflects some consensus of the community on these very important program issues, and that the TPX and ITER programs will benefit from these discussions. The title of the workshop was chosen to indicate both our knowledge and our uncertainty of MHD phenomena limiting (beta) and causing disruptions in tokamaks. The purpose was to bring together theorists and experimentalist in order to assess our current understanding of the external kink instability at high (beta) and to assess the potential for passive or active stabilization of the dominant modes. We also outlined the R&D needed for TPX and other future devices. Not only was the preworkshop theory clearly presented, but significant new theoretical results were described for the first time, emphasizing the roles of the resistivity of the cold edge plasma and of the plasma toroidicity in the stability criteria. Excellent reviews of the effects of the vessel walls on plasma stability were given as related to the D3-D, TFTR, JET, PBX-M, and HBT-EP experiments. These results are generally consistent with the more complete theory.
DOE

N94-24504# Massachusetts Inst. of Tech., Cambridge. Plasma Fusion Center.
PLASMA INITIATION IN A TOKAMAK WITH CONDUCTING SUPERSTRUCTURE: FIRST RESULTS FROM ALCATOR C-MOD
I. Hutchinson, R. Boivin, P. Bonoli, C. Fiore, J. Goetz, S. Golovato, R. Granetz, M. Greenwald, S. Horne, and A. Hubbard et al Jul. 1993 4 p Presented at the 20th European Conference on Controlled Fusion and Plasma Physics, Lisbon, Portugal, 26-30 Jul. 1993
(Contract DE-AC02-78ET-51013)
(DE94-001565; DOE/ET-51013/303; PFC/CP-93-1; CONF-930720-22)
Avail: CASI HC A01/MF A01

Alcator C-MOD is a compact high field tokamak with capability for high current shaping and closed and open diverters. Full tokamak operation was begun in May 1993 at 5T toroidal field, and plasmas lasting up to 0.4 seconds have been obtained so far. The tokamak's design includes a thick stainless-steel vacuum vessel that is toroidally continuous with resistance about 40 micro-Ohms. The stainless-steel superstructure supporting the toroidal field coil is even more massive, and likewise has no toroidal breaks, primarily because structural strength would suffer. As a result, very large toroidal eddy currents are induced in the structures, especially during current initiation when the loop voltage is high. Future large experiments, such as ITER, are likely to adopt design approaches with comparable conducting structures. Despite the large eddy currents, which can reach 1 MA in Alcator C-MOD, reliable plasma initiation has been established by appropriate adjustment of the time evolution of the coil currents to cancel the passive contribution and obtain the desired field structure. Detailed diagnosis of the full magnetic field structure is necessary to do the adjustment; the field structure is then known in some detail, and its effects on the shape and stability during the current ramp have been studied. Flat-top plasma currents are presently up to 0.4 MA, and elongated and diverted plasmas have been obtained, as well as more circular limited configurations.
DOE

N94-24519# Los Alamos National Lab., NM.
START-UP SIMULATIONS OF THE PULSAR PULSED TOKAMAK REACTOR
K. A. Werley and C. G. Bathke 1993 5 p Presented at the Symposium on Fusion Engineering, Hyannis, MA, 11-15 Oct. 1993
(Contract W-7405-eng-36)
(DE94-002634; LA-UR-93-3599; CONF-931018-56) Avail: CASI HC A01/MF A01

Start-up conditions are examined for a pulsed tokamak reactor that uses only inductively driven plasma current (and bootstrap current). A zero-dimensional (profile-averaged) model containing plasma power and particle balance equations is used to study several aspects of plasma start-up, including: (1) optimization of the start-up pathway; (2) tradeoffs of auxiliary start-up heating power versus start-up time; (3) volt-second consumption; (4) thermal stability of the operating point; (5) estimates of the diverter heat flux and temperature during the start-up transient; (6) the sensitivity of the available operating space to allowed values of the H confinement factor; and (7) partial-power operations.
DOE

N94-24546# Sandia National Labs., Albuquerque, NM.
THE CHEMISTRY OF PARTICULATE FORMATION IN FLUOROCARBON PLASMAS
Richard J. Buss and Willard A. Hareland 1993 16 p Presented at the North Atlantic Treaty Organization Advanced Research Workshop, Toulouse, France, 30 Aug. - 3 Sep. 1993
(Contract DE-AC04-94AL-85000)
(DE94-001500; SAND-93-2057C; CONF-9308151-2) Avail: CASI HC A03/MF A01

The production, suspension, and transport of fluorocarbon particulates in rf discharges have been studied using in situ laser light scattering and ex situ chemical analysis. The time evolution of the spatial distribution of suspended particles was obtained by 2-D imaging of the scattered light. The chemistry of the discharge was varied by the use of a range of pure fluorocarbon gases and mixtures with argon, oxygen, and hydrogen-containing molecules. The addition of hydrogen to a fluorocarbon discharge increases the rate of formation of particles, although these powders are found by FTIR to contain negligible hydrogen. Particle formation rates correlate with polymer deposition rates and are independent of apparatus history. It is proposed that this is a clear example of gas-phase rather than surface processes leading to particle nucleation and growth. DOE

N94-24623# National Inst. for Fusion Science, Nagoya (Japan).
DESIGN OF CENTRAL CONTROL SYSTEM FOR LARGE HELICAL DEVICE (LHD)
K. Yamazaki, H. Kaneko, S. Yamaguchi, K. Y. Watanabe, Y. Taniguchi, and O. Motojima et al Nov. 1993 16 p Presented at the International Conference on Accelerator and Large Experimental Physics Control Systems (ICALEPCS 1993), Berlin, Germany, 18-22 Oct. 1993
(NIFS-258) Avail: CASI HC A03/MF A01

The world's largest superconducting fusion machine, LHD (Large Helical Device), is under construction in Japan, aiming at steady state operations. Its basic control system consists of UNIX computers, FDDI/Ethernet LAN's, VME multiprocessors, and VxWorks real-time operating system. For flexible and reliable operations of the LHD machine, a cooperative distributed system with more than 30 pieces of experimental equipment is controlled by the central computer and the main timing system, and is supervised by the main protective interlock system. Intelligent control systems, such as applications of fuzzy logic and neural networks, are to be adopted for flexible feedback control of plasma configurations besides the classical PID control scheme. Design studies of the control system and related research and development programs with coil-plasma simulation systems are now being performed. The construction of the LHD Control Building on a new site will begin in 1995 after finishing the construction of the LHD Experimental Building, and the hardware construction of the LHD central control equipment will be started in 1996. A first plasma production by means of this control system is expected in 1997. Author (revised)

N94-24628# Los Alamos National Lab., NM.
TOKAMAK PHYSICS EXPERIMENT (TPX) COST AND PERFORMANCE TRADE STUDIES USING SUPERCODE
R. L. Miller, J. D. Galambos (Oak Ridge National Lab., TN.), S. W. Haney (Lawrence Livermore National Lab., CA.), L. J. Perkins (Lawrence Livermore National Lab., CA.), and J. Mandrekas (Georgia Inst. of Tech., Atlanta.) 1993 5 p Presented at the Symposium on Fusion Engineering, Hyannis, MA, 11-15 Oct. 1993
(Contracts W-7405-eng-36; DE-AC05-84OR-21400; W-7405-eng-48; DE-FG05-87ER-52141)
(DE94-002720; LA-UR-93-3677; CONF-931018-42) Avail: CASI HC A01/MF A01

The Tokamak Physics Experiment (TPX) has been proposed to demonstrate steady-state operation and to develop advanced performance in terms of beta and energy confinement. Major TPX cost drivers and the impact of physics and technology constraints and options on operating scenarios are identified. Key trade and sensitivity studies performed using SuperCode are summarized. DOE

N94-24746# General Atomics Technologies Corp., San Diego, CA.
MEASUREMENT OF ELECTRON TEMPERATURE AND DENSITY IN THE DIII-D NEUTRAL BEAM ION SOURCE ARC CHAMBER
D. H. Kellman, J. Busath, and R. Hong Oct. 1993 5 p Presented at the Symposium on Fusion Engineering, Hyannis, MA, 11-15 Oct. 1993
(Contract DE-AC03-89ER-51114)
(DE94-001099; GA-A-21398; CONF-931018-4) Avail: CASI HC A01/MF A01

A swept-bias Langmuir probe diagnostic was employed with the DIII-D neutral beam ion source in an effort to study the effects of filament temperature, arc power, and backstreaming energetic electrons on the electron temperature and density of the arc discharge inside the ion source arc chamber. The arc chamber contains six Langmuir probes biased with a negative dc voltage. These probes provide a feedback signal for regulation of the arc power supply, and give a relative indication of plasma uniformity within the arc chamber. For this study, one probe was reconnected to a voltage-sweeping power supply, and probe current versus voltage characteristics were generated. These characteristics provided the information necessary to calculate electron temperature and density. With arc discharge only, the results demonstrated that an filament temperature increases, so does electron density. Electron temperature decreases at a faster rate, however, as required to maintain constant ion maturation current (regulated by the arc power supply). The results also demonstrated that increasing arc power (through control of the arc power supply) results in higher electron temperature and density. Experiments were also performed with probe voltage sweeps during beam extraction, at various accelerator voltage levels and at different delay times after beam turn-on with a fixed acceleration voltage. These results indicated an increase in electron temperature and density as acceleration voltage is increased. However, nearly identical trends result when arc discharges are produced at the same parameter settings as during these beams, but without beam extraction. This indicates minimal influence of backstreaming energetic electrons on electron temperature and density in the arc chamber. Temperature and density also remain fairly constant over time during a long beam pulse. DOE

N94-24756# General Atomics Technologies Corp., San Diego, CA.
INVESTIGATION OF THE HEAT HANDLING CAPABILITIES OF DIII-D NEUTRAL BEAMLINE INTERNAL COMPONENTS
J. C. Phillips, C. B. Baxi, and R. Hong Oct. 1993 6 p Presented at the Symposium on Fusion Engineering, Hyannis, MA, 11-15 Oct. 1993
(Contract DE-AC03-89ER-51114)
(DE94-001107; GA-A-21409; CONF-931018-17) Avail: CASI HC A02/MF A01

The current D3-D neutral beam system is a nominal five second pulse length upgrade of a previous design rated for only 500 msec operation. While the ion sources are rated for 60 sec operation, in practice pulse lengths are limited both by the beamline internal components ability to handle the fraction of the power which is scraped off and by the power supplies ability to provide pulse lengths of greater than 5 sec. This paper examines the capability of the existing D3-D neutral beamline heat removing components both in terms of present and desired operating parameters. To date, at 2.5 MW per ion source, pulses are limited to 3.5 sec by beamline internal components, while at lower ratings of 2.0 MW per ion source, up to 5 sec pulses have been achieved. Recent advances and demonstration of the extraction of 3.5 MW per D3-D ion source give an even wider window of operating conditions. A full series of beamline thermocouple data has been collected to determine the heat loading and implied surface temperatures for the various D3-D neutral beamline internal components. These data will be presented along with an analysis of the needs for specific component upgrades, given a desire for 10 sec operation. DOE

N94-24949# Berkeley Research Associates, Inc., CA.
X RAY SIMULATOR THEORY SUPPORT Technical Report, 20 Oct. 1987 - 30 Oct. 1991
James L. Geary, Jr., Robert J. Kares, Lan-Lan Chen, and Nino R. Pereira 1 Nov. 1993 247 p
(Contract DNA001-88-C-0006)
(AD-A273613; BRA-92-WO24R; DNA-TR-92-6) Avail: CASI HC A11/MF A03

This report contains the theory, analyses and computations performed between 20 Oct. 1987 and 30 Oct. 1991 on plasma filled diodes, opening switches, and z-pinches. This includes the first quantitative estimate of plasma blowoff from surfaces in plasma opening switches, the first nine-dependent particle-in-cell simulation of a (one-dimensional) plasma opening switch (or plasma-filled diode), the first two-dimensional dynamical model of a plasma diode, and germinal reviews of z-pinch and vacuum spark research. DTIC

N94-25190*# Ohio State Univ., Columbus.
MECHANISMS OF ANODE POWER DEPOSITION IN A LOW PRESSURE FREE BURNING ARC Final Report
George C. Soulas and Roger M. Myers (Sverdrup Technology, Inc., Brook Park, OH.) Jan. 1994 28 p Presented at the 23rd International Electric Propulsion Conference, Seattle, WA, 13-16 Sep. 1993; sponsored by AIAA, AIDAA, DGLR, and JSASS
(Contract NAS3-25266; RTOP 506-42-31)
(NASA-CR-194442; E-8303; NAS 1.26:194442; IEPC-93-194) Avail: CASI HC A03/MF A01

Anode power deposition is a dominant power loss mechanism for arc jets and MPD thrusters. In this study, a free burning arc experiment was operated at pressures and current densities similar to those in arc jets and MPD thrusters in an attempt to identify the physics controlling this loss mechanism. Use of a free burning arc allowed for the isolation of

independent variables controlling anode power deposition and provided a convenient and flexible way to cover a broad range of currents, anode surface pressures, and applied magnetic field strengths and orientations using an argon gas. Test results showed that anode power deposition decreased with increasing anode surface pressure up to 6.7 Pa (0.05 torr) and then became insensitive to pressure. Anode power increased with increasing arc current while the electron number density near the anode surface increased linearity. Anode power also increased with increasing applied magnetic field strength due to an increasing anode fall voltage. Applied magnetic field orientation had an effect only at high currents and low anode surface pressures, where anode power decreased when applied field lines intercepted the anode surface. The results demonstrated that anode power deposition was dominated by the current carrying electrons and that the anode fall voltage was the largest contributor. Furthermore, the results showed that anode power deposition can be reduced by operating at increased anode pressures, reduced arc currents, and applied magnetic field strengths and with magnetic field lines intercepting the anode.
Author (revised)

N94-25241# Technische Univ., Eindhoven (Netherlands).
EXCITATION BALANCES AND TRANSPORT IN AN INDUCTIVELY COUPLED PLASMA Ph.D. Thesis
Franciscus Henricus Fey 1993 137 p
(ETN-94-95330) Avail: CASI HC A07/MF A02

A series of articles concerning the excitation balances, the transport processes, and their mutual influences in an Inductively Coupled Plasma (ICP) are presented. An ICP is a plasma that is fed with energy by means of an electromagnetic field. It is created in a torch that is placed inside an RF coil. A spectrochemical ICP is concentrated upon. The articles presented concern the following: an experimental study of the instantaneous and the delayed responses of line intensities to power interruption; the response of Li one line intensities to power interruption; a collisional radiative model of Li, which is extended with transport; a model for the evaporation of the droplets and a fluid model for the zone in which the droplets are injected; the characteristic features of free electrons in the active zone; the measurement of the drift velocity of the plasma and the corresponding energy losses. ESA

N94-25285 Technische Univ., Eindhoven (Netherlands).
A RELATIVISTIC THEORY ON WAVE PROPAGATION IN INHOMOGENEOUS MAGNETOPLASMAS Ph.D. Thesis
Maria Johanna vanBruggen-Kerkhof 1992 80 p Limited Reproducibility: More than 20% of this document may be affected by microfiche quality
(ETN-94-95322) Avail: CASI HC A05

Several problems of wave propagation in inhomogeneous plasmas are discussed. All the topics stem from the physics of fusion plasmas, such as those studied in tokamaks. The mathematical modeling of such a plasma, including both relativistic effects as well as the inhomogeneity of the plasma, is considered. Some elementary concepts from the theory of plasma physics and wave propagation are treated. Solution methods for the time independent Vlasov-Maxwell system for an inhomogeneous relativistic plasma are considered. The starting point is a plasma model that allows different temperatures for electrons and ions. The possibility of multiple ionization is also taken into account. Wave properties in a homogeneous magnetic field and then in an inhomogeneous magnetic field are considered. ESA

N94-25300# Technische Univ., Eindhoven (Netherlands).
MODELLING OF THERMAL ARGON PLASMAS Ph.D. Thesis
Daniel Anton Benoy 1993 153 p
(ETN-94-95363) Avail: CASI HC A08/MF A02

The construction of a two dimensional time independent plasma simulation model is described. Conditions for the validity of the hydrodynamic approach in the modeling of plasmas are considered. A cut-off procedure for numerical collisional radiative (CR) models is developed and is based on knowledge of the excitation flow in the collision dominated part of an atomic system as revealed by analytical models. The model is applied to ionizing and recombining argon plasma. A CR model, in which a hybrid cut-off technique is used, is applied to recombining plasmas to study the atomic state distribution and the recombination effect. The total radiative loss in atmospheric argon plasmas is calculated, admitting for deviation from local thermal equilibrium. The source terms of the particle, momentum, and energy transport equations are expressed in such a way that they can be used in the numerical model. Physical transport equations for the macroscopic description of thermal plasmas are formulated. ESA

N94-25327# Oxford Univ. (England). Dept. of Engineering Science.
FLUID VELOCITY AND ELECTROMAGNETIC FORCES MEASURED BY A ROTATING LANGMUIR PROBE IN THE SCRAPE OFF LAYER OF JFT-2M
B. M. Annaratone, T. Shoji (Japan Atomic Energy Research Inst., Tokai.), H. Maeda (Japan Atomic Energy Research Inst., Tokai.), S. Ohdachi (Tokyo Univ., Japan.), and H. Tamai (Japan Atomic Energy Research Inst., Tokai.) 1992 24 p Sponsored in part by Japan International Science and Technology Exchange Center, Japan
(OUEL-1968/92; ETN-94-95154) Avail: CASI HC A03/MF A01

Measurements obtained by the technique of an assembly of planar Langmuir probes rotating in the scrape off layer of JFT-2M are described. The probes scan the radial direction and can rotate 360 deg around a radius so measuring the direction of the magnetic field and of the density of current in the magnetic surfaces. Experiments with and without divertor biasing show different configurations of the electric fields and of the ion saturation current. Results show that: the probe identifies the direction of the local ion density of current; electrons flow in the verse opposite to the ion flux; the ion current has an angle respect to the magnetic field; the j by B force is always confining; with a divertor negative bias the toroidal current flows opposite to the main plasma current in a narrow layer where high radial electric fields appear. The estimate of the amplitude of the ion density of current is deduced from the ratio of the upstream to the downstream ion saturation current. The fluid equation for electrons and ions can, to some extent, be solved in steady state and the value of fluid velocity for the electrons and pressure gradient for the ions are calculated.
ESA

N94-25329# China Nuclear Information Centre, Beijing.
THE ANOMALOUS TRANSPORT CAUSED BY PARTICLES TRANSVERSE DRIFT
Mao-Quan Wang (Academia Sinica, Beijing, China.) Jan. 1992 11 p
(DE93-613685; CNIC-00569; ASIPP-0028) Avail: CASI HC A03/MF A01 (US Sales Only)

The plasma anomalous transport caused by particles transverse drift in a system has been completed, in which the magnetic surfaces are disrupted by a stochastic perturbation of magnetic field. In ergodic region the motion equation can be written in Langevin equation and diffusion coefficient D perpendicular can be obtained from Fokker-Planck model. Comparing with another diffusion coefficient D perpendicular derived by the diffusion of field lines in the quasilinear approximation, the D perpendicular obtained from Fokker-Planck model has the similar form and same order of magnitude. The two D perpendicular's are supplement to each other. Only when they are combined into one, will the result be completed. DOE

N94-25330# China Nuclear Information Centre, Beijing.
NUMERICAL SIMULATION AND ANALYSIS OF EXPERIMENTAL RESULTS ON STIMULATED RAMAN SCATTERING IN LASER-PLASMA HOHLRAUM TARGETS
Jia-Tai Zhang (Academia Sinica, Beijing, China.), Lin-Bao Xu (Academia Sinica, Beijing, China.), Tie-Qiang Chang (Academia Sinica, Beijing, China.), Shu-Gui Zhang (Academia Sinica, Beijing, China.), Xiao-Bo Nie (Academia Sinica, Beijing, China.), Shi-Hong Wang (Academia Sinica, Beijing, China.), and Wei-Xing Wang (Academia Sinica, Beijing, China.) Aug. 1991 16 p In CHINESE
(DE93-613719; CNIC-00513; IAPCM-0018) Avail: CASI HC A03/MF A01 (US Sales Only)

By using 3/2-D particle simulation code, the stimulated Raman scattering (SRS) in planar and Hohlraum targets is studied. Evaluations of linear growth rate of scattering electromagnetic waves and Langmuir waves and nonlinear saturation are obtained in detail. Other results such as electron distribution function, electron temperature, and the fraction of super hot-electrons produced by SRS are also given. The density distribution in the underdense coronal plasma region is determined by the analysis of SRS spectrum. These theoretical results are in agreement with experimental observations from the Shenguang-12 Nd-glass laser facility. DOE

N94-25331# China Nuclear Information Centre, Beijing.
LHCD (LOW HYBRID CURRENT DRIVE) EXPERIMENT ON THE HT-6B TOKAMAK
Jan. 1992 10 p Prepared in cooperation with Academia Sinica, Beijing, China
(DE93-613720; CNIC-00577; ASIPP-0030) Avail: CASI HC A02/MF A01 (US Sales Only)

LHCD (lower hybrid current drive) experiment was performed on the HT-6B tokamak recently. The RF (radio frequency) system consisted of a 100 kW, 2.45 GHz power source and a multi-junction antenna with relative narrow power spectrum. At relative high density, eta approximately = 0.2 (10(exp 19)m(exp -2) kA/kW) was achieved. The MHD modes and sawteeth were strongly affected by LHW (low hybrid wave). DOE

N94-25333 China Nuclear Information Centre, Beijing.
INVESTIGATION AND APPLICATION OF MICROWAVE ELECTRON CYCLOTRON RESONANCE PLASMA PHYSICAL VAPOUR DEPOSITION
Zhao-Xing Ren (Academia Sinica, Beijing, China.), Yan-Ya Sheng (Academia Sinica, Beijing, China.), Yi-Cai Shi (Academia Sinica, Beijing, China.), Hai-Hu Wen (Academia Sinica, Beijing, China.), and Xiao-Wen Cao (Academia Sinica, Beijing, China.) Jun. 1991 15 p Limited Reproducibility: More than 20% of this document may be affected by poor print
(DE93-613909; CNIC-00511; ASIPP-0027) Avail: Issuing Activity (Department of Energy (DOE)) (US Sales Only)

The evaporating deposition of Ti film and Cu film by using microwave electron cyclotron resonance (ECR) technique was investigated. It deposition rate was about 50 nm/min and the temperature of the substrate was 50 to approximately 150 C. The thin amorphous films with strong adherent force were obtained. The sputtering deposition with ECR plasma was studied by employing higher plasma density and ionicity and negative substrate potential to make YBaCuO superconducting film. Its film was compact and amorphous with a thickness of 1.0 micron and the deposition rate was about 10 nm/min. The results show that this technique can initiate a high density and high ionicity plasma at lower gas pressure (10(exp -2) to approximately 10(exp -3)Pa). This plasma is the most suitable plasma source in thin film deposition process and surface treatment technique. DOE

N94-25343# International Centre for Theoretical Physics, Trieste (Italy).
MODIFICATION IN THE KINETIC SOLUTION FOR MAGNETIZED PLASMAS
C. Y. Chen Sep. 1992 6 p
(DE93-613687; IC-92/274) Avail: CASI HC A02/MF A01 (US Sales Only)

By relating to the guiding-center drift equation, effective forces are introduced into the linearized Vlavov equation, which leads to modification in the standard kinetic solution for uniformly magnetized plasmas. In the newly-proposed formalism, all the convective (drift) currents induced by E x B(sub 0), nabla B and (n(center dot)nabla)n are properly formulated. DOE

N94-25344# China Nuclear Information Centre, Beijing.
EFFECT OF LHCD (LOW HYBRID CURRENT DRIVE) ON TEARING MODE INSTABILITY
Zheng-Ming Sheng (Academia Sinica, Beijing, China.), Nong Xiang (Academia Sinica, Beijing, China.), and Guo-Yang Yu (Academia Sinica, Beijing, China.) Jan. 1992 8 p
(DE93-613700; CNIC-00576; ASIPP-0029) Avail: CASI HC A02/MF A01 (US Sales Only)

Effect of LHCD (low hybrid current drive) on tearing mode instability is investigated through both kinetic and MHD approaches. In linear kinetic theory, the response of the fast electrons driven by LHCD to the tearing mode perturbations results in reductions of both the growth rate and the width of the perturbative layer of tearing mode in collisional as well as semi-collisional regimes. From MHD theory and LHCD simulation in tokamak geometry, it is shown that LHCD leads to both modification of the current profile and outward shift of the rational surfaces and hence to variation of (delta) of the tearing mode. Mostly LHCD plays a stabilizing role against tearing modes. However, under some conditions considered, LHCD can stabilize tearing modes in higher-q(sub a) plasma while destabilize it in lower-q(sub a) case, which is in a qualitative agreement with some experimental observation. DOE

N94-25439# Technische Univ., Eindhoven (Netherlands).
PLASMA SPRAYED THERMAL BARRIER COATINGS: PRODUCTION, CHARACTERIZATION AND TESTING Ph.D. Thesis
Adriaan Thomas Jacqu Verbeek 1992 253 p
(Contract IOP-TK-86.B051)
(ISBN-9-03-860082-8; ETN-94-95316) Avail: CASI HC A12/MF A03

A research program on thermal barrier coatings which covered the whole field of production, characterization, and testing of plasma sprayed thermal barrier coatings, consisting of a metallic bondcoat and a ceramic topcoat is described. The goal was to produce a thermal barrier coating with both a high thermal shock strength and a high erosion resistance. To obtain this goal, all factors influencing the characteristics and the properties of the ceramic topcoat were investigated by experiments on the basis of theoretical models. The behavior of single zirconia particles during the plasma spray process is described. The formation of cracks in plasma sprayed barrier coating is examined using acoustic emission evaluation, combined with the three point bending test. Results of thermal shock and erosion tests carried out on the different types of coatings are presented. ESA

N94-23655*# Northeastern Univ., Boston, MA. Dept. of Mechanical Engineering.
MIXING AND UNMIXEDNESS IN PLASMA JETS 1: NEAR-FIELD ANALYSIS
Olusegun J. Ilegbusi *In* NASA. Lewis Research Center, The Fifth Annual Thermal and Fluids Analysis Workshop Nov. 1993 p 307-328 (For primary document see N94-23634 06-34)
Avail: CASI HC A03/MF A04; 5 functional color pages

76 SOLID-STATE PHYSICS

Includes superconductivity.

For related information, see also *33 Electronics and Electrical Engineering* and *36 Lasers and Masers.*

N94-22717# Sandia National Labs., Albuquerque, NM.
ULTRAVIOLET PHOTOSULFIDATION OF III-V COMPOUND SEMICONDUCTORS FOR ELECTRONIC PASSIVATION
K. R. Zavadil, C. I. H. Ashby, A. J. Howard, and B. E. Hammons 1993 16 p Presented at the 40th National Symposium of the American Vacuum Society (AVS), Orlando, FL, 15-19 Nov. 1993
(Contract DE-AC04-94AL-85000)
(DE94-001417; SAND-93-1107C; CONF-9311104-2) Avail: CASI HC A03/MF A01

A new vacuum-compatible passivation technique for 3-5 compound semiconductors has been developed. Sulfur passivation of GaAs(100) is produced by ultraviolet photolytic deposition of a sulfide species from vapor phase elemental sulfur. Photoluminescence studies of the photosulfided GaAs reveal a degree of passivation greater than or equal to that produced by conventional (NH4)(sub 2)S solution treatment. X-ray Photoelectron Spectroscopy has shown that the sulfur resides on the surface as a single reduced sulfur species, either as sulfide of disulfide, indicating complete fragmentation of the S8 ring by UV light in proximity to the surface. The degree of photosulfidation depends strongly on surface preparation as demonstrated by the described surface oxide removal studies. DOE

N94-22730# Universiteit Twente, Enschede (Netherlands). Faculty of Applied Mathematics.
A NONLINEAR DEGENERATING PARABOLIC PROBLEM FROM THE THEORY OF TYPE 2 SUPERCONDUCTORS
B. H. Gilding and M. Vallentgoed Jan. 1993 39 p Sponsored by Netherlands Organization for Scientific Research
(MEMO-1112; ETN-94-94748) Avail: CASI HC A03/MF A01

A boundary value problem for a nonlinear partial differential equation is studied. This problem arises as a model for the current distribution in a multifilamentary wire in which the filaments consist of a type 2 superconducting material. The equation is ostensibly of parabolic type, but displays two types of degeneracy. The derivation of the model is explained. The existence and the uniqueness of a solution of the boundary value problem are proved. A comparison principle and some regularity results for its solution are established. The physical interpretation of the different results is discussed. ESA

N94-22864 Oak Ridge National Lab., TN.
HIGH-T(c) SUPERCONDUCTING SUPERLATTICES
R. F. Wood Jun. 1993 17 p Presented at the International Symposium on High-Tc Superconductivity and Its Applications, Cairo, Egypt, 4-16 Apr. 1993 Limited Reproducibility: More than 20% of this document may be affected by poor print
(Contract DE-AC05-84OR-21400)
(DE93-019200; CONF-9304191-3) Avail: Issuing Activity (Department of Energy (DOE))

Superlattices composed of YBa2CU3O7 and PrBa2Cu3O7 were studied extensively experimentally and several theoretical attempts to correlate the resistivity as a function of temperature with the superlattice structure have appeared in the literature. The theoretical interest in such structures comes about primarily because of insight into dimensionality effects, interlayer coupling, and interlayer charge redistribution in high-T(sub c) superconductors. On the experimental side, there are possibilities for device applications that are just now beginning to be explored. After an overview of the experimental work and a discussion of charge transfer calculations, a description of how the experimental data can be explained using a model that incorporates Kosterlitz-Thouless (vortex-antivortex unbinding) and Azlamazov-Larkin (fluctuation-enhanced conductivity) theories in the resistive transition region and charge-transfer effects, variable-range hopping, etc. in the normal state. Difficulty in disentangling charge transfer and dimensionality effects in determining the nominal transition temperature is pointed out and other mechanisms that influence the width of the resistive transition are considered. DOE

N94-22886# Argonne National Lab., IL.
HEAVY ION IRRADIATION OF BI-2223 SILVER-CLAD TAPES FOR SUPERCONDUCTING CURRENT DENSITY ENHANCEMENT
A. P. Malozcnoff (American Superconductor Corp., Watertown, MA.), W. L. Carter, G. N. Riley, Jr. (American Superconductor Corp., Watertown, MA.), R. Wheeler, IV, M. A. Kirk, L. Civale (International Business Machines Corp., Yorktown Heights, NY.), and A. D. Marwick (International Business Machines Corp., Yorktown Heights, NY.) 1993 8 p Presented at the International Cryogenic Engineering Conference and International Cryogenic Materials Conference, Albuquerque, NM, 12-16 Jul. 1993
(Contract W-31-109-eng-38)
(DE93-017416; ANL/MCT/CP-80158; CONF-930703-9) Avail: CASI HC A02/MF A01

Silver-clad composite tapes of Bi(Pb)SrCaCuO-2223 were irradiated with 1 GeV Au(23+) ions perpendicular to the tape plane, creating columnar tracks with 10 nm diameter. Detailed transmission electron microscopy shows continuous columns, but with variations in the track thickness of +/- 2 nm. Magnetic hysteresis measurements show substantial enhancement of superconducting current density at most temperatures and fields. Granular and nongranular models for the origin of the magnetic signals are discussed. The results indicate the potential for further performance improvement in high temperature superconducting wire technology, as well as limits in the high-field performance at 77 K. DOE

N94-22905# Laboratoire d'Automatique et d'Analyse des Systemes, Toulouse (France).
FLOATING WELL BASED DESIGN METHODOLOGY AIMED TO IMPROVE LATCH-UP IMMUNITY IN A CMOS/DMOS SMART POWER TECHNOLOGY Ph.D. Thesis - Toulouse Univ. [IMMUNITE AU 'LATCH-UP' D'UNE TECHNOLOGIE DE PUISSANCE INTELLIGENTE CMOS/DMOS BASEE SUR UN CONCEPT DE PUITS FLOTTANT ET APPLICATIONS]
Manuel PuigVidal 1993 188 p In FRENCH Sponsored in part by Conseil Regional Midi-Pyrenees, France; Ministere de la Recherche et de la Technologie, Paris, France; and PROMETHEUS/PROCHIP program
(LAAS-93093; ETN-94-95187) Avail: CASI HC A09/MF A02

In order to improve the latch up immunity of Complementary Metal Oxide Semiconductors/Diffusion Metal Oxide Semiconductor (CMOS/DMOS) technology, a low cost solution based on a floating well concept is proposed. The deep P(plus) diffusion inherent to a DMOS structure is used to realize a ring that surrounds the NMOS transistor in the P well and slightly overlaps the source diffusion. A CMOS/DMOS technology was developed and a test vehicle designed and realized. Improvements in both static and dynamic latch up immunity with regard to standard CMOS structure are demonstrated by the experimental results. NMOS transistor analysis shows the deep P(plus) ring efficiency in evacuating parasitic currents and proper transistor performance. Two applications, photodetector and temperature detector, based on a floating well concept are proposed and validated in 2 micrometers CMOS technology. ESA

N94-22912# Argonne National Lab., Idaho Falls, ID.
ELECTRICAL TRANSPORT IN La(2-x)Sr(x)CuO(4-y)
R. J. Thorn 1992 10 p
(Contract W-31-109-eng-38)
(DE93-040885; ANL/CHM/PP-77691) Avail: CASI HC A02/MF A01

Variations of resistivity with temperature and composition of La(2-x)Sr(x)CuO(4-y) reported by Awana can be described quantitatively by an equation based on small Fermi energies (approximately 10(exp -4) eV) and small gap energies (approximately 10(exp -2 eV). DOE

N94-22919# Oak Ridge National Lab., TN.
SPIN-POLARON THEORY OF HIGH-T(c) SUPERCONDUCTIVITY. 2: ELECTRONIC STRUCTURE OF THE CuO2 PLANES
R. F. Wood Jun. 1993 13 p Presented at the International Symposium on High-Tc Superconductivity and Its Applications, Cairo, Egypt, 4-16 Apr. 1993
(Contract DE-AC05-84OR-21400)
(DE93-019197; CONF-9304191-4) Avail: CASI HC A03/MF A01

After an introductory discussion of electronic structure calculations for the CuO2 planes in the copper-oxide based high-T(sub c) superconductors, the method suggested by Slater for studying antiferromagnetic (AF) metals is described. In this method, as applied here, the chemical unit cell is doubled to form a magnetic unit cell which contains one Cu ion with predominantly up spin and one with predominantly down spin. Down spins are kept off up-spin sites, and conversely, by the introduction of a Hubbard U term. As a result, the band structure obtained is typical of that for a Mott-Hubbard (M-H) or, more generally, a charge transfer insulator. Conductivity in the a-b plane results when holes are introduced into the M-H valence band. The band structure as a function of the parameters in Koster-Slater type calculations is discussed and the Fermi surface is described. A calculation of the delocalization energy for spin-polaron formation is carried out within the context of the band calculations. DOE

N94-22920 Argonne National Lab., IL.
THE DE HAAS-VAN ALPHEN MEASUREMENTS IN Ba(0.6)K(0.4)BiO3
R. G. Goodrich (Louisiana State Univ., Baton Rouge.), C. Grienier (Louisiana State Univ., Baton Rouge.), and D. Hall (Louisiana State Univ., Baton Rouge.) Aug. 1993 9 p Presented at the Conference on Spectroscopies in Novel Superconductors, Santa Fe, NM, 17-19 Mar. 1993 Limited Reproducibility: More than 20% of this document may be affected by poor print
(Contracts W-31-109-eng-38; W-7405-eng-36)
(DE93-041169; ANL/MSD/CP-80681; LA-UR-93-3127; CONF-930367-9)
Avail: Issuing Activity (Department of Energy (DOE))

Measurements of dHvA were made on the 32 K cubic superconductor Ba(0.6)K(0.4)BiO3 using a 50 Tesla pulsed field magnet at NHMFL (Los Alamos) and a 18 T superconducting magnet (LSU). Data were taken with the magnetic field aligned along the (001) direction, at 1.5 to 3.9 K. The pulsed fields were high enough to drive the system well into the normal state. Analysis shows that the frequencies of the observed dHvA oscillations arise from a several Fermi surface sheets. One cross section was nearly identical with that predicted by a new LDA calculation. DOE

N94-22921 Argonne National Lab., IL.
CHARACTERIZATION OF CCD-BASED IMAGING X RAY DETECTORS FOR DIFFRACTION EXPERIMENTS
I. Naday, S. Ross, M. Kanyo, E. Westbrook, and M. Westbrook 1993 5 p Presented at the Synchrotron Radiation Instrumentation, Gaithersburg, MD, 23-26 Aug. 1993 Limited Reproducibility: More than 20% of this document may be affected by poor print
(Contract W-31-109-eng-38)
(DE93-041343; ANL/ECT/CP-80138; CONF-930824-6) Avail: Issuing Activity (Department of Energy (DOE))

High resolution CCD-based imaging detectors are successfully used in

X ray diffraction experiments. Some of the detectors are commercially available, others have been developed by research groups around the world. Reliable comparison of the performance must be based on thorough testing of all relevant characteristics of these detectors. We describe methods of measurement of detector parameters such as conversion gain, linearity, uniformity, point spread function, geometrical uniformity, dark current, and detective quantum efficiency. As an example for the characterization, test results of a single module fiber optic taper/CCD X ray detector will be presented. The projected performance of a large area, array detector consisting of nine CCD's and fiberoptic taper modules, will be given. This new detector (the 'Gold' detector) will be installed on Beamline X8C at the Brookhaven National Laboratory at the NSLS Synchrotron. DOE

N94-22925# Los Alamos National Lab., NM.
SPIN-HOLE DOPING IN THE KONDO INSULATOR Ce3Bi4Pt3 STUDIED BY NEUTRON SCATTERING
A. Severing (Institut Laue-Langevin, Grenoble, France.), T. Perring (Rutherford Appleton Lab., Chilton, England.), J. D. Thompson, Z. Fisk, and P. C. Canfield 1993 11 p Presented at the International Conference on Strongly Correlated Electron Systems, La Jolla, CA, 16-19 Aug. 1993
(Contract W-7405-eng-36)
(DE93-040107; LA-UR-93-2949; CONF-930865-4) Avail: CASI HC A03/MF A01

To investigate the effect of non-magnetic impurities on gap formation and stability in Kondo insulators, we have performed inelastic neutron scattering experiments on (Ce(1-x)La(x))3Bi4Pt3, with x = 0.0, 0.1, 0.25 and 1.0. Data were collected at the Rutherford spallation source using incident neutron energies of 30 and 100 MeV and with the sample temperature fixed at 10K, well below (Delta)g/k(sub B). The gap edge, defined from the rapid onset of scattering intensity, decreases quadratically with La content. However, the energy (Delta)(sub g) at which the magnetic intensity reaches one-half its maximum value scales with x and the temperature T(sub max) at which the static susceptibility is maximum. (Delta)g/k(sub B)T(sub max) is independent of x and equal to 2.5 +/- 0.1, a value curiously close to the total angular momentum of Ce(3+). Three important conclusions are drawn from these observations: (1) As suggested theoretically, T(sub max) does provide a measure of the gap produced in the spin-excitation spectrum of Kondo insulators. (2) Creation of spin holes by thermal excitation or La substitution has comparable effects on the gap. (3) The existence of a spin gap even with significant perturbation in the Ce-sublattice periodicity suggests that coherence effects are not important for the existence of the gap and that spin dynamics are determined locally. DOE

N94-22926# California Univ., Berkeley. Lawrence Berkeley Lab.
PHYSICS WITH CHEMICALLY AND ISOTOPICALLY PURE SEMICONDUCTORS
E. E. Haller May 1993 26 p Presented at the JASOWIEC 1993, Warsaw, Poland, 24-28 May 1993
(Contract DE-AC03-76SF-00098)
(DE93-040120; LBL-34280; CONF-9305280-1) Avail: CASI HC A03/MF A01

Chemically and isotopically pure semiconductors offer a wealth of interesting physics. We review a number of impurity complexes which were discovered in ultrapure Germanium. They have led the way to the widely pursued studies of hydrogen in numerous semiconductors. Isotope related effects and processes include neutron transmutation doping, a technique used for a number of silicon and germanium devices. Isotopically pure and deliberately mixed crystals of germanium have been grown recently and have been used to study the dependence of the indirect bandgap and phonon properties on the mass and mass disorder of the nuclei. The large number of stable isotopes of the various semiconductors present a great potential for basic and applied studies. Semi-conductor isotope engineering may become a reality because of the new economic and political world order. DOE

N94-22927# Argonne National Lab., IL.
THE ELASTIC AND ELECTROMECHANICAL PROPERTIES OF BaTiO3 SINGLE CRYSTAL THROUGH THE FERROELECTRIC TRANSITION
Z. Li, M. Grimsditch, and S. K. Chan Jul. 1993 7 p Presented at the 8th International Meeting on Ferroelectricity, Gaithersburg, MD, 8-13 Aug. 1993
(Contract W-31-109-eng-38)
(DE94-001437; ANL/MSD/CP-78506; CONF-930852-3) Avail: CASI HC A02/MF A01

Using Brillouin scattering and impedance methods, the elastic, piezoelectric, and dielectric properties have been determined for monodomain single crystal BaTiO3 from 23 to 160 C. In the cubic phase (T greater than 130 C) only the compressional elastic constant C11 exhibits partial softening of about 6% upon cooling. During the tetragonal to cubic phase transition, most elastic constants show discontinuous changes; either stiffening or softening. These and other results are discussed in terms of precursive effects through the electromechanical interaction of the ferroelectric phase transformation. DOE

N94-22929# Argonne National Lab., IL.
ANISOTROPIC UNIAXIAL PRESSURE EFFECTS IN YBa2Cu3O(7-DELTA)
U. Welp, M. Grimsditch, S. Fleshler, W. Nessler, B. Veal, and G. W. Crabtree Oct. 1993 20 p Presented at the Physics and Chemistry of Molecular and Oxide Superconductors, Eugene, OR, 27-31 Jul. 1993
(Contract W-31-109-eng-38)
(DE94-001456; ANL/MSD/CP-80962; CONF-930710-4) Avail: CASI HC A03/MF A01

We present measurements of the uniaxial pressure dependence of T(sub c) of untwinned YBa2Cu3O(7-delta) crystals with various oxygen stoichiometries. For all samples investigated, T(sub c) decreases for pressure along a, increases for pressure along b, and, in oxygen deficient samples, increases strongly for pressure along c. These results are compared to the behavior found in the La(2-x)Sr(x)CuO4 and YBa2Cu4O8 systems. Neither the model of pressure induced charge transfer nor coupling to orthorhombic distortions can explain all the data. However, presence of singularities in electronic density of states close to Fermi energy is a possible origin of the observed behavior. Preliminary data on pressure dependence of c-axis and in-plane resistivities in twinned crystals are consistent with this view. DOE

N94-22938 Los Alamos National Lab., NM.
ORIENTATION IMAGING MICROSCOPY: NEW POSSIBILITIES FOR MICROSTRUCTURAL INVESTIGATIONS USING AUTOMATED BKD ANALYSIS
B. L. Adams, K. Kunze (Brigham Young Univ., Provo, UT.), D. J. Dingley (Bristol Univ., England.), and S. I. Wright 1993 13 p Presented at the International Conference on Textures of Materials, Clausthal, Germany, 20-24 Sep. 1993 Limited Reproducibility: More than 20% of this document may be affected by microfiche quality
(Contract W-7405-eng-36)
(DE94-000777; LA-UR-93-3268; CONF-9309231-2) Avail: CASI HC A03

A new microscopy, called orientation imaging microscopy, is described. Imaging results from precise measurements of local lattice orientation are rapidly obtained by backscattered Kikuchi diffraction. The hardware configuration of the microscope is described and a description of image formation presented. Applications to several materials of differing lattice structure are described. Connections of the microscopy with various aspects of modern texture analysis are emphasized. DOE

N94-22940# Los Alamos National Lab., NM.
COHERENCE LOST? NOT-SO-FAST ESCAPES FROM THE IN-PHASE ATTRACTOR OF A SET OF GLOBALLY COUPLED NONLINEAR OSCILLATORS
J. Theiler and S. Nichols (Georgia Inst. of Tech., Atlanta.) 1 Sep. 1993 17 p Presented at the Fluctuations and Order: The New Synthesis Workshop, Los Alamos, NM, 9-12 Sep. 1993
(Contract W-7405-eng-36)
(DE94-000799; LA-UR-93-3241; CONF-9309185-2) Avail: CASI HC A03/MF A01

The sensitivity to noise of the coherent (or in-phase) attractor for a set of N globally coupled maps is studied; these discrete-time maps are associated with the continuous-time equations of motion for a series array of Josephson junction oscillators. We investigate both geometrical properties of the basin of attraction in the large N limit, and the implications of this geometry on the average time for the system to 'escape' from the coherently oscillating mode. Our main results are that the attractor basin maintains a box-shaped 'core' of finite radius even as N approaches infinity, and that the in-phase attractor of a large N array is much less vulnerable to noise than are the out-of-phase attractors. DOE

N94-22941 Los Alamos National Lab., NM.
ANOMALOUS MAGNETORESISTANCE BEHAVIOR OF SUPERCONDUCTING Nd(2-x)Ce(x)CuO(4-y) SINGLE CRYSTAL
M. C. deAndrade, Y. Dalichaouch (California Univ., San Diego, La Jolla.), and M. B. Maple (California Univ., San Diego, La Jolla.) 1993 9 p Presented at the International Conference on Strongly Correlated Electronic Systems, San Diego, CA, 15-19 Aug. 1993 Limited Reproducibility: More than 20% of this document may be affected by microfiche quality
(Contract W-7405-eng-36)
(DE94-000806; LA-UR-93-3144; CONF-9308173-2) Avail: CASI HC A02

Magnetoresistance measurements on a superconducting Nd(2-x)Ce(x)CuO(4-y) single crystal with T(sub c) approximately 7 K were made with magnetic fields H applied parallel (H parallel c) and perpendicular (H perpendicular c) to the tetragonal c-axis. For H parallel c, the resistive superconductive transition curves exhibit a double transition at low temperatures and high magnetic fields. This double resistive transition has a maximum near T approximately 1.1 K, followed by an extremely sharp transition into the superconducting state. For applied fields of 1kOe, the resistivity first goes to zero, increases again to a finite value, and then goes through a second transition. In this region, the resistivity exhibits non-ohmic behavior for low current densities and ohmic behavior for larger measuring currents. The resistivity for H perpendicular c does not exhibit any anomalous behavior or a maximum for 0 less than or equal to H less than or equal to 60 kOe and 4 less than or equal to T less than or equal to 7 K. DOE

N94-22942 Los Alamos National Lab., NM.
A VALENCE-FLUCTUATION THEORY OF CUPRATE SUPERCONDUCTIVITY
B. H. Brandow 1993 5 p Presented at the International Conference on Strongly Correlated Electron Systems, La Jolla, CA, 16-19 Aug. 1993 Limited Reproducibility: More than 20% of this document may be affected by microfiche quality
(Contract W-7405-eng-36)
(DE94-000887; LA-UR-93-3329; CONF-930865-11) Avail: CASI HC A01

The concepts and formalism of valence fluctuation theory are applied to an Anderson lattice model of the CuO2 plane. Using a self-consistent variational treatment at the (1/N) level, for a finite-U lattice, we find adequate pairing attraction for realistic Hamiltonian parameters. Several unconventional features of the cuprate phenomenology are explained, including the extremely short coherence length, large resistivity, and strong gap anisotropy. DOE

N94-22946 Lawrence Livermore National Lab., CA.
HIGH PRESSURE HUGONIOT OF SAPPHIRE
D. Erskine Jul. 1993 5 p Presented at the 14th International Conference of the International Association for the Advancement of High Pressure Science and Technology, Colorado Springs, CO, 27 Jun. - 2 Jul. 1993 Limited Reproducibility: More than 20% of this document may be affected by microfiche quality
(Contract W-7405-eng-48)
(DE94-001048; UCRL-JC-113299; CONF-930676-59) Avail: CASI HC A01

The Hugoniot of sapphire was measured from 80 GPa to 340 GPa in shock wave experiments using projectiles accelerated by a two stage gas gun. Transit times of the shock waves were measured either optically with a streak camera or through electrical pin contacts. The Hugoniot in this pressure range fits U(sub s) = 8.74 + 0.96 U(sub p) in km/s. DOE

N94-22953# Sandia National Labs., Albuquerque, NM.
BRIDGMAN'S CONCERN
R. A. Graham 1993 10 p Presented at the 14th International Conference of the International Association for the Advancement of High Pressure Science and Technology, Colorado Springs, CO, 27 Jun. - 2 Jul. 1993
(Contract DE-AC04-76DP-00789)
(DE93-040900; SAND-93-1400C; CONF-930676-51) Avail: CASI HC A02/MF A01

In 1956 P.W. Bridgman published a letter to the editor in the Journal of Applied Physics reporting results of electrical resistance measurements on iron under static high pressure. The work was undertaken to verify the existence of a polymorphic phase transition at 130 kbar (13 GPa) reported in the same journal and year by the Los Alamos authors, Bancroft, Peterson and Minshall for high pressure, shock-compression loading. In his letter, Bridgman reported that he failed to find any evidence for the transition. Further, he raised some fundamental concerns as to the state of knowledge of shock-compression processes in solids. Later it was determined that Bridgman's static pressure scale was in error, and the shock observations became the basis for calibration of pressure values in static high pressure apparatuses. In spite of the error in pressure scales, Bridgman's concerns on descriptions of shock-compression processes were perceptive and have provided the basis for subsequent fundamental studies of shock-compressed solids. The present paper, written in response to receipt of the 1993 American Physical Society Shock-Compression Science Award, provides a brief contemporary assessment of those shock-compression issues which were the basis of Bridgman's 1956 concerns. DOE

N94-22957 Oak Ridge National Lab., TN.
LOW TEMPERATURE DIFFUSION OF HYDROGENIC SPECIES IN OXIDE CRYSTALS: RADIATION INDUCED DIFFUSION
Y. Chen and R. Gonzalez (Madrid Univ., Spain.) 1993 15 p Presented at the International Union of Materials Research Societies on Advanced Materials, Tokyo, Japan, 31 Aug. - 4 Sep. 1993 Limited Reproducibility: More than 20% of this document may be affected by microfiche quality
(Contract DE-AC05-84OR-21400)
(DE94-000374; CONF-9308122-9) Avail: Issuing Activity (Department of Energy (DOE))

Normally stable configurations of substitutional protons or deuterons in oxide crystal become highly unstable during ionizing radiation at room temperature, resulting in the displacements of these species. The cross section for radiation-induced-displacements of protons is exceedingly large and is a strong function of temperature. The displacement cross section of protons from cation sites is twice that of deuterons. Diffusion of these species can be induced at temperatures not otherwise possible by thermal means. For example, using electron irradiation near room temperature the O-H bond is readily broken and the hydrogenic species can be channeled along the c-axis in TiO2 by an applied electric field. Radiation induced displacements of protons from anion sites (hydride ions) at room temperature are also discussed. DOE

N94-22978 International Centre for Theoretical Physics, Trieste (Italy).
VACANCY FORMATION ENERGY OF LI(H, D) AND Na(H, D) SYSTEMS
A. K. M. A. Islam Jun. 1993 9 p Limited Reproducibility: More than 20% of this document may be affected by microfiche quality
(DE93-633452; IC-93/130) Avail: Issuing Activity (Department of Energy (DOE)) (US Sales Only)

Vacancy defect formation energy (Schottky defect) of lighter hydrides and deuterides of alkali metals are discussed with reference to conductivity measurements and the recent computer simulation calculations. An empirical relation with Debye temperature is found to yield values of Schottky defect formation energies of Li(H,D) systems in agreement with experiments. The relationship is also utilized to obtain the formation energies for Na(H,D) systems for which experimental values are available in the literature. DOE

N94-22990 Argonne National Lab., IL.
ATOMIC-SCALE STRUCTURE OF GRAIN BOUNDARIES: CORRELATIONS TO GRAIN BOUNDARY PROPERTIES
K. L. Merkle, M. I. Buckett, Y. Gao, S. J. Rozeveld, B. L. Vuchic, and D. Wolf Sep. 1993 7 p Presented at the International Union of Materials Research Societies on Advanced Materials, Tokyo, Japan, 31 Aug. - 4 Sep. 1993 Limited Reproducibility: More than 20% of this document may be affected by microfiche quality
(Contract W-31-109-eng-38)
(DE94-001289; ANL/MSD/CP-80905; CONF-9308122-10) Avail: CASI HC A02

It is generally believed that many properties of solid interfaces are ultimately determined by their structure and composition at the atomic level. We report here on work in two areas of grain boundary (GB) research in which structure-property correlations have been investigated recently. HREM observations in connection with computer modeling of GB's in fcc metals have given considerable insight into correlations between GB energy and atomic-scale GB structure. Efforts to understand and possibly control the supercurrent transport behavior across GB's in high-temperature superconductors require the combination of microstructure characterizations with investigations of electric transport properties. In both areas considerable progress is being made and has already lead to important insights concerning interfacial properties. DOE

N94-22993 Argonne National Lab., IL.
DESIGN OF MICROCHANNELS FOR CRYOSTABILIZATION OF HIGH TEMPERATURE SUPERCONDUCTING MAGNETS
Y. S. Cha, J. R. Hull, and R. C. Niemann 1993 23 p Presented at the Annual Winter Meeting of the ASME, New Orleans, LA, 28 Nov. - 3 Dec. 1993 Limited Reproducibility: More than 20% of this document may be affected by microfiche quality
(Contract W-31-109-eng-38)
(DE94-001324; ANL/MCT/CP-78916; CONF-931121-28) Avail: CASI HC A03

Microchannel cooling using subcooled liquid nitrogen is proposed to cryogenically stabilize high-temperature superconducting magnets. Various design constraints and parameters are identified and summarized. A graphical method is proposed for the design of microchannel systems. This graphical method helps to reduce the amount of work towards achieving optimum design for a specific application because there are a large number of parameters involved in the design of a microchannel system. The proposed graphical method are illustrated by three examples. The results show that a design window may appear for a given application. Any point within this window is an acceptable design. Another advantage of the graphical method is that, by selecting a design point, the design margin against various design contrains can be easily identified. Any two of the design variables can be selected as the independent variables. The choice depends on specific application and, to a certain extent, on individual preference. The three examples revealed that, for high current density applications, the most scattering constraints are the coolant temperature rise and the fin tip temperatures provided that a moderate pressure drop can be tolerated. DOE

N94-22994 Argonne National Lab., IL.
PROCESSING OF YBCO SUPERCONDUCTORS FOR IMPROVED LEVITATION FORCE
U. Balachandran and W. Zhong May 1993 5 p Presented at the Joint MMIJ/TMS International Conference on Processing Materials for Properties, Honolulu, HI, 7-10 Nov. 1993 Limited Reproducibility: More than 20% of this document may be affected by microfiche quality
(Contract W-31-109-eng-38)
(DE94-001326; ANL/ET/CP-78724; CONF-931103-4) Avail: CASI HC A01

One objective of the ANL superconductor program is to develop improved processing methods for production of YBCO superconductors with higher levitation forces suitable for low-friction, superconductor/permanent-magnet bearings and flywheel-energy-storage applications. From the standpoint of these applications, melt-processed bulk YBCO superconductors are of considerable interest. Levitation force and flux-pinning properties depend on microstructural features of the superconductors. We have added several chemical species to YBCO to alter the microstructure and have used a seeding technique to induce crystallization during melt processing. In this paper, we discuss the effects of various process parameters, additives, and a seeding technique on the properties of melt-processed bulk YBCO samples and compare the results with solid-state-sintered superconductors. DOE

N94-22995# Argonne National Lab., IL.
PHOTO-INDUCED ANTIFERROMAGNETIC INTERLAYER COUPLING IN Fe SUPERLATTICES WITH IRON SILICIDE SPACERS
J. E. Mattson, E. E. Fullerton, S. Kumar, S. R. Lee, C. H. Sowers, M. Grimsditch, S. D. Bader, and F. T. Parker (California Univ., San Diego, La Jolla.) Sep. 1993 22 p Presented at the 38th Annual Conference on Magnetism and Magnetic Materials, Minneapolis, MN, 15-18 Nov. 1993
(Contract W-31-109-eng-38)
(DE94-001345; ANL/MSD/CP-79360; CONF-931133-5) Avail: CASI HC A03/MF A01

Sputtered Fe/FeSi films possessing antiferromagnetic (AF) interlayer coupling at room temperature develop ferromagnetic remanence when cooled below 100K, but the AF coupling can be restored at low temperature by exposure to visible light of sufficient intensity (greater than 10 mW/mm(exp 2)). We attribute these effects to charge carriers in the FeSi spacer layer which, when thermally or photo-generated, are capable of communicating spin information between the Fe layers. DOE

N94-23006# Los Alamos National Lab., NM.
MUON SPIN RELAXATION STUDIES OF THE INTERPLAY BETWEEN MAGNETISM AND SUPERCONDUCTIVITY IN HEAVY FERMION SYSTEMS
R. H. Heffner 1993 15 p Presented at the 1993 Actinides, Santa Fe, NM, 19-24 Sep. 1993
(Contract W-7405-eng-36)
(DE94-000700; LA-UR-93-3449; CONF-930905-6) Avail: CASI HC A03/MF A01

The interplay between magnetism and superconductivity in heavy fermion systems is discussed and the role of muon spin relaxation in elucidating these properties is emphasized. Relevant properties of all six heavy fermion superconductors are briefly surveyed and instances where superconductivity and magnetism compete, coexist, and couple with one another are pointed out. Current theoretical concepts underlying these phenomena are highlighted. DOE

N94-23109 Amsterdam Univ. (Netherlands).
APPLICATION OF MAXIMUM ENTROPY AND IRREDUCIBLE CLUSTER INTEGRALS TO JOINT PROBABILITY DISTRIBUTIONS FOR X RAY STRUCTURE DETERMINATION Ph.D. Thesis
M. J. Kronenburg 5 Nov. 1992 89 p Sponsored by Netherlands Foundation for Chemical Research, and Nederlandse Organisatie voor WetenschAppelijk Onderzoek, The Hague Limited Reproducibility: More than 20% of this document may be affected by microfiche quality
(PB93-224152) Avail: CASI HC A05/MF A01

The physical theory of single crystal x-ray diffraction results in a Fourier transformation, as is demonstrated in section 1.1. Subject of the thesis is the derivation of joint probability distributions of the structure factors, and derivation of the corresponding estimates of invariants. The thesis provides a mathematical theory based on the maximum entropy method as applied in statistical gas theory. Using the maximum entropy method, combined with a mathematical tool from classical real gas theory, the irreducible cluster integrals, new expressions for joint probability distributions (jpd's) of invariant phase sums are derived. In chapter 2, a general outline of the standard derivation of jpd's is provided, and the importance of inequalities for jpd's is stressed. In chapter 3, Lagrange multipliers and general maximum entropy theory for continuous variables are introduced. In chapter 4, a theory for derivation of jpd's of structure factors based on maximum entropy theory is presented. In chapter 5, the normalization of crystallographic data is investigated in more detail. In chapter 6, the connection between jpd's and Patterson functions is stressed, and a new algorithm for iteratively finding better triplet values is outlined. NTIS

N94-23186# Sandia National Labs., Albuquerque, NM.
A QUALIFIED RADIATION HARDENED NONVOLATILE MEMORY FOR SPACE AND TACTICAL WEAPONS APPLICATIONS
J. Marthinuss (Westinghouse Electric Corp., Baltimore, MD.), D. Williams (Westinghouse Electric Corp., Baltimore, MD.), R. Bishop (Westinghouse Electric Corp., Baltimore, MD.), M. Jacunski (Westinghouse Electric Corp., Baltimore, MD.), D. Adams (Westinghouse Electric Corp., Baltimore, MD.), J. Jakubzcak, F. Gentry, R. McClintock, E. White, and J. Murray 1993 4 p Presented at the GOMAC 1993: Government Microcircuit Application Conference, New Orleans, LA, 1-4 Nov. 1993
(Contract DE-AC04-76DP-00789)
(DE94-001211; SAND-93-1965C; CONF-9311101-1) Avail: CASI HC A01/MF A01 (US Sales Only)

A radiation hardened 64K CMOS SONOS full featured EEPROM, W28C64, is available. A team of Sandia National Laboratories and Westinghouse Advanced Technology Division personnel successfully transitioned a development program into a production ready, radiation hardened nonvolatile memory product qualified for satellite (space), tactical weapons, and commercial systems. The part is software compatible with

commercial 64K EEPROMs and is presently being offered with Class B, Class S and commercial screening. A data sheet for W28C64 is available.
DOE

N94-23187 Argonne National Lab., IL.
MODIFICATIONS TO 8X8 DYNAMICAL THEORY: POLARIZATIONS REDEFINED ACCORDING TO X RAY DIFFRACTION CONVENTION
A. T. Macrander and R. C. Blasdell Sep. 1993 9 p Presented at the Synchrotron Radiation Instrumentation, Gaithersburg, MD, 23-26 Aug. 1993 Limited Reproducibility: More than 20% of this document may be affected by microfiche quality
(Contract W-31-109-eng-38)
(DE94-001290; ANL/XFD/CP-80251; CONF-930824-13) Avail: CASI HC A02

Dynamical x-ray diffraction theory can be cast in matrix form. In recent years, an 8x8 matrix theory was developed that treated asymmetric reflections from strained crystals. The polarization of the incident, specularly reflected, reflected diffracted, transmitted diffracted, and transmitted electromagnetic wave fields were all defined as s or p. That is, polarizations were defined with respect to the plane containing the incident beam direction and the surface normal. The authors present modifications of the theory to treat (sigma) and (pi) polarizations for Bragg diffraction from asymmetric planes, that is, for polarizations defined with respect to the plane containing the incident beam direction and the reciprocal lattice vector for Bragg diffraction. They present results of this theory for unstrained crystals in the inclined geometry. In this geometry, the incident beam wavevector, the reciprocal lattice vector, and the surface normal are not coplanar. The inclined crystal geometry appears promising for use in a high-heat-load monochromator for undulator radiation at the Advanced Photon Source. As expected, they find a weak (pi)-polarization component in the diffracted beam when the polarization of the incident beam is pure sigma. DOE

N94-23188 Argonne National Lab., IL.
PROPOSED ADDITIONS TO THE SHADOW RAY-TRACING CODE FOR GENERAL-ASYMMETRIC PERFECT-CRYSTAL OPTICS
R. C. Blasdell and A. T. Macrander Sep. 1993 14 p Presented at the Synchrotron Radiation Instrumentation, Gaithersburg, MD, 23-26 Aug. 1993 Limited Reproducibility: More than 20% of this document may be affected by microfiche quality
(Contract W-31-109-eng-38)
(DE94-001291; ANL/XFD/CP-80250; CONF-930824-14) Avail: CASI HC A03

The dynamical theory of the diffraction of x-rays from perfect crystals is traditionally expressed in terms of Maxwell's equations using a semi-classical theory originally due to Ewald and von Laue. Combining the work of Batterman and Cole, Caticha and Caticha-Ellis, and Zachariasen, a formalism is obtained that treats the general asymmetric, thick and thin crystal, Laue and Bragg cases within the second order dispersion surface approximation. The authors have implemented this formalism with thick Bragg crystal E-field boundary value conditions in several routines they have added to one of the Advanced Photon Source (APS) versions of the SHADOW ray-tracing code in order to provide the ability to ray trace inclined double-crystal monochromators and high-resolution backscattering analyzers. These additions have been submitted to the University of Wisconsin Center for X-Ray Lithography for consideration for inclusion in the next version of SHADOW. DOE

N94-23189# Argonne National Lab., IL.
GENERALIZED MELTING CRITERION FOR BEAM-INDUCED AMORPHIZATION
N. Q. Lam and Paul R. Okamoto Sep. 1993 22 p Presented at the 8th International Conference on Surface Modification of Metals By Ion Beams, Kanazawa, Japan, 13-17 Sep. 1993
(Contract W-31-109-eng-38)
(DE94-001333; ANL/MSD/CP-79942; CONF-9309251-1) Avail: CASI HC A03/MF A01

Recent studies have shown that the mean-square static atomic displacements provide a generic measure of the enthalpy stored in the lattice in the form of chemical and topological disorder, and that the effect of the displacements on the softening of shear elastic constants is identical to that of heating. This finding lends support to a generalized form of the Lindemann phenomenological melting criterion and leads to a natural interpretation of crystalline-to-amorphous transformations as defect-induced melting of metastable crystals driven beyond a critical state of disorder where the melting temperature falls below the glass-transition temperature. Application of the generalized Lindemann criterion to both the crystalline and amorphous phases indicates that the enthalpies of the two phases become identical when their shear moduli become equal. This thermoelastic rule provides a basis for predicting the relative susceptibility of compounds to amorphization in terms of their elastic properties as measured by Debye temperatures. The present approach can explain many of the basic findings on beam-induced amorphization of intermetallic compounds as well as amorphous phase formation associated with ion implantation, ion-beam mixing, and other solid-state processes. DOE

N94-23204# Sandia National Labs., Albuquerque, NM.
SENSORS FOR PROCESS CONTROL FOCUS TEAM REPORT
1993 10 p Presented at the Contamination Free Manufacturing Focus Technical Advisory Board Meeting, Austin, TX, 14-15 Jul. 1993
(Contract DE-AC04-76DP-00789)
(DE93-040897; SAND-93-1750C; CONF-9307140-1) Avail: CASI HC A02/MF A01

At the Semiconductor Technology Workshop, held in November 1992, the Semiconductor Industry Association (SIA) convened 179 semiconductor technology experts to assess the 15-year outlook for the semiconductor manufacturing industry. The output of the Workshop, a document entitled 'Semiconductor Technology: Workshop Working Group Reports,' contained an overall roadmap for the technology characteristics envisioned in integrated circuits (IC's) for the period 1992-2007. In addition, the document contained individual roadmaps for numerous key areas in IC manufacturing, such as film deposition, thermal processing, manufacturing systems, exposure technology, etc. The SIA Report did not contain a separate roadmap for contamination free manufacturing (CFM). A key component of CFM for the next 15 years is the use of sensors for (1) defect reduction, (2) improved product quality, (3) improved yield, (4) improved tool utilization through contamination reduction, and (5) real time process control in semiconductor fabrication. The objective of this Focus Team is to generate a Sensors for Process Control Roadmap. Implicit in this objective is the identification of gaps in current sensor technology so that research and development activity in the sensor industry can be stimulated to develop sensor systems capable of meeting the projected roadmap needs. Sensor performance features of interest include detection limit, specificity, sensitivity, ease of installation and maintenance, range, response time, accuracy, precision, ease and frequency of calibration, degree of automation, and adaptability to in-line process control applications. DOE

N94-23205# Boeing Defense and Space Group, Seattle, WA.
RESEARCH ON POLYCRYSTALLINE THIN-FILM CuInGaSe2 SOLAR CELLS
W. S. Chen, J. M. Stewart, R. A. Mickelsen, W. E. Devaney, and B. J. Stanbery Oct. 1993 25 p Prepared for Midwest Research Inst., Golden, CO
(Contract DE-AC02-83CH-10093)
(DE94-000203; NREL/TP-413-5835) Avail: CASI HC A03/MF A01

This report describes work to fabricate high-efficiency CdZnS/CuInGaSe2, thin-film solar cells and to develop improved transparent conductor window layers such as ZnO. The specific technical milestone for Phase 1 was to demonstrate an air mass (AM) 1.5 global 13% , 1-cm(exp 2) total-area CuInGaSe2 (CIGS) thin-film solar cell. For Phase 2, the objective was to demonstrate an AM1.5 global 13.5%, 1-cm(exp 2) total-area efficiency. We focused our activities on three areas. First, we modified the CIGS deposition system to double its substrate capacity. Second, we developed new tooling to enable investigation of a modified aqueous CdZnS process in which the goal was to improve the yield of this critical step in the device fabrication process. Third, we upgraded the ZnO sputtering system to improve its reliability and reproducibility. A dual rotatable cathode metallic source was installed, and the sputtering parameters were further optimized to improve ZnO's properties as a transparent conducting oxide (TCO). Combining the refined CdZnS process with CIGS from the newly fixtured deposition system enable us to fabricate and deliver a ZnO/Cd(0.08)Zn(0.20)S/CuIn(0.74)Ga(0.26)Se2 cell on alumina with I-V characteristics, as measured by NREL under standard test conditions, of 13.7% efficiency with V(proportional to) = 0.5458 V, J(sub sc) = 35.48 mA/cm(exp 2), FF = 0.688, and efficiency = 14.6%. DOE

N94-23214# Ames Lab., IA.
DENSITY FUNCTIONAL STUDIES: FIRST PRINCIPLES AND SEMI-EMPERICAL CALCULATIONS OF CLUSTERS AND SURFACES Ph.D. Thesis
S. Susan 30 Apr. 1993 165 p
(Contract W-7405-eng-82)
(DE94-002836; IS-T-1649) Avail: CASI HC A08/MF A02

Theoretical electronic structure techniques are used to analyze widely different systems from Si clusters to transition metal solids and surfaces. For the Si clusters, first principles density functional methods are used to investigate Si(sub N) for N=2-8. The goal is to understand the different types of bonding that can occur in such small clusters where the atomic coordination differs substantially from tetrahedral bonding; such uncoordinated structures can test approximate models of Si surfaces. For the transition metal systems, non-self-consistent electronic structure methods are used to understand the driving force for surface relaxations. In-depth analysis of results is presented and physical basis of surface relaxation within the theory is discussed. Limitations inherent in calculations of metal surface relaxation are addressed. Finally, in an effort to understand approximate methods, a novel non-self-consistent density functional electronic structure method is developed that is about 1000 times faster than more sophisticated methods; this method is tested for various systems including diatomics, mixed clusters, surfaces, and bulk lattices. DOE

N94-23222 Amsterdam Univ. (Netherlands).
Ga DELTA-DOPING LAYERS IN SILICON Ph.D. Thesis
P. M. Zagwijn 22 Feb. 1993 100 p Limited Reproducibility: More than 20% of this document may be affected by microfiche quality
(PB93-224632) Avail: CASI HC A05

Experimental studies of Ga delta-doping layers in silicon are described. The layers are mainly investigated by medium-energy ion scattering (MEIS). The measurement technique is greatly improved by the introduction of a new detection system for backscattered ions. In Chapter 1 the subject of delta-doping layers is introduced and the principles of MEIS are discussed. Compared with other surface science measurements techniques, it is shown that MEIS is an excellent technique to measure delta-doping profiles with high depth resolution. The design and the performance of the detection system are described in Chapter 2. Chapter 3 describes the fabrication of a Ga delta-doping layer in Si using a solid phase epitaxial growth (SPEG) method. The growth method is followed step-by-step by MEIS. In Chapter 4 the redistribution of Ga in amorphous silicon (a-Si) is investigated by MEIS. In Chapter 5 the incorporation of Ga in crystalline Si (c-Si) during the fabrication of delta-doping layers is studied in more detail. With the preparation method described, it is possible to bury a delta-doping Ga layer deep inside a Si crystal. NTIS

N94-23223# Amsterdam Univ. (Netherlands).
MAGNETIC RESONANCE STUDY OF ZINC-RELATED DEFECTS IN SILICON WITH OPTIMIZED EPR SPECTROMETER Ph.D. Thesis
H. E. Altink 25 Feb. 1993 116 p
(PB93-224640) Avail: CASI HC A06/MF A02

The work described can be divided into two major parts: the construction of a very sensitive electron paramagnetic resonance (EPR) spectrometer and EPR investigations with this spectrometer of silicon samples doped with zinc. In Chapter 1 the construction of the spectrometer is described where a lot of attention is paid to the noise sources and these were, where possible, removed or minimized. In Chapter 2 an overview of the electron nuclear double resonance (ENDOR) method is given. This method was not used in the investigations described. The work on zinc-related defects starts in Chapter 3 where the early results are presented and the chemical identification of two of these centers Si:ZnCu and Si:ZnCr are given. Chapter 4 is a review of the double acceptor zinc in silicon and data like solubility, diffusion, ionization levels, and acceptor states are given. In Chapter 5 the photo-EPR method is described, which in principal can give information of the energy level, and electron (or hole) capture processes, of the paramagnetic center under study. In Chapter 6 all new paramagnetic centers, that were found during these investigations are given in much more detail including details of the sample preparations. NTIS

N94-23428 Selskapet for Industriell og Teknisk Forskning, Trondheim (Norway). Div. of Applied Physics.
MAGNETIC PROPERTIES AND TRANSMISSION ELECTRON MICROSCOPY INVESTIGATIONS OF Nd-Fe-B-Co-Al MELT SPUN RIBBONS
S.-X. Zhou (Norges Tekniske Hoegskole, Trondheim.), G. Pettersen, and R. Hoeier Dec. 1992 14 p Limited Reproducibility: More than 20% of this document may be affected by microfiche quality
(PB93-201531; STF19-A92035) Avail: CASI HC A03

The magnetic properties and microstructure of ribbons with nominal composition Nd(0.165)(Fe(0.800) Co(0.120) Al(0.005) B(0.075))(0.835) were investigated using magnetic measurements and high resolution transmission electron microscopy (HRTEM). HRTEM observations show that the microstructure of ribbons with relative high coercivity (approximately 16kO(e)) is inhomogeneous. The grain size of the Nd2(Fe,Co)14B matrix phase, two intergranular phases have been observed. One of them is found to have the fcc structure with lattice constant of 5.4 +/- 0.1A. One lattice plane distance of the other phase is found to be 7.6 +/- 0.2A while its structure is still unknown. It is inferred that both phases act as pinning sites of domain walls. NTIS

N94-23432# Argonne National Lab., IL.
CONDUCTORS WITH SMALL FERMI ENERGIES AND SMALL GAP ENERGIES
R. J. Thorn 1993 16 p
(Contract W-31-109-eng-38)
(DE93-040887; ANL/CHM/PP-77001) Avail: CASI HC A03/MF A01

If the Fermi energy is of the order of meV's, the usual treatment of the density of free electrons is not valid, but use can be made of an averaged density of states that depends weakly on temperature, so that the temperature variation of the conductivity can be expressed by the equation: sigma is approximately CT(exp 1-s) 1n(((exp ((beta)E(sub f)) + 1)/2)(exp -(beta)(E(sub g) - E(sub f)) + 1)) in which E(sub f) is the Fermi energy, E(sub g) is the top of the energy gap for thermal activation, and s is the exponent of the temperature-dependent scattering. This equation serves to define a class of solids consisting of a microcomposite with a narrow conduction band for which E(sub f) of the order of ceV's or less and a thermal activated conduction for which E(sub g) is of the order of ceV's. It describes quantitatively the conductivity, (sigma)(T;(Delta)), for YBa2Cu3O(7-delta) and (sigma)(T;p) as the hydrostatic pressure p is varied for (kappa)-(BEDT-TTF)(sub 2)CuN(CN)(sub 2)Br. DOE

N94-23445 Selskapet for Industriell og Teknisk Forskning, Trondheim (Norway). Div. of Applied Physics.
SPECTROSCOPIC IR ELLIPSOMETRY OF 100 AND 001 ORIENTED YBa2Cu3O(7-DELTA) FILMS
E. Wold, J. Bremer (Norges Tekniske Hoegskole, Trondheim.), and O. Hunderi 22 Dec. 1992 17 p Limited Reproducibility: More than 20% of this document may be affected by microfiche quality
(PB93-201481; STF19-A92030) Avail: CASI HC A03/MF A01

A spectroscopic technique for IR ellipsometry has been developed. The method is based on a Mueller analysis of the optical system and the systematic application of correction routines for experimentally measured Fourier coefficients. The extinction ratio of the polarizers is not crucial for the measurements. Optical properties of micro-twinned 100(in brackets) and 001(in brackets) oriented YBa2Cu3O(7-delta) films have been studied. The two samples had a thickness of 300 nm and both were deposited on SrTiO3 substrates. The components of the out-of-plane and in-plane permittivity have been calculated through data inversion and effective-medium theories for anisotropic grains. NTIS

N94-23503 Selskapet for Industriell og Teknisk Forskning, Trondheim (Norway). Div. of Applied Physics.
OBSERVATION OF NON-CENTROSYMMETRY AND DETERMINATION OF POLARITY IN III-V SEMICONDUCTORS
K. Marthinsen and R. Hoeier (Norges Tekniske Hoegskole, Trondheim.) 8 Dec. 1992 5 p Limited Reproducibility: More than 20% of this document may be affected by microfiche quality
(PB93-201416; STF19-A92018) Avail: CASI HC A01

A simple method for determining polarity in III-V semiconductors is considered. It is based on comparison of two conjugate four-beam CBED patterns tilted away from the (011) zone axis. It is shown that with carefully chosen diffraction conditions strong effects of non-centrosymmetry may be observed both for GaAs and InP, and the polarity can be uniquely determined. The general conditions for strong asymmetry effects are that the structure factor magnitudes of the reflections involved are of the same size, and that the three-phase invariants involved are as close to + or - pi/2 as possible. The asymmetry effect is rather insensitive to thickness, but weakens as the thickness approaches the extinction lengths of the reflections involved. It is shown that the 200 structure factor for GaAs (sensitive to bonding) may be determined from the gap between the black lines in one of the 200 disks, if the other parameters can be controlled. However, the 200 structure factor is probably equally well determined from the strong variations in 2,0,0 oscillations itself using recently developed quantitative CBED methods. NTIS

N94-23535 Selskapet for Industriell og Teknisk Forskning, Trondheim (Norway). Div. of Applied Physics.

CHARACTERIZATION OF 3-D PARTICLE DISTRIBUTIONS AND EFFECTS ON RECRYSTALLIZATION STUDIED BY COMPUTER SIMULATION

J. M. Fridy (Aluminum Co. of America, Alcoa Center, PA.), K. Marthinsen, T. N. Rouns (Aluminum Co. of America, Alcoa Center, PA.), K. B. Lippert (Aluminum Co. of America, Alcoa Center, PA.), and E. Nes (Norges Tekniske Hoegskole, Trondheim.) 8 Dec. 1992 10 p Limited Reproducibility: More than 20% of this document may be affected by microfiche quality
(PB93-201408; STF19-A91017) Avail: Issuing Activity (National Technical Information Service (NTIS))

Artificial particle distributions in three dimensions with different degree of clustering have been generated and used as nucleation sites for the simulation of particle stimulated recrystallization with site saturation nucleation kinetics. The clustering has a strong effect on both the Avrami exponent and the resulting sectioned grain size distributions. The Avrami exponent decreases rapidly from the expected value of 3 with the degree of clustering. A value of less than 1.5 is obtained for the Avrami exponent with a strongly clustered distribution of nucleation sites. The size distributions of sectioned grain areas are considerably broadened with clustering, but are still far from the log-normal distributions observed experimentally. A computer program has been developed to generate particle distributions whose pair correlation functions (PCF) match experimentally measured PCF's. The procedure has been applied to an H19 gauge Al-alloy similar to 3004. The PCF's calculated exhibited clear anisotropy, especially in the longitudinal direction. However, when the particle distribution was used to define nucleation sites for the recrystallization simulations, the effects on the kinetics and resulting grain size distribution was not significantly different from random site saturated results. NTIS

N94-23766# Technische Univ., Delft (Netherlands).

PARTICLE SIZE MEASUREMENT FOR THE CONTROL OF INDUSTRIAL CRYSTALLIZERS Ph.D. Thesis

A. Boxman 1992 186 p
(PB94-119104; ISBN-90-6275-790-1) Copyright Avail: CASI HC A09/MF A02

The need for on-line sensors to monitor particulate processes is rapidly increasing. Such systems are a necessity to understand the complex phenomena of particle formation, growth, and breakage. Some aspects of the design of an on-line sensor for particle size analysis are discussed. The technique used is based on forward light scattering, which covers a size range from about 1 to 2,000 micrometers. The observations are used to develop a physical model and subsequently an effective control strategy for a 970 liter continuous crystallizer. The purpose of the controller is to manipulate the dynamics of the size distribution. Therefore, a firm relation between process inputs and outputs (i.e., the crystal size distribution) must first be established. Secondly, an intelligent interpretation of the recorded data, in this case a light scattering pattern, is required. Chapter headings include the following: Validation of Light Scattering Models for Polydisperse Particle Systems; Deconvolution Algorithm for the Recovery of Particle Size Distributions; Automated Measurement and Interpretation of Scattering Patterns; On-line Measurement of Crystal Size Distribution in Industrial Crystallizers. NTIS

N94-23769 Technische Univ., Eindhoven (Netherlands). Dept. of Mathematics and Computing Science.

REVIEW OF A VARIATIONAL METHOD APPLIED TO MAGNETOELASTIC BUCKLING PROBLEMS

A. A. F. vanDeVen Jun. 1993 16 p Limited Reproducibility: More than 20% of this document may be affected by microfiche quality
(PB94-111184; RANA-93-09) Avail: CASI HC A03

Magnetoelastic buckling theory, concerning ferromagnetic and superconducting systems, is reviewed. Special attention is given to a variational method, which yields a unified and direct solution for the buckling value. NTIS

N94-23795# Argonne National Lab., IL.

EXACT TRANSFORMATION OF THE ANISOTROPIC GINZBURG-LANDAU MODEL AND ITS CONSEQUENCES

R. A. Klemm Oct. 1993 50 p Presented at the Joint Summer Research Conferences in the Mathematical Sciences: Mathematics of Superconductivity, Seattle, WA, 24-30 Jul. 1993
(Contract W-31-109-eng-38)
(DE94-002208; ANL/MSD/CP-81086; CONF-930738-1) Avail: CASI HC A03/MF A01

Line energy of a single magnetic vortex at an arbitrary direction in an anisotropic superconductor is evaluated in three different phenomenological models: anisotropic London, anisotropic Ginzburg-Landau, and Lawrence-Doniach models. Vortex line energy in anisotropic London can be solved by Fourier transformation, but core cutoff is not present. Using the Klemm-Clem transformations of the free energy and vortex coordinates in the anisotropic Ginzburg-Landau model, a theorem relating shape of effective core cross-section in anisotropic London model to that in anisotropic Ginzburg-Landau model is presented. This theorem allows the anisotropic London model to be used in the entire regime H(sub c1) less than or equal to H much less than H(sub c2) regardless of anisotropy and field direction. Resulting lower critical field H(sub c1) ((theta)(sub H)) can exhibit a discontinuity, a kink, or monotonic angular dependence. The transformations are applied to the case of a core cross-section of a single vortex in Lawrence-Doniach model, and angular dependence of magnetic torque is calculated. The torque exhibits the expected dimensional crossover, having an angular dependence which reduces to an anisotropic Ginzburg-Landau superconductor near Tc, and to a lattice of decoupled, parallel Josephson junctions well below dimensional crossover temperature T*. In the vicinity of T*, however, dramatic oscillations in angular dependence of torque are predicted. DOE

N94-23805# Argonne National Lab., IL.

PULSED ION BEAM SURFACE ANALYSIS (PIBSA) AS A MEANS OF IN-SITU REAL-TIME ANALYSIS OF THIN FILMS DURING GROWTH

A. R Krauss, G. J. Lamich, D. M. Gruen, Y. Lin, R. P. H. Chang (Northwestern Univ., Evanston, IL.), O. Auciello (Microelectronics Center of North Carolina, Research Triangle Park.), and J. A. Schultz (Ionwerks, Houston, TX.) 1993 23 p Presented at the 40th National Symposium of the American Vacuum Society (AVS), Orlando, FL, 15-19 Nov. 1993
(Contract W-31-109-eng-38)
(DE94-001276; ANL/CHM/CP-80915; CONF-9311104-1) Avail: CASI HC A03/MF A01

Low energy (5-15 keV) pulsed ion beam surface analysis (PIBSA) comprises several different surface spectroscopies which provide a wide range of information relevant to growth of single and multi-component semiconductor, metal, and metal oxide thin films and layered structures. Ion beam methods have not been widely used as an in-situ monitor of thin film growth. PIBSA was developed as a non-destructive, in-situ, real-time probe of thin film composition and structure which does not physically interfere with deposition. Several PIBSA versions are exceptionally surface-specific, yet can yield high resolution data at ambient pressures in excess of 1 m Torr (4-5 orders of magnitude higher than conventional surface analytic methods). Therefore, PIBSA is ideal for studying ultra-thin layers and atomically abrupt interfaces. PIBSA instrumentation designed for use as an in-situ, real-time monitor of growth processes for single and multi-component thin films and layered structures is described. Representative data are shown for in-situ analysis of Pb and Zr layers at room temperature and high vacuum, as well as under conditions for growth of PZT perovskite films on MgO and RuO2 substrates. DOE

N94-23972* National Aeronautics and Space Administration. Pasadena Office, CA.
METHOD OF FORMING SILICON STRUCTURES WITH SELECTABLE OPTICAL CHARACTERISTICS Patent
Robert W. Fathauer, inventor (to NASA) (Jet Propulsion Lab., California Inst. of Tech., Pasadena.) and Leo Schowalter, inventor (to NASA) (Jet Propulsion Lab., California Inst. of Tech., Pasadena.) 28 Dec. 1993 5 p Filed 10 Jul. 1992 Supersedes N92-30102 (30 - 20, p 3559)
(NASA-Case-NPO-18625-1-CU; US-Patent-5,273,617; US-Patent-Appl-SN-912961; US-Patent-Class-156-613; US-Patent-Class-437-105; US-Patent-Class-437-200; Int-Patent-Class-C30B-23/02) Avail: US Patent and Trademark Office

Silicon and metal are coevaporated onto a silicon substrate in a molecular beam epitaxy system with a larger than stoichiometric amount of silicon so as to epitaxially grow particles of metal silicide embedded in a matrix of single crystal epitaxially grown silicon. The particles interact with incident photons by resonant optical absorption at the surface plasmon resonance frequency. Controlling the substrate temperature and deposition rate and time allows the aspect ratio of the particles to be tailored to desired wavelength photons and polarizations. The plasmon energy may decay as excited charge carriers or phonons, either of which can be monitored to indicate the amount of incident radiation at the selected frequency and polarization. Official Gazette of the U.S. Patent and Trademark Office

N94-24404# Christopher Newport Coll., Newport News, VA. Laser Photonics Lab.
INVESTIGATION OF THE OPTICAL AND LASER PROPERTIES OF Tm AND Ho IN YAG ANF YLF Final Report
Alexey A. Nikitichev (Academy of Sciences, USSR, Saint Petersburg.) Jan. 1994 37 p
(Rept-94-001) Avail: CASI HC A03/MF A01

The spectral-luminescence and laser properties of YAG and YLF crystals doped with Ho(3+) and Tm(3+) as active media for diode pumped lasers are examined. The processes of nonradiative excitation energy transfer (self-quenching sensitization and upconversion) providing the inverse population of working levels are studied. The intensity parameters are calculated for the YLF: Tm Crystal using the Judd-Offelt method. The energy transfer processes are experimentally studied in Ho(3+) and Tm(3+) doped YAG and YLF crystals. The spectroscopic amplifier model at laser diode pumping is proposed and optimization of the Ho(3+) and Tm(3+) concentrations is made. Author

N94-24517# Los Alamos National Lab., NM.
THE MECHANICAL PROPERTIES OF SINGLE CRYSTAL (ALPHA)-SI3N4
I. E. Reimanis, H. Suematsu, J. J. Petrovic, and T. E. Mitchell 1993 8 p Presented at the 1st Meeting of the Pacific Rim Ceramic Societies, Honolulu, HI, 7-10 Nov. 1993
(Contract W-7405-eng-36)
(DE94-002632; LA-UR-93-3531; CONF-931142-3) Avail: CASI HC A02/MF A01

The ambient and high temperature mechanical properties of single crystal alpha-Si3N4 synthesized by chemical vapor deposition are reported. Crack patterns in the as-grown crystals and around Vicker's indentations reveal that significant residual stresses develop during growth. Indentation studies indicate that the cleavage is essentially isotropic in alpha-Si3N4 at 25 C as well as at 1400 C. Transmission electron microscopy on crystals deformed at high temperatures, confirmed previous observation that high-temperature slip occurs primarily on the (1011)(bracket)1120(bracket) system. DOE

N94-24537 Princeton Univ., NJ.
PHOTOINDUCED CHARGE SEPARATION IN SOLID STATE AND MOLECULAR SYSTEMS
1993 10 p Limited Reproducibility: More than 20% of this document may be affected by microfiche quality
(Contract DE-FG02-85ER-13438)
(DE94-001727; DOE/ER-13438/T1) Avail: CASI HC A02

A critical theme has been to understand the role of intrinsic cyanometalate overlayers in modulating interfacial photoinduced charge transfer processes occurring at the Cd chalconide/aqueous ferri-ferrocyanide interface. Structural and charge transfer studies of (CdFe(CN)(sub 6))(sup 2-/1-) overlayers have been undertaken. It is reiterated that the focus of attention on the Cd ferrocyanide overlayer as a critical element in II-VI semiconductor based photoelectrochemical cells, is correct. A new project on metallization of solid supports, using photodeposition of Pt, has been initiated. A project has also been started in the area of visible light, molecular, charge transfer photochemistry. DOE

N94-24567# Oak Ridge National Lab., TN.
THE TORSION SPACE NUCLEIC ACIDS MOLECULAR MECHANICS PROGRAM DUPLEX: SURVEYING CONFORMATION SPACE BY POTENTIAL ENERGY MINIMIZATION
B. E. Hingerty and S. Broyde (New York Univ., New York.) 1993 11 p Presented at the 8th Conversation in the Discipline Biomolecular Stereodynamics, Albany, NY, Jun. 1993
(Contracts DE-AC05-84OR-21400; DE-FG02-90ER-60931)
(DE94-002441; CONF-9306237-4) Avail: CASI HC A03/MF A01

It has been 21 years since the inception of the program DUPLEX. Now that 'molecular modeling' (encompassing quantum mechanics, molecular mechanics and dynamics, and computer graphics) has become something of a trade, the time seems ripe for us to offer a brief perspective of our efforts since the beginnings of the field. The purpose in writing the program was to solve the crystal structure of Ca(++)-GpC, an RNA subunit for which x-ray diffraction data had been collected by T. Sato. No trial structure was available to aid us in solving the phase problem in the Fall of 1972, and we hoped to generate one by potential energy minimization. We hoped to compute not only the conformation of the GpC molecule, but also its packing scheme in the unit cell, a feat that had never before been performed for a nucleic acid subunit. Indeed, only one dinucleoside monophosphate crystal structure, that of UpA, had been previously solved, and its structure was very different from that of GpC. DOE

N94-24617*# Alabama Agricultural and Mechanical Coll., Normal. Dept. of Physics.
DIRECT OBSERVATION OF CRYSTAL GROWTH FROM SOLUTION USING OPTICAL INVESTIGATION OF A GROWING CRYSTAL FACE Annual Technical Report No. 1, 1 Jan. - 31 Dec. 1993
Ravindra Lal Feb. 1994 22 p
(Grant NAG3-1429)
(NASA-CR-195141; NAS 1.26:195141) Avail: CASI HC A03/MF A01

The first technical report for the period 1 Jan. 1993 till 31 Dec. 1993 for the research entitled, 'Direct observation of crystal growth from solution using Optical Investigation of a growing crystal Face' is presented. The work on the project did not start till 1 June 1993 due to the non-availability of the required personnel. The progress of the work during the period 1 June 1993 till the end of 1993 is described. Significant progress was made for testing various optical diagnostic techniques for monitoring crystal solution. Some of the techniques that are being tested are: heterodyne detection technique, in which changes in phase are measured as a interferometric function of time/crystal growth; a conventional technique, in which a fringe brightness is measured as a function of crystal growth/time; and a Mach-Zehnder interferometric technique in which a fringe brightness is measured as a function of time to obtain information on concentration changes. During the second year it will be decided to incorporate the best interferometric technique along with the ellipsometric technique, to obtain real time in-situ growth rate measurements. A laboratory mock-up of the first two techniques were made and tested. Author (revised)

N94-24624# Argonne National Lab., IL.
THERMOMECHANICAL PROCESSING OF Ag-CLAD Bi2Sr2CaCu2O(x) SUPERCONDUCTORS
C. T. Wu, K. C. Goretta, M. T. Lanagan, A. C. Biondo, and R. B. Poeppel Oct. 1993 13 p Presented at the Fall Meeting of the Minerals, Metals and Materials Society: Physical Metallurgy and Materials, Pittsburgh, PA, 17-21 Oct. 1993
(Contract W-31-109-eng-38)
(DE94-002347; ANL/ET/CP-78614; CONF-931009-8) Avail: CASI HC A03/MF A01

Bi2Sr2CaCu2O(x) (2212) powders were synthesized by solid-state reaction, loaded into Ag tubes, and processed into tapes by various combinations of drawing, rolling, and heat treatment. Critical current densities at 4.2 K of greater than 10(exp 5) A/sq cm were achieved from microstructures consisting of large, highly textured 2212 grains. Optimal microstructures were produced by specific mechanical-working conditions and heat-treatment schedules that incorporated solid-state and partial-melt sintering. The relationships between processing, microstructure, and critical current density are discussed. DOE

N94-24657# California Univ., Berkeley. Lawrence Berkeley Lab.
Ge-Au EUTECTIC BONDING OF Ge (100) SINGLE CRYSTALS
W. B. Knowlton, J. W. Beeman, J. H. Emes, D. Loretto, K. M. Itoh, and E. E. Haller Aug. 1993 6 p Presented at the 5th International Workshop on Low Temperature Particle Detectors, Berkeley, CA, 29 Jul. - 3 Aug. 1993
(Contract DE-AC03-76SF-00098)
(DE94-002281; LBL-34447; CONF-930751-1) Avail: CASI HC A02/MF A01

We present preliminary results on eutectic bonding between two (100) Ge single crystal surfaces using thin films of Au ranging from 900 A/surface and Pd (10% the thickness of Au). Following bonding, plan view optical microscopy (OM) of the cleaved interface of samples with Au thicknesses less than or = 500 A/surface show a eutectic morphology more conducive to phonon transmission through the bond interface. High resolution transmission electron microscopy (HRTEM) cross sectional interface studies of a 300 A/surface Au sample show group of zone axes (100) epitaxial growth of Ge. In sections of the bond, lattice continuity of the Ge is apparent through the interface. TEM studies also reveal group of zone axes (110) heteroepitaxial growth of Au with a Au-Ge lattice mismatch of less than 2%. Eutectic bonds with 200 A/surface Au have been attained with characterization pending. An optical polishing technique for Ge has been optimized to insure intimate contact between the Ge surfaces prior to bonding. Interferometry analysis of the optically polished Ge surface shows that surface height fluctuations lie within +/- 150 A across an interval of 1 mm. Characterization of phonon transmission through the interface is discussed with respect to low temperature detection of ballistic phonons. DOE

N94-24958# Yokohama National Univ. (Japan). Faculty of Engineering.
INFLUENCES OF NITROGEN ABSORPTION ON THE MAGNETIC PROPERTIES OF YFe2, YFe3 AND Y6Fe23
Isao Yamamoto, Fumitaka Sugaya, Satoshi Takabatake, Masuhiro Yamaguchi, Tsuneaki Goto, and Mikhail I. Bartashevich Feb. 1993 32 p Sponsored by Ministry of Education, Science and Culture, Tokyo, Japan and Inoue Science Foundation, Tokyo, Japan
(Rept-A-2654; JTN-94-80525) Avail: CASI HC A03/MF A01

The formation of the nitrides YFe2N(x), YFe3N(x) and Y6Fe23N(x) and their magnetic properties have been investigated. The nitrides are formed up to the composition of YFe2N(0.3), YFe3N(0.4) and Y6Fe23N6, retaining the original crystal structures. For all the compounds, nitrogen absorption leads to an apparent decrease in the low-field magnetization, whereas the Fe moment in high magnetic fields is not changed at all. The Curie temperature is almost independent of the nitrogen concentration although it varies by less than 1 percent. Anomalous dips in the magnetization-temperature curves occur around 230 K for Y6Fe23N(x) and around 200 K for YFe3N(x). These two nitrides also exhibit metamagnetic transitions at low temperatures. For Y6Fe23N5 the critical temperature above which the metamagnetism disappears is 250 K. The nitrogen-induced changes in the magnetic properties are explained by the modification of exchange interactions or the occurrence of strong local anisotropy. Author (NASDA)

N94-24959# Saitama Univ., Urawa (Japan). Dept. of Functional Material Science and Engineering.
THE ROLE OF EMITTER STATES IN MAGNETOTUNNELING THROUGH DOUBLE-BARRIER RESONANT-TUNNELING DIODES AT HIGH MAGNETIC FIELDS
Norihiko Kamata, Koji Yamada, Noboru Miura, and Laurence Eaves Mar. 1993 31 p
(Rept-A-2658; JTN-94-80529) Avail: CASI HC A03/MF A01

By applying pulsed high magnetic fields up to 40 T perpendicular (B(sub perpendicular)) and parallel (B(sub parallel) is parallel to I) to the current direction, a distinct role of emitter states in the magneto-tunneling processes through resonant tunneling diodes has been investigated. The B(sub perpendicular) dependence of the threshold voltage in current vs. voltage (one - five) curves has been explained consistently by tunneling from a combined magneto-electric state of a one-dimensional (1 D) emitter to that of a zero-dimensional (0 D) m well state. A drastic current decrease above B(sub parallel) = 10 T under constant applied voltage below the negative differential conductivity region together with multi-peaked one - five curves with hysteresis at above B(sub parallel) = 30 T was observed. These distinct features were analyzed by a self-consistent model of the charge build-up effect and the energy configuration of the 0 D emitter, 1 D emitter and 0 D well states. Author (NASDA)

N94-24960# Shizuoka Univ. (Japan). Dept. of General Education.
GGA STUDY OF THE MAGNETIC AND COHESIVE PROPERTIES OF bcc, fcc AND hcp Mn
Toshio Asada and Kiyoyuki Terakura Mar. 1993 17 p Sponsored by Ministry of Education, Science and Culture, Tokyo, Japan
(Rept-A-2662; JTN-94-80533) Avail: CASI HC A03/MF A01

Magnetic and cohesive properties of bcc (body centered cubic), fcc (face centered cubic), and ideal hcp (hexagonal closest packing) Mn are calculated by use of the Generalized Gradient Approximation (GGA) proposed by Perdew and Wang. Calculated results predict correctly an antiferromagnetic ground state for the fcc structure with lattice constant and magnetic moment in good agreements with experimental values. Investigation of the contribution to the free energy from lattice vibration by use of quasi-harmonic approximation removes apparent difficulties involving an hcp ground state in the calculated total energies of three structures. Author (NASDA)

N94-24978# Kyoto Univ., Sakyoku (Japan). Dept. of Physics.
ON SUPERCONDUCTIVITY OF ALPHA-(BEDT-TTF)2KHg(SCN)4
Hiroshi Ito, Hiroshi Kaneko, Takehiko Ishiguro, Hidehiko Ishimoto, Kimitoshi Kono, Sachio Horiuchi, Tokutaro Komatsu, and Gunji Saito Mar. 1993 18 p Sponsored by Ministry of Education, Science and Culture, Tokyo, Japan
(Rept-A-2660; JTN-94-80531) Avail: CASI HC A03/MF A01

The resistivity decrease in alpha-(BEDT (Bis(ethyleneclithio)) - TTF (Tetrathiafulvalene)) 2KHg(SCN)4 appearing in the temperature region below 300 mK was found to be suppressed by a magnetic fields of less than 0.1 T. The decrease in resistivity is due to the superconductivity occurring in a fibril-like structure. The observed behavior is in part due to the inhomogeneous molecular arrangement, but is also related to the subtle interplay between magnetism and superconductivity in this system. Author (NASDA)

N94-25024*# Christopher Newport Coll., Newport News, VA. Dept. of Physics.
EXCITED STATE DYNAMICS OF THULIUM IONS IN YTTRIUM ALUMINUM GARNETS
G. Armagan, A. M. Buoncristiani, and B. DiBartolo (Boston Coll., Chestnut Hill, MA.) 1991 10 p Repr. from Optic Materials (Elsevier Science Publishers B.V.) p 1-10
(Grants NAG1-796; NAG1-955)
(NASA-CR-195159; NAS 1.26:195159) Copyright Avail: CASI HC A02/MF A01

The processes that take place in the excited states of a trivalent Thulium (Tm) ion in an Yttrium Aluminum Garnet (YAG) crystal, being relevant to the use of this system for laser applications, have been the object of several studies. We have reexamined this system focusing our attention on the dynamics of Tm following its excitation in the H-3(sub 4) level. Under these conditions the system relaxes through a cross-relaxation process. H-3(sub 4) yields F-3(sub 4), H-3(sub 6) yields F-3(sub 4), whose rate depends upon both the concentration of the Tm ion and the temperature of the crystal. The excitation spectrum obtained by monitoring the 1.8 micron emission of Tm (due to the F-3(sub 4) yields H-3(sub 6) transition) indicates an increase in the contribution to this emission from the H-3(sub 4) level relative to the H-3(sub 5) level as the Tm concentration increases; this shows the increased role played by the H-3(sub 4) level in pumping the infrared emission. Correspondingly, the duration of the luminescence originating in the H-3(sub 4) level is shortened as the concentration of Tm increases. The concentration quenching of this lifetime can be fit to a model which assumes that the cross-relaxation is due to a dipole-dipole interaction; from this fit, the intrinsic Tm lifetime in the absence of cross relaxation can be derived. We have used this lifetime to calculate the rate of the cross-relaxation process. We have evaluated this rate as a function of the temperature and found it to be fastest at 77 K. We have also calculated the microscopic interaction parameters for the cross-relaxation process by using two independent experimental features: (1) the time evolution of the emission from the H-3(sub 4) level; and (2) the spectral overlap between the H-3(sub 4) yields F-3(sub 4) emission and the H-3(sub 6) yields F-3(sub 4) absorption. We have also considered the migration of excitation among the Tm ions in the F-3(sub 4) level and calculated the relevant microparameter by the use of the relevant spectral overlap. The data are consistent with the model in which the Tm ions, once excited into the H-3(sub 4) level decay by cross-relaxation to the F-3(sub 4), and then transfer rapidly their energy to other Tm ions. Author (revised)

N94-25025# Christopher Newport Coll., Newport News, VA. Laser Photonics Lab.

TWO MICRON STIMULATED EMISSION OF ACTIVATED INSULATING CRYSTALS

Alexander A. Kaminskii (Academy of Sciences, USSR, Moscow.) Jan. 1994 13 p

(Rept-94-002) Avail: CASI HC A03/MF A01

Two micron stimulated emission (SE) has potential for a variety of applications due to its relatively low physiological activity. Since the end of the 1960's, our laboratory has carried out systematic studies of crystalline laser materials that are suitable for 2 micron SE generation. Most of the research has focused on the generating properties of Ho(sup 3+), Tm(sup 3+), and Er(sup 3+) activator ions in different oxide and fluoride crystals with ordered and disordered structures. The crystals that were used in the spectroscopic and laser experiments were grown from the melt. Garnet Gd3Ga5O12 single crystals were grown by the Czochralski method using iridium crucibles. Alumina based crystals--garnets and perovskites--and fluoride crystals were grown by the Bridgman-Stockbarger method using molybdenum and graphite containers, respectively. A fluoridizing atmosphere was used for the latter processes. Two micron SE of these ions was realized by using new laser-action excitation schemes as well as through different laser pumping methods. Author (revised)

N94-25027 Materials Research Society, Pittsburg, PA.

FERROELECTRIC THIN FILMS 3

Edward R. Myers (National Semiconductor Corp., Santa Clara, CA.), Bruce A. Tuttle (Sandia National Labs., Albuquerque, NM.), Seshu B. Desu (Virginia Polytechnic Inst., Blacksburg.), and Poul K. Larsen (Philips Gloeilampenfabrieken N.V., Eindhoven, Netherlands.) 16 Apr. 1993 518 p Symposium held in San Francisco, CA, 13-16 Apr. 1993 Limited Reproducibility: More than 20% of this document may be affected by microfiche quality

(Contract N00014-93-I-0400)

(AD-A273394) Avail: Issuing Activity (Defense Technical Information Center (DTIC))

This symposium showcased the advancement in processing technology and basic scientific understanding of ferroelectric thin films. The conference highlighted the use of novel material science analysis techniques to characterize ferroelectric thin film materials and devices and to relate the nanoscale features and responses detected by these techniques to ferroelectric, electrooptic, and piezoelectric properties. Examples of newer material analysis techniques included atomic force microscopy, electron spin resonance, high resolution transmission electron microscopy, combined Rutherford backscattering-nuclear reaction analysis, and the use of optical interferometry to provide a three dimensional representation of field induced displacement. DTIC

N94-25059# Technische Univ., Eindhoven (Netherlands). Dept. of Physics.

QUANTUM TUNNELING TRANSPORT OF ELECTRONS IN DOUBLE-BARRIER HETEROSTRUCTURES: THEORY AND MODELING Ph.D. Thesis

Henricus Joseph Mari Noteborn 1993 177 p Sponsored by Netherlands Organization for the Advancement of Scientific Research

(ETN-94-95332) Avail: CASI HC A09/MF A02

The Double Barrier Resonant Tunneling (DBRT) diode model chosen to describe the heterofunction superlattices having two or more barriers is presented. Both the charge accumulation and depletion in the electrodes and the electrostatic feedback due to charge storage in the well are studied. The coherent tunneling method is described. Special emphasis is given to the determination of the position and width of the transmission peak. The theoretical background for the wave mechanical approach to tunneling in semiconductors is provided. Applications of the DBRT model are given. The stability of the current solutions obtained from the static model, its relation to the DBRT impedance, and the equivalent circuit that describes the diode are discussed. The application of quantizing magnetic fields, both perpendicular and parallel to the barriers, are covered. ESA

N94-25086# New Mexico Univ., Albuquerque. Dept. of Chemistry.

THE NANOMETER-SCALE MECHANICS OF GOLD FILMS Technical Report, 1 Aug. 1992 - 31 Jul. 1993

P. Tangyunyong, R. C. Thomas, J. E. Houston, T. A. Michalske, and R. M. Crooks 23 Nov. 1993 30 p

(Contract N00014-91-J-1991)

(AD-A273307; TR-7) Avail: CASI HC A03/MF A01

We have used interfacial force microscopy (IFM) to monitor the mechanical deformation of single nanometer-sized grains in Au thin films. Our results show that protruding grains, which represent early-stage delamination, display multiple deformation mechanisms including grain-boundary sliding and intragranular plasticity. The unprecedented load displacement control capability of the IFM provides data that is used for the first time to quantitatively distinguish and evaluate individual deformation processes. DTIC

N94-25093*# Eloret Corp., Palo Alto, CA.

SIMULATION STUDIES FOR SURFACES AND MATERIALS STRENGTH Final Technical Report, 1 May 1984 - 31 Jan. 1994

Timur Halicioglu and Grant D. Smith 7 Mar. 1994 14 p

(Contract NCC2-297)

(NASA-CR-195185; NAS 1.26:195185) Avail: CASI HC A03/MF A01

Computer simulation studies were conducted to investigate materials properties. All the calculations were carried out using atomic level simulation techniques which are based on semiempirical or model functions. During this project, functions with varying degrees of complexity were derived and employed in simulations. Investigations include covalently bonded materials as well as systems involving metal atoms. For small clusters calculated results provided information on various energy- and structure-related properties along with vibrational characteristics. Also, energy barriers for configurational transitions were calculated for selected cases. Simulation calculations for surfaces produced new results in areas related to surface energies, reconstructions and relaxations, surface defects, surface stresses as well as adsorption and nucleation processes. Simulations were also performed on bulk materials. Calculated results provided an atomic level understanding on energetics and structures of point defects, crystal stability, elastic properties, and materials strength for various systems. Calculations involving polymeric materials include studies of polar polymer melts and polymer/solid interfaces. Simulations employing specially developed codes provided significant information about energetics and conformational characteristics of different polymeric chains. Author (revised)

N94-25160# Pittsburgh Univ., PA. Surface Science Center.

SELECTED BIBLIOGRAPHY 2: DIAMOND SURFACE CHEMISTRY

Jian Wei, V. S. Smentkowski, and J. T. Yates, Jr. 30 Sep. 1993 226 p

(Grant AF-AFOSR-0364-89)

(AD-A273518; AFOSR-93-0850TR) Avail: CASI HC A11/MF A03

Key articles related to the surface chemistry of diamond crystals are presented in this 1993 update of an earlier compilation. The listings are arranged chronologically. The review extends up to mid-1993. This review will be useful to workers in the field of diamond film-growth chemistry even though the extensive film-growth literature has not been reviewed. DTIC

N94-25280# Technische Univ., Eindhoven (Netherlands). Low Temperature Physics Group.

TUNNELLING IN METALLIC CONTACTS ON HIGH-T(c) SUPERCONDUCTORS: A STORY OF CHARGE CARRIERS IN YBa2Cu3O(7-DELTA) AND Bi2CaSr2Cu2O(8+DELTA) Ph.D. Thesis

Henk Jan vanSchevicoven 1992 148 p Sponsored by Netherlands Foundation for Technical Sciences

(ISBN-9-03-860142-5; ETN-94-95304) Avail: CASI HC A07/MF A02

Electrical properties of contacts fabricated on the surface layer of polycrystalline YBCO and of single crystalline BiCaSCO are described. For polycrystalline YBCO pellets several fabrication methods are described, but only one method, silver paint on a gold layer deposited on the pellet, resulted in contacts yielding reproducible electrical characteristics after several thermal cycles of cooling down to 4.2K and warming up to room temperature. Other methods, such as bonding or (mechanical) point contacts, had the disadvantage of damaging the surface layer. The contacts to YBCO are relatively high ohmic and the associated voltages therefore are relatively high. As a result superconductive features are not visible. In fact, a model describing the contact as an N-I-N junction, predicts I-V curves that are in good agreement with the experiments, even though totally disregarding superconductivity. In contrast to the YBCO measurements, single crystalline BiCaSCO yields contacts that are relatively low ohmic. Superconductive features then become evident. The model used to describe the contacts of YBCO is extended to include Andreev reflection. This enables good agreement to be obtained with most of the electrical characteristics of contacts to BiCaSCO, but not with all. The merits of this model are critically evaluated. The main differences and similarities between contacts fabricated on the two superconductors are summarized. ESA

N94-25288# Autometric Corp., Inc., Alexandria, VA.
IMAGE ANALYSIS TECHNOLOGY APPLIED TO PROBLEMS IN CRYSTALLOGRAPHY Final Report, 1 Jul. 1991 - 30 Jun. 1992
Daniel Gordon 30 Jun. 1993 8 p
(Contract F49620-91-C-0058)
(AD-A273516; AFOSR-93-0865TR) Avail: CASI HC A02/MF A01

This work summarizes the procedures accomplished toward the objective of developing a demonstration capability (Proof-of-Concept) of three dimensional object modeling using close range photogrammetric techniques. Static stereo views and three-dimensional perspective scenes of crystals were to be developed using the same technology that is applied in displaying three dimensional earth surfaces. The work included the creation of close range photogrammetric capabilities to work along with various existing display capabilities. The imagery for this project was provided by the 3M Co. It was acquired using a Scanning Electron Microscope (SEM). The softcopy concept was demonstrated to the Office of Commercial Programs National Aeronautics and Space Administration at Autometric (Alexandria, VA headquarters). DTIC

N94-25297 Technische Univ., Eindhoven (Netherlands).
ON THE ORIGIN OF 1/f NOISE IN EPITAXIAL GaAs Ph.D. Thesis
Lin Ren 1993 110 p Sponsored by Netherlands Organization for the Advancement of Scientific Research Limited Reproducibility: More than 20% of this document may be affected by microfiche quality
(ISBN-9-09-006067-7; ETN-94-95334) Avail: CASI HC A06

A series of papers covering investigations into electrical 1/f noise is presented. Experimental results of 1/f noise and its temperature dependence in epitaxial n-GaAs, with the thickness and the dope concentration as parameters, are presented. A study of 1/f noise in Hall voltage of molecular beam epitaxy (MBE) grown n-GaAs is presented. A study of low frequency noise in electron irradiated n-GaAs epitaxial layers is presented. For the interpretation a simple formalism was needed which is presented. Investigations of 1/f noise in proton irradiated n-GaAs epitaxial layers are reported. A study of 1/f noise in an Al(x)Ga(1-x)As/GaAs heterostructure with a two dimensional gas is presented. ESA

N94-25332# China Nuclear Information Centre, Beijing.
INVESTIGATION OF THE SOLID-SOLID SURFACE ADSORPTION OF Eu2O3 ON AMORPHOUS Al2O3
Rong-Chuan Liu (Nanjing Univ., China.), Qi-Jie Yan (Nanjing Univ., China.), Hai-Hua Qi (Nanjing Univ., China.), Yuan-Fu Xia (Nanjing Univ., China.), Ya Zhai, J. Jiang (Saarland Univ., Saarbrucken, Germany.), and U. Gonser (Saarland Univ., Saarbrucken, Germany.) Nov. 1991 14 p
(DE93-613824; CNIC-00567; NU-0007) Avail: CASI HC A03/MF A01 (US Sales Only)

Solid-solid surface adsorption of Eu2O3 of amorphous Al2O3 was investigated by Moessbauer spectroscopy, x-ray diffraction analysis, and a Laser Raman Spectra. No x-ray diffraction peak of crystalline Eu2O3 can be found for all samples studied. With increasing Eu2O3 content the isomer shift and line width increase continuously and gradually approach to those of bulk Eu2O3. The Laser Raman Spectra show that two peaks at 998 and 1051 cm(exp -1) assigned to two-dimensional surface europium-oxygen species appear at Eu2O3 content of 18.7 wt.%. The peak at 1068 cm(exp -1) due to the surface species and another peak at 342 cm(exp -1) due to crystalline Eu2O3 content start to appear for the sample with Eu2O3 content of 36.5 wt.%. The dispersity of Eu2O3 on the surface of amorphous Al2O3 was compared with that of gamma-Al2O3, eta-Al2O3 and SiO2 gel. The change of isomer shift for the different support results from their distinct electronegativity. The results of these studies indicate that the structure of Eu2O3 dispersed onto the support surface depends on the structure of support and that there is an inductive effect of support on the structure of the Eu2O3. DOE

N94-25347# Technical Research Centre of Finland, Espoo. Reactor Lab.
DUAL-PURPOSE RTOF DIFFRACTOMETER FACILITY AT THE ET-RR-1 REACTOR
R. M. A. Maayouf, P. E. Hiismaeki, O. K. Antson, and A. T. Tiitta Nov. 1992 17 p
(VTT-TIED-1425; ISBN-9-51-384319-X; ETN-94-95257) Copyright Avail: CASI HC A03/MF A01

The reverse time of flight (RTOF) diffractometer facility, to be installed at the ET-RR-1 reactor, is discussed. The facility is a dual purpose instrument: it can be used for high resolution crystallography utilizing transmission diffraction technique and for strain measurements of technical components using a scattering geometry with a detector at 90 degrees. The RTOF diffractometer is an efficient tool for basic and applied research in material science. The proposed device allows transmission diffractometry and strain measurements. The resolution level at d equal to 2 angstroms for the transmission diffractometry is 0.2, and is 0.5 for strain diffractometry. The transmission geometry allows the resolution to be improved by a factor of three at a maximum. ESA

N94-25390 International Centre for Theoretical Physics, Trieste (Italy).
THE EFFECT OF A TRANSPORT CURRENT ON THE SURFACE BARRIER OF A UNIAXIAL ANISOTROPIC SUPERCONDUCTING SLAB
A. G. Saif Oct. 1992 9 p Limited Reproducibility: More than 20% of this document may be affected by microfiche quality
(DE93-617135; IC-92/360) Avail: CASI HC A02 (US Sales Only)

The role of a transport current on the annihilation of the surface barrier for high temperature type II superconducting infinite slab of arbitrary thickness is investigated. The London penetrating field, the vortex fields, and the Gibbs potential are calculated. The barrier depends on the external field strength, the value of the transport current flowing through the slab and the orientation of the external field. An agreement of our results with the previous one in some cases is found. DOE

N94-25391 International Centre for Theoretical Physics, Trieste (Italy).
EFFECTS OF A VIBRATING WIRE CARRYING DC CURRENT ON A MOVING TYPE 2 SUPERCONDUCTING SLAB OF ARBITRARY THICKNESS
A. G. Saif Oct. 1992 8 p Limited Reproducibility: More than 20% of this document may be affected by microfiche quality
(DE93-617136; IC-92/361) Avail: CASI HC A02 (US Sales Only)

A modified London equation is developed to study the system of a vibrating wire (two vibrating wires) carrying a direct current parallel to a moving type II superconducting infinite slab of arbitrary thickness. Exact solutions of the magnetic vector potential inside and outside the superconducting sample are obtained. Moreover, exact integral expression of power losses is obtained. These analytical solutions can be used for testing of the superconducting slabs in motion and the related problems of losses of moving superconductors. A good agreement with previous results is found in some limited cases. DOE

N94-25392 International Centre for Theoretical Physics, Trieste (Italy).
SURFACE BARRIER OF A UNIAXIAL ANISOTROPIC TYPE 2 SUPERCONDUCTING CYLINDER
A. G. Saif Oct. 1992 10 p Limited Reproducibility: More than 20% of this document may be affected by microfiche quality
(DE93-617137; IC-92/362) Avail: CASI HC A02 (US Sales Only)

The analytical solutions of the anisotropic London equation are developed for the cylindrical type II superconductors. By using these solutions (the London penetrating field and vortex fields), the Gibbs free energy and the superheating field are calculated. The annihilation of the surface barrier by the transport current is found. DOE

N94-25403 International Centre for Theoretical Physics, Trieste (Italy).
SIMULATION OF THE VORTEX MOTION IN THE HIGH T(c) SUPERCONDUCTORS
Jin-Ming Dong Nov. 1992 14 p Limited Reproducibility: More than 20% of this document may be affected by microfiche quality
(DE93-617138; IC-92/373) Avail: CASI HC A03 (US Sales Only)

One-d and 2D simulations of the single vortex dynamics in the presence of random pinning potential and periodical one were carried out. It is shown that the randomness of the pinning sites distribution does not have considerable effect on the transport properties such as I-V characteristics of the high T(sub c) superconductors, which was widely discussed in the approximation of a periodical pinning potential using analytical method. The randomness effect probably only reduces the vortex diffusing mobility more below the depinning current value, which is more obvious at lower temperature. DOE

N94-25412# Tokyo Univ. (Japan). Inst. for Solid State Physics.
MAGNETIC PROPERTIES OF NdCo3 AND ITS GAMMA PHASE HYDRIDE NdCo3H(4.1)
M. I. Bartashevich, K. Koui, T. Goto, M. Yamaguchi (Yokohama National Univ., Japan.), I. Yamamoto (Yokohama National Univ., Japan.), and F. Sugaya (Yokohama National Univ., Japan.) Feb. 1993 25 p Sponsored by Inoue Science Foundation, Tokyo, Japan and Ministry of Education, Science and Culture, Tokyo, Japan
(Rept-A-2655; JTN-94-80526) Avail: CASI HC A03/MF A01

Magnetization measurements have been carried out for an aligned powder sample NdCo3 and for an isotropic one of the hydride NdCo3H(4.1). NdCo3 is a ferromagnet with T(sub c) = 381 K and exhibits a spin reorientation transition of easy direction from the basal plane to the c-axis in the temperature range 220 to 255 K. NdCo3 shows a field induced phase transition in low fields below 0.7 T along the c-axis from the collinear to noncollinear structure at temperatures below 115 K. NdCo3H(4.1) is an antiferromagnet with T(sub N) = 214 K and exhibits a metamagnetic transition to the ferromagnetic structure in applied magnetic fields. The transition field of NdCo3H(4.1) is significantly decreased compared with the hydride with nonmagnetic Y instead of Nd by the positive exchange field acting on the Co sublattice from the Nd sublattice. Author (NASDA)

N94-25422 Israel Atomic Energy Commission, Beersheba. Nuclear Research Center.
TRANSIENT FLOWS OCCURRING DURING THE ACCELERATED CRUCIBLE ROTATION TECHNIQUE
Atara Horowitz and Yigal Horowitz (Ben Gurion Univ. of the Negev, Beersheva, Israel.) Nov. 1992 20 p Limited Reproducibility: More than 20% of this document may be affected by microfiche quality
(DE93-617049; NRCN-533) Avail: CASI HC A03 (US Sales Only)

The transient flows occurring after a change in the angular velocity of the cylindrical container are described. The dependence of the transient (known as spin-up or spin-down time) on experimental parameters as kinematic viscosity, cylinder dimensions, and the cylinder's initial and final angular velocities are elucidated by a review of the literature. It is emphasized that with large Rossby numbers the spin-up time is longer and the amount of fluid mixing is greater than small and moderate Rossby numbers. It is also elucidated that most crystal growth crucibles cannot be considered as infinitely-long cylinders for the evaluation of the fluid dynamics. DOE

N94-25423 International Centre for Theoretical Physics, Trieste (Italy).
ELECTRONIC STRUCTURE AND HIGH PRESSURE PHASE TRANSITION IN LaSb AND CeSb
S. Mathi Jaya and S. P. Sanyal Sep. 1992 20 p Limited Reproducibility: More than 20% of this document may be affected by microfiche quality
(DE93-617051; IC-92/287) Avail: CASI HC A03 (US Sales Only)

The electronic structure and high pressure structural phase transition in cerium and lanthanum antimonides were investigated using the tight binding Linear Muffin-Tin Orbitals (LMTO) method. The calculation of total energy reveals that the simple tetragonal structure is found to be stable at high pressures for both the compounds. In the case of LaSb, the calculated value of the equilibrium cell volume and the cell volume at which phase transition occurs are found to have a fairly good agreement with the experimental results. However, in the case of CeSb, the agreement is not as good as in LaSb. The most favored c/a value in the high pressure phase (simple tetragonal) for these compounds was also predicted. Further the calculated results on the electronic structure of these systems at the equilibrium as well as at the reduced cell volumes are presented. DOE

N94-25424 Joint Inst. for Nuclear Research, Dubna (USSR).
LATTICE DYNAMICS OF Ba(1-x)K(x)BiO3 AS STUDIED BY NEUTRON SCATTERING AND COMPUTER SIMULATION
A. V. Belushkin, A. V. Vagov, M. G. Zemlyanov, and P. P. Parshin 1991 15 p Limited Reproducibility: More than 20% of this document may be affected by microfiche quality
(DE93-617053; JINR-E-14-91-519) Avail: CASI HC A03 (US Sales Only)

A time-of-flight neutron inelastic scattering study of the lattice dynamics of Ba(1-x)K(x)BiO3 for x = 0.0 and x = 0.4 was performed for the temperatures 10, 80, and 290 K. No temperature effects were found for the generalized phonon density of states. The phonon spectrum of a superconducting sample reveals less in number van Hove singularities and softens in comparison with that of the nonsuperconducting one. On the basis of the simple model for interatomic potential the lattice dynamics of this system was calculated. Some features of the structural phase diagram and the optical spectroscopy data were explained using this model. The calculated phonon density of states was found to be in good agreement with experiment. DOE

N94-25425 Joint Inst. for Nuclear Research, Dubna (USSR). Lab. of Neutron Physics.
CRYSTAL FIELD IN Nd2CuO4
A. Yu. Muzychka, M. Divis, E. A. Goremychkin, I. Natkaniec, and I. L. Sashin 1991 15 p Limited Reproducibility: More than 20% of this document may be affected by microfiche quality
(DE93-617054; JINR-R-3-91-450) Avail: CASI HC A03 (US Sales Only)

On the base of magnetic inelastic neutron scattering on polycrystalline Nd2CuO4, the set of crystal electric field parameters was determined. These parameters satisfactorily describe both neutron spectra and experimental data on magnet susceptibility of monocrystal of this compound. Strong hybridization of ground and first excited multiplets was discovered. Predictional ability of the superposition model in nonmetals is confirmed. Quantitative significance of molecular field parameter was obtained. DOE

N94-25426 International Centre for Theoretical Physics, Trieste (Italy).
THE HALDANE ENERGY GAP OF A DOPED LINEAR-CHAIN HEISENBERG ANTIFERROMAGNET
Zhong-Yi Lu, Zhao-Bin Su, and Lu Yu Nov. 1992 14 p Limited Reproducibility: More than 20% of this document may be affected by microfiche quality
(DE93-617130; IC-92/378) Avail: CASI HC A03 (US Sales Only)

Using the valence-bond-solid (VBS) approach and the Schwinger boson mean field approximation, the dependence of the Haldane gap of a spin-1 linear chain Heisenberg antiferromagnet on impurity doping with different spins was studied. The impurity spins affect the singlet pairing order parameter (Delta) and the constraint factor (lambda). As a result, the Haldane gap is reduced by a factor approximately n(sub i)(sup 2/3), with n(sub i) as the impurity concentration, and eventually collapses at n(sub i) approximately 1/(xi) with (xi) as the VBS correlation length. This theoretical prediction can be verified by neutron scattering experiments. DOE

N94-25441# Wright Lab., Wright-Patterson AFB, OH.
STRUCTURE OF CHOLESTERYL-4-VINYLBENZOATE Final Report, 1 Jun. - 1 Aug. 1993
E. P. Socci (Virginia Univ. Hospital, Charlottesville.), B. L. Farmer (Virginia Univ. Hospital, Charlottesville.), M. L. Chabinyc (Dayton Univ., OH.), A. V. Fratini (Dayton Univ., OH.), T. J. Bunning, and W. W. Adams Aug. 1993 50 p
(AF Proj. 2422)
(AD-A273686; WL-TR-93-4088) Avail: CASI HC A03/MF A01

The structure of cholesteryl-4-vinylbenzoate was determined by x ray diffraction. The molecule is elongated, with the benzoate group oriented out of the plane of the tetracyclic core. Molecules pack antiparallel, with overlap between either aliphatic tails or tetracyclic cores. These two types of interactions (overlap) are similar to the two packing modes that coexist in the liquid crystalline phase. DTIC

N94-25447 International Centre for Theoretical Physics, Trieste (Italy).
EFFECT OF HIGH FREQUENCY FIELD ON THE TRANSPORT PROPERTIES OF SUPERLATTICE
S. Y. Mensah Oct. 1992 9 p Limited Reproducibility: More than 20% of this document may be affected by microfiche quality
(DE93-617047; IC-92/299) Avail: CASI HC A02 (US Sales Only)

Theoretical study of the transport properties of semiconductor superlattice (SL) in the presence of external electric field E(t) has been investigated with the help of Boltzmann's equation. The model adopted agrees fairly well with experimental work as well as Monte Carlo simulation. Among the phenomena observed are the induced self transparency, absolute negative conductivity and the negative differential conductivity. In the case of negative differential conductivity (NDC) it is observed that it does also occur under the a.c. and d.c electric field but appears only when (omega)(tau) is much less than than 1. It does appear in the vicinity where the d.c field E(sub 0) is equal to the amplitude of the a.c. field E(sub 1) and the peak decreases with an increase in E(sub 1). DOE

N94-25483 International Centre for Theoretical Physics, Trieste (Italy).
CONTRIBUTION OF ALL EXCITED STATES TO ZFS OF A (SUP 6) S-STATE
Wang Kangying Oct. 1992 11 p Limited Reproducibility: More than 20% of this document may be affected by microfiche quality
(DE93-617007; IC-92/348) Avail: CASI HC A03 (US Sales Only)

The rank-four spin-Hamiltonian parameter b(sup 0)(sub 4) and the rank-two term b(sup 0)(sub 2) of a 3d(sup 5) ion are examined by diagonalizing the complete energy matrices using SO mechanism in tetragonal symmetry. It is shown that the parameter b(sup 0)(sub 2) arises mainly from the interaction of a (sup 6)S-state with the spin quartets, but the calculation b(sup 0)(sub 4) must consider the contribution of the spin doublets. It makes no difference in the cubic field, where the quartets only play the role of a bridge. Numerical calculation for Mn(2+) ions in CaWO4 show that EPR zero-field splitting parameters might have uniformly been interpreted by using SO mechanism. DOE

N94-25515# Tokyo Univ. (Japan). Inst. for Solid State Physics.
MAGNETIC FIELD-INDUCED SADDLE POINT IN GaAs/AlGaAs SHORT PERIOD SUPERLATTICES
Satoshi Sasaki, Noboru Miura, and Yoshiji Horikoshi (Nippon Telegraph and Telephone Public Corp., Tokyo, Japan.) Feb. 1993 15 p
(Rept-A-2656; JTN-94-80527) Avail: CASI HC A03/MF A01

Interband magneto-absorption spectra of (GaAs)(6)/(Al(0.51)Ga(0.49)As)(6) = (6, 6) and (GaAs)(14)/(AlAs)(6) = (14, 6) under pulsed high magnetic fields up to 150 T was measured. In sample (6, 6), drastic broadening of the exciton peak due to a magnetic field-induced saddle point was observed when high magnetic fields were applied in the direction parallel to the layer planes and the cyclotron radius became smaller than the superlattice period. The line shape of the broadened exciton resonance was qualitatively understood as an effect of the Coulomb interaction between electrons and holes. The exciton binding energy of sample (6, 6) was estimated as 7.0 meV using the perturbational theory, which reflects an intermediate nature of the superlattice between bulk crystals and two-dimensional quantum wells. Author (NASDA)

N94-23664*# Pennsylvania State Univ., University Park. Dept. of Aerospace Engineering.
THREE-DIMENSIONAL SOLIDIFICATION AND MELTING USING MAGNETIC FIELD CONTROL
George S. Dulikravich and Vineet Ahuja *In* NASA. Lewis Research Center, The Fifth Annual Thermal and Fluids Analysis Workshop Nov. 1993 p 449-464 (For primary document see N94-23634 06-34)
Avail: CASI HC A03/MF A04; 5 functional color pages

N94-23686*# Kent State Univ., OH. Dept. of Mathematics and Computer Science.
APPLICATION OF MULTIGRID METHODS TO THE SOLUTION OF LIQUID CRYSTAL EQUATIONS ON A SIMD COMPUTER
Paul A. Farrell, Arden Ruttan, and Reinhardt R. Zeller *In* NASA. Langley Research Center, The Sixth Copper Mountain Conference on Multigrid Methods, Part 1 Nov. 1993 p 191-206 (For primary document see N94-23673 06-64)
(Grant DMR89-20147)
Avail: CASI HC A03/MF A03

N94-24344*# Alabama Univ., Huntsville. Center for Microgravity and Materials Research.
TEMPERATURE DEPENDENCE OF PROTEIN SOLUBILITY-DETERMINATION, APPLICATION TO CRYSTALLIZATION, AND GROWTH KINETICS STUDIES Abstract Only
Franz Rosenberger *In* NASA. Marshall Space Flight Center, Microgravity Studies of Organic and Polymeric Materials Dec. 1993 p 47 (For primary document see N94-24338 06-23)
Avail: CASI HC A01/MF A03

77 THERMODYNAMICS AND STATISTICAL PHYSICS

Includes quantum mechanics; theoretical physics; and Bose and Fermi statistics.

For related information see also *25 Inorganic and Physical Chemistry* and *34 Fluid Mechanics and Heat Transfer.*

N94-22709# Universiteit Twente, Enschede (Netherlands). Faculty of Applied Mathematics.
QUANTUM MECHANICS, LOCALITY AND REALISM
Jowi W. deRoever and Martin Streng Feb. 1993 21 p
(MEMO-1117; ETN-94-94757) Avail: CASI HC A03/MF A01

The question of whether the theory of quantum mechanics is a local realistic theory is addressed. The concept of locality is shown to be independent of the postulates of quantum mechanics. In particular, under the assumption that nature is local, the quantum mechanical predictions concerning experiments on correlated systems are shown to satisfy Bell's inequalities. ESA

N94-22719# Colorado State Univ., Fort Collins.
STUDY OF IMPROVED METHODS FOR PREDICTING CHEMICAL EQUILIBRIA
T. G. Lenz and J. D. Vaughan Sep. 1993 33 p
(Contract DE-FG02-86ER-13582)
(DE94-001647; DOE/ER-13582/T3) Avail: CASI HC A03/MF A01

The objective was to develop computational methods for equilibrium constants of Diels-Alder reactions in gas and liquid solution phases. The approach was to calculate standard enthalpies of formation at 298 K and standard thermodynamic functions for a range of temperatures for reactants and products, and then to calculate standard enthalpies, entropies, Gibbs free energies, and equilibrium constants at various temperatures. DOE

N94-22968 Centro Brasileiro de Pesquisas Fisicas, Rio de Janeiro.
ON SPONTANEOUS SYMMETRY BREAKING MECHANISM IN LIGHT-FRONT QUANTIZED FIELD THEORY
P. P. Srivastava 1992 11 p Limited Reproducibility: More than 20% of this document may be affected by microfiche quality
(DE93-633211; CBPF-NF-004/92) Avail: CASI HC A03 (US Sales Only)

Following the (standard) Dirac procedure, the spontaneous symmetry breaking in light-front quantized scalar field theory is described. The zero mode operator of the field is shown to commute with the nonzero mode operators, and thus may be looked upon as a background field. In the light-front framework a nonlocal constraint must be satisfied. The values of the background field at the tree level, as a consequence, are shown to follow from the minimization of the light-front energy functional. We are thus led to a description parallel to the one made in equal-time-framework where we appeal to physical considerations and minimize the energy. These values characterize the various (non-perturbative) vacua over which the corresponding physical sectors may be built by applying the non-zero mode operators. DOE

N94-23216# Lawrence Livermore National Lab., CA.
FULLY COUPLED NONLINEAR THERMOMECHANICAL ANALYSIS INCLUDING GENERAL CONTACT IN PALM2D
B. E. Engelmann and R. G. Whirley Oct. 1993 7 p Presented at the Annual Winter Meeting of the American Society of Mechanical Engineers,

New Orleans, LA, 28 Nov. - 3 Dec. 1993
(Contract W-7405-eng-48)
(DE94-001661; UCRL-JC-115418; CONF-931121-27) Avail: CASI HC A02/MF A01

Fully coupled thermomechanical analysis solves the thermal problem on the deforming geometry and incorporates thermal loads into the mechanical problem. In contrast, traditional thermal stress analysis is based on an uncoupled approach in which the thermal problem is solved on a fixed geometry, and the resulting temperatures are then used to load a mechanical problem. Thermal contact, in which heat flow paths depend on the mechanical deformations of adjacent surfaces, is a major component of many fully coupled thermomechanical analyses. This paper presents the development of a thermomechanical finite element formulation, including contact. The proposed approach accommodates arbitrarily large relative motions of contact surfaces, fully unstructured meshes, pressure-dependent contact resistance, conduction across small gaps, and approximate models for convection and radiation. The theory described herein has been implemented in the Lawrence Livermore National Laboratory public code PALM2D and has been used to solve a diverse set of thermomechanical problems. Examples illustrating the performance of this code on large deformation thermomechanical problems are presented and discussed. DOE

N94-23453 Los Alamos National Lab., NM.

CALCULATIONS OF BOSE-EINSTEIN CORRELATIONS FROM RELATIVISTIC QUANTUM MOLECULAR DYNAMICS

J. P. Sullivan, M. Berenguer, D. E. Fields, B. V. Jacak, M. Sarabura, J. Simon-Gillo, H. Sorge, H. vanHecke, and S. Pratt (Michigan State Univ., East Lansing.) 1993 5 p Presented at the 10th International Conference on Ultra-Relativistic Nucleus-Nucleus Collisions, Borlaenge, Sweden, 20-24 Jun. 1993 Limited Reproducibility: More than 20% of this document may be affected by poor print
(Contracts W-7405-eng-36; W-31-109-eng-38)
(DE94-000794; LA-UR-93-3334; CONF-930636-4) Avail: Issuing Activity (Department of Energy (DOE))

Bose-Einstein correlation functions which are in good agreement with pion data can be calculated from an event generator. Here, pion and (preliminary) kaon data from CERN experiment NA44 are compared to the calculations. The dynamics of 200 GeV/nucleon (sup 32)S + Pb collisions are calculated, without correlations due to interference patterns of a many-body wavefunction for identical particles, using the Relativistic Quantum Molecular Dynamics model (RQMD). The model is used to generate the phase-space coordinates of the emitted hadrons at the time they suffer their last strong interaction (freeze-out). Using the freeze-out position and momentum of pairs of randomly selected identical particles, a two-particle symmetrized wave-function is calculated and used to add two-body correlations. Details of the technique have been described previously. The method is similar to that used in the Spacer program. DOE

N94-24109*# Research Inst. for Advanced Computer Science, Moffett Field, CA.

ENERGY AND MAXIMUM NORM ESTIMATES FOR NONLINEAR CONSERVATION LAWS

Pelle Olsson and Joseph Oliger Jan. 1994 28 p
(Contract NAS2-13721)
(NASA-CR-195091; NAS 1.26:195091; RIACS-TR-94-01) Avail: CASI HC A03/MF A01

We have devised a technique that makes it possible to obtain energy estimates for initial-boundary value problems for nonlinear conservation laws. The two major tools to achieve the energy estimates are a certain splitting of the flux vector derivative f(u)(sub x), and a structural hypothesis, referred to as a cone condition, on the flux vector f(u). These hypotheses are fulfilled for many equations that occur in practice, such as the Euler equations of gas dynamics. It should be noted that the energy estimates are obtained without any assumptions on the gradient of the solution u. The results extend to weak solutions that are obtained as point wise limits of vanishing viscosity solutions. As a byproduct we obtain explicit expressions for the entropy function and the entropy flux of symmetrizable systems of conservation laws. Under certain circumstances the proposed technique can be applied repeatedly so as to yield estimates in the maximum norm. Author (revised)

N94-24516# Los Alamos National Lab., NM.

DENSITY ESTIMATION BY MAXIMUM QUANTUM ENTROPY

R. N. Silver, T. Wallstrom, and H. F. Martz 1993 14 p Presented at the Maximum Entropy and Bayesian Methods 1993, Santa Barbara, CA, 1-4 Aug. 1993
(Contract W-7405-eng-36)
(DE94-002626; LA-UR-93-3550; CONF-9308188-1) Avail: CASI HC A03/MF A01

A new Bayesian method for non-parametric density estimation is proposed, based on a mathematical analogy to quantum statistical physics. The mathematical procedure is related to maximum entropy methods for inverse problems and image reconstruction. The information divergence enforces global smoothing toward default models, convexity, positivity, extensivity and normalization. The novel feature is the replacement of classical entropy by quantum entropy, so that local smoothing is enforced by constraints on differential operators. The linear response of the estimate is proportional to the covariance. The hyperparameters are estimated by type-II maximum likelihood (evidence). The method is demonstrated on textbook data sets. DOE

N94-24532 Rutherford Appleton Lab., Chilton (England).

STITCHING THE YUKAWA QUILT

P. Ramond (Florida Univ., Gainesville.), R. G. Roberts, and G. G. Ross (Oxford Univ., England.) Mar. 1993 35 p Limited Reproducibility: More than 20% of this document may be affected by microfiche quality
(Contract DE-FG05-86ER-40272)
(PB93-204477; RAL-93-010; UFIFT-93-06) Avail: Issuing Activity (National Technical Information Service (NTIS))

The authors develop a systematic analysis of quark mass matrices which, starting with the measured values of quark masses and mixing angles, allows for a model independent search for all possible (symmetric or hermitian) mass matrices having texture zeroes at the unification scale. A survey of all six and five texture zero structures yields a total of five possible solutions which may be distinguished by improved measurements of the CKM matrix elements and which may readily be extended to include lepton masses with the Georgi-Jarlskog texture. The solutions naturally suggest a parameterization for the mass matrices based on a perturbative expansion and the authors present some speculations concerning the origin of such structure. NTIS

N94-24575 Technische Univ., Eindhoven (Netherlands). Dept. of Mathematics and Computing Science.

SOME MAXIMALITY RESULTS FOR EFFECT-VALUED MEASURES

S. V. Dorofeev and J. deGraaf Jun. 1993 28 p Limited Reproducibility: More than 20% of this document may be affected by poor print and microfiche quality
(PB94-111176; RANA-93-08) Avail: Issuing Activity (National Technical Information Service (NTIS))

An approach is provided to the theory of effect-valued measures taking their values in the positive operators on a Hilbert space. The concept of operator-valued measure is fundamental in modern theories of quantum measurements. In the paper we introduce and study relations of dominance and equivalence between two effect-valued measures and concepts of maximal and minimal effect-valued measures. Characterizations of maximal effect-valued measures are obtained in the discrete case and in the case of commutative range. As an example, we study the so-called Bargman measure which can be interpreted as a simultaneous non-ideal measurement of position and momentum. NTIS

N94-24777# Mississippi Univ., University. Physical Acoustics Research Lab.

A STUDY OF ELEMENT INTERACTION IN THERMOACOUSTIC ENGINES Annual Report, 1 Oct. 1992 - 30 Sep. 1993

Richard Raspet and Henry E. Bass 13 Nov. 1993 11 p
(Contract N00014-93-1-0077)
(AD-A273228; PARGUM-93-04) Avail: CASI HC A03/MF A01

The physical understanding of thermoacoustic engines has progressed rapidly in the past five years. The general performance of prime movers and refrigerators is now reasonably well understood and documented. There are, however, notable discrepancies between theory and experiment, especially at large acoustic amplitudes. The discrepancies are typically attributed to non-linear terms not included in the theory. Acoustic streaming is often mentioned as the culprit and this may well be the case. There is evidence, however, that interactions between elements in the engine are at least partially responsible for the differences. This is illustrated, for example, by Swift's observation that the heat exchanger appears to be effective over larger acoustic displacements than simple geometric arguments predict. Additional element interactions will arise when a thermoacoustic prime mover and a refrigerator are placed in the same acoustic cavity. This three year project centers on studies of different thermoacoustic element geometries. DTIC

N94-25028 California Univ., Berkeley. Dept. of Physics.

QUANTUM OPTICAL ASPECTS OF TOPOLOGICAL PHASES, SUCH AS BERRY'S PHASE Final Report, Jan. 1988 - Dec. 1991

Raymond Y. Chiao 10 Nov. 1993 6 p Limited Reproducibility: More than 20% of this document may be affected by microfiche quality
(Contract N00014-88-K-0126)
(AD-A273632) Avail: Issuing Activity (Defense Technical Information Center (DTIC))

The contract was for performing experiments on a recently discovered topological phase factor known as 'Berry's phase.' We proposed to examine this phase at both the quantum and classical levels, in its various manifestations. The goals of this contract were successfully accomplished; in particular, we succeeded in demonstrating this phase at the single photon level, thereby demonstrating that this phase did not originate at the classical level. Possible applications of this phase were explored. A two-photon light source, in the form a parametric down-converter of ultraviolet laser photons into highly correlated red photons was successfully constructed, and coincidence counting techniques were successfully applied to the detection of the conjugate signal and idler red photons. This formed the experimental basis for the examination of not only Berry's phase, but of the energy-time uncertainty relations, the Franson experiment, the measurement of the tunneling time of the photon, the quantum eraser, and other optical phenomena closely related to the Einstein-Podolsky-Rosen 'paradox.' DTIC

N94-25206 International Centre for Theoretical Physics, Trieste (Italy).

AN ATTEMPT AT A MACROREALISTIC QUANTUM WORLDVIEW

G. C. Ghirardi Nov. 1992 29 p Limited Reproducibility: More than 20% of this document may be affected by microfiche quality
(DE93-616821; IC-92/392) Avail: CASI HC A03 (US Sales Only)

Many scientists agree that various difficulties arise when one tries to build up a worldview incorporating some form of realism which can accommodate our knowledge about natural phenomena. Whether quantum mechanics (Q.M.), in the standard interpretation or in some of its more widely known and accepted variants, can be taken as a basis for such a program was investigated. Having pointed out that, in our opinion, this is not the case, an attempt to overcome the difficulties by accepting stochastic and nonlinear modifications of the evolution equation of the theory is presented. DOE

N94-25207 Joint Inst. for Nuclear Research, Dubna (USSR). Lab. of Nuclear Problems.

ON THE CONNECTION OF CLASSICAL MECHANICS, PHYSICAL KINETICS AND QUANTUM THEORY

V. I. Gordelij and A. E. Savelev 1991 16 p Limited Reproducibility: More than 20% of this document may be affected by microfiche quality
(DE93-616823; JINR-R-17-91-269) Avail: CASI HC A03 (US Sales Only)

The Schroedinger equation was generalized to consideration of the particles interaction with vacuum. The generalized Schroedinger ratio turned out to be a one-to-one correspondence between classical mechanics and physical kinetics. It is important that all results which follow from the Schroedinger equation are reproduced. The analytical solution of the generalized Schroedinger equation was found under the next conditions: (1) the potential external forces exerted over all parameters and with the whole space; and (2) classical mechanics Hamilton-Yacobi's equation has an ideal solution, i.e. the dependence of particle velocity on time only. The analytical solution of the generalized Schroedinger equation turned out to be coherent. The coherent properties of a wave function do not depend on symmetries by which the Hamiltonian determining the particle motion can be characterized. The investigation was performed at the Laboratory of Neutron Physics, JINR. DOE

N94-25257 Amsterdam Univ. (Netherlands). Faculteit der Natuur- en Sterrenkunde.

APPLICATIONS OF SUPERSYMMETRIC QUANTUM MECHANICS Ph.D. Thesis

Rachel Heloise Rietdijk 1992 115 p Sponsored by Stichting voor Fundamenteel Onderzoek der Materie, Netherlands Prepared in cooperation with Nationaal Inst. voor Kernfysica en Hoge Energiefysica, Amsterdam, Netherlands Limited Reproducibility: More than 20% of this document may be affected by microfiche quality
(ETN-94-95385) Avail: Issuing Activity (European Space Agency (ESA))

One of the simplest physical theories exhibiting supersymmetry, the spinning particle model, is considered. The symmetries of the spinning particle on an arbitrary Riemannian manifold are investigated. From the point of view of the one dimensional field theory global symmetries are looked for (that is constant on the world line) which correspond to conserved quantities which can be used to solve the equations of motion. Attention is also drawn to the application of supersymmetric quantum mechanical models (that is spinning particle models) defined on an arbitrary Riemannian manifold to the calculation of anomalies in quantum field theories defined on the same manifold. ESA

N94-25258# Amsterdam Univ. (Netherlands). Faculteit der Natuur- en Sterrenkunde.

ON BRST QUANTIZATION OF CONSTRAINED SYSTEMS Ph.D. Thesis

Wolfgang Kalau 1992 102 p Sponsored by Graduiertenfoerderung NRW, and Stichting voor Fundamenteel Onderzoek der Materie, Netherlands Prepared in cooperation with Nationaal Inst. voor Kernfysica en Hoge Energiefysica, Amsterdam, Netherlands
(ETN-94-95386) Avail: CASI HC A06/MF A02

The Hamiltonian analysis of a classical system with constraints is introduced and canonical quantization discussed. This method is illustrated by the example of Yang-Mills (YM) theory. The BRST quantization procedure is introduced and discussed for the case of YM theory. A formulation of general relativity, where the attempt is made to construct a system which avoids non-polynomial constraints without introducing complex variables, is presented. However, it turned out, that there are second class constraints. General aspects of BRST cohomology and a gauge fixing based on harmonic gauges are studied. The cohomology of a nontrivial example taken from the theory of higher spin particles is discussed. Systems with second class constraints are considered. The Gupta-Bleuler quantization method is introduced in order to formulate a necessary nontrivial condition for the applicability of this method to systems with second class constraints. A proof that this condition holds in any classical system is given. The BRST method is generalized to systems which allow for Gupta-Bleuler quantization. This method is applied to the four dimensional superparticle and developed to a system with an anomaly, two dimensional YM theory. The general structure of the cohomology for this system is discussed. The cohomology of SU(2)-YM theory is analyzed. ESA

N94-25336 International Centre for Theoretical Physics, Trieste (Italy).

THE 2D SUPERGRAVITY AND INTEGRABLE SYSTEMS

R. Ch. Rashkov Nov. 1992 10 p Limited Reproducibility: More than 20% of this document may be affected by microfiche quality
(DE93-616848; IC-92/372) Avail: CASI HC A02 (US Sales Only)

In this letter, we consider a realization of Osp (2/2) Kac-Moody algebra and its connection with the integrable systems. Integrable hierarchy based on the constrained Osp (2/2) connection is constructed. Using zero-curvature formulation we elucidate the connection between the integrable hierarchy and 2D supergravity. It is shown that super-Virasoro transformations are symmetries of our hierarchy. The analogies with W(sup 2)(sub 3) algebra are given. DOE

N94-25337 Joint Inst. for Nuclear Research, Dubna (USSR). Lab. of Theoretical Physics.

PHASE STRUCTURE OF THE TWO-DIMENSIONAL PHI(4) FIELD THEORY WITHIN THERMO-FIELD DYNAMICS

G. V. Efimov and S. N. Nedelko (Tomsk State Univ., USSR.) 1991 36 p Limited Reproducibility: More than 20% of this document may be affected by microfiche quality
(DE93-616850; JINR-E-2-91-464) Avail: CASI HC A03 (US Sales Only)

Phase structure of the two-dimensional phi(sup 4) field theory is investigated at arbitrary coupling constant and temperature. The critical values of the coupling constant and temperature, corresponding to symmetry rearrangement in the system, are calculated by the method of canonical transformations within the formalism of thermo-field dynamics. The Hamiltonians describing the system in each phase are obtained straightforwardly. DOE

N94-25339 Joint Inst. for Nuclear Research, Dubna (USSR). Lab. of Theoretical Physics.
DEVIATION EQUATIONS OF SYNGE AND SCHILD IN SPACES WITH AFFINE CONNECTION AND METRIC, AND EQUATIONS FOR GRAVITATIONAL WAVES DETECTORS
S. Manoff 1992 16 p Limited Reproducibility: More than 20% of this document may be affected by microfiche quality
(DE93-616852; JINR-E-2-92-19) Avail: CASI HC A03 (US Sales Only)

Deviation equation of Synge and Schild has been investigated in spaces with affine connection and metric. By means of a non-isotropic u vector field and the orthogonal to it, metric h(sub u), a projected deviation equation of Synge and Schild has been obtained for the orthogonal to u vector field. For a given non-isotropic, autoparallel, and normalized u vector field, this equation could have in some special cases the form of an oscillator equation. DOE

N94-25340 Weizmann Inst. of Science, Rehovoth (Israel). Dept. of Physics.
CORRELATIONS IN THE ACTIONS OF PERIODIC ORBITS DERIVED FROM QUANTUM CHAOS
N. Argaman, E. Doron, J. Keating (Manchester Univ., England.), A. Kitaev (Landau Inst. for Theoretical Physics, Moscow, USSR.), M. Sieber, and U. Smilansky Sep. 1992 11 p Limited Reproducibility: More than 20% of this document may be affected by microfiche quality
(DE93-616866; WIS-PH-92-73) Avail: CASI HC A03 (US Sales Only)

Based on semiclassical considerations, we derive universal expressions for a weighted two-point correlation function of actions of classical periodic orbits in chaotic systems. The derivation is based on the assumption that the semiclassical approximation succeeds in reproducing the results of Random Matrix Theory for the level statistics, even for times which exceed the Heisenberg time. A numerical study confirms the presence of these unexpected action correlations in three classically chaotic systems. We finally discuss the intimate relationship with the correlation between pairs of primes. DOE

N94-25416# Technical Research Centre of Finland, Espoo. Metals Lab.
HYDRIDE THERMODYNAMIC MACHINES [HYDRIDILAEMPOEVOIMAKONEET]
Seppo Taehtinen Oct. 1992 59 p In FINNISH Sponsored by Ministry of Trade and Industry, Finland; Technical Research Centre of Finland, Espoo; Imatran Voima Oy, Finland; and Rauma-Repola Oy, Tampere, Finland
(VTT-JULK-768; ISBN-951-38-4116-2; ETN-94-95241) Copyright Avail: CASI HC A04/MF A01

The operating principles of periodically operated thermodynamic machines based on connected metal hydride reaction beds are demonstrated. Temperature differences of 7.3 and 3.8 C for heating and cooling were measured for hydride heat pump operating at temperature levels of 20 and 80 C. For hydride heat transformer operating at temperature levels of 80 and 20 C the measured temperature differences were 8.9 and 5.6 C for heating and cooling. The continuous heating power of the hydride thermodynamic machine was 8.5 W/kg metal alloy. Based on the experimental results, the metal hydride reaction beds did not reach the chemical equilibrium during the operating cycles and measured dynamic equilibrium was used to evaluate the operation of the hydride thermodynamic machines. ESA

N94-25524 Air Force Inst. of Tech., Wright-Patterson AFB, OH.
EFFECT OF LONGITUDINAL VIBRATION ON THE CAPILLARY LIMIT OF A WRAPPED SCREEN WICK COPPER/WATER HEAT PIPE M.S. Thesis
Neil F. Huber Dec. 1993 103 p Limited Reproducibility: More than 20% of this document may be affected by microfiche quality
(AD-A273830; AFIT/GAE/ENY/93D-18) Avail: CASI HC A06

The effect of longitudinal vibration on the capillary limit of a copper/water heat pipe with a tightly wrapped screen wick was investigated. The capillary limit was measured over a range of operating temperatures under static conditions. A benchtop shaker was used to provide vibration in the longitudinal axis of the heat pipe. The capillary limit was measured at vibration frequencies of 10, 30, and 50 Hz. At each of these frequencies, tests were run at vibration amplitudes of 0.2 and 2.0 g. The pipe was maintained at a constant inclination angle and power throughput was increased until dryout occurred. The power throughput at dryout was considered the capillary limit. The measured capillary limit for each vibration test was compared to the static tests to determine the effect of the vibration. The results covered operating temperatures from 41.4 to 96.6 C. A vibration amplitude of 0.2 g caused a 2.3 percent decrease in the capillary limit. However, there is a 3.7 percent uncertainty in the data. A vibration amplitude of 2.0 g at 30 and 50 Hz caused a 9.6 and 6.1 percent degrade in capillary heat transport limit, respectively. At 2.0 g and 10 Hz, there is a 1.8 percent decrease in capillary heat transport limit. DTIC

N94-23646*# Nevada Univ., Reno. Dept. of Mechanical Engineering.
SECOND LAW ANALYSIS OF A CONVENTIONAL STEAM POWER PLANT
Geng Liu, Robert H. Turner, and Yunus A. Cengel *In* NASA. Lewis Research Center, The Fifth Annual Thermal and Fluids Analysis Workshop Nov. 1993 p 151-166 (For primary document see N94-23634 06-34)
Avail: CASI HC A03/MF A04; 5 functional color pages

80 SOCIAL SCIENCES (GENERAL)

Includes educational matters.

N94-23230*# National Aeronautics and Space Administration. John F. Kennedy Space Center, Cocoa Beach, FL.
NASA/ASEE SUMMER FACULTY FELLOWSHIP PROGRAM
E. Ramon Hosler, ed. (University of Central Florida, Orlando.), Carol Valdes, ed., and Tom Brown, ed. Oct. 1993 573 p Fellowship program held Merritt Island, FL, 1 Jun. - 6 Aug. 1993 Prepared in cooperation with the University of Central Florida, Orlando
(Grant NGT-60002)
(NASA-CR-194678; NAS 1.26:194678) Avail: CASI HC A24/MF A04

This document is a collection of technical reports on research conducted by the participants in the 1993 NASA/ASEE Summer Faculty Fellowship Program at KSC. The basic common objectives of the Program are: to further the professional knowledge of qualified engineering and science faculty members; to stimulate an exchange of ideas between participants and NASA; to enrich and refresh the research and teaching activities of participants' institutions; and to contribute to the research objectives of the NASA centers. 1993 topics include wide band fiber optic communications, a prototype expert/information system for examining environmental risks of KSC activities, alternatives to premise wiring using ATM and microcellular technologies, rack insertion end effector (RIEE) automation, FTIR quantification of industrial hydraulic fluids in perchloroethylene, switch configuration for migration to optical fiber network, and more. For individual titles, see N94-23231 through N94-23250.

N94-23231*# Towson State Univ., MD. Dept. of Physics.
WIDE BAND FIBER-OPTIC COMMUNICATIONS c32
Harry E. Bates *In* NASA. Kennedy Space Center, NASA/ASEE Summer Faculty Fellowship Program Oct. 1993 p 1-25 (For primary document see N94-23230 06-80)
Avail: CASI HC A03/MF A04

A number of optical communication lines are now in use at the Kennedy Space Center (KSC) for the transmission of voice, computer data and video signals. At the present time most of these channels utilize a single carrier wavelength centered near 1300 nm. As a result of previous work the bandwidth capacity of a number of these channels is being increased by transmitting another signal in the 1550 nm region on the same fiber. This is accomplished by means of wavelength division multiplexing (WDM). It is therefore important to understand the bandwidth properties of the installed fiber plant. This work developed new procedures for measuring the bandwidth of fibers in both the 1300nm and 1550nm region. In addition, a preliminary study of fiber links terminating in the Engineering Development Laboratory was completed. Author

N94-23232*# University of Central Florida, Orlando. Dept. of Mechanical and Aerospace Engineering.
CONTROL OF A SERPENTINE MANIPULATOR WITH COLLISION AVOIDANCE c37
Robert M. Byers *In* NASA. Kennedy Space Center, NASA/ASEE Summer Faculty Fellowship Program Oct. 1993 p 27-46 (For primary document see N94-23230 06-80)
Avail: CASI HC A03/MF A04

The robotics lab at the Kennedy Space Center is investigating the possibility of using a 'serpentine' manipulator for Shuttle inspection and payload processing. Serpentine manipulators are characterized by a large number of degrees of freedom giving them a high degree of redundancy. This redundancy allows them to be used to reach confined areas while avoiding collisions with their environment. In this paper, the author describes a new approach to controlling the joint rates for an n degree of freedom robot such that it moves its end effector to a desired position while simultaneously avoiding collision of any part of the robot arm with obstacles. Joint rates which move the end effector toward the target are found via a Lyapunov stability function. The gradient of an obstacle cost function indicates the direction toward obstacle collision in the joint space. The component of the end effector joint rates orthogonal to the obstacle gradient becomes the commanded joint rates. A notional eleven DOF model is used to numerically demonstrate the efficacy of the control law. Author

N94-23233*# Randolph-Macon Coll., Ashland, VA. Dept. of Chemistry.
EVALUATION OF INORGANIC ZINC-RICH PRIMERS USING ELECTROCHEMICAL IMPEDANCE SPECTROSCOPY (EIS) c25
Luz M. Calle *In* NASA. Kennedy Space Center, NASA/ASEE Summer Faculty Fellowship Program Oct. 1993 p 47-76 (For primary document see N94-23230 06-80)
Avail: CASI HC A03/MF A04

This investigation explores the use of Electrochemical Impedance Spectroscopy (EIS) in combination with beach exposure as a short term method for analyzing the performance of twenty-one zinc-rich primers. The twenty-one zinc-rich primers were: Carboline CZ-11, Ameron Devoe-Marine Catha-Coat 304, Briner V-65, Ameron D-21-9, Sherwin Williams Zinc Clad II, Carboline CZ-D7, Ameron D-4, Dupont Ganicin 347WB, Porter TQ-4374H, Inorganic Coatings IC-531, Subox Galvanox IV, Southern Coatings Chemtec 600, Glidden Glidzinc 5530, Byco SP-101, Tnemec 90E-75, Devoe Catha-Coat 302H, Glidden Glidzinc 5536, Koppers 701, Ameron D-21-5, Coronado 935-152, and Subox Galvanoz V. Data were also collected on galvanized steel for comparison purposes. A library of Bode magnitude plots was generated for each coating including curves for the initial time and after each week of atmospheric exposure as Beach Corrosion Test Site near the Space Shuttle launch pad at the Kennedy Space Center for up to three weeks. An examination of the variation of the Bode magnitude plots with atmospheric exposure revealed no clearly identifiable trend at this point that could distinguish between the good and the poor coatings. The test will be continued by including EIS measurements after six months and one year of atmospheric exposure. Author

N94-23234*# Florida Agricultural and Mechanical Univ., Tallahassee. Dept. of Industrial Engineering.
A FRAMEWORK FOR SFC/DC SYSTEM DATA ANALYSIS c66
Martha A. Centeno *In* NASA. Kennedy Space Center, NASA/ASEE Summer Faculty Fellowship Program Oct. 1993 p 77-90 (For primary document see N94-23230 06-80)
Avail: CASI HC A03/MF A04

The Shop Floor Control/Data Collection (SFC/DC) system is one of four major modules of the Integrated Work Control System being implemented at the NASA Kennedy Space Center. The SFC/DC system, which has been in operation approximately one and a half years, collects detailed information regarding the duration of tasks as well as work stoppages duration. This information needs to be effectively analyzed, so as be able to manage the shuttle processing activities under the continuous improvement philosophy. We have studied the contents and form of the SFC/DC database, and based on the results of such study, we have designed a Shop floor Modeling, Analysis, and Reporting Tool (SMART). SMART is a collection of compatible tools (off-the-shelf as well as customized C-based tools) that work cohesively to prepare inputs for the analysis models and process the various models. The feasibility of SMART has been demonstrated through an initial prototype. Author

N94-23235*# Florida Univ., Gainesville. Dept. of Electrical Engineering.
MASS PROPERTIES MEASUREMENT SYSTEM DYNAMICS c37
Keith L. Doty *In* NASA. Kennedy Space Center, NASA/ASEE Summer Faculty Fellowship Program Oct. 1993 p 91-110 (For primary document see N94-23230 06-80)
Avail: CASI HC A03/MF A04

The MPMS mechanism possess two revolute degrees-of-freedom and allows the user to measure the mass, center of gravity, and the inertia tensor of an unknown mass. The dynamics of the Mass Properties Measurement System (MPMS) from the Lagrangian approach to illustrate the dependency of the motion on the unknown parameters. Author

N94-23236*# Florida Univ., Gainesville. Dept. of Electrical Engineering.
MASS PROPERTIES MEASUREMENT SYSTEM: DYNAMICS AND STATICS MEASUREMENTS c37
Keith L. Doty *In* NASA. Kennedy Space Center, NASA/ASEE Summer Faculty Fellowship Program Oct. 1993 p 111-134 (For primary document see N94-23230 06-80)
Avail: CASI HC A03/MF A04

This report presents and interprets experimental data obtained from the Mass Properties Measurement System (MPMS). Statics measurements yield the center-of-gravity of an unknown mass and dynamics measurements yield its inertia matrix. Observations of the MPMS performance has lead us to specific design criteria and an understanding of MPMS limitations. Author

N94-23237*# Purdue Univ., West Lafayette, IN. Dept. of Agricultural Engineering.
A PROTOTYPE EXPERT/INFORMATION SYSTEM FOR EXAMINING ENVIRONMENTAL RISKS OF KSC ACTIVITIES c45
Bernard A. Engel *In* NASA. Kennedy Space Center, NASA/ASEE Summer Faculty Fellowship Program Oct. 1993 p 135-163 (For primary document see N94-23230 06-80)
Avail: CASI HC A03/MF A04

Protection of the environment and natural resources at the Kennedy Space Center (KSC) is of great concern. An expert/information system to replace the paper-based KSC Environmental Checklist was developed. The computer-based system requests information only as a required and supplies assistance as needed. The most comprehensive portion of the system provides information about endangered species habitat at KSC. This module uses geographic information system (GIS) data and tools, expert rules, color graphics, computer-based video, and hypertext to provide information. Author

N94-23238*# Pennsylvania State Univ., University Park. Dept. of Meteorology.
LIGHTNING STUDIES USING LDAR AND LLP DATA c47
Gregory S. Forbes *In* NASA. Kennedy Space Center, NASA/ASEE Summer Faculty Fellowship Program Oct. 1993 p 165-194 (For primary document see N94-23230 06-80)
Avail: CASI HC A03/MF A04

This study intercompared lightning data from LDAR and LLP systems in order to learn more about the spatial relationships between thunderstorm electrical discharges aloft and lightning strikes to the surface. The ultimate goal of the study is to provide information that can be used to improve the process of real-time detection and warning of lightning by weather forecasters who issue lightning advisories. The Lightning Detection and Ranging (LDAR) System provides data on electrical discharges from thunderstorms that includes cloud-ground flashes as well as lightning aloft (within cloud, cloud-to-cloud, and sometimes emanating from cloud to clear air outside or above cloud). The Lightning Location and Protection (LLP) system detects primarily ground strikes from lightning. Thunderstorms typically produce LDAR signals aloft prior to the first ground strike, so that knowledge of preferred positions of ground strikes relative to the LDAR data pattern from a thunderstorm could allow advance estimates of enhanced ground strike threat. Studies described in the report examine the position of LLP-detected ground strikes relative to the LDAR data pattern from the thunderstorms. The report also describes other potential approaches to the use of LDAR data in the detection and forecasting of lightning ground strikes. Author

N94-23239*# Michigan Univ., Ann Arbor. Dept. of Electrical Engineering.
REDUCED COST ALTERNATIVES TO PREMISE WIRING USING ATM AND MICROCELLULAR TECHNOLOGIES c33
Raghvendra R. Gejji *In* NASA. Kennedy Space Center, NASA/ASEE Summer Faculty Fellowship Program Oct. 1993 p 195-227 (For primary document see N94-23230 06-80)
Avail: CASI HC A03/MF A04

The cost of premises wiring keeps increasing due to personnel moves, new equipment, capacity upgrades etc. It would be desirable to have a wireless interface from the workstations to the fixed network, so as to minimize the wiring changes needed. New technologies such as microcellular personal communication systems are promising to bring down the cost of wireless communication. Another promising technology is Code Division Multiple Access (CDMA), which could dramatically increase the bandwidth available for wireless connections. In addition, Asynchronous Transfer Mode (ATM) technology is emerging as a technique for integrated management of voice, data, and video traffic on a single network. The focus of this investigation will be to assess the future utility of these new technologies for reducing the premise wiring cost at KSC. One of the issues to be studied is the cost comparison of 'old' versus 'new,' especially as time and technology progress. An additional issue for closer study is a feasible time-line for progress in technological capability. Author (revised)

N94-23240*# La Salle Univ., Philadelphia, PA. Management Dept.
COST BENEFITS OF ADVANCED SOFTWARE: A REVIEW OF METHODOLOGY USED AT KENNEDY SPACE CENTER c61
Prafulla N. Joglekar *In* NASA. Kennedy Space Center, NASA/ASEE Summer Faculty Fellowship Program Oct. 1993 p 229-268 (For primary document see N94-23230 06-80)
Avail: CASI HC A03/MF A04

To assist rational investments in advanced software, a formal, explicit, and multi-perspective cost-benefit analysis methodology is proposed. The methodology can be implemented through a six-stage process which is described and explained. The current practice of cost-benefit analysis at KSC is reviewed in the light of this methodology. The review finds that there is a vicious circle operating. Unsound methods lead to unreliable cost-benefit estimates. Unreliable estimates convince management that cost-benefit studies should not be taken seriously. Then, given external demands for cost-benefit estimates, management encourages software enginees to somehow come up with the numbers for their projects. Lacking the expertise needed to do a proper study, courageous software engineers with vested interests use ad hoc and unsound methods to generate some estimates. In turn, these estimates are unreliable, and the cycle continues. The proposed methodology should help KSC to break out of this cycle. Author (revised)

N94-23241*# University of Central Florida, Orlando. Dept. of Chemistry.
CHEMICAL CHARACTERIZATION OF SOME AEROBIC LIQUIDS IN CELSS c51
Brooks C. Madsen *In* NASA. Kennedy Space Center, NASA/ASEE Summer Faculty Fellowship Program Oct. 1993 p 269-299 (For primary document see N94-23230 06-80)
Avail: CASI HC A03/MF A04

Untreated aqueous soybean and wheat leachate and aerobically treated wheat leachate prepared from crop residues that are produced as a component of the Controlled Ecological Life Support System program designed to support long duration space missions were compared, and a general chemical characterization was accomplished. Solid phase extraction and high performance liquid chromatography were used to accomplish comparisons based on chromatographic and ultraviolet absorption properties of the components that are present. Specific compounds were not identified; however, general composition related to the initial presence of phenol-like compounds and their disappearance during aerobic treatment was explored. Author (revised)

N94-23242*# Tuskegee Inst., AL. Dept. of Mechanical Engineering.
RACK INSERTION END EFFECTOR (RIEE) AUTOMATION c37
Narasimha Malladi *In* NASA. Kennedy Space Center, NASA/ASEE Summer Faculty Fellowship Program Oct. 1993 p 301-326 (For primary document see N94-23230 06-80)
Avail: CASI HC A03/MF A04

NASA is developing a mechanism to manipulate and insert Racks into the Space Station Logistic modules. The mechanism consists of the following: a base with three motorized degrees of freedom, a 3 section motorized boom that goes from 15 to 44 feet in length, and a Rack Insertion End Effector (RIEE) with 5 hand wheels for precise alignment. The robotics section was tasked with the automation of the RIEE unit. In this report, for the automation of the RIEE unit, application of the Perceptics Vision System was conceptually developed to determine the position and orientation of the RIEE relative to the logistic module, and a MathCad program is written to display the needed displacements for precise alignment and final insertion of the Rack. The uniqueness of this report is that the whole report is in fact a MathCad program including text, derivations, and executable equations with example inputs and outputs. Author (revised)

N94-23243*# Puerto Rico Univ., Mayaguez. Dept. of Chemical Engineering.
FTIR QUANTIFICATION OF INDUSTRIAL HYDRAULIC FLUIDS IN PERCHLOROETHYLENE c27
Narinder K. Mehta *In* NASA. Kennedy Space Center, NASA/ASEE Summer Faculty Fellowship Program Oct. 1993 p 327-373 (For primary document see N94-23230 06-80)
Avail: CASI HC A03/MF A04

The purpose of this summer research project was to investigate whether perchloroethylene can be used as a solvent for the quantitative analysis of industrial hydraulic fluids by infrared spectroscopy employing Beer's law. Standard calibration curves using carbon-hydrogen stretching (generic) and ester absorption peaks were prepared for a series of standard dilutions at low ppm levels of concentration of seven hydraulic fluids in perchloroethylene. The absorbance spectras were recorded with 1.5-10 mm fixed and variable path length sample cells made of potassium bromide. The results indicate that using ester infrared spectral peak, it is possible to detect about 20 ppm of the hydraulic fluid in perchloroethylene. Author

N94-23244*# Puerto Rico Univ., Mayaguez. Dept. of Mechanical Engineering.
STRESS CORROSION CRACKING PROPERTIES OF 15-5PH STEEL c26
Ferdinand Rosa *In* NASA. Kennedy Space Center, NASA/ASEE Summer Faculty Fellowship Program Oct. 1993 p 375-402 (For primary document see N94-23230 06-80)
Avail: CASI HC A03/MF A04

Unexpected occurrence of failures, due to stress corrosion cracking (SCC) of structural components, indicate a need for improved characterization of materials and more advanced analytical procedures for reliably predicting structures performance. Accordingly, the purpose of this study was to determine the stress corrosion susceptibility of 15-5PH steel over a wide range of applied strain rates in a highly corrosive environment. The selected environment for this investigation was a highly acidified sodium chloride (NaCl) aqueous solution. The selected alloy for the study was a 15-5PH steel in the H900 condition. The slow strain rate technique was selected to test the metals specimens. Author (revised)

N94-23245*# Florida Inst. of Tech., Melbourne. Dept. of Mechanical and Aerospace Engineering.
INTERPRETATION OF DISCREPANCIES IN MASS SPECTROSCOPY DATA OBTAINED FROM DIFFERENT EXPERIMENTAL CONFIGURATIONS c25
John M. Russell *In* NASA. Kennedy Space Center, NASA/ASEE Summer Faculty Fellowship Program Oct. 1993 p 403-432 (For primary document see N94-23230 06-80)
Avail: CASI HC A03/MF A04

Many helium mass spectrometer leak detectors at KSC employ sampling systems that feature hand held sniffer probes. Authors of general leakage-testing literature recommend sniffer probes for leak location but not for quantitative leakage measurement. Their use in the latter application at KSC involves assumptions that may be subtle. The purpose of the research effort reported herein was to establish the significance of indicated leak rates displayed by sniffer-probe equipped leak detectors and to determine whether the use of alternative hardware or testing procedures may reduce the uncertainty of leakage measurements made with them. The report classifies probe-type sampling systems for helium leak detectors according to their internal plumbing (direct or branched), presents a basic analysis of the fluid dynamics in the sampling system in the branched-conduit case, describes the usual test method for measuring the internal supply-to-sample flowrate ratio (a.k.a permeation ratio), and describes a concept for a sponge-tipped probe whose external supply-to-sample flowrate ratio promises to be lower than that of a simple-ended probe. One conclusion is that the main source of uncertainty in the use of probe-type sampling systems for leakage measurement is uncertainty in the external supply-to-sample flowrate ratio. In contrast, the present method for measuring the internal supply-to-sample flowrate ratio is quantitative and satisfactory. The implication is that probes of lower external supply-to-sample flowrate ratio must be developed before this uncertainty may be reduced significantly. Author (revised)

N94-23246*# University of Central Florida, Orlando. Dept. of Industrial Engineering and Management Systems.
KSC MANAGEMENT TRAINING SYSTEM PROJECT c81
Jose A. Sepulveda *In* NASA. Kennedy Space Center, NASA/ASEE Summer Faculty Fellowship Program Oct. 1993 p 433-463 (For primary document see N94-23230 06-80)
Avail: CASI HC A03/MF A04

The stated objectives for the summer of 1993 were: to review the Individual Development Plan Surveys for 1994 in order to automate the analysis of the Needs Assessment effort; and to develop and implement evaluation methodologies to perform ongoing program-wide course-to-course assessment. This includes the following: to propose a methodology to develop and implement objective, performance-based assessment instruments for each training effort; to mechanize course evaluation forms and develop software to facilitate the data gathering, analysis, and reporting processes; and to implement the methodology, forms, and software in at lease one training course or seminar selected among those normally offered in the summer at KSC. Section two of this report addresses the work done in regard to the Individual Development Plan Surveys for 1994. Section three presents the methodology proposed to develop and implement objective, performance-based assessment instruments for each training course offered at KSC. Derived from text

N94-23247*# Wake Forest Univ., Winston-Salem, NC. Dept. of Mathematics and Computer Science.
EXPANDING THE KATE TOOLBOX c63
Stan J. Thomas *In* NASA. Kennedy Space Center, NASA/ASEE Summer Faculty Fellowship Program Oct. 1993 p 467-486 (For primary document see N94-23230 06-80)
Avail: CASI HC A03/MF A04

KATE (Knowledge-based Autonomous Test Engineer) is a model-based software system developed in the Artificial Intelligence Laboratory at the Kennedy Space Center for monitoring, fault detection, and control of launch vehicles and ground support systems. In order to bring KATE to the level of performance, functionality, and integratability needed for firing room applications, efforts are underway to implement KATE in the C++ programming language using an X-windows interface. Two programs which were designed and added to the collection of tools which comprise the KATE toolbox are described. The first tool, called the schematic viewer, gives the KATE user the capability to view digitized schematic drawings in the KATE environment. The second tool, called the model editor, gives the KATE model builder a tool for creating and editing knowledge base files. Design and implementation issues having to do with these two tools are discussed. It will be useful to anyone maintaining or extending either the schematic viewer or the model editor. Author (revised)

N94-23248*# University of Western Carolina, Cullowhee, NC. Dept. of Mathematics and Computer Science.
HURRICANE RISK ASSESSMENT: ROLLBACK OR RIDE OUT c47
Richard A. Wohlman *In* NASA. Kennedy Space Center, NASA/ASEE Summer Faculty Fellowship Program Oct. 1993 p 487-519 (For primary document see N94-23230 06-80)
Avail: CASI HC A03/MF A04

Winds in excess of 74.5 knots could cause severe damage to a space shuttle on the launch pad. Current plans exist for rollback to the Vehicle Assembly Building, but require 48 hour leadtime to implement. Decisions based upon cost/loss are evaluated to ascertain whether predetermined forecast probabilities for rollback/rideout decisions can be made far in advance of hurricane seasons for use in decision making. Author

N94-23249*# Purdue Univ., West Lafayette, IN. Engineering and Technology Dept.
FLAME TRENCH ANALYSIS OF NLS VEHICLES c15
Nuri Zeytinoglu *In* NASA. Kennedy Space Center, NASA/ASEE Summer Faculty Fellowship Program Oct. 1993 p 521-550 (For primary document see N94-23230 06-80)
Avail: CASI HC A03/MF A04

The present study takes the initial steps of establishing a better flame trench design criteria for future National Launch System vehicles. A three-dimensional finite element computer model for predicting the transient thermal and structural behavior of the flame trench walls was developed using both I-DEAS and MSC/NASTRAN software packages. The results of JANNAF Standardized Plume flowfield calculations of sea-level exhaust plume of the Space Shuttle Main Engine (SSME), Space Transportation Main Engine (STME), and Advanced Solid Rocket Motors (ASRM) were analyzed for different axial distances. The results of sample calculations, using the developed finite element model, are included. The further suggestions are also reported for enhancing the overall analysis of the flame trench model. Author (revised)

N94-23250*# Missouri Univ., Rolla. Dept. of Computer Science.
SWITCH CONFIGURATION FOR MIGRATION TO OPTICAL FIBER NETWORK c60
George W. Zobrist *In* NASA. Kennedy Space Center, NASA/ASEE Summer Faculty Fellowship Program Oct. 1993 p 551-579 (For primary document see N94-23230 06-80)
Avail: CASI HC A03/MF A04

The purpose is to investigate the migration of an Ethernet LAN segment to fiber optics. At the present time it is proposed to support a Fiber Distributed Data Interface (FDDI) backbone and to upgrade the VAX cluster to fiber optic interface. Possibly some workstations will have an FDDI interface. The remaining stations on the Ethernet LAN will be segmented. The rationale for migrating from the present Ethernet configuration to a fiber optic backbone is due to the increase in the number of workstations and the movement of applications to a windowing environment, extensive document transfers, and compute intensive applications. Author (revised)

N94-24225*# Interracial Council for Business Opportunity, New York, NY.
[ACTIVITIES INVOLVING AERONAUTICAL, SPACE SCIENCE, AND TECHNOLOGY SUPPORT FOR MINORITY INSTITUTIONS] Final Report
1993 4 p
(Contract NCCw-26)
(NASA-CR-195095; NAS 1.26:195095) Avail: CASI HC A01/MF A01

The Final Report addressed the activities with which the Interracial Council for Business Opportunity (ICBO) was involved over the past 12 months. ICBO was involved in the design and development of a CARES Student Tracking System Software (CARES). Cares is intended to provide an effective means of maintaining relevant current and historical information on NASA-funded students through a range of educational program initiatives. ICBP was extensively involved in the formation of a minority university consortium amd implementation of collaborative research activities by the consortium as part of NASA's Mission to Planet Earth/Earth Observing System. ICBO was involved in the formation of an HBCU/MI Consortium to facilitate technology transfer efforts to the small and minority business community in their respective regions. CASI

N94-24405*# Alabama Univ., Huntsville.
THE 1993 NASA/ASEE SUMMER FACULTY FELLOWSHIP PROGRAM Research Reports
Gerald R. Karr, ed., Charles R. Chappell, ed. (National Aeronautics and Space Administration. Marshall Space Flight Center, Huntsville, AL.), Frank Six, ed. (National Aeronautics and Space Administration. Marshall Space Flight Center, Huntsville, AL.), and L. Michael Freeman, ed. (Alabama Univ., Tuscaloosa.) NASA, Marshall Space Flight Center Nov. 1993 254 p Fellowship Program held in Huntsville, AL, 1 Jun. - 6 Aug. 1993 Prepared in cooperation with Alabama Univ., Tuscaloosa
(Grant NGT-01-008-021)
(NASA-CR-193862; NAS 1.26:193862) Avail: CASI HC A12/MF A03

For the 29th consecutive year, a NASA/ASEE Summer Faculty Fellowship Program was conducted at the Marshall Space Flight Center (MSFC). The program was conducted by the University of Alabama in Huntsville and

MSFC during the period of 6-1-93 through 8-6-93. Operated under the auspices of the American Society for Engineering Education, the MSFC program, as well as those at other NASA centers, was sponsored by the Office of Educational Affairs, NASA Headquarters, Washington, DC. The basic objectives of the programs, which are in the 30th year of operation nationally, are (1) to further the professional knowledge of qualified engineering and science faculty members; (2) to stimulate an exchange of ideas between participants and NASA; (3) to enrich and refresh the research and teaching activities of the participants' institution; and (4) to contribute to the research objectives of the NASA centers. For individual titles, see N94-24406 through N94-24455.

N94-24406*# Alabama Univ., Huntsville. Computer Science Dept.
INTEROPERABILITY THROUGH STANDARDIZATION: ELECTRONIC MAIL, AND X WINDOW SYSTEMS c82
Ashok T. Amin *In its* The 1993 NASA/ASEE Summer Faculty Fellowship Program Nov. 1993 5 p (For primary document see N94-24405 06-80)
Avail: CASI HC A01/MF A03

Since the introduction of computing machines, there has been continual advances in computer and communication technologies and approaching limits. The user interface has evolved from a row of switches, character based interface using teletype terminals and then video terminals, to present day graphical user interface. It is expected that next significant advances will come in the availability of services, such as electronic mail and directory services, as the standards for applications are developed and in the 'easy to use' interfaces, such as Graphical User Interface for example Window and X Window, which are being standardized. Various proprietary electronic mail (email) systems are in use within organizations at each center of NASA. Each system provides email services to users within an organization, however the support for email services across organizations and across centers exists at centers to a varying degree and is often easy to use. A recent NASA email initiative is intended 'to provide a simple way to send email across organizational boundaries without disruption of installed base.' The initiative calls for integration of existing organizational email systems through gateways connected by a message switch, supporting X.400 and SMTP protocols, to create a NASA wide email system and for implementation of NASA wide email directory services based on OSI standard X.500. A brief overview of MSFC efforts as a part of this initiative are described. Window based graphical user interfaces make computers easy to use. X window protocol has been developed at Massachusetts Institute of Technology in 1984/1985 to provide uniform window based interface in a distributed computing environment with heterogenous computers. It has since become a standard supported by a number of major manufacturers. Z Windows systems, terminals and workstations, and X Window applications are becoming available. However impact of its use in the Local Area Network environment on the network traffic are not well understood. It is expected that the use of X Windows systems will increase at MSFC especially for Unix based systems. An overview of X Window protocol is presented and its impact on the network traffic is examined. It is proposed that an analytical model of X Window systems in the network environment be developed and validated through the use of measurements to generate application and user profiles. Author

N94-24407*# Alabama Univ., Huntsville. Dept. of Industrial Engineering.
RISK IDENTIFICATION AND REDUCTION IN INTEGRATED PRODUCT TEAMS c65
Robert G. Batson *In its* The 1993 NASA/ASEE Summer Faculty Fellowship Program Nov. 1993 4 p (For primary document see N94-24405 06-80)
Avail: CASI HC A01/MF A03

This brief report summarizes research and planning conducted during Summer 1993 for MSFC on the subjects of risk identification, assessment, and management. Research findings are presented, citing useful references. The major output of this work, the AXAF-S Project Risk Management Plan is outlined. Author

N94-24408*# Alabama Univ., Huntsville. Dept. of Mechanical and Aerospace Engineering.
VISCOELASTIC ANALYSIS OF SEALS FOR EXTENDED SERVICE LIFE c37
Mark V. Bower *In its* The 1993 NASA/ASEE Summer Faculty Fellowship Program Nov. 1993 5 p (For primary document see N94-24405 06-80)
Avail: CASI HC A01/MF A03

The space station is being developed for a service life of up to thirty years. As a consequence, the design requirements for the seals to be used are unprecedented. Full scale testing to assure the selected seals can satisfy the design requirements are not feasible. As an alternative, a sub-scale test program (2) has been developed by MSFC to calibrate the analysis tools to be used to certify the proposed design. This research has been conducted in support of the MSFC Integrated Seal Test Program. The ultimate objective of this research is to correlate analysis and test results to qualify the analytical tools which in turn, are to be used to qualify the flight hardware. Seals are simple devices, in wide spread use. The most common type of seal is the O-ring. O-ring seals are typically rings of rubber with a circular cross section. The rings are placed between the surfaces to be sealed, usually in a groove of some design. The particular design may differ based on a number of different factors. This research is focused on O-rings that are staticly compressed by perpendicular clamping forces, commonly referred to as face seals. In this type of seal the O-ring is clamped between the sealing surfaces by loads perpendicular to the circular cross section. Author

N94-24409*# Columbia State Community Coll., TN. Computer Information Systems.
CAPE FOR CaPE c47
Joni Brooks *In* Alabama Univ., The 1993 NASA/ASEE Summer Faculty Fellowship Program Nov. 1993 5 p (For primary document see N94-24405 06-80)
Avail: CASI HC A01/MF A03

In an effort to improve short-term forecasting for the Kennedy Space Center region, Holle et al. (1992) investigated the effects of low level wind regimes on the distribution of cloud-to-ground lightning in central Florida. With a study period of 455 days, Holle et al. (1992) found 'southwest flow contributed 66 percent of the total network flashes while also occurring on the most days (142).' Relationships among mesoscale thermodynamic variables and precipitation and/or lightning have been addressed in previous studies in Canada and the Tennessee valley. Zawadzki et al. (1981) found 'soundings, surface pressure, temperature and humidity obtained from a standard observation network were correlated with rain rates given by raingages and radar.' Buechler et al. (1990) found 'a fair relationship between CAPE (convective available potential energy) and daily cloud-to-ground activity' with a correlation coefficient of $r = 0.68$. The present research will investigate the relationships among rainfall, cloud-to-ground (CG) lightning, CAPE, and low level wind flow using data collected during the CaPE (Convection and Precipitation/Electrification Experiment) field program. The CaPE field program was conducted in east central Florida from July 8, 1991 to August 18, 1991. Derived from text

N94-24410*# Armstrong State Coll., Savannah, GA. Dept. of Mathematics and Computer Science.
A REVIEW OF ISEAS DESIGN c61
Alex Bykat *In* Alabama Univ., The 1993 NASA/ASEE Summer Faculty Fellowship Program Nov. 1993 6 p (For primary document see N94-24405 06-80)
Avail: CASI HC A02/MF A03

The Space Station Freedom will offer facilities for experimentation and testing not available and not feasible or possible on earth. Due to a restricted space availability on board, the experimentation equipment and its organization will be frequently changing. This requires careful attention to electromagnetic compatibility between experimentation and other SSF equipment. To analyze the interactions between different equipment modules, a software system ISEAS is under development. Development of ISEAS was approached in two phases. In the 1st phase a PC version prototype of ISEAS was developed. In the 2nd phase, the PC prototype will be adapted to a VAX range of computers. The purpose of this paper is to review the design of the VAX version of ISEAS, and to recommend any suitable changes. Author

N94-24411*# Alabama Univ., Huntsville. Dept. of Civil and Environmental Engineering.
FINITE ELEMENT BASED ELECTRIC MOTOR DESIGN OPTIMIZATION c33

C. Warren Campbell *In its* The 1993 NASA/ASEE Summer Faculty Fellowship Program Nov. 1993 5 p (For primary document see N94-24405 06-80)
Avail: CASI HC A01/MF A03

The purpose of this effort was to develop a finite element code for the analysis and design of permanent magnet electric motors. These motors would drive electromechanical actuators in advanced rocket engines. The actuators would control fuel valves and thrust vector control systems. Refurbishing the hydraulic systems of the Space Shuttle after each flight is costly and time consuming. Electromechanical actuators could replace hydraulics, improve system reliability, and reduce down time. Author

N94-24412*# Marquette Univ., Milwaukee, WI. Dept. of Mechanical and Industrial Engineering.
CHARACTERISTICS OF PRODUCTS GENERATED BY SELECTIVE SINTERING AND STEREOLITHOGRAPHY RAPID PROTOTYPING PROCESSES **c27**
Vikram Cariapa *In* Alabama Univ., The 1993 NASA/ASEE Summer Faculty Fellowship Program Nov. 1993 5 p (For primary document see N94-24405 06-80)
Avail: CASI HC A01/MF A03

The trend in the modern global economy towards free market policies has motivated companies to use rapid prototyping technologies to not only reduce product development cycle time but also to maintain their competitive edge. A rapid prototyping technology is one which combines computer aided design with computer controlled tracking of focussed high energy source (eg. lasers, heat) on modern ceramic powders, metallic powders, plastics or photosensitive liquid resins in order to produce prototypes or models. At present, except for the process of shape melting, most rapid prototyping processes generate products that are only dimensionally similar to those of the desired end product. There is an urgent need, therefore, to enhance the understanding of the characteristics of these processes in order to realize their potential for production. Currently, the commercial market is dominated by four rapid prototyping processes, namely selective laser sintering, stereolithography, fused deposition modelling and laminated object manufacturing. This phase of the research has focussed on the selective laser sintering and stereolithography rapid prototyping processes. A theoretical model for these processes is under development. Different rapid prototyping sites supplied test specimens (based on ASTM 638-84, Type I) that have been measured and tested to provide a data base on surface finish, dimensional variation and ultimate tensile strength. Further plans call for developing and verifying the theoretical models by carefully designed experiments. This will be a joint effort between NASA and other prototyping centers to generate a larger database, thus encouraging more widespread usage by product designers. Author

N94-24413*# Oklahoma Univ., Norman. School of Electrical Engineering.
PERFORMANCE OF THE ENGINEERING ANALYSIS AND DATA SYSTEM 2 COMMON FILE SYSTEM **c82**
Linda S. DeBrunner *In* Alabama Univ., The 1993 NASA/ASEE Summer Faculty Fellowship Program Nov. 1993 5 p (For primary document see N94-24405 06-80)
Avail: CASI HC A01/MF A03

The Engineering Analysis and Data System (EADS) was used from April 1986 to July 1993 to support large scale scientific and engineering computation (e.g. computational fluid dynamics) at Marshall Space Flight Center. The need for an updated system resulted in a RFP in June 1991, after which a contract was awarded to Cray Grumman. EADS II was installed in February 1993, and by July 1993 most users were migrated. EADS II is a network of heterogeneous computer systems supporting scientific and engineering applications. The Common File System (CFS) is a key component of this system. The CFS provides a seamless, integrated environment to the users of EADS II including both disk and tape storage. UniTree software is used to implement this hierarchical storage management system. The performance of the CFS suffered during the early months of the production system. Several of the performance problems were traced to software bugs which have been corrected. Other problems were associated with hardware. However, the use of NFS in UniTree UCFM software limits the performance of the system. The performance issues related to the CFS have led to a need to develop a greater understanding of the CFS organization. This paper will first describe the EADS II with emphasis on the CFS. Then, a discussion of mass storage systems will be presented, and methods of measuring the performance of the Common File System will be outlined. Finally, areas for further study will be identified and conclusions will be drawn. Author

N94-24414*# Oklahoma Univ., Norman. School of Meteorology.
WATER CYCLE RESEARCH ASSOCIATED WITH THE CaPE HYDROMETEOROLOGY PROJECT (CHymP **c47**
Claude E. Duchon *In* Alabama Univ., The 1993 NASA/ASEE Summer Faculty Fellowship Program Nov. 1993 5 p (For primary document see N94-24405 06-80)
Avail: CASI HC A01/MF A03

One outgrowth of the Convection and Precipitation/Electrification (CaPE) experiment that took place in central Florida during July and August 1991 was the creation of the CaPE Hydrometeorology Project (CHymP). The principal goal of this project is to investigate the daily water cycle of the CaPE experimental area by analyzing the numerous land and atmosphere in situ and remotely sensed data sets that were generated during the 40-days of observations. The water cycle comprises the atmospheric branch. In turn, the atmospheric branch comprises precipitation leaving the base of the atmospheric volume under study, evaporation and transpiration entering the base, the net horizontal fluxes of water vapor and cloud water through the volume and the conversion of water vapor to cloud water and vice-versa. The sum of these components results in a time rate of change in the water and liquid water (or ice) content of the atmospheric volume. The components of the land branch are precipitation input to and evaporation and transpiration output from the surface, net horizontal fluxes of surface and subsurface water, the sum of which results in a time rate of change in surface and subsurface water mass. The objective of CHymP is to estimate these components in order to determine the daily water budget for a selected area within the CaPE domain. This work began in earnest in the summer of 1992 and continues. Even estimating all the budget components for one day is a complex and time consuming task. The discussions below provides a short summary of the rainfall quality assessment procedures followed by a plan for estimating the horizontal moisture flux. Author

N94-24415*# Alabama Univ., Huntsville. Mechanical and Aerospace Engineering Dept.
FOIL BEARINGS **c37**
David A. Elrod *In its* The 1993 NASA/ASEE Summer Faculty Fellowship Program Nov. 1993 5 p (For primary document see N94-24405 06-80)
Avail: CASI HC A01/MF A03

The rolling element bearings (REB's) which support many turbomachinery rotors offer high load capacity, low power requirements, and durability. Two disadvantages of REB's are: (1) rolling or sliding contact within the bearing has life-limiting consequences; and (2) REB's provide essentially no damping. The REB's in the Space Shuttle Main Engine (SSME) turbopumps must sustain high static and dynamic loads, at high speeds, with a cryogenic fluid as lubricant and coolant. The pump end ball bearings limit the life of the SSME high pressure oxygen turbopump (HPOTP). Compliant foil bearing (CFB) manufacturers have proposed replacing turbopump REB's with CFB's CFB's work well in aircraft air cycle machines, auxiliary power units, and refrigeration compressors. In a CFB, the rotor only contracts the foil support structure during start up and shut down. CFB damping is higher than REB damping. However, the load capacity of the CFB is low, compared to a REB. Furthermore, little stiffness and damping data exists for the CFB. A rotordynamic analysis for turbomachinery critical speeds and stability requires the input of bearing stiffness and damping coefficients. The two basic types of CFB are the tension-dominated bearing and the bending-dominated bearing. Many investigators have analyzed and measured characteristics of tension-dominated foil bearings, which are applied principally in magnetic tape recording. The bending-dominated CFB is used more in rotating machinery. This report describes the first phase of a structural analysis of a bending-dominated, multileaf CFB. A brief discussion of CFB literature is followed by a description and results of the present analysis. Author

N94-24416*# Alabama Univ., Huntsville. Dept. of Industrial and Systems Engineering.

DESIGN AND SPECIFICATION OF A CENTRALIZED MANUFACTURING DATA MANAGEMENT AND SCHEDULING SYSTEM **c81**

Phillip A. Farrington *In its* The 1993 NASA/ASEE Summer Faculty Fellowship Program Nov. 1993 6 p (For primary document see N94-24405 06-80)

Avail: CASI HC A02/MF A03

As was revealed in a previous study, the Materials and Processes Laboratory's Productivity Enhancement Complex (PEC) has a number of automated production areas/cells that are not effectively integrated, limiting the ability of users to readily share data. The recent decision to utilize the PEC for the fabrication of flight hardware has focused new attention on the problem and brought to light the need for an integrated data management and scheduling system. This report addresses this need by developing preliminary designs specifications for a centralized manufacturing data management and scheduling system for managing flight hardware fabrication in the PEC. This prototype system will be developed under the auspices of the Integrated Engineering Environment (IEE) Oversight team and the IEE Committee. At their recommendation the system specifications were based on the fabrication requirements of the AXAF-S Optical Bench. Author

N94-24417*# Alabama Univ., Huntsville. Dept. of MIS.

TECHNOLOGY UTILIZATION OFFICE DATA BASE ANALYSIS AND DESIGN **c82**

Stephen A. Floyd *In its* The 1993 NASA/ASEE Summer Faculty Fellowship Program Nov. 1993 5 p (For primary document see N94-24405 06-80)

Avail: CASI HC A01/MF A03

NASA Headquarters is placing a high priority on the transfer of NASA and NASA contractor developed technologies and expertise to the private sector and to other federal, state and local government organizations. The ultimate objective of these efforts is positive economic impact, an improved quality of life, and a more competitive U.S. posture in international markets. The Technology Utilization Office (TUO) currently serves seven states with its technology transfer efforts. Since 1989, the TUO has handled over one-thousand formal requests for NASA related technologies assistance. The technology transfer process requires promoting public awareness of NASA related soliciting requests for assistance, matching technologies to specific needs, assuring appropriate technology transfer, and monitoring and evaluating the process. Each of these activities have one very important aspect in common: the success of each is dissemination of appropriate high quality information. The purpose of the research was to establish the requirements and develop a preliminary design for a database system to increase the effectiveness and efficiency of the TUO's technology transfer function. The research was conducted following the traditional systems development life cycle methodology and was supported through the use of modern structured analysis techniques. The next section will describe the research and findings as conducted under the life cycle approach. Author

N94-24418*# Alabama A & M Univ., Huntsville. Dept. of Civil Engineering.

A STUDY OF THE CORE MODULE SIMULATOR FLOOR CAPABILITY **c39**

James W. Foreman *In* Alabama Univ., The 1993 NASA/ASEE Summer Faculty Fellowship Program Nov. 1993 4 p (For primary document see N94-24405 06-80)

Avail: CASI HC A01/MF A03

The floor of the Core Module Simulator (CMS) is required to support various combinations of dead load and live load during the testing process. Even though there is published data on the structural capability of the grating, it is not always evident if the combined loadings with joint loads will cause structural failure. Author

N94-24419*# Ohio Univ., Athens. Dept. of Industrial and Systems Engineering.

A MINIMUM COST TOLERANCE ALLOCATION METHOD FOR ROCKET ENGINES AND ROBUST ROCKET ENGINE DESIGN **c20**

Richard J. Gerth *In* Alabama Univ., The 1993 NASA/ASEE Summer Faculty Fellowship Program Nov. 1993 5 p (For primary document see N94-24405 06-80)

Avail: CASI HC A01/MF A03

Rocket engine design follows three phases: systems design, parameter design, and tolerance design. Systems design and parameter design are most effectively conducted in a concurrent engineering (CE) environment that utilize methods such as Quality Function Deployment and Taguchi methods. However, tolerance allocation remains an art driven by experience, handbooks, and rules of thumb. It was desirable to develop and optimization approach to tolerancing. The case study engine was the STME gas generator cycle. The design of the major components had been completed and the functional relationship between the component tolerances and system performance had been computed using the Generic Power Balance model. The system performance nominals (thrust, MR, and Isp) and tolerances were already specified, as were an initial set of component tolerances. However, the question was whether there existed an optimal combination of tolerances that would result in the minimum cost without any degradation in system performance. Author

N94-24420*# Auburn Univ., AL. Aerospace Engineering.

VALIDATION OF A NONINTRUSIVE OPTICAL TECHNIQUE FOR THE MEASUREMENT OF LIQUID MASS DISTRIBUTION IN A TWO-PHASE SPRAY **c74**

Roy Hartfield, Jr. *In* Alabama Univ., The 1993 NASA/ASEE Summer Faculty Fellowship Program Nov. 1993 5 p (For primary document see N94-24405 06-80)

Avail: CASI HC A01/MF A03

This work is the continuation of an optical technique development program initiated as part of the 1992 Summer Faculty Fellowship Program. The 1992 work consisted of the formulation and implementation of a technique ivolving the spatial deconvolution of fluorescence data from a uniformly illuminated, seeded densed spray to obtain quantitative measurements of the liquid density profiles. This measurement approach largely overcomes substantial scattering problems associated with other optical approaches for two-phase flows. However, to apply this measurement approach with confidence to unknown flows, the technique must be validated. Consequently, technique validation using classical grid patternator techniques has been focus of the current work. This work has included the design and construction of a patternator rig and the implementation of a test program designed for the comparison of patternator data with the deconvolved optical data. The flow field used for the validation is the plume of an axisymetric swirl coaxial LOX injector being considered for use in the Space Transportation System Main Engine. The flow facility is an improved version of the test rig which was constructed in 1992 for the initial technique development. This report includes a brief description of the optical measurement technique and the patternator rig and a presentation of the data comparisons. Author

N94-24421*# Alabama Univ., Tuscaloosa. Dept. of Aerospace Engineering.

IMPACT DAMAGE IN FILAMENT WOUND COMPOSITE BOTTLES **c24**

Alton L. Highsmith *In* Alabama Univ., The 1993 NASA/ASEE Summer Faculty Fellowship Program Nov. 1993 5 p (For primary document see N94-24405 06-80)

Avail: CASI HC A01/MF A03

Increasingly, composite materials are being used in advanced structural applications because of the significant weight savings they offer when compared to more traditional engineering materials. The higher cost of composites must be offset by the increased performance that results from reduced structural weight if these new materials are to be used effectively. At present, there is considerable interest in fabricating solid rocket motor cases out of composite materials, and capitalizing on the reduced structural weight to increase rocket performance. However, one of the difficulties that arises when composite materials are used is that composites can develop significant amounts of internal damage during low velocity impacts. Such low velocity impacts may be encountered in routine handling of a structural component like a rocket motor case. The ability to assess the reduction in structural integrity of composite motor cases that experience accidental impacts is essential if composite rocket motor cases are to be certified for manned flight. While experimental studies of the post-impact performance of filament wound composite motor cases haven been proven performed (2,3), scaling impact data from small specimens to full scale structures has proven difficult. If such a scaling methodology is to be achieved, an increased understanding of the damage processes which influence residual strength is required. The study described herein was part of an ongoing investigation of damage development and reduction of tensile strength in filament wound composites subjected to low velocity impacts. The present study, which focused on documenting the damage that develops in filament wound composites as a result of such impacts, included two distinct tasks. The first task was to experimentally assess impact damage in small, filament wound pressure bottles using x-ray radiography. The second task was to study the feasibility of using digital image processing techniques to assist in determining the 3-D distribution of damage from stereo x-ray pairs. Author

N94-24422*# Auburn Univ., AL. Dept. of Electrical Engineering.
OCTAVE: A MARSYAS POST-PROCESSOR FOR COMPUTER-AIDEED CONTROL SYSTEM DESIGN **c61**
A. Scottedward Hodel *In* Alabama Univ., The 1993 NASA/ASEE Summer Faculty Fellowship Program Nov. 1993 5 p (For primary document see N94-24405 06-80)
Avail: CASI HC A01/MF A03

MARSYAS is a computer-aided control system analysis package for the simulation and analysis of dynamic systems. In the summer of 1991 MARSYAS was updated to allow for the analysis of sampled-data systems in terms of frequency response, stability, etc. This update was continued during the summer of 1992 in order to extend further MARSYAS commands to the study of sampled data systems. Further work was done to examine the computation of openat transfer functions, root-locii and omega-plane frequency response plots. At the conclusion of the summer of 1992 work, it was proposed that control-system design capability be incorporated into the MARSYAS package. It was decided at that time to develop a separate 'stand-alone' computer-aided control system design (CACSD) package. This report is a brief description of such a package. Author

N94-24423*# Puerto Rico Univ., Mayaguez. Electrical and Computer Engineering Dept.
ON THE ANALYSIS OF CLEAR AIR RADAR ECHOES SEVERELY CONTAMINATED BY CLUTTER **c32**
H. Mario Ierkic *In* Alabama Univ., The 1993 NASA/ASEE Summer Faculty Fellowship Program Nov. 1993 6 p (For primary document see N94-24405 06-80)
Avail: CASI HC A02/MF A03

Many radar systems work in environments where clutter return overwhelm the atmospheric echoes. Sometimes by as much as 50 dB. At the Arecibo Observatory (AO), for example, clutter levels are conspicuously high. This situation greatly reduces its usefulness for lower atmospheric studies. It is not possible in general, to observe height profiles of the vertical component of the wind velocity. This parameter is important to understand planetary scale circulation, mountain and lee waves, turbulence, troprospheric and stratorspheric interactions and vertical transport of horizontal momentum. The topics discussed include the following: clutter propagation characteristics, knowledge-based spectral analysis system, and signal analysis system. Author

N94-24424*# Alabama Univ., Huntsville. Dept. of Electrical Engineering.
A COMPILATION OF TECHNOLOGY SPINOFFS FROM THE US SPACE SHUTTLE PROGRAM **c85**
David Jeff Jackson *In its* The 1993 NASA/ASEE Summer Faculty Fellowship Program Nov. 1993 5 p (For primary document see N94-24405 06-80)
Avail: CASI HC A01/MF A03

As the successful transfer of NASA-developed technology is a stated mission of NASA, the documentation of such transfer is vital in support of the program. The purpose of this report is to document technology transfer, i.e. 'spinoffs', from the U.S. Space Shuttle Program to the commercial sector. These spinoffs have their origin in the many scientific and engineering fields associated with the shuttle program and, as such, span many diverse commercial applications. These applications include, but are not limited to, consumer products, medicine, industrial productivity, manufacturing technology, public safety, resources management, materials processing, transportation, energy, computer technology, construction, and environmental applications. To aide to the generation of this technology spinoff list, significant effort was made to establish numerous and complementary sources of information. The primary sources of information used in compiling this list include: the NASA 'Spinoff' publication, NASA Tech Briefs, the Marshall Space Flight Center (MSFC) Technology Utilization (TU) Office, the NASA Center for Aerospace Information (CASI), the NASA COSMIC Software Center, and MSFC laboratory and contractor personnel. A complete listing of resources may be found in the bibliography of this report. Additionally, effort was made to insure that the obtained information was placed in electronic database form to insure that the subsequent updating would be feasible with minimal effort. Author

N94-24425*# Auburn Univ., AL. Materials Engineering.
WELD FRACTURE CRITERIA FOR COMPUTER SIMULATION **c26**
Wartan A. Jemian *In* Alabama Univ., The 1993 NASA/ASEE Summer Faculty Fellowship Program Nov. 1993 5 p (For primary document see N94-24405 06-80)
Avail: CASI HC A01/MF A03

Due to the complexity of welding, not all of the important factors are always properly considered and controlled. An automatic system is required. This report outlines a simulation method and all the important considerations to do this. As in many situations where a defect or failure has occurrred, it is freqently necessary to trouble shoot the system and eventually identify those factors that were neglected. This is expensive and time consuming. Very frequently the causes are materials-related that might have been anticipated. Computer simulation can automatically consider all important variables. The major goal of this presentation is to identify the proper relationship to design, processing and materials variables to welding. Author

N94-24426*# Alabama Univ., Huntsville. Dept. of Biological Sciences.
MEASURING THE DYNAMICS OF STRUCTURAL CHANGES IN BIOLOGICAL MACROMOLECULES FROM LIGHT SCATTERING DATA **c51**
Adriel D. Johnson *In its* The 1993 NASA/ASEE Summer Faculty Fellowship Program Nov. 1993 3 p (For primary document see N94-24405 06-80)
Avail: CASI HC A01/MF A03

Examining techniques to study the dynamics of structural changes in various molecules has been an ongoing goal of the space program. Knowing how these phenomena occur in biological systems is fundamental to understanding what is necessary for life to remain functional in the space environment. A hierarchy of biological organization is functionally described when cells join together small organic molecules to form larger and more complex molecules. Characterizing the architecture of a particular macromolecule helps determine how that molecule works in the living cell and is basic to the diversity of life. Understanding this arrangement involves the correlation of the structure of macromolecules with their functions. A light scattering photometer was developed for detecting continuous measurement of the angular spectrum of light scattered by dynamically changing systems. The analysis of light scattered by biological macromolecules can be used to determine concentration, size, shape, molecular weight, and structural changes of cells, such as erythrocytes. Some light scattering photometers can collect and store 120 angular scattering spectra per minute, with an angular resolution of 0.2 deg which can be displayed with computer graphics. The light scattering photometer does the following: functions to produce and detect scattered light; determines scatter angles; and collects, stores, and analyzes data. Author (revised)

N94-24427*# Colorado Univ., Boulder. Dept. of Aerospace Engineering Sciences.
WELD JOINT CONCEPTS FOR ON-ORBIT REPAIR OF SPACE STATION FREEDOM FLUID SYSTEM TUBE ASSEMBLIES **c37**
Steven D. Jolly *In* Alabama Univ., The 1993 NASA/ASEE Summer Faculty Fellowship Program Nov. 1993 5 p (For primary document see N94-24405 06-80)
Avail: CASI HC A01/MF A03

Because Space Station Freedom (SSF) is an independent satellite, not depending upon another spacecraft for power, attitude control, or thermal regulation, it has a variety of tubular, fluid-carrying assemblies on-board. The systems of interest in this analysis provide breathing air (oxygen and nitrogen), a working fluid (two-phase anhydrous ammonia) for thermal control, and a monopropellant (hydrazine) for station reboost. The tube assemblies run both internally and externally with respect to the habitats. They are found in up to 50 ft. continuous lengths constructed of mostly AISI 316L stainless steel tubing, but also including some Inconel 625 nickel-iron and Monel 400 nickel-copper alloy tubing. The outer diameters (OD) of the tubes range from 0.25-1.25 inches, and the wall thickness between 0.028-.095 inches. The system operational pressures range from 377 psi (for the thermal control system) to 3400 psi (for the high pressure oxygen and nitrogen supply lines in the ECLSS). SSF is designed for a fifteen to thirty year mission. It is likely that the tubular assemblies (TA's) will sustain damage or fail during this lifetime such that they require repair or replacement. The nature of the damage will be combinations of punctures, chips, scratches, and creases and may be cosmetic or actually leaking. The causes of these hypothetical problems are postulated to be: (1) faulty or fatigued fluid joints--both QD's and butt-welds; (2) micro-meteoroid impacts; (3) collison with another man-made object; and (4) over-pressure strain or burst (system origin). While the current NASA baseline may be to temporarily patch the lines by clamping metal c-sections over the defect, and then perform high pressure injection of a sealing compound, it is clear that permanent repair of the line(s) is necessary. This permanent repair could be to replace the entire TA in the segment, or perhaps the segment itself, both alternatives being extremely expensive and risky. The former would likely require extensive EVA to release TA clamps and pose great risk to other engineering subsystems, and the latter would require major de-servicing of the Station. Author (revised)

N94-24428*# Indiana Univ. of Pennsylvania, Indiana, PA. Physics Dept.
DIFFUSION ON Cu SURFACES c26
Majid Karimi *In* Alabama Univ., The 1993 NASA/ASEE Summer Faculty Fellowship Program Nov. 1993 5 p (For primary document see N94-24405 06-80)
Avail: CASI HC A01/MF A03

Understanding surface diffusion is essential in understanding surface phenomena, such as crystal growth, thin film growth, corrosion, physisorption, and chemisorption. Because of its importance, various experimental and theoretical efforts have been directed to understand this phenomena. The Field Ion Microscope (FIM) has been the major experimental tool for studying surface diffusion. FIM have been employed by various research groups to study surface diffusion of adatoms. Because of limitations of the FIM, such studies are only limited to a few surfaces: nickel, platinum, aluminum, iridium, tungsten, and rhodium. From the theoretical standpoint, various atomistic simulations are performed to study surface diffusion. In most of these calculations the Embedded Atom Method (EAM) along with the molecular static (MS) simulation are utilized. The EAM is a semi-empirical approach for modeling the interatomic interactions. The MS simulation is a technique for minimizing the total energy of a system of particles with respect to the positions of its particles. One of the objectives of this work is to develop the EAM functions for Cu and use them in conjunction with the molecular static (MS) simulation to study diffusion of a Cu atom on a perfect as well as stepped Cu(100) surfaces. This will provide a test of the validity of the EAM functions on Cu(100) surface and near the stepped environments. In particular, we construct a terrace-ledge-kink (TLK) model and calculate the migration energies of an atom on a terrace, near a ledge site, near a kink site, and going over a descending step. We have also calculated formation energies of an atom on the bare surface, a vacancy in the surface, a stepped surface, and a stepped-kink surface. Our results are compared with the available experimental and theoretical results. Author (revised)

N94-24429*# Alabama Univ., Huntsville. Dept. of Mathematical Sciences.
J-INTEGRAL PATCH FOR FINITE ELEMENT ANALYSIS OF DYNAMIC FRACTURE DUE TO IMPACT OF PRESSURE VESSELS c39
Boris I. Kunin *In its* The 1993 NASA/ASEE Summer Faculty Fellowship Program Nov. 1993 5 p (For primary document see N94-24405 06-80)
Avail: CASI HC A01/MF A03

Prediction of whether a pressurized cylinder will fail catastrophically when impacted by a projectile has important applications ranging from perforation of an airplane's skin by a failed turbine blade to meteorite impact of a space station habitation module. This report summarizes the accomplishment of one task for a project whose aim is to simulate numerically the outcome of a high velocity impact of pressure vessels. A finite element patch covering the vicinity of a growing crack has been constructed to estimate the J-integral (crack driving force) during the impact. Explicit expressions for the J-integral through the nodal values of displacement, strain, and stress have been written. The patch is to be used repeatedly to estimate the amount of crack growth during the time of the impact. The resulting crack size is to be compared to an estimated critical crack size for the pressurized cylinder. Author (revised)

N94-24430*# Alabama Univ., Huntsville. Dept. of Mechanical and Aerospace Engineering.
CFD SIMULATION OF COAXIAL INJECTORS c34
D. Brian Landrum *In its* The 1993 NASA/ASEE Summer Faculty Fellowship Program Nov. 1993 6 p (For primary document see N94-24405 06-80)
Avail: CASI HC A02/MF A03

The development of improved performance models for the Space Shuttle Main Engine (SSME) is an important, ongoing program at NASA MSFC. These models allow prediction of overall system performance, as well as analysis of run-time anomalies which might adversely affect engine performance or safety. Due to the complexity of the flow fields associated with the SSME, NASA has increasingly turned to Computational Fluid Dynamics (CFD) techniques as modeling tools. An important component of the SSME system is the fuel preburner, which consists of a cylindrical chamber with a plate containing 264 coaxial injector elements at one end. A fuel rich mixture of gaseous hydrogen and liquid oxygen is injected and combusted in the chamber. This process preheats the hydrogen fuel before it enters the main combustion chamber, powers the hydrogen turbo-pump, and provides a heat dump for nozzle cooling. Issues of interest include the temperature and pressure fields at the turbine inlet and the thermal compatibility between the preburner chamber and injector plate. Performance anomalies can occur due to incomplete combustion, blocked injector ports, etc. The performance model should include the capability to simulate the effects of these anomalies. The current approach to the numerical simulation of the SSME fuel preburner flow field is to use a global model based on the MSFC sponsored FNDS code. This code does not have the capabilities of modeling several aspects of the problem such as detailed modeling of the coaxial injectors. Therefore, an effort has been initiated to develop a detailed simulation of the preburner coaxial injectors and provide gas phase boundary conditions just downstream of the injector face as input to the FDNS code. This simulation should include three-dimensional geometric effects such as proximity of injectors to baffles and chamber walls and interaction between injectors. This report describes an investigation into the numerical simulation of GH2/LOX coaxial injectors. The following sections will discuss the physical aspects of injectors, the CFD code employed, and preliminary results of a simulation of a single coaxial injector for which experimental data is available. It is hoped that this work will lay the foundation for the development of a unique and useful tool to support the SSME program. Author (revised)

N94-24431*# Mississippi State Univ., State College. Dept. of Physics and Astronomy.
STRUCTURE IN GAMMA RAY BURST TIME PROFILES: CORRELATIONS WITH OTHER OBSERVABLES c93
John Patrick Lestrade *In* Alabama Univ., The 1993 NASA/ASEE Summer Faculty Fellowship Program Nov. 1993 5 p (For primary document see N94-24405 06-80)
Avail: CASI HC A01/MF A03

One of the current debates raging in the world of gamma-ray burst physics is whether the sources of these enigmatic bursts arise from a single or from multiple distributions. Several authors contend that the histograms of GRB observables imply the latter. The two most-likely candidate components are galactic and cosmological. For example, some researchers claim that a dip in the V/V max distribution is a result of such a two-component source distribution. Others have used a parameter called the 'burst variability' calculated by dividing the maximum count rate on the 64-msec timescale by that from the 1024-msec timescale to show that a correlation of this parameter with bursts brightness implies a two-component model. This method has met vigorous criticism. We have developed two parameters that measure the variability or structure in the time profiles of BATSE gamma-ray bursts. Both parameters ('structure' and 'spike height') are based on the statistics of 'runs up' and 'runs down.' In short, the structure parameter is the observed number of runs (at several lengths) minus the number expected in a chance distribution. The 'spike height' is the sum of all run heights minus the expected sum. These two are straight-forward to calculate, robust, and measure the variability over the complete profile--not just at the peak. We have applied this algorithm to the profiles of 156 GRB's. In this paper we present graphs of the two parameters as functions of the following: (1) burst duration, (2) burst hardness ratio, (3) V/V max, (4) source galactic longitude, and (5) source galactic latitude. We seek correlations as well as groupings in the data that might indicate a multi-component source distribution. Author (revised)

N94-24432*# East Carolina Univ., Greenville, NC. School of Human Environmental Sciences.
SPATIAL INTERPRETATION OF NASA'S MARSHALL SPACE FLIGHT CENTER PAYLOAD OPERATIONS CONTROL CENTER USING VIRTUAL REALITY TECHNOLOGY c14
Patricia F. Lindsey *In* Alabama Univ., The 1993 NASA/ASEE Summer Faculty Fellowship Program Nov. 1993 5 p (For primary document see N94-24405 06-80)
Avail: CASI HC A01/MF A03

In its search for higher level computer interfaces and more realistic electronic simulations for measurement and spatial analysis in human factors design, NASA at MSFC is evaluating the functionality of virtual reality (VR) technology. Virtual reality simulation generates a three dimensional environment in which the participant appears to be enveloped. It is a type of interactive simulation in which humans are not only involved, but included. Virtual reality technology is still in the experimental phase, but it appears to be the next logical step after computer aided three-dimensional animation in transferring the viewer from a passive to an active role in experiencing and evaluating an environment. There is great potential for using this new technology when designing environments for more successful interaction, both with the environment and with another participant in a remote location. At the University of North Carolina, a VR simulation of a the planned Sitterson Hall, revealed a flaw in the building's design that had not been observed during examination of the more traditional building plan simulation methods on paper and on computer aided design (CAD) work station. The virtual environment enables multiple participants in remote locations to come together and interact with one another and with the environment. Each participant is capable of seeing herself and the other participants and of interacting with them within the simulated environment.
Author (revised)

N94-24433*# Texas A&M Univ., College Station. Marine Engineering Dept.
NEURAL NETWORK-BASED CONTROL USING LYAPUNOV FUNCTIONS c63
Leon A. Luxemburg *In* Alabama Univ., The 1993 NASA/ASEE Summer Faculty Fellowship Program Nov. 1993 5 p (For primary document see N94-24405 06-80)
Avail: CASI HC A01/MF A03

We have successfully demonstrated how the problem of stabilization of plants can be reduced to a problem of approximation of functions. Neural networks have been shown to have approximating and interpolating properties. This approach is good for linear and nonlinear plants. Software has been generated to demonstrate this approach. Author

N94-24434*# Alabama Univ., Tuscaloosa. Aerospace Engineering Dept.
ACCESS TO SPACE STUDIES c15
James A. Martin *In* Alabama Univ., The 1993 NASA/ASEE Summer Faculty Fellowship Program Nov. 1993 4 p (For primary document see N94-24405 06-80)
Avail: CASI HC A01/MF A03

The National Aeronautics and Space Administration is currently considering possible directions in Earth-to-orbit vehicle development under a study called 'Access to Space.' This agency-wide study is considering commercial launch vehicles, human transportation, space station logistics, and other space transportation requirements over the next 40 years. Three options are being considered for human transportation: continued use of the Space Shuttle; development of a small personnel carrier (personnel logistics system (PLS)); or development of an advanced vehicle such as a single-stage-to-orbit (SSTO). Several studies related to the overall Access to Space study are reported in this document. Author (revised)

N94-24435*# New Mexico State Univ., Las Cruces. Astronomy Dept.
FLUX MEASUREMENTS USING THE BATSE SPECTROSCOPIC DETECTORS c93
Bernard McNamara *In* Alabama Univ., The 1993 NASA/ASEE Summer Faculty Fellowship Program Nov. 1993 5 p (For primary document see N94-24405 06-80)
Avail: CASI HC A01/MF A03

Among the Compton Gama-Ray Observatory instruments, the BATSE Spectroscopic Detectors (SD) have the distinction of being able to detect photons of energies less than about 20 keV. This is an interesting energy range for the examination of low mass X-ray binaries (LMXB's). In fact, Sco X-1, the prototype LMXB, is easily seen even in the raw BATSE spectroscopic data. The all-sky coverage afforded by these detectors offers a unique opportunity to monitor this source over time periods never before possible. The aim of this investigation was to test a number of ways in which both continous and discrete flux measurements can be obtained using the BATSE spectroscopic datasets. A instrumental description of a SD can be found in the Compton Workshop of Apr. 1989, this report will deal only with methods which can be used to analyze its datasets. Many of the items discussed below, particularly in regard to the earth occultation technique, have been developed, refined, and applied by the BATSE team to the reduction of BATSE LAD data. Code written as part of this project utilizes portions of that work. The following discussions will first address issues related to the reduction of SD datasets using the earth occultation technique. It will then discuss methods for the recovery of the flux history of strong sources while they are above the earth's limb. The report will conclude with recommended reduction procedures. Author (revised)

N94-24436*# Auburn Univ., AL. Department of Computer Science and Engineering.
INTEGRATION AND EVALUATION OF A SIMULATOR DESIGNED TO BE USED WITHIN A DYNAMIC PROTOTYPING ENVIRONMENT c14
Loretta A. Moore *In* Alabama Univ., The 1993 NASA/ASEE Summer Faculty Fellowship Program Nov. 1993 5 p (For primary document see N94-24405 06-80)
Avail: CASI HC A01/MF A03

The human computer interface (HCI) prototyping environment is designed to allow developers to rapidly prototype systems so that the interface and functionality of a system can be evaluated and iteratively refined early in the development process. This keeps development costs down by modifying the interface during the requirements definition phase, thus minimizing changes that need to be made during and after flight code development. Problems occur within a system when the user interface is not adequately developed and when designers and developers have an incomplete understanding of the system requirements. A process has been developed for prototyping on-board payload displays for Space Station Freedom. This prototyping process consists of five phases: identification of known requirements, analysis of the requirements, development of a formal design representation and specification, development of the prototype, and evaluation of the prototype. The actual development of the prototype involves prototyping the displays, developing a low fidelity simulator, building of an interface (or communication) between the displays and the simulator, integration of these components, and testing to ensure that the interface does what the developer expects. This research integrates and evaluates a software tool which has been developed to serve as a simulator within the prototyping environment. The tool is being evaluated to determine whether or not it meets the basic requirements which are needed for a low fidelity simulator within this environment. In order to evaluate the architecture and its components, a human computer interface for and a simulator of an automobile have been developed as a prototype. The individual components (i.e., the interface and simulator) have been developed, and the current research was designed to integrate and test the complete working system within the prototyping environment. The following sections will describe the architecture and components of the rapid prototyping environment, the development of a system to assess the environment, and the integration and evaluation of PERCNET.
Derived from text

N94-24437*# Alabama Univ., Huntsville. Dept. of Biological Sciences.
EVALUATION OF OVOSTATIN AND OVOSTATIN ASSAY c51
Debra M. Moriarity *In its* The 1993 NASA/ASEE Summer Faculty

Fellowship Program Nov. 1993 5 p (For primary document see N94-24405 06-80)
Avail: CASI HC A01/MF A03

Ovostatin is a 780,000 MW protein, originally isolated from chicken egg white, which is active as a protease inhibitor. Structural studies indicate that the protein is a tetramer of identical subunits of 165,000 MW which can be separated upon reduction with beta- mercaptoethanol. Chicken ovostatin is an inhibitor of metalloproteases such as collagenase and thermolysin, and of acid proteases such as pepsin and rennin. Ovostatin isolated from duck eggs and from crocodile eggs appears to be similar to chicken egg ovostatin, but with significant differences in structure and function. Duck ovostatin contains a reactive thiol ester which is not found in the chicken protein, and duck and crocodile ovostatin inhibit serine protease such as trypsin and chymotrypsin, while chicken ovostatin does not. Electron microscopy of ovostatin indicates that two subunits associated near the middle of each polypeptide to form a dimer with four arms. Two of these dimers then associate to produce a tetramer with eight arms, with the protease binding site near the center of the molecule. Upon binding of the protease, a conformational change causes all eight arms to curl toward the center of the molecule, effectively trapping the protease and sterically hindering access of the substrates to its active site. The structural organization and mechanism of action proposed for ovostatin are nearly identical to that proposed for alpha(sub 2)- macroglobulin, a serum protease inhibitor which may play an important role in regulation of proteases in animal tissues. Although the general arrangement of subunits appears to be the same for all ovostatins studied, some differences have been observed, with chicken ovostatin more closely resembling reptilian ovostatin than the duck protein. This is a surprising result, given the evolutionary relatedness of chickens and ducks. It is possible that the differences in structures may be due to deformed subunit arrangements which occur during the processing and fixing necessary for electron microscopy. Examination of the native structure of these proteins using X-ray crystallography would help clarify these discrepancies. Derived from text

N94-24438*# Alabama Univ., Huntsville. Dept. of Industrial Engineering.
EVALUATION OF COMPUTER-AIDED INSTRUCTION TECHNIQUES FOR THE CREW INTERFACE COORDINATION POSITION c53
Gary P. Moynihan *In its* The 1993 NASA/ASEE Summer Faculty Fellowship Program Nov. 1993 5 p (For primary document see N94-24405 06-80)
Avail: CASI HC A01/MF A03

The Crew Interface Coordinator (CIC) is responsible for real-time voice and procedural communication between the payload crew on the orbiter and the payload operations team on the ground. This function is dedicated to science activities and operations, and may also include some responsibilities for crew training. CIC training at Marshall Space Flight Center (MSFC) consists of mission-independent training, mission simulations, and line-organization training. As identified by Schneider, the program provides very good generic training; however position-specific training may be obtained in a very unstructured way. A computer-based training system, identified as Mac CIC, is currently under development to address this issue. Mac CIC is intended to provide an intermediate level of training in order to prepare the CIC for the more intensive mission simulations. Although originally intended as an intelligent tutoring system, Mac CIC currently exists as a hypertext-based application. The objectives of this research is to evaluate the current system and to provide both recommendations and a detailed plan for Mac CIC's evolution into an intelligent tutoring system. Derived from text

N94-24439*# Tuskegee Inst., AL.
ERROR CODING SIMULATIONS c32
Viveca K. Noble *In* Alabama Univ., The 1993 NASA/ASEE Summer Faculty Fellowship Program Nov. 1993 5 p (For primary document see N94-24405 06-80)
Avail: CASI HC A01/MF A03

There are various elements such as radio frequency interference (RFI) which may induce errors in data being transmitted via a satellite communication link. When a transmission is affected by interference or other error-causing elements, the transmitted data becomes indecipherable. It becomes necessary to implement techniques to recover from these disturbances. The objective of this research is to develop software which simulates error control circuits and evaluate the performance of these modules in various bit error rate environments. The results of the evaluation provide the engineer with information which helps determine the optimal error control scheme. The Consultative Committee for Space Data Systems (CCSDS) recommends the use of Reed-Solomon (RS) and convolutional encoders and Viterbi and RS decoders for error correction. The use of forward error correction techniques greatly reduces the received signal to noise needed for a certain desired bit error rate. The use of concatenated coding, e.g. inner convolutional code and outer RS code, provides even greater coding gain. The 16-bit cyclic redundancy check (CRC) code is recommended by CCSDS for error detection. Derived from text

N94-24440*# Texas A&M Univ., College Station. Mechanical Engineering Dept.
SIMULATION OF CRYOGENIC TURBOPUMP ANNULAR SEALS c37
Alan B. Palazzolo *In* Alabama Univ., The 1993 NASA/ASEE Summer Faculty Fellowship Program Nov. 1993 5 p (For primary document see N94-24405 06-80)
Avail: CASI HC A01/MF A03

San Andres employed the NBS software package MIPROPS to account for density's dependence on pressure in the simulation of liquid annular seals. His example on a LH2 seal showed a significant change in the mass coefficient compared to a constant density model. San Andres, Yang, and Childs extended this analysis by including the pressure and temperature dependence of density, specific heat, viscosity, volumetric expansion, and thermal conductivity in a coupled solution of the energy, momentum, and continuity equations. Their example showed very significant changes in stiffness and inertia for a high speed (38,000 rpm), large L/D ratio (0.5) LOX seal, as compared to their constant temperature results. The current research rederived the San Andres-Yang-Childs (SYC) analysis and extended it to include not only the Moody friction model of SYC but also the Hir's friction model. The derivation begins with obtaining the local differential equations of continuity, momentum, and energy conservation in the seal. These equations are averaged across the film thickness to obtain the resulting 'bulk flow' differential equations. Shear stress and convective heat loss through the stator (seal) and rotor are related to the Moody and Hir's friction factor model. The Holman analogy is employed to relate heat conduction in or out of the fluid film's boundary layer to the friction induced shear stress. Derived from text

N94-24441*# Alabama Univ., Huntsville. Dept. of Mechanical Engineering.
CONTROLLER MODELING AND EVALUATION FOR PCV ELECTRO-MECHANICAL ACTUATOR c37
Joey K. Parker *In its* The 1993 NASA/ASEE Summer Faculty Fellowship Program Nov. 1993 5 p (For primary document see N94-24405 06-80)
Avail: CASI HC A01/MF A03

Hydraulic actuators are currently used to operate the propellant control valves (PCV) for the space shuttle main engine (SSME) and other rocket engines. These actuators are characterized by large power to weight ratios, large force capabilities, and rapid accelerations, which favor their use in control valve applications. However, hydraulic systems are also characterized by susceptibility to contamination, which leads to frequent maintenance requirements. The Control Mechanisms Branch (EP34) of the Component Development Division of the Propulsion Laboratory at the Marshall Space Flight Center (MSFC) has been investigating the application of electromechanical actuators as replacements for the hydraulic units in PCV's over the last few years. This report deals with some testing and analysis of a PCV electromechanical actuator (EMA) designed and fabricated by HR Textron, Inc. This prototype actuator has undergone extensive testing by EP34 personnel since early 1993. At this time, the performance of the HR Textron PCV EMA does not meet requirements for position tracking. Derived from text

N94-24442*# Oakwood Coll., Huntsville, AL. Biology Dept.
THE MEASUREMENT AND ANALYSIS OF LEAF SPECTRAL REFLECTANCE OF TWO STANDS OF LOBLOLLY PINE POPULATIONS c43
Anthony D. Paul *In* Alabama Univ., The 1993 NASA/ASEE Summer Faculty Fellowship Program Nov. 1993 2 p (For primary document see N94-24405 06-80)
Avail: CASI HC A01/MF A03

My research was conducted under the mentorship of Dr. Jeff Luvall. I worked at Marshall from June 1 through August 6, 1993. My proposal is titled 'The Measurement and Analysis of Leaf Spectral Reflectance of Two Stands of Loblolly Pine Populations.' The populations for this study were chosen from a larger population of 31 families managed by the International Forest Seed Company, Odenville, Alabama. The technology for mobile ground base spectral detecting is new and therefore the majority of time, June 2 through July 9, was spent on learning the techniques of the Spectrometer 2 spectroradiometer used in the gathering of spectra information. The activities included in the learning process were as follows: calibration of the equipment, programming the associated computer for data management, operation of the spectral devices, and input and output of data. From July 12 through August 3 the time was spent on learning the 'STATGRAP' computer software. This software will be used in the analysis of the data retrieved by the Spectrometer 2 spectroradiometer. Dr. Greg Carter, at Stennis, a colleague of Dr. Luvall, has been conducting similar work with different instruments and procedures and has agreed to host us for a training session on data gathering and analysis. This visit, which has previously planned for July 9, 1993, but had to be postponed because of schedule conflicts, is now confirmed for August 18-22, 1993. This trip to Stennis will provide the knowledge for conducting the field operations in my study, i.e., gathering of data and file conversions.

Derived from text

N94-24443*# Alabama Univ., Huntsville. Dept. of Mathematical Sciences.

LRAT: LIGHTNING RADIATIVE TRANSFER **c47**

Dieudonne D. Phanord *In its* The 1993 NASA/ASEE Summer Faculty Fellowship Program Nov. 1993 5 p (For primary document see N94-24405 06-80)

Avail: CASI HC A01/MF A03

In this report, we extend to cloud physics the work done for single and multiple scattering of electromagnetic waves. We consider the scattering of light, visible or infrared, by a spherical cloud represented by a statistically homogeneous ensemble of configurations of N identical spherical water droplets whose centers are uniformly distributed in its volume V. The ensemble is specified by the average number rho of scatterers in unit volume and by rho f(R) with f(R) as the distribution function for separations R of pairs. The incident light, vector-phi(sub 0) a plane electromagnetic wave with harmonic time dependence, is from outside the cloud. The propagation parameter kappa(sub 0) and the index of refraction eta(sub 0) determine physically the medium outside the distribution of scatterers. We solve the interior problem separately to obtain the bulk parameters for the scatterer equivalent to the ensemble of spherical droplets. With the interior solution or the equivalent medium approach, the multiple scattering problem is reduced to that of an equivalent single scatterer excited from outside illumination. A dispersion relation which determines the bulk propagation parameter K and the bulk index of refraction eta of the cloud is given in terms of the vector equivalent scattering amplitude vector-G and the dyadic scattering amplitude tilde-g of the single object in isolation. Based on this transfer model we will have the ability to consider clouds composed of inhomogeneous distribution of water and/or ice particles and we will be able to take into account particle size distributions within the cloud. We will also be able to study the effects of cloud composition (i.e., particle shape, size, composition, orientation, location) on the polarization of the single or the multiple scattered waves. Finally, this study will provide a new starting point for studying the problem of lightning radiative transfer.

Derived from text

N94-24444*# Christian Brothers Coll., Memphis, TN. Mechanical Engineering Dept.

SPACE SHUTTLE MAIN ENGINE PERFORMANCE ANALYSIS **c20**

L. Michael Santi *In* Alabama Univ., The 1993 NASA/ASEE Summer Faculty Fellowship Program Nov. 1993 5 p (For primary document see N94-24405 06-80)

Avail: CASI HC A01/MF A03

For a number of years, NASA has relied primarily upon periodically updated versions of Rocketdyne's power balance model (PBM) to provide space shuttle main engine (SSME) steady-state performance prediction. A recent computational study indicated that PBM predictions do not satisfy fundamental energy conservation principles. More recently, SSME test results provided by the Technology Test Bed (TTB) program have indicated significant discrepancies between PBM flow and temperature predictions and TTB observations. Results of these investigations have diminished confidence in the predictions provided by PBM, and motivated the development of new computational tools for supporting SSME performance analysis. A multivariate least squares regression algorithm was developed and implemented during this effort in order to efficiently characterize TTB data. This procedure, called the 'gains model,' was used to approximate the variation of SSME performance parameters such as flow rate, pressure, temperature, speed, and assorted hardware characteristics in terms of six assumed independent influences. These six influences were engine power level, mixture ratio, fuel inlet pressure and temperature, and oxidizer inlet pressure and temperature. A BFGS optimization algorithm provided the base procedure for determining regression coefficients for both linear and full quadratic approximations of parameter variation. Statistical information relative to data deviation from regression derived relations was also computed. A new strategy for integrating test data with theoretical performance prediction was also investigated. The current integration procedure employed by PBM treats test data as pristine and adjusts hardware characteristics in a heuristic manner to achieve engine balance. Within PBM, this integration procedure is called 'data reduction.' By contrast, the new data integration procedure, termed 'reconciliation,' uses mathematical optimization techniques, and requires both measurement and balance uncertainty estimates. The reconciler attempts to select operational parameters that minimize the difference between theoretical prediction and observation. Selected values are further constrained to fall within measurement uncertainty limits and to satisfy fundamental physical relations (mass conservation, energy conservation, pressure drop relations, etc.) within uncertainty estimates for all SSME subsystems. The parameter selection problem described above is a traditional nonlinear programming problem. The reconciler employs a mixed penalty method to determine optimum values of SSME operating parameters associated with this problem formulation.

Derived from text

N94-24445*# Texas A&I Univ., Kingsville. Dept. of Electrical Engineering and Computer Science.

EVALUATION OF THE EFFICIENCY AND FAULT DENSITY OF SOFTWARE GENERATED BY CODE GENERATORS **c61**

Barbara Schreur *In* Alabama Univ., The 1993 NASA/ASEE Summer Faculty Fellowship Program Nov. 1993 4 p (For primary document see N94-24405 06-80)

Avail: CASI HC A01/MF A03

Flight computers and flight software are used for GN&C (guidance, navigation, and control), engine controllers, and avionics during missions. The software development requires the generation of a considerable amount of code. The engineers who generate the code make mistakes and the generation of a large body of code with high reliability requires considerable time. Computer-aided software engineering (CASE) tools are available which generates code automatically with inputs through graphical interfaces. These tools are referred to as code generators. In theory, code generators could write highly reliable code quickly and inexpensively. The various code generators offer different levels of reliability checking. Some check only the finished product while some allow checking of individual modules and combined sets of modules as well. Considering NASA's requirement for reliability, an in house manually generated code is needed. Furthermore, automatically generated code is reputed to be as efficient as the best manually generated code when executed. In house verification is warranted.

Derived from text

N94-24446*# Washington Univ., Saint Louis, MO. Dept. of Civil Engineering.

MICROMECHANICAL SIMULATION OF DAMAGE PROGRESSION IN CARBON PHENOLIC COMPOSITES **c24**

Kerry T. Slattery *In* Alabama Univ., The 1993 NASA/ASEE Summer Faculty Fellowship Program Nov. 1993 5 p (For primary document see N94-24405 06-80)

Avail: CASI HC A01/MF A03

Carbon/phenolic composites are used extensively as ablative insulating materials in the nozzle region of solid rocket motors. The current solid rocket motor (RSRM) on the space shuttle is fabricated from woven rayon cloth which is carbonized and then impregnated with the phenolic resin. These plies are layed up in the desired configuration and cured to form the finished part. During firing, the surface of the carbon/phenolic insulation is exposed to 5000 F gases from the rocket exhaust. The resin pyrolizes and the material chars to a depth which progresses with time. The rate of charring and erosion are generally predictable, and the insulation depth is designed to allow adequate safety margins over the firing time of the motor. However, anomalies in the properties and response of the carbon/phenolic materials can lead to severe material damage which may decrease safety margins to unacceptable levels. Three macro damage modes which were observed in fired nozzles are: ply lift, 'wedge out', and pocketing erosion. Ply lift occurs in materials with plies oriented nearly parallel to the surface. The damage occurs in a region below the charred material where material temperatures are relatively low - about 500 F. Wedge out occurs at the intersection of nozzle components whose plies are oriented at about 45 deg. The corner of the block of material breaks off along a ply interface. Pocketing erosion occurs in material with plies oriented normal to the surface. Thermal expansion is restrained in two directions resulting in large tensile strains and material failure normal to the surface. When a large section of material is removed as a result of damage, the insulation thickness is reduced which may lead to failure of the nozzle due to excessive heating of critical components. If these damage events cannot be prevented with certainty, the designer must increase the thickness of the insulator thus adding to both weight and cost. One of the difficulties in developing a full understanding of these macro damage mechanisms is that the loading environment and the material response to that environment are extremely complex. These types of damage are usually only observed in actual motor firings. Therefore, it is difficult and expensive to evaluate the reliability of new materials. Standard material tests which measure mechanical and thermal properties of test specimens can only provide a partial picture of how the material will respond in the service environment. The development of the ANALOG test procedure which can combine high heating rates and mechanical loads on a specimen will improve the understanding of the interactive effects of the various loads on the system. But a mechanistic model of material response which can account for the heterogeneity of the material, the progression of various micromechanical damage mechanisms, and the interaction of mechanical and thermal stresses on the material is required to accurately correlate material tests with response to service environments. A model based on fundamental damage mechanisms which is calibrated and verified under a variety of loading conditions will provide a general tool for predicting the response of rocket nozzles. The development of a micromechanical simulation technique was initiated and demonstrated to be effective for studying across-ply tensile failure of carbon/phenolic composites. Author (revised)

N94-24447*# Saint John Fisher Coll., Rochester, NY. Chemistry Dept.
A CHEMICAL SENSOR AND BIOSENSOR BASED TOTALLY AUTOMATED WATER QUALITY MONITOR FOR EXTENDED SPACE FLIGHT: STEP 1 c54
Robert S. Smith *In* Alabama Univ., The 1993 NASA/ASEE Summer Faculty Fellowship Program Nov. 1993 5 p (For primary document see N94-24405 06-80)
Avail: CASI HC A01/MF A03

The result of a literature search to consider what technologies should be represented in a totally automated water quality monitor for extended space flight is presented. It is the result of the first summer in a three year JOVE project. The next step will be to build a test platform at the Authors' school, St. John Fisher College. This will involve undergraduates in NASA related research. The test flow injection analysis system will be used to test the detection limit of sensors and the performance of sensors in groups. Sensor companies and research groups will be encouraged to produce sensors which are not currently available and are needed for this project. Author (revised)

N94-24448*# Wichita State Univ., KS. Dept. of Mechanical Engineering.
MICROSTRUCTURAL ANALYSIS OF THE 2195 ALUMINUM-LITHIUM ALLOY WELDS c26
George E. Talia *In* Alabama Univ., The 1993 NASA/ASEE Summer Faculty Fellowship Program Nov. 1993 5 p (For primary document see N94-24405 06-80)
Avail: CASI HC A01/MF A03

The principal objective of this research was to explain a tendency of 2195 Al-Li alloy to crack at elevated temperature during welding. Therefore, a study was made on the effect of welding and thermal treatment on the microstructure of Al-Li Alloy 2195. The critical roles of precipitates, boundaries, phases, and other features of the microstructure were inferred from the crack propagation paths and the morphology of fracture surface of the alloy with different microstructures. Particular emphasis was placed on the microstructures generated by the welding process and the mechanisms of crack propagation in such structures. Variation of the welding parameters and thermal treatments were used to alter the micro/macro structures, and they were characterized by optical and scanning electron microscopy. A theoretical model is proposed to explain changes in the microstructure of welded material. This model proposes a chemical reaction in which gases from the air (i.e., nitrogen) release hydrogen inside the alloy. Such a reaction could generate large internal stresses capable to induce porosity and crack-like delamination in the material. Author

N94-24449*# Pennsylvania State Univ., University Park. Dept. of Aerospace Engineering.
TORQUE EQUILIBRIUM ATTITUDES FOR THE SPACE STATION c18
Roger C. Thompson *In* Alabama Univ., The 1993 NASA/ASEE Summer Faculty Fellowship Program Nov. 1993 5 p (For primary document see N94-24405 06-80)
Avail: CASI HC A01/MF A03

All spacecraft orbiting in a low earth orbit (LEO) experience external torques due to environmental effects. Examples of these torques include those induced by aerodynamic, gravity-gradient, and solar forces. It is the gravity-gradient and aerodynamic torques that produce the greatest disturbances to the attitude of a spacecraft in LEO, and large asymmetric spacecraft, such as the space station, are affected to a greater degree because the magnitude of the torques will, in general, be larger in proportion to the moments of inertia. If left unchecked, these torques would cause the attitude of the space station to oscillate in a complex manner and the resulting motion would destroy the micro-gravity environment as well as prohibit the orbiter from docking. The application of control torques will maintain the proper attitude, but the controllers have limited momentum capacity. When any controller reaches its limit, propellant must then be used while the device is reset to a zero or negatively-biased momentum state. Consequently, the rate at which momentum is accumulated is a significant factor in the amount of propellant used and the frequency of resupply necessary to operate the station. A torque profile in which the area curve for a positive torque is not equal to the area under the curve for a negative torque is 'biased,' and the consequent momentum build-up about that axis is defined as secular momentum because it continues to grow with time. Conversely, when the areas are equal, the momentum is cyclic and bounded. A Torque Equilibrium Attitude (TEA) is thus defined as an attitude at which the external torques 'balance' each other as much as possible, and which will result in lower momentum growth in the controllers. Ideally, the positive and negative external moments experienced by a spacecraft at the TEA would exactly cancel each other out and small cyclic control torques would be required only for precise attitude control. Over time, the only momentum build-up in the controllers would be due to electro-mechanical losses within the device. However, the atmospheric torques are proportional to the density of the atmosphere and the density varies with the orbital position, time of day, time of year, and the solar cycle. In addition, there are unmodeled disturbances and uncertainties in the mass and inertias. Therefore, there is no constant attitude that will completely balance the environmental torques and the dynamic TEA cannot be solved in closed form. The objective of this research was to determine a method to calculate a dynamic TEA such that the rate of momentum build-up in the controllers would be minimized and to implement this method in the MATRIX(x) simulation software by Integrated Systems, Inc. Author

N94-24450*# Tuskegee Inst., AL. Chemical Engineering Dept.
PROPERTIES AND PROCESSING CHARACTERISTICS OF LOW DENSITY CARBON CLOTH PHENOLIC COMPOSITES c24
C. Jeff Wang *In* Alabama Univ., The 1993 NASA/ASEE Summer Faculty Fellowship Program Nov. 1993 5 p (For primary document see N94-24405 06-80)
Avail: CASI HC A01/MF A03

Ply-lift and pocketing are two critical anomalies of carbon cloth phenolic composites (CCPC) in rocket nozzle applications. Ply lift occurs at low temperatures when the A/P and in-plane permeabilities of the composite materials are still very low and in-plane porous paths are blocked. Pocketing occurs at elevated temperatures when in-plane permeability is reduced by the A/P compressive stress. The thermostructural response of CCPC in a rapid heating environment involves simultaneous heat, mass, and momentum transfer along with the degradation of phenolic resin in a multiphase system with temperature- and time-dependent material properties as well as dynamic processing conditions. Three temperature regions represent the consequent chemical reactions, material transformations, and property transitions, and provide a quick qualitative method for characterizing the thermostructural behavior of a CCPC. In order to optimize the FM5939 LDCCP (low density carbon cloth phenolic) for the nozzle performance required in the Advanced Solid Rocket Motor (ASRM) program, a fundamental study on LDCCP materials was conducted. The cured composite has a density of 1.0 +/- 0.5 gm/cc which includes 10 to 25 percent void volume. The weight percent of carbon microballoon is low (7-15 percent). However, they account for approximately one third of the volume and historically their percentages have not been controlled very tightly. In addition, the composite properties show no correlation with microballoon weight percent or fiber properties (e.g. fiber density or fiber moisture adsorption capacity). Test results concerning the ply-lift anomaly in the MNASA motor firings were: (1) Steeper ply angle (shorter path lenght) designs minimized/eliminated by lifting, (2) material with higher void volume ply lifted less frequently, (3) materials with high (greater than 9 percent) microballoon content had a higher rate of ply lifting, and (4) LDCCP materials failed at microballoon-resin interfaces. The objectives of this project are: (1) to investigate the effects of carbon microballoon and cabosil fillers as well as fiber heat treatment on plylift-related mechanical properties, (2) to develop a science-based thermostructural process model for the carbon phenolics. The model can be used in the future for the selection of the improved ASRM materials, (3) to develop the micro-failure mechanisms for the ply-lift initiation and propagation processes during the thermoelastic region of phenolic degradation, i.e. postcuring and devolatilization. Author (revised)

N94-24451*# Alabama A & M Univ., Huntsville. Dept. of Physics.

EFFECTS OF THERMAL-SOLUTAL CONVECTION ON TEMPERATURE AND SOLUTAL FIELDS UNDER VARIOUS GRAVITATIONAL ORIENTATIONS c29

Jai-Ching Wang *In* Alabama Univ., The 1993 NASA/ASEE Summer Faculty Fellowship Program Nov. 1993 5 p (For primary document see N94-24405 06-80)

Avail: CASI HC A01/MF A03

Semiconductor crystals such as Hg(1-x)CD(x)Te grown by unidirectional solidification Bridgmann method have shown compositional segregations in both the axial and radial directions. Due to the wide separation between the liquidus and the solidus of its pseudobinary phase diagram, there is a diffusion layer of higher HgTe content built up in the melt near the melt-solid interface which gives a solute concentration gradient in the axial direction. The value of effective diffusion coefficient calculated from fitting of the data to 1D model varies with Hg(1-x)Cd(x)Te growth conditions. This indicates that the growth condition of the Hg(1-x)Cd(x)Te is not purely diffusion controlled. Because of the higher thermal conductivity in the melt than that in the crystal in the growth system, there is a thermal leakage through the fused silica crucible wall near the melt-solid interface. This gives a thermal gradient in the radial direction. Hart, and Thorpe, Hutt and Soulsby have shown that under such conditon a fluid will become convectively unstable as a result of different diffusitivities of temperature and solute. It is quite important to understand the effects of this thermosolute convection on the compositonal segregation in both axial and radial directions in the unidirectionally solidified crystals under various gravitational directions. To reach this goal, we start with a simplified problem to study the effects of thermal-solutal convection on the temperature and solutal fields under various gravitional orientations. We begin by reviewing model governing equations. Author (revised)

N94-24452*# Alabama Univ., Tuscaloosa. Dept. of Aerospace Engineering.

USING NEURAL NETWORKS TO ASSIST IN OPAD DATA ANALYSIS c63

Kevin W. Whitaker *In* Alabama Univ., The 1993 NASA/ASEE Summer Faculty Fellowship Program Nov. 1993 5 p (For primary document see N94-24405 06-80)

Avail: CASI HC A01/MF A03

The space shuttle main engine (SSME) became the subject of plume emission spectroscopy in 1986 when researchers from NASA-Marshall Space Flight Center (MSFC), Arnold Engineering Development Center (AEDC), and Rocketdyne went to the SSME test stands at the NASA-Stennis Space Center and at Rocketdyne's Santa Susan Field Laboratory to optically observe the plume. Since then, plume spectral acquisitions have recorded many nominal tests and the qualitative spectral features of the SSME plume are now well established. Significant discoveries made with both wide-band and narrow-band plume emission spectroscopy systems led MSFC to promote the Optical Plume Anomaly Detection (OPAD) program with a goal of instrumenting all SSME test stands with customized spectrometer systems. A prototype OPAD system is now installed on the SSME Technology Test Bed (TTB) at MSFC. The OPAD system instrumentation consists of a broad-band, optical multiple-channel analyzer (OMA) and a narrow-band device called a polychrometer. The OMA is a high-resolution (1.5-2.0 Angstroms) 'super-spectrometer' covering the near-ultraviolet to near-infrared waveband (2800-7400 Angstroms), providing two scans per second. The polychrometer consists of sixteen narrow-band radiometers: fourteen monitoring discrete wavelengths of health and condition monitoring elements and two dedicated to monitoring background emissions. All sixteen channels are capable of providing 500 samples per second. To date, the prototype OPAD system has been used during 43 SSME firings on the TTB, collecting well over 250 megabytes of plume spectral data. One goal of OPAD data analysis is to determine interatively with the help of a computer code, SPECTRA4, developed at AEDC. Experience has shown that iteration with SPECTRA4 is an incredibly labor intensive task and not one to be performed by band. What is really needed is the 'inverse' of SPECTRA4 but the mathematical model for this inverse mapping is tenuous at best. However, the robustness of PSECTRA4 run in the 'forward' direction means that accurate input/output mappings can be obtained. If the mappings were inverted (i.e., input becomes output and output becomes input) then an 'inverse' of SPECTRA4 would be at hand but the 'model' would be specific to the data utilized and would in no way be general. Building a generalized model based upon known input/output mappings while ignoring the details of the governing physical model is possible through the use of a neural network. The research investigation described involves the development of a neural network to provide a generalized 'inverse' of SPECTRA4. The objectives of the research were to design an appropriate neural network architecture, train the network, and then evaluate its performance. Author (revised)

N94-24453*# Alabama Univ., Huntsville. Dept. of Physics and Center for Space Plasma and Aeronomic Research.

THE FAR ULTRAVIOLET (FUV) AURORAL IMAGER FOR THE INNER MAGNETOSPHERIC IMAGER (IMI) MISSION: OPTIONS c19

Gordon R. Wilson *In its* The 1993 NASA/ASEE Summer Faculty Fellowship Program Nov. 1993 5 p (For primary document see N94-24405 06-80)

Avail: CASI HC A01/MF A03

The change from an intermediate mission (cost ceiling of $300 million) to a solar-terrestrial probe class mission (cost ceiling of $150 million) will require some major changes in the configuration of the IMI mission. One option being considered is to move to a small spin-stabilized spacecraft (with no despun platform) which could be launched with a smaller Taurus or Conestoga class booster. Such a change in spacecraft type would not present any fundamental problems (other than restrictions on mass and power) for the He plus 304 A plasmasphere imager, the high and low energy neutral atom imagers, and the geocoronal imager, but would present a challenge for the FUV auroral imager since the original plan called for this instrument to operate from a despun platform. Since the FUV instrument is part of the core payload it cannot be dropped from the instrument complement without jeopardizing the science goals of the mission. A way must be found to keep this instrument and to allow it to accomplish most, if not all, of its science objectives. One of the subjects discussed are options for building an FUV instrument for a spinning spacecraft. Since a number of spinning spacecraft have carried auroral imagers, a range of techniques exists. In addition, the option of flying the FUV imager on a separate micro-satellite launched with the main IMI spacecraft or with a separate pegasus launch, was considered and is discussed. Author (revised)

N94-24454*# Tuskegee Inst., AL. Aerospace Science Engineering Dept.

EVALUATION OF ADVANCED MATERIALS THROUGH EXPERIMENTAL MECHANICS AND MODELLING c38

Yii-Ching Yang *In* Alabama Univ., The 1993 NASA/ASEE Summer Faculty Fellowship Program Nov. 1993 5 p (For primary document see N94-24405 06-80)
Avail: CASI HC A01/MF A03

Composite materials have been frequently used in aerospace vehicles. Very often defects are inherited during the manufacture and damages are inherited during the construction and services. It becomes critical to understand the mechanical behavior of such composite structure before it can be further used. One good example of these composite structures is the cylindrical bottle of solid rocket motor case with accidental impact damages. Since the replacement of this cylindrical bottle is expensive, it is valuable to know how the damages affects the material, and how it can be repaired. To reach this goal, the damage must be characterized and the stress/strain field must be carefully analyzed. First the damage area, due to impact, is surveyed and identified with a shearography technique which uses the principle of speckle shearing interferometry to measure displacement gradient. Within the damage area of a composite laminate, such as the bottle of solid rocket motor case, all layers are considered to be degraded. Once a lamina being degraded the stiffness as well as strength will be drastically decreased. It becomes a critical area of failure to the whole bottle. And hence the stress/strain field within and around a damage should be accurately evaluated for failure prediction. To investigate the stress/strain field around damages a Hybrid-Numerical method which combines experimental measurement and finite element analysis is used. It is known the stress or strain at the singular point can not be accurately measured by an experimental technique. Nevertheless, if the location is far away from the singular spot, the displacement can be found accurately. Since it reflects the true displacement field locally regardless of the boundary conditions, it is an excellent input data for a finite element analysis to replace the usually assumed boundary conditions. Therefore, the Hybrid-Numerical method is chosen to avoid the difficulty and to take advantage of both experimental technique and finite element analysis. Experimentally, the digital image correlation technique is employed to measure the displacement field. It is done by comparing two digitized images, before and after loading. Numerically, the finite element program, ABAQUS (version 5.2), is used to analyze the stress and strain field. It takes advantage of the high speed and huge memory size of modern supercomputer, CRAY Y-MP, at NASA Marshall Space Flight Center.
Author (revised)

N94-24455*# Mississippi State Univ., State College. Dept. of Physics and Astronomy.
USING CONTOUR MAPS TO SEARCH FOR RED-SHIFTED 511 keV FEATURES IN BATSE GRB SPECTRA c89
Peter G. Varmette *In* Alabama Univ., The 1993 NASA/ASEE Summer Faculty Fellowship Program Nov. 1993 5 p (For primary document see N94-24405 06-80)
Avail: CASI HC A01/MF A03

Since their discovery twenty years ago, the origin of gamma-ray bursts (GRB's) has remained an intriguing mystery. The quest to understand these objects has given rise to a plethora of competing theories. Several theories suggest that GRB's are galactic in origin while others suggest that GRB's are cosmological. One piece of evidence that might provide scientistis with a key to understanding the origin of GRB's may be whether or not spectral emission and absorption features exist in burst spectra. If the features exist and can be attributed to either cyclotron lines or to red-shifted 511 keV annihilation lines then credence would be given to those theories that support a galactic origin, i.e. near neutron stars. A method of searching for spectral features in burst spectra (BATSE HER data) is outlined.
Author (revised)

N94-24698 National Academy of Sciences - National Research Council, Washington, DC.
WOMEN SCIENTISTS AND ENGINEERS EMPLOYED IN INDUSTRY: WHY SO FEW? A REPORT BASED ON A CONFERENCE
1994 140 p
(ISBN-0-309-04991-1; LC-93-86930) Copyright Avail: Issuing Activity

Women comprise about 12 percent of the employed scientific and engineering (S&E) labor force in industry. While this is due in part to specific sub-fields selected by women, another significant contributing factor is the attrition rate for women scientists and engineers in industry, which is double that for men and substantially higher than for other employment sectors. These compelling facts led the Committee on Women in Science and Engineering (CWSE) of the National Research Council to plan a conference, 'Women Scientists and Engineers Employed in Industry: Why So Few?,' to examine the workplace environment for women pursuing careers in industry. The conference provided a forum for women scientists and engineers to share data and personal experiences to uncover the principal causes of underrepresentation of S&E women in industry and to explore effective strategies for change. In addition, representatives of five companies having established exemplary programs to recruit and retain women scientists and engineers - Aerospace Corporation, ALCOA, AT&T Bell Laboratories, Xerox Corporate Research and Technology, and Scios Nova - described strategies proven to be effective in removing barriers for women scientists and engineers.
Author (revised)

N94-25362*# Texas Southern Univ., Houston. Jesse H. Jones School of Business.
STRATEGIES FOR RECRUITING ADDITIONAL AFRICAN AMERICANS INTO THE NASA JSC SUMMER FACULTY FELLOWS PROGRAM
Ladelle M. Hyman *In* NASA. Johnson Space Center, National Aeronautics and Space Administration (NASA)/American Society for Engineering Education (ASEE) Summer Faculty Fellowship Program, 1993, Volume 1 Dec. 1993 15 p (For primary document see N94-25348 06-99)
Avail: CASI HC A03/MF A03

N94-25384*# Houston Univ., TX. Dept. of Curriculum and Instruction.
A MULTIMEDIA ADULT LITERACY PROGRAM: COMBINING NASA TECHNOLOGY, INSTRUCTIONAL DESIGN THEORY, AND AUTHENTIC LITERACY CONCEPTS
Jerry W. Willis *In* NASA. Johnson Space Center, National Aeronautics and Space Administration (NASA)/American Society for Engineering Education (ASEE) Summer Faculty Fellowship Program, 1993, Volume 2 Dec. 1993 13 p (For primary document see N94-25367 06-99)
Avail: CASI HC A03/MF A03

81 ADMINISTRATION AND MANAGEMENT

Includes management planning and research.

N94-22704# Universiteit Twente, Enschede (Netherlands). Faculty of Applied Mathematics.
PERSONNEL SHIFT ASSIGNMENT: EXISTENCE CONDITIONS AND NETWORK MODELS
Joeren vandenBerg and David M. Panton (University of South Australia, Pooraka.) Feb. 1993 21 p
(MEMO-1116; ETN-94-94752) Avail: CASI HC A03/MF A01

The personnel scheduling problem is known to be a five stage process in which the final stage involves the assignment of shifts to the days worked in the schedule. The existence conditions for both continuous and forward rotating shift assignments and heuristic network algorithms for the determination of such assignments are discussed. Results generated for a number of test problems demonstrate that the network devised to search for continous solutions produces these solutions in a high proportion of cases where such solutions are known to exist. For more general problems the algorithm is shown to be efficient in its ability to generate either continuous or rotating solutions.
ESA

N94-23563*# Aerojet-General Corp., Azusa, CA. Electronics Plant.
EARTH OBSERVING SYSTEM (EOS) ADVANCED MICROWAVE SOUNDING UNIT-A (AMSU-A) SCHEDULE PLAN Final Report
Jan. 1994 54 p
(Contract NAS5-32314)
(NASA-CR-194856; NAS 1.26:194856; Rept-10392) Avail: CASI HC A04/MF A01

This report describes Aerojet's methods and procedures used to control and administer contractual schedules for the EOS/AMSU-A program. Included are the master, intermediate, and detail schedules; critical path analysis; and the total program logic network diagrams.
Author (revised)

N94-23761# Vrije Univ., Brussels (Belgium).
FRAMEWORK FOR INTERACTIVE SOLVING OF META-CONSTRAINT

SATISFACTION PROBLEMS
F. J. Juengen and W. Kowalczyk Dec. 1992 24 p
(PB94-118825; IR-312) Avail: CASI HC A03/MF A01

This report presents a framework for solving Meta-Constraint Satisfaction Problems (MCSP's). The process of solving a MCSP interactively is viewed here as a user-driven search in an abstract search space. This search space consists of a collection of states which are represented by pairs of the form (set of constraints, partial valuation). The user can travel through the states by applying some transformations to states. To provide a better insight into the states, a number of their properties is measured and reported to the user. The goal of the search process is to find a state which satisfies some (implicit) meta-constraints. In particular, the result of the search process may consist of an incomplete (or even inconsistent) solution of a set of constraints. A special module, called Navigator, is used to allow the user to traverse the states already visited in an easy manner (these states are arranged in a tree). The usefulness of the framework is illustrated by an Interactive Project Scheduler. NTIS

N94-24528 Vrije Univ., Amsterdam (Netherlands). Faculteit der Wiskunde en Informatica.
MODULAR APPROACH TO PROJECT MANAGEMENT
Frederik-Jan Juengen and Wojciech Kowalczyk Dec. 1992 46 p Limited Reproducibility: More than 20% of this document may be affected by microfiche quality
(PB94-118833; IR-313) Avail: Issuing Activity (National Technical Information Service (NTIS))

The report provides a detailed analysis of project management. A number of desired functionalities of an 'ideal' project management system is identified and some suggestions are made concerning the implementations of these functionalities. Moreover, a methodology for developing complex systems for tasks like project management is outlined. The methodology is based on three principles: modularity, re-usability and incremental system development. The applicability of the methodology is illustrated by the development of a project management system. A number of generic modules have been implemented and configured into a powerful scheduling system for network planning, Interactive Project Scheduler (IPS). Two possible applications of the IPS have been discussed: in the building industry and software development projects. It is expected that our system will be extended by modules supporting other phases of project management, especially resources monitoring. NTIS

N94-24683# Naval Postgraduate School, Monterey, CA.
SEMATECH, A CASE STUDY: ANALYSIS OF A GOVERNMENT-INDUSTRY PARTNERSHIP M.S. Thesis
Robert M. Byron 23 Sep. 1993 109 p
(AD-A273166) Avail: CASI HC A06/MF A02

SEMATECH proponents argue that the SEMATECH consortium model represents future government-industry consortia. This thesis examines the Semiconductor Manufacturing Technology Initiative (SEMATECH). Analysis of SEMATECH includes the following: (1) its dissection as a consortium and as a government-industry venture; (2) the impact of SEMATECH on both semiconductor research and development (R&D) and the American chipmaking industry; and (3) the political implications of SEMATECH. SEMATECH is funded through the Advanced Research Programs Agency (ARPA). Federal support of the semiconductor industry via ARPA seems incompatible with Department of Defense interests. There are instances when federal support of R&D is justified. It seems doubtful that the semiconductor industry is one of those instances, but if it were, SEMATECH would not be the best way to channel government support. This thesis shows that SEMATECH is not responsible for the turnaround of the semiconductor industry; that SEMATECH is not an appropriate model for government-industry partnerships; and that federal funding of SEMATECH should cease. DTIC

N94-24708* National Aeronautics and Space Administration, Washington, DC.
MANAGEMENT. A BIBLIOGRAPHY FOR NASA MANAGERS
Washington Feb. 1994 72 p
(NASA-SP-7500(27); NAS 1.21:7500(27)) Avail: Issuing Activity

This bibliography lists 630 reports, articles, and other documents introduced into the NASA scientific and technical information system in 1992. Items are selected and grouped according to their usefulness to the manager as manager. Citations are grouped into ten subject categories: human factors and personnel issues; management theory and techniques; industrial management and manufacturing; robotics and expert systems; computers and information management; research and development; economics, costs, and markets; logistics and operations management; reliability and quality control; and legality, legislation, and policy. Author

N94-25076# Technische Univ., Eindhoven (Netherlands).
THE INCREASE OF THE CONTROLLABILITY OF PRODUCTION ORGANIZATIONS Ph.D. Thesis [HET VERGROTEN VAN DE BESTUURBAARHEID VAN PRODUKTIE-ORGANISATIES]
Petrus J. L. M. vanAmelsvoort 1992 188 p In DUTCH
(ISBN-9-03-860161-1; ETN-94-95291) Copyright Avail: CASI HC A09/MF A02

A model for the control structure of a flexible organization was developed, in view of the increased pressure on companies for higher demands with regard to efficiency, quality and flexibility. The model is based on the sociotechnical theory, in which attention is focused on the structure of production process in which the concept of a (semi)autonomous group plays an important role. In the process of developing the model, a number of gaps revealed in existing models were filled. A balance model of controllability based on the law of requisite variety was developed. The control model consists of autonomous teams that each control a particular part of the production process. Criteria were defined to determine the desired location of control possibilities. Proceeding on the basis of the principle of minimum possible division of labor, an efficient modular control structure is obtained. ESA

N94-25197*# National Aeronautics and Space Administration. Marshall Space Flight Center, Huntsville, AL.
NEW WAYS OF DOING BUSINESS (NWODB) COST QUANTIFICATION ANALYSIS Final Report
Joseph W. Hamaker and Russell L. Rosmait (Pittsburgh State Univ., KS.) Oct. 1992 30 p Presented at the Summer Faculty Fellowship Research Continuation Program, Huntsville, AL, Feb. 1994; sponsored by Alabama Univ. Prepared in cooperation with Applied Research, Inc., Huntsville, AL
(Grant NAG8-212)
(NASA-CR-195186; NAS 1.26:195186; UAH-5-30163) Avail: CASI HC A03/MF A01

The cost of designing, producing, and operating typical aerospace flight hardware is necessarily more expensive than most other human endeavors. Because of the more stringent environment of space, hardware designed to operate there will probably always be more expensive than similar hardware which is designed for less taxing environments. It is the thesis of this study that there are very significant improvements that can be made in the cost of aerospace flight hardware. Derived from text

N94-25235# Technische Univ., Eindhoven (Netherlands).
PRODUCTION CONTROL AND DEMAND MANAGEMENT IN CAPACITATED FLOW PROCESS INDUSTRIES Ph.D. Thesis
Jan Cornelis Fransoo 1993 134 p Sponsored by Netherlands Organization for Applied Scientific Research
(ISBN-9-03-860211-1; ETN-94-95299) Copyright Avail: CASI HC A07/MF A02

A single machine multiproduct production system under tight capacity constraints is studied. Focus is on the production control function in such a system. Both the managerial aspects and the scheduling aspects of the problem are addressed. The practical relevance of studying such a system originated from process industries. To enable a detailed analysis of production control in flow process industries to be made, the elementary flow process industries production system was defined. The production control concept developed was built up from a simple uncomplicated model to a more comprehensive and complicated model, links to the real life flow process industries environment being provided. The hierarchical structure of the specific concept developed was analyzed and its methodology studied in comparison with more general hierarchical approaches from the literature. The practical consequences of the concept and the necessary adjustment made to the concept on implementation in a glass factory are illustrated. ESA

N94-25279# Technische Univ., Eindhoven (Netherlands). Management Accounting Section.

RELEVANT COSTS OR FULL COSTS? EXPLAINING WHY MANAGERS USE CAPACITY COST ALLOCATIONS FOR SHORT TERM DECISIONS Ph.D. Thesis

Marcus Johannes F. Wouters 1993 222 p
(ISBN-9-06-215364-X; ETN-94-95303) Copyright Avail: CASI HC A10/MF A03

A study whose main purpose is to explain why managers would sometimes follow a full cost approach to capacity utilization decisions is reported. The usefulness for managers of allocating capacity costs to activities when capacity utilization decisions are made is investigated. Some systematic empirical evidence that managers do, in fact, follow a full cost approach to capacity utilization decisions is provided. A contribution to contemporary discussions, in the context of ABC, on the use of allocated costs for short term decision making, is made. It is noted that an activity yields a contribution margin and uses capacity. The latter consequence may lead to costs associated with foregone opportunities (because other activities cannot be implemented) or costs associated with additional capacity (because capacity expansion is required or because capacity reduction is obstructed). In a relevant cost approach these costs are compared with the contribution margin. In a full cost approach the contribution margin is related to an allocated share of the total capacity costs. ESA

N94-25283# Technische Univ., Eindhoven (Netherlands).

THROUGHPUT TIME CONTROL AND DUE DATE RELIABILITY IN TOOL AND DIE SHOPS Ph.D. Thesis

Antonius Maria vandeWakker 1993 289 p
(ISBN-9-03-860182-4; ETN-94-95349) Copyright Avail: CASI HC A13/MF A03

The results of a study into the production planning and control issues involved in manufacturing multiple discrete products in the component manufacturing units of tool and die shops are presented. Special attention is given to designing approaches to the following three planning and control decisions: due date assignment: how to be able to promise short and reliable throughput times; order release: when should the manufacturing unit receive an order; work sequencing: which manufacturing order should be given the highest priority at a given work station. The study focuses on designing a set of planning and control rules to be used as the basis for making the planning and control decisions mentioned above. These decision rules are intended to provide an optimal performance mix with respect to achieving a high level of due date reliability and a short average throughput time for assembly orders. ESA

N94-23246*# University of Central Florida, Orlando. Dept. of Industrial Engineering and Management Systems.

KSC MANAGEMENT TRAINING SYSTEM PROJECT

Jose A. Sepulveda *In* NASA. Kennedy Space Center, NASA/ASEE Summer Faculty Fellowship Program Oct. 1993 p 433-463 (For primary document see N94-23230 06-80)
Avail: CASI HC A03/MF A04

N94-23904*# National Aeronautics and Space Administration. Ames Research Center, Moffett Field, CA.

CONSTRAINT-BASED SCHEDULING

Monte Zweben *In* JPL, SpaceOps 1992: Proceedings of the Second International Symposium on Ground Data Systems for Space Mission Operations 1 Mar. 1993 p 477-484 (For primary document see N94-23832 06-66)
Avail: CASI HC A02/MF A10

N94-23938*# National Aeronautics and Space Administration. Goddard Space Flight Center, Greenbelt, MD.

MISSION AND SCIENCE ACTIVITY SCHEDULING LANGUAGE

Larry G. Hull *In* JPL, SpaceOps 1992: Proceedings of the Second International Symposium on Ground Data Systems for Space Mission Operations 1 Mar. 1993 p 697-702 (For primary document see N94-23832 06-66)
Avail: CASI HC A02/MF A10

N94-23963*# Jet Propulsion Lab., California Inst. of Tech., Pasadena.

RESOURCE ALLOCATION PLANNING WITH INTERNATIONAL COMPONENTS

Gene Burke, Ralph Durham, Frank Leppla, and David Porter (California Inst. of Tech., Pasadena.) *In its* SpaceOps 1992: Proceedings of the Second International Symposium on Ground Data Systems for Space Mission Operations 1 Mar. 1993 p 867-874 (For primary document see N94-23832 06-66)
Avail: CASI HC A02/MF A10

N94-23964*# National Aeronautics and Space Administration. Goddard Space Flight Center, Greenbelt, MD.

AN INTELLIGENT PLANNING AND SCHEDULING SYSTEM FOR THE HST SERVICING MISSIONS

Jay Johnson (Bendix Field Engineering Corp., Seabrook, MD.), Lynn Bogovich (Bendix Field Engineering Corp., Seabrook, MD.), Alan Tuchman (Bendix Field Engineering Corp., Seabrook, MD.), Andrew Kispert (Bendix Field Engineering Corp., Seabrook, MD.), Brenda Page (Bendix Field Engineering Corp., Seabrook, MD.), Christian Burkhardt (Bendix Field Engineering Corp., Seabrook, MD.), Ronald Littlefield (Bendix Field Engineering Corp., Seabrook, MD.), David McLean (Bendix Field Engineering Corp., Seabrook, MD.), William Potter, and William Ochs et al *In* JPL, SpaceOps 1992: Proceedings of the Second International Symposium on Ground Data Systems for Space Mission Operations 1 Mar. 1993 p 875-880 (For primary document see N94-23832 06-66)
(Contract NAS5-27772)
Avail: CASI HC A02/MF A10

N94-23965*# National Aeronautics and Space Administration. Goddard Space Flight Center, Greenbelt, MD.

SCHEDULING THE FUTURE NASA SPACE NETWORK: EXPERIENCES WITH A FLEXIBLE SCHEDULING PROTOTYPE

Nadine Happell (Stanford Telecommunications, Inc., Reston, VA.), Karen L. Moe, and Jay Minnix (Stanford Telecommunications, Inc., Reston, VA.) *In* JPL, SpaceOps 1992: Proceedings of the Second International Symposium on Ground Data Systems for Space Mission Operations 1 Mar. 1993 p 881-886 (For primary document see N94-23832 06-66)
Avail: CASI HC A02/MF A10

N94-23966*# National Aeronautics and Space Administration. Goddard Space Flight Center, Greenbelt, MD.

SOFTWARE REUSE IN SPACECRAFT PLANNING AND SCHEDULING SYSTEMS

David McLean (Bendix Field Engineering Corp., Seabrook, MD.), Alan Tuchman (Bendix Field Engineering Corp., Seabrook, MD.), Todd Broseghini (Bendix Field Engineering Corp., Seabrook, MD.), Wen Yen (Bendix Field Engineering Corp., Seabrook, MD.), Brenda Page (Bendix Field Engineering Corp., Seabrook, MD.), Jay Johnson (Bendix Field Engineering Corp., Seabrook, MD.), Lynn Bogovich (Bendix Field Engineering Corp., Seabrook, MD.), Chris Burkhardt (Bendix Field Engineering Corp., Seabrook, MD.), James McIntyre (Bendix Field Engineering Corp., Seabrook, MD.), and Scott Klein (Bendix Field Engineering Corp., Seabrook, MD.) et al *In* JPL, SpaceOps 1992: Proceedings of the Second International Symposium on Ground Data Systems for Space Mission Operations 1 Mar. 1993 p 887-892 (For primary document see N94-23832 06-66)
(Contract NAS5-27772)
Avail: CASI HC A02/MF A10

N94-23967*# Centre National d'Etudes Spatiales, Toulouse (France).

PLANNING: MANAGEMENT OF PREDICTABILITY AND UNCERTAINTY AND KEEPING ABREAST OF DEVELOPMENTS

Christophe Bastien-Thiry and Gerard Verfaillie *In* JPL, SpaceOps 1992: Proceedings of the Second International Symposium on Ground Data Systems for Space Mission Operations 1 Mar. 1993 p 893-898 (For primary document see N94-23832 06-66)
Avail: CASI HC A02/MF A10

N94-24416*# Alabama Univ., Huntsville. Dept. of Industrial and Systems Engineering.

DESIGN AND SPECIFICATION OF A CENTRALIZED MANUFACTURING DATA MANAGEMENT AND SCHEDULING SYSTEM

Phillip A. Farrington *In its* The 1993 NASA/ASEE Summer Faculty

Fellowship Program Nov. 1993 6 p (For primary document see N94-24405 06-80)
Avail: CASI HC A02/MF A03

N94-25361*# Houston Univ., TX. Dept. of Industrial Engineering.
INTEGRATED RISK MANAGEMENT
J. L. Hunsucker *In* NASA. Johnson Space Center, National Aeronautics and Space Administration (NASA)/American Society for Engineering Education (ASEE) Summer Faculty Fellowship Program, 1993, Volume 1 Dec. 1993 14 p (For primary document see N94-25348 06-99)
Avail: CASI HC A03/MF A03

N94-25373*# Minot State Univ., ND. College of Business.
A COMPARATIVE EVALUATION PLAN FOR THE MAINTENANCE, INVENTORY, AND LOGISTICS PLANNING (MILP) SYSTEM HUMAN-COMPUTER INTERFACE (HCI) Final Report
Scott P. Overmyer *In* NASA. Johnson Space Center, National Aeronautics and Space Administration (NASA)/American Society for Engineering Education (ASEE) Summer Faculty Fellowship Program, 1993, Volume 2 Dec. 1993 15 p (For primary document see N94-25367 06-99)
Avail: CASI HC A03/MF A03

82 DOCUMENTATION AND INFORMATION SCIENCE

Includes information management; information storage and retrieval technology; technical writing; graphic arts; and micrography.

For computer documentation see *61 Computer Programming and Software.*

N94-22734# Technical Research Centre of Finland, Espoo. Information Processing Lab.
OPEN EDI [AVOIN EDI]
Aija Palomaeki, Pasi Peuranen, and Jari Veijalainen Apr. 1992 72 p In FINNISH
(VTT-TIED-1353; ISBN-951-38-4166-9; ETN-94-94475) Copyright Avail: CASI HC A04/MF A01

Different kinds of organization autonomies and their practical effects on cooperation between organizations and on Electronic Data Interchange (EDI) between them are studied. The most obvious problems for organizations in their EDI activities currently concern the integration of EDI into existing data processing systems. Current standards give no solution to this practical problem, since attention is essentially directed to the description of data exchanged by organizations. A reference architecture developed to resolve these problems is proposed. The basic hypothesis of this architecture is that organization autonomy and in consequence choice of data processing system, are in no way restricted. On the other hand, an abstract local interface is defined between the standardized zone and local zone of organizations. The definition of this interface can be standardized as has been done in the OSI (Open Systems Interconnection) model, but the realization of the interface depends on the organizations themselves. ESA

N94-22863 Pacific Northwest Lab., Richland, WA.
TRANSLATIVE INTERFACE FOR DATA SHARING AND INTEGRATING: A PARADIGM FOR DISTRIBUTED DATA SYSTEMS
T. F. Maloney Apr. 1993 20 p Presented at the Sybase User's Conference, San Jose, CA, 28 Apr. 1993 Limited Reproducibility: More than 20% of this document may be affected by poor print and microfiche quality
(Contract DE-AC06-76RL-01830)
(DE93-018790; PNL-SA-21755; CONF-9304201-1) Avail: Issuing Activity (Department of Energy (DOE))

Typically, applications are built only after the database schema is available. To enable the application designer/programmer with the tools necessary to forge ahead without having to wait for the data schema definition, a change from traditional methodologies must take place. An alternate design methodology intended to bring applications on-line as soon as possible is proposed. Inmon's paradigm is looked at for decision support systems and tying it together with Martin's subject databases used in a distributed data system. DOE

N94-22875 Oak Ridge National Lab., TN. Carbon Dioxide Information Analysis Center.
CATALOG OF DATA BASES AND REPORTS
Jul. 1993 179 p Limited Reproducibility: More than 20% of this document may be affected by poor print
(Contract DE-AC05-84OR-21400)
(DE93-040597; ORNL/CDIAC-34/R3; ESDP-4048) Avail: Issuing Activity (Department of Energy (DOE))

Information about the many reports and other materials made available by the U.S. Department of Energy's (DOE's) Global Change Research Program (GCRP) is provided. It is divided into eight sections plus author and title indexes: U.S. Department of Energy Global Change Research Program Research plans and summaries, U.S. Department of Energy Global Change Research Program technical reports, U.S. Department of Energy Atmospheric Radiation Measurements (ARM) Program reports, other U.S. Department of Energy reports, CDIAC reports, CDAIC numeric data and computer model distribution, USDA reports on response of vegetation to carbon dioxide, and other publications. DOE

N94-22879# Grenoble-1 Univ. (France). Lab. de Genie Informatique.
AN INFORMATION RETRIEVAL LOGICAL MODEL APPLIED TO THE FORMALISM OF CONCEPTUAL GRAPHS: THE ELEN PROTOTYPE AND ITS EXPERIMENTATION ON A CORPUS OF SOFTWARE COMPONENTS Ph.D. Thesis [UN MODELE LOGIQUE DE RECHERCHE D'INFORMATIONS APPLIQUE AU FORMALISME DES GRAPHES CONCEPTUELS: LE PROTOTYPE ELEN ET SON EXPERIMENTATION SUR UN CORPUS DE COMPOSANTS LOGICIELS]
Jean-Pierre Chevallet 1992 195 p In FRENCH
(ETN-94-95162) Avail: CASI HC A09/MF A03

An information retrieval system was developed using a cluster indexing formalism based on the Sowa conceptual graphs. The purpose of the system was to retrieve accurate answers. The semantics was evaluated by a first order fuzzy model. An optimal research mechanism based on graph signatures is presented. The ELEN (French acronym for information retrieval and software engineering) prototype project is part of a main program involving the design and the development of database applications for software. ELEN is in fact a database for software. The software engineering aspects applying component research are reviewed. The logic model chosen is extended in order to satisfy the indexing formalism. Proposals, fuzzy and first order fuzzy modal logics are discussed. The indexing formalism, based on the knowledge of semantic networks and named conceptual graphs, are described. The results and the performance of the prototype system are discussed. ESA

N94-22880# Grenoble-1 Univ. (France). Lab. de Genie Informatique.
A GENERAL MODEL FOR DYNAMIC AND COMPLEX INFORMATION MANAGEMENT: THE ELEN PROTOTYPE OBJECT MANAGER FOR SOFTWARE ENGINEERING Ph.D. Thesis [UN MODELE GENERIQUE POUR LA GESTION DES INFORMATIONS COMPLEXES ET DYNAMIQUES: GESTIONNAIRE D'OBJETS DU PROTOTYPE ELEN DEDIE AU GENIE LOGICIEL]
Sahar Jarwah 1992 210 p In FRENCH
(ETN-94-95163) Avail: CASI HC A10/MF A03

The purpose of the study was to develop a tool to support large scale softwares. The ELEN (French acronym for information retrieval and software engineering) prototype is part of a program involving the design and the development of data base applications. ELEN is a software database for software. A general storage and management core which allows the integration of information sets and which uses declaratory tools is defined. The project manager is capable of specifying the searched development method or strategy. A data model for hypertext systems, capable of generating logic software information, is presented. The model uses object oriented semantics and integrates dynamic and static aspects of software engineering. Available object oriented data and procedures were used. The conditions required to activate and to control the object's behavior are summarized. ESA

N94-22934# Lawrence Livermore National Lab., CA.
STRUCTURE AND FLOW OF DATA THROUGH AN ENVIRONMENTAL DATA MANAGEMENT SYSTEM
C. S. Chamberlain and P. L. Cederwall Feb. 1993 7 p Presented at the HAZMACON 1993: Hazardous Materials Conference, San Jose, CA, 6-8 Apr. 1993
(Contract W-7405-eng-48)
(DE93-040487; UCRL-JC-111732; CONF-9304206-1) Avail: CASI HC A02/MF A01

Efficient data management is crucial to environmental investigations. The management system must provide for organized data tracking, storage, and retrieval of data essential to successful environmental management. Ultimately, the system is used as an environmental management tool for remediation decisionmaking. This paper will describe the structure and flow of data in the data management system used by the Environmental Restoration Division of the Environmental Protection Department of Lawrence Livermore National Laboratory (LLNL). The structure is based on three relational databases that are closely correlated. The first database handles sample tracking. The second database handles nondiscrete data, such as sample location, media, analytical results, and some geological information. These two databases are maintained on a VAX 63 10 with VMS, using INGRES relational database software. The third database handles nondiscrete data like graphic imaging flies and geophysical logs and will be run on an IPC Sparc, using INGRES. The flow of data, both hard copy and electronic, follows a model that tracks information from sampling plan through decisionmaking. The steps in the process include chain-of-custody (CoC) tracking of the sample, receipt of analytical results, application of quality control procedures, and electronic use of data in decision support tools, such as graphic imaging, model development and verification, or statistical analysis. DOE

N94-22944# Westinghouse Idaho Nuclear Co., Inc., Idaho Falls.
QUALITY DATA VALIDATION: COMPREHENSIVE APPROACH TO ENVIRONMENTAL DATA VALIDATION
L. A. Matejka, Jr. 1993 15 p Presented at the 20th American Society for Quality Control (ASQC) National Energy and Environmental Annual Conference, Indian Wells, CA, 19-22 Sep. 1993
(Contract DE-AC07-84ID-12435)
(DE94-000925; WINCO-11968; CONF-9309139-9) Avail: CASI HC A03/MF A01

Environmental data validation consists of an assessment of three major areas: analytical method validation; field procedures and documentation review; and evaluation of the level of achievement of data quality objectives based in part on PARCC parameters analysis and expected applications of data. A program utilizing matrix association of required levels of validation effort and analytical levels versus applications of this environmental data was developed in conjunction with DOE-ID guidance documents to implement actions under the Federal Facilities Agreement and Consent Order in effect at the Idaho National Engineering Laboratory. This was an effort to bring consistent quality to the INEL-wide Environmental Restoration Program and database in an efficient and cost-effective manner. This program, documenting all phases of the review process, is described here. DOE

N94-23095 Vrije Univ., Amsterdam (Netherlands). Faculteit der Wiskunde en Informatica.
FLEXIBLE FRAMEWORK FOR CONTINGENT INFORMATION SYSTEMS MODELLING
V. VanSwede and J. C. VanVliet Dec. 1992 32 p Limited Reproducibility: More than 20% of this document may be affected by microfiche quality
(PB93-220549; IR-310) Avail: CASI HC A03

The modelling of complex information systems requires that a large number of issues be dealt with. Most well-known development methods concentrate on a subset of these issues. The authors have developed a rich framework that aims to cover a much larger number of issues than is currently addressed. The framework can be used as a check list in composing project scenarios. The present article presents the framework and its rationale, and illustrates its use in classifying modelling techniques and extending existing development methods. NTIS

N94-23126# Sandia National Labs., Albuquerque, NM.
BIBLIOGRAPHIC RETRIEVAL SYSTEM (BARS), SANDIA SHOCK COMPRESSION (SSC) DATABASE SHOCK PHYSICS INDEX
W. Herrmann, T. J. Parker, and K. Mulholland (Career Services, Albuquerque, NM.) Sep. 1993 14 p
(Contract DE-AC04-94AL-85000)
(DE94-001679; SAND-93-1391) Avail: CASI HC A03/MF A01

The Bibliographic Retrieval System (BARS) is a database management system specially designed to retrieve bibliographic references. Two databases are available, (1) the Sandia Shock Compression (SSC) database which contains over 5600 references to the literature related to stress waves in solids and their applications, and (2) the Shock Physics Index (SPHINX) which includes over 6200 further references to stress waves in solids, material properties at intermediate and low rates, ballistic and hypervelocity impact, and explosive or shock fabrication methods. There is some overlap in the information in the two databases. DOE

N94-23127# Sandia National Labs., Albuquerque, NM.
BIBLIOGRAPHIC RETRIEVAL SYSTEM (BARS). SANDIA SHOCK COMPRESSION (SSC) DATABASE SHOCK PHYSICS INDEX (SPHINX) DATABASE. VOLUME 1: UNIX VERSION QUERY GUIDE CUSTOMIZED APPLICATION FOR INGRES
W. Herrmann, G. M. vonLaven (Advanced Software Engineering, Madison, AL.), and T. Parker (RE/SPEC, Inc., Albuquerque, NM.) Sep. 1993 19 p
(Contract DE-AC04-94AL-85000)
(DE94-001703; SAND-93-1422-Vol-1) Avail: CASI HC A03/MF A01

The Bibliographic Retrieval System (BARS) is a database management system specially designed to retrieve bibliographic references. Two databases are available, (1) the Sandia Shock Compression (SSC) database which contains over 5700 references to the literature related to stress waves in solids and their applications, and (2) the Shock Physics Index (SPHINX) which includes over 8000 further references to stress waves in solids, material properties at intermediate and low rates, ballistic and hypervelocity impact, and explosive or shock fabrication methods. There is some overlap in the information in the two databases. DOE

N94-23128# Sandia National Labs., Albuquerque, NM.
BIBLIOGRAPHIC RETRIEVAL SYSTEM (BARS), SANDIA SHOCK COMPRESSION (SSC) DATABASE, SHOCK PHYSICS INDEX (SPHINX) DATABASE, VOLUME 2: UNIX VERSION USER'S GUIDE
G. M. vonLaven (Advanced Software Engineering, Madison, AL.) and W. Herrmann Sep. 1993 65 p
(Contract DE-AC04-94AL-85000)
(DE94-001704; SAND-93-1422-Vol-2) Avail: CASI HC A04/MF A01

The Bibliographic Retrieval System (BARS) is a database management system specially designed to store and retrieve bibliographic references and track documents. The system uses INGRES to manage this database and user interface. It uses forms for journal articles, books, conference proceedings, theses, technical reports, letters, memos, visual aids, as well as miscellaneous forms which can be used for data sets or any other material which can be assigned an access or file number. Sorted output resulting from flexible BOOLEAN searches can be printed or saved in files which can be inserted in reference lists for use with word processors. DOE

N94-23150# Grenoble-1 Univ. (France). Lab. de Genie Informatique.
SPECIFICATIONS OF ETS, THE ENHANCED TRANSPORT SERVICE
Cristophe Diot, Patrick Cocquet (Dassalt Electronique, Saint Cloud, France.), and Didier Stunault (Dassalt Electronique, Saint Cloud, France.) 5 May 1992 66 p
(RR-907-I; ETN-93-94996) Avail: CASI HC A04/MF A01

Enhanced Transport Services (ETS) provided to the session layer at the boundary between session and transport layers of the OSI (Open Systems Interconnection) reference model is defined. ETS is structured as a service kernel backward compatible with ISO (International Standards Organization) 8072 service. Around this service kernel, optional service subsets will be added, depending on the application requirements: real time data transfer, voice and video transfer, etc. These specific service subsets will increase ETS flexibility and enlarge its range of applications. Synchronization, management, and automatic connection are examples of specific services required by the previous applications. The service kernel only is defined. Every time it is possible, this document adopts the ISO concepts and terminology. It has a structure which is similar to that of ISO

8072 in order to facilitate the comparison between the two documents.
ESA

N94-23190# Argonne National Lab., IL.
A SYSTEM FOR MANAGING INFORMATION AT ATLAS
I. R. Tilbrook 1993 12 p Presented at the 1993 Symposium of North-Eastern Accelerator Personnel (SNEAP), Rochester, NY, 22-25 Sep. 1993
(Contract W-31-109-eng-38)
(DE94-001337; ANL/PHY/CP-80830; CONF-9309262-1) Avail: CASI HC A03/MF A01

In response to a need for better management of maintenance and document information at the Argonne Tandem-Linear Accelerating System (ATLAS), the ATLAS Information Management System (AIMS) has been created. The system is based on the relational database model. The system's applications use the Alpha-4 relational database management system, a commercially available software package. The system's function and design are described.
DOE

N94-23289*# Lockheed Engineering and Sciences Co., Houston, TX.
SPACE STATION FREEDOM (SSF) DATA MANAGEMENT SYSTEM (DMS) PERFORMANCE MODEL DATA BASE
John R. Stovall Nov. 1993 128 p
(Contract NAS9-17900)
(NASA-CR-188270; NAS 1.26:188270; LESC-30966) Avail: CASI HC A07/MF A02

The purpose of this document was originally to be a working document summarizing Space Station Freedom (SSF) Data Management System (DMS) hardware and software design, configuration, performance and estimated loading data from a myriad of source documents such that the parameters provided could be used to build a dynamic performance model of the DMS. The document is published at this time as a close-out of the DMS performance modeling effort resulting from the Clinton Administration mandated Space Station Redesign. The DMS as documented in this report is no longer a part of the redesigned Space Station. The performance modeling effort was a joint undertaking between the National Aeronautics and Space Administration (NASA) Johnson Space Center (JSC) Flight Data Systems Division (FDSD) and the NASA Ames Research Center (ARC) Spacecraft Data Systems Research Branch. The scope of this document is limited to the DMS core network through the Man Tended Configuration (MTC) as it existed prior to the 1993 Clinton Administration mandated Space Station Redesign. Data is provided for the Standard Data Processors (SDP's), Multiplexer/Demultiplexers (MDM's) and Mass Storage Units (MSU's). Planned future releases would have added the additional hardware and software descriptions needed to describe the complete DMS. Performance and loading data through the Permanent Manned Configuration (PMC) was to have been included as it became available. No future releases of this document are presently planned pending completion of the present Space Station Redesign activities and task reassessment.
Derived from text

N94-23562*# National Aeronautics and Space Administration. Lewis Research Center, Cleveland, OH.
BIBLIOGRAPHY OF LEWIS RESEARCH CENTER TECHNICAL PUBLICATIONS ANNOUNCED IN 1992
Nov. 1993 440 p
(NASA-TM-106035; E-7602; NAS 1.15:106035) Avail: CASI HC A19/MF A04

This compilation of abstracts describes and indexes the technical reporting that resulted from the scientific and engineering work performed and managed by the Lewis Research Center in 1992. All the publications were announced in the 1992 issues of STAR (Scientific and Technical Aerospace Reports) and/or IAA (International Aerospace Abstracts). Included are research reports, journal articles, conference presentations, patents and patent applications, and theses.
Author (revised)

N94-23712* National Aeronautics and Space Administration, Washington, DC.
NASA PATENT ABSTRACTS BIBLIOGRAPHY: A CONTINUING BIBLIOGRAPHY. SECTION 2: INDEXES (SUPPLEMENT 44)
Jan. 1994 617 p
(NASA-SP-7039(44)-Sect-2; NAS 1.21:7039(44)-Sect-2) Avail: CASI HC A99

A subject index is provided for over 5500 patents and patent applications for the period May 1969 through December 1993. Additional indexes list personal authors, corporate authors, contract numbers, NASA case numbers, U.S. patent class numbers, U.S. patent numbers, and NASA accession numbers.
Author

N94-23741 National Defence Research Establishment, Linkoeping (Sweden). Huvudavelning foer Informationsteknologi.
STUDY OF METHODS AND STRUCTURES FOR HANDLING OF DIGITIZED MAPS FOR GEOGRAPHICAL INFORMATION SYSTEMS [STUDIE AV METODER OCH STRUKTURER FOER LAGRING OCH HANTERING AV DIGITALISERADE KARTOR FOER GEOGRAFISKA INFORMATIONSSYSTEM]
Erland Jungert Nov. 1992 19 p In SWEDISH See also PB90-227737 Limited Reproducibility: More than 20% of this document may be affected by microfiche quality
(PB93-204402; FOA-30078-3.4) Avail: Issuing Activity (National Technical Information Service (NTIS))

The report is the result of a study concerning the need for and the use of digitized maps in connection to crisis/emergency management. The work also includes a part concerned with different types of spatial data structures and their use in GIS.
NTIS

N94-23816# Technische Hogeschool Twente, Enschede (Netherlands). Dept. of Computer Science.
CONCEPTS AND TECHNIQUES FOR AN ACTIVE DATABASE APPROACH TO OFFICE PROCEDURE SUPPORT
P. W. P. J. Grefen 1993 28 p
(PB94-110749; Memo-Inf-93-25) Copyright Avail: CASI HC A03/MF A01

Administrative processes in office environments often consist of complex procedures specifying tasks to be executed and dependencies between them. Office automation systems support these office procedures by providing powerful and flexible transaction processing facilities. The report proposes a technique for office procedure support called 'automatic transaction invocation'. This technique makes use of standard active database concepts for the specification and implementation of complex office procedures. The technique provides separate high-level specification of transactions describing the elementary office tasks, and dependency rules between transactions describing the overall structure of the office procedure application, including detailed timing requirements. The concepts of the technique can easily be mapped onto a graph-based representation, allowing an attractive means for design and analysis of complex applications.
NTIS

N94-23971*# National Aeronautics and Space Administration, Washington, DC.
NASA PRINTING, DUPLICATING, AND COPYING MANAGEMENT HANDBOOK
Dec. 1993 55 p
(NASA-NHB-1490.5; NAS 1.18:1490.5) Avail: CASI HC A04/MF A01

This handbook provides information and procedures for the implementation of NASA policy and applicable laws and regulations relating to printing, duplicating, and copying. The topics addressed include a description of relevant laws and regulations, authorizations required, and responsible entities for NASA printing, duplicating, and copying. The policy of NASA is to ensure understanding and application of authority and responsibility on printing matters. Where necessary, the handbook clarifies the intent of basic laws and regulations applicable to NASA.
Derived from text

N94-24079*# National Aeronautics and Space Administration. Marshall Space Flight Center, Huntsville, AL.
FISCAL YEAR 1993 SCIENTIFIC AND TECHNICAL REPORTS, ARTICLES, PAPERS, AND PRESENTATIONS
Joyce E. Turner, comp. Oct. 1993 88 p
(NASA-TM-108423; NAS 1.15:108423) Avail: CASI HC A05/MF A01

This document presents formal NASA technical reports, papers published in technical journals, and presentations by MSFC personnel in FY93. It also includes papers of MSFC contractors. After being announced in STAR, all of the NASA series reports may be obtained from the National Technical Information Service, 5285 Port Royal Road, Springfield, VA 22161. The information in this report may be of value to the scientific and engineering community in determining what information has been published and what is available. Author

N94-24092# General Accounting Office, Washington, DC. National Security and International Affairs Div.

SPACE OPERATIONS: ARCHIVING SPACE SCIENCE DATA NEEDS FURTHER MANAGEMENT IMPROVEMENTS. REPORT TO THE CHAIRMAN, SUBCOMMITTEE ON INVESTIGATIONS AND OVERSIGHT, COMMITTEE ON SCIENCE, SPACE, AND TECHNOLOGY, HOUSE OF REPRESENTATIVES

Dec. 1993 25 p
(GAO/NSIAD-94-25; B-254957) Avail: CASI HC A03/MF A01; GAO, PO Box 6015, Gaithersburg, MD 20884-6015 HC

The National Aeronautics and Space Administration (NASA) creates long-term archives of scientific data from its space missions because of the potential importance of the data in future studies such as long-term analyses of the earth's environment. This report responds to the former Chairman's request that we review changes to NASA'S data archiving program since we last reported on the program in 1990. Our reports criticized the conditions of NASA'S data archives and pointed out that the archives were incomplete for many important missions and held no data for others. In summary, it is recommended that NASA improve the physical condition of its archives, obtain and restore all appropriate data from past missions, and revise its data management policies to ensure that all valuable data are adequately archived in the future. Our objectives were to determine if NASA had improved its data archiving policies and practices in response to our recommendations and whether there are other opportunities to improve that program. Author (revised)

N94-24099*# Stanford Univ., CA. Dept. of Electrical Engineering.

AstroMail: ELECTRONIC MAIL FOR THE ASTROPHYSICS COMMUNITY Final Report

Phillip H. Scherrer and Richard S. Bogart 20 May 1993 13 p
(Contract NAS5-30428; RTOP 506-59-11)
(NASA-CR-194877; NAS 1.26:194877) Avail: CASI HC A03/MF A01

As part of the NASA Science Internet User Support Services program, NASA Goddard was interested in R&D which could extend the SolarMail system developed by members of the Wilcox Space Observatory at Stanford University to support a larger astrophysics user community. Specific objectives of the R&D effort were to include: a clone of the existing SolarMail system with additional documentation, enabling a parallel mail system to be established by populating the database; a cloned version of SolarMail functioning with a user database similar to that of the High Energy Astrophysics Division (HEAD) of the American Astronomical Society; a report on the status and surveyed usage of SolarMail and its clones into an extendable distributed mail system to serve as the basis for AstroMail, including a draft declaration of policy; a prototype AstroMail system based on the above specifications and including at least SolarMail and one of its clones supporting a set of astronomy user databases as subsets; and a report on the status of the prototype AstroMail with recommendations for future modifications to AstroMail. Author

N94-24337*# National Aeronautics and Space Administration, Washington, DC.

NASA HIGH PERFORMANCE COMPUTING AND COMMUNICATIONS PROGRAM Annual Report, 1992

Lee Holcomb, Paul Smith, and Paul Hunter Dec. 1993 141 p
(NASA-TM-4554; NAS 1.15:4554) Avail: CASI HC A07/MF A02

The National Aeronautics and Space Administration's HPCC program is part of a new Presidential initiative aimed at producing a 1000-fold increase in supercomputing speed and a 100-fold improvement in available communications capability by 1997. As more advanced technologies are developed under the HPCC program, they will be used to solve NASA's 'Grand Challenge' problems, which include improving the design and simulation of advanced aerospace vehicles, allowing people at remote locations to communicate more effectively and share information, increasing scientist's abilities to model the Earth's climate and forecast global environmental trends, and improving the development of advanced spacecraft. NASA's HPCC program is organized into three projects which are unique to the agency's mission: the Computational Aerosciences (CAS) project, the Earth and Space Sciences (ESS) project, and the Remote Exploration and Experimentation (REE) project. An additional project, the Basic Research and Human Resources (BRHR) project exists to promote long term research in computer science and engineering and to increase the pool of trained personnel in a variety of scientific disciplines. This document presents an overview of the objectives and organization of these projects as well as summaries of individual research and development programs within each project. Author (revised)

N94-24501# Sandia National Labs., Albuquerque, NM.

FACT-BASED ENTERPRISE INFORMATION MANAGEMENT USING NIAM

G. Rivord 1993 13 p Presented at the 1993 Conference on Natural Language Information Analysis Methodology and Information System Design Methodology, Utrecht, Netherlands, 15-17 Sep. 1993
(Contract DE-AC04-76DP-00789)
(DE93-041135; SAND-93-1211C; CONF-9309238-2) Avail: CASI HC A03/MF A01

The effort to consolidate the 'islands of information' within an enterprise -- to manage information at the enterprise level rather than the department or sub-system level -- is known by many names, such as 'Information Resource Management' and 'Corporate Data Administration'. Here we will call it 'Enterprise Information Management' (EIM). This effort is becoming increasingly vital as the need for shared information grows, yet it is plagued by costly, time-consuming efforts that produce reams of hard-to-maintain documentation. The results are difficult to integrate, measure, or apply. Management needs a tool that can integrate models from diverse modeling efforts into a global knowledge base, produce metrics to clarify the value of the integration process, and provide a short, traceable route between information models and their physical implementations. The natural-language emphasis of NIAM makes it an ideal candidate for this tool. When integrated with enterprise-wide data administration, the collection of metrics, CASE tools that produce application code, and automated support tools, NIAM can effectively manage multiple Universes of Discourse (UOD). Prototypes of automated support tools, 'Fact Manager' and 'Fact Designer', will be discussed. DOE

N94-24552*# Research Inst. for Advanced Computer Science, Moffett Field, CA.

INCREASING LEVELS OF ASSISTANCE IN REFINEMENT OF KNOWLEDGE-BASED RETRIEVAL SYSTEMS

Catherine Baudin (National Aeronautics and Space Administration. Ames Research Center, Moffett Field, CA.), Smadar Kedar (Northwestern Univ., Evanston, IL.), and Barney Pell (National Aeronautics and Space Administration. Ames Research Center, Moffett Field, CA.) Feb. 1994 18 p
(Contract NAS2-13721)
(NASA-CR-195144; NAS 1.26:195144; RIACS-TR-94-03) Avail: CASI HC A03/MF A01

The task of incrementally acquiring and refining the knowledge and algorithms of a knowledge-based system in order to improve its performance over time is discussed. In particular, the design of DE-KART, a tool whose goal is to provide increasing levels of assistance in acquiring and refining indexing and retrieval knowledge for a knowledge-based retrieval system, is presented. DE-KART starts with knowledge that was entered manually, and increases its level of assistance in acquiring and refining that knowledge, both in terms of the increased level of automation in interacting with users, and in terms of the increased generality of the knowledge. DE-KART is at the intersection of machine learning and knowledge acquisition: it is a first step towards a system which moves along a continuum from interactive knowledge acquisition to increasingly automated machine learning as it acquires more knowledge and experience. Author (revised)

N94-24607 Sandia National Labs., Albuquerque, NM.

WASTE MINIMIZATION/POLLUTION PREVENTION AT R/D FACILITIES: A CRADLE-TO-GRAVE TRACKING AND INFORMATION SYSTEM THAT WILL BE IMPLEMENTED AT SANDIA NATIONAL LABORATORIES

M. W. Hollingsworth (Rinchem Co., Inc., Albuquerque, NM.), E. A. Kjeldgaard, and R. Navarrete (Bell Telephone Labs., Inc., Murray Hill, NJ.) 1993 6 p Presented at the Environmentally Conscious Manufacturing Congress 1993, Arlington, VA, 30 Aug. - 1 Sep. 1993 Limited Reproducibility: More

than 20% of this document may be affected by microfiche quality
(Contract DE-AC04-76DP-00789)
(DE93-040330; SAND-93-2031C; CONF-9308150-4) Avail: CASI HC A02

A comprehensive environment, safety, and health (ES&H) program allocates an extensive portion of its resources to information collection, management, and manipulation. Much of these resources are difficult to obtain and even more costly to ensure that they are sufficiently accurate; however, a system which collects information at the point which a process begins or a material enters a facility and maintains that information throughout its entire life-cycle is a more efficient approach to providing the data necessary to meet ES&H requirements. These data requirements for all the various groups within an ES&H program are associated with the properties and interactions among materials, personnel, facilities, hazards, waste, and processes. Although each group is charged with addressing a particular aspect of these properties and interactions, the information they require can be aggregated into a coherent set of common data fields. It is these common data fields that the Cradle-to-Grave Tracking and Information System (CGTIS) is designed to satisfy. Research and development laboratories such as Sandia National Laboratories (SNL) are diverse in nature and, therefore, present a complex challenge to ES&H professionals. The remainder of this paper will describe the CGTIS as envisioned and implemented at SNL, define the requirements of a complete CGTIS, and review the current status of each system module at SNL. DOE

N94-24642# Technische Univ., Delft (Netherlands). Faculty of Technical Mathematics and Informatics.

WORLD PROCESSOR: AN INTERFACE FOR TEXTUAL DISPLAY AND MANIPULATION IN VIRTUAL REALITY

Jouke Verlinden, Jay David Bolter, and C. vanderMast 1993 12 p
(PB94-118643; Rept-93-55) Copyright Avail: CASI HC A03/MF A01

We propose a Virtual Reality interface for creating and manipulating textual and hypertextual information. Many current hypertext systems include concept maps in two dimensions. Our system, called the World Processor, offers the user a three-dimensional concept map. It allows the user to move through the map while exploring existing objects and their associated texts and adding new objects and texts. We discuss a number of interface issues raised by three-dimensional hypertext and then describe the World Processor as an attempt to address some of these issues. Of particular interest in the World Processor interface are its point-and-shoot selection technique, its methods for reading and editing text in 3D, its widgets for creating and modifying conceptual objects, and its auditory as well as visual feedback. Possible applications for three-dimensional hypertext include CSCW (particularly collaborative writing) and authoring systems for computer-based training. NTIS

N94-24646 Technische Univ., Delft (Netherlands).

RITL: AN INFORMATION SYSTEM FOR APPLICATION REUSE-IN-THE-LARGE Ph.D. Thesis

HaiKuan Li 1993 243 p Limited Reproducibility: More than 20% of this document may be affected by microfiche quality
(PB94-119088; ISBN-90-6275-871-1) Copyright Avail: Issuing Activity (National Technical Information Service (NTIS))

This dissertation provides system developers with a set of methods for application reuse, particularly for application reuse-in-the-large. The idea of reuse-in-the-large, in contrast with that of traditional reuse (the reuse of small code components), aims at reusing large-grain components of information systems and, more importantly, the information about the creation of the components. Such kind of reuse reflects the requirements for developing large and complex applications. The methods for application reuse-in-the-large, as provided in this dissertation, include a method for reusing abstract data types and algorithm structures, a method for reusing system architectures and design templates, and a method for modeling, specification, management and manipulation of large-scale components. These methods are applied in an information system for application development and maintenance with reuse-in-the-large. NTIS

N94-24649*# National Aeronautics and Space Administration. Langley Research Center, Hampton, VA.

NASA/DOD AEROSPACE KNOWLEDGE DIFFUSION RESEARCH PROJECT. REPORT NUMBER 20: THE USE OF SELECTED INFORMATION PRODUCTS AND SERVICES BY US AEROSPACE ENGINEERS AND SCIENTISTS: RESULTS OF TWO SURVEYS

Thomas E. Pinelli, Rebecca O. Barclay (Rensselaer Polytechnic Inst., Troy, NY.), and John M. Kennedy (Indiana Univ., Bloomington.) Feb. 1994 62 p
(RTOP 505-90-00)
(NASA-TM-109022; NAS 1.15:109022) Avail: CASI HC A04/MF A01

The U.S. government technical report is a primary means by which the results of federally funded research and development (R&D) are transferred to the U.S. aerospace industry. However, little is known about this information product in terms of its actual use, importance, and value in the transfer of federally, funded R&D. To help establish a body of knowledge, the U.S. government technical report is being investigated as part of the NASA/DoD Aerospace Knowledge Diffusion Research Project. In this report, we summarize the literature on technical reports and provide a model that depicts the transfer of federally funded aerospace R&D via the U.S. government technical report. We present results from two surveys of our investigation of aerospace knowledge diffusion vis-a-vis the U.S. government technical report and close with a brief overview of on-going research into aerospace knowledge diffusion focusing on the role of the industry-affiliated information intermediary. Author (revised)

N94-24660*# National Aeronautics and Space Administration. Langley Research Center, Hampton, VA.

NADA/DOD AEROSPACE KNOWLEDGE DIFFUSION RESEARCH PROJECT. REPORT NUMBER 19: THE US GOVERNMENT TECHNICAL REPORT AND THE TRANSFER OF FEDERALLY FUNDED AEROSPACE R/D: AN ANALYSIS OF FIVE STUDIES

Thomas E. Pinelli, Rebecca O. Barclay (Rensselaer Polytechnic Inst., Troy, NY.), and John M. Kennedy (Indiana Univ., Bloomington.) Jan. 1994 115 p
(RTOP 505-90-00)
(NASA-TM-109061; NAS 1.15:109061) Avail: CASI HC A06/MF A02

The U.S. government technical report is a primary means by which the results of federally funded research and development are transferred to the U.S. aerospace industry. However, little is known about this information product in terms of its actual use, importance, and value in the transfer of federally funded R&D. To help establish a body of knowledge, the U.S. government technical report is being investigated as part of the 'NASA/DoD Aerospace Knowledge Diffusion Research Project'. In this report, we summarize the literature on technical reprts and provide a model that depicts the transfer of federally funded aerospace R&D via the U.S. government technical report. We present results from five studies of our investigation of aerospace knowledge diffusion vis-a-vis the U.S. government technical report and close with a brief overview of on-going research into the use of the U.S. government technical report as a rhetorical device for transferring federally funded aerospace R&D. Author

N94-24691# Georgia Inst. of Tech., Atlanta.

MODELING OF DATABASE CONSTRAINTS IN ACTIVE DATABASES Final Report, Jun. 1992 - Jun. 1993

S. B. Navathe and A. K. Tanaka Oct. 1993 59 p
(Contract F30602-92-C-0092)
(AD-A273484; RL-TR-93-189) Avail: CASI HC A04/MF A01

This report deals with the problems of specification, modeling, and enforcement of constraints in databases. The active database area is emerging as a viable alternative for implementation of large scale database applications, particularly those involving data that needs close monitoring and control due to its dynamic nature. Applications in monitoring of personnel, equipment materials, etc., need capabilities available in modern database systems. The entire area of command and control engineering is likely to benefit immensely from the emerging active database technology. This report presents an enhanced conceptual data model which is based on the popular entity relationship (ER) data model. This model has been enhanced with a capability of modeling active database behavior at a higher level than the event condition-action rules used in other systems. A high level specification language is presenting and then showing how it can be mapped into the facilities of an active commercial DBMS such as INGRES. This report addresses three different types of constraints: integrity constraints, the invariant properties of the model as constraints, and dynamic constraints that deal with a change of state that occurs during update operations. The facility described can be thought of as a part of the design tools that are needed to exploit the active capabilities in a database management system. DTIC

N94-24709*# National Aeronautics and Space Administration. Langley Research Center, Hampton, VA.
NASA/DOD AEROSPACE KNOWLEDGE DIFFUSION RESEARCH PROJECT. REPORT NUMBER 21: US AEROSPACE INDUSTRY LIBRARIANS AND TECHNICAL INFORMATION SPECIALISTS AS INFORMATION INTERMEDIARIES: RESULTS OF THE PHASE 2 SURVEY
Thomas E. Pinelli, Rebecca O. Barclay (Rensselaer Polytechnic Inst., Troy, NY.), and John M. Kennedy (Indiana Univ., Bloomington.) Feb. 1994 66 p
(RTOP 505-90-00)
(NASA-TM-109064; NAS 1.15:109064) Avail: CASI HC A04/MF A01

The U.S. government technical report is a primary means by which the results of federally funded research and development (R&D) are transferred to the U.S. aerospace industry. However, little is known about this information product in terms of its actual use, importance, and value in the transfer of federally funded R&D. To help establish a body of knowledge, the U.S. government technical report is being investigated as part of the NASA/DoD Aerospace Knowledge Diffusion Research Project. In this report, we summarize the literature on technical reports and provide a model that depicts the transfer of federally funded aerospace R&D via the U.S. government technical report. We present results from our investigation of aerospace knowledge diffusion vis-a-vis the U.S. government technical report, and present the results of research that investigated aerospace knowledge diffusion vis-a-vis U.S. aerospace industry librarians and technical information specialists as information intermediaries. Author (revised)

N94-24743 Technische Univ., Twente (Netherlands). Dept. of Computer Science.
CORRECT AND EFFICIENT INTERFACE FOR LOGICAL QUERY LANGUAGES WITH COMPLEX OBJECTS
M. Holsheimer, R. A. deBy, and H. Aiet-Kaci 1993 16 p Limited Reproducibility: More than 20% of this document may be affected by microfiche quality
(PB93-211175; Memo-INF-93-02) Copyright Avail: Issuing Activity (National Technical Information Service (NTIS))

The authors describe a formal design for a logical query language using psi-terms as data structures to interact effectively and efficiently with a relational database. The structure of psi-terms provides an adequate representation for so-called complex objects. They generalize conventional terms used in logic programming: they are typed attributed structures, ordered thanks to a subtype ordering. Unification of psi-terms is an effective means for integrating multiple inheritance and partial information into a deduction process. They define a compact database representation for psi-terms, representing part of the subtyping relation in the database as well. They describe a retrieval algorithm based on an abstract interpretation of the psi-term unification process and prove its formal correctness. The algorithm is efficient in that it incrementally retrieves only additional facts that are actually needed by a query, and never retrieves the same fact twice. NTIS

N94-24759*# National Aeronautics and Space Administration, Washington, DC.
THIRD ANNUAL FOREIGN ACQUISITIONS WORKSHOP: IMPROVING ACCESS TO FOREIGN GRAY LITERATURE
1993 214 p Workshop held in Crystal City, VA, 21-23 Sep. 1993
(NASA-TM-109683; NAS 1.15:109683) Avail: CASI HC A10/MF A03

The theme of the Third Annual Foreign Acquisitions Workshop was the acquisition of and access to foreign (non-U.S.) gray literature. Individual presentations addressed general topics related to the value and scope of gray literature, specialized and foreign gray-literature sources, intellectual property issues, and U.S. Federal Agency activities. Additional topics focused on electronic access and evaluation techniques and the current and potential uses of networking technology. The workshop papers are presented in their entirety or in abstract or outline form. Appendices include a listing of databases that include foreign gray literature, a bibliography, and a report on U.S.-Japan cooperation in the use of scientific and technical information. CASI

N94-24833 National Academy of Sciences - National Research Council, Washington, DC.
INFORMATION TECHNOLOGY IN THE SERVICE SOCIETY: A TWENTY-FIRST CENTURY LEVER
1994 281 p
(ISBN-0-309-04876-1; LC-92-85596) Copyright Avail: Issuing Activity

The use of information technology (IT), including computer and communications hardware as well as the software and associated services required to effectively use that hardware, has revolutionized the structure of management and the nature of competition in a variety of industries. IT is especially important in the service sector. Contrary to the widespread misconception of services as predominantly simple, labor-intensive and technically sophisticated firms in transportation, financial services, banking, insurance, retail and wholesale trade, telecommunications, health care, and professional and personal services. As IT becomes less expensive, more portable, better integrated and interconnected, and embedded in a wider variety of devices, new applications in these fields and whole new industries are likely to evolve and to have profound effects on industry structures, employment, and economic growth. The effectiveness with which IT is deployed in services strongly influences U.S. standards of living and competitiveness in world trade. This book includes chapters on the impact of IT at the macroeconomic level, the industry level, the enterprise level, and the activity level. Also included are chapters on improving decision making about IT, and IT in services: implications for public policy. Derived from text

N94-24946# Carnegie-Mellon Univ., Pittsburgh, PA. School of Computer Science.
A USAGE PROFILE AND EVALUATION OF A WIDE-AREA DISTRIBUTED FILE SYSTEM
Mirjana Spasojevic and M. Satyanarayanan Oct. 1993 18 p
(Contract MDA972-90-C-0036)
(AD-A273590) Avail: CASI HC A03/MF A01

The evolution of the Andrew File System (AFS) into a wide-area distributed file system has encouraged collaboration and information dissemination on a much broader scale than ever before. In this paper, we examine AFS as a provider of wide-area file services to over 80 organizations around the world. We discuss usage characteristic of AFS derived from empirical measurements of the system and from user responses to a questionnaire. Our observations indicate that AFS provides robust and efficient data access in its current configuration, thus confirming its viability as a design point for wide-area distributed file systems. DTIC

N94-25168*# National Aeronautics and Space Administration, Washington, DC.
NASA STI PROGRAM DATABASE: JOURNAL COVERAGE (1990-1992)
Mar. 1993 61 p
(NASA-TM-109720; NAS 1.15:109720) Avail: CASI HC A04/MF A01

Data are given in tabular form on the extent of recent journal accessions (1990-1992) to the NASA Scientific and Technical Information (STI) Database. Journals are presented by country in two ways: first by an alphabetical listing; and second, by the decreasing number of citations extracted from these journals during this period. An appendix containing a statistical summary is included. CASI

N94-25326# Oxford Univ. (England). Robotics Research Group.
HORATIO: LIBRARIES FOR VISION APPLICATIONS, RELEASE 2.0
Philip F. McLauchlan 15 Dec. 1992 77 p
(OUEL-1967/92; ETN-94-95153) Avail: CASI HC A05/MF A01

The Holistic Real Time Architecture for Transputer Image Operations (Horatio) is described. The Horatio vision system comprises a set of libraries written in ANSI C for either Sun workstations or transputers. The global library contains definitions and functions needed by most applications. There is also a maths library, a pipeline control library, a list manipulation library and an image library providing for manipulation and channel/stream/file input/output of two dimensional images. A graphics library allows images and other primitives to be displayed in an arbitary number of X-windows canvases. An image processing library contains source for image processing tools. The process library allows the creation of process pipelines and the tool library high level X-windows tools for creation of Horatio applications. Only the graphics and tool libraries are X-specific. ESA

N94-25485# Cranfield Inst. of Tech., Bedford (England). Applied Psychology Unit.

FACTORS INFLUENCING PERCEIVED USABILITY AND UTILITY OF LIBERTAS AT CRANFIELD: IMPLICATIONS FOR SYSTEM MODIFICATION AND USER EDUCATION

Peter Brooks Oct. 1992 53 p
(Cranfield-Aero-9212; ISBN-1-87-156450-6; ETN-94-95219) Avail: CASI HC A04/MF A01

A survey of user opinions towards and experience of Cranfield's Libertas library automation system was conducted in order to determine user attitudes towards the system, user characteristics which predict these attitudes, and the key areas for improvement in service provision. The survey included student and staff users of the academic library and the in-library and remote access of Libertas. The study identified that in general user perceptions of the utility and usability of the system are positive but indicate the need for improvements in system design and user education. It was found possible to predict more positive user attitudes on the basis of regularity and frequency of general system use and the use of the inter-library loan facility and certain catalog searching facilities. User characteristics such as demographic details and previous education and experience were not found to be associated with user attitudes toward the system. Six service change areas were identified from user opinion on recommended improvements and were concerned with additional functionality, system prompts, paper based information support, training, Boolean searching, and networking. Recommendations for service improvements in each of these areas are provided. ESA

N94-25487*# Maryland Univ., College Park. Coll. of Library and Information Sciences.

A COMPARISON OF BOOLEAN-BASED RETRIEVAL TO THE WAIS SYSTEM FOR RETRIEVAL OF AERONAUTICAL INFORMATION Final Report

Gary Marchionini and Diane Barlow Washington Mar. 1994 77 p Prepared for RMS Associates, Linthicum Heights, MD
(Contract NASw-4584)
(NASA-CR-4569; NAS 1.26:4569) Avail: CASI HC A05/MF A01

An evaluation of an information retrieval system using a Boolean-based retrieval engine and inverted file architecture and WAIS, which uses a vector-based engine, was conducted. Four research questions in aeronautical engineering were used to retrieve sets of citations from the NASA Aerospace Database which was mounted on a WAIS server and available through Dialog File 108 which served as the Boolean-based system (BBS). High recall and high precision searches were done in the BBS and terse and verbose queries were used in the WAIS condition. Precision values for the WAIS searches were consistently above the precision values for high recall BBS searches and consistently below the precision values for high precision BBS searches. Terse WAIS queries gave somewhat better precision performance than verbose WAIS queries. In every case, a small number of relevant documents retrieved by one system were not retrieved by the other, indicating the incomplete nature of the results from either retrieval system. Relevant documents in the WAIS searches were found to be randomly distributed in the retrieved sets rather than distributed by ranks. Advantages and limitations of both types of systems are discussed. Author

N94-25541*# Maryland Univ., College Park.

NACA COLLECTIONS: A DIRECTORY OF SIGNIFICANT COLLECTIONS OF THE DOCUMENTS OF THE NATIONAL ADVISORY COMMITTEE FOR AERONAUTICS

Ruth S. Smith Washington Mar. 1994 74 p Prepared for RMS Associates, Linthicum Heights, MD
(Contract NASw-4584)
(NASA-CR-195686; NAS 1.26:195686) Avail: CASI HC A04/MF A01

An alphabetical listing is given of 42 centers that hold National Advisory Committee for Aeronautics (NACA) documents. Information is given on the number of NACA holdings in paper copy, bound volumes, and microfiche. Additional information is given on the bibliographic records and availability. Author

N94-23597*# National Aeronautics and Space Administration. Goddard Space Flight Center, Greenbelt, MD.

SPDB (SCIENCE PROCESSING DATABASE): QUICK REFERENCE GUIDE

In its The Fifth Calibration/Data Product Validation Panel Meeting 1992 2 p (For primary document see N94-23595 06-43)
Avail: CASI HC A01/MF A04

N94-23886*# Jet Propulsion Lab., California Inst. of Tech., Pasadena.

MANAGEMENT OF INFORMATION FOR MISSION OPERATIONS USING AUTOMATED KEYWORD REFERENCING

Roger A. Davidson and Patrick S. Curran *In its* SpaceOps 1992: Proceedings of the Second International Symposium on Ground Data Systems for Space Mission Operations 1 Mar. 1993 p 349-354 (For primary document see N94-23832 06-66)
Avail: CASI HC A02/MF A10

N94-23899*# MATRA Marconi Space, Toulouse (France). Action de Recherche et Application MATRA IRIT en Interaction Homme Systeme.

A CROSS-DISCIPLINARY RESPONSE TO IMPROVE TEST ACTIVITIES: THE CORPORATE MEMORY CAPITALIZATION IN ARIANE4 TEST DOMAIN

Dinh Phuoc Vo, Christian Soler, N. Aussenac (Centre National de la Recherche Scientifique, Toulouse, France.), and D. Macchion (Centre National de la Recherche Scientifique, Toulouse, France.) *In* JPL, SpaceOps 1992: Proceedings of the Second International Symposium on Ground Data Systems for Space Mission Operations 1 Mar. 1993 p 441-450 (For primary document see N94-23832 06-66)
Avail: CASI HC A03/MF A10

N94-23937*# Technischer Uerberwachungs-Verein Rheinland e.V., Cologne (Germany).

SECURITY ASPECTS OF SPACE OPERATIONS DATA

Stefan Schmitz *In* JPL, SpaceOps 1992: Proceedings of the Second International Symposium on Ground Data Systems for Space Mission Operations 1 Mar. 1993 p 691-696 (For primary document see N94-23832 06-66)
Avail: CASI HC A02/MF A10

N94-23950*# Jet Propulsion Lab., California Inst. of Tech., Pasadena.

USING THE SPICE SYSTEM TO HELP PLAN AND INTERPRET SPACE SCIENCE OBSERVATIONS

Charles H. Acton, Jr. *In its* SpaceOps 1992: Proceedings of the Second International Symposium on Ground Data Systems for Space Mission Operations 1 Mar. 1993 p 781-786 (For primary document see N94-23832 06-66)
Avail: CASI HC A02/MF A10

N94-23951*# European Space Agency. European Space Operations Center, Darmstadt (Germany). Missions Operations Dept.

AN ENGINEERING DATABASE MANAGEMENT SYSTEM FOR SPACECRAFT OPERATIONS

Gregorio Cipollone, Michael H. McKay, and Joseph Paris (BIM SA/NV, Everberg, Belgium.) *In* JPL, SpaceOps 1992: Proceedings of the Second International Symposium on Ground Data Systems for Space Mission Operations 1 Mar. 1993 p 787-790 (For primary document see N94-23832 06-66)
Avail: CASI HC A01/MF A10

N94-23952*# Computer Resources International A/S (Denmark).

THE ESIS QUERY ENVIRONMENT PILOT PROJECT

Jens J. Fuchs, Alessandro Ciarlo (European Space Agency. ESRIN, Frascati, Italy.), and Stefano Benso (Compagnia Italiana Servizi Tecnici, Rome.) *In* JPL, SpaceOps 1992: Proceedings of the Second International Symposium on Ground Data Systems for Space Mission Operations 1 Mar. 1993 p 791-801 (For primary document see N94-23832 06-66)
Avail: CASI HC A03/MF A10

N94-23953*# Jet Propulsion Lab., California Inst. of Tech., Pasadena.

MARS OBSERVER DATA PRODUCTION, TRANSFER, AND ARCHIVAL: THE DATA PRODUCTION ASSEMBLY LINE

David B. Childs *In its* SpaceOps 1992: Proceedings of the Second

International Symposium on Ground Data Systems for Space Mission Operations 1 Mar. 1993 p 803-811 (For primary document see N94-23832 06-66)
Avail: CASI HC A02/MF A10

N94-23955*# Jet Propulsion Lab., California Inst. of Tech., Pasadena.
MULTIMISSION IMAGE PROCESSING AND SCIENCE DATA VISUALIZATION
William B. Green *In its* SpaceOps 1992: Proceedings of the Second International Symposium on Ground Data Systems for Space Mission Operations 1 Mar. 1993 p 819-821 (For primary document see N94-23832 06-66)
Avail: CASI HC A01/MF A10

N94-23956*# Centre National de la Recherche Scientifique, Toulouse (France). Inst. de Recherche en Informatique.
COMPRESSION FOR AN EFFECTIVE MANAGEMENT OF TELEMETRY DATA
J.-P. Arcangeli, M. Crochemore (Centre National de la Recherche Scientifique, Paris, France.), J.-N. Hourcastagnou (Centre National d'Etudes Spatiales, Toulouse, France.), and J.-E. Pin (Centre National de la Recherche Scientifique, Paris, France.) *In* JPL, SpaceOps 1992: Proceedings of the Second International Symposium on Ground Data Systems for Space Mission Operations 1 Mar. 1993 p 823-830 Sponsored in part by CNES (For primary document see N94-23832 06-66)
Avail: CASI HC A02/MF A10

N94-23957*# National Aeronautics and Space Administration, Washington, DC.
SPACE STATION FREEDOM GROUND DATA SYSTEM: DESIGN AND OPERATIONS
Richard A. Dunning, Jr. (Booz-Allen and Hamilton, Inc., Washington, DC.), Frederick W. Knops, III (Booz-Allen and Hamilton, Inc., Seabrook, MD.), Stanley A. Fishkind, and Michael P. Pasciuto *In* JPL, SpaceOps 1992: Proceedings of the Second International Symposium on Ground Data Systems for Space Mission Operations 1 Mar. 1993 p 831-836 (For primary document see N94-23832 06-66)
Avail: CASI HC A02/MF A10

N94-23958*# Defence Research Agency, Farnborough (England). Data Technology Section.
EARTH OBSERVATION ARCHIVE ACTIVITIES AT DRA FARNBOROUGH
M. D. Palmer and J. M. Williams (Serco Space Ltd., Southall, England.) *In* JPL, SpaceOps 1992: Proceedings of the Second International Symposium on Ground Data Systems for Space Mission Operations 1 Mar. 1993 p 837-840 (For primary document see N94-23832 06-66)
Avail: CASI HC A01/MF A10

N94-23959*# Compagnia Italiana Servizi Tecnici, Rome.
OPERATIONAL CHARACTERISATION OF REQUIREMENTS AND EARLY VALIDATION ENVIRONMENT FOR HIGH DEMANDING SPACE SYSTEMS
E. Barro, A. DelBufalo, and F. Rossi *In* JPL, SpaceOps 1992: Proceedings of the Second International Symposium on Ground Data Systems for Space Mission Operations 1 Mar. 1993 p 845-850 (For primary document see N94-23832 06-66)
Avail: CASI HC A02/MF A10

N94-24406*# Alabama Univ., Huntsville. Computer Science Dept.
INTEROPERABILITY THROUGH STANDARDIZATION: ELECTRONIC MAIL, AND X WINDOW SYSTEMS
Ashok T. Amin *In its* The 1993 NASA/ASEE Summer Faculty Fellowship Program Nov. 1993 5 p (For primary document see N94-24405 06-80)
Avail: CASI HC A01/MF A03

N94-24413*# Oklahoma Univ., Norman. School of Electrical Engineering.
PERFORMANCE OF THE ENGINEERING ANALYSIS AND DATA SYSTEM 2 COMMON FILE SYSTEM
Linda S. DeBrunner *In* Alabama Univ., The 1993 NASA/ASEE Summer Faculty Fellowship Program Nov. 1993 5 p (For primary document see N94-24405 06-80)
Avail: CASI HC A01/MF A03

N94-24417*# Alabama Univ., Huntsville. Dept. of MIS.
TECHNOLOGY UTILIZATION OFFICE DATA BASE ANALYSIS AND DESIGN
Stephen A. Floyd *In its* The 1993 NASA/ASEE Summer Faculty Fellowship Program Nov. 1993 5 p (For primary document see N94-24405 06-80)
Avail: CASI HC A01/MF A03

N94-25115*# National Aeronautics and Space Administration. Langley Research Center, Hampton, VA.
ADVANCED INFORMATION PROCESSING SYSTEM (AIPS)
Felix L. Pitts *In its* NASA LaRC Workshop on Guidance, Navigation, Controls, and Dynamics for Atmospheric Flight, 1993 Dec. 1993 p 533-547 (For primary document see N94-25096 06-01)
Avail: CASI HC A03/MF A04

N94-25123*# Purdue Univ., West Lafayette, IN. Center for Information and Numerical Data Analysis and Synthesis.
ESTABLISHMENT OF COMPUTERIZED NUMERICAL DATABASES ON THERMOPHYSICAL AND OTHER PROPERTIES OF MOLTEN AS WELL AS SOLID MATERIALS AND DATA EVALUATION AND VALIDATION FOR GENERATING RECOMMENDED RELIABLE REFERENCE DATA
C. Y. Ho *In* NASA. Lewis Research Center, Workshop on the Thermophysical Properties of Molten Materials Nov. 1993 p 51-68 (For primary document see N94-25120 06-26)
Avail: CASI HC A03/MF A03

N94-25366*# Florida State Univ., Tallahassee. Dept. of Computer Science.
CONSIDERATIONS REGARDING THE DEPLOYMENT OF HYPERMEDIA AT JSC
Charles J. Kacmar *In* NASA. Johnson Space Center, National Aeronautics and Space Administration (NASA)/American Society for Engineering Education (ASEE) Summer Faculty Fellowship Program, 1993, Volume 1 Dec. 1993 15 p (For primary document see N94-25348 06-99)
Avail: CASI HC A03/MF A03

N94-25496*# Technology Service Corp., Santa Monica, CA.
THE IRGen INFRARED DATA BASE MODELER
Uri Bernstein *In* NASA. Ames Research Center, Proceedings of the Workshop on Augmented Visual Display (AVID) Research Dec. 1993 p 99-120 (For primary document see N94-25490 06-54)
Avail: CASI HC A03/MF A04

83 ECONOMICS AND COST ANALYSIS

Includes cost effectiveness studies.

N94-23580 Rolls-Royce Ltd., Derby (England).
ENGINEERING FOR PROFITABILITY
Frank Turner 1992 11 p Presented at Sir Alfred Herbert Lecture, Institution of Electrical Engineers, London, United Kingdom, 18 Feb. 1992 Limited Reproducibility: More than 20% of this document may be affected by poor print
(PNR-90990; MISC-2693; ETN-93-93709) Copyright Avail: Issuing Activity (European Space Agency (ESA))

Engineering, and the ways it can be more focused on profitability and therefore on Britain's prosperity, are discussed. Profit is described as the financial gain which can only be achieved by reducing costs. The two major choices on how to achieve higher profit involve product differentiation and lower costs. The three major areas of product differentiation that could contribute to the profitability of a product are discussed: technical superiority, product integrity, and short time to market (i.e. available first). Areas in which lower costs can be addressed are also discussed: engineering plus manufacture, internal and external manufacture, and sales and support. Additionally, business education in engineering is discussed. ESA

N94-24477 Tilburg Univ. (Netherlands). Dept. of Economics.
SIMPLICIAL VARIABLE DIMENSION RESTART ALGORITHM TO FIND ECONOMIC EQUILIBRIA ON THE UNIT SIMPLEX USING n(n+1) RAYS
R. A. M. G. Joosten and A. J. J. Talman (Limburg State Univ., Maastricht, Netherlands.) 8 Jun. 1993 32 p Limited Reproducibility: More than 20% of this document may be affected by microfiche quality
(PB94-110541; FEW-608) Avail: Issuing Activity (National Technical Information Service (NTIS))

A new simplicial variable dimension restart algorithm is introduced to solve the zero point or equilibrium problem on the n-dimensional unit simplex S(sup n). The number of one-dimensional sets or rays along which the algorithm can leave the arbitrarily chosen starting point is n(n + 1). In case the algorithm is applied to find a general equilibrium price vector in an exchange economy with n + 1 commodities, it generates a piecewise linear path of prices, connecting the arbitrarily chosen starting price vector with an approximate equilibrium price vector. At an equilibrium price vector the excess demand of all commodities is zero. Along the path the price of a commodity is kept equal to the initial price if the excess demand of that commodity is neither minimal nor maximal. If the excess demand of a commodity becomes maximal, the price of that commodity is increased from its initial value, and if the excess demand becomes minimal, the price is decreased from its initial value. Also a new intersection theorem on S(sup n) is derived. NTIS

N94-23968*# Jet Propulsion Lab., California Inst. of Tech., Pasadena.
ESTIMATING THE DEEP SPACE NETWORK MODIFICATION COSTS TO PREPARE FOR FUTURE SPACE MISSIONS BY USING MAJOR COST DRIVERS
Donald S. Remer, Josef Sherif, and Harry R. Buchanan *In its* SpaceOps 1992: Proceedings of the Second International Symposium on Ground Data Systems for Space Mission Operations 1 Mar. 1993 p 899-904 (For primary document see N94-23832 06-66)
Avail: CASI HC A02/MF A10

84 LAW, POLITICAL SCIENCE AND SPACE POLICY

Includes NASA appropriation hearings; aviation law; space law and policy; international law; international cooperation; and patent policy.

N94-22748*# American Mobile Satellite Corp., Washington, DC.
US DOMESTIC AND INTERNATIONAL REGULATORY ISSUES
Lon C. Levin and Dennis C. Nash *In* JPL, Proceedings of the Third International Mobile Satellite Conference (IMSC 1993) 1993 p 67-72 (For primary document see N94-22735 06-32)
Avail: CASI HC A02/MF A06

N94-22749*# Anglin and Giaccherini, Playa del Rey, CA.
INTERNATIONAL ORGANIZATIONS TO ENABLE WORLD-WIDE MOBILE SATELLITE SERVICES
Richard L. Anglin, Jr. *In* JPL, Proceedings of the Third International Mobile Satellite Conference (IMSC 1993) 1993 p 73-78 (For primary document see N94-22735 06-32)
Avail: CASI HC A02/MF A06

N94-25066 Technology Strategies and Alliances, Menlo Park, CA.
DEFENSE AEROSPACE AND THE NEW WORLD ORDER
William J. Perry *In* National Academy of Engineering, The Future of Aerospace: Proceedings of a Symposium Held in Honor of Alexander H. Flax 1993 p 7-14 (For primary document see N94-25065 06-99)
Copyright Avail: Issuing Activity

85 URBAN TECHNOLOGY AND TRANSPORTATION

Includes applications of space technology to urban problems; technology transfer; technology assessment; and surface and mass transportation.

For related information see also *03 Air Transportation and Safety, 16 Space Transportation,* and *44 Energy Production and Conversion.*

N94-23526*# Space Foundation, Colorado Springs, CO.
SPACE TECHNOLOGY: A STUDY OF THE SIGNIFICANCE OF RECOGNITION FOR INNOVATORS OF SPINOFF TECHNOLOGIES. 1993 ACTIVITIES/1994, 1995 PLANS Annual Report
Jan. 1994 31 p
(Grant NAGw-3322)
(NASA-CR-194836; NAS 1.26:194836) Avail: CASI HC A03/MF A01

During the past 30 years as NASA has conducted technology transfer programs, it has gained considerable experience - particularly pertaining to the processes. However, three areas have not had much scrutiny: the examination of the contributions of the individuals who have developed successful spinoffs, the commercial success of the spinoffs themselves, and the degree to which they are understood by the public. In short, there has been limited evaluation to measure the success of technology transfer efforts mandated by Congress. Research conducted during the first year of a three-year NASA grant to the United States Space Foundation has taken the initial steps toward measuring the success of methodologies to accomplish that Congressionally-mandated technology transfer. In particular, the US Space Foundation, in cooperation with ARAC, technology transfer experts; JKA, a nationally recognized themed entertainment design company; and top evaluation consultants, inaugurated and evaluated a fresh approach including commercial practices to encourage, motivate, and energize technology transfer by: recognizing already successful efforts (Space Technology Hall of Fame Award), drawing potential business and industrial players into the process (Space Commerce Expo), and informing and motivating the general public (Space Technology Hall of Fame public venues). The first year's efforts are documented and directions for the future are outlined. Author (revised)

N94-23528*# Space Foundation, Colorado Springs, CO.
SPACE TECHNOLOGY: A STUDY OF THE SIGNIFICANCE OF RECOGNITION FOR INNOVATORS OF SPINOFF TECHNOLOGIES. COMMERCIAL SPACE EXPO-USA, 1993 Report, 1993
Aug. 1993 35 p
(Grant NAGw-3322)
(NASA-CR-194833; NAS 1.26:194833) Avail: CASI HC A03/MF A01

This is a report on the data collected at the Commercial Space Expo. The Expo was held 13-14 April 1993, in conjunction with the National Space Symposium. There were two modes of data gathering: surveys of expo registrants and exhibit feedback. In addition, exhibitors were interviewed to get their perspectives on the format of the expo and exhibits. Expo registrants were given a paper-pencil survey instrument at the beginning of the day and were asked to turn in the survey when they left for the day. Of the approximately 100 registrants, 22 surveys were returned. In the exhibit hall were five computers set up to collect people's reactions to specific exhibits. It was envisioned that people would react to each (or several) exhibits they visited. In fact, few people did this: almost everyone who visited a computer responded to one exhibit and did not stop by another computer. Therefore, we did not get a large number of responses for any particular exhibit. Nevertheless, there are some interesting data. Author (revised)

N94-23540*# Space Foundation, Colorado Springs, CO.
PROTOTYPE SPACE TECHNOLOGY HALL OF FAME EXHIBIT AT TECHNOLOGY 2003: ANALYSIS OF DATA FROM COMPUTER-BASED QUESTIONAIRE
Robert N. Ewell Jan. 1994 16 p Presented at the Technology 2003 Conference, Anaheim, CA, 7-9 Dec. 1993
(Grant NAGw-3322)
(NASA-CR-194834; NAS 1.26:194834) Avail: CASI HC A03/MF A01

The U.S. Space Foundation displayed its prototype Space Technology

Hall of Fame exhibit design at the Technology 2003 conference in Anaheim, CA, December 7-9, 1993. In order to sample public opinion on space technology in general and the exhibit in particular, a computer-based survey was set up as a part of the display. The data collected was analyzed. Author (revised)

N94-24312# Office of Technology Assessment, Washington, DC.
PROCEEDINGS OF TECHNOLOGY AND GOVERNANCE IN THE 1990'S
Apr. 1993 63 p Proceedings held in Washington, DC, 27 Jan. 1993
(PB93-192904; OTA-A-565) Avail: CASI HC A04/MF A01

On January 27, 1993, in celebration of OTA's twentieth anniversary, the agency's Congressional Technology Assessment Board hosted a one-day Forum on 'Technology and Governance in the 1990's' for members of Congress and key congressional staff. The Forum was designed to address several goals: to raise congressional and public awareness of the most critical issues faced by our nation and the world; to equip policymakers with an improved understanding of how best to deal with these issues; to show how technology is woven into socio-economic, domestic, and international policies; and to demonstrate the need to adapt the author's policies, methods of governance, and institutional mechanisms to this reality. NTIS

N94-24494*# Research Triangle Inst., Research Triangle Park, NC.
NASA TECHNOLOGY APPLICATIONS TEAM: APPLICATIONS OF AEROSPACE TECHNOLOGY Annual Report, Oct. 1992 - Sep. 1993
Sep. 1993 156 p
(Contract NASw-4367)
(NASA-CR-194775; NAS 1.26:194775; RTI/4321/Q4-93) Avail: CASI HC A08/MF A02

This report covers the activities of the Research Triangle Institute (RTI) Technology Applications Team for the period 1 October 1992 through 30 September 1993. The work reported herein was supported by the National Aeronautics and Space Administration (NASA), Contract No. NASW-4367. Highlights of the RTI Applications Team activities over the past year are presented in Section 1.0. The Team's progress in fulfilling the requirements of the contract is summarized in Section 2.0. In addition to our market-driven approach to applications project development, RTI has placed increased effort on activities to commercialize technologies developed at NASA Centers. These Technology Commercialization efforts are summarized in Section 3.0. New problem statements prepared by the Team in the reporting period are presented in Section 4.0. The Team's transfer activities for ongoing projects with the NASA Centers are presented in Section 5.0. Section 6.0 summarizes the status of four add-on tasks. Travel for the reporting period is described in Section 7.0. The RTI Team staff and consultants and their project responsibilities are listed in Appendix A. Appendix B includes Technology Opportunity Announcements and Spinoff! Sheets prepared by the Team while Appendix C contains a series of technology transfer articles prepared by the Team. Derived from text

N94-24496*# Space Foundation, Colorado Springs, CO.
SPACE TECHNOLOGY: A STUDY OF THE SIGNIFICANCE OF RECOGNITION FOR INNOVATORS OF SPINOFF TECHNOLOGIES. A CASE STUDY ON THE IMPACT OF THE SPACE TECHNOLOGY HALL OF FAME AWARD Research Report
Dec. 1993 24 p
(Grant NAGw-3322)
(NASA-CR-194835; NAS 1.26:194835) Avail: CASI HC A03/MF A01

This report represents the preliminary effort in studying the significance of recognition for innovators of spinoff technologies. The purpose of this initial year's effort in this area was to gather preliminary data and define the direction for the remainder of the research. This report focuses on the most recent recipients of the Hall of Fame Award, the developers of liquid-cooled garments. Liquid-cooled garments technology and its spinoffs were used as a case study to define and explore the factors involved in technology transfer and to consider the possible incentives in developing commercial applications including the Hall of Fame Award. Through interviews, views of award recipients were obtained on factors encouraging spinoffs as well as impediments to spinoffs. The researchers observed complex inter-relationships among the significant entities (government, individuals, large and small business), the importance of people, the importance of resource availability, and the significance of intrinsic motivation; drew preliminary conclusions pertaining to the direct and indirect influence of recognition like the Hall of Fame Award; and planned the direction for next year's follow-on research. Author

N94-24829*# Alabama Univ., Huntsville. Center for Automation and Robotics.
NASA TECH BRIEF EVALUATIONS
Gary L. Workman Feb. 1994 23 p
(Contract NCC8-18)
(NASA-CR-195150; NAS 1.26:195150; CAR-94-06) Avail: CASI HC A03/MF A01

A major step in transferring technology is to disseminate information about new developments to the appropriate sector(s). A useful vehicle for transferring technology from the government sector to industry has been demonstrated with the use of periodical and journal announcements to highlight technological achievements which may meet the needs of industries other than the one who developed the innovation. To meet this end, NASA has very successfully pursued the goal of identifying technical innovations through the national circulation publication; NASA Tech Briefs. At one time the Technology Utilization Offices of the various centers coordinated the selection of appropriate technologies through a common channel. In recent years, each NASA field center has undertaken the task of evaluating submittals for Tech Brief publication independently of the others. The University of Alabama in Huntsville was selected to assist MSFC in evaluating technology developed under the various programs managed by the NASA center for publication in the NASA Tech Briefs journal. The primary motivation for the NASA Tech Briefs publication is to bring to the attention of industry the various NASA technologies which, in general, have been developed for a specific aerospace requirement, but has application in other areas. Since there are a number of applications outside of NASA that can benefit from innovative concepts developed within the MSPC programs, the ability to transfer technology to other sectors is very high. In most cases, the innovator(s) are not always knowledgeable about other industries which might potentially benefit from their innovation. The evaluation process can therefore contribute to the list of potential users through a knowledgeable evaluator. Author (revised)

N94-25018*# National Aeronautics and Space Administration, Washington, DC.
SPINOFF 1993
James J. Haggerty 1993 142 p LIMITED REPRODUCIBILITY: More than 20% of this document may be affected by color photographs
(NASA-NP-211; NAS 1.83:211; ISBN-0-16-042100-4) Avail: CASI HC A07/MF A02; 133 functional color pages

This publication is intended to foster the aim of the NASA Technology Transfer Program by heightening awareness of the NASA technology available for reapplication and its potential for public benefit. The publication is organized in three main sections. Section 1 outlines NASA's mainline effort, the major programs that generate new technology and therefore replenish and expand the bank of knowledge available for transfer. Section 2 contains a representative sampling of spinoff products that resulted from secondary application of technology originally developed to meet mainline goals. Section 3 describes the various mechanisms NASA employs to stimulate technology transfer and lists, in an appendix, contact sources for further information about the Technology Transfer Program. Derived from text

N94-24424*# Alabama Univ., Huntsville. Dept. of Electrical Engineering.
A COMPILATION OF TECHNOLOGY SPINOFFS FROM THE US SPACE SHUTTLE PROGRAM
David Jeff Jackson *In its* The 1993 NASA/ASEE Summer Faculty Fellowship Program Nov. 1993 5 p (For primary document see N94-24405 06-80)
Avail: CASI HC A01/MF A03

88 SPACE SCIENCES (GENERAL)

N94-23536*# TRW Space Technology Labs., Redondo Beach, CA. Applied Technology Div.
GAS-GRAIN SIMULATION EXPERIMENT MODULE CONCEPTUAL DESIGN AND GAS-GRAIN SIMULATION FACILITY BREADBOARD DEVELOPMENT
James M. Zamel, Michael Petach, Nahum Gat, Jack Kropp, Christina Luong, and Michael Wolff Dec. 1993 131 p
(Contract NAS2-13408)
(NASA-CR-177632; A-94034; NAS 1.26:177632) Avail: CASI HC A07/MF A02

This report delineates the Option portion of the Phase A Gas-Grain Simulation Facility study. The conceptual design of a Gas-Grain Simulation Experiment Module (GGSEM) for Space Shuttle Middeck is discussed. In addition, a laboratory breadboard was developed during this study to develop a key function for the GGSEM and the GGSF, specifically, a solid particle cloud generating device. The breadboard design and test results are discussed and recommendations for further studies are included. The GGSEM is intended to fly on board a low earth orbit (LEO), manned platform. It will be used to perform a subset of the experiments planned for the GGSF for Space Station Freedom, as it can partially accommodate a number of the science experiments. The outcome of the experiments performed will provide an increased understanding of the operational requirements for the GGSF. The GGSEM will also act as a platform to accomplish technology development and proof-of-principle experiments for GGSF hardware, and to verify concepts and designs of hardware for GGSF. The GGSEM will allow assembled subsystems to be tested to verify facility level operation. The technology development that can be accommodated by the GGSEM includes: GGSF sample generation techniques, GGSF on-line diagnostics techniques, sample collection techniques, performance of various types of sensors for environmental monitoring, and some off-line diagnostics. Advantages and disadvantages of several LEO platforms available for GGSEM applications are identified and discussed. Several of the anticipated GGSF experiments require the deagglomeration and dispensing of dry solid particles into an experiment chamber. During the GGSF Phase A study, various techniques and devices available for the solid particle aerosol generator were reviewed. As a result of this review, solid particle deagglomeration and dispensing were identified as key undeveloped technologies in the GGSF design. A laboratory breadboard version of a solid particle generation system was developed and characterization tests performed. The breadboard hardware emulates the functions of the GGSF solid particle cloud generator in a ground laboratory environment, but with some modifications, can be used on other platforms. Author

N94-24644*# National Aeronautics and Space Administration. Lyndon B. Johnson Space Center, Houston, TX.
ORBITAL DEBRIS AND NEAR-EARTH ENVIRONMENTAL MANAGEMENT: A CHRONOLOGY
David S. F. Portree and Joseph P. Loftus, Jr. Dec. 1993 114 p
Sponsored by NASA. Washington
(NASA-RP-1320; S-747; NAS 1.61:1320) Avail: CASI HC A06/MF A02

This chronology covers the 32-year history of orbital debris and near-Earth environmental concerns. It tracks near-Earth environmental hazard creation, research, observation, experimentation, management, mitigation, protection, and policy-making, with emphasis on the orbital debris problem. Included are the Project West Ford experiments; Soviet ASAT tests and U.S. Delta upper stage explosions; the Ariane V16 explosion, U.N. treaties pertinent to near-Earth environmental problems, the PARCS tests; space nuclear power issues, the SPS/orbital debris link; Space Shuttle and space station orbital debris issues; the Solwind ASAT test; milestones in theory and modeling the Cosmos 954, Salyut 7, and Skylab reentries; the orbital debris/meteoroid research link; detection system development; orbital debris shielding development; popular culture and orbital debris; Solar Max results; LDEF results; orbital debris issues peculiar to geosynchronous orbit, including reboost policies and the stable plane; seminal papers, reports, and studies; the increasing effects of space activities on astronomy; and growing international awareness of the near-Earth environment. Author

N94-24832*# Advanced Research and Applications Corp., Sunnyvale, CA.
DEMONSTRATION OF THE FEASIBILITY OF AN INTEGRATED X RAY LABORATORY FOR PLANETARY EXPLORATION
E. D. Franco, J. A. Kerner, L. N. Koppel, and M. J. Boyle Dec. 1993 30 p
(Contract NAS2-13416)
(NASA-CR-177631; A-94033; NAS 1.26:177631) Avail: CASI HC A03/MF A01

The identification of minerals and elemental compositions is an important component in the geological and exobiological exploration of the solar system. X ray diffraction and fluorescence are common techniques for obtaining these data. The feasibility of combining these analytical techniques in an integrated x ray laboratory compatible with the volume, mass, and power constraints imposed by many planetary missions was demonstrated. Breadboard level hardware was developed to cover the range of diffraction lines produced by minerals, clays, and amorphous; and to detect the x ray fluorescence emissions of elements from carbon through uranium. These breadboard modules were fabricated and used to demonstrate the ability to detect elements and minerals. Additional effort is required to establish the detection limits of the breadboard modules and to integrate diffraction and fluorescence techniques into a single unit. It was concluded that this integrated x ray laboratory capability will be a valuable tool in the geological and exobiological exploration of the solar system. Author (revised)

N94-25006 Space Foundation, Colorado Springs, CO.
THE NINTH NATIONAL SPACE SYMPOSIUM
Beth Ann Lipskin, ed., Sara Patterson, ed., David A. Brescia, ed., Donna Burk, ed., Jack Flannery, ed., Pat St.John, ed., and Chuck Zimkas, ed. 1993 239 p Symposium held Colorado Springs, CO, 13-16 Apr. 1993 Original contains color illustrations
(ISBN-0-9616962-7-3) Copyright Avail: Issuing Activity; 4 functional color pages

Proceedings of the Ninth National Space Symposium held 13-16 April 1993 by the United States Space Foundation are presented. Presentations made at the symposium are included. Topics discussed include: Change, Challenge and Opportunity; Washington Insiders: National Space Policy and Budget Issues; Civil Space: a Vision for the Future; Space Power for an Expanded Vision; Unparalled Launch Vehicle Propulsion Capabilities; National Security Space Issues; Perspectives on the Air Force in Space; Future Technology: Space Propulsion, Earth Observation and International Cooperation; Achieving Efficient Space Transportation; the Future in Space Exploration; Kids, Parents and Teachers are into Space; and Public Congressional Forum on Space - International Space Issues. CASI

89 ASTRONOMY

Includes radio, gamma-ray, and infrared astronomy, and astrometry.

N94-23330*# Hughes STX, Inc., Greenbelt, MD.
VOYAGER OBSERVATIONS OF GLOBULAR CLUSTERS Final Report
5 Jan. 1994 8 p
(NASA Order S-97230-E)
(NASA-CR-194806; NAS 1.26:194806) Avail: CASI HC A02/MF A01

The objectives of this task are to direct and analyze the observations of globular clusters targets observed with the ultraviolet spectrometer on the Voyager spacecraft. The data analysis will be directed toward understanding the Voyager spectra or upper limits in terms of the expected properties of the hot stars in the globular clusters. One out of the four proposed targets was observed before the Voyager guest observer program was cancelled in early 1993. The observed target, NGC 6397, showed a spectrum characteristic of hot stars. However, further analysis showed that most of this emission was unlikely to be due to the hot post asymptotic giant branch cluster member ROB 162, and was probably due to dust-scattered light from unrelated foreground stars. Three types of analysis were performed to test the origin of the Voyager spectrum. First, the flux variations during the limit-cycle motion of the spacecraft motion were binned as a function of time; these showed no evidence of a point source response. Second, the Voyager spectrum were compared with an IUE spectrum of ROB 162; this showed that the Voyager flux was three times larger than

could be explained from this star alone. Finally, a Voyager background observation taken 26 arcminutes from the cluster center was analyzed; this showed that the observed spectrum intensity did not diminish as the Voyager aperture was moved away from the globular cluster center.
Derived from text

N94-23334*# Computer Sciences Corp., Greenbelt, MD. Astronomy Programs.
UV SPECTRAL VARIABILITY IN THE HERBIG Ae STAR HR 5999. 11: THE ACCRETION INTERPRETATION
M. R. Perez, C. A. Grady (Applied Research Corp., Landover, MD.), and P. S. The (Astronomical Inst., Amsterdam, Netherlands.) 2 Mar. 1993 11 p Submitted for publication
(Contracts NAS5-32059; NAS5-31841)
(NASA-CR-189313; NAS 1.26:189313) Avail: CASI HC A03/MF A01

We report recent IUE high- and low-dispersion observations with the IUE long wavelength camera (LWP) and short wavelength camera (SWP) of the Herbig Ae star HR 5999. We have found a dramatic change in the structure of the Mg II h and k lines (2795.5, 2802.7 A) along with some continuum flux excesses especially at the short end of the SWP camera. LWP high dispersion observations of HR 5999 obtained between 1979 and 1990, at times of comparatively low UV continuum fluxes, exhibit P Cygni type m profiles in the Mg II resonance doublet. In contrast, observations made from September 1990 through March 16-18, 1992, with high W continuum fluxes, present Mg II lines with reverse P Cygni profiles indicative of some active episodic accretion. Accreting gas can also be detected in the additional red wings of the various Fe II and Mn II absorption lines, with velocities up to +300-350 km/s (September 1990). By September 10, 1992 the Mg II profile had returned to the type III P Cygni profile similar to those from earlier spectra. The correlation between the presence of large column densities of accreting gas and the continuum light variations supports suggestions by several authors that HR 5999 is surrounded by an optically thick, viscously heated accretion disk. Detection of accreting gas in the line of sight to HR 5999 permits us to place constraints on our viewing geometry for this system. A discussion is included comparing the spectral and physical similarities between HR 5999 and the more evolved proto-planetary candidate system, beta Pictoris. Author (revised)

N94-23705# Chalmers Univ. of Technology, Goeteborg (Sweden).
100 GHz MAP OF 3C 446
M. S. Lerner (Onsala Space Observatory, Sweden.), L. B. Baath (Onsala Space Observatory, Sweden.), M. Inoue (Nobeyema Solar Radio Observatory, Japan.), S. Padin (Owens Valley Radio Observatory, Pasadena, CA.), A. E. E. Rogers (Northeast Radio Observatory Corp., Westford, Mass. Haystack Observatory.), M. C. H. Wright (California Univ., Berkeley.), A. Zensus (National Radio Astronomy Observatory, Socorro, NM.), D. C. Backer (California Univ., Berkeley.), R. S. Booth (Onsala Space Observatory, Sweden.), and J. E. Carlstrom (Owens Valley Radio Observatory, Pasadena, CA.) et al 1993 7 p Prepared in cooperation with Northeast Radio Observatory Corp., Westford, MA; Haystack Observatory, National Radio Astronomy Observatory, Socorro, NM; California Univ., Berkeley, and Owens Valley Radio Observatory, Pasadena, CA
(PB94-104882; REPT-93/67) Avail: CASI HC A02/MF A01

The first map made from 100 GHz VLBI observations of the quasar/BL Lac object 3C446 is presented. This map represents a 25-fold increase in resolution compared to earlier maps. The main conclusions are that the core of 3C446 is still almost unresolved at this frequency and that a jet extends several hundred microarcseconds at position angle about -142 deg. A comparison is also made with observations at other size scales.
NTIS

N94-24051*# Princeton Univ., NJ. Dept. of Astrophysical Sciences.
MODEL ATMOSPHERE ANALYSIS OF SELECTED LUMINOUS B STARS Final Report, 1 Oct. 1991 - 30 Sep. 1993
Edward L. Fitzpatrick, Massa (Applied Research Associates, Inc., Albuquerque, NM.), and Walgren (Computer Sciences Corp., El Segundo, CA.) 8 Feb. 1994 2 p
(Grant NAG5-1769)
(NASA-CR-195098; NAS 1.26:195098) Avail: CASI HC A01/MF A01

The general scientific goal of this program has been to determine whether the atmospheric structure of the B-type stars can be represented by the current generation of plane parallel, line-blanketed, LTE stellar atmosphere models sufficiently well to allow accurate effective temperatures and surface gravities to be deduced. The B stars cover a wide range of temperature and luminosity. For the hottest such stars (with T approximately 30,000 K) the applicability of the models may be compromised by departures from LTE in the stellar atmospheres ('non-LTE effects'). At the highest luminosities (the B 'super giants'), the models may be invalidated by departures from plane parallel geometry. Thus we seek to identify the temperature and luminosity range within which these effects are unimportant and where the models may be relied upon. Derived from text

N94-24521 Onsala Space Observatory (Sweden).
THE 1404+286: A NON-IDEAL CALIBRATOR FOR VLBI OBSERVATIONS
F. J. Zhang, L. B. Baath, and R. E. Spencer (Nuffield Radio Astronomy Labs., Jodrell Bank, England.) Aug. 1993 7 p Submitted for publication Limited Reproducibility: More than 20% of this document may be affected by microfiche quality
(PB94-104908; Rept-93/71) Avail: CASI HC A02

The radio source 1404+286 was observed with global VLBI arrays at 5 and 1.67 GHz in 1990.88 and 1991.45, respectively. High quality maps are presented in this paper, and show the source to be resolved at both frequencies with a core-jet like structure extending about 6 mas in position angle about -145 deg. The jet direction is similar in both maps. 1404+286 has often been used in the past as a flux density calibrator or a phase referencing source. The results show that this source is not an ideal calibrator on VLBI scales. NTIS

N94-24666*# Hughes STX, Inc., Lanham, MD.
UV-BRIGHT STARS IN GLOBULAR CLUSTERS
Wayne B. Landsman Jan. 1994 9 p
(NASA Order S-97230-E)
(NASA-CR-189324; NAS 1.26:189324) Avail: CASI HC A02/MF A01

This paper highlights globular cluster studies with Ultraviolet Imaging Telescope (UIT) in three areas: the discrepancy between observed ultraviolet HB magnitudes and predictions of theoretical HB models; the discovery of two hot subdwarfs in NGC 1851, a globular not previously known to contain such stars; and spectroscopic follow up of newly identified UV-bright stars in M79 and w Cen. I also present results of a recent observation of NGC 6397 with the Voyager ultraviolet spectrometer. Author

N94-24780 Onsala Space Observatory (Sweden).
INFRARED AND SiO MASER OBSERVATIONS OF OH/IR STARS
L. A. Nyman (European Southern Observatory, La Silla, Chile.), P. J. Hall (Anglo-Australian Observatory, Epping.), and T. LaBertre (Observatoire de Paris-Meudon, France.) 1993 24 p Submitted for publication Limited Reproducibility: More than 20% of this document may be affected by microfiche quality
(PB94-104890; Rept-93/70) Avail: CASI HC A03

The authors have performed quasisimultaneous infrared photometry and observations of the SiO 86 GHz (v=1, J=2-1) and SiO 43 GHz (v=1 and 2, J=1-0) maser emission from a sample of 44 OH/IR stars. In contrast to masers associated with Mira variables, the SiO 86 GHz integrated flux densities in OH/IR stars are weaker than those at 43 GHz, and the SiO 43 GHz (v=2) emission is often stronger than the SiO 43 GHz (v=1) emission. Results show that it is useful to divide the sample into two groups because of the difference in their SiO maser properties: sources with warm, thin envelopes (K - L less than 4), and sources with cooler, thicker envelopes (K - L greater than 4). In the warmer sources, the average 43 GHz/86 GHz integrated flux density ratio is of order 2, but in the cooler sources it is significantly larger, more than 10. NTIS

N94-24988*# Southwest Research Inst., San Antonio, TX. Instrumentation and Space Research Div.
[SO2 ON VENUS: A FINAL CROSS-CALIBRATION WITH PIONEER VENUS] Final Report
1 Mar. 1994 18 p
(Grant NAG5-1913; SwRI Proj. 15-5301)
(NASA-CR-195162; NAS 1.26:195162) Avail: CASI HC A03/MF A01

The three observing programs under NASA Grant NAG5-1913 are described. They are NSOSS, VEOEB, and PCOEB. The scientific objectives for the IUE observation program NSOSS were to: make the first ever UV observations of a near-earth asteroid (4179 Toutatis), an irregular satellite of Jupiter (Himalia), and the Saturnian satellite Hyperion; obtain the first radially-dependent information on the UV color of Saturn's rings; gather the uncontaminated UV spectra of Iapetus's bright and dark hemispheres; and obtain a spectrum of Titania to initiate the comparitive study of UV photometric properties in Uranian system. The VEOEB program studied Venus SO2, an important indicator of key processes in the Venus atmosphere and perhaps Venus surface. Based on past Pioneer Venus and IUE observations, significant SO2 variations have been interpreted as indicating that the long term atmospheric SO2 abundance may be related to large, episodic injections from the surface or interior of Venus. The PCOEB program studied the Pluto-Charon system, for which evidence of a variable UV light curve has been presented. This program is to complete the coverage of that UV light curve, since only approximately 26% has been observed. Derived from text

N94-25178*# Smithsonian Astrophysical Observatory, Cambridge, MA.
SHOCKED CLOUDS IN THE CYGNUS LOOP Final Report, 15 Feb. 1992 - 14 Feb. 1994
John C. Raymond Feb. 1994 4 p
(Grant NAG5-1870)
(NASA-CR-195190; NAS 1.26:195190) Avail: CASI HC A01/MF A01

This grant covers the analysis of ROSAT PSPC and HRI images of the Cygnus Loop, an elderly supernova remnant. The project, as proposed, includes not only the usual analysis of ROSAT data; the ROSAT data is being combined with optical and UV data, and new model calculations are being performed. The status is reported on optical imagery, echelle data, IUE data, ROSAT data, and the grain model. The major question being addressed is whether the blastwave-cloud interaction in the feature known as XA is basically a converging shock in a fairly large cloud or turbulent stripping of material from the edges of a smaller cloud. Derived from text

N94-25198*# Smithsonian Astrophysical Observatory, Cambridge, MA.
ROSAT OBSERVATIONS OF THE X RAY BINARY HD 154791 Final Report, 15 May 1992 - 14 Nov. 1993
Scott J. Kenyon Jan. 1994 7 p
(Grant NAG5-1980)
(NASA-CR-195189; NAS 1.26:195189) Avail: CASI HC A02/MF A01

We have been surveying the Taurus dark cloud for young stars using a variety of techniques. Two optical proper motion surveys identified 8 new pre-main sequence stars; an IRAS-based program discovered 6 new embedded sources and 4-6 new T Tauri stars. Finally, an optical objective prism survey found 12 new T Tauri stars. Our goal in this project is to examine and compare star formation in the dark clouds: Heiles cloud 2 (HCL2), L1537, L1538, and L1544. HCL2 is a very dense region actively forming young stars and contains 5-6 very young, deeply embedded sources; L1537 and L1538 have no known pre-main sequence stars; L1544 contains 7 optically visible T Tauri stars. These clouds appear roughly similar on optical sky survey plates. We would like to know why some of the clouds are active and why some are not. The first goal of the project is to survey the regions using IR photometry to identify very red pre-main sequence stars and X-ray imaging to identify solar-type young stars missed in the near-IR survey. We will follow up these observations with molecular line surveys to compare the conditions in various clouds with their star formation efficiencies. Author (revised)

N94-25269*# Smithsonian Astrophysical Observatory, Cambridge, MA.
INVESTIGATION RELATIVE TO THE ROENTGEN SATELLITE (ROSAT) Semiannual Report Nos. 4 and 5, 15 Oct. 1992 - 15 Oct. 1993
Martin S. Elvis, Francis A. Primini, Guiseppina Fabbiano, Daniel E. Harris, Christine Jones-Foreman, Ginevra Trinchieri, Leon Golub, Jay Bookbinder, Frederick D. Seward, and Martin V. Zombeck et al Jan. 1994 96 p
(Grant NAG5-1536)
(NASA-CR-195192; NAS 1.26:195192) Avail: CASI HC A05/MF A01

Reports include: High Resolution Observations of the Central Region of M31; The X-ray Emission of Low-X-ray-Luminosity Early-Type Galaxies: Gas Versus Compact Sources; Interaction Between Cluster Gas and Radio Features of Cygnus A; Hot Gas and Dark Halos in Early-Type Galaxies; A Gravitational Lens in X-rays - 0957+461; How Massive are Early-Type Galaxies?; Three Crab-Like SNR in the Large Magellanic Cloud; and Soft X-ray Emission from Boundary Layers in Cataclysmic Variables. Papers submitted to the Astrophysical Journal are attached. Derived from text

N94-25270*# Arizona State Univ., Tempe.
UV EXTINCTION AND IR EMISSION IN DIFFUSE H2 REGIONS Semiannual Status Report, 15 Aug. 1993 - 14 Feb. 1994
Per A. Aannestad 1994 8 p
(Grant NAG5-1743)
(NASA-CR-195194; NAS 1.26:195194) Avail: CASI HC A02/MF A01

During this period, much work was spent in an attempt to use theoretical UV line indices as a basis for spectral calibration of the program stars. Five line indices are shown as functions of effective temperature and log g, calculated with the spectral synthesis programs of Kurucz. Open stars and circles are observed values from Fanelli et al., using the spectral class-effective temperature calibration of Schmidt-Kaler. We conclude that these line indices may be used to determine an effective stellar temperature, but with uncertainties of approximately a few thousand degrees. Also, for the hotter stars, theoretical line opacities are systematically low compared to observations. We have also found that Kurucz's new models appear to represent hot stars very well, even at far-UV wavelengths. This is shown in an example where two spectra of mu Col (spectral class 09.5 V) are compared to a synthetic spectrum for T(sub eff) = 33,000 K, log g = 4.0. Also shown (uppermost curve) is an empirical estimate of the intrinsic flux distribution for 09.5 V stars from Papaj, Wegner, and Krelowski. Author (revised)

N94-25387*# National Aeronautics and Space Administration. Goddard Space Flight Center, Greenbelt, MD.
CATALOG OF INFRARED OBSERVATIONS, THIRD EDITION
Daniel Y. Gezari, Marion Schmitz (Jet Propulsion Lab., California Inst. of Tech., Pasadena.), Patricia S. Pitts (Computer Sciences Corp., Calverton, MD.), and Jaylee M. Mead Washington Jun. 1993 870 p
(RTOP 685-00-00)
(NASA-RP-1294; Rept-93A00689; NAS 1.61:1294) Avail: CASI HC A99/MF A10

The Far Infrared Supplement contains a subset of the data in the full Catalog of Infrared Observations (all observations at wavelengths greater than 4.6 microns). The Catalog of Infrared Observations (CIO), NASA RP-1294, is a compilation of infrared astronomical observational data obtained from an extensive literature search of scientific journals and major astronomical catalogs and surveys. The literature search is complete for years 1965 through 1990 in this Third Edition. The Catalog contains about 210,000 observations of roughly 20,000 individual sources and supporting appendices. The expanded Third Edition contains coded IRAS 4-band data for all CIO sources detected by IRAS. The appendices include an atlas of infrared source positions (also included in this volume), two bibliographies of Catalog listings, and an atlas of infrared spectral ranges. The complete CIO database is available to qualified users in printed, microfiche, and magnetic-tape formats. Author (revised)

N94-25458 Max-Planck-Inst. fuer Physik und Astrophysik, Garching (Germany). Werner-Heisenberg-Inst.
HIGH ENERGY GAMMA ASTRONOMY ABOVE 200 GeV
E. Lorenz Feb. 1993 23 p Presented at the 13th European Cosmic Ray Symposium, CERN, Geneva, Switzerland, 27-31 Jul. 1992 Limited Reproducibility: More than 20% of this document may be affected by microfiche quality
(MPI-PhE/93-04; ETN-94-95114) Copyright Avail: CASI HC A03

The status of high energy gamma ray astronomy above 2 x 10(exp 11) eV is reviewed. The main physics motivations for gamma astronomy are summarized. The importance of satellite observations and combined studies is discussed. Usual observation techniques are overviewed. In this energy range earth bound detectors can be used. New large area detectors with an increase in sensitivity became operational. The performance and the preliminary results from the leading experiments are presented. An outlook for the next generation detectors is given. ESA

N94-22850# Lockheed Aircraft Corp., Palo Alto, CA. Solar Physics Dept.
WHY PUT VISIBLE SOLAR TELESCOPES IN SPACE?
A. Title *In* ESA, Scientific Requirements for Future Solar-Physics Space Missions Jun. 1993 p 161-168 Original contains color illustrations
(For primary document see N94-22837 06-92)
Copyright Avail: CASI HC A02/MF A02; ESA, EPD, ESTEC, Noordwijk, Netherlands, HC

N94-23378 College de France, Paris.
INTERFEROMETRIC ASTRONOMY ON THE MOON
Antoine Labeyrie, Jean Jacques Kessis (Paris VII Univ., France.), and Jean Pierre Rambaut (Paris VII Univ., France.) *In* CNES, Missions, Technologies, and Design of Planetary Mobile Vehicles Jan. 1993 p 107-114 (For primary document see N94-23373 06-91)
Copyright Avail: Issuing Activity (CEPADUES-Editions, 111, rue Nicolas-Vaquelin, 31100 Toulouse, France)

N94-23942*# Computer Sciences Corp., Lanham, MD.
LONG TERM TRENDING OF ENGINEERING DATA FOR THE HUBBLE SPACE TELESCOPE
Ross M. Cox *In* JPL, SpaceOps 1992: Proceedings of the Second International Symposium on Ground Data Systems for Space Mission Operations 1 Mar. 1993 p 727-732 (For primary document see N94-23832 06-66)
Avail: CASI HC A02/MF A10

N94-24455*# Mississippi State Univ., State College. Dept. of Physics and Astronomy.
USING CONTOUR MAPS TO SEARCH FOR RED-SHIFTED 511 keV FEATURES IN BATSE GRB SPECTRA
Peter G. Varmette *In* Alabama Univ., The 1993 NASA/ASEE Summer Faculty Fellowship Program Nov. 1993 5 p (For primary document see N94-24405 06-80)
Avail: CASI HC A01/MF A03

90 ASTROPHYSICS

Includes cosmology; celestial mechanics; space plasmas; and interstellar and interplanetary gases and dust.
For related information see also *75 Plasma Physics.*

N94-23010# Fermi National Accelerator Lab., Batavia, IL.
THE CURRENT STATUS OF OBSERVATIONAL CONSTRAINTS ON COSMIC STRINGS
R. R. Caldwell 1993 7 p Presented at the Gravity and Relativistic Astrophysics, Waterloo, Ontario, 13-15 May 1993
(Contract DE-AC02-76CH-03000)
(DE94-001505; FNAL/C-93/196-A; CONF-9305199-2) Avail: CASI HC A02/MF A01

The observational restrictions on the cosmic string scenario for the formation of large scale structure are evaluated. The restrictions are due to the spectrum of gravitational radiation emitted by oscillating string loops, anisotropies in the cosmic microwave background caused by the strings, and evaporating black holes formed from collapsed cosmic string loops. It is shown that the only free parameter of the scenario, the cosmic string mass-per-unit-length, mu, is severely restricted. DOE

N94-23099# Institut des Hautes Etudes Scientifiques, Bures-sur-Yvette (France).
TENSOR-SCALAR COSMOLOGICAL MODELS AND THEIR RELAXATION TOWARD GENERAL RELATIVITY
Thibault Damour and Kenneth Nordtvedt Mar. 1993 34 p See also PB93-162543
(PB93-220796; IHES/P/93/16) Avail: CASI HC A03/MF A01

Cosmological models within general tensor-multi-scalar theories of gravity are studied. By isolating an autonomous evolution equation for the scalar fields, one shows that the expansion of the universe during the matter-dominated era tends to drive the scalar fields toward a minimum of the function alpha(phi) describing their coupling to matter, i.e. toward a state where the tensor-scalar theory becomes indistinguishable from general relativity. The two main parameters determining the efficiency of this natural attractor mechanism toward general relativity are the redshift at the beginning of the matter era (or equivalently the present cosmological matter density) and the curvature of the coupling function alpha(phi). Quantitative estimates for the present level of deviation from general relativity, as measured by the post-Newtonian parameters gamma-1, beta-1 and (G dot)/G, are derived, which give greater significance to future improvements of solar-system gravitational tests. NTIS

N94-23251*# Colorado Univ., Boulder. Lab. for Atmospheric and Space Physics.
EVOLUTION OF LARGE-SCALE PLASMA STRUCTURES IN COMETS: KINEMATICS AND PHYSICS Final Report
John C. Brandt Oct. 1993 42 p
(Grant NAGw-1387)
(NASA-CR-194777; NAS 1.26:194777) Avail: CASI HC A03/MF A01

Cometary and solar wind data from December 1985 through April 1986 are presented for the purpose of determining the solar wind conditions associated with comet plasma tail disconnection events (DE's). The cometary data are from The International Halley Watch Atlas of Large-Scale Phenomena (Brandt, Niedner, and Rahe, 1992). In addition, we present the kinematic analysis of 4 DE's, those of Dec. 13.5 and 31.2, 1985, and Feb. 21.7 and 28.7, 1986. The circumstances of these DE's clearly illustrate the need to analyze DE's in groups. In situ solar wind measurements from IMP-8, ICE, and PVO were used to construct the variation of solar wind speed, density, and dynamic pressure during this interval. Data from these same spacecraft plus Vega-1 were used to determine the time of 48 current sheet crossings. These data were fitted to heliospheric current sheet curves extrapolated from the corona into the heliosphere in order to determine the best-fit source surface radius for each Carrington rotation. Comparison of the solar wind conditions and 16 DE's in Halley's comet (the four DE's discussed in this paper and 12 DE's in the literature) leaves little doubt that DE's are associated primarily with crossings of the heliospheric current sheet and apparently not with any other property of the solar wind. If we assume that there is a single or primary physical mechanism and that Halley's DE's are representative, efforts at simulation should concentrate on conditions at current sheet crossings. The mechanisms consistent with this result are sunward magnetic reconnection and tailward magnetic reconnection, if tailward reconnection can be triggered by the sector boundary crossing. Author (revised)

N94-23499*# California Inst. of Tech., Pasadena. Div. of Geological and Planetary Sciences.
CORRELATED PETROGRAPHIC, ELECTRON MICROPROBE, AND ION MICROPROBE STUDIES OF SELECTED PRIMITIVE AND PROCESSED PHASE ASSEMBLAGES IN METEORITES Progress Report
Arden L. Albee 1 Sep. 1993 11 p
(Grant NAG9-185)
(NASA-CR-194827; NAS 1.26:194827) Avail: CASI HC A03/MF A01

During the past three years we have received support to continue our research in elucidating the formation and alteration histories of selected meteoritic materials by a combination of petrographic, trace element, and isotopic analyses employing optical and scanning electron microscopes and electron and ion microprobes. The awarded research funds enabled the P.I. to attend the annual LPSC, the co-I to devote approximately 15 percent of his time to the research proposed in the grant, and partial support for a visiting summer post-doctoral fellow to conduct electron microprobe analyses of meteoritic samples in our laboratory. The research funds, along with support from the NASA Education Initiative awarded to P.I. G. Wasserburg, enabled the co-I to continue a mentoring program with inner-city minority youth. The support enabled us to achieve significant results in the five projects that we proposed (in addition to the Education Initiative), namely: studies of the accretional and post-accretional alteration and thermal histories in CV meteorites, characterization of periclase-bearing Fremdlinge in CV meteorites, characterization of Ni-Pt-Ge-Te-rich Fremdlinge in CV meteorites in an attempt to determine the constraints they place on the petrogenetic and thermal histories of their host CAI's, correlated electron and ion microprobe studies of silicate and phosphate inclusions in the Colomera meteorite in an attempt to determine the petrogenesis of the IE iron meteorites, and development of improved instrumental and correction procedures for improved accuracy of analysis of meteoritic materials with the electron microprobe. This grant supported, in part or whole, 18 publications so far by our research team, with at least three more papers anticipated. The list of these publications is included. The details of the research results are briefly summarized. Derived from text

N94-23537*# New Mexico State Univ., Las Cruces. Dept. of Astronomy.
THE SOFT X RAY HALO OF THE SPIRAL GALAXY NGC4631
Rene A. M. Walterbos, Michael F. Steakley, Q. Daniel Wang (Colorado Univ., Boulder.), Colin A. Norman (Johns Hopkins Univ., Baltimore, MD.),

and Robert Braun (Netherlands Foundation for Radio Astronomy, Dwingelo.) 1994 5 p
(Grants NAG5-1924; NSF AST-91-23777)
(NASA-CR-194820; NAS 1.26:194820) Avail: CASI HC A01/MF A01

ROSAT PSPC observations of the close to edge-on spiral galaxy NGC4631 are presented. This vigorously star forming galaxy shows extented x ray emission perpendicular to the plane, out to about 6 to 8 kpc. The spatial extent is largest at soft x ray energies. The total x ray luminosity of hot gas can be easily supplied by star formation in the disk, and it is likely that the halo is due to outflow of hot gas from the inner disk. Spectral analysis of the x ray data shows that part of the halo emission may be quite cool, well below 10(exp 6)K. Implications of these results are briefly discussed. Author (revised)

N94-23812 Onsala Space Observatory (Sweden).
MOLECULAR ABUNDANCES IN THE ENVELOPES AROUND EVOLVED STARS
H. Olofsson 1993 24 p Submitted for publication Limited Reproducibility: More than 20% of this document may be affected by microfiche quality
(PB94-104916; Rept-93/75) Avail: Issuing Activity (National Technical Information Service (NTIS))

The circumstellar envelopes (CSE's) of stars on the Asymptotic Giant Branch (AGB) and beyond show a remarkably rich variety of different molecular species. However, only about a third of them have been detected in more than five sources. The relatively simple geometry and kinematics of the CSE's make it possible to use rather uncomplicated methods for estimating molecular abundances that are accurate to within a factor of about five or slightly worse in some cases. The methods have not yet reached the level of sophistication that allows the circumstellar data to be used to obtain detailed information about the elemental composition. However, the results on isotope ratios are already of high quality. It is clear that different molecular species behave differently as the object evolves, and there is good hope that one may eventually be able to use this as a kind of molecular line chronology for stellar evolution on and beyond the AGB. NTIS

N94-24522 Groningen Rijksuniv. (Netherlands). Dept. of Mathematics.
COMPARISON OF TIME INTEGRATION METHODS FOR THE EVOLUTION OF GALAXIES
W. deGraaf 1993 31 p Limited Reproducibility: More than 20% of this document may be affected by microfiche quality
(PB94-111671; W-9316) Avail: Issuing Activity (National Technical Information Service (NTIS))

In the simulation of the evolution of elliptical galaxies, Leap-Frog is currently the most frequently used time integration method. The question is whether other methods perform better than this classical method. Improvements may also be expected from the use of variable step-lengths. We compare Leap-Frog with several other methods, namely: a fourth-order Nystrom method, a symplectic method, and DOPRI-five and eight. DOPRI uses variable steps of its own accord. For the other methods we construct a variable step procedure ourselves. The comparison of the methods is carried out in three Hamiltonian test problems. NTIS

N94-24557# Virginia Univ., Charlottesville. Dept. of Astronomy.
CHROMOSPHERIC ACTIVITY IN AGOL BINARIES Annual Report, 1 Oct. 1992 - 30 Sep. 1993
Mercedes T. Richards 30 Sep. 1993 5 p
(Contract F49620-92-J-0024)
(AD-A273546; AFOSR-93-0858TR) Avail: CASI HC A01/MF A01

The PI continued her study of magnetic activity on the cool components in short-period Algol-type binaries. The rapid rotators typically display enhanced magnetic activity, variations in the brightness of the cool secondary, and changes in the orbital period of the binary which can be linked to changes in the polarity of the magnetic field of the cool star. The PI has compiled observational evidence of magnetic activity in 15 Algol binaries and found that there is a 12 ck of information on the cool stars in these binaries. The systems chosen had orbital periods typically less than 6 days since short-period rapid rotators are more likely to display magnetic activity than their long-period counterparts. The survey showed that although six of the chosen boundaries displayed evidence of variations in the brightness of the secondary, Persei is the only Algol binary for which there was strong evidence of starspot activity. DTIC

N94-24866# National Inst. for Fusion Science, Nagoya (Japan).
NONEQUILIBRIA IN THERMAL EMISSION FROM SUPERNOVA REMNANTS
Kuniaki Masai (Commissariat a l'Energie Atomique, Gif-sur-Yvette, France.) Dec. 1993 40 p Submitted for publication
(NIFS-264) Avail: CASI HC A03/MF A01

Nonequipartition between the electron and the ion temperatures, and nonequilibrium ionization are discussed in view of thermal X-ray emission from young supernova remnants (SNR's). For electron heating due to Coulomb collisions with ions in the postshock region, an analytical solution is derived for the electron temperature under the adiabatic condition. By Taylor expansion of the solution, we obtain the electron temperature as a function of the electron density, time, and the shock velocity or the shock temperature Ts. With equipartition time tEeq, the solution shows that the electron temperature increases to be approximately 0.1Ts and 0.3Ts in 10(exp -3)tEeq and 10(exp -2)tEeq, respectively. The result is applied to the self-similar solutions for SNR's in the adiabatic phase, i.e., the free expansion phase and the Sedov phase. For SNR's expanding into a uniform density medium, our results predict much slower variation of the electron temperature than the case of full equipartition within the shock. We show the electron temperature plateau on the shocked matter of an SNR, and give analytical expressions of the electron temperature and the resultant free-free luminosity. In the free expansion phase, the electron temperatures of the reverse- and the blast-shocked matter are close to each other in comparison with the case of full equipartition, and their ratio is nearly constant for the ejecta envelope steepness. This results in a larger difference in the free-free luminosities of the two shocks than the case of full equipartition. Ionization processes are discussed in the framework of eigenvalue problem to find the key matrix element which is a pivot of the transformation and gives the characteristic time constant. The ionization time approximately 10(exp 12) n(sub e)(exp -1)s for the electron density n(sub e), and has no systematic dependence either on the electron temperature or the atomic number. The emission from the shocked matter can scale as n(sub e)t, but its superposition on a t-old SNR expanding into a uniform density medium may be represented by a lower value than n(sub e)t expected from the ambient matter density and the age. Also the effect of the nonequilibria on the level populations is discussed in view of line emission processes. While innershell ionization followed by fluorescence lines is important in compression waves, radiative recombination followed by cascade lines is important in rarefaction waves. The rarefaction occurs and adiabatically cools the shocked matter rapidly when the shock wave breaks out of the dense circumstellar matter into the rarefied ambient medium. Author (revised)

N94-24867# National Inst. for Fusion Science, Nagoya (Japan).
X RAY ENHANCEMENT OF SN 1987A DUE TO INTERACTION WITH ITS RING-LIKE NEBULA
Kuniaki Masai (Commissariat a l'Energie Atomique, Gif-sur-Yvette, France.) and Kenichi Nomoto (Tokyo Univ., Japan.) Dec. 1993 29 p
(NIFS-265) Avail: CASI HC A03/MF A01

The progenitor of the supernova 1987A, Sk-69 202 probably had lost a few solar-M in its stellar wind in the past evolutionary track from the red supergiant through the blue supergiant. A part of the mass is thought to form the ring-like nebula surrounding SN 1987A by the interaction with the faster wind in the later blue supergiant stage, and the other must be left outside the ring. In 10-20 yr after the explosion, the expanding ejecta will catch up and collide with the ring. Shocks due to the collision will propagate into and heat up the ejecta, the ring, and the matter outside. The shocked matter will be a thermal X-ray source of temperature of several times 10(exp 7) K, and the X-ray luminosity will reach (0.4-1)x10(exp 37) erg s(exp -1) for the ring of 0.03-0.08 solar-M. The X-ray emission will last for a few decades with luminosity higher than 10(exp 36) erg s(exp -1) depending also on the density outside the ring. We predict the X-ray spectrum as well as the light curve with hydrodynamical calculations taking into account the light travel effect and the opacity of the unshocked ejecta. The epoch of the flare-up depends on the mass inside the ring, and earlier X-ray observations can give a constraint. We give the relations of the mass with the epoch and the pre-flare luminosity in an analytical way based on the self-similar solutions with nonequipartition in the electron and the ion temperatures. Accordingly, the ROSAT observation in 1991 suggests the collision with the ring in 20 yr after the explosion. Author (revised)

N94-24964*# Lunar and Planetary Inst., Houston, TX. Meteorite Working Group.

ANTARCTIC METEORITE LOCATION AND MAPPING PROJECT (AMLAMP): ANTARCTIC METEORITE LOCATION MAP SERIES EXPLANATORY TEXT AND USER'S GUIDE TO AMLAMP DATA

J. Schutt, B. Fessler, and W. A. Cassidy 1993 186 p
(Contract NASw-4574)
(NASA-CR-194841; NAS 1.26:194841; LPI-TR-93-07) Avail: CASI HC A09/MF A02

This technical report is an update to LPI Technical Report 89-02, which contained data and information that was current to May 1987. Since that time approximately 4000 new meteorites have been collected, mapped, and characterized, mainly from the numerous ice fields in the Allan Hills-David Glacier region, from the Pecora Escarpment and Moulton Escarpment in the Thiel Mountains-Patuxent region, the Wisconsin Range region, and from the Beardmore region. Meteorite location maps for ice fields from these regions have been produced and are available. This report includes explanatory texts for the maps of new areas and provides information on updates of maps of the areas covered in LPI Technical Report 89-02. Sketch maps and description of locales that have been searched and have yielded single or few meteorites are also included. The meteorite listings for all the ice fields have been updated to include any classification changes and new meteorites recovered from ice fields in the Allan Hills-David Glacier region since 1987. The text has been reorganized and minor errors in the original report have been corrected. Computing capabilities have improved immensely since the early days of this project. Current software and hardware allow easy access to data over computer networks. With various commercial software packages, the data can be used many different ways, including database creation, statistics, and mapping. The databases, explanatory texts, and the plotter files used to produce the meteorite location maps are available through a computer network. Information on how to access AMLAMP data, its formats, and ways it can be used are given in the User's Guide to AMLAMP Data section. Meteorite location maps and thematic maps may be ordered from the Lunar and Planetary Institute. Ordering information is given in Appendix A. Derived from text

N94-24973*# National Aeronautics and Space Administration, Washington, DC.

ULTRAVIOLET, VISIBLE, AND GRAVITY ASTROPHYSICS: A PLAN FOR THE 1990'S

1990 76 p Original contains color illustrations
(NASA-NP-152; NAS 1.83:152) Avail: CASI HC A05/MF A01; 30 functional color pages

NASA's Office of Space Science and Applications (OSSA) receives advice on scientific strategy and priorities from the U.S. National Academy of Sciences. Guidance to the OSSA Astrophysics Division, in particular, is provided by dedicated academy committees, ad hoc study groups, and, at ten-year intervals, by broadly mandated astronomy and astrophysics survey committees charged with making recommendations for the coming decade. Many of the academy's recommendations have important implications for the conduct of ultraviolet and visible-light astronomy from space. Moreover, these areas are now poised for an era of rapid growth. Through technological progress, ultraviolet astronomy has already risen from a novel observational technique four decades ago to the mainstream of astronomical research today. Recent developments in space technology and instrumentation have the potential to generate comparably dramatic strides in observational astronomy within the next ten years. In 1989, the Ultraviolet and Visible Astrophysics Branch of the OSSA Astrophysics Division recognized the need for a new, long-range plan that would implement the academy's recommendations in a way that yielded the most advantageous use of new technology. NASA's Ultraviolet, Visible, and Gravity Astrophysics Management Operations Working Group was asked to develop such a plan for the 1990's. Since the branch holds programmatic responsibility for space research in gravitational physics and relativity, as well as for ultraviolet and visible-light astrophysics, missions in those areas were also included. The working group met throughout 1989 and 1990 to survey current astrophysical problems, assess the potential of new technologies, examine prior academy recommendations, and develop the implementation plan. The present report is the product of those deliberations. Key astrophysical questions to be addressed cover topics such as the structure and evolution of the early universe, energetics of active galactic nuclei, stellar winds in massive stars, sources powered by accretion, composition and state of the interstellar medium, nature of the galactic halo, chromospheric activity in cool stars, and formation of stars and planetary systems. This document provides a review of these questions, program concerns, and the recommended implementation plan for the 1990's. Derived from text

N94-24976# Nobeyema Solar Radio Observatory (Japan).

MAGNETIC FIELD DISSIPATION AND CONTRACTION OF MOLECULAR CLOUDS

Takenori Nakano, Ryoichi Nishi, and Toyoharu Umebayashi 1993 11 p
(Rept-337; JTN-94-80523) Avail: CASI HC A03/MF A01

The magnetic flux phi of a cloud or a cloud core is 0.1 to one times the critical flux phi(sub cr) which is proportional to its mass M. The phi/M (or equivalently phi/phi(sub cr)) ratio for a cloud or a cloud core is several hundred to 10(exp 5) times greater than the ratio for magnetic stars with mean surface field of one to 30 kG. The dissipation of magnetic fields in clouds is complicated because they contain various kinds of charged particles (electrons, ions, and grains) whose degree of freezing to field lines vary widely and whose relative abundance changes drastically as the cloud contracts. With a quite general formalism applicable to such wide range of physical situation, the field dissipation in clouds containing ice-mantled grains were investigated, and existence of a decoupling density n(sub dec) with the flux loss time t(sub B) is less than the free-fall time t(sub f) only at the cloud density n(sub H) less than n(sub dec) or t(sub B) approximately equals (10 - 500)t(sub f)(phi(sub cr)/phi) (exp 2) at n(sub H) much less than n(sub dec) at least for phi approximately equal (1 - 0.1) phi(sub cr) was found. The value of n(sub dec) depends rather sensitively on the grain model and the minimum value found is four times 10(exp 9) cu cm including the cases of grains without ice mantles. Author (NASDA)

N94-24983# Nobeyema Solar Radio Observatory (Japan).

PROTOPLANETARY DISKS: THEORY AND OBSERVATION BY MILLIMETER AND SUB-MILLIMETER ARRAYS

Takenori Nakano 1993 5 p Sponsored by Ministry of Education, Science and Culture, Tokyo, Japan
(Rept-331; JTN-94-80518) Avail: CASI HC A01/MF A01

Existence of flattened disks around young stellar objects has been suggested by near-infrared and millimeter-wave observations. It is tempting to consider that these disks are related to planet formation and even to formation of a companion star and brown dwarfs. At least in the early stages these must be accretion disks slowly falling onto central stars. Assuming steady accretion with efficient angular momentum transport by magnetic torque, the disk structure was investigated and whether magnetic fields were really coupled well with the gas was checked. It was found that there was a 'decoupling' radius r(sub dec) inside which magnetic fields were decoupled from the gas. The value of r(sub dec) is of the order of 10(exp 2) (central star mass/solar mass) (exp 1/3) AU (Astronomical Unit) or greater depending on the accretion rate and magnetic field strength. The fragmentation which occurs around r(sub dec) and growth of fragments to a companion star and ejection of remaining fragments into galactic space which will finally become brown dwarfs are discussed. The scenario of planet formation developed by the Kyoto group is summarized. Finally such expected structure of protoplanetary disks was shown. Some stages of planet formation may be observed with millimeter and sub-millimeter arrays if approximately 0.1 arcsec resolution is attained. Author (NASDA)

N94-24985# Kyoto Univ., Sakyoku (Japan). Dept. of Astronomy.

CO-TO-H2 CONVERSION FACTOR IN DWARF IRREGULAR GALAXIES

Koji Ota, Akihiko Tomita, Mamoru Saito, Minoru Sasaki, and Naomasa Nakai 1993 18 p
(Rept-333; JTN-94-80520) Avail: CASI HC A03/MF A01

CO-12 (J = 1 - 0) observations of five nearby dwarf irregular galaxies were made with a beam size of 15 sec., which is comparable to the size of a giant molecular cloud in the galaxies. Star-forming regions and/or H(sub 1) clumps with a column density exceeding 10(exp 21) per sq cm, where molecular clouds tend to be detected, was observed. CO emission was detected toward two H(sub 1) clumps in NGC (New General Catalog of Nebulae and Clusters of Stars) 4214 and one clump in NGC 6822. For another three galaxies (IC (Index Catalog) 1613, Sex (Sextans) A, and GR 8) very low upper limits of the CO luminosity were obtained. The relation between the CO luminosities and the line widths of molecular clouds in twelve galaxies, including other previous observations with a beam size comparable to the size of a giant molecular cloud and/or complex, were examined. The general tendency of this relation is that the CO luminosity for the same line width decreases with decreasing metallicity (O/H) of a galaxy; that is, if the line width is an indicator of the mass of a molecular cloud, the CO-to-H2 conversion factor increases as the metallicity of a galaxy decreases. However, there is a large scatter in the CO luminosity among galaxies with the same metallicity; the conversion factors for dwarf irregular galaxies with the same metallicity are not always the same. The UV. (Ultraviolet) intensity in the star-forming region does not seem to be the main cause for this large scatter. Author (NASDA)

N94-24986# Nobeyema Solar Radio Observatory (Japan).
HIGH SPATIAL RESOLUTION OBSERVATIONS OF CO IN CRL 618
Katsunori M. Shibata, Shuji Deguchi, Naomi Hirano, Osamu Kameya, and Shinichi Tamura 1993 25 p Sponsored by Japanese Society for the Promotion of Science, Tokyo, Japan
(Rept-334; JTN-94-80521) Avail: CASI HC A03/MF A01

The aperture synthesis of the very young planetary nebula CRL 618 by CO-12 J = 1 - 0 line and continuum at 115.271 GHz with the Nobeyama Millimeter Array have been observed. The maps with the angular resolution of 3 sec. 6 times 3' sec. 5 show strong concentration of CO toward the ionized core with no clear evidence of a toroidal structure around the star nor along the axis of visible bipolar lobes. Velocity-channel maps show complex structures characterized by a spheroidal component weakly elongated to the east-west direction and a horn-like feature which looks to be spread from the center in a narrow opening angle. It seems difficult to interpret the maps by the simple model with a smooth outflow. The disk structure does not show up in the observation because of the smallness of the disk or obscuring by the surrounding thick spherical CO gas. The red wing component of a high velocity outflow was detected, but not the blue wing component. The red wing arises from the compact region, within 2 sec. from the ionized core, and suggests that the high velocity outflow occurs in a compact region centered on the ionized core. The 115 GHz continuum emission has been detected with the total flux density of 1.48 Jy and it is a point source centered on the ionized core. Author (NASDA)

N94-24987# Nobeyema Solar Radio Observatory (Japan).
THE NOBEYAMA MILLIMETER ARRAY SURVEY FOR PROTOPLANETARY DISKS AROUND PROTOSTAR CANDIDATES AND T TAURI STARS IN TAURUS
Nagayoshi Ohashi, Ryohei Kawabe, Masahiko Hayashi, and Masato Ishiguro 1993 11 p Sponsored by Japanese Society for the Promotion of Science, Tokyo, Japan
(Rept-336; JTN-94-80522) Avail: CASI HC A03/MF A01

The Nobeyama Millimeter Array Survey for protoplanetary disks has been made for 19 protostellar IRAS (Infrared Astronomical Satellite) sources in Taurus; 13 of them were optically invisible protostars and six were young T Tauri stars. 8 GHz continuum and CS (J = 2 - 1) line emission were observed simultaneously with spatial resolutions of 2 sec. 8 - 8 sec. 8 (360 AU (Astronomical Unit) - 1,200 AU). The continuum emission was detected from five out of six T Tauri stars and two out of 13 protostar candidates: the emission was not spatially resolved and was consistent with being originated from compact circumustellar disks. Extended CS emission was detected around two T Tauri stars and 11 protostar candidates. There is a remarkable tendency that the detectability for the 8 GHz continuum emission is small for protostar candidates. This tendency is explained if the mass of protoplanetary disks around protostars is not as large as that around T Tauri stars; the disk mass may increase with the increase of central stellar mass by dynamical accretion in the course of evolution from protostars to T Tauri stars. Author (NASDA)

N94-25210 International Centre for Theoretical Physics, Trieste (Italy).
A BRIEF HISTORY OF THE UNIVERSE
K. K. Sinha Oct. 1992 12 p Limited Reproducibility: More than 20% of this document may be affected by microfiche quality
(DE93-616843; IC-92/336) Avail: CASI HC A03 (US Sales Only)

The failure of the Big Bang Theory to explain the experimental (cosmological) data is well known. Attempts were made to give a new interpretation of the above theory to explain the existing cosmological problems and a brief history of the universe. DOE

N94-25211 International Centre for Theoretical Physics, Trieste (Italy).
CHOICE OF FILTERS FOR THE DETECTION OF GRAVITATIONAL WAVES FROM COALESCING BINARIES. 2: DETECTION IN COLOURED NOISE
S. V. Dhurandhar (Inter-University Centre for Astronomy and Astrophysics, Pune, India.) and B. S. Sathyaprakash Oct. 1992 33 p Limited Reproducibility: More than 20% of this document may be affected by microfiche quality
(DE93-616844; IC-92/345) Avail: CASI HC A03 (US Sales Only)

The problem of detecting gravitational wave signals embedded in colored noise from coalescing binary systems is discussed. The signal is assumed to be Newtonian and matched filtering techniques are employed to filter out the signal. The problem is discussed at first for a general power spectral density of the noise and then specific numerical results are obtained for the standard recycling case. Since the signal parameters are unknown, a bank of filters is needed to carry out the signal detection. The number of filters in a bank, the spacing between filters etc. is obtained for different values of the minimum strength of the signal relative to the threshold. An approximate analytical formula which relates the spacing between filters to the minimum strength is also presented. Finally, we discuss the problem of detection probabilities given a data train. DOE

N94-25212 International Centre for Theoretical Physics, Trieste (Italy).
A PARALLEL ALGORITHM FOR FILTERING GRAVITATIONAL WAVES FROM COALESCING BINARIES
B. S. Sathyaprakash and S. V. Dhurandhar (Inter-University Centre for Astronomy and Astrophysics, Pune, India.) Oct. 1992 24 p Limited Reproducibility: More than 20% of this document may be affected by microfiche quality
(DE93-616845; IC-92/346) Avail: CASI HC A03 (US Sales Only)

Coalescing binary stars are perhaps the most promising sources for the observation of gravitational waves with laser interferometric gravity wave detectors. The waveform from these sources can be predicted with sufficient accuracy for matched filtering techniques to be applied. A parallel algorithm for detecting signals from coalescing compact binaries by the method of matched filtering is presented. The details of its implementation on a 256-node connection machine consisting of a network of transputers are also reported. The results of our analysis indicate that parallel processing is a promising approach to on-line analysis of data from gravitational wave detectors to filter out coalescing binary signals. The algorithm described is quite general in that the kernel of the algorithm is applicable to any set of matched filters. DOE

N94-25215# International Centre for Theoretical Physics, Trieste (Italy).
COSMIC WAKE FIELDS
G. R. Dvali, V. I. Berezhiani, and S. Mahajan Nov. 1992 14 p
(DE93-616849; IC-92/396) Avail: CASI HC A03/MF A01 (US Sales Only)

The propagation of a spatially localized topological object (domain wall or the boundary of the expanding vacuum bubble) in the presence of an extra pseudogoldstone field is investigated. It is shown that, under certain conditions, the propagating domain wall can excite (in its wake) a strictly periodic comoving wave of the pseudogoldstone field. Some possible cosmological consequences of this rather general phenomenon are briefly discussed. DOE

N94-25265*# Applied Research Corp., Landover, MD.
OBSERVATIONAL STUDIES OF THE CLEARING PHASE IN PROTO-PLANETARY DISK SYSTEMS Annual Report, 19 Mar. 1993 - 18 Mar. 1994
Carol A. Grady 9 Mar. 1994 7 p
(Contract NASw-4756)
(NASA-CR-195182; NAS 1.26:195182; R93-217) Avail: CASI HC A02/MF A01

A summary of the work completed during the first year of a 5 year program to observationally study the clearing phase of proto-planetary disks is presented. Analysis of archival and current IUE data, together with supporting optical observations has resulted in the identification of 6 new proto-planetary disk systems associated with Herbig Ae/Be stars, the evolutionary precursors of the beta Pictoris system. These systems exhibit large amplitude light and optical color variations which enable us to identify additional systems which are viewed through their circumstellar disks including a number of classical T Tauri stars. On-going IUE observations of Herbig Ae/Be and T Tauri stars with this orientation have enabled us to detect bipolar emission plausibly associated with disk winds. Preliminary circumstellar extinction studies were completed for one star, UX Ori. Intercomparison of the available sample of edge-on systems, with stars ranging from 1-6 solar masses, suggests that the signatures of accreting gas, disk winds, and bipolar flows and the prominence of a dust-scattered light contribution to the integrated light of the system decreases with decreasing IR excess. Author (revised)

N94-23684*# Bowling Green State Univ., OH. Dept. of Physics and Astronomy.
A MIXED METHOD POISSON SOLVER FOR THREE-DIMENSIONAL SELF-GRAVITATING ASTROPHYSICAL FLUID DYNAMICAL SYSTEMS
Comer Duncan and Jim Jones (Colorado Univ., Denver.) *In* NASA. Langley Research Center, The Sixth Copper Mountain Conference on Multigrid Methods, Part 1 Nov. 1993 p 159-173 (For primary document see N94-23673 06-64)
Avail: CASI HC A03/MF A03

N94-25358*# Stockton State Coll., Pomona, NJ. Dept. of Geology and Environmental Studies.
A GEOCHEMICAL STUDY OF ACAPULCOITE AND LODRANITE METEORITES
Stephen W. Field *In* NASA. Johnson Space Center, National Aeronautics and Space Administration (NASA)/American Society for Engineering Education (ASEE) Summer Faculty Fellowship Program, 1993, Volume 1 Dec. 1993 13 p (For primary document see N94-25348 06-99)
Avail: CASI HC A03/MF A03

91 LUNAR AND PLANETARY EXPLORATION

Includes planetology; and manned and unmanned flights.
For spacecraft design or space stations see *18 Spacecraft Design, Testing and Performance.*

N94-23373 Centre National d'Etudes Spatiales, Toulouse (France).
MISSIONS, TECHNOLOGIES, AND DESIGN OF PLANETARY MOBILE VEHICLES [MISSIONS, TECHNOLOGIES ET CONCEPTION DES VEHICULES MOBILES PLANETAIRES]
Jan. 1993 522 p Conference held in Toulouse, France, Sep. 1992
(ISBN-2-85428-331-7; ETN-94-94439) Copyright Avail: Issuing Activity (CEPADUES-Editions, 111, rue Nicolas-Vaquelin, 31100 Toulouse, France)

Soviet and U.S. studies of planetary rovers are reported. The following topics are covered: mission definitions and requirements; mission analysis and system architecture; vehicle technologies and design; and robotics functions. For individual titles, see N94-23374 through N94-23427.

N94-23374 Academy of Sciences (USSR), Saint Petersburg.
SOVIET DEVELOPMENTS OF PLANET ROVERS IN PERIOD OF 1964 - 1990 c37
A. L. Kemurdjian, V. V. Gromov, I. F. Kazhukalo, G. V. Kozlov, V. I. Komissarov, G. N. Korepanov, B. N. Martinov, V. I. Malenkov, A. V. Mitskevich, and V. K. Mishkinyuk et al *In* CNES, Missions, Technologies, and Design of Planetary Mobile Vehicles Jan. 1993 p 25-43 (For primary document see N94-23373 06-91)
Copyright Avail: Issuing Activity (CEPADUES-Editions, 111, rue Nicolas-Vaquelin, 31100 Toulouse, France)

The history of Soviet planetary rovers, which were intended for work on the surface of planets and other heavenly bodies, is traced starting with Lunokhod 1, which was designed to survey the Moon. The equipment and methodology of ground tests which simulated lunar conditions--lunar vacuum, gravitation, and soil--are reported. Examples of planetary rovers which followed the Lunokhod program are given. These examples include machines of the following types: wheel walkers; machines that used skiing for locomotion; and two articulated modules. Planet rovers for Venus, Mars, and its satellite Phobos are addressed. The f ocus ison the performance of Marsokhod, the Mars rover. ESA

N94-23375* Jet Propulsion Lab., California Inst. of Tech., Pasadena.
PAST US STUDIES AND DEVELOPMENTS FOR PLANETARY ROVERS c37
James D. Burke (Planetary Society, Pasadena, CA.) *In* CNES, Missions, Technologies, and Design of Planetary Mobile Vehicles Jan. 1993 p 45-60 (For primary document see N94-23373 06-91)
Copyright Avail: Issuing Activity (CEPADUES-Editions, 111, rue Nicolas-Vaquelin, 31100 Toulouse, France)

The history of planetary rovers in the U.S. space program is outlined in the context of the goals, mission and spacecraft designs, and operations designs. The American lunar rover work has had three main stages. In the early sixties, the capacity of Surveyor lunar landers to deliver rovers with a mass of about 50 kg to the Moon was exploited. Several such machines were built and tested beginning in 1964 but none went to the Moon. A manned 400 kg short range rover was then developed. Three of these operated on the Moon in 1971 and 1972 as part of the Apollo 15, 16 and 17 missions. Following these Apollo successes, attempts were made to provide two kinds of follow on models: automated or dual mode (human carrying or not) rovers in the few hundred kg size class, and multi-ton mobile habitats that could carry humans on extended traverses. With the closing of both Soviet and American lunar exploration in the seventies, neither of these proposals succeeded. In parallel with these lunar developments, a lengthy technology program on Martian roving has gone on in the U.S., sometimes coming close to preproject status and sometimes fading away, but never quite being abandoned. As a result it is possible today to contemplate a wide range of lunar and Martian roving missions that could be made practical within a few years. However, with today's funding constraints none of the well studied, larger mission concepts appear to fit. Therefore new efforts are being made toward developing much smaller rovers taking advantage of new miniature techniques, not only in mobility systems but also in the scientific instruments that a small rover can carry. Illustrations are included. ESA

N94-23376* National Aeronautics and Space Administration. Lyndon B. Johnson Space Center, Houston, TX.
LUNAR SCIENCE STRATEGY: EXPLORING THE MOON WITH HUMANS AND MACHINES
Donald A. Morrison and Stephen J. Hoffman (Science Applications International Corp., Houston, TX.) *In* CNES, Missions, Technologies, and Design of Planetary Mobile Vehicles Jan. 1993 p 63-96 (For primary document see N94-23373 06-91)
Copyright Avail: Issuing Activity (CEPADUES-Editions, 111, rue Nicolas-Vaquelin, 31100 Toulouse, France)

Important scientific questions that can be addressed from the lunar surface are reviewed for a number of scientific disciplines. A successful strategy for human exploration of the Moon is outlined. It consists of several elements: thorough preparation; a means of extending the human reach; measurement of the mobility of both human and robotic components; and flexible technologies so as to be able to take the most effective path as successive decision points occur. Part of thorough preparation involves concurrent development of a set of science goals and objectives as well as a supporting information base; neither can evolve independently of the other. This matched set will drive the definition of missions and technologies used to satisfy the requirements of various science disciplines. No single site on the Moon will satisfy all requirements. Thus, global accessibility is a goal of the current Lunar and Mars Exploration Program science strategy. Human mobility on the surface is limited to a few kilometers without the use of vehicles. Unpressurized crew carrying rovers could take explorers to distances tens of kilometers from an outpost; the distance is primarily limited by health and safety concerns. Pressurized rovers could extend the range to hundreds of kilometers, but size, mass, and costs limit such vehicles to missions beyond current planning horizons. The establishment of several outposts instead of one would provide opportunities for effective use of the unique capabilities of humans. Extending the human reach to global dimensions may be accomplished through teleoperation or telepresence. The most effective mix of these techniques is a decision that will evolve as experience is gained on the surface. Planning and technology must be flexible enough to allow a variety of options to be selected. ESA

N94-23377* National Aeronautics and Space Administration. Lyndon B. Johnson Space Center, Houston, TX.
ROVER REQUIREMENTS FOR THE PLANET SURFACE SEGMENT OF THE SPACE EXPLORATION INITIATIVE **c37**
Barney B. Roberts and John F. Connolly *In* CNES, Missions, Technologies, and Design of Planetary Mobile Vehicles Jan. 1993 p 97-106 (For primary document see N94-23373 06-91)
Copyright Avail: Issuing Activity (CEPADUES-Editions, 111, rue Nicolas-Vaquelin, 31100 Toulouse, France)

Annotated requirements for rovers to be used for the First Lunar Outpost (FLO) of the Space Exploration Initiative (SEI) and for Mars missions are presented. The requirements are presented in the form of functions as opposed to performance. SEI surface systems will be required to execute many roving vehicle functions ranging from transporting humans to recovery and transporting raw materials to a processing plant. Some of the roving vehicles will be highly automated. These automation functions may include the following: teleoperated site survey and certification; teleoperation for repair; autonomous operations for resource location and mining; autonomous navigation and terrain traverse; and telerobotic scientific investigations. These requirements are complex, contradictory, and will be costly if they are not carefully analyzed and properly allocated to conceptual elements. Of greatest importance will be the iterative analysis of requirements and synergistic utilization of vehicle elements. ESA

N94-23378 College de France, Paris.
INTERFEROMETRIC ASTRONOMY ON THE MOON **c89**
Antoine Labeyrie, Jean Jacques Kessis (Paris VII Univ., France.), and Jean Pierre Rambaut (Paris VII Univ., France.) *In* CNES, Missions, Technologies, and Design of Planetary Mobile Vehicles Jan. 1993 p 107-114 (For primary document see N94-23373 06-91)
Copyright Avail: Issuing Activity (CEPADUES-Editions, 111, rue Nicolas-Vaquelin, 31100 Toulouse, France)

Optical interferometry, the art of achieving the angular resolution of a giant telescope by using many smaller elements, is introduced, and the principles of lunar interferometry are discussed. The proposed Lunar Optical Very Large Airay (LOVLA) is presented. LOVLA consists of telescopes which are mobile on six legs. Each reflects a narrow light beam towards a central station where all the images are superposed. Near the lunar poles, dark craters provide appropriate sites for such instruments. The array may expand to cover 10 km and include as many as 27 telescopes. The LOVLA concept, automated deployment and alignment, mechanical design, metrology and attitude sensors, optical train, and control are discussed. ESA

N94-23379 Yamaguchi Univ. (Japan). Faculty of Science.
ROBOTIC EXPLORATION OF MOON AND MARS
Y. Miura *In* CNES, Missions, Technologies, and Design of Planetary Mobile Vehicles Jan. 1993 p 115-124 Sponsored by the Japanese Monbusho (For primary document see N94-23373 06-91)
Copyright Avail: Issuing Activity (CEPADUES-Editions, 111, rue Nicolas-Vaquelin, 31100 Toulouse, France)

Results from robotic explorations of the Moon and Mars are summarized. The lunar and Martian soils and rocks can be identified by comparison with the standard data derived from mass spectral patterns of the 'remote sensing Secondary Ion Mass Spectrometry' (remote SIMS). Fine grained glassy materials show more complicated spectral patterns than those of hard crystalline rocks. This type of examination can be applied to analyze amorphous glassy materials and trace element compositions of the lunar and Martian soils and rocks. Experimental results from artificial and terrestrial impact craters suggest that the high density shocked or high pressure-type shocked phases of silica or carbon minerals can coexist with the amorphous glassy phases. Therefore, sophisticated instruments such as the remote SIMS for secondary ions, X-ray analyzers for X-ray diffraction and X-ray absorption coefficient, and polarized microscopy for optical images can be applied to find and collect new shocked crystalline minerals with amorphous phases on the Moon and Mars. ESA

N94-23380 Geological Survey, Menlo Park, CA.
SCIENCE STRATEGY FOR MARS EXPLORATION Abstract Only
Michael H. Carr *In* CNES, Missions, Technologies, and Design of Planetary Mobile Vehicles Jan. 1993 p 125-126 (For primary document see N94-23373 06-91)
Copyright Avail: Issuing Activity (CEPADUES-Editions, 111, rue Nicolas-Vaquelin, 31100 Toulouse, France)

During the 1990's Mars exploration is expected to change from dominantly orbital reconnaissance to surface reconnaissance. Systematic mapping of the planet by the Mars Observer and Mars-94 orbiters will effectively complete global orbital characterization. Any future orbital observations will likely focus on support of surface missions, both robotic and human. Robotic surface missions have two goals: to improve our scientific understanding of the planet, and to prepare the way for eventual human exploration. The course of Mars exploration in the first decade of the next century will partly depend on which of these two goals dominates. The main goals of Mars science are as follows: to determine the mode of formation of the solid planet and how it evolved to its present state; to determine the climatic history of the planet; and to determine the nature of any indigenous biologic activity, past or present. The science goals are best achieved by a mix of missions including a network, rover missions, and sample return missions, all with global access. Our focus is on the crucial role of rovers in fulfilling both scientific and human exploration goals. ESA

N94-23381 Academy of Sciences (USSR), Moscow. Inst. of Space Research.
MARS 96 SMALL ROVER: MISSION STRATEGY Abstract Only
V. V. Kerzhanovich and V. M. Linkin *In* CNES, Missions, Technologies, and Design of Planetary Mobile Vehicles Jan. 1993 p 127 (For primary document see N94-23373 06-91)
Copyright Avail: Issuing Activity (CEPADUES-Editions, 111, rue Nicolas-Vaquelin, 31100 Toulouse, France)

Mars is a favorite site for proposed planetary rover studies; it has the following characteristics: intriguing geology, surface features, and history; and an environment that is not terrbily hostile. For many years, 'Big Rover' was an essential element in the former Soviet space program. During the evolution of the current Soviet Mars project, it seemed attractive to include a rover. The idea was realized in 1990 when a small rover was included as a high risk experiment in the payload of the descent module. The main features of the mission and its science are presented and the limitations are analyzed. The further steps and improvements are foreseen. ESA

N94-23382 Centre National de la Recherche Scientifique, Caen (France). Centre de Geomorphologie.
A REFERENCE MARTIAN MISSION FOR A LONG RANGE ROVER
F. Costard, J. Achache (Institut de Physique du Globe, Paris, France.), J. P. Bibring (Institut d'Astrophysique, Paris, France.), M. Blanc (Observatoire de Midi-Pyresnees, Toulouse, France.), S. Coutin-Faye (Centre National d'Etudes Spatiales, Toulouse, France.), Y. Langevin (Institut d'Astrophysique, Paris, France.), P. Lognonne (Institut de Physique du Globe, Paris, France.), P. Masson (Paris-Sud Univ., Orsay, France.), D. Moura (Centre National d'Etudes Spatiales, Toulouse, France.), and F. Rocard (Centre National d'Etudes Spatiales, Toulouse, France.) *In* CNES, Missions, Technologies, and Design of Planetary Mobile Vehicles Jan. 1993 p 129-138 (For primary document see N94-23373 06-91)
Copyright Avail: Issuing Activity (CEPADUES-Editions, 111, rue Nicolas-Vaquelin, 31100 Toulouse, France)

The three basic rover missions currently under study by the French scientific community which will use the Automatic Planetary Rover are addressed. This rover will use two types of elements on the surface of Mars: delivering of fixed stations for seismology, magnetism, and meteorological measurements; and mobile vehicles for the study of a great diversity of terrains by means of geophysical profiling and in situ analysis. The French scientific objectives of the next Mars mission are presented. ESA

N94-23383 Jet Propulsion Lab., California Inst. of Tech., Wrightwood.
SCIENCE OBJECTIVES FOR SHORT-RANGE ROVERS ON MARS
M. P. Golombek *In* CNES, Missions, Technologies, and Design of Planetary Mobile Vehicles Jan. 1993 p 139-145 (For primary document see N94-23373 06-91)
Copyright Avail: Issuing Activity (CEPADUES-Editions, 111, rue Nicolas-Vaquelin, 31100 Toulouse, France)

The baseline small lander network mission MESUR (Mars Environmental Survey) is reviewed and the tasks that a microrover could do to improve the science return on such a mission are described. An early precursor small lander mission under study, called MESUR Pathfinder, and the science, technology, and mission engineering tasks that are being considered for the microrover are also described. A description of a microrover (instrumented with microsensors), which is applicable to a small Mars lander mission, is given. ESA

N94-23384 Babakin Engineering and Research Center, Moscow (Russia).
PROSPECTS FOR USING MOBILE VEHICLES IN MISSIONS TO MARS AND OTHER PLANETS
V. Kovtunenko, R. Kremnev, G. Rogovsky, and Y. Ivshchenko *In* CNES, Missions, Technologies, and Design of Planetary Mobile Vehicles Jan. 1993 p 149-160 (For primary document see N94-23373 06-91)
Copyright Avail: Issuing Activity (CEPADUES-Editions, 111, rue Nicolas-Vaquelin, 31100 Toulouse, France)

Automatic stations will play the main role in the Russian program of planetary research. Among these, the outstanding place is occupied by vehicles intended for surface investigations using contact methods. Such investigations may be performed as under stationary conditions and also by use of planetary mobile vehicles. Stationary stations can not provide research of macroevents over spacious terrains and can not gather the statistics necessary for comparative analyses of various geological and climatic zones, etc. All these tasks can be solved by use of planetary mobile vehicles: planetary rovers. The history of Soviet rovers is outlined. Planetary mobile vehicles in the program of Mars investigations are discussed looking into their problems and utilization (global mapping, soil sample gathering and investigation, search for landing site, and regions for investigation). Focus is on the Mars Rover and on a micro-Mars rover. The use of the Mars rover in the Mars sample return mission is considered. Planetary rover development trends (electronics, power support, chassis modifications) are outlined. Diagrams are included. ESA

N94-23385 Sternberg Astronomical Inst., Moscow (USSR).
THE MORPHOLOGY OF THE LUNAR SURFACE PARTS IN THE REGION OF WORK OF THE MOBILE GEOLOGICAL LABORATORY VEHICLE IN MARE IMBRIUM
J. F. Rodionova *In* CNES, Missions, Technologies, and Design of Planetary Mobile Vehicles Jan. 1993 p 161-165 (For primary document see N94-23373 06-91)
Copyright Avail: Issuing Activity (CEPADUES-Editions, 111, rue Nicolas-Vaquelin, 31100 Toulouse, France)

With the aim of building a manned lunar base at the beginning of the 21st century, the Imbrium basin, favored by its wide diversity of geological formations, was selected to be studied by a field crew of 6 to 8 members. They would travel a total distance of 4000 km and visit 29 separate locations in an attempt to characterize the processes involved in the formation and evolution of a variety of major lunar features. Sites chosen for this expedition are mentioned. Using previous data, the crater density distribution was studied. These results together with profiles and slope angles of several regions on the traverse of the mobile laboratory (constructed on the basis of maps) are presented. Mysterious features near crater Humason are identified and the possibility of them being natural caverns in the form of lava tubes is considered. ESA

N94-23386* Jet Propulsion Lab., California Inst. of Tech., Pasadena.
LUNAR ROVER NAVIGATION CONCEPTS
James D. Burke (Planetary Society, Pasadena, CA.) *In* CNES, Missions, Technologies, and Design of Planetary Mobile Vehicles Jan. 1993 p 167-179 Sponsored by NASA, Washington (For primary document see N94-23373 06-91)
Copyright Avail: Issuing Activity (CEPADUES-Editions, 111, rue Nicolas-Vaquelin, 31100 Toulouse, France)

With regard to the navigation of mobile lunar vehicles on the surface, candidate techniques are reviewed and progress of simulations and experiments made up to now are described. Progress that can be made through precursor investigations on Earth is considered. In the early seventies the problem was examined in a series of relevant tests made in the California desert. Meanwhile, Apollo rovers made short exploratory sorties and robotic Lunokhods traveled over modest distances on the Moon. In these early missions some of the required methods were demonstrated. The navigation problem for a lunar traverse can be viewed in three parts: to determine the starting point with enough accuracy to enable the desired mission; to determine the event sequence required to reach the site of each traverse objective; and to redetermine actual positions enroute. The navigator's first tool is a map made from overhead imagery. The Moon was almost completely photographed at moderate resolution by spacecraft launched in the sixties, but that data set provides imprecise topographic and selenodetic information. Therefore, more advanced orbital missions are now proposed as part of a resumed lunar exploration program. With the mapping coverage expected from such orbiters, it will be possible to use a combination of visual landmark navigation and external radio and optical references (Earth and Sun) to achieve accurate surface navigation almost everywhere on the near side of the Moon. On the far side and in permanently dark polar areas, there are interesting exploration targets where additional techniques will have to be used. ESA

N94-23387 Jet Propulsion Lab., California Inst. of Tech., Pasadena.
UNMANNED LUNAR ROVERS: UTILIZATION FOR EXPLORATION
J. B. Plescia, A. L. Lane, and D. P. Miller *In* CNES, Missions, Technologies, and Design of Planetary Mobile Vehicles Jan. 1993 p 181-192 (For primary document see N94-23373 06-91)
Copyright Avail: Issuing Activity (CEPADUES-Editions, 111, rue Nicolas-Vaquelin, 31100 Toulouse, France)

A small lunar rover and its use for lunar exploration are described. Constraints on a rover mission in the fields of communications, power, speed, navigation/hazard avoidance, and operational time are discussed. The rover design concept consistent with the constraints is described. The instruments to be used, again constrained by mass and power requirements, are listed. Three mission objectives are examined: geological exploration; resource assessment; and a geotechnical survey. It was determined that a small rover, with a mass of less than 60 kg and which would be compatible with being carried on the first Artemis lunar lander, could be built and could accomplish significant scientific exploration or the collection of engineering information. ESA

N94-23388* National Aeronautics and Space Administration. Langley Research Center, Hampton, VA.
EARLY LUNAR ROVER MISSION STUDIES
Vernon P. Gillespie *In* CNES, Missions, Technologies, and Design of Planetary Mobile Vehicles Jan. 1993 p 193-202 (For primary document see N94-23373 06-91)
Copyright Avail: Issuing Activity (CEPADUES-Editions, 111, rue Nicolas-Vaquelin, 31100 Toulouse, France)

Results of lunar mission studies aimed at developing mission goals and high level requirements are reported. A mission concept to meet the mission requirements was developed and the design of mission hardware was to follow. Mission concepts not only included operations analysis and plans but also fabrication and test planning, quality control measures, and project organization. The design of mission concepts and hardware identified issues that are not easily resolved. Although none of the issues identified appear to be unresolvable, many will be difficult to resolve within Space Exploration Initiative constraints. These issues discussed which appear to have the potential for negative project impact are rover mobility, power, imaging, telemanagment, and remote control. ESA

N94-23389 Tsukuba Space Center (Japan).
THE STUDY OF THE MOBILE LUNAR EXPLORER
T. Eto, M. Oda, Y. Kaneko, and T. Maeda *In* CNES, Missions, Technologies, and Design of Planetary Mobile Vehicles Jan. 1993 p 203-214 (For primary document see N94-23373 06-91)
Copyright Avail: Issuing Activity (CEPADUES-Editions, 111, rue Nicolas-Vaquelin, 31100 Toulouse, France)

The Japanese concept of the Lunar Mobile Explorer (LME), a robotic rover which employs second generation space robot technology, is presented. A single launch of H2 rocket will be used to send the rover to the lunar surface. An expendable lander is designed for this mission. After landing at a flat ground near the equator, the LME starts exploring tour toward polar region. It performs precise mapping along the touring course, collection of geological data, analysis of surface and subsurface materials, experimental processing of resources and technology demonstrations. The LME is equipped with an autonomous navigation and steering capability which is mounted by a human operator on the Earth for monitoring and teleoperation. The following are described with regard to the LME: mission requirements; landing point and tour route; vehicle system; system configuration; mass allocation; power constraints; driver guidance; navigation; locomotion mechanism; mission devices; communication; power; and development status. ESA

N94-23390 Hitachi Ltd., Yokohama (Japan). Space Systems Div.
THE ROBOTIC MARS ROVER
Toshihide Maeda, Kazuo Ohta (Tsukuba Space Center, Japan.), Yutaka Kaneko (National Space Development Agency, Tokyo, Japan.), Takao Eto (Rocket System Corp., Japan.), and Mitsushige Oda (Tsukuba Space Center, Japan.) *In* CNES, Missions, Technologies, and Design of Planetary Mobile Vehicles Jan. 1993 p 215-220 (For primary document see N94-23373 06-91)
Copyright Avail: Issuing Activity (CEPADUES-Editions, 111, rue Nicolas-Vaquelin, 31100 Toulouse, France)

MAME (Mars Mobile Explorer), a case study for the robotic Mars mission which will be launched by Japan's H2 launch vehicle, is presented. MAME is a six wheeler and powered by electricity from solar panel. MAME moves around the Martian surface and investigates the environmental conditions and composition of Martian surface. The mission and concept of this Mars rover are described. ESA

N94-23391 European Space Agency, Paris (France).
MISSION AND SYSTEM CONCEPTS FOR MARS ROBOTIC PRECURSOR MISSIONS
George E. N. Scoon and Martin Hechler *In* CNES, Missions, Technologies, and Design of Planetary Mobile Vehicles Jan. 1993 p 221-236 (For primary document see N94-23373 06-91)
Copyright Avail: Issuing Activity (CEPADUES-Editions, 111, rue Nicolas-Vaquelin, 31100 Toulouse, France)

Mission and system design concepts reflecting the status at about the midpoint of the Marsnet phase A study are reported. The objective of Marsnet is to place three to four small stations (approximately 80 kg) on the surface of Mars to perform scientific measurements in the areas of geophysics (seismology), geology, geochemistry, mineralogy, meteorology, and exobiology. The ESA Landers will constitute part of a global network to which NASA is planning to contribute up to 16 other stations. The Mars Global Network may be seen as a precursor to the exploration of Mars by mobile vehicles in terms of its scientific measurements. But, also, some aspects of mission and system design addressed may be applicable to more complex robotic missions to Mars, for example, the development and testing of feasible probe delivery concepts; the design of low mass, low power components, and solar arrays suited for the Mars environment; and the development of a low complexity mobile instrument deployment device. ESA

N94-23392 Centre National d'Etudes Spatiales, Toulouse (France).
MISSION AND SYSTEM DESIGN OF A LONG RANGE ROVER MISSION
Jacques Bernard, Frederic Bonneau, Francois-Xavier Chaffaut, and Jean Ciampi (Centre National d'Etudes Spatiales, Paris, France.) *In its* Missions, Technologies, and Design of Planetary Mobile Vehicles Jan. 1993 p 237-245 (For primary document see N94-23373 06-91)
Copyright Avail: Issuing Activity (CEPADUES-Editions, 111, rue Nicolas-Vaquelin, 31100 Toulouse, France)

The definition of the scientific mission of a planetary automatic vehicle on the surface of Mars (fixed stations positioning, profile measurements during traveling, and in situ analysis) identifies constraints on the mission analysis: exploration site location, vehicle mass, volume of data to transmit, duration of mission, interaction with the Earth, orbiter support etc. The mission analysis carried out for three launch opportunities in 1998, 2001 and 2003, for different families of orbits, a priori considered, selects orbits suited to these constraints. The scenarios and strategies of insertion around Mars, orbit positioning and vehicle deorbiting, were evaluated. The mission conditions and dust storms, conjunction, etc., were characterized. The location of vehicles on the surface of Mars (rover and stations) was evaluated, using different kind of measurement involving the spacecraft. The primary results are presented. ESA

N94-23393 Centre National de la Recherche Scientifique, Verrieres-Le Buisson (France). Service d'Aeronomie.
MARS SUBSURFACE SOUNDING WITH A GROUND PENETRATING RADAR
Y. Barbin, F. Nicollin (Rennes Univ., France.), F. Costard (Centre National de la Recherche Scientifique, Caen, France.), and W. Kofman (Centre National de la Recherche Scientifique, Grenoble, France.) *In* CNES, Missions, Technologies, and Design of Planetary Mobile Vehicles Jan. 1993 p 247-257 Sponsored by CNES (For primary document see N94-23373 06-91)
Copyright Avail: Issuing Activity (CEPADUES-Editions, 111, rue Nicolas-Vaquelin, 31100 Toulouse, France)

The general principles of Ground Penetrating Radars (GPR) applied to the Mars subsurface are presented. The case of the Mars 96 mission balloon GPR is studied. Work on the electromagnetic modeling of the Mars subsurface for GPR is shown. Accommodation guidelines for operating a GPR on a Planetary Automatic Vehicle are presented. ESA

N94-23394 Joanneum Research Centre, Graz (Austria).
DESCENT AND LANDING PHASE: VISION BASED ROBUST SPACECRAFT MOTION ESTIMATION AND ELEVATION MODELING
Gerhard Paar and Wolfgang Poelzleitner *In* CNES, Missions, Technologies, and Design of Planetary Mobile Vehicles Jan. 1993 p 259-272 (For primary document see N94-23373 06-91)
(Contract ESTEC-9195/90/NL/SF)
Copyright Avail: Issuing Activity (CEPADUES-Editions, 111, rue Nicolas-Vaquelin, 31100 Toulouse, France)

A technique for automatic elevation model computation, which uses a binocular camera system and an algorithm termed 'hierarchical feature vector matching' to derive an elevation model (or range map), as well as to compute the interframe correspondences for tracking, is introduced. It is robust in terms of geometric distortions between the stereo partners and relies on hierarchical image representations usable for the realtime demand during descent and landing. It is argued that this algorithm unifies the procedures of range estimation (stereo correspondence, tracking (interframe correspondence), and recognition (input/model correspondence). This technique is demonstrated using a physical model of the Mars surface and a binocular camera system with six geometrical degrees of freedom. This system provides a valuable tool to generate realistic test imagery for the mockup of a spacecraft approaching the landing site. The trajectory of the spacecraft can be predefined and is controlled by a computer interfaced to six motorized positioners. Several experiments that were defined to estimate the accuracy of the computer vision system are reported. ESA

N94-23395 Academy of Sciences (USSR), Moscow. Inst. of Space Research.
MARS 96 ROVER: SCIENCE, INSTRUMENTATION, AND CONTROL Abstract Only c37
V. M. Linkin and V. V. Kerzhanovich *In* CNES, Missions, Technologies, and Design of Planetary Mobile Vehicles Jan. 1993 p 273 (For primary document see N94-23373 06-91)
Copyright Avail: Issuing Activity (CEPADUES-Editions, 111, rue Nicolas-Vaquelin, 31100 Toulouse, France)

The scientific payload of the Mars rover project includes a large set of the instruments that can provide substantial improvement on the knowledge of Mars. Primary goals are surface studies: morphology, mineralogy, chemistry. Few instruments can investigate subsurface properties. Rovers will be used to study specific objects and to deploy instruments. A television system in pair with an onboard computer is planned for autonomous navigation. Limited command and data transmission through the satellite relay imposes restrictions on control methods. Control combines Earth based long term strategy planning with autonomous onboard short time local decisions. Special algorithms should be developed to control scientific instruments. ESA

N94-23396 Academy of Sciences (USSR), Moscow. Inst. of Space Research.
BALLOON EXPERIMENTS AT MARS 96 PROJECT Abstract Only
V. M. Linkin and V. V. Kerzhanovich *In* CNES, Missions, Technologies, and Design of Planetary Mobile Vehicles Jan. 1993 p 274 (For primary document see N94-23373 06-91)
Copyright Avail: Issuing Activity (CEPADUES-Editions, 111, rue Nicolas-Vaquelin, 31100 Toulouse, France)

The philosophy and details of the first Mars balloon flight mission are presented. The first Mars balloon flight initially scheduled for 1995 has been postponed to 1997. It will be inserted into the atmosphere of Mars from the Mars 96 orbiter. Its scientific program includes a number of experiments. During its flight, measurements of meteo parameters, magnetic field and altitude will be done; television-images with ultrahigh resolution and IR spectrums of the surface are planned. A guiderope, which serves to stabilize the night flight of the balloon near the surface, will be instrumented with subsurface radar and gamma spectrometer. Data from the balloon will be relayed through the Mars 96 orbiter and through Mars Observer. ESA

N94-23397 Babakin Engineering and Research Center, Moscow (Russia).
ROVER IN THE MARS 96 MISSION
A. Eremenko, B. Martinov, K. Pitchkhadze, V. Porotov, and V. Nagronyk *In* CNES, Missions, Technologies, and Design of Planetary Mobile Vehicles Jan. 1993 p 277-300 (For primary document see N94-23373 06-91)
Copyright Avail: Issuing Activity (CEPADUES-Editions, 111, rue Nicolas-Vaquelin, 31100 Toulouse, France)

The main data of the Mars-96 mission and performance of the Mars Rover (MR) which is the mission integral element are reported. The tasks of the Mars-96 mission are as follows: remote sensing from the Mars orbit of the various Mars regions in the different spectral bands; in situ investigations of the Martian atmosphere and surface parameters with the Balloon/Probe (BP) floating in the atmosphere; in situ contact investigations of the Mars surface and atmosphere, Martian soil on different depths, interaction of the atmosphere and soil along the MR route. With regard to the MR, the following are discussed: landing, destination, composition, systems functions, control, communication and program of operation, design, main performance. ESA

N94-23398* Jet Propulsion Lab., California Inst. of Tech., Pasadena.
THE NEW FAMILY OF JPL PLANETARY SURFACE VEHICLES c37
Donald B. Bickler *In* CNES, Missions, Technologies, and Design of Planetary Mobile Vehicles Jan. 1993 p 301-306 Sponsored by NASA, Washington (For primary document see N94-23373 06-91)
Copyright Avail: Issuing Activity (CEPADUES-Editions, 111, rue Nicolas-Vaquelin, 31100 Toulouse, France)

A new type of vehicle design named 'rocker-bogie' and later nicknamed 'Rocky', which has a free rocking bogie at the front of a master bogie, is presented. All Rocky design vehicles have the following in common: there are no springs or elastic members other than those used with tires; there is a single rigid body; they have very high ground clearence; all wheels are capable of being steered; the body is differentially connected between the left and right sides on a transverse axis. The basis of the design, a linkage system that distributes the weight among the wheels over a wide range of individual wheel elevations, and how this leads to superior obstacle climbing ability and superior bump performance, are explained. ESA

N94-23399 Fiat Spazio, Rome (Italy).
FEASIBILITY STUDY OF AN AUTOMATIC VEHICLE FOR PLANETARY EXPLORATION c37
C. Gerli, A. Murolo, R. Mugnuolo (Italian Space Agency, Matera.), E. Gallo (Telerobot, Genoa, Italy.), F. Cantatore (Telerobot, Genoa, Italy.), and L. Giardino (Tecnospazio S.p.A., Milan, Italy.) *In* CNES, Missions, Technologies, and Design of Planetary Mobile Vehicles Jan. 1993 p 307-312 (For primary document see N94-23373 06-91)
Copyright Avail: Issuing Activity (CEPADUES-Editions, 111, rue Nicolas-Vaquelin, 31100 Toulouse, France)

A study with the following objectives is reported: definition of the scientific objectives of a planetary exploration using a rover; definition of the planetary rover requirements; identification and characterization of the main subsystems of the rover; definition and critical areas and technological risks; and verification of the possibility on international cooperation on a planetary mission. The use of such a rover to investigate the Moon and Mars is focused upon. ESA

N94-23400 Centre National d'Etudes Spatiales, Toulouse (France).
ROVER: AUTONOMOUS CONCEPTS FOR MARS EXPLORATION c37
A. Baiget, B. Castets, H. Chochon, M. Hayard, H. Lamarre, and A. Lamothe *In its* Missions, Technologies, and Design of Planetary Mobile Vehicles Jan. 1993 p 313-326 Prepared in cooperation with Aerospatiale, Cannes, France; Alcatel Espace, Toulouse, France; Societe Generale de Constructions Electriques et Mecaniques Alsthon, Massy, France; and Societe d'Applications Generales d'Electricite et de Mecanique, Paris, France (For primary document see N94-23373 06-91)
Copyright Avail: Issuing Activity (CEPADUES-Editions, 111, rue Nicolas-Vaquelin, 31100 Toulouse, France)

The development of a mobile, autonomous vehicle that will be launched towards an unknown planet is considered. The rover significant constraints are: Ariane 5 compatibility, Earth/Mars transfer capability, 1000 km autonomous moving in Mars environment, on board localization, and maximum science capability. Two different types of subsystem were considered: classical subsystems (mechanical and mechanisms, thermal, telecommunications, power, onboard data processing) and robotics subsystem, (perception/navigation, autonomous displacement generation, autonomous localization). The needs of each subsystem were studied in terms of energy and data handling capability, in order to choose an on board architecture which best use the available capability, by means of specialized parts. A compromise must always be done between every subsystem in order to obtain the real need with respect to the goal, for example: between perception/navigation and the motion capability. A compromise must also be found between mechanical assembly and calibration need, which is a real problem. ESA

N94-23401* National Aeronautics and Space Administration. Lewis Research Center, Cleveland, OH.
ELECTRICAL POWER TECHNOLOGY FOR ROBOTIC PLANETARY ROVERS c33
C. P. Bankston (Jet Propulsion Lab., California Inst. of Tech., Pasadena.), M. Shirbacheh (Jet Propulsion Lab., California Inst. of Tech., Pasadena.), D. J. Bents, and J. M. Bozek *In* CNES, Missions, Technologies, and Design of Planetary Mobile Vehicles Jan. 1993 p 327-336 (For primary document see N94-23373 06-91)
Copyright Avail: Issuing Activity (CEPADUES-Editions, 111, rue Nicolas-Vaquelin, 31100 Toulouse, France)

Power technologies which will enable a range of robotic rover vehicle missions by the end of the 1990s and beyond are discussed. The electrical power system is the most critical system for reliability and life, since all other on board functions (mobility, navigation, command and data, communications, and the scientific payload instruments) require electrical power. The following are discussed: power generation, energy storage, power management and distribution, and thermal management. ESA

N94-23402 Tokyo Univ., Sagamihara (Japan). Inst. of Space and Astronautical Science.
DEVELOPMENT/DRILLING TEST OF AUGER BORING MACHINE ON BOARD MARS ROVER FOR MARS EXPLORATION c37
N. Kawashima, I. Nakatani, J. Kawaguchi, K. Saito (Nishimatsu Construction Co. Ltd., Tokyo, Japan.), M. Kojima (Nishimatsu Construction Co. Ltd., Tokyo, Japan.), and N. Fujii (Nagoya Univ., Japan.) *In* CNES, Missions, Technologies, and Design of Planetary Mobile Vehicles Jan. 1993 p 337-343 (For primary document see N94-23373 06-91)
Copyright Avail: Issuing Activity (CEPADUES-Editions, 111, rue Nicolas-Vaquelin, 31100 Toulouse, France)

A study was made on Mars exploration using a powerful Mars rover with a special emphasis on fabricating and testing of some model and of its subsystem. The major objective is set to search for water and organic material in the underground of Mars. An engineering model of a drilling machine to be on board and used for the sample collection in an extensive scientific exploration of Mars surface and underground was fabricated. As a drilling machine, auger boring was adopted. Though it cannot drill hard rocks, it is simple and easy to operate, because it does not require any liquid for lubrication and cooling. It has a capability of 1.5 m boring, requiring 1.15 kW electric power. The auger bit is surrounded with a metal cylindrical casing and the collected soil is stored in the space between the auger bit and the casing. A drilling test was performed using a simulated Mars soil. It has a layered structure, and between each layer, a thin sheet having a different color is inserted. The simulated soil was drilled and collected preserving the layer structure. It was verified that the sample can be collected with a vertical resolution of about 20 cm. The final goal of the drilling capability is set to 10 m drilling. ESA

N94-23403 Commissariat a l'Energie Atomique, Fontenay-aux-Roses (France). Robotics Unit.
MECHANICAL DESIGN OF A PLANETARY ROVER c37
F. Littmann, E. Villedieu, and J. M. Idasiak *In* CNES, Missions,

Technologies, and Design of Planetary Mobile Vehicles Jan. 1993 p 345-359 (For primary document see N94-23373 06-91)
Copyright Avail: Issuing Activity (CEPADUES-Editions, 111, rue Nicolas-Vaquelin, 31100 Toulouse, France)

The preliminary mechanical design studies of a planetary rover for the VAP (French acronym for automatic planetary rover) project with a light (100 kg) and a heavy (1000 kg) option are presented. The candidate locomotion concepts are compared and three main locomotion modes are selected: the rolling, walking and peristaltic modes. The peristaltic motion is obtained by sequential motion of parts of a vehicle. The rolling mode is chosen for simplicity and terrestrial experience, the existing planetary rovers based on the rolling mode are compared. An original four wheel drive vehicle with a peristaltic motion and a movable center of gravity is presented. ESA

N94-23404 Centre National d'Etudes Spatiales, Toulouse (France).
PLANETARY ROVER LOCOMOTION MECHANISMS c37
J. B. Mondier *In its* Missions, Technologies, and Design of Planetary Mobile Vehicles Jan. 1993 p 361-368 (For primary document see N94-23373 06-91)
Copyright Avail: Issuing Activity (CEPADUES-Editions, 111, rue Nicolas-Vaquelin, 31100 Toulouse, France)

The design of the most relevant mechanisms with respect to the robotics locomotion subsystem specifications of an exploration planetary rover is discussed. The mechanisms considered are the wheel setting and driving device, the axle rotary joints, the payload and axle translation apparatus. Constraints due to the surroundings are considered. ESA

N94-23405 Paris VII Univ. (France). Lab. de Robotique et Intelligence Artificielle.
CONCEPTUAL DESIGN AND ARCHITECTURE OF HEXAPOD ROBOTIC VEHICLES FOR THE (L)OVLA PROJECT c37
Jean-Jacques Kessis, Jean-Pierre Rambaut, and Antoine Labeyrie (College de France, Paris.) *In* CNES, Missions, Technologies, and Design of Planetary Mobile Vehicles Jan. 1993 p 369-375 (For primary document see N94-23373 06-91)
Copyright Avail: Issuing Activity (CEPADUES-Editions, 111, rue Nicolas-Vaquelin, 31100 Toulouse, France)

The current status of the design of the vehicle part of the Lunar Optical Very Large Array (LOVLA), which is to carry out optical interferometric astronomy on the Moon, is presented. Legs were chosen to deal with the LOVLA's mobility requirements. A frequent argument against legged solutions is the complexity of actuation and control. The problem of controlling the robot exhibits a wide mathematical indetermination. The gait concept, which provides neat and efficient means to reduce indermination, is described. The multilevel control architecture proposed is also described. ESA

N94-23406 Technische Univ., Munich (Germany). Lehrstuhl B fuer Mechanik.
WALKING MACHINES FOR SPACE c37
J. Eltze, H.-J. Weidemann, and F. Pfeiffer *In* CNES, Missions, Technologies, and Design of Planetary Mobile Vehicles Jan. 1993 p 377-384 (For primary document see N94-23373 06-91)
Copyright Avail: Issuing Activity (CEPADUES-Editions, 111, rue Nicolas-Vaquelin, 31100 Toulouse, France)

A study of a new walking machine model differing from existing walking machines both in geometry and control is presented. The main criteria used in the model are not technical principles as used in existing walking machines, but rather biological principles found in insects, the living prototypes of walking machines. The goal of this method is to obtain a harmonic gait which is very robust against disturbances and therefore is suitable to be used on uneven ground found on planets. The geometry, the kinematics and the kinetics of the walking machine model is introduced and the control is explained. Experimental results of this concept tested on a single laboratory leg are shown to prove the robustness of the controller. ESA

N94-23407 European Space Agency. European Space Research and Technology Center, ESTEC, Noordwijk (Netherlands). Robotics Section.
AUTOMATION TECHNOLOGY FOR REMOTE SAMPLE ACQUISITION c37
Anders Elfving *In* CNES, Missions, Technologies, and Design of Planetary Mobile Vehicles Jan. 1993 p 385-394 (For primary document see N94-23373 06-91)
Copyright Avail: Issuing Activity (CEPADUES-Editions, 111, rue Nicolas-Vaquelin, 31100 Toulouse, France)

Automation and robotics technology needs and the operational aspects applicable for planetary sample acquisition in general are discussed. In particular concepts for hybrid automation are highlighted. Special features of typical sampling tools, using the Rosetta mission as an example, are discussed and a control architecture in which this hybrid automation solution can be coordinatedly operated together with its hosting lander/rover vehicle is proposed. ESA

N94-23408 Swiss Center for Electronics and Microtechnology, Inc., Neuchatel.
ELECTRONIC PAYLOADS FOR MARTIAN MISSIONS: A PRELIMINARY ASSESSMENT OF TECHNOLOGIES
Michel E. Roulet and Jean-Luc Josset *In* CNES, Missions, Technologies, and Design of Planetary Mobile Vehicles Jan. 1993 p 395-403 (For primary document see N94-23373 06-91)
Copyright Avail: Issuing Activity (CEPADUES-Editions, 111, rue Nicolas-Vaquelin, 31100 Toulouse, France)

A preliminary assessment of design guidelines for electronic payloads that will be used on planetary missions where they will encounter extreme environmental conditions is presented. It shows different aspects related to electronic components on one hand and to mounting and assembly technologies on the other hand, focus is on silicon integrated circuits. Consideration is also given to theoretical semiconductor device physics in order to derive some guidelines for architectural design of analog and digital functional blocks or components. Even if some criticalities can be identified, it is obviously necessary to obtain a practical insight by realizing and testing electronic boards acting as representative test vehicles. The logic to implement this approach is presented and the dedicated cryogenic testing facilities, which are required to have a good test coverage, are described. ESA

N94-23409 Air Force Test Pilot School, Edwards AFB, CA.
CARBON MONOXIDE FUEL CELLS AS A SOURCE FOR MARS ROVER ELECTRIC POWER c33
Mitchell Burnside Clapp *In* CNES, Missions, Technologies, and Design of Planetary Mobile Vehicles Jan. 1993 p 405-409 (For primary document see N94-23373 06-91)
Copyright Avail: Issuing Activity (CEPADUES-Editions, 111, rue Nicolas-Vaquelin, 31100 Toulouse, France)

Electrochemical fuel cells which can efficiently provide electrical energy from chemical energy are considered. The possible use of carbon monoxide and oxygen obtained from the separation of the carbon dioxide in the Martian atmosphere to make electricity to power planetary rover vehicles on planet Mars is discussed. Although fuel cells are heavier than internal combustion engines of the same power output, they are potentially more reliable and efficient in the consumption of propellant. Depending on the mission model chosen for a planetary rover vehicle, fuel cells using the carbon monoxide and oxygen reaction offer a promising alternative to vehicle designers. ESA

N94-23410 Massachusetts Inst. of Tech., Cambridge. Artificial Intelligence Lab.
THE MASS OF MASSIVE ROVER SOFTWARE c61
David P. Miller *In* CNES, Missions, Technologies, and Design of Planetary Mobile Vehicles Jan. 1993 p 411-414 Prepared in cooperation with Jet Propulsion Lab., California Inst. of Tech., Pasadena (For primary document see N94-23373 06-91)
Copyright Avail: Issuing Activity (CEPADUES-Editions, 111, rue Nicolas-Vaquelin, 31100 Toulouse, France)

A planetary rover, like a spacecraft, must be fully self contained. Once launched, a rover can only receive information from its designers, and if solar powered, power from the Sun. As the distance from Earth increases, and the demands for power on the rover increase, there is a serious tradeoff between communication and computation. Both of these subsystems are very power hungry, and both can be the major driver of the rover's power subsystem, and therefore the minimum mass and size of the rover. This situation and software techniques that can be used to reduce the requirements on both communication and computation, allowing the overall robot mass to be greatly reduced, are discussed. ESA

N94-23411 Academy of Sciences (USSR), Saint Petersburg.
MACHINES FOR MOVING IN SOIL Abstract Only c37
V. V. Gromov and P. N. Brodsky *In* CNES, Missions, Technologies, and Design of Planetary Mobile Vehicles Jan. 1993 p 415 (For primary document see N94-23373 06-91)
Copyright Avail: Issuing Activity (CEPADUES-Editions, 111, rue Nicolas-Vaquelin, 31100 Toulouse, France)

A mode of motion in soil with the use of an impulse (impact) propulsor and tractive power assessments of the motion process are discussed; generalized relations are shown which allow to assess some structural parameters; the data of experimental tests are given. Various schemes for using the machines to move in soil are discussed, including the machines used in the scientific set of the Marsokhod according to the Mars 96 design. ESA

N94-23412 Centre National d'Etudes Spatiales, Toulouse (France).
THE MARS 96 BALLOON GUIDEROPE: AN AUTONOMOUS SYSTEM IN EXTREME ENVIRONMENT CONDITIONS c37
H. Laplace, M. Moreliere, and C. Gorse *In its* Missions, Technologies, and Design of Planetary Mobile Vehicles Jan. 1993 p 417-421 Prepared in cooperation with THARSYS, France (For primary document see N94-23373 06-91)
Copyright Avail: Issuing Activity (CEPADUES-Editions, 111, rue Nicolas-Vaquelin, 31100 Toulouse, France)

The Mars 96 balloon mission involves: an orbiting spacecraft, a descent module, and a balloon to which are attached a gondola with scientific experiments and a stabilizing element named guiderope. An overview of the guiderope mission and characteristics is given. The guiderope's primary mission is to stabilize the Mars balloon during the night, after its descent, in order to avoid the balloon and the gondola contacting the ground. The guiderope has a snake like shape to avoid snagging when dragged on the Martian surface. Its length is 7 m plus a 7 m cable tail. Its mass of 13.5 kg allows the guiderope to house various scientific payloads, management system and its initialization device, a transmitter, its antenna and the batteries. The duration of the mission is ten days after 10 months of transfer from Earth to Mars. ESA

N94-23413 Laboratoire d'Automatique et d'Analyse des Systemes, Toulouse (France).
THE REMOTE-OPERATED AUTONOMOUS-ROBOT CONCEPT: FROM DEEP SEA TO OUTER SPACE APPLICATIONS c37
Georges Giralt, Raja Chatila, and Rachid Alami *In* CNES, Missions, Technologies, and Design of Planetary Mobile Vehicles Jan. 1993 p 425-441 (For primary document see N94-23373 06-91)
Copyright Avail: Issuing Activity (CEPADUES-Editions, 111, rue Nicolas-Vaquelin, 31100 Toulouse, France)

Concepts of a generic architecture aimed to achieve task level teleprogramming and execution control of a remote intervention robot were developed in the framework of several domain oriented projects: deep sea intervention robots, the Advanced Mobile Robots (AMR) (EUREKA) project (public safety), and the Planetary Rover project VAP (French acronym) are developed. In this context, the functional architecture that implements the Remote-Operated Autonomous Robot (ROAR) concept is presented. The framework of the French Mars rover project VAP is used as an illustration of some crucial aspects discussed. ESA

N94-23414* National Aeronautics and Space Administration, Washington, DC.
EVOLVING DIRECTIONS IN NASA'S PLANETARY ROVER REQUIREMENTS AND TECHNOLOGY c37
C. R. Weisbin (Jet Propulsion Lab., California Inst. of Tech., Pasadena.), Mel Montemerlo, and W. Whittaker (Carnegie-Mellon Univ., Pittsburgh, PA.) *In* CNES, Missions, Technologies, and Design of Planetary Mobile Vehicles Jan. 1993 p 443-454 (For primary document see N94-23373 06-91)
Copyright Avail: Issuing Activity (CEPADUES-Editions, 111, rue Nicolas-Vaquelin, 31100 Toulouse, France)

The evolution of NASA's planning for planetary rovers (that is robotic vehicles which may be deployed on planetary bodies for exploration, science analysis, and construction) and some of the technology that was developed to achieve the desired capabilities is reviewed. The program is comprised of a variety of vehicle sizes and types in order to accommodate a range of potential user needs. This includes vehicles whose weight spans a few kilograms to several thousand kilograms; whose locomotion is implemented using wheels, tracks, and legs; and whose payloads vary from microinstruments to large scale assemblies for construction. Robotic vehicles and their associated control systems, developed in the late 1980's as part of a proposed Mars Rover Sample Return (MRSR) mission, are described. Goals suggested at the time for such a MRSR mission included navigating for one to two years across hundreds of kilometers of Martian surface; traversing a diversity of rugged, unknown terrain; collecting and analyzing a variety of samples; and bringing back selected samples to the lander for return to Earth. Current plans (considerably more modest) which have evolved both from technological 'lessons learned' in the previous period, and modified aspirations of NASA missions are presented. Some of the demonstrated capabilities of the developed machines and the technologies which made these capabilities possible are described. ESA

N94-23415 Tokyo Inst. of Tech. (Japan).
DUAL ROVER CONCEPT FOR MARS EXPLORATION c37
Y. Ohkami, K. Matsumoto (National Aerospace Lab., Tokyo, Japan.), and T. Yoshida (Shimizu Corp., Japan.) *In* CNES, Missions, Technologies, and Design of Planetary Mobile Vehicles Jan. 1993 p 455-464 (For primary document see N94-23373 06-91)
Copyright Avail: Issuing Activity (CEPADUES-Editions, 111, rue Nicolas-Vaquelin, 31100 Toulouse, France)

A concept composed of two identical vehicles connected by cable system is proposed for Mars exploration. Each vehicle is rather conventional with wheels, but the dual vehicle concept provides an outstanding capability, especially when either of them encounters an unexpected difficulty. This is just like a two person party of rock climbing. The leader vehicle can explore an unknown terrain at a risk of falling down or upset. The follower vehicle connected by an extensible cable moves very carefully according to the path exploited by the leader. If the vehicles are augmented by crane capability, it becomes possible to climb rocks whose size exceeds the limitation imposed by vehicle wheel radius, and also to recover from capture in a ditch. A fundamental concept is presented together with operation scenario for mountain climbing and waste land traveling. The key technology includes image processing, maintenance procedures, and hierarchy control under unknown environment. It is demonstrated by simulation that the dual vehicles corporation can do much more and provide increased reliability than the individual capability doubled. ESA

N94-23416 Academy of Sciences (USSR), Moscow. Inst. of Space Research.
RESULTS OF THE MOJAVE TESTS OF THE MARS 96 ROVER Abstract Only c37
V. M. Linkin, V. V. Kerzhanovich, A. I. Kemurdjian (Academy of Sciences, USSR, Saint Petersburg.), V. V. Gromov (Academy of Sciences, USSR, Saint Petersburg.), K. Pichkhaze (Babakin Engineering and Research Center, Moscow, Russia.), G. Rogovsky (Babakin Engineering and Research Center, Moscow, Russia.), L. Friedman (Planetary Society, Pasadena, CA.), and H. Schurmeier (Planetary Society, Pasadena, CA.) *In* CNES, Missions, Technologies, and Design of Planetary Mobile Vehicles Jan. 1993 p 465 (For primary document see N94-23373 06-91)
Copyright Avail: Issuing Activity (CEPADUES-Editions, 111, rue Nicolas-Vaquelin, 31100 Toulouse, France)

The self propelled undercarriage of the Mars 96 mission Marsokhod, a convertible three section joint structure moving to the wheel walking principle, is considered. Original conical cylindrical wheels provide a unique cross country ability both on loose friable soil and on a surface with critical relief conditions and accidental obstacles. The construction scheme of the self propelled undercarriage and its components and features of arrangement are discussed. Considerations concerning the problems of placing the scientific and service devices and power sources, and requirements for the latter, are indicated. New possibilities discovered for carrying out the scientific experiments are analyzed. Data of laboratory and field on the road tests are given. The main specifications are shown with the self propelled undercarriage and test pieces of the self propelled undercarriage. ESA

N94-23417 Academy of Sciences (USSR), Moscow. Inst. of Space Research.

MARS 96 ROVER: TECHNICAL VISION AND NAVIGATION Abstract Only c37

V. M. Linkin, V. V. Kerzhanovich, I. Sitenko, and S. Szalai (Hungarian Academy of Sciences, Budapest.) *In* CNES, Missions, Technologies, and Design of Planetary Mobile Vehicles Jan. 1993 p 466 (For primary document see N94-23373 06-91)
Copyright Avail: Issuing Activity (CEPADUES-Editions, 111, rue Nicolas-Vaquelin, 31100 Toulouse, France)

Two television (TV) systems are planned to be installed on the Mars 96 rover: linear panoramic and frame stereo. The first will permit high resolution 360 field of view image of surrounding landscape. Stereo frames will be written into onboard memory and after computer processing the three dimensional structure of the local surface will be restored. A number of algorithms are under development which should elaborate a safe pass for the rover. TV and TV navigation will also be used to find the objects for study with the instruments and to guide the rover to these objects. Another application of the rover and TV is foreseen: to deploy the instrument on the surface. It can be an antenna for electromagnetic sounding or special modules for seismic measurements. ESA

N94-23418 Academy of Sciences (USSR), Saint Petersburg.

MARSOHKOD MOVEMENT CONTROL Abstract Only c37

P. S. Sologub, S. V. Fedoseev, V. V. Gromov, and G. V. Kozlov *In* CNES, Missions, Technologies, and Design of Planetary Mobile Vehicles Jan. 1993 p 467 (For primary document see N94-23373 06-91)
Copyright Avail: Issuing Activity (CEPADUES-Editions, 111, rue Nicolas-Vaquelin, 31100 Toulouse, France)

The Marsokhod movement control, which ensures that the Marsokhod comes to a specified region, scientific investigations are carried out in the process of movement and the operation of the scientific devices during the scientific sessions, is discussed. The repertoire of the dataware required of the Marsokhod undercarriage and the tasks of the safety control system are disclosed for this Marsokhod. Possible methods for automatic driving of the undercarriage are discussed, and comparative assessments are produced; requirements are formulated for the computer complex. Practicability of the course indication system is shown in the absence of the magnetic field on Mars. Data are given which were obtained at the laboratory and proving ground tests of the Marsokhod undercarriage. ESA

N94-23419 Massachusetts Inst. of Tech., Cambridge. Artificial Intelligence Lab.

WALKING, JUMPING, AND TUMBLING: MORE THAN ONE WAY TO GET AROUND MARS Abstract Only c37

R. Brooks *In* CNES, Missions, Technologies, and Design of Planetary Mobile Vehicles Jan. 1993 p 469 (For primary document see N94-23373 06-91)
Copyright Avail: Issuing Activity (CEPADUES-Editions, 111, rue Nicolas-Vaquelin, 31100 Toulouse, France)

Smaller and novel alternatives to wheels or large legs as a means for moving small scientific packages around the Martian surface are proposed. These proposals include: walking robots on the scale of 2 kg down to a few grams; flea-like robots in the few gram range which make random ballistic motions in order to move around; tumbleweed like robots in the few gram range which rely on being blown around by Martian storms. Each of these approaches brings unique constraints to the types of science that can be done, the type of mission control that can be applied externally, the ways in which data can be communicated, and the options that can be employed for delivery to the surface. These questions are examined for each proposed means of locomotion, the technological bottlenecks are identified, and mission scenarios are examined. ESA

N94-23420 Academy of Sciences (USSR), Saint Petersburg.

PERSPECTIVE OF CREATION OF MEANS FOR COLLECTING INFORMATION CONCERNING TRANSPORT SITUATION Abstract Only c37

V. Mishkinyuk, I. Bolhovitinov, I. Kalyaev, V. Kuznetsov, and V. Noskov *In* CNES, Missions, Technologies, and Design of Planetary Mobile Vehicles Jan. 1993 p 471 (For primary document see N94-23373 06-91)
Copyright Avail: Issuing Activity (CEPADUES-Editions, 111, rue Nicolas-Vaquelin, 31100 Toulouse, France)

Some of the problems connected to the development of an autonomous command system for a Mars rover functioning in interactive mode are addressed. Results of a selection of the criteria of path optimization are cited; criteria are represented in the form of dimensionless parameters of energy or time expenditure for the movement along the investigated surface. Requirements of the set of onboard information systems are presented; these provide receiving information on time and energy expenditure within the range of sensivity of the onboard information systems. The functional arrangement of the systems for receiving information on surface geometric and mechanical characteristics is described. Various algorithms for information processing, model forming, and selection of optimal rover path, taking into account requirements cited, are considered. ESA

N94-23421 Canadian Space Agency, Ottawa (Ontario).

SENSING AND MODELLING CONCEPTS FOR AUTONOMOUS AND REMOTE MOBILE ROBOT CONTROL c37

S. K. Yeung, W. S. McMath, D. Necsulescu (Ottawa Univ., Ontario.), and E. M. Petriu (Ottawa Univ., Ontario.) *In* CNES, Missions, Technologies, and Design of Planetary Mobile Vehicles Jan. 1993 p 473-482 (For primary document see N94-23373 06-91)
(Contracts DSS-9F011-2-0923; DSS-9F011-2-0976)
Copyright Avail: Issuing Activity (CEPADUES-Editions, 111, rue Nicolas-Vaquelin, 31100 Toulouse, France)

Sensing functions and modeling concepts for autonomous and remote mobile robot control in an unstructured environment are discussed. Sensing methods for robot position recovery, object recognition, and tactile teleoperator feedback are presented. ESA

N94-23422 British Aerospace Public Ltd. Co., Bristol (England).

TOWARDS REAL-TIME STEREOVISION SYSTEMS FOR PLANETARY MISSIONS c37

Stephen Maxwell Parkes *In* CNES, Missions, Technologies, and Design of Planetary Mobile Vehicles Jan. 1993 p 483-498 (For primary document see N94-23373 06-91)
(Contract ESTEC-8741/90/NL/JG(SC))
Copyright Avail: Issuing Activity (CEPADUES-Editions, 111, rue Nicolas-Vaquelin, 31100 Toulouse, France)

Stereovision algorithms applicable to planetary mobile vehicles are considered. Stereovision systems have an important role to play in planetary exploration from digital elevation modeling of planetary surfaces to navigation of semiautonomous vehicles and control of robotic manipulators. Real time stereovision systems require very high processing power which can only be met by a heterogeneous multiprocessor processing architecture. The current and future processing technologies are examined together with the constraints on space-based electronic systems. The integrated multiprocessor system being developed for digital signal and image processing applications is described. ESA

N94-23423 Dassault-Breguet Aviation, Saint Cloud (France).

A DTM-BASED PATH PLANNING METHOD FOR PLANETARY ROVERS c37

R. Morlans and A. Liegeois (Montpellier Univ., France.) *In* CNES, Missions, Technologies, and Design of Planetary Mobile Vehicles Jan. 1993 p 499-507 (For primary document see N94-23373 06-91)
Copyright Avail: Issuing Activity (CEPADUES-Editions, 111, rue Nicolas-Vaquelin, 31100 Toulouse, France)

Algorithms that automatically find the feasible routes for a mobile robot in a partially known three dimensional environment are proposed. The system is especially devised keeping in mind a planetary rover mission. Starting with a low resolution digital terrain model (DTM), relevant points (saddle points) of the relief are first automatically extracted and a connected network of traversable lines is constructed in a 'structuralist' way: the starting points for the algorithm are the saddle points; the criteria, taking into account the smoothness and the slope of the constructed line, are used to compute the network iteratively. Lines and points of this network are used as arcs and nodes to create a search graph on which an A(star) algorithm is applied to find the optimal route minimizing traveling time or energy while insuring safety. This edge constrained solution serves to initiate shortcut finding laws allowing the vehicle to cross the regions bounded by the lines of the network. The motion across each region is characterized by a cost function computed from the elevation data: mean slope roughness. Examples using a 1000 by 1000 pixel DTM are given. ESA

N94-23424 M2A Engineering, Paris (France).

BOND GRAPH MODELING, SIMULATION, AND REFLEX CONTROL OF THE MARS PLANETARY AUTOMATIC VEHICLE c37

Maher Amara, Jean Pierre Friconneau (Nutech, Saint-Quetin-en-Yvelines, France.), and Alain Micaelli (Commissariat a l'Energie Atomique, Fontenay-aux-Roses, France.) *In* CNES, Missions, Technologies, and Design of Planetary Mobile Vehicles Jan. 1993 p 509-529 (For primary document see N94-23373 06-91)

Copyright Avail: Issuing Activity (CEPADUES-Editions, 111, rue Nicolas-Vaquelin, 31100 Toulouse, France)

The bond graph modeling, simulation, and reflex control study of the Planetary Automatic Vehicle are considered. A simulator derived from a complete bond graph model of the vehicle is presented. This model includes both knowledge and representation models of the mechanical structure, the floor contact, and the Mars site. The MACSYMEN (French acronym for aided design method of multi-energetic systems) is used and applied to study the input-output power transfers. The reflex control is then considered. Controller architecture and locomotion specificity are described. A numerical stage highlights some interesting results of the robot and the controller capabilities. ESA

N94-23425* Jet Propulsion Lab., California Inst. of Tech., Pasadena.

MOBILITY ANALYSIS, SIMULATION, AND SCALE MODEL TESTING FOR THE DESIGN OF WHEELED PLANETARY ROVERS c37

Randel A. Lindemann and Howard J. Eisen *In* CNES, Missions, Technologies, and Design of Planetary Mobile Vehicles Jan. 1993 p 531-536 Sponsored by NASA, Washington (For primary document see N94-23373 06-91)

Copyright Avail: Issuing Activity (CEPADUES-Editions, 111, rue Nicolas-Vaquelin, 31100 Toulouse, France)

The use of computer based techniques to model and simulate wheeled rovers on rough natural terrains is considered. Physical models of a prototype vehicle can be used to test the correlation of the simulations in scaled testing. The computer approaches include a quasi-static planar or two dimensional analysis and design tool based on the traction necessary for the vehicle to have imminent mobility. The computer program modeled a six by six wheel drive vehicle of original kinematic configuration, called the Rocker Bogie. The Rocker Bogie was optimized using the quasi-static software with respect to its articulation parameters prior to fabrication of a prototype. In another approach used, the dynamics of the Rocker Bogie vehicle in 3-D space was modeled on an engineering workstation using commercial software. The model included the complex and nonlinear interaction of the tire and terrain. The results of the investigation yielded numerical and graphical results of the rover traversing rough terrain on the earth, moon, and Mars. In addition, animations of the rover excursions were also generated. A prototype vehicle was then used in a series of testbed and field experiments. Correspondence was then established between the computer models and the physical model. The results indicated the utility of the quasi-static tool for configurational design, as well as the predictive ability of the 3-D simulation to model the dynamic behavior of the vehicle over short traverses. ESA

N94-23426 Grenoble-1 Univ. (France). Inst. IMAG.

PHYSICAL MODELING AND DYNAMIC SIMULATION OF PLANET VEHICLES: APPLICATION TO THE MOTION PREDICTION c37

Annie Luciani, Stephane Jimenez, and Christian Laugier *In* CNES, Missions, Technologies, and Design of Planetary Mobile Vehicles Jan. 1993 p 537-544 Sponsored in part by CNES and Rhone-Alps Region SHARP Project (For primary document see N94-23373 06-91)

Copyright Avail: Issuing Activity (CEPADUES-Editions, 111, rue Nicolas-Vaquelin, 31100 Toulouse, France)

Physical modeling to predict and control the motions of a planetary rover is considered. The approach presented is not only to incorporate dynamic constraints into geometrical modeling and reasoning, but rather, to design a complete physical model of the entire system: the robot in its physical natural context. Futhermore, with this model, the aim is firstly to evaluate and predict the possible motions of the robot according to its physics, and secondly to assess the feasible plans, according to these motion capabilities. The principles of the physically based modeler simulator Cordis-Anima are introduced. Different physically based models of vehicles, terrains, and terrain-terrain or vehicle-terrain interactions are explained. Given these models, the incorporation of strategical data, provided by a planing stage, into this modeled physical world, is discussed. The two possible directions that have been opened by this approach, the execution model and gestural programming of a planetary vehicle, are pointed out. ESA

N94-23427* Jet Propulsion Lab., California Inst. of Tech., Pasadena.

EXPERIMENTS WITH A SMALL BEHAVIOUR CONTROLLED PLANETARY ROVER c37

David P. Miller, Rajiv S. Desai, Erann Gat, Robert Ivlev, and John Loch *In* CNES, Missions, Technologies, and Design of Planetary Mobile Vehicles Jan. 1993 p 545-551 Sponsored by NASA, Washington (For primary document see N94-23373 06-91)

Copyright Avail: Issuing Activity (CEPADUES-Editions, 111, rue Nicolas-Vaquelin, 31100 Toulouse, France)

A series of experiments that were performed on the Rocky 3 robot is described. Rocky 3 is a small autonomous rover capable of navigating through rough outdoor terrain to a predesignated area, searching that area for soft soil, acquiring a soil sample, and depositing the sample in a container at its home base. The robot is programmed according to a reactive behavior control paradigm using the ALFA programming language. This style of programming produces robust autonomous performance while requiring significantly less computational resources than more traditional mobile robot control systems. The code for Rocky 3 runs on an eight bit processor and uses about ten k of memory. ESA

N94-23469# Sandia National Labs., Albuquerque, NM.

LUNAR EXPLORATION ROVER PROGRAM DEVELOPMENTS

P. R. Klarer 1993 8 p Presented at the SOAR 1993: Space Operations, Applications, and Research Conference, Houston, TX, 3-5 Aug. 1993

(Contract DE-AC04-76DP-00789)

(DE93-040759; SAND-93-1420C; CONF-9308159-2) Avail: CASI HC A02/MF A01

The Robotic All Terrain Lunar Exploration Rover (RATLER) design concept began at Sandia National Laboratories in late 1991 with a series of small, proof-of-principle, working scale models. The models proved the viability of the concept for high mobility through mechanical simplicity, and eventually received internal funding at Sandia National Laboratories for full scale, proof-of-concept prototype development. Whereas the proof-of-principle models demonstrated the mechanical design's capabilities for mobility, the full scale proof-of-concept design currently under development is intended to support field operations for experiments in telerobotics, autonomous robotic operations, telerobotic field geology, and advanced man-machine interface concepts. The development program's current status is described, including an outline of the program's work over the past year, recent accomplishments, and plans for follow-on development work. DOE

N94-24058*# Lunar and Planetary Inst., Houston, TX. Space and Life Sciences Directorate.

CATALOG OF APOLLO 17 ROCKS. VOLUME 1: STATIONS 2 AND 3 (SOUTH MASSIF)

Graham Ryder Jan. 1993 379 p

(Contract NASw-4574)

(NASA-CR-194854; LPI-CONTRIB-805; NAS 1.26:194854) Avail: CASI HC A17/MF A03

The Catalog of Apollo 17 Rocks is a set of volumes that characterize each of 334 individually numbered rock samples (79 larger than 100 g) in the Apollo 17 collection, showing what each sample is and what is known about it. Unconsolidated regolith samples are not included. The catalog is intended to be used by both researchers requiring sample allocations and a broad audience interested in Apollo 17 rocks. The volumes are arranged geographically, with separate volumes for the South Massif and Light Mantle, the North Massif, and two volumes for the mare plains. Within each volume, the samples are arranged in numerical order, closely corresponding with the sample collection stations. The present volume, for the South Massif and Light Mantle, describes the 55 individual rock fragments collected at Stations two, two-A, three, and LRV-five. Some were chipped from boulders, others collected as individual rocks, some by raking, and a few by picking from the soil in the processing laboratory. Information on sample collection, petrography, chemistry, stable and radiogenic isotopes, rock surface characteristics, physical properties, and curatorial processing is summarized and referenced as far as it is known up to early 1992. The intention has been to be comprehensive: to include all published studies of any kind that provide information on the sample, as well as some unpublished information. References which are primarily bulk interpretations of existing data or mere lists of samples are not generally included. Foreign language journals were not scrutinized, but little data appears to have been published only in such journals. We have attempted to be consistent in format across all of the volumes, and have used a common reference list that appears in all volumes. Where possible, ages based on Sr and Ar isotopes have been recalculated using the 'new' decay constants recommended by Steiger and Jager; however, in many of the reproduced diagrams the ages correspond with the 'old' decay constants. In this volume, mg' or Mg' = atomic Mg/(Mg +Fe). Derived from text

N94-24328*# Massachusetts Inst. of Tech., Cambridge. Research Lab. of Electronics.
VOYAGER PLANETARY RADIO ASTRONOMY STUDIES Final Report, 1 May 1985 - 30 Jun. 1993
David H. Staelin and Stephen S. Eikenberry 23 Dec. 1993 32 p
(Grant NAG5-537)
(NASA-CR-194776; NAS 1.26:194776) Avail: CASI HC A03/MF A01

Analysis of nonthermal radio emission data obtained by the Planetary Radio Astronomy (PRA) spectrometers on the Voyager 1 and 2 spacecraft was performed. This PRA data provided unique insights into the radio emission characteristics of the outer planets because of PRA's unique spectral response below the terrestrial ionospheric plasma frequency and its unprecedented proximity to the source. Of those results which were documented or published, this final report surveys only the highlights and cites references for more complete discussions. Unpublished results for Uranus, Neptune, and theoretical Ionian current distributions are presented at greater length. The most important conclusion to be drawn from these observations is that banded spectral emission is common to the radio emission below 1-2 MHz observed from all four Jovian planets. In every case multiple spectral features evolve on time scales of seconds to minutes. To the extent these features drift in frequency, they appear never to cross one another. The Neptunian spectral features appear to drift little or not at all, their evolution consisting principally of waxing and waning. Since other evidence strongly suggests that most or all of this radio emission is occurring near the local magnetospheric electron cyclotron frequency, this implies that this emission preferentially occurs at certain continually changing planetary radii. It remains unknown why certain radii might be favored, unless radial electric field components or other means serve to differentiate radially the magnetospheric plasma density, particle energy vectors, or particle coherence. Calculation of the spatial distribution and intensity of the Io-generated magnetospheric currents are also presented; these currents may be limited principally by wave impedance and local field strengths. Author (revised)

N94-24333*# California Univ., Los Angeles. Mechanical, Aerospace and Nuclear Engineering Dept.
PLANETARY AND ASTEROID MISSIONS. GETTING THERE: ANCHORING SPACECRAFT TO ASTEROIDS Final Report, 1992-1993
Rudolf X. Meyer and Joseph P. Melko 26 Jun. 1993 18 p
(Contract NASw-4435)
(NASA-CR-195493; NAS 1.26:195493) Avail: CASI HC A03/MF A01

In this hardware project, the students developed ideas for attaching objects to the surface of small moons or asteroids. A device was designed, and built in the university machine shop, that uses a projectile shot into concrete, thereby attaching a model spacecraft to the landing site. Author (revised)

N94-24363*# South Carolina Univ., Columbia. Dept. of Geological Sciences.
BASALTIC VOLCANISM AND ANCIENT PLANETARY CRUSTS Final Technical Report, 1 Jun. 1986 - 31 May 1993
John W. Shervais 31 May 1993 123 p
(Grant NAG9-169)
(NASA-CR-193151; NAS 1.26:193151) Avail: CASI HC A06/MF A02

The purpose of this project is to decipher the origin of rocks which form the ancient lunar crust. Our goal is to better understand how the moon evolved chemically and, more generally, the processes involved in the chemical fractionation of terrestrial planetoids. This research has implications for other planetary bodies besides the Moon, especially smaller planetoids which evolved early in the history of the solar system and are now thermally stable. The three main areas focused on in our work (lunar mare basalts, KREEP basalts, and plutonic rocks of the lunar highlands) provide complementary information on the lunar interior and the processes that formed it. For individual titles, see N94-24364 through N94-24373.

N94-24364*# South Carolina Univ., Columbia. Dept. of Geological Sciences.
HIGHLAND CRUST AT THE APOLLO 14 SITE: A REVIEW
John W. Shervais *In its* Basaltic Volcanism and Ancient Planetary Crusts 31 May 1993 10 p (For primary document see N94-24363 06-91)
Avail: CASI HC A02/MF A02

Recent petrologic studies of pristine nonmare samples from the Apollo 14 site have demonstrated the unique character of the western highlands crust. Many of the lithologies which occur here are not found at other highland sites or represent unique variations of more common lithologies. Rare highland samples found at the Apollo 12 site have petrologic and geochemical affinities with the Apollo 14 highland suite and the two sites taken together constitute what can be called the Western Highland Province. Rocks of the Western Highland Province are geochemically distinct from similar lithologies found at eastern highland sites (Apollo 15, Apollo 16, Apollo 17, and the Luna sites) -- a fact which adds further complications to current petrogenetic models for the lunar crust. Nonetheless, an understanding of how the Western Highlands Province formed and why it differs from highland crust in the east is crucial to our overall understanding of primordial lunar differentiation and petrogenesis. Derived from text

N94-24365*# Centenary Coll. of Louisiana, Shreveport. Dept. of Geology.
WHOLE ROCK MAJOR ELEMENT CHEMISTRY OF KREEP BASALT CLASTS IN LUNAR BRECCIA 15205: IMPLICATIONS FOR THE PETROGENESIS OF VOLCANIC KREEP BASALTS
Scott K. Vetter and John W. Shervais (South Carolina Univ., Columbia.) *In* South Carolina Univ., Basaltic Volcanism and Ancient Planetary Crusts 31 May 1993 4 p (For primary document see N94-24363 06-91)
Avail: CASI HC A01/MF A02

KREEP basalts are a major component of soils and regolith at the Apollo 15 site. Their origin is controversial: both endogenous (volcanic) and exogenous (impact melt) processes have been proposed, but it is now generally agreed that KREEP basalts are volcanic rocks derived from the nearby Apennine Bench formation. Because most pristine KREEP basalts are found only as small clasts in polymict lunar breccias, reliable chemical data are scarce. The primary aim of this study is to characterize the range in chemical composition of pristine KREEP basalt, and to use these data to decipher the petrogenesis of these unique volcanic rocks. Derived from text

N94-24366*# South Carolina Univ., Columbia. Dept. of Geological Sciences.
MAJOR ELEMENT CHEMISTRY OF APOLLO 14 MARE BASALT CLASTS AND HIGHLAND PLUTONIC CLASTS FROM LUNAR BRECCIA 14321: COMPARISON WITH NEUTRON ACTIVATION RESULTS
John W. Shervais and Scott K. Vetter (Centenary Coll. of Louisiana, Shreveport.) *In its* Basaltic Volcanism and Ancient Planetary Crusts 31 May 1993 2 p (For primary document see N94-24363 06-91)
Avail: CASI HC A01/MF A02

Studies of lithic components in lunar breccias have documented a wide variety of rock types and magma suites which are not found among large, discrete lunar samples. Rock types found exclusively or dominantly as clasts in breccias include KREEP basalts, VHK mare basalts, high-alumina mare basalts, olivine vitrophyres, alkali anorthosites, and magnesian anorthosites and troctolites. These miniature samples are crucial in petrogenetic studies of ancient mare basalts and the highlands crust of the western nearside, both of which have been battered by basin-forming impacts and no longer exist as distinct rock units. Derived from text

N94-24367*# South Carolina Univ., Columbia. Dept. of Geological Sciences.

AUTO-METASOMATISM OF THE WESTERN LUNAR HIGHLANDS: RESULT OF CLOSED SYSTEM FRACTIONATION AND MOBILIZATION OF A KREEPy TRAPPED LIQUID

John W. Shervais and Scott K. Vetter (Centenary Coll. of Louisiana, Shreveport.) *In its* Basaltic Volcanism and Ancient Planetary Crusts 31 May 1993 4 p (For primary document see N94-24363 06-91)
Avail: CASI HC A01/MF A02

The discovery of REE-rich phosphates (dominantly whitlockite) in pristine, non-mare rocks of the western lunar nearside (Apollo 14, Apollo 12, and most recently, Apollo 17) has created a paradox for lunar petrologists. These phases are found in feldspar-rich cumulates of both the Mg-suite and the Alkali suite, which differ significantly in their mineral chemistries and major element compositions. Despite the differences in host rock compositions, whitlockites in both suites have similar compositions, with LREE concentrations around 21,000 to 37,000 x chondrite. Simple modeling of possible parent magma compositions using the experimental whitlockite/liquid partition coefficients of Dickinson and Hess show that these REE concentrations are too high to form from normal lunar magmas, even those characterized as 'urKREEP.' Derived from text

N94-24368*# South Carolina Univ., Columbia. Dept. of Geological Sciences.

POLYTOPIC VECTOR ANALYSIS IN IGNEOUS PETROLOGY: APPLICATION TO LUNAR PETROGENESIS

John W. Shervais and R. Ehrlich *In its* Basaltic Volcanism and Ancient Planetary Crusts 31 May 1993 2 p (For primary document see N94-24363 06-91)
Avail: CASI HC A01/MF A02

Lunar samples represent a heterogeneous assemblage of rocks with complex inter-relationships that are difficult to decipher using standard petrogenetic approaches. These inter-relationships reflect several distinct petrogenetic trends as well as thermomechanical mixing of distinct components. Additional complications arise from the unequal quality of chemical analyses and from the fact that many samples (e.g., breccia clasts) are too small to be representative of the system from which they derived. Polytopic vector analysis (PVA) is a multi-variate procedure used as a tool for exploratory data analysis. PVA allows the analyst to classify samples and clarifies relationships among heterogenous samples with complex petrogenetic histories. It differs from orthogonal factor analysis in that it uses non-orthogonal multivariate sample vectors to extract sample endmember compositions. The output from a Q-mode (sample based) factor analysis is the initial step in PVA. The Q-mode analysis, using criteria established by Miesch and Klovan and Miesch, is used to determine the number of endmembers in the data system. The second step involves determination of endmembers and mixing proportions with all output expressed in the same geochemical variable as the input. The composition of endmembers is derived by analysis of the variability of the data set. Endmembers need not be present in the data set, nor is it necessary for their composition to be known a priori. A set of any endmembers defines a 'polytope' or classification figure (triangle for a three component system, tetrahedron for a four component system, a 'five-tope' in four dimensions for five component system, et cetera). Derived from text

N94-24369*# South Carolina Univ., Columbia. Dept. of Geological Sciences.

THE WESTERN HIGHLAND PROVINCE AT THE APOLLO 14 SITE

John W. Shervais *In its* Basaltic Volcanism and Ancient Planetary Crusts 31 May 1993 2 p (For primary document see N94-24363 06-91)
Avail: CASI HC A01/MF A02

Recent petrologic studies of pristine nonmare samples from the Apollo 14 site have demonstrated the unique character of the western highlands crust. Many of the lithologies which occur here are not found at other highland sites or represent unique variations of more common lithologies. Rare highland samples found at the Apollo 12 site have petrologic and geochemical affinities with the Apollo 14 highland suite, and the two sites taken together constitute what can be called the Western Highland Province. Rocks of the Western Highland Province are geochemically distinct from similar lithologies found at eastern highland sites (Apollo 15, Apollo 16, Apollo 17, and the Luna sites)--a fact which adds further complications to current petrogenetic models for the lunar crust. Nonetheless, and understanding of how the Western Highlands Province formed and why it differs from highland crust in the east is crucial to our overall understanding of primordial lunar differentiation and petrogenesis. Derived from text

N94-24370*# South Carolina Univ., Columbia. Dept. of Geological Sciences.

LUNAR MARE VOLCANISM: MIXING OF DISTINCT, MANTLE SOURCE REGIONS WITH KREEP-LIKE COMPONENT

John W. Shervais and Scott K. Vetter *In its* Basaltic Volcanism and Ancient Planetary Crusts 31 May 1993 2 p (For primary document see N94-24363 06-91)
Avail: CASI HC A01/MF A02

Mare basalts comprise less than 1% of the lunar crust, but they constitute our primary source of information on the moon's upper mantle. Compositional variations between mare basalt suites reflect variations in the mineralogical and geochemical composition of the lunar mantle which formed during early lunar differentiation (4.5-4.4 AE). Three broad suites of mare basalt are recognized: very low-Ti (VLT) basalts with TiO2 less than 1 wt%, low-Ti basalts with TiO2 = 2-4 wt%, and high-Ti basalts with TiO2 = 10-14 wt%. Important subgroups include the Apollo 12 ilmenite basalts (TiO2 = 5-6 wt%), aluminous low-Ti mare basalts (TiO2 = 2-4 wt%, Al2O3 = 10-14 wt%), and the newly discovered Very High potassium (VHK) aluminous low-Ti basalts, with K2O = 0.4-1.5 wt%. The mare basalt source region has geochemical characteristics complementary to the highlands crust and is generally thought to consist of mafic cumulates from the magma ocean which formed the felsic crust by feldspar flotation. The progressive enrichment of mare basalts in Fe/Mg, alkalis, and incompatible trace elements in the sequence VLT basalt yields low-Ti basalt yields high-Ti basalt is explained by the remelting of mafic cumulates formed at progressively shallower depths in the evolving magma ocean. This model is also consistent with the observed decrease in compatible element concentrations and the progressive increase in negative Eu anomalies. Derived from text

N94-24371*# South Carolina Univ., Columbia. Dept. of Geological Sciences.

A DYNAMIC MELTING MODEL FOR THE ORIGIN OF APOLLO 15 OLIVINE-NORMATIVE AND QUARTZ-NORMATIVE MARE BASALTS

Scott K. Vetter and John W. Shervais *In its* Basaltic Volcanism and Ancient Planetary Crusts 31 May 1993 2 p (For primary document see N94-24363 06-91)
Avail: CASI HC A01/MF A02

Early studies of mare basalts from the Apollo 15 site established that two distinct groups are represented: the olivine-normative basalts (ONB) and the quartz-normative basalts (QNB). The ONB and QNB suites are distinguished petrographically by their phenocryst assemblages (the ONB's are olivine-phyric, the QNB's are generally pyroxene-phyric) and chemically by their major element compositions: the QNB's are higher in SiO2 and MgO/FeO, and lower in FeO and TiO2 than ONB's with similar MgO contents. Experimental data show that the QNB suite is derived from a more magnesian, olivine-normative parent magma, a conclusion which is supported by the recent discovery of high-SiO2 olivine-normative basalt clasts in breccia 15498. The high-SiO2 ONB's fall on olivine control lines with primitive QNB's, and least-squares mixing calculations are consistent with the high-SiO2 ONB's being parantal to the more evolved QNB suite. These high-SiO2 ONB's are included as part of the 'QNB suite'. Our major element modeling results also are consistent with the conclusions of earlier studies which showed that the ONB and QNB suites cannot be related to one another by low pressure crystal fractionation. The combination of high Mg#, high SiO2, and low TiO2 in the QNB suite precludes a relationship to the ONB suite by simple removal of liquidus minerals (olivine and pigeonite). Despite these significant differences in petrography and major element composition, both groups have nearly identical trace element concentrations and chondrite-normalized abundance patterns. The major question to be addressed by any petrogenetic model for Apollo 15 mare basalts is how to form mare basalt suites with distinctly different major element characteristics but nearly identical trace element compositions. The similarity in trace element concentrations imply compositionally similar source regions and similar percent melting, but these conclusions are not easily reconciled with the observed differences in major element compositions, which require sources with distinct mineralogies or large differences in percent melt. Derived from text

N94-24372*# South Carolina Univ., Columbia. Dept. of Geological Sciences.

MELT ROCK COMPONENTS IN KREEPy BRECCIA 15205: PETROGRAPHY AND MINERAL CHEMISTRY OF KREEP BASALTS AND QUARTZ-NORMATIVE MARE BASALTS

John W. Shervais and Scott K. Vetter *In its* Basaltic Volcanism and Ancient Planetary Crusts 31 May 1993 2 p (For primary document see N94-24363 06-91)
Avail: CASI HC A01/MF A02

Many current models for the origin of lunar highland rocks feature as an essential component the assimilation of KREEPy material by primitive magmas parental to the Mg-rich suite and alkali suite plutonic rocks. Similar models have also been proposed for the origin of various mare basalt suites. However, any model which considers assimilation of KREEP an important petrologic process must sooner-or-later deal with the question: what is KREEP? Because pristine KREEP basalts are rare, and most known samples are small (e.g., 15382/15386), the geochemical variability of KREEP basalts is poorly known. Other KREEP compositions which are commonly used in these models include the hypothetical 'high-K KREEP' component of Warren and Wasson, which is derived from Apollo 14 soil data, and the 'superKREEP' quartz-monzodiorite 15405. Lunar breccia 15205 is a polymict regolith breccia that consists of approximately 20% KREEP basalt clasts and 20% quartz-normative basalt clasts in a KREEP-rich matrix. Bulk rock mixing calculations show that this sample comprises about 84% KREEP. The clasts range up to 1 cm in size, but most are considerably smaller. The primary aim is to characterize pristine KREEP basalts petrographically, to establish the range in chemical compositions of KREEP basalts, and to test models that were proposed for their origin. In addition, we may be able to extend the compositional range recognized in the quartz-normative basalt suite and cast some light on its origin as well. Preliminary whole rock geochemical data on the KREEP basalts are presented in a companion paper by M.M. Lindstrom and co-workers. Concentration is on petrography and mineral chemistry of these clasts, and the implications these data have for the origin of the different melt rock suites. Derived from text

N94-24373*# National Aeronautics and Space Administration. Lyndon B. Johnson Space Center, Houston, TX.

HETEROGENEITY IN SMALL ALIQUOTS OF APOLLLO 15 OLIVINE-NORMATIVE BASALT: IMPLICATIONS FOR BRECCIA CLAST STUDIES

Marilyn M. Lindstrom, John W. Shervais (South Carolina Univ., Columbia.), and Scott K. Vetter (South Carolina Univ., Columbia.) *In* South Carolina Univ., Basaltic Volcanism and Ancient Planetary Crusts 31 May 1993 2 p (For primary document see N94-24363 06-91)
Avail: CASI HC A01/MF A02

Most of the recent advances in lunar petrology are the direct result of breccia pull-apart studies, which have identified a wide array of new highland and mare basalt rock types that occur only as clasts within the breccias. These rocks show that the lunar crust is far more complex than suspected previously, and that processes such as magma mixing and wall-rock assimilation were important in its petrogenesis. These studies are based on the implicit assumption that the breccia clasts, which range in size from a few mm to several cm across, are representative of the parent rock from which they were derived. In many cases, the aliquot allocated for analysis may be only a few grain diameters across. While this problem is most acute for coarse-grained highland rocks, it can also cause considerable uncertainty in the analysis of mare basalt clasts. Similar problems arise with small aliquots of individual hand samples. Our study of sample heterogeneity in 9 samples of Apollo 15 olivine normative basalt (ONB) which exhibit a range in average grain size from coarse to fine are reported. Seven of these samples have not been analyzed previously, one has been analyzed by INAA only, and one has been analyzed by XRF+INAA. Our goal is to assess the effects of small aliquot size on the bulk chemistry of large mare basalt samples, and to extend this assessment to analyses of small breccia clasts. Derived from text

N94-24871*# Lunar and Planetary Inst., Houston, TX.

WORKSHOP ON ATMOSPHERIC TRANSPORT ON MARS

J. R. Barnes, ed. and R. M. Haberle, ed. 1993 52 p Workshop held in Corvallis, OR, 28-30 Jun. 1993; sponsored by Oregon State Univ. and Oregon Space Grant Consortium
(Contract NASw-4574)
(NASA-CR-194855; NAS 1.26:194855; LPI-TR-93-05) Avail: CASI HC A04/MF A01

On June 28-30, 1993, the Workshop on Atmospheric Transport on Mars was held in Corvallis, Oregon. The workshop was organized under the auspices of the MSATT (Mars Surface and Atmosphere Through Time) Program of NASA, and was jointly sponsored by the Lunar and Planetary Institute, Oregon State University, and the Oregon Space Grant Consortium. More than 50 scientists attended the workshop, which was the first such meeting to focus upon circulation processes in the Mars atmosphere. The timing of the workshop placed it almost on the eve of the arrival of Mars Observer at Mars, so that the presented papers gave a picture of the 'state of the art' in Mars atmospheric science just prior to the expected arrival of new data. The workshop highlighted a host of recent advances in atmospheric modeling and analysis - advances that will be relevant to any future observations. For individual titles, see N94-24872 through N94-24904.

N94-24872*# National Aeronautics and Space Administration. Goddard Inst. for Space Studies, New York, NY.

THE NASA/GISS MARS GENERAL CIRCULATION MODEL: PRELIMINARY EXPERIMENTS Abstract Only

Michael Allison, M. A. Chandler (University Corp. for Atmospheric Research, Boulder, CO.), A. D. DelGenio, A. Lacis, D. Rind, W. B. Rossow, L. D. Travis, and W. Zhou (Hughes STX, Inc., Greenbelt, MD.) *In* Lunar and Planetary Inst., Workshop on Atmospheric Transport on Mars 1993 p 5 (For primary document see N94-24871 06-91)
Avail: CASI HC A01/MF A01

The NASA/GISS Mars General Circulation Model (GCM) is an adapted version of the GISS Global Climate/Middle Atmosphere Model, specifically developed for the diagnostic validation and objective analysis of measured atmospheric temperatures from the Mars Observer Pressure Modulator Infrared Radiometer (PMIRR) experiment. The GISS Mars GCM has 23 vertical layers extending from the surface to approximately 80 km altitude, representing a vertical resolution of about 0.3 scale heights. The primitive (vertically hydrostatic) equations are solved in finite difference form on the Krakawa B grid, with a horizontal resolution of 8 deg x 10 deg (latitude-longitude). The model includes a diurnal solar cycle, heat transport within a two-layer ground, and a high-order 'slopes-scheme' for the advection of heat in the upper atmosphere. The radiative transfer scheme is based on the correlated k distribution method for the treatment of nongray gaseous absorption thermal emission, and multiple scattering, including options for suspended dust. A special feature of the model of particular importance for Mars is a parameterization of gravity-wave-induced drag incorporating orographic forcing, wind shear, convection, and radiative damping. The implementation of the GISS Mars model includes global maps of topography, roughness, and albedo. Derived from text

N94-24873*# California Inst. of Tech., Pasadena.

OPTIMAL GAINS FOR A SINGLE POLAR ORBITING SATELLITE Abstract Only c18

Don Banfield, A. P. Ingersoll, and C. L. Keppenne (Jet Propulsion Lab., California Inst. of Tech., Pasadena.) *In* Lunar and Planetary Inst., Workshop on Atmospheric Transport on Mars 1993 p 5-6 (For primary document see N94-24871 06-91)
Avail: CASI HC A01/MF A01

Gains are the spatial weighting of an observation in its neighborhood versus the local values of a model prediction. They are the key to data assimilation, as they are the direct measure of how the data are used to guide the model. As derived in the broad context of data assimilation by Kalman and in the context of meteorology, for example, by Rutherford, the optimal gains are functions of the prediction error covariances between the observation and analysis points. Kalman introduced a very powerful technique that allows one to calculate these optimal gains at the time of each observation. Unfortunately, this technique is both computationally expensive and often numerically unstable for dynamical systems of the magnitude of meteorological models, and thus is unsuited for use in PMIRR data assimilation. However, the optimal gains as calculated by a Kalman filter do reach a steady state for regular observing patterns like that of a satellite. In this steady state, the gains are constants in time, and thus could conceivably be computed off-line. These steady-state Kalman gains (i.e., Wiener gains) would yield optimal performance without the computational burden of true Kalman filtering. We proposed to use this type of constant-in-time Wiener gain for the assimilation of data from PMIRR and Mars Observer. Derived from text

N94-24874*# Oregon State Univ., Corvallis. Dept. of Atmospheric Science.

A DIAGNOSTIC MODEL TO ESTIMATE WINDS AND SMALL-SCALE DRAG FROM MARS OBSERVER PMIRR DATA Abstract Only

J. R. Barnes *In* Lunar and Planetary Inst., Workshop on Atmospheric Transport on Mars 1993 p 6 (For primary document see N94-24871 06-91)

Avail: CASI HC A01/MF A01

Theoretical and modeling studies indicate that small-scale drag due to breaking gravity waves is likely to be of considerable importance for the circulation in the middle atmospheric region (approximately 40-100 km altitude) on Mars. Recent earth-based spectroscopic observations have provided evidence for the existence of circulation features, in particular, a warm winter polar region, associated with gravity wave drag. Since the Mars Observer PMIRR experiment will obtain temperature profiles extending from the surface up to about 80 km altitude, it will be extensively sampling middle atmospheric regions in which gravity wave drag may play a dominant role. Estimating the drag then becomes crucial to the estimation of the atmospheric winds from the PMIRR-observed temperatures. An interative diagnostic model based upon one previously developed and tested with earth satellite temperature data will be applied to the PMIRR measurements to produce estimates of the small-scale zonal drag and three-dimensional wind fields in the Mars middle atmosphere. This model is based on the primitive equations, and can allow for time dependence (the time tendencies used may be based upon those computed in a Fast Fourier Mapping procedure). The small-scale zonal drag is estimated as the residual in the zonal momentum equation; the horizontal winds having first been estimated from the meridional momentum equation and the continuity equation. The scheme estimates the vertical motions from the thermodynamic equation, and thus needs estimates of the diabatic heating based upon the observed temperatures. The latter will be generated using a radiative model. It is hoped that the diagnostic scheme will be able to produce good estimates of the zonal gravity wave drag in the Mars middle atmosphere, estimates that can then be used in other diagnostic or assimilation efforts, as well as more theoretical studies. Author (revised)

N94-24875*# Oregon State Univ., Corvallis. Dept. of Atmospheric Science.

EDDY MIXING COEFFICIENT VALUES DERIVED FROM SIMULATIONS WITH THE NASA AMES MARS GCM Abstract Only

J. R. Barnes and Thomas D. Walsh *In* Lunar and Planetary Inst., Workshop on Atmospheric Transport on Mars 1993 p 6-7 (For primary document see N94-24871 06-91)

Avail: CASI HC A01/MF A01

Values of eddy mixing coefficients, especially that for vertical mixing, are of particular importance for various photochemical models of the Mars atmosphere, which are either globally or zonally averaged. These models represent atmospheric transport processes in terms of eddy diffusion. While this is not appropriate for the advective transport by the mean meridional circulation (in general, a part of the eddy diffusion tensor actually does represent advection--a 'correction' to the Eulerian-mean circulation), it can be applied to simulate both the small- and larger-scale eddy transports of an atmospheric constituent. An effort is underway to estimate values of the eddy mixing coefficients for the Mars atmosphere using circulation data generated with the NASA Ames Mars GCM. This model simulates the three-dimensional winds in the atmosphere, and these are then used as inputs for a tracer transport model. The latter model has previously been used in interactive dust transport experiments with the Ames GCM. Idealized tracer transport experiments, with a conservative or nearly conservative hypothetical tracer, are performed to generate data from which the eddy diffusion coefficients can be estimated. Carrying out matched pairs of tracer experiments, using two very different initial states, permits all four components of the diffusion tensor to be determined. A large number of GCM experiments have been conducted, spanning a range of seasons and atmospheric dust loading, allowing the eddy mixing coefficients to be estimated for a variety of atmospheric conditions. Author (revised)

N94-24876*# Arizona Univ., Tucson. Lunar and Planetary Lab.

MARS DUST-DRIVEN TIDES AND THEIR IMPACT ON THE THERMOSPHERE Abstract Only

Stephen W. Bougher and Richard W. Zurek (Jet Propulsion Lab., California Inst. of Tech., Pasadena.) *In* Lunar and Planetary Inst., Workshop on Atmospheric Transport on Mars 1993 p 7-9 (For primary document see N94-24871 06-91)

Avail: CASI HC A01/MF A01

It has been known since the early Mariner 6, 7, and 9 missions that dust loading of the lower atmosphere and the subsequent aerosol heating during dusty periods impacts the martian middle and upper atmospheres. A quantitative measure of this lower atmosphere forcing was obtained by the Viking 1 and 2 landers, from which observed amplitudes of semidiurnal surface-pressure oscillations were correlated with normal-incidence dust optical depths. It appears that the dominant semidiurnal mode is a good indicator of global dust content or mean dust optical depth, especially during dust storm events. A classical tidal model that reproduces the surface pressure oscillations measured by these Viking landers in 1977 was used to calculate tidal amplitudes and phases up to approximately 43 km. These tidal characteristics were calculated for various dust optical depth conditions ranging from typical dusty periods to global dust storm times. Reasonable extrapolations can be made to higher altitudes if one assumes that the vertically propagating tidal modes continue to grow without dissipation or breaking. It is very likely that gravity waves also play an important role in the structure and dynamics of the middle atmosphere of Mars, since the large topographical relief should produce vigorous gravity wave fluxes. Semidiurnal tidal modes, significantly enhanced by lower atmosphere dust-induced heating, may indeed propagate to the Mars thermosphere (approximately less than 100 km) before breaking and generating turbulence. The preferential enhancement of the semidiurnal tides during dust storm onset is primarily due to the elevation of the tidal heating source in a very dusty atmosphere. The (2,2) semidiurnal tidal tidal mode was shown to have the largest variation with dust optical depth, as measured by Viking lander instruments. Also, the (2,2) mode has the largest vertical wavelength of all the semidiurnal tidal modes, and thus is most likely to penetrate into the thermosphere before breaking and to modify the largely in situ solar-driven behavior otherwise expected. The tides may also be partially responsible for determining the height of the martian homopause (approximately 125 km). Derived from text

N94-24877*# Centre National de la Recherche Scientifique, Verrieres-Le Buisson (France). Service d'Aeronomie.

CLOUD, DUST, AND OZONE VERTICAL PROFILES FROM SOLAR OCCULTATION MEASUREMENTS: IMPLICATIONS FOR DYNAMICS Abstract Only

E. Chassefiere (Observatoire de Paris-Meudon, France.) and J. E. Blamont *In* Lunar and Planetary Inst., Workshop on Atmospheric Transport on Mars 1993 p 9-10 (For primary document see N94-24871 06-91)

Avail: CASI HC A01/MF A01

An instrument was designed for solar occultation measurements of the martian atmosphere from the Phobos spacecraft. It was composed of three different dispersive systems working in the ultraviolet (UV: 0.22-0.32 microns) for the measurement of O3 and aerosols, in the near infrared (NIR: 0.76 microns, 0.94 microns) for the detection of O2 and H2O, and in the infrared (IR: 1.9 microns, 3.7 microns) where CO2 and H2O were measured. A detailed description of the instrument may be found in the special issue of Nature. Its principle objective is to measure from the Phobos orbit the spectrum of the Sun, modified by atmospheric extinction, during sunset. The UV-NIR spot has an angular diameter of 1 arcmin, or approximately 3 km vertical resolution, and is located near the center of the solar disk. The IR field is about twice as large and its line of sight is shifted by 8.5 arcmin, or approximately 20 km, relative to the previous one. It is therefore located near the edge of the solar disk. Sampling times are generally 0.5, 1, and 2 s for IR, UV, and NIR channels respectively, corresponding to vertical excursions of the line of sight of 1, 2, and 4 km respectively under nominal conditions. The instrument operated from February 8 to March 26 (the martian equinox occurred on February 17). The latitude of the intersection of the Sun-spacecraft axis with the surface of Mars varied from -11 to +20, the seasonal date L(sub s) being in the range 0 - 20. All measurements were therefore made near northern spring equinox in equatorial regions. Due to an error in the pointing system, only partial results were obtained, the region below approximately equals 30 km altitude being never sounded by the UV-NIR spectrometer. On the contrary, nine complete occultations were obtained in the IR channels, whose line of sight was fortunately approximately equals 20 km below the UV-NIR axis. Author (revised)

N94-24878*# Colorado Univ., Boulder. Lab. for Atmospheric and Space Physics.

PARTICLE SIZES AND COMPOSITION OF MARS ATMOSPHERIC DUST BASED UPON VIKING AND MARINER 9 OBSERVATIONS Abstract Only

R. T. Clancy, S. W. Lee, and G. R. Gladstone (Southwest Research Inst., San Antonio, TX.) *In* Lunar and Planetary Inst., Workshop on Atmospheric Transport on Mars 1993 p 10-11 (For primary document see N94-24871 06-91)

Avail: CASI HC A01/MF A01

Mars atmospheric dust can play an important role in the thermal structure of the Mars atmosphere during periods of high dust loading. However, the radiative properties of Mars atmospheric dust remain uncertain due to uncertain definitions of the dust composition and size distribution. The analysis by Toon et al., of Mariner 9 IRIS spectra during the 1971-1972 global dust storm indicated a reasonable match between the modeled 9-micron absorption of montmorillinite and the observed 9-micron absorption. Toon et al. also determined that an effective (cross-section weighted) mean radius of 2.5 microns (R(sub mode) = 0.4 microns) provided a consistent fit of montmorillinite to the IRIS dust spectra at 9 microns. Pollack et al. analyzed Viking lander observations of atmospheric extinction and scattering at visible-near IR wavelengths (0.5-1.0 microns), and obtained consistency with the Toon et al. dust size distribution when the effects of nonspherical particle shapes were included. An additional, minor (1 percent) component of visible-ultraviolet absorbing material was required to model the derived visible (0.86) and ultraviolet (0.4-0.6) single-scattering albedos of the dust, since montmorillinite does not absorb sufficiently in this wavelength region. A combined analysis of the Viking IRTM and Mariner 9 observations was conducted to reassess the model of Mars atmospheric ultraviolet-to-infrared measurements of dust absorption and scattering. The optical constants for palagonite are incorporated in a doubling-adding radiative transfer model of the Mars atmosphere to simulate Mariner 9 IRIS spectra as well as the Viking IRTM IR band observations. Visible and ultraviolet single-scattering albedos based on the Hansen and Travis Mie scattering code were also derived. A tentative conclusion is that smaller dust particles (R(sub mode) = 0.15 microns, cross-section weighted mean R = 1.2 microns) composed of palagonite provide a much improved fit to the Mariner 9 IRIS spectra; agreement with the observed ratio of visible-to-infrared extinction opacities; and ultraviolet and visible single-scattering albedos comparable to their observed values. Author (revised)

N94-24879*# Reading Univ. (England). Dept. of Meteorology.

ASPECTS OF THE MARTIAN GLOBAL CIRCULATION Abstract Only

Michael Collins and I. N. James *In* Lunar and Planetary Inst., Workshop on Atmospheric Transport on Mars 1993 p 11-13 (For primary document see N94-24871 06-91)

Avail: CASI HC A01/MF A01

Recent advances in high-speed computers have given atmospheric scientists a new laboratory in which to work. Numerical models of the Earth's atmosphere and its dynamics have provided great insight. Given the lack of observations of the martian atmosphere it is natural to apply such models to help us understand aspects of, for instance, large-scale circulation patterns. A global circulation model of the Earth's atmosphere was modified for use with martian parameters and the relevant regimes of planetary flow were studied. Author (revised)

N94-24880*# National Aeronautics and Space Administration. Ames Research Center, Moffett Field, CA.

IMPACT OF THE CO2 AND H2O CLOUDS OF THE MARTIAN POLAR HOOD ON THE POLAR ENERGY BALANCE Abstract Only

Francois Forget and James B. Pollack *In* Lunar and Planetary Inst., Workshop on Atmospheric Transport on Mars 1993 p 13-14 (For primary document see N94-24871 06-91)

Avail: CASI HC A01/MF A01

Clouds covering extensive areas above the martian polar caps have regularly been observed during the fall and winter seasons of each hemisphere. These 'polar hoods' are thought to be made of H2O and CO2. In particular, the very cold temperatures observed during the polar night by Viking and Mariner 9 around both poles have been identified as CO2 clouds and several models, including GCM, have indicated that the CO2 can condense in the atmosphere at all polar latitudes. Estimating the impact of the polar hood clouds on the energy balance of the polar regions is necessary to model the CO2 cycle and address puzzling problems like the polar caps assymetry. For example, by altering the thermal radiation emitted to space, CO2 clouds alter the amount of CO2 that condenses during the fall and winter season. The complete set of Viking IRTM data was analyzed to define the spatial and temporal properties of the polar hoods, and how their presence affects the energy radiated by the atmosphere/caps system to space was estimated. The IRTM observations provide good spatial and temporal converage of both polar regions during fall, winter, and spring, when a combination of the first and the second Viking year is used. Only the IRTM brightness temperatures at 11, 15, and 20 microns are reliable at martian polar temperatures. To recover the integrated thermal fluxes from the IRTM data, a simple model of the polar hood, thought to consist of 'warm' H2O clouds lying above colder and opaque CO2 clouds was developed. Such a model is based on the analysis of the IRIS spectra, and is consistent with the IRTM data used. Author (revised)

N94-24881*# National Aeronautics and Space Administration. Ames Research Center, Moffett Field, CA.

MULTIANNUAL SIMULATIONS WITH THE MARS CLIMATE MODEL Abstract Only

R. M. Haberle, Howard C. Houben (Space Physics Research Inst., Sunnyvale, CA.), and R. E. Young *In* Lunar and Planetary Inst., Workshop on Atmospheric Transport on Mars 1993 p 14 (For primary document see N94-24871 06-91)

Avail: CASI HC A01/MF A01

The martian atmospheric circulaton for 10 Mars years was simulated using a simplified three-dimensional climate model that is briefly described below. Analysis of these simulations reveals several interesting behaviors not previously recognized in other three-dimensional models. The first concerns the potential for interannual variability in the martian climate system. It is now known from the aperiodic frequency of planet-encircling storms, as well as differences in atmospheric water vapor from one year to the next, that the real planet exhibits interannual variations. The results of our simulations also show significant interannual variability and, interestingly, that variability maximizes during southern spring, the dust storm season. A second and related finding is that transient eddies in the southern hemisphere during winter are indeed weaker than their northern hemisphere counterparts as was found in more sophisticated models. However, southern hemisphere eddy activity rises dramatically during spring and is greater than that in the northern hemisphere at any season. Author (revised)

N94-24882*# National Aeronautics and Space Administration. Ames Research Center, Moffett Field, CA.

REGARDING TRACER TRANSPORT IN MARS' WINTER ATMOSPHERE IN THE PRESENCE OF NEARLY STATIONARY, FORCED PLANETARY WAVES Abstract Only

Jeffrey L. Hollingsworth, R. M. Haberle, and Howard C. Houben (Space Physics Research Inst., Sunnyvale, CA.) *In* Lunar and Planetary Inst., Workshop on Atmospheric Transport on Mars 1993 p 14-15 (For primary document see N94-24871 06-91)

Avail: CASI HC A01/MF A01

Large-scale transport of volatiles and condensates on Mars, as well as atmospheric dust, is ultimately driven by the planet's global-scale atmospheric circulation. This circulation arises in part from the so-called mean meridional (Hadley) circulation that is associated with rising/poleward motion in low latitudes and sinking/equatorward motion in middle and high latitudes. Intimately connected to the mean circulation is an eddy-driven component due to large-scale wave activity in the planet's atmosphere. During winter this wave activity arises both from traveling weather systems (i.e., barotropic and baroclinic disturbances) and from 'forced' disturbances (e.g., the thermal tides and surface-forced planetary waves). Possible contributions to the effective (net) transport circulation from forced planetary waves are investigated. Author (revised)

N94-24883*# Space Physics Research Inst., Sunnyvale, CA.
ANALYZING MARTIAN WINDS AND TRACER CONCENTRATIONS USING MARS OBSERVER DATA Abstract Only
Howard C. Houben *In* Lunar and Planetary Inst., Workshop on Atmospheric Transport on Mars 1993 p 15-16 (For primary document see N94-24871 06-91)
Avail: CASI HC A01/MF A01

During the courses of a day, the Mars Observer spacecraft will acquire globally distributed profiles of the martian atmosphere. It is highly desirable that this data be assembled into synoptic weather maps (complete specifications of the atmospheric pressure, temperature, and winds at a given time), which can in turn be used as starting points in the study of many meteorological phenomena. Unfortunately, the special nature of the Mars Observer data presents several challenges above and beyond the usual difficult problem of data initialization. Mars Observer atmospheric data will consist almost exclusively of asynoptic vertical profiles of temperatures (or radiances) and pressures, whereas winds are generally in balance with horizontal gradients of these quantities (which will not be observed). It will therefore be necessary to resort to dynamical models to analyze the wind fields. As a rule, data assimilation into atmospheric models can result in the generation of spurious gravity waves, so special steps must be taken to suppress these. In addition, the asynoptic nature of the data will require a four-dimensional (space and time) data assimilation scheme. The problem is to find a full set of meteorological fields (winds and temperatures) such that, when marched forward in time in the model, they achieve a best fit (in the weighted least-squares sense) to the data. The proposed solution is to develop a model especially for the Mars Observer data assimilation problem. Gravity waves are filtered from the model by eliminating all divergence terms from the prognostic divergence equation. This leaves a diagnostic gradient wind relation between the rotational wind and the temperature field. The divergent wind is diagnosed as the wind required to maintain the gradient wind balance in the presence of the diabatic heating. The primitive equations of atmospheric dynamics (with three principal dependent variables) are thus reduced to a simpler system with a single prognostic equation for temperature - the variable that will be best observed. (This balance system was apparently first derived by Charney as a first-order Rossby number expansion of the equations of motion). Experience with a full primitive equation model of the martian atmosphere indicates that a further simplification is possible: at least for short-term integrations, the model can be linearized about the zonally symmetric basic state. Author (revised)

N94-24884*# Laboratoire de Meteorologie Dynamique, Paris (France).
THE ANNUAL PRESSURE CYCLE ON MARS: RESULTS FROM THE LMD MARTIAN ATMOSPHERIC GENERAL CIRCULATION MODEL Abstract Only
Frederic Hourdin, Francois Forget, and O. Talagrand *In* Lunar and Planetary Inst., Workshop on Atmospheric Transport on Mars 1993 p 16-17 (For primary document see N94-24871 06-91)
Avail: CASI HC A01/MF A01

We have been developing a General Circulation Model (GCM) of the martian atmosphere since 1989. The model has been described rather extensively elsewhere and only the main characteristics are given here. The dynamical part of the model, adapted from the LMD terrestrial climate model, is based on a finite-difference formulation of the classical 'primitive equations of meteorology.' The radiative transfer code includes absorption and emission by CO2 (carefully validated by comparison to line-by-line calculations) and dust in the thermal range and absorption and scattering by dust in the visible range. Other physical parameterizations are included: modeling of vertical turbulent mixing, dry convective adjustment (in order to prevent vertical unstable temperature profiles), and a multilayer model of the thermal conduction in the soil. Finally, the condensation-sublimation of CO2 is introduced through specification of a pressure-dependent condensation temperature. The atmospheric and surface temperatures are prevented from falling below this critical temperature by condensation and direct precipitation onto the surface of atmospheric CO2. The only prespecified spatial fields are the surface thermal inertia, albedo, and topography. Author (revised)

N94-24885*# Toledo Univ., OH. Dept. of Physics and Astronomy.
NORTHERN HEMISPHERE DUST STORMS ON MARS Abstract Only
P. B. James *In* Lunar and Planetary Inst., Workshop on Atmospheric Transport on Mars 1993 p 17 (For primary document see N94-24871 06-91)
Avail: CASI HC A01/MF A01

Dust storms in the northern hemisphere of Mars appear to be less common than the more familiar southern hemisphere storms, and essentially, no activity north of about 30 latittude has been documented. The data are, however, subject to an observational bias because Mars is near aphelion during oppositions, which occur during the most likely seasons for dust activity in the north. The amount of dust activity in the northern hemisphere is clearly very relevant to the role of atmospheric transport in the dust cycle. The classic global storms that occur during spring in the southern hemisphere are observed to transport dust from sources in the southern hemisphere to sinks or temporary depositories in the north. The question of whether atmospheric transport can close the dust cycle, i.e., return the dust to the southern hemisphere sources on some timescale, is clearly relevant to the solution of the puzzle of how the dust storm cycle is modulated, i.e., why storms occur in some years but not in others. There are data that suggest that the spring/early summer season in the northern hemisphere of Mars during the year following the major 1977 storms observed by Viking was very dusty. A number of observations of the vicinity of the receding north polar cap showed clear evidence of substantial dust activity in the sub-Arctic region. Author (revised)

N94-24886*# Oxford Univ. (England). Dept. of Physics.
THE INFLUENCE OF OROGRAPHY ON THE TRANSPORT OF ATMOSPHERIC CONSTITUENTS Abstract Only
Manoj M. Joshi, Stephen R. Lewis, and Peter L. Read *In* Lunar and Planetary Inst., Workshop on Atmospheric Transport on Mars 1993 p 18 (For primary document see N94-24871 06-91)
Avail: CASI HC A01/MF A01

Given the fact that martian orography varies over a range of two scale heights (cf., about one scale height on Earth), it is thought that on Mars some aspects of the circulation should be affected to a large degree by the presence of orography. Initial results from two numerical models are presented that illustrate the effect of orography on cross-equatorial transport on Mars. On Earth, western boundary currents are found not only in the oceans as one would expect, but also in the troposphere, the most notable example being the East African Jet, which has an important effect on the monsoon circulation of the Eastern Indian Ocean. Two models were used for this investigation: a simple GCM (hereafter referred to as the SGCM); and a simple one-level barotropic model (BM). The SGCM solves the hydrostatic primitive equations on a sphere by representing model variables by spherical harmonics in the horizontal, with nonlinear terms being calculated in grid-point space. In the vertical, the model uses the sigma coordinate system in finite-difference form. The model represents the radiative processes in the atmosphere by a Newtonian relaxation to a specified zonal mean temperature state and surface drag by Rayleigh friction in the lowest model level. Author (revised)

N94-24887*# Colorado Univ., Boulder. Lab. for Atmospheric and Space Physics.
TEMPORAL AND SPATIAL MAPPING OF SURFACE ALBEDO AND ATMOSPHERIC DUST OPACITY ON MARS Abstract Only
S. W. Lee, R. T. Clancy, and G. R. Gladstone (Southwest Research Inst., San Antonio, TX.) *In* Lunar and Planetary Inst., Workshop on Atmospheric Transport on Mars 1993 p 19 (For primary document see N94-24871 06-91)
Avail: CASI HC A01/MF A01

The Mariner 9 and Viking provided abundant evidence that eolian processes are active over much of the surface of Mars. Past studies have demonstrated that variations in regional albedo and wind-streak patterns are indicative of sediment transport through a region, while thermal inertia data (derived from the Viking Infrared Thermal Mapper (IRTM) dataset) are indicative of the degree of surface mantling by dust deposits. The visual and thermal data are therefore diagnostic of whether net erosion or deposition of dust-storm fallout is taking place currently and whether such processes have been active in a region over the long term. These previous investigations, however, have not attempted to correct for the effects of atmospheric dust loading on observations of the martian surface, so quantitative studies of current sediment transport rates have included large errors due to uncertainty in the magnitude of this 'atmospheric component' of the observations. We have developed a radiative transfer model that allows the atmospheric dust opacity to be determined from IRTM thermal observations. Corrections for the effects of atmospheric dust loading on observations of surface albedo can also be modeled. This approach to determining 'dust-corrected surface albedo' incorporates the atmospheric dust opacity, the single-scattering albedo and particle phase function of atmospheric dust, and the bidirectional reflectance of the surface, and it accounts for variable lighting and viewing geometry. Author (revised)

N94-24888*# Washington Univ., Seattle. Dept. of Atmospheric Sciences.
DYNAMICS OF THE ATMOSPHERE OF MARS: REVIEW OF SOME OUTSTANDING PROBLEMS Abstract Only
Conway B. Leovy *In* Lunar and Planetary Inst., Workshop on Atmospheric Transport on Mars 1993 p 19 (For primary document see N94-24871 06-91)
Avail: CASI HC A01/MF A01

Theoretical and modeling studies based on fragmentary data are responsible for our current level of understanding of the dynamics of Mars' atmosphere at the planetary scale. Largely because the boundary conditions and governing parameters are such that the large-scale circulation regime is similar to that or Earth, it has been possible to derive a remarkable amount of information from a relatively small number of observations. Nevertheless, the level of detail available from theoretical and modeling studies far exceeds the validation capability of existing data. Global observations from Mars Observer instruments are expected to go far to remedy this mismatch. This review will present and examine several outstanding dynamical questions, which Mars Observer measurements should help to answer. These include the following: What are the temporal and three-dimensional spatial distributions of thermal tides? What is the distribution of momentum flux divergence due to internal gravity waves? Are normal modes an important component of the general circulation? If so, how do they vary with season? Do normal modes contribute to the initiation of planetary-scale dust storms? What are the details of the global circulation response to large and rapid injections of dust? Current understanding of these problems, the potential role of Mars Observer observations for addressing them, and the implications of answers for our understanding of the present climate and past climate regimes will be discussed. Author (revised)

N94-24889*# Oxford Univ. (England). Dept. of Physics.
MODELING AND DATA ASSIMILATION FOR MARS OBSERVER Abstract Only
Stephen R. Lewis and Peter L. Read *In* Lunar and Planetary Inst., Workshop on Atmospheric Transport on Mars 1993 p 19-20 (For primary document see N94-24871 06-91)
Avail: CASI HC A01/MF A01

The Mars Observer mission will return a substantial set of meteorological data for the atmosphere of Mars, principally in the form of thermal infrared soundings from the Pressure Modulator Infrared Radiometer (PMIRR). The dataset will enable global studies of a range of dynamical and physical phenomena in the martian atmosphere. The solar orbital configuration of Mars Observer, however, means that the coverage of the martian atmosphere and surface by remote sounding instruments will be asynchronous. This leads to difficulties of interpretation when studying synoptic-scale phenomena with timescales of a few days. In an attempt to overcome such problems we propose to use data assimilation techniques, as currently employed for operational weather forecasting on the Earth, in conjunction with a Martian General Circulation Model (MGCM) that is under development at Oxford and Reading Universities. An overview of the model and assimilation scheme will be given, with reference to problems encountered so far in applying such methods to remote-sensing observations of the martian atmosphere. ESDU

N94-24890*# Wisconsin Univ., Madison. Space Science and Engineering Center.
MARS OPERATIONAL ENVIRONMENTAL SATELLITE (MOES): A POST-MARS OBSERVER DISCOVERY MISSION Abstract Only
Sanjay S. Limaye *In* Lunar and Planetary Inst., Workshop on Atmospheric Transport on Mars 1993 p 21-22 (For primary document see N94-24871 06-91)
Avail: CASI HC A01/MF A01

Mars Operational Environmental Satellite (MOES) is a Discovery concept mission that is designed to observe the global short-term weather phenomena on Mars in a systematic fashion. Even after the Mariner, Viking, and, soon, Mars Observer missions, crucial aspects of the martian atmosphere will remain unobserved systematically. Achieving a better understanding of the cycles of dust, water vapor, and ices on Mars requires detailed information about atmospheric transports of those quantities associated with the weather systems, particularly those arising in mid latitudes during fall and winter. It also requires a quantitive understanding of the processes responsible for the onset and evolution of dust storms on all scales. Whereas on Earth the system of geosynchronous and polar orbiting satellites provides continuous coverage of the weather systems, on Mars the time history of important events such as regional and global dust storms remains unobserved. To understand the transport of tracers in the martian atmosphere and particularly to identify their sources and sinks, it is necessary to have systematic global, synoptic observations that have yet to be attained. Clearly these requirements are not easy to achieve from a single spacecraft in orbit, but if we focus on specific regions of the planet, e.g., polar vs. low and mid latitudes, then it is possible to attain a nearly ideal coverage at a reasonable spatial and temporal resolution with a system of just two satellites. Mars Observer is about to yield good coverage of the polar latitudes, so we focus initially on the region not covered well in terms of diurnal coverage, and in terms of desired observations will provide the initial data for the numerical models of the martian weather and climate that can be verified only with better temporal and spatial data. Author

N94-24891*# Lowell Observatory, Flagstaff, AZ.
A STUDY OF CLOUD MOTIONS ON MARS. 2: SOME EXAMPLES OF OBSERVATIONS AND ANALYSES SINCE 1969 Abstract Only
Leonard J. Martin *In* Lunar and Planetary Inst., Workshop on Atmospheric Transport on Mars 1993 p 22-23 (For primary document see N94-24871 06-91)
Avail: CASI HC A01/MF A01

The purpose of this paper is to remind everyone of the varied database on cloud motions that exist but often is under-used in dynamical studies. Some striking examples of these cloud motions are described. Author

N94-24892*# Jet Propulsion Lab., California Inst. of Tech., Pasadena.
EVIDENCE FOR DUST TRANSPORT IN VIKING IR THERMAL MAPPER OPACITY DATA Abstract Only
Terry Z. Martin *In* Lunar and Planetary Inst., Workshop on Atmospheric Transport on Mars 1993 p 23-24 (For primary document see N94-24871 06-91)
Avail: CASI HC A01/MF A01

Global maps of 9-micron dust opacity derived from radiometric observations made by the Viking Orbiter IR Thermal Mapper instruments have revealed a wealth of new information about the distribution of airborne dust over 1.36 Mars years from 1976-1979. In particular, the changing dust distribution during major dust storms is of interest since the data provide a point of contact with both Earth-based observations of storm growth and with global circulation models. Derived from text

N94-24893*# National Aeronautics and Space Administration. Goddard Space Flight Center, Greenbelt, MD.
RETRIEVAL OF TEMPERATURE PROFILES FROM MARTIAN INFRARED SPECTRA Abstract Only
W. Wallace McMillan (National Academy of Sciences - National Research Council, Greenbelt, MD.), John C. Pearl, and Barney J. Conrath *In* Lunar and Planetary Inst., Workshop on Atmospheric Transport on Mars 1993 p 24-25 (For primary document see N94-24871 06-91)
Avail: CASI HC A01/MF A01

In theory, a thermal emission spectrum of Mars (220-1600 cm(exp -1)) contains a wealth of information about the composition and thermal structure of the atmosphere and surface. However, in practice, the ability to retrieve quantitative information from the spectrum is limited by a number of factors including (1) the ill-posed nature of the spectral inversion problem and the resulting nonuniqueness of all solutions; (2) assumptions built into any spectral inversion program; (3) uncertainties in surface pressure, temperature, and emissivity; and (4) uncertainties in the optical properties of atmospheric aerosols. Below, factors (1) and (2) are discussed as fundamental limitations on temperature retrievals from Mariner 9 Infrared Interferometer Spectrometer (IRIS) spectra. In preparation for the Mars Observer mission and the return of tens of thousands of infrared spectra per day from the Thermal Emission Spectrometer (TES), we have developed a fast inversion algorithm to retrieve temperature structure and aerosol opacity from the infrared spectra. The derived atmospheric models will be used to provide the atmospheric contribution to the TES spectra, so that the thermal emission spectra of the underlying surface can be determined for making mineralogical identifications. As a test of our algorithm, we are undertaking a systematic analysis of the entire Mariner 9 Infrared Interferometric Spectrometer (IRIS) dataset of 21,000 plus spectra. While portions of the IRIS dataset have been previously analyzed, the lack of a speedy and robust algorithm to invert the IRIS spectra to retrieve temperature profiles and aerosol opacities has been a major impediment to a truly comprehensive analysis. Author

N94-24894*# National Aeronautics and Space Administration. Ames Research Center, Moffett Field, CA.

DUST TRANSPORT IN THE MARTIAN ATMOSPHERE Abstract Only

James R. Murphy *In* Lunar and Planetary Inst., Workshop on Atmospheric Transport on Mars 1993 p 25-27 (For primary document see N94-24871 06-91)

Avail: CASI HC A01/MF A01

Dust in suspension within the martian atmosphere is an important driver of the atmospheric thermal and, ultimately, dynamical states. By virtue of its presence in the atmosphere, this suspended dust is susceptible to transport by the winds and thus the location from which dust is lifted from the surface is not necessarily the location at which it will return to the surface. Such surface dust lifting and subsequent transport, when accumulated over daily, seasonal and annual time intervals define the martian dust cycle. The atmospheric transport element (and equally surface lifting and redeposition) of this cycle is strongly dependent upon season and the quantity of dust in suspension. The seasonal dependence arises due to the dominance of particular components of the atmospheric circulation at particular locations (latitudes) at various times through the year. The dependence on dust abundance is due to the amount of dust available for transport, but it is also due to the influence that the dust has on the intensity of the circulation. As dust abundance and therefore its radiative influence increases, some components of the circulation intensity (Hadley circulation, thermal tides), while some components may decline in intensity (baroclinic waves, condensation flow). For these reasons, our ability to understand the martian dust cycle is dependent on our ability to define the contributions that various circulation components, under varying seasonal and dust-radiative forcings, play in the transport of dust around the planet. Author

N94-24895*# Wyoming Univ., Laramie. Dept. of Atmospheric Science.

THREE-DIMENSIONAL NUMERICAL SIMULATION OF NEAR-SURFACE FLOWS OVER THE MARTIAN NORTH POLAR CAP Abstract Only

Thomas R. Parish and A. D. Howard (Virginia Univ., Charlottesville.) *In* Lunar and Planetary Inst., Workshop on Atmospheric Transport on Mars 1993 p 27-30 (For primary document see N94-24871 06-91)

Avail: CASI HC A01/MF A01

Measurements made by Viking Lander VL-2 (48 N) have shown that the near-surface wind and temperature regime on Mars displays striking similarities to terrestrial counterparts. The diurnal radiative cycle is responsible for establishment of a well-defined thermal circulation in which downslope (Katabatic) flows prevail during the nighttime hours and weak upslope (anabatic) conditions prevail during the daytime. Previous work has indicated that the slope flows are much like those found on Earth, particularly the Katabatic winds, which show striking similarities to drainage flows observed over Antarctica. The low-level wind regime appears to be an important factor in the scouring of the martian landscape. The north polar cap shows evidence of eolian features such as dunes, frost streaks, and grooves from Viking imagery. The direction of the prevailing wind can in cases be inferred from the eolian features. We examine the thermally induced flows that result from the radiative heating and cooling of the martian north polar region using a comprehensive three-dimensional atmospheric mesoscale numerical model. The same model has been used previously for simulation of Antarctic Katabatic winds. The model equations are written in terrain-following coordinates to allow for irregular terrain; prognostic equations include the flux forms of the horizontal momentum equations, temperature, continuity. A surface energy budget equation is also incorporated in which the surface temperature is determined. Explicit parameterization of both terrestrial (longwave) and solar (shortwave) radiation is included. Turbulent transfer of heat and momentum in the martian atmosphere is assumed to follow the similarity expressions in the surface boundary layer on Earth. The terrain heights for the martian north polar region have been obtained from the U.S. Geological Survey map and digitized onto a 57x57 grid with a spacing of 75 km. The resulting terrain map is shown in Fig. 1. The vertical grid consists of 15 levels (delta equals 0.998, 0.99, 0.98, 0.97, 0.96, 0.94, 0.92, 0.90, 0.85, 0.775, 0.70, 0.60, 0.50, 0.30, 0.10). The high resolution in the lower atmosphere is necessary to capture details of the boundary layer flows. The lowest level corresponds to a height of approximately 20 m above the ground, the seconds level 100 m. Derived from text

N94-24896*# National Aeronautics and Space Administration. Ames Research Center, Moffett Field, CA.

THE ROLE OF ATMOSPHERIC HEAT TRANSPORT IN THE SEASONAL CARBON DIOXIDE CYCLE Abstract Only

James B. Pollack, R. M. Haberle, James R. Murphy, and J. Schaeffer (Sterling Software, Inc., Palo Alto, CA.) *In* Lunar and Planetary Inst., Workshop on Atmospheric Transport on Mars 1993 p 30 (For primary document see N94-24871 06-91)

Avail: CASI HC A01/MF A01

We have carried out numerical experiments with a general circulations model (GCM) and energy balance model of the martian atmosphere to define the importance of heat transported to the polar regions in determining the amount of CO2 condensed on the surface during the fall and winter seasons and the amount sublimated during the spring and summer seasons. In so doing, we performed both sensitivity experiments, in which the dust opacity was varied over the full range of its observed values, and annual simulations, in which the dust opacity varied continuously with seasonal data, in accord with measurements taken at the Viking landers. Dust opacity represents the key variable for determining the contribution of atmospheric heat advection to the energy budget in the polar regions. The amount of heat advected to the winter polar regions increases monotonically as the dust opacity at low and middle latitudes increases. However, the increase is sharpest between optical depths of 0 and 1 tends to level off at still higher optical depths. Heat advection is more important at times of CO2 condensation than CO2 sublimation, since the temperature gradients are much steeper in the winter hemisphere than in the summer hemisphere. Because dust opacity is much higher during northern winter than during southern winter, atmospheric heat advection reduces the amount of CO2 that condenses in the north by a much larger factor than it does in the south. Derived from text

N94-24897*# Observatoire de Paris-Meudon (France).

EDDY MIXING COEFFICIENT UPPER LIMIT DERIVED FROM THE PHOTOCHEMICAL BALANCE OF O2 Abstract Only

J. Rosenqvist and E. Chassefiere (Centre National de la Recherche Scientifique, Verrieres-Le Buisson, France.) *In* Lunar and Planetary Inst., Workshop on Atmospheric Transport on Mars 1993 p 30-32 (For primary document see N94-24871 06-91)

Avail: CASI HC A01/MF A01

This work is based on the study of the photochemical balance of molecular oxygen in the martian atmosphere by using a one-dimensional model of photochemical reactions involving species derived from CO2 and H2O. The model is basically similar to one used previously for the study of the regulation of CO on a global scale, but the chemical rates are taken from another source. In the present scheme, the regulation of molecular oxygen is studied over timescales of the order of its photochemical lifetime (approximately equals 30 yr), which is much shorter than typical escape timescales. Thus, the escape fluxes are fixed to the values given by 3 and 4. We examine the calculated equilibrium abundances of O2 for given thermal, eddy diffusion coefficients and H2O profiles. The thermal profile is taken from in the lower atmosphere. At higher levels, in order to include the diurnal and seasonal thermal profile variability, we have also used the IRTM data. In order to study the influence of both temperature and pressure profiles on the O2 mixing ratio, we have made several tests corresponding to different martian seasons. The results show that the influence of pressure and temperature is quantitatively weak compared to the one of K and of the water vapor density (H2O). Thus, in the following we have fixed the pressure at the surface to a value of 7 mbar and we have used unique standard thermal profile corresponding to a profile roughly averaged over the year, the season, and the day: T equal 205 K at 0 km altitude, 175 K at 25 km, and 145 K at 50 km. Author

N94-24898*# Jet Propulsion Lab., California Inst. of Tech., Pasadena.
DIAGNOSTIC CALCULATIONS OF THE CIRCULATION IN THE MARTIAN ATMOSPHERE Abstract Only
Michelle Santee and D. Crisp *In* Lunar and Planetary Inst., Workshop on Atmospheric Transport on Mars 1993 p 32-33 (For primary document see N94-24871 06-91)
Avail: CASI HC A01/MF A01

The circulation of the martian atmosphere during late southern summer is inferred from observed atmospheric temperature and dust distributions. We use global maps of temperature and dust optical depth (approximately 0-60 km) retrieved from a subset of the Mariner 9 IRIS thermal emission spectra spanning L(sub s) equals 343-348 deg. This thermal structure is characterized by a reversed meridional temperature gradient at altitudes above about 40 km, and temperatures that decrease from equator to pole at lower altitudes. Zonal-mean zonal winds are derived from the zonally averaged temperatures assuming gradient wind balance and midlatitude westerly jets with velocities of 80-90 m s(exp -1) near 50 km; in the southern tropics the winds are easterly with velocities of 40 m s(exp -1) near 50 km. The north-south atmospheric transport includes contributions from both the zonal mean meridional circulation and large-scale waves. Author

N94-24899*# Finnish Meteorological Inst., Helsinki. Dept. of Physics.
MARTIAN MESOSCALE CIRCULATIONS INDUCED BY VARIATIONS IN SURFACE OPTICAL AND THERMAL CHARACTERISTICS: A NUMERICAL STUDY Abstract Only
Tero Siili and H. Savijarvi (Helsinki Univ., Finland.) *In* Lunar and Planetary Inst., Workshop on Atmospheric Transport on Mars 1993 p 33-35 (For primary document see N94-24871 06-91)
Avail: CASI HC A01/MF A01

According to Mariner 9 and Viking observations the surface albedo and the thermal inertia of Mars' surface vary substantially, and fairly large gradients also occur. The Syrtis Major region is bounded in the west by high-albedo cratered terrain and in the east by Isidis Planitia, a high-albedo plateau. Sinus Meridiani, centered at 0 degrees W 5 degrees S, is almost surrounded by higher albedo regions with sharp boundaries, and Acidalia Planitia, between 10 and 50 degrees W and north of 35 degrees N, has sharp albedo boundaries to the east and west. Observational and modeling studies, e.g., on Australian dry salt lake coasts, have shown that discontinuities and gradients in surface properties can induce mesoscale circulations. We have used a version of the DMUH mesoscale model to simulate atmospheric circulations induced by variations in the reflectivity and in the thermal inertia of the martian surface. Author

N94-24900*# Centre National de la Recherche Scientifique, Verrieres-Le Buisson (France). Service d'Aeronomie.
TWO-DIMENSIONAL MODELING OF THERMAL INVERSION LAYERS IN THE MIDDLE ATMOSPHERE OF MARS Abstract Only
B. Theodore and E. Chassefiere *In* Lunar and Planetary Inst., Workshop on Atmospheric Transport on Mars 1993 p 35-37 (For primary document see N94-24871 06-91)
Avail: CASI HC A01/MF A01

There is some evidence that the thermal structure of the martian middle atmosphere may be altered in a significant way by the general circulation motions. Indeed, while it is well known that the circulation in the meridional plane is responsible for the reversal of the latitudinal thermal gradient at the solstice through the adiabatic heating due to sinking motions above the winter pole, here we want to emphasize that a likely by-product effect could be the formation of warm layers, mainly located in the winter hemisphere, and exhibiting an inversion of the vertical thermal gradient. Author

N94-24901*# Princeton Univ., NJ. Geophysical Fluid Dynamics Lab.
THREE-DIMENSIONAL NUMERICAL SIMULATION OF THERMAL TIDES IN THE MARTIAN ATMOSPHERE Abstract Only
R. John Wilson *In* Lunar and Planetary Inst., Workshop on Atmospheric Transport on Mars 1993 p 37-39 Prepared in cooperation with National Oceanic and Atmospheric Administration, Princeton, NJ (For primary document see N94-24871 06-91)
Avail: CASI HC A01/MF A01

Analysis of the Mariner 9 IRIS and Viking Orbiter IRTM temperature data and of the time series of surface pressure from the Viking landers has indicated that atmospheric thermal tides are a significant component of the martian general circulation. Classical tidal theory, considering only the Sun synchronous components, has been shown to at least roughly account for the amplitudes of the observed diurnal and semidirunal surface pressure oscillations. In particular, Zurek and Leovy have demonstrated that classical tidal theory can reproduce the observed dependence of the strength of the semidiurnal tide on aerosol optical depth. The high-amplitude topograph of Mars, however, can cause longitudinal distortions in the thermotidal forcing, leading to additional tidal modes that are not Sun synchronous. In particular, observation and theory have suggested the likely presence of a diurnal, zonal wavenumber-1 K wave. Hamilton and Garcia noted that the wavenumber-1 K normal mode has a period of close to 24 hr and may be detectable in surface pressure observations. Zurek has discussed the possibility of this mode being resonantly excited for various atmospheric temperature studies. The semidiurnal wavenumber-2 K mode, with roughly a 12-hr period, could also be resonantly excited. A numerical model with finite amplitude topography and a self-consistent thermotidal forcing resulting from the daily heat flux at the surface and atmospheric absorption of solar radiation by aerosols is used here to explore the influence of topography on martian thermal tides and to examine the possibility of Kelvin wave resonance. Derived from text

N94-24902*# National Aeronautics and Space Administration. Ames Research Center, Moffett Field, CA.
VERTICAL TRANSPORT OF WATER IN THE MARTIAN BOUNDARY LAYER Abstract Only
Aaron P. Zent, R. M. Haberle, and Howard C. Houben (Space Physics Research Inst., Sunnyvale, CA.) *In* Lunar and Planetary Inst., Workshop on Atmospheric Transport on Mars 1993 p 39-40 (For primary document see N94-24871 06-91)
Avail: CASI HC A01/MF A01

We are continuing our examination of the transport of H2O through the martian boundary layer, and we have written a one-dimensional numerical model of the exchange of H2O between the atmosphere and subsurface of Mars through the planetary boundary layer (PBL). Our goal is to explore the mechanisms of H2O exchange, and to elucidate the role played by the regolith in the local H2O budget. The atmospheric model includes effects of Coriolis, pressure gradient, and frictional forces for momentum, as well as radiation, sensible heat flux, and advection for heat. The model differs from Flasar and Goody by use of appropriate Viking-based physical constants and inclusion of the radiative effects of atmospheric dust. We specify the pressure gradient force or compute it from a simple slope model. The subsurface model accounts for conduction of heat and diffusion of H2O through a porous adsorbing medium in response to diurnal forcing. The model is initialized with depth-independent H2O concentrations (2 kg M(exp -3)) in the regolith, and a dry atmosphere. The model terminates when the atmospheric H2O column abundance stabilizes at 0.1 percent per sol. Derived from text

N94-24903*# National Aeronautics and Space Administration. Ames Research Center, Moffett Field, CA.
THE MARS AERIAL PLATFORM (MAP) MISSION Abstract Only
R. Zubrin (Martin Marietta Corp., Denver, CO.), T. Gamber (Martin Marietta Corp., Denver, CO.), Benton Clark (Martin Marietta Corp., Denver, CO.), R. M. Haberle, J. Cantrell (Utah State Univ., Logan.), and S. Price (Martin Marietta Corp., Denver, CO.) *In* Lunar and Planetary Inst., Workshop on Atmospheric Transport on Mars 1993 p 40-42 (For primary document see N94-24871 06-91)
Avail: CASI HC A01/MF A01

The Mars Aerial Platform (MAP) mission is a conceptual design for a low-cost, Discovery-class mission whose purpose would be to generate tens of thousands of very-high-resolution (20 cm/pixel) pictures of the martian surface, map the global circulation of the martian atmosphere, and examine the surface and subsurface with ground-penetrating radar, infrared spectroscopy, neutron spectroscopy, and other remote sensing techniques. The data would be acquired by instruments that are carried by balloons

flying at a nominal altitude of about 7 km over the martian surface. Because new balloon and microspacecraft technology is now available, the balloon probes could be quite long-lived, lasting hundreds or even thousands of days, producing an immense science harvest in the process. Together with the Mars Environmental Survey (MESUR) surface network science mission, MAP would revolutionize our knowledge of the Red Planet.
Author

N94-24904*# Jet Propulsion Lab., California Inst. of Tech., Pasadena.
MARS OBSERVER: APPLICATIONS TO ATMOSPHERIC TRANSPORT Abstract Only
Richard W. Zurek and Daniel J. McCleese *In* Lunar and Planetary Inst., Workshop on Atmospheric Transport on Mars 1993 p 42 (For primary document see N94-24871 06-91)
Avail: CASI HC A01/MF A01

The Pressure Modulator Infrared Radiometer (PMIRR) is an atmospheric sounder designed to observe temporal and spatial variations of water vapor and of dust suspended in the Mars atmosphere, to characterize the planetary-scale thermal structure and circulation of the atmosphere, and to quantify the polar radiative balance. These measurements are fundamental to understanding the seasonal cycles of dust, of water, and of CO2 on Mars and, in particular, to determining the role of atmospheric transport. Using measurements in eight narrow-band infrared spectral regions and one broadband visible channel, the PMIRR investigation teams at JPL and Oxford University will derive vertical profiles of atmospheric temperature, extinction due to suspended dust, and water vapor concentration, as well as locations of CO2 and H2O ice clouds. These data will be used in a variety of ways to address issues of atmospheric dynamics and transport. Three topics will be emphasized here: (1) the expected precision of the retrieved profiles of temperature, dust extinction, and water vapor, including plans for validating the profiles; (2) the observation strategy, designed to best use PMIRR's two-axis scan mirror, as deployed in the Mars Observer mapping orbit; and (3) approaches to mapping the atmospheric fields globally and the derivation of key meteorological fields related to estimating atmospheric transport.
Author

N94-24996*# Southern Methodist Univ., Dallas, TX. Dept. of Geological Sciences.
TECTONIC EVOLUTION OF MARS Final Technical Report, 1 May 1989 - 30 Apr. 1992
Roger J. Phillips 30 Apr. 1992 60 p
(Grant NAGw-1085)
(NASA-CR-194714; NAS 1.26:194714) Avail: CASI HC A04/MF A01

The Final Technical Report on tectonic evolution of Mars is presented. Two papers and an abstract are included. Topics addressed include: scientific rationale and requirements for a global seismic network on Mars, permanent uplift in magmatic systems with application to the Tharsis Region of Mars, and the geophysical signal of the Martian global dichotomy. For individual titles, see N94-24997 through N94-24997.

N94-24997*# Southern Methodist Univ., Dallas, TX. Dept. of Geological Sciences.
THE GEOPHYSICAL SIGNAL OF THE MARTIAN GLOBAL DICHOTOMY Abstract Only
Roger J. Phillips *In its* Tectonic Evolution of Mars 30 Apr. 1992 1 p (For primary document see N94-24996 06-91)
Avail: CASI HC A01/MF A01

A first-order tectonic question for Mars is the origin and nature of the global dichotomy (GD) separating approximately the northern and southern hemispheres of the planet. It is appropriate to focus on hypotheses for the origin of the GD as well as on geophysical models of related internal structure that are constrained by present-day observations. There are basic planetary scale observations that relate to the GD: (1) the dichotomy boundary separates two fundamentally different elevations on the planet, as the terrain to the north is lower by an average of about 3 km; (2) the boundary separates terrain of regionally distinct crater ages, heavily cratered (older) in the south and sparsely cratered (younger) in the north; (3) the amount of ancient crust apparently removed from north of the dichotomy boundary cannot be accounted for by simple surface erosion and deposition in the south, and the constraint becomes particularly severe if isostatic adjustment is presumed to have accompanied this process. This last point leads to the supposition that some type of interior process must have been responsible for the creation of the GD. An obvious way to create the observed elevation difference between the two hemispheres is with a thinner crust in the north, although a denser cust would also work. Hypotheses for producing a thinner northern crust include preferential sub-crustal erosion, a giant impact, and simply invoking the crustal thickness difference as a primordial feature of the planet. If the GD represents a fundamental change in the crustal thickness of Mars, then there should be geophysical evidence of this. The center-of-figure to center-of-mass offset of the planet may be related to the GD, but the Tharsis topography must certainly also contribute. If the Tharsis and GD effects can be separated, then a crustal thickness model can be tested, though the results will not be unique. The gravity field provides another geophysical constraint on GD models. A simple change in thickness of an isostatically compensated crust should show a characteristic gravity signal across the dichotomy boundary. There is a gravity anomaly that is clearly associated with the boundary in regions where the gravity signal is not cluttered by contributions from other features such as Tharsis and Elysium. The gravity signal has a complex spatial relationship with the boundary, and efforts are presently underway to model this anomaly.
Author (revised)

N94-25349*# LeTourneau Coll., Longview, TX. Div. of Natural Sciences.
DATA ANALYSIS AND INTERPRETATION OF LUNAR DUST EXOSPHERE
George A. Andrews, Jr. *In* NASA. Johnson Space Center, National Aeronautics and Space Administration (NASA)/American Society for Engineering Education (ASEE) Summer Faculty Fellowship Program, 1993, Volume 1 Dec. 1993 15 p (For primary document see N94-25348 06-99)
Avail: CASI HC A03/MF A03

N94-25355*# Houston Univ., Clear Lake, TX. School of Natural and Applied Sciences.
MEASURING TRACK DENSITIES IN LUNAR GRAINS BY IMAGE ANALYSIS
George E. Blanford *In* NASA. Johnson Space Center, National Aeronautics and Space Administration (NASA)/American Society for Engineering Education (ASEE) Summer Faculty Fellowship Program, 1993, Volume 1 Dec. 1993 10 p (For primary document see N94-25348 06-99)
Avail: CASI HC A02/MF A03

92 SOLAR PHYSICS

Includes solar activity, solar flares, solar radiation and sunspots. For related information see *93 Space Radiation.*

N94-22837# European Space Agency, Paris (France).
SCIENTIFIC REQUIREMENTS FOR FUTURE SOLAR-PHYSICS SPACE MISSIONS
P. Maltby, ed. (Oslo Univ., Norway.) and B. Battrick, ed. (European Space Agency. European Space Research and Technology Center, ESTEC, Noordwijk, Netherlands.) Noordwijk, Netherlands Jun. 1993 170 p
Workshop held in Norway Original contains color illustrations
(ESA-SP-1157; ISBN-9-29-092065-3; ETN-94-95194) Copyright Avail: CASI HC A08/MF A02; ESA, EPD, ESTEC, Noordwijk, Netherlands, HC

Key issues in solar astrophysics are addressed: some challenging problems of the structured and dynamical solar atmosphere; keys to understanding the corona; goals of ground based solar observations; and prospects for future solar wind missions. Prospects for future ground based solar observations and for improved instrumentation on future solar space missions are considered. ESA, NASA and Japanese solar physics projects are reviewed. The Coronas (complex orbital near Earth observations of solar activity) project is addressed. Prospects for very high resolution solar physics with the SIMURIS (solar, solar system, and stellar interferometric mission for ultrahigh resolution imaging and spectroscopy) are considered. Requirements for future solar physics missions with x-ray and ultraviolet instrumentation are given. Reasons for putting visible solar telescopes in space are also given. For individual titles, see N94-22838 through N94-22851.

N94-22838# National Center for Atmospheric Research, Boulder, CO. High-Altitude Observatory.
SOME CHALLENGING PROBLEMS OF THE STRUCTURED AND DYNAMICAL SOLAR ATMOSPHERE
B. W. Lites *In* ESA, Scientific Requirements for Future Solar-Physics Space Missions Jun. 1993 p 11-23 Sponsored by NSF Original contains color illustrations (For primary document see N94-22837 06-92)
Copyright Avail: CASI HC A03/MF A02; ESA, EPD, ESTEC, Noordwijk, Netherlands, HC

Several current but long standing problems of the solar photosphere are presented, along with suggestions which may help resolve them in the future. Particular emphasis is given to phenomena and processes involving the solar magnetic field. The problems addressed include the following: magnetostatics and magnetoconvection; chromospheric heating; solar oscillations; solar flare; and abundance variation in the corona/solar wind. These problems may best be addressed in the future by means of carefully coordinated ground and space based observations. ESA

N94-22839# Florence Univ. (Italy). Dept. of Astronomy and Space Science.
KEYS TO UNDERSTANDING THE CORONA
C. Chiuderi *In* ESA, Scientific Requirements for Future Solar-Physics Space Missions Jun. 1993 p 25-32 (For primary document see N94-22837 06-92)
Copyright Avail: CASI HC A02/MF A02; ESA, EPD, ESTEC, Noordwijk, Netherlands, HC

The theoretical understanding of the solar corona involves such different phenomena as the coronal heating and the occurrence of flares. It is argued that all of these phenomena could be seen as a manifestation of the same basic physics, the differences being a question of coherence. The theoretical work needed to support this view and its possible impact on future observational strategies are outlined. ESA

N94-22840# Kiepenheuer-Inst. fuer Sonnenphysik, Freiburg (Germany).
GOALS OF GROUND-BASED SOLAR OBSERVATIONS
W. Mattig *In* ESA, Scientific Requirements for Future Solar-Physics Space Missions Jun. 1993 p 33-41 Original contains color illustrations (For primary document see N94-22837 06-92)
Copyright Avail: CASI HC A02/MF A02; ESA, EPD, ESTEC, Noordwijk, Netherlands, HC

Advantages and disadvantages of ground based solar observations are discussed. Fruitful observations form spacecraft as well as from ground based observatories both require close and coordinated cooperation between observers and theoreticians. Advantages of ground based observations are the possibilities for studying long term variations (many years), even outside active regions, and the fact that large telescopes with complex instrumentation can be used. Disadvantages are the limitations on the usable wavelength region and the distorting influence of the Earth's atmosphere. Promising attempts to minimize these distortions have, however, been made by applying new technologies. Nevertheless, observations of very small structures (less than or equal to 0.2 arcsec) in the visible region over extended periods (many hours) will probably forever remain the domain of spaceborne instrumentation. ESA

N94-22841*# Bern Univ. (Switzerland). Physikalisches Inst.
PROSPECTS FOR FUTURE SOLAR-WIND MISSIONS
P. Bochsler and E. Moebius (New Hampshire Univ., Durham.) *In* ESA, Scientific Requirements for Future Solar-Physics Space Missions Jun. 1993 p 43-51 Sponsored in part by Swiss National Foundation for Scientific Research Original contains color illustrations (For primary document see N94-22837 06-92)
(Grant NAGw-2579)
Copyright Avail: CASI HC A02/MF A02; ESA, EPD, ESTEC, Noordwijk, Netherlands, HC

Possible activities and future goals for solar wind research in the post Soho era are discussed. Two major enterprises which will open up important fields in the future study of the Sun are addressed. The first deals with in situ study of the solar corona, a region that has not been accessible for direct study in the past. This exploratory work will include the coronal heating and the acceleration of the solar wind much closer to its origin and the determination of the charge states of a large number of ions as a diagnostic tool for fractionation processes in these regions. The second major goal will be the setting up of a baseline for the isotopic composition in the solar system by studying a sample from the Sun in detail. These studies will be complemented by a direct comparison with extra solar samples of interstellar pick up ions, which become accessible with the same instrumentation as is necessary for the detailed investigation of the solar wind's isotopic composition. In order to achieve these goals, advanced composition experiments are developed to investigate the solar wind with enhanced mass resolution, considerably increased geometrical factor, and improved time resolution. The placing of sophisticated mass/charge spectrometers, with the ability to investigate both charge and velocity distributions with enhanced time resolution, in the solar wind acceleration region, is also proposed. ESA

N94-22842# Oslo Univ. (Norway). Inst. for Theoretical Astrophysics.
PROSPECTS FOR FUTURE GROUND-BASED SOLAR OBSERVATIONS
O. Engvold *In* ESA, Scientific Requirements for Future Solar-Physics Space Missions Jun. 1993 p 55-65 (For primary document see N94-22837 06-92)
Copyright Avail: CASI HC A03/MF A02; ESA, EPD, ESTEC, Noordwijk, Netherlands, HC

The complementary aspects of solar ground based and space instrumentation are discussed and plans for future ground based solar observing facilities are reviewed. Prospects for high spatial resolution observations from the ground which are discussed are: correlation tracking, adaptive optics, and speckle interferometry. Plans for ground based solar instrumentation include polarimetry, coronagraphy, observations in infrared, helioseismology, monitoring of solar variability (synoptic studies), and telescopy. ESA

N94-22843# Paris XI Univ., Orsay (France). Inst. d'Astrophysique Spatiale.
PROSPECTS FOR IMPROVED INSTRUMENTATION ON FUTURE SOLAR SPACE MISSIONS
P. Lemaire *In* ESA, Scientific Requirements for Future Solar-Physics Space Missions Jun. 1993 p 67-77 Original contains color illustrations (For primary document see N94-22837 06-92)
Copyright Avail: CASI HC A03/MF A02; ESA, EPD, ESTEC, Noordwijk, Netherlands, HC

The status of space based instrumentation at the time of the Soho launch is summarized, the areas where improvements are foreseeable are examined, and an overview of the gains that can be achieved is presented. Special attention is paid to identifying intrinsic limitations related to classical mountings in the UV and EUV range. Some mountings are discussed, with their limitations, in the context of missions already proposed. The present capabilities of solar physics instrumentation in space are on the 1 arcsec angular resolution domain, with a resolving power near 30,000, and the ability to fit spectral line profiles and to establish line of sight velocities down to 1 km/s. Few rocket instruments have yet crossed the 1 arcsec angular resolution threshold. The goal of the next generation of solar instrumentation in space is to achieve 0.1 arcsec angular resolution whilst retaining the same spectral resolution and improving the temporal resolution. ESA

N94-22844# European Space Agency. European Space Research and Technology Center, ESTEC, Noordwijk (Netherlands). Space Science Dept.
SOLAR PHYSICS WITHIN ESA'S PLANNING
M. C. E. Huber *In its* Scientific Requirements for Future Solar-Physics Space Missions Jun. 1993 p 81-93 Original contains color illustrations (For primary document see N94-22837 06-92)
Copyright Avail: CASI HC A03/MF A02; ESA, EPD, ESTEC, Noordwijk, Netherlands, HC

The role of solar physics in past ESRO and ESA missions and mission studies is described. The preparation of 'Horizon 2000', which resulted in Soho becoming an approved project in ESA's scientific program, is discussed. The current studies of solar physics missions within ESA are reviewed, and 'rules' that should be kept in mind by European solar scientists planning a future mission are suggested. After a promising start in ESRO, with solar astronomy experiments being flown on two early satellites (ESRO 2 in 1968 and TD 1 in 1972), solar astronomers were not able to participate again in the ESRO/ESA programs until the Soho mission was approved in

1986. Nevertheless, in the meantime European solar astronomers developed a vigorous scientific endeavour by participating in national balloon, rocket and satellite programs and also serving as experimenters on, or by participating in the scientific operations of, NASA or ISAS (Japanese Institute of Space and Astronautical Science) satellite missions (OSO, Skylab, Yohkoh). In parallel, solar physics (if not solar astronomy) experiments continued to be flown on ESRO and ESA satellites. From the mid seventies, studies of solar astronomy missions began to reappear at ESA. It was then realized that pure solar astronomy would have little chance of being recommended for a mission by the ESA advisory structure, and that a wider scientific appeal was required. Accordingly, hybrid remote sensing and particle observatories began to appear. Soho was eventually successful, as it was proposed together with the Cluster space plasma physics mission to form a solar terrestrial science 'Cornerstone' for ESA's Horizon 2000 Long Term Scientific Program. It is also noted that a purely European solar physics mission is probably not viable either, another international partner is necessary. ESA

N94-22845*# National Aeronautics and Space Administration, Washington, DC.

SOLAR PHYSICS WITHIN NASA'S PLANNING

W. J. Wagner *In* ESA, Scientific Requirements for Future Solar-Physics Space Missions Jun. 1993 p 95-103 Original contains color illustrations (For primary document see N94-22837 06-92)

Copyright Avail: CASI HC A02/MF A02; ESA, EPD, ESTEC, Noordwijk, Netherlands, HC

A description of the new NASA headquarters science organization is provided. The track of a research concept is reviewed on its way to implementation by NASA. Six structural elements are available for use in establishing a concerted science program within the Agency. A list is given of the current active study areas of the NASA supported solar physics community. ESA

N94-22846# Tokyo Astronomical Observatory, Mitaka (Japan).

THE NEXT JAPANESE SOLAR SATELLITE

T. Hirayama *In* ESA, Scientific Requirements for Future Solar-Physics Space Missions Jun. 1993 p 105-113 (For primary document see N94-22837 06-92)

Copyright Avail: CASI HC A02/MF A02; ESA, EPD, ESTEC, Noordwijk, Netherlands, HC

Findings of the Yohkoh satellite about solar corona dynamics are described. Another mission planned by the Japanese solar team for around the year 2000 is addressed. The major objective of the next mission is to find the causes of the coronal dynamics discovered by Yohkoh, and to search for the mechanisms of the coronal and chromospheric heating by simultaneously observing the motions of photospheric magnetic flux tubes and the resultant heating and dynamics of the chromosphere and corona. For this purpose, it is proposed that the core instruments should consist of an optical telescope of less than or equal to 80 cm aperture and 0.1 to 0.2 arcsec resolution, and soft X-ray telescope(s) with resolution better than 1 arcsec. The former should have a magnetograph/Dopplergraph and H alpha plus CaK imagers. Once combined, it will be possible also to study the driving mechanisms of various phenomena such as spicules, fibrils and newly discovered x-ray jets, and prominences, sunspots, and needless to say flares. The objectives and necessary methods of observation are discussed. Only a very rough idea of the instrumentation is given, including some discussion of EUV and other instruments. The mission is expected to be conducted by an international team. ESA

N94-22847# Academy of Sciences (USSR), Moscow. Inst. of Terrestrial Magnetism and Radio Wave Propagation.

SOLAR PHYSICS AND THE CORONAS PROJECT Abstract Only

V. Oraevsky *In* ESA, Scientific Requirements for Future Solar-Physics Space Missions Jun. 1993 p 115-116 (For primary document see N94-22837 06-92)

Copyright Avail: CASI HC A01/MF A02; ESA, EPD, ESTEC, Noordwijk, Netherlands, HC

The three basic problems facing solar physics are addressed. These concern the internal structure of the Sun and the process of transfer of energy from the deeper layers towards the surface; the investigation of solar activity, its mechanism and its influence on the near Earth environment; and the transfer and storage of energy in the upper layers of the solar atmosphere, where the extremely high temperatures of the upper corona are yet to be explained. A future space project which hopes to shed a new light on these problems, the complex orbital near Earth observations of solar activity (Coronas) project and its scientific targets are considered. ESA

N94-22848# Centre National de la Recherche Scientifique, Verrieres-Le Buisson (France). Service d'Aeronomie.

PROSPECTS FOR VERY-HIGH-RESOLUTION SOLAR PHYSICS WITH THE SIMURIS INTEFEROMETRIC MISSION

L. Dame, M. Martic, and R. J. Rutten (Utrecht State Univ., Netherlands.) *In* ESA, Scientific Requirements for Future Solar-Physics Space Missions Jun. 1993 p 119-144 Original contains color illustrations (For primary document see N94-22837 06-92)

Copyright Avail: CASI HC A03/MF A02; ESA, EPD, ESTEC, Noordwijk, Netherlands, HC

The Simuris (Solar, Solar System, and Stellar Interferometric Mission for Ultrahigh Resolution Imaging and Spectroscopy) mission, its scientific objectives, instrument concepts and system design, are addressed. Simuris employs advanced interferometric techniques. Its payload includes two major instruments, which are the Solar Ultraviolet Network (SUN), an interferometric array of four 20 cm telescopes on a 2 m baseline, and the Imaging Fourier Transform Spectrometer (IFTS), which uses light from a 40 cm Gregory telescope. Both instruments have active pointing capabilities of 3 mas stability, and in addition SUN has an active cophasing control to 1/50th of a wavelength. EUV multilayer telescopes complete the payload for diagnostics of the very high temperature plasma. ESA

N94-22849# Mullard Space Science Lab., Dorking (England).

REQUIREMENTS FOR FUTURE SOLAR-PHYSICS MISSIONS WITH X RAY INSTRUMENTATION

J. L. Culhane *In* ESA, Scientific Requirements for Future Solar-Physics Space Missions Jun. 1993 p 147-159 Original contains color illustrations (For primary document see N94-22837 06-92)

Copyright Avail: CASI HC A03/MF A02; ESA, EPD, ESTEC, Noordwijk, Netherlands, HC

Several overall requirements for solar x-ray missions are stated and an outline of the underlying coronal physics is presented. The available techniques for x-ray imaging of the Sun are discussed and compared with reference to previous and ongoing missions. Solar x-ray spectroscopy is assessed in the same manner. Possible choices for future instruments in these two areas are discussed. X-rays are taken to lie broadly in the photon energy range 0.1 to 100 keV. Solar studies at these energies will be mainly concerned with high temperature coronal plasma and nonthermal radiation from particle beams produced in flares. ESA

N94-22850# Lockheed Aircraft Corp., Palo Alto, CA. Solar Physics Dept.

WHY PUT VISIBLE SOLAR TELESCOPES IN SPACE? c89

A. Title *In* ESA, Scientific Requirements for Future Solar-Physics Space Missions Jun. 1993 p 161-168 Original contains color illustrations (For primary document see N94-22837 06-92)

Copyright Avail: CASI HC A02/MF A02; ESA, EPD, ESTEC, Noordwijk, Netherlands, HC

The primary advantages of visible solar telescopes in space are discussed: spatial resolution, geometric stability, photometric accuracy, temporal evolution, and temporal completeness. Given these scientific requirements, factors yielded through image selection, real time and post processing, and adaptive optics from the ground, are addressed. The roles of space and ground based solar telescopes are discussed. ESA

N94-22851# Hulburt (E. O.) Center for Space Research, Washington, DC.

REQUIREMENTS FOR FUTURE SOLAR-PHYSICS MISSIONS THAT INCLUDE UV INSTRUMENTATION

G. E. Brueckner (Naval Research Lab., Washington, DC.) *In* ESA, Scientific Requirements for Future Solar-Physics Space Missions Jun. 1993 p 171-174 (For primary document see N94-22837 06-92)

Copyright Avail: CASI HC A01/MF A02; ESA, EPD, ESTEC, Noordwijk, Netherlands, HC

Reasons why UV solar physics has always been the centerpiece of solar research from space are given: ultraviolet solar radiation shortward of 300 nm is absorbed by the Earth's atmosphere and therefore, can only be explored from space; the solar UV is the dominant energy source of the upper Earth atmosphere; the outer solar atmosphere from the transition region into the corona emits most of its radiation in the ultraviolet. For these reasons, ultraviolet solar research can be divided into two categories: the measurement of solar ultraviolet irradiance with no spatial resolution for Earth atmosphere applications; and high spatial and spectral spectroscopy and imaging of the solar atmosphere for diagnostics of the solar plasma. ESA

N94-23020 Los Alamos National Lab., NM.
RECENT RESULTS FROM THE SOVIET-AMERICAN GALLIUM EXPERIMENT
O. L. Anosov, V. N. Gavrin, and E. L. Faizov (Academy of Sciences, USSR, Moscow.) 1993 4 p Presented at the 13th International Conference on Particles and Nuclei, Perugia, Italy, 27 Jun. - 3 Jul. 1993 Limited Reproducibility: More than 20% of this document may be affected by microfiche quality
(Contract W-7405-eng-36)
(DE94-000677; LA-UR-93-3488; CONF-930637-5) Avail: CASI HC A01

A radiochemical (Ga-71)-(Ge-71) experiment to determine the primary flux of neutrinos from the Sun began measurements of the solar neutrino flux at the Baksan Neutrino Observatory in 1990. The number of Ge-71 atoms extracted from 30 tons of gallium in 1990 and from 57 tons of gallium in 1991 was measured in twelve runs during the period of January 1990 to December 1991. The combined 1990 and 1991 data sets give a value of 58 + 17/-24 (stat) +/- 14 (syst) SNU. This is to be compared with 132 SNU predicted by the Standard Solar Model. DOE

N94-23276*# Lockheed Missiles and Space Co., Palo Alto, CA. Research Lab.
CORONAL ABUNDANCES AND THEIR VARIATION Semiannual Progress Report, Jun. - Dec. 1993
Julia L. R. Saba 15 Dec. 1993 5 p
(Contract NASw-4814)
(NASA-CR-194811; NAS 1.26:194811) Avail: CASI HC A01/MF A01

This contract supports the investigation of elemental abundances in the solar corona, principally through analysis of high-resolution soft x ray spectra from the Flat Crystal Spectrometer on NASA's Solar Maximum Mission. The goals of the study are a characterization of the mean values of relative abundances of elements accessible in the FCS data, and information on the extent and circumstances of their variability. A summation of the data analysis and reporting activities which occurred during the months of June to December 1993 is reported. Author (revised)

N94-23515# Los Alamos National Lab., NM.
ACCELERATOR-BASED NEUTRINO OSCILLATION SEARCHES
D. A. Whitehouse, R. Rameika, and N. Stanton 1993 7 p Presented at the Future Directions in Particle and Nuclear Physics at Multi-GeV Hadron Beam Facilities, Upton, NY, 4-6 Mar. 1993
(Contract W-7405-eng-36)
(DE94-000818; LA-UR-93-3408; CONF-930389-24) Avail: CASI HC A02/MF A01

This paper attempts to summarize the neutrino oscillation section of the Workshop on Future Directions in Particle and Nuclear Physics at Multi-GeV Hadron Beam Facilities. There were very lively discussions about the merits of the different oscillation channels, experiments, and facilities, but we believe a substantial consensus emerged. First, the next decade is one of great potential for discovery in neutrino physics, but it is also one of great peril. The possibility that neutrino oscillations explain the solar neutrino and atmospheric neutrino experiments, and the indirect evidence that Hot Dark Matter (HDM) in the form of light neutrinos might make up 30% of the mass of the universe, point to areas where accelerator-based experiments could play a crucial role in piecing together the puzzle. At the same time, the field faces a very uncertain future. The LSND experiment at LAMPF is the only funded neutrino oscillation experiment in the United States and it is threatened by the abrupt shutdown of LAMPF proposed for fiscal 1994. The future of neutrino physics at the Brookhaven National Laboratory AGS depends on the continuation of High Energy Physics (HEP) funding after the RHIC startup. Most proposed neutrino oscillation searches at Fermilab depend on the completion of the Main Injector project and on the construction of a new neutrino beamline, which is uncertain at this point. The proposed KAON facility at TRIUMF would provide a neutrino beam similar to that at the AGS but with a much increased intensity. The future of KAON is also uncertain. Despite the difficult obstacles present, there is a real possibility that we are on the verge of understanding the masses and mixings of the neutrinos. The physics importance of such a discovery cannot be overstated. The current experimental status and future possibilities are discussed. DOE

N94-23569*# Smithsonian Astrophysical Observatory, Cambridge, MA.
THE CALCULATION OF THEORETICAL CHROMOSPHERIC MODELS AND THE INTERPRETATION OF SOLAR SPECTRA FROM ROCKETS AND SPACECRAFT Final Report, 1 Jul. 1974 - 31 Dec. 1992
Eugene H. Avrett Dec. 1993 10 p
(Grant NsG-7054)
(NASA-CR-195083; NAS 1.26:195083) Avail: CASI HC A02/MF A01

Since the early 1970s we have been developing the extensive computer programs needed to construct models of the solar atmosphere and to calculate detailed spectra for use in the interpretation of solar observations. This research involves two major related efforts: work by Avrett and Loeser on the Pandora computer program for non-LTE modeling of the solar atmosphere including a wide range of physical processes, and work by Kurucz on the detailed synthesis of the solar spectrum based on opacity data for over 58 million atomic and molecular lines. Our goals are to determine models of the various features observed on the Sun (sunspots, different components of quiet and active regions, and flares) by means of physically realistic models, and to calculate detailed spectra at all wavelengths that match observations of those features. These two goals are interrelated: discrepancies between calculated and observed spectra are used to determine improvements in the structure of the models, and in the detailed physical processes used in both the model calculations and the spectrum calculations. The atmospheric models obtained in this way provide not only the depth variation of various atmospheric parameters, but also a description of the internal physical processes that are responsible for non-radiative heating, and for solar activity in general. Derived from text

N94-23626*# Colorado Univ., Boulder. Lab. for Atmospheric and Space Physics.
AN ANALYSIS OF SOLAR MESOSPHERIC TEMPERATURES FOR THE UPPER STRATOSPHERE AND MESOSPHERE Final Report
R. Todd Clancy and David W. Rusch Dec. 1993 57 p
(Grant NAGw-2130)
(NASA-CR-194861; NAS 1.26:194861) Avail: CASI HC A04/MF A01

We proposed to analyze Solar Mesosphere Explorer (SME) limb profiles of Rayleigh scattered solar flux at wavelengths of 304, 313, and 443 nm to retrieve atmospheric temperature profiles over the 40-65 km altitude region. These temperatures can be combined with the previous analysis of SME 296 nm limb radiances to construct a monthly average climatology of atmospheric temperatures over the 40-90 km, upper stratosphere-mesosphere region, with approximately 4 km vertical resolution. We proposed to investigate the detailed nature of the global temperature structure of this poorly measured region, based on these 1982-1986 SME temperatures. The average vertical structure of temperatures between the stratopause and mesopause has never been determined globally with vertical resolution sufficient to retrieve even scale-height structures. Hence, the SME temperatures provided a unique opportunity to study the detailed thermal structure of the mesosphere, in advance of Upper Atmosphere Research Satellite (UARS) measurements and the Thermosphere Ionosphere Mesosphere Energy and Dynamics (TIMED) mission. Author

N94-23738 National Geophysical Data Center, Boulder, CO.
SOLAR-GEOPHYSICAL DATA NUMBER 584, APRIL 1993. PART 1: (PROMPT REPORTS). DATA FOR FEBRUARY, MARCH, 1993, AND LATE DATA
H. E. Coffey Apr. 1993 145 p See also Part 2, PB93-198331 and PB93-188894 Limited Reproducibility: More than 20% of this document may be affected by microfiche quality
(PB93-198323; SGD-584-PT-1) Avail: Issuing Activity (National Technical Information Service (NTIS))

This document presents data for March 1993 on the following topics: solar-terrestrial environment; IUWDS alert periods (advance and worldwide); solar activity indices; solar flares; solar radio emission; and Stanford mean solar magnetic field. Data for February 1993 covers: solar active regions; sudden ionospheric disturbances; solar radio spectral observations; cosmic ray measurements by neutron monitor; and geomagnetic indices. NTIS

N94-23739 National Geophysical Data Center, Boulder, CO.
SOLAR-GEOPHYSICAL DATA NUMBER 584, APRIL 1993. PART 2: (COMPREHENSIVE REPORTS). DATA FOR OCTOBER 1992, AND MISCELLANEOUS
H. E. Coffey Apr. 1993 65 p See also Part 1, PB93-198323 and PB93-188902 Limited Reproducibility: More than 20% of this document may be affected by microfiche quality
(PB93-198331; SGD-584-PT-2) Avail: CASI HC A04

This document provides data for October 1992 on solar flares, solar radio bursts at fixed frequencies, solar x ray radiation from GOES satellite graphs, mass ejections from the sun, and active prominences and filaments. NTIS

N94-24094*# Alabama Univ., Huntsville.
[EXCITATION OF XUV RADIATION IN SOLAR FLARES] Final Report
A. Gordon Emslie Feb. 1992 4 p
(Grant NAG5-500)
(NASA-CR-193703; NAS 1.26:193703) Avail: CASI HC A01/MF A01

The goal of the proposed research was to understand the means by which XUV radiation in solar flares is excited, and to use this radiation as diagnostics of the energy release and transport processes occurring in the flare. Significant progress in both of these areas, as described, was made. Author (revised)

N94-24300*# Smithsonian Astrophysical Observatory, Cambridge, MA.
THE RESONANCE LINES OF MG2 AS DIAGNOSTICS OF THE UPPER SOLAR CHROMOSPHERE Final Report, 1 Nov. 1991 - 30 Apr. 1993
Eugene H. Avrett Jan. 1994 9 p
(Grant NAGw-2814)
(NASA-CR-195084; NAS 1.26:195084) Avail: CASI HC A02/MF A01

The resonance lines of singly ionized magnesium, the MgII h&k lines at about 280 nm, are two of the small number of lines in the solar spectrum that are optically thick in the chromospheric part of the solar atmosphere. Potentially these lines contain information on the initial temperature rise that occurs at the top of the photosphere. Unfortunately, few good observations of the lines exist due to their wavelength near 280 nm the ultraviolet. However, a fair number of observations (on the order of 200) are available from the data base of the UltraViolet Polarimeter and Spectrometer (UVSP) instrument that flew on board of NASA's Solar Maximum Mission (SMM) satellite. In addition, this data base contains a number of spectra that include the Mg I resonance line at (lambda)285.2nm, just longward of the h&k lines. The neutral magnesium line is not as strong as its ionic counterparts and samples slightly lower parts of the atmosphere. Its width is a sensitive diagnostic of the ionization balance between neutral and singly ionized magnesium, which determines the opacity scale (and formation height) of other diagnostically important MgI lines like the 457.1 nm intercombination line, the magnesium b lines and the infrared MgI emission lines near 12 microns. Analysis of the observed line profiles shows that it is necessary to include the effects of partial frequency redistribution (PRD) in the formation of the line as in the case of the h&k lines. This implies that the core of the line is very sensitive to the way scattering is treated in the modeling of the line, and in turn this allows us to separate the uncertain effects in the atomic data (viz. the Van der Waals broadening) from the uncertainties in the underlying atmospheric model. The main objective of this research was to compare observed spectra of the magnesium resonance lines against theoretical line profiles calculated from recent models of the solar atmosphere by Fontenla et al., hereafter called FAL. These models extend earlier solar models by Avrett et al. and provide yet a better match between observed and calculated spectra, in particular of the hydrogen Lyman line, by including the effects of ambipolar diffusion of hydrogen and helium in the mass and energy transport equations for the chromosphere-corona transition region. Although the transition region models can be built self-consistently (without additional observational input) once the proper boundary conditions are given at the top of the chromosphere, there are uncertainties in the models precisely because these boundary conditions are not well known. With the analysis of UVSP magnesium observations we strive to constrain these uncertainties. Author

N94-24461*# Alabama Univ., Huntsville.
SCIENTIFIC STUDY IN SOLAR AND PLASMA PHYSICS RELATIVE TO ROCKET AND BALLOON PROJECTS Final Report, 9 Dec. 1991 - 8 Dec. 1993
S. T. Wu 8 Dec. 1993 31 p
(Contract NAS8-38609)
(NASA-CR-193885; NAS 1.26:193885) Avail: CASI HC A03/MF A01

The goals of this research are to provide scientific and technical capabilities in the areas of solar and plasma physics contained in research programs and instrumentation development relative to current rocket and balloon projects; to develop flight instrumentation design, flight hardware, and flight program objectives and participate in peer reviews as appropriate; and to participate in solar-terrestrial physics modeling studies and analysis of flight data and provide theoretical investigations as required by these studies. Author (revised)

N94-24484*# Alabama Univ., Huntsville.
MODEL DEVELOPMENT FOR ULYSSES AND SOHO Final Report, 27 May - 27 Nov. 1993
S. T. Wu 27 Nov. 1993 43 p
(Contract NAS8-38609)
(NASA-CR-193884; NAS 1.26:193884) Avail: CASI HC A03/MF A01

The purpose of this research is to provide scientific expertise in solar physics and in the development and use of magnetohydrodynamic (MHD) models of coronal structures for the computation of Lyman alpha scattered radiation in these structures. The specific objectives will be to run MHD models with new boundary conditions and compute resulting scattered solar Lyman alpha intensities, guided by results from the first series of boundary conditions. Author (revised)

N94-24961# Tokyo Univ., Tanashi (Japan).
KAMIOKANDE RESULTS ON SOLAR NEUTRINOS AND A SUPERNOVA SEARCH
Y. Suzuki May 1993 11 p Presented at the International Symposium on Neutrino Astrophysics, Gifu, Japan, 19-22 Oct. 1992 See also A93-44876
(ICRR-Rept-294-93-6; JTN-94-80540) Avail: CASI HC A03/MF A01

The solar neutrino measurement extended till the end of August in 1992 gives almost entire coverage of the solar maximum in solar cycle 22. The observation shows the almost constant solar B-8-neutrino flux of Data/SSM (Standard Solar Model) = 0.49 +/- 0.04 +/- 0.06 on an average for the Kamiokande 2 and 3 data. The flux limit of the Hep neutrino is shown at first time. A stringent limit on solar anti-neutrinos that is less than 5.8 percent of the flux of B-8 neutrinos is obtained. A search for supernova neutrinos in the Kamiokande detector is briefly summarized and galactic supernova rate obtained is less than 0.54 SN (Supernova)/year for 4.26 years of observation. Author (NASDA)

N94-24962# Tokyo Univ., Tanashi (Japan). Inst. for Cosmic Ray Research.
SOLAR NEUTRINOS: REAL-TIME EXPERIMENTS
Yoji Totsuka Apr. 1993 21 p
(ICRR-Rept-293-93-5; JTN-94-80542) Avail: CASI HC A03/MF A01

This report outlines the principle of real-time solar neutrino detection experiments by detecting electrons with suitable target material, via Charged-Current (CC) reaction using conventional counting techniques developed in high-energy physics. Only B-8 neutrinos can be detected by minimum detectable energy of several MeV. The MSW (Mikheyev, Smirnov, Wolfenstein) effect not only distorts the energy spectrum but also induces new type of neutrinos, i.e. mu-neutrinos or tau-neutrinos. These neutrinos do not participate in the CC reaction. Therefore real-time experiment is to be sensitive to Neutral Current (NC) reactions. It is a challenge to eliminate environment background as much as possible and to lower the minimum detectable energy to several 100 keV, which will enable observation of Be-7 neutrinos. Target particles of real-time experiments currently running and under construction or planning are electron, deuteron, or argon. The relevant reactions corresponding to CC reaction and some relevant comments on the following targets are described: (1) electron target; (2) deuteron target; and (3) argon target. On-going experiment and future experiments for real-time neutron detection are also outlined. Author (NASDA)

N94-24989 National Geophysical Data Center, Boulder, CO.
SOLAR-GEOPHYSICAL DATA NUMBER 587, JULY 1993. PART 1: (PROMPT REPORTS). DATA FOR JUNE, MAY 1993, AND LATE DATA
Helen E. Coffey, ed. Jul. 1993 136 p See also PB93-232882 and PB93-216737 Limited Reproducibility: More than 20% of this document may be affected by microfiche quality
(PB93-232874; SGD-587-Pt-1) Avail: Issuing Activity (National Technical Information Service (NTIS))

Solar-Geophysical Data prompt reports for May and June 1993 are presented. Included are: Data for June 1993; Solar-Terrestrial Environment; IUWDS Alert Periods (Advance and Worldwide); Solar Activity Indices; Solar Flares; Solar Radio Emission; Stanford Mean Solar Magnetic Field; Data for May 1993; Solar Active Regions; Sudden Ionospheric Disturbances; Solar Radio Spectral Observations; Solar Radioheliograph - 164 MHz - Nancay; Cosmic Ray Measurements by Neutron Monitor; and Geomagnetic Indices. NTIS

N94-24990 National Geophysical Data Center, Boulder, CO.
SOLAR-GEOPHYSICAL DATA NUMBER 587, JULY 1993. PART 2: (COMPREHENSIVE REPORTS). DATA FOR JANUARY 1993, AND MISCELLANEOUS
Helen E. Coffey, ed. Jul. 1993 45 p See also PB93-232874 and PB93-216745 Limited Reproducibility: More than 20% of this document may be affected by microfiche quality
(PB93-232882; SGD-587-Pt-2) Avail: CASI HC A03

Solar-Geophysical Data cmprehensive reports for January 1993 are presented. Included are: Data for January 1993; Solar Flares; Solar Radio Bursts at Fixed Frequencies; Solar X Ray Radiation from GOES Satellite Graphs; Mass Ejections from the Sun; Active Prominences and Filaments; and IMP-8 Solar Wind Plot. NTIS

N94-24991# National Geophysical Data Center, Boulder, CO.
SOLAR-GEOPHYSICAL DATA NUMBER 588, AUGUST 1993. PART 1: (PROMPT REPORTS). DATA FOR JULY, JUNE 1993, AND LATE DATA
H. E. Coffey Aug. 1993 128 p See also PB94-109105 and PB93-232874
(PB94-109089; SGD-588-Pt-1) Avail: CASI HC A07/MF A02

Solar-Geophysical Data prompt reports for July, and June 1993 are presented. Included are: Data for July 1993; Solar-Terrestrial Environment; IUWDS Alert Periods (Advance and Worldwide); Solar Activity Indices; Solar Flares; Solar Radio Emission; Stanford Mean Solar Magnetic Field; Data for June 1993; Solar Active Regions; Sudden Ionospheric Disturbances; Solar Radio Spectral Observations; Solar Radioheliograph - 164 MHz - Nancay; Cosmic Ray Measurements by Neutron Monitor; and Geomagnetic Indices. NTIS

N94-24992# National Geophysical Data Center, Boulder, CO.
SOLAR-GEOPHYSICAL DATA NUMBER 588, AUGUST 1993. PART 2: (COMPREHENSIVE REPORTS). DATA FOR FEBRUARY 1993, AND MISCELLANEOUS
H. E. Coffey Aug. 1993 71 p See also PB94-109089 and PB93-232882
(PB94-109105; SGD-588-Pt-2) Avail: CASI HC A04/MF A01

Solar-Geophysical Data comprehensive reports for Bebruary 1993 are presented. Included are: Data for February 1993; Solar Flares; Solar Radio Bursts at Fixed Frequencies; Solar X Ray Radiation from GOES Satellite Graphs; Mass Ejections from the Sun; and Active Prominences and Filaments. NTIS

N94-24993# National Geophysical Data Center, Boulder, CO.
SOLAR-GEOPHYSICAL DATA NUMBER 589, SEPTEMBER 1993. PART 1: (PROMPT REPORTS). DATA FOR AUGUST, JULY 1993, AND LATE DATA
H. E. Coffey Sep. 1993 129 p See also PB94-117405 and PB94-109089
(PB94-117082; SGD-589-Pt-1) Avail: CASI HC A07/MF A02

Contents: Data for August 1993; Solar-Terrestrial Environment; IUWDS Alert Periods (Advance and Worldwide); Solar Activity Indices; Solar Flares; Solar Radio Emission; Stanford Mean Solar Magnetic Field. NTIS

N94-24994# National Geophysical Data Center, Boulder, CO.
SOLAR-GEOPHYSICAL DATA NUMBER 589, SEPTEMBER 1993. PART 2: (COMPREHENSIVE REPORTS). DATA FOR MARCH 1993, AND MISCELLANEOUS
H. E. Coffey Sep. 1993 77 p See also PB94-117082 and PB94-109105
(PB94-117405; SGD-589-PT-2) Avail: CASI HC A05/MF A01

Contents: Solar Flares; H-alpha Solar Flare Groups; Intervals of No Flare Patrol Observation; Number of Solar Flares August 1966-present; Solar Radio Bursts at Fixed Frequencies; Solar X-Ray Radiation from GOES Satellite Graphs; Mass Ejections from the Sun; Active Prominences and Filaments; Solar Irradiance (Unavailable at time of publication); and IMP-8 Solar Wind Plot (Unavailable at time of publication). NTIS

N94-25031 Louisiana State Univ., Baton Rouge. Dept. of Physics and Astronomy.
SOLAR FLARES AND MAGNETOSPHERIC PARTICLES: INVESTIGATIONS BASED UPON THE ONR-602 AND ONR-604 EXPERIMENTS Quarterly Report No. 4
John P. Wefel and T. G. Guzik 30 Nov. 1993 23 p Limited Reproducibility: More than 20% of this document may be affected by microfiche quality
(Contract N00014-90-J-1466)
(AD-A273639) Avail: CASI HC A03

This performance report covers work accomplished under ONR Grant N00014-90-J-1466 related to the radiation environment in near-earth space. The goal of the research is to measure and describe, quantitatively, the geospace radiation environment in which men and spacecraft must survive and function. The tools for this investigation are the data returned by the ONR-602 and ONR-604 experiments, both flown under the auspices of ONR and the Air Force Space Test Program, augmented by correlative databases of both space-based and ground-based data. The investigation involves data analysis, modeling, and applications to a variety of space equipment and environments. This report builds upon the detailed technical report and the previous performance reports. For the current period, the principal effort was in modeling of the anomalous component, determining the modulation level during the CRRES mission, and studying the quiet-time particle access to the magnetosphere. DTIC

N94-25264*# Alabama Univ., Huntsville. Dept. of Mechanical and Aerospace Engineering.
ON THE PHYSICS OF WAVES IN THE SOLAR ATMOSPHERE: WAVE HEATING AND WIND ACCELERATION Semiannual Report, period ending Mar. 1994
Z. E. Musielak Mar. 1994 7 p
(Grant NAG8-839)
(NASA-CR-195197; NAS 1.26:195197) Avail: CASI HC A02/MF A01

This paper presents work performed on the generation and physics of acoustic waves in the solar atmosphere. The investigators have incorporated spatial and temporal turbulent energy spectra in a newly corrected version of the Lighthill-Stein theory of acoustic wave generation in order to calculate the acoustic wave energy fluxes generated in the solar convective zone. The investigators have also revised and improved the treatment of the generation of magnetic flux tube waves, which can carry energy along the tubes far away from the region of their origin, and have calculated the tube wave energy fluxes for the sun. They also examine the transfer of the wave energy originated in the solar convective zone to the outer atmospheric layers through computation of wave propagation and dissipation in highly nonhomogeneous solar atmosphere. These waves may efficiently heat the solar atmosphere and the heating will be especially significant in the chromospheric network. It is also shown that the role played by Alfven waves in solar wind acceleration and coronal hole heating is dominant. The second part of the project concerned investigation of wave propagation in highly inhomogeneous stellar atmospheres using an approach based on an analytic tool developed by Musielak, Fontenla, and Moore. In addition, a new technique based on Dirac equations has been developed to investigate coupling between different MHD waves propagating in stratified stellar atmospheres. CASI

N94-25275*# Solar Physics Research Corp., Tucson, AZ.
SOLAR MAGNETIC CYCLE

Karen L. Harvey 1993 17 p
(Contract NASw-4721)
(NASA-CR-195202; NAS 1.26:195202) Avail: CASI HC A03/MF A01

Using NSO/KP magnetograms, the pattern and rate of the emergence of magnetic flux and the development of the large-scale patterns of unipolar fields are considered in terms of the solar magnetic cycle. Magnetic flux emerges in active regions at an average rate of 2 x 10(exp 21) Mx/day, approximately 10 times the estimated rate in ephemeral regions. Observations are presented that demonstrate that the large-scale unipolar fields originate in active regions and activity nests. For cycle 21, the net contribution of ephemeral regions to the axial dipole moment of the Sun is positive, and is of opposite sign to that of active regions. Its amplitude is smaller by a factor of 6, assuming an average lifetime of ephemeral regions of 8 hours. Active regions larger than 4500 Mm(sup 2) are the primary contributor to the cycle variation of Sun's axial dipole moment. Author (revised)

93 SPACE RADIATION

Includes cosmic radiation; and inner and outer earth's radiation belts.

For biological effects of radiation see *52 Aerospace Medicine*. For theory see *73 Nuclear and High-Energy Physics*.

N94-22947*# Washington Univ., Saint Louis, MO. Dept. of Physics.
TWO POPULATIONS AND MODELS OF GAMMA RAY BURSTS
J. I. Katz 20 Jul. 1993 19 p Repr. from The Astrophysical Journal, v. 422, no. 49, 10 Feb. 1994
(Grant NAGw-2918)
(NASA-CR-194762; NAS 1.26:194762) Avail: CASI HC A03/MF A01

Gamma-ray burst statistics are best explained by a source population at cosmological distances, while spectroscopy and intensity histories of some individual bursts imply an origin on Galactic neutron stars. To resolve this inconsistency I suggest the presence of two populations, one at cosmological distances and the other Galactic. I build on ideas of Shemi and Piran (1990) and of Rees and Mesozaros (1992) involving the interaction of fireball debris with surrounding clouds to explain the observed intensity histories in bursts at cosmological distances. The distances to the Galactic population are undetermined because they are too few to affect the statistics of intensity and direction; I explain them as resulting from magnetic reconnection in neutron star magnetospheres. An appendix describes the late evolution of the debris as a relativistic blast wave. Author

N94-24695 Bubble Technology Industries, Inc., Chalk River (Ontario).
TO PERFORM A PROOF-OF-CONCEPT STUDY ON THE USE OF SUPERHEATED DROP DETECTORS FOR THE MEASUREMENT OF LET SPECTRA IN SPACE ENVIRONMENTS Final Report
R. A. Noulty, S. Hoffman, M. L. Larabie, J. L. Jevcak, B. Campbell, T. Clifford, T. McLean, and H. Ing 1992 92 p
(Contract W7714-0-9393/01-ST)
(BTI-92/3-31; CTN-94-60900) Avail: Micromedia Ltd., Technical Information Centre, 165 Hotel de Ville, Place du Portage, Phase 2, Hull, Quebec J8X 3X2, Canada

Research was conducted with the ultimate aim of developing a linear energy transfer (LET) spectrometer suitable for measurement of space radiation, in order to quantify the effect of cosmic rays on electronic components. For measuring the LET spectrum sensed by electronic components, the technical problem is the low penetration of many extraterrestrial radiations of interest. The chosen approach to this problem involves encapsulating individual droplets of the medium that forms the sensitive sites of the bubble detectors. In the research, fluorinated compounds suitable for micro-encapsulation were determined along with the various polymers useful for encapsulating those compounds. Encapsulation processes including complex coacervation, interfacial polymerization, spray drying, and suspension polymerization were evaluated. The capabilities of the capsules to detect neutrons and heavy ions were tested. Thin layer detectors were also fabricated and tested. The results indicate that it is possible to surround a superheated freon droplet with an amount of material thin enough to allow penetration of a heavy ion, and that thin-bubble detectors are capable of detecting He-4 ions and neutrons. Problems with excess drying in vacuum and lowering of effective superheat still have to be overcome. CISTI

N94-25091*# Harvard Coll. Observatory, Cambridge, MA. Center for Astrophysics.
NEUTRON STAR MERGERS AND GAMMA-RAY BURSTS Final Technical Report, period ending 31 Dec. 1993
Ramesh Narayan 1993 6 p
(Grant NAG5-1904)
(NASA-CR-195176; NAS 1.26:195176) Avail: CASI HC A02/MF A01

Under the support of grant NAG 5-1904, we have carried out research on several topics related to gamma-ray bursts (GRB's). In our proposal, we stated that we would study three topics: (1) fireball evolution; (2) neutron star mergers; and (3) statistics of bursts. We have completed a significant amount of work in each of these areas. Resulting papers from this work are presented. Author (revised)

N94-25199*# Alabama Univ., Huntsville.
[AN ANALYSIS OF GAMMA RAY BURST TIME HISTORIES] Final Report
John Patrick Lestrade and Gerald R. Karr Feb. 1994 4 p Presented at the Summer Faculty Fellowship Research Continuation Program, Huntsville, AL, Feb. 1994; sponsored by Alabama Univ.
(Grant NAG8-212)
(NASA-CR-195191; NAS 1.26:195191; UAH-5-30166) Avail: CASI HC A01/MF A01

Gamma ray burst time histories, ranging in durations from milliseconds to thousands of seconds, are as varied as the number of bursts. They show a wide array of structures from those that are very smooth to those that contain a seemingly uncountable number of spikes riding on top of other spikes. These profiles have tantalized researchers for years - they obviously hold important information on the nature of GRB's, but to date no one has been successful in analyzing them. For the past year the author has been working on algorithms to analyze these data. Two approaches have been followed in this investigation. The first is an attempt to quantify the amount of structure, or spikiness, in a profile. The second involves applying the latest theorems on chaos and fractals with the aim of extracting useful information from what seems to be a random collection of shot noise. Author (revised)

N94-25260*# National Center for Atmospheric Research, Boulder, CO. High Altitude Observatory.
THE SOLAR SPECTRAL IRRADIANCES FROM X RAY TO RADIO WAVELENGTHS
O. R. White 1993 9 p
(Contract NASw-4721)
(NASA-CR-195203; NAS 1.26:195203) Avail: CASI HC A02/MF A01

Sources of new measurements of the solar EUV, UV, and visible spectrum are presented together with discussion of formation of the solar spectrum as a problem in stellar atmospheres. Agreement between the data and a modern synthetic spectrum shows that observed radiative variability is a minor perturbation on a photosphere in radiative equilibrium and local thermodynamic equilibrium (LTE). Newly observed solar variability in 1992 defines a magnetic episode on the Sun closely associated with changes in both spectral irradiances and the total irradiance. This episode offers the opportunity to track the relationship between radiation and magnetic flux evolution. Author

N94-25459 Max-Planck-Inst. fuer Physik und Astrophysik, Garching (Germany). Werner-Heisenberg-Inst.
SUPERCONDUCTING COSMIC STRINGS NEAR THE ELECTROWEAK SCALE AND COSMIC-RAY PROPAGATION
R. Plaga Feb. 1993 10 p Submitted for publication Limited Reproducibility: More than 20% of this document may be affected by microfiche quality
(MPI-PhE/93-05; ETN-94-95115) Copyright Avail: CASI HC A02

A method to search for superconducting cosmic strings with a symmetry breaking mass scale near the electroweak scale from experimental data is described. Strings in the galaxy act as scattering centers because of their coherent and bounded magnetic field. In this case they contribute to the diffusion of galactic cosmic rays. The rigidity dependence of the string induced diffusion coefficient is very specific. The search for superconducting strings can be performed by studying the diffusion properties of low energy galactic cosmic rays. Particle emission by galactic strings near the electroweak scale is discussed. Gamma ray emission from galactic strings near the electroweak scale have not been detected up to now. Further experiments are required. ESA

N94-24431*# Mississippi State Univ., State College. Dept. of Physics and Astronomy.
STRUCTURE IN GAMMA RAY BURST TIME PROFILES: CORRELATIONS WITH OTHER OBSERVABLES
John Patrick Lestrade *In* Alabama Univ., The 1993 NASA/ASEE Summer Faculty Fellowship Program Nov. 1993 5 p (For primary document see N94-24405 06-80)
Avail: CASI HC A01/MF A03

N94-24435*# New Mexico State Univ., Las Cruces. Astronomy Dept.
FLUX MEASUREMENTS USING THE BATSE SPECTROSCOPIC DETECTORS
Bernard McNamara *In* Alabama Univ., The 1993 NASA/ASEE Summer Faculty Fellowship Program Nov. 1993 5 p (For primary document see N94-24405 06-80)
Avail: CASI HC A01/MF A03

99 GENERAL

N94-22893# Loyola Coll., Baltimore, MD. International Technology Research Inst.
ADVANCED DISPLAY TECHNOLOGIES IN RUSSIA, UKRAINE, AND BELARUS. VIEWGRAPHS
Michael J. DeHaemer and Geoffrey M. Holdridge, ed. 1994 157 p Workshop held in Arlington, VA, 3 Feb. 1994 Sponsored in part by NSF and ARPA
Copyright Avail: CASI HC A08/MF A02

Viewgraphs from a workshop on advanced display technologies in Russia, Ukraine, and Belarus are presented. The workshop was sponsored by the National Science Foundation Advanced Research Projects Agency and the World Technology Evaluation Center at Loyola College. Topics covered include: non-emissive display technology, non-emissive display materials, emissive display technology and materials, infrastructure, and business issues. CASI

N94-23135*# National Aeronautics and Space Administration. Lewis Research Center, Cleveland, OH.
LEWIS RESEARCH CENTER R AND D FACILITIES
Jun. 1991 55 p Original contains color illustrations
(NASA-TM-109400; NAS 1.15:109400) Avail: CASI HC A04/MF A01; 51 functional color pages

The NASA Lewis Research Center (LeRC) defines and develops advanced technology for high priority national needs. The work of the Center is directed toward new propulsion, power, and communications technologies for application to aeronautics and space, so that U.S. leadership in these areas is ensured. The end product is knowledge, usually in a report, that is made fully available to potential users--the aircraft engine industry, the energy industry, the automotive industry, the space industry, and other NASA centers. In addition to offices and laboratories for almost every kind of physical research in such fields as fluid mechanics, physics, materials, fuels, combustion, thermodynamics, lubrication, heat transfer, and electronics, LeRC has a variety of engineering test cells for experiments with components such as compressors, pumps, conductors, turbines, nozzles, and controls. A number of large facilities can simulate the operating environment for a complete system: altitude chambers for aircraft engines; large supersonic wind tunnels for advanced airframes and propulsion systems; space simulation chambers for electric rockets or spacecraft; and a 420-foot-deep zero-gravity facility for microgravity experiments. Some problems are amenable to detection and solution only in the complete system and at essentially full scale. By combining basic research in pertinent disciplines and generic technologies with applied research on components and complete systems, LeRC has become one of the most productive centers in its field in the world. This brochure describes a number of the facilities that provide LeRC with its exceptional capabilities. Author (revised)

N94-23333*# National Aeronautics and Space Administration, Washington, DC.
THE BIRTH OF NASA: THE DIARY OF T. KEITH GLENNAN
Thomas Keith Glennan and J. D. Hunley, ed. 1993 421 p *Its* NASA History Series Original contains color illustrations
(NASA-SP-4105; NAS 1.21:4105; LC-93-31238; ISBN-0-16-041936-0)
Avail: CASI HC A18/MF A04; SOD HC

In this book, part diary and recollection, T. Keith Glennan--the first administrator of NASA--relates the story of how he and others both inside and outside of the agency worked within the circumstances created by the Sputnik crisis to plan and organize a viable space program that ultimately put 12 Americans on the Moon. In the process, Glennan also reveals a great deal about Eisenhower as a human. Derived from text

N94-23336# Nagoya Univ. (Japan).
SOLAR-TERRESTRIAL ENVIRONMENTAL LABORATORY Annual Report, 1 Apr. 1992 - 31 Mar. 1993
31 Mar. 1993 33 p Original contains color illustrations
Avail: CASI HC A03/MF A01

The Solar-Terrestrial Environment (STE) Laboratory was established in June 1990 as one of the research institutes attached to Nagoya University for promoting cooperative research on the solar-terrestrial environment. The former Research Institute of Atmospherics and the Cosmic-Ray Research Laboratory, School of Science, were merged to create the new laboratory. Several cooperative projects under the Solar Terrestrial Energy Program (STEP), International Global Atmospheric Chemistry (IGBP) program, and a domestic research program on the global environment were set up at approximately the same time as the start of the STE Laboratory. These research projects aim at understanding solar-terrestrial environment changes relevant to the objective of our institute. We have participated in these programs, carrying out several observations in collaboration with other institutions. Most of the observations have been carried out as international cooperative research projects, not only at the observation sites of the STE Laboratory in Japan, but also at 25 other observation points situated in the United States, Canada, Russia, Australia, New Zealand, France, Norway, Sweden, Indonesia, Papua New Guinea, Peru, Bolivia, and Brazil. These observations continuously monitor geomagnetic variations, ULF and VLF waves, auroras, minor atmospheric constituents, aerosols, solar wind, solar neutrons and cosmic rays. It is important to embark on research programs which have long-term prospects and international cooperation to increase our understanding of the global aspect of the solar-terrestrial environment. At present, we have agreements with 14 foreign institutions, to develop academic exchange and cooperation in the field of solar-terrestrial studies. Observations from the Raman scattering lidar, installed in 1991, started in July, 1993. This sophisticated lidar system is used for monitoring aerosols and some gaseous components, such as H2O and CO2 and will be open to use for collaborative research work. Construction of a new UHF antenna was completed at Agematsu, Nagano, to make up a four-antenna system for the measurement of solar wind plasmas by using the interplanetary scintillation method. The new antenna will not only improve the capability of solar wind observations in the vicinity of the sun, but also make it possible to measure random velocities which are expected to impart additional acceleration to the solar wind. To promote collaborative research activity in the field of solar-terrestrial environmental science, efforts were made to establish an on-line connection between the STE Laboratory and other institutions. A new network system, STEnet, in the laboratory is connected to the Japanese inter-university network known as N1 and the Internet via TISN (Total International Science Network), which supports both NSI/DECnet (SPAN) and Academic Internet. Derived from text

N94-23572# Office of Technology Assessment, Washington, DC.
CONTRIBUTIONS OF DOE WEAPONS LABS AND NIST TO SEMICONDUTOR TECHNOLOGY
Avtar S. Oberai and Elizabeth Sheley, ed. Sep. 1993 91 p
(OTA-ITE-585; ISBN-0-16-042095-4) Avail: CASI HC A05/MF A01; SOD HC

The debate over whether and how to expand the missions of the DOE labs has raised questions of how to coordinate these new activities with those of labs and agencies that already have responsibility for civilian technology policy - principally the National Institute of Standards and Technology of the Department of Commerce. NIST has emerged in the last few years as one of the federal government's major players in civilian technology advancement through, for example, management of the new and well-regarded Advanced Technology Program. This Report examines how NIST and DOE weapons laboratories could contribute to advances in semiconductor technology aimed specifically at civilian applications. Semiconductor technology was chosen as an example of a technology focus for a civilian technology initiative, primarily because the industry had already developed a set of comprehensive technology road maps and the federal labs had substantial expertise in the area. The Report was requested as a follow-on assessment to OTA's work on the implications for the U.S. civilian economy at the end of the Cold War. That work consists of two reports: After the Cold War: Living With Lower Defense Spending, and Defense Conversion: Redirecting R&D. The former considered the effects on defense workers, defense-dependent communities, and defense companies, and suggested policy options to ease transitions for those affected by cutbacks. The latter examined how the R&D institutions whose primary missions were defense-related could contribute to national well-being under a broader concept of national security. Author (revised)

N94-24493*# Florida Inst. of Tech., Melbourne. Dept. of Physics and Space Sciences.
JOVE NASA-FIT PROGRAM: MICROGRAVITY AND AERONOMY PROJECTS Semiannual Status Report, 24 May 1993 - 24 Jan. 1994
James D. Patterson, James G. Mantovani, and Hamid K. Rassoul 25 Jan. 1994 57 p
(Grant NAG8-195)
(NASA-CR-195121; NAS 1.26:195121) Avail: CASI HC A04/MF A01

This semi-annual status report is divided into two sections: Scanning Tunneling Microscopy Lab and Aeronomy Lab. The Scanning Tunneling Microscopy (STM) research involves studying solar cell materials using the STM built at Florida Tech using a portion of our initial Jove equipment funding. One result of the participation in the FSEC project will be to design and build an STM system which is portable. This could serve as a prototype STM system which might be used on the Space Shuttle during a Spacelab mission, or onboard the proposed Space Station. The scanning tunneling microscope is only able to image the surface structure of electrically conductive crystals; by building an atomic force microscope (AFM) the surface structure of any sample, regardless of its conductivity, will be able to be imaged. With regards to the Aeronomy Lab, a total of four different mesospheric oxygen emission codes were created to calculate the intensity along the line of sight of the shuttle observations for 2972A, Herzberg I, Herzberg II, and Chamberlain bands. The thermosphere-ionosphere coupling project was completed with two major accomplishments: collection of 500 data points on modulation of neutral wind with geophysical variables, and establishment of constraints on behavior of the height of the ionosphere as a result of interaction between geophysical and geometrical factors. The magnetotail plasma project has been centered around familiarization with the subject in the form of a literature search and preprocessing of IMP-8 data. Derived from text

N94-24584*# National Aeronautics and Space Administration. Lyndon B. Johnson Space Center, Houston, TX.
SUDDENLY, TOMORROW CAME... A HISTORY OF THE JOHNSON SPACE CENTER
Henry C. Dethloff 1993 425 p *Its* NASA history series Original contains color illustrations
(NASA-SP-4307; NAS 1.21:4307; LC-93-86012) Avail: CASI HC A18/MF A04; 4 functional color pages

This book chronicles the history of the Johnson Space Center into 17 chapters with a forward written by Donald K. Slayton. Photographs and illustrations are provided. This book becomes part of the NASA history series. CASI

N94-24585*# National Aeronautics and Space Administration, Washington, DC.
JAPANESE AEROSPACE SCIENCE AND TECHNOLOGY 1992. A BIBLIOGRAPHY WITH INDEXES
Washington May 1993 1017 p
(NASA-SP-7104; NAS 1.21:7104) Avail: CASI HC A99/MF A10

This report contains 4271 annotated references to reports and journal articles of Japaness intellectual origin entered into the NASA scientific and technical information system during 1992. Representative subject areas of interest include: adaptive control, antireflection coatings, fiber reinforced composites, gallium arsenide lasers, laser interferometry, reduced gravity (microgravity), and VHSIC (circuits). Author

N94-25003*# Research Inst. for Advanced Computer Science, Moffett Field, CA.
RIACS/USRA Annual Report, 1993
Joseph Oliger 1993 40 p
(Contract NAS2-13721)
(NASA-CR-195117; NAS 1.26:195117) Avail: CASI HC A03/MF A01

The Research Institute for Advanced Computer Science (RIACS) was established by the Universities Space Research Association (USRA) at the NASA Ames Research Center (ARC) on 6 June 1983. RIACS is privately operated by USRA, a consortium of universities with research programs in the aerospace sciences, under contract with NASA. The primary mission of RIACS is to provide research and expertise in computer science and scientific computing to support the scientific missions of NASA ARC. The research carried out at RIACS must change its emphasis from year to year in response to NASA ARC's changing needs and technological opportunities. A flexible scientific staff is provided through a university faculty visitor program, a post doctoral program, and a student visitor program. Not only does this provide appropriate expertise but it also introduces scientists outside of NASA to NASA problems. A small group of core RIACS staff provides continuity and interacts with an ARC technical monitor and scientific advisory group to determine the RIACS mission. RIACS activities are reviewed and monitored by a USRA advisory council and ARC technical monitor. Research at RIACS is currently being done in the following areas: Parallel Computing, Advanced Methods for Scientific Computing, High Performance Networks and Technology, and Learning Systems. Parallel compiler techniques, adaptive numerical methods for flows in complicated geometries, and optimization were identified as important problems to investigate for ARC's involvement in the Computational Grand Challenges of the next decade. Author (revised)

N94-25065 National Academy of Engineering, Washington, DC.
THE FUTURE OF AEROSPACE: PROCEEDINGS OF A SYMPOSIUM HELD IN HONOR OF ALEXANDER H. FLAX
1993 83 p Symposium was held in Washington, DC, 28 Feb. 1992
(LC-93-83945; ISBN-0-309-04881-8) Copyright Avail: Issuing Activity

This volume consists of papers and speakers' remarks presented during a symposium entitled 'The Future of Aerospace,' held Feb. 28, 1992. Topics covered include the defense industry and the new world order, the future of manned spaceflight, the current outlook for the aviation industry, applying technology to new airplane development, and the future of rotary wing aircraft. For individual titles, see N94-25066 through N94-25070.

N94-25066 Technology Strategies and Alliances, Menlo Park, CA.
DEFENSE AEROSPACE AND THE NEW WORLD ORDER c84
William J. Perry *In* National Academy of Engineering, The Future of Aerospace: Proceedings of a Symposium Held in Honor of Alexander H. Flax 1993 p 7-14 (For primary document see N94-25065 06-99)
Copyright Avail: Issuing Activity

With the end of the Cold War, the aerospace industry is faced with serious challenges in maintaining a capable defense industrial base while considerable downsizing occurs. This paper covers the unique military technologies that allowed U.S. military forces to prevail during the Persian Gulf War, such as C3I, defense suppression, and precision-guided weapons, and the author's recommendations on how the government and aerospace industry should plan to maintain such capabilities in the future. CASI

N94-25067* National Aeronautics and Space Administration. Lyndon B. Johnson Space Center, Houston, TX.
THE FUTURE OF MANNED SPACEFLIGHT c12
Aaron Cohen *In* National Academy of Engineering, The Future of Aerospace: Proceedings of a Symposium Held in Honor of Alexander H. Flax 1993 p 15-27 (For primary document see N94-25065 06-99)
Copyright Avail: Issuing Activity

This paper examines the future of manned spaceflight in context of past accomplishments and possible future benefits of space exploration.

Three technological advances mentioned are a device called the rotating wall vessel, also known as the 'bioreactor,' which allows the study of the growth of cells in three dimensions; the use of microgravity to produce high-quality electronic, magnetic, and superconducting thin films; and mining of helium-3 from the lunar surface for use in future fusion reactions with deuterium. The author then makes recommendations on how NASA should meet the challenges of manned spaceflight. CASI

N94-25068 General Electric Co., Cincinnati, OH. Aircraft Engines.
AVIATION: THE TIMELESS INDUSTRY c01
Brian H. Rowe *In* National Academy of Engineering, The Future of Aerospace: Proceedings of a Symposium Held in Honor of Alexander H. Flax 1993 p 29-36 (For primary document see N94-25065 06-99)
Copyright Avail: Issuing Activity

From an engineering perspective, we may be entering the most exciting, rewarding, and interesting time during which one can work in the U.S. air transportation industry. At the same time, we may be entering a period of steadily declining U.S. leadership in civil aeronautics - if we allow ourselves to become complacent. This paradox stems from the fact that world airline economics are in dreadful shape, even though opportunities for technical advances in civil aviation abound. To maintain our leadership in this environment, we must shift our focus from 'high-tech' to cost-conscious designs made possible through concurrent engineering, coupled with better-than-ever customer support. Derived from text

N94-25069 Boeing Co., Seattle, WA.
HIGH-ORDER TECHNOLOGY: APPLYING TECHNICAL EXCELLENCE TO NEW AIRPLANE DEVELOPMENT c05
Albertus D. Welliver *In* National Academy of Engineering, The Future of Aerospace: Proceedings of a Symposium Held in Honor of Alexander H. Flax 1993 p 37-44 (For primary document see N94-25065 06-99)
Copyright Avail: Issuing Activity

There is a misconception today about what technology really is. Technology has now come to mean specific things: fault-tolerant computers, portable satellite phones, featherweight composite materials. But these individual items, however important they may be, are not examples of the true meaning of the word technology. Instead, these are examples of technical excellence. A higher form of technology is at work behind these specific pieces of equipment: the technology based on human experience, wisdom, and judgment. In aviation, the ultimate technology means listening to the customer and adding value to the airplane. In Boeing's design process, every new technology development must earn its way onto an airplane by adding value in one of three ways: increased safety, improved operational efficiency and economic utility, and greater customer satisfaction. Higher-order technology, the technology of knowing how to apply examples of technical excellence, is now shaping the development of two exciting classes of airplane. One is the development of large subsonic transports, including the potential for new airplanes larger than any current commercial transports. The other is the prospect of a high-speed civil transport (HSCT). Although these two categories of airplane are very different, they do have one thing in common: A successful design will depend on how technical excellence is applied to the satisfaction of the customer. By themselves, individual examples of technical excellence will not produce a winning design. A good airplane is the result of good decisions, not just good components. Derived from text

N94-25070 Army Aviation Systems Command, Moffett Field, CA. Advanced Systems Research and Analysis Office.
THE FUTURE OF ROTARY-WING AIRCRAFT c05
Richard M. Carlson *In* National Academy of Engineering, The Future of Aerospace: Proceedings of a Symposium Held in Honor of Alexander H. Flax 1993 p 45-63 (For primary document see N94-25065 06-99)
Copyright Avail: Issuing Activity

Advances in rotary wing aircraft technology will improve performance of future helicopters in three broad mission segments, defined as vertical takeoff and landing, horizontal flight, and hovering flight. This paper addresses technologies associated with these three mission segments in the areas of propulsion, rotary-wing aerodynamics, and materials and structures. The paper also examines the economic outlook for rotary wing aircraft in future commercial and military markets. CASI

N94-25075# Air Force Office of Scientific Research, Bolling AFB, Washington, DC.
RESEARCH INTERESTS AND BROAD AGENCY ANNOUNCEMENT 94-1 OF THE AIR FORCE OFFICE OF SCIENTIFIC RESEARCH Annual Report
1 Oct. 1993 46 p See also N93-18985
(AD-A273410; AFOSR-TR-93-0848; AFOSR-PAM-70-1; AD-A258806)
Avail: CASI HC A03/MF A01

The Air Force Office of Scientific Research (AFOSR) manages all basic research conducted by the U.S. Air Force. To accomplish this task, AFOSR solicits proposals for research through a general Broad Agency Announcement (BAA) and through specialized BAA's published in the Commerce Business Daily. This general BAA outlines the Air Force Defense Research Sciences Program and is reprinted in Section 4, Proposal Guidance, for your convenience. AFSOR invites proposals for basic research in many broad areas. Section 2 of this pamphlet describes those areas in greater detail. DTIC

N94-25348*# National Aeronautics and Space Administration. Lyndon B. Johnson Space Center, Houston, TX.
NATIONAL AERONAUTICS AND SPACE ADMINISTRATION (NASA)/AMERICAN SOCIETY FOR ENGINEERING EDUCATION (ASEE) SUMMER FACULTY FELLOWSHIP PROGRAM, 1993, VOLUME 1
William A. Hyman, ed. (Texas A&M Univ., College Station.) and Stanley H. Goldstein, ed. Dec. 1993 237 p Fellowship program held in Houston, TX, 1993; sponsored by NASA
(Grant NGT-44-001-800)
(NASA-CR-188271-Vol-1; NAS 1.26:188271-Vol-1) Avail: CASI HC A11/MF A03

The JSC NASA/ASEE Summer Faculty Fellowship Program was conducted by Texas A&M University and JSC. The objectives of the program, which began nationally in 1964 and at JSC in 1965, are as follows: (1) to further the professional knowledge of qualified engineering and science faculty members; (2) to stimulate an exchange of ideas between participants and NASA; (3) to enrich and refresh the research and teaching activities of participants' institutions; and (4) to contribute to the research objectives of the NASA centers. Each faculty fellow spent at least 10 weeks at JSC engaged in a research project in collaboration with a NASA/JSC colleague. This document is a compilation of the final reports on the research projects completed by the faculty fellows during the summer of 1993. For individual titles, see N94-25349 through N94-25366.

N94-25349*# LeTourneau Coll., Longview, TX. Div. of Natural Sciences.
DATA ANALYSIS AND INTERPRETATION OF LUNAR DUST EXOSPHERE c91
George A. Andrews, Jr. *In* NASA. Johnson Space Center, National Aeronautics and Space Administration (NASA)/American Society for Engineering Education (ASEE) Summer Faculty Fellowship Program, 1993, Volume 1 Dec. 1993 15 p (For primary document see N94-25348 06-99)
Avail: CASI HC A03/MF A03

The lunar horizon glow observed by Apollo astronauts and recorded during the Surveyor missions is believed to result from the scattering of sunlight off lunar fines suspended in a dust layer above the lunar surface. For scale heights of tens of kilometers, theory and astronaut's observations suggest that the size of the dust particles will be smaller than 0.1 microns in radius and will act as Rayleigh scatters. This means that the dust scattered light will be 100 percent polarized at a 90 degree scattering angle and will depend on wavelength to the inverse fourth power ('bluing'). Believing these signatures to be observable from ground based telescopes, observational data in the form of CCD images has been collected from McDonald Observatory's 36 in. telescope, and the reduction and analysis of this data is the focus of the present report. Author (revised)

N94-25350*# Texas Technological Univ., Lubbock. Dept. of Mechanical Engineering.
MODELLING THE SHUTTLE REMOTE MANIPULATOR SYSTEM: ANOTHER FLEXIBLE MODEL c37
Alan A. Barhorst *In* NASA. Johnson Space Center, National Aeronautics and Space Administration (NASA)/American Society for Engineering Education (ASEE) Summer Faculty Fellowship Program, 1993, Volume 1

Dec. 1993 17 p (For primary document see N94-25348 06-99)
Avail: CASI HC A03/MF A03

High fidelity elastic system modeling algorithms are discussed. The particular system studied is the Space Shuttle Remote Manipulator System (RMS) undergoing full articulated motion. The model incorporates flexibility via a methodology the author has been developing. The technique is based in variational principles, so rigorous boundary condition generation and weak formulations for the associated partial differential equations are realized, yet the analyst need not integrate by parts. The methodology is formulated using vector-dyad notation with minimal use of tensor notation, therefore the technique is believed to be affable to practicing engineers. The objectives of this work are as follows: (1) determine the efficacy of the modeling method; and (2) determine if the method affords an analyst advantages in the overall modeling and simulation task. Generated out of necessity were Mathematica algorithms that quasi-automate the modeling procedure and simulation development. The project was divided into sections as follows: (1) model development of a simplified manipulator; (2) model development of the full-freedom RMS including a flexible movable base on a six degree of freedom orbiter (a rigid-body is attached to the manipulator end-effector); (3) simulation development for item 2; and (4) comparison to the currently used model of the flexible RMS in the Structures and Mechanics Division of NASA JSC. At the time of the writing of this report, items 3 and 4 above were not complete. Author (revised)

N94-25351*# Mount Holyoke Coll., South Hadley, MA. Dept. of Biological Sciences.

THE ROLE OF VISUAL CONTEXT IN MANUAL TARGET LOCALIZATION c53

Susan R. Barry *In* NASA. Johnson Space Center, National Aeronautics and Space Administration (NASA)/American Society for Engineering Education (ASEE) Summer Faculty Fellowship Program, 1993, Volume 1 Dec. 1993 14 p (For primary document see N94-25348 06-99)
Avail: CASI HC A03/MF A03

During space flight and immediately after return to the 1-g environment of earth, astronauts experience perceptual and sensory-motor disturbances. These changes result from adaptation of the astronaut to the microgravity environment of space. During space flight, sensory information from the eyes, limbs, and vestibular organs is reinterpreted by the central nervous system in order to produce appropriate body movements in the microgravity. This adaptation takes several days to develop. Upon return to earth, the changes in the sensory-motor system are no longer appropriate to a 1-g environment. Over several days, the astronaut must re-adapt to the terrestrial environment. Alterations in sensory-motor function may affect eye-head-hand coordination and, thus, the crewmember's ability to manually locate objects in extrapersonal space. Previous reports have demonstrated that crewmembers have difficulty in estimating joint and limb position and in pointing to memorized target positions on orbit and immediately postflight. The ability to point at or reach toward an object or perform other manual tasks is essential for safe Shuttle operation and may be compromised particularly during re-entry and landing sequences and during possible emergency egress from the Shuttle. An understanding of eye-head-hand coordination and the changes produced during space flight is necessary to develop effective countermeasures. This summer's project formed part of the study of the sensory cues use in the manual localization of objects. Author (revised)

N94-25352*# Louisiana Tech Univ., Ruston. Dept. of Electrical Engineering.

PARALLEL PROCESSING METHODS FOR SPACE BASED POWER SYSTEMS c20

F. C. Berry *In* NASA. Johnson Space Center, National Aeronautics and Space Administration (NASA)/American Society for Engineering Education (ASEE) Summer Faculty Fellowship Program, 1993, Volume 1 Dec. 1993 15 p (For primary document see N94-25348 06-99)
Avail: CASI HC A03/MF A03

This report presents a method for doing load-flow analysis of a power system by using a decomposition approach. The power system for the Space Shuttle is used as a basis to build a model for the load-flow analysis. To test the decomposition method for doing load-flow analysis, simulations were performed on power systems of 16, 25, 34, 43, 52, 61, 70, and 79 nodes. Each of the power systems was divided into subsystems and simulated under steady-state conditions. The results from these tests have been found to be as accurate as tests performed using a standard serial simulator. The division of the power systems into different subsystems was done by assigning a processor to each area. There were 13 transputers available, therefore, up to 13 different subsystems could be simulated at the same time. This report has preliminary results for a load-flow analysis using a decomposition principal. The report shows that the decomposition algorithm for load-flow analysis is well suited for parallel processing and provides increases in the speed of execution. Author

N94-25353*# Southern Vital Records Center, Inc., Flora, MS. Dept. of Computer Science.

A PROTOTYPE TO AUTOMATE THE VIDEO SUBSYSTEM ROUTING FOR THE VIDEO DISTRIBUTION SUBSYSTEM OF SPACE STATION FREEDOM c32

Jessie M. Bethly Betz *In* NASA. Johnson Space Center, National Aeronautics and Space Administration (NASA)/American Society for Engineering Education (ASEE) Summer Faculty Fellowship Program, 1993, Volume 1 Dec. 1993 10 p (For primary document see N94-25348 06-99)
Avail: CASI HC A02/MF A03

The Video Distribution Subsystem (VDS) for Space Station Freedom provides onboard video communications. The VDS includes three major functions: external video switching; internal video switching; and sync and control generation. The Video Subsystem Routing (VSR) is a part of the VDS Manager Computer Software Configuration Item (VSM/CSCI). The VSM/CSCI is the software which controls and monitors the VDS equipment. VSR activates, terminates, and modifies video services in response to Tier-1 commands to connect video sources to video destinations. VSR selects connection paths based on availability of resources and updates the video routing lookup tables. This project involves investigating the current methodology to automate the Video Subsystem Routing and developing and testing a prototype as 'proof of concept' for designers. Author (revised)

N94-25354*# Nebraska Univ., Omaha. Dept. of Industrial and Management Systems Engineering.

INVESTIGATION OF HAND CAPABILITIES UNDER A VARIETY OF PERFORMANCE CONDITIONS AND AN ATTEMPT TO EXPLAIN PERFORMANCE DIFFERENCES c54

Ram R. Bishu and Lisa Bronkema *In* NASA. Johnson Space Center, National Aeronautics and Space Administration (NASA)/American Society for Engineering Education (ASEE) Summer Faculty Fellowship Program, 1993, Volume 1 Dec. 1993 14 p (For primary document see N94-25348 06-99)
Avail: CASI HC A03/MF A03

Human capabilities such as dexterity, manipulability, and tactile perception are unique and render the hands as a very versatile, effective and a multipurpose tool. This is especially true for environments such as the EVA environment. However, with the use of the protective EVA gloves, there is much evidence to suggest that human performance decreases. In order to determine the nature and cause of this performance decrement, several performance tests were run which studied the effects of gloves on strength, tactile feedback, and range of motion. Tactile sensitivity was measured as a function of grip strength, and the results are discussed. Equipment which was developed to measure finger range of motion along with corresponding finger strength values is discussed. The results of these studies have useful implications for improved glove design. Author (revised)

N94-25355*# Houston Univ., Clear Lake, TX. School of Natural and Applied Sciences.

MEASURING TRACK DENSITIES IN LUNAR GRAINS BY IMAGE ANALYSIS c91

George E. Blanford *In* NASA. Johnson Space Center, National Aeronautics and Space Administration (NASA)/American Society for Engineering Education (ASEE) Summer Faculty Fellowship Program, 1993, Volume 1 Dec. 1993 10 p (For primary document see N94-25348 06-99)
Avail: CASI HC A02/MF A03

We have developed techniques to use digitized scanning electron micrographs and computer image analysis programs to measure track densities in lunar soil grains. Tracks were formed by highly ionizing solar energetic particles and cosmic rays during near surface exposure on the

Moon. The track densities are related to the exposure conditions (depth and time). Distributions of the number of grains as a function of their track densities can reveal the modality of soil maturation. We used a sample that had already been etched in 6 N NaOH at 118 C for 15 h to reveal tracks. We determined that back-scattered electron images taken at 50 percent contrast and approximately 49.8 percent brightness produced suitable high contrast images for analysis. We ascertained gray-scale thresholds of interest: 0-230 for tracks, 231 for masked regions, and 232-255 for background. We found no need to set an upper size limit for distinguishing tracks. We did use lower limits to exclude noise: 16 pixels at 15000x, 4 pixels at 10000x, 2 pixels at 6800x, and 0 pixels at 4600x. We used computer counting and measurement of area to obtain track densities. We found an excellent correlation with manual measurements for track densities below 1x10(exp 8) sq cm. For track densities between 1x10(exp 8) sq cm to 1x10(exp 9) sq cm, we found that a regression formula using the percentage area covered by tracks gave good agreement with manual measurements. Finally we used these new techniques to obtain a track density distribution that gave more detail and was more rapidly obtained than using manual techniques 15 years ago. Author (revised)

N94-25356*# Texas A&M Univ., Galveston. Maritime System Engineering.

UNIFIED APPROACH FOR INCOMPRESSIBLE FLOWS c34

Tyne-Hsien Chang *In* NASA. Johnson Space Center, National Aeronautics and Space Administration (NASA)/American Society for Engineering Education (ASEE) Summer Faculty Fellowship Program, 1993, Volume 1 Dec. 1993 6 p (For primary document see N94-25348 06-99)
Avail: CASI HC A02/MF A03

An unified approach for solving both compressible and incompressible flows was investigated in this study. The difference in CFD code development between incompressible and compressible flows is due to the mathematical characteristics. However, if one can modify the continuity equation for incompressible flows by introducing pseudocompressibility, the governing equations for incompressible flows would have the same mathematical characters as compressible flows. The application of a compressible flow code to solve incompressible flows becomes feasible. Among numerical algorithms developed for compressible flows, the Centered Total Variation Diminishing (CTVD) schemes possess better mathematical properties to damp out the spurious oscillations while providing high-order accuracy for high speed flows. It leads us to believe that CTVD schemes can equally well solve incompressible flows. In this study, the governing equations for incompressible flows include the continuity equation and momentum equations. The continuity equation is modified by adding a time-derivative of the pressure term containing the artificial compressibility. The modified continuity equation together with the unsteady momentum equations forms a hyperbolic-parabolic type of time-dependent system of equations. The continuity equation is modified by adding a time-derivative of the pressure term containing the artificial compressibility. The modified continuity equation together with the unsteady momentum equations forms a hyperbolic-parabolic type of time-dependent system of equations. Thus, the CTVD schemes can be implemented. In addition, the boundary conditions including physical and numerical boundary conditions must be properly specified to obtain accurate solution. The CFD code for this research is currently in progress. Flow past a circular cylinder will be used for numerical experiments to determine the accuracy and efficiency of the code before applying this code to more specific applications. Author (revised)

N94-25357*# Texas A&M Univ., College Station. Bioengineering Program.

NON-INVASIVE OPTICAL DETECTION OF GLUCOSE IN CELL CULTURE NUTRIENT MEDIUM c51

Gerald L. Cote *In* NASA. Johnson Space Center, National Aeronautics and Space Administration (NASA)/American Society for Engineering Education (ASEE) Summer Faculty Fellowship Program, 1993, Volume 1 Dec. 1993 11 p (For primary document see N94-25348 06-99)
Avail: CASI HC A03/MF A03

The objective of the proposed research was to begin the development of a non-invasive optical sensor for measuring glucose concentration in the output medium of cell cultures grown in a unique NASA bioreactor referred to as an integrated rotating-wall vessel (IRWV). The input, a bovine serum based nutrient media, has a known glucose concentration. The cells within the bioreactor digest a portion of the glucose. Thus, the non-invasive optical sensor is needed to monitor the decrease in glucose due to cellular consumption since the critical parameters for sustained cellular productivity are glucose and pH. Previous glucose sensing techniques have used chemical reactions to quantify the glucose concentration. Chemical reactions, however, cannot provide for continuous, real time, non-invasive measurement as is required in this application. Our effort while in the fellowship program was focused on the design, optical setup, and testing of one bench top prototype non-invasive optical sensor using a mid-infrared absorption spectroscopy technique. Glucose has a fundamental vibrational absorption peak in the mid-infrared wavelength range at 9.6 micron. Preliminary absorption data using a CO2 laser were collected at this wavelength for water based glucose solutions at different concentrations and one bovine serum based nutrient medium (GTSF) with added glucose. The results showed near linear absorption responses for the glucose-in-water data with resolutions as high at 108 mg/dl and as low as 10 mg/dl. The nutrient medium had a resolution of 291 mg/dl. The variability of the results was due mainly to thermal and polarization drifts of the laser while the decrease in sensitivity to glucose in the nutrient medium was expected due to the increase in the number of confounders present in the nutrient medium. A multispectral approach needs to be used to compensate for these confounders. The CO2 laser used for these studies was wavelength tunable (9.2 to 10.8 micrometers), however, it was to unstable across wavelengths to test the multispectral approach. From this research, further NASA support was obtained to continue the work throughout the year in which a more stable light source will be used at smaller, near-infrared, wavelengths. It is anticipated that a more compact, non-invasive, optical glucose sensor will be realized which can be used with a bioreactor on future space shuttle missions. It is also anticipated that a multispectral optical sensor may be used to determine the concentration of other molecules needed within the NASA bioreactor, such as fructose and galactose. Author

N94-25358*# Stockton State Coll., Pomona, NJ. Dept. of Geology and Environmental Studies.

A GEOCHEMICAL STUDY OF ACAPULCOITE AND LODRANITE METEORITES c90

Stephen W. Field *In* NASA. Johnson Space Center, National Aeronautics and Space Administration (NASA)/American Society for Engineering Education (ASEE) Summer Faculty Fellowship Program, 1993, Volume 1 Dec. 1993 13 p (For primary document see N94-25348 06-99)
Avail: CASI HC A03/MF A03

Lodranites and acapulcoites (primitive achondrites) are two classes of meteorites with geochemical signatures similar to chondrite meteorites. Lodranites and acapulcoites, however, have few or none of the chondrules characteristic of the chondrites. Texturally the primitive achondrites appear to have been recystallized though planetary igneous or metamorphic processes. A study of five primitive achondrites, two lodranites, two acapulcoites, and one supposedly intermediate acapulcoite/lodranite, were analyzed petrographically and geochemically to determine the igneous and metamorphic processes which have affected them. Acapulcoites show little evidence of melt extraction. The geochemistry of lodranite samples indicates silicate and metal/sulfide melts were removed from the rocks. The mineralogy and geochemistry of the intermediate meteorite suggest the rock is a metal rich acapulcoite and not a lodranite. Author

N94-25359*# Tulane Univ., New Orleans, LA. Dept. of Mechanical Engineering.

LOADING, ELECTROMYOGRAPH, AND MOTION DURING EXERCISE c52

Fernando Figueroa *In* NASA. Johnson Space Center, National Aeronautics and Space Administration (NASA)/American Society for Engineering Education (ASEE) Summer Faculty Fellowship Program, 1993, Volume 1 Dec. 1993 11 p (For primary document see N94-25348 06-99)
Avail: CASI HC A03/MF A03

A system is being developed to gather kineto-dynamic data for a study to determine the load vectors applied to bone during exercise on equipment similar to that used in space. This information will quantify bone loading for exercise countermeasures development. Decreased muscle loading and external loading of bone during weightlessness results in cancellous bone loss of 1 percent per month in the lower extremities and 2 percent per month in the calcaneous. It is hypothesized that loading bone appropriately during exercise may prevent the bone loss. The system consists of an ergometer instrumented to provide position of the pedal (foot), pedaling forces on the foot (on the sagittal plane), and force on the seat. Accelerometers attached to the limbs will provide acceleration. These data will be used as input to an analytical model of the limb to determine forces on the bones and on groups of muscles. EMG signals from activity in the muscles will also be used in conjunction with the equations of mechanics of motion to be able to discern forces exerted by specific muscles. The tasks to be carried out include: design of various mechanical components to mount transducers, specification of mechanical components, specification of position transducers, development of a scheme to control the data acquisition instruments (TEAC recorder and optical encoder board), development of a dynamic model of the limbs in motion, and development of an overall scheme for data collection analysis and presentation. At the present time, all the hardware components of the system are operational, except for a computer board to gather position data from the pedals and crank. This board, however, may be put to use by anyone with background in computer based instrumentation. The software components are not all done. Software to transfer data recorded from the EMG measurements is operational, software to drive the optical encoder card is mostly done. The equations to model the kinematics and dynamics of motion of the limbs have been developed, but they have not yet been implemented in software. Aside from the development of the hardware and software components of the system, the methodology to use accelerometers and encoders and the formulation of the appropriate equations are an important contribution to the area of biomechanics, particularly in space applications. Author

N94-25360*# Wyoming Univ., Laramie. Dept. of Computer Science.

FAILURE DETECTION AND RECOVERY IN THE ASSEMBLY/CONTINGENCY SUBSYSTEM **c32**

Rex E. Gantenbein *In* NASA. Johnson Space Center, National Aeronautics and Space Administration (NASA)/American Society for Engineering Education (ASEE) Summer Faculty Fellowship Program, 1993, Volume 1 Dec. 1993 15 p (For primary document see N94-25348 06-99)

Avail: CASI HC A03/MF A03

The Assembly/Contingency Subsystem (ACS) is the primary communications link on board the Space Station. Any failure in a component of this system or in the external devices through which it communicates with ground-based systems will isolate the Station. The ACS software design includes a failure management capability (ACFM) that provides protocols for failure detection, isolation, and recovery (FDIR). The the ACFM design requirements as outlined in the current ACS software requirements specification document are reviewed. The activities carried out in this review include: (1) an informal, but thorough, end-to-end failure mode and effects analysis of the proposed software architecture for the ACFM; and (2) a prototype of the ACFM software, implemented as a C program under the UNIX operating system. The purpose of this review is to evaluate the FDIR protocols specified in the ACS design and the specifications themselves in light of their use in implementing the ACFM. The basis of failure detection in the ACFM is the loss of signal between the ground and the Station, which (under the appropriate circumstances) will initiate recovery to restore communications. This recovery involves the reconfiguration of the ACS to either a backup set of components or to a degraded communications mode. The initiation of recovery depends largely on the criticality of the failure mode, which is defined by tables in the ACFM and can be modified to provide a measure of flexibility in recovery procedures. Author

N94-25361*# Houston Univ., TX. Dept. of Industrial Engineering.

INTEGRATED RISK MANAGEMENT **c81**

J. L. Hunsucker *In* NASA. Johnson Space Center, National Aeronautics and Space Administration (NASA)/American Society for Engineering Education (ASEE) Summer Faculty Fellowship Program, 1993, Volume 1 Dec. 1993 14 p (For primary document see N94-25348 06-99)

Avail: CASI HC A03/MF A03

The purpose of this report is to first present a basis or foundation for the building of an integrated risk management plan and them to present the plan. The integration referred to is across both the temporal and the hierarchical dimensions. Complexity, consequence, and credibility seem to be driving the need for the consideration of risk. Reduction of personal bias and reproducibility of the decision making process seem to be driving the consideration of a formal risk plan. While risk can be used as either a selection tool or a control tool, this paper concentrates on the selection usage. Risk relies on stated purpose. The tightness of the definition of purpose and success is directly reflected in the definition and control of risk. Much of a risk management plan could be designed by the answers to the questions of why, what, who, when, and where. However, any plan must provide the following information about a threat or risk: likelihood, consequence, predictability, reliability, and reproducibility. While the environment at NASA is seen as warm, but not hot, for the introduction of a risk program, some encouragement is seen if the following problems are addressed: no champion, no commitment of resource, confused definitions, lack of direction and focus, a hard sell, NASA culture, many choices of assessment methods, and cost. The plan is designed to follow the normal method of doing work and is structured to follow either the work break down structure or a functional structure very well. The parts of the plan include: defining purpose and success, initial threat assessment, initial risk assessment, reconciling threats and parameters, putting part of the information down and factoring the information back into the decision process as it comes back up, and developing inferences. Two major suggestions are presented. One is to build an office of risk management to be used as a resource by managers in doing the risk process. Another is to form a pilot program to try out the details in the plan and modify the method where needed. Author

N94-25362*# Texas Southern Univ., Houston. Jesse H. Jones School of Business.

STRATEGIES FOR RECRUITING ADDITIONAL AFRICAN AMERICANS INTO THE NASA JSC SUMMER FACULTY FELLOWS PROGRAM **c80**

Ladelle M. Hyman *In* NASA. Johnson Space Center, National Aeronautics and Space Administration (NASA)/American Society for Engineering Education (ASEE) Summer Faculty Fellowship Program, 1993, Volume 1 Dec. 1993 15 p (For primary document see N94-25348 06-99)

Avail: CASI HC A03/MF A03

African Americans have participated sporadically in the NASA JSC Summer Faculty Fellows Program--none in 1992 and four in 1993. There is a pool of African Americans who are both qualified to provide services and willing to participate in initiatives which support technologies required for future JSC programs. They can provide human support and handle mission operations, spacecraft systems, planet surface systems, and management tools. Most of these faculty teach at historically black colleges and universities (HBCU's). This research will document the current recruitment system, critique it, and develop a strategy which will facilitate the diversification of the NASA JSC Summer Faculty Fellows Program. While NASA currently mails notices to HBCU's, such notices have generated few applications from, and fewer selections of, targeted faculty. To increase the participation of African Americans in the NASA JSC Summer Faculty Fellows Program, this participant will prepare a strategy which includes a document which identifies HBCU-targeted faculty and enumerates more formally extensive and intensive communication procedures. A fifteen-minute panel discussion, which will include a video, will be delivered during the annual meeting of the American Society for Engineering Education (ASEE) to be held in Edmonton, Alberta, Canada, June 26-29, 1994. An announcement letter will be mailed to targeted faculty; follow-up telephone calls and personal visits will be made and a checklist flowchart will be completed by key NASA personnel or designee. Although initially limited to NASA JSC's recruitment of African Americans, this strategy may be broadened to include other NASA sites and other targeted minority groups. Author

N94-25363*# Houston Univ., TX. College of Technology.

IMAGE REMAPPING STRATEGIES APPLIED AS PROTHESES FOR THE VISUALLY IMPAIRED **c54**

Curtis D. Johnson *In* NASA. Johnson Space Center, National Aeronautics and Space Administration (NASA)/American Society for Engineering Education (ASEE) Summer Faculty Fellowship Program, 1993, Volume 1 Dec. 1993 11 p (For primary document see N94-25348 06-99)

Avail: CASI HC A03/MF A03

Maculopathy and retinitis pigmentosa (rp) are two vision defects which render the afflicted person with impaired ability to read and recognize visual patterns. For some time there has been interest and work on the use of image remapping techniques to provide a visual aid for individuals with these impairments. The basic concept is to remap an image according to some mathematical transformation such that the image is warped around a maculopathic defect (scotoma) or within the rp foveal region of retinal

sensitivity. NASA/JSC has been pursuing this research using angle invariant transformations with testing of the resulting remapping using subjects and facilities of the University of Houston, College of Optometry. Testing is facilitated by use of a hardware device, the Programmable Remapper, to provide the remapping of video images. This report presents the results of studies of alternative remapping transformations with the objective of improving subject reading rates and pattern recognition. In particular a form of conformal transformation was developed which provides for a smooth warping of an image around a scotoma. In such a case it is shown that distortion of characters and lines of characters is minimized which should lead to enhanced character recognition. In addition studies were made of alternative transformations which, although not conformal, provide for similar low character distortion remapping. A second, non-conformal transformation was studied for remapping of images to aid rp impairments. In this case a transformation was investigated which allows remapping of a vision field into a circular area representing the foveal retina region. The size and spatial representation of the image are selectable. It is shown that parametric adjustments allow for a wide variation of how a visual field is presented to the sensitive retina. This study also presents some preliminary considerations of how a prosthetic device could be implemented in a practical sense, vis-a-vis, size, weight and portability.
Author

N94-25364*# Houston Univ., TX. Dept. of Mathematics.
NEAR SURFACE ANALYSIS c46
Gordon G. Johnson *In* NASA. Johnson Space Center, National Aeronautics and Space Administration (NASA)/American Society for Engineering Education (ASEE) Summer Faculty Fellowship Program, 1993, Volume 1 Dec. 1993 11 p (For primary document see N94-25348 06-99)
Avail: CASI HC A03/MF A03

This is a study to assist in the understanding of earth near surface structure. Higher order moments are used to detect the density distribution as well as to seek patterns found in geological structures. It is shown how higher order moments at points outside a mass structure are determined as well as how to recover the mass distribution from the higher order moments. It is interesting to note that the first moment at a point P outside the mass structure, V(sub O)(P), is the entire mass and the second moment, V(sub 1)(P), is the potential at P due to the mass structure. Usually only the mass and the potential function are used to determine the density distribution in a body. An infinite function sequence (V(sub n)(P))(sub n=0)(sup infinity) is required to uniquely determine the density distribution.
Author (revised)

N94-25365*# New Mexico State Univ., Las Cruces. Dept. of Mechanical Engineering.
INFLUENCE OF TEST CONFIGURATION ON THE COMBUSTION CHARACTERISTICS OF POLYMERS AS IGNITION SOURCES c25
Howard L. Julien *In* NASA. Johnson Space Center, National Aeronautics and Space Administration (NASA)/American Society for Engineering Education (ASEE) Summer Faculty Fellowship Program, 1993, Volume 1 Dec. 1993 13 p (For primary document see N94-25348 06-99)
Avail: CASI HC A03/MF A03

The experimental evaluation of polymers as ignition sources for metals was accomplished at the NASA White Sands Test Facility (WSTF) using a standard promoted combustion test. These tests involve the transient burning of materials in high-pressure oxygen environments. They have provided data from which design decisions can be made; data include video recordings of ignition and non-ignition for specific combinations of metals and polymers. Other tests provide the measured compositions of combustion products for polymers at select burn times and an empirical basis for estimating burn rates. With the current test configuration, the detailed analysis of test results requires modeling a three-dimensional, transient convection process involving fluid motion, thermal conduction and convection, the diffusion of chemical species, and the erosion of sample surface. At the high pressure extremes, it even requires the analysis of turbulent, transient convection where the physics of the problem are not well known and the computation requirements are not practical at this time. An alternative test configuration that can be analyzed with a relatively-simple convection model was developed during the summer period. The principal change constitutes replacing a large-diameter polymer disk at the end of the metal test rod with coaxial polymer cylinders that have a diameter nearer to that of the metal rod. The experimental objective is to assess the importance of test geometries on the promotion of metal ignition by testing with different lengths of the polymer and, with an extended effort, to analyze the surface combustion in the redesigned promoted combustion tests through analytical modeling of the process. The analysis shall use the results of cone-calorimeter tests of the polymer material to model primary chemical reactions and, with proper design of the promoted combustion test, modeling of the convection process could be conveniently limited to a quasi-steady boundary layer analysis where the economical solution of parabolic equations is involved. The products for the summer period are: (1) a conceptual-level redesign of the test apparatus, and (2) the development and use of an approximate integral boundary layer analysis to demonstrate the influence of geometry changes prior to testing. A computer code STAN5, an accurate numerical boundary layer model whose earlier versions were developed for the NASA Lewis Research Center by the Fellow, also was installed and validated on the WSTF and New Mexico State University computer systems as a starting point in the development of a more detailed fluid mechanics and combustion model.
Author (revised)

N94-25366*# Florida State Univ., Tallahassee. Dept. of Computer Science.
CONSIDERATIONS REGARDING THE DEPLOYMENT OF HYPERMEDIA AT JSC c82
Charles J. Kacmar *In* NASA. Johnson Space Center, National Aeronautics and Space Administration (NASA)/American Society for Engineering Education (ASEE) Summer Faculty Fellowship Program, 1993, Volume 1 Dec. 1993 15 p (For primary document see N94-25348 06-99)
Avail: CASI HC A03/MF A03

Electronic documents and systems are becoming the primary means of managing information for ground and space operations at NASA. These documents will utilize hypertext and hypermedia technologies to aid users in structuring and accessing information. Documents will be composed of static and dynamic data consisting of user-defined annotations and hypermedia links. The report consists of three major sections. First, it provides an overview of hypermedia and surveys the use of hypermedia throughout JSC. Second, it briefly describes a prototypical hypermedia system that was developed in conjunction with this work. This system was constructed to demonstrate various hypermedia features and to serve as a platform for supporting the electronic documentation needs for the MIDAS system developed by the Intelligent Systems Branch of the Automation and Robotics Division (Pac92). Third, it discusses emerging hypermedia technologies which have either been untapped by vendors or present significant challenges to the Agency.
Author

N94-25367*# National Aeronautics and Space Administration. Lyndon B. Johnson Space Center, Houston, TX.
NATIONAL AERONAUTICS AND SPACE ADMINISTRATION (NASA)/AMERICAN SOCIETY FOR ENGINEERING EDUCATION (ASEE) SUMMER FACULTY FELLOWSHIP PROGRAM, 1993, VOLUME 2
William A. Hyman, ed. (Texas A&M Univ., College Station.) and Stanley H. Goldstein, ed. Dec. 1993 243 p Fellowship program held in Houston, TX, 1993; sponsored by NASA
(Grant NGT-44-001-800)
(NASA-CR-188271-Vol-2; NAS 1.26:188271-Vol-2) Avail: CASI HC A11/MF A03

The JSC NASA/ASEE Summer Faculty Fellowship Program was conducted by Texas A&M University and JSC. The objectives of the program, which began nationally in 1964 and at JSC in 1965, are (1) to further the professional knowledge of qualified engineering and science faculty members; (2) to stimulate an exchange of ideas between participants and NASA; (3) to enrich and refresh the research and teaching activities of participant's institutions; and (4) to contribute to the research objectives of the NASA centers. Each faculty fellow spent at least 10 weeks at JSC engaged in a research project in collaboration with a NASA/JSC colleague. A compilation of the final reports on the research projects completed by the faculty fellows during the summer of 1993 is presented. For individual titles, see N94-25368 through N94-25384.

N94-25368*# Houston Univ., Clear Lake, TX. Div. of Biology.
DESIGN AND TESTING OF A UNIQUE RANDOMIZED GRAVITY, CONTINUOUS FLOW BIOREACTOR c51
Carroll B. Lassiter *In* NASA. Johnson Space Center, National Aeronautics and Space Administration (NASA)/American Society for Engineering

Education (ASEE) Summer Faculty Fellowship Program, 1993, Volume 2 Dec. 1993 15 p (For primary document see N94-25367 06-99)
Avail: CASI HC A03/MF A03

A rotating, null gravity simulator, or Couette bioreactor was successfully used for the culture of mammalian cells in a simulated microgravity environment. Two limited studies using Lipomyces starkeyi and Streptomyces clavuligerus were also conducted under conditions of simulated weightlessness. Although these studies with microorganisms showed promising preliminary results, oxygen limitations presented significant limitations in studying the biochemical and cultural characteristics of these cell types. Microbial cell systems such as bacteria and yeast promise significant potential as investigative models to study the effects of microgravity on membrane transport, as well as substrate induction of inactive enzyme systems. Additionally, the smaller size of the microorganisms should further reduce the gravity induced oscillatory particle motion and thereby improve the microgravity simulation on earth. Focus is on the unique conceptual design, and subsequent development of a rotating bioreactor that is compatible with the culture and investigation of microgravity effects on microbial systems. The new reactor design will allow testing of highly aerobic cell types under simulated microgravity conditions. The described reactor affords a mechanism for investigating the long term effects of reduced gravity on cellular respiration, membrane transfer, ion exchange, and substrate conversions. It offers the capability of dynamically altering nutrients, oxygenation, pH, carbon dioxide, and substrate concentration without disturbing the microgravity simulation, or Couette flow, of the reactor. All progeny of the original cell inoculum may be acclimated to the simulated microgravity in the absence of a substrate or nutrient. The reactor has the promise of allowing scientists to probe the long term effects of weightlessness on cell interactions in plants, bacteria, yeast, and fungi. The reactor is designed to have a flow field growth chamber with uniform shear stress, yet transfer high concentrations of oxygen into the culture medium. The system described allows for continuous, on line sampling for production of product without disturbing fluid and particle dynamics in the reaction chamber. It provides for the introduction of substrate, or control substances after cell adaptation to simulated microgravity has been accomplished. The reactor system provides for the nondisruptive, continuous flow replacement of nutrient and removal of product. On line monitoring and control of growth conditions such as pH and nutrient status are provided. A rotating distribution valve allows cessation of growth chamber rotation, thereby preserving the simulated microgravity conditions over longer periods of time. Author (revised)

N94-25369*# Wyoming Univ., Laramie. Dept. of Computer Science.
AN EVALUATION OF THREE-DIMENSIONAL SENSORS FOR THE EXTRAVEHICULAR ACTIVITY HELPER/RETREIVER c54
Michael Magee *In* NASA. Johnson Space Center, National Aeronautics and Space Administration (NASA)/American Society for Engineering Education (ASEE) Summer Faculty Fellowship Program, 1993, Volume 2 Dec. 1993 8 p (For primary document see N94-25367 06-99)
Avail: CASI HC A02/MF A03

The Extravehicular Activity Retriever/Helper (EVAHR) is a robotic device currently under development at the NASA Johnson Space Center that is designed to fetch objects or to assist in retrieving an astronaut who may have become inadvertently de-tethered. The EVAHR will be required to exhibit a high degree of intelligent autonomous operation and will base much of its reasoning upon information obtained from one or more three-dimensional sensors that it will carry and control. At the highest level of visual cognition and reasoning, the EVAHR will be required to detect objects, recognize them, and estimate their spatial orientation and location. The recognition phase and estimation of spatial pose will depend on the ability of the vision system to reliably extract geometric features of the objects such as whether the surface topologies observed are planar or curved and the spatial relationships between the component surfaces. In order to achieve these tasks, accurate sensing of the operational environment and objects in the environment will therefore be critical. The qualitative and quantitative results of empirical studies of three sensors that are capable of providing three-dimensional information to the EVAHR, but using completely different hardware approaches are documented. The first of these devices is a phase shift laser with an effective operating range (ambiguity interval) of approximately 15 meters. The second sensor is a laser triangulation system designed to operate at much closer range and to provide higher resolution images. The third sensor is a dual camera stereo imaging system from which range images can also be obtained. The remainder of the report characterizes the strengths and weaknesses of each of these systems relative to quality of data extracted and how different object characteristics affect sensor operation. Author

N94-25370*# Rice Univ., Houston, TX. Dept. of Mechanical Engineering and Materials Science.
DEVELOPMENT OF PROGRAMMABLE ARTIFICIAL NEURAL NETWORKS c63
Andrew J. Meade *In* NASA. Johnson Space Center, National Aeronautics and Space Administration (NASA)/American Society for Engineering Education (ASEE) Summer Faculty Fellowship Program, 1993, Volume 2 Dec. 1993 14 p (For primary document see N94-25367 06-99)
Avail: CASI HC A03/MF A03

Conventionally programmed digital computers can process numbers with great speed and precision, but do not easily recognize patterns or imprecise or contradictory data. Instead of being programmed in the conventional sense, artificial neural networks are capable of self-learning through exposure to repeated examples. However, the training of an ANN can be a time consuming and unpredictable process. A general method is being developed to mate the adaptability of the ANN with the speed and precision of the digital computer. This method was successful in building feedforward networks that can approximate functions and their partial derivatives from examples in a single iteration. The general method also allows the formation of feedforward networks that can approximate the solution to nonlinear ordinary and partial differential equations to desired accuracy without the need of examples. It is believed that continued research will produce artificial neural networks that can be used with confidence in practical scientific computing and engineering applications.
Author (revised)

N94-25371*# Purdue Univ., West Lafayette, IN. Dept. of Agricultural Engineering.
ROBOTICS IN A CONTROLLED, ECOLOGICAL LIFE SUPPORT SYSTEM c54
Gaines E. Miles and Kimberly J. Krom *In* NASA. Johnson Space Center, National Aeronautics and Space Administration (NASA)/American Society for Engineering Education (ASEE) Summer Faculty Fellowship Program, 1993, Volume 2 Dec. 1993 27 p (For primary document see N94-25367 06-99)
Avail: CASI HC A03/MF A03

Controlled, Ecological Life Support Systems (CELSS) that utilize plants to provide food, water and oxygen could consume considerable amounts of labor unless crop production, recovery and processing are automated. Robotic manipulators equipped with special end-effectors and programmed to perform the sensing and materials handling tasks would minimize the amount of astronaut labor required. The Human Rated Test Facility (HRTF) planned for Johnson Space Center could discover and demonstrate techniques of crop production which can be reliably integrated with machinery to minimize labor requirements. Before the physical components (shelves, lighting fixtures, etc.) can be selected, a systems analysis must be performed to determine which alternative processes should be followed and how the materials handling tasks should be automated. Given that the current procedures used to grow crops in a CELSS may not be the best methods to automate, then what are the alternatives? How may plants be grown, harvested, processed for food, and the inedible components recycled? What commercial technologies current exist? What research efforts are underway to develop new technologies which might satisfy the need for automation in a CELSS? The answers to these questions should prove enlightening and provide some of the information necessary to perform the systems analysis. The planting, culturing, gathering, threshing and separation, food processing, and recovery of inedible portions of wheat were studied. The basic biological and materials handling processes of each task are defined and discussed. Current practices at Johnson Space Center and other NASA centers are described and compared to common production practices in the plant production industry. Technologies currently being researched which might be applicable are identified and illustrated. Finally, based on this knowledge, several scenarios are proposed for automating the tasks for wheat. Author

N94-25372*# Virginia Commonwealth Univ., Richmond. Dept. of Mathematical Sciences.

MODELLING EARLY FAILURES IN SPACE STATION FREEDOM **c38**

Sharon E. Navard *In* NASA. Johnson Space Center, National Aeronautics and Space Administration (NASA)/American Society for Engineering Education (ASEE) Summer Faculty Fellowship Program, 1993, Volume 2 Dec. 1993 13 p (For primary document see N94-25367 06-99)

Avail: CASI HC A03/MF A03

A major problem encountered in planning for Space Station Freedom is the amount of maintenance that will be required. To predict the failure rates of components and systems aboard Space Station Freedom, the logical approach is to use data obtained from previously flown spacecraft. In order to determine the mechanisms that are driving the failures, models can be proposed, and then checked to see if they adequately fit the observed failure data obtained from a large variety of satellites. For this particular study, failure data and truncation times were available for satellites launched between 1976 and 1984; no data past 1984 was available. The study was limited to electrical subsystems and assemblies, which were studied to determine if they followed a model resulting from a mixture of exponential distributions. Author

N94-25373*# Minot State Univ., ND. College of Business.

A COMPARATIVE EVALUATION PLAN FOR THE MAINTENANCE, INVENTORY, AND LOGISTICS PLANNING (MILP) SYSTEM HUMAN-COMPUTER INTERFACE (HCI) Final Report **c81**

Scott P. Overmyer *In* NASA. Johnson Space Center, National Aeronautics and Space Administration (NASA)/American Society for Engineering Education (ASEE) Summer Faculty Fellowship Program, 1993, Volume 2 Dec. 1993 15 p (For primary document see N94-25367 06-99)

Avail: CASI HC A03/MF A03

The primary goal of this project was to develop a tailored and effective approach to the design and evaluation of the human-computer interface (HCI) to the Maintenance, Inventory and Logistics Planning (MILP) System in support of the Mission Operations Directorate (MOD). An additional task that was undertaken was to assist in the review of Ground Displays for Space Station Freedom (SSF) by attending the Ground Displays Interface Group (GDIG), and commenting on the preliminary design for these displays. Based upon data gathered over the 10 week period, this project has hypothesized that the proper HCI concept for navigating through maintenance databases for large space vehicles is one based upon a spatial, direct manipulation approach. This dialogue style can be then coupled with a traditional text-based DBMS, after the user has determined the general nature and location of the information needed. This conclusion is in contrast with the currently planned HCI for MILP which uses a traditional form-fill-in dialogue style for all data access and retrieval. In order to resolve this difference in HCI and dialogue styles, it is recommended that comparative evaluation be performed which combines the use of both subjective and objective metrics to determine the optimal (performance-wise) and preferred approach for end users. The proposed plan has been outlined in the previous paragraphs and is available in its entirety in the Technical Report associated with this project. Further, it is suggested that several of the more useful features of the Maintenance Operations Management System (MOMS), especially those developed by the end-users, be incorporated into MILP to save development time and money. Author

N94-25374*# Tarrant County Junior Coll., Fort Worth, TX. Computer Science Dept.

MODELING AND ANALYSIS OF SELECTED SPACE STATION COMMUNICATIONS AND TRACKING SUBSYSTEMS **c32**

Elmer Raydean Richmond *In* NASA. Johnson Space Center, National Aeronautics and Space Administration (NASA)/American Society for Engineering Education (ASEE) Summer Faculty Fellowship Program, 1993, Volume 2 Dec. 1993 15 p (For primary document see N94-25367 06-99)

Avail: CASI HC A03/MF A03

The Communications and Tracking System on board Space Station Freedom (SSF) provides space-to-ground, space-to-space, audio, and video communications, as well as tracking data reception and processing services. Each major category of service is provided by a communications subsystem which is controlled and monitored by software. Among these subsystems, the Assembly/Contingency Subsystem (ACS) and the Space-to-Ground Subsystem (SGS) provide communications with the ground via the Tracking and Data Relay Satellite (TDRS) System. The ACS is effectively SSF's command link, while the SGS is primarily intended as the data link for SSF payloads. The research activities of this project focused on the ACS and SGS antenna management algorithms identified in the Flight System Software Requirements (FSSR) documentation, including: (1) software modeling and evaluation of antenna management (positioning) algorithms; and (2) analysis and investigation of selected variables and parameters of these antenna management algorithms i.e., descriptions and definitions of ranges, scopes, and dimensions. In a related activity, to assist those responsible for monitoring the development of this flight system software, a brief summary of software metrics concepts, terms, measures, and uses was prepared. Author

N94-25375*# Bevill State Community Coll., Fayette, AL. Chemistry Dept.

INVESTIGATING PYROLYSIS/INCINERATION AS A METHOD OF RESOURCE RECOVERY FROM SOLID WASTE **c54**

Bobby J. Robertson and Christopher S. LeMay *In* NASA. Johnson Space Center, National Aeronautics and Space Administration (NASA)/American Society for Engineering Education (ASEE) Summer Faculty Fellowship Program, 1993, Volume 2 Dec. 1993 11 p (For primary document see N94-25367 06-99)

Avail: CASI HC A03/MF A03

Pyrolysis/incineration (P/I) is a physicochemical method for the generation of recoverable resources from solid waste materials such as inedible plant biomass (IPB), paper, plastics, cardboard, etc. P/I permits the collection of numerous gases with a minimal amount of solid residue. Pyrolysis, also known as starved air incineration, is usually conducted at relatively high temperatures (greater than 500 deg C) in the absence of oxygen. Incineration is conducted at lower temperatures in the presence of oxygen. The primary purpose of this study was to design, construct, and test a model P/I. The system design includes safety requirements for temperature and pressure. The objectives of this study were: (1) to design and construct a P/I system for incorporation with the Hybrid Regenerative Water Recovery System; (2) to initiate testing of the P/I system; (3) to collect and analyze P/I system data; (4) to consider test variables; and (5) to determine the feasibility of P/I as an effective method of resource recovery. A P/I system for the recovery of reuseable resources from solid waste materials was designed, constructed, and tested. Since a large amount of inedible plant biomass (IPB) will be generated in a space-based habitat on the lunar surface and Mars, IPB was the primary waste material tested in the system. Analysis of the effluent gases was performed to determine which gases could be used in a life support system. Author

N94-25376*# Saint Louis Univ., MO. School of Nursing.

DEVELOPMENT OF A MODEL TO ASSESS ORTHOSTATIC RESPONSES **c52**

Marilyn Rubin *In* NASA. Johnson Space Center, National Aeronautics and Space Administration (NASA)/American Society for Engineering Education (ASEE) Summer Faculty Fellowship Program, 1993, Volume 2 Dec. 1993 15 p (For primary document see N94-25367 06-99)

Avail: CASI HC A03/MF A03

A major change for crewmembers during weightlessness in microgravity is the redistribution of body fluids from the legs into the abdomen, thorax, and head. The fluids continue to be sequestered in these areas throughout the flight. Upon reentry into gravity on landing, these same body fluids are displaced again to their normal locations, however, not without hazardous incidence to the crewmembers. The problem remains that upon landing, crewmembers are subject to orthostasis, that is, the blood flowing into the legs reduces the blood supply to the brain and may result in the crewmember fainting. The purpose of this study was to develop a model of testing orthostatic responses of blood pressure regulating mechanisms of the cardiovascular system, when challenged, to maintain blood pressure to the brain. To accomplish this, subjects' responses were assessed as they proceeded from the supine position of progressive head-up tilt positions of 30 deg, 60 deg, and 90 deg angles. A convenience sample consisted of 21 subjects, females (N=11) and males (N=10), selected from a list of potential subjects available through the NASA subject screening office. The methodology included all non-invasive measurements of blood pressure, heart rate, echocardiograms, cardiac output, cardiac stroke volume, fluid shifts in the thorax, ventricular ejection and velocity times, and skin blood perfusion. The Fischer statistical analysis was done of all data with the significance level at .05. Significant differences were demonstrated in many instances of changes of posture for all variables. Based on the significance of the findings of this study, this model for assessing orthostatic responses does provide an adequate challenge to the blood pressure regulatory systems. While individuals may use different adaptations to incremental changes in gravity, the subjects, in aggregate, demonstrated significant adaptive cardiovascular changes to orthostatic challenges which were presented to them. Author

N94-25377*# Memphis State Univ., TN. Dept. of Electrical Engineering.
DIGITAL DATA, COMPOSITE VIDEO MULTIPLEXER AND DEMULTIPLEXER BOARDS FOR AN IBM PC/AT COMPATIBLE COMPUTER **c60**
Dean Lance Smith *In* NASA. Johnson Space Center, National Aeronautics and Space Administration (NASA)/American Society for Engineering Education (ASEE) Summer Faculty Fellowship Program, 1993, Volume 2 Dec. 1993 5 p (For primary document see N94-25367 06-99)
Avail: CASI HC A01/MF A03

Work continued on the design of two IBM PC/AT compatible computer interface boards. The boards will permit digital data to be transmitted over a composite video channel from the Orbiter. One board combines data with a composite video signal. The other board strips the data from the video signal. Author

N94-25378*# Akron Univ., OH. Biomedical Engineering.
EVALUATION OF BIOIMPEDANCE FOR THE MEASUREMENT OF PHYSIOLOGIC VARIABLES AS RELATED TO HEMODYNAMIC STUDIES IN SPACE FLIGHT **c52**
Bruce C. Taylor *In* NASA. Johnson Space Center, National Aeronautics and Space Administration (NASA)/American Society for Engineering Education (ASEE) Summer Faculty Fellowship Program, 1993, Volume 2 Dec. 1993 15 p (For primary document see N94-25367 06-99)
Avail: CASI HC A03/MF A03

Orthostatic intolerance, following space flight, has received substantial attention because of the possibility that it compromises astronaut safety and reduces the ability of astronauts to function at peak performance levels upon return to a one-g environment. Many pre- and post-flight studies are performed to evaluate changes in hemodynamic responses to orthostatic challenges after shuttle missions. The purpose of this present project is to validate bioimpedance as a means to acquire stroke volume and other hemodynamic information in these studies. In this study, ten male and ten female subjects were subjected to simultaneous measurements of thoracic bioimpedance and Doppler ultrasonic velocimetry under supine, 10 degree head down and 30 degree head up conditions. Paired measurements were made during six periods of five seconds breath holding, over a two minute period, for each of the three positions. Stroke volume was calculated by three bioimpedance techniques and ultrasonic Doppler. Author (revised)

N94-25379*# Colorado Univ., Colorado Springs. Dept. of Electrical Engineering.
CONCEPTUAL COMMUNICATIONS SYSTEM DESIGN IN THE 25.25-27.5 AND 37.0-40.5 GHz FREQUENCY BANDS **c32**
Michael W. Thompson *In* NASA. Johnson Space Center, National Aeronautics and Space Administration (NASA)/American Society for Engineering Education (ASEE) Summer Faculty Fellowship Program, 1993, Volume 2 Dec. 1993 15 p (For primary document see N94-25367 06-99)
Avail: CASI HC A03/MF A03

Future space applications are likely to rely heavily on Ka-band frequencies (20-40 GHz) for communications traffic. Many space research activities are now conducted using S-band and X-band frequencies, which are becoming congested and require a degree of pre-coordination. In addition to providing relief from frequency congestion, Ka-band technologies offer potential size, weight, and power savings when compared to lower frequency bands. The use of the 37.0-37.5 and 40.0-40.5 GHz bands for future planetary missions was recently approved at the 1992 World Administrative Radio Conference (WARC-92). WARC-92 also allocated the band 25.25-27.5 GHz to the Intersatellite Service on a primary basis to accommodate Data Relay Satellite return link requirements. Intersatellite links are defined to be between artificial satellites and thus a communication link with the surface of a planetary body, such as the moon, and a relay satellite orbiting that body are not permitted in this frequency band. This report provides information about preliminary communications system concepts for forward and return links for earth-Mars and earth-lunar links using the 37.0-37.5 (return link) and 40.0-40.5 (forward link) GHz frequency bands. In this study we concentrate primarily on a conceptual system for communications between earth and a single lunar surface terminal (LST), and between earth and a single Mars surface terminal (MST). Due to large space losses, these links have the most stringent link requirements for an overall interplanetary system. The earth ground station is assumed to be the Deep Space Network (DSN) using either 34 meter or 70 meter antennas. We also develop preliminary communications concepts for a space-to-space system operating at near 26 GHz. Space-to-space applications can encompass a variety of operating conditions, and we consider several 'typical' scenarios described in more detail later in this report. Among these scenarios are vehicle-to-vehicle communications, vehicle-to-geosyncronous satellite (GEO) communications, and GEO-to-GEO communications. Additional details about both the interplanetary and space-to-space communications systems are provided in an 'expanded' final report which has been submitted to the Tracking and Communications Division (TCD) at the NASA Johnson Space Center. Author (revised)

N94-25380*# Alabama Univ., Huntsville. Dept. of Engineering Science and Mechanics.
LOADING, ELECTROMYOGRAPH, AND MOTION DURING EXERCISE **c52**
Beth A. Todd *In* NASA. Johnson Space Center, National Aeronautics and Space Administration (NASA)/American Society for Engineering Education (ASEE) Summer Faculty Fellowship Program, 1993, Volume 2 Dec. 1993 11 p (For primary document see N94-25367 06-99)
Avail: CASI HC A03/MF A03

A bicycle ergometer system has been developed to determine forces acting in specific muscles and muscle groups for both cycling and isometric exercise. The bicycle has been instrumented with encoders, accelerometers, and load cells. A harnessing system has been developed to keep subjects in place during isometric exercise. EMG data will also be collected with electrodes attached to various muscles on the subject's leg. Data has been collected for static loading and will be collected for cycling in both an earth-based laboratory and on the KC-135. Once the data is analyzed, the forces will be entered into finite element models of bones of the lower extremities. A finite element model of the tibia-fibula has been generated from the experimental subject's MRI data. The linear elastic isoparametric brick elements representing the bones are connected by linear elastic isoparametric shell elements placed at the locations of ligaments. Models will be generated for the calcaneus and the femur. Material properties for the various tissues will be taken from the literature. The experimentally determined muscle forces will be applied to the models to determine the stress distribution which is created in the bones. Author

N94-25381*# Amarillo Coll., TX. Electronics Technology Dept.
MODELING OF THE GROUND-TO-SSFMB LINK NETWORKING FEATURES USING SPW **c32**
John C. Watson *In* NASA. Johnson Space Center, National Aeronautics and Space Administration (NASA)/American Society for Engineering Education (ASEE) Summer Faculty Fellowship Program, 1993, Volume 2 Dec. 1993 15 p (For primary document see N94-25367 06-99)
Avail: CASI HC A03/MF A03

This report describes the modeling and simulation of the networking features of the ground-to-Space Station Freedom manned base (SSFMB) link using COMDISCO signal processing work-system (SPW). The networking features modeled include the implementation of Consultative Committee for Space Data Systems (CCSDS) protocols in the multiplexing of digitized audio and core data into virtual channel data units (VCDU's) in the control center complex and the demultiplexing of VCDU's in the onboard baseband signal processor. The emphasis of this work has been placed on techniques for modeling the CCSDS networking features using SPW. The objectives for developing the SPW models are to test the suitability of SPW for modeling networking features and to develop SPW simulation models of the control center complex and space station baseband signal processor for use in end-to-end testing of the ground-to-SSFMB S-band single access forward (SSAF) link. Author (revised)

N94-25382*# Southeastern Oklahoma State Univ., Durant. Computer Science/Information Systems Dept.

SOFTWARE ENGINEERING METHODOLOGIES AND TOOLS **c61**

Lawrence M. Wilcox *In* NASA. Johnson Space Center, National Aeronautics and Space Administration (NASA)/American Society for Engineering Education (ASEE) Summer Faculty Fellowship Program, 1993, Volume 2 Dec. 1993 15 p (For primary document see N94-25367 06-99)
Avail: CASI HC A03/MF A03

Over the years many engineering disciplines have developed, including chemical, electronic, etc. Common to all engineering disciplines is the use of rigor, models, metrics, and predefined methodologies. Recently, a new engineering discipline has appeared on the scene, called software engineering. For over thirty years computer software has been developed and the track record has not been good. Software development projects often miss schedules, are over budget, do not give the user what is wanted, and produce defects. One estimate is there are one to three defects per 1000 lines of deployed code. More and more systems are requiring larger and more complex software for support. As this requirement grows, the software development problems grow exponentially. It is believed that software quality can be improved by applying engineering principles. Another compelling reason to bring the engineering disciplines to software development is productivity. It has been estimated that productivity of producing software has only increased one to two percent a year in the last thirty years. Ironically, the computer and its software have contributed significantly to the industry-wide productivity, but computer professionals have done a poor job of using the computer to do their job. Engineering disciplines and methodologies are now emerging supported by software tools that address the problems of software development. This paper addresses some of the current software engineering methodologies as a backdrop for the general evaluation of computer assisted software engineering (CASE) tools from actual installation of and experimentation with some specific tools. Author (revised)

N94-25383*# Cincinnati Univ., OH. Dept. of Aerospace Engineering.

SPACE STATION FLEXIBLE DYNAMICS UNDER PLUME IMPINGEMENT **c18**

Trevor Williams *In* NASA. Johnson Space Center, National Aeronautics and Space Administration (NASA)/American Society for Engineering Education (ASEE) Summer Faculty Fellowship Program, 1993, Volume 2 Dec. 1993 14 p (For primary document see N94-25367 06-99)
Avail: CASI HC A03/MF A03

Assembly of the Space Station requires numerous construction flights by the Space Shuttle. A particularly challenging problem is that of control of each intermediate station configuration when the shuttle orbiter is approaching it to deliver the next component. The necessary braking maneuvers cause orbiter thruster plumes to impinge on the station, especially its solar arrays. This in turn causes both overall attitude errors and excitation of flexible-body vibration modes. These plume loads are predicted to lead to CMG saturation during the approach of the orbiter to the SC-5 station configuration, necessitating the use of the station RCS jets for desaturation. They are also expected to lead to significant excitation of solar array vibrations. It is therefore of great practical importance to investigate the effects of plume loads on the flexible dynamics of station configuration SC-5 as accurately as possible. However, this system possesses a great many flexible modes (89 below 5 rad/s), making analysis time-consuming and complicated. Model reduction techniques can be used to overcome this problem, reducing the system model to one which retains only the significant dynamics, i.e. those which are strongly excited by the control inputs or plume disturbance forces and which strongly couple with the measured outputs. The particular technique to be used in this study is the subsystem balancing approach which was previously developed by the present investigator. This method is very efficient computationally. Furthermore, it gives accurate results even for the difficult case where the structure has many closed-spaced natural frequencies, when standard modal truncation can give misleading results. Station configuration SC-5 is a good example of such a structure. Author (revised)

N94-25384*# Houston Univ., TX. Dept. of Curriculum and Instruction.

A MULTIMEDIA ADULT LITERACY PROGRAM: COMBINING NASA TECHNOLOGY, INSTRUCTIONAL DESIGN THEORY, AND AUTHENTIC LITERACY CONCEPTS **c80**

Jerry W. Willis *In* NASA. Johnson Space Center, National Aeronautics and Space Administration (NASA)/American Society for Engineering Education (ASEE) Summer Faculty Fellowship Program, 1993, Volume 2 Dec. 1993 13 p (For primary document see N94-25367 06-99)
Avail: CASI HC A03/MF A03

For a number of years, the Software Technology Branch of the Information Systems Directorate has been involved in the application of cutting edge hardware and software technologies to instructional tasks related to NASA projects. The branch has developed intelligent computer aided training shells, instructional applications of virtual reality and multimedia, and computer-based instructional packages that use fuzzy logic for both instructional and diagnostic decision making. One outcome of the work on space-related technology-supported instruction has been the creation of a significant pool of human talent in the branch with current expertise on the cutting edges of instructional technologies. When the human talent is combined with advanced technologies for graphics, sound, video, CD-ROM, and high speed computing, the result is a powerful research and development group that both contributes to the applied foundations of instructional technology and creates effective instructional packages that take advantage of a range of advanced technologies. Several branch projects are currently underway that combine NASA-developed expertise to significant instructional problems in public education. The branch, for example, has developed intelligent computer aided software to help high school students learn physics and staff are currently working on a project to produce educational software for young children with language deficits. This report deals with another project, the adult literacy tutor. Unfortunately, while there are a number of computer-based instructional packages available for adult literacy instruction, most of them are based on the same instructional models that failed these students when they were in school. The teacher-centered, discrete skill and drill-oriented, instructional strategies, even when they are supported by color computer graphics and animation, that form the foundation for most of the computer-based literacy packages currently on the market may not be the most effective or most desirable way to use computer technology in literacy programs. This project is developing a series of instructional packages that are based on a different instructional model - authentic instruction. The instructional development model used to create these packages is also different. Instead of using the traditional five stage linear, sequential model based on behavioral learning theory, the project uses the recursive, reflective design and development model (R2D2) that is based on cognitive learning theory, particularly the social constructivism of Vygotsky, and an epistemology based on critical theory. Using alternative instructional and instructional development theories, the result of the summer faculty fellowship is LiteraCity, a multimedia adult literacy instructional package that is a simulation of finding and applying for a job. The program, which is about 120 megabytes, is distributed on CD-ROM.
Author (revised)

SUBJECT INDEX

SCIENTIFIC AND TECHNICAL AEROSPACE REPORTS VOLUME 32 NUMBER 6

Typical Subject Index Listing

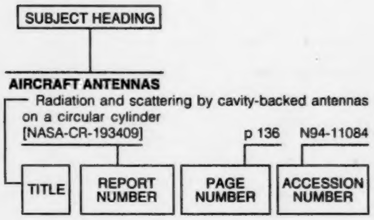

The subject heading is a key to the subject content of the document. Titles, report numbers, and accession numbers of pertinent documents are provided under each subject heading. When the title is insufficiently descriptive of the document content, a title extension is added, separated from the title by three hyphens. The report number helps to indicate the type of document cited (e.g., NASA report, NASA translation, NASA contractor report). The accession number is the number by which the document abstracts are arranged in this journal and by which the document is sold or requested. The page number helps you locate the citation in the abstract section. The titles, with title extensions if present, are arranged under each subject heading in ascending accession number order. The subject headings have been selected from the latest revision of the *NASA Thesaurus*.

A

A STARS
UV spectral variability in the Herbig Ae star HR 5999. 11: The accretion interpretation
[NASA-CR-189313] p 2599 N94-23334
Observational studies of the clearing phase in proto-planetary disk systems
[NASA-CR-195182] p 2604 N94-25265
ABERRATION
Polarization analysis of a balloon-borne solar magnetograph
[NASA-CR-193908] p 2345 N94-24852
ABLATION
The internal structure and dynamics of the railgun plasma armature between infinitely wide ablating rails
[DE94-001473] p 2198 N94-23208
Computational model of surface ablation from tokamak disruptions
[DE94-002204] p 2550 N94-23474
Pellet ablation in the large helical device
[NIFS-260] p 2551 N94-24358
ABLATIVE MATERIALS
Micromechanical simulation of damage progression in carbon phenolic composites p 2231 N94-24446
ABORT APPARATUS
Regulated drag area parachute
[AD-D015992] p 2170 N94-25051
ABORT TRAJECTORIES
Optimal RTLS abort trajectories for an HL-20 personnel launch vehicle p 2165 N94-25114
ABRASION RESISTANCE
A preliminary evaluation of the phosphazene resin PPZ
[AD-A273674] p 2263 N94-25410
ABSORBERS (MATERIALS)
High energy collimating fine grids for HESP program
[NASA-CR-189317] p 2209 N94-24767
ABSORPTION COOLING
Enhanced absorption cycle computer model
[DE94-001997] p 2271 N94-23793
ABSORPTION SPECTRA
Algorithm-development activities
[NASA-CR-193225] p 2420 N94-23538
Development of an analytical-numerical model to predict radiant emission or absorption
[NASA-CR-194860] p 2453 N94-23624
Radiative forcing calculations for SF6 and CH4 using a correlated k-distribution transmission model
[DE94-001855] p 2397 N94-23700
Using contour maps to search for red-shifted 511 keV features in BATSE GRB spectra p 2585 N94-24455
ABSORPTION SPECTROSCOPY
Tropospheric Ozone Lidar Intercomparison Experiment, TROLIX 1991
[MPIM-102] p 2402 N94-24108
Doppler global velocimetry: Development of a flight research instrumentation system for application to non-intrusive measurements of the flow field
[NASA-CR-191490] p 2344 N94-24360
Non-invasive optical detection of glucose in cell culture nutrient medium p 2422 N94-25357
ABSORPTIVITY
Algorithm-development activities
[NASA-CR-193225] p 2420 N94-23538
ABSTRACTS
Bibliography of Lewis Research Center technical publications announced in 1992
[NASA-TM-106035] p 2590 N94-23562
Aircraft flight safety: A bibliography
[AGARD-R-805] p 2173 N94-24091
ABUNDANCE
Coronal abundances and their variation
[NASA-CR-194811] p 2626 N94-23276
Molecular abundances in the envelopes around evolved stars
[PB94-104916] p 2602 N94-23812
AC GENERATORS
Controllability of free-piston Stirling engine/linear alternator driving a dynamic load
[NASA-TM-106497] p 2521 N94-24302
ACCELERATED LIFE TESTS
Review of super Ni/Cd cell designs and performance
p 2391 N94-23348
Airport pavement test machine design and cost study
[DOT/FAA/CT-93/51] p 2192 N94-24072
ACCELERATION (PHYSICS)
An investigation into acceleration determination for airborne gravimetry using the global positioning system
[ISBN-0-315-59470-5] p 2175 N94-24176
ACCELERATION STRESSES (PHYSIOLOGY)
Artificial gravity in space flight
[AD-A273420] p 2427 N94-24928
ACCELEROMETERS
The pre-development of the Aristoteles calibration mechanism p 2209 N94-24006
Integrated accelerometer assembly
[CA-PATENT-1322107] p 2344 N94-24184
ACCEPTOR MATERIALS
Magnetic resonance study of zinc-related defects in silicon with optimized EPR spectrometer
[PB93-224640] p 2561 N94-23223
ACCESS TIME
Design and implementation issues of end-to-end protocols in high-speed networks
[PB94-110905] p 2467 N94-23752
ACCIDENTS
Continuum representations of cellular solids
[DE94-001706] p 2375 N94-23217
ACCRETION DISKS
UV spectral variability in the Herbig Ae star HR 5999. 11: The accretion interpretation
[NASA-CR-189313] p 2599 N94-23334
Protoplanetary disks: Theory and observation by millimeter and sub-millimeter arrays
[REPT-331] p 2603 N94-24983
Observational studies of the clearing phase in proto-planetary disk systems
[NASA-CR-195182] p 2604 N94-25265
ACCUMULATIONS
Synthesis of passive microwave and radar altimeter data for estimating accumulation rates of polar snow
[NASA-CR-194864] p 2382 N94-23573
ACCURACY
Accuracy control in Monte Carlo radiative calculations
p 2321 N94-23639
ACETIC ACID
Scanning probe lithography. 2: Selective chemical vapor deposition of copper into scanning tunneling microscope-defined patterns
[AD-A273304] p 2547 N94-25144
ACETYLENE
Polydiacetylene thin films for nonlinear optical applications p 2225 N94-24347
Metal-catalyzed alkynylation of brominated polyphenylenes: Thermoset precursors of high density monolithic glassy carbon
[AD-A273232] p 2259 N94-24789
ACID RAIN
Chemistry on the mesoscale: Modeling and measurement issues p 2413 N94-24390
ACIDS
Curing phthalonitriles with acid
[AD-D015996] p 2261 N94-25054
ACOUSTIC ATTENUATION
JAPE 91: Influence of terrain masking of the acoustic propagation of helicopter noise p 2528 N94-24214
Comparison between 1-minute and 15-minute averages of turbulence parameters p 2528 N94-24218
ACOUSTIC DUCTS
The acoustic and instability waves of jets confined inside an acoustically lined rectangular duct
[NASA-CR-191586] p 2334 N94-24602
ACOUSTIC EMISSION
Acoustic target detection and classification using neural networks p 2529 N94-24221
Investigation of the effects of manufacturing variations and materials on fatigue crack detection methods in gear teeth
[NASA-CR-195093] p 2373 N94-24769
ACOUSTIC FREQUENCIES
Ground characterization for JAPE
p 2527 N94-24213
Some subjects in digital audio, noise shaping, sample rate conversion, dynamic range compression and testing
[ISBN-9-09-005162-7] p 2530 N94-25220
ACOUSTIC IMPEDANCE
Ground characterization for JAPE
p 2527 N94-24213
Comparisons of calculated and measured helicopter noise near instrument hill p 2528 N94-24215
ACOUSTIC INSTABILITY
The acoustic and instability waves of jets confined inside an acoustically lined rectangular duct
[NASA-CR-191586] p 2334 N94-24602
ACOUSTIC MEASUREMENT
JAPE 91: Influence of terrain masking of the acoustic propagation of helicopter noise p 2528 N94-24214
Preliminary analysis of amplitude and phase fluctuations in the JAPE multiple tone data to distances of 500 meters p 2528 N94-24216
Fiber optic detection of ultrasound and its application to cure monitoring
[ISBN-0-315-83424-2] p 2544 N94-24466
Global acoustic mapping of ocean temperatures (GAMOT)
[AD-A273387] p 2418 N94-24719
Investigation of the effects of manufacturing variations and materials on fatigue crack detection methods in gear teeth
[NASA-CR-195093] p 2373 N94-24769
ACOUSTIC PROPAGATION
Diffraction analysis of transient acoustic waves: Half-plane in a layered medium
[PB94-110988] p 2526 N94-23726
Joint Acoustic Propagation Experiment (JAPE-91) Workshop
[NASA-CP-3231] p 2526 N94-24207
Joint Acoustic Propagation Experiment (JAPE)
p 2527 N94-24208

Some results gained from JAPE: An overview p 2527 N94-24209

Intercomparison of remote and balloon-borne sensors operated at JAPE-91 p 2527 N94-24210

Effects of atmospheric variations on acoustic system performance p 2527 N94-24211

Comparison of measured and predicted pure tone propagation levels from JAPE-1: An evaluation of the performance of ASOPRAT p 2527 N94-24212

Ground characterization for JAPE p 2527 N94-24213

JAPE 91: Influence of terrain masking of the acoustic propagation of helicopter noise p 2528 N94-24214

Comparisons of calculated and measured helicopter noise near instrument hill p 2528 N94-24215

Preliminary analysis of amplitude and phase fluctuations in the JAPE multiple tone data to distances of 500 meters p 2528 N94-24216

Dimensional analysis of acoustically propagated signals p 2528 N94-24217

Beamforming in an acoustic shadow p 2528 N94-24219

Analysis of passive acoustic ranging of helicopters from the joint acoustic propagation experiment p 2529 N94-24220

Acoustic target detection and classification using neural networks p 2529 N94-24221

Measurements and modeling of multitone, low-frequency acoustic data from the Arraial do Cabo range [AD-A273406] p 2530 N94-25073

On the physics of waves in the solar atmosphere: Wave heating and wind acceleration [NASA-CR-195197] p 2628 N94-25264

Analysis of modal evolution caused by a weakly range-dependent seabed in shallow water and its application to inversion for geoacoustic properties [AD-A273656] p 2419 N94-25435

ACOUSTIC PROPERTIES

Measurements and modeling of multitone, low-frequency acoustic data from the Arraial do Cabo range [AD-A273406] p 2530 N94-25073

ACOUSTIC SCATTERING

Classical scattering theory of waves from the view point of an eigenvalue problem and application to target identification [DE94-000472] p 2525 N94-23206

Effects of atmospheric variations on acoustic system performance p 2527 N94-24211

JAPE 91: Influence of terrain masking of the acoustic propagation of helicopter noise p 2528 N94-24214

Comparisons of calculated and measured helicopter noise near instrument hill p 2528 N94-24215

Preprocessor and adaptive beamformer for linear-frequency modulation active signals [AD-D016008] p 2302 N94-25048

ACOUSTIC SOUNDING

Intercomparison of remote and balloon-borne sensors operated at JAPE-91 p 2527 N94-24210

ACOUSTIC VELOCITY

Fiber optic detection of laser generated ultrasound for materials characterization [ISBN-0-315-83541-9] p 2541 N94-22891

Development of a droplet breakup model considering aerodynamic and droplet collision effects p 2213 N94-23045

Normal zone propagation and thermal hydraulic quenchback in a cable-in-conduit superconductor [DE94-002457] p 2271 N94-24568

Development and validation of RNG methodology for compressible turbulence [AD-A273469] p 2337 N94-24929

ACOUSTICS

Acoustic and optical investigations of superfluid He-3 [PB93-224889] p 2523 N94-23101

Joint Acoustic Propagation Experiment (JAPE) p 2527 N94-24208

Some results gained from JAPE: An overview p 2527 N94-24209

A study of element interaction in thermoacoustic engines [AD-A273228] p 2569 N94-24777

ACOUSTO-OPTICS

Advanced technology for a satellite multichannel demultiplexer/demodulator [NASA-CR-194435] p 2202 N94-23631

ACRYLATES

Feasibility study: Monodisperse polymer particles containing laser-excitable dyes p 2225 N94-24350

ACRYLIC ACID

Convective instabilities in traveling fronts of addition polymerization p 2226 N94-24352

ACRYLIC RESINS

Microstructure of styrene methyl methacrylate copolymers grafted onto polybutadiene seeds [ETN-94-95360] p 2262 N94-25225

ACTINIDE SERIES

Thermochemistry of the actinides [DE94-000895] p 2231 N94-22943

ACTINIDE SERIES COMPOUNDS

Thermochemistry of the actinides [DE94-000895] p 2231 N94-22943

ACTIVATION ENERGY

A novel method for determination of transport parameters of H2 and O2 in PEMFCs [DE94-001492] p 2389 N94-22962

Thermally activated low temperature creep and primary water stress corrosion cracking of NiCrFe alloys [DE94-001756] p 2241 N94-23219

ACTIVE CONTROL

Aeroelastic, aeromechanical and vibration problems in helicopters p 2154 N94-24244

LSS systems planning and performance program [NASA-CR-193882] p 2196 N94-24309

Influence of active controls on the design process of a large transport aircraft p 2178 N94-24323

Active control of buildings during earthquakes [NASA-TM-109033] p 2271 N94-24473

Active control of oscillatory lift forces on a circular cylinder [AD-A273243] p 2338 N94-25140

Modeling of a large undamped space structure using time domain techniques [AD-A273828] p 2206 N94-25523

ACTS

Internetworking satellite and local exchange networks for personal communications applications p 2276 N94-22755

ACTS broadband aeronautical experiment p 2279 N94-22771

ACTS mobile SATCOM experiments p 2280 N94-22774

ACTS advanced system concepts and experimentation p 2280 N94-22780

K-band mobile propagation measurements using ACTS p 2283 N94-22792

Channel and terminal description of the ACTS mobile terminal p 2284 N94-22802

K- and Ka-band mobile-vehicular satellite-tracking reflector antenna system for the NASA ACTS mobile terminal p 2289 N94-22831

An active K/Ka-band antenna array for the NASA ACTS mobile terminal p 2289 N94-22832

Supercomputer networking for space science applications [NASA-CR-194876] p 2465 N94-23085

ACTUATORS

A structural design methodology for large angle articulated trusses considering realistic joint modeling p 2376 N94-23560

A comparison of two multi-variable integrator windup protection schemes [NASA-CR-194436] p 2190 N94-23590

The Fifth European Space Mechanisms and Tribology Symposium [ESA-SP-334] p 2355 N94-23985

Low melting temperature alloy deployment mechanism p 2356 N94-23997

Periscope mechanism for SWAN instrument p 2357 N94-24000

Opening mechanism for ISO/CVV cover release p 2357 N94-24001

An Earth observation telescope refocusing mechanism p 2359 N94-24014

Inter orbit link antenna pointing mechanisms design using standard actuators p 2359 N94-24016

Precision Displacement Mechanism (PDM) p 2360 N94-24026

Development of a Low-Temperature Gear Motor (LOG) p 2361 N94-24032

A novel rotary actuator for spacecraft p 2361 N94-24034

Design and performances of electromagnetic initiators for space mechanisms: An alternative to pyrotechnic system p 2315 N94-24037

Recharge mechanism based on shape memory alloy p 2362 N94-24039

Controller modeling and evaluation for PCV electro-mechanical actuator p 2371 N94-24441

Design and application of electromechanical actuators for deep space missions [NASA-CR-195134] p 2365 N94-24842

Collocated tunable wavenumber sensor/actuators for smart structures [AD-A273697] p 2314 N94-25488

ADA (PROGRAMMING LANGUAGE)

Update of GRASP/Ada reverse engineering tools for Ada [NASA-CR-193890] p 2455 N94-24111

The Adam language: Ada extended with support for multiway activities [NASA-CR-4565] p 2456 N94-24480

An automated tool to facilitate code translation for software fault tree analysis [AD-A273205] p 2457 N94-24556

ADAPTERS

Precision drive and speed reduction device [AD-D016004] p 2367 N94-25046

ADAPTIVE CONTROL

Adaptive data rate control TDMA systems as a rain attenuation compensation technique p 2287 N94-22821

A novel process monitoring and control system based on a neural manufacturing concept [DE94-001516] p 2471 N94-23011

Real-time dynamics and control strategies for space operations of flexible structures [NASA-CR-194794] p 2203 N94-23618

Adaptive nonlinear polynomial neural networks for control of boundary layer/structural interaction [NASA-CR-189645] p 2525 N94-23698

Identification of integrated airframe: Propulsion effects on an F-15 aircraft for application to drag minimization [NASA-TM-4532] p 2188 N94-24106

Change-point detection and adaptive control of time-varying systems [AD-A273509] p 2475 N94-24943

Probabilistic assessment of smart composite structures [NASA-TM-106358] p 2378 N94-25188

Genetic algorithms in control systems engineering [RR-470] p 2463 N94-25315

Adaptive predictive control of the benchmark plant [OUEL-1972/93] p 2477 N94-25470

ADAPTIVE FILTERS

Maximum likelihood modal parameter identification and realization of stochastic systems p 2157 N94-24265

Linear and nonlinear adaptive filtering and their application to speech intelligibility enhancement [ISBN-9-09-005342-5] p 2304 N94-25292

ADAPTIVE OPTICS

Sodium-layer laser guide stars [DE93-019621] p 2349 N94-23490

Low power ground-based laser illumination for electric propulsion applications [NASA-CR-194444] p 2219 N94-23555

ADDITION RESINS

A preliminary evaluation of the phosphazene resin PPZ [AD-A273674] p 2263 N94-25410

ADDITIVES

Processing of YBCO superconductors for improved levitation force [DE94-001326] p 2559 N94-22994

Polyimide processing additives [NASA-CASE-LAR-13669-2] p 2252 N94-23079

New method for increasing machine service-life, phase 2 [PB93-200707] p 2354 N94-23533

Capillary electrokinetic separations with optical detection [DE94-001639] p 2233 N94-23716

Overcharge and overdischarge protection of ambient temperature secondary lithium cells [NASA-CASE-NPO-18343-1-CU] p 2310 N94-23823

Numerical simulation of non-Newtonian free shear flows p 2331 N94-24160

Isothiazolone volatility study of a water bottom from fuel treated with Kathon (tm) FP1.5 biocide [AD-A273165] p 2266 N94-24728

The effects of zinc borate addition on the flammability characteristics of polyester, vinyl ester, and epoxy glass reinforced plastics [AD-A273164] p 2262 N94-25136

ADENOSINE TRIPHOSPHATE

The evolution of energy-transducing systems. Studies with an extremely halophilic archaebacterium [NASA-CR-193803] p 2422 N94-24807

The evolution of energy-transducing systems. Studies with archaebacteria [NASA-CR-195129] p 2422 N94-24811

ADHESION

Selective hydrogen separation by palladium-based composite membranes [PB93-201671] p 2254 N94-23431

Static adhesion in preloaded contacts subjected to long-term vacuum exposure p 2363 N94-24043

Laser-deposited biocompatible films and methods and apparatuses for producing same [AD-D016017] p 2350 N94-24952

ADHESION TESTS
Evaluation of the fracture resistance and durability of adhesive bonded joints p 2160 N94-24278

ADHESIVE BONDING
Computer based expert system for battle damage repair of composite structures p 2157 N94-24262
Evaluation of the fracture resistance and durability of adhesive bonded joints p 2160 N94-24278
High temperature adhesive
[AD-D016019] p 2258 N94-24737
Ultrasonic process for curing adhesives
[AD-A273175] p 2259 N94-24788

ADHESIVES
Computer based expert system for battle damage repair of composite structures p 2157 N94-24262
High temperature adhesive
[AD-D016019] p 2258 N94-24737
Ultrasonic process for curing adhesives
[AD-A273175] p 2259 N94-24788

ADIABATIC CONDITIONS
Analytical skin friction and heat transfer formula for compressible internal flows
[NASA-CR-191185] p 2170 N94-25173

ADIABATIC FLOW
Analytical skin friction and heat transfer formula for compressible internal flows
[NASA-CR-191185] p 2170 N94-25173

ADJOINTS
Boundary layer receptivity and control
p 2327 N94-24141
Signatures of selfadjoint pencils
[PB94-111127] p 2457 N94-24599

ADSORPTION
Ordered organic thin films self-assembled from the vapor phase p 2223 N94-24339
Diffusion on Cu surfaces p 2251 N94-24428
Adsorption, desorption, and decomposition of HCl and HBr on Ge(100): Competitive pairingand near-first-order desorption kinetics
[AD-A273504] p 2235 N94-24790
Investigation of the solid-solid surface adsorption of Eu2O3 on amorphous Al2O3
[DE93-613824] p 2566 N94-25332
Use of scanning tunneling microscope in corrosion studies
[VTT-TIED-1416] p 2250 N94-25346

ADVANCED LAUNCH SYSTEM (STS)
Approximate optimal guidance for the advanced launch system
[NASA-CR-4568] p 2198 N94-24752
Advanced launch system. Advanced development oxidizer turbopump program
[NASA-CR-193920] p 2367 N94-25174

ADVANCED SOLID ROCKET MOTOR (STS)
Flame trench analysis of NLS vehicles
p 2199 N94-23249
Properties and processing characteristics of low density carbon cloth phenolic composites p 2231 N94-24450
Analysis and effects of the advanced solid rocket motor on the Space Shuttle elements
[NASA-CR-193879] p 2200 N94-24664

ADVANCED VERY HIGH RESOLUTION RADIOMETER
An AVHRR cloud classification database typed by experts
[AD-A273560] p 2416 N94-25162

ADVECTION
A geometric weighted elliptic grid regeneration method for 3D unstructured ALE hydrodynamics
[DE94-000309] p 2448 N94-22980
Locally modified Bott-scheme for highly convective flows
[MPIM-99] p 2400 N94-23157
A two-dimensional dispersion module for the TOUGH2 simulator
[DE94-002262] p 2335 N94-24655

AERIAL PHOTOGRAPHY
Optical component MAC Europe ground truth report: Flevoland 1991 (Netherlands)
[BCRS-92-27] p 2382 N94-23177
Application of ERS-1 active microwave instrumentation data to remote sensing of snow
[PB93-224756] p 2382 N94-23224

AERIAL RECONNAISSANCE
Imaging System (INEL) T805 prototype
[DE94-002807] p 2382 N94-23492
UAV current technology and future trends
p 2154 N94-24245

AEROACOUSTICS
Refraction of high frequency noise in an arbitrary jet flow
[NASA-TM-106465] p 2525 N94-23464
Unsteady jet flow computation towards noise prediction
[NASA-CR-194449] p 2153 N94-23553
Sound radiation due to boundary layer transition
p 2332 N94-24163
Variability of measured sonic boom signatures. Volume 1: Technical report
[NASA-CR-191483-VOL-1] p 2526 N94-24172
Variability of measured sonic boom signatures. Volume 2: Data report
[NASA-CR-191483-VOL-2] p 2526 N94-24173
Validation of the ROTAC code for the rotor noise prediction
[PB93-204311] p 2529 N94-24514
Fan noise research at NASA
[NASA-TM-106512] p 2530 N94-25172
The ISL rotor bench
[ISL-R-108/92] p 2185 N94-25301
Study of the blade/vortex interaction: Acoustics, aerodynamics and models
[ISL-R-104/92] p 2340 N94-25463

AEROBES
Chemical characterization of some aerobic liquids in CELSS p 2422 N94-23241

AERODYNAMIC CHARACTERISTICS
Aerodynamic models for performance calculations of modern technology propellers p 2161 N94-24285
An experimental investigation of a Mach 3.0 high-speed civil transport at supersonic speeds
[NASA-TP-3365] p 2169 N94-24311
NASA/USRA advanced design program
[NASA-CR-195548] p 2180 N94-24492
Aerodynamic characteristics and pressure distributions for an executive-jet baseline airfoil section
[NASA-TM-4529] p 2169 N94-24586
Supersonic aerodynamic characteristics of a circular body Earth-to-Orbit vehicle
[NASA-TM-4533] p 2170 N94-24716
Weasel works SA-150: Design study of a 100 to 150 passenger transport aircraft
[NASA-CR-195489] p 2183 N94-24975
NASA LaRC Workshop on Guidance, Navigation, Controls, and Dynamics for Atmospheric Flight, 1993
[NASA-CP-10127] p 2162 N94-25096
X-31 aerodynamic characteristics determined from flight data p 2164 N94-25109
Nonlinear aerodynamic modeling using multivariate orthogonal functions p 2164 N94-25110
Modeling transonic aerodynamic response using nonlinear systems theory for use with modern control theory p 2164 N94-25112
Aircraft maneuvers for the evaluation of flying qualities and agility. Volume 2: Maneuver descriptions and section guide
[AD-A273685] p 2185 N94-25440

AERODYNAMIC CONFIGURATIONS
The airplane: A simulated commercial air transportation study
[NASA-CR-195525] p 2182 N94-24837
Numerical flow simulation for complete vehicle configurations
[AD-A273588] p 2170 N94-24849
The Bunny: A simulated commercial air transportation study
[NASA-CR-195537] p 2183 N94-25001
Effect of aeroelastic-propulsive interactions on flight dynamics of a hypersonic vehicle p 2164 N94-25113

AERODYNAMIC DRAG
Experimental study of a turbulent boundary layer in presence of external manipulators of NACA 0009 profile in the transonic regime
[ISBN-0-315-57633-2] p 2333 N94-24177
Design of a resistojet for Space Station Freedom
[NASA-CR-195506] p 2221 N94-24979

AERODYNAMIC FORCES
LinAir: A multi-element discrete vortex Weissinger aerodynamic prediction method
[NASA-TM-108786] p 2167 N94-23557
Torque equilibrium attitudes for the Space Station
p 2208 N94-24449
Nonlinear equations of motion for a panel subject to external loads
[AD-A273142] p 2170 N94-24773

AERODYNAMIC HEAT TRANSFER
Stagnation region heat transfer: The influence of turbulence parameters, Reynolds number and body shape
[NASA-TM-106504] p 2334 N94-24481

AERODYNAMIC HEATING
Prediction of three sigma maximum dispersed density for aerospace applications p 2207 N94-23654
Thermal-fluid analysis of the fill and drain operations of a cryrogenic fuel tank
[NASA-TM-104273] p 2334 N94-24495
Analysis and effects of the advanced solid rocket motor on the Space Shuttle elements
[NASA-CR-193879] p 2200 N94-24664

AERODYNAMIC INTERFERENCE
Aerodynamic characteristics and pressure distributions for an executive-jet baseline airfoil section
[NASA-TM-4529] p 2169 N94-24586
A numerical study of airplanes flying in proximity
[AD-A273373] p 2173 N94-24718

AERODYNAMIC LOADS
Computation of the loads on the AH-1/OLS model rotor in forward flight and comparison with wind tunnel tests
[ISL-CO-230/92] p 2176 N94-23146
Leading-edge votex-system details obtained on F-106B aircraft using a rotating vapor screen and surface techniques
[NASA-TP-3374] p 2166 N94-23512
Issac, Jason Cherian ses in transonic flow
[NASA-CR-194837] p 2167 N94-24052
Validation of the ROTAC code for the rotor noise prediction
[PB93-204311] p 2529 N94-24514

AERODYNAMIC NOISE
Refraction of high frequency noise in an arbitrary jet flow
[NASA-TM-106465] p 2525 N94-23464
Sound radiation due to boundary layer transition
p 2332 N94-24163
The radiated noise from isotropic turbulence revisited
[NASA-CR-191547] p 2333 N94-24356
Fan noise research at NASA
[NASA-TM-106512] p 2530 N94-25172

AERODYNAMIC STABILITY
Radially constructed cruciform parachute
[CA-PATENT-1323021] p 2168 N94-24182
NASA advanced design program. Design and analysis of a radio-controlled flying wing aircraft
[NASA-CR-195515] p 2180 N94-24589
A numerical study of airplanes flying in proximity
[AD-A273373] p 2173 N94-24718
Wind tunnel test of a variable-diameter tiltrotor (VDTR) model
[NASA-CR-177629] p 2181 N94-24796
Aeroelastic response and stability of tiltrotors with elastically-coupled composite rotor blades
[NASA-TM-108758] p 2182 N94-24953

AERODYNAMIC STALLING
An experimental investigation of the effect of upper surface blowing on dynamic stall
[NASA-CR-194863] p 2165 N94-22894
Computational study of GA(W)-1: Airfoil near stall
[PB93-226249] p 2165 N94-23116
Compressibility effects on dynamic stall of airfoils undergoing rapid transient pitching motion
[NASA-TM-109681] p 2167 N94-23975
Thrust vectoring theory, laboratory and flight tests
p 2155 N94-24251
Effect of an extendable slat on the stall behavior of a VR-12 airfoil
[NASA-TP-3407] p 2171 N94-25187

AERODYNAMICS
Local grid refinement method for the euler equations
[PB93-223329] p 2317 N94-22985
JPRS report: Science and technology. Central Eurasia: Space
[JPRS-USP-93-006] p 2194 N94-23015
Two-dimensional Navier-Stokes computations of subsonic and supersonic flows through turbine cascades
[PB93-226223] p 2317 N94-23114
Control algorithms for effective operation of variable-speed wind turbines
[DE94-002607] p 2394 N94-23704
Aeronautical engineering: A continuing bibliography with indexes (supplement 298)
[NASA-SP-7037(298)] p 2153 N94-23711
Aeronautical engineering: A continuing bibliography with indexes (supplement 299)
[NASA-SP-7037(299)] p 2153 N94-23973
Roles, uses, and benefits of general aviation aircraft in aerospace engineering education
[NASA-TM-106463] p 2153 N94-24100
Numerical simulation of non-Newtonian free shear flows p 2331 N94-24160
Integrated Airframe Design Technology
[AGARD-R-794] p 2177 N94-24313
Research in progress and other activities of the Institute for Computer Applications in Science and Engineering
[NASA-CR-191576] p 2444 N94-25090
Effect of aeroelastic-propulsive interactions on flight dynamics of a hypersonic vehicle p 2164 N94-25113
State-of-the-art engineering aeroprediction methods with emphasis on new semiempirical techniques for predicting nonlinear aerodynamics on complete missile configurations
[AD-A273680] p 2171 N94-25411

AEROELASTICITY
Issac, Jason Cherian ses in transonic flow
[NASA-CR-194837] p 2167 N94-24052
Aeroelastic, aeromechanical and vibration problems in helicopters p 2154 N94-24244
Current and future design methods for large transport aircraft p 2179 N94-24324

Structural dynamics division research and technology accomplishments for FY 1993 and plans for FY 1994 [NASA-TM-109036] p 2169 N94-24576
Nonlinear equations of motion for a panel subject to external loads [AD-A273142] p 2170 N94-24773
Wind tunnel test of a variable-diameter tiltrotor (VDTR) model [NASA-CR-177629] p 2181 N94-24796
Aeroelastic response and stability of tiltrotors with elastically-coupled composite rotor blades [NASA-TM-108758] p 2182 N94-24953
Effect of aeroelastic-propulsive interactions on flight dynamics of a hypersonic vehicle p 2164 N94-25113

AEROGELS
Carbon aerogels: An update on structure, properties, and applications [DE94-001528] p 2252 N94-22931

AERONAUTICAL ENGINEERING
Aeronautical engineering: A continuing bibliography with indexes (supplement 298) [NASA-SP-7037(298)] p 2153 N94-23711
Aeronautical engineering: A continuing bibliography with indexes (supplement 299) [NASA-SP-7037(299)] p 2153 N94-23973
Frameworks for integrated airframe design p 2178 N94-24318
The process network in the design and manufacturing of aircraft p 2178 N94-24319
Japanese aerospace science and technology 1992. A bibliography with indexes [NASA-SP-7104] p 2631 N94-24585
NACA collections: A directory of significant collections of the documents of the National Advisory Committee for Aeronautics [NASA-CR-195686] p 2594 N94-25541

AERONAUTICAL SATELLITES
ACTS broadband aeronautical experiment p 2279 N94-22771

AERONOMY
JOVE NASA-FIT program: Microgravity and aeronomy projects [NASA-CR-195121] p 2631 N94-24493

AEROSOLS
Particle formation in a laser-heated aerosol reactor. Application to silicon and silicon nitride synthesis [PB93-217982] p 2347 N94-22982
Gas-grain simulation experiment module conceptual design and gas-grain simulation facility breadboard development [NASA-CR-177632] p 2598 N94-23536
Cloud-free aerosol optical depth determination over oceans from satellite radiometry [DE94-001897] p 2386 N94-23779
Participation in TOMS missions [NASA-CR-195110] p 2398 N94-24078
Session on coupled atmospheric/chemistry coupled models p 2414 N94-24398
Cloud, dust, and ozone vertical profiles from solar occultation measurements: Implications for dynamics p 2617 N94-24877
Results from the VISA project [AD-A273752] p 2406 N94-25540

AEROSPACE ENGINEERING
JPRS report: Science and technology. Central Eurasia: Space [JPRS-USP-93-006] p 2194 N94-23015
Shell buckling research at Delft, 1976 - 1992 [PB93-224442] p 2375 N94-23221
GPHS-RTG's in support of the Cassini mission [DE94-001445] p 2218 N94-23459
Space technology: A study of the significance of recognition for innovators of spinoff technologies. 1993 activities/1994, 1995 plans [NASA-CR-194836] p 2596 N94-23526
Space technology: A study of the significance of recognition for innovators of spinoff technologies. Commercial Space Expo-USA, 1993 [NASA-CR-194833] p 2596 N94-23528
NASA patent abstracts bibliography: A continuing bibliography. Section 2: Indexes (supplement 44) [NASA-SP-7039(44)-SECT-2] p 2590 N94-23712
National Institute of Standards and Technology Conference on Reducing the Cost of Space Infrastructure and Operations. Part 2: Topical papers [PB94-113487] p 2194 N94-23819
Long term trending of engineering data for the Hubble Space Telescope p 2516 N94-23942
Fiscal year 1993 scientific and technical reports, articles, papers, and presentations [NASA-TM-108423] p 2590 N94-24079
Roles, uses, and benefits of general aviation aircraft in aerospace engineering education [NASA-TM-106463] p 2153 N94-24100
Probabilistic simulation of concurrent engineering of propulsion systems p 2177 N94-24317
The process network in the design and manufacturing of aircraft p 2178 N94-24319
NASA high performance computing and communications program [NASA-TM-4554] p 2591 N94-24337
The 1993 NASA/ASEE Summer Faculty Fellowship Program [NASA-CR-193862] p 2574 N94-24405
NASA technology applications team: Applications of aerospace technology [NASA-CR-194775] p 2597 N94-24494
Space Technology: A study of the significance of recognition for innovators of spinoff technologies. A case study on the impact of the space technology hall of fame award [NASA-CR-194835] p 2597 N94-24496
Japanese aerospace science and technology 1992. A bibliography with indexes [NASA-SP-7104] p 2631 N94-24585
NASA/DOD Aerospace Knowledge Diffusion Research Project. Report number 20: The use of selected information products and services by US aerospace engineers and scientists: Results of two surveys [NASA-TM-109022] p 2592 N94-24649
NADA/DOD Aerospace Knowledge Diffusion Research Project. Report number 19: The US government technical report and the transfer of federally funded aerospace R/D: An analysis of five studies [NASA-TM-109061] p 2592 N94-24660
Integrated design and manufacturing for the high speed civil transport [NASA-CR-195511] p 2182 N94-24968
Spinoff 1993 [NASA-NP-211] p 2597 N94-25018
NASA LaRC Workshop on Guidance, Navigation, Controls, and Dynamics for Atmospheric Flight, 1993 [NASA-CP-10127] p 2162 N94-25096

AEROSPACE ENVIRONMENTS
The possible effects of the natural and induced space environment on the optical and thermal properties of EOS surfaces p 2207 N94-23596
Measuring the dynamics of structural changes in biological macromolecules from light scattering data p 2422 N94-24426

AEROSPACE INDUSTRY
Review of the probabilistic failure analysis methodology and other probabilistic approaches for application in aerospace structural design [NASA-TP-3434] p 2376 N94-23342
Prototype Space Technology Hall of Fame exhibit at Technology 2003: Analysis of data from computer-based questionaire [NASA-CR-194834] p 2596 N94-23540
Proceedings of the NIST Conference on Reducing the Cost of Space Infrastructure and Operations: Part 1: Oral presentations and discussion [PB94-111374] p 2194 N94-23770
Applications of CFD codes and supercomputers to aircraft design activities p 2177 N94-24316
Frameworks for integrated airframe design p 2178 N94-24318
NASA/DOD Aerospace Knowledge Diffusion Research Project. Report number 20: The use of selected information products and services by US aerospace engineers and scientists: Results of two surveys [NASA-TM-109022] p 2592 N94-24649
NADA/DOD Aerospace Knowledge Diffusion Research Project. Report number 19: The US government technical report and the transfer of federally funded aerospace R/D: An analysis of five studies [NASA-TM-109061] p 2592 N94-24660
The Future of Aerospace: Proceedings of a symposium held in honor of Alexander H. Flax [LC-93-83945] p 2631 N94-25065
Defense aerospace and the new world order p 2596 N94-25066

AEROSPACE MEDICINE
Increasing accuracy in the assessment of motion sickness: A construct methodology [NASA-TM-108797] p 2420 N94-23088
Cardiopulmonary Aspects in Aerospace Medicine [AGARD-LS-189] p 2423 N94-23313
Cardiovascular and pulmonary disease in NATO aircrew: An overview p 2423 N94-23314
Screening for asymptomatic coronary heart disease p 2423 N94-23315
Aeromedical disposition for coronary artery disease p 2423 N94-23316
Primary prevention of coronary heart disease p 2423 N94-23317
Aeromedical disposition of Arrhythmias and electrocardiographic findings in aircrew p 2423 N94-23318
Echocardiographic screening of aircrew candidates p 2424 N94-23319
Echocardiographic findings in trained aircrew: The effect of +Gz on cardiac structure (working group 18) p 2424 N94-23320
Aortic valve disease p 2424 N94-23322
Aeromedical implications of mitral valve prolapse p 2424 N94-23323
Sarcoidosis and the aviator p 2425 N94-23325
Spontaneous pneumothorax, cysts and bullae p 2425 N94-23326
Asthma in aircrew p 2425 N94-23327
Arterial hypertension and the aviator p 2425 N94-23328
Cytokines and immune surveillance in humans [NASA-CR-194801] p 2425 N94-23331
Fluid-loading solutions and plasma volume: Astro-ade and salt tablets with water [NASA-TP-3456] p 2426 N94-23544
Vision impairment and corrective considerations of civil airmen [DOT/FAA/AM-93/21] p 2426 N94-23623
Visual Problems in Night Operations [AGARD-LS-187] p 2431 N94-23976
Index to FAA Office of Aviation Medicine Reports: 1961 through 1993 [DOT/FAA/AM-94/1] p 2426 N94-24093
EEG and chaos: Description of underlying dynamics and its relation to dissociative states [NASA-CR-195171] p 2428 N94-24799
Specification list and function structure for a full-body dynamometer to be used aboard Space Station Freedom [NASA-CR-195508] p 2439 N94-24835
Evaluation of bioimpedance for the measurement of physiologic variables as related to hemodynamic studies in space flight p 2427 N94-25378
Loading, electromyograph, and motion during exercise p 2427 N94-25380

AEROSPACE PLANES
A conceptual design of an unmanned test vehicle using an airbreathing propulsion system [NASA-CR-195550] p 2189 N94-25085

AEROSPACE SAFETY
Develop advanced nonlinear signal analysis topographical mapping system [NASA-CR-195128] p 2388 N94-24827

AEROSPACE SCIENCES
JPRS report: Science and technology. Central Eurasia: Space [JPRS-USP-93-006] p 2194 N94-23015
Parallel unstructured grid generation for computational aerosciences [NASA-CR-192244] p 2466 N94-23483
Prototype Space Technology Hall of Fame exhibit at Technology 2003: Analysis of data from computer-based questionaire [NASA-CR-194834] p 2596 N94-23540
Fiscal year 1993 scientific and technical reports, articles, papers, and presentations [NASA-TM-108423] p 2590 N94-24079
The Ninth National Space Symposium [ISBN-0-9616962-7-3] p 2598 N94-25006

AEROSPACE SYSTEMS
JPRS report: Science and technology. Central Eurasia: Space [JPRS-USP-93-006] p 2194 N94-23015
A reference model for space data system interconnection services p 2305 N94-23847
ATOS-1: Designing the infrastructure for an advanced spacecraft operations system p 2197 N94-23849
NASA/Goddard Space Flight Center's testbed for CCSDS compatible systems p 2197 N94-23855
Distributed computing environments for future space control systems p 2464 N94-23911
Operational characterisation of requirements and early validation environment for high demanding space systems p 2519 N94-23959
The 1993 NASA/ASEE Summer Faculty Fellowship Program [NASA-CR-193862] p 2574 N94-24405

AEROSPACE TECHNOLOGY TRANSFER
Aerospace applications of batteries p 2390 N94-23346
A compilation of technology spinoffs from the US Space Shuttle Program p 2578 N94-24424
NASA technology applications team: Applications of aerospace technology [NASA-CR-194775] p 2597 N94-24494
Space Technology: A study of the significance of recognition for innovators of spinoff technologies. A case study on the impact of the space technology hall of fame award [NASA-CR-194835] p 2597 N94-24496

NASA/DOD Aerospace Knowledge Diffusion Research Project. Report number 20: The use of selected information products and services by US aerospace engineers and scientists: Results of two surveys
[NASA-TM-109022] p 2592 N94-24649

NASA/DOD Aerospace Knowledge Diffusion Research Project. Report number 21: US aerospace industry librarians and technical information specialists as information intermediaries: Results of the phase 2 survey
[NASA-TM-109064] p 2593 N94-24709

Iowa satellite project ISAT-1
[NASA-CR-195517] p 2206 N94-24838

Spinoff 1993
[NASA-NP-211] p 2597 N94-25018

AEROSPACE VEHICLES

NASA high performance computing and communications program
[NASA-TM-4554] p 2591 N94-24337

Evaluation of advanced materials through experimental mechanics and modelling p 2374 N94-24454

AEROTHERMODYNAMICS

Effects of shock strength on shock turbulence interaction p 2332 N94-24165

AFRICA

The AGRHYMET data communications project
p 2280 N94-22776

AFTERGLOWS

Diffusion in electronegative discharges with magnetic fields
[AD-A273826] p 2304 N94-25521

AGE FACTOR

Chronic obstructive pulmonary disease
p 2425 N94-23324

AGING (MATERIALS)

Time dependent behavior of a graphite/thermoplastic composite and the effects of stress and physical aging
[NASA-TM-109047] p 2228 N94-23280

Effect of irradiation on the stress corrosion cracking behavior of Alloy X-750 and Alloy 625
[DE94-001759] p 2244 N94-23792

Proceedings of the 12th International Congress: Corrosion Control for Low-Cost Reliability. Volume 3B: Corrosion: Specific issues
[AD-A273664] p 2251 N94-25451

AGRICULTURE

Groundtruth collection for the JPL-SAR and ERS-1 campaign in Flevoland and Veluwe, Netherlands, 1991
[PB93-230654] p 2386 N94-23755

Manual on measurement of methane and nitrous oxide emissions from agriculture
[DE93-616429] p 2399 N94-25167

AILERONS

Cockpit control system conceptual design
[NASA-CR-195543] p 2190 N94-24551

Aircraft wing structural detail design (wing, aileron, flaps, and subsystems)
[NASA-CR-195487] p 2183 N94-24974

AIR BAG RESTRAINT DEVICES

Projected effectiveness of airbag supplemental restraint systems in US Army helicopter cockpits
[AD-A273250] p 2174 N94-25141

AIR BREATHING BOOSTERS

Conceptual design of a two stage to orbit spacecraft
[NASA-CR-195536] p 2204 N94-24620

AIR BREATHING ENGINES

A conceptual design of an unmanned test vehicle using an airbreathing propulsion system
[NASA-CR-195550] p 2189 N94-25085

Hypersonic vehicle control law development using H(infinity) and micron-synthesis p 2163 N94-25104

AIR CONDITIONING

US Department of Energy phaseout of CFC-refrigerants
[DE94-001668] p 2397 N94-23016

AIR CONDITIONING EQUIPMENT

Fault detection in HVAC systems using fuzzy models
[OUEL-1977/93] p 2373 N94-25475

AIR FILTERS

Microbiological analysis of debris from Space Transportation System (STS)-55 Spacelab D-2
[NASA-CR-193883] p 2421 N94-24310

AIR FLOW

Flow quality studies of the NASA Lewis Research Center Icing Research Tunnel diffuser
[NASA-TM-106311] p 2192 N94-23091

Calibration of HYPULSE for hypervelocity air flows corresponding to flight Mach numbers 13.5, 15, and 17
[NASA-CR-191578] p 2192 N94-23564

The 3-D CFD modeling of gas turbine combustor-integral bleed flow interaction p 2189 N94-23658

The 3-D numerical study of airflow in the compressor/combustor prediffuser and dump diffuser of an industrial gas turbine p 2324 N94-23660

Zone fire modeling with natural building flows and a zero order shaft model
[PB94-112166] p 2270 N94-23735

AIR JETS

Effect of delta tabs on mixing and axis switching in jets from asymmetric nozzles
[NASA-TM-106450] p 2167 N94-23592

AIR LAND INTERACTIONS

Methodology for the assessment of surface resistance and soil water storage variability at mesoscale based on remote sensing measurements. A case study with HAPEX-EFEDA data. UNESCO-International Hydrological Program 4
[PB94-111721] p 2386 N94-23734

Coupled land surface/hydrologic/atmospheric models
p 2413 N94-24387

Session on coupled land surface/hydrological/atmospheric models
p 2414 N94-24395

AIR LAUNCHING

Design of an airborne launch vehicle for an air launched space booster
[NASA-CR-195534] p 2198 N94-24860

GRYPHON: Air launched space booster
[NASA-CR-195497] p 2199 N94-25022

AIR LOCKS

An opening mechanism for the scientific airlock outer hatch p 2360 N94-24027

AIR NAVIGATION

An overview of a generic multi-sensor integrated navigation system design
[CTN-94-60916] p 2174 N94-24120

Differential GPS for air transport: Status
p 2162 N94-25100

Application of aircraft navigation sensors to enhanced vision systems p 2176 N94-25495

AIR POLLUTION

US Department of Energy phaseout of CFC-refrigerants
[DE94-001668] p 2397 N94-23016

Reduction of nitric oxide over platinum, rhodium and platinum-rhodium single crystal surfaces
[PB93-230092] p 2232 N94-23482

Exploratory report nickel and nickel compounds
[PB93-223998] p 2242 N94-23496

Exploratory report antimony and antimony compounds
[PB93-224004] p 2397 N94-23497

Estimation of delays and emissions at four-way junctions with different forms of regulation, principally four-way mandatory stop
[PB94-105236] p 2398 N94-23813

Alternative control techniques document: NOx emissions from stationary reciprocating internal combustion engines
[PB94-104494] p 2398 N94-24476

EPA's survey of in-use driving patterns: Implications for mobile source emission inventories
[PB94-118502] p 2399 N94-24525

Carbon and hydrogen isotope composition and C-14 concentration in methane from sources and from the atmosphere: Implications for a global methane budget
[NASA-CR-195166] p 2399 N94-25092

Manual on measurement of methane and nitrous oxide emissions from agriculture
[DE93-616429] p 2399 N94-25167

Preceedings of the 12th International Congress: Corrosion Control for Low-Cost Reliability. Volume 2: Process Industries Plant Operations
[AD-A273662] p 2251 N94-25449

Results from the VISA project
[AD-A273752] p 2406 N94-25540

AIR QUALITY

Federal alternative fuel program light duty vehicle operations
[DE93-040663] p 2264 N94-22878

US Department of Energy phaseout of CFC-refrigerants
[DE94-001668] p 2397 N94-23016

EPA's survey of in-use driving patterns: Implications for mobile source emission inventories
[PB94-118502] p 2399 N94-24525

AIR SAMPLING

Carbon and hydrogen isotope composition and C-14 concentration in methane from sources and from the atmosphere: Implications for a global methane budget
[NASA-CR-195166] p 2399 N94-25092

AIR TRAFFIC

Conflict-free trajectory planning for air traffic control automation
[NASA-TM-108790] p 2174 N94-25272

AIR TRAFFIC CONTROL

The FAA satellite communications program
p 2279 N94-22772

Airport surface operations requirements analysis
[NASA-CR-191508] p 2172 N94-23288

An examination of the operational error database for air route traffic control centers
[DOT/FAA/AM-93/22] p 2175 N94-24472

ASR-9 microburst detection algorithm
[AD-A273591] p 2415 N94-24850

Aircraft accident report: In-flight loss of propeller blade and uncontrolled collision with terrain Mitsubishi MU-2B-60, N86SD, Zwingle, Iowa, 19 April 1993
[PB93-910409] p 2174 N94-25175

Conflict-free trajectory planning for air traffic control automation
[NASA-TM-108790] p 2174 N94-25272

Automation and cognition in air traffic control: An empirical investigation
[DOT/FAA/AM-94/3] p 2176 N94-25444

AIR TRAFFIC CONTROLLERS (PERSONNEL)

Harmonisation of man-machine interface experiments in the context of the development of PHARE advanced tools
[PB93-204725] p 2430 N94-23744

An examination of the operational error database for air route traffic control centers
[DOT/FAA/AM-93/22] p 2175 N94-24472

AIR TRANSPORTATION

NASA/USRA University Advanced Design Program, 1992-1993. The Diamondback: A simulated commercial air transportation study
[NASA-CR-195523] p 2180 N94-24462

Information systems strategy in air transport
[AD-A273125] p 2173 N94-24781

The airplane: A simulated commercial air transportation study
[NASA-CR-195525] p 2182 N94-24837

The Bunny: A simulated commercial air transportation study
[NASA-CR-195537] p 2183 N94-25001

The Gold Rush: A simulated commercial air transportation study
[NASA-CR-195528] p 2184 N94-25002

Aviation: The timeless industry p 2165 N94-25068

US general aviation: The ingredients for a renaissance. A vision and technology strategy for US industry, NASA, FAA, universities p 2162 N94-25097

Differential GPS for air transport: Status
p 2162 N94-25100

AIR WATER INTERACTIONS

Monte Carlo climate change forecasts with a global coupled ocean-atmosphere model
[MPIM-97] p 2407 N94-23156

Modes of ocean variability in the tropical Pacific as derived from Geosat altimetry
[MPIM-103] p 2382 N94-23158

Climate variability in a coupled GCM. Part 2: The Indian Ocean and monsoon
[MPIM-104] p 2401 N94-23159

Coupled land surface/hydrologic/atmospheric models
p 2413 N94-24387

Techniques and resources for storm-scale numerical weather prediction p 2414 N94-24392

Observational and modeling studies of heat, moisture, precipitation and global-scale circulation patterns
[NASA-CR-195148] p 2415 N94-24485

AIRBORNE EQUIPMENT

An overview of a generic multi-sensor integrated navigation system design
[CTN-94-60916] p 2174 N94-24120

Analysis and surveillance performance at Chicago O'Hare Airport
[DOT/FAA/RD-92/29] p 2175 N94-24127

AIRBORNE RADAR

The 94 GHz MMW imaging radar system
p 2306 N94-25493

AIRBORNE SURVEILLANCE RADAR

CF-18 AN/ALQ-126B-MG 13 IIP interface to the DREO Electronic Warfare Engagement Simulation Facility
[DREO-TN-93-4] p 2296 N94-24118

AIRBORNE/SPACEBORNE COMPUTERS

Towards the formal specification of the requirements and design of a processor interface unit: HOL listings
[NASA-CR-191465] p 2466 N94-23252

Formal methods and digital systems validation for airborne systems
[NASA-CR-4551] p 2468 N94-23293

Magellan spacecraft and memory state tracking: Lessons learned, future thoughts p 2207 N94-23865

Spacecraft crew procedures from paper to computers
p 2433 N94-24188

Advanced avionics architecture and technology review. Executive summary and volume 1: Avionics tech nology. Volume 2: Avionics systems engineering
[AD-A273630] p 2186 N94-24733

AIRCRAFT ACCIDENT INVESTIGATION

Aircraft accident report: Inadvertent in-flight slat deployment, China Eastern Airlines Flight 583, McDonnell Douglas MD-11, B-2171, 950 nautical miles south of Shemya, Alaska, 6 April 1993
[PB93-910408] p 2172 N94-23579

Aircraft accident report: In-flight engine separation. Japan Airlines, Inc., flight 46E, Boeing 747-121, N473EV, Anchorage, Alaska, 31 March 1993
[PB93-410407] p 2173 N94-24062

Aircraft accident report: In-flight loss of propeller blade and uncontrolled collision with terrain Mitsubishi MU-2B-60, N86SD, Zwingle, Iowa, 19 April 1993
[PB93-910409] p 2174 N94-25175

Aircraft accident/incident summary report: Controlled flight into terrain GP Express Airlines, Inc., N115GP Beechcraft C-99, Shelton, Nebraska, 28 April 1993
[PB94-910401] p 2174 N94-25273

AIRCRAFT ACCIDENTS

Development and experimental validation of computational methods to simulate abnormal thermal and structural environments
[DE94-000554] p 2268 N94-23000

Aircraft accident report: Inadvertent in-flight slat deployment, China Eastern Airlines Flight 583, McDonnell Douglas MD-11, B-2171, 950 nautical miles south of Shemya, Alaska, 6 April 1993
[PB93-910408] p 2172 N94-23579

Aircraft accident report: In-flight engine separation. Japan Airlines, Inc., flight 46E, Boeing 747-121, N473EV, Anchorage, Alaska, 31 March 1993
[PB93-410407] p 2173 N94-24062

Annual review of aircraft accident data. US general aviation calendar year 1990
[PB94-126869] p 2173 N94-24841

Projected effectiveness of airbag supplemental restraint systems in US Army helicopter cockpits
[AD-A273250] p 2174 N94-25141

Aircraft accident report: In-flight loss of propeller blade and uncontrolled collision with terrain Mitsubishi MU-2B-60, N86SD, Zwingle, Iowa, 19 April 1993
[PB93-910409] p 2174 N94-25175

Aircraft accident/incident summary report: Controlled flight into terrain GP Express Airlines, Inc., N115GP Beechcraft C-99, Shelton, Nebraska, 28 April 1993
[PB94-910401] p 2174 N94-25273

AIRCRAFT ANTENNAS

L-band mobile terminal antennas for helicopters
p 2289 N94-22835

Aeronautical satellite antenna steering using magnetic field sensors p 2289 N94-22836

Advanced electromagnetic methods for aerospace vehicles
[NASA-CR-195111] p 2365 N94-24699

AIRCRAFT APPROACH SPACING

An examination of the operational error database for air route traffic control centers
[DOT/FAA/AM-93/22] p 2175 N94-24472

AIRCRAFT CARRIERS

Design project: LONGBOW supersonic interceptor
[NASA-CR-195510] p 2180 N94-24581

AIRCRAFT COMMUNICATION

ACTS broadband aeronautical experiment
p 2279 N94-22771

The FAA satellite communications program
p 2279 N94-22772

Canadian aeronautical mobile data trials
p 2279 N94-22773

Cockpit weather graphics using mobile satellite communications p 2280 N94-22775

AIRCRAFT COMPARTMENTS

Full-scale fire testing of seat component materials
[AD-A273499] p 2174 N94-24941

AIRCRAFT CONFIGURATIONS

Design project: LONGBOW supersonic interceptor
[NASA-CR-195510] p 2180 N94-24581

Configuration development study of the OSU 1 hypersonic research vehicle
[NASA-CR-195522] p 2181 N94-24591

The cetaceopteryx: A global range military transport aircraft
[NASA-CR-195519] p 2181 N94-24711

Conceptual design proposal: HUGO global range/mobility transport aircraft
[NASA-CR-195501] p 2181 N94-24787

VLCT-13: A commercial transport for the 21st Century
[NASA-CR-195492] p 2181 N94-24803

The airplane: A simulated commercial air transportation study
[NASA-CR-195525] p 2182 N94-24837

Numerical flow simulation for complete vehicle configurations
[AD-A273588] p 2170 N94-24849

A global range military transport: The ostrich
[NASA-CR-195494] p 2183 N94-24972

Weasel works SA-150: Design study of a 100 to 150 passenger transport aircraft
[NASA-CR-195489] p 2183 N94-24975

The RTL-46: A simulated commercial air transportation study
[NASA-CR-195524] p 2184 N94-25017

AIRCRAFT CONSTRUCTION MATERIALS

An evaluation of Compton scatter imaging using COMSCAN
[DREP-TM-93-38] p 2372 N94-24136

Feasibility study of shot-peening modeling
[CTN-94-60926] p 2244 N94-24170

Introduction of Ceramics into Aerospace Structural Composites
[AGARD-R-795] p 2255 N94-24228

Post buckling behaviour of stiffened composite panels loaded in cyclic compression and shear
p 2157 N94-24260

Test methods for composites: A status report. Volume 1: Tension test methods
[AD-A273501] p 2230 N94-24942

Establishment of computerized numerical databases on thermophysical and other properties of molten as well as solid materials and data evaluation and validation for generating recommended reliable reference data
p 2246 N94-25123

AIRCRAFT CONTROL

Identification of integrated airframe: Propulsion effects on an F-15 aircraft for application to drag minimization
[NASA-TM-4532] p 2188 N94-24106

The 33rd Israel Annual Conference on Aviation and Astronautics
[ITN-94-85227] p 2153 N94-24241

Influence of active controls on the design process of a large transport aircraft p 2178 N94-24323

Cockpit control system conceptual design
[NASA-CR-195543] p 2190 N94-24551

Determination of the stability and control derivatives of the NASA F/A-18 HARV using flight data
[NASA-CR-194838] p 2190 N94-24804

NASA LaRC Workshop on Guidance, Navigation, Controls, and Dynamics for Atmospheric Flight, 1993
[NASA-CP-10127] p 2162 N94-25096

Aircraft digital flight control technical review
p 2163 N94-25106

Development of high-angle-of-attack nose-down pitch control margin design guidelines for combat aircraft
p 2164 N94-25107

X-31 aerodynamic characteristics determined from flight data p 2164 N94-25109

Nonlinear aerodynamic modeling using multivariate orthogonal functions p 2164 N94-25110

Feedback control laws for highly maneuverable aircraft
[NASA-CR-195195] p 2190 N94-25176

Proceedings of the Workshop on Augmented Visual Display (AVID) Research
[NASA-CP-10128] p 2439 N94-25490

AIRCRAFT DESIGN

Pilot-vehicle interface
[DOT/FAA/CT-92/21] p 2430 N94-23083

Summary of lift and lift/cruise fan powered lift concept technology
[NASA-CR-177619] p 2176 N94-23489

An engineering code to analyze hypersonic thermal management systems p 2320 N94-23636

The 33rd Israel Annual Conference on Aviation and Astronautics
[ITN-94-85227] p 2153 N94-24241

New features in Computational Fluid Dynamics (CFD) technology at the TASHAN Engineering Center at IAI
p 2155 N94-24249

Continuous gust response and sensitivity derivatives using state-space models p 2161 N94-24287

Integrated Airframe Design Technology
[AGARD-R-794] p 2177 N94-24313

New computing systems, future computing environment, and their implications on structural analysis and design
p 2177 N94-24314

Applications of CFD codes and supercomputers to aircraft design activities p 2177 N94-24316

The process network in the design and manufacturing of aircraft p 2178 N94-24319

Application of concurrent engineering principles to aircraft structural design p 2178 N94-24321

Some practical problems in multidisciplinary design and optimisation p 2178 N94-24322

Influence of active controls on the design process of a large transport aircraft p 2178 N94-24323

Current and future design methods for large transport aircraft p 2179 N94-24324

The integration of design and manufacturing processes at Alenia DVD p 2179 N94-24325

Trends of design methodology of airframe
p 2179 N94-24327

Aircraft empennage structural detail design
[NASA-CR-195496] p 2179 N94-24332

JB-300: An advanced medium size transport for 2005
[NASA-CR-195499] p 2179 N94-24401

NASA/USRA University Advanced Design Program, 1992-1993. The Diamondback: A simulated commercial air transportation study
[NASA-CR-195523] p 2180 N94-24462

NASA/USRA advanced design program
[NASA-CR-195548] p 2180 N94-24492

Aircraft wing structure detail design
[NASA-CR-195485] p 2180 N94-24498

Structural dynamics division research and technology accomplishments for FY 1993 and plans for FY 1994
[NASA-TM-109036] p 2169 N94-24576

The cetaceopteryx: A global range military transport aircraft
[NASA-CR-195519] p 2181 N94-24711

Conceptual design proposal: HUGO global range/mobility transport aircraft
[NASA-CR-195501] p 2181 N94-24787

VLCT-13: A commercial transport for the 21st Century
[NASA-CR-195492] p 2181 N94-24803

The Blue Emu
[NASA-CR-195535] p 2182 N94-24817

The airplane: A simulated commercial air transportation study
[NASA-CR-195525] p 2182 N94-24837

Design of an airborne launch vehicle for an air launched space booster
[NASA-CR-195534] p 2198 N94-24860

Dumbo heavy lifter aircraft
[NASA-CR-195500] p 2182 N94-24915

Cockpit control system
[NASA-CR-195488] p 2190 N94-24957

The AC-120: The advanced commercial transport
[NASA-CR-195491] p 2182 N94-24966

Integrated design and manufacturing for the high speed civil transport
[NASA-CR-195511] p 2182 N94-24968

Aircraft empennage structural detail design
[NASA-CR-195486] p 2183 N94-24969

Sabot high speed interceptor AE 4273 aircraft design
[NASA-CR-195495] p 2183 N94-24971

A global range military transport: The ostrich
[NASA-CR-195494] p 2183 N94-24972

Aircraft wing structural detail design (wing, aileron, flaps, and subsystems)
[NASA-CR-195487] p 2183 N94-24974

Weasel works SA-150: Design study of a 100 to 150 passenger transport aircraft
[NASA-CR-195489] p 2183 N94-24975

The Bunny: A simulated commercial air transportation study
[NASA-CR-195537] p 2183 N94-25001

The Gold Rush: A simulated commercial air transportation study
[NASA-CR-195528] p 2184 N94-25002

The Triton: Design concepts and methods
[NASA-CR-195542] p 2184 N94-25004

The RTL-46: A simulated commercial air transportation study
[NASA-CR-195524] p 2184 N94-25017

Design project: Viper
[NASA-CR-195484] p 2184 N94-25021

The Future of Aerospace: Proceedings of a symposium held in honor of Alexander H. Flax
[LC-93-83945] p 2631 N94-25065

High-order technology: Applying technical excellence to new airplane development p 2185 N94-25069

A conceptual design of an unmanned test vehicle using an airbreathing propulsion system
[NASA-CR-195550] p 2189 N94-25085

AIRCRAFT DETECTION

Device for the selective detection of objects
[CA-PATENT-1-308-179] p 2544 N94-24489

AIRCRAFT ENGINES

Vibration isolating engine mount
[CA-PATENT-1-320-710] p 2353 N94-23215

Rolls-Royce in perspective: Past, present and future
[PNR-90882] p 2187 N94-23519

The RB211: The first 25 years
[PNR-90977] p 2187 N94-23570

Internal combustion engine with a central crankshaft and integral tandem annular pistons
[CA-PATENT-1-320-878] p 2363 N94-24055

Aircraft accident report: In-flight engine separation. Japan Airlines, Inc., flight 46E, Boeing 747-121, N473EV, Anchorage, Alaska, 31 March 1993
[PB93-410407] p 2173 N94-24062

A colour image processing algorithm to identify copper-based particles in filter debris samples
[DREP-TM-93-19] p 2455 N94-24122

The 33rd Israel Annual Conference on Aviation and Astronautics
[ITN-94-85227] p 2153 N94-24241

Gas turbine and operating method of the same
[CA-PATENT-APPL-SN-2043039] p 2188 N94-24490
Effect of power system technology and mission requirements on high altitude long endurance aircraft
[NASA-CR-194455] p 2189 N94-25200

AIRCRAFT GUIDANCE
Airport surface operations requirements analysis
[NASA-CR-191508] p 2172 N94-23288

AIRCRAFT HAZARDS
Aircraft accident report: In-flight engine separation. Japan Airlines, Inc., flight 46E, Boeing 747-121, N473EV, Anchorage, Alaska, 31 March 1993
[PB93-410407] p 2173 N94-24062
Aviation Weather Program (AWP)
p 2411 N94-24380
Annual review of aircraft accident data. US general aviation calendar year 1990
[PB94-126869] p 2173 N94-24841
Full-scale fire testing of seat component materials
[AD-A273499] p 2174 N94-24941

AIRCRAFT ICING
Characteristics of surface roughness associated with leading edge ice accretion
[NASA-TM-106459] p 2166 N94-23522
Close-up analysis of inflight ice accretion
[NASA-TM-106457] p 2172 N94-23523
Rime-, mixed- and glaze-ice evaluations of three scaling laws
[NASA-TM-106461] p 2173 N94-24047

AIRCRAFT INDUSTRY
Applications of CFD codes and supercomputers to aircraft design activities p 2177 N94-24316
The Future of Aerospace: Proceedings of a symposium held in honor of Alexander H. Flax
[LC-93-83945] p 2631 N94-25065
Aviation: The timeless industry p 2165 N94-25068

AIRCRAFT INSTRUMENTS
Pilot-vehicle interface
[DOT/FAA/CT-92/21] p 2430 N94-23083
Evaluation of the UH-1N instrument panel
[AD-A273145] p 2186 N94-24774

AIRCRAFT LANDING
Airport pavement test machine design and cost study
[DOT/FAA/CT-93/51] p 2192 N94-24072
Optical information in landing scenes
p 2442 N94-25511

AIRCRAFT MAINTENANCE
A colour image processing algorithm to identify copper-based particles in filter debris samples
[DREP-TM-93-19] p 2455 N94-24122
Repair of cracked aluminum aircraft structure with composite patches p 2156 N94-24259
Computer based expert system for battle damage repair of composite structures p 2157 N94-24262

AIRCRAFT MANEUVERS
Thrust vectoring theory, laboratory and flight tests
p 2155 N94-24251
Combined 1991 and 1992 Robinson-22B (R-22) parking test results
[AD-A273550] p 2193 N94-24559
Development of high-angle-of-attack nose-down pitch control margin design guidelines for combat aircraft
p 2164 N94-25107
Aircraft maneuvers for the evaluation of flying qualities and agility. Volume 2: Maneuver descriptions and section guide
[AD-A273685] p 2185 N94-25440

AIRCRAFT MODELS
An overview of a model rotor icing test in the NASA Lewis Icing Research Tunnel
[NASA-TM-106471] p 2166 N94-23299
NASA/USRA University Advanced Design Program, 1992-1993. The Diamondback: A simulated commercial air transportation study
[NASA-CR-195523] p 2180 N94-24462
The RTL-46: A simulated commercial air transportation study
[NASA-CR-195524] p 2184 N94-25017

AIRCRAFT NOISE
JAPE 91: Influence of terrain masking of the acoustic propagation of helicopter noise p 2528 N94-24214
Comparisons of calculated and measured helicopter noise near instrument hill p 2528 N94-24215
Exercise keevil: Noise levels of six military helicopters
[PB93-210722] p 2529 N94-25026
The ISL rotor bench
[ISL-R-108/92] p 2185 N94-25301

AIRCRAFT PARTS
Flush head fastener
[CA-PATENT-1308581] p 2364 N94-24175
The airplane: A simulated commercial air transportation study
[NASA-CR-195525] p 2182 N94-24837
Proceedings of the 12th International Congress: Corrosion Control for Low-Cost Reliability. Volume 5A: Corrosion: General issues
[AD-A273666] p 2250 N94-25406

AIRCRAFT PERFORMANCE
Identification of integrated airframe: Propulsion effects on an F-15 aircraft for application to drag minimization
[NASA-TM-4532] p 2188 N94-24106
S-2E Tracker maritime patrol aircraft re-engine and system upgrade program p 2158 N94-24270
Conceptual design proposal: HUGO global range/mobility transport aircraft
[NASA-CR-195501] p 2181 N94-24787
The Blue Emu
[NASA-CR-195535] p 2182 N94-24817
Dumbo heavy lifter aircraft
[NASA-CR-195500] p 2182 N94-24915
A global range military transport: The ostrich
[NASA-CR-195494] p 2183 N94-24972
Design project: Viper
[NASA-CR-195484] p 2184 N94-25021
High lift aerodynamics
[NASA-CR-195183] p 2184 N94-25268
Aircraft maneuvers for the evaluation of flying qualities and agility. Volume 2: Maneuver descriptions and section guide
[AD-A273685] p 2185 N94-25440

AIRCRAFT PILOTS
Screening for asymptomatic coronary heart disease
p 2423 N94-23315
Aeromedical disposition for coronary artery disease
p 2423 N94-23316
Aeromedical disposition of Arrhythmias and electrocardiographic findings in aircrew
p 2423 N94-23318
Sarcoidosis and the aviator p 2425 N94-23325
Arterial hypertension and the aviator
p 2425 N94-23328
Vision impairment and corrective considerations of civil airmen
[DOT/FAA/AM-93/21] p 2426 N94-23623
In flight mission planning in the Copilote Electronique
p 2522 N94-25015

AIRCRAFT POWER SUPPLIES
Highly-reliable fly-by-light/power-by-wire technology
p 2162 N94-25099

AIRCRAFT PRODUCTION
The integration of design and manufacturing processes at Alenia DVD p 2179 N94-24325
The Blue Emu
[NASA-CR-195535] p 2182 N94-24817

AIRCRAFT PRODUCTION COSTS
C-17 lot 3 production contract
[AD-A273180] p 2174 N94-25153

AIRCRAFT SAFETY
Cockpit weather graphics using mobile satellite communications p 2280 N94-22775
Development and experimental validation of computational methods to simulate abnormal thermal and structural environments
[DE94-000554] p 2268 N94-23000
Airport surface operations requirements analysis
[NASA-CR-191508] p 2172 N94-23288
Initial evaluation of burn characteristics of phenolic foam runway brake arrestor material
[DOT/FAA/CT-TN93/7] p 2253 N94-23335
Aircraft accident report: Inadvertent in-flight slat deployment, China Eastern Airlines Flight 583, McDonnell Douglas MD-11, B-2171, 950 nautical miles south of Shemya, Alaska, 6 April 1993
[PB93-910408] p 2172 N94-23579
Dispersion of fire suppression agents discharged from high pressure vessels: Establishing initial/boundary conditions for the flow outside the vessel
[PB94-103660] p 2172 N94-23810
Rime-, mixed- and glaze-ice evaluations of three scaling laws
[NASA-TM-106461] p 2173 N94-24047
Aircraft accident report: In-flight engine separation. Japan Airlines, Inc., flight 46E, Boeing 747-121, N473EV, Anchorage, Alaska, 31 March 1993
[PB93-410407] p 2173 N94-24062
Aircraft flight safety: A bibliography
[AGARD-R-805] p 2173 N94-24091
Aviation Weather Program (AWP)
p 2411 N94-24380
Aircraft evacuation testing: Research and technology issues
[PB94-107620] p 2173 N94-24750
Annual review of aircraft accident data. US general aviation calendar year 1990
[PB94-126869] p 2173 N94-24841
Aviation system safety risk management tool analysis. Volume 2: Appendices
[AD-A273502] p 2173 N94-24864
Full-scale fire testing of seat component materials
[AD-A273499] p 2174 N94-24941

AIRCRAFT SPECIFICATIONS
A global range military transport: The ostrich
[NASA-CR-195494] p 2183 N94-24972
Design project: Viper
[NASA-CR-195484] p 2184 N94-25021

AIRCRAFT STABILITY
NASA advanced design program. Design and analysis of a radio-controlled flying wing aircraft
[NASA-CR-195515] p 2180 N94-24589
A numerical study of airplanes flying in proximity
[AD-A273373] p 2173 N94-24718
Determination of the stability and control derivatives of the NASA F/A-18 HARV using flight data
[NASA-CR-194838] p 2190 N94-24804

AIRCRAFT STRUCTURES
Adaptive nonlinear polynomial neural networks for control of boundary layer/structural interaction
[NASA-CR-189645] p 2525 N94-23698
A prediction method for the compressive strength of impact damaged composite laminates
[CTN-94-60925] p 2229 N94-24137
Flush head fastener
[CA-PATENT-1308581] p 2364 N94-24175
The 33rd Israel Annual Conference on Aviation and Astronautics
[ITN-94-85227] p 2153 N94-24241
Repair of cracked aluminum aircraft structure with composite patches p 2156 N94-24259
Development of a damage tolerance tool to analyze multiple-site damage in aircraft structure
p 2157 N94-24261
Computer based expert system for battle damage repair of composite structures p 2157 N94-24262
Integrated stress and strength analysis of airplane structures using the data processing tool ISSY
p 2178 N94-24320
Application of concurrent engineering principles to aircraft structural design p 2178 N94-24321
Some practical problems in multidisciplinary design and optimisation p 2178 N94-24322
Aircraft empennage structural detail design
[NASA-CR-195496] p 2179 N94-24332
Aircraft wing structure detail design
[NASA-CR-195485] p 2180 N94-24498
NASA advanced design program. Design and analysis of a radio-controlled flying wing aircraft
[NASA-CR-195515] p 2180 N94-24589
Ultrasonic process for curing adhesives
[AD-A273175] p 2259 N94-24788
Test methods for composites: A status report. Volume 1: Tension test methods
[AD-A273501] p 2230 N94-24942
Aircraft empennage structural detail design
[NASA-CR-195486] p 2183 N94-24969
The Bunny: A simulated commercial air transportation study
[NASA-CR-195537] p 2183 N94-25001
The Gold Rush: A simulated commercial air transportation study
[NASA-CR-195528] p 2184 N94-25002
Test methods for composites: A status report. Volume 3: Shear test methods
[AD-A273561] p 2230 N94-25163

AIRCRAFT WAKES
A new experimental apparatus for the study of the unsteady flowfield over an airfoil in pitching and heaving motions using laser Doppler anemometry
[ISL-CO-229/92] p 2165 N94-23149
LDA measurements of the unsteady near wake behind an airfoil undergoing transient and periodic pitching motions
[ISL-CO-215/92] p 2165 N94-23161
Feasibility of detecting aircraft wake vortices using passive microwave radiometers
[NASA-CR-191553] p 2343 N94-23498
CFD assessment of orifice aspect ratio and mass flow ratio on jet mixing in rectangular ducts
[NASA-TM-106434] p 2187 N94-24082

AIRDROPS
Radially constructed cruciform parachute
[CA-PATENT-1323021] p 2168 N94-24182

AIRFIELD SURFACE MOVEMENTS
System for automatic transportation of aircraft on the ground
[CA-PATENT-1-322-361] p 2193 N94-24785

AIRFOIL OSCILLATIONS
Aeroelastic, aeromechanical and vibration problems in helicopters p 2154 N94-24244
The influence of elastic pitch variations on helicopter flight mechanics p 2161 N94-24286
Effect of an extendable slat on the stall behavior of a VR-12 airfoil
[NASA-TP-3407] p 2171 N94-25187

AIRFOIL PROFILES

Issac, Jason Cherian ses in transonic flow [NASA-CR-194837] p 2167 N94-24052

Aerodynamic characteristics and pressure distributions for an executive-jet baseline airfoil section [NASA-TM-4529] p 2169 N94-24586

AIRFOILS

Computational study of GA(W)-1: Airfoil near stall [PB93-226249] p 2165 N94-23116

Turbine engine with induced pre-swirl at the compressor inlet [CA-PATENT-1-317-467] p 2186 N94-23253

Characteristics of surface roughness associated with leading edge ice accretion [NASA-TM-106459] p 2166 N94-23522

An analytic study of a two-phase laminar airfoil in simulated heavy rain p 2171 N94-23661

Compressible turbulent flow simulation with a multigrid multiblock method p 2342 N94-23694

Compressibility effects on dynamic stall of airfoils undergoing rapid transient pitching motion [NASA-TM-109681] p 2167 N94-23975

Issac, Jason Cherian ses in transonic flow [NASA-CR-194837] p 2167 N94-24052

Toward large eddy simulation of turbulent flow over an airfoil p 2172 N94-24150

Discrete sensitivity derivatives of the Navier-Stokes equations with a parallel Krylov solver [NASA-TM-106481] p 2265 N94-24301

Effect of an extendable slat on the stall behavior of a VR-12 airfoil [NASA-TP-3407] p 2171 N94-25187

AIRFRAME MATERIALS

The 33rd Israel Annual Conference on Aviation and Astronautics [ITN-94-85227] p 2153 N94-24241

AIRFRAMES

Lewis Research Center R and D Facilities [NASA-TM-109400] p 2630 N94-23135

Integrated Airframe Design Technology [AGARD-R-794] p 2177 N94-24313

Frameworks for integrated airframe design p 2178 N94-24318

AIRLINE OPERATIONS

Information systems strategy in air transport [AD-A273125] p 2173 N94-24781

The Blue Emu [NASA-CR-195535] p 2182 N94-24817

AIRLOCK MODULES

An opening mechanism for the scientific airlock outer hatch p 2360 N94-24027

AIRPORT SURFACE DETECTION EQUIPMENT

Airport surface operations requirements analysis [NASA-CR-191508] p 2172 N94-23288

AIRPORTS

Airport surface operations requirements analysis [NASA-CR-191508] p 2172 N94-23288

Performance of prefabricated geocomposite subdrainage system in an airport runway [DOT/FAA/RD-93/23] p 2192 N94-23303

System for automatic transportation of aircraft on the ground [CA-PATENT-1-322-361] p 2193 N94-24785

ASR-9 microburst detection algorithm [AD-A273591] p 2415 N94-24850

AIRSPACE

Conflict-free trajectory planning for air traffic control automation [NASA-TM-108790] p 2174 N94-25272

AIRSPEED

Characteristics of surface roughness associated with leading edge ice accretion [NASA-TM-106459] p 2166 N94-23522

AIRY FUNCTION

Stability analysis of anisotropic conical shells [PB94-119054] p 2377 N94-24645

ALBEDO

Participation in TOMS missions [NASA-CR-195110] p 2398 N94-24078

Temporal and spatial mapping of surface albedo and atmospheric dust opacity on Mars p 2619 N94-24887

Martian mesoscale circulations induced by variations in surface optical and thermal characteristics: A numerical study p 2622 N94-24899

ALBUMINS

Temperature dependence of protein solubility-determination, application to crystallization, and growth kinetics studies p 2224 N94-24344

ALGAE

Literature study on: Remote Fraunhofer luminescence detection of algal bloom in marine environments [BCRS-92-25] p 2417 N94-23176

Factors affecting the identification of phytoplankton groups by means of remote sensing [NASA-TM-108799] p 2387 N94-24403

ALGEBRA

Tool sharing: An application of max-algebra, part 2 [MEMO-1122] p 2478 N94-22710

Tool sharing: An application of max-algebra, part 1 [MEMO-1108] p 2478 N94-22726

Median stabilization degree of a median algebra [PB93-220010] p 2479 N94-23093

Differential algebraic equations [PB93-237618] p 2481 N94-23455

Relational algebra and equational proofs [PB94-110822] p 2486 N94-23724

Sequential composition, action prefixes and process prefix [PB94-101433] p 2488 N94-24539

Coadjoint orbits and conformal field theory [DE94-002285] p 2523 N94-24658

Algebraic-geometric codes and their decoding algorithms [ETN-94-95294] p 2491 N94-25079

Data structures and amortized complexity in a functional setting [ETN-94-95307] p 2476 N94-25290

Extension problem for generalized multi-monogenic functions in Clifford analysis [DE93-616818] p 2493 N94-25433

ALGORITHMS

On dynamic input-output linearization of discrete-time nonlinear systems [MEMO-1123] p 2447 N94-22711

Algorithms for speech coding systems based on linear prediction [EUT-92-E-260] p 2447 N94-22731

On the numeric integration of dynamic attitude equations [NASA-CR-194788] p 2448 N94-23073

The explicit computation of integration algorithms and first integrals for ordinary differential equations with polynomials coefficients using trees [NASA-CR-194787] p 2448 N94-23074

Linear algorithm for flattening list graphs [PB93-220648] p 2448 N94-23097

On the numerical computation of invariant manifolds [W-9306] p 2480 N94-23140

A reliable algorithm for optimal control synthesis [NASA-CR-194809] p 2472 N94-23332

A DTM-based path planning method for planetary rovers p 2370 N94-23423

A knowledge based system for scientific data visualization [NASA-CR-194879] p 2452 N94-23507

A working algorithm to isolate integrable surfaces in E cubed [SSCL-PREPRINT-761] p 2452 N94-23518

The computation of R(sub 0) for discrete-time epidemic models with dynamic heterogeneity [CWI-AM-R9301] p 2420 N94-23521

Algorithm-development activities [NASA-CR-193225] p 2420 N94-23538

Implementation and evaluation of the new wind algorithm in NASA's 50 MHz doppler radar wind profiler [NASA-CR-194880] p 2408 N94-23576

A comparative study of computational solutions to flow over a backward-facing step p 2326 N94-23670

Implementing abstract multigrid or multilevel methods p 2483 N94-23682

A multilevel adaptive projection method for unsteady incompressible flow p 2341 N94-23690

Control algorithms for effective operation of variable-speed wind turbines [DE94-002607] p 2394 N94-23704

Algorithm on addition chains with restricted memory [PB94-118692] p 2454 N94-23759

Exercises in multiprogramming [PB94-101458] p 2454 N94-23768

Typechecker for bijective pure type systems [PB94-110814] p 2454 N94-23817

The instant sequencing task: Toward constraint-checking a complex spacecraft command sequence interactively p 2504 N94-23875

Participation in TOMS missions [NASA-CR-195110] p 2398 N94-24078

System for Anomaly and Failure Detection (SAFD) system development [NASA-CR-193907] p 2372 N94-24174

Satellite autonomous navigation and orbit determination using magnetometers p 2156 N94-24258

Maximum likelihood modal parameter identification and realization of stochastic systems p 2157 N94-24265

Failure-proof estimation under conditions of lack of information p 2158 N94-24267

Structure in gamma ray burst time profiles: Correlations with other observables p 2579 N94-24431

MERILL: An equational reasoning system in standard ML: A user guide (prerelease version 0.4) [PB93-204501] p 2456 N94-24534

An efficient data assimilation algorithm with a gaussian covariance structure [AD-A273152] p 2418 N94-24671

ASR-9 microburst detection algorithm [AD-A273591] p 2415 N94-24850

New directions in network flows [AD-A273467] p 2468 N94-24939

Algebraic-geometric codes and their decoding algorithms [ETN-94-95294] p 2491 N94-25079

Development and application of new algorithms for the simulation of viscous compressible flows with moving bodies in three dimensions [AD-A273514] p 2338 N94-25157

An AVHRR cloud classification database typed by experts [AD-A273560] p 2416 N94-25162

An analysis of gamma ray burst time histories [NASA-CR-195191] p 2629 N94-25199

Data structures and amortized complexity in a functional setting [ETN-94-95307] p 2476 N94-25290

Unwrapping the phase response functions for nonlinear systems [RR-465] p 2462 N94-25311

Two-dimensional pattern analysis and classification using a complex orthogonal estimation algorithm [RR-475] p 2463 N94-25321

Kernels of anti-causal operators and the multivariable generalized predictive control problem [MATHS-REPT-A-191] p 2476 N94-25428

Advances in generalized and constrained generalized predictive control with application to a dynamometer model [MATHS-REPT-A-192] p 2476 N94-25429

New algorithm for minimizing (chi)(sup 2) functionals with constraints [DE93-616800] p 2463 N94-25432

Active camera calibration for a head-eye platform using a variable state dimension filter [OUEL-1975/93] p 2346 N94-25472

Validation of vision-based range estimation algorithms using helicopter flight data p 2442 N94-25506

ALIGNMENT

Rack Insertion End Effector (RIEE) automation p 2368 N94-23242

Hubble Space Telescope high speed photometer orbital verification [NASA-CR-189333] p 2204 N94-24226

ALKALI METALS

Vacancy formation energy of Li(H, D) and Na(H, D) systems [DE93-633452] p 2558 N94-22978

ALKALIES

Auto-metasomatism of the western lunar highlands: Result of closed system fractionation and mobilization of a KREEPy trapped liquid p 2615 N94-24367

ALKANES

Interactions between organized, surface-confined monolayers and vapor-phase probe molecules. 7: Comparison of self-assemblying organomercaptan monolayers deposited on gold from liquid and vapor phases [AD-A273196] p 2535 N94-24555

Synthesis and characterization of two-dimensional molecular recognition interfaces [AD-A273177] p 2536 N94-24729

ALKENES

Dispersion of Rh/Cu in a sol-gel matrix. Highly chemo- and stereoselective catalyst for the reduction of alkynes to Z-alkenes [AD-A273306] p 2262 N94-25145

ALKYL COMPOUNDS

STM studies of LB deposited alkyl substituted polyaniline and its corresponding monomer [AD-A273553] p 2257 N94-24562

Dispersion of Rh/Cu in a sol-gel matrix. Highly chemo- and stereoselective catalyst for the reduction of alkynes to Z-alkenes [AD-A273306] p 2262 N94-25145

ALKYNES

Metal-catalyzed alkynylation of brominated polyphenylenes: Thermoset precursors of high density monolithic glassy carbon [AD-A273232] p 2259 N94-24789

Metal-catalyzed alkynylation of (Bromophenyl)Oligophenylenes: A rapid route to thermoset precursors of high density monolithic glass-like carbon [AD-A273219] p 2260 N94-24863

Dispersion of Rh/Cu in a sol-gel matrix. Highly chemo- and stereoselective catalyst for the reduction of alkynes to Z-alkenes [AD-A273306] p 2262 N94-25145

ALL-WEATHER LANDING SYSTEMS
The 94 GHz MMW imaging radar system
p 2306 N94-25493
ALLOCATIONS
Generalized concavity in cooperative game theory: Characterizations in terms of the core
[MEMO-1121] p 2497 N94-22708
Irreducible core of a minimum cost spanning tree game
[PB94-110962] p 2489 N94-24653
ALLOYING
Internal friction associated with dislocation relaxations in virgin martensite
[PB93-226280] p 2240 N94-23119
Alloys for hydrogen storage in nickel/hydrogen and nickel/metal hydride batteries p 2391 N94-23353
Large-scale production of Si(0.8)Ge(0.2) thermoelectric alloys by mechanical alloying
[DE94-000695] p 2243 N94-23753
ALLOYS
Symposium on diffusion in ordered alloys
[AD-A273643] p 2245 N94-25033
ALPHA PARTICLES
Fusion plasma theory project summaries
[DE94-001712] p 2551 N94-23808
ALTERNATIVES
Reduced cost alternatives to premise wiring using ATM and microcellular technologies p 2314 N94-23239
ALTIMETRY
Application of aircraft navigation sensors to enhanced vision systems p 2176 N94-25495
ALTITUDE
Trends in mobile satellite communication
p 2278 N94-22763
ALTITUDE CONTROL
Design of a resistojet for Space Station Freedom
[NASA-CR-195506] p 2221 N94-24979
ALTITUDE SIMULATION
Lewis Research Center R and D Facilities
[NASA-TM-109400] p 2630 N94-23135
The effect of high altitude pressure on the power and efficiency of an airborne two-stroke engine
p 2155 N94-24253
Altitude simulation facility for testing large space motors p 2156 N94-24255
Temperature measurement using infrared imaging systems during turbine engine altitude testing
[NASA-TM-105871] p 2193 N94-25184
ALTITUDE TESTS
The effect of high altitude pressure on the power and efficiency of an airborne two-stroke engine
p 2155 N94-24253
ALUMINUM
Influence of sintering atmospheres on the aluminum sintering characteristics
[DE93-632412] p 2239 N94-22965
Analysis and test of low profile aluminum aerospace tank dome
[NASA-TP-3442] p 2375 N94-23294
Plasma ARC keyhole welding of aluminum
[PB93-201606] p 2353 N94-23449
SALI chemical analysis of provided samples
[NASA-CR-194138] p 2232 N94-23524
Repair of cracked aluminum aircraft structure with composite patches p 2156 N94-24259
Procedures for determining MATMOD-4V material constants
[DE94-002638] p 2245 N94-24520
Crashworthiness analysis using advanced material models in DYNA3D
[DE94-002988] p 2229 N94-24632
Ignition and combustion characteristics of metallized propellants, phase 2
[NASA-CR-195107] p 2266 N94-24700
Excitation mechanisms for XUV and x ray lasers
[DE93-617006] p 2351 N94-25482
ALUMINUM ALLOYS
Chromate-free talc chemical conversion coatings for aluminum alloys
[DE94-001567] p 2238 N94-22932
Damage under monotonic or cyclic loads of new AlSiFe alloys prepared by the Osprey (tm) process
[ISAL-93-0008] p 2239 N94-22972
Interplay of magnetic and superconducting heavy fermion ground states
[DE94-000680] p 2240 N94-23003
New extensions in the development of deformation processed metal-metal matrix composites
[DE94-000692] p 2227 N94-23004
Development of small punch testing technique and its application to evaluation of mechanical properties degradation
[DE94-001193] p 2375 N94-23184
Magnetic properties and transmission electron microscopy investigations of Nd-Fe-B-Co-Al melt spun ribbons
[PB93-201531] p 2561 N94-23428
Quantitative analysis in the Al-Mg-Si system with small amounts of Mg and Si
[PB93-201499] p 2241 N94-23446
Theory of extrusion: Advances and challenges
[PB93-201572] p 2241 N94-23447
Plasma ARC keyhole welding of aluminum
[PB93-201606] p 2353 N94-23449
Multilayer relaxation and surface structure of ordered alloys
[NASA-TM-106433] p 2243 N94-23578
High temperature, oxidation resistant noble metal-Al alloy thermocouple
[NASA-CASE-LEW-15515-1] p 2343 N94-23826
Segregation and oxidation studies of Al-Li and Al-Mg alloys
[ISBN-0-315-83993-7] p 2244 N94-24469
Investigate zero-stress replicated optics
[NASA-CR-193889] p 2545 N94-24665
Ultrasonic process for curing adhesives
[AD-A273175] p 2259 N94-24788
Preceedings of the 12th International Congress: Corrosion Control for Low-Cost Reliability. Volume 3A: Corrosion: Specific issues
[AD-A273663] p 2251 N94-25450
Proceedings of the 12th International Congress: Corrosion Control for Low-Cost Reliability. Volume 3B: Corrosion: Specific issues
[AD-A273664] p 2251 N94-25451
The mechanical property data base from an Air Force/Industry Cooperative Test Program on advanced aluminum alloys (7064 and CW67)
[AD-A273741] p 2251 N94-25531
ALUMINUM COMPOUNDS
Electrochemical sulfur passivation of visible (approximately 670nm) AlGaInP lasers
[DE94-002293] p 2350 N94-24659
ALUMINUM GALLIUM ARSENIDES
Manufacturing and characterization of GaAs/AlGaAs multiple quantumwell ridge waveguide lasers
[EUT-92-E-265] p 2348 N94-23168
Planar varactor frequency multiplier devices with blocking barrier
[NASA-CASE-NPO-18428-1-CU] p 2310 N94-23821
Magnetic field-induced saddle point in GaAs/AlGaAs short period superlattices
[REPT-A-2656] p 2568 N94-25515
ALUMINUM NITRIDES
Preparation and properties of translucent gamma-aluminium oxynitride
[ETN-94-95305] p 2263 N94-25281
ALUMINUM OXIDES
Glass-ceramic Li-Al-Si-O composition and process for its production
[CA-PATENT-APPL-SN-2043757] p 2254 N94-24129
Preparation and properties of translucent gamma-aluminium oxynitride
[ETN-94-95305] p 2263 N94-25281
Investigation of the solid-solid surface adsorption of Eu2O3 on amorphous Al2O3
[DE93-613824] p 2566 N94-25332
ALUMINUM SILICATES
Discontinuous phase formation and selective attack of SiC materials exposed to low oxygen partial pressure environments
[DE93-040161] p 2231 N94-22933
ALUMINUM-LITHIUM ALLOYS
Microstructural analysis of the 2195 aluminum-lithium alloy welds p 2251 N94-24448
AMAZON REGION (SOUTH AMERICA)
Effect of land use change on the carbon cycle in Amazon soils
[NASA-CR-195168] p 2399 N94-24853
Human impacts on soil carbon dynamics of deep-rooted Amazonian forests
[NASA-CR-195127] p 2399 N94-24861
AMBIENT TEMPERATURE
Status of the development of rechargeable lithium cells p 2392 N94-23354
AMBIPOLAR DIFFUSION
Diffusion in electronegative discharges with magnetic fields
[AD-A273826] p 2304 N94-25521
AMERICIUM
A survey of metallurgical research on several actinides
[DE94-002643] p 2245 N94-24747
AMIDES
The electrochemistry of the solvated electron: A study of its properties and of its applications
[ETN-94-95313] p 2236 N94-25296
AMINES
Curing phthalonitrile resins with acid and amine
[AD-D016021] p 2258 N94-24721
AMINO ACIDS
Capillary electrophoresis of biomolecules: Theory, instrumentation and applications
[ETN-94-95297] p 2236 N94-25233
AMMONIA
Contaminant effects in solid oxide fuel cells
[DE94-002963] p 2395 N94-23785
AMMONIUM COMPOUNDS
Integrated hydrometallurgical jarosite treatment
[PB93-217990] p 2232 N94-22983
AMORPHOUS MATERIALS
Development of small punch testing technique and its application to evaluation of mechanical properties degradation
[DE94-001193] p 2375 N94-23184
Generalized melting criterion for beam-induced amorphization
[DE94-001333] p 2560 N94-23189
Disorder effects on small-polaron formation and hopping
[DE94-001205] p 2534 N94-23804
Synthesis of soluble halogenated polyphenylenes: Mechanism for the coupling halogenated lithiobenzenes
[AD-A273547] p 2257 N94-24558
Demonstration of the feasibility of an integrated x ray laboratory for planetary exploration
[NASA-CR-177631] p 2598 N94-24832
Solid state synthesis of Fe-B-Si alloys
[VTT-PUBS-118] p 2250 N94-25316
Investigation of the solid-solid surface adsorption of Eu2O3 on amorphous Al2O3
[DE93-613824] p 2566 N94-25332
Investigation and application of microwave electron cyclotron resonance plasma physical vapour deposition
[DE93-613909] p 2555 N94-25333
AMORPHOUS SILICON
Ga delta-doping layers in silicon
[PB93-224632] p 2561 N94-23222
Amorphous silicon PVMaT, phase 2A
[DE93-018221] p 2390 N94-23295
AMPLIFIER DESIGN
Broadband linearisation of high-efficiency power amplifiers p 2275 N94-22747
AMPLIFIERS
Field emitter array
[AD-D016023] p 2303 N94-25150
AMPLITUDE MODULATION
An optical ASK and FSK phase diversity transmission system
[EUT-92-E-268] p 2542 N94-23171
Modulation characteristics of a high-power semiconductor Master Oscillator Power Amplifier (MOPA)
[NASA-TM-104577] p 2308 N94-23281
Preliminary analysis of amplitude and phase fluctuations in the JAPE multiple tone data to distances of 500 meters p 2528 N94-24216
AMPOULES
Numerical modeling of physical vapor transport under microgravity conditions: Effect of thermal creep and stress p 2223 N94-24340
ANALOG CIRCUITS
APLAC: An object-oriented analog circuit simulator and design tool. 6.1 system simulations manual
[PB93-224871] p 2450 N94-23226
CADBIT 2: Computer-aided design for built-in test, volume 1
[AD-A273702] p 2463 N94-25455
CADBIT 2: Computer-aided design for built-in test, volume 2
[AD-A273703] p 2463 N94-25456
ANALOG COMPUTERS
High speed electronic analog computers using low-gain amplifiers
[AD-D015974] p 2446 N94-25034
MOS analog memory with injection capacitors
[AD-D015990] p 2312 N94-25050
ANALOG SIMULATION
Mixed analog-digital description and simulation: Proposition for VHDL-analogue
[RR-908-I] p 2450 N94-23180
ANALOG TO DIGITAL CONVERTERS
CAMAC throughput of a new RISC-based data acquisition computer at the DIII-D tokamak
[DE94-001113] p 2550 N94-23182
Study of methods and structures for handling of digitized maps for geographical information systems
[PB93-204402] p 2590 N94-23741
ANALYSIS (MATHEMATICS)
Probabilistic methods in problems of applied analysis
[PB94-110681] p 2495 N94-24571
ANALYTIC FUNCTIONS
On the Gibbs phenomenon 3: Recovering exponential accuracy in a sub-interval from a spectral partial sum of a piecewise analytic function
[NASA-CR-191560] p 2480 N94-23278

Genericity of stabilizability for time-delay systems
[PB93-237725] p 2475 N94-24762

ANALYTICAL CHEMISTRY

Fifty years of continuous improvement: What has DOE done for analytical chemistry?
[DE94-002539] p 2234 N94-24548

Proceedings of the 12th International Congress: Corrosion Control for Low-Cost Reliability. Volume 5B: Corrosion: General issues
[AD-A273667] p 2250 N94-25407

ANALYZERS

A study of non-ideal focus properties of 30 deg parallel plate energy analyzers
[NIFS-263] p 2311 N94-24457

ANCHORS (FASTENERS)

A system for the challenging task of collecting samples from a comet surface p 2358 N94-24007

Planetary and asteroid missions. Getting there: Anchoring spacecraft to asteroids
[NASA-CR-195493] p 2614 N94-24333

ANECHOIC CHAMBERS

Head related transfer function pseudo-stereophony
[NASA-CASE-ARC-11919-1-NP] p 2525 N94-23312

ANEMOMETERS

Improvement of system properties of a pulsed laser Doppler anemometer with respect to an optical amplifier
[DLR-FB-93-19] p 2547 N94-25305

ANESTHESIA

The adaptive resonance theory network: (Clustering-) behaviour in relation with brainstem auditory evoked potential patterns
[EUT-92-E-264] p 2470 N94-22877

ANGLE OF ATTACK

An experimental investigation of a Mach 3.0 high-speed civil transport at supersonic speeds
[NASA-TP-3365] p 2169 N94-24311

Determination of the stability and control derivatives of the NASA F/A-18 HARV using flight data
[NASA-CR-194838] p 2190 N94-24804

Development of high-angle-of-attack nose-down pitch control margin design guidelines for combat aircraft
p 2164 N94-25107

Robust, nonlinear, high angle-of-attack control design for a supermaneuverable vehicle p 2164 N94-25108

X-31 aerodynamic characteristics determined from flight data p 2164 N94-25109

Nonlinear aerodynamic modeling using multivariate orthogonal functions p 2164 N94-25110

A study of roll attractor and wing rock of delta wings at high angles of attack p 2164 N94-25111

Effect of an extendable slat on the stall behavior of a VR-12 airfoil
[NASA-TP-3407] p 2171 N94-25187

State-of-the-art engineering aeroprediction methods with emphasis on new semiempirical techniques for predicting nonlinear aerodynamics on complete missile configurations
[AD-A273680] p 2171 N94-25411

ANGLES (GEOMETRY)

Fiber optical angular sensor: Literature study and experimental results
[PB93-204345] p 2545 N94-24529

Off-design performance of crenulated blades in a linear compressor cascade
[AD-A273744] p 2340 N94-25534

ANGULAR DISTRIBUTION

Strong interactions studies with medium energy probes
[DE94-001446] p 2540 N94-23791

ANGULAR MOMENTUM

Evaluation of uranium transitions for isotopically-selective laser induced fluorescence with diode lasers (technical report for ST064)
[DE94-002000] p 2347 N94-22974

The low noise momentum wheel MW-X: EM design and predicted properties p 2360 N94-24024

Momentum management and torque distribution
p 2159 N94-24272

Proton spin: The role of quark-gluon and hadron degrees of freedom
[DE93-616867] p 2538 N94-25341

ANGULAR VELOCITY

Momentum management and torque distribution
p 2159 N94-24272

Heterodyne array for measurement of target velocity
[AD-D016025] p 2545 N94-24722

Transient flows occurring during the accelerated crucible rotation technique
[DE93-617049] p 2567 N94-25422

ANILINE

Di(hydroxyphenyl)- 1,2,4-triazole monomers
[NASA-CASE-LAR-14440-2] p 2252 N94-23075

STM studies of LB deposited alkyl substituted polyaniline and its corresponding monomer
[AD-A273553] p 2257 N94-24562

ANIMALS

ELF communications system ecological monitoring program
[AD-A273456] p 2299 N94-24676

ANIONS

Reactivity of ambident anions in the gas phase
[PB93-232189] p 2533 N94-23713

Effects of ionizing radiation on modern ion exchange materials
[DE94-001569] p 2535 N94-24505

Free energy profiles for Li(+) and I(-) ions approaching Pt(100) surface: A molecular dynamics study
[AD-A273455] p 2536 N94-24675

ANISOTROPIC MEDIA

Time-domain analysis of conduction and displacement current distributions in inhomogeneous and anisotropic layered media
[PB94-111036] p 2403 N94-24592

ANISOTROPIC SHELLS

Stability analysis of anisotropic conical shells
[PB94-119054] p 2377 N94-24645

ANISOTROPY

Anisotropic uniaxial pressure effects in YBa2Cu3O(7-delta)
[DE94-001456] p 2557 N94-22929

A technique to measure rotordynamic coefficients in hydrostatic bearings p 2215 N94-23061

Polarizability of gyrotropic sphere
[PB93-225019] p 2524 N94-23131

Characterization of 3-D particle distributions and effects on recrystallization studied by computer simulation
[PB93-201408] p 2562 N94-23535

Exact transformation of the anisotropic Ginzburg-Landau model and its consequences
[DE94-002208] p 2562 N94-23795

Damage tolerance of pressurized graphite/epoxy tape cylinders under uniaxial and biaxial loading
[NASA-CR-195101] p 2377 N94-24587

Metallic multilayers: Experimental investigation of magnetic anisotropy and magnetic interlayer coupling
[ETN-94-95364] p 2250 N94-25242

The effect of a transport current on the surface barrier of a uniaxial anisotropic superconducting slab
[DE93-617135] p 2566 N94-25390

Surface barrier of a uniaxial anisotropic type 2 superconducting cylinder
[DE93-617137] p 2566 N94-25392

ANNEALING

Development of small punch testing technique and its application to evaluation of mechanical properties degradation
[DE94-001193] p 2375 N94-23184

The effects of texture and strain on the r-va lue of heavy gauge tantalum plate
[DE94-000690] p 2242 N94-23541

Characterization of the microstructure of Nb-1wt.%Zr-0.1wt.%C tubes as affected by thermomechanical processing
[NASA-TM-106381] p 2242 N94-23550

Polymer morphologh p 2226 N94-24353

ANNIHILATION REACTIONS

Strong interactions studies with medium energy probes
[DE94-001446] p 2540 N94-23791

The effect of a transport current on the surface barrier of a uniaxial anisotropic superconducting slab
[DE93-617135] p 2566 N94-25390

ANNUAL VARIATIONS

Modes of ocean variability in the tropical Pacific as derived from Geosat altimetry
[MPIM-103] p 2382 N94-23158

Climate variability in a coupled GCM. Part 2: The Indian Ocean and monsoon
[MPIM-104] p 2401 N94-23159

Modal structure of variations in the tropical climate system. Part 2: Origins of the low-frequency mode
[MPIM-96] p 2407 N94-23199

The effect of sub-surface volume scattering on the accuracy of ice-sheet altimeter retracking algorithms
[NASA-CR-194825] p 2386 N94-24060

Multiannual simulations with the Mars climate model
p 2618 N94-24881

The role of atmospheric heat transport in the seasonal carbon dioxide cycle p 2621 N94-24896

Eddy mixing coefficient upper limit derived from the photochemical balance of O2 p 2621 N94-24897

ANNULAR FLOW

Response of an anchored annular cylindrical liquid layer to various axial excitations in zero-gravity
[LRT-WE-9-FB-3-1992] p 2266 N94-23195

ANODES

High energy density aluminum-oxygen cell
p 2393 N94-23363

A high performance H2-Cl2 fuel cell for space power applications p 2394 N94-23366

Investigation of a subsonic-arc-attachment thruster using segmented anodes
[NASA-TM-106419] p 2219 N94-23531

Arc electrode interaction study
[NASA-CR-195096] p 2310 N94-24070

Mechanisms of anode power deposition in a low pressure free burning arc
[NASA-CR-194442] p 2553 N94-25190

ANOMALIES

Galileo spacecraft anomaly and safing recovery
p 2207 N94-23864

Magellan spacecraft and memory state tracking: Lessons learned, future thoughts p 2207 N94-23865

CFD simulation of coaxial injectors
p 2342 N94-24430

ANTARCTIC REGIONS

A solar photovoltaic power system for use in Antarctica
[NASA-TM-106417] p 2395 N94-24071

Antarctic Meteorite Location and Mapping Project (AMLAMP): Antarctic meteorite location map series explanatory text and user's guide to AMLAMP data
[NASA-CR-194841] p 2603 N94-24964

ANTENNA ARRAYS

Adaptive digital beamforming for a CDMA mobile communications payload p 2274 N94-22743

Adaptive array antenna for satellite cellular and direct broadcast communications p 2275 N94-22745

Low cost antennas for MSAT vehicular applications
p 2289 N94-22830

An active K/Ka-band antenna array for the NASA ACTS mobile terminal p 2289 N94-22832

Calibration block for digital beam forming antenna
[PB93-204550] p 2294 N94-23773

A constrained optimization technique for arbitrary antenna arrays and various performance indices
[ISBN-0-315-59455-1] p 2297 N94-24179

Evaluation of EHF multi-beam adaptive arrays
[CTN-94-60898] p 2297 N94-24296

Spatial frequency multiplier with active linearly tapered slot antenna array
[NASA-TM-106494] p 2310 N94-24308

Calibration network intended for phase-array antennas at 3 GHz
[PB93-204352] p 2297 N94-24530

Layered parallel interface for an active antenna array
[AD-D016002] p 2301 N94-25045

ANTENNA COMPONENTS

Spatial frequency multiplier with active linearly tapered slot antenna array
[NASA-TM-106494] p 2310 N94-24308

Layered parallel interface for an active antenna array
[AD-D016002] p 2301 N94-25045

ANTENNA COUPLERS

Calibration block for digital beam forming antenna
[PB93-204550] p 2294 N94-23773

ANTENNA DESIGN

Electrical performance of wire mesh for spacecraft deployable reflector antennas p 2275 N94-22744

Adaptive array antenna for satellite cellular and direct broadcast communications p 2275 N94-22745

Geostationary payload concepts for personal satellite communications p 2278 N94-22765

Applicability of different onboard routing and processing techniques to mobile satellite systems
p 2278 N94-22767

Study of LEO-SAT microwave link for broad-band mobile satellite communication system p 2279 N94-22769

Low cost antennas for MSAT vehicular applications
p 2289 N94-22830

K- and Ka-band mobile-vehicular satellite-tracking reflector antenna system for the NASA ACTS mobile terminal p 2289 N94-22831

An active K/Ka-band antenna array for the NASA ACTS mobile terminal p 2289 N94-22832

Microstrip monopulse antenna for land mobile communications p 2289 N94-22833

Isolated and coupled superquadric loop antennas for mobile communications applications
p 2289 N94-22834

Rigorous analysis of thick microstrip antennas and wire antennas embedded in a substrate
[EUT-92-E-263] p 2290 N94-22876

Experimental modification and identification of the DSS-13 antenna control system model
p 2291 N94-23260

Performance of the X-/Ka/KABLE-band dichroic plate in the DSS-13 beam waveguide antenna
p 2291 N94-23261

The down, release, and deployment of the RADARSAT SAR antenna p 2305 N94-23986

A constrained optimization technique for arbitrary antenna arrays and various performance indices
[ISBN-0-315-59455-1] p 2297 N94-24179

Integrated reflector antenna design and analysis
[NASA-CR-195164] p 2300 N94-24678

Advanced electromagnetic methods for aerospace vehicles
[NASA-CR-195111] p 2365 N94-24699
Feasibility study of a synthesis procedure for array feeds to improve radiation performance of large distorted reflector antennas
[NASA-CR-195167] p 2301 N94-25005

ANTENNA FEEDS
Data relay system satellite: The development of an antenna pointing mechanism for the inter-orbit link antenna p 2359 N94-24015
Inter orbit link antenna pointing mechanisms design using standard actuators p 2359 N94-24016

ANTENNA RADIATION PATTERNS
Study of LEO-SAT microwave link for broad-band mobile satellite communication system p 2279 N94-22769
Low cost antennas for MSAT vehicular applications p 2289 N94-22830
A constrained optimization technique for arbitrary antenna arrays and various performance indices
[ISBN-0-315-59455-1] p 2297 N94-24179
Advanced electromagnetic methods for aerospace vehicles
[NASA-CR-195111] p 2365 N94-24699
Feasibility study of a synthesis procedure for array feeds to improve radiation performance of large distorted reflector antennas
[NASA-CR-195167] p 2301 N94-25005
Method and apparatus of generating sum or difference signals corresponding to an apparent beam in a monopulse radar system
[AD-D015998] p 2302 N94-25056

ANTHROPOMETRY
Hand controller commonality evaluation process p 2435 N94-24197
Establishing a relationship between maximum torque production of isolated joints to simulate EVA ratchet push-pull maneuver: A case study p 2437 N94-24206
Development of a force feedback anthropomorphic teleoperation input device for control of robot hands
[NASA-CR-195109] p 2437 N94-24329
Concepts and embodiment design of a reentry recumbent seating system for the NASA Space Shuttle
[NASA-CR-195504] p 2438 N94-24667
Conceptual design of an astronaut hand anthropometry device
[NASA-CR-195490] p 2439 N94-24956

ANTIBODIES
Monoclonal antibodies directed against surface molecules of multicell spheroids
[NASA-CR-195102] p 2420 N94-23633

ANTIFERROMAGNETISM
Spin-polaron theory of high-T(c) superconductivity. 2: Electronic structure of the CuO2 planes
[DE93-019197] p 2556 N94-22919
Spin-hole doping in the Kondo insulator Ce3Bi4Pt3 studied by neutron scattering
[DE93-040107] p 2557 N94-22925
Photo-induced antiferromagnetic interlayer coupling in Fe superlattices with iron silicide spacers
[DE94-001345] p 2559 N94-22995
The renormalization group for flag manifolds
[DE93-616846] p 2491 N94-25213
The Haldane energy gap of a doped linear-chain Heisenberg antiferromagnet
[DE93-617130] p 2567 N94-25426

ANTIMATTER
A scalar-vector model of quark-antiquark interaction under linear confinement
[DE93-616871] p 2538 N94-25317

ANTIMONIDES
Electronic structure and high pressure phase transition in LaSb and CeSb
[DE93-617051] p 2567 N94-25423

ANTIMONY
Exploratory report antimony and antimony compounds
[PB93-224004] p 2397 N94-23497

ANTIMONY COMPOUNDS
Exploratory report antimony and antimony compounds
[PB93-224004] p 2397 N94-23497

ANTIREFLECTION COATINGS
A new automatic design method to develop multilayer thin film devices for high power laser applications
[DE93-632490] p 2347 N94-22967
Design refinement of multilayer optical thin film devices with two optimization techniques
[DE93-634228] p 2542 N94-22979
Inertial confinement fusion
[DE94-002602] p 2551 N94-23703
Analysis for the computational modeling of finite cladding and lossy coating effects in fibers
[PB94-111085] p 2544 N94-23732
Tunable lasers pumped by visible laser diodes
[AD-D016000] p 2350 N94-25044

ANTISUBMARINE WARFARE AIRCRAFT
S-2E Tracker maritime patrol aircraft re-engine and system upgrade program p 2158 N94-24270

AORTA
Aortic valve disease p 2424 N94-23322

APERTURES
A comparison of free-space and fiber mixer performances
[AD-A273558] p 2547 N94-25161

APHELIONS
Northern hemisphere dust storms on Mars p 2619 N94-24885

APOGEES
Kalman filtering applied to real-time monitoring of apogee maneuvers p 2196 N94-23923

APOLLO LUNAR EXPERIMENT MODULE
Catalog of Apollo experiment operations
[NASA-RP-1317] p 2194 N94-23292

APOLLO LUNAR SURFACE EXPERIMENTS PACKAGE
Catalog of Apollo experiment operations
[NASA-RP-1317] p 2194 N94-23292

APOLLO 17 FLIGHT
Catalog of Apollo 17 rocks. Volume 1: Stations 2 and 3 (South Massif)
[NASA-CR-194854] p 2613 N94-24058

APPLICATIONS OF MATHEMATICS
Discrete applied mathematics
[AD-A273552] p 2488 N94-24561

APPLICATIONS PROGRAMS (COMPUTERS)
Transient analysis of circuits including frequency-dependent components using transgyrator and convolution
[PB93-225001] p 2308 N94-23130
A system for managing information at ATLAS
[DE94-001337] p 2590 N94-23190
Programming in Fortran M
[DE94-000541] p 2450 N94-23207
Advanced X ray Astrophysics Facility-Imaging (AXAF-I) thermal analyses using Integrated Thermal Analysis System (ITAS) program p 2320 N94-23635
Some useful innovations with TRASYS and SINDA-85 p 2322 N94-23647
Enhanced absorption cycle computer model
[DE94-001997] p 2271 N94-23793
SPOT4 Operational Control Center (CMP) p 2197 N94-23856
A quick uplink, expandable executable for the NSSC-1 of the Hubble Space Telescope p 2305 N94-23859
ASPT software source code: ASPT application software package, host component
[CTN-94-60907] p 2455 N94-24116
ASPT software source code: ASPT signal excision software package
[CTN-94-60904] p 2296 N94-24133
ASPT software source code: ASPT application software package, VME-C30 component
[CTN-94-60906] p 2455 N94-24135
Three dimensional study of an airplane wing and its wake in the subsonic regime
[ISBN-0-315-58963-9] p 2168 N94-24178
Using computer graphics to design Space Station Freedom viewing p 2434 N94-24191
ACES spectral display software: Software description
[SK-1600-99-003] p 2455 N94-24297
PROPWR: A versatile tool for 1/3 octave processing and narrowband line tracking
[DREA-TC-93-303] p 2297 N94-24298
Integrated stress and strength analysis of airplane structures using the data processing tool ISSY p 2178 N94-24320
Some practical problems in multidisciplinary design and optimisation p 2178 N94-24322
MERILL: An equational reasoning system in standard ML: A user guide (prerelease version 0.4)
[PB93-204501] p 2456 N94-24534
The HEC NexGen software development project
[AD-A273512] p 2460 N94-24822
Parametric uncertainty reduction in robust multivariable control
[AD-A273412] p 2460 N94-24927
Modeling and analysis of selected space station communications and tracking subsystems p 2306 N94-25374
A multimedia adult literacy program: Combining NASA technology, instructional design theory, and authentic literacy concepts p 2585 N94-25384

APPROXIMATION
Loss probabilities in batch-arrival bulk-service queues with finite capacity
[MEMO-1106] p 2493 N94-22724
Asymptotic analysis: Working note no. 3, boundary layers
[DE94-002299] p 2318 N94-23213
Out of plane gradients in laminated composites
[NASA-CR-194875] p 2228 N94-23566
On the differentiation matrix for Daubechies-based wavelets on an interval
[NASA-CR-191582] p 2487 N94-24291
Center for modeling of turbulence and transition: Research briefs, 1993
[NASA-TM-106383] p 2333 N94-24336
A comparison of approximate interval estimators for the Bernoulli parameter
[NASA-CR-191585] p 2458 N94-24680
Approximate optimal guidance for the advanced launch system
[NASA-CR-4568] p 2198 N94-24752
Approximation to nonlinear equations using nonlinear rational models
[RR-448] p 2492 N94-25306
Liapunov stability in chemical engineering
[MATHS-REPT-A-184] p 2236 N94-25427

AQUEOUS SOLUTIONS
Preparing polymeric matrix composites using an aqueous slurry technique
[NASA-CASE-LAR-14771-1] p 2252 N94-23076
Stress corrosion cracking properties of 15-5PH steel p 2251 N94-23244
Measurement of interfacial tension by use of pendant drop video techniques
[DE93-000168] p 2345 N94-24831

ARC DISCHARGES
Measurement of electron temperature and density in the DIII-D neutral beam ion source arc chamber
[DE94-001099] p 2553 N94-24746

ARC JET ENGINES
Investigation of a subsonic-arc-attachment thruster using segmented anodes
[NASA-TM-106419] p 2219 N94-23531
Arc electrode interaction study
[NASA-CR-195096] p 2310 N94-24070
Mechanisms of anode power deposition in a low pressure free burning arc
[NASA-CR-194442] p 2553 N94-25190

ARC WELDING
Weldability of Accelerated-Cooled (AcC) high strength TMCP steel X80
[VTT-TIED-1413] p 2251 N94-25419

ARCHAEBACTERIA
The evolution of energy-transducing systems. Studies with an extremely halophilic archaebacterium
[NASA-CR-193803] p 2422 N94-24807
The evolution of energy-transducing systems. Studies with archaebacteria
[NASA-CR-195129] p 2422 N94-24811

ARCHES
Global dynamic stability of a shallow arch by poincare-like simple cell mapping p 2160 N94-24280

ARCHITECTURE
Wind climate and urban geometry
[ISBN-9-03-860132-8] p 2416 N94-25261

ARCHITECTURE (COMPUTERS)
Design of integrated architectures for low level image processing
[ETN-94-95183] p 2445 N94-22901
Representation and specification of architectures for heterogeneous internetworking: Using a knowledge based approach
[LAAS-93088] p 2445 N94-22903
AMICAL: An aid for architectural synthesis and exploration of control circuits
[ETN-94-95177] p 2308 N94-23154
Automated parallelization of timed Petri-net simulations
[NASA-CR-191574] p 2451 N94-23341
Implementing the space shuttle data processing system with the space generic open avionics architecture
[NASA-CR-188254] p 2199 N94-23571
Advanced design concepts for open distributed systems development
[PB94-110897] p 2454 N94-23751
Concepts and techniques for an active database approach to office procedure support
[PB94-110749] p 2590 N94-23816
Telerobotic rendezvous and docking vision system architecture
[NASA-CR-191329] p 2204 N94-23828
An OSI architecture for the deep space network p 2305 N94-23848
The Ulysses spacecraft control and monitoring concepts and realities p 2502 N94-23862
Making adaptable systems work for mission operations: A case study p 2506 N94-23883
High performance, low cost, self-contained, multipurpose PC based ground systems p 2516 N94-23943
The design of a standard message passing interface for distributed memory concurrent computers
[DE94-002536] p 2446 N94-24536
High-performance computing and communications
[DE94-002215] p 2457 N94-24566

Optical wavelet transform processor
[AD-A273625] p 2546 N94-24731
Advanced avionics architecture and technology review. Executive summary and volume 1: Avionics tech nology. Volume 2: Avionics systems engineering
[AD-A273630] p 2186 N94-24733
The HEC NexGen software development project
[AD-A273512] p 2460 N94-24822
Study on fine grain dynamic dataflow computer
[REPT-946] p 2446 N94-24981
Ground based mission planning systems
p 2522 N94-25014
The design of the EMPS multiprocessor executive for distributed computing
[ETN-94-95336] p 2468 N94-25062
Advanced Information Processing System (AIPS)
p 2165 N94-25115
Appendix A: Proposed statement of work, 1994
p 2272 N94-25194
Design of a walking robot
[NASA-CR-195200] p 2367 N94-25274
Transputer benchmarks and performance comparisons with other computing machines
[RR-467] p 2446 N94-25312
Advanced control structures: A transputer-based multi-robot system
[RR-468] p 2446 N94-25313
Horatio: Libraries for vision applications, release 2.0
[OUEL-1967/92] p 2593 N94-25326
The transputer
[AD-A273688] p 2446 N94-25438

ARCTIC REGIONS
National Academy of Sciences-Academy of Sciences of the USSR Workshop on the Mechanics of Ice and its Applications
[AD-A273338] p 2419 N94-25088

ARGON
Radiative properties of molecular nitrogen ions produced by helium Penning ionization and argon effects
[NASA-CR-195126] p 2534 N94-24487

ARGON PLASMA
Modelling of thermal argon plasmas
[ETN-94-95363] p 2554 N94-25300

ARIANE LAUNCH VEHICLE
A cross-disciplinary response to improve test activities: The corporate memory capitalization in Ariane4 test domain p 2508 N94-23899
Liquid rocket propulsion Retrospective and prospects
p 2154 N94-24243

ARMATURES
The internal structure and dynamics of the railgun plasma armature between infinitely wide ablating rails
[DE94-001473] p 2198 N94-23208
Design and application of electromechanical actuators for deep space missions
[NASA-CR-195134] p 2365 N94-24842

ARRHYTHMIA
Aeromedical disposition of Arrhythmias and electrocardiographic findings in aircrew
p 2423 N94-23318
Sarcoidosis and the aviator p 2425 N94-23325

ARTERIES
Aeromedical disposition for coronary artery disease
p 2423 N94-23316
Arterial hypertension and the aviator
p 2425 N94-23328

ARTERIOSCLEROSIS
Primary prevention of coronary heart disease
p 2423 N94-23317

ARTIFICIAL GRAVITY
Artificial gravity in space flight
[AD-A273420] p 2427 N94-24928

ARTIFICIAL HEART VALVES
Image processing for acquisition of fluid rest time in the running of an artificial heart valve p 2316 N94-22858

ARTIFICIAL INTELLIGENCE
Artificial neural networks: Application to the optical recognition of music partitions
[ETN-94-95166] p 2470 N94-22884
Interpretation of evolutive environment by a multisensory perception machine
[LAAS-93111] p 2471 N94-22907
A novel process monitoring and control system based on a neural manufacturing concept
[DE94-001516] p 2471 N94-23011
Nuclear propulsion control and health monitoring
p 2217 N94-23071
Glossary knowledge engineering
[NLR-TP-91435-U] p 2471 N94-23137
Expanding the KATE toolbox p 2477 N94-23247
Link monitor and control operator assistant: A prototype demonstrating semiautomated monitor and control
p 2292 N94-23267
Neural network research in Finland. Symposium
[PB93-224822] p 2472 N94-23463
A review of European applications of artificial intelligence to space
[NASA-TM-108769] p 2453 N94-23568
Arc consistency problem: An exercise in parallel programming with shared objects
[PB94-110590] p 2466 N94-23706
Logic of capabilities
[PB94-110715] p 2473 N94-23747
Epistemic logic for defeasible reasoning using a meta-level architecture metaphor
[PB94-110723] p 2473 N94-23748
Design and specification of a generic task model for solving boolean constraint satisfaction problems
[PB94-118841] p 2486 N94-23762
Structured constraint satisfaction
[PB94-119039] p 2497 N94-23764
Two applications of a generic task model for solving boolean constraint satisfaction problems
[PB94-119047] p 2487 N94-23765
ATOS-1: Designing the infrastructure for an advanced spacecraft operations system p 2197 N94-23849
Mission activities planning for a Hermes mission by means of AI-technology p 2502 N94-23858
Influence of a new generation of operations support systems on current spacecraft operations philosophy: The users feedback p 2507 N94-23894
PILOT: An intelligent distributed operations support system p 2508 N94-23895
Combining real-time monitoring and knowledge-based analysis in MARVEL p 2477 N94-23900
Constraint-based scheduling p 2510 N94-23904
Intelligent tutoring and aiding in satellite ground control p 2443 N94-23929
An intelligent planning and scheduling system for the HST servicing missions p 2520 N94-23964
Software reuse in spacecraft planning and scheduling systems p 2520 N94-23966
Making intelligent systems team players: Additional case studies
[NASA-TM-104786] p 2473 N94-24068
Evaluation of computer-aided instruction techniques for the crew interface coordination position
p 2429 N94-24438
Compositional architecture for simple design formally specified in DESIRE
[PB94-119013] p 2474 N94-24543
Human-like robots for space and hazardous environments
[NASA-CR-195549] p 2365 N94-24703
In flight mission planning in the Copilote Electronique
p 2522 N94-25015
ROSAT mission planning using artificial intelligence methods
[DLR-FB-93-14] p 2476 N94-25345
The use of knowledge systems
[ETN-94-95318] p 2477 N94-25431

ARTIFICIAL SATELLITES
SIMSAT: An object oriented architecture for real-time satellite simulation p 2197 N94-23940
Satellite situation report, volume 33, number 4
[NASA-TM-109677] p 2205 N94-24824
Iowa satellite project ISAT-1
[NASA-CR-195517] p 2206 N94-24838
Mars Operational Environmental Satellite (MOES): A post-Mars Observer discovery mission
p 2620 N94-24890
Steady motions of rigid body satellites in a central gravitational field
[AD-A273742] p 2206 N94-25532

ASCENT
Analysis and effects of the advanced solid rocket motor on the Space Shuttle elements
[NASA-CR-193879] p 2200 N94-24664

ASIA
JPRS report: Science and technology. Central Eurasia: Space
[JPRS-USP-93-006] p 2194 N94-23015

ASPECT RATIO
Optimization of orifice geometry for cross-flow mixing in a cylindrical duct
[NASA-TM-106436] p 2481 N94-23593
Issac, Jason Cherian ses in transonic flow
[NASA-CR-194837] p 2167 N94-24052
CFD assessment of orifice aspect ratio and mass flow ratio on jet mixing in rectangular ducts
[NASA-TM-106434] p 2187 N94-24082
Vibrations of variable cross section Timoshenko beams p 2160 N94-24279
The Triton Design concepts and methods
[NASA-CR-195542] p 2184 N94-25004

ASSAYING
Evaluation of ovostatin and ovostatin assay
p 2422 N94-24437

ASSESSMENTS
Increasing accuracy in the assessment of motion sickness: A construct methodology
[NASA-TM-108797] p 2420 N94-23088

ASSIMILATION
Next generation initiation techniques
p 2412 N94-24383
Examples of data assimilation in mesoscale models
p 2412 N94-24384
An efficient data assimilation algorithm with a gaussian covariance structure
[AD-A273152] p 2418 N94-24671
Modeling and data assimilation for Mars Observer
p 2620 N94-24889

ASTEROID MISSIONS
Planetary and asteroid missions. Getting there: Anchoring spacecraft to asteroids
[NASA-CR-195493] p 2614 N94-24333
Near Earth asteroid rendezvous
[NASA-CR-195518] p 2195 N94-24808

ASTEROIDS
Planetary and asteroid missions. Getting there: Anchoring spacecraft to asteroids
[NASA-CR-195493] p 2614 N94-24333

ASTHMA
Asthma in aircrew p 2425 N94-23327

ASTRONAUT PERFORMANCE
Transfer of perceptual adaptation to space sickness: What enhances an individual's ability to adapt?
[NASA-CR-188256] p 2427 N94-24227
The role of visual context in manual target localization
p 2429 N94-25351

ASTRONAUTS
Crew interface analysis: Selected articles on space human factors research, 1987 - 1991
[NASA-TM-104756] p 2433 N94-24185
Concepts and embodiment design of a reentry recumbent seating system for the NASA Space Shuttle
[NASA-CR-195504] p 2438 N94-24667

ASTRONOMICAL CATALOGS
Catalog of infrared observations, third edition
[NASA-RP-1294] p 2600 N94-25387

ASTRONOMICAL INTERFEROMETRY
Prospects for very-high-resolution solar physics with the Simuris inteferometric mission p 2625 N94-22848
LOLA: Lunar Optical Long-baseline Array. 1992-1993 space design
[NASA-CR-195533] p 2298 N94-24582
LOITA: Lunar Optical/Infrared Telescope Array
[NASA-CR-195532] p 2546 N94-24816

ASTRONOMICAL MAPS
100 GHz map of 3C 446
[PB94-104882] p 2599 N94-23705
The 1404+286: A non-ideal calibrator for VLBI observations
[PB94-104908] p 2599 N94-24521

ASTRONOMICAL MODELS
Tensor-scalar cosmological models and their relaxation toward general relativity
[PB93-220796] p 2601 N94-23099
Optical model analyses of galactic cosmic ray fragmentation in hydrogen targets
[NASA-TP-3404] p 2540 N94-23509
The scattering and collision of gravitational waves in Friedmann-Robertson-Walker open universes
[MATHS-REPT-A-193] p 2406 N94-25430

ASTRONOMICAL OBSERVATORIES
Lunar science strategy: Exploring the Moon with humans and machines p 2605 N94-23376
Opening mechanism for ISO/CVV cover release
p 2357 N94-24001
Report on operations of the Air Force Geophysics Laboratory infrared array spectrometer
[AD-A273800] p 2406 N94-25535

ASTRONOMICAL PHOTOMETRY
Hubble Space Telescope high speed photometer orbital verification
[NASA-CR-189333] p 2204 N94-24226
Infrared and SiO maser observations of OH/IR stars
[PB94-104890] p 2599 N94-24780

ASTRONOMICAL SATELLITES
The next Japanese solar satellite
p 2625 N94-22846
Solar physics and the Coronas project
p 2625 N94-22847
The Submillimeter Wave Astronomy Satellite (SWAS) solar array system p 2361 N94-24029

ASTRONOMICAL SPECTROSCOPY
Flux measurements using the BATSE spectroscopic detectors p 2580 N94-24435
Report on operations of the Air Force Geophysics Laboratory infrared array spectrometer
[AD-A273800] p 2406 N94-25535

ASTRONOMY
Some challenging problems of the structured and dynamical solar atmosphere p 2624 N94-22838

Prospects for future solar-wind missions
p 2624 N94-22841

ASTROPHYSICS

Semiempirical studies of atomic structure
[DE94-001588] p 2531 N94-22937

AstroMail: Electronic mail for the astrophysics community
[NASA-CR-194877] p 2591 N94-24099

Ultraviolet, visible, and gravity astrophysics: A plan for the 1990's
[NASA-NP-152] p 2603 N94-24973

ASYMMETRY

A measurement of the forward-backward asymmetry and sin(sup 2)(theta)(sub W) from the process Z(sup 0) (yields) (mu)(sup +)(mu)(sup (minus)) at (radical)s = 1.8 TeV
[DE94-001908] p 2532 N94-23018

Proposed additions to the SHADOW ray-tracing code for general-asymmetric perfect-crystal optics
[DE94-001291] p 2560 N94-23188

On the effect of the damping coefficients on the trajectories of symmetric and non-symmetric stores
p 2155 N94-24250

ASYMPTOTIC METHODS

Loss probabilities in batch-arrival bulk-service queues with finite capacity
[MEMO-1106] p 2493 N94-22724

Energy estimates and asymptotic analysis in the theory of shells
[PB93-225738] p 2374 N94-23113

Asymptotic analysis: Working note no. 3, boundary layers
[DE94-002299] p 2318 N94-23213

ASYMPTOTIC PROPERTIES

Control of the internal stresses in plane elasticity
[PB93-225514] p 2374 N94-23112

Stability behavior of systems obtained by index-reduction
[PB93-237709] p 2481 N94-23439

Asymptotic confidence intervals for the length of the shortt under random censoring
[PB93-237816] p 2494 N94-23774

ASYMPTOTIC SERIES

Asymptotic analysis: Working note no. 3, boundary layers
[DE94-002299] p 2318 N94-23213

Maximal type test statistics based on conditional processes
[PB94-111614] p 2494 N94-23771

Bounds and asymptotic expansions for solutions of the free boundary problems related to sequential decision versions of a bioequivalence problem
[AD-A273551] p 2495 N94-24560

Stable non-Gaussian diffusive profiles
[PB93-238053] p 2489 N94-24610

Approximate optimal guidance for the advanced launch system
[NASA-CR-4568] p 2198 N94-24752

ATHLETES

Left ventricular hypertrophy and athlete's heart
p 2424 N94-23321

ATLAS LAUNCH VEHICLES

Liquid rocket propulsion: Retrospective and prospects
p 2154 N94-24243

ATMOSPHERIC ATTENUATION

Adaptive data rate control TDMA systems as a rain attenuation compensation technique
p 2287 N94-22821

ATMOSPHERIC BOUNDARY LAYER

Methodology for the assessment of surface resistance and soil water storage variability at mesoscale based on remote sensing measurements. A case study with HAPEX-EFEDA data. UNESCO-International Hydrological Program 4
[PB94-111721] p 2386 N94-23734

ATMOSPHERIC CHEMISTRY

Solar-terrestrial environmental laboratory
p 2630 N94-23336

Radiative forcing calculations for SF6 and CH4 using a correlated k-distribution transmission model
[DE94-001855] p 2397 N94-23700

Molecular abundances in the envelopes around evolved stars
[PB94-104916] p 2602 N94-23812

The atmospheric effects of stratospheric aircraft: A third program report
[NASA-RP-1313] p 2398 N94-24104

Report of the proceedings of the Colloquium and Workshop on Multiscale Coupled Modeling
[NASA-CP-3217] p 2410 N94-24374

Grand challenge scientific questions in coupled modeling p 2412 N94-24382

Chemistry on the mesoscale: Modeling and measurement issues p 2413 N94-24390

Session on coupled atmospheric/chemistry coupled models p 2414 N94-24398

Measurement of HO2 and other trace gases in the stratosphere using a high resolution far-infrared spectrometer
[NASA-CR-195173] p 2404 N94-24738

Eddy mixing coefficient upper limit derived from the photochemical balance of O2 p 2621 N94-24897

ATMOSPHERIC CIRCULATION

Atmospheric numerical modeling resource enhancement and model convective parameterization/scale interaction studies
[NASA-CR-194769] p 2400 N94-23124

Atmospheric flow in heterogeneous vegetated regions
[W-9303] p 2401 N94-23175

Scientific investigations of atmospheric processes
[NASA-CR-194805] p 2401 N94-23271

Diagnostic budgets of analyzed and modelled tropical plumes
[NASA-CR-194853] p 2409 N94-23621

Implementation of a state of the art automated system for the production of cloud/water vapor motion winds from geostationary satellites
[NASA-CR-195087] p 2410 N94-24125

Scientific goals of the Cooperative Multiscale Experiment (CME) p 2411 N94-24381

Parameterization of sub-grid scale convection
p 2413 N94-24386

The role of radiation in mesoscale flows: Physics, parameterizations, codes p 2413 N94-24389

Joint sessions on moisture processes and cumulus parameterization p 2414 N94-24393

Session on cumulus parameterization
p 2414 N94-24394

CAPE for CaPE p 2416 N94-24409

Observational and modeling studies of heat, moisture, precipitation and global-scale circulation patterns
[NASA-CR-195148] p 2415 N94-24485

Northern hemisphere tropospheric mid-latitude circulation after violent volcanic eruptions
[MPIM-107] p 2403 N94-24491

Workshop on Atmospheric Transport on Mars
[NASA-CR-194855] p 2616 N94-24871

The NASA/GISS Mars general circulation model: Preliminary experiments p 2616 N94-24872

A diagnostic model to estimate winds and small-scale drag from Mars Observer PMIRR data
p 2617 N94-24874

Eddy mixing coefficient values derived from simulations with the NASA Ames Mars GCM p 2617 N94-24875

Aspects of the Martian global circulation
p 2618 N94-24879

Regarding tracer transport in Mars' winter atmosphere in the presence of nearly stationary, forced planetary waves p 2618 N94-24882

Northern hemisphere dust storms on Mars
p 2619 N94-24885

Modeling and data assimilation for Mars Observer
p 2620 N94-24889

A study of cloud motions on Mars. 2: Some examples of observations and analyses since 1969
p 2620 N94-24891

Evidence for dust transport in Viking IR thermal mapper opacity data p 2620 N94-24892

Dust transport in the Martian atmosphere
p 2621 N94-24894

Three-dimensional numerical simulation of near-surface flows over the Martian north polar cap
p 2621 N94-24895

Diagnostic calculations of the circulation in the Martian atmosphere p 2622 N94-24898

Martian mesoscale circulations induced by variations in surface optical and thermal characteristics: A numerical study p 2622 N94-24899

Three-dimensional numerical simulation of thermal tides in the Martian atmosphere p 2622 N94-24901

The Mars Aerial Platform (MAP) mission
p 2622 N94-24903

Mars Observer: Applications to atmospheric transport
p 2623 N94-24904

A nighttime structure model of atmospheric optical turbulence, c2(n), derived from thermosonde and high resolution rawinsonde measurements
[AD-A273803] p 2406 N94-25537

ATMOSPHERIC COMPOSITION

Overview of global greenhouse effects
[DE93-041165] p 2396 N94-22887

In situ detection of tropospheric OH, HO2, NO2, and NO by laser-induced fluorescence in detection chambers at reduced pressures
[NASA-CR-194810] p 2397 N94-23277

Cloud-free aerosol optical depth determination over oceans from satellite radiometry
[DE94-001897] p 2386 N94-23779

High precision double four bar linkage mechanism for interferometric linear scanning p 2359 N94-24013

Ethylene trace-gas techniques for high-speed flows
[NASA-TM-106491] p 2169 N94-24335

Chemistry on the mesoscale: Modeling and measurement issues p 2413 N94-24390

Session on coupled land surface/hydrological/atmospheric models
p 2414 N94-24395

Design of a vehicle based system to prevent ozone loss
[NASA-CR-195498] p 2180 N94-24479

Mesospheric and lower thermospheric winds, temperatures densities, and volume emission rates
[NASA-CR-195147] p 2403 N94-24486

Measurement of HO2 and other trace gases in the stratosphere using a high resolution far-infrared spectrometer
[NASA-CR-195173] p 2404 N94-24738

Particle sizes and composition of Mars atmospheric dust based upon Viking and Mariner 9 observations
p 2618 N94-24878

Regarding tracer transport in Mars' winter atmosphere in the presence of nearly stationary, forced planetary waves p 2618 N94-24882

The influence of orography on the transport of atmospheric constituents p 2619 N94-24886

Carbon and hydrogen isotope composition and C-14 concentration in methane from sources and from the atmosphere: Implications for a global methane budget
[NASA-CR-195166] p 2399 N94-25092

ATMOSPHERIC CORRECTION

Optimization of techniques to reconstruct images disturbed by atmospheric turbulence in the near infra-red
[PB93-199784] p 2298 N94-24630

ATMOSPHERIC DENSITY

Prediction of three sigma maximum dispersed density for aerospace applications p 2207 N94-23654

ATMOSPHERIC EFFECTS

Goals of ground-based solar observations
p 2624 N94-22840

Evaluation of inorganic zinc-rich primers using Electrochemical Impedance Spectroscopy (EIS)
p 2237 N94-23233

Optical subnet concepts for the deep space network
p 2292 N94-23269

SeaWiFS technical report series. Volume 11: Analysis of selected orbit propagation models for the SeaWiFS mission
[NASA-TM-104566-VOL-11] p 2417 N94-23338

Diffuse panel studies: Conclusions
p 2384 N94-23606

The atmospheric effects of stratospheric aircraft: A third program report
[NASA-RP-1313] p 2398 N94-24104

A small satellite design for deep space network testing and training
[NASA-CR-195526] p 2205 N94-24702

Embodiment design for a multipropellant resistojet
[NASA-CR-195505] p 2221 N94-24834

Preceedings of the 12th International Congress: Corrosion Control for Low-Cost Reliability. Volume 2: Process Industries Plant Operations
[AD-A273662] p 2251 N94-25449

ATMOSPHERIC ELECTRICITY

Lightning, atmospheric electricity, and climate change
[DE94-002003] p 2408 N94-23471

ATMOSPHERIC ENTRY

Analysis and effects of the advanced solid rocket motor on the Space Shuttle elements
[NASA-CR-193879] p 2200 N94-24864

ATMOSPHERIC GENERAL CIRCULATION MODELS

Estimates of monthly mean soil moisture for 1979-1989
[NASA-TM-104571] p 2407 N94-23132

Climate variability in a coupled GCM. Part 2: The Indian Ocean and monsoon
[MPIM-104] p 2401 N94-23159

Modal structure of variations in the tropical climate system. Part 2: Origins of the low-frequency mode
[MPIM-96] p 2407 N94-23199

On testing two major cumulus parameterization schemes using the CSU regional atmospheric modeling system
[DE94-000703] p 2407 N94-23284

A regional analysis of cloudy mean spherical albedo over the marine stratocumulus region and the tropical Atlantic Ocean
[NASA-CR-194771] p 2409 N94-24049

Session on modeling of radiative transfer processes
p 2414 N94-24397

The NASA/GISS Mars general circulation model: Preliminary experiments p 2616 N94-24872

Optimal gains for a single polar orbiting satellite
p 2208 N94-24873

Eddy mixing coefficient values derived from simulations with the NASA Ames Mars GCM p 2617 N94-24875

The annual pressure cycle on Mars: Results from the LMD Martian atmospheric general circulation model
p 2619 N94-24884

ATMOSPHERIC MODELS

NOAA Federal/State Cooperative Program in Atmospheric Modification Research. Collected publication titles and abstracts [PB93-198125] p 2396 N94-22913

Atmospheric numerical modeling resource enhancement and model convective parameterization/scale interaction studies [NASA-CR-194769] p 2400 N94-23124

Monte Carlo climate change forecasts with a global coupled ocean-atmosphere model [MPIM-97] p 2407 N94-23156

Locally modified Bott-scheme for highly convective flows [MPIM-99] p 2400 N94-23157

Atmospheric flow in heterogeneous vegetated regions [W-9303] p 2401 N94-23175

Scientific investigations of atmospheric processes [NASA-CR-194805] p 2401 N94-23271

Modelling TOVS radiances of synoptic systems [NASA-CR-194847] p 2408 N94-23620

Diagnostic budgets of analyzed and modelled tropical plumes [NASA-CR-194853] p 2409 N94-23621

Radiative forcing calculations for SF6 and CH4 using a correlated k-distribution transmission model [DE94-001855] p 2397 N94-23700

Cloud-free aerosol optical depth determination over oceans from satellite radiometry [DE94-001897] p 2386 N94-23779

Model atmosphere analysis of selected luminous B stars [NASA-CR-195098] p 2599 N94-24051

Participation in TOMS missions [NASA-CR-195110] p 2398 N94-24078

Report of the proceedings of the Colloquium and Workshop on Multiscale Coupled Modeling [NASA-CP-3217] p 2410 N94-24374

Atmospheric Radiation Measurement (ARM)/CART site p 2411 N94-24379

Scientific goals of the Cooperative Multiscale Experiment (CME) p 2411 N94-24381

Grand challenge scientific questions in coupled modeling p 2412 N94-24382

Next generation initiation techniques p 2412 N94-24383

Examples of data assimilation in mesoscale models p 2412 N94-24384

Measurement and modeling of moist processes p 2413 N94-24385

Parameterization of sub-grid scale convection p 2413 N94-24386

Coupled land surface/hydrologic/atmospheric models p 2413 N94-24387

Incorporation of the planetary boundary layer in atmospheric models p 2413 N94-24388

The role of radiation in mesoscale flows: Physics, parameterizations, codes p 2413 N94-24389

Chemistry on the mesoscale: Modeling and measurement issues p 2413 N94-24390

Validation of mesoscale models p 2413 N94-24391

Joint sessions on moisture processes and cumulus parameterization p 2414 N94-24393

Session on cumulus parameterization p 2414 N94-24394

Session on coupled land surface/hydrological/atmospheric models p 2414 N94-24395

Joint sessions on modeling of boundary layer and radiative transfer processes p 2414 N94-24396

Session on coupled atmospheric/chemistry coupled models p 2414 N94-24398

Session on validation of coupled models p 2414 N94-24399

Session on techniques and resources for storm-scale numerical weather prediction p 2415 N94-24400

LRAT: Lightning Radiative Transfer p 2416 N94-24443

Workshop on Atmospheric Transport on Mars [NASA-CR-194855] p 2616 N94-24871

Particle sizes and composition of Mars atmospheric dust based upon Viking and Mariner 9 observations p 2618 N94-24878

Aspects of the Martian global circulation p 2618 N94-24879

Multiannual simulations with the Mars climate model p 2618 N94-24881

Analyzing Martian winds and tracer concentrations using Mars Observer data p 2619 N94-24883

Evidence for dust transport in Viking IR thermal mapper opacity data p 2620 N94-24892

Retrieval of temperature profiles from Martian infrared spectra p 2620 N94-24893

Three-dimensional numerical simulation of near-surface flows over the Martian north polar cap p 2621 N94-24895

Two-dimensional modeling of thermal inversion layers in the middle atmosphere of Mars p 2622 N94-24900

Three-dimensional numerical simulation of thermal tides in the Martian atmosphere p 2622 N94-24901

Observed and Navy operational global model climatologies of synoptic disturbances over the tropical western Pacific during winter 1991-1992 [AD-A273400] p 2416 N94-25071

Collection and evaluation of numerical models with the aim to investigate the impact of aircraft emissions [DLR-MITT-93-06] p 2400 N94-25414

A nighttime structure model of atmospheric optical turbulence, c2(n), derived from thermosonde and high resolution rawinsonde measurements [AD-A273803] p 2406 N94-25537

Results from the VISA project [AD-A273752] p 2406 N94-25540

ATMOSPHERIC MOISTURE

Atmospheric moisture fields derived by satellite observations over the tropical Pacific Ocean [NASA-CR-194852] p 2408 N94-23542

Uncertainties in climate data sets [NASA-CR-194848] p 2408 N94-23577

Modelling TOVS radiances of synoptic systems [NASA-CR-194847] p 2408 N94-23620

MAMS data for the Convection and Moisture Experiment (CAMEX) [NASA-TM-108435] p 2409 N94-24080

GEWEX Water Vapor Project (GVaP) p 2411 N94-24378

Measurement and modeling of moist processes p 2413 N94-24385

Joint sessions on moisture processes and cumulus parameterization p 2414 N94-24393

Water cycle research associated with the CaPE hydrometeorology project (CHymP p 2416 N94-24414

Observational and modeling studies of heat, moisture, precipitation and global-scale circulation patterns [NASA-CR-195148] p 2415 N94-24485

Vertical transport of water in the Martian boundary layer p 2622 N94-24902

ATMOSPHERIC OPTICS

Sodium-layer laser guide stars [DE93-019621] p 2349 N94-23490

Temporal and spatial mapping of surface albedo and atmospheric dust opacity on Mars p 2619 N94-24887

ATMOSPHERIC PHYSICS

The role of radiation in mesoscale flows: Physics, parameterizations, codes p 2413 N94-24389

ATMOSPHERIC PRESSURE

Three-dimensional numerical simulation of thermal tides in the Martian atmosphere p 2622 N94-24901

Mars Observer: Applications to atmospheric transport p 2623 N94-24904

ATMOSPHERIC RADIATION

Atmospheric Radiation Measurement (ARM)/CART site p 2411 N94-24379

ATMOSPHERIC REFRACTION

IRIG radar calibration catalog. Version 2: The IRIG error model reference for radar calibrations [AD-A273344] p 2303 N94-25155

ATMOSPHERIC SCATTERING

Micro pulse laser radar [NASA-CASE-GSC-13493-1] p 2294 N94-23827

Particle sizes and composition of Mars atmospheric dust based upon Viking and Mariner 9 observations p 2618 N94-24878

ATMOSPHERIC SOUNDING

A field evaluation of remote sensor measurements of wind, temperature, and moisture for ARM integrated sounding system research [DE94-000565] p 2381 N94-23001

Atmospheric moisture fields derived by satellite observations over the tropical Pacific Ocean [NASA-CR-194852] p 2408 N94-23542

Uncertainties in climate data sets [NASA-CR-194848] p 2408 N94-23577

Convective organization in the Pacific ITCZ: Merging OLR, TOVS, and SSM/I information [NASA-CR-194850] p 2408 N94-23619

Interferometer scan unit mechanism definition p 2358 N94-24012

Intercomparison of remote and balloon-borne sensors operated at JAPE-91 p 2527 N94-24210

Joint sessions on moisture processes and cumulus parameterization p 2414 N94-24393

Investigation of passive atmospheric sounding using millimeter and submillimeter wavelength channels [NASA-CR-194858] p 2404 N94-24843

Electromagnetic interference impact of the proposed emitters for the High Frequency Active Auroral Research Program (HAARP) [AD-A273401] p 2301 N94-24926

Northern Exposure 1992: An investigation of transauroral HF radio skywave propagation [AD-A273363] p 2303 N94-25089

ATMOSPHERIC TEMPERATURE

An analysis of solar mesospheric temperatures for the upper stratosphere and mesosphere [NASA-CR-194861] p 2626 N94-23626

Comparison between 1-minute and 15-minute averages of turbulence parameters p 2528 N94-24218

Mesospheric and lower thermospheric winds, temperatures densities, and volume emission rates [NASA-CR-195147] p 2403 N94-24486

The NASA/GISS Mars general circulation model: Preliminary experiments p 2616 N94-24872

Analyzing Martian winds and tracer concentrations using Mars Observer data p 2619 N94-24883

The annual pressure cycle on Mars: Results from the LMD Martian atmospheric general circulation model p 2619 N94-24884

Retrieval of temperature profiles from Martian infrared spectra p 2620 N94-24893

Dust transport in the Martian atmosphere p 2621 N94-24894

Three-dimensional numerical simulation of near-surface flows over the Martian north polar cap p 2621 N94-24895

Diagnostic calculations of the circulation in the Martian atmosphere p 2622 N94-24898

Two-dimensional modeling of thermal inversion layers in the middle atmosphere of Mars p 2622 N94-24900

Three-dimensional numerical simulation of thermal tides in the Martian atmosphere p 2622 N94-24901

Mars Observer: Applications to atmospheric transport p 2623 N94-24904

Thermistor controlled current source versatile temperature sensor [AD-D015979] p 2345 N94-25037

A nighttime structure model of atmospheric optical turbulence, c2(n), derived from thermosonde and high resolution rawinsonde measurements [AD-A273803] p 2406 N94-25537

ATMOSPHERIC TIDES

Mars dust-driven tides and their impact on the thermosphere p 2617 N94-24876

Three-dimensional numerical simulation of thermal tides in the Martian atmosphere p 2622 N94-24901

ATMOSPHERIC TURBULENCE

A review of the Workshop on Fatigue Life Methodologies for Wind Turbines [DE94-002039] p 2394 N94-23472

Joint Acoustic Propagation Experiment (JAPE) p 2527 N94-24208

Comparison between 1-minute and 15-minute averages of turbulence parameters p 2528 N94-24218

Beamforming in an acoustic shadow p 2528 N94-24219

Continuous gust response and sensitivity derivatives using state-space models p 2161 N94-24287

Optimization of techniques to reconstruct images disturbed by atmospheric turbulence in the near infra-red [PB93-199784] p 2298 N94-24630

A nighttime structure model of atmospheric optical turbulence, c2(n), derived from thermosonde and high resolution rawinsonde measurements [AD-A273803] p 2406 N94-25537

ATOMIC BEAMS

Method and apparatus for producing a thermal atomic oxygen beam [NASA-CASE-LEW-15614-1] p 2534 N94-23825

Optical spin polarization and state-sensitive detection of a cesium atomic beam [ATR-92(8436)-1] p 2534 N94-24077

Matter-wave interferometry with laser cooled atoms [AD-A273249] p 2536 N94-24717

ATOMIC CLUSTERS

Density functional studies: First principles and semi-emperical calculations of clusters and surfaces [DE94-002836] p 2561 N94-23214

ATOMIC COLLISIONS

Report of the Joint Seminar on Solid State Physics, Atomic and Molecular Physics, and Materials Science in the Energy Region of Tandem Accelerators [DE93-508268] p 2548 N94-22924

Optical spin polarization and state-sensitive detection of a cesium atomic beam [ATR-92(8436)-1] p 2534 N94-24077

Ultracold atoms in traps and fountains [ETN-94-95325] p 2537 N94-25239

Intramultiplet mixing for Ne(**)(3p)+He at superthermal energies [ETN-94-95327] p 2538 N94-25240

Modelling of thermal argon plasmas [ETN-94-95363] p 2554 N94-25300

ATOMIC FORCE MICROSCOPY

Condensed-phase thermal decomposition of TATB investigated by Atomic Force Microscopy (AFM) and Simultaneous Thermogravimetric Modulated Beam Mass Spectrometry (STMBMS) [DE94-000396] p 2232 N94-23298

ATOMIC INTERACTIONS
Optical spin polarization and state-sensitive detection of a cesium atomic beam [ATR-92(8436)-1] p 2534 N94-24077
Diffusion on Cu surfaces p 2251 N94-24428
ATOMIC PHYSICS
Report of the Joint Seminar on Solid State Physics, Atomic and Molecular Physics, and Materials Science in the Energy Region of Tandem Accelerators [DE93-508268] p 2548 N94-22924
Theoretical atomic physics for fusion [DE94-000712] p 2533 N94-23543
ATOMIC RECOMBINATION
Modelling of thermal argon plasmas [ETN-94-95363] p 2554 N94-25300
ATOMIC STRUCTURE
Atomic probes of surface structure and dynamics [DE94-001651] p 2530 N94-22720
Spin-polaron theory of high-T(c) superconductivity. 2: Electronic structure of the CuO2 planes [DE93-019197] p 2556 N94-22919
Semiempirical studies of atomic structure [DE94-001588] p 2531 N94-22937
Relativistic configuration interaction calculation of the correlation energies of highly-charged ions [DE94-001055] p 2532 N94-22988
Density functional studies: First principles and semi-emperical calculations of clusters and surfaces [DE94-002836] p 2561 N94-23214
Polydiacetylene thin films for nonlinear optical applications p 2225 N94-24347
A survey of metallurgical research on several actinides [DE94-002643] p 2245 N94-24747
The structure and catalytic properties of supported platinum catalysts [ETN-94-95357] p 2236 N94-25250
Electronic structure and high pressure phase transition in LaSb and CeSb [DE93-617051] p 2567 N94-25423
ATOMIZING
Fundamental rocket injector/spray programs at the Phillips Laboratory p 2211 N94-23039
Shear coaxial injector instability mechanisms p 2213 N94-23047
Ignition and combustion characteristics of metallized propellants, phase 2 [NASA-CR-195107] p 2266 N94-24700
ATOMS
Matter-wave interferometry with laser cooled atoms [AD-A273249] p 2536 N94-24717
ATROPHY
Skeletal muscle metabolism in hypokinetic rats [NASA-CR-195082] p 2420 N94-24124
ATTACK AIRCRAFT
Birdstrike resistant crew enclosure program [AD-A273700] p 2463 N94-25453
ATTENUATION COEFFICIENTS
Optical properties and emissivities of liquid metals and alloys p 2248 N94-25129
ATTENUATORS
Flight solar calibrations using the Mirror Attenuator Mosaic (MAM): Low scattering mirror p 2384 N94-23602
ATTITUDE (INCLINATION)
Decentralized autonomous attitude determination using an inertially stabilized payload p 2157 N94-24264
ATTITUDE CONTROL
Torque equilibrium attitudes for the Space Station p 2208 N94-24449
An Earth albedo model: A mathematical model for the radiant energy input to an orbiting spacecraft due to the diffuse reflectance of solar radiation from the Earth below [NASA-TM-104596] p 2195 N94-24497
Near Earth asteroid rendezvous [NASA-CR-195518] p 2195 N94-24808
ATTITUDE STABILITY
Numerical simulation of Ulysses nutation p 2207 N94-24017
AUDIO DATA
Aeronautical audio broadcasting via satellite p 2274 N94-22741
Some subjects in digital audio, noise shaping, sample rate conversion, dynamic range compression and testing [ISBN-9-09-005162-7] p 2530 N94-25220
Modeling of the ground-to-SSFMB link networking features using SPW p 2306 N94-25381
AUDIO EQUIPMENT
Effects of atmospheric variations on acoustic system performance p 2527 N94-24211
AUDIO SIGNALS
The HDTV digital audio matrix [BBC-RD-1993/9] p 2295 N94-24085
Linear and nonlinear adaptive filtering and their application to speech intelligibility enhancement [ISBN-9-09-005342-5] p 2304 N94-25292
AUDITORY PERCEPTION
Auditory spectro-temporal pattern analysis [AD-A273554] p 2427 N94-24865
On the auditory discrimination of spectral shape [ETN-94-95306] p 2530 N94-25289
AUDITORY SIGNALS
Head related transfer function pseudo-stereophony [NASA-CASE-ARC-11919-1-NP] p 2525 N94-23312
Dimensional analysis of acoustically propagated signals p 2528 N94-24217
Auditory spectro-temporal pattern analysis [AD-A273554] p 2427 N94-24865
AUDITORY STIMULI
On the auditory discrimination of spectral shape [ETN-94-95306] p 2530 N94-25289
AUGER SPECTROSCOPY
Grain-boundary microchemistry and intergranular cracking of irradiated austenitic stainless steel [DE94-000466] p 2242 N94-23457
AUGMENTATION
Reliability enhancement of Navier-Stokes codes through convergence enhancement p 2216 N94-23064
AURORAL ZONES
High latitude cusp signature observations for southward IMF B sub Z [AD-A273801] p 2406 N94-25536
AURORAS
Computer assisted analysis of auroral images obtained from high altitude polar satellites [NASA-CR-194873] p 2400 N94-23084
PULSAUR 2 [NASA-CR-194832] p 2209 N94-23484
Electromagnetic interference impact of the proposed emitters for the High Frequency Active Auroral Research Program (HAARP) [AD-A273401] p 2301 N94-24926
AUSTENITE
Tensile properties of 21-6-9 stainless steel at elevated temperatures [DE94-001852] p 2240 N94-23017
AUSTENITIC STAINLESS STEELS
Grain-boundary microchemistry and intergranular cracking of irradiated austenitic stainless steel [DE94-000466] p 2242 N94-23457
AUTOCORRELATION
Composite sequences for rapid acquisition of direct-sequence spread spectrum signals [CTN-94-60901] p 2300 N94-24696
Direct measurement of turbulent dissipation rate using dual laser doppler velocimeters [AD-A273740] p 2340 N94-25530
AUTOMATA THEORY
A method for the general simultaneous full decomposition of sequential machines: Algorithms and implementation [EUT-92-E-267] p 2445 N94-23170
PROGRIL: A language for the definition of protocol grammars [EUT-93-E-270] p 2449 N94-23172
Viewing hybrid systems as products of control systems and automata [NASA-CR-194792] p 2472 N94-23300
Fixed points and shift cycles in cellular automata [RR-459] p 2492 N94-25309
AUTOMATED RADAR TERMINAL SYSTEM
Analysis and surveillance performance at Chicago O'Hare Airport [DOT/FAA/RD-92/29] p 2175 N94-24127
AUTOMATIC CONTROL
Viewing hybrid systems as products of control systems and automata [NASA-CR-194792] p 2472 N94-23300
A reference Martian mission for a long range rover p 2606 N94-23382
Feasibility study of an automatic vehicle for planetary exploration p 2369 N94-23399
Rover: Autonomous concepts for Mars exploration p 2369 N94-23400
Mechanical design of a planetary rover p 2369 N94-23403
Automation technology for remote sample acquisition p 2369 N94-23407
Marsohkod movement control p 2370 N94-23418
Perspective of creation of means for collecting information concerning transport situation p 2370 N94-23420
Sensing and modelling concepts for autonomous and remote mobile robot control p 2370 N94-23421
Bond graph modeling, simulation, and reflex control of the Mars planetary automatic vehicle p 2370 N94-23424
Operations concepts for Mars missions with multiple mobile spacecraft p 2501 N94-23852
Real-time automated failure identification in the Control Center Complex (CCC) p 2272 N94-23892
PILOT: An intelligent distributed operations support system p 2508 N94-23895
NASDA knowledge-based network planning system p 2508 N94-23898
Expert diagnostics system as a part of analysis software for power mission operations p 2516 N94-23944
Autonomous Space Processor for Orbital Debris (ASPOD) [NASA-CR-195521] p 2204 N94-24621
Conflict-free trajectory planning for air traffic control automation [NASA-TM-108790] p 2174 N94-25272
Automation and cognition in air traffic control: An empirical investigation [DOT/FAA/AM-94/3] p 2176 N94-25444
Automatic pressure control system for the Wright Laboratory Compressor Research Facility [AD-A273827] p 2194 N94-25522
AUTOMATIC FLIGHT CONTROL
UAV current technology and future trends p 2154 N94-24245
AUTOMATIC FREQUENCY CONTROL
A pattern jitter free AFC scheme for mobile satellite systems p 2285 N94-22809
AUTOMATIC LANDING CONTROL
Infrared sensors and systems for enhanced vision/autonomous landing applications p 2439 N94-25491
AUTOMATIC WEATHER STATIONS
The evaluation of ASOS for the Kennedy Space Center's Shuttle Landing Facility [NASA-CR-195685] p 2416 N94-25271
AUTOMATION
System for automatic transportation of aircraft on the ground [CA-PATENT-1-322-361] p 2193 N94-24785
AUTOMOBILE ENGINES
Rolls-Royce in perspective: Past, present and future [PNR-90882] p 2187 N94-23519
AUTOMOBILE FUELS
Federal alternative fuel program light duty vehicle operations [DE93-040663] p 2264 N94-22878
New methane chemistry synthesis of materials for reversible uptake and useful functionalization of methane [PB94-112786] p 2233 N94-23801
AUTOMOBILES
Federal alternative fuel program light duty vehicle operations [DE93-040663] p 2264 N94-22878
Method for simulating a vehicle shock test: Design and realization of the required implementation tools [ECL-92-14] p 2352 N94-22885
EPA's survey of in-use driving patterns: Implications for mobile source emission inventories [PB94-118502] p 2399 N94-24525
AUTOMORPHISMS
Number of moduli of families of curves on toric surfaces [PB93-230381] p 2479 N94-23121
Algebraic-geometric codes and their decoding algorithms [ETN-94-95294] p 2491 N94-25079
AUTONOMOUS NAVIGATION
Perception and 3D environment modeling for mobile robot autonomous navigation [LAAS-93117] p 2471 N94-22908
UAV current technology and future trends p 2154 N94-24245
Satellite autonomous navigation and orbit determination using magnetometers p 2156 N94-24258
Design of a wheeled articulating land rover [NASA-CR-195520] p 2365 N94-24806
Overall system concepts in mission planning p 2521 N94-25009
AUTONOMY
Open EDI [VTT-TIED-1353] p 2588 N94-22734
The Mars 96 balloon guiderope: An autonomous system in extreme environment conditions p 2369 N94-23412
The remote-operated autonomous-robot concept: From deep sea to outer space applications p 2370 N94-23413
Experiments with a small behaviour controlled planetary rover p 2371 N94-23427
Decentralized autonomous attitude determination using an inertially stabilized payload p 2157 N94-24264
Human-like robots for space and hazardous environments [NASA-CR-195549] p 2365 N94-24703
Design of a walking robot [NASA-CR-195200] p 2367 N94-25274
An evaluation of three-dimensional sensors for the extravehicular activity helper/retreiver p 2444 N94-25369

AUTOREGRESSIVE PROCESSES
Temporal aggregation in a periodically integrated autoregressive process
[PB93-230480] p 2479 N94-23122
Two-dimensional pattern analysis and classification using a complex orthogonal estimation algorithm
[RR-475] p 2463 N94-25321
Parametric and nonparametric discriminants for regional earthquakes and explosions
[AD-A273807] p 2406 N94-25538

AUXILIARY POWER SOURCES
Development of a power electronics unit for the Space Station plasma contactor
[NASA-TM-106486] p 2222 N94-25201

AUXILIARY PROPULSION
Power console development for NASA's electric propulsion outreach program
[NASA-TM-106428] p 2218 N94-23372

AVIATION METEOROLOGY
Aviation Weather Program (AWP)
p 2411 N94-24380
The evaluation of ASOS for the Kennedy Space Center's Shuttle Landing Facility
[NASA-CR-195685] p 2416 N94-25271

AVIONICS
Implementing the space shuttle data processing system with the space generic open avionics architecture
[NASA-CR-188254] p 2199 N94-23571
S-2E Tracker maritime patrol aircraft re-engine and system upgrade program p 2158 N94-24270
Advanced avionics architecture and technology review. Executive summary and volume 1: Avionics tech nology. Volume 2: Avionics systems engineering
[AD-A273630] p 2186 N94-24733
New Advances in Mission Planning and Rehearsal Systems
[AGARD-LS-192] p 2521 N94-25008
Overall system concepts in mission planning
p 2521 N94-25009
Future space transportation system architecture avionics requirements p 2162 N94-25098
New Technologies for Space Avionics, 1993
[NASA-CR-195157] p 2272 N94-25193
Appendix A: Proposed statement of work, 1994
p 2272 N94-25194

AXIAL FLOW
Effect of delta tabs on mixing and axis switching in jets from asymmetric nozzles
[NASA-TM-106450] p 2167 N94-23592
Hydrodynamics of stirred gas-liquid dispersions
[ETN-94-95368] p 2339 N94-25254

AXIAL FLOW TURBINES
Two-dimensional Navier-Stokes computations of subsonic and supersonic flows through turbine cascades
[PB93-226223] p 2317 N94-23114

AXIAL LOADS
Damage tolerance of pressurized graphite/epoxy tape cylinders under uniaxial and biaxial loading
[NASA-CR-195101] p 2377 N94-24587

AXIAL STRAIN
Constitutive modelling of fiber-reinforced concrete under uniaxial tensile loading
[VTT-JULK-774] p 2379 N94-25385

AXIAL STRESS
Damage tolerance of pressurized graphite/epoxy tape cylinders under uniaxial and biaxial loading
[NASA-CR-195101] p 2377 N94-24587
Assessment of impact damage of composite rocket motor cases
[NASA-CR-195143] p 2220 N94-24595

AXIOMS
On the reduced game property for and the axiomatization of the tau-value
[MEMO-1128] p 2497 N94-22716
Reduced game properties of egalitarian division rules for cooperative games
[PB94-111689] p 2521 N94-24523

AXISYMMETRIC BODIES
Development of a code for wall contour design in the transonic region of axisymmetric and square nozzles
[NASA-CR-194857] p 2167 N94-23625

AXISYMMETRIC FLOW
Supersonic minimum length nozzle design for dense gases p 2171 N94-23656
BEM solution for the simulation of axisymmetric viscous sintering
[PB93-237717] p 2336 N94-24761
Analytical skin friction and heat transfer formula for compressible internal flows
[NASA-CR-191185] p 2170 N94-25173

B

B STARS
Model atmosphere analysis of selected luminous B stars
[NASA-CR-195098] p 2599 N94-24051
Observational studies of the clearing phase in proto-planetary disk systems
[NASA-CR-195182] p 2604 N94-25265

B-2 AIRCRAFT
B-2 bomber: Assessment of DOD's response to mandated certifications and reports
[AD-A273179] p 2184 N94-25152

BACKGROUND RADIATION
The current status of observational constraints on cosmic strings
[DE94-001505] p 2601 N94-23010

BACKSCATTERING
Analysis of a proposed Compton backscatter imaging technique
[DE93-040537] p 2371 N94-22935
Examination of the physical, electrical, and microwave evolution of water into young sea ice
[AD-A273559] p 2418 N94-24918
Use of microwave polarimetry to enhance SAR images of the ocean surface
[AD-A273568] p 2419 N94-24944
Measuring track densities in lunar grains by image analysis p 2623 N94-25355

BACKWARD FACING STEPS
A comparative study of computational solutions to flow over a backward-facing step p 2326 N94-23670
Computation of turbulent flows over backward and forward-facing steps using a near-wall Reynolds stress model p 2172 N94-24145

BACTERIA
Investigation of evolution-related aspects of bacterial rhodopsins
[NASA-CR-194826] p 2420 N94-23501
Microbiological analysis of debris from Space Transportation System (STS)-55 Spacelab D-2
[NASA-CR-193883] p 2421 N94-24310
Factors affecting the identification of phytoplankton groups by means of remote sensing
[NASA-TM-108799] p 2387 N94-24403
Symbiosis in marine luminous bacteria
[AD-A273540] p 2422 N94-24791
The evolution of energy-transducing systems. Studies with an extremely halophilic archaebacterium
[NASA-CR-193803] p 2422 N94-24807
Design and testing of a unique randomized gravity, continuous flow bioreactor p 2423 N94-25368

BAFFLES
Shock-induced turbulent flow in baffle systems
[DE94-001532] p 2319 N94-23470
Flight solar calibrations using the Mirror Attenuator Mosaic (MAM): Low scattering mirror
p 2384 N94-23602
Responses of a finite baffled plate subject to turbulent and mean flow excitations
[NASA-CR-191570] p 2334 N94-24605

BALANCE
The role of atmospheric heat transport in the seasonal carbon dioxide cycle p 2621 N94-24896

BALANCING
Balancing for unstable nonlinear systems
[MEMO-1118] p 2469 N94-22705

BALL BEARINGS
Tribological characteristics of ball bearings lubricated with a sputtered molybdenum disulphide film in a vacuum under a high thrust load p 2355 N94-23992
In-vacuum performance of Fomblin Z25-lubricated, 52100 steel bearings with TiC-coated balls
p 2358 N94-24011
An Earth observation telescope refocusing mechanism
p 2359 N94-24014
The development of dry-lubricated ceramic cages
p 2363 N94-24045

BALLISTIC RANGES
Advanced ballistic range technology
[NASA-CR-195198] p 2165 N94-25169

BALLISTIC TRAJECTORIES
Comparison of c.t.s. based prediction of store trajectory with flight test data p 2158 N94-24268

BALLOON FLIGHT
Results of the 1993 NASA/JPL balloon flight solar cell calibration program
[NASA-CR-195158] p 2395 N94-24563

BALLOON SOUNDING
Balloon experiments at Mars 96 project
p 2608 N94-23396

BALLOON-BORNE INSTRUMENTS
The Mars 96 balloon guiderope: An autonomous system in extreme environment conditions p 2369 N94-23412
Intercomparison of remote and balloon-borne sensors operated at JAPE-91 p 2527 N94-24210
Results of the 1993 NASA/JPL balloon flight solar cell calibration program
[NASA-CR-195158] p 2395 N94-24563
Polarization analysis of a balloon-borne solar magnetograph
[NASA-CR-193908] p 2345 N94-24852

BANACH SPACE
Lacunary series as quadratic differentials in conformal dynamics
[PB93-238061] p 2481 N94-23547
Multigrid method for integral equations and automatic programs p 2464 N94-23696
The least energy critical set
[DE93-616820] p 2493 N94-25434

BAND STRUCTURE OF SOLIDS
A valence-fluctuation theory of cuprate superconductivity
[DE94-000887] p 2558 N94-22942

BANDPASS FILTERS
Radar target discrimination systems using artificial neural network topology
[AD-D015984] p 2301 N94-25041

BANDWIDTH
Wide band fiber-optic communications
p 2304 N94-23231
Experimental modification and identification of the DSS-13 antenna control system model
p 2291 N94-23260
Theoretical investigation of variable periodicity (graded) multilayers for hard x ray applications
[NASA-CR-194824] p 2543 N94-23502
Reducing video frame rate increases remote optimal focus time
[NASA-TM-104018] p 2431 N94-23970

BARIUM COMPOUNDS
The elastic and electromechanical properties of BaTiO3 single crystal through the ferroelectric transition
[DE94-001437] p 2557 N94-22927

BARIUM ION CLOUDS
Artificial plasma experiments. Chemical release observations associated with the CRRES program
[NASA-CR-194871] p 2550 N94-23565

BARIUM OXIDES
The de Haas-van Alphen measurements in Ba(0.6)K(0.4)BiO3
[DE93-041169] p 2556 N94-22920

BAROCLINIC WAVES
Global ocean modeling on the Connection Machine
[DE94-000888] p 2417 N94-23517

BAROTROPIC FLOW
Global ocean modeling on the Connection Machine
[DE94-000888] p 2417 N94-23517
An adaptive multigrid model for hurricane track prediction p 2416 N94-23687

BAROTROPISM
Nonlinear dynamics applied to atmospheric prediction
[AD-A273437] p 2404 N94-24674

BARRIER LAYERS
Planar varactor frequency multiplier devices with blocking barrier
[NASA-CASE-NPO-18428-1-CU] p 2310 N94-23821

BARS
Analysis of the effects of wake passage on heat transfer in a linear turbine cascade
[AD-A273729] p 2339 N94-25446

BARYONS
A quark structure of hadrons and nuclei
[DE93-616872] p 2539 N94-25474

BASALT
Basaltic Volcanism and Ancient Planetary Crusts
[NASA-CR-193151] p 2614 N94-24363
Whole rock major element chemistry of KREEP basalt clasts in lunar breccia 15205: Implications for the petrogenesis of volcanic KREEP basalts
p 2614 N94-24365
Major element chemistry of Apollo 14 mare basalt clasts and highland plutonic clasts from lunar breccia 14321: Comparison with neutron activation results
p 2614 N94-24366
Lunar mare volcanism: Mixing of distinct, mantle source regions with KREEP-like component
p 2615 N94-24370
A dynamic melting model for the origin of Apollo 15 olivine-normative and quartz-normative mare basalts
p 2615 N94-24371

BATHS
Detection of velocity in high temperature liquid metals
p 2247 N94-25127

BAYES THEOREM
On non-informativeness in a classical Bayesian inference problem
[MEMO-COSOR-92-35] p 2494 N94-23143

Bayesian decision theory with imprecise prior probabilities applied to replacement problems
[PB93-237634] p 2481 N94-23456
Decision making with imprecise probabilities
[PB94-111622] p 2494 N94-23772
Density estimation by maximum quantum entropy
[DE94-002626] p 2569 N94-24516
Bounds and asymptotic expansions for solutions of the free boundary problems related to sequential decision versions of a bioequivalence problem
[AD-A273551] p 2495 N94-24560

BCH CODES
Box codes of lengths 48 and 72 p 2292 N94-23265

BEACONS
Sodium-layer laser guide stars
[DE93-019621] p 2349 N94-23490

BEAM INJECTION
Investigation of the heat handling capabilities of DIII-D neutral beamline internal components
[DE94-001107] p 2553 N94-24756

BEAM SPLITTERS
Design refinement of multilayer optical thin film devices with two optimization techniques
[DE93-634228] p 2542 N94-22979

BEAM WAVEGUIDES
Performance of the X-/Ka/KABLE-band dichroic plate in the DSS-13 beam waveguide antenna
p 2291 N94-23261

BEAMFORMING
Adaptive digital beamforming for a CDMA mobile communications payload p 2274 N94-22743
Adaptive array antenna for satellite cellular and direct broadcast communications p 2275 N94-22745
Geostationary payload concepts for personal satellite communications p 2278 N94-22765
Study of LEO-SAT microwave link for broad-band mobile satellite communication system p 2279 N94-22769
Characterization of germanium stripe x ray lasers
[DE93-019629] p 2347 N94-22867
Calibration block for digital beam forming antenna
[PB93-204550] p 2294 N94-23773
Effects of atmospheric variations on acoustic system performance p 2527 N94-24211
Beamforming in an acoustic shadow
p 2528 N94-24219
Layered parallel interface for an active antenna array
[AD-D016002] p 2301 N94-25045
Preprocessor and adaptive beamformer for linear-frequency modulation active signals
[AD-D016008] p 2302 N94-25048

BEAMS (SUPPORTS)
Inverse dynamics of a rigid rod system as a simplified model of flexible beam p 2160 N94-24281

BEARINGS
The Fifth European Space Mechanisms and Tribology Symposium
[ESA-SP-334] p 2355 N94-23985
Interferometer scan unit mechanism definition
p 2358 N94-24012
The development of dry-lubricated ceramic cages
p 2363 N94-24045
Wear reduction in ceramic bearings by surface generated pyrolytic carbon continuously replenished by ethylene gas
[NASA-CR-189214] p 2364 N94-24090
Flex bearing UUEC, volume 2
[NASA-CR-193901] p 2365 N94-24588
Influence of backup bearings and support structure dynamics on the behavior of rotors with active supports
[NASA-CR-195106] p 2365 N94-24751

BELLMAN THEORY
Approximate optimal guidance for the advanced launch system
[NASA-CR-4568] p 2198 N94-24752

BENDING
Energy estimates and asymptotic analysis in the theory of shells
[PB93-225738] p 2374 N94-23113
Vectorization and parallelization of the finite strip method for dynamic Mindlin plate problems
p 2483 N94-23679
Vibrations of variable cross section Timoshenko beams p 2160 N94-24279
Nonlinear analysis using a modal based reduction technique p 2161 N94-24288
Fiber optical angular sensor: Literature study and experimental results
[PB93-204345] p 2545 N94-24529
Buckling of circular cylindrical shells subjected to combined loads (axial compression, normal pressure, bending and transverse shear loading)
[PB93-215358] p 2378 N94-24745

BENDING FATIGUE
Investigation of the effects of manufacturing variations and materials on fatigue crack detection methods in gear teeth
[NASA-CR-195093] p 2373 N94-24769

BENDING VIBRATION
Vibrations of variable cross section Timoshenko beams p 2160 N94-24279
Inverse dynamics of a rigid rod system as a simplified model of flexible beam p 2160 N94-24281

BENZENE
Dispersion of Rh/Cu in a sol-gel matrix. Highly chemo- and stereoselective catalyst for the reduction of alkynes to Z-alkenes
[AD-A273306] p 2262 N94-25145

BERYLLIUM ALLOYS
Interplay of magnetic and superconducting heavy fermion ground states
[DE94-000680] p 2240 N94-23003

BESSEL FUNCTIONS
A theorem regarding roots of the zero-order Bessel function of the first kind p 2325 N94-23667
Analysis for the computational modeling of finite cladding and lossy coating effects in fibers
[PB94-111085] p 2544 N94-23732
Probabilistic methods in problems of applied analysis
[PB94-110681] p 2495 N94-24571

BETHE-SALPETER EQUATION
A scalar-vector model of quark-antiquark interaction under linear confinement
[DE93-616871] p 2538 N94-25317

BIAS
Temporal behavior of the electron density profile during limiter biasing in the HYBTOK-2 tokamak
[NIFS-257] p 2552 N94-24456

BIBLIOGRAPHIES
Bibliographic Retrieval System (BARS), Sandia Shock Compression (SSC) database Shock Physics Index
[DE94-001679] p 2589 N94-23126
Bibliographic Retrieval System (BARS). Sandia Shock Compression (SSC) database Shock Physics Index (SPHINX) database. Volume 1: UNIX version query guide customized application for INGRES
[DE94-001703] p 2589 N94-23127
Bibliographic Retrieval System (BARS), Sandia Shock Compression (SSC) database, Shock Physics Index (SPHINX) database, Volume 2: UNIX version user's guide
[DE94-001704] p 2589 N94-23128
Bibliography of Lewis Research Center technical publications announced in 1992
[NASA-TM-106035] p 2590 N94-23562
Aeronautical engineering: A continuing bibliography with indexes (supplement 298)
[NASA-SP-7037(298)] p 2153 N94-23711
NASA patent abstracts bibliography: A continuing bibliography. Section 2: Indexes (supplement 44)
[NASA-SP-7039(44)-SECT-2] p 2590 N94-23712
Aeronautical engineering: A continuing bibliography with indexes (supplement 299)
[NASA-SP-7037(299)] p 2153 N94-23973
Aircraft flight safety: A bibliography
[AGARD-R-805] p 2173 N94-24091
Japanese aerospace science and technology 1992. A bibliography with indexes
[NASA-SP-7104] p 2631 N94-24585
Management. A bibliography for NASA managers
[NASA-SP-7500(27)] p 2586 N94-24708
Selected bibliography 2: Diamond surface chemistry
[AD-A273518] p 2565 N94-25160

BIG BANG COSMOLOGY
A brief history of the universe
[DE93-616843] p 2604 N94-25210

BIMETALS
Organometallic chemistry of bimetallic compounds
[DE94-002313] p 2238 N94-22897

BINARY ALLOYS
New extensions in the development of deformation processed metal-metal matrix composites
[DE94-000692] p 2227 N94-23004
Multilayer relaxation and surface structure of ordered alloys
[NASA-TM-106433] p 2243 N94-23578
Crystal growth of organics for nonlinear optical applications p 2225 N94-24348
Segregation and oxidation studies of Al-Li and Al-Mg alloys
[ISBN-0-315-83993-7] p 2244 N94-24469

BINARY CODES
Box codes of lengths 48 and 72 p 2292 N94-23265
Binary block codes for correcting asymmetric or unidirectional errors
[ETN-94-95337] p 2460 N94-25063
On chain coding of line drawings
[ISBN-9-06-275778-2] p 2462 N94-25252

BINARY DATA
Box codes of lengths 48 and 72 p 2292 N94-23265
Simulation of adjacent channel interference in a UHF satellite system
[AD-A273147] p 2299 N94-24669

BINARY MIXTURES
Comparison of numerical simulation and experimental data for steam-in-place sterilization
p 2326 N94-23669
Microscopic dynamics in dense helium-neon mixtures: Neutron scattering, kinetic theory and computer simulations
[ISBN-9-07-386105-5] p 2537 N94-25228

BINARY PHASE SHIFT KEYING
Low cost coherent demodulation for mobile satellite terminals p 2284 N94-22803
Estimation of frequency offset in mobile satellite modems p 2285 N94-22807
Transmission over EHF mobile satellite channels
p 2287 N94-22820

BINARY STARS
Chromospheric activity in agol binaries
[AD-A273546] p 2602 N94-24557
Choice of filters for the detection of gravitational waves from coalescing binaries. 2: Detection in coloured noise
[DE93-616844] p 2604 N94-25211
A parallel algorithm for filtering gravitational waves from coalescing binaries
[DE93-616845] p 2604 N94-25212

BINDERS (MATERIALS)
Selection of polymer binders and fabrication of SiC fiber-reinforced reaction-bonded silicon nitride matrix composites
[NASA-CR-194874] p 2255 N94-24223
Collocated tunable wavenumber sensor/actuators for smart structures
[AD-A273697] p 2314 N94-25488

BINOMIALS
A comparison of approximate interval estimators for the Bernoulli parameter
[NASA-CR-191585] p 2458 N94-24680

BIOASTRONAUTICS
Cytokines and immune surveillance in humans
[NASA-CR-194801] p 2425 N94-23331
Crew interface analysis: Selected articles on space human factors research, 1987 - 1991
[NASA-TM-104756] p 2433 N94-24185
Specification list and function structure for a full-body dynamometer to be used aboard Space Station Freedom
[NASA-CR-195508] p 2439 N94-24835
Conceptual design of an astronaut hand anthropometry device
[NASA-CR-195490] p 2439 N94-24956
Evaluation of bioimpedance for the measurement of physiologic variables as related to hemodynamic studies in space flight p 2427 N94-25378
Loading, electromyograph, and motion during exercise
p 2427 N94-25380

BIOCHEMISTRY
Capillary electrophoresis of biomolecules: Theory, instrumentation and applications
[ETN-94-95297] p 2236 N94-25233

BIOCONVERSION
Considerations in implementing integrated biomass energy systems in developing countries
[DE93-018720] p 2395 N94-24499

BIODEGRADABILITY
Aqueous alkaline cleaners: An alternative to organic solvents
[AD-A273510] p 2260 N94-24848

BIODYNAMICS
Use of infrared telemetry as part of a nonintrusive inflight data collection system to collect human factors data
p 2434 N94-24193
Hand controller commonality evaluation process
p 2435 N94-24197
Development of biomechanical models for human factors evaluations p 2437 N94-24205
Establishing a relationship between maximum torque production of isolated joints to simulate EVA ratchet push-pull maneuver: A case study p 2437 N94-24206

BIOELECTRIC POTENTIAL
Electrophysiology of the rat nucleus accumbens: Local circuitry, neuromodulation and synaptic plasticity
[PB93-232254] p 2420 N94-23454

BIOFEEDBACK
Autogenic-feedback training: A potential treatment for post-flight orthostatic intolerance in aerospace crews
[NASA-TM-108785] p 2426 N94-24102

BIOINSTRUMENTATION
A chemical sensor and biosensor based totally automated water quality monitor for extended space flight: Step 1 p 2443 N94-24447

Evaluation of bioimpedance for the measurement of physiologic variables as related to hemodynamic studies in space flight p 2427 N94-25378

BIOLOGICAL EFFECTS
Research for electric energy systems
[DE94-001839] p 2293 N94-23719

BIOLOGICAL EVOLUTION
SETI: Search for extraterrestrial intelligence. An international interdisciplinary seminar, star days
[PB93-230597] p 2444 N94-23754
The evolution of energy-transducing systems. Studies with an extremely halophilic archaebacterium
[NASA-CR-193803] p 2422 N94-24807

BIOLOGY
A biological survey for the nation
[LC-93-85920] p 2421 N94-24704

BIOMASS
Considerations in implementing integrated biomass energy systems in developing countries
[DE93-018720] p 2395 N94-24499
Nutrients and light as factors controlling phytoplankton biomass on the Dutch continental shelf (North Sea), 1988-1990
[PB94-111143] p 2418 N94-24601
Investigating pyrolysis/incineration as a method of resource recovery from solid waste
p 2444 N94-25375

BIOMASS ENERGY PRODUCTION
Considerations in implementing integrated biomass energy systems in developing countries
[DE93-018720] p 2395 N94-24499

BIOREACTORS
Non-invasive optical detection of glucose in cell culture nutrient medium p 2422 N94-25357
Design and testing of a unique randomized gravity, continuous flow bioreactor p 2423 N94-25368

BIPOLAR TRANSISTORS
Electrochemical sulfur passivation of visible (approximately 670nm) AlGaInP lasers
[DE94-002293] p 2350 N94-24659
Method of fabricating a receptor-based sensor
[AD-D016026] p 2344 N94-24723
The 5th Engineering Foundation Conference: Advanced Heterostructure Transistors
[AD-A273508] p 2312 N94-24819
Method for fabricating self-aligned gate diffused junction field effect transistor
[AD-D015975] p 2312 N94-25035
On the characterization and optimization of high-speed silicon bipolar transistors
[ETN-94-95367] p 2313 N94-25253

BIRD-AIRCRAFT COLLISIONS
Birdstrike resistant crew enclosure program
[AD-A273700] p 2463 N94-25453

BIREFRINGENT FILTERS
A theoretical investigation of electrically tunable birefringent optical filters as the special discriminator in hyperspectral imaging systems
[AD-A273743] p 2547 N94-25533

BISMUTH ALLOYS
Spin-hole doping in the Kondo insulator Ce3Bi4Pt3 studied by neutron scattering
[DE93-040107] p 2557 N94-22925

BISMUTH OXIDES
The de Haas-van Alphen measurements in Ba(0.6)K(0.4)BiO3
[DE93-041169] p 2556 N94-22920

BIT ERROR RATE
Asynchronous timing and Doppler recovery in DSP based DPSK modems for fixed and mobile satellite applications p 2285 N94-22805
Performance of the unique-word-reverse-modulation type demodulator for mobile satellite communications
p 2286 N94-22813
DS-SSMA capacity for a mobile satellite system
p 2286 N94-22814
Diversity reception for advanced multi-satellite networks: A CDMA approach p 2286 N94-22816
Pseudo-coherent demodulation for mobile satellite systems p 2287 N94-22819
Error coding simulations p 2306 N94-24439
Bounds and simulation results of 32-ary and 64-ary quadrature amplitude modulation for broadband-ISDN via satellite
[NASA-TM-106484] p 2202 N94-25095
On chain coding of line drawings
[ISBN-9-06-275778-2] p 2462 N94-25252
DCT quantization matrices visually optimized for individual images p 2442 N94-25509

BIT SYNCHRONIZATION
Improved frame synchronization schemes for INMARSAT-B/M SCPC and TDM channels
p 2285 N94-22806

BIVARIATE ANALYSIS
Setting test limits under prescribed consumer loss
[MEMO-1107] p 2478 N94-22725

BL LACERTAE OBJECTS
100 GHz map of 3C 446
[PB94-104882] p 2599 N94-23705

BLACK BODY RADIATION
Activities of NIST (National Inst. of Standards and Technology) p 2384 N94-23605

BLADE SLAP NOISE
Unstructured adaptive mesh computations of rotorcraft high-speed impulsive noise
[NASA-CR-195090] p 2529 N94-24307
Validation of the ROTAC code for the rotor noise prediction
[PB93-204311] p 2529 N94-24514
Study of the blade/vortex interaction: Acoustics, aerodynamics and models
[ISL-R-104/92] p 2340 N94-25463

BLADE TIPS
Bent-tip blade for aircraft rotary-wing
[CA-PATENT-1-315-259] p 2176 N94-23254
Aerodynamic models for performance calculations of modern technology propellers p 2161 N94-24285
Unstructured adaptive mesh computations of rotorcraft high-speed impulsive noise
[NASA-CR-195090] p 2529 N94-24307

BLADE-VORTEX INTERACTION
Validation of the ROTAC code for the rotor noise prediction
[PB93-204311] p 2529 N94-24514
Study of the blade/vortex interaction: Acoustics, aerodynamics and models
[ISL-R-104/92] p 2340 N94-25463

BLASIUS FLOW
Boundary layer receptivity and control
p 2327 N94-24141

BLAST LOADS
The plastic response of a cylindrical shell subjected to an internal blast wave with a finite width shock front
p 2154 N94-24246

BLOCK COPOLYMERS
Reaction of isocyanates with carboxylic acids and its application to polymer synthesis
[PB94-118858] p 2254 N94-23763
Center for advanced electrical and structural polymers
[AD-A273415] p 2259 N94-24783
Morphology of highly textured polyethylene/polyethylene- propylene semicrystalline diblock copolymers
[AD-A273683] p 2263 N94-25413

BLOCK DIAGRAMS
Binary block codes for correcting asymmetric or unidirectional errors
[ETN-94-95337] p 2460 N94-25063

BLOOD FLOW
Image processing for acquisition of fluid rest time in the running of an artificial heart valve p 2316 N94-22858
Development of a model to assess orthostatic responses p 2427 N94-25376

BLOOD PLASMA
Fluid-loading solutions and plasma volume: Astro-ade and salt tablets with water
[NASA-TP-3456] p 2426 N94-23544

BLOOD PRESSURE
Development of a model to assess orthostatic responses p 2427 N94-25376

BLOWING
Vortex generation and wave-vortex interaction over a concave plate with roughness and suction
[NASA-CR-191589] p 2337 N94-24869

BLUNT BODIES
Stability of hypersonic flow of a detonable gas mixture in the stagnation region of a blunt body and a forward facing step p 2154 N94-24248

BODY CENTERED CUBIC LATTICES
The effects of texture and strain on the r-va lue of heavy gauge tantalum plate
[DE94-000690] p 2242 N94-23541

BODY FLUIDS
Fluid-loading solutions and plasma volume: Astro-ade and salt tablets with water
[NASA-TP-3456] p 2426 N94-23544

BODY-WING AND TAIL CONFIGURATIONS
The cetaceopteryx: A global range military transport aircraft
[NASA-CR-195519] p 2181 N94-24711
The airplane: A simulated commercial air transportation study
[NASA-CR-195525] p 2182 N94-24837

BOLTED JOINTS
Computer based expert system for battle damage repair of composite structures p 2157 N94-24262

BOLTS
Split spline screw
[NASA-CASE-GSC-13434-1] p 2352 N94-23082

BOLTZMANN TRANSPORT EQUATION
Effect of high frequency field on the transport properties of superlattice
[DE93-617047] p 2568 N94-25447

BOLTZMANN-VLASOV EQUATION
Modification in the kinetic solution for magnetized plasmas
[DE93-613687] p 2555 N94-25343

BOMBER AIRCRAFT
Birdstrike resistant crew enclosure program
[AD-A273700] p 2463 N94-25453

BOND GRAPHS
Bond graph modeling, simulation, and reflex control of the Mars planetary automatic vehicle
p 2370 N94-23424

BONDED JOINTS
Final postflight hardware evaluation report RSRM-28 (STS-53)
[NASA-CR-193902] p 2200 N94-24112
Attachment methods in composite joints - analysis of test results by controlled experiments method
p 2158 N94-24269
Evaluation of the fracture resistance and durability of adhesive bonded joints p 2160 N94-24278
Postflight hardware evaluation 360T021 (RSRM-21, STS-45), revision A
[NASA-CR-193904] p 2201 N94-24965

BONDING
Particle formation in a laser-heated aerosol reactor. Application to silicon and silicon nitride synthesis
[PB93-217982] p 2347 N94-22982

BONE DEMINERALIZATION
Loading, electromyograph, and motion during exercise
p 2427 N94-25359

BONES
Loading, electromyograph, and motion during exercise
p 2427 N94-25359

BOOLEAN ALGEBRA
Phased-mission system analysis using Boolean algebraic methods
[NASA-CR-191564] p 2451 N94-23340
Design and specification of a generic task model for solving boolean constraint satisfaction problems
[PB94-118841] p 2486 N94-23762
Structured constraint satisfaction
[PB94-119039] p 2497 N94-23764
Two applications of a generic task model for solving boolean constraint satisfaction problems
[PB94-119047] p 2487 N94-23765
Expert system rule-base evaluation using real-time parallel processing
[AD-A273701] p 2469 N94-25454

BOOLEAN FUNCTIONS
Logic synthesis on programmable networks
[ETN-94-95174] p 2449 N94-23151
Design and specification of a generic task model for solving boolean constraint satisfaction problems
[PB94-118841] p 2486 N94-23762
Two applications of a generic task model for solving boolean constraint satisfaction problems
[PB94-119047] p 2487 N94-23765
Area-power-delay trade-off in logic synthesis
[ISBN-9-09-005332-8] p 2461 N94-25080

BOOMS (EQUIPMENT)
Stiffening of deployable space booms: Automated Protein Crystal Growth Facility
[NASA-CR-195547] p 2196 N94-24820

BOOSTER ROCKET ENGINES
STE thrust chamber technology: Main injector technology program and nozzle Advanced Development Program (ADP)
[NASA-CR-193919] p 2221 N94-25019
GRYPHON: Air launched space booster
[NASA-CR-195497] p 2199 N94-25022

BOOSTER ROCKETS
Design of an airborne launch vehicle for an air launched space booster
[NASA-CR-195534] p 2198 N94-24860

BORATES
The effects of zinc borate addition on the flammability characteristics of polyester, vinyl ester, and epoxy glass reinforced plastics
[AD-A273164] p 2262 N94-25136

BOREHOLES
Decomposition of multi-component measurements into P and S waves
[ISBN-9-09-005197-X] p 2405 N94-25251

BORING MACHINES
Development/drilling test of auger boring machine on board Mars rover for Mars exploration
p 2369 N94-23402

BORON ALLOYS
Magnetic properties and transmission electron microscopy investigations of Nd-Fe-B-Co-Al melt spun ribbons
[PB93-201531] p 2561 N94-23428

BORON ISOTOPES

Synthesis and in-vivo detection of boronated compounds for use in BNCT
[DE94-001899] p 2233 N94-23780

BOSON FIELDS

The Haldane energy gap of a doped linear-chain Heisenberg antiferromagnet
[DE93-617130] p 2567 N94-25426

BOSONS

A measurement of the forward-backward asymmetry and sin(sup 2)(theta)(sub W) from the process Z(sup 0) (yields) (mu)(sup +)(mu)(sup (minus)) at (radical)s = 1.8 TeV
[DE94-001908] p 2532 N94-23018

Photon-photon collisions at the next linear collider: Theory
[DE93-041025] p 2534 N94-23803

Cosmic wake fields
[DE93-616849] p 2604 N94-25215

The determination of the branching ratios of the Z(zero) boson into heavy quarks using neural networks
[ETN-94-95381] p 2538 N94-25246

BOTTLES

Impact damage in filament wound composite bottles
p 2231 N94-24421

BOUNDARIES

High strain rate superplasticity in metals and composites
[DE94-001521] p 2229 N94-24547

Stability of premixed laminar flames in a stagnation point flow to general disturbances
[AD-A273429] p 2234 N94-24673

Nonlinear dynamics applied to atmospheric prediction
[AD-A273437] p 2404 N94-24674

BOUNDARY CONDITIONS

Coupled frequencies of a hydroelastic rectangular system
[LRT-WE-9-FB-4-1992] p 2375 N94-23196

The theoretical accuracy of Runge-Kutta time discretizations for the initial boundary value problem: A careful study of the boundary error
[NASA-CR-191561] p 2480 N94-23272

Out of plane gradients in laminated composites
[NASA-CR-194875] p 2228 N94-23566

A direct approach to finding unknown boundary conditions in steady heat conduction
p 2322 N94-23645

Convection equation modeling: A non-iterative direct matrix solution algorithm for use with SINDA
p 2323 N94-23651

An analytic study of a two-phase laminar airfoil in simulated heavy rain p 2171 N94-23661

An application of small-gap equations in sealing devices p 2325 N94-23668

Response-coefficient method for heat-conduction transients with time-dependent inputs
p 2326 N94-23671

Multigrid and cyclic reduction applied to the Helmholtz equation p 2304 N94-23676

Study of a local absorbing boundary condition for the modeling of an infinite external domain in the time-domain finite-element package FEMAXT
[PB94-111002] p 2294 N94-23728

Inverse dynamics of a rigid rod system as a simplified model of flexible beam p 2160 N94-24281

Dynamics of the atmosphere of Mars: Review of some outstanding problems p 2620 N94-24888

Modelling the Shuttle Remote Manipulator System: Another flexible model p 2371 N94-25350

Unified approach for incompressible flows
p 2342 N94-25356

BOUNDARY ELEMENT METHOD

A direct approach to finding unknown boundary conditions in steady heat conduction
p 2322 N94-23645

Unsteady three-dimensional thermal field prediction in turbine blades using nonlinear BEM
p 2325 N94-23665

A dual reciprocal boundary element formulation for viscous flows p 2325 N94-23666

BEM solution for the simulation of axisymmetric viscous sintering
[PB93-237717] p 2336 N94-24761

BOUNDARY INTEGRAL METHOD

Classical scattering theory of waves from the view point of an eigenvalue problem and application to target identification
[DE94-000472] p 2525 N94-23206

BOUNDARY LAYER CONTROL

Drag reduction at a plane wall p 2327 N94-24140

Boundary layer receptivity and control
p 2327 N94-24141

Large-eddy simulation of flow in a plane, asymmetric diffuser p 2328 N94-24147

Coherent structures over grooved surfaces
[ETN-94-95308] p 2339 N94-25291

BOUNDARY LAYER EQUATIONS

Multigrid methods for a semilinear PDE in the theory of pseudoplastic fluids p 2341 N94-23689

BOUNDARY LAYER FLOW

Measurement of kinematically unstationary separated flows p 2315 N94-22854

Fundamental and experimental studies on the catalytic combustion of methane
[PB94-112661] p 2233 N94-23736

Optimal feedback control of turbulent channel flow
p 2327 N94-24139

On the large eddy simulation of turbulent flows in complex geometry p 2329 N94-24148

An analysis for high Reynolds number inviscid/viscid interactions in cascades
[NASA-CR-4519] p 2169 N94-24606

Turbulence models and Reynolds analogy for two-dimensional supersonic compression ramp flow
[NASA-TM-106474] p 2337 N94-25119

Detailed description of two calculation programs for incompressible, steady state boundary layer flows, applied to determine the aerodynamic characteristics of NACA12 and OA312 foils at low Reynolds numbers
[ISL-N-604/92] p 2171 N94-25461

BOUNDARY LAYER SEPARATION

Evaluation of turbulence models in the PARC code for transonic diffuser flows
[NASA-TM-106391] p 2168 N94-24084

Large-eddy simulation of flow in a plane, asymmetric diffuser p 2328 N94-24147

Advanced ballistic range technology
[NASA-CR-195198] p 2165 N94-25169

BOUNDARY LAYER STABILITY

Relationship between transition and modes of instability in supersonic boundary layers
[NASA-CR-4562] p 2336 N94-24725

BOUNDARY LAYER TRANSITION

Sound radiation due to boundary layer transition
p 2332 N94-24163

Workshop on Computational Turbulence Modeling
[NASA-CP-10130] p 2333 N94-24460

Aerodynamic characteristics and pressure distributions for an executive-jet baseline airfoil section
[NASA-TM-4529] p 2169 N94-24586

Computational fluid mechanics
[NASA-CR-194765] p 2337 N94-24859

Vortex generation and wave-vortex interaction over a concave plate with roughness and suction
[NASA-CR-191589] p 2337 N94-24869

BOUNDARY LAYERS

Measurement of kinematically unstationary separated flows p 2315 N94-22854

The use of near-wall hot-wire probes for time-resolved skin-friction measurements p 2316 N94-22857

Efficiency and reliability enhancements in propulsion flowfield modeling p 2215 N94-23055

Asymptotic analysis: Working note no. 3, boundary layers
[DE94-002299] p 2318 N94-23213

Computation of turbulent flows over backward and forward-facing steps using a near-wall Reynolds stress model p 2172 N94-24145

Large eddy simulation of a boundary layer with concave streamwise curvature p 2328 N94-24146

Sound radiation due to boundary layer transition
p 2332 N94-24163

GEWEX Cloud Systems Study (GCSS)
p 2411 N94-24377

A vorticity dynamics based model for the turbulent dissipation: Model development and validation
[NASA-TM-106177] p 2336 N94-24713

Computational fluid mechanics
[NASA-CR-194765] p 2337 N94-24859

BOUNDARY VALUE PROBLEMS

A nonlinear degenerating parabolic problem from the theory of type 2 superconductors
[MEMO-1112] p 2555 N94-22730

Asymptotic analysis: Working note no. 3, boundary layers
[DE94-002299] p 2318 N94-23213

The theoretical accuracy of Runge-Kutta time discretizations for the initial boundary value problem: A careful study of the boundary error
[NASA-CR-191561] p 2480 N94-23272

Uniform convergence of multigrid V-cycle iterations for indefinite and nonsymmetric problems
p 2482 N94-23677

Wavelet multiresolution analyses adapted for the fast solution of boundary value ordinary differential equations
p 2485 N94-23691

A nonconforming multigrid method using conforming subspaces p 2485 N94-23695

Error due to the stopping of the Newton iteration in implicit linear multistep methods
[PB94-101425] p 2487 N94-23786

Energy and maximum norm estimates for nonlinear conservation laws
[NASA-CR-195091] p 2569 N94-24109

Bounds and asymptotic expansions for solutions of the free boundary problems related to sequential decision versions of a bioequivalence problem
[AD-A273551] p 2495 N94-24560

Stability analysis of anisotropic conical shells
[PB94-119054] p 2377 N94-24645

Characteristic method for one-dimensional scalar hyperbolic conservation laws with stiff source terms
[PB93-237675] p 2491 N94-24954

The state space method for integro-differential equations of convolution type with rational matrix symbols
[ETN-94-95379] p 2491 N94-25244

BRAGG ANGLE

Modifications to 8x8 dynamical theory: Polarizations redefined according to x ray diffraction convention
[DE94-001290] p 2560 N94-23187

Proposed additions to the SHADOW ray-tracing code for general-asymmetric perfect-crystal optics
[DE94-001291] p 2560 N94-23188

BRAGG CELLS

Advanced technology for a satellite multichannel demultiplexer/demodulator
[NASA-CR-194435] p 2202 N94-23631

BRAIN

Static image method for computing the electric potential due to sources in a layered sphere
[PB93-224970] p 2308 N94-23105

Electrophysiology of the rat nucleus accumbens: Local circuitry, neuromodulation and synaptic plasticity
[PB93-232254] p 2420 N94-23454

Interaction of tacrine at M(1) and M(2) cholinoceptors in guinea pig brain p 2421 N94-24294

BRAKES (FOR ARRESTING MOTION)

Electromagnetic brake/clutch device
[NASA-CASE-GSC-13502-1] p 2354 N94-23969

Studies of Shuttle orbiter arrestment system
[NASA-TP-3370] p 2177 N94-24304

BRANCHING (MATHEMATICS)

The cusp horseshoe and its bifurcations in the unfolding of an inclination-flip homoclinic orbit
[W-9307] p 2480 N94-23141

The determination of the branching ratios of the Z(zero) boson into heavy quarks using neural networks
[ETN-94-95381] p 2538 N94-25246

BRASSES

Laser soldering of Sn plated brass integrator assembly housings
[DE94-001149] p 2270 N94-23790

BRAYTON CYCLE

Utilization of recently developed codes for high power Brayton and Rankine cycle power systems
p 2222 N94-23641

BRAZIL

Human impacts on soil carbon dynamics of deep-rooted Amazonian forests
[NASA-CR-195127] p 2399 N94-24861

BRAZING

Determination of the compatibility between structural alloys and molten metals at high temperatures
[DE94-000954] p 2241 N94-23434

BREADBOARD MODELS

Gas-grain simulation experiment module conceptual design and gas-grain simulation facility breadboard development
[NASA-CR-177632] p 2598 N94-23536

Micro-gravity compatible drive (MGCD)
p 2355 N94-23988

BREATHING APPARATUS

Computer control of an electro-mechancial regulator for providing positive pressure breathing and an electronic G-valve for human +Gz research
[DCIEM-93-05] p 2437 N94-24299

BRECCIA

Whole rock major element chemistry of KREEP basalt clasts in lunar breccia 15205: Implications for the petrogenesis of volcanic KREEP basalts
p 2614 N94-24365

Major element chemistry of Apollo 14 mare basalt clasts and highland plutonic clasts from lunar breccia 14321: Comparison with neutron activation results
p 2614 N94-24366

Polytopic vector analysis in igneous petrology: Application to lunar petrogenesis p 2615 N94-24368

BREEDING (REPRODUCTION)

Generalized linear mixed models and their application in plant breeding research
[ETN-94-95335] p 2460 N94-25061

BREMSSTRAHLUNG

Low p(sub T) photon production in proton-nucleus collisions at 18 GeV/c
[DE94-001380] p 2532 N94-23007

BRIDGMAN METHOD

Two micron stimulated emission of activated insulating crystals
[REPT-94-002] p 2565 N94-25025

BRIGHTNESS

Luminance-brightness mapping: The missing decades
[ETN-94-95351] p 2428 N94-25298

BRIGHTNESS DISCRIMINATION

Luminance-brightness mapping: The missing decades
[ETN-94-95351] p 2428 N94-25298

BRIGHTNESS TEMPERATURE

Synthesis of passive microwave and radar altimeter data for estimating accumulation rates of polar snow
[NASA-CR-194864] p 2382 N94-23573

An investigation of current and future satellite and in-situ data for the remote sensing of the land surface energy balance
[NASA-CR-195138] p 2387 N94-24596

Investigation of passive atmospheric sounding using millimeter and submillimeter wavelength channels
[NASA-CR-194858] p 2404 N94-24843

BRILLOUIN EFFECT

The elastic and electromechanical properties of BaTiO3 single crystal through the ferroelectric transition
[DE94-001437] p 2557 N94-22927

BRILLOUIN ZONES

Lattice dynamics of Ba(1-x)K(x)BiO3 as studied by neutron scattering and computer simulation
[DE93-617053] p 2567 N94-25424

BRITTLE MATERIALS

Evaluation of multiaxial fracture models for technical ceramics
[ISBN-9-03-860192-1] p 2263 N94-25299

BRITTLENESS

Effects of neutron irradiation and hydrogen on ductile-brittle transition temperatures of V-Cr-Ti alloys
[DE94-001466] p 2240 N94-23009

Micromechanical failure modes in brittle matrix composites p 2255 N94-24232

BROADBAND

Broadband linearisation of high-efficiency power amplifiers p 2275 N94-22747

ACTS broadband aeronautical experiment
p 2279 N94-22771

Measurement of multipath delay profile in land mobile satellite channels p 2283 N94-22793

Propagation model for the Land Mobile Satellite channel in urban environments p 2283 N94-22796

Multi-ion, multi-event test of ion cyclotron resonance heating
[NASA-CR-194859] p 2540 N94-23495

Wide bandwidth differential amplifier
[AD-D015985] p 2303 N94-25217

BROADCASTING

Worldwide survey of direct-to-listener digital audio delivery systems development since WARC-1992
p 2273 N94-22736

ESA personal communications and digital audio broadcasting systems based on non-geostationary satellites p 2273 N94-22737

Direct broadcast satellite-radio, space-segment/receiver tradeoffs p 2273 N94-22738

Direct broadcast satellite-radio, receiver development
p 2273 N94-22739

Utilizing a TDRS satellite for direct broadcast satellite-radio propagation experiments and demonstrations p 2274 N94-22740

Aeronautical audio broadcasting via satellite
p 2274 N94-22741

The possibilities for mobile and fixed services in the 20/30 GHz frequency bands p 2276 N94-22752

Design and implementation considerations of a MSAT packet data network p 2280 N94-22778

Satellite communications systems and technology. Volume 1: Analytical chapters
[NASA-TM-109398] p 2293 N94-23627

An introduction to digital modulation and OFDM techniques
[BBC-RD-1993/10] p 2295 N94-24086

BROKEN SYMMETRY

On spontaneous symmetry breaking mechanism in light-front quantized field theory
[DE93-633211] p 2568 N94-22968

Flavor changing strings and domain walls
[DE93-633217] p 2532 N94-22970

Defects in electro-optically active polymer solids
p 2223 N94-24342

Cosmic wake fields
[DE93-616849] p 2604 N94-25215

Phase structure of the two-dimensional phi(4) field theory within thermo-field dynamics
[DE93-616850] p 2570 N94-25337

Superconducting cosmic strings near the electroweak scale and cosmic-ray propagation
[MPI-PHE/93-05] p 2629 N94-25459

BROMIDES

Metal-catalyzed alkynylation of brominated polyphenylenes: Thermoset precursors of high density monolithic glassy carbon
[AD-A273232] p 2259 N94-24789

Adsorption, desorption, and decomposition of HCl and HBr on Ge(100): Competitive pairingand near-first-order desorption kinetics
[AD-A273504] p 2235 N94-24790

Metal-catalyzed alkynylation of (Bromophenyl)Oligophenylenes: A rapid route to thermoset precursors of high density monolithic glass-like carbon
[AD-A273219] p 2260 N94-24863

BROMINATION

A method to remove intercalates from bromine and iodine intercalated carbon fibers
[NASA-TM-106443] p 2222 N94-23591

Metal-catalyzed alkynylation of brominated polyphenylenes: Thermoset precursors of high density monolithic glassy carbon
[AD-A273232] p 2259 N94-24789

BRONCHI

Chronic obstructive pulmonary disease
p 2425 N94-23324

Asthma in aircrew p 2425 N94-23327

BROWNIAN MOVEMENTS

Bounds and asymptotic expansions for solutions of the free boundary problems related to sequential decision versions of a bioequivalence problem
[AD-A273551] p 2495 N94-24560

BRUSH SEALS

Brush seals for cryogenic applications
p 2216 N94-23063

BSCCO SUPERCONDUCTORS

Heavy ion irradiation of Bi-2223 silver-clad tapes for superconducting current density enhancement
[DE93-017416] p 2556 N94-22886

Thermomechanical processing of Ag-clad Bi2Sr2CaCu2O(x) superconductors
[DE94-002347] p 2563 N94-24624

BUCKLING

Shell buckling research at Delft, 1976 - 1992
[PB93-224442] p 2375 N94-23221

Review of a variational method applied to magnetoelastic buckling problems
[PB94-111184] p 2562 N94-23769

Post buckling behaviour of stiffened composite panels loaded in cyclic compression and shear
p 2157 N94-24260

Global dynamic stability of a shallow arch by poincare-like simple cell mapping p 2160 N94-24280

Structural design criteria for filament-wound composite shells
[NASA-CR-195125] p 2229 N94-24402

Stability analysis of anisotropic conical shells
[PB94-119054] p 2377 N94-24645

Buckling of circular cylindrical shells subjected to combined loads (axial compression, normal pressure, bending and transverse shear loading)
[PB93-215358] p 2378 N94-24745

BUDGETING

Proceedings of the NIST Conference on Reducing the Cost of Space Infrastructure and Operations: Part 1: Oral presentations and discussion
[PB94-111374] p 2194 N94-23770

Strategies in transition p 2498 N94-23833

Toward lowering the cost of mission operations
p 2519 N94-23960

New mission requirements methodologies for services provided by the Office of Space Communications
p 2519 N94-23961

BUFFER STORAGE

Loss probabilities in batch-arrival bulk-service queues with finite capacity
[MEMO-1106] p 2493 N94-22724

Fast simulation of packet loss rates in a shared buffer communications switch
[NASA-CR-191556] p 2457 N94-24638

BUILDINGS

A prediction model of signal degradation in LMSS for urban areas p 2284 N94-22797

Zone fire modeling with natural building flows and a zero order shaft model
[PB94-112166] p 2270 N94-23735

Active control of buildings during earthquakes
[NASA-TM-109033] p 2271 N94-24473

Collaborating with our customers: NIST building and fire research laboratory
[PB94-110194] p 2272 N94-24955

Wind climate and urban geometry
[ISBN-9-03-860132-8] p 2416 N94-25261

BUOYANCY

Survival suit for submarine personnel: Summary of evaluation studies
[PB93-204634] p 2430 N94-23743

BURAN SPACE SHUTTLE

Liquid rocket propulsion: Retrospective and prospects
p 2154 N94-24243

BURNERS

Characterization and durability testing of plasma-sprayed zirconia-yttria and hafnia-yttria thermal barrier coatings. Part 2: Effect of spray parameters on the performance of several hafnia-yttria and zirconia-yttria coatings
[NASA-TP-3296] p 2242 N94-23467

BURNING RATE

Theory and computation of optimal low- and medium-thrust transfers
[NASA-CR-194812] p 2217 N94-23275

Calculation of flame spread on lining materials by the field model KAMELEON. Project 5 of the EUREFIC fire research programme
[PB93-201614] p 2268 N94-23450

Burning rate of double-base propellant in the presence of plasma p 2155 N94-24252

Solid rocket combustion simulator technology using the hybrid rocket for simulation
[NASA-CR-195142] p 2265 N94-24578

Influence of test configuration on the combustion characteristics of polymers as ignition sources
p 2238 N94-25365

BURNOUT

Reburning rich-lean kinetics
[PB93-220887] p 2232 N94-23100

Modal test of the Brazilian satellite launcher (VLS) configuration burn-out of the first stage
p 2156 N94-24257

BUSHINGS

The development of the SOHO SUMER mechanisms
p 2361 N94-24028

BUTADIENE

Particle nucleation and growth in butadiene emulsion polymerization
[ETN-94-95300] p 2262 N94-25236

BY-PRODUCTS

Reduction of hydrocarbon impurities in 200 l/h helium liquefier-refrigerator system
[NIFS-259] p 2271 N94-24459

C

C (PROGRAMMING LANGUAGE)

Horatio: Libraries for vision applications, release 2.0
[OUEL-1967/92] p 2593 N94-25326

C BAND

Precipitation measurement using SIR-C: A feasibility study. Investigation at nadir
[NASA-CR-195103] p 2410 N94-24126

C++ (PROGRAMMING LANGUAGE)

An object-oriented approach for parallel self adaptive mesh refinement on block structured grids
p 2469 N94-23697

CADMIUM

Integrated hydrometallurgical jarosite treatment
[PB93-217990] p 2232 N94-22983

CADMIUM COMPOUNDS

Photoinduced charge separation in solid state and molecular systems
[DE94-001727] p 2563 N94-24537

CADMIUM TELLURIDES

Magnetic resonance studies of 3d transition metal impurities in compound semiconductors
[PB93-232197] p 2243 N94-23714

Thin film cadmium telluride photovoltaic cells
[DE94-000201] p 2395 N94-24509

CALCIUM TUNGSTATES

Contribution of all excited states to ZFS of a (sup 6) S-state
[DE93-617007] p 2568 N94-25483

CALCULUS

Simple calculus of finite probabilistic processes
[PB93-223782] p 2493 N94-23108

Relational algebra and equational proofs
[PB94-110822] p 2486 N94-23724

Sequential composition, action prefixes and process prefix
[PB94-101433] p 2488 N94-24539

Combinatory reduction systems: Introduction and survey
[PB94-110582] p 2457 N94-24570

A type-theoretic approach to higher-order modules with sharing
[AD-A273566] p 2458 N94-24693

CALIBRATING

Eye-gaze control of the computer interface: Discrimination of zoom intent
[DE94-000480] p 2429 N94-22997

FTIR quantification of industrial hydraulic fluids in perchloroethylene p 2264 N94-23243

Calibration of HYPULSE for hypervelocity air flows corresponding to flight Mach numbers 13.5, 15, and 17 [NASA-CR-191578] p 2192 N94-23564

The Fifth Calibration/Data Product Validation Panel Meeting [NASA-TM-108270] p 2383 N94-23595

Cross-calibration survey (VISNIR) p 2383 N94-23599

MODIS calibration p 2383 N94-23600

Flight solar calibrations using the Mirror Attenuator Mosaic (MAM): Low scattering mirror p 2384 N94-23602

Activities of NIST (National Inst. of Standards and Technology) p 2384 N94-23605

Calibration of a helium-cooled infrared spatial radiometer and grating spectrometer p 2384 N94-23607

Infrared calibration p 2384 N94-23608

Concept of ASTER calibration requirement p 2384 N94-23609

VNIR and SWIR transfer radiometers developed at NRLM for preflight laboratory cross-calibration p 2385 N94-23610

In-flight cross-calibration of ASTER/TIR and MODIS-N p 2385 N94-23611

ASTER TIR subsystem and calibration p 2385 N94-23612

Calibration block for digital beam forming antenna [PB93-204550] p 2294 N94-23773

Digital test signal generation: An accurate SNR calibration approach for the DSN p 2305 N94-23912

Doppler global velocimetry: Development of a flight research instrumentation system for application to non-intrusive measurements of the flow field [NASA-CR-191490] p 2344 N94-24360

Improved pressure measurement system for calibration of the NASA LeRC 10x10 supersonic wind tunnel [NASA-TM-106470] p 2344 N94-24362

The 1404+286: A non-ideal calibrator for VLBI observations [PB94-104908] p 2599 N94-24521

Calibration network intended for phase-array antennas at 3 GHz [PB93-204352] p 2297 N94-24530

Results of the 1993 NASA/JPL balloon flight solar cell calibration program [NASA-CR-195158] p 2395 N94-24563

Hubble Space Telescope high speed photometer science verification test report [NASA-CR-189322] p 2205 N94-24710

Analysis of SOFCAL calibration data [NASA-CR-193910] p 2345 N94-25000

Active camera calibration for a head-eye platform using a variable state dimension filter [OUEL-1975/93] p 2346 N94-25472

CALIFORNIUM

A survey of metallurgical research on several actinides [DE94-002643] p 2245 N94-24747

CALORIMETERS

Fire safety engineering research in Norway [PB93-201630] p 2268 N94-23429

Calculation of flame spread on lining materials by the field model KAMELEON. Project 5 of the EUREFIC fire research programme [PB93-201614] p 2268 N94-23450

Analysis of SOFCAL calibration data [NASA-CR-193910] p 2345 N94-25000

CAMERAS

Stereo for gazing and converging cameras. Part 1: Basic geometry [OUEL-1915/92] p 2343 N94-23162

Speech versus manual control of camera functions during a telerobotic task p 2436 N94-24199

The effects of spatially displaced visual feedback on remote manipulator performance p 2436 N94-24201

Preliminary design of a satellite observation system for Space Station Freedom [NASA-CR-195514] p 2209 N94-24840

Active camera calibration for a head-eye platform using a variable state dimension filter [OUEL-1975/93] p 2346 N94-25472

Simulation of a passive millimeter wave sensor p 2346 N94-25499

Multiple-camera/motion stereoscopy for range estimation in helicopter flight p 2441 N94-25505

A model-based approach for detection of objects in low resolution passive-millimeter wave images p 2442 N94-25507

CAMOUFLAGE

Experimental evaluation of camouflage effectiveness in the thermal infrared [FEL-93-A043] p 2381 N94-22896

CANARD CONFIGURATIONS

Dumbo heavy lifter aircraft [NASA-CR-195500] p 2182 N94-24915

The AC-120: The advanced commercial transport [NASA-CR-195491] p 2182 N94-24966

CANCER

Annual research progress report, fiscal year 1992. Volume 2: Department of Clinical Investigation [AD-A273584] p 2427 N94-24945

CANONICAL FORMS

Infinite divisible and stable distributions modulo 1 [PB94-110640] p 2495 N94-23815

Wiener-Hopf factorization of rational matrix functions in terms of realizations: An alternative version [ETN-94-95380] p 2491 N94-25245

CAPACITANCE

Calibration network intended for phase-array antennas at 3 GHz [PB93-204352] p 2297 N94-24530

Carbon supercapacitors [DE94-002652] p 2311 N94-24748

CAPACITORS

Limiting factors for carbon based chemical double layer capacitors p 2394 N94-23365

Carbon supercapacitors [DE94-002652] p 2311 N94-24748

MOS analog memory with injection capacitors [AD-D015990] p 2312 N94-25050

CAPE KENNEDY LAUNCH COMPLEX

A prototype expert/information system for examining environmental risks of KSC activities p 2400 N94-23237

CAPILLARY FLOW

Interpretation of discrepancies in mass spectroscopy data obtained from different experimental configurations p 2237 N94-23245

Mathematical addenda to Hopper's model of plane stokes flow driven by capillarity on a free surface [PB93-237691] p 2480 N94-23438

Capillary electrokinetic separations with optical detection [DE94-001639] p 2233 N94-23716

Effect of longitudinal vibration on the capillary limit of a wrapped screen wick copper/water heat pipe [AD-A273830] p 2571 N94-25524

CAPILLARY TUBES

Transient studies of capillary-induced flow p 2325 N94-23662

Electrophoresis in open capillaries: Some fundamental aspects [ETN-94-95290] p 2236 N94-25232

Capillary electrophoresis of biomolecules: Theory, instrumentation and applications [ETN-94-95297] p 2236 N94-25233

CARBIDES

Characterization of the microstructure of Nb-1wt.%Zr-0.1wt.%C tubes as affected by thermomechanical processing [NASA-TM-106381] p 2242 N94-23550

CARBOHYDRATE METABOLISM

Skeletal muscle metabolism in hypokinetic rats [NASA-CR-195082] p 2420 N94-24124

CARBON

Carbon aerogels: An update on structure, properties, and applications [DE94-001528] p 2252 N94-22931

Limiting factors for carbon based chemical double layer capacitors p 2394 N94-23365

Hairy carbon electrodes studied by cyclic voltammetry and battery discharge testing p 2394 N94-23367

Theoretical considerations for Reaction-Formed Silicon Carbide (RFSC) formation by molten silicon infiltration into slurry-derived preforms [NASA-TM-106414] p 2222 N94-23500

Wear reduction in ceramic bearings by surface generated pyrolytic carbon continuously replenished by ethylene gas [NASA-CR-189214] p 2364 N94-24090

Carbon supercapacitors [DE94-002652] p 2311 N94-24748

CARBON ARCS

A review of wiring system safety in space power systems [NASA-CR-194439] p 2203 N94-23632

CARBON COMPOUNDS

New tribocoating combination for vacuum operation p 2355 N94-23990

Laboratory detection of C5S by pulsed-discharge-nozzle Fourier-transform microwave spectroscopy [JTN-94-80519] p 2235 N94-24984

CARBON CYCLE

Effect of land use change on the carbon cycle in Amazon soils [NASA-CR-195168] p 2399 N94-24853

Human impacts on soil carbon dynamics of deep-rooted Amazonian forests [NASA-CR-195127] p 2399 N94-24861

CARBON DIOXIDE

Feasibility study on a CO2 global recycling system using natural energy [DE94-714889] p 2397 N94-23026

Performance of the Carbon Dioxide Information Analysis Center (CDIAC) [DE94-002190] p 2397 N94-23794

Radiative properties of molecular nitrogen ions produced by helium Penning ionization and argon effects [NASA-CR-195126] p 2534 N94-24487

Effect of land use change on the carbon cycle in Amazon soils [NASA-CR-195168] p 2399 N94-24853

Cloud, dust, and ozone vertical profiles from solar occultation measurements: Implications for dynamics p 2617 N94-24877

Impact of the CO2 and H2O clouds of the Martian polar hood on the polar energy balance p 2618 N94-24880

The annual pressure cycle on Mars: Results from the LMD Martian atmospheric general circulation model p 2619 N94-24884

The role of atmospheric heat transport in the seasonal carbon dioxide cycle p 2621 N94-24896

CARBON DIOXIDE LASERS

Remote vibration measurements at a sud aviation alouette 3 helicopter with a CW CO2-laser system [AD-A273818] p 2190 N94-25516

CARBON FIBER REINFORCED PLASTICS

The use of expanding monomers in carbon fibre composites [ISBN-0-315-83550-8] p 2226 N94-22890

Optimization of laminate orientation to enhance failure properties [ISBN-0-315-83539-7] p 2227 N94-22892

Preparing polymeric matrix composites using an aqueous slurry technique [NASA-CASE-LAR-14771-1] p 2252 N94-23076

Intelligent Material Systems and Structures (IMSS). Part 5: Fiber optic registration of deformation in carbon laminates 91/92 [PB93-204600] p 2544 N94-23723

CARBON FIBERS

A method to remove intercalates from bromine and iodine intercalated carbon fibers [NASA-TM-106443] p 2222 N94-23591

CARBON ISOTOPES

Carbon and hydrogen isotope composition and C-14 concentration in methane from sources and from the atmosphere: Implications for a global methane budget [NASA-CR-195166] p 2399 N94-25092

CARBON MONOXIDE

High-resolution soft x ray photoionization studies of selected molecules [DE94-000568] p 2532 N94-23002

Reburning rich-lean kinetics [PB93-220887] p 2232 N94-23100

Carbon monoxide fuel cells as a source for Mars rover electric power p 2314 N94-23409

Evaluation of reducing gas turbine emissions through hydrogen-enhanced steam-injected combustion [PB94-109873] p 2187 N94-23709

CO-to-H2 conversion factor in dwarf irregular galaxies [REPT-333] p 2603 N94-24985

High spatial resolution observations of CO in CRL 618 [REPT-334] p 2604 N94-24986

CARBON TETRACHLORIDE

Thermoelectric cooled, purge-and-trap device for enhancing the utility of fiber optic VOC sensors [DE94-001772] p 2541 N94-22722

CARBON 13

Effect of land use change on the carbon cycle in Amazon soils [NASA-CR-195168] p 2399 N94-24853

CARBON 14

Effect of land use change on the carbon cycle in Amazon soils [NASA-CR-195168] p 2399 N94-24853

Carbon and hydrogen isotope composition and C-14 concentration in methane from sources and from the atmosphere: Implications for a global methane budget [NASA-CR-195166] p 2399 N94-25092

Manual on measurement of methane and nitrous oxide emissions from agriculture [DE93-616429] p 2399 N94-25167

CARBON-PHENOLIC COMPOSITES

Micromechanical simulation of damage progression in carbon phenolic composites p 2231 N94-24446

Properties and processing characteristics of low density carbon cloth phenolic composites p 2231 N94-24450

CARBONACEOUS CHONDRITES

Correlated petrographic, electron microprobe, and ion microprobe studies of selected primitive and processed phase assemblages in meteorites [NASA-CR-194827] p 2601 N94-23499

CARBONATES

Advanced research and technology development of MCFCs [DE94-001918] p 2389 N94-22723

Overview of molten carbonate fuel cell technology development
[DE94-001911] p 2394 N94-23781

CARBORANE
Synthesis and in-vivo detection of boronated compounds for use in BNCT
[DE94-001899] p 2233 N94-23780

CARBOXYLIC ACIDS
Reaction of isocyanates with carboxylic acids and its application to polymer synthesis
[PB94-118858] p 2254 N94-23763

CARDIAC OUTPUT
Responses to LBNP in men with varying profiles of strength and aerobic capacity: Implications for flight crews
[NASA-TP-3346] p 2426 N94-23530

CARDIAC VENTRICLES
Echocardiographic findings in trained aircrew: The effect of +Gz on cardiac structure (working group 18)
p 2424 N94-23320
Left ventricular hypertrophy and athlete's heart
p 2424 N94-23321

CARDIOLOGY
Cardiovascular and pulmonary disease in NATO aircrew: An overview p 2423 N94-23314
Screening for asymptomatic coronary heart disease
p 2423 N94-23315
Left ventricular hypertrophy and athlete's heart
p 2424 N94-23321

CARDIOVASCULAR SYSTEM
Cardiovascular and pulmonary disease in NATO aircrew: An overview p 2423 N94-23314
Sarcoidosis and the aviator p 2425 N94-23325
Arterial hypertension and the aviator
p 2425 N94-23328
Responses to LBNP in men with varying profiles of strength and aerobic capacity: Implications for flight crews
[NASA-TP-3346] p 2426 N94-23530
Autogenic-feedback training: A potential treatment for post-flight orthostatic intolerance in aerospace crews
[NASA-TM-108785] p 2426 N94-24102
Development of a model to assess orthostatic responses p 2427 N94-25376

CARGO AIRCRAFT
Conceptual design proposal: HUGO global range/mobility transport aircraft
[NASA-CR-195501] p 2181 N94-24787
Dumbo heavy lifter aircraft
[NASA-CR-195500] p 2182 N94-24915
A global range military transport: The ostrich
[NASA-CR-195494] p 2183 N94-24972

CARRIER DENSITY (SOLID STATE)
Transparent conducting thin films for spacecraft applications
[NASA-TM-106466] p 2218 N94-23370

CARRIER FREQUENCIES
Estimation of frequency offset in mobile satellite modems p 2285 N94-22807
Theoretical and simulated performance for a novel frequency estimation technique p 2285 N94-22808
A pattern jitter free AFC scheme for mobile satellite systems p 2285 N94-22809
Dual frequency optical carrier technique for transmission of reference frequencies in dispersive media
[NASA-CASE-NPO-18007-2-CU] p 2543 N94-23270

CARRIER MOBILITY
Large-scale production of Si(0.8)Ge(0.2) thermoelectric alloys by mechanical alloying
[DE94-000695] p 2243 N94-23753

CARRIER TO NOISE RATIOS
Analysis of open-loop conical scan pointing error and variance estimators p 2291 N94-23263

CARTESIAN COORDINATES
A mixed method Poisson solver for three-dimensional self-gravitating astrophysical fluid dynamical systems
p 2484 N94-23684
Finite-element method for computing three-dimensional electromagnetic fields in inhomogeneous media (1993)
[PB94-111101] p 2298 N94-24637

CARTS
Preliminary results on time-varying feedback stabilization of a nonholonomic car-like mobile robot
[INRIA-RR-1512] p 2475 N94-24963

CASCADE FLOW
Two-dimensional Navier-Stokes computations of subsonic and supersonic flows through turbine cascades
[PB93-226223] p 2317 N94-23114
Analysis of the effects of wake passage on heat transfer in a linear turbine cascade
[AD-A273729] p 2339 N94-25446

CASSINI MISSION
GPHS-RTG's in support of the Cassini mission
[DE94-001445] p 2218 N94-23459
Development of the Cassini Ground Data System in a multimission environment p 2500 N94-23845
Distributed science operations for JPL planetary missions p 2500 N94-23850
Science planning and sequencing for Cassini
p 2504 N94-23871

CASTING
Materials Science and Engineering
[DE94-003018] p 2228 N94-23493
The importance of properties in modeling
p 2246 N94-25121

CATALOGS (PUBLICATIONS)
Catalog of data bases and reports
[DE93-040597] p 2588 N94-22875
Catalog of Apollo experiment operations
[NASA-RP-1317] p 2194 N94-23292
Satellite situation report, volume 33, number 4
[NASA-TM-109677] p 2205 N94-24824

CATALYSIS
Advances in direct oxidation methanol fuel cells
p 2393 N94-23361
Fundamental and experimental studies on the catalytic combustion of methane
[PB94-112661] p 2233 N94-23736
Reaction of isocyanates with carboxylic acids and its application to polymer synthesis
[PB94-118858] p 2254 N94-23763
Metal-catalyzed alkynylation of (Bromophenyl)Oligophenylenes: A rapid route to thermoset precursors of high density monolithic glass-like carbon
[AD-A273219] p 2260 N94-24863
Design of novel catalysts for the partial oxidation of methane to methanol
[PB94-114212] p 2235 N94-24920

CATALYSTS
Composite fiber structures for catalysts and electrodes
p 2393 N94-23364
Hairy carbon electrodes studied by cyclic voltammetry and battery discharge testing p 2394 N94-23367
Development of durable high-temperature catalysts for natural gas combustion
[PB93-226447] p 2232 N94-23477
Reduction of nitric oxide over platinum, rhodium and platinum-rhodium single crystal surfaces
[PB93-230092] p 2232 N94-23482
New methane chemistry synthesis of materials for reversible uptake and useful functionalization of methane
[PB94-112786] p 2233 N94-23801
Fundamental study of NO(x) control in catalytic combustion
[PB94-112323] p 2398 N94-23818
Metal-catalyzed alkynylation of brominated polyphenylenes: Thermoset precursors of high density monolithic glassy carbon
[AD-A273232] p 2259 N94-24789
Design of novel catalysts for the partial oxidation of methane to methanol
[PB94-114212] p 2235 N94-24920
Dispersion of Rh/Cu in a sol-gel matrix. Highly chemo- and stereoselective catalyst for the reduction of alkynes to Z-alkenes
[AD-A273306] p 2262 N94-25145
The structure and catalytic properties of supported platinum catalysts
[ETN-94-95357] p 2236 N94-25250

CATALYTIC ACTIVITY
Fundamental study of NO(x) control in catalytic combustion
[PB94-112323] p 2398 N94-23818
The structure and catalytic properties of supported platinum catalysts
[ETN-94-95357] p 2236 N94-25250

CATASTROPHE THEORY
The Hamiltonian double-zero eigenvalue
[W-9304] p 2479 N94-23138

CATHODES
Novel two-stage selenization methods for fabrication of thin-film CIS cells and submodules
[DE94-000220] p 2390 N94-23296
A high performance H2-Cl2 fuel cell for space power applications p 2394 N94-23366
Power console development for NASA's electric propulsion outreach program
[NASA-TM-106428] p 2218 N94-23372
Arc electrode interaction study
[NASA-CR-195096] p 2310 N94-24070
In situ and ex situ spectroelectrochemical and x ray absorption studies on rechargeable, chemically-modified and other MnO2 materials
[DE94-001387] p 2234 N94-24545

CATHODIC COATINGS
Arc electrode interaction study
[NASA-CR-195096] p 2310 N94-24070
Proceedings of the 12th International Congress: Corrosion Control for Low-Cost Reliability. Volume 4: Oil/Gas Pipeline
[AD-A273665] p 2250 N94-25405
Proceedings of the 12th International Congress: Corrosion Control for Low-Cost Reliability. Volume 5A: Corrosion: General issues
[AD-A273666] p 2250 N94-25406

CATIONS
Effects of ionizing radiation on modern ion exchange materials
[DE94-001569] p 2535 N94-24505
Free energy profiles for Li(+) and I(-) ions approaching Pt(100) surface: A molecular dynamics study
[AD-A273455] p 2536 N94-24675
Electrochemical and electronic properties of neural and oxidized soluble orthogonally-fused thiophene oligomers
[AD-A273283] p 2260 N94-24815

CAUCHY PROBLEM
Periodic nonlinear Schroedinger equation and invariant measures
[PB93-238012] p 2487 N94-23775
Cauchy problem for periodic KDV-type equations
[PB93-238020] p 2487 N94-23776
A numerical investigation of the artificial compressibility method for the solution of the Navier-Stokes equations
[CRANFIELD-AERO-9213] p 2340 N94-25486

CAUCHY-RIEMANN EQUATIONS
Extension problem for generalized multi-monogenic functions in Clifford analysis
[DE93-616818] p 2493 N94-25433

CAVITATION FLOW
Computational fluid dynamic modelling of cavitation
p 2215 N94-23060
Hydro-elastic analysis using a selection of commercial analysis programs
[PB94-118734] p 2376 N94-24478

CAVITIES
Spontaneous pneumothorax, cysts and bullae
p 2425 N94-23326
Experimental cavity pressure measurements at subsonic and transonic speeds. Static-pressure results
[NASA-TP-3358] p 2169 N94-24464

CAVITY RESONATORS
Optimization of energy transfer in microwave electrothermal thrusters p 2216 N94-23065
CFD modeling of microwave electrothermal thrusters
p 2216 N94-23066
An active antenna for ELF magnetic fields
p 2303 N94-25192

CELESTIAL MECHANICS
Comparison of time integration methods for the evolution of galaxies
[PB94-111671] p 2602 N94-24522

CELL CATHODES
Advanced research and technology development of MCFCs
[DE94-001918] p 2389 N94-22723
Overcharge and overdischarge protection of ambient temperature secondary lithium cells
[NASA-CASE-NPO-18343-1-CU] p 2310 N94-23823

CELLS (BIOLOGY)
Cellular and tissue injury during nonfreezing cold injury and frostbite
[AD-A270883] p 2423 N94-22732
Measuring the dynamics of structural changes in biological macromolecules from light scattering data
p 2422 N94-24426
Photonic technology for implementation of generalizable neural networks: A synthetic approach
[AD-A273497] p 2474 N94-24622
An exploratory stochastic model for toxic effects on cells
[AD-A273438] p 2422 N94-25146
Non-invasive optical detection of glucose in cell culture nutrient medium p 2422 N94-25357
Design and testing of a unique randomized gravity, continuous flow bioreactor p 2423 N94-25368

CELLULOSE
Composite fiber structures for catalysts and electrodes
p 2393 N94-23364

CEMENTS
Alternatives for reinforcement: Fiber composites
[VTT-TIED-1412] p 2230 N94-25386

CENTAUR LAUNCH VEHICLE
Liquid rocket propulsion: Retrospective and prospects
p 2154 N94-24243

CENTER OF GRAVITY
Mass properties measurement system dynamics
p 2368 N94-23235
Mass properties measurement system: Dynamics and statics measurements p 2368 N94-23236

CENTER OF MASS
Mass properties measurement system dynamics
p 2368 N94-23235

CENTRAL NERVOUS SYSTEM
A statistical analysis of recent Naval Experimental Diving Unit (NEDU) single-depth human exposures to 100 percent oxygen at pressure
[AD-A273488] p 2427 N94-24950

CENTRAL PROCESSING UNITS
ATOS-1: Designing the infrastructure for an advanced spacecraft operations system p 2197 N94-23849
Transputer benchmarks and performance comparisons with other computing machines
[RR-467] p 2446 N94-25312

CENTRIFUGAL COMPRESSORS
Gas turbine and operating method of the same
[CA-PATENT-APPL-SN-2043039] p 2188 N94-24490

CERAMIC COATINGS
Fire-resistant barriers for composite materials
[AD-D016014] p 2230 N94-24735
An x ray diffraction investigation of alpha-Al2O2 addition to Yttria Stabilized Zirconia (YSZ) thermal barrier coatings subject to destabilizing vanadium pentoxide (V2O5) exposure
[AD-A273403] p 2261 N94-25072
Plasma sprayed thermal barrier coatings: Production, characterization and testing
[ISBN-9-03-860082-8] p 2555 N94-25439

CERAMIC FIBERS
Development of silicon nitride composites with continuous fiber reinforcement
[DE94-001996] p 2227 N94-23022
Ceramic silicon-boron-carbon fibers from organic silicon-boron-polymers
[NASA-CASE-ARC-11956-1-SB] p 2253 N94-23311
An overview on the main available ceramic composites and their processing routes p 2255 N94-24229

CERAMIC MATRIX COMPOSITES
A numerical analysis of crack propagation in microcracking ceramic and ceramic composites
[DE94-001192] p 2253 N94-23183
Engine materials characterization and damage monitoring by using x ray technologies
[NASA-TP-3328] p 2372 N94-24074
Glass-ceramic Li-Al-Si-O composition and process for its production
[CA-PATENT-APPL-SN-2043757] p 2254 N94-24129
Introduction of Ceramics into Aerospace Structural Composites
[AGARD-R-795] p 2255 N94-24228
An overview on the main available ceramic composites and their processing routes p 2255 N94-24229
Ceramic matrix composites: Challenges and opportunities p 2255 N94-24230
Interface evaluation in ceramic composites
p 2255 N94-24231
Micromechanical failure modes in brittle matrix composites p 2255 N94-24232
Micromechanical characterization of ceramic-matrix composites using the instrumented microindentation technique p 2256 N94-24233
Role of interfaces on the cyclic fatigue behaviour of ceramic matrix composites p 2256 N94-24234
Mechanical behavior of CMCs: Crack growth resistance and creep aspects p 2256 N94-24235
Microstructure and micromechanical behaviour of CMCs p 2256 N94-24236
Ceramic matrix composite parts design
p 2256 N94-24237
CMC design consequences p 2256 N94-24238
Integrated approach in modelling, testing, and design of gradient-CVI derived CMC components
p 2256 N94-24239
Ultrasonic nondestructive evaluation as a tool for the development of aerospace structural ceramic composites p 2257 N94-24240
The effects of anisotropy on the nonlinear behavior of bridged cracks in long strips
[NASA-CR-194453] p 2377 N94-24604
Nanodesigning of hierarchical multifunctional ceramics
[AD-A273466] p 2257 N94-24677

CERAMICS
Gas-pressure forming of superplastic ceramic sheet
[DE94-001520] p 2252 N94-22930
Particle formation in a laser-heated aerosol reactor. Application to silicon and silicon nitride synthesis
[PB93-217982] p 2347 N94-22982
A numerical analysis of crack propagation in microcracking ceramic and ceramic composites
[DE94-001192] p 2253 N94-23183
Development of small punch testing technique and its application to evaluation of mechanical properties degradation
[DE94-001193] p 2375 N94-23184
Theoretical considerations for Reaction-Formed Silicon Carbide (RFSC) formation by molten silicon infiltration into slurry-derived preforms
[NASA-TM-106414] p 2222 N94-23500
Combustion synthesis and engineering of nanoparticles for electronic, structural and superconductor applications
[DE94-001865] p 2254 N94-23720
Development of a theory of the wear of ceramics
[DE94-002773] p 2254 N94-23783
Metal-mullite reactions
[DE94-002038] p 2244 N94-23811
The tribology of some MoS2-lubricated engineering ceramics p 2356 N94-23993
Wear reduction in ceramic bearings by surface generated pyrolytic carbon continuously replenished by ethylene gas
[NASA-CR-189214] p 2364 N94-24090
Introduction of Ceramics into Aerospace Structural Composites
[AGARD-R-795] p 2255 N94-24228
Integrated approach in modelling, testing, and design of gradient-CVI derived CMC components
p 2256 N94-24239
Superconducting energy storage
[DE94-002248] p 2395 N94-24654
Nanodesigning of hierarchical multifunctional ceramics
[AD-A273466] p 2257 N94-24677
Durability evaluation of ceramic components using CARES/LIFE
[NASA-TM-106475] p 2258 N94-24682
Ferroelectric thin films 3
[AD-A273394] p 2565 N94-25027
Conformal method of fabricating and optical waveguide on a semiconductor substrate
[AD-D015988] p 2546 N94-25043
Nuclear magnetic resonance imaging with short gradient pulses
[AD-D016006] p 2537 N94-25047
An x ray diffraction investigation of alpha-Al2O2 addition to Yttria Stabilized Zirconia (YSZ) thermal barrier coatings subject to destabilizing vanadium pentoxide (V2O5) exposure
[AD-A273403] p 2261 N94-25072
Preparation and properties of translucent gamma-aluminium oxynitride
[ETN-94-95305] p 2263 N94-25281
Evaluation of multiaxial fracture models for technical ceramics
[ISBN-9-03-860192-1] p 2263 N94-25299
Critical currents in YBaCuO-ceramics
[DE93-617140] p 2263 N94-25404
The complete stress field due to a dislocation located anywhere in two bonded quarter planes
[OUEL-1990/93] p 2379 N94-25478
The pressure loaded volumetric ceramic receiver 500 kW version design and construction
[DLR-MITT-93-02] p 2396 N94-25479

CEREBRAL CORTEX
Customizable VLSI artificial neural network chips based on a novel technology
[DE94-001418] p 2307 N94-23008

CERIUM
Spin-hole doping in the Kondo insulator Ce3Bi4Pt3 studied by neutron scattering
[DE93-040107] p 2557 N94-22925

CERIUM COMPOUNDS
Electronic structure and high pressure phase transition in LaSb and CeSb
[DE93-617051] p 2567 N94-25423

CERIUM OXIDES
Anomalous magnetoresistance behavior of superconducting Nd(2-x)Ce(x)CuO(4-y) single crystal
[DE94-000806] p 2558 N94-22941

CERMETS
Low-gravity electrodeposition and growth of polymer thin films with large third-order optical nonlinearities by electrochemical processes for devices: Thiophene-based polymers p 2225 N94-24346

CERTIFICATION
Formal methods and digital systems validation for airborne systems
[NASA-CR-4551] p 2466 N94-23293
Aircraft evacuation testing: Research and technology issues
[PB94-107620] p 2173 N94-24750
Pilot-vehicle interface handbook, chapter 19. Volume 2: Digital systems validation
[DOT/FAA/CT-88/10-VOL-2] p 2438 N94-24830

CESIUM IODIDES
CsI(Tl)-photodiode detectors for spectroscopy at low radiation levels
[MPI-PHE/92-22] p 2314 N94-25457

CHAINS
Algorithm on addition chains with restricted memory
[PB94-118692] p 2454 N94-23759

CHANGE DETECTION
VLSI-based video event triggering for image data compression
[NASA-TM-106500] p 2345 N94-25116

CHANNEL FLOW
Turbulent separated flows above an obstacle in an open channel p 2316 N94-22859
Flow visualization study in high aspect ratio cooling channels for rocket engines p 2213 N94-23049
CFD analyses of coolant channel flowfields
p 2214 N94-23050
Optimal feedback control of turbulent channel flow
p 2327 N94-24139
Large eddy simulation of a boundary layer with concave streamwise curvature p 2328 N94-24146
Dynamic localization and second-order subgrid-scale models in large eddy simulations of channel flow
p 2329 N94-24149
Direct simulation of isothermal-wall supersonic channel flow p 2172 N94-24164
A vorticity dynamics based model for the turbulent dissipation: Model development and validation
[NASA-TM-106177] p 2336 N94-24713

CHANNELS (DATA TRANSMISSION)
Land mobile satellite propagation measurements in Japan using ETS-V satellite p 2282 N94-22790
Measurements on the satellite-mobile channel at L and S bands p 2282 N94-22791
Measurement of multipath delay profile in land mobile satellite channels p 2283 N94-22793
Improved frame synchronization schemes for INMARSAT-B/M SCPC and TDM channels
p 2285 N94-22806
A protocol for satellite access via use of spot-beams
p 2286 N94-22811
System services and architecture of the TMI satellite mobile data system p 2286 N94-22817
Transmission over EHF mobile satellite channels
p 2287 N94-22820
Low rate data bus general specification for the NOAA-OPQ polar orbiting environmental satellites and EUMETSAT polar satellite systems
[NASA-TM-109408] p 2208 N94-23480
High-rate data link general specification for the NOAA-OPQ polar orbiting environmental satellites and EUMETSAT satellite systems
[NASA-TM-109384] p 2208 N94-23481

CHAOS
Chaos in plasma simulation and experiment
[DE94-001574] p 2549 N94-22963
Chaotic phenomena in plasma, 2
[DE93-508286] p 2549 N94-22964
Chaos and simple determinism in reversed field pinch plasmas: Nonlinear analysis of numerical simulation and experimental data
[DE94-001575] p 2550 N94-23211
On the estimation of the correlation dimension and its application to radar reflector discrimination
[NASA-CR-4564] p 2309 N94-23304
Lacunary series as quadratic differentials in conformal dynamics
[PB93-238061] p 2481 N94-23547
EEG and chaos: Description of underlying dynamics and its relation to dissociative states
[NASA-CR-195171] p 2428 N94-24799
Validating identified nonlinear models with chaotic dynamics
[RR-469] p 2523 N94-25314
Controlling regular and chaotic dynamics in the Duffing-Ueda oscillator
[RR-477] p 2523 N94-25323
Correlations in the actions of periodic orbits derived from quantum chaos
[DE93-616866] p 2571 N94-25340

CHARACTER RECOGNITION
Image remapping strategies applied as protheses for the visually impaired p 2444 N94-25363

CHARACTERIZATION
Chemical characterization of some aerobic liquids in CELSS p 2422 N94-23241
Joint Acoustic Propagation Experiment (JAPE-91) Workshop
[NASA-CP-3231] p 2526 N94-24207
Ground characterization for JAPE
p 2527 N94-24213
Seafloor characterization/Galapagos propagating rift
[AD-A273586] p 2419 N94-25165
Metallic multilayers: Experimental investigation of magnetic anisotropy and magnetic interlayer coupling
[ETN-94-95364] p 2250 N94-25242
The structure and catalytic properties of supported platinum catalysts
[ETN-94-95357] p 2236 N94-25250

CHARGE CARRIERS
Photo-induced antiferromagnetic interlayer coupling in Fe superlattices with iron silicide spacers
[DE94-001345] p 2559 N94-22995

CHARGE COUPLED DEVICES
Characterization of CCD-based imaging x ray detectors for diffraction experiments
[DE93-041343] p 2556 N94-22921
Development of a power electronics unit for the Space Station plasma contactor
[NASA-TM-106486] p 2222 N94-25201
Data analysis and interpretation of lunar dust exosphere p 2623 N94-25349
CHARGE EXCHANGE
Pions and neutrinos as probes of the nucleon and nuclear few-body system
[DE93-040127] p 2531 N94-22928
CHARGE TRANSFER
High-T(c) superconducting superlattices
[DE93-019200] p 2556 N94-22864
Pions and neutrinos as probes of the nucleon and nuclear few-body system
[DE93-040127] p 2531 N94-22928
Anisotropic uniaxial pressure effects in YBa2Cu3O(7-delta)
[DE94-001456] p 2557 N94-22929
Strong interactions studies with medium energy probes
[DE94-001446] p 2540 N94-23791
Photoinduced charge separation in solid state and molecular systems
[DE94-001727] p 2563 N94-24537
CHARGED PARTICLES
Measuring electrically charged particle fluxes in space using a fiber optic loop sensor
[NASA-CR-191328] p 2544 N94-23829
CHARM (PARTICLE PHYSICS)
Strong interactions studies with medium energy probes
[DE94-001446] p 2540 N94-23791
CHARPY IMPACT TEST
Irradiation damage behavior of low alloy steel wrought and weld materials
[DE94-000519] p 2239 N94-22999
Development of small punch testing technique and its application to evaluation of mechanical properties degradation
[DE94-001193] p 2375 N94-23184
Weldability of Accelerated-Cooled (AcC) high strength TMCP steel X80
[VTT-TIED-1413] p 2251 N94-25419
CHARRING
Laser soldering of Sn plated brass integrator assembly housings
[DE94-001149] p 2270 N94-23790
Postflight hardware evaluation RSRM-29 (STS-54). Appendix D: Nozzle postfire data
[NASA-CR-193898] p 2199 N94-24057
Micromechanical simulation of damage progression in carbon phenolic composites p 2231 N94-24446
CHEBYSHEV APPROXIMATION
Implementation and parallelization of fast matrix multiplication for a fast Legendre transform
[DE94-002184] p 2478 N94-22975
On the Gibbs phenomenon 3: Recovering exponential accuracy in a sub-interval from a spectral partial sum of a piecewise analytic function
[NASA-CR-191560] p 2480 N94-23278
Relaxation schemes for Chebyshev spectral multigrid methods p 2484 N94-23688
Generalized Gaussian quadrature rules for systems of arbitrary functions
[AD-A273610] p 2491 N94-24947
CHECKOUT
SATCOM simulator speeds MSS deployment and lowers costs p 2287 N94-22822
CHEMICAL ANALYSIS
Correlated petrographic, electron microprobe, and ion microprobe studies of selected primitive and processed phase assemblages in meteorites
[NASA-CR-194827] p 2601 N94-23499
SALI chemical analysis of provided samples
[NASA-CR-194138] p 2232 N94-23524
Chemically sensitive interfaces on SAW devices
[DE94-001832] p 2526 N94-23718
An analytical ultra-high vacuum tribometer for solid lubricant studies p 2361 N94-24033
Polytopic vector analysis in igneous petrology: Application to lunar petrogenesis p 2615 N94-24368
The chemistry of particulate formation in fluorocarbon plasmas
[DE94-001500] p 2552 N94-24546
Fifty years of continuous improvement: What has DOE done for analytical chemistry?
[DE94-002539] p 2234 N94-24548
Bioregenerative life support systems for microgravity
[NASA-CR-195516] p 2422 N94-24810
The evolution of energy-transducing systems. Studies with archaebacteria
[NASA-CR-195129] p 2422 N94-24811
CHEMICAL BONDS
Particle formation in a laser-heated aerosol reactor. Application to silicon and silicon nitride synthesis
[PB93-217982] p 2347 N94-22982
Density functional studies: First principles and semi-emperical calculations of clusters and surfaces
[DE94-002836] p 2561 N94-23214
Planar poly(p-phenylene) derivatives: Ladder formation for maximization of extended conjugation
[AD-A273220] p 2260 N94-24922
CHEMICAL COMPOSITION
Relationship of microstructure and mechanical properties for V-Cr-Ti alloys
[DE94-001431] p 2238 N94-22718
Coronal abundances and their variation
[NASA-CR-194811] p 2626 N94-23276
Molecular abundances in the envelopes around evolved stars
[PB94-104916] p 2602 N94-23812
Catalog of Apollo 17 rocks. Volume 1: Stations 2 and 3 (South Massif)
[NASA-CR-194854] p 2613 N94-24058
Whole rock major element chemistry of KREEP basalt clasts in lunar breccia 15205: Implications for the petrogenesis of volcanic KREEP basalts
p 2614 N94-24365
Melt rock components in KREEPy breccia 15205: Petrography and mineral chemistry of KREEP basalts and quartz-normative mare basalts p 2616 N94-24372
Demonstration of the feasibility of an integrated x ray laboratory for planetary exploration
[NASA-CR-177631] p 2598 N94-24832
CHEMICAL EFFECTS
Effects of ionizing radiation on modern ion exchange materials
[DE94-001569] p 2535 N94-24505
CHEMICAL ENGINEERING
Liapunov stability in chemical engineering
[MATHS-REPT-A-184] p 2236 N94-25427
CHEMICAL EQUILIBRIUM
Study of improved methods for predicting chemical equilibria
[DE94-001647] p 2568 N94-22719
Development of durable high-temperature catalysts for natural gas combustion
[PB93-226447] p 2232 N94-23477
CHEMICAL EVOLUTION
SETI: Search for extraterrestrial intelligence. An international interdisciplinary seminar, star days
[PB93-230597] p 2444 N94-23754
CHEMICAL FRACTIONATION
Basaltic Volcanism and Ancient Planetary Crusts
[NASA-CR-193151] p 2614 N94-24363
CHEMICAL PROPERTIES
Chemically sensitive interfacial force microscopy: Contact potential measurements of self-assembling monolayer films
[AD-A273135] p 2234 N94-24772
Investigation of the ultrafiltration technique using military greases
[AD-A273633] p 2261 N94-25029
CHEMICAL PROPULSION
NASA Propulsion Engineering Research Center, volume 2
[NASA-CR-194719-VOL-2] p 2209 N94-23028
Performance assessment of low pressure nuclear thermal propulsion p 2217 N94-23070
CHEMICAL REACTIONS
Economics of electron beam and electrical discharge processing for post-combustion NO(x) control in internal combustion engines
[DE93-019574] p 2351 N94-22865
Organometallic chemistry of bimetallic compounds
[DE94-002313] p 2238 N94-22897
Di(hydroxyphenyl)- 1,2,4-triazole monomers
[NASA-CASE-LAR-14440-2] p 2252 N94-23075
Reburning rich-lean kinetics
[PB93-220887] p 2232 N94-23100
Phase transformations in Cu-Zr multilayers
[DE94-000393] p 2241 N94-23297
Reduction of nitric oxide over platinum, rhodium and platinum-rhodium single crystal surfaces
[PB93-230092] p 2232 N94-23482
Reactivity of ambident anions in the gas phase
[PB93-232189] p 2533 N94-23713
Energy transfer in solid explosives
[DE94-001523] p 2265 N94-23778
Metal-mullite reactions
[DE94-002038] p 2244 N94-23811
Hot hydrogen testing of metallic turbo pump materials
[NASA-CR-193880] p 2244 N94-24066
Fracture kinetics analysis of empirical and semi-empirical corrosion fatigue relations p 2159 N94-24277
Convective instabilities in traveling fronts of addition polymerization p 2226 N94-24352
The chemistry of particulate formation in fluorocarbon plasmas
[DE94-001500] p 2552 N94-24546
Chemically sensitive interfacial force microscopy: Contact potential measurements of self-assembling monolayer films
[AD-A273135] p 2234 N94-24772
Collection and evaluation of numerical models with the aim to investigate the impact of aircraft emissions
[DLR-MITT-93-06] p 2400 N94-25414
Preceedings of the 12th International Congress: Corrosion Control for Low-Cost Reliability. Volume 2: Process Industries Plant Operations
[AD-A273662] p 2251 N94-25449
CHEMICAL REACTORS
Particle formation in a laser-heated aerosol reactor. Application to silicon and silicon nitride synthesis
[PB93-217982] p 2347 N94-22982
CHEMICAL VAPOR INFILTRATION
An overview on the main available ceramic composites and their processing routes p 2255 N94-24229
CMC design consequences p 2256 N94-24238
Integrated approach in modelling, testing, and design of gradient-CVI derived CMC components
p 2256 N94-24239
CHEMICAL WARFARE
Operation Friction: Development and introduction of personal cooling for CH124 Sea King aircrew
[DCIEM-93-06] p 2433 N94-24119
CHEMILUMINESCENCE
Capillary electrokinetic separations with optical detection
[DE94-001639] p 2233 N94-23716
CHEMISORPTION
Diffusion on Cu surfaces p 2251 N94-24428
Adsorption, desorption, and decomposition of HCl and HBr on Ge(100): Competitive pairingand near-first-order desorption kinetics
[AD-A273504] p 2235 N94-24790
CHEMOTHERAPY
Synthesis and in-vivo detection of boronated compounds for use in BNCT
[DE94-001899] p 2233 N94-23780
CHEST
Spontaneous pneumothorax, cysts and bullae
p 2425 N94-23326
CHICKENS
Evaluation of ovostatin and ovostatin assay
p 2422 N94-24437
CHINA
Activities of Academia Sinica
[DE93-614529] p 2541 N94-25335
CHIPS (ELECTRONICS)
A CDMA synchronisation scheme
p 2285 N94-22810
Towards the formal specification of the requirements and design of a processor interface unit: HOL listings
[NASA-CR-191465] p 2466 N94-23252
The HDTV digital audio matrix
[BBC-RD-1993/9] p 2295 N94-24085
SEMATECH, a case study: Analysis of a government-industry partnership
[AD-A273166] p 2586 N94-24683
Crosstalk analysis of synchronous and asynchronous optical chip interconnects with direct detection
[AD-A273261] p 2311 N94-24685
CHIRAL DYNAMICS
Proceedings of the 1993 Bi-Isotropics Workshop on Novel Microwave Materials
[PB93-224772] p 2290 N94-23225
Weak interactions in a bilocal chiral theory
[DE93-616887] p 2539 N94-25477
CHIRP SIGNALS
Choice of filters for the detection of gravitational waves from coalescing binaries. 2: Detection in coloured noise
[DE93-616844] p 2604 N94-25211
CHLORIDES
Investigation of evolution-related aspects of bacterial rhodopsins
[NASA-CR-194826] p 2420 N94-23501
CHLORINE
A high performance H2-Cl2 fuel cell for space power applications p 2394 N94-23366
Structures of Cl(-)(H2O)(n) and F(-)(H2O)(n) (n equal to 2,3...15) clusters: Molecular dynamics computer simulations
[AD-A273474] p 2537 N94-24940
CHLORINE COMPOUNDS
FTIR quantification of industrial hydraulic fluids in perchloroethylene p 2264 N94-23243
CHLOROFLUOROCARBONS
US Department of Energy phaseout of CFC-refrigerants
[DE94-001668] p 2397 N94-23016

Design of a vehicle based system to prevent ozone loss
[NASA-CR-195498] p 2180 N94-24479
Ozone depletion, paradigms, and politics
[DE94-001600] p 2398 N94-24506

CHLOROPHYLLS
Algorithm-development activities
[NASA-CR-193225] p 2420 N94-23538

CHOLESTEROL
Structure of cholesteryl-4-vinylbenzoate
[AD-A273686] p 2567 N94-25441

CHOLINE
Interaction of tacrine at M(1) and M(2) cholinoceptors in guinea pig brain p 2421 N94-24294

CHOLINERGICS
Interaction of tacrine at M(1) and M(2) cholinoceptors in guinea pig brain p 2421 N94-24294

CHROMIUM ALLOYS
Relationship of microstructure and mechanical properties for V-Cr-Ti alloys
[DE94-001431] p 2238 N94-22718
Effect of neutron irradiation on tensile properties of V-Cr-Ti alloys
[DE94-001433] p 2240 N94-23194
Effect of hydrogen exposure on a Cu-8 Cr-4 Nb alloy
[NASA-TM-106429] p 2243 N94-23556
Electrochemical behavior of ion-plated TiN and Cu-Cr coatings
[AD-A273411] p 2235 N94-24784

CHROMOSPHERE
Some challenging problems of the structured and dynamical solar atmosphere p 2624 N94-22838
The calculation of theoretical chromospheric models and the interpretation of solar spectra from rockets and spacecraft
[NASA-CR-195083] p 2626 N94-23569
Excitation of XUV radiation in solar flares
[NASA-CR-193703] p 2627 N94-24094
The resonance lines of MG2 as diagnostics of the upper solar chromosphere
[NASA-CR-195084] p 2627 N94-24300
Chromospheric activity in agol binaries
[AD-A273546] p 2602 N94-24557

CHRONOLOGY
Orbital debris and near-Earth environmental management: A chronology
[NASA-RP-1320] p 2598 N94-24644

CINEMATOGRAPHY
Quantitative assessment of human motion using video motion analysis p 2436 N94-24203

CIRCUIT BOARDS
PULSAUR 2
[NASA-CR-194832] p 2209 N94-23484
Digital data, composite video multiplexer and demultiplexer boards for an IBM PC/AT compatible computer p 2447 N94-25377
CADBIT 2: Computer-aided design for built-in test, volume 1
[AD-A273702] p 2463 N94-25455
CADBIT 2: Computer-aided design for built-in test, volume 2
[AD-A273703] p 2463 N94-25456

CIRCUIT PROTECTION
A review of wiring system safety in space power systems
[NASA-CR-194439] p 2203 N94-23632

CIRCUIT RELIABILITY
Formal verification of digital circuits described in VHDL
[ETN-94-95165] p 2306 N94-22883
A review of wiring system safety in space power systems
[NASA-CR-194439] p 2203 N94-23632

CIRCUITS
Progress on the design of a data push architecture for an array of optimized time tagging pixels
[DE93-041011] p 2307 N94-22955
Performance analysis of the combined EDS maglev propulsion, levitation, and guidance system
[DE94-001346] p 2352 N94-22996
Calibration block for digital beam forming antenna
[PB93-204550] p 2294 N94-23773
Worst case analysis: Earth sensor assembly for the tropical rainfall measuring mission observatory
[NASA-CR-189320] p 2311 N94-24754
From circuit to signal: Development of a piecewise linear simulator
[ISBN-9-09-005713-7] p 2462 N94-25263

CIRCULAR CYLINDERS
Buckling of circular cylindrical shells subjected to combined loads (axial compression, normal pressure, bending and transverse shear loading)
[PB93-215358] p 2378 N94-24745
Unified approach for incompressible flows
p 2342 N94-25356

CIRCULAR ORBITS
Global coverage Mobile Satellite Systems: System availability versus channel propagation impairments
p 2284 N94-22798
Steady motions of rigid body satellites in a central gravitational field
[AD-A273742] p 2206 N94-25532

CIRCULAR POLARIZATION
Germanium x ray phase plates for the production of circularly polarized x rays
[DE94-002908] p 2545 N94-24550

CITIES
Electromagnetic field strength prediction in an urban environment: A useful tool for the planning of LMSS
p 2283 N94-22795
Propagation model for the Land Mobile Satellite channel in urban environments p 2283 N94-22796
A prediction model of signal degradation in LMSS for urban areas p 2284 N94-22797
Urban/rural application of weather radar for flow forecasting. Proceedings of the Informal CEc -Workshop
[PB93-220135] p 2407 N94-23129

CIVIL AVIATION
Simplified, inverse, ejector design tool
[NASA-CR-194438] p 2166 N94-23511
Vision impairment and corrective considerations of civil airmen
[DOT/FAA/AM-93/21] p 2426 N94-23623
The atmospheric effects of stratospheric aircraft: A third program report
[NASA-RP-1313] p 2398 N94-24104
An experimental investigation of a Mach 3.0 high-speed civil transport at supersonic speeds
[NASA-TP-3365] p 2169 N94-24311
Information systems strategy in air transport
[AD-A273125] p 2173 N94-24781
Annual review of aircraft accident data. US general aviation calendar year 1990
[PB94-126869] p 2173 N94-24841
Aviation: The timeless industry p 2165 N94-25068
US general aviation: The ingredients for a renaissance. A vision and technology strategy for US industry, NASA, FAA, universities p 2162 N94-25097

CLADDING
Evaluation of inorganic zinc-rich primers using Electrochemical Impedance Spectroscopy (EIS)
p 2237 N94-23233
Weld cladding of hard surfaces
[PB93-201598] p 2353 N94-23448
Fiber optic temperature sensor using a Y2O2S:Eu thermographic phosphor
[DE94-000331] p 2543 N94-23461
Analysis for the computational modeling of finite cladding and lossy coating effects in fibers
[PB94-111085] p 2544 N94-23732

CLAMPS
Multipurpose clamping device with electrical connector for in orbit attachment of payloads p 2361 N94-24035
Analysis of impactor residues in tray clamps from the Long Duration Exposure Facility. Part 2: Clamps from Bay B of the satellite
[NASA-TM-104784] p 2386 N94-24095

CLASSICAL MECHANICS
On the connection of classical mechanics, physical kinetics and quantum theory
[DE93-616823] p 2570 N94-25207

CLASSIFICATIONS
Security aspects of space operations data
p 2515 N94-23937
Method for selection of wavelength bands for multispectral classification
[PB93-204378] p 2388 N94-24741
Evaluation of the use of remote-sensing data to identify crop types and estimate irrigated acreage, Uvalde and Medina Counties, Texas, 1989
[PB93-193159] p 2388 N94-24809
An AVHRR cloud classification database typed by experts
[AD-A273560] p 2416 N94-25162
Remote vibration measurements at a sud aviation alouette 3 helicopter with a CW CO2-laser system
[AD-A273818] p 2190 N94-25516

CLASSIFIERS
Preliminary analysis of the JAPE ground vehicle test data with an artificial neural network classifier
p 2529 N94-24222

CLAYS
Demonstration of the feasibility of an integrated x ray laboratory for planetary exploration
[NASA-CR-177631] p 2598 N94-24832
Drying deformable media: Kinetics, shrinkage and stresses
[ETN-94-95314] p 2236 N94-25302

CLEANERS
Aqueous alkaline cleaners: An alternative to organic solvents
[AD-A273510] p 2260 N94-24848

CLEANING
Aqueous alkaline cleaners: An alternative to organic solvents
[AD-A273510] p 2260 N94-24848

CLEARANCES
Combined 1991 and 1992 Robinson-22B (R-22) parking test results
[AD-A273550] p 2193 N94-24559

CLIMATE
Overview of global greenhouse effects
[DE93-041165] p 2396 N94-22887
Climate variability in a coupled GCM. Part 2: The Indian Ocean and monsoon
[MPIM-104] p 2401 N94-23159
Modal structure of variations in the tropical climate system. Part 2: Origins of the low-frequency mode
[MPIM-96] p 2407 N94-23199
Uncertainties in climate data sets
[NASA-CR-194848] p 2408 N94-23577
Northern hemisphere tropospheric mid-latitude circulation after violent volcanic eruptions
[MPIM-107] p 2403 N94-24491
Multiannual simulations with the Mars climate model
p 2618 N94-24881

CLIMATE CHANGE
Catalog of data bases and reports
[DE93-040597] p 2588 N94-22875
Overview of global greenhouse effects
[DE93-041165] p 2396 N94-22887
Monte Carlo climate change forecasts with a global coupled ocean-atmosphere model
[MPIM-97] p 2407 N94-23156
Lightning, atmospheric electricity, and climate change
[DE94-002003] p 2408 N94-23471
GEWEX p 2385 N94-23614
Performance of the Carbon Dioxide Information Analysis Center (CDIAC)
[DE94-002190] p 2397 N94-23794
Mission operations update for the restructured Earth Observing System (EOS) mission p 2499 N94-23839
GEWEX Continental-scale International Project (GCIP)
p 2411 N94-24376
Snow modeling, water resources, climate change
[PB93-201770] p 2399 N94-24633
Manual on measurement of methane and nitrous oxide emissions from agriculture
[DE93-616429] p 2399 N94-25167
Collection and evaluation of numerical models with the aim to investigate the impact of aircraft emissions
[DLR-MITT-93-06] p 2400 N94-25414

CLIMATOLOGY
Monte Carlo climate change forecasts with a global coupled ocean-atmosphere model
[MPIM-97] p 2407 N94-23156
Modes of ocean variability in the tropical Pacific as derived from Geosat altimetry
[MPIM-103] p 2382 N94-23158
Climate variability in a coupled GCM. Part 2: The Indian Ocean and monsoon
[MPIM-104] p 2401 N94-23159
Evaluating NOAA satellite products for global climate monitoring p 2384 N94-23604
Cloud-free aerosol optical depth determination over oceans from satellite radiometry
[DE94-001897] p 2386 N94-23779
GEWEX Continental-scale International Project (GCIP)
p 2411 N94-24376
GEWEX Cloud Systems Study (GCSS)
p 2411 N94-24377
GEWEX Water Vapor Project (GVaP)
p 2411 N94-24378
Atmospheric Radiation Measurement (ARM)/CART site p 2411 N94-24379
Scientific goals of the Cooperative Multiscale Experiment (CME) p 2411 N94-24381
Coupled land surface/hydrologic/atmospheric models
p 2413 N94-24387
Observational case studies and diagnostic analyses of long-lived large-amplitude inertia-gravity waves
[AD-A273545] p 2404 N94-24794
The annual pressure cycle on Mars: Results from the LMD Martian atmospheric general circulation model
p 2619 N94-24884
Observed and Navy operational global model climatologies of synoptic disturbances over the tropical western Pacific during winter 1991-1992
[AD-A273400] p 2416 N94-25071
Wind climate and urban geometry
[ISBN-9-03-860132-8] p 2416 N94-25261

CLINICAL MEDICINE
Arterial hypertension and the aviator
p 2425 N94-23328

Autogenic-feedback training: A potential treatment for post-flight orthostatic intolerance in aerospace crews [NASA-TM-108785] p 2426 N94-24102

Annual research progress report, fiscal year 1992. Volume 2: Department of Clinical Investigation [AD-A273584] p 2427 N94-24945

CLOCKS

Asynchronous timing and Doppler recovery in DSP based DPSK modems for fixed and mobile satellite applications p 2285 N94-22805

CLOSED ECOLOGICAL SYSTEMS

Chemical characterization of some aerobic liquids in CELSS p 2422 N94-23241

Recent advances in SPE (tm) water electrolyzer p 2393 N94-23362

Microbial biofilm formation and its consequences for the CELSS program [NASA-CR-195146] p 2438 N94-24706

Bioregenerative life support systems for microgravity [NASA-CR-195516] p 2422 N94-24810

Robotics in a controlled, ecological life support system p 2444 N94-25371

CLOSURE LAW

Reliability in second moment turbulence closures revisited [NASA-TM-106469] p 2326 N94-24063

Toward modeling wingtip vortices p 2171 N94-24142

CLOUD COVER

Convective organization in the Pacific ITCZ: Merging OLR, TOVS, and SSM/I information [NASA-CR-194850] p 2408 N94-23619

Atmospheric Radiation Measurement (ARM)/CART site p 2411 N94-24379

Session on modeling of radiative transfer processes p 2414 N94-24397

Session on coupled atmospheric/chemistry coupled models p 2414 N94-24398

Impact of the CO2 and H2O clouds of the Martian polar hood on the polar energy balance p 2618 N94-24880

CLOUD PHYSICS

NOAA Federal/State Cooperative Program in Atmospheric Modification Research. Collected publication titles and abstracts [PB93-198125] p 2396 N94-22913

A regional analysis of cloudy mean spherical albedo over the marine stratocumulus region and the tropical Atlantic Ocean [NASA-CR-194771] p 2409 N94-24049

GEWEX Cloud Systems Study (GCSS) p 2411 N94-24377

Joint sessions on moisture processes and cumulus parameterization p 2414 N94-24393

Session on cumulus parameterization p 2414 N94-24394

LRAT: Lightning Radiative Transfer p 2416 N94-24443

A study of cloud motions on Mars. 2: Some examples of observations and analyses since 1969 p 2620 N94-24891

CLOUD SEEDING

NOAA Federal/State Cooperative Program in Atmospheric Modification Research. Collected publication titles and abstracts [PB93-198125] p 2396 N94-22913

CLOUDS

Cloud, dust, and ozone vertical profiles from solar occultation measurements: Implications for dynamics p 2617 N94-24877

Shocked clouds in the Cygnus Loop [NASA-CR-195190] p 2600 N94-25178

CLOUDS (METEOROLOGY)

Chemistry on the mesoscale: Modeling and measurement issues p 2413 N94-24390

Further studies to extend and test the area-time-integral technique applied to satellite data [NASA-CR-195132] p 2415 N94-24705

A study of cloud motions on Mars. 2: Some examples of observations and analyses since 1969 p 2620 N94-24891

An AVHRR cloud classification database typed by experts [AD-A273560] p 2416 N94-25162

CLUSTER ANALYSIS

The adaptive resonance theory network: (Clustering-) behaviour in relation with brainstem auditory evoked potential patterns [EUT-92-E-264] p 2470 N94-22877

Process and representation in graphical displays p 2433 N94-24187

Designers' models of the human-computer interface p 2433 N94-24188

CLUTCHES

Electromagnetic brake/clutch device [NASA-CASE-GSC-13502-1] p 2354 N94-23969

CLUTTER

Precipitation measurement using SIR-C: A feasibility study [NASA-CR-195104] p 2409 N94-24048

Estimation of the rain signal in the presence of large surface clutter [NASA-CR-195105] p 2409 N94-24087

Precipitation measurement using SIR-C: A feasibility study. Investigation at nadir [NASA-CR-195103] p 2410 N94-24126

On the analysis of clear air radar echoes severely contaminated by clutter p 2306 N94-24423

Radar target discrimination by spectrum analysis [AD-D015982] p 2301 N94-25040

Radar target discrimination systems using artificial neural network topology [AD-D015984] p 2301 N94-25041

CMOS

Floating well based design methodology aimed to improve latch-up immunity in a CMOS/DMOS smart power technology [LAAS-93093] p 2556 N94-22905

A qualified radiation hardened nonvolatile memory for space and tactical weapons applications [DE94-001211] p 2559 N94-23186

COAGULATION

On the stability of the process of formation of combustion generated particles by coagulation and simultaneous shrinkage due to particle oxidation p 2159 N94-24274

The influence of flow type, particle type and gravity on orthokinetic coagulation [ETN-94-95333] p 2267 N94-25060

COAL DERIVED GASES

Contaminant effects in solid oxide fuel cells [DE94-002963] p 2395 N94-23785

COALESCING

BEM solution for the simulation of axisymmetric viscous sintering [PB93-237717] p 2336 N94-24761

COASTAL WATER

Nutrients and light as factors controlling phytoplankton biomass on the Dutch continental shelf (North Sea), 1988-1990 [PB94-111143] p 2418 N94-24601

COASTS

Analysis of vulnerability to the impacts of sea level rise: A case study for The Netherlands [PB94-111150] p 2399 N94-24573

COATING

Total light loss optic spectroscopy: Progress towards a fiber optic Raman organic vapor sensor [DE94-002545] p 2234 N94-24549

Birdstrike resistant crew enclosure program [AD-A273700] p 2463 N94-25453

COATINGS

Transparent conducting thin films for spacecraft applications [NASA-TM-106466] p 2218 N94-23370

Infrared analysis of vapor phase deposited tricresylphosphate (TCP) [NASA-TM-106423] p 2253 N94-23371

COAXIAL FLOW

A modelling of the noise from simple co-axial jets. Part 2: In a simulated flightstream [ISVR-TR-226] p 2525 N94-22959

COBALT ALLOYS

New extensions in the development of deformation processed metal-metal matrix composites [DE94-000692] p 2227 N94-23004

Magnetic properties and transmission electron microscopy investigations of Nd-Fe-B-Co-Al melt spun ribbons [PB93-201531] p 2561 N94-23428

Metal band drives in spacecraft mechanisms p 2355 N94-23987

Robotic weld overlay coatings for erosion control [DE94-002665] p 2258 N94-24749

Comparative M-H characteristics of 1-5 and 2-17 type samarium-cobalt permanent magnets to 300 C [NASA-CR-194440] p 2312 N94-24870

COBALT COMPOUNDS

Magnetic properties of NdCo3 and its gamma phase hydride NdCo3H(4.1) [REPT-A-2655] p 2567 N94-25412

COBALT OXIDES

Applications of x ray absorption fine structure to the in situ study of the effect of cobalt in nickel hydrous oxide electrodes for fuel cells and rechargeable batteries p 2391 N94-23347

COCKPITS

Pilot-vehicle interface [DOT/FAA/CT-92/21] p 2430 N94-23083

Cockpit/NVG visual integration issues p 2432 N94-23983

Cockpit control system conceptual design [NASA-CR-195543] p 2190 N94-24551

Pilot-vehicle interface handbook, chapter 19. Volume 2: Digital systems validation [DOT/FAA/CT-88/10-VOL-2] p 2438 N94-24830

Cockpit control system [NASA-CR-195488] p 2190 N94-24957

Projected effectiveness of airbag supplemental restraint systems in US Army helicopter cockpits [AD-A273250] p 2174 N94-25141

Expert system rule-base evaluation using real-time parallel processing [AD-A273701] p 2469 N94-25454

CODE DIVISION MULTIPLE ACCESS

Adaptive digital beamforming for a CDMA mobile communications payload p 2274 N94-22743

A European mobile satellite system concept exploiting CDMA and OBP p 2279 N94-22768

ROCSAT-1 telecommunication experiments p 2279 N94-22770

ACTS advanced system concepts and experimentation p 2280 N94-22780

Odyssey personal communications satellite system p 2282 N94-22787

First satellite mobile communication trials using BLQS-CDMA p 2284 N94-22801

A CDMA synchronisation scheme p 2285 N94-22810

Diversity reception for advanced multi-satellite networks: A CDMA approach p 2286 N94-22816

Handover aspects for a Low Earth Orbit (LEO) CDMA Land Mobile Satellite (LMS) system p 2288 N94-22824

Reduced cost alternatives to premise wiring using ATM and microcellular technologies p 2314 N94-23239

CODERS

A high quality voice coder with integrated echo canceller and voice activity detector for mobile satellite applications p 2286 N94-22812

High resolution encoder-motor used in the orbital spin scan radiometer, GOES VAS satellites p 2209 N94-24038

Encoders for space applications p 2363 N94-24046

Error coding simulations p 2306 N94-24439

Evaluation of the efficiency and fault density of software generated by code generators p 2465 N94-24445

A constrained joint source/channel coder design and vector quantization of nonstationary sources [NASA-CR-195145] p 2301 N94-24707

A soft robot interface [OUEL-1948/92] p 2463 N94-25468

CODES

Algebraic-geometric codes and their decoding algorithms [ETN-94-95294] p 2491 N94-25079

CODING

A high quality voice coder with integrated echo canceller and voice activity detector for mobile satellite applications p 2286 N94-22812

Box codes of lengths 48 and 72 p 2292 N94-23265

Error coding simulations p 2306 N94-24439

A constrained joint source/channel coder design and vector quantization of nonstationary sources [NASA-CR-195145] p 2301 N94-24707

Algebraic-geometric codes and their decoding algorithms [ETN-94-95294] p 2491 N94-25079

On chain coding of line drawings [ISBN-9-06-275778-2] p 2462 N94-25252

COEFFICIENT OF FRICTION

Contact analysis of rough rail surfaces p 2270 N94-23589

New pin-on-disk equipment for vacuum tribometry p 2360 N94-24023

An analytical ultra-high vacuum tribometer for solid lubricant studies p 2361 N94-24033

An assessment of solid lubricant films for use in high temperature space applications p 2363 N94-24044

COEFFICIENTS

A technique to measure rotordynamic coefficients in hydrostatic bearings p 2215 N94-23061

Multigrid methods for differential equations with highly oscillatory coefficients p 2484 N94-23685

COERCIVITY

Magnetic properties and transmission electron microscopy investigations of Nd-Fe-B-Co-Al melt spun ribbons [PB93-201531] p 2561 N94-23428

Comparative M-H characteristics of 1-5 and 2-17 type samarium-cobalt permanent magnets to 300 C [NASA-CR-194440] p 2312 N94-24870

COGNITION

Multi-sensoral approach to night flight: Perceptive and Cognitive limitations p 2432 N94-23981

Automation and cognition in air traffic control: An empirical investigation [DOT/FAA/AM-94/3] p 2176 N94-25444

COGNITIVE PSYCHOLOGY
Epistemic logic for defeasible reasoning using a meta-level architecture metaphor
[PB94-110723] p 2473 N94-23748
Mental images p 2429 N94-23980
Process and representation in graphical displays
p 2433 N94-24187
The use of analytical models in human-computer interface design p 2434 N94-24190
Automation and cognition in air traffic control: An empirical investigation
[DOT/FAA/AM-94/3] p 2176 N94-25444

COHERENCE
Ray and wave optics modeling of laboratory x ray lasers
[DE93-019940] p 2541 N94-22868

COHERENT RADAR
High latitude cusp signature observations for southward IMF B sub Z
[AD-A273801] p 2406 N94-25536

COHERENT RADIATION
High-order sum and difference-frequency generation in helium
[DE94-001064] p 2348 N94-23181

COLD DRAWING
Characterization of the microstructure of Nb-1wt.%Zr-0.1wt.%C tubes as affected by thermomechanical processing
[NASA-TM-106381] p 2242 N94-23550

COLD FLOW TESTS
SSME fuel preburner injector characterization
p 2211 N94-23037
Dual-bell altitude compensating nozzles
p 2215 N94-23057

COLD PLASMAS
Computational model of surface ablation from tokamak disruptions
[DE94-002204] p 2550 N94-23474
Stabilization of the external kink and other MHD issues
[DE94-001541] p 2552 N94-24502

COLD WATER
Survival suit for submarine personnel: Summary of evaluation studies
[PB93-204634] p 2430 N94-23743

COLD WEATHER
Cellular and tissue injury during nonfreezing cold injury and frostbite
[AD-A270883] p 2423 N94-22732

COLD WELDING
Static adhesion in preloaded contacts subjected to long-term vacuum exposure p 2363 N94-24043

COLD WORKING
Lubrication in cold rolling: Numerical simulation using multigrid techniques
[ISBN-9-09-005313-1] p 2262 N94-25230

COLLIMATORS
High energy collimating fine grids for HESP program
[NASA-CR-189317] p 2209 N94-24767

COLLISION AVOIDANCE
Control of a serpentine manipulator with collision avoidance p 2368 N94-23232

COLLISION PARAMETERS
Intramultiplet mixing for Ne(**)(3p)+He at superthermal energies
[ETN-94-95327] p 2538 N94-25240

COLLISIONAL PLASMAS
Characterization of heat transport and radiation hydrodynamics in collisional laser plasmas using collective Thomson scattering
[DE94-001502] p 2349 N94-23209

COLLISIONS
Method for simulating a vehicle shock test: Design and realization of the required implementation tools
[ECL-92-14] p 2352 N94-22885
Development of a droplet breakup model considering aerodynamic and droplet collision effects
p 2213 N94-23045

COLLOIDS
Nanodesigning of hierarchical multifunctional ceramics
[AD-A273466] p 2257 N94-24677

COLONIES
Symbiosis in marine luminous bacteria
[AD-A273540] p 2422 N94-24791

COLOR
Some background information on perceptual color matching pertinent to computer applications
[PB93-200327] p 2445 N94-23788
Automating a human factors evaluation of graphical user interfaces for NASA applications: An update on CHIMES
p 2443 N94-23936
Investigation on interval edge-coloring of graphs
[PB94-110913] p 2488 N94-24541

COLOR TELEVISION
Orbital docking system centerline color television camera system test
[NASA-TM-104783] p 2205 N94-24625

COLOR VISION
Some background information on perceptual color matching pertinent to computer applications
[PB93-200327] p 2445 N94-23788

COLORIMETRY
Some background information on perceptual color matching pertinent to computer applications
[PB93-200327] p 2445 N94-23788

COLUMBUS SPACE STATION
Mission activities planning for a Hermes mission by means of AI-technology p 2502 N94-23858
Columbus system support for telescience operations
p 2505 N94-23877
The Columbus logistics support at the APMC: Requirements and implementation aspects
p 2515 N94-23935

COMBINATORIAL ANALYSIS
Thermal analysis of combinatorial solid geometry models using SINDA p 2323 N94-23650
The Third Twente Workshop on Graphs and Combinatorial Optimization
[PB94-110947] p 2486 N94-23722
Discrete applied mathematics
[AD-A273552] p 2488 N94-24561
Combinatory reduction systems: Introduction and survey
[PB94-110582] p 2457 N94-24570
The Third Twente Workshop on Graphs and Combinatorial Optimization: Abstracts and late extended abstracts
[PB94-110954] p 2489 N94-24652
Sensitivity analysis of list scheduling heuristics
[PB93-237766] p 2468 N94-24764

COMBUSTIBLE FLOW
An experimental study of characteristic combustion-driven flows for CFD validation
p 2212 N94-23040
Study of streamwise vorticity-stirred combustion
[NASA-CR-194450] p 2234 N94-24565
Conservation equations for reacting gas flow
[PB94-111168] p 2334 N94-24574
HYPULSE combustor analysis
[NASA-CR-191579] p 2336 N94-24771

COMBUSTION
Evaporation and combustion of LOX under supercritical and subcritical conditions p 2211 N94-23035
Reburning rich-lean kinetics
[PB93-220887] p 2232 N94-23100
Calculation of flame spread on lining materials by the field model KAMELEON. Project 5 of the EUREFIC fire research programme
[PB93-201614] p 2268 N94-23450
Evaluation of reducing gas turbine emissions through hydrogen-enhanced steam-injected combustion
[PB94-109873] p 2187 N94-23709
Extinguishment of combustible porous solids by water droplets
[PB93-198893] p 2270 N94-23740
Energy transfer in solid explosives
[DE94-001523] p 2265 N94-23778
Multiple shock initiation of LX-17
[DE94-001524] p 2265 N94-23807
Modelling the ignition of boron/titanium particles
p 2159 N94-24273

COMBUSTION CHAMBERS
CFD analyses of combustor and nozzle flowfields
p 2210 N94-23033
Axisymmetric single shear element combustion instability experiment p 2213 N94-23044
Numerical investigation of two- and three-dimensional heat transfer in expander cycle engines
p 2213 N94-23048
Computational Fluid Dynamics (CFD) applications in rocket propulsion analysis and design
p 2214 N94-23054
Shock tunnel studies of scramjet phenomena, supplement 7
[NASA-CR-191572] p 2319 N94-23513
Shock tunnel studies of scramjet phenomena, supplement 8
[NASA-CR-191573] p 2320 N94-23532
The 3-D CFD modeling of gas turbine combustor-integral bleed flow interaction p 2189 N94-23658
The 3-D numerical study of airflow in the compressor/combustor prediffuser and dump diffuser of an industrial gas turbine p 2324 N94-23660
Evaluation of reducing gas turbine emissions through hydrogen-enhanced steam-injected combustion
[PB94-109873] p 2187 N94-23709
Fundamental and experimental studies on the catalytic combustion of methane
[PB94-112661] p 2233 N94-23736
Altitude simulation facility for testing large space motors p 2156 N94-24255
Multiple flames in counterflow spray combustion
p 2161 N94-24284
CFD simulation of coaxial injectors
p 2342 N94-24430
Heat transfer in rocket engine combustion chambers and regeneratively cooled nozzles
[NASA-CR-195094] p 2220 N94-24471
STE thrust chamber technology: Main injector technology program and nozzle Advanced Development Program (ADP)
[NASA-CR-193919] p 2221 N94-25019

COMBUSTION CHEMISTRY
Fundamental limitations of non-thermal plasma processing for internal combustion engine NO(x) control
[DE93-019622] p 2351 N94-22866
Laser diagnostics for small rockets
p 2210 N94-23032
Fundamental study of NO(x) control in catalytic combustion
[PB94-112323] p 2398 N94-23818
Multiple flames in counterflow spray combustion
p 2161 N94-24284
HYPULSE combustor analysis
[NASA-CR-191579] p 2336 N94-24771
Influence of test configuration on the combustion characteristics of polymers as ignition sources
p 2238 N94-25365

COMBUSTION EFFICIENCY
Theory and computation of optimal low- and medium-thrust transfers
[NASA-CR-194812] p 2217 N94-23275
STE thrust chamber technology: Main injector technology program and nozzle Advanced Development Program (ADP)
[NASA-CR-193919] p 2221 N94-25019

COMBUSTION PHYSICS
Fundamental limitations of non-thermal plasma processing for internal combustion engine NO(x) control
[DE93-019622] p 2351 N94-22866
Laser diagnostics for small rockets
p 2210 N94-23032
Fundamental rocket injector/spray programs at the Phillips Laboratory p 2211 N94-23039
Numerical parametric studies of spray combustion instability p 2212 N94-23041
The ignition temperature of solid explosives exposed to a fire
[DE94-001047] p 2265 N94-23436
Field models: Their present and future application in fire safety engineering
[PB93-201622] p 2269 N94-23506
Shock tunnel studies of scramjet phenomena, supplement 7
[NASA-CR-191572] p 2319 N94-23513
Shock tunnel studies of scramjet phenomena, supplement 8
[NASA-CR-191573] p 2320 N94-23532
The combustion program at CTR
p 2237 N94-24155
Experimental investigation of ignition of boron/titanium composite particles p 2159 N94-24275

COMBUSTION PRODUCTS
Economics of electron beam and electrical discharge processing for post-combustion NO(x) control in internal combustion engines
[DE93-019574] p 2351 N94-22865
Fundamental limitations of non-thermal plasma processing for internal combustion engine NO(x) control
[DE93-019622] p 2351 N94-22866
Reburning rich-lean kinetics
[PB93-220887] p 2232 N94-23100
Evaluation of reducing gas turbine emissions through hydrogen-enhanced steam-injected combustion
[PB94-109873] p 2187 N94-23709
Fundamental study of NO(x) control in catalytic combustion
[PB94-112323] p 2398 N94-23818
On the stability of the process of formation of combustion generated particles by coagulation and simultaneous shrinkage due to particle oxidation p 2159 N94-24274
Alternative control techniques document: NOx emissions from stationary reciprocating internal combustion engines
[PB94-104494] p 2398 N94-24476
EPA's survey of in-use driving patterns: Implications for mobile source emission inventories
[PB94-118502] p 2399 N94-24525
The effects of zinc borate addition on the flammability characteristics of polyester, vinyl ester, and epoxy glass reinforced plastics
[AD-A273164] p 2262 N94-25136
Influence of test configuration on the combustion characteristics of polymers as ignition sources
p 2238 N94-25365

COMBUSTION STABILITY

Fundamental rocket injector/spray programs at the Phillips Laboratory p 2211 N94-23039

Numerical parametric studies of spray combustion instability p 2212 N94-23041

Spray formation processes of impinging jet injectors p 2212 N94-23042

Inherent stability of central element coaxial liquid-liquid injectors p 2212 N94-23043

Axisymmetric single shear element combustion instability experiment p 2213 N94-23044

Development of a computational testbed for numerical simulation of combustion instability p 2213 N94-23046

Shear coaxial injector instability mechanisms p 2213 N94-23047

On the stability of the process of formation of combustion generated particles by coagulation and simultaneous shrinkage due to particle oxidation p 2159 N94-24274

Multiple flames in counterflow spray combustion p 2161 N94-24284

Stability of premixed laminar flames in a stagnation point flow to general disturbances [AD-A273429] p 2234 N94-24673

STE thrust chamber technology: Main injector technology program and nozzle Advanced Development Program (ADP) [NASA-CR-193919] p 2221 N94-25019

Research in progress and other activities of the Institute for Computer Applications in Science and Engineering [NASA-CR-191576] p 2444 N94-25090

COMBUSTION SYNTHESIS

Combustion synthesis and engineering of nanoparticles for electronic, structural and superconductor applications [DE94-001865] p 2254 N94-23720

COMET NUCLEI

A system for the challenging task of collecting samples from a comet surface p 2358 N94-24007

COMET TAILS

Evolution of large-scale plasma structures in comets: Kinematics and physics [NASA-CR-194777] p 2601 N94-23251

COMMAND AND CONTROL

OASIS-CC presentation p 2385 N94-23613

Operations concepts for Mars missions with multiple mobile spacecraft p 2501 N94-23852

EOS ground data systems: A description and interface overview p 2517 N94-23948

Modeling of database constraints in active databases [AD-A273484] p 2592 N94-24691

COMMAND GUIDANCE

Intelligent systems and advanced user interfaces for design, operation, and maintenance of command management systems [NASA-CR-195172] p 2459 N94-24797

COMMERCE

First satellite mobile communication trials using BLQS-CDMA p 2284 N94-22801

The Electronics Quality/Reliability Center: Lessons learned from partnering with industry [DE94-001501] p 2309 N94-23777

Research interests and broad agency announcement 94-1 of the Air Force Office of Scientific Research [AD-A273410] p 2632 N94-25075

COMMERCIAL AIRCRAFT

Aircraft accident report: Inadvertent in-flight slat deployment, China Eastern Airlines Flight 583, McDonnell Douglas MD-11, B-2171, 950 nautical miles south of Shemya, Alaska, 6 April 1993 [PB93-910408] p 2172 N94-23579

JB-300: An advanced medium size transport for 2005 [NASA-CR-195499] p 2179 N94-24401

Information systems strategy in air transport [AD-A273125] p 2173 N94-24781

The AC-120: The advanced commercial transport [NASA-CR-195491] p 2182 N94-24966

Integrated design and manufacturing for the high speed civil transport [NASA-CR-195511] p 2182 N94-24968

The RTL-46: A simulated commercial air transportation study [NASA-CR-195524] p 2184 N94-25017

High-order technology: Applying technical excellence to new airplane development p 2185 N94-25069

COMMUNICATING

Sequential composition, action prefixes and process prefix [PB94-101433] p 2488 N94-24539

COMMUNICATION

PROGRIL: A language for the definition of protocol grammars [EUT-93-E-270] p 2449 N94-23172

Delay-insensitive communication [ETN-94-95315] p 2304 N94-25303

COMMUNICATION EQUIPMENT

Linear time algorithm to schedule trees with communication delays optimally on two machines [PB93-237782] p 2451 N94-23441

Three, four, five, six or the complexity of scheduling with communication delays [PB94-111630] p 2467 N94-23767

COMMUNICATION NETWORKS

Transparent data service with multiple wireless access p 2276 N94-22754

Internetworking satellite and local exchange networks for personal communications applications p 2276 N94-22755

Power attenuation characteristics as switch-over criterion in personal satellite mobile communications p 2277 N94-22756

Integration of mobile satellite and cellular systems p 2277 N94-22757

Interworking evolution of mobile satellite and terrestrial networks p 2277 N94-22758

Interworking and integration of the Inmarsat Standard-M with Pan-European GSM system p 2277 N94-22759

Architectures and protocols for an integrated satellite-terrestrial mobile system p 2277 N94-22760

Handover procedures in integrated satellite and terrestrial mobile systems p 2277 N94-22761

MSAT and cellular hybrid networking p 2278 N94-22762

A system architecture for an advanced Canadian wideband mobile satellite system p 2278 N94-22766

ACTS broadband aeronautical experiment p 2279 N94-22771

EUTELTRACS: The European experience on mobile satellite services p 2281 N94-22781

Systems implications of L-band fade data statistics for LEO mobile systems p 2284 N94-22799

Handover aspects for a Low Earth Orbit (LEO) CDMA Land Mobile Satellite (LMS) system p 2288 N94-22824

Study on networking issues of medium earth orbit satellite communications systems p 2288 N94-22825

The design and networking of dynamic satellite constellations for global mobile communication systems p 2288 N94-22826

Low earth orbit satellite/terrestrial mobile service compatibility p 2288 N94-22827

Generation of modules for control communication circuits: A design study used in the framework of the safe vehicle PROMETHEUS [ETN-94-95171] p 2308 N94-23165

Reduced cost alternatives to premise wiring using ATM and microcellular technologies p 2314 N94-23239

Automated parallelization of timed Petri-net simulations [NASA-CR-191574] p 2451 N94-23341

MITS architecture V1.0 [PB93-201762] p 2452 N94-23451

Source spacing in B-ISDN [PB93-201747] p 2293 N94-23508

Mean-value of product-form stochastic Petri net models of slotted-ring systems [PB94-110871] p 2494 N94-23749

Design and implementation issues of end-to-end protocols in high-speed networks [PB94-110905] p 2467 N94-23752

Multi-access laser communications terminal [NASA-CR-191251] p 2295 N94-23830

SpaceOps 1992: Proceedings of the Second International Symposium on Ground Data Systems for Space Mission Operations [NASA-CR-194486] p 2497 N94-23832

The space operations at CNES p 2498 N94-23837

A reference model for space data system interconnection services p 2305 N94-23847

The application of automated operations at the Institutional Processing Center p 2509 N94-23901

NASDA's Advanced On-Line System (ADOLIS) p 2509 N94-23903

Applications of CCSDS recommendations to Integrated Ground Data Systems (IGDS) p 2510 N94-23906

Resource allocation planning with international components p 2520 N94-23963

Scheduling the future NASA Space Network: Experiences with a flexible scheduling prototype p 2520 N94-23965

Radio communication and wave propagation. A visit to the Netherlands in December 1992 [PB93-204360] p 2297 N94-24531

A simulation and evaluation of NATO Standardization Agreement (STANAG) 4214 [AD-A273195] p 2297 N94-24554

Fast simulation of packet loss rates in a shared buffer communications switch [NASA-CR-191556] p 2457 N94-24638

Service description of communication systems supporting multi-media multi-user applications [PB94-110855] p 2299 N94-24650

Bounds and simulation results of 32-ary and 64-ary quadrature amplitude modulation for broadband-ISDN via satellite [NASA-TM-106484] p 2202 N94-25095

First results from the Fennoscandian GPS networks p 2405 N94-25204

Failure detection and recovery in the assembly/contingency subsystem p 2306 N94-25360

COMMUNICATION SATELLITES

SAW based systems for mobile communications satellites p 2275 N94-22746

Use of negotiated rulemaking in developing technical rules for low-Earth orbit mobile satellite systems p 2276 N94-22750

Integration of mobile satellite and cellular systems p 2277 N94-22757

Interworking evolution of mobile satellite and terrestrial networks p 2277 N94-22758

Interworking and integration of the Inmarsat Standard-M with Pan-European GSM system p 2277 N94-22759

Architectures and protocols for an integrated satellite-terrestrial mobile system p 2277 N94-22760

Trends in mobile satellite communication p 2278 N94-22763

Optimizing space constellations for mobile satellite systems p 2278 N94-22764

Geostationary payload concepts for personal satellite communications p 2278 N94-22765

A system architecture for an advanced Canadian wideband mobile satellite system p 2278 N94-22766

Applicability of different onboard routing and processing techniques to mobile satellite systems p 2278 N94-22767

ROCSAT-1 telecommunication experiments p 2279 N94-22770

ACTS advanced system concepts and experimentation p 2280 N94-22780

EUTELTRACS: The European experience on mobile satellite services p 2281 N94-22781

The ORBCOMM data communications system p 2281 N94-22782

Mobilesat (tm): A world first p 2281 N94-22783

The Iridium (tm) system: Personal communications anytime, anyplace p 2281 N94-22785

Odyssey personal communications satellite system p 2282 N94-22787

The European Mobile System (EMS) p 2282 N94-22789

Land mobile satellite propagation measurements in Japan using ETS-V satellite p 2282 N94-22790

Measurements on the satellite-mobile channel at L and S bands p 2282 N94-22791

A study of satellite motion-induced multipath phenomena p 2283 N94-22794

Electromagnetic field strength prediction in an urban environment: A useful tool for the planning of LMSS p 2283 N94-22795

Propagation model for the Land Mobile Satellite channel in urban environments p 2283 N94-22796

Systems implications of L-band fade data statistics for LEO mobile systems p 2284 N94-22799

Low cost coherent demodulation for mobile satellite terminals p 2284 N94-22803

SATCOM simulator speeds MSS deployment and lowers costs p 2287 N94-22822

Advanced mobile satellite communications using COMETS satellite in MM-wave and Ka-band p 2288 N94-22829

Power beaming to space using a nuclear reactor-pumped laser [DE94-001208] p 2348 N94-23185

Satellite communications systems and technology. Volume 2: Site reports [NASA-TM-109399] p 2293 N94-23628

Future trends in NASA space operations p 2498 N94-23836

Worldwide vessel locating and tracking system, volume 1 [PB93-193217] p 2175 N94-24474

Preliminary far-field plume sputtering characterization of the Stationary Plasma Thruster (SPT-100) [NASA-TM-106464] p 2221 N94-24766

COMMUNICATION THEORY

Delay-insensitive communication [ETN-94-95315] p 2304 N94-25303

COMPATIBILITY

Determination of the compatibility between structural alloys and molten metals at high temperatures [DE94-000954] p 2241 N94-23434

Development testing of the two-watt RTG heat source and Hastelloy-S/T-111 alloy compatibility studies [DE94-002875] p 2243 N94-23784

NASA/Goddard Space Flight Center's testbed for CCSDS compatible systems p 2197 N94-23855

COMPENSATORS

Discrete-time H(infinity) control problem with strictly proper measurement feedback
[NASA-CR-195089] p 2473 N94-24542

Automatic pressure control system for the Wright Laboratory Compressor Research Facility
[AD-A273827] p 2194 N94-25522

COMPILERS

Code generation for the attribute evaluator of the protocol engine grammar processor unit
[EUT-93-E-271] p 2450 N94-23173

Object distribution in orca using compile-time and run-time techniques
[PB94-110574] p 2453 N94-23745

Micro SIL-1 simulator
[PB94-110889] p 2454 N94-23750

Runtime support and compilation methods for user-specified data distributions
[NASA-CR-191587] p 2458 N94-24679

Optimizing parallelization
[AD-A273565] p 2467 N94-24692

An integrated runtime and compile-time approach for parallelizing structured and block structured applications
[NASA-CR-191554] p 2458 N94-24740

RIACS/USRA
[NASA-CR-195117] p 2631 N94-25003

COMPLEX SYSTEMS

Automated parallelization of timed Petri-net simulations
[NASA-CR-191574] p 2451 N94-23341

COMPLEX VARIABLES

Edge detection using a complex wavelet
[AD-A273699] p 2493 N94-25452

COMPONENT RELIABILITY

Long term trending of engineering data for the Hubble Space Telescope p 2516 N94-23942

Reliable redundant device for mechanisms
p 2361 N94-24030

Viscous rotary damper p 2361 N94-24031

A minimum cost tolerance allocation method for rocket engines and robust rocket engine design
p 2222 N94-24419

Aviation system safety risk management tool analysis. Volume 2: Appendices
[AD-A273502] p 2173 N94-24864

An x ray diffraction investigation of alpha-Al2O2 addition to Yttria Stabilized Zirconia (YSZ) thermal barrier coatings subject to destabilizing vanadium pentoxide (V2O5) exposure
[AD-A273403] p 2261 N94-25072

Computerized testing system software conversion and development: Identifying software and hardware portability issues and solutions
[AD-A273489] p 2462 N94-25287

COMPOSITE MATERIALS

Counterrotating aircraft propulsor blades
[CA-PATENT-1-319-357] p 2186 N94-23255

Time dependent behavior of a graphite/thermoplastic composite and the effects of stress and physical aging
[NASA-TM-109047] p 2228 N94-23280

An evaluation of Compton scatter imaging using COMSCAN
[DREP-TM-93-38] p 2372 N94-24136

Attachment methods in composite joints - analysis of test results by controlled experiments method
p 2158 N94-24269

S-2E Tracker maritime patrol aircraft re-engine and system upgrade program p 2158 N94-24270

Modelling the ignition of boron/titanium particles
p 2159 N94-24273

Experimental investigation of ignition of boron/titanium composite particles p 2159 N94-24275

Nonlinear analysis using a modal based reduction technique p 2161 N94-24288

Evaluation of advanced materials through experimental mechanics and modelling p 2374 N94-24454

High strain rate superplasticity in metals and composites
[DE94-001521] p 2229 N94-24547

Polythiophene derivative with a side chain chromophore as photovoltaic and photorefractive materials
[AD-A273245] p 2260 N94-24813

Center for Analysis of Heterogeneous and Nonlinear Media
[AD-A273515] p 2230 N94-25158

Alternatives for reinforcement: Fiber composites
[VTT-TIED-1412] p 2230 N94-25386

Proceedings of the 12th International Congress: Corrosion Control for Low-Cost Reliability. Volume 5A: Corrosion: General issues
[AD-A273666] p 2250 N94-25406

Composites and textile reinforcement
[VTT-TIED-1424] p 2231 N94-25420

Application of body fitted-coordinates in heat conduction problems
[ETN-94-95338] p 2340 N94-25484

COMPOSITE STRUCTURES

Composite fiber structures for catalysts and electrodes
p 2393 N94-23364

Holographic testing of composite propfans for a cruise missile wind tunnel model
[NASA-TM-105271] p 2187 N94-23545

Computer based expert system for battle damage repair of composite structures p 2157 N94-24262

Attachment methods in composite joints - analysis of test results by controlled experiments method
p 2158 N94-24269

The process network in the design and manufacturing of aircraft p 2178 N94-24319

Structural design criteria for filament-wound composite shells
[NASA-CR-195125] p 2229 N94-24402

Assessment of impact damage of composite rocket motor cases
[NASA-CR-195143] p 2220 N94-24595

Stability analysis of anisotropic conical shells
[PB94-119054] p 2377 N94-24645

Advanced electromagnetic methods for aerospace vehicles
[NASA-CR-195111] p 2365 N94-24699

Dynamic analysis of pretwisted elastically-coupled rotor blades
[NASA-TM-109070] p 2378 N94-24839

Aeroelastic response and stability of tiltrotors with elastically-coupled composite rotor blades
[NASA-TM-108758] p 2182 N94-24953

Probabilistic assessment of smart composite structures
[NASA-TM-106358] p 2378 N94-25188

Alternatives for reinforcement: Fiber composites
[VTT-TIED-1412] p 2230 N94-25386

COMPRESSED GAS

Picosecond High Pressure Gas Switch experiment
[DE93-040853] p 2307 N94-22950

COMPRESSIBILITY

Control of the internal stresses in plane elasticity
[PB93-225514] p 2374 N94-23112

Heat pipe vapor dynamics
[NASA-CR-194217] p 2327 N94-24096

Buckling of circular cylindrical shells subjected to combined loads (axial compression, normal pressure, bending and transverse shear loading)
[PB93-215358] p 2378 N94-24745

Unified approach for incompressible flows
p 2342 N94-25356

A numerical investigation of the artificial compressibility method for the solution of the Navier-Stokes equations
[CRANFIELD-AERO-9213] p 2340 N94-25486

COMPRESSIBILITY EFFECTS

Compressibility effects on dynamic stall of airfoils undergoing rapid transient pitching motion
[NASA-TM-109681] p 2167 N94-23975

Direct simulation of isothermal-wall supersonic channel flow p 2172 N94-24164

Development and validation of RNG methodology for compressible turbulence
[AD-A273469] p 2337 N94-24929

COMPRESSIBLE BOUNDARY LAYER

Development and validation of RNG methodology for compressible turbulence
[AD-A273469] p 2337 N94-24929

COMPRESSIBLE FLOW

A multigrid multiblock solver for compressible turbulent flow
[MEMO-1125] p 2315 N94-22713

An F2D analysis of the Flow Instability Test (FIT) experiment
[DE94-001420] p 2217 N94-23193

A representation for the turbulent mass flux contribution to Reynolds-stress and two-equation closures for compressible turbulence
[NASA-CR-191569] p 2319 N94-23302

An implicit numerical scheme for the simulation of internal viscous flows on unstructured grids
[NASA-TM-106437] p 2481 N94-23554

Compressible turbulent flow simulation with a multigrid multiblock method p 2342 N94-23694

Issac, Jason Cherian ses in transonic flow
[NASA-CR-194837] p 2167 N94-24052

Heat pipe vapor dynamics
[NASA-CR-194217] p 2327 N94-24096

Direct simulation of isothermal-wall supersonic channel flow p 2172 N94-24164

Carrying the mass flux terms exactly in the first and second moment equations of compressible turbulence
[NASA-CR-191568] p 2335 N94-24712

Development and validation of RNG methodology for compressible turbulence
[AD-A273469] p 2337 N94-24929

Development and application of new algorithms for the simulation of viscous compressible flows with moving bodies in three dimensions
[AD-A273514] p 2338 N94-25157

Unified approach for incompressible flows
p 2342 N94-25356

COMPRESSIBLE FLUIDS

Local grid refinement method for the euler equations
[PB93-223329] p 2317 N94-22985

COMPRESSION LOADS

Post buckling behaviour of stiffened composite panels loaded in cyclic compression and shear
p 2157 N94-24260

Properties and processing characteristics of low density carbon cloth phenolic composites p 2231 N94-24450

COMPRESSION RATIO

Integer cosine transform compression for Galileo at Jupiter: A preliminary look p 2292 N94-23266

COMPRESSION TESTS

A prediction method for the compressive strength of impact damaged composite laminates
[CTN-94-60925] p 2229 N94-24137

Post buckling behaviour of stiffened composite panels loaded in cyclic compression and shear
p 2157 N94-24260

Structural design criteria for filament-wound composite shells
[NASA-CR-195125] p 2229 N94-24402

Test methods for composites: A status report. Volume 2: Compression test methods
[AD-A273522] p 2230 N94-24779

COMPRESSIVE STRENGTH

Developments in materials for high-field magnets
[DE94-000761] p 2307 N94-22987

A prediction method for the compressive strength of impact damaged composite laminates
[CTN-94-60925] p 2229 N94-24137

Humidity effects on soluble core mechanical and thermal properties (polyvinyl alcohol/microballoon composite) type CG extendospheres, volume 2
[NASA-CR-193893] p 2229 N94-24224

. Test methods for composites: A status report. Volume 2: Compression test methods
[AD-A273522] p 2230 N94-24779

The mechanical property data base from an Air Force/Industry Cooperative Test Program on advanced aluminum alloys (7064 and CW67)
[AD-A273741] p 2251 N94-25531

COMPRESSOR BLADES

Off-design performance of crenulated blades in a linear compressor cascade
[AD-A273744] p 2340 N94-25534

COMPRESSOR ROTORS

Analysis and characteristics of compressor stall precursor signals in forward and AFT swept high speed compressor
[AD-A273820] p 2171 N94-25517

COMPRESSORS

Measurement of kinematically unstationary separated flows p 2315 N94-22854

Magnetic power piston fluid compressor
[NASA-CASE-GSC-13565-1] p 2354 N94-23831

Reduction of hydrocarbon impurities in 200 l/h helium liquefier-refrigerator system
[NIFS-259] p 2271 N94-24459

Analysis and characteristics of compressor stall precursor signals in forward and AFT swept high speed compressor
[AD-A273820] p 2171 N94-25517

Automatic pressure control system for the Wright Laboratory Compressor Research Facility
[AD-A273827] p 2194 N94-25522

COMPTON EFFECT

Analysis of a proposed Compton backscatter imaging technique
[DE93-040537] p 2371 N94-22935

An evaluation of Compton scatter imaging using COMSCAN
[DREP-TM-93-38] p 2372 N94-24136

COMPUTATION

The explicit computation of integration algorithms and first integrals for ordinary differential equations with polynomials coefficients using trees
[NASA-CR-194787] p 2448 N94-23074

On the numerical computation of invariant manifolds
[W-9306] p 2480 N94-23140

Runtime support and compilation methods for user-specified data distributions
[NASA-CR-191587] p 2458 N94-24679

Efficiency of subset selection of an epsilon-best uniform population relative to selection of the best one
[PB93-237741] p 2490 N94-24763

Computing techniques in mission planning
p 2522 N94-25012

COMPUTATIONAL ASTROPHYSICS

A mixed method Poisson solver for three-dimensional self-gravitating astrophysical fluid dynamical systems p 2484 N94-23684

COMPUTATIONAL FLUID DYNAMICS

Local grid refinement method for the euler equations [PB93-223329] p 2317 N94-22985

CFD analyses of combustor and nozzle flowfields p 2210 N94-23033

Numerical parametric studies of spray combustion instability p 2212 N94-23041

Numerical investigation of two- and three-dimensional heat transfer in expander cycle engines p 2213 N94-23048

CFD analyses of coolant channel flowfields p 2214 N94-23050

Heat transfer in rocket combustion chambers p 2214 N94-23051

Computational Fluid Dynamics (CFD) applications in rocket propulsion analysis and design p 2214 N94-23054

Computation of propulsion-related flowfields using unstructured adaptive meshes p 2215 N94-23056

Computational fluid dynamic modelling of cavitation p 2215 N94-23060

CFD modeling of microwave electrothermal thrusters p 2216 N94-23066

Two-dimensional Navier-Stokes computations of subsonic and supersonic flows through turbine cascades [PB93-226223] p 2317 N94-23114

POISs3: A 3D poisson smoother of structured grids [PB93-226231] p 2318 N94-23115

Computational study of GA(W)-1: Airfoil near stall [PB93-226249] p 2165 N94-23116

Locally modified Bott-scheme for highly convective flows [MPIM-99] p 2400 N94-23157

Field models: Their present and future application in fire safety engineering [PB93-201622] p 2269 N94-23506

Unsteady jet flow computation towards noise prediction [NASA-CR-194449] p 2153 N94-23553

An implicit numerical scheme for the simulation of internal viscous flows on unstructured grids [NASA-TM-106437] p 2481 N94-23554

LinAir: A multi-element discrete vortex Weissinger aerodynamic prediction method [NASA-TM-108786] p 2167 N94-23557

Prediction of pressure drop in fluid tuned mounts using analytical and computational techniques p 2321 N94-23643

The 3-D CFD modeling of gas turbine combustor-integral bleed flow interaction p 2189 N94-23658

The 3-D numerical study of airflow in the compressor/combustor prediffuser and dump diffuser of an industrial gas turbine p 2324 N94-23660

An analytic study of a two-phase laminar airfoil in simulated heavy rain p 2171 N94-23661

An application of small-gap equations in sealing devices p 2325 N94-23668

Comparison of numerical simulation and experimental data for steam-in-place sterilization p 2326 N94-23669

A comparative study of computational solutions to flow over a backward-facing step p 2326 N94-23670

Upwind MacCormack Euler solver with non-equilibrium chemistry p 2326 N94-23672

The Sixth Copper Mountain Conference on Multigrid Methods, part 1 [NASA-CP-3224-PT-1] p 2482 N94-23673

A mixed method Poisson solver for three-dimensional self-gravitating astrophysical fluid dynamical systems p 2484 N94-23684

An object-oriented approach for parallel self adaptive mesh refinement on block structured grids p 2469 N94-23697

Efficient interpolation of velocity and flux components defined on 2- and 3-dimensional non-cartesian grids [PB94-118619] p 2486 N94-23757

Thermohydrodynamic analysis of cryogenic liquid turbulent flow fluid film bearings [NASA-CR-194869] p 2363 N94-24081

CFD assessment of orifice aspect ratio and mass flow ratio on jet mixing in rectangular ducts [NASA-TM-106434] p 2187 N94-24082

New concepts for Reynolds stress transport equation modeling of inhomogeneous flows p 2171 N94-24143

Turbulence modeling for non-equilibrium flows p 2328 N94-24144

Computation of turbulent flows over backward and forward-facing steps using a near-wall Reynolds stress model p 2172 N94-24145

Large eddy simulation of a boundary layer with concave streamwise curvature p 2328 N94-24146

Large-eddy simulation of flow in a plane, asymmetric diffuser p 2328 N94-24147

On the large eddy simulation of turbulent flows in complex geometry p 2329 N94-24148

Investigation of the asymptotic state of rotating turbulence using large-eddy simulation p 2330 N94-24152

A large eddy simulation scheme for turbulent reacting flows p 2330 N94-24154

A transport equation for the scalar dissipation in reacting flows with variable density: First results p 2331 N94-24157

The production of premixed flame surface area in turbulent shear flow p 2237 N94-24158

On streak spacing in wall-bounded turbulent flows p 2331 N94-24159

Numerical simulation of non-Newtonian free shear flows p 2331 N94-24160

Direct simulation of isothermal-wall supersonic channel flow p 2172 N94-24164

Effects of shock strength on shock turbulence interaction p 2332 N94-24165

Computation of large-scale statistics in decaying isotropic turbulence p 2332 N94-24167

On the dynamics of approximating schemes for dissipative nonlinear equations p 2332 N94-24168

New features in Computational Fluid Dynamics (CFD) technology at the TASHAN Engineering Center at IAI p 2155 N94-24249

Discrete sensitivity derivatives of the Navier-Stokes equations with a parallel Krylov solver [NASA-TM-106481] p 2265 N94-24301

Integrated Airframe Design Technology [AGARD-R-794] p 2177 N94-24313

Applications of CFD codes and supercomputers to aircraft design activities p 2177 N94-24316

Modeling dynamically coupled fluid-duct systems with finite line elements [NASA-CR-193909] p 2376 N94-24359

CFD simulation of coaxial injectors p 2342 N94-24430

Workshop on Computational Turbulence Modeling [NASA-CP-10130] p 2333 N94-24460

Heat transfer in rocket engine combustion chambers and regeneratively cooled nozzles [NASA-CR-195094] p 2220 N94-24471

Radiative properties of molecular nitrogen ions produced by helium Penning ionization and argon effects [NASA-CR-195126] p 2534 N94-24487

Validation of the ROTAC code for the rotor noise prediction [PB93-204311] p 2529 N94-24514

Conservation equations for reacting gas flow [PB94-111168] p 2334 N94-24574

Solution of the discretized incompressible Navier-Stokes equations with iterative methods [PB94-118635] p 2335 N94-24641

A numerical study of airplanes flying in proximity [AD-A273373] p 2173 N94-24718

An integrated runtime and compile-time approach for parallelizing structured and block structured applications [NASA-CR-191554] p 2458 N94-24740

HYPULSE combustor analysis [NASA-CR-191579] p 2336 N94-24771

Projection techniques for iterative solution of A(bar x) equals (bar b) with successive right-hand sides [NASA-CR-191571] p 2490 N94-24836

Numerical flow simulation for complete vehicle configurations [AD-A273588] p 2170 N94-24849

Numerical solutions of the complete Navier-Stokes equations [NASA-CR-194780] p 2337 N94-24858

Computational fluid mechanics [NASA-CR-194765] p 2337 N94-24859

Vortex generation and wave-vortex interaction over a concave plate with roughness and suction [NASA-CR-191589] p 2337 N94-24869

Triangular spectral elements for incompressible fluid flow [NASA-CR-191588] p 2490 N94-24914

A finite-element-based perturbation model for the rotordynamic analysis of shrouded pump impellers: Part 1: Model development and applications [NASA-CR-193916] p 2366 N94-24998

A finite-element-based perturbation model for the rotordynamic analysis of shrouded pump impellers: Part 2: User's guide [NASA-CR-193917] p 2366 N94-24999

Research in progress and other activities of the Institute for Computer Applications in Science and Engineering [NASA-CR-191576] p 2444 N94-25090

LES, DNS and RANS for the analysis of high-speed turbulent reacting flows [NASA-CR-195196] p 2337 N94-25094

Modeling transonic aerodynamic response using nonlinear systems theory for use with modern control theory p 2164 N94-25112

Active control of oscillatory lift forces on a circular cylinder [AD-A273243] p 2338 N94-25140

Development and application of new algorithms for the simulation of viscous compressible flows with moving bodies in three dimensions [AD-A273514] p 2338 N94-25157

Advanced ballistic range technology [NASA-CR-195198] p 2165 N94-25169

A continuing search for a near-perfect numerical flux scheme. Part 1: AUSM+ [NASA-TM-106524] p 2338 N94-25180

Improving diffusing S-duct performance by secondary flow control [NASA-TM-106492] p 2170 N94-25182

Two-dimensional CFD modeling of wave rotor flow dynamics [NASA-TM-106261] p 2189 N94-25185

Hydrodynamics of stirred gas-liquid dispersions [ETN-94-95368] p 2339 N94-25254

High lift aerodynamics [NASA-CR-195183] p 2184 N94-25268

Detailed description of two calculation programs for incompressible, steady state boundary layer flows, applied to determine the aerodynamic characteristics of NACA12 and OA312 foils at low Reynolds numbers [ISL-N-604/92] p 2171 N94-25461

Study of the blade/vortex interaction: Acoustics, aerodynamics and models [ISL-R-104/92] p 2340 N94-25463

An adaptive streamline diffusion finite element method for hyperbolic systems in gas dynamics [PREPRINT-688] p 2340 N94-25466

A numerical investigation of the artificial compressibility method for the solution of the Navier-Stokes equations [CRANFIELD-AERO-9213] p 2340 N94-25486

COMPUTATIONAL GEOMETRY

Parallel unstructured grid generation for computational aerosciences [NASA-CR-192244] p 2466 N94-23483

COMPUTATIONAL GRIDS

A geometric weighted elliptic grid regeneration method for 3D unstructured ALE hydrodynamics [DE94-000309] p 2448 N94-22980

Local grid refinement method for the euler equations [PB93-223329] p 2317 N94-22985

Computation of propulsion-related flowfields using unstructured adaptive meshes p 2215 N94-23056

Two-dimensional Navier-Stokes computations of subsonic and supersonic flows through turbine cascades [PB93-226223] p 2317 N94-23114

POISs3: A 3D poisson smoother of structured grids [PB93-226231] p 2318 N94-23115

Computational study of GA(W)-1: Airfoil near stall [PB93-226249] p 2165 N94-23116

Simulation of unsteady flows through stator and rotor blades of a gas turbine using the Chimera method p 2323 N94-23652

The Sixth Copper Mountain Conference on Multigrid Methods, part 1 [NASA-CP-3224-PT-1] p 2482 N94-23673

FAS multigrid calculations of three dimensional flow using non-staggered grids p 2341 N94-23675

Uniform convergence of multigrid V-cycle iterations for indefinite and nonsymmetric problems p 2482 N94-23677

An adaptive multigrid model for hurricane track prediction p 2416 N94-23687

A multilevel adaptive projection method for unsteady incompressible flow p 2341 N94-23690

A comparison of locally adaptive multigrid methods: LDC, FAC and FIC p 2485 N94-23692

Compressible turbulent flow simulation with a multigrid multiblock method p 2342 N94-23694

An object-oriented approach for parallel self adaptive mesh refinement on block structured grids p 2469 N94-23697

Efficient interpolation of velocity and flux components defined on 2- and 3-dimensional non-cartesian grids [PB94-118619] p 2486 N94-23757

On the dynamics of some grid adaption schemes [NASA-CR-195092] p 2454 N94-24110

Toward large eddy simulation of turbulent flow over an airfoil p 2172 N94-24150

Unstructured grid large eddy simulation of wall bounded turbulent flows p 2329 N94-24151

Unstructured adaptive mesh computations of rotorcraft high-speed impulsive noise [NASA-CR-195090] p 2529 N94-24307

Implementation of the Baldwin-Barth turbulence model into the ZETA code and its diagnosis [NASA-CR-194795] p 2335 N94-24640

Solution of the discretized incompressible Navier-Stokes equations with iterative methods
[PB94-118635] p 2335 N94-24641

Numerical flow simulation for complete vehicle configurations
[AD-A273588] p 2170 N94-24849

COMPUTER AIDED DESIGN

A new automatic design method to develop multilayer thin film devices for high power laser applications
[DE93-632490] p 2347 N94-22967

Hypermedia support for engineering design system
[PB93-226256] p 2449 N94-23117

AMICAL: An aid for architectural synthesis and exploration of control circuits
[ETN-94-95177] p 2308 N94-23154

APLAC: An object-oriented analog circuit simulator and design tool. 6.1 system simulations manual
[PB93-224871] p 2450 N94-23226

Object oriented simulation implementation in support of robust system design
[DE93-011687] p 2452 N94-23488

Development of a code for wall contour design in the transonic region of axisymmetric and square nozzles
[NASA-CR-194857] p 2167 N94-23625

Some useful innovations with TRASYS and SINDA-85
p 2322 N94-23647

Development of biomechanical models for human factors evaluations p 2437 N94-24205

New features in Computational Fluid Dynamics (CFD) technology at the TASHAN Engineering Center at IAI
p 2155 N94-24249

Integrated Airframe Design Technology
[AGARD-R-794] p 2177 N94-24313

The process network in the design and manufacturing of aircraft p 2178 N94-24319

Application of concurrent engineering principles to aircraft structural design p 2178 N94-24321

Some practical problems in multidisciplinary design and optimisation p 2178 N94-24322

Current and future design methods for large transport aircraft p 2179 N94-24324

The integration of design and manufacturing processes at Alenia DVD p 2179 N94-24325

Trends of design methodology of airframe
p 2179 N94-24327

Characteristics of products generated by selective sintering and stereolithography rapid prototyping processes p 2264 N94-24412

Octave: A MARSYAS post-processor for computer-aideed control system design
p 2465 N94-24422

Evaluation of the efficiency and fault density of software generated by code generators p 2465 N94-24445

Computer modeling of plasma flow switches-high current switching on Procyon
[DE93-040189] p 2311 N94-24500

Compositional architecture for simple design formally specified in DESIRE
[PB94-119013] p 2474 N94-24543

NASA advanced design program. Design and analysis of a radio-controlled flying wing aircraft
[NASA-CR-195515] p 2180 N94-24589

The use of design automation software by government-contracted architect/engineer firms: A status report
[AD-A273181] p 2459 N94-24812

Merits and limitations of optimality criteria method for structural optimization
[NASA-TP-3373] p 2378 N94-24845

Parametric uncertainty reduction in robust multivariable control
[AD-A273412] p 2460 N94-24927

Area-power-delay trade-off in logic synthesis
[ISBN-9-09-005332-8] p 2461 N94-25080

From circuit to signal: Development of a piecewise linear simulator
[ISBN-9-09-005713-7] p 2462 N94-25263

Software engineering methodologies and tools
p 2465 N94-25382

CADBIT 2: Computer-aided design for built-in test, volume 1
[AD-A273702] p 2463 N94-25455

CADBIT 2: Computer-aided design for built-in test, volume 2
[AD-A273703] p 2463 N94-25456

COMPUTER AIDED MANUFACTURING

Plan generation for flexible assembly systems
[PB93-217974] p 2267 N94-22981

The process network in the design and manufacturing of aircraft p 2178 N94-24319

The integration of design and manufacturing processes at Alenia DVD p 2179 N94-24325

DARPA DICE manufacturing optimization
[AD-A273345] p 2461 N94-25156

COMPUTER AIDED MAPPING

Study of methods and structures for handling of digitized maps for geographical information systems
[PB93-204402] p 2590 N94-23741

COMPUTER AIDED TOMOGRAPHY

Nondestructive evaluations
[DE94-003020] p 2373 N94-24613

COMPUTER ANIMATION

Visualization of results from meteorological simulations on CRAY
[PB93-201358] p 2451 N94-23443

Development of biomechanical models for human factors evaluations p 2437 N94-24205

COMPUTER ASSISTED INSTRUCTION

Intelligent tutoring and aiding in satellite ground control p 2443 N94-23929

Operational training for the mission operations at the Brazilian National Institute for Space Research (INPE)
p 2429 N94-23933

Training: Plugging the information gaps
p 2429 N94-23934

Evaluation of computer-aided instruction techniques for the crew interface coordination position
p 2429 N94-24438

World processor: An interface for textual display and manipulation in virtual reality
[PB94-118643] p 2592 N94-24642

Understanding and facilitating discovery learning in computer-based simulation environment
[ISBN-9-03-860242-1] p 2462 N94-25219

A multimedia adult literacy program: Combining NASA technology, instructional design theory, and authentic literacy concepts p 2585 N94-25384

COMPUTER DESIGN

A novel process monitoring and control system based on a neural manufacturing concept
[DE94-001516] p 2471 N94-23011

New computing systems, future computing environment, and their implications on structural analysis and design
p 2177 N94-24314

Optical wavelet transform processor
[AD-A273625] p 2546 N94-24731

Study on fine grain dynamic dataflow computer
[REPT-946] p 2446 N94-24981

COMPUTER GRAPHICS

VTGRAPH:Computer graphics program using ReGIS mode
[DE94-600342] p 2448 N94-23024

Switch configuration for migration to optical fiber network p 2447 N94-23250

Image pattern recognition supporting interactive analysis and graphical visualization
[NASA-CR-194878] p 2451 N94-23369

GLview user's guide
[PB93-201366] p 2452 N94-23444

Simultaneous simulation and visualization using DGL
[PB93-201341] p 2453 N94-23534

Experience with parametric binary dissection
[NASA-CR-191552] p 2473 N94-23558

Framework for interactive solving of meta-constraint satisfaction problems
[PB94-118825] p 2585 N94-23761

GSMS and space views: Advanced spacecraft monitoring tools p 2507 N94-23890

The mission events graphic generator software: A small tool with big results p 2464 N94-23893

Night vision goggle illusions and visual training
p 2432 N94-23984

Using computer graphics to design Space Station Freedom viewing p 2434 N94-24191

ACES spectral display software: Software description
[SK-1600-99-003] p 2455 N94-24297

The torsion space nucleic acids molecular mechanics program DUPLEX: Surveying conformation space by potential energy minimization
[DE94-002441] p 2563 N94-24567

World processor: An interface for textual display and manipulation in virtual reality
[PB94-118643] p 2592 N94-24642

Tools for visualizing landscape pattern for large geographic areas
[DE94-001121] p 2388 N94-24757

CADBIT 2: Computer-aided design for built-in test, volume 2
[AD-A273703] p 2463 N94-25456

COMPUTER INFORMATION SECURITY

Security aspects of space operations data
p 2515 N94-23937

Special signature schemes
[ETN-94-95296] p 2446 N94-25081

COMPUTER NETWORKS

Using satellite communications for a mobile computer network p 2280 N94-22777

Design and implementation considerations of a MSAT packet data network p 2280 N94-22778

Distributed Operating Systems and Mach. Proceedings of the Spring 1992 Graduate Seminar on Distributed Systems
[PB93-224905] p 2449 N94-23103

Specifications of ETS, the Enhanced Transport Service
[RR-907-I] p 2589 N94-23150

A parallel PROLOG system for distributed memory multiprocessor
[ETN-94-95173] p 2465 N94-23167

Reduced cost alternatives to premise wiring using ATM and microcellular technologies p 2314 N94-23239

Mean-value of product-form stochastic Petri net models of slotted-ring systems
[PB94-110871] p 2494 N94-23749

Design and implementation issues of end-to-end protocols in high-speed networks
[PB94-110905] p 2467 N94-23752

Applications of CCSDS recommendations to Integrated Ground Data Systems (IGDS) p 2510 N94-23906

Distributed computing environments for future space control systems p 2464 N94-23911

Deep Space Network (DSN), Network Operations Control Center (NOCC) computer-human interfaces
p 2447 N94-23917

Telemetry ground system development via the component approach p 2203 N94-23949

An engineering database management system for spacecraft operations p 2517 N94-23951

An investigation of requirements traceability to support systems development
[AD-A273167] p 2458 N94-24684

Evolving neural network connectivity
[AD-A273134] p 2490 N94-24921

A usage profile and evaluation of a wide-area distributed file system
[AD-A273590] p 2593 N94-24946

COMPUTER PROGRAMMING

VTGRAPH:Computer graphics program using ReGIS mode
[DE94-600342] p 2448 N94-23024

Software for scientific visualization: State of the art and experiences
[PB93-225183] p 2449 N94-23111

Code generation for the attribute evaluator of the protocol engine grammar processor unit
[EUT-93-E-271] p 2450 N94-23173

FEMAX finite-element package for computing three-dimensional time-domain electromagnetic fields in inhomogeneous media
[PB94-111093] p 2294 N94-23733

Object distribution in orca using compile-time and run-time techniques
[PB94-110574] p 2453 N94-23745

Micro SIL-1 simulator
[PB94-110889] p 2454 N94-23750

Making tomorrow's mistakes today: Evolutionary prototyping for risk reduction and shorter development time p 2197 N94-23902

Software reuse in spacecraft planning and scheduling systems p 2520 N94-23966

SAO mission support software and data standards, version 1.0
[NASA-CR-193906] p 2454 N94-24050

Update of GRASP/Ada reverse engineering tools for Ada
[NASA-CR-193890] p 2455 N94-24111

Evaluation of the efficiency and fault density of software generated by code generators p 2465 N94-24445

Verification and validation of models
[PB94-110566] p 2456 N94-24507

A methodology for software cost estimation using machine learning techniques
[AD-A273158] p 2459 N94-24775

Evolving neural network connectivity
[AD-A273134] p 2490 N94-24921

Reengineering real-time software systems
[AD-A273408] p 2461 N94-25074

Models of trace theory systems
[ETN-94-95361] p 2468 N94-25226

Failure detection and recovery in the assembly/contingency subsystem p 2306 N94-25360

Software engineering methodologies and tools
p 2465 N94-25382

COMPUTER PROGRAMS

Algorithms for speech coding systems based on linear prediction
[EUT-92-E-260] p 2447 N94-22731

Proof test of the computer program BUCKY for plasticity problems
[NASA-TP-3444] p 2374 N94-22960

Users manual for the Chameleon parallel programming tools
[DE94-001934] p 2465 N94-22973

Software for scientific visualization: State of the art and experiences [PB93-225183] p 2449 N94-23111
Tools reference manual for a Requirements Specification Language (RSL), version 2.0 [NASA-CR-191461] p 2445 N94-23125
Atmospheric flow in heterogeneous vegetated regions [W-9303] p 2401 N94-23175
Towards the formal specification of the requirements and design of a processor interface unit: HOL listings [NASA-CR-191465] p 2466 N94-23252
CRRES microelectronics package flight data analysis [NASA-TP-3423] p 2540 N94-23273
Image pattern recognition supporting interactive analysis and graphical visualization [NASA-CR-194878] p 2451 N94-23369
Experiments with a small behaviour controlled planetary rover p 2371 N94-23427
Transient Ejector Analysis (TEA) code user's guide [NASA-TM-106310] p 2186 N94-23466
Theoretical studies of a molecular beam generator [NASA-CR-194779] p 2540 N94-23485
OASIS-CC presentation p 2385 N94-23613
Validating a large geophysical data set: Experiences with satellite-derived cloud parameters p 2385 N94-23615
Experience of the JPL Exploratory Data Analysis Team at validating HIRS2/MSU cloud parameters p 2385 N94-23616
The Fifth Annual Thermal and Fluids Analysis Workshop [NASA-CP-10122] p 2320 N94-23634
A comparison of TSS and TRASYS in form factor calculation p 2321 N94-23638
Utilization of recently developed codes for high power Brayton and Rankine cycle power systems p 2222 N94-23641
Thermal analysis of combinatorial solid geometry models using SINDA p 2323 N94-23650
Convection equation modeling: A non-iterative direct matrix solution algorithm for use with SINDA p 2323 N94-23651
Micro SIL-1 simulator [PB94-110889] p 2454 N94-23750
Design and implementation issues of end-to-end protocols in high-speed networks [PB94-110905] p 2467 N94-23752
Mission planning for Shuttle Imaging Radar-C (SIR-C) with a real-time interactive planning software p 2305 N94-23842
SCOS2: ESA's new generation of mission control systems p 2197 N94-23851
The application of automated operations at the Institutional Processing Center p 2509 N94-23901
Multimission image processing and science data visualization p 2518 N94-23955
From requirements to acceptance tests p 2464 N94-23962
SAO mission support software and data standards, version 1.0 [NASA-CR-193906] p 2454 N94-24050
Quantitative assessment of human motion using video motion analysis p 2436 N94-24203
New features in Computational Fluid Dynamics (CFD) technology at the TASHAN Engineering Center at IAI p 2155 N94-24249
A review of ISEAS design p 2465 N94-24410
High-performance computing and communications [DE94-002215] p 2457 N94-24566
Comparison of HF groundwave propagation models [AD-A273146] p 2299 N94-24668
The use of design automation software by government-contracted architect/engineer firms: A status report [AD-A273181] p 2459 N94-24812
COSMIC monthly progress report [NASA-CR-195153] p 2460 N94-25023
Computerized testing system software conversion and development: Identifying software and hardware portability issues and solutions [AD-A273489] p 2462 N94-25287
Failure detection and recovery in the assembly/contingency subsystem p 2306 N94-25360

COMPUTER STORAGE DEVICES
A qualified radiation hardened nonvolatile memory for space and tactical weapons applications [DE94-001211] p 2559 N94-23186
Performance of the engineering analysis and data system 2 common file system p 2576 N94-24413
Field emitter array memory device [AD-D016015] p 2311 N94-24736
MOS analog memory with injection capacitors [AD-D015990] p 2312 N94-25050

COMPUTER SYSTEMS DESIGN
Definition and realization of a formal verification tool of LUSTRE programs: The LESAR system [ETN-94-95164] p 2447 N94-22882
Resolution of Markov models on distributed memory machines [ETN-94-95182] p 2444 N94-22900
AMICAL: An aid for architectural synthesis and exploration of control circuits [ETN-94-95177] p 2308 N94-23154
SPOT4 Operational Control Center (CMP) p 2197 N94-23856
Distributed computing environments for future space control systems p 2464 N94-23911
Making intelligent systems team players: Additional case studies [NASA-TM-104786] p 2473 N94-24068
New computing systems, future computing environment, and their implications on structural analysis and design p 2177 N94-24314
Performance of the engineering analysis and data system 2 common file system p 2576 N94-24413
Extension of the critical path method [PB94-118817] p 2488 N94-24527
Real-time process logic [PB94-101441] p 2446 N94-24540
An investigation of requirements traceability to support systems development [AD-A273167] p 2458 N94-24684
Study on fine grain dynamic dataflow computer [REPT-946] p 2446 N94-24981
Mission rehearsal in the SOF-ATS program p 2522 N94-25016
The design of the EMPS multiprocessor executive for distributed computing [ETN-94-95336] p 2468 N94-25062
Designing parallel programs of parameterized granularity [ETN-94-95302] p 2468 N94-25278
A design method for parallel programs [ETN-94-95331] p 2469 N94-25282

COMPUTER SYSTEMS PERFORMANCE
Resolution of Markov models on distributed memory machines [ETN-94-95182] p 2444 N94-22900
ACOS: The performance based approach to build a parallel complex object server [PB93-223816] p 2465 N94-22986
Advanced Information Processing System (AIPS) p 2165 N94-25115

COMPUTER SYSTEMS PROGRAMS
ACOS: The performance based approach to build a parallel complex object server [PB93-223816] p 2465 N94-22986
A type declarative system for PROLOG [ETN-94-95178] p 2449 N94-23155
Design and implementation issues of end-to-end protocols in high-speed networks [PB94-110905] p 2467 N94-23752
A quick uplink, expandable executable for the NSSC-1 of the Hubble Space Telescope p 2305 N94-23859
High-performance computing and communications [DE94-002215] p 2457 N94-24566
An investigation of requirements traceability to support systems development [AD-A273167] p 2458 N94-24684

COMPUTER SYSTEMS SIMULATION
The TOPSIM 4 graphic user interface [ESA-STM-247] p 2450 N94-23228

COMPUTER TECHNIQUES
Computer assisted analysis of auroral images obtained from high altitude polar satellites [NASA-CR-194873] p 2400 N94-23084
Hypermedia support for engineering design system [PB93-226256] p 2449 N94-23117
A prototype expert/information system for examining environmental risks of KSC activities p 2400 N94-23237
Analysis for the computational modeling of finite cladding and lossy coating effects in fibers [PB94-111085] p 2544 N94-23732
Framework for interactive solving of meta-constraint satisfaction problems [PB94-118825] p 2585 N94-23761
Concepts and techniques for an active database approach to office procedure support [PB94-110749] p 2590 N94-23816
Operational characterisation of requirements and early validation environment for high demanding space systems p 2519 N94-23959
Early manufacturing considerations in design p 2177 N94-24315
Octave: A MARSYAS post-processor for computer-aideed control system design p 2465 N94-24422
Modular approach to project management [PB94-118833] p 2586 N94-24528
RITL: An information system for application reuse-in-the-large [PB94-119088] p 2592 N94-24646
The HEC NexGen software development project [AD-A273512] p 2460 N94-24822
Mission planning and mission rehearsal systems: Displays and other interactive techniques p 2522 N94-25013
Research in progress and other activities of the Institute for Computer Applications in Science and Engineering [NASA-CR-191576] p 2444 N94-25090
Measuring track densities in lunar grains by image analysis p 2623 N94-25355

COMPUTER VISION
Stereo for gazing and converging cameras. Part 1: Basic geometry [OUEL-1915/92] p 2343 N94-23162
Descent and landing phase: Vision based robust spacecraft motion estimation and elevation modeling p 2608 N94-23394
Mars 96 rover: Technical vision and navigation p 2370 N94-23417
Towards real-time stereovision systems for planetary missions p 2370 N94-23422
Remote sensing, imaging, and signal engineering [DE94-003021] p 2382 N94-23494
Telerobotic rendezvous and docking vision system architecture [NASA-CR-191329] p 2204 N94-23828
Multi-sensoral approach to night flight: Perceptive and Cognitive limitations p 2432 N94-23981
Method for selection of wavelength bands for multispectral classification [PB93-204378] p 2388 N94-24741
Object recognition through image understanding for an autonomous mobile robot [AD-A273206] p 2475 N94-24862
Proceedings of the Workshop on Augmented Visual Display (AVID) Research [NASA-CP-10128] p 2439 N94-25490
Enhanced image capture through fusion p 2346 N94-25502

COMPUTERIZED SIMULATION
Development of a multilayer interference simulation program for MSS systems p 2287 N94-22823
Characterization of germanium stripe x ray lasers [DE93-019629] p 2347 N94-22867
Novel fringe scanning/Fourier transform method of synthetic imaging [DE93-018936] p 2542 N94-22917
Development and experimental validation of computational methods to simulate abnormal thermal and structural environments [DE94-000554] p 2268 N94-23000
Texture gradient effects in tantalum [DE94-000689] p 2240 N94-23021
Nuclear propulsion control and health monitoring p 2217 N94-23071
Software for scientific visualization: State of the art and experiences [PB93-225183] p 2449 N94-23111
APLAC: An object-oriented analog circuit simulator and design tool. 6.1 system simulations manual [PB93-224871] p 2450 N94-23226
Flame trench analysis of NLS vehicles p 2199 N94-23249
Mobility analysis, simulation, and scale model testing for the design of wheeled planetary rovers p 2370 N94-23425
Visualization of results from meteorological simulations on CRAY [PB93-201358] p 2451 N94-23443
GLview user's guide [PB93-201366] p 2452 N94-23444
Calculation of flame spread on lining materials by the field model KAMELEON. Project 5 of the EUREFIC fire research programme [PB93-201614] p 2268 N94-23450
Tracking sharp interface of two fluids by the CIP (Cubic-Interpolated Propagation) scheme [DE93-508322] p 2319 N94-23460
Computational model of surface ablation from tokamak disruptions [DE94-002204] p 2550 N94-23474
Object oriented simulation implementation in support of robust system design [DE93-011687] p 2452 N94-23488
Dynamic ray tracing and its application in triangulated media [DE94-000875] p 2402 N94-23516
Global ocean modeling on the Connection Machine [DE94-000888] p 2417 N94-23517
The use of transition region characteristics to improve the numerical simulation of heat transfer in bypass transitional flows [NASA-TM-106445] p 2320 N94-23525
Simultaneous simulation and visualization using DGL [PB93-201341] p 2453 N94-23534

Characterization of 3-D particle distributions and effects on recrystallization studied by computer simulation [PB93-201408] p 2562 N94-23535

An implicit numerical scheme for the simulation of internal viscous flows on unstructured grids [NASA-TM-106437] p 2481 N94-23554

A comparison of TSS and TRASYS in form factor calculation p 2321 N94-23638

Analysis of high vacuum systems using SINDA'85 p 2322 N94-23648

Features of a SINDA/FLUINT model of a liquid oxygen supply line p 2322 N94-23649

Simulation of unsteady flows through stator and rotor blades of a gas turbine using the Chimera method p 2323 N94-23652

Experimental and analytical study of cryogenic propellant boiloff to develop and verify alternate pressurization concepts for Space Shuttle external tank using a scaled down tank p 2266 N94-23657

Radar stimulator interface protocol, preliminary interface design and Doppler Beam Sharpening implementation [DE94-002567] p 2453 N94-23701

Control algorithms for effective operation of variable-speed wind turbines [DE94-002607] p 2394 N94-23704

Transition system specifications in stalk format with bisimulation as a congruence [PB94-110608] p 2453 N94-23707

Zone fire modeling with natural building flows and a zero order shaft model [PB94-112166] p 2270 N94-23735

Micro SIL-1 simulator [PB94-110889] p 2454 N94-23750

Enhanced absorption cycle computer model [DE94-001997] p 2271 N94-23793

SIMSAT: An object oriented architecture for real-time satellite simulation p 2197 N94-23940

Operational characterisation of requirements and early validation environment for high demanding space systems p 2519 N94-23959

Heat pipe cooled heat rejection subsystem modelling for nuclear electric propulsion [NASA-CR-191132] p 2219 N94-24061

Annual research briefs, 1993 — Center for Turbulence Research [NASA-CR-194755] p 2327 N94-24138

Unstructured grid large eddy simulation of wall bounded turbulent flows p 2329 N94-24151

Tensoral for post-processing users and simulation authors p 2333 N94-24169

The use of analytical models in human-computer interface design p 2434 N94-24190

Using computer graphics to design Space Station Freedom viewing p 2434 N94-24191

Simulation of the human-telerobot interface on the Space Station p 2436 N94-24202

Establishing a relationship between maximum torque production of isolated joints to simulate EVA ratchet push-pull maneuver: A case study p 2437 N94-24206

The effect of high altitude pressure on the power and efficiency of an airborne two-stroke engine p 2155 N94-24253

Evaluation of EHF multi-beam adaptive arrays [CTN-94-60898] p 2297 N94-24296

Probabilistic simulation of concurrent engineering of propulsion systems p 2177 N94-24317

Multi-disciplinary coupling for integrated design of propulsion systems p 2179 N94-24326

NASA high performance computing and communications program [NASA-TM-4554] p 2591 N94-24337

A study of the core module simulator floor capability p 2380 N94-24418

Weld fracture criteria for computer simulation p 2251 N94-24425

Spatial interpretation of NASA's Marshall Space Flight Center Payload Operations Control Center using virtual reality technology p 2198 N94-24432

Error coding simulations p 2306 N94-24439

Micromechanical simulation of damage progression in carbon phenolic composites p 2231 N94-24446

Systems engineering: A formal approach. Part 4: Analysis methods [PB94-101417] p 2271 N94-24475

Computer modeling of plasma flow switches-high current switching on Procyon [DE93-040189] p 2311 N94-24500

Systems engineering: A formal approach. Part 3: Modeling methods [PB94-101409] p 2456 N94-24513

Start-up simulations of the PULSAR pulsed tokamak reactor [DE94-002634] p 2552 N94-24519

A simulation and evaluation of NATO Standardization Agreement (STANAG) 4214 [AD-A273195] p 2297 N94-24554

Recent developments in the mathematical modelling and physical understanding of transport and dispersion in aquatic systems, with special reference to tidal waters [PB94-111135] p 2418 N94-24600

Crashworthiness analysis using advanced material models in DYNA3D [DE94-002988] p 2229 N94-24632

Fast simulation of packet loss rates in a shared buffer communications switch [NASA-CR-191556] p 2457 N94-24638

A two-dimensional dispersion module for the TOUGH2 simulator [DE94-002262] p 2335 N94-24655

The HEC NexGen software development project [AD-A273512] p 2460 N94-24822

Design of orbital debris shields for oblique hypervelocity impact [NASA-CR-195152] p 2205 N94-24828

Numerical flow simulation for complete vehicle configurations [AD-A273588] p 2170 N94-24849

Three-dimensional numerical simulation of near-surface flows over the Martian north polar cap p 2621 N94-24895

The role of atmospheric heat transport in the seasonal carbon dioxide cycle p 2621 N94-24896

Triangular spectral elements for incompressible fluid flow [NASA-CR-191588] p 2490 N94-24914

Structures of Cl(-)(H2O)(n) and F(-)(H2O)(n) (n equal to 2,3...15) clusters: Molecular dynamics computer simulations [AD-A273474] p 2537 N94-24940

Computer simulation of low energy scattering [ETN-94-95326] p 2537 N94-25082

PLANET: A hierarchical network simulator [ISBN-9-09-005693-9] p 2313 N94-25083

Simulation studies for surfaces and materials strength [NASA-CR-195185] p 2565 N94-25093

Understanding and facilitating discovery learning in computer-based simulation environment [ISBN-9-03-860242-1] p 2462 N94-25219

Microscopic dynamics in dense helium-neon mixtures: Neutron scattering, kinetic theory and computer simulations [ISBN-9-07-386105-5] p 2537 N94-25228

Numerical simulation and analysis of experimental results on stimulated Raman scattering in laser-plasma Hohlraum targets [DE93-613719] p 2554 N94-25330

Lattice dynamics of Ba(1-x)K(x)BiO3 as studied by neutron scattering and computer simulation [DE93-617053] p 2567 N94-25424

Expert system rule-base evaluation using real-time parallel processing [AD-A273701] p 2469 N94-25454

The IRGen infrared data base modeler p 2440 N94-25496

Advanced radiometric and interferometric milimeter-wave scene simulations p 2306 N94-25498

Engineering workstation: Sensor modeling p 2441 N94-25500

COMPUTERS

ACOS: The performance based approach to build a parallel complex object server [PB93-223816] p 2465 N94-22986

CAMAC throughput of a new RISC-based data acquisition computer at the DIII-D tokamak [DE94-001113] p 2550 N94-23182

Information technology in the service society: A twenty-first century lever [ISBN-0-309-04876-1] p 2593 N94-24833

Computerized testing system software conversion and development: Identifying software and hardware portability issues and solutions [AD-A273489] p 2462 N94-25287

CONCATENATED CODES

Separable concatenated codes with iterative map decoding for Rician fading channels p 2286 N94-22815

CONCAVITY

Generalized concavity in cooperative game theory: Characterizations in terms of the core [MEMO-1121] p 2497 N94-22708

CONCENTRATION (COMPOSITION)

Quantitative analysis in the Al-Mg-Si system with small amounts of Mg and Si [PB93-201499] p 2241 N94-23446

Exploratory report nickel and nickel compounds [PB93-223998] p 2242 N94-23496

Exploratory report antimony and antimony compounds [PB93-224004] p 2397 N94-23497

Algorithm-development activities [NASA-CR-193225] p 2420 N94-23538

Bioregenerative life support systems for microgravity [NASA-CR-195516] p 2422 N94-24810

CONCENTRATORS

The hexagonal compound parabolic concentrator design and construction [DLR-MITT-93-03] p 2396 N94-25464

CONCENTRICITY

Precision drive and speed reduction device [AD-D016004] p 2367 N94-25046

CONCRETE STRUCTURES

Alternatives for reinforcement: Fiber composites [VTT-TIED-1412] p 2230 N94-25386

CONCRETES

Impacts: NIST Building and Fire Research Laboratory (technical and societal) [PB94-113420] p 2270 N94-23737

Constitutive modelling of fiber-reinforced concrete under uniaxial tensile loading [VTT-JULK-774] p 2379 N94-25385

Frost effects on the microstructure of high strength concrete, and methods for their analysis [VTT-PUBS-126] p 2379 N94-25529

CONCURRENT PROCESSING

Causal labeled transition systems: A new approach for describing the behavior of concurrent systems [LAAS-93179] p 2447 N94-22911

Simultaneous simulation and visualization using DGL [PB93-201341] p 2453 N94-23534

Models of trace theory systems [ETN-94-95361] p 2468 N94-25226

CONDUCTING POLYMERS

The electrolyte challenge for a direct methanol-air polymer electrolyte fuel cell operating at temperatures up to 200 C p 2393 N94-23360

Template synthesis of electronically conductive polymers [AD-A273673] p 2263 N94-25409

CONDUCTION BANDS

Conductors with small Fermi energies and small gap energies [DE93-040887] p 2561 N94-23432

CONDUCTIVE HEAT TRANSFER

Local grid refinement method for the euler equations [PB93-223329] p 2317 N94-22985

Conductors with small Fermi energies and small gap energies [DE93-040887] p 2561 N94-23432

A direct approach to finding unknown boundary conditions in steady heat conduction p 2322 N94-23645

A theorem regarding roots of the zero-order Bessel function of the first kind p 2325 N94-23667

Response-coefficient method for heat-conduction transients with time-dependent inputs p 2326 N94-23671

Normal zone propagation and thermal hydraulic quenchback in a cable-in-conduit superconductor [DE94-002457] p 2271 N94-24568

An extended laser flash technique for thermal diffusivity measurement of high-temperature materials p 2238 N94-25132

Application of body fitted-coordinates in heat conduction problems [ETN-94-95338] p 2340 N94-25484

CONDUCTORS

Transient analysis of conducting half-plane problem with noncausal scattering image [PB93-225027] p 2524 N94-23110

Conductors with small Fermi energies and small gap energies [DE93-040887] p 2561 N94-23432

Mitigation of EMI/RFI produced by a 1.2 kW uninterruptible power supply [AD-A273149] p 2299 N94-24670

Shielded Coil Electrodynamic Propulsion (SCEP). A feasibility study [AD-A273824] p 2314 N94-25539

CONFERENCES

Proceedings of the Third International Mobile Satellite Conference (IMSC 1993) [NASA-CR-194516] p 2273 N94-22735

Proceedings of Workshop on Laser Diagnostics in Fluid Mechanics and Combustion [AD-A272808] p 2347 N94-22914

Proceedings of the Fifth Users Meeting for the Advanced Photon Source [DE93-040692] p 2531 N94-22948

New welding and finishing procedures [DE94-602022] p 2352 N94-23025

NASA Propulsion Engineering Research Center, volume 2 [NASA-CR-194719-VOL-2] p 2209 N94-23028

Distributed Operating Systems and Mach. Proceedings of the Spring 1992 Graduate Seminar on Distributed Systems [PB93-224905] p 2449 N94-23103

Urban/rural application of weather radar for flow forecasting. Proceedings of the Informal CEc -Workshop
[PB93-220135] p 2407 N94-23129

Proceedings of the 1993 Bi-Isotropics Workshop on Novel Microwave Materials
[PB93-224772] p 2290 N94-23225

Deployable video conference table
[NASA-CASE-ARC-11950-1] p 2192 N94-23310

Echocardiographic findings in trained aircrew: The effect of +Gz on cardiac structure (working group 18)
p 2424 N94-23320

Space Electrochemical Research and Technology
[NASA-CP-3228] p 2390 N94-23345

Neural network research in Finland. Symposium
[PB93-224822] p 2472 N94-23463

Space technology: A study of the significance of recognition for innovators of spinoff technologies. Commercial Space Expo-USA, 1993
[NASA-CR-194833] p 2596 N94-23528

Prototype Space Technology Hall of Fame exhibit at Technology 2003: Analysis of data from computer-based questionaire
[NASA-CR-194834] p 2596 N94-23540

The Fifth Annual Thermal and Fluids Analysis Workshop
[NASA-CP-10122] p 2320 N94-23634

The Sixth Copper Mountain Conference on Multigrid Methods, part 1
[NASA-CP-3224-PT-1] p 2482 N94-23673

Physics of iron
[DE94-002002] p 2402 N94-23721

Proceedings of the NIST Conference on Reducing the Cost of Space Infrastructure and Operations: Part 1: Oral presentations and discussion
[PB94-111374] p 2194 N94-23770

National Institute of Standards and Technology Conference on Reducing the Cost of Space Infrastructure and Operations. Part 2: Topical papers
[PB94-113487] p 2194 N94-23819

SpaceOps 1992: Proceedings of the Second International Symposium on Ground Data Systems for Space Mission Operations
[NASA-CR-194486] p 2497 N94-23832

The Fifth European Space Mechanisms and Tribology Symposium
[ESA-SP-334] p 2355 N94-23985

Introduction of Ceramics into Aerospace Structural Composites
[AGARD-R-795] p 2255 N94-24228

The 33rd Israel Annual Conference on Aviation and Astronautics
[ITN-94-85227] p 2153 N94-24241

Proceedings of Technology and Governance in the 1990's
[PB93-192904] p 2597 N94-24312

Report of the proceedings of the Colloquium and Workshop on Multiscale Coupled Modeling
[NASA-CP-3217] p 2410 N94-24374

The 7th Annual National Conference of Black Physics Students p 2524 N94-24583

The Third Twente Workshop on Graphs and Combinatorial Optimization: Abstracts and late extended abstracts
[PB94-110954] p 2489 N94-24652

Stability of premixed laminar flames in a stagnation point flow to general disturbances
[AD-A273429] p 2234 N94-24673

Women scientists and engineers employed in industry: Why so few? A report based on a conference
[ISBN-0-309-04991-1] p 2585 N94-24698

The 5th Engineering Foundation Conference: Advanced Heterostructure Transistors
[AD-A273508] p 2312 N94-24819

Statistical methods in physical oceanography
[AD-A273612] p 2419 N94-24948

The Ninth National Space Symposium
[ISBN-0-9616962-7-3] p 2598 N94-25006

Ferroelectric thin films 3
[AD-A273394] p 2565 N94-25027

The Future of Aerospace: Proceedings of a symposium held in honor of Alexander H. Flax
[LC-93-83945] p 2631 N94-25065

National Academy of Sciences-Academy of Sciences of the USSR Workshop on the Mechanics of Ice and its Applications
[AD-A273338] p 2419 N94-25088

Proceedings of the 12th International Congress: Corrosion Control for Low-Cost Reliability. Volume 1: Coatings
[AD-A273661] p 2251 N94-25448

Proceedings of the 12th International Congress: Corrosion Control for Low-Cost Reliability. Volume 3B: Corrosion: Specific issues
[AD-A273664] p 2251 N94-25451

CONFIDENCE LIMITS

Subset selection for the best of two populations: Tables of the expected subset size
[PB93-237857] p 2494 N94-23546

Asymptotic confidence intervals for the length of the shortt under random censoring
[PB93-237816] p 2494 N94-23774

Subset selection with a generalized selection goal based on a loss function
[PB94-111192] p 2494 N94-23798

A comparison of approximate interval estimators for the Bernoulli parameter
[NASA-CR-191585] p 2458 N94-24680

CONFIGURATION INTERACTION

Relativistic configuration interaction calculation of the correlation energies of highly-charged ions
[DE94-001055] p 2532 N94-22988

CONFIGURATION MANAGEMENT

Guide to software configuration management
[ESA-PSS-05-09-ISSUE-1] p 2450 N94-23229

Planning: Management of predictability and uncertainty and keeping abreast of developments
p 2520 N94-23967

CONFINEMENT

Overview of the ATF stellarator program
[DE94-000371] p 2550 N94-23462

The role of the radial electric field in confinement and transport in H-mode and VH-mode discharges in the DIII-D tokamak
[DE94-002746] p 2551 N94-23782

Fusion plasma theory project summaries
[DE94-001712] p 2551 N94-23808

Solutions of the 2-D Helmoholtz equation for optical waveguides
[DE93-616840] p 2547 N94-25209

A scalar-vector model of quark-antiquark interaction under linear confinement
[DE93-616871] p 2538 N94-25317

CONFORMAL MAPPING

Computation of the loads on the AH-1/OLS model rotor in forward flight and comparison with wind tunnel tests
[ISL-CO-230/92] p 2176 N94-23146

Coadjoint orbits and conformal field theory
[DE94-002285] p 2523 N94-24658

Super Beltrami differentials and N equal to 4 superconformal anomalies
[DE93-613047] p 2491 N94-25166

Image remapping strategies applied as protheses for the visually impaired p 2444 N94-25363

CONGENITAL ANOMALIES

Echocardiographic screening of aircrew candidates
p 2424 N94-23319

CONGRESSIONAL REPORTS

Federal alternative fuel program light duty vehicle operations
[DE93-040663] p 2264 N94-22878

Proceedings of Technology and Governance in the 1990's
[PB93-192904] p 2597 N94-24312

CONGRUENCES

Transition system specifications in stalk format with bisimulation as a congruence
[PB94-110608] p 2453 N94-23707

CONICAL FLOW

Design project: LONGBOW supersonic interceptor
[NASA-CR-195510] p 2180 N94-24581

CONICAL SCANNING

Analysis of open-loop conical scan pointing error and variance estimators p 2291 N94-23263

CONICAL SHELLS

Stability analysis of anisotropic conical shells
[PB94-119054] p 2377 N94-24645

CONIFERS

The measurement and analysis of leaf spectral reflectance of two stands of loblolly pine populations
p 2389 N94-24442

CONJUGATE GRADIENT METHOD

Extending substructure based iterative solvers to multiple load and repeated analyses
[NASA-CR-194822] p 2466 N94-23504

An implicit numerical scheme for the simulation of internal viscous flows on unstructured grids
[NASA-TM-106437] p 2481 N94-23554

A matrix analysis of conjugate gradient algorithms
[DE94-002546] p 2454 N94-23796

CONJUGATION

Planar poly(p-phenylene) derivatives: Ladder formation for maximization of extended conjugation
[AD-A273220] p 2260 N94-24922

CONSERVATION EQUATIONS

Conservation equations for reacting gas flow
[PB94-111168] p 2334 N94-24574

CONSERVATION LAWS

Nonlocal models in continuum mechanics
[DE93-040146] p 2316 N94-22870

An implicit numerical scheme for the simulation of internal viscous flows on unstructured grids
[NASA-TM-106437] p 2481 N94-23554

Energy and maximum norm estimates for nonlinear conservation laws
[NASA-CR-195091] p 2569 N94-24109

Characteristic method for one-dimensional scalar hyperbolic conservation laws with stiff source terms
[PB93-237675] p 2491 N94-24954

CONSTELLATIONS

Odyssey personal communications satellite system
p 2282 N94-22787

CONSTITUTIVE EQUATIONS

Nonlocal models in continuum mechanics
[DE93-040146] p 2316 N94-22870

On the deformation kinetics constitutive law of plastic deformation: The rate equation p 2161 N94-24289

Constitutive modelling of fiber-reinforced concrete under uniaxial tensile loading
[VTT-JULK-774] p 2379 N94-25385

CONSTRAINTS

The instant sequencing task: Toward constraint-checking a complex spacecraft command sequence interactively p 2504 N94-23875

Planning: Management of predictability and uncertainty and keeping abreast of developments
p 2520 N94-23967

Modeling of database constraints in active databases
[AD-A273484] p 2592 N94-24691

On BRST quantization of constrained systems
[ETN-94-95386] p 2570 N94-25258

CONSTRUCTION

Limiting factors for carbon based chemical double layer capacitors p 2394 N94-23365

Accelerator-based neutrino oscillation searches
[DE94-000818] p 2626 N94-23515

A simulation system for Space Station extravehicular activity p 2434 N94-24192

Collaborating with our customers: NIST building and fire research laboratory
[PB94-110194] p 2272 N94-24955

CONTACT POTENTIALS

Chemically sensitive interfacial force microscopy: Contact potential measurements of self-assembling monolayer films
[AD-A273135] p 2234 N94-24772

CONTACT RESISTANCE

Advanced research and technology development of MCFCs
[DE94-001918] p 2389 N94-22723

Fully coupled nonlinear thermomechanical analysis including general contact in PALM2D
[DE94-001661] p 2568 N94-23216

CONTACTORS

Development of a power electronics unit for the Space Station plasma contactor
[NASA-TM-106486] p 2222 N94-25201

CONTAINERLESS MELTS

Workshop on the Thermophysical Properties of Molten Materials
[NASA-CP-10121] p 2246 N94-25120

CONTAMINANTS

Contaminant effects in solid oxide fuel cells
[DE94-002963] p 2395 N94-23785

CONTAMINATION

The possible effects of the natural and induced space environment on the optical and thermal properties of EOS surfaces p 2207 N94-23596

Microbial biofilm formation and its consequences for the CELSS program
[NASA-CR-195146] p 2438 N94-24706

CONTINENTAL SHELVES

Nutrients and light as factors controlling phytoplankton biomass on the Dutch continental shelf (North Sea), 1988-1990
[PB94-111143] p 2418 N94-24601

CONTINUITY (MATHEMATICS)

Introduction to a behavioral approach for continuous time systems
[ETN-94-95301] p 2492 N94-25277

CONTINUITY EQUATION

A multigrid solver for the semiconductor equations
p 2482 N94-23674

Unified approach for incompressible flows
p 2342 N94-25356

CONTINUOUS RADIATION

Measurements and modeling of multitone, low-frequency accustic data from the Arraial do Cabo range
[AD-A273406] p 2530 N94-25073

Remote vibration measurements at a sud aviation alouette 3 helicopter with a CW CO2-laser system
[AD-A273818] p 2190 N94-25516

CONTINUUM MECHANICS

Nonlocal models in continuum mechanics
[DE93-040146] p 2316 N94-22870

Conservation equations for reacting gas flow
[PB94-111168] p 2334 N94-24574

CONTINUUMS

Continuum representations of cellular solids
[DE94-001706] p 2375 N94-23217

CONTOURS

Development of a code for wall contour design in the transonic region of axisymmetric and square nozzles
[NASA-CR-194857] p 2167 N94-23625

CONTRACT MANAGEMENT

B-2 bomber: Assessment of DOD's response to mandated certifications and reports
[AD-A273179] p 2184 N94-25152

C-17 lot 3 production contract
[AD-A273180] p 2174 N94-25153

CONTRACTORS

Panel to review EOSDIS plans
[NASA-CR-195088] p 2387 N94-24303

CONTRAROTATING PROPELLERS

Counterrotating aircraft propulsor blades
[CA-PATENT-1-319-357] p 2186 N94-23255

CONTROL BOARDS

Programmable display pushbuttons on the Space Station's telerobot control panel p 2435 N94-24198

Evaluation of the UH-1N instrument panel
[AD-A273145] p 2186 N94-24774

CONTROL EQUIPMENT

Design of central control system for Large Helical Device (LHD)
[NIFS-258] p 2553 N94-24623

Cockpit control system
[NASA-CR-195488] p 2190 N94-24957

CONTROL MOMENT GYROSCOPES

Results of a laboratory experiment that tests rotating unbalanced-mass devices for scanning gimbaled payloads and free-flying spacecraft
[NASA-TP-3458] p 2269 N94-23574

CONTROL SIMULATION

Operating the Daisy facility to perform control experiments
[ISBN-0-315-83554-0] p 2196 N94-22889

Stability questions in predictive control
[OUEL-1970/93] p 2477 N94-25469

Adaptive predictive control of the benchmark plant
[OUEL-1972/93] p 2477 N94-25470

CONTROL STABILITY

How much integral action can a control system tolerate?
[OUEL-1923/92] p 2471 N94-23147

Reduced-order modelling and control of a class of systems for which balanced truncation is Hankel-norm optimal
[OUEL-1922/92] p 2472 N94-23163

Control of a serpentine manipulator with collision avoidance p 2368 N94-23232

Design of a new high-performance pointing controller for the Hubble Space Telescope
[NASA-CR-193891] p 2364 N94-24088

Control of nonlinear systems represented in quasilinear form
[NASA-CR-194840] p 2475 N94-24760

Parametric uncertainty reduction in robust multivariable control
[AD-A273412] p 2460 N94-24927

Aircraft digital flight control technical review
p 2163 N94-25106

Stability questions in predictive control
[OUEL-1970/93] p 2477 N94-25469

CONTROL SURFACES

Supersonic aerodynamic characteristics of a circular body Earth-to-Orbit vehicle
[NASA-TM-4533] p 2170 N94-24716

CONTROL SYSTEMS DESIGN

A novel process monitoring and control system based on a neural manufacturing concept
[DE94-001516] p 2471 N94-23011

Nuclear propulsion control and health monitoring
p 2217 N94-23071

How much integral action can a control system tolerate?
[OUEL-1923/92] p 2471 N94-23147

The Telecommunications and Data Acquisition Report
[NASA-CR-194766] p 2290 N94-23256

Experimental modification and identification of the DSS-13 antenna control system model
p 2291 N94-23260

Link monitor and control operator assistant: A prototype demonstrating semiautomated monitor and control
p 2292 N94-23267

Beam-waveguide antenna servo design issues for tracking low earth-orbiting satellites
p 2292 N94-23268

Viewing hybrid systems as products of control systems and automata
[NASA-CR-194792] p 2472 N94-23300

A reliable algorithm for optimal control synthesis
[NASA-CR-194809] p 2472 N94-23332

Conceptual design and architecture of hexapod robotic vehicles for the (L)OVLA project p 2369 N94-23405

Walking machines for space p 2369 N94-23406

Marsohkod movement control p 2370 N94-23418

Perspective of creation of means for collecting information concerning transport situation
p 2370 N94-23420

Bond graph modeling, simulation, and reflex control of the Mars planetary automatic vehicle
p 2370 N94-23424

A comparison of two multi-variable integrator windup protection schemes
[NASA-CR-194436] p 2190 N94-23590

Thrust vectoring theory, laboratory and flight tests
p 2155 N94-24251

LSS systems planning and performance program
[NASA-CR-193882] p 2196 N94-24309

Finite element based electric motor design optimization p 2315 N94-24411

Octave: A MARSYAS post-processor for computer-aideed control system design
p 2465 N94-24422

A homotopy algorithm for digital optimal projection control GASD-HADOC
[NASA-CR-193881] p 2456 N94-24470

Active control of buildings during earthquakes
[NASA-TM-109033] p 2271 N94-24473

Alternative control techniques document: NOx emissions from stationary reciprocating internal combustion engines
[PB94-104494] p 2398 N94-24476

Cockpit control system conceptual design
[NASA-CR-195543] p 2190 N94-24551

Robust stability of second-order systems
[NASA-CR-195175] p 2488 N94-24564

Design of central control system for Large Helical Device (LHD)
[NIFS-258] p 2553 N94-24623

The experimental physics and industrial control system architecture: Past, present, and future
[DE94-002639] p 2457 N94-24626

Human-like robots for space and hazardous environments
[NASA-CR-195549] p 2365 N94-24703

Controlled invariance of nonlinear systems: Nonexact forms speak louder than exact forms
[PB93-237790] p 2475 N94-24755

Control of nonlinear systems represented in quasilinear form
[NASA-CR-194840] p 2475 N94-24760

Design of a wheeled articulating land rover
[NASA-CR-195520] p 2365 N94-24806

Intelligent control of chemical vapor deposition processes
[AD-A273356] p 2261 N94-24937

Cockpit control system
[NASA-CR-195488] p 2190 N94-24957

NASA LaRC Workshop on Guidance, Navigation, Controls, and Dynamics for Atmospheric Flight, 1993
[NASA-CP-10127] p 2162 N94-25096

Parametric uncertainty modeling for application to robust control p 2163 N94-25103

Feedback control laws for highly maneuverable aircraft
[NASA-CR-195195] p 2190 N94-25176

New Technologies for Space Avionics, 1993
[NASA-CR-195157] p 2272 N94-25193

Practical evaluation of robust control for a class of nonlinear mechanical dynamic systems
[ISBN-9-03-860092-5] p 2475 N94-25224

Genetic algorithms in control systems engineering
[RR-470] p 2463 N94-25315

CONTROL THEORY

Balancing for unstable nonlinear systems
[MEMO-1118] p 2469 N94-22705

Nonlinear state space H(sub infinity) control theory
[MEMO-1119] p 2469 N94-22706

On dynamic input-output linearization of discrete-time nonlinear systems
[MEMO-1123] p 2447 N94-22711

Identification for robust control using an H(sub infinity) norm
[EUT-92-E-261] p 2470 N94-22873

Real-time dynamics and control strategies for space operations of flexible structures
[NASA-CR-194794] p 2203 N94-23618

Coordinate-free interpretations of the optimal costs for Lq problems subject to implicit systems
[PB94-118700] p 2473 N94-23760

Drag reduction at a plane wall p 2327 N94-24140

Next generation initiation techniques
p 2412 N94-24383

A homotopy algorithm for digital optimal projection control GASD-HADOC
[NASA-CR-193881] p 2456 N94-24470

Discrete-time H(infinity) control problem with strictly proper measurement feedback
[NASA-CR-195089] p 2473 N94-24542

Japanese aerospace science and technology 1992. A bibliography with indexes
[NASA-SP-7104] p 2631 N94-24585

Squaring-down and the problems of almost-zeros for continuous-time systems
[PB93-237758] p 2489 N94-24608

Discrete time minimum entropy H(infinity) control problem
[PB93-237808] p 2474 N94-24609

Asymptotic correctors: The LTR
[PB93-199701] p 2474 N94-24627

Controlled invariance of nonlinear systems: Nonexact forms speak louder than exact forms
[PB93-237790] p 2475 N94-24755

Control of nonlinear systems represented in quasilinear form
[NASA-CR-194840] p 2475 N94-24760

Genericity of stabilizability for time-delay systems
[PB93-237725] p 2475 N94-24762

NASA LaRC Workshop on Guidance, Navigation, Controls, and Dynamics for Atmospheric Flight, 1993
[NASA-CP-10127] p 2162 N94-25096

Hypersonic vehicle control law development using H(infinity) and micron-synthesis p 2163 N94-25104

Robust, nonlinear, high angle-of-attack control design for a supermaneuverable vehicle p 2164 N94-25108

Modeling transonic aerodynamic response using nonlinear systems theory for use with modern control theory p 2164 N94-25112

Optimal RTLS abort trajectories for an HL-20 personnel launch vehicle p 2165 N94-25114

Feedback control laws for highly maneuverable aircraft
[NASA-CR-195195] p 2190 N94-25176

MIMO system identification for H(infinity) robust control: A frequency domain approach with minimum error bounds
[ETN-94-95354] p 2476 N94-25262

On-line control of dynamic systems using feedforward neural networks
[RR-457] p 2476 N94-25307

The phase response of nonlinear systems
[RR-458] p 2476 N94-25308

Kernels of anti-causal operators and the multivariable generalized predictive control problem
[MATHS-REPT-A-191] p 2476 N94-25428

Advances in generalized and constrained generalized predictive control with application to a dynamometer model
[MATHS-REPT-A-192] p 2476 N94-25429

CONTROL UNITS (COMPUTERS)

AMICAL: An aid for architectural synthesis and exploration of control circuits
[ETN-94-95177] p 2308 N94-23154

CONTROL VALVES

Computer control of an electro-mechancial regulator for providing positive pressure breathing and an electronic G-valve for human +Gz research
[DCIEM-93-05] p 2437 N94-24299

Controller modeling and evaluation for PCV electro-mechanical actuator p 2371 N94-24441

Electro-rheological control valve
[AD-D015997] p 2367 N94-25055

CONTROLLABILITY

Controllability of free-piston Stirling engine/linear alternator driving a dynamic load
[NASA-TM-106497] p 2521 N94-24302

CONTROLLED ATMOSPHERES

Influence of sintering atmospheres on the aluminum sintering characteristics
[DE93-632412] p 2239 N94-22965

A pressurized thermogravimetric analyzer for use in studies of gas/solid systems
[DE94-001224] p 2342 N94-22989

CONTROLLED FUSION

Massachusetts Institute of Technology Plasma Fusion Center 1992-1993 report to the President
[DE94-001725] p 2548 N94-22721

CONTROLLERS

Nuclear propulsion control and health monitoring
p 2217 N94-23071

Spline screw multiple rotations mechanism
[NASA-CASE-GSC-13452-1] p 2352 N94-23078

A comparison of two multi-variable integrator windup protection schemes
[NASA-CR-194436] p 2190 N94-23590

Adaptive nonlinear polynomial neural networks for control of boundary layer/structural interaction
[NASA-CR-189645] p 2525 N94-23698

Particle size measurement for the control of industrial crystallizers
[PB94-119104] p 2562 N94-23766
Design of a new high-performance pointing controller for the Hubble Space Telescope
[NASA-CR-193891] p 2364 N94-24088
Hand controller commonality evaluation process
p 2435 N94-24197
Aircraft empennage structural detail design
[NASA-CR-195496] p 2179 N94-24332
Neural network-based control using Lyapunov functions p 2477 N94-24433
Controller modeling and evaluation for PCV electro-mechanical actuator p 2371 N94-24441
Torque equilibrium attitudes for the Space Station
p 2208 N94-24449
A homotopy algorithm for digital optimal projection control GASD-HADOC
[NASA-CR-193881] p 2456 N94-24470
Active control of buildings during earthquakes
[NASA-TM-109033] p 2271 N94-24473
Discrete-time H(infinity) control problem with strictly proper measurement feedback
[NASA-CR-195089] p 2473 N94-24542
Discrete time minimum entropy H(infinity) control problem
[PB93-237808] p 2474 N94-24609
The experimental physics and industrial control system architecture: Past, present, and future
[DE94-002639] p 2457 N94-24626
Control of nonlinear systems represented in quasilinear form
[NASA-CR-194840] p 2475 N94-24760
The H(sub infinity) optimal controller design and reduction for the inertial hold mode of the attitude control system of the XTE spacecraft
[NASA-CR-195137] p 2366 N94-24846
Exploiting structure: Introduction and motivation
[NASA-CR-195136] p 2490 N94-24847
Parametric uncertainty reduction in robust multivariable control
[AD-A273412] p 2460 N94-24927
On-line evaluation of multiloop digital controller performance p 2163 N94-25105
Robust, nonlinear, high angle-of-attack control design for a supermaneuverable vehicle p 2164 N94-25108
Development of a power electronics unit for the Space Station plasma contactor
[NASA-TM-106486] p 2222 N94-25201
Practical evaluation of robust control for a class of nonlinear mechanical dynamic systems
[ISBN-9-03-860092-5] p 2475 N94-25224
Automatic pressure control system for the Wright Laboratory Compressor Research Facility
[AD-A273827] p 2194 N94-25522
Flight controller design using mixed H2/H infinity optimization with a singular H infinity constraint
[AD-A273831] p 2191 N94-25525

CONVECTION
Atmospheric numerical modeling resource enhancement and model convective parameterization/scale interaction studies
[NASA-CR-194769] p 2400 N94-23124
A method to simulate viscous diffusion of vorticity by convective transport of vortices at a non-solenoidal velocity
[DE94-001777] p 2318 N94-23220
On testing two major cumulus parameterization schemes using the CSU regional atmospheric modeling system
[DE94-000703] p 2407 N94-23284
Convective organization in the Pacific ITCZ: Merging OLR, TOVS, and SSM/I information
[NASA-CR-194850] p 2408 N94-23619
Convection equation modeling: A non-iterative direct matrix solution algorithm for use with SINDA
p 2323 N94-23651
A dual reciprocal boundary element formulation for viscous flows p 2325 N94-23666
Miniature convection cooled plug-type heat flux gauges
[NASA-TM-106483] p 2344 N94-24069
MAMS data for the Convection and Moisture Experiment (CAMEX)
[NASA-TM-108435] p 2409 N94-24080
Convective instabilities in traveling fronts of addition polymerization p 2226 N94-24352
Polymer morphologh p 2226 N94-24353
Parameterization of sub-grid scale convection
p 2413 N94-24386
Chemistry on the mesoscale: Modeling and measurement issues p 2413 N94-24390
CAPE for CaPE p 2416 N94-24409
Effects of thermal-solutal convection on temperature and solutal fields under various gravitational orientations
p 2267 N94-24451

CONVECTION-DIFFUSION EQUATION
On the dynamics of some grid adaption schemes
[NASA-CR-195092] p 2454 N94-24110

CONVECTIVE FLOW
Atmospheric numerical modeling resource enhancement and model convective parameterization/scale interaction studies
[NASA-CR-194769] p 2400 N94-23124
A dual reciprocal boundary element formulation for viscous flows p 2325 N94-23666
Comparison of numerical simulation and experimental data for steam-in-place sterilization
p 2326 N94-23669
Scientific goals of the Cooperative Multiscale Experiment (CME) p 2411 N94-24381
Grand challenge scientific questions in coupled modeling p 2412 N94-24382
Parameterization of sub-grid scale convection
p 2413 N94-24386

CONVECTIVE HEAT TRANSFER
Numerical investigation of two- and three-dimensional heat transfer in expander cycle engines
p 2213 N94-23048
Solution of mixed convection heat transfer from isothermal in-line fins p 2321 N94-23644
Features of a SINDA/FLUINT model of a liquid oxygen supply line p 2322 N94-23649
Prediction of three sigma maximum dispersed density for aerospace applications p 2207 N94-23654
A theorem regarding roots of the zero-order Bessel function of the first kind p 2325 N94-23667
The annual pressure cycle on Mars: Results from the LMD Martian atmospheric general circulation model
p 2619 N94-24884
Analysis of the effects of wake passage on heat transfer in a linear turbine cascade
[AD-A273729] p 2339 N94-25446

CONVERGENCE
Reliability enhancement of Navier-Stokes codes through convergence enhancement p 2216 N94-23064
Incomplete corrections in nonlinear problems
[PB93-225746] p 2479 N94-23106
Nested Krylov methods and preserving the orthogonality p 2483 N94-23681
Multigrid methods for differential equations with highly oscillatory coefficients p 2484 N94-23685
A comparison of locally adaptive multigrid methods: LDC, FAC and FIC p 2485 N94-23692
A nonconforming multigrid method using conforming subspaces p 2485 N94-23695
Infinite divisible and stable distributions modulo 1
[PB94-110640] p 2495 N94-23815
Combinatory reduction systems: Introduction and survey
[PB94-110582] p 2457 N94-24570

CONVERGENT NOZZLES
CFD modeling of microwave electrothermal thrusters
p 2216 N94-23066

CONVERGENT-DIVERGENT NOZZLES
Efficiency and reliability enhancements in propulsion flowfield modeling p 2215 N94-23055
Computation of propulsion-related flowfields using unstructured adaptive meshes p 2215 N94-23056
Theoretical studies of a molecular beam generator
[NASA-CR-194779] p 2540 N94-23485

CONVEXITY
Split spline screw
[NASA-CASE-GSC-13434-1] p 2352 N94-23082
Characterization of measures with a convex range: A generalization of Lyapounov's theorem
[PB93-220523] p 2523 N94-23094
Characterization of measures with a convex matrix-k-range
[PB93-220655] p 2479 N94-23098

CONVOLUTION INTEGRALS
The state space method for integro-differential equations of convolution type with rational matrix symbols
[ETN-94-95379] p 2491 N94-25244

COOL STARS
Chromospheric activity in agol binaries
[AD-A273546] p 2602 N94-24557

COOLANTS
SP-100 heat transport technology development
[DE94-000769] p 2218 N94-23452

COOLERS
Thermoelectric cooled, purge-and-trap device for enhancing the utility of fiber optic VOC sensors
[DE94-001772] p 2541 N94-22722

COOLING
Design of microchannels for cryostabilization of high temperature superconducting magnets
[DE94-001324] p 2559 N94-22993
Determination of the compatibility between structural alloys and molten metals at high temperatures
[DE94-000954] p 2241 N94-23434
SP-100 heat transport technology development
[DE94-000769] p 2218 N94-23452
Matter-wave interferometry with laser cooled atoms
[AD-A273249] p 2536 N94-24717
Flow and temperature distribution in a naturally stratified thermal storage tank
[AD-A273511] p 2336 N94-24821

COOLING SYSTEMS
The design of a turbine vane cooling system used in the topping cycle
[OUEL-1963/92] p 2353 N94-23164
Operation Friction: Development and introduction of personal cooling for CH124 Sea King aircrew
[DCIEM-93-06] p 2433 N94-24119
Hydride thermodynamic machines
[VTT-JULK-768] p 2571 N94-25416

COORDINATE TRANSFORMATIONS
Aeronautical satellite antenna steering using magnetic field sensors p 2289 N94-22836

COORDINATES
Tools for visualizing landscape pattern for large geographic areas
[DE94-001121] p 2388 N94-24757

COPOLYMERIZATION
Microstructure of styrene methyl methacrylate copolymers grafted onto polybutadiene seeds
[ETN-94-95360] p 2262 N94-25225

COPOLYMERS
Pyroelectric sensors in copolymer integrated on silicon
[LAAS-93044] p 2342 N94-22902
Reaction of isocyanates with carboxylic acids and its application to polymer synthesis
[PB94-118858] p 2254 N94-23763
Effects of ionizing radiation on modern ion exchange materials
[DE94-001569] p 2535 N94-24505
Polythiophene derivative with a side chain chromophore as photovoltaic and photorefractive materials
[AD-A273245] p 2260 N94-24813

COPPER
Strength, acoustic evaluation and metallurgy of diffusion bonds
[DE94-001804] p 2243 N94-23717
Metal-catalyzed alkynylation of brominated polyphenylenes: Thermoset precursors of high density monolithic glassy carbon
[AD-A273232] p 2259 N94-24789
Scanning probe lithography. 2: Selective chemical vapor deposition of copper into scanning tunneling microscope-defined patterns
[AD-A273304] p 2547 N94-25144
Dispersion of Rh/Cu in a sol-gel matrix. Highly chemo- and stereoselective catalyst for the reduction of alkynes to Z-alkenes
[AD-A273306] p 2262 N94-25145

COPPER ALLOYS
Irradiation damage behavior of low alloy steel wrought and weld materials
[DE94-000519] p 2239 N94-22999
New extensions in the development of deformation processed metal-metal matrix composites
[DE94-000692] p 2227 N94-23004
Phase transformations in Cu-Zr multilayers
[DE94-000393] p 2241 N94-23297
Effect of hydrogen exposure on a Cu-8 Cr-4 Nb alloy
[NASA-TM-106429] p 2243 N94-23556
Multilayer relaxation and surface structure of ordered alloys
[NASA-TM-106433] p 2243 N94-23578
Electrochemical behavior of ion-plated TiN and Cu-Cr coatings
[AD-A273411] p 2235 N94-24784

COPPER OXIDES
Spin-polaron theory of high-T(c) superconductivity. 2: Electronic structure of the CuO2 planes
[DE93-019197] p 2556 N94-22919
Anomalous magnetoresistance behavior of superconducting Nd(2-x)Ce(x)CuO(4-y) single crystal
[DE94-000806] p 2558 N94-22941
A valence-fluctuation theory of cuprate superconductivity
[DE94-000887] p 2558 N94-22942

COPPER SELENIDES
Novel two-stage selenization methods for fabrication of thin-film CIS cells and submodules
[DE94-000220] p 2390 N94-23296

CORE FLOW
Steady induction effects in geomagnetism. Part 1C: Geomagnetic estimation of steady surficial core motions: Application to the definitive geomagnetic reference field models
[NASA-TP-3272-PT-1C] p 2403 N94-24465

CORE SAMPLING
A system for the challenging task of collecting samples from a comet surface p 2358 N94-24007

CORONARY ARTERY DISEASE

Cardiopulmonary Aspects in Aerospace Medicine [AGARD-LS-189] p 2423 N94-23313

Aeromedical disposition for coronary artery disease p 2423 N94-23316

Primary prevention of coronary heart disease p 2423 N94-23317

CORONAS

Flue gas cleaning by pulse corona streamer [EUT-93-E-272] p 2268 N94-23174

CORRECTION

A complete public archive for the Einstein IPC [NASA-CR-189316] p 2453 N94-23559

CORRELATION

Correlation function estimator performance in non-Gaussian spherically invariant random processes [AD-A273498] p 2496 N94-24951

Detection of velocity in high temperature liquid metals p 2247 N94-25127

First results from the Fennoscandian GPS networks p 2405 N94-25204

Direct measurement of turbulent dissipation rate using dual laser doppler velocimeters [AD-A273740] p 2340 N94-25530

CORRELATION COEFFICIENTS

Synthesis of passive microwave and radar altimeter data for estimating accumulation rates of polar snow [NASA-CR-194864] p 2382 N94-23573

Radar target discrimination systems using artificial neural network topology [AD-D015984] p 2301 N94-25041

CORROSION

Vaporization behavior of non-stoichiometric refractory carbide materials and direct observations of the vapor phase using laser diagnostics [DE93-040094] p 2348 N94-23203

Evaluation of inorganic zinc-rich primers using Electrochemical Impedance Spectroscopy (EIS) p 2237 N94-23233

Statistical procedures for corrosion studies [PB93-199412] p 2244 N94-23802

Diffusion on Cu surfaces p 2251 N94-24428

Use of scanning tunneling microscope in corrosion studies [VTT-TIED-1416] p 2250 N94-25346

Proceedings of the 12th International Congress: Corrosion Control for Low-Cost Reliability. Volume 6: Electric Power Industry [AD-A273668] p 2250 N94-25408

A preliminary evaluation of the phosphazene resin PPZ [AD-A273674] p 2263 N94-25410

Preceedings of the 12th International Congress: Corrosion Control for Low-Cost Reliability. Volume 2: Process Industries Plant Operations [AD-A273662] p 2251 N94-25449

Preceedings of the 12th International Congress: Corrosion Control for Low-Cost Reliability. Volume 3A: Corrosion: Specific issues [AD-A273663] p 2251 N94-25450

Proceedings of the 12th International Congress: Corrosion Control for Low-Cost Reliability. Volume 3B: Corrosion: Specific issues [AD-A273664] p 2251 N94-25451

CORROSION PREVENTION

Chromate-free talc chemical conversion coatings for aluminum alloys [DE94-001567] p 2238 N94-22932

Statistical procedures for corrosion studies [PB93-199412] p 2244 N94-23802

Proceedings of the 12th International Congress: Corrosion Control for Low-Cost Reliability. Volume 4: Oil/Gas Pipeline [AD-A273665] p 2250 N94-25405

Proceedings of the 12th International Congress: Corrosion Control for Low-Cost Reliability. Volume 5A: Corrosion: General issues [AD-A273666] p 2250 N94-25406

Proceedings of the 12th International Congress: Corrosion Control for Low-Cost Reliability. Volume 5B: Corrosion: General issues [AD-A273667] p 2250 N94-25407

Proceedings of the 12th International Congress: Corrosion Control for Low-Cost Reliability. Volume 6: Electric Power Industry [AD-A273668] p 2250 N94-25408

Proceedings of the 12th International Congress: Corrosion Control for Low-Cost Reliability. Volume 1: Coatings [AD-A273661] p 2251 N94-25448

Preceedings of the 12th International Congress: Corrosion Control for Low-Cost Reliability. Volume 2: Process Industries Plant Operations [AD-A273662] p 2251 N94-25449

Preceedings of the 12th International Congress: Corrosion Control for Low-Cost Reliability. Volume 3A: Corrosion: Specific issues [AD-A273663] p 2251 N94-25450

Proceedings of the 12th International Congress: Corrosion Control for Low-Cost Reliability. Volume 3B: Corrosion: Specific issues [AD-A273664] p 2251 N94-25451

CORROSION RESISTANCE

Chromate-free talc chemical conversion coatings for aluminum alloys [DE94-001567] p 2238 N94-22932

Evaluation of inorganic zinc-rich primers using Electrochemical Impedance Spectroscopy (EIS) p 2237 N94-23233

New method for increasing machine service-life, phase 2 [PB93-200707] p 2354 N94-23533

Feasibility study of shot-peening modeling [CTN-94-60926] p 2244 N94-24170

Electrochemical behavior of ion-plated TiN and Cu-Cr coatings [AD-A273411] p 2235 N94-24784

Proceedings of the 12th International Congress: Corrosion Control for Low-Cost Reliability. Volume 4: Oil/Gas Pipeline [AD-A273665] p 2250 N94-25405

Proceedings of the 12th International Congress: Corrosion Control for Low-Cost Reliability. Volume 5A: Corrosion: General issues [AD-A273666] p 2250 N94-25406

Proceedings of the 12th International Congress: Corrosion Control for Low-Cost Reliability. Volume 5B: Corrosion: General issues [AD-A273667] p 2250 N94-25407

Proceedings of the 12th International Congress: Corrosion Control for Low-Cost Reliability. Volume 6: Electric Power Industry [AD-A273668] p 2250 N94-25408

Proceedings of the 12th International Congress: Corrosion Control for Low-Cost Reliability. Volume 1: Coatings [AD-A273661] p 2251 N94-25448

Preceedings of the 12th International Congress: Corrosion Control for Low-Cost Reliability. Volume 2: Process Industries Plant Operations [AD-A273662] p 2251 N94-25449

Preceedings of the 12th International Congress: Corrosion Control for Low-Cost Reliability. Volume 3A: Corrosion: Specific issues [AD-A273663] p 2251 N94-25450

Proceedings of the 12th International Congress: Corrosion Control for Low-Cost Reliability. Volume 3B: Corrosion: Specific issues [AD-A273664] p 2251 N94-25451

CORROSION TESTS

Electrochemical behavior of ion-plated TiN and Cu-Cr coatings [AD-A273411] p 2235 N94-24784

CORRUGATING

Rail Corrugations [ILR-BER-59] p 2269 N94-23581

A rail corrugation theory which allows for contact patch size p 2269 N94-23582

A rail joint: The possible initiator of corrugation? p 2269 N94-23583

A linear model for corrugation and its limit of validity p 2269 N94-23584

Lateral high frequency oscillations and stability of a wheel rolling on a flexible track p 2269 N94-23585

Wear characteristics of technical dry rolling/sliding systems with relations to corrugation problems p 2269 N94-23586

Surface analysis of corrugated rail treads p 2270 N94-23587

Surface observations of stick-slip oscillations in tightly conformal wheel/rail contacts p 2270 N94-23588

COSMIC DUST

The three-dimensional structure of the infrared cirrus [NASA-CR-194870] p 2410 N94-24097

Report on operations of the Air Force Geophysics Laboratory infrared array spectrometer [AD-A273800] p 2406 N94-25535

COSMIC RAYS

Solar-geophysical data number 584, April 1993. Part 1: (Prompt reports). Data for February, March, 1993, and late data [PB93-198323] p 2626 N94-23738

Analysis of SOFCAL calibration data [NASA-CR-193910] p 2345 N94-25000

Solar flares and magnetospheric particles: Investigations based upon the ONR-602 and ONR-604 experiments [AD-A273639] p 2628 N94-25031

Measuring track densities in lunar grains by image analysis p 2623 N94-25355

COSMOLOGY

Two populations and models of gamma ray bursts [NASA-CR-194762] p 2629 N94-22947

The current status of observational constraints on cosmic strings [DE94-001505] p 2601 N94-23010

Tensor-scalar cosmological models and their relaxation toward general relativity [PB93-220796] p 2601 N94-23099

Structure in gamma ray burst time profiles: Correlations with other observables p 2579 N94-24431

Cosmic wake fields [DE93-616849] p 2604 N94-25215

The scattering and collision of gravitational waves in Friedmann-Robertson-Walker open universes [MATHS-REPT-A-193] p 2406 N94-25430

COST ANALYSIS

US Department of Energy phaseout of CFC-refrigerants [DE94-001668] p 2397 N94-23016

Life cycle cost modeling of conceptual space vehicles [NASA-CR-194813] p 2203 N94-23329

Coordinate-free interpretations of the optimal costs for Lq problems subject to implicit systems [PB94-118700] p 2473 N94-23760

Proceedings of the NIST Conference on Reducing the Cost of Space Infrastructure and Operations: Part 1: Oral presentations and discussion [PB94-111374] p 2194 N94-23770

Estimating the Deep Space Network modification costs to prepare for future space missions by using major cost drivers p 2520 N94-23968

A minimum cost tolerance allocation method for rocket engines and robust rocket engine design p 2222 N94-24419

Tokamak Physics Experiment (TPX) cost and performance trade studies using supercode [DE94-002720] p 2553 N94-24628

The cetaceopteryx: A global range military transport aircraft [NASA-CR-195519] p 2181 N94-24711

Advanced launch system. Advanced development oxidizer turbopump program [NASA-CR-193920] p 2367 N94-25174

Relevant costs or full costs? Explaining why managers use capacity cost allocations for short term decisions [ISBN-9-06-215364-X] p 2587 N94-25279

COST EFFECTIVENESS

Cost benefits of advanced software: A review of methodology used at Kennedy Space Center p 2464 N94-23240

Echocardiographic screening of aircrew candidates p 2424 N94-23319

A minimum cost tolerance allocation method for rocket engines and robust rocket engine design p 2222 N94-24419

Overview of the status and progress in photovoltaics research in the United States [DE94-000981] p 2395 N94-24512

PERCIVAL mission to Mars [NASA-CR-195541] p 2195 N94-24995

Aviation: The timeless industry p 2165 N94-25068

COST ESTIMATES

US Department of Energy phaseout of CFC-refrigerants [DE94-001668] p 2397 N94-23016

Cost benefits of advanced software: A review of methodology used at Kennedy Space Center p 2464 N94-23240

Life cycle cost modeling of conceptual space vehicles [NASA-CR-194813] p 2203 N94-23329

Low power ground-based laser illumination for electric propulsion applications [NASA-CR-194444] p 2219 N94-23555

Estimating the Deep Space Network modification costs to prepare for future space missions by using major cost drivers p 2520 N94-23968

A methodology for software cost estimation using machine learning techniques [AD-A273158] p 2459 N94-24775

C-17 lot 3 production contract [AD-A273180] p 2174 N94-25153

COST REDUCTION

SATCOM simulator speeds MSS deployment and lowers costs p 2287 N94-22822

Reduced cost alternatives to premise wiring using ATM and microcellular technologies p 2314 N94-23239

Task 1: Health management demonstration. Task 2: Process management environment and support of enterprise integration. Task 3: New algorithm development in the PME [NASA-CR-188268] p 2430 N94-23290

Amorphous silicon PVMaT, phase 2A [DE93-018221] p 2390 N94-23295

Review of the probabilistic failure analysis methodology and other probabilistic approaches for application in aerospace structural design [NASA-TP-3434] p 2376 N94-23342
Engineering for profitability [PNR-90990] p 2595 N94-23580
Proceedings of the NIST Conference on Reducing the Cost of Space Infrastructure and Operations: Part 1: Oral presentations and discussion [PB94-111374] p 2194 N94-23770
National Institute of Standards and Technology Conference on Reducing the Cost of Space Infrastructure and Operations. Part 2: Topical papers [PB94-113487] p 2194 N94-23819
Strategies in transition p 2498 N94-23833
Future trends in NASA space operations p 2498 N94-23836
Toward lowering the cost of mission operations p 2519 N94-23960
Evaluation of turbulence models in the PARC code for transonic diffuser flows [NASA-TM-106391] p 2168 N94-24084
The Far Ultraviolet (FUV) auroral imager for the Inner Magnetospheric Imager (IMI) mission: Options p 2209 N94-24453
Advanced avionics architecture and technology review. Executive summary and volume 1: Avionics tech nology. Volume 2: Avionics systems engineering [AD-A273630] p 2186 N94-24733
New Technologies for Space Avionics, 1993 [NASA-CR-195157] p 2272 N94-25193
Appendix A: Proposed statement of work, 1994 p 2272 N94-25194
New Ways Of Doing Business (NWODB) cost quantification analysis [NASA-CR-195186] p 2586 N94-25197
Proceedings of the 12th International Congress: Corrosion Control for Low-Cost Reliability. Volume 6: Electric Power Industry [AD-A273668] p 2250 N94-25408

COSTS
Generalized concavity in cooperative game theory: Characterizations in terms of the core [MEMO-1121] p 2497 N94-22708
KSC management training system project p 2574 N94-23246
Engineering for profitability [PNR-90990] p 2595 N94-23580
A multilevel cost-space approach to solving the balanced long transportation problem p 2483 N94-23678
Toward lowering the cost of mission operations p 2519 N94-23960
Estimating the Deep Space Network modification costs to prepare for future space missions by using major cost drivers p 2520 N94-23968
Tokamak Physics Experiment (TPX) cost and performance trade studies using supercode [DE94-002720] p 2553 N94-24628
Aqueous alkaline cleaners: An alternative to organic solvents [AD-A273510] p 2260 N94-24848

COUCHES
Concepts and embodiment design of a reentry recumbent seating system for the NASA Space Shuttle [NASA-CR-195504] p 2438 N94-24667
Design of a recumbent seating system [NASA-CR-195503] p 2438 N94-24786

COUETTE FLOW
On streak spacing in wall-bounded turbulent flows p 2331 N94-24159
The influence of flow type, particle type and gravity on orthokinetic coagulation [ETN-94-95333] p 2267 N94-25060

COUGH
Asthma in aircrew p 2425 N94-23327

COULOMB POTENTIAL
Localized excitations in competing bond-order-wave, charge-density-wave and spin-density-wave systems. 2: Competing charge-density-wave and spin-density-wave [DE93-617131] p 2538 N94-25388

COUNTER ROTATION
Two stage turbine for rockets p 2215 N94-23059
Measurements and modeling of flow structure in the wake of a low profile wishbone vortex generator [NASA-TM-106468] p 2166 N94-23465

COUNTERFLOW
Extinguishment of combustible porous solids by water droplets [PB93-198893] p 2270 N94-23740
Transient phenomena in laminar spray combustion p 2160 N94-24282
Multiple flames in counterflow spray combustion p 2161 N94-24284

COUNTERMEASURES
Security aspects of space operations data p 2515 N94-23937

COUPLED MODES
Generalized three-dimensional simulation of ferruled coupled-cavity traveling-wave-tube dispersion and impedance characteristics [NASA-TP-3389] p 2310 N94-24056

COUPLERS
Internally folded scalable laser [AD-D015978] p 2350 N94-25216

COUPLING
Coupled frequencies of a hydroelastic rectangular system [LRT-WE-9-FB-4-1992] p 2375 N94-23196
Metallic multilayers: Experimental investigation of magnetic anisotropy and magnetic interlayer coupling [ETN-94-95364] p 2250 N94-25242

COUPLINGS
Space Station Freedom coupling tasks: An evaluation of their telerobotic and EVA compatibility p 2436 N94-24200

COVALENCE
Particle formation in a laser-heated aerosol reactor. Application to silicon and silicon nitride synthesis [PB93-217982] p 2347 N94-22982

COVARIANCE
First order conditions for the maximum likelihood estimation of an exact ARMA model [PB94-110533] p 2495 N94-23814
The radiated noise from isotropic turbulence revisited [NASA-CR-191547] p 2333 N94-24356
Rao-Blackwell theorem in stereology and some counterexamples [PB94-111713] p 2496 N94-24639
An efficient data assimilation algorithm with a gaussian covariance structure [AD-A273152] p 2418 N94-24671
Optimal gains for a single polar orbiting satellite p 2208 N94-24873

CRACK CLOSURE
Fatigue life and crack growth prediction methodology [NASA-TM-109044] p 2228 N94-23279
Analysis of local delaminations caused by angle ply matrix cracks [NASA-TM-109052] p 2228 N94-24083

CRACK INITIATION
Development of a damage tolerance tool to analyze multiple-site damage in aircraft structure p 2157 N94-24261

CRACK OPENING DISPLACEMENT
Elevated temperature crack propagation [NASA-TM-106490] p 2377 N94-24715

CRACK PROPAGATION
Fatigue crack growth rate studies of medium sulfur low alloy steels tested in high temperature water [DE93-040437] p 2238 N94-22861
Fracture simulations via massively parallel molecular dynamics [DE93-040159] p 2374 N94-22871
Fundamentals of fatigue analysis [PB93-226264] p 2374 N94-23118
A numerical analysis of crack propagation in microcracking ceramic and ceramic composites [DE94-001192] p 2253 N94-23183
Thermally activated low temperature creep and primary water stress corrosion cracking of NiCrFe alloys [DE94-001756] p 2241 N94-23219
Fatigue life and crack growth prediction methodology [NASA-TM-109044] p 2228 N94-23279
Mechanical behavior of CMCs: Crack growth resistance and creep aspects p 2256 N94-24235
Repair of cracked aluminum aircraft structure with composite patches p 2156 N94-24259
Development of a damage tolerance tool to analyze multiple-site damage in aircraft structure p 2157 N94-24261
Fracture kinetics analysis of empirical and semi-empirical corrosion fatigue relations p 2159 N94-24277
J-integral patch for finite element analysis of dynamic fracture due to impact of pressure vessels p 2381 N94-24429
Microstructural analysis of the 2195 aluminum-lithium alloy welds p 2251 N94-24448
Prediction of thermal cycling induced cracking in polmer matrix composites [NASA-CR-195135] p 2229 N94-24579
The effects of anisotropy on the nonlinear behavior of bridged cracks in long strips [NASA-CR-194453] p 2377 N94-24604
Durability evaluation of ceramic components using CARES/LIFE [NASA-TM-106475] p 2258 N94-24682
Elevated temperature crack propagation [NASA-TM-106490] p 2377 N94-24715
Investigation of the effects of manufacturing variations and materials on fatigue crack detection methods in gear teeth [NASA-CR-195093] p 2373 N94-24769
Environmentally assisted cracking of high strength beta titanium alloys [AD-A273598] p 2245 N94-24823
FRANC2D: A two-dimensional crack propagation simulator. Version 2.7: User's guide [NASA-CR-4572] p 2246 N94-25118
The mechanical property data base from an Air Force/Industry Cooperative Test Program on advanced aluminum alloys (7064 and CW67) [AD-A273741] p 2251 N94-25531

CRACK TIPS
Fracture simulations via massively parallel molecular dynamics [DE93-040159] p 2374 N94-22871
Analysis of Alloy 600 and X-750 stress corrosion cracks [DE94-001578] p 2238 N94-22936
Environmentally assisted cracking of high strength beta titanium alloys [AD-A273598] p 2245 N94-24823

CRACKING (FRACTURING)
Fundamentals of fatigue analysis [PB93-226264] p 2374 N94-23118
Weld cladding of hard surfaces [PB93-201598] p 2353 N94-23448
The mechanical properties of single crystal (alpha)-Si3N4 [DE94-002632] p 2563 N94-24517
Three-dimensional, inelastic response of single-edge notch bend specimens subjected to impact loading [AD-A273302] p 2378 N94-25143
Matrix fatigue cracking mechanisms of alpha(2) TMC for hypersonic applications [NASA-TM-106506] p 2230 N94-25186
Evaluation of multiaxial fracture models for technical ceramics [ISBN-9-03-860192-1] p 2263 N94-25299
Ring nuclei of strain for bonded dissimilar elastic half spaces with particular application to axisymmetric crack problems [OUEL-1966/92] p 2379 N94-25325
Constitutive modelling of fiber-reinforced concrete under uniaxial tensile loading [VTT-JULK-774] p 2379 N94-25385
Preceedings of the 12th International Congress: Corrosion Control for Low-Cost Reliability. Volume 3A: Corrosion: Specific issues [AD-A273663] p 2251 N94-25450

CRACKS
Analysis of Alloy 600 and X-750 stress corrosion cracks [DE94-001578] p 2238 N94-22936
Thermally activated low temperature creep and primary water stress corrosion cracking of NiCrFe alloys [DE94-001756] p 2241 N94-23219
Analysis of local delaminations caused by angle ply matrix cracks [NASA-TM-109052] p 2228 N94-24083
J-integral patch for finite element analysis of dynamic fracture due to impact of pressure vessels p 2381 N94-24429

CRASHES
Method for simulating a vehicle shock test: Design and realization of the required implementation tools [ECL-92-14] p 2352 N94-22885
Development and experimental validation of computational methods to simulate abnormal thermal and structural environments [DE94-000554] p 2268 N94-23000
Aircraft accident report: In-flight loss of propeller blade and uncontrolled collision with terrain Mitsubishi MU-2B-60, N86SD, Zwingle, Iowa, 19 April 1993 [PB93-910409] p 2174 N94-25175
Aircraft accident/incident summary report: Controlled flight into terrain GP Express Airlines, Inc., N115GP Beechcraft C-99, Shelton, Nebraska, 28 April 1993 [PB94-910401] p 2174 N94-25273

CRASHWORTHINESS
Crashworthiness analysis using advanced material models in DYNA3D [DE94-002988] p 2229 N94-24632

CRAY COMPUTERS
Radar stimulator interface protocol, preliminary interface design and Doppler Beam Sharpening implementation [DE94-002567] p 2453 N94-23701
High-performance computing and communications [DE94-002215] p 2457 N94-24566

CREEP ANALYSIS
Creep deformation characteristics of ductile discontinuous fiber reinforced composites [DE94-000697] p 2227 N94-23005

CREEP PROPERTIES
Relationship of microstructure and mechanical properties for V-Cr-Ti alloys [DE94-001431] p 2238 N94-22718

Creep deformation characteristics of ductile discontinuous fiber reinforced composites
[DE94-000697] p 2227 N94-23005

Thermally activated low temperature creep and primary water stress corrosion cracking of NiCrFe alloys
[DE94-001756] p 2241 N94-23219

Time dependent behavior of a graphite/thermoplastic composite and the effects of stress and physical aging
[NASA-TM-109047] p 2228 N94-23280

Introduction of Ceramics into Aerospace Structural Composites
[AGARD-R-795] p 2255 N94-24228

Mechanical behavior of CMCs: Crack growth resistance and creep aspects p 2256 N94-24235

Numerical modeling of physical vapor transport under microgravity conditions: Effect of thermal creep and stress p 2223 N94-24340

Strength and life of pressure vessels subjected to impacts and thermomechanical GFRP loading
[VTT-JULK-771] p 2379 N94-25418

CREEP STRENGTH

Effect of hydrogen exposure on a Cu-8 Cr-4 Nb alloy
[NASA-TM-106429] p 2243 N94-23556

Strength and life of pressure vessels subjected to impacts and thermomechanical GFRP loading
[VTT-JULK-771] p 2379 N94-25418

CREEP TESTS

On the deformation kinetics constitutive law of plastic deformation: The rate equation p 2161 N94-24289

CREW PROCEDURES (INFLIGHT)

Spacecraft crew procedures from paper to computers
p 2433 N94-24186

CRITERIA

Generalized melting criterion for beam-induced amorphization
[DE94-001333] p 2560 N94-23189

CRITICAL LOADING

Determination of fiber-matrix interface failure parameters from off-axis tests
[NASA-TM-109043] p 2241 N94-23274

CRITICAL PATH METHOD

Extension of the critical path method
[PB94-118817] p 2488 N94-24527

CRITICAL TEMPERATURE

LOX droplet vaporization in a supercritical forced convective environment p 2211 N94-23034

Phase structure of the two-dimensional phi(4) field theory within thermo-field dynamics
[DE93-616850] p 2570 N94-25337

CRITICAL VELOCITY

Control algorithms for effective operation of variable-speed wind turbines
[DE94-002607] p 2394 N94-23704

CROP GROWTH

Manual on measurement of methane and nitrous oxide emissions from agriculture
[DE93-616429] p 2399 N94-25167

Robotics in a controlled, ecological life support system
p 2444 N94-25371

CROP IDENTIFICATION

Evaluation of the use of remote-sensing data to identify crop types and estimate irrigated acreage, Uvalde and Medina Counties, Texas, 1989
[PB93-193159] p 2388 N94-24809

CROSS CORRELATION

Cross-calibration survey (VISNIR)
p 2383 N94-23599

In-flight cross-calibration of ASTER/TIR and MODIS-N
p 2385 N94-23611

CROSS COUPLING

Synthesis of molecular wires by a novel divergent/convergent approach
[AD-A273332] p 2537 N94-25087

CROSS FLOW

An experimental study of the flow field surrounding a subsonic jet in a cross flow
[NASA-CR-194770] p 2317 N94-23072

An implicit numerical scheme for the simulation of internal viscous flows on unstructured grids
[NASA-TM-106437] p 2481 N94-23554

Optimization of orifice geometry for cross-flow mixing in a cylindrical duct
[NASA-TM-106436] p 2481 N94-23593

Study of transient behavior of finned coil heat exchangers p 2321 N94-23642

CFD assessment of orifice aspect ratio and mass flow ratio on jet mixing in rectangular ducts
[NASA-TM-106434] p 2187 N94-24082

Mixing characteristics of directly opposed rows of jets injected normal to a crossflow in a rectangular duct
[NASA-TM-106477] p 2188 N94-24594

CROSS RELAXATION

Excited state dynamics of thulium ions in yttrium aluminum garnets
[NASA-CR-195159] p 2564 N94-25024

CROSSLINKING

Phenylethynl-terminated poly(arylene ethers)
[NASA-CASE-LAR-14797-1] p 2253 N94-23307

Ceramic silicon-boron-carbon fibers from organic silicon-boron-polymers
[NASA-CASE-ARC-11956-1-SB] p 2253 N94-23311

Dipolar relaxation in a second-order nonlinear optical interpenetrating polymer network
[AD-A273626] p 2258 N94-24732

Metal-catalyzed alkynylation of brominated polyphenylenes: Thermoset precursors of high density monolithic glassy carbon
[AD-A273232] p 2259 N94-24789

Polythiophene derivative with a side chain chromophore as photovoltaic and photorefractive materials
[AD-A273245] p 2260 N94-24813

CROSSTALK

Simulation of adjacent channel interference in a UHF satellite system
[AD-A273147] p 2299 N94-24669

Crosstalk analysis of synchronous and asynchronous optical chip interconnects with direct detection
[AD-A273261] p 2311 N94-24685

CRRES (SATELLITE)

CRRES microelectronics package flight data analysis
[NASA-TP-3423] p 2540 N94-23273

Artificial plasma experiments. Chemical release observations associated with the CRRES program
[NASA-CR-194871] p 2550 N94-23565

The CRRES time history data base: All sensors
[AD-A273737] p 2207 N94-25542

CRUCIBLES

Determination of the compatibility between structural alloys and molten metals at high temperatures
[DE94-000954] p 2241 N94-23434

Transient flows occurring during the accelerated crucible rotation technique
[DE93-617049] p 2567 N94-25422

CRUDE OIL

Measurement of interfacial tension by use of pendant drop video techniques
[DE93-000168] p 2345 N94-24831

CRUISE MISSILES

Holographic testing of composite propfans for a cruise missile wind tunnel model
[NASA-TM-105271] p 2187 N94-23545

CRUSHING

Continuum representations of cellular solids
[DE94-001706] p 2375 N94-23217

CRUSTAL FRACTURES

Electromagnetic field changes as a precursory phenomena of earthquakes and volcanic eruptions
[REPT-157] p 2405 N94-24980

Measurement and Interpretation of Crustal Deformation Rates Associated with Postglacial Rebound
[NASA-CR-195193] p 2405 N94-25203

CRYOGENIC COOLING

Cryogenic, low-noise high electron mobility transistor amplifiers for the Deep Space Network
p 2291 N94-23262

Calibration of a helium-cooled infrared spatial radiometer and grating spectrometer p 2384 N94-23607

CRYOGENIC EQUIPMENT

Foil bearing research at Penn State
p 2215 N94-23058

Brush seals for cryogenic applications
p 2216 N94-23063

Reduction of hydrocarbon impurities in 200 l/h helium liquefier-refrigerator system
[NIFS-259] p 2271 N94-24459

CRYOGENIC FLUID STORAGE

Analysis and test of low profile aluminum aerospace tank dome
[NASA-TP-3442] p 2375 N94-23294

Thermodynamic models for bounding pressurant mass requirements of cryogenic tanks
[NASA-TM-106476] p 2346 N94-25202

CRYOGENIC FLUIDS

Computational fluid dynamic modelling of cavitation
p 2215 N94-23060

Thermohydrodynamic analysis of cryogenic liquid turbulent flow fluid film bearings
[NASA-CR-194869] p 2363 N94-24081

Electro-rheology fluids and liquid fuel flow
[AD-A273640] p 2337 N94-25032

CRYOGENIC TEMPERATURE

Developments in materials for high-field magnets
[DE94-000761] p 2307 N94-22987

Precision Displacement Mechanism (PDM)
p 2360 N94-24026

Development of a Low-Temperature Gear Motor (LOG) p 2361 N94-24032

CRYOGENICS

Contamination control and plume assessment of low-energy thrusters
[NASA-TM-104585] p 2218 N94-23343

Experimental and analytical study of cryogenic propellant boiloff to develop and verify alternate pressurization concepts for Space Shuttle external tank using a scaled down tank p 2266 N94-23657

Simulation of cryogenic turbopump annular seals
p 2371 N94-24440

Thermal-fluid analysis of the fill and drain operations of a cryrogenic fuel tank
[NASA-TM-104273] p 2334 N94-24495

CRYOPUMPING

Performance characteristics of the DIII-D advanced divertor cryopump
[DE94-002745] p 2354 N94-23797

CRYOSTATS

Opening mechanism for ISO/CVV cover release
p 2357 N94-24001

CRYPTOGRAPHY

Special signature schemes
[ETN-94-95296] p 2446 N94-25081

CRYSTAL DEFECTS

Report of the Joint Seminar on Solid State Physics, Atomic and Molecular Physics, and Materials Science in the Energy Region of Tandem Accelerators
[DE93-508268] p 2548 N94-22924

Discontinuous phase formation and selective attack of SiC materials exposed to low oxygen partial pressure environments
[DE93-040161] p 2231 N94-22933

Magnetic resonance study of zinc-related defects in silicon with optimized EPR spectrometer
[PB93-224640] p 2561 N94-23223

Defects in electro-optically active polymer solids
p 2223 N94-24342

Thermophysical property sensitivity effects in steel solidification p 2246 N94-25122

Improved magnetostrictive transducer drive elements achieved by reduction of crystalline defects and improved crystalline orientation
[AD-A273391] p 2313 N94-25276

CRYSTAL FIELD THEORY

Structure and energetics of high index Fe, Al, Cu and Ni surfaces using equivalent crystal theory
[NASA-TM-106408] p 2249 N94-25171

Crystal field in Nd2CuO4
[DE93-617054] p 2567 N94-25425

Contribution of all excited states to ZFS of a (sup 6) S-state
[DE93-617007] p 2568 N94-25483

CRYSTAL GROWTH

The study of dopant segregation behavior during the growth of GaAs in microgravity
[NASA-CR-193905] p 2267 N94-23549

Three-dimensional solidification and melting using magnetic field control p 2325 N94-23664

Inertial confinement fusion
[DE94-002602] p 2551 N94-23703

Particle size measurement for the control of industrial crystallizers
[PB94-119104] p 2562 N94-23766

Numerical modeling of physical vapor transport under microgravity conditions: Effect of thermal creep and stress p 2223 N94-24340

Temperature dependence of protein solubility-determination, application to crystallization, and growth kinetics studies p 2224 N94-24344

Crystal growth of organics for nonlinear optical applications p 2225 N94-24348

Diffusion on Cu surfaces p 2251 N94-24428

The mechanical properties of single crystal (alpha)-Si3N4
[DE94-002632] p 2563 N94-24517

Direct observation of crystal growth from solution using optical investigation of a growing crystal face
[NASA-CR-195141] p 2563 N94-24617

Transient flows occurring during the accelerated crucible rotation technique
[DE93-617049] p 2567 N94-25422

CRYSTAL LATTICES

Modifications to 8x8 dynamical theory: Polarizations redefined according to x ray diffraction convention
[DE94-001290] p 2560 N94-23187

GGA study of the magnetic and cohesive properties of bcc, fcc and hcp Mn
[REPT-A-2662] p 2564 N94-24960

Symposium on diffusion in ordered alloys
[AD-A273643] p 2245 N94-25033

CRYSTAL OPTICS

Proposed additions to the SHADOW ray-tracing code for general-asymmetric perfect-crystal optics
[DE94-001291] p 2560 N94-23188

Investigation of the optical and laser properties of Tm and Ho in YAG anf YLF
[REPT-94-001] p 2563 N94-24404

CRYSTAL STRUCTURE

Bridgman's concern
[DE93-040900] p 2558 N94-22953

Application of maximum entropy and irreducible cluster integrals to joint probability distributions for x ray structure determination
[PB93-224152] p 2559 N94-23109
Perturbation theory in electron diffraction
[PB93-201424] p 2533 N94-23505
Defects in electro-optically active polymer solids
p 2223 N94-24342
The torsion space nucleic acids molecular mechanics program DUPLEX: Surveying conformation space by potential energy minimization
[DE94-002441] p 2563 N94-24567
Thermal phase behavior of metal surfaces: X-ray scattering studies of Pt(001)
[DE94-002991] p 2245 N94-24612
Direct observation of crystal growth from solution using optical investigation of a growing crystal face
[NASA-CR-195141] p 2563 N94-24617
Simulation studies for surfaces and materials strength
[NASA-CR-195185] p 2565 N94-25093
Structure and energetics of high index Fe, Al, Cu and Ni surfaces using equivalent crystal theory
[NASA-TM-106408] p 2249 N94-25171
Preparation and properties of translucent gamma-aluminium oxynitride
[ETN-94-95305] p 2263 N94-25281
Investigation of the solid-solid surface adsorption of Eu2O3 on amorphous Al2O3
[DE93-613824] p 2566 N94-25332
Structure of cholesteryl-4-vinylbenzoate
[AD-A273686] p 2567 N94-25441

CRYSTAL SURFACES
Ge-Au eutectic bonding of Ge (100) single crystals
[DE94-002281] p 2564 N94-24657
Structure and energetics of high index Fe, Al, Cu and Ni surfaces using equivalent crystal theory
[NASA-TM-106408] p 2249 N94-25171

CRYSTALLINITY
Polydiacetylene thin films for nonlinear optical applications p 2225 N94-24347
Two micron stimulated emission of activated insulating crystals
[REPT-94-002] p 2565 N94-25025

CRYSTALLITES
Combustion synthesis and engineering of nanoparticles for electronic, structural and superconductor applications
[DE94-001865] p 2254 N94-23720

CRYSTALLIZATION
Processing of YBCO superconductors for improved levitation force
[DE94-001326] p 2559 N94-22994
Temperature dependence of protein solubility-determination, application to crystallization, and growth kinetics studies p 2224 N94-24344

CRYSTALLOGRAPHY
Orientation imaging microscopy: New possibilities for microstructural investigations using automated BKD analysis
[DE94-000777] p 2557 N94-22938
Application of maximum entropy and irreducible cluster integrals to joint probability distributions for x ray structure determination
[PB93-224152] p 2559 N94-23109
Observation of non-centrosymmetry and determination of polarity in III-V semiconductors
[PB93-201416] p 2561 N94-23503
Image analysis technology applied to problems in crystallography
[AD-A273516] p 2566 N94-25288
Dual-purpose RTOF diffractometer facility at the ET-RR-1 reactor
[VTT-TIED-1425] p 2566 N94-25347
Morphology of highly textured polyethylene/polyethylene- propylene semicrystalline diblock copolymers
[AD-A273683] p 2263 N94-25413

CRYSTALS
Anisotropic uniaxial pressure effects in YBa2Cu3O(7-delta)
[DE94-001456] p 2557 N94-22929
Low temperature diffusion of hydrogenic species in oxide crystals: Radiation induced diffusion
[DE94-000374] p 2558 N94-22957
Modifications to 8x8 dynamical theory: Polarizations redefined according to x ray diffraction convention
[DE94-001290] p 2560 N94-23187
Perturbation theory in electron diffraction
[PB93-201424] p 2533 N94-23505
Inertial confinement fusion
[DE94-002602] p 2551 N94-23703
The statistics of sputtering
[DE94-001128] p 2243 N94-23715
Particle size measurement for the control of industrial crystallizers
[PB94-119104] p 2562 N94-23766
Modeling of PCG fluid dynamics: Salient results
p 2224 N94-24345
GGA study of the magnetic and cohesive properties of bcc, fcc and hcp Mn
[REPT-A-2662] p 2564 N94-24960
Excited state dynamics of thulium ions in yttrium aluminum garnets
[NASA-CR-195159] p 2564 N94-25024
Selected bibliography 2: Diamond surface chemistry
[AD-A273518] p 2565 N94-25160
Image analysis technology applied to problems in crystallography
[AD-A273516] p 2566 N94-25288

CUBES (MATHEMATICS)
Median stabilization degree of a median algebra
[PB93-220010] p 2479 N94-23093

CULTURE TECHNIQUES
Non-invasive optical detection of glucose in cell culture nutrient medium p 2422 N94-25357

CUMULATIVE DAMAGE
Damage under monotonic or cyclic loads of new AlSiFe alloys prepared by the Osprey (tm) process
[ISAL-93-0008] p 2239 N94-22972
Contribution to the interface micromechanical study and to the damage fundamental phenomena in glass fiber epoxy resin model composites
[ISAL-93-0027] p 2227 N94-23133

CUMULUS CLOUDS
On testing two major cumulus parameterization schemes using the CSU regional atmospheric modeling system
[DE94-000703] p 2407 N94-23284
Joint sessions on moisture processes and cumulus parameterization p 2414 N94-24393
Session on cumulus parameterization
p 2414 N94-24394

CURIE TEMPERATURE
Influences of nitrogen absorption on the magnetic properties of YFe2, YFe3 and Y6Fe23
[REPT-A-2654] p 2564 N94-24958

CURING
Phenylethynl-terminated poly(arylene ethers)
[NASA-CASE-LAR-14797-1] p 2253 N94-23307
Fiber optic detection of ultrasound and its application to cure monitoring
[ISBN-0-315-83424-2] p 2544 N94-24466
Curing phthalonitrile resins with acid and amine
[AD-D016021] p 2258 N94-24721
Ultrasonic process for curing adhesives
[AD-A273175] p 2259 N94-24788
Curing phthalonitriles with acid
[AD-D015996] p 2261 N94-25054
A preliminary evaluation of the phosphazene resin PPZ
[AD-A273674] p 2263 N94-25410

CURIUM
A survey of metallurgical research on several actinides
[DE94-002643] p 2245 N94-24747

CURRENT ALGEBRA
Off-critical W(infinity) and Virasoro algebras as dynamical symmetries of the integrable models
[DE93-633215] p 2478 N94-22969
The 2D supergravity and integrable systems
[DE93-616848] p 2570 N94-25336

CURRENT DENSITY
Heavy ion irradiation of Bi-2223 silver-clad tapes for superconducting current density enhancement
[DE93-017416] p 2556 N94-22886
High energy density aluminum-oxygen cell
p 2393 N94-23363
A high performance H2-Cl2 fuel cell for space power applications p 2394 N94-23366
Stationary plasma thruster plume characteristics
[NASA-CR-194454] p 2219 N94-24361
Mechanisms of anode power deposition in a low pressure free burning arc
[NASA-CR-194442] p 2553 N94-25190

CURRENT DISTRIBUTION
A nonlinear degenerating parabolic problem from the theory of type 2 superconductors
[MEMO-1112] p 2555 N94-22730
Rigorous analysis of thick microstrip antennas and wire antennas embedded in a substrate
[EUT-92-E-263] p 2290 N94-22876
Voyager planetary radio astronomy studies
[NASA-CR-194776] p 2614 N94-24328
Time-domain analysis of conduction and displacement current distributions in inhomogeneous and anisotropic layered media
[PB94-111036] p 2403 N94-24592

CURRENT SHEETS
Evolution of large-scale plasma structures in comets: Kinematics and physics
[NASA-CR-194777] p 2601 N94-23251

CURVATURE
Bent-tip blade for aircraft rotary-wing
[CA-PATENT-1-315-259] p 2176 N94-23254
Large eddy simulation of a boundary layer with concave streamwise curvature p 2328 N94-24146
Studies on the implementation of normals and curvatures. Part 1: The first or mean curvature
[DE94-001546] p 2488 N94-24503

CURVED PANELS
Radially constructed cruciform parachute
[CA-PATENT-1323021] p 2168 N94-24182

CURVES (GEOMETRY)
Number of moduli of families of curves on toric surfaces
[PB93-230381] p 2479 N94-23121

CUSPS (MATHEMATICS)
The cusp horseshoe and its bifurcations in the unfolding of an inclination-flip homoclinic orbit
[W-9307] p 2480 N94-23141

CYANIDES
Photoinduced charge separation in solid state and molecular systems
[DE94-001727] p 2563 N94-24537

CYCLES
Tool sharing: An application of max-algebra, part 1
[MEMO-1108] p 2478 N94-22726
Long cycles in graphs with prescribed toughness and minimum degree
[MEMO-1109] p 2478 N94-22727
The role of atmospheric heat transport in the seasonal carbon dioxide cycle p 2621 N94-24896

CYCLIC AMP
On the mechanism of action of 3',5'-cyclic adenosine monophosphate: A study of four- and five-coordinated phosphorus compounds, modelling the activated state of cAMP
[ISBN-9-03-860222-7] p 2226 N94-25238

CYCLIC COMPOUNDS
Scanning probe lithography. 2: Selective chemical vapor deposition of copper into scanning tunneling microscope-defined patterns
[AD-A273304] p 2547 N94-25144

CYCLIC LOADS
Damage under monotonic or cyclic loads of new AlSiFe alloys prepared by the Osprey (tm) process
[ISAL-93-0008] p 2239 N94-22972
A review of the Workshop on Fatigue Life Methodologies for Wind Turbines
[DE94-002039] p 2394 N94-23472
Role of interfaces on the cyclic fatigue behaviour of ceramic matrix composites p 2256 N94-24234
Post buckling behaviour of stiffened composite panels loaded in cyclic compression and shear
p 2157 N94-24260
Mean stress models for low cycle fatigue of a nickel-base superalloy p 2159 N94-24276
Matrix fatigue cracking mechanisms of alpha(2) TMC for hypersonic applications
[NASA-TM-106506] p 2230 N94-25186

CYCLOTRON FREQUENCY
Voyager planetary radio astronomy studies
[NASA-CR-194776] p 2614 N94-24328

CYCLOTRON RADIATION
Investigation and application of microwave electron cyclotron resonance plasma physical vapour deposition
[DE93-613909] p 2555 N94-25333

CYCLOTRON RESONANCE
Multi-ion, multi-event test of ion cyclotron resonance heating
[NASA-CR-194859] p 2540 N94-23495
Reactivity of ambident anions in the gas phase
[PB93-232189] p 2533 N94-23713
Investigation and application of microwave electron cyclotron resonance plasma physical vapour deposition
[DE93-613909] p 2555 N94-25333

CYCLOTRON RESONANCE DEVICES
Massachusetts Institute of Technology Plasma Fusion Center 1992-1993 report to the President
[DE94-001725] p 2548 N94-22721

CYLINDRICAL BODIES
Damage tolerance of pressurized graphite/epoxy tape cylinders under uniaxial and biaxial loading
[NASA-CR-195101] p 2377 N94-24587
Surface barrier of a uniaxial anisotropic type 2 superconducting cylinder
[DE93-617137] p 2566 N94-25392
Transient flows occurring during the accelerated crucible rotation technique
[DE93-617049] p 2567 N94-25422

CYLINDRICAL CHAMBERS
CFD simulation of coaxial injectors
p 2342 N94-24430

CYLINDRICAL SHELLS
Energy estimates and asymptotic analysis in the theory of shells
[PB93-225738] p 2374 N94-23113
Shell buckling research at Delft, 1976 - 1992
[PB93-224442] p 2375 N94-23221

The plastic response of a cylindrical shell subjected to an internal blast wave with a finite width shock front
p 2154 N94-24246

Structural design criteria for filament-wound composite shells
[NASA-CR-195125] p 2229 N94-24402

CORSS: Cylinder Optimization of Rings, Skin, and Stringers
[NASA-TP-3457] p 2490 N94-24727

Buckling of circular cylindrical shells subjected to combined loads (axial compression, normal pressure, bending and transverse shear loading)
[PB93-215358] p 2378 N94-24745

CYSTS

Spontaneous pneumothorax, cysts and bullae
p 2425 N94-23326

CYTOMETRY

Monoclonal antibodies directed against surface molecules of multicell spheroids
[NASA-CR-195102] p 2420 N94-23633

CZOCHRALSKI METHOD

Two micron stimulated emission of activated insulating crystals
[REPT-94-002] p 2565 N94-25025

D

DAMAGE

Pressure wall patch
[NASA-CASE-MFS-28724-1] p 2203 N94-23824

Engine materials characterization and damage monitoring by using x ray technologies
[NASA-TP-3328] p 2372 N94-24074

DAMAGE ASSESSMENT

Debris/Ice/TPS assessment and integrated photographic analysis for Shuttle Mission STS-61
[NASA-TM-109195] p 2199 N94-24059

Final postflight hardware evaluation report RSRM-32 (STS-57)
[NASA-CR-193903] p 2200 N94-24065

Development of a damage tolerance tool to analyze multiple-site damage in aircraft structure
p 2157 N94-24261

Computer based expert system for battle damage repair of composite structures p 2157 N94-24262

Assessment of impact damage of composite rocket motor cases
[NASA-CR-195143] p 2220 N94-24595

Nondestructive evaluations
[DE94-003020] p 2373 N94-24613

Postflight hardware evaluation (RSRM-29, STS-54)
[NASA-CR-193895] p 2201 N94-24802

DAMKOHLER NUMBER

Transient phenomena in laminar spray combustion
p 2160 N94-24282

Multiple flames in counterflow spray combustion
p 2161 N94-24284

DAMPING

Low melting temperature alloy deployment mechanism
p 2356 N94-23997

On the effect of the damping coefficients on the trajectories of symmetric and non-symmetric stores
p 2155 N94-24250

Foil bearings p 2371 N94-24415

DATA ACQUISITION

Federal alternative fuel program light duty vehicle operations
[DE93-040663] p 2264 N94-22878

CAMAC throughput of a new RISC-based data acquisition computer at the DIII-D tokamak
[DE94-001113] p 2550 N94-23182

SeaWiFS technical report series. Volume 11: Analysis of selected orbit propagation models for the SeaWiFS mission
[NASA-TM-104566-VOL-11] p 2417 N94-23338

The national geomagnetic initiative
[LC-93-85739] p 2401 N94-23344

Cross-calibration survey (VISNIR)
p 2383 N94-23599

Evaluating NOAA satellite products for global climate monitoring p 2384 N94-23604

ASTER TIR subsystem and calibration
p 2385 N94-23612

OASIS-CC presentation p 2385 N94-23613

Groundtruth collection for the JPL-SAR and ERS-1 campaign in Flevoland and Veluwe, Netherlands, 1991
[PB93-230654] p 2386 N94-23755

Commonality of flight control systems for support of European telecommunications missions
p 2304 N94-23834

Development of the Cassini Ground Data System in a multimission environment p 2500 N94-23845

Distributed science operations for JPL planetary missions p 2500 N94-23850

The Ulysses spacecraft control and monitoring concepts and realities p 2502 N94-23862

A review of mission planning systems
p 2503 N94-23866

Techniques and software for optimum and efficient mission science sequence development
p 2504 N94-23872

A packet-based concept for spacecraft command planning p 2504 N94-23873

Mars Observer screen display design for a multimission environment p 2197 N94-23888

The evolving trend in spacecraft health analysis
p 2202 N94-23946

Using the SPICE system to help plan and interpret space science observations p 2517 N94-23950

Mars Observer data production, transfer, and archival: The data production assembly line p 2518 N94-23953

Space Station Freedom ground data system: Design and operations p 2518 N94-23957

The Olympus PAX, measurement of mechanism induced vibration p 2362 N94-24041

ASPT software source code: ASPT application software package, host component
[CTN-94-60907] p 2455 N94-24116

Use of infrared telemetry as part of a nonintrusive inflight data collection system to collect human factors data
p 2434 N94-24193

The experimental physics and industrial control system architecture: Past, present, and future
[DE94-002639] p 2457 N94-24626

Near-surface seismic imaging
[PB94-119096] p 2404 N94-24647

Investigation of the heat handling capabilities of DIII-D neutral beamline internal components
[DE94-001107] p 2553 N94-24756

Design and simulation of EVA tools for first servicing mission of HST
[NASA-CR-194784] p 2439 N94-24857

VLSI-based video event triggering for image data compression
[NASA-TM-106500] p 2345 N94-25116

The data-acquisition and second level trigger system for ZEUS calorimeter
[ETN-94-95384] p 2541 N94-25256

DATA BASE MANAGEMENT SYSTEMS

Translative interface for data sharing and integrating: A paradigm for distributed data systems
[DE93-018790] p 2588 N94-22863

A general model for dynamic and complex information management: The ELEN prototype object manager for software engineering
[ETN-94-95163] p 2588 N94-22880

Structure and flow of data through an environmental data management system
[DE93-040487] p 2589 N94-22934

ACOS: The performance based approach to build a parallel complex object server
[PB93-223816] p 2465 N94-22986

Bibliographic Retrieval System (BARS), Sandia Shock Compression (SSC) database Shock Physics Index
[DE94-001679] p 2589 N94-23126

Bibliographic Retrieval System (BARS). Sandia Shock Compression (SSC) database Shock Physics Index (SPHINX) database. Volume 1: UNIX version query guide customized application for INGRES
[DE94-001703] p 2589 N94-23127

Bibliographic Retrieval System (BARS), Sandia Shock Compression (SSC) database, Shock Physics Index (SPHINX) database, Volume 2: UNIX version user's guide
[DE94-001704] p 2589 N94-23128

A system for managing information at ATLAS
[DE94-001337] p 2590 N94-23190

A framework for SFC/DC system data analysis
p 2523 N94-23234

An engineering database management system for spacecraft operations p 2517 N94-23951

The ESIS query environment pilot project
p 2518 N94-23952

Compression for an effective management of telemetry data p 2518 N94-23956

From requirements to acceptance tests
p 2464 N94-23962

Space operations: Archiving space science data needs further management improvements. Report to the Chairman, Subcommittee on Investigations and Oversight, Committee on Science, Space, and Technology, House of Representatives
[GAO/NSIAD-94-25] p 2591 N94-24092

Activities involving aeronautical, space science, and technology support for minority institutions
[NASA-CR-195095] p 2574 N94-24225

Fact-based enterprise information management using NIAM
[DE93-041135] p 2591 N94-24501

Waste minimization/pollution prevention at R/D facilities: A cradle-to-grave tracking and information system that will be implemented at Sandia National Laboratories
[DE93-040330] p 2591 N94-24607

Modeling of database constraints in active databases
[AD-A273484] p 2592 N94-24691

Correct and efficient interface for logical query languages with complex objects
[PB93-211175] p 2593 N94-24743

DATA BASES

Translative interface for data sharing and integrating: A paradigm for distributed data systems
[DE93-018790] p 2588 N94-22863

Catalog of data bases and reports
[DE93-040597] p 2588 N94-22875

Structure and flow of data through an environmental data management system
[DE93-040487] p 2589 N94-22934

ACOS: The performance based approach to build a parallel complex object server
[PB93-223816] p 2465 N94-22986

Bibliographic Retrieval System (BARS), Sandia Shock Compression (SSC) database Shock Physics Index
[DE94-001679] p 2589 N94-23126

Bibliographic Retrieval System (BARS). Sandia Shock Compression (SSC) database Shock Physics Index (SPHINX) database. Volume 1: UNIX version query guide customized application for INGRES
[DE94-001703] p 2589 N94-23127

Bibliographic Retrieval System (BARS), Sandia Shock Compression (SSC) database, Shock Physics Index (SPHINX) database, Volume 2: UNIX version user's guide
[DE94-001704] p 2589 N94-23128

A system for managing information at ATLAS
[DE94-001337] p 2590 N94-23190

A framework for SFC/DC system data analysis
p 2523 N94-23234

Space Station Freedom (SSF) Data Management System (DMS) performance model data base
[NASA-CR-188270] p 2590 N94-23289

Task 1: Health management demonstration. Task 2: Process management environment and support of enterprise integration. Task 3: New algorithm development in the PME
[NASA-CR-188268] p 2430 N94-23290

An overview of a model rotor icing test in the NASA Lewis Icing Research Tunnel
[NASA-TM-106471] p 2166 N94-23299

MITS architecture V1.0
[PB93-201762] p 2452 N94-23451

Development of durable high-temperature catalysts for natural gas combustion
[PB93-226447] p 2232 N94-23477

The Fifth Calibration/Data Product Validation Panel Meeting
[NASA-TM-108270] p 2383 N94-23595

SPDB (science processing database): Quick reference guide p 2383 N94-23597

TOVS Pathfinder product validation and intercomparison p 2384 N94-23603

Validating a large geophysical data set: Experiences with satellite-derived cloud parameters p 2385 N94-23615

An overview of the UARS data validation effort
p 2386 N94-23617

Multi-set extended relational algebra: A formal approach to a practical issue
[PB94-110830] p 2486 N94-23725

Concepts and techniques for an active database approach to office procedure support
[PB94-110749] p 2590 N94-23816

The evolving trend in spacecraft health analysis
p 2202 N94-23946

An engineering database management system for spacecraft operations p 2517 N94-23951

The ESIS query environment pilot project
p 2518 N94-23952

Compression for an effective management of telemetry data p 2518 N94-23956

New mission requirements methodologies for services provided by the Office of Space Communications
p 2519 N94-23961

From requirements to acceptance tests
p 2464 N94-23962

AstroMail: Electronic mail for the astrophysics community
[NASA-CR-194877] p 2591 N94-24099

Tensoral for post-processing users and simulation authors p 2333 N94-24169

Previous experience in manned space flight: A survey of human factors lessons learned p 2435 N94-24196

Joint Acoustic Propagation Experiment (JAPE)
p 2527 N94-24208

Panel to review EOSDIS plans
[NASA-CR-195088] p 2387 N94-24303

Application of concurrent engineering principles to aircraft structural design p 2178 N94-24321
Technology utilization office data base analysis and design p 2577 N94-24417
MERILL: An equational reasoning system in standard ML: A user guide (prerelease version 0.4)
[PB93-204501] p 2456 N94-24534
Systems engineering: A formal approach. Part 2: Frameworks
[PB94-101391] p 2489 N94-24615
Modeling of database constraints in active databases
[AD-A273484] p 2592 N94-24691
Correct and efficient interface for logical query languages with complex objects
[PB93-211175] p 2593 N94-24743
Rice cultivation and methane emission: Documentation of distributed geographic data sets
[NASA-TM-104595] p 2381 N94-24800
A study of cloud motions on Mars. 2: Some examples of observations and analyses since 1969
p 2620 N94-24891
Ground based mission planning systems
p 2522 N94-25014
Mission rehearsal in the SOF-ATS program
p 2522 N94-25016
Establishment of computerized numerical databases on thermophysical and other properties of molten as well as solid materials and data evaluation and validation for generating recommended reliable reference data
p 2246 N94-25123
NASA STI program database: Journal coverage (1990-1992)
[NASA-TM-109720] p 2593 N94-25168
The IRGen infrared data base modeler
p 2440 N94-25496
The CRRES time history data base: All sensors
[AD-A273737] p 2207 N94-25542

DATA COMPRESSION
Integer cosine transform compression for Galileo at Jupiter: A preliminary look p 2292 N94-23266
Neural network research in Finland. Symposium
[PB93-224822] p 2472 N94-23463
Material data representation of hysteresis loops for Hastelloy X using artificial neural networks
[NASA-TM-105990] p 2376 N94-23551
Compression for an effective management of telemetry data p 2518 N94-23956
A constrained joint source/channel coder design and vector quantization of nonstationary sources
[NASA-CR-195145] p 2301 N94-24707
New directions in network flows
[AD-A273467] p 2468 N94-24939
HORACE: Presentation-level protocol standard for digital transmission of monochrome television images
[AD-A273395] p 2197 N94-25064

DATA CORRELATION
Evaluating NOAA satellite products for global climate monitoring p 2384 N94-23604

DATA FLOW ANALYSIS
A dataflow analysis tool for parallel processing of algorithms
[NASA-TM-109054] p 2448 N94-23086
Source spacing in B-ISDN
[PB93-201747] p 2293 N94-23508
Validation activities for LOTOS based on static data flow analysis
[PB94-110863] p 2459 N94-24758
Study on fine grain dynamic dataflow computer
[REPT-946] p 2446 N94-24981

DATA INTEGRATION
Convective organization in the Pacific ITCZ: Merging OLR, TOVS, and SSM/I information
[NASA-CR-194850] p 2408 N94-23619
Space Shuttle Main Engine performance analysis
p 2222 N94-24444
Optimal gains for a single polar orbiting satellite
p 2208 N94-24873
Sensor fusion display evaluation using information integration models in enhanced/synthetic vision applications p 2443 N94-25512

DATA LINKS
Measurement of multipath delay profile in land mobile satellite channels p 2283 N94-22793
System services and architecture of the TMI satellite mobile data system p 2286 N94-22817
Handover aspects for a Low Earth Orbit (LEO) CDMA Land Mobile Satellite (LMS) system
p 2288 N94-22824
Command/telemetry bus general specification for the NOAA-OPQ polar orbiting environmental satellites and EUMETSAT polar satellite systems
[NASA-TM-109407] p 2208 N94-23479
Multi-access laser communications terminal
[NASA-CR-191251] p 2295 N94-23830
Representing operations procedures using temporal dependency networks p 2305 N94-23914
Situation management in the Link Monitor and Control Operator Assistant (LMCOA) p 2305 N94-23915
Experimental verification of an acoustic telemetry link between an Aurora and CFAV quest
[DREA-TC-93-304] p 2202 N94-24121
New Advances in Mission Planning and Rehearsal Systems
[AGARD-LS-192] p 2521 N94-25008
Failure detection and recovery in the assembly/contingency subsystem p 2306 N94-25360
Conceptual communications system design in the 25.25-27.5 and 37.0-40.5 GHz frequency bands
p 2306 N94-25379
Modeling of the ground-to-SSFMB link networking features using SPW p 2306 N94-25381

DATA MANAGEMENT
Structure and flow of data through an environmental data management system
[DE93-040487] p 2589 N94-22934
Quality data validation: Comprehensive approach to environmental data validation
[DE94-000925] p 2589 N94-22944
A framework for SFC/DC system data analysis
p 2523 N94-23234
Space Station Freedom (SSF) Data Management System (DMS) performance model data base
[NASA-CR-188270] p 2590 N94-23289
GEWEX p 2385 N94-23614
SpaceOps 1992: Proceedings of the Second International Symposium on Ground Data Systems for Space Mission Operations
[NASA-CR-194486] p 2497 N94-23832
Distributed science operations for JPL planetary missions p 2500 N94-23850
A MOS for all seasons p 2505 N94-23879
Mission and science activity scheduling language
p 2515 N94-23938
The evolving trend in spacecraft health analysis
p 2202 N94-23946
Mars Observer data production, transfer, and archival: The data production assembly line p 2518 N94-23953
Compression for an effective management of telemetry data p 2518 N94-23956
Space Station Freedom ground data system: Design and operations p 2518 N94-23957
Earth observation archive activities at DRA Farnborough p 2519 N94-23958
From requirements to acceptance tests
p 2464 N94-23962
Scheduling the future NASA Space Network: Experiences with a flexible scheduling prototype
p 2520 N94-23965
Space operations: Archiving space science data needs further management improvements. Report to the Chairman, Subcommittee on Investigations and Oversight, Committee on Science, Space, and Technology, House of Representatives
[GAO/NSIAD-94-25] p 2591 N94-24092
Decentralized autonomous attitude determination using an inertially stabilized payload p 2157 N94-24264
Session on techniques and resources for storm-scale numerical weather prediction p 2415 N94-24400
Design and specification of a centralized manufacturing data management and scheduling system
p 2577 N94-24416

DATA PROCESSING
VIERS-1, phase 3
[BCRS-92-24] p 2381 N94-23145
Code generation for the attribute evaluator of the protocol engine grammar processor unit
[EUT-93-E-271] p 2450 N94-23173
Implementing the space shuttle data processing system with the space generic open avionics architecture
[NASA-CR-188254] p 2199 N94-23571
Radar stimulator interface protocol, preliminary interface design and Doppler Beam Sharpening implementation
[DE94-002567] p 2453 N94-23701
A reference model for space data system interconnection services p 2305 N94-23847
Preparing the DSN operations concepts
p 2501 N94-23853
Object-oriented technologies in a multi-mission data system p 2506 N94-23885
VMPLOT: A versatile analysis tool for mission operations p 2507 N94-23891
The application of automated operations at the Institutional Processing Center p 2509 N94-23901
The advanced orbiting systems testbed program: Results to date p 2197 N94-23907
Verification of technical elements of the advanced spacecraft based upon the CCSDS recommendation
p 2207 N94-23910
MERCATOR: Methods and Realization for Control of the Attitude and the Orbit of spacecraft
p 2202 N94-23925
Using SFOC to fly the Magellan Venus mapping mission p 2516 N94-23941
The evolving trend in spacecraft health analysis
p 2202 N94-23946
Telemetry ground system development via the component approach p 2203 N94-23949
Using the SPICE system to help plan and interpret space science observations p 2517 N94-23950
Mars Observer data production, transfer, and archival: The data production assembly line p 2518 N94-23953
Activities involving aeronautical, space science, and technology support for minority institutions
[NASA-CR-195095] p 2574 N94-24225
Integrated stress and strength analysis of airplane structures using the data processing tool ISSY
p 2178 N94-24320
Next generation initiation techniques
p 2412 N94-24383
Using neural networks to assist in OPAD data analysis
p 2477 N94-24452
Near-surface seismic imaging
[PB94-119096] p 2404 N94-24647
New Advances in Mission Planning and Rehearsal Systems
[AGARD-LS-192] p 2521 N94-25008
Advanced Information Processing System (AIPS)
p 2165 N94-25115
Downward extrapolation of multi-component seismic data
[ISBN-9-09-005213-5] p 2405 N94-25229
The L3 visualization system and its use in the Z(zero) line shape analysis
[ETN-94-95382] p 2537 N94-25231
Decomposition of multi-component measurements into P and S waves
[ISBN-9-09-005197-X] p 2405 N94-25251

DATA PROCESSING EQUIPMENT
Implementing the space shuttle data processing system with the space generic open avionics architecture
[NASA-CR-188254] p 2199 N94-23571
MERCATOR: Methods and Realization for Control of the Attitude and the Orbit of spacecraft
p 2202 N94-23925

DATA REDUCTION
Uncertainties in climate data sets
[NASA-CR-194848] p 2408 N94-23577
Object-oriented technologies in a multi-mission data system p 2506 N94-23885
VMPLOT: A versatile analysis tool for mission operations p 2507 N94-23891
Long term trending of engineering data for the Hubble Space Telescope p 2516 N94-23942
Tensoral for post-processing users and simulation authors p 2333 N94-24169
Space Shuttle Main Engine performance analysis
p 2222 N94-24444
Using neural networks to assist in OPAD data analysis
p 2477 N94-24452
Measurement of HO2 and other trace gases in the stratosphere using a high resolution far-infrared spectrometer
[NASA-CR-195173] p 2404 N94-24738

DATA RETRIEVAL
SPDB (science processing database): Quick reference guide p 2383 N94-23597
TOVS Pathfinder product validation and intercomparison p 2384 N94-23603
From requirements to acceptance tests
p 2464 N94-23962
A usage profile and evaluation of a wide-area distributed file system
[AD-A273590] p 2593 N94-24946

DATA SAMPLING
Quality data validation: Comprehensive approach to environmental data validation
[DE94-000925] p 2589 N94-22944

DATA SIMULATION
The evolving trend in spacecraft health analysis
p 2202 N94-23946

DATA STORAGE
Structure and flow of data through an environmental data management system
[DE93-040487] p 2589 N94-22934
The Fifth Calibration/Data Product Validation Panel Meeting
[NASA-TM-108270] p 2383 N94-23595
Validating a large geophysical data set: Experiences with satellite-derived cloud parameters p 2385 N94-23615
Mars Observer data production, transfer, and archival: The data production assembly line p 2518 N94-23953
Compression for an effective management of telemetry data p 2518 N94-23956
Earth observation archive activities at DRA Farnborough p 2519 N94-23958

Space operations: Archiving space science data needs further management improvements. Report to the Chairman, Subcommittee on Investigations and Oversight, Committee on Science, Space, and Technology, House of Representatives
[GAO/NSIAD-94-25] p 2591 N94-24092
Performance of the engineering analysis and data system 2 common file system p 2576 N94-24413

DATA STRUCTURES
The explicit computation of integration algorithms and first integrals for ordinary differential equations with polynomials coefficients using trees
[NASA-CR-194787] p 2448 N94-23074
Using genetic algorithms for scheduling data flow graphs
[EUT-92-E-266] p 2449 N94-23169
SeaWiFS technical report series. Volume 9: The simulated SeaWiFS data set, version 1
[NASA-TM-104566-VOL-9] p 2417 N94-23291
An object-oriented approach for parallel self adaptive mesh refinement on block structured grids
p 2469 N94-23697
Multi-set extended relational algebra: A formal approach to a practical issue
[PB94-110830] p 2486 N94-23725
Study of methods and structures for handling of digitized maps for geographical information systems
[PB93-204402] p 2590 N94-23741
Security aspects of space operations data
p 2515 N94-23937
Activities involving aeronautical, space science, and technology support for minority institutions
[NASA-CR-195095] p 2574 N94-24225
RITL: An information system for application reuse-in-the-large
[PB94-119088] p 2592 N94-24646
Runtime support and compilation methods for user-specified data distributions
[NASA-CR-191587] p 2458 N94-24679
A type-theoretic approach to higher-order modules with sharing
[AD-A273566] p 2458 N94-24693
Correct and efficient interface for logical query languages with complex objects
[PB93-211175] p 2593 N94-24743
From circuit to signal: Development of a piecewise linear simulator
[ISBN-9-09-005713-7] p 2462 N94-25263
Data structures and amortized complexity in a functional setting
[ETN-94-95307] p 2476 N94-25290
Expert system rule-base evaluation using real-time parallel processing
[AD-A273701] p 2469 N94-25454

DATA SYSTEMS
Design and implementation considerations of a MSAT packet data network p 2280 N94-22778
System services and architecture of the TMI satellite mobile data system p 2286 N94-22817
Translative interface for data sharing and integrating: A paradigm for distributed data systems
[DE93-018790] p 2588 N94-22863
NASA/ASEE Summer Faculty Fellowship Program
[NASA-CR-194678] p 2571 N94-23230
SeaWiFS technical report series. Volume 9: The simulated SeaWiFS data set, version 1
[NASA-TM-104566-VOL-9] p 2417 N94-23291
A complete public archive for the Einstein IPC
[NASA-CR-189316] p 2453 N94-23559
SpaceOps 1992: Proceedings of the Second International Symposium on Ground Data Systems for Space Mission Operations
[NASA-CR-194486] p 2497 N94-23832
Commonality of flight control systems for support of European telecommunications missions
p 2304 N94-23834
Mission operations update for the restructured Earth Observing System (EOS) mission p 2499 N94-23839
Development of the Cassini Ground Data System in a multimission environment p 2500 N94-23845
A reference model for space data system interconnection services p 2305 N94-23847
NASDA satellite mission operation system and operations p 2501 N94-23854
NASA/Goddard Space Flight Center's testbed for CCSDS compatible systems p 2197 N94-23855
Ground data system for Space Flyer Unit (SFU)
p 2207 N94-23860
The Mars mapper science and mission planning tool
p 2503 N94-23867
A MOS for all seasons p 2505 N94-23879
Making adaptable systems work for mission operations: A case study p 2506 N94-23883
An approach to the design of operations systems
p 2506 N94-23884
Mars Observer screen display design for a multimission environment p 2197 N94-23888
Influence of a new generation of operations support systems on current spacecraft operations philosophy: The users feedback p 2507 N94-23894
Making tomorrow's mistakes today: Evolutionary prototyping for risk reduction and shorter development time p 2197 N94-23902
Applications of CCSDS recommendations to Integrated Ground Data Systems (IGDS) p 2510 N94-23906
The advanced orbiting systems testbed program: Results to date p 2197 N94-23907
Verification of technical elements of the advanced spacecraft based upon the CCSDS recommendation
p 2207 N94-23910
Security aspects of space operations data
p 2515 N94-23937
Using SFOC to fly the Magellan Venus mapping mission p 2516 N94-23941
EOS ground data systems: A description and interface overview p 2517 N94-23948
Telemetry ground system development via the component approach p 2203 N94-23949
Space Station Freedom ground data system: Design and operations p 2518 N94-23957
SAO mission support software and data standards, version 1.0
[NASA-CR-193906] p 2454 N94-24050
Panel to review EOSDIS plans
[NASA-CR-195088] p 2387 N94-24303
Performance of the engineering analysis and data system 2 common file system p 2576 N94-24413
Worldwide vessel locating and tracking system, volume 1
[PB93-193217] p 2175 N94-24474
A usage profile and evaluation of a wide-area distributed file system
[AD-A273590] p 2593 N94-24946

DATA TRANSFER (COMPUTERS)
Open EDI
[VTT-TIED-1353] p 2588 N94-22734
Specifications of ETS, the Enhanced Transport Service
[RR-907-I] p 2589 N94-23150
OASIS-CC presentation p 2385 N94-23613
Reliable transfer of data from ground to space
p 2305 N94-23908

DATA TRANSMISSION
Open EDI
[VTT-TIED-1353] p 2588 N94-22734
Proceedings of the Third International Mobile Satellite Conference (IMSC 1993)
[NASA-CR-194516] p 2273 N94-22735
Internetworking satellite and local exchange networks for personal communications applications
p 2276 N94-22755
ROCSAT-1 telecommunication experiments
p 2279 N94-22770
Canadian aeronautical mobile data trials
p 2279 N94-22773
The AGRHYMET data communications project
p 2280 N94-22776
The ORBCOMM data communications system
p 2281 N94-22782
Specifications of ETS, the Enhanced Transport Service
[RR-907-I] p 2589 N94-23150
An optical ASK and FSK phase diversity transmission system
[EUT-92-E-268] p 2542 N94-23171
PROGRIL: A language for the definition of protocol grammars
[EUT-93-E-270] p 2449 N94-23172
Reduced cost alternatives to premise wiring using ATM and microcellular technologies p 2314 N94-23239
High-rate data link general specification for the NOAA-OPQ polar orbiting environmental satellites and EUMETSAT satellite systems
[NASA-TM-109384] p 2208 N94-23481
A reference model for space data system interconnection services p 2305 N94-23847
AMFESYS: Modelling and diagnosis functions for operations support p 2506 N94-23887
Verification of technical elements of the advanced spacecraft based upon the CCSDS recommendation
p 2207 N94-23910
The ESIS query environment pilot project
p 2518 N94-23952
Mars Observer data production, transfer, and archival: The data production assembly line p 2518 N94-23953
The European Space Agency standard for space packet utilisation p 2203 N94-23954
Space Station Freedom ground data system: Design and operations p 2518 N94-23957
A small satellite design for deep space network testing and training
[NASA-CR-195526] p 2205 N94-24702
A constrained joint source/channel coder design and vector quantization of nonstationary sources
[NASA-CR-195145] p 2301 N94-24707
Modeling of the ground-to-SSFMB link networking features using SPW p 2306 N94-25381

DEBONDING (MATERIALS)
Creep deformation characteristics of ductile discontinuous fiber reinforced composites
[DE94-000697] p 2227 N94-23005
Interface evaluation in ceramic composites
p 2255 N94-24231

DEBRIS
Debris/Ice/TPS assessment and integrated photographic analysis for Shuttle Mission STS-61
[NASA-TM-109195] p 2199 N94-24059
Microbiological analysis of debris from Space Transportation System (STS)-55 Spacelab D-2
[NASA-CR-193883] p 2421 N94-24310

DECAY
Decay of swirl in turbulent pipe flows
[ETN-94-95353] p 2339 N94-25248

DECISION MAKING
Task 1: Health management demonstration. Task 2: Process management environment and support of enterprise integration. Task 3: New algorithm development in the PME
[NASA-CR-188268] p 2430 N94-23290
Decision making with imprecise probabilities
[PB94-111622] p 2494 N94-23772
Human factors of mission planning systems: Theory and concepts p 2521 N94-25010
An implementation of the REpresentation and MAintenance of Process knowledge (REMAP) model in the knowledge-based software assistant concept demonstration system
[AD-A273207] p 2461 N94-25138
Relevant costs or full costs? Explaining why managers use capacity cost allocations for short term decisions
[ISBN-9-06-215364-X] p 2587 N94-25279
Throughput time control and due date reliability in tool and die shops
[ISBN-9-03-860182-4] p 2587 N94-25283
Transputer benchmarks and performance comparisons with other computing machines
[RR-467] p 2446 N94-25312
Integrated risk management p 2588 N94-25361
Quality metrics for sensor images
p 2443 N94-25513
Solving the ranking and selection indifference-zone formulation for normal distributions using computer software
[AD-A273821] p 2496 N94-25518
On finding optimal policies for Markov decision chains: A unifying framework for mean-variance-tradeoffs
[TW-92-13] p 2497 N94-25528

DECISION THEORY
Bayesian decision theory with imprecise prior probabilities applied to replacement problems
[PB93-237634] p 2481 N94-23456
Decision making with imprecise probabilities
[PB94-111622] p 2494 N94-23772
On finding optimal policies for Markov decision chains: A unifying framework for mean-variance-tradeoffs
[TW-92-13] p 2497 N94-25528

DECODING
Separable concatenated codes with iterative map decoding for Rician fading channels
p 2286 N94-22815
Compression for an effective management of telemetry data p 2518 N94-23956
Conveying digital data in noisy, unstable, multipath environments
[AD-D015980] p 2301 N94-25038
Algebraic-geometric codes and their decoding algorithms
[ETN-94-95294] p 2491 N94-25079

DECOMPOSITION
A method for the general simultaneous full decomposition of sequential machines: Algorithms and implementation
[EUT-92-E-267] p 2445 N94-23170
Domain decomposition methods for nonconforming finite element spaces of Lagrange-type
p 2483 N94-23680
Multi-grid domain decomposition approach for solution of Navier-Stokes equations in primitive variable form
p 2341 N94-23693
Adsorption, desorption, and decomposition of HCl and HBr on Ge(100): Competitive pairingand near-first-order desorption kinetics
[AD-A273504] p 2235 N94-24790
Computing techniques in mission planning
p 2522 N94-25012

Decomposition of multi-component measurements into P and S waves
[ISBN-9-09-005197-X] p 2405 N94-25251
Parallel processing methods for space based power systems p 2222 N94-25352

DECOUPLING
Decoupling problems around a trajectory: From linearity to nonlinearity
[MEMO-1115] p 2469 N94-22703

DEEP SPACE
The remote-operated autonomous-robot concept: From deep sea to outer space applications
p 2370 N94-23413

DEEP SPACE NETWORK
The Telecommunications and Data Acquisition Report
[NASA-CR-194766] p 2290 N94-23256
Cryogenic, low-noise high electron mobility transistor amplifiers for the Deep Space Network
p 2291 N94-23262
Analysis of open-loop conical scan pointing error and variance estimators p 2291 N94-23263
Link monitor and control operator assistant: A prototype demonstrating semiautomated monitor and control
p 2292 N94-23267
Optical subnet concepts for the deep space network
p 2292 N94-23269
An improved gravity model for Mars: Goddard Mars Model-1 (GMM-1)
[NASA-TM-104584] p 2401 N94-23282
An OSI architecture for the deep space network
p 2305 N94-23848
Preparing the DSN operations concepts
p 2501 N94-23853
Radioastron flight operations p 2502 N94-23861
Digital test signal generation: An accurate SNR calibration approach for the DSN p 2305 N94-23912
Representing operations procedures using temporal dependency networks p 2305 N94-23914
Situation management in the Link Monitor and Control Operator Assistant (LMCOA) p 2305 N94-23915
Using Mach threads to control DSN operational sequences p 2477 N94-23916
Deep Space Network (DSN), Network Operations Control Center (NOCC) computer-human interfaces
p 2447 N94-23917
Operability engineering in the Deep Space Network
p 2514 N94-23930
Estimating the Deep Space Network modification costs to prepare for future space missions by using major cost drivers p 2520 N94-23968
The Jet Propulsion Laboratory space exploration: Past, present and future p 2153 N94-24242
A small satellite design for deep space network testing and training
[NASA-CR-195526] p 2205 N94-24702

DEEP WATER
The remote-operated autonomous-robot concept: From deep sea to outer space applications
p 2370 N94-23413

DEFECTS
Vacancy formation energy of Li(H, D) and Na(H, D) systems
[DE93-633452] p 2558 N94-22978
Interactions between organized, surface-confined monolayers and vapor-phase probe molecules. 7: Comparison of self-assemblying organomercaptan monolayers deposited on gold from liquid and vapor phases
[AD-A273196] p 2535 N94-24555
Image remapping strategies applied as protheses for the visually impaired p 2444 N94-25363

DEFENSE INDUSTRY
Frameworks for integrated airframe design
p 2178 N94-24318
The Future of Aerospace: Proceedings of a symposium held in honor of Alexander H. Flax
[LC-93-83945] p 2631 N94-25065
Defense aerospace and the new world order
p 2596 N94-25066

DEFENSE PROGRAM
Frameworks for integrated airframe design
p 2178 N94-24318
Information systems strategy in air transport
[AD-A273125] p 2173 N94-24781
Aqueous alkaline cleaners: An alternative to organic solvents
[AD-A273510] p 2260 N94-24848
Research interests and broad agency announcement 94-1 of the Air Force Office of Scientific Research
[AD-A273410] p 2632 N94-25075
B-2 bomber: Assessment of DOD's response to mandated certifications and reports
[AD-A273179] p 2184 N94-25152

DEFINITION
Definitions in use by the visible and near-infrared, and thermal working groups p 2383 N94-23598

DEFLAGRATION
Investigations on detonation shock dynamics and related topics
[DE94-002570] p 2326 N94-23809

DEFORESTATION
Human impacts on soil carbon dynamics of deep-rooted Amazonian forests
[NASA-CR-195127] p 2399 N94-24861

DEFORMATION
Gas-pressure forming of superplastic ceramic sheet
[DE94-001520] p 2252 N94-22930
Design of a surface deformation measuring instrument for the Surface Tension Driven Convection Experiment (STDCE-2)
[NASA-CR-194758] p 2343 N94-23285
Intelligent Material Systems and Structures (IMSS). Part 5: Fiber optic registration of deformation in carbon laminates 91/92
[PB93-204600] p 2544 N94-23723
Real-time holographic endoscopy
[ISL-CO-203/92] p 2343 N94-24054
Post buckling behaviour of stiffened composite panels loaded in cyclic compression and shear
p 2157 N94-24260
Stability analysis of anisotropic conical shells
[PB94-119054] p 2377 N94-24645
Development of a nondestructive vibration technique for bond assessment of Space Shuttle tiles
[NASA-CR-195163] p 2201 N94-24919
The measurement of the film thickness and the roughness deformation of lubricated elastomers
[ETN-94-95293] p 2261 N94-25078
The nanometer-scale mechanics of gold films
[AD-A273307] p 2565 N94-25086

DEGRADATION
A prediction model of signal degradation in LMSS for urban areas p 2284 N94-22797
Hot hydrogen testing of metallic turbo pump materials
[NASA-CR-193880] p 2244 N94-24066
Viscoelastic analysis of seals for extended service life
p 2371 N94-24408
Properties and processing characteristics of low density carbon cloth phenolic composites p 2231 N94-24450

DEGREES OF FREEDOM
Control of a serpentine manipulator with collision avoidance p 2368 N94-23232
Rack Insertion End Effector (RIEE) automation
p 2368 N94-23242
Proton spin: The role of quark-gluon and hadron degrees of freedom
[DE93-616867] p 2538 N94-25341

DEIMOS
A mission to Mercury and a mission to the moons of Mars
[NASA-CR-195530] p 2195 N94-24619

DELAMINATING
Analysis of local delaminations caused by angle ply matrix cracks
[NASA-TM-109052] p 2228 N94-24083
The nanometer-scale mechanics of gold films
[AD-A273307] p 2565 N94-25086

DELAY
Investigations into deployment complications of the ERS-1 SAR antenna p 2305 N94-23996
Delay-insensitive communication
[ETN-94-95315] p 2304 N94-25303

DELTA FUNCTION
Ga delta-doping layers in silicon
[PB93-224632] p 2561 N94-23222

DELTA LAUNCH VEHICLE
Liquid rocket propulsion: Retrospective and prospects
p 2154 N94-24243

DELTA WINGS
Lift augmentation on a delta wing via leading edge fences and the Gurney flap
[NASA-CR-194793] p 2168 N94-24103
Supersonic aerodynamic characteristics of a circular body Earth-to-Orbit vehicle
[NASA-TM-4533] p 2170 N94-24716
A study of roll attractor and wing rock of delta wings at high angles of attack p 2164 N94-25111

DEMAGNETIZATION
Comparative M-H characteristics of 1-5 and 2-17 type samarium-cobalt permanent magnets to 300 C
[NASA-CR-194440] p 2312 N94-24870

DEMAND (ECONOMICS)
Simplicial variable dimension restart algorithm to find economic equilibria on the unit simplex using n(n+1) rays
[PB94-110541] p 2596 N94-24477
US general aviation: The ingredients for a renaissance. A vision and technology strategy for US industry, NASA, FAA, universities p 2162 N94-25097

DEMODULATION
Low cost coherent demodulation for mobile satellite terminals p 2284 N94-22803
Pseudo-coherent demodulation for mobile satellite systems p 2287 N94-22819
Analysis of time-diversity combining methods for frequency-hopped signals
[CU-DOE-92-09] p 2300 N94-24694
Modulation and synchronization technique for MF-TDMA system
[NASA-CR-194448] p 2304 N94-25266

DEMODULATORS
Performance of the unique-word-reverse-modulation type demodulator for mobile satellite communications
p 2286 N94-22813
Pseudo-coherent demodulation for mobile satellite systems p 2287 N94-22819
Advanced technology for a satellite multichannel demultiplexer/demodulator
[NASA-CR-194435] p 2202 N94-23631

DEMOGRAPHY
Vision impairment and corrective considerations of civil airmen
[DOT/FAA/AM-93/21] p 2426 N94-23623

DEMULTIPLEXING
Advanced technology for a satellite multichannel demultiplexer/demodulator
[NASA-CR-194435] p 2202 N94-23631
Modulation and synchronization technique for MF-TDMA system
[NASA-CR-194448] p 2304 N94-25266
Modeling of the ground-to-SSFMB link networking features using SPW p 2306 N94-25381

DENSITY DISTRIBUTION
Measuring track densities in lunar grains by image analysis p 2623 N94-25355
Near surface analysis p 2407 N94-25364

DENSITY MEASUREMENT
Stationary plasma thruster plume characteristics
[NASA-CR-194454] p 2219 N94-24361

DEOXYRIBONUCLEIC ACID
Applications of the Aurora parallel PROLOG system to computational molecular biology
[DE93-041166] p 2420 N94-23468
Capillary electrophoresis of biomolecules: Theory, instrumentation and applications
[ETN-94-95297] p 2236 N94-25233

DEPLOYMENT
Deployable video conference table
[NASA-CASE-ARC-11950-1] p 2192 N94-23310
Aircraft accident report: Inadvertent in-flight slat deployment, China Eastern Airlines Flight 583, McDonnell Douglas MD-11, B-2171, 950 nautical miles south of Shemya, Alaska, 6 April 1993
[PB93-910408] p 2172 N94-23579
Primary deployment mechanism for the European Polar Platform p 2207 N94-23995
Investigations into deployment complications of the ERS-1 SAR antenna p 2305 N94-23996
Low melting temperature alloy deployment mechanism
p 2356 N94-23997
Nearly uniform deployment/retrieval strategy for space tether systems p 2156 N94-24256

DEPOLYMERIZATION
Solid rocket combustion simulator technology using the hybrid rocket for simulation
[NASA-CR-195142] p 2265 N94-24578

DEPOSITION
Ultraviolet photosulfidation of III-V compound semiconductors for electronic passivation
[DE94-001417] p 2555 N94-22717
Novel two-stage selenization methods for fabrication of thin-film CIS cells and submodules
[DE94-000220] p 2390 N94-23296
Pulsed Ion Beam Surface Analysis (PIBSA) as a means of in-situ real-time analysis of thin films during growth
[DE94-001276] p 2562 N94-23805
Mechanisms of anode power deposition in a low pressure free burning arc
[NASA-CR-194442] p 2553 N94-25190

DEPOSITS
Temporal and spatial mapping of surface albedo and atmospheric dust opacity on Mars p 2619 N94-24887

DEPTH
Effect of land use change on the carbon cycle in Amazon soils
[NASA-CR-195168] p 2399 N94-24853
A statistical analysis of recent Naval Experimental Diving Unit (NEDU) single-depth human exposures to 100 percent oxygen at pressure
[AD-A273488] p 2427 N94-24950

DESERTS
The AGRHYMET data communications project
p 2280 N94-22776

DESIGN ANALYSIS
The design and networking of dynamic satellite constellations for global mobile communication systems
p 2288 N94-22826

Design refinement of multilayer optical thin film devices with two optimization techniques
[DE93-634228] p 2542 N94-22979

Design of microchannels for cryostabilization of high temperature superconducting magnets
[DE94-001324] p 2559 N94-22993

Shell buckling research at Delft, 1976 - 1992
[PB93-224442] p 2375 N94-23221

Flame trench analysis of NLS vehicles
p 2199 N94-23249

A reliable algorithm for optimal control synthesis
[NASA-CR-194809] p 2472 N94-23332

Status of the development of rechargeable lithium cells p 2392 N94-23354

Composite material impregnation unit
[NASA-TM-107751] p 2254 N94-23486

Object oriented simulation implementation in support of robust system design
[DE93-011687] p 2452 N94-23488

Simplified, inverse, ejector design tool
[NASA-CR-194438] p 2166 N94-23511

Generic mission planning concepts for space astronomy missions p 2505 N94-23878

Automating a human factors evaluation of graphical user interfaces for NASA applications: An update on CHIMES
p 2443 N94-23936

Specifying design conservatism: Worst case versus probabilistic analysis p 2374 N94-23939

A novel rotary actuator for spacecraft
p 2361 N94-24034

Sensorless, brushless motor to drive a sealed freon-ammonia pump p 2315 N94-24036

The use of analytical models in human-computer interface design p 2434 N94-24190

CMC design consequences p 2256 N94-24238

Integrated Airframe Design Technology
[AGARD-R-794] p 2177 N94-24313

New computing systems, future computing environment, and their implications on structural analysis and design
p 2177 N94-24314

Early manufacturing considerations in design
p 2177 N94-24315

Probabilistic simulation of concurrent engineering of propulsion systems p 2177 N94-24317

The process network in the design and manufacturing of aircraft p 2178 N94-24319

Application of concurrent engineering principles to aircraft structural design p 2178 N94-24321

Viscoelastic analysis of seals for extended service life
p 2371 N94-24408

A review of ISEAS design p 2465 N94-24410

Finite element based electric motor design optimization p 2315 N94-24411

Design and specification of a centralized manufacturing data management and scheduling system
p 2577 N94-24416

Technology utilization office data base analysis and design p 2577 N94-24417

Controller modeling and evaluation for PCV electro-mechanical actuator p 2371 N94-24441

LOLA: Lunar Optical Long-baseline Array. 1992-1993 space design
[NASA-CR-195533] p 2298 N94-24582

An investigation of requirements traceability to support systems development
[AD-A273167] p 2458 N94-24684

The cetaceopteryx: A global range military transport aircraft
[NASA-CR-195519] p 2181 N94-24711

Pre-design study of a general purpose vehicle simulator platform
[PB93-215366] p 2193 N94-24739

Design and application of electromechanical actuators for deep space missions
[NASA-CR-195134] p 2365 N94-24842

Weasel works SA-150: Design study of a 100 to 150 passenger transport aircraft
[NASA-CR-195489] p 2183 N94-24975

The Bunny: A simulated commercial air transportation study
[NASA-CR-195537] p 2183 N94-25001

The Gold Rush: A simulated commercial air transportation study
[NASA-CR-195528] p 2184 N94-25002

Human factors of mission planning systems: Theory and concepts p 2521 N94-25010

Development of high-angle-of-attack nose-down pitch control margin design guidelines for combat aircraft
p 2164 N94-25107

DESIGN TO COST

PERCIVAL mission to Mars
[NASA-CR-195541] p 2195 N94-24995

DESORPTION

Adsorption, desorption, and decomposition of HCl and HBr on Ge(100): Competitive pairingand near-first-order desorption kinetics
[AD-A273504] p 2235 N94-24790

DESTABILIZATION

Effect of LHCD (low hybrid current drive) on tearing mode instability
[DE93-613700] p 2555 N94-25344

DETECTION

Lightning studies using LDAR and LLP data
p 2416 N94-23238

Screening for asymptomatic coronary heart disease
p 2423 N94-23315

Feasibility of detecting aircraft wake vortices using passive microwave radiometers
[NASA-CR-191553] p 2343 N94-23498

Orbital Signature Analyzer (OSA): A spacecraft health/safety monitoring and analysis tool
p 2203 N94-23947

A chemical sensor and biosensor based totally automated water quality monitor for extended space flight: Step 1 p 2443 N94-24447

The measurement of the film thickness and the roughness deformation of lubricated elastomers
[ETN-94-95293] p 2261 N94-25078

A model-based approach for detection of objects in low resolution passive-millimeter wave images
p 2442 N94-25507

DETECTORS

Deviation equations of Synge and Schild in spaces with affine connection and metric, and equations for gravitational waves detectors
[DE93-616852] p 2571 N94-25339

DETONABLE GAS MIXTURES

Stability of hypersonic flow of a detonable gas mixture in the stagnation region of a blunt body and a forward facing step p 2154 N94-24248

DETONATION

The ignition temperature of solid explosives exposed to a fire
[DE94-001047] p 2265 N94-23436

Multiple shock initiation of LX-17
[DE94-001524] p 2265 N94-23807

Investigations on detonation shock dynamics and related topics
[DE94-002570] p 2326 N94-23809

Stability of hypersonic flow of a detonable gas mixture in the stagnation region of a blunt body and a forward facing step p 2154 N94-24248

DETONATION WAVES

Investigations on detonation shock dynamics and related topics
[DE94-002570] p 2326 N94-23809

DEUTERIDES

Vacancy formation energy of Li(H, D) and Na(H, D) systems
[DE93-633452] p 2558 N94-22978

DEUTERIUM

Pellet ablation in the large helical device
[NIFS-260] p 2551 N94-24358

DEUTERIUM COMPOUNDS

High-resolution soft x ray photoionization studies of selected molecules
[DE94-000568] p 2532 N94-23002

DEXTRANS

Capillary electrokinetic separations with optical detection
[DE94-001639] p 2233 N94-23716

DIAMOND FILMS

The in situ observation of epitaxial diamond thin film nucleation and growth using emission electron microscopy
[AD-A273698] p 2263 N94-25489

DIAMONDS

Intelligent control of chemical vapor deposition processes
[AD-A273356] p 2261 N94-24937

Selected bibliography 2: Diamond surface chemistry
[AD-A273518] p 2565 N94-25160

Temperature dependent performance of Coplanar Waveguide (CPW) on substrates of various materials
[NASA-TM-106505] p 2313 N94-25170

DIASTOLIC PRESSURE

Autogenic-feedback training: A potential treatment for post-flight orthostatic intolerance in aerospace crews
[NASA-TM-108785] p 2426 N94-24102

DIATOMIC MOLECULES

Energy transfer in solid explosives
[DE94-001523] p 2265 N94-23778

DICARBOXYLIC ACIDS

Reaction of isocyanates with carboxylic acids and its application to polymer synthesis
[PB94-118858] p 2254 N94-23763

DICHOTOMIES

The geophysical signal of the martian global dichotomy p 2623 N94-24997

DICHROISM

Performance of the X-/Ka/KABLE-band dichroic plate in the DSS-13 beam waveguide antenna
p 2291 N94-23261

Mueller matrix analysis of infrared ellipsometry
[PB93-201549] p 2544 N94-23629

DIELECTRIC PROPERTIES

The elastic and electromechanical properties of BaTiO3 single crystal through the ferroelectric transition
[DE94-001437] p 2557 N94-22927

Mueller matrix analysis of infrared ellipsometry
[PB93-201549] p 2544 N94-23629

Multigrid and cyclic reduction applied to the Helmholtz equation p 2304 N94-23676

DIELECTRICS

Fabrication of sub-40-nm p-n junctions for 0.18 micron MOS device applications using a cluster-tool-compatible, nanosecond thermal doping technique
[DE94-001608] p 2309 N94-23520

DIELS-ALDER REACTIONS

Study of improved methods for predicting chemical equilibria
[DE94-001647] p 2568 N94-22719

Synthesis of soluble halogenated polyphenylenes: Mechanism for the coupling halogenated lithiobenzenes
[AD-A273547] p 2257 N94-24558

DIESEL ENGINES

Development of high temperature liquid lubricants for low-heat rejection: Heavy duty diesel engines
[NASA-CR-191197] p 2258 N94-24753

DIFFERENTIAL AMPLIFIERS

High speed electronic analog computers using low-gain amplifiers
[AD-D015974] p 2446 N94-25034

Wide bandwidth differential amplifier
[AD-D015985] p 2303 N94-25217

DIFFERENTIAL CALCULUS

Differential algebraic equations
[PB93-237618] p 2481 N94-23455

On the differentiation matrix for Daubechies-based wavelets on an interval
[NASA-CR-191582] p 2487 N94-24291

Discrete sensitivity derivatives of the Navier-Stokes equations with a parallel Krylov solver
[NASA-TM-106481] p 2265 N94-24301

DIFFERENTIAL EQUATIONS

Coherence lost? Not-so-fast escapes from the in-phase attractor of a set of globally coupled nonlinear oscillators
[DE94-000799] p 2557 N94-22940

On the numeric integration of dynamic attitude equations
[NASA-CR-194788] p 2448 N94-23073

The explicit computation of integration algorithms and first integrals for ordinary differential equations with polynomials coefficients using trees
[NASA-CR-194787] p 2448 N94-23074

Differential algebraic equations
[PB93-237618] p 2481 N94-23455

Response-coefficient method for heat-conduction transients with time-dependent inputs
p 2326 N94-23671

Multigrid methods for differential equations with highly oscillatory coefficients p 2484 N94-23685

Error due to the stopping of the Newton iteration in implicit linear multistep methods
[PB94-101425] p 2487 N94-23786

Neural network-based control using Lyapunov functions p 2477 N94-24433

Simulation of cryogenic turbopump annular seals
p 2371 N94-24440

Comparison of time integration methods for the evolution of galaxies
[PB94-111671] p 2602 N94-24522

Stable non-Gaussian diffusive profiles
[PB93-238053] p 2489 N94-24610

Super Beltrami differentials and N equal to 4 superconformal anomalies
[DE93-613047] p 2491 N94-25166

The state space method for integro-differential equations of convolution type with rational matrix symbols
[ETN-94-95379] p 2491 N94-25244

Liapunov stability in chemical engineering
[MATHS-REPT-A-184] p 2236 N94-25427

DIFFERENTIAL GEOMETRY

On the numeric integration of dynamic attitude equations
[NASA-CR-194788] p 2448 N94-23073

Studies on the implementation of normals and curvatures. Part 1: The first or mean curvature
[DE94-001546] p 2488 N94-24503

DIFFERENTIAL INTERFEROMETRY

Interferometry in rarefied gas flows
[ISL-CO-207/92] p 2318 N94-23160

DIFFERENTIAL PRESSURE
Nonlinear equations of motion for a panel subject to external loads
[AD-A273142] p 2170 N94-24773
DIFFRACTION
A prediction model of signal degradation in LMSS for urban areas p 2284 N94-22797
Modifications to 8x8 dynamical theory: Polarizations redefined according to x ray diffraction convention
[DE94-001290] p 2560 N94-23187
DIFFRACTION PATTERNS
X ray diffraction analysis of electrodeposited beta-tantalum
[AD-A273254] p 2249 N94-25142
DIFFRACTOMETERS
Dual-purpose RTOF diffractometer facility at the ET-RR-1 reactor
[VTT-TIED-1425] p 2566 N94-25347
DIFFUSE RADIATION
Uncertainty analysis of diffuse-gray radiation enclosure problems: A hypersensitive case study
p 2320 N94-23637
An Earth albedo model: A mathematical model for the radiant energy input to an orbiting spacecraft due to the diffuse reflectance of solar radiation from the Earth below
[NASA-TM-104596] p 2195 N94-24497
DIFFUSERS
Numerical analysis of a vortex controlled diffuser
p 2324 N94-23659
The 3-D numerical study of airflow in the compressor/combustor prediffuser and dump diffuser of an industrial gas turbine p 2324 N94-23660
DIFFUSION
Low temperature diffusion of hydrogenic species in oxide crystals: Radiation induced diffusion
[DE94-000374] p 2558 N94-22957
Diffusion of hydrogen in iron oxides
[DE93-632430] p 2239 N94-22966
A method to simulate viscous diffusion of vorticity by convective transport of vortices at a non-solenoidal velocity
[DE94-001777] p 2318 N94-23220
Fabrication of sub-40-nm p-n junctions for 0.18 micron MOS device applications using a cluster-tool-compatible, nanosecond thermal doping technique
[DE94-001608] p 2309 N94-23520
Convective instabilities in traveling fronts of addition polymerization p 2226 N94-24352
Effects of thermal-solutal convection on temperature and solutal fields under various gravitational orientations
p 2267 N94-24451
Symposium on diffusion in ordered alloys
[AD-A273643] p 2245 N94-25033
DIFFUSION COEFFICIENT
Eddy mixing coefficient values derived from simulations with the NASA Ames Mars GCM p 2617 N94-24875
Drying deformable media: Kinetics, shrinkage and stresses
[ETN-94-95314] p 2236 N94-25302
Diffusion in electronegative discharges with magnetic fields
[AD-A273826] p 2304 N94-25521
DIFFUSION FLAMES
Evaporation and combustion of LOX under supercritical and subcritical conditions p 2211 N94-23035
Efficiency and reliability enhancements in propulsion flowfield modeling p 2215 N94-23055
Extinguishment of combustible porous solids by water droplets
[PB93-198893] p 2270 N94-23740
Transient phenomena in laminar spray combustion
p 2160 N94-24282
Multiple flames in counterflow spray combustion
p 2161 N94-24284
DIFFUSION THEORY
Applications of the homogenization method to flow and transport in porous media
[BER-9110] p 2340 N94-25467
DIFFUSION WELDING
Gas-pressure forming of superplastic ceramic sheet
[DE94-001520] p 2252 N94-22930
Strength, acoustic evaluation and metallurgy of diffusion bonds
[DE94-001804] p 2243 N94-23717
DIFFUSIVITY
Stable non-Gaussian diffusive profiles
[PB93-238053] p 2489 N94-24610
Derivation of the macroscopic rate equations for the driven diffusive Ising model at pair level of approximation
[DE93-616839] p 2524 N94-25208
DIGITAL COMPUTERS
Verification of synchronous sequential numerical material systems: Application of the LUSTRE language and of the LESAR verification tool
[ETN-94-95181] p 2447 N94-22899
Development of programmable artificial neural networks p 2477 N94-25370
DIGITAL DATA
ASTER TIR subsystem and calibration
p 2385 N94-23612
The Mars mapper science and mission planning tool
p 2503 N94-23867
Conveying digital data in noisy, unstable, multipath environments
[AD-D015980] p 2301 N94-25038
Some subjects in digital audio, noise shaping, sample rate conversion, dynamic range compression and testing
[ISBN-9-09-005162-7] p 2530 N94-25220
Digital data, composite video multiplexer and demultiplexer boards for an IBM PC/AT compatible computer p 2447 N94-25377
DIGITAL ELECTRONICS
Multidisciplinary specification and design of microelectronics in products
[EUT-93-E-269] p 2308 N94-23136
PLANET: A hierarchical network simulator
[ISBN-9-09-005693-9] p 2313 N94-25083
CADBIT 2: Computer-aided design for built-in test, volume 1
[AD-A273702] p 2463 N94-25455
DIGITAL SIMULATION
Mixed analog-digital description and simulation: Proposition for VHDL-analogue
[RR-908-I] p 2450 N94-23180
DIGITAL SYSTEMS
ESA personal communications and digital audio broadcasting systems based on non-geostationary satellites p 2273 N94-22737
Direct broadcast satellite-radio, receiver development
p 2273 N94-22739
Pilot-vehicle interface
[DOT/FAA/CT-92/21] p 2430 N94-23083
Formal methods and digital systems validation for airborne systems
[NASA-CR-4551] p 2466 N94-23293
Micro SIL-1 simulator
[PB94-110889] p 2454 N94-23750
An introduction to digital modulation and OFDM techniques
[BBC-RD-1993/10] p 2295 N94-24086
A homotopy algorithm for digital optimal projection control GASD-HADOC
[NASA-CR-193881] p 2456 N94-24470
Mitigation of EMI/RFI produced by a 1.2 kW uninterruptible power supply
[AD-A273149] p 2299 N94-24670
Pilot-vehicle interface handbook, chapter 19. Volume 2: Digital systems validation
[DOT/FAA/CT-88/10-VOL-2] p 2438 N94-24830
On-line evaluation of multiloop digital controller performance p 2163 N94-25105
Aircraft digital flight control technical review
p 2163 N94-25106
DIGITAL TECHNIQUES
Spur-reduced digital sinusoid synthesis
p 2291 N94-23264
The HDTV digital audio matrix
[BBC-RD-1993/9] p 2295 N94-24085
An introduction to digital modulation and OFDM techniques
[BBC-RD-1993/10] p 2295 N94-24086
Special signature schemes
[ETN-94-95296] p 2446 N94-25081
On chain coding of line drawings
[ISBN-9-06-275778-2] p 2462 N94-25252
DIGITAL TELEVISION
HORACE: Presentation-level protocol standard for digital transmission of monochrome television images
[AD-A273395] p 2197 N94-25064
DIISOCYANATES
Reaction of isocyanates with carboxylic acids and its application to polymer synthesis
[PB94-118858] p 2254 N94-23763
DILUTION
Optimization of orifice geometry for cross-flow mixing in a cylindrical duct
[NASA-TM-106436] p 2481 N94-23593
DIMENSIONAL MEASUREMENT
Particle size measurement for the control of industrial crystallizers
[PB94-119104] p 2562 N94-23766
DIMERS
Synthesis of molecular wires by a novel divergent/convergent approach
[AD-A273332] p 2537 N94-25087
DIRAC EQUATION
Relativistic configuration interaction calculation of the correlation energies of highly-charged ions
[DE94-001055] p 2532 N94-22988
DIRECT BROADCAST SATELLITES
Utilizing a TDRS satellite for direct broadcast satellite-radio propagation experiments and demonstrations p 2274 N94-22740
Adaptive array antenna for satellite cellular and direct broadcast communications p 2275 N94-22745
DIRECT CURRENT
Laser energized high voltage direct current power supply
[AD-D015977] p 2312 N94-25036
A vibrating wire parallel to a type 2 superconducting slab of arbitrary thickness
[DE93-617134] p 2525 N94-25389
Effects of a vibrating wire carrying DC current on a moving type 2 superconducting slab of arbitrary thickness
[DE93-617136] p 2566 N94-25391
DIRECTIONAL ANTENNAS
A study of satellite motion-induced multipath phenomena p 2283 N94-22794
Aeronautical satellite antenna steering using magnetic field sensors p 2289 N94-22836
Experimental verification of an acoustic telemetry link between an Aurora and CFAV quest
[DREA-TC-93-304] p 2202 N94-24121
DIRECTIONAL COUPLERS
Calibration network intended for phase-array antennas at 3 GHz
[PB93-204352] p 2297 N94-24530
DIRECTIONAL SOLIDIFICATION (CRYSTALS)
Microgravity sciences application visiting scientist program
[NASA-CR-194804] p 2267 N94-23287
Effects of thermal-solutal convection on temperature and solutal fields under various gravitational orientations
p 2267 N94-24451
DIRECTIONAL STABILITY
Supersonic aerodynamic characteristics of a circular body Earth-to-Orbit vehicle
[NASA-TM-4533] p 2170 N94-24716
DIRECTORIES
NACA collections: A directory of significant collections of the documents of the National Advisory Committee for Aeronautics
[NASA-CR-195686] p 2594 N94-25541
DIRICHLET PROBLEM
Multigrid and cyclic reduction applied to the Helmholtz equation p 2304 N94-23676
DISCONNECT DEVICES
Electromagnetic brake/clutch device
[NASA-CASE-GSC-13502-1] p 2354 N94-23969
DISCRETE FUNCTIONS
Characterizations of shift-invariant distributions based on summation modulo one
[PB93-237824] p 2481 N94-23442
DCT quantization matrices visually optimized for individual images p 2442 N94-25509
DISCRIMINANT ANALYSIS (STATISTICS)
Eye-gaze control of the computer interface: Discrimination of zoom intent
[DE94-000480] p 2429 N94-22997
DISCRIMINATION
Parametric and nonparametric discriminants for regional earthquakes and explosions
[AD-A273807] p 2406 N94-25538
DISCRIMINATORS
A theoretical investigation of electrically tunable birefringent optical filters as the special discriminator in hyperspectral imaging systems
[AD-A273743] p 2547 N94-25533
DISEASES
Sarcoidosis and the aviator p 2425 N94-23325
DISILICIDES
Design of a resistojet for Space Station Freedom
[NASA-CR-195506] p 2221 N94-24979
DISLOCATIONS (MATERIALS)
Ring nuclei of strain for bonded dissimilar elastic half spaces with particular application to axisymmetric crack problems
[OUEL-1966/92] p 2379 N94-25325
The complete stress field due to a dislocation located anywhere in two bonded quarter planes
[OUEL-1990/93] p 2379 N94-25478
DISPERSING
Mechanisms of droplet formation
[ISBN-9-06-275765-0] p 2338 N94-25227
DISPERSION
Recent developments in the mathematical modelling and physical understanding of transport and dispersion in aquatic systems, with special reference to tidal waters
[PB94-111135] p 2418 N94-24600
DISPERSIONS
Effect of initial droplet-size distributions on fuel-vapor profiles in a shear-layer flow p 2160 N94-24283

DISPLACEMENT
Perception and 3D environment modeling for mobile robot autonomous navigation
[LAAS-93117] p 2471 N94-22908

DISPLAY DEVICES
Cockpit weather graphics using mobile satellite communications p 2280 N94-22775
Advanced display technologies in Russia, Ukraine, and Belarus. Viewgraphs p 2630 N94-22893
Pilot-vehicle interface
[DOT/FAA/CT-92/21] p 2430 N94-23083
The Mars mapper science and mission planning tool
p 2503 N94-23867
Mars Observer screen display design for a multimission environment p 2197 N94-23888
Multimission image processing and science data visualization p 2518 N94-23955
Night operations p 2431 N94-23977
Process and representation in graphical displays
p 2433 N94-24187
Evaluation of the UH-1N instrument panel
[AD-A273145] p 2186 N94-24774
Mission planning and mission rehearsal systems: Displays and other interactive techniques
p 2522 N94-25013
Future space transportation system architecture avionics requirements p 2162 N94-25098
Proceedings of the Workshop on Augmented Visual Display (AVID) Research
[NASA-CP-10128] p 2439 N94-25490
Optical information in landing scenes
p 2442 N94-25511
Sensor fusion display evaluation using information integration models in enhanced/synthetic vision applications p 2443 N94-25512
Quality metrics for sensor images
p 2443 N94-25513
Evaluation of image quality p 2443 N94-25514

DISRUPTING
Microinjection of the Yersinia YopE cytotoxin in mammalian cells induces actin microfilament disruption
[FOA-B-40418-4.4] p 2421 N94-24290

DISSIPATION
Nonlinear ion-mixing-mode particle transport in the dissipative trapped electron regime
[DE94-000989] p 2533 N94-23435
Shock-induced turbulent flow in baffle systems
[DE94-001532] p 2319 N94-23470
A transport equation for the scalar dissipation in reacting flows with variable density: First results
p 2331 N94-24157
Direct measurement of turbulent dissipation rate using dual laser doppler velocimeters
[AD-A273740] p 2340 N94-25530

DISSOCIATION
Adsorption, desorption, and decomposition of HCl and HBr on Ge(100): Competitive pairingand near-first-order desorption kinetics
[AD-A273504] p 2235 N94-24790

DISSOLVING
Use of scanning tunneling microscope in corrosion studies
[VTT-TIED-1416] p 2250 N94-25346

DISTORTION
Vibrations of variable cross section Timoshenko beams p 2160 N94-24279

DISTRIBUTED AMPLIFIERS
Spatial frequency multiplier with active linearly tapered slot antenna array
[NASA-TM-106494] p 2310 N94-24308

DISTRIBUTED FEEDBACK LASERS
InGaAsP/InP based 1.3/1.55 micron vertical cavity surface emitting lasers for wavelength division multiplexed high speed distributed computing, phase 1
[AD-A271081] p 2348 N94-23123

DISTRIBUTED PROCESSING
Translative interface for data sharing and integrating: A paradigm for distributed data systems
[DE93-018790] p 2588 N94-22863
Resolution of Markov models on distributed memory machines
[ETN-94-95182] p 2444 N94-22900
Distributed Operating Systems and Mach. Proceedings of the Spring 1992 Graduate Seminar on Distributed Systems
[PB93-224905] p 2449 N94-23103
Modeling parallelism and synchronization
[ETN-94-95179] p 2465 N94-23134
A parallel PROLOG system for distributed memory multiprocessor
[ETN-94-95173] p 2465 N94-23167
Advanced design concepts for open distributed systems development
[PB94-110897] p 2454 N94-23751
PILOT: An intelligent distributed operations support system p 2508 N94-23895
Customizing graphical user interface technology for spacecraft control centers p 2510 N94-23905
Distributed computing environments for future space control systems p 2464 N94-23911
Mission and science activity scheduling language
p 2515 N94-23938
A programming environment for distributed complex computing. An overview of the Framework for Interdisciplinary Design Optimization (FIDO) project. NASA Langley TOPS exhibit H120b
[NASA-TM-109058] p 2457 N94-24603
Design of central control system for Large Helical Device (LHD)
[NIFS-258] p 2553 N94-24623
The experimental physics and industrial control system architecture: Past, present, and future
[DE94-002639] p 2457 N94-24626
A usage profile and evaluation of a wide-area distributed file system
[AD-A273590] p 2593 N94-24946
The design of the EMPS multiprocessor executive for distributed computing
[ETN-94-95336] p 2468 N94-25062
Design and implementation of a distributed version of the NASA Engine Performance Program
[NASA-CR-194475] p 2462 N94-25179
A design method for parallel programs
[ETN-94-95331] p 2469 N94-25282
Parallel processing methods for space based power systems p 2222 N94-25352

DISTRIBUTION FUNCTIONS
A prediction model of signal degradation in LMSS for urban areas p 2284 N94-22797
Limiting distribution of fractional parts of extreme order statistics
[PB93-237733] p 2494 N94-23440
Development and application of an empirical probability distribution for the prediction error of re-entry body maximum dynamic pressure p 2207 N94-23653
Asymptotic confidence intervals for the length of the shortt under random censoring
[PB93-237816] p 2494 N94-23774
Infinite divisible and stable distributions modulo 1
[PB94-110640] p 2495 N94-23815
Tail processes under heavy random censorship with applications
[PB94-110632] p 2495 N94-24508
Integral equations for the microstructures of supercritical fluids
[DE94-002460] p 2535 N94-24569
Polynomials orthogonal with respect to an inner product involving differences
[PB94-110731] p 2489 N94-24572
Durability evaluation of ceramic components using CARES/LIFE
[NASA-TM-106475] p 2258 N94-24682
Efficiency of subset selection of an epsilon-best uniform population relative to selection of the best one
[PB93-237741] p 2490 N94-24763
Generalized linear mixed models and their application in plant breeding research
[ETN-94-95335] p 2460 N94-25061

DISULFIDES
Status of the development of rechargeable lithium cells p 2392 N94-23354

DIURNAL VARIATIONS
A study of satellite motion-induced multipath phenomena p 2283 N94-22794

DIVERGENCE
Diagnostic budgets of analyzed and modelled tropical plumes
[NASA-CR-194853] p 2409 N94-23621
Multi-grid domain decomposition approach for solution of Navier-Stokes equations in primitive variable form
p 2341 N94-23693

DIVERTERS
Massachusetts Institute of Technology Plasma Fusion Center 1992-1993 report to the President
[DE94-001725] p 2548 N94-22721
Assessment of stellarators as reactors
[DE93-017775] p 2548 N94-22916
Superconducting magnet system for the TPX Tokamak
[DE94-001535] p 2549 N94-23013
Performance characteristics of the DIII-D advanced divertor cryopump
[DE94-002745] p 2354 N94-23797
Proposal of Modular Heliotron: Advanced modular helical system compatible with closed helical divertor
[NIFS-261] p 2552 N94-24458
Plasma initiation in a tokamak with conducting superstructure: First results from Alcator C-MOD
[DE94-001565] p 2552 N94-24504

DIVING (UNDERWATER)
A statistical analysis of recent Naval Experimental Diving Unit (NEDU) single-depth human exposures to 100 percent oxygen at pressure
[AD-A273488] p 2427 N94-24950

DOCUMENTATION
Fiscal year 1993 scientific and technical reports, articles, papers, and presentations
[NASA-TM-108423] p 2590 N94-24079

DOCUMENTS
NACA collections: A directory of significant collections of the documents of the National Advisory Committee for Aeronautics
[NASA-CR-195686] p 2594 N94-25541

DOMAIN WALL
Flavor changing strings and domain walls
[DE93-633217] p 2532 N94-22970

DOPED CRYSTALS
Polycrystalline thin film materials and devices
[DE93-018213] p 2389 N94-22862
Physics with chemically and isotopically pure semiconductors
[DE93-040120] p 2557 N94-22926
Ga delta-doping layers in silicon
[PB93-224632] p 2561 N94-23222
Magnetic resonance study of zinc-related defects in silicon with optimized EPR spectrometer
[PB93-224640] p 2561 N94-23223
Transparent conducting thin films for spacecraft applications
[NASA-TM-106466] p 2218 N94-23370
Fabrication of sub-40-nm p-n junctions for 0.18 micron MOS device applications using a cluster-tool-compatible, nanosecond thermal doping technique
[DE94-001608] p 2309 N94-23520
The study of dopant segregation behavior during the growth of GaAs in microgravity
[NASA-CR-193905] p 2267 N94-23549
Combustion synthesis and engineering of nanoparticles for electronic, structural and superconductor applications
[DE94-001865] p 2254 N94-23720
Large-scale production of Si(0.8)Ge(0.2) thermoelectric alloys by mechanical alloying
[DE94-000695] p 2243 N94-23753
Development of infrared sensors using energy transfer/energy upconversion processes: Study of laser excited fluorescence in rare Earth ion doped crystals
[NASA-TM-108437] p 2233 N94-24073
Investigation of the optical and laser properties of Tm and Ho in YAG anf YLF
[REPT-94-001] p 2563 N94-24404
In situ and ex situ spectroelectrochemical and x ray absorption studies on rechargeable, chemically-modified and other MnO2 materials
[DE94-001387] p 2234 N94-24545
Polythiophene derivative with a side chain chromophore as photovoltaic and photorefractive materials
[AD-A273245] p 2260 N94-24813
The Haldane energy gap of a doped linear-chain Heisenberg antiferromagnet
[DE93-617130] p 2567 N94-25426

DOPPLER EFFECT
Electromagnetic field strength prediction in an urban environment: A useful tool for the planning of LMSS
p 2283 N94-22795
A comparison between coherent and noncoherent mobile systems in large Doppler shift, delay spread, and C/I environment p 2287 N94-22818
SFOLDA: A semiconductor LDA for measurements in complex flows p 2316 N94-22856
Radar stimulator interface protocol, preliminary interface design and Doppler Beam Sharpening implementation
[DE94-002567] p 2453 N94-23701

DOPPLER NAVIGATION
Navigation of space VLBI missions: Radioastron and VSOP p 2513 N94-23926

DOPPLER RADAR
Urban/rural application of weather radar for flow forecasting. Proceedings of the Informal CEc -Workshop
[PB93-220135] p 2407 N94-23129
An improved gravity model for Mars: Goddard Mars Model-1 (GMM-1)
[NASA-TM-104584] p 2401 N94-23282
Implementation and evaluation of the new wind algorithm in NASA's 50 MHz doppler radar wind profiler
[NASA-CR-194880] p 2408 N94-23576
IRIG radar calibration catalog. Version 2: The IRIG error model reference for radar calibrations
[AD-A273344] p 2303 N94-25155
Improvement of system properties of a pulsed laser Doppler anemometer with respect to an optical amplifier
[DLR-FB-93-19] p 2547 N94-25305

DOSIMETERS
Experimental characterization of the AFIT Neutron Facility
[AD-A273822] p 2539 N94-25519

DOUBLE BASE PROPELLANTS
Burning rate of double-base propellant in the presence of plasma p 2155 N94-24252
DOWNLINKING
The provision of spectrum for feeder links of non-geostationary mobile satellites
p 2276 N94-22751
K-band mobile propagation measurements using ACTS p 2283 N94-22792
Analysis of open-loop conical scan pointing error and variance estimators p 2291 N94-23263
DRAG
Embodiment design for a multipropellant resistojet
[NASA-CR-195505] p 2221 N94-24834
A diagnostic model to estimate winds and small-scale drag from Mars Observer PMIRR data
p 2617 N94-24874
DRAG REDUCTION
Optimal feedback control of turbulent channel flow
p 2327 N94-24139
Drag reduction at a plane wall p 2327 N94-24140
Boundary layer receptivity and control
p 2327 N94-24141
Experimental study of a turbulent boundary layer in presence of external manipulators of NACA 0009 profile in the transonic regime
[ISBN-0-315-57633-2] p 2333 N94-24177
The Triton: Design concepts and methods
[NASA-CR-195542] p 2184 N94-25004
Coherent structures over grooved surfaces
[ETN-94-95308] p 2339 N94-25291
DRAINAGE
Urban/rural application of weather radar for flow forecasting. Proceedings of the Informal CEc -Workshop
[PB93-220135] p 2407 N94-23129
Performance of prefabricated geocomposite subdrainage system in an airport runway
[DOT/FAA/RD-93/23] p 2192 N94-23303
DRAINAGE PATTERNS
Performance of prefabricated geocomposite subdrainage system in an airport runway
[DOT/FAA/RD-93/23] p 2192 N94-23303
DRILLING
Development/drilling test of auger boring machine on board Mars rover for Mars exploration
p 2369 N94-23402
DRONE AIRCRAFT
UAV current technology and future trends
p 2154 N94-24245
Generic drone control system
[AD-D015993] p 2184 N94-25052
DROP SIZE
Development of a droplet breakup model considering aerodynamic and droplet collision effects
p 2213 N94-23045
Shear coaxial injector instability mechanisms
p 2213 N94-23047
Effect of initial droplet-size distributions on fuel-vapor profiles in a shear-layer flow p 2160 N94-24283
Mechanisms of droplet formation
[ISBN-9-06-275765-0] p 2338 N94-25227
Infrared sensors and systems for enhanced vision/autonomous landing applications
p 2439 N94-25491
DROPS (LIQUIDS)
Droplet turbulence interactions under subcritical and supercritical conditions p 2211 N94-23036
Fundamental rocket injector/spray programs at the Phillips Laboratory p 2211 N94-23039
Numerical parametric studies of spray combustion instability p 2212 N94-23041
Development of a droplet breakup model considering aerodynamic and droplet collision effects
p 2213 N94-23045
Development of a computational testbed for numerical simulation of combustion instability
p 2213 N94-23046
Liquid oscillations in a spherical system with sliding edges boundary by two conical solid surfaces in zero-gravity
[LRT-WE-9-FB-5-1992] p 2318 N94-23197
Forced vibrations of a non-viscous drop
[MPIS-24/1992] p 2318 N94-23198
An overview of a model rotor icing test in the NASA Lewis Icing Research Tunnel
[NASA-TM-106471] p 2166 N94-23299
Mechanisms of droplet formation
[ISBN-9-06-275765-0] p 2338 N94-25227
DRY FRICTION
Wear characteristics of technical dry rolling/sliding systems with relations to corrugation problems
p 2269 N94-23586
DRYING
Composite fiber structures for catalysts and electrodes
p 2393 N94-23364
Drying deformable media: Kinetics, shrinkage and stresses
[ETN-94-95314] p 2236 N94-25302
DUCTED FAN ENGINES
NASA advanced design program. Design and analysis of a radio-controlled flying wing aircraft
[NASA-CR-195515] p 2180 N94-24589
DUCTED FANS
Summary of lift and lift/cruise fan powered lift concept technology
[NASA-CR-177619] p 2176 N94-23489
DUCTED FLOW
Turbulent separated flows above an obstacle in an open channel p 2316 N94-22859
Zone fire modeling with natural building flows and a zero order shaft model
[PB94-112166] p 2270 N94-23735
Modeling dynamically coupled fluid-duct systems with finite line elements
[NASA-CR-193909] p 2376 N94-24359
DUCTILE-BRITTLE TRANSITION
Effects of neutron irradiation and hydrogen on ductile-brittle transition temperatures of V-Cr-Ti alloys
[DE94-001466] p 2240 N94-23009
DUCTILITY
Relationship of microstructure and mechanical properties for V-Cr-Ti alloys
[DE94-001431] p 2238 N94-22718
Creep deformation characteristics of ductile discontinuous fiber reinforced composites
[DE94-000697] p 2227 N94-23005
Effects of neutron irradiation and hydrogen on ductile-brittle transition temperatures of V-Cr-Ti alloys
[DE94-001466] p 2240 N94-23009
Mean stress models for low cycle fatigue of a nickel-base superalloy p 2159 N94-24276
DUCTS
Computation of flows in a turn-around duct and a turbine cascade using advanced turbulence models
p 2216 N94-23062
Modeling dynamically coupled fluid-duct systems with finite line elements
[NASA-CR-193909] p 2376 N94-24359
DUFFING DIFFERENTIAL EQUATION
Controlling regular and chaotic dynamics in the Duffing-Ueda oscillator
[RR-477] p 2523 N94-25323
DURABILITY
Characterization and durability testing of plasma-sprayed zirconia-yttria and hafnia-yttria thermal barrier coatings. Part 2: Effect of spray parameters on the performance of several hafnia-yttria and zirconia-yttria coatings
[NASA-TP-3296] p 2242 N94-23467
Evaluation of the fracture resistance and durability of adhesive bonded joints p 2160 N94-24278
Foil bearings p 2371 N94-24415
Durability evaluation of ceramic components using CARES/LIFE
[NASA-TM-106475] p 2258 N94-24682
DUST
Flames in dusty mixtures: Their structure and stability
[NASA-CR-191567] p 2317 N94-23089
Mars dust-driven tides and their impact on the thermosphere p 2617 N94-24876
Cloud, dust, and ozone vertical profiles from solar occultation measurements: Implications for dynamics
p 2617 N94-24877
Particle sizes and composition of Mars atmospheric dust based upon Viking and Mariner 9 observations
p 2618 N94-24878
The annual pressure cycle on Mars: Results from the LMD Martian atmospheric general circulation model
p 2619 N94-24884
Northern hemisphere dust storms on Mars
p 2619 N94-24885
Dynamics of the atmosphere of Mars: Review of some outstanding problems p 2620 N94-24888
Mars Operational Environmental Satellite (MOES): A post-Mars Observer discovery mission
p 2620 N94-24890
Evidence for dust transport in Viking IR thermal mapper opacity data p 2620 N94-24892
Dust transport in the Martian atmosphere
p 2621 N94-24894
The role of atmospheric heat transport in the seasonal carbon dioxide cycle p 2621 N94-24896
Diagnostic calculations of the circulation in the Martian atmosphere p 2622 N94-24898
DUST STORMS
Mars dust-driven tides and their impact on the thermosphere p 2617 N94-24876
Northern hemisphere dust storms on Mars
p 2619 N94-24885
Temporal and spatial mapping of surface albedo and atmospheric dust opacity on Mars p 2619 N94-24887
Mars Operational Environmental Satellite (MOES): A post-Mars Observer discovery mission
p 2620 N94-24890
Evidence for dust transport in Viking IR thermal mapper opacity data p 2620 N94-24892
DWARF GALAXIES
CO-to-H2 conversion factor in dwarf irregular galaxies
[REPT-333] p 2603 N94-24985
DYADICS
Polarizability of gyrotropic sphere
[PB93-225019] p 2524 N94-23131
DYE LASERS
In situ detection of tropospheric OH, HO2, NO2, and NO by laser-induced fluorescence in detection chambers at reduced pressures
[NASA-CR-194810] p 2397 N94-23277
Sodium-layer laser guide stars
[DE93-019621] p 2349 N94-23490
DYES
Feasibility study: Monodisperse polymer particles containing laser-excitable dyes p 2225 N94-24350
DYNAMIC CHARACTERISTICS
Experimental modification and identification of the DSS-13 antenna control system model
p 2291 N94-23260
Global dynamic stability of a shallow arch by poincare-like simple cell mapping p 2160 N94-24280
Develop advanced nonlinear signal analysis topographical mapping system
[NASA-CR-195128] p 2388 N94-24827
Dynamic measurements of thermophysical properties of metals and alloys at high temperatures by subsecond pulse heating techniques p 2247 N94-25124
DYNAMIC CONTROL
Contribution to geometric and dynamic modeling of parallel robots
[LAAS-93089] p 2470 N94-22904
An architecture for teleprogramming autonomous mobile robots at task level
[LAAS-93107] p 2470 N94-22906
Real-time dynamics and control strategies for space operations of flexible structures
[NASA-CR-194794] p 2203 N94-23618
Temperature dependence of protein solubility-determination, application to crystallization, and growth kinetics studies p 2224 N94-24344
Robust, nonlinear, high angle-of-attack control design for a supermaneuverable vehicle p 2164 N94-25108
Modeling of a large undamped space structure using time domain techniques
[AD-A273828] p 2206 N94-25523
DYNAMIC LOADS
A technique to measure rotordynamic coefficients in hydrostatic bearings p 2215 N94-23061
Role of interfaces on the cyclic fatigue behaviour of ceramic matrix composites p 2256 N94-24234
Controllability of free-piston Stirling engine/linear alternator driving a dynamic load
[NASA-TM-106497] p 2521 N94-24302
Foil bearings p 2371 N94-24415
DYNAMIC MODELS
Space Station Freedom (SSF) Data Management System (DMS) performance model data base
[NASA-CR-188270] p 2590 N94-23289
Viewing hybrid systems as products of control systems and automata
[NASA-CR-194792] p 2472 N94-23300
Heat pipe vapor dynamics
[NASA-CR-194217] p 2327 N94-24096
Large eddy simulation of a boundary layer with concave streamwise curvature p 2328 N94-24146
Dynamic localization and second-order subgrid-scale models in large eddy simulations of channel flow
p 2329 N94-24149
A large eddy simulation scheme for turbulent reacting flows p 2330 N94-24154
A dynamic melting model for the origin of Apollo 15 olivine-normative and quartz-normative mare basalts
p 2615 N94-24371
An exploratory stochastic model for toxic effects on cells
[AD-A273438] p 2422 N94-25146
Timed coloured Petri nets and their application to logistics
[ETN-94-95310] p 2522 N94-25293
Simulation of a passive millimeter wave sensor
p 2346 N94-25499
DYNAMIC PRESSURE
Development and application of an empirical probability distribution for the prediction error of re-entry body maximum dynamic pressure p 2207 N94-23653
DYNAMIC PROGRAMMING
General optimal stopping theorems for semi-Markov processes
[PB93-214989] p 2496 N94-24744

Approximate optimal guidance for the advanced launch system [NASA-CR-4568] p 2198 N94-24752

Class of strong valid inequalities for the discrete lot-sizing and scheduling problem [PB93-237774] p 2459 N94-24765

DYNAMIC RESPONSE

Proof test of the computer program BUCKY for plasticity problems [NASA-TP-3444] p 2374 N94-22960

Lectures on magnetohydrodynamical drives [PB93-224962] p 2308 N94-23104

Extending substructure based iterative solvers to multiple load and repeated analyses [NASA-CR-194822] p 2466 N94-23504

Issac, Jason Cherian ses in transonic flow [NASA-CR-194837] p 2167 N94-24052

Thermohydrodynamic analysis of cryogenic liquid turbulent flow fluid film bearings [NASA-CR-194869] p 2363 N94-24081

LSS systems planning and performance program [NASA-CR-193882] p 2196 N94-24309

Procedures for determining MATMOD-4V material constants [DE94-002638] p 2245 N94-24520

Responses of a finite baffled plate subject to turbulent and mean flow excitations [NASA-CR-191570] p 2334 N94-24605

Admittance model for the shuttle remote manipulator system in four configurations [NASA-CR-4555] p 2474 N94-24635

Aeroelastic response and stability of tiltrotors with elastically-coupled composite rotor blades [NASA-TM-108758] p 2182 N94-24953

The phase response of nonlinear systems [RR-458] p 2476 N94-25308

Frequency response functions for nonlinear rational models [RR-471] p 2492 N94-25318

Space Station flexible dynamics under plume impingement p 2208 N94-25383

DYNAMIC STABILITY

Global dynamic stability of a shallow arch by poincare-like simple cell mapping p 2160 N94-24280

Controllability of free-piston Stirling engine/linear alternator driving a dynamic load [NASA-TM-106497] p 2521 N94-24302

DYNAMIC STRUCTURAL ANALYSIS

Development and experimental validation of computational methods to simulate abnormal thermal and structural environments [DE94-000554] p 2268 N94-23000

Extending substructure based iterative solvers to multiple load and repeated analyses [NASA-CR-194822] p 2466 N94-23504

Real-time dynamics and control strategies for space operations of flexible structures [NASA-CR-194794] p 2203 N94-23618

Modal test of the Brazilian satellite launcher (VLS) configuration burn-out of the first stage p 2156 N94-24257

Modeling dynamically coupled fluid-duct systems with finite line elements [NASA-CR-193909] p 2376 N94-24359

Structural dynamics division research and technology accomplishments for FY 1993 and plans for FY 1994 [NASA-TM-109036] p 2169 N94-24576

Influence of backup bearings and support structure dynamics on the behavior of rotors with active supports [NASA-CR-195106] p 2365 N94-24751

Aeroelastic response and stability of tiltrotors with elastically-coupled composite rotor blades [NASA-TM-108758] p 2182 N94-24953

Space Station flexible dynamics under plume impingement p 2208 N94-25383

DYNAMIC TESTS

Modeling of a large undamped space structure using time domain techniques [AD-A273828] p 2206 N94-25523

DYNAMICAL SYSTEMS

On the numeric integration of dynamic attitude equations [NASA-CR-194788] p 2448 N94-23073

Chaos and simple determinism in reversed field pinch plasmas: Nonlinear analysis of numerical simulation and experimental data [DE94-001575] p 2550 N94-23211

Lacunary series as quadratic differentials in conformal dynamics [PB93-238061] p 2481 N94-23547

When an infinitely-renormalizable endomorphism of the interval can be smoothed [PB93-238087] p 2481 N94-23548

A mixed method Poisson solver for three-dimensional self-gravitating astrophysical fluid dynamical systems p 2484 N94-23684

Dimensional analysis of acoustically propagated signals p 2528 N94-24217

Global dynamic stability of a shallow arch by poincare-like simple cell mapping p 2160 N94-24280

Systems engineering: A formal approach. Part 2: Frameworks [PB94-101391] p 2489 N94-24615

Change-point detection and adaptive control of time-varying systems [AD-A273509] p 2475 N94-24943

Practical evaluation of robust control for a class of nonlinear mechanical dynamic systems [ISBN-9-03-860092-5] p 2475 N94-25224

On-line control of dynamic systems using feedforward neural networks [RR-457] p 2476 N94-25307

The phase response of nonlinear systems [RR-458] p 2476 N94-25308

Validating identified nonlinear models with chaotic dynamics [RR-469] p 2523 N94-25314

Controlling regular and chaotic dynamics in the Duffing-Ueda oscillator [RR-477] p 2523 N94-25323

DYNAMICS

Mass properties measurement system dynamics p 2368 N94-23235

Mass properties measurement system: Dynamics and statics measurements p 2368 N94-23236

DYNAMOMETERS

NASA project 1: Full-body dynamometer [NASA-CR-195507] p 2438 N94-24331

Specification list and function structure for a full-body dynamometer to be used aboard Space Station Freedom [NASA-CR-195508] p 2439 N94-24835

DYSPROSIUM

Improved magnetostrictive transducer drive elements achieved by reduction of crystalline defects and improved crystalline orientation [AD-A273391] p 2313 N94-25276

E

E REGION

High latitude cusp signature observations for southward IMF B sub Z [AD-A273801] p 2406 N94-25536

EARTH ALBEDO

Nimbus-7 Total Ozone Mapping Spectrometer (TOMS) data products user's guide [NASA-RP-1323] p 2410 N94-24355

An Earth albedo model: A mathematical model for the radiant energy input to an orbiting spacecraft due to the diffuse reflectance of solar radiation from the Earth below [NASA-TM-104596] p 2195 N94-24497

EARTH ATMOSPHERE

On testing two major cumulus parameterization schemes using the CSU regional atmospheric modeling system [DE94-000703] p 2407 N94-23284

Cloud-free aerosol optical depth determination over oceans from satellite radiometry [DE94-001897] p 2386 N94-23779

Results from the VISA project [AD-A273752] p 2406 N94-25540

EARTH CORE

Steady induction effects in geomagnetism. Part 1C: Geomagnetic estimation of steady surficial core motions: Application to the definitive geomagnetic reference field models [NASA-TP-3272-PT-1C] p 2403 N94-24465

EARTH CRUST

Electromagnetic field changes as a precursory phenomena of earthquakes and volcanic eruptions [REPT-157] p 2405 N94-24980

Seafloor characterization/Galapagos propagating rift [AD-A273586] p 2419 N94-25165

EARTH IONOSPHERE

Solar-terrestrial environmental laboratory p 2630 N94-23336

The national geomagnetic initiative [LC-93-85739] p 2401 N94-23344

Artificial plasma experiments. Chemical release observations associated with the CRRES program [NASA-CR-194871] p 2550 N94-23565

Electromagnetic interference impact of the proposed emitters for the High Frequency Active Auroral Research Program (HAARP) [AD-A273401] p 2301 N94-24926

Magnetic Earth Ionosphere Resonant Frequencies [NASA-CR-195131] p 2303 N94-25191

An active antenna for ELF magnetic fields p 2303 N94-25192

EARTH MAGNETOSPHERE

Solar-terrestrial environmental laboratory p 2630 N94-23336

The national geomagnetic initiative [LC-93-85739] p 2401 N94-23344

Artificial plasma experiments. Chemical release observations associated with the CRRES program [NASA-CR-194871] p 2550 N94-23565

The Far Ultraviolet (FUV) auroral imager for the Inner Magnetospheric Imager (IMI) mission: Options p 2209 N94-24453

Solar flares and magnetospheric particles: Investigations based upon the ONR-602 and ONR-604 experiments [AD-A273639] p 2628 N94-25031

EARTH MANTLE

Measurement and Interpretation of Crustal Deformation Rates Associated with Postglacial Rebound [NASA-CR-195193] p 2405 N94-25203

Constraining proposed combinations of ice history and Earth rheology using VLBI determined baseline length rates in North America p 2405 N94-25205

EARTH MOVEMENTS

GPS survey of the western Tien Shan [NASA-CR-195174] p 2175 N94-24826

EARTH OBSERVATIONS (FROM SPACE)

GEWEX p 2385 N94-23614

NASDA's view of ground control in mission operations p 2305 N94-23835

The space operations at CNES p 2498 N94-23837

Mission planning for an Earth observation low Earth orbiter: ERS-1 p 2503 N94-23868

Earth observation archive activities at DRA Farnborough p 2519 N94-23958

The pre-development of the Aristoteles calibration mechanism p 2209 N94-24006

Precipitation measurement using SIR-C: A feasibility study. Investigation at nadir [NASA-CR-195103] p 2410 N94-24126

EARTH OBSERVING SYSTEM (EOS)

Earth Observing System (EOS) Advanced Microwave Sounding Unit-A (AMSU-A) schedule plan [NASA-CR-194856] p 2585 N94-23563

The Fifth Calibration/Data Product Validation Panel Meeting [NASA-TM-108270] p 2383 N94-23595

The possible effects of the natural and induced space environment on the optical and thermal properties of EOS surfaces p 2207 N94-23596

SPDB (science processing database): Quick reference guide p 2383 N94-23597

Definitions in use by the visible and near-infrared, and thermal working groups p 2383 N94-23598

Cross-calibration survey (VISNIR) p 2383 N94-23599

MODIS calibration p 2383 N94-23600

Eos cross-calibration radiometers p 2383 N94-23601

Activities of NIST (National Inst. of Standards and Technology) p 2384 N94-23605

Concept of ASTER calibration requirement p 2384 N94-23609

VNIR and SWIR transfer radiometers developed at NRLM for preflight laboratory cross-calibration p 2385 N94-23610

Mission operations update for the restructured Earth Observing System (EOS) mission p 2499 N94-23839

ASTER, a multinational Earth observing concept p 2389 N94-23840

Applications of CCSDS recommendations to Integrated Ground Data Systems (IGDS) p 2510 N94-23906

EOS ground data systems: A description and interface overview p 2517 N94-23948

Panel to review EOSDIS plans [NASA-CR-195088] p 2387 N94-24303

EARTH ORBITAL ENVIRONMENTS

Use of negotiated rulemaking in developing technical rules for low-Earth orbit mobile satellite systems p 2276 N94-22750

Global coverage Mobile Satellite Systems: System availability versus channel propagation impairments p 2284 N94-22798

Systems implications of L-band fade data statistics for LEO mobile systems p 2284 N94-22799

Analysis of impactor residues in tray clamps from the Long Duration Exposure Facility. Part 2: Clamps from Bay B of the satellite [NASA-TM-104784] p 2386 N94-24095

Orbital debris and near-Earth environmental management: A chronology [NASA-RP-1320] p 2598 N94-24644

Solar flares and magnetospheric particles: Investigations based upon the ONR-602 and ONR-604 experiments [AD-A273639] p 2628 N94-25031

EARTH ORBITS

Low earth orbit satellite/terrestrial mobile service compatibility p 2288 N94-22827

Impedance measurements on a spiral-wound nickel/metal hydride cell cycled in a simulated Leo orbit
p 2392 N94-23355
Torque equilibrium attitudes for the Space Station
p 2208 N94-24449
GRYPHON: Air launched space booster
[NASA-CR-195497] p 2199 N94-25022

EARTH RADIATION BUDGET
A regional analysis of cloudy mean spherical albedo over the marine stratocumulus region and the tropical Atlantic Ocean
[NASA-CR-194771] p 2409 N94-24049

EARTH RADIATION BUDGET EXPERIMENT
Flight solar calibrations using the Mirror Attenuator Mosaic (MAM): Low scattering mirror
p 2384 N94-23602

EARTH RESOURCES
Mapping Tomorrow's Resources: A symposium on the uses of remote sensing, Geographic Information Systems (GIS), and Global Positioning Systems (GPS) for natural resources management p 2387 N94-24357

EARTH SCIENCES
Image pattern recognition supporting interactive analysis and graphical visualization
[NASA-CR-194878] p 2451 N94-23369
Mission operations update for the restructured Earth Observing System (EOS) mission p 2499 N94-23839
NASA high performance computing and communications program
[NASA-TM-4554] p 2591 N94-24337

EARTH SURFACE
Atmospheric flow in heterogeneous vegetated regions
[W-9303] p 2401 N94-23175
Lightning, atmospheric electricity, and climate change
[DE94-002003] p 2408 N94-23471
Session on coupled land surface/hydrological/atmospheric models
p 2414 N94-24395
An investigation of current and future satellite and in-situ data for the remote sensing of the land surface energy balance
[NASA-CR-195138] p 2387 N94-24596
Image analysis technology applied to problems in crystallography
[AD-A273516] p 2566 N94-25288
Near surface analysis p 2407 N94-25364

EARTH TERMINALS
Low cost coherent demodulation for mobile satellite terminals p 2284 N94-22803
Optical subnet concepts for the deep space network
p 2292 N94-23269

EARTHQUAKE DAMAGE
Active control of buildings during earthquakes
[NASA-TM-109033] p 2271 N94-24473

EARTHQUAKES
Active control of buildings during earthquakes
[NASA-TM-109033] p 2271 N94-24473
Parametric and nonparametric discriminants for regional earthquakes and explosions
[AD-A273807] p 2406 N94-25538

ECCENTRICITY
Validation of a second generation conspicuity meter
[IZF-1993-A-11] p 2542 N94-22895

ECHOCARDIOGRAPHY
Echocardiographic screening of aircrew candidates
p 2424 N94-23319
Echocardiographic findings in trained aircrew: The effect of +Gz on cardiac structure (working group 18)
p 2424 N94-23320

ECHOES
Preprocessor and adaptive beamformer for linear-frequency modulation active signals
[AD-D016008] p 2302 N94-25048

ECLIPTIC
Ulysses log 1992 p 2502 N94-23863

ECOLOGY
Analysis of vulnerability to the impacts of sea level rise: A case study for The Netherlands
[PB94-111150] p 2399 N94-24573

ECONOMETRICS
Temporal aggregation in a periodically integrated autoregressive process
[PB93-230480] p 2479 N94-23122
First order conditions for the maximum likelihood estimation of an exact ARMA model
[PB94-110533] p 2495 N94-23814

ECONOMIC ANALYSIS
A practical system for regional mobile satellite services p 2288 N94-22828
Simplicial variable dimension restart algorithm to find economic equilibria on the unit simplex using n(n+1) rays
[PB94-110541] p 2596 N94-24477
The future of rotary-wing aircraft p 2185 N94-25070

ECONOMIC FACTORS
Proceedings of Technology and Governance in the 1990's
[PB93-192904] p 2597 N94-24312
Considerations in implementing integrated biomass energy systems in developing countries
[DE93-018720] p 2395 N94-24499
The airplane: A simulated commercial air transportation study
[NASA-CR-195525] p 2182 N94-24837

ECONOMIC IMPACT
Information technology in the service society: A twenty-first century lever
[ISBN-0-309-04876-1] p 2593 N94-24833

ECOSYSTEMS
Human impacts on soil carbon dynamics of deep-rooted Amazonian forests
[NASA-CR-195127] p 2399 N94-24861

EDDY CURRENTS
Structural analysis of a superconducting central solenoid for the Tokamak Physics Experiment
[DE94-001536] p 2549 N94-23014
Preliminary eddy current modelling for the large angle magnetic suspension test fixture
[NASA-CR-194772] p 2192 N94-23539
Plasma initiation in a tokamak with conducting superstructure: First results from Alcator C-MOD
[DE94-001565] p 2552 N94-24504

EDDY VISCOSITY
Turbulence modeling for non-equilibrium flows
p 2328 N94-24144
Large eddy simulation of a boundary layer with concave streamwise curvature p 2328 N94-24146
A vorticity dynamics based model for the turbulent dissipation: Model development and validation
[NASA-TM-106177] p 2336 N94-24713
Turbulence models and Reynolds analogy for two-dimensional supersonic compression ramp flow
[NASA-TM-106474] p 2337 N94-25119

EDGE DETECTION
Object recognition through image understanding for an autonomous mobile robot
[AD-A273206] p 2475 N94-24862
Edge detection using a complex wavelet
[AD-A273699] p 2493 N94-25452

EDGES
Investigation on interval edge-coloring of graphs
[PB94-110913] p 2488 N94-24541
Edge elements, their advantages and disadvantages
[PB94-111069] p 2298 N94-24593
Finite-element modelling of three-dimensional electromagnetic fields using edge and nodal elements
[PB94-111077] p 2298 N94-24597
Tools for visualizing landscape pattern for large geographic areas
[DE94-001121] p 2388 N94-24757

EDITING
World processor: An interface for textual display and manipulation in virtual reality
[PB94-118643] p 2592 N94-24642

EDUCATION
KSC management training system project
p 2574 N94-23246
Operational training for the mission operations at the Brazilian National Institute for Space Research (INPE)
p 2429 N94-23933
Training: Plugging the information gaps
p 2429 N94-23934
Roles, uses, and benefits of general aviation aircraft in aerospace engineering education
[NASA-TM-106463] p 2153 N94-24100
Evaluation of computer-aided instruction techniques for the crew interface coordination position
p 2429 N94-24438
The 7th Annual National Conference of Black Physics Students p 2524 N94-24583
Design of an airborne launch vehicle for an air launched space booster
[NASA-CR-195534] p 2198 N94-24860
Magnetic Earth Ionosphere Resonant Frequencies
[NASA-CR-195131] p 2303 N94-25191
Understanding and facilitating discovery learning in computer-based simulation environment
[ISBN-9-03-860242-1] p 2462 N94-25219

EFFICIENCY
Sensorless, brushless motor to drive a sealed freon-ammonia pump p 2315 N94-24036

EGGS
Evaluation of ovostatin and ovostatin assay
p 2422 N94-24437

EIGENVALUES
Tool sharing: An application of max-algebra, part 2
[MEMO-1122] p 2478 N94-22710
Tool sharing: An application of max-algebra, part 1
[MEMO-1108] p 2478 N94-22726
The Hamiltonian double-zero eigenvalue
[W-9304] p 2479 N94-23138
Classical scattering theory of waves from the view point of an eigenvalue problem and application to target identification
[DE94-000472] p 2525 N94-23206
A matrix analysis of conjugate gradient algorithms
[DE94-002546] p 2454 N94-23796
Infinite divisible and stable distributions modulo 1
[PB94-110640] p 2495 N94-23815
Tool sharing, part 3
[PB94-111697] p 2467 N94-24524

EIGENVECTORS
Multi-grid domain decomposition approach for solution of Navier-Stokes equations in primitive variable form
p 2341 N94-23693
Infinite divisible and stable distributions modulo 1
[PB94-110640] p 2495 N94-23815
Maximum likelihood modal parameter identification and realization of stochastic systems p 2157 N94-24265
Nonlinear analysis using a modal based reduction technique p 2161 N94-24288

EJECTORS
Transient Ejector Analysis (TEA) code user's guide
[NASA-TM-106310] p 2186 N94-23466
Simplified, inverse, ejector design tool
[NASA-CR-194438] p 2166 N94-23511

ELASTIC ANISOTROPY
Aeroelastic response and stability of tiltrotors with elastically-coupled composite rotor blades
[NASA-TM-108758] p 2182 N94-24953

ELASTIC BUCKLING
Nonlinear analysis using a modal based reduction technique p 2161 N94-24288

ELASTIC PROPERTIES
The elastic and electromechanical properties of BaTiO3 single crystal through the ferroelectric transition
[DE94-001437] p 2557 N94-22927
Foil bearing research at Penn State
p 2215 N94-23058
Brush seals for cryogenic applications
p 2216 N94-23063
Control of the internal stresses in plane elasticity
[PB93-225514] p 2374 N94-23112
Generalized melting criterion for beam-induced amorphization
[DE94-001333] p 2560 N94-23189
Continuum representations of cellular solids
[DE94-001706] p 2375 N94-23217
Global dynamic stability of a shallow arch by poincare-like simple cell mapping p 2160 N94-24280
Aerodynamic models for performance calculations of modern technology propellers p 2161 N94-24285
The influence of elastic pitch variations on helicopter flight mechanics p 2161 N94-24286
Center for Analysis of Heterogeneous and Nonlinear Media
[AD-A273515] p 2230 N94-25158
Ring nuclei of strain for bonded dissimilar elastic half spaces with particular application to axisymmetric crack problems
[OUEL-1966/92] p 2379 N94-25325

ELASTIC SCATTERING
Application and development of the Schwinger multichannel scattering theory and the partial differential equation theory of electron-molecule scattering
[NASA-CR-194774] p 2536 N94-24798
Relativistic hadrons in an external field
[ETN-94-95387] p 2538 N94-25259

ELASTIC WAVES
Similarity in wave propagation under a global relaxation law
[PB94-111028] p 2524 N94-23730
Analysis of time-domain acoustic wavefields in horizontally continuously layered configurations based on the modified Cagniard method
[PB94-111044] p 2524 N94-23731

ELASTOMERS
The measurement of the film thickness and the roughness deformation of lubricated elastomers
[ETN-94-95293] p 2261 N94-25078

ELECTRIC ARCS
The internal structure and dynamics of the railgun plasma armature between infinitely wide ablating rails
[DE94-001473] p 2198 N94-23208
Investigation of a subsonic-arc-attachment thruster using segmented anodes
[NASA-TM-106419] p 2219 N94-23531
Measurement of electron temperature and density in the DIII-D neutral beam ion source arc chamber
[DE94-001099] p 2553 N94-24746

ELECTRIC BATTERIES
Electric and hybrid vehicles program
[DE93-040664] p 2352 N94-22881
Pushing technology to satisfy world applications
[DE94-001365] p 2353 N94-23191

Applications of x ray absorption fine structure to the in situ study of the effect of cobalt in nickel hydrous oxide electrodes for fuel cells and rechargeable batteries
p 2391 N94-23347
Ovonic nickel metal hydride batteries for space applications p 2391 N94-23352
Limiting factors for carbon based chemical double layer capacitors p 2394 N94-23365
Hairy carbon electrodes studied by cyclic voltammetry and battery discharge testing p 2394 N94-23367
In situ and ex situ spectroelectrochemical and x ray absorption studies on rechargeable, chemically-modified and other MnO2 materials
[DE94-001387] p 2234 N94-24545

ELECTRIC BRIDGES
Bridge type optoelectronic sample and hold circuit
[AD-D015986] p 2312 N94-25042

ELECTRIC CHARGE
Overcharge and overdischarge protection of ambient temperature secondary lithium cells
[NASA-CASE-NPO-18343-1-CU] p 2310 N94-23823

ELECTRIC CONNECTORS
Connector mechanisms in compliance with extreme space conditions p 2360 N94-24025
Multipurpose clamping device with electrical connector for in orbit attachment of payloads p 2361 N94-24035
Design and testing of ubitron amplifier tubes
[AD-A273297] p 2311 N94-24818

ELECTRIC CONTACTS
Tunnelling in metallic contacts on high-T(c) superconductors: A story of charge carriers in YBa2Cu3O(7-delta) and Bi2CaSr2Cu2O(8+delta)
[ISBN-9-03-860142-5] p 2565 N94-25280
Mesoscopic phenomena in metallic point contacts
[ETN-94-95371] p 2313 N94-25286

ELECTRIC CURRENT
Performance evaluation of the Russian SPT-100 thruster at NASA LeRC
[NASA-TM-106401] p 2219 N94-23630
A multigrid solver for the semiconductor equations
p 2482 N94-23674
Thermistor controlled current source versatile temperature sensor
[AD-D015979] p 2345 N94-25037
The effect of a transport current on the surface barrier of a uniaxial anisotropic superconducting slab
[DE93-617135] p 2566 N94-25390

ELECTRIC DISCHARGES
Diffusion in electronegative discharges with magnetic fields
[AD-A273826] p 2304 N94-25521

ELECTRIC ENERGY STORAGE
High power density proton exchange membrane fuel cells p 2393 N94-23359
Thermal control system for Space Station Freedom photovoltaic power module
[NASA-TM-105650] p 2205 N94-24825

ELECTRIC FIELDS
Static image method for computing the electric potential due to sources in a layered sphere
[PB93-224970] p 2308 N94-23105
The role of the radial electric field in confinement and transport in H-mode and VH-mode discharges in the DIII-D tokamak
[DE94-002746] p 2551 N94-23782
Voyager planetary radio astronomy studies
[NASA-CR-194776] p 2614 N94-24328
Electric field-mediated processing of polymer blend solutions p 2223 N94-24341
A study of non-ideal focus properties of 30 deg parallel plate energy analyzers
[NIFS-263] p 2311 N94-24457
Time-domain analysis of conduction and displacement current distributions in inhomogeneous and anisotropic layered media
[PB94-111036] p 2403 N94-24592
Electro-rheology fluids and liquid fuel flow
[AD-A273640] p 2337 N94-25032
Mechanisms of droplet formation
[ISBN-9-06-275765-0] p 2338 N94-25227
Effect of high frequency field on the transport properties of superlattice
[DE93-617047] p 2568 N94-25447

ELECTRIC FILTERS
A theoretical investigation of electrically tunable birefringent optical filters as the special discriminator in hyperspectral imaging systems
[AD-A273743] p 2547 N94-25533

ELECTRIC HYBRID VEHICLES
Electric and hybrid vehicles program
[DE93-040664] p 2352 N94-22881

ELECTRIC MOTOR VEHICLES
Electric and hybrid vehicles program
[DE93-040664] p 2352 N94-22881
Pushing technology to satisfy world applications
[DE94-001365] p 2353 N94-23191

Crashworthiness analysis using advanced material models in DYNA3D
[DE94-002988] p 2229 N94-24632

ELECTRIC MOTORS
Low noise electric motor p 2315 N94-23989
Sensorless, brushless motor to drive a sealed freon-ammonia pump p 2315 N94-24036
Finite element based electric motor design optimization p 2315 N94-24411

ELECTRIC NETWORKS
Transient analysis of circuits including frequency-dependent components using transgyrator and convolution
[PB93-225001] p 2308 N94-23130

ELECTRIC POTENTIAL
Static image method for computing the electric potential due to sources in a layered sphere
[PB93-224970] p 2308 N94-23105
Thermodynamics of nickel-cadmium and nickel-hydrogen batteries p 2391 N94-23349
Power console development for NASA's electric propulsion outreach program
[NASA-TM-106428] p 2218 N94-23372
Investigation of a subsonic-arc-attachment thruster using segmented anodes
[NASA-TM-106419] p 2219 N94-23531
Performance evaluation of the Russian SPT-100 thruster at NASA LeRC
[NASA-TM-106401] p 2219 N94-23630
Lightning tests and analyses of tunnel bond straps and shielded cables on the Space Shuttle solid rocket booster
[NASA-CR-193921] p 2200 N94-24801
Thermistor controlled current source versatile temperature sensor
[AD-D015979] p 2345 N94-25037
Dynamic measurements of thermophysical properties of metals and alloys at high temperatures by subsecond pulse heating techniques p 2247 N94-25124

ELECTRIC POWER
Electrical power technology for robotic planetary rovers p 2314 N94-23401

ELECTRIC PROPULSION
Electric and hybrid vehicles program
[DE93-040664] p 2352 N94-22881
NASA Propulsion Engineering Research Center, volume 2
[NASA-CR-194719-VOL-2] p 2209 N94-23028
Power console development for NASA's electric propulsion outreach program
[NASA-TM-106428] p 2218 N94-23372
Carbon monoxide fuel cells as a source for Mars rover electric power p 2314 N94-23409
Investigation of a subsonic-arc-attachment thruster using segmented anodes
[NASA-TM-106419] p 2219 N94-23531
Shielded Coil Electrodynamic Propulsion (SCEP). A feasibility study
[AD-A273824] p 2314 N94-25539

ELECTRIC ROCKET ENGINES
Performance evaluation of the Russian SPT-100 thruster at NASA LeRC
[NASA-TM-106401] p 2219 N94-23630
Numerical simulation of cylindrical, self-field MPD thrusters with multiple propellants
[NASA-CR-194458] p 2220 N94-24714

ELECTRIC WIRE
Magnetic shielding of interplanetary spacecraft against solar flare radiation
[NASA-CR-195539] p 2204 N94-24334

ELECTRICAL ENGINEERING
Engineering for profitability
[PNR-90990] p 2595 N94-23580

ELECTRICAL FAULTS
Probabilistic methods in problems of applied analysis
[PB94-110681] p 2495 N94-24571

ELECTRICAL IMPEDANCE
Evaluation of inorganic zinc-rich primers using Electrochemical Impedance Spectroscopy (EIS)
p 2237 N94-23233
Impedance measurements on a spiral-wound nickel/metal hydride cell cycled in a simulated Leo orbit
p 2392 N94-23355
Advanced electromagnetic methods for aerospace vehicles
[NASA-CR-195111] p 2365 N94-24699
Evaluation of bioimpedance for the measurement of physiologic variables as related to hemodynamic studies in space flight p 2427 N94-25378

ELECTRICAL INSULATION
Developments in materials for high-field magnets
[DE94-000761] p 2307 N94-22987
Simple estimate of stored energy and conductor insulation voltage-withstand requirements for advanced solenoid magnet designs
[DE93-041048] p 2307 N94-23019

A review of wiring system safety in space power systems
[NASA-CR-194439] p 2203 N94-23632
Thermal control system for SSF sensor/electronics
[SAND-92-0652C] p 2321 N94-23640
Research for electric energy systems
[DE94-001839] p 2293 N94-23719
Field emitter array
[AD-D016023] p 2303 N94-25150

ELECTRICAL MEASUREMENT
Measuring electrically charged particle fluxes in space using a fiber optic loop sensor
[NASA-CR-191328] p 2544 N94-23829
Chemically sensitive interfacial force microscopy: Contact potential measurements of self-assembling monolayer films
[AD-A273135] p 2234 N94-24772
Very low frequency and low frequency transmitting antenna parameter monitoring system
[AD-D015989] p 2302 N94-25049

ELECTRICAL PROPERTIES
Atomic-scale structure of grain boundaries: Correlations to grain boundary properties
[DE94-001289] p 2558 N94-22990
Status of the development of rechargeable lithium cells p 2392 N94-23354
Instrument interface description for NOAA 2000 instruments with European morning spacecraft and/or NOAA-OPQ spacecraft
[NASA-TM-109406] p 2208 N94-23478
Time-domain analysis of conduction and displacement current distributions in inhomogeneous and anisotropic layered media
[PB94-111036] p 2403 N94-24592
Center for advanced electrical and structural polymers
[AD-A273415] p 2259 N94-24783
Electrochemical and electronic properties of neural and oxidized soluble orthogonally-fused thiophene oligomers
[AD-A273283] p 2260 N94-24815
Ferroelectric thin films 3
[AD-A273394] p 2565 N94-25027
Tunnelling in metallic contacts on high-T(c) superconductors: A story of charge carriers in YBa2Cu3O(7-delta) and Bi2CaSr2Cu2O(8+delta)
[ISBN-9-03-860142-5] p 2565 N94-25280
Mesoscopic phenomena in metallic point contacts
[ETN-94-95371] p 2313 N94-25286

ELECTRICAL RESISTANCE
Bridgman's concern
[DE93-040900] p 2558 N94-22953
Generic microelectronic smart sensor platform for detection of toxic, hazardous, and flammable gases
[DE93-017626] p 2343 N94-23200
Design of a resistojet for Space Station Freedom
[NASA-CR-195506] p 2221 N94-24979
Mesoscopic phenomena in metallic point contacts
[ETN-94-95371] p 2313 N94-25286

ELECTRICAL RESISTIVITY
High-T(c) superconducting superlattices
[DE93-019200] p 2556 N94-22864
Electrical transport in La(2-x)Sr(x)CuO(4-y)
[DE93-040685] p 2556 N94-22912
Carbon aerogels: An update on structure, properties, and applications
[DE94-001528] p 2252 N94-22931
Developments in materials for high-field magnets
[DE94-000761] p 2307 N94-22987
Simple estimate of stored energy and conductor insulation voltage-withstand requirements for advanced solenoid magnet designs
[DE93-041048] p 2307 N94-23019
Transparent conducting thin films for spacecraft applications
[NASA-TM-106466] p 2218 N94-23370
Non-volatile, solid state bistable electrical switch
[NASA-CASE-NPO-17621-1-CU] p 2309 N94-23820
Comparison of HF groundwave propagation models
[AD-A273146] p 2299 N94-24668
Performance of inverse photoemission spectrometer with a new bandpass photon detector of narrow bandwidth and high sensitivity
[REPT-A-2659] p 2345 N94-24977
Dynamic measurements of thermophysical properties of metals and alloys at high temperatures by subsecond pulse heating techniques p 2247 N94-25124
Proceedings of the 12th International Congress: Corrosion Control for Low-Cost Reliability. Volume 6: Electric Power Industry
[AD-A273668] p 2250 N94-25408
Template synthesis of electronically conductive polymers
[AD-A273673] p 2263 N94-25409
Effect of high frequency field on the transport properties of superlattice
[DE93-617047] p 2568 N94-25447

ELECTRO-OPTICAL EFFECT
Photo-induced and electrooptic properties of $(Pb,La)(Zr,Ti)O_3$ films for optical memories
[DE93-019820] p 2542 N94-23202
Ultrastructure processing of macromolecular materials
[AD-A273413] p 2258 N94-24782

ELECTRO-OPTICS
A fully automated stage for optical waveguide measurements
[AD-A273042] p 2542 N94-22915
Defects in electro-optically active polymer solids
p 2223 N94-24342
Nonlinear optical thin films p 2225 N94-24349
Optimization of microscopic and macroscopic second order optical nonlinearities p 2226 N94-24354
Photonic technology for implementation of generalizable neural networks: A synthetic approach
[AD-A273497] p 2474 N94-24622
Crosstalk analysis of synchronous and asynchronous optical chip interconnects with direct detection
[AD-A273261] p 2311 N94-24685
Dipolar relaxation in a second-order nonlinear optical interpenetrating polymer network
[AD-A273626] p 2258 N94-24732
Ferroelectric thin films 3
[AD-A273394] p 2565 N94-25027
Wide bandwidth differential amplifier
[AD-D015985] p 2303 N94-25217

ELECTROCARDIOGRAPHY
Aeromedical disposition of Arrhythmias and electrocardiographic findings in aircrew
p 2423 N94-23318
Echocardiographic screening of aircrew candidates
p 2424 N94-23319
Left ventricular hypertrophy and athlete's heart
p 2424 N94-23321

ELECTROCATALYSTS
PEM regenerative fuel cells p 2392 N94-23358

ELECTROCHEMICAL CELLS
High power density proton exchange membrane fuel cells p 2393 N94-23359

ELECTROCHEMICAL CORROSION
Electrochemical behavior of ion-plated TiN and Cu-Cr coatings
[AD-A273411] p 2235 N94-24784
Proceedings of the 12th International Congress: Corrosion Control for Low-Cost Reliability. Volume 1: Coatings
[AD-A273661] p 2251 N94-25448
Preceedings of the 12th International Congress: Corrosion Control for Low-Cost Reliability. Volume 3A: Corrosion: Specific issues
[AD-A273663] p 2251 N94-25450

ELECTROCHEMICAL OXIDATION
Diffusion of hydrogen in iron oxides
[DE93-632430] p 2239 N94-22966
Low-gravity electrodeposition and growth of polymer thin films with large third-order optical nonlinearities by electrochemical processes for devices: Thiophene-based polymers p 2225 N94-24346

ELECTROCHEMISTRY
Space Electrochemical Research and Technology
[NASA-CP-3228] p 2390 N94-23345
In situ and ex situ spectroelectrochemical and x ray absorption studies on rechargeable, chemically-modified and other MnO_2 materials
[DE94-001387] p 2234 N94-24545
Electrochemical sulfur passivation of visible (approximately 670nm) AlGaInP lasers
[DE94-002293] p 2350 N94-24659
Electrochemical behavior of ion-plated TiN and Cu-Cr coatings
[AD-A273411] p 2235 N94-24784
Electrochemically mediated polymerization of 2-pentadecylaniline confined to a planar liquid-liquid interface
[AD-A273541] p 2259 N94-24792
Electrochemical and electronic properties of neural and oxidized soluble orthogonally-fused thiophene oligomers
[AD-A273283] p 2260 N94-24815
The electrochemistry of the solvated electron: A study of its properties and of its applications
[ETN-94-95313] p 2236 N94-25296
Use of scanning tunneling microscope in corrosion studies
[VTT-TIED-1416] p 2250 N94-25346
Proceedings of the 12th International Congress: Corrosion Control for Low-Cost Reliability. Volume 5B: Corrosion: General issues
[AD-A273667] p 2250 N94-25407
Proceedings of the 12th International Congress: Corrosion Control for Low-Cost Reliability. Volume 6: Electric Power Industry
[AD-A273668] p 2250 N94-25408
Proceedings of the 12th International Congress: Corrosion Control for Low-Cost Reliability. Volume 1: Coatings
[AD-A273661] p 2251 N94-25448
Preceedings of the 12th International Congress: Corrosion Control for Low-Cost Reliability. Volume 2: Process Industries Plant Operations
[AD-A273662] p 2251 N94-25449

ELECTRODE MATERIALS
Overcharge and overdischarge protection of ambient temperature secondary lithium cells
[NASA-CASE-NPO-18343-1-CU] p 2310 N94-23823
Arc electrode interaction study
[NASA-CR-195096] p 2310 N94-24070

ELECTRODEPOSITION
Applications of x ray absorption fine structure to the in situ study of the effect of cobalt in nickel hydrous oxide electrodes for fuel cells and rechargeable batteries
p 2391 N94-23347
Low-gravity electrodeposition and growth of polymer thin films with large third-order optical nonlinearities by electrochemical processes for devices: Thiophene-based polymers p 2225 N94-24346
X ray diffraction analysis of electrodeposited beta-tantalum
[AD-A273254] p 2249 N94-25142
Proceedings of the 12th International Congress: Corrosion Control for Low-Cost Reliability. Volume 1: Coatings
[AD-A273661] p 2251 N94-25448

ELECTRODES
High specific energy, high capacity nickel-hydrogen cell design p 2391 N94-23350
High surface area, low weight composite nickel fiber electrodes p 2391 N94-23351
NASA Lewis advanced IPV nickel-hydrogen technology p 2392 N94-23356
PEM regenerative fuel cells p 2392 N94-23358
High power density proton exchange membrane fuel cells p 2393 N94-23359
Composite fiber structures for catalysts and electrodes
p 2393 N94-23364
Hairy carbon electrodes studied by cyclic voltammetry and battery discharge testing p 2394 N94-23367
Field emitter array memory device
[AD-D016015] p 2311 N94-24736

ELECTRODYNAMICS
Data analysis and theoretical studies of the upper mesosphere and lower thermosphere
[NASA-CR-195108] p 2402 N94-24089
Shielded Coil Electrodynamic Propulsion (SCEP). A feasibility study
[AD-A273824] p 2314 N94-25539

ELECTROENCEPHALOGRAPHY
Static image method for computing the electric potential due to sources in a layered sphere
[PB93-224970] p 2308 N94-23105
EEG and chaos: Description of underlying dynamics and its relation to dissociative states
[NASA-CR-195171] p 2428 N94-24799

ELECTROFORMING
Investigate zero-stress replicated optics
[NASA-CR-193889] p 2545 N94-24665

ELECTROKINETICS
Capillary electrokinetic separations with optical detection
[DE94-001639] p 2233 N94-23716

ELECTROLUMINESCENCE
Ultrastructure processing of macromolecular materials
[AD-A273413] p 2258 N94-24782

ELECTROLYSIS
Primary and secondary electrical space power based on advanced PEM systems p 2392 N94-23357
PEM regenerative fuel cells p 2392 N94-23358
Recent advances in SPE (tm) water electrolyzer
p 2393 N94-23362

ELECTROLYTE METABOLISM
Fluid-loading solutions and plasma volume: Astro-ade and salt tablets with water
[NASA-TP-3456] p 2426 N94-23544

ELECTROLYTES
NASA Lewis advanced IPV nickel-hydrogen technology p 2392 N94-23356
High energy density aluminum-oxygen cell
p 2393 N94-23363
Fluid-loading solutions and plasma volume: Astro-ade and salt tablets with water
[NASA-TP-3456] p 2426 N94-23544

ELECTROLYTIC CELLS
The electrolyte challenge for a direct methanol-air polymer electrolyte fuel cell operating at temperatures up to 200 C p 2393 N94-23360
Advances in direct oxidation methanol fuel cells
p 2393 N94-23361
A high performance H_2-Cl_2 fuel cell for space power applications p 2394 N94-23366
Carbon supercapacitors
[DE94-002652] p 2311 N94-24748

ELECTROMAGNETIC ABSORPTION
Study of a local absorbing boundary condition for the modeling of an infinite external domain in the time-domain finite-element package FEMAXT
[PB94-111002] p 2294 N94-23728
Magnetic field-induced saddle point in GaAs/AlGaAs short period superlattices
[REPT-A-2656] p 2568 N94-25515

ELECTROMAGNETIC COMPATIBILITY
Compatibility relations and the finite-element formulation of electromagnetic field problems
[PB94-110996] p 2294 N94-23727
FEMAX finite-element package for computing three-dimensional time-domain electromagnetic fields in inhomogeneous media
[PB94-111093] p 2294 N94-23733
A review of ISEAS design p 2465 N94-24410
Finite-element method for computing three-dimensional electromagnetic fields in inhomogeneous media (1993)
[PB94-111101] p 2298 N94-24637

ELECTROMAGNETIC FIELDS
Electromagnetic field strength prediction in an urban environment: A useful tool for the planning of LMSS
p 2283 N94-22795
Gauge invariance and the electromagnetic current of composite pions
[DE93-040869] p 2532 N94-22952
Transient analysis of conducting half-plane problem with noncausal scattering image
[PB93-225027] p 2524 N94-23110
Research for electric energy systems
[DE94-001839] p 2293 N94-23719
Compatibility relations and the finite-element formulation of electromagnetic field problems
[PB94-110996] p 2294 N94-23727
Study of a local absorbing boundary condition for the modeling of an infinite external domain in the time-domain finite-element package FEMAXT
[PB94-111002] p 2294 N94-23728
FEMAX finite-element package for computing three-dimensional time-domain electromagnetic fields in inhomogeneous media
[PB94-111093] p 2294 N94-23733
Design and performances of electromagnetic initiators for space mechanisms: An alternative to pyrotechnic system p 2315 N94-24037
Edge elements, their advantages and disadvantages
[PB94-111069] p 2298 N94-24593
Finite-element modelling of three-dimensional electromagnetic fields using edge and nodal elements
[PB94-111077] p 2298 N94-24597
Finite-element method for computing three-dimensional electromagnetic fields in inhomogeneous media (1993)
[PB94-111101] p 2298 N94-24637
ELF communications system ecological monitoring program
[AD-A273456] p 2299 N94-24676
Effect of high frequency field on the transport properties of superlattice
[DE93-617047] p 2568 N94-25447

ELECTROMAGNETIC INTERACTIONS
Photon-photon collisions at the next linear collider: Theory
[DE93-041025] p 2534 N94-23803
A comparison of in-bore projectile motion from an electromagnetic railgun versus that of a conventional cannon barrel
[AD-A273473] p 2198 N94-24690

ELECTROMAGNETIC INTERFERENCE
Simulation of adjacent channel interference in a UHF satellite system
[AD-A273147] p 2299 N94-24669
Mitigation of EMI/RFI produced by a 1.2 kW uninterruptible power supply
[AD-A273149] p 2299 N94-24670
Integrated reflector antenna design and analysis
[NASA-CR-195164] p 2300 N94-24678
Electrochemical behavior of ion-plated TiN and Cu-Cr coatings
[AD-A273411] p 2235 N94-24784
Electromagnetic interference impact of the proposed emitters for the High Frequency Active Auroral Research Program (HAARP)
[AD-A273401] p 2301 N94-24926
Highly-reliable fly-by-light/power-by-wire technology
p 2162 N94-25099
Contribution to the study of HF converters radiated disturbances
[ECL-92-34] p 2313 N94-25421

ELECTROMAGNETIC MEASUREMENT
Fluid velocity and electromagnetic forces measured by a rotating Langmuir probe in the scrape off layer of JFT-2M
[OUEL-1968/92] p 2554 N94-25327

ELECTROMAGNETIC NOISE
System for cancelling phase noise in an interferometric fiber optic sensor arrangement
[AD-D015994] p 2345 N94-25053
On the origin of 1/f noise in epitaxial GaAs
[ISBN-9-09-006067-7] p 2566 N94-25297
ELECTROMAGNETIC PULSES
Mitigation of EMI/RFI produced by a 1.2 kW uninterruptible power supply
[AD-A273149] p 2299 N94-24670
ELECTROMAGNETIC PUMPS
SP-100 heat transport technology development
[DE94-000769] p 2218 N94-23452
ELECTROMAGNETIC RADIATION
Similarity in wave propagation under a global relaxation law
[PB94-111028] p 2524 N94-23730
Analysis of time-domain acoustic wavefields in horizontally continuously layered configurations based on the modified Cagniard method
[PB94-111044] p 2524 N94-23731
Electromagnetic field changes as a precursory phenomena of earthquakes and volcanic eruptions
[REPT-157] p 2405 N94-24980
Numerical simulation and analysis of experimental results on stimulated Raman scattering in laser-plasma Hohlraum targets
[DE93-613719] p 2554 N94-25330
Contribution to the study of HF converters radiated disturbances
[ECL-92-34] p 2313 N94-25421
ELECTROMAGNETIC SCATTERING
Propagation model for the Land Mobile Satellite channel in urban environments p 2283 N94-22796
Transient analysis of conducting half-plane problem with noncausal scattering image
[PB93-225027] p 2524 N94-23110
Classical scattering theory of waves from the view point of an eigenvalue problem and application to target identification
[DE94-000472] p 2525 N94-23206
Electromagnetic scattering by inhomogeneous objects. Solution methods based upon reciprocity theorems of time-convolution and time-correlation type
[PB94-111010] p 2294 N94-23729
ELECTROMAGNETIC SHIELDING
Electrochemical behavior of ion-plated TiN and Cu-Cr coatings
[AD-A273411] p 2235 N94-24784
Shielded Coil Electrodynamic Propulsion (SCEP). A feasibility study
[AD-A273824] p 2314 N94-25539
ELECTROMAGNETIC SPECTRA
Magnetic field-induced saddle point in GaAs/AlGaAs short period superlattices
[REPT-A-2656] p 2568 N94-25515
ELECTROMAGNETISM
Proceedings of the 1993 Bi-Isotropics Workshop on Novel Microwave Materials
[PB93-224772] p 2290 N94-23225
Advanced electromagnetic methods for aerospace vehicles
[NASA-CR-195111] p 2365 N94-24699
ELECTROMAGNETS
Preliminary eddy current modelling for the large angle magnetic suspension test fixture
[NASA-CR-194772] p 2192 N94-23539
The use of harmonics in 3-D magnetic fields
[DE94-002274] p 2299 N94-24656
Compact free electron lasers for medical applications
[AD-A273609] p 2350 N94-24934
ELECTROMECHANICAL DEVICES
Electromagnetic brake/clutch device
[NASA-CASE-GSC-13502-1] p 2354 N94-23969
Finite element based electric motor design optimization p 2315 N94-24411
Controller modeling and evaluation for PCV electro-mechanical actuator p 2371 N94-24441
Design and application of electromechanical actuators for deep space missions
[NASA-CR-195134] p 2365 N94-24842
ELECTROMECHANICS
The elastic and electromechanical properties of BaTiO3 single crystal through the ferroelectric transition
[DE94-001437] p 2557 N94-22927
A comparison of in-bore projectile motion from an electromagnetic railgun versus that of a conventional cannon barrel
[AD-A273473] p 2198 N94-24690
ELECTROMYOGRAPHY
Loading, electromyograph, and motion during exercise
p 2427 N94-25359
Loading, electromyograph, and motion during exercise
p 2427 N94-25380
ELECTRON AVALANCHE
MOS analog memory with injection capacitors
[AD-D015990] p 2312 N94-25050
ELECTRON BEAMS
Properties of the transfer matrices of deflecting magnet systems for free electron laser
[DE93-508257] p 2347 N94-22922
The CEBAF beam loss sensors
[CEBAF-PR-93-032] p 2540 N94-24662
A research of possibility for negative muon production by a low energy electron beam accompanying ion beam
[NIFS-266] p 2536 N94-24868
High precision x ray lithographic masks
[AD-A273342] p 2346 N94-25154
ELECTRON CYCLOTRON HEATING
Analysis and experiments of a whistler-wave plasma thruster
[DE94-001533] p 2209 N94-23012
Overview of the ATF stellarator program
[DE94-000371] p 2550 N94-23462
ELECTRON DENSITY (CONCENTRATION)
Picosecond High Pressure Gas Switch experiment
[DE93-040853] p 2307 N94-22950
Characterization of heat transport and radiation hydrodynamics in collisional laser plasmas using collective Thomson scattering
[DE94-001502] p 2349 N94-23209
Density functional studies: First principles and semi-emperical calculations of clusters and surfaces
[DE94-002836] p 2561 N94-23214
Nonlinear ion-mixing-mode particle transport in the dissipative trapped electron regime
[DE94-000989] p 2533 N94-23435
Measurement of electron temperature and density in the DIII-D neutral beam ion source arc chamber
[DE94-001099] p 2553 N94-24746
Mechanisms of anode power deposition in a low pressure free burning arc
[NASA-CR-194442] p 2553 N94-25190
ELECTRON DENSITY PROFILES
Temporal behavior of the electron density profile during limiter biasing in the HYBTOK-2 tokamak
[NIFS-257] p 2552 N94-24456
ELECTRON DIFFRACTION
Inelastic electron scattering from surfaces
[DE94-001368] p 2531 N94-22733
Orientation imaging microscopy: New possibilities for microstructural investigations using automated BKD analysis
[DE94-000777] p 2557 N94-22938
Perturbation theory in electron diffraction
[PB93-201424] p 2533 N94-23505
ELECTRON DISTRIBUTION
Analysis and experiments of a whistler-wave plasma thruster
[DE94-001533] p 2209 N94-23012
ELECTRON EMISSION
Limits on high-order harmonic generation from single-atom calculations
[DE93-019950] p 2531 N94-22869
Electron spectroscopic studies of the neutralization of slow multicharged ions during interactions with a metal surface
[DE93-041046] p 2532 N94-22956
Field emitter array memory device
[AD-D016015] p 2311 N94-24736
ELECTRON ENERGY
Inelastic electron scattering from surfaces
[DE94-001368] p 2531 N94-22733
Electron spectroscopic studies of the neutralization of slow multicharged ions during interactions with a metal surface
[DE93-041046] p 2532 N94-22956
High-order sum and difference-frequency generation in helium
[DE94-001064] p 2348 N94-23181
Nonlinear ion-mixing-mode particle transport in the dissipative trapped electron regime
[DE94-000989] p 2533 N94-23435
Stationary plasma thruster plume characteristics
[NASA-CR-194454] p 2219 N94-24361
Measurement of electron temperature and density in the DIII-D neutral beam ion source arc chamber
[DE94-001099] p 2553 N94-24746
Nonequilibria in thermal emission from supernova remnants
[NIFS-264] p 2602 N94-24866
ELECTRON GUNS
Design and testing of ubitron amplifier tubes
[AD-A273297] p 2311 N94-24818
Performance of inverse photoemission spectrometer with a new bandpass photon detector of narrow bandwidth and high sensitivity
[REPT-A-2659] p 2345 N94-24977
ELECTRON IRRADIATION
On the origin of 1/f noise in epitaxial GaAs
[ISBN-9-09-006067-7] p 2566 N94-25297
ELECTRON MICROSCOPES
Scanning probe surface modification
[AD-A273178] p 2346 N94-25151
ELECTRON MICROSCOPY
Phase transformations in Cu-Zr multilayers
[DE94-000393] p 2241 N94-23297
The in situ observation of epitaxial diamond thin film nucleation and growth using emission electron microscopy
[AD-A273698] p 2263 N94-25489
ELECTRON PARAMAGNETIC RESONANCE
Magnetic resonance study of zinc-related defects in silicon with optimized EPR spectrometer
[PB93-224640] p 2561 N94-23223
Magnetic resonance studies of 3d transition metal impurities in compound semiconductors
[PB93-232197] p 2243 N94-23714
Contribution of all excited states to ZFS of a (sup 6) S-state
[DE93-617007] p 2568 N94-25483
ELECTRON PHONON INTERACTIONS
Localized excitations in competing bond-order-wave, charge-density-wave and spin-density-wave systems. 2: Competing charge-density-wave and spin-density-wave
[DE93-617131] p 2538 N94-25388
ELECTRON SCATTERING
Inelastic electron scattering from surfaces
[DE94-001368] p 2531 N94-22733
Perturbation theory in electron diffraction
[PB93-201424] p 2533 N94-23505
Theoretical atomic physics for fusion
[DE94-000712] p 2533 N94-23543
Application and development of the Schwinger multichannel scattering theory and the partial differential equation theory of electron-molecule scattering
[NASA-CR-194774] p 2536 N94-24798
High precision x ray lithographic masks
[AD-A273342] p 2346 N94-25154
ELECTRON SPECTROSCOPY
Grain-boundary microchemistry and intergranular cracking of irradiated austenitic stainless steel
[DE94-000466] p 2242 N94-23457
Low mass muon pair production in 450 GeV p-Be collisions
[PB94-110699] p 2533 N94-23746
Activities of Academia Sinica
[DE93-614529] p 2541 N94-25335
ELECTRON SPIN
Spin-polaron theory of high-T(c) superconductivity. 2: Electronic structure of the CuO2 planes
[DE93-019197] p 2556 N94-22919
Spin fluctuations in an ordered Heisenberg ferromagnet with dipolar interactions
[PB93-204493] p 2524 N94-24533
ELECTRON STATES
Anisotropic uniaxial pressure effects in YBa2Cu3O(7-delta)
[DE94-001456] p 2557 N94-22929
ELECTRON TRANSFER
Disorder effects on small-polaron formation and hopping
[DE94-001205] p 2534 N94-23804
Mesoscopic phenomena in metallic point contacts
[ETN-94-95371] p 2313 N94-25286
ELECTRON TRANSITIONS
Intramultiplet mixing for Ne(**)(3p)+He at superthermal energies
[ETN-94-95327] p 2538 N94-25240
ELECTRON TUNNELING
The role of emitter states in magnetotunneling through double-barrier resonant-tunneling diodes at high magnetic fields
[REPT-A-2658] p 2564 N94-24959
Quantum tunneling transport of electrons in double-barrier heterostructures: Theory and modeling
[ETN-94-95332] p 2565 N94-25059
ELECTRON-POSITRON PAIRS
Progress report for the UCSD experimental HEP group
[DE94-001357] p 2533 N94-23699
New evaluation of hadronic contributions to the anomalous magnetic moment of charged leptons
[DE93-634394] p 2536 N94-24844
ELECTRONIC CONTROL
Open EDI
[VTT-TIED-1353] p 2588 N94-22734
Computer control of an electro-mechancial regulator for providing positive pressure breathing and an electronic G-valve for human +Gz research
[DCIEM-93-05] p 2437 N94-24299
ELECTRONIC COUNTERMEASURES
CF-18 AN/ALQ-126B-MG 13 IIP interface to the DREO Electronic Warfare Engagement Simulation Facility
[DREO-TN-93-4] p 2296 N94-24118

ELECTRONIC EQUIPMENT
Electronic payloads for Martian missions: A preliminary assessment of technologies p 2610 N94-23408
The Electronics Quality/Reliability Center: Lessons learned from partnering with industry
[DE94-001501] p 2309 N94-23777
Laser soldering of Sn plated brass integrator assembly housings
[DE94-001149] p 2270 N94-23790
Worst case analysis: Earth sensor assembly for the tropical rainfall measuring mission observatory
[NASA-CR-189320] p 2311 N94-24754
PLANET: A hierarchical network simulator
[ISBN-9-09-005693-9] p 2313 N94-25083
Computerized testing system software conversion and development: Identifying software and hardware portability issues and solutions
[AD-A273489] p 2462 N94-25287

ELECTRONIC EQUIPMENT TESTS
Characterization of CCD-based imaging x ray detectors for diffraction experiments
[DE93-041343] p 2556 N94-22921
Experimental verification of an acoustic telemetry link between an Aurora and CFAV quest
[DREA-TC-93-304] p 2202 N94-24121
On the characterization and optimization of high-speed silicon bipolar transistors
[ETN-94-95367] p 2313 N94-25253
CADBIT 2: Computer-aided design for built-in test, volume 1
[AD-A273702] p 2463 N94-25455
CADBIT 2: Computer-aided design for built-in test, volume 2
[AD-A273703] p 2463 N94-25456

ELECTRONIC MAIL
AstroMail: Electronic mail for the astrophysics community
[NASA-CR-194877] p 2591 N94-24099
Interoperability through standardization: Electronic mail, and X Window systems p 2575 N94-24406

ELECTRONIC PACKAGING
Transient analysis of circuits including frequency-dependent components using transgyrator and convolution
[PB93-225001] p 2308 N94-23130

ELECTRONIC WARFARE
CF-18 AN/ALQ-126B-MG 13 IIP interface to the DREO Electronic Warfare Engagement Simulation Facility
[DREO-TN-93-4] p 2296 N94-24118

ELECTRONS
Nonlinear ion-mixing-mode particle transport in the dissipative trapped electron regime
[DE94-000989] p 2533 N94-23435
The electrochemistry of the solvated electron: A study of its properties and of its applications
[ETN-94-95313] p 2236 N94-25296

ELECTROPHORESIS
Capillary electrokinetic separations with optical detection
[DE94-001639] p 2233 N94-23716
Electrophoresis in open capillaries: Some fundamental aspects
[ETN-94-95290] p 2236 N94-25232
Capillary electrophoresis of biomolecules: Theory, instrumentation and applications
[ETN-94-95297] p 2236 N94-25233

ELECTROPHYSIOLOGY
Electrophysiology of the rat nucleus accumbens: Local circuitry, neuromodulation and synaptic plasticity
[PB93-232254] p 2420 N94-23454

ELECTROPLATING
Molten salt reactor for potentiostatic electroplating
[AD-D016020] p 2258 N94-24720

ELECTRORHEOLOGICAL FLUIDS
Electro-rheology fluids and liquid fuel flow
[AD-A273640] p 2337 N94-25032
Electro-rheological control valve
[AD-D015997] p 2367 N94-25055

ELECTROSTATIC PROBES
Active probing of plasma edge turbulence and feedback studies on the Texas Experimental Tokamak (TEXT)
[DE94-001017] p 2548 N94-22945
Stationary plasma thruster plume characteristics
[NASA-CR-194454] p 2219 N94-24361
Scanning probe surface modification
[AD-A273178] p 2346 N94-25151
Fluid velocity and electromagnetic forces measured by a rotating Langmuir probe in the scrape off layer of JFT-2M
[OUEL-1968/92] p 2554 N94-25327

ELECTROSTATICS
Static image method for computing the electric potential due to sources in a layered sphere
[PB93-224970] p 2308 N94-23105
Nonlinear ion-mixing-mode particle transport in the dissipative trapped electron regime
[DE94-000989] p 2533 N94-23435
A study on electrostatic quadrupole lenses and their application technologies
[REPT-948] p 2546 N94-24982
Electrostatic levitation technology for thermophysical properties of molten materials p 2238 N94-25135

ELEMENTARY PARTICLE INTERACTIONS
A scalar-vector model of quark-antiquark interaction under linear confinement
[DE93-616871] p 2538 N94-25317
Proton spin: The role of quark-gluon and hadron degrees of freedom
[DE93-616867] p 2538 N94-25341
On the hadron formation time in pion-nucleus interaction
[DE93-616879] p 2539 N94-25476

ELEMENTARY PARTICLES
Activities of Academia Sinica
[DE93-614529] p 2541 N94-25335

ELEVATION
Synthesis of passive microwave and radar altimeter data for estimating accumulation rates of polar snow
[NASA-CR-194864] p 2382 N94-23573
The effect of sub-surface volume scattering on the accuracy of ice-sheet altimeter retracking algorithms
[NASA-CR-194825] p 2386 N94-24060

ELLIPSES
A rational elliptic surface related to the question of expressing squares as sum of consecutive squares
[W-9305] p 2479 N94-23139

ELLIPSOIDS
Mathematical addenda to Hopper's model of plane stokes flow driven by capillarity on a free surface
[PB93-237691] p 2480 N94-23438

ELLIPSOMETERS
Mueller matrix analysis of infrared ellipsometry
[PB93-201549] p 2544 N94-23629

ELLIPSOMETRY
Spectroscopic IR ellipsometry of 100 and 001 oriented YBa2Cu3O(7-delta) films
[PB93-201481] p 2561 N94-23445
Mueller matrix analysis of infrared ellipsometry
[PB93-201549] p 2544 N94-23629
Direct observation of crystal growth from solution using optical investigation of a growing crystal face
[NASA-CR-195141] p 2563 N94-24617
Optical properties and emissivities of liquid metals and alloys p 2248 N94-25129

ELLIPTIC DIFFERENTIAL EQUATIONS
Nonlinear smoothing for random fields
[MEMO-1110] p 2493 N94-22728
Uniform convergence of multigrid V-cycle iterations for indefinite and nonsymmetric problems
p 2482 N94-23677
Domain decomposition methods for nonconforming finite element spaces of Lagrange-type
p 2483 N94-23680
Numerical solution of flame sheet problems with and without multigrid methods p 2237 N94-23683
Relaxation schemes for Chebyshev spectral multigrid methods p 2484 N94-23688
A comparison of locally adaptive multigrid methods: LDC, FAC and FIC p 2485 N94-23692
The least energy critical set
[DE93-616820] p 2493 N94-25434
Applications of the homogenization method to flow and transport in porous media
[BER-9110] p 2340 N94-25467

ELLIPTIC FUNCTIONS
A rational elliptic surface related to the question of expressing squares as sum of consecutive squares
[W-9305] p 2479 N94-23139

ELLIPTICAL GALAXIES
Comparison of time integration methods for the evolution of galaxies
[PB94-111671] p 2602 N94-24522

ELONGATION
Effect of neutron irradiation on tensile properties of V-Cr-Ti alloys
[DE94-001433] p 2240 N94-23194

EMBEDDED COMPUTER SYSTEMS
Expert system rule-base evaluation using real-time parallel processing
[AD-A273701] p 2469 N94-25454

EMBEDDING
Towards the formal specification of the requirements and design of a processor interface unit
[NASA-CR-4521] p 2467 N94-24463

EMBRITTLEMENT
Development of small punch testing technique and its application to evaluation of mechanical properties degradation
[DE94-001193] p 2375 N94-23184
Fracture kinetics analysis of empirical and semi-empirical corrosion fatigue relations p 2159 N94-24277

EMERGENCIES
Aircraft evacuation testing: Research and technology issues
[PB94-107620] p 2173 N94-24750

EMISSION SPECTRA
1993 annual report for the Phaedrus-T RF current drive experiments
[DE94-001369] p 2550 N94-23192
Development of an analytical-numerical model to predict radiant emission or absorption
[NASA-CR-194860] p 2453 N94-23624
Using neural networks to assist in OPAD data analysis
p 2477 N94-24452
Infrared and SiO maser observations of OH/IR stars
[PB94-104890] p 2599 N94-24780
Retrieval of temperature profiles from Martian infrared spectra p 2620 N94-24893
An AVHRR cloud classification database typed by experts
[AD-A273560] p 2416 N94-25162
UV extinction and IR emission in diffuse H2 regions
[NASA-CR-195194] p 2600 N94-25270
Report on operations of the Air Force Geophysics Laboratory infrared array spectrometer
[AD-A273800] p 2406 N94-25535

EMISSIVITY
Experimental evaluation of camouflage effectiveness in the thermal infrared
[FEL-93-A043] p 2361 N94-22896
Spatial and temporal variability of soil temperature, moisture and surface soil properties
[NASA-CR-194109] p 2401 N94-23337
Containerless measurements on liquids at high temperatures p 2238 N94-25125
Liquidus temperature and optical properties measurement by containerless techniques
p 2247 N94-25126

EMITTERS
Electromagnetic interference impact of the proposed emitters for the High Frequency Active Auroral Research Program (HAARP)
[AD-A273401] p 2301 N94-24926
The role of emitter states in magnetotunneling through double-barrier resonant-tunneling diodes at high magnetic fields
[REPT-A-2658] p 2564 N94-24959
Field emitter array
[AD-D016023] p 2303 N94-25150

EMPHYSEMA
Chronic obstructive pulmonary disease
p 2425 N94-23324

EMPLOYEE RELATIONS
Perceptions of organizational support and affectivity as predictors of job satisfaction
[DOT/FAA/AM-94/2] p 2429 N94-25442

EMPLOYMENT
Women scientists and engineers employed in industry: Why so few? A report based on a conference
[ISBN-0-309-04991-1] p 2585 N94-24698

EMULSIONS
Feasibility study: Monodisperse polymer particles containing laser-excitable dyes p 2225 N94-24350
Particle nucleation and growth in butadiene emulsion polymerization
[ETN-94-95300] p 2262 N94-25236

ENCAPSULATING
To perform a proof-of-concept study on the use of superheated drop detectors for the measurement of LET spectra in space environments
[BTI-92/3-31] p 2629 N94-24695

ENCLOSURE
Birdstrike resistant crew enclosure program
[AD-A273700] p 2463 N94-25453

END EFFECTORS
Spline screw multiple rotations mechanism
[NASA-CASE-GSC-13452-1] p 2352 N94-23078
NASA/ASEE Summer Faculty Fellowship Program
[NASA-CR-194678] p 2571 N94-23230
Control of a serpentine manipulator with collision avoidance p 2368 N94-23232
Rack Insertion End Effector (RIEE) automation
p 2368 N94-23242
Development of a force feedback anthropomorphic teleoperation input device for control of robot hands
[NASA-CR-195109] p 2437 N94-24329
Autonomous Space Processor for Orbital Debris (ASPOD)
[NASA-CR-195521] p 2204 N94-24621
Admittance model for the shuttle remote manipulator system in four configurations
[NASA-CR-4555] p 2474 N94-24635
Modelling the Shuttle Remote Manipulator System: Another flexible model p 2371 N94-25350

END-TO-END DATA SYSTEMS
The advanced orbiting systems testbed program: Results to date p 2197 N94-23907
ENDOSCOPES
Real-time holographic endoscopy
[ISL-CO-203/92] p 2343 N94-24054
ENERGETIC PARTICLES
Measuring track densities in lunar grains by image analysis p 2623 N94-25355
ENERGY ABSORPTION
Radiative forcing calculations for SF6 and CH4 using a correlated k-distribution transmission model
[DE94-001855] p 2397 N94-23700
ENERGY BUDGETS
Methodology for the assessment of surface resistance and soil water storage variability at mesoscale based on remote sensing measurements. A case study with HAPEX-EFEDA data. UNESCO-International Hydrological Program 4
[PB94-111721] p 2386 N94-23734
An investigation of current and future satellite and in-situ data for the remote sensing of the land surface energy balance
[NASA-CR-195138] p 2387 N94-24596
The role of atmospheric heat transport in the seasonal carbon dioxide cycle p 2621 N94-24896
ENERGY CONSERVATION
Preliminary study concerning development of petroleum-substitution energy integration technology
[DE94-714902] p 2264 N94-23027
ENERGY CONSUMPTION
Snow modeling, water resources, climate change
[PB93-201770] p 2399 N94-24633
ENERGY CONVERSION
Second law analysis of a conventional steam power plant p 2322 N94-23646
Overview of molten carbonate fuel cell technology development
[DE94-001911] p 2394 N94-23781
Recharge mechanism based on shape memory alloy
p 2362 N94-24039
ENERGY CONVERSION EFFICIENCY
Lectures on magnetohydrodynamical drives
[PB93-224962] p 2308 N94-23104
High-order sum and difference-frequency generation in helium
[DE94-001064] p 2348 N94-23181
Novel two-stage selenization methods for fabrication of thin-film CIS cells and submodules
[DE94-000220] p 2390 N94-23296
Low power ground-based laser illumination for electric propulsion applications
[NASA-CR-194444] p 2219 N94-23555
A solar photovoltaic power system for use in Antarctica
[NASA-TM-106417] p 2395 N94-24071
Spatial frequency multiplier with active linearly tapered slot antenna array
[NASA-TM-106494] p 2310 N94-24308
ENERGY DISSIPATION
Quantitative analysis in the Al-Mg-Si system with small amounts of Mg and Si
[PB93-201499] p 2241 N94-23446
Data analysis and theoretical studies of the upper mesosphere and lower thermosphere
[NASA-CR-195108] p 2402 N94-24089
Energy transfer and constrained simulations in isotropic turbulence p 2330 N94-24153
Magnetic field dissipation and contraction of molecular clouds
[REPT-337] p 2603 N94-24976
Computer simulation of low energy scattering
[ETN-94-95326] p 2537 N94-25082
ENERGY DISTRIBUTION
Solar neutrinos: Real-time experiments
[ICRR-REPT-293-93-5] p 2627 N94-24962
ENERGY GAPS (SOLID STATE)
A valence-fluctuation theory of cuprate superconductivity
[DE94-000887] p 2558 N94-22942
Localized excitations in competing bond-order-wave, charge-density-wave and spin-density-wave systems. 2: Competing charge-density-wave and spin-density-wave
[DE93-617131] p 2538 N94-25388
The Haldane energy gap of a doped linear-chain Heisenberg antiferromagnet
[DE93-617130] p 2567 N94-25426
ENERGY LEVELS
Semiempirical studies of atomic structure
[DE94-001588] p 2531 N94-22937
Evaluation of uranium transitions for isotopically-selective laser induced fluorescence with diode lasers (technical report for ST064)
[DE94-002000] p 2347 N94-22974
GGA study of the magnetic and cohesive properties of bcc, fcc and hcp Mn
[REPT-A-2662] p 2564 N94-24960
ENERGY METHODS
Energy estimates and asymptotic analysis in the theory of shells
[PB93-225738] p 2374 N94-23113
ENERGY OF FORMATION
Vacancy formation energy of Li(H, D) and Na(H, D) systems
[DE93-633452] p 2558 N94-22978
Diffusion on Cu surfaces p 2251 N94-24428
ENERGY POLICY
Federal alternative fuel program light duty vehicle operations
[DE93-040663] p 2264 N94-22878
Feasibility study on a CO2 global recycling system using natural energy
[DE94-714889] p 2397 N94-23026
ENERGY SPECTRA
Electron spectroscopic studies of the neutralization of slow multicharged ions during interactions with a metal surface
[DE93-041046] p 2532 N94-22956
Energy transfer and constrained simulations in isotropic turbulence p 2330 N94-24153
Analysis of SOFCAL calibration data
[NASA-CR-193910] p 2345 N94-25000
Radar target discrimination by spectrum analysis
[AD-D015982] p 2301 N94-25040
Examination of the response capacity of a silicon pixel detector for ions and molecules in the energy area 100 to 300 keV
[MPE-241] p 2346 N94-25415
CsI(Tl)-photodiode detectors for spectroscopy at low radiation levels
[MPI-PHE/92-22] p 2314 N94-25457
High energy gamma astronomy above 200 GeV
[MPI-PHE/93-04] p 2600 N94-25458
ENERGY STORAGE
Picosecond High Pressure Gas Switch experiment
[DE93-040853] p 2307 N94-22950
Primary and secondary electrical space power based on advanced PEM systems p 2392 N94-23357
Limiting factors for carbon based chemical double layer capacitors p 2394 N94-23365
Flow and temperature distribution in a naturally stratified thermal storage tank
[AD-A273511] p 2336 N94-24821
Metal hydride storage
[VTT-JULK-769] p 2396 N94-25417
ENERGY TECHNOLOGY
Catalog of data bases and reports
[DE93-040597] p 2588 N94-22875
Preliminary study concerning development of petroleum-substitution energy integration technology
[DE94-714902] p 2264 N94-23027
Electrical power technology for robotic planetary rovers p 2314 N94-23401
Considerations in implementing integrated biomass energy systems in developing countries
[DE93-018720] p 2395 N94-24499
ENERGY TRANSFER
Optimization of energy transfer in microwave electrothermal thrusters p 2216 N94-23065
Energy transfer in solid explosives
[DE94-001523] p 2265 N94-23778
Data analysis and theoretical studies of the upper mesosphere and lower thermosphere
[NASA-CR-195108] p 2402 N94-24089
Energy transfer and constrained simulations in isotropic turbulence p 2330 N94-24153
Investigation of the optical and laser properties of Tm and Ho in YAG anf YLF
[REPT-94-001] p 2563 N94-24404
Thermodynamic models for bounding pressurant mass requirements of cryogenic tanks
[NASA-TM-106476] p 2346 N94-25202
Infrared fluorescence studies of electronic-to-vibrational energy transfer in a Br2:NO system
[AD-A273727] p 2539 N94-25443
ENGINE AIRFRAME INTEGRATION
Vibration isolating engine mount
[CA-PATENT-1-320-710] p 2353 N94-23215
Integrated design and manufacturing for the high speed civil transport
[NASA-CR-195511] p 2182 N94-24968
ENGINE CONTROL
Controllability of free-piston Stirling engine/linear alternator driving a dynamic load
[NASA-TM-106497] p 2521 N94-24302
ENGINE COOLANTS
CFD analyses of coolant channel flowfields
p 2214 N94-23050
ENGINE DESIGN
Rolls-Royce in perspective: Past, present and future
[PNR-90882] p 2187 N94-23519
The RB211: The first 25 years
[PNR-90977] p 2187 N94-23570
Internal combustion engine with a central crankshaft and integral tandem annular pistons
[CA-PATENT-1-320-878] p 2363 N94-24055
Gas turbine and operating method of the same
[CA-PATENT-APPL-SN-2043039] p 2188 N94-24490
Advanced launch system. Advanced development oxidizer turbopump program
[NASA-CR-193920] p 2367 N94-25174
Design and implementation of a distributed version of the NASA Engine Performance Program
[NASA-CR-194475] p 2462 N94-25179
ENGINE FAILURE
System for Anomaly and Failure Detection (SAFD) system development
[NASA-CR-193907] p 2372 N94-24174
ENGINE MONITORING INSTRUMENTS
Nuclear propulsion control and health monitoring
p 2217 N94-23071
Development of an analytical-numerical model to predict radiant emission or absorption
[NASA-CR-194860] p 2453 N94-23624
ENGINE NOISE
Fan noise research at NASA
[NASA-TM-106512] p 2530 N94-25172
ENGINE PARTS
Engine materials characterization and damage monitoring by using x ray technologies
[NASA-TP-3328] p 2372 N94-24074
An x ray diffraction investigation of alpha-Al2O2 addition to Yttria Stabilized Zirconia (YSZ) thermal barrier coatings subject to destabilizing vanadium pentoxide (V2O5) exposure
[AD-A273403] p 2261 N94-25072
ENGINE TESTS
Performance evaluation of the Russian SPT-100 thruster at NASA LeRC
[NASA-TM-106401] p 2219 N94-23630
System for Anomaly and Failure Detection (SAFD) system development
[NASA-CR-193907] p 2372 N94-24174
Thrust vectoring theory, laboratory and flight tests
p 2155 N94-24251
The effect of high altitude pressure on the power and efficiency of an airborne two-stroke engine
p 2155 N94-24253
Altitude simulation facility for testing large space motors p 2156 N94-24255
Preliminary far-field plume sputtering characterization of the Stationary Plasma Thruster (SPT-100)
[NASA-TM-106464] p 2221 N94-24766
Develop advanced nonlinear signal analysis topographical mapping system
[NASA-CR-194785] p 2389 N94-24856
Temperature measurement using infrared imaging systems during turbine engine altitude testing
[NASA-TM-105871] p 2193 N94-25184
Power electronics development for the SPT-100 thruster
[NASA-TM-106488] p 2221 N94-25189
ENGINEERING MANAGEMENT
Cost benefits of advanced software: A review of methodology used at Kennedy Space Center
p 2464 N94-23240
Mission engineering p 2505 N94-23881
An engineering database management system for spacecraft operations p 2517 N94-23951
The integration of design and manufacturing processes at Alenia DVD p 2179 N94-24325
Advanced Capability Exhaust Systems/Integrated Product Development for advanced nozzles (ACES/IPD)
[AD-A273209] p 2189 N94-24776
Reuse-Driven Software Processes Guidebook, version 02.00.03
[AD-A273644] p 2461 N94-25148
New Technologies for Space Avionics, 1993
[NASA-CR-195157] p 2272 N94-25193
Appendix B: Rapid development approaches for system engineering and design p 2272 N94-25195
Appendix C: Rapid development approaches for system engineering and design p 2272 N94-25196
Software engineering methodologies and tools
p 2465 N94-25382
ENGINEERS
Women scientists and engineers employed in industry: Why so few? A report based on a conference
[ISBN-0-309-04991-1] p 2585 N94-24698
ENTHALPY
Thermochemistry of the actinides
[DE94-000895] p 2231 N94-22943

Calibration of HYPULSE for hypervelocity air flows corresponding to flight Mach numbers 13.5, 15, and 17
[NASA-CR-191578] p 2192 N94-23564
Convection equation modeling: A non-iterative direct matrix solution algorithm for use with SINDA
p 2323 N94-23651
A theorem regarding roots of the zero-order Bessel function of the first kind p 2325 N94-23667
Improved gas core propulsion model
[DE94-000929] p 2220 N94-24511
Dynamic measurements of thermophysical properties of metals and alloys at high temperatures by subsecond pulse heating techniques p 2247 N94-25124
Containerless measurements on liquids at high temperatures p 2238 N94-25125
A thermodynamic approach to obtain materials properties for engineering applications
p 2248 N94-25131

ENTRAINMENT
Simplified, inverse, ejector design tool
[NASA-CR-194438] p 2166 N94-23511

ENTROPY
Thermochemistry of the actinides
[DE94-000895] p 2231 N94-22943
Density estimation by maximum quantum entropy
[DE94-002626] p 2569 N94-24516
Discrete time minimum entropy H(infinity) control problem
[PB93-237808] p 2474 N94-24609

ENVIRONMENT EFFECTS
Exploratory report nickel and nickel compounds
[PB93-223998] p 2242 N94-23496
Exploratory report antimony and antimony compounds
[PB93-224004] p 2397 N94-23497
Artificial plasma experiments. Chemical release observations associated with the CRRES program
[NASA-CR-194871] p 2550 N94-23565
The possible effects of the natural and induced space environment on the optical and thermal properties of EOS surfaces p 2207 N94-23596
Analysis of vulnerability to the impacts of sea level rise: A case study for The Netherlands
[PB94-111150] p 2399 N94-24573
Orbital debris and near-Earth environmental management: A chronology
[NASA-RP-1320] p 2598 N94-24644

ENVIRONMENT MANAGEMENT
Structure and flow of data through an environmental data management system
[DE93-040487] p 2589 N94-22934
Orbital debris and near-Earth environmental management: A chronology
[NASA-RP-1320] p 2598 N94-24644

ENVIRONMENT POLLUTION
Proceedings of the 12th International Congress: Corrosion Control for Low-Cost Reliability. Volume 5B: Corrosion: General issues
[AD-A273667] p 2250 N94-25407

ENVIRONMENT PROTECTION
A prototype expert/information system for examining environmental risks of KSC activities
p 2400 N94-23237
Ozone depletion, paradigms, and politics
[DE94-001600] p 2398 N94-24506

ENVIRONMENT SIMULATION
SATCOM simulator speeds MSS deployment and lowers costs p 2287 N94-22822
A white paper: NASA virtual environment research, applications, and technology
[NASA-TM-109682] p 2428 N94-24855

ENVIRONMENT SIMULATORS
Safety guidelines for the operation of the DREO 10 m EMP simulator DREMPS
[DREO-TN-93-5] p 2193 N94-24117
TEM cell safety report
[DREO-TN-93-9] p 2193 N94-24123

ENVIRONMENTAL CONTROL
Feasibility study on a CO2 global recycling system using natural energy
[DE94-714889] p 2397 N94-23026
Weld joint concepts for on-orbit repair of Space Station Freedom fluid system tube assemblies
p 2371 N94-24427

ENVIRONMENTAL LABORATORIES
Solar-terrestrial environmental laboratory
p 2630 N94-23336

ENVIRONMENTAL MONITORING
Quality data validation: Comprehensive approach to environmental data validation
[DE94-000925] p 2589 N94-22944
A prototype expert/information system for examining environmental risks of KSC activities
p 2400 N94-23237
Lightning, atmospheric electricity, and climate change
[DE94-002003] p 2408 N94-23471
Low rate data bus general specification for the NOAA-OPQ polar orbiting environmental satellites and EUMETSAT polar satellite systems
[NASA-TM-109408] p 2208 N94-23480
Mission operations update for the restructured Earth Observing System (EOS) mission p 2499 N94-23839
The measurement and analysis of leaf spectral reflectance of two stands of loblolly pine populations
p 2389 N94-24442
EPA's survey of in-use driving patterns: Implications for mobile source emission inventories
[PB94-118502] p 2399 N94-24525
Manual on measurement of methane and nitrous oxide emissions from agriculture
[DE93-616429] p 2399 N94-25167

ENVIRONMENTAL RESEARCH SATELLITES
Low rate data bus general specification for the NOAA-OPQ polar orbiting environmental satellites and EUMETSAT polar satellite systems
[NASA-TM-109408] p 2208 N94-23480
High-rate data link general specification for the NOAA-OPQ polar orbiting environmental satellites and EUMETSAT satellite systems
[NASA-TM-109384] p 2208 N94-23481

ENVIRONMENTAL SURVEYS
Aqueous alkaline cleaners: An alternative to organic solvents
[AD-A273510] p 2260 N94-24848
Soil pollution at former industrial sites, the heritage of 150 years of industrial development in Noord-Brabant, The Netherlands
[ISBN-9-09-005758-7] p 2400 N94-25223

ENVIRONMENTAL TESTS
Impedance measurements on a spiral-wound nickel/metal hydride cell cycled in a simulated Leo orbit
p 2392 N94-23355

ENZYME ACTIVITY
The evolution of energy-transducing systems. Studies with archaebacteria
[NASA-CR-195129] p 2422 N94-24811

ENZYMES
The evolution of energy-transducing systems. Studies with an extremely halophilic archaebacterium
[NASA-CR-193803] p 2422 N94-24807
On the mechanism of action of 3',5'-cyclic adenosine monophosphate: A study of four- and five-coordinated phosphorus compounds, modelling the activated state of cAMP
[ISBN-9-03-860222-7] p 2226 N94-25238

ENZYMOLOGY
The evolution of energy-transducing systems. Studies with archaebacteria
[NASA-CR-195129] p 2422 N94-24811
On the mechanism of action of 3',5'-cyclic adenosine monophosphate: A study of four- and five-coordinated phosphorus compounds, modelling the activated state of cAMP
[ISBN-9-03-860222-7] p 2226 N94-25238

EPIDEMIOLOGY
The computation of R(sub 0) for discrete-time epidemic models with dynamic heterogeneity
[CWI-AM-R9301] p 2420 N94-23521

EPITAXY
Ge-Au eutectic bonding of Ge (100) single crystals
[DE94-002281] p 2564 N94-24657
Adsorption, desorption, and decomposition of HCl and HBr on Ge(100): Competitive pairingand near-first-order desorption kinetics
[AD-A273504] p 2235 N94-24790
The in situ observation of epitaxial diamond thin film nucleation and growth using emission electron microscopy
[AD-A273698] p 2263 N94-25489

EPOXY COMPOUNDS
Ultrasonic process for curing adhesives
[AD-A273175] p 2259 N94-24788

EPOXY MATRIX COMPOSITES
The use of expanding monomers in carbon fibre composites
[ISBN-0-315-83550-8] p 2226 N94-22890
Contribution to the interface micromechanical study and to the damage fundamental phenomena in glass fiber epoxy resin model composites
[ISAL-93-0027] p 2227 N94-23133

EPOXY RESINS
Fiber optic detection of ultrasound and its application to cure monitoring
[ISBN-0-315-83424-2] p 2544 N94-24466
Dipolar relaxation in a second-order nonlinear optical interpenetrating polymer network
[AD-A273626] p 2258 N94-24732
Ultrasonic process for curing adhesives
[AD-A273175] p 2259 N94-24788

EQUATIONS OF MOTION
Coherence lost? Not-so-fast escapes from the in-phase attractor of a set of globally coupled nonlinear oscillators
[DE94-000799] p 2557 N94-22940
On the numeric integration of dynamic attitude equations
[NASA-CR-194788] p 2448 N94-23073
Projectile transverse motion and stability in electromagnetic induction launchers
[DE94-001557] p 2198 N94-23210
Differential algebraic equations
[PB93-237618] p 2481 N94-23455
Comparison of time integration methods for the evolution of galaxies
[PB94-111671] p 2602 N94-24522
Nonlinear equations of motion for a panel subject to external loads
[AD-A273142] p 2170 N94-24773
The Casimir energy of the rigid string with massive ends
[DE93-616851] p 2492 N94-25338
Numerical analysis of the motion of a rigid body with an attached spring-mass-damper
[AD-A273825] p 2379 N94-25520
Steady motions of rigid body satellites in a central gravitational field
[AD-A273742] p 2206 N94-25532

EQUATIONS OF STATE
Tool sharing: An application of max-algebra, part 2
[MEMO-1122] p 2478 N94-22710
Tool sharing: An application of max-algebra, part 1
[MEMO-1108] p 2478 N94-22726
Physics of iron
[DE94-002002] p 2402 N94-23721

EQUILIBRIUM EQUATIONS
Product forms as a solution base for queueing systems
[MEMO-COSOR-92-37] p 2477 N94-25526

EQUIPMENT SPECIFICATIONS
Analog communication transmitter and receiver test procedures
[AD-A273423] p 2300 N94-24687

EQUIPOTENTIALS
On the transverse size of a fast moving nucleon
[DE93-616891] p 2539 N94-25481

EQUIVALENT CIRCUITS
Transient analysis of circuits including frequency-dependent components using transgyrator and convolution
[PB93-225001] p 2308 N94-23130
Carbon supercapacitors
[DE94-002652] p 2311 N94-24748

ERGODIC PROCESS
Algorithm on addition chains with restricted memory
[PB94-118692] p 2454 N94-23759
Uniform limit theorems for marked point processes
[PB94-118726] p 2488 N94-24526
Correlation function estimator performance in non-Gaussian spherically invariant random processes
[AD-A273498] p 2496 N94-24951
The anomalous transport caused by particles transverse drift
[DE93-613685] p 2554 N94-25329

ERGOMETERS
Loading, electromyograph, and motion during exercise
p 2427 N94-25380

EROSION
The possible effects of the natural and induced space environment on the optical and thermal properties of EOS surfaces p 2207 N94-23596
Postflight hardware evaluation RSRM-29 (STS-54). Appendix D: Nozzle postfire data
[NASA-CR-193898] p 2199 N94-24057
Arc electrode interaction study
[NASA-CR-195096] p 2310 N94-24070
Temporal and spatial mapping of surface albedo and atmospheric dust opacity on Mars p 2619 N94-24887
Plasma sprayed thermal barrier coatings: Production, characterization and testing
[ISBN-9-03-860082-8] p 2555 N94-25439

ERROR ANALYSIS
Analysis of open-loop conical scan pointing error and variance estimators p 2291 N94-23263
Spur-reduced digital sinusoid synthesis
p 2291 N94-23264
Uncertainties in climate data sets
[NASA-CR-194848] p 2408 N94-23577
Development and application of an empirical probability distribution for the prediction error of re-entry body maximum dynamic pressure p 2207 N94-23653
Study of a local absorbing boundary condition for the modeling of an infinite external domain in the time-domain finite-element package FEMAXT
[PB94-111002] p 2294 N94-23728

Error due to the stopping of the Newton iteration in implicit linear multistep methods
[PB94-101425] p 2487 N94-23786
Coding for frequency hopped spread spectrum satellite communications
[ECE-91-1] p 2296 N94-24132
An examination of the operational error database for air route traffic control centers
[DOT/FAA/AM-93/22] p 2175 N94-24472
Parametric uncertainty reduction in robust multivariable control
[AD-A273412] p 2460 N94-24927
Correlation function estimator performance in non-Gaussian spherically invariant random processes
[AD-A273498] p 2496 N94-24951
IRIG radar calibration catalog. Version 2: The IRIG error model reference for radar calibrations
[AD-A273344] p 2303 N94-25155
An adaptive streamline diffusion finite element method for hyperbolic systems in gas dynamics
[PREPRINT-688] p 2340 N94-25466

ERROR CORRECTING CODES
Coding for frequency hopped spread spectrum satellite communications
[ECE-91-1] p 2296 N94-24132
Coding for frequency hopped spread spectrum satellite communications
[ECE-92-1] p 2300 N94-24697
Binary block codes for correcting asymmetric or unidirectional errors
[ETN-94-95337] p 2460 N94-25063

ERROR DETECTION CODES
Contribution to the evaluation of efficiency of a microprocessor functional test
[ETN-94-95176] p 2445 N94-23153
Design and implementation issues of end-to-end protocols in high-speed networks
[PB94-110905] p 2467 N94-23752
Error coding simulations p 2306 N94-24439
Validation activities for LOTOS based on static data flow analysis
[PB94-110863] p 2459 N94-24758
Binary block codes for correcting asymmetric or unidirectional errors
[ETN-94-95337] p 2460 N94-25063

ERROR SIGNALS
Conveying digital data in noisy, unstable, multipath environments
[AD-D015980] p 2301 N94-25038

ERRORS
Magellan spacecraft and memory state tracking: Lessons learned, future thoughts p 2207 N94-23865
Mission operations and command assurance: Instilling quality into flight operations p 2374 N94-23932

ERS-1 (ESA SATELLITE)
VIERS-1, phase 3
[BCRS-92-24] p 2381 N94-23145
Mission planning for an Earth observation low Earth orbiter: ERS-1 p 2503 N94-23868
Investigations into deployment complications of the ERS-1 SAR antenna p 2305 N94-23996

ERYTHROCYTES
Measuring the dynamics of structural changes in biological macromolecules from light scattering data
p 2422 N94-24426

ESCAPE SYSTEMS
Reach performance while wearing the Space Shuttle launch and entry suit during exposure to launch accelerations p 2436 N94-24204
Regulated drag area parachute
[AD-D015992] p 2170 N94-25051

ESTERS
Planar poly(p-phenylene) derivatives: Ladder formation for maximization of extended conjugation
[AD-A273220] p 2260 N94-24922
Structure of cholesteryl-4-vinylbenzoate
[AD-A273686] p 2567 N94-25441

ESTIMATES
Energy estimates and asymptotic analysis in the theory of shells
[PB93-225738] p 2374 N94-23113
Estimates of monthly mean soil moisture for 1979-1989
[NASA-TM-104571] p 2407 N94-23132
Energy and maximum norm estimates for nonlinear conservation laws
[NASA-CR-195091] p 2569 N94-24109

ESTIMATING
Estimates of monthly mean soil moisture for 1979-1989
[NASA-TM-104571] p 2407 N94-23132
Chronic obstructive pulmonary disease
p 2425 N94-23324
Density estimation by maximum quantum entropy
[DE94-002626] p 2569 N94-24516

Two-stage versus sequential sample-size determination in regression analysis of simulation experiments
[PB94-110558] p 2495 N94-24634

ESTUARIES
Recent developments in the mathematical modelling and physical understanding of transport and dispersion in aquatic systems, with special reference to tidal waters
[PB94-111135] p 2418 N94-24600

ETALONS
Nonlinear optical thin films p 2225 N94-24349

ETHERS
Phenylethynl-terminated poly(arylene ethers)
[NASA-CASE-LAR-14797-1] p 2253 N94-23307

ETHYL COMPOUNDS
The evolution of energy-transducing systems. Studies with archaebacteria
[NASA-CR-195129] p 2422 N94-24811
Synthesis of molecular wires by a novel divergent/convergent approach
[AD-A273332] p 2537 N94-25087

ETHYLENE
Wear reduction in ceramic bearings by surface generated pyrolytic carbon continuously replenished by ethylene gas
[NASA-CR-189214] p 2364 N94-24090
Ethylene trace-gas techniques for high-speed flows
[NASA-TM-106491] p 2169 N94-24335

ETHYLENE COMPOUNDS
FTIR quantification of industrial hydraulic fluids in perchloroethylene p 2264 N94-23243

ETIOLOGY
Sarcoidosis and the aviator p 2425 N94-23325

EUKARYOTES
Microinjection of the Yersinia YopE cytotoxin in mammalian cells induces actin microfilament disruption
[FOA-B-40418-4.4] p 2421 N94-24290

EULER BUCKLING
Inverse dynamics of a rigid rod system as a simplified model of flexible beam p 2160 N94-24281

EULER EQUATIONS OF MOTION
Local grid refinement method for the euler equations
[PB93-223329] p 2317 N94-22985
Upwind MacCormack Euler solver with non-equilibrium chemistry p 2326 N94-23672
Energy transfer and constrained simulations in isotropic turbulence p 2330 N94-24153
Inverse dynamics of a rigid rod system as a simplified model of flexible beam p 2160 N94-24281
Characteristic method for one-dimensional scalar hyperbolic conservation laws with stiff source terms
[PB93-237675] p 2491 N94-24954
A continuing search for a near-perfect numerical flux scheme. Part 1: AUSM+
[NASA-TM-106524] p 2338 N94-25180

EULER-LAGRANGE EQUATION
Solution of mixed convection heat transfer from isothermal in-line fins p 2321 N94-23644

EURECA (ESA)
A user view of the EURECA ground segment
p 2499 N94-23844
The EURECA telecommanding chain: Experience with packet telecommand and telemetry systems
p 2305 N94-23909

EUROPE
JPRS report: Science and technology. Central Eurasia: Space
[JPRS-USP-93-006] p 2194 N94-23015
Satellite communications systems and technology. Executive Summary
[NASA-TM-109388] p 2293 N94-23622
Satellite communications systems and technology. Volume 1: Analytical chapters
[NASA-TM-109398] p 2293 N94-23627

EUROPEAN SPACE AGENCY
Solar physics within ESA's planning
p 2624 N94-22844
Guide to software configuration management
[ESA-PSS-05-09-ISSUE-1] p 2450 N94-23229
Commonality of flight control systems for support of European telecommunications missions
p 2304 N94-23834
SCOS2: ESA's new generation of mission control systems p 2197 N94-23851

EUROPEAN SPACE PROGRAMS
Solar physics within ESA's planning
p 2624 N94-22844
A review of European applications of artificial intelligence to space
[NASA-TM-108789] p 2453 N94-23568

EUROPIUM COMPOUNDS
Spin fluctuations in an ordered Heisenberg ferromagnet with dipolar interactions
[PB93-204493] p 2524 N94-24533
Investigation of the solid-solid surface adsorption of Eu2O3 on amorphous Al2O3
[DE93-613824] p 2566 N94-25332

EUTECTIC ALLOYS
Metal-mullite reactions
[DE94-002038] p 2244 N94-23811

EUTECTICS
Metal-mullite reactions
[DE94-002038] p 2244 N94-23811
Ge-Au eutectic bonding of Ge (100) single crystals
[DE94-002281] p 2564 N94-24657

EUTROPHICATION
Nutrients and light as factors controlling phytoplankton biomass on the Dutch continental shelf (North Sea), 1988-1990
[PB94-111143] p 2418 N94-24601

EVACUATING (TRANSPORTATION)
Aircraft evacuation testing: Research and technology issues
[PB94-107620] p 2173 N94-24750

EVALUATION
The Automated Instrumentation and Monitoring System (AIMS) reference manual
[NASA-TM-108795] p 2452 N94-23510

EVAPORATION
Experimental and analytical study of cryogenic propellant boiloff to develop and verify alternate pressurization concepts for Space Shuttle external tank using a scaled down tank p 2266 N94-23657
Methodology for the assessment of surface resistance and soil water storage variability at mesoscale based on remote sensing measurements. A case study with HAPEX-EFEDA data. UNESCO-International Hydrological Program 4
[PB94-111721] p 2386 N94-23734
Effect of initial droplet-size distributions on fuel-vapor profiles in a shear-layer flow p 2160 N94-24283

EVAPORATION RATE
Evaporation and combustion of LOX under supercritical and subcritical conditions p 2211 N94-23035

EVAPOTRANSPIRATION
Estimates of monthly mean soil moisture for 1979-1989
[NASA-TM-104571] p 2407 N94-23132
Coupled land surface/hydrologic/atmospheric models
p 2413 N94-24387
Human impacts on soil carbon dynamics of deep-rooted Amazonian forests
[NASA-CR-195127] p 2399 N94-24861

EVOKED RESPONSE (PSYCHOPHYSIOLOGY)
Electrophysiology of the rat nucleus accumbens: Local circuitry, neuromodulation and synaptic plasticity
[PB93-232254] p 2420 N94-23454

EXCIMER LASERS
Fabrication of sub-40-nm p-n junctions for 0.18 micron MOS device applications using a cluster-tool-compatible, nanosecond thermal doping technique
[DE94-001608] p 2309 N94-23520
Exciplex laser study: Discharge and magnetic switching systems
[PB93-199768] p 2349 N94-24629

EXCITATION
Inelastic electron scattering from surfaces
[DE94-001368] p 2531 N94-22733
Experimental and theoretical features of strong suppression and shifting phenomena in odd-photon resonant excitations and stimulated emissions
[DE94-000341] p 2535 N94-24510
Application and development of the Schwinger multichannel scattering theory and the partial differential equation theory of electron-molecule scattering
[NASA-CR-194774] p 2536 N94-24798
Excited state dynamics of thulium ions in yttrium aluminum garnets
[NASA-CR-195159] p 2564 N94-25024
Localized excitations in competing bond-order-wave, charge-density-wave and spin-density-wave systems. 2: Competing charge-density-wave and spin-density-wave
[DE93-617131] p 2538 N94-25388
Excitation mechanisms for XUV and x ray lasers
[DE93-617006] p 2351 N94-25482

EXCLUSION
Exercises in multiprogramming
[PB94-101458] p 2454 N94-23768

EXERCISE PHYSIOLOGY
Responses to LBNP in men with varying profiles of strength and aerobic capacity: Implications for flight crews
[NASA-TP-3346] p 2426 N94-23530
Exercise, exercise training, and the immune system. A compendium of research (1902-1991)
[NASA-TM-108778] p 2426 N94-23575
Loading, electromyograph, and motion during exercise
p 2427 N94-25380

EXHAUST EMISSION
Estimation of delays and emissions at four-way junctions with different forms of regulation, principally four-way mandatory stop
[PB94-105236] p 2398 N94-23813

Alternative control techniques document: NOx emissions from stationary reciprocating internal combustion engines
[PB94-104494] p 2398 N94-24476
EPA's survey of in-use driving patterns: Implications for mobile source emission inventories
[PB94-118502] p 2399 N94-24525
Embodiment design for a multipropellant resistojet
[NASA-CR-195505] p 2221 N94-24834

EXHAUST GASES
Development of an analytical-numerical model to predict radiant emission or absorption
[NASA-CR-194860] p 2453 N94-23624
Alternative control techniques document: NOx emissions from stationary reciprocating internal combustion engines
[PB94-104494] p 2398 N94-24476
Collection and evaluation of numerical models with the aim to investigate the impact of aircraft emissions
[DLR-MITT-93-06] p 2400 N94-25414

EXHAUST NOZZLES
Advanced Capability Exhaust Systems/Integrated Product Development for advanced nozzles (ACES/IPD)
[AD-A273209] p 2189 N94-24776

EXHAUST SYSTEMS
Analysis of high vacuum systems using SINDA'85
p 2322 N94-23648
Advanced Capability Exhaust Systems/Integrated Product Development for advanced nozzles (ACES/IPD)
[AD-A273209] p 2189 N94-24776

EXISTENCE THEOREMS
Personnel shift assignment: Existence conditions and network models
[MEMO-1116] p 2585 N94-22704

EXOBIOLOGY
SETI: Search for extraterrestrial intelligence. An international interdisciplinary seminar, star days
[PB93-230597] p 2444 N94-23754
Measuring the dynamics of structural changes in biological macromolecules from light scattering data
p 2422 N94-24426

EXOSPHERE
Data analysis and interpretation of lunar dust exosphere p 2623 N94-25349

EXOTHERMIC REACTIONS
Modelling the ignition of boron/titanium particles
p 2159 N94-24273
Experimental investigation of ignition of boron/titanium composite particles p 2159 N94-24275

EXPELLANTS
Thermodynamic models for bounding pressurant mass requirements of cryogenic tanks
[NASA-TM-106476] p 2346 N94-25202

EXPERIMENT DESIGN
Gas-grain simulation experiment module conceptual design and gas-grain simulation facility breadboard development
[NASA-CR-177632] p 2598 N94-23536
Harmonisation of man-machine interface experiments in the context of the development of PHARE advanced tools
[PB93-204725] p 2430 N94-23744
Integrating payload design, planning, and control in the Dutch Utilisation Centre p 2207 N94-23869
Attachment methods in composite joints - analysis of test results by controlled experiments method
p 2158 N94-24269
Verification and validation of models
[PB94-110566] p 2456 N94-24507
Design and application of electromechanical actuators for deep space missions
[NASA-CR-195134] p 2365 N94-24842
Designs with a small number of runs for factorial experiments
[ISBN-9-03-860162-X] p 2462 N94-25237

EXPERT SYSTEMS
Glossary knowledge engineering
[NLR-TP-91435-U] p 2471 N94-23137
A prototype expert/information system for examining environmental risks of KSC activities
p 2400 N94-23237
Two applications of a generic task model for solving boolean constraint satisfaction problems
[PB94-119047] p 2487 N94-23765
NASDA knowledge-based network planning system
p 2508 N94-23898
A cross-disciplinary response to improve test activities: The corporate memory capitalization in Ariane4 test domain p 2508 N94-23899
Combining real-time monitoring and knowledge-based analysis in MARVEL p 2477 N94-23900
TOPEX/Poseidon precision orbit determination production and expert system p 2196 N94-23920
A real-time navigation monitoring expert system for the Space Shuttle Mission Control Center
p 2202 N94-23921
Expert diagnostics system as a part of analysis software for power mission operations p 2516 N94-23944
GenSAA: A tool for advancing satellite monitoring with graphical expert systems p 2516 N94-23945
An intelligent planning and scheduling system for the HST servicing missions p 2520 N94-23964
Computer based expert system for battle damage repair of composite structures p 2157 N94-24262
Evaluation of computer-aided instruction techniques for the crew interface coordination position
p 2429 N94-24438
Non-brittleness of a DESIRE-model for an office assignment task
[PB94-119021] p 2489 N94-24643
The use of knowledge systems
[ETN-94-95318] p 2477 N94-25431
Expert system rule-base evaluation using real-time parallel processing
[AD-A273701] p 2469 N94-25454

EXPLORER SATELLITES
SAMPEX payload operation control center implementation p 2197 N94-23843
The H(sub infinity) optimal controller design and reduction for the inertial hold mode of the attitude control system of the XTE spacecraft
[NASA-CR-195137] p 2366 N94-24846

EXPLOSIONS
The ignition temperature of solid explosives exposed to a fire
[DE94-001047] p 2265 N94-23436
Multiple shock initiation of LX-17
[DE94-001524] p 2265 N94-23807
The plastic response of a cylindrical shell subjected to an internal blast wave with a finite width shock front
p 2154 N94-24246

EXPLOSIVES
The ignition temperature of solid explosives exposed to a fire
[DE94-001047] p 2265 N94-23436
Energy transfer in solid explosives
[DE94-001523] p 2265 N94-23778

EXPOSURE
Survival suit for submarine personnel: Summary of evaluation studies
[PB93-204634] p 2430 N94-23743

EXTERNAL STORE SEPARATION
On the effect of the damping coefficients on the trajectories of symmetric and non-symmetric stores
p 2155 N94-24250
Comparison of c.t.s. based prediction of store trajectory with flight test data p 2158 N94-24268

EXTERNAL STORES
On the effect of the damping coefficients on the trajectories of symmetric and non-symmetric stores
p 2155 N94-24250

EXTERNAL TANKS
Experimental and analytical study of cryogenic propellant boiloff to develop and verify alternate pressurization concepts for Space Shuttle external tank using a scaled down tank p 2266 N94-23657
National Institute of Standards and Technology Conference on Reducing the Cost of Space Infrastructure and Operations. Part 2: Topical papers
[PB94-113487] p 2194 N94-23819
Debris/Ice/TPS assessment and integrated photographic analysis for Shuttle Mission STS-61
[NASA-TM-109195] p 2199 N94-24059

EXTRAPOLATION
On the deformation kinetics constitutive law of plastic deformation: The rate equation p 2161 N94-24289

EXTRATERRESTRIAL INTELLIGENCE
SETI: Search for extraterrestrial intelligence. An international interdisciplinary seminar, star days
[PB93-230597] p 2444 N94-23754

EXTRATERRESTRIAL LIFE
SETI: Search for extraterrestrial intelligence. An international interdisciplinary seminar, star days
[PB93-230597] p 2444 N94-23754

EXTRATERRESTRIAL RADIATION
The possible effects of the natural and induced space environment on the optical and thermal properties of EOS surfaces p 2207 N94-23596
Solar flares and magnetospheric particles: Investigations based upon the ONR-602 and ONR-604 experiments
[AD-A273639] p 2628 N94-25031

EXTRAVEHICULAR ACTIVITY
Proceedings of the NIST Conference on Reducing the Cost of Space Infrastructure and Operations: Part 1: Oral presentations and discussion
[PB94-111374] p 2194 N94-23770
National Institute of Standards and Technology Conference on Reducing the Cost of Space Infrastructure and Operations. Part 2: Topical papers
[PB94-113487] p 2194 N94-23819
A simulation system for Space Station extravehicular activity p 2434 N94-24192
Space Station Freedom coupling tasks: An evaluation of their telerobotic and EVA compatibility
p 2436 N94-24200
Design and simulation of EVA tools for first servicing mission of HST
[NASA-CR-194784] p 2439 N94-24857
Investigation of hand capabilities under a variety of performance conditions and an attempt to explain performance differences p 2444 N94-25354
An evaluation of three-dimensional sensors for the extravehicular activity helper/retreiver
p 2444 N94-25369

EXTREME ULTRAVIOLET RADIATION
Imaging XUV spectroscopy of a Z-pinch plasma in the former Soviet Union
[DE93-040849] p 2549 N94-22949
High-order sum and difference-frequency generation in helium
[DE94-001064] p 2348 N94-23181
Excitation of XUV radiation in solar flares
[NASA-CR-193703] p 2627 N94-24094
The solar spectral irradiances from x ray to radio wavelengths
[NASA-CR-195203] p 2629 N94-25260
Excitation mechanisms for XUV and x ray lasers
[DE93-617006] p 2351 N94-25482

EXTREMELY HIGH FREQUENCIES
Use of the 30/20 GHz band by multipurpose satellite systems p 2276 N94-22753
ACTS advanced system concepts and experimentation p 2280 N94-22780
DS-SSMA capacity for a mobile satellite system
p 2286 N94-22814
Transmission over EHF mobile satellite channels
p 2287 N94-22820
Adaptive data rate control TDMA systems as a rain attenuation compensation technique
p 2287 N94-22821
Advanced mobile satellite communications using COMETS satellite in MM-wave and Ka-band
p 2288 N94-22829
K- and Ka-band mobile-vehicular satellite-tracking reflector antenna system for the NASA ACTS mobile terminal p 2289 N94-22831
An active K/Ka-band antenna array for the NASA ACTS mobile terminal p 2289 N94-22832
Performance of the X-/Ka/KABLE-band dichroic plate in the DSS-13 beam waveguide antenna
p 2291 N94-23261
Cryogenic, low-noise high electron mobility transistor amplifiers for the Deep Space Network
p 2291 N94-23262
Analysis of open-loop conical scan pointing error and variance estimators p 2291 N94-23263
A small satellite design for deep space network testing and training
[NASA-CR-195526] p 2205 N94-24702
Conceptual communications system design in the 25.25-27.5 and 37.0-40.5 GHz frequency bands
p 2306 N94-25379

EXTREMELY LOW FREQUENCIES
An active antenna for ELF magnetic fields
p 2303 N94-25192

EXTREMELY LOW RADIO FREQUENCIES
ELF communications system ecological monitoring program
[AD-A273456] p 2299 N94-24676

EXTRUDING
Theory of extrusion: Advances and challenges
[PB93-201572] p 2241 N94-23447
Characterization of the microstructure of Nb-1wt.%Zr-0.1wt.%C tubes as affected by thermomechanical processing
[NASA-TM-106381] p 2242 N94-23550

EYE PROTECTION
Micro pulse laser radar
[NASA-CASE-GSC-13493-1] p 2294 N94-23827

F

F REGION
High latitude cusp signature observations for southward IMF B sub Z
[AD-A273801] p 2406 N94-25536

F-106 AIRCRAFT
Leading-edge votex-system details obtained on F-106B aircraft using a rotating vapor screen and surface techniques
[NASA-TP-3374] p 2166 N94-23512

F-15 AIRCRAFT
Identification of integrated airframe: Propulsion effects on an F-15 aircraft for application to drag minimization
[NASA-TM-4532] p 2188 N94-24106

F-16 AIRCRAFT
Flight controller design using mixed H2/H infinity optimization with a singular H infinity constraint
[AD-A273831] p 2191 N94-25525
F-18 AIRCRAFT
A photogrammetric solution to a particular problem
[NASA-TP-3415] p 2381 N94-22961
Determination of the stability and control derivatives of the NASA F/A-18 HARV using flight data
[NASA-CR-194838] p 2190 N94-24804
Development of high-angle-of-attack nose-down pitch control margin design guidelines for combat aircraft
p 2164 N94-25107
Nonlinear aerodynamic modeling using multivariate orthogonal functions p 2164 N94-25110
FABRICATION
Development of silicon nitride composites with continuous fiber reinforcement
[DE94-001996] p 2227 N94-23022
Preparing polymeric matrix composites using an aqueous slurry technique
[NASA-CASE-LAR-14771-1] p 2252 N94-23076
Novel two-stage selenization methods for fabrication of thin-film CIS cells and submodules
[DE94-000220] p 2390 N94-23296
GPHS-RTG's in support of the Cassini mission
[DE94-001445] p 2218 N94-23459
Tunnelling in metallic contacts on high-T(c) superconductors: A story of charge carriers in YBa2Cu3O(7-delta) and Bi2CaSr2Cu2O(8+delta)
[ISBN-9-03-860142-5] p 2565 N94-25280
Composites and textile reinforcement
[VTT-TIED-1424] p 2231 N94-25420
FABRICS
Composites and textile reinforcement
[VTT-TIED-1424] p 2231 N94-25420
FACE CENTERED CUBIC LATTICES
Multilayer relaxation and surface structure of ordered alloys
[NASA-TM-106433] p 2243 N94-23578
FACSIMILE COMMUNICATION
The Iridium (tm) system: Personal communications anytime, anyplace p 2281 N94-22785
FACTORIAL DESIGN
Designs with a small number of runs for factorial experiments
[ISBN-9-03-860162-X] p 2462 N94-25237
FACTORIALS
Generalized concavity in cooperative game theory: Characterizations in terms of the core
[MEMO-1121] p 2497 N94-22708
FACTORIZATION
Logic synthesis on programmable networks
[ETN-94-95174] p 2449 N94-23151
Squaring-down and the problems of almost-zeros for continuous-time systems
[PB93-237758] p 2489 N94-24608
Wiener-Hopf factorization of rational matrix functions in terms of realizations: An alternative version
[ETN-94-95380] p 2491 N94-25245
FADING
Transmission over EHF mobile satellite channels
p 2287 N94-22820
High specific energy, high capacity nickel-hydrogen cell design p 2391 N94-23350
FAIL-SAFE SYSTEMS
Electro-rheological control valve
[AD-D015997] p 2367 N94-25055
FAILURE
Ceramic matrix composites: Challenges and opportunities p 2255 N94-24230
Failure-proof estimation under conditions of lack of information p 2158 N94-24267
Diagnosing process faults using neural network models
[DE94-002633] p 2473 N94-24518
FAILURE ANALYSIS
Time-frequency domain analysis of vibration signals for machinery diagnostics.(4): Interpretation using image processing techniques
[OUEL-1953/92] p 2353 N94-23178
Review of the probabilistic failure analysis methodology and other probabilistic approaches for application in aerospace structural design
[NASA-TP-3434] p 2376 N94-23342
Materials Science and Engineering
[DE94-003018] p 2228 N94-23493
Galileo spacecraft anomaly and safing recovery
p 2207 N94-23864
Real-time automated failure identification in the Control Center Complex (CCC) p 2272 N94-23892
Micromechanical failure modes in brittle matrix composites p 2255 N94-24232
Role of interfaces on the cyclic fatigue behaviour of ceramic matrix composites p 2256 N94-24234
Failure-proof estimation under conditions of lack of information p 2158 N94-24267
A study of the core module simulator floor capability
p 2380 N94-24418
Micromechanical simulation of damage progression in carbon phenolic composites p 2231 N94-24446
Evaluation of advanced materials through experimental mechanics and modelling p 2374 N94-24454
Diagnosing process faults using neural network models
[DE94-002633] p 2473 N94-24518
Reliability analysis of a repairable dependent parallel system
[ETN-94-95312] p 2373 N94-25295
Failure detection and recovery in the assembly/contingency subsystem p 2306 N94-25360
Modelling early failures in Space Station Freedom
p 2374 N94-25372
FAILURE MODES
Optimization of laminate orientation to enhance failure properties
[ISBN-0-315-83539-7] p 2227 N94-22892
Analysis and test of low profile aluminum aerospace tank dome
[NASA-TP-3442] p 2375 N94-23294
Micromechanical failure modes in brittle matrix composites p 2255 N94-24232
Post buckling behaviour of stiffened composite panels loaded in cyclic compression and shear
p 2157 N94-24260
Pilot-vehicle interface handbook, chapter 19. Volume 2: Digital systems validation
[DOT/FAA/CT-88/10-VOL-2] p 2438 N94-24830
Failure detection and recovery in the assembly/contingency subsystem p 2306 N94-25360
FALLOUT
Towards a new radiation protection organization
[FOA-C-40304-4.3] p 2437 N94-24292
FAN BLADES
Holographic testing of composite propfans for a cruise missile wind tunnel model
[NASA-TM-105271] p 2187 N94-23545
FAR FIELDS
Unsteady jet flow computation towards noise prediction
[NASA-CR-194449] p 2153 N94-23553
Toward modeling wingtip vortices
p 2171 N94-24142
Unstructured adaptive mesh computations of rotorcraft high-speed impulsive noise
[NASA-CR-195090] p 2529 N94-24307
FAR INFRARED RADIATION
Catalog of infrared observations, third edition
[NASA-RP-1294] p 2600 N94-25387
FAR ULTRAVIOLET RADIATION
Method and apparatus for producing a thermal atomic oxygen beam
[NASA-CASE-LEW-15614-1] p 2534 N94-23825
FARM CROPS
Integrated use of hydrological modelling and remote sensing in the province of Drenthe (The Netherlands): Possibilities and restrictions
[REPT-61] p 2382 N94-23148
Groundtruth collection for the JPL-SAR and ERS-1 campaign in Flevoland and Veluwe, Netherlands, 1991
[PB93-230654] p 2386 N94-23755
Evaluation of the use of remote-sensing data to identify crop types and estimate irrigated acreage, Uvalde and Medina Counties, Texas, 1989
[PB93-193159] p 2388 N94-24809
FAST FOURIER TRANSFORMATIONS
Estimation of frequency offset in mobile satellite modems p 2285 N94-22807
Transient analysis of circuits including frequency-dependent components using transgyrator and convolution
[PB93-225001] p 2308 N94-23130
The detection performance of a long-term spectral integrator using normalized and quantized data
[DREP-TM-93-11] p 2455 N94-24130
Fast fourier transforms of piecewise constant functions
[AD-A272648] p 2456 N94-24535
An active antenna for ELF magnetic fields
p 2303 N94-25192
FASTENERS
Split spline screw
[NASA-CASE-GSC-13434-1] p 2352 N94-23082
Docking mechanisms: An overview of different systems p 2357 N94-24004
Flush head fastener
[CA-PATENT-1308581] p 2364 N94-24175
FATIGUE (MATERIALS)
Fatigue crack growth rate studies of medium sulfur low alloy steels tested in high temperature water
[DE93-040437] p 2238 N94-22861
Fundamentals of fatigue analysis
[PB93-226264] p 2374 N94-23118
Thermal fatigue: A literature review
[PB93-226306] p 2375 N94-23120
A review of the Workshop on Fatigue Life Methodologies for Wind Turbines
[DE94-002039] p 2394 N94-23472
Control algorithms for effective operation of variable-speed wind turbines
[DE94-002607] p 2394 N94-23704
Introduction of Ceramics into Aerospace Structural Composites
[AGARD-R-795] p 2255 N94-24228
Repair of cracked aluminum aircraft structure with composite patches p 2156 N94-24259
Fracture kinetics analysis of empirical and semi-empirical corrosion fatigue relations p 2159 N94-24277
Variable amplitude fatigue, modelling and testing
[PB93-204469] p 2378 N94-24742
Matrix fatigue cracking mechanisms of alpha(2) TMC for hypersonic applications
[NASA-TM-106506] p 2230 N94-25186
FATIGUE LIFE
Fundamentals of fatigue analysis
[PB93-226264] p 2374 N94-23118
Thermal fatigue: A literature review
[PB93-226306] p 2375 N94-23120
Fatigue life and crack growth prediction methodology
[NASA-TM-109044] p 2228 N94-23279
A review of the Workshop on Fatigue Life Methodologies for Wind Turbines
[DE94-002039] p 2394 N94-23472
Feasibility study of shot-peening modeling
[CTN-94-60926] p 2244 N94-24170
Development of a damage tolerance tool to analyze multiple-site damage in aircraft structure
p 2157 N94-24261
Durability evaluation of ceramic components using CARES/LIFE
[NASA-TM-106475] p 2258 N94-24682
Variable amplitude fatigue, modelling and testing
[PB93-204469] p 2378 N94-24742
Investigation of the effects of manufacturing variations and materials on fatigue crack detection methods in gear teeth
[NASA-CR-195093] p 2373 N94-24769
Matrix fatigue cracking mechanisms of alpha(2) TMC for hypersonic applications
[NASA-TM-106506] p 2230 N94-25186
FATIGUE TESTING MACHINES
Investigation of the effects of manufacturing variations and materials on fatigue crack detection methods in gear teeth
[NASA-CR-195093] p 2373 N94-24769
FATIGUE TESTS
Optimization of laminate orientation to enhance failure properties
[ISBN-0-315-83539-7] p 2227 N94-22892
Development of a damage tolerance tool to analyze multiple-site damage in aircraft structure
p 2157 N94-24261
Application of fault detection techniques to spiral bevel gear fatigue data
[NASA-TM-106467] p 2364 N94-24483
FAULT DETECTION
Real-time automated failure identification in the Control Center Complex (CCC) p 2272 N94-23892
Long term trending of engineering data for the Hubble Space Telescope p 2516 N94-23942
GenSAA: A tool for advancing satellite monitoring with graphical expert systems p 2516 N94-23945
System for Anomaly and Failure Detection (SAFD) system development
[NASA-CR-193907] p 2372 N94-24174
Application of fault detection techniques to spiral bevel gear fatigue data
[NASA-TM-106467] p 2364 N94-24483
The CEBAF beam loss sensors
[CEBAF-PR-93-032] p 2540 N94-24662
Develop advanced nonlinear signal analysis topographical mapping system
[NASA-CR-194785] p 2389 N94-24856
Fault detection in HVAC systems using fuzzy models
[OUEL-1977/93] p 2373 N94-25475
FAULT TOLERANCE
Distributed Operating Systems and Mach. Proceedings of the Spring 1992 Graduate Seminar on Distributed Systems
[PB93-224905] p 2449 N94-23103
Towards the formal specification of the requirements and design of a processor interface unit: HOL listings
[NASA-CR-191465] p 2466 N94-23252
Fault tolerant onboard packet switch architecture for communication satellites: Shared memory per beam approach
[NASA-TM-106397] p 2201 N94-23567

Operations concepts for Mars missions with multiple mobile spacecraft p 2501 N94-23852
Galileo spacecraft anomaly and safing recovery p 2207 N94-23864
Towards the formal verification of the requirements and design of a processor interface unit [NASA-CR-4522] p 2467 N94-24075
Towards the formal specification of the requirements and design of a processor interface unit [NASA-CR-4521] p 2467 N94-24463
Parametric uncertainty reduction in robust multivariable control [AD-A273412] p 2460 N94-24927
Future space transportation system architecture avionics requirements p 2162 N94-25098
Advanced Information Processing System (AIPS) p 2165 N94-25115
Design and implementation of a distributed version of the NASA Engine Performance Program [NASA-CR-194475] p 2462 N94-25179
Appendix A: Proposed statement of work, 1994 p 2272 N94-25194

FAULT TREES
An automated tool to facilitate code translation for software fault tree analysis [AD-A273205] p 2457 N94-24556

FEASIBILITY
Feasibility study of an automatic vehicle for planetary exploration p 2369 N94-23399

FEASIBILITY ANALYSIS
Precipitation measurement using SIR-C: A feasibility study [NASA-CR-195104] p 2409 N94-24048
VLCT-13: A commercial transport for the 21st Century [NASA-CR-195492] p 2181 N94-24803

FEEDBACK
Active probing of plasma edge turbulence and feedback studies on the Texas Experimental Tokamak (TEXT) [DE94-001017] p 2548 N94-22945
Data analysis and theoretical studies of the upper mesosphere and lower thermosphere [NASA-CR-195108] p 2402 N94-24089
A mixed map/variable structure observer for target tracking p 2157 N94-24263
The effects of optical feedback on polarization of vertical cavity surface emitting lasers [AD-A273728] p 2351 N94-25445

FEEDBACK CONTROL
Nonlinear state space H(sub infinity) control theory [MEMO-1119] p 2469 N94-22706
Feedback linearization of parametrized nonlinear time-varying systems [MEMO-1126] p 2470 N94-22714
A CDMA synchronisation scheme p 2285 N94-22810
Microstrip monopulse antenna for land mobile communications p 2289 N94-22833
Link monitor and control operator assistant: A prototype demonstrating semiautomated monitor and control p 2292 N94-23267
Adaptive nonlinear polynomial neural networks for control of boundary layer/structural interaction [NASA-CR-189645] p 2525 N94-23698
The effects of spatially displaced visual feedback on remote manipulator performance p 2436 N94-24201
Discrete-time H(infinity) control problem with strictly proper measurement feedback [NASA-CR-195089] p 2473 N94-24542
Robust stability of second-order systems [NASA-CR-195175] p 2488 N94-24564
Autonomous Space Processor for Orbital Debris (ASPOD) [NASA-CR-195521] p 2204 N94-24621
Design of central control system for Large Helical Device (LHD) [NIFS-258] p 2553 N94-24623
Controlled invariance of nonlinear systems: Nonexact forms speak louder than exact forms [PB93-237790] p 2475 N94-24755
Genericity of stabilizability for time-delay systems [PB93-237725] p 2475 N94-24762
Preliminary results on time-varying feedback stabilization of a nonholonomic car-like mobile robot [INRIA-RR-1512] p 2475 N94-24963
High speed electronic analog computers using low-gain amplifiers [AD-D015974] p 2446 N94-25034
Active control of oscillatory lift forces on a circular cylinder [AD-A273243] p 2338 N94-25140
Feedback control laws for highly maneuverable aircraft [NASA-CR-195195] p 2190 N94-25176
Stability questions in predictive control [OUEL-1970/93] p 2477 N94-25469

FEEDFORWARD CONTROL
Beam-waveguide antenna servo design issues for tracking low earth-orbiting satellites p 2292 N94-23268
Evolving neural network connectivity [AD-A273134] p 2490 N94-24921
Development of programmable artificial neural networks p 2477 N94-25370

FELDSPARS
Lunar mare volcanism: Mixing of distinct, mantle source regions with KREEP-like component p 2615 N94-24370

FEMALES
Women scientists and engineers employed in industry: Why so few? A report based on a conference [ISBN-0-309-04991-1] p 2585 N94-24698

FERMI SURFACES
Spin-polaron theory of high-T(c) superconductivity. 2: Electronic structure of the CuO2 planes [DE93-019197] p 2556 N94-22919
The de Haas-van Alphen measurements in Ba(0.6)K(0.4)BiO3 [DE93-041169] p 2556 N94-22920
A valence-fluctuation theory of cuprate superconductivity [DE94-000887] p 2558 N94-22942

FERMI-DIRAC STATISTICS
Conductors with small Fermi energies and small gap energies [DE93-040887] p 2561 N94-23432

FERMIONS
Interplay of magnetic and superconducting heavy fermion ground states [DE94-000680] p 2240 N94-23003

FERRITES
Integrated hydrometallurgical jarosite treatment [PB93-217990] p 2232 N94-22983

FERROELECTRICITY
Ferroelectric thin films 3 [AD-A273394] p 2565 N94-25027

FERROMAGNETIC MATERIALS
Review of a variational method applied to magnetoelastic buckling problems [PB94-111184] p 2562 N94-23769
Compact free electron lasers for medical applications [AD-A273609] p 2350 N94-24934
Magnetic properties of NdCo3 and its gamma phase hydride NdCo3H(4.1) [REPT-A-2655] p 2567 N94-25412

FERROMAGNETISM
Review of a variational method applied to magnetoelastic buckling problems [PB94-111184] p 2562 N94-23769
Spin fluctuations in an ordered Heisenberg ferromagnet with dipolar interactions [PB93-204493] p 2524 N94-24533

FIBER COMPOSITES
Creep deformation characteristics of ductile discontinuous fiber reinforced composites [DE94-000697] p 2227 N94-23005
Development of silicon nitride composites with continuous fiber reinforcement [DE94-001996] p 2227 N94-23022
High surface area, low weight composite nickel fiber electrodes p 2391 N94-23351
Composite material impregnation unit [NASA-TM-107751] p 2254 N94-23486
Selection of polymer binders and fabrication of SiC fiber-reinforced reaction-bonded silicon nitride matrix composites [NASA-CR-194874] p 2255 N94-24223
Micromechanical characterization of ceramic-matrix composites using the instrumented microindentation technique p 2256 N94-24233
Role of interfaces on the cyclic fatigue behaviour of ceramic matrix composites p 2256 N94-24234
Structural design criteria for filament-wound composite shells [NASA-CR-195125] p 2229 N94-24402
Crashworthiness analysis using advanced material models in DYNA3D [DE94-002988] p 2229 N94-24632
Fire-resistant barriers for composite materials [AD-D016014] p 2230 N94-24735
Test methods for composites: A status report. Volume 2: Compression test methods [AD-A273522] p 2230 N94-24779
Test methods for composites: A status report. Volume 1: Tension test methods [AD-A273501] p 2230 N94-24942
Test methods for composites: A status report. Volume 3: Shear test methods [AD-A273561] p 2230 N94-25163
Alternatives for reinforcement: Fiber composites [VTT-TIED-1412] p 2230 N94-25386

FIBER OPTICS
Thermoelectric cooled, purge-and-trap device for enhancing the utility of fiber optic VOC sensors [DE94-001772] p 2541 N94-22722
InGaAsP/InP based 1.3/1.55 micron vertical cavity surface emitting lasers for wavelength division multiplexed high speed distributed computing, phase 1 [AD-A271081] p 2348 N94-23123
NASA/ASEE Summer Faculty Fellowship Program [NASA-CR-194678] p 2571 N94-23230
Wide band fiber-optic communications p 2304 N94-23231
Switch configuration for migration to optical fiber network p 2447 N94-23250
Laser light scattering instrument advanced technology development [NASA-CR-194803] p 2349 N94-23286
Fiber optic temperature sensor using a Y2O2S:Eu thermographic phosphor [DE94-000331] p 2543 N94-23461
A lower bound for routing on a completely connected optical communication parallel computer [DE93-040752] p 2466 N94-23491
Intelligent Material Systems and Structures (IMSS). Part 5: Fiber optic registration of deformation in carbon laminates 91/92 [PB93-204600] p 2544 N94-23723
Measuring electrically charged particle fluxes in space using a fiber optic loop sensor [NASA-CR-191328] p 2544 N94-23829
Optimization of microscopic and macroscopic second order optical nonlinearities p 2226 N94-24354
Fiber optical angular sensor: Literature study and experimental results [PB93-204345] p 2545 N94-24529
Total light loss optic spectroscopy: Progress towards a fiber optic Raman organic vapor sensor [DE94-002545] p 2234 N94-24549
Method and apparatus for the non-invasive measurement of pressure inside pipes using a fiber optic interferometer sensor [AD-D016013] p 2344 N94-24734
Layered parallel interface for an active antenna array [AD-D016002] p 2301 N94-25045
System for cancelling phase noise in an interferometric fiber optic sensor arrangement [AD-D015994] p 2345 N94-25053
Highly-reliable fly-by-light/power-by-wire technology p 2162 N94-25099
Wide bandwidth differential amplifier [AD-D015985] p 2303 N94-25217

FIBER STRENGTH
Test methods for composites: A status report. Volume 2: Compression test methods [AD-A273522] p 2230 N94-24779

FIELD COILS
Plasma initiation in a tokamak with conducting superstructure: First results from Alcator C-MOD [DE94-001565] p 2552 N94-24504

FIELD EFFECT TRANSISTORS
Microwave analog frequency dividers: Design, modeling and realization [LAAS-93139] p 2307 N94-22909
Electrochemical sulfur passivation of visible (approximately 670nm) AlGaInP lasers [DE94-002293] p 2350 N94-24659
The 5th Engineering Foundation Conference: Advanced Heterostructure Transistors [AD-A273508] p 2312 N94-24819

FIELD EMISSION
Field emitter array memory device [AD-D016015] p 2311 N94-24736

FIELD OF VIEW
Night vision devices and characteristics p 2432 N94-23982

FIELD STRENGTH
Electromagnetic field strength prediction in an urban environment: A useful tool for the planning of LMSS p 2283 N94-22795

FIELD THEORY (ALGEBRA)
Off-critical W(infinity) and Virasoro algebras as dynamical symmetries of the integrable models [DE93-633215] p 2478 N94-22969
Applications of supersymmetric quantum mechanics [ETN-94-95385] p 2570 N94-25257

FIELD THEORY (PHYSICS)
On spontaneous symmetry breaking mechanism in light-front quantized field theory [DE93-633211] p 2568 N94-22968
Coadjoint orbits and conformal field theory [DE94-002285] p 2523 N94-24658
Super Beltrami differentials and N equal to 4 superconformal anomalies [DE93-613047] p 2491 N94-25166
Cosmic wake fields [DE93-616849] p 2604 N94-25215

Phase structure of the two-dimensional phi(4) field theory within thermo-field dynamics
[DE93-616850] p 2570 N94-25337

FIGHTER AIRCRAFT
Echocardiographic findings in trained aircrew: The effect of +Gz on cardiac structure (working group 18)
p 2424 N94-23320
Advanced Capability Exhaust Systems/Integrated Product Development for advanced nozzles (ACES/IPD)
[AD-A273209] p 2189 N94-24776
Sabot high speed interceptor AE 4273 aircraft design
[NASA-CR-195495] p 2183 N94-24971
Robust, nonlinear, high angle-of-attack control design for a supermaneuverable vehicle p 2164 N94-25108
Birdstrike resistant crew enclosure program
[AD-A273700] p 2463 N94-25453

FILAMENT WINDING
Structural design criteria for filament-wound composite shells
[NASA-CR-195125] p 2229 N94-24402
Impact damage in filament wound composite bottles
p 2231 N94-24421

FILE MAINTENANCE (COMPUTERS)
Using the SPICE system to help plan and interpret space science observations p 2517 N94-23950
From requirements to acceptance tests
p 2464 N94-23962

FILM COOLING
Heat transfer in rocket combustion chambers
p 2214 N94-23051

FILM THICKNESS
The measurement of the film thickness and the roughness deformation of lubricated elastomers
[ETN-94-95293] p 2261 N94-25078

FILTRATION
Investigation of the ultrafiltration technique using military greases
[AD-A273633] p 2261 N94-25029

FINANCE
Engineering for profitability
[PNR-90990] p 2595 N94-23580

FINANCIAL MANAGEMENT
Strategies in transition p 2498 N94-23833

FINE STRUCTURE
Applications of x ray absorption fine structure to the in situ study of the effect of cobalt in nickel hydrous oxide electrodes for fuel cells and rechargeable batteries
p 2391 N94-23347
Center for advanced electrical and structural polymers
[AD-A273415] p 2259 N94-24783
Intramultiplet mixing for Ne(**)(3p)+He at superthermal energies
[ETN-94-95327] p 2538 N94-25240

FINES
Data analysis and interpretation of lunar dust exosphere p 2623 N94-25349

FINGERS
Fingered bola body, bola with same, and methods of use
[NASA-CASE-MSC-21967-1] p 2354 N94-23822

FINITE DIFFERENCE THEORY
Isolated and coupled superquadric loop antennas for mobile communications applications
p 2289 N94-22834
Field models: Their present and future application in fire safety engineering
[PB93-201622] p 2269 N94-23506
A comparative study of computational solutions to flow over a backward-facing step p 2326 N94-23670
The Sixth Copper Mountain Conference on Multigrid Methods, part 1
[NASA-CP-3224-PT-1] p 2482 N94-23673
Application of multigrid methods to the solution of liquid crystal equations on a SIMD computer
p 2484 N94-23686
Efficient interpolation of velocity and flux components defined on 2- and 3-dimensional non-cartesian grids
[PB94-118619] p 2486 N94-23757
On the dynamics of some grid adaption schemes
[NASA-CR-195092] p 2454 N94-24110
On the dynamics of approximating schemes for dissipative nonlinear equations p 2332 N94-24168
Balanced truncation is Hankel-norm optimal when used to approximate a finite-difference model of a parabolic PDE
[OUEL-1921/92] p 2492 N94-25324

FINITE ELEMENT METHOD
Texture gradient effects in tantalum
[DE94-000689] p 2240 N94-23021
A numerical analysis of crack propagation in microcracking ceramic and ceramic composites
[DE94-001192] p 2253 N94-23183
Continuum representations of cellular solids
[DE94-001706] p 2375 N94-23217
Out of plane gradients in laminated composites
[NASA-CR-194875] p 2228 N94-23566
Comparison of numerical simulation and experimental data for steam-in-place sterilization
p 2326 N94-23669
A comparative study of computational solutions to flow over a backward-facing step p 2326 N94-23670
The Sixth Copper Mountain Conference on Multigrid Methods, part 1
[NASA-CP-3224-PT-1] p 2482 N94-23673
A multigrid solver for the semiconductor equations
p 2482 N94-23674
Vectorization and parallelization of the finite strip method for dynamic Mindlin plate problems
p 2483 N94-23679
Domain decomposition methods for nonconforming finite element spaces of Lagrange-type
p 2483 N94-23680
A nonconforming multigrid method using conforming subspaces p 2485 N94-23695
Compatibility relations and the finite-element formulation of electromagnetic field problems
[PB94-110996] p 2294 N94-23727
Study of a local absorbing boundary condition for the modeling of an infinite external domain in the time-domain finite-element package FEMAXT
[PB94-111002] p 2294 N94-23728
FEMAX finite-element package for computing three-dimensional time-domain electromagnetic fields in inhomogeneous media
[PB94-111093] p 2294 N94-23733
Analysis of local delaminations caused by angle ply matrix cracks
[NASA-TM-109052] p 2228 N94-24083
On the dynamics of approximating schemes for dissipative nonlinear equations p 2332 N94-24168
Modal test of the Brazilian satellite launcher (VLS) configuration burn-out of the first stage
p 2156 N94-24257
Modeling dynamically coupled fluid-duct systems with finite line elements
[NASA-CR-193909] p 2376 N94-24359
Structural design criteria for filament-wound composite shells
[NASA-CR-195125] p 2229 N94-24402
Finite element based electric motor design optimization p 2315 N94-24411
J-integral patch for finite element analysis of dynamic fracture due to impact of pressure vessels
p 2381 N94-24429
Evaluation of advanced materials through experimental mechanics and modelling p 2374 N94-24454
Hydro-elastic analysis using a selection of commercial analysis programs
[PB94-118734] p 2376 N94-24478
Studies on the implementation of normals and curvatures. Part 1: The first or mean curvature
[DE94-001546] p 2488 N94-24503
Edge elements, their advantages and disadvantages
[PB94-111069] p 2298 N94-24593
Finite-element modelling of three-dimensional electromagnetic fields using edge and nodal elements
[PB94-111077] p 2298 N94-24597
Crashworthiness analysis using advanced material models in DYNA3D
[DE94-002988] p 2229 N94-24632
Finite-element method for computing three-dimensional electromagnetic fields in inhomogeneous media (1993)
[PB94-111101] p 2298 N94-24637
Solution of the discretized incompressible Navier-Stokes equations with iterative methods
[PB94-118635] p 2335 N94-24641
Influence of backup bearings and support structure dynamics on the behavior of rotors with active supports
[NASA-CR-195106] p 2365 N94-24751
Dynamic analysis of pretwisted elastically-coupled rotor blades
[NASA-TM-109070] p 2378 N94-24839
A finite-element-based perturbation model for the rotordynamic analysis of shrouded pump impellers: Part 1: Model development and applications
[NASA-CR-193916] p 2366 N94-24998
A finite-element-based perturbation model for the rotordynamic analysis of shrouded pump impellers: Part 2: User's guide
[NASA-CR-193917] p 2366 N94-24999
FRANC2D: A two-dimensional crack propagation simulator. Version 2.7: User's guide
[NASA-CR-4572] p 2246 N94-25118
Three-dimensional, inelastic response of single-edge notch bend specimens subjected to impact loading
[AD-A273302] p 2378 N94-25143
NASA/Army rotorcraft transmission research, a review of recent significant accomplishments
[NASA-TM-106508] p 2367 N94-25181
Loading, electromyograph, and motion during exercise
p 2427 N94-25380
An adaptive streamline diffusion finite element method for hyperbolic systems in gas dynamics
[PREPRINT-688] p 2340 N94-25466

FINITE VOLUME METHOD
Local grid refinement method for the euler equations
[PB93-223329] p 2317 N94-22985
Locally modified Bott-scheme for highly convective flows
[MPIM-99] p 2400 N94-23157
An implicit numerical scheme for the simulation of internal viscous flows on unstructured grids
[NASA-TM-106437] p 2481 N94-23554
Solution of the discretized incompressible Navier-Stokes equations with iterative methods
[PB94-118635] p 2335 N94-24641

FINNED BODIES
Study of transient behavior of finned coil heat exchangers p 2321 N94-23642

FINS
Solution of mixed convection heat transfer from isothermal in-line fins p 2321 N94-23644
Supersonic aerodynamic characteristics of a circular body Earth-to-Orbit vehicle
[NASA-TM-4533] p 2170 N94-24716

FIR FILTERS
Adaptive noise cancellation using recurrent radial basis function networks
[RR-472] p 2313 N94-25319

FIRE DAMAGE
Initial evaluation of burn characteristics of phenolic foam runway brake arrestor material
[DOT/FAA/CT-TN93/7] p 2253 N94-23335

FIRE EXTINGUISHERS
Extinguishment of enclosed gas fires with water sprays
[PB93-201663] p 2268 N94-23430
Extinguishment of combustible porous solids by water droplets
[PB93-198893] p 2270 N94-23740
Dispersion of fire suppression agents discharged from high pressure vessels: Establishing initial/boundary conditions for the flow outside the vessel
[PB94-103660] p 2172 N94-23810

FIRE FIGHTING
Extinguishment of enclosed gas fires with water sprays
[PB93-201663] p 2268 N94-23430

FIRE PREVENTION
Fire safety engineering research in Norway
[PB93-201630] p 2268 N94-23429
Extinguishment of enclosed gas fires with water sprays
[PB93-201663] p 2268 N94-23430
Impacts: NIST Building and Fire Research Laboratory (technical and societal)
[PB94-113420] p 2270 N94-23737
Dispersion of fire suppression agents discharged from high pressure vessels: Establishing initial/boundary conditions for the flow outside the vessel
[PB94-103660] p 2172 N94-23810
Full-scale fire testing of seat component materials
[AD-A273499] p 2174 N94-24941
Collaborating with our customers: NIST building and fire research laboratory
[PB94-110194] p 2272 N94-24955

FIREBALLS
Neutron star mergers and gamma-ray bursts
[NASA-CR-195176] p 2629 N94-25091

FIRES
Development and experimental validation of computational methods to simulate abnormal thermal and structural environments
[DE94-000554] p 2268 N94-23000
Fire safety engineering research in Norway
[PB93-201630] p 2268 N94-23429
Extinguishment of enclosed gas fires with water sprays
[PB93-201663] p 2268 N94-23430
The ignition temperature of solid explosives exposed to a fire
[DE94-001047] p 2265 N94-23436
Field models: Their present and future application in fire safety engineering
[PB93-201622] p 2269 N94-23506
Zone fire modeling with natural building flows and a zero order shaft model
[PB94-112166] p 2270 N94-23735
Impacts: NIST Building and Fire Research Laboratory (technical and societal)
[PB94-113420] p 2270 N94-23737
Full-scale fire testing of seat component materials
[AD-A273499] p 2174 N94-24941

FITTING
A multigrid solver for the semiconductor equations
p 2482 N94-23674

FIXED POINTS (MATHEMATICS)
Fixed points and shift cycles in cellular automata [RR-459] p 2492 N94-25309
FIXED WINGS
Three dimensional study of an airplane wing and its wake in the subsonic regime [ISBN-0-315-58963-9] p 2168 N94-24178
FLAME PROPAGATION
Mechanism and enhancement of flame stabilization [DE94-002181] p 2232 N94-23023
Flame trench analysis of NLS vehicles p 2199 N94-23249
Initial evaluation of burn characteristics of phenolic foam runway brake arrestor material [DOT/FAA/CT-TN93/7] p 2253 N94-23335
Fire safety engineering research in Norway [PB93-201630] p 2268 N94-23429
Calculation of flame spread on lining materials by the field model KAMELEON. Project 5 of the EUREFIC fire research programme [PB93-201614] p 2268 N94-23450
Field models: Their present and future application in fire safety engineering [PB93-201622] p 2269 N94-23506
Extinguishment of combustible porous solids by water droplets [PB93-198893] p 2270 N94-23740
Burning rate of double-base propellant in the presence of plasma p 2155 N94-24252
Transient phenomena in laminar spray combustion p 2160 N94-24282
Study of streamwise vorticity-stirred combustion [NASA-CR-194450] p 2234 N94-24565
FLAME RETARDANTS
Initial evaluation of burn characteristics of phenolic foam runway brake arrestor material [DOT/FAA/CT-TN93/7] p 2253 N94-23335
Extinguishment of combustible porous solids by water droplets [PB93-198893] p 2270 N94-23740
Fire-resistant barriers for composite materials [AD-D016014] p 2230 N94-24735
The effects of zinc borate addition on the flammability characteristics of polyester, vinyl ester, and epoxy glass reinforced plastics [AD-A273164] p 2262 N94-25136
FLAME STABILITY
Mechanism and enhancement of flame stabilization [DE94-002181] p 2232 N94-23023
Flames in dusty mixtures: Their structure and stability [NASA-CR-191567] p 2317 N94-23089
Transient phenomena in laminar spray combustion p 2160 N94-24282
Modelling of premixed laminar flames [ETN-94-95317] p 2236 N94-25284
FLAME TEMPERATURE
Evaluation of reducing gas turbine emissions through hydrogen-enhanced steam-injected combustion [PB94-109873] p 2187 N94-23709
FLAMES
Flames in dusty mixtures: Their structure and stability [NASA-CR-191567] p 2317 N94-23089
Numerical solution of flame sheet problems with and without multigrid methods p 2237 N94-23683
A transport equation for the scalar dissipation in reacting flows with variable density: First results p 2331 N94-24157
FLAMMABILITY
Initial evaluation of burn characteristics of phenolic foam runway brake arrestor material [DOT/FAA/CT-TN93/7] p 2253 N94-23335
Calculation of flame spread on lining materials by the field model KAMELEON. Project 5 of the EUREFIC fire research programme [PB93-201614] p 2268 N94-23450
Impacts: NIST Building and Fire Research Laboratory (technical and societal) [PB94-113420] p 2270 N94-23737
Full-scale fire testing of seat component materials [AD-A273499] p 2174 N94-24941
The effects of zinc borate addition on the flammability characteristics of polyester, vinyl ester, and epoxy glass reinforced plastics [AD-A273164] p 2262 N94-25136
FLAPPING
Lift augmentation on a delta wing via leading edge fences and the Gurney flap [NASA-CR-194793] p 2168 N94-24103
Reduction of structural loads using maneuver load control on the Advanced Fighter Technology Integration (AFTI)/F-111 mission adaptive wing [NASA-TM-4526] p 2166 N94-24295
FLASHING (VAPORIZING)
An extended laser flash technique for thermal diffusivity measurement of high-temperature materials p 2238 N94-25132
Microwave techniques for physical property measurements p 2238 N94-25134
FLAT PLATES
Efficiency and reliability enhancements in propulsion flowfield modeling p 2215 N94-23055
Multigrid methods for a semilinear PDE in the theory of pseudoplastic fluids p 2341 N94-23689
Relationship between transition and modes of instability in supersonic boundary layers [NASA-CR-4562] p 2336 N94-24725
FLATTENING
Linear algorithm for flattening list graphs [PB93-220648] p 2448 N94-23097
FLAVOR (PARTICLE PHYSICS)
Flavor changing strings and domain walls [DE93-633217] p 2532 N94-22970
Heavy flavour physics at LEP [NIKHEF-H/92-19] p 2539 N94-25465
FLEXIBILITY
Modelling the Shuttle Remote Manipulator System: Another flexible model p 2371 N94-25350
FLEXIBLE BODIES
Ulysses log 1992 p 2502 N94-23863
The Columbus solar array mechanisms p 2356 N94-23994
FLEXIBLE SPACECRAFT
Operating the Daisy facility to perform control experiments [ISBN-0-315-83554-0] p 2196 N94-22889
Real-time dynamics and control strategies for space operations of flexible structures [NASA-CR-194794] p 2203 N94-23618
Space Station flexible dynamics under plume impingement p 2208 N94-25383
Modeling of a large undamped space structure using time domain techniques [AD-A273828] p 2206 N94-25523
FLEXING
Inverse dynamics of a rigid rod system as a simplified model of flexible beam p 2160 N94-24281
FLIGHT CHARACTERISTICS
Identification of integrated airframe: Propulsion effects on an F-15 aircraft for application to drag minimization [NASA-TM-4532] p 2188 N94-24106
Aircraft maneuvers for the evaluation of flying qualities and agility. Volume 2: Maneuver descriptions and section guide [AD-A273685] p 2185 N94-25440
FLIGHT CLOTHING
Physiological protection for aircrew at high altitudes: A review of the literature [DCIEM-93-13] p 2432 N94-24114
Operation Friction: Development and introduction of personal cooling for CH124 Sea King aircrew [DCIEM-93-06] p 2433 N94-24119
FLIGHT CONDITIONS
Identification of integrated airframe: Propulsion effects on an F-15 aircraft for application to drag minimization [NASA-TM-4532] p 2188 N94-24106
Aviation Weather Program (AWP) p 2411 N94-24380
FLIGHT CONTROL
Commonality of flight control systems for support of European telecommunications missions p 2304 N94-23834
Magellan spacecraft and memory state tracking: Lessons learned, future thoughts p 2207 N94-23865
A real-time navigation monitoring expert system for the Space Shuttle Mission Control Center p 2202 N94-23921
Cockpit control system conceptual design [NASA-CR-195543] p 2190 N94-24551
Pilot-vehicle interface handbook, chapter 19. Volume 2: Digital systems validation [DOT/FAA/CT-88/10-VOL-2] p 2438 N94-24830
Cockpit control system [NASA-CR-195488] p 2190 N94-24957
Aircraft digital flight control technical review p 2163 N94-25106
Robust, nonlinear, high angle-of-attack control design for a supermaneuverable vehicle p 2164 N94-25108
Flight controller design using mixed H2/H infinity optimization with a singular H infinity constraint [AD-A273831] p 2191 N94-25525
FLIGHT CREWS
Echocardiographic screening of aircrew candidates p 2424 N94-23319
Echocardiographic findings in trained aircrew: The effect of +Gz on cardiac structure (working group 18) p 2424 N94-23320
Left ventricular hypertrophy and athlete's heart p 2424 N94-23321
Aortic valve disease p 2424 N94-23322
Aeromedical implications of mitral valve prolapse p 2424 N94-23323
Asthma in aircrew p 2425 N94-23327
Arterial hypertension and the aviator p 2425 N94-23328
Perception in flight: Shape and motion perception, space perception, spatial orientation, and visual vestibular interaction p 2429 N94-23979
New Advances in Mission Planning and Rehearsal Systems [AGARD-LS-192] p 2521 N94-25008
Human factors of mission planning systems: Theory and concepts p 2521 N94-25010
Human factors of mission planning systems: Applications and implementation p 2522 N94-25011
Ground based mission planning systems p 2522 N94-25014
Mission rehearsal in the SOF-ATS program p 2522 N94-25016
Birdstrike resistant crew enclosure program [AD-A273700] p 2463 N94-25453
Image processing for flight crew enhanced situation awareness p 2442 N94-25508
FLIGHT ENVELOPES
S-2E Tracker maritime patrol aircraft re-engine and system upgrade program p 2158 N94-24270
Robust, nonlinear, high angle-of-attack control design for a supermaneuverable vehicle p 2164 N94-25108
FLIGHT HAZARDS
Close-up analysis of inflight ice accretion [NASA-TM-106457] p 2172 N94-23523
Perception in flight: Shape and motion perception, space perception, spatial orientation, and visual vestibular interaction p 2429 N94-23979
Aircraft accident report: In-flight engine separation. Japan Airlines, Inc., flight 46E, Boeing 747-121, N473EV, Anchorage, Alaska, 31 March 1993 [PB93-410407] p 2173 N94-24062
Aviation Weather Program (AWP) p 2411 N94-24380
FLIGHT INSTRUMENTS
Pilot-vehicle interface [DOT/FAA/CT-92/21] p 2430 N94-23083
Distributed science operations for JPL planetary missions p 2500 N94-23850
Evaluation of the UH-1N instrument panel [AD-A273145] p 2186 N94-24774
FLIGHT MANAGEMENT SYSTEMS
Mission operations and command assurance: Instilling quality into flight operations p 2374 N94-23932
Appendix A: Proposed statement of work, 1994 p 2272 N94-25194
FLIGHT MECHANICS
The influence of elastic pitch variations on helicopter flight mechanics p 2161 N94-24286
FLIGHT OPERATIONS
OASIS-CC presentation p 2385 N94-23613
Radioastron flight operations p 2502 N94-23861
A MOS for all seasons p 2505 N94-23879
An operations concept methodology to achieve low-cost mission operations p 2505 N94-23880
Object-oriented technologies in a multi-mission data system p 2506 N94-23885
The FOT tool kit concept p 2507 N94-23889
GSMS and space views: Advanced spacecraft monitoring tools p 2507 N94-23890
The application of total quality management principles to spacecraft mission operations p 2374 N94-23931
Mission operations and command assurance: Instilling quality into flight operations p 2374 N94-23932
Operational training for the mission operations at the Brazilian National Institute for Space Research (INPE) p 2429 N94-23933
Security aspects of space operations data p 2515 N94-23937
Using SFOC to fly the Magellan Venus mapping mission p 2516 N94-23941
Expert diagnostics system as a part of analysis software for power mission operations p 2516 N94-23944
The evolving trend in spacecraft health analysis p 2202 N94-23946
An engineering database management system for spacecraft operations p 2517 N94-23951
Multimission image processing and science data visualization p 2518 N94-23955
Engineering workstation: Sensor modeling p 2441 N94-25500
FLIGHT PATHS
Multiple-camera/motion stereoscopy for range estimation in helicopter flight p 2441 N94-25505
FLIGHT PLANS
Aviation Weather Program (AWP) p 2411 N94-24380
In flight mission planning in the Copilote Electronique p 2522 N94-25015
FLIGHT SAFETY
Canadian aeronautical mobile data trials p 2279 N94-22773

Cockpit weather graphics using mobile satellite communications p 2280 N94-22775

Aircraft accident report: Inadvertent in-flight slat deployment, China Eastern Airlines Flight 583, McDonnell Douglas MD-11, B-2171, 950 nautical miles south of Shemya, Alaska, 6 April 1993
[PB93-910408] p 2172 N94-23579

An analytic study of a two-phase laminar airfoil in simulated heavy rain p 2171 N94-23661

Aircraft accident report: In-flight engine separation. Japan Airlines, Inc., flight 46E, Boeing 747-121, N473EV, Anchorage, Alaska, 31 March 1993
[PB93-410407] p 2173 N94-24062

Aircraft flight safety: A bibliography
[AGARD-R-805] p 2173 N94-24091

Aviation Weather Program (AWP)
p 2411 N94-24380

A numerical study of airplanes flying in proximity
[AD-A273373] p 2173 N94-24718

Projected effectiveness of airbag supplemental restraint systems in US Army helicopter cockpits
[AD-A273250] p 2174 N94-25141

Aircraft accident/incident summary report: Controlled flight into terrain GP Express Airlines, Inc., N115GP Beechcraft C-99, Shelton, Nebraska, 28 April 1993
[PB94-910401] p 2174 N94-25273

Multiple-camera/motion stereoscopy for range estimation in helicopter flight p 2441 N94-25505

FLIGHT SIMULATION

Transfer of perceptual adaptation to space sickness: What enhances an individual's ability to adapt?
[NASA-CR-188256] p 2427 N94-24227

Pre-design study of a general purpose vehicle simulator platform
[PB93-215366] p 2193 N94-24739

Mission rehearsal in the SOF-ATS program
p 2522 N94-25016

Future directions in flight simulation: A user perspective p 2162 N94-25101

A simulation study of control and display requirements for zero-experience general aviation pilots
p 2163 N94-25102

FLIGHT SIMULATORS

Transfer of perceptual adaptation to space sickness: What enhances an individual's ability to adapt?
[NASA-CR-188256] p 2427 N94-24227

Pilot evaluation system p 2158 N94-24266

Pre-design study of a general purpose vehicle simulator platform
[PB93-215366] p 2193 N94-24739

Mission rehearsal in the SOF-ATS program
p 2522 N94-25016

Future directions in flight simulation: A user perspective p 2162 N94-25101

A simulation study of control and display requirements for zero-experience general aviation pilots
p 2163 N94-25102

FLIGHT STABILITY TESTS

Roles, uses, and benefits of general aviation aircraft in aerospace engineering education
[NASA-TM-106463] p 2153 N94-24100

FLIGHT SURGEONS

Cardiopulmonary Aspects in Aerospace Medicine
[AGARD-LS-189] p 2423 N94-23313

Cardiovascular and pulmonary disease in NATO aircrew: An overview p 2423 N94-23314

Aeromedical disposition of Arrhythmias and electrocardiographic findings in aircrew
p 2423 N94-23318

FLIGHT TESTS

Roles, uses, and benefits of general aviation aircraft in aerospace engineering education
[NASA-TM-106463] p 2153 N94-24100

Comparison of c.t.s. based prediction of store trajectory with flight test data p 2158 N94-24268

Reduction of structural loads using maneuver load control on the Advanced Fighter Technology Integration (AFTI)/F-111 mission adaptive wing
[NASA-TM-4526] p 2168 N94-24295

Trends of design methodology of airframe
p 2179 N94-24327

Doppler global velocimetry: Development of a flight research instrumentation system for application to non-intrusive measurements of the flow field
[NASA-CR-191490] p 2344 N94-24360

Determination of the stability and control derivatives of the NASA F/A-18 HARV using flight data
[NASA-CR-194838] p 2190 N94-24804

Development of high-angle-of-attack nose-down pitch control margin design guidelines for combat aircraft
p 2164 N94-25107

X-31 aerodynamic characteristics determined from flight data p 2164 N94-25109

Aircraft accident/incident summary report: Controlled flight into terrain GP Express Airlines, Inc., N115GP Beechcraft C-99, Shelton, Nebraska, 28 April 1993
[PB94-910401] p 2174 N94-25273

Aircraft maneuvers for the evaluation of flying qualities and agility. Volume 2: Maneuver descriptions and section guide
[AD-A273685] p 2185 N94-25440

Synthetic vision system flight test results and lessons learned p 2429 N94-25492

FLIGHT TIME

General aviation activity survey
[AD-A273284] p 2162 N94-24923

FLIGHT TRAINING

Pilot evaluation system p 2158 N94-24266

Mission rehearsal in the SOF-ATS program
p 2522 N94-25016

FLIR DETECTORS

Infrared sensors and systems for enhanced vision/autonomous landing applications
p 2439 N94-25491

FLOATING

Survival suit for submarine personnel: Summary of evaluation studies
[PB93-204634] p 2430 N94-23743

FLOODS

Urban/rural application of weather radar for flow forecasting. Proceedings of the Informal CEc -Workshop
[PB93-220135] p 2407 N94-23129

FLOORS

A study of the core module simulator floor capability
p 2380 N94-24418

FLOW CHARACTERISTICS

CFD analyses of coolant channel flowfields
p 2214 N94-23050

Heat transfer in rocket combustion chambers
p 2214 N94-23051

Polyimide processing additives
[NASA-CASE-LAR-13669-2] p 2252 N94-23079

Analysis of high vacuum systems using SINDA'85
p 2322 N94-23648

Mixing and unmixedness in plasma jets 1: Near-field analysis p 2323 N94-23655

Supersonic minimum length nozzle design for dense gases p 2171 N94-23656

Toward large eddy simulation of turbulent flow over an airfoil p 2172 N94-24150

Aerodynamic characteristics and pressure distributions for an executive-jet baseline airfoil section
[NASA-TM-4529] p 2169 N94-24586

FLOW DISTORTION

Local isotropy in distorted turbulent boundary layers at high Reynolds number p 2332 N94-24166

FLOW DISTRIBUTION

Small rocket flowfield diagnostic chambers
p 2210 N94-23030

Laser diagnostics for small rockets
p 2210 N94-23032

CFD analyses of combustor and nozzle flowfields
p 2210 N94-23033

An experimental study of characteristic combustion-driven flows for CFD validation
p 2212 N94-23040

Numerical investigation of two- and three-dimensional heat transfer in expander cycle engines
p 2213 N94-23048

CFD analyses of coolant channel flowfields
p 2214 N94-23050

Heat transfer in rocket combustion chambers
p 2214 N94-23051

Efficiency and reliability enhancements in propulsion flowfield modeling p 2215 N94-23055

Computation of propulsion-related flowfields using unstructured adaptive meshes p 2215 N94-23056

Dual-bell altitude compensating nozzles
p 2215 N94-23057

An experimental study of the flow field surrounding a subsonic jet in a cross flow
[NASA-CR-194770] p 2317 N94-23072

Flow quality studies of the NASA Lewis Research Center Icing Research Tunnel diffuser
[NASA-TM-106311] p 2192 N94-23091

A new experimental apparatus for the study of the unsteady flowfield over an airfoil in pitching and heaving motions using laser Doppler anemometry
[ISL-CO-229/92] p 2165 N94-23149

LDA measurements of the unsteady near wake behind an airfoil undergoing transient and periodic pitching motions
[ISL-CO-215/92] p 2165 N94-23161

Atmospheric flow in heterogeneous vegetated regions
[W-9303] p 2401 N94-23175

Measurements and modeling of flow structure in the wake of a low profile wishbone vortex generator
[NASA-TM-106468] p 2166 N94-23465

The 3-D CFD modeling of gas turbine combustor-integral bleed flow interaction p 2189 N94-23658

Numerical analysis of a vortex controlled diffuser
p 2324 N94-23659

The 3-D numerical study of airflow in the compressor/combustor prediffuser and dump diffuser of an industrial gas turbine p 2324 N94-23660

A multilevel adaptive projection method for unsteady incompressible flow p 2341 N94-23690

Estimation of delays and emissions at four-way junctions with different forms of regulation, principally four-way mandatory stop
[PB94-105236] p 2398 N94-23813

Toward large eddy simulation of turbulent flow over an airfoil p 2172 N94-24150

A large eddy simulation scheme for turbulent reacting flows p 2330 N94-24154

A transport equation for the scalar dissipation in reacting flows with variable density: First results
p 2331 N94-24157

On streak spacing in wall-bounded turbulent flows
p 2331 N94-24159

Ethylene trace-gas techniques for high-speed flows
[NASA-TM-106491] p 2169 N94-24335

The radiated noise from isotropic turbulence revisited
[NASA-CR-191547] p 2333 N94-24356

Doppler global velocimetry: Development of a flight research instrumentation system for application to non-intrusive measurements of the flow field
[NASA-CR-191490] p 2344 N94-24360

Validation of a nonintrusive optical technique for the measurement of liquid mass distribution in a two-phase spray p 2548 N94-24420

HYPULSE combustor analysis
[NASA-CR-191579] p 2336 N94-24771

Flow and temperature distribution in a naturally stratified thermal storage tank
[AD-A273511] p 2336 N94-24821

Thermophysical property sensitivity effects in steel solidification p 2246 N94-25122

Sub-sonic flow about a slender profile in a tunnel having perforated walls
[AD-A273184] p 2170 N94-25137

Hydrodynamics of stirred gas-liquid dispersions
[ETN-94-95368] p 2339 N94-25254

Study of the blade/vortex interaction: Acoustics, aerodynamics and models
[ISL-R-104/92] p 2340 N94-25463

FLOW EQUATIONS

Atmospheric flow in heterogeneous vegetated regions
[W-9303] p 2401 N94-23175

An implicit numerical scheme for the simulation of internal viscous flows on unstructured grids
[NASA-TM-106437] p 2481 N94-23554

A dual reciprocal boundary element formulation for viscous flows p 2325 N94-23666

Numerical solution of flame sheet problems with and without multigrid methods p 2237 N94-23683

Energy and maximum norm estimates for nonlinear conservation laws
[NASA-CR-195091] p 2569 N94-24109

New features in Computational Fluid Dynamics (CFD) technology at the TASHAN Engineering Center at IAI
p 2155 N94-24249

Simulation of cryogenic turbopump annular seals
p 2371 N94-24440

Conservation equations for reacting gas flow
[PB94-111168] p 2334 N94-24574

FLOW GEOMETRY

Simplified, inverse, ejector design tool
[NASA-CR-194438] p 2166 N94-23511

Optimization of orifice geometry for cross-flow mixing in a cylindrical duct
[NASA-TM-106436] p 2481 N94-23593

The 3-D numerical study of airflow in the compressor/combustor prediffuser and dump diffuser of an industrial gas turbine p 2324 N94-23660

Multi-grid domain decomposition approach for solution of Navier-Stokes equations in primitive variable form
p 2341 N94-23693

FLOW MEASUREMENT

Measurement of kinematically unstationary separated flows p 2315 N94-22854

An experimental study of characteristic combustion-driven flows for CFD validation
p 2212 N94-23040

Probe shapes that measure time-averaged streamwise momentum and cross-stream turbulence intensity
[NASA-CASE-ARC-11934-1] p 2317 N94-23077

Flow quality studies of the NASA Lewis Research Center Icing Research Tunnel diffuser
[NASA-TM-106311] p 2192 N94-23091

Measurements and modeling of flow structure in the wake of a low profile wishbone vortex generator
[NASA-TM-106468] p 2166 N94-23465

On the determination of local instantaneous averages in particulate flow measurements p 2325 N94-23663
Vortical structure in a forced plane mixing layer p 2331 N94-24162
Joint Acoustic Propagation Experiment (JAPE-91) Workshop [NASA-CP-3231] p 2526 N94-24207
Measurement of the volume mass by spontaneous Raman scattering. Study of turbulent fluctuations of mixing in a subsonic free jet. Measurements in supersonic wind tunnels [ISL-R-102/92] p 2339 N94-25462

FLOW STABILITY
Performance assessment of low pressure nuclear thermal propulsion p 2217 N94-23070
An F2D analysis of the Flow Instability Test (FIT) experiment [DE94-001420] p 2217 N94-23193
Numerical simulation of non-Newtonian free shear flows p 2331 N94-24160
Transition to turbulence in an elliptic vortex p 2331 N94-24161
Stability of hypersonic flow of a detonable gas mixture in the stagnation region of a blunt body and a forward facing step p 2154 N94-24248
Implementation of the Baldwin-Barth turbulence model into the ZETA code and its diagnosis [NASA-CR-194795] p 2335 N94-24640
Analysis and characteristics of compressor stall precursor signals in forward and AFT swept high speed compressor [AD-A273620] p 2171 N94-25517

FLOW VELOCITY
Computational Fluid Dynamics (CFD) applications in rocket propulsion analysis and design p 2214 N94-23054
Two stage turbine for rockets p 2215 N94-23059
Interpretation of discrepancies in mass spectroscopy data obtained from different experimental configurations p 2237 N94-23245
Measurements and modeling of flow structure in the wake of a low profile wishbone vortex generator [NASA-TM-106468] p 2166 N94-23465
Studies of two phase flow [NASA-CR-195099] p 2267 N94-23594
On the determination of local instantaneous averages in particulate flow measurements p 2325 N94-23663

FLOW VISUALIZATION
Image processing for acquisition of fluid rest time in the running of an artificial heart valve p 2316 N94-22858
A photogrammetric solution to a particular problem [NASA-TP-3415] p 2381 N94-22961
Image analysis applications to mixing phenomena and turbulent dispersions [ECL-92-29] p 2317 N94-22971
Flow visualization study in high aspect ratio cooling channels for rocket engines p 2213 N94-23049
Experimental investigation of generic three-dimensional sidewall-compression scramjet inlets at Mach 6 in tetrafluoromethane [NASA-TM-4497] p 2319 N94-23339
Shock-induced turbulent flow in baffle systems [DE94-001532] p 2319 N94-23470
Leading-edge votex-system details obtained on F-106B aircraft using a rotating vapor screen and surface techniques [NASA-TP-3374] p 2166 N94-23512
Effect of delta tabs on mixing and axis switching in jets from asymmetric nozzles [NASA-TM-106450] p 2167 N94-23592
Simulation of unsteady flows through stator and rotor blades of a gas turbine using the Chimera method p 2323 N94-23652
Stretch-induced quenching in flame-vortex interactions p 2237 N94-24156
Study of streamwise vorticity-stirred combustion [NASA-CR-194450] p 2234 N94-24565
Implementation of the Baldwin-Barth turbulence model into the ZETA code and its diagnosis [NASA-CR-194795] p 2335 N94-24640
Interactive control in turbulent shear layers [AD-A273544] p 2336 N94-24793
Forces on an oscillating cylinder and related fluid flow phenomena [ISBN-9-09-005589-4] p 2338 N94-25243
High lift aerodynamics [NASA-CR-195183] p 2184 N94-25268

FLUE GASES
Reburning rich-lean kinetics [PB93-220887] p 2232 N94-23100
Flue gas cleaning by pulse corona streamer [EUT-93-E-272] p 2268 N94-23174

FLUENCE
Effect of irradiation on the stress corrosion cracking behavior of Alloy X-750 and Alloy 625 [DE94-001759] p 2244 N94-23792
Experimental characterization of the AFIT Neutron Facility [AD-A273822] p 2539 N94-25519

FLUID DYNAMICS
Activities report to NATO [ETN-94-95047] p 2318 N94-23227
Design of a surface deformation measuring instrument for the Surface Tension Driven Convection Experiment (STDCE-2) [NASA-CR-194758] p 2343 N94-23285
Mathematical addenda to Hopper's model of plane stokes flow driven by capillarity on a free surface [PB93-237691] p 2480 N94-23438
Modeling of PCG fluid dynamics: Salient results p 2224 N94-24345
Development and validation of RNG methodology for compressible turbulence [AD-A273469] p 2337 N94-24929
Center for Analysis of Heterogeneous and Nonlinear Media [AD-A273515] p 2230 N94-25158
Transient flows occurring during the accelerated crucible rotation technique [DE93-617049] p 2567 N94-25422
Automatic pressure control system for the Wright Laboratory Compressor Research Facility [AD-A273827] p 2194 N94-25522

FLUID FILLED SHELLS
Coupled frequencies of a hydroelastic rectangular system [LRT-WE-9-FB-4-1992] p 2375 N94-23196

FLUID FILMS
Foil bearing research at Penn State p 2215 N94-23058
A technique to measure rotordynamic coefficients in hydrostatic bearings p 2215 N94-23061
Thermohydrodynamic analysis of cryogenic liquid turbulent flow fluid film bearings [NASA-CR-194869] p 2363 N94-24081
Surface-induced static undulations in multilayer films of liquid-crystalline polymers [AD-A273517] p 2262 N94-25159

FLUID FLOW
Probe systems for measuring static pressure and turbulence intensity in fluid streams [NASA-CASE-ARC-11935-1] p 2319 N94-23306
Tracking sharp interface of two fluids by the CIP (Cubic-Interpolated Propagation) scheme [DE93-508322] p 2319 N94-23460
Numerical solution of flame sheet problems with and without multigrid methods p 2237 N94-23683
Numerical flow simulation for complete vehicle configurations [AD-A273588] p 2170 N94-24849
Electro-rheological control valve [AD-D015997] p 2367 N94-25055
The importance of properties in modeling p 2246 N94-25121
Forces on an oscillating cylinder and related fluid flow phenomena [ISBN-9-09-005589-4] p 2338 N94-25243
Transient flows occurring during the accelerated crucible rotation technique [DE93-617049] p 2567 N94-25422
Applications of the homogenization method to flow and transport in porous media [BER-9110] p 2340 N94-25467

FLUID JETS
Measurement of intact-core length of atomizing liquid jets by image deconvolution p 2210 N94-23029
Numerical parametric studies of spray combustion instability p 2212 N94-23041
Spray formation processes of impinging jet injectors p 2212 N94-23042
CFD assessment of orifice aspect ratio and mass flow ratio on jet mixing in rectangular ducts [NASA-TM-106434] p 2187 N94-24082

FLUID MECHANICS
Proceedings of Workshop on Laser Diagnostics in Fluid Mechanics and Combustion [AD-A272808] p 2347 N94-22914
Lewis Research Center R and D Facilities [NASA-TM-109400] p 2630 N94-23135
A method to simulate viscous diffusion of vorticity by convective transport of vortices at a non-solenoidal velocity [DE94-001777] p 2318 N94-23220
Tracking sharp interface of two fluids by the CIP (Cubic-Interpolated Propagation) scheme [DE93-508322] p 2319 N94-23460
The Fifth Annual Thermal and Fluids Analysis Workshop [NASA-CP-10122] p 2320 N94-23634

FLUID PRESSURE
Prediction of pressure drop in fluid tuned mounts using analytical and computational techniques p 2321 N94-23643

FLUORESCENCE
Literature study on: Remote Fraunhofer luminescence detection of algal bloom in marine environments [BCRS-92-25] p 2417 N94-23176
Monoclonal antibodies directed against surface molecules of multicell spheroids [NASA-CR-195102] p 2420 N94-23633
Infrared fluorescence studies of electronic-to-vibrational energy transfer in a Br2:NO system [AD-A273727] p 2539 N94-25443

FLUORIDES
Thermochemistry of the actinides [DE94-000895] p 2231 N94-22943

FLUORINE
A method to remove intercalates from bromine and iodine intercalated carbon fibers [NASA-TM-106443] p 2222 N94-23591
Structures of Cl(-)(H2O)(n) and F(-)(H2O)(n) (n equal to 2,3...15) clusters: Molecular dynamics computer simulations [AD-A273474] p 2537 N94-24940

FLUORO COMPOUNDS
Tribological behaviour of fluorinated resins and polyimide resins sliding over a metallic surface in liquid nitrogen p 2355 N94-23991

FLUOROCARBONS
Reactivity of ambident anions in the gas phase [PB93-232189] p 2533 N94-23713
The chemistry of particulate formation in fluorocarbon plasmas [DE94-001500] p 2552 N94-24546

FLUTTER
Aeroelastic response and stability of tiltrotors with elastically-coupled composite rotor blades [NASA-TM-108758] p 2182 N94-24953

FLUTTER ANALYSIS
Issac, Jason Cherian ses in transonic flow [NASA-CR-194837] p 2167 N94-24052

FLUX (RATE)
Solar neutrinos: Real-time experiments [ICRR-REPT-293-93-5] p 2627 N94-24962

FLUX DENSITY
Spatial and temporal variability of soil temperature, moisture and surface soil properties [NASA-CR-194109] p 2401 N94-23337
High power density proton exchange membrane fuel cells p 2393 N94-23359
High energy density aluminum-oxygen cell p 2393 N94-23363
A high performance H2-Cl2 fuel cell for space power applications p 2394 N94-23366
Research for electric energy systems [DE94-001839] p 2293 N94-23719

FLUX PINNING
Simulation of the vortex motion in the high T(c) superconductors [DE93-617138] p 2567 N94-25403

FLUX VECTOR SPLITTING
Upwind MacCormack Euler solver with non-equilibrium chemistry p 2326 N94-23672

FLY BY LIGHT CONTROL
Highly-reliable fly-by-light/power-by-wire technology p 2162 N94-25099

FOAMS
Initial evaluation of burn characteristics of phenolic foam runway brake arrestor material [DOT/FAA/CT-TN93/7] p 2253 N94-23335

FOCUSING
Reducing video frame rate increases remote optimal focus time [NASA-TM-104018] p 2431 N94-23970
An Earth observation telescope refocusing mechanism p 2359 N94-24014

FOG
Infrared sensors and systems for enhanced vision/autonomous landing applications p 2439 N94-25491

FOIL BEARINGS
Foil bearing research at Penn State p 2215 N94-23058
Foil bearings p 2371 N94-24415

FOKKER-PLANCK EQUATION
Derivation of the macroscopic rate equations for the driven diffusive Ising model at pair level of approximation [DE93-616839] p 2524 N94-25208
The anomalous transport caused by particles transverse drift [DE93-613685] p 2554 N94-25329

FOLDING STRUCTURES
Reliable redundant device for mechanisms p 2361 N94-24030

FOOD

Multigrid and cyclic reduction applied to the Helmholtz equation p 2304 N94-23676

FORCE DISTRIBUTION

Forces on an oscillating cylinder and related fluid flow phenomena [ISBN-9-09-005589-4] p 2338 N94-25243

FORCED VIBRATION

Forced vibrations of a non-viscous drop [MPIS-24/1992] p 2318 N94-23198

Identification of integrated airframe: Propulsion effects on an F-15 aircraft for application to drag minimization [NASA-TM-4532] p 2188 N94-24106

Mechanisms of droplet formation [ISBN-9-06-275765-0] p 2338 N94-25227

FORESTS

Groundtruth collection for the JPL-SAR and ERS-1 campaign in Flevoland and Veluwe, Netherlands, 1991 [PB93-230654] p 2386 N94-23755

Effect of land use change on the carbon cycle in Amazon soils [NASA-CR-195168] p 2399 N94-24853

Human impacts on soil carbon dynamics of deep-rooted Amazonian forests [NASA-CR-195127] p 2399 N94-24861

FORM FACTORS

Gauge invariance and the electromagnetic current of composite pions [DE93-040869] p 2532 N94-22952

A comparison of TSS and TRASYS in form factor calculation p 2321 N94-23638

New evaluation of hadronic contributions to the anomalous magnetic moment of charged leptons [DE93-634394] p 2536 N94-24844

FORMALDEHYDE

Design of novel catalysts for the partial oxidation of methane to methanol [PB94-114212] p 2235 N94-24920

FORMALISM

Towards the formal verification of the requirements and design of a processor interface unit [NASA-CR-4522] p 2467 N94-24075

FORTRAN

Dynamic data distributions in Vienna Fortran [NASA-CR-191575] p 2448 N94-23092

Programming in Fortran M [DE94-000541] p 2450 N94-23207

Transient Ejector Analysis (TEA) code user's guide [NASA-TM-106310] p 2186 N94-23466

FORWARD SCATTERING

Particle size measurement for the control of industrial crystallizers [PB94-119104] p 2562 N94-23766

FOSSIL FUELS

New methane chemistry synthesis of materials for reversible uptake and useful functionalization of methane [PB94-112786] p 2233 N94-23801

FOUR-WAVE MIXING

Spatiotemporal behavior and nonlinear dynamics in a phase conjugate resonator [NASA-CR-4567] p 2543 N94-23529

FOURIER ANALYSIS

On the asymptotically uniform distribution modulo 1 of extreme order statistics [MEMO-COSOR-91-38-REV] p 2493 N94-23142

FOURIER SERIES

On the Gibbs phenomenon 3: Recovering exponential accuracy in a sub-interval from a spectral partial sum of a piecewise analytic function [NASA-CR-191560] p 2480 N94-23278

Fast fourier transforms of piecewise constant functions [AD-A272648] p 2456 N94-24535

FOURIER TRANSFORMATION

Novel fringe scanning/Fourier transform method of synthetic imaging [DE93-018936] p 2542 N94-22917

Application of maximum entropy and irreducible cluster integrals to joint probability distributions for x ray structure determination [PB93-224152] p 2559 N94-23109

Wavelet multiresolution analyses adapted for the fast solution of boundary value ordinary differential equations p 2485 N94-23691

Reactivity of ambident anions in the gas phase [PB93-232189] p 2533 N94-23713

FOVEA

Evaluation of visual acuity with Gen 3 night vision goggles [NASA-TM-108792] p 2431 N94-23974

Image remapping strategies applied as protheses for the visually impaired p 2444 N94-25363

FRACTALS

Chaos and simple determinism in reversed field pinch plasmas: Nonlinear analysis of numerical simulation and experimental data [DE94-001575] p 2550 N94-23211

On the estimation of the correlation dimension and its application to radar reflector discrimination [NASA-CR-4564] p 2309 N94-23304

Fractal geometry in physics [AD-A273271] p 2523 N94-24936

Behavior of the intermittency exponents and a quark-gluon plasma formation in the heavy ion collisions [DE93-616869] p 2541 N94-25342

FRACTIONATION

Auto-metasomatism of the western lunar highlands: Result of closed system fractionation and mobilization of a KREEPy trapped liquid p 2615 N94-24367

FRACTOGRAPHY

Discontinuous phase formation and selective attack of SiC materials exposed to low oxygen partial pressure environments [DE93-040161] p 2231 N94-22933

FRACTURE MECHANICS

Fracture simulations via massively parallel molecular dynamics [DE93-040159] p 2374 N94-22871

Fundamentals of fatigue analysis [PB93-226264] p 2374 N94-23118

A numerical analysis of crack propagation in microcracking ceramic and ceramic composites [DE94-001192] p 2253 N94-23183

Stress corrosion cracking properties of 15-5PH steel p 2251 N94-23244

Feasibility study of shot-peening modeling [CTN-94-60926] p 2244 N94-24170

Micromechanical failure modes in brittle matrix composites p 2255 N94-24232

Role of interfaces on the cyclic fatigue behaviour of ceramic matrix composites p 2256 N94-24234

Fracture kinetics analysis of empirical and semi-empirical corrosion fatigue relations p 2159 N94-24277

The mechanical properties of single crystal (alpha)-Si3N4 [DE94-002632] p 2563 N94-24517

The effects of anisotropy on the nonlinear behavior of bridged cracks in long strips [NASA-CR-194453] p 2377 N94-24604

Investigation of the effects of manufacturing variations and materials on fatigue crack detection methods in gear teeth [NASA-CR-195093] p 2373 N94-24769

Environmentally assisted cracking of high strength beta titanium alloys [AD-A273598] p 2245 N94-24823

FRANC2D: A two-dimensional crack propagation simulator. Version 2.7: User's guide [NASA-CR-4572] p 2246 N94-25118

Three-dimensional, inelastic response of single-edge notch bend specimens subjected to impact loading [AD-A273302] p 2378 N94-25143

Evaluation of multiaxial fracture models for technical ceramics [ISBN-9-03-860192-1] p 2263 N94-25299

Preceedings of the 12th International Congress: Corrosion Control for Low-Cost Reliability. Volume 3A: Corrosion: Specific issues [AD-A273663] p 2251 N94-25450

FRACTURE STRENGTH

Mechanical behavior of CMCs: Crack growth resistance and creep aspects p 2256 N94-24235

Ceramic matrix composite parts design p 2256 N94-24237

Evaluation of the fracture resistance and durability of adhesive bonded joints p 2160 N94-24278

Evaluation of multiaxial fracture models for technical ceramics [ISBN-9-03-860192-1] p 2263 N94-25299

The mechanical property data base from an Air Force/Industry Cooperative Test Program on advanced aluminum alloys (7064 and CW67) [AD-A273741] p 2251 N94-25531

FRACTURES (MATERIALS)

Repair of cracked aluminum aircraft structure with composite patches p 2156 N94-24259

FRACTURING

Analysis of local delaminations caused by angle ply matrix cracks [NASA-TM-109052] p 2228 N94-24083

J-integral patch for finite element analysis of dynamic fracture due to impact of pressure vessels p 2381 N94-24429

Damage tolerance of pressurized graphite/epoxy tape cylinders under uniaxial and biaxial loading [NASA-CR-195101] p 2377 N94-24587

Elevated temperature crack propagation [NASA-TM-106490] p 2377 N94-24715

FRAGMENTATION

Optical model analyses of galactic cosmic ray fragmentation in hydrogen targets [NASA-TP-3404] p 2540 N94-23509

FRAMES

Deployable video conference table [NASA-CASE-ARC-11950-1] p 2192 N94-23310

FRAUNHOFER LINES

Literature study on: Remote Fraunhofer luminescence detection of algal bloom in marine environments [BCRS-92-25] p 2417 N94-23176

FREDHOLM EQUATIONS

Multigrid method for integral equations and automatic programs p 2464 N94-23696

FREE ATMOSPHERE

Session on modeling of radiative transfer processes p 2414 N94-24397

FREE BOUNDARIES

The characterization of reaction-convection-diffusion processes by travelling waves [MEMO-1111] p 2273 N94-22729

Bounds and asymptotic expansions for solutions of the free boundary problems related to sequential decision versions of a bioequivalence problem [AD-A273551] p 2495 N94-24560

FREE ELECTRON LASERS

Properties of the transfer matrices of deflecting magnet systems for free electron laser [DE93-508257] p 2347 N94-22922

Inverse free electron laser beat-wave accelerator research [DE94-002597] p 2349 N94-23702

Design and testing of ubitron amplifier tubes [AD-A273297] p 2311 N94-24818

Compact free electron lasers for medical applications [AD-A273609] p 2350 N94-24934

Activities of Academia Sinica [DE93-614529] p 2541 N94-25335

FREE ELECTRONS

Conductors with small Fermi energies and small gap energies [DE93-040887] p 2561 N94-23432

Excitation balances and transport in an inductively coupled plasma [ETN-94-95330] p 2554 N94-25241

FREE ENERGY

Application of multigrid methods to the solution of liquid crystal equations on a SIMD computer p 2484 N94-23686

Free energy profiles for Li(+) and I(-) ions approaching Pt(100) surface: A molecular dynamics study [AD-A273455] p 2536 N94-24675

Thermophysical properties of simple liquid metals: A brief review of theory p 2248 N94-25130

FREE FLOW

Effect of delta tabs on mixing and axis switching in jets from asymmetric nozzles [NASA-TM-106450] p 2167 N94-23592

New concepts for Reynolds stress transport equation modeling of inhomogeneous flows p 2171 N94-24143

Measurements of the influence of integral length scale on stagnation region heat transfer [NASA-TM-106503] p 2338 N94-25183

FREE MOLECULAR FLOW

Prediction of three sigma maximum dispersed density for aerospace applications p 2207 N94-23654

FREE RADICALS

Design of a vehicle based system to prevent ozone loss [NASA-CR-195498] p 2180 N94-24479

FREE VIBRATION

Nonlinear analysis using a modal based reduction technique p 2161 N94-24288

FRENCH SPACE PROGRAM

A reference Martian mission for a long range rover p 2606 N94-23382

The space operations at CNES p 2498 N94-23837

FREQUENCIES

Coupled frequencies of a hydroelastic rectangular system [LRT-WE-9-FB-4-1992] p 2375 N94-23196

Solid state Time Base Corrector (TBC) [AD-D015981] p 2312 N94-25039

FREQUENCY CONVERTERS

Some subjects in digital audio, noise shaping, sample rate conversion, dynamic range compression and testing [ISBN-9-09-005162-7] p 2530 N94-25220

FREQUENCY DISCRIMINATORS

A pattern jitter free AFC scheme for mobile satellite systems p 2285 N94-22809

FREQUENCY DISTRIBUTION

Radar target discrimination systems using artificial neural network topology [AD-D015984] p 2301 N94-25041

FREQUENCY DIVIDERS
Microwave analog frequency dividers: Design, modeling and realization
[LAAS-93139] p 2307 N94-22909
FREQUENCY DIVISION MULTIPLE ACCESS
Aeronautical audio broadcasting via satellite
p 2274 N94-22741
FREQUENCY DIVISION MULTIPLEXING
An introduction to digital modulation and OFDM techniques
[BBC-RD-1993/10] p 2295 N94-24086
FREQUENCY HOPPING
Coding for frequency hopped spread spectrum satellite communications
[ECE-91-1] p 2296 N94-24132
Evaluation of EHF multi-beam adaptive arrays
[CTN-94-60898] p 2297 N94-24296
Analysis of time-diversity combining methods for frequency-hopped signals
[CU-DOE-92-09] p 2300 N94-24694
Coding for frequency hopped spread spectrum satellite communications
[ECE-92-1] p 2300 N94-24697
FREQUENCY MODULATION
Power attenuation characteristics as switch-over criterion in personal satellite mobile communications
p 2277 N94-22756
Theoretical and simulated performance for a novel frequency estimation technique p 2285 N94-22808
Modulation characteristics of a high-power semiconductor Master Oscillator Power Amplifier (MOPA)
[NASA-TM-104577] p 2308 N94-23281
Preprocessor and adaptive beamformer for linear-frequency modulation active signals
[AD-D016008] p 2302 N94-25048
System for cancelling phase noise in an interferometric fiber optic sensor arrangement
[AD-D015994] p 2345 N94-25053
FREQUENCY MULTIPLIERS
Planar varactor frequency multiplier devices with blocking barrier
[NASA-CASE-NPO-18428-1-CU] p 2310 N94-23821
Spatial frequency multiplier with active linearly tapered slot antenna array
[NASA-TM-106494] p 2310 N94-24308
FREQUENCY RANGES
A pattern jitter free AFC scheme for mobile satellite systems p 2285 N94-22809
MIMO system identification for H(infinity) robust control: A frequency domain approach with minimum error bounds
[ETN-94-95354] p 2476 N94-25262
On the auditory discrimination of spectral shape
[ETN-94-95306] p 2530 N94-25289
Frequency response functions for nonlinear rational models
[RR-471] p 2492 N94-25318
FREQUENCY RESPONSE
Unwrapping the phase response functions for nonlinear systems
[RR-465] p 2462 N94-25311
FREQUENCY SCANNING
Novel fringe scanning/Fourier transform method of synthetic imaging
[DE93-018936] p 2542 N94-22917
FREQUENCY SHIFT
Estimation of frequency offset in mobile satellite modems p 2285 N94-22807
Theoretical and simulated performance for a novel frequency estimation technique p 2285 N94-22808
Experimental and theoretical features of strong suppression and shifting phenomena in odd-photon resonant excitations and stimulated emissions
[DE94-000341] p 2535 N94-24510
Ultracold atoms in traps and fountains
[ETN-94-95325] p 2537 N94-25239
FREQUENCY SHIFT KEYING
An optical ASK and FSK phase diversity transmission system
[EUT-92-E-268] p 2542 N94-23171
Coding for frequency hopped spread spectrum satellite communications
[ECE-91-1] p 2296 N94-24132
Simulation of adjacent channel interference in a UHF satellite system
[AD-A273147] p 2299 N94-24669
Analysis of time-diversity combining methods for frequency-hopped signals
[CU-DOE-92-09] p 2300 N94-24694
Coding for frequency hopped spread spectrum satellite communications
[ECE-92-1] p 2300 N94-24697
Very low frequency and low frequency transmitting antenna parameter monitoring system
[AD-D015989] p 2302 N94-25049
FREQUENCY STABILITY
Direct digital RF synthesis and modulation for MSAT mobile applications p 2285 N94-22804
Progress toward ultra-stable lasers for use in space
[NASA-TM-109678] p 2349 N94-24488
FREQUENCY SYNTHESIZERS
Spur-reduced digital sinusoid synthesis
p 2291 N94-23264
FRICTION
New tribocoating combination for vacuum operation
p 2355 N94-23990
Tribological behaviour of fluorinated resins and polyimide resins sliding over a metallic surface in liquid nitrogen
p 2355 N94-23991
Simulation of cryogenic turbopump annular seals
p 2371 N94-24440
FRICTION FACTOR
Development of a theory of the wear of ceramics
[DE94-002773] p 2254 N94-23783
Simulation of cryogenic turbopump annular seals
p 2371 N94-24440
FRICTION MEASUREMENT
New pin-on-disk equipment for vacuum tribometry
p 2360 N94-24023
An analytical ultra-high vacuum tribometer for solid lubricant studies p 2361 N94-24033
Skin friction measurement in complex flows using thin oil film techniques
[NASA-CR-194872] p 2327 N94-24098
FRONTS (METEOROLOGY)
ASR-9 microburst detection algorithm
[AD-A273591] p 2415 N94-24850
FROST DAMAGE
Frost effects on the microstructure of high strength concrete, and methods for their analysis
[VTT-PUBS-126] p 2379 N94-25529
FROSTBITE
Cellular and tissue injury during nonfreezing cold injury and frostbite
[AD-A270883] p 2423 N94-22732
FUEL CELL POWER PLANTS
Mathematical modeling of MCFC cells/stacks and networks
[DE94-001914] p 2390 N94-23212
Overview of molten carbonate fuel cell technology development
[DE94-001911] p 2394 N94-23781
FUEL CELLS
Advanced research and technology development of MCFCs
[DE94-001918] p 2389 N94-22723
A novel method for determination of transport parameters of H2 and O2 in PEMFCs
[DE94-001492] p 2389 N94-22962
Preliminary study concerning development of petroleum-substitution energy integration technology
[DE94-714902] p 2264 N94-23027
Modelling of solid polymer and direct methanol fuel cells: Phenomenological equations and analytical solutions
[PB93-224897] p 2390 N94-23102
Mathematical modeling of MCFC cells/stacks and networks
[DE94-001914] p 2390 N94-23212
Space Electrochemical Research and Technology
[NASA-CP-3228] p 2390 N94-23345
Applications of x ray absorption fine structure to the in situ study of the effect of cobalt in nickel hydrous oxide electrodes for fuel cells and rechargeable batteries
p 2391 N94-23347
High power density proton exchange membrane fuel cells p 2393 N94-23359
The electrolyte challenge for a direct methanol-air polymer electrolyte fuel cell operating at temperatures up to 200 C p 2393 N94-23360
Advances in direct oxidation methanol fuel cells
p 2393 N94-23361
High energy density aluminum-oxygen cell
p 2393 N94-23363
A high performance H2-Cl2 fuel cell for space power applications p 2394 N94-23366
Carbon monoxide fuel cells as a source for Mars rover electric power p 2314 N94-23409
Overview of molten carbonate fuel cell technology development
[DE94-001911] p 2394 N94-23781
Contaminant effects in solid oxide fuel cells
[DE94-002963] p 2395 N94-23785
FUEL COMBUSTION
Development of durable high-temperature catalysts for natural gas combustion
[PB93-226447] p 2232 N94-23477
Shock tunnel studies of scramjet phenomena, supplement 7
[NASA-CR-191572] p 2319 N94-23513
Shock tunnel studies of scramjet phenomena, supplement 8
[NASA-CR-191573] p 2320 N94-23532
Fundamental and experimental studies on the catalytic combustion of methane
[PB94-112661] p 2233 N94-23736
Multiple flames in counterflow spray combustion
p 2161 N94-24284
Solid rocket combustion simulator technology using the hybrid rocket for simulation
[NASA-CR-195142] p 2265 N94-24578
FUEL CONSUMPTION
Theory and computation of optimal low- and medium-thrust transfers
[NASA-CR-194812] p 2217 N94-23275
S-2E Tracker maritime patrol aircraft re-engine and system upgrade program p 2158 N94-24270
General aviation activity survey
[AD-A273284] p 2162 N94-24923
FUEL CONTAMINATION
Isothiazolone volatility study of a water bottom from fuel treated with Kathon (tm) FP1.5 biocide
[AD-A273165] p 2266 N94-24728
FUEL FLOW
Heat transfer in rocket combustion chambers
p 2214 N94-23051
CFD simulation of coaxial injectors
p 2342 N94-24430
Thermal-fluid analysis of the fill and drain operations of a cryrogenic fuel tank
[NASA-TM-104273] p 2334 N94-24495
STE thrust chamber technology: Main injector technology program and nozzle Advanced Development Program (ADP)
[NASA-CR-193919] p 2221 N94-25019
FUEL INJECTION
SSME fuel preburner injector characterization
p 2211 N94-23037
Axisymmetric single shear element combustion instability experiment p 2213 N94-23044
Heat transfer in rocket combustion chambers
p 2214 N94-23051
Transient phenomena in laminar spray combustion
p 2160 N94-24282
Pellet ablation in the large helical device
[NIFS-260] p 2551 N94-24358
Validation of a nonintrusive optical technique for the measurement of liquid mass distribution in a two-phase spray p 2548 N94-24420
HYPULSE combustor analysis
[NASA-CR-191579] p 2336 N94-24771
FUEL SPRAYS
Transient phenomena in laminar spray combustion
p 2160 N94-24282
Effect of initial droplet-size distributions on fuel-vapor profiles in a shear-layer flow p 2160 N94-24283
Validation of a nonintrusive optical technique for the measurement of liquid mass distribution in a two-phase spray p 2548 N94-24420
FUEL SYSTEMS
Isothiazolone volatility study of a water bottom from fuel treated with Kathon (tm) FP1.5 biocide
[AD-A273165] p 2266 N94-24728
FUEL TANKS
Thermal-fluid analysis of the fill and drain operations of a cryrogenic fuel tank
[NASA-TM-104273] p 2334 N94-24495
FUEL TESTS
HYPULSE combustor analysis
[NASA-CR-191579] p 2336 N94-24771
FUELS
Multiple flames in counterflow spray combustion
p 2161 N94-24284
An x ray diffraction investigation of alpha-Al2O2 addition to Yttria Stabilized Zirconia (YSZ) thermal barrier coatings subject to destabilizing vanadium pentoxide (V2O5) exposure
[AD-A273403] p 2261 N94-25072
FULLERENES
SALI chemical analysis of provided samples
[NASA-CR-194138] p 2232 N94-23524
Capillary electrokinetic separations with optical detection
[DE94-001639] p 2233 N94-23716
Potent solvents for C60 and their utility for the rapid acquisition of 13CNMR data for fullerenes
[AD-A273349] p 2235 N94-24925
FUNCTIONAL ANALYSIS
Logarithm of probability measures and infinite divisibility of sub-stable random vectors
[PB94-118627] p 2486 N94-23758
FUNCTIONAL DESIGN SPECIFICATIONS
Development of the Cassini Ground Data System in a multimission environment p 2500 N94-23845

Operational characterisation of requirements and early validation environment for high demanding space systems p 2519 N94-23959

Design of a recumbent seating system
[NASA-CR-195503] p 2438 N94-24786

Specification list and function structure for a full-body dynamometer to be used aboard Space Station Freedom
[NASA-CR-195508] p 2439 N94-24835

FUNCTIONALS

Density functional studies: First principles and semi-emperical calculations of clusters and surfaces
[DE94-002836] p 2561 N94-23214

Infinitely divisible processes and their nonlinear functionals; a study of their structural, statistical and sample path properties and their prediction problems
[AD-A273468] p 2496 N94-25147

New algorithm for minimizing (chi)(sup 2) functionals with constraints
[DE93-616800] p 2463 N94-25432

The least energy critical set
[DE93-616820] p 2493 N94-25434

FUNCTIONS (MATHEMATICS)

Wiener-Hopf factorization of rational matrix functions in terms of realizations: An alternative version
[ETN-94-95380] p 2491 N94-25245

Adaptive noise cancellation using recurrent radial basis function networks
[RR-472] p 2313 N94-25319

Extension problem for generalized multi-monogenic functions in Clifford analysis
[DE93-616818] p 2493 N94-25433

FURNACES

Determination of the compatibility between structural alloys and molten metals at high temperatures
[DE94-000954] p 2241 N94-23434

FUSELAGES

Aircraft empennage structural detail design
[NASA-CR-195496] p 2179 N94-24332

The Triton: Design concepts and methods
[NASA-CR-195542] p 2184 N94-25004

FUSION REACTORS

Design of central control system for Large Helical Device (LHD)
[NIFS-258] p 2553 N94-24623

FUZZY SETS

An information retrieval logical model applied to the formalism of conceptual graphs: The ELEN prototype and its experimentation on a corpus of software components
[ETN-94-95162] p 2588 N94-22879

FUZZY SYSTEMS

VLSI-based video event triggering for image data compression
[NASA-TM-106500] p 2345 N94-25116

Fault detection in HVAC systems using fuzzy models
[OUEL-1977/93] p 2373 N94-25475

G

G STARS

ROSAT observations of the x ray binary HD 154791
[NASA-CR-195189] p 2600 N94-25198

GADOLINIUM

Synthesis and in-vivo detection of boronated compounds for use in BNCT
[DE94-001899] p 2233 N94-23780

GALACTIC COSMIC RAYS

Optical model analyses of galactic cosmic ray fragmentation in hydrogen targets
[NASA-TP-3404] p 2540 N94-23509

Superconducting cosmic strings near the electroweak scale and cosmic-ray propagation
[MPI-PHE/93-05] p 2629 N94-25459

GALACTIC EVOLUTION

Comparison of time integration methods for the evolution of galaxies
[PB94-111671] p 2602 N94-24522

GALACTIC HALOS

The soft x ray halo of the spiral galaxy NGC4631
[NASA-CR-194820] p 2601 N94-23537

GALERKIN METHOD

Isolated and coupled superquadric loop antennas for mobile communications applications
p 2289 N94-22834

Wavelet multiresolution analyses adapted for the fast solution of boundary value ordinary differential equations
p 2485 N94-23691

FEMAX finite-element package for computing three-dimensional time-domain electromagnetic fields in inhomogeneous media
[PB94-111093] p 2294 N94-23733

On the dynamics of approximating schemes for dissipative nonlinear equations p 2332 N94-24168

Responses of a finite baffled plate subject to turbulent and mean flow excitations
[NASA-CR-191570] p 2334 N94-24605

GALILEO PROJECT

Galileo spacecraft anomaly and safing recovery
p 2207 N94-23864

GALILEO SPACECRAFT

Galileo spacecraft anomaly and safing recovery
p 2207 N94-23864

Techniques and software for optimum and efficient mission science sequence development
p 2504 N94-23872

GALLIUM

Ga delta-doping layers in silicon
[PB93-224632] p 2561 N94-23222

GALLIUM ARSENIDE LASERS

Manufacturing and characterization of GaAs/AlGaAs multiple quantumwell ridge waveguide lasers
[EUT-92-E-265] p 2348 N94-23168

GALLIUM ARSENIDES

InGaAsP/InP based 1.3/1.55 micron vertical cavity surface emitting lasers for wavelength division multiplexed high speed distributed computing, phase 1
[AD-A271081] p 2348 N94-23123

Observation of non-centrosymmetry and determination of polarity in III-V semiconductors
[PB93-201416] p 2561 N94-23503

The study of dopant segregation behavior during the growth of GaAs in microgravity
[NASA-CR-193905] p 2267 N94-23549

Magnetic resonance studies of 3d transition metal impurities in compound semiconductors
[PB93-232197] p 2243 N94-23714

Photonic technology for implementation of generalizable neural networks: A synthetic approach
[AD-A273497] p 2474 N94-24622

On the origin of 1/f noise in epitaxial GaAs
[ISBN-9-09-006067-7] p 2566 N94-25297

GALLIUM COMPOUNDS

Electrochemical sulfur passivation of visible (approximately 670nm) AlGaInP lasers
[DE94-002293] p 2350 N94-24659

GALLIUM ISOTOPES

Recent results from the Soviet-American Gallium Experiment
[DE94-000677] p 2626 N94-23020

GALLIUM PHOSPHIDES

Magnetic resonance studies of 3d transition metal impurities in compound semiconductors
[PB93-232197] p 2243 N94-23714

GAME THEORY

On some approximately balanced combinatorial cooperative games
[MEMO-1113] p 2493 N94-22702

Generalized concavity in cooperative game theory: Characterizations in terms of the core
[MEMO-1121] p 2497 N94-22708

On the reduced game property for and the axiomatization of the tau-value
[MEMO-1128] p 2497 N94-22716

The Third Twente Workshop on Graphs and Combinatorial Optimization
[PB94-110947] p 2486 N94-23722

Egalitarian non-average contribution method for cooperative games
[PB94-111705] p 2497 N94-23800

Reduced game properties of egalitarian division rules for cooperative games
[PB94-111689] p 2521 N94-24523

Irreducible core of a minimum cost spanning tree game
[PB94-110962] p 2489 N94-24653

GAMMA RAY ASTRONOMY

An analysis of gamma ray burst time histories
[NASA-CR-195191] p 2629 N94-25199

High energy gamma astronomy above 200 GeV
[MPI-PHE/93-04] p 2600 N94-25458

GAMMA RAY BURSTS

Two populations and models of gamma ray bursts
[NASA-CR-194762] p 2629 N94-22947

Structure in gamma ray burst time profiles: Correlations with other observables p 2579 N94-24431

Using contour maps to search for red-shifted 511 keV features in BATSE GRB spectra p 2585 N94-24455

Neutron star mergers and gamma-ray bursts
[NASA-CR-195176] p 2629 N94-25091

An analysis of gamma ray burst time histories
[NASA-CR-195191] p 2629 N94-25199

GAMMA RAY OBSERVATORY

Structure in gamma ray burst time profiles: Correlations with other observables p 2579 N94-24431

Flux measurements using the BATSE spectroscopic detectors p 2580 N94-24435

GAMMA RAY SPECTROMETERS

New concepts for HgI2 scintillator gamma ray spectroscopy
[NASA-CR-194819] p 2233 N94-24113

GAMMA RAY TELESCOPES

High energy gamma astronomy above 200 GeV
[MPI-PHE/93-04] p 2600 N94-25458

GANGLIA

Electrophysiology of the rat nucleus accumbens: Local circuitry, neuromodulation and synaptic plasticity
[PB93-232254] p 2420 N94-23454

GAPS

An application of small-gap equations in sealing devices p 2325 N94-23668

GARNETS

Two micron stimulated emission of activated insulating crystals
[REPT-94-002] p 2565 N94-25025

GAS ANALYSIS

Generic microelectronic smart sensor platform for detection of toxic, hazardous, and flammable gases
[DE93-017626] p 2343 N94-23200

Rice cultivation and methane emission: Documentation of distributed geographic data sets
[NASA-TM-104595] p 2381 N94-24800

GAS BEARINGS

Design of gas bearing systems for precision applications
[ISBN-9-03-860112-3] p 2367 N94-25249

GAS CHROMATOGRAPHY

Evaporation and combustion of LOX under supercritical and subcritical conditions p 2211 N94-23035

Reduction of hydrocarbon impurities in 200 l/h helium liquefier-refrigerator system
[NIFS-259] p 2271 N94-24459

Isothiazolone volatility study of a water bottom from fuel treated with Kathon (tm) FP1.5 biocide
[AD-A273165] p 2266 N94-24728

GAS COMPOSITION

Evaporation and combustion of LOX under supercritical and subcritical conditions p 2211 N94-23035

Hot hydrogen testing of metallic turbo pump materials
[NASA-CR-193880] p 2244 N94-24066

GAS COOLING

Ultracold atoms in traps and fountains
[ETN-94-95325] p 2537 N94-25239

GAS DENSITY

Supersonic minimum length nozzle design for dense gases p 2171 N94-23656

Reduction of hydrocarbon impurities in 200 l/h helium liquefier-refrigerator system
[NIFS-259] p 2271 N94-24459

The effects of zinc borate addition on the flammability characteristics of polyester, vinyl ester, and epoxy glass reinforced plastics
[AD-A273164] p 2262 N94-25136

GAS DETECTORS

Robust, wide-range hydrogen sensor for use in commercial, space, and government applications
[DE93-040902] p 2342 N94-22954

Interpretation of discrepancies in mass spectroscopy data obtained from different experimental configurations
p 2237 N94-23245

Total light loss optic spectroscopy: Progress towards a fiber optic Raman organic vapor sensor
[DE94-002545] p 2234 N94-24549

GAS DISCHARGES

Flue gas cleaning by pulse corona streamer
[EUT-93-E-272] p 2268 N94-23174

Microwave excitation of pulsed high pressure gas discharge lasers
[DLR-FB-93-12] p 2351 N94-25304

GAS DYNAMICS

Molecular gas dynamics applied to low-thrust propulsion p 2214 N94-23053

Interpretation of discrepancies in mass spectroscopy data obtained from different experimental configurations
p 2237 N94-23245

A multilevel adaptive projection method for unsteady incompressible flow p 2341 N94-23690

Heat pipe vapor dynamics
[NASA-CR-194217] p 2327 N94-24096

Energy and maximum norm estimates for nonlinear conservation laws
[NASA-CR-195091] p 2569 N94-24109

An investigation on a new technique to improve the performance of the shock tube/tunnel testing in the equilibrium interface condition p 2154 N94-24247

Characteristic method for one-dimensional scalar hyperbolic conservation laws with stiff source terms
[PB93-237675] p 2491 N94-24954

Microscopic dynamics in dense helium-neon mixtures: Neutron scattering, kinetic theory and computer simulations
[ISBN-9-07-386105-5] p 2537 N94-25228

An adaptive streamline diffusion finite element method for hyperbolic systems in gas dynamics
[PREPRINT-688] p 2340 N94-25466

GAS FLOW
Picosecond High Pressure Gas Switch experiment
[DE93-040853] p 2307 N94-22950
Local grid refinement method for the euler equations
[PB93-223329] p 2317 N94-22985
Interferometry in rarefied gas flows
[ISL-CO-207/92] p 2318 N94-23160
An F2D analysis of the Flow Instability Test (FIT) experiment
[DE94-001420] p 2217 N94-23193
Vaporization behavior of non-stoichiometric refractory carbide materials and direct observations of the vapor phase using laser diagnostics
[DE93-040094] p 2348 N94-23203
Analysis of high vacuum systems using SINDA'85
p 2322 N94-23648
Supersonic minimum length nozzle design for dense gases p 2171 N94-23656
Conservation equations for reacting gas flow
[PB94-111168] p 2334 N94-24574
Molten salt reactor for potentiostatic electroplating
[AD-D016020] p 2258 N94-24720
Sub-sonic flow about a slender profile in a tunnel having perforated walls
[AD-A273184] p 2170 N94-25137
A continuing search for a near-perfect numerical flux scheme. Part 1: AUSM+
[NASA-TM-106524] p 2338 N94-25180

GAS GENERATORS
Computational Fluid Dynamics (CFD) applications in rocket propulsion analysis and design
p 2214 N94-23054
A minimum cost tolerance allocation method for rocket engines and robust rocket engine design
p 2222 N94-24419

GAS GIANT PLANETS
Voyager planetary radio astronomy studies
[NASA-CR-194776] p 2614 N94-24328

GAS GUNS
Multiple shock initiation of LX-17
[DE94-001524] p 2265 N94-23807

GAS INJECTION
Shear coaxial injector instability mechanisms
p 2213 N94-23047
Mixing characteristics of directly opposed rows of jets injected normal to a crossflow in a rectangular duct
[NASA-TM-106477] p 2188 N94-24594

GAS IONIZATION
Radiative properties of molecular nitrogen ions produced by helium Penning ionization and argon effects
[NASA-CR-195126] p 2534 N94-24487

GAS JETS
Refraction of high frequency noise in an arbitrary jet flow
[NASA-TM-106465] p 2525 N94-23464
Optimization of orifice geometry for cross-flow mixing in a cylindrical duct
[NASA-TM-106436] p 2481 N94-23593

GAS LASERS
Fabrication of sub-40-nm p-n junctions for 0.18 micron MOS device applications using a cluster-tool-compatible, nanosecond thermal doping technique
[DE94-001608] p 2309 N94-23520

GAS MIXTURES
Discontinuous phase formation and selective attack of SiC materials exposed to low oxygen partial pressure environments
[DE93-040161] p 2231 N94-22933
Transient phenomena in laminar spray combustion
p 2160 N94-24282
The chemistry of particulate formation in fluorocarbon plasmas
[DE94-001500] p 2552 N94-24546
Microscopic dynamics in dense helium-neon mixtures: Neutron scattering, kinetic theory and computer simulations
[ISBN-9-07-386105-5] p 2537 N94-25228

GAS PIPES
Demonstration of polyscann ultrasonic butt-fusion inspection system for polyethylene pipes
[AD-A273279] p 2373 N94-24814

GAS PRESSURE
Gas-pressure forming of superplastic ceramic sheet
[DE94-001520] p 2252 N94-22930
Thermodynamics of nickel-cadmium and nickel-hydrogen batteries p 2391 N94-23349
Investigation and application of microwave electron cyclotron resonance plasma physical vapour deposition
[DE93-613909] p 2555 N94-25333

GAS STREAMS
A pressurized thermogravimetric analyzer for use in studies of gas/solid systems
[DE94-001224] p 2342 N94-22989

Effect of initial droplet-size distributions on fuel-vapor profiles in a shear-layer flow p 2160 N94-24283

GAS TRANSPORT
Vaporization behavior of non-stoichiometric refractory carbide materials and direct observations of the vapor phase using laser diagnostics
[DE93-040094] p 2348 N94-23203
Chemistry on the mesoscale: Modeling and measurement issues p 2413 N94-24390

GAS TUNGSTEN ARC WELDING
Use of photostress to characterize the mechanical behavior of weldments
[NASA-CR-195201] p 2378 N94-25267

GAS TURBINE ENGINES
Vibration isolating engine mount
[CA-PATENT-1-320-710] p 2353 N94-23215
Turbine engine with induced pre-swirl at the compressor inlet
[CA-PATENT-1-317-467] p 2186 N94-23253
Seal assembly
[CA-PATENT-163126888] p 2364 N94-24128
Probabilistic simulation of concurrent engineering of propulsion systems p 2177 N94-24317
Gas turbine and operating method of the same
[CA-PATENT-APPL-SN-2043039] p 2188 N94-24490
Study of streamwise vorticity-stirred combustion
[NASA-CR-194450] p 2234 N94-24565
An x ray diffraction investigation of alpha-Al2O2 addition to Yttria Stabilized Zirconia (YSZ) thermal barrier coatings subject to destabilizing vanadium pentoxide (V2O5) exposure
[AD-A273403] p 2261 N94-25072

GAS TURBINES
Brush seals for cryogenic applications
p 2216 N94-23063
Two-dimensional Navier-Stokes computations of subsonic and supersonic flows through turbine cascades
[PB93-226223] p 2317 N94-23114
Optimization of orifice geometry for cross-flow mixing in a cylindrical duct
[NASA-TM-106436] p 2481 N94-23593
Simulation of unsteady flows through stator and rotor blades of a gas turbine using the Chimera method
p 2323 N94-23652
The 3-D CFD modeling of gas turbine combustor-integral bleed flow interaction p 2189 N94-23658
The 3-D numerical study of airflow in the compressor/combustor prediffuser and dump diffuser of an industrial gas turbine p 2324 N94-23660
Evaluation of reducing gas turbine emissions through hydrogen-enhanced steam-injected combustion
[PB94-109873] p 2187 N94-23709
Gas turbine and operating method of the same
[CA-PATENT-APPL-SN-2043039] p 2188 N94-24490
Analysis of the effects of wake passage on heat transfer in a linear turbine cascade
[AD-A273729] p 2339 N94-25446

GAS VALVES
Pressure wall patch
[NASA-CASE-MFS-28724-1] p 2203 N94-23824

GAS VISCOSITY
Local grid refinement method for the euler equations
[PB93-223329] p 2317 N94-22985

GAS-ION INTERACTIONS
Reactivity of ambident anions in the gas phase
[PB93-232189] p 2533 N94-23713

GAS-LIQUID INTERACTIONS
The 2-D polymerized Langmuir-Blodgett films studied by STM
[AD-A273542] p 2261 N94-24930

GAS-METAL INTERACTIONS
Effect of hydrogen exposure on a Cu-8 Cr-4 Nb alloy
[NASA-TM-106429] p 2243 N94-23556

GAS-SOLID INTERFACES
A method for recognition of frequency cells in a cylinder flow influenced by wall effects p 2316 N94-22860

GASEOUS DIFFUSION
Comparison of numerical simulation and experimental data for steam-in-place sterilization
p 2326 N94-23669
Ethylene trace-gas techniques for high-speed flows
[NASA-TM-106491] p 2169 N94-24335
An adaptive streamline diffusion finite element method for hyperbolic systems in gas dynamics
[PREPRINT-688] p 2340 N94-25466

GATES (CIRCUITS)
Method for fabricating self-aligned gate diffused junction field effect transistor
[AD-D015975] p 2312 N94-25035

GAUGE INVARIANCE
Gauge invariance and the electromagnetic current of composite pions
[DE93-040869] p 2532 N94-22952
Off-critical W(infinity) and Virasoro algebras as dynamical symmetries of the integrable models
[DE93-633215] p 2478 N94-22969

The 2D supergravity and integrable systems
[DE93-616848] p 2570 N94-25336
Proton spin: The role of quark-gluon and hadron degrees of freedom
[DE93-616867] p 2538 N94-25341

GAUGE THEORY
On BRST quantization of constrained systems
[ETN-94-95386] p 2570 N94-25258

GEAR TEETH
Thermal vacuum performance of cycloid and harmonic gearboxes with solid (MoS2) and liquid (Braycote 601) lubrication p 2358 N94-24009
Application of fault detection techniques to spiral bevel gear fatigue data
[NASA-TM-106467] p 2364 N94-24483
Investigation of the effects of manufacturing variations and materials on fatigue crack detection methods in gear teeth
[NASA-CR-195093] p 2373 N94-24769

GEARS
Time-frequency domain analysis of vibration signals for machinery diagnostics.(4): Interpretation using image processing techniques
[OUEL-1953/92] p 2353 N94-23178
Thermal vacuum performance of cycloid and harmonic gearboxes with solid (MoS2) and liquid (Braycote 601) lubrication p 2358 N94-24009
Development of gears for space use
p 2360 N94-24021
Development of a Low-Temperature Gear Motor (LOG) p 2361 N94-24032
Application of fault detection techniques to spiral bevel gear fatigue data
[NASA-TM-106467] p 2364 N94-24483

GELLED ROCKET PROPELLANTS
A theoretical evaluation of aluminum gel propellant two-phase flow losses on vehicle performance
p 2210 N94-23031
Ignition and combustion characteristics of metallized propellants, phase 2
[NASA-CR-195107] p 2266 N94-24700

GENERAL AVIATION AIRCRAFT
Roles, uses, and benefits of general aviation aircraft in aerospace engineering education
[NASA-TM-106463] p 2153 N94-24100
Annual review of aircraft accident data. US general aviation calendar year 1990
[PB94-126869] p 2173 N94-24641
General aviation activity survey
[AD-A273284] p 2162 N94-24923
US general aviation: The ingredients for a renaissance. A vision and technology strategy for US industry, NASA, FAA, universities p 2162 N94-25097
A simulation study of control and display requirements for zero-experience general aviation pilots
p 2163 N94-25102

GENES
Investigation of evolution-related aspects of bacterial rhodopsins
[NASA-CR-194826] p 2420 N94-23501

GENETIC ALGORITHMS
Using genetic algorithms for scheduling data flow graphs
[EUT-92-E-266] p 2449 N94-23169
A methodology for software cost estimation using machine learning techniques
[AD-A273158] p 2459 N94-24775
High-level connectionist models
[AD-A273638] p 2468 N94-25030
Genetic algorithms in control systems engineering
[RR-470] p 2463 N94-25315
Genetic-based motion planning for articulated robotic manipulators
[RR-476] p 2368 N94-25322

GENETIC CODE
Microinjection of the Yersinia YopE cytotoxin in mammalian cells induces actin microfilament disruption
[FOA-B-40418-4.4] p 2421 N94-24290

GENETICS
Applications of the Aurora parallel PROLOG system to computational molecular biology
[DE93-041166] p 2420 N94-23468

GEOCHEMISTRY
Whole rock major element chemistry of KREEP basalt clasts in lunar breccia 15205: Implications for the petrogenesis of volcanic KREEP basalts
p 2614 N94-24365
The western highland province at the Apollo 14 site
p 2615 N94-24369
Lunar mare volcanism: Mixing of distinct, mantle source regions with KREEP-like component
p 2615 N94-24370
Reactive trace metals as indicators of subduction and ventilation processes in the ocean
[AD-A273585] p 2419 N94-25164

A geochemical study of acapulcoite and lodranite meteorites p 2605 N94-25358

GEODESY

An improved gravity model for Mars: Goddard Mars Model-1 (GMM-1)
[NASA-TM-104584] p 2401 N94-23282

GEODETIC SURVEYS

GPS survey of the western Tien Shan
[NASA-CR-195174] p 2175 N94-24826

GEODYNAMICS

GPS survey of the western Tien Shan
[NASA-CR-195174] p 2175 N94-24826

Constraining proposed combinations of ice history and Earth rheology using VLBI determined baseline length rates in North America p 2405 N94-25205

GEOELECTRICITY

Electromagnetic field changes as a precursory phenomena of earthquakes and volcanic eruptions
[REPT-157] p 2405 N94-24980

GEOGRAPHIC INFORMATION SYSTEMS

A prototype expert/information system for examining environmental risks of KSC activities
p 2400 N94-23237

Study of methods and structures for handling of digitized maps for geographical information systems
[PB93-204402] p 2590 N94-23741

Mapping Tomorrow's Resources: A symposium on the uses of remote sensing, Geographic Information Systems (GIS), and Global Positioning Systems (GPS) for natural resources management p 2387 N94-24357

Tools for visualizing landscape pattern for large geographic areas
[DE94-001121] p 2388 N94-24757

GEOLOGICAL FAULTS

Seafloor characterization/Galapagos propagating rift
[AD-A273586] p 2419 N94-25165

GEOLOGICAL SURVEYS

The AGRHYMET data communications project
p 2280 N94-22776

The national geomagnetic initiative
[LC-93-85739] p 2401 N94-23344

ASTER, a multinational Earth observing concept
p 2389 N94-23840

Near-surface seismic imaging
[PB94-119096] p 2404 N94-24647

GPS survey of the western Tien Shan
[NASA-CR-195174] p 2175 N94-24826

GEOMAGNETIC LATITUDE

Satellite autonomous navigation and orbit determination using magnetometers p 2156 N94-24258

GEOMAGNETISM

Aeronautical satellite antenna steering using magnetic field sensors p 2289 N94-22836

Solar-terrestrial environmental laboratory
p 2630 N94-23336

The national geomagnetic initiative
[LC-93-85739] p 2401 N94-23344

Solar-geophysical data number 584, April 1993. Part 1: (Prompt reports). Data for February, March, 1993, and late data
[PB93-198323] p 2626 N94-23738

Steady induction effects in geomagnetism. Part 1C: Geomagnetic estimation of steady surficial core motions: Application to the definitive geomagnetic reference field models
[NASA-TP-3272-PT-1C] p 2403 N94-24465

Geomagnetic field models incorporating physical constraints on the secular variation
[NASA-CR-195165] p 2405 N94-24854

Shielded Coil Electrodynamic Propulsion (SCEP). A feasibility study
[AD-A273824] p 2314 N94-25539

GEOMETRICAL ACOUSTICS

Refraction of high frequency noise in an arbitrary jet flow
[NASA-TM-106465] p 2525 N94-23464

GEOMETRICAL OPTICS

Ray and wave optics modeling of laboratory x ray lasers
[DE93-019940] p 2541 N94-22868

High-frequency techniques for RCS prediction of plate geometries and a physical optics/equivalent currents model for the RCS of trihedral corner reflectors, parts 1 and 2
[NASA-CR-195140] p 2298 N94-24616

Feasibility study of a synthesis procedure for array feeds to improve radiation performance of large distorted reflector antennas
[NASA-CR-195167] p 2301 N94-25005

GEOMETRICAL THEORY OF DIFFRACTION

Propagation model for the Land Mobile Satellite channel in urban environments p 2283 N94-22796

High-frequency techniques for RCS prediction of plate geometries and a physical optics/equivalent currents model for the RCS of trihedral corner reflectors, parts 1 and 2
[NASA-CR-195140] p 2298 N94-24616

GEOMETRY

Algebraic-geometric codes and their decoding algorithms
[ETN-94-95294] p 2491 N94-25079

GEOMORPHOLOGY

The morphology of the lunar surface parts in the region of work of the mobile geological laboratory vehicle in Mare Imbrium p 2607 N94-23385

Hydraulics and morphology of mountain rivers: A literature survey. Communications on hydraulic and geotechnical engineering
[PB94-110772] p 2388 N94-24636

GEOPHYSICAL FLUIDS

Steady induction effects in geomagnetism. Part 1C: Geomagnetic estimation of steady surficial core motions: Application to the definitive geomagnetic reference field models
[NASA-TP-3272-PT-1C] p 2403 N94-24465

GEOPHYSICS

Time-domain analysis of conduction and displacement current distributions in inhomogeneous and anisotropic layered media
[PB94-111036] p 2403 N94-24592

Rao-Blackwell theorem in stereology and some counterexamples
[PB94-111713] p 2496 N94-24639

Near-surface seismic imaging
[PB94-119096] p 2404 N94-24647

Solar-geophysical data number 587, July 1993. Part 1: (Prompt reports). Data for June, May 1993, and late data
[PB93-232874] p 2628 N94-24989

Solar-geophysical data number 587, July 1993. Part 2: (Comprehensive reports). Data for January 1993, and miscellaneous
[PB93-232882] p 2628 N94-24990

Solar-geophysical data number 588, August 1993. Part 1: (Prompt reports). Data for July, June 1993, and late data
[PB94-109089] p 2628 N94-24991

Solar-geophysical data number 588, August 1993. Part 2: (Comprehensive reports). Data for February 1993, and miscellaneous
[PB94-109105] p 2628 N94-24992

Solar-geophysical data number 589, September 1993. Part 1: (Prompt reports). Data for August, July 1993, and late data
[PB94-117082] p 2628 N94-24993

Solar-geophysical data number 589, September 1993. Part 2: (Comprehensive reports). Data for March 1993, and miscellaneous
[PB94-117405] p 2628 N94-24994

The geophysical signal of the martian global dichotomy p 2623 N94-24997

Measurement and Interpretation of Crustal Deformation Rates Associated with Postglacial Rebound
[NASA-CR-195193] p 2405 N94-25203

Report on operations of the Air Force Geophysics Laboratory infrared array spectrometer
[AD-A273800] p 2406 N94-25535

GEOPOTENTIAL

Electromagnetic field changes as a precursory phenomena of earthquakes and volcanic eruptions
[REPT-157] p 2405 N94-24980

GEOSYNCHRONOUS ORBITS

Trends in mobile satellite communication
p 2278 N94-22763

Geostationary payload concepts for personal satellite communications p 2278 N94-22765

Global coverage Mobile Satellite Systems: System availability versus channel propagation impairments
p 2284 N94-22798

New approaches for tracking earth orbiters using modified GPS ground receivers p 2196 N94-23258

CNES organization for station positioning of geostationary satellites p 2501 N94-23857

The geo-control system for station keeping and colocation of geostationary satellites
p 2464 N94-23927

HISPASAT launch and early operations phases: Computation and monitoring of geostationary satellite positioning p 2514 N94-23928

Reactive thrust cruise for a geosynchronous satellite with minimum fuel consumption p 2158 N94-24271

GEOTECHNICAL ENGINEERING

Unmanned lunar rovers: Utilization for exploration
p 2607 N94-23387

GERMANIUM

Physics with chemically and isotopically pure semiconductors
[DE93-040120] p 2557 N94-22928

Germanium x ray phase plates for the production of circularly polarized x rays
[DE94-002908] p 2545 N94-24550

Ge-Au eutectic bonding of Ge (100) single crystals
[DE94-002281] p 2564 N94-24657

Adsorption, desorption, and decomposition of HCl and HBr on Ge(100): Competitive pairingand near-first-order desorption kinetics
[AD-A273504] p 2235 N94-24790

GERMANIUM ALLOYS

Magnetic phases in UNiGe
[DE94-000793] p 2239 N94-22939

Large-scale production of Si(0.8)Ge(0.2) thermoelectric alloys by mechanical alloying
[DE94-000695] p 2243 N94-23753

GERMANIUM ISOTOPES

Recent results from the Soviet-American Gallium Experiment
[DE94-000677] p 2626 N94-23020

GIBBS FREE ENERGY

Surface barrier of a uniaxial anisotropic type 2 superconducting cylinder
[DE93-617137] p 2566 N94-25392

GIBBS PHENOMENON

On the Gibbs phenomenon 3: Recovering exponential accuracy in a sub-interval from a spectral partial sum of a piecewise analytic function
[NASA-CR-191560] p 2480 N94-23278

GIMBALS

Results of a laboratory experiment that tests rotating unbalanced-mass devices for scanning gimbaled payloads and free-flying spacecraft
[NASA-TP-3458] p 2269 N94-23574

Inter orbit link antenna pointing mechanisms design using standard actuators p 2359 N94-24016

GLACIOLOGY

Measurement and Interpretation of Crustal Deformation Rates Associated with Postglacial Rebound
[NASA-CR-195193] p 2405 N94-25203

Constraining proposed combinations of ice history and Earth rheology using VLBI determined baseline length rates in North America p 2405 N94-25205

GLASS

The structure and spin dynamics of lanthanide-bearing silicate glasses
[DE94-001320] p 2252 N94-22992

Micromechanical failure modes in brittle matrix composites p 2255 N94-24232

BEM solution for the simulation of axisymmetric viscous sintering
[PB93-237717] p 2336 N94-24761

GLASS FIBER REINFORCED PLASTICS

Contribution to the interface micromechanical study and to the damage fundamental phenomena in glass fiber epoxy resin model composites
[ISAL-93-0027] p 2227 N94-23133

Surface and interfacial properties of polymer blends. A literature survey
[PB93-230191] p 2254 N94-23561

Strength and life of pressure vessels subjected to impacts and thermomechanical GFRP loading
[VTT-JULK-771] p 2379 N94-25418

GLASS FIBERS

Glass-ceramic Li-Al-Si-O composition and process for its production
[CA-PATENT-APPL-SN-2043757] p 2254 N94-24129

Total light loss optic spectroscopy: Progress towards a fiber optic Raman organic vapor sensor
[DE94-002545] p 2234 N94-24549

GLASS LASERS

Inertial confinement fusion
[DE94-002602] p 2551 N94-23703

GLASS TRANSITION TEMPERATURE

Generalized melting criterion for beam-induced amorphization
[DE94-001333] p 2560 N94-23189

Di(hydroxyphenyl)- benzimidazole monomers
[NASA-CASE-LAR-14643-2] p 2253 N94-23305

Synthesis of soluble halogenated polyphenylenes: Mechanism for the coupling halogenated lithiobenzenes
[AD-A273547] p 2257 N94-24558

GLASSY CARBON

Metal-catalyzed alkynylation of brominated polyphenylenes: Thermoset precursors of high density monolithic glassy carbon
[AD-A273232] p 2259 N94-24789

Metal-catalyzed alkynylation of (Bromophenyl)Oligophenylenes: A rapid route to thermoset precursors of high density monolithic glass-like carbon
[AD-A273219] p 2260 N94-24863

GLIDE PATHS

Optical information in landing scenes
p 2442 N94-25511

GLOBAL POSITIONING SYSTEM
The Telecommunications and Data Acquisition Report
[NASA-CR-194766] p 2290 N94-23256
A review of GPS-based tracking techniques for TDRS orbit determination p 2196 N94-23257
New approaches for tracking earth orbiters using modified GPS ground receivers p 2196 N94-23258
Improved thermal force modeling for GPS satellites
p 2207 N94-23259
An investigation into acceleration determination for airborne gravimetry using the global positioning system
[ISBN-0-315-59470-5] p 2175 N94-24176
Mapping Tomorrow's Resources: A symposium on the uses of remote sensing, Geographic Information Systems (GIS), and Global Positioning Systems (GPS) for natural resources management p 2387 N94-24357
GPS survey of the western Tien Shan
[NASA-CR-195174] p 2175 N94-24826
Differential GPS for air transport: Status
p 2162 N94-25100
Measurement and Interpretation of Crustal Deformation Rates Associated with Postglacial Rebound
[NASA-CR-195193] p 2405 N94-25203
First results from the Fennoscandian GPS networks
p 2405 N94-25204
Application of aircraft navigation sensors to enhanced vision systems p 2176 N94-25495

GLOBAL TRACKING NETWORK
Worldwide vessel locating and tracking system, volume 1
[PB93-193217] p 2175 N94-24474

GLOBAL WARMING
Monte Carlo climate change forecasts with a global coupled ocean-atmosphere model
[MPIM-97] p 2407 N94-23156
Lightning, atmospheric electricity, and climate change
[DE94-002003] p 2408 N94-23471
Radiative forcing calculations for SF6 and CH4 using a correlated k-distribution transmission model
[DE94-001855] p 2397 N94-23700

GLOBULAR CLUSTERS
Voyager observations of globular clusters
[NASA-CR-194806] p 2598 N94-23330
UV-bright stars in globular clusters
[NASA-CR-189324] p 2599 N94-24666

GLOVES
Investigation of hand capabilities under a variety of performance conditions and an attempt to explain performance differences p 2444 N94-25354

GLUCOSE
Non-invasive optical detection of glucose in cell culture nutrient medium p 2422 N94-25357

GLUONS
The status of glueballs
[DE93-040040] p 2531 N94-22923
The Casimir energy of the rigid string with massive ends
[DE93-616851] p 2492 N94-25338
Proton spin: The role of quark-gluon and hadron degrees of freedom
[DE93-616867] p 2538 N94-25341
On the hadron formation time in pion-nucleus interaction
[DE93-616879] p 2539 N94-25476

GOES SATELLITES
Solar-geophysical data number 584, April 1993. Part 2: (Comprehensive reports). Data for October 1992, and miscellaneous
[PB93-198331] p 2627 N94-23739
High resolution encoder-motor used in the orbital spin scan radiometer, GOES VAS satellites
p 2209 N94-24038

GOGGLES
Evaluation of visual acuity with Gen 3 night vision goggles
[NASA-TM-108792] p 2431 N94-23974
Night operations p 2431 N94-23977
Night vision devices and characteristics
p 2432 N94-23982
Cockpit/NVG visual integration issues
p 2432 N94-23983
Night vision goggle illusions and visual training
p 2432 N94-23984

GOLD
The statistics of sputtering
[DE94-001128] p 2243 N94-23715
Interactions between organized, surface-confined monolayers and vapor-phase probe molecules. 7: Comparison of self-assemblying organomercaptan monolayers deposited on gold from liquid and vapor phases
[AD-A273196] p 2535 N94-24555
Ge-Au eutectic bonding of Ge (100) single crystals
[DE94-002281] p 2564 N94-24657
Investigate zero-stress replicated optics
[NASA-CR-193889] p 2545 N94-24665
Chemically sensitive interfacial force microscopy: Contact potential measurements of self-assembling monolayer films
[AD-A273135] p 2234 N94-24772
The nanometer-scale mechanics of gold films
[AD-A273307] p 2565 N94-25086

GOLD ALLOYS
Multilayer relaxation and surface structure of ordered alloys
[NASA-TM-106433] p 2243 N94-23578

GOVERNMENT/INDUSTRY RELATIONS
The Electronics Quality/Reliability Center: Lessons learned from partnering with industry
[DE94-001501] p 2309 N94-23777
NASA technology applications team: Applications of aerospace technology
[NASA-CR-194775] p 2597 N94-24494
SEMATECH, a case study: Analysis of a government-industry partnership
[AD-A273166] p 2586 N94-24683
NASA/DOD Aerospace Knowledge Diffusion Research Project. Report number 21: US aerospace industry librarians and technical information specialists as information intermediaries: Results of the phase 2 survey
[NASA-TM-109064] p 2593 N94-24709
Defense aerospace and the new world order
p 2596 N94-25066

GOVERNMENTS
Making government work: Electronic delivery of Federal services
[OTA-TCT-578] p 2290 N94-23081

GRADIENTS
Application of multigrid methods to the solution of liquid crystal equations on a SIMD computer
p 2484 N94-23686
Studies on the implementation of normals and curvatures. Part 1: The first or mean curvature
[DE94-001546] p 2488 N94-24503

GRAFTING
Microstructure of styrene methyl methacrylate copolymers grafted onto polybutadiene seeds
[ETN-94-95360] p 2262 N94-25225

GRAIN BOUNDARIES
Polycrystalline thin film materials and devices
[DE93-018213] p 2389 N94-22862
Atomic-scale structure of grain boundaries: Correlations to grain boundary properties
[DE94-001289] p 2558 N94-22990
Grain-boundary microchemistry and intergranular cracking of irradiated austenitic stainless steel
[DE94-000466] p 2242 N94-23457
Defects in electro-optically active polymer solids
p 2223 N94-24342

GRAIN SIZE
Characterization of 3-D particle distributions and effects on recrystallization studied by computer simulation
[PB93-201408] p 2562 N94-23535
High strain rate superplasticity in metals and composites
[DE94-001521] p 2229 N94-24547

GRAMMARS
PROGRIL: A language for the definition of protocol grammars
[EUT-93-E-270] p 2449 N94-23172
Code generation for the attribute evaluator of the protocol engine grammar processor unit
[EUT-93-E-271] p 2450 N94-23173

GRAND UNIFIED THEORY
Towards a theory of quark and lepton masses
[DE94-001726] p 2533 N94-23218
Stitching the Yukawa quilt
[PB93-204477] p 2569 N94-24532

GRAPH THEORY
Toughness and triangle-free graphs
[MEMO-1127] p 2478 N94-22715
Median stabilization degree of a median algebra
[PB93-220010] p 2479 N94-23093
Linear algorithm for flattening list graphs
[PB93-220648] p 2448 N94-23097
The p-ranks of Latin square graphs
[PB93-230498] p 2479 N94-23107
Structures of tetrahedrization: A mathematical and algorithmical point of view
[ETN-94-95172] p 2480 N94-23166
Experience with parametric binary dissection
[NASA-CR-191552] p 2473 N94-23558
The Third Twente Workshop on Graphs and Combinatorial Optimization
[PB94-110947] p 2486 N94-23722
Toughness in Hamiltonicity in almost claw-free graphs
[MEMO-1114] p 2487 N94-24053
Investigation on interval edge-coloring of graphs
[PB94-110913] p 2488 N94-24541
Criterion for some Hamiltonian graphs to be hamilton-connected
[PB94-110921] p 2489 N94-24651
The Third Twente Workshop on Graphs and Combinatorial Optimization: Abstracts and late extended abstracts
[PB94-110954] p 2489 N94-24652
Irreducible core of a minimum cost spanning tree game
[PB94-110962] p 2489 N94-24653
Fixed points and shift cycles in cellular automata
[RR-459] p 2492 N94-25309

GRAPHICAL USER INTERFACE
The TOPSIM 4 graphic user interface
[ESA-STM-247] p 2450 N94-23228
GLview user's guide
[PB93-201366] p 2452 N94-23444
The Mars mapper science and mission planning tool
p 2503 N94-23867
Customizing graphical user interface technology for spacecraft control centers p 2510 N94-23905
XRTD: An X-Windows based, real-time radiometric display and analysis system p 2305 N94-23922
Intelligent tutoring and aiding in satellite ground control p 2443 N94-23929
Automating a human factors evaluation of graphical user interfaces for NASA applications: An update on CHIMES
p 2443 N94-23936
Automated system function allocation and display format: Task information processing requirements
p 2434 N94-24189
Interoperability through standardization: Electronic mail, and X Window systems p 2575 N94-24406
Integration and evaluation of a simulator designed to be used within a dynamic prototyping environment
p 2198 N94-24436
World processor: An interface for textual display and manipulation in virtual reality
[PB94-118643] p 2592 N94-24642
Analyzing the properties of user interface software
[AD-A273601] p 2460 N94-24933

GRAPHITE-EPOXY COMPOSITES
Fiber optic detection of laser generated ultrasound for materials characterization
[ISBN-0-315-83541-9] p 2541 N94-22891
Analysis of local delaminations caused by angle ply matrix cracks
[NASA-TM-109052] p 2228 N94-24083
A prediction method for the compressive strength of impact damaged composite laminates
[CTN-94-60925] p 2229 N94-24137
Repair of cracked aluminum aircraft structure with composite patches p 2156 N94-24259
Post buckling behaviour of stiffened composite panels loaded in cyclic compression and shear
p 2157 N94-24260
Fiber optic detection of ultrasound and its application to cure monitoring
[ISBN-0-315-83424-2] p 2544 N94-24466
Damage tolerance of pressurized graphite/epoxy tape cylinders under uniaxial and biaxial loading
[NASA-CR-195101] p 2377 N94-24587
Test methods for composites: A status report. Volume 2: Compression test methods
[AD-A273522] p 2230 N94-24779
Test methods for composites: A status report. Volume 3: Shear test methods
[AD-A273561] p 2230 N94-25163

GRAPHS (CHARTS)
Toughness and triangle-free graphs
[MEMO-1127] p 2478 N94-22715
Long cycles in graphs with prescribed toughness and minimum degree
[MEMO-1109] p 2478 N94-22727
Linear algorithm for flattening list graphs
[PB93-220648] p 2448 N94-23097
The p-ranks of Latin square graphs
[PB93-230498] p 2479 N94-23107
Using genetic algorithms for scheduling data flow graphs
[EUT-92-E-266] p 2449 N94-23169
Toughness in Hamiltonicity in almost claw-free graphs
[MEMO-1114] p 2487 N94-24053
Process and representation in graphical displays
p 2433 N94-24187

GRASSLANDS
Groundtruth collection for the JPL-SAR and ERS-1 campaign in Flevoland and Veluwe, Netherlands, 1991
[PB93-230654] p 2386 N94-23755

GRATINGS (SPECTRA)
Calibration of a helium-cooled infrared spatial radiometer and grating spectrometer p 2384 N94-23607

GRAVIMETRY
An investigation into acceleration determination for airborne gravimetry using the global positioning system
[ISBN-0-315-59470-5] p 2175 N94-24176

GRAVITATION
Tensor-scalar cosmological models and their relaxation toward general relativity
[PB93-220796] p 2601 N94-23099
GRAVITATIONAL COLLAPSE
The current status of observational constraints on cosmic strings
[DE94-001505] p 2601 N94-23010
GRAVITATIONAL EFFECTS
Echocardiographic findings in trained aircrew: The effect of +Gz on cardiac structure (working group 18)
p 2424 N94-23320
Reach performance while wearing the Space Shuttle launch and entry suit during exposure to launch accelerations p 2436 N94-24204
Modeling of PCG fluid dynamics: Salient results
p 2224 N94-24345
The influence of flow type, particle type and gravity on orthokinetic coagulation
[ETN-94-95333] p 2267 N94-25060
The role of visual context in manual target localization
p 2429 N94-25351
Development of a model to assess orthostatic responses p 2427 N94-25376
GRAVITATIONAL FIELDS
An improved gravity model for Mars: Goddard Mars Model-1 (GMM-1)
[NASA-TM-104584] p 2401 N94-23282
A mixed method Poisson solver for three-dimensional self-gravitating astrophysical fluid dynamical systems
p 2484 N94-23684
The pre-development of the Aristoteles calibration mechanism p 2209 N94-24006
Steady motions of rigid body satellites in a central gravitational field
[AD-A273742] p 2206 N94-25532
GRAVITATIONAL PHYSIOLOGY
Echocardiographic findings in trained aircrew: The effect of +Gz on cardiac structure (working group 18)
p 2424 N94-23320
Responses to LBNP in men with varying profiles of strength and aerobic capacity: Implications for flight crews
[NASA-TP-3346] p 2426 N94-23530
Artificial gravity in space flight
[AD-A273420] p 2427 N94-24928
The role of visual context in manual target localization
p 2429 N94-25351
Loading, electromyograph, and motion during exercise
p 2427 N94-25359
GRAVITATIONAL WAVES
The current status of observational constraints on cosmic strings
[DE94-001505] p 2601 N94-23010
Choice of filters for the detection of gravitational waves from coalescing binaries. 2: Detection in coloured noise
[DE93-616844] p 2604 N94-25211
A parallel algorithm for filtering gravitational waves from coalescing binaries
[DE93-616845] p 2604 N94-25212
Deviation equations of Synge and Schild in spaces with affine connection and metric, and equations for gravitational waves detectors
[DE93-616852] p 2571 N94-25339
The scattering and collision of gravitational waves in Friedmann-Robertson-Walker open universes
[MATHS-REPT-A-193] p 2406 N94-25430
GRAVITY GRADIOMETERS
The pre-development of the Aristoteles calibration mechanism p 2209 N94-24006
GRAVITY WAVES
Hamiltonian approach to fairly low and long gravity waves
[PB94-111119] p 2404 N94-24598
Observational case studies and diagnostic analyses of long-lived large-amplitude inertia-gravity waves
[AD-A273545] p 2404 N94-24794
A diagnostic model to estimate winds and small-scale drag from Mars Observer PMIRR data
p 2617 N94-24874
Three-dimensional numerical simulation of thermal tides in the Martian atmosphere p 2622 N94-24901
GREASES
Tribological characterization of spatial wet lubricants under vacuum p 2264 N94-24010
BLAST, a new lubricant screening tester for space oils and greases p 2362 N94-24042
Investigation of the ultrafiltration technique using military greases
[AD-A273633] p 2261 N94-25029
GREEN'S FUNCTIONS
Rigorous analysis of thick microstrip antennas and wire antennas embedded in a substrate
[EUT-92-E-263] p 2290 N94-22876
Unsteady three-dimensional thermal field prediction in turbine blades using nonlinear BEM
p 2325 N94-23665
Fast fourier transforms of piecewise constant functions
[AD-A272648] p 2456 N94-24535
Advanced electromagnetic methods for aerospace vehicles
[NASA-CR-195111] p 2365 N94-24699
On a new functional integral formalism for Hubbard model
[DE93-614017] p 2492 N94-25334
Weak interactions in a bilocal chiral theory
[DE93-616887] p 2539 N94-25477
GREENHOUSE EFFECT
Catalog of data bases and reports
[DE93-040597] p 2568 N94-22875
Overview of global greenhouse effects
[DE93-041165] p 2396 N94-22887
Radiative forcing calculations for SF6 and CH4 using a correlated k-distribution transmission model
[DE94-001855] p 2397 N94-23700
Cloud-free aerosol optical depth determination over oceans from satellite radiometry
[DE94-001897] p 2386 N94-23779
Manual on measurement of methane and nitrous oxide emissions from agriculture
[DE93-616429] p 2399 N94-25167
GRID GENERATION (MATHEMATICS)
A geometric weighted elliptic grid regeneration method for 3D unstructured ALE hydrodynamics
[DE94-000309] p 2448 N94-22980
Computation of propulsion-related flowfields using unstructured adaptive meshes p 2215 N94-23056
POISs3: A 3D poisson smoother of structured grids
[PB93-226231] p 2318 N94-23115
Tracking sharp interface of two fluids by the CIP (Cubic-Interpolated Propagation) scheme
[DE93-508322] p 2319 N94-23460
Parallel unstructured grid generation for computational aerosciences
[NASA-CR-192244] p 2466 N94-23483
Simulation of unsteady flows through stator and rotor blades of a gas turbine using the Chimera method
p 2323 N94-23652
The Sixth Copper Mountain Conference on Multigrid Methods, part 1
[NASA-CP-3224-PT-1] p 2482 N94-23673
FAS multigrid calculations of three dimensional flow using non-staggered grids p 2341 N94-23675
A comparison of locally adaptive multigrid methods: LDC, FAC and FIC p 2485 N94-23692
An object-oriented approach for parallel self adaptive mesh refinement on block structured grids
p 2469 N94-23697
Unstructured grid large eddy simulation of wall bounded turbulent flows p 2329 N94-24151
Unstructured adaptive mesh computations of rotorcraft high-speed impulsive noise
[NASA-CR-195090] p 2529 N94-24307
Implementation of the Baldwin-Barth turbulence model into the ZETA code and its diagnosis
[NASA-CR-194795] p 2335 N94-24640
A two-dimensional dispersion module for the TOUGH2 simulator
[DE94-002262] p 2335 N94-24655
Advanced electromagnetic methods for aerospace vehicles
[NASA-CR-195111] p 2365 N94-24699
An integrated runtime and compile-time approach for parallelizing structured and block structured applications
[NASA-CR-191554] p 2458 N94-24740
Numerical flow simulation for complete vehicle configurations
[AD-A273588] p 2170 N94-24849
FRANC2D: A two-dimensional crack propagation simulator. Version 2.7: User's guide
[NASA-CR-4572] p 2246 N94-25118
Development and application of new algorithms for the simulation of viscous compressible flows with moving bodies in three dimensions
[AD-A273514] p 2338 N94-25157
Application of body fitted-coordinates in heat conduction problems
[ETN-94-95338] p 2340 N94-25484
GROUND BASED CONTROL
Graphical programming: A systems approach for telerobotic servicing of space assets
[DE93-019016] p 2472 N94-23201
NASDA's view of ground control in mission operations
p 2305 N94-23835
The space operations at CNES p 2498 N94-23837
Common front end systems for Space Shuttle and Space Station control centers at Johnson Space Center
p 2305 N94-23838
ASTER, a multinational Earth observing concept
p 2389 N94-23840
Ground operation of robotics on Space Station Freedom p 2371 N94-23841
SAMPEX payload operation control center implementation p 2197 N94-23843
A user view of the EURECA ground segment
p 2499 N94-23844
SPOT satellite family: Past, present, and future of the operations in the mission and control center
p 2500 N94-23846
A reference model for space data system interconnection services p 2305 N94-23847
Distributed science operations for JPL planetary missions p 2500 N94-23850
SCOS2: ESA's new generation of mission control systems p 2197 N94-23851
Operations concepts for Mars missions with multiple mobile spacecraft p 2501 N94-23852
Preparing the DSN operations concepts
p 2501 N94-23853
NASDA satellite mission operation system and operations p 2501 N94-23854
NASA/Goddard Space Flight Center's testbed for CCSDS compatible systems p 2197 N94-23855
SPOT4 Operational Control Center (CMP)
p 2197 N94-23856
Ground data system for Space Flyer Unit (SFU)
p 2207 N94-23860
Radioastron flight operations p 2502 N94-23861
Management of information for mission operations using automated keyword referencing p 2506 N94-23886
AMFESYS: Modelling and diagnosis functions for operations support p 2506 N94-23887
Mars Observer screen display design for a multimission environment p 2197 N94-23888
The FOT tool kit concept p 2507 N94-23889
GSMS and space views: Advanced spacecraft monitoring tools p 2507 N94-23890
VMPLOT: A versatile analysis tool for mission operations p 2507 N94-23891
The mission events graphic generator software: A small tool with big results p 2464 N94-23893
Customizing graphical user interface technology for spacecraft control centers p 2510 N94-23905
Reliable transfer of data from ground to space
p 2305 N94-23908
Kalman filtering applied to real-time monitoring of apogee maneuvers p 2196 N94-23923
MERCATOR: Methods and Realization for Control of the Attitude and the Orbit of spacecraft
p 2202 N94-23925
HISPASAT launch and early operations phases: Computation and monitoring of geostationary satellite positioning p 2514 N94-23928
Intelligent tutoring and aiding in satellite ground control p 2443 N94-23929
Operational training for the mission operations at the Brazilian National Institute for Space Research (INPE)
p 2429 N94-23933
GenSAA: A tool for advancing satellite monitoring with graphical expert systems p 2516 N94-23945
EOS ground data systems: A description and interface overview p 2517 N94-23948
Telemetry ground system development via the component approach p 2203 N94-23949
GROUND CREWS
Evaluation of computer-aided instruction techniques for the crew interface coordination position
p 2429 N94-24438
GROUND OPERATIONAL SUPPORT SYSTEM
Making adaptable systems work for mission operations: A case study p 2506 N94-23883
An approach to the design of operations systems
p 2506 N94-23884
GROUND STATE
Ultracold atoms in traps and fountains
[ETN-94-95325] p 2537 N94-25239
GROUND STATIONS
Implementation of a system to provide mobile satellite services in North America p 2281 N94-22784
INMARSAT's personal communicator system
p 2282 N94-22788
A protocol for satellite access via use of spot-beams
p 2286 N94-22811
NASDA satellite mission operation system and operations p 2501 N94-23854
Ground data system for Space Flyer Unit (SFU)
p 2207 N94-23860
Customizing graphical user interface technology for spacecraft control centers p 2510 N94-23905
The Columbus logistics support at the APMC: Requirements and implementation aspects
p 2515 N94-23935

GROUND SUPPORT EQUIPMENT
Implementation of a system to provide mobile satellite services in North America p 2281 N94-22784
GPHS-RTG's in support of the Cassini mission
[DE94-001445] p 2218 N94-23459
GROUND SUPPORT SYSTEMS
INMARSAT's personal communicator system
p 2282 N94-22788
System services and architecture of the TMI satellite mobile data system p 2286 N94-22817
Expanding the KATE toolbox p 2477 N94-23247
SpaceOps 1992: Proceedings of the Second International Symposium on Ground Data Systems for Space Mission Operations
[NASA-CR-194486] p 2497 N94-23832
Commonality of flight control systems for support of European telecommunications missions
p 2304 N94-23834
The space operations at CNES p 2498 N94-23837
Ground operation of robotics on Space Station Freedom p 2371 N94-23841
A user view of the EURECA ground segment
p 2499 N94-23844
Development of the Cassini Ground Data System in a multimission environment p 2500 N94-23845
SPOT satellite family: Past, present, and future of the operations in the mission and control center
p 2500 N94-23846
A reference model for space data system interconnection services p 2305 N94-23847
Distributed science operations for JPL planetary missions p 2500 N94-23850
Operations concepts for Mars missions with multiple mobile spacecraft p 2501 N94-23852
Preparing the DSN operations concepts
p 2501 N94-23853
NASDA satellite mission operation system and operations p 2501 N94-23854
NASA/Goddard Space Flight Center's testbed for CCSDS compatible systems p 2197 N94-23855
SPOT4 Operational Control Center (CMP)
p 2197 N94-23856
Columbus system support for telescience operations
p 2505 N94-23877
Using Mach threads to control DSN operational sequences p 2477 N94-23916
Deep Space Network (DSN), Network Operations Control Center (NOCC) computer-human interfaces
p 2447 N94-23917
A real-time navigation monitoring expert system for the Space Shuttle Mission Control Center
p 2202 N94-23921
XRTD: An X-Windows based, real-time radiometric display and analysis system p 2305 N94-23922
The Columbus logistics support at the APMC: Requirements and implementation aspects
p 2515 N94-23935
Using SFOC to fly the Magellan Venus mapping mission p 2516 N94-23941
High performance, low cost, self-contained, multipurpose PC based ground systems
p 2516 N94-23943
Space Station Freedom ground data system: Design and operations p 2518 N94-23957
New mission requirements methodologies for services provided by the Office of Space Communications
p 2519 N94-23961
Resource allocation planning with international components p 2520 N94-23963
Scheduling the future NASA Space Network: Experiences with a flexible scheduling prototype
p 2520 N94-23965
Iowa satellite project ISAT-1
[NASA-CR-195517] p 2206 N94-24838
GROUND TESTS
Development of the Cassini Ground Data System in a multimission environment p 2500 N94-23845
LSS systems planning and performance program
[NASA-CR-193882] p 2196 N94-24309
GROUND TRUTH
Optical component MAC Europe ground truth report: Flevoland 1991 (Netherlands)
[BCRS-92-27] p 2382 N94-23177
Uncertainties in climate data sets
[NASA-CR-194848] p 2408 N94-23577
Groundtruth collection for the JPL-SAR and ERS-1 campaign in Flevoland and Veluwe, Netherlands, 1991
[PB93-230654] p 2386 N94-23755
GROUND WAVE PROPAGATION
Comparison of HF groundwave propagation models
[AD-A273146] p 2299 N94-24668
GROUND-AIR-GROUND COMMUNICATION
Power attenuation characteristics as switch-over criterion in personal satellite mobile communications
p 2277 N94-22756
Integration of mobile satellite and cellular systems
p 2277 N94-22757
New mission requirements methodologies for services provided by the Office of Space Communications
p 2519 N94-23961
GROUP DYNAMICS
Egalitarian non-average contribution method for cooperative games
[PB94-111705] p 2497 N94-23800
GROUP THEORY
Orbit spaces over commutative rings and projectives as semi-isomorphisms
[DE93-616822] p 2493 N94-25473
GUIDANCE (MOTION)
A tracking sonar sensor for vehicle guidance
[OUEL-1956/92] p 2472 N94-23179
NASA LaRC Workshop on Guidance, Navigation, Controls, and Dynamics for Atmospheric Flight, 1993
[NASA-CP-10127] p 2162 N94-25096
GUIDANCE SENSORS
A tracking sonar sensor for vehicle guidance
[OUEL-1956/92] p 2472 N94-23179
GUIDE VANES
Gas turbine and operating method of the same
[CA-PATENT-APPL-SN-2043039] p 2188 N94-24490
GUINEA PIGS
Interaction of tacrine at M(1) and M(2) cholinoceptors in guinea pig brain p 2421 N94-24294
GULF OF MEXICO
An efficient data assimilation algorithm with a gaussian covariance structure
[AD-A273152] p 2418 N94-24671
GULF STREAM
Vertical motion in the SYNOP central array
[AD-A273593] p 2418 N94-24795
GUN LAUNCHERS
Projectile transverse motion and stability in electromagnetic induction launchers
[DE94-001557] p 2198 N94-23210
GUN PROPELLANTS
The internal structure and dynamics of the railgun plasma armature between infinitely wide ablating rails
[DE94-001473] p 2198 N94-23208
Burning rate of double-base propellant in the presence of plasma p 2155 N94-24252
GUNS (ORDNANCE)
A comparison of in-bore projectile motion from an electromagnetic railgun versus that of a conventional cannon barrel
[AD-A273473] p 2198 N94-24690
GUST LOADS
A review of the Workshop on Fatigue Life Methodologies for Wind Turbines
[DE94-002039] p 2394 N94-23472
Continuous gust response and sensitivity derivatives using state-space models p 2161 N94-24287
GUSTS
ASR-9 microburst detection algorithm
[AD-A273591] p 2415 N94-24850
GYROTROPISM
Polarizability of gyrotropic sphere
[PB93-225019] p 2524 N94-23131

H

H ALPHA LINE
Solar-geophysical data number 589, September 1993. Part 2: (Comprehensive reports). Data for March 1993, and miscellaneous
[PB94-117405] p 2628 N94-24994
H II REGIONS
UV extinction and IR emission in diffuse H2 regions
[NASA-CR-195194] p 2600 N94-25270
H LINES
UV spectral variability in the Herbig Ae star HR 5999. 11: The accretion interpretation
[NASA-CR-189313] p 2599 N94-23334
The resonance lines of MG2 as diagnostics of the upper solar chromosphere
[NASA-CR-195084] p 2627 N94-24300
H-INFINITY CONTROL
Nonlinear state space H(sub infinity) control theory
[MEMO-1119] p 2469 N94-22706
Nonlinear systems which have finite-dimensional H(sub infinity) suboptimal central controllers
[MEMO-1120] p 2469 N94-22707
Identification for robust control using an H(sub infinity) norm
[EUT-92-E-261] p 2470 N94-22673
Reduced-order modelling and control of a class of systems for which balanced truncation is Hankel-norm optimal
[OUEL-1922/92] p 2472 N94-23163
Squaring-down and the problems of almost-zeros for continuous-time systems
[PB93-237758] p 2489 N94-24608
Discrete time minimum entropy H(infinity) control problem
[PB93-237808] p 2474 N94-24609
Asymptotic correctors: The LTR
[PB93-199701] p 2474 N94-24627
The H(sub infinity) optimal controller design and reduction for the inertial hold mode of the attitude control system of the XTE spacecraft
[NASA-CR-195137] p 2366 N94-24846
Exploiting structure: Introduction and motivation
[NASA-CR-195136] p 2490 N94-24847
Parametric uncertainty reduction in robust multivariable control
[AD-A273412] p 2460 N94-24927
HABITABILITY
Crew interface analysis: Selected articles on space human factors research, 1987 - 1991
[NASA-TM-104756] p 2433 N94-24185
HADRONS
Low p(sub T) photon production in proton-nucleus collisions at 18 GeV/c
[DE94-001380] p 2532 N94-23007
Calculations of Bose-Einstein correlations from Relativistic Quantum Molecular Dynamics
[DE94-000794] p 2569 N94-23453
B-quark production at hadron colliders
[DE94-001459] p 2534 N94-23806
Proton spin: The role of quark-gluon and hadron degrees of freedom
[DE93-616867] p 2538 N94-25341
A quark structure of hadrons and nuclei
[DE93-616872] p 2539 N94-25474
On the hadron formation time in pion-nucleus interaction
[DE93-616879] p 2539 N94-25476
Weak interactions in a bilocal chiral theory
[DE93-616887] p 2539 N94-25477
HALF PLANES
Transient analysis of conducting half-plane problem with noncausal scattering image
[PB93-225027] p 2524 N94-23110
HALF SPACES
Diffraction analysis of transient acoustic waves: Half-plane in a layered medium
[PB94-110988] p 2526 N94-23726
Ring nuclei of strain for bonded dissimilar elastic half spaces with particular application to axisymmetric crack problems
[OUEL-1966/92] p 2379 N94-25325
HALIDES
Adsorption, desorption, and decomposition of HCl and HBr on Ge(100): Competitive pairingand near-first-order desorption kinetics
[AD-A273504] p 2235 N94-24790
HALLEY'S COMET
Evolution of large-scale plasma structures in comets: Kinematics and physics
[NASA-CR-194777] p 2601 N94-23251
HAMILTON-JACOBI EQUATION
Approximate optimal guidance for the advanced launch system
[NASA-CR-4568] p 2198 N94-24752
HAMILTONIAN FUNCTIONS
Long cycles in graphs with prescribed toughness and minimum degree
[MEMO-1109] p 2478 N94-22727
Relativistic configuration interaction calculation of the correlation energies of highly-charged ions
[DE94-001055] p 2532 N94-22988
The Hamiltonian double-zero eigenvalue
[W-9304] p 2479 N94-23138
Toughness in Hamiltonicity in almost claw-free graphs
[MEMO-1114] p 2487 N94-24053
Comparison of time integration methods for the evolution of galaxies
[PB94-111671] p 2602 N94-24522
Hamiltonian approach to fairly low and long gravity waves
[PB94-111119] p 2404 N94-24598
Criterion for some Hamiltonian graphs to be hamilton-connected
[PB94-110921] p 2489 N94-24651
Thermophysical properties of simple liquid metals: A brief review of theory p 2248 N94-25130
Phase structure of the two-dimensional phi(4) field theory within thermo-field dynamics
[DE93-616850] p 2570 N94-25337
The Casimir energy of the rigid string with massive ends
[DE93-616851] p 2492 N94-25338
Contribution of all excited states to ZFS of a (sup 6) S-state
[DE93-617007] p 2568 N94-25483

HAND (ANATOMY)
Conceptual design of an astronaut hand anthropometry device
[NASA-CR-195490] p 2439 N94-24956

HANDBOOKS
NASA printing, duplicating, and copying management handbook
[NASA-NHB-1490.5] p 2590 N94-23971
Pilot-vehicle interface handbook, chapter 19. Volume 2: Digital systems validation
[DOT/FAA/CT-88/10-VOL-2] p 2438 N94-24830

HANDWRITING
On chain coding of line drawings
[ISBN-9-06-275778-2] p 2462 N94-25252

HANKEL FUNCTIONS
Reduced-order modelling and control of a class of systems for which balanced truncation is Hankel-norm optimal
[OUEL-1922/92] p 2472 N94-23163
Balanced truncation is Hankel-norm optimal when used to approximate a finite-difference model of a parabolic PDE
[OUEL-1921/92] p 2492 N94-25324

HARDNESS
Development of small punch testing technique and its application to evaluation of mechanical properties degradation
[DE94-001193] p 2375 N94-23184

HARDWARE
Experiments with a small behaviour controlled planetary rover p 2371 N94-23427
The Fifth European Space Mechanisms and Tribology Symposium
[ESA-SP-334] p 2355 N94-23985
Primary deployment mechanism for the European Polar Platform p 2207 N94-23995
The Olympus PAX, measurement of mechanism induced vibration p 2362 N94-24041
Postflight hardware evaluation 360T021 (RSRM-21, STS-45), revision A
[NASA-CR-193904] p 2201 N94-24965
Postflight hardware evaluation RSRM-29 (STS-54). Case, seals, and joints PFORs, appendix B
[NASA-CR-193899] p 2367 N94-25020
Computerized testing system software conversion and development: Identifying software and hardware portability issues and solutions
[AD-A273489] p 2462 N94-25287
A soft robot interface
[OUEL-1948/92] p 2463 N94-25468

HARDWARE DESCRIPTION LANGUAGES
Formal verification of digital circuits described in VHDL
[ETN-94-95165] p 2306 N94-22883
Micro SIL-1 simulator
[PB94-110889] p 2454 N94-23750

HARMONIC ANALYSIS
Finite-element modelling of three-dimensional electromagnetic fields using edge and nodal elements
[PB94-111077] p 2298 N94-24597

HARMONIC EXCITATION
Response of an anchored annular cylindrical liquid layer to various axial excitations in zero-gravity
[LRT-WE-9-FB-3-1992] p 2266 N94-23195

HARMONIC FUNCTIONS
Vectorization and parallelization of the finite strip method for dynamic Mindlin plate problems
p 2483 N94-23679

HARMONIC GENERATIONS
Limits on high-order harmonic generation from single-atom calculations
[DE93-019950] p 2531 N94-22869
High-order sum and difference-frequency generation in helium
[DE94-001064] p 2348 N94-23181
Inertial confinement fusion
[DE94-002602] p 2551 N94-23703
Prediction of nonlinear optical properties of organic materials. General theoretical considerations
p 2224 N94-24343
Nonlinear dynamical control of lasers
[AD-A273359] p 2350 N94-24938

HARMONICS
High-order sum and difference-frequency generation in helium
[DE94-001064] p 2348 N94-23181
The use of harmonics in 3-D magnetic fields
[DE94-002274] p 2299 N94-24656

HARTREE APPROXIMATION
Excitation mechanisms for XUV and x ray lasers
[DE93-617006] p 2351 N94-25482

HASTELLOY (TRADEMARK)
Material data representation of hysteresis loops for Hastelloy X using artificial neural networks
[NASA-TM-105990] p 2376 N94-23551
Development testing of the two-watt RTG heat source and Hastelloy-S/T-111 alloy compatibility studies
[DE94-002875] p 2243 N94-23784

HATCHES
An opening mechanism for the scientific airlock outer hatch p 2360 N94-24027

HEAD DOWN TILT
Responses to LBNP in men with varying profiles of strength and aerobic capacity: Implications for flight crews
[NASA-TP-3346] p 2426 N94-23530

HEAD MOVEMENT
Predictive head movement tracking using innovations generated by Kalman filters
[ISBN-0-315-83371-8] p 2427 N94-24467

HEAD-UP DISPLAYS
Cockpit/NVG visual integration issues
p 2432 N94-23983

HEALTH
Waste minimization/pollution prevention at R/D facilities: A cradle-to-grave tracking and information system that will be implemented at Sandia National Laboratories
[DE93-040330] p 2591 N94-24607

HEALTH PHYSICS
Experimental characterization of the AFIT Neutron Facility
[AD-A273822] p 2539 N94-25519

HEART
Primary prevention of coronary heart disease
p 2423 N94-23317
Echocardiographic screening of aircrew candidates
p 2424 N94-23319
Echocardiographic findings in trained aircrew: The effect of +Gz on cardiac structure (working group 18)
p 2424 N94-23320
Left ventricular hypertrophy and athlete's heart
p 2424 N94-23321
Aortic valve disease p 2424 N94-23322
Aeromedical implications of mitral valve prolapse
p 2424 N94-23323
Sarcoidosis and the aviator p 2425 N94-23325

HEART DISEASES
Cardiopulmonary Aspects in Aerospace Medicine
[AGARD-LS-189] p 2423 N94-23313
Cardiovascular and pulmonary disease in NATO aircrew: An overview p 2423 N94-23314
Screening for asymptomatic coronary heart disease
p 2423 N94-23315
Aeromedical disposition of Arrhythmias and electrocardiographic findings in aircrew
p 2423 N94-23318
Aortic valve disease p 2424 N94-23322

HEART FUNCTION
Cardiopulmonary Aspects in Aerospace Medicine
[AGARD-LS-189] p 2423 N94-23313
Echocardiographic screening of aircrew candidates
p 2424 N94-23319
Aeromedical implications of mitral valve prolapse
p 2424 N94-23323

HEART VALVES
Aortic valve disease p 2424 N94-23322
Aeromedical implications of mitral valve prolapse
p 2424 N94-23323
Nondestructive evaluations
[DE94-003020] p 2373 N94-24613

HEAT AFFECTED ZONE
New welding and finishing procedures
[DE94-602022] p 2352 N94-23025
Flex bearing UUEC, volume 2
[NASA-CR-193901] p 2365 N94-24588

HEAT BUDGET
Physics of iron
[DE94-002002] p 2402 N94-23721

HEAT ENGINES
A study of element interaction in thermoacoustic engines
[AD-A273228] p 2569 N94-24777

HEAT EXCHANGERS
Assessment of an SP-100 bi-modal propulsion and power system
[DE94-000889] p 2218 N94-23433
Study of transient behavior of finned coil heat exchangers p 2321 N94-23642
A theorem regarding roots of the zero-order Bessel function of the first kind p 2325 N94-23667
A study of element interaction in thermoacoustic engines
[AD-A273228] p 2569 N94-24777

HEAT FLUX
Fully coupled nonlinear thermomechanical analysis including general contact in PALM2D
[DE94-001661] p 2568 N94-23216
Performance characteristics of the DIII-D advanced divertor cryopump
[DE94-002745] p 2354 N94-23797
Miniature convection cooled plug-type heat flux gauges
[NASA-TM-106483] p 2344 N94-24069
Heat pipe vapor dynamics
[NASA-CR-194217] p 2327 N94-24096
Session on modeling of radiative transfer processes
p 2414 N94-24397
Heat transfer and flow structure in end-wall boundary layers
[AD-A273470] p 2335 N94-24689

HEAT MEASUREMENT
Phase transformations in Cu-Zr multilayers
[DE94-000393] p 2241 N94-23297
Microwave techniques for physical property measurements p 2238 N94-25134

HEAT PIPES
Heat pipe cooled heat rejection subsystem modelling for nuclear electric propulsion
[NASA-CR-191132] p 2219 N94-24061
Heat pipe vapor dynamics
[NASA-CR-194217] p 2327 N94-24096
Effect of longitudinal vibration on the capillary limit of a wrapped screen wick copper/water heat pipe
[AD-A273830] p 2571 N94-25524

HEAT PUMPS
Enhanced absorption cycle computer model
[DE94-001997] p 2271 N94-23793

HEAT RESISTANT ALLOYS
Tensile properties of 21-6-9 stainless steel at elevated temperatures
[DE94-001852] p 2240 N94-23017
Determination of the compatibility between structural alloys and molten metals at high temperatures
[DE94-000954] p 2241 N94-23434
Material data representation of hysteresis loops for Hastelloy X using artificial neural networks
[NASA-TM-105990] p 2376 N94-23551
Hot hydrogen testing of metallic turbo pump materials
[NASA-CR-193880] p 2244 N94-24066
Mean stress models for low cycle fatigue of a nickel-base superalloy p 2159 N94-24276
The importance of properties in modeling
p 2246 N94-25121
An overview of the measurements of thermophysical properties and some results on molten superalloys and semiconductors p 2248 N94-25128
Proceedings of the 12th International Congress: Corrosion Control for Low-Cost Reliability. Volume 1: Coatings
[AD-A273661] p 2251 N94-25448
Preceedings of the 12th International Congress: Corrosion Control for Low-Cost Reliability. Volume 3A: Corrosion: Specific issues
[AD-A273663] p 2251 N94-25450
Proceedings of the 12th International Congress: Corrosion Control for Low-Cost Reliability. Volume 3B: Corrosion: Specific issues
[AD-A273664] p 2251 N94-25451

HEAT SINKS
Thermoelectric cooled, purge-and-trap device for enhancing the utility of fiber optic VOC sensors
[DE94-001772] p 2541 N94-22722

HEAT SOURCES
Development of a theory of the wear of ceramics
[DE94-002773] p 2254 N94-23783
Development testing of the two-watt RTG heat source and Hastelloy-S/T-111 alloy compatibility studies
[DE94-002875] p 2243 N94-23784

HEAT TRANSFER
Small rocket flowfield diagnostic chambers
p 2210 N94-23030
Flow visualization study in high aspect ratio cooling channels for rocket engines p 2213 N94-23049
CFD analyses of coolant channel flowfields
p 2214 N94-23050
Heat transfer in rocket combustion chambers
p 2214 N94-23051
Characterization of heat transport and radiation hydrodynamics in collisional laser plasmas using collective Thomson scattering
[DE94-001502] p 2349 N94-23209
Assessment of an SP-100 bi-modal propulsion and power system
[DE94-000889] p 2218 N94-23433
SP-100 heat transport technology development
[DE94-000769] p 2218 N94-23452
Field models: Their present and future application in fire safety engineering
[PB93-201622] p 2269 N94-23506
The use of transition region characteristics to improve the numerical simulation of heat transfer in bypass transitional flows
[NASA-TM-106445] p 2320 N94-23525
Convection equation modeling: A non-iterative direct matrix solution algorithm for use with SINDA
p 2323 N94-23651

Mixing and unmixedness in plasma jets 1: Near-field analysis p 2323 N94-23655

Heat transfer in rocket engine combustion chambers and regeneratively cooled nozzles
[NASA-CR-195094] p 2220 N94-24471

Thermal-fluid analysis of the fill and drain operations of a cryogenic fuel tank
[NASA-TM-104273] p 2334 N94-24495

Solid rocket combustion simulator technology using the hybrid rocket for simulation
[NASA-CR-195142] p 2265 N94-24578

Heat transfer and flow structure in end-wall boundary layers
[AD-A273470] p 2335 N94-24689

Relationship between transition and modes of instability in supersonic boundary layers
[NASA-CR-4562] p 2336 N94-24725

Investigation of the heat handling capabilities of DIII-D neutral beamline internal components
[DE94-001107] p 2553 N94-24756

The role of atmospheric heat transport in the seasonal carbon dioxide cycle p 2621 N94-24896

The importance of properties in modeling
p 2246 N94-25121

Analytical skin friction and heat transfer formula for compressible internal flows
[NASA-CR-191185] p 2170 N94-25173

Measurements of the influence of integral length scale on stagnation region heat transfer
[NASA-TM-106503] p 2338 N94-25183

Effect of longitudinal vibration on the capillary limit of a wrapped screen wick copper/water heat pipe
[AD-A273830] p 2571 N94-25524

HEAT TRANSFER COEFFICIENTS

Experimental and analytical study of cryogenic propellant boiloff to develop and verify alternate pressurization concepts for Space Shuttle external tank using a scaled down tank p 2266 N94-23657

Response-coefficient method for heat-conduction transients with time-dependent inputs
p 2326 N94-23671

HEAT TRANSMISSION

An F2D analysis of the Flow Instability Test (FIT) experiment
[DE94-001420] p 2217 N94-23193

Fully coupled nonlinear thermomechanical analysis including general contact in PALM2D
[DE94-001661] p 2568 N94-23216

Fire safety engineering research in Norway
[PB93-201630] p 2268 N94-23429

HEAT TREATMENT

Discontinuous phase formation and selective attack of SiC materials exposed to low oxygen partial pressure environments
[DE93-040161] p 2231 N94-22933

Internal friction associated with dislocation relaxations in virgin martensite
[PB93-226280] p 2240 N94-23119

Characterization of the microstructure of Nb-1wt.%Zr-0.1wt.%C tubes as affected by thermomechanical processing
[NASA-TM-106381] p 2242 N94-23550

Properties and processing characteristics of low density carbon cloth phenolic composites p 2231 N94-24450

Investigate zero-stress replicated optics
[NASA-CR-193889] p 2545 N94-24665

Use of photostress to characterize the mechanical behavior of weldments
[NASA-CR-195201] p 2378 N94-25267

HEATERS

Design of a resistojet for Space Station Freedom
[NASA-CR-195506] p 2221 N94-24979

HEATING

Multigrid and cyclic reduction applied to the Helmholtz equation p 2304 N94-23676

HEATING EQUIPMENT

Hydride thermodynamic machines
[VTT-JULK-768] p 2571 N94-25416

HEAVY IONS

Heavy ion irradiation of Bi-2223 silver-clad tapes for superconducting current density enhancement
[DE93-017416] p 2556 N94-22886

Semiempirical studies of atomic structure
[DE94-001588] p 2531 N94-22937

A study of non-ideal focus properties of 30 deg parallel plate energy analyzers
[NIFS-263] p 2311 N94-24457

Behavior of the intermittency exponents and a quark-gluon plasma formation in the heavy ion collisions
[DE93-616869] p 2541 N94-25342

HEAVY NUCLEI

Behavior of the intermittency exponents and a quark-gluon plasma formation in the heavy ion collisions
[DE93-616869] p 2541 N94-25342

HEISENBERG THEORY

Spin fluctuations in an ordered Heisenberg ferromagnet with dipolar interactions
[PB93-204493] p 2524 N94-24533

HELICAL ANTENNAS

Low cost antennas for MSAT vehicular applications
p 2289 N94-22830

L-band mobile terminal antennas for helicopters
p 2289 N94-22835

HELICAL WINDINGS

Overview of the ATF stellarator program
[DE94-000371] p 2550 N94-23462

HELICOPTER DESIGN

Aeroelastic, aeromechanical and vibration problems in helicopters p 2154 N94-24244

The future of rotary-wing aircraft p 2185 N94-25070

HELICOPTER PERFORMANCE

The future of rotary-wing aircraft p 2185 N94-25070

Remote vibration measurements at a sud aviation alouette 3 helicopter with a CW CO2-laser system
[AD-A273818] p 2190 N94-25516

HELICOPTER PROPELLER DRIVE

NASA/Army rotorcraft transmission research, a review of recent significant accomplishments
[NASA-TM-106508] p 2367 N94-25181

HELICOPTERS

L-band mobile terminal antennas for helicopters
p 2289 N94-22835

An overview of a model rotor icing test in the NASA Lewis Icing Research Tunnel
[NASA-TM-106471] p 2166 N94-23299

Analysis of passive acoustic ranging of helicopters from the joint acoustic propagation experiment
p 2529 N94-24220

Unstructured adaptive mesh computations of rotorcraft high-speed impulsive noise
[NASA-CR-195090] p 2529 N94-24307

Validation of the ROTAC code for the rotor noise prediction
[PB93-204311] p 2529 N94-24514

Advanced electromagnetic methods for aerospace vehicles
[NASA-CR-195111] p 2365 N94-24699

A parametric study of harmonic rotor hub loads
[NASA-CR-4558] p 2181 N94-24726

Projected effectiveness of airbag supplemental restraint systems in US Army helicopter cockpits
[AD-A273250] p 2174 N94-25141

The ISL rotor bench
[ISL-R-108/92] p 2185 N94-25301

Multiple-camera/motion stereoscopy for range estimation in helicopter flight p 2441 N94-25505

Validation of vision-based range estimation algorithms using helicopter flight data p 2442 N94-25506

HELIOSPHERE

Solar-terrestrial environmental laboratory
p 2630 N94-23336

HELIOTRONS

Pellet ablation in the large helical device
[NIFS-260] p 2551 N94-24358

Proposal of Modular Heliotron: Advanced modular helical system compatible with closed helical divertor
[NIFS-261] p 2552 N94-24458

HELIPORTS

Combined 1991 and 1992 Robinson-22B (R-22) parking test results
[AD-A273550] p 2193 N94-24559

HELIUM

Atomic probes of surface structure and dynamics
[DE94-001651] p 2530 N94-22720

CFD modeling of microwave electrothermal thrusters
p 2216 N94-23066

High-order sum and difference-frequency generation in helium
[DE94-001064] p 2348 N94-23181

Interpretation of discrepancies in mass spectroscopy data obtained from different experimental configurations
p 2237 N94-23245

Reduction of hydrocarbon impurities in 200 l/h helium liquefier-refrigerator system
[NIFS-259] p 2271 N94-24459

Radiative properties of molecular nitrogen ions produced by helium Penning ionization and argon effects
[NASA-CR-195126] p 2534 N94-24487

Normal zone propagation and thermal hydraulic quenchback in a cable-in-conduit superconductor
[DE94-002457] p 2271 N94-24568

Intramultiplet mixing for Ne(**)(3p) + He at superthermal energies
[ETN-94-95327] p 2538 N94-25240

HELIUM IONS

Multi-ion, multi-event test of ion cyclotron resonance heating
[NASA-CR-194859] p 2540 N94-23495

HELIUM ISOTOPES

Acoustic and optical investigations of superfluid He-3
[PB93-224889] p 2523 N94-23101

HELMET MOUNTED DISPLAYS

A simulation system for Space Station extravehicular activity p 2434 N94-24192

HELMHOLTZ EQUATIONS

Multigrid and cyclic reduction applied to the Helmholtz equation p 2304 N94-23676

Hamiltonian approach to fairly low and long gravity waves
[PB94-111119] p 2404 N94-24598

Solutions of the 2-D Helmoholtz equation for optical waveguides
[DE93-616840] p 2547 N94-25209

HEMODYNAMIC RESPONSES

Evaluation of bioimpedance for the measurement of physiologic variables as related to hemodynamic studies in space flight p 2427 N94-25378

HERMES MANNED SPACEPLANE

HERA (Hermes robot arm) overview
p 2357 N94-24005

HERMITIAN POLYNOMIAL

Application and development of the Schwinger multichannel scattering theory and the partial differential equation theory of electron-molecule scattering
[NASA-CR-194774] p 2536 N94-24798

Generalized Gaussian quadrature rules for systems of arbitrary functions
[AD-A273610] p 2491 N94-24947

HETEROCYCLIC COMPOUNDS

Ordered organic thin films self-assembled from the vapor phase p 2223 N94-24339

HETERODYNING

A low noise 665 GHz SIS quasi-particle waveguide receiver
[NASA-CR-194735] p 2296 N94-24105

A comparison of free-space and fiber mixer performances
[AD-A273558] p 2547 N94-25161

HETEROGENEITY

The computation of R(sub 0) for discrete-time epidemic models with dynamic heterogeneity
[CWI-AM-R9301] p 2420 N94-23521

Heterogeneity in small aliquots of Apolllo 15 olivine-normative basalt: Implications for breccia clast studies p 2616 N94-24373

In situ and ex situ spectroelectrochemical and x ray absorption studies on rechargeable, chemically-modified and other MnO2 materials
[DE94-001387] p 2234 N94-24545

Two-point PADE approximants for Stieltjes series
p 2490 N94-24768

Center for Analysis of Heterogeneous and Nonlinear Media
[AD-A273515] p 2230 N94-25158

HETEROJUNCTION DEVICES

Polycrystalline thin film materials and devices
[DE93-018213] p 2389 N94-22862

Electrochemical sulfur passivation of visible (approximately 670nm) AlGaInP lasers
[DE94-002293] p 2350 N94-24659

HETEROJUNCTIONS

Planar varactor frequency multiplier devices with blocking barrier
[NASA-CASE-NPO-18428-1-CU] p 2310 N94-23821

HEURISTIC METHODS

Personnel shift assignment: Existence conditions and network models
[MEMO-1116] p 2585 N94-22704

Structured constraint satisfaction
[PB94-119039] p 2497 N94-23764

Sensitivity analysis of list scheduling heuristics
[PB93-237766] p 2468 N94-24764

Computing techniques in mission planning
p 2522 N94-25012

HIERARCHIES

Computing techniques in mission planning
p 2522 N94-25012

HIGH ALTITUDE

New approaches for tracking earth orbiters using modified GPS ground receivers p 2196 N94-23258

Effect of power system technology and mission requirements on high altitude long endurance aircraft
[NASA-CR-194455] p 2189 N94-25200

HIGH ASPECT RATIO

Flow visualization study in high aspect ratio cooling channels for rocket engines p 2213 N94-23049

HIGH DEFINITION TELEVISION

The HDTV digital audio matrix
[BBC-RD-1993/9] p 2295 N94-24085

HIGH ELECTRON MOBILITY TRANSISTORS

Cryogenic, low-noise high electron mobility transistor amplifiers for the Deep Space Network
p 2291 N94-23262

HIGH ENERGY INTERACTIONS
Accelerator-based neutrino oscillation searches
[DE94-000818] p 2626 N94-23515
Progress report for the UCSD experimental HEP group
[DE94-001357] p 2533 N94-23699
Electro-weak, QCD and top physics at the Tevatron
[DE94-002304] p 2535 N94-24611
Activities of Academia Sinica
[DE93-614529] p 2541 N94-25335

HIGH FIELD MAGNETS
Developments in materials for high-field magnets
[DE94-000761] p 2307 N94-22987

HIGH FREQUENCIES
Refraction of high frequency noise in an arbitrary jet flow
[NASA-TM-106465] p 2525 N94-23464
Radar signature related radome techniques for flush-mounted HF-, VHF- and, UHF communication antennas
[PB93-204618] p 2294 N94-23742
Comparison of HF groundwave propagation models
[AD-A273146] p 2299 N94-24668
Simulation of adjacent channel interference in a UHF satellite system
[AD-A273147] p 2299 N94-24669
Electromagnetic interference impact of the proposed emitters for the High Frequency Active Auroral Research Program (HAARP)
[AD-A273401] p 2301 N94-24926
Effect of high frequency field on the transport properties of superlattice
[DE93-617047] p 2568 N94-25447

HIGH LEVEL LANGUAGES
Modeling of database constraints in active databases
[AD-A273484] p 2592 N94-24691

HIGH POLYMERS
Numerical simulation of non-Newtonian free shear flows p 2331 N94-24160

HIGH POWER LASERS
A new automatic design method to develop multilayer thin film devices for high power laser applications
[DE93-632490] p 2347 N94-22967
Power beaming to space using a nuclear reactor-pumped laser
[DE94-001208] p 2348 N94-23185

HIGH PRESSURE
High pressure Hugoniot of sapphire
[DE94-001048] p 2558 N94-22946
Development testing of the two-watt RTG heat source and Hastelloy-S/T-111 alloy compatibility studies
[DE94-002875] p 2243 N94-23784
Miniature convection cooled plug-type heat flux gauges
[NASA-TM-106483] p 2344 N94-24069
Convective instabilities in traveling fronts of addition polymerization p 2226 N94-24352

HIGH RESOLUTION
Prospects for future ground-based solar observations
p 2624 N94-22842
Prospects for very-high-resolution solar physics with the Simuris inteferometric mission p 2625 N94-22848
SeaWiFS technical report series. Volume 11: Analysis of selected orbit propagation models for the SeaWiFS mission
[NASA-TM-104566-VOL-11] p 2417 N94-23338
ASTER, a multinational Earth observing concept
p 2389 N94-23840
Reducing video frame rate increases remote optimal focus time
[NASA-TM-104018] p 2431 N94-23970

HIGH REYNOLDS NUMBER
A multilevel adaptive projection method for unsteady incompressible flow p 2341 N94-23690
Local isotropy in distorted turbulent boundary layers at high Reynolds number p 2332 N94-24166
Computation of large-scale statistics in decaying isotropic turbulence p 2332 N94-24167
Discrete sensitivity derivatives of the Navier-Stokes equations with a parallel Krylov solver
[NASA-TM-106481] p 2265 N94-24301
The radiated noise from isotropic turbulence revisited
[NASA-CR-191547] p 2333 N94-24356
An analysis for high Reynolds number inviscid/viscid interactions in cascades
[NASA-CR-4519] p 2169 N94-24606
High lift aerodynamics
[NASA-CR-195183] p 2184 N94-25268

HIGH SPEED
Integration and test of high-speed transmitter electronics for free-space laser communications
[NASA-TM-106295] p 2295 N94-24101
Hubble Space Telescope high speed photometer science verification test report
[NASA-CR-189322] p 2205 N94-24710

HIGH SPEED PHOTOGRAPHY
Debris/Ice/TPS assessment and integrated photographic analysis for Shuttle Mission STS-61
[NASA-TM-109195] p 2199 N94-24059

HIGH STRENGTH
Ceramic silicon-boron-carbon fibers from organic silicon-boron-polymers
[NASA-CASE-ARC-11956-1-SB] p 2253 N94-23311
Test methods for composites: A status report. Volume 2: Compression test methods
[AD-A273522] p 2230 N94-24779
Test methods for composites: A status report. Volume 1: Tension test methods
[AD-A273501] p 2230 N94-24942

HIGH STRENGTH ALLOYS
Environmentally assisted cracking of high strength beta titanium alloys
[AD-A273598] p 2245 N94-24823

HIGH STRENGTH STEELS
Fatigue crack growth rate studies of medium sulfur low alloy steels tested in high temperature water
[DE93-040437] p 2238 N94-22861
Irradiation damage behavior of low alloy steel wrought and weld materials
[DE94-000519] p 2239 N94-22999
New welding and finishing procedures
[DE94-602022] p 2352 N94-23025
Thermal fatigue: A literature review
[PB93-226306] p 2375 N94-23120
Weldability of Accelerated-Cooled (AcC) high strength TMCP steel X80
[VTT-TIED-1413] p 2251 N94-25419

HIGH TEMPERATURE
Ceramic silicon-boron-carbon fibers from organic silicon-boron-polymers
[NASA-CASE-ARC-11956-1-SB] p 2253 N94-23311
Elevated temperature crack propagation
[NASA-TM-106490] p 2377 N94-24715
High temperature adhesive
[AD-D016019] p 2258 N94-24737
Containerless measurements on liquids at high temperatures p 2238 N94-25125
Detection of velocity in high temperature liquid metals
p 2247 N94-25127
Microwave techniques for physical property measurements p 2238 N94-25134

HIGH TEMPERATURE ENVIRONMENTS
Determination of the compatibility between structural alloys and molten metals at high temperatures
[DE94-000954] p 2241 N94-23434
Microstructural analysis of the 2195 aluminum-lithium alloy welds p 2251 N94-24448
Surface compositional variations of Mo-47Re alloy as a function of temperature
[NASA-TP-3402] p 2245 N94-25117
Dynamic measurements of thermophysical properties of metals and alloys at high temperatures by subsecond pulse heating techniques p 2247 N94-25124

HIGH TEMPERATURE GASES
Development of durable high-temperature catalysts for natural gas combustion
[PB93-226447] p 2232 N94-23477

HIGH TEMPERATURE LUBRICANTS
Development of high temperature liquid lubricants for low-heat rejection: Heavy duty diesel engines
[NASA-CR-191197] p 2258 N94-24753

HIGH TEMPERATURE PLASMAS
A relativistic theory on wave propagation in inhomogeneous magnetoplasmas
[ETN-94-95322] p 2554 N94-25285

HIGH TEMPERATURE RESEARCH
An extended laser flash technique for thermal diffusivity measurement of high-temperature materials
p 2238 N94-25132

HIGH TEMPERATURE SUPERCONDUCTORS
High-T(c) superconducting superlattices
[DE93-019200] p 2556 N94-22864
Electrical transport in La(2-x)Sr(x)CuO(4-y)
[DE93-040885] p 2556 N94-22912
Spin-polaron theory of high-T(c) superconductivity. 2: Electronic structure of the CuO2 planes
[DE93-019197] p 2556 N94-22919
The de Haas-van Alphen measurements in Ba(0.6)K(0.4)BiO3
[DE93-041169] p 2556 N94-22920
Report of the Joint Seminar on Solid State Physics, Atomic and Molecular Physics, and Materials Science in the Energy Region of Tandem Accelerators
[DE93-508268] p 2548 N94-22924
Anomalous magnetoresistance behavior of superconducting Nd(2-x)Ce(x)CuO(4-y) single crystal
[DE94-000806] p 2558 N94-22941
Atomic-scale structure of grain boundaries: Correlations to grain boundary properties
[DE94-001289] p 2558 N94-22990
Design of microchannels for cryostabilization of high temperature superconducting magnets
[DE94-001324] p 2559 N94-22993
Exact transformation of the anisotropic Ginzburg-Landau model and its consequences
[DE94-002208] p 2562 N94-23795
Magnetic shielding of interplanetary spacecraft against solar flare radiation
[NASA-CR-195539] p 2204 N94-24334
Tunnelling in metallic contacts on high-T(c) superconductors: A story of charge carriers in YBa2Cu3O(7-delta) and Bi2CaSr2Cu2O(8+delta)
[ISBN-9-03-860142-5] p 2565 N94-25280
The effect of a transport current on the surface barrier of a uniaxial anisotropic superconducting slab
[DE93-617135] p 2566 N94-25390
Surface barrier of a uniaxial anisotropic type 2 superconducting cylinder
[DE93-617137] p 2566 N94-25392
Simulation of the vortex motion in the high T(c) superconductors
[DE93-617138] p 2567 N94-25403

HIGH TEMPERATURE TESTS
Phase transformations in Cu-Zr multilayers
[DE94-000393] p 2241 N94-23297
An assessment of solid lubricant films for use in high temperature space applications p 2363 N94-24044
Hot hydrogen testing of metallic turbo pump materials
[NASA-CR-193880] p 2244 N94-24066

HIGH VOLTAGES
Laser energized high voltage direct current power supply
[AD-D015977] p 2312 N94-25036

HIGHLANDS
Highland crust at the Apollo 14 site: A review
p 2614 N94-24364
Auto-metasomatism of the western lunar highlands: Result of closed system fractionation and mobilization of a KREEPy trapped liquid p 2615 N94-24367
The western highland province at the Apollo 14 site
p 2615 N94-24369

HIGHLY MANEUVERABLE AIRCRAFT
Development of high-angle-of-attack nose-down pitch control margin design guidelines for combat aircraft
p 2164 N94-25107
Feedback control laws for highly maneuverable aircraft
[NASA-CR-195195] p 2190 N94-25176

HILBERT SPACE
Mathematical addenda to Hopper's model of plane stokes flow driven by capillarity on a free surface
[PB93-237691] p 2480 N94-23438
Quasiconformal mappings, operators on Hilbert space, and local formulae for characteristic classes
[PB93-238079] p 2488 N94-24536
Some maximality results for effect-valued measures
[PB94-111176] p 2569 N94-24575
Signatures of selfadjoint pencils
[PB94-111127] p 2457 N94-24599

HILBERT TRANSFORMATION
Direct digital RF synthesis and modulation for MSAT mobile applications p 2285 N94-22804

HINGES
Deployable video conference table
[NASA-CASE-ARC-11950-1] p 2192 N94-23310
Primary deployment mechanism for the European Polar Platform p 2207 N94-23995
Development steps on the basis of test with the LOCSTAR reflector deployment mechanism
p 2356 N94-23998
Preloaded launch locking devices for SILEX
p 2358 N94-24008
An opening mechanism for the scientific airlock outer hatch p 2360 N94-24027

HIPPOCAMPUS
Electrophysiology of the rat nucleus accumbens: Local circuitry, neuromodulation and synaptic plasticity
[PB93-232254] p 2420 N94-23454

HISTOGRAMS
Structure in gamma ray burst time profiles: Correlations with other observables p 2579 N94-24431

HISTORIES
The history of development of molybdenum alloys for structural applications
[DE94-000389] p 2239 N94-22958
The birth of NASA: The diary of T. Keith Glennan
[NASA-SP-4105] p 2630 N94-23333
Soviet developments of planet rovers in period of 1964 - 1990 p 2369 N94-23374
Past US studies and developments for planetary rovers p 2369 N94-23375
Rolls-Royce in perspective: Past, present and future
[PNR-90882] p 2187 N94-23519
The RB211: The first 25 years
[PNR-90977] p 2187 N94-23570

Suddenly, tomorrow came... A history of the Johnson Space Center
[NASA-SP-4307] p 2631 N94-24584
The evolution of the laser: A systems perspective on science, technology and society
[ETN-94-95319] p 2351 N94-25218

HOHLRAUMS
Numerical simulation and analysis of experimental results on stimulated Raman scattering in laser-plasma Hohlraum targets
[DE93-613719] p 2554 N94-25330

HOLDERS
Fingered bola body, bola with same, and methods of use
[NASA-CASE-MSC-21967-1] p 2354 N94-23822
Docking mechanisms: An overview of different systems p 2357 N94-24004
Multipurpose clamping device with electrical connector for in orbit attachment of payloads p 2361 N94-24035

HOLES (MECHANICS)
Condensed-phase thermal decomposition of TATB investigated by Atomic Force Microscopy (AFM) and Simultaneous Thermogravimetric Modulated Beam Mass Spectrometry (STMBMS)
[DE94-000396] p 2232 N94-23298
Pressure wall patch
[NASA-CASE-MFS-28724-1] p 2203 N94-23824

HOLLOW CATHODES
Development of a power electronics unit for the Space Station plasma contactor
[NASA-TM-106486] p 2222 N94-25201

HOLMIUM
Investigation of the optical and laser properties of Tm and Ho in YAG anf YLF
[REPT-94-001] p 2563 N94-24404

HOLOGRAPHIC INTERFEROMETRY
Spatiotemporal behavior and nonlinear dynamics in a phase conjugate resonator
[NASA-CR-4567] p 2543 N94-23529
Real-time holographic endoscopy
[ISL-CO-203/92] p 2343 N94-24054

HOLOGRAPHY
Holographic testing of composite propfans for a cruise missile wind tunnel model
[NASA-TM-105271] p 2187 N94-23545

HOMOGENEOUS TURBULENCE
On the large eddy simulation of turbulent flows in complex geometry p 2329 N94-24148

HOMOGENIZING
Multigrid methods for differential equations with highly oscillatory coefficients p 2484 N94-23685

HOMOLOGY
On BRST quantization of constrained systems
[ETN-94-95386] p 2570 N94-25258

HOMOTOPY THEORY
Theory and computation of optimal low- and medium-thrust transfers
[NASA-CR-194812] p 2217 N94-23275
A homotopy algorithm for digital optimal projection control GASD-HADOC
[NASA-CR-193881] p 2456 N94-24470

HONEYCOMB STRUCTURES
Continuum representations of cellular solids
[DE94-001706] p 2375 N94-23217

HOOKS
Fingered bola body, bola with same, and methods of use
[NASA-CASE-MSC-21967-1] p 2354 N94-23822

HORMONE METABOLISMS
Skeletal muscle metabolism in hypokinetic rats
[NASA-CR-195082] p 2420 N94-24124

HORN ANTENNAS
Advanced electromagnetic methods for aerospace vehicles
[NASA-CR-195111] p 2365 N94-24699

HORSEPOWER
The Triton: Design concepts and methods
[NASA-CR-195542] p 2184 N94-25004

HORSESHOE VORTICES
LinAir: A multi-element discrete vortex Weissinger aerodynamic prediction method
[NASA-TM-108786] p 2167 N94-23557

HOT STARS
Voyager observations of globular clusters
[NASA-CR-194806] p 2598 N94-23330
UV-bright stars in globular clusters
[NASA-CR-189324] p 2599 N94-24666

HOT-WIRE ANEMOMETERS
The use of near-wall hot-wire probes for time-resolved skin-friction measurements p 2316 N94-22857
A method for recognition of frequency cells in a cylinder flow influenced by wall effects p 2316 N94-22860

HOUSINGS
Laser soldering of Sn plated brass integrator assembly housings
[DE94-001149] p 2270 N94-23790
Magnetic power piston fluid compressor
[NASA-CASE-GSC-13565-1] p 2354 N94-23831

HTPB PROPELLANTS
Design considerations of hybrid rockets
p 2156 N94-24254

HUBBLE SPACE TELESCOPE
A quick uplink, expandable executable for the NSSC-1 of the Hubble Space Telescope p 2305 N94-23859
The mission events graphic generator software: A small tool with big results p 2464 N94-23893
An intelligent planning and scheduling system for the HST servicing missions p 2520 N94-23964
Design of a new high-performance pointing controller for the Hubble Space Telescope
[NASA-CR-193891] p 2364 N94-24088
Hubble Space Telescope high speed photometer orbital verification
[NASA-CR-189333] p 2204 N94-24226
Hubble Space Telescope high speed photometer science verification test report
[NASA-CR-189322] p 2205 N94-24710

HUBS
A parametric study of harmonic rotor hub loads
[NASA-CR-4558] p 2181 N94-24726

HUGONIOT EQUATION OF STATE
High pressure Hugoniot of sapphire
[DE94-001048] p 2558 N94-22946

HUMAN BEHAVIOR
Activity Catalog Tool (ACT) user manual, version 2.0
[NASA-CR-177634] p 2430 N94-23527

HUMAN BODY
Quantitative assessment of human motion using video motion analysis p 2436 N94-24203
Development of biomechanical models for human factors evaluations p 2437 N94-24205

HUMAN CENTRIFUGES
Artificial gravity in space flight
[AD-A273420] p 2427 N94-24928

HUMAN FACTORS ENGINEERING
Eye-gaze control of the computer interface: Discrimination of zoom intent
[DE94-000480] p 2429 N94-22997
Pilot-vehicle interface
[DOT/FAA/CT-92/21] p 2430 N94-23083
Harmonisation of man-machine interface experiments in the context of the development of PHARE advanced tools
[PB93-204725] p 2430 N94-23744
SpaceOps 1992: Proceedings of the Second International Symposium on Ground Data Systems for Space Mission Operations
[NASA-CR-194486] p 2497 N94-23832
Automating a human factors evaluation of graphical user interfaces for NASA applications: An update on CHIMES
p 2443 N94-23936
Reducing video frame rate increases remote optimal focus time
[NASA-TM-104018] p 2431 N94-23970
Visual Problems in Night Operations
[AGARD-LS-187] p 2431 N94-23976
Crew interface analysis: Selected articles on space human factors research, 1987 - 1991
[NASA-TM-104756] p 2433 N94-24185
Designers' models of the human-computer interface
p 2433 N94-24188
The use of analytical models in human-computer interface design p 2434 N94-24190
Using computer graphics to design Space Station Freedom viewing p 2434 N94-24191
Use of infrared telemetry as part of a nonintrusive inflight data collection system to collect human factors data
p 2434 N94-24193
Performing speech recognition research with hypercard p 2306 N94-24194
Previous experience in manned space flight: A survey of human factors lessons learned p 2435 N94-24196
Hand controller commonality evaluation process
p 2435 N94-24197
Programmable display pushbuttons on the Space Station's telerobot control panel p 2435 N94-24198
Simulation of the human-telerobot interface on the Space Station p 2436 N94-24202
Development of biomechanical models for human factors evaluations p 2437 N94-24205
Establishing a relationship between maximum torque production of isolated joints to simulate EVA ratchet push-pull maneuver: A case study p 2437 N94-24206
NASA project 1: Full-body dynamometer
[NASA-CR-195507] p 2438 N94-24331
An examination of the operational error database for air route traffic control centers
[DOT/FAA/AM-93/22] p 2175 N94-24472
Concepts and embodiment design of a reentry recumbent seating system for the NASA Space Shuttle
[NASA-CR-195504] p 2438 N94-24667
Evaluation of the UH-1N instrument panel
[AD-A273145] p 2186 N94-24774
Design of a recumbent seating system
[NASA-CR-195503] p 2438 N94-24786
Pilot-vehicle interface handbook, chapter 19. Volume 2: Digital systems validation
[DOT/FAA/CT-88/10-VOL-2] p 2438 N94-24830
A white paper: NASA virtual environment research, applications, and technology
[NASA-TM-109682] p 2428 N94-24855
Conceptual design of an astronaut hand anthropometry device
[NASA-CR-195490] p 2439 N94-24956
Cockpit control system
[NASA-CR-195488] p 2190 N94-24957
New Advances in Mission Planning and Rehearsal Systems
[AGARD-LS-192] p 2521 N94-25008
Human factors of mission planning systems: Theory and concepts p 2521 N94-25010
Human factors of mission planning systems: Applications and implementation p 2522 N94-25011
A simulation study of control and display requirements for zero-experience general aviation pilots
p 2163 N94-25102

HUMAN PERFORMANCE
Harmonisation of man-machine interface experiments in the context of the development of PHARE advanced tools
[PB93-204725] p 2430 N94-23744
Crew interface analysis: Selected articles on space human factors research, 1987 - 1991
[NASA-TM-104756] p 2433 N94-24185
Quantitative assessment of human motion using video motion analysis p 2436 N94-24203
Reach performance while wearing the Space Shuttle launch and entry suit during exposure to launch accelerations p 2436 N94-24204
Development of biomechanical models for human factors evaluations p 2437 N94-24205
Establishing a relationship between maximum torque production of isolated joints to simulate EVA ratchet push-pull maneuver: A case study p 2437 N94-24206
Pilot evaluation system p 2158 N94-24266
An examination of the operational error database for air route traffic control centers
[DOT/FAA/AM-93/22] p 2175 N94-24472
Human factors of mission planning systems: Theory and concepts p 2521 N94-25010
Investigation of hand capabilities under a variety of performance conditions and an attempt to explain performance differences p 2444 N94-25354

HUMAN REACTIONS
Automated system function allocation and display format: Task information processing requirements
p 2434 N94-24189

HUMAN-COMPUTER INTERFACE
Eye-gaze control of the computer interface: Discrimination of zoom intent
[DE94-000480] p 2429 N94-22997
The TOPSIM 4 graphic user interface
[ESA-STM-247] p 2450 N94-23228
MITS architecture V1.0
[PB93-201762] p 2452 N94-23451
Activity Catalog Tool (ACT) user manual, version 2.0
[NASA-CR-177634] p 2430 N94-23527
Harmonisation of man-machine interface experiments in the context of the development of PHARE advanced tools
[PB93-204725] p 2430 N94-23744
Deep Space Network (DSN), Network Operations Control Center (NOCC) computer-human interfaces
p 2447 N94-23917
Making intelligent systems team players: Additional case studies
[NASA-TM-104786] p 2473 N94-24068
CF-18 AN/ALQ-126B-MG 13 IIP interface to the DREO Electronic Warfare Engagement Simulation Facility
[DREO-TN-93-4] p 2296 N94-24118
Activities involving aeronautical, space science, and technology support for minority institutions
[NASA-CR-195095] p 2574 N94-24225
A review of ISEAS design p 2465 N94-24410
Integration and evaluation of a simulator designed to be used within a dynamic prototyping environment
p 2198 N94-24436
World processor: An interface for textual display and manipulation in virtual reality
[PB94-118643] p 2592 N94-24642
Analyzing the properties of user interface software
[AD-A273601] p 2460 N94-24933
A comparative evaluation plan for the Maintenance, Inventory, and Logistics Planning (MILP) System Human-Computer Interface (HCI) p 2588 N94-25373

HUMIDITY
Humidity effects on soluble core mechanical and thermal properties (polyvinyl alcohol/microballoon composite) type CG extendospheres, volume 2
[NASA-CR-193893] p 2229 N94-24224

HURRICANES
Hurricane risk assessment: Rollback or ride out
p 2416 N94-23248
An adaptive multigrid model for hurricane track prediction p 2416 N94-23687
Implementation of a state of the art automated system for the production of cloud/water vapor motion winds from geostationary satellites
[NASA-CR-195087] p 2410 N94-24125

HYBRID PROPELLANT ROCKET ENGINES
Design considerations of hybrid rockets
p 2156 N94-24254
Solid rocket combustion simulator technology using the hybrid rocket for simulation
[NASA-CR-195142] p 2265 N94-24578

HYBRID PROPULSION
Electric and hybrid vehicles program
[DE93-040664] p 2352 N94-22881
NASA Propulsion Engineering Research Center, volume 2
[NASA-CR-194719-VOL-2] p 2209 N94-23028

HYDRAULIC CONTROL
Electro-rheological control valve
[AD-D015997] p 2367 N94-25055

HYDRAULIC FLUIDS
FTIR quantification of industrial hydraulic fluids in perchloroethylene p 2264 N94-23243

HYDRAULICS
Modeling dynamically coupled fluid-duct systems with finite line elements
[NASA-CR-193909] p 2376 N94-24359

HYDRAZIDES
Di(hydroxyphenyl)- 1,2,4-triazole monomers
[NASA-CASE-LAR-14440-2] p 2252 N94-23075

HYDRIDES
Magnetic properties of NdCo3 and its gamma phase hydride NdCo3H(4.1)
[REPT-A-2655] p 2567 N94-25412

HYDROCARBON FUELS
Configuration development study of the OSU 1 hypersonic research vehicle
[NASA-CR-195522] p 2181 N94-24591

HYDROCARBONS
Reduction of hydrocarbon impurities in 200 l/h helium liquefier-refrigerator system
[NIFS-259] p 2271 N94-24459
Design of a vehicle based system to prevent ozone loss
[NASA-CR-195498] p 2180 N94-24479
Near-surface seismic imaging
[PB94-119096] p 2404 N94-24647
Potent solvents for C60 and their utility for the rapid acquisition of 13CNMR data for fullerenes
[AD-A273349] p 2235 N94-24925

HYDROCHLORIDES
Di(hydroxyphenyl)- 1,2,4-triazole monomers
[NASA-CASE-LAR-14440-2] p 2252 N94-23075

HYDRODYNAMICS
A geometric weighted elliptic grid regeneration method for 3D unstructured ALE hydrodynamics
[DE94-000309] p 2448 N94-22980
Characterization of heat transport and radiation hydrodynamics in collisional laser plasmas using collective Thomson scattering
[DE94-001502] p 2349 N94-23209
HERACLITUS, phase 1. Harbour Entrance of Rotterdam Radar based Current Related Information for Traffic Guidance of Ships: Feasibility of deriving current profile data from sea surface observations in the Rotterdam (Netherlands) port entrance
[BCRS-93-04] p 2417 N94-24107
A two-dimensional dispersion module for the TOUGH2 simulator
[DE94-002262] p 2335 N94-24655
The hydrodynamics of a moving fluid-liquid contact line
[ETN-94-95352] p 2339 N94-25247
Hydrodynamics of stirred gas-liquid dispersions
[ETN-94-95368] p 2339 N94-25254
Coherent structures over grooved surfaces
[ETN-94-95308] p 2339 N94-25291

HYDROELASTICITY
Coupled frequencies of a hydroelastic rectangular system
[LRT-WE-9-FB-4-1992] p 2375 N94-23196

HYDROELECTRICITY
Snow modeling, water resources, climate change
[PB93-201770] p 2399 N94-24633

HYDROGEN
Analysis of Alloy 600 and X-750 stress corrosion cracks
[DE94-001578] p 2238 N94-22936
Robust, wide-range hydrogen sensor for use in commercial, space, and government applications
[DE93-040902] p 2342 N94-22954
A novel method for determination of transport parameters of H2 and O2 in PEMFCs
[DE94-001492] p 2389 N94-22962
Diffusion of hydrogen in iron oxides
[DE93-632430] p 2239 N94-22966
Effects of neutron irradiation and hydrogen on ductile-brittle transition temperatures of V-Cr-Ti alloys
[DE94-001466] p 2240 N94-23009
Axisymmetric single shear element combustion instability experiment p 2213 N94-23044
Generic microelectronic smart sensor platform for detection of toxic, hazardous, and flammable gases
[DE93-017626] p 2343 N94-23200
Selective hydrogen separation by palladium-based composite membranes
[PB93-201671] p 2254 N94-23431
Assessment of an SP-100 bi-modal propulsion and power system
[DE94-000889] p 2218 N94-23433
Optical model analyses of galactic cosmic ray fragmentation in hydrogen targets
[NASA-TP-3404] p 2540 N94-23509
Hot hydrogen testing of metallic turbo pump materials
[NASA-CR-193880] p 2244 N94-24066
Pellet ablation in the large helical device
[NIFS-260] p 2551 N94-24358
Environmentally assisted cracking of high strength beta titanium alloys
[AD-A273598] p 2245 N94-24823
Surface compositional variations of Mo-47Re alloy as a function of temperature
[NASA-TP-3402] p 2245 N94-25117
UV extinction and IR emission in diffuse H2 regions
[NASA-CR-195194] p 2600 N94-25270
Proceedings of the 12th International Congress: Corrosion Control for Low-Cost Reliability. Volume 4: Oil/Gas Pipeline
[AD-A273665] p 2250 N94-25405
Metal hydride storage
[VTT-JULK-769] p 2396 N94-25417

HYDROGEN CHLORIDES
Adsorption, desorption, and decomposition of HCl and HBr on Ge(100): Competitive pairingand near-first-order desorption kinetics
[AD-A273504] p 2235 N94-24790

HYDROGEN COMPOUNDS
Adsorption, desorption, and decomposition of HCl and HBr on Ge(100): Competitive pairingand near-first-order desorption kinetics
[AD-A273504] p 2235 N94-24790

HYDROGEN EMBRITTLEMENT
Analysis of Alloy 600 and X-750 stress corrosion cracks
[DE94-001578] p 2238 N94-22936
Effects of neutron irradiation and hydrogen on ductile-brittle transition temperatures of V-Cr-Ti alloys
[DE94-001466] p 2240 N94-23009
Effect of hydrogen exposure on a Cu-8 Cr-4 Nb alloy
[NASA-TM-106429] p 2243 N94-23556
Environmentally assisted cracking of high strength beta titanium alloys
[AD-A273598] p 2245 N94-24823
Proceedings of the 12th International Congress: Corrosion Control for Low-Cost Reliability. Volume 4: Oil/Gas Pipeline
[AD-A273665] p 2250 N94-25405
Proceedings of the 12th International Congress: Corrosion Control for Low-Cost Reliability. Volume 2: Process Industries Plant Operations
[AD-A273662] p 2251 N94-25449

HYDROGEN FUELS
Configuration development study of the OSU 1 hypersonic research vehicle
[NASA-CR-195522] p 2181 N94-24591

HYDROGEN ISOTOPES
Carbon and hydrogen isotope composition and C-14 concentration in methane from sources and from the atmosphere: Implications for a global methane budget
[NASA-CR-195166] p 2399 N94-25092

HYDROGEN MASERS
Ultracold atoms in traps and fountains
[ETN-94-95325] p 2537 N94-25239

HYDROGEN OXYGEN ENGINES
Laser diagnostics for small rockets
p 2210 N94-23032
CFD analyses of combustor and nozzle flowfields
p 2210 N94-23033
Two stage turbine for rockets p 2215 N94-23059
Validation of a nonintrusive optical technique for the measurement of liquid mass distribution in a two-phase spray p 2548 N94-24420
STE thrust chamber technology: Main injector technology program and nozzle Advanced Development Program (ADP)
[NASA-CR-193919] p 2221 N94-25019

HYDROGEN PRODUCTION
Recent advances in SPE (tm) water electrolyzer
p 2393 N94-23362

HYDROGEN RECOMBINATIONS
Performance assessment of low pressure nuclear thermal propulsion p 2217 N94-23070

HYDROGEN SULFIDE
High-resolution soft x ray photoionization studies of selected molecules
[DE94-000568] p 2532 N94-23002

HYDROGENATION
Organometallic chemistry of bimetallic compounds
[DE94-002313] p 2238 N94-22897

HYDROLOGICAL CYCLE
GEWEX p 2385 N94-23614
GEWEX Water Vapor Project (GVaP)
p 2411 N94-24378
Measurement and modeling of moist processes
p 2413 N94-24385
Snow modeling, water resources, climate change
[PB93-201770] p 2399 N94-24633

HYDROLOGY
Urban/rural application of weather radar for flow forecasting. Proceedings of the Informal CEc -Workshop
[PB93-220135] p 2407 N94-23129
Methodology for the assessment of surface resistance and soil water storage variability at mesoscale based on remote sensing measurements. A case study with HAPEX-EFEDA data. UNESCO-International Hydrological Program 4
[PB94-111721] p 2386 N94-23734
Coupled land surface/hydrologic/atmospheric models
p 2413 N94-24387
Joint sessions on moisture processes and cumulus parameterization p 2414 N94-24393
Hydraulics and morphology of mountain rivers: A literature survey. Communications on hydraulic and geotechnical engineering
[PB94-110772] p 2388 N94-24636
Human impacts on soil carbon dynamics of deep-rooted Amazonian forests
[NASA-CR-195127] p 2399 N94-24861

HYDROLOGY MODELS
Urban/rural application of weather radar for flow forecasting. Proceedings of the Informal CEc -Workshop
[PB93-220135] p 2407 N94-23129
Integrated use of hydrological modelling and remote sensing in the province of Drenthe (The Netherlands): Possibilities and restrictions
[REPT-61] p 2382 N94-23148
Report of the proceedings of the Colloquium and Workshop on Multiscale Coupled Modeling
[NASA-CP-3217] p 2410 N94-24374
GEWEX Continental-scale International Project (GCiP)
p 2411 N94-24376
Measurement and modeling of moist processes
p 2413 N94-24385
Coupled land surface/hydrologic/atmospheric models
p 2413 N94-24387
Session on coupled land surface/hydrological/atmospheric models
p 2414 N94-24395

HYDROLYSIS
On the mechanism of action of 3',5'-cyclic adenosine monophosphate: A study of four- and five-coordinated phosphorus compounds, modelling the activated state of cAMP
[ISBN-9-03-860222-7] p 2226 N94-25238

HYDROMETALLURGY
Integrated hydrometallurgical jarosite treatment
[PB93-217990] p 2232 N94-22983

HYDROMETEOROLOGY
Water cycle research associated with the CaPE hydrometeorology project (CHymP p 2416 N94-24414

HYDROPHONES
Preprocessor and adaptive beamformer for linear-frequency modulation active signals
[AD-D016008] p 2302 N94-25048

HYDROSTATICS
A technique to measure rotordynamic coefficients in hydrostatic bearings p 2215 N94-23061
The influence of orography on the transport of atmospheric constituents p 2619 N94-24886

HYDROTHERMAL SYSTEMS
Reactive trace metals as indicators of subduction and ventilation processes in the ocean
[AD-A273585] p 2419 N94-25164

HYDROXYL COMPOUNDS
Di(hydroxyphenyl)- 1,2,4-triazole monomers
[NASA-CASE-LAR-14440-2] p 2252 N94-23075
HYDROXYL EMISSION
Infrared and SiO maser observations of OH/IR stars
[PB94-104890] p 2599 N94-24780
HYPERBOLIC DIFFERENTIAL EQUATIONS
Characteristic method for one-dimensional scalar hyperbolic conservation laws with stiff source terms
[PB93-237675] p 2491 N94-24954
HYPERBOLIC FUNCTIONS
An adaptive streamline diffusion finite element method for hyperbolic systems in gas dynamics
[PREPRINT-688] p 2340 N94-25466
Arbitrary-order numerical schemes for linear hyperbolic systems
[CRANFIELD-AERO-9211] p 2523 N94-25480
HYPERCUBE MULTIPROCESSORS
Discrete sensitivity derivatives of the Navier-Stokes equations with a parallel Krylov solver
[NASA-TM-106481] p 2265 N94-24301
HYPERFINE STRUCTURE
The nanostructure of multilayered films: A NMR study
[ETN-94-95347] p 2262 N94-25222
A scalar-vector model of quark-antiquark interaction under linear confinement
[DE93-616871] p 2538 N94-25317
HYPERPLANES
The fundamental group of the complement of complexified real arrangements
[DE93-616847] p 2491 N94-25214
HYPERSONIC AIRCRAFT
NASA/USRA advanced design program
[NASA-CR-195548] p 2180 N94-24492
HYPERSONIC FLIGHT
NASA/USRA advanced design program
[NASA-CR-195548] p 2180 N94-24492
Advanced ballistic range technology
[NASA-CR-195198] p 2165 N94-25169
HYPERSONIC FLOW
Shock tunnel studies of scramjet phenomena, supplement 7
[NASA-CR-191572] p 2319 N94-23513
Shock tunnel studies of scramjet phenomena, supplement 8
[NASA-CR-191573] p 2320 N94-23532
Stability of hypersonic flow of a detonable gas mixture in the stagnation region of a blunt body and a forward facing step p 2154 N94-24248
Radiative properties of molecular nitrogen ions produced by helium Penning ionization and argon effects
[NASA-CR-195126] p 2534 N94-24487
HYPULSE combustor analysis
[NASA-CR-191579] p 2336 N94-24771
HYPERSONIC SHOCK
An investigation on a new technique to improve the performance of the shock tube/tunnel testing in the equilibrium interface condition p 2154 N94-24247
HYPERSONIC VEHICLES
An engineering code to analyze hypersonic thermal management systems p 2320 N94-23636
Configuration development study of the OSU 1 hypersonic research vehicle
[NASA-CR-195522] p 2181 N94-24591
Hypersonic vehicle control law development using H(infinity) and micron-synthesis p 2163 N94-25104
Effect of aeroelastic-propulsive interactions on flight dynamics of a hypersonic vehicle p 2164 N94-25113
HYPERSONICS
NASA/USRA advanced design program
[NASA-CR-195548] p 2180 N94-24492
Design project: LONGBOW supersonic interceptor
[NASA-CR-195510] p 2180 N94-24581
HYPERTENSION
Arterial hypertension and the aviator
p 2425 N94-23328
HYPERVELOCITY FLOW
Calibration of HYPULSE for hypervelocity air flows corresponding to flight Mach numbers 13.5, 15, and 17
[NASA-CR-191578] p 2192 N94-23564
HYPERVELOCITY IMPACT
Bibliographic Retrieval System (BARS), Sandia Shock Compression (SSC) database Shock Physics Index
[DE94-001679] p 2589 N94-23126
Design of orbital debris shields for oblique hypervelocity impact
[NASA-CR-195152] p 2205 N94-24828
HYPERVELOCITY PROJECTILES
The internal structure and dynamics of the railgun plasma armature between infinitely wide ablating rails
[DE94-001473] p 2198 N94-23208
HYPERVELOCITY WIND TUNNELS
An investigation on a new technique to improve the performance of the shock tube/tunnel testing in the equilibrium interface condition p 2154 N94-24247
HYPOTENSION
Evaluation of bioimpedance for the measurement of physiologic variables as related to hemodynamic studies in space flight p 2427 N94-25378
HYPOTHERMIA
Survival suit for submarine personnel: Summary of evaluation studies
[PB93-204634] p 2430 N94-23743
HYPOXIA
Physiological protection for aircrew at high altitudes: A review of the literature
[DCIEM-93-13] p 2432 N94-24114
HYSTERESIS
Photo-induced and electrooptic properties of (Pb,La)(Zr,Ti)O3 films for optical memories
[DE93-019820] p 2542 N94-23202
Material data representation of hysteresis loops for Hastelloy X using artificial neural networks
[NASA-TM-105990] p 2376 N94-23551

I

ICE
Characteristics of surface roughness associated with leading edge ice accretion
[NASA-TM-106459] p 2166 N94-23522
Close-up analysis of inflight ice accretion
[NASA-TM-106457] p 2172 N94-23523
Mars Operational Environmental Satellite (MOES): A post-Mars Observer discovery mission
p 2620 N94-24890
ICE ENVIRONMENTS
A solar photovoltaic power system for use in Antarctica
[NASA-TM-106417] p 2395 N94-24071
ICE FORMATION
Flow quality studies of the NASA Lewis Research Center Icing Research Tunnel diffuser
[NASA-TM-106311] p 2192 N94-23091
An overview of a model rotor icing test in the NASA Lewis Icing Research Tunnel
[NASA-TM-106471] p 2166 N94-23299
Characteristics of surface roughness associated with leading edge ice accretion
[NASA-TM-106459] p 2166 N94-23522
Close-up analysis of inflight ice accretion
[NASA-TM-106457] p 2172 N94-23523
Rime-, mixed- and glaze-ice evaluations of three scaling laws
[NASA-TM-106461] p 2173 N94-24047
Debris/Ice/TPS assessment and integrated photographic analysis for Shuttle Mission STS-61
[NASA-TM-109195] p 2199 N94-24059
Debris/ice/TPS assessment and integrated photographic analysis for Shuttle mission STS-58
[NASA-TM-109194] p 2200 N94-24577
Examination of the physical, electrical, and microwave evolution of water into young sea ice
[AD-A273559] p 2418 N94-24918
National Academy of Sciences-Academy of Sciences of the USSR Workshop on the Mechanics of Ice and its Applications
[AD-A273338] p 2419 N94-25088
ICE MAPPING
The effect of sub-surface volume scattering on the accuracy of ice-sheet altimeter retracking algorithms
[NASA-CR-194825] p 2386 N94-24060
IDEAL GAS
Local grid refinement method for the euler equations
[PB93-223329] p 2317 N94-22985
Direct simulation of isothermal-wall supersonic channel flow p 2172 N94-24164
IGNITION
Multiple shock initiation of LX-17
[DE94-001524] p 2265 N94-23807
Experimental investigation of ignition of boron/titanium composite particles p 2159 N94-24275
Transient phenomena in laminar spray combustion
p 2160 N94-24282
IGNITION TEMPERATURE
The ignition temperature of solid explosives exposed to a fire
[DE94-001047] p 2265 N94-23436
Calculation of flame spread on lining materials by the field model KAMELEON. Project 5 of the EUREFIC fire research programme
[PB93-201614] p 2268 N94-23450
ILLUMINATING
Evaluation of visual acuity with Gen 3 night vision goggles
[NASA-TM-108792] p 2431 N94-23974
Illumination requirements for operating a space remote manipulator p 2435 N94-24195
ILLUSIONS
Night vision goggle illusions and visual training
p 2432 N94-23984
ILMENITE
Lunar mare volcanism: Mixing of distinct, mantle source regions with KREEP-like component
p 2615 N94-24370
IMAGE ANALYSIS
Artificial neural networks: Application to the optical recognition of music partitions
[ETN-94-95166] p 2470 N94-22884
Image analysis applications to mixing phenomena and turbulent dispersions
[ECL-92-29] p 2317 N94-22971
Computer assisted analysis of auroral images obtained from high altitude polar satellites
[NASA-CR-194873] p 2400 N94-23084
Image pattern recognition supporting interactive analysis and graphical visualization
[NASA-CR-194878] p 2451 N94-23369
A complete public archive for the Einstein IPC
[NASA-CR-189316] p 2453 N94-23559
Method for selection of wavelength bands for multispectral classification
[PB93-204378] p 2388 N94-24741
Image analysis technology applied to problems in crystallography
[AD-A273516] p 2566 N94-25288
Measuring track densities in lunar grains by image analysis p 2623 N94-25355
Validation of vision-based range estimation algorithms using helicopter flight data p 2442 N94-25506
A model-based approach for detection of objects in low resolution passive-millimeter wave images
p 2442 N94-25507
Frost effects on the microstructure of high strength concrete, and methods for their analysis
[VTT-PUBS-126] p 2379 N94-25529
IMAGE CLASSIFICATION
Hyperspectral imagery classification using a backpropagation neural network
[AD-A273615] p 2545 N94-24730
Evaluation of the use of remote-sensing data to identify crop types and estimate irrigated acreage, Uvalde and Medina Counties, Texas, 1989
[PB93-193159] p 2388 N94-24809
IMAGE CONTRAST
Validation of a second generation conspicuity meter
[IZF-1993-A-11] p 2542 N94-22895
IMAGE CORRELATORS
Evaluation of advanced materials through experimental mechanics and modelling p 2374 N94-24454
IMAGE ENHANCEMENT
Use of microwave polarimetry to enhance SAR images of the ocean surface
[AD-A273568] p 2419 N94-24944
Engineering workstation: Sensor modeling
p 2441 N94-25500
Image fusion p 2441 N94-25501
Enhanced image capture through fusion
p 2346 N94-25502
Radar E-O image fusion p 2306 N94-25503
IMAGE INTENSIFIERS
Evaluation of visual acuity with Gen 3 night vision goggles
[NASA-TM-108792] p 2431 N94-23974
Night vision devices and characteristics
p 2432 N94-23982
Night vision goggle illusions and visual training
p 2432 N94-23984
IMAGE MOTION COMPENSATION
Multiple-camera/motion stereoscopy for range estimation in helicopter flight p 2441 N94-25505
IMAGE PROCESSING
Image processing for acquisition of fluid rest time in the running of an artificial heart valve p 2316 N94-22858
Design of integrated architectures for low level image processing
[ETN-94-95183] p 2445 N94-22901
Novel fringe scanning/Fourier transform method of synthetic imaging
[DE93-018936] p 2542 N94-22917
Analysis of a proposed Compton backscatter imaging technique
[DE93-040537] p 2371 N94-22935
Computer assisted analysis of auroral images obtained from high altitude polar satellites
[NASA-CR-194873] p 2400 N94-23084
Time-frequency domain analysis of vibration signals for machinery diagnostics.(4): Interpretation using image processing techniques
[OUEL-1953/92] p 2353 N94-23178
Integer cosine transform compression for Galileo at Jupiter: A preliminary look p 2292 N94-23266
Neural network research in Finland. Symposium
[PB93-224822] p 2472 N94-23463

Imaging System (INEL) T805 prototype
[DE94-002807] p 2382 N94-23492
Remote sensing, imaging, and signal engineering
[DE94-003021] p 2382 N94-23494
Characteristics of surface roughness associated with leading edge ice accretion
[NASA-TM-106459] p 2166 N94-23522
Holographic testing of composite propfans for a cruise missile wind tunnel model
[NASA-TM-105271] p 2187 N94-23545
A complete public archive for the Einstein IPC
[NASA-CR-189316] p 2453 N94-23559
Mission planning for Shuttle Imaging Radar-C (SIR-C) with a real-time interactive planning software
p 2305 N94-23842
Multimission image processing and science data visualization p 2518 N94-23955
A colour image processing algorithm to identify copper-based particles in filter debris samples
[DREP-TM-93-19] p 2455 N94-24122
Impact damage in filament wound composite bottles
p 2231 N94-24421
Optimization of techniques to reconstruct images disturbed by atmospheric turbulence in the near infra-red
[PB93-199784] p 2298 N94-24630
Investigation of Raman beam cleanup and phase conjugation
[AD-A273157] p 2545 N94-24672
Optical wavelet transform processor
[AD-A273625] p 2546 N94-24731
VLSI-based video event triggering for image data compression
[NASA-TM-106500] p 2345 N94-25116
Horatio: Libraries for vision applications, release 2.0
[OUEL-1967/92] p 2593 N94-25326
Edge detection using a complex wavelet
[AD-A273699] p 2493 N94-25452
Active camera calibration for a head-eye platform using a variable state dimension filter
[OUEL-1975/93] p 2346 N94-25472
Proceedings of the Workshop on Augmented Visual Display (AVID) Research
[NASA-CP-10128] p 2439 N94-25490
The Radar Image Generation (RIG) model
p 2306 N94-25497
Engineering workstation: Sensor modeling
p 2441 N94-25500
Image fusion p 2441 N94-25501
Enhanced image capture through fusion
p 2346 N94-25502
Radar E-O image fusion p 2306 N94-25503
Expansion-based passive ranging
p 2176 N94-25504
Validation of vision-based range estimation algorithms using helicopter flight data p 2442 N94-25506
A model-based approach for detection of objects in low resolution passive-millimeter wave images
p 2442 N94-25507
Image processing for flight crew enhanced situation awareness p 2442 N94-25508
DCT quantization matrices visually optimized for individual images p 2442 N94-25509
Report on operations of the Air Force Geophysics Laboratory infrared array spectrometer
[AD-A273800] p 2406 N94-25535

IMAGE RECONSTRUCTION
Integer cosine transform compression for Galileo at Jupiter: A preliminary look p 2292 N94-23266
Optimization of techniques to reconstruct images disturbed by atmospheric turbulence in the near infra-red
[PB93-199784] p 2298 N94-24630
Sensor fusion display evaluation using information integration models in enhanced/synthetic vision applications p 2443 N94-25512

IMAGE RESOLUTION
Experience with parametric binary dissection
[NASA-CR-191552] p 2473 N94-23558
Night vision devices and characteristics
p 2432 N94-23982
Hubble Space Telescope high speed photometer orbital verification
[NASA-CR-189333] p 2204 N94-24226
Extracting projective information from single views of 3D point sets
[OUEL-1973/93] p 2464 N94-25471
Evaluation of image quality p 2443 N94-25514

IMAGES
Mental images p 2429 N94-23980
HORACE: Presentation-level protocol standard for digital transmission of monochrome television images
[AD-A273395] p 2197 N94-25064

IMAGING RADAR
The 94 GHz MMW imaging radar system
p 2306 N94-25493

IMAGING SPECTROMETERS
Prospects for very-high-resolution solar physics with the Simuris inteferometric mission p 2625 N94-22848
Optical component MAC Europe ground truth report: Flevoland 1991 (Netherlands)
[BCRS-92-27] p 2382 N94-23177
MODIS calibration p 2383 N94-23600
Concept of ASTER calibration requirement
p 2384 N94-23609

IMAGING TECHNIQUES
Novel fringe scanning/Fourier transform method of synthetic imaging
[DE93-018936] p 2542 N94-22917
Characterization of CCD-based imaging x ray detectors for diffraction experiments
[DE93-041343] p 2556 N94-22921
Analysis of a proposed Compton backscatter imaging technique
[DE93-040537] p 2371 N94-22935
Orientation imaging microscopy: New possibilities for microstructural investigations using automated BKD analysis
[DE94-000777] p 2557 N94-22938
Measurement of intact-core length of atomizing liquid jets by image deconvolution p 2210 N94-23029
Time-frequency domain analysis of vibration signals for machinery diagnostics.(4): Interpretation using image processing techniques
[OUEL-1953/92] p 2353 N94-23178
Imaging System (INEL) T805 prototype
[DE94-002807] p 2382 N94-23492
Remote sensing, imaging, and signal engineering
[DE94-003021] p 2382 N94-23494
Advanced X ray Astrophysics Facility-Imaging (AXAF-I) thermal analyses using Integrated Thermal Analysis System (ITAS) program p 2320 N94-23635
Synthesis and in-vivo detection of boronated compounds for use in BNCT
[DE94-001899] p 2233 N94-23780
ASTER, a multinational Earth observing concept
p 2389 N94-23840
Mission planning for Shuttle Imaging Radar-C (SIR-C) with a real-time interactive planning software
p 2305 N94-23842
Estimation of the rain signal in the presence of large surface clutter
[NASA-CR-195105] p 2409 N94-24087
Precipitation measurement using SIR-C: A feasibility study. Investigation at nadir
[NASA-CR-195103] p 2410 N94-24126
JOVE NASA-FIT program: Microgravity and aeronomy projects
[NASA-CR-195121] p 2631 N94-24493
Near-surface seismic imaging
[PB94-119096] p 2404 N94-24647
Preliminary design of a satellite observation system for Space Station Freedom
[NASA-CR-195514] p 2209 N94-24840
The Mars Aerial Platform (MAP) mission
p 2622 N94-24903
Development of a nondestructive vibration technique for bond assessment of Space Shuttle tiles
[NASA-CR-195163] p 2201 N94-24919
Conceptual design of an astronaut hand anthropometry device
[NASA-CR-195490] p 2439 N94-24956
Nuclear magnetic resonance imaging with short gradient pulses
[AD-D016006] p 2537 N94-25047
Temperature measurement using infrared imaging systems during turbine engine altitude testing
[NASA-TM-105871] p 2193 N94-25184
Synthetic vision system flight test results and lessons learned p 2429 N94-25492
Passive millimeter-wave imaging p 2306 N94-25494
The Radar Image Generation (RIG) model
p 2306 N94-25497
Advanced radiometric and interferometric milimeter-wave scene simulations p 2306 N94-25498

IMIDES
Polyimide processing additives
[NASA-CASE-LAR-13669-2] p 2252 N94-23079
The evolution of energy-transducing systems. Studies with archaebacteria
[NASA-CR-195129] p 2422 N94-24811

IMINES
Planar poly(p-phenylene) derivatives: Ladder formation for maximization of extended conjugation
[AD-A273220] p 2260 N94-24922

IMMUNE SYSTEMS
Cytokines and immune surveillance in humans
[NASA-CR-194801] p 2425 N94-23331
Exercise, exercise training, and the immune system. A compendium of research (1902-1991)
[NASA-TM-108778] p 2426 N94-23575

IMMUNOASSAY
Monoclonal antibodies directed against surface molecules of multicell spheroids
[NASA-CR-195102] p 2420 N94-23633

IMMUNOLOGY
Cytokines and immune surveillance in humans
[NASA-CR-194801] p 2425 N94-23331
Exercise, exercise training, and the immune system. A compendium of research (1902-1991)
[NASA-TM-108778] p 2426 N94-23575
Monoclonal antibodies directed against surface molecules of multicell spheroids
[NASA-CR-195102] p 2420 N94-23633

IMPACT DAMAGE
Analysis of impactor residues in tray clamps from the Long Duration Exposure Facility. Part 2: Clamps from Bay B of the satellite
[NASA-TM-104784] p 2386 N94-24095
A prediction method for the compressive strength of impact damaged composite laminates
[CTN-94-60925] p 2229 N94-24137
Impact damage in filament wound composite bottles
p 2231 N94-24421
J-integral patch for finite element analysis of dynamic fracture due to impact of pressure vessels
p 2381 N94-24429
Assessment of impact damage of composite rocket motor cases
[NASA-CR-195143] p 2220 N94-24595

IMPACT LOADS
Continuum representations of cellular solids
[DE94-001706] p 2375 N94-23217
Development testing of the two-watt RTG heat source and Hastelloy-S/T-111 alloy compatibility studies
[DE94-002875] p 2243 N94-23784
Assessment of impact damage of composite rocket motor cases
[NASA-CR-195143] p 2220 N94-24595
Projected effectiveness of airbag supplemental restraint systems in US Army helicopter cockpits
[AD-A273250] p 2174 N94-25141

IMPACT PREDICTION
Comparison of c.t.s. based prediction of store trajectory with flight test data p 2158 N94-24268

IMPACT STRENGTH
Three-dimensional, inelastic response of single-edge notch bend specimens subjected to impact loading
[AD-A273302] p 2378 N94-25143
Strength and life of pressure vessels subjected to impacts and thermomechanical GFRP loading
[VTT-JULK-771] p 2379 N94-25418

IMPACT TESTS
Method for simulating a vehicle shock test: Design and realization of the required implementation tools
[ECL-92-14] p 2352 N94-22885
High pressure Hugoniot of sapphire
[DE94-001048] p 2558 N94-22946
Assessment of impact damage of composite rocket motor cases
[NASA-CR-195143] p 2220 N94-24595
Three-dimensional, inelastic response of single-edge notch bend specimens subjected to impact loading
[AD-A273302] p 2378 N94-25143

IMPEDANCE
Generalized three-dimensional simulation of ferruled coupled-cavity traveling-wave-tube dispersion and impedance characteristics
[NASA-TP-3389] p 2310 N94-24056

IMPEDANCE MEASUREMENT
Impedance measurements on a spiral-wound nickel/metal hydride cell cycled in a simulated Leo orbit
p 2392 N94-23355

IMPELLERS
Computational Fluid Dynamics (CFD) applications in rocket propulsion analysis and design
p 2214 N94-23054
Hydrodynamics of stirred gas-liquid dispersions
[ETN-94-95368] p 2339 N94-25254

IMPINGEMENT
Optimal Space Station solar array gimbal angle determination via radial basis function neural networks
[NASA-TM-106482] p 2195 N94-24482

IMPREGNATING
Composite material impregnation unit
[NASA-TM-107751] p 2254 N94-23486

IMPROVEMENT
Prospects for improved instrumentation on future solar space missions p 2624 N94-22843

IMPURITIES
Physics with chemically and isotopically pure semiconductors
[DE93-040120] p 2557 N94-22926
Magnetic resonance studies of 3d transition metal impurities in compound semiconductors
[PB93-232197] p 2243 N94-23714

Reduction of hydrocarbon impurities in 200 l/h helium liquefier-refrigerator system
[NIFS-259] p 2271 N94-24459

IN SITU MEASUREMENT
Pulsed Ion Beam Surface Analysis (PIBSA) as a means of in-situ real-time analysis of thin films during growth
[DE94-001276] p 2562 N94-23805
Engine materials characterization and damage monitoring by using x ray technologies
[NASA-TP-3328] p 2372 N94-24074
An investigation of current and future satellite and in-situ data for the remote sensing of the land surface energy balance
[NASA-CR-195138] p 2387 N94-24596
Direct observation of crystal growth from solution using optical investigation of a growing crystal face
[NASA-CR-195141] p 2563 N94-24617

IN-FLIGHT MONITORING
The Olympus PAX, measurement of mechanism induced vibration p 2362 N94-24041

INCIDENCE
Off-design performance of crenulated blades in a linear compressor cascade
[AD-A273744] p 2340 N94-25534

INCINERATORS
Investigating pyrolysis/incineration as a method of resource recovery from solid waste
p 2444 N94-25375

INCLUSIONS
Correlated petrographic, electron microprobe, and ion microprobe studies of selected primitive and processed phase assemblages in meteorites
[NASA-CR-194827] p 2601 N94-23499

INCOHERENT SCATTER RADAR
Electromagnetic interference impact of the proposed emitters for the High Frequency Active Auroral Research Program (HAARP)
[AD-A273401] p 2301 N94-24926

INCOHERENT SCATTERING
Electromagnetic interference impact of the proposed emitters for the High Frequency Active Auroral Research Program (HAARP)
[AD-A273401] p 2301 N94-24926

INCOMPRESSIBLE FLOW
Global ocean modeling on the Connection Machine
[DE94-000888] p 2417 N94-23517
Numerical analysis of a vortex controlled diffuser
p 2324 N94-23659
A dual reciprocal boundary element formulation for viscous flows p 2325 N94-23666
FAS multigrid calculations of three dimensional flow using non-staggered grids p 2341 N94-23675
A multilevel adaptive projection method for unsteady incompressible flow p 2341 N94-23690
Multi-grid domain decomposition approach for solution of Navier-Stokes equations in primitive variable form
p 2341 N94-23693
Drag reduction at a plane wall p 2327 N94-24140
Numerical simulation of non-Newtonian free shear flows p 2331 N94-24160
Solution of the discretized incompressible Navier-Stokes equations with iterative methods
[PB94-118635] p 2335 N94-24641
Triangular spectral elements for incompressible fluid flow
[NASA-CR-191588] p 2490 N94-24914
Sub-sonic flow about a slender profile in a tunnel having perforated walls
[AD-A273184] p 2170 N94-25137
Analytical skin friction and heat transfer formula for compressible internal flows
[NASA-CR-191185] p 2170 N94-25173
Unified approach for incompressible flows
p 2342 N94-25356
Detailed description of two calculation programs for incompressible, steady state boundary layer flows, applied to determine the aerodynamic characteristics of NACA12 and OA312 foils at low Reynolds numbers
[ISL-N-604/92] p 2171 N94-25461

INCOMPRESSIBLE FLUIDS
Forced vibrations of a non-viscous drop
[MPIS-24/1992] p 2318 N94-23198
An application of small-gap equations in sealing devices p 2325 N94-23668
Hydro-elastic analysis using a selection of commercial analysis programs
[PB94-118734] p 2376 N94-24478
Triangular spectral elements for incompressible fluid flow
[NASA-CR-191588] p 2490 N94-24914

INCONEL (TRADEMARK)
Effect of irradiation on the stress corrosion cracking behavior of Alloy X-750 and Alloy 625
[DE94-001759] p 2244 N94-23792

Performance characteristics of the DIII-D advanced divertor cryopump
[DE94-002745] p 2354 N94-23797

INDEPENDENT VARIABLES
Subset selection for the best of two populations: Tables of the expected subset size
[PB93-237857] p 2494 N94-23546

INDEXES (DOCUMENTATION)
An information retrieval logical model applied to the formalism of conceptual graphs: The ELEN prototype and its experimentation on a corpus of software components
[ETN-94-95162] p 2588 N94-22879
Aeronautical engineering: A continuing bibliography with indexes (supplement 298)
[NASA-SP-7037(298)] p 2153 N94-23711
Aeronautical engineering: A continuing bibliography with indexes (supplement 299)
[NASA-SP-7037(299)] p 2153 N94-23973

INDIUM ARSENIDES
InGaAsP/InP based 1.3/1.55 micron vertical cavity surface emitting lasers for wavelength division multiplexed high speed distributed computing, phase 1
[AD-A271081] p 2348 N94-23123

INDIUM COMPOUNDS
LPCVD of InN on GaAs(110) using HN3 and TMIn: Comparison with Si(100) results
[AD-A273555] p 2235 N94-24917

INDIUM PHOSPHIDES
InGaAsP/InP based 1.3/1.55 micron vertical cavity surface emitting lasers for wavelength division multiplexed high speed distributed computing, phase 1
[AD-A271081] p 2348 N94-23123
Observation of non-centrosymmetry and determination of polarity in III-V semiconductors
[PB93-201416] p 2561 N94-23503
Electrochemical sulfur passivation of visible (approximately 670nm) AlGaInP lasers
[DE94-002293] p 2350 N94-24659

INDOOR AIR POLLUTION
Microbiological analysis of debris from Space Transportation System (STS)-55 Spacelab D-2
[NASA-CR-193883] p 2421 N94-24310

INDUCTANCE
An active antenna for ELF magnetic fields
p 2303 N94-25192

INDUCTION MOTORS
Lectures on magnetohydrodynamical drives
[PB93-224962] p 2308 N94-23104
Controllability of free-piston Stirling engine/linear alternator driving a dynamic load
[NASA-TM-106497] p 2521 N94-24302
Design and application of electromechanical actuators for deep space missions
[NASA-CR-195134] p 2365 N94-24842

INDUSTRIAL AREAS
Extinguishment of enclosed gas fires with water sprays
[PB93-201663] p 2268 N94-23430

INDUSTRIAL MANAGEMENT
The increase of the controllability of production organizations
[ISBN-9-03-860161-1] p 2586 N94-25076

INDUSTRIAL WASTES
Aqueous alkaline cleaners: An alternative to organic solvents
[AD-A273510] p 2260 N94-24848
Soil pollution at former industrial sites, the heritage of 150 years of industrial development in Noord-Brabant, The Netherlands
[ISBN-9-09-005758-7] p 2400 N94-25223

INDUSTRIES
Rolls-Royce in perspective: Past, present and future
[PNR-90882] p 2187 N94-23519
Satellite communications systems and technology. Volume 2: Site reports
[NASA-TM-109399] p 2293 N94-23628
Ozone depletion, paradigms, and politics
[DE94-001600] p 2398 N94-24506
What makes industries believe in formal methods
[PB94-110848] p 2272 N94-24648
Information technology in the service society: A twenty-first century lever
[ISBN-0-309-04876-1] p 2593 N94-24833

INELASTIC COLLISIONS
Intramultiplet mixing for Ne(**)(3p) + He at superthermal energies
[ETN-94-95327] p 2538 N94-25240

INELASTIC SCATTERING
Atomic probes of surface structure and dynamics
[DE94-001651] p 2530 N94-22720
Inelastic electron scattering from surfaces
[DE94-001368] p 2531 N94-22733
Spin-hole doping in the Kondo insulator Ce3Bi4Pt3 studied by neutron scattering
[DE93-040107] p 2557 N94-22925

The structure and spin dynamics of lanthanide-bearing silicate glasses
[DE94-001320] p 2252 N94-22992
Perturbation theory in electron diffraction
[PB93-201424] p 2533 N94-23505
Computer simulation of low energy scattering
[ETN-94-95326] p 2537 N94-25082
Lattice dynamics of Ba(1-x)K(x)BiO3 as studied by neutron scattering and computer simulation
[DE93-617053] p 2567 N94-25424
Crystal field in Nd2CuO4
[DE93-617054] p 2567 N94-25425

INEQUALITIES
Class of strong valid inequalities for the discrete lot-sizing and scheduling problem
[PB93-237774] p 2459 N94-24765

INERTIA
Mass properties measurement system dynamics
p 2368 N94-23235
Reactive thrust cruise for a geosynchronous satellite with minimum fuel consumption p 2158 N94-24271

INERTIAL CONFINEMENT FUSION
An antiproton driver for ICF propulsion
p 2217 N94-23069
Inertial confinement fusion
[DE94-002602] p 2551 N94-23703

INERTIAL NAVIGATION
Application of aircraft navigation sensors to enhanced vision systems p 2176 N94-25495
Expansion-based passive ranging
p 2176 N94-25504

INERTIAL PLATFORMS
Decentralized autonomous attitude determination using an inertially stabilized payload p 2157 N94-24264

INFERENCE
On non-informativeness in a classical Bayesian inference problem
[MEMO-COSOR-92-35] p 2494 N94-23143
Typechecker for bijective pure type systems
[PB94-110814] p 2454 N94-23817

INFILTRATION
Theoretical considerations for Reaction-Formed Silicon Carbide (RFSC) formation by molten silicon infiltration into slurry-derived preforms
[NASA-TM-106414] p 2222 N94-23500

INFORMATION
Mission planning and mission rehearsal systems: Displays and other interactive techniques
p 2522 N94-25013

INFORMATION DISSEMINATION
Performance of the Carbon Dioxide Information Analysis Center (CDIAC)
[DE94-002190] p 2397 N94-23794
The ESIS query environment pilot project
p 2518 N94-23952
Fact-based enterprise information management using NIAM
[DE93-041135] p 2591 N94-24501
NASA/DOD Aerospace Knowledge Diffusion Research Project. Report number 20: The use of selected information products and services by US aerospace engineers and scientists: Results of two surveys
[NASA-TM-109022] p 2592 N94-24649
NADA/DOD Aerospace Knowledge Diffusion Research Project. Report number 19: The US government technical report and the transfer of federally funded aerospace R/D: An analysis of five studies
[NASA-TM-109061] p 2592 N94-24660
NASA/DOD Aerospace Knowledge Diffusion Research Project. Report number 21: US aerospace industry librarians and technical information specialists as information intermediaries: Results of the phase 2 survey
[NASA-TM-109064] p 2593 N94-24709
Third Annual Foreign Acquisitions Workshop: Improving Access to Foreign Gray Literature
[NASA-TM-109683] p 2593 N94-24759
NASA tech brief evaluations
[NASA-CR-195150] p 2597 N94-24829
COSMIC monthly progress report
[NASA-CR-195153] p 2460 N94-25023
National Aeronautics and Space Administration (NASA)/American Society for Engineering Education (ASEE) Summer Faculty Fellowship Program, 1993, volume 1
[NASA-CR-188271-VOL-1] p 2632 N94-25348

INFORMATION FLOW
An engineering database management system for spacecraft operations p 2517 N94-23951
Validation activities for LOTOS based on static data flow analysis
[PB94-110863] p 2459 N94-24758
Specification list and function structure for a full-body dynamometer to be used aboard Space Station Freedom
[NASA-CR-195508] p 2439 N94-24835

Human factors of mission planning systems: Applications and implementation p 2522 N94-25011
Mission planning and mission rehearsal systems: Displays and other interactive techniques
p 2522 N94-25013

INFORMATION MANAGEMENT
An information retrieval logical model applied to the formalism of conceptual graphs: The ELEN prototype and its experimentation on a corpus of software components
[ETN-94-95162] p 2588 N94-22879
A general model for dynamic and complex information management: The ELEN prototype object manager for software engineering
[ETN-94-95163] p 2588 N94-22880
Making government work: Electronic delivery of Federal services
[OTA-TCT-578] p 2290 N94-23081
A system for managing information at ATLAS
[DE94-001337] p 2590 N94-23190
Performance of the Carbon Dioxide Information Analysis Center (CDIAC)
[DE94-002190] p 2397 N94-23794
Management of information for mission operations using automated keyword referencing p 2506 N94-23886
EOS ground data systems: A description and interface overview p 2517 N94-23948
Earth observation archive activities at DRA Farnborough p 2519 N94-23958
Fact-based enterprise information management using NIAM
[DE93-041135] p 2591 N94-24501
Waste minimization/pollution prevention at R/D facilities: A cradle-to-grave tracking and information system that will be implemented at Sandia National Laboratories
[DE93-040330] p 2591 N94-24607
COSMIC monthly progress report
[NASA-CR-195153] p 2460 N94-25023
Considerations regarding the deployment of hypermedia at JSC p 2595 N94-25366
NACA collections: A directory of significant collections of the documents of the National Advisory Committee for Aeronautics
[NASA-CR-195686] p 2594 N94-25541

INFORMATION PROCESSING (BIOLOGY)
Investigation of time and intensity effects in operator workload and performance
[CTN-94-60927] p 2433 N94-24171
Process and representation in graphical displays
p 2433 N94-24187
Automated system function allocation and display format: Task information processing requirements
p 2434 N94-24189

INFORMATION RETRIEVAL
An information retrieval logical model applied to the formalism of conceptual graphs: The ELEN prototype and its experimentation on a corpus of software components
[ETN-94-95162] p 2588 N94-22879
Hypermedia support for engineering design system
[PB93-226256] p 2449 N94-23117
Bibliographic Retrieval System (BARS), Sandia Shock Compression (SSC) database Shock Physics Index
[DE94-001679] p 2589 N94-23126
Bibliographic Retrieval System (BARS). Sandia Shock Compression (SSC) database Shock Physics Index (SPHINX) database. Volume 1: UNIX version query guide customized application for INGRES
[DE94-001703] p 2589 N94-23127
Bibliographic Retrieval System (BARS), Sandia Shock Compression (SSC) database, Shock Physics Index (SPHINX) database, Volume 2: UNIX version user's guide
[DE94-001704] p 2589 N94-23128
SPDB (science processing database): Quick reference guide p 2383 N94-23597
Management of information for mission operations using automated keyword referencing p 2506 N94-23886
The ESIS query environment pilot project
p 2518 N94-23952
Increasing levels of assistance in refinement of knowledge-based retrieval systems
[NASA-CR-195144] p 2591 N94-24552
Correct and efficient interface for logical query languages with complex objects
[PB93-211175] p 2593 N94-24743
Considerations regarding the deployment of hypermedia at JSC p 2595 N94-25366
Factors influencing perceived usability and utility of LIBERTAS at Cranfield: Implications for system modification and user education
[CRANFIELD-AERO-9212] p 2594 N94-25485
A comparison of Boolean-based retrieval to the WAIS system for retrieval of aeronautical information
[NASA-CR-4569] p 2594 N94-25487

INFORMATION SYSTEMS
Structure and flow of data through an environmental data management system
[DE93-040487] p 2589 N94-22934
Making government work: Electronic delivery of Federal services
[OTA-TCT-578] p 2290 N94-23081
Flexible framework for contingent information systems modelling
[PB93-220549] p 2589 N94-23095
Specifications of ETS, the Enhanced Transport Service
[RR-907-I] p 2589 N94-23150
NASA/ASEE Summer Faculty Fellowship Program
[NASA-CR-194678] p 2571 N94-23230
MITS architecture V1.0
[PB93-201762] p 2452 N94-23451
Systems engineering: A formal approach. Part 1: System concepts
[PB93-225308] p 2268 N94-23476
Object distribution in orca using compile-time and run-time techniques
[PB94-110574] p 2453 N94-23745
Performance of the Carbon Dioxide Information Analysis Center (CDIAC)
[DE94-002190] p 2397 N94-23794
Mission operations update for the restructured Earth Observing System (EOS) mission p 2499 N94-23839
A reference model for space data system interconnection services p 2305 N94-23847
Management of information for mission operations using automated keyword referencing p 2506 N94-23886
The application of automated operations at the Institutional Processing Center p 2509 N94-23901
Applications of CCSDS recommendations to Integrated Ground Data Systems (IGDS) p 2510 N94-23906
The evolving trend in spacecraft health analysis
p 2202 N94-23946
Using the SPICE system to help plan and interpret space science observations p 2517 N94-23950
The ESIS query environment pilot project
p 2518 N94-23952
Spacecraft crew procedures from paper to computers
p 2433 N94-24186
A simulation system for Space Station extravehicular activity p 2434 N94-24192
Panel to review EOSDIS plans
[NASA-CR-195088] p 2387 N94-24303
The 1993 NASA/ASEE Summer Faculty Fellowship Program
[NASA-CR-193862] p 2574 N94-24405
Increasing levels of assistance in refinement of knowledge-based retrieval systems
[NASA-CR-195144] p 2591 N94-24552
Waste minimization/pollution prevention at R/D facilities: A cradle-to-grave tracking and information system that will be implemented at Sandia National Laboratories
[DE93-040330] p 2591 N94-24607
RITL: An information system for application reuse-in-the-large
[PB94-119088] p 2592 N94-24646
A biological survey for the nation
[LC-93-85920] p 2421 N94-24704
Third Annual Foreign Acquisitions Workshop: Improving Access to Foreign Gray Literature
[NASA-TM-109683] p 2593 N94-24759
Information systems strategy in air transport
[AD-A273125] p 2173 N94-24781
Information technology in the service society: A twenty-first century lever
[ISBN-0-309-04876-1] p 2593 N94-24833
Advanced Information Processing System (AIPS)
p 2165 N94-25115
Establishment of computerized numerical databases on thermophysical and other properties of molten as well as solid materials and data evaluation and validation for generating recommended reliable reference data
p 2246 N94-25123
NASA STI program database: Journal coverage (1990-1992)
[NASA-TM-109720] p 2593 N94-25168
Considerations regarding the deployment of hypermedia at JSC p 2595 N94-25366
A comparison of Boolean-based retrieval to the WAIS system for retrieval of aeronautical information
[NASA-CR-4569] p 2594 N94-25487

INFORMATION TRANSFER
Source spacing in B-ISDN
[PB93-201747] p 2293 N94-23508
An engineering database management system for spacecraft operations p 2517 N94-23951
NASA/DOD Aerospace Knowledge Diffusion Research Project. Report number 20: The use of selected information products and services by US aerospace engineers and scientists: Results of two surveys
[NASA-TM-109022] p 2592 N94-24649
Third Annual Foreign Acquisitions Workshop: Improving Access to Foreign Gray Literature
[NASA-TM-109683] p 2593 N94-24759
National Aeronautics and Space Administration (NASA)/American Society for Engineering Education (ASEE) Summer Faculty Fellowship Program, 1993, volume 2
[NASA-CR-188271-VOL-2] p 2636 N94-25367

INFRARED ASTRONOMY
The three-dimensional structure of the infrared cirrus
[NASA-CR-194870] p 2410 N94-24097
Infrared and SiO maser observations of OH/IR stars
[PB94-104890] p 2599 N94-24780
Catalog of infrared observations, third edition
[NASA-RP-1294] p 2600 N94-25387
Report on operations of the Air Force Geophysics Laboratory infrared array spectrometer
[AD-A273800] p 2406 N94-25535

INFRARED ASTRONOMY SATELLITE
Catalog of infrared observations, third edition
[NASA-RP-1294] p 2600 N94-25387

INFRARED CIRRUS (ASTRONOMY)
The three-dimensional structure of the infrared cirrus
[NASA-CR-194870] p 2410 N94-24097

INFRARED DETECTORS
Pyroelectric sensors in copolymer integrated on silicon
[LAAS-93044] p 2342 N94-22902
Development of infrared sensors using energy transfer/energy upconversion processes: Study of laser excited fluorescence in rare Earth ion doped crystals
[NASA-TM-108437] p 2233 N94-24073
The IRGen infrared data base modeler
p 2440 N94-25496
Report on operations of the Air Force Geophysics Laboratory infrared array spectrometer
[AD-A273800] p 2406 N94-25535

INFRARED IMAGERY
ASTER TIR subsystem and calibration
p 2385 N94-23612
Thermal analysis of combinatorial solid geometry models using SINDA p 2323 N94-23650
Hyperspectral imagery classification using a backpropagation neural network
[AD-A273615] p 2545 N94-24730
Temperature measurement using infrared imaging systems during turbine engine altitude testing
[NASA-TM-105871] p 2193 N94-25184
The IRGen infrared data base modeler
p 2440 N94-25496

INFRARED INSTRUMENTS
Mueller matrix analysis of infrared ellipsometry
[PB93-201549] p 2544 N94-23629
Temperature measurement using infrared imaging systems during turbine engine altitude testing
[NASA-TM-105871] p 2193 N94-25184

INFRARED INTERFEROMETERS
Interferometer scan unit mechanism definition
p 2358 N94-24012
High precision double four bar linkage mechanism for interferometric linear scanning p 2359 N94-24013
Retrieval of temperature profiles from Martian infrared spectra p 2620 N94-24893

INFRARED LASERS
Development of infrared sensors using energy transfer/energy upconversion processes: Study of laser excited fluorescence in rare Earth ion doped crystals
[NASA-TM-108437] p 2233 N94-24073
Infrared and SiO maser observations of OH/IR stars
[PB94-104890] p 2599 N94-24780

INFRARED PHOTOMETRY
Infrared and SiO maser observations of OH/IR stars
[PB94-104890] p 2599 N94-24780

INFRARED RADIATION
Infrared analysis of vapor phase deposited tricresylphosphate (TCP)
[NASA-TM-106423] p 2253 N94-23371
Mueller matrix analysis of infrared ellipsometry
[PB93-201549] p 2544 N94-23629
ASTER, a multinational Earth observing concept
p 2389 N94-23840
The three-dimensional structure of the infrared cirrus
[NASA-CR-194870] p 2410 N94-24097
Use of infrared telemetry as part of a nonintrusive inflight data collection system to collect human factors data
p 2434 N94-24193
Infrared fluorescence studies of electronic-to-vibrational energy transfer in a Br2:NO system
[AD-A273727] p 2539 N94-25443
Infrared sensors and systems for enhanced vision/autonomous landing applications
p 2439 N94-25491
The IRGen infrared data base modeler
p 2440 N94-25496
Report on operations of the Air Force Geophysics Laboratory infrared array spectrometer
[AD-A273800] p 2406 N94-25535

INFRARED RADIOMETERS
A field evaluation of remote sensor measurements of wind, temperature, and moisture for ARM integrated sounding system research
[DE94-000565] p 2381 N94-23001
Activities of NIST (National Inst. of Standards and Technology) p 2384 N94-23605
Calibration of a helium-cooled infrared spatial radiometer and grating spectrometer p 2384 N94-23607
Concept of ASTER calibration requirement
p 2384 N94-23609
ASTER TIR subsystem and calibration
p 2385 N94-23612
Modeling and data assimilation for Mars Observer
p 2620 N94-24889
INFRARED SCANNERS
A combined Earth scanner and momentum wheel for attitude determination and control of small spacecraft
p 2208 N94-24022
A fifteen years lifetime mechanism for an infrared Earth sensor p 2362 N94-24040
Device for the selective detection of objects
[CA-PATENT-1-308-179] p 2544 N94-24489
INFRARED SIGNATURES
Experimental evaluation of camouflage effectiveness in the thermal infrared
[FEL-93-A043] p 2381 N94-22896
Calibration of a helium-cooled infrared spatial radiometer and grating spectrometer p 2384 N94-23607
Advanced Capability Exhaust Systems/Integrated Product Development for advanced nozzles (ACES/IPD)
[AD-A273209] p 2189 N94-24776
INFRARED SOURCES (ASTRONOMY)
The three-dimensional structure of the infrared cirrus
[NASA-CR-194870] p 2410 N94-24097
INFRARED SPACE OBSERVATORY (ISO)
Opening mechanism for ISO/CVV cover release
p 2357 N94-24001
Design and performances of electromagnetic initiators for space mechanisms: An alternative to pyrotechnic system p 2315 N94-24037
INFRARED SPECTRA
FTIR quantification of industrial hydraulic fluids in perchloroethylene p 2264 N94-23243
Particle sizes and composition of Mars atmospheric dust based upon Viking and Mariner 9 observations
p 2618 N94-24878
Retrieval of temperature profiles from Martian infrared spectra p 2620 N94-24893
Catalog of infrared observations, third edition
[NASA-RP-1294] p 2600 N94-25387
Report on operations of the Air Force Geophysics Laboratory infrared array spectrometer
[AD-A273800] p 2406 N94-25535
INFRARED SPECTROMETERS
Optical component MAC Europe ground truth report: Flevoland 1991 (Netherlands)
[BCRS-92-27] p 2382 N94-23177
Calibration of a helium-cooled infrared spatial radiometer and grating spectrometer p 2384 N94-23607
High precision double four bar linkage mechanism for interferometric linear scanning p 2359 N94-24013
Hyperspectral imagery classification using a backpropagation neural network
[AD-A273615] p 2545 N94-24730
Retrieval of temperature profiles from Martian infrared spectra p 2620 N94-24893
Report on operations of the Air Force Geophysics Laboratory infrared array spectrometer
[AD-A273800] p 2406 N94-25535
INFRARED SPECTROSCOPY
FTIR quantification of industrial hydraulic fluids in perchloroethylene p 2264 N94-23243
Spectroscopic IR ellipsometry of 100 and 001 oriented YBa2Cu3O(7-delta) films
[PB93-201481] p 2561 N94-23445
Non-invasive optical detection of glucose in cell culture nutrient medium p 2422 N94-25357
Report on operations of the Air Force Geophysics Laboratory infrared array spectrometer
[AD-A273800] p 2406 N94-25535
INFRARED STARS
Infrared and SiO maser observations of OH/IR stars
[PB94-104890] p 2599 N94-24780
INFRARED TELESCOPES
Precision Displacement Mechanism (PDM)
p 2360 N94-24026
Report on operations of the Air Force Geophysics Laboratory infrared array spectrometer
[AD-A273800] p 2406 N94-25535
INFRARED WINDOWS
Surface modification of sapphire for enhanced infrared window performance
[DE94-000333] p 2543 N94-23458
INGOTS
Characterization of the microstructure of Nb-1wt.%Zr-0.1wt.%C tubes as affected by thermomechanical processing
[NASA-TM-106381] p 2242 N94-23550
INHIBITORS
Evaluation of ovostatin and ovostatin assay
p 2422 N94-24437
The evolution of energy-transducing systems. Studies with archaebacteria
[NASA-CR-195129] p 2422 N94-24811
INHOMOGENEITY
Electromagnetic scattering by inhomogeneous objects. Solution methods based upon reciprocity theorems of time-convolution and time-correlation type
[PB94-111010] p 2294 N94-23729
Finite-element method for computing three-dimensional electromagnetic fields in inhomogeneous media (1993)
[PB94-111101] p 2298 N94-24637
Two-point PADE approximants for Stieltjes series
p 2490 N94-24768
A relativistic theory on wave propagation in inhomogeneous magnetoplasmas
[ETN-94-95322] p 2554 N94-25285
INJECTION
Evaluation of reducing gas turbine emissions through hydrogen-enhanced steam-injected combustion
[PB94-109873] p 2187 N94-23709
Microinjection of the Yersinia YopE cytotoxin in mammalian cells induces actin microfilament disruption
[FOA-B-40418-4.4] p 2421 N94-24290
Design of a vehicle based system to prevent ozone loss
[NASA-CR-195498] p 2180 N94-24479
INJECTORS
SSME fuel preburner injector characterization
p 2211 N94-23037
Small rocket research and technology
p 2211 N94-23038
Fundamental rocket injector/spray programs at the Phillips Laboratory p 2211 N94-23039
Inherent stability of central element coaxial liquid-liquid injectors p 2212 N94-23043
Validation of a nonintrusive optical technique for the measurement of liquid mass distribution in a two-phase spray p 2548 N94-24420
CFD simulation of coaxial injectors
p 2342 N94-24430
HYPULSE combustor analysis
[NASA-CR-191579] p 2336 N94-24771
STE thrust chamber technology: Main injector technology program and nozzle Advanced Development Program (ADP)
[NASA-CR-193919] p 2221 N94-25019
INJURIES
Cellular and tissue injury during nonfreezing cold injury and frostbite
[AD-A270883] p 2423 N94-22732
INLET FLOW
Flow quality studies of the NASA Lewis Research Center Icing Research Tunnel diffuser
[NASA-TM-106311] p 2192 N94-23091
Turbine engine with induced pre-swirl at the compressor inlet
[CA-PATENT-1-317-467] p 2186 N94-23253
Experimental investigation of generic three-dimensional sidewall-compression scramjet inlets at Mach 6 in tetrafluoromethane
[NASA-TM-4497] p 2319 N94-23339
Improving diffusing S-duct performance by secondary flow control
[NASA-TM-106492] p 2170 N94-25182
Two-dimensional CFD modeling of wave rotor flow dynamics
[NASA-TM-106261] p 2189 N94-25185
INLET NOZZLES
Optimization of energy transfer in microwave electrothermal thrusters p 2216 N94-23065
Seal assembly
[CA-PATENT-163126888] p 2364 N94-24128
INORGANIC MATERIALS
Crystal growth of organics for nonlinear optical applications p 2225 N94-24348
INPUT
On dynamic input-output linearization of discrete-time nonlinear systems
[MEMO-1123] p 2447 N94-22711
A mixed map/variable structure observer for target tracking p 2157 N94-24263
INPUT/OUTPUT ROUTINES
Designing parallel programs of parameterized granularity
[ETN-94-95302] p 2468 N94-25278
INSERTS
Rack Insertion End Effector (RIEE) automation
p 2368 N94-23242
INSTRUCTION SETS (COMPUTERS)
CAMAC throughput of a new RISC-based data acquisition computer at the DIII-D tokamak
[DE94-001113] p 2550 N94-23182
INSTRUCTORS
Strategies for recruiting additional African Americans into the NASA JSC summer faculty fellows program
p 2585 N94-25362
INSTRUMENT COMPENSATION
MODIS calibration p 2383 N94-23600
Flight solar calibrations using the Mirror Attenuator Mosaic (MAM): Low scattering mirror
p 2384 N94-23602
Calibration of a helium-cooled infrared spatial radiometer and grating spectrometer p 2384 N94-23607
Infrared calibration p 2384 N94-23608
In-flight cross-calibration of ASTER/TIR and MODIS-N
p 2385 N94-23611
INSTRUMENT ERRORS
Strain gage measurement errors in the transient heating of structural components
[NASA-TM-104274] p 2376 N94-23487
INSULATION
Postflight hardware evaluation RSRM-29 (STS-54). Appendix E: Insulation postfire data
[NASA-CR-193897] p 2200 N94-24067
INSULATORS
Spin-hole doping in the Kondo insulator Ce3Bi4Pt3 studied by neutron scattering
[DE93-040107] p 2557 N94-22925
INTAKE SYSTEMS
Thrust vectoring theory, laboratory and flight tests
p 2155 N94-24251
INTEGERS
Subset selection with a generalized selection goal based on a loss function
[PB94-111192] p 2494 N94-23798
INTEGRAL EQUATIONS
A dual reciprocal boundary element formulation for viscous flows p 2325 N94-23666
Multigrid method for integral equations and automatic programs p 2464 N94-23696
Integral equations for the microstructures of supercritical fluids
[DE94-002460] p 2535 N94-24569
On a new functional integral formalism for Hubbard model
[DE93-614017] p 2492 N94-25334
INTEGRALS
The explicit computation of integration algorithms and first integrals for ordinary differential equations with polynomials coefficients using trees
[NASA-CR-194787] p 2448 N94-23074
Application of maximum entropy and irreducible cluster integrals to joint probability distributions for x ray structure determination
[PB93-224152] p 2559 N94-23109
INTEGRATED CIRCUITS
Design of integrated architectures for low level image processing
[ETN-94-95183] p 2445 N94-22901
Floating well based design methodology aimed to improve latch-up immunity in a CMOS/DMOS smart power technology
[LAAS-93093] p 2556 N94-22905
Transient analysis of circuits including frequency-dependent components using transgyrator and convolution
[PB93-225001] p 2308 N94-23130
Generation of modules for control communication circuits: A design study used in the framework of the safe vehicle PROMETHEUS
[ETN-94-95171] p 2308 N94-23165
Mixed analog-digital description and simulation: Proposition for VHDL-analogue
[RR-908-I] p 2450 N94-23180
Sensors for process control Focus Team report
[DE93-040897] p 2560 N94-23204
Electronic payloads for Martian missions: A preliminary assessment of technologies p 2610 N94-23408
Fabrication of sub-40-nm p-n junctions for 0.18 micron MOS device applications using a cluster-tool-compatible, nanosecond thermal doping technique
[DE94-001608] p 2309 N94-23520
Integration and test of high-speed transmitter electronics for free-space laser communications
[NASA-TM-106295] p 2295 N94-24101
Nonlinear optical thin films p 2225 N94-24349
Crosstalk analysis of synchronous and asynchronous optical chip interconnects with direct detection
[AD-A273261] p 2311 N94-24685
MOS analog memory with injection capacitors
[AD-D015990] p 2312 N94-25050

INTEGRATED ENERGY SYSTEMS
Considerations in implementing integrated biomass energy systems in developing countries
[DE93-018720] p 2395 N94-24499
INTEGRATED LIBRARY SYSTEMS
Factors influencing perceived usability and utility of LIBERTAS at Cranfield: Implications for system modification and user education
[CRANFIELD-AERO-9212] p 2594 N94-25485
INTEGRATED MISSION CONTROL CENTER
Common front end systems for Space Shuttle and Space Station control centers at Johnson Space Center
p 2305 N94-23838
ASTER, a multinational Earth observing concept
p 2389 N94-23840
Manned Space-laboratories Control Center (MSCC) operations concept p 2505 N94-23882
Orbital Signature Analyzer (OSA): A spacecraft health/safety monitoring and analysis tool
p 2203 N94-23947
INTEGRATED OPTICS
Optimization of microscopic and macroscopic second order optical nonlinearities p 2226 N94-24354
INTEGRATORS
A comparison of two multi-variable integrator windup protection schemes
[NASA-CR-194436] p 2190 N94-23590
The detection performance of a long-term spectral integrator using normalized and quantized data
[DREP-TM-93-11] p 2455 N94-24130
INTERACTIONAL AERODYNAMICS
Comparison of c.t.s. based prediction of store trajectory with flight test data p 2158 N94-24268
INTERACTIVE CONTROL
Extension of the critical path method
[PB94-118817] p 2488 N94-24527
INTERATOMIC FORCES
Lattice dynamics of Ba(1-x)K(x)BiO3 as studied by neutron scattering and computer simulation
[DE93-617053] p 2567 N94-25424
INTERCALATION
A method to remove intercalates from bromine and iodine intercalated carbon fibers
[NASA-TM-106443] p 2222 N94-23591
INTERFACIAL ENERGY
Atomic-scale structure of grain boundaries: Correlations to grain boundary properties
[DE94-001289] p 2558 N94-22990
INTERFACIAL TENSION
Response of an anchored annular cylindrical liquid layer to various axial excitations in zero-gravity
[LRT-WE-9-FB-3-1992] p 2266 N94-23195
Determination of fiber-matrix interface failure parameters from off-axis tests
[NASA-TM-109043] p 2241 N94-23274
Mathematical addenda to Hopper's model of plane stokes flow driven by capillarity on a free surface
[PB93-237691] p 2480 N94-23438
Surface and interfacial properties of polymer blends. A literature survey
[PB93-230191] p 2254 N94-23561
Measurement of interfacial tension by use of pendant drop video techniques
[DE93-000168] p 2345 N94-24831
Containerless measurements on liquids at high temperatures p 2238 N94-25125
Surface chemistry of liquid metals
p 2249 N94-25133
INTERFEROMETERS
Mueller matrix analysis of infrared ellipsometry
[PB93-201549] p 2544 N94-23629
LOLA: Lunar Optical Long-baseline Array. 1992-1993 space design
[NASA-CR-195533] p 2298 N94-24582
Matter-wave interferometry with laser cooled atoms
[AD-A273249] p 2536 N94-24717
LOITA: Lunar Optical/Infrared Telescope Array
[NASA-CR-195532] p 2546 N94-24816
System for cancelling phase noise in an interferometric fiber optic sensor arrangement
[AD-D015994] p 2345 N94-25053
INTERFEROMETRY
Interferometric astronomy on the Moon
p 2601 N94-23378
Intelligent Material Systems and Structures (IMSS). Part 5: Fiber optic registration of deformation in carbon laminates 91/92
[PB93-204600] p 2544 N94-23723
Direct observation of crystal growth from solution using optical investigation of a growing crystal face
[NASA-CR-195141] p 2563 N94-24617
Optimization of techniques to reconstruct images disturbed by atmospheric turbulence in the near infra-red
[PB93-199784] p 2298 N94-24630
White-light, pressure, and temperature interferopolarimetric sensor featuring optical fibers
[PB93-199792] p 2545 N94-24631
Matter-wave interferometry with laser cooled atoms
[AD-A273249] p 2536 N94-24717
Retrieval of temperature profiles from Martian infrared spectra p 2620 N94-24893
System for cancelling phase noise in an interferometric fiber optic sensor arrangement
[AD-D015994] p 2345 N94-25053
Advanced radiometric and interferometric milimeter-wave scene simulations p 2306 N94-25498
INTERFERON
Cytokines and immune surveillance in humans
[NASA-CR-194801] p 2425 N94-23331
INTERGRANULAR CORROSION
Grain-boundary microchemistry and intergranular cracking of irradiated austenitic stainless steel
[DE94-000466] p 2242 N94-23457
INTERLAMINAR STRESS
Out of plane gradients in laminated composites
[NASA-CR-194875] p 2228 N94-23566
INTERLAYERS
Photo-induced antiferromagnetic interlayer coupling in Fe superlattices with iron silicide spacers
[DE94-001345] p 2559 N94-22995
INTERMETALLICS
Evaluation of A5Si3Z(x) intermetallics for use as high temperature structural materials
[DE93-041127] p 2227 N94-22977
Generalized melting criterion for beam-induced amorphization
[DE94-001333] p 2560 N94-23189
Multilayer relaxation and surface structure of ordered alloys
[NASA-TM-106433] p 2243 N94-23578
Symposium on diffusion in ordered alloys
[AD-A273643] p 2245 N94-25033
Improved magnetostrictive transducer drive elements achieved by reduction of crystalline defects and improved crystalline orientation
[AD-A273391] p 2313 N94-25276
INTERMITTENCY
Behavior of the intermittency exponents and a quark-gluon plasma formation in the heavy ion collisions
[DE93-616869] p 2541 N94-25342
INTERMOLECULAR FORCES
Theoretical studies of a molecular beam generator
[NASA-CR-194779] p 2540 N94-23485
INTERNAL COMBUSTION ENGINES
Economics of electron beam and electrical discharge processing for post-combustion NO(x) control in internal combustion engines
[DE93-019574] p 2351 N94-22865
Fundamental limitations of non-thermal plasma processing for internal combustion engine NO(x) control
[DE93-019622] p 2351 N94-22866
Internal combustion engine with a central crankshaft and integral tandem annular pistons
[CA-PATENT-1-320-878] p 2363 N94-24055
Alternative control techniques document: NOx emissions from stationary reciprocating internal combustion engines
[PB94-104494] p 2398 N94-24476
INTERNAL FRICTION
Internal friction associated with dislocation relaxations in virgin martensite
[PB93-226280] p 2240 N94-23119
INTERNAL PRESSURE
Analysis and test of low profile aluminum aerospace tank dome
[NASA-TP-3442] p 2375 N94-23294
Development testing of the two-watt RTG heat source and Hastelloy-S/T-111 alloy compatibility studies
[DE94-002875] p 2243 N94-23784
INTERNATIONAL COOPERATION
International organizations to enable world-wide mobile satellite services p 2275 N94-22749
Advanced display technologies in Russia, Ukraine, and Belarus. Viewgraphs p 2630 N94-22893
Satellite communications systems and technology. Executive Summary
[NASA-TM-109388] p 2293 N94-23622
Resource allocation planning with international components p 2520 N94-23963
The Ninth National Space Symposium
[ISBN-0-9616962-7-3] p 2598 N94-25006
INTERNATIONAL LAW
US domestic and international regulatory issues
p 2275 N94-22748
Proceedings of Technology and Governance in the 1990's
[PB93-192904] p 2597 N94-24312
INTERNETS
AstroMail: Electronic mail for the astrophysics community
[NASA-CR-194877] p 2591 N94-24099
INTERPLANETARY COMMUNICATION
Conceptual communications system design in the 25.25-27.5 and 37.0-40.5 GHz frequency bands
p 2306 N94-25379
INTERPLANETARY MAGNETIC FIELDS
High latitude cusp signature observations for southward IMF B sub Z
[AD-A273801] p 2406 N94-25536
INTERPLANETARY SPACE
An antiproton driver for ICF propulsion
p 2217 N94-23069
INTERPLANETARY SPACECRAFT
A packet-based concept for spacecraft command planning p 2504 N94-23873
Expert diagnostics system as a part of analysis software for power mission operations p 2516 N94-23944
Magnetic shielding of interplanetary spacecraft against solar flare radiation
[NASA-CR-195539] p 2204 N94-24334
Preliminary design of a universal Martian lander
[NASA-CR-195529] p 2206 N94-25007
INTERPOLATION
Impiementing abstract multigrid or multilevel methods
p 2483 N94-23682
Efficient interpolation of velocity and flux components defined on 2- and 3-dimensional non-cartesian grids
[PB94-118619] p 2486 N94-23757
On the deformation kinetics constitutive law of plastic deformation: The rate equation p 2161 N94-24289
Solving the ranking and selection indifference-zone formulation for normal distributions using computer software
[AD-A273821] p 2496 N94-25518
INTERPROCESSOR COMMUNICATION
Programming in Fortran M
[DE94-000541] p 2450 N94-23207
Linear time algorithm to schedule trees with communication delays optimally on two machines
[PB93-237782] p 2451 N94-23441
Three, four, five, six or the complexity of scheduling with communication delays
[PB94-111630] p 2467 N94-23767
An OSI architecture for the deep space network
p 2305 N94-23848
Interoperability through standardization: Electronic mail, and X Window systems p 2575 N94-24406
The design of a standard message passing interface for distributed memory concurrent computers
[DE94-002536] p 2446 N94-24538
Runtime support and compilation methods for user-specified data distributions
[NASA-CR-191587] p 2458 N94-24679
Performance measurements of the multimedia testbed on Mach 3.0: Experience writing real-time device drivers, servers, and applications
[AD-A273600] p 2460 N94-24932
Digital data, composite video multiplexer and demultiplexer boards for an IBM PC/AT compatible computer p 2447 N94-25377
INTERSECTIONS
Estimation of delays and emissions at four-way junctions with different forms of regulation, principally four-way mandatory stop
[PB94-105236] p 2398 N94-23813
INTERSTELLAR CHEMISTRY
Molecular abundances in the envelopes around evolved stars
[PB94-104916] p 2602 N94-23812
INTERSTELLAR COMMUNICATION
SETI: Search for extraterrestrial intelligence. An international interdisciplinary seminar, star days
[PB93-230597] p 2444 N94-23754
INTERSTELLAR MAGNETIC FIELDS
Magnetic field dissipation and contraction of molecular clouds
[REPT-337] p 2603 N94-24976
INTERSTELLAR MATTER
Molecular abundances in the envelopes around evolved stars
[PB94-104916] p 2602 N94-23812
The three-dimensional structure of the infrared cirrus
[NASA-CR-194870] p 2410 N94-24097
Magnetic field dissipation and contraction of molecular clouds
[REPT-337] p 2603 N94-24976
Protoplanetary disks: Theory and observation by millimeter and sub-millimeter arrays
[REPT-331] p 2603 N94-24983
The Nobeyama millimeter array survey for protoplanetary disks around protostar candidates and T Tauri stars in Taurus
[REPT-336] p 2604 N94-24987

INTERSTELLAR SPACECRAFT
Voyager uplink planning in the interstellar mission era
p 2305 N94-23870
INTERSTELLAR TRAVEL
Voyager uplink planning in the interstellar mission era
p 2305 N94-23870
INTERSTITIALS
Evaluation of A5Si3Z(x) intermetallics for use as high temperature structural materials
[DE93-041127] p 2227 N94-22977
Magnetic resonance studies of 3d transition metal impurities in compound semiconductors
[PB93-232197] p 2243 N94-23714
INTERTROPICAL CONVERGENT ZONES
Observational and modeling studies of heat, moisture, precipitation and global-scale circulation patterns
[NASA-CR-195148] p 2415 N94-24485
INTRAMOLECULAR STRUCTURES
Microstructure of styrene methyl methacrylate copolymers grafted onto polybutadiene seeds
[ETN-94-95360] p 2262 N94-25225
INVARIANCE
Characterizations of shift-invariant distributions based on summation modulo one
[PB93-237824] p 2481 N94-23442
Correlation function estimator performance in non-Gaussian spherically invariant random processes
[AD-A273498] p 2496 N94-24951
INVERSE KINEMATICS
Control of a serpentine manipulator with collision avoidance p 2368 N94-23232
Inverse dynamics of a rigid rod system as a simplified model of flexible beam p 2160 N94-24281
Robust stability of second-order systems
[NASA-CR-195175] p 2488 N94-24564
INVERSIONS
Robust, nonlinear, high angle-of-attack control design for a supermaneuverable vehicle p 2164 N94-25108
On the inversion of the n-dimensional Laplace transform
[RR-461] p 2492 N94-25310
INVISCID FLOW
Local grid refinement method for the euler equations
[PB93-223329] p 2317 N94-22985
Forced vibrations of a non-viscous drop
[MPIS-24/1992] p 2318 N94-23198
An implicit numerical scheme for the simulation of internal viscous flows on unstructured grids
[NASA-TM-106437] p 2481 N94-23554
Upwind MacCormack Euler solver with non-equilibrium chemistry p 2326 N94-23672
Compressible turbulent flow simulation with a multigrid multiblock method p 2342 N94-23694
An analysis for high Reynolds number inviscid/viscid interactions in cascades
[NASA-CR-4519] p 2169 N94-24606
IODINE COMPOUNDS
New concepts for HgI2 scintillator gamma ray spectroscopy
[NASA-CR-194819] p 2233 N94-24113
ION ACOUSTIC WAVES
Characterization of heat transport and radiation hydrodynamics in collisional laser plasmas using collective Thomson scattering
[DE94-001502] p 2349 N94-23209
ION BEAMS
Semiempirical studies of atomic structure
[DE94-001588] p 2531 N94-22937
Electron spectroscopic studies of the neutralization of slow multicharged ions during interactions with a metal surface
[DE93-041046] p 2532 N94-22956
Generalized melting criterion for beam-induced amorphization
[DE94-001333] p 2560 N94-23189
Pulsed Ion Beam Surface Analysis (PIBSA) as a means of in-situ real-time analysis of thin films during growth
[DE94-001276] p 2562 N94-23805
A study of non-ideal focus properties of 30 deg parallel plate energy analyzers
[NIFS-263] p 2311 N94-24457
Measurement of electron temperature and density in the DIII-D neutral beam ion source arc chamber
[DE94-001099] p 2553 N94-24746
A research of possibility for negative muon production by a low energy electron beam accompanying ion beam
[NIFS-266] p 2536 N94-24868
ION CURRENTS
Stationary plasma thruster plume characteristics
[NASA-CR-194454] p 2219 N94-24361
ION CYCLOTRON RADIATION
Overview of the ATF stellarator program
[DE94-000371] p 2550 N94-23462
Multi-ion, multi-event test of ion cyclotron resonance heating
[NASA-CR-194859] p 2540 N94-23495
ION DENSITY (CONCENTRATION)
Fluid velocity and electromagnetic forces measured by a rotating Langmuir probe in the scrape off layer of JFT-2M
[OUEL-1968/92] p 2554 N94-25327
ION DISTRIBUTION
Multi-ion, multi-event test of ion cyclotron resonance heating
[NASA-CR-194859] p 2540 N94-23495
ION ENGINES
Preliminary far-field plume sputtering characterization of the Stationary Plasma Thruster (SPT-100)
[NASA-TM-106464] p 2221 N94-24766
Performance of the NASA cm ion thruster
[NASA-TM-106426] p 2221 N94-24770
ION EXCHANGING
A novel method for determination of transport parameters of H2 and O2 in PEMFCs
[DE94-001492] p 2389 N94-22962
Effects of ionizing radiation on modern ion exchange materials
[DE94-001569] p 2535 N94-24505
ION IMPLANTATION
Generalized melting criterion for beam-induced amorphization
[DE94-001333] p 2560 N94-23189
Surface modification of sapphire for enhanced infrared window performance
[DE94-000333] p 2543 N94-23458
Fabrication of sub-40-nm p-n junctions for 0.18 micron MOS device applications using a cluster-tool-compatible, nanosecond thermal doping technique
[DE94-001608] p 2309 N94-23520
ION IRRADIATION
Heavy ion irradiation of Bi-2223 silver-clad tapes for superconducting current density enhancement
[DE93-017416] p 2556 N94-22886
ION MICROSCOPES
Diffusion on Cu surfaces p 2251 N94-24428
ION PLATING
Electrochemical behavior of ion-plated TiN and Cu-Cr coatings
[AD-A273411] p 2235 N94-24784
ION PROPULSION
Power console development for NASA's electric propulsion outreach program
[NASA-TM-106428] p 2218 N94-23372
Preliminary far-field plume sputtering characterization of the Stationary Plasma Thruster (SPT-100)
[NASA-TM-106464] p 2221 N94-24766
Performance of the NASA cm ion thruster
[NASA-TM-106426] p 2221 N94-24770
ION SCATTERING
Ga delta-doping layers in silicon
[PB93-224632] p 2561 N94-23222
Computer simulation of low energy scattering
[ETN-94-95326] p 2537 N94-25082
ION SELECTIVE ELECTRODES
Bioregenerative life support systems for microgravity
[NASA-CR-195516] p 2422 N94-24810
ION SOURCES
Measurement of electron temperature and density in the DIII-D neutral beam ion source arc chamber
[DE94-001099] p 2553 N94-24746
Investigation of the heat handling capabilities of DIII-D neutral beamline internal components
[DE94-001107] p 2553 N94-24756
Diffusion in electronegative discharges with magnetic fields
[AD-A273826] p 2304 N94-25521
ION TEMPERATURE
Nonlinear ion-mixing-mode particle transport in the dissipative trapped electron regime
[DE94-000989] p 2533 N94-23435
IONIC COLLISIONS
Theoretical atomic physics for fusion
[DE94-000712] p 2533 N94-23543
The statistics of sputtering
[DE94-001128] p 2243 N94-23715
Behavior of the intermittency exponents and a quark-gluon plasma formation in the heavy ion collisions
[DE93-616869] p 2541 N94-25342
IONIZATION
Theoretical atomic physics for fusion
[DE94-000712] p 2533 N94-23543
Analysis of SOFCAL calibration data
[NASA-CR-193910] p 2345 N94-25000
IONIZATION POTENTIALS
High-order sum and difference-frequency generation in helium
[DE94-001064] p 2348 N94-23181
IONIZED GASES
Reactivity of ambident anions in the gas phase
[PB93-232189] p 2533 N94-23713
IONIZING RADIATION
Low temperature diffusion of hydrogenic species in oxide crystals: Radiation induced diffusion
[DE94-000374] p 2558 N94-22957
Effects of ionizing radiation on modern ion exchange materials
[DE94-001569] p 2535 N94-24505
IONOGRAMS
High latitude cusp signature observations for southward IMF B sub Z
[AD-A273801] p 2406 N94-25536
IONOSPHERIC NOISE
Electromagnetic field changes as a precursory phenomena of earthquakes and volcanic eruptions
[REPT-157] p 2405 N94-24980
IONOSPHERIC PROPAGATION
Electromagnetic interference impact of the proposed emitters for the High Frequency Active Auroral Research Program (HAARP)
[AD-A273401] p 2301 N94-24926
Northern Exposure 1992: An investigation of transauroral HF radio skywave propagation
[AD-A273363] p 2303 N94-25089
IONS
Relativistic configuration interaction calculation of the correlation energies of highly-charged ions
[DE94-001055] p 2532 N94-22988
The statistics of sputtering
[DE94-001128] p 2243 N94-23715
Computer modeling of nonlinearities
p 2458 N94-24661
Free energy profiles for Li(+) and I(-) ions approaching Pt(100) surface: A molecular dynamics study
[AD-A273455] p 2536 N94-24675
Bioregenerative life support systems for microgravity
[NASA-CR-195516] p 2422 N94-24810
Two micron stimulated emission of activated insulating crystals
[REPT-94-002] p 2565 N94-25025
IRIDIUM
Advanced materials for radiation-cooled rockets
p 2214 N94-23052
IRIDIUM COMPOUNDS
PEM regenerative fuel cells p 2392 N94-23358
IRON
Photo-induced antiferromagnetic interlayer coupling in Fe superlattices with iron silicide spacers
[DE94-001345] p 2559 N94-22995
Physics of iron
[DE94-002002] p 2402 N94-23721
IRON ALLOYS
Development of small punch testing technique and its application to evaluation of mechanical properties degradation
[DE94-001193] p 2375 N94-23184
Magnetic properties and transmission electron microscopy investigations of Nd-Fe-B-Co-Al melt spun ribbons
[PB93-201531] p 2561 N94-23428
Robotic weld overlay coatings for erosion control
[DE94-002665] p 2258 N94-24749
Improved magnetostrictive transducer drive elements achieved by reduction of crystalline defects and improved crystalline orientation
[AD-A273391] p 2313 N94-25276
Solid state synthesis of Fe-B-Si alloys
[VTT-PUBS-118] p 2250 N94-25316
Preceedings of the 12th International Congress: Corrosion Control for Low-Cost Reliability. Volume 3A: Corrosion: Specific issues
[AD-A273663] p 2251 N94-25450
IRON COMPOUNDS
Photoinduced charge separation in solid state and molecular systems
[DE94-001727] p 2563 N94-24537
Influences of nitrogen absorption on the magnetic properties of YFe2, YFe3 and Y6Fe23
[REPT-A-2654] p 2564 N94-24958
IRON METEORITES
Correlated petrographic, electron microprobe, and ion microprobe studies of selected primitive and processed phase assemblages in meteorites
[NASA-CR-194827] p 2601 N94-23499
IRON OXIDES
Advanced research and technology development of MCFCs
[DE94-001918] p 2389 N94-22723
Diffusion of hydrogen in iron oxides
[DE93-632430] p 2239 N94-22966
IRRADIANCE
The solar spectral irradiances from x ray to radio wavelengths
[NASA-CR-195203] p 2629 N94-25260

IRRADIATION
Grain-boundary microchemistry and intergranular cracking of irradiated austenitic stainless steel
[DE94-000466] p 2242 N94-23457
IRREGULAR VARIABLE STARS
UV spectral variability in the Herbig Ae star HR 5999. 11: The accretion interpretation
[NASA-CR-189313] p 2599 N94-23334
IRRIGATION
Evaluation of the use of remote-sensing data to identify crop types and estimate irrigated acreage, Uvalde and Medina Counties, Texas, 1989
[PB93-193159] p 2388 N94-24809
ISING MODEL
Off-critical W(infinity) and Virasoro algebras as dynamical symmetries of the integrable models
[DE93-633215] p 2478 N94-22969
Derivation of the macroscopic rate equations for the driven diffusive Ising model at pair level of approximation
[DE93-616839] p 2524 N94-25208
ISOCYANATES
Reaction of isocyanates with carboxylic acids and its application to polymer synthesis
[PB94-118858] p 2254 N94-23763
ISOMERS
Investigation of the solid-solid surface adsorption of Eu2O3 on amorphous Al2O3
[DE93-613824] p 2566 N94-25332
ISOMORPHISM
Domain decomposition methods for nonconforming finite element spaces of Lagrange-type
p 2483 N94-23680
ISOTOPE EFFECT
Physics with chemically and isotopically pure semiconductors
[DE93-040120] p 2557 N94-22926
Evaluation of uranium transitions for isotopically-selective laser induced fluorescence with diode lasers (technical report for ST064)
[DE94-002000] p 2347 N94-22974
ISOTOPES
Prospects for future solar-wind missions
p 2624 N94-22841
Physics with chemically and isotopically pure semiconductors
[DE93-040120] p 2557 N94-22926
ISOTROPIC MEDIA
Investigation of the asymptotic state of rotating turbulence using large-eddy simulation
p 2330 N94-24152
ISOTROPIC TURBULENCE
A representation for the turbulent mass flux contribution to Reynolds-stress and two-equation closures for compressible turbulence
[NASA-CR-191569] p 2319 N94-23302
Energy transfer and constrained simulations in isotropic turbulence p 2330 N94-24153
Effects of shock strength on shock turbulence interaction p 2332 N94-24165
Local isotropy in distorted turbulent boundary layers at high Reynolds number p 2332 N94-24166
Computation of large-scale statistics in decaying isotropic turbulence p 2332 N94-24167
The radiated noise from isotropic turbulence revisited
[NASA-CR-191547] p 2333 N94-24356
ITERATION
Incomplete corrections in nonlinear problems
[PB93-225746] p 2479 N94-23106
Uniform convergence of multigrid V-cycle iterations for indefinite and nonsymmetric problems
p 2482 N94-23677
Nested Krylov methods and preserving the orthogonality p 2483 N94-23681
Error due to the stopping of the Newton iteration in implicit linear multistep methods
[PB94-101425] p 2487 N94-23786
Generic mission planning concepts for space astronomy missions p 2505 N94-23878
ITERATIVE SOLUTION
Extending substructure based iterative solvers to multiple load and repeated analyses
[NASA-CR-194822] p 2466 N94-23504
Perturbation theory in electron diffraction
[PB93-201424] p 2533 N94-23505
Application of multigrid methods to the solution of liquid crystal equations on a SIMD computer
p 2484 N94-23686
A matrix analysis of conjugate gradient algorithms
[DE94-002546] p 2454 N94-23796
Solution of the discretized incompressible Navier-Stokes equations with iterative methods
[PB94-118635] p 2335 N94-24641
Projection techniques for iterative solution of A(bar x) equals (bar b) with successive right-hand sides
[NASA-CR-191571] p 2490 N94-24836
IUE
SO2 on Venus: A final cross-calibration with Pioneer Venus
[NASA-CR-195162] p 2599 N94-24988
Observational studies of the clearing phase in proto-planetary disk systems
[NASA-CR-195182] p 2604 N94-25265

J

J INTEGRAL
J-integral patch for finite element analysis of dynamic fracture due to impact of pressure vessels
p 2381 N94-24429
JACKETS
Fiber optic temperature sensor using a Y2O2S:Eu thermographic phosphor
[DE94-000331] p 2543 N94-23461
JAMMERS
CF-18 AN/ALQ-126B-MG 13 IIP interface to the DREO Electronic Warfare Engagement Simulation Facility
[DREO-TN-93-4] p 2296 N94-24118
JAMMING
Coding for frequency hopped spread spectrum satellite communications
[ECE-91-1] p 2296 N94-24132
Evaluation of EHF multi-beam adaptive arrays
[CTN-94-60898] p 2297 N94-24296
Coding for frequency hopped spread spectrum satellite communications
[ECE-92-1] p 2300 N94-24697
JAPAN
Satellite communications systems and technology. Executive Summary
[NASA-TM-109388] p 2293 N94-23622
Satellite communications systems and technology. Volume 1: Analytical chapters
[NASA-TM-109398] p 2293 N94-23627
JAPANESE SPACE PROGRAM
The next Japanese solar satellite
p 2625 N94-22846
The study of the mobile lunar explorer
p 2607 N94-23389
NASDA's view of ground control in mission operations
p 2305 N94-23835
NASDA's Advanced On-Line System (ADOLIS)
p 2509 N94-23903
Japanese aerospace science and technology 1992. A bibliography with indexes
[NASA-SP-7104] p 2631 N94-24585
JAPANESE SPACECRAFT
Advanced mobile satellite communications using COMETS satellite in MM-wave and Ka-band
p 2288 N94-22829
The next Japanese solar satellite
p 2625 N94-22846
NASDA satellite mission operation system and operations p 2501 N94-23854
Japanese aerospace science and technology 1992. A bibliography with indexes
[NASA-SP-7104] p 2631 N94-24585
JET AIRCRAFT
Sabot high speed interceptor AE 4273 aircraft design
[NASA-CR-195495] p 2183 N94-24971
A global range military transport: The ostrich
[NASA-CR-195494] p 2183 N94-24972
C-17 lot 3 production contract
[AD-A273180] p 2174 N94-25153
Birdstrike resistant crew enclosure program
[AD-A273700] p 2463 N94-25453
JET AIRCRAFT NOISE
A modelling of the noise from simple co-axial jets. Part 2: In a simulated flightstream
[ISVR-TR-226] p 2525 N94-22959
Refraction of high frequency noise in an arbitrary jet flow
[NASA-TM-106465] p 2525 N94-23464
Variability of measured sonic boom signatures. Volume 1: Technical report
[NASA-CR-191483-VOL-1] p 2526 N94-24172
Variability of measured sonic boom signatures. Volume 2: Data report
[NASA-CR-191483-VOL-2] p 2526 N94-24173
Fan noise research at NASA
[NASA-TM-106512] p 2530 N94-25172
The effects of profiles on supersonic jet noise
[NASA-CR-195184] p 2530 N94-25177
JET ENGINE FUELS
Initial evaluation of burn characteristics of phenolic foam runway brake arrestor material
[DOT/FAA/CT-TN93/7] p 2253 N94-23335
JET FLOW
A modelling of the noise from simple co-axial jets. Part 2: In a simulated flightstream
[ISVR-TR-226] p 2525 N94-22959
Spray formation processes of impinging jet injectors
p 2212 N94-23042
An experimental study of the flow field surrounding a subsonic jet in a cross flow
[NASA-CR-194770] p 2317 N94-23072
Refraction of high frequency noise in an arbitrary jet flow
[NASA-TM-106465] p 2525 N94-23464
Unsteady jet flow computation towards noise prediction
[NASA-CR-194449] p 2153 N94-23553
Mixing characteristics of directly opposed rows of jets injected normal to a crossflow in a rectangular duct
[NASA-TM-106477] p 2188 N94-24594
JET IMPINGEMENT
Spray formation processes of impinging jet injectors
p 2212 N94-23042
JET MIXING FLOW
Effect of delta tabs on mixing and axis switching in jets from asymmetric nozzles
[NASA-TM-106450] p 2167 N94-23592
Optimization of orifice geometry for cross-flow mixing in a cylindrical duct
[NASA-TM-106436] p 2481 N94-23593
CFD assessment of orifice aspect ratio and mass flow ratio on jet mixing in rectangular ducts
[NASA-TM-106434] p 2187 N94-24082
Mixing characteristics of directly opposed rows of jets injected normal to a crossflow in a rectangular duct
[NASA-TM-106477] p 2188 N94-24594
JET NOZZLES
Thrust vectoring theory, laboratory and flight tests
p 2155 N94-24251
JET STREAMS (METEOROLOGY)
Diagnostic budgets of analyzed and modelled tropical plumes
[NASA-CR-194853] p 2409 N94-23621
JFET
Method for fabricating self-aligned gate diffused junction field effect transistor
[AD-D015975] p 2312 N94-25035
JOINED WINGS
NASA/USRA University Advanced Design Program, 1992-1993. The Diamondback: A simulated commercial air transportation study
[NASA-CR-195523] p 2180 N94-24462
JOINTS (JUNCTIONS)
Attachment methods in composite joints - analysis of test results by controlled experiments method
p 2158 N94-24269
Ultrasonic process for curing adhesives
[AD-A273175] p 2259 N94-24788
JOSEPHSON JUNCTIONS
Coherence lost? Not-so-fast escapes from the in-phase attractor of a set of globally coupled nonlinear oscillators
[DE94-000799] p 2557 N94-22940
A low noise 665 GHz SIS quasi-particle waveguide receiver
[NASA-CR-194735] p 2296 N94-24105
JOURNAL BEARINGS
Foil bearing research at Penn State
p 2215 N94-23058
A technique to measure rotordynamic coefficients in hydrostatic bearings p 2215 N94-23061
Thermohydrodynamic analysis of cryogenic liquid turbulent flow fluid film bearings
[NASA-CR-194869] p 2363 N94-24081
JUPITER (PLANET)
The Jet Propulsion Laboratory space exploration: Past, present and future p 2153 N94-24242

K

K LINES
UV spectral variability in the Herbig Ae star HR 5999. 11: The accretion interpretation
[NASA-CR-189313] p 2599 N94-23334
The resonance lines of MG2 as diagnostics of the upper solar chromosphere
[NASA-CR-195084] p 2627 N94-24300
K-EPSILON TURBULENCE MODEL
Computation of flows in a turn-around duct and a turbine cascade using advanced turbulence models
p 2216 N94-23062
A representation for the turbulent mass flux contribution to Reynolds-stress and two-equation closures for compressible turbulence
[NASA-CR-191569] p 2319 N94-23302
Field models: Their present and future application in fire safety engineering
[PB93-201622] p 2269 N94-23506
The use of transition region characteristics to improve the numerical simulation of heat transfer in bypass transitional flows
[NASA-TM-106445] p 2320 N94-23525

Numerical analysis of a vortex controlled diffuser p 2324 N94-23659

A comparative study of computational solutions to flow over a backward-facing step p 2326 N94-23670

Evaluation of turbulence models in the PARC code for transonic diffuser flows [NASA-TM-106391] p 2168 N94-24084

Carrying the mass flux terms exactly in the first and second moment equations of compressible turbulence [NASA-CR-191568] p 2335 N94-24712

Turbulence models and Reynolds analogy for two-dimensional supersonic compression ramp flow [NASA-TM-106474] p 2337 N94-25119

KALMAN FILTERS

Kalman filtering applied to real-time monitoring of apogee maneuvers p 2196 N94-23923

An overview of a generic multi-sensor integrated navigation system design [CTN-94-60916] p 2174 N94-24120

Decentralized autonomous attitude determination using an inertially stabilized payload p 2157 N94-24264

Failure-proof estimation under conditions of lack of information p 2158 N94-24267

Predictive head movement tracking using innovations generated by Kalman filters [ISBN-0-315-83371-8] p 2427 N94-24467

X-31 aerodynamic characteristics determined from flight data p 2164 N94-25109

Active camera calibration for a head-eye platform using a variable state dimension filter [OUEL-1975/93] p 2346 N94-25472

Expansion-based passive ranging p 2176 N94-25504

Multiple-camera/motion stereoscopy for range estimation in helicopter flight p 2441 N94-25505

Validation of vision-based range estimation algorithms using helicopter flight data p 2442 N94-25506

KAONS

Calculations of Bose-Einstein correlations from Relativistic Quantum Molecular Dynamics [DE94-000794] p 2569 N94-23453

New evaluation of hadronic contributions to the anomalous magnetic moment of charged leptons [DE93-634394] p 2536 N94-24844

KERNEL FUNCTIONS

Specifications of ETS, the Enhanced Transport Service [RR-907-I] p 2589 N94-23150

KINEMATICS

Normal forms of kinematic singularities of 3R robot manipulators [MEMO-1124] p 2469 N94-22712

Mass properties measurement system dynamics p 2368 N94-23235

Walking machines for space p 2369 N94-23406

KINETIC ENERGY

Mass properties measurement system dynamics p 2368 N94-23235

Shock-induced turbulent flow in baffle systems [DE94-001532] p 2319 N94-23470

Effects of shock strength on shock turbulence interaction p 2332 N94-24165

Computation of large-scale statistics in decaying isotropic turbulence p 2332 N94-24167

KINETIC THEORY

Microscopic dynamics in dense helium-neon mixtures: Neutron scattering, kinetic theory and computer simulations [ISBN-9-07-386105-5] p 2537 N94-25228

KINETICS

Walking machines for space p 2369 N94-23406

On the connection of classical mechanics, physical kinetics and quantum theory [DE93-616823] p 2570 N94-25207

Modification in the kinetic solution for magnetized plasmas [DE93-613687] p 2555 N94-25343

Effect of LHCD (low hybrid current drive) on tearing mode instability [DE93-613700] p 2555 N94-25344

KLYSTRONS

Design and testing of ubitron amplifier tubes [AD-A273297] p 2311 N94-24818

KNOWLEDGE BASED SYSTEMS

Representation and specification of architectures for heterogeneous internetworking: Using a knowledge based approach [LAAS-93088] p 2445 N94-22903

Expanding the KATE toolbox p 2477 N94-23247

Link monitor and control operator assistant: A prototype demonstrating semiautomated monitor and control p 2292 N94-23267

A knowledge based system for scientific data visualization [NASA-CR-194879] p 2452 N94-23507

ATOS-1: Designing the infrastructure for an advanced spacecraft operations system p 2197 N94-23849

The Advanced Technology Operations System: ATOS p 2508 N94-23897

NASDA knowledge-based network planning system p 2508 N94-23898

A cross-disciplinary response to improve test activities: The corporate memory capitalization in Ariane4 test domain p 2508 N94-23899

Combining real-time monitoring and knowledge-based analysis in MARVEL p 2477 N94-23900

Representing operations procedures using temporal dependency networks p 2305 N94-23914

Situation management in the Link Monitor and Control Operator Assistant (LMCOA) p 2305 N94-23915

Automating a human factors evaluation of graphical user interfaces for NASA applications: An update on CHIMES p 2443 N94-23936

On the analysis of clear air radar echoes severely contaminated by clutter p 2306 N94-24423

Increasing levels of assistance in refinement of knowledge-based retrieval systems [NASA-CR-195144] p 2591 N94-24552

Intelligent systems and advanced user interfaces for design, operation, and maintenance of command management systems [NASA-CR-195172] p 2459 N94-24797

Declarative Object Manipulation Environment (DOME): Alpha version [AD-A273233] p 2460 N94-24935

An implementation of the REpresentation and MAintenance of Process knowledge (REMAP) model in the knowledge-based software assistant concept demonstration system [AD-A273207] p 2461 N94-25138

ROSAT mission planning using artificial intelligence methods [DLR-FB-93-14] p 2476 N94-25345

The use of knowledge systems [ETN-94-95318] p 2477 N94-25431

Expert system rule-base evaluation using real-time parallel processing [AD-A273701] p 2469 N94-25454

KNOWLEDGE BASES (ARTIFICIAL INTELLIGENCE)

In flight mission planning in the Copilote Electronique p 2522 N94-25015

Considerations regarding the deployment of hypermedia at JSC p 2595 N94-25366

The use of knowledge systems [ETN-94-95318] p 2477 N94-25431

KNOWLEDGE REPRESENTATION

Representation and specification of architectures for heterogeneous internetworking: Using a knowledge based approach [LAAS-93088] p 2445 N94-22903

Understanding and facilitating discovery learning in computer-based simulation environment [ISBN-9-03-860242-1] p 2462 N94-25219

KOLMOGOROV THEORY

On the large eddy simulation of turbulent flows in complex geometry p 2329 N94-24148

Local isotropy in distorted turbulent boundary layers at high Reynolds number p 2332 N94-24166

KORTEWEG-DEVRIES EQUATION

Cauchy problem for periodic KDV-type equations [PB93-238020] p 2487 N94-23776

KREEP

Basaltic Volcanism and Ancient Planetary Crusts [NASA-CR-193151] p 2614 N94-24363

Whole rock major element chemistry of KREEP basalt clasts in lunar breccia 15205: Implications for the petrogenesis of volcanic KREEP basalts p 2614 N94-24365

Major element chemistry of Apollo 14 mare basalt clasts and highland plutonic clasts from lunar breccia 14321: Comparison with neutron activation results p 2614 N94-24366

Auto-metasomatism of the western lunar highlands: Result of closed system fractionation and mobilization of a KREEPy trapped liquid p 2615 N94-24367

Melt rock components in KREEPy breccia 15205: Petrography and mineral chemistry of KREEP basalts and quartz-normative mare basalts p 2616 N94-24372

L

LABORATORIES

Contributions of DOE weapons labs and NIST to semicondutor technology [OTA-ITE-585] p 2630 N94-23572

Satellite communications systems and technology. Volume 2: Site reports [NASA-TM-109399] p 2293 N94-23628

Waste minimization/pollution prevention at R/D facilities: A cradle-to-grave tracking and information system that will be implemented at Sandia National Laboratories [DE93-040330] p 2591 N94-24607

Collaborating with our customers: NIST building and fire research laboratory [PB94-110194] p 2272 N94-24955

LABORATORY EQUIPMENT

Determination of the compatibility between structural alloys and molten metals at high temperatures [DE94-000954] p 2241 N94-23434

Stiffening of deployable space booms: Automated Protein Crystal Growth Facility [NASA-CR-195547] p 2196 N94-24820

LAGRANGE MULTIPLIERS

Application of maximum entropy and irreducible cluster integrals to joint probability distributions for x ray structure determination [PB93-224152] p 2559 N94-23109

Stability behavior of systems obtained by index-reduction [PB93-237709] p 2481 N94-23439

LAGRANGIAN FUNCTION

Mass properties measurement system dynamics p 2368 N94-23235

The renormalization group for flag manifolds [DE93-616846] p 2491 N94-25213

Cosmic wake fields [DE93-616849] p 2604 N94-25215

Weak interactions in a bilocal chiral theory [DE93-616887] p 2539 N94-25477

LAMINAR FLOW

Transient phenomena in laminar spray combustion p 2160 N94-24282

Stability of premixed laminar flames in a stagnation point flow to general disturbances [AD-A273429] p 2234 N94-24673

The influence of flow type, particle type and gravity on orthokinetic coagulation [ETN-94-95333] p 2267 N94-25060

LAMINATES

Theoretical studies of wave propagation in multilayered piezoelectric media [DE93-040273] p 2371 N94-22872

Optimization of laminate orientation to enhance failure properties [ISBN-0-315-83539-7] p 2227 N94-22892

Preparing polymeric matrix composites using an aqueous slurry technique [NASA-CASE-LAR-14771-1] p 2252 N94-23076

Method of determining shear stress employing a monomer-polymer laminate structure [NASA-CASE-LAR-14654-2] p 2375 N94-23308

Materials Science and Engineering [DE94-003018] p 2228 N94-23493

Out of plane gradients in laminated composites [NASA-CR-194875] p 2228 N94-23566

Intelligent Material Systems and Structures (IMSS). Part 5: Fiber optic registration of deformation in carbon laminates 91/92 [PB93-204600] p 2544 N94-23723

Analysis of local delaminations caused by angle ply matrix cracks [NASA-TM-109052] p 2228 N94-24083

A prediction method for the compressive strength of impact damaged composite laminates [CTN-94-60925] p 2229 N94-24137

Prediction of thermal cycling induced cracking in polmer matrix composites [NASA-CR-195135] p 2229 N94-24579

Composites and textile reinforcement [VTT-TIED-1424] p 2231 N94-25420

Collocated tunable wavenumber sensor/actuators for smart structures [AD-A273697] p 2314 N94-25488

LAND MOBILE SATELLITE SERVICE

The MSAT spacecraft of Telesat Mobile Inc. p 2207 N94-22742

Evolution of INMARSAT systems and applications: The land mobile experience p 2280 N94-22779

EUTELTRACS: The European experience on mobile satellite services p 2281 N94-22781

The ORBCOMM data communications system p 2281 N94-22782

Mobilesat (tm): A world first p 2281 N94-22783

Implementation of a system to provide mobile satellite services in North America p 2281 N94-22784

Land mobile satellite propagation measurements in Japan using ETS-V satellite p 2282 N94-22790

Measurements on the satellite-mobile channel at L and S bands p 2282 N94-22791

K-band mobile propagation measurements using ACTS p 2283 N94-22792

Measurement of multipath delay profile in land mobile satellite channels p 2283 N94-22793

Propagation model for the Land Mobile Satellite channel in urban environments p 2283 N94-22796
A prediction model of signal degradation in LMSS for urban areas p 2284 N94-22797
Global coverage Mobile Satellite Systems: System availability versus channel propagation impairments p 2284 N94-22798

LAND USE
Groundtruth collection for the JPL-SAR and ERS-1 campaign in Flevoland and Veluwe, Netherlands, 1991 [PB93-230654] p 2386 N94-23755
Effect of land use change on the carbon cycle in Amazon soils [NASA-CR-195168] p 2399 N94-24853

LANDAU DAMPING
Characterization of heat transport and radiation hydrodynamics in collisional laser plasmas using collective Thomson scattering [DE94-001502] p 2349 N94-23209

LANDAU-GINZBURG EQUATIONS
Exact transformation of the anisotropic Ginzburg-Landau model and its consequences [DE94-002208] p 2562 N94-23795

LANDING AIDS
The evaluation of ASOS for the Kennedy Space Center's Shuttle Landing Facility [NASA-CR-195685] p 2416 N94-25271
Application of aircraft navigation sensors to enhanced vision systems p 2176 N94-25495
Radar E-O image fusion p 2306 N94-25503
A model-based approach for detection of objects in low resolution passive-millimeter wave images p 2442 N94-25507
Image processing for flight crew enhanced situation awareness p 2442 N94-25508

LANDING GEAR
Landing gear with swivelling beam [CA-PATENT-1323020] p 2176 N94-24181
Studies of Shuttle orbiter arrestment system [NASA-TP-3370] p 2177 N94-24304
VLCT-13: A commercial transport for the 21st Century [NASA-CR-195492] p 2181 N94-24803

LANDING LOADS
Projected effectiveness of airbag supplemental restraint systems in US Army helicopter cockpits [AD-A273250] p 2174 N94-25141

LANDING RADAR
The 94 GHz MMW imaging radar system p 2306 N94-25493

LANDING SIMULATION
Descent and landing phase: Vision based robust spacecraft motion estimation and elevation modeling p 2608 N94-23394

LANGEVIN FORMULA
The anomalous transport caused by particles transverse drift [DE93-613685] p 2554 N94-25329

LANGMUIR-BLODGETT FILMS
The 2-D polymerized Langmuir-Blodgett films studied by STM [AD-A273542] p 2261 N94-24930

LANGUAGES
Logic of capabilities [PB94-110715] p 2473 N94-23747

LANTHANUM COMPOUNDS
Electronic structure and high pressure phase transition in LaSb and CeSb [DE93-617051] p 2567 N94-25423

LAPLACE TRANSFORMATION
Analysis of time-domain acoustic wavefields in horizontally continuously layered configurations based on the modified Cagniard method [PB94-111044] p 2524 N94-23731
On the inversion of the n-dimensional Laplace transform [RR-461] p 2492 N94-25310

LARGE SPACE STRUCTURES
Operating the Daisy facility to perform control experiments [ISBN-0-315-83554-0] p 2196 N94-22889
Real-time dynamics and control strategies for space operations of flexible structures [NASA-CR-194794] p 2203 N94-23618
LSS systems planning and performance program [NASA-CR-193882] p 2196 N94-24309
Modeling of a large undamped space structure using time domain techniques [AD-A273828] p 2206 N94-25523

LASER ABLATION
Laser ablation and deposition of metals [ETN-94-95311] p 2351 N94-25294

LASER ANEMOMETERS
Turbulence sensors for separated flows: Current capabilities, future requirements p 2315 N94-22853
SFOLDA: A semiconductor LDA for measurements in complex flows p 2316 N94-22856

LASER APPLICATIONS
Proceedings of Workshop on Laser Diagnostics in Fluid Mechanics and Combustion [AD-A272808] p 2347 N94-22914
A new automatic design method to develop multilayer thin film devices for high power laser applications [DE93-632490] p 2347 N94-22967
Evaluation of uranium transitions for isotopically-selective laser induced fluorescence with diode lasers (technical report for ST064) [DE94-002000] p 2347 N94-22974
Particle formation in a laser-heated aerosol reactor. Application to silicon and silicon nitride synthesis [PB93-217982] p 2347 N94-22982
Laser diagnostics for small rockets p 2210 N94-23032
InGaAsP/InP based 1.3/1.55 micron vertical cavity surface emitting lasers for wavelength division multiplexed high speed distributed computing, phase 1 [AD-A271081] p 2348 N94-23123
Vaporization behavior of non-stoichiometric refractory carbide materials and direct observations of the vapor phase using laser diagnostics [DE93-040094] p 2348 N94-23203
Sodium-layer laser guide stars [DE93-019621] p 2349 N94-23490
Particle size measurement for the control of industrial crystallizers [PB94-119104] p 2562 N94-23766
Laser soldering of Sn plated brass integrator assembly housings [DE94-001149] p 2270 N94-23790
Integration and test of high-speed transmitter electronics for free-space laser communications [NASA-TM-106295] p 2295 N94-24101
Conceptual design of a device to measure hand swelling in a micro-gravity environment [NASA-CR-195509] p 2437 N94-24330
Progress toward ultra-stable lasers for use in space [NASA-TM-109678] p 2349 N94-24488
Nondestructive evaluations [DE94-003020] p 2373 N94-24613
Development of a nondestructive vibration technique for bond assessment of Space Shuttle tiles [NASA-CR-195163] p 2201 N94-24919
Excited state dynamics of thulium ions in yttrium aluminum garnets [NASA-CR-195159] p 2564 N94-25024
An extended laser flash technique for thermal diffusivity measurement of high-temperature materials p 2238 N94-25132
The evolution of the laser: A systems perspective on science, technology and society [ETN-94-95319] p 2351 N94-25218
Ultracold atoms in traps and fountains [ETN-94-95325] p 2537 N94-25239
Non-invasive optical detection of glucose in cell culture nutrient medium p 2422 N94-25357
Excitation mechanisms for XUV and x ray lasers [DE93-617006] p 2351 N94-25482

LASER ARRAYS
InGaAsP/InP based 1.3/1.55 micron vertical cavity surface emitting lasers for wavelength division multiplexed high speed distributed computing, phase 1 [AD-A271081] p 2348 N94-23123
Manufacturing and characterization of GaAs/AlGaAs multiple quantumwell ridge waveguide lasers [EUT-92-E-265] p 2348 N94-23168

LASER BEAMS
Limits on high-order harmonic generation from single-atom calculations [DE93-019950] p 2531 N94-22869
Laser light scattering instrument advanced technology development [NASA-CR-194803] p 2349 N94-23286
Fabrication of sub-40-nm p-n junctions for 0.18 micron MOS device applications using a cluster-tool-compatible, nanosecond thermal doping technique [DE94-001608] p 2309 N94-23520
Particle size measurement for the control of industrial crystallizers [PB94-119104] p 2562 N94-23766
Temporal behavior of the electron density profile during limiter biasing in the HYBTOK-2 tokamak [NIFS-257] p 2552 N94-24456
Matter-wave interferometry with laser cooled atoms [AD-A273249] p 2536 N94-24717

LASER CAVITIES
InGaAsP/InP based 1.3/1.55 micron vertical cavity surface emitting lasers for wavelength division multiplexed high speed distributed computing, phase 1 [AD-A271081] p 2348 N94-23123
Computer modeling of nonlinearities p 2458 N94-24661
Internally folded scalable laser [AD-D015978] p 2350 N94-25216
The effects of optical feedback on polarization of vertical cavity surface emitting lasers [AD-A273728] p 2351 N94-25445

LASER DOPPLER VELOCIMETERS
An experimental study of characteristic combustion-driven flows for CFD validation p 2212 N94-23040
An experimental study of the flow field surrounding a subsonic jet in a cross flow [NASA-CR-194770] p 2317 N94-23072
A new experimental apparatus for the study of the unsteady flowfield over an airfoil in pitching and heaving motions using laser Doppler anemometry [ISL-CO-229/92] p 2165 N94-23149
LDA measurements of the unsteady near wake behind an airfoil undergoing transient and periodic pitching motions [ISL-CO-215/92] p 2165 N94-23161
Output optics for laser velocimeters [NASA-CASE-ARC-11889-1-SB] p 2543 N94-23309
Doppler global velocimetry: Development of a flight research instrumentation system for application to non-intrusive measurements of the flow field [NASA-CR-191490] p 2344 N94-24360
Direct measurement of turbulent dissipation rate using dual laser doppler velocimeters [AD-A273740] p 2340 N94-25530

LASER FUSION
Inertial confinement fusion [DE94-002602] p 2551 N94-23703

LASER HEATING
Particle formation in a laser-heated aerosol reactor. Application to silicon and silicon nitride synthesis [PB93-217982] p 2347 N94-22982

LASER INDUCED FLUORESCENCE
Evaluation of uranium transitions for isotopically-selective laser induced fluorescence with diode lasers (technical report for ST064) [DE94-002000] p 2347 N94-22974
Vaporization behavior of non-stoichiometric refractory carbide materials and direct observations of the vapor phase using laser diagnostics [DE93-040094] p 2348 N94-23203
In situ detection of tropospheric OH, HO2, NO2, and NO by laser-induced fluorescence in detection chambers at reduced pressures [NASA-CR-194810] p 2397 N94-23277

LASER INTERFEROMETRY
Japanese aerospace science and technology 1992. A bibliography with indexes [NASA-SP-7104] p 2631 N94-24585
Quantum optical aspects of topological phases, such as Berry's phase [AD-A273632] p 2570 N94-25028

LASER MATERIALS
Development of infrared sensors using energy transfer/energy upconversion processes: Study of laser excited fluorescence in rare Earth ion doped crystals [NASA-TM-108437] p 2233 N94-24073
Two micron stimulated emission of activated insulating crystals [REPT-94-002] p 2565 N94-25025
Excitation mechanisms for XUV and x ray lasers [DE93-617006] p 2351 N94-25482

LASER OUTPUTS
Fabrication of sub-40-nm p-n junctions for 0.18 micron MOS device applications using a cluster-tool-compatible, nanosecond thermal doping technique [DE94-001608] p 2309 N94-23520
Feasibility study: Monodisperse polymer particles containing laser-excitable dyes p 2225 N94-24350
Exciplex laser study: Discharge and magnetic switching systems [PB93-199768] p 2349 N94-24629
Temporal model of an optically pumped co-doped solid state laser [NASA-TM-109680] p 2350 N94-24851
A comparison of free-space and fiber mixer performances [AD-A273558] p 2547 N94-25161

LASER PLASMAS
Characterization of germanium stripe x ray lasers [DE93-019629] p 2347 N94-22867
Characterization of heat transport and radiation hydrodynamics in collisional laser plasmas using collective Thomson scattering [DE94-001502] p 2349 N94-23209

LASER POWER BEAMING
Power beaming to space using a nuclear reactor-pumped laser [DE94-001208] p 2348 N94-23185
Low power ground-based laser illumination for electric propulsion applications [NASA-CR-194444] p 2219 N94-23555
WISPER: Wirless Space Power Experiment [NASA-CR-195538] p 2396 N94-24701

LASER PROPULSION

Advanced space propulsion concepts p 2216 N94-23067

Low power ground-based laser illumination for electric propulsion applications [NASA-CR-194444] p 2219 N94-23555

LASER PUMPING

Power beaming to space using a nuclear reactor-pumped laser [DE94-001208] p 2348 N94-23185

Investigation of the optical and laser properties of Tm and Ho in YAG anf YLF [REPT-94-001] p 2563 N94-24404

Nonlinear dynamical control of lasers [AD-A273359] p 2350 N94-24938

Two micron stimulated emission of activated insulating crystals [REPT-94-002] p 2565 N94-25025

Tunable lasers pumped by visible laser diodes [AD-D016000] p 2350 N94-25044

Internally folded scalable laser [AD-D015978] p 2350 N94-25216

LASER SPECTROSCOPY

Evaluation of uranium transitions for isotopically-selective laser induced fluorescence with diode lasers (technical report for ST064) [DE94-002000] p 2347 N94-22974

Doppler global velocimetry: Development of a flight research instrumentation system for application to non-intrusive measurements of the flow field [NASA-CR-191490] p 2344 N94-24360

LASER STABILITY

Inverse free electron laser beat-wave accelerator research [DE94-002597] p 2349 N94-23702

Inertial confinement fusion [DE94-002602] p 2551 N94-23703

Progress toward ultra-stable lasers for use in space [NASA-TM-109678] p 2349 N94-24488

LASER TARGETS

Numerical simulation and analysis of experimental results on stimulated Raman scattering in laser-plasma Hohlraum targets [DE93-613719] p 2554 N94-25330

LASERS

Crosstalk analysis of synchronous and asynchronous optical chip interconnects with direct detection [AD-A273261] p 2311 N94-24685

Internally folded scalable laser [AD-D015978] p 2350 N94-25216

The evolution of the laser: A systems perspective on science, technology and society [ETN-94-95319] p 2351 N94-25218

LASING

Characterization of germanium stripe x ray lasers [DE93-019629] p 2347 N94-22867

Power beaming to space using a nuclear reactor-pumped laser [DE94-001208] p 2348 N94-23185

Excitation mechanisms for XUV and x ray lasers [DE93-617006] p 2351 N94-25482

LATCH-UP

Floating well based design methodology aimed to improve latch-up immunity in a CMOS/DMOS smart power technology [LAAS-93093] p 2556 N94-22905

LATCHES

Low melting temperature alloy deployment mechanism p 2356 N94-23997

Docking mechanisms: An overview of different systems p 2357 N94-24004

Microwelding due to random vibration p 2359 N94-24019

LATE STARS

Infrared and SiO maser observations of OH/IR stars [PB94-104890] p 2599 N94-24780

LATERAL CONTROL

Feedback control laws for highly maneuverable aircraft [NASA-CR-195195] p 2190 N94-25176

LATERAL STABILITY

Lateral high frequency oscillations and stability of a wheel rolling on a flexible track p 2269 N94-23585

Determination of the stability and control derivatives of the NASA F/A-18 HARV using flight data [NASA-CR-194838] p 2190 N94-24804

X-31 aerodynamic characteristics determined from flight data p 2164 N94-25109

LATITUDE

Effect of power system technology and mission requirements on high altitude long endurance aircraft [NASA-CR-194455] p 2189 N94-25200

LATTICE VIBRATIONS

Lattice dynamics of Ba(1-x)K(x)BiO3 as studied by neutron scattering and computer simulation [DE93-617053] p 2567 N94-25424

LATTICES (MATHEMATICS)

A rational elliptic surface related to the question of expressing squares as sum of consecutive squares [W-9305] p 2479 N94-23139

LAUNCH VEHICLES

Expanding the KATE toolbox p 2477 N94-23247

Analysis and test of low profile aluminum aerospace tank dome [NASA-TP-3442] p 2375 N94-23294

Life cycle cost modeling of conceptual space vehicles [NASA-CR-194813] p 2203 N94-23329

National Institute of Standards and Technology Conference on Reducing the Cost of Space Infrastructure and Operations. Part 2: Topical papers [PB94-113487] p 2194 N94-23819

Modal test of the Brazilian satellite launcher (VLS) configuration burn-out of the first stage p 2156 N94-24257

Access to space studies p 2199 N94-24434

Design of an airborne launch vehicle for an air launched space booster [NASA-CR-195534] p 2198 N94-24860

Space transfer vehicle concepts and requirements. Volume 4: Summary of special studies [NASA-CR-193918] p 2201 N94-24970

Optimal RTLS abort trajectories for an HL-20 personnel launch vehicle p 2165 N94-25114

LAW (JURISPRUDENCE)

Using satellite communications for a mobile computer network p 2280 N94-22777

NASA printing, duplicating, and copying management handbook [NASA-NHB-1490.5] p 2590 N94-23971

LAWS

NASA printing, duplicating, and copying management handbook [NASA-NHB-1490.5] p 2590 N94-23971

LAYOUTS

Pilot-vehicle interface [DOT/FAA/CT-92/21] p 2430 N94-23083

Pilot-vehicle interface handbook, chapter 19. Volume 2: Digital systems validation [DOT/FAA/CT-88/10-VOL-2] p 2438 N94-24830

LEACHING

Chemical characterization of some aerobic liquids in CELSS p 2422 N94-23241

LEAD ZIRCONATE TITANATES

Photo-induced and electrooptic properties of (Pb,La)(Zr,Ti)O3 films for optical memories [DE93-019820] p 2542 N94-23202

LEADING EDGE SLATS

Aircraft accident report: Inadvertent in-flight slat deployment, China Eastern Airlines Flight 583, McDonnell Douglas MD-11, B-2171, 950 nautical miles south of Shemya, Alaska, 6 April 1993 [PB93-910408] p 2172 N94-23579

LEADING EDGE SWEEP

Experimental investigation of generic three-dimensional sidewall-compression scramjet inlets at Mach 6 in tetrafluoromethane [NASA-TM-4497] p 2319 N94-23339

LEADING EDGES

Leading-edge votex-system details obtained on F-106B aircraft using a rotating vapor screen and surface techniques [NASA-TP-3374] p 2166 N94-23512

Characteristics of surface roughness associated with leading edge ice accretion [NASA-TM-106459] p 2166 N94-23522

Compressibility effects on dynamic stall of airfoils undergoing rapid transient pitching motion [NASA-TM-109681] p 2167 N94-23975

Lift augmentation on a delta wing via leading edge fences and the Gurney flap [NASA-CR-194793] p 2168 N94-24103

Stagnation region heat transfer: The influence of turbulence parameters, Reynolds number and body shape [NASA-TM-106504] p 2334 N94-24481

Measurements of the influence of integral length scale on stagnation region heat transfer [NASA-TM-106503] p 2338 N94-25183

Effect of an extendable slat on the stall behavior of a VR-12 airfoil [NASA-TP-3407] p 2171 N94-25187

Analysis and characteristics of compressor stall precursor signals in forward and AFT swept high speed compressor [AD-A273820] p 2171 N94-25517

LEAF AREA INDEX

Session on coupled land surface/hydrological/atmospheric models p 2414 N94-24395

LEAKAGE

Robust, wide-range hydrogen sensor for use in commercial, space, and government applications [DE93-040902] p 2342 N94-22954

Brush seals for cryogenic applications p 2216 N94-23063

Interpretation of discrepancies in mass spectroscopy data obtained from different experimental configurations p 2237 N94-23245

Viscous rotary damper p 2361 N94-24031

Electrochemical sulfur passivation of visible (approximately 670nm) AlGaInP lasers [DE94-002293] p 2350 N94-24659

LEARNING THEORY

Understanding and facilitating discovery learning in computer-based simulation environment [ISBN-9-03-860242-1] p 2462 N94-25219

LEAST SQUARES METHOD

Two-stage versus sequential sample-size determination in regression analysis of simulation experiments [PB94-110558] p 2495 N94-24634

Adaptive predictive control of the benchmark plant [OUEL-1972/93] p 2477 N94-25470

Modeling of a large undamped space structure using time domain techniques [AD-A273828] p 2206 N94-25523

LEAVES

The measurement and analysis of leaf spectral reflectance of two stands of loblolly pine populations p 2389 N94-24442

LECTURES

Cardiopulmonary Aspects in Aerospace Medicine [AGARD-LS-189] p 2423 N94-23313

Visual Problems in Night Operations [AGARD-LS-187] p 2431 N94-23976

LEGENDRE FUNCTIONS

Implementation and parallelization of fast matrix multiplication for a fast Legendre transform [DE94-002184] p 2478 N94-22975

On the Gibbs phenomenon 3: Recovering exponential accuracy in a sub-interval from a spectral partial sum of a piecewise analytic function [NASA-CR-191560] p 2480 N94-23278

LENS DESIGN

A study on electrostatic quadrupole lenses and their application technologies [REPT-948] p 2546 N94-24982

LENSES

Output optics for laser velocimeters [NASA-CASE-ARC-11889-1-SB] p 2543 N94-23309

Vision impairment and corrective considerations of civil airmen [DOT/FAA/AM-93/21] p 2426 N94-23623

LENTICULAR BODIES

Internal friction associated with dislocation relaxations in virgin martensite [PB93-226280] p 2240 N94-23119

LEPTONS

Towards a theory of quark and lepton masses [DE94-001726] p 2533 N94-23218

Low mass muon pair production in 450 GeV p-Be collisions [PB94-110699] p 2533 N94-23746

Stitching the Yukawa quilt [PB93-204477] p 2569 N94-24532

LEVITATION

Processing of YBCO superconductors for improved levitation force [DE94-001326] p 2559 N94-22994

Performance analysis of the combined EDS maglev propulsion, levitation, and guidance system [DE94-001346] p 2352 N94-22996

Electrostatic levitation technology for thermophysical properties of molten materials p 2238 N94-25135

LIAPUNOV FUNCTIONS

Control of a serpentine manipulator with collision avoidance p 2368 N94-23232

Continuous gust response and sensitivity derivatives using state-space models p 2161 N94-24287

Neural network-based control using Lyapunov functions p 2477 N94-24433

Liapunov stability in chemical engineering [MATHS-REPT-A-184] p 2236 N94-25427

LIBRARIES

NASA/DOD Aerospace Knowledge Diffusion Research Project. Report number 21: US aerospace industry librarians and technical information specialists as information intermediaries: Results of the phase 2 survey [NASA-TM-109064] p 2593 N94-24709

Factors influencing perceived usability and utility of LIBERTAS at Cranfield: Implications for system modification and user education [CRANFIELD-AERO-9212] p 2594 N94-25485

NACA collections: A directory of significant collections of the documents of the National Advisory Committee for Aeronautics
[NASA-CR-195686] p 2594 N94-25541

LIE GROUPS
A working algorithm to isolate integrable surfaces in E cubed
[SSCL-PREPRINT-761] p 2452 N94-23518
Coadjoint orbits and conformal field theory
[DE94-002285] p 2523 N94-24658
On BRST quantization of constrained systems
[ETN-94-95386] p 2570 N94-25258

LIFE (DURABILITY)
Small rocket research and technology
p 2211 N94-23038
Strength and life of pressure vessels subjected to impacts and thermomechanical GFRP loading
[VTT-JULK-771] p 2379 N94-25418

LIFE CYCLE COSTS
US Department of Energy phaseout of CFC-refrigerants
[DE94-001668] p 2397 N94-23016
Task 1: Health management demonstration. Task 2: Process management environment and support of enterprise integration. Task 3: New algorithm development in the PME
[NASA-CR-188268] p 2430 N94-23290
Life cycle cost modeling of conceptual space vehicles
[NASA-CR-194813] p 2203 N94-23329
National Institute of Standards and Technology Conference on Reducing the Cost of Space Infrastructure and Operations. Part 2: Topical papers
[PB94-113487] p 2194 N94-23819
New Technologies for Space Avionics, 1993
[NASA-CR-195157] p 2272 N94-25193

LIFE RAFTS
Survival suit for submarine personnel: Summary of evaluation studies
[PB93-204634] p 2430 N94-23743

LIFE SUPPORT SYSTEMS
Chemical characterization of some aerobic liquids in CELSS p 2422 N94-23241
Weld joint concepts for on-orbit repair of Space Station Freedom fluid system tube assemblies
p 2371 N94-24427

LIFT
A numerical study of airplanes flying in proximity
[AD-A273373] p 2173 N94-24718
Active control of oscillatory lift forces on a circular cylinder
[AD-A273243] p 2338 N94-25140
High lift aerodynamics
[NASA-CR-195183] p 2184 N94-25268

LIFT AUGMENTATION
Lift augmentation on a delta wing via leading edge fences and the Gurney flap
[NASA-CR-194793] p 2168 N94-24103

LIFT DRAG RATIO
The Triton: Design concepts and methods
[NASA-CR-195542] p 2184 N94-25004

LIFT FANS
Summary of lift and lift/cruise fan powered lift concept technology
[NASA-CR-177619] p 2176 N94-23489

LIFTING ROTORS
The ISL rotor bench
[ISL-R-108/92] p 2185 N94-25301

LIGHT ADAPTATION
DCT quantization matrices visually optimized for individual images p 2442 N94-25509

LIGHT AIRCRAFT
Design project: Viper
[NASA-CR-195484] p 2184 N94-25021

LIGHT AMPLIFIERS
Investigation of Raman beam cleanup and phase conjugation
[AD-A273157] p 2545 N94-24672
Design and testing of ubitron amplifier tubes
[AD-A273297] p 2311 N94-24818
Improvement of system properties of a pulsed laser Doppler anemometer with respect to an optical amplifier
[DLR-FB-93-19] p 2547 N94-25305

LIGHT BEAMS
Output optics for laser velocimeters
[NASA-CASE-ARC-11889-1-SB] p 2543 N94-23309
Method and apparatus for the non-invasive measurement of pressure inside pipes using a fiber optic interferometer sensor
[AD-D016013] p 2344 N94-24734

LIGHT CURVE
SO2 on Venus: A final cross-calibration with Pioneer Venus
[NASA-CR-195162] p 2599 N94-24988

LIGHT MODULATION
A fully automated stage for optical waveguide measurements
[AD-A273042] p 2542 N94-22915

LIGHT SCATTERING
Laser diagnostics for small rockets
p 2210 N94-23032
Laser light scattering instrument advanced technology development
[NASA-CR-194803] p 2349 N94-23286
Flight solar calibrations using the Mirror Attenuator Mosaic (MAM): Low scattering mirror
p 2384 N94-23602
Particle size measurement for the control of industrial crystallizers
[PB94-119104] p 2562 N94-23766
Measuring the dynamics of structural changes in biological macromolecules from light scattering data
p 2422 N94-24426
LRAT: Lightning Radiative Transfer
p 2416 N94-24443
The chemistry of particulate formation in fluorocarbon plasmas
[DE94-001500] p 2552 N94-24546
Investigation of Raman beam cleanup and phase conjugation
[AD-A273157] p 2545 N94-24672
Ultrastructure processing of macromolecular materials
[AD-A273413] p 2258 N94-24782
Numerical simulation and analysis of experimental results on stimulated Raman scattering in laser-plasma Hohlraum targets
[DE93-613719] p 2554 N94-25330

LIGHT SCATTERING METERS
Laser light scattering instrument advanced technology development
[NASA-CR-194803] p 2349 N94-23286

LIGHT SOURCES
Laser energized high voltage direct current power supply
[AD-D015977] p 2312 N94-25036

LIGHT TRANSMISSION
Dual frequency optical carrier technique for transmission of reference frequencies in dispersive media
[NASA-CASE-NPO-18007-2-CU] p 2543 N94-23270
Design and implementation issues of end-to-end protocols in high-speed networks
[PB94-110905] p 2467 N94-23752

LIGHT-CONE EXPANSION
On spontaneous symmetry breaking mechanism in light-front quantized field theory
[DE93-633211] p 2568 N94-22968

LIGHTHILL GAS MODEL
Sound radiation due to boundary layer transition
p 2332 N94-24163

LIGHTING EQUIPMENT
Cockpit/NVG visual integration issues
p 2432 N94-23983

LIGHTNING
Lightning studies using LDAR and LLP data
p 2416 N94-23238
Lightning, atmospheric electricity, and climate change
[DE94-002003] p 2408 N94-23471
CAPE for CaPE p 2416 N94-24409
LRAT: Lightning Radiative Transfer
p 2416 N94-24443
Lightning tests and analyses of tunnel bond straps and shielded cables on the Space Shuttle solid rocket booster
[NASA-CR-193921] p 2200 N94-24801

LIMITERS (FUSION REACTORS)
Temporal behavior of the electron density profile during limiter biasing in the HYBTOK-2 tokamak
[NIFS-257] p 2552 N94-24456

LIMITS (MATHEMATICS)
Setting test limits under prescribed consumer loss
[MEMO-1107] p 2478 N94-22725
Infinite divisible and stable distributions modulo 1
[PB94-110640] p 2495 N94-23815
Uniform limit theorems for marked point processes
[PB94-118726] p 2488 N94-24526

LINE CURRENT
Transient analysis of conducting half-plane problem with noncausal scattering image
[PB93-225027] p 2524 N94-23110

LINE SPECTRA
Molecular abundances in the envelopes around evolved stars
[PB94-104916] p 2602 N94-23812

LINEAR ACCELERATORS
A system for managing information at ATLAS
[DE94-001337] p 2590 N94-23190
The CEBAF beam loss sensors
[CEBAF-PR-93-032] p 2540 N94-24662
Activities of Academia Sinica
[DE93-614529] p 2541 N94-25335

LINEAR CIRCUITS
APLAC: An object-oriented analog circuit simulator and design tool. 6.1 system simulations manual
[PB93-224871] p 2450 N94-23226

LINEAR ENERGY TRANSFER (LET)
To perform a proof-of-concept study on the use of superheated drop detectors for the measurement of LET spectra in space environments
[BTI-92/3-31] p 2629 N94-24695

LINEAR EQUATIONS
Multigrid method for integral equations and automatic programs p 2464 N94-23696

LINEAR PREDICTION
Algorithms for speech coding systems based on linear prediction
[EUT-92-E-260] p 2447 N94-22731
Psychophysical and signal-processing aspects of speech representation
[ETN-94-95292] p 2302 N94-25077

LINEAR PROGRAMMING
The Third Twente Workshop on Graphs and Combinatorial Optimization
[PB94-110947] p 2486 N94-23722

LINEAR QUADRATIC GAUSSIAN CONTROL
Balancing for unstable nonlinear systems
[MEMO-1118] p 2469 N94-22705
A homotopy algorithm for digital optimal projection control GASD-HADOC
[NASA-CR-193881] p 2456 N94-24470
Flight controller design using mixed H2/H infinity optimization with a singular H infinity constraint
[AD-A273831] p 2191 N94-25525

LINEAR QUADRATIC REGULATOR
Operating the Daisy facility to perform control experiments
[ISBN-0-315-83554-0] p 2196 N94-22889

LINEAR SYSTEMS
Reduced-order modelling and control of a class of systems for which balanced truncation is Hankel-norm optimal
[OUEL-1922/92] p 2472 N94-23163
Nested Krylov methods and preserving the orthogonality p 2483 N94-23681
Coordinate-free interpretations of the optimal costs for Lq problems subject to implicit systems
[PB94-118700] p 2473 N94-23760
Neural network-based control using Lyapunov functions p 2477 N94-24433
The state space method for integro-differential equations of convolution type with rational matrix symbols
[ETN-94-95379] p 2491 N94-25244
From circuit to signal: Development of a piecewise linear simulator
[ISBN-9-09-005713-7] p 2462 N94-25263
Arbitrary-order numerical schemes for linear hyperbolic systems
[CRANFIELD-AERO-9211] p 2523 N94-25480

LINEAR TRANSFORMATIONS
Orbit spaces over commutative rings and projectives as semi-isomorphisms
[DE93-616822] p 2493 N94-25473

LINEARIZATION
Decoupling problems around a trajectory: From linearity to nonlinearity
[MEMO-1115] p 2469 N94-22703
On dynamic input-output linearization of discrete-time nonlinear systems
[MEMO-1123] p 2447 N94-22711
Feedback linearization of parametrized nonlinear time-varying systems
[MEMO-1126] p 2470 N94-22714
Broadband linearisation of high-efficiency power amplifiers p 2275 N94-22747

LINKAGES
Docking mechanisms: An overview of different systems p 2357 N94-24004
High precision double four bar linkage mechanism for interferometric linear scanning p 2359 N94-24013

LIPIDS
Primary prevention of coronary heart disease
p 2423 N94-23317
Synthesis and in-vivo detection of boronated compounds for use in BNCT
[DE94-001899] p 2233 N94-23780

LIQUID ALLOYS
Optical properties and emissivities of liquid metals and alloys p 2248 N94-25129

LIQUID ATOMIZATION
Measurement of intact-core length of atomizing liquid jets by image deconvolution p 2210 N94-23029
A theoretical evaluation of aluminum gel propellant two-phase flow losses on vehicle performance
p 2210 N94-23031
Spray formation processes of impinging jet injectors
p 2212 N94-23042

LIQUID CHROMATOGRAPHY
Capillary electrokinetic separations with optical detection [DE94-001639] p 2233 N94-23716
LIQUID CRYSTALS
Method of determining shear stress employing a monomer-polymer laminate structure [NASA-CASE-LAR-14654-2] p 2375 N94-23308
Application of multigrid methods to the solution of liquid crystal equations on a SIMD computer p 2484 N94-23686
Ultrastructure processing of macromolecular materials [AD-A273413] p 2258 N94-24782
Center for advanced electrical and structural polymers [AD-A273415] p 2259 N94-24783
Surface-induced static undulations in multilayer films of liquid-crystalline polymers [AD-A273517] p 2262 N94-25159
Structure of cholesteryl-4-vinylbenzoate [AD-A273686] p 2567 N94-25441
LIQUID FUELS
Electro-rheology fluids and liquid fuel flow [AD-A273640] p 2337 N94-25032
LIQUID INJECTION
Inherent stability of central element coaxial liquid-liquid injectors p 2212 N94-23043
LIQUID LEVELS
Thermodynamic models for bounding pressurant mass requirements of cryogenic tanks [NASA-TM-106476] p 2346 N94-25202
LIQUID METALS
SP-100 heat transport technology development [DE94-000769] p 2218 N94-23452
Workshop on the Thermophysical Properties of Molten Materials [NASA-CP-10121] p 2246 N94-25120
Detection of velocity in high temperature liquid metals p 2247 N94-25127
Optical properties and emissivities of liquid metals and alloys p 2248 N94-25129
Thermophysical properties of simple liquid metals: A brief review of theory p 2248 N94-25130
Surface chemistry of liquid metals p 2249 N94-25133
LIQUID NITROGEN
Design of microchannels for cryostabilization of high temperature superconducting magnets [DE94-001324] p 2559 N94-22993
Experimental and analytical study of cryogenic propellant boiloff to develop and verify alternate pressurization concepts for Space Shuttle external tank using a scaled down tank p 2266 N94-23657
Tribological behaviour of fluorinated resins and polyimide resins sliding over a metallic surface in liquid nitrogen p 2355 N94-23991
LIQUID OXYGEN
LOX droplet vaporization in a supercritical forced convective environment p 2211 N94-23034
Evaporation and combustion of LOX under supercritical and subcritical conditions p 2211 N94-23035
Axisymmetric single shear element combustion instability experiment p 2213 N94-23044
Shear coaxial injector instability mechanisms p 2213 N94-23047
Computational Fluid Dynamics (CFD) applications in rocket propulsion analysis and design p 2214 N94-23054
Features of a SINDA/FLUINT model of a liquid oxygen supply line p 2322 N94-23649
Design considerations of hybrid rockets p 2156 N94-24254
Validation of a nonintrusive optical technique for the measurement of liquid mass distribution in a two-phase spray p 2548 N94-24420
Advanced launch system. Advanced development oxidizer turbopump program [NASA-CR-193920] p 2367 N94-25174
LIQUID PHASES
High strain rate superplasticity in metals and composites [DE94-001521] p 2229 N94-24547
LIQUID PROPELLANT ROCKET ENGINES
Measurement of intact-core length of atomizing liquid jets by image deconvolution p 2210 N94-23029
LOX droplet vaporization in a supercritical forced convective environment p 2211 N94-23034
Droplet turbulence interactions under subcritical and supercritical conditions p 2211 N94-23036
Fundamental rocket injector/spray programs at the Phillips Laboratory p 2211 N94-23039
Numerical parametric studies of spray combustion instability p 2212 N94-23041
Spray formation processes of impinging jet injectors p 2212 N94-23042
Inherent stability of central element coaxial liquid-liquid injectors p 2212 N94-23043
Flow visualization study in high aspect ratio cooling channels for rocket engines p 2213 N94-23049
Heat transfer in rocket combustion chambers p 2214 N94-23051
Computational Fluid Dynamics (CFD) applications in rocket propulsion analysis and design p 2214 N94-23054
Liquid rocket propulsion: Retrospective and prospects p 2154 N94-24243
Heat transfer in rocket engine combustion chambers and regeneratively cooled nozzles [NASA-CR-195094] p 2220 N94-24471
Ignition and combustion characteristics of metallized propellants, phase 2 [NASA-CR-195107] p 2266 N94-24700
LIQUID ROCKET PROPELLANTS
Development of a computational testbed for numerical simulation of combustion instability p 2213 N94-23046
Recent advances in SPE (tm) water electrolyzer p 2393 N94-23362
Assessment of an SP-100 bi-modal propulsion and power system [DE94-000889] p 2218 N94-23433
LIQUID SURFACES
Measurement of intact-core length of atomizing liquid jets by image deconvolution p 2210 N94-23029
Response of an anchored annular cylindrical liquid layer to various axial excitations in zero-gravity [LRT-WE-9-FB-3-1992] p 2266 N94-23195
Design of a surface deformation measuring instrument for the Surface Tension Driven Convection Experiment (STDCE-2) [NASA-CR-194758] p 2343 N94-23285
LIQUID-GAS MIXTURES
Hydrodynamics of stirred gas-liquid dispersions [ETN-94-95368] p 2339 N94-25254
LIQUID-LIQUID INTERFACES
Electrochemically mediated polymerization of 2-pentadecylaniline confined to a planar liquid-liquid interface [AD-A273541] p 2259 N94-24792
The hydrodynamics of a moving fluid-liquid contact line [ETN-94-95352] p 2339 N94-25247
LIQUID-SOLID INTERFACES
Liquid oscillations in a spherical system with sliding edges boundary by two conical solid surfaces in zero-gravity [LRT-WE-9-FB-5-1992] p 2318 N94-23197
Effects of thermal-solutal convection on temperature and solutal fields under various gravitational orientations p 2267 N94-24451
Surface-induced static undulations in multilayer films of liquid-crystalline polymers [AD-A273517] p 2262 N94-25159
The hydrodynamics of a moving fluid-liquid contact line [ETN-94-95352] p 2339 N94-25247
LIQUID-VAPOR EQUILIBRIUM
Effect of initial droplet-size distributions on fuel-vapor profiles in a shear-layer flow p 2160 N94-24283
LIQUID-VAPOR INTERFACES
The 2-D polymerized Langmuir-Blodgett films studied by STM [AD-A273542] p 2261 N94-24930
LIQUIDS
Containerless measurements on liquids at high temperatures p 2238 N94-25125
LIQUIDUS
Containerless measurements on liquids at high temperatures p 2238 N94-25125
Liquidus temperature and optical properties measurement by containerless techniques p 2247 N94-25126
LITERATURE
Third Annual Foreign Acquisitions Workshop: Improving Access to Foreign Gray Literature [NASA-TM-109683] p 2593 N94-24759
LITHIUM
SP-100 heat transport technology development [DE94-000769] p 2218 N94-23452
LITHIUM ALLOYS
Segregation and oxidation studies of Al-Li and Al-Mg alloys [ISBN-0-315-83993-7] p 2244 N94-24469
LITHIUM HYDRIDES
Vacancy formation energy of Li(H, D) and Na(H, D) systems [DE93-633452] p 2558 N94-22978
LITHIUM OXIDES
Overcharge and overdischarge protection of ambient temperature secondary lithium cells [NASA-CASE-NPO-18343-1-CU] p 2310 N94-23823
Glass-ceramic Li-Al-Si-O composition and process for its production [CA-PATENT-APPL-SN-2043757] p 2254 N94-24129
LITHIUM SULFUR BATTERIES
Status of the development of rechargeable lithium cells p 2392 N94-23354
LITHOGRAPHY
Proposed additions to the SHADOW ray-tracing code for general-asymmetric perfect-crystal optics [DE94-001291] p 2560 N94-23188
Fabrication of sub-40-nm p-n junctions for 0.18 micron MOS device applications using a cluster-tool-compatible, nanosecond thermal doping technique [DE94-001608] p 2309 N94-23520
Characteristics of products generated by selective sintering and stereolithography rapid prototyping processes p 2264 N94-24412
Scanning probe lithography. 2: Selective chemical vapor deposition of copper into scanning tunneling microscope-defined patterns [AD-A273304] p 2547 N94-25144
High precision x ray lithographic masks [AD-A273342] p 2346 N94-25154
LITHOLOGY
Highland crust at the Apollo 14 site: A review p 2614 N94-24364
The western highland province at the Apollo 14 site p 2615 N94-24369
Seafloor characterization/Galapagos propagating rift [AD-A273586] p 2419 N94-25165
LITHOSPHERE
The national geomagnetic initiative [LC-93-85739] p 2401 N94-23344
LIVER
In vitro system for studying metabolism of environmental chemicals in human cells [AD-A273427] p 2421 N94-24688
LOAD DISTRIBUTION (FORCES)
Global dynamic stability of a shallow arch by poincare-like simple cell mapping p 2160 N94-24280
Reduction of structural loads using maneuver load control on the Advanced Fighter Technology Integration (AFTI)/F-111 mission adaptive wing [NASA-TM-4526] p 2168 N94-24295
LOADING RATE
Humidity effects on soluble core mechanical and thermal properties (polyvinyl alcohol/microballoon composite) type CG extendospheres, volume 2 [NASA-CR-193893] p 2229 N94-24224
LOADS (FORCES)
Split spline screw [NASA-CASE-GSC-13434-1] p 2352 N94-23082
A study of the core module simulator floor capability p 2380 N94-24418
Buckling of circular cylindrical shells subjected to combined loads (axial compression, normal pressure, bending and transverse shear loading) [PB93-215358] p 2378 N94-24745
Loading, electromyograph, and motion during exercise p 2427 N94-25359
Loading, electromyograph, and motion during exercise p 2427 N94-25380
LOCAL AREA NETWORKS
Supercomputer networking for space science applications [NASA-CR-194876] p 2465 N94-23085
Switch configuration for migration to optical fiber network p 2447 N94-23250
SPOT4 Operational Control Center (CMP) p 2197 N94-23856
The evolving trend in spacecraft health analysis p 2202 N94-23946
The experimental physics and industrial control system architecture: Past, present, and future [DE94-002639] p 2457 N94-24626
Ground based mission planning systems p 2522 N94-25014
LOCAL SCIENTIFIC SURVEY MODULE
Using the SPICE system to help plan and interpret space science observations p 2517 N94-23950
LOCAL THERMODYNAMIC EQUILIBRIUM
Model atmosphere analysis of selected luminous B stars [NASA-CR-195098] p 2599 N94-24051
The solar spectral irradiances from x ray to radio wavelengths [NASA-CR-195203] p 2629 N94-25260
LOCKS (FASTENERS)
Preloaded launch locking devices for SILEX p 2358 N94-24008
LOCOMOTION
Mechanical design of a planetary rover p 2369 N94-23403
Planetary rover locomotion mechanisms p 2369 N94-23404

Walking, jumping, and tumbling: More than one way to get around Mars p 2370 N94-23419
Physical modeling and dynamic simulation of planet vehicles: Application to the motion prediction p 2371 N94-23426

LOGARITHMS
Logarithm of probability measures and infinite divisibility of sub-stable random vectors [PB94-118627] p 2486 N94-23758

LOGIC CIRCUITS
Formal verification of digital circuits described in VHDL [ETN-94-95165] p 2306 N94-22883
Logic synthesis on programmable networks [ETN-94-95174] p 2449 N94-23151
CADBIT 2: Computer-aided design for built-in test, volume 1 [AD-A273702] p 2463 N94-25455
CADBIT 2: Computer-aided design for built-in test, volume 2 [AD-A273703] p 2463 N94-25456

LOGIC DESIGN
A method for the general simultaneous full decomposition of sequential machines: Algorithms and implementation [EUT-92-E-267] p 2445 N94-23170
Towards the formal specification of the requirements and design of a processor interface unit: HOL listings [NASA-CR-191465] p 2466 N94-23252

LOGIC PROGRAMMING
An information retrieval logical model applied to the formalism of conceptual graphs: The ELEN prototype and its experimentation on a corpus of software components [ETN-94-95162] p 2588 N94-22879
Interpretation of evolutive environment by a multisensory perception machine [LAAS-93111] p 2471 N94-22907
Asynchronous rendezvous in distributed logic programming [PB93-220614] p 2448 N94-23096
Logic synthesis on programmable networks [ETN-94-95174] p 2449 N94-23151
Applications of the Aurora parallel PROLOG system to computational molecular biology [DE93-041166] p 2420 N94-23468
Transition system specifications in stalk format with bisimulation as a congruence [PB94-110608] p 2453 N94-23707
Combinatory reduction systems: Introduction and survey [PB94-110582] p 2457 N94-24570
Area-power-delay trade-off in logic synthesis [ISBN-9-09-005332-8] p 2461 N94-25080

LOGISTICS
The Columbus logistics support at the APMC: Requirements and implementation aspects p 2515 N94-23935
Timed coloured Petri nets and their application to logistics [ETN-94-95310] p 2522 N94-25293
A comparative evaluation plan for the Maintenance, Inventory, and Logistics Planning (MILP) System Human-Computer Interface (HCI) p 2588 N94-25373

LOGISTICS MANAGEMENT
A framework for SFC/DC system data analysis p 2523 N94-23234

LONG DURATION EXPOSURE FACILITY
Analysis of impactor residues in tray clamps from the Long Duration Exposure Facility. Part 2: Clamps from Bay B of the satellite [NASA-TM-104784] p 2386 N94-24095

LONG DURATION SPACE FLIGHT
Concepts and embodiment design of a reentry recumbent seating system for the NASA Space Shuttle [NASA-CR-195504] p 2438 N94-24667

LONG TERM EFFECTS
A fifteen years lifetime mechanism for an infrared Earth sensor p 2362 N94-24040
Static adhesion in preloaded contacts subjected to long-term vacuum exposure p 2363 N94-24043
Design and testing of a unique randomized gravity, continuous flow bioreactor p 2423 N94-25368

LONGITUDINAL CONTROL
A combined Earth scanner and momentum wheel for attitude determination and control of small spacecraft p 2208 N94-24022
Feedback control laws for highly maneuverable aircraft [NASA-CR-195195] p 2190 N94-25176

LONGITUDINAL STABILITY
Determination of the stability and control derivatives of the NASA F/A-18 HARV using flight data [NASA-CR-194838] p 2190 N94-24804
Effect of aeroelastic-propulsive interactions on flight dynamics of a hypersonic vehicle p 2164 N94-25113

LOOP ANTENNAS
Isolated and coupled superquadric loop antennas for mobile communications applications p 2289 N94-22834

LOOP TRANSFER RECOVERY
Asymptotic correctors: The LTR [PB93-199701] p 2474 N94-24627

LOOPS
Material data representation of hysteresis loops for Hastelloy X using artificial neural networks [NASA-TM-105990] p 2376 N94-23551

LORENTZ TRANSFORMATIONS
On the transverse size of a fast moving nucleon [DE93-616891] p 2539 N94-25481

LOSSES
Momentum loss in proton-nucleus and nucleus-nucleus collisions [NASA-TP-3405] p 2540 N94-24305

LOUDNESS
Variability of measured sonic boom signatures. Volume 1: Technical report [NASA-CR-191483-VOL-1] p 2526 N94-24172
Variability of measured sonic boom signatures. Volume 2: Data report [NASA-CR-191483-VOL-2] p 2526 N94-24173

LOUDSPEAKERS
Comparison of measured and predicted pure tone propagation levels from JAPE-1: An evaluation of the performance of ASOPRAT p 2527 N94-24212

LOUVERS
Solution of mixed convection heat transfer from isothermal in-line fins p 2321 N94-23644

LOW ALTITUDE
Regulated drag area parachute [AD-D015992] p 2170 N94-25051

LOW ASPECT RATIO
Off-design performance of crenulated blades in a linear compressor cascade [AD-A273744] p 2340 N94-25534

LOW CARBON STEELS
Crashworthiness analysis using advanced material models in DYNA3D [DE94-002988] p 2229 N94-24632

LOW COST
The Westinghouse Series 1000 Mobile Phone: Technology and applications p 2284 N94-22800
Low cost coherent demodulation for mobile satellite terminals p 2284 N94-22803
Low cost antennas for MSAT vehicular applications p 2289 N94-22830
Microstrip monopulse antenna for land mobile communications p 2289 N94-22833
L-band mobile terminal antennas for helicopters p 2289 N94-22835
An x ray diffraction investigation of alpha-Al2O2 addition to Yttria Stabilized Zirconia (YSZ) thermal barrier coatings subject to destabilizing vanadium pentoxide (V2O5) exposure [AD-A273403] p 2261 N94-25072
Preceedings of the 12th International Congress: Corrosion Control for Low-Cost Reliability. Volume 2: Process Industries Plant Operations [AD-A273662] p 2251 N94-25449

LOW CURRENTS
LHCD (low hybrid current drive) experiment on the HT-6B tokamak [DE93-613720] p 2555 N94-25331
Effect of LHCD (low hybrid current drive) on tearing mode instability [DE93-613700] p 2555 N94-25344

LOW FREQUENCIES
Modal structure of variations in the tropical climate system. Part 2: Origins of the low-frequency mode [MPIM-96] p 2407 N94-23199
Multi-ion, multi-event test of ion cyclotron resonance heating [NASA-CR-194859] p 2540 N94-23495
Nonlinear dynamics applied to atmospheric prediction [AD-A273437] p 2404 N94-24674
Very low frequency and low frequency transmitting antenna parameter monitoring system [AD-D015989] p 2302 N94-25049
Measurements and modeling of multitone, low-frequency acoustic data from the Arraial do Cabo range [AD-A273406] p 2530 N94-25073
Improved magnetostrictive transducer drive elements achieved by reduction of crystalline defects and improved crystalline orientation [AD-A273391] p 2313 N94-25276

LOW MOLECULAR WEIGHTS
Polyimide processing additives [NASA-CASE-LAR-13669-2] p 2252 N94-23079
Center for advanced electrical and structural polymers [AD-A273415] p 2259 N94-24783

LOW NOISE
Cryogenic, low-noise high electron mobility transistor amplifiers for the Deep Space Network p 2291 N94-23262

LOW PRESSURE
Discontinuous phase formation and selective attack of SiC materials exposed to low oxygen partial pressure environments [DE93-040161] p 2231 N94-22933
Performance assessment of low pressure nuclear thermal propulsion p 2217 N94-23070
LPCVD of InN on GaAs(110) using HN3 and TMIn: Comparison with Si(100) results [AD-A273555] p 2235 N94-24917
Mechanisms of anode power deposition in a low pressure free burning arc [NASA-CR-194442] p 2553 N94-25190

LOW REYNOLDS NUMBER
The use of transition region characteristics to improve the numerical simulation of heat transfer in bypass transitional flows [NASA-TM-106445] p 2320 N94-23525
Evaluation of turbulence models in the PARC code for transonic diffuser flows [NASA-TM-106391] p 2168 N94-24084
On streak spacing in wall-bounded turbulent flows p 2331 N94-24159
Detailed description of two calculation programs for incompressible, steady state boundary layer flows, applied to determine the aerodynamic characteristics of NACA12 and OA312 foils at low Reynolds numbers [ISL-N-604/92] p 2171 N94-25461

LOW TEMPERATURE
Low temperature diffusion of hydrogenic species in oxide crystals: Radiation induced diffusion [DE94-000374] p 2558 N94-22957
Thermally activated low temperature creep and primary water stress corrosion cracking of NiCrFe alloys [DE94-001756] p 2241 N94-23219

LOW THRUST
Theory and computation of optimal low- and medium-thrust transfers [NASA-CR-194812] p 2217 N94-23275
Design of a resistojet for Space Station Freedom [NASA-CR-195506] p 2221 N94-24979

LOW THRUST PROPULSION
Molecular gas dynamics applied to low-thrust propulsion p 2214 N94-23053

LOW VISIBILITY
Airport surface operations requirements analysis [NASA-CR-191508] p 2172 N94-23288

LOW VOLTAGE
Limiting factors for carbon based chemical double layer capacitors p 2394 N94-23365

LOWER BODY NEGATIVE PRESSURE
Responses to LBNP in men with varying profiles of strength and aerobic capacity: Implications for flight crews [NASA-TP-3346] p 2426 N94-23530

LUBRICANT TESTS
An analytical ultra-high vacuum tribometer for solid lubricant studies p 2361 N94-24033
BLAST, a new lubricant screening tester for space oils and greases p 2362 N94-24042
An assessment of solid lubricant films for use in high temperature space applications p 2363 N94-24044
The development of dry-lubricated ceramic cages p 2363 N94-24045
Development of high temperature liquid lubricants for low-heat rejection: Heavy duty diesel engines [NASA-CR-191197] p 2258 N94-24753

LUBRICANTS
New method for increasing machine service-life, phase 2 [PB93-200707] p 2354 N94-23533
New pin-on-disk equipment for vacuum tribometry p 2360 N94-24023

LUBRICATING OILS
Tribological characterization of spatial wet lubricants under vacuum p 2264 N94-24010
In-vacuum performance of Fomblin Z25-lubricated, 52100 steel bearings with TiC-coated balls p 2358 N94-24011
BLAST, a new lubricant screening tester for space oils and greases p 2362 N94-24042
A colour image processing algorithm to identify copper-based particles in filter debris samples [DREP-TM-93-19] p 2455 N94-24122

LUBRICATION
Lewis Research Center R and D Facilities [NASA-TM-109400] p 2630 N94-23135
New method for increasing machine service-life, phase 2 [PB93-200707] p 2354 N94-23533
An application of small-gap equations in sealing devices p 2325 N94-23668

Development of a theory of the wear of ceramics [DE94-002773] p 2254 N94-23783

Tribological characteristics of ball bearings lubricated with a sputtered molybdenum disulphide film in a vacuum under a high thrust load p 2355 N94-23992

The tribology of some MoS2-lubricated engineering ceramics p 2356 N94-23993

Thermal vacuum performance of cycloid and harmonic gearboxes with solid (MoS2) and liquid (Braycote 601) lubrication p 2358 N94-24009

Wear reduction in ceramic bearings by surface generated pyrolytic carbon continuously replenished by ethylene gas [NASA-CR-189214] p 2364 N94-24090

Investigation of the ultrafiltration technique using military greases [AD-A273633] p 2261 N94-25029

LUMINANCE

Validation of a second generation conspicuity meter [IZF-1993-A-11] p 2542 N94-22895

Evaluation of visual acuity with Gen 3 night vision goggles [NASA-TM-108792] p 2431 N94-23974

Night vision devices and characteristics p 2432 N94-23982

Luminance-brightness mapping: The missing decades [ETN-94-95351] p 2428 N94-25298

LUMINESCENCE

Symbiosis in marine luminous bacteria [AD-A273540] p 2422 N94-24791

Data analysis and interpretation of lunar dust exosphere p 2623 N94-25349

LUMINOSITY

Search for the top quark and other new particles at D0 [DE94-001220] p 2535 N94-24515

LUNAR BASED EQUIPMENT

Interferometric astronomy on the Moon p 2601 N94-23378

Conceptual design and architecture of hexapod robotic vehicles for the (L)OVLA project p 2369 N94-23405

LOITA: Lunar Optical/Infrared Telescope Array [NASA-CR-195532] p 2546 N94-24816

LUNAR BASES

Power beaming to space using a nuclear reactor-pumped laser [DE94-001208] p 2348 N94-23185

Design of a lunar propellant processing facility. NASA/USRA advanced program [NASA-CR-195502] p 2266 N94-24618

Space transfer vehicle concepts and requirements. Volume 4: Summary of special studies [NASA-CR-193918] p 2201 N94-24970

LUNAR COMMUNICATION

Conceptual communications system design in the 25.25-27.5 and 37.0-40.5 GHz frequency bands p 2306 N94-25379

LUNAR COMPOSITION

Basaltic Volcanism and Ancient Planetary Crusts [NASA-CR-193151] p 2614 N94-24363

LUNAR CRATERS

The morphology of the lunar surface parts in the region of work of the mobile geological laboratory vehicle in Mare Imbrium p 2607 N94-23385

LUNAR CRUST

Basaltic Volcanism and Ancient Planetary Crusts [NASA-CR-193151] p 2614 N94-24363

Highland crust at the Apollo 14 site: A review p 2614 N94-24364

Whole rock major element chemistry of KREEP basalt clasts in lunar breccia 15205: Implications for the petrogenesis of volcanic KREEP basalts p 2614 N94-24365

Major element chemistry of Apollo 14 mare basalt clasts and highland plutonic clasts from lunar breccia 14321: Comparison with neutron activation results p 2614 N94-24366

The western highland province at the Apollo 14 site p 2615 N94-24369

Lunar mare volcanism: Mixing of distinct, mantle source regions with KREEP-like component p 2615 N94-24370

Heterogeneity in small aliquots of Apolllo 15 olivine-normative basalt: Implications for breccia clast studies p 2616 N94-24373

LUNAR DUST

Data analysis and interpretation of lunar dust exosphere p 2623 N94-25349

LUNAR EXPLORATION

The birth of NASA: The diary of T. Keith Glennan [NASA-SP-4105] p 2630 N94-23333

Lunar science strategy: Exploring the Moon with humans and machines p 2605 N94-23376

Robotic exploration of Moon and Mars p 2606 N94-23379

The morphology of the lunar surface parts in the region of work of the mobile geological laboratory vehicle in Mare Imbrium p 2607 N94-23385

Unmanned lunar rovers: Utilization for exploration p 2607 N94-23387

Early lunar rover mission studies p 2607 N94-23388

Lunar exploration rover program developments [DE93-040759] p 2613 N94-23469

LUNAR GEOLOGY

Lunar science strategy: Exploring the Moon with humans and machines p 2605 N94-23376

The morphology of the lunar surface parts in the region of work of the mobile geological laboratory vehicle in Mare Imbrium p 2607 N94-23385

Catalog of Apollo 17 rocks. Volume 1: Stations 2 and 3 (South Massif) [NASA-CR-194854] p 2613 N94-24058

Highland crust at the Apollo 14 site: A review p 2614 N94-24364

Major element chemistry of Apollo 14 mare basalt clasts and highland plutonic clasts from lunar breccia 14321: Comparison with neutron activation results p 2614 N94-24366

Auto-metasomatism of the western lunar highlands: Result of closed system fractionation and mobilization of a KREEPy trapped liquid p 2615 N94-24367

Polytopic vector analysis in igneous petrology: Application to lunar petrogenesis p 2615 N94-24368

The western highland province at the Apollo 14 site p 2615 N94-24369

LUNAR LANDING MODULES

Lunar transportation system [NASA-CR-195540] p 2365 N94-24805

Extended duration lunar lander [NASA-CR-195527] p 2206 N94-24916

LUNAR LANDING SITES

Auto-metasomatism of the western lunar highlands: Result of closed system fractionation and mobilization of a KREEPy trapped liquid p 2615 N94-24367

LUNAR MANTLE

Lunar mare volcanism: Mixing of distinct, mantle source regions with KREEP-like component p 2615 N94-24370

LUNAR MARIA

Basaltic Volcanism and Ancient Planetary Crusts [NASA-CR-193151] p 2614 N94-24363

Major element chemistry of Apollo 14 mare basalt clasts and highland plutonic clasts from lunar breccia 14321: Comparison with neutron activation results p 2614 N94-24366

Auto-metasomatism of the western lunar highlands: Result of closed system fractionation and mobilization of a KREEPy trapped liquid p 2615 N94-24367

Lunar mare volcanism: Mixing of distinct, mantle source regions with KREEP-like component p 2615 N94-24370

LUNAR MINING

Design of a lunar propellant processing facility. NASA/USRA advanced program [NASA-CR-195502] p 2266 N94-24618

LUNAR OBSERVATORIES

Interferometric astronomy on the Moon p 2601 N94-23378

LOLA: Lunar Optical Long-baseline Array. 1992-1993 space design [NASA-CR-195533] p 2298 N94-24582

LOITA: Lunar Optical/Infrared Telescope Array [NASA-CR-195532] p 2546 N94-24816

LUNAR RESOURCES

Design of a lunar propellant processing facility. NASA/USRA advanced program [NASA-CR-195502] p 2266 N94-24618

LUNAR ROCKS

Catalog of Apollo 17 rocks. Volume 1: Stations 2 and 3 (South Massif) [NASA-CR-194854] p 2613 N94-24058

Highland crust at the Apollo 14 site: A review p 2614 N94-24364

Polytopic vector analysis in igneous petrology: Application to lunar petrogenesis p 2615 N94-24368

The western highland province at the Apollo 14 site p 2615 N94-24369

Heterogeneity in small aliquots of Apolllo 15 olivine-normative basalt: Implications for breccia clast studies p 2616 N94-24373

LUNAR ROVING VEHICLES

Catalog of Apollo experiment operations [NASA-RP-1317] p 2194 N94-23292

Missions, Technologies, and Design of Planetary Mobile Vehicles [ISBN-2-85428-331-7] p 2605 N94-23373

Past US studies and developments for planetary rovers p 2369 N94-23375

Lunar science strategy: Exploring the Moon with humans and machines p 2605 N94-23376

Rover requirements for the planet surface segment of the space exploration initiative p 2369 N94-23377

Lunar rover navigation concepts p 2607 N94-23386

Unmanned lunar rovers: Utilization for exploration p 2607 N94-23387

Early lunar rover mission studies p 2607 N94-23388

The study of the mobile lunar explorer p 2607 N94-23389

Lunar exploration rover program developments [DE93-040759] p 2613 N94-23469

Some useful innovations with TRASYS and SINDA-85 p 2322 N94-23647

LUNAR SOIL

Highland crust at the Apollo 14 site: A review p 2614 N94-24364

Whole rock major element chemistry of KREEP basalt clasts in lunar breccia 15205: Implications for the petrogenesis of volcanic KREEP basalts p 2614 N94-24365

Major element chemistry of Apollo 14 mare basalt clasts and highland plutonic clasts from lunar breccia 14321: Comparison with neutron activation results p 2614 N94-24366

Polytopic vector analysis in igneous petrology: Application to lunar petrogenesis p 2615 N94-24368

Measuring track densities in lunar grains by image analysis p 2623 N94-25355

LUNAR SURFACE

Catalog of Apollo experiment operations [NASA-RP-1317] p 2194 N94-23292

Rover requirements for the planet surface segment of the space exploration initiative p 2369 N94-23377

The morphology of the lunar surface parts in the region of work of the mobile geological laboratory vehicle in Mare Imbrium p 2607 N94-23385

Design of a walking robot [NASA-CR-195200] p 2367 N94-25274

LUNAR TOPOGRAPHY

The morphology of the lunar surface parts in the region of work of the mobile geological laboratory vehicle in Mare Imbrium p 2607 N94-23385

LUNAR TRAJECTORIES

Lunar transportation system [NASA-CR-195540] p 2365 N94-24805

LUNGS

Spontaneous pneumothorax, cysts and bullae p 2425 N94-23326

LUNOKHOD LUNAR ROVING VEHICLES

Soviet developments of planet rovers in period of 1964 - 1990 p 2369 N94-23374

LYMAN ALPHA RADIATION

Model development for Ulysses and SOHO [NASA-CR-193884] p 2627 N94-24484

LYSOZYME

Temperature dependence of protein solubility-determination, application to crystallization, and growth kinetics studies p 2224 N94-24344

M

MACH NUMBER

Calibration of HYPULSE for hypervelocity air flows corresponding to flight Mach numbers 13.5, 15, and 17 [NASA-CR-191578] p 2192 N94-23564

Evaluation of turbulence models in the PARC code for transonic diffuser flows [NASA-TM-106391] p 2168 N94-24084

Direct simulation of isothermal-wall supersonic channel flow p 2172 N94-24164

Effects of shock strength on shock turbulence interaction p 2332 N94-24165

An experimental investigation of a Mach 3.0 high-speed civil transport at supersonic speeds [NASA-TP-3365] p 2169 N94-24311

The radiated noise from isotropic turbulence revisited [NASA-CR-191547] p 2333 N94-24356

Experimental cavity pressure measurements at subsonic and transonic speeds. Static-pressure results [NASA-TP-3358] p 2169 N94-24464

Validation of the ROTAC code for the rotor noise prediction [PB93-204311] p 2529 N94-24514

Relationship between transition and modes of instability in supersonic boundary layers [NASA-CR-4562] p 2336 N94-24725

MACHINE LEARNING

Artificial neural networks: Application to the optical recognition of music partitions [ETN-94-95166] p 2470 N94-22884

Increasing levels of assistance in refinement of knowledge-based retrieval systems [NASA-CR-195144] p 2591 N94-24552

A methodology for software cost estimation using machine learning techniques [AD-A273158] p 2459 N94-24775

High-level connectionist models [AD-A273638] p 2468 N94-25030

MACHINE TOOLS

Machines for moving in soil p 2369 N94-23411

JBK-75 stainless steel machinability study [DE94-002268] p 2242 N94-23475

Composite material impregnation unit [NASA-TM-107751] p 2254 N94-23486

Tool sharing, part 3 [PB94-111697] p 2467 N94-24524

Research experience for undergraduates in robotics and materials [AD-A273659] p 2368 N94-25436

MACHINE-INDEPENDENT PROGRAMS

Dynamic data distributions in Vienna Fortran [NASA-CR-191575] p 2448 N94-23092

MACHINERY

Vibrational power transmission analysis of machinery installations in ships with the objective of noise reduction [ISVR-TR-216] p 2363 N94-24076

MACHINING

JBK-75 stainless steel machinability study [DE94-002268] p 2242 N94-23475

MACINTOSH PERSONAL COMPUTERS

Activity Catalog Tool (ACT) user manual, version 2.0 [NASA-CR-177634] p 2430 N94-23527

Performing speech recognition research with hypercard p 2306 N94-24194

MACROMOLECULES

Polymer morphologh p 2226 N94-24353

Ultrastructure processing of macromolecular materials [AD-A273413] p 2258 N94-24782

Center for advanced electrical and structural polymers [AD-A273415] p 2259 N94-24783

MACROSCOPIC EQUATIONS

Derivation of the macroscopic rate equations for the driven diffusive Ising model at pair level of approximation [DE93-616839] p 2524 N94-25208

MAGELLAN SPACECRAFT (NASA)

Magellan spacecraft and memory state tracking: Lessons learned, future thoughts p 2207 N94-23865

VMPLOT: A versatile analysis tool for mission operations p 2507 N94-23891

Using SFOC to fly the Magellan Venus mapping mission p 2516 N94-23941

MAGMA

Lunar mare volcanism: Mixing of distinct, mantle source regions with KREEP-like component p 2615 N94-24370

The transition from diapirism to dike intrusion: Implications for planetary volcanism [NASA-CR-195133] p 2403 N94-24580

MAGNESIUM

The resonance lines of MG2 as diagnostics of the upper solar chromosphere [NASA-CR-195084] p 2627 N94-24300

MAGNESIUM ALLOYS

New extensions in the development of deformation processed metal-metal matrix composites [DE94-000692] p 2227 N94-23004

Quantitative analysis in the Al-Mg-Si system with small amounts of Mg and Si [PB93-201499] p 2241 N94-23446

Segregation and oxidation studies of Al-Li and Al-Mg alloys [ISBN-0-315-83993-7] p 2244 N94-24469

MAGNESIUM FLUORIDES

SALI chemical analysis of provided samples [NASA-CR-194138] p 2232 N94-23524

MAGNET COILS

Developments in materials for high-field magnets [DE94-000761] p 2307 N94-22987

Study of a system for producing a pulsed magnetic field (B 2T) with a frequency of 50 Hz [ISL-N-601/92] p 2314 N94-25460

MAGNETIC ANOMALIES

A scalar-vector model of quark-antiquark interaction under linear confinement [DE93-616871] p 2538 N94-25317

MAGNETIC BEARINGS

The low noise momentum wheel MW-X: EM design and predicted properties p 2360 N94-24024

Superconducting energy storage [DE94-002248] p 2395 N94-24654

MAGNETIC COILS

Assessment of stellarators as reactors [DE93-017775] p 2548 N94-22916

Performance analysis of the combined EDS maglev propulsion, levitation, and guidance system [DE94-001346] p 2352 N94-22996

Proposal of Modular Heliotron: Advanced modular helical system compatible with closed helical divertor [NIFS-261] p 2552 N94-24458

The use of harmonics in 3-D magnetic fields [DE94-002274] p 2299 N94-24656

MAGNETIC CONTROL

A scalar-vector model of quark-antiquark interaction under linear confinement [DE93-616871] p 2538 N94-25317

MAGNETIC DISPERSION

Magnetic field dissipation and contraction of molecular clouds [REPT-337] p 2603 N94-24976

MAGNETIC EFFECTS

The structure and spin dynamics of lanthanide-bearing silicate glasses [DE94-001320] p 2252 N94-22992

Steady induction effects in geomagnetism. Part 1C: Geomagnetic estimation of steady surficial core motions: Application to the definitive geomagnetic reference field models [NASA-TP-3272-PT-1C] p 2403 N94-24465

MAGNETIC ENERGY STORAGE

Superconducting energy storage [DE94-002248] p 2395 N94-24654

MAGNETIC FIELD CONFIGURATIONS

Plasma initiation in a tokamak with conducting superstructure: First results from Alcator C-MOD [DE94-001565] p 2552 N94-24504

MAGNETIC FIELD RECONNECTION

Two populations and models of gamma ray bursts [NASA-CR-194762] p 2629 N94-22947

Reduction of the anode fall in a coaxial plasma thruster with an applied magnetic nozzle [DE94-000670] p 2218 N94-23283

MAGNETIC FIELDS

The de Haas-van Alphen measurements in Ba(0.6)K(0.4)BiO3 [DE93-041169] p 2556 N94-22920

Simple estimate of stored energy and conductor insulation voltage-withstand requirements for advanced solenoid magnet designs [DE93-041048] p 2307 N94-23019

Reduction of the anode fall in a coaxial plasma thruster with an applied magnetic nozzle [DE94-000670] p 2218 N94-23283

Three-dimensional solidification and melting using magnetic field control p 2325 N94-23664

Application of multigrid methods to the solution of liquid crystal equations on a SIMD computer p 2484 N94-23686

Research for electric energy systems [DE94-001839] p 2293 N94-23719

Review of a variational method applied to magnetoelastic buckling problems [PB94-111184] p 2562 N94-23769

Exact transformation of the anisotropic Ginzburg-Landau model and its consequences [DE94-002208] p 2562 N94-23795

Magnetic power piston fluid compressor [NASA-CASE-GSC-13565-1] p 2354 N94-23831

Magnetic shielding of interplanetary spacecraft against solar flare radiation [NASA-CR-195539] p 2204 N94-24334

The use of harmonics in 3-D magnetic fields [DE94-002274] p 2299 N94-24656

Compact free electron lasers for medical applications [AD-A273609] p 2350 N94-24934

The role of emitter states in magnetotunneling through double-barrier resonant-tunneling diodes at high magnetic fields [REPT-A-2658] p 2564 N94-24959

On superconductivity of alpha-(BEDT-TTF)2KHg(SCN)4 [REPT-A-2660] p 2564 N94-24978

An active antenna for ELF magnetic fields p 2303 N94-25192

The nanostructure of multilayered films: A NMR study [ETN-94-95347] p 2262 N94-25222

A relativistic theory on wave propagation in inhomogeneous magnetoplasmas [ETN-94-95322] p 2554 N94-25285

The anomalous transport caused by particles transverse drift [DE93-613685] p 2554 N94-25329

Study of a system for producing a pulsed magnetic field (B 2T) with a frequency of 50 Hz [ISL-N-601/92] p 2314 N94-25460

Magnetic field-induced saddle point in GaAs/AlGaAs short period superlattices [REPT-A-2656] p 2568 N94-25515

Diffusion in electronegative discharges with magnetic fields [AD-A273826] p 2304 N94-25521

Shielded Coil Electrodynamic Propulsion (SCEP). A feasibility study [AD-A273824] p 2314 N94-25539

MAGNETIC FLUX

Research for electric energy systems [DE94-001839] p 2293 N94-23719

Exact transformation of the anisotropic Ginzburg-Landau model and its consequences [DE94-002208] p 2562 N94-23795

Magnetic field dissipation and contraction of molecular clouds [REPT-337] p 2603 N94-24976

Mechanisms of anode power deposition in a low pressure free burning arc [NASA-CR-194442] p 2553 N94-25190

Solar magnetic cycle [NASA-CR-195202] p 2628 N94-25275

The Casimir energy of the rigid string with massive ends [DE93-616851] p 2492 N94-25338

Diffusion in electronegative discharges with magnetic fields [AD-A273826] p 2304 N94-25521

MAGNETIC INDUCTION

Projectile transverse motion and stability in electromagnetic induction launchers [DE94-001557] p 2198 N94-23210

Excitation balances and transport in an inductively coupled plasma [ETN-94-95330] p 2554 N94-25241

MAGNETIC LENSES

The use of harmonics in 3-D magnetic fields [DE94-002274] p 2299 N94-24656

A study on electrostatic quadrupole lenses and their application technologies [REPT-948] p 2546 N94-24982

MAGNETIC LEVITATION VEHICLES

Vehicle/guideway interaction and ride comfort in maglev systems [DE94-001319] p 2352 N94-22991

Performance analysis of the combined EDS maglev propulsion, levitation, and guidance system [DE94-001346] p 2352 N94-22996

MAGNETIC MATERIALS

Influences of nitrogen absorption on the magnetic properties of YFe2, YFe3 and Y6Fe23 [REPT-A-2654] p 2564 N94-24958

Metallic multilayers: Experimental investigation of magnetic anisotropy and magnetic interlayer coupling [ETN-94-95364] p 2250 N94-25242

MAGNETIC MEASUREMENT

Aeronautical satellite antenna steering using magnetic field sensors p 2289 N94-22836

Heavy ion irradiation of Bi-2223 silver-clad tapes for superconducting current density enhancement [DE93-017416] p 2556 N94-22886

Magnetic properties and transmission electron microscopy investigations of Nd-Fe-B-Co-Al melt spun ribbons [PB93-201531] p 2561 N94-23428

Research for electric energy systems [DE94-001839] p 2293 N94-23719

Some theoretical problems of magnetic diagnostics in tokamaks and stellarators [NIFS-262] p 2551 N94-24306

MAGNETIC MOMENTS

A scalar-vector model of quark-antiquark interaction under linear confinement [DE93-616871] p 2538 N94-25317

MAGNETIC PERMEABILITY

Magnetic phases in UNiGe [DE94-000793] p 2239 N94-22939

Crystal field in Nd2CuO4 [DE93-617054] p 2567 N94-25425

MAGNETIC PROPERTIES

The de Haas-van Alphen measurements in Ba(0.6)K(0.4)BiO3 [DE93-041169] p 2556 N94-22920

The structure and spin dynamics of lanthanide-bearing silicate glasses [DE94-001320] p 2252 N94-22992

Muon spin relaxation studies of the interplay between magnetism and superconductivity in heavy fermion systems [DE94-000700] p 2559 N94-23006

Magnetic properties and transmission electron microscopy investigations of Nd-Fe-B-Co-Al melt spun ribbons [PB93-201531] p 2561 N94-23428

Instrument interface description for NOAA 2000 instruments with European morning spacecraft and/or NOAA-OPQ spacecraft [NASA-TM-109406] p 2208 N94-23478

Influences of nitrogen absorption on the magnetic properties of YFe2, YFe3 and Y6Fe23 [REPT-A-2654] p 2564 N94-24958

Magnetic properties of NdCo3 and its gamma phase hydride NdCo3H(4.1) [REPT-A-2655] p 2567 N94-25412

MAGNETIC RELAXATION
Muon spin relaxation studies of the interplay between magnetism and superconductivity in heavy fermion systems
[DE94-000700] p 2559 N94-23006
Dipolar relaxation in a second-order nonlinear optical interpenetrating polymer network
[AD-A273626] p 2258 N94-24732
MAGNETIC RESONANCE
Magnetic resonance studies of 3d transition metal impurities in compound semiconductors
[PB93-232197] p 2243 N94-23714
MAGNETIC SHIELDING
Magnetic shielding of interplanetary spacecraft against solar flare radiation
[NASA-CR-195539] p 2204 N94-24334
MAGNETIC SIGNATURES
Polarization analysis of a balloon-borne solar magnetograph
[NASA-CR-193908] p 2345 N94-24852
MAGNETIC STORMS
Data analysis and theoretical studies of the upper mesosphere and lower thermosphere
[NASA-CR-195108] p 2402 N94-24089
MAGNETIC SUSPENSION
Vehicle/guideway interaction and ride comfort in maglev systems
[DE94-001319] p 2352 N94-22991
Performance analysis of the combined EDS maglev propulsion, levitation, and guidance system
[DE94-001346] p 2352 N94-22996
Preliminary eddy current modelling for the large angle magnetic suspension test fixture
[NASA-CR-194772] p 2192 N94-23539
MAGNETIC SWITCHING
Exciplex laser study: Discharge and magnetic switching systems
[PB93-199768] p 2349 N94-24629
MAGNETIC VARIATIONS
Chromospheric activity in agol binaries
[AD-A273546] p 2602 N94-24557
High latitude cusp signature observations for southward IMF B sub Z
[AD-A273801] p 2406 N94-25536
MAGNETICALLY TRAPPED PARTICLES
Ultracold atoms in traps and fountains
[ETN-94-95325] p 2537 N94-25239
MAGNETIZATION
Magnetic phases in UNiGe
[DE94-000793] p 2239 N94-22939
Spin fluctuations in an ordered Heisenberg ferromagnet with dipolar interactions
[PB93-204493] p 2524 N94-24533
Influences of nitrogen absorption on the magnetic properties of YFe2, YFe3 and Y6Fe23
[REPT-A-2654] p 2564 N94-24958
Metallic multilayers: Experimental investigation of magnetic anisotropy and magnetic interlayer coupling
[ETN-94-95364] p 2250 N94-25242
Modification in the kinetic solution for magnetized plasmas
[DE93-613687] p 2555 N94-25343
Critical currents in YBaCuO-ceramics
[DE93-617140] p 2263 N94-25404
Magnetic properties of NdCo3 and its gamma phase hydride NdCo3H(4.1)
[REPT-A-2655] p 2567 N94-25412
MAGNETOHYDRODYNAMIC FLOW
Three-dimensional solidification and melting using magnetic field control p 2325 N94-23664
Scientific study in solar and plasma physics relative to rocket and balloon projects
[NASA-CR-193885] p 2627 N94-24461
MAGNETOHYDRODYNAMIC STABILITY
Fluctuations and confinement in ATF
[DE94-000485] p 2549 N94-22998
Optimization of energy transfer in microwave electrothermal thrusters p 2216 N94-23065
Investigation of a subsonic-arc-attachment thruster using segmented anodes
[NASA-TM-106419] p 2219 N94-23531
Stabilization of the external kink and other MHD issues
[DE94-001541] p 2552 N94-24502
Plasma initiation in a tokamak with conducting superstructure: First results from Alcator C-MOD
[DE94-001565] p 2552 N94-24504
Effect of LHCD (low hybrid current drive) on tearing mode instability
[DE93-613700] p 2555 N94-25344
MAGNETOHYDRODYNAMIC TURBULENCE
On the physics of waves in the solar atmosphere: Wave heating and wind acceleration
[NASA-CR-195197] p 2628 N94-25264
MAGNETOHYDRODYNAMIC WAVES
On the physics of waves in the solar atmosphere: Wave heating and wind acceleration
[NASA-CR-195197] p 2628 N94-25264
MAGNETOHYDRODYNAMICS
Plasma research in the Madison Symmetric Torus (MST)
[DE94-002318] p 2549 N94-22976
Lectures on magnetohydrodynamical drives
[PB93-224962] p 2308 N94-23104
The internal structure and dynamics of the railgun plasma armature between infinitely wide ablating rails
[DE94-001473] p 2198 N94-23208
Evolution of large-scale plasma structures in comets: Kinematics and physics
[NASA-CR-194777] p 2601 N94-23251
Scientific study in solar and plasma physics relative to rocket and balloon projects
[NASA-CR-193885] p 2627 N94-24461
Model development for Ulysses and SOHO
[NASA-CR-193884] p 2627 N94-24484
Stabilization of the external kink and other MHD issues
[DE94-001541] p 2552 N94-24502
Modelling of thermal argon plasmas
[ETN-94-95363] p 2554 N94-25300
LHCD (low hybrid current drive) experiment on the HT-6B tokamak
[DE93-613720] p 2555 N94-25331
Effect of LHCD (low hybrid current drive) on tearing mode instability
[DE93-613700] p 2555 N94-25344
MAGNETOMETERS
Polarization analysis of a balloon-borne solar magnetograph
[NASA-CR-193908] p 2345 N94-24852
MAGNETOPLASMADYNAMICS
Reduction of the anode fall in a coaxial plasma thruster with an applied magnetic nozzle
[DE94-000670] p 2218 N94-23283
Numerical simulation of cylindrical, self-field MPD thrusters with multiple propellants
[NASA-CR-194458] p 2220 N94-24714
MAGNETORESISTIVITY
Magnetic phases in UNiGe
[DE94-000793] p 2239 N94-22939
Anomalous magnetoresistance behavior of superconducting Nd(2-x)Ce(x)CuO(4-y) single crystal
[DE94-000806] p 2558 N94-22941
MAGNETOSTATICS
Some challenging problems of the structured and dynamical solar atmosphere p 2624 N94-22838
MAGNETOSTRICTION
Review of a variational method applied to magnetoelastic buckling problems
[PB94-111184] p 2562 N94-23769
Improved magnetostrictive transducer drive elements achieved by reduction of crystalline defects and improved crystalline orientation
[AD-A273391] p 2313 N94-25276
MAGNETRONS
Novel two-stage selenization methods for fabrication of thin-film CIS cells and submodules
[DE94-000220] p 2390 N94-23296
Inverse free electron laser beat-wave accelerator research
[DE94-002597] p 2349 N94-23702
MAGNONS
Spin fluctuations in an ordered Heisenberg ferromagnet with dipolar interactions
[PB93-204493] p 2524 N94-24533
Localized excitations in competing bond-order-wave, charge-density-wave and spin-density-wave systems. 2: Competing charge-density-wave and spin-density-wave
[DE93-617131] p 2538 N94-25388
MAIN SEQUENCE STARS
ROSAT observations of the x ray binary HD 154791
[NASA-CR-195189] p 2600 N94-25198
MAINTENANCE
Constraint-based scheduling p 2510 N94-23904
Reliability analysis of a repairable dependent parallel system
[ETN-94-95312] p 2373 N94-25295
MALES
Aeromedical disposition for coronary artery disease
p 2423 N94-23316
Aeromedical implications of mitral valve prolapse
p 2424 N94-23323
Spontaneous pneumothorax, cysts and bullae
p 2425 N94-23326
MAN MACHINE SYSTEMS
Link monitor and control operator assistant: A prototype demonstrating semiautomated monitor and control
p 2292 N94-23267
Lunar exploration rover program developments
[DE93-040759] p 2613 N94-23469
Activity Catalog Tool (ACT) user manual, version 2.0
[NASA-CR-177634] p 2430 N94-23527
Intelligent tutoring and aiding in satellite ground control p 2443 N94-23929
Programmable display pushbuttons on the Space Station's telerobot control panel p 2435 N94-24198
Simulation of the human-telerobot interface on the Space Station p 2436 N94-24202
Intelligent systems and advanced user interfaces for design, operation, and maintenance of command management systems
[NASA-CR-195172] p 2459 N94-24797
Human factors of mission planning systems: Theory and concepts p 2521 N94-25010
Mission planning and mission rehearsal systems: Displays and other interactive techniques
p 2522 N94-25013
Sensor fusion display evaluation using information integration models in enhanced/synthetic vision applications p 2443 N94-25512
Quality metrics for sensor images
p 2443 N94-25513
MAN TENDED FREE FLYERS
Mission activities planning for a Hermes mission by means of AI-technology p 2502 N94-23858
MAN-COMPUTER INTERFACE
AGENDA: A task organizer and scheduler
p 2504 N94-23876
NASDA's Advanced On-Line System (ADOLIS)
p 2509 N94-23903
Customizing graphical user interface technology for spacecraft control centers p 2510 N94-23905
Operability engineering in the Deep Space Network
p 2514 N94-23930
Crew interface analysis: Selected articles on space human factors research, 1987 - 1991
[NASA-TM-104756] p 2433 N94-24185
Process and representation in graphical displays
p 2433 N94-24187
Designers' models of the human-computer interface
p 2433 N94-24188
Automated system function allocation and display format: Task information processing requirements
p 2434 N94-24189
The use of analytical models in human-computer interface design p 2434 N94-24190
Performing speech recognition research with hypercard p 2306 N94-24194
MANAGEMENT
Management. A bibliography for NASA managers
[NASA-SP-7500(27)] p 2586 N94-24708
Defense aerospace and the new world order
p 2596 N94-25086
MANAGEMENT ANALYSIS
Relevant costs or full costs? Explaining why managers use capacity cost allocations for short term decisions
[ISBN-9-06-215364-X] p 2587 N94-25279
MANAGEMENT INFORMATION SYSTEMS
A system for managing information at ATLAS
[DE94-001337] p 2590 N94-23190
Management. A bibliography for NASA managers
[NASA-SP-7500(27)] p 2586 N94-24708
Aviation system safety risk management tool analysis. Volume 2: Appendices
[AD-A273502] p 2173 N94-24864
COSMIC monthly progress report
[NASA-CR-195153] p 2460 N94-25023
MANAGEMENT METHODS
New mission requirements methodologies for services provided by the Office of Space Communications
p 2519 N94-23961
Early manufacturing considerations in design
p 2177 N94-24315
Extension of the critical path method
[PB94-118817] p 2488 N94-24527
Management. A bibliography for NASA managers
[NASA-SP-7500(27)] p 2586 N94-24708
Reuse-Driven Software Processes Guidebook, version 02.00.03
[AD-A273644] p 2461 N94-25148
Appendix B: Rapid development approaches for system engineering and design p 2272 N94-25195
Appendix C: Rapid development approaches for system engineering and design p 2272 N94-25196
Relevant costs or full costs? Explaining why managers use capacity cost allocations for short term decisions
[ISBN-9-06-215364-X] p 2587 N94-25279
Throughput time control and due date reliability in tool and die shops
[ISBN-9-03-860182-4] p 2587 N94-25283
Integrated risk management p 2588 N94-25361
Strategies for recruiting additional African Americans into the NASA JSC summer faculty fellows program
p 2585 N94-25362

MANAGEMENT PLANNING

Cost benefits of advanced software: A review of methodology used at Kennedy Space Center p 2464 N94-23240

New mission requirements methodologies for services provided by the Office of Space Communications p 2519 N94-23961

Software reuse in spacecraft planning and scheduling systems p 2520 N94-23966

Risk identification and reduction in integrated product teams p 2497 N94-24407

Management. A bibliography for NASA managers [NASA-SP-7500(27)] p 2586 N94-24708

Design and application of electromechanical actuators for deep space missions [NASA-CR-195134] p 2365 N94-24842

The future of manned spaceflight p 2195 N94-25067

Integrated risk management p 2588 N94-25361

MANAGEMENT SYSTEMS

Structure and flow of data through an environmental data management system [DE93-040487] p 2589 N94-22934

A system for managing information at ATLAS [DE94-001337] p 2590 N94-23190

KSC management training system project p 2574 N94-23246

Space Station Freedom (SSF) Data Management System (DMS) performance model data base [NASA-CR-188270] p 2590 N94-23289

GEWEX p 2385 N94-23614

An engineering code to analyze hypersonic thermal management systems p 2320 N94-23636

Columbus system support for telescience operations p 2505 N94-23877

Real-time automated failure identification in the Control Center Complex (CCC) p 2272 N94-23892

Performance of the engineering analysis and data system 2 common file system p 2576 N94-24413

Design and specification of a centralized manufacturing data management and scheduling system p 2577 N94-24416

Modular approach to project management [PB94-118833] p 2586 N94-24528

Intelligent systems and advanced user interfaces for design, operation, and maintenance of command management systems [NASA-CR-195172] p 2459 N94-24797

The use of design automation software by government-contracted architect/engineer firms: A status report [AD-A273181] p 2459 N94-24812

A comparative evaluation plan for the Maintenance, Inventory, and Logistics Planning (MILP) System Human-Computer Interface (HCI) p 2588 N94-25373

MANEUVERABILITY

Thrust vectoring theory, laboratory and flight tests p 2155 N94-24251

MANGANESE

GGA study of the magnetic and cohesive properties of bcc, fcc and hcp Mn [REPT-A-2662] p 2564 N94-24960

MANGANESE COMPOUNDS

Magnetic resonance studies of 3d transition metal impurities in compound semiconductors [PB93-232197] p 2243 N94-23714

MANGANESE IONS

Contribution of all excited states to ZFS of a (sup 6) S-state [DE93-617007] p 2568 N94-25483

MANGANIN (TRADEMARK)

Multiple shock initiation of LX-17 [DE94-001524] p 2265 N94-23807

MANIFOLDS (MATHEMATICS)

On the numerical computation of invariant manifolds [W-9306] p 2480 N94-23140

When an infinitely-renormalizable endomorphism of the interval can be smoothed [PB93-238087] p 2481 N94-23548

Non-trivial examples of real isolated singularity at the origin [PB94-110939] p 2487 N94-23787

Quasiconformal mappings, operators on Hilbert space, and local formulae for characteristic classes [PB93-238079] p 2488 N94-24536

The renormalization group for flag manifolds [DE93-616846] p 2491 N94-25213

MANIPULATORS

Normal forms of kinematic singularities of 3R robot manipulators [MEMO-1124] p 2469 N94-22712

Graphical programming: A systems approach for telerobotic servicing of space assets [DE93-019016] p 2472 N94-23201

NASA/ASEE Summer Faculty Fellowship Program [NASA-CR-194678] p 2571 N94-23230

Control of a serpentine manipulator with collision avoidance p 2368 N94-23232

Micro-gravity compatible drive (MGCD) p 2355 N94-23988

Illumination requirements for operating a space remote manipulator p 2435 N94-24195

Robust stability of second-order systems [NASA-CR-195175] p 2488 N94-24564

Genetic-based motion planning for articulated robotic manipulators [RR-476] p 2368 N94-25322

Modelling the Shuttle Remote Manipulator System: Another flexible model p 2371 N94-25350

Robotics in a controlled, ecological life support system p 2444 N94-25371

MANNED MARS MISSIONS

Manned Mars mission on-orbit operations FTS capabilities assessment [NASA-CR-189328] p 2430 N94-23080

Power generation technology options for a Mars mission [NASA-TM-106451] p 2220 N94-24681

Preliminary design of a universal Martian lander [NASA-CR-195529] p 2206 N94-25007

MANNED ORBITAL LABORATORIES

Docking mechanisms: An overview of different systems p 2357 N94-24004

MANNED REENTRY

Concepts and embodiment design of a reentry recumbent seating system for the NASA Space Shuttle [NASA-CR-195504] p 2438 N94-24667

MANNED SPACE FLIGHT

An antiproton driver for ICF propulsion p 2217 N94-23069

The birth of NASA: The diary of T. Keith Glennan [NASA-SP-4105] p 2630 N94-23333

Space tourism: A flight of fantasy or the next major space product? Paper session 3: Products [NASA-TM-109385] p 2194 N94-23710

Crew interface analysis: Selected articles on space human factors research, 1987 - 1991 [NASA-TM-104756] p 2433 N94-24185

Previous experience in manned space flight: A survey of human factors lessons learned p 2435 N94-24196

Suddenly, tomorrow came... A history of the Johnson Space Center [NASA-SP-4307] p 2631 N94-24584

The future of manned spaceflight p 2195 N94-25067

MANNED SPACECRAFT

Suddenly, tomorrow came... A history of the Johnson Space Center [NASA-SP-4307] p 2631 N94-24584

MANPOWER

Personnel shift assignment: Existence conditions and network models [MEMO-1116] p 2585 N94-22704

MANUAL CONTROL

Reducing video frame rate increases remote optimal focus time [NASA-TM-104018] p 2431 N94-23970

Speech versus manual control of camera functions during a telerobotic task p 2436 N94-24199

MANUALS

Tools reference manual for a Requirements Specification Language (RSL), version 2.0 [NASA-CR-191461] p 2445 N94-23125

Bibliographic Retrieval System (BARS), Sandia Shock Compression (SSC) database, Shock Physics Index (SPHINX) database, Volume 2: UNIX version user's guide [DE94-001704] p 2589 N94-23128

Manual on measurement of methane and nitrous oxide emissions from agriculture [DE93-616429] p 2399 N94-25167

MANUFACTURING

Progress in phases 2 and 3 of the Photovoltaic Manufacturing Technology Project (PVMaT) [DE94-000206] p 2389 N94-22888

A novel process monitoring and control system based on a neural manufacturing concept [DE94-001516] p 2471 N94-23011

Sensors for process control Focus Team report [DE93-040897] p 2560 N94-23204

Amorphous silicon PVMaT, phase 2A [DE93-018221] p 2390 N94-23295

SP-100 heat transport technology development [DE94-000769] p 2218 N94-23452

Engineering for profitability [PNR-90990] p 2595 N94-23580

The Electronics Quality/Reliability Center: Lessons learned from partnering with industry [DE94-001501] p 2309 N94-23777

Integrated Airframe Design Technology [AGARD-R-794] p 2177 N94-24313

Early manufacturing considerations in design p 2177 N94-24315

Applications of CFD codes and supercomputers to aircraft design activities p 2177 N94-24316

Frameworks for integrated airframe design p 2178 N94-24318

Design and specification of a centralized manufacturing data management and scheduling system p 2577 N94-24416

SEMATECH, a case study: Analysis of a government-industry partnership [AD-A273166] p 2586 N94-24683

The Blue Emu [NASA-CR-195535] p 2182 N94-24817

Production control and demand management in capacitated flow process industries [ISBN-9-03-860211-1] p 2586 N94-25235

MANY BODY PROBLEM

Method for simulating a vehicle shock test: Design and realization of the required implementation tools [ECL-92-14] p 2352 N94-22885

Pions and neutrinos as probes of the nucleon and nuclear few-body system [DE93-040127] p 2531 N94-22928

Calculations of Bose-Einstein correlations from Relativistic Quantum Molecular Dynamics [DE94-000794] p 2569 N94-23453

MANY ELECTRON EFFECTS

Semiempirical studies of atomic structure [DE94-001588] p 2531 N94-22937

MAPPING

Relational algebra and equational proofs [PB94-110822] p 2486 N94-23724

MAPS

Study of methods and structures for handling of digitized maps for geographical information systems [PB93-204402] p 2590 N94-23741

The Mars mapper science and mission planning tool p 2503 N94-23867

Antarctic Meteorite Location and Mapping Project (AMLAMP): Antarctic meteorite location map series explanatory text and user's guide to AMLAMP data [NASA-CR-194841] p 2603 N94-24964

MARINE BIOLOGY

Nutrients and light as factors controlling phytoplankton biomass on the Dutch continental shelf (North Sea), 1988-1990 [PB94-111143] p 2418 N94-24601

MARINE ENVIRONMENTS

Diffraction analysis of transient acoustic waves: Half-plane in a layered medium [PB94-110988] p 2526 N94-23726

Recent developments in the mathematical modelling and physical understanding of transport and dispersion in aquatic systems, with special reference to tidal waters [PB94-111135] p 2418 N94-24600

Environmentally assisted cracking of high strength beta titanium alloys [AD-A273598] p 2245 N94-24823

MARINE METEOROLOGY

A regional analysis of cloudy mean spherical albedo over the marine stratocumulus region and the tropical Atlantic Ocean [NASA-CR-194771] p 2409 N94-24049

MARINE TECHNOLOGY

Fire safety engineering research in Norway [PB93-201630] p 2268 N94-23429

MARINER SPACECRAFT

Mars Operational Environmental Satellite (MOES): A post-Mars Observer discovery mission p 2620 N94-24890

MARITIME SATELLITES

Evolution of INMARSAT systems and applications: The land mobile experience p 2280 N94-22779

INMARSAT's personal communicator system p 2282 N94-22788

Low cost coherent demodulation for mobile satellite terminals p 2284 N94-22803

Improved frame synchronization schemes for INMARSAT-B/M SCPC and TDM channels p 2285 N94-22806

MARKOV CHAINS

Resolution of Markov models on distributed memory machines [ETN-94-95182] p 2444 N94-22900

Modeling parallelism and synchronization [ETN-94-95179] p 2465 N94-23134

Control algorithms for effective operation of variable-speed wind turbines [DE94-002607] p 2394 N94-23704

General optimal stopping theorems for semi-Markov processes [PB93-214989] p 2496 N94-24744

On finding optimal policies for Markov decision chains: A unifying framework for mean-variance-tradeoffs [TW-92-13] p 2497 N94-25528

MARKOV PROCESSES
Product forms as a solution base for queueing systems [MEMO-COSOR-92-37] p 2477 N94-25526
MARS (PLANET)
An improved gravity model for Mars: Goddard Mars Model-1 (GMM-1) [NASA-TM-104584] p 2401 N94-23282
Robotic exploration of Moon and Mars p 2606 N94-23379
Science strategy for Mars exploration p 2606 N94-23380
Mars 96 small rover: Mission strategy p 2606 N94-23381
A reference Martian mission for a long range rover p 2606 N94-23382
Science objectives for short-range rovers on Mars p 2606 N94-23383
Prospects for using mobile vehicles in missions to Mars and other planets p 2607 N94-23384
The robotic Mars rover p 2608 N94-23390
Mission and system concepts for Mars robotic precursor missions p 2608 N94-23391
Mission and system design of a long range rover mission p 2608 N94-23392
Mars subsurface sounding with a ground penetrating radar p 2608 N94-23393
Balloon experiments at Mars 96 project p 2608 N94-23396
Rover: Autonomous concepts for Mars exploration p 2369 N94-23400
Mechanical design of a planetary rover p 2369 N94-23403
Dual rover concept for Mars exploration p 2370 N94-23415
Mars 96 rover: Technical vision and navigation p 2370 N94-23417
Marsohkod movement control p 2370 N94-23418
The influence of orography on the transport of atmospheric constituents p 2619 N94-24886
Retrieval of temperature profiles from Martian infrared spectra p 2620 N94-24893
Three-dimensional numerical simulation of near-surface flows over the Martian north polar cap p 2621 N94-24895
MARS ATMOSPHERE
Workshop on Atmospheric Transport on Mars [NASA-CR-194855] p 2616 N94-24871
The NASA/GISS Mars general circulation model: Preliminary experiments p 2616 N94-24872
Optimal gains for a single polar orbiting satellite p 2208 N94-24873
A diagnostic model to estimate winds and small-scale drag from Mars Observer PMIRR data p 2617 N94-24874
Eddy mixing coefficient values derived from simulations with the NASA Ames Mars GCM p 2617 N94-24875
Mars dust-driven tides and their impact on the thermosphere p 2617 N94-24876
Cloud, dust, and ozone vertical profiles from solar occultation measurements: Implications for dynamics p 2617 N94-24877
Particle sizes and composition of Mars atmospheric dust based upon Viking and Mariner 9 observations p 2618 N94-24878
Aspects of the Martian global circulation p 2618 N94-24879
Impact of the CO2 and H2O clouds of the Martian polar hood on the polar energy balance p 2618 N94-24880
Multiannual simulations with the Mars climate model p 2618 N94-24881
Regarding tracer transport in Mars' winter atmosphere in the presence of nearly stationary, forced planetary waves p 2618 N94-24882
Analyzing Martian winds and tracer concentrations using Mars Observer data p 2619 N94-24883
The annual pressure cycle on Mars: Results from the LMD Martian atmospheric general circulation model p 2619 N94-24884
Northern hemisphere dust storms on Mars p 2619 N94-24885
Dynamics of the atmosphere of Mars: Review of some outstanding problems p 2620 N94-24888
Modeling and data assimilation for Mars Observer p 2620 N94-24889
Mars Operational Environmental Satellite (MOES): A post-Mars Observer discovery mission p 2620 N94-24890
A study of cloud motions on Mars. 2: Some examples of observations and analyses since 1969 p 2620 N94-24891
Evidence for dust transport in Viking IR thermal mapper opacity data p 2620 N94-24892
Retrieval of temperature profiles from Martian infrared spectra p 2620 N94-24893
Dust transport in the Martian atmosphere p 2621 N94-24894
The role of atmospheric heat transport in the seasonal carbon dioxide cycle p 2621 N94-24896
Eddy mixing coefficient upper limit derived from the photochemical balance of O2 p 2621 N94-24897
Diagnostic calculations of the circulation in the Martian atmosphere p 2622 N94-24898
Martian mesoscale circulations induced by variations in surface optical and thermal characteristics: A numerical study p 2622 N94-24899
Two-dimensional modeling of thermal inversion layers in the middle atmosphere of Mars p 2622 N94-24900
Three-dimensional numerical simulation of thermal tides in the Martian atmosphere p 2622 N94-24901
Vertical transport of water in the Martian boundary layer p 2622 N94-24902
The Mars Aerial Platform (MAP) mission p 2622 N94-24903
Mars Observer: Applications to atmospheric transport p 2623 N94-24904
MARS ENVIRONMENT
Particle sizes and composition of Mars atmospheric dust based upon Viking and Mariner 9 observations p 2618 N94-24878
Multiannual simulations with the Mars climate model p 2618 N94-24881
Northern hemisphere dust storms on Mars p 2619 N94-24885
Mars Operational Environmental Satellite (MOES): A post-Mars Observer discovery mission p 2620 N94-24890
MARS LANDING
Descent and landing phase: Vision based robust spacecraft motion estimation and elevation modeling p 2608 N94-23394
Rover in the Mars 96 mission p 2609 N94-23397
MARS OBSERVER
Distributed science operations for JPL planetary missions p 2500 N94-23850
The Mars mapper science and mission planning tool p 2503 N94-23867
An approach to the design of operations systems p 2506 N94-23884
Mars Observer screen display design for a multimission environment p 2197 N94-23888
Mars Observer data production, transfer, and archival: The data production assembly line p 2518 N94-23953
Modeling and data assimilation for Mars Observer p 2620 N94-24889
Mars Operational Environmental Satellite (MOES): A post-Mars Observer discovery mission p 2620 N94-24890
Mars Observer: Applications to atmospheric transport p 2623 N94-24904
MARS PROBES
Mars 1994/1996: The French navigation tasks p 2195 N94-23924
MARS SAMPLE RETURN MISSIONS
Science strategy for Mars exploration p 2606 N94-23380
Operations concepts for Mars missions with multiple mobile spacecraft p 2501 N94-23852
MARS SURFACE
Missions, Technologies, and Design of Planetary Mobile Vehicles [ISBN-2-85428-331-7] p 2605 N94-23373
Rover requirements for the planet surface segment of the space exploration initiative p 2369 N94-23377
The robotic Mars rover p 2608 N94-23390
Mars subsurface sounding with a ground penetrating radar p 2608 N94-23393
Descent and landing phase: Vision based robust spacecraft motion estimation and elevation modeling p 2608 N94-23394
Mars 96 rover: Science, instrumentation, and control p 2369 N94-23395
Rover in the Mars 96 mission p 2609 N94-23397
Development/drilling test of auger boring machine on board Mars rover for Mars exploration p 2369 N94-23402
Planetary rover locomotion mechanisms p 2369 N94-23404
Machines for moving in soil p 2369 N94-23411
The Mars 96 balloon guiderope: An autonomous system in extreme environment conditions p 2369 N94-23412
Walking, jumping, and tumbling: More than one way to get around Mars p 2370 N94-23419
Perspective of creation of means for collecting information concerning transport situation p 2370 N94-23420
The Mars mapper science and mission planning tool p 2503 N94-23867
Impact of the CO2 and H2O clouds of the Martian polar hood on the polar energy balance p 2618 N94-24880
Temporal and spatial mapping of surface albedo and atmospheric dust opacity on Mars p 2619 N94-24887
Mars Operational Environmental Satellite (MOES): A post-Mars Observer discovery mission p 2620 N94-24890
Dust transport in the Martian atmosphere p 2621 N94-24894
Three-dimensional numerical simulation of near-surface flows over the Martian north polar cap p 2621 N94-24895
Martian mesoscale circulations induced by variations in surface optical and thermal characteristics: A numerical study p 2622 N94-24899
Three-dimensional numerical simulation of thermal tides in the Martian atmosphere p 2622 N94-24901
Vertical transport of water in the Martian boundary layer p 2622 N94-24902
The Mars Aerial Platform (MAP) mission p 2622 N94-24903
Tectonic Evolution of Mars [NASA-CR-194714] p 2623 N94-24996
The geophysical signal of the martian global dichotomy p 2623 N94-24997
MARTENSITE
Internal friction associated with dislocation relaxations in virgin martensite [PB93-226280] p 2240 N94-23119
MASERS
Infrared and SiO maser observations of OH/IR stars [PB94-104890] p 2599 N94-24780
MASKING
Joint Acoustic Propagation Experiment (JAPE) p 2527 N94-24208
JAPE 91: Influence of terrain masking of the acoustic propagation of helicopter noise p 2528 N94-24214
Auditory spectro-temporal pattern analysis [AD-A273554] p 2427 N94-24865
MASS
Mass properties measurement system dynamics p 2368 N94-23235
Mass properties measurement system: Dynamics and statics measurements p 2368 N94-23236
MASS DISTRIBUTION
Validation of a nonintrusive optical technique for the measurement of liquid mass distribution in a two-phase spray p 2548 N94-24420
Near surface analysis p 2407 N94-25364
MASS FLOW
A representation for the turbulent mass flux contribution to Reynolds-stress and two-equation closures for compressible turbulence [NASA-CR-191569] p 2319 N94-23302
CFD assessment of orifice aspect ratio and mass flow ratio on jet mixing in rectangular ducts [NASA-TM-106434] p 2187 N94-24082
Ethylene trace-gas techniques for high-speed flows [NASA-TM-106491] p 2169 N94-24335
MASS FLOW RATE
Two stage turbine for rockets p 2215 N94-23059
Simplified, inverse, ejector design tool [NASA-CR-194438] p 2166 N94-23511
Ethylene trace-gas techniques for high-speed flows [NASA-TM-106491] p 2169 N94-24335
Carrying the mass flux terms exactly in the first and second moment equations of compressible turbulence [NASA-CR-191568] p 2335 N94-24712
Measurement of the volume mass by spontaneous Raman scattering. Study of turbulent fluctuations of mixing in a subsonic free jet. Measurements in supersonic wind tunnels [ISL-R-102/92] p 2339 N94-25462
MASS SPECTROMETERS
Prospects for future solar-wind missions p 2624 N94-22841
Interpretation of discrepancies in mass spectroscopy data obtained from different experimental configurations p 2237 N94-23245
Multi-ion, multi-event test of ion cyclotron resonance heating [NASA-CR-194859] p 2540 N94-23495
Reactivity of ambident anions in the gas phase [PB93-232189] p 2533 N94-23713
MASS SPECTROSCOPY
Interpretation of discrepancies in mass spectroscopy data obtained from different experimental configurations p 2237 N94-23245
Condensed-phase thermal decomposition of TATB investigated by Atomic Force Microscopy (AFM) and Simultaneous Thermogravimetric Modulated Beam Mass Spectrometry (STMBMS) [DE94-000396] p 2232 N94-23298
Fifty years of continuous improvement: What has DOE done for analytical chemistry? [DE94-002539] p 2234 N94-24548

Isothiazolone volatility study of a water bottom from fuel treated with Kathon (tm) FP1.5 biocide
[AD-A273165] p 2266 N94-24728

MASS TRANSFER

A novel method for determination of transport parameters of H2 and O2 in PEMFCs
[DE94-001492] p 2389 N94-22962

MATCHED FILTERS

Choice of filters for the detection of gravitational waves from coalescing binaries. 2: Detection in coloured noise
[DE93-616844] p 2604 N94-25211

A parallel algorithm for filtering gravitational waves from coalescing binaries
[DE93-616845] p 2604 N94-25212

MATERIALS HANDLING

Robotics in a controlled, ecological life support system
p 2444 N94-25371

MATERIALS TESTS

Ceramic matrix composite parts design
p 2256 N94-24237

On the deformation kinetics constitutive law of plastic deformation: The rate equation p 2161 N94-24289

MATHEMATICAL LOGIC

Making some issues of implicit knowledge explicit
[PB93-220606] p 2478 N94-22984

Logic of capabilities
[PB94-110715] p 2473 N94-23747

Epistemic logic for defeasible reasoning using a meta-level architecture metaphor
[PB94-110723] p 2473 N94-23748

Typechecker for bijective pure type systems
[PB94-110814] p 2454 N94-23817

Real-time process logic
[PB94-101441] p 2446 N94-24540

PLANET: A hierarchical network simulator
[ISBN-9-09-005693-9] p 2313 N94-25083

MATHEMATICAL MODELS

On some approximately balanced combinatorial cooperative games
[MEMO-1113] p 2493 N94-22702

Personnel shift assignment: Existence conditions and network models
[MEMO-1116] p 2585 N94-22704

Nonlinear state space H(sub infinity) control theory
[MEMO-1119] p 2469 N94-22706

Nonlinear systems which have finite-dimensional H(sub infinity) suboptimal central controllers
[MEMO-1120] p 2469 N94-22707

Normal forms of kinematic singularities of 3R robot manipulators
[MEMO-1124] p 2469 N94-22712

Feedback linearization of parametrized nonlinear time-varying systems
[MEMO-1126] p 2470 N94-22714

Nonlocal models in continuum mechanics
[DE93-040146] p 2316 N94-22870

Identification for robust control using an H(sub infinity) norm
[EUT-92-E-261] p 2470 N94-22873

Method for simulating a vehicle shock test: Design and realization of the required implementation tools
[ECL-92-14] p 2352 N94-22885

Causal labeled transition systems: A new approach for describing the behavior of concurrent systems
[LAAS-93179] p 2447 N94-22911

Small rocket flowfield diagnostic chambers
p 2210 N94-23030

A theoretical evaluation of aluminum gel propellant two-phase flow losses on vehicle performance
p 2210 N94-23031

LOX droplet vaporization in a supercritical forced convective environment p 2211 N94-23034

Evaporation and combustion of LOX under supercritical and subcritical conditions p 2211 N94-23035

CFD modeling of microwave electrothermal thrusters
p 2216 N94-23066

Nuclear propulsion control and health monitoring
p 2217 N94-23071

Flames in dusty mixtures: Their structure and stability
[NASA-CR-191567] p 2317 N94-23089

Modelling of solid polymer and direct methanol fuel cells: Phenomenological equations and analytical solutions
[PB93-224897] p 2390 N94-23102

Atmospheric numerical modeling resource enhancement and model convective parameterization/scale interaction studies
[NASA-CR-194769] p 2400 N94-23124

Atmospheric flow in heterogeneous vegetated regions
[W-9303] p 2401 N94-23175

Mathematical modeling of MCFC cells/stacks and networks
[DE94-001914] p 2390 N94-23212

Experimental modification and identification of the DSS-13 antenna control system model
p 2291 N94-23260

Viewing hybrid systems as products of control systems and automata
[NASA-CR-194792] p 2472 N94-23300

The ignition temperature of solid explosives exposed to a fire
[DE94-001047] p 2265 N94-23436

Mathematical addenda to Hopper's model of plane stokes flow driven by capillarity on a free surface
[PB93-237691] p 2480 N94-23438

Differential algebraic equations
[PB93-237618] p 2481 N94-23455

Bayesian decision theory with imprecise prior probabilities applied to replacement problems
[PB93-237634] p 2481 N94-23456

Mechanical and thermal buckling analysis of sandwich panels under different edge conditions
[NASA-TM-4535] p 2228 N94-23514

The computation of R(sub 0) for discrete-time epidemic models with dynamic heterogeneity
[CWI-AM-R9301] p 2420 N94-23521

Preliminary eddy current modelling for the large angle magnetic suspension test fixture
[NASA-CR-194772] p 2192 N94-23539

Material data representation of hysteresis loops for Hastelloy X using artificial neural networks
[NASA-TM-105990] p 2376 N94-23551

A linear model for corrugation and its limit of validity
p 2269 N94-23584

Development of an analytical-numerical model to predict radiant emission or absorption
[NASA-CR-194860] p 2453 N94-23624

Thermal control system for SSF sensor/electronics
[SAND-92-0652C] p 2321 N94-23640

Study of transient behavior of finned coil heat exchangers p 2321 N94-23642

A direct approach to finding unknown boundary conditions in steady heat conduction
p 2322 N94-23645

Some useful innovations with TRASYS and SINDA-85
p 2322 N94-23647

Features of a SINDA/FLUINT model of a liquid oxygen supply line p 2322 N94-23649

Convection equation modeling: A non-iterative direct matrix solution algorithm for use with SINDA
p 2323 N94-23651

An analytic study of a two-phase laminar airfoil in simulated heavy rain p 2171 N94-23661

An adaptive multigrid model for hurricane track prediction p 2416 N94-23687

Similarity in wave propagation under a global relaxation law
[PB94-111028] p 2524 N94-23730

Structured constraint satisfaction
[PB94-119039] p 2497 N94-23764

Two applications of a generic task model for solving boolean constraint satisfaction problems
[PB94-119047] p 2487 N94-23765

Investigations on detonation shock dynamics and related topics
[DE94-002570] p 2326 N94-23809

Dispersion of fire suppression agents discharged from high pressure vessels: Establishing initial/boundary conditions for the flow outside the vessel
[PB94-103660] p 2172 N94-23810

Boundary layer receptivity and control
p 2327 N94-24141

The use of analytical models in human-computer interface design p 2434 N94-24190

Integrated approach in modelling, testing, and design of gradient-CVI derived CMC components
p 2256 N94-24239

New features in Computational Fluid Dynamics (CFD) technology at the TASHAN Engineering Center at IAI
p 2155 N94-24249

Development of a damage tolerance tool to analyze multiple-site damage in aircraft structure
p 2157 N94-24261

Aerodynamic models for performance calculations of modern technology propellers p 2161 N94-24285

Integrated stress and strength analysis of airplane structures using the data processing tool ISSY
p 2178 N94-24320

Trends of design methodology of airframe
p 2179 N94-24327

Numerical modeling of physical vapor transport under microgravity conditions: Effect of thermal creep and stress p 2223 N94-24340

GEWEX Cloud Systems Study (GCSS)
p 2411 N94-24377

Parameterization of sub-grid scale convection
p 2413 N94-24386

Coupled land surface/hydrologic/atmospheric models
p 2413 N94-24387

Session on validation of coupled models
p 2414 N94-24399

A study of the core module simulator floor capability
p 2380 N94-24418

A minimum cost tolerance allocation method for rocket engines and robust rocket engine design
p 2222 N94-24419

Using neural networks to assist in OPAD data analysis
p 2477 N94-24452

Evaluation of advanced materials through experimental mechanics and modelling p 2374 N94-24454

An Earth albedo model: A mathematical model for the radiant energy input to an orbiting spacecraft due to the diffuse reflectance of solar radiation from the Earth below
[NASA-TM-104596] p 2195 N94-24497

Improved gas core propulsion model
[DE94-000929] p 2220 N94-24511

Diagnosing process faults using neural network models
[DE94-002633] p 2473 N94-24518

The transition from diapirism to dike intrusion: Implications for planetary volcanism
[NASA-CR-195133] p 2403 N94-24580

Edge elements, their advantages and disadvantages
[PB94-111069] p 2298 N94-24593

Finite-element modelling of three-dimensional electromagnetic fields using edge and nodal elements
[PB94-111077] p 2298 N94-24597

Recent developments in the mathematical modelling and physical understanding of transport and dispersion in aquatic systems, with special reference to tidal waters
[PB94-111135] p 2418 N94-24600

Crashworthiness analysis using advanced material models in DYNA3D
[DE94-002988] p 2229 N94-24632

Non-brittleness of a DESIRE-model for an office assignment task
[PB94-119021] p 2489 N94-24643

A two-dimensional dispersion module for the TOUGH2 simulator
[DE94-002262] p 2335 N94-24655

An efficient data assimilation algorithm with a gaussian covariance structure
[AD-A273152] p 2418 N94-24671

Temporal model of an optically pumped co-doped solid state laser
[NASA-TM-109680] p 2350 N94-24851

Vertical transport of water in the Martian boundary layer p 2622 N94-24902

Exercise keevil: Noise levels of six military helicopters
[PB93-210722] p 2529 N94-25026

Parametric uncertainty modeling for application to robust control p 2163 N94-25103

A study of roll attractor and wing rock of delta wings at high angles of attack p 2164 N94-25111

The importance of properties in modeling
p 2246 N94-25121

Thermophysical property sensitivity effects in steel solidification p 2246 N94-25122

A thermodynamic approach to obtain materials properties for engineering applications
p 2248 N94-25131

An exploratory stochastic model for toxic effects on cells
[AD-A273438] p 2422 N94-25146

First results from the Fennoscandian GPS networks
p 2405 N94-25204

Designs with a small number of runs for factorial experiments
[ISBN-9-03-860162-X] p 2462 N94-25237

Introduction to a behavioral approach for continuous time systems
[ETN-94-95301] p 2492 N94-25277

Modelling of premixed laminar flames
[ETN-94-95317] p 2236 N94-25284

Validating identified nonlinear models with chaotic dynamics
[RR-469] p 2523 N94-25314

Ring nuclei of strain for bonded dissimilar elastic half spaces with particular application to axisymmetric crack problems
[OUEL-1966/92] p 2379 N94-25325

On a new functional integral formalism for Hubbard model
[DE93-614017] p 2492 N94-25334

The Casimir energy of the rigid string with massive ends
[DE93-616851] p 2492 N94-25338

Deviation equations of Synge and Schild in spaces with affine connection and metric, and equations for gravitational waves detectors
[DE93-616852] p 2571 N94-25339

Loading, electromyograph, and motion during exercise
p 2427 N94-25359

Influence of test configuration on the combustion characteristics of polymers as ignition sources
p 2238 N94-25365

Modelling early failures in Space Station Freedom
p 2374 N94-25372
Edge detection using a complex wavelet
[AD-A273699] p 2493 N94-25452
Fault detection in HVAC systems using fuzzy models
[OUEL-1977/93] p 2373 N94-25475
Quality metrics for sensor images
p 2443 N94-25513
Shielded Coil Electrodynamic Propulsion (SCEP). A feasibility study
[AD-A273824] p 2314 N94-25539

MATHEMATICAL PROGRAMMING
Simplicial variable dimension restart algorithm to find economic equilibria on the unit simplex using n(n+1) rays
[PB94-110541] p 2596 N94-24477
CORSS: Cylinder Optimization of Rings, Skin, and Stringers
[NASA-TP-3457] p 2490 N94-24727
Evolving recurrent perceptrons
[AD-A273241] p 2496 N94-24778
Determining neural network hidden layer size using evolutionary programming
[AD-A273242] p 2475 N94-25139
Data structures and amortized complexity in a functional setting
[ETN-94-95307] p 2476 N94-25290

MATRICES (MATHEMATICS)
Properties of the transfer matrices of deflecting magnet systems for free electron laser
[DE93-508257] p 2347 N94-22922
Implementation and parallelization of fast matrix multiplication for a fast Legendre transform
[DE94-002184] p 2478 N94-22975
On the Daubechies-based wavelet differentiation matrix
[NASA-CR-191583] p 2479 N94-23090
Characterization of measures with a convex matrix-k-range
[PB93-220655] p 2479 N94-23098
The p-ranks of Latin square graphs
[PB93-230498] p 2479 N94-23107
Implementing abstract multigrid or multilevel methods
p 2483 N94-23682
The Third Twente Workshop on Graphs and Combinatorial Optimization
[PB94-110947] p 2486 N94-23722
Coordinate-free interpretations of the optimal costs for Lq problems subject to implicit systems
[PB94-118700] p 2473 N94-23760
A matrix analysis of conjugate gradient algorithms
[DE94-002546] p 2454 N94-23796
The HDTV digital audio matrix
[BBC-RD-1993/9] p 2295 N94-24085
On the differentiation matrix for Daubechies-based wavelets on an interval
[NASA-CR-191582] p 2487 N94-24291
Stitching the Yukawa quilt
[PB93-204477] p 2569 N94-24532
Conveying digital data in noisy, unstable, multipath environments
[AD-D015980] p 2301 N94-25038
Designs with a small number of runs for factorial experiments
[ISBN-9-03-860162-X] p 2462 N94-25237
A reachability test for systems over polynomial rings using Groebner bases
[MEMO-COSOR-92-38] p 2493 N94-25527

MATRIX MATERIALS
Determination of fiber-matrix interface failure parameters from off-axis tests
[NASA-TM-109043] p 2241 N94-23274
Time dependent behavior of a graphite/thermoplastic composite and the effects of stress and physical aging
[NASA-TM-109047] p 2228 N94-23280
Test methods for composites: A status report. Volume 2: Compression test methods
[AD-A273522] p 2230 N94-24779
Test methods for composites: A status report. Volume 1: Tension test methods
[AD-A273501] p 2230 N94-24942
Test methods for composites: A status report. Volume 3: Shear test methods
[AD-A273561] p 2230 N94-25163

MATRIX METHODS
Maximum likelihood modal parameter identification and realization of stochastic systems p 2157 N94-24265

MATRIX THEORY
Modifications to 8x8 dynamical theory: Polarizations redefined according to x ray diffraction convention
[DE94-001290] p 2560 N94-23187

MATTER-ANTIMATTER PROPULSION
An antiproton driver for ICF propulsion
p 2217 N94-23069

MAXIMUM ENTROPY METHOD
Application of maximum entropy and irreducible cluster integrals to joint probability distributions for x ray structure determination
[PB93-224152] p 2559 N94-23109
Density estimation by maximum quantum entropy
[DE94-002626] p 2569 N94-24516

MAXIMUM LIKELIHOOD ESTIMATES
Nonlinear smoothing for random fields
[MEMO-1110] p 2493 N94-22728
Pseudo-coherent demodulation for mobile satellite systems p 2287 N94-22819
First order conditions for the maximum likelihood estimation of an exact ARMA model
[PB94-110533] p 2495 N94-23814
Maximum likelihood modal parameter identification and realization of stochastic systems p 2157 N94-24265
Density estimation by maximum quantum entropy
[DE94-002626] p 2569 N94-24516
Determination of the stability and control derivatives of the NASA F/A-18 HARV using flight data
[NASA-CR-194838] p 2190 N94-24804
A statistical analysis of recent Naval Experimental Diving Unit (NEDU) single-depth human exposures to 100 percent oxygen at pressure
[AD-A273488] p 2427 N94-24950
X-31 aerodynamic characteristics determined from flight data p 2164 N94-25109

MAXIMUM USABLE FREQUENCY
Northern Exposure 1992: An investigation of transauroral HF radio skywave propagation
[AD-A273363] p 2303 N94-25089

MAXWELL EQUATION
Proposed additions to the SHADOW ray-tracing code for general-asymmetric perfect-crystal optics
[DE94-001291] p 2560 N94-23188
Compatibility relations and the finite-element formulation of electromagnetic field problems
[PB94-110996] p 2294 N94-23727
Study of a local absorbing boundary condition for the modeling of an infinite external domain in the time-domain finite-element package FEMAXT
[PB94-111002] p 2294 N94-23728
Analysis for the computational modeling of finite cladding and lossy coating effects in fibers
[PB94-111085] p 2544 N94-23732
Finite-element method for computing three-dimensional electromagnetic fields in inhomogeneous media (1993)
[PB94-111101] p 2298 N94-24637

MCDONNELL AIRCRAFT
Numerical flow simulation for complete vehicle configurations
[AD-A273588] p 2170 N94-24849

MCDONNELL DOUGLAS AIRCRAFT
Aircraft accident report: Inadvertent in-flight slat deployment, China Eastern Airlines Flight 583, McDonnell Douglas MD-11, B-2171, 950 nautical miles south of Shemya, Alaska, 6 April 1993
[PB93-910408] p 2172 N94-23579

MEAN
Estimates of monthly mean soil moisture for 1979-1989
[NASA-TM-104571] p 2407 N94-23132

MEAN SQUARE VALUES
Development and validation of RNG methodology for compressible turbulence
[AD-A273469] p 2337 N94-24929

MEASURE AND INTEGRATION
The explicit computation of integration algorithms and first integrals for ordinary differential equations with polynomials coefficients using trees
[NASA-CR-194787] p 2448 N94-23074
Characterization of measures with a convex range: A generalization of Lyapounov's theorem
[PB93-220523] p 2523 N94-23094
Characterization of measures with a convex matrix-k-range
[PB93-220655] p 2479 N94-23098
Response-coefficient method for heat-conduction transients with time-dependent inputs
p 2326 N94-23671
On the continuity of limit capacity of central Cantor sets
[DE93-613022] p 2523 N94-25328

MEASUREMENT
Mass properties measurement system: Dynamics and statics measurements p 2368 N94-23236

MEASURING INSTRUMENTS
Thermoelectric cooled, purge-and-trap device for enhancing the utility of fiber optic VOC sensors
[DE94-001772] p 2541 N94-22722
Unmanned lunar rovers: Utilization for exploration
p 2607 N94-23387
Measuring electrically charged particle fluxes in space using a fiber optic loop sensor
[NASA-CR-191328] p 2544 N94-23829
New pin-on-disk equipment for vacuum tribometry
p 2360 N94-24023
An analytical ultra-high vacuum tribometer for solid lubricant studies p 2361 N94-24033
Miniature convection cooled plug-type heat flux gauges
[NASA-TM-106483] p 2344 N94-24069
The CEBAF beam loss sensors
[CEBAF-PR-93-032] p 2540 N94-24662
Chemically sensitive interfacial force microscopy: Contact potential measurements of self-assembling monolayer films
[AD-A273135] p 2234 N94-24772
Bioregenerative life support systems for microgravity
[NASA-CR-195516] p 2422 N94-24810
Measurement of interfacial tension by use of pendant drop video techniques
[DE93-000168] p 2345 N94-24831
Conceptual design of an astronaut hand anthropometry device
[NASA-CR-195490] p 2439 N94-24956
Very low frequency and low frequency transmitting antenna parameter monitoring system
[AD-D015989] p 2302 N94-25049

MECHANICAL DEVICES
Metal band drives in spacecraft mechanisms
p 2355 N94-23987
Low melting temperature alloy deployment mechanism
p 2356 N94-23997

MECHANICAL DRIVES
Lectures on magnetohydrodynamical drives
[PB93-224962] p 2308 N94-23104
The Fifth European Space Mechanisms and Tribology Symposium
[ESA-SP-334] p 2355 N94-23985
Micro-gravity compatible drive (MGCD)
p 2355 N94-23988
Development steps on the basis of test with the LOCSTAR reflector deployment mechanism
p 2356 N94-23998
Ultra-clean high-precision mechanisms for the SUMER EUV spectrometer on SOHO p 2356 N94-23999
Periscope mechanism for SWAN instrument
p 2357 N94-24000
Thermal vacuum performance of cycloid and harmonic gearboxes with solid (MoS2) and liquid (Braycote 601) lubrication p 2358 N94-24009
Reliable redundant device for mechanisms
p 2361 N94-24030
Viscous rotary damper p 2361 N94-24031
Recharge mechanism based on shape memory alloy
p 2362 N94-24039

MECHANICAL ENGINEERING
Stiffening of deployable space booms: Automated Protein Crystal Growth Facility
[NASA-CR-195547] p 2196 N94-24820
Design of gas bearing systems for precision applications
[ISBN-9-03-860112-3] p 2367 N94-25249

MECHANICAL IMPEDANCE
Low melting temperature alloy deployment mechanism
p 2356 N94-23997
Development steps on the basis of test with the LOCSTAR reflector deployment mechanism
p 2356 N94-23998

MECHANICAL PROPERTIES
The history of development of molybdenum alloys for structural applications
[DE94-000389] p 2239 N94-22958
Evaluation of A5Si3Z(x) intermetallics for use as high temperature structural materials
[DE93-041127] p 2227 N94-22977
Development of small punch testing technique and its application to evaluation of mechanical properties degradation
[DE94-001193] p 2375 N94-23184
Instrument interface description for NOAA 2000 instruments with European morning spacecraft and/or NOAA-OPQ spacecraft
[NASA-TM-109406] p 2208 N94-23478
Materials Science and Engineering
[DE94-003018] p 2228 N94-23493
The effects of texture and strain on the r-va lue of heavy gauge tantalum plate
[DE94-000690] p 2242 N94-23541
The mechanical properties of single crystal (alpha)-Si3N4
[DE94-002632] p 2563 N94-24517
A survey of metallurgical research on several actinides
[DE94-002643] p 2245 N94-24747
Environmentally assisted cracking of high strength beta titanium alloys
[AD-A273598] p 2245 N94-24823

An x ray diffraction investigation of alpha-Al2O2 addition to Yttria Stabilized Zirconia (YSZ) thermal barrier coatings subject to destabilizing vanadium pentoxide (V2O5) exposure
[AD-A273403] p 2261 N94-25072
The nanometer-scale mechanics of gold films
[AD-A273307] p 2565 N94-25086
Simulation studies for surfaces and materials strength
[NASA-CR-195185] p 2565 N94-25093
Surface compositional variations of Mo-47Re alloy as a function of temperature
[NASA-TP-3402] p 2245 N94-25117
Preparation and properties of translucent gamma-aluminium oxynitride
[ETN-94-95305] p 2263 N94-25281
Alternatives for reinforcement: Fiber composites
[VTT-TIED-1412] p 2230 N94-25386

MECHANICAL SHOCK
US tag for ISO/TC 108 mechanical vibration and shock: Minutes of the accredited Standards Committee on Mechanical Vibration and Shock, S2
[AD-A273015] p 2376 N94-23789

MEDICAL ELECTRONICS
The adaptive resonance theory network: (Clustering-) behaviour in relation with brainstem auditory evoked potential patterns
[EUT-92-E-264] p 2470 N94-22877

MEDICAL EQUIPMENT
Compact free electron lasers for medical applications
[AD-A273609] p 2350 N94-24934

MEDICAL SERVICES
Annual research progress report, fiscal year 1992. Volume 2: Department of Clinical Investigation
[AD-A273584] p 2427 N94-24945

MELT SPINNING
Ceramic silicon-boron-carbon fibers from organic silicon-boron-polymers
[NASA-CASE-ARC-11956-1-SB] p 2253 N94-23311

MELTING
Processing of YBCO superconductors for improved levitation force
[DE94-001326] p 2559 N94-22994
Generalized melting criterion for beam-induced amorphization
[DE94-001333] p 2560 N94-23189
Three-dimensional solidification and melting using magnetic field control p 2325 N94-23664
A dynamic melting model for the origin of Apollo 15 olivine-normative and quartz-normative mare basalts
p 2615 N94-24371
Detection of velocity in high temperature liquid metals
p 2247 N94-25127

MELTING POINTS
Low melting temperature alloy deployment mechanism
p 2356 N94-23997
High strain rate superplasticity in metals and composites
[DE94-001521] p 2229 N94-24547
Synthesis of soluble halogenated polyphenylenes: Mechanism for the coupling halogenated lithiobenzenes
[AD-A273547] p 2257 N94-24558
Metal-catalyzed alkynylation of brominated polyphenylenes: Thermoset precursors of high density monolithic glassy carbon
[AD-A273232] p 2259 N94-24789

MELTS (CRYSTAL GROWTH)
Theoretical considerations for Reaction-Formed Silicon Carbide (RFSC) formation by molten silicon infiltration into slurry-derived preforms
[NASA-TM-106414] p 2222 N94-23500
Three-dimensional solidification and melting using magnetic field control p 2325 N94-23664

MEMBRANE STRUCTURES
High power density proton exchange membrane fuel cells p 2393 N94-23359
Advances in direct oxidation methanol fuel cells
p 2393 N94-23361

MEMBRANES
Cellular and tissue injury during nonfreezing cold injury and frostbite
[AD-A270883] p 2423 N94-22732
A novel method for determination of transport parameters of H2 and O2 in PEMFCs
[DE94-001492] p 2389 N94-22962
Primary and secondary electrical space power based on advanced PEM systems p 2392 N94-23357
PEM regenerative fuel cells p 2392 N94-23358
A high performance H2-Cl2 fuel cell for space power applications p 2394 N94-23366
Selective hydrogen separation by palladium-based composite membranes
[PB93-201671] p 2254 N94-23431

MEMORY (COMPUTERS)
Dynamic data distributions in Vienna Fortran
[NASA-CR-191575] p 2448 N94-23092
Distributed Operating Systems and Mach. Proceedings of the Spring 1992 Graduate Seminar on Distributed Systems
[PB93-224905] p 2449 N94-23103
Fault tolerant onboard packet switch architecture for communication satellites: Shared memory per beam approach
[NASA-TM-106397] p 2201 N94-23567
Vectorization and parallelization of the finite strip method for dynamic Mindlin plate problems
p 2483 N94-23679
Design and implementation issues of end-to-end protocols in high-speed networks
[PB94-110905] p 2467 N94-23752
Algorithm on addition chains with restricted memory
[PB94-118692] p 2454 N94-23759
Non-volatile, solid state bistable electrical switch
[NASA-CASE-NPO-17621-1-CU] p 2309 N94-23820
A quick uplink, expandable executable for the NSSC-1 of the Hubble Space Telescope p 2305 N94-23859
Magellan spacecraft and memory state tracking: Lessons learned, future thoughts p 2207 N94-23865
The design of a standard message passing interface for distributed memory concurrent computers
[DE94-002536] p 2446 N94-24538
Crosstie random access memory element having associated read/write circuitry
[AD-D016027] p 2446 N94-24724
MOS analog memory with injection capacitors
[AD-D015990] p 2312 N94-25050

MENTAL PERFORMANCE
Mental images p 2429 N94-23980
Investigation of time and intensity effects in operator workload and performance
[CTN-94-60927] p 2433 N94-24171
Automated system function allocation and display format: Task information processing requirements
p 2434 N94-24189
EEG and chaos: Description of underlying dynamics and its relation to dissociative states
[NASA-CR-195171] p 2428 N94-24799
Human factors of mission planning systems: Theory and concepts p 2521 N94-25010

MERCURY (PLANET)
A mission to Mercury and a mission to the moons of Mars
[NASA-CR-195530] p 2195 N94-24619

MERCURY CADMIUM TELLURIDES
Effects of thermal-solutal convection on temperature and solutal fields under various gravitational orientations
p 2267 N94-24451

MERCURY COMPOUNDS
New concepts for HgI2 scintillator gamma ray spectroscopy
[NASA-CR-194819] p 2233 N94-24113

MERIDIONAL FLOW
Observed and Navy operational global model climatologies of synoptic disturbances over the tropical western Pacific during winter 1991-1992
[AD-A273400] p 2416 N94-25071

MEROMORPHIC FUNCTIONS
Controlled invariance of nonlinear systems: Nonexact forms speak louder than exact forms
[PB93-237790] p 2475 N94-24755

MESOMETEOROLOGY
United States Weather Research Program (USWRP)
p 2411 N94-24375
Validation of mesoscale models p 2413 N94-24391
Session on validation of coupled models
p 2414 N94-24399

MESON RESONANCE
On the hadron formation time in pion-nucleus interaction
[DE93-616879] p 2539 N94-25476

MESON-NUCLEON INTERACTIONS
Pions and neutrinos as probes of the nucleon and nuclear few-body system
[DE93-040127] p 2531 N94-22928
Momentum and coordinate space three-nucleon potentials
[DE93-040868] p 2531 N94-22951

MESONS
Low mass muon pair production in 450 GeV p-Be collisions
[PB94-110699] p 2533 N94-23746
Strong interactions studies with medium energy probes
[DE94-001446] p 2540 N94-23791
Relativistic hadrons in an external field
[ETN-94-95387] p 2538 N94-25259
A quark structure of hadrons and nuclei
[DE93-616872] p 2539 N94-25474
Weak interactions in a bilocal chiral theory
[DE93-616887] p 2539 N94-25477
On the transverse size of a fast moving nucleon
[DE93-616891] p 2539 N94-25481

MESOSCALE PHENOMENA
Scientific investigations of atmospheric processes
[NASA-CR-194805] p 2401 N94-23271
Methodology for the assessment of surface resistance and soil water storage variability at mesoscale based on remote sensing measurements. A case study with HAPEX-EFEDA data. UNESCO-International Hydrological Program 4
[PB94-111721] p 2386 N94-23734
Report of the proceedings of the Colloquium and Workshop on Multiscale Coupled Modeling
[NASA-CP-3217] p 2410 N94-24374
United States Weather Research Program (USWRP)
p 2411 N94-24375
Scientific goals of the Cooperative Multiscale Experiment (CME) p 2411 N94-24381
Grand challenge scientific questions in coupled modeling p 2412 N94-24382
Examples of data assimilation in mesoscale models
p 2412 N94-24384
Measurement and modeling of moist processes
p 2413 N94-24385
Parameterization of sub-grid scale convection
p 2413 N94-24386
Coupled land surface/hydrologic/atmospheric models
p 2413 N94-24387
Incorporation of the planetary boundary layer in atmospheric models p 2413 N94-24388
The role of radiation in mesoscale flows: Physics, parameterizations, codes p 2413 N94-24389
Chemistry on the mesoscale: Modeling and measurement issues p 2413 N94-24390
Validation of mesoscale models p 2413 N94-24391
Techniques and resources for storm-scale numerical weather prediction p 2414 N94-24392
Session on cumulus parameterization
p 2414 N94-24394
Joint sessions on modeling of boundary layer and radiative transfer processes p 2414 N94-24396
Session on modeling of radiative transfer processes
p 2414 N94-24397
Session on validation of coupled models
p 2414 N94-24399
Session on techniques and resources for storm-scale numerical weather prediction p 2415 N94-24400
Vertical motion in the SYNOP central array
[AD-A273593] p 2418 N94-24795
Three-dimensional numerical simulation of near-surface flows over the Martian north polar cap
p 2621 N94-24895
Martian mesoscale circulations induced by variations in surface optical and thermal characteristics: A numerical study p 2622 N94-24899

MESOSPHERE
An analysis of solar mesospheric temperatures for the upper stratosphere and mesosphere
[NASA-CR-194861] p 2626 N94-23626
Data analysis and theoretical studies of the upper mesosphere and lower thermosphere
[NASA-CR-195108] p 2402 N94-24089
Mesospheric and lower thermospheric winds, temperatures densities, and volume emission rates
[NASA-CR-195147] p 2403 N94-24486

MESSAGE PROCESSING
EUTELTRACS: The European experience on mobile satellite services p 2281 N94-22781
Users manual for the Chameleon parallel programming tools
[DE94-001934] p 2465 N94-22973
Arc consistency problem: An exercise in parallel programming with shared objects
[PB94-110590] p 2466 N94-23706
The design of a standard message passing interface for distributed memory concurrent computers
[DE94-002536] p 2446 N94-24538
Special signature schemes
[ETN-94-95296] p 2446 N94-25081

MESSAGES
A packet-based concept for spacecraft command planning p 2504 N94-23873
The design of a standard message passing interface for distributed memory concurrent computers
[DE94-002536] p 2446 N94-24538

METABOLISM
In vitro system for studying metabolism of environmental chemicals in human cells
[AD-A273427] p 2421 N94-24688

METAL AIR BATTERIES
High energy density aluminum-oxygen cell
p 2393 N94-23363

METAL BONDING
Gas-pressure forming of superplastic ceramic sheet
[DE94-001520] p 2252 N94-22930
Ge-Au eutectic bonding of Ge (100) single crystals
[DE94-002281] p 2564 N94-24657

METAL CLUSTERS
Simulation studies for surfaces and materials strength
[NASA-CR-195185] p 2565 N94-25093
METAL COATINGS
Structural characterization and thermal cycling behaviour of EB-PVD thermal barrier coating systems
[ISBN-0-315-83365-3] p 2257 N94-24468
Robotic weld overlay coatings for erosion control
[DE94-002665] p 2258 N94-24749
Electrochemical behavior of ion-plated TiN and Cu-Cr coatings
[AD-A273411] p 2235 N94-24784
Laser ablation and deposition of metals
[ETN-94-95311] p 2351 N94-25294
Plasma sprayed thermal barrier coatings: Production, characterization and testing
[ISBN-9-03-860082-8] p 2555 N94-25439
Proceedings of the 12th International Congress: Corrosion Control for Low-Cost Reliability. Volume 1: Coatings
[AD-A273661] p 2251 N94-25448
Proceedings of the 12th International Congress: Corrosion Control for Low-Cost Reliability. Volume 3B: Corrosion: Specific issues
[AD-A273664] p 2251 N94-25451
METAL COMBUSTION
Influence of test configuration on the combustion characteristics of polymers as ignition sources
p 2238 N94-25365
METAL CUTTING
JBK-75 stainless steel machinability study
[DE94-002268] p 2242 N94-23475
METAL FATIGUE
Fatigue life and crack growth prediction methodology
[NASA-TM-109044] p 2228 N94-23279
Mean stress models for low cycle fatigue of a nickel-base superalloy p 2159 N94-24276
Elevated temperature crack propagation
[NASA-TM-106490] p 2377 N94-24715
Variable amplitude fatigue, modelling and testing
[PB93-204469] p 2378 N94-24742
The mechanical property data base from an Air Force/Industry Cooperative Test Program on advanced aluminum alloys (7064 and CW67)
[AD-A273741] p 2251 N94-25531
METAL FIBERS
Composite fiber structures for catalysts and electrodes
p 2393 N94-23364
Surface and interfacial properties of polymer blends. A literature survey
[PB93-230191] p 2254 N94-23561
METAL FILMS
Selective hydrogen separation by palladium-based composite membranes
[PB93-201671] p 2254 N94-23431
Soft x ray optics by pulsed laser deposition
[NASA-CR-195139] p 2546 N94-24967
The nanometer-scale mechanics of gold films
[AD-A273307] p 2565 N94-25086
Laser ablation and deposition of metals
[ETN-94-95311] p 2351 N94-25294
METAL FOILS
Foil bearing research at Penn State
p 2215 N94-23058
Phase transformations in Cu-Zr multilayers
[DE94-000393] p 2241 N94-23297
METAL GRINDING
JBK-75 stainless steel machinability study
[DE94-002268] p 2242 N94-23475
METAL HYDRIDES
Ovonic nickel metal hydride batteries for space applications p 2391 N94-23352
Alloys for hydrogen storage in nickel/hydrogen and nickel/metal hydride batteries p 2391 N94-23353
Impedance measurements on a spiral-wound nickel/metal hydride cell cycled in a simulated Leo orbit
p 2392 N94-23355
Hydride thermodynamic machines
[VTT-JULK-768] p 2571 N94-25416
Metal hydride storage
[VTT-JULK-769] p 2396 N94-25417
METAL IONS
Excited state dynamics of thulium ions in yttrium aluminum garnets
[NASA-CR-195159] p 2564 N94-25024
Excitation mechanisms for XUV and x ray lasers
[DE93-617006] p 2351 N94-25482
METAL MATRIX COMPOSITES
New extensions in the development of deformation processed metal-metal matrix composites
[DE94-000692] p 2227 N94-23004
Materials Science and Engineering
[DE94-003018] p 2228 N94-23493
Engine materials characterization and damage monitoring by using x ray technologies
[NASA-TP-3328] p 2372 N94-24074
High strain rate superplasticity in metals and composites
[DE94-001521] p 2229 N94-24547
Crashworthiness analysis using advanced material models in DYNA3D
[DE94-002988] p 2229 N94-24632
Matrix fatigue cracking mechanisms of alpha(2) TMC for hypersonic applications
[NASA-TM-106506] p 2230 N94-25186
METAL OXIDE SEMICONDUCTORS
Fabrication of sub-40-nm p-n junctions for 0.18 micron MOS device applications using a cluster-tool-compatible, nanosecond thermal doping technique
[DE94-001608] p 2309 N94-23520
METAL OXIDES
Development of durable high-temperature catalysts for natural gas combustion
[PB93-226447] p 2232 N94-23477
Pulsed Ion Beam Surface Analysis (PIBSA) as a means of in-situ real-time analysis of thin films during growth
[DE94-001276] p 2562 N94-23805
Surface compositional variations of Mo-47Re alloy as a function of temperature
[NASA-TP-3402] p 2245 N94-25117
Investigation of the solid-solid surface adsorption of Eu2O3 on amorphous Al2O3
[DE93-613824] p 2566 N94-25332
METAL PLATES
Performance of the X-/Ka/KABLE-band dichroic plate in the DSS-13 beam waveguide antenna
p 2291 N94-23261
The effects of texture and strain on the r-va lue of heavy gauge tantalum plate
[DE94-000690] p 2242 N94-23541
METAL PROPELLANTS
Experimental investigation of ignition of boron/titanium composite particles p 2159 N94-24275
Ignition and combustion characteristics of metallized propellants, phase 2
[NASA-CR-195107] p 2266 N94-24700
METAL SHEETS
Weld cladding of hard surfaces
[PB93-201598] p 2353 N94-23448
METAL SHELLS
Foil bearing research at Penn State
p 2215 N94-23058
METAL SURFACES
Inelastic electron scattering from surfaces
[DE94-001368] p 2531 N94-22733
Chromate-free talc chemical conversion coatings for aluminum alloys
[DE94-001567] p 2238 N94-22932
Density functional studies: First principles and semi-emperical calculations of clusters and surfaces
[DE94-002836] p 2561 N94-23214
Thermal phase behavior of metal surfaces: X-ray scattering studies of Pt(001)
[DE94-002991] p 2245 N94-24612
Free energy profiles for Li(+) and I(-) ions approaching Pt(100) surface: A molecular dynamics study
[AD-A273455] p 2536 N94-24675
Use of scanning tunneling microscope in corrosion studies
[VTT-TIED-1416] p 2250 N94-25346
Proceedings of the 12th International Congress: Corrosion Control for Low-Cost Reliability. Volume 5A: Corrosion: General issues
[AD-A273666] p 2250 N94-25406
Proceedings of the 12th International Congress: Corrosion Control for Low-Cost Reliability. Volume 1: Coatings
[AD-A273661] p 2251 N94-25448
METAL VAPORS
Artificial plasma experiments. Chemical release observations associated with the CRRES program
[NASA-CR-194871] p 2550 N94-23565
The reaction mechanism of W-CVD in Si
[ETN-94-95329] p 2261 N94-25084
METAL-GAS SYSTEMS
Diffusion of hydrogen in iron oxides
[DE93-632430] p 2239 N94-22966
METAL-METAL BONDING
Organometallic chemistry of bimetallic compounds
[DE94-002313] p 2238 N94-22897
Strength, acoustic evaluation and metallurgy of diffusion bonds
[DE94-001804] p 2243 N94-23717
METAL-WATER REACTIONS
Proceedings of the 12th International Congress: Corrosion Control for Low-Cost Reliability. Volume 5B: Corrosion: General issues
[AD-A273667] p 2250 N94-25407
METALLIZING
Low-gravity electrodeposition and growth of polymer thin films with large third-order optical nonlinearities by electrochemical processes for devices: Thiophene-based polymers p 2225 N94-24346
Robotic weld overlay coatings for erosion control
[DE94-002665] p 2258 N94-24749
METALLOGRAPHY
Influence of sintering atmospheres on the aluminum sintering characteristics
[DE93-632412] p 2239 N94-22965
Determination of the compatibility between structural alloys and molten metals at high temperatures
[DE94-000954] p 2241 N94-23434
Large-scale production of Si(0.8)Ge(0.2) thermoelectric alloys by mechanical alloying
[DE94-000695] p 2243 N94-23753
Robotic weld overlay coatings for erosion control
[DE94-002665] p 2258 N94-24749
METALLURGY
Irradiation damage behavior of low alloy steel wrought and weld materials
[DE94-000519] p 2239 N94-22999
New extensions in the development of deformation processed metal-metal matrix composites
[DE94-000692] p 2227 N94-23004
METALS
Development of an analytical-numerical model to predict radiant emission or absorption
[NASA-CR-194860] p 2453 N94-23624
Variable amplitude fatigue, modelling and testing
[PB93-204469] p 2378 N94-24742
A thermodynamic approach to obtain materials properties for engineering applications
p 2248 N94-25131
Three-dimensional, inelastic response of single-edge notch bend specimens subjected to impact loading
[AD-A273302] p 2378 N94-25143
METAMORPHISM (GEOLOGY)
A geochemical study of acapulcoite and lodranite meteorites p 2605 N94-25358
METASTABLE STATE
Generalized melting criterion for beam-induced amorphization
[DE94-001333] p 2560 N94-23189
Electrochemical behavior of ion-plated TiN and Cu-Cr coatings
[AD-A273411] p 2235 N94-24784
Excitation mechanisms for XUV and x ray lasers
[DE93-617006] p 2351 N94-25482
METEORITES
Antarctic Meteorite Location and Mapping Project (AMLAMP): Antarctic meteorite location map series explanatory text and user's guide to AMLAMP data
[NASA-CR-194841] p 2603 N94-24964
METEORITIC COMPOSITION
Correlated petrographic, electron microprobe, and ion microprobe studies of selected primitive and processed phase assemblages in meteorites
[NASA-CR-194827] p 2601 N94-23499
A geochemical study of acapulcoite and lodranite meteorites p 2605 N94-25358
METEOROLOGICAL CHARTS
Analyzing Martian winds and tracer concentrations using Mars Observer data p 2619 N94-24883
METEOROLOGICAL PARAMETERS
Atmospheric numerical modeling resource enhancement and model convective parameterization/scale interaction studies
[NASA-CR-194769] p 2400 N94-23124
An adaptive multigrid model for hurricane track prediction p 2416 N94-23687
Joint Acoustic Propagation Experiment (JAPE)
p 2527 N94-24208
Some results gained from JAPE: An overview
p 2527 N94-24209
Intercomparison of remote and balloon-borne sensors operated at JAPE-91 p 2527 N94-24210
Comparison of measured and predicted pure tone propagation levels from JAPE-1: An evaluation of the performance of ASOPRAT p 2527 N94-24212
GEWEX Cloud Systems Study (GCSS)
p 2411 N94-24377
Grand challenge scientific questions in coupled modeling p 2412 N94-24382
Session on cumulus parameterization
p 2414 N94-24394
Modeling and data assimilation for Mars Observer
p 2620 N94-24889
The evaluation of ASOS for the Kennedy Space Center's Shuttle Landing Facility
[NASA-CR-195685] p 2416 N94-25271
METEOROLOGICAL RADAR
Urban/rural application of weather radar for flow forecasting. Proceedings of the Informal CEc -Workshop
[PB93-220135] p 2407 N94-23129

Implementation and evaluation of the new wind algorithm in NASA's 50 MHz doppler radar wind profiler
[NASA-CR-194880] p 2408 N94-23576
Estimation of the rain signal in the presence of large surface clutter
[NASA-CR-195105] p 2409 N94-24087
Further studies to extend and test the area-time-integral technique applied to satellite data
[NASA-CR-195132] p 2415 N94-24705
ASR-9 microburst detection algorithm
[AD-A273591] p 2415 N94-24850

METEOROLOGICAL SATELLITES
The AGRHYMET data communications project
p 2280 N94-22776
An AVHRR cloud classification database typed by experts
[AD-A273560] p 2416 N94-25162

METEOROLOGY
Locally modified Bott-scheme for highly convective flows
[MPIM-99] p 2400 N94-23157
Visualization of results from meteorological simulations on CRAY
[PB93-201358] p 2451 N94-23443
Atmospheric moisture fields derived by satellite observations over the tropical Pacific Ocean
[NASA-CR-194852] p 2408 N94-23542
Implementation and evaluation of the new wind algorithm in NASA's 50 MHz doppler radar wind profiler
[NASA-CR-194880] p 2408 N94-23576
Uncertainties in climate data sets
[NASA-CR-194848] p 2408 N94-23577
Convective organization in the Pacific ITCZ: Merging OLR, TOVS, and SSM/I information
[NASA-CR-194850] p 2408 N94-23619
Methodology for the assessment of surface resistance and soil water storage variability at mesoscale based on remote sensing measurements. A case study with HAPEX-EFEDA data. UNESCO-International Hydrological Program 4
[PB94-111721] p 2386 N94-23734
MAMS data for the Convection and Moisture Experiment (CAMEX)
[NASA-TM-108435] p 2409 N94-24080
Report of the proceedings of the Colloquium and Workshop on Multiscale Coupled Modeling
[NASA-CP-3217] p 2410 N94-24374
GEWEX Water Vapor Project (GVaP)
p 2411 N94-24378

METEOSAT SATELLITE
Instrument interface description for NOAA 2000 instruments with European morning spacecraft and/or NOAA-OPQ spacecraft
[NASA-TM-109406] p 2208 N94-23478
Command/telemetry bus general specification for the NOAA-OPQ polar orbiting environmental satellites and EUMETSAT polar satellite systems
[NASA-TM-109407] p 2208 N94-23479

METHANATION
New methane chemistry synthesis of materials for reversible uptake and useful functionalization of methane
[PB94-112786] p 2233 N94-23801

METHANE
Radiative forcing calculations for SF6 and CH4 using a correlated k-distribution transmission model
[DE94-001855] p 2397 N94-23700
Fundamental and experimental studies on the catalytic combustion of methane
[PB94-112661] p 2233 N94-23736
New methane chemistry synthesis of materials for reversible uptake and useful functionalization of methane
[PB94-112786] p 2233 N94-23801
Fundamental study of NO(x) control in catalytic combustion
[PB94-112323] p 2398 N94-23818
Rice cultivation and methane emission: Documentation of distributed geographic data sets
[NASA-TM-104595] p 2381 N94-24800
Design of novel catalysts for the partial oxidation of methane to methanol
[PB94-114212] p 2235 N94-24920
Carbon and hydrogen isotope composition and C-14 concentration in methane from sources and from the atmosphere: Implications for a global methane budget
[NASA-CR-195166] p 2399 N94-25092
Manual on measurement of methane and nitrous oxide emissions from agriculture
[DE93-616429] p 2399 N94-25167

METHOD OF CHARACTERISTICS
Supersonic minimum length nozzle design for dense gases p 2171 N94-23656

METHOD OF MOMENTS
Isolated and coupled superquadric loop antennas for mobile communications applications
p 2289 N94-22834
Rigorous analysis of thick microstrip antennas and wire antennas embedded in a substrate
[EUT-92-E-263] p 2290 N94-22876

METHYL ALCOHOL
Modelling of solid polymer and direct methanol fuel cells: Phenomenological equations and analytical solutions
[PB93-224897] p 2390 N94-23102
The electrolyte challenge for a direct methanol-air polymer electrolyte fuel cell operating at temperatures up to 200 C p 2393 N94-23360
Advances in direct oxidation methanol fuel cells
p 2393 N94-23361
New methane chemistry synthesis of materials for reversible uptake and useful functionalization of methane
[PB94-112786] p 2233 N94-23801
Design of novel catalysts for the partial oxidation of methane to methanol
[PB94-114212] p 2235 N94-24920

METHYL COMPOUNDS
Feasibility study: Monodisperse polymer particles containing laser-excitable dyes p 2225 N94-24350
Potent solvents for C60 and their utility for the rapid acquisition of 13CNMR data for fullerenes
[AD-A273349] p 2235 N94-24925
The electrochemistry of the solvated electron: A study of its properties and of its applications
[ETN-94-95313] p 2236 N94-25296

METRIC SPACE
Median stabilization degree of a median algebra
[PB93-220010] p 2479 N94-23093
Medians and steiner trees
[PB94-110616] p 2486 N94-23708
On the continuity of limit capacity of central Cantor sets
[DE93-613022] p 2523 N94-25328

MICHELSON INTERFEROMETERS
Fiber optic detection of laser generated ultrasound for materials characterization
[ISBN-0-315-83541-9] p 2541 N94-22891
Fiber optic detection of ultrasound and its application to cure monitoring
[ISBN-0-315-83424-2] p 2544 N94-24466

MICROBALLOONS
Properties and processing characteristics of low density carbon cloth phenolic composites p 2231 N94-24450

MICROBIOLOGY
Microbiological analysis of debris from Space Transportation System (STS)-55 Spacelab D-2
[NASA-CR-193883] p 2421 N94-24310
Microbial biofilm formation and its consequences for the CELSS program
[NASA-CR-195146] p 2438 N94-24706
Proceedings of the 12th International Congress: Corrosion Control for Low-Cost Reliability. Volume 5B: Corrosion: General issues
[AD-A273667] p 2250 N94-25407
Proceedings of the 12th International Congress: Corrosion Control for Low-Cost Reliability. Volume 6: Electric Power Industry
[AD-A273668] p 2250 N94-25408

MICROCHANNELS
Design of microchannels for cryostabilization of high temperature superconducting magnets
[DE94-001324] p 2559 N94-22993

MICROCRACKS
A numerical analysis of crack propagation in microcracking ceramic and ceramic composites
[DE94-001192] p 2253 N94-23183
Micromechanical failure modes in brittle matrix composites p 2255 N94-24232

MICROELECTRONICS
Multidisciplinary specification and design of microelectronics in products
[EUT-93-E-269] p 2308 N94-23136
Generic microelectronic smart sensor platform for detection of toxic, hazardous, and flammable gases
[DE93-017626] p 2343 N94-23200
CRRES microelectronics package flight data analysis
[NASA-TP-3423] p 2540 N94-23273

MICROFIBERS
Microinjection of the Yersinia YopE cytotoxin in mammalian cells induces actin microfilament disruption
[FOA-B-40418-4.4] p 2421 N94-24290

MICROGRAVITY
Lewis Research Center R and D Facilities
[NASA-TM-109400] p 2630 N94-23135
Microgravity sciences application visiting scientist program
[NASA-CR-194804] p 2267 N94-23287
High power density proton exchange membrane fuel cells p 2393 N94-23359
Responses to LBNP in men with varying profiles of strength and aerobic capacity: Implications for flight crews
[NASA-TP-3346] p 2426 N94-23530
The study of dopant segregation behavior during the growth of GaAs in microgravity
[NASA-CR-193905] p 2267 N94-23549
Studies of two phase flow
[NASA-CR-195099] p 2267 N94-23594
Micro-gravity compatible drive (MGCD)
p 2355 N94-23988
The development of the HERA Test Facility (HTF)
p 2197 N94-24020
Roles, uses, and benefits of general aviation aircraft in aerospace engineering education
[NASA-TM-106463] p 2153 N94-24100
Autogenic-feedback training: A potential treatment for post-flight orthostatic intolerance in aerospace crews
[NASA-TM-108785] p 2426 N94-24102
Conceptual design of a device to measure hand swelling in a micro-gravity environment
[NASA-CR-195509] p 2437 N94-24330
NASA project 1: Full-body dynamometer
[NASA-CR-195507] p 2438 N94-24331
Microgravity Studies of Organic and Polymeric Materials
[NASA-CP-3250] p 2223 N94-24338
Numerical modeling of physical vapor transport under microgravity conditions: Effect of thermal creep and stress p 2223 N94-24340
Low-gravity electrodeposition and growth of polymer thin films with large third-order optical nonlinearities by electrochemical processes for devices: Thiophene-based polymers p 2225 N94-24346
Processing of semicrystalline polymers
p 2226 N94-24351
Polymer morphologh p 2226 N94-24353
Measuring the dynamics of structural changes in biological macromolecules from light scattering data
p 2422 N94-24426
Torque equilibrium attitudes for the Space Station
p 2208 N94-24449
Effects of thermal-solutal convection on temperature and solutal fields under various gravitational orientations
p 2267 N94-24451
JOVE NASA-FIT program: Microgravity and aeronomy projects
[NASA-CR-195121] p 2631 N94-24493
Japanese aerospace science and technology 1992. A bibliography with indexes
[NASA-SP-7104] p 2631 N94-24585
Concepts and embodiment design of a reentry recumbent seating system for the NASA Space Shuttle
[NASA-CR-195504] p 2438 N94-24667
Artificial gravity in space flight
[AD-A273420] p 2427 N94-24928
The role of visual context in manual target localization
p 2429 N94-25351
Loading, electromyograph, and motion during exercise
p 2427 N94-25359
Development of a model to assess orthostatic responses p 2427 N94-25376

MICROHARDNESS
Contribution to the interface micromechanical study and to the damage fundamental phenomena in glass fiber epoxy resin model composites
[ISAL-93-0027] p 2227 N94-23133
Robotic weld overlay coatings for erosion control
[DE94-002665] p 2258 N94-24749

MICROMECHANICS
Determination of fiber-matrix interface failure parameters from off-axis tests
[NASA-TM-109043] p 2241 N94-23274
Micromechanical failure modes in brittle matrix composites p 2255 N94-24232
Micromechanical characterization of ceramic-matrix composites using the instrumented microindentation technique p 2256 N94-24233
Role of interfaces on the cyclic fatigue behaviour of ceramic matrix composites p 2256 N94-24234
Microstructure and micromechanical behaviour of CMCs p 2256 N94-24236
Micromechanical simulation of damage progression in carbon phenolic composites p 2231 N94-24446
Environmentally assisted cracking of high strength beta titanium alloys
[AD-A273598] p 2245 N94-24823

MICROORGANISMS
Microbial biofilm formation and its consequences for the CELSS program
[NASA-CR-195146] p 2438 N94-24706
Symbiosis in marine luminous bacteria
[AD-A273540] p 2422 N94-24791

MICROPHONES
Head related transfer function pseudo-stereophony
[NASA-CASE-ARC-11919-1-NP] p 2525 N94-23312

Comparison of measured and predicted pure tone propagation levels from JAPE-1: An evaluation of the performance of ASOPRAT p 2527 N94-24212

MICROPOROSITY

Template synthesis of electronically conductive polymers
[AD-A273673] p 2263 N94-25409

MICROPROCESSORS

Installation of an artificial neural network on distributed memory microprocessors
[ETN-94-95175] p 2471 N94-23152

Contribution to the evaluation of efficiency of a microprocessor functional test
[ETN-94-95176] p 2445 N94-23153

Towards the formal specification of the requirements and design of a processor interface unit: HOL listings
[NASA-CR-191465] p 2466 N94-23252

Design and implementation issues of end-to-end protocols in high-speed networks
[PB94-110905] p 2467 N94-23752

Towards the formal verification of the requirements and design of a processor interface unit
[NASA-CR-4522] p 2467 N94-24075

Towards the formal specification of the requirements and design of a processor interface unit
[NASA-CR-4521] p 2467 N94-24463

Crosstie random access memory element having associated read/write circuitry
[AD-D016027] p 2446 N94-24724

The transputer
[AD-A273688] p 2446 N94-25438

MICROSCOPY

Orientation imaging microscopy: New possibilities for microstructural investigations using automated BKD analysis
[DE94-000777] p 2557 N94-22938

Chemically sensitive interfacial force microscopy: Contact potential measurements of self-assembling monolayer films
[AD-A273135] p 2234 N94-24772

The nanometer-scale mechanics of gold films
[AD-A273307] p 2565 N94-25086

MICROSTRIP ANTENNAS

An active K/Ka-band antenna array for the NASA ACTS mobile terminal p 2289 N94-22832

Microstrip monopulse antenna for land mobile communications p 2289 N94-22833

Rigorous analysis of thick microstrip antennas and wire antennas embedded in a substrate
[EUT-92-E-263] p 2290 N94-22876

A constrained optimization technique for arbitrary antenna arrays and various performance indices
[ISBN-0-315-59455-1] p 2297 N94-24179

MICROSTRUCTURE

Relationship of microstructure and mechanical properties for V-Cr-Ti alloys
[DE94-001431] p 2238 N94-22718

Carbon aerogels: An update on structure, properties, and applications
[DE94-001528] p 2252 N94-22931

Orientation imaging microscopy: New possibilities for microstructural investigations using automated BKD analysis
[DE94-000777] p 2557 N94-22938

The history of development of molybdenum alloys for structural applications
[DE94-000389] p 2239 N94-22958

Damage under monotonic or cyclic loads of new AlSiFe alloys prepared by the Osprey (tm) process
[ISAL-93-0008] p 2239 N94-22972

Atomic-scale structure of grain boundaries: Correlations to grain boundary properties
[DE94-001289] p 2558 N94-22990

Texture gradient effects in tantalum
[DE94-000689] p 2240 N94-23021

Internal friction associated with dislocation relaxations in virgin martensite
[PB93-226280] p 2240 N94-23119

Magnetic properties and transmission electron microscopy investigations of Nd-Fe-B-Co-Al melt spun ribbons
[PB93-201531] p 2561 N94-23428

Theory of extrusion: Advances and challenges
[PB93-201572] p 2241 N94-23447

Characterization of the microstructure of Nb-1wt.%Zr-0.1wt.%C tubes as affected by thermomechanical processing
[NASA-TM-106381] p 2242 N94-23550

Strength, acoustic evaluation and metallurgy of diffusion bonds
[DE94-001804] p 2243 N94-23717

Combustion synthesis and engineering of nanoparticles for electronic, structural and superconductor applications
[DE94-001865] p 2254 N94-23720

Large-scale production of Si(0.8)Ge(0.2) thermoelectric alloys by mechanical alloying
[DE94-000695] p 2243 N94-23753

Metal-mullite reactions
[DE94-002038] p 2244 N94-23811

Catalog of Apollo 17 rocks. Volume 1: Stations 2 and 3 (South Massif)
[NASA-CR-194854] p 2613 N94-24058

Microstructure and micromechanical behaviour of CMCs p 2256 N94-24236

Ordered organic thin films self-assembled from the vapor phase p 2223 N94-24339

Defects in electro-optically active polymer solids
p 2223 N94-24342

Microstructural analysis of the 2195 aluminum-lithium alloy welds p 2251 N94-24448

Integral equations for the microstructures of supercritical fluids
[DE94-002460] p 2535 N94-24569

Ultrastructure processing of macromolecular materials
[AD-A273413] p 2258 N94-24782

Thermophysical property sensitivity effects in steel solidification p 2246 N94-25122

Microstructure of styrene methyl methacrylate copolymers grafted onto polybutadiene seeds
[ETN-94-95360] p 2262 N94-25225

Evaluation of multiaxial fracture models for technical ceramics
[ISBN-9-03-860192-1] p 2263 N94-25299

Frost effects on the microstructure of high strength concrete, and methods for their analysis
[VTT-PUBS-126] p 2379 N94-25529

MICROWAVE AMPLIFIERS

Cryogenic, low-noise high electron mobility transistor amplifiers for the Deep Space Network
p 2291 N94-23262

MICROWAVE ANTENNAS

K- and Ka-band mobile-vehicular satellite-tracking reflector antenna system for the NASA ACTS mobile terminal p 2289 N94-22831

An active K/Ka-band antenna array for the NASA ACTS mobile terminal p 2289 N94-22832

MICROWAVE CIRCUITS

Microwave analog frequency dividers: Design, modeling and realization
[LAAS-93139] p 2307 N94-22909

Spatial frequency multiplier with active linearly tapered slot antenna array
[NASA-TM-106494] p 2310 N94-24308

MICROWAVE COUPLING

Microwave excitation of pulsed high pressure gas discharge lasers
[DLR-FB-93-12] p 2351 N94-25304

MICROWAVE IMAGERY

Investigation of passive atmospheric sounding using millimeter and submillimeter wavelength channels
[NASA-CR-194858] p 2404 N94-24843

Passive millimeter-wave imaging p 2306 N94-25494

Advanced radiometric and interferometric milimeter-wave scene simulations p 2306 N94-25498

A model-based approach for detection of objects in low resolution passive-millimeter wave images
p 2442 N94-25507

MICROWAVE POWER BEAMING

WISPER: Wirless Space Power Experiment
[NASA-CR-195538] p 2396 N94-24701

MICROWAVE RADIOMETERS

A field evaluation of remote sensor measurements of wind, temperature, and moisture for ARM integrated sounding system research
[DE94-000565] p 2381 N94-23001

Application of ERS-1 active microwave instrumentation data to remote sensing of snow
[PB93-224756] p 2382 N94-23224

Feasibility of detecting aircraft wake vortices using passive microwave radiometers
[NASA-CR-191553] p 2343 N94-23498

Investigation of passive atmospheric sounding using millimeter and submillimeter wavelength channels
[NASA-CR-194858] p 2404 N94-24843

MICROWAVE RESONANCE

Investigation and application of microwave electron cyclotron resonance plasma physical vapour deposition
[DE93-613909] p 2555 N94-25333

MICROWAVE SCATTERING

Overview of the ATF stellarator program
[DE94-000371] p 2550 N94-23462

Use of microwave polarimetry to enhance SAR images of the ocean surface
[AD-A273568] p 2419 N94-24944

MICROWAVE SENSORS

Mission planning for an Earth observation low Earth orbiter: ERS-1 p 2503 N94-23868

MICROWAVE SOUNDING

Earth Observing System (EOS) Advanced Microwave Sounding Unit-A (AMSU-A) schedule plan
[NASA-CR-194856] p 2585 N94-23563

MICROWAVE SPECTRA

Laboratory detection of C5S by pulsed-discharge-nozzle Fourier-transform microwave spectroscopy
[JTN-94-80519] p 2235 N94-24984

MICROWAVES

Optimization of energy transfer in microwave electrothermal thrusters p 2216 N94-23065

CFD modeling of microwave electrothermal thrusters
p 2216 N94-23066

Proceedings of the 1993 Bi-Isotropics Workshop on Novel Microwave Materials
[PB93-224772] p 2290 N94-23225

Synthesis of passive microwave and radar altimeter data for estimating accumulation rates of polar snow
[NASA-CR-194864] p 2382 N94-23573

Multigrid and cyclic reduction applied to the Helmholtz equation p 2304 N94-23676

Microwave techniques for physical property measurements p 2238 N94-25134

Microwave excitation of pulsed high pressure gas discharge lasers
[DLR-FB-93-12] p 2351 N94-25304

MIDDLE ATMOSPHERE

Two-dimensional modeling of thermal inversion layers in the middle atmosphere of Mars p 2622 N94-24900

MIE SCATTERING

Particle sizes and composition of Mars atmospheric dust based upon Viking and Mariner 9 observations
p 2618 N94-24878

MILITARY HELICOPTERS

Night operations p 2431 N94-23977

Evaluation of the UH-1N instrument panel
[AD-A273145] p 2186 N94-24774

Exercise keevil: Noise levels of six military helicopters
[PB93-210722] p 2529 N94-25026

MILITARY OPERATIONS

Night operations p 2431 N94-23977

Safety guidelines for the operation of the DREO 10 m EMP simulator DREMPS
[DREO-TN-93-5] p 2193 N94-24117

Operation Friction: Development and introduction of personal cooling for CH124 Sea King aircrew
[DCIEM-93-06] p 2433 N94-24119

Overall system concepts in mission planning
p 2521 N94-25009

Human factors of mission planning systems: Applications and implementation p 2522 N94-25011

Ground based mission planning systems
p 2522 N94-25014

In flight mission planning in the Copilote Electronique
p 2522 N94-25015

Mission rehearsal in the SOF-ATS program
p 2522 N94-25016

MILITARY TECHNOLOGY

Operation Friction: Development and introduction of personal cooling for CH124 Sea King aircrew
[DCIEM-93-06] p 2433 N94-24119

UAV current technology and future trends
p 2154 N94-24245

Design project: LONGBOW supersonic interceptor
[NASA-CR-195510] p 2180 N94-24581

Advanced avionics architecture and technology review. Executive summary and volume 1: Avionics tech nology. Volume 2: Avionics systems engineering
[AD-A273630] p 2186 N94-24733

Information systems strategy in air transport
[AD-A273125] p 2173 N94-24781

Overall system concepts in mission planning
p 2521 N94-25009

Research interests and broad agency announcement 94-1 of the Air Force Office of Scientific Research
[AD-A273410] p 2632 N94-25075

MILLIMETER WAVES

Adaptive data rate control TDMA systems as a rain attenuation compensation technique
p 2287 N94-22821

Advanced mobile satellite communications using COMETS satellite in MM-wave and Ka-band
p 2288 N94-22829

Planar varactor frequency multiplier devices with blocking barrier
[NASA-CASE-NPO-18428-1-CU] p 2310 N94-23821

Investigation of passive atmospheric sounding using millimeter and submillimeter wavelength channels
[NASA-CR-194858] p 2404 N94-24843

Passive millimeter-wave imaging p 2306 N94-25494

Advanced radiometric and interferometric milimeter-wave scene simulations p 2306 N94-25498

Simulation of a passive millimeter wave sensor
p 2346 N94-25499

A model-based approach for detection of objects in low resolution passive-millimeter wave images p 2442 N94-25507

MIMD (COMPUTERS)

The design of a standard message passing interface for distributed memory concurrent computers [DE94-002536] p 2446 N94-24538

MIMO (CONTROL SYSTEMS)

A homotopy algorithm for digital optimal projection control GASD-HADOC [NASA-CR-193881] p 2456 N94-24470

MIMO system identification for H(infinity) robust control: A frequency domain approach with minimum error bounds [ETN-94-95354] p 2476 N94-25262

Flight controller design using mixed H2/H infinity optimization with a singular H infinity constraint [AD-A273831] p 2191 N94-25525

MINERALOGY

Highland crust at the Apollo 14 site: A review p 2614 N94-24364

Whole rock major element chemistry of KREEP basalt clasts in lunar breccia 15205: Implications for the petrogenesis of volcanic KREEP basalts p 2614 N94-24365

Lunar mare volcanism: Mixing of distinct, mantle source regions with KREEP-like component p 2615 N94-24370

A geochemical study of acapulcoite and lodranite meteorites p 2605 N94-25358

MINERALS

Integrated hydrometallurgical jarosite treatment [PB93-217990] p 2232 N94-22983

Demonstration of the feasibility of an integrated x ray laboratory for planetary exploration [NASA-CR-177631] p 2598 N94-24832

MINIATURIZATION

Laser light scattering instrument advanced technology development [NASA-CR-194803] p 2349 N94-23286

MINICOMPUTERS

Fifty years of continuous improvement: What has DOE done for analytical chemistry? [DE94-002539] p 2234 N94-24548

MINIMAX TECHNIQUE

Tool sharing: An application of max-algebra, part 2 [MEMO-1122] p 2478 N94-22710

Tool sharing: An application of max-algebra, part 1 [MEMO-1108] p 2478 N94-22726

The least energy critical set [DE93-616820] p 2493 N94-25434

MINIMUM DRAG

Identification of integrated airframe: Propulsion effects on an F-15 aircraft for application to drag minimization [NASA-TM-4532] p 2188 N94-24106

MINORITIES

Strategies for recruiting additional African Americans into the NASA JSC summer faculty fellows program p 2585 N94-25362

MINORITY CARRIERS

Polycrystalline thin film materials and devices [DE93-018213] p 2389 N94-22862

MIR SPACE STATION

Orbital docking system centerline color television camera system test [NASA-TM-104783] p 2205 N94-24625

Concepts and embodiment design of a reentry recumbent seating system for the NASA Space Shuttle [NASA-CR-195504] p 2438 N94-24667

MIRA VARIABLES

Infrared and SiO maser observations of OH/IR stars [PB94-104890] p 2599 N94-24780

MIRRORS

Theoretical investigation of variable periodicity (graded) multilayers for hard x ray applications [NASA-CR-194824] p 2543 N94-23502

SALI chemical analysis of provided samples [NASA-CR-194138] p 2232 N94-23524

Flight solar calibrations using the Mirror Attenuator Mosaic (MAM): Low scattering mirror p 2384 N94-23602

Investigate zero-stress replicated optics [NASA-CR-193889] p 2545 N94-24665

MISS DISTANCE

Comparison of c.t.s. based prediction of store trajectory with flight test data p 2158 N94-24268

MISSILE CONFIGURATIONS

Holographic testing of composite propfans for a cruise missile wind tunnel model [NASA-TM-105271] p 2187 N94-23545

State-of-the-art engineering aeroprediction methods with emphasis on new semiempirical techniques for predicting nonlinear aerodynamics on complete missile configurations [AD-A273680] p 2171 N94-25411

MISSILE CONTROL

A mixed map/variable structure observer for target tracking p 2157 N94-24263

MISSILE RANGES

Joint Acoustic Propagation Experiment (JAPE-91) Workshop [NASA-CP-3231] p 2526 N94-24207

MISSILE TESTS

Comparison of c.t.s. based prediction of store trajectory with flight test data p 2158 N94-24268

MISSILE TRAJECTORIES

Comparison of c.t.s. based prediction of store trajectory with flight test data p 2158 N94-24268

MISSILES

An overview on the main available ceramic composites and their processing routes p 2255 N94-24229

MISSION ADAPTIVE WINGS

Reduction of structural loads using maneuver load control on the Advanced Fighter Technology Integration (AFTI)/F-111 mission adaptive wing [NASA-TM-4526] p 2168 N94-24295

MISSION PLANNING

Solar physics within ESA's planning p 2624 N94-22844

Lunar science strategy: Exploring the Moon with humans and machines p 2605 N94-23376

Mars 96 small rover: Mission strategy p 2606 N94-23381

A reference Martian mission for a long range rover p 2606 N94-23382

Early lunar rover mission studies p 2607 N94-23388

The robotic Mars rover p 2608 N94-23390

Mission and system concepts for Mars robotic precursor missions p 2608 N94-23391

Mission and system design of a long range rover mission p 2608 N94-23392

Balloon experiments at Mars 96 project p 2608 N94-23396

Evolving directions in NASA's planetary rover requirements and technology p 2370 N94-23414

Walking, jumping, and tumbling: More than one way to get around Mars p 2370 N94-23419

Strategies in transition p 2498 N94-23833

Mission operations update for the restructured Earth Observing System (EOS) mission p 2499 N94-23839

Mission planning for Shuttle Imaging Radar-C (SIR-C) with a real-time interactive planning software p 2305 N94-23842

ATOS-1: Designing the infrastructure for an advanced spacecraft operations system p 2197 N94-23849

Operations concepts for Mars missions with multiple mobile spacecraft p 2501 N94-23852

NASDA satellite mission operation system and operations p 2501 N94-23854

Mission activities planning for a Hermes mission by means of AI-technology p 2502 N94-23858

A review of mission planning systems p 2503 N94-23866

The Mars mapper science and mission planning tool p 2503 N94-23867

Mission planning for an Earth observation low Earth orbiter: ERS-1 p 2503 N94-23868

Integrating payload design, planning, and control in the Dutch Utilisation Centre p 2207 N94-23869

Voyager uplink planning in the interstellar mission era p 2305 N94-23870

Science planning and sequencing for Cassini p 2504 N94-23871

Techniques and software for optimum and efficient mission science sequence development p 2504 N94-23872

A packet-based concept for spacecraft command planning p 2504 N94-23873

Connecting science and operations: The operations coordinator p 2504 N94-23874

The instant sequencing task: Toward constraint-checking a complex spacecraft command sequence interactively p 2504 N94-23875

AGENDA: A task organizer and scheduler p 2504 N94-23876

Generic mission planning concepts for space astronomy missions p 2505 N94-23878

A MOS for all seasons p 2505 N94-23879

An operations concept methodology to achieve low-cost mission operations p 2505 N94-23880

Mission engineering p 2505 N94-23881

Manned Space-laboratories Control Center (MSCC) operations concept p 2505 N94-23882

Making adaptable systems work for mission operations: A case study p 2506 N94-23883

An approach to the design of operations systems p 2506 N94-23884

Management of information for mission operations using automated keyword referencing p 2506 N94-23886

The FOT tool kit concept p 2507 N94-23889

GSMS and space views: Advanced spacecraft monitoring tools p 2507 N94-23890

Influence of a new generation of operations support systems on current spacecraft operations philosophy: The users feedback p 2507 N94-23894

The Advanced Technology Operations System: ATOS p 2508 N94-23897

Mission and science activity scheduling language p 2515 N94-23938

Toward lowering the cost of mission operations p 2519 N94-23960

New mission requirements methodologies for services provided by the Office of Space Communications p 2519 N94-23961

An intelligent planning and scheduling system for the HST servicing missions p 2520 N94-23964

Software reuse in spacecraft planning and scheduling systems p 2520 N94-23966

Planning: Management of predictability and uncertainty and keeping abreast of developments p 2520 N94-23967

Estimating the Deep Space Network modification costs to prepare for future space missions by using major cost drivers p 2520 N94-23968

The Far Ultraviolet (FUV) auroral imager for the Inner Magnetospheric Imager (IMI) mission: Options p 2209 N94-24453

A mission to Mercury and a mission to the moons of Mars [NASA-CR-195530] p 2195 N94-24619

Power generation technology options for a Mars mission [NASA-TM-106451] p 2220 N94-24681

WISPER: Wirless Space Power Experiment [NASA-CR-195538] p 2396 N94-24701

Near Earth asteroid rendezvous [NASA-CR-195518] p 2195 N94-24808

Ultraviolet, visible, and gravity astrophysics: A plan for the 1990's [NASA-NP-152] p 2603 N94-24973

PERCIVAL mission to Mars [NASA-CR-195541] p 2195 N94-24995

New Advances in Mission Planning and Rehearsal Systems [AGARD-LS-192] p 2521 N94-25008

Overall system concepts in mission planning p 2521 N94-25009

Human factors of mission planning systems: Theory and concepts p 2521 N94-25010

Human factors of mission planning systems: Applications and implementation p 2522 N94-25011

Computing techniques in mission planning p 2522 N94-25012

Mission planning and mission rehearsal systems: Displays and other interactive techniques p 2522 N94-25013

Ground based mission planning systems p 2522 N94-25014

In flight mission planning in the Copilote Electronique p 2522 N94-25015

Effect of power system technology and mission requirements on high altitude long endurance aircraft [NASA-CR-194455] p 2189 N94-25200

ROSAT mission planning using artificial intelligence methods [DLR-FB-93-14] p 2476 N94-25345

A comparative evaluation plan for the Maintenance, Inventory, and Logistics Planning (MILP) System Human-Computer Interface (HCI) p 2588 N94-25373

MIXERS

A comparison of free-space and fiber mixer performances [AD-A273558] p 2547 N94-25161

MIXING

Ethylene trace-gas techniques for high-speed flows [NASA-TM-106491] p 2169 N94-24335

MIXING LAYERS (FLUIDS)

Image analysis applications to mixing phenomena and turbulent dispersions [ECL-92-29] p 2317 N94-22971

Small rocket flowfield diagnostic chambers p 2210 N94-23030

A random distribution reacting mixing layer model [NASA-CR-194445] p 2187 N94-23552

Numerical simulation of non-Newtonian free shear flows p 2331 N94-24160

Vortical structure in a forced plane mixing layer p 2331 N94-24162

Measurement of the volume mass by spontaneous Raman scattering. Study of turbulent fluctuations of mixing in a subsonic free jet. Measurements in supersonic wind tunnels [ISL-R-102/92] p 2339 N94-25462

MIXING LENGTH FLOW THEORY

Turbulence modeling for non-equilibrium flows p 2328 N94-24144

MIXING RATIOS
Eddy mixing coefficient upper limit derived from the photochemical balance of O2 p 2621 N94-24897
MIXTURES
Ultrastructure processing of macromolecular materials [AD-A273413] p 2258 N94-24782
MOBILE COMMUNICATION SYSTEMS
Proceedings of the Third International Mobile Satellite Conference (IMSC 1993) [NASA-CR-194516] p 2273 N94-22735
Worldwide survey of direct-to-listener digital audio delivery systems development since WARC-1992 p 2273 N94-22736
ESA personal communications and digital audio broadcasting systems based on non-geostationary satellites p 2273 N94-22737
Utilizing a TDRS satellite for direct broadcast satellite-radio propagation experiments and demonstrations p 2274 N94-22740
Aeronautical audio broadcasting via satellite p 2274 N94-22741
The MSAT spacecraft of Telesat Mobile Inc. p 2207 N94-22742
Adaptive digital beamforming for a CDMA mobile communications payload p 2274 N94-22743
Electrical performance of wire mesh for spacecraft deployable reflector antennas p 2275 N94-22744
Adaptive array antenna for satellite cellular and direct broadcast communications p 2275 N94-22745
SAW based systems for mobile communications satellites p 2275 N94-22746
US domestic and international regulatory issues p 2275 N94-22748
International organizations to enable world-wide mobile satellite services p 2275 N94-22749
Use of negotiated rulemaking in developing technical rules for low-Earth orbit mobile satellite systems p 2276 N94-22750
The provision of spectrum for feeder links of non-geostationary mobile satellites p 2276 N94-22751
The possibilities for mobile and fixed services in the 20/30 GHz frequency bands p 2276 N94-22752
Use of the 30/20 GHz band by multipurpose satellite systems p 2276 N94-22753
Power attenuation characteristics as switch-over criterion in personal satellite mobile communications p 2277 N94-22756
Integration of mobile satellite and cellular systems p 2277 N94-22757
Interworking evolution of mobile satellite and terrestrial networks p 2277 N94-22758
Interworking and integration of the Inmarsat Standard-M with Pan-European GSM system p 2277 N94-22759
Architectures and protocols for an integrated satellite-terrestrial mobile system p 2277 N94-22760
Handover procedures in integrated satellite and terrestrial mobile systems p 2277 N94-22761
MSAT and cellular hybrid networking p 2278 N94-22762
Trends in mobile satellite communication p 2278 N94-22763
Optimizing space constellations for mobile satellite systems p 2278 N94-22764
A system architecture for an advanced Canadian wideband mobile satellite system p 2278 N94-22766
Applicability of different onboard routing and processing techniques to mobile satellite systems p 2278 N94-22767
A European mobile satellite system concept exploiting CDMA and OBP p 2279 N94-22768
Study of LEO-SAT microwave link for broad-band mobile satellite communication system p 2279 N94-22769
The FAA satellite communications program p 2279 N94-22772
Canadian aeronautical mobile data trials p 2279 N94-22773
ACTS mobile SATCOM experiments p 2280 N94-22774
Cockpit weather graphics using mobile satellite communications p 2280 N94-22775
Using satellite communications for a mobile computer network p 2280 N94-22777
Design and implementation considerations of a MSAT packet data network p 2280 N94-22778
ACTS advanced system concepts and experimentation p 2280 N94-22780
The Iridium (tm) system: Personal communications anytime, anyplace p 2281 N94-22785
The Globalstar mobile satellite system for worldwide personal communications p 2282 N94-22786
Odyssey personal communications satellite system p 2282 N94-22787
INMARSAT's personal communicator system p 2282 N94-22788
The European Mobile System (EMS) p 2282 N94-22789
Electromagnetic field strength prediction in an urban environment: A useful tool for the planning of LMSS p 2283 N94-22795
Systems implications of L-band fade data statistics for LEO mobile systems p 2284 N94-22799
The Westinghouse Series 1000 Mobile Phone: Technology and applications p 2284 N94-22800
First satellite mobile communication trials using BLQS-CDMA p 2284 N94-22801
Channel and terminal description of the ACTS mobile terminal p 2284 N94-22802
Low cost coherent demodulation for mobile satellite terminals p 2284 N94-22803
Asynchronous timing and Doppler recovery in DSP based DPSK modems for fixed and mobile satellite applications p 2285 N94-22805
Estimation of frequency offset in mobile satellite modems p 2285 N94-22807
A pattern jitter free AFC scheme for mobile satellite systems p 2285 N94-22809
A CDMA synchronisation scheme p 2285 N94-22810
A high quality voice coder with integrated echo canceller and voice activity detector for mobile satellite applications p 2286 N94-22812
Performance of the unique-word-reverse-modulation type demodulator for mobile satellite communications p 2286 N94-22813
Diversity reception for advanced multi-satellite networks: A CDMA approach p 2286 N94-22816
System services and architecture of the TMI satellite mobile data system p 2286 N94-22817
A comparison between coherent and noncoherent mobile systems in large Doppler shift, delay spread, and C/I environment p 2287 N94-22818
Pseudo-coherent demodulation for mobile satellite systems p 2287 N94-22819
Transmission over EHF mobile satellite channels p 2287 N94-22820
Adaptive data rate control TDMA systems as a rain attenuation compensation technique p 2287 N94-22821
SATCOM simulator speeds MSS deployment and lowers costs p 2287 N94-22822
Development of a multilayer interference simulation program for MSS systems p 2287 N94-22823
Handover aspects for a Low Earth Orbit (LEO) CDMA Land Mobile Satellite (LMS) system p 2288 N94-22824
Study on networking issues of medium earth orbit satellite communications systems p 2288 N94-22825
The design and networking of dynamic satellite constellations for global mobile communication systems p 2288 N94-22826
Low earth orbit satellite/terrestrial mobile service compatibility p 2288 N94-22827
A practical system for regional mobile satellite services p 2288 N94-22828
Advanced mobile satellite communications using COMETS satellite in MM-wave and Ka-band p 2288 N94-22829
Low cost antennas for MSAT vehicular applications p 2289 N94-22830
K- and Ka-band mobile-vehicular satellite-tracking reflector antenna system for the NASA ACTS mobile terminal p 2289 N94-22831
An active K/Ka-band antenna array for the NASA ACTS mobile terminal p 2289 N94-22832
Microstrip monopulse antenna for land mobile communications p 2289 N94-22833
Isolated and coupled superquadric loop antennas for mobile communications applications p 2289 N94-22834
L-band mobile terminal antennas for helicopters p 2289 N94-22835
Satellite communications systems and technology. Volume 1: Analytical chapters [NASA-TM-109398] p 2293 N94-23627
MOBILITY
Conceptual design and architecture of hexapod robotic vehicles for the (L)OVLA project p 2369 N94-23405
Mobility analysis, simulation, and scale model testing for the design of wheeled planetary rovers p 2370 N94-23425
Preliminary results on time-varying feedback stabilization of a nonholonomic car-like mobile robot [INRIA-RR-1512] p 2475 N94-24963
MODAL RESPONSE
Modal test of the Brazilian satellite launcher (VLS) configuration burn-out of the first stage p 2156 N94-24257
Maximum likelihood modal parameter identification and realization of stochastic systems p 2157 N94-24265
MODELS
An experimental investigation of the effect of upper surface blowing on dynamic stall [NASA-CR-194863] p 2165 N94-22894
Flexible framework for contingent information systems modelling [PB93-220549] p 2589 N94-23095
Designers' models of the human-computer interface p 2433 N94-24188
Systems engineering: A formal approach. Part 3: Modeling methods [PB94-101409] p 2456 N94-24513
MODEMS
Asynchronous timing and Doppler recovery in DSP based DPSK modems for fixed and mobile satellite applications p 2285 N94-22805
Estimation of frequency offset in mobile satellite modems p 2285 N94-22807
A comparison between coherent and noncoherent mobile systems in large Doppler shift, delay spread, and C/I environment p 2287 N94-22818
MODULARITY
Laser light scattering instrument advanced technology development [NASA-CR-194803] p 2349 N94-23286
Modular approach to project management [PB94-118833] p 2586 N94-24528
A type-theoretic approach to higher-order modules with sharing [AD-A273566] p 2458 N94-24693
MODULATION
Direct digital RF synthesis and modulation for MSAT mobile applications p 2285 N94-22804
An introduction to digital modulation and OFDM techniques [BBC-RD-1993/10] p 2295 N94-24086
Automatic modulation recognition based on spatial pattern classification using artificial neural networks [CTN-94-60897] p 2296 N94-24115
Modulation and synchronization technique for MF-TDMA system [NASA-CR-194448] p 2304 N94-25266
MOISTURE
Humidity effects on soluble core mechanical and thermal properties (polyvinyl alcohol/microballoon composite) type CG extendospheres, volume 2 [NASA-CR-193893] p 2229 N94-24224
MOISTURE CONTENT
An overview of a model rotor icing test in the NASA Lewis Icing Research Tunnel [NASA-TM-106471] p 2166 N94-23299
Spatial and temporal variability of soil temperature, moisture and surface soil properties [NASA-CR-194109] p 2401 N94-23337
Methodology for the assessment of surface resistance and soil water storage variability at mesoscale based on remote sensing measurements. A case study with HAPEX-EFEDA data. UNESCO-International Hydrological Program 4 [PB94-111721] p 2386 N94-23734
Groundtruth collection for the JPL-SAR and ERS-1 campaign in Flevoland and Veluwe, Netherlands, 1991 [PB93-230654] p 2386 N94-23755
Water cycle research associated with the CaPE hydrometeorology project (CHymP p 2416 N94-24414
Drying deformable media: Kinetics, shrinkage and stresses [ETN-94-95314] p 2236 N94-25302
MOLECULAR BEAM EPITAXY
Ga delta-doping layers in silicon [PB93-224632] p 2561 N94-23222
Method of forming silicon structures with selectable optical characteristics [NASA-CASE-NPO-18625-1-CU] p 2563 N94-23972
On the origin of 1/f noise in epitaxial GaAs [ISBN-9-09-006067-7] p 2566 N94-25297
MOLECULAR BEAMS
Theoretical studies of a molecular beam generator [NASA-CR-194779] p 2540 N94-23485
MOLECULAR BIOLOGY
Applications of the Aurora parallel PROLOG system to computational molecular biology [DE93-041166] p 2420 N94-23468
MOLECULAR CLOUDS
Magnetic field dissipation and contraction of molecular clouds [REPT-337] p 2603 N94-24976
CO-to-H2 conversion factor in dwarf irregular galaxies [REPT-333] p 2603 N94-24985
High spatial resolution observations of CO in CRL 618 [REPT-334] p 2604 N94-24986
The Nobeyama millimeter array survey for protoplanetary disks around protostar candidates and T Tauri stars in Taurus [REPT-336] p 2604 N94-24987

MOLECULAR DIFFUSION
A two-dimensional dispersion module for the TOUGH2 simulator
[DE94-002262] p 2335 N94-24655
MOLECULAR DYNAMICS
Fracture simulations via massively parallel molecular dynamics
[DE93-040159] p 2374 N94-22871
Calculations of Bose-Einstein correlations from Relativistic Quantum Molecular Dynamics
[DE94-000794] p 2569 N94-23453
Momentum loss in proton-nucleus and nucleus-nucleus collisions
[NASA-TP-3405] p 2540 N94-24305
The torsion space nucleic acids molecular mechanics program DUPLEX: Surveying conformation space by potential energy minimization
[DE94-002441] p 2563 N94-24567
Integral equations for the microstructures of supercritical fluids
[DE94-002460] p 2535 N94-24569
Free energy profiles for Li(+) and I(-) ions approaching Pt(100) surface: A molecular dynamics study
[AD-A273455] p 2536 N94-24675
Structures of Cl(-)(H2O)(n) and F(-)(H2O)(n) (n equal to 2,3...15) clusters: Molecular dynamics computer simulations
[AD-A273474] p 2537 N94-24940
MOLECULAR EXCITATION
Contribution of all excited states to ZFS of a (sup 6) S-state
[DE93-617007] p 2568 N94-25483
MOLECULAR FLOW
Molecular gas dynamics applied to low-thrust propulsion p 2214 N94-23053
MOLECULAR GASES
Molecular abundances in the envelopes around evolved stars
[PB94-104916] p 2602 N94-23812
MOLECULAR INTERACTIONS
Integral equations for the microstructures of supercritical fluids
[DE94-002460] p 2535 N94-24569
MOLECULAR IONS
Examination of the response capacity of a silicon pixel detector for ions and molecules in the energy area 100 to 300 keV
[MPE-241] p 2346 N94-25415
MOLECULAR SPECTROSCOPY
Laboratory detection of C5S by pulsed-discharge-nozzle Fourier-transform microwave spectroscopy
[JTN-94-80519] p 2235 N94-24984
CO-to-H2 conversion factor in dwarf irregular galaxies
[REPT-333] p 2603 N94-24985
High spatial resolution observations of CO in CRL 618
[REPT-334] p 2604 N94-24986
The Nobeyama millimeter array survey for protoplanetary disks around protostar candidates and T Tauri stars in Taurus
[REPT-336] p 2604 N94-24987
MOLECULAR STRUCTURE
Measuring the dynamics of structural changes in biological macromolecules from light scattering data
p 2422 N94-24426
Interactions between organized, surface-confined monolayers and vapor-phase probe molecules. 7: Comparison of self-assemblying organomercaptan monolayers deposited on gold from liquid and vapor phases
[AD-A273196] p 2535 N94-24555
Center for advanced electrical and structural polymers
[AD-A273415] p 2259 N94-24783
Synthesis of molecular wires by a novel divergent/convergent approach
[AD-A273332] p 2537 N94-25087
On the mechanism of action of 3',5'-cyclic adenosine monophosphate: A study of four- and five-coordinated phosphorus compounds, modelling the activated state of cAMP
[ISBN-9-03-860222-7] p 2226 N94-25238
Contribution of all excited states to ZFS of a (sup 6) S-state
[DE93-617007] p 2568 N94-25483
MOLECULAR WEIGHT
Phenylethynl-terminated poly(arylene ethers)
[NASA-CASE-LAR-14797-1] p 2253 N94-23307
Measuring the dynamics of structural changes in biological macromolecules from light scattering data
p 2422 N94-24426
MOLECULES
Measuring the dynamics of structural changes in biological macromolecules from light scattering data
p 2422 N94-24426
Interactions between organized, surface-confined monolayers and vapor-phase probe molecules. 7: Comparison of self-assemblying organomercaptan monolayers deposited on gold from liquid and vapor phases
[AD-A273196] p 2535 N94-24555
Synthesis and characterization of two-dimensional molecular recognition interfaces
[AD-A273177] p 2536 N94-24729
MOLTEN SALTS
Molten salt reactor for potentiostatic electroplating
[AD-D016020] p 2258 N94-24720
X ray diffraction analysis of electrodeposited beta-tantalum
[AD-A273254] p 2249 N94-25142
MOLYBDENUM
Soft x ray optics by pulsed laser deposition
[NASA-CR-195139] p 2546 N94-24967
Surface compositional variations of Mo-47Re alloy as a function of temperature
[NASA-TP-3402] p 2245 N94-25117
MOLYBDENUM ALLOYS
The history of development of molybdenum alloys for structural applications
[DE94-000389] p 2239 N94-22958
Evaluation of A5Si3Z(x) intermetallics for use as high temperature structural materials
[DE93-041127] p 2227 N94-22977
MOLYBDENUM COMPOUNDS
Design of a resistojet for Space Station Freedom
[NASA-CR-195506] p 2221 N94-24979
MOLYBDENUM SULFIDES
Tribological characteristics of ball bearings lubricated with a sputtered molybdenum disulphide film in a vacuum under a high thrust load p 2355 N94-23992
The tribology of some MoS2-lubricated engineering ceramics p 2356 N94-23993
MOMENTS OF INERTIA
Torque equilibrium attitudes for the Space Station
p 2208 N94-24449
Numerical analysis of the motion of a rigid body with an attached spring-mass-damper
[AD-A273825] p 2379 N94-25520
MOMENTUM
Momentum and coordinate space three-nucleon potentials
[DE93-040868] p 2531 N94-22951
Momentum loss in proton-nucleus and nucleus-nucleus collisions
[NASA-TP-3405] p 2540 N94-24305
On the hadron formation time in pion-nucleus interaction
[DE93-616879] p 2539 N94-25476
MOMENTUM THEORY
Momentum loss in proton-nucleus and nucleus-nucleus collisions
[NASA-TP-3405] p 2540 N94-24305
Unified approach for incompressible flows
p 2342 N94-25356
MOMENTUM TRANSFER
Momentum loss in proton-nucleus and nucleus-nucleus collisions
[NASA-TP-3405] p 2540 N94-24305
Proton spin: The role of quark-gluon and hadron degrees of freedom
[DE93-616867] p 2538 N94-25341
MONAURAL SIGNALS
Head related transfer function pseudo-stereophony
[NASA-CASE-ARC-11919-1-NP] p 2525 N94-23312
MONITORS
Generic microelectronic smart sensor platform for detection of toxic, hazardous, and flammable gases
[DE93-017626] p 2343 N94-23200
Particle size measurement for the control of industrial crystallizers
[PB94-119104] p 2562 N94-23766
Mars Observer screen display design for a multimission environment p 2197 N94-23888
MONOCHROMATORS
Modifications to 8x8 dynamical theory: Polarizations redefined according to x ray diffraction convention
[DE94-001290] p 2560 N94-23187
Proposed additions to the SHADOW ray-tracing code for general-asymmetric perfect-crystal optics
[DE94-001291] p 2560 N94-23188
MONOMERS
The use of expanding monomers in carbon fibre composites
[ISBN-0-315-83550-8] p 2226 N94-22890
Di(hydroxyphenyl)- 1,2,4-triazole monomers
[NASA-CASE-LAR-14440-2] p 2252 N94-23075
Di(hydroxyphenyl)- benzimidazole monomers
[NASA-CASE-LAR-14643-2] p 2253 N94-23305
Phenylethynl-terminated poly(arylene ethers)
[NASA-CASE-LAR-14797-1] p 2253 N94-23307
Method of determining shear stress employing a monomer-polymer laminate structure
[NASA-CASE-LAR-14654-2] p 2375 N94-23308
Reaction of isocyanates with carboxylic acids and its application to polymer synthesis
[PB94-118858] p 2254 N94-23763
STM studies of LB deposited alkyl substituted polyaniline and its corresponding monomer
[AD-A273553] p 2257 N94-24562
High temperature adhesive
[AD-D016019] p 2258 N94-24737
Synthesis of polyphenylenes via Bergman cyclization of enediyne monomers
[AD-A273298] p 2260 N94-24924
Curing phthalonitriles with acid
[AD-D015996] p 2261 N94-25054
Synthesis of molecular wires by a novel divergent/convergent approach
[AD-A273332] p 2537 N94-25087
MONOMOLECULAR FILMS
Chemically sensitive interfaces on SAW devices
[DE94-001832] p 2526 N94-23718
Synthesis and characterization of two-dimensional molecular recognition interfaces
[AD-A273177] p 2536 N94-24729
MONOPROPELLANTS
Weld joint concepts for on-orbit repair of Space Station Freedom fluid system tube assemblies
p 2371 N94-24427
MONOPULSE ANTENNAS
Microstrip monopulse antenna for land mobile communications p 2289 N94-22833
Beam-waveguide antenna servo design issues for tracking low earth-orbiting satellites
p 2292 N94-23268
MONOPULSE RADAR
Method and apparatus of generating sum or difference signals corresponding to an apparent beam in a monopulse radar system
[AD-D015998] p 2302 N94-25056
Method and apparatus for determining target elevation angle, altitude and range, and the like in a monopulse radar system with reduced multipath errors
[AD-D016005] p 2302 N94-25058
MONSOONS
Climate variability in a coupled GCM. Part 2: The Indian Ocean and monsoon
[MPIM-104] p 2401 N94-23159
MONTE CARLO METHOD
Analysis of a proposed Compton backscatter imaging technique
[DE93-040537] p 2371 N94-22935
Coherence lost? Not-so-fast escapes from the in-phase attractor of a set of globally coupled nonlinear oscillators
[DE94-000799] p 2557 N94-22940
Molecular gas dynamics applied to low-thrust propulsion p 2214 N94-23053
Monte Carlo climate change forecasts with a global coupled ocean-atmosphere model
[MPIM-97] p 2407 N94-23156
Accuracy control in Monte Carlo radiative calculations
p 2321 N94-23639
Thermal analysis of combinatorial solid geometry models using SINDA p 2323 N94-23650
Integral equations for the microstructures of supercritical fluids
[DE94-002460] p 2535 N94-24569
Bounds and simulation results of 32-ary and 64-ary quadrature amplitude modulation for broadband-ISDN via satellite
[NASA-TM-106484] p 2202 N94-25095
Effect of high frequency field on the transport properties of superlattice
[DE93-617047] p 2568 N94-25447
On the hadron formation time in pion-nucleus interaction
[DE93-616879] p 2539 N94-25476
MOORING
Vertical motion in the SYNOP central array
[AD-A273593] p 2418 N94-24795
MORPHOLOGY
Electric field-mediated processing of polymer blend solutions p 2223 N94-24341
Polymer morphologh p 2226 N94-24353
Hydraulics and morphology of mountain rivers: A literature survey. Communications on hydraulic and geotechnical engineering
[PB94-110772] p 2388 N94-24636
Morphology of highly textured polyethylene/polyethylene- propylene semicrystalline diblock copolymers
[AD-A273683] p 2263 N94-25413
MOSAICS
Flight solar calibrations using the Mirror Attenuator Mosaic (MAM): Low scattering mirror
p 2384 N94-23602

MOSSBAUER EFFECT
Investigation of the solid-solid surface adsorption of Eu2O3 on amorphous Al2O3
[DE93-613824] p 2566 N94-25332

MOTION PERCEPTION
Perception in flight: Shape and motion perception, space perception, spatial orientation, and visual vestibular interaction p 2429 N94-23979
Extracting heading and temporal range from optic flow: Human performance issues p 2442 N94-25510

MOTION SICKNESS
Increasing accuracy in the assessment of motion sickness: A construct methodology
[NASA-TM-108797] p 2420 N94-23088
Perception in flight: Shape and motion perception, space perception, spatial orientation, and visual vestibular interaction p 2429 N94-23979
Transfer of perceptual adaptation to space sickness: What enhances an individual's ability to adapt?
[NASA-CR-188256] p 2427 N94-24227

MOTION SIMULATION
Reach performance while wearing the Space Shuttle launch and entry suit during exposure to launch accelerations p 2436 N94-24204

MOTION SIMULATORS
Future directions in flight simulation: A user perspective p 2162 N94-25101

MOTION STABILITY
Projectile transverse motion and stability in electromagnetic induction launchers
[DE94-001557] p 2198 N94-23210

MOUNTAINS
Hydraulics and morphology of mountain rivers: A literature survey. Communications on hydraulic and geotechnical engineering
[PB94-110772] p 2388 N94-24636
GPS survey of the western Tien Shan
[NASA-CR-195174] p 2175 N94-24826

MSAT
The MSAT spacecraft of Telesat Mobile Inc. p 2207 N94-22742
MSAT and cellular hybrid networking p 2278 N94-22762
Design and implementation considerations of a MSAT packet data network p 2280 N94-22778
The Westinghouse Series 1000 Mobile Phone: Technology and applications p 2284 N94-22800
Direct digital RF synthesis and modulation for MSAT mobile applications p 2285 N94-22804
A practical system for regional mobile satellite services p 2288 N94-22828
Low cost antennas for MSAT vehicular applications p 2289 N94-22830

MULLITES
Metal-mullite reactions
[DE94-002038] p 2244 N94-23811

MULTICHANNEL COMMUNICATION
Electrical performance of wire mesh for spacecraft deployable reflector antennas p 2275 N94-22744
Fault tolerant onboard packet switch architecture for communication satellites: Shared memory per beam approach
[NASA-TM-106397] p 2201 N94-23567
Advanced technology for a satellite multichannel demultiplexer/demodulator
[NASA-CR-194435] p 2202 N94-23631

MULTIGRID METHODS
A multigrid multiblock solver for compressible turbulent flow
[MEMO-1125] p 2315 N94-22713
Local grid refinement method for the euler equations
[PB93-223329] p 2317 N94-22985
The Sixth Copper Mountain Conference on Multigrid Methods, part 1
[NASA-CP-3224-PT-1] p 2482 N94-23673
A multigrid solver for the semiconductor equations p 2482 N94-23674
FAS multigrid calculations of three dimensional flow using non-staggered grids p 2341 N94-23675
Multigrid and cyclic reduction applied to the Helmholtz equation p 2304 N94-23676
Uniform convergence of multigrid V-cycle iterations for indefinite and nonsymmetric problems p 2482 N94-23677
A multilevel cost-space approach to solving the balanced long transportation problem p 2483 N94-23678
Domain decomposition methods for nonconforming finite element spaces of Lagrange-type p 2483 N94-23680
Implementing abstract multigrid or multilevel methods p 2483 N94-23682
Numerical solution of flame sheet problems with and without multigrid methods p 2237 N94-23683
A mixed method Poisson solver for three-dimensional self-gravitating astrophysical fluid dynamical systems p 2484 N94-23684
Multigrid methods for differential equations with highly oscillatory coefficients p 2484 N94-23685
Application of multigrid methods to the solution of liquid crystal equations on a SIMD computer p 2484 N94-23686
An adaptive multigrid model for hurricane track prediction p 2416 N94-23687
Relaxation schemes for Chebyshev spectral multigrid methods p 2484 N94-23688
Multigrid methods for a semilinear PDE in the theory of pseudoplastic fluids p 2341 N94-23689
A comparison of locally adaptive multigrid methods: LDC, FAC and FIC p 2485 N94-23692
Compressible turbulent flow simulation with a multigrid multiblock method p 2342 N94-23694
A nonconforming multigrid method using conforming subspaces p 2485 N94-23695
Multigrid method for integral equations and automatic programs p 2464 N94-23696
Toward large eddy simulation of turbulent flow over an airfoil p 2172 N94-24150
An integrated runtime and compile-time approach for parallelizing structured and block structured applications
[NASA-CR-191554] p 2458 N94-24740
Lubrication in cold rolling: Numerical simulation using multigrid techniques
[ISBN-9-09-005313-1] p 2262 N94-25230

MULTIMEDIA
Transparent data service with multiple wireless access p 2276 N94-22754
Internetworking satellite and local exchange networks for personal communications applications p 2276 N94-22755
NASDA's Advanced On-Line System (ADOLIS) p 2509 N94-23903
Service description of communication systems supporting multi-media multi-user applications
[PB94-110855] p 2299 N94-24650
Performance measurements of the multimedia testbed on Mach 3.0: Experience writing real-time device drivers, servers, and applications
[AD-A273600] p 2460 N94-24932
Considerations regarding the deployment of hypermedia at JSC p 2595 N94-25366
A multimedia adult literacy program: Combining NASA technology, instructional design theory, and authentic literacy concepts p 2585 N94-25384

MULTIPATH TRANSMISSION
Adaptive digital beamforming for a CDMA mobile communications payload p 2274 N94-22743
ROCSAT-1 telecommunication experiments p 2279 N94-22770
Land mobile satellite propagation measurements in Japan using ETS-V satellite p 2282 N94-22790
K-band mobile propagation measurements using ACTS p 2283 N94-22792
Measurement of multipath delay profile in land mobile satellite channels p 2283 N94-22793
A study of satellite motion-induced multipath phenomena p 2283 N94-22794
Diversity reception for advanced multi-satellite networks: A CDMA approach p 2286 N94-22816
Transmission over EHF mobile satellite channels p 2287 N94-22820
Global acoustic mapping of ocean temperatures (GAMOT)
[AD-A273387] p 2418 N94-24719
Conveying digital data in noisy, unstable, multipath environments
[AD-D015980] p 2301 N94-25038
Measurements and modeling of multitone, low-frequency acoustic data from the Arraial do Cabo range
[AD-A273406] p 2530 N94-25073
Northern Exposure 1992: An investigation of transauroral HF radio skywave propagation
[AD-A273363] p 2303 N94-25089

MULTIPLE ACCESS
Transparent data service with multiple wireless access p 2276 N94-22754
A protocol for satellite access via use of spot-beams p 2286 N94-22811
DS-SSMA capacity for a mobile satellite system p 2286 N94-22814
Multi-access laser communications terminal
[NASA-CR-191251] p 2295 N94-23830

MULTIPLE DOCKING ADAPTERS
Docking mechanisms: An overview of different systems p 2357 N94-24004

MULTIPLEXING
InGaAsP/InP based 1.3/1.55 micron vertical cavity surface emitting lasers for wavelength division multiplexed high speed distributed computing, phase 1
[AD-A271081] p 2348 N94-23123
Design and implementation issues of end-to-end protocols in high-speed networks
[PB94-110905] p 2467 N94-23752
Digital data, composite video multiplexer and demultiplexer boards for an IBM PC/AT compatible computer p 2447 N94-25377
Modeling of the ground-to-SSFMB link networking features using SPW p 2306 N94-25381

MULTIPLICATION
Implementation and parallelization of fast matrix multiplication for a fast Legendre transform
[DE94-002184] p 2478 N94-22975

MULTIPLIERS
Radar target discrimination systems using artificial neural network topology
[AD-D015984] p 2301 N94-25041

MULTIPROCESSING (COMPUTERS)
A dataflow analysis tool for parallel processing of algorithms
[NASA-TM-109054] p 2448 N94-23086
Distributed Operating Systems and Mach. Proceedings of the Spring 1992 Graduate Seminar on Distributed Systems
[PB93-224905] p 2449 N94-23103
Installation of an artificial neural network on distributed memory microprocessors
[ETN-94-95175] p 2471 N94-23152
A parallel PROLOG system for distributed memory multiprocessor
[ETN-94-95173] p 2465 N94-23167
Towards real-time stereovision systems for planetary missions p 2370 N94-23422
Linear time algorithm to schedule trees with communication delays optimally on two machines
[PB93-237782] p 2451 N94-23441
Preemptive scheduling in a two-stage multiprocessor flow shop is Np-hard
[PB94-111648] p 2467 N94-23756
Three, four, five, six or the complexity of scheduling with communication delays
[PB94-111630] p 2467 N94-23767
Mission planning for Shuttle Imaging Radar-C (SIR-C) with a real-time interactive planning software p 2305 N94-23842
The design of the EMPS multiprocessor executive for distributed computing
[ETN-94-95336] p 2468 N94-25062
Multiprocessor scheduling with communication delays
[ETN-94-95346] p 2468 N94-25221

MULTIPROGRAMMING
Exercises in multiprogramming
[PB94-101458] p 2454 N94-23768

MULTISENSOR APPLICATIONS
Multi-sensoral approach to night flight: Perceptive and Cognitive limitations p 2432 N94-23981
Radar E-O image fusion p 2306 N94-25503

MULTISPECTRAL BAND SCANNERS
Method for selection of wavelength bands for multispectral classification
[PB93-204378] p 2388 N94-24741

MULTISPECTRAL PHOTOGRAPHY
MAMS data for the Convection and Moisture Experiment (CAMEX)
[NASA-TM-108435] p 2409 N94-24080

MULTISTAGE ROCKET VEHICLES
Modal test of the Brazilian satellite launcher (VLS) configuration burn-out of the first stage p 2156 N94-24257

MULTISTATIC RADAR
Calibration network intended for phase-array antennas at 3 GHz
[PB93-204352] p 2297 N94-24530

MULTIVARIABLE CONTROL
Reduced-order modelling and control of a class of systems for which balanced truncation is Hankel-norm optimal
[OUEL-1922/92] p 2472 N94-23163
A reliable algorithm for optimal control synthesis
[NASA-CR-194809] p 2472 N94-23332
Parametric uncertainty reduction in robust multivariable control
[AD-A273412] p 2460 N94-24927
On-line evaluation of multiloop digital controller performance p 2163 N94-25105
Kernels of anti-causal operators and the multivariable generalized predictive control problem
[MATHS-REPT-A-191] p 2476 N94-25428

MULTIVARIATE STATISTICAL ANALYSIS
Parametric uncertainty reduction in robust multivariable control
[AD-A273412] p 2460 N94-24927
Topics in probability and dynamics
[AD-A273543] p 2496 N94-24931

MUON SPIN ROTATION
Interplay of magnetic and superconducting heavy fermion ground states
[DE94-000680] p 2240 N94-23003
Muon spin relaxation studies of the interplay between magnetism and superconductivity in heavy fermion systems
[DE94-000700] p 2559 N94-23006

MUONS
A measurement of the forward-backward asymmetry and sin(sup 2)(theta)(sub W) from the process Z(sup 0) (yields) (mu)(sup +)(mu)(sup (minus)) at (radical)s = 1.8 TeV
[DE94-001908] p 2532 N94-23018
Low mass muon pair production in 450 GeV p-Be collisions
[PB94-110699] p 2533 N94-23746
New evaluation of hadronic contributions to the anomalous magnetic moment of charged leptons
[DE93-634394] p 2536 N94-24844
A research of possibility for negative muon production by a low energy electron beam accompanying ion beam
[NIFS-266] p 2536 N94-24868
The L3 visualization system and its use in the Z(zero) line shape analysis
[ETN-94-95382] p 2537 N94-25231

MUSCLES
Cellular and tissue injury during nonfreezing cold injury and frostbite
[AD-A270883] p 2423 N94-22732
Left ventricular hypertrophy and athlete's heart
p 2424 N94-23321
Skeletal muscle metabolism in hypokinetic rats
[NASA-CR-195082] p 2420 N94-24124
Microinjection of the Yersinia YopE cytotoxin in mammalian cells induces actin microfilament disruption
[FOA-B-40418-4.4] p 2421 N94-24290
Loading, electromyograph, and motion during exercise
p 2427 N94-25359
Loading, electromyograph, and motion during exercise
p 2427 N94-25380

MUSCULAR STRENGTH
Responses to LBNP in men with varying profiles of strength and aerobic capacity: Implications for flight crews
[NASA-TP-3346] p 2426 N94-23530
NASA project 1: Full-body dynamometer
[NASA-CR-195507] p 2438 N94-24331

MUSCULOSKELETAL SYSTEM
Skeletal muscle metabolism in hypokinetic rats
[NASA-CR-195082] p 2420 N94-24124

N

NAP-OF-THE-EARTH NAVIGATION
Multiple-camera/motion stereoscopy for range estimation in helicopter flight p 2441 N94-25505

NARROWBAND
Conductors with small Fermi energies and small gap energies
[DE93-040887] p 2561 N94-23432
Investigation of Raman beam cleanup and phase conjugation
[AD-A273157] p 2545 N94-24672

NASA PROGRAMS
NASA patent abstracts bibliography: A continuing bibliography. Section 2: Indexes (supplement 44)
[NASA-SP-7039(44)-SECT-2] p 2590 N94-23712
NASA printing, duplicating, and copying management handbook
[NASA-NHB-1490.5] p 2590 N94-23971
NASA high performance computing and communications program
[NASA-TM-4554] p 2591 N94-24337
A compilation of technology spinoffs from the US Space Shuttle Program p 2578 N94-24424
Access to space studies p 2199 N94-24434
Suddenly, tomorrow came... A history of the Johnson Space Center
[NASA-SP-4307] p 2631 N94-24584
NASA/DOD Aerospace Knowledge Diffusion Research Project. Report number 20: The use of selected information products and services by US aerospace engineers and scientists: Results of two surveys
[NASA-TM-109022] p 2592 N94-24649
Management. A bibliography for NASA managers
[NASA-SP-7500(27)] p 2586 N94-24708
NASA tech brief evaluations
[NASA-CR-195150] p 2597 N94-24829
NASA STI program database: Journal coverage (1990-1992)
[NASA-TM-109720] p 2593 N94-25168
National Aeronautics and Space Administration (NASA)/American Society for Engineering Education (ASEE) Summer Faculty Fellowship Program, 1993, volume 1
[NASA-CR-188271-VOL-1] p 2632 N94-25348
Strategies for recruiting additional African Americans into the NASA JSC summer faculty fellows program
p 2585 N94-25362

NASA SPACE PROGRAMS
Solar physics within NASA's planning
p 2625 N94-22845
The birth of NASA: The diary of T. Keith Glennan
[NASA-SP-4105] p 2630 N94-23333
Past US studies and developments for planetary rovers p 2369 N94-23375
Strategies in transition p 2498 N94-23833
Future trends in NASA space operations
p 2498 N94-23836
Ultraviolet, visible, and gravity astrophysics: A plan for the 1990's
[NASA-NP-152] p 2603 N94-24973
The future of manned spaceflight
p 2195 N94-25067
New Ways Of Doing Business (NWODB) cost quantification analysis
[NASA-CR-195186] p 2586 N94-25197

NATIONAL AEROSPACE PLANE PROGRAM
A conceptual design of an unmanned test vehicle using an airbreathing propulsion system
[NASA-CR-195550] p 2189 N94-25085

NATIONAL AIRSPACE SYSTEM
Conflict-free trajectory planning for air traffic control automation
[NASA-TM-108790] p 2174 N94-25272

NATIONAL LAUNCH VEHICLE PROGRAM
Flame trench analysis of NLS vehicles
p 2199 N94-23249

NATURAL GAS
Development of durable high-temperature catalysts for natural gas combustion
[PB93-226447] p 2232 N94-23477
Evaluation of reducing gas turbine emissions through hydrogen-enhanced steam-injected combustion
[PB94-109873] p 2187 N94-23709
Fundamental and experimental studies on the catalytic combustion of methane
[PB94-112661] p 2233 N94-23736
Fundamental study of NO(x) control in catalytic combustion
[PB94-112323] p 2398 N94-23818
Near-surface seismic imaging
[PB94-119096] p 2404 N94-24647
Modelling of premixed laminar flames
[ETN-94-95317] p 2236 N94-25284

NAVIER-STOKES EQUATION
A multigrid multiblock solver for compressible turbulent flow
[MEMO-1125] p 2315 N94-22713
CFD analyses of combustor and nozzle flowfields
p 2210 N94-23033
Heat transfer in rocket combustion chambers
p 2214 N94-23051
Computational fluid dynamic modelling of cavitation
p 2215 N94-23060
Reliability enhancement of Navier-Stokes codes through convergence enhancement p 2216 N94-23064
CFD modeling of microwave electrothermal thrusters
p 2216 N94-23066
Two-dimensional Navier-Stokes computations of subsonic and supersonic flows through turbine cascades
[PB93-226223] p 2317 N94-23114
POISs3: A 3D poisson smoother of structured grids
[PB93-226231] p 2318 N94-23115
Computational study of GA(W)-1: Airfoil near stall
[PB93-226249] p 2165 N94-23116
Tracking sharp interface of two fluids by the CIP (Cubic-Interpolated Propagation) scheme
[DE93-508322] p 2319 N94-23460
Unsteady jet flow computation towards noise prediction
[NASA-CR-194449] p 2153 N94-23553
An implicit numerical scheme for the simulation of internal viscous flows on unstructured grids
[NASA-TM-106437] p 2481 N94-23554
Numerical analysis of a vortex controlled diffuser
p 2324 N94-23659
An application of small-gap equations in sealing devices p 2325 N94-23668
A comparative study of computational solutions to flow over a backward-facing step p 2326 N94-23670
Multi-grid domain decomposition approach for solution of Navier-Stokes equations in primitive variable form
p 2341 N94-23693
Efficient interpolation of velocity and flux components defined on 2- and 3-dimensional non-cartesian grids
[PB94-118619] p 2486 N94-23757
Drag reduction at a plane wall p 2327 N94-24140
On the large eddy simulation of turbulent flows in complex geometry p 2329 N94-24148
Transition to turbulence in an elliptic vortex
p 2331 N94-24161
On the dynamics of approximating schemes for dissipative nonlinear equations p 2332 N94-24168
Discrete sensitivity derivatives of the Navier-Stokes equations with a parallel Krylov solver
[NASA-TM-106481] p 2265 N94-24301
Implementation of the Baldwin-Barth turbulence model into the ZETA code and its diagnosis
[NASA-CR-194795] p 2335 N94-24640
Solution of the discretized incompressible Navier-Stokes equations with iterative methods
[PB94-118635] p 2335 N94-24641
Carrying the mass flux terms exactly in the first and second moment equations of compressible turbulence
[NASA-CR-191568] p 2335 N94-24712
Numerical solutions of the complete Navier-Stokes equations
[NASA-CR-194780] p 2337 N94-24858
Computational fluid mechanics
[NASA-CR-194765] p 2337 N94-24859
Triangular spectral elements for incompressible fluid flow
[NASA-CR-191588] p 2490 N94-24914
Turbulence models and Reynolds analogy for two-dimensional supersonic compression ramp flow
[NASA-TM-106474] p 2337 N94-25119
Development and application of new algorithms for the simulation of viscous compressible flows with moving bodies in three dimensions
[AD-A273514] p 2338 N94-25157
A continuing search for a near-perfect numerical flux scheme. Part 1: AUSM+
[NASA-TM-106524] p 2338 N94-25180
Two-dimensional CFD modeling of wave rotor flow dynamics
[NASA-TM-106261] p 2189 N94-25185
A numerical investigation of the artificial compressibility method for the solution of the Navier-Stokes equations
[CRANFIELD-AERO-9213] p 2340 N94-25486

NAVIGATION
HERACLITUS, phase 1. Harbour Entrance of Rotterdam Radar based Current Related Information for Traffic Guidance of Ships: Feasibility of deriving current profile data from sea surface observations in the Rotterdam (Netherlands) port entrance
[BCRS-93-04] p 2417 N94-24107
NASA LaRC Workshop on Guidance, Navigation, Controls, and Dynamics for Atmospheric Flight, 1993
[NASA-CP-10127] p 2162 N94-25096

NAVIGATION AIDS
Lunar rover navigation concepts p 2607 N94-23386
Expansion-based passive ranging
p 2176 N94-25504

NAVIGATION INSTRUMENTS
An overview of a generic multi-sensor integrated navigation system design
[CTN-94-60916] p 2174 N94-24120
Application of aircraft navigation sensors to enhanced vision systems p 2176 N94-25495

NAVY
Design project: LONGBOW supersonic interceptor
[NASA-CR-195510] p 2180 N94-24581
ELF communications system ecological monitoring program
[AD-A273456] p 2299 N94-24676
Observed and Navy operational global model climatologies of synoptic disturbances over the tropical western Pacific during winter 1991-1992
[AD-A273400] p 2416 N94-25071

NEAR FIELDS
Mixing and unmixedness in plasma jets 1: Near-field analysis p 2323 N94-23655
Toward modeling wingtip vortices
p 2171 N94-24142
Unstructured adaptive mesh computations of rotorcraft high-speed impulsive noise
[NASA-CR-195090] p 2529 N94-24307

NEAR INFRARED RADIATION
Optimization of techniques to reconstruct images disturbed by atmospheric turbulence in the near infra-red
[PB93-199784] p 2298 N94-24630

NEBULAE
X ray enhancement of SN 1987A due to interaction with its ring-like nebula
[NIFS-265] p 2602 N94-24867

NEGATIVE FEEDBACK
High speed electronic analog computers using low-gain amplifiers
[AD-D015974] p 2446 N94-25034

NEGATIVE IONS
Semiempirical studies of atomic structure
[DE94-001588] p 2531 N94-22937

Diffusion in electronegative discharges with magnetic fields
[AD-A273826] p 2304 N94-25521
NEODYMIUM ALLOYS
Magnetic properties and transmission electron microscopy investigations of Nd-Fe-B-Co-Al melt spun ribbons
[PB93-201531] p 2561 N94-23428
NEODYMIUM COMPOUNDS
Anomalous magnetoresistance behavior of superconducting Nd(2-x)Ce(x)CuO(4-y) single crystal
[DE94-000806] p 2558 N94-22941
Magnetic properties of NdCo3 and its gamma phase hydride NdCo3H(4.1)
[REPT-A-2655] p 2567 N94-25412
NEODYMIUM LASERS
Progress toward ultra-stable lasers for use in space
[NASA-TM-109678] p 2349 N94-24488
Numerical simulation and analysis of experimental results on stimulated Raman scattering in laser-plasma Hohlraum targets
[DE93-613719] p 2554 N94-25330
NEON
Intramultiplet mixing for Ne(**)(3p)+He at superthermal energies
[ETN-94-95327] p 2538 N94-25240
NEPTUNE (PLANET)
The Jet Propulsion Laboratory space exploration: Past, present and future p 2153 N94-24242
NEPTUNIUM
A survey of metallurgical research on several actinides
[DE94-002643] p 2245 N94-24747
NERVOUS SYSTEM
Electrophysiology of the rat nucleus accumbens: Local circuitry, neuromodulation and synaptic plasticity
[PB93-232254] p 2420 N94-23454
Photonic technology for implementation of generalizable neural networks: A synthetic approach
[AD-A273497] p 2474 N94-24622
NETHERLANDS
Exploratory report nickel and nickel compounds
[PB93-223998] p 2242 N94-23496
Exploratory report antimony and antimony compounds
[PB93-224004] p 2397 N94-23497
Analysis of vulnerability to the impacts of sea level rise: A case study for The Netherlands
[PB94-111150] p 2399 N94-24573
Soil pollution at former industrial sites, the heritage of 150 years of industrial development in Noord-Brabant, The Netherlands
[ISBN-9-09-005758-7] p 2400 N94-25223
NETS
Studies of Shuttle orbiter arrestment system
[NASA-TP-3370] p 2177 N94-24304
NETWORK ANALYSIS
Handover procedures in integrated satellite and terrestrial mobile systems p 2277 N94-22761
MSAT and cellular hybrid networking
p 2278 N94-22762
Trends in mobile satellite communication
p 2278 N94-22763
A system architecture for an advanced Canadian wideband mobile satellite system p 2278 N94-22766
Transient analysis of circuits including frequency-dependent components using transgyrator and convolution
[PB93-225001] p 2308 N94-23130
Mathematical modeling of MCFC cells/stacks and networks
[DE94-001914] p 2390 N94-23212
Extension of the critical path method
[PB94-118817] p 2488 N94-24527
Modular approach to project management
[PB94-118833] p 2586 N94-24528
Irreducible core of a minimum cost spanning tree game
[PB94-110962] p 2489 N94-24653
New directions in network flows
[AD-A273467] p 2468 N94-24939
NETWORK CONTROL
Interworking evolution of mobile satellite and terrestrial networks p 2277 N94-22758
Interworking and integration of the Inmarsat Standard-M with Pan-European GSM system p 2277 N94-22759
Architectures and protocols for an integrated satellite-terrestrial mobile system p 2277 N94-22760
Handover procedures in integrated satellite and terrestrial mobile systems p 2277 N94-22761
Optimizing space constellations for mobile satellite systems p 2278 N94-22764
ACTS mobile SATCOM experiments
p 2280 N94-22774
The ORBCOMM data communications system
p 2281 N94-22782
System services and architecture of the TMI satellite mobile data system p 2286 N94-22817
Study on networking issues of medium earth orbit satellite communications systems p 2288 N94-22825
Specifications of ETS, the Enhanced Transport Service
[RR-907-I] p 2589 N94-23150
Source spacing in B-ISDN
[PB93-201747] p 2293 N94-23508
NASDA satellite mission operation system and operations p 2501 N94-23854
NASDA knowledge-based network planning system
p 2508 N94-23898
Deep Space Network (DSN), Network Operations Control Center (NOCC) computer-human interfaces
p 2447 N94-23917
EOS ground data systems: A description and interface overview p 2517 N94-23948
NEURAL NETS
The adaptive resonance theory network: (Clustering-) behaviour in relation with brainstem auditory evoked potential patterns
[EUT-92-E-264] p 2470 N94-22877
Artificial neural networks: Application to the optical recognition of music partitions
[ETN-94-95166] p 2470 N94-22884
Customizable VLSI artificial neural network chips based on a novel technology
[DE94-001418] p 2307 N94-23008
A novel process monitoring and control system based on a neural manufacturing concept
[DE94-001516] p 2471 N94-23011
Installation of an artificial neural network on distributed memory microprocessors
[ETN-94-95175] p 2471 N94-23152
Neural network research in Finland. Symposium
[PB93-224822] p 2472 N94-23463
Material data representation of hysteresis loops for Hastelloy X using artificial neural networks
[NASA-TM-105990] p 2376 N94-23551
Adaptive nonlinear polynomial neural networks for control of boundary layer/structural interaction
[NASA-CR-189645] p 2525 N94-23698
Automatic modulation recognition based on spatial pattern classification using artificial neural networks
[CTN-94-60897] p 2296 N94-24115
Acoustic target detection and classification using neural networks p 2529 N94-24221
Preliminary analysis of the JAPE ground vehicle test data with an artificial neural network classifier
p 2529 N94-24222
Neural network-based control using Lyapunov functions p 2477 N94-24433
Using neural networks to assist in OPAD data analysis
p 2477 N94-24452
Optimal Space Station solar array gimbal angle determination via radial basis function neural networks
[NASA-TM-106482] p 2195 N94-24482
Diagnosing process faults using neural network models
[DE94-002633] p 2473 N94-24518
Systematic construction of trigonometric neural networks
[PB93-200228] p 2474 N94-24544
Photonic technology for implementation of generalizable neural networks: A synthetic approach
[AD-A273497] p 2474 N94-24622
Hyperspectral imagery classification using a backpropagation neural network
[AD-A273615] p 2545 N94-24730
A methodology for software cost estimation using machine learning techniques
[AD-A273158] p 2459 N94-24775
Evolving recurrent perceptrons
[AD-A273241] p 2496 N94-24778
Evolving neural network connectivity
[AD-A273134] p 2490 N94-24921
High-level connectionist models
[AD-A273638] p 2468 N94-25030
Radar target discrimination systems using artificial neural network topology
[AD-D015984] p 2301 N94-25041
Determining neural network hidden layer size using evolutionary programming
[AD-A273242] p 2475 N94-25139
The determination of the branching ratios of the Z(zero) boson into heavy quarks using neural networks
[ETN-94-95381] p 2538 N94-25246
On-line control of dynamic systems using feedforward neural networks
[RR-457] p 2476 N94-25307
Development of programmable artificial neural networks p 2477 N94-25370
NEURONS
Customizable VLSI artificial neural network chips based on a novel technology
[DE94-001418] p 2307 N94-23008
NEUROPHYSIOLOGY
Electrophysiology of the rat nucleus accumbens: Local circuitry, neuromodulation and synaptic plasticity
[PB93-232254] p 2420 N94-23454
NEUROTRANSMITTERS
Electrophysiology of the rat nucleus accumbens: Local circuitry, neuromodulation and synaptic plasticity
[PB93-232254] p 2420 N94-23454
NEUTRAL BEAMS
IPP Prague Contributions to the IAEA Technical Committee Meeting on Research Using Small Tokamaks
[IPPCZ-329] p 2551 N94-24293
Investigation of the heat handling capabilities of DIII-D neutral beamline internal components
[DE94-001107] p 2553 N94-24756
NEUTRINO BEAMS
Accelerator-based neutrino oscillation searches
[DE94-000818] p 2626 N94-23515
NEUTRINOS
Pions and neutrinos as probes of the nucleon and nuclear few-body system
[DE93-040127] p 2531 N94-22928
Accelerator-based neutrino oscillation searches
[DE94-000818] p 2626 N94-23515
Kamiokande results on solar neutrinos and a supernova search
[ICRR-REPT-294-93-6] p 2627 N94-24961
NEUTRON COUNTERS
Experimental characterization of the AFIT Neutron Facility
[AD-A273822] p 2539 N94-25519
NEUTRON DIFFRACTION
The structure and spin dynamics of lanthanide-bearing silicate glasses
[DE94-001320] p 2252 N94-22992
Dual-purpose RTOF diffractometer facility at the ET-RR-1 reactor
[VTT-TIED-1425] p 2566 N94-25347
NEUTRON IRRADIATION
Effects of neutron irradiation and hydrogen on ductile-brittle transition temperatures of V-Cr-Ti alloys
[DE94-001466] p 2240 N94-23009
Development of small punch testing technique and its application to evaluation of mechanical properties degradation
[DE94-001193] p 2375 N94-23184
Effect of neutron irradiation on tensile properties of V-Cr-Ti alloys
[DE94-001433] p 2240 N94-23194
NEUTRON SCATTERING
Spin-hole doping in the Kondo insulator Ce3Bi4Pt3 studied by neutron scattering
[DE93-040107] p 2557 N94-22925
The structure and spin dynamics of lanthanide-bearing silicate glasses
[DE94-001320] p 2252 N94-22992
Microscopic dynamics in dense helium-neon mixtures: Neutron scattering, kinetic theory and computer simulations
[ISBN-9-07-386105-5] p 2537 N94-25228
Lattice dynamics of Ba(1-x)K(x)BiO3 as studied by neutron scattering and computer simulation
[DE93-617053] p 2567 N94-25424
Crystal field in Nd2CuO4
[DE93-617054] p 2567 N94-25425
The Haldane energy gap of a doped linear-chain Heisenberg antiferromagnet
[DE93-617130] p 2567 N94-25426
NEUTRON SPECTRA
Crystal field in Nd2CuO4
[DE93-617054] p 2567 N94-25425
Experimental characterization of the AFIT Neutron Facility
[AD-A273822] p 2539 N94-25519
NEUTRON STARS
Neutron star mergers and gamma-ray bursts
[NASA-CR-195176] p 2629 N94-25091
NEUTRONS
Polarized structure functions of the nucleon in the resonance region
[CEBAF-PR-94-001] p 2540 N94-24663
Experimental characterization of the AFIT Neutron Facility
[AD-A273822] p 2539 N94-25519
NEWTON METHODS
Error due to the stopping of the Newton iteration in implicit linear multistep methods
[PB94-101425] p 2487 N94-23786
Generalized Gaussian quadrature rules for systems of arbitrary functions
[AD-A273610] p 2491 N94-24947
NEWTONIAN FLUIDS
An application of small-gap equations in sealing devices p 2325 N94-23668

NICHROME (TRADEMARK)
Wear reduction in ceramic bearings by surface generated pyrolytic carbon continuously replenished by ethylene gas
[NASA-CR-189214] p 2364 N94-24090
NICKEL
High surface area, low weight composite nickel fiber electrodes p 2391 N94-23351
Exploratory report nickel and nickel compounds
[PB93-223998] p 2242 N94-23496
Strength, acoustic evaluation and metallurgy of diffusion bonds
[DE94-001804] p 2243 N94-23717
NICKEL ALLOYS
Magnetic phases in UNiGe
[DE94-000793] p 2239 N94-22939
Generic microelectronic smart sensor platform for detection of toxic, hazardous, and flammable gases
[DE93-017626] p 2343 N94-23200
Material data representation of hysteresis loops for Hastelloy X using artificial neural networks
[NASA-TM-105990] p 2376 N94-23551
Multilayer relaxation and surface structure of ordered alloys
[NASA-TM-106433] p 2243 N94-23578
Mean stress models for low cycle fatigue of a nickel-base superalloy p 2159 N94-24276
Structural characterization and thermal cycling behaviour of EB-PVD thermal barrier coating systems
[ISBN-0-315-83365-3] p 2257 N94-24468
Investigate zero-stress replicated optics
[NASA-CR-193889] p 2545 N94-24665
Robotic weld overlay coatings for erosion control
[DE94-002665] p 2258 N94-24749
NICKEL CADMIUM BATTERIES
Aerospace applications of batteries
p 2390 N94-23346
Review of super Ni/Cd cell designs and performance
p 2391 N94-23348
Thermodynamics of nickel-cadmium and nickel-hydrogen batteries p 2391 N94-23349
NICKEL COMPOUNDS
Ovonic nickel metal hydride batteries for space applications p 2391 N94-23352
Alloys for hydrogen storage in nickel/hydrogen and nickel/metal hydride batteries p 2391 N94-23353
Exploratory report nickel and nickel compounds
[PB93-223998] p 2242 N94-23496
NICKEL HYDROGEN BATTERIES
Thermodynamics of nickel-cadmium and nickel-hydrogen batteries p 2391 N94-23349
High specific energy, high capacity nickel-hydrogen cell design p 2391 N94-23350
High surface area, low weight composite nickel fiber electrodes p 2391 N94-23351
Alloys for hydrogen storage in nickel/hydrogen and nickel/metal hydride batteries p 2391 N94-23353
Impedance measurements on a spiral-wound nickel/metal hydride cell cycled in a simulated Leo orbit
p 2392 N94-23355
NASA Lewis advanced IPV nickel-hydrogen technology p 2392 N94-23356
NICKEL OXIDES
Applications of x ray absorption fine structure to the in situ study of the effect of cobalt in nickel hydrous oxide electrodes for fuel cells and rechargeable batteries
p 2391 N94-23347
NICKEL STEELS
Irradiation damage behavior of low alloy steel wrought and weld materials
[DE94-000519] p 2239 N94-22999
NIGHT
A nighttime structure model of atmospheric optical turbulence, c2(n), derived from thermosonde and high resolution rawinsonde measurements
[AD-A273803] p 2406 N94-25537
NIGHT FLIGHTS (AIRCRAFT)
Visual Problems in Night Operations
[AGARD-LS-187] p 2431 N94-23976
NIGHT VISION
Evaluation of visual acuity with Gen 3 night vision goggles
[NASA-TM-108792] p 2431 N94-23974
Visual Problems in Night Operations
[AGARD-LS-187] p 2431 N94-23976
Night operations p 2431 N94-23977
Physical aspects of the visual stimulus
p 2431 N94-23978
Perception in flight: Shape and motion perception, space perception, spatial orientation, and visual vestibular interaction p 2429 N94-23979
Mental images p 2429 N94-23980
Multi-sensoral approach to night flight: Perceptive and Cognitive limitations p 2432 N94-23981
Night vision devices and characteristics
p 2432 N94-23982
Cockpit/NVG visual integration issues
p 2432 N94-23983
Night vision goggle illusions and visual training
p 2432 N94-23984
NIOBIUM
Welding of niobium to stainless
[DE94-003365] p 2365 N94-24614
NIOBIUM ALLOYS
New extensions in the development of deformation processed metal-metal matrix composites
[DE94-000692] p 2227 N94-23004
Characterization of the microstructure of Nb-1wt.%Zr-0.1wt.%C tubes as affected by thermomechanical processing
[NASA-TM-106381] p 2242 N94-23550
Effect of hydrogen exposure on a Cu-8 Cr-4 Nb alloy
[NASA-TM-106429] p 2243 N94-23556
NITRIDES
LPCVD of InN on GaAs(110) using HN3 and TMIn: Comparison with Si(100) results
[AD-A273555] p 2235 N94-24917
Influences of nitrogen absorption on the magnetic properties of YFe2, YFe3 and Y6Fe23
[REPT-A-2654] p 2564 N94-24958
NITRIDING
Selection of polymer binders and fabrication of SiC fiber-reinforced reaction-bonded silicon nitride matrix composites
[NASA-CR-194874] p 2255 N94-24223
NITRILES
Curing phthalonitrile resins with acid and amine
[AD-D016021] p 2258 N94-24721
Curing phthalonitriles with acid
[AD-D015996] p 2261 N94-25054
NITROGEN
Reburning rich-lean kinetics
[PB93-220887] p 2232 N94-23100
NITROGEN IONS
Electron spectroscopic studies of the neutralization of slow multicharged ions during interactions with a metal surface
[DE93-041046] p 2532 N94-22956
Radiative properties of molecular nitrogen ions produced by helium Penning ionization and argon effects
[NASA-CR-195126] p 2534 N94-24487
NITROGEN OXIDES
Economics of electron beam and electrical discharge processing for post-combustion NO(x) control in internal combustion engines
[DE93-019574] p 2351 N94-22865
Fundamental limitations of non-thermal plasma processing for internal combustion engine NO(x) control
[DE93-019622] p 2351 N94-22866
Reburning rich-lean kinetics
[PB93-220887] p 2232 N94-23100
Flue gas cleaning by pulse corona streamer
[EUT-93-E-272] p 2268 N94-23174
Evaluation of reducing gas turbine emissions through hydrogen-enhanced steam-injected combustion
[PB94-109873] p 2187 N94-23709
Fundamental study of NO(x) control in catalytic combustion
[PB94-112323] p 2398 N94-23818
Alternative control techniques document: NOx emissions from stationary reciprocating internal combustion engines
[PB94-104494] p 2398 N94-24476
NITROGEN 15
Manual on measurement of methane and nitrous oxide emissions from agriculture
[DE93-616429] p 2399 N94-25167
NITROUS OXIDES
Manual on measurement of methane and nitrous oxide emissions from agriculture
[DE93-616429] p 2399 N94-25167
NOAA SATELLITES
Instrument interface description for NOAA 2000 instruments with European morning spacecraft and/or NOAA-OPQ spacecraft
[NASA-TM-109406] p 2208 N94-23478
Command/telemetry bus general specification for the NOAA-OPQ polar orbiting environmental satellites and EUMETSAT polar satellite systems
[NASA-TM-109407] p 2208 N94-23479
Evaluating NOAA satellite products for global climate monitoring p 2384 N94-23604
NODULES
Sarcoidosis and the aviator p 2425 N94-23325
NOISE INTENSITY
Spatial frequency multiplier with active linearly tapered slot antenna array
[NASA-TM-106494] p 2310 N94-24308
Exercise keevil: Noise levels of six military helicopters
[PB93-210722] p 2529 N94-25026
NOISE MEASUREMENT
Validation of the ROTAC code for the rotor noise prediction
[PB93-204311] p 2529 N94-24514
Fan noise research at NASA
[NASA-TM-106512] p 2530 N94-25172
On the origin of 1/f noise in epitaxial GaAs
[ISBN-9-09-006067-7] p 2566 N94-25297
The ISL rotor bench
[ISL-R-108/92] p 2185 N94-25301
NOISE PREDICTION
A modelling of the noise from simple co-axial jets. Part 2: In a simulated flightstream
[ISVR-TR-226] p 2525 N94-22959
Unsteady jet flow computation towards noise prediction
[NASA-CR-194449] p 2153 N94-23553
NOISE PREDICTION (AIRCRAFT)
Validation of the ROTAC code for the rotor noise prediction
[PB93-204311] p 2529 N94-24514
NOISE PROPAGATION
JAPE 91: Influence of terrain masking of the acoustic propagation of helicopter noise p 2528 N94-24214
NOISE REDUCTION
Estimation of frequency offset in mobile satellite modems p 2285 N94-22807
Low noise electric motor p 2315 N94-23989
Vibrational power transmission analysis of machinery installations in ships with the objective of noise reduction
[ISVR-TR-216] p 2363 N94-24076
Fan noise research at NASA
[NASA-TM-106512] p 2530 N94-25172
Adaptive noise cancellation using recurrent radial basis function networks
[RR-472] p 2313 N94-25319
NOISE SPECTRA
Laser linewidth measurement in the presence of RIN and using the recirculating self heterodyne method
[EUT-92-E-262] p 2347 N94-22874
A modelling of the noise from simple co-axial jets. Part 2: In a simulated flightstream
[ISVR-TR-226] p 2525 N94-22959
Ground characterization for JAPE
p 2527 N94-24213
Some subjects in digital audio, noise shaping, sample rate conversion, dynamic range compression and testing
[ISBN-9-09-005162-7] p 2530 N94-25220
Study of the blade/vortex interaction: Acoustics, aerodynamics and models
[ISL-R-104/92] p 2340 N94-25463
NOISE TEMPERATURE
Cryogenic, low-noise high electron mobility transistor amplifiers for the Deep Space Network
p 2291 N94-23262
NONADIABATIC CONDITIONS
Nonlinear ion-mixing-mode particle transport in the dissipative trapped electron regime
[DE94-000989] p 2533 N94-23435
NONCONDENSABLE GASES
Thermodynamic models for bounding pressurant mass requirements of cryogenic tanks
[NASA-TM-106476] p 2346 N94-25202
NONDESTRUCTIVE TESTS
Theoretical studies of wave propagation in multilayered piezoelectric media
[DE93-040273] p 2371 N94-22872
Strength, acoustic evaluation and metallurgy of diffusion bonds
[DE94-001804] p 2243 N94-23717
An evaluation of Compton scatter imaging using COMSCAN
[DREP-TM-93-38] p 2372 N94-24136
Ultrasonic nondestructive evaluation as a tool for the development of aerospace structural ceramic composites p 2257 N94-24240
Nondestructive evaluations
[DE94-003020] p 2373 N94-24613
Investigation of the effects of manufacturing variations and materials on fatigue crack detection methods in gear teeth
[NASA-CR-195093] p 2373 N94-24769
Demonstration of polyscann ultrasonic butt-fusion inspection system for polyethylene pipes
[AD-A273279] p 2373 N94-24814
Development of a nondestructive vibration technique for bond assessment of Space Shuttle tiles
[NASA-CR-195163] p 2201 N94-24919
Nuclear magnetic resonance imaging with short gradient pulses
[AD-D016006] p 2537 N94-25047
NONEQUILIBRIUM FLOW
Upwind MacCormack Euler solver with non-equilibrium chemistry p 2326 N94-23672

Radiative properties of molecular nitrogen ions produced by helium Penning ionization and argon effects
[NASA-CR-195126] p 2534 N94-24487

NONEQUILIBRIUM IONIZATION

Nonequilibria in thermal emission from supernova remnants
[NIFS-264] p 2602 N94-24866

NONEQUILIBRIUM PLASMAS

Modelling of thermal argon plasmas
[ETN-94-95363] p 2554 N94-25300

NONFLAMMABLE MATERIALS

Fire-resistant barriers for composite materials
[AD-D016014] p 2230 N94-24735

NONINTRUSIVE MEASUREMENT

An experimental study of characteristic combustion-driven flows for CFD validation
p 2212 N94-23040

Design of a surface deformation measuring instrument for the Surface Tension Driven Convection Experiment (STDCE-2)
[NASA-CR-194758] p 2343 N94-23285

Doppler global velocimetry: Development of a flight research instrumentation system for application to non-intrusive measurements of the flow field
[NASA-CR-191490] p 2344 N94-24360

Temperature measurement using infrared imaging systems during turbine engine altitude testing
[NASA-TM-105871] p 2193 N94-25184

Non-invasive optical detection of glucose in cell culture nutrient medium p 2422 N94-25357

NONLINEAR EQUATIONS

Nonlinear smoothing for random fields
[MEMO-1110] p 2493 N94-22728

The characterization of reaction-convection-diffusion processes by travelling waves
[MEMO-1111] p 2273 N94-22729

Incomplete corrections in nonlinear problems
[PB93-225746] p 2479 N94-23106

On the estimation of the correlation dimension and its application to radar reflector discrimination
[NASA-CR-4564] p 2309 N94-23304

Periodic nonlinear Schroedinger equation and invariant measures
[PB93-238012] p 2487 N94-23775

Error due to the stopping of the Newton iteration in implicit linear multistep methods
[PB94-101425] p 2487 N94-23786

On the dynamics of some grid adaption schemes
[NASA-CR-195092] p 2454 N94-24110

On the dynamics of approximating schemes for dissipative nonlinear equations p 2332 N94-24168

Global dynamic stability of a shallow arch by poincare-like simple cell mapping p 2160 N94-24280

Stable non-Gaussian diffusive profiles
[PB93-238053] p 2489 N94-24610

Stability analysis of anisotropic conical shells
[PB94-119054] p 2377 N94-24645

Nonlinear equations of motion for a panel subject to external loads
[AD-A273142] p 2170 N94-24773

Approximation to nonlinear equations using nonlinear rational models
[RR-448] p 2492 N94-25306

NONLINEAR EVOLUTION EQUATIONS

Cauchy problem for periodic KDV-type equations
[PB93-238020] p 2487 N94-23776

NONLINEAR FEEDBACK

Adaptive nonlinear polynomial neural networks for control of boundary layer/structural interaction
[NASA-CR-189645] p 2525 N94-23698

NONLINEAR FILTERS

Evolving recurrent perceptrons
[AD-A273241] p 2496 N94-24778

NONLINEAR OPTICS

A fully automated stage for optical waveguide measurements
[AD-A273042] p 2542 N94-22915

Microgravity sciences application visiting scientist program
[NASA-CR-194804] p 2267 N94-23287

Spatiotemporal behavior and nonlinear dynamics in a phase conjugate resonator
[NASA-CR-4567] p 2543 N94-23529

Inertial confinement fusion
[DE94-002602] p 2551 N94-23703

Prediction of nonlinear optical properties of organic materials. General theoretical considerations
p 2224 N94-24343

Low-gravity electrodeposition and growth of polymer thin films with large third-order optical nonlinearities by electrochemical processes for devices: Thiophene-based polymers p 2225 N94-24346

Polydiacetylene thin films for nonlinear optical applications p 2225 N94-24347

Crystal growth of organics for nonlinear optical applications p 2225 N94-24348

Nonlinear optical thin films p 2225 N94-24349

Optimization of microscopic and macroscopic second order optical nonlinearities p 2226 N94-24354

Dipolar relaxation in a second-order nonlinear optical interpenetrating polymer network
[AD-A273626] p 2258 N94-24732

Ultrastructure processing of macromolecular materials
[AD-A273413] p 2258 N94-24782

Center for advanced electrical and structural polymers
[AD-A273415] p 2259 N94-24783

NONLINEAR PROGRAMMING

A structural design decomposition method utilizing substructuring
[NASA-TM-107750] p 2376 N94-23368

PLANET: A hierarchical network simulator
[ISBN-9-09-005693-9] p 2313 N94-25083

NONLINEAR SYSTEMS

Decoupling problems around a trajectory: From linearity to nonlinearity
[MEMO-1115] p 2469 N94-22703

Balancing for unstable nonlinear systems
[MEMO-1118] p 2469 N94-22705

Nonlinear state space H(sub infinity) control theory
[MEMO-1119] p 2469 N94-22706

Nonlinear systems which have finite-dimensional H(sub infinity) suboptimal central controllers
[MEMO-1120] p 2469 N94-22707

On dynamic input-output linearization of discrete-time nonlinear systems
[MEMO-1123] p 2447 N94-22711

Feedback linearization of parametrized nonlinear time-varying systems
[MEMO-1126] p 2470 N94-22714

Probabilistic analysis of mechanical systems
[DE93-041145] p 2371 N94-22918

Chaos and simple determinism in reversed field pinch plasmas: Nonlinear analysis of numerical simulation and experimental data
[DE94-001575] p 2550 N94-23211

Viewing hybrid systems as products of control systems and automata
[NASA-CR-194792] p 2472 N94-23300

On the estimation of the correlation dimension and its application to radar reflector discrimination
[NASA-CR-4564] p 2309 N94-23304

Nonlinear analysis using a modal based reduction technique p 2161 N94-24288

Neural network-based control using Lyapunov functions p 2477 N94-24433

Discrete applied mathematics
[AD-A273552] p 2488 N94-24561

Robust stability of second-order systems
[NASA-CR-195175] p 2488 N94-24564

Hamiltonian approach to fairly low and long gravity waves
[PB94-111119] p 2404 N94-24598

Control of nonlinear systems represented in quasilinear form
[NASA-CR-194840] p 2475 N94-24760

Nonlinear dynamical control of lasers
[AD-A273359] p 2350 N94-24938

System for producing synchronized signals
[AD-D016003] p 2302 N94-25057

Modeling transonic aerodynamic response using nonlinear systems theory for use with modern control theory p 2164 N94-25112

Center for Analysis of Heterogeneous and Nonlinear Media
[AD-A273515] p 2230 N94-25158

Practical evaluation of robust control for a class of nonlinear mechanical dynamic systems
[ISBN-9-03-860092-5] p 2475 N94-25224

Approximation to nonlinear equations using nonlinear rational models
[RR-448] p 2492 N94-25306

The phase response of nonlinear systems
[RR-458] p 2476 N94-25308

On the inversion of the n-dimensional Laplace transform
[RR-461] p 2492 N94-25310

Unwrapping the phase response functions for nonlinear systems
[RR-465] p 2462 N94-25311

Validating identified nonlinear models with chaotic dynamics
[RR-469] p 2523 N94-25314

Frequency response functions for nonlinear rational models
[RR-471] p 2492 N94-25318

Relationship between the structure and performance of identified nonlinear polynomial models
[RR-474] p 2492 N94-25320

NONLINEARITY

Theoretical and simulated performance for a novel frequency estimation technique p 2285 N94-22808

Chaos in plasma simulation and experiment
[DE94-001574] p 2549 N94-22963

Computation of flows in a turn-around duct and a turbine cascade using advanced turbulence models
p 2216 N94-23062

Fully coupled nonlinear thermomechanical analysis including general contact in PALM2D
[DE94-001661] p 2568 N94-23216

Nonlinear ion-mixing-mode particle transport in the dissipative trapped electron regime
[DE94-000989] p 2533 N94-23435

Tracking sharp interface of two fluids by the CIP (Cubic-Interpolated Propagation) scheme
[DE93-508322] p 2319 N94-23460

Implementing abstract multigrid or multilevel methods
p 2483 N94-23682

Energy and maximum norm estimates for nonlinear conservation laws
[NASA-CR-195091] p 2569 N94-24109

Prediction of nonlinear optical properties of organic materials. General theoretical considerations
p 2224 N94-24343

Optimization of microscopic and macroscopic second order optical nonlinearities p 2226 N94-24354

Diagnosing process faults using neural network models
[DE94-002633] p 2473 N94-24518

Computer modeling of nonlinearities
p 2458 N94-24661

Nonlinear dynamics applied to atmospheric prediction
[AD-A273437] p 2404 N94-24674

Robust, nonlinear, high angle-of-attack control design for a supermaneuverable vehicle p 2164 N94-25108

Nonlinear aerodynamic modeling using multivariate orthogonal functions p 2164 N94-25110

Infinitely divisible processes and their nonlinear functionals; a study of their structural, statistical and sample path properties and their prediction problems
[AD-A273468] p 2496 N94-25147

NONNEWTONIAN FLUIDS

Multigrid methods for a semilinear PDE in the theory of pseudoplastic fluids p 2341 N94-23689

NONTHERMAL RADIATION

Voyager planetary radio astronomy studies
[NASA-CR-194776] p 2614 N94-24328

NORMAL DENSITY FUNCTIONS

Setting test limits under prescribed consumer loss
[MEMO-1107] p 2478 N94-22725

Subset selection for the best of two populations: Tables of the expected subset size
[PB93-237857] p 2494 N94-23546

A random distribution reacting mixing layer model
[NASA-CR-194445] p 2187 N94-23552

Solving the ranking and selection indifference-zone formulation for normal distributions using computer software
[AD-A273821] p 2496 N94-25518

NORMAL SHOCK WAVES

Stability of hypersonic flow of a detonable gas mixture in the stagnation region of a blunt body and a forward facing step p 2154 N94-24248

NORMALIZING (STATISTICS)

The detection performance of a long-term spectral integrator using normalized and quantized data
[DREP-TM-93-11] p 2455 N94-24130

NORMS

Identification for robust control using an H(sub infinity) norm
[EUT-92-E-261] p 2470 N94-22873

NORTH AMERICA

Implementation of a system to provide mobile satellite services in North America p 2281 N94-22784

NORTH ATLANTIC TREATY ORGANIZATION (NATO)

Activities report to NATO
[ETN-94-95047] p 2318 N94-23227

Cardiovascular and pulmonary disease in NATO aircrew: An overview p 2423 N94-23314

NORTH SEA

Nutrients and light as factors controlling phytoplankton biomass on the Dutch continental shelf (North Sea), 1988-1990
[PB94-111143] p 2418 N94-24601

NORTHERN HEMISPHERE

Northern hemisphere tropospheric mid-latitude circulation after violent volcanic eruptions
[MPIM-107] p 2403 N94-24491

Northern hemisphere dust storms on Mars
p 2619 N94-24885

An AVHRR cloud classification database typed by experts
[AD-A273560] p 2416 N94-25162

NORWAY

Fire safety engineering research in Norway
[PB93-201630] p 2268 N94-23429

NOSE FINS
Supersonic aerodynamic characteristics of a circular body Earth-to-Orbit vehicle [NASA-TM-4533] p 2170 N94-24716

NOTCH STRENGTH
Three-dimensional, inelastic response of single-edge notch bend specimens subjected to impact loading [AD-A273302] p 2378 N94-25143

NOTCH TESTS
Micromechanical characterization of ceramic-matrix composites using the instrumented microindentation technique p 2256 N94-24233

NOTCHES
Off-design performance of crenulated blades in a linear compressor cascade [AD-A273744] p 2340 N94-25534

NOWCASTING
An efficient data assimilation algorithm with a gaussian covariance structure [AD-A273152] p 2418 N94-24671

NOZZLE DESIGN
Dual-bell altitude compensating nozzles p 2215 N94-23057
Development of a code for wall contour design in the transonic region of axisymmetric and square nozzles [NASA-CR-194857] p 2167 N94-23625
Supersonic minimum length nozzle design for dense gases p 2171 N94-23656
Final postflight hardware evaluation report RSRM-28 (STS-53) [NASA-CR-193902] p 2200 N94-24112

NOZZLE EFFICIENCY
Postflight hardware evaluation RSRM-29 (STS-54). Appendix C: Nozzle PFORs [NASA-CR-193894] p 2219 N94-24064

NOZZLE FLOW
Molecular gas dynamics applied to low-thrust propulsion p 2214 N94-23053
Dual-bell altitude compensating nozzles p 2215 N94-23057
Two stage turbine for rockets p 2215 N94-23059
Theoretical studies of a molecular beam generator [NASA-CR-194779] p 2540 N94-23485
Effect of delta tabs on mixing and axis switching in jets from asymmetric nozzles [NASA-TM-106450] p 2167 N94-23592
Ignition and combustion characteristics of metallized propellants, phase 2 [NASA-CR-195107] p 2266 N94-24700

NOZZLE GEOMETRY
Dual-bell altitude compensating nozzles p 2215 N94-23057
Effect of delta tabs on mixing and axis switching in jets from asymmetric nozzles [NASA-TM-106450] p 2167 N94-23592

NOZZLE WALLS
Development of a code for wall contour design in the transonic region of axisymmetric and square nozzles [NASA-CR-194857] p 2167 N94-23625

NOZZLES
Postflight hardware evaluation RSRM-29 (STS-54). Case, seals, and joints PFORs, appendix B [NASA-CR-193899] p 2367 N94-25020

NUCLEAR CHEMISTRY
Fifty years of continuous improvement: What has DOE done for analytical chemistry? [DE94-002539] p 2234 N94-24548

NUCLEAR ELECTRIC PROPULSION
Advanced nuclear thermal propulsion concepts p 2217 N94-23068
Utilization of recently developed codes for high power Brayton and Rankine cycle power systems p 2222 N94-23641
Heat pipe cooled heat rejection subsystem modelling for nuclear electric propulsion [NASA-CR-191132] p 2219 N94-24061

NUCLEAR EXPLOSIONS
Parametric and nonparametric discriminants for regional earthquakes and explosions [AD-A273807] p 2406 N94-25538

NUCLEAR FUEL ELEMENTS
An F2D analysis of the Flow Instability Test (FIT) experiment [DE94-001420] p 2217 N94-23193

NUCLEAR FUELS
Pellet ablation in the large helical device [NIFS-260] p 2551 N94-24358

NUCLEAR INTERACTIONS
Momentum loss in proton-nucleus and nucleus-nucleus collisions [NASA-TP-3405] p 2540 N94-24305
Behavior of the intermittency exponents and a quark-gluon plasma formation in the heavy ion collisions [DE93-616869] p 2541 N94-25342

NUCLEAR MAGNETIC RESONANCE
Magnetic resonance studies of 3d transition metal impurities in compound semiconductors [PB93-232197] p 2243 N94-23714
Synthesis and in-vivo detection of boronated compounds for use in BNCT [DE94-001699] p 2233 N94-23780
Nuclear magnetic resonance imaging with short gradient pulses [AD-D016006] p 2537 N94-25047
The nanostructure of multilayered films: A NMR study [ETN-94-95347] p 2262 N94-25222
Microstructure of styrene methyl methacrylate copolymers grafted onto polybutadiene seeds [ETN-94-95360] p 2262 N94-25225
On the mechanism of action of 3',5'-cyclic adenosine monophosphate: A study of four- and five-coordinated phosphorus compounds, modelling the activated state of cAMP [ISBN-9-03-860222-7] p 2226 N94-25238

NUCLEAR MODELS
Momentum loss in proton-nucleus and nucleus-nucleus collisions [NASA-TP-3405] p 2540 N94-24305

NUCLEAR PHYSICS
Accelerator-based neutrino oscillation searches [DE94-000818] p 2626 N94-23515
Polarized structure functions of the nucleon in the resonance region [CEBAF-PR-94-001] p 2540 N94-24663

NUCLEAR POWER REACTORS
Power generation technology options for a Mars mission [NASA-TM-106451] p 2220 N94-24681

NUCLEAR PROPULSION
NASA Propulsion Engineering Research Center, volume 2 [NASA-CR-194719-VOL-2] p 2209 N94-23028
Advanced nuclear thermal propulsion concepts p 2217 N94-23068
Performance assessment of low pressure nuclear thermal propulsion p 2217 N94-23070
Nuclear propulsion control and health monitoring p 2217 N94-23071
Improved gas core propulsion model [DE94-000929] p 2220 N94-24511

NUCLEAR REACTIONS
Ferroelectric thin films 3 [AD-A273394] p 2565 N94-25027

NUCLEAR ROCKET ENGINES
Nuclear propulsion control and health monitoring p 2217 N94-23071

NUCLEAR WEAPONS
A qualified radiation hardened nonvolatile memory for space and tactical weapons applications [DE94-001211] p 2559 N94-23186
Nondestructive evaluations [DE94-003020] p 2373 N94-24613

NUCLEATION
Microgravity sciences application visiting scientist program [NASA-CR-194804] p 2267 N94-23287
Characterization of 3-D particle distributions and effects on recrystallization studied by computer simulation [PB93-201408] p 2562 N94-23535
Temperature dependence of protein solubility-determination, application to crystallization, and growth kinetics studies p 2224 N94-24344
Polymer morphologh p 2226 N94-24353
The chemistry of particulate formation in fluorocarbon plasmas [DE94-001500] p 2552 N94-24546
Containerless measurements on liquids at high temperatures p 2238 N94-25125
Particle nucleation and growth in butadiene emulsion polymerization [ETN-94-95300] p 2262 N94-25236
The in situ observation of epitaxial diamond thin film nucleation and growth using emission electron microscopy [AD-A273698] p 2263 N94-25489

NUCLEI
A quark structure of hadrons and nuclei [DE93-616872] p 2539 N94-25474
On the hadron formation time in pion-nucleus interaction [DE93-616879] p 2539 N94-25476

NUCLEI (NUCLEAR PHYSICS)
Momentum loss in proton-nucleus and nucleus-nucleus collisions [NASA-TP-3405] p 2540 N94-24305

NUCLEIC ACIDS
The torsion space nucleic acids molecular mechanics program DUPLEX: Surveying conformation space by potential energy minimization [DE94-002441] p 2563 N94-24567

NUCLEON-NUCLEON INTERACTIONS
Momentum and coordinate space three-nucleon potentials [DE93-040868] p 2531 N94-22951
On the transverse size of a fast moving nucleon [DE93-616891] p 2539 N94-25481

NUCLEONS
Pions and neutrinos as probes of the nucleon and nuclear few-body system [DE93-040127] p 2531 N94-22928
Momentum and coordinate space three-nucleon potentials [DE93-040868] p 2531 N94-22951
Polarized structure functions of the nucleon in the resonance region [CEBAF-PR-94-001] p 2540 N94-24663
On the transverse size of a fast moving nucleon [DE93-616891] p 2539 N94-25481

NUMBER THEORY
A rational elliptic surface related to the question of expressing squares as sum of consecutive squares [W-9305] p 2479 N94-23139

NUMERICAL ANALYSIS
A numerical analysis of crack propagation in microcracking ceramic and ceramic composites [DE94-001192] p 2253 N94-23183
Chaos and simple determinism in reversed field pinch plasmas: Nonlinear analysis of numerical simulation and experimental data [DE94-001575] p 2550 N94-23211
Study of transient behavior of finned coil heat exchangers p 2321 N94-23642
Solution of mixed convection heat transfer from isothermal in-line fins p 2321 N94-23644
Unsteady three-dimensional thermal field prediction in turbine blades using nonlinear BEM p 2325 N94-23665
Temporal model of an optically pumped co-doped solid state laser [NASA-TM-109680] p 2350 N94-24851
Research in progress and other activities of the Institute for Computer Applications in Science and Engineering [NASA-CR-191576] p 2444 N94-25090
Space Station flexible dynamics under plume impingement p 2208 N94-25383
Numerical analysis of the motion of a rigid body with an attached spring-mass-damper [AD-A273825] p 2379 N94-25520

NUMERICAL CONTROL
K- and Ka-band mobile-vehicular satellite-tracking reflector antenna system for the NASA ACTS mobile terminal p 2289 N94-22831
Link monitor and control operator assistant: A prototype demonstrating semiautomated monitor and control p 2292 N94-23267
A reliable algorithm for optimal control synthesis [NASA-CR-194809] p 2472 N94-23332
Imaging System (INEL) T805 prototype [DE94-002807] p 2382 N94-23492
Calibration block for digital beam forming antenna [PB93-204550] p 2294 N94-23773
Characteristics of products generated by selective sintering and stereolithography rapid prototyping processes p 2264 N94-24412
Octave: A MARSYAS post-processor for computer-aideed control system design p 2465 N94-24422
The experimental physics and industrial control system architecture: Past, present, and future [DE94-002639] p 2457 N94-24626
Bioregenerative life support systems for microgravity [NASA-CR-195516] p 2422 N94-24810
NASA/Army rotorcraft transmission research, a review of recent significant accomplishments [NASA-TM-106508] p 2367 N94-25181
Research experience for undergraduates in robotics and materials [AD-A273659] p 2368 N94-25436

NUMERICAL INTEGRATION
On the numeric integration of dynamic attitude equations [NASA-CR-194788] p 2448 N94-23073
Comparison of time integration methods for the evolution of galaxies [PB94-111671] p 2602 N94-24522

NUMERICAL STABILITY
Stability behavior of systems obtained by index-reduction [PB93-237709] p 2481 N94-23439
Infinite divisible and stable distributions modulo 1 [PB94-110640] p 2495 N94-23815
Dynamic localization and second-order subgrid-scale models in large eddy simulations of channel flow p 2329 N94-24149

Octave: A MARSYAS post-processor for computer-aideed control system design
p 2465 N94-24422
Exploiting structure: Introduction and motivation
[NASA-CR-195136] p 2490 N94-24847

NUMERICAL WEATHER FORECASTING
Monte Carlo climate change forecasts with a global coupled ocean-atmosphere model
[MPIM-97] p 2407 N94-23156
Hurricane risk assessment: Rollback or ride out
p 2416 N94-23248
Visualization of results from meteorological simulations on CRAY
[PB93-201358] p 2451 N94-23443
Modelling TOVS radiances of synoptic systems
[NASA-CR-194847] p 2408 N94-23620
Implementation of a state of the art automated system for the production of cloud/water vapor motion winds from geostationary satellites
[NASA-CR-195087] p 2410 N94-24125
GEWEX Cloud Systems Study (GCSS)
p 2411 N94-24377
Validation of mesoscale models p 2413 N94-24391
Techniques and resources for storm-scale numerical weather prediction p 2414 N94-24392
Session on cumulus parameterization
p 2414 N94-24394
Session on techniques and resources for storm-scale numerical weather prediction p 2415 N94-24400

NUTATION
Ulysses log 1992 p 2502 N94-23863
Numerical simulation of Ulysses nutation
p 2207 N94-24017

NUTATION DAMPERS
Reactive thrust cruise for a geosynchronous satellite with minimum fuel consumption p 2158 N94-24271
Numerical analysis of the motion of a rigid body with an attached spring-mass-damper
[AD-A273825] p 2379 N94-25520

NUTRIENTS
Microbial biofilm formation and its consequences for the CELSS program
[NASA-CR-195146] p 2438 N94-24706

O

O RING SEALS
Viscoelastic analysis of seals for extended service life
p 2371 N94-24408
Postflight hardware evaluation RSRM-29 (STS-54). Case, seals, and joints PFORs, appendix B
[NASA-CR-193899] p 2367 N94-25020

OBJECT-ORIENTED PROGRAMMING
A general model for dynamic and complex information management: The ELEN prototype object manager for software engineering
[ETN-94-95163] p 2588 N94-22880
Asynchronous rendezvous in distributed logic programming
[PB93-220614] p 2448 N94-23096
APLAC: An object-oriented analog circuit simulator and design tool. 6.1 system simulations manual
[PB93-224871] p 2450 N94-23226
An object-oriented approach for parallel self adaptive mesh refinement on block structured grids
p 2469 N94-23697
Object-oriented technologies in a multi-mission data system p 2506 N94-23885
Using Mach threads to control DSN operational sequences p 2477 N94-23916
SIMSAT: An object oriented architecture for real-time satellite simulation p 2197 N94-23940
Telemetry ground system development via the component approach p 2203 N94-23949
A simulation and evaluation of NATO Standardization Agreement (STANAG) 4214
[AD-A273195] p 2297 N94-24554
Declarative Object Manipulation Environment (DOME): Alpha version
[AD-A273233] p 2460 N94-24935

OBSTACLE AVOIDANCE
Object recognition through image understanding for an autonomous mobile robot
[AD-A273206] p 2475 N94-24862

OCEAN BOTTOM
Reactive trace metals as indicators of subduction and ventilation processes in the ocean
[AD-A273585] p 2419 N94-25164
Seafloor characterization/Galapagos propagating rift
[AD-A273586] p 2419 N94-25165
Analysis of modal evolution caused by a weakly range-dependent seabed in shallow water and its application to inversion for geoacoustic properties
[AD-A273656] p 2419 N94-25435

OCEAN CURRENTS
HERACLITUS, phase 1. Harbour Entrance of Rotterdam Radar based Current Related Information for Traffic Guidance of Ships: Feasibility of deriving current profile data from sea surface observations in the Rotterdam (Netherlands) port entrance
[BCRS-93-04] p 2417 N94-24107
An efficient data assimilation algorithm with a gaussian covariance structure
[AD-A273152] p 2418 N94-24671
Vertical motion in the SYNOP central array
[AD-A273593] p 2418 N94-24795

OCEAN DATA ACQUISITIONS SYSTEMS
SeaWiFS technical report series. Volume 9: The simulated SeaWiFS data set, version 1
[NASA-TM-104566-VOL-9] p 2417 N94-23291

OCEAN DYNAMICS
GEWEX Continental-scale International Project (GCIP)
p 2411 N94-24376
Statistical methods in physical oceanography
[AD-A273612] p 2419 N94-24948

OCEAN MODELS
VIERS-1, phase 3
[BCRS-92-24] p 2381 N94-23145
Monte Carlo climate change forecasts with a global coupled ocean-atmosphere model
[MPIM-97] p 2407 N94-23156
Climate variability in a coupled GCM. Part 2: The Indian Ocean and monsoon
[MPIM-104] p 2401 N94-23159
Modal structure of variations in the tropical climate system. Part 2: Origins of the low-frequency mode
[MPIM-96] p 2407 N94-23199
Global ocean modeling on the Connection Machine
[DE94-000888] p 2417 N94-23517
HERACLITUS, phase 1. Harbour Entrance of Rotterdam Radar based Current Related Information for Traffic Guidance of Ships: Feasibility of deriving current profile data from sea surface observations in the Rotterdam (Netherlands) port entrance
[BCRS-93-04] p 2417 N94-24107
Techniques and resources for storm-scale numerical weather prediction p 2414 N94-24392
An efficient data assimilation algorithm with a gaussian covariance structure
[AD-A273152] p 2418 N94-24671
Global acoustic mapping of ocean temperatures (GAMOT)
[AD-A273387] p 2418 N94-24719
Vertical motion in the SYNOP central array
[AD-A273593] p 2418 N94-24795
Statistical methods in physical oceanography
[AD-A273612] p 2419 N94-24948
Seafloor characterization/Galapagos propagating rift
[AD-A273586] p 2419 N94-25165

OCEAN SURFACE
Modes of ocean variability in the tropical Pacific as derived from Geosat altimetry
[MPIM-103] p 2382 N94-23158
Global ocean modeling on the Connection Machine
[DE94-000888] p 2417 N94-23517
The effect of sub-surface volume scattering on the accuracy of ice-sheet altimeter retracking algorithms
[NASA-CR-194825] p 2386 N94-24060
Factors affecting the identification of phytoplankton groups by means of remote sensing
[NASA-TM-108799] p 2387 N94-24403
Free-surface/vorticity interaction
[AD-A273263] p 2335 N94-24686
Use of microwave polarimetry to enhance SAR images of the ocean surface
[AD-A273568] p 2419 N94-24944

OCEAN TEMPERATURE
Global acoustic mapping of ocean temperatures (GAMOT)
[AD-A273387] p 2418 N94-24719

OCEANOGRAPHY
Global acoustic mapping of ocean temperatures (GAMOT)
[AD-A273387] p 2418 N94-24719
Vertical motion in the SYNOP central array
[AD-A273593] p 2418 N94-24795
Statistical methods in physical oceanography
[AD-A273612] p 2419 N94-24948
Active control of oscillatory lift forces on a circular cylinder
[AD-A273243] p 2338 N94-25140

OCTAVES
Artificial neural networks: Application to the optical recognition of music partitions
[ETN-94-95166] p 2470 N94-22884

OFFICE AUTOMATION
Concepts and techniques for an active database approach to office procedure support
[PB94-110749] p 2590 N94-23816

OFFSHORE PLATFORMS
Fire safety engineering research in Norway
[PB93-201630] p 2268 N94-23429

OIL EXPLORATION
Near-surface seismic imaging
[PB94-119096] p 2404 N94-24647

OIL RECOVERY
Measurement of interfacial tension by use of pendant drop video techniques
[DE93-000168] p 2345 N94-24831

OILS
New methane chemistry synthesis of materials for reversible uptake and useful functionalization of methane
[PB94-112786] p 2233 N94-23801
Skin friction measurement in complex flows using thin oil film techniques
[NASA-CR-194872] p 2327 N94-24098

OLIGOMERS
Electrochemical and electronic properties of neural and oxidized soluble orthogonally-fused thiophene oligomers
[AD-A273283] p 2260 N94-24815
Metal-catalyzed alkynylation of (Bromophenyl)Oligophenylenes: A rapid route to thermoset precursors of high density monolithic glass-like carbon
[AD-A273219] p 2260 N94-24863
Synthesis of molecular wires by a novel divergent/convergent approach
[AD-A273332] p 2537 N94-25087

OLIVINE
A dynamic melting model for the origin of Apollo 15 olivine-normative and quartz-normative mare basalts
p 2615 N94-24371

OMNIDIRECTIONAL ANTENNAS
L-band mobile terminal antennas for helicopters
p 2289 N94-22835

ON-LINE SYSTEMS
Translative interface for data sharing and integrating: A paradigm for distributed data systems
[DE93-018790] p 2588 N94-22863
A novel process monitoring and control system based on a neural manufacturing concept
[DE94-001516] p 2471 N94-23011
SPDB (science processing database): Quick reference guide p 2383 N94-23597
Particle size measurement for the control of industrial crystallizers
[PB94-119104] p 2562 N94-23766
Columbus system support for telescience operations
p 2505 N94-23877
NASDA's Advanced On-Line System (ADOLIS)
p 2509 N94-23903
Intelligent tutoring and aiding in satellite ground control p 2443 N94-23929
On-line evaluation of multiloop digital controller performance p 2163 N94-25105
On-line control of dynamic systems using feedforward neural networks
[RR-457] p 2476 N94-25307
Proceedings of the 12th International Congress: Corrosion Control for Low-Cost Reliability. Volume 6: Electric Power Industry
[AD-A273668] p 2250 N94-25408
CADBIT 2: Computer-aided design for built-in test, volume 1
[AD-A273702] p 2463 N94-25455
CADBIT 2: Computer-aided design for built-in test, volume 2
[AD-A273703] p 2463 N94-25456
Factors influencing perceived usability and utility of LIBERTAS at Cranfield: Implications for system modification and user education
[CRANFIELD-AERO-9212] p 2594 N94-25485

ONBOARD DATA PROCESSING
SAW based systems for mobile communications satellites p 2275 N94-22746
Applicability of different onboard routing and processing techniques to mobile satellite systems
p 2278 N94-22767
A European mobile satellite system concept exploiting CDMA and OBP p 2279 N94-22768
Cockpit weather graphics using mobile satellite communications p 2280 N94-22775
Towards real-time stereovision systems for planetary missions p 2370 N94-23422
Fault tolerant onboard packet switch architecture for communication satellites: Shared memory per beam approach
[NASA-TM-106397] p 2201 N94-23567
Advanced technology for a satellite multichannel demultiplexer/demodulator
[NASA-CR-194435] p 2202 N94-23631
UAV current technology and future trends
p 2154 N94-24245

Decentralized autonomous attitude determination using an inertially stabilized payload p 2157 N94-24264
Modulation and synchronization technique for MF-TDMA system
[NASA-CR-194448] p 2304 N94-25266

OPERATING COSTS
Future trends in NASA space operations
p 2498 N94-23836
Design of an airborne launch vehicle for an air launched space booster
[NASA-CR-195534] p 2198 N94-24860
The Bunny: A simulated commercial air transportation study
[NASA-CR-195537] p 2183 N94-25001

OPERATING SYSTEMS (COMPUTERS)
ACOS: The performance based approach to build a parallel complex object server
[PB93-223816] p 2465 N94-22986
Distributed Operating Systems and Mach. Proceedings of the Spring 1992 Graduate Seminar on Distributed Systems
[PB93-224905] p 2449 N94-23103
Performance measurements of the multimedia testbed on Mach 3.0: Experience writing real-time device drivers, servers, and applications
[AD-A273600] p 2460 N94-24932
Analyzing the properties of user interface software
[AD-A273601] p 2460 N94-24933
The design of the EMPS multiprocessor executive for distributed computing
[ETN-94-95336] p 2468 N94-25062

OPERATIONAL AMPLIFIERS
Fifty years of continuous improvement: What has DOE done for analytical chemistry?
[DE94-002539] p 2234 N94-24548
High speed electronic analog computers using low-gain amplifiers
[AD-D015974] p 2446 N94-25034

OPERATIONAL HAZARDS
Safety guidelines for the operation of the DREO 10 m EMP simulator DREMPS
[DREO-TN-93-5] p 2193 N94-24117

OPERATIONAL PROBLEMS
Operability engineering in the Deep Space Network
p 2514 N94-23930
An examination of the operational error database for air route traffic control centers
[DOT/FAA/AM-93/22] p 2175 N94-24472

OPERATIONS RESEARCH
Tool sharing: An application of max-algebra, part 2
[MEMO-1122] p 2478 N94-22710
A multilevel cost-space approach to solving the balanced long transportation problem p 2483 N94-23678
Design and specification of a generic task model for solving boolean constraint satisfaction problems
[PB94-116841] p 2486 N94-23762
Verification and validation of models
[PB94-110566] p 2456 N94-24507
Tool sharing, part 3
[PB94-111697] p 2467 N94-24524
Throughput time control and due date reliability in tool and die shops
[ISBN-9-03-860182-4] p 2587 N94-25283

OPERATOR PERFORMANCE
Pushing technology to satisfy world applications
[DE94-001365] p 2353 N94-23191
Operability engineering in the Deep Space Network
p 2514 N94-23930
Investigation of time and intensity effects in operator workload and performance
[CTN-94-60927] p 2433 N94-24171

OPERATORS (MATHEMATICS)
Note on the use of spherical vectorfields in Clifford analysis
[PB93-237667] p 2480 N94-23437
A comparison of locally adaptive multigrid methods: LDC, FAC and FIC p 2485 N94-23692
Tensoral for post-processing users and simulation authors p 2333 N94-24169
Some maximality results for effect-valued measures
[PB94-111176] p 2569 N94-24575
Signatures of selfadjoint pencils
[PB94-111127] p 2457 N94-24599
Downward extrapolation of multi-component seismic data
[ISBN-9-09-005213-5] p 2405 N94-25229
Introduction to a behavioral approach for continuous time systems
[ETN-94-95301] p 2492 N94-25277

OPERATORS (PERSONNEL)
Operational training for the mission operations at the Brazilian National Institute for Space Research (INPE)
p 2429 N94-23933

OPHTHALMOLOGY
Vision impairment and corrective considerations of civil airmen
[DOT/FAA/AM-93/21] p 2426 N94-23623

OPTICAL COMMUNICATION
Laser linewidth measurement in the presence of RIN and using the recirculating self heterodyne method
[EUT-92-E-262] p 2347 N94-22874
InGaAsP/InP based 1.3/1.55 micron vertical cavity surface emitting lasers for wavelength division multiplexed high speed distributed computing, phase 1
[AD-A271081] p 2348 N94-23123
Wide band fiber-optic communications
p 2304 N94-23231
Optical subnet concepts for the deep space network
p 2292 N94-23269
A lower bound for routing on a completely connected optical communication parallel computer
[DE93-040752] p 2466 N94-23491
Analysis for the computational modeling of finite cladding and lossy coating effects in fibers
[PB94-111085] p 2544 N94-23732
Measuring electrically charged particle fluxes in space using a fiber optic loop sensor
[NASA-CR-191328] p 2544 N94-23829
Multi-access laser communications terminal
[NASA-CR-191251] p 2295 N94-23830
Preloaded launch locking devices for SILEX
p 2358 N94-24008
Integration and test of high-speed transmitter electronics for free-space laser communications
[NASA-TM-106295] p 2295 N94-24101
Optimization of microscopic and macroscopic second order optical nonlinearities p 2226 N94-24354
Japanese aerospace science and technology 1992. A bibliography with indexes
[NASA-SP-7104] p 2631 N94-24585
Crosstalk analysis of synchronous and asynchronous optical chip interconnects with direct detection
[AD-A273261] p 2311 N94-24685

OPTICAL COMPUTERS
Optical wavelet transform processor
[AD-A273625] p 2546 N94-24731

OPTICAL CORRECTION PROCEDURE
A study on electrostatic quadrupole lenses and their application technologies
[REPT-948] p 2546 N94-24982

OPTICAL COUPLING
An optical ASK and FSK phase diversity transmission system
[EUT-92-E-268] p 2542 N94-23171

OPTICAL DATA PROCESSING
Encoders for space applications p 2363 N94-24046

OPTICAL DISKS
Earth observation archive activities at DRA Farnborough p 2519 N94-23958

OPTICAL EMISSION SPECTROSCOPY
Fifty years of continuous improvement: What has DOE done for analytical chemistry?
[DE94-002539] p 2234 N94-24548
Total light loss optic spectroscopy: Progress towards a fiber optic Raman organic vapor sensor
[DE94-002545] p 2234 N94-24549

OPTICAL EQUIPMENT
Measuring electrically charged particle fluxes in space using a fiber optic loop sensor
[NASA-CR-191328] p 2544 N94-23829
Mesospheric and lower thermospheric winds, temperatures densities, and volume emission rates
[NASA-CR-195147] p 2403 N94-24486
Germanium x ray phase plates for the production of circularly polarized x rays
[DE94-002908] p 2545 N94-24550
Heterodyne array for measurement of target velocity
[AD-D016025] p 2545 N94-24722
A study on electrostatic quadrupole lenses and their application technologies
[REPT-948] p 2546 N94-24982
Solutions of the 2-D Helmoholtz equation for optical waveguides
[DE93-616840] p 2547 N94-25209

OPTICAL FIBERS
SFOLDA: A semiconductor LDA for measurements in complex flows p 2316 N94-22856
Fiber optic detection of laser generated ultrasound for materials characterization
[ISBN-0-315-83541-9] p 2541 N94-22891
NASA/ASEE Summer Faculty Fellowship Program
[NASA-CR-194678] p 2571 N94-23230
Output optics for laser velocimeters
[NASA-CASE-ARC-11889-1-SB] p 2543 N94-23309
Fiber optic temperature sensor using a Y2O2S:Eu thermographic phosphor
[DE94-000331] p 2543 N94-23461
Analysis for the computational modeling of finite cladding and lossy coating effects in fibers
[PB94-111085] p 2544 N94-23732
Measuring electrically charged particle fluxes in space using a fiber optic loop sensor
[NASA-CR-191328] p 2544 N94-23829
Fiber optic detection of ultrasound and its application to cure monitoring
[ISBN-0-315-83424-2] p 2544 N94-24466
Fiber optical angular sensor: Literature study and experimental results
[PB93-204345] p 2545 N94-24529
Total light loss optic spectroscopy: Progress towards a fiber optic Raman organic vapor sensor
[DE94-002545] p 2234 N94-24549
White-light, pressure, and temperature interferopolarimetric sensor featuring optical fibers
[PB93-199792] p 2545 N94-24631
Layered parallel interface for an active antenna array
[AD-D016002] p 2301 N94-25045

OPTICAL FILTERS
Design refinement of multilayer optical thin film devices with two optimization techniques
[DE93-634228] p 2542 N94-22979
Germanium x ray phase plates for the production of circularly polarized x rays
[DE94-002908] p 2545 N94-24550
Investigation of Raman beam cleanup and phase conjugation
[AD-A273157] p 2545 N94-24672

OPTICAL FLOW (IMAGE ANALYSIS)
Extracting heading and temporal range from optic flow: Human performance issues p 2442 N94-25510
Optical information in landing scenes
p 2442 N94-25511

OPTICAL HETERODYNING
Laser linewidth measurement in the presence of RIN and using the recirculating self heterodyne method
[EUT-92-E-262] p 2347 N94-22874

OPTICAL MATERIALS
A fully automated stage for optical waveguide measurements
[AD-A273042] p 2542 N94-22915
Crystal growth of organics for nonlinear optical applications p 2225 N94-24348
Nonlinear optical thin films p 2225 N94-24349
Optimization of microscopic and macroscopic second order optical nonlinearities p 2226 N94-24354
Dipolar relaxation in a second-order nonlinear optical interpenetrating polymer network
[AD-A273626] p 2258 N94-24732
Ultrastructure processing of macromolecular materials
[AD-A273413] p 2258 N94-24782

OPTICAL MEASUREMENT
A fully automated stage for optical waveguide measurements
[AD-A273042] p 2542 N94-22915
Acoustic and optical investigations of superfluid He-3
[PB93-224889] p 2523 N94-23101
Capillary electrokinetic separations with optical detection
[DE94-001639] p 2233 N94-23716
Validation of a nonintrusive optical technique for the measurement of liquid mass distribution in a two-phase spray p 2548 N94-24420
Mesospheric and lower thermospheric winds, temperatures densities, and volume emission rates
[NASA-CR-195147] p 2403 N94-24486
Method and apparatus for the non-invasive measurement of pressure inside pipes using a fiber optic interferometer sensor
[AD-D016013] p 2344 N94-24734
A comparison of free-space and fiber mixer performances
[AD-A273558] p 2547 N94-25161
Non-invasive optical detection of glucose in cell culture nutrient medium p 2422 N94-25357

OPTICAL MEASURING INSTRUMENTS
Design of a surface deformation measuring instrument for the Surface Tension Driven Convection Experiment (STDCE-2)
[NASA-CR-194758] p 2343 N94-23285
Fiber optical angular sensor: Literature study and experimental results
[PB93-204345] p 2545 N94-24529
LOLA: Lunar Optical Long-baseline Array. 1992-1993 space design
[NASA-CR-195533] p 2298 N94-24582
Method and apparatus for the non-invasive measurement of pressure inside pipes using a fiber optic interferometer sensor
[AD-D016013] p 2344 N94-24734
System for cancelling phase noise in an interferometric fiber optic sensor arrangement
[AD-D015994] p 2345 N94-25053

Non-invasive optical detection of glucose in cell culture nutrient medium p 2422 N94-25357

OPTICAL MEMORY (DATA STORAGE)
A novel process monitoring and control system based on a neural manufacturing concept [DE94-001516] p 2471 N94-23011
Photo-induced and electrooptic properties of (Pb,La)(Zr,Ti)O3 films for optical memories [DE93-019820] p 2542 N94-23202
Earth observation archive activities at DRA Farnborough p 2519 N94-23958

OPTICAL POLARIZATION
Optical spin polarization and state-sensitive detection of a cesium atomic beam [ATR-92(8436)-1] p 2534 N94-24077
The effects of optical feedback on polarization of vertical cavity surface emitting lasers [AD-A273728] p 2351 N94-25445

OPTICAL PROPERTIES
A new automatic design method to develop multilayer thin film devices for high power laser applications [DE93-632490] p 2347 N94-22967
Interferometry in rarefied gas flows [ISL-CO-207/92] p 2318 N94-23160
Transparent conducting thin films for spacecraft applications [NASA-TM-106466] p 2218 N94-23370
Spectroscopic IR ellipsometry of 100 and 001 oriented YBa2Cu3O(7-delta) films [PB93-201481] p 2561 N94-23445
The possible effects of the natural and induced space environment on the optical and thermal properties of EOS surfaces p 2207 N94-23596
Method of forming silicon structures with selectable optical characteristics [NASA-CASE-NPO-18625-1-CU] p 2563 N94-23972
Night vision devices and characteristics p 2432 N94-23982
Cockpit/NVG visual integration issues p 2432 N94-23983
Prediction of nonlinear optical properties of organic materials. General theoretical considerations p 2224 N94-24343
Center for advanced electrical and structural polymers [AD-A273415] p 2259 N94-24783
Retrieval of temperature profiles from Martian infrared spectra p 2620 N94-24893
A study on electrostatic quadrupole lenses and their application technologies [REPT-948] p 2546 N94-24982
Liquidus temperature and optical properties measurement by containerless techniques p 2247 N94-25126
Optical properties and emissivities of liquid metals and alloys p 2248 N94-25129
Preparation and properties of translucent gamma-aluminium oxynitride [ETN-94-95305] p 2263 N94-25281
Results from the VISA project [AD-A273752] p 2406 N94-25540

OPTICAL PUMPING
Optical spin polarization and state-sensitive detection of a cesium atomic beam [ATR-92(8436)-1] p 2534 N94-24077
Experimental and theoretical features of strong suppression and shifting phenomena in odd-photon resonant excitations and stimulated emissions [DE94-000341] p 2535 N94-24510
Computer modeling of nonlinearities p 2458 N94-24661
Temporal model of an optically pumped co-doped solid state laser [NASA-TM-109680] p 2350 N94-24851

OPTICAL PYROMETERS
Fiber optic temperature sensor using a Y2O2S:Eu thermographic phosphor [DE94-000331] p 2543 N94-23461

OPTICAL RADAR
Micro pulse laser radar [NASA-CASE-GSC-13493-1] p 2294 N94-23827
Tropospheric Ozone Lidar Intercomparison Experiment, TROLIX 1991 [MPIM-102] p 2402 N94-24108
Nonlinear dynamical control of lasers [AD-A273359] p 2350 N94-24938
A comparison of free-space and fiber mixer performances [AD-A273558] p 2547 N94-25161
Improvement of system properties of a pulsed laser Doppler anemometer with respect to an optical amplifier [DLR-FB-93-19] p 2547 N94-25305
Results from the VISA project [AD-A273752] p 2406 N94-25540

OPTICAL RESONANCE
The resonance lines of MG2 as diagnostics of the upper solar chromosphere [NASA-CR-195084] p 2627 N94-24300

OPTICAL SCANNERS
Microstructural analysis of the 2195 aluminum-lithium alloy welds p 2251 N94-24448

OPTICAL SWITCHING
The effects of optical feedback on polarization of vertical cavity surface emitting lasers [AD-A273728] p 2351 N94-25445

OPTICAL THICKNESS
Cloud-free aerosol optical depth determination over oceans from satellite radiometry [DE94-001897] p 2386 N94-23779
Participation in TOMS missions [NASA-CR-195110] p 2398 N94-24078
Mars dust-driven tides and their impact on the thermosphere p 2617 N94-24876

OPTICAL WAVEGUIDES
A fully automated stage for optical waveguide measurements [AD-A273042] p 2542 N94-22915
Conformal method of fabricating and optical waveguide on a semiconductor substrate [AD-D015988] p 2546 N94-25043
Solutions of the 2-D Helmoholtz equation for optical waveguides [DE93-616840] p 2547 N94-25209

OPTIMAL CONTROL
A mixed H2/H(infinity) function for a discrete time system [MEMO-COSOR-92-36] p 2480 N94-23144
A reliable algorithm for optimal control synthesis [NASA-CR-194809] p 2472 N94-23332
Coordinate-free interpretations of the optimal costs for Lq problems subject to implicit systems [PB94-118700] p 2473 N94-23760
Identification of integrated airframe: Propulsion effects on an F-15 aircraft for application to drag minimization [NASA-TM-4532] p 2188 N94-24106
Optimal feedback control of turbulent channel flow p 2327 N94-24139
Approximate optimal guidance for the advanced launch system [NASA-CR-4568] p 2198 N94-24752
Control of nonlinear systems represented in quasilinear form [NASA-CR-194840] p 2475 N94-24760
Optimal RTLS abort trajectories for an HL-20 personnel launch vehicle p 2165 N94-25114
Genetic algorithms in control systems engineering [RR-470] p 2463 N94-25315
Flight controller design using mixed H2/H infinity optimization with a singular H infinity constraint [AD-A273831] p 2191 N94-25525

OPTIMIZATION
The Westinghouse Series 1000 Mobile Phone: Technology and applications p 2284 N94-22800
A mixed H2/H(infinity) function for a discrete time system [MEMO-COSOR-92-36] p 2480 N94-23144
A structural design decomposition method utilizing substructuring [NASA-TM-107750] p 2376 N94-23368
Object oriented simulation implementation in support of robust system design [DE93-011687] p 2452 N94-23488
An engineering code to analyze hypersonic thermal management systems p 2320 N94-23636
Low noise electric motor p 2315 N94-23989
A constrained optimization technique for arbitrary antenna arrays and various performance indices [ISBN-0-315-59455-1] p 2297 N94-24179
Application of concurrent engineering principles to aircraft structural design p 2178 N94-24321
Current and future design methods for large transport aircraft p 2179 N94-24324
Trends of design methodology of airframe p 2179 N94-24327
Next generation initiation techniques p 2412 N94-24383
Discrete applied mathematics [AD-A273552] p 2488 N94-24561
A programming environment for distributed complex computing. An overview of the Framework for Interdisciplinary Design Optimization (FIDO) project. NASA Langley TOPS exhibit H120b [NASA-TM-109058] p 2457 N94-24603
Tokamak Physics Experiment (TPX) cost and performance trade studies using supercode [DE94-002720] p 2553 N94-24628
The Third Twente Workshop on Graphs and Combinatorial Optimization: Abstracts and late extended abstracts [PB94-110954] p 2489 N94-24652
Runtime support and compilation methods for user-specified data distributions [NASA-CR-191587] p 2458 N94-24679
Sensitivity analysis of list scheduling heuristics [PB93-237766] p 2468 N94-24764
Merits and limitations of optimality criteria method for structural optimization [NASA-TP-3373] p 2378 N94-24845
RIACS/USRA [NASA-CR-195117] p 2631 N94-25003
Computing techniques in mission planning p 2522 N94-25012
On the characterization and optimization of high-speed silicon bipolar transistors [ETN-94-95367] p 2313 N94-25253
MIMO system identification for H(infinity) robust control: A frequency domain approach with minimum error bounds [ETN-94-95354] p 2476 N94-25262
New algorithm for minimizing (chi)(sup 2) functionals with constraints [DE93-616800] p 2463 N94-25432

OPTOELECTRONIC DEVICES
Visual Problems in Night Operations [AGARD-LS-187] p 2431 N94-23976
Ferroelectric thin films 3 [AD-A273394] p 2565 N94-25027
Bridge type optoelectronic sample and hold circuit [AD-D015986] p 2312 N94-25042
Radar E-O image fusion p 2306 N94-25503

OPTOMETRY
Image remapping strategies applied as protheses for the visually impaired p 2444 N94-25363

ORBIT CALCULATION
A review of GPS-based tracking techniques for TDRS orbit determination p 2196 N94-23257
New approaches for tracking earth orbiters using modified GPS ground receivers p 2196 N94-23258
Improved thermal force modeling for GPS satellites p 2207 N94-23259
Real-time on-board orbit determination with DORIS p 2196 N94-23919
TOPEX/Poseidon precision orbit determination production and expert system p 2196 N94-23920
Kalman filtering applied to real-time monitoring of apogee maneuvers p 2196 N94-23923
Navigation of space VLBI missions: Radioastron and VSOP p 2513 N94-23926
The geo-control system for station keeping and colocation of geostationary satellites p 2464 N94-23927
Comparison of time integration methods for the evolution of galaxies [PB94-111671] p 2602 N94-24522

ORBIT INSERTION
MERCATOR: Methods and Realization for Control of the Attitude and the Orbit of spacecraft p 2202 N94-23925
HISPASAT launch and early operations phases: Computation and monitoring of geostationary satellite positioning p 2514 N94-23928

ORBIT PERTURBATION
Improved thermal force modeling for GPS satellites p 2207 N94-23259

ORBIT TRANSFER VEHICLES
Power beaming to space using a nuclear reactor-pumped laser [DE94-001208] p 2348 N94-23185
Lunar transportation system [NASA-CR-195540] p 2365 N94-24805
Space transfer vehicle concepts and requirements. Volume 4: Summary of special studies [NASA-CR-193918] p 2201 N94-24970

ORBITAL ASSEMBLY
Manned Mars mission on-orbit operations FTS capabilities assessment [NASA-CR-189328] p 2430 N94-23080

ORBITAL ELEMENTS
SeaWiFS technical report series. Volume 11: Analysis of selected orbit propagation models for the SeaWiFS mission [NASA-TM-104566-VOL-11] p 2417 N94-23338

ORBITAL MANEUVERS
MERCATOR: Methods and Realization for Control of the Attitude and the Orbit of spacecraft p 2202 N94-23925
The geo-control system for station keeping and colocation of geostationary satellites p 2464 N94-23927
HISPASAT launch and early operations phases: Computation and monitoring of geostationary satellite positioning p 2514 N94-23928

ORBITAL MECHANICS
Improved thermal force modeling for GPS satellites p 2207 N94-23259

CNES organization for station positioning of geostationary satellites p 2501 N94-23857
Steady motions of rigid body satellites in a central gravitational field
[AD-A273742] p 2206 N94-25532

ORBITAL POSITION ESTIMATION
A review of GPS-based tracking techniques for TDRS orbit determination p 2196 N94-23257
New approaches for tracking earth orbiters using modified GPS ground receivers p 2196 N94-23258
Real-time on-board orbit determination with DORIS p 2196 N94-23919
TOPEX/Poseidon precision orbit determination production and expert system p 2196 N94-23920
Satellite autonomous navigation and orbit determination using magnetometers p 2156 N94-24258

ORBITAL RENDEZVOUS
Telerobotic rendezvous and docking vision system architecture
[NASA-CR-191329] p 2204 N94-23828

ORBITAL RESONANCES (CELESTIAL MECHANICS)
The design and networking of dynamic satellite constellations for global mobile communication systems p 2288 N94-22826

ORBITAL SERVICING
Graphical programming: A systems approach for telerobotic servicing of space assets
[DE93-019016] p 2472 N94-23201
Ground operation of robotics on Space Station Freedom p 2371 N94-23841
An intelligent planning and scheduling system for the HST servicing missions p 2520 N94-23964
Illumination requirements for operating a space remote manipulator p 2435 N94-24195

ORBITAL WORKERS
A simulation system for Space Station extravehicular activity p 2434 N94-24192

ORBITS
Correlations in the actions of periodic orbits derived from quantum chaos
[DE93-616866] p 2571 N94-25340
Orbit spaces over commutative rings and projectives as semi-isomorphisms
[DE93-616822] p 2493 N94-25473

ORDER-DISORDER TRANSFORMATIONS
Disorder effects on small-polaron formation and hopping
[DE94-001205] p 2534 N94-23804
Two micron stimulated emission of activated insulating crystals
[REPT-94-002] p 2565 N94-25025

ORGANIC COMPOUNDS
Ordered organic thin films self-assembled from the vapor phase p 2223 N94-24339
On superconductivity of alpha-(BEDT-TTF)2KHg(SCN)4
[REPT-A-2660] p 2564 N94-24978

ORGANIC LIQUIDS
Electrochemically mediated polymerization of 2-pentadecylaniline confined to a planar liquid-liquid interface
[AD-A273541] p 2259 N94-24792

ORGANIC MATERIALS
Algorithm-development activities
[NASA-CR-193225] p 2420 N94-23538
Microgravity Studies of Organic and Polymeric Materials
[NASA-CP-3250] p 2223 N94-24338
Prediction of nonlinear optical properties of organic materials. General theoretical considerations p 2224 N94-24343
Crystal growth of organics for nonlinear optical applications p 2225 N94-24348
Test methods for composites: A status report. Volume 1: Tension test methods
[AD-A273501] p 2230 N94-24942
Test methods for composites: A status report. Volume 3: Shear test methods
[AD-A273561] p 2230 N94-25163

ORGANIZATIONS
International organizations to enable world-wide mobile satellite services p 2275 N94-22749
Towards a new radiation protection organization
[FOA-C-40304-4.3] p 2437 N94-24292
SEMATECH, a case study: Analysis of a government-industry partnership
[AD-A273166] p 2586 N94-24683

ORGANOMETALLIC COMPOUNDS
Organometallic chemistry of bimetallic compounds
[DE94-002313] p 2238 N94-22897
Synthesis and in-vivo detection of boronated compounds for use in BNCT
[DE94-001899] p 2233 N94-23780

Scanning probe lithography. 2: Selective chemical vapor deposition of copper into scanning tunneling microscope-defined patterns
[AD-A273304] p 2547 N94-25144

ORIFICE FLOW
Dispersion of fire suppression agents discharged from high pressure vessels: Establishing initial/boundary conditions for the flow outside the vessel
[PB94-103660] p 2172 N94-23810

ORIFICES
Shock-induced turbulent flow in baffle systems
[DE94-001532] p 2319 N94-23470
Optimization of orifice geometry for cross-flow mixing in a cylindrical duct
[NASA-TM-106436] p 2481 N94-23593
CFD assessment of orifice aspect ratio and mass flow ratio on jet mixing in rectangular ducts
[NASA-TM-106434] p 2187 N94-24082

OROGRAPHY
GPS survey of the western Tien Shan
[NASA-CR-195174] p 2175 N94-24826
The influence of orography on the transport of atmospheric constituents p 2619 N94-24886

ORTHOGONAL FUNCTIONS
Polynomials orthogonal with respect to an inner product involving differences
[PB94-110731] p 2489 N94-24572
Responses of a finite baffled plate subject to turbulent and mean flow excitations
[NASA-CR-191570] p 2334 N94-24605
Nonlinear aerodynamic modeling using multivariate orthogonal functions p 2164 N94-25110
Two-dimensional pattern analysis and classification using a complex orthogonal estimation algorithm
[RR-475] p 2463 N94-25321

ORTHOGONAL MULTIPLEXING THEORY
An introduction to digital modulation and OFDM techniques
[BBC-RD-1993/10] p 2295 N94-24086

ORTHOGONALITY
Nested Krylov methods and preserving the orthogonality p 2483 N94-23681

ORTHONORMAL FUNCTIONS
Deviation equations of Synge and Schild in spaces with affine connection and metric, and equations for gravitational waves detectors
[DE93-616852] p 2571 N94-25339

ORTHOSTATIC TOLERANCE
Autogenic-feedback training: A potential treatment for post-flight orthostatic intolerance in aerospace crews
[NASA-TM-108785] p 2426 N94-24102
Development of a model to assess orthostatic responses p 2427 N94-25376
Evaluation of bioimpedance for the measurement of physiologic variables as related to hemodynamic studies in space flight p 2427 N94-25378

ORTHOTROPIC PLATES
Nonlinear equations of motion for a panel subject to external loads
[AD-A273142] p 2170 N94-24773

OSCILLATING CYLINDERS
Forces on an oscillating cylinder and related fluid flow phenomena
[ISBN-9-09-005589-4] p 2338 N94-25243

OSCILLATIONS
The current status of observational constraints on cosmic strings
[DE94-001505] p 2601 N94-23010
Accelerator-based neutrino oscillation searches
[DE94-000818] p 2626 N94-23515
Lateral high frequency oscillations and stability of a wheel rolling on a flexible track p 2269 N94-23585
Surface observations of stick-slip oscillations in tightly conformal wheel/rail contacts p 2270 N94-23588
Multigrid methods for differential equations with highly oscillatory coefficients p 2484 N94-23685
Nonlinear dynamics applied to atmospheric prediction
[AD-A273437] p 2404 N94-24674

OSCILLATORS
Coherence lost? Not-so-fast escapes from the in-phase attractor of a set of globally coupled nonlinear oscillators
[DE94-000799] p 2557 N94-22940
Modulation characteristics of a high-power semiconductor Master Oscillator Power Amplifier (MOPA)
[NASA-TM-104577] p 2308 N94-23281
Controlling regular and chaotic dynamics in the Duffing-Ueda oscillator
[RR-477] p 2523 N94-25323
Deviation equations of Synge and Schild in spaces with affine connection and metric, and equations for gravitational waves detectors
[DE93-616852] p 2571 N94-25339

OUTPUT
On dynamic input-output linearization of discrete-time nonlinear systems
[MEMO-1123] p 2447 N94-22711

OVERPRESSURE
Variability of measured sonic boom signatures. Volume 1: Technical report
[NASA-CR-191483-VOL-1] p 2526 N94-24172
Variability of measured sonic boom signatures. Volume 2: Data report
[NASA-CR-191483-VOL-2] p 2526 N94-24173

OXIDATION
Discontinuous phase formation and selective attack of SiC materials exposed to low oxygen partial pressure environments
[DE93-040161] p 2231 N94-22933
Influence of sintering atmospheres on the aluminum sintering characteristics
[DE93-632412] p 2239 N94-22965
Modelling of solid polymer and direct methanol fuel cells: Phenomenological equations and analytical solutions
[PB93-224897] p 2390 N94-23102
Advances in direct oxidation methanol fuel cells p 2393 N94-23361
The possible effects of the natural and induced space environment on the optical and thermal properties of EOS surfaces p 2207 N94-23596
Fundamental and experimental studies on the catalytic combustion of methane
[PB94-112661] p 2233 N94-23736
On the stability of the process of formation of combustion generated particles by coagulation and simultaneous shrinkage due to particle oxidation p 2159 N94-24274
Segregation and oxidation studies of Al-Li and Al-Mg alloys
[ISBN-0-315-83993-7] p 2244 N94-24469
Design of novel catalysts for the partial oxidation of methane to methanol
[PB94-114212] p 2235 N94-24920

OXIDATION RESISTANCE
Evaluation of A5Si3Z(x) intermetallics for use as high temperature structural materials
[DE93-041127] p 2227 N94-22977
Advanced materials for radiation-cooled rockets p 2214 N94-23052
New method for increasing machine service-life, phase 2
[PB93-200707] p 2354 N94-23533
High temperature, oxidation resistant noble metal-Al alloy thermocouple
[NASA-CASE-LEW-15515-1] p 2343 N94-23826

OXIDATION-REDUCTION REACTIONS
Electrochemically mediated polymerization of 2-pentadecylaniline confined to a planar liquid-liquid interface
[AD-A273541] p 2259 N94-24792

OXIDES
Low temperature diffusion of hydrogenic species in oxide crystals: Radiation induced diffusion
[DE94-000374] p 2558 N94-22957
The structure and spin dynamics of lanthanide-bearing silicate glasses
[DE94-001320] p 2252 N94-22992
PEM regenerative fuel cells p 2392 N94-23358
Contaminant effects in solid oxide fuel cells
[DE94-002963] p 2395 N94-23785

OXIDIZERS
Multiple flames in counterflow spray combustion p 2161 N94-24284
Advanced launch system. Advanced development oxidizer turbopump program
[NASA-CR-193920] p 2367 N94-25174

OXYGEN
A novel method for determination of transport parameters of H2 and O2 in PEMFCs
[DE94-001492] p 2389 N94-22962
Eddy mixing coefficient upper limit derived from the photochemical balance of O2 p 2621 N94-24897
Design of novel catalysts for the partial oxidation of methane to methanol
[PB94-114212] p 2235 N94-24920
A statistical analysis of recent Naval Experimental Diving Unit (NEDU) single-depth human exposures to 100 percent oxygen at pressure
[AD-A273488] p 2427 N94-24950
The effects of zinc borate addition on the flammability characteristics of polyester, vinyl ester, and epoxy glass reinforced plastics
[AD-A273164] p 2262 N94-25136

OXYGEN ATOMS
Method and apparatus for producing a thermal atomic oxygen beam
[NASA-CASE-LEW-15614-1] p 2534 N94-23825

OXYGEN FLUORIDES
Research for electric energy systems
[DE94-001839] p 2293 N94-23719

OXYGEN IONS
Multi-ion, multi-event test of ion cyclotron resonance heating
[NASA-CR-194859] p 2540 N94-23495
OXYGEN PRODUCTION
Recent advances in SPE (tm) water electrolyzer
p 2393 N94-23362
Nutrients and light as factors controlling phytoplankton biomass on the Dutch continental shelf (North Sea), 1988-1990
[PB94-111143] p 2418 N94-24601
OXYGEN SPECTRA
JOVE NASA-FIT program: Microgravity and aeronomy projects
[NASA-CR-195121] p 2631 N94-24493
OXYGENATION
Fatigue crack growth rate studies of medium sulfur low alloy steels tested in high temperature water
[DE93-040437] p 2238 N94-22861
OZONE
Overview of global greenhouse effects
[DE93-041165] p 2396 N94-22887
High precision double four bar linkage mechanism for interferometric linear scanning p 2359 N94-24013
Participation in TOMS missions
[NASA-CR-195110] p 2398 N94-24078
Tropospheric Ozone Lidar Intercomparison Experiment, TROLIX 1991
[MPIM-102] p 2402 N94-24108
Nimbus-7 Total Ozone Mapping Spectrometer (TOMS) data products user's guide
[NASA-RP-1323] p 2410 N94-24355
Design of a vehicle based system to prevent ozone loss
[NASA-CR-195498] p 2180 N94-24479
Ozone depletion, paradigms, and politics
[DE94-001600] p 2398 N94-24506
Cloud, dust, and ozone vertical profiles from solar occultation measurements: Implications for dynamics
p 2617 N94-24877
OZONE DEPLETION
US Department of Energy phaseout of CFC-refrigerants
[DE94-001668] p 2397 N94-23016
Ozone depletion, paradigms, and politics
[DE94-001600] p 2398 N94-24506
OZONOSPHERE
Ozone depletion, paradigms, and politics
[DE94-001600] p 2398 N94-24506

P

P WAVES
Downward extrapolation of multi-component seismic data
[ISBN-9-09-005213-5] p 2405 N94-25229
Decomposition of multi-component measurements into P and S waves
[ISBN-9-09-005197-X] p 2405 N94-25251
P-N JUNCTIONS
Method for fabricating self-aligned gate diffused junction field effect transistor
[AD-D015975] p 2312 N94-25035
PACIFIC OCEAN
Observed and Navy operational global model climatologies of synoptic disturbances over the tropical western Pacific during winter 1991-1992
[AD-A273400] p 2416 N94-25071
PACKET SWITCHING
Design and implementation considerations of a MSAT packet data network p 2280 N94-22778
Fault tolerant onboard packet switch architecture for communication satellites: Shared memory per beam approach
[NASA-TM-106397] p 2201 N94-23567
Fast simulation of packet loss rates in a shared buffer communications switch
[NASA-CR-191556] p 2457 N94-24638
PACKET TRANSMISSION
Design and implementation considerations of a MSAT packet data network p 2280 N94-22778
The EURECA telecommanding chain: Experience with packet telecommand and telemetry systems
p 2305 N94-23909
Modeling of the ground-to-SSFMB link networking features using SPW p 2306 N94-25381
PACKETS (COMMUNICATION)
Design and implementation considerations of a MSAT packet data network p 2280 N94-22778
A packet-based concept for spacecraft command planning p 2504 N94-23873
AMFESYS: Modelling and diagnosis functions for operations support p 2506 N94-23887
The European Space Agency standard for space packet utilisation p 2203 N94-23954
Fast simulation of packet loss rates in a shared buffer communications switch
[NASA-CR-191556] p 2457 N94-24638
PACKING DENSITY
The 2-D polymerized Langmuir-Blodgett films studied by STM
[AD-A273542] p 2261 N94-24930
PADE APPROXIMATION
Unsteady jet flow computation towards noise prediction
[NASA-CR-194449] p 2153 N94-23553
Two-point PADE approximants for Stieltjes series
p 2490 N94-24768
PAIR PRODUCTION
Low mass muon pair production in 450 GeV p-Be collisions
[PB94-110699] p 2533 N94-23746
Photon-photon collisions at the next linear collider: Theory
[DE93-041025] p 2534 N94-23803
PALLADIUM
Selective hydrogen separation by palladium-based composite membranes
[PB93-201671] p 2254 N94-23431
Fundamental and experimental studies on the catalytic combustion of methane
[PB94-112661] p 2233 N94-23736
Metal-catalyzed alkynylation of brominated polyphenylenes: Thermoset precursors of high density monolithic glassy carbon
[AD-A273232] p 2259 N94-24789
PALLADIUM ALLOYS
Interplay of magnetic and superconducting heavy fermion ground states
[DE94-000680] p 2240 N94-23003
Generic microelectronic smart sensor platform for detection of toxic, hazardous, and flammable gases
[DE93-017626] p 2343 N94-23200
PANEL METHOD (FLUID DYNAMICS)
A numerical study of airplanes flying in proximity
[AD-A273373] p 2173 N94-24718
PANELS
Out of plane gradients in laminated composites
[NASA-CR-194875] p 2228 N94-23566
Adaptive nonlinear polynomial neural networks for control of boundary layer/structural interaction
[NASA-CR-189645] p 2525 N94-23698
The Columbus solar array mechanisms
p 2356 N94-23994
Post buckling behaviour of stiffened composite panels loaded in cyclic compression and shear
p 2157 N94-24260
Nonlinear equations of motion for a panel subject to external loads
[AD-A273142] p 2170 N94-24773
Evaluation of the UH-1N instrument panel
[AD-A273145] p 2186 N94-24774
PARABOLIC DIFFERENTIAL EQUATIONS
The characterization of reaction-convection-diffusion processes by travelling waves
[MEMO-1111] p 2273 N94-22729
A nonlinear degenerating parabolic problem from the theory of type 2 superconductors
[MEMO-1112] p 2555 N94-22730
Balanced truncation is Hankel-norm optimal when used to approximate a finite-difference model of a parabolic PDE
[OUEL-1921/92] p 2492 N94-25324
Applications of the homogenization method to flow and transport in porous media
[BER-9110] p 2340 N94-25467
PARABOLIC REFLECTORS
Development steps on the basis of test with the LOCSTAR reflector deployment mechanism
p 2356 N94-23998
PARACHUTES
Radially constructed cruciform parachute
[CA-PATENT-1323021] p 2168 N94-24182
PARADOXES
On non-informativeness in a classical Bayesian inference problem
[MEMO-COSOR-92-35] p 2494 N94-23143
PARALLEL COMPUTERS
Users manual for the Chameleon parallel programming tools
[DE94-001934] p 2465 N94-22973
Modeling parallelism and synchronization
[ETN-94-95179] p 2465 N94-23134
Linear time algorithm to schedule trees with communication delays optimally on two machines
[PB93-237782] p 2451 N94-23441
Applications of the Aurora parallel PROLOG system to computational molecular biology
[DE93-041166] p 2420 N94-23468
The instant sequencing task: Toward constraint-checking a complex spacecraft command sequence interactively p 2504 N94-23875
Discrete sensitivity derivatives of the Navier-Stokes equations with a parallel Krylov solver
[NASA-TM-106481] p 2265 N94-24301
High-performance computing and communications
[DE94-002215] p 2457 N94-24566
Transputer benchmarks and performance comparisons with other computing machines
[RR-467] p 2446 N94-25312
PARALLEL FLOW
Refraction of high frequency noise in an arbitrary jet flow
[NASA-TM-106465] p 2525 N94-23464
PARALLEL PLATES
A study of non-ideal focus properties of 30 deg parallel plate energy analyzers
[NIFS-263] p 2311 N94-24457
PARALLEL PROCESSING (COMPUTERS)
Contribution to geometric and dynamic modeling of parallel robots
[LAAS-93089] p 2470 N94-22904
Users manual for the Chameleon parallel programming tools
[DE94-001934] p 2465 N94-22973
Implementation and parallelization of fast matrix multiplication for a fast Legendre transform
[DE94-002184] p 2478 N94-22975
ACOS: The performance based approach to build a parallel complex object server
[PB93-223816] p 2465 N94-22986
Asynchronous rendezvous in distributed logic programming
[PB93-220614] p 2448 N94-23096
Incomplete corrections in nonlinear problems
[PB93-225746] p 2479 N94-23106
Programming in Fortran M
[DE94-000541] p 2450 N94-23207
Automated parallelization of timed Petri-net simulations
[NASA-CR-191574] p 2451 N94-23341
Linear time algorithm to schedule trees with communication delays optimally on two machines
[PB93-237782] p 2451 N94-23441
A lower bound for routing on a completely connected optical communication parallel computer
[DE93-040752] p 2466 N94-23491
Extending substructure based iterative solvers to multiple load and repeated analyses
[NASA-CR-194822] p 2466 N94-23504
Experience with parametric binary dissection
[NASA-CR-191552] p 2473 N94-23558
Real-time dynamics and control strategies for space operations of flexible structures
[NASA-CR-194794] p 2203 N94-23618
Vectorization and parallelization of the finite strip method for dynamic Mindlin plate problems
p 2483 N94-23679
An object-oriented approach for parallel self adaptive mesh refinement on block structured grids
p 2469 N94-23697
Multi-set extended relational algebra: A formal approach to a practical issue
[PB94-110830] p 2486 N94-23725
Advanced design concepts for open distributed systems development
[PB94-110897] p 2454 N94-23751
Preemptive scheduling in a two-stage multiprocessor flow shop is Np-hard
[PB94-111648] p 2467 N94-23756
Three, four, five, six or the complexity of scheduling with communication delays
[PB94-111630] p 2467 N94-23767
High performance, low cost, self-contained, multipurpose PC based ground systems
p 2516 N94-23943
Decentralized autonomous attitude determination using an inertially stabilized payload p 2157 N94-24264
The design of a standard message passing interface for distributed memory concurrent computers
[DE94-002536] p 2446 N94-24538
High-performance computing and communications
[DE94-002215] p 2457 N94-24566
A programming environment for distributed complex computing. An overview of the Framework for Interdisciplinary Design Optimization (FIDO) project. NASA Langley TOPS exhibit H120b
[NASA-TM-109058] p 2457 N94-24603
Runtime support and compilation methods for user-specified data distributions
[NASA-CR-191587] p 2458 N94-24679
Optimizing parallelization
[AD-A273565] p 2467 N94-24692
Sensitivity analysis of list scheduling heuristics
[PB93-237766] p 2468 N94-24764

RIACS/USRA
[NASA-CR-195117] p 2631 N94-25003
A parallel algorithm for filtering gravitational waves from coalescing binaries
[DE93-616845] p 2604 N94-25212
Multiprocessor scheduling with communication delays
[ETN-94-95346] p 2468 N94-25221
Designing parallel programs of parameterized granularity
[ETN-94-95302] p 2468 N94-25278
A design method for parallel programs
[ETN-94-95331] p 2469 N94-25282
Parallel processing methods for space based power systems p 2222 N94-25352
The transputer
[AD-A273688] p 2446 N94-25438
Expert system rule-base evaluation using real-time parallel processing
[AD-A273701] p 2469 N94-25454

PARALLEL PROGRAMMING
Users manual for the Chameleon parallel programming tools
[DE94-001934] p 2465 N94-22973
Installation of an artificial neural network on distributed memory microprocessors
[ETN-94-95175] p 2471 N94-23152
Applications of the Aurora parallel PROLOG system to computational molecular biology
[DE93-041166] p 2420 N94-23468
The Automated Instrumentation and Monitoring System (AIMS) reference manual
[NASA-TM-108795] p 2452 N94-23510
Arc consistency problem: An exercise in parallel programming with shared objects
[PB94-110590] p 2466 N94-23706
Object distribution in orca using compile-time and run-time techniques
[PB94-110574] p 2453 N94-23745
NASA high performance computing and communications program
[NASA-TM-4554] p 2591 N94-24337
The Adam language: Ada extended with support for multiway activities
[NASA-CR-4565] p 2456 N94-24480
An integrated runtime and compile-time approach for parallelizing structured and block structured applications
[NASA-CR-191554] p 2458 N94-24740
Design and implementation of a distributed version of the NASA Engine Performance Program
[NASA-CR-194475] p 2462 N94-25179
Designing parallel programs of parameterized granularity
[ETN-94-95302] p 2468 N94-25278
A design method for parallel programs
[ETN-94-95331] p 2469 N94-25282
Parallel processing methods for space based power systems p 2222 N94-25352

PARAMETER IDENTIFICATION
Identification for robust control using an H(sub infinity) norm
[EUT-92-E-261] p 2470 N94-22873
Failure-proof estimation under conditions of lack of information p 2158 N94-24267
A comparison of approximate interval estimators for the Bernoulli parameter
[NASA-CR-191585] p 2458 N94-24680
Determination of the stability and control derivatives of the NASA F/A-18 HARV using flight data
[NASA-CR-194838] p 2190 N94-24804
Advanced ballistic range technology
[NASA-CR-195198] p 2165 N94-25169
Frequency response functions for nonlinear rational models
[RR-471] p 2492 N94-25318

PARAMETERIZATION
Atmospheric numerical modeling resource enhancement and model convective parameterization/scale interaction studies
[NASA-CR-194769] p 2400 N94-23124
On testing two major cumulus parameterization schemes using the CSU regional atmospheric modeling system
[DE94-000703] p 2407 N94-23284
Parameterization of sub-grid scale convection
p 2413 N94-24386
Session on cumulus parameterization
p 2414 N94-24394
Joint sessions on modeling of boundary layer and radiative transfer processes p 2414 N94-24396
Super Beltrami differentials and N equal to 4 superconformal anomalies
[DE93-613047] p 2491 N94-25166
MIMO system identification for H(infinity) robust control: A frequency domain approach with minimum error bounds
[ETN-94-95354] p 2476 N94-25262
Designing parallel programs of parameterized granularity
[ETN-94-95302] p 2468 N94-25278

PARKING ORBITS
Prediction of three sigma maximum dispersed density for aerospace applications p 2207 N94-23654

PARTIAL DIFFERENTIAL EQUATIONS
A working algorithm to isolate integrable surfaces in E cubed
[SSCL-PREPRINT-761] p 2452 N94-23518
A dual reciprocal boundary element formulation for viscous flows p 2325 N94-23666
A theorem regarding roots of the zero-order Bessel function of the first kind p 2325 N94-23667
Implementing abstract multigrid or multilevel methods
p 2483 N94-23682
Multigrid methods for a semilinear PDE in the theory of pseudoplastic fluids p 2341 N94-23689
Wavelet multiresolution analyses adapted for the fast solution of boundary value ordinary differential equations
p 2485 N94-23691
An object-oriented approach for parallel self adaptive mesh refinement on block structured grids
p 2469 N94-23697
On the dynamics of approximating schemes for dissipative nonlinear equations p 2332 N94-24168
Global dynamic stability of a shallow arch by poincare-like simple cell mapping p 2160 N94-24280
Modelling the Shuttle Remote Manipulator System: Another flexible model p 2371 N94-25350
Development of programmable artificial neural networks p 2477 N94-25370

PARTIAL PRESSURE
Discontinuous phase formation and selective attack of SiC materials exposed to low oxygen partial pressure environments
[DE93-040161] p 2231 N94-22933

PARTICLE ACCELERATOR TARGETS
An antiproton driver for ICF propulsion
p 2217 N94-23069

PARTICLE ACCELERATORS
Report of the Joint Seminar on Solid State Physics, Atomic and Molecular Physics, and Materials Science in the Energy Region of Tandem Accelerators
[DE93-508268] p 2548 N94-22924
Search for the top quark and other new particles at D0
[DE94-001220] p 2535 N94-24515
Electro-weak, QCD and top physics at the Tevatron
[DE94-002304] p 2535 N94-24611
Welding of niobium to stainless
[DE94-003365] p 2365 N94-24614
The L3 visualization system and its use in the Z(zero) line shape analysis
[ETN-94-95382] p 2537 N94-25231

PARTICLE COLLISIONS
Low p(sub T) photon production in proton-nucleus collisions at 18 GeV/c
[DE94-001380] p 2532 N94-23007
A measurement of the forward-backward asymmetry and sin(sup 2)(theta)(sub W) from the process Z(sup 0) (yields) (mu)(sup +)(mu)(sup (minus)) at (radical)s = 1.8 TeV
[DE94-001908] p 2532 N94-23018
Calculations of Bose-Einstein correlations from Relativistic Quantum Molecular Dynamics
[DE94-000794] p 2569 N94-23453
Low mass muon pair production in 450 GeV p-Be collisions
[PB94-110699] p 2533 N94-23746
Photon-photon collisions at the next linear collider: Theory
[DE93-041025] p 2534 N94-23803
Search for the top quark and other new particles at D0
[DE94-001220] p 2535 N94-24515
Electro-weak, QCD and top physics at the Tevatron
[DE94-002304] p 2535 N94-24611
Analysis of SOFCAL calibration data
[NASA-CR-193910] p 2345 N94-25000

PARTICLE DENSITY (CONCENTRATION)
The influence of flow type, particle type and gravity on orthokinetic coagulation
[ETN-94-95333] p 2267 N94-25060

PARTICLE DIFFUSION
Recent developments in the mathematical modelling and physical understanding of transport and dispersion in aquatic systems, with special reference to tidal waters
[PB94-111135] p 2418 N94-24600

PARTICLE EMISSION
Superconducting cosmic strings near the electroweak scale and cosmic-ray propagation
[MPI-PHE/93-05] p 2629 N94-25459

PARTICLE ENERGY
Examination of the response capacity of a silicon pixel detector for ions and molecules in the energy area 100 to 300 keV
[MPE-241] p 2346 N94-25415

PARTICLE FLUX DENSITY
Measuring electrically charged particle fluxes in space using a fiber optic loop sensor
[NASA-CR-191328] p 2544 N94-23829

PARTICLE IMAGE VELOCIMETRY
Droplet turbulence interactions under subcritical and supercritical conditions p 2211 N94-23036

PARTICLE INTERACTIONS
Electron spectroscopic studies of the neutralization of slow multicharged ions during interactions with a metal surface
[DE93-041046] p 2532 N94-22956
Computer modeling of nonlinearities
p 2458 N94-24661
Thermophysical properties of simple liquid metals: A brief review of theory p 2248 N94-25130
On the connection of classical mechanics, physical kinetics and quantum theory
[DE93-616823] p 2570 N94-25207

PARTICLE MASS
Low mass muon pair production in 450 GeV p-Be collisions
[PB94-110699] p 2533 N94-23746
Stitching the Yukawa quilt
[PB93-204477] p 2569 N94-24532

PARTICLE PRODUCTION
B-quark production at hadron colliders
[DE94-001459] p 2534 N94-23806
A research of possibility for negative muon production by a low energy electron beam accompanying ion beam
[NIFS-266] p 2536 N94-24868
Bottom quark production at the Z resonance
[ISBN-9-09-006217-3] p 2538 N94-25255
Behavior of the intermittency exponents and a quark-gluon plasma formation in the heavy ion collisions
[DE93-616869] p 2541 N94-25342
On the hadron formation time in pion-nucleus interaction
[DE93-616879] p 2539 N94-25476

PARTICLE SIZE DISTRIBUTION
Development of a droplet breakup model considering aerodynamic and droplet collision effects
p 2213 N94-23045
Characterization of 3-D particle distributions and effects on recrystallization studied by computer simulation
[PB93-201408] p 2562 N94-23535
Gas-grain simulation experiment module conceptual design and gas-grain simulation facility breadboard development
[NASA-CR-177632] p 2598 N94-23536
Particle size measurement for the control of industrial crystallizers
[PB94-119104] p 2562 N94-23766
On the stability of the process of formation of combustion generated particles by coagulation and simultaneous shrinkage due to particle oxidation p 2159 N94-24274
Effect of initial droplet-size distributions on fuel-vapor profiles in a shear-layer flow p 2160 N94-24283
Low-gravity electrodeposition and growth of polymer thin films with large third-order optical nonlinearities by electrochemical processes for devices: Thiophene-based polymers p 2225 N94-24346
LRAT: Lightning Radiative Transfer
p 2416 N94-24443
The influence of flow type, particle type and gravity on orthokinetic coagulation
[ETN-94-95333] p 2267 N94-25060
Mechanisms of droplet formation
[ISBN-9-06-275765-0] p 2338 N94-25227

PARTICLE SPIN
Polarized structure functions of the nucleon in the resonance region
[CEBAF-PR-94-001] p 2540 N94-24663
Proton spin: The role of quark-gluon and hadron degrees of freedom
[DE93-616867] p 2538 N94-25341
A quark structure of hadrons and nuclei
[DE93-616872] p 2539 N94-25474

PARTICLE THEORY
Towards a theory of quark and lepton masses
[DE94-001726] p 2533 N94-23218
Applications of supersymmetric quantum mechanics
[ETN-94-95385] p 2570 N94-25257
Correlations in the actions of periodic orbits derived from quantum chaos
[DE93-616866] p 2571 N94-25340
Heavy flavour physics at LEP
[NIKHEF-H/92-19] p 2539 N94-25465

PARTICULATE SAMPLING
Bioregenerative life support systems for microgravity
[NASA-CR-195516] p 2422 N94-24810

PARTICULATES
Composite fiber structures for catalysts and electrodes p 2393 N94-23364
On the determination of local instantaneous averages in particulate flow measurements p 2325 N94-23663
Particle size measurement for the control of industrial crystallizers [PB94-119104] p 2562 N94-23766
On the stability of the process of formation of combustion generated particles by coagulation and simultaneous shrinkage due to particle oxidation p 2159 N94-24274
The chemistry of particulate formation in fluorocarbon plasmas [DE94-001500] p 2552 N94-24546

PARTITIONS (MATHEMATICS)
Characterization of measures with a convex matrix-k-range [PB93-220655] p 2479 N94-23098
A knowledge based system for scientific data visualization [NASA-CR-194879] p 2452 N94-23507
Experience with parametric binary dissection [NASA-CR-191552] p 2473 N94-23558

PARTITIONS (STRUCTURES)
Continuum representations of cellular solids [DE94-001706] p 2375 N94-23217

PARTONS
Proton spin: The role of quark-gluon and hadron degrees of freedom [DE93-616867] p 2538 N94-25341

PASCAL (PROGRAMMING LANGUAGE)
Algorithms for speech coding systems based on linear prediction [EUT-92-E-260] p 2447 N94-22731

PASSENGER AIRCRAFT
JB-300: An advanced medium size transport for 2005 [NASA-CR-195499] p 2179 N94-24401
NASA/USRA University Advanced Design Program, 1992-1993. The Diamondback: A simulated commercial air transportation study [NASA-CR-195523] p 2180 N94-24462
The airplane: A simulated commercial air transportation study [NASA-CR-195525] p 2182 N94-24837
The AC-120: The advanced commercial transport [NASA-CR-195491] p 2182 N94-24966
Weasel works SA-150: Design study of a 100 to 150 passenger transport aircraft [NASA-CR-195489] p 2183 N94-24975
The Bunny: A simulated commercial air transportation study [NASA-CR-195537] p 2183 N94-25001
The Gold Rush: A simulated commercial air transportation study [NASA-CR-195528] p 2184 N94-25002
The RTL-46: A simulated commercial air transportation study [NASA-CR-195524] p 2184 N94-25017
High-order technology: Applying technical excellence to new airplane development p 2185 N94-25069

PASSENGERS
Aircraft evacuation testing: Research and technology issues [PB94-107620] p 2173 N94-24750

PASSIVITY
Ultraviolet photosulfidation of III-V compound semiconductors for electronic passivation [DE94-001417] p 2555 N94-22717
Chromate-free talc chemical conversion coatings for aluminum alloys [DE94-001567] p 2238 N94-22932
Electrochemical sulfur passivation of visible (approximately 670nm) AlGaInP lasers [DE94-002293] p 2350 N94-24659

PATENT POLICY
NASA patent abstracts bibliography: A continuing bibliography. Section 2: Indexes (supplement 44) [NASA-SP-7039(44)-SECT-2] p 2590 N94-23712

PATHOGENESIS
Asthma in aircrew p 2425 N94-23327

PATROLS
Using satellite communications for a mobile computer network p 2280 N94-22777

PATTERN RECOGNITION
The adaptive resonance theory network: (Clustering-) behaviour in relation with brainstem auditory evoked potential patterns [EUT-92-E-264] p 2470 N94-22877
Artificial neural networks: Application to the optical recognition of music partitions [ETN-94-95166] p 2470 N94-22884
Image pattern recognition supporting interactive analysis and graphical visualization [NASA-CR-194878] p 2451 N94-23369
Sensing and modelling concepts for autonomous and remote mobile robot control p 2370 N94-23421
Neural network research in Finland. Symposium [PB93-224822] p 2472 N94-23463
Imaging System (INEL) T805 prototype [DE94-002807] p 2382 N94-23492
Joint Acoustic Propagation Experiment (JAPE) p 2527 N94-24208
Heterodyne array for measurement of target velocity [AD-D016025] p 2545 N94-24722
Method for selection of wavelength bands for multispectral classification [PB93-204378] p 2388 N94-24741
Object recognition through image understanding for an autonomous mobile robot [AD-A273206] p 2475 N94-24862
Image remapping strategies applied as protheses for the visually impaired p 2444 N94-25363
An evaluation of three-dimensional sensors for the extravehicular activity helper/retreiver p 2444 N94-25369
Extracting projective information from single views of 3D point sets [OUEL-1973/93] p 2464 N94-25471
Parametric and nonparametric discriminants for regional earthquakes and explosions [AD-A273807] p 2406 N94-25538

PAVEMENTS
Performance of prefabricated geocomposite subdrainage system in an airport runway [DOT/FAA/RD-93/23] p 2192 N94-23303
Airport pavement test machine design and cost study [DOT/FAA/CT-93/51] p 2192 N94-24072

PAYLOAD CONTROL
SAMPEX payload operation control center implementation p 2197 N94-23843
Integrating payload design, planning, and control in the Dutch Utilisation Centre p 2207 N94-23869
Customizing graphical user interface technology for spacecraft control centers p 2510 N94-23905
Spatial interpretation of NASA's Marshall Space Flight Center Payload Operations Control Center using virtual reality technology p 2198 N94-24432

PAYLOADS
Geostationary payload concepts for personal satellite communications p 2278 N94-22765
Results of a laboratory experiment that tests rotating unbalanced-mass devices for scanning gimbaled payloads and free-flying spacecraft [NASA-TP-3458] p 2269 N94-23574
A review of mission planning systems p 2503 N94-23866
Recharge mechanism based on shape memory alloy p 2362 N94-24039
Satellite situation report, volume 33, number 4 [NASA-TM-109677] p 2205 N94-24824
Effect of power system technology and mission requirements on high altitude long endurance aircraft [NASA-CR-194455] p 2189 N94-25200

PELLETS
Pellet ablation in the large helical device [NIFS-260] p 2551 N94-24358

PENCIL BEAMS
Analysis of a proposed Compton backscatter imaging technique [DE93-040537] p 2371 N94-22935

PENDULUMS
Integrated accelerometer assembly [CA-PATENT-1322107] p 2344 N94-24184

PENNING EFFECT
Radiative properties of molecular nitrogen ions produced by helium Penning ionization and argon effects [NASA-CR-195126] p 2534 N94-24487

PEPTIDES
The evolution of energy-transducing systems. Studies with archaebacteria [NASA-CR-195129] p 2422 N94-24811
Capillary electrophoresis of biomolecules: Theory, instrumentation and applications [ETN-94-95297] p 2236 N94-25233

PERCEPTION
Transfer of perceptual adaptation to space sickness: What enhances an individual's ability to adapt? [NASA-CR-188256] p 2427 N94-24227
Perceptions of organizational support and affectivity as predictors of job satisfaction [DOT/FAA/AM-94/2] p 2429 N94-25442

PERCEPTUAL ERRORS
Perception in flight: Shape and motion perception, space perception, spatial orientation, and visual vestibular interaction p 2429 N94-23979
Night vision goggle illusions and visual training p 2432 N94-23984
Mechanisms of eye-hand coordination [AD-A273687] p 2428 N94-25437
DCT quantization matrices visually optimized for individual images p 2442 N94-25509

PERFORATED PLATES
Performance of the X-/Ka/KABLE-band dichroic plate in the DSS-13 beam waveguide antenna p 2291 N94-23261

PERFORMANCE PREDICTION
Proof test of the computer program BUCKY for plasticity problems [NASA-TP-3444] p 2374 N94-22960
Foil bearing research at Penn State p 2215 N94-23058
Computational fluid dynamic modelling of cavitation p 2215 N94-23060
Mathematical modeling of MCFC cells/stacks and networks [DE94-001914] p 2390 N94-23212
Optical subnet concepts for the deep space network p 2292 N94-23269
Investigation of time and intensity effects in operator workload and performance [CTN-94-60927] p 2433 N94-24171
Pilot evaluation system p 2158 N94-24266
Aerodynamic models for performance calculations of modern technology propellers p 2161 N94-24285
CFD simulation of coaxial injectors p 2342 N94-24430
Space Shuttle Main Engine performance analysis p 2222 N94-24444
Tokamak Physics Experiment (TPX) cost and performance trade studies using supercode [DE94-002720] p 2553 N94-24628
Design and implementation of a distributed version of the NASA Engine Performance Program [NASA-CR-194475] p 2462 N94-25179
Transputer benchmarks and performance comparisons with other computing machines [RR-467] p 2446 N94-25312
Relationship between the structure and performance of identified nonlinear polynomial models [RR-474] p 2492 N94-25320
State-of-the-art engineering aeroprediction methods with emphasis on new semiempirical techniques for predicting nonlinear aerodynamics on complete missile configurations [AD-A273680] p 2171 N94-25411

PERFORMANCE TESTS
Electric and hybrid vehicles program [DE93-040664] p 2352 N94-22881
A field evaluation of remote sensor measurements of wind, temperature, and moisture for ARM integrated sounding system research [DE94-000565] p 2381 N94-23001
Contribution to the evaluation of efficiency of a microprocessor functional test [ETN-94-95176] p 2445 N94-23153
Results of the Mojave tests of the Mars 96 rover p 2370 N94-23416
Performance evaluation of the Russian SPT-100 thruster at NASA LeRC [NASA-TM-106401] p 2219 N94-23630
In-vacuum performance of Fomblin Z25-lubricated, 52100 steel bearings with TiC-coated balls p 2358 N94-24011
Data relay system satellite: The development of an antenna pointing mechanism for the inter-orbit link antenna p 2359 N94-24015
Development of gears for space use p 2360 N94-24021
Design and performances of electromagnetic initiators for space mechanisms: An alternative to pyrotechnic system p 2315 N94-24037
BLAST, a new lubricant screening tester for space oils and greases p 2362 N94-24042
Roles, uses, and benefits of general aviation aircraft in aerospace engineering education [NASA-TM-106463] p 2153 N94-24100
Experimental verification of an acoustic telemetry link between an Aurora and CFAV quest [DREA-TC-93-304] p 2202 N94-24121
The effects of spatially displaced visual feedback on remote manipulator performance p 2436 N94-24201
Analog communication transmitter and receiver test procedures [AD-A273423] p 2300 N94-24687
Hubble Space Telescope high speed photometer science verification test report [NASA-CR-189322] p 2205 N94-24710
Lightning tests and analyses of tunnel bond straps and shielded cables on the Space Shuttle solid rocket booster [NASA-CR-193921] p 2200 N94-24801
Design and simulation of EVA tools for first servicing mission of HST [NASA-CR-194784] p 2439 N94-24857

Performance measurements of the multimedia testbed on Mach 3.0: Experience writing real-time device drivers, servers, and applications
[AD-A273600] p 2460 N94-24932

Power electronics development for the SPT-100 thruster
[NASA-TM-106488] p 2221 N94-25189

The evaluation of ASOS for the Kennedy Space Center's Shuttle Landing Facility
[NASA-CR-195685] p 2416 N94-25271

Investigation of hand capabilities under a variety of performance conditions and an attempt to explain performance differences p 2444 N94-25354

Hydride thermodynamic machines
[VTT-JULK-768] p 2571 N94-25416

Evaluation of image quality p 2443 N94-25514

PERICLASE

Correlated petrographic, electron microprobe, and ion microprobe studies of selected primitive and processed phase assemblages in meteorites
[NASA-CR-194827] p 2601 N94-23499

PERIODIC FUNCTIONS

On the Daubechies-based wavelet differentiation matrix
[NASA-CR-191583] p 2479 N94-23090

Temporal aggregation in a periodically integrated autoregressive process
[PB93-230480] p 2479 N94-23122

Periodic nonlinear Schroedinger equation and invariant measures
[PB93-238012] p 2487 N94-23775

Cauchy problem for periodic KDV-type equations
[PB93-238020] p 2487 N94-23776

PERIODIC VARIATIONS

Forced vibrations of a non-viscous drop
[MPIS-24/1992] p 2318 N94-23198

Theoretical investigation of variable periodicity (graded) multilayers for hard x ray applications
[NASA-CR-194824] p 2543 N94-23502

Correlations in the actions of periodic orbits derived from quantum chaos
[DE93-616866] p 2571 N94-25340

PERIODICALS

NASA STI program database: Journal coverage (1990-1992)
[NASA-TM-109720] p 2593 N94-25168

PERISCOPES

Periscope mechanism for SWAN instrument
p 2357 N94-24000

PERMANENT MAGNETS

Finite element based electric motor design optimization p 2315 N94-24411

Design and application of electromechanical actuators for deep space missions
[NASA-CR-195134] p 2365 N94-24842

Comparative M-H characteristics of 1-5 and 2-17 type samarium-cobalt permanent magnets to 300 C
[NASA-CR-194440] p 2312 N94-24870

PERMITTIVITY

Polarizability of gyrotropic sphere
[PB93-225019] p 2524 N94-23131

Spectroscopic IR ellipsometry of 100 and 001 oriented YBa2Cu3O(7-delta) films
[PB93-201481] p 2561 N94-23445

Mueller matrix analysis of infrared ellipsometry
[PB93-201549] p 2544 N94-23629

Temperature dependent performance of Coplanar Waveguide (CPW) on substrates of various materials
[NASA-TM-106505] p 2313 N94-25170

PEROVSKITES

Fundamental study of NO(x) control in catalytic combustion
[PB94-112323] p 2398 N94-23818

PEROXIDES

In situ detection of tropospheric OH, HO2, NO2, and NO by laser-induced fluorescence in detection chambers at reduced pressures
[NASA-CR-194810] p 2397 N94-23277

Measurement of HO2 and other trace gases in the stratosphere using a high resolution far-infrared spectrometer
[NASA-CR-195173] p 2404 N94-24738

PERSONAL COMPUTERS

Some background information on perceptual color matching pertinent to computer applications
[PB93-200327] p 2445 N94-23788

High performance, low cost, self-contained, multipurpose PC based ground systems
p 2516 N94-23943

PERSONNEL

Survival suit for submarine personnel: Summary of evaluation studies
[PB93-204634] p 2430 N94-23743

NASA/DOD Aerospace Knowledge Diffusion Research Project. Report number 21: US aerospace industry librarians and technical information specialists as information intermediaries: Results of the phase 2 survey
[NASA-TM-109064] p 2593 N94-24709

Aircraft digital flight control technical review
p 2163 N94-25106

PERSONNEL DEVELOPMENT

Women scientists and engineers employed in industry: Why so few? A report based on a conference
[ISBN-0-309-04991-1] p 2585 N94-24698

PERSONNEL MANAGEMENT

Women scientists and engineers employed in industry: Why so few? A report based on a conference
[ISBN-0-309-04991-1] p 2585 N94-24698

PERSONNEL SELECTION

Strategies for recruiting additional African Americans into the NASA JSC summer faculty fellows program
p 2585 N94-25362

PERTURBATION

Decoupling problems around a trajectory: From linearity to nonlinearity
[MEMO-1115] p 2469 N94-22703

Contribution to the study of HF converters radiated disturbances
[ECL-92-34] p 2313 N94-25421

PERTURBATION THEORY

Projectile transverse motion and stability in electromagnetic induction launchers
[DE94-001557] p 2198 N94-23210

Perturbation theory in electron diffraction
[PB93-201424] p 2533 N94-23505

Reactivity of ambident anions in the gas phase
[PB93-232189] p 2533 N94-23713

Approximate optimal guidance for the advanced launch system
[NASA-CR-4568] p 2198 N94-24752

A finite-element-based perturbation model for the rotordynamic analysis of shrouded pump impellers: Part 1: Model development and applications
[NASA-CR-193916] p 2366 N94-24998

A finite-element-based perturbation model for the rotordynamic analysis of shrouded pump impellers: Part 2: User's guide
[NASA-CR-193917] p 2366 N94-24999

On a new functional integral formalism for Hubbard model
[DE93-614017] p 2492 N94-25334

PESTICIDES

Isothiazolone volatility study of a water bottom from fuel treated with Kathon (tm) FP1.5 biocide
[AD-A273165] p 2266 N94-24728

PETRI NETS

Automated parallelization of timed Petri-net simulations
[NASA-CR-191574] p 2451 N94-23341

Mean-value of product-form stochastic Petri net models of slotted-ring systems
[PB94-110871] p 2494 N94-23749

Operational characterisation of requirements and early validation environment for high demanding space systems p 2519 N94-23959

Systems engineering: A formal approach. Part 4: Analysis methods
[PB94-101417] p 2271 N94-24475

Systems engineering: A formal approach. Part 2: Frameworks
[PB94-101391] p 2489 N94-24615

Timed coloured Petri nets and their application to logistics
[ETN-94-95310] p 2522 N94-25293

PETROGRAPHY

Catalog of Apollo 17 rocks. Volume 1: Stations 2 and 3 (South Massif)
[NASA-CR-194854] p 2613 N94-24058

A dynamic melting model for the origin of Apollo 15 olivine-normative and quartz-normative mare basalts
p 2615 N94-24371

Melt rock components in KREEPy breccia 15205: Petrography and mineral chemistry of KREEP basalts and quartz-normative mare basalts p 2616 N94-24372

A geochemical study of acapulcoite and lodranite meteorites p 2605 N94-25358

PETROLOGY

Correlated petrographic, electron microprobe, and ion microprobe studies of selected primitive and processed phase assemblages in meteorites
[NASA-CR-194827] p 2601 N94-23499

Highland crust at the Apollo 14 site: A review
p 2614 N94-24364

Whole rock major element chemistry of KREEP basalt clasts in lunar breccia 15205: Implications for the petrogenesis of volcanic KREEP basalts
p 2614 N94-24365

Polytopic vector analysis in igneous petrology: Application to lunar petrogenesis p 2615 N94-24368

The western highland province at the Apollo 14 site
p 2615 N94-24369

A dynamic melting model for the origin of Apollo 15 olivine-normative and quartz-normative mare basalts
p 2615 N94-24371

Melt rock components in KREEPy breccia 15205: Petrography and mineral chemistry of KREEP basalts and quartz-normative mare basalts p 2616 N94-24372

Heterogeneity in small aliquots of Apollo 15 olivine-normative basalt: Implications for breccia clast studies p 2616 N94-24373

PHARMACOLOGY

Electrophoresis in open capillaries: Some fundamental aspects
[ETN-94-95290] p 2236 N94-25232

PHASE CONJUGATION

Spatiotemporal behavior and nonlinear dynamics in a phase conjugate resonator
[NASA-CR-4567] p 2543 N94-23529

Investigation of Raman beam cleanup and phase conjugation
[AD-A273157] p 2545 N94-24672

Quantum optical aspects of topological phases, such as Berry's phase
[AD-A273632] p 2570 N94-25028

PHASE DEVIATION

Phase linearity of the 914H coupled-cavity traveling wave tube
[NASA-CR-191056] p 2290 N94-23087

PHASE DIAGRAMS

Physics of iron
[DE94-002002] p 2402 N94-23721

Lattice dynamics of Ba(1-x)K(x)BiO3 as studied by neutron scattering and computer simulation
[DE93-617053] p 2567 N94-25424

PHASE LOCKED SYSTEMS

An optical ASK and FSK phase diversity transmission system
[EUT-92-E-268] p 2542 N94-23171

PHASE MATCHING

High-order sum and difference-frequency generation in helium
[DE94-001064] p 2348 N94-23181

PHASE MODULATION

Preliminary analysis of amplitude and phase fluctuations in the JAPE multiple tone data to distances of 500 meters p 2528 N94-24216

PHASE SHIFT

Modulation characteristics of a high-power semiconductor Master Oscillator Power Amplifier (MOPA)
[NASA-TM-104577] p 2308 N94-23281

Develop advanced nonlinear signal analysis topographical mapping system
[NASA-CR-194785] p 2389 N94-24856

The phase response of nonlinear systems
[RR-458] p 2476 N94-25308

Unwrapping the phase response functions for nonlinear systems
[RR-465] p 2462 N94-25311

PHASE SHIFT KEYING

Asynchronous timing and Doppler recovery in DSP based DPSK modems for fixed and mobile satellite applications p 2285 N94-22805

Theoretical and simulated performance for a novel frequency estimation technique p 2285 N94-22808

Pseudo-coherent demodulation for mobile satellite systems p 2287 N94-22819

Coding for frequency hopped spread spectrum satellite communications
[ECE-91-1] p 2296 N94-24132

Simulation of adjacent channel interference in a UHF satellite system
[AD-A273147] p 2299 N94-24669

Coding for frequency hopped spread spectrum satellite communications
[ECE-92-1] p 2300 N94-24697

PHASE TRANSFORMATIONS

The elastic and electromechanical properties of BaTiO3 single crystal through the ferroelectric transition
[DE94-001437] p 2557 N94-22927

Bridgman's concern
[DE93-040900] p 2558 N94-22953

Phase transformations in Cu-Zr multilayers
[DE94-000393] p 2241 N94-23297

Processing of semicrystalline polymers
p 2226 N94-24351

Thermal phase behavior of metal surfaces: X-ray scattering studies of Pt(001)
[DE94-002991] p 2245 N94-24612

Dynamic measurements of thermophysical properties of metals and alloys at high temperatures by subsecond pulse heating techniques p 2247 N94-25124

Center for Analysis of Heterogeneous and Nonlinear Media
[AD-A273515] p 2230 N94-25158
Phase structure of the two-dimensional phi(4) field theory within thermo-field dynamics
[DE93-616850] p 2570 N94-25337
Electronic structure and high pressure phase transition in LaSb and CeSb
[DE93-617051] p 2567 N94-25423

PHASED ARRAYS
Adaptive digital beamforming for a CDMA mobile communications payload p 2274 N94-22743
Calibration block for digital beam forming antenna
[PB93-204550] p 2294 N94-23773
Calibration network intended for phase-array antennas at 3 GHz
[PB93-204352] p 2297 N94-24530

PHENOLIC RESINS
Initial evaluation of burn characteristics of phenolic foam runway brake arrestor material
[DOT/FAA/CT-TN93/7] p 2253 N94-23335

PHENOMENOLOGY
Thermally activated low temperature creep and primary water stress corrosion cracking of NiCrFe alloys
[DE94-001756] p 2241 N94-23219

PHENYLS
Di(hydroxyphenyl)- 1,2,4-triazole monomers
[NASA-CASE-LAR-14440-2] p 2252 N94-23075
Metal-catalyzed alkynylation of (Bromophenyl)Oligophenylenes: A rapid route to thermoset precursors of high density monolithic glass-like carbon
[AD-A273219] p 2260 N94-24863
Planar poly(p-phenylene) derivatives: Ladder formation for maximization of extended conjugation
[AD-A273220] p 2260 N94-24922

PHOBOS
A mission to Mercury and a mission to the moons of Mars
[NASA-CR-195530] p 2195 N94-24619

PHONEMES
On the quality of synthetic speech evaluation and improvements
[ETN-94-95298] p 2304 N94-25234

PHONONS
Energy transfer in solid explosives
[DE94-001523] p 2265 N94-23776
Lattice dynamics of Ba(1-x)K(x)BiO3 as studied by neutron scattering and computer simulation
[DE93-617053] p 2567 N94-25424

PHOSPHATES
Infrared analysis of vapor phase deposited tricresylphosphate (TCP)
[NASA-TM-106423] p 2253 N94-23371
Auto-metasomatism of the western lunar highlands: Result of closed system fractionation and mobilization of a KREEPy trapped liquid p 2615 N94-24367

PHOSPHAZENE
A preliminary evaluation of the phosphazene resin PPZ
[AD-A273674] p 2263 N94-25410

PHOSPHORS
Fiber optic temperature sensor using a Y2O2S:Eu thermographic phosphor
[DE94-000331] p 2543 N94-23461

PHOSPHORUS COMPOUNDS
The electrochemistry of the solvated electron: A study of its properties and of its applications
[ETN-94-95313] p 2236 N94-25296

PHOTOCHEMICAL REACTIONS
Chemistry on the mesoscale: Modeling and measurement issues p 2413 N94-24390
Photoinduced charge separation in solid state and molecular systems
[DE94-001727] p 2563 N94-24537
Eddy mixing coefficient upper limit derived from the photochemical balance of O2 p 2621 N94-24897

PHOTODIODES
Micro pulse laser radar
[NASA-CASE-GSC-13493-1] p 2294 N94-23827
CsI(Tl)-photodiode detectors for spectroscopy at low radiation levels
[MPI-PHE/92-22] p 2314 N94-25457

PHOTOELECTRIC EMISSION
Limits on high-order harmonic generation from single-atom calculations
[DE93-019950] p 2531 N94-22869
Performance of inverse photoemission spectrometer with a new bandpass photon detector of narrow bandwidth and high sensitivity
[REPT-A-2659] p 2345 N94-24977
The in situ observation of epitaxial diamond thin film nucleation and growth using emission electron microscopy
[AD-A273698] p 2263 N94-25489

PHOTOELECTROCHEMICAL DEVICES
Photoinduced charge separation in solid state and molecular systems
[DE94-001727] p 2563 N94-24537

PHOTOELECTRON SPECTROSCOPY
An analytical ultra-high vacuum tribometer for solid lubricant studies p 2361 N94-24033
LPCVD of InN on GaAs(110) using HN3 and TMIn: Comparison with Si(100) results
[AD-A273555] p 2235 N94-24917

PHOTOGRAMMETRY
A photogrammetric solution to a particular problem
[NASA-TP-3415] p 2381 N94-22961
Quantitative assessment of human motion using video motion analysis p 2436 N94-24203
Reach performance while wearing the Space Shuttle launch and entry suit during exposure to launch accelerations p 2436 N94-24204
Image analysis technology applied to problems in crystallography
[AD-A273516] p 2566 N94-25288

PHOTOGRAPHIC EMULSIONS
Analysis of SOFCAL calibration data
[NASA-CR-193910] p 2345 N94-25000

PHOTOGRAPHIC MEASUREMENT
Debris/ice/TPS assessment and integrated photographic analysis for Shuttle mission STS-58
[NASA-TM-109194] p 2200 N94-24577

PHOTOGRAPHIC RECORDING
Debris/Ice/TPS assessment and integrated photographic analysis for Shuttle Mission STS-61
[NASA-TM-109195] p 2199 N94-24059

PHOTOGRAPHY
Close-up analysis of inflight ice accretion
[NASA-TM-106457] p 2172 N94-23523

PHOTOINTERPRETATION
Integrated use of hydrological modelling and remote sensing in the province of Drenthe (The Netherlands): Possibilities and restrictions
[REPT-61] p 2382 N94-23148

PHOTOIONIZATION
Limits on high-order harmonic generation from single-atom calculations
[DE93-019950] p 2531 N94-22869
High-resolution soft x ray photoionization studies of selected molecules
[DE94-000568] p 2532 N94-23002
SALI chemical analysis of provided samples
[NASA-CR-194138] p 2232 N94-23524

PHOTOLUMINESCENCE
Ultraviolet photosulfidation of III-V compound semiconductors for electronic passivation
[DE94-001417] p 2555 N94-22717

PHOTOLYSIS
Ultraviolet photosulfidation of III-V compound semiconductors for electronic passivation
[DE94-001417] p 2555 N94-22717
Infrared fluorescence studies of electronic-to-vibrational energy transfer in a Br2:NO system
[AD-A273727] p 2539 N94-25443

PHOTOMAPPING
Enhanced image capture through fusion
p 2346 N94-25502

PHOTOMETERS
New concepts for HgI2 scintillator gamma ray spectroscopy
[NASA-CR-194819] p 2233 N94-24113
Hubble Space Telescope high speed photometer orbital verification
[NASA-CR-189333] p 2204 N94-24226
Hubble Space Telescope high speed photometer science verification test report
[NASA-CR-189322] p 2205 N94-24710

PHOTOMULTIPLIER TUBES
The CEBAF beam loss sensors
[CEBAF-PR-93-032] p 2540 N94-24662
Performance of inverse photoemission spectrometer with a new bandpass photon detector of narrow bandwidth and high sensitivity
[REPT-A-2659] p 2345 N94-24977

PHOTON BEAMS
Proceedings of the Fifth Users Meeting for the Advanced Photon Source
[DE93-040692] p 2531 N94-22948

PHOTONICS
Photonic technology for implementation of generalizable neural networks: A synthetic approach
[AD-A273497] p 2474 N94-24622

PHOTONS
Low p(sub T) photon production in proton-nucleus collisions at 18 GeV/c
[DE94-001380] p 2532 N94-23007
Photon-photon collisions at the next linear collider: Theory
[DE93-041025] p 2534 N94-23803
Flux measurements using the BATSE spectroscopic detectors p 2580 N94-24435
Electro-weak, QCD and top physics at the Tevatron
[DE94-002304] p 2535 N94-24611
Quantum optical aspects of topological phases, such as Berry's phase
[AD-A273632] p 2570 N94-25028

PHOTOPRODUCTION
Low p(sub T) photon production in proton-nucleus collisions at 18 GeV/c
[DE94-001380] p 2532 N94-23007
Electro-weak, QCD and top physics at the Tevatron
[DE94-002304] p 2535 N94-24611

PHOTOSPHERE
The solar spectral irradiances from x ray to radio wavelengths
[NASA-CR-195203] p 2629 N94-25260

PHOTOSTRESSES
Use of photostress to characterize the mechanical behavior of weldments
[NASA-CR-195201] p 2378 N94-25267

PHOTOVOLTAIC CELLS
Novel two-stage selenization methods for fabrication of thin-film CIS cells and submodules
[DE94-000220] p 2390 N94-23296
A solar photovoltaic power system for use in Antarctica
[NASA-TM-106417] p 2395 N94-24071
Overview of the status and progress in photovoltaics research in the United States
[DE94-000981] p 2395 N94-24512
Laser energized high voltage direct current power supply
[AD-D015977] p 2312 N94-25036
Effect of power system technology and mission requirements on high altitude long endurance aircraft
[NASA-CR-194455] p 2189 N94-25200

PHOTOVOLTAIC CONVERSION
Polycrystalline thin film materials and devices
[DE93-018213] p 2389 N94-22862
Progress in phases 2 and 3 of the Photovoltaic Manufacturing Technology Project (PVMaT)
[DE94-000206] p 2389 N94-22888
Preliminary study concerning development of petroleum-substitution energy integration technology
[DE94-714902] p 2264 N94-23027
Amorphous silicon PVMaT, phase 2A
[DE93-018221] p 2390 N94-23295
Low power ground-based laser illumination for electric propulsion applications
[NASA-CR-194444] p 2219 N94-23555
A solar photovoltaic power system for use in Antarctica
[NASA-TM-106417] p 2395 N94-24071
Overview of the status and progress in photovoltaics research in the United States
[DE94-000981] p 2395 N94-24512

PHOTOVOLTAIC EFFECT
Polythiophene derivative with a side chain chromophore as photovoltaic and photorefractive materials
[AD-A273245] p 2260 N94-24813

PHYSICAL EXAMINATIONS
Echocardiographic screening of aircrew candidates
p 2424 N94-23319

PHYSICAL EXERCISE
Exercise, exercise training, and the immune system. A compendium of research (1902-1991)
[NASA-TM-108778] p 2426 N94-23575
NASA project 1: Full-body dynamometer
[NASA-CR-195507] p 2438 N94-24331
Loading, electromyograph, and motion during exercise
p 2427 N94-25359

PHYSICAL OPTICS
High-frequency techniques for RCS prediction of plate geometries and a physical optics/equivalent currents model for the RCS of trihedral corner reflectors, parts 1 and 2
[NASA-CR-195140] p 2298 N94-24616
Feasibility study of a synthesis procedure for array feeds to improve radiation performance of large distorted reflector antennas
[NASA-CR-195167] p 2301 N94-25005
The Radar Image Generation (RIG) model
p 2306 N94-25497

PHYSICAL PROPERTIES
Mass properties measurement system dynamics
p 2368 N94-23235
Mass properties measurement system: Dynamics and statics measurements p 2368 N94-23236

PHYSICAL SCIENCES
The 7th Annual National Conference of Black Physics Students p 2524 N94-24583

PHYSICS
Fractal geometry in physics
[AD-A273271] p 2523 N94-24936

PHYSIOCHEMISTRY
Stability of premixed laminar flames in a stagnation point flow to general disturbances
[AD-A273429] p 2234 N94-24673

PHYSIOLOGICAL EFFECTS
Aeromedical disposition for coronary artery disease p 2423 N94-23316
Exercise, exercise training, and the immune system. A compendium of research (1902-1991)
[NASA-TM-108778] p 2426 N94-23575
Transfer of perceptual adaptation to space sickness: What enhances an individual's ability to adapt?
[NASA-CR-188256] p 2427 N94-24227

PHYSIOLOGICAL RESPONSES
Increasing accuracy in the assessment of motion sickness: A construct methodology
[NASA-TM-108797] p 2420 N94-23088
Cytokines and immune surveillance in humans
[NASA-CR-194801] p 2425 N94-23331
Physiological protection for aircrew at high altitudes: A review of the literature
[DCIEM-93-13] p 2432 N94-24114
ELF communications system ecological monitoring program
[AD-A273456] p 2299 N94-24676
The role of visual context in manual target localization p 2429 N94-25351

PHYSIOLOGICAL TESTS
Cardiopulmonary Aspects in Aerospace Medicine
[AGARD-LS-189] p 2423 N94-23313
Aortic valve disease p 2424 N94-23322
Aeromedical implications of mitral valve prolapse p 2424 N94-23323
Evaluation of bioimpedance for the measurement of physiologic variables as related to hemodynamic studies in space flight p 2427 N94-25378
Mechanisms of eye-hand coordination
[AD-A273687] p 2428 N94-25437

PHYSIOLOGY
Visual Problems in Night Operations
[AGARD-LS-187] p 2431 N94-23976
Use of infrared telemetry as part of a nonintrusive inflight data collection system to collect human factors data p 2434 N94-24193
ELF communications system ecological monitoring program
[AD-A273456] p 2299 N94-24676

PHYTOPLANKTON
Factors affecting the identification of phytoplankton groups by means of remote sensing
[NASA-TM-108799] p 2387 N94-24403
Nutrients and light as factors controlling phytoplankton biomass on the Dutch continental shelf (North Sea), 1988-1990
[PB94-111143] p 2418 N94-24601

PI-ELECTRONS
Planar poly(p-phenylene) derivatives: Ladder formation for maximization of extended conjugation
[AD-A273220] p 2260 N94-24922

PIEZOELECTRICITY
Theoretical studies of wave propagation in multilayered piezoelectric media
[DE93-040273] p 2371 N94-22872
Ferroelectric thin films 3
[AD-A273394] p 2565 N94-25027

PILOT INDUCED OSCILLATION
Aircraft digital flight control technical review p 2163 N94-25106

PILOT PERFORMANCE
Pilot-vehicle interface
[DOT/FAA/CT-92/21] p 2430 N94-23083
Pilot evaluation system p 2158 N94-24266
Combined 1991 and 1992 Robinson-22B (R-22) parking test results
[AD-A273550] p 2193 N94-24559
Extracting heading and temporal range from optic flow: Human performance issues p 2442 N94-25510
Sensor fusion display evaluation using information integration models in enhanced/synthetic vision applications p 2443 N94-25512
Quality metrics for sensor images p 2443 N94-25513

PILOT PLANTS
Statistical procedures for corrosion studies
[PB93-199412] p 2244 N94-23802

PILOT SELECTION
Cardiopulmonary Aspects in Aerospace Medicine
[AGARD-LS-189] p 2423 N94-23313
Screening for asymptomatic coronary heart disease p 2423 N94-23315
Aeromedical disposition for coronary artery disease p 2423 N94-23316
Echocardiographic screening of aircrew candidates p 2424 N94-23319
Aortic valve disease p 2424 N94-23322
Asthma in aircrew p 2425 N94-23327

PILOT TRAINING
Pilot evaluation system p 2158 N94-24266
A simulation study of control and display requirements for zero-experience general aviation pilots p 2163 N94-25102

PILOTLESS AIRCRAFT
A conceptual design of an unmanned test vehicle using an airbreathing propulsion system
[NASA-CR-195550] p 2189 N94-25085

PINTLES
Inherent stability of central element coaxial liquid-liquid injectors p 2212 N94-23043

PIONEER VENUS SPACECRAFT
SO2 on Venus: A final cross-calibration with Pioneer Venus
[NASA-CR-195162] p 2599 N94-24988

PIONS
Pions and neutrinos as probes of the nucleon and nuclear few-body system
[DE93-040127] p 2531 N94-22926
Gauge invariance and the electromagnetic current of composite pions
[DE93-040869] p 2532 N94-22952
Low p(sub T) photon production in proton-nucleus collisions at 18 GeV/c
[DE94-001380] p 2532 N94-23007
Calculations of Bose-Einstein correlations from Relativistic Quantum Molecular Dynamics
[DE94-000794] p 2569 N94-23453
New evaluation of hadronic contributions to the anomalous magnetic moment of charged leptons
[DE93-634394] p 2536 N94-24844
On the hadron formation time in pion-nucleus interaction
[DE93-616879] p 2539 N94-25476

PIPE FLOW
Features of a SINDA/FLUINT model of a liquid oxygen supply line p 2322 N94-23649
Comparison of numerical simulation and experimental data for steam-in-place sterilization p 2326 N94-23669
Heat pipe vapor dynamics
[NASA-CR-194217] p 2327 N94-24096
Modeling dynamically coupled fluid-duct systems with finite line elements
[NASA-CR-193909] p 2376 N94-24359
Interactive control in turbulent shear layers
[AD-A273544] p 2336 N94-24793
Decay of swirl in turbulent pipe flows
[ETN-94-95353] p 2339 N94-25248

PIPELINES
Demonstration of polyscann ultrasonic butt-fusion inspection system for polyethylene pipes
[AD-A273279] p 2373 N94-24814
Proceedings of the 12th International Congress: Corrosion Control for Low-Cost Reliability. Volume 4: Oil/Gas Pipeline
[AD-A273665] p 2250 N94-25405

PIPES (TUBES)
Characterization of the microstructure of Nb-1wt.%Zr-0.1wt.%C tubes as affected by thermomechanical processing
[NASA-TM-106381] p 2242 N94-23550
Statistical procedures for corrosion studies
[PB93-199412] p 2244 N94-23802
Weld joint concepts for on-orbit repair of Space Station Freedom fluid system tube assemblies p 2371 N94-24427
Method and apparatus for the non-invasive measurement of pressure inside pipes using a fiber optic interferometer sensor
[AD-D016013] p 2344 N94-24734
Strength and life of pressure vessels subjected to impacts and thermomechanical GFRP loading
[VTT-JULK-771] p 2379 N94-25418

PISTON ENGINES
Internal combustion engine with a central crankshaft and integral tandem annular pistons
[CA-PATENT-1-320-878] p 2363 N94-24055
The effect of high altitude pressure on the power and efficiency of an airborne two-stroke engine p 2155 N94-24253
Controllability of free-piston Stirling engine/linear alternator driving a dynamic load
[NASA-TM-106497] p 2521 N94-24302

PISTON THEORY
Nonlinear equations of motion for a panel subject to external loads
[AD-A273142] p 2170 N94-24773

PITCH (INCLINATION)
LDA measurements of the unsteady near wake behind an airfoil undergoing transient and periodic pitching motions
[ISL-CO-215/92] p 2165 N94-23161
The influence of elastic pitch variations on helicopter flight mechanics p 2161 N94-24286

PITCHING MOMENTS
Compressibility effects on dynamic stall of airfoils undergoing rapid transient pitching motion
[NASA-TM-109681] p 2167 N94-23975
A numerical study of airplanes flying in proximity
[AD-A273373] p 2173 N94-24718

PITTING
Use of scanning tunneling microscope in corrosion studies
[VTT-TIED-1416] p 2250 N94-25346

PIXELS
Progress on the design of a data push architecture for an array of optimized time tagging pixels
[DE93-041011] p 2307 N94-22955

PLANAR STRUCTURES
Modifications to 8x8 dynamical theory: Polarizations redefined according to x ray diffraction convention
[DE94-001290] p 2560 N94-23187
Planar poly(p-phenylene) derivatives: Ladder formation for maximization of extended conjugation
[AD-A273220] p 2260 N94-24922

PLANE STRAIN
Morphology of highly textured polyethylene/polyethylene- propylene semicrystalline diblock copolymers
[AD-A273683] p 2263 N94-25413

PLANE WAVES
Proceedings of the 1993 Bi-Isotropics Workshop on Novel Microwave Materials
[PB93-224772] p 2290 N94-23225
LRAT: Lightning Radiative Transfer p 2416 N94-24443

PLANETARY BASES
Preliminary design of a universal Martian lander
[NASA-CR-195529] p 2206 N94-25007

PLANETARY BOUNDARY LAYER
Incorporation of the planetary boundary layer in atmospheric models p 2413 N94-24388
Joint sessions on moisture processes and cumulus parameterization p 2414 N94-24393
Joint sessions on modeling of boundary layer and radiative transfer processes p 2414 N94-24396
Session on coupled atmospheric/chemistry coupled models p 2414 N94-24398
Vertical transport of water in the Martian boundary layer p 2622 N94-24902

PLANETARY CRUSTS
Basaltic Volcanism and Ancient Planetary Crusts
[NASA-CR-193151] p 2614 N94-24363
The geophysical signal of the martian global dichotomy p 2623 N94-24997

PLANETARY ENVIRONMENTS
Electronic payloads for Martian missions: A preliminary assessment of technologies p 2610 N94-23408

PLANETARY EVOLUTION
Basaltic Volcanism and Ancient Planetary Crusts
[NASA-CR-193151] p 2614 N94-24363
Protoplanetary disks: Theory and observation by millimeter and sub-millimeter arrays
[REPT-331] p 2603 N94-24983
The Nobeyama millimeter array survey for protoplanetary disks around protostar candidates and T Tauri stars in Taurus
[REPT-336] p 2604 N94-24987
Tectonic Evolution of Mars
[NASA-CR-194714] p 2623 N94-24996

PLANETARY GEOLOGY
An improved gravity model for Mars: Goddard Mars Model-1 (GMM-1)
[NASA-TM-104584] p 2401 N94-23282
Robotic exploration of Moon and Mars p 2606 N94-23379
The geophysical signal of the martian global dichotomy p 2623 N94-24997

PLANETARY LANDING
Past US studies and developments for planetary rovers p 2369 N94-23375
Planetary and asteroid missions. Getting there: Anchoring spacecraft to asteroids
[NASA-CR-195493] p 2614 N94-24333

PLANETARY MAPPING
Science strategy for Mars exploration p 2606 N94-23380
Evidence for dust transport in Viking IR thermal mapper opacity data p 2620 N94-24892
The Mars Aerial Platform (MAP) mission p 2622 N94-24903

PLANETARY METEOROLOGY
Workshop on Atmospheric Transport on Mars
[NASA-CR-194855] p 2616 N94-24871
The NASA/GISS Mars general circulation model: Preliminary experiments p 2616 N94-24872
Optimal gains for a single polar orbiting satellite p 2208 N94-24873

A diagnostic model to estimate winds and small-scale drag from Mars Observer PMIRR data
p 2617 N94-24874

Eddy mixing coefficient values derived from simulations with the NASA Ames Mars GCM p 2617 N94-24875

Mars dust-driven tides and their impact on the thermosphere p 2617 N94-24876

PLANETARY NEBULAE

High spatial resolution observations of CO in CRL 618
[REPT-334] p 2604 N94-24986

PLANETARY SURFACES

The new family of JPL planetary surface vehicles
p 2369 N94-23398

Automation technology for remote sample acquisition
p 2369 N94-23407

Evolving directions in NASA's planetary rover requirements and technology p 2370 N94-23414

Towards real-time stereovision systems for planetary missions p 2370 N94-23422

A DTM-based path planning method for planetary rovers p 2370 N94-23423

Mobility analysis, simulation, and scale model testing for the design of wheeled planetary rovers
p 2370 N94-23425

The transition from diapirism to dike intrusion: Implications for planetary volcanism
[NASA-CR-195133] p 2403 N94-24580

PLANETARY TEMPERATURE

Three-dimensional numerical simulation of near-surface flows over the Martian north polar cap
p 2621 N94-24895

PLANETARY WAVES

Global acoustic mapping of ocean temperatures (GAMOT)
[AD-A273387] p 2418 N94-24719

Regarding tracer transport in Mars' winter atmosphere in the presence of nearly stationary, forced planetary waves p 2618 N94-24882

Two-dimensional modeling of thermal inversion layers in the middle atmosphere of Mars p 2622 N94-24900

PLANTS (BOTANY)

ELF communications system ecological monitoring program
[AD-A273456] p 2299 N94-24676

Generalized linear mixed models and their application in plant breeding research
[ETN-94-95335] p 2460 N94-25061

PLASMA ARC WELDING

Plasma ARC keyhole welding of aluminum
[PB93-201606] p 2353 N94-23449

Robotic weld overlay coatings for erosion control
[DE94-002665] p 2258 N94-24749

PLASMA CHEMISTRY

Excitation balances and transport in an inductively coupled plasma
[ETN-94-95330] p 2554 N94-25241

PLASMA CLOUDS

Artificial plasma experiments. Chemical release observations associated with the CRRES program
[NASA-CR-194871] p 2550 N94-23565

PLASMA COMPOSITION

Fusion plasma theory project summaries
[DE94-001712] p 2551 N94-23808

PLASMA CONTROL

Massachusetts Institute of Technology Plasma Fusion Center 1992-1993 report to the President
[DE94-001725] p 2548 N94-22721

Active probing of plasma edge turbulence and feedback studies on the Texas Experimental Tokamak (TEXT)
[DE94-001017] p 2548 N94-22945

Plasma research in the Madison Symmetric Torus (MST)
[DE94-002318] p 2549 N94-22976

Fluctuations and confinement in ATF
[DE94-000485] p 2549 N94-22998

Structural analysis of a superconducting central solenoid for the Tokamak Physics Experiment
[DE94-001536] p 2549 N94-23014

Overview of the ATF stellarator program
[DE94-000371] p 2550 N94-23462

The role of the radial electric field in confinement and transport in H-mode and VH-mode discharges in the DIII-D tokamak
[DE94-002746] p 2551 N94-23782

Fusion plasma theory project summaries
[DE94-001712] p 2551 N94-23808

IPP Prague Contributions to the IAEA Technical Committee Meeting on Research Using Small Tokamaks
[IPPCZ-329] p 2551 N94-24293

Temporal behavior of the electron density profile during limiter biasing in the HYBTOK-2 tokamak
[NIFS-257] p 2552 N94-24456

Proposal of Modular Heliotron: Advanced modular helical system compatible with closed helical divertor
[NIFS-261] p 2552 N94-24458

Computer modeling of plasma flow switches-high current switching on Procyon
[DE93-040189] p 2311 N94-24500

Stabilization of the external kink and other MHD issues
[DE94-001541] p 2552 N94-24502

Start-up simulations of the PULSAR pulsed tokamak reactor
[DE94-002634] p 2552 N94-24519

Design of central control system for Large Helical Device (LHD)
[NIFS-258] p 2553 N94-24623

PLASMA CURRENTS

Active probing of plasma edge turbulence and feedback studies on the Texas Experimental Tokamak (TEXT)
[DE94-001017] p 2548 N94-22945

1993 annual report for the Phaedrus-T RF current drive experiments
[DE94-001369] p 2550 N94-23192

Computer modeling of plasma flow switches-high current switching on Procyon
[DE93-040189] p 2311 N94-24500

Plasma initiation in a tokamak with conducting superstructure: First results from Alcator C-MOD
[DE94-001565] p 2552 N94-24504

Start-up simulations of the PULSAR pulsed tokamak reactor
[DE94-002634] p 2552 N94-24519

LHCD (low hybrid current drive) experiment on the HT-6B tokamak
[DE93-613720] p 2555 N94-25331

PLASMA DENSITY

Fluctuations and confinement in ATF
[DE94-000485] p 2549 N94-22998

Analysis and experiments of a whistler-wave plasma thruster
[DE94-001533] p 2209 N94-23012

PLASMA DIAGNOSTICS

Massachusetts Institute of Technology Plasma Fusion Center 1992-1993 report to the President
[DE94-001725] p 2548 N94-22721

Prospects for very-high-resolution solar physics with the Simuris inteferometric mission p 2625 N94-22848

Characterization of heat transport and radiation hydrodynamics in collisional laser plasmas using collective Thomson scattering
[DE94-001502] p 2349 N94-23209

Some theoretical problems of magnetic diagnostics in tokamaks and stellarators
[NIFS-262] p 2551 N94-24306

Pellet ablation in the large helical device
[NIFS-260] p 2551 N94-24358

A study of non-ideal focus properties of 30 deg parallel plate energy analyzers
[NIFS-263] p 2311 N94-24457

Plasma initiation in a tokamak with conducting superstructure: First results from Alcator C-MOD
[DE94-001565] p 2552 N94-24504

The chemistry of particulate formation in fluorocarbon plasmas
[DE94-001500] p 2552 N94-24546

Measurement of electron temperature and density in the DIII-D neutral beam ion source arc chamber
[DE94-001099] p 2553 N94-24746

PLASMA DIFFUSION

The anomalous transport caused by particles transverse drift
[DE93-613685] p 2554 N94-25329

PLASMA DIODES

X ray simulator theory support
[AD-A273613] p 2553 N94-24949

PLASMA DRIFT

Excitation balances and transport in an inductively coupled plasma
[ETN-94-95330] p 2554 N94-25241

The anomalous transport caused by particles transverse drift
[DE93-613685] p 2554 N94-25329

Modification in the kinetic solution for magnetized plasmas
[DE93-613687] p 2555 N94-25343

PLASMA DYNAMICS

Chaos in plasma simulation and experiment
[DE94-001574] p 2549 N94-22963

Chaos and simple determinism in reversed field pinch plasmas: Nonlinear analysis of numerical simulation and experimental data
[DE94-001575] p 2550 N94-23211

Start-up simulations of the PULSAR pulsed tokamak reactor
[DE94-002634] p 2552 N94-24519

PLASMA ELECTRODES

Reduction of the anode fall in a coaxial plasma thruster with an applied magnetic nozzle
[DE94-000670] p 2218 N94-23283

PLASMA ENGINES

Optimization of energy transfer in microwave electrothermal thrusters p 2216 N94-23065

CFD modeling of microwave electrothermal thrusters
p 2216 N94-23066

Advanced space propulsion concepts
p 2216 N94-23067

Stationary plasma thruster plume characteristics
[NASA-CR-194454] p 2219 N94-24361

Power electronics development for the SPT-100 thruster
[NASA-TM-106488] p 2221 N94-25189

PLASMA EQUILIBRIUM

Some theoretical problems of magnetic diagnostics in tokamaks and stellarators
[NIFS-262] p 2551 N94-24306

PLASMA GENERATORS

Burning rate of double-base propellant in the presence of plasma p 2155 N94-24252

PLASMA GUNS

Computational model of surface ablation from tokamak disruptions
[DE94-002204] p 2550 N94-23474

PLASMA HEATING

Massachusetts Institute of Technology Plasma Fusion Center 1992-1993 report to the President
[DE94-001725] p 2548 N94-22721

Plasma research in the Madison Symmetric Torus (MST)
[DE94-002318] p 2549 N94-22976

Analysis and experiments of a whistler-wave plasma thruster
[DE94-001533] p 2209 N94-23012

Structural analysis of a superconducting central solenoid for the Tokamak Physics Experiment
[DE94-001536] p 2549 N94-23014

Overview of the ATF stellarator program
[DE94-000371] p 2550 N94-23462

Multi-ion, multi-event test of ion cyclotron resonance heating
[NASA-CR-194859] p 2540 N94-23495

PLASMA JETS

Massachusetts Institute of Technology Plasma Fusion Center 1992-1993 report to the President
[DE94-001725] p 2548 N94-22721

CAMAC throughput of a new RISC-based data acquisition computer at the DIII-D tokamak
[DE94-001113] p 2550 N94-23182

Mixing and unmixedness in plasma jets 1: Near-field analysis p 2323 N94-23655

PLASMA OSCILLATIONS

Temporal behavior of the electron density profile during limiter biasing in the HYBTOK-2 tokamak
[NIFS-257] p 2552 N94-24456

LHCD (low hybrid current drive) experiment on the HT-6B tokamak
[DE93-613720] p 2555 N94-25331

Effect of LHCD (low hybrid current drive) on tearing mode instability
[DE93-613700] p 2555 N94-25344

PLASMA PHYSICS

1993 annual report for the Phaedrus-T RF current drive experiments
[DE94-001369] p 2550 N94-23192

Fusion plasma theory project summaries
[DE94-001712] p 2551 N94-23808

IPP Prague Contributions to the IAEA Technical Committee Meeting on Research Using Small Tokamaks
[IPPCZ-329] p 2551 N94-24293

Modification in the kinetic solution for magnetized plasmas
[DE93-613687] p 2555 N94-25343

PLASMA POTENTIALS

1993 annual report for the Phaedrus-T RF current drive experiments
[DE94-001369] p 2550 N94-23192

Stationary plasma thruster plume characteristics
[NASA-CR-194454] p 2219 N94-24361

PLASMA PRESSURE

Investigation and application of microwave electron cyclotron resonance plasma physical vapour deposition
[DE93-613909] p 2555 N94-25333

PLASMA PROBES

Temporal behavior of the electron density profile during limiter biasing in the HYBTOK-2 tokamak
[NIFS-257] p 2552 N94-24456

A study of non-ideal focus properties of 30 deg parallel plate energy analyzers
[NIFS-263] p 2311 N94-24457

PLASMA PROPULSION

Performance evaluation of the Russian SPT-100 thruster at NASA LeRC
[NASA-TM-106401] p 2219 N94-23630

Numerical simulation of cylindrical, self-field MPD thrusters with multiple propellants
[NASA-CR-194458] p 2220 N94-24714

Power electronics development for the SPT-100 thruster
[NASA-TM-106488] p 2221 N94-25189

PLASMA RADIATION
Method and apparatus for producing a thermal atomic oxygen beam
[NASA-CASE-LEW-15614-1] p 2534 N94-23825
X ray simulator theory support
[AD-A273613] p 2553 N94-24949

PLASMA SHEATHS
Chaotic phenomena in plasma, 2
[DE93-508286] p 2549 N94-22964
Computational model of surface ablation from tokamak disruptions
[DE94-002204] p 2550 N94-23474

PLASMA SPRAYING
Selective hydrogen separation by palladium-based composite membranes
[PB93-201671] p 2254 N94-23431
Characterization and durability testing of plasma-sprayed zirconia-yttria and hafnia-yttria thermal barrier coatings. Part 2: Effect of spray parameters on the performance of several hafnia-yttria and zirconia-yttria coatings
[NASA-TP-3296] p 2242 N94-23467
Plasma sprayed thermal barrier coatings: Production, characterization and testing
[ISBN-9-03-860082-8] p 2555 N94-25439

PLASMA TEMPERATURE
Imaging XUV spectroscopy of a Z-pinch plasma in the former Soviet Union
[DE93-040849] p 2549 N94-22949

PLASMA TURBULENCE
Active probing of plasma edge turbulence and feedback studies on the Texas Experimental Tokamak (TEXT)
[DE94-001017] p 2548 N94-22945
Chaos in plasma simulation and experiment
[DE94-001574] p 2549 N94-22963
Chaos and simple determinism in reversed field pinch plasmas: Nonlinear analysis of numerical simulation and experimental data
[DE94-001575] p 2550 N94-23211
Nonlinear ion-mixing-mode particle transport in the dissipative trapped electron regime
[DE94-000989] p 2533 N94-23435
Multi-ion, multi-event test of ion cyclotron resonance heating
[NASA-CR-194859] p 2540 N94-23495
The role of the radial electric field in confinement and transport in H-mode and VH-mode discharges in the DIII-D tokamak
[DE94-002746] p 2551 N94-23782

PLASMA WAVES
Active probing of plasma edge turbulence and feedback studies on the Texas Experimental Tokamak (TEXT)
[DE94-001017] p 2548 N94-22945
Chaotic phenomena in plasma, 2
[DE93-508286] p 2549 N94-22964
Multi-ion, multi-event test of ion cyclotron resonance heating
[NASA-CR-194859] p 2540 N94-23495
A relativistic theory on wave propagation in inhomogeneous magnetoplasmas
[ETN-94-95322] p 2554 N94-25285
Numerical simulation and analysis of experimental results on stimulated Raman scattering in laser-plasma Hohlraum targets
[DE93-613719] p 2554 N94-25330
LHCD (low hybrid current drive) experiment on the HT-6B tokamak
[DE93-613720] p 2555 N94-25331

PLASMAS (PHYSICS)
Massachusetts Institute of Technology Plasma Fusion Center 1992-1993 report to the President
[DE94-001725] p 2548 N94-22721
Semiempirical studies of atomic structure
[DE94-001588] p 2531 N94-22937
The internal structure and dynamics of the railgun plasma armature between infinitely wide ablating rails
[DE94-001473] p 2198 N94-23208
Overview of the ATF stellarator program
[DE94-000371] p 2550 N94-23462
Artificial plasma experiments. Chemical release observations associated with the CRRES program
[NASA-CR-194871] p 2550 N94-23565
Stationary plasma thruster plume characteristics
[NASA-CR-194454] p 2219 N94-24361
The chemistry of particulate formation in fluorocarbon plasmas
[DE94-001500] p 2552 N94-24546
X ray simulator theory support
[AD-A273613] p 2553 N94-24949
Excitation balances and transport in an inductively coupled plasma
[ETN-94-95330] p 2554 N94-25241
The anomalous transport caused by particles transverse drift
[DE93-613685] p 2554 N94-25329
Behavior of the intermittency exponents and a quark-gluon plasma formation in the heavy ion collisions
[DE93-616869] p 2541 N94-25342
Effect of LHCD (low hybrid current drive) on tearing mode instability
[DE93-613700] p 2555 N94-25344
Excitation mechanisms for XUV and x ray lasers
[DE93-617006] p 2351 N94-25482
Diffusion in electronegative discharges with magnetic fields
[AD-A273826] p 2304 N94-25521

PLASMASPHERE
The Far Ultraviolet (FUV) auroral imager for the Inner Magnetospheric Imager (IMI) mission: Options
p 2209 N94-24453

PLASTIC DEFORMATION
Analysis of Alloy 600 and X-750 stress corrosion cracks
[DE94-001578] p 2238 N94-22936
Proof test of the computer program BUCKY for plasticity problems
[NASA-TP-3444] p 2374 N94-22960
Damage under monotonic or cyclic loads of new AlSiFe alloys prepared by the Osprey (tm) process
[ISAL-93-0008] p 2239 N94-22972
The plastic response of a cylindrical shell subjected to an internal blast wave with a finite width shock front
p 2154 N94-24246
On the deformation kinetics constitutive law of plastic deformation: The rate equation p 2161 N94-24289
Procedures for determining MATMOD-4V material constants
[DE94-002638] p 2245 N94-24520

PLASTIC PROPERTIES
Gas-pressure forming of superplastic ceramic sheet
[DE94-001520] p 2252 N94-22930
Texture gradient effects in tantalum
[DE94-000689] p 2240 N94-23021
Mean stress models for low cycle fatigue of a nickel-base superalloy p 2159 N94-24276
The nanometer-scale mechanics of gold films
[AD-A273307] p 2565 N94-25086

PLATE THEORY
Vectorization and parallelization of the finite strip method for dynamic Mindlin plate problems
p 2483 N94-23679
Nonlinear analysis using a modal based reduction technique p 2161 N94-24288
Nonlinear equations of motion for a panel subject to external loads
[AD-A273142] p 2170 N94-24773

PLATES (STRUCTURAL MEMBERS)
Hydro-elastic analysis using a selection of commercial analysis programs
[PB94-118734] p 2376 N94-24478
Responses of a finite baffled plate subject to turbulent and mean flow excitations
[NASA-CR-191570] p 2334 N94-24605

PLATING
Investigate zero-stress replicated optics
[NASA-CR-193889] p 2545 N94-24665

PLATINUM
High power density proton exchange membrane fuel cells p 2393 N94-23359
Fundamental and experimental studies on the catalytic combustion of methane
[PB94-112661] p 2233 N94-23736
Thermal phase behavior of metal surfaces: X-ray scattering studies of Pt(001)
[DE94-002991] p 2245 N94-24612
The structure and catalytic properties of supported platinum catalysts
[ETN-94-95357] p 2236 N94-25250

PLATINUM ALLOYS
Reduction of nitric oxide over platinum, rhodium and platinum-rhodium single crystal surfaces
[PB93-230092] p 2232 N94-23482

PLATINUM OXIDES
PEM regenerative fuel cells p 2392 N94-23358

PLOTTING
VTGRAPH:Computer graphics program using ReGIS mode
[DE94-600342] p 2448 N94-23024

PLUMES
Molecular gas dynamics applied to low-thrust propulsion p 2214 N94-23053
Contamination control and plume assessment of low-energy thrusters
[NASA-TM-104585] p 2218 N94-23343
Diagnostic budgets of analyzed and modelled tropical plumes
[NASA-CR-194853] p 2409 N94-23621
Stationary plasma thruster plume characteristics
[NASA-CR-194454] p 2219 N94-24361
Optimal Space Station solar array gimbal angle determination via radial basis function neural networks
[NASA-TM-106482] p 2195 N94-24482
Analysis and effects of the advanced solid rocket motor on the Space Shuttle elements
[NASA-CR-193879] p 2200 N94-24664

PLUTONIUM
A survey of metallurgical research on several actinides
[DE94-002643] p 2245 N94-24747

PLY ORIENTATION
Optimization of laminate orientation to enhance failure properties
[ISBN-0-315-83539-7] p 2227 N94-22892
Analysis of local delaminations caused by angle ply matrix cracks
[NASA-TM-109052] p 2228 N94-24083

PNEUMOTHORAX
Spontaneous pneumothorax, cysts and bullae
p 2425 N94-23326

POINT SOURCES
Static image method for computing the electric potential due to sources in a layered sphere
[PB93-224970] p 2308 N94-23105
Electromagnetic scattering by inhomogeneous objects. Solution methods based upon reciprocity theorems of time-convolution and time-correlation type
[PB94-111010] p 2294 N94-23729

POINT TO POINT COMMUNICATION
MITS architecture V1.0
[PB93-201762] p 2452 N94-23451
The design of a standard message passing interface for distributed memory concurrent computers
[DE94-002536] p 2446 N94-24538

POINTING CONTROL SYSTEMS
Ultra-clean high-precision mechanisms for the SUMER EUV spectrometer on SOHO p 2356 N94-23999
Data relay system satellite: The development of an antenna pointing mechanism for the inter-orbit link antenna p 2359 N94-24015
Inter orbit link antenna pointing mechanisms design using standard actuators p 2359 N94-24016
Design of a new high-performance pointing controller for the Hubble Space Telescope
[NASA-CR-193891] p 2364 N94-24088
Optimal Space Station solar array gimbal angle determination via radial basis function neural networks
[NASA-TM-106482] p 2195 N94-24482

POISSON DENSITY FUNCTIONS
Loss probabilities in batch-arrival bulk-service queues with finite capacity
[MEMO-1106] p 2493 N94-22724
Probabilistic methods in problems of applied analysis
[PB94-110681] p 2495 N94-24571

POISSON EQUATION
A mixed method Poisson solver for three-dimensional self-gravitating astrophysical fluid dynamical systems
p 2484 N94-23684
Comparison of time integration methods for the evolution of galaxies
[PB94-111671] p 2602 N94-24522
Triangular spectral elements for incompressible fluid flow
[NASA-CR-191588] p 2490 N94-24914

POISSON RATIO
Humidity effects on soluble core mechanical and thermal properties (polyvinyl alcohol/microballoon composite) type CG extendospheres, volume 2
[NASA-CR-193893] p 2229 N94-24224

POLAR CAPS
Impact of the CO2 and H2O clouds of the Martian polar hood on the polar energy balance p 2618 N94-24880
High latitude cusp signature observations for southward IMF B sub Z
[AD-A273801] p 2406 N94-25536

POLAR ORBITS
Mission planning for an Earth observation low Earth orbiter: ERS-1 p 2503 N94-23868

POLAR REGIONS
Three-dimensional numerical simulation of near-surface flows over the Martian north polar cap
p 2621 N94-24895
The role of atmospheric heat transport in the seasonal carbon dioxide cycle p 2621 N94-24896

POLARIMETRY
White-light, pressure, and temperature interferopolarimetric sensor featuring optical fibers
[PB93-199792] p 2545 N94-24631
Use of microwave polarimetry to enhance SAR images of the ocean surface
[AD-A273568] p 2419 N94-24944
Liquidus temperature and optical properties measurement by containerless techniques
p 2247 N94-25126

Optical properties and emissivities of liquid metals and alloys p 2248 N94-25129

POLARITY

Observation of non-centrosymmetry and determination of polarity in III-V semiconductors
[PB93-201416] p 2561 N94-23503

POLARIZATION (CHARGE SEPARATION)

Photoinduced charge separation in solid state and molecular systems
[DE94-001727] p 2563 N94-24537

POLARIZATION (SPIN ALIGNMENT)

Polarized structure functions of the nucleon in the resonance region
[CEBAF-PR-94-001] p 2540 N94-24663

POLARIZATION CHARACTERISTICS

Optical properties and emissivities of liquid metals and alloys p 2248 N94-25129

POLARIZERS

Mueller matrix analysis of infrared ellipsometry
[PB93-201549] p 2544 N94-23629

GOLF mechanisms p 2357 N94-24003

POLARONS

Spin-polaron theory of high-T(c) superconductivity. 2: Electronic structure of the CuO2 planes
[DE93-019197] p 2556 N94-22919

Disorder effects on small-polaron formation and hopping
[DE94-001205] p 2534 N94-23804

POLICE

Using satellite communications for a mobile computer network p 2280 N94-22777

POLICIES

Proceedings of the Third International Mobile Satellite Conference (IMSC 1993)
[NASA-CR-194516] p 2273 N94-22735

US domestic and international regulatory issues
p 2275 N94-22748

Use of negotiated rulemaking in developing technical rules for low-Earth orbit mobile satellite systems
p 2276 N94-22750

NASA printing, duplicating, and copying management handbook
[NASA-NHB-1490.5] p 2590 N94-23971

Proceedings of Technology and Governance in the 1990's
[PB93-192904] p 2597 N94-24312

Orbital debris and near-Earth environmental management: A chronology
[NASA-RP-1320] p 2598 N94-24644

POLISHING

Ge-Au eutectic bonding of Ge (100) single crystals
[DE94-002281] p 2564 N94-24657

POLLUTION

Soil pollution at former industrial sites, the heritage of 150 years of industrial development in Noord-Brabant, The Netherlands
[ISBN-9-09-005758-7] p 2400 N94-25223

POLLUTION CONTROL

Economics of electron beam and electrical discharge processing for post-combustion NO(x) control in internal combustion engines
[DE93-019574] p 2351 N94-22865

Fundamental limitations of non-thermal plasma processing for internal combustion engine NO(x) control
[DE93-019622] p 2351 N94-22866

Reduction of nitric oxide over platinum, rhodium and platinum-rhodium single crystal surfaces
[PB93-230092] p 2232 N94-23482

POLLUTION MONITORING

Estimation of delays and emissions at four-way junctions with different forms of regulation, principally four-way mandatory stop
[PB94-105236] p 2398 N94-23813

EPA's survey of in-use driving patterns: Implications for mobile source emission inventories
[PB94-118502] p 2399 N94-24525

Manual on measurement of methane and nitrous oxide emissions from agriculture
[DE93-616429] p 2399 N94-25167

POLLUTION TRANSPORT

Carbon and hydrogen isotope composition and C-14 concentration in methane from sources and from the atmosphere: Implications for a global methane budget
[NASA-CR-195166] p 2399 N94-25092

Collection and evaluation of numerical models with the aim to investigate the impact of aircraft emissions
[DLR-MITT-93-06] p 2400 N94-25414

POLYAMIDE RESINS

Polyimide processing additives
[NASA-CASE-LAR-13669-2] p 2252 N94-23079

Reaction of isocyanates with carboxylic acids and its application to polymer synthesis
[PB94-118858] p 2254 N94-23763

POLYBENZIMIDAZOLE

Di(hydroxyphenyl)- benzimidazole monomers
[NASA-CASE-LAR-14643-2] p 2253 N94-23305

POLYBUTADIENE

Microstructure of styrene methyl methacrylate copolymers grafted onto polybutadiene seeds
[ETN-94-95360] p 2262 N94-25225

POLYCARBONATES

A preliminary evaluation of the phosphazene resin PPZ
[AD-A273674] p 2263 N94-25410

Birdstrike resistant crew enclosure program
[AD-A273700] p 2463 N94-25453

POLYCRYSTALS

Polycrystalline thin film materials and devices
[DE93-018213] p 2389 N94-22862

Chromate-free talc chemical conversion coatings for aluminum alloys
[DE94-001567] p 2238 N94-22932

Orientation imaging microscopy: New possibilities for microstructural investigations using automated BKD analysis
[DE94-000777] p 2557 N94-22938

Research on polycrystalline thin-film CuInGaSe2 solar cells
[DE94-000203] p 2560 N94-23205

Defects in electro-optically active polymer solids
p 2223 N94-24342

POLYETHYLENE TEREPHTHALATE

Processing of semicrystalline polymers
p 2226 N94-24351

A preliminary evaluation of the phosphazene resin PPZ
[AD-A273674] p 2263 N94-25410

POLYETHYLENES

Demonstration of polyscann ultrasonic butt-fusion inspection system for polyethylene pipes
[AD-A273279] p 2373 N94-24814

POLYGONS

Number of moduli of families of curves on toric surfaces
[PB93-230381] p 2479 N94-23121

Tools for visualizing landscape pattern for large geographic areas
[DE94-001121] p 2388 N94-24757

POLYHEDRONS

Extracting projective information from single views of 3D point sets
[OUEL-1973/93] p 2464 N94-25471

POLYIMIDE RESINS

Tribological behaviour of fluorinated resins and polyimide resins sliding over a metallic surface in liquid nitrogen
p 2355 N94-23991

POLYIMIDES

Polyimide processing additives
[NASA-CASE-LAR-13669-2] p 2252 N94-23079

POLYMER BLENDS

Surface and interfacial properties of polymer blends. A literature survey
[PB93-230191] p 2254 N94-23561

Electric field-mediated processing of polymer blend solutions p 2223 N94-24341

Processing of semicrystalline polymers
p 2226 N94-24351

Ultrastructure processing of macromolecular materials
[AD-A273413] p 2258 N94-24782

Center for advanced electrical and structural polymers
[AD-A273415] p 2259 N94-24783

Simulation studies for surfaces and materials strength
[NASA-CR-195185] p 2565 N94-25093

POLYMER CHEMISTRY

Reaction of isocyanates with carboxylic acids and its application to polymer synthesis
[PB94-118858] p 2254 N94-23763

Synthesis of molecular wires by a novel divergent/convergent approach
[AD-A273332] p 2537 N94-25087

Influence of test configuration on the combustion characteristics of polymers as ignition sources
p 2238 N94-25365

POLYMER MATRIX COMPOSITES

Materials Science and Engineering
[DE94-003018] p 2228 N94-23493

Prediction of thermal cycling induced cracking in polmer matrix composites
[NASA-CR-195135] p 2229 N94-24579

POLYMERIC FILMS

Chemically sensitive interfaces on SAW devices
[DE94-001832] p 2526 N94-23718

Ordered organic thin films self-assembled from the vapor phase p 2223 N94-24339

Electric field-mediated processing of polymer blend solutions p 2223 N94-24341

Low-gravity electrodeposition and growth of polymer thin films with large third-order optical nonlinearities by electrochemical processes for devices: Thiophene-based polymers p 2225 N94-24346

Nonlinear optical thin films p 2225 N94-24349

Proceedings of the 12th International Congress: Corrosion Control for Low-Cost Reliability. Volume 1: Coatings
[AD-A273661] p 2251 N94-25448

POLYMERIZATION

Surface and interfacial properties of polymer blends. A literature survey
[PB93-230191] p 2254 N94-23561

Reaction of isocyanates with carboxylic acids and its application to polymer synthesis
[PB94-118858] p 2254 N94-23763

Prediction of nonlinear optical properties of organic materials. General theoretical considerations
p 2224 N94-24343

Polydiacetylene thin films for nonlinear optical applications p 2225 N94-24347

Feasibility study: Monodisperse polymer particles containing laser-excitable dyes p 2225 N94-24350

Convective instabilities in traveling fronts of addition polymerization p 2226 N94-24352

Synthesis of soluble halogenated polyphenylenes: Mechanism for the coupling halogenated lithiobenzenes
[AD-A273547] p 2257 N94-24558

STM studies of LB deposited alkyl substituted polyaniline and its corresponding monomer
[AD-A273553] p 2257 N94-24562

Curing phthalonitrile resins with acid and amine
[AD-D016021] p 2258 N94-24721

Electrochemically mediated polymerization of 2-pentadecylaniline confined to a planar liquid-liquid interface
[AD-A273541] p 2259 N94-24792

The 2-D polymerized Langmuir-Blodgett films studied by STM
[AD-A273542] p 2261 N94-24930

Synthesis of molecular wires by a novel divergent/convergent approach
[AD-A273332] p 2537 N94-25087

Particle nucleation and growth in butadiene emulsion polymerization
[ETN-94-95300] p 2262 N94-25236

POLYMERS

Method of determining shear stress employing a monomer-polymer laminate structure
[NASA-CASE-LAR-14654-2] p 2375 N94-23308

Selection of polymer binders and fabrication of SiC fiber-reinforced reaction-bonded silicon nitride matrix composites
[NASA-CR-194874] p 2255 N94-24223

Microgravity Studies of Organic and Polymeric Materials
[NASA-CP-3250] p 2223 N94-24338

Planar poly(p-phenylene) derivatives: Ladder formation for maximization of extended conjugation
[AD-A273220] p 2260 N94-24922

POLYMETHYL METHACRYLATE

Extinguishment of combustible porous solids by water droplets
[PB93-198893] p 2270 N94-23740

POLYMORPHISM

A type declarative system for PROLOG
[ETN-94-95178] p 2449 N94-23155

POLYNOMIALS

On the Daubechies-based wavelet differentiation matrix
[NASA-CR-191583] p 2479 N94-23090

Mathematical addenda to Hopper's model of plane stokes flow driven by capillarity on a free surface
[PB93-237691] p 2480 N94-23438

Adaptive nonlinear polynomial neural networks for control of boundary layer/structural interaction
[NASA-CR-189645] p 2525 N94-23698

Systematic construction of trigonometric neural networks
[PB93-200228] p 2474 N94-24544

Polynomials orthogonal with respect to an inner product involving differences
[PB94-110731] p 2489 N94-24572

On BRST quantization of constrained systems
[ETN-94-95386] p 2570 N94-25258

Relationship between the structure and performance of identified nonlinear polynomial models
[RR-474] p 2492 N94-25320

A reachability test for systems over polynomial rings using Groebner bases
[MEMO-COSOR-92-38] p 2493 N94-25527

POLYPHENYLS

Synthesis of soluble halogenated polyphenylenes: Mechanism for the coupling halogenated lithiobenzenes
[AD-A273547] p 2257 N94-24558

Metal-catalyzed alkynylation of brominated polyphenylenes: Thermoset precursors of high density monolithic glassy carbon
[AD-A273232] p 2259 N94-24789

Synthesis of polyphenylenes via Bergman cyclization of enediyne monomers [AD-A273298] p 2260 N94-24924

POLYSTYRENE

Feasibility study: Monodisperse polymer particles containing laser-excitable dyes p 2225 N94-24350

POLYTOPES

Number of moduli of families of curves on toric surfaces [PB93-230381] p 2479 N94-23121

Polytopic vector analysis in igneous petrology: Application to lunar petrogenesis p 2615 N94-24368

POLYURETHANE RESINS

Reaction of isocyanates with carboxylic acids and its application to polymer synthesis [PB94-118858] p 2254 N94-23763

POPULATIONS

Aeromedical disposition for coronary artery disease p 2423 N94-23316

Primary prevention of coronary heart disease p 2423 N94-23317

Aeromedical implications of mitral valve prolapse p 2424 N94-23323

Sarcoidosis and the aviator p 2425 N94-23325

Subset selection for the best of two populations: Tables of the expected subset size [PB93-237857] p 2494 N94-23546

Subset selection with a generalized selection goal based on a loss function [PB94-111192] p 2494 N94-23798

Some generalized subset selection procedures [PB94-111655] p 2487 N94-23799

Factors affecting the identification of phytoplankton groups by means of remote sensing [NASA-TM-108799] p 2387 N94-24403

Efficiency of subset selection of an epsilon-best uniform population relative to selection of the best one [PB93-237741] p 2490 N94-24763

An exploratory stochastic model for toxic effects on cells [AD-A273438] p 2422 N94-25146

Solving the ranking and selection indifference-zone formulation for normal distributions using computer software [AD-A273821] p 2496 N94-25518

POROSITY

Influence of sintering atmospheres on the aluminum sintering characteristics [DE93-632412] p 2239 N94-22965

Modelling the ignition of boron/titanium particles p 2159 N94-24273

Method of fabricating a receptor-based sensor [AD-D016026] p 2344 N94-24723

Laser-deposited biocompatible films and methods and apparatuses for producing same [AD-D016017] p 2350 N94-24952

POROUS MATERIALS

Carbon aerogels: An update on structure, properties, and applications [DE94-001528] p 2252 N94-22931

Extinguishment of combustible porous solids by water droplets [PB93-198893] p 2270 N94-23740

Investigations on detonation shock dynamics and related topics [DE94-002570] p 2326 N94-23809

Applications of the homogenization method to flow and transport in porous media [BER-9110] p 2340 N94-25467

PORTABLE EQUIPMENT

Compact free electron lasers for medical applications [AD-A273609] p 2350 N94-24934

POSEIDON SATELLITE

TOPEX/Poseidon precision orbit determination production and expert system p 2196 N94-23920

POSITION (LOCATION)

Joint Acoustic Propagation Experiment (JAPE) p 2527 N94-24208

Worldwide vessel locating and tracking system, volume 1 [PB93-193217] p 2175 N94-24474

The role of visual context in manual target localization p 2429 N94-25351

Mechanisms of eye-hand coordination [AD-A273687] p 2428 N94-25437

POSITION ERRORS

A review of GPS-based tracking techniques for TDRS orbit determination p 2196 N94-23257

POSITION INDICATORS

EUTELTRACS: The European experience on mobile satellite services p 2281 N94-22781

Lightning studies using LDAR and LLP data p 2416 N94-23238

POSITION SENSING

Sensing and modelling concepts for autonomous and remote mobile robot control p 2370 N94-23421

Autonomous Space Processor for Orbital Debris (ASPOD) [NASA-CR-195521] p 2204 N94-24621

POSITIONING

CNES organization for station positioning of geostationary satellites p 2501 N94-23857

MERCATOR: Methods and Realization for Control of the Attitude and the Orbit of spacecraft p 2202 N94-23925

HISPASAT launch and early operations phases: Computation and monitoring of geostationary satellite positioning p 2514 N94-23928

Differential GPS for air transport: Status p 2162 N94-25100

POSITIONING DEVICES (MACHINERY)

Precision Displacement Mechanism (PDM) p 2360 N94-24026

System for automatic transportation of aircraft on the ground [CA-PATENT-1-322-361] p 2193 N94-24785

POSTFLIGHT ANALYSIS

Postflight hardware evaluation RSRM-29 (STS-54). Appendix D: Nozzle postfire data [NASA-CR-193898] p 2199 N94-24057

Postflight hardware evaluation RSRM-29 (STS-54). Appendix C: Nozzle PFORs [NASA-CR-193894] p 2219 N94-24064

Final postflight hardware evaluation report RSRM-32 (STS-57) [NASA-CR-193903] p 2200 N94-24065

Postflight hardware evaluation RSRM-29 (STS-54). Appendix E: Insulation postfire data [NASA-CR-193897] p 2200 N94-24067

Final postflight hardware evaluation report RSRM-28 (STS-53) [NASA-CR-193902] p 2200 N94-24112

Postflight hardware evaluation (RSRM-29, STS-54) [NASA-CR-193895] p 2201 N94-24802

Postflight hardware evaluation 360T021 (RSRM-21, STS-45), revision A [NASA-CR-193904] p 2201 N94-24965

Postflight hardware evaluation RSRM-29 (STS-54). Case, seals, and joints PFORs, appendix B [NASA-CR-193899] p 2367 N94-25020

POSTLAUNCH REPORTS

Final postflight hardware evaluation report RSRM-32 (STS-57) [NASA-CR-193903] p 2200 N94-24065

POSTMISSION ANALYSIS (SPACECRAFT)

Debris/Ice/TPS assessment and integrated photographic analysis for Shuttle Mission STS-61 [NASA-TM-109195] p 2199 N94-24059

Postflight hardware evaluation (RSRM-29, STS-54) [NASA-CR-193895] p 2201 N94-24802

POTABLE WATER

Statistical procedures for corrosion studies [PB93-199412] p 2244 N94-23802

POTASSIUM HYDROXIDES

NASA Lewis advanced IPV nickel-hydrogen technology p 2392 N94-23356

POTASSIUM OXIDES

The de Haas-van Alphen measurements in Ba(0.6)K(0.4)BiO3 [DE93-041169] p 2556 N94-22920

POTENTIAL ENERGY

Mechanical and thermal buckling analysis of sandwich panels under different edge conditions [NASA-TM-4535] p 2228 N94-23514

CAPE for CaPE p 2416 N94-24409

The torsion space nucleic acids molecular mechanics program DUPLEX: Surveying conformation space by potential energy minimization [DE94-002441] p 2563 N94-24567

Free energy profiles for Li(+) and I(-) ions approaching Pt(100) surface: A molecular dynamics study [AD-A273455] p 2536 N94-24675

POTENTIAL FIELDS

Comparison of time integration methods for the evolution of galaxies [PB94-111671] p 2602 N94-24522

POTENTIAL FLOW

Computational fluid dynamic modelling of cavitation p 2215 N94-23060

A dual reciprocal boundary element formulation for viscous flows p 2325 N94-23666

Doppler global velocimetry: Development of a flight research instrumentation system for application to non-intrusive measurements of the flow field [NASA-CR-191490] p 2344 N94-24360

POWDER (PARTICLES)

Development of silicon nitride composites with continuous fiber reinforcement [DE94-001996] p 2227 N94-23022

Theoretical considerations for Reaction-Formed Silicon Carbide (RFSC) formation by molten silicon infiltration into slurry-derived preforms [NASA-TM-106414] p 2222 N94-23500

Magnetic power piston fluid compressor [NASA-CASE-GSC-13565-1] p 2354 N94-23831

Modelling the ignition of boron/titanium particles p 2159 N94-24273

Experimental investigation of ignition of boron/titanium composite particles p 2159 N94-24275

Thermomechanical processing of Ag-clad Bi2Sr2CaCu2O(x) superconductors [DE94-002347] p 2563 N94-24624

POWDER METALLURGY

Solid state synthesis of Fe-B-Si alloys [VTT-PUBS-118] p 2250 N94-25316

The mechanical property data base from an Air Force/Industry Cooperative Test Program on advanced aluminum alloys (7064 and CW67) [AD-A273741] p 2251 N94-25531

POWDERED ALUMINUM

Influence of sintering atmospheres on the aluminum sintering characteristics [DE93-632412] p 2239 N94-22965

POWER AMPLIFIERS

Broadband linearisation of high-efficiency power amplifiers p 2275 N94-22747

Modulation characteristics of a high-power semiconductor Master Oscillator Power Amplifier (MOPA) [NASA-TM-104577] p 2308 N94-23281

Design and testing of ubitron amplifier tubes [AD-A273297] p 2311 N94-24818

Bounds and simulation results of 32-ary and 64-ary quadrature amplitude modulation for broadband-ISDN via satellite [NASA-TM-106484] p 2202 N94-25095

POWER BEAMING

Power beaming to space using a nuclear reactor-pumped laser [DE94-001208] p 2348 N94-23185

POWER CONDITIONING

Development of a power electronics unit for the Space Station plasma contactor [NASA-TM-106486] p 2222 N94-25201

Parallel processing methods for space based power systems p 2222 N94-25352

POWER EFFICIENCY

Second law analysis of a conventional steam power plant p 2322 N94-23646

The effect of high altitude pressure on the power and efficiency of an airborne two-stroke engine p 2155 N94-24253

POWER GAIN

Design and testing of ubitron amplifier tubes [AD-A273297] p 2311 N94-24818

POWER LINES

Mitigation of EMI/RFI produced by a 1.2 kW uninterruptible power supply [AD-A273149] p 2299 N94-24670

POWER LOSS

Effects of a vibrating wire carrying DC current on a moving type 2 superconducting slab of arbitrary thickness [DE93-617136] p 2566 N94-25391

POWER PLANTS

Second law analysis of a conventional steam power plant p 2322 N94-23646

POWER SPECTRA

Propagation model for the Land Mobile Satellite channel in urban environments p 2283 N94-22796

Laser linewidth measurement in the presence of RIN and using the recirculating self heterodyne method [EUT-92-E-262] p 2347 N94-22874

Continuous gust response and sensitivity derivatives using state-space models p 2161 N94-24287

PROPWR: A versatile tool for 1/3 octave processing and narrowband line tracking [DREA-TC-93-303] p 2297 N94-24298

Composite sequences for rapid acquisition of direct-sequence spread spectrum signals [CTN-94-60901] p 2300 N94-24696

Choice of filters for the detection of gravitational waves from coalescing binaries. 2: Detection in coloured noise [DE93-616844] p 2604 N94-25211

POWER SUPPLIES

Power generation technology options for a Mars mission [NASA-TM-106451] p 2220 N94-24681

POWER SUPPLY CIRCUITS

Power electronics development for the SPT-100 thruster [NASA-TM-106488] p 2221 N94-25189

POWER TRANSMISSION
Vibrational power transmission analysis of machinery installations in ships with the objective of noise reduction
[ISVR-TR-216] p 2363 N94-24076
POWERED LIFT AIRCRAFT
Summary of lift and lift/cruise fan powered lift concept technology
[NASA-CR-177619] p 2176 N94-23489
PRANDTL NUMBER
Computational fluid mechanics
[NASA-CR-194765] p 2337 N94-24859
PREBURNERS
SSME fuel preburner injector characterization
p 2211 N94-23037
CFD simulation of coaxial injectors
p 2342 N94-24430
PRECIPITATES
Relationship of microstructure and mechanical properties for V-Cr-Ti alloys
[DE94-001431] p 2238 N94-22718
Potent solvents for C60 and their utility for the rapid acquisition of 13CNMR data for fullerenes
[AD-A273349] p 2235 N94-24925
PRECIPITATION (METEOROLOGY)
NOAA Federal/State Cooperative Program in Atmospheric Modification Research. Collected publication titles and abstracts
[PB93-198125] p 2396 N94-22913
Scientific investigations of atmospheric processes
[NASA-CR-194805] p 2401 N94-23271
Precipitation measurement using SIR-C: A feasibility study
[NASA-CR-195104] p 2409 N94-24048
Water cycle research associated with the CaPE hydrometeorology project (CHymP p 2416 N94-24414
Observational and modeling studies of heat, moisture, precipitation and global-scale circulation patterns
[NASA-CR-195148] p 2415 N94-24485
Observational case studies and diagnostic analyses of long-lived large-amplitude inertia-gravity waves
[AD-A273545] p 2404 N94-24794
PRECIPITATION HARDENING
Effect of irradiation on the stress corrosion cracking behavior of Alloy X-750 and Alloy 625
[DE94-001759] p 2244 N94-23792
PRECISION
Precision drive and speed reduction device
[AD-D016004] p 2367 N94-25046
Design of gas bearing systems for precision applications
[ISBN-9-03-860112-3] p 2367 N94-25249
PRECONDITIONING
An implicit numerical scheme for the simulation of internal viscous flows on unstructured grids
[NASA-TM-106437] p 2481 N94-23554
PREDICATE LOGIC
Design and specification of a generic task model for solving boolean constraint satisfaction problems
[PB94-118841] p 2486 N94-23762
PREDICTION ANALYSIS TECHNIQUES
Electromagnetic field strength prediction in an urban environment: A useful tool for the planning of LMSS
p 2283 N94-22795
Fatigue life and crack growth prediction methodology
[NASA-TM-109044] p 2228 N94-23279
Physical modeling and dynamic simulation of planet vehicles: Application to the motion prediction
p 2371 N94-23426
Transient Ejector Analysis (TEA) code user's guide
[NASA-TM-106310] p 2186 N94-23466
Development of an analytical-numerical model to predict radiant emission or absorption
[NASA-CR-194860] p 2453 N94-23624
Examples of data assimilation in mesoscale models
p 2412 N94-24384
Predictive head movement tracking using innovations generated by Kalman filters
[ISBN-0-315-83371-8] p 2427 N94-24467
Further studies to extend and test the area-time-integral technique applied to satellite data
[NASA-CR-195132] p 2415 N94-24705
The hydrodynamics of a moving fluid-liquid contact line
[ETN-94-95352] p 2339 N94-25247
Kernels of anti-causal operators and the multivariable generalized predictive control problem
[MATHS-REPT-A-191] p 2476 N94-25428
Advances in generalized and constrained generalized predictive control with application to a dynamometer model
[MATHS-REPT-A-192] p 2476 N94-25429
Fault detection in HVAC systems using fuzzy models
[OUEL-1977/93] p 2373 N94-25475
PREDICTIONS
Screening for asymptomatic coronary heart disease
p 2423 N94-23315
The ignition temperature of solid explosives exposed to a fire
[DE94-001047] p 2265 N94-23436
Stability questions in predictive control
[OUEL-1970/93] p 2477 N94-25469
Adaptive predictive control of the benchmark plant
[OUEL-1972/93] p 2477 N94-25470
PREDICTOR-CORRECTOR METHODS
An adaptive streamline diffusion finite element method for hyperbolic systems in gas dynamics
[PREPRINT-688] p 2340 N94-25466
PREFLIGHT OPERATIONS
Constraint-based scheduling p 2510 N94-23904
PREFORMS
Composite fiber structures for catalysts and electrodes
p 2393 N94-23364
Theoretical considerations for Reaction-Formed Silicon Carbide (RFSC) formation by molten silicon infiltration into slurry-derived preforms
[NASA-TM-106414] p 2222 N94-23500
PRELAUNCH TESTS
Constraint-based scheduling p 2510 N94-23904
PREMIXED FLAMES
Mechanism and enhancement of flame stabilization
[DE94-002181] p 2232 N94-23023
Stretch-induced quenching in flame-vortex interactions
p 2237 N94-24156
The production of premixed flame surface area in turbulent shear flow p 2237 N94-24158
Experimental investigation of ignition of boron/titanium composite particles p 2159 N94-24275
Stability of premixed laminar flames in a stagnation point flow to general disturbances
[AD-A273429] p 2234 N94-24673
Modelling of premixed laminar flames
[ETN-94-95317] p 2236 N94-25284
PREPARATION
Preparation and properties of translucent gamma-aluminium oxynitride
[ETN-94-95305] p 2263 N94-25281
PREPOLYMERS
High temperature adhesive
[AD-D016019] p 2258 N94-24737
Curing phthalonitriles with acid
[AD-D015996] p 2261 N94-25054
PREPREGS
Preparing polymeric matrix composites using an aqueous slurry technique
[NASA-CASE-LAR-14771-1] p 2252 N94-23076
Composite material impregnation unit
[NASA-TM-107751] p 2254 N94-23486
PRESBYOPIA
Vision impairment and corrective considerations of civil airmen
[DOT/FAA/AM-93/21] p 2426 N94-23623
PRESIDENTIAL REPORTS
Advanced nuclear thermal propulsion concepts
p 2217 N94-23068
PRESSURE DEPENDENCE
Anisotropic uniaxial pressure effects in YBa2Cu3O(7-delta)
[DE94-001456] p 2557 N94-22929
Bridgman's concern
[DE93-040900] p 2558 N94-22953
Physics of iron
[DE94-002002] p 2402 N94-23721
The effect of high altitude pressure on the power and efficiency of an airborne two-stroke engine
p 2155 N94-24253
PRESSURE DISTRIBUTION
Computational fluid dynamic modelling of cavitation
p 2215 N94-23060
An experimental study of the flow field surrounding a subsonic jet in a cross flow
[NASA-CR-194770] p 2317 N94-23072
Probe systems for measuring static pressure and turbulence intensity in fluid streams
[NASA-CASE-ARC-11935-1] p 2319 N94-23306
Experimental investigation of generic three-dimensional sidewall-compression scramjet inlets at Mach 6 in tetrafluoromethane
[NASA-TM-4497] p 2319 N94-23339
The 3-D CFD modeling of gas turbine combustor-integral bleed flow interaction p 2189 N94-23658
FAS multigrid calculations of three dimensional flow using non-staggered grids p 2341 N94-23675
Evaluation of turbulence models in the PARC code for transonic diffuser flows
[NASA-TM-106391] p 2168 N94-24084
CFD simulation of coaxial injectors
p 2342 N94-24430
Aerodynamic characteristics and pressure distributions for an executive-jet baseline airfoil section
[NASA-TM-4529] p 2169 N94-24586
Eddy mixing coefficient upper limit derived from the photochemical balance of O2 p 2621 N94-24897
Three-dimensional numerical simulation of thermal tides in the Martian atmosphere p 2622 N94-24901
PRESSURE DROP
Prediction of pressure drop in fluid tuned mounts using analytical and computational techniques
p 2321 N94-23643
Solution of mixed convection heat transfer from isothermal in-line fins p 2321 N94-23644
PRESSURE EFFECTS
Anisotropic uniaxial pressure effects in YBa2Cu3O(7-delta)
[DE94-001456] p 2557 N94-22929
Performance evaluation of the Russian SPT-100 thruster at NASA LeRC
[NASA-TM-106401] p 2219 N94-23630
PRESSURE GRADIENTS
Heat transfer and flow structure in end-wall boundary layers
[AD-A273470] p 2335 N94-24689
Fluid velocity and electromagnetic forces measured by a rotating Langmuir probe in the scrape off layer of JFT-2M
[OUEL-1968/92] p 2554 N94-25327
PRESSURE MEASUREMENT
Experimental Methods in Separated Flows
[ILR-MITT-260(1991)] p 2315 N94-22852
Pressure oscillation measurements in turbulent flows
p 2316 N94-22855
The use of near-wall hot-wire probes for time-resolved skin-friction measurements p 2316 N94-22857
Probe shapes that measure time-averaged streamwise momentum and cross-stream turbulence intensity
[NASA-CASE-ARC-11934-1] p 2317 N94-23077
Probe systems for measuring static pressure and turbulence intensity in fluid streams
[NASA-CASE-ARC-11935-1] p 2319 N94-23306
Calibration of HYPULSE for hypervelocity air flows corresponding to flight Mach numbers 13.5, 15, and 17
[NASA-CR-191578] p 2192 N94-23564
Improved pressure measurement system for calibration of the NASA LeRC 10x10 supersonic wind tunnel
[NASA-TM-106470] p 2344 N94-24362
Experimental cavity pressure measurements at subsonic and transonic speeds. Static-pressure results
[NASA-TP-3358] p 2169 N94-24464
White-light, pressure, and temperature interferopolarimetric sensor featuring optical fibers
[PB93-199792] p 2545 N94-24631
Method and apparatus for the non-invasive measurement of pressure inside pipes using a fiber optic interferometer sensor
[AD-D016013] p 2344 N94-24734
Analysis of the effects of wake passage on heat transfer in a linear turbine cascade
[AD-A273729] p 2339 N94-25446
PRESSURE MODULATOR RADIOMETERS
Modeling and data assimilation for Mars Observer
p 2620 N94-24889
PRESSURE OSCILLATIONS
Pressure oscillation measurements in turbulent flows
p 2316 N94-22855
Three-dimensional numerical simulation of thermal tides in the Martian atmosphere p 2622 N94-24901
PRESSURE PULSES
Magnetic power piston fluid compressor
[NASA-CASE-GSC-13565-1] p 2354 N94-23831
PRESSURE RECOVERY
Improving diffusing S-duct performance by secondary flow control
[NASA-TM-106492] p 2170 N94-25182
PRESSURE REDUCTION
Experimental and analytical study of cryogenic propellant boiloff to develop and verify alternate pressurization concepts for Space Shuttle external tank using a scaled down tank p 2266 N94-23657
PRESSURE REGULATORS
Computer control of an electro-mechancial regulator for providing positive pressure breathing and an electronic G-valve for human +Gz research
[DCIEM-93-05] p 2437 N94-24299
The pressure loaded volumetric ceramic receiver 500 kW version design and construction
[DLR-MITT-93-02] p 2396 N94-25479
PRESSURE SENSORS
Probe shapes that measure time-averaged streamwise momentum and cross-stream turbulence intensity
[NASA-CASE-ARC-11934-1] p 2317 N94-23077
Probe systems for measuring static pressure and turbulence intensity in fluid streams
[NASA-CASE-ARC-11935-1] p 2319 N94-23306
White-light, pressure, and temperature interferopolarimetric sensor featuring optical fibers
[PB93-199792] p 2545 N94-24631

PRESSURE VESSELS
A pressurized thermogravimetric analyzer for use in studies of gas/solid systems
[DE94-001224] p 2342 N94-22989
Dispersion of fire suppression agents discharged from high pressure vessels: Establishing initial/boundary conditions for the flow outside the vessel
[PB94-103660] p 2172 N94-23810
J-integral patch for finite element analysis of dynamic fracture due to impact of pressure vessels
p 2381 N94-24429
Plasma initiation in a tokamak with conducting superstructure: First results from Alcator C-MOD
[DE94-001565] p 2552 N94-24504
Metal hydride storage
[VTT-JULK-769] p 2396 N94-25417
Strength and life of pressure vessels subjected to impacts and thermomechanical GFRP loading
[VTT-JULK-771] p 2379 N94-25418
PRESSURIZED CABINS
Pressure wall patch
[NASA-CASE-MFS-28724-1] p 2203 N94-23824
PRESSURIZING
Thermodynamic models for bounding pressurant mass requirements of cryogenic tanks
[NASA-TM-106476] p 2346 N94-25202
PREVENTION
Primary prevention of coronary heart disease
p 2423 N94-23317
Waste minimization/pollution prevention at R/D facilities: A cradle-to-grave tracking and information system that will be implemented at Sandia National Laboratories
[DE93-040330] p 2591 N94-24607
PRIMERS (COATINGS)
Evaluation of inorganic zinc-rich primers using Electrochemical Impedance Spectroscopy (EIS)
p 2237 N94-23233
PRIMITIVE EQUATIONS
An efficient data assimilation algorithm with a gaussian covariance structure
[AD-A273152] p 2418 N94-24671
A diagnostic model to estimate winds and small-scale drag from Mars Observer PMIRR data
p 2617 N94-24874
The influence of orography on the transport of atmospheric constituents p 2619 N94-24886
PRINTED CIRCUITS
CADBIT 2: Computer-aided design for built-in test, volume 1
[AD-A273702] p 2463 N94-25455
CADBIT 2: Computer-aided design for built-in test, volume 2
[AD-A273703] p 2463 N94-25456
PRINTING
NASA printing, duplicating, and copying management handbook
[NASA-NHB-1490.5] p 2590 N94-23971
PROBABILITY DENSITY FUNCTIONS
Numerical solutions of the complete Navier-Stokes equations
[NASA-CR-194780] p 2337 N94-24858
Probabilistic assessment of smart composite structures
[NASA-TM-106358] p 2378 N94-25188
PROBABILITY DISTRIBUTION FUNCTIONS
Characterizations of shift-invariant distributions based on summation modulo one
[PB93-237824] p 2481 N94-23442
PROBABILITY THEORY
On some approximately balanced combinatorial cooperative games
[MEMO-1113] p 2493 N94-22702
Probabilistic analysis of mechanical systems
[DE93-041145] p 2371 N94-22918
Simple calculus of finite probabilistic processes
[PB93-223782] p 2493 N94-23108
Application of maximum entropy and irreducible cluster integrals to joint probability distributions for x ray structure determination
[PB93-224152] p 2559 N94-23109
On non-informativeness in a classical Bayesian inference problem
[MEMO-COSOR-92-35] p 2494 N94-23143
Review of the probabilistic failure analysis methodology and other probabilistic approaches for application in aerospace structural design
[NASA-TP-3434] p 2376 N94-23342
Bayesian decision theory with imprecise prior probabilities applied to replacement problems
[PB93-237634] p 2481 N94-23456
Development and application of an empirical probability distribution for the prediction error of re-entry body maximum dynamic pressure p 2207 N94-23653
Mean-value of product-form stochastic Petri net models of slotted-ring systems
[PB94-110871] p 2494 N94-23749
Logarithm of probability measures and infinite divisibility of sub-stable random vectors
[PB94-118627] p 2486 N94-23758
Decision making with imprecise probabilities
[PB94-111622] p 2494 N94-23772
Asymptotic confidence intervals for the length of the shortt under random censoring
[PB93-237816] p 2494 N94-23774
Subset selection with a generalized selection goal based on a loss function
[PB94-111192] p 2494 N94-23798
Some generalized subset selection procedures
[PB94-111655] p 2487 N94-23799
Specifying design conservatism: Worst case versus probabilistic analysis p 2374 N94-23939
Probabilistic simulation of concurrent engineering of propulsion systems p 2177 N94-24317
Uniform limit theorems for marked point processes
[PB94-118726] p 2488 N94-24526
Integral equations for the microstructures of supercritical fluids
[DE94-002460] p 2535 N94-24569
Probabilistic methods in problems of applied analysis
[PB94-110681] p 2495 N94-24571
Mitigation of EMI/RFI produced by a 1.2 kW uninterruptible power supply
[AD-A273149] p 2299 N94-24670
Topics in probability and dynamics
[AD-A273543] p 2496 N94-24931
Infinitely divisible processes and their nonlinear functionals; a study of their structural, statistical and sample path properties and their prediction problems
[AD-A273468] p 2496 N94-25147
Solving the ranking and selection indifference-zone formulation for normal distributions using computer software
[AD-A273821] p 2496 N94-25518
PROBLEM SOLVING
Framework for interactive solving of meta-constraint satisfaction problems
[PB94-118825] p 2585 N94-23761
Design and specification of a generic task model for solving boolean constraint satisfaction problems
[PB94-118841] p 2486 N94-23762
Two applications of a generic task model for solving boolean constraint satisfaction problems
[PB94-119047] p 2487 N94-23765
Egalitarian non-average contribution method for cooperative games
[PB94-111705] p 2497 N94-23800
Non-brittleness of a DESIRE-model for an office assignment task
[PB94-119021] p 2489 N94-24643
Introduction to a behavioral approach for continuous time systems
[ETN-94-95301] p 2492 N94-25277
PROCEDURES
An analysis of traditional operational testing to project how testing will be conducted in the future
[AD-A273189] p 2372 N94-24553
Aircraft digital flight control technical review
p 2163 N94-25106
PROCESS CONTROL (INDUSTRY)
Tool sharing: An application of max-algebra, part 2
[MEMO-1122] p 2478 N94-22710
Sensors for process control Focus Team report
[DE93-040697] p 2560 N94-23204
Intelligent control of chemical vapor deposition processes
[AD-A273356] p 2261 N94-24937
Production control and demand management in capacitated flow process industries
[ISBN-9-03-860211-1] p 2586 N94-25235
MIMO system identification for H(infinity) robust control: A frequency domain approach with minimum error bounds
[ETN-94-95354] p 2476 N94-25262
PRODUCT DEVELOPMENT
Multidisciplinary specification and design of microelectronics in products
[EUT-93-E-269] p 2308 N94-23136
Rolls-Royce in perspective: Past, present and future
[PNR-90882] p 2187 N94-23519
The RB211: The first 25 years
[PNR-90977] p 2187 N94-23570
Overview of molten carbonate fuel cell technology development
[DE94-001911] p 2394 N94-23781
Training: Plugging the information gaps
p 2429 N94-23934
Roles, uses, and benefits of general aviation aircraft in aerospace engineering education
[NASA-TM-106463] p 2153 N94-24100
Early manufacturing considerations in design
p 2177 N94-24315
Frameworks for integrated airframe design
p 2178 N94-24318
Characteristics of products generated by selective sintering and stereolithography rapid prototyping processes p 2264 N94-24412
High-order technology: Applying technical excellence to new airplane development p 2185 N94-25069
Reuse-Driven Software Processes Guidebook, version 02.00.03
[AD-A273644] p 2461 N94-25148
New Technologies for Space Avionics, 1993
[NASA-CR-195157] p 2272 N94-25193
Appendix B: Rapid development approaches for system engineering and design p 2272 N94-25195
Appendix C: Rapid development approaches for system engineering and design p 2272 N94-25196
A multimedia adult literacy program: Combining NASA technology, instructional design theory, and authentic literacy concepts p 2585 N94-25384
PRODUCTION COSTS
Amorphous silicon PVMaT, phase 2A
[DE93-018221] p 2390 N94-23295
New Ways Of Doing Business (NWODB) cost quantification analysis
[NASA-CR-195186] p 2586 N94-25197
PRODUCTION ENGINEERING
Making tomorrow's mistakes today: Evolutionary prototyping for risk reduction and shorter development time p 2197 N94-23902
Tool sharing, part 3
[PB94-111697] p 2467 N94-24524
What makes industries believe in formal methods
[PB94-110848] p 2272 N94-24648
The increase of the controllability of production organizations
[ISBN-9-03-860161-1] p 2586 N94-25076
Throughput time control and due date reliability in tool and die shops
[ISBN-9-03-860182-4] p 2587 N94-25283
PRODUCTION MANAGEMENT
The application of automated operations at the Institutional Processing Center p 2509 N94-23901
The integration of design and manufacturing processes at Alenia DVD p 2179 N94-24325
The increase of the controllability of production organizations
[ISBN-9-03-860161-1] p 2586 N94-25076
New Ways Of Doing Business (NWODB) cost quantification analysis
[NASA-CR-195186] p 2586 N94-25197
Production control and demand management in capacitated flow process industries
[ISBN-9-03-860211-1] p 2586 N94-25235
PRODUCTION PLANNING
Class of strong valid inequalities for the discrete lot-sizing and scheduling problem
[PB93-237774] p 2459 N94-24765
Production control and demand management in capacitated flow process industries
[ISBN-9-03-860211-1] p 2586 N94-25235
PROGRAM VERIFICATION (COMPUTERS)
Definition and realization of a formal verification tool of LUSTRE programs: The LESAR system
[ETN-94-95164] p 2447 N94-22882
Proof test of the computer program BUCKY for plasticity problems
[NASA-TP-3444] p 2374 N94-22960
Formal methods and digital systems validation for airborne systems
[NASA-CR-4551] p 2466 N94-23293
Micro SIL-1 simulator
[PB94-110889] p 2454 N94-23750
Towards the formal verification of the requirements and design of a processor interface unit
[NASA-CR-4522] p 2467 N94-24075
Verification and validation of models
[PB94-110566] p 2456 N94-24507
Validation activities for LOTOS based on static data flow analysis
[PB94-110863] p 2459 N94-24750
Analyzing the properties of user interface software
[AD-A273601] p 2460 N94-24933
DARPA DICE manufacturing optimization
[AD-A273345] p 2461 N94-25156
Computerized testing system software conversion and development: Identifying software and hardware portability issues and solutions
[AD-A273489] p 2462 N94-25287
PROGRAMMABLE LOGIC DEVICES
Logic synthesis on programmable networks
[ETN-94-95174] p 2449 N94-23151
PROGRAMMERS
Designers' models of the human-computer interface
p 2433 N94-24188

PROGRAMMING (SCHEDULING)
Modular approach to project management
[PB94-118833] p 2586 N94-24528
PROGRAMMING ENVIRONMENTS
MITS architecture V1.0
[PB93-201762] p 2452 N94-23451
A programming environment for distributed complex computing. An overview of the Framework for Interdisciplinary Design Optimization (FIDO) project. NASA Langley TOPS exhibit H120b
[NASA-TM-109058] p 2457 N94-24603
PROGRAMMING LANGUAGES
Definition and realization of a formal verification tool of LUSTRE programs: The LESAR system
[ETN-94-95164] p 2447 N94-22882
Asynchronous rendezvous in distributed logic programming
[PB93-220614] p 2448 N94-23096
Tools reference manual for a Requirements Specification Language (RSL), version 2.0
[NASA-CR-191461] p 2445 N94-23125
PROGRIL: A language for the definition of protocol grammars
[EUT-93-E-270] p 2449 N94-23172
Arc consistency problem: An exercise in parallel programming with shared objects
[PB94-110590] p 2466 N94-23706
Transition system specifications in stalk format with bisimulation as a congruence
[PB94-110608] p 2453 N94-23707
Object distribution in orca using compile-time and run-time techniques
[PB94-110574] p 2453 N94-23745
Mission and science activity scheduling language
p 2515 N94-23938
Tensoral for post-processing users and simulation authors p 2333 N94-24169
Sequential composition, action prefixes and process prefix
[PB94-101433] p 2488 N94-24539
Correct and efficient interface for logical query languages with complex objects
[PB93-211175] p 2593 N94-24743
PROJECT MANAGEMENT
Progress in phases 2 and 3 of the Photovoltaic Manufacturing Technology Project (PVMaT)
[DE94-000206] p 2389 N94-22888
Flexible framework for contingent information systems modelling
[PB93-220549] p 2589 N94-23095
A framework for SFC/DC system data analysis
p 2523 N94-23234
Earth Observing System (EOS) Advanced Microwave Sounding Unit-A (AMSU-A) schedule plan
[NASA-CR-194856] p 2585 N94-23563
Framework for interactive solving of meta-constraint satisfaction problems
[PB94-118825] p 2585 N94-23761
Mission engineering p 2505 N94-23881
Manned Space-laboratories Control Center (MSCC) operations concept p 2505 N94-23882
An approach to the design of operations systems
p 2506 N94-23884
Mission operations and command assurance: Instilling quality into flight operations p 2374 N94-23932
Frameworks for integrated airframe design
p 2178 N94-24318
Risk identification and reduction in integrated product teams p 2497 N94-24407
Spatial interpretation of NASA's Marshall Space Flight Center Payload Operations Control Center using virtual reality technology p 2198 N94-24432
Extension of the critical path method
[PB94-118817] p 2488 N94-24527
Modular approach to project management
[PB94-118833] p 2586 N94-24528
A methodology for software cost estimation using machine learning techniques
[AD-A273158] p 2459 N94-24775
New Ways Of Doing Business (NWODB) cost quantification analysis
[NASA-CR-195186] p 2586 N94-25197
PROJECT PLANNING
Manned Space-laboratories Control Center (MSCC) operations concept p 2505 N94-23882
PROJECT SETI
SETI: Search for extraterrestrial intelligence. An international interdisciplinary seminar, star days
[PB93-230597] p 2444 N94-23754
PROJECTILES
Projectile transverse motion and stability in electromagnetic induction launchers
[DE94-001557] p 2198 N94-23210
A comparison of in-bore projectile motion from an electromagnetic railgun versus that of a conventional cannon barrel
[AD-A273473] p 2198 N94-24690
PROJECTION
Projection techniques for iterative solution of A(bar x) equals (bar b) with successive right-hand sides
[NASA-CR-191571] p 2490 N94-24836
PROJECTIVE GEOMETRY
Orbit spaces over commutative rings and projectives as semi-isomorphisms
[DE93-616822] p 2493 N94-25473
PROLOG (PROGRAMMING LANGUAGE)
A type declarative system for PROLOG
[ETN-94-95178] p 2449 N94-23155
A parallel PROLOG system for distributed memory multiprocessor
[ETN-94-95173] p 2465 N94-23167
Applications of the Aurora parallel PROLOG system to computational molecular biology
[DE93-041166] p 2420 N94-23468
Declarative Object Manipulation Environment (DOME): Alpha version
[AD-A273233] p 2460 N94-24935
PROP-FAN TECHNOLOGY
Holographic testing of composite propfans for a cruise missile wind tunnel model
[NASA-TM-105271] p 2187 N94-23545
Aerodynamic models for performance calculations of modern technology propellers p 2161 N94-24285
Dumbo heavy lifter aircraft
[NASA-CR-195500] p 2182 N94-24915
PROPAGATION VELOCITY
Normal zone propagation and thermal hydraulic quenchback in a cable-in-conduit superconductor
[DE94-002457] p 2271 N94-24568
Arbitrary-order numerical schemes for linear hyperbolic systems
[CRANFIELD-AERO-9211] p 2523 N94-25480
PROPELLANT COMBUSTION
A theoretical evaluation of aluminum gel propellant two-phase flow losses on vehicle performance
p 2210 N94-23031
Laser diagnostics for small rockets
p 2210 N94-23032
CFD analyses of combustor and nozzle flowfields
p 2210 N94-23033
LOX droplet vaporization in a supercritical forced convective environment p 2211 N94-23034
Development of a computational testbed for numerical simulation of combustion instability
p 2213 N94-23046
Numerical investigation of two- and three-dimensional heat transfer in expander cycle engines
p 2213 N94-23048
Two stage turbine for rockets p 2215 N94-23059
The Jet Propulsion Laboratory space exploration: Past, present and future p 2153 N94-24242
Burning rate of double-base propellant in the presence of plasma p 2155 N94-24252
Ignition and combustion characteristics of metallized propellants, phase 2
[NASA-CR-195107] p 2266 N94-24700
PROPELLANT GRAINS
Design considerations of hybrid rockets
p 2156 N94-24254
PROPELLANT STORAGE
New methane chemistry synthesis of materials for reversible uptake and useful functionalization of methane
[PB94-112786] p 2233 N94-23801
Design of a lunar propellant processing facility. NASA/USRA advanced program
[NASA-CR-195502] p 2266 N94-24618
PROPELLANTS
Experimental and analytical study of cryogenic propellant boiloff to develop and verify alternate pressurization concepts for Space Shuttle external tank using a scaled down tank p 2266 N94-23657
Numerical simulation of cylindrical, self-field MPD thrusters with multiple propellants
[NASA-CR-194458] p 2220 N94-24714
PROPELLER BLADES
Counterrotating aircraft propulsor blades
[CA-PATENT-1-319-357] p 2186 N94-23255
Wing mounted unducted fan engine
[CA-PATENT-1323353] p 2188 N94-24180
Aerodynamic models for performance calculations of modern technology propellers p 2161 N94-24285
Aircraft accident report: In-flight loss of propeller blade and uncontrolled collision with terrain Mitsubishi MU-2B-60, N86SD, Zwingle, Iowa, 19 April 1993
[PB93-910409] p 2174 N94-25175
PROPELLER EFFICIENCY
Aerodynamic models for performance calculations of modern technology propellers p 2161 N94-24285
PROPELLER FANS
Holographic testing of composite propfans for a cruise missile wind tunnel model
[NASA-TM-105271] p 2187 N94-23545
PROPELLERS
Aerodynamic models for performance calculations of modern technology propellers p 2161 N94-24285
Hydro-elastic analysis using a selection of commercial analysis programs
[PB94-118734] p 2376 N94-24478
PROPOSALS
Research interests and broad agency announcement 94-1 of the Air Force Office of Scientific Research
[AD-A273410] p 2632 N94-25075
PROPULSION
The 1993 NASA/ASEE Summer Faculty Fellowship Program
[NASA-CR-193862] p 2574 N94-24405
PROPULSION SYSTEM CONFIGURATIONS
Analysis and experiments of a whistler-wave plasma thruster
[DE94-001533] p 2209 N94-23012
Efficiency and reliability enhancements in propulsion flowfield modeling p 2215 N94-23055
Performance assessment of low pressure nuclear thermal propulsion p 2217 N94-23070
Lewis Research Center R and D Facilities
[NASA-TM-109400] p 2630 N94-23135
Assessment of an SP-100 bi-modal propulsion and power system
[DE94-000889] p 2218 N94-23433
Heat pipe cooled heat rejection subsystem modelling for nuclear electric propulsion
[NASA-CR-191132] p 2219 N94-24061
Probabilistic simulation of concurrent engineering of propulsion systems p 2177 N94-24317
Multi-disciplinary coupling for integrated design of propulsion systems p 2179 N94-24326
Center for modeling of turbulence and transition: Research briefs, 1993
[NASA-TM-106383] p 2333 N94-24336
VLCT-13: A commercial transport for the 21st Century
[NASA-CR-195492] p 2181 N94-24803
The Blue Emu
[NASA-CR-195535] p 2182 N94-24817
Extended duration lunar lander
[NASA-CR-195527] p 2206 N94-24916
Space transfer vehicle concepts and requirements. Volume 4: Summary of special studies
[NASA-CR-193918] p 2201 N94-24970
Effect of aeroelastic-propulsive interactions on flight dynamics of a hypersonic vehicle p 2164 N94-25113
Shielded Coil Electrodynamic Propulsion (SCEP). A feasibility study
[AD-A273824] p 2314 N94-25539
PROPULSION SYSTEM PERFORMANCE
Analysis and experiments of a whistler-wave plasma thruster
[DE94-001533] p 2209 N94-23012
Small rocket research and technology
p 2211 N94-23038
Performance assessment of low pressure nuclear thermal propulsion p 2217 N94-23070
Assessment of an SP-100 bi-modal propulsion and power system
[DE94-000889] p 2218 N94-23433
Performance evaluation of the Russian SPT-100 thruster at NASA LeRC
[NASA-TM-106401] p 2219 N94-23630
Center for modeling of turbulence and transition: Research briefs, 1993
[NASA-TM-106383] p 2333 N94-24336
A minimum cost tolerance allocation method for rocket engines and robust rocket engine design
p 2222 N94-24419
Space Shuttle Main Engine performance analysis
p 2222 N94-24444
Ignition and combustion characteristics of metallized propellants, phase 2
[NASA-CR-195107] p 2266 N94-24700
Performance of the NASA cm ion thruster
[NASA-TM-106426] p 2221 N94-24770
A conceptual design of an unmanned test vehicle using an airbreathing propulsion system
[NASA-CR-195550] p 2189 N94-25085
Effect of aeroelastic-propulsive interactions on flight dynamics of a hypersonic vehicle p 2164 N94-25113
Shielded Coil Electrodynamic Propulsion (SCEP). A feasibility study
[AD-A273824] p 2314 N94-25539
PROPYLENE
Morphology of highly textured polyethylene/polyethylene- propylene semicrystalline diblock copolymers
[AD-A273683] p 2263 N94-25413

PROSTHETIC DEVICES

Image remapping strategies applied as protheses for the visually impaired p 2444 N94-25363

PROTEASE

Evaluation of ovostatin and ovostatin assay p 2422 N94-24437

PROTECTION

Lightning studies using LDAR and LLP data p 2416 N94-23238

PROTECTIVE CLOTHING

Survival suit for submarine personnel: Summary of evaluation studies [PB93-204634] p 2430 N94-23743

Operation Friction: Development and introduction of personal cooling for CH124 Sea King aircrew [DCIEM-93-06] p 2433 N94-24119

PROTECTIVE COATINGS

Advanced research and technology development of MCFCs [DE94-001918] p 2389 N94-22723

Chromate-free talc chemical conversion coatings for aluminum alloys [DE94-001567] p 2238 N94-22932

Advanced materials for radiation-cooled rockets p 2214 N94-23052

Counterrotating aircraft propulsor blades [CA-PATENT-1-319-357] p 2186 N94-23255

Fiber optic temperature sensor using a Y2O2S:Eu thermographic phosphor [DE94-000331] p 2543 N94-23461

Characterization and durability testing of plasma-sprayed zirconia-yttria and hafnia-yttria thermal barrier coatings. Part 2: Effect of spray parameters on the performance of several hafnia-yttria and zirconia-yttria coatings [NASA-TP-3296] p 2242 N94-23467

Diffuse panel studies: Conclusions p 2384 N94-23606

New tribocoating combination for vacuum operation p 2355 N94-23990

Tribological characteristics of ball bearings lubricated with a sputtered molybdenum disulphide film in a vacuum under a high thrust load p 2355 N94-23992

In-vacuum performance of Fomblin Z25-lubricated, 52100 steel bearings with TiC-coated balls p 2358 N94-24011

Structural characterization and thermal cycling behaviour of EB-PVD thermal barrier coating systems [ISBN-0-315-83365-3] p 2257 N94-24468

Robotic weld overlay coatings for erosion control [DE94-002665] p 2258 N94-24749

The reaction mechanism of W-CVD in Si [ETN-94-95329] p 2261 N94-25084

Proceedings of the 12th International Congress: Corrosion Control for Low-Cost Reliability. Volume 4: Oil/Gas Pipeline [AD-A273665] p 2250 N94-25405

Proceedings of the 12th International Congress: Corrosion Control for Low-Cost Reliability. Volume 5A: Corrosion: General issues [AD-A273666] p 2250 N94-25406

A preliminary evaluation of the phosphazene resin PPZ [AD-A273674] p 2263 N94-25410

Proceedings of the 12th International Congress: Corrosion Control for Low-Cost Reliability. Volume 1: Coatings [AD-A273661] p 2251 N94-25448

Preceedings of the 12th International Congress: Corrosion Control for Low-Cost Reliability. Volume 2: Process Industries Plant Operations [AD-A273662] p 2251 N94-25449

Proceedings of the 12th International Congress: Corrosion Control for Low-Cost Reliability. Volume 3B: Corrosion: Specific issues [AD-A273664] p 2251 N94-25451

PROTEIN CRYSTAL GROWTH

Microgravity sciences application visiting scientist program [NASA-CR-194804] p 2267 N94-23287

Modeling of PCG fluid dynamics: Salient results p 2224 N94-24345

Stiffening of deployable space booms: Automated Protein Crystal Growth Facility [NASA-CR-195547] p 2196 N94-24820

PROTEIN METABOLISM

Skeletal muscle metabolism in hypokinetic rats [NASA-CR-195082] p 2420 N94-24124

PROTEINS

Microgravity sciences application visiting scientist program [NASA-CR-194804] p 2267 N94-23287

Microinjection of the Yersinia YopE cytotoxin in mammalian cells induces actin microfilament disruption [FOA-B-40418-4.4] p 2421 N94-24290

Evaluation of ovostatin and ovostatin assay p 2422 N94-24437

In vitro system for studying metabolism of environmental chemicals in human cells [AD-A273427] p 2421 N94-24688

PROTOCOL (COMPUTERS)

Land mobile satellite propagation measurements in Japan using ETS-V satellite p 2282 N94-22790

A protocol for satellite access via use of spot-beams p 2286 N94-22811

System services and architecture of the TMI satellite mobile data system p 2286 N94-22817

Representation and specification of architectures for heterogeneous internetworking: Using a knowledge based approach [LAAS-93088] p 2445 N94-22903

Generation of modules for control communication circuits: A design study used in the framework of the safe vehicle PROMETHEUS [ETN-94-95171] p 2308 N94-23165

PROGRIL: A language for the definition of protocol grammars [EUT-93-E-270] p 2449 N94-23172

Code generation for the attribute evaluator of the protocol engine grammar processor unit [EUT-93-E-271] p 2450 N94-23173

MITS architecture V1.0 [PB93-201762] p 2452 N94-23451

Command/telemetry bus general specification for the NOAA-OPQ polar orbiting environmental satellites and EUMETSAT polar satellite systems [NASA-TM-109407] p 2208 N94-23479

Low rate data bus general specification for the NOAA-OPQ polar orbiting environmental satellites and EUMETSAT polar satellite systems [NASA-TM-109408] p 2208 N94-23480

High-rate data link general specification for the NOAA-OPQ polar orbiting environmental satellites and EUMETSAT satellite systems [NASA-TM-109384] p 2208 N94-23481

Source spacing in B-ISDN [PB93-201747] p 2293 N94-23508

Radar stimulator interface protocol, preliminary interface design and Doppler Beam Sharpening implementation [DE94-002567] p 2453 N94-23701

Design and implementation issues of end-to-end protocols in high-speed networks [PB94-110905] p 2467 N94-23752

A reference model for space data system interconnection services p 2305 N94-23847

Reliable transfer of data from ground to space p 2305 N94-23908

The EURECA telecommanding chain: Experience with packet telecommand and telemetry systems p 2305 N94-23909

Verification of technical elements of the advanced spacecraft based upon the CCSDS recommendation p 2207 N94-23910

Real-time process logic [PB94-101441] p 2446 N94-24540

Optimizing parallelization [AD-A273565] p 2467 N94-24692

Validation activities for LOTOS based on static data flow analysis [PB94-110863] p 2459 N94-24758

HORACE: Presentation-level protocol standard for digital transmission of monochrome television images [AD-A273395] p 2197 N94-25064

Models of trace theory systems [ETN-94-95361] p 2468 N94-25226

Failure detection and recovery in the assembly/contingency subsystem p 2306 N94-25360

PROTON IRRADIATION

On the origin of 1/f noise in epitaxial GaAs [ISBN-9-09-006067-7] p 2566 N94-25297

PROTONS

A novel method for determination of transport parameters of H2 and O2 in PEMFCs [DE94-001492] p 2389 N94-22962

Low p(sub T) photon production in proton-nucleus collisions at 18 GeV/c [DE94-001380] p 2532 N94-23007

Primary and secondary electrical space power based on advanced PEM systems p 2392 N94-23357

PEM regenerative fuel cells p 2392 N94-23358

High power density proton exchange membrane fuel cells p 2393 N94-23359

A high performance H2-Cl2 fuel cell for space power applications p 2394 N94-23366

Investigation of evolution-related aspects of bacterial rhodopsins [NASA-CR-194826] p 2420 N94-23501

Low mass muon pair production in 450 GeV p-Be collisions [PB94-110699] p 2533 N94-23746

Momentum loss in proton-nucleus and nucleus-nucleus collisions [NASA-TP-3405] p 2540 N94-24305

Polarized structure functions of the nucleon in the resonance region [CEBAF-PR-94-001] p 2540 N94-24663

Activities of Academia Sinica [DE93-614529] p 2541 N94-25335

Proton spin: The role of quark-gluon and hadron degrees of freedom [DE93-616867] p 2538 N94-25341

PROTOPLANETS

Protoplanetary disks: Theory and observation by millimeter and sub-millimeter arrays [REPT-331] p 2603 N94-24983

The Nobeyama millimeter array survey for protoplanetary disks around protostar candidates and T Tauri stars in Taurus [REPT-336] p 2604 N94-24987

Observational studies of the clearing phase in proto-planetary disk systems [NASA-CR-195182] p 2604 N94-25265

PROTOTYPES

Direct broadcast satellite-radio, receiver development p 2273 N94-22739

The Automated Instrumentation and Monitoring System (AIMS) reference manual [NASA-TM-108795] p 2452 N94-23510

Harmonisation of man-machine interface experiments in the context of the development of PHARE advanced tools [PB93-204725] p 2430 N94-23744

Making tomorrow's mistakes today: Evolutionary prototyping for risk reduction and shorter development time p 2197 N94-23902

Performing speech recognition research with hypercard p 2306 N94-24194

Characteristics of products generated by selective sintering and stereolithography rapid prototyping processes p 2264 N94-24412

Integration and evaluation of a simulator designed to be used within a dynamic prototyping environment p 2198 N94-24436

A prototype to automate the video subsystem routing for the video distribution subsystem of Space Station Freedom p 2306 N94-25353

PROVING

Validating identified nonlinear models with chaotic dynamics [RR-469] p 2523 N94-25314

PSYCHOACOUSTICS

On the auditory discrimination of spectral shape [ETN-94-95306] p 2530 N94-25289

PSYCHOLOGICAL EFFECTS

Transfer of perceptual adaptation to space sickness: What enhances an individual's ability to adapt? [NASA-CR-188256] p 2427 N94-24227

PSYCHOMETRICS

EEG and chaos: Description of underlying dynamics and its relation to dissociative states [NASA-CR-195171] p 2428 N94-24799

PSYCHOPHYSICS

Physical aspects of the visual stimulus p 2431 N94-23978

Luminance-brightness mapping: The missing decades [ETN-94-95351] p 2428 N94-25298

Extracting heading and temporal range from optic flow: Human performance issues p 2442 N94-25510

PSYCHOPHYSIOLOGY

EEG and chaos: Description of underlying dynamics and its relation to dissociative states [NASA-CR-195171] p 2428 N94-24799

PUBLIC RELATIONS

Space technology: A study of the significance of recognition for innovators of spinoff technologies. 1993 activities/1994, 1995 plans [NASA-CR-194836] p 2596 N94-23526

PULSE COMMUNICATION

Worldwide survey of direct-to-listener digital audio delivery systems development since WARC-1992 p 2273 N94-22736

Direct broadcast satellite-radio, receiver development p 2273 N94-22739

Utilizing a TDRS satellite for direct broadcast satellite-radio propagation experiments and demonstrations p 2274 N94-22740

Adaptive digital beamforming for a CDMA mobile communications payload p 2274 N94-22743

Transparent data service with multiple wireless access p 2276 N94-22754

APLAC: An object-oriented analog circuit simulator and design tool. 6.1 system simulations manual [PB93-224871] p 2450 N94-23226

Source spacing in B-ISDN [PB93-201747] p 2293 N94-23508

PULSE COMPRESSION
Microwave excitation of pulsed high pressure gas discharge lasers
[DLR-FB-93-12] p 2351 N94-25304
PULSE GENERATORS
Safety guidelines for the operation of the DREO 10 m EMP simulator DREMPS
[DREO-TN-93-5] p 2193 N94-24117
TEM cell safety report
[DREO-TN-93-9] p 2193 N94-24123
Computer modeling of plasma flow switches-high current switching on Procyon
[DE93-040189] p 2311 N94-24500
Study of a system for producing a pulsed magnetic field (B 2T) with a frequency of 50 Hz
[ISL-N-601/92] p 2314 N94-25460
PULSE HEATING
Dynamic measurements of thermophysical properties of metals and alloys at high temperatures by subsecond pulse heating techniques p 2247 N94-25124
PULSE POSITION MODULATION
Integration and test of high-speed transmitter electronics for free-space laser communications
[NASA-TM-106295] p 2295 N94-24101
PULSED LASER DEPOSITION
Laser-deposited biocompatible films and methods and apparatuses for producing same
[AD-D016017] p 2350 N94-24952
Soft x ray optics by pulsed laser deposition
[NASA-CR-195139] p 2546 N94-24967
Laser ablation and deposition of metals
[ETN-94-95311] p 2351 N94-25294
PULSED LASERS
Micro pulse laser radar
[NASA-CASE-GSC-13493-1] p 2294 N94-23827
Exciplex laser study: Discharge and magnetic switching systems
[PB93-199768] p 2349 N94-24629
Laser-deposited biocompatible films and methods and apparatuses for producing same
[AD-D016017] p 2350 N94-24952
Microwave excitation of pulsed high pressure gas discharge lasers
[DLR-FB-93-12] p 2351 N94-25304
PULSES
Flue gas cleaning by pulse corona streamer
[EUT-93-E-272] p 2268 N94-23174
PULTRUSION
Composites and textile reinforcement
[VTT-TIED-1424] p 2231 N94-25420
PUMP IMPELLERS
Computational Fluid Dynamics (CFD) applications in rocket propulsion analysis and design
p 2214 N94-23054
A finite-element-based perturbation model for the rotordynamic analysis of shrouded pump impellers: Part 1: Model development and applications
[NASA-CR-193916] p 2366 N94-24998
A finite-element-based perturbation model for the rotordynamic analysis of shrouded pump impellers: Part 2: User's guide
[NASA-CR-193917] p 2366 N94-24999
PUMPS
Sensorless, brushless motor to drive a sealed freon-ammonia pump p 2315 N94-24036
PURIFICATION
Physics with chemically and isotopically pure semiconductors
[DE93-040120] p 2557 N94-22926
New method for increasing machine service-life, phase 2
[PB93-200707] p 2354 N94-23533
PYLONS
Aircraft accident report: In-flight engine separation. Japan Airlines, Inc., flight 46E, Boeing 747-121, N473EV, Anchorage, Alaska, 31 March 1993
[PB93-410407] p 2173 N94-24062
PYROELECTRICITY
Pyroelectric sensors in copolymer integrated on silicon
[LAAS-93044] p 2342 N94-22902
PYROLYSIS
Atomic probes of surface structure and dynamics
[DE94-001651] p 2530 N94-22720
Ceramic silicon-boron-carbon fibers from organic silicon-boron-polymers
[NASA-CASE-ARC-11956-1-SB] p 2253 N94-23311
CMC design consequences p 2256 N94-24238
Investigating pyrolysis/incineration as a method of resource recovery from solid waste
p 2444 N94-25375
PYROLYTIC GRAPHITE
Wear reduction in ceramic bearings by surface generated pyrolytic carbon continuously replenished by ethylene gas
[NASA-CR-189214] p 2364 N94-24090

Q

QUADRATURE AMPLITUDE MODULATION
Bounds and simulation results of 32-ary and 64-ary quadrature amplitude modulation for broadband-ISDN via satellite
[NASA-TM-106484] p 2202 N94-25095
QUADRATURE PHASE SHIFT KEYING
A comparison between coherent and noncoherent mobile systems in large Doppler shift, delay spread, and C/I environment p 2287 N94-22818
Detection and analysis of unbalanced QPSK in Gaussian noise, version 1.0
[DREO-12-020.1] p 2296 N94-24131
QUADRATURES
Generalized Gaussian quadrature rules for systems of arbitrary functions
[AD-A273610] p 2491 N94-24947
Correlation function estimator performance in non-Gaussian spherically invariant random processes
[AD-A273498] p 2496 N94-24951
QUALITY CONTROL
Quality data validation: Comprehensive approach to environmental data validation
[DE94-000925] p 2589 N94-22944
Sensors for process control Focus Team report
[DE93-040897] p 2560 N94-23204
The use of design automation software by government-contracted architect/engineer firms: A status report
[AD-A273181] p 2459 N94-24812
Demonstration of polyscann ultrasonic butt-fusion inspection system for polyethylene pipes
[AD-A273279] p 2373 N94-24814
New Ways Of Doing Business (NWODB) cost quantification analysis
[NASA-CR-195186] p 2586 N94-25197
Software engineering methodologies and tools
p 2465 N94-25382
QUANTITATIVE ANALYSIS
Generic microelectronic smart sensor platform for detection of toxic, hazardous, and flammable gases
[DE93-017626] p 2343 N94-23200
FTIR quantification of industrial hydraulic fluids in perchloroethylene p 2264 N94-23243
Interpretation of discrepancies in mass spectroscopy data obtained from different experimental configurations
p 2237 N94-23245
Quantitative analysis in the Al-Mg-Si system with small amounts of Mg and Si
[PB93-201499] p 2241 N94-23446
Real-time holographic endoscopy
[ISL-CO-203/92] p 2343 N94-24054
QUANTUM CHROMODYNAMICS
The status of glueballs
[DE93-040040] p 2531 N94-22923
Momentum and coordinate space three-nucleon potentials
[DE93-040868] p 2531 N94-22951
Strong interactions studies with medium energy probes
[DE94-001446] p 2540 N94-23791
Photon-photon collisions at the next linear collider: Theory
[DE93-041025] p 2534 N94-23803
Electro-weak, QCD and top physics at the Tevatron
[DE94-002304] p 2535 N94-24611
New evaluation of hadronic contributions to the anomalous magnetic moment of charged leptons
[DE93-634394] p 2536 N94-24844
Relativistic hadrons in an external field
[ETN-94-95387] p 2538 N94-25259
A quark structure of hadrons and nuclei
[DE93-616872] p 2539 N94-25474
On the transverse size of a fast moving nucleon
[DE93-616891] p 2539 N94-25481
QUANTUM ELECTRONICS
Quantum tunneling transport of electrons in double-barrier heterostructures: Theory and modeling
[ETN-94-95332] p 2565 N94-25059
QUANTUM MECHANICS
Quantum mechanics, locality and realism
[MEMO-1117] p 2568 N94-22709
Limits on high-order harmonic generation from single-atom calculations
[DE93-019950] p 2531 N94-22869
The torsion space nucleic acids molecular mechanics program DUPLEX: Surveying conformation space by potential energy minimization
[DE94-002441] p 2563 N94-24567
An attempt at a macrorealistic quantum worldview
[DE93-616821] p 2570 N94-25206
Intramultiplet mixing for Ne(**)(3p)+He at superthermal energies
[ETN-94-95327] p 2538 N94-25240
Applications of supersymmetric quantum mechanics
[ETN-94-95385] p 2570 N94-25257
Correlations in the actions of periodic orbits derived from quantum chaos
[DE93-616866] p 2571 N94-25340
QUANTUM NUMBERS
Evaluation of uranium transitions for isotopically-selective laser induced fluorescence with diode lasers (technical report for ST064)
[DE94-002000] p 2347 N94-22974
QUANTUM OPTICS
Quantum optical aspects of topological phases, such as Berry's phase
[AD-A273632] p 2570 N94-25028
QUANTUM STATISTICS
Calculations of Bose-Einstein correlations from Relativistic Quantum Molecular Dynamics
[DE94-000794] p 2569 N94-23453
Ultracold atoms in traps and fountains
[ETN-94-95325] p 2537 N94-25239
QUANTUM THEORY
Quantum mechanics, locality and realism
[MEMO-1117] p 2568 N94-22709
On spontaneous symmetry breaking mechanism in light-front quantized field theory
[DE93-633211] p 2568 N94-22968
Flavor changing strings and domain walls
[DE93-633217] p 2532 N94-22970
Coadjoint orbits and conformal field theory
[DE94-002285] p 2523 N94-24658
Quantum optical aspects of topological phases, such as Berry's phase
[AD-A273632] p 2570 N94-25028
On the connection of classical mechanics, physical kinetics and quantum theory
[DE93-616823] p 2570 N94-25207
Applications of supersymmetric quantum mechanics
[ETN-94-95385] p 2570 N94-25257
QUANTUM WELLS
Manufacturing and characterization of GaAs/AlGaAs multiple quantumwell ridge waveguide lasers
[EUT-92-E-265] p 2348 N94-23168
QUARK MODELS
Gauge invariance and the electromagnetic current of composite pions
[DE93-040869] p 2532 N94-22952
A measurement of the forward-backward asymmetry and sin(sup 2)(theta)(sub W) from the process Z(sup 0) (yields) (mu)(sup +)(mu)(sup (minus)) at (radical)s = 1.8 TeV
[DE94-001908] p 2532 N94-23018
A quark structure of hadrons and nuclei
[DE93-616872] p 2539 N94-25474
On the hadron formation time in pion-nucleus interaction
[DE93-616879] p 2539 N94-25476
QUARKS
The status of glueballs
[DE93-040040] p 2531 N94-22923
Towards a theory of quark and lepton masses
[DE94-001726] p 2533 N94-23218
Progress report for the UCSD experimental HEP group
[DE94-001357] p 2533 N94-23699
Strong interactions studies with medium energy probes
[DE94-001446] p 2540 N94-23791
B-quark production at hadron colliders
[DE94-001459] p 2534 N94-23806
Search for the top quark and other new particles at D0
[DE94-001220] p 2535 N94-24515
Stitching the Yukawa quilt
[PB93-204477] p 2569 N94-24532
Electro-weak, QCD and top physics at the Tevatron
[DE94-002304] p 2535 N94-24611
The determination of the branching ratios of the Z(zero) boson into heavy quarks using neural networks
[ETN-94-95381] p 2538 N94-25246
Bottom quark production at the Z resonance
[ISBN-9-09-006217-3] p 2538 N94-25255
A scalar-vector model of quark-antiquark interaction under linear confinement
[DE93-616871] p 2538 N94-25317
The Casimir energy of the rigid string with massive ends
[DE93-616851] p 2492 N94-25338
Proton spin: The role of quark-gluon and hadron degrees of freedom
[DE93-616867] p 2538 N94-25341
Heavy flavour physics at LEP
[NIKHEF-H/92-19] p 2539 N94-25465
A quark structure of hadrons and nuclei
[DE93-616872] p 2539 N94-25474
On the hadron formation time in pion-nucleus interaction
[DE93-616879] p 2539 N94-25476

QUARTZ
A dynamic melting model for the origin of Apollo 15 olivine-normative and quartz-normative mare basalts
p 2615 N94-24371

QUASARS
100 GHz map of 3C 446
[PB94-104882] p 2599 N94-23705

QUENCHING (COOLING)
Stretch-induced quenching in flame-vortex interactions
p 2237 N94-24156

QUERY LANGUAGES
Multi-set extended relational algebra: A formal approach to a practical issue
[PB94-110830] p 2486 N94-23725
The ESIS query environment pilot project
p 2518 N94-23952
Correct and efficient interface for logical query languages with complex objects
[PB93-211175] p 2593 N94-24743
A comparison of Boolean-based retrieval to the WAIS system for retrieval of aeronautical information
[NASA-CR-4569] p 2594 N94-25487

QUEUEING THEORY
Loss probabilities in batch-arrival bulk-service queues with finite capacity
[MEMO-1106] p 2493 N94-22724
Uniform limit theorems for marked point processes
[PB94-118726] p 2488 N94-24526
Fast simulation of packet loss rates in a shared buffer communications switch
[NASA-CR-191556] p 2457 N94-24638
Data structures and amortized complexity in a functional setting
[ETN-94-95307] p 2476 N94-25290
Product forms as a solution base for queueing systems
[MEMO-COSOR-92-37] p 2477 N94-25526

R

RACKS (GEARS)
Metal band drives in spacecraft mechanisms
p 2355 N94-23987

RADAR
Image processing for flight crew enhanced situation awareness p 2442 N94-25508

RADAR ANTENNAS
Calibration block for digital beam forming antenna
[PB93-204550] p 2294 N94-23773
The down, release, and deployment of the RADARSAT SAR antenna p 2305 N94-23986
Calibration network intended for phase-array antennas at 3 GHz
[PB93-204352] p 2297 N94-24530

RADAR BEAMS
Method and apparatus of generating sum or difference signals corresponding to an apparent beam in a monopulse radar system
[AD-D015998] p 2302 N94-25056

RADAR CORNER REFLECTORS
High-frequency techniques for RCS prediction of plate geometries and a physical optics/equivalent currents model for the RCS of trihedral corner reflectors, parts 1 and 2
[NASA-CR-195140] p 2298 N94-24616

RADAR CROSS SECTIONS
High-frequency techniques for RCS prediction of plate geometries and a physical optics/equivalent currents model for the RCS of trihedral corner reflectors, parts 1 and 2
[NASA-CR-195140] p 2298 N94-24616

RADAR DATA
Further studies to extend and test the area-time-integral technique applied to satellite data
[NASA-CR-195132] p 2415 N94-24705

RADAR DETECTION
Mars subsurface sounding with a ground penetrating radar p 2608 N94-23393
ASR-9 microburst detection algorithm
[AD-A273591] p 2415 N94-24850
Radar E-O image fusion p 2306 N94-25503

RADAR ECHOES
On the analysis of clear air radar echoes severely contaminated by clutter p 2306 N94-24423

RADAR IMAGERY
Mission planning for Shuttle Imaging Radar-C (SIR-C) with a real-time interactive planning software
p 2305 N94-23842
Free-surface/vorticity interaction
[AD-A273263] p 2335 N94-24686
Use of microwave polarimetry to enhance SAR images of the ocean surface
[AD-A273568] p 2419 N94-24944
Edge detection using a complex wavelet
[AD-A273699] p 2493 N94-25452
Synthetic vision system flight test results and lessons learned p 2429 N94-25492
The Radar Image Generation (RIG) model
p 2306 N94-25497
Radar E-O image fusion p 2306 N94-25503

RADAR MEASUREMENT
Mars subsurface sounding with a ground penetrating radar p 2608 N94-23393
HERACLITUS, phase 1. Harbour Entrance of Rotterdam Radar based Current Related Information for Traffic Guidance of Ships: Feasibility of deriving current profile data from sea surface observations in the Rotterdam (Netherlands) port entrance
[BCRS-93-04] p 2417 N94-24107
Mesospheric and lower thermospheric winds, temperatures densities, and volume emission rates
[NASA-CR-195147] p 2403 N94-24486

RADAR REFLECTORS
On the estimation of the correlation dimension and its application to radar reflector discrimination
[NASA-CR-4564] p 2309 N94-23304

RADAR SIGNATURES
Radar signature related radome techniques for flush-mounted HF-, VHF- and, UHF communication antennas
[PB93-204618] p 2294 N94-23742
High latitude cusp signature observations for southward IMF B sub Z
[AD-A273801] p 2406 N94-25536

RADAR TARGETS
Radar target discrimination by spectrum analysis
[AD-D015982] p 2301 N94-25040
Radar target discrimination systems using artificial neural network topology
[AD-D015984] p 2301 N94-25041

RADAR TRACKING
An improved gravity model for Mars: Goddard Mars Model-1 (GMM-1)
[NASA-TM-104584] p 2401 N94-23282
Method and apparatus for determining target elevation angle, altitude and range, and the like in a monopulse radar system with reduced multipath errors
[AD-D016005] p 2302 N94-25058
IRIG radar calibration catalog. Version 2: The IRIG error model reference for radar calibrations
[AD-A273344] p 2303 N94-25155

RADARSAT
The down, release, and deployment of the RADARSAT SAR antenna p 2305 N94-23986

RADIAL FLOW
Two-dimensional Navier-Stokes computations of subsonic and supersonic flows through turbine cascades
[PB93-226223] p 2317 N94-23114

RADIANCE
Algorithm-development activities
[NASA-CR-193225] p 2420 N94-23538
VNIR and SWIR transfer radiometers developed at NRLM for preflight laboratory cross-calibration
p 2365 N94-23610
Modelling TOVS radiances of synoptic systems
[NASA-CR-194847] p 2408 N94-23620
Evaluation of visual acuity with Gen 3 night vision goggles
[NASA-TM-108792] p 2431 N94-23974
The IRGen infrared data base modeler
p 2440 N94-25496

RADIANT FLUX DENSITY
Physical aspects of the visual stimulus
p 2431 N94-23978
An extended laser flash technique for thermal diffusivity measurement of high-temperature materials
p 2238 N94-25132

RADIANT HEATING
Strain gage measurement errors in the transient heating of structural components
[NASA-TM-104274] p 2376 N94-23487

RADIATION BELTS
Solar flares and magnetospheric particles: Investigations based upon the ONR-602 and ONR-604 experiments
[AD-A273639] p 2628 N94-25031
The CRRES time history data base: All sensors
[AD-A273737] p 2207 N94-25542

RADIATION COUNTERS
A measurement of the forward-backward asymmetry and sin(sup 2)(theta)(sub W) from the process Z(sup 0) (yields) (mu)(sup +)(mu)(sup (minus)) at (radical)s = 1.8 TeV
[DE94-001908] p 2532 N94-23018
Examination of the response capacity of a silicon pixel detector for ions and molecules in the energy area 100 to 300 keV
[MPE-241] p 2346 N94-25415

RADIATION DAMAGE
Irradiation damage behavior of low alloy steel wrought and weld materials
[DE94-000519] p 2239 N94-22999

RADIATION DETECTORS
Electro-weak, QCD and top physics at the Tevatron
[DE94-002304] p 2535 N94-24611
To perform a proof-of-concept study on the use of superheated drop detectors for the measurement of LET spectra in space environments
[BTI-92/3-31] p 2629 N94-24695
High energy gamma astronomy above 200 GeV
[MPI-PHE/93-04] p 2600 N94-25458

RADIATION EFFECTS
Report of the Joint Seminar on Solid State Physics, Atomic and Molecular Physics, and Materials Science in the Energy Region of Tandem Accelerators
[DE93-508268] p 2548 N94-22924
Low temperature diffusion of hydrogenic species in oxide crystals: Radiation induced diffusion
[DE94-000374] p 2558 N94-22957
A new automatic design method to develop multilayer thin film devices for high power laser applications
[DE93-632490] p 2347 N94-22967
Effects of neutron irradiation and hydrogen on ductile-brittle transition temperatures of V-Cr-Ti alloys
[DE94-001466] p 2240 N94-23009
Advanced materials for radiation-cooled rockets
p 2214 N94-23052
Development of small punch testing technique and its application to evaluation of mechanical properties degradation
[DE94-001193] p 2375 N94-23184
Generalized melting criterion for beam-induced amorphization
[DE94-001333] p 2560 N94-23189
Grain-boundary microchemistry and intergranular cracking of irradiated austenitic stainless steel
[DE94-000466] p 2242 N94-23457
Surface modification of sapphire for enhanced infrared window performance
[DE94-000333] p 2543 N94-23458
Research for electric energy systems
[DE94-001839] p 2293 N94-23719
Effect of irradiation on the stress corrosion cracking behavior of Alloy X-750 and Alloy 625
[DE94-001759] p 2244 N94-23792
The role of radiation in mesoscale flows: Physics, parameterizations, codes p 2413 N94-24389
Effects of ionizing radiation on modern ion exchange materials
[DE94-001569] p 2535 N94-24505
Highly-reliable fly-by-light/power-by-wire technology
p 2162 N94-25099
The CRRES time history data base: All sensors
[AD-A273737] p 2207 N94-25542

RADIATION HARDENING
A qualified radiation hardened nonvolatile memory for space and tactical weapons applications
[DE94-001211] p 2559 N94-23186

RADIATION MEASUREMENT
Atmospheric Radiation Measurement (ARM)/CART site p 2411 N94-24379

RADIATION PRESSURE
Contribution to the study of HF converters radiated disturbances
[ECL-92-34] p 2313 N94-25421

RADIATION PROTECTION
Towards a new radiation protection organization
[FOA-C-40304-4.3] p 2437 N94-24292

RADIATION SHIELDING
GOLF mechanisms p 2357 N94-24003
Magnetic shielding of interplanetary spacecraft against solar flare radiation
[NASA-CR-195539] p 2204 N94-24334

RADIATION TOLERANCE
Effects of ionizing radiation on modern ion exchange materials
[DE94-001569] p 2535 N94-24505

RADIATION TRANSPORT
Computational model of surface ablation from tokamak disruptions
[DE94-002204] p 2550 N94-23474
Improved gas core propulsion model
[DE94-000929] p 2220 N94-24511

RADIATIVE HEAT TRANSFER
Flames in dusty mixtures: Their structure and stability
[NASA-CR-191567] p 2317 N94-23089
Fully coupled nonlinear thermomechanical analysis including general contact in PALM2D
[DE94-001661] p 2568 N94-23216
Accuracy control in Monte Carlo radiative calculations
p 2321 N94-23639
Ignition and combustion characteristics of metallized propellants, phase 2
[NASA-CR-195107] p 2266 N94-24700

RADIATIVE TRANSFER
Modelling TOVS radiances of synoptic systems
[NASA-CR-194847] p 2408 N94-23620

Development of an analytical-numerical model to predict radiant emission or absorption
[NASA-CR-194860] p 2453 N94-23624
Thermal analysis of combinatorial solid geometry models using SINDA p 2323 N94-23650
Radiative forcing calculations for SF6 and CH4 using a correlated k-distribution transmission model
[DE94-001855] p 2397 N94-23700
Participation in TOMS missions
[NASA-CR-195110] p 2398 N94-24078
Atmospheric Radiation Measurement (ARM)/CART site p 2411 N94-24379
Session on modeling of radiative transfer processes
p 2414 N94-24397
LRAT: Lightning Radiative Transfer
p 2416 N94-24443
The annual pressure cycle on Mars: Results from the LMD Martian atmospheric general circulation model
p 2619 N94-24884
Temporal and spatial mapping of surface albedo and atmospheric dust opacity on Mars p 2619 N94-24887

RADICALS
Potent solvents for C60 and their utility for the rapid acquisition of 13CNMR data for fullerenes
[AD-A273349] p 2235 N94-24925
Dispersion of Rh/Cu in a sol-gel matrix. Highly chemo- and stereoselective catalyst for the reduction of alkynes to Z-alkenes
[AD-A273306] p 2262 N94-25145

RADIO ALTIMETERS
Synthesis of passive microwave and radar altimeter data for estimating accumulation rates of polar snow
[NASA-CR-194864] p 2382 N94-23573

RADIO ANTENNAS
The MSAT spacecraft of Telesat Mobile Inc.
p 2207 N94-22742
Very low frequency and low frequency transmitting antenna parameter monitoring system
[AD-D015989] p 2302 N94-25049

RADIO ASTRONOMY
Molecular abundances in the envelopes around evolved stars
[PB94-104916] p 2602 N94-23812
Voyager planetary radio astronomy studies
[NASA-CR-194776] p 2614 N94-24328
Infrared and SiO maser observations of OH/IR stars
[PB94-104890] p 2599 N94-24780
Investigation relative to the Roentgen Satellite (ROSAT)
[NASA-CR-195192] p 2600 N94-25269

RADIO ATTENUATION
Power attenuation characteristics as switch-over criterion in personal satellite mobile communications
p 2277 N94-22756

RADIO COMMUNICATION
The MSAT spacecraft of Telesat Mobile Inc.
p 2207 N94-22742
Power attenuation characteristics as switch-over criterion in personal satellite mobile communications
p 2277 N94-22756
Evolution of INMARSAT systems and applications: The land mobile experience p 2280 N94-22779
EUTELTRACS: The European experience on mobile satellite services p 2281 N94-22781
System services and architecture of the TMI satellite mobile data system p 2286 N94-22817
Pseudo-coherent demodulation for mobile satellite systems p 2287 N94-22819
Handover aspects for a Low Earth Orbit (LEO) CDMA Land Mobile Satellite (LMS) system
p 2288 N94-22824
Radio communication and wave propagation. A visit to the Netherlands in December 1992
[PB93-204360] p 2297 N94-24531
Conceptual communications system design in the 25.25-27.5 and 37.0-40.5 GHz frequency bands
p 2306 N94-25379

RADIO CONTROL
NASA advanced design program. Design and analysis of a radio-controlled flying wing aircraft
[NASA-CR-195515] p 2180 N94-24589

RADIO EMISSION
Voyager planetary radio astronomy studies
[NASA-CR-194776] p 2614 N94-24328

RADIO EQUIPMENT
Mitigation of EMI/RFI produced by a 1.2 kW uninterruptible power supply
[AD-A273149] p 2299 N94-24670
ELF communications system ecological monitoring program
[AD-A273456] p 2299 N94-24676

RADIO FREQUENCIES
Aeronautical audio broadcasting via satellite
p 2274 N94-22741
The MSAT spacecraft of Telesat Mobile Inc.
p 2207 N94-22742
Direct digital RF synthesis and modulation for MSAT mobile applications p 2285 N94-22804
Separable concatenated codes with iterative map decoding for Rician fading channels
p 2286 N94-22815
1993 annual report for the Phaedrus-T RF current drive experiments
[DE94-001369] p 2550 N94-23192

RADIO FREQUENCY INTERFERENCE
Diversity reception for advanced multi-satellite networks: A CDMA approach p 2286 N94-22816
Development of a multilayer interference simulation program for MSS systems p 2287 N94-22823
A method for interference mitigation in space communications scheduling p 2305 N94-23918
Analysis and surveillance performance at Chicago O'Hare Airport
[DOT/FAA/RD-92/29] p 2175 N94-24127
Error coding simulations p 2306 N94-24439
Simulation of adjacent channel interference in a UHF satellite system
[AD-A273147] p 2299 N94-24669

RADIO JETS (ASTRONOMY)
The 1404+286: A non-ideal calibrator for VLBI observations
[PB94-104908] p 2599 N94-24521

RADIO OBSERVATION
CO-to-H2 conversion factor in dwarf irregular galaxies
[REPT-333] p 2603 N94-24985
High spatial resolution observations of CO in CRL 618
[REPT-334] p 2604 N94-24986
The Nobeyama millimeter array survey for protoplanetary disks around protostar candidates and T Tauri stars in Taurus
[REPT-336] p 2604 N94-24987

RADIO RECEIVERS
Direct broadcast satellite-radio, space-segment/receiver tradeoffs p 2273 N94-22738
Direct broadcast satellite-radio, receiver development
p 2273 N94-22739
Measurements on the satellite-mobile channel at L and S bands p 2282 N94-22791
A study of satellite motion-induced multipath phenomena p 2283 N94-22794
A comparison between coherent and noncoherent mobile systems in large Doppler shift, delay spread, and C/I environment p 2287 N94-22818
A low noise 665 GHz SIS quasi-particle waveguide receiver
[NASA-CR-194735] p 2296 N94-24105
Northern Exposure 1992: An investigation of transauroral HF radio skywave propagation
[AD-A273363] p 2303 N94-25089

RADIO RELAY SYSTEMS
Satellite communications system
[CA-PATENT-APPL-SN-2053597] p 2297 N94-24183

RADIO SIGNALS
Mitigation of EMI/RFI produced by a 1.2 kW uninterruptible power supply
[AD-A273149] p 2299 N94-24670

RADIO SOURCES (ASTRONOMY)
100 GHz map of 3C 446
[PB94-104882] p 2599 N94-23705
The 1404+286: A non-ideal calibrator for VLBI observations
[PB94-104908] p 2599 N94-24521

RADIO TELEMETRY
The advanced orbiting systems testbed program: Results to date p 2197 N94-23907
Experimental verification of an acoustic telemetry link between an Aurora and CFAV quest
[DREA-TC-93-304] p 2202 N94-24121

RADIO TELESCOPES
Radioastron flight operations p 2502 N94-23861

RADIO TRANSMISSION
An introduction to digital modulation and OFDM techniques
[BBC-RD-1993/10] p 2295 N94-24086
Radio communication and wave propagation. A visit to the Netherlands in December 1992
[PB93-204360] p 2297 N94-24531
Comparison of HF groundwave propagation models
[AD-A273146] p 2299 N94-24668
Mitigation of EMI/RFI produced by a 1.2 kW uninterruptible power supply
[AD-A273149] p 2299 N94-24670
Northern Exposure 1992: An investigation of transauroral HF radio skywave propagation
[AD-A273363] p 2303 N94-25089
Conceptual communications system design in the 25.25-27.5 and 37.0-40.5 GHz frequency bands
p 2306 N94-25379

RADIO TRANSMITTERS
ELF communications system ecological monitoring program
[AD-A273456] p 2299 N94-24676

RADIO WAVES
Comparison of HF groundwave propagation models
[AD-A273146] p 2299 N94-24668

RADIOACTIVE DECAY
Low p(sub T) photon production in proton-nucleus collisions at 18 GeV/c
[DE94-001380] p 2532 N94-23007
Heavy flavour physics at LEP
[NIKHEF-H/92-19] p 2539 N94-25465
Weak interactions in a bilocal chiral theory
[DE93-616887] p 2539 N94-25477

RADIOCHEMISTRY
Fifty years of continuous improvement: What has DOE done for analytical chemistry?
[DE94-002539] p 2234 N94-24548

RADIOGRAPHY
Measurement of intact-core length of atomizing liquid jets by image deconvolution p 2210 N94-23029
An evaluation of Compton scatter imaging using COMSCAN
[DREP-TM-93-38] p 2372 N94-24136

RADIOISOTOPE BATTERIES
Development testing of the two-watt RTG heat source and Hastelloy-S/T-111 alloy compatibility studies
[DE94-002875] p 2243 N94-23784

RADIOMETERS
Eos cross-calibration radiometers
p 2383 N94-23601
Flight solar calibrations using the Mirror Attenuator Mosaic (MAM): Low scattering mirror
p 2384 N94-23602
Infrared calibration p 2384 N94-23608
VNIR and SWIR transfer radiometers developed at NRLM for preflight laboratory cross-calibration
p 2385 N94-23610
In-flight cross-calibration of ASTER/TIR and MODIS-N
p 2385 N94-23611
ASTER, a multinational Earth observing concept
p 2389 N94-23840
High resolution encoder-motor used in the orbital spin scan radiometer, GOES VAS satellites
p 2209 N94-24038
Evidence for dust transport in Viking IR thermal mapper opacity data p 2620 N94-24892
An AVHRR cloud classification database typed by experts
[AD-A273560] p 2416 N94-25162
Advanced radiometric and interferometric milimeter-wave scene simulations p 2306 N94-25498

RADIOSONDES
Intercomparison of remote and balloon-borne sensors operated at JAPE-91 p 2527 N94-24210
Observed and Navy operational global model climatologies of synoptic disturbances over the tropical western Pacific during winter 1991-1992
[AD-A273400] p 2416 N94-25071
A nighttime structure model of atmospheric optical turbulence, c2(n), derived from thermosonde and high resolution rawinsonde measurements
[AD-A273803] p 2406 N94-25537

RADOME MATERIALS
Radar signature related radome techniques for flush-mounted HF-, VHF- and, UHF communication antennas
[PB93-204618] p 2294 N94-23742

RADOMES
Radar signature related radome techniques for flush-mounted HF-, VHF- and, UHF communication antennas
[PB93-204618] p 2294 N94-23742

RAIL TRANSPORTATION
Vehicle/guideway interaction and ride comfort in maglev systems
[DE94-001319] p 2352 N94-22991
Performance analysis of the combined EDS maglev propulsion, levitation, and guidance system
[DE94-001346] p 2352 N94-22996
Rail Corrugations
[ILR-BER-59] p 2269 N94-23581
A rail corrugation theory which allows for contact patch size p 2269 N94-23582
A rail joint: The possible initiator of corrugation?
p 2269 N94-23583
A linear model for corrugation and its limit of validity
p 2269 N94-23584
Lateral high frequency oscillations and stability of a wheel rolling on a flexible track p 2269 N94-23585
Wear characteristics of technical dry rolling/sliding systems with relations to corrugation problems
p 2269 N94-23586
Surface analysis of corrugated rail treads
p 2270 N94-23587
Surface observations of stick-slip oscillations in tightly conformal wheel/rail contacts p 2270 N94-23588
Contact analysis of rough rail surfaces
p 2270 N94-23589

RAILGUN ACCELERATORS
The internal structure and dynamics of the railgun plasma armature between infinitely wide ablating rails
[DE94-001473] p 2198 N94-23208
A comparison of in-bore projectile motion from an electromagnetic railgun versus that of a conventional cannon barrel
[AD-A273473] p 2198 N94-24690
RAILS
Rail Corrugations
[ILR-BER-59] p 2269 N94-23581
A rail corrugation theory which allows for contact patch size p 2269 N94-23582
A rail joint: The possible initiator of corrugation?
p 2269 N94-23583
A linear model for corrugation and its limit of validity
p 2269 N94-23584
Lateral high frequency oscillations and stability of a wheel rolling on a flexible track p 2269 N94-23585
Wear characteristics of technical dry rolling/sliding systems with relations to corrugation problems
p 2269 N94-23586
Surface analysis of corrugated rail treads
p 2270 N94-23587
Surface observations of stick-slip oscillations in tightly conformal wheel/rail contacts p 2270 N94-23588
Contact analysis of rough rail surfaces
p 2270 N94-23589
RAIN
Adaptive data rate control TDMA systems as a rain attenuation compensation technique
p 2287 N94-22821
An analytic study of a two-phase laminar airfoil in simulated heavy rain p 2171 N94-23661
Estimation of the rain signal in the presence of large surface clutter
[NASA-CR-195105] p 2409 N94-24087
Precipitation measurement using SIR-C: A feasibility study. Investigation at nadir
[NASA-CR-195103] p 2410 N94-24126
CAPE for CaPE p 2416 N94-24409
Water cycle research associated with the CaPE hydrometeorology project (CHymP p 2416 N94-24414
Further studies to extend and test the area-time-integral technique applied to satellite data
[NASA-CR-195132] p 2415 N94-24705
Worst case analysis: Earth sensor assembly for the tropical rainfall measuring mission observatory
[NASA-CR-189320] p 2311 N94-24754
Human impacts on soil carbon dynamics of deep-rooted Amazonian forests
[NASA-CR-195127] p 2399 N94-24861
RAMAN SPECTRA
Numerical simulation and analysis of experimental results on stimulated Raman scattering in laser-plasma Hohlraum targets
[DE93-613719] p 2554 N94-25330
Measurement of the volume mass by spontaneous Raman scattering. Study of turbulent fluctuations of mixing in a subsonic free jet. Measurements in supersonic wind tunnels
[ISL-R-102/92] p 2339 N94-25462
RAMAN SPECTROSCOPY
Materials Science and Engineering
[DE94-003018] p 2228 N94-23493
Total light loss optic spectroscopy: Progress towards a fiber optic Raman organic vapor sensor
[DE94-002545] p 2234 N94-24549
Nondestructive evaluations
[DE94-003020] p 2373 N94-24613
Investigation of Raman beam cleanup and phase conjugation
[AD-A273157] p 2545 N94-24672
RANDOM ACCESS MEMORY
Crosstie random access memory element having associated read/write circuitry
[AD-D016027] p 2446 N94-24724
RANDOM NOISE
Asynchronous timing and Doppler recovery in DSP based DPSK modems for fixed and mobile satellite applications p 2285 N94-22805
Separable concatenated codes with iterative map decoding for Rician fading channels
p 2286 N94-22815
A mixed map/variable structure observer for target tracking p 2157 N94-24263
An analysis of gamma ray burst time histories
[NASA-CR-195191] p 2629 N94-25199
RANDOM NUMBERS
Two-stage versus sequential sample-size determination in regression analysis of simulation experiments
[PB94-110558] p 2495 N94-24634
RANDOM PROCESSES
Logarithm of probability measures and infinite divisibility of sub-stable random vectors
[PB94-118627] p 2486 N94-23758
Correlation function estimator performance in non-Gaussian spherically invariant random processes
[AD-A273498] p 2496 N94-24951
RANDOM SAMPLING
Rao-Blackwell theorem in stereology and some counterexamples
[PB94-111713] p 2496 N94-24639
RANDOM VARIABLES
On the asymptotically uniform distribution modulo 1 of extreme order statistics
[MEMO-COSOR-91-38-REV] p 2493 N94-23142
Limiting distribution of fractional parts of extreme order statistics
[PB93-237733] p 2494 N94-23440
Characterizations of shift-invariant distributions based on summation modulo one
[PB93-237824] p 2481 N94-23442
Subset selection for the best of two populations: Tables of the expected subset size
[PB93-237857] p 2494 N94-23546
Subset selection with a generalized selection goal based on a loss function
[PB94-111192] p 2494 N94-23798
Some generalized subset selection procedures
[PB94-111655] p 2487 N94-23799
Infinite divisible and stable distributions modulo 1
[PB94-110640] p 2495 N94-23815
A comparison of approximate interval estimators for the Bernoulli parameter
[NASA-CR-191585] p 2458 N94-24680
Efficiency of subset selection of an epsilon-best uniform population relative to selection of the best one
[PB93-237741] p 2490 N94-24763
Topics in probability and dynamics
[AD-A273543] p 2496 N94-24931
RANDOM VIBRATION
Microwelding due to random vibration
p 2359 N94-24019
RANDOM WALK
Coherence lost? Not-so-fast escapes from the in-phase attractor of a set of globally coupled nonlinear oscillators
[DE94-000799] p 2557 N94-22940
RANGE ERRORS
Comparison of c.t.s. based prediction of store trajectory with flight test data p 2158 N94-24268
RANGE FINDERS
Expansion-based passive ranging
p 2176 N94-25504
RANGEFINDING
EUTELTRACS: The European experience on mobile satellite services p 2281 N94-22781
Lightning studies using LDAR and LLP data
p 2416 N94-23238
Object recognition through image understanding for an autonomous mobile robot
[AD-A273206] p 2475 N94-24862
Method and apparatus for determining target elevation angle, altitude and range, and the like in a monopulse radar system with reduced multipath errors
[AD-D016005] p 2302 N94-25058
Expansion-based passive ranging
p 2176 N94-25504
Multiple-camera/motion stereoscopy for range estimation in helicopter flight p 2441 N94-25505
Validation of vision-based range estimation algorithms using helicopter flight data p 2442 N94-25506
RANKINE CYCLE
Utilization of recently developed codes for high power Brayton and Rankine cycle power systems
p 2222 N94-23641
RANKING
Solving the ranking and selection indifference-zone formulation for normal distributions using computer software
[AD-A273821] p 2496 N94-25518
RARE EARTH ELEMENTS
Development of infrared sensors using energy transfer/energy upconversion processes: Study of laser excited fluorescence in rare Earth ion doped crystals
[NASA-TM-108437] p 2233 N94-24073
RAREFIED GASES
Interferometry in rarefied gas flows
[ISL-CO-207/92] p 2318 N94-23160
RASTER SCANNING
Results of a laboratory experiment that tests rotating unbalanced-mass devices for scanning gimbaled payloads and free-flying spacecraft
[NASA-TP-3458] p 2269 N94-23574
RATIONAL FUNCTIONS
A rational elliptic surface related to the question of expressing squares as sum of consecutive squares
[W-9305] p 2479 N94-23139
Mathematical addenda to Hopper's model of plane stokes flow driven by capillarity on a free surface
[PB93-237691] p 2480 N94-23438
Approximation to nonlinear equations using nonlinear rational models
[RR-448] p 2492 N94-25306
RATIOS
The computation of R(sub 0) for discrete-time epidemic models with dynamic heterogeneity
[CWI-AM-R9301] p 2420 N94-23521
RATS
Electrophysiology of the rat nucleus accumbens: Local circuitry, neuromodulation and synaptic plasticity
[PB93-232254] p 2420 N94-23454
Skeletal muscle metabolism in hypokinetic rats
[NASA-CR-195082] p 2420 N94-24124
In vitro system for studying metabolism of environmental chemicals in human cells
[AD-A273427] p 2421 N94-24688
RAWINSONDES
A nighttime structure model of atmospheric optical turbulence, c2(n), derived from thermosonde and high resolution rawinsonde measurements
[AD-A273803] p 2406 N94-25537
RAY TRACING
Electromagnetic field strength prediction in an urban environment: A useful tool for the planning of LMSS
p 2283 N94-22795
Proposed additions to the SHADOW ray-tracing code for general-asymmetric perfect-crystal optics
[DE94-001291] p 2560 N94-23188
Refraction of high frequency noise in an arbitrary jet flow
[NASA-TM-106465] p 2525 N94-23464
Theoretical investigation of variable periodicity (graded) multilayers for hard x ray applications
[NASA-CR-194824] p 2543 N94-23502
Dynamic ray tracing and its application in triangulated media
[DE94-000875] p 2402 N94-23516
Accuracy control in Monte Carlo radiative calculations
p 2321 N94-23639
RAYLEIGH DISTRIBUTION
Control algorithms for effective operation of variable-speed wind turbines
[DE94-002607] p 2394 N94-23704
RAYLEIGH SCATTERING
Data analysis and interpretation of lunar dust exosphere p 2623 N94-25349
RAYLEIGH-RITZ METHOD
Mechanical and thermal buckling analysis of sandwich panels under different edge conditions
[NASA-TM-4535] p 2228 N94-23514
RC CIRCUITS
Carbon supercapacitors
[DE94-002652] p 2311 N94-24748
REACTING FLOW
Numerical parametric studies of spray combustion instability p 2212 N94-23041
A random distribution reacting mixing layer model
[NASA-CR-194445] p 2187 N94-23552
Upwind MacCormack Euler solver with non-equilibrium chemistry p 2326 N94-23672
Fundamental and experimental studies on the catalytic combustion of methane
[PB94-112661] p 2233 N94-23736
A large eddy simulation scheme for turbulent reacting flows p 2330 N94-24154
The combustion program at CTR
p 2237 N94-24155
A transport equation for the scalar dissipation in reacting flows with variable density: First results
p 2331 N94-24157
Workshop on Computational Turbulence Modeling
[NASA-CP-10130] p 2333 N94-24460
Conservation equations for reacting gas flow
[PB94-111168] p 2334 N94-24574
Numerical solutions of the complete Navier-Stokes equations
[NASA-CR-194780] p 2337 N94-24858
LES, DNS and RANS for the analysis of high-speed turbulent reacting flows
[NASA-CR-195196] p 2337 N94-25094
REACTION BONDING
Selection of polymer binders and fabrication of SiC fiber-reinforced reaction-bonded silicon nitride matrix composites
[NASA-CR-194874] p 2255 N94-24223
REACTION KINETICS
Study of improved methods for predicting chemical equilibria
[DE94-001647] p 2568 N94-22719
A novel method for determination of transport parameters of H2 and O2 in PEMFCs
[DE94-001492] p 2389 N94-22962
Integrated hydrometallurgical jarosite treatment
[PB93-217990] p 2232 N94-22983
Reburning rich-lean kinetics
[PB93-220887] p 2232 N94-23100

Modelling of solid polymer and direct methanol fuel cells: Phenomenological equations and analytical solutions [PB93-224897] p 2390 N94-23102

Alloys for hydrogen storage in nickel/hydrogen and nickel/metal hydride batteries p 2391 N94-23353

Reaction of isocyanates with carboxylic acids and its application to polymer synthesis [PB94-118858] p 2254 N94-23763

Selection of polymer binders and fabrication of SiC fiber-reinforced reaction-bonded silicon nitride matrix composites [NASA-CR-194874] p 2255 N94-24223

Fracture kinetics analysis of empirical and semi-empirical corrosion fatigue relations p 2159 N94-24277

Adsorption, desorption, and decomposition of HCl and HBr on Ge(100): Competitive pairingand near-first-order desorption kinetics [AD-A273504] p 2235 N94-24790

Eddy mixing coefficient upper limit derived from the photochemical balance of O2 p 2621 N94-24897

Reactive trace metals as indicators of subduction and ventilation processes in the ocean [AD-A273585] p 2419 N94-25164

REACTION PRODUCTS

Condensed-phase thermal decomposition of TATB investigated by Atomic Force Microscopy (AFM) and Simultaneous Thermogravimetric Modulated Beam Mass Spectrometry (STMBMS) [DE94-000396] p 2232 N94-23298

Metal-mullite reactions [DE94-002038] p 2244 N94-23811

REACTION TIME

Automated system function allocation and display format: Task information processing requirements p 2434 N94-24189

REACTION WHEELS

A combined Earth scanner and momentum wheel for attitude determination and control of small spacecraft p 2208 N94-24022

The low noise momentum wheel MW-X: EM design and predicted properties p 2360 N94-24024

Reactive thrust cruise for a geosynchronous satellite with minimum fuel consumption p 2158 N94-24271

Momentum management and torque distribution p 2159 N94-24272

REACTIVITY

Reburning rich-lean kinetics [PB93-220887] p 2232 N94-23100

Reactivity of ambident anions in the gas phase [PB93-232189] p 2533 N94-23713

Fundamental and experimental studies on the catalytic combustion of methane [PB94-112661] p 2233 N94-23736

Chemically sensitive interfacial force microscopy: Contact potential measurements of self-assembling monolayer films [AD-A273135] p 2234 N94-24772

Reactive trace metals as indicators of subduction and ventilation processes in the ocean [AD-A273585] p 2419 N94-25164

REACTOR DESIGN

Design and testing of a unique randomized gravity, continuous flow bioreactor p 2423 N94-25368

REACTOR MATERIALS

Effects of neutron irradiation and hydrogen on ductile-brittle transition temperatures of V-Cr-Ti alloys [DE94-001466] p 2240 N94-23009

Performance assessment of low pressure nuclear thermal propulsion p 2217 N94-23070

REACTOR TECHNOLOGY

Start-up simulations of the PULSAR pulsed tokamak reactor [DE94-002634] p 2552 N94-24519

READERS

Harmonisation of man-machine interface experiments in the context of the development of PHARE advanced tools [PB93-204725] p 2430 N94-23744

READING

A multimedia adult literacy program: Combining NASA technology, instructional design theory, and authentic literacy concepts p 2585 N94-25384

READOUT

Progress on the design of a data push architecture for an array of optimized time tagging pixels [DE93-041011] p 2307 N94-22955

REAL GASES

Application of maximum entropy and irreducible cluster integrals to joint probability distributions for x ray structure determination [PB93-224152] p 2559 N94-23109

REAL TIME OPERATION

A novel process monitoring and control system based on a neural manufacturing concept [DE94-001516] p 2471 N94-23011

Urban/rural application of weather radar for flow forecasting. Proceedings of the Informal CEc -Workshop [PB93-220135] p 2407 N94-23129

CAMAC throughput of a new RISC-based data acquisition computer at the DIII-D tokamak [DE94-001113] p 2550 N94-23182

Towards real-time stereovision systems for planetary missions p 2370 N94-23422

Mission planning for Shuttle Imaging Radar-C (SIR-C) with a real-time interactive planning software p 2305 N94-23842

SAMPEX payload operation control center implementation p 2197 N94-23843

PILOT: An intelligent distributed operations support system p 2508 N94-23895

Combining real-time monitoring and knowledge-based analysis in MARVEL p 2477 N94-23900

Real-time on-board orbit determination with DORIS p 2196 N94-23919

A real-time navigation monitoring expert system for the Space Shuttle Mission Control Center p 2202 N94-23921

XRTD: An X-Windows based, real-time radiometric display and analysis system p 2305 N94-23922

Kalman filtering applied to real-time monitoring of apogee maneuvers p 2196 N94-23923

SIMSAT: An object oriented architecture for real-time satellite simulation p 2197 N94-23940

Real-time holographic endoscopy [ISL-CO-203/92] p 2343 N94-24054

Making intelligent systems team players: Additional case studies [NASA-TM-104786] p 2473 N94-24068

Doppler global velocimetry: Development of a flight research instrumentation system for application to non-intrusive measurements of the flow field [NASA-CR-191490] p 2344 N94-24360

Real-time process logic [PB94-101441] p 2446 N94-24540

ASR-9 microburst detection algorithm [AD-A273591] p 2415 N94-24850

Performance measurements of the multimedia testbed on Mach 3.0: Experience writing real-time device drivers, servers, and applications [AD-A273600] p 2460 N94-24932

Reengineering real-time software systems [AD-A273408] p 2461 N94-25074

On chain coding of line drawings [ISBN-9-06-275778-2] p 2462 N94-25252

Non-invasive optical detection of glucose in cell culture nutrient medium p 2422 N94-25357

Proceedings of the 12th International Congress: Corrosion Control for Low-Cost Reliability. Volume 6: Electric Power Industry [AD-A273668] p 2250 N94-25408

Expert system rule-base evaluation using real-time parallel processing [AD-A273701] p 2469 N94-25454

REATTACHED FLOW

A comparative study of computational solutions to flow over a backward-facing step p 2326 N94-23670

Computation of turbulent flows over backward and forward-facing steps using a near-wall Reynolds stress model p 2172 N94-24145

RECEIVERS

Systems implications of L-band fade data statistics for LEO mobile systems p 2284 N94-22799

Low cost coherent demodulation for mobile satellite terminals p 2284 N94-22803

An optical ASK and FSK phase diversity transmission system [EUT-92-E-268] p 2542 N94-23171

Integration and test of high-speed transmitter electronics for free-space laser communications [NASA-TM-106295] p 2295 N94-24101

Effects of atmospheric variations on acoustic system performance p 2527 N94-24211

Comparison of measured and predicted pure tone propagation levels from JAPE-1: An evaluation of the performance of ASOPRAT p 2527 N94-24212

Simulation of adjacent channel interference in a UHF satellite system [AD-A273147] p 2299 N94-24669

Measurements and modeling of multitone, low-frequency acoustic data from the Arraial do Cabo range [AD-A273406] p 2530 N94-25073

RECEPTION DIVERSITY

Diversity reception for advanced multi-satellite networks: A CDMA approach p 2286 N94-22816

Isolated and coupled superquadric loop antennas for mobile communications applications p 2289 N94-22834

RECIPROCITY THEOREM

Electromagnetic scattering by inhomogeneous objects. Solution methods based upon reciprocity theorems of time-convolution and time-correlation type [PB94-111010] p 2294 N94-23729

RECIRCULATIVE FLUID FLOW

A comparative study of computational solutions to flow over a backward-facing step p 2326 N94-23670

RECOIL ATOMS

Optical spin polarization and state-sensitive detection of a cesium atomic beam [ATR-92(8436)-1] p 2534 N94-24077

RECOMMENDATIONS

Ultraviolet, visible, and gravity astrophysics: A plan for the 1990's [NASA-NP-152] p 2603 N94-24973

RECONNAISSANCE

Design project: LONGBOW supersonic interceptor [NASA-CR-195510] p 2180 N94-24581

RECONNAISSANCE AIRCRAFT

UAV current technology and future trends p 2154 N94-24245

S-2E Tracker maritime patrol aircraft re-engine and system upgrade program p 2158 N94-24270

RECORDS MANAGEMENT

Fact-based enterprise information management using NIAM [DE93-041135] p 2591 N94-24501

RECOVERY

Galileo spacecraft anomaly and safing recovery p 2207 N94-23864

RECOVERY PARACHUTES

Regulated drag area parachute [AD-D015992] p 2170 N94-25051

RECRYSTALLIZATION

Characterization of 3-D particle distributions and effects on recrystallization studied by computer simulation [PB93-201408] p 2562 N94-23535

RECTANGULAR PANELS

Nonlinear equations of motion for a panel subject to external loads [AD-A273142] p 2170 N94-24773

RECURSIVE FUNCTIONS

Mean-value of product-form stochastic Petri net models of slotted-ring systems [PB94-110871] p 2494 N94-23749

The Adam language: Ada extended with support for multiway activities [NASA-CR-4565] p 2456 N94-24480

RECYCLING

Feasibility study on a CO2 global recycling system using natural energy [DE94-714889] p 2397 N94-23026

RED SHIFT

Using contour maps to search for red-shifted 511 keV features in BATSE GRB spectra p 2585 N94-24455

REDUCTION (CHEMISTRY)

Dispersion of Rh/Cu in a sol-gel matrix. Highly chemo- and stereoselective catalyst for the reduction of alkynes to Z-alkenes [AD-A273306] p 2262 N94-25145

The electrochemistry of the solvated electron: A study of its properties and of its applications [ETN-94-95313] p 2236 N94-25296

REDUNDANT COMPONENTS

Reliable redundant device for mechanisms p 2361 N94-24030

Reliability analysis of a repairable dependent parallel system [ETN-94-95312] p 2373 N94-25295

REED-SOLOMON CODES

Box codes of lengths 48 and 72 p 2292 N94-23265

REELS

Nearly uniform deployment/retrieval strategy for space tether systems p 2156 N94-24256

REENTRY EFFECTS

Analysis and effects of the advanced solid rocket motor on the Space Shuttle elements [NASA-CR-193879] p 2200 N94-24664

REENTRY VEHICLES

Development and application of an empirical probability distribution for the prediction error of re-entry body maximum dynamic pressure p 2207 N94-23653

REFINING

Proceedings of the 12th International Congress: Corrosion Control for Low-Cost Reliability. Volume 4: Oil/Gas Pipeline [AD-A273665] p 2250 N94-25405

REFLECTANCE

Spatial and temporal variability of soil temperature, moisture and surface soil properties [NASA-CR-194109] p 2401 N94-23337

Theoretical investigation of variable periodicity (graded) multilayers for hard x ray applications [NASA-CR-194824] p 2543 N94-23502

Nimbus-7 Total Ozone Mapping Spectrometer (TOMS) data products user's guide
[NASA-RP-1323] p 2410 N94-24355

REFLECTION

An Earth albedo model: A mathematical model for the radiant energy input to an orbiting spacecraft due to the diffuse reflectance of solar radiation from the Earth below
[NASA-TM-104596] p 2195 N94-24497

The Radar Image Generation (RIG) model
p 2306 N94-25497

REFLECTOR ANTENNAS

Electrical performance of wire mesh for spacecraft deployable reflector antennas p 2275 N94-22744

K- and Ka-band mobile-vehicular satellite-tracking reflector antenna system for the NASA ACTS mobile terminal p 2289 N94-22831

Integrated reflector antenna design and analysis
[NASA-CR-195164] p 2300 N94-24678

Feasibility study of a synthesis procedure for array feeds to improve radiation performance of large distorted reflector antennas
[NASA-CR-195167] p 2301 N94-25005

REFRACTION

Refraction of high frequency noise in an arbitrary jet flow
[NASA-TM-106465] p 2525 N94-23464

REFRACTIVITY

Design refinement of multilayer optical thin film devices with two optimization techniques
[DE93-634228] p 2542 N94-22979

Dimensional analysis of acoustically propagated signals p 2528 N94-24217

Conformal method of fabricating and optical waveguide on a semiconductor substrate
[AD-D015988] p 2546 N94-25043

Liquidus temperature and optical properties measurement by containerless techniques
p 2247 N94-25126

Optical properties and emissivities of liquid metals and alloys p 2248 N94-25129

REFRACTORY COATINGS

Molten salt reactor for potentiostatic electroplating
[AD-D016020] p 2258 N94-24720

REFRACTORY MATERIALS

Evaluation of A5Si3Z(x) intermetallics for use as high temperature structural materials
[DE93-041127] p 2227 N94-22977

Small rocket research and technology
p 2211 N94-23038

Advanced materials for radiation-cooled rockets
p 2214 N94-23052

Vaporization behavior of non-stoichiometric refractory carbide materials and direct observations of the vapor phase using laser diagnostics
[DE93-040094] p 2348 N94-23203

Preceedings of the 12th International Congress: Corrosion Control for Low-Cost Reliability. Volume 2: Process Industries Plant Operations
[AD-A273662] p 2251 N94-25449

Preceedings of the 12th International Congress: Corrosion Control for Low-Cost Reliability. Volume 3A: Corrosion: Specific issues
[AD-A273663] p 2251 N94-25450

REFRACTORY METAL ALLOYS

An extended laser flash technique for thermal diffusivity measurement of high-temperature materials
p 2238 N94-25132

REFRACTORY METALS

New extensions in the development of deformation processed metal-metal matrix composites
[DE94-000692] p 2227 N94-23004

The effects of texture and strain on the r-va lue of heavy gauge tantalum plate
[DE94-000690] p 2242 N94-23541

REFRIGERANTS

US Department of Energy phaseout of CFC-refrigerants
[DE94-001668] p 2397 N94-23016

REFRIGERATING

US Department of Energy phaseout of CFC-refrigerants
[DE94-001668] p 2397 N94-23016

REFRIGERATORS

A study of element interaction in thermoacoustic engines
[AD-A273228] p 2569 N94-24777

REGENERATIVE COOLING

Flow visualization study in high aspect ratio cooling channels for rocket engines p 2213 N94-23049

Effect of hydrogen exposure on a Cu-8 Cr-4 Nb alloy
[NASA-TM-106429] p 2243 N94-23556

Heat transfer in rocket engine combustion chambers and regeneratively cooled nozzles
[NASA-CR-195094] p 2220 N94-24471

REGENERATIVE FUEL CELLS

Primary and secondary electrical space power based on advanced PEM systems p 2392 N94-23357

PEM regenerative fuel cells p 2392 N94-23358

Effect of power system technology and mission requirements on high altitude long endurance aircraft
[NASA-CR-194455] p 2189 N94-25200

REGOLITH

Whole rock major element chemistry of KREEP basalt clasts in lunar breccia 15205: Implications for the petrogenesis of volcanic KREEP basalts
p 2614 N94-24365

Design of a lunar propellant processing facility. NASA/USRA advanced program
[NASA-CR-195502] p 2266 N94-24618

Vertical transport of water in the Martian boundary layer p 2622 N94-24902

REGRESSION ANALYSIS

Atmospheric moisture fields derived by satellite observations over the tropical Pacific Ocean
[NASA-CR-194852] p 2408 N94-23542

Maximal type test statistics based on conditional processes
[PB94-111614] p 2494 N94-23771

First order conditions for the maximum likelihood estimation of an exact ARMA model
[PB94-110533] p 2495 N94-23814

Verification and validation of models
[PB94-110566] p 2456 N94-24507

Two-stage versus sequential sample-size determination in regression analysis of simulation experiments
[PB94-110558] p 2495 N94-24634

Generalized linear mixed models and their application in plant breeding research
[ETN-94-95335] p 2460 N94-25061

REGRESSION COEFFICIENTS

Space Shuttle Main Engine performance analysis
p 2222 N94-24444

REGULATIONS

US domestic and international regulatory issues
p 2275 N94-22748

Use of negotiated rulemaking in developing technical rules for low-Earth orbit mobile satellite systems
p 2276 N94-22750

NASA printing, duplicating, and copying management handbook
[NASA-NHB-1490.5] p 2590 N94-23971

REINFORCED PLASTICS

Fire-resistant barriers for composite materials
[AD-D016014] p 2230 N94-24735

Composites and textile reinforcement
[VTT-TIED-1424] p 2231 N94-25420

REINFORCED PLATES

Out of plane gradients in laminated composites
[NASA-CR-194875] p 2228 N94-23566

Post buckling behaviour of stiffened composite panels loaded in cyclic compression and shear
p 2157 N94-24260

REINFORCED SHELLS

Post buckling behaviour of stiffened composite panels loaded in cyclic compression and shear
p 2157 N94-24260

CORSS: Cylinder Optimization of Rings, Skin, and Stringers
[NASA-TP-3457] p 2490 N94-24727

REINFORCEMENT RINGS

CORSS: Cylinder Optimization of Rings, Skin, and Stringers
[NASA-TP-3457] p 2490 N94-24727

REINFORCING FIBERS

Creep deformation characteristics of ductile discontinuous fiber reinforced composites
[DE94-000697] p 2227 N94-23005

Development of silicon nitride composites with continuous fiber reinforcement
[DE94-001996] p 2227 N94-23022

Determination of fiber-matrix interface failure parameters from off-axis tests
[NASA-TM-109043] p 2241 N94-23274

Interface evaluation in ceramic composites
p 2255 N94-24231

CMC design consequences p 2256 N94-24238

Constitutive modelling of fiber-reinforced concrete under uniaxial tensile loading
[VTT-JULK-774] p 2379 N94-25385

Alternatives for reinforcement: Fiber composites
[VTT-TIED-1412] p 2230 N94-25386

The pressure loaded volumetric ceramic receiver 500 kW version design and construction
[DLR-MITT-93-02] p 2396 N94-25479

RELATIVISTIC PARTICLES

Relativistic hadrons in an external field
[ETN-94-95387] p 2538 N94-25259

RELATIVISTIC PLASMAS

A relativistic theory on wave propagation in inhomogeneous magnetoplasmas
[ETN-94-95322] p 2554 N94-25285

RELATIVISTIC THEORY

A relativistic theory on wave propagation in inhomogeneous magnetoplasmas
[ETN-94-95322] p 2554 N94-25285

RELATIVITY

Tensor-scalar cosmological models and their relaxation toward general relativity
[PB93-220796] p 2601 N94-23099

On BRST quantization of constrained systems
[ETN-94-95386] p 2570 N94-25258

RELAXATION (MECHANICS)

Structure and energetics of high index Fe, Al, Cu and Ni surfaces using equivalent crystal theory
[NASA-TM-106408] p 2249 N94-25171

RELAXATION METHOD (MATHEMATICS)

Relaxation schemes for Chebyshev spectral multigrid methods p 2484 N94-23688

RELAXATION TIME

Dipolar relaxation in a second-order nonlinear optical interpenetrating polymer network
[AD-A273626] p 2258 N94-24732

RELAY SATELLITES

The Olympus PAX, measurement of mechanism induced vibration p 2362 N94-24041

RELIABILITY

Efficiency and reliability enhancements in propulsion flowfield modeling p 2215 N94-23055

Connector mechanisms in compliance with extreme space conditions p 2360 N94-24025

Embodiment design for a multipropellant resistojet
[NASA-CR-195505] p 2221 N94-24834

RELIABILITY ANALYSIS

Phased-mission system analysis using Boolean algebraic methods
[NASA-CR-191564] p 2451 N94-23340

Specifying design conservatism: Worst case versus probabilistic analysis p 2374 N94-23939

Aviation system safety risk management tool analysis. Volume 2: Appendices
[AD-A273502] p 2173 N94-24864

Reliability analysis of a repairable dependent parallel system
[ETN-94-95312] p 2373 N94-25295

RELIABILITY ENGINEERING

Reliability enhancement of Navier-Stokes codes through convergence enhancement p 2216 N94-23064

Contribution to the evaluation of efficiency of a microprocessor functional test
[ETN-94-95176] p 2445 N94-23153

Aviation system safety risk management tool analysis. Volume 2: Appendices
[AD-A273502] p 2173 N94-24864

Preceedings of the 12th International Congress: Corrosion Control for Low-Cost Reliability. Volume 3A: Corrosion: Specific issues
[AD-A273663] p 2251 N94-25450

Fault detection in HVAC systems using fuzzy models
[OUEL-1977/93] p 2373 N94-25475

RELIEF MAPS

Using contour maps to search for red-shifted 511 keV features in BATSE GRB spectra p 2585 N94-24455

REMANENCE

Photo-induced antiferromagnetic interlayer coupling in Fe superlattices with iron silicide spacers
[DE94-001345] p 2559 N94-22995

Comparative M-H characteristics of 1-5 and 2-17 type samarium-cobalt permanent magnets to 300 C
[NASA-CR-194440] p 2312 N94-24870

REMOTE CONTROL

Mars 96 rover: Science, instrumentation, and control
p 2369 N94-23395

The remote-operated autonomous-robot concept: From deep sea to outer space applications
p 2370 N94-23413

Sensing and modelling concepts for autonomous and remote mobile robot control p 2370 N94-23421

The European Space Agency standard for space packet utilisation p 2203 N94-23954

Crew interface analysis: Selected articles on space human factors research, 1987 - 1991
[NASA-TM-104756] p 2433 N94-24185

UAV current technology and future trends
p 2154 N94-24245

Generic drone control system
[AD-D015993] p 2184 N94-25052

REMOTE HANDLING

System for automatic transportation of aircraft on the ground
[CA-PATENT-1-322-361] p 2193 N94-24785

REMOTE MANIPULATOR SYSTEM

Illumination requirements for operating a space remote manipulator p 2435 N94-24195

Programmable display pushbuttons on the Space Station's telerobot control panel p 2435 N94-24198
The effects of spatially displaced visual feedback on remote manipulator performance p 2436 N94-24201
Admittance model for the shuttle remote manipulator system in four configurations
[NASA-CR-4555] p 2474 N94-24635
Modelling the Shuttle Remote Manipulator System: Another flexible model p 2371 N94-25350

REMOTE SENSING
The AGRHYMET data communications project
p 2280 N94-22776
A field evaluation of remote sensor measurements of wind, temperature, and moisture for ARM integrated sounding system research
[DE94-000565] p 2381 N94-23001
Integrated use of hydrological modelling and remote sensing in the province of Drenthe (The Netherlands): Possibilities and restrictions
[REPT-61] p 2382 N94-23148
Literature study on: Remote Fraunhofer luminescence detection of algal bloom in marine environments
[BCRS-92-25] p 2417 N94-23176
Optical component MAC Europe ground truth report: Flevoland 1991 (Netherlands)
[BCRS-92-27] p 2382 N94-23177
Application of ERS-1 active microwave instrumentation data to remote sensing of snow
[PB93-224756] p 2382 N94-23224
SeaWiFS technical report series. Volume 9: The simulated SeaWiFS data set, version 1
[NASA-TM-104566-VOL-9] p 2417 N94-23291
SeaWiFS technical report series. Volume 11: Analysis of selected orbit propagation models for the SeaWiFS mission
[NASA-TM-104566-VOL-11] p 2417 N94-23338
Rover in the Mars 96 mission p 2609 N94-23397
Lunar exploration rover program developments
[DE93-040759] p 2613 N94-23469
Remote sensing, imaging, and signal engineering
[DE94-003021] p 2382 N94-23494
The Fifth Calibration/Data Product Validation Panel Meeting
[NASA-TM-108270] p 2383 N94-23595
ASTER TIR subsystem and calibration
p 2385 N94-23612
Methodology for the assessment of surface resistance and soil water storage variability at mesoscale based on remote sensing measurements. A case study with HAPEX-EFEDA data. UNESCO-International Hydrological Program 4
[PB94-111721] p 2386 N94-23734
NASDA's view of ground control in mission operations
p 2305 N94-23835
SPOT satellite family: Past, present, and future of the operations in the mission and control center
p 2500 N94-23846
SPOT4 Operational Control Center (CMP)
p 2197 N94-23856
Mission planning for an Earth observation low Earth orbiter: ERS-1 p 2503 N94-23868
MAMS data for the Convection and Moisture Experiment (CAMEX)
[NASA-TM-108435] p 2409 N94-24080
Estimation of the rain signal in the presence of large surface clutter
[NASA-CR-195105] p 2409 N94-24087
Roles, uses, and benefits of general aviation aircraft in aerospace engineering education
[NASA-TM-106463] p 2153 N94-24100
Intercomparison of remote and balloon-borne sensors operated at JAPE-91 p 2527 N94-24210
Preliminary analysis of the JAPE ground vehicle test data with an artificial neural network classifier
p 2529 N94-24222
Optimization of microscopic and macroscopic second order optical nonlinearities p 2226 N94-24354
Mapping Tomorrow's Resources: A symposium on the uses of remote sensing, Geographic Information Systems (GIS), and Global Positioning Systems (GPS) for natural resources management p 2387 N94-24357
Factors affecting the identification of phytoplankton groups by means of remote sensing
[NASA-TM-108799] p 2387 N94-24403
The measurement and analysis of leaf spectral reflectance of two stands of loblolly pine populations
p 2389 N94-24442
An investigation of current and future satellite and in-situ data for the remote sensing of the land surface energy balance
[NASA-CR-195138] p 2387 N94-24596
Nondestructive evaluations
[DE94-003020] p 2373 N94-24613
Hyperspectral imagery classification using a backpropagation neural network
[AD-A273615] p 2545 N94-24730
Method for selection of wavelength bands for multispectral classification
[PB93-204378] p 2388 N94-24741
Evaluation of the use of remote-sensing data to identify crop types and estimate irrigated acreage, Uvalde and Medina Counties, Texas, 1989
[PB93-193159] p 2388 N94-24809
Investigation of passive atmospheric sounding using millimeter and submillimeter wavelength channels
[NASA-CR-194858] p 2404 N94-24843
Feasibility study of a synthesis procedure for array feeds to improve radiation performance of large distorted reflector antennas
[NASA-CR-195167] p 2301 N94-25005
Remote vibration measurements at a sud aviation alouette 3 helicopter with a CW CO2-laser system
[AD-A273818] p 2190 N94-25516

REMOTE SENSORS
A field evaluation of remote sensor measurements of wind, temperature, and moisture for ARM integrated sounding system research
[DE94-000565] p 2381 N94-23001
PULSAUR 2
[NASA-CR-194832] p 2209 N94-23484
MODIS calibration p 2383 N94-23600
Eos cross-calibration radiometers
p 2383 N94-23601
Activities of NIST (National Inst. of Standards and Technology) p 2384 N94-23605
A fifteen years lifetime mechanism for an infrared Earth sensor p 2362 N94-24040
Intercomparison of remote and balloon-borne sensors operated at JAPE-91 p 2527 N94-24210

REMOTELY PILOTED VEHICLES
Decentralized autonomous attitude determination using an inertially stabilized payload p 2157 N94-24264
Overall system concepts in mission planning
p 2521 N94-25009
Generic drone control system
[AD-D015993] p 2184 N94-25052

RENORMALIZATION GROUP METHODS
Development and validation of RNG methodology for compressible turbulence
[AD-A273469] p 2337 N94-24929
The renormalization group for flag manifolds
[DE93-616846] p 2491 N94-25213

REPETITION
Two-stage versus sequential sample-size determination in regression analysis of simulation experiments
[PB94-110558] p 2495 N94-24634

REPORTS
Activities report to NATO
[ETN-94-95047] p 2318 N94-23227
Fiscal year 1993 scientific and technical reports, articles, papers, and presentations
[NASA-TM-108423] p 2590 N94-24079
NASA/DOD Aerospace Knowledge Diffusion Research Project. Report number 21: US aerospace industry librarians and technical information specialists as information intermediaries: Results of the phase 2 survey
[NASA-TM-109064] p 2593 N94-24709

REPRODUCTION (COPYING)
NASA printing, duplicating, and copying management handbook
[NASA-NHB-1490.5] p 2590 N94-23971

REQUIREMENTS
The next Japanese solar satellite
p 2625 N94-22846
Requirements for future solar-physics missions that include UV instrumentation p 2625 N94-22851
Tools reference manual for a Requirements Specification Language (RSL), version 2.0
[NASA-CR-191461] p 2445 N94-23125
Rover requirements for the planet surface segment of the space exploration initiative p 2369 N94-23377
Electronic payloads for Martian missions: A preliminary assessment of technologies p 2610 N94-23408
An approach to the design of operations systems
p 2506 N94-23884
The Columbus logistics support at the APMC: Requirements and implementation aspects
p 2515 N94-23935

RESEARCH
The national geomagnetic initiative
[LC-93-85739] p 2401 N94-23344
Bibliography of Lewis Research Center technical publications announced in 1992
[NASA-TM-106035] p 2590 N94-23562
Index to FAA Office of Aviation Medicine Reports: 1961 through 1993
[DOT/FAA/AM-94/1] p 2426 N94-24093
RIACS/USRA
[NASA-CR-195117] p 2631 N94-25003
Research interests and broad agency announcement 94-1 of the Air Force Office of Scientific Research
[AD-A273410] p 2632 N94-25075
National Aeronautics and Space Administration (NASA)/American Society for Engineering Education (ASEE) Summer Faculty Fellowship Program, 1993, volume 2
[NASA-CR-188271-VOL-2] p 2636 N94-25367

RESEARCH AIRCRAFT
Close-up analysis of inflight ice accretion
[NASA-TM-106457] p 2172 N94-23523
A conceptual design of an unmanned test vehicle using an airbreathing propulsion system
[NASA-CR-195550] p 2189 N94-25085
X-31 aerodynamic characteristics determined from flight data p 2164 N94-25109
Nonlinear aerodynamic modeling using multivariate orthogonal functions p 2164 N94-25110

RESEARCH AND DEVELOPMENT
Progress in phases 2 and 3 of the Photovoltaic Manufacturing Technology Project (PVMaT)
[DE94-000206] p 2389 N94-22888
JPRS report: Science and technology. Central Eurasia: Space
[JPRS-USP-93-006] p 2194 N94-23015
NASA Propulsion Engineering Research Center, volume 2
[NASA-CR-194719-VOL-2] p 2209 N94-23028
Activities report to NATO
[ETN-94-95047] p 2318 N94-23227
Bibliography of Lewis Research Center technical publications announced in 1992
[NASA-TM-106035] p 2590 N94-23562
The RB211: The first 25 years
[PNR-90977] p 2187 N94-23570
Contributions of DOE weapons labs and NIST to semicondutor technology
[OTA-ITE-585] p 2630 N94-23572
Satellite communications systems and technology. Volume 1: Analytical chapters
[NASA-TM-109398] p 2293 N94-23627
Fiscal year 1993 scientific and technical reports, articles, papers, and presentations
[NASA-TM-108423] p 2590 N94-24079
Proceedings of Technology and Governance in the 1990's
[PB93-192904] p 2597 N94-24312
NASA high performance computing and communications program
[NASA-TM-4554] p 2591 N94-24337
Radio communication and wave propagation. A visit to the Netherlands in December 1992
[PB93-204360] p 2297 N94-24531
Structural dynamics division research and technology accomplishments for FY 1993 and plans for FY 1994
[NASA-TM-109036] p 2169 N94-24576
Nondestructive evaluations
[DE94-003020] p 2373 N94-24613
NASA/DOD Aerospace Knowledge Diffusion Research Project. Report number 20: The use of selected information products and services by US aerospace engineers and scientists: Results of two surveys
[NASA-TM-109022] p 2592 N94-24649
NADA/DOD Aerospace Knowledge Diffusion Research Project. Report number 19: The US government technical report and the transfer of federally funded aerospace R/D: An analysis of five studies
[NASA-TM-109061] p 2592 N94-24660
Research interests and broad agency announcement 94-1 of the Air Force Office of Scientific Research
[AD-A273410] p 2632 N94-25075
National Aeronautics and Space Administration (NASA)/American Society for Engineering Education (ASEE) Summer Faculty Fellowship Program, 1993, volume 1
[NASA-CR-188271-VOL-1] p 2632 N94-25348

RESEARCH FACILITIES
Satellite communications systems and technology. Volume 2: Site reports
[NASA-TM-109399] p 2293 N94-23628
Suddenly, tomorrow came... A history of the Johnson Space Center
[NASA-SP-4307] p 2631 N94-24584
Advanced ballistic range technology
[NASA-CR-195198] p 2165 N94-25169
Activities of Academia Sinica
[DE93-614529] p 2541 N94-25335
Automatic pressure control system for the Wright Laboratory Compressor Research Facility
[AD-A273827] p 2194 N94-25522

RESEARCH MANAGEMENT
Satellite communications systems and technology. Volume 2: Site reports
[NASA-TM-109399] p 2293 N94-23628

Collaborating with our customers: NIST building and fire research laboratory [PB94-110194] p 2272 N94-24955

RESEARCH PROJECTS

Fiscal year 1993 scientific and technical reports, articles, papers, and presentations [NASA-TM-108423] p 2590 N94-24079

GRYPHON: Air launched space booster [NASA-CR-195497] p 2199 N94-25022

National Aeronautics and Space Administration (NASA)/American Society for Engineering Education (ASEE) Summer Faculty Fellowship Program, 1993, volume 2 [NASA-CR-188271-VOL-2] p 2636 N94-25367

RESEARCH VEHICLES

Configuration development study of the OSU 1 hypersonic research vehicle [NASA-CR-195522] p 2181 N94-24591

Design of a wheeled articulating land rover [NASA-CR-195520] p 2365 N94-24806

RESERVOIRS

Near-surface seismic imaging [PB94-119096] p 2404 N94-24647

RESIDUAL GAS

Hot hydrogen testing of metallic turbo pump materials [NASA-CR-193880] p 2244 N94-24066

RESIDUAL STRESS

Control of the internal stresses in plane elasticity [PB93-225514] p 2374 N94-23112

Analysis of local delaminations caused by angle ply matrix cracks [NASA-TM-109052] p 2228 N94-24083

Dynamic localization and second-order subgrid-scale models in large eddy simulations of channel flow p 2329 N94-24149

Feasibility study of shot-peening modeling [CTN-94-60926] p 2244 N94-24170

Birdstrike resistant crew enclosure program [AD-A273700] p 2463 N94-25453

RESIDUES

Chemical characterization of some aerobic liquids in CELSS p 2422 N94-23241

Analysis of impactor residues in tray clamps from the Long Duration Exposure Facility. Part 2: Clamps from Bay B of the satellite [NASA-TM-104784] p 2386 N94-24095

RESIN TRANSFER MOLDING

Composites and textile reinforcement [VTT-TIED-1424] p 2231 N94-25420

RESINS

Curing phthalonitrile resins with acid and amine [AD-D016021] p 2258 N94-24721

RESISTOJET ENGINES

Embodiment design for a multipropellant resistojet [NASA-CR-195505] p 2221 N94-24834

Design of a resistojet for Space Station Freedom [NASA-CR-195506] p 2221 N94-24979

RESONANCE

Analysis and experiments of a whistler-wave plasma thruster [DE94-001533] p 2209 N94-23012

An active antenna for ELF magnetic fields p 2303 N94-25192

Bottom quark production at the Z resonance [ISBN-9-09-006217-3] p 2538 N94-25255

RESONANCE LINES

Semiempirical studies of atomic structure [DE94-001588] p 2531 N94-22937

The resonance lines of MG2 as diagnostics of the upper solar chromosphere [NASA-CR-195084] p 2627 N94-24300

RESONANT FREQUENCIES

Liquid oscillations in a spherical system with sliding edges boundary by two conical solid surfaces in zero-gravity [LRT-WE-9-FB-5-1992] p 2318 N94-23197

Vibrations of variable cross section Timoshenko beams p 2160 N94-24279

The H(sub infinity) optimal controller design and reduction for the inertial hold mode of the attitude control system of the XTE spacecraft [NASA-CR-195137] p 2366 N94-24846

Magnetic Earth Ionosphere Resonant Frequencies [NASA-CR-195131] p 2303 N94-25191

An active antenna for ELF magnetic fields p 2303 N94-25192

RESONANT TUNNELING

Quantum tunneling transport of electrons in double-barrier heterostructures: Theory and modeling [ETN-94-95332] p 2565 N94-25059

RESONATORS

Spatiotemporal behavior and nonlinear dynamics in a phase conjugate resonator [NASA-CR-4567] p 2543 N94-23529

Internally folded scalable laser [AD-D015978] p 2350 N94-25216

RESOURCE ALLOCATION

Resource allocation planning with international components p 2520 N94-23963

RESOURCES MANAGEMENT

Planning: Management of predictability and uncertainty and keeping abreast of developments p 2520 N94-23967

Mapping Tomorrow's Resources: A symposium on the uses of remote sensing, Geographic Information Systems (GIS), and Global Positioning Systems (GPS) for natural resources management p 2387 N94-24357

A biological survey for the nation [LC-93-85920] p 2421 N94-24704

The HEC NexGen software development project [AD-A273512] p 2460 N94-24822

Investigating pyrolysis/incineration as a method of resource recovery from solid waste p 2444 N94-25375

RESPIRATORY SYSTEM

Chronic obstructive pulmonary disease p 2425 N94-23324

RETINA

Physical aspects of the visual stimulus p 2431 N94-23978

RETRIEVAL

Nearly uniform deployment/retrieval strategy for space tether systems p 2156 N94-24256

REUSABLE SPACECRAFT

An assessment of solid lubricant films for use in high temperature space applications p 2363 N94-24044

Conceptual design of a two stage to orbit spacecraft [NASA-CR-195536] p 2204 N94-24620

REVERSE ENGINEERING

Update of GRASP/Ada reverse engineering tools for Ada [NASA-CR-193890] p 2455 N94-24111

REVERSE FIELD PINCH

Chaos in plasma simulation and experiment [DE94-001574] p 2549 N94-22963

Plasma research in the Madison Symmetric Torus (MST) [DE94-002318] p 2549 N94-22976

Chaos and simple determinism in reversed field pinch plasmas: Nonlinear analysis of numerical simulation and experimental data [DE94-001575] p 2550 N94-23211

REYNOLDS EQUATION

New concepts for Reynolds stress transport equation modeling of inhomogeneous flows p 2171 N94-24143

Carrying the mass flux terms exactly in the first and second moment equations of compressible turbulence [NASA-CR-191568] p 2335 N94-24712

REYNOLDS NUMBER

A method to simulate viscous diffusion of vorticity by convective transport of vortices at a non-solenoidal velocity [DE94-001777] p 2318 N94-23220

Unstructured grid large eddy simulation of wall bounded turbulent flows p 2329 N94-24151

Energy transfer and constrained simulations in isotropic turbulence p 2330 N94-24153

Stagnation region heat transfer: The influence of turbulence parameters, Reynolds number and body shape [NASA-TM-106504] p 2334 N94-24481

Interactive control in turbulent shear layers [AD-A273544] p 2336 N94-24793

Active control of oscillatory lift forces on a circular cylinder [AD-A273243] p 2338 N94-25140

REYNOLDS STRESS

Turbulence sensors for separated flows: Current capabilities, future requirements p 2315 N94-22853

Computation of flows in a turn-around duct and a turbine cascade using advanced turbulence models p 2216 N94-23062

A representation for the turbulent mass flux contribution to Reynolds-stress and two-equation closures for compressible turbulence [NASA-CR-191569] p 2319 N94-23302

Reliability in second moment turbulence closures revisited [NASA-TM-106469] p 2326 N94-24063

Toward modeling wingtip vortices p 2171 N94-24142

New concepts for Reynolds stress transport equation modeling of inhomogeneous flows p 2171 N94-24143

Turbulence modeling for non-equilibrium flows p 2328 N94-24144

Computation of turbulent flows over backward and forward-facing steps using a near-wall Reynolds stress model p 2172 N94-24145

Dynamic localization and second-order subgrid-scale models in large eddy simulations of channel flow p 2329 N94-24149

Sound radiation due to boundary layer transition p 2332 N94-24163

Effects of shock strength on shock turbulence interaction p 2332 N94-24165

Local isotropy in distorted turbulent boundary layers at high Reynolds number p 2332 N94-24166

Implementation of the Baldwin-Barth turbulence model into the ZETA code and its diagnosis [NASA-CR-194795] p 2335 N94-24640

Carrying the mass flux terms exactly in the first and second moment equations of compressible turbulence [NASA-CR-191568] p 2335 N94-24712

RHENIUM

Advanced materials for radiation-cooled rockets p 2214 N94-23052

Surface compositional variations of Mo-47Re alloy as a function of temperature [NASA-TP-3402] p 2245 N94-25117

RHEOLOGY

Electro-rheology fluids and liquid fuel flow [AD-A273640] p 2337 N94-25032

Constraining proposed combinations of ice history and Earth rheology using VLBI determined baseline length rates in North America p 2405 N94-25205

RHODIUM

Dispersion of Rh/Cu in a sol-gel matrix. Highly chemo- and stereoselective catalyst for the reduction of alkynes to Z-alkenes [AD-A273306] p 2262 N94-25145

RHODIUM ALLOYS

Reduction of nitric oxide over platinum, rhodium and platinum-rhodium single crystal surfaces [PB93-230092] p 2232 N94-23482

RIBLETS

Coherent structures over grooved surfaces [ETN-94-95308] p 2339 N94-25291

RIBONUCLEIC ACIDS

The torsion space nucleic acids molecular mechanics program DUPLEX: Surveying conformation space by potential energy minimization [DE94-002441] p 2563 N94-24567

RICCATI EQUATION

A mixed H2/H(infinity) function for a discrete time system [MEMO-COSOR-92-36] p 2480 N94-23144

Coordinate-free interpretations of the optimal costs for Lq problems subject to implicit systems [PB94-118700] p 2473 N94-23760

Control of nonlinear systems represented in quasilinear form [NASA-CR-194840] p 2475 N94-24760

RICE

Rice cultivation and methane emission: Documentation of distributed geographic data sets [NASA-TM-104595] p 2381 N94-24800

RIEMANN MANIFOLD

Lacunary series as quadratic differentials in conformal dynamics [PB93-238061] p 2481 N94-23547

Applications of supersymmetric quantum mechanics [ETN-94-95385] p 2570 N94-25257

Deviation equations of Synge and Schild in spaces with affine connection and metric, and equations for gravitational waves detectors [DE93-616852] p 2571 N94-25339

RIGID STRUCTURES

A structural design decomposition method utilizing substructuring [NASA-TM-107750] p 2376 N94-23368

Pressure wall patch [NASA-CASE-MFS-28724-1] p 2203 N94-23824

Numerical analysis of the motion of a rigid body with an attached spring-mass-damper [AD-A273825] p 2379 N94-25520

RINGS (MATHEMATICS)

Orbit spaces over commutative rings and projectives as semi-isomorphisms [DE93-616822] p 2493 N94-25473

RISK

Aeromedical disposition for coronary artery disease p 2423 N94-23316

Arterial hypertension and the aviator p 2425 N94-23328

Risk identification and reduction in integrated product teams p 2497 N94-24407

In vitro system for studying metabolism of environmental chemicals in human cells [AD-A273427] p 2421 N94-24688

A statistical analysis of recent Naval Experimental Diving Unit (NEDU) single-depth human exposures to 100 percent oxygen at pressure [AD-A273488] p 2427 N94-24950

Integrated risk management p 2588 N94-25361

RIVERS
Hydraulics and morphology of mountain rivers: A literature survey. Communications on hydraulic and geotechnical engineering
[PB94-110772] p 2388 N94-24636
RL-10 ENGINES
Extended duration lunar lander
[NASA-CR-195527] p 2206 N94-24916
RLC CIRCUITS
Study of a system for producing a pulsed magnetic field (B 2T) with a frequency of 50 Hz
[ISL-N-601/92] p 2314 N94-25460
ROADS
Estimation of delays and emissions at four-way junctions with different forms of regulation, principally four-way mandatory stop
[PB94-105236] p 2398 N94-23813
ROBOT ARMS
Control of a serpentine manipulator with collision avoidance p 2368 N94-23232
Telerobotic rendezvous and docking vision system architecture
[NASA-CR-191329] p 2204 N94-23828
HERA (Hermes robot arm) overview
p 2357 N94-24005
The development of the HERA Test Facility (HTF)
p 2197 N94-24020
Robust stability of second-order systems
[NASA-CR-195175] p 2488 N94-24564
Autonomous Space Processor for Orbital Debris (ASPOD)
[NASA-CR-195521] p 2204 N94-24621
Human-like robots for space and hazardous environments
[NASA-CR-195549] p 2365 N94-24703
Research experience for undergraduates in robotics and materials
[AD-A273659] p 2368 N94-25436
ROBOT CONTROL
Normal forms of kinematic singularities of 3R robot manipulators
[MEMO-1124] p 2469 N94-22712
Control of a serpentine manipulator with collision avoidance p 2368 N94-23232
Rack Insertion End Effector (RIEE) automation
p 2368 N94-23242
The robotic Mars rover p 2608 N94-23390
Sensing and modelling concepts for autonomous and remote mobile robot control p 2370 N94-23421
Bond graph modeling, simulation, and reflex control of the Mars planetary automatic vehicle
p 2370 N94-23424
Experiments with a small behaviour controlled planetary rover p 2371 N94-23427
Telerobotic rendezvous and docking vision system architecture
[NASA-CR-191329] p 2204 N94-23828
Ground operation of robotics on Space Station Freedom p 2371 N94-23841
Development of a force feedback anthropomorphic teleoperation input device for control of robot hands
[NASA-CR-195109] p 2437 N94-24329
Autonomous Space Processor for Orbital Debris (ASPOD)
[NASA-CR-195521] p 2204 N94-24621
Human-like robots for space and hazardous environments
[NASA-CR-195549] p 2365 N94-24703
Preliminary results on time-varying feedback stabilization of a nonholonomic car-like mobile robot
[INRIA-RR-1512] p 2475 N94-24963
Advanced control structures: A transputer-based multi-robot system
[RR-468] p 2446 N94-25313
ROBOT DYNAMICS
Normal forms of kinematic singularities of 3R robot manipulators
[MEMO-1124] p 2469 N94-22712
Motion planning for a non-holonomic mobile in a dynamic workspace
[ETN-94-95180] p 2470 N94-22898
Contribution to geometric and dynamic modeling of parallel robots
[LAAS-93089] p 2470 N94-22904
An architecture for teleprogramming autonomous mobile robots at task level
[LAAS-93107] p 2470 N94-22906
Perception and 3D environment modeling for mobile robot autonomous navigation
[LAAS-93117] p 2471 N94-22908
Walking, jumping, and tumbling: More than one way to get around Mars p 2370 N94-23419
Perspective of creation of means for collecting information concerning transport situation
p 2370 N94-23420
Sensing and modelling concepts for autonomous and remote mobile robot control p 2370 N94-23421
Physical modeling and dynamic simulation of planet vehicles: Application to the motion prediction
p 2371 N94-23426
Human-like robots for space and hazardous environments
[NASA-CR-195549] p 2365 N94-24703
Preliminary results on time-varying feedback stabilization of a nonholonomic car-like mobile robot
[INRIA-RR-1512] p 2475 N94-24963
Advanced control structures: A transputer-based multi-robot system
[RR-468] p 2446 N94-25313
Genetic-based motion planning for articulated robotic manipulators
[RR-476] p 2368 N94-25322
ROBOT SENSORS
An evaluation of three-dimensional sensors for the extravehicular activity helper/retreiver
p 2444 N94-25369
ROBOTICS
Normal forms of kinematic singularities of 3R robot manipulators
[MEMO-1124] p 2469 N94-22712
Motion planning for a non-holonomic mobile in a dynamic workspace
[ETN-94-95180] p 2470 N94-22898
Contribution to geometric and dynamic modeling of parallel robots
[LAAS-93089] p 2470 N94-22904
Plan generation for flexible assembly systems
[PB93-217974] p 2267 N94-22981
Spline screw multiple rotations mechanism
[NASA-CASE-GSC-13452-1] p 2352 N94-23078
Split spline screw
[NASA-CASE-GSC-13434-1] p 2352 N94-23082
NASA/ASEE Summer Faculty Fellowship Program
[NASA-CR-194678] p 2571 N94-23230
Rack Insertion End Effector (RIEE) automation
p 2368 N94-23242
Missions, Technologies, and Design of Planetary Mobile Vehicles
[ISBN-2-85428-331-7] p 2605 N94-23373
The study of the mobile lunar explorer
p 2607 N94-23389
The robotic Mars rover p 2608 N94-23390
Electrical power technology for robotic planetary rovers p 2314 N94-23401
Mechanical design of a planetary rover
p 2369 N94-23403
Conceptual design and architecture of hexapod robotic vehicles for the (L)OVLA project p 2369 N94-23405
Automation technology for remote sample acquisition
p 2369 N94-23407
Evolving directions in NASA's planetary rover requirements and technology p 2370 N94-23414
Towards real-time stereovision systems for planetary missions p 2370 N94-23422
Mobility analysis, simulation, and scale model testing for the design of wheeled planetary rovers
p 2370 N94-23425
Lunar exploration rover program developments
[DE93-040759] p 2613 N94-23469
The instant sequencing task: Toward constraint-checking a complex spacecraft command sequence interactively p 2504 N94-23875
The Fifth European Space Mechanisms and Tribology Symposium
[ESA-SP-334] p 2355 N94-23985
Multipurpose clamping device with electrical connector for in orbit attachment of payloads p 2361 N94-24035
Human-like robots for space and hazardous environments
[NASA-CR-195549] p 2365 N94-24703
Design of a wheeled articulating land rover
[NASA-CR-195520] p 2365 N94-24806
Object recognition through image understanding for an autonomous mobile robot
[AD-A273206] p 2475 N94-24862
Design of a walking robot
[NASA-CR-195200] p 2367 N94-25274
Advanced control structures: A transputer-based multi-robot system
[RR-468] p 2446 N94-25313
An evaluation of three-dimensional sensors for the extravehicular activity helper/retreiver
p 2444 N94-25369
Robotics in a controlled, ecological life support system
p 2444 N94-25371
Research experience for undergraduates in robotics and materials
[AD-A273659] p 2368 N94-25436
ROBOTS
Normal forms of kinematic singularities of 3R robot manipulators
[MEMO-1124] p 2469 N94-22712
Plan generation for flexible assembly systems
[PB93-217974] p 2267 N94-22981
Graphical programming: A systems approach for telerobotic servicing of space assets
[DE93-019016] p 2472 N94-23201
Missions, Technologies, and Design of Planetary Mobile Vehicles
[ISBN-2-85428-331-7] p 2605 N94-23373
Lunar science strategy: Exploring the Moon with humans and machines p 2605 N94-23376
Robotic exploration of Moon and Mars
p 2606 N94-23379
Mission and system concepts for Mars robotic precursor missions p 2608 N94-23391
Planetary rover locomotion mechanisms
p 2369 N94-23404
The remote-operated autonomous-robot concept: From deep sea to outer space applications
p 2370 N94-23413
Walking, jumping, and tumbling: More than one way to get around Mars p 2370 N94-23419
Sensing and modelling concepts for autonomous and remote mobile robot control p 2370 N94-23421
Experiments with a small behaviour controlled planetary rover p 2371 N94-23427
Human-like robots for space and hazardous environments
[NASA-CR-195549] p 2365 N94-24703
Design of a wheeled articulating land rover
[NASA-CR-195520] p 2365 N94-24806
Object recognition through image understanding for an autonomous mobile robot
[AD-A273206] p 2475 N94-24862
Preliminary results on time-varying feedback stabilization of a nonholonomic car-like mobile robot
[INRIA-RR-1512] p 2475 N94-24963
Design of a walking robot
[NASA-CR-195200] p 2367 N94-25274
A soft robot interface
[OUEL-1948/92] p 2463 N94-25468
ROBUSTNESS (MATHEMATICS)
Nonlinear state space H(sub infinity) control theory
[MEMO-1119] p 2469 N94-22706
Identification for robust control using an H(sub infinity) norm
[EUT-92-E-261] p 2470 N94-22873
A reliable algorithm for optimal control synthesis
[NASA-CR-194809] p 2472 N94-23332
Descent and landing phase: Vision based robust spacecraft motion estimation and elevation modeling
p 2608 N94-23394
Failure-proof estimation under conditions of lack of information p 2158 N94-24267
Parametric uncertainty reduction in robust multivariable control
[AD-A273412] p 2460 N94-24927
Parametric uncertainty modeling for application to robust control p 2163 N94-25103
Robust, nonlinear, high angle-of-attack control design for a supermaneuverable vehicle p 2164 N94-25108
Practical evaluation of robust control for a class of nonlinear mechanical dynamic systems
[ISBN-9-03-860092-5] p 2475 N94-25224
ROCK INTRUSIONS
The transition from diapirism to dike intrusion: Implications for planetary volcanism
[NASA-CR-195133] p 2403 N94-24580
ROCKET ENGINE CASES
Impact damage in filament wound composite bottles
p 2231 N94-24421
Evaluation of advanced materials through experimental mechanics and modelling p 2374 N94-24454
Assessment of impact damage of composite rocket motor cases
[NASA-CR-195143] p 2220 N94-24595
Lightning tests and analyses of tunnel bond straps and shielded cables on the Space Shuttle solid rocket booster
[NASA-CR-193921] p 2200 N94-24801
ROCKET ENGINE DESIGN
Dual-bell altitude compensating nozzles
p 2215 N94-23057
Liquid rocket propulsion: Retrospective and prospects
p 2154 N94-24243
A minimum cost tolerance allocation method for rocket engines and robust rocket engine design
p 2222 N94-24419
Performance of the NASA cm ion thruster
[NASA-TM-106426] p 2221 N94-24770
ROCKET ENGINES
Small rocket research and technology
p 2211 N94-23038

An experimental study of characteristic combustion-driven flows for CFD validation p 2212 N94-23040
Efficiency and reliability enhancements in propulsion flowfield modeling p 2215 N94-23055
Brush seals for cryogenic applications p 2216 N94-23063
Reduction of the anode fall in a coaxial plasma thruster with an applied magnetic nozzle [DE94-000670] p 2218 N94-23283
An overview on the main available ceramic composites and their processing routes p 2255 N94-24229
The 33rd Israel Annual Conference on Aviation and Astronautics [ITN-94-85227] p 2153 N94-24241
A minimum cost tolerance allocation method for rocket engines and robust rocket engine design p 2222 N94-24419
Controller modeling and evaluation for PCV electro-mechanical actuator p 2371 N94-24441
Conceptual design of a two stage to orbit spacecraft [NASA-CR-195536] p 2204 N94-24620

ROCKET EXHAUST
Flame trench analysis of NLS vehicles p 2199 N94-23249
Development of an analytical-numerical model to predict radiant emission or absorption [NASA-CR-194860] p 2453 N94-23624
Using neural networks to assist in OPAD data analysis p 2477 N94-24452
Preliminary far-field plume sputtering characterization of the Stationary Plasma Thruster (SPT-100) [NASA-TM-106464] p 2221 N94-24766

ROCKET NOZZLES
Two stage turbine for rockets p 2215 N94-23059
Postflight hardware evaluation RSRM-29 (STS-54). Appendix D: Nozzle postfire data [NASA-CR-193898] p 2199 N94-24057
Postflight hardware evaluation RSRM-29 (STS-54). Appendix C: Nozzle PFORs [NASA-CR-193894] p 2219 N94-24064
Final postflight hardware evaluation report RSRM-32 (STS-57) [NASA-CR-193903] p 2200 N94-24065
Postflight hardware evaluation RSRM-29 (STS-54). Appendix E: Insulation postfire data [NASA-CR-193897] p 2200 N94-24067
Properties and processing characteristics of low density carbon cloth phenolic composites p 2231 N94-24450
Postflight hardware evaluation 360T021 (RSRM-21, STS-45), revision A [NASA-CR-193904] p 2201 N94-24965

ROCKET PROPELLANTS
Design of a lunar propellant processing facility. NASA/USRA advanced program [NASA-CR-195502] p 2266 N94-24618
Embodiment design for a multipropellant resistojet [NASA-CR-195505] p 2221 N94-24834

RODS
Inverse dynamics of a rigid rod system as a simplified model of flexible beam p 2160 N94-24281

ROLL
A study of roll attractor and wing rock of delta wings at high angles of attack p 2164 N94-25111

ROLL FORMING
Weld cladding of hard surfaces [PB93-201598] p 2353 N94-23448
Lubrication in cold rolling: Numerical simulation using multigrid techniques [ISBN-9-09-005313-1] p 2262 N94-25230

ROLLER BEARINGS
NASA/Army rotorcraft transmission research, a review of recent significant accomplishments [NASA-TM-106508] p 2367 N94-25181

ROLLERS
Electromagnetic brake/clutch device [NASA-CASE-GSC-13502-1] p 2354 N94-23969

ROLLING CONTACT LOADS
Rail Corrugations [ILR-BER-59] p 2269 N94-23581
A rail corrugation theory which allows for contact patch size p 2269 N94-23582
A rail joint: The possible initiator of corrugation? p 2269 N94-23583
A linear model for corrugation and its limit of validity p 2269 N94-23584
Lateral high frequency oscillations and stability of a wheel rolling on a flexible track p 2269 N94-23585
Wear characteristics of technical dry rolling/sliding systems with relations to corrugation problems p 2269 N94-23586
Surface observations of stick-slip oscillations in tightly conformal wheel/rail contacts p 2270 N94-23588
Contact analysis of rough rail surfaces p 2270 N94-23589

ROLLING MOMENTS
Wear characteristics of technical dry rolling/sliding systems with relations to corrugation problems p 2269 N94-23586

RONCHI TEST
Design of a surface deformation measuring instrument for the Surface Tension Driven Convection Experiment (STDCE-2) [NASA-CR-194758] p 2343 N94-23285

ROOM TEMPERATURE
Selective hydrogen separation by palladium-based composite membranes [PB93-201671] p 2254 N94-23431
Laser-deposited biocompatible films and methods and apparatuses for producing same [AD-D016017] p 2350 N94-24952

ROOT-MEAN-SQUARE ERRORS
Integer cosine transform compression for Galileo at Jupiter: A preliminary look p 2292 N94-23266
Development and validation of RNG methodology for compressible turbulence [AD-A273469] p 2337 N94-24929

ROOTS OF EQUATIONS
A theorem regarding roots of the zero-order Bessel function of the first kind p 2325 N94-23667

ROSAT MISSION
Shocked clouds in the Cygnus Loop [NASA-CR-195190] p 2600 N94-25178
ROSAT observations of the x ray binary HD 154791 [NASA-CR-195189] p 2600 N94-25198
Investigation relative to the Roentgen Satellite (ROSAT) [NASA-CR-195192] p 2600 N94-25269
ROSAT mission planning using artificial intelligence methods [DLR-FB-93-14] p 2476 N94-25345

ROTARY WING AIRCRAFT
The future of rotary-wing aircraft p 2185 N94-25070
NASA/Army rotorcraft transmission research, a review of recent significant accomplishments [NASA-TM-106508] p 2367 N94-25181

ROTARY WINGS
Bent-tip blade for aircraft rotary-wing [CA-PATENT-1-315-259] p 2176 N94-23254
An overview of a model rotor icing test in the NASA Lewis Icing Research Tunnel [NASA-TM-106471] p 2166 N94-23299
The influence of elastic pitch variations on helicopter flight mechanics p 2161 N94-24286
Validation of the ROTAC code for the rotor noise prediction [PB93-204311] p 2529 N94-24514
Wind tunnel test of a variable-diameter tiltrotor (VDTR) model [NASA-CR-177629] p 2181 N94-24796
Dynamic analysis of pretwisted elastically-coupled rotor blades [NASA-TM-109070] p 2378 N94-24839
Study of the blade/vortex interaction: Acoustics, aerodynamics and models [ISL-R-104/92] p 2340 N94-25463

ROTATING FLUIDS
Acoustic and optical investigations of superfluid He-3 [PB93-224889] p 2523 N94-23101
Investigation of the asymptotic state of rotating turbulence using large-eddy simulation p 2330 N94-24152
Transient flows occurring during the accelerated crucible rotation technique [DE93-617049] p 2567 N94-25422

ROTATING SHAFTS
Viscous rotary damper p 2361 N94-24031
A novel rotary actuator for spacecraft p 2361 N94-24034

ROTATING STALLS
Analysis and characteristics of compressor stall precursor signals in forward and AFT swept high speed compressor [AD-A273820] p 2171 N94-25517

ROTATION
Spline screw multiple rotations mechanism [NASA-CASE-GSC-13452-1] p 2352 N94-23078
Projectile transverse motion and stability in electromagnetic induction launchers [DE94-001557] p 2198 N94-23210
Results of a laboratory experiment that tests rotating unbalanced-mass devices for scanning gimbaled payloads and free-flying spacecraft [NASA-TP-3458] p 2269 N94-23574

ROTATIONAL SPECTRA
Laboratory detection of C5S by pulsed-discharge-nozzle Fourier-transform microwave spectroscopy [JTN-94-80519] p 2235 N94-24984
CO-to-H2 conversion factor in dwarf irregular galaxies [REPT-333] p 2603 N94-24985
The Nobeyama millimeter array survey for protoplanetary disks around protostar candidates and T Tauri stars in Taurus [REPT-336] p 2604 N94-24987

ROTATIONAL STATES
Radiative properties of molecular nitrogen ions produced by helium Penning ionization and argon effects [NASA-CR-195126] p 2534 N94-24487

ROTOR AERODYNAMICS
Computation of the loads on the AH-1/OLS model rotor in forward flight and comparison with wind tunnel tests [ISL-CO-230/92] p 2176 N94-23146
The influence of elastic pitch variations on helicopter flight mechanics p 2161 N94-24286
Validation of the ROTAC code for the rotor noise prediction [PB93-204311] p 2529 N94-24514
A parametric study of harmonic rotor hub loads [NASA-CR-4558] p 2181 N94-24726
Two-dimensional CFD modeling of wave rotor flow dynamics [NASA-TM-106261] p 2189 N94-25185
Study of the blade/vortex interaction: Acoustics, aerodynamics and models [ISL-R-104/92] p 2340 N94-25463

ROTOR BLADES
The influence of elastic pitch variations on helicopter flight mechanics p 2161 N94-24286
Dynamic analysis of pretwisted elastically-coupled rotor blades [NASA-TM-109070] p 2378 N94-24839

ROTOR BLADES (TURBOMACHINERY)
Simulation of unsteady flows through stator and rotor blades of a gas turbine using the Chimera method p 2323 N94-23652

ROTOR BODY INTERACTIONS
Influence of backup bearings and support structure dynamics on the behavior of rotors with active supports [NASA-CR-195106] p 2365 N94-24751

ROTOR DYNAMICS
A technique to measure rotordynamic coefficients in hydrostatic bearings p 2215 N94-23061
A parametric study of harmonic rotor hub loads [NASA-CR-4558] p 2181 N94-24726
Influence of backup bearings and support structure dynamics on the behavior of rotors with active supports [NASA-CR-195106] p 2365 N94-24751
Aeroelastic response and stability of tiltrotors with elastically-coupled composite rotor blades [NASA-TM-108758] p 2182 N94-24953
A finite-element-based perturbation model for the rotordynamic analysis of shrouded pump impellers: Part 1: Model development and applications [NASA-CR-193916] p 2366 N94-24998
A finite-element-based perturbation model for the rotordynamic analysis of shrouded pump impellers: Part 2: User's guide [NASA-CR-193917] p 2366 N94-24999

ROTOR SPEED
An overview of a model rotor icing test in the NASA Lewis Icing Research Tunnel [NASA-TM-106471] p 2166 N94-23299

ROTORS
Sensorless, brushless motor to drive a sealed freon-ammonia pump p 2315 N94-24036
Influence of backup bearings and support structure dynamics on the behavior of rotors with active supports [NASA-CR-195106] p 2365 N94-24751
Two-dimensional CFD modeling of wave rotor flow dynamics [NASA-TM-106261] p 2189 N94-25185
Analysis and characteristics of compressor stall precursor signals in forward and AFT swept high speed compressor [AD-A273820] p 2171 N94-25517

ROVING VEHICLES
Missions, Technologies, and Design of Planetary Mobile Vehicles [ISBN-2-85428-331-7] p 2605 N94-23373
Soviet developments of planet rovers in period of 1964 - 1990 p 2369 N94-23374
Rover requirements for the planet surface segment of the space exploration initiative p 2369 N94-23377
Robotic exploration of Moon and Mars p 2606 N94-23379
Science strategy for Mars exploration p 2606 N94-23380
Mars 96 small rover: Mission strategy p 2606 N94-23381
A reference Martian mission for a long range rover p 2606 N94-23382
Science objectives for short-range rovers on Mars p 2606 N94-23383
Prospects for using mobile vehicles in missions to Mars and other planets p 2607 N94-23384
The robotic Mars rover p 2608 N94-23390

Mission and system design of a long range rover mission p 2608 N94-23392
Mars 96 rover: Science, instrumentation, and control p 2369 N94-23395
Rover in the Mars 96 mission p 2609 N94-23397
The new family of JPL planetary surface vehicles p 2369 N94-23398
Feasibility study of an automatic vehicle for planetary exploration p 2369 N94-23399
Rover: Autonomous concepts for Mars exploration p 2369 N94-23400
Electrical power technology for robotic planetary rovers p 2314 N94-23401
Development/drilling test of auger boring machine on board Mars rover for Mars exploration p 2369 N94-23402
Mechanical design of a planetary rover p 2369 N94-23403
Planetary rover locomotion mechanisms p 2369 N94-23404
Carbon monoxide fuel cells as a source for Mars rover electric power p 2314 N94-23409
The mass of massive rover software p 2464 N94-23410
Machines for moving in soil p 2369 N94-23411
Evolving directions in NASA's planetary rover requirements and technology p 2370 N94-23414
Dual rover concept for Mars exploration p 2370 N94-23415
Results of the Mojave tests of the Mars 96 rover p 2370 N94-23416
Mars 96 rover: Technical vision and navigation p 2370 N94-23417
Marsohkod movement control p 2370 N94-23418
Walking, jumping, and tumbling: More than one way to get around Mars p 2370 N94-23419
Perspective of creation of means for collecting information concerning transport situation p 2370 N94-23420
Sensing and modelling concepts for autonomous and remote mobile robot control p 2370 N94-23421
Towards real-time stereovision systems for planetary missions p 2370 N94-23422
A DTM-based path planning method for planetary rovers p 2370 N94-23423
Bond graph modeling, simulation, and reflex control of the Mars planetary automatic vehicle p 2370 N94-23424
Mobility analysis, simulation, and scale model testing for the design of wheeled planetary rovers p 2370 N94-23425
Physical modeling and dynamic simulation of planet vehicles: Application to the motion prediction p 2371 N94-23426
Experiments with a small behaviour controlled planetary rover p 2371 N94-23427
Operations concepts for Mars missions with multiple mobile spacecraft p 2501 N94-23852
Human-like robots for space and hazardous environments [NASA-CR-195549] p 2365 N94-24703
Design of a wheeled articulating land rover [NASA-CR-195520] p 2365 N94-24806

RUBIDIUM
Matter-wave interferometry with laser cooled atoms [AD-A273249] p 2536 N94-24717

RUDDERS
Cockpit control system conceptual design [NASA-CR-195543] p 2190 N94-24551

RUN TIME (COMPUTERS)
Linear time algorithm to schedule trees with communication delays optimally on two machines [PB93-237782] p 2451 N94-23441
Object distribution in orca using compile-time and run-time techniques [PB94-110574] p 2453 N94-23745
Runtime support and compilation methods for user-specified data distributions [NASA-CR-191587] p 2458 N94-24679

RUNGE-KUTTA METHOD
A multigrid multiblock solver for compressible turbulent flow [MEMO-1125] p 2315 N94-22713
Computation of propulsion-related flowfields using unstructured adaptive meshes p 2215 N94-23056
Reliability enhancement of Navier-Stokes codes through convergence enhancement p 2216 N94-23064
The theoretical accuracy of Runge-Kutta time discretizations for the initial boundary value problem: A careful study of the boundary error [NASA-CR-191561] p 2480 N94-23272
Differential algebraic equations [PB93-237618] p 2481 N94-23455
Compressible turbulent flow simulation with a multigrid multiblock method p 2342 N94-23694

RUNWAY CONDITIONS
The 94 GHz MMW imaging radar system p 2306 N94-25493

RUNWAYS
Performance of prefabricated geocomposite subdrainage system in an airport runway [DOT/FAA/RD-93/23] p 2192 N94-23303
Airport pavement test machine design and cost study [DOT/FAA/CT-93/51] p 2192 N94-24072

RUPTURING
Mechanical behavior of CMCs: Crack growth resistance and creep aspects p 2256 N94-24235
Ceramic matrix composite parts design p 2256 N94-24237

RURAL AREAS
Urban/rural application of weather radar for flow forecasting. Proceedings of the Informal CEc -Workshop [PB93-220135] p 2407 N94-23129

RUSSIAN FEDERATION
Satellite communications systems and technology. Executive Summary [NASA-TM-109388] p 2293 N94-23622
Satellite communications systems and technology. Volume 1: Analytical chapters [NASA-TM-109398] p 2293 N94-23627

S

S WAVES
Measurements and modeling of multitone, low-frequency acoustic data from the Arraial do Cabo range [AD-A273406] p 2530 N94-25073
Downward extrapolation of multi-component seismic data [ISBN-9-09-005213-5] p 2405 N94-25229
Decomposition of multi-component measurements into P and S waves [ISBN-9-09-005197-X] p 2405 N94-25251
Parametric and nonparametric discriminants for regional earthquakes and explosions [AD-A273807] p 2406 N94-25538

S-2 AIRCRAFT
S-2E Tracker maritime patrol aircraft re-engine and system upgrade program p 2158 N94-24270

SADDLE POINTS
The cusp horseshoe and its bifurcations in the unfolding of an inclination-flip homoclinic orbit [W-9307] p 2480 N94-23141
Magnetic field-induced saddle point in GaAs/AlGaAs short period superlattices [REPT-A-2656] p 2568 N94-25515

SADDLES
The cusp horseshoe and its bifurcations in the unfolding of an inclination-flip homoclinic orbit [W-9307] p 2480 N94-23141

SAFETY
GPHS-RTG's in support of the Cassini mission [DE94-001445] p 2218 N94-23459
Impacts: NIST Building and Fire Research Laboratory (technical and societal) [PB94-113420] p 2270 N94-23737
An automated tool to facilitate code translation for software fault tree analysis [AD-A273205] p 2457 N94-24556
Waste minimization/pollution prevention at R/D facilities: A cradle-to-grave tracking and information system that will be implemented at Sandia National Laboratories [DE93-040330] p 2591 N94-24607

SAFETY DEVICES
Composite material impregnation unit [NASA-TM-107751] p 2254 N94-23486
Reach performance while wearing the Space Shuttle launch and entry suit during exposure to launch accelerations p 2436 N94-24204
Studies of Shuttle orbiter arrestment system [NASA-TP-3370] p 2177 N94-24304

SAFETY FACTORS
Specifying design conservatism: Worst case versus probabilistic analysis p 2374 N94-23939

SAFETY MANAGEMENT
Safety guidelines for the operation of the DREO 10 m EMP simulator DREMPS [DREO-TN-93-5] p 2193 N94-24117
TEM cell safety report [DREO-TN-93-9] p 2193 N94-24123
Collaborating with our customers: NIST building and fire research laboratory [PB94-110194] p 2272 N94-24955

SALINITY
A two-dimensional dispersion module for the TOUGH2 simulator [DE94-002262] p 2335 N94-24655
Examination of the physical, electrical, and microwave evolution of water into young sea ice [AD-A273559] p 2418 N94-24918

SAMARIUM
Comparative M-H characteristics of 1-5 and 2-17 type samarium-cobalt permanent magnets to 300 C [NASA-CR-194440] p 2312 N94-24870

SAMPLERS
Automation technology for remote sample acquisition p 2369 N94-23407

SAMPLING
Subset selection with a generalized selection goal based on a loss function [PB94-111192] p 2494 N94-23798
Verification and validation of models [PB94-110566] p 2456 N94-24507
Two-stage versus sequential sample-size determination in regression analysis of simulation experiments [PB94-110558] p 2495 N94-24634

SANDWICH STRUCTURES
Mechanical and thermal buckling analysis of sandwich panels under different edge conditions [NASA-TM-4535] p 2228 N94-23514

SAPPHIRE
High pressure Hugoniot of sapphire [DE94-001048] p 2558 N94-22946
Surface modification of sapphire for enhanced infrared window performance [DE94-000333] p 2543 N94-23458

SARSAT
The space operations at CNES p 2498 N94-23837

SATELLITE ALTIMETRY
Modes of ocean variability in the tropical Pacific as derived from Geosat altimetry [MPIM-103] p 2382 N94-23158
The effect of sub-surface volume scattering on the accuracy of ice-sheet altimeter retracking algorithms [NASA-CR-194825] p 2386 N94-24060

SATELLITE ANTENNAS
Investigations into deployment complications of the ERS-1 SAR antenna p 2305 N94-23996
Data relay system satellite: The development of an antenna pointing mechanism for the inter-orbit link antenna p 2359 N94-24015

SATELLITE ATTITUDE CONTROL
A combined Earth scanner and momentum wheel for attitude determination and control of small spacecraft p 2208 N94-24022
Reactive thrust cruise for a geosynchronous satellite with minimum fuel consumption p 2158 N94-24271
Momentum management and torque distribution p 2159 N94-24272
The H(sub infinity) optimal controller design and reduction for the inertial hold mode of the attitude control system of the XTE spacecraft [NASA-CR-195137] p 2366 N94-24846

SATELLITE COMMUNICATION
ESA personal communications and digital audio broadcasting systems based on non-geostationary satellites p 2273 N94-22737
Direct broadcast satellite-radio, space-segment/receiver tradeoffs p 2273 N94-22738
Electrical performance of wire mesh for spacecraft deployable reflector antennas p 2275 N94-22744
US domestic and international regulatory issues p 2275 N94-22748
International organizations to enable world-wide mobile satellite services p 2275 N94-22749
The possibilities for mobile and fixed services in the 20/30 GHz frequency bands p 2276 N94-22752
Use of the 30/20 GHz band by multipurpose satellite systems p 2276 N94-22753
Interworking and integration of the Inmarsat Standard-M with Pan-European GSM system p 2277 N94-22759
MSAT and cellular hybrid networking p 2278 N94-22762
Trends in mobile satellite communication p 2278 N94-22763
Optimizing space constellations for mobile satellite systems p 2278 N94-22764
Geostationary payload concepts for personal satellite communications p 2278 N94-22765
Applicability of different onboard routing and processing techniques to mobile satellite systems p 2278 N94-22767
Study of LEO-SAT microwave link for broad-band mobile satellite communication system p 2279 N94-22769
ROCSAT-1 telecommunication experiments p 2279 N94-22770
ACTS broadband aeronautical experiment p 2279 N94-22771
The FAA satellite communications program p 2279 N94-22772
ACTS mobile SATCOM experiments p 2280 N94-22774

Cockpit weather graphics using mobile satellite communications p 2280 N94-22775
Using satellite communications for a mobile computer network p 2280 N94-22777
Evolution of INMARSAT systems and applications: The land mobile experience p 2280 N94-22779
ACTS advanced system concepts and experimentation p 2280 N94-22780
EUTELTRACS: The European experience on mobile satellite services p 2281 N94-22781
The ORBCOMM data communications system p 2281 N94-22782
Implementation of a system to provide mobile satellite services in North America p 2281 N94-22784
The Iridium (tm) system: Personal communications anytime, anyplace p 2281 N94-22785
The Globalstar mobile satellite system for worldwide personal communications p 2282 N94-22786
Odyssey personal communications satellite system p 2282 N94-22787
INMARSAT's personal communicator system p 2282 N94-22788
The European Mobile System (EMS) p 2282 N94-22789
Land mobile satellite propagation measurements in Japan using ETS-V satellite p 2282 N94-22790
Measurements on the satellite-mobile channel at L and S bands p 2282 N94-22791
K-band mobile propagation measurements using ACTS p 2283 N94-22792
Measurement of multipath delay profile in land mobile satellite channels p 2283 N94-22793
A study of satellite motion-induced multipath phenomena p 2283 N94-22794
Electromagnetic field strength prediction in an urban environment: A useful tool for the planning of LMSS p 2283 N94-22795
Propagation model for the Land Mobile Satellite channel in urban environments p 2283 N94-22796
The Westinghouse Series 1000 Mobile Phone: Technology and applications p 2284 N94-22800
First satellite mobile communication trials using BLQS-CDMA p 2284 N94-22801
Channel and terminal description of the ACTS mobile terminal p 2284 N94-22802
Low cost coherent demodulation for mobile satellite terminals p 2284 N94-22803
Asynchronous timing and Doppler recovery in DSP based DPSK modems for fixed and mobile satellite applications p 2285 N94-22805
Improved frame synchronization schemes for INMARSAT-B/M SCPC and TDM channels p 2285 N94-22806
Estimation of frequency offset in mobile satellite modems p 2285 N94-22807
A pattern jitter free AFC scheme for mobile satellite systems p 2285 N94-22809
A CDMA synchronisation scheme p 2285 N94-22810
A protocol for satellite access via use of spot-beams p 2286 N94-22811
A high quality voice coder with integrated echo canceller and voice activity detector for mobile satellite applications p 2286 N94-22812
Performance of the unique-word-reverse-modulation type demodulator for mobile satellite communications p 2286 N94-22813
Transmission over EHF mobile satellite channels p 2287 N94-22820
Adaptive data rate control TDMA systems as a rain attenuation compensation technique p 2287 N94-22821
Development of a multilayer interference simulation program for MSS systems p 2287 N94-22823
Study on networking issues of medium earth orbit satellite communications systems p 2288 N94-22825
The design and networking of dynamic satellite constellations for global mobile communication systems p 2288 N94-22826
Low earth orbit satellite/terrestrial mobile service compatibility p 2288 N94-22827
A practical system for regional mobile satellite services p 2288 N94-22828
Supercomputer networking for space science applications
[NASA-CR-194876] p 2465 N94-23085
Phase linearity of the 914H coupled-cavity traveling wave tube
[NASA-CR-191056] p 2290 N94-23087
Satellite communications systems and technology. Executive Summary
[NASA-TM-109388] p 2293 N94-23622
Satellite communications systems and technology. Volume 1: Analytical chapters
[NASA-TM-109398] p 2293 N94-23627
Satellite communications systems and technology. Volume 2: Site reports
[NASA-TM-109399] p 2293 N94-23628
Advanced technology for a satellite multichannel demultiplexer/demodulator
[NASA-CR-194435] p 2202 N94-23631
Multi-access laser communications terminal
[NASA-CR-191251] p 2295 N94-23830
Commonality of flight control systems for support of European telecommunications missions p 2304 N94-23834
The European Space Agency standard for space packet utilisation p 2203 N94-23954
Generalized three-dimensional simulation of ferruled coupled-cavity traveling-wave-tube dispersion and impedance characteristics
[NASA-TP-3389] p 2310 N94-24056
Satellite communications system
[CA-PATENT-APPL-SN-2053597] p 2297 N94-24183
The 33rd Israel Annual Conference on Aviation and Astronautics
[ITN-94-85227] p 2153 N94-24241
Error coding simulations p 2306 N94-24439
Comparison of HF groundwave propagation models
[AD-A273146] p 2299 N94-24668
Simulation of adjacent channel interference in a UHF satellite system
[AD-A273147] p 2299 N94-24669
Bounds and simulation results of 32-ary and 64-ary quadrature amplitude modulation for broadband-ISDN via satellite
[NASA-TM-106484] p 2202 N94-25095
Conceptual communications system design in the 25.25-27.5 and 37.0-40.5 GHz frequency bands p 2306 N94-25379
Modeling of the ground-to-SSFMB link networking features using SPW p 2306 N94-25381

SATELLITE CONFIGURATIONS
Mobilesat (tm): A world first p 2281 N94-22783

SATELLITE CONSTELLATIONS
Optimizing space constellations for mobile satellite systems p 2278 N94-22764
The design and networking of dynamic satellite constellations for global mobile communication systems p 2288 N94-22826

SATELLITE CONTROL
Commonality of flight control systems for support of European telecommunications missions p 2304 N94-23834
SPOT4 Operational Control Center (CMP) p 2197 N94-23856
A quick uplink, expandable executable for the NSSC-1 of the Hubble Space Telescope p 2305 N94-23859
NASDA knowledge-based network planning system p 2508 N94-23898
Kalman filtering applied to real-time monitoring of apogee maneuvers p 2196 N94-23923
MERCATOR: Methods and Realization for Control of the Attitude and the Orbit of spacecraft p 2202 N94-23925
The geo-control system for station keeping and colocation of geostationary satellites p 2464 N94-23927
Operational training for the mission operations at the Brazilian National Institute for Space Research (INPE) p 2429 N94-23933
GenSAA: A tool for advancing satellite monitoring with graphical expert systems p 2516 N94-23945
Iowa satellite project ISAT-1
[NASA-CR-195517] p 2206 N94-24838

SATELLITE DESIGN
Aeronautical audio broadcasting via satellite p 2274 N94-22741
A system architecture for an advanced Canadian wideband mobile satellite system p 2278 N94-22766
GPHS-RTG's in support of the Cassini mission
[DE94-001445] p 2218 N94-23459
An engineering database management system for spacecraft operations p 2517 N94-23951
A combined Earth scanner and momentum wheel for attitude determination and control of small spacecraft p 2208 N94-24022
The Submillimeter Wave Astronomy Satellite (SWAS) solar array system p 2361 N94-24029
The 33rd Israel Annual Conference on Aviation and Astronautics
[ITN-94-85227] p 2153 N94-24241
NPS alternate techsat satellite, design project for AE-4871
[NASA-CR-195512] p 2204 N94-24590
A small satellite design for deep space network testing and training
[NASA-CR-195526] p 2205 N94-24702
Iowa satellite project ISAT-1
[NASA-CR-195517] p 2206 N94-24838
Preliminary design of a satellite observation system for Space Station Freedom
[NASA-CR-195514] p 2209 N94-24840

SATELLITE DOPPLER POSITIONING
Mars 1994/1996: The French navigation tasks p 2195 N94-23924
Navigation of space VLBI missions: Radioastron and VSOP p 2513 N94-23926

SATELLITE GROUND SUPPORT
A European mobile satellite system concept exploiting CDMA and OBP p 2279 N94-22768
Kalman filtering applied to real-time monitoring of apogee maneuvers p 2196 N94-23923
The European Space Agency standard for space packet utilisation p 2203 N94-23954

SATELLITE GUIDANCE
Real-time on-board orbit determination with DORIS p 2196 N94-23919
TOPEX/Poseidon precision orbit determination production and expert system p 2196 N94-23920

SATELLITE IMAGERY
The AGRHYMET data communications project p 2280 N94-22776
Computer assisted analysis of auroral images obtained from high altitude polar satellites
[NASA-CR-194873] p 2400 N94-23084
Application of ERS-1 active microwave instrumentation data to remote sensing of snow
[PB93-224756] p 2382 N94-23224
SeaWiFS technical report series. Volume 11: Analysis of selected orbit propagation models for the SeaWiFS mission
[NASA-TM-104566-VOL-11] p 2417 N94-23338
Image pattern recognition supporting interactive analysis and graphical visualization
[NASA-CR-194878] p 2451 N94-23369
The Far Ultraviolet (FUV) auroral imager for the Inner Magnetospheric Imager (IMI) mission: Options p 2209 N94-24453
An AVHRR cloud classification database typed by experts
[AD-A273560] p 2416 N94-25162

SATELLITE INSTRUMENTS
Instrument interface description for NOAA 2000 instruments with European morning spacecraft and/or NOAA-OPQ spacecraft
[NASA-TM-109406] p 2208 N94-23478
Command/telemetry bus general specification for the NOAA-OPQ polar orbiting environmental satellites and EUMETSAT polar satellite systems
[NASA-TM-109407] p 2208 N94-23479
Low rate data bus general specification for the NOAA-OPQ polar orbiting environmental satellites and EUMETSAT polar satellite systems
[NASA-TM-109408] p 2208 N94-23480
Earth Observing System (EOS) Advanced Microwave Sounding Unit-A (AMSU-A) schedule plan
[NASA-CR-194856] p 2585 N94-23563
Mission planning for an Earth observation low Earth orbiter: ERS-1 p 2503 N94-23868
Science planning and sequencing for Cassini p 2504 N94-23871
Connecting science and operations: The operations coordinator p 2504 N94-23874
A combined Earth scanner and momentum wheel for attitude determination and control of small spacecraft p 2208 N94-24022
Hubble Space Telescope high speed photometer science verification test report
[NASA-CR-189322] p 2205 N94-24710
High energy collimating fine grids for HESP program
[NASA-CR-189317] p 2209 N94-24767

SATELLITE NAVIGATION SYSTEMS
Satellite autonomous navigation and orbit determination using magnetometers p 2156 N94-24258
Differential GPS for air transport: Status p 2162 N94-25100

SATELLITE NETWORKS
Internetworking satellite and local exchange networks for personal communications applications p 2276 N94-22755
Integration of mobile satellite and cellular systems p 2277 N94-22757
Interworking evolution of mobile satellite and terrestrial networks p 2277 N94-22758
Interworking and integration of the Inmarsat Standard-M with Pan-European GSM system p 2277 N94-22759
Architectures and protocols for an integrated satellite-terrestrial mobile system p 2277 N94-22760
Handover procedures in integrated satellite and terrestrial mobile systems p 2277 N94-22761
Optimizing space constellations for mobile satellite systems p 2278 N94-22764
A system architecture for an advanced Canadian wideband mobile satellite system p 2278 N94-22766

Applicability of different onboard routing and processing techniques to mobile satellite systems p 2278 N94-22767

The ORBCOMM data communications system p 2281 N94-22782

Implementation of a system to provide mobile satellite services in North America p 2281 N94-22784

The Iridium (tm) system: Personal communications anytime, anyplace p 2281 N94-22785

The Globalstar mobile satellite system for worldwide personal communications p 2282 N94-22786

The European Mobile System (EMS) p 2282 N94-22789

Global coverage Mobile Satellite Systems: System availability versus channel propagation impairments p 2284 N94-22798

First satellite mobile communication trials using BLQS-CDMA p 2284 N94-22801

Improved frame synchronization schemes for INMARSAT-B/M SCPC and TDM channels p 2285 N94-22806

Diversity reception for advanced multi-satellite networks: A CDMA approach p 2286 N94-22816

Development of a multilayer interference simulation program for MSS systems p 2287 N94-22823

Handover aspects for a Low Earth Orbit (LEO) CDMA Land Mobile Satellite (LMS) system p 2288 N94-22824

Study on networking issues of medium earth orbit satellite communications systems p 2288 N94-22825

The design and networking of dynamic satellite constellations for global mobile communication systems p 2288 N94-22826

Low earth orbit satellite/terrestrial mobile service compatibility p 2288 N94-22827

A practical system for regional mobile satellite services p 2288 N94-22828

Multi-access laser communications terminal [NASA-CR-191251] p 2295 N94-23830

SATELLITE OBSERVATION

The AGRHYMET data communications project p 2280 N94-22776

Land mobile satellite propagation measurements in Japan using ETS-V satellite p 2282 N94-22790

SeaWiFS technical report series. Volume 9: The simulated SeaWiFS data set, version 1 [NASA-TM-104566-VOL-9] p 2417 N94-23291

Atmospheric moisture fields derived by satellite observations over the tropical Pacific Ocean [NASA-CR-194852] p 2408 N94-23542

Evaluating NOAA satellite products for global climate monitoring p 2384 N94-23604

Validating a large geophysical data set: Experiences with satellite-derived cloud parameters p 2385 N94-23615

Experience of the JPL Exploratory Data Analysis Team at validating HIRS2/MSU cloud parameters p 2385 N94-23616

An overview of the UARS data validation effort p 2386 N94-23617

SPOT4 Operational Control Center (CMP) p 2197 N94-23856

AGENDA: A task organizer and scheduler p 2504 N94-23876

The effect of sub-surface volume scattering on the accuracy of ice-sheet altimeter retracking algorithms [NASA-CR-194825] p 2386 N94-24060

Factors affecting the identification of phytoplankton groups by means of remote sensing [NASA-TM-108799] p 2387 N94-24403

Further studies to extend and test the area-time-integral technique applied to satellite data [NASA-CR-195132] p 2415 N94-24705

Optimal gains for a single polar orbiting satellite p 2208 N94-24873

SATELLITE ORBITS

The design and networking of dynamic satellite constellations for global mobile communication systems p 2288 N94-22826

Low earth orbit satellite/terrestrial mobile service compatibility p 2288 N94-22827

Improved thermal force modeling for GPS satellites p 2207 N94-23259

Real-time on-board orbit determination with DORIS p 2196 N94-23919

SATELLITE ORIENTATION

Momentum management and torque distribution p 2159 N94-24272

SATELLITE PERTURBATION

SeaWiFS technical report series. Volume 11: Analysis of selected orbit propagation models for the SeaWiFS mission [NASA-TM-104566-VOL-11] p 2417 N94-23338

Numerical simulation of Ulysses nutation p 2207 N94-24017

Spacecraft vibrations due to mechanisms; measurements from Olympus on-station p 2207 N94-24018

SATELLITE POWER TRANSMISSION

WISPER: Wirless Space Power Experiment [NASA-CR-195538] p 2396 N94-24701

Iowa satellite project ISAT-1 [NASA-CR-195517] p 2206 N94-24838

SATELLITE ROTATION

Momentum management and torque distribution p 2159 N94-24272

SATELLITE SOUNDING

Atmospheric moisture fields derived by satellite observations over the tropical Pacific Ocean [NASA-CR-194852] p 2408 N94-23542

Uncertainties in climate data sets [NASA-CR-194848] p 2408 N94-23577

TOVS Pathfinder product validation and intercomparison p 2384 N94-23603

Experience of the JPL Exploratory Data Analysis Team at validating HIRS2/MSU cloud parameters p 2385 N94-23616

Convective organization in the Pacific ITCZ: Merging OLR, TOVS, and SSM/I information [NASA-CR-194850] p 2408 N94-23619

Cloud-free aerosol optical depth determination over oceans from satellite radiometry [DE94-001897] p 2386 N94-23779

Implementation of a state of the art automated system for the production of cloud/water vapor motion winds from geostationary satellites [NASA-CR-195087] p 2410 N94-24125

SATELLITE TRACKING

K- and Ka-band mobile-vehicular satellite-tracking reflector antenna system for the NASA ACTS mobile terminal p 2289 N94-22831

Microstrip monopulse antenna for land mobile communications p 2289 N94-22833

Aeronautical satellite antenna steering using magnetic field sensors p 2289 N94-22836

The Telecommunications and Data Acquisition Report [NASA-CR-194766] p 2290 N94-23256

A review of GPS-based tracking techniques for TDRS orbit determination p 2196 N94-23257

New approaches for tracking earth orbiters using modified GPS ground receivers p 2196 N94-23258

Beam-waveguide antenna servo design issues for tracking low earth-orbiting satellites p 2292 N94-23268

Ground data system for Space Flyer Unit (SFU) p 2207 N94-23860

Radioastron flight operations p 2502 N94-23861

Navigation of space VLBI missions: Radioastron and VSOP p 2513 N94-23926

Worldwide vessel locating and tracking system, volume 1 [PB93-193217] p 2175 N94-24474

SATELLITE TRANSMISSION

Design and implementation considerations of a MSAT packet data network p 2280 N94-22778

The ORBCOMM data communications system p 2281 N94-22782

The Iridium (tm) system: Personal communications anytime, anyplace p 2281 N94-22785

K-band mobile propagation measurements using ACTS p 2283 N94-22792

Measurement of multipath delay profile in land mobile satellite channels p 2283 N94-22793

A study of satellite motion-induced multipath phenomena p 2283 N94-22794

Electromagnetic field strength prediction in an urban environment: A useful tool for the planning of LMSS p 2283 N94-22795

Iowa satellite project ISAT-1 [NASA-CR-195517] p 2206 N94-24838

SATELLITE-BORNE INSTRUMENTS

Prospects for improved instrumentation on future solar space missions p 2624 N94-22843

The next Japanese solar satellite p 2625 N94-22846

Interferometer scan unit mechanism definition p 2358 N94-24012

SATURN (PLANET)

Science planning and sequencing for Cassini p 2504 N94-23871

The Jet Propulsion Laboratory space exploration: Past, present and future p 2153 N94-24242

SAWTOOTH WAVEFORMS

LHCD (low hybrid current drive) experiment on the HT-6B tokamak [DE93-613720] p 2555 N94-25331

SCALARS

A transport equation for the scalar dissipation in reacting flows with variable density: First results p 2331 N94-24157

SCALE HEIGHT

The influence of orography on the transport of atmospheric constituents p 2619 N94-24886

Data analysis and interpretation of lunar dust exosphere p 2623 N94-25349

SCALE MODELS

Extinguishment of enclosed gas fires with water sprays [PB93-201663] p 2268 N94-23430

SCALING LAWS

Strong interactions studies with medium energy probes [DE94-001446] p 2540 N94-23791

Rime-, mixed- and glaze-ice evaluations of three scaling laws [NASA-TM-106461] p 2173 N94-24047

SCANNERS

Results of a laboratory experiment that tests rotating unbalanced-mass devices for scanning gimbaled payloads and free-flying spacecraft [NASA-TP-3458] p 2269 N94-23574

Interferometer scan unit mechanism definition p 2358 N94-24012

High precision double four bar linkage mechanism for interferometric linear scanning p 2359 N94-24013

SCANNING

Feasibility study of a synthesis procedure for array feeds to improve radiation performance of large distorted reflector antennas [NASA-CR-195167] p 2301 N94-25005

SCANNING ELECTRON MICROSCOPY

Influence of sintering atmospheres on the aluminum sintering characteristics [DE93-632412] p 2239 N94-22965

Microstructural analysis of the 2195 aluminum-lithium alloy welds p 2251 N94-24448

LPCVD of InN on GaAs(110) using HN3 and TMIn: Comparison with Si(100) results [AD-A273555] p 2235 N94-24917

Scanning probe surface modification [AD-A273178] p 2346 N94-25151

SCANNING TUNNELING MICROSCOPY

JOVE NASA-FIT program: Microgravity and aeronomy projects [NASA-CR-195121] p 2631 N94-24493

The 2-D polymerized Langmuir-Blodgett films studied by STM [AD-A273542] p 2261 N94-24930

Scanning probe lithography. 2: Selective chemical vapor deposition of copper into scanning tunneling microscope-defined patterns [AD-A273304] p 2547 N94-25144

Use of scanning tunneling microscope in corrosion studies [VTT-TIED-1416] p 2250 N94-25346

SCATTERING

Conductors with small Fermi energies and small gap energies [DE93-040887] p 2561 N94-23432

Momentum loss in proton-nucleus and nucleus-nucleus collisions [NASA-TP-3405] p 2540 N94-24305

Integral equations for the microstructures of supercritical fluids [DE94-002460] p 2535 N94-24569

Behavior of the intermittency exponents and a quark-gluon plasma formation in the heavy ion collisions [DE93-616869] p 2541 N94-25342

SCATTERING AMPLITUDE

Momentum and coordinate space three-nucleon potentials [DE93-040868] p 2531 N94-22951

Application and development of the Schwinger multichannel scattering theory and the partial differential equation theory of electron-molecule scattering [NASA-CR-194774] p 2536 N94-24798

SCATTERING CROSS SECTIONS

Inelastic electron scattering from surfaces [DE94-001368] p 2531 N94-22733

Pions and neutrinos as probes of the nucleon and nuclear few-body system [DE93-040127] p 2531 N94-22928

B-quark production at hadron colliders [DE94-001459] p 2534 N94-23806

Optical spin polarization and state-sensitive detection of a cesium atomic beam [ATR-92(8436)-1] p 2534 N94-24077

SCATTERING FUNCTIONS

Propagation model for the Land Mobile Satellite channel in urban environments p 2283 N94-22796

SCENE ANALYSIS

Extracting heading and temporal range from optic flow: Human performance issues p 2442 N94-25510

Optical information in landing scenes p 2442 N94-25511

SCHEDULES

Linear time algorithm to schedule trees with communication delays optimally on two machines [PB93-237782] p 2451 N94-23441

Earth Observing System (EOS) Advanced Microwave Sounding Unit-A (AMSU-A) schedule plan [NASA-CR-194856] p 2585 N94-23563

Preemptive scheduling in a two-stage multiprocessor flow shop is Np-hard [PB94-111648] p 2467 N94-23756

Three, four, five, six or the complexity of scheduling with communication delays [PB94-111630] p 2467 N94-23767

The mission events graphic generator software: A small tool with big results p 2464 N94-23893

ESSOPE: Towards S/C operations with reactive schedule planning p 2508 N94-23896

Panel to review EOSDIS plans [NASA-CR-195088] p 2387 N94-24303

SCHEDULING

Personnel shift assignment: Existence conditions and network models [MEMO-1116] p 2585 N94-22704

Using genetic algorithms for scheduling data flow graphs [EUT-92-E-266] p 2449 N94-23169

Linear time algorithm to schedule trees with communication delays optimally on two machines [PB93-237782] p 2451 N94-23441

Preemptive scheduling in a two-stage multiprocessor flow shop is Np-hard [PB94-111648] p 2467 N94-23756

Framework for interactive solving of meta-constraint satisfaction problems [PB94-118825] p 2585 N94-23761

Three, four, five, six or the complexity of scheduling with communication delays [PB94-111630] p 2467 N94-23767

Mission planning for an Earth observation low Earth orbiter: ERS-1 p 2503 N94-23868

Integrating payload design, planning, and control in the Dutch Utilisation Centre p 2207 N94-23869

Techniques and software for optimum and efficient mission science sequence development p 2504 N94-23872

Connecting science and operations: The operations coordinator p 2504 N94-23874

AGENDA: A task organizer and scheduler p 2504 N94-23876

NASDA knowledge-based network planning system p 2508 N94-23898

Constraint-based scheduling p 2510 N94-23904

A method for interference mitigation in space communications scheduling p 2305 N94-23918

Mission and science activity scheduling language p 2515 N94-23938

An intelligent planning and scheduling system for the HST servicing missions p 2520 N94-23964

Scheduling the future NASA Space Network: Experiences with a flexible scheduling prototype p 2520 N94-23965

Software reuse in spacecraft planning and scheduling systems p 2520 N94-23966

Planning: Management of predictability and uncertainty and keeping abreast of developments p 2520 N94-23967

Design and specification of a centralized manufacturing data management and scheduling system p 2577 N94-24416

Compositional architecture for simple design formally specified in DESIRE [PB94-119013] p 2474 N94-24543

Sensitivity analysis of list scheduling heuristics [PB93-237766] p 2468 N94-24764

Class of strong valid inequalities for the discrete lot-sizing and scheduling problem [PB93-237774] p 2459 N94-24765

Multiprocessor scheduling with communication delays [ETN-94-95346] p 2468 N94-25221

Conflict-free trajectory planning for air traffic control automation [NASA-TM-108790] p 2174 N94-25272

ROSAT mission planning using artificial intelligence methods [DLR-FB-93-14] p 2476 N94-25345

SCHLIEREN PHOTOGRAPHY

An experimental study of the flow field surrounding a subsonic jet in a cross flow [NASA-CR-194770] p 2317 N94-23072

SCHMIDT NUMBER

A random distribution reacting mixing layer model [NASA-CR-194445] p 2187 N94-23552

SCHROEDINGER EQUATION

Periodic nonlinear Schroedinger equation and invariant measures [PB93-238012] p 2487 N94-23775

On the connection of classical mechanics, physical kinetics and quantum theory [DE93-616823] p 2570 N94-25207

SCIENTIFIC SATELLITES

Connecting science and operations: The operations coordinator p 2504 N94-23874

Mission engineering p 2505 N94-23881

SCIENTIFIC VISUALIZATION

Software for scientific visualization: State of the art and experiences [PB93-225183] p 2449 N94-23111

Visualization of results from meteorological simulations on CRAY [PB93-201358] p 2451 N94-23443

GLview user's guide [PB93-201366] p 2452 N94-23444

A knowledge based system for scientific data visualization [NASA-CR-194879] p 2452 N94-23507

Simultaneous simulation and visualization using DGL [PB93-201341] p 2453 N94-23534

Multimission image processing and science data visualization p 2518 N94-23955

A white paper: NASA virtual environment research, applications, and technology [NASA-TM-109682] p 2428 N94-24855

SCIENTISTS

Women scientists and engineers employed in industry: Why so few? A report based on a conference [ISBN-0-309-04991-1] p 2585 N94-24698

SCINTILLATION COUNTERS

New concepts for Hgl2 scintillator gamma ray spectroscopy [NASA-CR-194819] p 2233 N94-24113

The L3 visualization system and its use in the Z(zero) line shape analysis [ETN-94-95382] p 2537 N94-25231

Bottom quark production at the Z resonance [ISBN-9-09-006217-3] p 2538 N94-25255

The data-acquisition and second level trigger system for ZEUS calorimeter [ETN-94-95384] p 2541 N94-25256

CsI(Tl)-photodiode detectors for spectroscopy at low radiation levels [MPI-PHE/92-22] p 2314 N94-25457

SCREW DISLOCATIONS

Internal friction associated with dislocation relaxations in virgin martensite [PB93-226280] p 2240 N94-23119

SCREWS

Spline screw multiple rotations mechanism [NASA-CASE-GSC-13452-1] p 2352 N94-23078

Split spline screw [NASA-CASE-GSC-13434-1] p 2352 N94-23082

SEA ICE

The effect of sub-surface volume scattering on the accuracy of ice-sheet altimeter retracking algorithms [NASA-CR-194825] p 2386 N94-24060

Examination of the physical, electrical, and microwave evolution of water into young sea ice [AD-A273559] p 2418 N94-24918

National Academy of Sciences-Academy of Sciences of the USSR Workshop on the Mechanics of Ice and its Applications [AD-A273338] p 2419 N94-25088

SEA LEVEL

Modes of ocean variability in the tropical Pacific as derived from Geosat altimetry [MPIM-103] p 2382 N94-23158

Analysis of vulnerability to the impacts of sea level rise: A case study for The Netherlands [PB94-111150] p 2399 N94-24573

SEA WATER

Symbiosis in marine luminous bacteria [AD-A273540] p 2422 N94-24791

SEALING

Viscoelastic analysis of seals for extended service life p 2371 N94-24408

SEALS (STOPPERS)

An application of small-gap equations in sealing devices p 2325 N94-23668

Viscous rotary damper p 2361 N94-24031

Seal assembly [CA-PATENT-163126888] p 2364 N94-24128

Simulation of cryogenic turbopump annular seals p 2371 N94-24440

SEARCH PROFILES

A comparison of Boolean-based retrieval to the WAIS system for retrieval of aeronautical information [NASA-CR-4569] p 2594 N94-25487

SEARCH RADAR

Method and apparatus for determining target elevation angle, altitude and range, and the like in a monopulse radar system with reduced multipath errors [AD-D016005] p 2302 N94-25058

SEAS

Survival suit for submarine personnel: Summary of evaluation studies [PB93-204634] p 2430 N94-23743

SEATS

Design of a recumbent seating system [NASA-CR-195503] p 2438 N94-24786

Full-scale fire testing of seat component materials [AD-A273499] p 2174 N94-24941

SECONDARY FLOW

CFD analyses of coolant channel flowfields p 2214 N94-23050

Improving diffusing S-duct performance by secondary flow control [NASA-TM-106492] p 2170 N94-25182

SECULAR VARIATIONS

Geomagnetic field models incorporating physical constraints on the secular variation [NASA-CR-195165] p 2405 N94-24854

SEDIMENT TRANSPORT

Hydraulics and morphology of mountain rivers: A literature survey. Communications on hydraulic and geotechnical engineering [PB94-110772] p 2388 N94-24636

Temporal and spatial mapping of surface albedo and atmospheric dust opacity on Mars p 2619 N94-24887

SEDIMENTS

Hydraulics and morphology of mountain rivers: A literature survey. Communications on hydraulic and geotechnical engineering [PB94-110772] p 2388 N94-24636

SEISMIC WAVES

Dynamic ray tracing and its application in triangulated media [DE94-000875] p 2402 N94-23516

Near-surface seismic imaging [PB94-119096] p 2404 N94-24647

Downward extrapolation of multi-component seismic data [ISBN-9-09-005213-5] p 2405 N94-25229

Decomposition of multi-component measurements into P and S waves [ISBN-9-09-005197-X] p 2405 N94-25251

Parametric and nonparametric discriminants for regional earthquakes and explosions [AD-A273807] p 2406 N94-25538

SEISMOGRAMS

Dynamic ray tracing and its application in triangulated media [DE94-000875] p 2402 N94-23516

SEISMOLOGY

Seafloor characterization/Galapagos propagating rift [AD-A273586] p 2419 N94-25165

SELECTION

Some generalized subset selection procedures [PB94-111655] p 2487 N94-23799

Solving the ranking and selection indifference-zone formulation for normal distributions using computer software [AD-A273821] p 2496 N94-25518

SELECTIVE FADING

Measurement of multipath delay profile in land mobile satellite channels p 2283 N94-22793

SELECTIVE SURFACES

Radar signature related radome techniques for flush-mounted HF-, VHF- and, UHF communication antennas [PB93-204618] p 2294 N94-23742

SELF ORGANIZING SYSTEMS

The adaptive resonance theory network: (Clustering-) behaviour in relation with brainstem auditory evoked potential patterns [EUT-92-E-264] p 2470 N94-22877

Evolving recurrent perceptrons [AD-A273241] p 2496 N94-24778

SEMANTICS

Formal verification of digital circuits described in VHDL [ETN-94-95165] p 2306 N94-22883

Asynchronous rendezvous in distributed logic programming [PB93-220614] p 2448 N94-23096

Transition system specifications in stalk format with bisimulation as a congruence [PB94-110608] p 2453 N94-23707

Multi-set extended relational algebra: A formal approach to a practical issue [PB94-110830] p 2486 N94-23725

Logic of capabilities [PB94-110715] p 2473 N94-23747

Design and specification of a generic task model for solving boolean constraint satisfaction problems [PB94-118841] p 2486 N94-23762

SEMICONDUCTOR DEVICES

A qualified radiation hardened nonvolatile memory for space and tactical weapons applications [DE94-001211] p 2559 N94-23186

Sensors for process control Focus Team report
[DE93-040897] p 2560 N94-23204
CRRES microelectronics package flight data analysis
[NASA-TP-3423] p 2540 N94-23273
A multigrid solver for the semiconductor equations
p 2482 N94-23674

SEMICONDUCTOR DIODES
Tunable lasers pumped by visible laser diodes
[AD-D016000] p 2350 N94-25044

SEMICONDUCTOR LASERS
SFOLDA: A semiconductor LDA for measurements in complex flows p 2316 N94-22856
Laser linewidth measurement in the presence of RIN and using the recirculating self heterodyne method
[EUT-92-E-262] p 2347 N94-22874
Evaluation of uranium transitions for isotopically-selective laser induced fluorescence with diode lasers (technical report for ST064)
[DE94-002000] p 2347 N94-22974
InGaAsP/InP based 1.3/1.55 micron vertical cavity surface emitting lasers for wavelength division multiplexed high speed distributed computing, phase 1
[AD-A271081] p 2348 N94-23123
Electrochemical sulfur passivation of visible (approximately 670nm) AlGaInP lasers
[DE94-002293] p 2350 N94-24659
Matter-wave interferometry with laser cooled atoms
[AD-A273249] p 2536 N94-24717
Tunable lasers pumped by visible laser diodes
[AD-D016000] p 2350 N94-25044
The effects of optical feedback on polarization of vertical cavity surface emitting lasers
[AD-A273728] p 2351 N94-25445

SEMICONDUCTORS (MATERIALS)
Ultraviolet photosulfidation of III-V compound semiconductors for electronic passivation
[DE94-001417] p 2555 N94-22717
Report of the Joint Seminar on Solid State Physics, Atomic and Molecular Physics, and Materials Science in the Energy Region of Tandem Accelerators
[DE93-508268] p 2548 N94-22924
Physics with chemically and isotopically pure semiconductors
[DE93-040120] p 2557 N94-22926
Sensors for process control Focus Team report
[DE93-040897] p 2560 N94-23204
Modulation characteristics of a high-power semiconductor Master Oscillator Power Amplifier (MOPA)
[NASA-TM-104577] p 2308 N94-23281
Microgravity sciences application visiting scientist program
[NASA-CR-194804] p 2267 N94-23287
Observation of non-centrosymmetry and determination of polarity in III-V semiconductors
[PB93-201416] p 2561 N94-23503
Contributions of DOE weapons labs and NIST to semicondutor technology
[OTA-ITE-585] p 2630 N94-23572
A multigrid solver for the semiconductor equations
p 2482 N94-23674
Magnetic resonance studies of 3d transition metal impurities in compound semiconductors
[PB93-232197] p 2243 N94-23714
Disorder effects on small-polaron formation and hopping
[DE94-001205] p 2534 N94-23804
Pulsed Ion Beam Surface Analysis (PIBSA) as a means of in-situ real-time analysis of thin films during growth
[DE94-001276] p 2562 N94-23805
Effects of thermal-solutal convection on temperature and solutal fields under various gravitational orientations
p 2267 N94-24451
Ge-Au eutectic bonding of Ge (100) single crystals
[DE94-002281] p 2564 N94-24657
Electrochemical sulfur passivation of visible (approximately 670nm) AlGaInP lasers
[DE94-002293] p 2350 N94-24659
SEMATECH, a case study: Analysis of a government-industry partnership
[AD-A273166] p 2586 N94-24683
Method of fabricating a receptor-based sensor
[AD-D016026] p 2344 N94-24723
The 5th Engineering Foundation Conference: Advanced Heterostructure Transistors
[AD-A273508] p 2312 N94-24819
LPCVD of InN on GaAs(110) using HN3 and TMIn: Comparison with Si(100) results
[AD-A273555] p 2235 N94-24917
Conformal method of fabricating and optical waveguide on a semiconductor substrate
[AD-D015968] p 2546 N94-25043
An overview of the measurements of thermophysical properties and some results on molten superalloys and semiconductors p 2248 N94-25128
Effect of high frequency field on the transport properties of superlattice
[DE93-617047] p 2568 N94-25447

SENSORIMOTOR PERFORMANCE
The role of visual context in manual target localization
p 2429 N94-25351
Mechanisms of eye-hand coordination
[AD-A273687] p 2428 N94-25437

SENSORY DISCRIMINATION
Auditory spectro-temporal pattern analysis
[AD-A273554] p 2427 N94-24865
On the auditory discrimination of spectral shape
[ETN-94-95306] p 2530 N94-25289

SENSORY PERCEPTION
Interpretation of evolutive environment by a multisensory perception machine
[LAAS-93111] p 2471 N94-22907
A white paper: NASA virtual environment research, applications, and technology
[NASA-TM-109682] p 2428 N94-24855

SEPARATED FLOW
Experimental Methods in Separated Flows
[ILR-MITT-260(1991)] p 2315 N94-22852
Turbulence sensors for separated flows: Current capabilities, future requirements p 2315 N94-22853
Measurement of kinematically unstationary separated flows p 2315 N94-22854
Pressure oscillation measurements in turbulent flows
p 2316 N94-22855
Turbulent separated flows above an obstacle in an open channel p 2316 N94-22859
A method for recognition of frequency cells in a cylinder flow influenced by wall effects p 2316 N94-22860
Leading-edge votex-system details obtained on F-106B aircraft using a rotating vapor screen and surface techniques
[NASA-TP-3374] p 2166 N94-23512
Computation of turbulent flows over backward and forward-facing steps using a near-wall Reynolds stress model p 2172 N94-24145
Large-eddy simulation of flow in a plane, asymmetric diffuser p 2328 N94-24147
Implementation of the Baldwin-Barth turbulence model into the ZETA code and its diagnosis
[NASA-CR-194795] p 2335 N94-24640
A vorticity dynamics based model for the turbulent dissipation: Model development and validation
[NASA-TM-106177] p 2336 N94-24713

SEPARATORS
Capillary electrokinetic separations with optical detection
[DE94-001639] p 2233 N94-23716
Systematic construction of trigonometric neural networks
[PB93-200228] p 2474 N94-24544

SEPTUM
Aortic valve disease p 2424 N94-23322

SEQUENCING
Science planning and sequencing for Cassini
p 2504 N94-23871
A packet-based concept for spacecraft command planning p 2504 N94-23873
The instant sequencing task: Toward constraint-checking a complex spacecraft command sequence interactively p 2504 N94-23875
AGENDA: A task organizer and scheduler
p 2504 N94-23876

SEQUENTIAL ANALYSIS
On the asymptotically uniform distribution modulo 1 of extreme order statistics
[MEMO-COSOR-91-38-REV] p 2493 N94-23142

SEQUENTIAL COMPUTERS
A method for the general simultaneous full decomposition of sequential machines: Algorithms and implementation
[EUT-92-E-267] p 2445 N94-23170
Transputer benchmarks and performance comparisons with other computing machines
[RR-467] p 2446 N94-25312

SERIES (MATHEMATICS)
Incomplete corrections in nonlinear problems
[PB93-225746] p 2479 N94-23106

SERIES EXPANSION
Approximate optimal guidance for the advanced launch system
[NASA-CR-4568] p 2198 N94-24752

SERUMS
Non-invasive optical detection of glucose in cell culture nutrient medium p 2422 N94-25357

SERVICE LIFE
NASA Lewis advanced IPV nickel-hydrogen technology p 2392 N94-23356
New method for increasing machine service-life, phase 2
[PB93-200707] p 2354 N94-23533
Impacts: NIST Building and Fire Research Laboratory (technical and societal)
[PB94-113420] p 2270 N94-23737
Viscoelastic analysis of seals for extended service life
p 2371 N94-24408
Performance of the NASA cm ion thruster
[NASA-TM-106426] p 2221 N94-24770
Embodiment design for a multipropellant resistojet
[NASA-CR-195505] p 2221 N94-24834
General aviation activity survey
[AD-A273284] p 2162 N94-24923
Reliability analysis of a repairable dependent parallel system
[ETN-94-95312] p 2373 N94-25295
Modelling early failures in Space Station Freedom
p 2374 N94-25372
Proceedings of the 12th International Congress: Corrosion Control for Low-Cost Reliability. Volume 5B: Corrosion: General issues
[AD-A273667] p 2250 N94-25407

SERVICES
Service description of communication systems supporting multi-media multi-user applications
[PB94-110855] p 2299 N94-24650

SERVOMECHANISMS
Plan generation for flexible assembly systems
[PB93-217974] p 2267 N94-22981
Beam-waveguide antenna servo design issues for tracking low earth-orbiting satellites
p 2292 N94-23268
The Columbus solar array mechanisms
p 2356 N94-23994
GOLF mechanisms p 2357 N94-24003
High precision double four bar linkage mechanism for interferometric linear scanning p 2359 N94-24013

SET THEORY
Generalized concavity in cooperative game theory: Characterizations in terms of the core
[MEMO-1121] p 2497 N94-22708
Making some issues of implicit knowledge explicit
[PB93-220606] p 2478 N94-22984
Median stabilization degree of a median algebra
[PB93-220010] p 2479 N94-23093
Characterization of measures with a convex range: A generalization of Lyapounov's theorem
[PB93-220523] p 2523 N94-23094
Linear algorithm for flattening list graphs
[PB93-220648] p 2448 N94-23097
How much integral action can a control system tolerate?
[OUEL-1923/92] p 2471 N94-23147
When an infinitely-renormalizable endomorphism of the interval can be smoothed
[PB93-238087] p 2481 N94-23548
Medians and steiner trees
[PB94-110616] p 2486 N94-23708
Relational algebra and equational proofs
[PB94-110822] p 2486 N94-23724
Multi-set extended relational algebra: A formal approach to a practical issue
[PB94-110830] p 2486 N94-23725
Subset selection with a generalized selection goal based on a loss function
[PB94-111192] p 2494 N94-23798
Some generalized subset selection procedures
[PB94-111655] p 2487 N94-23799
Infinite divisible and stable distributions modulo 1
[PB94-110640] p 2495 N94-23815
Reduced game properties of egalitarian division rules for cooperative games
[PB94-111689] p 2521 N94-24523
On the continuity of limit capacity of central Cantor sets
[DE93-613022] p 2523 N94-25328
The least energy critical set
[DE93-616820] p 2493 N94-25434

SEYFERT GALAXIES
The 1404+286: A non-ideal calibrator for VLBI observations
[PB94-104908] p 2599 N94-24521

SHAFTS (MACHINE ELEMENTS)
A technique to measure rotordynamic coefficients in hydrostatic bearings p 2215 N94-23061
Spline screw multiple rotations mechanism
[NASA-CASE-GSC-13452-1] p 2352 N94-23078
An overview of a model rotor icing test in the NASA Lewis Icing Research Tunnel
[NASA-TM-106471] p 2166 N94-23299
Zone fire modeling with natural building flows and a zero order shaft model
[PB94-112166] p 2270 N94-23735
Electromagnetic brake/clutch device
[NASA-CASE-GSC-13502-1] p 2354 N94-23969
Opening mechanism for ISO/CVV cover release
p 2357 N94-24001

Precision drive and speed reduction device
[AD-D016004] p 2367 N94-25046

SHALLOW WATER

Measurements and modeling of multitone, low-frequency acoustic data from the Arraial do Cabo range
[AD-A273406] p 2530 N94-25073

Analysis of modal evolution caused by a weakly range-dependent seabed in shallow water and its application to inversion for geoacoustic properties
[AD-A273656] p 2419 N94-25435

SHAPE MEMORY ALLOYS

Recharge mechanism based on shape memory alloy
p 2362 N94-24039

SHAPES

Gas-pressure forming of superplastic ceramic sheet
[DE94-001520] p 2252 N94-22930

Perception in flight: Shape and motion perception, space perception, spatial orientation, and visual vestibular interaction p 2429 N94-23979

Polymer morphologh p 2226 N94-24353

SHEAR FLOW

The role of the radial electric field in confinement and transport in H-mode and VH-mode discharges in the DIII-D tokamak
[DE94-002746] p 2551 N94-23782

The production of premixed flame surface area in turbulent shear flow p 2237 N94-24158

Numerical simulation of non-Newtonian free shear flows p 2331 N94-24160

Local isotropy in distorted turbulent boundary layers at high Reynolds number p 2332 N94-24166

A vorticity dynamics based model for the turbulent dissipation: Model development and validation
[NASA-TM-106177] p 2336 N94-24713

SHEAR LAYERS

A random distribution reacting mixing layer model
[NASA-CR-194445] p 2187 N94-23552

Effect of initial droplet-size distributions on fuel-vapor profiles in a shear-layer flow p 2160 N94-24283

Interactive control in turbulent shear layers
[AD-A273544] p 2336 N94-24793

The effects of profiles on supersonic jet noise
[NASA-CR-195184] p 2530 N94-25177

SHEAR PROPERTIES

Control of the internal stresses in plane elasticity
[PB93-225514] p 2374 N94-23112

Dynamic analysis of pretwisted elastically-coupled rotor blades
[NASA-TM-109070] p 2378 N94-24839

Test methods for composites: A status report. Volume 3: Shear test methods
[AD-A273561] p 2230 N94-25163

SHEAR STRENGTH

Relationship of microstructure and mechanical properties for V-Cr-Ti alloys
[DE94-001431] p 2238 N94-22718

The mechanical property data base from an Air Force/Industry Cooperative Test Program on advanced aluminum alloys (7064 and CW67)
[AD-A273741] p 2251 N94-25531

SHEAR STRESS

The use of near-wall hot-wire probes for time-resolved skin-friction measurements p 2316 N94-22857

Method of determining shear stress employing a monomer-polymer laminate structure
[NASA-CASE-LAR-14654-2] p 2375 N94-23308

Skin friction measurement in complex flows using thin oil film techniques
[NASA-CR-194872] p 2327 N94-24098

Role of interfaces on the cyclic fatigue behaviour of ceramic matrix composites p 2256 N94-24234

Post buckling behaviour of stiffened composite panels loaded in cyclic compression and shear
p 2157 N94-24260

Evaluation of the fracture resistance and durability of adhesive bonded joints p 2160 N94-24278

Use of photostress to characterize the mechanical behavior of weldments
[NASA-CR-195201] p 2378 N94-25267

SHELL THEORY

Energy estimates and asymptotic analysis in the theory of shells
[PB93-225738] p 2374 N94-23113

SHELLS (STRUCTURAL FORMS)

Counterrotating aircraft propulsor blades
[CA-PATENT-1-319-357] p 2186 N94-23255

SHELTERS

Manned Mars mission on-orbit operations FTS capabilities assessment
[NASA-CR-189328] p 2430 N94-23080

SHIP HULLS

Hydro-elastic analysis using a selection of commercial analysis programs
[PB94-118734] p 2376 N94-24478

SHIPS

HERACLITUS, phase 1. Harbour Entrance of Rotterdam Radar based Current Related Information for Traffic Guidance of Ships: Feasibility of deriving current profile data from sea surface observations in the Rotterdam (Netherlands) port entrance
[BCRS-93-04] p 2417 N94-24107

Free-surface/vorticity interaction
[AD-A273263] p 2335 N94-24686

SHOCK ABSORBERS

Preloaded launch locking devices for SILEX
p 2358 N94-24008

Landing gear with swivelling beam
[CA-PATENT-1323020] p 2176 N94-24181

Design of a recumbent seating system
[NASA-CR-195503] p 2438 N94-24786

SHOCK FRONTS

Energy transfer in solid explosives
[DE94-001523] p 2265 N94-23778

The plastic response of a cylindrical shell subjected to an internal blast wave with a finite width shock front
p 2154 N94-24246

The scattering and collision of gravitational waves in Friedmann-Robertson-Walker open universes
[MATHS-REPT-A-193] p 2406 N94-25430

SHOCK LOADS

Bridgman's concern
[DE93-040900] p 2558 N94-22953

Bibliographic Retrieval System (BARS), Sandia Shock Compression (SSC) database Shock Physics Index
[DE94-001679] p 2589 N94-23126

Bibliographic Retrieval System (BARS). Sandia Shock Compression (SSC) database Shock Physics Index (SPHINX) database. Volume 1: UNIX version query guide customized application for INGRES
[DE94-001703] p 2589 N94-23127

Bibliographic Retrieval System (BARS), Sandia Shock Compression (SSC) database, Shock Physics Index (SPHINX) database, Volume 2: UNIX version user's guide
[DE94-001704] p 2589 N94-23128

SHOCK TESTS

Method for simulating a vehicle shock test: Design and realization of the required implementation tools
[ECL-92-14] p 2352 N94-22885

SHOCK TUBES

An investigation on a new technique to improve the performance of the shock tube/tunnel testing in the equilibrium interface condition p 2154 N94-24247

SHOCK TUNNELS

Shock tunnel studies of scramjet phenomena, supplement 7
[NASA-CR-191572] p 2319 N94-23513

Shock tunnel studies of scramjet phenomena, supplement 8
[NASA-CR-191573] p 2320 N94-23532

An investigation on a new technique to improve the performance of the shock tube/tunnel testing in the equilibrium interface condition p 2154 N94-24247

SHOCK WAVE INTERACTION

Experimental investigation of generic three-dimensional sidewall-compression scramjet inlets at Mach 6 in tetrafluoromethane
[NASA-TM-4497] p 2319 N94-23339

Effects of shock strength on shock turbulence interaction p 2332 N94-24165

Shocked clouds in the Cygnus Loop
[NASA-CR-195190] p 2600 N94-25178

Two-dimensional CFD modeling of wave rotor flow dynamics
[NASA-TM-106261] p 2189 N94-25185

The scattering and collision of gravitational waves in Friedmann-Robertson-Walker open universes
[MATHS-REPT-A-193] p 2406 N94-25430

SHOCK WAVE PROPAGATION

The scattering and collision of gravitational waves in Friedmann-Robertson-Walker open universes
[MATHS-REPT-A-193] p 2406 N94-25430

SHOCK WAVES

High pressure Hugoniot of sapphire
[DE94-001048] p 2558 N94-22946

Bibliographic Retrieval System (BARS), Sandia Shock Compression (SSC) database Shock Physics Index
[DE94-001679] p 2589 N94-23126

Bibliographic Retrieval System (BARS). Sandia Shock Compression (SSC) database Shock Physics Index (SPHINX) database. Volume 1: UNIX version query guide customized application for INGRES
[DE94-001703] p 2589 N94-23127

Bibliographic Retrieval System (BARS), Sandia Shock Compression (SSC) database, Shock Physics Index (SPHINX) database, Volume 2: UNIX version user's guide
[DE94-001704] p 2589 N94-23128

Shock-induced turbulent flow in baffle systems
[DE94-001532] p 2319 N94-23470

Calibration of HYPULSE for hypervelocity air flows corresponding to flight Mach numbers 13.5, 15, and 17
[NASA-CR-191578] p 2192 N94-23564

Energy transfer in solid explosives
[DE94-001523] p 2265 N94-23778

Multiple shock initiation of LX-17
[DE94-001524] p 2265 N94-23807

Heat pipe vapor dynamics
[NASA-CR-194217] p 2327 N94-24096

Effects of shock strength on shock turbulence interaction p 2332 N94-24165

Scientific study in solar and plasma physics relative to rocket and balloon projects
[NASA-CR-193885] p 2627 N94-24461

Characteristic method for one-dimensional scalar hyperbolic conservation laws with stiff source terms
[PB93-237675] p 2491 N94-24954

A continuing search for a near-perfect numerical flux scheme. Part 1: AUSM+
[NASA-TM-106524] p 2338 N94-25180

SHORT TAKEOFF AIRCRAFT

Aircraft digital flight control technical review
p 2163 N94-25106

SHORT WAVE RADIATION

Cloud-free aerosol optical depth determination over oceans from satellite radiometry
[DE94-001897] p 2386 N94-23779

SHOT PEENING

Feasibility study of shot-peening modeling
[CTN-94-60926] p 2244 N94-24170

SHRINKAGE

The use of expanding monomers in carbon fibre composites
[ISBN-0-315-83550-8] p 2226 N94-22890

Drying deformable media: Kinetics, shrinkage and stresses
[ETN-94-95314] p 2236 N94-25302

SHUTTLE IMAGING RADAR

Mission planning for Shuttle Imaging Radar-C (SIR-C) with a real-time interactive planning software
p 2305 N94-23842

Precipitation measurement using SIR-C: A feasibility study
[NASA-CR-195104] p 2409 N94-24048

Precipitation measurement using SIR-C: A feasibility study. Investigation at nadir
[NASA-CR-195103] p 2410 N94-24126

SICKNESSES

Chronic obstructive pulmonary disease
p 2425 N94-23324

SIDEBANDS

Direct digital RF synthesis and modulation for MSAT mobile applications p 2285 N94-22804

SIGNAL ANALYSIS

Automatic modulation recognition based on spatial pattern classification using artificial neural networks
[CTN-94-60897] p 2296 N94-24115

Detection and analysis of unbalanced QPSK in Gaussian noise, version 1.0
[DREO-12-020.1] p 2296 N94-24131

On the analysis of clear air radar echoes severely contaminated by clutter p 2306 N94-24423

Develop advanced nonlinear signal analysis topographical mapping system
[NASA-CR-195128] p 2388 N94-24827

Develop advanced nonlinear signal analysis topographical mapping system
[NASA-CR-194785] p 2389 N94-24856

SIGNAL ANALYZERS

Dimensional analysis of acoustically propagated signals p 2528 N94-24217

Some subjects in digital audio, noise shaping, sample rate conversion, dynamic range compression and testing
[ISBN-9-09-005162-7] p 2530 N94-25220

SIGNAL DETECTION

Detection and analysis of unbalanced QPSK in Gaussian noise, version 1.0
[DREO-12-020.1] p 2296 N94-24131

Effects of atmospheric variations on acoustic system performance p 2527 N94-24211

Auditory spectro-temporal pattern analysis
[AD-A273554] p 2427 N94-24865

Evolving neural network connectivity
[AD-A273134] p 2490 N94-24921

Choice of filters for the detection of gravitational waves from coalescing binaries. 2: Detection in coloured noise
[DE93-616844] p 2604 N94-25211

A parallel algorithm for filtering gravitational waves from coalescing binaries
[DE93-616845] p 2604 N94-25212

SIGNAL DETECTORS

The detection performance of a long-term spectral integrator using normalized and quantized data
[DREP-TM-93-11] p 2455 N94-24130

SIGNAL DISTORTION

Night vision devices and characteristics p 2432 N94-23982

SIGNAL ENCODING

Algorithms for speech coding systems based on linear prediction [EUT-92-E-260] p 2447 N94-22731

Encoders for space applications p 2363 N94-24046

SIGNAL FADING

Power attenuation characteristics as switch-over criterion in personal satellite mobile communications p 2277 N94-22756

ROCSAT-1 telecommunication experiments p 2279 N94-22770

Land mobile satellite propagation measurements in Japan using ETS-V satellite p 2282 N94-22790

K-band mobile propagation measurements using ACTS p 2283 N94-22792

Electromagnetic field strength prediction in an urban environment: A useful tool for the planning of LMSS p 2283 N94-22795

Systems implications of L-band fade data statistics for LEO mobile systems p 2284 N94-22799

Asynchronous timing and Doppler recovery in DSP based DPSK modems for fixed and mobile satellite applications p 2285 N94-22805

Separable concatenated codes with iterative map decoding for Rician fading channels p 2286 N94-22815

Diversity reception for advanced multi-satellite networks: A CDMA approach p 2286 N94-22816

SIGNAL GENERATORS

SATCOM simulator speeds MSS deployment and lowers costs p 2287 N94-22822

Digital test signal generation: An accurate SNR calibration approach for the DSN p 2305 N94-23912

System for producing synchronized signals [AD-D016003] p 2302 N94-25057

SIGNAL MEASUREMENT

The detection performance of a long-term spectral integrator using normalized and quantized data [DREP-TM-93-11] p 2455 N94-24130

SIGNAL PROCESSING

Algorithms for speech coding systems based on linear prediction [EUT-92-E-260] p 2447 N94-22731

Cockpit weather graphics using mobile satellite communications p 2280 N94-22775

Odyssey personal communications satellite system p 2282 N94-22787

Asynchronous timing and Doppler recovery in DSP based DPSK modems for fixed and mobile satellite applications p 2285 N94-22805

Performance of the unique-word-reverse-modulation type demodulator for mobile satellite communications p 2286 N94-22813

Progress on the design of a data push architecture for an array of optimized time tagging pixels [DE93-041011] p 2307 N94-22955

A dataflow analysis tool for parallel processing of algorithms [NASA-TM-109054] p 2448 N94-23086

Spur-reduced digital sinusoid synthesis p 2291 N94-23264

System identification using a wavelet-based approach [DE94-002191] p 2293 N94-23473

Fault tolerant onboard packet switch architecture for communication satellites: Shared memory per beam approach [NASA-TM-106397] p 2201 N94-23567

The HDTV digital audio matrix [BBC-RD-1993/9] p 2295 N94-24085

Automatic modulation recognition based on spatial pattern classification using artificial neural networks [CTN-94-60897] p 2296 N94-24115

ASPT software source code: ASPT signal excision software package [CTN-94-60904] p 2296 N94-24133

ASPT software source code: Development system package, library component [CTN-94-60905] p 2455 N94-24134

ASPT software source code: ASPT application software package, VME-C30 component [CTN-94-60906] p 2455 N94-24135

Dimensional analysis of acoustically propagated signals p 2528 N94-24217

PROPWR: A versatile tool for 1/3 octave processing and narrowband line tracking [DREA-TC-93-303] p 2297 N94-24298

Device for the selective detection of objects [CA-PATENT-1-308-179] p 2544 N94-24489

Nondestructive evaluations [DE94-003020] p 2373 N94-24613

Heterodyne array for measurement of target velocity [AD-D016025] p 2545 N94-24722

Crosstie random access memory element having associated read/write circuitry [AD-D016027] p 2446 N94-24724

Conveying digital data in noisy, unstable, multipath environments [AD-D015980] p 2301 N94-25038

Bridge type optoelectronic sample and hold circuit [AD-D015986] p 2312 N94-25042

Preprocessor and adaptive beamformer for linear-frequency modulation active signals [AD-D016008] p 2302 N94-25048

System for cancelling phase noise in an interferometric fiber optic sensor arrangement [AD-D015994] p 2345 N94-25053

Method and apparatus of generating sum or difference signals corresponding to an apparent beam in a monopulse radar system [AD-D015998] p 2302 N94-25056

Method and apparatus for determining target elevation angle, altitude and range, and the like in a monopulse radar system with reduced multipath errors [AD-D016005] p 2302 N94-25058

Psychophysical and signal-processing aspects of speech representation [ETN-94-95292] p 2302 N94-25077

Wide bandwidth differential amplifier [AD-D015985] p 2303 N94-25217

Some subjects in digital audio, noise shaping, sample rate conversion, dynamic range compression and testing [ISBN-9-09-005162-7] p 2530 N94-25220

On the quality of synthetic speech evaluation and improvements [ETN-94-95298] p 2304 N94-25234

Linear and nonlinear adaptive filtering and their application to speech intelligibility enhancement [ISBN-9-09-005342-5] p 2304 N94-25292

Adaptive noise cancellation using recurrent radial basis function networks [RR-472] p 2313 N94-25319

Digital data, composite video multiplexer and demultiplexer boards for an IBM PC/AT compatible computer p 2447 N94-25377

Modeling of the ground-to-SSFMB link networking features using SPW p 2306 N94-25381

SIGNAL RECEPTION

Layered parallel interface for an active antenna array [AD-D016002] p 2301 N94-25045

SIGNAL TO NOISE RATIOS

Estimation of frequency offset in mobile satellite modems p 2285 N94-22807

Theoretical and simulated performance for a novel frequency estimation technique p 2285 N94-22808

DS-SSMA capacity for a mobile satellite system p 2286 N94-22814

Beam-waveguide antenna servo design issues for tracking low earth-orbiting satellites p 2292 N94-23268

Digital test signal generation: An accurate SNR calibration approach for the DSN p 2305 N94-23912

Precipitation measurement using SIR-C: A feasibility study [NASA-CR-195104] p 2409 N94-24048

Precipitation measurement using SIR-C: A feasibility study. Investigation at nadir [NASA-CR-195103] p 2410 N94-24126

Detection and analysis of unbalanced QPSK in Gaussian noise, version 1.0 [DREO-12-020.1] p 2296 N94-24131

Mitigation of EMI/RFI produced by a 1.2 kW uninterruptible power supply [AD-A273149] p 2299 N94-24670

Improvement of system properties of a pulsed laser Doppler anemometer with respect to an optical amplifier [DLR-FB-93-19] p 2547 N94-25305

SIGNAL TRANSMISSION

Measurement of multipath delay profile in land mobile satellite channels p 2283 N94-22793

Wide band fiber-optic communications p 2304 N94-23231

Preliminary analysis of amplitude and phase fluctuations in the JAPE multiple tone data to distances of 500 meters p 2528 N94-24216

Layered parallel interface for an active antenna array [AD-D016002] p 2301 N94-25045

SIGNATURES

Development of a nondestructive vibration technique for bond assessment of Space Shuttle tiles [NASA-CR-195163] p 2201 N94-24919

Special signature schemes [ETN-94-95296] p 2446 N94-25081

SIGNS AND SYMPTOMS

Screening for asymptomatic coronary heart disease p 2423 N94-23315

SIKORSKY AIRCRAFT

Wind tunnel test of a variable-diameter tiltrotor (VDTR) model [NASA-CR-177629] p 2181 N94-24796

SILICATES

The structure and spin dynamics of lanthanide-bearing silicate glasses [DE94-001320] p 2252 N94-22992

SILICIDES

Evaluation of A5Si3Z(x) intermetallics for use as high temperature structural materials [DE93-041127] p 2227 N94-22977

Photo-induced antiferromagnetic interlayer coupling in Fe superlattices with iron silicide spacers [DE94-001345] p 2559 N94-22995

Method of forming silicon structures with selectable optical characteristics [NASA-CASE-NPO-18625-1-CU] p 2563 N94-23972

SILICON

Density functional studies: First principles and semi-emperical calculations of clusters and surfaces [DE94-002836] p 2561 N94-23214

Magnetic resonance study of zinc-related defects in silicon with optimized EPR spectrometer [PB93-224640] p 2561 N94-23223

Quantitative analysis in the Al-Mg-Si system with small amounts of Mg and Si [PB93-201499] p 2241 N94-23446

Method of forming silicon structures with selectable optical characteristics [NASA-CASE-NPO-18625-1-CU] p 2563 N94-23972

Photonic technology for implementation of generalizable neural networks: A synthetic approach [AD-A273497] p 2474 N94-24622

Temperature dependent performance of Coplanar Waveguide (CPW) on substrates of various materials [NASA-TM-106505] p 2313 N94-25170

SILICON ALLOYS

Large-scale production of Si(0.8)Ge(0.2) thermoelectric alloys by mechanical alloying [DE94-000695] p 2243 N94-23753

SILICON CARBIDES

Discontinuous phase formation and selective attack of SiC materials exposed to low oxygen partial pressure environments [DE93-040161] p 2231 N94-22933

Theoretical considerations for Reaction-Formed Silicon Carbide (RFSC) formation by molten silicon infiltration into slurry-derived preforms [NASA-TM-106414] p 2222 N94-23500

An overview on the main available ceramic composites and their processing routes p 2255 N94-24229

Ceramic matrix composites: Challenges and opportunities p 2255 N94-24230

SILICON COMPOUNDS

Disilane LPCVD deposited silicon films: Deposition mechanisms, properties and capability of making transistors on thin films [LAAS-93156] p 2252 N94-22910

SILICON DIOXIDE

Glass-ceramic Li-Al-Si-O composition and process for its production [CA-PATENT-APPL-SN-2043757] p 2254 N94-24129

SILICON NITRIDES

Particle formation in a laser-heated aerosol reactor. Application to silicon and silicon nitride synthesis [PB93-217982] p 2347 N94-22982

Development of silicon nitride composites with continuous fiber reinforcement [DE94-001996] p 2227 N94-23022

Wear reduction in ceramic bearings by surface generated pyrolytic carbon continuously replenished by ethylene gas [NASA-CR-189214] p 2364 N94-24090

Selection of polymer binders and fabrication of SiC fiber-reinforced reaction-bonded silicon nitride matrix composites [NASA-CR-194874] p 2255 N94-24223

The mechanical properties of single crystal (alpha)-Si3N4 [DE94-002632] p 2563 N94-24517

SILICON RADIATION DETECTORS

Examination of the response capacity of a silicon pixel detector for ions and molecules in the energy area 100 to 300 keV [MPE-241] p 2346 N94-25415

SILICON TRANSISTORS

Disilane LPCVD deposited silicon films: Deposition mechanisms, properties and capability of making transistors on thin films [LAAS-93156] p 2252 N94-22910

SILICONES

Viscous rotary damper p 2361 N94-24031

SILVER
Thermomechanical processing of Ag-clad Bi2Sr2CaCu2O(x) superconductors
[DE94-002347] p 2563 N94-24624
SILVER ZINC BATTERIES
Aerospace applications of batteries
p 2390 N94-23346
SIMD (COMPUTERS)
Application of multigrid methods to the solution of liquid crystal equations on a SIMD computer
p 2484 N94-23686
SIMULATION
New welding and finishing procedures
[DE94-602022] p 2352 N94-23025
Robust stability of second-order systems
[NASA-CR-195175] p 2488 N94-24564
Solid rocket combustion simulator technology using the hybrid rocket for simulation
[NASA-CR-195142] p 2265 N94-24578
Admittance model for the shuttle remote manipulator system in four configurations
[NASA-CR-4555] p 2474 N94-24635
Numerical simulation of cylindrical, self-field MPD thrusters with multiple propellants
[NASA-CR-194458] p 2220 N94-24714
BEM solution for the simulation of axisymmetric viscous sintering
[PB93-237717] p 2336 N94-24761
Simulation of the vortex motion in the high T(c) superconductors
[DE93-617138] p 2567 N94-25403
SIMULATORS
Physical modeling and dynamic simulation of planet vehicles: Application to the motion prediction
p 2371 N94-23426
Micro SIL-1 simulator
[PB94-110889] p 2454 N94-23750
SIMSAT: An object oriented architecture for real-time satellite simulation p 2197 N94-23940
CF-18 AN/ALQ-126B-MG 13 IIP interface to the DREO Electronic Warfare Engagement Simulation Facility
[DREO-TN-93-4] p 2296 N94-24118
A study of the core module simulator floor capability
p 2380 N94-24418
Integration and evaluation of a simulator designed to be used within a dynamic prototyping environment
p 2198 N94-24436
A two-dimensional dispersion module for the TOUGH2 simulator
[DE94-002262] p 2335 N94-24655
X ray simulator theory support
[AD-A273613] p 2553 N94-24949
SINE WAVES
Spur-reduced digital sinusoid synthesis
p 2291 N94-23264
SINGLE CHANNEL PER CARRIER TRANSMISSION
Improved frame synchronization schemes for INMARSAT-B/M SCPC and TDM channels
p 2285 N94-22806
SINGLE CRYSTALS
The elastic and electromechanical properties of BaTiO3 single crystal through the ferroelectric transition
[DE94-001437] p 2557 N94-22927
Anomalous magnetoresistance behavior of superconducting Nd(2-x)Ce(x)CuO(4-y) single crystal
[DE94-000806] p 2558 N94-22941
Application of maximum entropy and irreducible cluster integrals to joint probability distributions for x ray structure determination
[PB93-224152] p 2559 N94-23109
Proposed additions to the SHADOW ray-tracing code for general-asymmetric perfect-crystal optics
[DE94-001291] p 2560 N94-23188
Reduction of nitric oxide over platinum, rhodium and platinum-rhodium single crystal surfaces
[PB93-230092] p 2232 N94-23482
Inertial confinement fusion
[DE94-002602] p 2551 N94-23703
Polymer morpholoqh p 2226 N94-24353
The mechanical properties of single crystal (alpha)-Si3N4
[DE94-002632] p 2563 N94-24517
Ge-Au eutectic bonding of Ge (100) single crystals
[DE94-002281] p 2564 N94-24657
Two micron stimulated emission of activated insulating crystals
[REPT-94-002] p 2565 N94-25025
SINGLE STAGE TO ORBIT VEHICLES
Access to space studies p 2199 N94-24434
Configuration development study of the OSU 1 hypersonic research vehicle
[NASA-CR-195522] p 2181 N94-24591
A conceptual design of an unmanned test vehicle using an airbreathing propulsion system
[NASA-CR-195550] p 2189 N94-25065
Hypersonic vehicle control law development using H(infinity) and micron-synthesis p 2163 N94-25104
SINGULAR INTEGRAL EQUATIONS
The effects of anisotropy on the nonlinear behavior of bridged cracks in long strips
[NASA-CR-194453] p 2377 N94-24604
SINGULARITY (MATHEMATICS)
Normal forms of kinematic singularities of 3R robot manipulators
[MEMO-1124] p 2469 N94-22712
Coordinate-free interpretations of the optimal costs for Lq problems subject to implicit systems
[PB94-118700] p 2473 N94-23760
Non-trivial examples of real isolated singularity at the origin
[PB94-110939] p 2487 N94-23787
SINTERING
Influence of sintering atmospheres on the aluminum sintering characteristics
[DE93-632412] p 2239 N94-22965
Particle formation in a laser-heated aerosol reactor. Application to silicon and silicon nitride synthesis
[PB93-217982] p 2347 N94-22982
Composite fiber structures for catalysts and electrodes
p 2393 N94-23364
Combustion synthesis and engineering of nanoparticles for electronic, structural and superconductor applications
[DE94-001865] p 2254 N94-23720
Modelling the ignition of boron/titanium particles
p 2159 N94-24273
Characteristics of products generated by selective sintering and stereolithography rapid prototyping processes p 2264 N94-24412
Thermomechanical processing of Ag-clad Bi2Sr2CaCu2O(x) superconductors
[DE94-002347] p 2563 N94-24624
BEM solution for the simulation of axisymmetric viscous sintering
[PB93-237717] p 2336 N94-24761
Solid state synthesis of Fe-B-Si alloys
[VTT-PUBS-118] p 2250 N94-25316
SIS (SUPERCONDUCTORS)
A low noise 665 GHz SIS quasi-particle waveguide receiver
[NASA-CR-194735] p 2296 N94-24105
SISO (CONTROL SYSTEMS)
Flight controller design using mixed H2/H infinity optimization with a singular H infinity constraint
[AD-A273831] p 2191 N94-25525
SIZE DISTRIBUTION
Particle size measurement for the control of industrial crystallizers
[PB94-119104] p 2562 N94-23766
Infrared sensors and systems for enhanced vision/autonomous landing applications
p 2439 N94-25491
SKIN FRICTION
The use of near-wall hot-wire probes for time-resolved skin-friction measurements p 2316 N94-22857
Skin friction measurement in complex flows using thin oil film techniques
[NASA-CR-194872] p 2327 N94-24098
Analytical skin friction and heat transfer formula for compressible internal flows
[NASA-CR-191185] p 2170 N94-25173
SKY WAVES
Northern Exposure 1992: An investigation of transauroral HF radio skywave propagation
[AD-A273363] p 2303 N94-25089
SLABS
A vibrating wire parallel to a type 2 superconducting slab of arbitrary thickness
[DE93-617134] p 2525 N94-25389
The effect of a transport current on the surface barrier of a uniaxial anisotropic superconducting slab
[DE93-617135] p 2566 N94-25390
Effects of a vibrating wire carrying DC current on a moving type 2 superconducting slab of arbitrary thickness
[DE93-617136] p 2566 N94-25391
SLAGS
Detection of velocity in high temperature liquid metals
p 2247 N94-25127
SLIDING FRICTION
Wear characteristics of technical dry rolling/sliding systems with relations to corrugation problems
p 2269 N94-23586
Surface observations of stick-slip oscillations in tightly conformal wheel/rail contacts p 2270 N94-23588
Development of a theory of the wear of ceramics
[DE94-002773] p 2254 N94-23783
Development of gears for space use
p 2360 N94-24021
Wear reduction in ceramic bearings by surface generated pyrolytic carbon continuously replenished by ethylene gas
[NASA-CR-189214] p 2364 N94-24090
SLOT ANTENNAS
Radar signature related radome techniques for flush-mounted HF-, VHF- and, UHF communication antennas
[PB93-204618] p 2294 N94-23742
Spatial frequency multiplier with active linearly tapered slot antenna array
[NASA-TM-106494] p 2310 N94-24308
SLURRIES
Preparing polymeric matrix composites using an aqueous slurry technique
[NASA-CASE-LAR-14771-1] p 2252 N94-23076
Composite fiber structures for catalysts and electrodes
p 2393 N94-23364
Theoretical considerations for Reaction-Formed Silicon Carbide (RFSC) formation by molten silicon infiltration into slurry-derived preforms
[NASA-TM-106414] p 2222 N94-23500
SLURRY PROPELLANTS
Electro-rheology fluids and liquid fuel flow
[AD-A273640] p 2337 N94-25032
SMALL SCIENTIFIC SATELLITES
WISPER: Wirless Space Power Experiment
[NASA-CR-195538] p 2396 N94-24701
SMART STRUCTURES
Intelligent Material Systems and Structures (IMSS). Part 5: Fiber optic registration of deformation in carbon laminates 91/92
[PB93-204600] p 2544 N94-23723
Probabilistic assessment of smart composite structures
[NASA-TM-106358] p 2378 N94-25188
SMOKE
Chronic obstructive pulmonary disease
p 2425 N94-23324
Field models: Their present and future application in fire safety engineering
[PB93-201622] p 2269 N94-23506
Zone fire modeling with natural building flows and a zero order shaft model
[PB94-112166] p 2270 N94-23735
The effects of zinc borate addition on the flammability characteristics of polyester, vinyl ester, and epoxy glass reinforced plastics
[AD-A273164] p 2262 N94-25136
SMOOTHING
Nonlinear smoothing for random fields
[MEMO-1110] p 2493 N94-22728
POISs3: A 3D poisson smoother of structured grids
[PB93-226231] p 2318 N94-23115
A nonconforming multigrid method using conforming subspaces p 2485 N94-23695
SNOW
Close-up analysis of inflight ice accretion
[NASA-TM-106457] p 2172 N94-23523
Synthesis of passive microwave and radar altimeter data for estimating accumulation rates of polar snow
[NASA-CR-194864] p 2382 N94-23573
Snow modeling, water resources, climate change
[PB93-201770] p 2399 N94-24633
SNOW COVER
Application of ERS-1 active microwave instrumentation data to remote sensing of snow
[PB93-224756] p 2382 N94-23224
SOBOLEV SPACE
Polynomials orthogonal with respect to an inner product involving differences
[PB94-110731] p 2489 N94-24572
SOCIAL FACTORS
Proceedings of Technology and Governance in the 1990's
[PB93-192904] p 2597 N94-24312
SOCIOLOGY
The evolution of the laser: A systems perspective on science, technology and society
[ETN-94-95319] p 2351 N94-25218
SODIUM CHLORIDES
Stress corrosion cracking properties of 15-5PH steel
p 2251 N94-23244
SODIUM HYDRIDES
Vacancy formation energy of Li(H, D) and Na(H, D) systems
[DE93-633452] p 2558 N94-22978
SODIUM HYDROXIDES
Aqueous alkaline cleaners: An alternative to organic solvents
[AD-A273510] p 2260 N94-24848
SOFTENING
Mean stress models for low cycle fatigue of a nickel-base superalloy p 2159 N94-24276

SOFTWARE ENGINEERING
An information retrieval logical model applied to the formalism of conceptual graphs: The ELEN prototype and its experimentation on a corpus of software components
[ETN-94-95162] p 2588 N94-22879
A general model for dynamic and complex information management: The ELEN prototype object manager for software engineering
[ETN-94-95163] p 2588 N94-22880
Definition and realization of a formal verification tool of LUSTRE programs: The LESAR system
[ETN-94-95164] p 2447 N94-22882
Software for scientific visualization: State of the art and experiences
[PB93-225183] p 2449 N94-23111
Guide to software configuration management
[ESA-PSS-05-09-ISSUE-1] p 2450 N94-23229
Cost benefits of advanced software: A review of methodology used at Kennedy Space Center
p 2464 N94-23240
Formal methods and digital systems validation for airborne systems
[NASA-CR-4551] p 2466 N94-23293
ATOS-1: Designing the infrastructure for an advanced spacecraft operations system p 2197 N94-23849
SPOT4 Operational Control Center (CMP)
p 2197 N94-23856
The Ulysses spacecraft control and monitoring concepts and realities p 2502 N94-23862
The Mars mapper science and mission planning tool
p 2503 N94-23867
VMPLOT: A versatile analysis tool for mission operations p 2507 N94-23891
The Advanced Technology Operations System: ATOS
p 2508 N94-23897
Making tomorrow's mistakes today: Evolutionary prototyping for risk reduction and shorter development time p 2197 N94-23902
SAO mission support software and data standards, version 1.0
[NASA-CR-193906] p 2454 N94-24050
Update of GRASP/Ada reverse engineering tools for Ada
[NASA-CR-193890] p 2455 N94-24111
Designers' models of the human-computer interface
p 2433 N94-24188
New computing systems, future computing environment, and their implications on structural analysis and design
p 2177 N94-24314
Integration and evaluation of a simulator designed to be used within a dynamic prototyping environment
p 2198 N94-24436
Evaluation of the efficiency and fault density of software generated by code generators p 2465 N94-24445
Hydro-elastic analysis using a selection of commercial analysis programs
[PB94-118734] p 2376 N94-24478
High-performance computing and communications
[DE94-002215] p 2457 N94-24566
An investigation of requirements traceability to support systems development
[AD-A273167] p 2458 N94-24684
A type-theoretic approach to higher-order modules with sharing
[AD-A273566] p 2458 N94-24693
A methodology for software cost estimation using machine learning techniques
[AD-A273158] p 2459 N94-24775
Intelligent systems and advanced user interfaces for design, operation, and maintenance of command management systems
[NASA-CR-195172] p 2459 N94-24797
The use of design automation software by government-contracted architect/engineer firms: A status report
[AD-A273181] p 2459 N94-24812
Reengineering real-time software systems
[AD-A273408] p 2461 N94-25074
Future directions in flight simulation: A user perspective p 2162 N94-25101
An implementation of the REpresentation and MAintenance of Process knowledge (REMAP) model in the knowledge-based software assistant concept demonstration system
[AD-A273207] p 2461 N94-25138
Reuse-Driven Software Processes Guidebook, version 02.00.03
[AD-A273644] p 2461 N94-25148
Reuse Adoption Guidebook, version 02.00.05
[AD-A273652] p 2461 N94-25149
Computerized testing system software conversion and development: Identifying software and hardware portability issues and solutions
[AD-A273489] p 2462 N94-25287
A prototype to automate the video subsystem routing for the video distribution subsystem of Space Station Freedom p 2306 N94-25353
Software engineering methodologies and tools
p 2465 N94-25382
A multimedia adult literacy program: Combining NASA technology, instructional design theory, and authentic literacy concepts p 2585 N94-25384
CADBIT 2: Computer-aided design for built-in test, volume 1
[AD-A273702] p 2463 N94-25455
CADBIT 2: Computer-aided design for built-in test, volume 2
[AD-A273703] p 2463 N94-25456
SOFTWARE RELIABILITY
Evaluation of the efficiency and fault density of software generated by code generators p 2465 N94-24445
A type-theoretic approach to higher-order modules with sharing
[AD-A273566] p 2458 N94-24693
SOFTWARE REUSE
Software reuse in spacecraft planning and scheduling systems p 2520 N94-23966
RITL: An information system for application reuse-in-the-large
[PB94-119088] p 2592 N94-24646
Intelligent systems and advanced user interfaces for design, operation, and maintenance of command management systems
[NASA-CR-195172] p 2459 N94-24797
Analyzing the properties of user interface software
[AD-A273601] p 2460 N94-24933
Reengineering real-time software systems
[AD-A273408] p 2461 N94-25074
Reuse-Driven Software Processes Guidebook, version 02.00.03
[AD-A273644] p 2461 N94-25148
Reuse Adoption Guidebook, version 02.00.05
[AD-A273652] p 2461 N94-25149
SOFTWARE TOOLS
A general model for dynamic and complex information management: The ELEN prototype object manager for software engineering
[ETN-94-95163] p 2588 N94-22880
Definition and realization of a formal verification tool of LUSTRE programs: The LESAR system
[ETN-94-95164] p 2447 N94-22882
Verification of synchronous sequential numerical material systems: Application of the LUSTRE language and of the LESAR verification tool
[ETN-94-95181] p 2447 N94-22899
Users manual for the Chameleon parallel programming tools
[DE94-001934] p 2465 N94-22973
A dataflow analysis tool for parallel processing of algorithms
[NASA-TM-109054] p 2448 N94-23086
Tools reference manual for a Requirements Specification Language (RSL), version 2.0
[NASA-CR-191461] p 2445 N94-23125
The TOPSIM 4 graphic user interface
[ESA-STM-247] p 2450 N94-23228
A framework for SFC/DC system data analysis
p 2523 N94-23234
The Automated Instrumentation and Monitoring System (AIMS) reference manual
[NASA-TM-108795] p 2452 N94-23510
Activity Catalog Tool (ACT) user manual, version 2.0
[NASA-CR-177634] p 2430 N94-23527
Simultaneous simulation and visualization using DGL
[PB93-201341] p 2453 N94-23534
Mean-value of product-form stochastic Petri net models of slotted-ring systems
[PB94-110871] p 2494 N94-23749
Magellan spacecraft and memory state tracking: Lessons learned, future thoughts p 2207 N94-23865
Integrating payload design, planning, and control in the Dutch Utilisation Centre p 2207 N94-23869
Making adaptable systems work for mission operations: A case study p 2506 N94-23883
The FOT tool kit concept p 2507 N94-23889
VMPLOT: A versatile analysis tool for mission operations p 2507 N94-23891
The mission events graphic generator software: A small tool with big results p 2464 N94-23893
Using SFOC to fly the Magellan Venus mapping mission p 2516 N94-23941
Expert diagnostics system as a part of analysis software for power mission operations p 2516 N94-23944
GenSAA: A tool for advancing satellite monitoring with graphical expert systems p 2516 N94-23945
From requirements to acceptance tests
p 2464 N94-23962
Software reuse in spacecraft planning and scheduling systems p 2520 N94-23966
Integration and evaluation of a simulator designed to be used within a dynamic prototyping environment
p 2198 N94-24436
Evaluation of the efficiency and fault density of software generated by code generators p 2465 N94-24445
Fact-based enterprise information management using NIAM
[DE93-041135] p 2591 N94-24501
MERILL: An equational reasoning system in standard ML: A user guide (prerelease version 0.4)
[PB93-204501] p 2456 N94-24534
An automated tool to facilitate code translation for software fault tree analysis
[AD-A273205] p 2457 N94-24556
High-performance computing and communications
[DE94-002215] p 2457 N94-24566
Timed coloured Petri nets and their application to logistics
[ETN-94-95310] p 2522 N94-25293
Genetic algorithms in control systems engineering
[RR-470] p 2463 N94-25315
Software engineering methodologies and tools
p 2465 N94-25382
CADBIT 2: Computer-aided design for built-in test, volume 1
[AD-A273702] p 2463 N94-25455
CADBIT 2: Computer-aided design for built-in test, volume 2
[AD-A273703] p 2463 N94-25456
SOHO MISSION
Ultra-clean high-precision mechanisms for the SUMER EUV spectrometer on SOHO p 2356 N94-23999
Width modulator mechanism for spectrometer entrance slits p 2357 N94-24002
GOLF mechanisms p 2357 N94-24003
The development of the SOHO SUMER mechanisms
p 2361 N94-24028
Examination of the response capacity of a silicon pixel detector for ions and molecules in the energy area 100 to 300 keV
[MPE-241] p 2346 N94-25415
SOIL MOISTURE
Estimates of monthly mean soil moisture for 1979-1989
[NASA-TM-104571] p 2407 N94-23132
Spatial and temporal variability of soil temperature, moisture and surface soil properties
[NASA-CR-194109] p 2401 N94-23337
Methodology for the assessment of surface resistance and soil water storage variability at mesoscale based on remote sensing measurements. A case study with HAPEX-EFEDA data. UNESCO-International Hydrological Program 4
[PB94-111721] p 2386 N94-23734
Groundtruth collection for the JPL-SAR and ERS-1 campaign in Flevoland and Veluwe, Netherlands, 1991
[PB93-230654] p 2386 N94-23755
Session on coupled land surface/hydrological/atmospheric models
p 2414 N94-24395
SOIL SCIENCE
Spatial and temporal variability of soil temperature, moisture and surface soil properties
[NASA-CR-194109] p 2401 N94-23337
SOILS
Machines for moving in soil p 2369 N94-23411
Effect of land use change on the carbon cycle in Amazon soils
[NASA-CR-195168] p 2399 N94-24853
Human impacts on soil carbon dynamics of deep-rooted Amazonian forests
[NASA-CR-195127] p 2399 N94-24861
SOL-GEL PROCESSES
Photo-induced and electrooptic properties of (Pb,La)(Zr,Ti)O3 films for optical memories
[DE93-019820] p 2542 N94-23202
Glass-ceramic Li-Al-Si-O composition and process for its production
[CA-PATENT-APPL-SN-2043757] p 2254 N94-24129
Conformal method of fabricating and optical waveguide on a semiconductor substrate
[AD-D015988] p 2546 N94-25043
SOLAR ACTIVITY
Solar-geophysical data number 584, April 1993. Part 1: (Prompt reports). Data for February, March, 1993, and late data
[PB93-198323] p 2626 N94-23738
Solar-geophysical data number 584, April 1993. Part 2: (Comprehensive reports). Data for October 1992, and miscellaneous
[PB93-198331] p 2627 N94-23739
Solar-geophysical data number 589, September 1993. Part 1: (Prompt reports). Data for August, July 1993, and late data
[PB94-117082] p 2628 N94-24993

SOLAR ARRAYS

The Fifth European Space Mechanisms and Tribology Symposium
[ESA-SP-334] p 2355 N94-23985

The Columbus solar array mechanisms
p 2356 N94-23994

Primary deployment mechanism for the European Polar Platform p 2207 N94-23995

The Submillimeter Wave Astronomy Satellite (SWAS) solar array system p 2361 N94-24029

Design of a new high-performance pointing controller for the Hubble Space Telescope
[NASA-CR-193891] p 2364 N94-24088

Optimal Space Station solar array gimbal angle determination via radial basis function neural networks
[NASA-TM-106482] p 2195 N94-24482

Thermal control system for Space Station Freedom photovoltaic power module
[NASA-TM-105650] p 2205 N94-24825

SOLAR ATMOSPHERE

Some challenging problems of the structured and dynamical solar atmosphere p 2624 N94-22838

Goals of ground-based solar observations
p 2624 N94-22840

Why put visible solar telescopes in space?
p 2600 N94-22850

The calculation of theoretical chromospheric models and the interpretation of solar spectra from rockets and spacecraft
[NASA-CR-195083] p 2626 N94-23569

An analysis of solar mesospheric temperatures for the upper stratosphere and mesosphere
[NASA-CR-194861] p 2626 N94-23626

The resonance lines of MG2 as diagnostics of the upper solar chromosphere
[NASA-CR-195084] p 2627 N94-24300

On the physics of waves in the solar atmosphere: Wave heating and wind acceleration
[NASA-CR-195197] p 2628 N94-25264

SOLAR CELLS

Polycrystalline thin film materials and devices
[DE93-018213] p 2389 N94-22862

Feasibility study on a CO2 global recycling system using natural energy
[DE94-714889] p 2397 N94-23026

Research on polycrystalline thin-film CuInGaSe2 solar cells
[DE94-000203] p 2560 N94-23205

Amorphous silicon PVMaT, phase 2A
[DE93-018221] p 2390 N94-23295

Novel two-stage selenization methods for fabrication of thin-film CIS cells and submodules
[DE94-000220] p 2390 N94-23296

Transparent conducting thin films for spacecraft applications
[NASA-TM-106466] p 2218 N94-23370

JOVE NASA-FIT program: Microgravity and aeronomy projects
[NASA-CR-195121] p 2631 N94-24493

Thin film cadmium telluride photovoltaic cells
[DE94-000201] p 2395 N94-24509

Results of the 1993 NASA/JPL balloon flight solar cell calibration program
[NASA-CR-195158] p 2395 N94-24563

SOLAR COLLECTORS

Preliminary study concerning development of petroleum-substitution energy integration technology
[DE94-714902] p 2264 N94-23027

The hexagonal compound parabolic concentrator design and construction
[DLR-MITT-93-03] p 2396 N94-25464

The pressure loaded volumetric ceramic receiver 500 kW version design and construction
[DLR-MITT-93-02] p 2396 N94-25479

SOLAR CONVECTION (ASTRONOMY)

On the physics of waves in the solar atmosphere: Wave heating and wind acceleration
[NASA-CR-195197] p 2628 N94-25264

SOLAR CORONA

Scientific Requirements for Future Solar-Physics Space Missions
[ESA-SP-1157] p 2623 N94-22837

Keys to understanding the corona
p 2624 N94-22839

Prospects for future solar-wind missions
p 2624 N94-22841

The next Japanese solar satellite
p 2625 N94-22846

Solar physics and the Coronas project
p 2625 N94-22847

Requirements for future solar-physics missions with x ray instrumentation p 2625 N94-22849

Coronal abundances and their variation
[NASA-CR-194811] p 2626 N94-23276

Model development for Ulysses and SOHO
[NASA-CR-193884] p 2627 N94-24484

SOLAR CYCLES

Solar magnetic cycle
[NASA-CR-195202] p 2628 N94-25275

SOLAR ENERGY

Feasibility study on a CO2 global recycling system using natural energy
[DE94-714889] p 2397 N94-23026

Preliminary study concerning development of petroleum-substitution energy integration technology
[DE94-714902] p 2264 N94-23027

Power generation technology options for a Mars mission
[NASA-TM-106451] p 2220 N94-24681

SOLAR FLARES

Some challenging problems of the structured and dynamical solar atmosphere p 2624 N94-22838

The next Japanese solar satellite
p 2625 N94-22846

Excitation of XUV radiation in solar flares
[NASA-CR-193703] p 2627 N94-24094

Magnetic shielding of interplanetary spacecraft against solar flare radiation
[NASA-CR-195539] p 2204 N94-24334

Solar-geophysical data number 587, July 1993. Part 1: (Prompt reports). Data for June, May 1993, and late data
[PB93-232874] p 2628 N94-24989

Solar-geophysical data number 587, July 1993. Part 2: (Comprehensive reports). Data for January 1993, and miscellaneous
[PB93-232882] p 2628 N94-24990

Solar-geophysical data number 588, August 1993. Part 1: (Prompt reports). Data for July, June 1993, and late data
[PB94-109089] p 2628 N94-24991

Solar-geophysical data number 588, August 1993. Part 2: (Comprehensive reports). Data for February 1993, and miscellaneous
[PB94-109105] p 2628 N94-24992

Solar-geophysical data number 589, September 1993. Part 1: (Prompt reports). Data for August, July 1993, and late data
[PB94-117082] p 2628 N94-24993

Solar-geophysical data number 589, September 1993. Part 2: (Comprehensive reports). Data for March 1993, and miscellaneous
[PB94-117405] p 2628 N94-24994

Solar flares and magnetospheric particles: Investigations based upon the ONR-602 and ONR-604 experiments
[AD-A273639] p 2628 N94-25031

SOLAR FLUX

An analysis of solar mesospheric temperatures for the upper stratosphere and mesosphere
[NASA-CR-194861] p 2626 N94-23626

Numerical simulation of Ulysses nutation
p 2207 N94-24017

Kamiokande results on solar neutrinos and a supernova search
[ICRR-REPT-294-93-6] p 2627 N94-24961

Solar neutrinos: Real-time experiments
[ICRR-REPT-293-93-5] p 2627 N94-24962

SOLAR INSTRUMENTS

Polarization analysis of a balloon-borne solar magnetograph
[NASA-CR-193908] p 2345 N94-24852

SOLAR MAGNETIC FIELD

Solar-geophysical data number 584, April 1993. Part 1: (Prompt reports). Data for February, March, 1993, and late data
[PB93-198323] p 2626 N94-23738

Solar-geophysical data number 587, July 1993. Part 1: (Prompt reports). Data for June, May 1993, and late data
[PB93-232874] p 2628 N94-24989

Solar-geophysical data number 588, August 1993. Part 1: (Prompt reports). Data for July, June 1993, and late data
[PB94-109089] p 2628 N94-24991

Solar-geophysical data number 589, September 1993. Part 1: (Prompt reports). Data for August, July 1993, and late data
[PB94-117082] p 2628 N94-24993

Solar magnetic cycle
[NASA-CR-195202] p 2628 N94-25275

SOLAR MAXIMUM MISSION

Coronal abundances and their variation
[NASA-CR-194811] p 2626 N94-23276

SOLAR NEUTRINOS

Recent results from the Soviet-American Gallium Experiment
[DE94-000677] p 2626 N94-23020

Accelerator-based neutrino oscillation searches
[DE94-000818] p 2626 N94-23515

Solar neutrinos: Real-time experiments
[ICRR-REPT-293-93-5] p 2627 N94-24962

SOLAR OPTICAL TELESCOPE

Width modulator mechanism for spectrometer entrance slits p 2357 N94-24002

SOLAR OSCILLATIONS

Some challenging problems of the structured and dynamical solar atmosphere p 2624 N94-22838

SOLAR PHYSICS

Scientific Requirements for Future Solar-Physics Space Missions
[ESA-SP-1157] p 2623 N94-22837

Some challenging problems of the structured and dynamical solar atmosphere p 2624 N94-22838

Keys to understanding the corona
p 2624 N94-22839

Goals of ground-based solar observations
p 2624 N94-22840

Prospects for future ground-based solar observations
p 2624 N94-22842

Prospects for improved instrumentation on future solar space missions p 2624 N94-22843

Solar physics within ESA's planning
p 2624 N94-22844

Solar physics within NASA's planning
p 2625 N94-22845

The next Japanese solar satellite
p 2625 N94-22846

Solar physics and the Coronas project
p 2625 N94-22847

Prospects for very-high-resolution solar physics with the Simuris inteferometric mission p 2625 N94-22848

Requirements for future solar-physics missions with x ray instrumentation p 2625 N94-22849

Why put visible solar telescopes in space?
p 2600 N94-22850

Requirements for future solar-physics missions that include UV instrumentation p 2625 N94-22851

The calculation of theoretical chromospheric models and the interpretation of solar spectra from rockets and spacecraft
[NASA-CR-195083] p 2626 N94-23569

Solar-geophysical data number 584, April 1993. Part 1: (Prompt reports). Data for February, March, 1993, and late data
[PB93-198323] p 2626 N94-23738

Solar-geophysical data number 584, April 1993. Part 2: (Comprehensive reports). Data for October 1992, and miscellaneous
[PB93-198331] p 2627 N94-23739

Model development for Ulysses and SOHO
[NASA-CR-193884] p 2627 N94-24484

Solar-geophysical data number 587, July 1993. Part 1: (Prompt reports). Data for June, May 1993, and late data
[PB93-232874] p 2628 N94-24989

Solar-geophysical data number 587, July 1993. Part 2: (Comprehensive reports). Data for January 1993, and miscellaneous
[PB93-232882] p 2628 N94-24990

Solar-geophysical data number 588, August 1993. Part 1: (Prompt reports). Data for July, June 1993, and late data
[PB94-109089] p 2628 N94-24991

Solar-geophysical data number 588, August 1993. Part 2: (Comprehensive reports). Data for February 1993, and miscellaneous
[PB94-109105] p 2628 N94-24992

Solar-geophysical data number 589, September 1993. Part 1: (Prompt reports). Data for August, July 1993, and late data
[PB94-117082] p 2628 N94-24993

Solar-geophysical data number 589, September 1993. Part 2: (Comprehensive reports). Data for March 1993, and miscellaneous
[PB94-117405] p 2628 N94-24994

On the physics of waves in the solar atmosphere: Wave heating and wind acceleration
[NASA-CR-195197] p 2628 N94-25264

SOLAR POWERED AIRCRAFT

Effect of power system technology and mission requirements on high altitude long endurance aircraft
[NASA-CR-194455] p 2189 N94-25200

SOLAR PROMINENCES

Solar-geophysical data number 589, September 1993. Part 2: (Comprehensive reports). Data for March 1993, and miscellaneous
[PB94-117405] p 2628 N94-24994

SOLAR PROTONS

Magnetic shielding of interplanetary spacecraft against solar flare radiation
[NASA-CR-195539] p 2204 N94-24334

SOLAR RADIATION

Flight solar calibrations using the Mirror Attenuator Mosaic (MAM): Low scattering mirror
p 2384 N94-23602

Solar-geophysical data number 589, September 1993. Part 2: (Comprehensive reports). Data for March 1993, and miscellaneous
[PB94-117405] p 2628 N94-24994

The hexagonal compound parabolic concentrator design and construction
[DLR-MITT-93-03] p 2396 N94-25464

SOLAR RADIO BURSTS
Solar-geophysical data number 584, April 1993. Part 2: (Comprehensive reports). Data for October 1992, and miscellaneous
[PB93-198331] p 2627 N94-23739
Solar-geophysical data number 587, July 1993. Part 2: (Comprehensive reports). Data for January 1993, and miscellaneous
[PB93-232882] p 2628 N94-24990
Solar-geophysical data number 588, August 1993. Part 2: (Comprehensive reports). Data for February 1993, and miscellaneous
[PB94-109105] p 2628 N94-24992
Solar-geophysical data number 589, September 1993. Part 1: (Prompt reports). Data for August, July 1993, and late data
[PB94-117082] p 2628 N94-24993
Solar-geophysical data number 589, September 1993. Part 2: (Comprehensive reports). Data for March 1993, and miscellaneous
[PB94-117405] p 2628 N94-24994

SOLAR RADIO EMISSION
Solar-geophysical data number 584, April 1993. Part 1: (Prompt reports). Data for February, March, 1993, and late data
[PB93-198323] p 2626 N94-23738
Solar-geophysical data number 587, July 1993. Part 1: (Prompt reports). Data for June, May 1993, and late data
[PB93-232874] p 2628 N94-24989
Solar-geophysical data number 588, August 1993. Part 1: (Prompt reports). Data for July, June 1993, and late data
[PB94-109089] p 2628 N94-24991
Solar-geophysical data number 589, September 1993. Part 1: (Prompt reports). Data for August, July 1993, and late data
[PB94-117082] p 2628 N94-24993

SOLAR SENSORS
An Earth albedo model: A mathematical model for the radiant energy input to an orbiting spacecraft due to the diffuse reflectance of solar radiation from the Earth below
[NASA-TM-104596] p 2195 N94-24497

SOLAR SPECTRA
The calculation of theoretical chromospheric models and the interpretation of solar spectra from rockets and spacecraft
[NASA-CR-195083] p 2626 N94-23569
The resonance lines of MG2 as diagnostics of the upper solar chromosphere
[NASA-CR-195084] p 2627 N94-24300
The solar spectral irradiances from x ray to radio wavelengths
[NASA-CR-195203] p 2629 N94-25260

SOLAR SPECTROMETERS
Prospects for improved instrumentation on future solar space missions p 2624 N94-22843
Prospects for very-high-resolution solar physics with the Simuris inteferometric mission p 2625 N94-22848
Ultra-clean high-precision mechanisms for the SUMER EUV spectrometer on SOHO p 2356 N94-23999
Periscope mechanism for SWAN instrument
p 2357 N94-24000
Width modulator mechanism for spectrometer entrance slits p 2357 N94-24002
The development of the SOHO SUMER mechanisms
p 2361 N94-24028
High energy collimating fine grids for HESP program
[NASA-CR-189317] p 2209 N94-24767

SOLAR SYSTEM
Tensor-scalar cosmological models and their relaxation toward general relativity
[PB93-220796] p 2601 N94-23099

SOLAR SYSTEM EVOLUTION
Correlated petrographic, electron microprobe, and ion microprobe studies of selected primitive and processed phase assemblages in meteorites
[NASA-CR-194827] p 2601 N94-23499
A brief history of the universe
[DE93-616843] p 2604 N94-25210

SOLAR TEMPERATURE
An analysis of solar mesospheric temperatures for the upper stratosphere and mesosphere
[NASA-CR-194861] p 2626 N94-23626

SOLAR TERRESTRIAL INTERACTIONS
Solar-terrestrial environmental laboratory
p 2630 N94-23336
Solar-geophysical data number 584, April 1993. Part 1: (Prompt reports). Data for February, March, 1993, and late data
[PB93-198323] p 2626 N94-23738
Scientific study in solar and plasma physics relative to rocket and balloon projects
[NASA-CR-193885] p 2627 N94-24461
Solar-geophysical data number 587, July 1993. Part 1: (Prompt reports). Data for June, May 1993, and late data
[PB93-232874] p 2628 N94-24989
Solar-geophysical data number 588, August 1993. Part 1: (Prompt reports). Data for July, June 1993, and late data
[PB94-109089] p 2628 N94-24991

SOLAR WIND
Scientific Requirements for Future Solar-Physics Space Missions
[ESA-SP-1157] p 2623 N94-22837
Some challenging problems of the structured and dynamical solar atmosphere p 2624 N94-22838
Prospects for future solar-wind missions
p 2624 N94-22841
Evolution of large-scale plasma structures in comets: Kinematics and physics
[NASA-CR-194777] p 2601 N94-23251
Scientific study in solar and plasma physics relative to rocket and balloon projects
[NASA-CR-193885] p 2627 N94-24461
Solar-geophysical data number 589, September 1993. Part 2: (Comprehensive reports). Data for March 1993, and miscellaneous
[PB94-117405] p 2628 N94-24994
On the physics of waves in the solar atmosphere: Wave heating and wind acceleration
[NASA-CR-195197] p 2628 N94-25264
High latitude cusp signature observations for southward IMF B sub Z
[AD-A273801] p 2406 N94-25536

SOLAR X-RAYS
Solar-geophysical data number 584, April 1993. Part 2: (Comprehensive reports). Data for October 1992, and miscellaneous
[PB93-198331] p 2627 N94-23739
Solar-geophysical data number 589, September 1993. Part 2: (Comprehensive reports). Data for March 1993, and miscellaneous
[PB94-117405] p 2628 N94-24994

SOLDERED JOINTS
Laser soldering of Sn plated brass integrator assembly housings
[DE94-001149] p 2270 N94-23790

SOLDERING
Laser soldering of Sn plated brass integrator assembly housings
[DE94-001149] p 2270 N94-23790

SOLDERS
Laser soldering of Sn plated brass integrator assembly housings
[DE94-001149] p 2270 N94-23790

SOLENOIDS
Structural analysis of a superconducting central solenoid for the Tokamak Physics Experiment
[DE94-001536] p 2549 N94-23014

SOLID ELECTROLYTES
Modelling of solid polymer and direct methanol fuel cells: Phenomenological equations and analytical solutions
[PB93-224897] p 2390 N94-23102
High power density proton exchange membrane fuel cells p 2393 N94-23359
The electrolyte challenge for a direct methanol-air polymer electrolyte fuel cell operating at temperatures up to 200 C p 2393 N94-23360
Advances in direct oxidation methanol fuel cells
p 2393 N94-23361

SOLID LUBRICANTS
New tribocoating combination for vacuum operation
p 2355 N94-23990
Tribological characteristics of ball bearings lubricated with a sputtered molybdenum disulphide film in a vacuum under a high thrust load p 2355 N94-23992
The tribology of some MoS2-lubricated engineering ceramics p 2356 N94-23993
Development of gears for space use
p 2360 N94-24021
An analytical ultra-high vacuum tribometer for solid lubricant studies p 2361 N94-24033
An assessment of solid lubricant films for use in high temperature space applications p 2363 N94-24044
The development of dry-lubricated ceramic cages
p 2363 N94-24045

SOLID PROPELLANT COMBUSTION
Design considerations of hybrid rockets
p 2156 N94-24254
Modelling the ignition of boron/titanium particles
p 2159 N94-24273

SOLID PROPELLANT IGNITION
Modelling the ignition of boron/titanium particles
p 2159 N94-24273

SOLID PROPELLANT ROCKET ENGINES
Final postflight hardware evaluation report RSRM-28 (STS-53)
[NASA-CR-193902] p 2200 N94-24112
Impact damage in filament wound composite bottles
p 2231 N94-24421
Micromechanical simulation of damage progression in carbon phenolic composites p 2231 N94-24446

SOLID PROPELLANTS
Burning rate of double-base propellant in the presence of plasma p 2155 N94-24252
Modelling the ignition of boron/titanium particles
p 2159 N94-24273
Experimental investigation of ignition of boron/titanium composite particles p 2159 N94-24275

SOLID STATE
In situ and ex situ spectroelectrochemical and x ray absorption studies on rechargeable, chemically-modified and other MnO2 materials
[DE94-001387] p 2234 N94-24545
Thermomechanical processing of Ag-clad Bi2Sr2CaCu2O(x) superconductors
[DE94-002347] p 2563 N94-24624
Solid state Time Base Corrector (TBC)
[AD-D015981] p 2312 N94-25039

SOLID STATE DEVICES
Non-volatile, solid state bistable electrical switch
[NASA-CASE-NPO-17621-1-CU] p 2309 N94-23820
Mesoscopic phenomena in metallic point contacts
[ETN-94-95371] p 2313 N94-25286

SOLID STATE LASERS
Micro pulse laser radar
[NASA-CASE-GSC-13493-1] p 2294 N94-23827
Computer modeling of nonlinearities
p 2458 N94-24661
Temporal model of an optically pumped co-doped solid state laser
[NASA-TM-109680] p 2350 N94-24851
Nonlinear dynamical control of lasers
[AD-A273359] p 2350 N94-24938
Laser energized high voltage direct current power supply
[AD-D015977] p 2312 N94-25036

SOLID WASTES
Investigating pyrolysis/incineration as a method of resource recovery from solid waste
p 2444 N94-25375

SOLID-SOLID INTERFACES
Contribution to the interface micromechanical study and to the damage fundamental phenomena in glass fiber epoxy resin model composites
[ISAL-93-0027] p 2227 N94-23133
Interface evaluation in ceramic composites
p 2255 N94-24231
Chemically sensitive interfacial force microscopy: Contact potential measurements of self-assembling monolayer films
[AD-A273135] p 2234 N94-24772

SOLIDIFICATION
Three-dimensional solidification and melting using magnetic field control p 2325 N94-23664
Workshop on the Thermophysical Properties of Molten Materials
[NASA-CP-10121] p 2246 N94-25120
Thermophysical property sensitivity effects in steel solidification p 2246 N94-25122
A thermodynamic approach to obtain materials properties for engineering applications
p 2248 N94-25131

SOLUBILITY
Di(hydroxyphenyl)- benzimidazole monomers
[NASA-CASE-LAR-14643-2] p 2253 N94-23305
Humidity effects on soluble core mechanical and thermal properties (polyvinyl alcohol/microballoon composite) type CG extendospheres, volume 2
[NASA-CR-193893] p 2229 N94-24224
Temperature dependence of protein solubility-determination, application to crystallization, and growth kinetics studies p 2224 N94-24344
Ultrastructure processing of macromolecular materials
[AD-A273413] p 2258 N94-24782
Center for advanced electrical and structural polymers
[AD-A273415] p 2259 N94-24783

SOLVATION
Structures of Cl(-)(H2O)(n) and F(-)(H2O)(n) (n equal to 2,3...15) clusters: Molecular dynamics computer simulations
[AD-A273474] p 2537 N94-24940
The electrochemistry of the solvated electron: A study of its properties and of its applications
[ETN-94-95313] p 2236 N94-25296

SOLVENTS
FTIR quantification of industrial hydraulic fluids in perchloroethylene p 2264 N94-23243
Phenylethynl-terminated poly(arylene ethers)
[NASA-CASE-LAR-14797-1] p 2253 N94-23307

Selection of polymer binders and fabrication of SiC fiber-reinforced reaction-bonded silicon nitride matrix composites

[NASA-CR-194874] p 2255 N94-24223

Ozone depletion, paradigms, and politics

[DE94-001600] p 2398 N94-24506

Aqueous alkaline cleaners: An alternative to organic solvents

[AD-A273510] p 2260 N94-24848

Potent solvents for C60 and their utility for the rapid acquisition of 13CNMR data for fullerenes

[AD-A273349] p 2235 N94-24925

SONAR

A tracking sonar sensor for vehicle guidance

[OUEL-1956/92] p 2472 N94-23179

Improved magnetostrictive transducer drive elements achieved by reduction of crystalline defects and improved crystalline orientation

[AD-A273391] p 2313 N94-25276

SONIC ANEMOMETERS

Comparison between 1-minute and 15-minute averages of turbulence parameters p 2528 N94-24218

SONIC BOOMS

Variability of measured sonic boom signatures. Volume 1: Technical report

[NASA-CR-191483-VOL-1] p 2526 N94-24172

Variability of measured sonic boom signatures. Volume 2: Data report

[NASA-CR-191483-VOL-2] p 2526 N94-24173

SOS (SEMICONDUCTORS)

Laser energized high voltage direct current power supply

[AD-D015977] p 2312 N94-25036

SOUND DETECTING AND RANGING

Ground characterization for JAPE

p 2527 N94-24213

JAPE 91: Influence of terrain masking of the acoustic propagation of helicopter noise p 2528 N94-24214

Acoustic target detection and classification using neural networks p 2529 N94-24221

Preliminary analysis of the JAPE ground vehicle test data with an artificial neural network classifier

p 2529 N94-24222

SOUND FIELDS

Beamforming in an acoustic shadow

p 2528 N94-24219

SOUND GENERATORS

Joint Acoustic Propagation Experiment (JAPE-91) Workshop

[NASA-CP-3231] p 2526 N94-24207

Joint Acoustic Propagation Experiment (JAPE)

p 2527 N94-24208

Some results gained from JAPE: An overview

p 2527 N94-24209

Effects of atmospheric variations on acoustic system performance p 2527 N94-24211

SOUND PRESSURE

Variability of measured sonic boom signatures. Volume 1: Technical report

[NASA-CR-191483-VOL-1] p 2526 N94-24172

Variability of measured sonic boom signatures. Volume 2: Data report

[NASA-CR-191483-VOL-2] p 2526 N94-24173

JAPE 91: Influence of terrain masking of the acoustic propagation of helicopter noise p 2528 N94-24214

SOUND PROPAGATION

Some results gained from JAPE: An overview

p 2527 N94-24209

Comparison of measured and predicted pure tone propagation levels from JAPE-1: An evaluation of the performance of ASOPRAT p 2527 N94-24212

Comparisons of calculated and measured helicopter noise near instrument hill p 2528 N94-24215

Preliminary analysis of amplitude and phase fluctuations in the JAPE multiple tone data to distances of 500 meters p 2528 N94-24216

Analysis of modal evolution caused by a weakly range-dependent seabed in shallow water and its application to inversion for geoacoustic properties

[AD-A273656] p 2419 N94-25435

SOUND RANGING

Some results gained from JAPE: An overview

p 2527 N94-24209

SOUND TRANSMISSION

Global acoustic mapping of ocean temperatures (GAMOT)

[AD-A273387] p 2418 N94-24719

Measurements and modeling of multitone, low-frequency acoustic data from the Arraial do Cabo range

[AD-A273406] p 2530 N94-25073

SOUND WAVES

Classical scattering theory of waves from the view point of an eigenvalue problem and application to target identification

[DE94-000472] p 2525 N94-23206

Chemically sensitive interfaces on SAW devices

[DE94-001832] p 2526 N94-23718

Similarity in wave propagation under a global relaxation law

[PB94-111028] p 2524 N94-23730

Analysis of time-domain acoustic wavefields in horizontally continuously layered configurations based on the modified Cagniard method

[PB94-111044] p 2524 N94-23731

Preliminary analysis of amplitude and phase fluctuations in the JAPE multiple tone data to distances of 500 meters p 2528 N94-24216

Dimensional analysis of acoustically propagated signals p 2528 N94-24217

Unstructured adaptive mesh computations of rotorcraft high-speed impulsive noise

[NASA-CR-195090] p 2529 N94-24307

The acoustic and instability waves of jets confined inside an acoustically lined rectangular duct

[NASA-CR-191586] p 2334 N94-24602

Responses of a finite baffled plate subject to turbulent and mean flow excitations

[NASA-CR-191570] p 2334 N94-24605

Global acoustic mapping of ocean temperatures (GAMOT)

[AD-A273387] p 2418 N94-24719

Preprocessor and adaptive beamformer for linear-frequency modulation active signals

[AD-D016008] p 2302 N94-25048

SOUNDING

Mars subsurface sounding with a ground penetrating radar p 2608 N94-23393

SOUNDING ROCKETS

PULSAUR 2

[NASA-CR-194832] p 2209 N94-23484

SOUTHERN HEMISPHERE

Northern hemisphere dust storms on Mars

p 2619 N94-24885

SOYBEANS

Chemical characterization of some aerobic liquids in CELSS p 2422 N94-23241

SPACE ADAPTATION SYNDROME

Transfer of perceptual adaptation to space sickness: What enhances an individual's ability to adapt?

[NASA-CR-188256] p 2427 N94-24227

SPACE CHARGE

Inverse free electron laser beat-wave accelerator research

[DE94-002597] p 2349 N94-23702

SPACE COMMERCIALIZATION

Space tourism: A flight of fantasy or the next major space product? Paper session 3: Products

[NASA-TM-109385] p 2194 N94-23710

National Institute of Standards and Technology Conference on Reducing the Cost of Space Infrastructure and Operations. Part 2: Topical papers

[PB94-113487] p 2194 N94-23819

Access to space studies p 2199 N94-24434

NASA technology applications team: Applications of aerospace technology

[NASA-CR-194775] p 2597 N94-24494

Design of a lunar propellant processing facility. NASA/USRA advanced program

[NASA-CR-195502] p 2266 N94-24618

SPACE COMMUNICATION

The Telecommunications and Data Acquisition Report

[NASA-CR-194766] p 2290 N94-23256

Optical subnet concepts for the deep space network

p 2292 N94-23269

Future trends in NASA space operations

p 2498 N94-23836

A reference model for space data system interconnection services p 2305 N94-23847

Reliable transfer of data from ground to space

p 2305 N94-23908

Verification of technical elements of the advanced spacecraft based upon the CCSDS recommendation

p 2207 N94-23910

Digital test signal generation: An accurate SNR calibration approach for the DSN p 2305 N94-23912

A method for interference mitigation in space communications scheduling p 2305 N94-23918

New mission requirements methodologies for services provided by the Office of Space Communications

p 2519 N94-23961

Resource allocation planning with international components p 2520 N94-23963

Scheduling the future NASA Space Network: Experiences with a flexible scheduling prototype

p 2520 N94-23965

Failure detection and recovery in the assembly/contingency subsystem p 2306 N94-25360

SPACE DEBRIS

Power beaming to space using a nuclear reactor-pumped laser

[DE94-001208] p 2348 N94-23185

The possible effects of the natural and induced space environment on the optical and thermal properties of EOS surfaces p 2207 N94-23596

Debris/ice/TPS assessment and integrated photographic analysis for Shuttle mission STS-58

[NASA-TM-109194] p 2200 N94-24577

Orbital debris and near-Earth environmental management: A chronology

[NASA-RP-1320] p 2598 N94-24644

Satellite situation report, volume 33, number 4

[NASA-TM-109677] p 2205 N94-24824

Design of orbital debris shields for oblique hypervelocity impact

[NASA-CR-195152] p 2205 N94-24828

SPACE ENVIRONMENT SIMULATION

Altitude simulation facility for testing large space motors p 2156 N94-24255

SPACE ERECTABLE STRUCTURES

Reliable redundant device for mechanisms

p 2361 N94-24030

SPACE EXPLORATION

Advanced nuclear thermal propulsion concepts

p 2217 N94-23068

Rover requirements for the planet surface segment of the space exploration initiative p 2369 N94-23377

Science strategy for Mars exploration

p 2606 N94-23380

Prospects for using mobile vehicles in missions to Mars and other planets p 2607 N94-23384

The robotic Mars rover p 2608 N94-23390

Mission and system concepts for Mars robotic precursor missions p 2608 N94-23391

Mission and system design of a long range rover mission p 2608 N94-23392

Mars 96 rover: Science, instrumentation, and control

p 2369 N94-23395

Balloon experiments at Mars 96 project

p 2608 N94-23396

Feasibility study of an automatic vehicle for planetary exploration p 2369 N94-23399

Electrical power technology for robotic planetary rovers p 2314 N94-23401

Walking machines for space p 2369 N94-23406

The mass of massive rover software

p 2464 N94-23410

Dual rover concept for Mars exploration

p 2370 N94-23415

Results of the Mojave tests of the Mars 96 rover

p 2370 N94-23416

The Jet Propulsion Laboratory space exploration: Past, present and future p 2153 N94-24242

NASA high performance computing and communications program

[NASA-TM-4554] p 2591 N94-24337

The 1993 NASA/ASEE Summer Faculty Fellowship Program

[NASA-CR-193862] p 2574 N94-24405

Demonstration of the feasibility of an integrated x ray laboratory for planetary exploration

[NASA-CR-177631] p 2598 N94-24832

The Ninth National Space Symposium

[ISBN-0-9616962-7-3] p 2598 N94-25006

The future of manned spaceflight

p 2195 N94-25067

SPACE FLIGHT

Mission engineering p 2505 N94-23881

Transfer of perceptual adaptation to space sickness: What enhances an individual's ability to adapt?

[NASA-CR-188256] p 2427 N94-24227

SPACE FLIGHT STRESS

Transfer of perceptual adaptation to space sickness: What enhances an individual's ability to adapt?

[NASA-CR-188256] p 2427 N94-24227

Artificial gravity in space flight

[AD-A273420] p 2427 N94-24928

SPACE HABITATS

Proceedings of the NIST Conference on Reducing the Cost of Space Infrastructure and Operations: Part 1: Oral presentations and discussion

[PB94-111374] p 2194 N94-23770

National Institute of Standards and Technology Conference on Reducing the Cost of Space Infrastructure and Operations. Part 2: Topical papers

[PB94-113487] p 2194 N94-23819

Crew interface analysis: Selected articles on space human factors research, 1987 - 1991

[NASA-TM-104756] p 2433 N94-24185

Preliminary design of a universal Martian lander

[NASA-CR-195529] p 2206 N94-25007

SPACE LABORATORIES

Manned Space-laboratories Control Center (MSCC) operations concept p 2505 N94-23882

SPACE MAINTENANCE

An intelligent planning and scheduling system for the HST servicing missions p 2520 N94-23964

A simulation system for Space Station extravehicular activity p 2434 N94-24192
Design and simulation of EVA tools for first servicing mission of HST [NASA-CR-194784] p 2439 N94-24857

SPACE MISSIONS
Prospects for improved instrumentation on future solar space missions p 2624 N94-22843
Solar physics within NASA's planning p 2625 N94-22845
The next Japanese solar satellite p 2625 N94-22846
Prospects for very-high-resolution solar physics with the Simuris inteferometric mission p 2625 N94-22848
Requirements for future solar-physics missions with x ray instrumentation p 2625 N94-22849
Requirements for future solar-physics missions that include UV instrumentation p 2625 N94-22851
Mission and system concepts for Mars robotic precursor missions p 2608 N94-23391
Mission and system design of a long range rover mission p 2608 N94-23392
Electronic payloads for Martian missions: A preliminary assessment of technologies p 2610 N94-23408
OASIS-CC presentation p 2385 N94-23613
Commonality of flight control systems for support of European telecommunications missions p 2304 N94-23834
NASDA's view of ground control in mission operations p 2305 N94-23835
Future trends in NASA space operations p 2498 N94-23836
The space operations at CNES p 2498 N94-23837
Common front end systems for Space Shuttle and Space Station control centers at Johnson Space Center p 2305 N94-23838
Distributed science operations for JPL planetary missions p 2500 N94-23850
SCOS2: ESA's new generation of mission control systems p 2197 N94-23851
NASDA satellite mission operation system and operations p 2501 N94-23854
Mission activities planning for a Hermes mission by means of AI-technology p 2502 N94-23858
A review of mission planning systems p 2503 N94-23866
Techniques and software for optimum and efficient mission science sequence development p 2504 N94-23872
A packet-based concept for spacecraft command planning p 2504 N94-23873
Connecting science and operations: The operations coordinator p 2504 N94-23874
The instant sequencing task: Toward constraint-checking a complex spacecraft command sequence interactively p 2504 N94-23875
Generic mission planning concepts for space astronomy missions p 2505 N94-23878
A MOS for all seasons p 2505 N94-23879
An operations concept methodology to achieve low-cost mission operations p 2505 N94-23880
The Advanced Technology Operations System: ATOS p 2508 N94-23897
The application of total quality management principles to spacecraft mission operations p 2374 N94-23931
Mission operations and command assurance: Instilling quality into flight operations p 2374 N94-23932
Security aspects of space operations data p 2515 N94-23937
Mission and science activity scheduling language p 2515 N94-23938
Expert diagnostics system as a part of analysis software for power mission operations p 2516 N94-23944
Planning: Management of predictability and uncertainty and keeping abreast of developments p 2520 N94-23967
Estimating the Deep Space Network modification costs to prepare for future space missions by using major cost drivers p 2520 N94-23968
Space operations: Archiving space science data needs further management improvements. Report to the Chairman, Subcommittee on Investigations and Oversight, Committee on Science, Space, and Technology, House of Representatives [GAO/NSIAD-94-25] p 2591 N94-24092
Use of infrared telemetry as part of a nonintrusive inflight data collection system to collect human factors data p 2434 N94-24193
A mission to Mercury and a mission to the moons of Mars [NASA-CR-195530] p 2195 N94-24619
Ultraviolet, visible, and gravity astrophysics: A plan for the 1990's [NASA-NP-152] p 2603 N94-24973

SPACE NAVIGATION
Real-time on-board orbit determination with DORIS p 2196 N94-23919
TOPEX/Poseidon precision orbit determination production and expert system p 2196 N94-23920
A real-time navigation monitoring expert system for the Space Shuttle Mission Control Center p 2202 N94-23921
XRTD: An X-Windows based, real-time radiometric display and analysis system p 2305 N94-23922
Navigation of space VLBI missions: Radioastron and VSOP p 2513 N94-23926
Satellite autonomous navigation and orbit determination using magnetometers p 2156 N94-24258

SPACE OBSERVATIONS (FROM EARTH)
Scientific Requirements for Future Solar-Physics Space Missions [ESA-SP-1157] p 2623 N94-22837
Goals of ground-based solar observations p 2624 N94-22840
Prospects for future ground-based solar observations p 2624 N94-22842
Kamiokande results on solar neutrinos and a supernova search [ICRR-REPT-294-93-6] p 2627 N94-24961
Solar neutrinos: Real-time experiments [ICRR-REPT-293-93-5] p 2627 N94-24962
CO-to-H2 conversion factor in dwarf irregular galaxies [REPT-333] p 2603 N94-24985
High spatial resolution observations of CO in CRL 618 [REPT-334] p 2604 N94-24986

SPACE PERCEPTION
Perception and 3D environment modeling for mobile robot autonomous navigation [LAAS-93117] p 2471 N94-22908
Perception in flight: Shape and motion perception, space perception, spatial orientation, and visual vestibular interaction p 2429 N94-23979
Extracting heading and temporal range from optic flow: Human performance issues p 2442 N94-25510

SPACE PLASMAS
Prospects for very-high-resolution solar physics with the Simuris inteferometric mission p 2625 N94-22848
Evolution of large-scale plasma structures in comets: Kinematics and physics [NASA-CR-194777] p 2601 N94-23251
Development of a power electronics unit for the Space Station plasma contactor [NASA-TM-106486] p 2222 N94-25201

SPACE PLATFORMS
Ground data system for Space Flyer Unit (SFU) p 2207 N94-23860

SPACE POWER REACTORS
An F2D analysis of the Flow Instability Test (FIT) experiment [DE94-001420] p 2217 N94-23193
Assessment of an SP-100 bi-modal propulsion and power system [DE94-000889] p 2218 N94-23433
SP-100 heat transport technology development [DE94-000769] p 2218 N94-23452

SPACE PROCESSING
Processing of semicrystalline polymers p 2226 N94-24351

SPACE PROGRAMS
Solar physics and the Coronas project p 2625 N94-22847
National Institute of Standards and Technology Conference on Reducing the Cost of Space Infrastructure and Operations. Part 2: Topical papers [PB94-113487] p 2194 N94-23819

SPACE RENDEZVOUS
Manned Mars mission on-orbit operations FTS capabilities assessment [NASA-CR-189328] p 2430 N94-23080

SPACE SHUTTLE BOOSTERS
Debris/Ice/TPS assessment and integrated photographic analysis for Shuttle Mission STS-61 [NASA-TM-109195] p 2199 N94-24059
Final postflight hardware evaluation report RSRM-32 (STS-57) [NASA-CR-193903] p 2200 N94-24065
Lightning tests and analyses of tunnel bond straps and shielded cables on the Space Shuttle solid rocket booster [NASA-CR-193921] p 2200 N94-24801
Postflight hardware evaluation (RSRM-29, STS-54) [NASA-CR-193895] p 2201 N94-24802

SPACE SHUTTLE MAIN ENGINE
SSME fuel preburner injector characterization p 2211 N94-23037
Flame trench analysis of NLS vehicles p 2199 N94-23249
Development of an analytical-numerical model to predict radiant emission or absorption [NASA-CR-194860] p 2453 N94-23624
System for Anomaly and Failure Detection (SAFD) system development [NASA-CR-193907] p 2372 N94-24174
CFD simulation of coaxial injectors p 2342 N94-24430
Space Shuttle Main Engine performance analysis p 2222 N94-24444
Using neural networks to assist in OPAD data analysis p 2477 N94-24452
Develop advanced nonlinear signal analysis topographical mapping system [NASA-CR-195128] p 2388 N94-24827

SPACE SHUTTLE MISSIONS
Mission planning for Shuttle Imaging Radar-C (SIR-C) with a real-time interactive planning software p 2305 N94-23842
Final postflight hardware evaluation report RSRM-32 (STS-57) [NASA-CR-193903] p 2200 N94-24065

SPACE SHUTTLE ORBITERS
A real-time navigation monitoring expert system for the Space Shuttle Mission Control Center p 2202 N94-23921
Debris/Ice/TPS assessment and integrated photographic analysis for Shuttle Mission STS-61 [NASA-TM-109195] p 2199 N94-24059
Studies of Shuttle orbiter arrestment system [NASA-TP-3370] p 2177 N94-24304
Orbital docking system centerline color television camera system test [NASA-TM-104783] p 2205 N94-24625
Development of a nondestructive vibration technique for bond assessment of Space Shuttle tiles [NASA-CR-195163] p 2201 N94-24919

SPACE SHUTTLE PAYLOADS
Mission planning for Shuttle Imaging Radar-C (SIR-C) with a real-time interactive planning software p 2305 N94-23842
The EURECA telecommanding chain: Experience with packet telecommand and telemetry systems p 2305 N94-23909

SPACE SHUTTLES
Hurricane risk assessment: Rollback or ride out p 2416 N94-23248
Implementing the space shuttle data processing system with the space generic open avionics architecture [NASA-CR-188254] p 2199 N94-23571
Common front end systems for Space Shuttle and Space Station control centers at Johnson Space Center p 2305 N94-23838
Ground data system for Space Flyer Unit (SFU) p 2207 N94-23860
Constraint-based scheduling p 2510 N94-23904
Liquid rocket propulsion: Retrospective and prospects p 2154 N94-24243
A compilation of technology spinoffs from the US Space Shuttle Program p 2578 N94-24424
Debris/ice/TPS assessment and integrated photographic analysis for Shuttle mission STS-58 [NASA-TM-109194] p 2200 N94-24577
Supersonic aerodynamic characteristics of a circular body Earth-to-Orbit vehicle [NASA-TM-4533] p 2170 N94-24716
Parallel processing methods for space based power systems p 2222 N94-25352

SPACE STATION FREEDOM
Space Station Freedom (SSF) Data Management System (DMS) performance model data base [NASA-CR-188270] p 2590 N94-23289
Thermal control system for SSF sensor/electronics [SAND-92-0652C] p 2321 N94-23640
Ground operation of robotics on Space Station Freedom p 2371 N94-23841
Space Station Freedom ground data system: Design and operations p 2518 N94-23957
Connector mechanisms in compliance with extreme space conditions p 2360 N94-24025
Spacecraft crew procedures from paper to computers p 2433 N94-24186
Using computer graphics to design Space Station Freedom viewing p 2434 N94-24191
A simulation system for Space Station extravehicular activity p 2434 N94-24192
Space Station Freedom coupling tasks: An evaluation of their telerobotic and EVA compatibility p 2436 N94-24200
Simulation of the human-telerobot interface on the Space Station p 2436 N94-24202
Weld joint concepts for on-orbit repair of Space Station Freedom fluid system tube assemblies p 2371 N94-24427
Optimal Space Station solar array gimbal angle determination via radial basis function neural networks [NASA-TM-106482] p 2195 N94-24482

Thermal control system for Space Station Freedom photovoltaic power module
[NASA-TM-105650] p 2205 N94-24825
Preliminary design of a satellite observation system for Space Station Freedom
[NASA-CR-195514] p 2209 N94-24840
Design of a resistojet for Space Station Freedom
[NASA-CR-195506] p 2221 N94-24979
A prototype to automate the video subsystem routing for the video distribution subsystem of Space Station Freedom p 2306 N94-25353
Modelling early failures in Space Station Freedom
p 2374 N94-25372
Modeling and analysis of selected space station communications and tracking subsystems
p 2306 N94-25374
Space Station flexible dynamics under plume impingement p 2208 N94-25383

SPACE STATION PAYLOADS
Columbus system support for telescience operations
p 2505 N94-23877

SPACE STATION POWER SUPPLIES
Thermal control system for Space Station Freedom photovoltaic power module
[NASA-TM-105650] p 2205 N94-24825

SPACE STATION STRUCTURES
Space Station flexible dynamics under plume impingement p 2208 N94-25383

SPACE STATIONS
Proceedings of the NIST Conference on Reducing the Cost of Space Infrastructure and Operations: Part 1: Oral presentations and discussion
[PB94-111374] p 2194 N94-23770
Common front end systems for Space Shuttle and Space Station control centers at Johnson Space Center
p 2305 N94-23838
Torque equilibrium attitudes for the Space Station
p 2208 N94-24449
Embodiment design for a multipropellant resistojet
[NASA-CR-195505] p 2221 N94-24834
Development of a power electronics unit for the Space Station plasma contactor
[NASA-TM-106486] p 2222 N94-25201
Failure detection and recovery in the assembly/contingency subsystem p 2306 N94-25360

SPACE STORAGE
Small rocket research and technology
p 2211 N94-23038

SPACE SUITS
Reach performance while wearing the Space Shuttle launch and entry suit during exposure to launch accelerations p 2436 N94-24204

SPACE TOOLS
Design and simulation of EVA tools for first servicing mission of HST
[NASA-CR-194784] p 2439 N94-24857

SPACE TRANSPORTATION
Flame trench analysis of NLS vehicles
p 2199 N94-23249
Proceedings of the NIST Conference on Reducing the Cost of Space Infrastructure and Operations: Part 1: Oral presentations and discussion
[PB94-111374] p 2194 N94-23770
National Institute of Standards and Technology Conference on Reducing the Cost of Space Infrastructure and Operations. Part 2: Topical papers
[PB94-113487] p 2194 N94-23819
The 1993 NASA/ASEE Summer Faculty Fellowship Program
[NASA-CR-193862] p 2574 N94-24405
Access to space studies p 2199 N94-24434
Lunar transportation system
[NASA-CR-195540] p 2365 N94-24805
Space transfer vehicle concepts and requirements. Volume 4: Summary of special studies
[NASA-CR-193918] p 2201 N94-24970
The Ninth National Space Symposium
[ISBN-0-9616962-7-3] p 2598 N94-25006

SPACE TRANSPORTATION SYSTEM
A minimum cost tolerance allocation method for rocket engines and robust rocket engine design
p 2222 N94-24419
Validation of a nonintrusive optical technique for the measurement of liquid mass distribution in a two-phase spray p 2548 N94-24420
Future space transportation system architecture avionics requirements p 2162 N94-25098

SPACE TRANSPORTATION SYSTEM FLIGHTS
Common front end systems for Space Shuttle and Space Station control centers at Johnson Space Center
p 2305 N94-23838
Debris/Ice/TPS assessment and integrated photographic analysis for Shuttle Mission STS-61
[NASA-TM-109195] p 2199 N94-24059
Debris/ice/TPS assessment and integrated photographic analysis for Shuttle mission STS-58
[NASA-TM-109194] p 2200 N94-24577
Postflight hardware evaluation (RSRM-29, STS-54)
[NASA-CR-193895] p 2201 N94-24802

SPACE WEAPONS
A qualified radiation hardened nonvolatile memory for space and tactical weapons applications
[DE94-001211] p 2559 N94-23186

SPACE-TIME FUNCTIONS
Introduction to a behavioral approach for continuous time systems
[ETN-94-95301] p 2492 N94-25277
The scattering and collision of gravitational waves in Friedmann-Robertson-Walker open universes
[MATHS-REPT-A-193] p 2406 N94-25430

SPACEBORNE ASTRONOMY
Scientific Requirements for Future Solar-Physics Space Missions
[ESA-SP-1157] p 2623 N94-22837
Prospects for future ground-based solar observations
p 2624 N94-22842
Interferometric astronomy on the Moon
p 2601 N94-23378
Generic mission planning concepts for space astronomy missions p 2505 N94-23878
Hubble Space Telescope high speed photometer orbital verification
[NASA-CR-189333] p 2204 N94-24226
Structure in gamma ray burst time profiles: Correlations with other observables p 2579 N94-24431
LOLA: Lunar Optical Long-baseline Array. 1992-1993 space design
[NASA-CR-195533] p 2298 N94-24582
LOITA: Lunar Optical/Infrared Telescope Array
[NASA-CR-195532] p 2546 N94-24816
Investigation relative to the Roentgen Satellite (ROSAT)
[NASA-CR-195192] p 2600 N94-25269

SPACEBORNE EXPERIMENTS
Design of a surface deformation measuring instrument for the Surface Tension Driven Convection Experiment (STDCE-2)
[NASA-CR-194758] p 2343 N94-23285
PULSAUR 2
[NASA-CR-194832] p 2209 N94-23484
Columbus system support for telescience operations
p 2505 N94-23877
Spacecraft vibrations due to mechanisms; measurements from Olympus on-station
p 2207 N94-24018
Modeling of PCG fluid dynamics: Salient results
p 2224 N94-24345
Progress toward ultra-stable lasers for use in space
[NASA-TM-109678] p 2349 N94-24488

SPACEBORNE LASERS
Progress toward ultra-stable lasers for use in space
[NASA-TM-109678] p 2349 N94-24488

SPACEBORNE TELESCOPES
Scientific Requirements for Future Solar-Physics Space Missions
[ESA-SP-1157] p 2623 N94-22837
Prospects for improved instrumentation on future solar space missions p 2624 N94-22843
The next Japanese solar satellite
p 2625 N94-22846
Why put visible solar telescopes in space?
p 2600 N94-22850
Radioastron flight operations p 2502 N94-23861
An Earth observation telescope refocusing mechanism
p 2359 N94-24014
Precision Displacement Mechanism (PDM)
p 2360 N94-24026
LOLA: Lunar Optical Long-baseline Array. 1992-1993 space design
[NASA-CR-195533] p 2298 N94-24582
LOITA: Lunar Optical/Infrared Telescope Array
[NASA-CR-195532] p 2546 N94-24816

SPACECRAFT ANTENNAS
Electrical performance of wire mesh for spacecraft deployable reflector antennas p 2275 N94-22744
Precision Displacement Mechanism (PDM)
p 2360 N94-24026

SPACECRAFT BREAKUP
Orbital debris and near-Earth environmental management: A chronology
[NASA-RP-1320] p 2598 N94-24644

SPACECRAFT COMMUNICATION
Future trends in NASA space operations
p 2498 N94-23836
A user view of the EURECA ground segment
p 2499 N94-23844
The EURECA telecommanding chain: Experience with packet telecommand and telemetry systems
p 2305 N94-23909
Representing operations procedures using temporal dependency networks p 2305 N94-23914
Situation management in the Link Monitor and Control Operator Assistant (LMCOA) p 2305 N94-23915
Using Mach threads to control DSN operational sequences p 2477 N94-23916
Modeling and analysis of selected space station communications and tracking subsystems
p 2306 N94-25374

SPACECRAFT COMPONENTS
Metal band drives in spacecraft mechanisms
p 2355 N94-23987
Development of gears for space use
p 2360 N94-24021

SPACECRAFT CONFIGURATIONS
Supersonic aerodynamic characteristics of a circular body Earth-to-Orbit vehicle
[NASA-TM-4533] p 2170 N94-24716
Near Earth asteroid rendezvous
[NASA-CR-195518] p 2195 N94-24808

SPACECRAFT CONSTRUCTION MATERIALS
Diffuse panel studies: Conclusions
p 2384 N94-23606
Establishment of computerized numerical databases on thermophysical and other properties of molten as well as solid materials and data evaluation and validation for generating recommended reliable reference data
p 2246 N94-25123

SPACECRAFT CONTAMINATION
Contamination control and plume assessment of low-energy thrusters
[NASA-TM-104585] p 2218 N94-23343
Microbiological analysis of debris from Space Transportation System (STS)-55 Spacelab D-2
[NASA-CR-193883] p 2421 N94-24310
Preliminary far-field plume sputtering characterization of the Stationary Plasma Thruster (SPT-100)
[NASA-TM-106464] p 2221 N94-24766

SPACECRAFT CONTROL
A user view of the EURECA ground segment
p 2499 N94-23844
SCOS2: ESA's new generation of mission control systems p 2197 N94-23851
Operations concepts for Mars missions with multiple mobile spacecraft p 2501 N94-23852
NASA/Goddard Space Flight Center's testbed for CCSDS compatible systems p 2197 N94-23855
The Ulysses spacecraft control and monitoring concepts and realities p 2502 N94-23862
The instant sequencing task: Toward constraint-checking a complex spacecraft command sequence interactively p 2504 N94-23875
AGENDA: A task organizer and scheduler
p 2504 N94-23876
A MOS for all seasons p 2505 N94-23879
AMFESYS: Modelling and diagnosis functions for operations support p 2506 N94-23887
ESSOPE: Towards S/C operations with reactive schedule planning p 2508 N94-23896
Customizing graphical user interface technology for spacecraft control centers p 2510 N94-23905
Automatic tools for system testing
p 2197 N94-23913
XRTD: An X-Windows based, real-time radiometric display and analysis system p 2305 N94-23922
The application of total quality management principles to spacecraft mission operations p 2374 N94-23931
Space Station Freedom ground data system: Design and operations p 2518 N94-23957
The 33rd Israel Annual Conference on Aviation and Astronautics
[ITN-94-85227] p 2153 N94-24241
Weld joint concepts for on-orbit repair of Space Station Freedom fluid system tube assemblies
p 2371 N94-24427
An Earth albedo model: A mathematical model for the radiant energy input to an orbiting spacecraft due to the diffuse reflectance of solar radiation from the Earth below
[NASA-TM-104596] p 2195 N94-24497

SPACECRAFT DEFENSE
An engineering code to analyze hypersonic thermal management systems p 2320 N94-23636

SPACECRAFT DESIGN
Life cycle cost modeling of conceptual space vehicles
[NASA-CR-194813] p 2203 N94-23329
Soviet developments of planet rovers in period of 1964 - 1990 p 2369 N94-23374
Past US studies and developments for planetary rovers p 2369 N94-23375
Integrating payload design, planning, and control in the Dutch Utilisation Centre p 2207 N94-23869
A packet-based concept for spacecraft command planning p 2504 N94-23873
Long term trending of engineering data for the Hubble Space Telescope p 2516 N94-23942

An opening mechanism for the scientific airlock outer hatch p 2360 N94-24027
Crew interface analysis: Selected articles on space human factors research, 1987 - 1991
[NASA-TM-104756] p 2433 N94-24185
Conceptual design of a two stage to orbit spacecraft
[NASA-CR-195536] p 2204 N94-24620
WISPER: Wirless Space Power Experiment
[NASA-CR-195538] p 2396 N94-24701
Supersonic aerodynamic characteristics of a circular body Earth-to-Orbit vehicle
[NASA-TM-4533] p 2170 N94-24716
Lunar transportation system
[NASA-CR-195540] p 2365 N94-24805
Near Earth asteroid rendezvous
[NASA-CR-195518] p 2195 N94-24808
Extended duration lunar lander
[NASA-CR-195527] p 2206 N94-24916
PERCIVAL mission to Mars
[NASA-CR-195541] p 2195 N94-24995
Preliminary design of a universal Martian lander
[NASA-CR-195529] p 2206 N94-25007
GRYPHON: Air launched space booster
[NASA-CR-195497] p 2199 N94-25022

SPACECRAFT DOCKING
Manned Mars mission on-orbit operations FTS capabilities assessment
[NASA-CR-189328] p 2430 N94-23080
Telerobotic rendezvous and docking vision system architecture
[NASA-CR-191329] p 2204 N94-23828
Docking mechanisms: An overview of different systems p 2357 N94-24004
Orbital docking system centerline color television camera system test
[NASA-TM-104783] p 2205 N94-24625

SPACECRAFT ELECTRONIC EQUIPMENT
Advanced mobile satellite communications using COMETS satellite in MM-wave and Ka-band
p 2288 N94-22829

SPACECRAFT ENVIRONMENTS
Connector mechanisms in compliance with extreme space conditions p 2360 N94-24025

SPACECRAFT GUIDANCE
A real-time navigation monitoring expert system for the Space Shuttle Mission Control Center
p 2202 N94-23921
Space Station Freedom ground data system: Design and operations p 2518 N94-23957
Satellite autonomous navigation and orbit determination using magnetometers p 2156 N94-24258
Intelligent systems and advanced user interfaces for design, operation, and maintenance of command management systems
[NASA-CR-195172] p 2459 N94-24797

SPACECRAFT INSTRUMENTS
Distributed science operations for JPL planetary missions p 2500 N94-23850
A packet-based concept for spacecraft command planning p 2504 N94-23873
An Earth albedo model: A mathematical model for the radiant energy input to an orbiting spacecraft due to the diffuse reflectance of solar radiation from the Earth below
[NASA-TM-104596] p 2195 N94-24497

SPACECRAFT LAUNCHING
Channel and terminal description of the ACTS mobile terminal p 2284 N94-22802
Hurricane risk assessment: Rollback or ride out
p 2416 N94-23248
GPHS-RTG's in support of the Cassini mission
[DE94-001445] p 2218 N94-23459
Galileo spacecraft anomaly and safing recovery
p 2207 N94-23864
A MOS for all seasons p 2505 N94-23879
HISPASAT launch and early operations phases: Computation and monitoring of geostationary satellite positioning p 2514 N94-23928
Preloaded launch locking devices for SILEX
p 2358 N94-24008
Reach performance while wearing the Space Shuttle launch and entry suit during exposure to launch accelerations p 2436 N94-24204
Design of an airborne launch vehicle for an air launched space booster
[NASA-CR-195534] p 2198 N94-24860

SPACECRAFT MAINTENANCE
Graphical programming: A systems approach for telerobotic servicing of space assets
[DE93-019016] p 2472 N94-23201
Task 1: Health management demonstration. Task 2: Process management environment and support of enterprise integration. Task 3: New algorithm development in the PME
[NASA-CR-188268] p 2430 N94-23290
Life cycle cost modeling of conceptual space vehicles
[NASA-CR-194813] p 2203 N94-23329
Ground operation of robotics on Space Station Freedom p 2371 N94-23841
A simulation system for Space Station extravehicular activity p 2434 N94-24192
Illumination requirements for operating a space remote manipulator p 2435 N94-24195
Weld joint concepts for on-orbit repair of Space Station Freedom fluid system tube assemblies
p 2371 N94-24427
A comparative evaluation plan for the Maintenance, Inventory, and Logistics Planning (MILP) System Human-Computer Interface (HCI) p 2588 N94-25373

SPACECRAFT MANEUVERS
XRTD: An X-Windows based, real-time radiometric display and analysis system p 2305 N94-23922
Kalman filtering applied to real-time monitoring of apogee maneuvers p 2196 N94-23923

SPACECRAFT PERFORMANCE
Orbital Signature Analyzer (OSA): A spacecraft health/safety monitoring and analysis tool
p 2203 N94-23947

SPACECRAFT POSITION INDICATORS
Satellite autonomous navigation and orbit determination using magnetometers p 2156 N94-24258

SPACECRAFT POWER SUPPLIES
Power beaming to space using a nuclear reactor-pumped laser
[DE94-001208] p 2348 N94-23185
Aerospace applications of batteries
p 2390 N94-23346
Review of super Ni/Cd cell designs and performance
p 2391 N94-23348
Impedance measurements on a spiral-wound nickel/metal hydride cell cycled in a simulated Leo orbit
p 2392 N94-23355
NASA Lewis advanced IPV nickel-hydrogen technology p 2392 N94-23356
Primary and secondary electrical space power based on advanced PEM systems p 2392 N94-23357
A high performance H2-Cl2 fuel cell for space power applications p 2394 N94-23366
The mass of massive rover software
p 2464 N94-23410
Assessment of an SP-100 bi-modal propulsion and power system
[DE94-000889] p 2218 N94-23433
GPHS-RTG's in support of the Cassini mission
[DE94-001445] p 2218 N94-23459
Low power ground-based laser illumination for electric propulsion applications
[NASA-CR-194444] p 2219 N94-23555
A review of wiring system safety in space power systems
[NASA-CR-194439] p 2203 N94-23632
The Submillimeter Wave Astronomy Satellite (SWAS) solar array system p 2361 N94-24029
Near Earth asteroid rendezvous
[NASA-CR-195518] p 2195 N94-24808
Extended duration lunar lander
[NASA-CR-195527] p 2206 N94-24916
Parallel processing methods for space based power systems p 2222 N94-25352

SPACECRAFT PROPULSION
Advanced space propulsion concepts
p 2216 N94-23067
Advanced nuclear thermal propulsion concepts
p 2217 N94-23068
An antiproton driver for ICF propulsion
p 2217 N94-23069
Lewis Research Center R and D Facilities
[NASA-TM-109400] p 2630 N94-23135
Ovonic nickel metal hydride batteries for space applications p 2391 N94-23352
Assessment of an SP-100 bi-modal propulsion and power system
[DE94-000889] p 2218 N94-23433
The 33rd Israel Annual Conference on Aviation and Astronautics
[ITN-94-85227] p 2153 N94-24241
NPS alternate techsat satellite, design project for AE-4871
[NASA-CR-195512] p 2204 N94-24590
Numerical simulation of cylindrical, self-field MPD thrusters with multiple propellants
[NASA-CR-194458] p 2220 N94-24714
Near Earth asteroid rendezvous
[NASA-CR-195518] p 2195 N94-24808
Embodiment design for a multipropellant resistojet
[NASA-CR-195505] p 2221 N94-24834

SPACECRAFT RADIATORS
Heat pipe cooled heat rejection subsystem modelling for nuclear electric propulsion
[NASA-CR-191132] p 2219 N94-24061

SPACECRAFT REENTRY
Development and application of an empirical probability distribution for the prediction error of re-entry body maximum dynamic pressure p 2207 N94-23653

SPACECRAFT RELIABILITY
Task 1: Health management demonstration. Task 2: Process management environment and support of enterprise integration. Task 3: New algorithm development in the PME
[NASA-CR-188268] p 2430 N94-23290
The development of the SOHO SUMER mechanisms
p 2361 N94-24028
Reliable redundant device for mechanisms
p 2361 N94-24030
Develop advanced nonlinear signal analysis topographical mapping system
[NASA-CR-195128] p 2388 N94-24827

SPACECRAFT SHIELDING
Magnetic shielding of interplanetary spacecraft against solar flare radiation
[NASA-CR-195539] p 2204 N94-24334
Design of orbital debris shields for oblique hypervelocity impact
[NASA-CR-195152] p 2205 N94-24828

SPACECRAFT STABILITY
Numerical simulation of Ulysses nutation
p 2207 N94-24017
Spacecraft vibrations due to mechanisms; measurements from Olympus on-station
p 2207 N94-24018

SPACECRAFT STRUCTURES
The Submillimeter Wave Astronomy Satellite (SWAS) solar array system p 2361 N94-24029
Reliable redundant device for mechanisms
p 2361 N94-24030
Extended duration lunar lander
[NASA-CR-195527] p 2206 N94-24916

SPACECRAFT SURVIVABILITY
Development and application of an empirical probability distribution for the prediction error of re-entry body maximum dynamic pressure p 2207 N94-23653

SPACECRAFT TEMPERATURE
A comparison of TSS and TRASYS in form factor calculation p 2321 N94-23638

SPACECRAFT TRACKING
SpaceOps 1992: Proceedings of the Second International Symposium on Ground Data Systems for Space Mission Operations
[NASA-CR-194486] p 2497 N94-23832
Future trends in NASA space operations
p 2498 N94-23836
Magellan spacecraft and memory state tracking: Lessons learned, future thoughts p 2207 N94-23865
GSMS and space views: Advanced spacecraft monitoring tools p 2507 N94-23890
VMPLOT: A versatile analysis tool for mission operations p 2507 N94-23891
Combining real-time monitoring and knowledge-based analysis in MARVEL p 2477 N94-23900
Resource allocation planning with international components p 2520 N94-23963
Scheduling the future NASA Space Network: Experiences with a flexible scheduling prototype
p 2520 N94-23965
Modeling and analysis of selected space station communications and tracking subsystems
p 2306 N94-25374

SPACECRAFT TRAJECTORIES
Nearly uniform deployment/retrieval strategy for space tether systems p 2156 N94-24256

SPACECREWS
Mission activities planning for a Hermes mission by means of AI-technology p 2502 N94-23858
Crew interface analysis: Selected articles on space human factors research, 1987 - 1991
[NASA-TM-104756] p 2433 N94-24185
Use of infrared telemetry as part of a nonintrusive inflight data collection system to collect human factors data
p 2434 N94-24193
Illumination requirements for operating a space remote manipulator p 2435 N94-24195
Reach performance while wearing the Space Shuttle launch and entry suit during exposure to launch accelerations p 2436 N94-24204
Development of biomechanical models for human factors evaluations p 2437 N94-24205

SPACELAB
Microbiological analysis of debris from Space Transportation System (STS)-55 Spacelab D-2
[NASA-CR-193883] p 2421 N94-24310

SPALLATION
Optical model analyses of galactic cosmic ray fragmentation in hydrogen targets
[NASA-TP-3404] p 2540 N94-23509

SPATIAL DISTRIBUTION

Lightning studies using LDAR and LLP data p 2416 N94-23238

Spatial and temporal variability of soil temperature, moisture and surface soil properties [NASA-CR-194109] p 2401 N94-23337

Tools for visualizing landscape pattern for large geographic areas [DE94-001121] p 2388 N94-24757

Dynamics of the atmosphere of Mars: Review of some outstanding problems p 2620 N94-24888

Seafloor characterization/Galapagos propagating rift [AD-A273586] p 2419 N94-25165

SPATIAL FILTERING

Electromagnetic field strength prediction in an urban environment: A useful tool for the planning of LMSS p 2283 N94-22795

Characterization of germanium stripe x ray lasers [DE93-019629] p 2347 N94-22867

SPATIAL RESOLUTION

Prospects for future ground-based solar observations p 2624 N94-22842

ASTER, a multinational Earth observing concept p 2389 N94-23840

Evaluation of image quality p 2443 N94-25514

SPECIFIC HEAT

Magnetic phases in UNiGe [DE94-000793] p 2239 N94-22939

Dynamic measurements of thermophysical properties of metals and alloys at high temperatures by subsecond pulse heating techniques p 2247 N94-25124

A thermodynamic approach to obtain materials properties for engineering applications p 2248 N94-25131

Microwave techniques for physical property measurements p 2238 N94-25134

SPECIFIC IMPULSE

Analysis and experiments of a whistler-wave plasma thruster [DE94-001533] p 2209 N94-23012

CFD modeling of microwave electrothermal thrusters p 2216 N94-23066

Design considerations of hybrid rockets p 2156 N94-24254

SPECIFICATIONS

Setting test limits under prescribed consumer loss [MEMO-1107] p 2478 N94-22725

Tools reference manual for a Requirements Specification Language (RSL), version 2.0 [NASA-CR-191461] p 2445 N94-23125

Specifications of ETS, the Enhanced Transport Service [RR-907-I] p 2589 N94-23150

Towards the formal specification of the requirements and design of a processor interface unit: HOL listings [NASA-CR-191465] p 2466 N94-23252

Towards the formal verification of the requirements and design of a processor interface unit [NASA-CR-4522] p 2467 N94-24075

Design and specification of a centralized manufacturing data management and scheduling system p 2577 N94-24416

SPECTRA

Factors affecting the identification of phytoplankton groups by means of remote sensing [NASA-TM-108799] p 2387 N94-24403

SPECTRAL BANDS

ASTER, a multinational Earth observing concept p 2389 N94-23840

Excitation mechanisms for XUV and x ray lasers [DE93-617006] p 2351 N94-25482

SPECTRAL EMISSION

Voyager planetary radio astronomy studies [NASA-CR-194776] p 2614 N94-24328

Using contour maps to search for red-shifted 511 keV features in BATSE GRB spectra p 2585 N94-24455

Liquidus temperature and optical properties measurement by containerless techniques p 2247 N94-25126

Optical properties and emissivities of liquid metals and alloys p 2248 N94-25129

SPECTRAL LINE WIDTH

Investigation of the solid-solid surface adsorption of Eu2O3 on amorphous Al2O3 [DE93-613824] p 2566 N94-25332

SPECTRAL METHODS

Rigorous analysis of thick microstrip antennas and wire antennas embedded in a substrate [EUT-92-E-263] p 2290 N94-22876

Relaxation schemes for Chebyshev spectral multigrid methods p 2484 N94-23688

Multi-grid domain decomposition approach for solution of Navier-Stokes equations in primitive variable form p 2341 N94-23693

On the dynamics of approximating schemes for dissipative nonlinear equations p 2332 N94-24168

Triangular spectral elements for incompressible fluid flow [NASA-CR-191588] p 2490 N94-24914

SPECTRAL REFLECTANCE

Optical component MAC Europe ground truth report: Flevoland 1991 (Netherlands) [BCRS-92-27] p 2382 N94-23177

The measurement and analysis of leaf spectral reflectance of two stands of loblolly pine populations p 2389 N94-24442

SPECTROMETERS

Magnetic resonance study of zinc-related defects in silicon with optimized EPR spectrometer [PB93-224640] p 2561 N94-23223

Measurement of HO2 and other trace gases in the stratosphere using a high resolution far-infrared spectrometer [NASA-CR-195173] p 2404 N94-24738

Performance of inverse photoemission spectrometer with a new bandpass photon detector of narrow bandwidth and high sensitivity [REPT-A-2659] p 2345 N94-24977

Experimental characterization of the AFIT Neutron Facility [AD-A273822] p 2539 N94-25519

SPECTRORADIOMETERS

Concept of ASTER calibration requirement p 2384 N94-23609

The measurement and analysis of leaf spectral reflectance of two stands of loblolly pine populations p 2389 N94-24442

SPECTROSCOPIC ANALYSIS

Spectroscopic IR ellipsometry of 100 and 001 oriented YBa2Cu3O(7-delta) films [PB93-201481] p 2561 N94-23445

Ultrastructure processing of macromolecular materials [AD-A273413] p 2258 N94-24782

Electrochemical behavior of ion-plated TiN and Cu-Cr coatings [AD-A273411] p 2235 N94-24784

Investigation of the solid-solid surface adsorption of Eu2O3 on amorphous Al2O3 [DE93-613824] p 2566 N94-25332

SPECTROSCOPY

Inelastic electron scattering from surfaces [DE94-001368] p 2531 N94-22733

Flue gas cleaning by pulse corona streamer [EUT-93-E-272] p 2268 N94-23174

Evaluation of inorganic zinc-rich primers using Electrochemical Impedance Spectroscopy (EIS) p 2237 N94-23233

Strong interactions studies with medium energy probes [DE94-001446] p 2540 N94-23791

On the mechanism of action of 3',5'-cyclic adenosine monophosphate: A study of four- and five-coordinated phosphorus compounds, modelling the activated state of cAMP [ISBN-9-03-860222-7] p 2226 N94-25238

CsI(Tl)-photodiode detectors for spectroscopy at low radiation levels [MPI-PHE/92-22] p 2314 N94-25457

SPECTRUM ANALYSIS

Laser linewidth measurement in the presence of RIN and using the recirculating self heterodyne method [EUT-92-E-262] p 2347 N94-22874

Electron spectroscopic studies of the neutralization of slow multicharged ions during interactions with a metal surface [DE93-041046] p 2532 N94-22956

The soft x ray halo of the spiral galaxy NGC4631 [NASA-CR-194820] p 2601 N94-23537

A rail joint: The possible initiator of corrugation? p 2269 N94-23583

Data analysis and theoretical studies of the upper mesosphere and lower thermosphere [NASA-CR-195108] p 2402 N94-24089

An investigation into acceleration determination for airborne gravimetry using the global positioning system [ISBN-0-315-59470-5] p 2175 N94-24176

ACES spectral display software: Software description [SK-1600-99-003] p 2455 N94-24297

On the analysis of clear air radar echoes severely contaminated by clutter p 2306 N94-24423

The measurement and analysis of leaf spectral reflectance of two stands of loblolly pine populations p 2389 N94-24442

Optical wavelet transform processor [AD-A273625] p 2546 N94-24731

Method for selection of wavelength bands for multispectral classification [PB93-204378] p 2388 N94-24741

Laboratory detection of C5S by pulsed-discharge-nozzle Fourier-transform microwave spectroscopy [JTN-94-80519] p 2235 N94-24984

Radar target discrimination by spectrum analysis [AD-D015982] p 2301 N94-25040

On the hadron formation time in pion-nucleus interaction [DE93-616879] p 2539 N94-25476

High latitude cusp signature observations for southward IMF B sub Z [AD-A273801] p 2406 N94-25536

SPEECH

Algorithms for speech coding systems based on linear prediction [EUT-92-E-260] p 2447 N94-22731

SPEECH RECOGNITION

Performing speech recognition research with hypercard p 2306 N94-24194

Psychophysical and signal-processing aspects of speech representation [ETN-94-95292] p 2302 N94-25077

On the quality of synthetic speech evaluation and improvements [ETN-94-95298] p 2304 N94-25234

Linear and nonlinear adaptive filtering and their application to speech intelligibility enhancement [ISBN-9-09-005342-5] p 2304 N94-25292

SPEED CONTROL

Gas turbine and operating method of the same [CA-PATENT-APPL-SN-2043039] p 2188 N94-24490

SPHERES

Static image method for computing the electric potential due to sources in a layered sphere [PB93-224970] p 2308 N94-23105

Polarizability of gyrotropic sphere [PB93-225019] p 2524 N94-23131

Fingered bola body, bola with same, and methods of use [NASA-CASE-MSC-21967-1] p 2354 N94-23822

BEM solution for the simulation of axisymmetric viscous sintering [PB93-237717] p 2336 N94-24761

Experimental characterization of the AFIT Neutron Facility [AD-A273822] p 2539 N94-25519

SPHERICAL COORDINATES

Note on the use of spherical vectorfields in Clifford analysis [PB93-237667] p 2480 N94-23437

SPHEROIDS

Monoclonal antibodies directed against surface molecules of multicell spheroids [NASA-CR-195102] p 2420 N94-23633

SPIN DYNAMICS

The structure and spin dynamics of lanthanide-bearing silicate glasses [DE94-001320] p 2252 N94-22992

Spin fluctuations in an ordered Heisenberg ferromagnet with dipolar interactions [PB93-204493] p 2524 N94-24533

SPIN EXCHANGE

Derivation of the macroscopic rate equations for the driven diffusive Ising model at pair level of approximation [DE93-616839] p 2524 N94-25208

SPIN RESONANCE

Polarized structure functions of the nucleon in the resonance region [CEBAF-PR-94-001] p 2540 N94-24663

SPIN-LATTICE RELAXATION

Interplay of magnetic and superconducting heavy fermion ground states [DE94-000680] p 2240 N94-23003

SPIRAL ANTENNAS

Low cost antennas for MSAT vehicular applications p 2289 N94-22830

SPIRAL GALAXIES

The soft x ray halo of the spiral galaxy NGC4631 [NASA-CR-194820] p 2601 N94-23537

SPLINE FUNCTIONS

Relativistic configuration interaction calculation of the correlation energies of highly-charged ions [DE94-001055] p 2532 N94-22988

SPLINES

Spline screw multiple rotations mechanism [NASA-CASE-GSC-13452-1] p 2352 N94-23078

Split spline screw [NASA-CASE-GSC-13434-1] p 2352 N94-23082

SPOT (FRENCH SATELLITE)

The space operations at CNES p 2498 N94-23837

SPOT satellite family: Past, present, and future of the operations in the mission and control center p 2500 N94-23846

SPOT4 Operational Control Center (CMP) p 2197 N94-23856

AGENDA: A task organizer and scheduler p 2504 N94-23876

Real-time on-board orbit determination with DORIS p 2196 N94-23919

SPRAY CHARACTERISTICS
Droplet turbulence interactions under subcritical and supercritical conditions p 2211 N94-23036
Development of a droplet breakup model considering aerodynamic and droplet collision effects p 2213 N94-23045
Shear coaxial injector instability mechanisms p 2213 N94-23047
SPRAY NOZZLES
Extinguishment of enclosed gas fires with water sprays [PB93-201663] p 2268 N94-23430
SPRAYED COATINGS
Characterization and durability testing of plasma-sprayed zirconia-yttria and hafnia-yttria thermal barrier coatings. Part 2: Effect of spray parameters on the performance of several hafnia-yttria and zirconia-yttria coatings [NASA-TP-3296] p 2242 N94-23467
Plasma sprayed thermal barrier coatings: Production, characterization and testing [ISBN-9-03-860082-8] p 2555 N94-25439
SPRAYERS
Development of a droplet breakup model considering aerodynamic and droplet collision effects p 2213 N94-23045
Extinguishment of enclosed gas fires with water sprays [PB93-201663] p 2268 N94-23430
Validation of a nonintrusive optical technique for the measurement of liquid mass distribution in a two-phase spray p 2548 N94-24420
SPRAYING
Droplet turbulence interactions under subcritical and supercritical conditions p 2211 N94-23036
Numerical parametric studies of spray combustion instability p 2212 N94-23041
SPREAD SPECTRUM TRANSMISSION
ACTS advanced system concepts and experimentation p 2280 N94-22780
Odyssey personal communications satellite system p 2282 N94-22787
DS-SSMA capacity for a mobile satellite system p 2286 N94-22814
Coding for frequency hopped spread spectrum satellite communications [ECE-91-1] p 2296 N94-24132
Analysis of time-diversity combining methods for frequency-hopped signals [CU-DOE-92-09] p 2300 N94-24694
Composite sequences for rapid acquisition of direct-sequence spread spectrum signals [CTN-94-60901] p 2300 N94-24696
Coding for frequency hopped spread spectrum satellite communications [ECE-92-1] p 2300 N94-24697
SPUTNIK SATELLITES
The birth of NASA: The diary of T. Keith Glennan [NASA-SP-4105] p 2630 N94-23333
SPUTTERING
Research on polycrystalline thin-film CuInGaSe2 solar cells [DE94-000203] p 2560 N94-23205
Novel two-stage selenization methods for fabrication of thin-film CIS cells and submodules [DE94-000220] p 2390 N94-23296
Selective hydrogen separation by palladium-based composite membranes [PB93-201671] p 2254 N94-23431
The statistics of sputtering [DE94-001128] p 2243 N94-23715
Thin film cadmium telluride photovoltaic cells [DE94-000201] p 2395 N94-24509
Preliminary far-field plume sputtering characterization of the Stationary Plasma Thruster (SPT-100) [NASA-TM-106464] p 2221 N94-24766
Investigation and application of microwave electron cyclotron resonance plasma physical vapour deposition [DE93-613909] p 2555 N94-25333
STABILITY
Stable non-Gaussian diffusive profiles [PB93-238053] p 2489 N94-24610
Numerical analysis of the motion of a rigid body with an attached spring-mass-damper [AD-A273825] p 2379 N94-25520
STABILITY DERIVATIVES
LinAir: A multi-element discrete vortex Weissinger aerodynamic prediction method [NASA-TM-108786] p 2167 N94-23557
STABILITY TESTS
Stability analysis of anisotropic conical shells [PB94-119054] p 2377 N94-24645
Stability of premixed laminar flames in a stagnation point flow to general disturbances [AD-A273429] p 2234 N94-24673
STABILIZATION
Median stabilization degree of a median algebra [PB93-220010] p 2479 N94-23093
Stabilization of the external kink and other MHD issues [DE94-001541] p 2552 N94-24502
Genericity of stabilizability for time-delay systems [PB93-237725] p 2475 N94-24762
Preliminary results on time-varying feedback stabilization of a nonholonomic car-like mobile robot [INRIA-RR-1512] p 2475 N94-24963
STAGGERING
FAS multigrid calculations of three dimensional flow using non-staggered grids p 2341 N94-23675
STAGNATION POINT
Stability of hypersonic flow of a detonable gas mixture in the stagnation region of a blunt body and a forward facing step p 2154 N94-24248
Stagnation region heat transfer: The influence of turbulence parameters, Reynolds number and body shape [NASA-TM-106504] p 2334 N94-24481
Stability of premixed laminar flames in a stagnation point flow to general disturbances [AD-A273429] p 2234 N94-24673
Measurements of the influence of integral length scale on stagnation region heat transfer [NASA-TM-106503] p 2338 N94-25183
STAGNATION PRESSURE
Probe shapes that measure time-averaged streamwise momentum and cross-stream turbulence intensity [NASA-CASE-ARC-11934-1] p 2317 N94-23077
STAINLESS STEELS
Tensile properties of 21-6-9 stainless steel at elevated temperatures [DE94-001852] p 2240 N94-23017
Stress corrosion cracking properties of 15-5PH steel p 2251 N94-23244
Grain-boundary microchemistry and intergranular cracking of irradiated austenitic stainless steel [DE94-000466] p 2242 N94-23457
JBK-75 stainless steel machinability study [DE94-002268] p 2242 N94-23475
Weld joint concepts for on-orbit repair of Space Station Freedom fluid system tube assemblies p 2371 N94-24427
Welding of niobium to stainless [DE94-003365] p 2365 N94-24614
Preceedings of the 12th International Congress: Corrosion Control for Low-Cost Reliability. Volume 3A: Corrosion: Specific issues [AD-A273663] p 2251 N94-25450
Proceedings of the 12th International Congress: Corrosion Control for Low-Cost Reliability. Volume 3B: Corrosion: Specific issues [AD-A273664] p 2251 N94-25451
STANDARD DEVIATION
Estimates of monthly mean soil moisture for 1979-1989 [NASA-TM-104571] p 2407 N94-23132
STANDARDIZATION
High-rate data link general specification for the NOAA-OPQ polar orbiting environmental satellites and EUMETSAT satellite systems [NASA-TM-109384] p 2208 N94-23481
Definitions in use by the visible and near-infrared, and thermal working groups p 2383 N94-23598
Activities of NIST (National Inst. of Standards and Technology) p 2384 N94-23605
NASA/Goddard Space Flight Center's testbed for CCSDS compatible systems p 2197 N94-23855
Interoperability through standardization: Electronic mail, and X Window systems p 2575 N94-24406
A simulation and evaluation of NATO Standardization Agreement (STANAG) 4214 [AD-A273195] p 2297 N94-24554
Solid state Time Base Corrector (TBC) [AD-D015981] p 2312 N94-25039
STANDARDS
Guide to software configuration management [ESA-PSS-05-09-ISSUE-1] p 2450 N94-23229
Impacts: NIST Building and Fire Research Laboratory (technical and societal) [PB94-113420] p 2270 N94-23737
US tag for ISO/TC 108 mechanical vibration and shock: Minutes of the accredited Standards Committee on Mechanical Vibration and Shock, S2 [AD-A273015] p 2376 N94-23789
STANDING WAVE RATIOS
Phase linearity of the 914H coupled-cavity traveling wave tube [NASA-CR-191056] p 2290 N94-23087
STAR FORMATION
ROSAT observations of the x ray binary HD 154791 [NASA-CR-195189] p 2600 N94-25198
STATE ESTIMATION
A mixed map/variable structure observer for target tracking p 2157 N94-24263
STATIC CHARACTERISTICS
Extending substructure based iterative solvers to multiple load and repeated analyses [NASA-CR-194822] p 2466 N94-23504
STATIC LOADS
Foil bearings p 2371 N94-24415
Nonlinear equations of motion for a panel subject to external loads [AD-A273142] p 2170 N94-24773
STATIC PRESSURE
Bridgman's concern [DE93-040900] p 2558 N94-22953
Probe systems for measuring static pressure and turbulence intensity in fluid streams [NASA-CASE-ARC-11935-1] p 2319 N94-23306
Experimental cavity pressure measurements at subsonic and transonic speeds. Static-pressure results [NASA-TP-3358] p 2169 N94-24464
STATIC TESTS
Optimization of laminate orientation to enhance failure properties [ISBN-0-315-83539-7] p 2227 N94-22892
Summary of lift and lift/cruise fan powered lift concept technology [NASA-CR-177619] p 2176 N94-23489
Effect of longitudinal vibration on the capillary limit of a wrapped screen wick copper/water heat pipe [AD-A273830] p 2571 N94-25524
STATICS
Mass properties measurement system: Dynamics and statics measurements p 2368 N94-23236
STATIONKEEPING
CNES organization for station positioning of geostationary satellites p 2501 N94-23857
The geo-control system for station keeping and colocation of geostationary satellites p 2464 N94-23927
Nearly uniform deployment/retrieval strategy for space tether systems p 2156 N94-24256
STATISTICAL ANALYSIS
Application of maximum entropy and irreducible cluster integrals to joint probability distributions for x ray structure determination [PB93-224152] p 2559 N94-23109
Maximal type test statistics based on conditional processes [PB94-111614] p 2494 N94-23771
Decision making with imprecise probabilities [PB94-111622] p 2494 N94-23772
Asymptotic confidence intervals for the length of the shortt under random censoring [PB93-237816] p 2494 N94-23774
Some generalized subset selection procedures [PB94-111655] p 2487 N94-23799
Specifying design conservatism: Worst case versus probabilistic analysis p 2374 N94-23939
Computation of large-scale statistics in decaying isotropic turbulence p 2332 N94-24167
Attachment methods in composite joints - analysis of test results by controlled experiments method p 2158 N94-24269
Verification and validation of models [PB94-110566] p 2456 N94-24507
Tail processes under heavy random censorship with applications [PB94-110632] p 2495 N94-24508
A comparison of approximate interval estimators for the Bernoulli parameter [NASA-CR-191585] p 2458 N94-24680
Annual review of aircraft accident data. US general aviation calendar year 1990 [PB94-126869] p 2173 N94-24841
Statistical methods in physical oceanography [AD-A273612] p 2419 N94-24948
A statistical analysis of recent Naval Experimental Diving Unit (NEDU) single-depth human exposures to 100 percent oxygen at pressure [AD-A273488] p 2427 N94-24950
Correlation function estimator performance in non-Gaussian spherically invariant random processes [AD-A273498] p 2496 N94-24951
Neutron star mergers and gamma-ray bursts [NASA-CR-195176] p 2629 N94-25091
NASA STI program database: Journal coverage (1990-1992) [NASA-TM-109720] p 2593 N94-25168
Designs with a small number of runs for factorial experiments [ISBN-9-03-860162-X] p 2462 N94-25237
Solving the ranking and selection indifference-zone formulation for normal distributions using computer software [AD-A273821] p 2496 N94-25518

A nighttime structure model of atmospheric optical turbulence, c2(n), derived from thermosonde and high resolution rawinsonde measurements
[AD-A273803] p 2406 N94-25537

STATISTICAL CORRELATION
Correlations in the actions of periodic orbits derived from quantum chaos
[DE93-616866] p 2571 N94-25340

STATISTICAL DECISION THEORY
Bayesian decision theory with imprecise prior probabilities applied to replacement problems
[PB93-237634] p 2481 N94-23456

STATISTICAL DISTRIBUTIONS
Limiting distribution of fractional parts of extreme order statistics
[PB93-237733] p 2494 N94-23440
Maximal type test statistics based on conditional processes
[PB94-111614] p 2494 N94-23771
Infinite divisible and stable distributions modulo 1
[PB94-110640] p 2495 N94-23815
A comparison of approximate interval estimators for the Bernoulli parameter
[NASA-CR-191585] p 2458 N94-24680
Infinitely divisible processes and their nonlinear functionals; a study of their structural, statistical and sample path properties and their prediction problems
[AD-A273468] p 2496 N94-25147

STATISTICAL MECHANICS
Fracture simulations via massively parallel molecular dynamics
[DE93-040159] p 2374 N94-22871

STATOR BLADES
Simulation of unsteady flows through stator and rotor blades of a gas turbine using the Chimera method
p 2323 N94-23652

STEADY FLOW
Detailed description of two calculation programs for incompressible, steady state boundary layer flows, applied to determine the aerodynamic characteristics of NACA12 and OA312 foils at low Reynolds numbers
[ISL-N-604/92] p 2171 N94-25461

STEADY STATE
On the estimation of the correlation dimension and its application to radar reflector discrimination
[NASA-CR-4564] p 2309 N94-23304
A direct approach to finding unknown boundary conditions in steady heat conduction
p 2322 N94-23645
A theorem regarding roots of the zero-order Bessel function of the first kind p 2325 N94-23667
Numerical solution of flame sheet problems with and without multigrid methods p 2237 N94-23683
Enhanced absorption cycle computer model
[DE94-001997] p 2271 N94-23793
Space Shuttle Main Engine performance analysis
p 2222 N94-24444

STEAM
Second law analysis of a conventional steam power plant p 2322 N94-23646
Evaluation of reducing gas turbine emissions through hydrogen-enhanced steam-injected combustion
[PB94-109873] p 2187 N94-23709

STEEL STRUCTURES
Fire safety engineering research in Norway
[PB93-201630] p 2268 N94-23429

STEELS
Thermal fatigue: A literature review
[PB93-226306] p 2375 N94-23120
Weld cladding of hard surfaces
[PB93-201598] p 2353 N94-23448
Impacts: NIST Building and Fire Research Laboratory (technical and societal)
[PB94-113420] p 2270 N94-23737
Wear reduction in ceramic bearings by surface generated pyrolytic carbon continuously replenished by ethylene gas
[NASA-CR-189214] p 2364 N94-24090
Thermophysical property sensitivity effects in steel solidification p 2246 N94-25122
Proceedings of the 12th International Congress: Corrosion Control for Low-Cost Reliability. Volume 1: Coatings
[AD-A273661] p 2251 N94-25448

STEERABLE ANTENNAS
Adaptive array antenna for satellite cellular and direct broadcast communications p 2275 N94-22745

STEERING
Aeronautical satellite antenna steering using magnetic field sensors p 2289 N94-22836
Cockpit control system conceptual design
[NASA-CR-195543] p 2190 N94-24551

STELLAR ATMOSPHERES
Molecular abundances in the envelopes around evolved stars
[PB94-104916] p 2602 N94-23812
Model atmosphere analysis of selected luminous B stars
[NASA-CR-195098] p 2599 N94-24051
The solar spectral irradiances from x ray to radio wavelengths
[NASA-CR-195203] p 2629 N94-25260

STELLAR ENVELOPES
Molecular abundances in the envelopes around evolved stars
[PB94-104916] p 2602 N94-23812
X ray enhancement of SN 1987A due to interaction with its ring-like nebula
[NIFS-265] p 2602 N94-24867
Observational studies of the clearing phase in proto-planetary disk systems
[NASA-CR-195182] p 2604 N94-25265

STELLAR EVOLUTION
Molecular abundances in the envelopes around evolved stars
[PB94-104916] p 2602 N94-23812

STELLAR LUMINOSITY
Model atmosphere analysis of selected luminous B stars
[NASA-CR-195098] p 2599 N94-24051

STELLAR MAGNETIC FIELDS
Protoplanetary disks: Theory and observation by millimeter and sub-millimeter arrays
[REPT-331] p 2603 N94-24983

STELLAR MAGNETOSPHERES
Two populations and models of gamma ray bursts
[NASA-CR-194762] p 2629 N94-22947

STELLAR MASS
Observational studies of the clearing phase in proto-planetary disk systems
[NASA-CR-195182] p 2604 N94-25265

STELLAR MASS ACCRETION
UV spectral variability in the Herbig Ae star HR 5999. 11: The accretion interpretation
[NASA-CR-189313] p 2599 N94-23334
Protoplanetary disks: Theory and observation by millimeter and sub-millimeter arrays
[REPT-331] p 2603 N94-24983

STELLAR MASS EJECTION
Solar-geophysical data number 584, April 1993. Part 2: (Comprehensive reports). Data for October 1992, and miscellaneous
[PB93-198331] p 2627 N94-23739
Molecular abundances in the envelopes around evolved stars
[PB94-104916] p 2602 N94-23812
Solar-geophysical data number 587, July 1993. Part 2: (Comprehensive reports). Data for January 1993, and miscellaneous
[PB93-232882] p 2628 N94-24990
Solar-geophysical data number 589, September 1993. Part 2: (Comprehensive reports). Data for March 1993, and miscellaneous
[PB94-117405] p 2628 N94-24994

STELLAR MODELS
The calculation of theoretical chromospheric models and the interpretation of solar spectra from rockets and spacecraft
[NASA-CR-195083] p 2626 N94-23569
Model atmosphere analysis of selected luminous B stars
[NASA-CR-195098] p 2599 N94-24051
Model development for Ulysses and SOHO
[NASA-CR-193884] p 2627 N94-24484

STELLAR OCCULTATION
Cloud, dust, and ozone vertical profiles from solar occultation measurements: Implications for dynamics
p 2617 N94-24877

STELLAR RADIATION
Nonequilibria in thermal emission from supernova remnants
[NIFS-264] p 2602 N94-24866
X ray enhancement of SN 1987A due to interaction with its ring-like nebula
[NIFS-265] p 2602 N94-24867

STELLAR SPECTRA
Voyager observations of globular clusters
[NASA-CR-194806] p 2598 N94-23330
Molecular abundances in the envelopes around evolved stars
[PB94-104916] p 2602 N94-23812
Infrared and SiO maser observations of OH/IR stars
[PB94-104890] p 2599 N94-24780

STELLAR STRUCTURE
Model development for Ulysses and SOHO
[NASA-CR-193884] p 2627 N94-24484

STELLAR TEMPERATURE
Model atmosphere analysis of selected luminous B stars
[NASA-CR-195098] p 2599 N94-24051
UV extinction and IR emission in diffuse H2 regions
[NASA-CR-195194] p 2600 N94-25270

STELLAR WINDS
X ray enhancement of SN 1987A due to interaction with its ring-like nebula
[NIFS-265] p 2602 N94-24867

STELLARATORS
Assessment of stellarators as reactors
[DE93-017775] p 2548 N94-22916
Overview of the ATF stellarator program
[DE94-000371] p 2550 N94-23462
Some theoretical problems of magnetic diagnostics in tokamaks and stellarators
[NIFS-262] p 2551 N94-24306
Pellet ablation in the large helical device
[NIFS-260] p 2551 N94-24358
Proposal of Modular Heliotron: Advanced modular helical system compatible with closed helical divertor
[NIFS-261] p 2552 N94-24458

STEPPING MOTORS
The development of the SOHO SUMER mechanisms
p 2361 N94-24028
Development of a Low-Temperature Gear Motor (LOG) p 2361 N94-24032

STEREOPHONICS
Head related transfer function pseudo-stereophony
[NASA-CASE-ARC-11919-1-NP] p 2525 N94-23312

STEREOSCOPIC VISION
Stereo for gazing and converging cameras. Part 1: Basic geometry
[OUEL-1915/92] p 2343 N94-23162
Towards real-time stereovision systems for planetary missions p 2370 N94-23422

STEREOSCOPY
Multiple-camera/motion stereoscopy for range estimation in helicopter flight p 2441 N94-25505

STERILIZATION
Comparison of numerical simulation and experimental data for steam-in-place sterilization
p 2326 N94-23669

STIELTJES INTEGRAL
On the asymptotically uniform distribution modulo 1 of extreme order statistics
[MEMO-COSOR-91-38-REV] p 2493 N94-23142
Two-point PADE approximants for Stieltjes series
p 2490 N94-24768

STIFFENING
Post buckling behaviour of stiffened composite panels loaded in cyclic compression and shear
p 2157 N94-24260
Stiffening of deployable space booms: Automated Protein Crystal Growth Facility
[NASA-CR-195547] p 2196 N94-24820

STIFFNESS
Ceramic matrix composite parts design
p 2256 N94-24237
Ultrasonic nondestructive evaluation as a tool for the development of aerospace structural ceramic composites p 2257 N94-24240
Post buckling behaviour of stiffened composite panels loaded in cyclic compression and shear
p 2157 N94-24260
Attachment methods in composite joints - analysis of test results by controlled experiments method
p 2158 N94-24269
Precision drive and speed reduction device
[AD-D016004] p 2367 N94-25046

STIFFNESS MATRIX
A multigrid solver for the semiconductor equations
p 2482 N94-23674
Wavelet multiresolution analyses adapted for the fast solution of boundary value ordinary differential equations
p 2485 N94-23691
Vibrations of variable cross section Timoshenko beams p 2160 N94-24279

STIMULATED EMISSION
Experimental and theoretical features of strong suppression and shifting phenomena in odd-photon resonant excitations and stimulated emissions
[DE94-000341] p 2535 N94-24510
Computer modeling of nonlinearities
p 2458 N94-24661
Two micron stimulated emission of activated insulating crystals
[REPT-94-002] p 2565 N94-25025
Numerical simulation and analysis of experimental results on stimulated Raman scattering in laser-plasma Hohlraum targets
[DE93-613719] p 2554 N94-25330

STIMULATION
Radar stimulator interface protocol, preliminary interface design and Doppler Beam Sharpening implementation
[DE94-002567] p 2453 N94-23701
Convective instabilities in traveling fronts of addition polymerization p 2226 N94-24352

STIRLING CYCLE
Controllability of free-piston Stirling engine/linear alternator driving a dynamic load
[NASA-TM-106497] p 2521 N94-24302
STIRRING
Hydrodynamics of stirred gas-liquid dispersions
[ETN-94-95368] p 2339 N94-25254
STOCHASTIC PROCESSES
Nonlinear smoothing for random fields
[MEMO-1110] p 2493 N94-22728
Mean-value of product-form stochastic Petri net models of slotted-ring systems
[PB94-110871] p 2494 N94-23749
A mixed map/variable structure observer for target tracking p 2157 N94-24263
Maximum likelihood modal parameter identification and realization of stochastic systems p 2157 N94-24265
Uniform limit theorems for marked point processes
[PB94-118726] p 2488 N94-24526
Probabilistic methods in problems of applied analysis
[PB94-110681] p 2495 N94-24571
Evolving neural network connectivity
[AD-A273134] p 2490 N94-24921
Change-point detection and adaptive control of time-varying systems
[AD-A273509] p 2475 N94-24943
Statistical methods in physical oceanography
[AD-A273612] p 2419 N94-24948
Determining neural network hidden layer size using evolutionary programming
[AD-A273242] p 2475 N94-25139
An exploratory stochastic model for toxic effects on cells
[AD-A273438] p 2422 N94-25146
An attempt at a macrorealistic quantum worldview
[DE93-616821] p 2570 N94-25206
Approximation to nonlinear equations using nonlinear rational models
[RR-448] p 2492 N94-25306
The anomalous transport caused by particles transverse drift
[DE93-613685] p 2554 N94-25329
STOICHIOMETRY
Laser-deposited biocompatible films and methods and apparatuses for producing same
[AD-D016017] p 2350 N94-24952
STOKES FLOW
Mathematical addenda to Hopper's model of plane stokes flow driven by capillarity on a free surface
[PB93-237691] p 2480 N94-23438
BEM solution for the simulation of axisymmetric viscous sintering
[PB93-237717] p 2336 N94-24761
STOPPING
General optimal stopping theorems for semi-Markov processes
[PB93-214989] p 2496 N94-24744
STORABLE PROPELLANTS
Small rocket research and technology
p 2211 N94-23038
STORAGE BATTERIES
Space Electrochemical Research and Technology
[NASA-CP-3228] p 2390 N94-23345
Primary and secondary electrical space power based on advanced PEM systems p 2392 N94-23357
High energy density aluminum-oxygen cell
p 2393 N94-23363
Overcharge and overdischarge protection of ambient temperature secondary lithium cells
[NASA-CASE-NPO-18343-1-CU] p 2310 N94-23823
STORAGE RINGS (PARTICLE ACCELERATORS)
Proceedings of the Fifth Users Meeting for the Advanced Photon Source
[DE93-040692] p 2531 N94-22948
STORAGE STABILITY
NASA Lewis advanced IPV nickel-hydrogen technology p 2392 N94-23356
STORAGE TANKS
Analysis and test of low profile aluminum aerospace tank dome
[NASA-TP-3442] p 2375 N94-23294
Flow and temperature distribution in a naturally stratified thermal storage tank
[AD-A273511] p 2336 N94-24821
Thermodynamic models for bounding pressurant mass requirements of cryogenic tanks
[NASA-TM-106476] p 2346 N94-25202
Metal hydride storage
[VTT-JULK-769] p 2396 N94-25417
STORMS
United States Weather Research Program (USWRP)
p 2411 N94-24375
STRAIN DISTRIBUTION
Ceramic matrix composites: Challenges and opportunities p 2255 N94-24230
Use of photostress to characterize the mechanical behavior of weldments
[NASA-CR-195201] p 2378 N94-25267
STRAIN ENERGY RELEASE RATE
Analysis of local delaminations caused by angle ply matrix cracks
[NASA-TM-109052] p 2228 N94-24083
STRAIN GAGES
Strain gage measurement errors in the transient heating of structural components
[NASA-TM-104274] p 2376 N94-23487
STRAIN HARDENING
Use of photostress to characterize the mechanical behavior of weldments
[NASA-CR-195201] p 2378 N94-25267
STRAIN MEASUREMENT
Strain gage measurement errors in the transient heating of structural components
[NASA-TM-104274] p 2376 N94-23487
Intelligent Material Systems and Structures (IMSS). Part 5: Fiber optic registration of deformation in carbon laminates 91/92
[PB93-204600] p 2544 N94-23723
Dual-purpose RTOF diffractometer facility at the ET-RR-1 reactor
[VTT-TIED-1425] p 2566 N94-25347
STRAIN RATE
Tensile properties of 21-6-9 stainless steel at elevated temperatures
[DE94-001852] p 2240 N94-23017
Stress corrosion cracking properties of 15-5PH steel
p 2251 N94-23244
Theory of extrusion: Advances and challenges
[PB93-201572] p 2241 N94-23447
Dynamic localization and second-order subgrid-scale models in large eddy simulations of channel flow
p 2329 N94-24149
On the deformation kinetics constitutive law of plastic deformation: The rate equation p 2161 N94-24289
Procedures for determining MATMOD-4V material constants
[DE94-002638] p 2245 N94-24520
High strain rate superplasticity in metals and composites
[DE94-001521] p 2229 N94-24547
Three-dimensional, inelastic response of single-edge notch bend specimens subjected to impact loading
[AD-A273302] p 2378 N94-25143
STRANGE ATTRACTORS
On the estimation of the correlation dimension and its application to radar reflector discrimination
[NASA-CR-4564] p 2309 N94-23304
STRAPS
Lightning tests and analyses of tunnel bond straps and shielded cables on the Space Shuttle solid rocket booster
[NASA-CR-193921] p 2200 N94-24801
STRATOCUMULUS CLOUDS
A regional analysis of cloudy mean spherical albedo over the marine stratocumulus region and the tropical Atlantic Ocean
[NASA-CR-194771] p 2409 N94-24049
STRATOSPHERE
An analysis of solar mesospheric temperatures for the upper stratosphere and mesosphere
[NASA-CR-194861] p 2626 N94-23626
The atmospheric effects of stratospheric aircraft: A third program report
[NASA-RP-1313] p 2398 N94-24104
Measurement of HO2 and other trace gases in the stratosphere using a high resolution far-infrared spectrometer
[NASA-CR-195173] p 2404 N94-24738
Carbon and hydrogen isotope composition and C-14 concentration in methane from sources and from the atmosphere: Implications for a global methane budget
[NASA-CR-195166] p 2399 N94-25092
Collection and evaluation of numerical models with the aim to investigate the impact of aircraft emissions
[DLR-MITT-93-06] p 2400 N94-25414
STREAM FUNCTIONS (FLUIDS)
Transition to turbulence in an elliptic vortex
p 2331 N94-24161
STRESS ANALYSIS
Computation of flows in a turn-around duct and a turbine cascade using advanced turbulence models
p 2216 N94-23062
Control of the internal stresses in plane elasticity
[PB93-225514] p 2374 N94-23112
Internal friction associated with dislocation relaxations in virgin martensite
[PB93-226280] p 2240 N94-23119
A numerical analysis of crack propagation in microcracking ceramic and ceramic composites
[DE94-001192] p 2253 N94-23183
Fully coupled nonlinear thermomechanical analysis including general contact in PALM2D
[DE94-001661] p 2568 N94-23216
Determination of fiber-matrix interface failure parameters from off-axis tests
[NASA-TM-109043] p 2241 N94-23274
Out of plane gradients in laminated composites
[NASA-CR-194875] p 2228 N94-23566
Contact analysis of rough rail surfaces
p 2270 N94-23589
Dynamic localization and second-order subgrid-scale models in large eddy simulations of channel flow
p 2329 N94-24149
Integrated stress and strength analysis of airplane structures using the data processing tool ISSY
p 2178 N94-24320
Buckling of circular cylindrical shells subjected to combined loads (axial compression, normal pressure, bending and transverse shear loading)
[PB93-215358] p 2378 N94-24745
FRANC2D: A two-dimensional crack propagation simulator. Version 2.7: User's guide
[NASA-CR-4572] p 2246 N94-25118
The complete stress field due to a dislocation located anywhere in two bonded quarter planes
[OUEL-1990/93] p 2379 N94-25478
STRESS CORROSION
Analysis of Alloy 600 and X-750 stress corrosion cracks
[DE94-001578] p 2238 N94-22936
Fracture kinetics analysis of empirical and semi-empirical corrosion fatigue relations p 2159 N94-24277
Preceedings of the 12th International Congress: Corrosion Control for Low-Cost Reliability. Volume 2: Process Industries Plant Operations
[AD-A273662] p 2251 N94-25449
Preceedings of the 12th International Congress: Corrosion Control for Low-Cost Reliability. Volume 3A: Corrosion: Specific issues
[AD-A273663] p 2251 N94-25450
STRESS CORROSION CRACKING
Analysis of Alloy 600 and X-750 stress corrosion cracks
[DE94-001578] p 2238 N94-22936
Thermally activated low temperature creep and primary water stress corrosion cracking of NiCrFe alloys
[DE94-001756] p 2241 N94-23219
NASA/ASEE Summer Faculty Fellowship Program
[NASA-CR-194678] p 2571 N94-23230
Stress corrosion cracking properties of 15-5PH steel
p 2251 N94-23244
Grain-boundary microchemistry and intergranular cracking of irradiated austenitic stainless steel
[DE94-000466] p 2242 N94-23457
Effect of irradiation on the stress corrosion cracking behavior of Alloy X-750 and Alloy 625
[DE94-001759] p 2244 N94-23792
Feasibility study of shot-peening modeling
[CTN-94-60926] p 2244 N94-24170
Microstructure and micromechanical behaviour of CMCs p 2256 N94-24236
STRESS CYCLES
Fundamentals of fatigue analysis
[PB93-226264] p 2374 N94-23118
Review of super Ni/Cd cell designs and performance
p 2391 N94-23348
STRESS DISTRIBUTION
A numerical analysis of crack propagation in microcracking ceramic and ceramic composites
[DE94-001192] p 2253 N94-23183
Development of a theory of the wear of ceramics
[DE94-002773] p 2254 N94-23783
Ceramic matrix composites: Challenges and opportunities p 2255 N94-24230
Interface evaluation in ceramic composites
p 2255 N94-24231
Fracture kinetics analysis of empirical and semi-empirical corrosion fatigue relations p 2159 N94-24277
The complete stress field due to a dislocation located anywhere in two bonded quarter planes
[OUEL-1990/93] p 2379 N94-25478
STRESS FUNCTIONS
Stability analysis of anisotropic conical shells
[PB94-119054] p 2377 N94-24645
STRESS INTENSITY FACTORS
Fatigue life and crack growth prediction methodology
[NASA-TM-109044] p 2228 N94-23279
Effect of irradiation on the stress corrosion cracking behavior of Alloy X-750 and Alloy 625
[DE94-001759] p 2244 N94-23792
FRANC2D: A two-dimensional crack propagation simulator. Version 2.7: User's guide
[NASA-CR-4572] p 2246 N94-25118

STRESS MEASUREMENT
Method of determining shear stress employing a monomer-polymer laminate structure
[NASA-CASE-LAR-14654-2] p 2375 N94-23308
Skin friction measurement in complex flows using thin oil film techniques
[NASA-CR-194872] p 2327 N94-24098
Feasibility study of shot-peening modeling
[CTN-94-60926] p 2244 N94-24170
Alternatives for reinforcement: Fiber composites
[VTT-TIED-1412] p 2230 N94-25386
STRESS RELAXATION
Thermally activated low temperature creep and primary water stress corrosion cracking of NiCrFe alloys
[DE94-001756] p 2241 N94-23219
On the deformation kinetics constitutive law of plastic deformation: The rate equation p 2161 N94-24289
STRESS TENSORS
On the large eddy simulation of turbulent flows in complex geometry p 2329 N94-24148
Super Beltrami differentials and N equal to 4 superconformal anomalies
[DE93-613047] p 2491 N94-25166
STRESS WAVES
Bibliographic Retrieval System (BARS), Sandia Shock Compression (SSC) database Shock Physics Index
[DE94-001679] p 2589 N94-23126
Bibliographic Retrieval System (BARS). Sandia Shock Compression (SSC) database Shock Physics Index (SPHINX) database. Volume 1: UNIX version query guide customized application for INGRES
[DE94-001703] p 2589 N94-23127
STRESS-STRAIN DIAGRAMS
Constitutive modelling of fiber-reinforced concrete under uniaxial tensile loading
[VTT-JULK-774] p 2379 N94-25385
STRESS-STRAIN RELATIONSHIPS
The effects of texture and strain on the r-va lue of heavy gauge tantalum plate
[DE94-000690] p 2242 N94-23541
Material data representation of hysteresis loops for Hastelloy X using artificial neural networks
[NASA-TM-105990] p 2376 N94-23551
Microstructure and micromechanical behaviour of CMCs p 2256 N94-24236
Mean stress models for low cycle fatigue of a nickel-base superalloy p 2159 N94-24276
Evaluation of advanced materials through experimental mechanics and modelling p 2374 N94-24454
Test methods for composites: A status report. Volume 3: Shear test methods
[AD-A273561] p 2230 N94-25163
STRESSES
Drying deformable media: Kinetics, shrinkage and stresses
[ETN-94-95314] p 2236 N94-25302
STRETCHING
Intelligent Material Systems and Structures (IMSS). Part 5: Fiber optic registration of deformation in carbon laminates 91/92
[PB93-204600] p 2544 N94-23723
STRIATION
Temperature dependence of protein solubility-determination, application to crystallization, and growth kinetics studies p 2224 N94-24344
STRING THEORY
Flavor changing strings and domain walls
[DE93-633217] p 2532 N94-22970
The current status of observational constraints on cosmic strings
[DE94-001505] p 2601 N94-23010
The Casimir energy of the rigid string with massive ends
[DE93-616851] p 2492 N94-25338
Superconducting cosmic strings near the electroweak scale and cosmic-ray propagation
[MPI-PHE/93-05] p 2629 N94-25459
On the hadron formation time in pion-nucleus interaction
[DE93-616879] p 2539 N94-25476
STRINGERS
CORSS: Cylinder Optimization of Rings, Skin, and Stringers
[NASA-TP-3457] p 2490 N94-24727
STRIP MINING
Manned Mars mission on-orbit operations FTS capabilities assessment
[NASA-CR-189328] p 2430 N94-23080
STROKE VOLUME
Evaluation of bioimpedance for the measurement of physiologic variables as related to hemodynamic studies in space flight p 2427 N94-25378
STROUHAL NUMBER
Computational fluid mechanics
[NASA-CR-194765] p 2337 N94-24859
STRUCTURAL ANALYSIS
Probabilistic analysis of mechanical systems
[DE93-041145] p 2371 N94-22918
Structural analysis of a superconducting central solenoid for the Tokamak Physics Experiment
[DE94-001536] p 2549 N94-23014
Review of the probabilistic failure analysis methodology and other probabilistic approaches for application in aerospace structural design
[NASA-TP-3434] p 2376 N94-23342
A structural design decomposition method utilizing substructuring
[NASA-TM-107750] p 2376 N94-23368
A review of the Workshop on Fatigue Life Methodologies for Wind Turbines
[DE94-002039] p 2394 N94-23472
A prediction method for the compressive strength of impact damaged composite laminates
[CTN-94-60925] p 2229 N94-24137
New computing systems, future computing environment, and their implications on structural analysis and design p 2177 N94-24314
Integrated stress and strength analysis of airplane structures using the data processing tool ISSY p 2178 N94-24320
Structural design criteria for filament-wound composite shells
[NASA-CR-195125] p 2229 N94-24402
A study of the core module simulator floor capability p 2380 N94-24418
Hydro-elastic analysis using a selection of commercial analysis programs
[PB94-118734] p 2376 N94-24478
Stability analysis of anisotropic conical shells
[PB94-119054] p 2377 N94-24645
CORSS: Cylinder Optimization of Rings, Skin, and Stringers
[NASA-TP-3457] p 2490 N94-24727
Pre-design study of a general purpose vehicle simulator platform
[PB93-215366] p 2193 N94-24739
Conceptual design proposal: HUGO global range/mobility transport aircraft
[NASA-CR-195501] p 2181 N94-24787
Aircraft empennage structural detail design
[NASA-CR-195486] p 2183 N94-24969
Probabilistic assessment of smart composite structures
[NASA-TM-106358] p 2378 N94-25188
STRUCTURAL DESIGN
The history of development of molybdenum alloys for structural applications
[DE94-000389] p 2239 N94-22958
Control of the internal stresses in plane elasticity
[PB93-225514] p 2374 N94-23112
Review of the probabilistic failure analysis methodology and other probabilistic approaches for application in aerospace structural design
[NASA-TP-3434] p 2376 N94-23342
A structural design decomposition method utilizing substructuring
[NASA-TM-107750] p 2376 N94-23368
Strain gage measurement errors in the transient heating of structural components
[NASA-TM-104274] p 2376 N94-23487
A structural design methodology for large angle articulated trusses considering realistic joint modeling p 2376 N94-23560
An Earth observation telescope refocusing mechanism p 2359 N94-24014
The Submillimeter Wave Astronomy Satellite (SWAS) solar array system p 2361 N94-24029
CMC design consequences p 2256 N94-24238
Integrated approach in modelling, testing, and design of gradient-CVI derived CMC components p 2256 N94-24239
Aeroelastic, aeromechanical and vibration problems in helicopters p 2154 N94-24244
Application of concurrent engineering principles to aircraft structural design p 2178 N94-24321
Some practical problems in multidisciplinary design and optimisation p 2178 N94-24322
Current and future design methods for large transport aircraft p 2179 N94-24324
Impact damage in filament wound composite bottles p 2231 N94-24421
Active control of buildings during earthquakes
[NASA-TM-109033] p 2271 N94-24473
Pre-design study of a general purpose vehicle simulator platform
[PB93-215366] p 2193 N94-24739
Design of a recumbent seating system
[NASA-CR-195503] p 2438 N94-24786
Merits and limitations of optimality criteria method for structural optimization
[NASA-TP-3373] p 2378 N94-24845
Aircraft empennage structural detail design
[NASA-CR-195486] p 2183 N94-24969
Aircraft wing structural detail design (wing, aileron, flaps, and subsystems)
[NASA-CR-195487] p 2183 N94-24974
STRUCTURAL DESIGN CRITERIA
The Columbus solar array mechanisms p 2356 N94-23994
Primary deployment mechanism for the European Polar Platform p 2207 N94-23995
HERA (Hermes robot arm) overview p 2357 N94-24005
Preloaded launch locking devices for SILEX p 2358 N94-24008
The development of the HERA Test Facility (HTF) p 2197 N94-24020
The low noise momentum wheel MW-X: EM design and predicted properties p 2360 N94-24024
The Submillimeter Wave Astronomy Satellite (SWAS) solar array system p 2361 N94-24029
Multipurpose clamping device with electrical connector for in orbit attachment of payloads p 2361 N94-24035
Continuous gust response and sensitivity derivatives using state-space models p 2161 N94-24287
Structural design criteria for filament-wound composite shells
[NASA-CR-195125] p 2229 N94-24402
Merits and limitations of optimality criteria method for structural optimization
[NASA-TP-3373] p 2378 N94-24845
STRUCTURAL ENGINEERING
Impacts: NIST Building and Fire Research Laboratory (technical and societal)
[PB94-113420] p 2270 N94-23737
LSS systems planning and performance program
[NASA-CR-193882] p 2196 N94-24309
Frameworks for integrated airframe design p 2178 N94-24318
STRUCTURAL FAILURE
Probabilistic analysis of mechanical systems
[DE93-041145] p 2371 N94-22918
A study of the core module simulator floor capability p 2380 N94-24418
Impact damage in filament wound composite bottles p 2231 N94-24421
J-integral patch for finite element analysis of dynamic fracture due to impact of pressure vessels p 2381 N94-24429
STRUCTURAL MEMBERS
Inverse dynamics of a rigid rod system as a simplified model of flexible beam p 2160 N94-24281
Reduction of structural loads using maneuver load control on the Advanced Fighter Technology Integration (AFTI)/F-111 mission adaptive wing
[NASA-TM-4526] p 2168 N94-24295
STRUCTURAL RELIABILITY
Impacts: NIST Building and Fire Research Laboratory (technical and societal)
[PB94-113420] p 2270 N94-23737
STRUCTURAL STRAIN
Mean stress models for low cycle fatigue of a nickel-base superalloy p 2159 N94-24276
STRUCTURAL VIBRATION
Adaptive nonlinear polynomial neural networks for control of boundary layer/structural interaction
[NASA-CR-189645] p 2525 N94-23698
Control algorithms for effective operation of variable-speed wind turbines
[DE94-002607] p 2394 N94-23704
Microwelding due to random vibration p 2359 N94-24019
Vibrational power transmission analysis of machinery installations in ships with the objective of noise reduction
[ISVR-TR-216] p 2363 N94-24076
Responses of a finite baffled plate subject to turbulent and mean flow excitations
[NASA-CR-191570] p 2334 N94-24805
Influence of backup bearings and support structure dynamics on the behavior of rotors with active supports
[NASA-CR-195106] p 2365 N94-24751
Space Station flexible dynamics under plume impingement p 2208 N94-25383
Modeling of a large undamped space structure using time domain techniques
[AD-A273828] p 2206 N94-25523
STRUTS
Continuum representations of cellular solids
[DE94-001706] p 2375 N94-23217
Design of a recumbent seating system
[NASA-CR-195503] p 2438 N94-24786
STUDENTS
Design of an airborne launch vehicle for an air launched space booster
[NASA-CR-195534] p 2198 N94-24860
The Triton: Design concepts and methods
[NASA-CR-195542] p 2184 N94-25004

Magnetic Earth Ionosphere Resonant Frequencies
[NASA-CR-195131] p 2303 N94-25191

STYRENES

Microstructure of styrene methyl methacrylate copolymers grafted onto polybutadiene seeds
[ETN-94-95360] p 2262 N94-25225

SUBDUCTION (GEOLOGY)

Reactive trace metals as indicators of subduction and ventilation processes in the ocean
[AD-A273585] p 2419 N94-25164

SUBDWARF STARS

UV-bright stars in globular clusters
[NASA-CR-189324] p 2599 N94-24666

SUBLIMATION

On the stability of the process of formation of combustion generated particles by coagulation and simultaneous shrinkage due to particle oxidation p 2159 N94-24274

SUBMILLIMETER WAVES

Investigation of passive atmospheric sounding using millimeter and submillimeter wavelength channels
[NASA-CR-194858] p 2404 N94-24843

SUBROUTINE LIBRARIES (COMPUTERS)

Users manual for the Chameleon parallel programming tools
[DE94-001934] p 2465 N94-22973

ASPT software source code: Development system package, library component
[CTN-94-60905] p 2455 N94-24134

Horatio: Libraries for vision applications, release 2.0
[OUEL-1967/92] p 2593 N94-25326

SUBROUTINES

Implementation of the Baldwin-Barth turbulence model into the ZETA code and its diagnosis
[NASA-CR-194795] p 2335 N94-24640

SUBSONIC FLOW

An experimental study of the flow field surrounding a subsonic jet in a cross flow
[NASA-CR-194770] p 2317 N94-23072

Two-dimensional Navier-Stokes computations of subsonic and supersonic flows through turbine cascades
[PB93-226223] p 2317 N94-23114

Computational study of GA(W)-1: Airfoil near stall
[PB93-226249] p 2165 N94-23116

Refraction of high frequency noise in an arbitrary jet flow
[NASA-TM-106465] p 2525 N94-23464

Unsteady jet flow computation towards noise prediction
[NASA-CR-194449] p 2153 N94-23553

Three dimensional study of an airplane wing and its wake in the subsonic regime
[ISBN-0-315-58963-9] p 2168 N94-24178

Development and validation of RNG methodology for compressible turbulence
[AD-A273469] p 2337 N94-24929

Sub-sonic flow about a slender profile in a tunnel having perforated walls
[AD-A273184] p 2170 N94-25137

A numerical investigation of the artificial compressibility method for the solution of the Navier-Stokes equations
[CRANFIELD-AERO-9213] p 2340 N94-25486

Off-design performance of crenulated blades in a linear compressor cascade
[AD-A273744] p 2340 N94-25534

SUBSONIC SPEED

Experimental cavity pressure measurements at subsonic and transonic speeds. Static-pressure results
[NASA-TP-3358] p 2169 N94-24464

Nonlinear aerodynamic modeling using multivariate orthogonal functions p 2164 N94-25110

SUBSTITUTES

US Department of Energy phaseout of CFC-refrigerants
[DE94-001668] p 2397 N94-23016

Ozone depletion, paradigms, and politics
[DE94-001600] p 2398 N94-24506

SUBSTRATES

Theoretical studies of wave propagation in multilayered piezoelectric media
[DE93-040273] p 2371 N94-22872

Novel two-stage selenization methods for fabrication of thin-film CIS cells and submodules
[DE94-000220] p 2390 N94-23296

Method of determining shear stress employing a monomer-polymer laminate structure
[NASA-CASE-LAR-14654-2] p 2375 N94-23308

Hairy carbon electrodes studied by cyclic voltammetry and battery discharge testing p 2394 N94-23367

Infrared analysis of vapor phase deposited tricresylphosphate (TCP)
[NASA-TM-106423] p 2253 N94-23371

Method of forming silicon structures with selectable optical characteristics
[NASA-CASE-NPO-18625-1-CU] p 2563 N94-23972

Chemically sensitive interfacial force microscopy: Contact potential measurements of self-assembling monolayer films
[AD-A273135] p 2234 N94-24772

Laser-deposited biocompatible films and methods and apparatuses for producing same
[AD-D016017] p 2350 N94-24952

Field emitter array
[AD-D016023] p 2303 N94-25150

SUBSTRUCTURES

Extending substructure based iterative solvers to multiple load and repeated analyses
[NASA-CR-194822] p 2466 N94-23504

SUCTION

Vortex generation and wave-vortex interaction over a concave plate with roughness and suction
[NASA-CR-191589] p 2337 N94-24869

SUD AVIATION AIRCRAFT

Remote vibration measurements at a sud aviation alouette 3 helicopter with a CW CO2-laser system
[AD-A273818] p 2190 N94-25516

SUDDEN IONOSPHERIC DISTURBANCES

Solar-geophysical data number 584, April 1993. Part 1: (Prompt reports). Data for February, March, 1993, and late data
[PB93-198323] p 2626 N94-23738

Solar-geophysical data number 587, July 1993. Part 1: (Prompt reports). Data for June, May 1993, and late data
[PB93-232874] p 2628 N94-24989

SULFATES

Integrated hydrometallurgical jarosite treatment
[PB93-217990] p 2232 N94-22983

Cloud-free aerosol optical depth determination over oceans from satellite radiometry
[DE94-001897] p 2386 N94-23779

SULFIDATION

Ultraviolet photosulfidation of III-V compound semiconductors for electronic passivation
[DE94-001417] p 2555 N94-22717

SULFIDES

High-resolution soft x ray photoionization studies of selected molecules
[DE94-000568] p 2532 N94-23002

Spin fluctuations in an ordered Heisenberg ferromagnet with dipolar interactions
[PB93-204493] p 2524 N94-24533

Laboratory detection of C5S by pulsed-discharge-nozzle Fourier-transform microwave spectroscopy
[JTN-94-80519] p 2235 N94-24984

SULFUR

Electrochemical sulfur passivation of visible (approximately 670nm) AlGaInP lasers
[DE94-002293] p 2350 N94-24659

SULFUR DIOXIDES

Participation in TOMS missions
[NASA-CR-195110] p 2398 N94-24078

Nimbus-7 Total Ozone Mapping Spectrometer (TOMS) data products user's guide
[NASA-RP-1323] p 2410 N94-24355

SO2 on Venus: A final cross-calibration with Pioneer Venus
[NASA-CR-195162] p 2599 N94-24988

SULFUR FLUORIDES

Radiative forcing calculations for SF6 and CH4 using a correlated k-distribution transmission model
[DE94-001855] p 2397 N94-23700

Research for electric energy systems
[DE94-001839] p 2293 N94-23719

SULFUR HEXAFLUORIDE

High-resolution soft x ray photoionization studies of selected molecules
[DE94-000568] p 2532 N94-23002

SUN

The calculation of theoretical chromospheric models and the interpretation of solar spectra from rockets and spacecraft
[NASA-CR-195083] p 2626 N94-23569

SUPERCOMPUTERS

Supercomputer networking for space science applications
[NASA-CR-194876] p 2465 N94-23085

Applications of CFD codes and supercomputers to aircraft design activities p 2177 N94-24316

High-performance computing and communications
[DE94-002215] p 2457 N94-24566

SUPERCONDUCTING CAVITY RESONATORS

Welding of niobium to stainless
[DE94-003365] p 2365 N94-24614

SUPERCONDUCTING FILMS

Spectroscopic IR ellipsometry of 100 and 001 oriented YBa2Cu3O(7-delta) films
[PB93-201481] p 2561 N94-23445

Investigation and application of microwave electron cyclotron resonance plasma physical vapour deposition
[DE93-613909] p 2555 N94-25333

SUPERCONDUCTING MAGNETS

Assessment of stellarators as reactors
[DE93-017775] p 2548 N94-22916

Design of microchannels for cryostabilization of high temperature superconducting magnets
[DE94-001324] p 2559 N94-22993

Superconducting magnet system for the TPX Tokamak
[DE94-001535] p 2549 N94-23013

Structural analysis of a superconducting central solenoid for the Tokamak Physics Experiment
[DE94-001536] p 2549 N94-23014

Simple estimate of stored energy and conductor insulation voltage-withstand requirements for advanced solenoid magnet designs
[DE93-041048] p 2307 N94-23019

A system for managing information at ATLAS
[DE94-001337] p 2590 N94-23190

Normal zone propagation and thermal hydraulic quenchback in a cable-in-conduit superconductor
[DE94-002457] p 2271 N94-24568

SUPERCONDUCTING SUPER COLLIDER

B-quark production at hadron colliders
[DE94-001459] p 2534 N94-23806

The use of harmonics in 3-D magnetic fields
[DE94-002274] p 2299 N94-24656

SUPERCONDUCTIVITY

Anomalous magnetoresistance behavior of superconducting Nd(2-x)Ce(x)CuO(4-y) single crystal
[DE94-000806] p 2558 N94-22941

A valence-fluctuation theory of cuprate superconductivity
[DE94-000887] p 2558 N94-22942

Interplay of magnetic and superconducting heavy fermion ground states
[DE94-000680] p 2240 N94-23003

Muon spin relaxation studies of the interplay between magnetism and superconductivity in heavy fermion systems
[DE94-000700] p 2559 N94-23006

Structural analysis of a superconducting central solenoid for the Tokamak Physics Experiment
[DE94-001536] p 2549 N94-23014

Exact transformation of the anisotropic Ginzburg-Landau model and its consequences
[DE94-002208] p 2562 N94-23795

Reduction of hydrocarbon impurities in 200 l/h helium liquefier-refrigerator system
[NIFS-259] p 2271 N94-24459

Superconducting energy storage
[DE94-002248] p 2395 N94-24654

On superconductivity of alpha-(BEDT-TTF)2KHg(SCN)4
[REPT-A-2660] p 2564 N94-24978

Tunnelling in metallic contacts on high-T(c) superconductors: A story of charge carriers in YBa2Cu3O(7-delta) and Bi2CaSr2Cu2O(8+delta)
[ISBN-9-03-860142-5] p 2565 N94-25280

Lattice dynamics of Ba(1-x)K(x)BiO3 as studied by neutron scattering and computer simulation
[DE93-617053] p 2567 N94-25424

Superconducting cosmic strings near the electroweak scale and cosmic-ray propagation
[MPI-PHE/93-05] p 2629 N94-25459

SUPERCONDUCTORS

A nonlinear degenerating parabolic problem from the theory of type 2 superconductors
[MEMO-1112] p 2555 N94-22730

Interplay of magnetic and superconducting heavy fermion ground states
[DE94-000680] p 2240 N94-23003

Muon spin relaxation studies of the interplay between magnetism and superconductivity in heavy fermion systems
[DE94-000700] p 2559 N94-23006

Normal zone propagation and thermal hydraulic quenchback in a cable-in-conduit superconductor
[DE94-002457] p 2271 N94-24568

Thermomechanical processing of Ag-clad Bi2Sr2CaCu2O(x) superconductors
[DE94-002347] p 2563 N94-24624

Superconducting energy storage
[DE94-002248] p 2395 N94-24654

On superconductivity of alpha-(BEDT-TTF)2KHg(SCN)4
[REPT-A-2660] p 2564 N94-24978

A vibrating wire parallel to a type 2 superconducting slab of arbitrary thickness
[DE93-617134] p 2525 N94-25389

Effects of a vibrating wire carrying DC current on a moving type 2 superconducting slab of arbitrary thickness
[DE93-617136] p 2566 N94-25391

SUPERCRITICAL AIRFOILS

JB-300: An advanced medium size transport for 2005
[NASA-CR-195499] p 2179 N94-24401

SUPERCRITICAL FLUIDS
Integral equations for the microstructures of supercritical fluids [DE94-002460] p 2535 N94-24569
SUPERCRITICAL WINGS
Reduction of structural loads using maneuver load control on the Advanced Fighter Technology Integration (AFTI)/F-111 mission adaptive wing [NASA-TM-4526] p 2168 N94-24295
SUPERFLUIDITY
Acoustic and optical investigations of superfluid He-3 [PB93-224889] p 2523 N94-23101
SUPERGRAVITY
The 2D supergravity and integrable systems [DE93-616848] p 2570 N94-25336
SUPERHEATING
Surface barrier of a uniaxial anisotropic type 2 superconducting cylinder [DE93-617137] p 2566 N94-25392
SUPERHIGH FREQUENCIES
The provision of spectrum for feeder links of non-geostationary mobile satellites p 2276 N94-22751
Measurements on the satellite-mobile channel at L and S bands p 2282 N94-22791
K-band mobile propagation measurements using ACTS p 2283 N94-22792
Performance of the X-/Ka/KABLE-band dichroic plate in the DSS-13 beam waveguide antenna p 2291 N94-23261
Precipitation measurement using SIR-C: A feasibility study. Investigation at nadir [NASA-CR-195103] p 2410 N94-24126
A small satellite design for deep space network testing and training [NASA-CR-195526] p 2205 N94-24702
SUPERLATTICES
High-T(c) superconducting superlattices [DE93-019200] p 2556 N94-22864
Report of the Joint Seminar on Solid State Physics, Atomic and Molecular Physics, and Materials Science in the Energy Region of Tandem Accelerators [DE93-508268] p 2548 N94-22924
Photo-induced antiferromagnetic interlayer coupling in Fe superlattices with iron silicide spacers [DE94-001345] p 2559 N94-22995
Quantum tunneling transport of electrons in double-barrier heterostructures: Theory and modeling [ETN-94-95332] p 2565 N94-25059
Effect of high frequency field on the transport properties of superlattice [DE93-617047] p 2568 N94-25447
SUPERNOVA REMNANTS
Nonequilibria in thermal emission from supernova remnants [NIFS-264] p 2602 N94-24866
X ray enhancement of SN 1987A due to interaction with its ring-like nebula [NIFS-265] p 2602 N94-24867
Shocked clouds in the Cygnus Loop [NASA-CR-195190] p 2600 N94-25178
Investigation relative to the Roentgen Satellite (ROSAT) [NASA-CR-195192] p 2600 N94-25269
SUPERNOVA 1987A
X ray enhancement of SN 1987A due to interaction with its ring-like nebula [NIFS-265] p 2602 N94-24867
SUPERNOVAE
Kamiokande results on solar neutrinos and a supernova search [ICRR-REPT-294-93-6] p 2627 N94-24961
SUPERPLASTICITY
Gas-pressure forming of superplastic ceramic sheet [DE94-001520] p 2252 N94-22930
Materials Science and Engineering [DE94-003018] p 2228 N94-23493
High strain rate superplasticity in metals and composites [DE94-001521] p 2229 N94-24547
The nanometer-scale mechanics of gold films [AD-A273307] p 2565 N94-25086
SUPERSONIC AIRCRAFT
Sabot high speed interceptor AE 4273 aircraft design [NASA-CR-195495] p 2183 N94-24971
SUPERSONIC BOUNDARY LAYERS
Relationship between transition and modes of instability in supersonic boundary layers [NASA-CR-4562] p 2336 N94-24725
SUPERSONIC COMBUSTION
Proceedings of Workshop on Laser Diagnostics in Fluid Mechanics and Combustion [AD-A272808] p 2347 N94-22914
SUPERSONIC COMBUSTION RAMJET ENGINES
Experimental investigation of generic three-dimensional sidewall-compression scramjet inlets at Mach 6 in tetrafluoromethane [NASA-TM-4497] p 2319 N94-23339
Shock tunnel studies of scramjet phenomena, supplement 7 [NASA-CR-191572] p 2319 N94-23513
Shock tunnel studies of scramjet phenomena, supplement 8 [NASA-CR-191573] p 2320 N94-23532
NASA/USRA advanced design program [NASA-CR-195548] p 2180 N94-24492
HYPULSE combustor analysis [NASA-CR-191579] p 2336 N94-24771
Effect of aeroelastic-propulsive interactions on flight dynamics of a hypersonic vehicle p 2164 N94-25113
SUPERSONIC FLIGHT
An experimental investigation of a Mach 3.0 high-speed civil transport at supersonic speeds [NASA-TP-3365] p 2169 N94-24311
SUPERSONIC FLOW
Two-dimensional Navier-Stokes computations of subsonic and supersonic flows through turbine cascades [PB93-226223] p 2317 N94-23114
Direct simulation of isothermal-wall supersonic channel flow p 2172 N94-24164
Effects of shock strength on shock turbulence interaction p 2332 N94-24165
Numerical solutions of the complete Navier-Stokes equations [NASA-CR-194780] p 2337 N94-24858
Development and validation of RNG methodology for compressible turbulence [AD-A273469] p 2337 N94-24929
Turbulence models and Reynolds analogy for two-dimensional supersonic compression ramp flow [NASA-TM-106474] p 2337 N94-25119
SUPERSONIC JET FLOW
Refraction of high frequency noise in an arbitrary jet flow [NASA-TM-106465] p 2525 N94-23464
The acoustic and instability waves of jets confined inside an acoustically lined rectangular duct [NASA-CR-191586] p 2334 N94-24602
The effects of profiles on supersonic jet noise [NASA-CR-195184] p 2530 N94-25177
SUPERSONIC NOZZLES
Supersonic minimum length nozzle design for dense gases p 2171 N94-23656
SUPERSONIC TRANSPORTS
Simplified, inverse, ejector design tool [NASA-CR-194438] p 2166 N94-23511
The atmospheric effects of stratospheric aircraft: A third program report [NASA-RP-1313] p 2398 N94-24104
Discrete sensitivity derivatives of the Navier-Stokes equations with a parallel Krylov solver [NASA-TM-106481] p 2265 N94-24301
An experimental investigation of a Mach 3.0 high-speed civil transport at supersonic speeds [NASA-TP-3365] p 2169 N94-24311
Integrated design and manufacturing for the high speed civil transport [NASA-CR-195511] p 2182 N94-24968
High-order technology: Applying technical excellence to new airplane development p 2185 N94-25069
SUPERSONIC TURBINES
Computation of flows in a turn-around duct and a turbine cascade using advanced turbulence models p 2216 N94-23062
Two-dimensional Navier-Stokes computations of subsonic and supersonic flows through turbine cascades [PB93-226223] p 2317 N94-23114
SUPERSONIC WIND TUNNELS
Lewis Research Center R and D Facilities [NASA-TM-109400] p 2630 N94-23135
Improved pressure measurement system for calibration of the NASA LeRC 10x10 supersonic wind tunnel [NASA-TM-106470] p 2344 N94-24362
SUPERSONICS
Integrated design and manufacturing for the high speed civil transport [NASA-CR-195511] p 2182 N94-24968
SUPERSYMMETRY
Stitching the Yukawa quilt [PB93-204477] p 2569 N94-24532
Super Beltrami differentials and N equal to 4 superconformal anomalies [DE93-613047] p 2491 N94-25166
Applications of supersymmetric quantum mechanics [ETN-94-95385] p 2570 N94-25257
The 2D supergravity and integrable systems [DE93-616848] p 2570 N94-25336
SUPPORT SYSTEMS
Hypermedia support for engineering design system [PB93-226256] p 2449 N94-23117
Object oriented simulation implementation in support of robust system design [DE93-011687] p 2452 N94-23488
ATOS-1: Designing the infrastructure for an advanced spacecraft operations system p 2197 N94-23849
Influence of a new generation of operations support systems on current spacecraft operations philosophy: The users feedback p 2507 N94-23894
PILOT: An intelligent distributed operations support system p 2508 N94-23895
The Advanced Technology Operations System: ATOS p 2508 N94-23897
Telemetry ground system development via the component approach p 2203 N94-23949
Multi-sensoral approach to night flight: Perceptive and Cognitive limitations p 2432 N94-23981
Towards the formal specification of the requirements and design of a processor interface unit [NASA-CR-4521] p 2467 N94-24463
An investigation of requirements traceability to support systems development [AD-A273167] p 2458 N94-24684
SUPPORTS
Landing gear with swivelling beam [CA-PATENT-1323020] p 2176 N94-24181
SURFACE ACOUSTIC WAVE DEVICES
SAW based systems for mobile communications satellites p 2275 N94-22746
Chemically sensitive interfaces on SAW devices [DE94-001832] p 2526 N94-23718
SURFACE CRACKS
Matrix fatigue cracking mechanisms of alpha(2) TMC for hypersonic applications [NASA-TM-106506] p 2230 N94-25186
SURFACE DEFECTS
Surface modification of sapphire for enhanced infrared window performance [DE94-000333] p 2543 N94-23458
Design of novel catalysts for the partial oxidation of methane to methanol [PB94-114212] p 2235 N94-24920
Simulation studies for surfaces and materials strength [NASA-CR-195185] p 2565 N94-25093
SURFACE DIFFUSION
Diffusion on Cu surfaces p 2251 N94-24428
SURFACE DISTORTION
Feasibility study of a synthesis procedure for array feeds to improve radiation performance of large distorted reflector antennas [NASA-CR-195167] p 2301 N94-25005
SURFACE EMITTING LASERS
InGaAsP/InP based 1.3/1.55 micron vertical cavity surface emitting lasers for wavelength division multiplexed high speed distributed computing, phase 1 [AD-A271081] p 2348 N94-23123
The effects of optical feedback on polarization of vertical cavity surface emitting lasers [AD-A273728] p 2351 N94-25445
SURFACE ENERGY
Multilayer relaxation and surface structure of ordered alloys [NASA-TM-106433] p 2243 N94-23578
An investigation of current and future satellite and in-situ data for the remote sensing of the land surface energy balance [NASA-CR-195138] p 2387 N94-24596
Simulation studies for surfaces and materials strength [NASA-CR-195185] p 2565 N94-25093
Structure and energetics of high index Fe, Al, Cu and Ni surfaces using equivalent crystal theory [NASA-TM-106408] p 2249 N94-25171
SURFACE FINISHING
Weld cladding of hard surfaces [PB93-201598] p 2353 N94-23448
JBK-75 stainless steel machinability study [DE94-002268] p 2242 N94-23475
SURFACE IONIZATION
SALI chemical analysis of provided samples [NASA-CR-194138] p 2232 N94-23524
SURFACE LAYERS
Free energy profiles for Li(+) and I(-) ions approaching Pt(100) surface: A molecular dynamics study [AD-A273455] p 2536 N94-24675
Surface compositional variations of Mo-47Re alloy as a function of temperature [NASA-TP-3402] p 2245 N94-25117
Metallic multilayers: Experimental investigation of magnetic anisotropy and magnetic interlayer coupling [ETN-94-95364] p 2250 N94-25242
Tunnelling in metallic contacts on high-T(c) superconductors: A story of charge carriers in YBa2Cu3O(7-delta) and Bi2CaSr2Cu2O(8+delta) [ISBN-9-03-860142-5] p 2565 N94-25280

SURFACE NAVIGATION
Lunar rover navigation concepts p 2607 N94-23386
Mars 96 rover: Science, instrumentation, and control
p 2369 N94-23395
Mars 96 rover: Technical vision and navigation
p 2370 N94-23417
Marsohkod movement control p 2370 N94-23418
Experiments with a small behaviour controlled planetary rover p 2371 N94-23427
Mars 1994/1996: The French navigation tasks
p 2195 N94-23924
Worldwide vessel locating and tracking system, volume 1
[PB93-193217] p 2175 N94-24474
Design of a wheeled articulating land rover
[NASA-CR-195520] p 2365 N94-24806
SURFACE PROPERTIES
Atomic probes of surface structure and dynamics
[DE94-001651] p 2530 N94-22720
Influence of sintering atmospheres on the aluminum sintering characteristics
[DE93-632412] p 2239 N94-22965
SALI chemical analysis of provided samples
[NASA-CR-194138] p 2232 N94-23524
Surface and interfacial properties of polymer blends. A literature survey
[PB93-230191] p 2254 N94-23561
Chemically sensitive interfaces on SAW devices
[DE94-001832] p 2526 N94-23718
Coupled land surface/hydrologic/atmospheric models
p 2413 N94-24387
Thermal phase behavior of metal surfaces: X-ray scattering studies of Pt(001)
[DE94-002991] p 2245 N94-24612
Martian mesoscale circulations induced by variations in surface optical and thermal characteristics: A numerical study p 2622 N94-24899
A thermodynamic approach to obtain materials properties for engineering applications
p 2248 N94-25131
Scanning probe surface modification
[AD-A273178] p 2346 N94-25151
Selected bibliography 2: Diamond surface chemistry
[AD-A273518] p 2565 N94-25160
Use of scanning tunneling microscope in corrosion studies
[VTT-TIED-1416] p 2250 N94-25346
SURFACE REACTIONS
SALI chemical analysis of provided samples
[NASA-CR-194138] p 2232 N94-23524
Chemically sensitive interfaces on SAW devices
[DE94-001832] p 2526 N94-23718
Fundamental and experimental studies on the catalytic combustion of methane
[PB94-112661] p 2233 N94-23736
Selection of polymer binders and fabrication of SiC fiber-reinforced reaction-bonded silicon nitride matrix composites
[NASA-CR-194874] p 2255 N94-24223
Synthesis and characterization of two-dimensional molecular recognition interfaces
[AD-A273177] p 2536 N94-24729
Chemically sensitive interfacial force microscopy: Contact potential measurements of self-assembling monolayer films
[AD-A273135] p 2234 N94-24772
Adsorption, desorption, and decomposition of HCl and HBr on Ge(100): Competitive pairingand near-first-order desorption kinetics
[AD-A273504] p 2235 N94-24790
Surface chemistry of liquid metals
p 2249 N94-25133
Selected bibliography 2: Diamond surface chemistry
[AD-A273518] p 2565 N94-25160
SURFACE ROUGHNESS
Characteristics of surface roughness associated with leading edge ice accretion
[NASA-TM-106459] p 2166 N94-23522
A rail joint: The possible initiator of corrugation?
p 2269 N94-23583
Surface analysis of corrugated rail treads
p 2270 N94-23587
Contact analysis of rough rail surfaces
p 2270 N94-23589
Groundtruth collection for the JPL-SAR and ERS-1 campaign in Flevoland and Veluwe, Netherlands, 1991
[PB93-230654] p 2386 N94-23755
Interface evaluation in ceramic composites
p 2255 N94-24231
Vortex generation and wave-vortex interaction over a concave plate with roughness and suction
[NASA-CR-191589] p 2337 N94-24869
Examination of the physical, electrical, and microwave evolution of water into young sea ice
[AD-A273559] p 2418 N94-24918
The measurement of the film thickness and the roughness deformation of lubricated elastomers
[ETN-94-95293] p 2261 N94-25078
Surface-induced static undulations in multilayer films of liquid-crystalline polymers
[AD-A273517] p 2262 N94-25159
Analytical skin friction and heat transfer formula for compressible internal flows
[NASA-CR-191185] p 2170 N94-25173
SURFACE TEMPERATURE
Evaporation and combustion of LOX under supercritical and subcritical conditions p 2211 N94-23035
Spatial and temporal variability of soil temperature, moisture and surface soil properties
[NASA-CR-194109] p 2401 N94-23337
Lightning, atmospheric electricity, and climate change
[DE94-002003] p 2408 N94-23471
Synthesis of passive microwave and radar altimeter data for estimating accumulation rates of polar snow
[NASA-CR-194864] p 2382 N94-23573
An investigation of current and future satellite and in-situ data for the remote sensing of the land surface energy balance
[NASA-CR-195138] p 2387 N94-24596
Heat transfer and flow structure in end-wall boundary layers
[AD-A273470] p 2335 N94-24689
Investigation of the heat handling capabilities of DIII-D neutral beamline internal components
[DE94-001107] p 2553 N94-24756
Examination of the physical, electrical, and microwave evolution of water into young sea ice
[AD-A273559] p 2418 N94-24918
An extended laser flash technique for thermal diffusivity measurement of high-temperature materials
p 2238 N94-25132
The IRGen infrared data base modeler
p 2440 N94-25496
SURFACE TREATMENT
Diffusion of hydrogen in iron oxides
[DE93-632430] p 2239 N94-22966
Surface modification of sapphire for enhanced infrared window performance
[DE94-000333] p 2543 N94-23458
Repair of cracked aluminum aircraft structure with composite patches p 2156 N94-24259
Low-gravity electrodeposition and growth of polymer thin films with large third-order optical nonlinearities by electrochemical processes for devices: Thiophene-based polymers p 2225 N94-24346
Ge-Au eutectic bonding of Ge (100) single crystals
[DE94-002281] p 2564 N94-24657
Investigation and application of microwave electron cyclotron resonance plasma physical vapour deposition
[DE93-613909] p 2555 N94-25333
Proceedings of the 12th International Congress: Corrosion Control for Low-Cost Reliability. Volume 1: Coatings
[AD-A273661] p 2251 N94-25448
SURFACE VEHICLES
EUTELTRACS: The European experience on mobile satellite services p 2281 N94-22781
Perception and 3D environment modeling for mobile robot autonomous navigation
[LAAS-93117] p 2471 N94-22908
Mars 1994/1996: The French navigation tasks
p 2195 N94-23924
SURFACE WATER
Performance of prefabricated geocomposite subdrainage system in an airport runway
[DOT/FAA/RD-93/23] p 2192 N94-23303
Free energy profiles for Li(+) and I(-) ions approaching Pt(100) surface: A molecular dynamics study
[AD-A273455] p 2536 N94-24675
SURFACE WAVES
Global ocean modeling on the Connection Machine
[DE94-000888] p 2417 N94-23517
Hydro-elastic analysis using a selection of commercial analysis programs
[PB94-118734] p 2376 N94-24478
SURFACTANTS
Measurement of interfacial tension by use of pendant drop video techniques
[DE93-000168] p 2345 N94-24831
SURVEILLANCE RADAR
Analysis and surveillance performance at Chicago O'Hare Airport
[DOT/FAA/RD-92/29] p 2175 N94-24127
SURVEYS
Space technology: A study of the significance of recognition for innovators of spinoff technologies. Commercial Space Expo-USA, 1993
[NASA-CR-194833] p 2596 N94-23528
Prototype Space Technology Hall of Fame exhibit at Technology 2003: Analysis of data from computer-based questionaire
[NASA-CR-194834] p 2596 N94-23540
Cross-calibration survey (VISNIR)
p 2383 N94-23599
Verification and validation of models
[PB94-110566] p 2456 N94-24507
Hydraulics and morphology of mountain rivers: A literature survey. Communications on hydraulic and geotechnical engineering
[PB94-110772] p 2388 N94-24636
NASA/DOD Aerospace Knowledge Diffusion Research Project. Report number 20: The use of selected information products and services by US aerospace engineers and scientists: Results of two surveys
[NASA-TM-109022] p 2592 N94-24649
A biological survey for the nation
[LC-93-85920] p 2421 N94-24704
Evaluation of the UH-1N instrument panel
[AD-A273145] p 2186 N94-24774
General aviation activity survey
[AD-A273284] p 2162 N94-24923
Perceptions of organizational support and affectivity as predictors of job satisfaction
[DOT/FAA/AM-94/2] p 2429 N94-25442
SURVIVAL
Survival suit for submarine personnel: Summary of evaluation studies
[PB93-204634] p 2430 N94-23743
Aircraft evacuation testing: Research and technology issues
[PB94-107620] p 2173 N94-24750
SUSPENSION SYSTEMS (VEHICLES)
Vehicle/guideway interaction and ride comfort in maglev systems
[DE94-001319] p 2352 N94-22991
Vibration isolating engine mount
[CA-PATENT-1-320-710] p 2353 N94-23215
SWELLING
High specific energy, high capacity nickel-hydrogen cell design p 2391 N94-23350
Conceptual design of a device to measure hand swelling in a micro-gravity environment
[NASA-CR-195509] p 2437 N94-24330
SWEPT WINGS
Reduction of structural loads using maneuver load control on the Advanced Fighter Technology Integration (AFTI)/F-111 mission adaptive wing
[NASA-TM-4526] p 2168 N94-24295
SWIRLING
Decay of swirl in turbulent pipe flows
[ETN-94-95353] p 2339 N94-25248
SWITCHES
Picosecond High Pressure Gas Switch experiment
[DE93-040853] p 2307 N94-22950
Switch configuration for migration to optical fiber network p 2447 N94-23250
Viewing hybrid systems as products of control systems and automata
[NASA-CR-194792] p 2472 N94-23300
Non-volatile, solid state bistable electrical switch
[NASA-CASE-NPO-17621-1-CU] p 2309 N94-23820
Computer modeling of plasma flow switches-high current switching on Procyon
[DE93-040189] p 2311 N94-24500
X ray simulator theory support
[AD-A273613] p 2553 N94-24949
SWITCHING
Picosecond High Pressure Gas Switch experiment
[DE93-040853] p 2307 N94-22950
Viewing hybrid systems as products of control systems and automata
[NASA-CR-194792] p 2472 N94-23300
A prototype to automate the video subsystem routing for the video distribution subsystem of Space Station Freedom p 2306 N94-25353
SWITCHING CIRCUITS
Mobilesat (tm): A world first p 2281 N94-22783
Exciplex laser study: Discharge and magnetic switching systems
[PB93-199768] p 2349 N94-24629
Contribution to the study of HF converters radiated disturbances
[ECL-92-34] p 2313 N94-25421
Study of a system for producing a pulsed magnetic field (B 2T) with a frequency of 50 Hz
[ISL-N-601/92] p 2314 N94-25460
SYMBIOSIS
Symbiosis in marine luminous bacteria
[AD-A273540] p 2422 N94-24791
SYMBOLIC PROGRAMMING
ATOS-1: Designing the infrastructure for an advanced spacecraft operations system p 2197 N94-23849

SYMBOLS

Conveying digital data in noisy, unstable, multipath environments [AD-D015980] p 2301 N94-25038

SYMMETRICAL BODIES

On the effect of the damping coefficients on the trajectories of symmetric and non-symmetric stores p 2155 N94-24250

SYMMETRY

Transient analysis of conducting half-plane problem with noncausal scattering image [PB93-225027] p 2524 N94-23110

Observation of non-centrosymmetry and determination of polarity in III-V semiconductors [PB93-201416] p 2561 N94-23503

A working algorithm to isolate integrable surfaces in E cubed [SSCL-PREPRINT-761] p 2452 N94-23518

On BRST quantization of constrained systems [ETN-94-95386] p 2570 N94-25258

Weak interactions in a bilocal chiral theory [DE93-616887] p 2539 N94-25477

SYNAPSES

Customizable VLSI artificial neural network chips based on a novel technology [DE94-001418] p 2307 N94-23008

Electrophysiology of the rat nucleus accumbens: Local circuitry, neuromodulation and synaptic plasticity [PB93-232254] p 2420 N94-23454

SYNCHRONISM

Asynchronous timing and Doppler recovery in DSP based DPSK modems for fixed and mobile satellite applications p 2285 N94-22805

A CDMA synchronisation scheme p 2285 N94-22810

DS-SSMA capacity for a mobile satellite system p 2286 N94-22814

Incomplete corrections in nonlinear problems [PB93-225746] p 2479 N94-23106

Modeling parallelism and synchronization [ETN-94-95179] p 2465 N94-23134

Solid state Time Base Corrector (TBC) [AD-D015981] p 2312 N94-25039

System for producing synchronized signals [AD-D016003] p 2302 N94-25057

Modulation and synchronization technique for MF-TDMA system [NASA-CR-194448] p 2304 N94-25266

SYNCHRONOUS MOTORS

Design and application of electromechanical actuators for deep space missions [NASA-CR-195134] p 2365 N94-24842

SYNCHRONOUS PLATFORMS

Geostationary payload concepts for personal satellite communications p 2278 N94-22765

Global coverage Mobile Satellite Systems: System availability versus channel propagation impairments p 2284 N94-22798

A practical system for regional mobile satellite services p 2288 N94-22828

Advanced mobile satellite communications using COMETS satellite in MM-wave and Ka-band p 2288 N94-22829

CNES organization for station positioning of geostationary satellites p 2501 N94-23857

SYNCHRONOUS SATELLITES

The provision of spectrum for feeder links of non-geostationary mobile satellites p 2276 N94-22751

Multi-access laser communications terminal [NASA-CR-191251] p 2295 N94-23830

Commonality of flight control systems for support of European telecommunications missions p 2304 N94-23834

The geo-control system for station keeping and colocation of geostationary satellites p 2464 N94-23927

HISPASAT launch and early operations phases: Computation and monitoring of geostationary satellite positioning p 2514 N94-23928

SYNCHROTRON RADIATION

Proceedings of the Fifth Users Meeting for the Advanced Photon Source [DE93-040692] p 2531 N94-22948

Activities of Academia Sinica [DE93-614529] p 2541 N94-25335

SYNCHROTRONS

Inverse free electron laser beat-wave accelerator research [DE94-002597] p 2349 N94-23702

Low mass muon pair production in 450 GeV p-Be collisions [PB94-110699] p 2533 N94-23746

SYNOPTIC METEOROLOGY

Modelling TOVS radiances of synoptic systems [NASA-CR-194847] p 2408 N94-23620

Mesospheric and lower thermospheric winds, temperatures densities, and volume emission rates [NASA-CR-195147] p 2403 N94-24486

Analyzing Martian winds and tracer concentrations using Mars Observer data p 2619 N94-24883

Observed and Navy operational global model climatologies of synoptic disturbances over the tropical western Pacific during winter 1991-1992 [AD-A273400] p 2416 N94-25071

The evaluation of ASOS for the Kennedy Space Center's Shuttle Landing Facility [NASA-CR-195685] p 2416 N94-25271

SYNTAX

Design and specification of a generic task model for solving boolean constraint satisfaction problems [PB94-118841] p 2486 N94-23762

SYNTHESIS (CHEMISTRY)

Particle formation in a laser-heated aerosol reactor. Application to silicon and silicon nitride synthesis [PB93-217982] p 2347 N94-22982

Di(hydroxyphenyl)- 1,2,4-triazole monomers [NASA-CASE-LAR-14440-2] p 2252 N94-23075

Reaction of isocyanates with carboxylic acids and its application to polymer synthesis [PB94-118858] p 2254 N94-23763

Synthesis and in-vivo detection of boronated compounds for use in BNCT [DE94-001899] p 2233 N94-23780

New methane chemistry synthesis of materials for reversible uptake and useful functionalization of methane [PB94-112786] p 2233 N94-23801

Synthesis of soluble halogenated polyphenylenes: Mechanism for the coupling halogenated lithiobenzenes [AD-A273547] p 2257 N94-24558

Metal-catalyzed alkynylation of (Bromophenyl)Oligophenylenes: A rapid route to thermoset precursors of high density monolithic glass-like carbon [AD-A273219] p 2260 N94-24863

SYNTHETIC APERTURE RADAR

Optical component MAC Europe ground truth report: Flevoland 1991 (Netherlands) [BCRS-92-27] p 2382 N94-23177

Application of ERS-1 active microwave instrumentation data to remote sensing of snow [PB93-224756] p 2382 N94-23224

Mission planning for Shuttle Imaging Radar-C (SIR-C) with a real-time interactive planning software p 2305 N94-23842

The down, release, and deployment of the RADARSAT SAR antenna p 2305 N94-23986

Investigations into deployment complications of the ERS-1 SAR antenna p 2305 N94-23996

Precipitation measurement using SIR-C: A feasibility study. Investigation at nadir [NASA-CR-195103] p 2410 N94-24126

Free-surface/vorticity interaction [AD-A273263] p 2335 N94-24686

Use of microwave polarimetry to enhance SAR images of the ocean surface [AD-A273568] p 2419 N94-24944

Edge detection using a complex wavelet [AD-A273699] p 2493 N94-25452

The Radar Image Generation (RIG) model p 2306 N94-25497

SYSTEM EFFECTIVENESS

Automatic tools for system testing p 2197 N94-23913

SYSTEM FAILURES

A review of wiring system safety in space power systems [NASA-CR-194439] p 2203 N94-23632

A cross-disciplinary response to improve test activities: The corporate memory capitalization in Ariane4 test domain p 2508 N94-23899

System for Anomaly and Failure Detection (SAFD) system development [NASA-CR-193907] p 2372 N94-24174

Diagnosing process faults using neural network models [DE94-002633] p 2473 N94-24518

Develop advanced nonlinear signal analysis topographical mapping system [NASA-CR-195128] p 2388 N94-24827

Reliability analysis of a repairable dependent parallel system [ETN-94-95312] p 2373 N94-25295

SYSTEM GENERATED ELECTROMAGNETIC PULSES

Safety guidelines for the operation of the DREO 10 m EMP simulator DREMPS [DREO-TN-93-5] p 2193 N94-24117

TEM cell safety report [DREO-TN-93-9] p 2193 N94-24123

SYSTEM IDENTIFICATION

Experimental modification and identification of the DSS-13 antenna control system model p 2291 N94-23260

System identification using a wavelet-based approach [DE94-002191] p 2293 N94-23473

SYSTEMS ANALYSIS

APLAC: An object-oriented analog circuit simulator and design tool. 6.1 system simulations manual [PB93-224871] p 2450 N94-23226

A framework for SFC/DC system data analysis p 2523 N94-23234

Phased-mission system analysis using Boolean algebraic methods [NASA-CR-191564] p 2451 N94-23340

Systems engineering: A formal approach. Part 1: System concepts [PB93-225308] p 2268 N94-23476

GenSAA: A tool for advancing satellite monitoring with graphical expert systems p 2516 N94-23945

Operational characterisation of requirements and early validation environment for high demanding space systems p 2519 N94-23959

A review of ISEAS design p 2465 N94-24410

Systems engineering: A formal approach. Part 4: Analysis methods [PB94-101417] p 2271 N94-24475

Systems engineering: A formal approach. Part 3: Modeling methods [PB94-101409] p 2456 N94-24513

Analyzing the properties of user interface software [AD-A273601] p 2460 N94-24933

Expert system rule-base evaluation using real-time parallel processing [AD-A273701] p 2469 N94-25454

SYSTEMS COMPATIBILITY

Low earth orbit satellite/terrestrial mobile service compatibility p 2288 N94-22827

SYSTEMS ENGINEERING

SATCOM simulator speeds MSS deployment and lowers costs p 2287 N94-22822

Prospects for very-high-resolution solar physics with the Simuris inteferometric mission p 2625 N94-22848

Flexible framework for contingent information systems modelling [PB93-220549] p 2589 N94-23095

How much integral action can a control system tolerate? [OUEL-1923/92] p 2471 N94-23147

The design of a turbine vane cooling system used in the topping cycle [OUEL-1963/92] p 2353 N94-23164

Missions, Technologies, and Design of Planetary Mobile Vehicles [ISBN-2-85428-331-7] p 2605 N94-23373

The study of the mobile lunar explorer p 2607 N94-23389

The robotic Mars rover p 2608 N94-23390

Mission and system concepts for Mars robotic precursor missions p 2608 N94-23391

The new family of JPL planetary surface vehicles p 2369 N94-23398

Electronic payloads for Martian missions: A preliminary assessment of technologies p 2610 N94-23408

The Mars 96 balloon guiderope: An autonomous system in extreme environment conditions p 2369 N94-23412

Dual rover concept for Mars exploration p 2370 N94-23415

Bond graph modeling, simulation, and reflex control of the Mars planetary automatic vehicle p 2370 N94-23424

Systems engineering: A formal approach. Part 1: System concepts [PB93-225308] p 2268 N94-23476

A review of wiring system safety in space power systems [NASA-CR-194439] p 2203 N94-23632

Advanced design concepts for open distributed systems development [PB94-110897] p 2454 N94-23751

Design and specification of a generic task model for solving boolean constraint satisfaction problems [PB94-118841] p 2486 N94-23762

Automatic tools for system testing p 2197 N94-23913

Using Mach threads to control DSN operational sequences p 2477 N94-23916

Deep Space Network (DSN), Network Operations Control Center (NOCC) computer-human interfaces p 2447 N94-23917

A real-time navigation monitoring expert system for the Space Shuttle Mission Control Center p 2202 N94-23921

XRTD: An X-Windows based, real-time radiometric display and analysis system p 2305 N94-23922

Operability engineering in the Deep Space Network p 2514 N94-23930

Training: Plugging the information gaps p 2429 N94-23934

An overview of a generic multi-sensor integrated navigation system design
[CTN-94-60916] p 2174 N94-24120

Technology utilization office data base analysis and design p 2577 N94-24417

A minimum cost tolerance allocation method for rocket engines and robust rocket engine design p 2222 N94-24419

Systems engineering: A formal approach. Part 4: Analysis methods
[PB94-101417] p 2271 N94-24475

Systems engineering: A formal approach. Part 3: Modeling methods
[PB94-101409] p 2456 N94-24513

An automated tool to facilitate code translation for software fault tree analysis
[AD-A273205] p 2457 N94-24556

Systems engineering: A formal approach. Part 2: Frameworks
[PB94-101391] p 2489 N94-24615

RITL: An information system for application reuse-in-the-large
[PB94-119088] p 2592 N94-24646

What makes industries believe in formal methods
[PB94-110848] p 2272 N94-24648

An investigation of requirements traceability to support systems development
[AD-A273167] p 2458 N94-24684

Advanced avionics architecture and technology review. Executive summary and volume 1: Avionics tech nology. Volume 2: Avionics systems engineering
[AD-A273630] p 2186 N94-24733

Intelligent systems and advanced user interfaces for design, operation, and maintenance of command management systems
[NASA-CR-195172] p 2459 N94-24797

Integrated design and manufacturing for the high speed civil transport
[NASA-CR-195511] p 2182 N94-24968

Reuse-Driven Software Processes Guidebook, version 02.00.03
[AD-A273644] p 2461 N94-25148

New Technologies for Space Avionics, 1993
[NASA-CR-195157] p 2272 N94-25193

Appendix A: Proposed statement of work, 1994 p 2272 N94-25194

Appendix B: Rapid development approaches for system engineering and design p 2272 N94-25195

Appendix C: Rapid development approaches for system engineering and design p 2272 N94-25196

Design of gas bearing systems for precision applications
[ISBN-9-03-860112-3] p 2367 N94-25249

A soft robot interface
[OUEL-1948/92] p 2463 N94-25468

Stability questions in predictive control
[OUEL-1970/93] p 2477 N94-25469

SYSTEMS INTEGRATION

Channel and terminal description of the ACTS mobile terminal p 2284 N94-22802

Low earth orbit satellite/terrestrial mobile service compatibility p 2288 N94-22827

Resource allocation planning with international components p 2520 N94-23963

Cockpit/NVG visual integration issues p 2432 N94-23983

Integration and test of high-speed transmitter electronics for free-space laser communications
[NASA-TM-106295] p 2295 N94-24101

Integrated Airframe Design Technology
[AGARD-R-794] p 2177 N94-24313

Multi-disciplinary coupling for integrated design of propulsion systems p 2179 N94-24326

Declarative Object Manipulation Environment (DOME): Alpha version
[AD-A273233] p 2460 N94-24935

Passive millimeter-wave imaging p 2306 N94-25494

SYSTEMS MANAGEMENT

A framework for SFC/DC system data analysis p 2523 N94-23234

Link monitor and control operator assistant: A prototype demonstrating semiautomated monitor and control p 2292 N94-23267

SYSTEMS SIMULATION

SATCOM simulator speeds MSS deployment and lowers costs p 2287 N94-22822

Causal labeled transition systems: A new approach for describing the behavior of concurrent systems
[LAAS-93179] p 2447 N94-22911

Mathematical modeling of MCFC cells/stacks and networks
[DE94-001914] p 2390 N94-23212

A simulation system for Space Station extravehicular activity p 2434 N94-24192

From circuit to signal: Development of a piecewise linear simulator
[ISBN-9-09-005713-7] p 2462 N94-25263

SYSTOLIC PRESSURE

Autogenic-feedback training: A potential treatment for post-flight orthostatic intolerance in aerospace crews
[NASA-TM-108785] p 2426 N94-24102

T

T TAURI STARS

The Nobeyama millimeter array survey for protoplanetary disks around protostar candidates and T Tauri stars in Taurus
[REPT-336] p 2604 N94-24987

ROSAT observations of the x ray binary HD 154791
[NASA-CR-195189] p 2600 N94-25198

Observational studies of the clearing phase in proto-planetary disk systems
[NASA-CR-195182] p 2604 N94-25265

TABLES (DATA)

NASA STI program database: Journal coverage (1990-1992)
[NASA-TM-109720] p 2593 N94-25168

TABS (CONTROL SURFACES)

Effect of delta tabs on mixing and axis switching in jets from asymmetric nozzles
[NASA-TM-106450] p 2167 N94-23592

TACHYONS

The Casimir energy of the rigid string with massive ends
[DE93-616851] p 2492 N94-25338

TACTILE DISCRIMINATION

Investigation of hand capabilities under a variety of performance conditions and an attempt to explain performance differences p 2444 N94-25354

TAIL ASSEMBLIES

Aircraft empennage structural detail design
[NASA-CR-195496] p 2179 N94-24332

Aircraft empennage structural detail design
[NASA-CR-195486] p 2183 N94-24969

TAILLESS AIRCRAFT

NASA advanced design program. Design and analysis of a radio-controlled flying wing aircraft
[NASA-CR-195515] p 2180 N94-24589

TALC

Chromate-free talc chemical conversion coatings for aluminum alloys
[DE94-001567] p 2238 N94-22932

TANKS (COMBAT VEHICLES)

Preliminary analysis of the JAPE ground vehicle test data with an artificial neural network classifier p 2529 N94-24222

TANTALUM

Texture gradient effects in tantalum
[DE94-000689] p 2240 N94-23021

The effects of texture and strain on the r-va lue of heavy gauge tantalum plate
[DE94-000690] p 2242 N94-23541

X ray diffraction analysis of electrodeposited beta-tantalum
[AD-A273254] p 2249 N94-25142

TARGET ACQUISITION

Experimental evaluation of camouflage effectiveness in the thermal infrared
[FEL-93-A043] p 2381 N94-22896

Analysis of passive acoustic ranging of helicopters from the joint acoustic propagation experiment p 2529 N94-24220

Acoustic target detection and classification using neural networks p 2529 N94-24221

TARGET RECOGNITION

Imaging System (INEL) T805 prototype
[DE94-002807] p 2382 N94-23492

UAV current technology and future trends p 2154 N94-24245

Object recognition through image understanding for an autonomous mobile robot
[AD-A273206] p 2475 N94-24862

Radar target discrimination by spectrum analysis
[AD-D015982] p 2301 N94-25040

TARGETS

A mixed map/variable structure observer for target tracking p 2157 N94-24263

TASK COMPLEXITY

Pilot evaluation system p 2158 N94-24266

TASK PLANNING (ROBOTICS)

An architecture for teleprogramming autonomous mobile robots at task level
[LAAS-93107] p 2470 N94-22906

A system for the challenging task of collecting samples from a comet surface p 2358 N94-24007

Admittance model for the shuttle remote manipulator system in four configurations
[NASA-CR-4555] p 2474 N94-24635

TASKS

The role of visual context in manual target localization p 2429 N94-25351

TATB

Condensed-phase thermal decomposition of TATB investigated by Atomic Force Microscopy (AFM) and Simultaneous Thermogravimetric Modulated Beam Mass Spectrometry (STMBMS)
[DE94-000396] p 2232 N94-23298

TAURUS CONSTELLATION

ROSAT observations of the x ray binary HD 154791
[NASA-CR-195189] p 2600 N94-25198

TAXIING

System for automatic transportation of aircraft on the ground
[CA-PATENT-1-322-361] p 2193 N94-24785

TAYLOR SERIES

Application of body fitted-coordinates in heat conduction problems
[ETN-94-95338] p 2340 N94-25484

TDR SATELLITES

Utilizing a TDRS satellite for direct broadcast satellite-radio propagation experiments and demonstrations p 2274 N94-22740

A review of GPS-based tracking techniques for TDRS orbit determination p 2196 N94-23257

A method for interference mitigation in space communications scheduling p 2305 N94-23918

Modeling and analysis of selected space station communications and tracking subsystems p 2306 N94-25374

TEARING MODES (PLASMAS)

Effect of LHCD (low hybrid current drive) on tearing mode instability
[DE93-613700] p 2555 N94-25344

TECHNOLOGIES

Prototype Space Technology Hall of Fame exhibit at Technology 2003: Analysis of data from computer-based questionaire
[NASA-CR-194834] p 2596 N94-23540

TECHNOLOGY ASSESSMENT

Advanced display technologies in Russia, Ukraine, and Belarus. Viewgraphs p 2630 N94-22893

Making government work: Electronic delivery of Federal services
[OTA-TCT-578] p 2290 N94-23081

A review of European applications of artificial intelligence to space
[NASA-TM-108789] p 2453 N94-23568

Satellite communications systems and technology. Executive Summary
[NASA-TM-109388] p 2293 N94-23622

Satellite communications systems and technology. Volume 2: Site reports
[NASA-TM-109399] p 2293 N94-23628

Overview of molten carbonate fuel cell technology development
[DE94-001911] p 2394 N94-23781

A fifteen years lifetime mechanism for an infrared Earth sensor p 2362 N94-24040

Proceedings of Technology and Governance in the 1990's
[PB93-192904] p 2597 N94-24312

Overview of the status and progress in photovoltaics research in the United States
[DE94-000981] p 2395 N94-24512

Advanced avionics architecture and technology review. Executive summary and volume 1: Avionics tech nology. Volume 2: Avionics systems engineering
[AD-A273630] p 2186 N94-24733

The future of rotary-wing aircraft p 2185 N94-25070

US general aviation: The ingredients for a renaissance. A vision and technology strategy for US industry, NASA, FAA, universities p 2162 N94-25097

TECHNOLOGY TRANSFER

Space technology: A study of the significance of recognition for innovators of spinoff technologies. 1993 activities/1994, 1995 plans
[NASA-CR-194836] p 2596 N94-23526

Space technology: A study of the significance of recognition for innovators of spinoff technologies. Commercial Space Expo-USA, 1993
[NASA-CR-194833] p 2596 N94-23528

Contributions of DOE weapons labs and NIST to semicondutor technology
[OTA-ITE-585] p 2630 N94-23572

Proceedings of the NIST Conference on Reducing the Cost of Space Infrastructure and Operations: Part 1: Oral presentations and discussion
[PB94-111374] p 2194 N94-23770

The Electronics Quality/Reliability Center: Lessons learned from partnering with industry
[DE94-001501] p 2309 N94-23777

National Institute of Standards and Technology Conference on Reducing the Cost of Space Infrastructure and Operations. Part 2: Topical papers [PB94-113487] p 2194 N94-23819
Object-oriented technologies in a multi-mission data system p 2506 N94-23885
Activities involving aeronautical, space science, and technology support for minority institutions [NASA-CR-195095] p 2574 N94-24225
Technology utilization office data base analysis and design p 2577 N94-24417
A compilation of technology spinoffs from the US Space Shuttle Program p 2578 N94-24424
NASA tech brief evaluations [NASA-CR-195150] p 2597 N94-24829
Collaborating with our customers: NIST building and fire research laboratory [PB94-110194] p 2272 N94-24955
Spinoff 1993 [NASA-NP-211] p 2597 N94-25018
National Academy of Sciences-Academy of Sciences of the USSR Workshop on the Mechanics of Ice and its Applications [AD-A273338] p 2419 N94-25088
Advanced Information Processing System (AIPS) p 2165 N94-25115
Reuse Adoption Guidebook, version 02.00.05 [AD-A273652] p 2461 N94-25149
Wind climate and urban geometry [ISBN-9-03-860132-8] p 2416 N94-25261
National Aeronautics and Space Administration (NASA)/American Society for Engineering Education (ASEE) Summer Faculty Fellowship Program, 1993, volume 1 [NASA-CR-188271-VOL-1] p 2632 N94-25348

TECHNOLOGY UTILIZATION
The history of development of molybdenum alloys for structural applications [DE94-000389] p 2239 N94-22958
Power beaming to space using a nuclear reactor-pumped laser [DE94-001208] p 2348 N94-23185
Pushing technology to satisfy world applications [DE94-001365] p 2353 N94-23191
Influence of a new generation of operations support systems on current spacecraft operations philosophy: The users feedback p 2507 N94-23894
Technology utilization office data base analysis and design p 2577 N94-24417
NASA technology applications team: Applications of aerospace technology [NASA-CR-194775] p 2597 N94-24494
Space Technology: A study of the significance of recognition for innovators of spinoff technologies. A case study on the impact of the space technology hall of fame award [NASA-CR-194835] p 2597 N94-24496
Power generation technology options for a Mars mission [NASA-TM-106451] p 2220 N94-24681
NASA tech brief evaluations [NASA-CR-195150] p 2597 N94-24829
A white paper: NASA virtual environment research, applications, and technology [NASA-TM-109682] p 2428 N94-24855
Spinoff 1993 [NASA-NP-211] p 2597 N94-25018
High-order technology: Applying technical excellence to new airplane development p 2185 N94-25069

TECTONICS
GPS survey of the western Tien Shan [NASA-CR-195174] p 2175 N94-24826
Tectonic Evolution of Mars [NASA-CR-194714] p 2623 N94-24996
The geophysical signal of the martian global dichotomy p 2623 N94-24997

TELECOMMUNICATION
Global coverage Mobile Satellite Systems: System availability versus channel propagation impairments p 2284 N94-22798
Channel and terminal description of the ACTS mobile terminal p 2284 N94-22802
Code generation for the attribute evaluator of the protocol engine grammar processor unit [EUT-93-E-271] p 2450 N94-23173
The TOPSIM 4 graphic user interface [ESA-STM-247] p 2450 N94-23228
Advanced design concepts for open distributed systems development [PB94-110897] p 2454 N94-23751
A simulation and evaluation of NATO Standardization Agreement (STANAG) 4214 [AD-A273195] p 2297 N94-24554
Service description of communication systems supporting multi-media multi-user applications [PB94-110855] p 2299 N94-24650
ELF communications system ecological monitoring program [AD-A273456] p 2299 N94-24676
Analog communication transmitter and receiver test procedures [AD-A273423] p 2300 N94-24687

TELECONFERENCING
Deployable video conference table [NASA-CASE-ARC-11950-1] p 2192 N94-23310

TELEMETRY
Command/telemetry bus general specification for the NOAA-OPQ polar orbiting environmental satellites and EUMETSAT polar satellite systems [NASA-TM-109407] p 2208 N94-23479
SpaceOps 1992: Proceedings of the Second International Symposium on Ground Data Systems for Space Mission Operations [NASA-CR-194486] p 2497 N94-23832
Common front end systems for Space Shuttle and Space Station control centers at Johnson Space Center p 2305 N94-23838
SAMPEX payload operation control center implementation p 2197 N94-23843
A reference model for space data system interconnection services p 2305 N94-23847
NASDA satellite mission operation system and operations p 2501 N94-23854
NASA/Goddard Space Flight Center's testbed for CCSDS compatible systems p 2197 N94-23855
The Ulysses spacecraft control and monitoring concepts and realities p 2502 N94-23862
Ulysses log 1992 p 2502 N94-23863
Magellan spacecraft and memory state tracking: Lessons learned, future thoughts p 2207 N94-23865
A MOS for all seasons p 2505 N94-23879
AMFESYS: Modelling and diagnosis functions for operations support p 2506 N94-23887
GSMS and space views: Advanced spacecraft monitoring tools p 2507 N94-23890
ESSOPE: Towards S/C operations with reactive schedule planning p 2508 N94-23896
Combining real-time monitoring and knowledge-based analysis in MARVEL p 2477 N94-23900
Making tomorrow's mistakes today: Evolutionary prototyping for risk reduction and shorter development time p 2197 N94-23902
The EURECA telecommanding chain: Experience with packet telecommand and telemetry systems p 2305 N94-23909
Using SFOC to fly the Magellan Venus mapping mission p 2516 N94-23941
High performance, low cost, self-contained, multipurpose PC based ground systems p 2516 N94-23943
Expert diagnostics system as a part of analysis software for power mission operations p 2516 N94-23944
GenSAA: A tool for advancing satellite monitoring with graphical expert systems p 2516 N94-23945
The evolving trend in spacecraft health analysis p 2202 N94-23946
Orbital Signature Analyzer (OSA): A spacecraft health/safety monitoring and analysis tool p 2203 N94-23947
Telemetry ground system development via the component approach p 2203 N94-23949
The European Space Agency standard for space packet utilisation p 2203 N94-23954
Compression for an effective management of telemetry data p 2518 N94-23956
Use of infrared telemetry as part of a nonintrusive inflight data collection system to collect human factors data p 2434 N94-24193

TELEOPERATORS
Manned Mars mission on-orbit operations FTS capabilities assessment [NASA-CR-189328] p 2430 N94-23080
Telerobotic rendezvous and docking vision system architecture [NASA-CR-191329] p 2204 N94-23828
SAMPEX payload operation control center implementation p 2197 N94-23843
Columbus system support for telescience operations p 2505 N94-23877
Mars 1994/1996: The French navigation tasks p 2195 N94-23924
Connector mechanisms in compliance with extreme space conditions p 2360 N94-24025
Precision Displacement Mechanism (PDM) p 2360 N94-24026
Crew interface analysis: Selected articles on space human factors research, 1987 - 1991 [NASA-TM-104756] p 2433 N94-24185
Hand controller commonality evaluation process p 2435 N94-24197
Programmable display pushbuttons on the Space Station's telerobot control panel p 2435 N94-24198
Space Station Freedom coupling tasks: An evaluation of their telerobotic and EVA compatibility p 2436 N94-24200
The effects of spatially displaced visual feedback on remote manipulator performance p 2436 N94-24201
Development of a force feedback anthropomorphic teleoperation input device for control of robot hands [NASA-CR-195109] p 2437 N94-24329

TELEPHONES
The Iridium (tm) system: Personal communications anytime, anyplace p 2281 N94-22785
The Globalstar mobile satellite system for worldwide personal communications p 2282 N94-22786
Odyssey personal communications satellite system p 2282 N94-22787

TELEPHONY
Mobilesat (tm): A world first p 2281 N94-22783
INMARSAT's personal communicator system p 2282 N94-22788
A high quality voice coder with integrated echo canceller and voice activity detector for mobile satellite applications p 2286 N94-22812

TELEROBOTICS
An architecture for teleprogramming autonomous mobile robots at task level [LAAS-93107] p 2470 N94-22906
Manned Mars mission on-orbit operations FTS capabilities assessment [NASA-CR-189328] p 2430 N94-23080
Graphical programming: A systems approach for telerobotic servicing of space assets [DE93-019016] p 2472 N94-23201
The remote-operated autonomous-robot concept: From deep sea to outer space applications p 2370 N94-23413
Lunar exploration rover program developments [DE93-040759] p 2613 N94-23469
Ground operation of robotics on Space Station Freedom p 2371 N94-23841
Hand controller commonality evaluation process p 2435 N94-24197
Programmable display pushbuttons on the Space Station's telerobot control panel p 2435 N94-24198
Speech versus manual control of camera functions during a telerobotic task p 2436 N94-24199
Space Station Freedom coupling tasks: An evaluation of their telerobotic and EVA compatibility p 2436 N94-24200
The effects of spatially displaced visual feedback on remote manipulator performance p 2436 N94-24201
Simulation of the human-telerobot interface on the Space Station p 2436 N94-24202

TELESCOPES
Multi-access laser communications terminal [NASA-CR-191251] p 2295 N94-23830
ASTER, a multinational Earth observing concept p 2389 N94-23840
Data analysis and interpretation of lunar dust exosphere p 2623 N94-25349

TELEVISION CAMERAS
Orbital docking system centerline color television camera system test [NASA-TM-104783] p 2205 N94-24625

TELEVISION SYSTEMS
Mars 96 rover: Technical vision and navigation p 2370 N94-23417
Reducing video frame rate increases remote optimal focus time [NASA-TM-104018] p 2431 N94-23970
HORACE: Presentation-level protocol standard for digital transmission of monochrome television images [AD-A273395] p 2197 N94-25064

TELEVISION TRANSMISSION
HORACE: Presentation-level protocol standard for digital transmission of monochrome television images [AD-A273395] p 2197 N94-25064

TELLURIC CURRENTS
The influence of orography on the transport of atmospheric constituents p 2619 N94-24886

TEMPERATE REGIONS
Nonlinear dynamics applied to atmospheric prediction [AD-A273437] p 2404 N94-24674

TEMPERATURE CONTROL
An engineering code to analyze hypersonic thermal management systems p 2320 N94-23636
Thermal control system for SSF sensor/electronics [SAND-92-0652C] p 2321 N94-23640
Utilization of recently developed codes for high power Brayton and Rankine cycle power systems p 2222 N94-23641
Hubble Space Telescope high speed photometer orbital verification [NASA-CR-189333] p 2204 N94-24226
Temperature dependence of protein solubility-determination, application to crystallization, and growth kinetics studies p 2224 N94-24344

Weld joint concepts for on-orbit repair of Space Station Freedom fluid system tube assemblies
p 2371 N94-24427
Near Earth asteroid rendezvous
[NASA-CR-195518] p 2195 N94-24808
Thermal control system for Space Station Freedom photovoltaic power module
[NASA-TM-105650] p 2205 N94-24825
Thermistor controlled current source versatile temperature sensor
[AD-D015979] p 2345 N94-25037

TEMPERATURE DEPENDENCE
Electrical transport in La(2-x)Sr(x)CuO(4-y)
[DE93-040885] p 2556 N94-22912
Low temperature diffusion of hydrogenic species in oxide crystals: Radiation induced diffusion
[DE94-000374] p 2558 N94-22957
Effects of neutron irradiation and hydrogen on ductile-brittle transition temperatures of V-Cr-Ti alloys
[DE94-001466] p 2240 N94-23009
Tensile properties of 21-6-9 stainless steel at elevated temperatures
[DE94-001852] p 2240 N94-23017
Thermally activated low temperature creep and primary water stress corrosion cracking of NiCrFe alloys
[DE94-001756] p 2241 N94-23219
Conductors with small Fermi energies and small gap energies
[DE93-040887] p 2561 N94-23432
Physics of iron
[DE94-002002] p 2402 N94-23721
Disorder effects on small-polaron formation and hopping
[DE94-001205] p 2534 N94-23804
Temperature dependence of protein solubility-determination, application to crystallization, and growth kinetics studies p 2224 N94-24344
The mechanical properties of single crystal (alpha)-Si3N4
[DE94-002632] p 2563 N94-24517
Surface compositional variations of Mo-47Re alloy as a function of temperature
[NASA-TP-3402] p 2245 N94-25117

TEMPERATURE DISTRIBUTION
A random distribution reacting mixing layer model
[NASA-CR-194445] p 2187 N94-23552
An analysis of solar mesospheric temperatures for the upper stratosphere and mesosphere
[NASA-CR-194861] p 2626 N94-23626
A direct approach to finding unknown boundary conditions in steady heat conduction
p 2322 N94-23645
Convection equation modeling: A non-iterative direct matrix solution algorithm for use with SINDA
p 2323 N94-23651
Experimental and analytical study of cryogenic propellant boiloff to develop and verify alternate pressurization concepts for Space Shuttle external tank using a scaled down tank p 2266 N94-23657
Unsteady three-dimensional thermal field prediction in turbine blades using nonlinear BEM
p 2325 N94-23665
Flow and temperature distribution in a naturally stratified thermal storage tank
[AD-A273511] p 2336 N94-24821
Diagnostic calculations of the circulation in the Martian atmosphere p 2622 N94-24898
Two-dimensional modeling of thermal inversion layers in the middle atmosphere of Mars p 2622 N94-24900
Mars Observer: Applications to atmospheric transport
p 2623 N94-24904
Thermophysical property sensitivity effects in steel solidification p 2246 N94-25122
Hydride thermodynamic machines
[VTT-JULK-768] p 2571 N94-25416

TEMPERATURE EFFECTS
Discontinuous phase formation and selective attack of SiC materials exposed to low oxygen partial pressure environments
[DE93-040161] p 2231 N94-22933
Development of a computational testbed for numerical simulation of combustion instability
p 2213 N94-23046
Shear coaxial injector instability mechanisms
p 2213 N94-23047
Thermodynamics of nickel-cadmium and nickel-hydrogen batteries p 2391 N94-23349
A method to remove intercalates from bromine and iodine intercalated carbon fibers
[NASA-TM-106443] p 2222 N94-23591
Development of a theory of the wear of ceramics
[DE94-002773] p 2254 N94-23783
Laser soldering of Sn plated brass integrator assembly housings
[DE94-001149] p 2270 N94-23790
The mechanical properties of single crystal (alpha)-Si3N4
[DE94-002632] p 2563 N94-24517
Prediction of thermal cycling induced cracking in polmer matrix composites
[NASA-CR-195135] p 2229 N94-24579
Flex bearing UUEC, volume 2
[NASA-CR-193901] p 2365 N94-24588
Thermal phase behavior of metal surfaces: X-ray scattering studies of Pt(001)
[DE94-002991] p 2245 N94-24612
Crashworthiness analysis using advanced material models in DYNA3D
[DE94-002988] p 2229 N94-24632
Relationship between transition and modes of instability in supersonic boundary layers
[NASA-CR-4562] p 2336 N94-24725
Dipolar relaxation in a second-order nonlinear optical interpenetrating polymer network
[AD-A273626] p 2258 N94-24732
Measurement of electron temperature and density in the DIII-D neutral beam ion source arc chamber
[DE94-001099] p 2553 N94-24746
The role of atmospheric heat transport in the seasonal carbon dioxide cycle p 2621 N94-24896
On superconductivity of alpha-(BEDT-TTF)2KHg(SCN)4
[REPT-A-2660] p 2564 N94-24978
Lattice dynamics of Ba(1-x)K(x)BiO3 as studied by neutron scattering and computer simulation
[DE93-617053] p 2567 N94-25424

TEMPERATURE GRADIENTS
Experimental evaluation of camouflage effectiveness in the thermal infrared
[FEL-93-A043] p 2381 N94-22896
Nonlinear ion-mixing-mode particle transport in the dissipative trapped electron regime
[DE94-000989] p 2533 N94-23435
Modelling TOVS radiances of synoptic systems
[NASA-CR-194847] p 2408 N94-23620
A nighttime structure model of atmospheric optical turbulence, c2(n), derived from thermosonde and high resolution rawinsonde measurements
[AD-A273803] p 2406 N94-25537

TEMPERATURE INVERSIONS
Two-dimensional modeling of thermal inversion layers in the middle atmosphere of Mars p 2622 N94-24900

TEMPERATURE MEASUREMENT
A field evaluation of remote sensor measurements of wind, temperature, and moisture for ARM integrated sounding system research
[DE94-000565] p 2381 N94-23001
Droplet turbulence interactions under subcritical and supercritical conditions p 2211 N94-23036
Fiber optic temperature sensor using a Y2O2S:Eu thermographic phosphor
[DE94-000331] p 2543 N94-23461
High temperature, oxidation resistant noble metal-Al alloy thermocouple
[NASA-CASE-LEW-15515-1] p 2343 N94-23826
Comparison between 1-minute and 15-minute averages of turbulence parameters p 2528 N94-24218
White-light, pressure, and temperature interferopolarimetric sensor featuring optical fibers
[PB93-199792] p 2545 N94-24631
Measurement of electron temperature and density in the DIII-D neutral beam ion source arc chamber
[DE94-001099] p 2553 N94-24746
Containerless measurements on liquids at high temperatures p 2238 N94-25125
Liquidus temperature and optical properties measurement by containerless techniques
p 2247 N94-25126
Temperature measurement using infrared imaging systems during turbine engine altitude testing
[NASA-TM-105871] p 2193 N94-25184
Hydride thermodynamic machines
[VTT-JULK-768] p 2571 N94-25416
Analysis of the effects of wake passage on heat transfer in a linear turbine cascade
[AD-A273729] p 2339 N94-25446

TEMPERATURE PROFILES
A pressurized thermogravimetric analyzer for use in studies of gas/solid systems
[DE94-001224] p 2342 N94-22989
Spatial and temporal variability of soil temperature, moisture and surface soil properties
[NASA-CR-194109] p 2401 N94-23337
An analysis of solar mesospheric temperatures for the upper stratosphere and mesosphere
[NASA-CR-194861] p 2626 N94-23626
Retrieval of temperature profiles from Martian infrared spectra p 2620 N94-24893
Examination of the physical, electrical, and microwave evolution of water into young sea ice
[AD-A273559] p 2418 N94-24918

TEMPERATURE SENSORS
Fiber optic temperature sensor using a Y2O2S:Eu thermographic phosphor
[DE94-000331] p 2543 N94-23461
White-light, pressure, and temperature interferopolarimetric sensor featuring optical fibers
[PB93-199792] p 2545 N94-24631
Thermistor controlled current source versatile temperature sensor
[AD-D015979] p 2345 N94-25037

TEMPORAL DISTRIBUTION
Spatial and temporal variability of soil temperature, moisture and surface soil properties
[NASA-CR-194109] p 2401 N94-23337
Dynamics of the atmosphere of Mars: Review of some outstanding problems p 2620 N94-24888
An analysis of gamma ray burst time histories
[NASA-CR-195191] p 2629 N94-25199

TEMPORAL RESOLUTION
Dimensional analysis of acoustically propagated signals p 2528 N94-24217
Temporal behavior of the electron density profile during limiter biasing in the HYBTOK-2 tokamak
[NIFS-257] p 2552 N94-24456
Dynamic measurements of thermophysical properties of metals and alloys at high temperatures by subsecond pulse heating techniques p 2247 N94-25124
Evaluation of image quality p 2443 N94-25514

TENSILE DEFORMATION
The effects of texture and strain on the r-va lue of heavy gauge tantalum plate
[DE94-000690] p 2242 N94-23541

TENSILE PROPERTIES
Tensile properties of 21-6-9 stainless steel at elevated temperatures
[DE94-001852] p 2240 N94-23017
Effect of neutron irradiation on tensile properties of V-Cr-Ti alloys
[DE94-001433] p 2240 N94-23194
The effects of texture and strain on the r-va lue of heavy gauge tantalum plate
[DE94-000690] p 2242 N94-23541
Ceramic matrix composites: Challenges and opportunities p 2255 N94-24230
Test methods for composites: A status report. Volume 3: Shear test methods
[AD-A273561] p 2230 N94-25163

TENSILE STRENGTH
Humidity effects on soluble core mechanical and thermal properties (polyvinyl alcohol/microballoon composite) type CG extendospheres, volume 2
[NASA-CR-193893] p 2229 N94-24224
Assessment of impact damage of composite rocket motor cases
[NASA-CR-195143] p 2220 N94-24595
The mechanical property data base from an Air Force/Industry Cooperative Test Program on advanced aluminum alloys (7064 and CW67)
[AD-A273741] p 2251 N94-25531

TENSILE STRESS
Fracture simulations via massively parallel molecular dynamics
[DE93-040159] p 2374 N94-22871
Tensile properties of 21-6-9 stainless steel at elevated temperatures
[DE94-001852] p 2240 N94-23017

TENSILE TESTS
Stress corrosion cracking properties of 15-5PH steel
p 2251 N94-23244
Time dependent behavior of a graphite/thermoplastic composite and the effects of stress and physical aging
[NASA-TM-109047] p 2228 N94-23280
Grain-boundary microchemistry and intergranular cracking of irradiated austenitic stainless steel
[DE94-000466] p 2242 N94-23457
Effect of hydrogen exposure on a Cu-8 Cr-4 Nb alloy
[NASA-TM-106429] p 2243 N94-23556
Test methods for composites: A status report. Volume 1: Tension test methods
[AD-A273501] p 2230 N94-24942

TENSOR ANALYSIS
Tensoral for post-processing users and simulation authors p 2333 N94-24169

TENSORS
Mass properties measurement system dynamics
p 2368 N94-23235
Tensoral for post-processing users and simulation authors p 2333 N94-24169

TERBIUM
Improved magnetostrictive transducer drive elements achieved by reduction of crystalline defects and improved crystalline orientation
[AD-A273391] p 2313 N94-25276

TERMINAL BALLISTICS
Bibliographic Retrieval System (BARS), Sandia Shock Compression (SSC) database Shock Physics Index [DE94-001679] p 2589 N94-23126
TERMINOLOGY
Glossary knowledge engineering [NLR-TP-91435-U] p 2471 N94-23137
Definitions in use by the visible and near-infrared, and thermal working groups p 2383 N94-23598
TERRAIN
K-band mobile propagation measurements using ACTS p 2283 N94-22792
Mobility analysis, simulation, and scale model testing for the design of wheeled planetary rovers p 2370 N94-23425
Joint Acoustic Propagation Experiment (JAPE) p 2527 N94-24208
Tools for visualizing landscape pattern for large geographic areas [DE94-001121] p 2388 N94-24757
TEST CHAMBERS
Dual-bell altitude compensating nozzles p 2215 N94-23057
Automatic pressure control system for the Wright Laboratory Compressor Research Facility [AD-A273827] p 2194 N94-25522
TEST EQUIPMENT
Airport pavement test machine design and cost study [DOT/FAA/CT-93/51] p 2192 N94-24072
An analysis of traditional operational testing to project how testing will be conducted in the future [AD-A273189] p 2372 N94-24553
TEST FACILITIES
The development of the HERA Test Facility (HTF) p 2197 N94-24020
TEM cell safety report [DREO-TN-93-9] p 2193 N94-24123
Altitude simulation facility for testing large space motors p 2156 N94-24255
LSS systems planning and performance program [NASA-CR-193882] p 2196 N94-24309
An analysis of traditional operational testing to project how testing will be conducted in the future [AD-A273189] p 2372 N94-24553
Collaborating with our customers: NIST building and fire research laboratory [PB94-110194] p 2272 N94-24955
TEST STANDS
NASA/Goddard Space Flight Center's testbed for CCSDS compatible systems p 2197 N94-23855
Design and application of electromechanical actuators for deep space missions [NASA-CR-195134] p 2365 N94-24842
Performance measurements of the multimedia testbed on Mach 3.0: Experience writing real-time device drivers, servers, and applications [AD-A273600] p 2460 N94-24932
The ISL rotor bench [ISL-R-108/92] p 2185 N94-25301
TEST VEHICLES
High energy density aluminum-oxygen cell p 2393 N94-23363
TESTS
Automatic tools for system testing p 2197 N94-23913
TETHERED SATELLITES
Nearly uniform deployment/retrieval strategy for space tether systems p 2156 N94-24256
TETHERING
Fingered bola body, bola with same, and methods of use [NASA-CASE-MSC-21967-1] p 2354 N94-23822
TETHERLINES
Nearly uniform deployment/retrieval strategy for space tether systems p 2156 N94-24256
TETRAHEDRONS
Structures of tetrahedrization: A mathematical and algorithmical point of view [ETN-94-95172] p 2480 N94-23166
TEXTILES
Composites and textile reinforcement [VTT-TIED-1424] p 2231 N94-25420
TEXTS
World processor: An interface for textual display and manipulation in virtual reality [PB94-118643] p 2592 N94-24642
TEXTURES
Texture gradient effects in tantalum [DE94-000689] p 2240 N94-23021
The effects of texture and strain on the r-va lue of heavy gauge tantalum plate [DE94-000690] p 2242 N94-23541
THALLIUM
CsI(Tl)-photodiode detectors for spectroscopy at low radiation levels [MPI-PHE/92-22] p 2314 N94-25457
THEOREM PROVING
Combinatory reduction systems: Introduction and survey [PB94-110582] p 2457 N94-24570
Exploiting structure: Introduction and motivation [NASA-CR-195136] p 2490 N94-24847
On the inversion of the n-dimensional Laplace transform [RR-461] p 2492 N94-25310
Extension problem for generalized multi-monogenic functions in Clifford analysis [DE93-616818] p 2493 N94-25433
A reachability test for systems over polynomial rings using Groebner bases [MEMO-COSOR-92-38] p 2493 N94-25527
THEOREMS
On the numerical computation of invariant manifolds [W-9306] p 2480 N94-23140
The cusp horseshoe and its bifurcations in the unfolding of an inclination-flip homoclinic orbit [W-9307] p 2480 N94-23141
A theorem regarding roots of the zero-order Bessel function of the first kind p 2325 N94-23667
The Third Twente Workshop on Graphs and Combinatorial Optimization [PB94-110947] p 2486 N94-23722
Egalitarian non-average contribution method for cooperative games [PB94-111705] p 2497 N94-23800
Tail processes under heavy random censorship with applications [PB94-110632] p 2495 N94-24508
Reduced game properties of egalitarian division rules for cooperative games [PB94-111689] p 2521 N94-24523
Tool sharing, part 3 [PB94-111697] p 2467 N94-24524
Polynomials orthogonal with respect to an inner product involving differences [PB94-110731] p 2489 N94-24572
THEORETICAL PHYSICS
Towards a theory of quark and lepton masses [DE94-001726] p 2533 N94-23218
Theoretical atomic physics for fusion [DE94-000712] p 2533 N94-23543
Heavy flavour physics at LEP [NIKHEF-H/92-19] p 2539 N94-25465
Orbit spaces over commutative rings and projectives as semi-isomorphisms [DE93-616822] p 2493 N94-25473
THERMAL ABSORPTION
The annual pressure cycle on Mars: Results from the LMD Martian atmospheric general circulation model p 2619 N94-24884
THERMAL ANALYSIS
A pressurized thermogravimetric analyzer for use in studies of gas/solid systems [DE94-001224] p 2342 N94-22989
Fully coupled nonlinear thermomechanical analysis including general contact in PALM2D [DE94-001661] p 2568 N94-23216
Improved thermal force modeling for GPS satellites p 2207 N94-23259
Mechanical and thermal buckling analysis of sandwich panels under different edge conditions [NASA-TM-4535] p 2228 N94-23514
The Fifth Annual Thermal and Fluids Analysis Workshop [NASA-CP-10122] p 2320 N94-23634
Advanced X ray Astrophysics Facility-Imaging (AXAF-I) thermal analyses using Integrated Thermal Analysis System (ITAS) program p 2320 N94-23635
Uncertainty analysis of diffuse-gray radiation enclosure problems: A hypersensitive case study p 2320 N94-23637
A comparison of TSS and TRASYS in form factor calculation p 2321 N94-23638
Accuracy control in Monte Carlo radiative calculations p 2321 N94-23639
Some useful innovations with TRASYS and SINDA-85 p 2322 N94-23647
Analysis of high vacuum systems using SINDA'85 p 2322 N94-23648
Thermal analysis of combinatorial solid geometry models using SINDA p 2323 N94-23650
Unsteady three-dimensional thermal field prediction in turbine blades using nonlinear BEM p 2325 N94-23665
Response-coefficient method for heat-conduction transients with time-dependent inputs p 2326 N94-23671
Thermal-fluid analysis of the fill and drain operations of a cryogenic fuel tank [NASA-TM-104273] p 2334 N94-24495
THERMAL BLOOMING
Internally folded scalable laser [AD-D015978] p 2350 N94-25216
THERMAL BUCKLING
Mechanical and thermal buckling analysis of sandwich panels under different edge conditions [NASA-TM-4535] p 2228 N94-23514
THERMAL CONDUCTIVITY
Fully coupled nonlinear thermomechanical analysis including general contact in PALM2D [DE94-001661] p 2568 N94-23216
Fire safety engineering research in Norway [PB93-201630] p 2268 N94-23429
Uncertainty analysis of diffuse-gray radiation enclosure problems: A hypersensitive case study p 2320 N94-23637
Features of a SINDA/FLUINT model of a liquid oxygen supply line p 2322 N94-23649
THERMAL CONTROL COATINGS
Characterization and durability testing of plasma-sprayed zirconia-yttria and hafnia-yttria thermal barrier coatings. Part 2: Effect of spray parameters on the performance of several hafnia-yttria and zirconia-yttria coatings [NASA-TP-3296] p 2242 N94-23467
Structural characterization and thermal cycling behaviour of EB-PVD thermal barrier coating systems [ISBN-0-315-83365-3] p 2257 N94-24468
An x ray diffraction investigation of alpha-Al2O2 addition to Yttria Stabilized Zirconia (YSZ) thermal barrier coatings subject to destabilizing vanadium pentoxide (V2O5) exposure [AD-A273403] p 2261 N94-25072
THERMAL CYCLING TESTS
Structural characterization and thermal cycling behaviour of EB-PVD thermal barrier coating systems [ISBN-0-315-83365-3] p 2257 N94-24468
Prediction of thermal cycling induced cracking in polmer matrix composites [NASA-CR-195135] p 2229 N94-24579
Synthesis of polyphenylenes via Bergman cyclization of enediyne monomers [AD-A273298] p 2260 N94-24924
THERMAL DECOMPOSITION
Condensed-phase thermal decomposition of TATB investigated by Atomic Force Microscopy (AFM) and Simultaneous Thermogravimetric Modulated Beam Mass Spectrometry (STMBMS) [DE94-000396] p 2232 N94-23298
THERMAL DEGRADATION
Electrochemical sulfur passivation of visible (approximately 670nm) AlGaInP lasers [DE94-002293] p 2350 N94-24659
THERMAL DIFFUSION
Eddy mixing coefficient upper limit derived from the photochemical balance of O2 p 2621 N94-24897
THERMAL DIFFUSIVITY
Characterization and durability testing of plasma-sprayed zirconia-yttria and hafnia-yttria thermal barrier coatings. Part 2: Effect of spray parameters on the performance of several hafnia-yttria and zirconia-yttria coatings [NASA-TP-3296] p 2242 N94-23467
Containerless measurements on liquids at high temperatures p 2238 N94-25125
An extended laser flash technique for thermal diffusivity measurement of high-temperature materials p 2238 N94-25132
Microwave techniques for physical property measurements p 2238 N94-25134
THERMAL DISSOCIATION
Atomic probes of surface structure and dynamics [DE94-001651] p 2530 N94-22720
THERMAL EMISSION
Imaging XUV spectroscopy of a Z-pinch plasma in the former Soviet Union [DE93-040849] p 2549 N94-22949
ASTER, a multinational Earth observing concept p 2389 N94-23840
Nonequilibria in thermal emission from supernova remnants [NIFS-264] p 2602 N94-24868
Temporal and spatial mapping of surface albedo and atmospheric dust opacity on Mars p 2619 N94-24887
Retrieval of temperature profiles from Martian infrared spectra p 2620 N94-24893
THERMAL ENERGY
Second law analysis of a conventional steam power plant p 2322 N94-23646
Ulysses log 1992 p 2502 N94-23863
Infrared sensors and systems for enhanced vision/autonomous landing applications p 2439 N94-25491

THERMAL ENVIRONMENTS
Development and experimental validation of computational methods to simulate abnormal thermal and structural environments
[DE94-000554] p 2268 N94-23000
THERMAL EXPANSION
Developments in materials for high-field magnets
[DE94-000761] p 2307 N94-22987
Humidity effects on soluble core mechanical and thermal properties (polyvinyl alcohol/microballoon composite) type CG extendospheres, volume 2
[NASA-CR-193893] p 2229 N94-24224
Dynamic measurements of thermophysical properties of metals and alloys at high temperatures by subsecond pulse heating techniques p 2247 N94-25124
THERMAL FATIGUE
Thermal fatigue: A literature review
[PB93-226306] p 2375 N94-23120
Elevated temperature crack propagation
[NASA-TM-106490] p 2377 N94-24715
THERMAL INSULATION
Features of a SINDA/FLUINT model of a liquid oxygen supply line p 2322 N94-23649
Micromechanical simulation of damage progression in carbon phenolic composites p 2231 N94-24446
Thermal-fluid analysis of the fill and drain operations of a cryogenic fuel tank
[NASA-TM-104273] p 2334 N94-24495
THERMAL MAPPING
Temporal and spatial mapping of surface albedo and atmospheric dust opacity on Mars p 2619 N94-24887
Evidence for dust transport in Viking IR thermal mapper opacity data p 2620 N94-24892
Eddy mixing coefficient upper limit derived from the photochemical balance of O2 p 2621 N94-24897
Diagnostic calculations of the circulation in the Martian atmosphere p 2622 N94-24898
THERMAL PLASMAS
Analysis and experiments of a whistler-wave plasma thruster
[DE94-001533] p 2209 N94-23012
Modelling of thermal argon plasmas
[ETN-94-95363] p 2554 N94-25300
THERMAL PROTECTION
NASA/USRA advanced design program
[NASA-CR-195548] p 2180 N94-24492
Debris/ice/TPS assessment and integrated photographic analysis for Shuttle mission STS-58
[NASA-TM-109194] p 2200 N94-24577
Configuration development study of the OSU 1 hypersonic research vehicle
[NASA-CR-195522] p 2181 N94-24591
Development of a nondestructive vibration technique for bond assessment of Space Shuttle tiles
[NASA-CR-195163] p 2201 N94-24919
Plasma sprayed thermal barrier coatings: Production, characterization and testing
[ISBN-9-03-860082-8] p 2555 N94-25439
Effect of longitudinal vibration on the capillary limit of a wrapped screen wick copper/water heat pipe
[AD-A273830] p 2571 N94-25524
THERMAL RADIATION
Improved thermal force modeling for GPS satellites
p 2207 N94-23259
Uncertainty analysis of diffuse-gray radiation enclosure problems: A hypersensitive case study
p 2320 N94-23637
The IRGen infrared data base modeler
p 2440 N94-25496
THERMAL RESISTANCE
Advanced materials for radiation-cooled rockets
p 2214 N94-23052
THERMAL SHOCK
Plasma sprayed thermal barrier coatings: Production, characterization and testing
[ISBN-9-03-860082-8] p 2555 N94-25439
THERMAL STABILITY
Shear coaxial injector instability mechanisms
p 2213 N94-23047
Condensed-phase thermal decomposition of TATB investigated by Atomic Force Microscopy (AFM) and Simultaneous Thermogravimetric Modulated Beam Mass Spectrometry (STMBMS)
[DE94-000396] p 2232 N94-23298
Ceramic silicon-boron-carbon fibers from organic silicon-boron-polymers
[NASA-CASE-ARC-11956-1-SB] p 2253 N94-23311
A method to remove intercalates from bromine and iodine intercalated carbon fibers
[NASA-TM-106443] p 2222 N94-23591
Hubble Space Telescope high speed photometer orbital verification
[NASA-CR-189333] p 2204 N94-24226
An overview on the main available ceramic composites and their processing routes p 2255 N94-24229
CMC design consequences p 2256 N94-24238
Preparation and properties of translucent gamma-aluminium oxynitride
[ETN-94-95305] p 2263 N94-25281
THERMAL STRESSES
Thermal fatigue: A literature review
[PB93-226306] p 2375 N94-23120
Fully coupled nonlinear thermomechanical analysis including general contact in PALM2D
[DE94-001661] p 2568 N94-23216
Analysis of local delaminations caused by angle ply matrix cracks
[NASA-TM-109052] p 2228 N94-24083
Numerical modeling of physical vapor transport under microgravity conditions: Effect of thermal creep and stress p 2223 N94-24340
Strength and life of pressure vessels subjected to impacts and thermomechanical GFRP loading
[VTT-JULK-771] p 2379 N94-25418
THERMAL VACUUM TESTS
Thermal control system for SSF sensor/electronics
[SAND-92-0652C] p 2321 N94-23640
THERMISTORS
Thermistor controlled current source versatile temperature sensor
[AD-D015979] p 2345 N94-25037
THERMOCHEMISTRY
Thermochemistry of the actinides
[DE94-000895] p 2231 N94-22943
THERMOCLINES
Vertical motion in the SYNOP central array
[AD-A273593] p 2418 N94-24795
Flow and temperature distribution in a naturally stratified thermal storage tank
[AD-A273511] p 2336 N94-24821
THERMOCOUPLES
High temperature, oxidation resistant noble metal-Al alloy thermocouple
[NASA-CASE-LEW-15515-1] p 2343 N94-23826
Investigation of the heat handling capabilities of DIII-D neutral beamline internal components
[DE94-001107] p 2553 N94-24756
THERMODYNAMIC CYCLES
Enhanced absorption cycle computer model
[DE94-001997] p 2271 N94-23793
THERMODYNAMIC EFFICIENCY
CFD modeling of microwave electrothermal thrusters
p 2216 N94-23066
The effect of high altitude pressure on the power and efficiency of an airborne two-stroke engine
p 2155 N94-24253
THERMODYNAMIC EQUILIBRIUM
Thermodynamic models for bounding pressurant mass requirements of cryogenic tanks
[NASA-TM-106476] p 2346 N94-25202
THERMODYNAMIC PROPERTIES
Particle formation in a laser-heated aerosol reactor. Application to silicon and silicon nitride synthesis
[PB93-217982] p 2347 N94-22982
Heat transfer in rocket combustion chambers
p 2214 N94-23051
Thermodynamics of nickel-cadmium and nickel-hydrogen batteries p 2391 N94-23349
Instrument interface description for NOAA 2000 instruments with European morning spacecraft and/or NOAA-OPQ spacecraft
[NASA-TM-109406] p 2208 N94-23478
The possible effects of the natural and induced space environment on the optical and thermal properties of EOS surfaces p 2207 N94-23596
Enhanced absorption cycle computer model
[DE94-001997] p 2271 N94-23793
Humidity effects on soluble core mechanical and thermal properties (polyvinyl alcohol/microballoon composite) type CG extendospheres, volume 2
[NASA-CR-193893] p 2229 N94-24224
Coupled land surface/hydrologic/atmospheric models
p 2413 N94-24387
A study of element interaction in thermoacoustic engines
[AD-A273228] p 2569 N94-24777
Flow and temperature distribution in a naturally stratified thermal storage tank
[AD-A273511] p 2336 N94-24821
Thermophysical properties of simple liquid metals: A brief review of theory p 2248 N94-25130
THERMODYNAMICS
Study of improved methods for predicting chemical equilibria
[DE94-001647] p 2568 N94-22719
Computational fluid dynamic modelling of cavitation
p 2215 N94-23060
Lewis Research Center R and D Facilities
[NASA-TM-109400] p 2630 N94-23135
Alloys for hydrogen storage in nickel/hydrogen and nickel/metal hydride batteries p 2391 N94-23353
Effect of hydrogen exposure on a Cu-8 Cr-4 Nb alloy
[NASA-TM-106429] p 2243 N94-23556
Second law analysis of a conventional steam power plant p 2322 N94-23646
Improved gas core propulsion model
[DE94-000929] p 2220 N94-24511
Integral equations for the microstructures of supercritical fluids
[DE94-002460] p 2535 N94-24569
Stable non-Gaussian diffusive profiles
[PB93-238053] p 2489 N94-24610
Thermodynamic models for bounding pressurant mass requirements of cryogenic tanks
[NASA-TM-106476] p 2346 N94-25202
Phase structure of the two-dimensional phi(4) field theory within thermo-field dynamics
[DE93-616850] p 2570 N94-25337
Hydride thermodynamic machines
[VTT-JULK-768] p 2571 N94-25416
THERMOELECTRIC GENERATORS
SP-100 heat transport technology development
[DE94-000769] p 2218 N94-23452
Development testing of the two-watt RTG heat source and Hastelloy-S/T-111 alloy compatibility studies
[DE94-002875] p 2243 N94-23784
THERMOELECTRIC MATERIALS
Large-scale production of Si(0.8)Ge(0.2) thermoelectric alloys by mechanical alloying
[DE94-000695] p 2243 N94-23753
THERMOELECTRICITY
Thermoelectric cooled, purge-and-trap device for enhancing the utility of fiber optic VOC sensors
[DE94-001772] p 2541 N94-22722
Large-scale production of Si(0.8)Ge(0.2) thermoelectric alloys by mechanical alloying
[DE94-000695] p 2243 N94-23753
THERMOGRAPHY
Fiber optic temperature sensor using a Y2O2S:Eu thermographic phosphor
[DE94-000331] p 2543 N94-23461
THERMOGRAVIMETRY
A pressurized thermogravimetric analyzer for use in studies of gas/solid systems
[DE94-001224] p 2342 N94-22989
Potent solvents for C60 and their utility for the rapid acquisition of 13CNMR data for fullerenes
[AD-A273349] p 2235 N94-24925
THERMOMECHANICAL TREATMENT
Characterization of the microstructure of Nb-1wt.%Zr-0.1wt.%C tubes as affected by thermomechanical processing
[NASA-TM-106381] p 2242 N94-23550
Thermomechanical processing of Ag-clad Bi2Sr2CaCu2O(x) superconductors
[DE94-002347] p 2563 N94-24624
THERMOPHYSICAL PROPERTIES
Workshop on the Thermophysical Properties of Molten Materials
[NASA-CP-10121] p 2246 N94-25120
Thermophysical property sensitivity effects in steel solidification p 2246 N94-25122
Establishment of computerized numerical databases on thermophysical and other properties of molten as well as solid materials and data evaluation and validation for generating recommended reliable reference data
p 2246 N94-25123
Dynamic measurements of thermophysical properties of metals and alloys at high temperatures by subsecond pulse heating techniques p 2247 N94-25124
An overview of the measurements of thermophysical properties and some results on molten superalloys and semiconductors p 2248 N94-25128
Thermophysical properties of simple liquid metals: A brief review of theory p 2248 N94-25130
Microwave techniques for physical property measurements p 2238 N94-25134
Electrostatic levitation technology for thermophysical properties of molten materials p 2238 N94-25135
THERMOPLASTIC RESINS
Surface and interfacial properties of polymer blends. A literature survey
[PB93-230191] p 2254 N94-23561
THERMOPLASTICITY
Full-scale fire testing of seat component materials
[AD-A273499] p 2174 N94-24941
THERMOSETTING RESINS
Metal-catalyzed alkynylation of brominated polyphenylenes: Thermoset precursors of high density monolithic glassy carbon
[AD-A273232] p 2259 N94-24789
Metal-catalyzed alkynylation of (Bromophenyl)Oligophenylenes: A rapid route to thermoset precursors of high density monolithic glass-like carbon
[AD-A273219] p 2260 N94-24863

THERMOSPHERE
Data analysis and theoretical studies of the upper mesosphere and lower thermosphere
[NASA-CR-195108] p 2402 N94-24089
Mesospheric and lower thermospheric winds, temperatures densities, and volume emission rates
[NASA-CR-195147] p 2403 N94-24486
THICK PLATES
Performance of the X-/Ka/KABLE-band dichroic plate in the DSS-13 beam waveguide antenna
p 2291 N94-23261
THICKNESS
Echocardiographic findings in trained aircrew: The effect of +Gz on cardiac structure (working group 18)
p 2424 N94-23320
Left ventricular hypertrophy and athlete's heart
p 2424 N94-23321
Examination of the physical, electrical, and microwave evolution of water into young sea ice
[AD-A273559] p 2418 N94-24918
THIN FILMS
Advanced research and technology development of MCFCs
[DE94-001918] p 2389 N94-22723
Polycrystalline thin film materials and devices
[DE93-018213] p 2389 N94-22862
Disilane LPCVD deposited silicon films: Deposition mechanisms, properties and capability of making transistors on thin films
[LAAS-93156] p 2252 N94-22910
A new automatic design method to develop multilayer thin film devices for high power laser applications
[DE93-632490] p 2347 N94-22967
Design refinement of multilayer optical thin film devices with two optimization techniques
[DE93-634228] p 2542 N94-22979
Customizable VLSI artificial neural network chips based on a novel technology
[DE94-001418] p 2307 N94-23008
A novel process monitoring and control system based on a neural manufacturing concept
[DE94-001516] p 2471 N94-23011
Generic microelectronic smart sensor platform for detection of toxic, hazardous, and flammable gases
[DE93-017626] p 2343 N94-23200
Research on polycrystalline thin-film CuInGaSe2 solar cells
[DE94-000203] p 2560 N94-23205
Amorphous silicon PVMaT, phase 2A
[DE93-018221] p 2390 N94-23295
Novel two-stage selenization methods for fabrication of thin-film CIS cells and submodules
[DE94-000220] p 2390 N94-23296
Transparent conducting thin films for spacecraft applications
[NASA-TM-106466] p 2218 N94-23370
Infrared analysis of vapor phase deposited tricresylphosphate (TCP)
[NASA-TM-106423] p 2253 N94-23371
Selective hydrogen separation by palladium-based composite membranes
[PB93-201671] p 2254 N94-23431
Pulsed Ion Beam Surface Analysis (PIBSA) as a means of in-situ real-time analysis of thin films during growth
[DE94-001276] p 2562 N94-23805
Skin friction measurement in complex flows using thin oil film techniques
[NASA-CR-194872] p 2327 N94-24098
Ordered organic thin films self-assembled from the vapor phase p 2223 N94-24339
Low-gravity electrodeposition and growth of polymer thin films with large third-order optical nonlinearities by electrochemical processes for devices: Thiophene-based polymers p 2225 N94-24346
Polydiacetylene thin films for nonlinear optical applications p 2225 N94-24347
Nonlinear optical thin films p 2225 N94-24349
Diffusion on Cu surfaces p 2251 N94-24428
Thin film cadmium telluride photovoltaic cells
[DE94-000201] p 2395 N94-24509
Ge-Au eutectic bonding of Ge (100) single crystals
[DE94-002281] p 2564 N94-24657
Electrochemically mediated polymerization of 2-pentadecylaniline confined to a planar liquid-liquid interface
[AD-A273541] p 2259 N94-24792
Ferroelectric thin films 3
[AD-A273394] p 2565 N94-25027
The nanometer-scale mechanics of gold films
[AD-A273307] p 2565 N94-25086
The nanostructure of multilayered films: A NMR study
[ETN-94-95347] p 2262 N94-25222
Metallic multilayers: Experimental investigation of magnetic anisotropy and magnetic interlayer coupling
[ETN-94-95364] p 2250 N94-25242
Laser ablation and deposition of metals
[ETN-94-95311] p 2351 N94-25294
Investigation and application of microwave electron cyclotron resonance plasma physical vapour deposition
[DE93-613909] p 2555 N94-25333
Template synthesis of electronically conductive polymers
[AD-A273673] p 2263 N94-25409
THIN WALLED SHELLS
Energy estimates and asymptotic analysis in the theory of shells
[PB93-225738] p 2374 N94-23113
The plastic response of a cylindrical shell subjected to an internal blast wave with a finite width shock front
p 2154 N94-24246
THIOLS
Interactions between organized, surface-confined monolayers and vapor-phase probe molecules. 7: Comparison of self-assemblying organomercaptan monolayers deposited on gold from liquid and vapor phases
[AD-A273196] p 2535 N94-24555
Synthesis and characterization of two-dimensional molecular recognition interfaces
[AD-A273177] p 2536 N94-24729
Chemically sensitive interfacial force microscopy: Contact potential measurements of self-assembling monolayer films
[AD-A273135] p 2234 N94-24772
THOMSON SCATTERING
1993 annual report for the Phaedrus-T RF current drive experiments
[DE94-001369] p 2550 N94-23192
Characterization of heat transport and radiation hydrodynamics in collisional laser plasmas using collective Thomson scattering
[DE94-001502] p 2349 N94-23209
THREE AXIS STABILIZATION
Decentralized autonomous attitude determination using an inertially stabilized payload p 2157 N94-24264
THREE DIMENSIONAL BODIES
Extracting projective information from single views of 3D point sets
[OUEL-1973/93] p 2464 N94-25471
THREE DIMENSIONAL FLOW
Efficiency and reliability enhancements in propulsion flowfield modeling p 2215 N94-23055
Development and application of new algorithms for the simulation of viscous compressible flows with moving bodies in three dimensions
[AD-A273514] p 2338 N94-25157
THREE DIMENSIONAL MODELS
Mobility analysis, simulation, and scale model testing for the design of wheeled planetary rovers
p 2370 N94-23425
A structural design methodology for large angle articulated trusses considering realistic joint modeling
p 2376 N94-23560
Unsteady three-dimensional thermal field prediction in turbine blades using nonlinear BEM
p 2325 N94-23665
Analysis of time-domain acoustic wavefields in horizontally continuously layered configurations based on the modified Cagniard method
[PB94-111044] p 2524 N94-23731
Generalized three-dimensional simulation of ferruled coupled-cavity traveling-wave-tube dispersion and impedance characteristics
[NASA-TP-3389] p 2310 N94-24056
Conceptual design of a device to measure hand swelling in a micro-gravity environment
[NASA-CR-195509] p 2437 N94-24330
Recent developments in the mathematical modelling and physical understanding of transport and dispersion in aquatic systems, with special reference to tidal waters
[PB94-111135] p 2418 N94-24600
Multiannual simulations with the Mars climate model
p 2618 N94-24881
Three-dimensional numerical simulation of near-surface flows over the Martian north polar cap
p 2621 N94-24895
Image analysis technology applied to problems in crystallography
[AD-A273516] p 2566 N94-25288
THREE DIMENSIONAL MOTION
Quantitative assessment of human motion using video motion analysis p 2436 N94-24203
Heat transfer and flow structure in end-wall boundary layers
[AD-A273470] p 2335 N94-24689
THRESHOLD VOLTAGE
Generic microelectronic smart sensor platform for detection of toxic, hazardous, and flammable gases
[DE93-017626] p 2343 N94-23200
The role of emitter states in magnetotunneling through double-barrier resonant-tunneling diodes at high magnetic fields
[REPT-A-2658] p 2564 N94-24959
THRUST BEARINGS
Spline screw multiple rotations mechanism
[NASA-CASE-GSC-13452-1] p 2352 N94-23078
THRUST CHAMBERS
Small rocket flowfield diagnostic chambers
p 2210 N94-23030
An experimental study of characteristic combustion-driven flows for CFD validation
p 2212 N94-23040
Numerical investigation of two- and three-dimensional heat transfer in expander cycle engines
p 2213 N94-23048
Advanced materials for radiation-cooled rockets
p 2214 N94-23052
Effect of hydrogen exposure on a Cu-8 Cr-4 Nb alloy
[NASA-TM-106429] p 2243 N94-23556
STE thrust chamber technology: Main injector technology program and nozzle Advanced Development Program (ADP)
[NASA-CR-193919] p 2221 N94-25019
THRUST VECTOR CONTROL
Thrust vectoring theory, laboratory and flight tests
p 2155 N94-24251
Development of high-angle-of-attack nose-down pitch control margin design guidelines for combat aircraft
p 2164 N94-25107
THRUSTORS
Optimization of energy transfer in microwave electrothermal thrusters p 2216 N94-23065
CFD modeling of microwave electrothermal thrusters
p 2216 N94-23066
Advanced space propulsion concepts
p 2216 N94-23067
Stationary plasma thruster plume characteristics
[NASA-CR-194454] p 2219 N94-24361
THULIUM
Investigation of the optical and laser properties of Tm and Ho in YAG anf YLF
[REPT-94-001] p 2563 N94-24404
Excited state dynamics of thulium ions in yttrium aluminum garnets
[NASA-CR-195159] p 2564 N94-25024
THUNDERSTORMS
Lightning studies using LDAR and LLP data
p 2416 N94-23238
TIDES
Dynamics of the atmosphere of Mars: Review of some outstanding problems p 2620 N94-24888
TILES
Development of a nondestructive vibration technique for bond assessment of Space Shuttle tiles
[NASA-CR-195163] p 2201 N94-24919
TILT ROTOR AIRCRAFT
Wind tunnel test of a variable-diameter tiltrotor (VDTR) model
[NASA-CR-177629] p 2181 N94-24796
Aeroelastic response and stability of tiltrotors with elastically-coupled composite rotor blades
[NASA-TM-108758] p 2182 N94-24953
TILTING ROTORS
Aeroelastic response and stability of tiltrotors with elastically-coupled composite rotor blades
[NASA-TM-108758] p 2182 N94-24953
TIME CONSTANT
Rime-, mixed- and glaze-ice evaluations of three scaling laws
[NASA-TM-106461] p 2173 N94-24047
TIME DEPENDENCE
Feedback linearization of parametrized nonlinear time-varying systems
[MEMO-1126] p 2470 N94-22714
The theoretical accuracy of Runge-Kutta time discretizations for the initial boundary value problem: A careful study of the boundary error
[NASA-CR-191561] p 2480 N94-23272
Time dependent behavior of a graphite/thermoplastic composite and the effects of stress and physical aging
[NASA-TM-109047] p 2228 N94-23280
Response-coefficient method for heat-conduction transients with time-dependent inputs
p 2326 N94-23671
Computation of large-scale statistics in decaying isotropic turbulence p 2332 N94-24167
A statistical analysis of recent Naval Experimental Diving Unit (NEDU) single-depth human exposures to 100 percent oxygen at pressure
[AD-A273488] p 2427 N94-24950
Preliminary results on time-varying feedback stabilization of a nonholonomic car-like mobile robot
[INRIA-RR-1512] p 2475 N94-24963

TIME DIVISION MULTIPLE ACCESS
Adaptive data rate control TDMA systems as a rain attenuation compensation technique
p 2287 N94-22821
Modulation and synchronization technique for MF-TDMA system
[NASA-CR-194448] p 2304 N94-25266
TIME DIVISION MULTIPLEXING
Improved frame synchronization schemes for INMARSAT-B/M SCPC and TDM channels
p 2285 N94-22806
TIME LAG
Measurement of multipath delay profile in land mobile satellite channels p 2283 N94-22793
Linear time algorithm to schedule trees with communication delays optimally on two machines
[PB93-237782] p 2451 N94-23441
Genericity of stabilizability for time-delay systems
[PB93-237725] p 2475 N94-24762
Develop advanced nonlinear signal analysis topographical mapping system
[NASA-CR-194785] p 2389 N94-24856
TIME MEASUREMENT
Solid state Time Base Corrector (TBC)
[AD-D015981] p 2312 N94-25039
TIME OF FLIGHT SPECTROMETERS
Dual-purpose RTOF diffractometer facility at the ET-RR-1 reactor
[VTT-TIED-1425] p 2566 N94-25347
TIME OPTIMAL CONTROL
Throughput time control and due date reliability in tool and die shops
[ISBN-9-03-860182-4] p 2587 N94-25283
TIME SERIES ANALYSIS
A review of the Workshop on Fatigue Life Methodologies for Wind Turbines
[DE94-002039] p 2394 N94-23472
First order conditions for the maximum likelihood estimation of an exact ARMA model
[PB94-110533] p 2495 N94-23814
Dimensional analysis of acoustically propagated signals p 2528 N94-24217
TIME SIGNALS
Progress on the design of a data push architecture for an array of optimized time tagging pixels
[DE93-041011] p 2307 N94-22955
TIMING DEVICES
Modulation and synchronization technique for MF-TDMA system
[NASA-CR-194448] p 2304 N94-25266
TIMOSHENKO BEAMS
Vibrations of variable cross section Timoshenko beams p 2160 N94-24279
TIN OXIDES
Surface chemistry of liquid metals
p 2249 N94-25133
TIP SPEED
An overview of a model rotor icing test in the NASA Lewis Icing Research Tunnel
[NASA-TM-106471] p 2166 N94-23299
TIP VANES
The design of a turbine vane cooling system used in the topping cycle
[OUEL-1963/92] p 2353 N94-23164
TIROS SATELLITES
TOVS Pathfinder product validation and intercomparison p 2384 N94-23603
TISSUES (BIOLOGY)
Cellular and tissue injury during nonfreezing cold injury and frostbite
[AD-A270883] p 2423 N94-22732
TITAN
Science planning and sequencing for Cassini
p 2504 N94-23871
TITAN LAUNCH VEHICLES
Liquid rocket propulsion: Retrospective and prospects
p 2154 N94-24243
TITANATES
The elastic and electromechanical properties of BaTiO3 single crystal through the ferroelectric transition
[DE94-001437] p 2557 N94-22927
TITANIUM ALLOYS
Relationship of microstructure and mechanical properties for V-Cr-Ti alloys
[DE94-001431] p 2238 N94-22718
Evaluation of A5Si3Z(x) intermetallics for use as high temperature structural materials
[DE93-041127] p 2227 N94-22977
New extensions in the development of deformation processed metal-metal matrix composites
[DE94-000692] p 2227 N94-23004
Effect of neutron irradiation on tensile properties of V-Cr-Ti alloys
[DE94-001433] p 2240 N94-23194
Environmentally assisted cracking of high strength beta titanium alloys
[AD-A273598] p 2245 N94-24823
Matrix fatigue cracking mechanisms of alpha(2) TMC for hypersonic applications
[NASA-TM-106506] p 2230 N94-25186
TITANIUM BORIDES
Experimental investigation of ignition of boron/titanium composite particles p 2159 N94-24275
TITANIUM CARBIDES
In-vacuum performance of Fomblin Z25-lubricated, 52100 steel bearings with TiC-coated balls
p 2358 N94-24011
TITANIUM COMPOUNDS
Status of the development of rechargeable lithium cells p 2392 N94-23354
TITANIUM NITRIDES
Electrochemical behavior of ion-plated TiN and Cu-Cr coatings
[AD-A273411] p 2235 N94-24784
TOBACCO
Chronic obstructive pulmonary disease
p 2425 N94-23324
TOKAMAK DEVICES
Massachusetts Institute of Technology Plasma Fusion Center 1992-1993 report to the President
[DE94-001725] p 2548 N94-22721
Active probing of plasma edge turbulence and feedback studies on the Texas Experimental Tokamak (TEXT)
[DE94-001017] p 2548 N94-22945
Superconducting magnet system for the TPX Tokamak
[DE94-001535] p 2549 N94-23013
Structural analysis of a superconducting central solenoid for the Tokamak Physics Experiment
[DE94-001536] p 2549 N94-23014
CAMAC throughput of a new RISC-based data acquisition computer at the DIII-D tokamak
[DE94-001113] p 2550 N94-23182
1993 annual report for the Phaedrus-T RF current drive experiments
[DE94-001369] p 2550 N94-23192
Chaos and simple determinism in reversed field pinch plasmas: Nonlinear analysis of numerical simulation and experimental data
[DE94-001575] p 2550 N94-23211
Nonlinear ion-mixing-mode particle transport in the dissipative trapped electron regime
[DE94-000989] p 2533 N94-23435
Computational model of surface ablation from tokamak disruptions
[DE94-002204] p 2550 N94-23474
The role of the radial electric field in confinement and transport in H-mode and VH-mode discharges in the DIII-D tokamak
[DE94-002746] p 2551 N94-23782
Performance characteristics of the DIII-D advanced divertor cryopump
[DE94-002745] p 2354 N94-23797
Fusion plasma theory project summaries
[DE94-001712] p 2551 N94-23808
IPP Prague Contributions to the IAEA Technical Committee Meeting on Research Using Small Tokamaks
[IPPCZ-329] p 2551 N94-24293
Some theoretical problems of magnetic diagnostics in tokamaks and stellarators
[NIFS-262] p 2551 N94-24306
Pellet ablation in the large helical device
[NIFS-260] p 2551 N94-24358
Temporal behavior of the electron density profile during limiter biasing in the HYBTOK-2 tokamak
[NIFS-257] p 2552 N94-24456
Stabilization of the external kink and other MHD issues
[DE94-001541] p 2552 N94-24502
Plasma initiation in a tokamak with conducting superstructure: First results from Alcator C-MOD
[DE94-001565] p 2552 N94-24504
Start-up simulations of the PULSAR pulsed tokamak reactor
[DE94-002634] p 2552 N94-24519
Tokamak Physics Experiment (TPX) cost and performance trade studies using supercode
[DE94-002720] p 2553 N94-24628
Investigation of the heat handling capabilities of DIII-D neutral beamline internal components
[DE94-001107] p 2553 N94-24756
Fluid velocity and electromagnetic forces measured by a rotating Langmuir probe in the scrape off layer of JFT-2M
[OUEL-1968/92] p 2554 N94-25327
LHCD (low hybrid current drive) experiment on the HT-6B tokamak
[DE93-613720] p 2555 N94-25331
Effect of LHCD (low hybrid current drive) on tearing mode instability
[DE93-613700] p 2555 N94-25344
TOLERANCES (MECHANICS)
Damage tolerance of pressurized graphite/epoxy tape cylinders under uniaxial and biaxial loading
[NASA-CR-195101] p 2377 N94-24587
TOLLMIEN-SCHLICHTING WAVES
Computational fluid mechanics
[NASA-CR-194765] p 2337 N94-24859
TOOLS
A system for the challenging task of collecting samples from a comet surface p 2358 N94-24007
TOPEX
TOPEX/Poseidon precision orbit determination production and expert system p 2196 N94-23920
TOPOGRAPHY
A DTM-based path planning method for planetary rovers p 2370 N94-23423
Nonlinear dynamics applied to atmospheric prediction
[AD-A273437] p 2404 N94-24674
Tools for visualizing landscape pattern for large geographic areas
[DE94-001121] p 2388 N94-24757
Seafloor characterization/Galapagos propagating rift
[AD-A273586] p 2419 N94-25165
TOPOLOGY
Supercomputer networking for space science applications
[NASA-CR-194876] p 2465 N94-23085
Structures of tetrahedrization: A mathematical and algorithmical point of view
[ETN-94-95172] p 2480 N94-23166
Lacunary series as quadratic differentials in conformal dynamics
[PB93-238061] p 2481 N94-23547
When an infinitely-renormalizable endomorphism of the interval can be smoothed
[PB93-238087] p 2481 N94-23548
Non-trivial examples of real isolated singularity at the origin
[PB94-110939] p 2487 N94-23787
Tools for visualizing landscape pattern for large geographic areas
[DE94-001121] p 2388 N94-24757
Quantum optical aspects of topological phases, such as Berry's phase
[AD-A273632] p 2570 N94-25028
Radar target discrimination systems using artificial neural network topology
[AD-D015984] p 2301 N94-25041
The fundamental group of the complement of complexified real arrangements
[DE93-616847] p 2491 N94-25214
TOPPING CYCLE ENGINES
The design of a turbine vane cooling system used in the topping cycle
[OUEL-1963/92] p 2353 N94-23164
TOROIDAL PLASMAS
Chaos in plasma simulation and experiment
[DE94-001574] p 2549 N94-22963
Plasma research in the Madison Symmetric Torus (MST)
[DE94-002318] p 2549 N94-22976
Fluctuations and confinement in ATF
[DE94-000485] p 2549 N94-22998
Superconducting magnet system for the TPX Tokamak
[DE94-001535] p 2549 N94-23013
1993 annual report for the Phaedrus-T RF current drive experiments
[DE94-001369] p 2550 N94-23192
Fusion plasma theory project summaries
[DE94-001712] p 2551 N94-23808
Pellet ablation in the large helical device
[NIFS-260] p 2551 N94-24358
Stabilization of the external kink and other MHD issues
[DE94-001541] p 2552 N94-24502
Plasma initiation in a tokamak with conducting superstructure: First results from Alcator C-MOD
[DE94-001565] p 2552 N94-24504
TORQUE
Spline screw multiple rotations mechanism
[NASA-CASE-GSC-13452-1] p 2352 N94-23078
A novel rotary actuator for spacecraft
p 2361 N94-24034
Establishing a relationship between maximum torque production of isolated joints to simulate EVA ratchet push-pull maneuver: A case study p 2437 N94-24206
The effect of high altitude pressure on the power and efficiency of an airborne two-stroke engine
p 2155 N94-24253
Torque equilibrium attitudes for the Space Station
p 2208 N94-24449

TORQUE MOTORS
Low melting temperature alloy deployment mechanism
p 2356 N94-23997
Development of a Low-Temperature Gear Motor (LOG) p 2361 N94-24032
High resolution encoder-motor used in the orbital spin scan radiometer, GOES VAS satellites
p 2209 N94-24038

TORSION
The torsion space nucleic acids molecular mechanics program DUPLEX: Surveying conformation space by potential energy minimization
[DE94-002441] p 2563 N94-24567

TORUSES
Plasma research in the Madison Symmetric Torus (MST)
[DE94-002318] p 2549 N94-22976
Number of moduli of families of curves on toric surfaces
[PB93-230381] p 2479 N94-23121

TOTAL ENERGY SYSTEMS
Diffusion on Cu surfaces p 2251 N94-24428

TOTAL OZONE MAPPING SPECTROMETER
Participation in TOMS missions
[NASA-CR-195110] p 2398 N94-24078
Nimbus-7 Total Ozone Mapping Spectrometer (TOMS) data products user's guide
[NASA-RP-1323] p 2410 N94-24355

TOTAL QUALITY MANAGEMENT
The application of total quality management principles to spacecraft mission operations p 2374 N94-23931
Mission operations and command assurance: Instilling quality into flight operations p 2374 N94-23932

TOUCH
Mechanisms of eye-hand coordination
[AD-A273687] p 2428 N94-25437

TOXICITY
Exploratory report nickel and nickel compounds
[PB93-223998] p 2242 N94-23496
Exploratory report antimony and antimony compounds
[PB93-224004] p 2397 N94-23497
In vitro system for studying metabolism of environmental chemicals in human cells
[AD-A273427] p 2421 N94-24688
A statistical analysis of recent Naval Experimental Diving Unit (NEDU) single-depth human exposures to 100 percent oxygen at pressure
[AD-A273488] p 2427 N94-24950
The effects of zinc borate addition on the flammability characteristics of polyester, vinyl ester, and epoxy glass reinforced plastics
[AD-A273164] p 2262 N94-25136
An exploratory stochastic model for toxic effects on cells
[AD-A273438] p 2422 N94-25146

TOXINS AND ANTITOXINS
An exploratory stochastic model for toxic effects on cells
[AD-A273438] p 2422 N94-25146

TRACE CONTAMINANTS
Ethylene trace-gas techniques for high-speed flows
[NASA-TM-106491] p 2169 N94-24335

TRACE ELEMENTS
Ethylene trace-gas techniques for high-speed flows
[NASA-TM-106491] p 2169 N94-24335
A dynamic melting model for the origin of Apollo 15 olivine-normative and quartz-normative mare basalts
p 2615 N94-24371
Measurement of HO2 and other trace gases in the stratosphere using a high resolution far-infrared spectrometer
[NASA-CR-195173] p 2404 N94-24738
Rice cultivation and methane emission: Documentation of distributed geographic data sets
[NASA-TM-104595] p 2381 N94-24800
Reactive trace metals as indicators of subduction and ventilation processes in the ocean
[AD-A273585] p 2419 N94-25164

TRACKING (POSITION)
A tracking sonar sensor for vehicle guidance
[OUEL-1956/92] p 2472 N94-23179
An adaptive multigrid model for hurricane track prediction p 2416 N94-23687
A mixed map/variable structure observer for target tracking p 2157 N94-24263
Predictive head movement tracking using innovations generated by Kalman filters
[ISBN-0-315-83371-8] p 2427 N94-24467

TRACKING FILTERS
Predictive head movement tracking using innovations generated by Kalman filters
[ISBN-0-315-83371-8] p 2427 N94-24467

TRACKING NETWORKS
Resource allocation planning with international components p 2520 N94-23963
Scheduling the future NASA Space Network: Experiences with a flexible scheduling prototype
p 2520 N94-23965

TRACKING STATIONS
NASDA satellite mission operation system and operations p 2501 N94-23854
Radioastron flight operations p 2502 N94-23861

TRADEOFFS
Squaring-down and the problems of almost-zeros for continuous-time systems
[PB93-237758] p 2489 N94-24608
Tokamak Physics Experiment (TPX) cost and performance trade studies using supercode
[DE94-002720] p 2553 N94-24628

TRAFFIC
Estimation of delays and emissions at four-way junctions with different forms of regulation, principally four-way mandatory stop
[PB94-105236] p 2398 N94-23813

TRAILING EDGE FLAPS
Reduction of structural loads using maneuver load control on the Advanced Fighter Technology Integration (AFTI)/F-111 mission adaptive wing
[NASA-TM-4526] p 2168 N94-24295

TRAILING EDGES
Off-design performance of crenulated blades in a linear compressor cascade
[AD-A273744] p 2340 N94-25534

TRAINING AIRCRAFT
Aircraft wing structure detail design
[NASA-CR-195485] p 2180 N94-24498
Cockpit control system
[NASA-CR-195488] p 2190 N94-24957
Aircraft wing structural detail design (wing, aileron, flaps, and subsystems)
[NASA-CR-195487] p 2183 N94-24974
Design project: Viper
[NASA-CR-195484] p 2184 N94-25021

TRAINING DEVICES
Intelligent tutoring and aiding in satellite ground control p 2443 N94-23929
Aircraft empennage structural detail design
[NASA-CR-195496] p 2179 N94-24332
Cockpit control system conceptual design
[NASA-CR-195543] p 2190 N94-24551

TRAINING EVALUATION
KSC management training system project
p 2574 N94-23246

TRAJECTORIES
Decoupling problems around a trajectory: From linearity to nonlinearity
[MEMO-1115] p 2469 N94-22703

TRAJECTORY ANALYSIS
Path planning by querying persistent stores of trajectory segments
[NASA-CR-194789] p 2451 N94-23301
On the effect of the damping coefficients on the trajectories of symmetric and non-symmetric stores
p 2155 N94-24250
Comparison of c.t.s. based prediction of store trajectory with flight test data p 2158 N94-24268
NASA/USRA advanced design program
[NASA-CR-195548] p 2180 N94-24492
NASA LaRC Workshop on Guidance, Navigation, Controls, and Dynamics for Atmospheric Flight, 1993
[NASA-CP-10127] p 2162 N94-25096

TRAJECTORY CONTROL
Marsohkod movement control p 2370 N94-23418

TRAJECTORY MEASUREMENT
Comparison of c.t.s. based prediction of store trajectory with flight test data p 2158 N94-24268

TRAJECTORY OPTIMIZATION
Perspective of creation of means for collecting information concerning transport situation
p 2370 N94-23420
A DTM-based path planning method for planetary rovers p 2370 N94-23423
Approximate optimal guidance for the advanced launch system
[NASA-CR-4568] p 2198 N94-24752
Optimal RTLS abort trajectories for an HL-20 personnel launch vehicle p 2165 N94-25114

TRAJECTORY PLANNING
Motion planning for a non-holonomic mobile in a dynamic workspace
[ETN-94-95180] p 2470 N94-22898
Path planning by querying persistent stores of trajectory segments
[NASA-CR-194789] p 2451 N94-23301
Perspective of creation of means for collecting information concerning transport situation
p 2370 N94-23420
A DTM-based path planning method for planetary rovers p 2370 N94-23423
Physical modeling and dynamic simulation of planet vehicles: Application to the motion prediction
p 2371 N94-23426
Conflict-free trajectory planning for air traffic control automation
[NASA-TM-108790] p 2174 N94-25272

TRANSDUCERS
Improved magnetostrictive transducer drive elements achieved by reduction of crystalline defects and improved crystalline orientation
[AD-A273391] p 2313 N94-25276

TRANSFER FUNCTIONS
Head related transfer function pseudo-stereophony
[NASA-CASE-ARC-11919-1-NP] p 2525 N94-23312
Squaring-down and the problems of almost-zeros for continuous-time systems
[PB93-237758] p 2489 N94-24608
Exploiting structure: Introduction and motivation
[NASA-CR-195136] p 2490 N94-24847

TRANSFER ORBITS
Theory and computation of optimal low- and medium-thrust transfers
[NASA-CR-194812] p 2217 N94-23275
Assessment of an SP-100 bi-modal propulsion and power system
[DE94-000889] p 2218 N94-23433
HISPASAT launch and early operations phases: Computation and monitoring of geostationary satellite positioning p 2514 N94-23928

TRANSFORMATIONS (MATHEMATICS)
Implementation and parallelization of fast matrix multiplication for a fast Legendre transform
[DE94-002184] p 2478 N94-22975
Integer cosine transform compression for Galileo at Jupiter: A preliminary look p 2292 N94-23266
System identification using a wavelet-based approach
[DE94-002191] p 2293 N94-23473
Relational algebra and equational proofs
[PB94-110822] p 2486 N94-23724
Exact transformation of the anisotropic Ginzburg-Landau model and its consequences
[DE94-002208] p 2562 N94-23795
Quasiconformal mappings, operators on Hilbert space, and local formulae for characteristic classes
[PB93-238079] p 2488 N94-24536
Optical wavelet transform processor
[AD-A273625] p 2546 N94-24731
Deviation equations of Synge and Schild in spaces with affine connection and metric, and equations for gravitational waves detectors
[DE93-616852] p 2571 N94-25339
DCT quantization matrices visually optimized for individual images p 2442 N94-25509

TRANSIENT HEATING
Strain gage measurement errors in the transient heating of structural components
[NASA-TM-104274] p 2376 N94-23487
Advanced X ray Astrophysics Facility-Imaging (AXAF-I) thermal analyses using Integrated Thermal Analysis System (ITAS) program p 2320 N94-23635
Response-coefficient method for heat-conduction transients with time-dependent inputs
p 2326 N94-23671

TRANSIENT RESPONSE
Transient analysis of circuits including frequency-dependent components using transgyrator and convolution
[PB93-225001] p 2308 N94-23130

TRANSISTOR AMPLIFIERS
Cryogenic, low-noise high electron mobility transistor amplifiers for the Deep Space Network
p 2291 N94-23262

TRANSISTORS
Floating well based design methodology aimed to improve latch-up immunity in a CMOS/DMOS smart power technology
[LAAS-93093] p 2556 N94-22905
Fabrication of sub-40-nm p-n junctions for 0.18 micron MOS device applications using a cluster-tool-compatible, nanosecond thermal doping technique
[DE94-001608] p 2309 N94-23520

TRANSITION FLOW
Transition to turbulence in an elliptic vortex
p 2331 N94-24161
Vortical structure in a forced plane mixing layer
p 2331 N94-24162
Sound radiation due to boundary layer transition
p 2332 N94-24163
Center for modeling of turbulence and transition: Research briefs, 1993
[NASA-TM-106383] p 2333 N94-24336
Workshop on Computational Turbulence Modeling
[NASA-CP-10130] p 2333 N94-24460
Relationship between transition and modes of instability in supersonic boundary layers
[NASA-CR-4562] p 2336 N94-24725

Computational fluid mechanics
[NASA-CR-194765] p 2337 N94-24859

TRANSITION METALS

Vaporization behavior of non-stoichiometric refractory carbide materials and direct observations of the vapor phase using laser diagnostics
[DE93-040094] p 2348 N94-23203

Density functional studies: First principles and semi-emperical calculations of clusters and surfaces
[DE94-002836] p 2561 N94-23214

Magnetic resonance studies of 3d transition metal impurities in compound semiconductors
[PB93-232197] p 2243 N94-23714

New methane chemistry synthesis of materials for reversible uptake and useful functionalization of methane
[PB94-112786] p 2233 N94-23801

TRANSITION POINTS

Effects of neutron irradiation and hydrogen on ductile-brittle transition temperatures of V-Cr-Ti alloys
[DE94-001466] p 2240 N94-23009

TRANSITION TEMPERATURE

Anisotropic uniaxial pressure effects in YBa2Cu3O(7-delta)
[DE94-001456] p 2557 N94-22929

Anomalous magnetoresistance behavior of superconducting Nd(2-x)Ce(x)CuO(4-y) single crystal
[DE94-000806] p 2558 N94-22941

Irradiation damage behavior of low alloy steel wrought and weld materials
[DE94-000519] p 2239 N94-22999

Effects of neutron irradiation and hydrogen on ductile-brittle transition temperatures of V-Cr-Ti alloys
[DE94-001466] p 2240 N94-23009

Development of small punch testing technique and its application to evaluation of mechanical properties degradation
[DE94-001193] p 2375 N94-23184

TRANSLATING

Projectile transverse motion and stability in electromagnetic induction launchers
[DE94-001557] p 2198 N94-23210

An automated tool to facilitate code translation for software fault tree analysis
[AD-A273205] p 2457 N94-24556

TRANSMISSION ELECTRON MICROSCOPY

Magnetic properties and transmission electron microscopy investigations of Nd-Fe-B-Co-Al melt spun ribbons
[PB93-201531] p 2561 N94-23428

Ge-Au eutectic bonding of Ge (100) single crystals
[DE94-002281] p 2564 N94-24657

TRANSMISSION LINES

Layered parallel interface for an active antenna array
[AD-D016002] p 2301 N94-25045

Temperature dependent performance of Coplanar Waveguide (CPW) on substrates of various materials
[NASA-TM-106505] p 2313 N94-25170

TRANSMISSION LOSS

Comparison of HF groundwave propagation models
[AD-A273146] p 2299 N94-24668

Design and testing of ubitron amplifier tubes
[AD-A273297] p 2311 N94-24818

TRANSMISSION RATE (COMMUNICATIONS)

Adaptive data rate control TDMA systems as a rain attenuation compensation technique
p 2287 N94-22821

Compression for an effective management of telemetry data p 2518 N94-23956

Reducing video frame rate increases remote optimal focus time
[NASA-TM-104018] p 2431 N94-23970

A small satellite design for deep space network testing and training
[NASA-CR-195526] p 2205 N94-24702

Delay-insensitive communication
[ETN-94-95315] p 2304 N94-25303

TRANSMISSIONS (MACHINE ELEMENTS)

Metal band drives in spacecraft mechanisms
p 2355 N94-23987

NASA/Army rotorcraft transmission research, a review of recent significant accomplishments
[NASA-TM-106508] p 2367 N94-25161

TRANSMITTER RECEIVERS

The Globalstar mobile satellite system for worldwide personal communications p 2282 N94-22786

Integration and test of high-speed transmitter electronics for free-space laser communications
[NASA-TM-106295] p 2295 N94-24101

Analog communication transmitter and receiver test procedures
[AD-A273423] p 2300 N94-24687

Layered parallel interface for an active antenna array
[AD-D016002] p 2301 N94-25045

Method and apparatus of generating sum or difference signals corresponding to an apparent beam in a monopulse radar system
[AD-D015998] p 2302 N94-25056

TRANSMITTERS

Systems implications of L-band fade data statistics for LEO mobile systems p 2284 N94-22799

Performance of the unique-word-reverse-modulation type demodulator for mobile satellite communications
p 2286 N94-22813

TRANSONIC COMPRESSORS

Analysis and characteristics of compressor stall precursor signals in forward and AFT swept high speed compressor
[AD-A273820] p 2171 N94-25517

TRANSONIC FLOW

Issac, Jason Cherian ses in transonic flow
[NASA-CR-194837] p 2167 N94-24052

Evaluation of turbulence models in the PARC code for transonic diffuser flows
[NASA-TM-106391] p 2168 N94-24084

Experimental study of a turbulent boundary layer in presence of external manipulators of NACA 0009 profile in the transonic regime
[ISBN-0-315-57633-2] p 2333 N94-24177

TRANSONIC NOZZLES

Development of a code for wall contour design in the transonic region of axisymmetric and square nozzles
[NASA-CR-194857] p 2167 N94-23625

TRANSONIC SPEED

Experimental cavity pressure measurements at subsonic and transonic speeds. Static-pressure results
[NASA-TP-3358] p 2169 N94-24464

TRANSPARENCE

Transparent conducting thin films for spacecraft applications
[NASA-TM-106466] p 2218 N94-23370

TRANSPIRATION

Integrated use of hydrological modelling and remote sensing in the province of Drenthe (The Netherlands): Possibilities and restrictions
[REPT-61] p 2382 N94-23148

TRANSPONDERS

ROCSAT-1 telecommunication experiments
p 2279 N94-22770

Odyssey personal communications satellite system
p 2282 N94-22787

TRANSPORT AIRCRAFT

Pilot-vehicle interface
[DOT/FAA/CT-92/21] p 2430 N94-23083

Influence of active controls on the design process of a large transport aircraft p 2178 N94-24323

Current and future design methods for large transport aircraft p 2179 N94-24324

JB-300: An advanced medium size transport for 2005
[NASA-CR-195499] p 2179 N94-24401

NASA/USRA University Advanced Design Program, 1992-1993. The Diamondback: A simulated commercial air transportation study
[NASA-CR-195523] p 2180 N94-24462

The cetaceopteryx: A global range military transport aircraft
[NASA-CR-195519] p 2181 N94-24711

Conceptual design proposal: HUGO global range/mobility transport aircraft
[NASA-CR-195501] p 2181 N94-24787

Pilot-vehicle interface handbook, chapter 19. Volume 2: Digital systems validation
[DOT/FAA/CT-88/10-VOL-2] p 2438 N94-24830

Dumbo heavy lifter aircraft
[NASA-CR-195500] p 2182 N94-24915

The AC-120: The advanced commercial transport
[NASA-CR-195491] p 2182 N94-24966

A global range military transport: The ostrich
[NASA-CR-195494] p 2183 N94-24972

Weasel works SA-150: Design study of a 100 to 150 passenger transport aircraft
[NASA-CR-195489] p 2183 N94-24975

The RTL-46: A simulated commercial air transportation study
[NASA-CR-195524] p 2184 N94-25017

C-17 lot 3 production contract
[AD-A273180] p 2174 N94-25153

TRANSPORT PROPERTIES

Atomic-scale structure of grain boundaries: Correlations to grain boundary properties
[DE94-001289] p 2558 N94-22990

Modelling of solid polymer and direct methanol fuel cells: Phenomenological equations and analytical solutions
[PB93-224897] p 2390 N94-23102

Investigation of evolution-related aspects of bacterial rhodopsins
[NASA-CR-194826] p 2420 N94-23501

Comparison of numerical simulation and experimental data for steam-in-place sterilization
p 2326 N94-23669

Two-point PADE approximants for Stieltjes series
p 2490 N94-24768

Evidence for dust transport in Viking IR thermal mapper opacity data p 2620 N94-24892

Dust transport in the Martian atmosphere
p 2621 N94-24894

Modelling of thermal argon plasmas
[ETN-94-95363] p 2554 N94-25300

Effect of high frequency field on the transport properties of superlattice
[DE93-617047] p 2568 N94-25447

TRANSPORT THEORY

Numerical modeling of physical vapor transport under microgravity conditions: Effect of thermal creep and stress p 2223 N94-24340

Conservation equations for reacting gas flow
[PB94-111168] p 2334 N94-24574

The transition from diapirism to dike intrusion: Implications for planetary volcanism
[NASA-CR-195133] p 2403 N94-24580

The anomalous transport caused by particles transverse drift
[DE93-613685] p 2554 N94-25329

Collection and evaluation of numerical models with the aim to investigate the impact of aircraft emissions
[DLR-MITT-93-06] p 2400 N94-25414

Applications of the homogenization method to flow and transport in porous media
[BER-9110] p 2340 N94-25467

TRANSPORTATION

A multilevel cost-space approach to solving the balanced long transportation problem p 2483 N94-23678

TRANSPUTERS

A parallel PROLOG system for distributed memory multiprocessor
[ETN-94-95173] p 2465 N94-23167

High performance, low cost, self-contained, multipurpose PC based ground systems
p 2516 N94-23943

Transputer benchmarks and performance comparisons with other computing machines
[RR-467] p 2446 N94-25312

Advanced control structures: A transputer-based multi-robot system
[RR-468] p 2446 N94-25313

Horatio: Libraries for vision applications, release 2.0
[OUEL-1967/92] p 2593 N94-25326

Parallel processing methods for space based power systems p 2222 N94-25352

The transputer
[AD-A273688] p 2446 N94-25438

TRANSVERSE ACCELERATION

A comparison of in-bore projectile motion from an electromagnetic railgun versus that of a conventional cannon barrel
[AD-A273473] p 2198 N94-24690

TRAPPED PARTICLES

Fluctuations and confinement in ATF
[DE94-000485] p 2549 N94-22998

TRAVELING SALESMAN PROBLEM

On some approximately balanced combinatorial cooperative games
[MEMO-1113] p 2493 N94-22702

TRAVELING WAVE AMPLIFIERS

Inverse free electron laser beat-wave accelerator research
[DE94-002597] p 2349 N94-23702

TRAVELING WAVE TUBES

Phase linearity of the 914H coupled-cavity traveling wave tube
[NASA-CR-191056] p 2290 N94-23087

Generalized three-dimensional simulation of ferruled coupled-cavity traveling-wave-tube dispersion and impedance characteristics
[NASA-TP-3389] p 2310 N94-24056

TRAVELING WAVES

The characterization of reaction-convection-diffusion processes by travelling waves
[MEMO-1111] p 2273 N94-22729

Inverse free electron laser beat-wave accelerator research
[DE94-002597] p 2349 N94-23702

TREADS

Rail Corrugations
[ILR-BER-59] p 2269 N94-23581

Surface analysis of corrugated rail treads
p 2270 N94-23587

TREES (MATHEMATICS)

Causal labeled transition systems: A new approach for describing the behavior of concurrent systems
[LAAS-93179] p 2447 N94-22911

The explicit computation of integration algorithms and first integrals for ordinary differential equations with polynomials coefficients using trees
[NASA-CR-194787] p 2448 N94-23074

Medians and steiner trees
[PB94-110616] p 2486 N94-23708
The Third Twente Workshop on Graphs and Combinatorial Optimization
[PB94-110947] p 2486 N94-23722
Irreducible core of a minimum cost spanning tree game
[PB94-110962] p 2489 N94-24653
Data structures and amortized complexity in a functional setting
[ETN-94-95307] p 2476 N94-25290

TREND ANALYSIS
Long term trending of engineering data for the Hubble Space Telescope p 2516 N94-23942

TRIANGLES
Toughness and triangle-free graphs
[MEMO-1127] p 2478 N94-22715

TRIANGULATION
Structures of tetrahedrization: A mathematical and algorithmical point of view
[ETN-94-95172] p 2480 N94-23166
Dynamic ray tracing and its application in triangulated media
[DE94-000875] p 2402 N94-23516
An implicit numerical scheme for the simulation of internal viscous flows on unstructured grids
[NASA-TM-106437] p 2481 N94-23554
Expansion-based passive ranging
p 2176 N94-25504

TRIATOMIC MOLECULES
Energy transfer in solid explosives
[DE94-001523] p 2265 N94-23778

TRIBOLOGY
A rail corrugation theory which allows for contact patch size p 2269 N94-23582
A linear model for corrugation and its limit of validity
p 2269 N94-23584
Lateral high frequency oscillations and stability of a wheel rolling on a flexible track p 2269 N94-23585
Surface analysis of corrugated rail treads
p 2270 N94-23587
Surface observations of stick-slip oscillations in tightly conformal wheel/rail contacts p 2270 N94-23588
Contact analysis of rough rail surfaces
p 2270 N94-23589
An application of small-gap equations in sealing devices p 2325 N94-23668
The Fifth European Space Mechanisms and Tribology Symposium
[ESA-SP-334] p 2355 N94-23985
New tribocoating combination for vacuum operation
p 2355 N94-23990
Tribological behaviour of fluorinated resins and polyimide resins sliding over a metallic surface in liquid nitrogen
p 2355 N94-23991
Tribological characteristics of ball bearings lubricated with a sputtered molybdenum disulphide film in a vacuum under a high thrust load p 2355 N94-23992
The tribology of some MoS2-lubricated engineering ceramics p 2356 N94-23993
HERA (Hermes robot arm) overview
p 2357 N94-24005
Thermal vacuum performance of cycloid and harmonic gearboxes with solid (MoS2) and liquid (Braycote 601) lubrication p 2358 N94-24009
Tribological characterization of spatial wet lubricants under vacuum p 2264 N94-24010
In-vacuum performance of Fomblin Z25-lubricated, 52100 steel bearings with TiC-coated balls
p 2358 N94-24011
Development of gears for space use
p 2360 N94-24021
New pin-on-disk equipment for vacuum tribometry
p 2360 N94-24023
An analytical ultra-high vacuum tribometer for solid lubricant studies p 2361 N94-24033
An assessment of solid lubricant films for use in high temperature space applications p 2363 N94-24044
The development of dry-lubricated ceramic cages
p 2363 N94-24045
Investigation of the ultrafiltration technique using military greases
[AD-A273633] p 2261 N94-25029
Lubrication in cold rolling: Numerical simulation using multigrid techniques
[ISBN-9-09-005313-1] p 2262 N94-25230

TRIGGER CIRCUITS
VLSI-based video event triggering for image data compression
[NASA-TM-106500] p 2345 N94-25116
The data-acquisition and second level trigger system for ZEUS calorimeter
[ETN-94-95384] p 2541 N94-25256

TRIGONOMETRIC FUNCTIONS
Systematic construction of trigonometric neural networks
[PB93-200228] p 2474 N94-24544

TRIMERS
Electrochemical and electronic properties of neural and oxidized soluble orthogonally-fused thiophene oligomers
[AD-A273283] p 2260 N94-24815

TRIVALENT IONS
Excited state dynamics of thulium ions in yttrium aluminum garnets
[NASA-CR-195159] p 2564 N94-25024

TROPICAL METEOROLOGY
Diagnostic budgets of analyzed and modelled tropical plumes
[NASA-CR-194853] p 2409 N94-23621
Observational and modeling studies of heat, moisture, precipitation and global-scale circulation patterns
[NASA-CR-195148] p 2415 N94-24485
Observed and Navy operational global model climatologies of synoptic disturbances over the tropical western Pacific during winter 1991-1992
[AD-A273400] p 2416 N94-25071

TROPICAL REGIONS
Modal structure of variations in the tropical climate system. Part 2: Origins of the low-frequency mode
[MPIM-96] p 2407 N94-23199
Atmospheric moisture fields derived by satellite observations over the tropical Pacific Ocean
[NASA-CR-194852] p 2408 N94-23542
Convective organization in the Pacific ITCZ: Merging OLR, TOVS, and SSM/I information
[NASA-CR-194850] p 2408 N94-23619
A regional analysis of cloudy mean spherical albedo over the marine stratocumulus region and the tropical Atlantic Ocean
[NASA-CR-194771] p 2409 N94-24049
Worst case analysis: Earth sensor assembly for the tropical rainfall measuring mission observatory
[NASA-CR-189320] p 2311 N94-24754
Human impacts on soil carbon dynamics of deep-rooted Amazonian forests
[NASA-CR-195127] p 2399 N94-24861

TROPOSPHERE
In situ detection of tropospheric OH, HO2, NO2, and NO by laser-induced fluorescence in detection chambers at reduced pressures
[NASA-CR-194810] p 2397 N94-23277
Tropospheric Ozone Lidar Intercomparison Experiment, TROLIX 1991
[MPIM-102] p 2402 N94-24108
Implementation of a state of the art automated system for the production of cloud/water vapor motion winds from geostationary satellites
[NASA-CR-195087] p 2410 N94-24125
Northern hemisphere tropospheric mid-latitude circulation after violent volcanic eruptions
[MPIM-107] p 2403 N94-24491
The influence of orography on the transport of atmospheric constituents p 2619 N94-24886

TRUSSES
A structural design methodology for large angle articulated trusses considering realistic joint modeling
p 2376 N94-23560

TUMORS
Monoclonal antibodies directed against surface molecules of multicell spheroids
[NASA-CR-195102] p 2420 N94-23633
Annual research progress report, fiscal year 1992. Volume 2: Department of Clinical Investigation
[AD-A273584] p 2427 N94-24945

TUNABLE LASERS
Compact free electron lasers for medical applications
[AD-A273609] p 2350 N94-24934
Tunable lasers pumped by visible laser diodes
[AD-D016000] p 2350 N94-25044

TUNGSTEN
High energy collimating fine grids for HESP program
[NASA-CR-189317] p 2209 N94-24767

TUNGSTEN FLUORIDES
The reaction mechanism of W-CVD in Si
[ETN-94-95329] p 2261 N94-25084

TUNING
Compact free electron lasers for medical applications
[AD-A273609] p 2350 N94-24934
A theoretical investigation of electrically tunable birefringent optical filters as the special discriminator in hyperspectral imaging systems
[AD-A273743] p 2547 N94-25533

TUNNEL DIODES
The role of emitter states in magnetotunneling through double-barrier resonant-tunneling diodes at high magnetic fields
[REPT-A-2658] p 2564 N94-24959

TURBINE BLADES
Two stage turbine for rockets p 2215 N94-23059
The use of transition region characteristics to improve the numerical simulation of heat transfer in bypass transitional flows
[NASA-TM-106445] p 2320 N94-23525
Unsteady three-dimensional thermal field prediction in turbine blades using nonlinear BEM
p 2325 N94-23665
Nondestructive evaluations
[DE94-003020] p 2373 N94-24613

TURBINE PUMPS
SSME fuel preburner injector characterization
p 2211 N94-23037
Computational Fluid Dynamics (CFD) applications in rocket propulsion analysis and design
p 2214 N94-23054
Two stage turbine for rockets p 2215 N94-23059
Brush seals for cryogenic applications
p 2216 N94-23063
Foil bearings p 2371 N94-24415
Simulation of cryogenic turbopump annular seals
p 2371 N94-24440
Advanced launch system. Advanced development oxidizer turbopump program
[NASA-CR-193920] p 2367 N94-25174

TURBINES
Computation of flows in a turn-around duct and a turbine cascade using advanced turbulence models
p 2216 N94-23062

TURBOCOMPRESSORS
Turbine engine with induced pre-swirl at the compressor inlet
[CA-PATENT-1-317-467] p 2186 N94-23253
The 3-D numerical study of airflow in the compressor/combustor prediffuser and dump diffuser of an industrial gas turbine p 2324 N94-23660
Analysis and characteristics of compressor stall precursor signals in forward and AFT swept high speed compressor
[AD-A273820] p 2171 N94-25517
Off-design performance of crenulated blades in a linear compressor cascade
[AD-A273744] p 2340 N94-25534

TURBOFAN AIRCRAFT
Conceptual design proposal: HUGO global range/mobility transport aircraft
[NASA-CR-195501] p 2181 N94-24787

TURBOFAN ENGINES
Rolls-Royce in perspective: Past, present and future
[PNR-90882] p 2187 N94-23519
The RB211: The first 25 years
[PNR-90977] p 2187 N94-23570
A comparison of two multi-variable integrator windup protection schemes
[NASA-CR-194436] p 2190 N94-23590
JB-300: An advanced medium size transport for 2005
[NASA-CR-195499] p 2179 N94-24401
Fan noise research at NASA
[NASA-TM-106512] p 2530 N94-25172

TURBOFANS
Fan noise research at NASA
[NASA-TM-106512] p 2530 N94-25172

TURBOMACHINERY
Foil bearing research at Penn State
p 2215 N94-23058
An analysis for high Reynolds number inviscid/viscid interactions in cascades
[NASA-CR-4519] p 2169 N94-24606

TURBOPROP ENGINES
Wing mounted unducted fan engine
[CA-PATENT-1323353] p 2188 N94-24180
S-2E Tracker maritime patrol aircraft re-engine and system upgrade program p 2158 N94-24270
The AC-120: The advanced commercial transport
[NASA-CR-195491] p 2182 N94-24966

TURBULENCE
Droplet turbulence interactions under subcritical and supercritical conditions p 2211 N94-23036
Computation of flows in a turn-around duct and a turbine cascade using advanced turbulence models
p 2216 N94-23062
Probe shapes that measure time-averaged streamwise momentum and cross-stream turbulence intensity
[NASA-CASE-ARC-11934-1] p 2317 N94-23077
Computational study of GA(W)-1: Airfoil near stall
[PB93-226249] p 2165 N94-23116
Probe systems for measuring static pressure and turbulence intensity in fluid streams
[NASA-CASE-ARC-11935-1] p 2319 N94-23306
The use of transition region characteristics to improve the numerical simulation of heat transfer in bypass transitional flows
[NASA-TM-106445] p 2320 N94-23525
Aircraft accident report: In-flight engine separation. Japan Airlines, Inc., flight 46E, Boeing 747-121, N473EV, Anchorage, Alaska, 31 March 1993
[PB93-410407] p 2173 N94-24062

Annual research briefs, 1993 — Center for Turbulence Research
[NASA-CR-194755] p 2327 N94-24138
Stretch-induced quenching in flame-vortex interactions p 2237 N94-24156
On streak spacing in wall-bounded turbulent flows p 2331 N94-24159
Transition to turbulence in an elliptic vortex p 2331 N94-24161
Vortical structure in a forced plane mixing layer p 2331 N94-24162
Sound radiation due to boundary layer transition p 2332 N94-24163
Direct simulation of isothermal-wall supersonic channel flow p 2172 N94-24164
Tensoral for post-processing users and simulation authors p 2333 N94-24169
Center for modeling of turbulence and transition: Research briefs, 1993
[NASA-TM-106383] p 2333 N94-24336
Workshop on Computational Turbulence Modeling
[NASA-CP-10130] p 2333 N94-24460
Development and validation of RNG methodology for compressible turbulence
[AD-A273469] p 2337 N94-24929
High lift aerodynamics
[NASA-CR-195183] p 2184 N94-25268

TURBULENCE EFFECTS
Evaluation of turbulence models in the PARC code for transonic diffuser flows
[NASA-TM-106391] p 2168 N94-24084
Variability of measured sonic boom signatures. Volume 1: Technical report
[NASA-CR-191483-VOL-1] p 2526 N94-24172
Variability of measured sonic boom signatures. Volume 2: Data report
[NASA-CR-191483-VOL-2] p 2526 N94-24173
Effects of atmospheric variations on acoustic system performance p 2527 N94-24211
Stagnation region heat transfer: The influence of turbulence parameters, Reynolds number and body shape
[NASA-TM-106504] p 2334 N94-24481

TURBULENCE METERS
Experimental Methods in Separated Flows
[ILR-MITT-260(1991)] p 2315 N94-22852
Turbulence sensors for separated flows: Current capabilities, future requirements p 2315 N94-22853

TURBULENCE MODELS
Reliability in second moment turbulence closures revisited
[NASA-TM-106469] p 2326 N94-24063
Evaluation of turbulence models in the PARC code for transonic diffuser flows
[NASA-TM-106391] p 2168 N94-24084
Annual research briefs, 1993 — Center for Turbulence Research
[NASA-CR-194755] p 2327 N94-24138
Toward modeling wingtip vortices p 2171 N94-24142
New concepts for Reynolds stress transport equation modeling of inhomogeneous flows p 2171 N94-24143
Turbulence modeling for non-equilibrium flows p 2328 N94-24144
Computation of turbulent flows over backward and forward-facing steps using a near-wall Reynolds stress model p 2172 N94-24145
Large eddy simulation of a boundary layer with concave streamwise curvature p 2328 N94-24146
Large-eddy simulation of flow in a plane, asymmetric diffuser p 2328 N94-24147
The combustion program at CTR p 2237 N94-24155
Computation of large-scale statistics in decaying isotropic turbulence p 2332 N94-24167
Center for modeling of turbulence and transition: Research briefs, 1993
[NASA-TM-106383] p 2333 N94-24336
Workshop on Computational Turbulence Modeling
[NASA-CP-10130] p 2333 N94-24460
Implementation of the Baldwin-Barth turbulence model into the ZETA code and its diagnosis
[NASA-CR-194795] p 2335 N94-24640
A vorticity dynamics based model for the turbulent dissipation: Model development and validation
[NASA-TM-106177] p 2336 N94-24713
Computational fluid mechanics
[NASA-CR-194765] p 2337 N94-24859
LES, DNS and RANS for the analysis of high-speed turbulent reacting flows
[NASA-CR-195196] p 2337 N94-25094
Development and application of new algorithms for the simulation of viscous compressible flows with moving bodies in three dimensions
[AD-A273514] p 2338 N94-25157
Decay of swirl in turbulent pipe flows
[ETN-94-95353] p 2339 N94-25248

TURBULENT BOUNDARY LAYER
Measurements and modeling of flow structure in the wake of a low profile wishbone vortex generator
[NASA-TM-106468] p 2166 N94-23485
An analytic study of a two-phase laminar airfoil in simulated heavy rain p 2171 N94-23661
Adaptive nonlinear polynomial neural networks for control of boundary layer/structural interaction
[NASA-CR-189645] p 2525 N94-23698
Optimal feedback control of turbulent channel flow p 2327 N94-24139
Boundary layer receptivity and control p 2327 N94-24141
New concepts for Reynolds stress transport equation modeling of inhomogeneous flows p 2171 N94-24143
Local isotropy in distorted turbulent boundary layers at high Reynolds number p 2332 N94-24166
Experimental study of a turbulent boundary layer in presence of external manipulators of NACA 0009 profile in the transonic regime
[ISBN-0-315-57633-2] p 2333 N94-24177
Experimental cavity pressure measurements at subsonic and transonic speeds. Static-pressure results
[NASA-TP-3358] p 2169 N94-24464
Heat transfer and flow structure in end-wall boundary layers
[AD-A273470] p 2335 N94-24689
Interactive control in turbulent shear layers
[AD-A273544] p 2336 N94-24793
Coherent structures over grooved surfaces
[ETN-94-95308] p 2339 N94-25291

TURBULENT COMBUSTION
A random distribution reacting mixing layer model
[NASA-CR-194445] p 2187 N94-23552
The combustion program at CTR p 2237 N94-24155
Stretch-induced quenching in flame-vortex interactions p 2237 N94-24156
A transport equation for the scalar dissipation in reacting flows with variable density: First results p 2331 N94-24157
Study of streamwise vorticity-stirred combustion
[NASA-CR-194450] p 2234 N94-24565
Numerical solutions of the complete Navier-Stokes equations
[NASA-CR-194780] p 2337 N94-24858

TURBULENT DIFFUSION
Eddy mixing coefficient values derived from simulations with the NASA Ames Mars GCM p 2617 N94-24875
Eddy mixing coefficient upper limit derived from the photochemical balance of O2 p 2621 N94-24897

TURBULENT FLOW
A multigrid multiblock solver for compressible turbulent flow
[MEMO-1125] p 2315 N94-22713
Experimental Methods in Separated Flows
[ILR-MITT-260(1991)] p 2315 N94-22852
Turbulence sensors for separated flows: Current capabilities, future requirements p 2315 N94-22853
Measurement of kinematically unstationary separated flows p 2315 N94-22854
Pressure oscillation measurements in turbulent flows p 2316 N94-22855
SFOLDA: A semiconductor LDA for measurements in complex flows p 2316 N94-22856
The use of near-wall hot-wire probes for time-resolved skin-friction measurements p 2316 N94-22857
Turbulent separated flows above an obstacle in an open channel p 2316 N94-22859
A photogrammetric solution to a particular problem
[NASA-TP-3415] p 2381 N94-22961
Efficiency and reliability enhancements in propulsion flowfield modeling p 2215 N94-23055
Computation of flows in a turn-around duct and a turbine cascade using advanced turbulence models p 2216 N94-23062
Shock-induced turbulent flow in baffle systems
[DE94-001532] p 2319 N94-23470
The use of transition region characteristics to improve the numerical simulation of heat transfer in bypass transitional flows
[NASA-TM-106445] p 2320 N94-23525
The 3-D CFD modeling of gas turbine combustor-integral bleed flow interaction p 2189 N94-23658
A comparative study of computational solutions to flow over a backward-facing step p 2326 N94-23670
Compressible turbulent flow simulation with a multigrid multiblock method p 2342 N94-23694
Reliability in second moment turbulence closures revisited
[NASA-TM-106469] p 2326 N94-24063
Thermohydrodynamic analysis of cryogenic liquid turbulent flow fluid film bearings
[NASA-CR-194869] p 2363 N94-24081
Annual research briefs, 1993 — Center for Turbulence Research
[NASA-CR-194755] p 2327 N94-24138
Optimal feedback control of turbulent channel flow p 2327 N94-24139
Drag reduction at a plane wall p 2327 N94-24140
Toward modeling wingtip vortices p 2171 N94-24142
Computation of turbulent flows over backward and forward-facing steps using a near-wall Reynolds stress model p 2172 N94-24145
On the large eddy simulation of turbulent flows in complex geometry p 2329 N94-24148
Toward large eddy simulation of turbulent flow over an airfoil p 2172 N94-24150
Unstructured grid large eddy simulation of wall bounded turbulent flows p 2329 N94-24151
Investigation of the asymptotic state of rotating turbulence using large-eddy simulation p 2330 N94-24152
Energy transfer and constrained simulations in isotropic turbulence p 2330 N94-24153
A large eddy simulation scheme for turbulent reacting flows p 2330 N94-24154
The combustion program at CTR p 2237 N94-24155
Stretch-induced quenching in flame-vortex interactions p 2237 N94-24156
A transport equation for the scalar dissipation in reacting flows with variable density: First results p 2331 N94-24157
The production of premixed flame surface area in turbulent shear flow p 2237 N94-24158
On streak spacing in wall-bounded turbulent flows p 2331 N94-24159
Direct simulation of isothermal-wall supersonic channel flow p 2172 N94-24164
Effects of shock strength on shock turbulence interaction p 2332 N94-24165
Local isotropy in distorted turbulent boundary layers at high Reynolds number p 2332 N94-24166
Computation of large-scale statistics in decaying isotropic turbulence p 2332 N94-24167
Joint Acoustic Propagation Experiment (JAPE-91) Workshop
[NASA-CP-3231] p 2526 N94-24207
Center for modeling of turbulence and transition: Research briefs, 1993
[NASA-TM-106383] p 2333 N94-24336
Workshop on Computational Turbulence Modeling
[NASA-CP-10130] p 2333 N94-24460
Responses of a finite baffled plate subject to turbulent and mean flow excitations
[NASA-CR-191570] p 2334 N94-24605
Implementation of the Baldwin-Barth turbulence model into the ZETA code and its diagnosis
[NASA-CR-194795] p 2335 N94-24640
Carrying the mass flux terms exactly in the first and second moment equations of compressible turbulence
[NASA-CR-191568] p 2335 N94-24712
Interactive control in turbulent shear layers
[AD-A273544] p 2336 N94-24793
Numerical solutions of the complete Navier-Stokes equations
[NASA-CR-194780] p 2337 N94-24858
Development and validation of RNG methodology for compressible turbulence
[AD-A273469] p 2337 N94-24929
The influence of flow type, particle type and gravity on orthokinetic coagulation
[ETN-94-95333] p 2267 N94-25060
LES, DNS and RANS for the analysis of high-speed turbulent reacting flows
[NASA-CR-195196] p 2337 N94-25094
The effects of profiles on supersonic jet noise
[NASA-CR-195184] p 2530 N94-25177
Measurements of the influence of integral length scale on stagnation region heat transfer
[NASA-TM-106503] p 2338 N94-25183
Measurement of the volume mass by spontaneous Raman scattering. Study of turbulent fluctuations of mixing in a subsonic free jet. Measurements in supersonic wind tunnels
[ISL-R-102/92] p 2339 N94-25462
Direct measurement of turbulent dissipation rate using dual laser doppler velocimeters
[AD-A273740] p 2340 N94-25530

TURBULENT HEAT TRANSFER
Turbulence models and Reynolds analogy for two-dimensional supersonic compression ramp flow
[NASA-TM-106474] p 2337 N94-25119

TURBULENT JETS
Spray formation processes of impinging jet injectors p 2212 N94-23042
Transient Ejector Analysis (TEA) code user's guide
[NASA-TM-106310] p 2186 N94-23466

TURBULENT MIXING
Shock-induced turbulent flow in baffle systems
[DE94-001532] p 2319 N94-23470
A random distribution reacting mixing layer model
[NASA-CR-194445] p 2187 N94-23552
Eddy mixing coefficient values derived from simulations with the NASA Ames Mars GCM p 2617 N94-24875

TURBULENT WAKES
LDA measurements of the unsteady near wake behind an airfoil undergoing transient and periodic pitching motions
[ISL-CO-215/92] p 2165 N94-23161
Decay of swirl in turbulent pipe flows
[ETN-94-95353] p 2339 N94-25248
High lift aerodynamics
[NASA-CR-195183] p 2184 N94-25268

TURING MACHINES
Verification of synchronous sequential numerical material systems: Application of the LUSTRE language and of the LESAR verification tool
[ETN-94-95181] p 2447 N94-22899

TVD SCHEMES
Unified approach for incompressible flows
p 2342 N94-25356

TWO DIMENSIONAL FLOW
A theoretical evaluation of aluminum gel propellant two-phase flow losses on vehicle performance
p 2210 N94-23031
Two-dimensional Navier-Stokes computations of subsonic and supersonic flows through turbine cascades
[PB93-226223] p 2317 N94-23114
Upwind MacCormack Euler solver with non-equilibrium chemistry p 2326 N94-23672
Numerical simulation of non-Newtonian free shear flows p 2331 N94-24160
Transition to turbulence in an elliptic vortex
p 2331 N94-24161
Turbulence models and Reynolds analogy for two-dimensional supersonic compression ramp flow
[NASA-TM-106474] p 2337 N94-25119
Two-dimensional CFD modeling of wave rotor flow dynamics
[NASA-TM-106261] p 2189 N94-25185

TWO DIMENSIONAL MODELS
An F2D analysis of the Flow Instability Test (FIT) experiment
[DE94-001420] p 2217 N94-23193
X ray simulator theory support
[AD-A273613] p 2553 N94-24949
Modelling of premixed laminar flames
[ETN-94-95317] p 2236 N94-25284
Modelling of thermal argon plasmas
[ETN-94-95363] p 2554 N94-25300
Two-dimensional pattern analysis and classification using a complex orthogonal estimation algorithm
[RR-475] p 2463 N94-25321

TWO FLUID MODELS
Mixing and unmixedness in plasma jets 1: Near-field analysis p 2323 N94-23655
Three-dimensional solidification and melting using magnetic field control p 2325 N94-23664

TWO PHASE FLOW
A theoretical evaluation of aluminum gel propellant two-phase flow losses on vehicle performance
p 2210 N94-23031
Numerical parametric studies of spray combustion instability p 2212 N94-23041
Performance assessment of low pressure nuclear thermal propulsion p 2217 N94-23070
Studies of two phase flow
[NASA-CR-195099] p 2267 N94-23594
An analytic study of a two-phase laminar airfoil in simulated heavy rain p 2171 N94-23661
Three-dimensional solidification and melting using magnetic field control p 2325 N94-23664
Dispersion of fire suppression agents discharged from high pressure vessels: Establishing initial/boundary conditions for the flow outside the vessel
[PB94-103660] p 2172 N94-23810
Validation of a nonintrusive optical technique for the measurement of liquid mass distribution in a two-phase spray p 2548 N94-24420
Ignition and combustion characteristics of metallized propellants, phase 2
[NASA-CR-195107] p 2266 N94-24700

TWO STAGE TURBINES
Two stage turbine for rockets p 2215 N94-23059

U

U BENDS
Analysis of Alloy 600 and X-750 stress corrosion cracks
[DE94-001578] p 2238 N94-22936

U.S.S.R. SPACE PROGRAM
Soviet developments of planet rovers in period of 1964 - 1990 p 2369 N94-23374
Mars 96 small rover: Mission strategy
p 2606 N94-23381
Radioastron flight operations p 2502 N94-23861

UH-1 HELICOPTER
Aviation system safety risk management tool analysis. Volume 2: Appendices
[AD-A273502] p 2173 N94-24864

UH-60A HELICOPTER
Aviation system safety risk management tool analysis. Volume 2: Appendices
[AD-A273502] p 2173 N94-24864

ULTRAHIGH FREQUENCIES
The European Mobile System (EMS)
p 2282 N94-22789
Measurements on the satellite-mobile channel at L and S bands p 2282 N94-22791
K-band mobile propagation measurements using ACTS p 2283 N94-22792
Systems implications of L-band fade data statistics for LEO mobile systems p 2284 N94-22799
Microstrip monopulse antenna for land mobile communications p 2289 N94-22833
L-band mobile terminal antennas for helicopters
p 2289 N94-22835
Radar signature related radome techniques for flush-mounted HF-, VHF- and, UHF communication antennas
[PB93-204618] p 2294 N94-23742
Simulation of adjacent channel interference in a UHF satellite system
[AD-A273147] p 2299 N94-24669
Electromagnetic interference impact of the proposed emitters for the High Frequency Active Auroral Research Program (HAARP)
[AD-A273401] p 2301 N94-24926

ULTRAHIGH VACUUM
An analytical ultra-high vacuum tribometer for solid lubricant studies p 2361 N94-24033
Surface chemistry of liquid metals
p 2249 N94-25133

ULTRASONIC FLAW DETECTION
Nondestructive evaluations
[DE94-003020] p 2373 N94-24613
Demonstration of polyscann ultrasonic butt-fusion inspection system for polyethylene pipes
[AD-A273279] p 2373 N94-24814

ULTRASONIC SCANNERS
Conceptual design of a device to measure hand swelling in a micro-gravity environment
[NASA-CR-195509] p 2437 N94-24330

ULTRASONIC TESTS
Fiber optic detection of laser generated ultrasound for materials characterization
[ISBN-0-315-83541-9] p 2541 N94-22891
Acoustic and optical investigations of superfluid He-3
[PB93-224889] p 2523 N94-23101
Strength, acoustic evaluation and metallurgy of diffusion bonds
[DE94-001804] p 2243 N94-23717
Ultrasonic nondestructive evaluation as a tool for the development of aerospace structural ceramic composites p 2257 N94-24240
Fiber optic detection of ultrasound and its application to cure monitoring
[ISBN-0-315-83424-2] p 2544 N94-24466

ULTRASONIC WAVE TRANSDUCERS
Fiber optic detection of ultrasound and its application to cure monitoring
[ISBN-0-315-83424-2] p 2544 N94-24466

ULTRASONICS
Ultrasonic process for curing adhesives
[AD-A273175] p 2259 N94-24788

ULTRAVIOLET ABSORPTION
In situ and ex situ spectroelectrochemical and x ray absorption studies on rechargeable, chemically-modified and other MnO2 materials
[DE94-001387] p 2234 N94-24545

ULTRAVIOLET ASTRONOMY
Scientific Requirements for Future Solar-Physics Space Missions
[ESA-SP-1157] p 2623 N94-22837
Requirements for future solar-physics missions that include UV instrumentation p 2625 N94-22851
Voyager observations of globular clusters
[NASA-CR-194806] p 2598 N94-23330
UV spectral variability in the Herbig Ae star HR 5999. 11: The accretion interpretation
[NASA-CR-189313] p 2599 N94-23334
The resonance lines of MG2 as diagnostics of the upper solar chromosphere
[NASA-CR-195084] p 2627 N94-24300
UV-bright stars in globular clusters
[NASA-CR-189324] p 2599 N94-24666
Ultraviolet, visible, and gravity astrophysics: A plan for the 1990's
[NASA-NP-152] p 2603 N94-24973
Shocked clouds in the Cygnus Loop
[NASA-CR-195190] p 2600 N94-25178

ULTRAVIOLET DETECTORS
Electrophoresis in open capillaries: Some fundamental aspects
[ETN-94-95290] p 2236 N94-25232

ULTRAVIOLET RADIATION
The possible effects of the natural and induced space environment on the optical and thermal properties of EOS surfaces p 2207 N94-23596
UV extinction and IR emission in diffuse H2 regions
[NASA-CR-195194] p 2600 N94-25270

ULTRAVIOLET SPECTRA
Voyager observations of globular clusters
[NASA-CR-194806] p 2598 N94-23330
UV spectral variability in the Herbig Ae star HR 5999. 11: The accretion interpretation
[NASA-CR-189313] p 2599 N94-23334
SO2 on Venus: A final cross-calibration with Pioneer Venus
[NASA-CR-195162] p 2599 N94-24988

ULTRAVIOLET SPECTROMETERS
The development of the SOHO SUMER mechanisms
p 2361 N94-24028

ULTRAVIOLET SPECTROSCOPY
Width modulator mechanism for spectrometer entrance slits p 2357 N94-24002

ULTRAVIOLET TELESCOPES
UV-bright stars in globular clusters
[NASA-CR-189324] p 2599 N94-24666

ULYSSES MISSION
The Ulysses spacecraft control and monitoring concepts and realities p 2502 N94-23862
Ulysses log 1992 p 2502 N94-23863
Numerical simulation of Ulysses nutation
p 2207 N94-24017

UNDERGROUND EXPLOSIONS
Parametric and nonparametric discriminants for regional earthquakes and explosions
[AD-A273807] p 2406 N94-25538

UNDERWATER ACOUSTICS
Diffraction analysis of transient acoustic waves: Half-plane in a layered medium
[PB94-110988] p 2526 N94-23726
Measurements and modeling of multitone, low-frequency acoustic data from the Arraial do Cabo range
[AD-A273406] p 2530 N94-25073
Analysis of modal evolution caused by a weakly range-dependent seabed in shallow water and its application to inversion for geoacoustic properties
[AD-A273656] p 2419 N94-25435

UNIQUENESS
Multigrid methods for a semilinear PDE in the theory of pseudoplastic fluids p 2341 N94-23689

UNITED STATES
Making government work: Electronic delivery of Federal services
[OTA-TCT-578] p 2290 N94-23081

UNIVERSE
Tensor-scalar cosmological models and their relaxation toward general relativity
[PB93-220796] p 2601 N94-23099
A brief history of the universe
[DE93-616843] p 2604 N94-25210

UNIVERSITIES
Magnetic Earth Ionosphere Resonant Frequencies
[NASA-CR-195131] p 2303 N94-25191
National Aeronautics and Space Administration (NASA)/American Society for Engineering Education (ASEE) Summer Faculty Fellowship Program, 1993, volume 1
[NASA-CR-188271-VOL-1] p 2632 N94-25348

UNIVERSITY PROGRAM
Roles, uses, and benefits of general aviation aircraft in aerospace engineering education
[NASA-TM-106463] p 2153 N94-24100
NPS alternate techsat satellite, design project for AE-4871
[NASA-CR-195512] p 2204 N94-24590
A mission to Mercury and a mission to the moons of Mars
[NASA-CR-195530] p 2195 N94-24619
VLCT-13: A commercial transport for the 21st Century
[NASA-CR-195492] p 2181 N94-24803
Stiffening of deployable space booms: Automated Protein Crystal Growth Facility
[NASA-CR-195547] p 2196 N94-24820
Design of an airborne launch vehicle for an air launched space booster
[NASA-CR-195534] p 2198 N94-24860
RIACS/USRA
[NASA-CR-195117] p 2631 N94-25003

The Triton: Design concepts and methods
[NASA-CR-195542] p 2184 N94-25004
Activities of Academia Sinica
[DE93-614529] p 2541 N94-25335
National Aeronautics and Space Administration (NASA)/American Society for Engineering Education (ASEE) Summer Faculty Fellowship Program, 1993, volume 1
[NASA-CR-188271-VOL-1] p 2632 N94-25348
Strategies for recruiting additional African Americans into the NASA JSC summer faculty fellows program
p 2585 N94-25362
Image remapping strategies applied as protheses for the visually impaired p 2444 N94-25363
National Aeronautics and Space Administration (NASA)/American Society for Engineering Education (ASEE) Summer Faculty Fellowship Program, 1993, volume 2
[NASA-CR-188271-VOL-2] p 2636 N94-25367

UNIX (OPERATING SYSTEM)
CADBIT 2: Computer-aided design for built-in test, volume 1
[AD-A273702] p 2463 N94-25455
CADBIT 2: Computer-aided design for built-in test, volume 2
[AD-A273703] p 2463 N94-25456

UNMANNED SPACECRAFT
PERCIVAL mission to Mars
[NASA-CR-195541] p 2195 N94-24995

UNSTEADY AERODYNAMICS
Compressibility effects on dynamic stall of airfoils undergoing rapid transient pitching motion
[NASA-TM-109681] p 2167 N94-23975
Issac, Jason Cherian ses in transonic flow
[NASA-CR-194837] p 2167 N94-24052
An analysis for high Reynolds number inviscid/viscid interactions in cascades
[NASA-CR-4519] p 2169 N94-24606
Nonlinear equations of motion for a panel subject to external loads
[AD-A273142] p 2170 N94-24773

UNSTEADY FLOW
Measurement of kinematically unstationary separated flows p 2315 N94-22854
A new experimental apparatus for the study of the unsteady flowfield over an airfoil in pitching and heaving motions using laser Doppler anemometry
[ISL-CO-229/92] p 2165 N94-23149
Unsteady jet flow computation towards noise prediction
[NASA-CR-194449] p 2153 N94-23553
Simulation of unsteady flows through stator and rotor blades of a gas turbine using the Chimera method
p 2323 N94-23652
Transient studies of capillary-induced flow
p 2325 N94-23662
A multilevel adaptive projection method for unsteady incompressible flow p 2341 N94-23690
Compressibility effects on dynamic stall of airfoils undergoing rapid transient pitching motion
[NASA-TM-109681] p 2167 N94-23975
Sound radiation due to boundary layer transition
p 2332 N94-24163
Free-surface/vorticity interaction
[AD-A273263] p 2335 N94-24686
Computational fluid mechanics
[NASA-CR-194765] p 2337 N94-24859
Two-dimensional CFD modeling of wave rotor flow dynamics
[NASA-TM-106261] p 2189 N94-25185

UNSTEADY STATE
Unsteady three-dimensional thermal field prediction in turbine blades using nonlinear BEM
p 2325 N94-23665

UPGRADING
S-2E Tracker maritime patrol aircraft re-engine and system upgrade program p 2158 N94-24270

UPLINKING
The provision of spectrum for feeder links of non-geostationary mobile satellites
p 2276 N94-22751
A quick uplink, expandable executable for the NSSC-1 of the Hubble Space Telescope p 2305 N94-23859
Voyager uplink planning in the interstellar mission era
p 2305 N94-23870
Reliable transfer of data from ground to space
p 2305 N94-23908
The EURECA telecommanding chain: Experience with packet telecommand and telemetry systems
p 2305 N94-23909

UPPER ATMOSPHERE
Prediction of three sigma maximum dispersed density for aerospace applications p 2207 N94-23654

UPPER ATMOSPHERE RESEARCH SATELLITE (UARS)
An overview of the UARS data validation effort
p 2386 N94-23617

UPPER STAGE ROCKET ENGINES
Two stage turbine for rockets p 2215 N94-23059

UPPER SURFACE BLOWING
An experimental investigation of the effect of upper surface blowing on dynamic stall
[NASA-CR-194863] p 2165 N94-22894

UPWIND SCHEMES (MATHEMATICS)
Locally modified Bott-scheme for highly convective flows
[MPIM-99] p 2400 N94-23157
Upwind MacCormack Euler solver with non-equilibrium chemistry p 2326 N94-23672
A continuing search for a near-perfect numerical flux scheme. Part 1: AUSM+
[NASA-TM-106524] p 2338 N94-25180

URANIUM
Evaluation of uranium transitions for isotopically-selective laser induced fluorescence with diode lasers (technical report for ST064)
[DE94-002000] p 2347 N94-22974

URANIUM ALLOYS
Magnetic phases in UNiGe
[DE94-000793] p 2239 N94-22939
Interplay of magnetic and superconducting heavy fermion ground states
[DE94-000680] p 2240 N94-23003

URANIUM ISOTOPES
Evaluation of uranium transitions for isotopically-selective laser induced fluorescence with diode lasers (technical report for ST064)
[DE94-002000] p 2347 N94-22974

URANUS (PLANET)
The Jet Propulsion Laboratory space exploration: Past, present and future p 2153 N94-24242

URBAN PLANNING
Wind climate and urban geometry
[ISBN-9-03-860132-8] p 2416 N94-25261

USER MANUALS (COMPUTER PROGRAMS)
Users manual for the Chameleon parallel programming tools
[DE94-001934] p 2465 N94-22973
Programming in Fortran M
[DE94-000541] p 2450 N94-23207
GLview user's guide
[PB93-201366] p 2452 N94-23444
The Automated Instrumentation and Monitoring System (AIMS) reference manual
[NASA-TM-108795] p 2452 N94-23510
Activity Catalog Tool (ACT) user manual, version 2.0
[NASA-CR-177634] p 2430 N94-23527
SPDB (science processing database): Quick reference guide p 2383 N94-23597
Automatic modulation recognition based on spatial pattern classification using artificial neural networks
[CTN-94-60897] p 2296 N94-24115
MERILL: An equational reasoning system in standard ML: A user guide (prerelease version 0.4)
[PB93-204501] p 2456 N94-24534
DARPA DICE manufacturing optimization
[AD-A273345] p 2461 N94-25156

USER REQUIREMENTS
Proceedings of the Third International Mobile Satellite Conference (IMSC 1993)
[NASA-CR-194516] p 2273 N94-22735
Canadian aeronautical mobile data trials
p 2279 N94-22773
The Westinghouse Series 1000 Mobile Phone: Technology and applications p 2284 N94-22800
Software for scientific visualization: State of the art and experiences
[PB93-225183] p 2449 N94-23111
Training: Plugging the information gaps
p 2429 N94-23934
From requirements to acceptance tests
p 2464 N94-23962
The use of analytical models in human-computer interface design p 2434 N94-24190
Worldwide vessel locating and tracking system, volume 1
[PB93-193217] p 2175 N94-24474
A usage profile and evaluation of a wide-area distributed file system
[AD-A273590] p 2593 N94-24946
Human factors of mission planning systems: Applications and implementation p 2522 N94-25011
Factors influencing perceived usability and utility of LIBERTAS at Cranfield: Implications for system modification and user education
[CRANFIELD-AERO-9212] p 2594 N94-25485

UTILITIES
Statistical procedures for corrosion studies
[PB93-199412] p 2244 N94-23802
Superconducting energy storage
[DE94-002248] p 2395 N94-24654

UTILIZATION
Prospects for using mobile vehicles in missions to Mars and other planets p 2607 N94-23384
Unmanned lunar rovers: Utilization for exploration
p 2607 N94-23387

V

V/STOL AIRCRAFT
Transient Ejector Analysis (TEA) code user's guide
[NASA-TM-106310] p 2186 N94-23466

VACUUM CHAMBERS
New pin-on-disk equipment for vacuum tribometry
p 2360 N94-24023

VACUUM EFFECTS
Static adhesion in preloaded contacts subjected to long-term vacuum exposure p 2363 N94-24043

VACUUM SYSTEMS
Analysis of high vacuum systems using SINDA'85
p 2322 N94-23648

VACUUM TESTS
Tribological characterization of spatial wet lubricants under vacuum p 2264 N94-24010
In-vacuum performance of Fomblin Z25-lubricated, 52100 steel bearings with TiC-coated balls
p 2358 N94-24011

VALENCE
A valence-fluctuation theory of cuprate superconductivity
[DE94-000887] p 2558 N94-22942

VALIDITY
TOVS Pathfinder product validation and intercomparison p 2384 N94-23603
Validating a large geophysical data set: Experiences with satellite-derived cloud parameters p 2385 N94-23615
Experience of the JPL Exploratory Data Analysis Team at validating HIRS2/MSU cloud parameters
p 2385 N94-23616
An overview of the UARS data validation effort
p 2386 N94-23617

VANADIUM ALLOYS
Relationship of microstructure and mechanical properties for V-Cr-Ti alloys
[DE94-001431] p 2238 N94-22718
Effect of neutron irradiation on tensile properties of V-Cr-Ti alloys
[DE94-001433] p 2240 N94-23194

VAPOR DEPOSITION
Disilane LPCVD deposited silicon films: Deposition mechanisms, properties and capability of making transistors on thin films
[LAAS-93156] p 2252 N94-22910
Particle formation in a laser-heated aerosol reactor. Application to silicon and silicon nitride synthesis
[PB93-217982] p 2347 N94-22982
Ordered organic thin films self-assembled from the vapor phase p 2223 N94-24339
Structural characterization and thermal cycling behaviour of EB-PVD thermal barrier coating systems
[ISBN-0-315-83365-3] p 2257 N94-24468
Thin film cadmium telluride photovoltaic cells
[DE94-000201] p 2395 N94-24509
Photoinduced charge separation in solid state and molecular systems
[DE94-001727] p 2563 N94-24537
LPCVD of InN on GaAs(110) using HN3 and TMIn: Comparison with Si(100) results
[AD-A273555] p 2235 N94-24917
Intelligent control of chemical vapor deposition processes
[AD-A273356] p 2261 N94-24937
The reaction mechanism of W-CVD in Si
[ETN-94-95329] p 2261 N94-25084
Scanning probe lithography. 2: Selective chemical vapor deposition of copper into scanning tunneling microscope-defined patterns
[AD-A273304] p 2547 N94-25144
Investigation and application of microwave electron cyclotron resonance plasma physical vapour deposition
[DE93-613909] p 2555 N94-25333
The in situ observation of epitaxial diamond thin film nucleation and growth using emission electron microscopy
[AD-A273698] p 2263 N94-25489

VAPOR PHASES
Ultraviolet photosulfidation of III-V compound semiconductors for electronic passivation
[DE94-001417] p 2555 N94-22717
High-resolution soft x ray photoionization studies of selected molecules
[DE94-000568] p 2532 N94-23002
Vaporization behavior of non-stoichiometric refractory carbide materials and direct observations of the vapor phase using laser diagnostics
[DE93-040094] p 2348 N94-23203

Infrared analysis of vapor phase deposited tricresylphosphate (TCP)
[NASA-TM-106423] p 2253 N94-23371

Numerical modeling of physical vapor transport under microgravity conditions: Effect of thermal creep and stress p 2223 N94-24340

CFD simulation of coaxial injectors
p 2342 N94-24430

VAPOR PRESSURE

Experimental and analytical study of cryogenic propellant boiloff to develop and verify alternate pressurization concepts for Space Shuttle external tank using a scaled down tank p 2266 N94-23657

VAPORIZING

LOX droplet vaporization in a supercritical forced convective environment p 2211 N94-23034

Evaporation and combustion of LOX under supercritical and subcritical conditions p 2211 N94-23035

Droplet turbulence interactions under subcritical and supercritical conditions p 2211 N94-23036

Fundamental rocket injector/spray programs at the Phillips Laboratory p 2211 N94-23039

Development of a computational testbed for numerical simulation of combustion instability
p 2213 N94-23046

Vaporization behavior of non-stoichiometric refractory carbide materials and direct observations of the vapor phase using laser diagnostics
[DE93-040094] p 2348 N94-23203

VAPORS

Wear reduction in ceramic bearings by surface generated pyrolytic carbon continuously replenished by ethylene gas
[NASA-CR-189214] p 2364 N94-24090

VARACTOR DIODES

Planar varactor frequency multiplier devices with blocking barrier
[NASA-CASE-NPO-18428-1-CU] p 2310 N94-23821

VARIABILITY

Estimates of monthly mean soil moisture for 1979-1989
[NASA-TM-104571] p 2407 N94-23132

Convective organization in the Pacific ITCZ: Merging OLR, TOVS, and SSM/I information
[NASA-CR-194850] p 2408 N94-23619

GEWEX Water Vapor Project (GVaP)
p 2411 N94-24378

Two-stage versus sequential sample-size determination in regression analysis of simulation experiments
[PB94-110558] p 2495 N94-24634

VARIANCE (STATISTICS)

Analysis of open-loop conical scan pointing error and variance estimators p 2291 N94-23263

Two-stage versus sequential sample-size determination in regression analysis of simulation experiments
[PB94-110558] p 2495 N94-24634

Correlation function estimator performance in non-Gaussian spherically invariant random processes
[AD-A273498] p 2496 N94-24951

VARIATIONAL PRINCIPLES

A geometric weighted elliptic grid regeneration method for 3D unstructured ALE hydrodynamics
[DE94-000309] p 2448 N94-22980

Forced vibrations of a non-viscous drop
[MPIS-24/1992] p 2318 N94-23198

Application and development of the Schwinger multichannel scattering theory and the partial differential equation theory of electron-molecule scattering
[NASA-CR-194774] p 2536 N94-24798

Modelling the Shuttle Remote Manipulator System: Another flexible model p 2371 N94-25350

VARIATIONS

Measurement of the volume mass by spontaneous Raman scattering. Study of turbulent fluctuations of mixing in a subsonic free jet. Measurements in supersonic wind tunnels
[ISL-R-102/92] p 2339 N94-25462

VAX COMPUTERS

The Ulysses spacecraft control and monitoring concepts and realities p 2502 N94-23862

VECTOR ANALYSIS

Characterization of measures with a convex matrix-k-range
[PB93-220655] p 2479 N94-23098

Note on the use of spherical vectorfields in Clifford analysis
[PB93-237667] p 2480 N94-23437

Polytopic vector analysis in igneous petrology: Application to lunar petrogenesis p 2615 N94-24368

VECTOR DOMINANCE MODEL

New evaluation of hadronic contributions to the anomalous magnetic moment of charged leptons
[DE93-634394] p 2536 N94-24844

VECTOR MESONS

Momentum and coordinate space three-nucleon potentials
[DE93-040868] p 2531 N94-22951

Gauge invariance and the electromagnetic current of composite pions
[DE93-040869] p 2532 N94-22952

VECTOR PROCESSING (COMPUTERS)

Algorithm on addition chains with restricted memory
[PB94-118692] p 2454 N94-23759

VECTOR QUANTIZATION

A constrained joint source/channel coder design and vector quantization of nonstationary sources
[NASA-CR-195145] p 2301 N94-24707

VECTOR SPACES

Characterization of measures with a convex range: A generalization of Lyapounov's theorem
[PB93-220523] p 2523 N94-23094

The cusp horseshoe and its bifurcations in the unfolding of an inclination-flip homoclinic orbit
[W-9307] p 2480 N94-23141

Note on the use of spherical vectorfields in Clifford analysis
[PB93-237667] p 2480 N94-23437

The fundamental group of the complement of complexified real arrangements
[DE93-616847] p 2491 N94-25214

Deviation equations of Synge and Schild in spaces with affine connection and metric, and equations for gravitational waves detectors
[DE93-616852] p 2571 N94-25339

VECTORS (MATHEMATICS)

Implementation and parallelization of fast matrix multiplication for a fast Legendre transform
[DE94-002184] p 2478 N94-22975

Nested Krylov methods and preserving the orthogonality p 2483 N94-23681

Logarithm of probability measures and infinite divisibility of sub-stable random vectors
[PB94-118627] p 2486 N94-23758

VEGETATION

The AGRHYMET data communications project
p 2280 N94-22776

Atmospheric flow in heterogeneous vegetated regions
[W-9303] p 2401 N94-23175

Effect of land use change on the carbon cycle in Amazon soils
[NASA-CR-195168] p 2399 N94-24853

Human impacts on soil carbon dynamics of deep-rooted Amazonian forests
[NASA-CR-195127] p 2399 N94-24861

VEGETATION GROWTH

Microbial biofilm formation and its consequences for the CELSS program
[NASA-CR-195146] p 2438 N94-24706

VEGETATIVE INDEX

Session on coupled land surface/hydrological/atmospheric models
p 2414 N94-24395

VEHICLE WHEELS

Landing gear with swivelling beam
[CA-PATENT-1323020] p 2176 N94-24181

VELOCITY DISTRIBUTION

Turbulent separated flows above an obstacle in an open channel p 2316 N94-22859

Shear coaxial injector instability mechanisms
p 2213 N94-23047

A representation for the turbulent mass flux contribution to Reynolds-stress and two-equation closures for compressible turbulence
[NASA-CR-191569] p 2319 N94-23302

Measurements and modeling of flow structure in the wake of a low profile wishbone vortex generator
[NASA-TM-106468] p 2166 N94-23465

A random distribution reacting mixing layer model
[NASA-CR-194445] p 2187 N94-23552

Solution of mixed convection heat transfer from isothermal in-line fins p 2321 N94-23644

Evaluation of turbulence models in the PARC code for transonic diffuser flows
[NASA-TM-106391] p 2168 N94-24084

Vortical structure in a forced plane mixing layer
p 2331 N94-24162

Stagnation region heat transfer: The influence of turbulence parameters, Reynolds number and body shape
[NASA-TM-106504] p 2334 N94-24481

A two-dimensional dispersion module for the TOUGH2 simulator
[DE94-002262] p 2335 N94-24655

A diagnostic model to estimate winds and small-scale drag from Mars Observer PMIRR data
p 2617 N94-24874

The effects of profiles on supersonic jet noise
[NASA-CR-195184] p 2530 N94-25177

VELOCITY MEASUREMENT

Experimental Methods in Separated Flows
[ILR-MITT-260(1991)] p 2315 N94-22852

Pressure oscillation measurements in turbulent flows
p 2316 N94-22855

SFOLDA: A semiconductor LDA for measurements in complex flows p 2316 N94-22856

An experimental study of characteristic combustion-driven flows for CFD validation
p 2212 N94-23040

Studies of two phase flow
[NASA-CR-195099] p 2267 N94-23594

On the determination of local instantaneous averages in particulate flow measurements p 2325 N94-23663

Vortical structure in a forced plane mixing layer
p 2331 N94-24162

Doppler global velocimetry: Development of a flight research instrumentation system for application to non-intrusive measurements of the flow field
[NASA-CR-191490] p 2344 N94-24360

Heterodyne array for measurement of target velocity
[AD-D016025] p 2545 N94-24722

Detection of velocity in high temperature liquid metals
p 2247 N94-25127

Direct measurement of turbulent dissipation rate using dual laser doppler velocimeters
[AD-A273740] p 2340 N94-25530

VENTILATION

Reactive trace metals as indicators of subduction and ventilation processes in the ocean
[AD-A273585] p 2419 N94-25164

VENTS

Design of a resistojet for Space Station Freedom
[NASA-CR-195506] p 2221 N94-24979

Reactive trace metals as indicators of subduction and ventilation processes in the ocean
[AD-A273585] p 2419 N94-25164

VENUS (PLANET)

SO2 on Venus: A final cross-calibration with Pioneer Venus
[NASA-CR-195162] p 2599 N94-24988

VENUS ATMOSPHERE

SO2 on Venus: A final cross-calibration with Pioneer Venus
[NASA-CR-195162] p 2599 N94-24988

VENUS SURFACE

SO2 on Venus: A final cross-calibration with Pioneer Venus
[NASA-CR-195162] p 2599 N94-24988

VERTICAL DISTRIBUTION

Cloud, dust, and ozone vertical profiles from solar occultation measurements: Implications for dynamics
p 2617 N94-24877

Results from the VISA project
[AD-A273752] p 2406 N94-25540

VERTICAL LANDING

Summary of lift and lift/cruise fan powered lift concept technology
[NASA-CR-177619] p 2176 N94-23489

VERTICAL MOTION

Vertical motion in the SYNOP central array
[AD-A273593] p 2418 N94-24795

VERTICAL TAKEOFF

Summary of lift and lift/cruise fan powered lift concept technology
[NASA-CR-177619] p 2176 N94-23489

VERY HIGH FREQUENCIES

The ORBCOMM data communications system
p 2281 N94-22782

Radar signature related radome techniques for flush-mounted HF-, VHF- and, UHF communication antennas
[PB93-204618] p 2294 N94-23742

VERY LARGE ARRAY (VLA)

Interferometric astronomy on the Moon
p 2601 N94-23378

Conceptual design and architecture of hexapod robotic vehicles for the (L)OVLA project p 2369 N94-23405

VERY LARGE SCALE INTEGRATION

Customizable VLSI artificial neural network chips based on a novel technology
[DE94-001418] p 2307 N94-23008

Mixed analog-digital description and simulation: Proposition for VHDL-analogue
[RR-908-I] p 2450 N94-23180

Area-power-delay trade-off in logic synthesis
[ISBN-9-09-005332-8] p 2461 N94-25080

VERY LONG BASE INTERFEROMETRY

Radioastron flight operations p 2502 N94-23861

Navigation of space VLBI missions: Radioastron and VSOP p 2513 N94-23926

The 1404+286: A non-ideal calibrator for VLBI observations
[PB94-104908] p 2599 N94-24521

LOITA: Lunar Optical/Infrared Telescope Array
[NASA-CR-195532] p 2546 N94-24816

Constraining proposed combinations of ice history and Earth rheology using VLBI determined baseline length rates in North America p 2405 N94-25205

VERY LOW FREQUENCIES

Very low frequency and low frequency transmitting antenna parameter monitoring system [AD-D015989] p 2302 N94-25049

VESTIBULES

Perception in flight: Shape and motion perception, space perception, spatial orientation, and visual vestibular interaction p 2429 N94-23979

The role of visual context in manual target localization p 2429 N94-25351

VHSIC (CIRCUITS)

Formal verification of digital circuits described in VHDL [ETN-94-95165] p 2306 N94-22883

Micro SIL-1 simulator [PB94-110889] p 2454 N94-23750

Japanese aerospace science and technology 1992. A bibliography with indexes [NASA-SP-7104] p 2631 N94-24585

VIBRATION

Time-frequency domain analysis of vibration signals for machinery diagnostics.(4): Interpretation using image processing techniques [OUEL-1953/92] p 2353 N94-23178

Energy transfer in solid explosives [DE94-001523] p 2265 N94-23778

US tag for ISO/TC 108 mechanical vibration and shock: Minutes of the accredited Standards Committee on Mechanical Vibration and Shock, S2 [AD-A273015] p 2376 N94-23789

Vibrational power transmission analysis of machinery installations in ships with the objective of noise reduction [ISVR-TR-216] p 2363 N94-24076

Aeroelastic, aeromechanical and vibration problems in helicopters p 2154 N94-24244

Development of a nondestructive vibration technique for bond assessment of Space Shuttle tiles [NASA-CR-195163] p 2201 N94-24919

A vibrating wire parallel to a type 2 superconducting slab of arbitrary thickness [DE93-617134] p 2525 N94-25389

Effects of a vibrating wire carrying DC current on a moving type 2 superconducting slab of arbitrary thickness [DE93-617136] p 2566 N94-25391

Remote vibration measurements at a sud aviation alouette 3 helicopter with a CW CO2-laser system [AD-A273818] p 2190 N94-25516

Modeling of a large undamped space structure using time domain techniques [AD-A273828] p 2206 N94-25523

Effect of longitudinal vibration on the capillary limit of a wrapped screen wick copper/water heat pipe [AD-A273830] p 2571 N94-25524

VIBRATION DAMPING

Vibration isolating engine mount [CA-PATENT-1-320-710] p 2353 N94-23215

Low noise electric motor p 2315 N94-23989

Vibrational power transmission analysis of machinery installations in ships with the objective of noise reduction [ISVR-TR-216] p 2363 N94-24076

Aeroelastic, aeromechanical and vibration problems in helicopters p 2154 N94-24244

Numerical analysis of the motion of a rigid body with an attached spring-mass-damper [AD-A273825] p 2379 N94-25520

VIBRATION EFFECTS

Microwelding due to random vibration p 2359 N94-24019

Modeling of PCG fluid dynamics: Salient results p 2224 N94-24345

Effect of longitudinal vibration on the capillary limit of a wrapped screen wick copper/water heat pipe [AD-A273830] p 2571 N94-25524

VIBRATION ISOLATORS

Vibration isolating engine mount [CA-PATENT-1-320-710] p 2353 N94-23215

Prediction of pressure drop in fluid tuned mounts using analytical and computational techniques p 2321 N94-23643

The low noise momentum wheel MW-X: EM design and predicted properties p 2360 N94-24024

Vibrational power transmission analysis of machinery installations in ships with the objective of noise reduction [ISVR-TR-216] p 2363 N94-24076

Modeling of PCG fluid dynamics: Salient results p 2224 N94-24345

VIBRATION MEASUREMENT

Spacecraft vibrations due to mechanisms; measurements from Olympus on-station p 2207 N94-24018

The Olympus PAX, measurement of mechanism induced vibration p 2362 N94-24041

Remote vibration measurements at a sud aviation alouette 3 helicopter with a CW CO2-laser system [AD-A273818] p 2190 N94-25516

VIBRATION METERS

Spacecraft vibrations due to mechanisms; measurements from Olympus on-station p 2207 N94-24018

The Olympus PAX, measurement of mechanism induced vibration p 2362 N94-24041

VIBRATION MODE

Microwelding due to random vibration p 2359 N94-24019

Maximum likelihood modal parameter identification and realization of stochastic systems p 2157 N94-24265

Development of a nondestructive vibration technique for bond assessment of Space Shuttle tiles [NASA-CR-195163] p 2201 N94-24919

Space Station flexible dynamics under plume impingement p 2208 N94-25383

VIBRATION TESTS

Data relay system satellite: The development of an antenna pointing mechanism for the inter-orbit link antenna p 2359 N94-24015

Remote vibration measurements at a sud aviation alouette 3 helicopter with a CW CO2-laser system [AD-A273818] p 2190 N94-25516

Effect of longitudinal vibration on the capillary limit of a wrapped screen wick copper/water heat pipe [AD-A273830] p 2571 N94-25524

VIBRATIONAL STATES

Radiative properties of molecular nitrogen ions produced by helium Penning ionization and argon effects [NASA-CR-195126] p 2534 N94-24487

VIBRATORY LOADS

A parametric study of harmonic rotor hub loads [NASA-CR-4558] p 2181 N94-24726

VIDEO COMMUNICATION

Deployable video conference table [NASA-CASE-ARC-11950-1] p 2192 N94-23310

A constrained joint source/channel coder design and vector quantization of nonstationary sources [NASA-CR-195145] p 2301 N94-24707

A protctype to automate the video subsystem routing for the video distribution subsystem of Space Station Freedom p 2306 N94-25353

VIDEO COMPRESSION

VLSI-based video event triggering for image data compression [NASA-TM-106500] p 2345 N94-25116

VIDEO DATA

Close-up analysis of inflight ice accretion [NASA-TM-106457] p 2172 N94-23523

Measurement of interfacial tension by use of pendant drop video techniques [DE93-000168] p 2345 N94-24831

Preliminary design of a satellite observation system for Space Station Freedom [NASA-CR-195514] p 2209 N94-24840

VLSI-based video event triggering for image data compression [NASA-TM-106500] p 2345 N94-25116

VIDEO EQUIPMENT

Preliminary design of a satellite observation system for Space Station Freedom [NASA-CR-195514] p 2209 N94-24840

Conceptual design of an astronaut hand anthropometry device [NASA-CR-195490] p 2439 N94-24956

VIDEO SIGNALS

Image processing for acquisition of fluid rest time in the running of an artificial heart valve p 2316 N94-22858

Reducing video frame rate increases remote optimal focus time [NASA-TM-104018] p 2431 N94-23970

Solid state Time Base Corrector (TBC) [AD-D015981] p 2312 N94-25039

Digital data, composite video multiplexer and demultiplexer boards for an IBM PC/AT compatible computer p 2447 N94-25377

VIEWING

Using the SPICE system to help plan and interpret space science observations p 2517 N94-23950

Using computer graphics to design Space Station Freedom viewing p 2434 N94-24191

Illumination requirements for operating a space remote manipulator p 2435 N94-24195

VIKING MARS PROGRAM

Mars Operational Environmental Satellite (MOES): A post-Mars Observer discovery mission p 2620 N94-24890

VINYL POLYMERS

Humidity effects on soluble core mechanical and thermal properties (polyvinyl alcohol/microballoon composite) type CG extendospheres, volume 2 [NASA-CR-193893] p 2229 N94-24224

VIRTUAL REALITY

Spatial interpretation of NASA's Marshall Space Flight Center Payload Operations Control Center using virtual reality technology p 2198 N94-24432

World processor: An interface for textual display and manipulation in virtual reality [PB94-118643] p 2592 N94-24642

A white paper: NASA virtual environment research, applications, and technology [NASA-TM-109682] p 2428 N94-24855

VISCOELASTICITY

Nonlocal models in continuum mechanics [DE93-040146] p 2316 N94-22870

Numerical simulation of non-Newtonian free shear flows p 2331 N94-24160

Viscoelastic analysis of seals for extended service life p 2371 N94-24408

VISCOPLASTICITY

Theory of extrusion: Advances and challenges [PB93-201572] p 2241 N94-23447

VISCOSITY

Local grid refinement method for the euler equations [PB93-223329] p 2317 N94-22985

Polyimide processing additives [NASA-CASE-LAR-13669-2] p 2252 N94-23079

A multilevel adaptive projection method for unsteady incompressible flow p 2341 N94-23690

Direct simulation of isothermal-wall supersonic channel flow p 2172 N94-24164

Electro-rheology fluids and liquid fuel flow [AD-A273640] p 2337 N94-25032

Containerless measurements on liquids at high temperatures p 2238 N94-25125

VISCOUS DAMPING

Viscous rotary damper p 2361 N94-24031

VISCOUS FLOW

Molecular gas dynamics applied to low-thrust propulsion p 2214 N94-23053

Two-dimensional Navier-Stokes computations of subsonic and supersonic flows through turbine cascades [PB93-226223] p 2317 N94-23114

Transient Ejector Analysis (TEA) code user's guide [NASA-TM-106310] p 2186 N94-23466

An implicit numerical scheme for the simulation of internal viscous flows on unstructured grids [NASA-TM-106437] p 2481 N94-23554

A dual reciprocal boundary element formulation for viscous flows p 2325 N94-23666

Heat pipe vapor dynamics [NASA-CR-194217] p 2327 N94-24096

Drag reduction at a plane wall p 2327 N94-24140

Transition to turbulence in an elliptic vortex p 2331 N94-24161

An analysis for high Reynolds number inviscid/viscid interactions in cascades [NASA-CR-4519] p 2169 N94-24606

Carrying the mass flux terms exactly in the first and second moment equations of compressible turbulence [NASA-CR-191568] p 2335 N94-24712

Development and application of new algorithms for the simulation of viscous compressible flows with moving bodies in three dimensions [AD-A273514] p 2338 N94-25157

VISCOUS FLUIDS

Nonlinear dynamics applied to atmospheric prediction [AD-A273437] p 2404 N94-24674

The hydrodynamics of a moving fluid-liquid contact line [ETN-94-95352] p 2339 N94-25247

VISIBILITY

Validation of a second generation conspicuity meter [IZF-1993-A-11] p 2542 N94-22895

A model-based approach for detection of objects in low resolution passive-millimeter wave images p 2442 N94-25507

Results from the VISA project [AD-A273752] p 2406 N94-25540

VISIBLE INFRARED SPIN SCAN RADIOMETER

Interferometer scan unit mechanism definition p 2358 N94-24012

VISION

Vision impairment and corrective considerations of civil airmen [DOT/FAA/AM-93/21] p 2426 N94-23623

Image remapping strategies applied as protheses for the visually impaired p 2444 N94-25363

VISUAL ACUITY

Evaluation of visual acuity with Gen 3 night vision goggles [NASA-TM-108792] p 2431 N94-23974

Cockpit/NVG visual integration issues p 2432 N94-23983

VISUAL CONTROL

Eye-gaze control of the computer interface: Discrimination of zoom intent [DE94-000480] p 2429 N94-22997

The effects of spatially displaced visual feedback on remote manipulator performance p 2436 N94-24201

VISUAL DISCRIMINATION
Quality metrics for sensor images p 2443 N94-25513

VISUAL OBSERVATION
Observational studies of the clearing phase in proto-planetary disk systems [NASA-CR-195182] p 2604 N94-25265

VISUAL PERCEPTION
Validation of a second generation conspicuity meter [IZF-1993-A-11] p 2542 N94-22895
A knowledge based system for scientific data visualization [NASA-CR-194879] p 2452 N94-23507
Some background information on perceptual color matching pertinent to computer applications [PB93-200327] p 2445 N94-23788
Visual Problems in Night Operations [AGARD-LS-187] p 2431 N94-23976
Multi-sensoral approach to night flight: Perceptive and Cognitive limitations p 2432 N94-23981
Cockpit/NVG visual integration issues p 2432 N94-23983
Night vision goggle illusions and visual training p 2432 N94-23984
Luminance-brightness mapping: The missing decades [ETN-94-95351] p 2428 N94-25298
Synthetic vision system flight test results and lessons learned p 2429 N94-25492
Extracting heading and temporal range from optic flow: Human performance issues p 2442 N94-25510
Optical information in landing scenes p 2442 N94-25511

VISUAL STIMULI
Physical aspects of the visual stimulus p 2431 N94-23978

VISUAL TASKS
Automated system function allocation and display format: Task information processing requirements p 2434 N94-24189

VOICE COMMUNICATION
Proceedings of the Third International Mobile Satellite Conference (IMSC 1993) [NASA-CR-194516] p 2273 N94-22735
ROCSAT-1 telecommunication experiments p 2279 N94-22770
Mobilesat (tm): A world first p 2281 N94-22783
First satellite mobile communication trials using BLQS-CDMA p 2284 N94-22801
A protocol for satellite access via use of spot-beams p 2286 N94-22811
Performance of the unique-word-reverse-modulation type demodulator for mobile satellite communications p 2286 N94-22813
On the quality of synthetic speech evaluation and improvements [ETN-94-95298] p 2304 N94-25234

VOICE CONTROL
Speech versus manual control of camera functions during a telerobotic task p 2436 N94-24199

VOICE DATA PROCESSING
A high quality voice coder with integrated echo canceller and voice activity detector for mobile satellite applications p 2286 N94-22812
Linear and nonlinear adaptive filtering and their application to speech intelligibility enhancement [ISBN-9-09-005342-5] p 2304 N94-25292

VOIDS
Analysis of a proposed Compton backscatter imaging technique [DE93-040537] p 2371 N94-22935
Analysis of Alloy 600 and X-750 stress corrosion cracks [DE94-001578] p 2238 N94-22936

VOLATILITY
Isothiazolone volatility study of a water bottom from fuel treated with Kathon (tm) FP1.5 biocide [AD-A273165] p 2266 N94-24728

VOLCANOES
Northern hemisphere tropospheric mid-latitude circulation after violent volcanic eruptions [MPIM-107] p 2403 N94-24491
Electromagnetic field changes as a precursory phenomena of earthquakes and volcanic eruptions [REPT-157] p 2405 N94-24980

VOLCANOLOGY
Basaltic Volcanism and Ancient Planetary Crusts [NASA-CR-193151] p 2614 N94-24363
Lunar mare volcanism: Mixing of distinct, mantle source regions with KREEP-like component p 2615 N94-24370
Northern hemisphere tropospheric mid-latitude circulation after violent volcanic eruptions [MPIM-107] p 2403 N94-24491
The transition from diapirism to dike intrusion: Implications for planetary volcanism [NASA-CR-195133] p 2403 N94-24580
Seafloor characterization/Galapagos propagating rift [AD-A273586] p 2419 N94-25165

VOLT-AMPERE CHARACTERISTICS
The role of emitter states in magnetotunneling through double-barrier resonant-tunneling diodes at high magnetic fields [REPT-A-2658] p 2564 N94-24959

VOLTAGE REGULATORS
Electrochemical sulfur passivation of visible (approximately 670nm) AlGaInP lasers [DE94-002293] p 2350 N94-24659
Laser energized high voltage direct current power supply [AD-D015977] p 2312 N94-25036

VOLTERRA EQUATIONS
Modeling transonic aerodynamic response using nonlinear systems theory for use with modern control theory p 2164 N94-25112

VOLUME
The effect of sub-surface volume scattering on the accuracy of ice-sheet altimeter retracking algorithms [NASA-CR-194825] p 2386 N94-24060

VORTEX GENERATORS
A method for recognition of frequency cells in a cylinder flow influenced by wall effects p 2316 N94-22860
Measurements and modeling of flow structure in the wake of a low profile wishbone vortex generator [NASA-TM-106468] p 2166 N94-23465
Vortex generation and wave-vortex interaction over a concave plate with roughness and suction [NASA-CR-191589] p 2337 N94-24869
Improving diffusing S-duct performance by secondary flow control [NASA-TM-106492] p 2170 N94-25182

VORTEX LATTICE METHOD
Computation of the loads on the AH-1/OLS model rotor in forward flight and comparison with wind tunnel tests [ISL-CO-230/92] p 2176 N94-23146
LinAir: A multi-element discrete vortex Weissinger aerodynamic prediction method [NASA-TM-108786] p 2167 N94-23557

VORTEX SHEDDING
Active control of oscillatory lift forces on a circular cylinder [AD-A273243] p 2338 N94-25140

VORTEX SHEETS
The acoustic and instability waves of jets confined inside an acoustically lined rectangular duct [NASA-CR-191586] p 2334 N94-24602
The effects of profiles on supersonic jet noise [NASA-CR-195184] p 2530 N94-25177

VORTICES
A photogrammetric solution to a particular problem [NASA-TP-3415] p 2381 N94-22961
Acoustic and optical investigations of superfluid He-3 [PB93-224889] p 2523 N94-23101
A method to simulate viscous diffusion of vorticity by convective transport of vortices at a non-solenoidal velocity [DE94-001777] p 2318 N94-23220
Measurements and modeling of flow structure in the wake of a low profile wishbone vortex generator [NASA-TM-106468] p 2166 N94-23465
Feasibility of detecting aircraft wake vortices using passive microwave radiometers [NASA-CR-191553] p 2343 N94-23498
Leading-edge votex-system details obtained on F-106B aircraft using a rotating vapor screen and surface techniques [NASA-TP-3374] p 2166 N94-23512
LinAir: A multi-element discrete vortex Weissinger aerodynamic prediction method [NASA-TM-108786] p 2167 N94-23557
Numerical analysis of a vortex controlled diffuser p 2324 N94-23659
Compressibility effects on dynamic stall of airfoils undergoing rapid transient pitching motion [NASA-TM-109681] p 2167 N94-23975
Toward modeling wingtip vortices p 2171 N94-24142
Large eddy simulation of a boundary layer with concave streamwise curvature p 2328 N94-24146
Dynamic localization and second-order subgrid-scale models in large eddy simulations of channel flow p 2329 N94-24149
Toward large eddy simulation of turbulent flow over an airfoil p 2172 N94-24150
Unstructured grid large eddy simulation of wall bounded turbulent flows p 2329 N94-24151
Investigation of the asymptotic state of rotating turbulence using large-eddy simulation p 2330 N94-24152
A large eddy simulation scheme for turbulent reacting flows p 2330 N94-24154
Stretch-induced quenching in flame-vortex interactions p 2237 N94-24156
On streak spacing in wall-bounded turbulent flows p 2331 N94-24159
Numerical simulation of non-Newtonian free shear flows p 2331 N94-24160
Transition to turbulence in an elliptic vortex p 2331 N94-24161
Vortical structure in a forced plane mixing layer p 2331 N94-24162
Free-surface/vorticity interaction [AD-A273263] p 2335 N94-24686
Vortex generation and wave-vortex interaction over a concave plate with roughness and suction [NASA-CR-191589] p 2337 N94-24869
Eddy mixing coefficient upper limit derived from the photochemical balance of O2 p 2621 N94-24897
Simulation of the vortex motion in the high T(c) superconductors [DE93-617138] p 2567 N94-25403
A nighttime structure model of atmospheric optical turbulence, c2(n), derived from thermosonde and high resolution rawinsonde measurements [AD-A273803] p 2406 N94-25537

VORTICITY
A method to simulate viscous diffusion of vorticity by convective transport of vortices at a non-solenoidal velocity [DE94-001777] p 2318 N94-23220
Measurements and modeling of flow structure in the wake of a low profile wishbone vortex generator [NASA-TM-106468] p 2166 N94-23465
LinAir: A multi-element discrete vortex Weissinger aerodynamic prediction method [NASA-TM-108786] p 2167 N94-23557
Effect of delta tabs on mixing and axis switching in jets from asymmetric nozzles [NASA-TM-106450] p 2167 N94-23592
Diagnostic budgets of analyzed and modelled tropical plumes [NASA-CR-194853] p 2409 N94-23621
Transition to turbulence in an elliptic vortex p 2331 N94-24161
Vortical structure in a forced plane mixing layer p 2331 N94-24162
Study of streamwise vorticity-stirred combustion [NASA-CR-194450] p 2234 N94-24565
Nonlinear dynamics applied to atmospheric prediction [AD-A273437] p 2404 N94-24674
Free-surface/vorticity interaction [AD-A273263] p 2335 N94-24686

VORTICITY EQUATIONS
An adaptive multigrid model for hurricane track prediction p 2416 N94-23687
A vorticity dynamics based model for the turbulent dissipation: Model development and validation [NASA-TM-106177] p 2336 N94-24713

VOYAGER PROJECT
Voyager uplink planning in the interstellar mission era p 2305 N94-23870
Techniques and software for optimum and efficient mission science sequence development p 2504 N94-23872

VOYAGER 1 SPACECRAFT
The Jet Propulsion Laboratory space exploration: Past, present and future p 2153 N94-24242

VOYAGER 2 SPACECRAFT
The Jet Propulsion Laboratory space exploration: Past, present and future p 2153 N94-24242

VSAT (NETWORK)
A European mobile satellite system concept exploiting CDMA and OBP p 2279 N94-22768
Modulation and synchronization technique for MF-TDMA system [NASA-CR-194448] p 2304 N94-25266

W

WAKES
Measurements and modeling of flow structure in the wake of a low profile wishbone vortex generator [NASA-TM-106468] p 2166 N94-23465
Three dimensional study of an airplane wing and its wake in the subsonic regime [ISBN-0-315-58963-9] p 2168 N94-24178
Free-surface/vorticity interaction [AD-A273263] p 2335 N94-24686
Analysis of the effects of wake passage on heat transfer in a linear turbine cascade [AD-A273729] p 2339 N94-25446

WALKING MACHINES
Walking machines for space p 2369 N94-23406

Design of a walking robot [NASA-CR-195200] p 2367 N94-25274

WALL FLOW

Experimental Methods in Separated Flows [ILR-MITT-260(1991)] p 2315 N94-22852

A method for recognition of frequency cells in a cylinder flow influenced by wall effects p 2316 N94-22860

Numerical investigation of two- and three-dimensional heat transfer in expander cycle engines p 2213 N94-23048

Flow visualization study in high aspect ratio cooling channels for rocket engines p 2213 N94-23049

Computation of flows in a turn-around duct and a turbine cascade using advanced turbulence models p 2216 N94-23062

Development of a code for wall contour design in the transonic region of axisymmetric and square nozzles [NASA-CR-194857] p 2167 N94-23625

Supersonic minimum length nozzle design for dense gases p 2171 N94-23656

Unstructured grid large eddy simulation of wall bounded turbulent flows p 2329 N94-24151

Sub-sonic flow about a slender profile in a tunnel having perforated walls [AD-A273184] p 2170 N94-25137

Analytical skin friction and heat transfer formula for compressible internal flows [NASA-CR-191185] p 2170 N94-25173

WALL TEMPERATURE

Numerical investigation of two- and three-dimensional heat transfer in expander cycle engines p 2213 N94-23048

Flow visualization study in high aspect ratio cooling channels for rocket engines p 2213 N94-23049

WALLS

Pressure wall patch [NASA-CASE-MFS-28724-1] p 2203 N94-23824

WARFARE

Night operations p 2431 N94-23977

WARNING SYSTEMS

Robust, wide-range hydrogen sensor for use in commercial, space, and government applications [DE93-040902] p 2342 N94-22954

Lightning studies using LDAR and LLP data p 2416 N94-23238

Towards a new radiation protection organization [FOA-C-40304-4.3] p 2437 N94-24292

WASTE DISPOSAL

Aqueous alkaline cleaners: An alternative to organic solvents [AD-A273510] p 2260 N94-24848

WASTE ENERGY UTILIZATION

Investigating pyrolysis/incineration as a method of resource recovery from solid waste p 2444 N94-25375

WASTE TREATMENT

Investigating pyrolysis/incineration as a method of resource recovery from solid waste p 2444 N94-25375

WASTE UTILIZATION

Investigating pyrolysis/incineration as a method of resource recovery from solid waste p 2444 N94-25375

WATER

Analysis of Alloy 600 and X-750 stress corrosion cracks [DE94-001578] p 2238 N94-22936

Recent advances in SPE (tm) water electrolyzer p 2393 N94-23362

Extinguishment of enclosed gas fires with water sprays [PB93-201663] p 2268 N94-23430

Extinguishment of combustible porous solids by water droplets [PB93-198893] p 2270 N94-23740

GEWEX Continental-scale International Project (GCIP) p 2411 N94-24376

Water cycle research associated with the CaPE hydrometeorology project (CHymP p 2416 N94-24414

Impact of the CO2 and H2O clouds of the Martian polar hood on the polar energy balance p 2618 N94-24880

Vertical transport of water in the Martian boundary layer p 2622 N94-24902

Examination of the physical, electrical, and microwave evolution of water into young sea ice [AD-A273559] p 2418 N94-24918

WATER BALANCE

An investigation of current and future satellite and in-situ data for the remote sensing of the land surface energy balance [NASA-CR-195138] p 2387 N94-24596

WATER CIRCULATION

Recent developments in the mathematical modelling and physical understanding of transport and dispersion in aquatic systems, with special reference to tidal waters [PB94-111135] p 2418 N94-24600

WATER COLOR

Algorithm-development activities [NASA-CR-193225] p 2420 N94-23538

Factors affecting the identification of phytoplankton groups by means of remote sensing [NASA-TM-108799] p 2387 N94-24403

WATER FLOW

Performance of prefabricated geocomposite subdrainage system in an airport runway [DOT/FAA/RD-93/23] p 2192 N94-23303

Transient studies of capillary-induced flow p 2325 N94-23662

WATER IMMERSION

Transient studies of capillary-induced flow p 2325 N94-23662

WATER MANAGEMENT

High power density proton exchange membrane fuel cells p 2393 N94-23359

WATER POLLUTION

Chemical characterization of some aerobic liquids in CELSS p 2422 N94-23241

Exploratory report nickel and nickel compounds [PB93-223998] p 2242 N94-23496

Exploratory report antimony and antimony compounds [PB93-224004] p 2397 N94-23497

WATER QUALITY

Statistical procedures for corrosion studies [PB93-199412] p 2244 N94-23802

A chemical sensor and biosensor based totally automated water quality monitor for extended space flight: Step 1 p 2443 N94-24447

WATER RESOURCES

GEWEX Continental-scale International Project (GCIP) p 2411 N94-24376

Snow modeling, water resources, climate change [PB93-201770] p 2399 N94-24633

The HEC NexGen software development project [AD-A273512] p 2460 N94-24822

WATER TREATMENT

Statistical procedures for corrosion studies [PB93-199412] p 2244 N94-23802

WATER VAPOR

Implementation of a state of the art automated system for the production of cloud/water vapor motion winds from geostationary satellites [NASA-CR-195087] p 2410 N94-24125

GEWEX Water Vapor Project (GVaP) p 2411 N94-24378

Water cycle research associated with the CaPE hydrometeorology project (CHymP p 2416 N94-24414

Mars Operational Environmental Satellite (MOES): A post-Mars Observer discovery mission p 2620 N94-24890

Mars Observer: Applications to atmospheric transport p 2623 N94-24904

WATER WAVES

VIERS-1, phase 3 [BCRS-92-24] p 2381 N94-23145

Investigation of passive atmospheric sounding using millimeter and submillimeter wavelength channels [NASA-CR-194858] p 2404 N94-24843

WATERSHEDS

Urban/rural application of weather radar for flow forecasting. Proceedings of the Informal CEc -Workshop [PB93-220135] p 2407 N94-23129

WAVE ATTENUATION

Similarity in wave propagation under a global relaxation law [PB94-111028] p 2524 N94-23730

Fiber optical angular sensor: Literature study and experimental results [PB93-204345] p 2545 N94-24529

Temperature dependent performance of Coplanar Waveguide (CPW) on substrates of various materials [NASA-TM-106505] p 2313 N94-25170

WAVE DIFFRACTION

Electromagnetic field strength prediction in an urban environment: A useful tool for the planning of LMSS p 2283 N94-22795

Transient analysis of conducting half-plane problem with noncausal scattering image [PB93-225027] p 2524 N94-23110

Diffraction analysis of transient acoustic waves: Half-plane in a layered medium [PB94-110988] p 2526 N94-23726

WAVE DISPERSION

Similarity in wave propagation under a global relaxation law [PB94-111028] p 2524 N94-23730

Analysis for the computational modeling of finite cladding and lossy coating effects in fibers [PB94-111085] p 2544 N94-23732

WAVE EQUATIONS

Classical scattering theory of waves from the view point of an eigenvalue problem and application to target identification [DE94-000472] p 2525 N94-23206

Multigrid and cyclic reduction applied to the Helmholtz equation p 2304 N94-23676

Similarity in wave propagation under a global relaxation law [PB94-111028] p 2524 N94-23730

Decomposition of multi-component measurements into P and S waves [ISBN-9-09-005197-X] p 2405 N94-25251

WAVE FRONT DEFORMATION

Sodium-layer laser guide stars [DE93-019621] p 2349 N94-23490

WAVE FRONTS

Spatiotemporal behavior and nonlinear dynamics in a phase conjugate resonator [NASA-CR-4567] p 2543 N94-23529

Convective instabilities in traveling fronts of addition polymerization p 2226 N94-24352

WAVE FUNCTIONS

Calculations of Bose-Einstein correlations from Relativistic Quantum Molecular Dynamics [DE94-000794] p 2569 N94-23453

Weak interactions in a bilocal chiral theory [DE93-616887] p 2539 N94-25477

WAVE GENERATION

On the physics of waves in the solar atmosphere: Wave heating and wind acceleration [NASA-CR-195197] p 2628 N94-25264

WAVE INTERACTION

Vortex generation and wave-vortex interaction over a concave plate with roughness and suction [NASA-CR-191589] p 2337 N94-24869

WAVE PROPAGATION

The characterization of reaction-convection-diffusion processes by travelling waves [MEMO-1111] p 2273 N94-22729

Ray and wave optics modeling of laboratory x ray lasers [DE93-019940] p 2541 N94-22868

Theoretical studies of wave propagation in multilayered piezoelectric media [DE93-040273] p 2371 N94-22872

Tracking sharp interface of two fluids by the CIP (Cubic-Interpolated Propagation) scheme [DE93-508322] p 2319 N94-23460

Shock-induced turbulent flow in baffle systems [DE94-001532] p 2319 N94-23470

Similarity in wave propagation under a global relaxation law [PB94-111028] p 2524 N94-23730

Analysis of time-domain acoustic wavefields in horizontally continuously layered configurations based on the modified Cagniard method [PB94-111044] p 2524 N94-23731

Generalized three-dimensional simulation of ferruled coupled-cavity traveling-wave-tube dispersion and impedance characteristics [NASA-TP-3389] p 2310 N94-24056

Radio communication and wave propagation. A visit to the Netherlands in December 1992 [PB93-204360] p 2297 N94-24531

Near-surface seismic imaging [PB94-119096] p 2404 N94-24647

Downward extrapolation of multi-component seismic data [ISBN-9-09-005213-5] p 2405 N94-25229

Decomposition of multi-component measurements into P and S waves [ISBN-9-09-005197-X] p 2405 N94-25251

A relativistic theory on wave propagation in inhomogeneous magnetoplasmas [ETN-94-95322] p 2554 N94-25285

Arbitrary-order numerical schemes for linear hyperbolic systems [CRANFIELD-AERO-9211] p 2523 N94-25480

WAVE SCATTERING

The effect of sub-surface volume scattering on the accuracy of ice-sheet altimeter retracking algorithms [NASA-CR-194825] p 2386 N94-24060

The scattering and collision of gravitational waves in Friedmann-Robertson-Walker open universes [MATHS-REPT-A-193] p 2406 N94-25430

WAVEGUIDE ANTENNAS

The Telecommunications and Data Acquisition Report [NASA-CR-194766] p 2290 N94-23256

Performance of the X-/Ka/KABLE-band dichroic plate in the DSS-13 beam waveguide antenna p 2291 N94-23261

Beam-waveguide antenna servo design issues for tracking low earth-orbiting satellites p 2292 N94-23268

WAVEGUIDE LASERS
Manufacturing and characterization of GaAs/AlGaAs multiple quantumwell ridge waveguide lasers
[EUT-92-E-265] p 2348 N94-23168
WAVEGUIDES
Generalized three-dimensional simulation of ferruled coupled-cavity traveling-wave-tube dispersion and impedance characteristics
[NASA-TP-3389] p 2310 N94-24056
A low noise 665 GHz SIS quasi-particle waveguide receiver
[NASA-CR-194735] p 2296 N94-24105
Total light loss optic spectroscopy: Progress towards a fiber optic Raman organic vapor sensor
[DE94-002545] p 2234 N94-24549
Temperature dependent performance of Coplanar Waveguide (CPW) on substrates of various materials
[NASA-TM-106505] p 2313 N94-25170
WAVELENGTH DIVISION MULTIPLEXING
Wide band fiber-optic communications
p 2304 N94-23231
WAVELET ANALYSIS
On the Daubechies-based wavelet differentiation matrix
[NASA-CR-191583] p 2479 N94-23090
System identification using a wavelet-based approach
[DE94-002191] p 2293 N94-23473
Wavelet multiresolution analyses adapted for the fast solution of boundary value ordinary differential equations
p 2485 N94-23691
On the differentiation matrix for Daubechies-based wavelets on an interval
[NASA-CR-191582] p 2487 N94-24291
Optical wavelet transform processor
[AD-A273625] p 2546 N94-24731
Edge detection using a complex wavelet
[AD-A273699] p 2493 N94-25452
WAVERIDERS
Design project: LONGBOW supersonic interceptor
[NASA-CR-195510] p 2180 N94-24581
Sabot high speed interceptor AE 4273 aircraft design
[NASA-CR-195495] p 2183 N94-24971
WEAK INTERACTIONS (FIELD THEORY)
Photon-photon collisions at the next linear collider: Theory
[DE93-041025] p 2534 N94-23803
New evaluation of hadronic contributions to the anomalous magnetic moment of charged leptons
[DE93-634394] p 2536 N94-24844
Weak interactions in a bilocal chiral theory
[DE93-616887] p 2539 N94-25477
WEAPON SYSTEMS
A qualified radiation hardened nonvolatile memory for space and tactical weapons applications
[DE94-001211] p 2559 N94-23186
Early manufacturing considerations in design
p 2177 N94-24315
WEAPONS DEVELOPMENT
Advanced Capability Exhaust Systems/Integrated Product Development for advanced nozzles (ACES/IPD)
[AD-A273209] p 2189 N94-24776
WEAR
New method for increasing machine service-life, phase 2
[PB93-200707] p 2354 N94-23533
A rail corrugation theory which allows for contact patch size p 2269 N94-23582
A linear model for corrugation and its limit of validity
p 2269 N94-23584
Surface analysis of corrugated rail treads
p 2270 N94-23587
Development of a theory of the wear of ceramics
[DE94-002773] p 2254 N94-23783
New tribocoating combination for vacuum operation
p 2355 N94-23990
Wear reduction in ceramic bearings by surface generated pyrolytic carbon continuously replenished by ethylene gas
[NASA-CR-189214] p 2364 N94-24090
WEAR RESISTANCE
JBK-75 stainless steel machinability study
[DE94-002268] p 2242 N94-23475
Wear reduction in ceramic bearings by surface generated pyrolytic carbon continuously replenished by ethylene gas
[NASA-CR-189214] p 2364 N94-24090
Development of high temperature liquid lubricants for low-heat rejection: Heavy duty diesel engines
[NASA-CR-191197] p 2258 N94-24753
A preliminary evaluation of the phosphazene resin PPZ
[AD-A273674] p 2263 N94-25410
WEAR TESTS
A colour image processing algorithm to identify copper-based particles in filter debris samples
[DREP-TM-93-19] p 2455 N94-24122
WEATHER
Cockpit weather graphics using mobile satellite communications p 2280 N94-22775
Aircraft accident report: In-flight engine separation. Japan Airlines, Inc., flight 46E, Boeing 747-121, N473EV, Anchorage, Alaska, 31 March 1993
[PB93-410407] p 2173 N94-24062
United States Weather Research Program (USWRP)
p 2411 N94-24375
Aviation Weather Program (AWP)
p 2411 N94-24380
ASR-9 microburst detection algorithm
[AD-A273591] p 2415 N94-24850
WEATHER FORECASTING
Urban/rural application of weather radar for flow forecasting. Proceedings of the Informal CEc -Workshop
[PB93-220135] p 2407 N94-23129
Lightning studies using LDAR and LLP data
p 2416 N94-23238
United States Weather Research Program (USWRP)
p 2411 N94-24375
Aviation Weather Program (AWP)
p 2411 N94-24380
Scientific goals of the Cooperative Multiscale Experiment (CME) p 2411 N94-24381
Examples of data assimilation in mesoscale models
p 2412 N94-24384
Session on validation of coupled models
p 2414 N94-24399
CAPE for CaPE p 2416 N94-24409
Modeling and data assimilation for Mars Observer
p 2620 N94-24889
Observed and Navy operational global model climatologies of synoptic disturbances over the tropical western Pacific during winter 1991-1992
[AD-A273400] p 2416 N94-25071
WEATHER MODIFICATION
NOAA Federal/State Cooperative Program in Atmospheric Modification Research. Collected publication titles and abstracts
[PB93-198125] p 2396 N94-22913
WEIBULL DENSITY FUNCTIONS
Durability evaluation of ceramic components using CARES/LIFE
[NASA-TM-106475] p 2258 N94-24682
WEIGHT ANALYSIS
NASA/USRA advanced design program
[NASA-CR-195548] p 2180 N94-24492
WEIGHT MEASUREMENT
Mass properties measurement system dynamics
p 2368 N94-23235
Mass properties measurement system: Dynamics and statics measurements p 2368 N94-23236
WEIGHT REDUCTION
NASA Lewis advanced IPV nickel-hydrogen technology p 2392 N94-23356
The mass of massive rover software
p 2464 N94-23410
WEIGHTING FUNCTIONS
Optimal gains for a single polar orbiting satellite
p 2208 N94-24873
The Casimir energy of the rigid string with massive ends
[DE93-616851] p 2492 N94-25338
WEIGHTLESSNESS
Response of an anchored annular cylindrical liquid layer to various axial excitations in zero-gravity
[LRT-WE-9-FB-3-1992] p 2266 N94-23195
Liquid oscillations in a spherical system with sliding edges boundary by two conical solid surfaces in zero-gravity
[LRT-WE-9-FB-5-1992] p 2318 N94-23197
Artificial gravity in space flight
[AD-A273420] p 2427 N94-24928
Loading, electromyograph, and motion during exercise
p 2427 N94-25359
Development of a model to assess orthostatic responses p 2427 N94-25376
WEIGHTLESSNESS SIMULATION
Design and testing of a unique randomized gravity, continuous flow bioreactor p 2423 N94-25368
WELD STRENGTH
Strength, acoustic evaluation and metallurgy of diffusion bonds
[DE94-001804] p 2243 N94-23717
Weldability of Accelerated-Cooled (AcC) high strength TMCP steel X80
[VTT-TIED-1413] p 2251 N94-25419
WELD TESTS
Plasma ARC keyhole welding of aluminum
[PB93-201606] p 2353 N94-23449
Use of photostress to characterize the mechanical behavior of weldments
[NASA-CR-195201] p 2378 N94-25267
WELDABILITY
Weldability of Accelerated-Cooled (AcC) high strength TMCP steel X80
[VTT-TIED-1413] p 2251 N94-25419
WELDED JOINTS
Plasma ARC keyhole welding of aluminum
[PB93-201606] p 2353 N94-23449
Strength, acoustic evaluation and metallurgy of diffusion bonds
[DE94-001804] p 2243 N94-23717
Weld joint concepts for on-orbit repair of Space Station Freedom fluid system tube assemblies
p 2371 N94-24427
Microstructural analysis of the 2195 aluminum-lithium alloy welds p 2251 N94-24448
Use of photostress to characterize the mechanical behavior of weldments
[NASA-CR-195201] p 2378 N94-25267
Weldability of Accelerated-Cooled (AcC) high strength TMCP steel X80
[VTT-TIED-1413] p 2251 N94-25419
WELDING
New welding and finishing procedures
[DE94-602022] p 2352 N94-23025
Weld cladding of hard surfaces
[PB93-201598] p 2353 N94-23448
Microwelding due to random vibration
p 2359 N94-24019
Weld fracture criteria for computer simulation
p 2251 N94-24425
Microstructural analysis of the 2195 aluminum-lithium alloy welds p 2251 N94-24448
Welding of niobium to stainless
[DE94-003365] p 2365 N94-24614
The importance of properties in modeling
p 2246 N94-25121
WETTING
An analytic study of a two-phase laminar airfoil in simulated heavy rain p 2171 N94-23661
WHEAT
Chemical characterization of some aerobic liquids in CELSS p 2422 N94-23241
WHEELS
A rail corrugation theory which allows for contact patch size p 2269 N94-23582
Surface observations of stick-slip oscillations in tightly conformal wheel/rail contacts p 2270 N94-23588
WHISTLERS
Analysis and experiments of a whistler-wave plasma thruster
[DE94-001533] p 2209 N94-23012
WHITE NOISE
Nonlinear smoothing for random fields
[MEMO-1110] p 2493 N94-22728
Separable concatenated codes with iterative map decoding for Rician fading channels
p 2286 N94-22815
Coherence lost? Not-so-fast escapes from the in-phase attractor of a set of globally coupled nonlinear oscillators
[DE94-000799] p 2557 N94-22940
A mixed H2/H(infinity) function for a discrete time system
[MEMO-COSOR-92-36] p 2480 N94-23144
Detection and analysis of unbalanced QPSK in Gaussian noise, version 1.0
[DREO-12-020.1] p 2296 N94-24131
WICKS
Effect of longitudinal vibration on the capillary limit of a wrapped screen wick copper/water heat pipe
[AD-A273830] p 2571 N94-25524
WIDEBAND COMMUNICATION
NASA/ASEE Summer Faculty Fellowship Program
[NASA-CR-194678] p 2571 N94-23230
Wide band fiber-optic communications
p 2304 N94-23231
Northern Exposure 1992: An investigation of transauroral HF radio skywave propagation
[AD-A273363] p 2303 N94-25089
WIENER HOPF EQUATIONS
Diffraction analysis of transient acoustic waves: Half-plane in a layered medium
[PB94-110988] p 2526 N94-23726
Wiener-Hopf factorization of rational matrix functions in terms of realizations: An alternative version
[ETN-94-95380] p 2491 N94-25245
WIGGLER MAGNETS
Properties of the transfer matrices of deflecting magnet systems for free electron laser
[DE93-508257] p 2347 N94-22922
Inverse free electron laser beat-wave accelerator research
[DE94-002597] p 2349 N94-23702
Compact free electron lasers for medical applications
[AD-A273609] p 2350 N94-24934

WIND (METEOROLOGY)
The AGRHYMET data communications project
p 2280 N94-22776
Implementation of a state of the art automated system for the production of cloud/water vapor motion winds from geostationary satellites
[NASA-CR-195087] p 2410 N94-24125
A diagnostic model to estimate winds and small-scale drag from Mars Observer PMIRR data
p 2617 N94-24874
Analyzing Martian winds and tracer concentrations using Mars Observer data p 2619 N94-24883
Three-dimensional numerical simulation of near-surface flows over the Martian north polar cap
p 2621 N94-24895
Wind climate and urban geometry
[ISBN-9-03-860132-8] p 2416 N94-25261
WIND DIRECTION
Combined 1991 and 1992 Robinson-22B (R-22) parking test results
[AD-A273550] p 2193 N94-24559
WIND EFFECTS
CAPE for CaPE p 2416 N94-24409
WIND MEASUREMENT
A field evaluation of remote sensor measurements of wind, temperature, and moisture for ARM integrated sounding system research
[DE94-000565] p 2381 N94-23001
WIND PROFILES
Implementation and evaluation of the new wind algorithm in NASA's 50 MHz doppler radar wind profiler
[NASA-CR-194880] p 2408 N94-23576
CAPE for CaPE p 2416 N94-24409
Analyzing Martian winds and tracer concentrations using Mars Observer data p 2619 N94-24883
WIND SHEAR
ASR-9 microburst detection algorithm
[AD-A273591] p 2415 N94-24850
WIND TUNNEL APPARATUS
Doppler global velocimetry: Development of a flight research instrumentation system for application to non-intrusive measurements of the flow field
[NASA-CR-191490] p 2344 N94-24360
WIND TUNNEL CALIBRATION
Improved pressure measurement system for calibration of the NASA LeRC 10x10 supersonic wind tunnel
[NASA-TM-106470] p 2344 N94-24362
WIND TUNNEL MODELS
Holographic testing of composite propfans for a cruise missile wind tunnel model
[NASA-TM-105271] p 2187 N94-23545
WIND TUNNEL STABILITY TESTS
Supersonic aerodynamic characteristics of a circular body Earth-to-Orbit vehicle
[NASA-TM-4533] p 2170 N94-24716
WIND TUNNEL TESTS
An experimental study of the flow field surrounding a subsonic jet in a cross flow
[NASA-CR-194770] p 2317 N94-23072
Summary of lift and lift/cruise fan powered lift concept technology
[NASA-CR-177619] p 2176 N94-23489
Holographic testing of composite propfans for a cruise missile wind tunnel model
[NASA-TM-105271] p 2187 N94-23545
Compressibility effects on dynamic stall of airfoils undergoing rapid transient pitching motion
[NASA-TM-109681] p 2167 N94-23975
Lift augmentation on a delta wing via leading edge fences and the Gurney flap
[NASA-CR-194793] p 2168 N94-24103
Vortical structure in a forced plane mixing layer
p 2331 N94-24162
Local isotropy in distorted turbulent boundary layers at high Reynolds number p 2332 N94-24166
An experimental investigation of a Mach 3.0 high-speed civil transport at supersonic speeds
[NASA-TP-3365] p 2169 N94-24311
Aerodynamic characteristics and pressure distributions for an executive-jet baseline airfoil section
[NASA-TM-4529] p 2169 N94-24586
Wind tunnel test of a variable-diameter tiltrotor (VDTR) model
[NASA-CR-177629] p 2181 N94-24796
Measurements of the influence of integral length scale on stagnation region heat transfer
[NASA-TM-106503] p 2338 N94-25183
Measurement of the volume mass by spontaneous Raman scattering. Study of turbulent fluctuations of mixing in a subsonic free jet. Measurements in supersonic wind tunnels
[ISL-R-102/92] p 2339 N94-25462
Off-design performance of crenulated blades in a linear compressor cascade
[AD-A273744] p 2340 N94-25534
WIND TUNNELS
Automatic pressure control system for the Wright Laboratory Compressor Research Facility
[AD-A273827] p 2194 N94-25522
WIND TURBINES
A review of the Workshop on Fatigue Life Methodologies for Wind Turbines
[DE94-002039] p 2394 N94-23472
Control algorithms for effective operation of variable-speed wind turbines
[DE94-002607] p 2394 N94-23704
WIND VELOCITY
VIERS-1, phase 3
[BCRS-92-24] p 2381 N94-23145
Control algorithms for effective operation of variable-speed wind turbines
[DE94-002607] p 2394 N94-23704
Comparison between 1-minute and 15-minute averages of turbulence parameters p 2528 N94-24218
A nighttime structure model of atmospheric optical turbulence, c2(n), derived from thermosonde and high resolution rawinsonde measurements
[AD-A273803] p 2406 N94-25537
WIND VELOCITY MEASUREMENT
Implementation and evaluation of the new wind algorithm in NASA's 50 MHz doppler radar wind profiler
[NASA-CR-194880] p 2408 N94-23576
Implementation of a state of the art automated system for the production of cloud/water vapor motion winds from geostationary satellites
[NASA-CR-195087] p 2410 N94-24125
WINDOWS (COMPUTER PROGRAMS)
XRTD: An X-Windows based, real-time radiometric display and analysis system p 2305 N94-23922
Interoperability through standardization: Electronic mail, and X Window systems p 2575 N94-24406
Horatio: Libraries for vision applications, release 2.0
[OUEL-1967/92] p 2593 N94-25326
WINDS ALOFT
Mesospheric and lower thermospheric winds, temperatures densities, and volume emission rates
[NASA-CR-195147] p 2403 N94-24486
WINDSHIELDS
Cockpit/NVG visual integration issues
p 2432 N94-23983
Birdstrike resistant crew enclosure program
[AD-A273700] p 2463 N94-25453
WING FLAPS
Aircraft wing structural detail design (wing, aileron, flaps, and subsystems)
[NASA-CR-195487] p 2183 N94-24974
WING NACELLE CONFIGURATIONS
An experimental investigation of a Mach 3.0 high-speed civil transport at supersonic speeds
[NASA-TP-3365] p 2169 N94-24311
WING PLANFORMS
The Triton: Design concepts and methods
[NASA-CR-195542] p 2184 N94-25004
WING PROFILES
The Gold Rush: A simulated commercial air transportation study
[NASA-CR-195528] p 2184 N94-25002
WING TIPS
Bent-tip blade for aircraft rotary-wing
[CA-PATENT-1-315-259] p 2176 N94-23254
Toward modeling wingtip vortices
p 2171 N94-24142
WINGS
An experimental investigation of the effect of upper surface blowing on dynamic stall
[NASA-CR-194863] p 2165 N94-22894
POISs3: A 3D poisson smoother of structured grids
[PB93-226231] p 2318 N94-23115
Leading-edge votex-system details obtained on F-106B aircraft using a rotating vapor screen and surface techniques
[NASA-TP-3374] p 2166 N94-23512
LinAir: A multi-element discrete vortex Weissinger aerodynamic prediction method
[NASA-TM-108786] p 2167 N94-23557
Aircraft wing structure detail design
[NASA-CR-195485] p 2180 N94-24498
Aircraft wing structural detail design (wing, aileron, flaps, and subsystems)
[NASA-CR-195487] p 2183 N94-24974
WIRE
Wear reduction in ceramic bearings by surface generated pyrolytic carbon continuously replenished by ethylene gas
[NASA-CR-189214] p 2364 N94-24090
A vibrating wire parallel to a type 2 superconducting slab of arbitrary thickness
[DE93-617134] p 2525 N94-25389
Effects of a vibrating wire carrying DC current on a moving type 2 superconducting slab of arbitrary thickness
[DE93-617136] p 2566 N94-25391
WIRE CLOTH
Electrical performance of wire mesh for spacecraft deployable reflector antennas p 2275 N94-22744
WIRELESS COMMUNICATION
Odyssey personal communications satellite system
p 2282 N94-22787
Reduced cost alternatives to premise wiring using ATM and microcellular technologies p 2314 N94-23239
WIRING
NASA/ASEE Summer Faculty Fellowship Program
[NASA-CR-194678] p 2571 N94-23230
Reduced cost alternatives to premise wiring using ATM and microcellular technologies p 2314 N94-23239
A review of wiring system safety in space power systems
[NASA-CR-194439] p 2203 N94-23632
Lightning tests and analyses of tunnel bond straps and shielded cables on the Space Shuttle solid rocket booster
[NASA-CR-193921] p 2200 N94-24801
WORKING FLUIDS
Enhanced absorption cycle computer model
[DE94-001997] p 2271 N94-23793
Weld joint concepts for on-orbit repair of Space Station Freedom fluid system tube assemblies
p 2371 N94-24427
WORKLOADS (PSYCHOPHYSIOLOGY)
Investigation of time and intensity effects in operator workload and performance
[CTN-94-60927] p 2433 N94-24171
Pilot evaluation system p 2158 N94-24266
An examination of the operational error database for air route traffic control centers
[DOT/FAA/AM-93/22] p 2175 N94-24472
New Advances in Mission Planning and Rehearsal Systems
[AGARD-LS-192] p 2521 N94-25008
Human factors of mission planning systems: Theory and concepts p 2521 N94-25010
Multiple-camera/motion stereoscopy for range estimation in helicopter flight p 2441 N94-25505
WORKSTATIONS
Deployable video conference table
[NASA-CASE-ARC-11950-1] p 2192 N94-23310
The Automated Instrumentation and Monitoring System (AIMS) reference manual
[NASA-TM-108795] p 2452 N94-23510
Customizing graphical user interface technology for spacecraft control centers p 2510 N94-23905
High performance, low cost, self-contained, multipurpose PC based ground systems
p 2516 N94-23943
CADBIT 2: Computer-aided design for built-in test, volume 1
[AD-A273702] p 2463 N94-25455
CADBIT 2: Computer-aided design for built-in test, volume 2
[AD-A273703] p 2463 N94-25456
Engineering workstation: Sensor modeling
p 2441 N94-25500

X

X RAY ABSORPTION
Applications of x ray absorption fine structure to the in situ study of the effect of cobalt in nickel hydrous oxide electrodes for fuel cells and rechargeable batteries
p 2391 N94-23347
In situ and ex situ spectroelectrochemical and x ray absorption studies on rechargeable, chemically-modified and other MnO2 materials
[DE94-001387] p 2234 N94-24545
X RAY ANALYSIS
Phase transformations in Cu-Zr multilayers
[DE94-000393] p 2241 N94-23297
Evaluation of ovostatin and ovostatin assay
p 2422 N94-24437
X RAY ASTRONOMY
Excitation of XUV radiation in solar flares
[NASA-CR-193703] p 2627 N94-24094
Shocked clouds in the Cygnus Loop
[NASA-CR-195190] p 2600 N94-25178
Investigation relative to the Roentgen Satellite (ROSAT)
[NASA-CR-195192] p 2600 N94-25269
X RAY ASTROPHYSICS FACILITY
Advanced X ray Astrophysics Facility-Imaging (AXAF-I) thermal analyses using Integrated Thermal Analysis System (ITAS) program p 2320 N94-23635

SAO mission support software and data standards, version 1.0
[NASA-CR-193906] p 2454 N94-24050

X RAY BINARIES
Flux measurements using the BATSE spectroscopic detectors p 2580 N94-24435
ROSAT observations of the x ray binary HD 154791
[NASA-CR-195189] p 2600 N94-25198

X RAY DENSITY MEASUREMENT
Engine materials characterization and damage monitoring by using x ray technologies
[NASA-TP-3328] p 2372 N94-24074

X RAY DETECTORS
Characterization of CCD-based imaging x ray detectors for diffraction experiments
[DE93-041343] p 2556 N94-22921

X RAY DIFFRACTION
Characterization of CCD-based imaging x ray detectors for diffraction experiments
[DE93-041343] p 2556 N94-22921
Application of maximum entropy and irreducible cluster integrals to joint probability distributions for x ray structure determination
[PB93-224152] p 2559 N94-23109
Modifications to 8x8 dynamical theory: Polarizations redefined according to x ray diffraction convention
[DE94-001290] p 2560 N94-23187
Proposed additions to the SHADOW ray-tracing code for general-asymmetric perfect-crystal optics
[DE94-001291] p 2560 N94-23188
Demonstration of the feasibility of an integrated x ray laboratory for planetary exploration
[NASA-CR-177631] p 2598 N94-24832
An x ray diffraction investigation of alpha-Al2O2 addition to Yttria Stabilized Zirconia (YSZ) thermal barrier coatings subject to destabilizing vanadium pentoxide (V2O5) exposure
[AD-A273403] p 2261 N94-25072
X ray diffraction analysis of electrodeposited beta-tantalum
[AD-A273254] p 2249 N94-25142

X RAY FLUORESCENCE
Demonstration of the feasibility of an integrated x ray laboratory for planetary exploration
[NASA-CR-177631] p 2598 N94-24832

X RAY IMAGERY
Requirements for future solar-physics missions with x ray instrumentation p 2625 N94-22849

X RAY INSPECTION
Engine materials characterization and damage monitoring by using x ray technologies
[NASA-TP-3328] p 2372 N94-24074
An evaluation of Compton scatter imaging using COMSCAN
[DREP-TM-93-38] p 2372 N94-24136

X RAY LASERS
Characterization of germanium stripe x ray lasers
[DE93-019629] p 2347 N94-22867
Ray and wave optics modeling of laboratory x ray lasers
[DE93-019940] p 2541 N94-22868
Inertial confinement fusion
[DE94-002602] p 2551 N94-23703
Excitation mechanisms for XUV and x ray lasers
[DE93-617006] p 2351 N94-25482

X RAY OPTICS
Ray and wave optics modeling of laboratory x ray lasers
[DE93-019940] p 2541 N94-22868
Theoretical investigation of variable periodicity (graded) multilayers for hard x ray applications
[NASA-CR-194824] p 2543 N94-23502
Germanium x ray phase plates for the production of circularly polarized x rays
[DE94-002908] p 2545 N94-24550
Investigate zero-stress replicated optics
[NASA-CR-193889] p 2545 N94-24665
Soft x ray optics by pulsed laser deposition
[NASA-CR-195139] p 2546 N94-24967

X RAY SCATTERING
Thermal phase behavior of metal surfaces: X-ray scattering studies of Pt(001)
[DE94-002991] p 2245 N94-24612

X RAY SOURCES
The soft x ray halo of the spiral galaxy NGC4631
[NASA-CR-194820] p 2601 N94-23537
X ray simulator theory support
[AD-A273613] p 2553 N94-24949
Investigation relative to the Roentgen Satellite (ROSAT)
[NASA-CR-195192] p 2600 N94-25269

X RAY SPECTRA
High-resolution soft x ray photoionization studies of selected molecules
[DE94-000568] p 2532 N94-23002
1993 annual report for the Phaedrus-T RF current drive experiments
[DE94-001369] p 2550 N94-23192

X RAY SPECTROSCOPY
Requirements for future solar-physics missions with x ray instrumentation p 2625 N94-22849
Imaging XUV spectroscopy of a Z-pinch plasma in the former Soviet Union
[DE93-040849] p 2549 N94-22949
Investigate zero-stress replicated optics
[NASA-CR-193889] p 2545 N94-24665
LPCVD of InN on GaAs(110) using HN3 and TMIn: Comparison with Si(100) results
[AD-A273555] p 2235 N94-24917
The structure and catalytic properties of supported platinum catalysts
[ETN-94-95357] p 2236 N94-25250

X RAY TIMING EXPLORER
The H(sub infinity) optimal controller design and reduction for the inertial hold mode of the attitude control system of the XTE spacecraft
[NASA-CR-195137] p 2366 N94-24846

X RAYS
IPP Prague Contributions to the IAEA Technical Committee Meeting on Research Using Small Tokamaks
[IPPCZ-329] p 2551 N94-24293
High energy collimating fine grids for HESP program
[NASA-CR-189317] p 2209 N94-24767
Nonequilibria in thermal emission from supernova remnants
[NIFS-264] p 2602 N94-24866
X ray enhancement of SN 1987A due to interaction with its ring-like nebula
[NIFS-265] p 2602 N94-24867
High precision x ray lithographic masks
[AD-A273342] p 2346 N94-25154
Excitation mechanisms for XUV and x ray lasers
[DE93-617006] p 2351 N94-25482

XENON
Contamination control and plume assessment of low-energy thrusters
[NASA-TM-104585] p 2218 N94-23343
Power console development for NASA's electric propulsion outreach program
[NASA-TM-106428] p 2218 N94-23372
Performance evaluation of the Russian SPT-100 thruster at NASA LeRC
[NASA-TM-106401] p 2219 N94-23630
Performance of the NASA cm ion thruster
[NASA-TM-106426] p 2221 N94-24770

XENON CHLORIDE LASERS
Microwave excitation of pulsed high pressure gas discharge lasers
[DLR-FB-93-12] p 2351 N94-25304

Y

YAG LASERS
Investigation of the optical and laser properties of Tm and Ho in YAG anf YLF
[REPT-94-001] p 2563 N94-24404
Progress toward ultra-stable lasers for use in space
[NASA-TM-109678] p 2349 N94-24488

YANG-MILLS THEORY
On BRST quantization of constrained systems
[ETN-94-95386] p 2570 N94-25258

YBCO SUPERCONDUCTORS
Anisotropic uniaxial pressure effects in YBa2Cu3O(7-delta)
[DE94-001456] p 2557 N94-22929
Processing of YBCO superconductors for improved levitation force
[DE94-001326] p 2559 N94-22994
Conductors with small Fermi energies and small gap energies
[DE93-040887] p 2561 N94-23432
Spectroscopic IR ellipsometry of 100 and 001 oriented YBa2Cu3O(7-delta) films
[PB93-201481] p 2561 N94-23445
Investigation and application of microwave electron cyclotron resonance plasma physical vapour deposition
[DE93-613909] p 2555 N94-25333
Critical currents in YBaCuO-ceramics
[DE93-617140] p 2263 N94-25404

YEAST
Design and testing of a unique randomized gravity, continuous flow bioreactor p 2423 N94-25368

YIELD
Setting test limits under prescribed consumer loss
[MEMO-1107] p 2478 N94-22725

YIELD STRENGTH
Relationship of microstructure and mechanical properties for V-Cr-Ti alloys
[DE94-001431] p 2238 N94-22718
Effect of neutron irradiation on tensile properties of V-Cr-Ti alloys
[DE94-001433] p 2240 N94-23194
Use of photostress to characterize the mechanical behavior of weldments
[NASA-CR-195201] p 2378 N94-25267

YLF LASERS
Investigation of the optical and laser properties of Tm and Ho in YAG anf YLF
[REPT-94-001] p 2563 N94-24404

YTTRIA-STABILIZED ZIRCONIA
Combustion synthesis and engineering of nanoparticles for electronic, structural and superconductor applications
[DE94-001865] p 2254 N94-23720
An x ray diffraction investigation of alpha-Al2O2 addition to Yttria Stabilized Zirconia (YSZ) thermal barrier coatings subject to destabilizing vanadium pentoxide (V2O5) exposure
[AD-A273403] p 2261 N94-25072

YTTRIUM ALLOYS
New extensions in the development of deformation processed metal-metal matrix composites
[DE94-000692] p 2227 N94-23004

YTTRIUM COMPOUNDS
Influences of nitrogen absorption on the magnetic properties of YFe2, YFe3 and Y6Fe23
[REPT-A-2654] p 2564 N94-24958

YTTRIUM OXIDES
Processing of YBCO superconductors for improved levitation force
[DE94-001326] p 2559 N94-22994
An x ray diffraction investigation of alpha-Al2O2 addition to Yttria Stabilized Zirconia (YSZ) thermal barrier coatings subject to destabilizing vanadium pentoxide (V2O5) exposure
[AD-A273403] p 2261 N94-25072

YTTRIUM-ALUMINUM GARNET
Excited state dynamics of thulium ions in yttrium aluminum garnets
[NASA-CR-195159] p 2564 N94-25024

YUKAWA POTENTIAL
Stitching the Yukawa quilt
[PB93-204477] p 2569 N94-24532
On the transverse size of a fast moving nucleon
[DE93-616891] p 2539 N94-25481

Z

ZETA PINCH
Imaging XUV spectroscopy of a Z-pinch plasma in the former Soviet Union
[DE93-040849] p 2549 N94-22949
Computer modeling of plasma flow switches-high current switching on Procyon
[DE93-040189] p 2311 N94-24500
X ray simulator theory support
[AD-A273613] p 2553 N94-24949

ZINC
Integrated hydrometallurgical jarosite treatment
[PB93-217990] p 2232 N94-22983
Magnetic resonance study of zinc-related defects in silicon with optimized EPR spectrometer
[PB93-224640] p 2561 N94-23223
Evaluation of inorganic zinc-rich primers using Electrochemical Impedance Spectroscopy (EIS)
p 2237 N94-23233
The effects of zinc borate addition on the flammability characteristics of polyester, vinyl ester, and epoxy glass reinforced plastics
[AD-A273164] p 2262 N94-25136

ZINC COATINGS
Evaluation of inorganic zinc-rich primers using Electrochemical Impedance Spectroscopy (EIS)
p 2237 N94-23233

ZIRCONIUM ALLOYS
Phase transformations in Cu-Zr multilayers
[DE94-000393] p 2241 N94-23297

ZIRCONIUM OXIDES
An x ray diffraction investigation of alpha-Al2O2 addition to Yttria Stabilized Zirconia (YSZ) thermal barrier coatings subject to destabilizing vanadium pentoxide (V2O5) exposure
[AD-A273403] p 2261 N94-25072

ZONAL FLOW (METEOROLOGY)
Diagnostic calculations of the circulation in the Martian atmosphere p 2622 N94-24898

PERSONAL AUTHOR INDEX

Typical Personal Author Index Listing

ALEXOPOULOS, JIM S. .... p 436 N94-12023

PERSONAL AUTHOR
PAGE NUMBER
ACCESSION NUMBER

Listings in this index are arranged alphabetically by personal author. The page number helps you locate the citation in the abstract section. The accession number denotes the number by which the citation is identified.

A

AAGESEN, FINN ARVE .... p 2293 N94-23508
AAMNES, KETIL .... p 2451 N94-23443
p 2452 N94-23444
p 2453 N94-23534
AANNESTAD, PER A. .... p 2600 N94-25270
AARTS, HARRY F. M. .... p 2489 N94-24653
ABARBANEL, SAUL .... p 2480 N94-23272
ABBE, B. S. .... p 2284 N94-22802
ABBE, BRIAN S. .... p 2279 N94-22771
p 2280 N94-22774
p 2280 N94-22780
ABBINK, HENRY C. .... p 2344 N94-24184
ABBOTT, DAVID R. .... p 2364 N94-24128
ABBOTT, DEAN W. .... p 2525 N94-23698
ABEND, KENNETH .... p 2275 N94-22745
ABERLE, JAMES T. .... p 2365 N94-24699
ABERNATHY, D. L. .... p 2245 N94-24612
ABOWD, GREGORY .... p 2460 N94-24933
ABRAHAM, F. F. .... p 2374 N94-22871
ABRAMOVITZ, IRWIN J. .... p 2202 N94-23631
ABRAMS-BLAKEMORE, BRUCE p 2391 N94-23348
ABUSALI, P. A. M. .... p 2207 N94-23259
ACHACHE, J. .... p 2606 N94-23382
ACKERMANS, MARIETTE THEODORA
p 2236 N94-25232
ACTON, CHARLES H., JR. .... p 2517 N94-23950
ADAM, SUSAN C. .... p 2435 N94-24197
ADAMS, B. L. .... p 2557 N94-22938
ADAMS, D. .... p 2559 N94-23186
p 2230 N94-24942
p 2230 N94-25163
ADAMS, D. F. .... p 2230 N94-24779
ADAMS, RICHARD J. .... p 2164 N94-25108
ADAMS, W. W. .... p 2567 N94-25441
ADAMSON, A. P. .... p 2188 N94-24180
ADAN, IVO J. B. F. .... p 2477 N94-25526
ADKINS, SEAN .... p 2206 N94-25007
ADRIAN, KENNETH .... p 2183 N94-24974
AERDTS, ANNA MARIA .... p 2262 N94-25225
AFFELD, K. .... p 2316 N94-22858
AGAN, M. J. .... p 2284 N94-22802
AGAN, MARTIN J. .... p 2279 N94-22771
AGARWAL, A. .... p 2286 N94-22817
AGARWAL, S. K. .... p 2398 N94-23818
AGATONOVIC, P. .... p 2256 N94-24239
AGRAVANTE, H. .... p 2306 N94-25498
AGRAWAL, AJAY K. .... p 2324 N94-23660
AGRAWAL, GAGAN .... p 2458 N94-24740
AGRAWAL, O. P. .... p 2325 N94-23667
AGUIAR, JOHN .... p 2183 N94-24972
AGUIRRE, L. A. .... p 2492 N94-25320
AGUIRRE, LUIS A. .... p 2523 N94-25314
p 2523 N94-25323
AGUIRRE, M. .... p 2209 N94-24006
AHAMAD, ATIQ .... p 2409 N94-24048
p 2409 N94-24087
p 2410 N94-24126
AHLIN, LARS .... p 2297 N94-24531
AHMAD, ZIUDDIN .... p 2410 N94-24355
AHMED, R. .... p 2375 N94-23294
AHN, SOONHO .... p 2393 N94-23364
AHUJA, VINEET .... p 2325 N94-23664
AHUMADA, AL .... p 2443 N94-25513
AIBEL, DAVID W. .... p 2272 N94-25193
AIET-KACI, H. .... p 2593 N94-24743
AIHARA, SHIN ICHI .... p 2493 N94-22728
AIT-AHMED, MOURAD .... p 2470 N94-22904
AJAMI, ALFRED M. .... p 2354 N94-23533
AJMANI, KUMUD .... p 2265 N94-24301
AKAU, R. L. .... p 2321 N94-23640
AKINC, M. .... p 2227 N94-22977
AKSAY, ILHAN A. .... p 2257 N94-24677
AKSNES, E. .... p 2254 N94-23431
AKYUZLU, K. M. .... p 2266 N94-23657
AL-HASHEL, WALEED .... p 2183 N94-24971
ALAI, H. .... p 2357 N94-24005
ALAM, JAVED .... p 2376 N94-23551
ALAMERI, MOHAMED .... p 2180 N94-24498
ALAMI, RACHID .... p 2370 N94-23413
ALBANO, R. K. .... p 2542 N94-22917
ALBE, F. .... p 2343 N94-24054
ALBEE, ARDEN L. .... p 2601 N94-23499
ALBERS, W. .... p 2478 N94-22725
ALCENIUS, TIMOTHY .... p 2167 N94-23625
ALDHAHIR, A. .... p 2487 N94-23787
ALDO, ANDREW C. .... p 2171 N94-23656
ALDRICH, C. H. .... p 2453 N94-23701
ALEKSOFF, CARL C. .... p 2546 N94-24731
ALEXANDER, S. .... p 2203 N94-23618
ALHORN, D. C. .... p 2269 N94-23574
ALKALAJ, LEON J. .... p 2504 N94-23875
ALKEMA, KEVIN .... p 2183 N94-24975
ALLARD, F. .... p 2502 N94-23858
ALLEN, G. A. .... p 2320 N94-23532
ALLEN, G. A., JR. .... p 2319 N94-23513
ALLEN, KEVIN S. .... p 2339 N94-25446
ALLISON, DENNIS O. .... p 2169 N94-24586
ALLISON, MICHAEL .... p 2616 N94-24872
ALLNUTT, R. M. .... p 2283 N94-22794
ALLRED, R. E. .... p 2526 N94-23718
ALMAZAN, P. PLANAS .... p 2321 N94-23639
ALON, YAIR .... p 2306 N94-25493
ALTINK, H. E. .... p 2561 N94-23223
ALTMAN, SYLVIA I. .... p 2175 N94-24127
ALTUNIN, K. R. .... p 2502 N94-23861
ALTUNIN, V. I. .... p 2502 N94-23861
ALVAREZ, L. S. .... p 2291 N94-23263
ALVIN, K. F. .... p 2203 N94-23618
AMADOR, ARTHUR V. .... p 2504 N94-23875
AMALBERTI, RENE .... p 2429 N94-23980
p 2432 N94-23981
AMARA, MAHER .... p 2370 N94-23424
AMARAKOON, V. R. W. .... p 2254 N94-23720
AMIN, ASHOK T. .... p 2575 N94-24406
AMINE, HICHAM .... p 2307 N94-22909
AMOS, DAVID A. .... p 2175 N94-24474
AMUNDSEN, R. M. .... p 2349 N94-24488
AMUNDSEN, RUTH M. .... p 2322 N94-23647
ANANASSO, F. .... p 2282 N94-22789
ANANI, ANABA .... p 2391 N94-23353
ANCELLET, GERARD .... p 2402 N94-24108
ANDERBERG, NILS-ERIC .... p 2193 N94-24785
ANDERSEN, GERALD .... p 2184 N94-25017
ANDERSON, COLLIN D. .... p 2247 N94-25126
ANDERSON, DAVID B. .... p 2460 N94-24932
ANDERSON, DAVID N. .... p 2173 N94-24047
ANDERSON, EVERETT B. .... p 2394 N94-23366
ANDERSON, M. J. .... p 2356 N94-23993
p 2363 N94-24044
ANDERSON, O. .... p 2402 N94-23721
ANDERSON, P. .... p 2214 N94-23051
ANDERSON, W. E. .... p 2212 N94-23042
p 2293 N94-23719
ANDERSSON, TORBJOERN .... p 2357 N94-24001
ANDRE, ANTHONY D. .... p 2430 N94-23527
ANDRES, LUIS SAN .... p 2363 N94-24081
ANDREW, WILLIAM V. .... p 2365 N94-24699
ANDREWS, AUSTIN L. .... p 2189 N94-24776
ANDREWS, GEORGE A., JR. .... p 2623 N94-25349
ANDRIANOV, IGOR .... p 2490 N94-24768
ANGEL, S. M. .... p 2541 N94-22722
p 2234 N94-24549
ANGELINO, R. .... p 2477 N94-23900
ANGLIN, RICHARD L., JR. .... p 2275 N94-22749
ANGOLD, NIGEL .... p 2502 N94-23862
ANGOT, PHILIPPE .... p 2485 N94-23692
ANNARATONE, B. M. .... p 2554 N94-25327
ANOSOV, O. L. .... p 2626 N94-23020
ANSPAUGH, B. E. .... p 2395 N94-24563
ANTONIO, MARK R. .... p 2391 N94-23347
ANTSON, O. K. .... p 2566 N94-25347
APITULEY, ARNOUD .... p 2402 N94-24108
APPARAO, K. V. S. R. .... p 2347 N94-22967
p 2542 N94-22979
ARAIZA, JOE .... p 2205 N94-24702
ARAJ, A. .... p 2301 N94-24707
ARAKAKI, YOSHIYA .... p 2283 N94-22793
ARAKI, NORIYUKI .... p 2288 N94-22825
ARBOCZ, J. .... p 2375 N94-23221
ARCANGELI, J.-P. .... p 2518 N94-23956
ARCHER, D. .... p 2390 N94-23212
ARGAMAN, N. .... p 2571 N94-25340
ARGROW, BRIAN M. .... p 2171 N94-23656
ARGYROPOULOS, S. A. .... p 2247 N94-25127
ARMAGAN, G. .... p 2458 N94-24661
p 2564 N94-25024
ARMIGER, SCOTT C. .... p 2204 N94-24620
ARRINGTON, E. ALLEN .... p 2192 N94-23091
ARRITT, RAY .... p 2413 N94-24387
ARRUBBAN, M. M. .... p 2351 N94-25482
ASABE, YOSHIYUKI .... p 2405 N94-24980
ASADA, TOSHIO .... p 2564 N94-24960
ASHBY, C. I. H. .... p 2555 N94-22717
p 2350 N94-24659
ASHBY, S. F. .... p 2454 N94-23796
ASHLEY, A. T. .... p 2202 N94-24121
ASRATIAN, A. S. .... p 2488 N94-24541
p 2489 N94-24651
ASSENBAUM, MICHEL .... p 2401 N94-23159
ASSOUFID, L. .... p 2545 N94-24550
ATHANASIU, I. .... p 2466 N94-23706
ATHOUSAKE, ROXANNE .... p 2190 N94-24957
p 2183 N94-24969
ATIF, KARIM .... p 2465 N94-23134
ATKINSON, R. J. .... p 2409 N94-24060
ATLAS, E. .... p 2307 N94-22955
ATREYA, ARVIND .... p 2270 N94-23740
ATTENBOROUGH, KEITH .... p 2527 N94-24213
ATTIA, ALAN I. .... p 2310 N94-23823
AUCIELLO, O. .... p 2562 N94-23805
AUERKARI, PERTTI .... p 2379 N94-25418
AUSSENAC, N. .... p 2508 N94-23899
AUTEN, T. A. .... p 2238 N94-22861
AVISSAR, RONI .... p 2413 N94-24387
AVRETT, EUGENE H. .... p 2626 N94-23569
p 2627 N94-24300
AYER, TIMOTHY C. .... p 2169 N94-24606
AZAIEZ, J. .... p 2331 N94-24160
AZBOUCHE, A. .... p 2448 N94-23024
AZOR, RUTH .... p 2159 N94-24272

B

BAAKLINI, GEORGE Y. .... p 2372 N94-24074
BAATH, L. B. .... p 2599 N94-23705
p 2599 N94-24521
BABIC, NIKOLA .... p 2206 N94-24916
BACHMANN, BERNHARD .... p 2482 N94-23674
BACKER, D. C. .... p 2599 N94-23705
BACON, DAVID .... p 2414 N94-24392
BADDELEY, A. J. .... p 2496 N94-24639
BADER, S. D. .... p 2559 N94-22995
BAETEN, J. C. M. .... p 2488 N94-24539
p 2446 N94-24540
BAGCHI, ARUNABHA .... p 2493 N94-22728
BAGIAN, JAMES P. .... p 2436 N94-24204
BAGIAN, TANDI .... p 2433 N94-24185
BAGNASCHI, LUCA L. .... p 2157 N94-24263
BAHRAMI, KHOSROW A. .... p 2516 N94-23944
BAIGET, A. .... p 2369 N94-23400
BAILEY, M. D. .... p 2501 N94-23853

BAILEY, T. S. .... p 2261 N94-24930
BAILIN, SIDNEY C. .... p 2443 N94-23936
BAIN, D. B. .... p 2187 N94-24082
BAIZE, LIONEL .... p 2464 N94-23962
BAKER, MATT .... p 2180 N94-24581
BAKKEN, L. N. .... p 2533 N94-23505
BAKKEN, P. M. .... p 2278 N94-22767
BAKKER, ANDRIES .... p 2339 N94-25254
BAKOS, R. J. .... p 2319 N94-23513
p 2320 N94-23532
BAL, H. E. .... p 2466 N94-23706
BAL, HANS E. .... p 2453 N94-23745
BALA, GREGORY A. .... p 2345 N94-24831
BALACHANDRAN, U. .... p 2559 N94-22994
BALANIS, CONSTANTINE A. .... p 2298 N94-24616
p 2365 N94-24699
BALANON, WILL .... p 2181 N94-24803
BALAS, GARY J. .... p 2190 N94-25176
BALDOCCHI, BOB .... p 2183 N94-24971
BALLANTYNE, M. J. .... p 2433 N94-24119
BALLARINI, R. .... p 2377 N94-24604
BANDELT, H. J. .... p 2479 N94-23093
BANFIELD, DON .... p 2208 N94-24873
BANKS, BRUCE A. .... p 2534 N94-23825
BANKS, MARTIN S. .... p 2442 N94-25510
BANKS, S. P. .... p 2492 N94-25309
p 2492 N94-25310
BANKSTON, C. P. .... p 2314 N94-23401
BAO, JOHNNY .... p 2221 N94-24834
BAR-ITZHACK, ITZHACK Y. .... p 2156 N94-24258
BARAKAT, M. .... p 2289 N94-22830
BARANOWSKY, PATRICK W., II p 2278 N94-22762
BARBEE, T. W., JR. .... p 2241 N94-23297
BARBIER, CHRISTIAN .... p 2196 N94-23923
BARBIN, Y. .... p 2608 N94-23393
BARBIS, A. .... p 2359 N94-24013
BARCLAY, REBECCA O. .... p 2592 N94-24649
p 2592 N94-24660
p 2593 N94-24709
BARHO, R. .... p 2305 N94-23996
BARHORST, ALAN A. .... p 2371 N94-25350
BARKER, JOHN L. .... p 2383 N94-23600
BARLOW, DIANE .... p 2594 N94-25487
BARMATZ, M. .... p 2238 N94-25134
BARNES, J. R. .... p 2616 N94-24871
p 2617 N94-24874
p 2617 N94-24875
BARNES, VALERIE B. .... p 2504 N94-23873
BARNETT, KEVIN D. .... p 2309 N94-23304
BARNETT, MARK .... p 2169 N94-24606
BARNETT, TIMOTHY P. .... p 2407 N94-23199
BARNIV, YAIR .... p 2176 N94-25504
BARON, J. .... p 2157 N94-24262
BARR, THOMAS H. .... p 2509 N94-23901
BARRO, E. .... p 2519 N94-23959
BARRON, ROGER L. .... p 2525 N94-23698
BARROS, E. .... p 2156 N94-24257
BARROWS, LINDA H. .... p 2426 N94-23544
BARRY, SUSAN R. .... p 2429 N94-25351
BARTASHEVICH, M. I. .... p 2567 N94-25412
BARTASHEVICH, MIKHAIL I. .... p 2564 N94-24958
BARTLETT, DAVE .... p 2272 N94-25193
BARTON, S. K. .... p 2282 N94-22791
BARTSCH, KNUT .... p 2375 N94-23120
BARTUCCA, FRANCESCO .... p 2286 N94-22814
BASILE, G. .... p 2357 N94-24002
BASILIO, RALPH R. .... p 2207 N94-23864
BASKHARONE, ERIAN A. .... p 2366 N94-24998
p 2366 N94-24999
BASOL, B. M. .... p 2390 N94-23296
BASS, HENRY E. .... p 2527 N94-24212
p 2528 N94-24215
p 2569 N94-24777
BASS, LEN .... p 2460 N94-24933
BASTIAANSSEN, W. G. M. .... p 2386 N94-23734
BASTIEN-THIRY, CHRISTOPHE . p 2520 N94-23967
BATER, R. .... p 2305 N94-23909
BATES, HARRY E. .... p 2304 N94-23231
BATES, JOHN J. .... p 2384 N94-23604
BATHER, JOHN .... p 2495 N94-24560
BATHKE, C. G. .... p 2552 N94-24519
BATRA, RAJESH .... p 2266 N94-24618
BATSON, ROBERT G. .... p 2497 N94-24407
BATTOCCHIO, L. .... p 2515 N94-23935
BATTRICK, B. .... p 2623 N94-22837
BAUDIN, CATHERINE .... p 2591 N94-24552
BAUER, D. .... p 2478 N94-22715
p 2478 N94-22727
BAUER, HELMUT F. .... p 2266 N94-23195
p 2375 N94-23196
p 2318 N94-23197
BAUTISTA, J. J. .... p 2291 N94-23262
BAVINCK, H. .... p 2489 N94-24572
BAXI, C. B. .... p 2354 N94-23797
p 2553 N94-24756
BEACH, EDWARD .... p 2510 N94-23905
BEACH, M. A. .... p 2288 N94-22824
BEAL, PAMELA .... p 2181 N94-24803
BEATON, ROBERT M. .... p 2521 N94-25009
BEAUDOIN, A. J. .... p 2240 N94-23021
BECKER, CHRISTOPHER H. .... p 2232 N94-23524
BECKER, GUNNAR R. .... p 2527 N94-24209
BECKER, H. A. .... p 2341 N94-23675
BECONNE, JEAN-PAUL .... p 2342 N94-22902
BEEMAN, J. W. .... p 2564 N94-24657
BEGAULT, DURAND R. .... p 2525 N94-23312
BEHRENDT, D. R. .... p 2222 N94-23500
BEHRENS, R., JR. .... p 2232 N94-23298
BEIGLEMAN, Z. .... p 2161 N94-24286
BEIRLANT, JAN .... p 2494 N94-23771
p 2494 N94-23774
BEKEFI, GEORGE .... p 2350 N94-24934
BELANGER, M. .... p 2285 N94-22805
BELCASTRO, CHRISTINE M. .... p 2163 N94-25103
BELL, D. .... p 2273 N94-22739
BELL, DAVID E. .... p 2304 N94-25521
BELL, JASON .... p 2266 N94-24618
BELLAN, JOSETTE .... p 2153 N94-24242
BELUSHKIN, A. V. .... p 2567 N94-25424
BELYAKOV, V. A. .... p 2539 N94-25481
BEN-YAKAR, ADELA .... p 2156 N94-24254
BENAMAR, M. A. .... p 2448 N94-23024
BENDER, STANLEY I. .... p 2353 N94-23215
BENEDICTO, J. .... p 2273 N94-22737
p 2278 N94-22765
p 2278 N94-22767
BENEDICTO, XAVIER .... p 2288 N94-22826
BENFORD, D. J. .... p 2296 N94-24105
BENGTSON, R. D. .... p 2548 N94-22945
BENGTSSON, JAN-PETER .... p 2544 N94-23723
BENJAMIN, STAN .... p 2412 N94-24384
p 2413 N94-24391
BENJAMIN, T. G. .... p 2389 N94-22723
BENKOVITZ, C. M. .... p 2386 N94-23779
BENNATI, S. .... p 2374 N94-23112
BENNETT, DAVID W. .... p 2275 N94-22747
BENOUALI, N. .... p 2448 N94-23024
BENOY, DANIEL ANTON .... p 2554 N94-25300
BENSO, STEFANO .... p 2518 N94-23952
BENSON, RICHARD D. .... p 2500 N94-23850
BENTS, D. J. .... p 2314 N94-23401
BERENGUER, M. .... p 2569 N94-23453
BERETTA, G. B. .... p 2445 N94-23788
BEREZHIANI, V. I. .... p 2604 N94-25215
BERG, TIM .... p 2183 N94-24971
BERGQUIST, AKE .... p 2294 N94-23742
BERGSTRA, J. A. .... p 2488 N94-24539
p 2446 N94-24540
BERGSTROEM, STEN .... p 2399 N94-24633
BERGWERFF, HANS .... p 2402 N94-24108
BERKANE, BACHIR .... p 2447 N94-22899
BERKE, LASZLO .... p 2376 N94-23551
p 2378 N94-24845
BERKELAAR, MICHEL R. C. M. .. p 2461 N94-25080
BERKENBOSCH, A. C. .... p 2491 N94-24954
BERKLEY, WILLIAM E. .... p 2431 N94-23977
p 2432 N94-23984
BERKOVITZ, AVRAHAM .... p 2159 N94-24276
BERKOWITZ, C. M. .... p 2386 N94-23779
BERKOWITZ, M. .... p 2537 N94-24940
BERKOWITZ, MAX L. .... p 2536 N94-24675
BERLOWITZ, ILAN .... p 2158 N94-24270
BERMUDEZBELKYS, S. .... p 2239 N94-22965
BERNARD, JACQUES .... p 2608 N94-23392
p 2195 N94-23924
BERNHARD, RONALD P. .... p 2386 N94-24095
BERNS, D. .... p 2310 N94-24070
BERNS, DARREN H. .... p 2219 N94-23531
BERNSTEIN, URI .... p 2440 N94-25496
BERRY, B. F. .... p 2529 N94-25026
BERRY, F. C. .... p 2222 N94-25352
BERRY, MARK H. .... p 2303 N94-25217
BERTENYI, E. .... p 2207 N94-22742
BERTHIAS, J.-P. .... p 2196 N94-23919
BERTHIER, Y. .... p 2264 N94-24010
BERTOLOTTI, FABIO .... p 2337 N94-24869
BERTRAND, R. M. .... p 2544 N94-23732
BETZ, JESSIE M. BETHLY .... p 2306 N94-25353
BEWLEY, THOMAS .... p 2327 N94-24139
BHARGAVA, V. K. .... p 2296 N94-24132
p 2300 N94-24697
BHARTIA, P. K. .... p 2410 N94-24355
BHAT, P. C. .... p 2535 N94-24515
BHAT, T. R. S. .... p 2530 N94-25177
BHATTACHARJEE, A. .... p 2349 N94-23702
BHATTARAI, H. N. .... p 2493 N94-25473
BHUMRALKAR, CHANDRAKANT p 2411 N94-24375
BIAGLOW, JAMES .... p 2211 N94-23038
p 2214 N94-23052
BIALKE, BILL .... p 2208 N94-24022
BIBRING, J. P. .... p 2606 N94-23382
BICAK, JIRI .... p 2406 N94-25430
BICKLER, DONALD B. .... p 2369 N94-23398
BIDEK, MALEINA C. .... p 2337 N94-25119
BIERSCHWALE, JOHN M. .... p 2435 N94-24197
p 2436 N94-24199
p 2436 N94-24200
BIGGAR, STUART F. .... p 2383 N94-23601
BIGLIERI, EZIO .... p 2286 N94-22814
BILLICA, LINDA W. .... p 2354 N94-23822
BILLINGS, S. A. .... p 2492 N94-25306
p 2476 N94-25308
p 2462 N94-25311
p 2523 N94-25314
p 2492 N94-25318
p 2313 N94-25319
p 2492 N94-25320
p 2463 N94-25321
p 2523 N94-25323
BINDAL, P. .... p 2547 N94-25209
BINER, S. B. .... p 2227 N94-23005
p 2253 N94-23183
BINGERT, J. .... p 2242 N94-23541
BINKOWSKI, FRANK .... p 2413 N94-24390
BIONDO, A. C. .... p 2563 N94-24624
BIRD, ROBERT W. .... p 2260 N94-24848
BIRKMIRE, R. W. .... p 2389 N94-22862
BIRTCHER, CRAIG R. .... p 2365 N94-24699
BISHOP, R. .... p 2559 N94-23186
BISHU, RAM R. .... p 2444 N94-25354
BISWAS, RUPAK .... p 2529 N94-24307
BIZKARGUENAGA, A. .... p 2358 N94-24008
BLACK, D. C. .... p 2218 N94-23283
BLACK, STEVE .... p 2272 N94-25193
BLAKE, I. F. .... p 2296 N94-24132
p 2300 N94-24697
BLAMONT, J. E. .... p 2617 N94-24877
BLANC, M. .... p 2606 N94-23382
BLANFORD, GEORGE E. .... p 2623 N94-25355
BLANKEN, H. M. .... p 2465 N94-22986
BLASDELL, R. C. .... p 2560 N94-23187
p 2560 N94-23188
BLAWZDZIEWICZ, JERZY .... p 2490 N94-24768
BLISS, DAVID A. .... p 2504 N94-23872
BLOEMEN, PASCAL JEAN HENRI
p 2250 N94-25242
BLOKS, R. H. J. .... p 2449 N94-23172
p 2450 N94-23173
BLOOM, S. .... p 2407 N94-23132
BLUMENTHAL, PHILIP Z. .... p 2344 N94-24362
BOBIN, L. .... p 2339 N94-25462
BOCHSLER, P. .... p 2624 N94-22841
BODIE, J. .... p 2296 N94-24131
BODWELL, CHARLES .... p 2206 N94-25007
BOEGGILD, CARL EGEDE .... p 2399 N94-24633
BOESENBERG, JENS .... p 2402 N94-24108
BOETZ, H. E. .... p 2190 N94-25516
BOGART, RICHARD S. .... p 2591 N94-24099
BOGOVICH, LYNN .... p 2520 N94-23964
p 2520 N94-23966
BOHN, R. G. .... p 2395 N94-24509
BOIVIN, R. .... p 2552 N94-24504
BOKHARI, SHAHID H. .... p 2473 N94-23558
BOKHOVE, H. .... p 2209 N94-24006
BOL, R. N. .... p 2446 N94-24540
BOLHOVITINOV, I. .... p 2370 N94-23420
BOLTER, JAY DAVID .... p 2592 N94-24642
BOLTON, PAUL .... p 2195 N94-24995
BONCZ, P. .... p 2448 N94-23097
BOND, THOMAS H. .... p 2166 N94-23299
BONESCHANSCHER, N. .... p 2267 N94-22981
BONGRAND, L. .... p 2363 N94-24046
BONNEAU, FREDERIC .... p 2608 N94-23392
p 2195 N94-23924
BONOLI, P. .... p 2552 N94-24504
BONT, P. F. H. .... p 2242 N94-23496
p 2397 N94-23497
BOOKBINDER, JAY .... p 2600 N94-25269
BOOKER, CECILIA .... p 2183 N94-24972
BOOM, WILLEM .... p 2538 N94-25240
BOONE, ROD .... p 2184 N94-25268
BOOTH, R. S. .... p 2599 N94-23705
BOSART, LANCE F. .... p 2404 N94-24794
BOSHUIZEN, FRANS A. .... p 2496 N94-24744
BOSLOOPER, E. C. .... p 2207 N94-24017
BOSSERT, J. E. .... p 2407 N94-23284
BOSSI, L. L. M. .... p 2433 N94-24119
BOSTIAN, CHARLES W. .... p 2293 N94-23622
p 2293 N94-23627
p 2293 N94-23628
BOSWIJK, H. P. .... p 2479 N94-23122
BOTHWELL, GRAHAM W. .... p 2389 N94-23840
BOTTCHER, C. .... p 2525 N94-23206
BOTTEMA, MARCEL .... p 2416 N94-25261
BOUBEKEUR, AHMED .... p 2445 N94-22901
BOUCHET, LAURENT .... p 2449 N94-23151
BOUGHER, STEPHEN W. .... p 2617 N94-24876
BOUMAN, B. A. M. .... p 2382 N94-23177

BOURGAIN, JEAN	p 2487	N94-23775
	p 2487	N94-23776
BOURY, D.	p 2256	N94-24237
BOVING, H. J.	p 2358	N94-24011
BOWEN, BARRY C.	p 2199	N94-24059
	p 2200	N94-24577
BOWEN, J. H.	p 2187	N94-23709
BOWEN, ROBERT	p 2276	N94-22753
BOWEN, ROBERT R.	p 2276	N94-22751
BOWER, MARK V.	p 2371	N94-24408
BOWERS, R. L.	p 2311	N94-24500
BOWLES, MIKE W.	p 2278	N94-22763
BOWMAN, W. J.	p 2325	N94-23662
BOXMAN, A.	p 2562	N94-23766
BOYD, IAIN D.	p 2214	N94-23053
BOYLE, M. J.	p 2598	N94-24832
BOZEK, J. M.	p 2314	N94-23401
BOZEK, JOHN M.	p 2220	N94-24681
BOZET, JEAN-LUC	p 2355	N94-23991
BOZZOLO, GUILLERMO	p 2243	N94-23578
	p 2249	N94-25171
BRAAKMAN, H. W. T.	p 2361	N94-24035
BRAAM, B. C.	p 2209	N94-24006
	p 2361	N94-24035
BRACKENRIDGE, KENNETH	p 2304	N94-23676
BRADLEY, ARTHUR	p 2431	N94-23974
BRAMBLE, JAMES H.	p 2482	N94-23677
BRANDON, JAY	p 2166	N94-23512
BRANDON, WILLIAM T.	p 2293	N94-23622
	p 2293	N94-23627
	p 2293	N94-23628
BRANDOW, B. H.	p 2558	N94-22942
BRANDS, J. J. A. M.	p 2493	N94-23142
BRANDT, JOHN C.	p 2601	N94-23251
BRASE, J. M.	p 2382	N94-23494
BRAUN, ROBERT	p 2601	N94-23537
BRAVINA, L. V.	p 2539	N94-25476
BREEDIN, SARAH D.	p 2433	N94-24188
BREISACHER, KEVIN J.	p 2213	N94-23044
BREMER, J.	p 2561	N94-23445
	p 2544	N94-23629
BRESCIA, DAVID A.	p 2598	N94-25006
BRESCIANINI, C.	p 2320	N94-23532
BRICMONT, J.	p 2489	N94-24610
BRIDGER, K.	p 2314	N94-25488
BRILLHART, MARK V.	p 2226	N94-24351
BRINDISI, ANTHONY E.	p 2364	N94-24175
BRITCHER, COLIN	p 2192	N94-23539
BRITTON, DORIS L.	p 2392	N94-23356
BRITTON, RANDALL K.	p 2166	N94-23299
BRIVKALNS, CHAD	p 2181	N94-24711
BROADBENT, S.	p 2430	N94-23744
BRODSKY, P. N.	p 2369	N94-23411
BRODSKY, S. J.	p 2534	N94-23803
BROEDERS, NICOLAAS LAMBERTUS H. L.		
	p 2226	N94-25238
BROER, HENK W.	p 2479	N94-23138
BROERSMA, H. J.	p 2478	N94-22727
	p 2487	N94-24053
BROM, G.	p 2339	N94-25462
BROMMUNDT, E.	p 2269	N94-23585
BRONKEMA, LISA	p 2444	N94-25354
BRONTE, DANIEL	p 2298	N94-24582
BROOKS, BARRY	p 2438	N94-24667
BROOKS, JONI	p 2416	N94-24409
BROOKS, PETER	p 2594	N94-25485
BROOKS, R.	p 2370	N94-23419
BROSEGHINI, TODD	p 2520	N94-23966
BROSI, FRED	p 2305	N94-23908
BROSNAN, STEPHEN J.	p 2344	N94-24360
BROT, A.	p 2157	N94-24261
BROTINI, M.	p 2359	N94-24013
BROUSSE, PASCAL	p 2514	N94-23928
BROWN, JAMES H.	p 2406	N94-25537
BROWN, RHONDA	p 2179	N94-24332
	p 2190	N94-24551
	p 2184	N94-25004
BROWN, T. G.	p 2549	N94-23013
BROWN, TOM	p 2571	N94-23230
BROWNING, R.	p 2346	N94-25154
BROYDE, S.	p 2563	N94-24567
BRUCKART, JAMES E.	p 2174	N94-25141
BRUCKER, G. J.	p 2540	N94-23273
BRUECKNER, G. E.	p 2625	N94-22851
BRUEGGE, CAROL J.	p 2383	N94-23598
	p 2383	N94-23599
BRUNE, WILLIAM H.	p 2397	N94-23277
BRUNEAU, B.	p 2359	N94-24016
BRUNO, KRISTIN J.	p 2374	N94-23932
BRUNS, H. C.	p 2549	N94-22949
BRUSSAARD, G.	p 2283	N94-22795
BRUZZONI, P.	p 2239	N94-22966
BRYANT, LARRY	p 2505	N94-23879
BRYANT, ROBERT F.	p 2461	N94-25156
BRYANT, ROBERT G.	p 2253	N94-23307
BU, Y.	p 2235	N94-24917
BUCCI, GREG	p 2184	N94-25268
BUCHANAN, HARRY R.	p 2520	N94-23968
BUCHER, ALLEN W.	p 2207	N94-23865
	p 2507	N94-23891
	p 2516	N94-23941
BUCHHEIT, R. G.	p 2238	N94-22932
BUCHHOLZ, MARK D.	p 2168	N94-24103
BUCK, O.	p 2243	N94-23717
BUCKETT, M. I.	p 2558	N94-22990
BUCKMASTER, J.	p 2317	N94-23089
BUDERER, G.	p 2314	N94-25460
BUEKER, C.	p 2382	N94-23177
BUELOW, PHILIP E. O.	p 2215	N94-23055
BUENO, J. I.	p 2360	N94-24026
BUESCHER, K. L.	p 2473	N94-24518
BUICK, F.	p 2437	N94-24299
BUKSA, J. J.	p 2218	N94-23433
	p 2218	N94-23452
BULSARI, A.	p 2472	N94-23463
BUNKER, DEBORAH	p 2180	N94-24479
BUNNING, T. J.	p 2567	N94-25441
BUONCRISTIANI, A. M.	p 2349	N94-24488
	p 2458	N94-24661
	p 2350	N94-24851
	p 2564	N94-25024
BUONOMO, S.	p 2284	N94-22798
BURCAT, ALEXANDER	p 2153	N94-24241
BURCH, ROBERT	p 2210	N94-23029
BURCH, ROBERT L.	p 2213	N94-23048
BURCHAM, KAREN L.	p 2279	N94-22772
BURCHILL, PETER J.	p 2258	N94-24721
BURGER, M. J.	p 2229	N94-24632
BURGESS, DOUGLAS W.	p 2175	N94-24127
BURGESS, S. C.	p 2207	N94-23995
BURK, DONNA	p 2598	N94-25006
BURKE, GENE	p 2520	N94-23963
BURKE, JAMES D.	p 2369	N94-23375
	p 2607	N94-23386
BURKE, W. R.	p 2450	N94-23228
	p 2355	N94-23985
BURKERT, VOLKER D.	p 2540	N94-24663
BURKHARDT, CHRIS	p 2520	N94-23966
BURKHARDT, CHRISTIAN	p 2520	N94-23964
BURKS, HAROLD D.	p 2252	N94-23079
BURLIEGH, SCOTT	p 2197	N94-23902
BURNS, ALAN	p 2402	N94-24089
BURNS, MAUREEN E.	p 2193	N94-25184
BURRELL, K. H.	p 2551	N94-23782
BURT, PETER J.	p 2346	N94-25502
BURTON, LAWRENCE W.	p 2198	N94-24690
BURTON, ROBERT, JR.	p 2496	N94-24931
BURTON, RUSSELL R.	p 2427	N94-24928
BUSATH, J.	p 2553	N94-24746
BUSCHE, GREGORY C.	p 2278	N94-22763
BUSH, G. S.	p 2305	N94-23986
BUSH, JOY	p 2203	N94-23947
BUSS, RICHARD J.	p 2552	N94-24546
BUTLER, LAWRENCE	p 2353	N94-23215
BUTT, D. P.	p 2231	N94-22933
	p 2348	N94-23203
BUTTERFIELD, C. P.	p 2394	N94-23472
BUTTRILL, CAREY S.	p 2162	N94-25096
BUTTSWORTH, D.	p 2319	N94-23513
BUTTSWORTH, D. R.	p 2320	N94-23532
BUURMAN, HENDRIK WILLEM	p 2462	N94-25263
BUVAT, D.	p 2359	N94-24016
BYERS, ROBERT M.	p 2368	N94-23232
BYKAT, ALEX	p 2465	N94-24410
BYRON, ROBERT M.	p 2586	N94-24683

C

CABE, GREG	p 2209	N94-24840
CABELLO, JEAN	p 2338	N94-25157
CABOT, WILLIAM H.	p 2329	N94-24149
CAHAN, BORIS	p 2393	N94-23360
CAHELA, DONALD R.	p 2393	N94-23364
CAI, Y.	p 2352	N94-22991
CALDWELL, R. R.	p 2601	N94-23010
CALEF, D. F.	p 2265	N94-23778
CALKOEN, C.	p 2381	N94-23145
CALLE, LUZ M.	p 2237	N94-23233
CALLEJA, JOHN	p 2192	N94-23564
CALTAGIRONE, JEAN-PAUL	p 2485	N94-23692
CAMBON, CLAUDE	p 2330	N94-24152
CAMERON, LOUIS IAN	p 2196	N94-22889
CAMERON, S. M.	p 2349	N94-23209
CAMP, B. H.	p 2522	N94-25014
CAMPAGNA, DAVE	p 2272	N94-25193
CAMPAN, GENEVIEVE	p 2202	N94-23925
CAMPBELL, B.	p 2629	N94-24695
CAMPBELL, BRYAN	p 2184	N94-25268
CAMPBELL, C. WARREN	p 2315	N94-24411
CAMPBELL, G. L.	p 2354	N94-23797
CAMPBELL, J. MATT	p 2266	N94-24618
CAMPION, G.	p 2470	N94-22714
CANFIELD, P. C.	p 2557	N94-22925
CANNON, B. D.	p 2347	N94-22974
CANNON, M. R.	p 2326	N94-23670
CANTATORE, F.	p 2369	N94-23399
CANTIN, MARC R.	p 2371	N94-23841
CANTRELL, J.	p 2622	N94-24903
CANU, C.	p 2515	N94-23935
CAO, XIAO-WEN	p 2555	N94-25333
CAPALDI, RUSSELL J.	p 2215	N94-23061
CAPSTAFF, JOSEPH G.	p 2180	N94-24581
CARDELINO, B.	p 2224	N94-24343
CARDELINO, B. H.	p 2223	N94-24338
CARDER, KENDALL L.	p 2420	N94-23538
CAREY, TIM	p 2287	N94-22822
CARIAPA, VIKRAM	p 2264	N94-24412
CARLI, B.	p 2359	N94-24013
CARLSON, RICHARD M.	p 2185	N94-25070
CARLSTROM, J. E.	p 2599	N94-23705
CARLTON, DOUGLAS	p 2507	N94-23890
CARLTON, MAGDI	p 2447	N94-23917
CARMONA, R. L. R.	p 2156	N94-24257
CARNES, BEN L.	p 2529	N94-24222
CARNES, BENNY L.	p 2527	N94-24208
	p 2529	N94-24220
CARPEN, LEENA	p 2250	N94-25346
CARPENTER, MARK H.	p 2480	N94-23272
CARPENTER, R. L.	p 2422	N94-25146
CARPER, RICHARD D.	p 2197	N94-23855
CARPINO, MARC	p 2215	N94-23058
CARR, FRED	p 2412	N94-24384
CARR, MICHAEL H.	p 2606	N94-23380
CARROLL, GERARD P.	p 2344	N94-24734
CARROLL, JOHN B.	p 2335	N94-24686
CARTER, MATT	p 2206	N94-24916
CARTER, P.	p 2288	N94-22824
CARTER, W. L.	p 2556	N94-22886
CARTWRIGHT, LLOYD	p 2528	N94-24216
CASEY, C. P.	p 2238	N94-22897
CASEY, LARRY	p 2281	N94-22785
CASH, TOM	p 2266	N94-24618
CASPI, S.	p 2299	N94-24656
CASSIDY, W. A.	p 2603	N94-24964
CASSINGHAM, RANDY	p 2273	N94-22735
CASTELLI, VINCENT	p 2230	N94-24735
CASTETS, B.	p 2369	N94-23400
CASTRO, HENRY	p 2197	N94-23902
CASTRO, JONATHAN P.	p 2277	N94-22756
CASTRONUOVO, M.	p 2430	N94-23083
	p 2438	N94-24830
CATALDO, ROBERT L.	p 2220	N94-24681
CATLOW, C. R. A.	p 2235	N94-24920
CAVANAUGH, JOSEPH E.	p 2406	N94-25538
CAVANAUGH, KEVIN J.	p 2483	N94-23678
CAZES, ALEX	p 2155	N94-24250
CEBE, PEGGY	p 2226	N94-24351
CEBULA, RICHARD P.	p 2410	N94-24355
CEDERBERG, MARK	p 2251	N94-25419
CEDERWALL, P. L.	p 2589	N94-22934
CELIO, P. V.	p 2423	N94-23316
	p 2423	N94-23318
	p 2424	N94-23320
	p 2424	N94-23323
CELLUCCI, RICHARD L.	p 2525	N94-23698
CENGEL, YUNUS A.	p 2322	N94-23646
CENTENO, MARTHA A.	p 2523	N94-23234
CENTURIONI, D. X.	p 2243	N94-23753
CESS, ROBERT D.	p 2413	N94-24389
CEYLAN, TAMER	p 2326	N94-23671
CEZAIRLIYAN, ARED	p 2247	N94-25124
CHA, Y. S.	p 2559	N94-22993
CHABINYC, M. L.	p 2567	N94-25441
CHAFFAUT, FRANCOIS-XAVIER	p 2608	N94-23392
CHAFIN, ROY L.	p 2506	N94-23884
	p 2197	N94-23888
CHAILAPAKUL, O.	p 2535	N94-24555
	p 2536	N94-24729
CHAKRABARTY, S.	p 2538	N94-25317
	p 2539	N94-25474
CHALLINGSWORTH, MARK L.	p 2391	N94-23349
CHAMBERLAIN, A.	p 2256	N94-24236
CHAMBERLAIN, C. S.	p 2589	N94-22934
CHAMIS, C. C.	p 2177	N94-24317
	p 2179	N94-24326
CHAMIS, CHRISTOS C.	p 2378	N94-25188
CHAMPIGNEUX, G.	p 2522	N94-25015
CHAN, KWONG K.	p 2368	N94-25322
CHAN, S. K.	p 2557	N94-22927
CHAN, VINCENT W. S.	p 2293	N94-23622
	p 2293	N94-23627
	p 2293	N94-23628
CHAN, Y. C.	p 2534	N94-24077
CHANCE, KELLEY V.	p 2404	N94-24738
CHANDLEE, GEORGE O.	p 2435	N94-24195
	p 2435	N94-24196
CHANDLER, M. A.	p 2616	N94-24872

CHANDRASEKHARA, M. S. p 2167 N94-23975
CHANEY, JOANNE p 2298 N94-24582
CHANG, A. O. T. p 2476 N94-25428
CHANG, B.-C. p 2163 N94-25103
CHANG, C.-P. p 2416 N94-25071
CHANG, CHENG-SHANG p 2457 N94-24638
CHANG, CHING-T. p 2312 N94-25042
CHANG, EDWARD S. p 2499 N94-23839
CHANG, J. F. p 2279 N94-22770
CHANG, R. P. H. p 2562 N94-23805
CHANG, TIE-QIANG p 2554 N94-25330
CHANG, TYNE-HSIEN p 2342 N94-25356
CHANG, Y. AUSTIN p 2248 N94-25131
CHAO, CHIN p 2198 N94-24860
CHAPLIN, M. R. p 2549 N94-23013
CHAPLINE, G. p 2307 N94-23008
CHAPMAN, BARBARA p 2448 N94-23092
CHAPMAN, PAUL C. p 2285 N94-22806
CHAPPELL, CHARLES R. p 2574 N94-24405
CHARLES, TERRI L. p 2207 N94-23654
CHARLESWORTH, ARTHUR p 2456 N94-24480
CHASNOV, JEFFREY R. p 2330 N94-24152
p 2332 N94-24167
CHASSEFIERE, E. p 2617 N94-24877
p 2621 N94-24897
p 2622 N94-24900
CHATERJEE, S. p 2230 N94-24779
p 2230 N94-24942
p 2230 N94-25163
CHATILA, RAJA p 2370 N94-23413
CHEN, BEN M. p 2473 N94-24542
CHEN, C. Y. p 2555 N94-25343
CHEN, D. Y. p 2189 N94-23658
CHEN, FRANK C. p 2417 N94-23291
CHEN, HSIN-CHU p 2483 N94-23679
CHEN, J. C. p 2291 N94-23261
CHEN, J. I. p 2258 N94-24732
CHEN, JING-HONG p 2225 N94-24350
CHEN, JUDY D. p 2417 N94-23291
CHEN, LAN-LAN p 2553 N94-24949
CHEN, M. H. p 2532 N94-22988
CHEN, PI-FUAY p 2545 N94-24730
CHEN, Q. p 2296 N94-24132
p 2300 N94-24697
CHEN, S. S. p 2352 N94-22991
CHEN, TIMOTHY S. p 2253 N94-23311
CHEN, W. S. p 2560 N94-23205
CHEN, WENTAO p 2478 N94-22975
CHEN, Y. p 2558 N94-22957
CHEN, Y. C. p 2301 N94-24707
CHENG, G. p 2214 N94-23051
CHENG, K. T. p 2532 N94-22988
CHERMANT, J. L. p 2256 N94-24235
CHERNOFF, HERMAN p 2495 N94-24560
CHERRETTE, ALAN R. p 2278 N94-22763
CHERUBINI, G. p 2357 N94-24002
CHESTA, L. p 2179 N94-24325
CHESTNUTT, DAVID p 2526 N94-24207
CHEUNG, FAN-BILL p 2210 N94-23029
p 2213 N94-23048
CHEUNG, K.-M. p 2292 N94-23266
CHEVALLET, JEAN-PIERRE p 2588 N94-22879
CHEVALLIER, Y. p 2361 N94-24033
CHIANG, PI-REN p 2217 N94-23069
CHIAO, RAYMOND Y. p 2570 N94-25028
CHIAVERINI, M. p 2217 N94-23069
CHIBA, ISAMU p 2279 N94-22769
CHIEN, HUAL-TE p 2371 N94-22872
CHILD, ANDREW D. p 2259 N94-24792
CHILDERS, BROOKS A. p 2166 N94-23512
CHILDS, DAVID B. p 2518 N94-23953
CHILOSI, THIERRY p 2221 N94-24834
CHIMA, RODRICK V. p 2189 N94-25185
CHIN, BRYAN p 2244 N94-24066
CHING, CHANG Y. p 2338 N94-25183
CHING, JASON p 2413 N94-24390
CHINNERY, ANNE E. p 2379 N94-25520
CHINTAWONGVANICH, PRASAN p 2527 N94-24211
CHIPMAN, RUSSELL A. p 2345 N94-24852
CHITTIBABU, K. G. p 2260 N94-24813
CHIUDERI, C. p 2624 N94-22839
CHLOND, ANDREAS p 2400 N94-23157
CHOCHON, H. p 2369 N94-23400
CHOI, C. S. p 2242 N94-23541
CHOI, HAECHEON p 2327 N94-24139
p 2172 N94-24150
CHOI, K.-Y. p 2216 N94-23064
CHOI, RICH p 2198 N94-24860
CHOUDHURY, ALOK p 2458 N94-24679
CHOUINARD, J.-Y. p 2287 N94-22820
CHOW, SANGUAN p 2197 N94-23902
CHOW, SHUI-NEE p 2479 N94-23138
CHOWDHRY, RAJIV S. p 2163 N94-25104
CHRISEY, DOUGLAS H. p 2350 N94-24952
CHRISTENSEN, M. p 2300 N94-24678
CHU, ROSE W. p 2443 N94-23929
CHU, T. H. p 2279 N94-22770
CHUANG, C.-H. p 2217 N94-23275
p 2488 N94-24564
CHUDEJ, CHRIS p 2438 N94-24667
CHUJO, WATARU p 2279 N94-22769
CHUNG, C. D. p 2279 N94-22770
CHUNG, DEBORAH D. L. p 2394 N94-23367
CHUNG, H. M. p 2240 N94-23009
p 2242 N94-23457
CHUNG, HYOSANG p 2408 N94-23542
CHURCHILL, DEAN p 2413 N94-24389
CIAMPI, JEAN p 2608 N94-23392
CIARLO, ALESSANDRO p 2518 N94-23952
CIARPALLINI, PAOLA p 2404 N94-24738
CIONI, R. p 2283 N94-22796
CIPOLLONE, GREGORIO p 2517 N94-23951
CIRES, ALFREDO p 2189 N94-24776
CITRIN, ELIZABETH A. p 2305 N94-23859
CITROLO, J. C. p 2549 N94-23013
CITURS, KEVIN D. p 2185 N94-25440
CIVALE, L. p 2556 N94-22886
CLANCY, DANIEL J. p 2195 N94-24482
CLANCY, R. T. p 2618 N94-24878
p 2619 N94-24887
CLANCY, R. TODD p 2626 N94-23626
CLANTON, S. E. p 2322 N94-23648
CLAPP, MITCHELL BURNSIDE p 2314 N94-23409
CLAPPER, M. L. p 2365 N94-24588
CLARK, BENTON p 2622 N94-24903
CLARK, W. A. p 2430 N94-23290
CLARKE, AMANDA p 2184 N94-25002
CLARKE, DAVID W. p 2477 N94-25469
p 2477 N94-25470
CLAUS, S. J. p 2229 N94-24402
CLAUSSEN, MATTHIAS p 2457 N94-24626
CLAVENNA, MICHAEL p 2205 N94-24702
CLEVERS, J. G. P. W. p 2382 N94-23177
CLIFFORD, T. p 2629 N94-24695
CLUITMANS, L. J. M. p 2449 N94-23169
CLUITMANS, P. J. M. p 2470 N94-22877
COCHRAN, H. D. p 2535 N94-24569
COCKS, FRANKLIN H. p 2204 N94-24334
COCQUET, PATRICK p 2589 N94-23150
COE, THOMAS EDDY p 2408 N94-23620
COELHODACOSTA, ROSVELTER JOAO
p 2447 N94-22911
COETSEE, JOSEF A. p 2475 N94-24760
COFFEY, H. E. p 2626 N94-23738
p 2627 N94-23739
p 2628 N94-24991
p 2628 N94-24992
p 2628 N94-24993
p 2628 N94-24994
COFFEY, H. T. p 2352 N94-22991
p 2352 N94-22996
COFFEY, HELEN E. p 2628 N94-24989
p 2628 N94-24990
COGGINS, JAMES M. p 2451 N94-23369
COGLEY, ALLEN p 2365 N94-24703
COHEN, AARON p 2195 N94-25067
COHEN, GERALD C. p 2445 N94-23125
p 2466 N94-23252
p 2467 N94-24075
p 2467 N94-24463
COHEN, MARC M. p 2192 N94-23310
COHEN, R. E. p 2263 N94-25413
COHEN, SCOTT p 2198 N94-24860
COHEN, STEPHEN M. p 2235 N94-24790
COHEN, TS. p 2158 N94-24268
COHEN, Y. p 2156 N94-24255
COHN, STEVE p 2412 N94-24383
COLCY, JEAN-NOEL p 2281 N94-22781
COLEMAN, GARY N. p 2172 N94-24164
COLINA-MORLES, ELIEZER p 2476 N94-25307
COLLINS, EMMANUEL G., JR. p 2456 N94-24470
COLLINS, JOHN p 2266 N94-24618
COLLINS, MICHAEL p 2618 N94-24879
COLLINS, WILLIAM E. p 2426 N94-24093
COLOZZA, ANTHONY p 2395 N94-24071
COLOZZA, ANTHONY J. p 2189 N94-25200
COLZI, E. p 2286 N94-22816
COMBS, LISA p 2190 N94-24957
COMBS, LISA M. p 2183 N94-24969
COMEAUX, MICHAEL p 2183 N94-24975
COMPAAN, C. D. p 2395 N94-24509
COMPOSTIZO, C. p 2360 N94-24027
CONLEY, MICHAEL P. p 2311 N94-24754
CONLON, MARK p 2529 N94-24221
CONNELL, JOHN W. p 2252 N94-23075
p 2253 N94-23305
CONNELLY, BRIAN p 2284 N94-22800
CONNES, ALAIN p 2488 N94-24536
CONNOLLY, JOHN F. p 2369 N94-23377
CONOVER, D. R. p 2397 N94-23016
CONRATH, BARNEY J. p 2620 N94-24893
CONSTABLE, CATHERINE p 2405 N94-24854
CONVERTINO, VICTOR A. p 2426 N94-23530
CONWAY, B. E. p 2234 N94-24545
COOK, B. A. p 2243 N94-23753
COOK, GREG J. p 2527 N94-24210
COOK, T. M. p 2265 N94-23807
COOK, WOODROW L. p 2176 N94-23489
COOKE, D. H. p 2187 N94-23709
COOLEN, F. P. A. p 2494 N94-23143
p 2481 N94-23456
p 2494 N94-23772
COON, S. A. p 2531 N94-22951
COOPER, JOEL P. p 2262 N94-25145
COOPER, L. P. p 2292 N94-23267
COOPER, L. Y. p 2172 N94-23810
COOPER, LYNNE P. p 2305 N94-23848
p 2305 N94-23914
COOPER, PAUL p 2281 N94-22783
COQUELET, D. p 2359 N94-24019
CORAZZA, G. E. p 2277 N94-22761
CORBETT, W. p 2343 N94-23200
CORBITT, T. S. p 2346 N94-25151
CORBITT, THOMAS S. p 2547 N94-25144
CORDS, D. p 2307 N94-22955
CORLESS, R. F. p 2350 N94-24659
CORNISH, IAN J. p 2446 N94-25312
CORNWELL, DONALD MITCHELL, JR.
p 2308 N94-23281
CORONADO, PATRICK L. p 2417 N94-23338
CORREVON, M. p 2315 N94-23989
CORRIGAN, D. A. p 2391 N94-23352
CORY, DAVID G. p 2537 N94-25047
COSPER, DONNA p 2206 N94-24916
COSTARD, F. p 2606 N94-23382
p 2608 N94-23393
COSTE, P. p 2360 N94-24026
COSTE, P. A. p 2358 N94-24007
COSTELLO, MICHAEL J. p 2340 N94-25534
COSTER, M. J. p 2454 N94-23759
COTE, GERALD L. p 2422 N94-25357
COTELL, CATHERINE M. p 2350 N94-24952
COTTON, MATT p 2181 N94-24803
COTTON, WILLIAM p 2411 N94-24381
p 2413 N94-24385
p 2414 N94-24393
COURAGE, W. M. G. p 2209 N94-24006
COURS, JEFFREY T. p 2462 N94-25179
COUTIN-FAYE, S. p 2606 N94-23382
COVELL, PETER F. p 2169 N94-24311
COWAN, R. S. p 2254 N94-23783
COWINGS, PATRICIA S. p 2420 N94-23088
p 2426 N94-24102
COWLEY, W. G. p 2285 N94-22807
COWSAR, LAWRENCE C. p 2483 N94-23680
COX, ROSS M. p 2516 N94-23942
COY, E. B. p 2211 N94-23036
COYLE, A. J. p 2494 N94-23749
COYLE, JOHN M. p 2178 N94-24321
CRABTREE, G. W. p 2557 N94-22929
CRAIG, A. D. p 2278 N94-22767
p 2279 N94-22768
CRANE, J. K. p 2348 N94-23181
CRAVEY, W. R. p 2307 N94-22950
CRAWFORD, T. M. p 2542 N94-22917
CRAWLEY, LINDA p 2281 N94-22783
CRAXTON, R. S. p 2541 N94-22868
CREIGHTON, J. R. p 2265 N94-23436
CREWS, JOHN H., JR. p 2241 N94-23274
CRISE, A. p 2449 N94-23111
CRISP, D. p 2622 N94-24898
CRIST, R. p 2289 N94-22832
CROCHEMORE, M. p 2518 N94-23956
CROOK, ANDREW p 2414 N94-24392
CROOKS, R. M. p 2526 N94-23718
p 2535 N94-24555
p 2536 N94-24729
p 2234 N94-24772
p 2565 N94-25086
p 2346 N94-25151
CROOKS, RICHARD M. p 2547 N94-25144
CROSIAR, C. L. p 2416 N94-25162
CROSS, JAMES H., II p 2455 N94-24111
CROUCH, P. E. p 2448 N94-23073
p 2448 N94-23074
CROWELL, JAMES A. p 2442 N94-25510
CROYLE, SCOTT p 2438 N94-24786
CROZIER, STEWART p 2285 N94-22804
CROZIER, STEWART N. p 2285 N94-22808
CRUSE, THOMAS p 2196 N94-24820
CRUZ-ORIVE, L. M. p 2496 N94-24639
CUBASCH, U. p 2407 N94-23156
CULHANE, J. L. p 2625 N94-22849
CULLEN, CIONAITH J. p 2288 N94-22826
CULLEN, J. A. p 2415 N94-24850
CUMMINGS, J. W. p 2550 N94-23182
CUMMINGS, RAMONA p 2320 N94-23635
CUNNINGHAM, J. M. p 2356 N94-23993

CURBILLON, LAURENT p 2359 N94-24015
CURRAN, CHRISTINE p 2298 N94-24582
CURRAN, PATRICK p 2423 N94-22732
CURRAN, PATRICK S. p 2506 N94-23884
p 2506 N94-23886
CURTIS, L. J. p 2531 N94-22937
CUSHMAN, PAULA P. p 2400 N94-23124
CZERWINSKI, MARY P. p 2434 N94-24189

D

DABBS, D. M. p 2257 N94-24677
DAHL, I. p 2254 N94-23431
DAHLEH, MUNTHER A. p 2472 N94-23163
DAIGLE, GILLES p 2528 N94-24219
DAILEY, BRIAN p 2266 N94-24618
DAILEY, J. p 2217 N94-23069
DALE, ALLEN p 2181 N94-24796
DALESIO, JOHN p 2457 N94-24626
DALESIO, LEO R. p 2457 N94-24626
DALEY, P. F. p 2541 N94-22722
DALICHAOUCH, Y. p 2558 N94-22941
DAM-JOHANSEN, K. p 2232 N94-23100
DAME, L. p 2625 N94-22848
DAMEN, A. A. H. p 2470 N94-22873
DAMERIS, MARTIN p 2400 N94-25414
DAMOUR, THIBAULT p 2601 N94-23099
DANE, J. H. p 2401 N94-23337
DANIEL, A. M. p 2256 N94-24236
DANIEL, RICHARD A. p 2301 N94-25038
DANILSONS, MARKUS p 2544 N94-23723
DANNENBERG, ROGER B. p 2460 N94-24932
DANYLUK, S. p 2238 N94-22718
DARMET, AGNES p 2480 N94-23166
DARROY, JEAN MICHEL p 2507 N94-23894
DAS, UMESH C. p 2403 N94-24592
DASILVEIRA, D. D. p 2156 N94-24257
DATTA, RAVI p 2285 N94-22804
DAUTEUIL, MARK p 2182 N94-24837
DAVENPORT, OTHA B. p 2163 N94-25106
DAVIDHEISER, R. p 2306 N94-25498
DAVIDHEISER, ROGER A. p 2306 N94-25494
DAVIDSON, ERIC A. p 2399 N94-24853
p 2399 N94-24861
DAVIDSON, J. R. p 2382 N94-23492
DAVIDSON, ROGER A. p 2506 N94-23886
DAVIES, N. GEORGE p 2281 N94-22784
DAVILA, CELSO V. p 2299 N94-24668
DAVIS, ANDREW MICHAEL p 2541 N94-22891
DAVIS, CURT H. p 2382 N94-23573
p 2386 N94-24060
DAVIS, DARRYL W. p 2460 N94-24822
DAVIS, DAVID O. p 2169 N94-24335
DAVIS, J. BRADLEY p 2199 N94-24059
p 2200 N94-24577
DAVIS, J. L. p 2405 N94-25205
DAVIS, JAMES L. p 2405 N94-25203
DAVIS, JOANNA F. p 2257 N94-24558
DAVIS, L. C. p 2364 N94-24090
DAVIS, LAWRENCE D. p 2456 N94-24470
DAVIS, MICHAEL p 2463 N94-25455
p 2463 N94-25456
DAVIS, PAMELA A. p 2177 N94-24304
DAWES, PETER W. p 2353 N94-23215
DEAN, RICHARD A. p 2276 N94-22754
DEANDRADE, M. C. p 2558 N94-22941
DEBATIN, KURT p 2304 N94-23834
DEBE, M. K. p 2223 N94-24339
DEBOER, FREDERIC p 2196 N94-23923
DEBROUWER, GILES p 2179 N94-24401
DEBRUNNER, LINDA S. p 2576 N94-24413
DEBY, R. A. p 2486 N94-23725
p 2593 N94-24743
DECHANT, LAWRENCE J. p 2166 N94-23511
p 2170 N94-25173
DECKER, HARRY J. p 2364 N94-24483
DECLUE, MARK J. p 2475 N94-24862
DEELEN, C. p 2417 N94-24107
DEGALLAIX, BERNARD p 2470 N94-22906
DEGAUDENZI, R. p 2286 N94-22816
DEGEORGES, CHARLES p 2203 N94-23947
DEGIORGIO, CHRIS p 2184 N94-25002
DEGLINNOCENTI, S. p 2374 N94-23112
DEGRAAF, J. p 2480 N94-23437
p 2480 N94-23438
p 2569 N94-24575
DEGRAAF, W. p 2602 N94-24522
DEGROH, KIM K. p 2218 N94-23370
DEGRONCKEL, HONORE ALPHONSUS MARIA
p 2262 N94-25222
DEGROOT, NICOLO p 2538 N94-25246
DEGROOT, WILHELMUS A. p 2210 N94-23032
DEGUCHI, SHUJI p 2604 N94-24986
DEHAEMER, MICHAEL J. p 2630 N94-22893
DEHOFF, P. H. p 2439 N94-24857
DEHOOP, A. T. p 2524 N94-23730
p 2524 N94-23731
DEHOOP, ADRIANUS T. p 2403 N94-24592
DEHUGUES, P. PLANTIN p 2171 N94-25187
DEJAGER, ABRAHAM GILLES p 2475 N94-25224
DEJONG, M. C. M. p 2420 N94-23521
DEJONGE, CORA p 2402 N94-24108
DEKOGEL, E. p 2486 N94-23724
DEKROM, W. H. C. p 2542 N94-23171
DELAGRANGE, ARTHUR D. p 2446 N94-25034
DELANGE, RICK p 2236 N94-25284
DELAPORTE, P. p 2349 N94-24629
DELAROSA, JOSE p 2438 N94-24786
DELBUFALO, A. p 2519 N94-23959
DELCAMPO, F. p 2360 N94-24026
DELEIJER, F. p 2542 N94-23171
DELGENIO, A. D. p 2616 N94-24872
DELGENIO, ANTHONY p 2385 N94-23616
DELL, JAMES p 2272 N94-23892
DELLIN, THEODORE A. p 2309 N94-23777
DELLIPRISCOLI, F. p 2277 N94-22760
DELNICK, F. M. p 2311 N94-24748
DELOBETTE, DAMIEN p 2195 N94-23924
DELOREY, DENNIS E. p 2207 N94-25542
DELRE, E. p 2277 N94-22760
DELVALLE, J. C. p 2289 N94-22833
DEMAN, IVAN p 2284 N94-22801
DEMPSEY, BARRY J. p 2192 N94-23303
DEMUTH, S. p 2218 N94-23433
DENDY, MICHAEL J. p 2196 N94-24309
DENNIS, ROBERT FOSTER p 2317 N94-23072
DENSMORE, ART p 2289 N94-22831
p 2289 N94-22832
DEOGHURIA, S. p 2539 N94-25474
DEOLAZABAL, I. p 2360 N94-24027
DERBER, JOHN p 2412 N94-24383
DERBER, JOHN C. p 2418 N94-24671
DEROEVER, JOWI W. p 2568 N94-22709
DERRIEN, MICHEL p 2176 N94-24181
DERUITER, WILLEM p 2351 N94-25218
DESAI, RAJIV S. p 2371 N94-23427
DESCALZI, DOUG p 2182 N94-24817
DESCH, PAUL B. p 2391 N94-23353
DESHPANDE, MANISH p 2215 N94-23060
DESOPPER, ANDRE p 2176 N94-23254
DESPRAIRIES, ARNAUD p 2514 N94-23928
DESTURLER, ERIC p 2483 N94-23681
DESU, SESHU B. p 2565 N94-25027
DETHLOFF, HENRY C. p 2631 N94-24584
DEVADIGA, SADASHIVA p 2442 N94-25507
DEVALK, C. F. p 2417 N94-24107
DEVANEY, W. E. p 2560 N94-23205
DEVANY, CHRIS p 2438 N94-24667
DEVELYN, MARK P. p 2235 N94-24790
DEVIEUX, CARRIE L. p 2284 N94-22799
DEVINK, E. P. p 2448 N94-23096
p 2453 N94-23707
DEVRIES, I. p 2418 N94-24601
DEXTER, A. L. p 2373 N94-25475
DHAR, S. K. p 2391 N94-23352
DHURANDHAR, S. V. p 2604 N94-25211
p 2604 N94-25212
DIAK, GEORGE R. p 2387 N94-24596
DIAS, WILLIAM C. p 2501 N94-23852
DIAZ, A. p 2260 N94-24815
DIAZ, ALPHONSO V. p 2498 N94-23833
DIAZ, MANUEL F. p 2435 N94-24197
DIBARTOLO, B. p 2564 N94-25024
DIBERNARDO, G. p 2283 N94-22796
DIBIASO, T. p 2390 N94-23295
DICKERSON, RUSSELL p 2413 N94-24390
DICKMAN, OLA p 2544 N94-23723
DIEHL, H. T. p 2535 N94-24611
DIEKMANN, O. p 2420 N94-23521
DIJKSMA, AAD p 2457 N94-24599
DILORENZO, MATHEW p 2365 N94-24806
DIMOS, D. p 2542 N94-23202
DINGLEY, D. J. p 2557 N94-22938
DIOT, CRISTOPHE p 2589 N94-23150
DISCHLI, B. p 2343 N94-24054
DISHMAN, ROBERT p 2180 N94-24581
DISSANAYAKE, A. p 2283 N94-22794
DIVIS, M. p 2567 N94-25425
DIVSALAR, D. p 2289 N94-22835
DIVSALAR, DARIUSH p 2287 N94-22819
DJIRAR, S. p 2492 N94-25309
DO, DUNG p 2253 N94-23335
DOBER, DAVE p 2183 N94-24971
DOBSON, B. J. p 2363 N94-24076
DODD, DAVID p 2462 N94-25287
DODDS, GORDON I. p 2446 N94-25313
DODDS, ROBERT H., JR. p 2378 N94-25143
DOHAN, Y. p 2360 N94-24025
DOHERTY, MICHAEL P. p 2222 N94-23641
DOHI, TOMOHIRO p 2286 N94-22813
DOLINAR, S. p 2292 N94-23266
DON, WAI-SUN p 2480 N94-23272
DONADO, R. A. p 2389 N94-22723
DONAHUE, BERNARD A. p 2260 N94-24848
DONG, JIN-MING p 2567 N94-25403
DONKER, J. C. p 2471 N94-23137
DONNET, C. p 2361 N94-24033
DORKO, MICHAEL A. p 2297 N94-24554
DOROFEEV, S. V. p 2569 N94-24575
DORON, E. p 2571 N94-25340
DOTHEY, MICHEL p 2284 N94-22801
DOTY, KEITH L. p 2368 N94-23235
p 2368 N94-23236
DOUGHTY, GLEN E. p 2217 N94-23070
DOUGLAS, CRAIG C. p 2483 N94-23682
p 2237 N94-23683
DOWLING, KEVIN p 2367 N94-25274
DOWNS, ROBERT p 2183 N94-24974
DOYLE, E. J. p 2551 N94-23782
DOYLE, JAMES p 2414 N94-24392
DRESHFIELD, ROBERT L. p 2243 N94-23556
DRESNER, L. p 2307 N94-23019
p 2271 N94-24568
DRESSELHAUS, ELIOT p 2333 N94-24169
DREWIEN, C. A. p 2238 N94-22932
DRIESSEN, T. S. H. p 2497 N94-23800
p 2521 N94-24523
DRIESSEN, THEO S. H. p 2497 N94-22708
p 2497 N94-22716
DRIESSEN, THEODORE S. H. p 2489 N94-24653
DROEGEMEIER, KELVIN p 2414 N94-24392
p 2415 N94-24400
DROEGKAMP, M. p 2178 N94-24321
DRUCKER, ELLIOTT H. p 2277 N94-22757
DRUEN, WILLIAM M. p 2200 N94-24801
DRUMMOND, COLIN K. p 2186 N94-23466
DRUMMOND, J. E. p 2168 N94-24084
DRUMMOND, MARK p 2453 N94-23568
DUBBELDAY, WADAD B. p 2312 N94-25036
DUBE, E. p 2448 N94-22980
DUBNICKA, S. p 2536 N94-24844
DUBNICKOVA, A. Z. p 2536 N94-24844
DUCHON, CLAUDE E. p 2416 N94-24414
DUFOUR, MARTIAL p 2289 N94-22836
DUKOWICZ, J. K. p 2417 N94-23517
DULAC, JEAN p 2501 N94-23857
DULIKRAVICH, G. S. p 2216 N94-23064
DULIKRAVICH, GEORGE S. p 2322 N94-23645
p 2325 N94-23664
p 2325 N94-23665
DUMONT, BRIAN p 2198 N94-24860
DUNBAR, CHRISTIAN p 2184 N94-25017
DUNBRACK, HARRY p 2183 N94-24971
DUNCAN, COMER p 2484 N94-23684
DUNG, LE p 2493 N94-25434
DUNN, C. E. p 2196 N94-23258
DUNNING, RICHARD A., JR. p 2518 N94-23957
DUPONT, J. N. p 2258 N94-24749
DURAN, DAVID p 2182 N94-24966
DURAN, G. p 2390 N94-23295
DURAN, R. S. p 2257 N94-24562
p 2262 N94-25159
DURAN, RANDOLPH S. p 2259 N94-24792
p 2261 N94-24930
DURBIN, PAUL A. p 2328 N94-24144
DURHAM, DAVID M. p 2207 N94-23864
DURHAM, RALPH p 2520 N94-23963
DURRANT-WHYTE, HUGH F. p 2472 N94-23179
DURSTON, DONALD A. p 2167 N94-23557
DUTTA, SANTANU p 2284 N94-22803
DUTTON, KEVIN p 2165 N94-25114
DVALI, G. p 2532 N94-22970
DVALI, G. R. p 2604 N94-25215
DYER, RUTH p 2365 N94-24703
DZENITIS, JOHN M. p 2354 N94-23822

E

EAVES, LAURENCE p 2564 N94-24959
EBELING, CHARLES p 2203 N94-23329
EBERHARD, CAROL D. p 2209 N94-24767
ECHEVARRIA, J. J. p 2358 N94-24008
ECKARDT, T. p 2360 N94-24024
ECKELMANN, H. p 2316 N94-22860
ECKSTEIN, M. C. p 2464 N94-23927
EDELSON, B. I. p 2465 N94-23085
EDELSON, BURTON I. p 2293 N94-23622
p 2293 N94-23627
p 2293 N94-23628
EDNER, HANS p 2402 N94-24108
EDVARSON, KAY p 2437 N94-24292
EDWARDS, C. D. p 2196 N94-23258
EDWARDS, MARK B. p 2176 N94-25444
EDWARDS, R. M. p 2217 N94-23071
EFIMOV, G. V. p 2570 N94-25337
EFTEKHARI, ABE p 2375 N94-23308

EGGEN, JOSEPHUS HUBERTUS p 2304 N94-25234
EGGERS, AAD P. p 2197 N94-24020
EHRLICH, R. p 2615 N94-24368
EHST, D. p 2550 N94-23474
EIDSON, THOMAS M. p 2457 N94-24603
EIKENBERRY, STEPHEN S. p 2614 N94-24328
EINARSSON, KRISTINN p 2399 N94-24633
EINMAHL, JOHN H. J. p 2494 N94-23771
p 2494 N94-23774
p 2495 N94-24508
EIROLA, T. p 2479 N94-23106
EISEN, HOWARD J. p 2370 N94-23425
EISENBERGER, MOSHE p 2160 N94-24279
EISENLOHR, H. p 2316 N94-22860
EKROOT, L. p 2292 N94-23266
EKROOT, LAURA p 2277 N94-22757
EL-SHARAWY, EL-BUDAWY p 2365 N94-24699
EL-SHERBINI, T. M. p 2351 N94-25482
ELBAND, DAVID M. p 2184 N94-25052
ELFVING, ANDERS p 2369 N94-23407
ELGERSMA, F. p 2232 N94-22983
ELIA, C. p 2286 N94-22816
ELIEENS, A. p 2448 N94-23096
ELISSA, M. G. p 2321 N94-23642
ELLIOTT, SUSAN p 2195 N94-24995
ELLIS, COLLEEN p 2182 N94-24915
ELLIS, DAVID L. p 2243 N94-23556
ELLIS, JOHN p 2522 N94-25016
ELLIS, JORDAN p 2513 N94-23926
ELLIS, T. W. p 2227 N94-23004
ELLISON, A. J. G. p 2252 N94-22992
ELLMAN, ALVIN p 2447 N94-23917
ELMER, K. R. p 2526 N94-24172
p 2526 N94-24173
ELROD, DAVID A. p 2371 N94-24415
ELSTON, SIDNEY B. p 2186 N94-23255
ELSWORTH, D. T. p 2340 N94-25486
ELTZE, J. p 2369 N94-23406
ELVIS, MARTIN S. p 2600 N94-25269
EMANUELSON, R. H. p 2238 N94-22861
EMES, J. H. p 2564 N94-24657
EMIG, J. A. p 2549 N94-22949
EMIN, D. p 2534 N94-23804
EMSLIE, A. GORDON p 2627 N94-24094
ENDO, YASUKI p 2235 N94-24984
ENGEL, BERNARD A. p 2400 N94-23237
ENGEL, G. p 2161 N94-24285
ENGELHARDT, W. p 2356 N94-23999
p 2361 N94-24028
ENGELHAUPT, DARELL p 2545 N94-24665
ENGELMANN, B. E. p 2568 N94-23216
ENGELUND, WALT p 2162 N94-25098
ENGELUND, WALTER C. p 2170 N94-24716
ENGLISH, NICOLE p 2181 N94-24711
ENGQUIST, BJORN p 2484 N94-23685
ENGVOLD, O. p 2624 N94-22842
ENNS, PHIL p 2399 N94-24525
ENOMOTO, YUJI p 2405 N94-24980
EPHREMIDES, ANTHONY p 2286 N94-22811
EPSTEIN, B. p 2155 N94-24249
EPSTEIN, MIKAEL p 2231 N94-25420
ERAUSQUIN, RICK p 2184 N94-25268
EREMENKO, A. p 2609 N94-23397
ERMUTLU, M. E. p 2524 N94-23110
ERN, ALEXANDRE p 2237 N94-23683
ERSKINE, D. p 2558 N94-22946
ESCOBAR, J. p 2357 N94-24003
ESPARBES, BERNARD p 2363 N94-24055
ESPOSTO, FRANK JOSEPH p 2244 N94-24469
ESTABROOK, POLLY p 2277 N94-22757
p 2279 N94-22771
ETO, T. p 2607 N94-23389
ETO, TAKAO p 2608 N94-23390
ETZLER, C.-C. p 2356 N94-23998
EVANS, A. G. p 2255 N94-24230
EVANS, B. G. p 2277 N94-22759
p 2286 N94-22812
EVANS, BARRY p 2288 N94-22826
EVERETT, R. A., JR. p 2228 N94-23279
EVERS, B. p 2178 N94-24320
EWELL, ROBERT N. p 2596 N94-23540
EZERS, ROLANDS p 2300 N94-24694

F

FABBIANO, GUISEPPINA p 2600 N94-25269
FABBRIZZI, F. p 2359 N94-24013
FAHRENTHOLD, ERIC P. p 2205 N94-24828
FAIGLE, U. p 2493 N94-22702
p 2486 N94-23722
p 2489 N94-24652
FAIZOV, E. L. p 2626 N94-23020
FALCONER, ALLAN p 2387 N94-24357
FANG, DAINING p 2159 N94-24276
FANG, GANG p 2460 N94-25063
FARAZIAN, K. p 2289 N94-22835
FARE, THOMAS L. p 2344 N94-24723
FARHAT, CHARBEL p 2466 N94-23504
FARIS, FARIS p 2304 N94-25266
FARMER, B. L. p 2567 N94-25441
FARMER, R. p 2214 N94-23051
FARRELL, JOSEPH B. p 2297 N94-24298
FARRELL, PAUL A. p 2484 N94-23686
FARRINGTON, PHILLIP A. p 2577 N94-24416
FATHAUER, ROBERT W. p 2563 N94-23972
FATIG, MICHAEL p 2505 N94-23881
p 2507 N94-23889
FAULKNER, SEAN p 2300 N94-24696
FAURE-GEORS, ALINE p 2257 N94-24468
FAVRE, E. p 2315 N94-23989
FAVRE, MICHEL p 2465 N94-23167
FAYYAD, KRISTINA E. p 2305 N94-23914
FEDOSEEV, S. V. p 2370 N94-23418
FEELEY, T. S. p 2198 N94-24752
FEHER, KAMILO p 2287 N94-22818
FEILLARD, PASCAL p 2227 N94-23133
FEIT, M. D. p 2541 N94-22868
FELDHUHN, A. p 2158 N94-24268
FELDMAN, MARK p 2228 N94-23280
FELKAI, R. p 2361 N94-24030
FELLER, H. G. p 2270 N94-23587
FENG, JINZHANG p 2214 N94-23050
p 2215 N94-23060
FENZI, M. p 2358 N94-24007
FERGUSON, KEITH p 2298 N94-24582
FERGUSON, N. S. p 2207 N94-24018
FERGUSON, S. W. p 2209 N94-23012
FERNALD, NANCY p 2272 N94-25193
FERNANDEZ, FELIX E. p 2546 N94-24967
FERRANTE, JOHN p 2243 N94-23578
p 2249 N94-25171
FERRI, PAOLO p 2499 N94-23844
FERRO, RICHARD E. p 2391 N94-23351
FESSLER, B. p 2603 N94-24964
FETCENKO, M. A. p 2391 N94-23352
FEY, FRANCISCUS HENRICUS A. G.
p 2554 N94-25241
FICK, GREGORY p 2180 N94-24581
FIEDLER, JENS p 2402 N94-24108
FIELD, STEPHEN W. p 2605 N94-25358
FIELDS, D. E. p 2569 N94-23453
FIGUEROA, FERNANDO p 2427 N94-25359
FINCKENOR, J. p 2490 N94-24727
FINLAYSON, R. D. p 2372 N94-24136
FINNERTY, DANIEL F. p 2504 N94-23871
FIORE, C. p 2552 N94-24504
FIRESTONE, ELAINE R. p 2417 N94-23291
p 2417 N94-23338
FISCHER, PAUL F. p 2490 N94-24836
FISCHL, ROBERT p 2163 N94-25103
FISHER, GENE L. p 2445 N94-23125
FISHER, M. J. p 2525 N94-22959
FISHER, S. p 2215 N94-23057
FISHKIND, STANLEY A. p 2518 N94-23957
FISK, Z. p 2557 N94-22925
FITZPATRICK, EDWARD L. p 2599 N94-24051
FLACCAVENTO, M. p 2179 N94-24325
FLAMAND, L. p 2264 N94-24010
FLANAGAN, M. J. p 2291 N94-23264
FLANNERY, JACK p 2598 N94-25006
FLATAU, P. J. p 2413 N94-24389
FLATAU, PIOTR p 2414 N94-24397
FLATLEY, THOMAS W. p 2195 N94-24497
FLECHSIG, DREW E. p 2202 N94-23631
FLEDEL, S. p 2158 N94-24268
FLEMING, P. J. p 2463 N94-25315
FLEMING, REX p 2413 N94-24385
FLEMING, TERENCE F. p 2436 N94-24200
FLEMMING, ROBERT J. p 2166 N94-23299
FLESHLER, S. p 2557 N94-22929
FLESNER, LARRY D. p 2312 N94-25036
FLETCHER, MALISE p 2202 N94-23921
FLINK, INGELA p 2437 N94-24292
FLINT, ERIC p 2298 N94-24582
FLORIE, C. p 2154 N94-24246
FLOWERS, GEORGE T. p 2365 N94-24751
FLOYD, STEPHEN A. p 2577 N94-24417
FLUEGEL, MORITZ p 2407 N94-23199
FLYNN, MICHAEL p 2400 N94-23084
FOKKEMA, DIEDERIK R. p 2483 N94-23681
FOLEY, GLENN T. p 2305 N94-23859
FOLKERTS, L. p 2532 N94-22956
FOLTZ, M. F. p 2232 N94-23298
FONSECA, C. M. p 2463 N94-25315
FOOTE, BRANT p 2411 N94-24380
FORBES, GREGORY S. p 2416 N94-23238
FOREMAN, JAMES W. p 2380 N94-24418
FOREMAN, TIM p 2538 N94-25255
FORGET, FRANCOIS p 2618 N94-24880
p 2619 N94-24884
FORMAN, MICHAEL p 2516 N94-23943
FORNEY, G. P. p 2270 N94-23735
FORSBERG, AAKE p 2421 N94-24290
FORSTER, D. J. p 2358 N94-24009
FORSYTH, D. A. p 2464 N94-25471
FORTNEY, SUZANNE M. p 2426 N94-23544
FOSTER, I. p 2450 N94-23207
FOSTER, JOHN V. p 2164 N94-25107
FOSTERVOLL, H. p 2353 N94-23449
FOX, GEOFFREY p 2458 N94-24679
FOYLE, DAVID C. p 2443 N94-25512
FRAICHARD, THIERRY p 2470 N94-22898
FRANCE, ANGELIQUE p 2266 N94-24618
FRANCO, E. D. p 2598 N94-24832
FRANK, BERNARD J. p 2171 N94-25517
FRANK, BILL p 2414 N94-24394
FRANK, H. p 2393 N94-23361
FRANK, M. R. p 2532 N94-22952
FRANK, WILLIAM p 2413 N94-24386
FRANKHAUSER, CHRIS p 2181 N94-24591
FRANSES, P. H. p 2479 N94-23122
FRANSOO, JAN CORNELIS p 2586 N94-25235
FRATINI, A. V. p 2567 N94-25441
FRATTER, ISABELLE p 2504 N94-23876
FRAZIER, D. O. p 2223 N94-24338
FRAZIER, EDWARD p 2209 N94-24767
FREBIE, CHRISTOPHER P. p 2244 N94-23802
FREDERICK, C. O. p 2269 N94-23582
FREDERICKSON, CARL K. p 2527 N94-24212
FREEMAN, L. MICHAEL p 2574 N94-24405
FREIDBERG, J. P. p 2552 N94-24502
FREISE, JON p 2365 N94-24703
FRERIKS, IVO. L. p 2533 N94-23713
FRERIKS, L. W. p 2470 N94-22877
FRERKING, MARGARET A. p 2310 N94-23821
FRESE, M. H. p 2198 N94-23208
FREY, MARY ANNE BASSETT p 2426 N94-23530
FREYDEFONT, M. p 2316 N94-22858
FREYTAG, E. K. p 2307 N94-22950
FRICK, STEPHEN N. p 2180 N94-24581
FRICKE, S. K. p 2401 N94-23282
FRICONNEAU, JEAN PIERRE p 2370 N94-23424
FRIDY, J. M. p 2562 N94-23535
FRIED, L. E. p 2265 N94-23778
FRIEDMAN, GARY p 2197 N94-23902
FRIEDMAN, H. W. p 2349 N94-23490
FRIEDMAN, L. p 2370 N94-23416
FRIEDMANN, PERETZ P. p 2154 N94-24244
FRIEDRICH, R. p 2316 N94-22859
FRIM, J. p 2433 N94-24119
FROSTIG, Y. p 2157 N94-24260
FRYDLENDER, HERVE p 2471 N94-23152
FRYE, ROBERT E. p 2280 N94-22774
FRYSZ, CHRISTINE A. p 2394 N94-23367
FU, C. Y. p 2307 N94-23008
FU, CHI YUNG p 2471 N94-23011
FUCHS, JENS J. p 2518 N94-23952
FUECHSEL, CHARLES F. p 2498 N94-23836
FUJII, N. p 2369 N94-23402
FUJII, SEIICHI p 2207 N94-23910
FUJISAWA, A. p 2311 N94-24457
FUJISAWA, MASAMI p 2345 N94-24977
FUJISE, MASAYUKI p 2279 N94-22769
FUJIWARA, M. p 2508 N94-23898
FUKUSADA, KATSUAKI p 2271 N94-24459
FULLER, DANA K. p 2176 N94-25444
FULLERTON, E. E. p 2559 N94-22995
FULTON, DAVID p 2183 N94-25001
FULTON, SCOTT R. p 2416 N94-23687
p 2484 N94-23688
FULZ, BRENT p 2245 N94-25033
FUNAKI, Y. p 2497 N94-23800
p 2521 N94-24523
FUNG, C. F. p 2313 N94-25319
FUNG, INEZ p 2381 N94-24800
FURA, DAVID A. p 2466 N94-23252
p 2467 N94-24075
p 2467 N94-24463
FURUHAMA, YOJI p 2279 N94-22769

G

GABB, TIMOTHY P. p 2230 N94-25186
GABRIEL, KARIN M. p 2263 N94-25410
GAHILL, PATRICIA p 2174 N94-24941
GAL-OR, BENJAMIN p 2155 N94-24251
GALAMBOS, J. D. p 2553 N94-24628
GALI, S. p 2157 N94-24262
GALILI, N. p 2160 N94-24281
GALKA, EDMUND p 2184 N94-25002
GALLAGHER, CHRIS p 2209 N94-24840
GALLAGHER, PATRICK p 2183 N94-25001
GALLAY, G. p 2359 N94-24019
GALLE, BO p 2402 N94-24108
GALLO, E. p 2369 N94-23399
GALLO, FRANK G. p 2430 N94-23080

GALLUS, H. E. p 2315 N94-22854
GAMBER, T. p 2622 N94-24903
GAMBRELL, S. C., JR. p 2378 N94-25267
GANTENBEIN, REX E. p 2306 N94-25360
GANY, A. p 2159 N94-24275
GANY, ALON p 2159 N94-24273
GAO, FENG p 2330 N94-24154
GAO, Y. p 2558 N94-22990
GARBEY, M. p 2318 N94-23213
GARBOS, RAY p 2272 N94-25193
GARCEAU, MICHAEL p 2529 N94-24307
GARCIA, GRAHAM A. p 2312 N94-25050
GARCIA, Q. p 2289 N94-22833
GARCIA, R. p 2214 N94-23054
GARCIAMARIRRODRIGA, C. p 2207 N94-24017
GARDINER, FREDERICK P. p 2481 N94-23547
GARDINER, J. G. p 2282 N94-22791
p 2288 N94-22827
GARDNER, C. p 2193 N94-24123
GARDNER, C. L. p 2193 N94-24117
GAREAU, WILL p 2266 N94-24618
GARRARD, WILLIAM L. p 2190 N94-25176
GARRETT, W. R. p 2535 N94-24510
GARROWAY, ALLEN N. p 2537 N94-25047
GARZA, DAVID p 2206 N94-24916
GARZA, JOSE p 2221 N94-24979
GASIEWSKI, ALBIN J. p 2404 N94-24843
GASKIN, DAVID E. p 2206 N94-25007
GASSER, MAX G. p 2354 N94-23831
GAT, ERANN p 2371 N94-23427
GAT, NAHUM p 2598 N94-23536
GATES, THOMAS S. p 2228 N94-23280
GAUGER, J. R. p 2299 N94-24676
GAUMET, DANIEL p 2363 N94-24046
GAUSTAD, JOHN E. p 2410 N94-24097
GAVER, D. P. p 2422 N94-25146
GAVIRA, J. p 2361 N94-24035
GAVRIN, V. N. p 2626 N94-23020
GAWRONSKI, W. K. p 2291 N94-23260
p 2292 N94-23268
GAYDA, JOHN p 2230 N94-25186
GAZDA, J. p 2238 N94-22718
GAZZE, C. p 2217 N94-23069
GEARY, JAMES L., JR. p 2553 N94-24949
GEDWILL, MICHAEL G. p 2343 N94-23826
GEELEN, P. p 2486 N94-23762
p 2487 N94-23765
GEELEN, PIETER p 2489 N94-24643
GEER, R. E. p 2262 N94-25159
GEERING, H. P. p 2157 N94-24263
GEERTS, T. p 2473 N94-23760
GEJJI, RAGHVENDRA R. p 2314 N94-23239
GEKAT, FRANK p 2351 N94-25304
GELB, ALAN p 2394 N94-23366
GELLER, GARY N. p 2389 N94-23840
GENIESSE, PETE p 2182 N94-24837
GENNSER, MIKAEL p 2430 N94-23743
GENTRY, F. p 2559 N94-23186
GEORGE, DAREN p 2438 N94-24786
GEORGIADIS, N. J. p 2326 N94-23670
p 2168 N94-24084
GEORGOPOULOS, APOSTOLOS P.
p 2428 N94-25437
GERENCSER, DIANE p 2323 N94-23650
GERLI, C. p 2369 N94-23399
GERMAN, JOHN p 2399 N94-24525
GEROPP, D. p 2315 N94-22853
GERRASSY, J. p 2157 N94-24262
GERRETSEN, A. p 2417 N94-24107
GERRISH, HARROLD P., JR. p 2217 N94-23070
GERSBACH, JIM p 2197 N94-23902
GERTH, RICHARD J. p 2222 N94-24419
GERVASIO, DOMINIC p 2393 N94-23360
GERWIN, R. A. p 2218 N94-23283
GEURTS, BERNARD p 2342 N94-23694
GEURTS, BERNARD J. p 2315 N94-22713
GEVARGIZ, J. p 2273 N94-22739
GEZARI, DANIEL Y. p 2600 N94-25387
GHAFFARIAN, BENNY p 2320 N94-23635
GHAN, S. J. p 2386 N94-23779
GHANI, NASIR p 2296 N94-24115
GHEONDEA, AURELIAN p 2457 N94-24599
GHEZ, P. p 2298 N94-24630
GHIRARDI, G. C. p 2570 N94-25206
GHOSAL, SANDIP p 2329 N94-24148
GIAMEI, A. F. p 2246 N94-25121
GIANCOLA, PETER p 2510 N94-23905
GIANNETTI, F. p 2286 N94-22816
GIARDINO, L. p 2369 N94-23399
GIBBONS, D. W. p 2393 N94-23363
GIBBS, D. p 2245 N94-24612
GIBIN, MAURICIUS p 2198 N94-24860
GIBSON, E. D. p 2227 N94-23004
GIBSON, STEVEN p 2510 N94-23905
GIESE, R. F. p 2395 N94-24654
GIESING, J. P. p 2179 N94-24324
GIFFORD, P. R. p 2391 N94-23352
GILBERT, TIMOTHY p 2183 N94-24975
GILDING, B. H. p 2273 N94-22729
p 2555 N94-22730
GILL, S. p 2358 N94-24009
p 2358 N94-24011
p 2362 N94-24042
p 2363 N94-24043
GILLAN, DOUGLAS J. p 2433 N94-24187
p 2433 N94-24188
GILLESPIE, VERNON P. p 2607 N94-23388
GILLETT, JOHN p 2182 N94-24817
GINGER, KATHRYN M. p 2409 N94-24049
GIRALT, GEORGES p 2370 N94-23413
GIRARDEY, C. C. p 2284 N94-22802
GIULIANI, JAMES E. p 2213 N94-23049
GIUNTA, TONY p 2298 N94-24582
GIVI, PEYMAN p 2337 N94-25094
GJESSING, YNGVAR p 2399 N94-24633
GLADSTONE, G. R. p 2618 N94-24878
p 2619 N94-24887
GLARBORG, P. p 2232 N94-23100
GLASKOV, S. A. p 2170 N94-25137
GLASS, K. C. p 2433 N94-24119
GLECKLER, MARK p 2266 N94-24618
GLEIN, RANDALL p 2288 N94-22828
GLENNAN, THOMAS KEITH p 2630 N94-23333
GLOGOWSKI, M. p 2213 N94-23047
GNEMMI, P. p 2529 N94-24514
p 2185 N94-25301
p 2340 N94-25463
GODET, M. p 2264 N94-24010
GOERZ, D. A. p 2307 N94-22950
GOETZ, J. p 2552 N94-24504
GOHIL, P. p 2551 N94-23782
GOKHALE, D. p 2286 N94-22817
GOLDBERG, E. p 2158 N94-24268
GOLDBERG, J. H. p 2429 N94-22997
GOLDBERG, L. A. p 2466 N94-23491
GOLDHIRSH, JULIUS p 2283 N94-22792
GOLDSBERRY, BETTY S. p 2434 N94-24191
GOLDSTEIN, JOSEPH A. p 2303 N94-25089
GOLDSTEIN, STANLEY H. p 2632 N94-25348
p 2636 N94-25367
GOLDSTON, R. J. p 2552 N94-24502
GOLISH, MICHAEL L. p 2459 N94-24812
GOLLIHER, ERIC p 2321 N94-23638
GOLOMBEK, M. P. p 2606 N94-23383
GOLOVATO, S. p 2552 N94-24504
GOLSHAN, N. p 2289 N94-22835
GOLSHAN, NASSER p 2273 N94-22738
p 2273 N94-22739
GOLUB, LEON p 2600 N94-25269
GOMINA, M. p 2256 N94-24235
GONG, LESLIE p 2334 N94-24495
GONNER, J. p 2464 N94-23927
GONSER, U. p 2566 N94-25332
GONZALEZ, ELOY p 2206 N94-24916
GONZALEZ, R. p 2558 N94-22957
GONZALEZVALLEJO, J. J. p 2357 N94-24004
GOODINE, DAVID p 2206 N94-24916
GOODMAN, L. S. p 2432 N94-24114
GOODRICH, KENT p 2418 N94-24671
GOODRICH, R. G. p 2556 N94-22920
GOODWIN, JASON p 2221 N94-24834
GOOKIN, DEBRA J. p 2303 N94-25217
GORDELIJ, V. I. p 2570 N94-25207
GORDON, CARLTON p 2182 N94-24817
GORDON, DANIEL p 2566 N94-25288
GOREMYCHKIN, E. A. p 2567 N94-25425
GORETTA, K. C. p 2563 N94-24624
GORSE, C. p 2369 N94-23412
GOTO, T. p 2567 N94-25412
GOTO, TSUNEAKI p 2564 N94-24958
GOTTESMAN, T. p 2158 N94-24269
GOTTLIEB, DAVID p 2480 N94-23272
p 2480 N94-23278
GOULD, RICHARD D. p 2340 N94-25530
GOULD, S. G. p 2356 N94-23993
GOUWELEEUW, J. p 2523 N94-23094
p 2479 N94-23098
GOUWELEEUW, JOSE M. p 2496 N94-24744
GRABOWSKI, KENNETH S. p 2350 N94-24952
GRADY, C. A. p 2599 N94-23334
GRADY, CAROL A. p 2604 N94-25265
GRAF, HANS-F. p 2403 N94-24491
GRAHAM, EARL E. p 2253 N94-23371
GRAHAM, KATHERINE p 2179 N94-24401
GRAHAM, NICHOLAS E. p 2407 N94-23199
GRAHAM, R. A. p 2558 N94-22953
GRAHAM, RONALD E. p 2195 N94-24482
GRANDMAISON, E. W. p 2341 N94-23675
GRANETZ, R. p 2552 N94-24504
GRANGER-GALLEGOS, STEPHANIE
p 2385 N94-23615
p 2385 N94-23616
GRANNAN, WILLIAM p 2183 N94-25001
GRANT, K. E. p 2397 N94-23700
GRANT, T. J. p 2207 N94-23869
GRAS, RENE p 2355 N94-23991
GRASS, ALAIN p 2363 N94-24046
GRATTAROLA, M. p 2362 N94-24039
GRAVELY, BEN p 2204 N94-23828
GRAY, G. T., III p 2240 N94-23021
GRAY, GARY p 2424 N94-23319
p 2425 N94-23327
GRAY, GARY W. p 2423 N94-23314
GRAY, HENRY F. p 2311 N94-24736
p 2303 N94-25150
GREEN, A. K. p 2156 N94-24259
GREEN, CAROL E. p 2421 N94-24688
GREEN, M. L. H. p 2233 N94-23801
GREEN, STEVE p 2174 N94-25272
GREEN, WILLIAM B. p 2518 N94-23955
GREENBERG, J. B. p 2160 N94-24282
p 2161 N94-24284
GREENE, A. E. p 2311 N94-24500
GREENE, RICHARD F. p 2303 N94-25150
GREENFIELD, S. C. p 2211 N94-23036
GREENISEN, MICHAEL p 2437 N94-24206
GREENISEN, MICHAEL C. p 2436 N94-24204
GREENLEAF, J. E. p 2426 N94-23575
GREENWALD, M. p 2552 N94-24504
GREFEN, P. W. P. J. p 2486 N94-23725
p 2590 N94-23816
GREGG, WATSON W. p 2417 N94-23291
p 2417 N94-23338
GREGORY, IRENE M. p 2163 N94-25104
GREGORY, JOHN C. p 2345 N94-25000
GRELL, GEORG p 2413 N94-24386
p 2414 N94-24392
GRENDA, JEFFREY p 2213 N94-23046
GRIENIER, C. p 2556 N94-22920
GRIFFIN, ERNEST p 2182 N94-24966
GRIFFIN, L. W. p 2214 N94-23054
GRIFFITHS, JERRY B. p 2406 N94-25430
GRIMSDITCH, M. p 2557 N94-22927
p 2557 N94-22929
p 2559 N94-22995
GROCE, JOHN L. p 2172 N94-23288
GROEBNER, R. J. p 2551 N94-23782
GROENAS, S. p 2451 N94-23443
GROENEN, PAULUS ADRIANUS CORNELIS
p 2261 N94-25084
GROENEWALD, GILBERT JOSEPH
p 2491 N94-25245
GROENEWEG, J. p 2487 N94-23786
GROENEWEG, JOHN F. p 2530 N94-25172
GROMOV, V. V. p 2369 N94-23374
p 2369 N94-23411
p 2370 N94-23416
p 2370 N94-23418
GROPP, WILLIAM p 2465 N94-22973
GROSS-THEBING, ARNOLD p 2269 N94-23584
GROSSMAN, A. S. p 2397 N94-23700
GROSSMAN, G. p 2271 N94-23793
GROSSMAN, R. L. p 2472 N94-23300
GROSSMAN, ROBERT p 2448 N94-23073
p 2448 N94-23074
GROSSMAN, ROBERT L. p 2451 N94-23301
GROTEN, M. p 2347 N94-22874
GRUEBEL, G. p 2245 N94-24612
GRUEN, D. M. p 2562 N94-23805
GRUFFMAN, STIG p 2544 N94-23723
GU, YU HUA p 2304 N94-25292
GUAY, J. p 2260 N94-24815
GUFFIN, O. T. p 2505 N94-23878
GUGERTY, LEO p 2434 N94-24190
GUI-ZHANG, TU p 2452 N94-23518
GUIBORD, A. p 2286 N94-22817
GUIBORD, ARTHUR F. p 2280 N94-22778
GUILLORY, A. R. p 2409 N94-24080
GULAKOWSKI, STEVE p 2181 N94-24787
GULLIVER, T. A. p 2296 N94-24132
GUNAWAN, MARY p 2206 N94-25007
GUNTER, WILLIAM D. p 2543 N94-23309
GUO, EDWARD H. p 2192 N94-24072
GUPTILL, JAMES D. p 2378 N94-24845
GUSTAFSON, DAVID p 2365 N94-24703
GUTIERREZ-LUACES, BENITO O.
p 2305 N94-23912
GUTKNECHT, M. H. p 2454 N94-23796
GUZIK, T. G. p 2628 N94-25031
GYEKENYESI, JOHN P. p 2258 N94-24682

H

HA, ANHHOANG p 2272 N94-23892
HAAG, THOMAS W. p 2219 N94-23630
p 2221 N94-24770
HAAK, K. F. I. p 2526 N94-23726

HAAS, H. A. p 2418 N94-24601
HABERBUSCH, MARK S. p 2346 N94-25202
HABERLE, R. M. p 2616 N94-24871
p 2618 N94-24881
p 2618 N94-24882
p 2621 N94-24896
p 2622 N94-24902
p 2622 N94-24903
HABETS, L. C. G. J. M. p 2475 N94-24762
p 2493 N94-25527
HABIB, SHAHID p 2390 N94-23346
HABREKKE, T. p 2353 N94-23448
HACHA, THOMAS H. p 2205 N94-24825
HADDOW, C. R. p 2503 N94-23866
HAEFFNER, D. R. p 2545 N94-24550
HAEME, T. p 2382 N94-23224
HAENNINEN, HANNU p 2375 N94-23120
HAERTIG, J. p 2176 N94-23146
p 2529 N94-24514
p 2185 N94-25301
p 2340 N94-25463
HAGER, E. PAUL p 2293 N94-23622
p 2293 N94-23627
p 2293 N94-23628
HAGGERTY, JAMES J. p 2597 N94-25018
HAGGERTY, JOHN S. p 2255 N94-24223
HAGGETT, R. D. p 2266 N94-24728
HAGUE, J. R. p 2353 N94-23191
HAHN, H. T. p 2229 N94-24402
HAIME, GREGORY CARLO p 2405 N94-25229
HAINAUT, JEAN-PIERRE p 2176 N94-24181
HAINES, B. J. p 2196 N94-23257
p 2196 N94-23258
HAINES, RICHARD F. p 2431 N94-23970
HAITHCOCK, STEPHEN p 2184 N94-25021
HAJEK, B. F. p 2401 N94-23337
HAJEN, G. p 2502 N94-23858
HALANI, A. p 2390 N94-23296
HALICIOGLU, TIMUR p 2565 N94-25093
HALL, D. p 2556 N94-22920
HALL, J. p 2371 N94-22935
HALL, J. R. p 2519 N94-23961
HALL, JOSEPH W. p 2427 N94-24865
HALL, L. J. p 2533 N94-23218
HALL, M. M., JR. p 2241 N94-23219
HALL, MELISSA p 2179 N94-24332
p 2190 N94-24551
HALL, P. J. p 2599 N94-24780
HALLER, E. E. p 2557 N94-22926
p 2564 N94-24657
HALLIKAINEN, M. p 2382 N94-23224
HALPERT, G. p 2392 N94-23354
p 2393 N94-23361
HALPERT, GERALD p 2310 N94-23823
HAMADA, Y. p 2311 N94-24457
HAMAKER, JOSEPH W. p 2586 N94-25197
HAMBOURGER, PAUL p 2218 N94-23370
HAMER, PAUL p 2502 N94-23862
HAMILTON, CHARLES p 2266 N94-24618
HAMILTON, DOUG p 2195 N94-24995
HAMILTON, JAMES M. p 2331 N94-24159
HAMLEY, JOHN A. p 2219 N94-23630
p 2221 N94-25189
p 2222 N94-25201
HAMMER, PETER L. p 2488 N94-24561
HAMMILTON, D. B. p 2173 N94-24864
HAMMONS, B. E. p 2555 N94-22717
HAMMOUD, AHMAD N. p 2203 N94-23632
HAMPDEN-SMITH, M. J. p 2346 N94-25151
HAMPDEN-SMITH, MARK J. p 2547 N94-25144
HAMPTON, LAWRENCE p 2253 N94-23335
HAMPTON, TOM p 2365 N94-24703
HANDSCHUH, ROBERT F. p 2364 N94-24483
HANEY, S. W. p 2553 N94-24628
HANIGOFSKY, J. A. p 2227 N94-23022
HANNA, GREGORY J. p 2334 N94-24495
HANNA, KEITH p 2346 N94-25502
HANNULA, HEIKKI p 2357 N94-24000
HANSEN, SCOTT D. p 2528 N94-24217
HANSON, RANDY L. p 2285 N94-22806
HANYALOGLU, BENGI p 2253 N94-23371
HAPPELL, NADINE p 2520 N94-23965
HARA, HIDEO p 2509 N94-23903
p 2207 N94-23910
HARA, M. p 2257 N94-24562
p 2261 N94-24930
HARABIN, A. L. p 2427 N94-24950
HARARI, D. p 2154 N94-24245
HARARI, R. p 2155 N94-24253
HARDESTY, A. J. p 2426 N94-23575
HARELAND, WILLARD A. p 2552 N94-24546
HARI, YASUKO p 2345 N94-24977
HARPER, ROBERT p 2458 N94-24693
HARRINGA, J. L. p 2243 N94-23753
HARRINGTON, GALE A. p 2458 N94-24684
HARRINGTON, RICHARD F. p 2343 N94-23498
HARRIS, A. L. p 2529 N94-25026
HARRIS, DANIEL E. p 2600 N94-25269
HARRIS, DAVID R. p 2272 N94-25193
HARRIS, J. H. p 2549 N94-22998
HARRIS, JENNIFER A. p 2516 N94-23944
HARRIS, RANDALL L., SR. p 2442 N94-25507
HARRISON, L. p 2430 N94-23083
p 2438 N94-24830
HART, NICK p 2282 N94-22788
HARTFIELD, ROY, JR. p 2548 N94-24420
HARTMANN, ROBERT p 2346 N94-25415
HARTWIG, H. p 2356 N94-23999
p 2361 N94-24028
HARVEY, BOB p 2184 N94-25004
HARVEY, KAREN L. p 2628 N94-25275
HARVEY, ROBERT p 2179 N94-24332
p 2190 N94-24551
HARVEY, T. JEFFREY p 2361 N94-24034
HASHIMOTO, HIROSHI p 2405 N94-24980
HASHIMOTO, KOUICHI p 2206 N94-25007
HASKEW, TIM A. p 2365 N94-24842
HASKINS, ROBERT D. p 2385 N94-23615
p 2385 N94-23616
HASSAN, H. A. p 2337 N94-24858
p 2337 N94-24859
HASSANEIN, A. p 2550 N94-23474
HASSENZAHL, W. V. p 2549 N94-23013
HASSON, SCOTT p 2437 N94-24206
HASSUN, ROLAND p 2287 N94-22822
HASTI, D. p 2389 N94-22888
HATLELID, JOHN E. p 2281 N94-22785
HAUGLI, HANS-C. p 2282 N94-22788
HAUSS, B. I. p 2306 N94-25498
HAUSS, BRUCE p 2306 N94-25494
HAVELA, L. p 2239 N94-22939
HAVELOCK, DAVID p 2528 N94-24219
HAVENER, C. C. p 2532 N94-22956
HAVERKORT, B. R. p 2494 N94-23749
HAWKINS, JOSEPH p 2396 N94-24701
HAWKS, MICHAEL R. p 2539 N94-25443
HAYARD, M. p 2369 N94-23400
HAYASHI, MASAHIKO p 2604 N94-24987
HAYDEN, S. Z. p 2238 N94-22861
HAYES, PATRICK M. p 2408 N94-23619
HAYHOE, GORDON F. p 2192 N94-24072
HE, AI-FANG p 2483 N94-23679
HE, CHENGJIAN p 2181 N94-24726
HE, J. L. p 2352 N94-22996
HEAD, N. C. p 2197 N94-23851
HEARN, TERRY p 2280 N94-22778
HEBERLEIN, J. p 2310 N94-24070
HECHLER, MARTIN p 2608 N94-23391
HECZKO, OLEG p 2250 N94-25316
HEDBY, GUNNAR p 2297 N94-24531
HEDGLEY, DAVID R., JR. p 2381 N94-22961
HEDSTROM, J. C. p 2392 N94-23357
HEEMSTRADEGROOT, S. M. p 2467 N94-23752
HEESTERBEEK, J. A. P. p 2420 N94-23521
HEFFNER, R. H. p 2240 N94-23003
p 2559 N94-23006
HEGEDUS, S. S. p 2389 N94-22862
HEGERL, G. p 2407 N94-23156
HEIDELBERGER, PHILIP p 2457 N94-24638
HEIJENK, G. J. p 2299 N94-24650
HEIKKILAE, P. p 2308 N94-23130
HEIM, J. R. p 2549 N94-23013
p 2549 N94-23014
HEINBOCKEL, JOHN p 2540 N94-23485
HEINO, M. p 2254 N94-23561
HEINRICH, JUAN C. p 2325 N94-23668
HEISER, TERRY p 2183 N94-24974
HELANDER, JOHANNES p 2449 N94-23103
HELFAND, DAVID J. p 2453 N94-23559
HELLAND, STEPHEN M. p 2344 N94-24362
HELLBACH, A. p 2407 N94-23156
HELLER, E. J. p 2530 N94-22720
HELLMAN, ROLF p 2437 N94-24292
HELM, M. p 2299 N94-24656
HELM, NEIL R. p 2293 N94-23622
p 2293 N94-23627
p 2293 N94-23628
HEMINK, W. C. p 2361 N94-24035
HEMPELMANN, KLAUS p 2269 N94-23584
HENDERSON, DIANE p 2419 N94-24948
HENDERSON, W. p 2494 N94-23749
HENDRICKS, E. W. p 2338 N94-25140
HENELY, STEVEN J. p 2284 N94-22803
HENINS, I. p 2218 N94-23283
HENNINGS, ELSA J. p 2170 N94-25051
HENRIKSSON, P. p 2398 N94-23813
HENSHALL, G. A. p 2240 N94-23017
p 2241 N94-23434
HENSON, VAN EMDEN p 2483 N94-23678
p 2341 N94-23689
HEPNER, S. A. R. p 2157 N94-24263
HEPPNER, RICHARD A. p 2207 N94-23596
HERAKOVICH, CARL T. p 2228 N94-23566
HERBEN, M. H. A. J. p 2283 N94-22795
HERD, MELVIN D. p 2345 N94-24831
HERGENROTHER, PAUL M. p 2252 N94-23075
p 2253 N94-23305
p 2253 N94-23307
HERLIHY, MAURICE p 2467 N94-24692
HERMAN, JAY R. p 2410 N94-24355
HERNANDEZ, GLORIA p 2169 N94-24311
HERNANDEZ, J. A. p 2549 N94-22949
HERRMANN, PHILIPPE CHARLES
p 2405 N94-25251
HERRMANN, W. p 2589 N94-23126
p 2589 N94-23127
p 2589 N94-23128
HERSHKOWITZ, N. p 2550 N94-23192
HERWIG, L. O. p 2389 N94-22888
HESBACH, THOMAS D., JR. p 2180 N94-24479
HESS, RALPH M. p 2258 N94-24720
HESSE, J. M. p 2397 N94-23497
HESSEL, MICHAEL I., JR. p 2422 N94-24810
HESTERMAN, T. W. p 2178 N94-24321
HEUSER, W. RANDY p 2305 N94-23848
HEVENOR, RICHARD A. p 2493 N94-25452
HEWETT, CHARLES A. p 2312 N94-25035
HICKS, DANIEL p 2528 N94-24216
HIGASHI, K. p 2229 N94-24547
HIGHSMITH, ALTON L. p 2231 N94-24421
HIGMAN, K. p 2217 N94-23069
HIISMAEKI, P. E. p 2566 N94-25347
HIJKOOP, G. p 2209 N94-24006
HILDENBRAND, DONALD L. p 2232 N94-23477
HILJANEN, M. p 2254 N94-23561
HILL, D. C. p 2327 N94-24140
p 2327 N91-24141
HILL, GERALD M. p 2221 N94-25189
p 2222 N94-25201
HILL, JEFFREY O. p 2457 N94-24626
HILL, M. A. p 2307 N94-22987
HILL, RANDALL W., JR. p 2305 N94-23915
HILLER, R. E. p 2365 N94-24614
HILLS, D. A. p 2379 N94-25478
HINEDI, S. p 2289 N94-22835
HINGERTY, B. E. p 2563 N94-24567
HINGST, W. R. p 2166 N94-23465
HINKLE, CATHY p 2438 N94-24786
HINNANT, HOWARD E. p 2378 N94-24839
HINTERMANN, H. E. p 2355 N94-23990
p 2360 N94-24023
HINTERMANN, H.-E. p 2358 N94-24011
HIPP, P. A. p 2229 N94-24402
HIRAHARA, YASUHIRO p 2235 N94-24984
HIRANO, NAOMI p 2604 N94-24986
HIRATA, NOBUYUKI p 2509 N94-23903
HIRAYAMA, T. p 2625 N94-22846
HIRST, EDWARD p 2206 N94-24916
HITCHCOCK, MICHAEL F. p 2177 N94-24315
HITCHENS, G. DUNCAN p 2393 N94-23359
HO, C. Y. p 2246 N94-25123
HODEL, A. SCOTTEDWARD p 2465 N94-24422
HODGE, B. K. p 2320 N94-23637
HOECK, H. p 2407 N94-23156
HOEDE, C. p 2486 N94-23722
p 2489 N94-24652
HOEG, PER p 2406 N94-25536
HOEIER, R. p 2561 N94-23428
p 2241 N94-23446
p 2561 N94-23503
p 2533 N94-23505
HOEKJE, S. J. p 2245 N94-25117
HOEKMAN, D. H. p 2386 N94-23734
HOELZL, G. p 2269 N94-23583
HOFFLER, G. WYCKLIFFE p 2426 N94-23530
HOFFMAN, C. M. p 2531 N94-22928
HOFFMAN, ERIC p 2183 N94-24972
HOFFMAN, R. C. p 2244 N94-23792
HOFFMAN, S. p 2629 N94-24695
HOFFMAN, STEPHEN J. p 2605 N94-23376
HOFFREN, J. p 2165 N94-23116
HOISINGTON, CHARLES M. p 2417 N94-23338
HOLBROOK, B. p 2307 N94-22955
HOLCOMB, LEE p 2591 N94-24337
HOLDEMAN, J. D. p 2481 N94-23593
p 2187 N94-24082
p 2188 N94-24594
HOLDER, BARBARA E. p 2506 N94-23883
HOLDRIDGE, GEOFFREY M. p 2630 N94-22893
HOLIAN, B. L. p 2374 N94-22871
HOLLAND, SCOTT D. p 2319 N94-23339
HOLLANSWORTH, JAMES E. p 2274 N94-22740
HOLLINGSWORTH, JEFFREY L. p 2618 N94-24882
HOLLINGSWORTH, M. W. p 2591 N94-24607
HOLLIS, P. p 2320 N94-23532
HOLMES, BRUCE p 2162 N94-25097
HOLMES, DWIGHT P. p 2519 N94-23961
HOLSHEIMER, M. p 2593 N94-24743

HOLSTI-MIETTINEN, R. p 2254 N94-23561
HOLTROP, K. L. p 2354 N94-23797
HOLWEG, PHILIPPUS ANTONIUS MARIA
p 2313 N94-25286
HOLZER, TONY p 2463 N94-25455
p 2463 N94-25456
HOMBURG, A. J. p 2480 N94-23140
HOMBURG, ALE JAN p 2480 N94-23141
HOMSY, G. M. p 2331 N94-24160
HONDA, T. p 2360 N94-24021
HONG, R. p 2553 N94-24746
p 2553 N94-24756
HONGWEI, HUI p 2227 N94-22892
HONKURA, YOSHIMORI p 2405 N94-24980
HONTALAS, PHILIP p 2452 N94-23510
HOOGEVEEN, J. A. p 2467 N94-23756
p 2467 N94-23767
HOOKER, STANFORD B. p 2417 N94-23291
p 2417 N94-23338
HOOPER, E. B. p 2209 N94-23012
HOPKINS, MARK A. p 2170 N94-24773
HOPMAN, J. p 2209 N94-24006
HORIKOSHI, YOSHIJI p 2568 N94-25515
HORIUCHI, SACHIO p 2564 N94-24978
HORN, M. p 2215 N94-23057
HORNE, S. p 2552 N94-24504
HORNUNG, ULRICH p 2340 N94-25467
HOROWITZ, ATARA p 2567 N94-25422
HOROWITZ, YIGAL p 2567 N94-25422
HORSLEY, KEVIN B. p 2204 N94-24620
HORTON, CHARLES R. p 2275 N94-22745
HORVATH, JOAN C. p 2504 N94-23875
HOSKIN, CHERYLYNN N. p 2426 N94-23544
HOSLER, E. RAMON p 2571 N94-23230
HOU, X. p 2299 N94-24650
HOUBEN, HOWARD C. p 2618 N94-24881
p 2618 N94-24882
p 2619 N94-24883
p 2622 N94-24902
HOURCASTAGNOU, J.-N. p 2518 N94-23956
HOURDIN, FREDERIC p 2619 N94-24884
HOUSER, DONALD R. p 2373 N94-24769
HOUSNER, JERROLD M. p 2177 N94-24314
HOUSTON, J. E. p 2234 N94-24772
p 2565 N94-25086
HOUWINK, R. p 2178 N94-24322
HOVAN, SCOT A. p 2221 N94-24770
HOWARD, A. D. p 2621 N94-24895
HOWARD, A. J. p 2555 N94-22717
p 2350 N94-24659
HOWARD, DEAN D. p 2302 N94-25056
p 2302 N94-25058
HOWARD, LAURA p 2205 N94-24825
HOWE, STEVEN D. p 2217 N94-23068
HOWELL, E. I. p 2243 N94-23784
HOWELL, LOUIS H. p 2341 N94-23690
HOWERTON, EVERETT B. p 2180 N94-24479
HOYT, R. P. p 2218 N94-23283
HREINSSON, G. p 2180 N94-24479
HSIAO, CHIA-CHUN p 2211 N94-23034
HSIEH, P. p 2454 N94-24050
HSIEH, W. H. p 2211 N94-23035
HSU, MING-TA S. p 2253 N94-23311
HSU, YU-KAO p 2171 N94-23661
HU, A. p 2426 N94-23575
HU, FANG Q. p 2334 N94-24602
HUANG, C-K. p 2392 N94-23354
HUANG, CHEN-KUO p 2310 N94-23823
HUANG, YING p 2497 N94-25528
HUBBARD, A. p 2552 N94-24504
HUBER, M. C. E. p 2624 N94-22844
HUBER, NEIL F. p 2571 N94-25524
HUBER, T. p 2218 N94-23433
HUBINETTE, SVEIN p 2186 N94-23253
HUDSON, E. A. p 2532 N94-23002
HUDSON, ROBERT D. p 2398 N94-24078
HUESCHEN, RICHARD M. p 2162 N94-25100
HUFF, J. R. p 2392 N94-23357
HUFF, T. L. p 2421 N94-24310
HUGHES, C. D. p 2276 N94-22752
HUGHES, FRANK J. p 2461 N94-25138
HUGHES, I. G. p 2532 N94-22956
HUGHES, JAMES p 2183 N94-24974
HUGHES, PETER M. p 2516 N94-23945
HUIJBERTS, H. J. C. p 2475 N94-24755
HUIJSKENS, F. p 2542 N94-23171
HULL, BRIAN J. p 2194 N94-25522
HULL, DAVID H. p 2424 N94-23321
p 2424 N94-23322
p 2425 N94-23324
p 2425 N94-23325
p 2425 N94-23326
p 2425 N94-23328
HULL, J. R. p 2559 N94-22993
HULL, LARRY G. p 2515 N94-23938
HUMPHRIES, M. E. p 2207 N94-23995
HUNDERI, O. p 2561 N94-23445
HUNG, CHING-CHEH p 2218 N94-23370
p 2222 N94-23591
HUNLEY, J. D. p 2630 N94-23333
HUNNIFORD, MICHAEL p 2182 N94-24837
HUNSAKER, C. T. p 2388 N94-24757
HUNSUCKER, J. L. p 2588 N94-25361
HUNT, GEOFFREY H. p 2522 N94-25013
HUNT, JAMES B. p 2373 N94-24814
HUNT, STEPHAN p 2457 N94-24626
HUNT, WILLIAM p 2181 N94-24591
HUNTER, DAVID G. p 2371 N94-23841
HUNTER, PAUL p 2591 N94-24337
HUNTER, T. R. p 2296 N94-24105
HUOMO, HEIKKI p 2357 N94-24000
HUTCHINGS, G. J. p 2235 N94-24920
HUTCHINSON, I. p 2552 N94-24504
HUTT, JOHN J. p 2211 N94-23037
HWANG, YUAN-SHIN p 2458 N94-24679
HYATT, A. W. p 2354 N94-23797
HYMAN, LADELLE M. p 2585 N94-25362
HYMAN, WILLIAM A. p 2632 N94-25348
p 2636 N94-25367
HYSINGER, CHRISTOPHER L. p 2437 N94-24330

I

IANNUCCI, P. p 2277 N94-22760
IBU, ILAN p 2159 N94-24273
IDASIAK, J. M. p 2369 N94-23403
IERKIC, H. MARIO p 2306 N94-24423
IGNATIUS, EVE p 2452 N94-23507
IGUCHI, H. p 2311 N94-24457
IHARA, HIROKAZU p 2510 N94-23906
IKEGAMI, TETSUSHI p 2283 N94-22793
ILEGBUSI, OLUSEGUN J. p 2323 N94-23655
ILMONIEMI, R. J. p 2308 N94-23105
IMAN, RONALD L. p 2398 N94-24506
INAMDAR, ROHIT p 2244 N94-24066
INDEST, A. W. p 2417 N94-23291
p 2417 N94-23338
ING, H. p 2629 N94-24695
INGERSOLL, A. P. p 2208 N94-24873
INGRAFFEA, ANTHONY p 2246 N94-25118
INOUE, M. p 2599 N94-23705
INTRONE, ROB p 2323 N94-23650
INUKAI, THOMAS p 2304 N94-25266
IORIO, VINCENT M. p 2367 N94-25055
IRELAND, P. T. p 2353 N94-23164
IRWIN, GEORGE W. p 2446 N94-25313
ISAKOW, MICHAEL p 2157 N94-24264
ISHIDO, TSUNEO p 2405 N94-24980
ISHIGURO, MASATO p 2604 N94-24987
ISHIGURO, TAKEHIKO p 2564 N94-24978
ISHIMOTO, HIDEHIKO p 2564 N94-24978
ISLAM, A. K. M. A. p 2558 N94-22978
ISLER, R. C. p 2549 N94-22998
ISOBE, SHUNKICHI p 2288 N94-22829
ISON, JIM p 2179 N94-24401
ISSAC, JASON CHERION p 2167 N94-24052
ISSACCI, FARROKH p 2327 N94-24096
ITO, HIROSHI p 2564 N94-24978
ITO, YASUHIKO p 2288 N94-22825
ITOH, K. M. p 2564 N94-24657
IVARNEZ, ROLAND p 2498 N94-23837
IVLEV, ROBERT p 2371 N94-23427
IVSHCHENKO, Y. p 2607 N94-23384
IWANCZYK, JAN S. p 2233 N94-24113
IZADIAN, JAMAL S. p 2287 N94-22823

J

JACAK, B. V. p 2569 N94-23453
JACKSON, BRUCE p 2162 N94-25101
JACKSON, C. G. R. p 2426 N94-23575
JACKSON, DAVID JEFF p 2578 N94-24424
JACKSON, STEWART W. p 2430 N94-23080
JACKSON, T. p 2317 N94-23089
JACKSON, THOMAS p 2234 N94-24673
JACOBS, H. R. p 2213 N94-23045
JACOBS, P. A. p 2422 N94-25146
JACOBS, P. A. M. p 2381 N94-22896
JACOBSEN, LARRY p 2384 N94-23607
p 2384 N94-23608
JACOBY, B. p 2371 N94-22935
JACUNSKI, M. p 2559 N94-23186
JADUSZLIWER, B. p 2534 N94-24077
JAEAESKELAEINEN, V. p 2382 N94-23224
JAEHNE, B. p 2381 N94-23145
JAGLOWSKI, ADAM J. p 2263 N94-25410
JAKUBZCAK, J. p 2559 N94-23186
JALDEHAG, R. T. K. p 2405 N94-25204
JAMES, I. N. p 2618 N94-24879
JAMES, P. B. p 2619 N94-24885
JAMESON, LELAND p 2479 N94-23090
p 2487 N94-24291
JAMET, JEAN p 2254 N94-24129
JAMNEJAD, VAHRAZ p 2289 N94-22831
JANG, B. W. p 2398 N94-23818
JANOSIK, LESLEY A. p 2258 N94-24682
JANOWITZ, J. p 2430 N94-23083
p 2438 N94-24830
JANSEN, JOHANNES p 2460 N94-25061
JANSEN, KENNETH p 2329 N94-24151
JANSSEN, H. p 2381 N94-23145
JANUS, J. A. p 2242 N94-23496
JARDIN, S. C. p 2552 N94-24502
JARWAH, SAHAR p 2588 N94-22880
JAWERTH, BJOERN p 2485 N94-23691
JAYA, S. MATHI p 2567 N94-25423
JAYLES, C. p 2196 N94-23919
JEDLOVEC, G. J. p 2409 N94-24080
JEDREY, T. C. p 2284 N94-22802
JEDREY, THOMAS C. p 2279 N94-22771
p 2280 N94-22774
JEMIAN, WARTAN A. p 2251 N94-24425
JENG, R. J. p 2258 N94-24732
JENKINS, B. K. p 2474 N94-24622
JENKINS, JAMES P. p 2428 N94-24855
JENNINGS, RAYMOND D. p 2293 N94-23622
p 2293 N94-23627
p 2293 N94-23628
JENSEN, BRIAN J. p 2253 N94-23307
JENSEN, D. W. p 2229 N94-24402
JENSEN, DEAN G. p 2435 N94-24197
JENSEN, MICHAEL A. p 2289 N94-22834
JERO, PAUL D. p 2255 N94-24231
JERRUM, M. p 2466 N94-23491
JEVCAK, J. L. p 2629 N94-24695
JIANG, J. p 2566 N94-25332
JIANG, JIAN-PING p 2443 N94-23936
JIMENEZ, JAVIER p 2330 N94-24153
JIMENEZ, STEPHANE p 2371 N94-23426
JIN, Y. p 2292 N94-23265
JOGLEKAR, PRAFULLA N. p 2464 N94-23240
JOHANNSEN, KLAUS G. p 2278 N94-22763
JOHANSON, GARY A. p 2281 N94-22784
JOHANSSON, J. M. p 2405 N94-25204
JOHE, C. p 2529 N94-24514
p 2185 N94-25301
p 2340 N94-25463
JOHN, JASMIN p 2381 N94-24800
JOHN, JENS A. p 2260 N94-24924
JOHNS, SIMON p 2284 N94-22801
JOHNSON, ADRIEL D. p 2422 N94-24426
JOHNSON, BRADLEY A. p 2391 N94-23351
JOHNSON, C. p 2394 N94-23365
JOHNSON, C. D. p 2364 N94-24088
JOHNSON, CURTIS D. p 2444 N94-25363
JOHNSON, DAVID G. p 2404 N94-24738
JOHNSON, GORDON G. p 2407 N94-25364
JOHNSON, JAY p 2520 N94-23964
p 2520 N94-23966
JOHNSON, JOHN R. p 2391 N94-23353
JOHNSON, N. L. p 2316 N94-22870
JOHNSON, RAQUEL p 2206 N94-25007
JOHNSON, THOMAS D., JR. p 2166 N94-23512
JOHNSON, W. R. p 2532 N94-22988
JOHNSON, WALTER W. p 2442 N94-25511
JOHNSTON, N. J. p 2254 N94-23486
JOHNSTON, NORMAN J. p 2252 N94-23076
JOHNSTON, TOM p 2181 N94-24787
JOLLY, STEVEN D. p 2371 N94-24427
JONES-FOREMAN, CHRISTINE p 2600 N94-25269
JONES, CHRIS E. p 2226 N94-24352
JONES, DONALD A. p 2332 N94-24168
JONES, JASON p 2205 N94-24702
JONES, JIM p 2484 N94-23684
JONES, L. p 2314 N94-25488
JONES, M. p 2503 N94-23866
JONES, P. ALAN p 2361 N94-24034
JONES, R. D. p 2473 N94-24518
JONES, RICHARD A. p 2187 N94-23552
JONES, ROBERT L., III p 2448 N94-23086
JONES, S. p 2266 N94-23657
JONES, S. B. p 2397 N94-23794
JONES, T. p 2277 N94-22758
JONES, T. V. p 2353 N94-23164
JONG, JEN-YI p 2389 N94-24856
JONGEJANS, A. p 2282 N94-22789
p 2289 N94-22833
JONSSON, H. p 2530 N94-22720
JOOSTEN, R. A. M. G. p 2596 N94-24477
JORDAN, PAUL R., III p 2525 N94-23698
JORDEN, ROB p 2198 N94-24860
JORGENSON, PHILIP C. E. p 2481 N94-23554
JOSHI, G. p 2187 N94-23709
JOSHI, M. C. p 2526 N94-24172
p 2526 N94-24173
JOSHI, MANOJ M. p 2619 N94-24886

JOSLIN, D. L. .... p 2543 N94-23458
JOSSET, JEAN-LUC .... p 2610 N94-23408
JOWERS, STEVEN .... p 2272 N94-23892
JOYNER, R. W. .... p 2235 N94-24920
JOZWIAK, LECH .... p 2445 N94-23170
JUAREZ, VINCE .... p 2179 N94-24401
JUCKS, KENNETH W. .... p 2404 N94-24738
JUENGEN, F. J. .... p 2585 N94-23761
p 2488 N94-24527
JUENGEN, FREDERIK-JAN .... p 2586 N94-24528
JULIEN, HOWARD L. .... p 2238 N94-25365
JUMPER, JOHN M. .... p 2209 N94-24038
JUNGE, MARTINA M. .... p 2401 N94-23159
JUNGERT, ERLAND .... p 2590 N94-23741

K

KAASHOEK, M. FRANS .... p 2453 N94-23745
KAASSCHIETER, E. F. .... p 2491 N94-24954
KABALKA, G. W. .... p 2233 N94-23780
KACMAR, CHARLES J. .... p 2595 N94-25366
KADOTA, K. .... p 2552 N94-24456
KAFALAS, JAMES A. .... p 2267 N94-23549
KAFKA, CYNTHIA M. .... p 2262 N94-25145
KAHLBAUM, WILLIAM W. .... p 2346 N94-25499
KAHN, PETER B. .... p 2500 N94-23850
KAHN, RALPH .... p 2385 N94-23615
p 2385 N94-23616
KAIN, JACK .... p 2413 N94-24386
KAISER, MARY K. .... p 2431 N94-23974
p 2439 N94-25490
p 2442 N94-25510
KALAU, WOLFGANG .... p 2570 N94-25258
KALINOVSKIJ, YU. L. .... p 2539 N94-25477
KALLENBERG, L. C. M. .... p 2497 N94-25528
KALLENBERG, W. C. M. .... p 2478 N94-22725
KALLIES, W. .... p 2539 N94-25477
KALOUSEK, J. .... p 2270 N94-23588
KALTENBACH, HANS-JAKOB .... p 2328 N94-24147
KALTZ, T. .... p 2213 N94-23047
KALYAEV, I. .... p 2370 N94-23420
KAMALIAN, R. R. .... p 2488 N94-24541
KAMATA, NORIHIKO .... p 2564 N94-24959
KAMATH, M. .... p 2260 N94-24813
KAMEDA, J. .... p 2375 N94-23184
KAMEYA, OSAMU .... p 2604 N94-24986
KAMINSKII, A. A. .... p 2458 N94-24661
KAMINSKII, ALEXANDER A. .... p 2565 N94-25025
KANEKO, H. .... p 2553 N94-24623
KANEKO, HIROSHI .... p 2564 N94-24978
KANEKO, Y. .... p 2607 N94-23389
KANEKO, YUTAKA .... p 2608 N94-23390
KANG, YIMIN .... p 2484 N94-23688
KANGYING, WANG .... p 2568 N94-25483
KANKAM, M. DAVID .... p 2521 N94-24302
KANYO, M. .... p 2556 N94-22921
KAO, C. Y. J. .... p 2407 N94-23284
KAPANIA, RAKESH K. .... p 2167 N94-24052
KAPER, H. G. .... p 2318 N94-23213
KAPUR, V. K. .... p 2390 N94-23296
KARAM, FOUAD G. .... p 2280 N94-22778
KARAS, STEPHEN .... p 2438 N94-24786
KARASAWA, YOSHIO .... p 2284 N94-22797
KARASZ, FRANK E. .... p 2258 N94-24782
p 2259 N94-24783
KARES, ROBERT J. .... p 2553 N94-24949
KARIMI, MAJID .... p 2251 N94-24428
KARNIADAKIS, G. E. .... p 2337 N94-24929
KAROUTA, F. .... p 2348 N94-23168
KARPEL, MORDECHAY .... p 2161 N94-24287
KARPUR, PRASANNA .... p 2257 N94-24240
KARR, GERALD R. .... p 2574 N94-24405
p 2629 N94-25199
KARTTUNEN, MIKKO .... p 2231 N94-25420
KARUCHRO, Z. .... p 2157 N94-24262
KARYADI, E. .... p 2378 N94-24745
KARYAMPUDI, MOHAN .... p 2413 N94-24386
KASAI, YASUKO .... p 2235 N94-24984
KASCHMITTER, J. L. .... p 2252 N94-22931
KASHIHARA, SHINICHIROU .... p 2271 N94-24459
KASSNER, T. F. .... p 2242 N94-23457
KASTURI, RANGACHAR .... p 2442 N94-25507
KATNIK, GREGORY N. .... p 2199 N94-24059
p 2200 N94-24577
KATO, HATSUHIKO .... p 2510 N94-23906
KATOSHEVSKI, D. .... p 2160 N94-24283
KATZ, J. I. .... p 2629 N94-22947
KATZ, U. .... p 2156 N94-24255
KAUFELER, J. F. .... p 2197 N94-23851
KAUFELER, J.-F. .... p 2508 N94-23897
p 2203 N94-23954
KAUFMANN, L. M. F. .... p 2348 N94-23168
KAUPPINEN, PENTTI .... p 2379 N94-25418
KAURANEN, P. S. .... p 2390 N94-23102
KAVANAGH, FRANK E. .... p 2290 N94-23087
KAWABATA, KAZUAKI .... p 2279 N94-22769
KAWABE, RYOHEI .... p 2604 N94-24987
KAWAGUCHI, J. .... p 2369 N94-23402
KAWAGUCHI, KENTARO .... p 2235 N94-24984
KAWAI, Y. .... p 2549 N94-22964
KAWASHIMA, N. .... p 2369 N94-23402
p 2360 N94-24021
KAZEMI, TAHMINEH .... p 2181 N94-24711
KAZHUKALO, I. F. .... p 2369 N94-23374
KAZMAN, RICK .... p 2460 N94-24933
KAZUMATA, YUKIO .... p 2548 N94-22924
KEARNS, J. J. .... p 2244 N94-23792
KEATING, J. .... p 2571 N94-25340
KEDAR, SMADAR .... p 2591 N94-24552
KEELTY, M. .... p 2278 N94-22766
KEENER, ED .... p 2182 N94-24817
KEHR, JOACHIM .... p 2505 N94-23882
KEICHER, D. M. .... p 2270 N94-23790
KELLEHER, P. .... p 2277 N94-22758
KELLER, TEDDY M. .... p 2258 N94-24721
p 2258 N94-24737
p 2261 N94-25054
KELLMAN, D. H. .... p 2553 N94-24746
KELLOCK, STEVE J. .... p 2499 N94-23844
KELLY, ANGELITA CASTRO .... p 2499 N94-23839
KELLY, G. M. .... p 2319 N94-23513
KELLY, MARK .... p 2180 N94-24581
KELLY, MICHAEL A. .... p 2459 N94-24775
KELLY, P. .... p 2379 N94-25478
KEMPKA, S. N. .... p 2318 N94-23220
KEMURDJIAN, A. I. .... p 2370 N94-23416
KEMURDJIAN, A. L. .... p 2369 N94-23374
KENDALL, STEVEN C. .... p 2461 N94-25138
KENINGTON, PETER B. .... p 2275 N94-22747
KENNEDY, BRUCE W. .... p 2527 N94-24208
KENNEDY, EDWARD J. .... p 2303 N94-25089
KENNEDY, JOHN M. .... p 2592 N94-24649
p 2592 N94-24660
p 2593 N94-24709
KENSKY, E. T. .... p 2542 N94-22915
KENYON, SCOTT J. .... p 2600 N94-25198
KEPING, YAN .... p 2268 N94-23174
KEPPENNE, C. L. .... p 2208 N94-24873
KERANS, RONALD J. .... p 2255 N94-24231
KERN, LYNN R. .... p 2184 N94-25052
KERN, W. .... p 2493 N94-22702
KERNER, J. A. .... p 2598 N94-24832
KERR, J. RICHARD .... p 2439 N94-25491
KERSEY, ALAN D. .... p 2345 N94-25053
KERSHAW, R. P. .... p 2241 N94-23434
KERSNER, R. .... p 2273 N94-22729
KERTZSCHER, U. .... p 2316 N94-22859
KERZHANOVICH, V. V. .... p 2606 N94-23381
p 2369 N94-23395
p 2608 N94-23396
p 2370 N94-23416
p 2370 N94-23417
KESSIS, JEAN JACQUES .... p 2601 N94-23378
KESSIS, JEAN-JACQUES .... p 2369 N94-23405
KESSLER, WILLIAM C. .... p 2177 N94-24315
KETELAARS, ANTONIUS ADRIANUS J.
p 2236 N94-25302
KETIKYAN, A. ZH. .... p 2463 N94-25432
KEVENAAR, THOMAS ANDREAS MARIA
p 2313 N94-25083
KEYSER, DANIEL .... p 2404 N94-24794
KHADRA, KHODOR .... p 2485 N94-23692
KHALILOLLAHI, AMIR .... p 2321 N94-23643
p 2321 N94-23644
KHAN, AKHTAR M. .... p 2226 N94-24352
KHAN, FERDOUS .... p 2540 N94-24305
KHAVARAN, ABBAS .... p 2525 N94-23464
KHODADADI, J. M. .... p 2238 N94-25132
KHOSID, S. .... p 2159 N94-24274
KIANG, Y. W. .... p 2279 N94-22770
KIEFFER, HUGH H. .... p 2383 N94-23598
KIFLE, MULI .... p 2202 N94-25095
KILCOYNE, M. K. .... p 2348 N94-23123
KILLEEN, TIMOTHY L. .... p 2402 N94-24089
p 2403 N94-24486
KIM, J. .... p 2389 N94-22962
KIM, JOHN J. .... p 2331 N94-24159
KIM, SUNGHYUN .... p 2391 N94-23347
KIM, Y. .... p 2227 N94-22977
KIM, YONG-IN .... p 2479 N94-23138
KIMURA, S. G. .... p 2187 N94-23709
KINNEY, RALPH A. .... p 2543 N94-23502
KINSEY, KENNETH E. .... p 2257 N94-24558
KIRBY, SARAH .... p 2272 N94-23892
KIRCHNER, INGO .... p 2403 N94-24491
KIRK, M. A. .... p 2556 N94-22886
KIRKPATRICK, RUSSELL L. .... p 2202 N94-23946
KIRULUTA, ANDREW MUWANGA
p 2427 N94-24467
KISELEV, A. V. .... p 2538 N94-25341
KISPERT, ANDREW .... p 2520 N94-23964
KITAEV, A. .... p 2571 N94-25340
KIVITY, Y. .... p 2154 N94-24246
KJELDGAARD, E. A. .... p 2591 N94-24607
KLARER, P. R. .... p 2613 N94-23469
KLEIJNEN, JACK P. C. .... p 2456 N94-24507
p 2495 N94-24634
KLEIN, M. .... p 2465 N94-22986
KLEIN, SCOTT .... p 2520 N94-23966
KLEINROCK, MARTIN C. .... p 2419 N94-25165
KLEINSCHMIDT, P. D. .... p 2231 N94-22943
KLEMM, R. A. .... p 2562 N94-23795
KLOMPSTRA, MARTIN .... p 2470 N94-22873
KLOP, J. W. .... p 2457 N94-24570
KLOSKO, STEVEN .... p 2196 N94-23920
KLOSTERMAN, JOHN .... p 2323 N94-23650
KLOTE, J. H. .... p 2270 N94-23735
KLUIT, PETER M. .... p 2539 N94-25465
KNAUER, CHAD .... p 2184 N94-25268
KNIGHT, ROY W. .... p 2223 N94-24340
KNIGHTON, JAMES E. .... p 2385 N94-23615
KNILL, DUANE .... p 2298 N94-24582
KNOLL, M. .... p 2343 N94-23200
KNOLL, W. .... p 2257 N94-24562
KNOPS, FREDERICK W., III .... p 2518 N94-23957
KNOTHE, K. .... p 2270 N94-23589
KNOTHE, KLAUS .... p 2269 N94-23581
p 2269 N94-23584
KNOWLTON, W. B. .... p 2564 N94-24657
KO, SUNG HO .... p 2172 N94-24145
KO, WILLIAM L. .... p 2228 N94-23514
KOBERSTEIN, DAVE .... p 2287 N94-22822
KOBISTEK, ROBERT J. .... p 2243 N94-23578
KOBLENTS, B. .... p 2285 N94-22805
KOCH, STEVE .... p 2413 N94-24385
p 2413 N94-24391
KOCH, STEVEN .... p 2412 N94-24382
KOCH, STEVEN E. .... p 2410 N94-24374
KOCHER, H. R. .... p 2360 N94-24023
KOE, ERIC C. .... p 2204 N94-24620
KOEKER, I. .... p 2356 N94-23998
KOELMAN, R. J. .... p 2479 N94-23121
KOENIG, M. .... p 2316 N94-22860
KOERBER, G. .... p 2165 N94-23149
p 2165 N94-23161
KOFINAS, P. .... p 2263 N94-25413
KOFMAN, W. .... p 2608 N94-23393
KOHN, ROBERT .... p 2230 N94-25158
KOHOUT, LISA L. .... p 2395 N94-24071
KOJIMA, M. .... p 2369 N94-23402
KOKOLIOS, ALEX .... p 2164 N94-25109
KOKOTOFF, DAVID .... p 2365 N94-24699
KOKUBU, HIROSHI .... p 2480 N94-23141
KOLCZYNSKI, RAYMOND J. .... p 2346 N94-25502
KOLEN, A. W. J. .... p 2468 N94-24764
KOLEN, ANTOON .... p 2459 N94-24765
KOLITZ, STEPHAN E. .... p 2521 N94-25009
p 2522 N94-25012
KOLLER, F. .... p 2361 N94-24031
KOMATSU, SHIGENORI .... p 2509 N94-23903
KOMATSU, TOKUTARO .... p 2564 N94-24978
KOMINE, HIROSHI .... p 2344 N94-24360
KOMISSAROV, E. V. .... p 2463 N94-25432
KOMISSAROV, V. I. .... p 2369 N94-23374
KONCAK, KYLE .... p 2184 N94-25021
KONDOZ, A. M. .... p 2286 N94-22812
KONG, F. M. .... p 2252 N94-22931
KONISHI, YOSHIHIKO .... p 2279 N94-22769
KONO, KIMITOSHI .... p 2564 N94-24978
KOOI, J. W. .... p 2296 N94-24105
KOOLS, JACQUES CONSTANT STEFAN
p 2351 N94-25294
KOPEL, KIM .... p 2181 N94-24711
KOPPEL, L. N. .... p 2598 N94-24832
KORDESCH, MARTIN E. .... p 2263 N94-25489
KOREPANOV, G. N. .... p 2369 N94-23374
KORINKO, J. J. .... p 2244 N94-23792
KOROTKIKH, V. L. .... p 2539 N94-25476
KORSUNSKY, ALEXANDER M. .... p 2379 N94-25325
KORY, CAROL L. .... p 2310 N94-24056
KORZUN, RONALD W. .... p 2364 N94-24128
KOSANCHICK, MELVIN, III .... p 2181 N94-24591
KOSEK, J. .... p 2393 N94-23361
KOSLOSKY, JACK .... p 2197 N94-23843
KOSTER, M. P. .... p 2209 N94-24006
KOSUGI, S. .... p 2508 N94-23898
KOTOWSKI, M. .... p 2551 N94-23703
KOTTA, U. .... p 2447 N94-22711
KOTTHAUS, RAINER .... p 2314 N94-25457
KOUI, K. .... p 2567 N94-25412
KOUVARITAKIS, B. .... p 2476 N94-25428
p 2476 N94-25429
KOVTUNENKO, V. .... p 2607 N94-23384
KOWALCZYK, W. .... p 2585 N94-23761
p 2486 N94-23762
p 2487 N94-23765
KOWALCZYK, WOJCIECH .... p 2586 N94-24528

KOZLOV, G. V. p 2369 N94-23374
p 2370 N94-23418
KRAIMER, MARTIN p 2457 N94-24626
KRAMAR, JAMES p 2183 N94-24972
KRAMMER, J. p 2178 N94-24319
KRANTZ, TIMOTHY L. p 2367 N94-25181
KRASNOSELSKII, A. M. p 2479 N94-23106
KRASNOSELSKII, M. A. p 2479 N94-23106
KRASODOMSKI, H. p 2238 N94-22936
KRAUSE, S. p 2223 N94-24341
KRAUSS, A. R p 2562 N94-23805
KRAUSZ, A. S. p 2159 N94-24277
p 2161 N94-24289
KRAUSZ, K. p 2159 N94-24277
p 2161 N94-24289
KREJSA, EUGENE A. p 2525 N94-23464
KREMER, P. p 2297 N94-24296
KREMNEV, R. p 2607 N94-23384
KRENKEL, W. p 2256 N94-24238
KRESSEL, I. p 2157 N94-24262
KRESTOS, DEAN M. p 2261 N94-25072
KRISHNAN, SHANKAR p 2248 N94-25129
KRISTENSEN, P. G. p 2232 N94-23100
KROGER, SETH p 2181 N94-24711
KROLL, J. T. p 2481 N94-23593
KROM, KIMBERLY J. p 2444 N94-25371
KRONENBURG, M. J. p 2559 N94-23109
KROPP, JACK p 2598 N94-23536
KRUEGER, ARLIN J. p 2410 N94-24355
KRUEGER, DAVID L. p 2460 N94-24927
KRUEGER, STEVE p 2413 N94-24388
KRUIS, F. E. p 2347 N94-22982
KRUPA, MARTIN p 2480 N94-23141
KRUTZ, ROBERT W., JR. p 2436 N94-24204
KRUTZER, LAMBERTUS LEONARDUS MARIE
p 2267 N94-25060
KRUYER, WILLIAM B. p 2423 N94-23315
p 2423 N94-23317
KU, HWAR-CHING p 2341 N94-23693
KUCHNIR, M. p 2365 N94-24614
KUERTEN, HANS p 2342 N94-23694
KUERTEN, HANS G. M. p 2315 N94-22713
KUHL, A. L. p 2319 N94-23470
KUIJPER, ANDRE BAUKE p 2491 N94-25244
KUKKO, HEIKKI p 2379 N94-25529
KULANDER, K. C. p 2531 N94-22869
KULKARNI, S. p 2373 N94-24613
KULLAA, JYRKI p 2379 N94-25385
KUMAR, J. p 2258 N94-24732
p 2260 N94-24813
KUMAR, S. p 2559 N94-22995
KUNIN, BORIS I. p 2381 N94-24429
KUNZ, G. J. p 2406 N94-25540
KUNZE, K. p 2557 N94-22938
KUO, BILL p 2413 N94-24391
p 2414 N94-24399
KUO, K. K. p 2211 N94-23035
KUO, KENNETH p 2210 N94-23029
KUO, N. R. p 2501 N94-23853
KUPIAINEN, A. p 2489 N94-24610
KURBATOV, V. S. p 2463 N94-25432
KUSUNOSE, KINICHIRO p 2405 N94-24980
KUTEEV, BORIS V. p 2551 N94-24358
KUWATA, MASATO p 2479 N94-23139
KUWATA, YURI p 2405 N94-24980
KUZNETSOV, N. A. p 2479 N94-23106
KUZNETSOV, V. p 2370 N94-23420
KWAK, DO Y. p 2482 N94-23677
KWAN, ROBERT p 2273 N94-22735
p 2293 N94-23622
KWAN, ROBERT K. p 2293 N94-23627
p 2293 N94-23628
KWAN, SONNY p 2463 N94-25455
p 2463 N94-25456
KWARTA, JENNIFER S. p 2204 N94-24620
KYLE, K. R. p 2541 N94-22722
p 2234 N94-24549

L

LAAN, D. J. p 2178 N94-24322
LABEAUME, SERGE p 2296 N94-24118
LABERTRE, T. p 2599 N94-24780
LABEYRIE, ANTOINE p 2601 N94-23378
p 2369 N94-23405
LABRUYERE, G. p 2361 N94-24031
LABRUYERE, GILLES p 2359 N94-24015
LACHANCE, ROGER p 2186 N94-23253
LACIS, A. p 2616 N94-24372
LACKEY, W. J. p 2227 N94-23022
LACONTI, ANTHONY B. p 2392 N94-23358
p 2393 N94-23361
LADD, D. M. p 2338 N94-25140
LADOUCEUR, RICHARD J. p 2314 N94-25539
LAFE, OLU p 2325 N94-23666
LAGER, IOAN p 2298 N94-24637
LAHTAKIA, MERCEDES p 2413 N94-24387
LAI, C. C. p 2407 N94-23284
LAKSHMINARAYANA, B. p 2216 N94-23062
LAL, RAVINDRA p 2563 N94-24617
LAM, N. Q. p 2560 N94-23189
LAMAR, JOHN E. p 2166 N94-23512
LAMARRE, H. p 2369 N94-23400
LAMBA, JAYDEEP J. p 2260 N94-24922
LAMICH, G. J. p 2562 N94-23805
LAMICQ, P. p 2256 N94-24237
LAMOTHE, A. p 2369 N94-23400
LAMOUR, R. p 2481 N94-23439
LANAGAN, M. T. p 2563 N94-24624
LANCHO, M. p 2357 N94-24003
LAND, T. A. p 2232 N94-23298
LANDAU, UZIEL p 2393 N94-23360
LANDRUM, D. BRIAN p 2342 N94-24430
LANDSHOF, JOHN A. p 2504 N94-23874
LANDSMAN, WAYNE B. p 2599 N94-24666
LANE, A. L. p 2607 N94-23387
LANG, D. D. p 2549 N94-23013
LANG, STEPHEN p 2527 N94-24211
LANGEVIN, Y. p 2606 N94-23382
LANGRY, K. C. p 2541 N94-22722
LANIER, N. E. p 2549 N94-22949
LANU, MATTI p 2230 N94-25386
LANZI, R. JAMES p 2207 N94-23653
LAPEAN, J. p 2301 N94-25005
LAPLACE, H. p 2369 N94-23412
LAPOINTE, LINDA J. p 2461 N94-25156
LAPOINTE, MICHAEL R. p 2216 N94-23067
p 2219 N94-23555
p 2220 N94-24714
LARABIE, M. L. p 2629 N94-24695
LARNAC, GUY p 2254 N94-24129
LARSEN, NATHAN F. p 2529 N94-24222
LARSEN, POUL K. p 2565 N94-25027
LARSON, R. G. p 2472 N94-23300
LARSON, STEVEN A. p 2389 N94-23840
LARSSON, AKE p 2430 N94-23743
LARSSON, CURT p 2545 N94-24529
LARSSON, TOR p 2437 N94-24292
LASHER, WILLIAM C. p 2321 N94-23643
p 2326 N94-23669
LASLETT, L. J. p 2299 N94-24656
LASLEY, MARY L. p 2426 N94-23530
LASSAHN, G. D. p 2382 N94-23492
LASSAHN, GORDON D. p 2345 N94-24831
LASSITER, CARROLL B. p 2423 N94-25368
LATELLA, D. p 2493 N94-23108
LATIF, MOJIB p 2382 N94-23158
p 2401 N94-23159
p 2407 N94-23199
LAU, KAI-HUNG p 2232 N94-23477
LAU, WAI-MAN p 2421 N94-24294
LAU, Y. X. H. p 2463 N94-25468
LAUDERDALE, JACK p 2197 N94-23843
LAUE, H. A. p 2508 N94-23897
LAUER, J. L. p 2364 N94-24090
LAUGHON, G. J. p 2354 N94-23797
LAUGIER, CHRISTIAN p 2371 N94-23426
LAURITSEN, JANET p 2272 N94-23892
LAVADOUX, M. p 2359 N94-24014
LAW, B. p 2307 N94-23008
p 2471 N94-23011
LAWLER, KATHLEEN p 2182 N94-24837
LE, XUAN-TRANG p 2209 N94-24840
LEBO, M. R. p 2244 N94-23792
LEBOEUF, RICHARD L. p 2331 N94-24162
LEBOVITZ, H. p 2157 N94-24262
LEDBETTER, K. W. p 2519 N94-23960
LEDBETTER, KENNETH W. p 2505 N94-23880
LEDER, A. p 2315 N94-22853
LEDUC, H. G. p 2296 N94-24105
LEE, CHANG OCK p 2485 N94-23695
LEE, D. E. p 2321 N94-23640
LEE, HOSAE p 2464 N94-23696
LEE, L. F. p 2292 N94-23267
LEE, L. L. p 2535 N94-24569
LEE, LORRINE p 2197 N94-23902
LEE, LORRINE F. p 2305 N94-23915
LEE, M. p 2275 N94-22746
LEE, PAUL S. C. p 2306 N94-25494
LEE, RICHARD Q. p 2310 N94-24308
LEE, ROBERT B., III p 2384 N94-23602
LEE, S. R. p 2559 N94-22995
LEE, S. W. p 2300 N94-24678
p 2618 N94-24878
p 2619 N94-24887
LEE, SANGSAN p 2332 N94-24165
LEE, Y. W. p 2235 N94-24784
LEEMIS, LAWRENCE p 2458 N94-24680
LEGGETT, DAVID B. p 2163 N94-25106
LEHMANN, P. p 2314 N94-25460
LEHNA, H. p 2269 N94-23586
LEHTIMAEKI, R. p 2318 N94-23115
LEI, XINGLIN p 2405 N94-24980
LEIBEE, JACK p 2464 N94-23893
LEIBOVICH, H. p 2156 N94-24259
p 2160 N94-24278
LEIBOWITZ, HERSCHEL W. p 2429 N94-23979
LEIDHOLM, C. p 2390 N94-23296
LEISSLER, GEORGE W. p 2242 N94-23467
LEMAIRE, P. p 2624 N94-22843
LEMAY, CHRISTOPHER S. p 2444 N94-25375
LEMKE, MAX p 2469 N94-23697
LEMOGNE, T. p 2361 N94-24033
LEMOINE, F. G. p 2401 N94-23282
LENSELINK, H. p 2154 N94-24246
LENSTRA, J. K. p 2467 N94-23756
p 2467 N94-23767
LENZ, T. G. p 2568 N94-22719
LEONARD, B. P. p 2168 N94-24084
LEONARD, ROBERT E., JR. p 2516 N94-23941
LEOVY, CONWAY B. p 2620 N94-24888
LEPPLA, FRANK p 2520 N94-23963
LERCH, F. J. p 2401 N94-23282
LERNER, M. S. p 2599 N94-23705
LESLIE, THOMAS M. p 2225 N94-24349
LESNEWSKI, DAVID p 2190 N94-24957
p 2183 N94-24969
LESSARD, OSCAR J. p 2539 N94-25519
LESTRADE, JOHN PATRICK p 2579 N94-24431
p 2629 N94-25199
LESUER, D. R. p 2228 N94-23493
LETOURNEAU, JEAN p 2186 N94-23253
LETT, PAT p 2205 N94-24702
LEURS, C. P. W. p 2361 N94-24035
LEVAN, P. D. p 2406 N94-25535
LEVCHENKO, B. B. p 2541 N94-25342
LEVERSON, DENIS p 2288 N94-22828
LEVESQUE, ALLEN H. p 2276 N94-22754
LEVESQUE, DANIEL p 2298 N94-24582
LEVESQUE, MICHAEL E. p 2506 N94-23883
LEVI, D. p 2452 N94-23518
LEVIN, B. F. p 2258 N94-24749
LEVIN, E. M. p 2156 N94-24256
LEVIN, LON C. p 2275 N94-22748
LEVITAS, J. p 2160 N94-24280
LEWIS, JAMES L., JR. p 2434 N94-24191
LEWIS, M. H. p 2256 N94-24236
LEWIS, N. p 2238 N94-22936
LEWIS, R. A. p 2217 N94-23069
LEWIS, ROBERT p 2433 N94-24187
LEWIS, STEPHEN R. p 2619 N94-24886
p 2620 N94-24889
LEWIS, STEVEN p 2457 N94-24626
LHALLABI, T. p 2491 N94-25166
LI, G. p 2296 N94-24132
p 2300 N94-24697
LI, H. S. p 2279 N94-22770
LI, HAIKUAN p 2592 N94-24646
LI, L. p 2258 N94-24732
p 2260 N94-24813
LI, RAY p 2206 N94-24916
LI, Y. Y. p 2239 N94-22999
LI, Z. p 2557 N94-22927
LIANG, D. F. p 2174 N94-24120
LIAO, JIANQIAO p 2433 N94-24171
LIBAI, A. p 2160 N94-24281
LICHTEN, S. M. p 2196 N94-23257
p 2196 N94-23258
LIEBERT, CURT H. p 2344 N94-24069
LIEGEOIS, A. p 2370 N94-23423
LIEN, T. K. p 2355 N94-23988
LIENEWEG, UDO p 2310 N94-23821
LIGHTFOOT, A. p 2255 N94-24223
LIGLER, FRANCES S. p 2344 N94-24723
LILLEY, GEOFFREY M. p 2333 N94-24356
LILLEY, STEWART p 2195 N94-24995
LILLIBRIDGE, MARK p 2458 N94-24693
LIMAYE, SANJAY S. p 2620 N94-24890
LIMBER, MARK p 2418 N94-24671
LIN, H. D. p 2279 N94-22770
LIN, K. T. p 2283 N94-22794
LIN, M. C. p 2235 N94-24917
LIN, X.-A. p 2325 N94-23667
LIN, Y. p 2562 N94-23805
LINDELL, I. p 2524 N94-23131
LINDELL, I. V. p 2524 N94-23110
LINDEMANN, RANDEL A. p 2370 N94-23425
LINDENBAUM, S. J. p 2531 N94-22923
LINDERSSON, KJELL p 2544 N94-23723
LINDSAY, CURT p 2183 N94-24971
LINDSEY, MARTIN p 2206 N94-24916
LINDSEY, PATRICIA F. p 2198 N94-24432
LINDSTROM, MARILYN M. p 2616 N94-24373
LINDSTROM, SCOTT S. p 2418 N94-24795
LINICK, SUSAN H. p 2305 N94-23870
LINKIN, V. M. p 2606 N94-23381
p 2369 N94-23395
p 2608 N94-23396

p 2370 N94-23416
p 2370 N94-23417
LINNALUOTO, S. p 2444 N94-23754
LIOU, MENG-SING p 2338 N94-25180
LIOU, WILLIAM W. p 2333 N94-24336
p 2336 N94-24713
LIPINSKI, R. J. p 2348 N94-23185
LIPPERT, BUDDY O. p 2434 N94-24191
LIPPERT, K. B. p 2562 N94-23535
LIPSKIN, BETH ANN p 2598 N94-25006
LISCINSKY, D. S. p 2188 N94-24594
LISSAUER, D. p 2532 N94-23007
LISSOL, PETER p 2192 N94-23310
LISTGARTEN, SHERRY p 2452 N94-23510
LITES, B. W. p 2624 N94-22838
LITT, MORTON p 2393 N94-23360
LITTLEFIELD, RONALD p 2520 N94-23964
LITTMANN, F. p 2369 N94-23403
LIU, GENG p 2322 N94-23646
LIU, KUN p 2462 N94-25252
LIU, RONG-CHUAN p 2566 N94-25332
LIU, SIUYING RAYMOND p 2543 N94-23529
LIUKKONEN, J. p 2450 N94-23226
LIZANICH, PAUL J. p 2295 N94-24101
LO, MARTIN W. p 2503 N94-23867
LOCH, JOHN p 2371 N94-23427
LOCKE, PAUL A. p 2281 N94-22782
LOCKWOOD, JAMES C. p 2302 N94-25048
LOCKYER, PAUL p 2503 N94-23868
LODGE, J. H. p 2286 N94-22815
LOEHMAN, RONALD E. p 2244 N94-23811
LOESCH, RENA M. p 2311 N94-24685
LOFTUS, JOSEPH P., JR. p 2598 N94-24644
LOGALBO, P. p 2273 N94-22737
LOGAN, R. W. p 2229 N94-24632
LOGNONNE, P. p 2606 N94-23382
LOHNER, RAINOLD p 2338 N94-25157
LOIGOM, VILLEM p 2308 N94-23104
LONDON, R. A. p 2541 N94-22868
LONG, WILLIAM H. p 2344 N94-24360
LOO, JAMES p 2296 N94-24118
LOOBY, BRENT p 2438 N94-24667
LOOMIS, B. A. p 2238 N94-22718
p 2240 N94-23009
p 2240 N94-23194
LOONG, C. K. p 2252 N94-22992
LOOS, B. p 2242 N94-23496
p 2397 N94-23497
LORBER, PETER p 2181 N94-24796
LORENZ, E. p 2600 N94-25458
LORETTO, D. p 2564 N94-24657
LOTT, J. A. p 2350 N94-24659
LOUGHIN, S. p 2243 N94-23753
LOUIE, JOHN J. p 2506 N94-23885
LOVESEY, STEPHEN W. p 2524 N94-24533
LOW, SCOTT L. p 2335 N94-24640
LOWE, T. C. p 2245 N94-24520
LOY, T. p 2316 N94-22859
LOYENS, LUDOVICUS DANIEL JOSEPH C.
p 2469 N94-25282
LU, LI-DAI p 2438 N94-24331
LU, ZHONG-YI p 2567 N94-25426
LUCIANI, ANNIE p 2371 N94-23426
LUCK, ROGELIO p 2320 N94-23637
LUCZAK, EDWARD C. p 2516 N94-23945
LUDLAGE, J. H. A. p 2489 N94-24608
p 2474 N94-24609
LUE, J. W. p 2271 N94-24568
LUGT, PIETER MARTIN p 2262 N94-25230
LUKE, JAMES P. p 2191 N94-25525
LUMLEY, JOHN L. p 2326 N94-24063
LUND, THOMAS S. p 2328 N94-24146
LUNDGREN, THOMAS S. p 2331 N94-24161
LUNDIN, ENRICO p 2437 N94-24292
LUNDIN, JAN-ERIK p 2544 N94-24489
LUO, ERDING p 2484 N94-23685
LUO, H. A. p 2377 N94-24604
LUO, J. p 2216 N94-23062
LUOMA, G. A. p 2455 N94-24122
LUONG, CHRISTINA p 2598 N94-23536
LUPISELLA, MARK p 2464 N94-23893
LUPPES, R. p 2401 N94-23175
LUSK, E. L. p 2420 N94-23468
LUSTIG, J. p 2156 N94-24255
LUTHER, R. F. p 2244 N94-23792
LUXEMBURG, LEON A. p 2477 N94-24433
LUZDEMATEO, MARIA p 2284 N94-22801
LY, UY-LOI p 2472 N94-23332
LYNCH, DANA H. p 2543 N94-23309
LYNN, SEAN R. p 2180 N94-24479
LYON, DONALD p 2298 N94-24582
LYON, J. F. p 2548 N94-22916
p 2550 N94-23462
LYTTON, DAVID W. p 2505 N94-23877

M

MA, CHANGXUE p 2302 N94-25077
MA, J. p 2491 N94-24947
MAAG, CARL R. p 2207 N94-23596
MAAYOUF, R. M. A. p 2566 N94-25347
MACCAULY, LINDA E. p 2201 N94-24965
MACCHION, D. p 2508 N94-23899
MACCONOCHIE, IAN O. p 2170 N94-24716
MACDONALD, DIGBY D. p 2391 N94-23349
MACDONALD, J. W. p 2202 N94-24121
MACDONNELL, DAVID p 2206 N94-25007
MACGOWAN, B. J. p 2347 N94-22867
p 2551 N94-23703
MACKAMUL, K. p 2390 N94-23295
MACKENZIE, P. D. p 2466 N94-23491
MACKOWSKI, DANIEL W. p 2223 N94-24340
MACOUGHTRY, WILLIAM p 2519 N94-23961
MACRANDER, A. T. p 2560 N94-23187
p 2560 N94-23188
MADDEN, M. J. p 2356 N94-23997
MADDOCKS, M. C. D. p 2295 N94-24086
MADHUKAR, ANUPAM p 2474 N94-24622
MADILL, DONALD H. p 2285 N94-22806
MADRID, G. p 2500 N94-23845
MADSEN, BROOKS C. p 2422 N94-23241
MAEDA, H. p 2554 N94-25327
MAEDA, T. p 2607 N94-23389
MAEDA, TOSHIHIDE p 2608 N94-23390
MAERZ, R. p 2481 N94-23439
MAESTRELLO, LUCIO p 2334 N94-24605
MAGEE, MICHAEL p 2444 N94-25369
MAGNI, J. F. p 2474 N94-24627
MAGNUSSEN, B. F. p 2269 N94-23506
MAH, G. R. p 2280 N94-22776
MAHAJAN, S. p 2604 N94-25215
MAHDAVI, M. A. p 2354 N94-23797
MAHLE, CHRISTOPH E. p 2293 N94-23622
p 2293 N94-23627
p 2293 N94-23628
MAHMOT, RON p 2197 N94-23843
MAHMOT, RONALD p 2510 N94-23905
MAHON, RITA p 2545 N94-24672
MAIDA, JAMES p 2437 N94-24205
p 2437 N94-24206
MAIER-REIMER, E. p 2407 N94-23156
MAIER-REIMER, ERNST p 2401 N94-23159
MAILHOT, JOCELYN p 2413 N94-24385
MAILLAT, M. p 2355 N94-23990
p 2360 N94-24023
MAINGI, R. p 2354 N94-23797
MAKARIOU, C. C. p 2354 N94-23797
MAKOWSKI, M. A. p 2209 N94-23012
MALAVE-SANABRIA, TANIA p 2218 N94-23370
MALEKI, LUTFOLLAH p 2543 N94-23270
MALENKOV, V. I. p 2369 N94-23374
MALIN, JANE T. p 2473 N94-24068
MALKIN, I. p 2156 N94-24255
MALLA, R. P. p 2196 N94-23257
MALLADI, NARASIMHA p 2368 N94-23242
MALLON, BOB p 2180 N94-24498
MALOAN, J. p 2437 N94-24299
MALONE, R. C. p 2417 N94-23517
MALONEY, T. F. p 2588 N94-22863
MALOZCNOFF, A. P. p 2556 N94-22886
MALTBY, P. p 2623 N94-22837
MANAHAN, MEERA p 2433 N94-24186
MANAHAN, ORLANDO p 2183 N94-24972
MANDELBROT, BENOIT B. p 2523 N94-24936
MANDL, DANIEL p 2197 N94-23843
p 2507 N94-23890
p 2203 N94-23947
MANDREKAS, J. p 2553 N94-24628
MANI, S. p 2307 N94-22955
MANKO, DAVID J. p 2393 N94-23359
MANN, J. ADIN, JR. p 2249 N94-25133
MANNINEN, A. p 2523 N94-23101
MANNING, CAROL A. p 2176 N94-25444
MANOBIANCO, JOHN p 2416 N94-25271
MANOBIANCO, JOHN T. p 2408 N94-23576
MANOFF, S. p 2571 N94-25339
MANSELL, JUSTIN D. p 2222 N94-25201
MANSOUR, N. N. p 2331 N94-24161
MANSOUR, NAGI N. p 2330 N94-24152
MANTEL, T. p 2331 N94-24157
MANTEUFFEL, T. A. p 2482 N94-23673
MANTOVANI, JAMES G. p 2631 N94-24493
MANYIKA, JAMES M. p 2472 N94-23179
MANZELLA, DAVID H. p 2219 N94-24361
MAO, WEIZHEN p 2451 N94-23341
MAPLE, M. B. p 2558 N94-22941
MARANDA, B. H. p 2455 N94-24130
MARCELIN, G. p 2398 N94-23818
MARCHELLO, J. M. p 2254 N94-23486
MARCHIONINI, GARY p 2594 N94-25487
MARCZYK, J. p 2357 N94-24003
MARDER, A. R. p 2258 N94-24749
MARDER, SETH R. p 2226 N94-24354
MARGERUM, EUGENE A. p 2493 N94-25452
MARK, MARTIN B. p 2547 N94-25161
MARKEY, JIM p 2399 N94-24525
MARKOSKY, L. A. p 2532 N94-23018
MARMOLEJO, JOSE A. p 2434 N94-24192
MAROLEWSKI, T. A. p 2258 N94-24753
MARRION, CHRISTOPHER J. p 2393 N94-23364
MARSH, S. FREDRIC p 2535 N94-24505
MARSHALL, MADELEINE H. p 2504 N94-23874
MARSHALL, ORANGE S., JR. p 2373 N94-24814
MARSHALL, T. C. p 2349 N94-23702
MARSTON, P. C. p 2278 N94-22767
MARTHINSEN, K. p 2561 N94-23503
p 2533 N94-23505
p 2562 N94-23535
MARTHINUSS, J. p 2559 N94-23186
MARTIC, M. p 2625 N94-22848
MARTIN, BOB p 2383 N94-23598
MARTIN, C. p 2289 N94-22833
MARTIN, C. R. p 2263 N94-25409
MARTIN, DANIEL p 2510 N94-23906
MARTIN, DAVID C. p 2223 N94-24342
MARTIN, J. M. p 2361 N94-24033
MARTIN, JAMES A. p 2199 N94-24434
MARTIN, JENNIFER p 2183 N94-25001
MARTIN, LEONARD J. p 2620 N94-24891
MARTIN, PHILIPPE p 2470 N94-22884
MARTIN, S. J. p 2526 N94-23718
MARTIN, SCOTT p 2158 N94-24270
MARTIN, TERRY Z. p 2620 N94-24892
MARTIN, THOMAS J. p 2322 N94-23645
p 2325 N94-23665
MARTINET, BERNARD p 2445 N94-23153
MARTINEZ, A. p 2357 N94-24003
MARTINEZ, ANDREW O. p 2420 N94-23633
MARTINOV, B. p 2609 N94-23397
MARTINOV, B. N. p 2369 N94-23374
MARTNER, B. E. p 2381 N94-23001
MARTURUNKAKUL, S. p 2258 N94-24732
MARTZ, H. F. p 2569 N94-24516
MARUSCHEK, JOSEPH W. p 2310 N94-24056
MARWICK, A. D. p 2556 N94-22886
MASAD, JAMAL A. p 2336 N94-24725
MASAI, KUNIAKI p 2602 N94-24866
p 2602 N94-24867
MASERJIAN, JOSEPH p 2310 N94-23821
MASKALICK, N. J. p 2395 N94-23785
MASON, A. J. p 2295 N94-24085
MASSA p 2599 N94-24051
MASSON, P. p 2606 N94-23382
MASTEJ, NICOLE p 2183 N94-25001
MASUDA, KAORU p 2271 N94-24459
MASULLO, S. p 2515 N94-23935
MATEJKA, L. A., JR. p 2589 N94-22944
MATHES, KAREN L. p 2426 N94-23530
MATIKAS, THEODORE E. p 2257 N94-24240
MATOVIC, D. p 2341 N94-23675
MATSUDO, TAKASHI p 2284 N94-22797
MATSUMOTO, K. p 2370 N94-23415
MATTEIS, RICHARD M., JR. p 2202 N94-23631
MATTERN, DUANE p 2190 N94-23590
MATTHEIJ, R. M. M. p 2481 N94-23439
MATTHEWS, B. L. p 2178 N94-24321
MATTHEWS, BRIAN p 2456 N94-24534
MATTHEWS, ELAINE p 2381 N94-24800
MATTIG, W. p 2624 N94-22840
MATTSON, J. E. p 2559 N94-22995
MATUSKA, DAVID p 2181 N94-24796
MATYAS, R. p 2277 N94-22758
MAUGHAN, J. R. p 2187 N94-23709
MAURER, ALEXA p 2209 N94-24840
MAUS, DARYL p 2355 N94-23987
MAVRIPLIS, C. p 2490 N94-24914
MAY, R. p 2540 N94-24662
MAYER, S. T. p 2252 N94-22931
MAYFIELD, M. J. p 2394 N94-23781
MAYO, R. M. p 2218 N94-23283
MAZELSKY, R. p 2225 N94-24348
MCALISTER, K. W. p 2171 N94-25187
MCALISTER, KENNETH W. p 2543 N94-23309
MCATEE, AARON p 2183 N94-24971
MCBANE, DOUG p 2181 N94-24787
MCBREEN, J. p 2389 N94-22962
p 2234 N94-24545
MCCANDLESS, B. E. p 2389 N94-22862
MCCARTHY, A. M. p 2309 N94-23520
MCCARTY, JON G. p 2232 N94-23477
MCCATTY, STEPHEN A. p 2392 N94-23358
MCCLEESE, DANIEL J. p 2623 N94-24904
MCCLINTOCK, R. p 2559 N94-23186
MCCONNAUGHEY, P. K. p 2214 N94-23054
MCCORMICK, S. F. p 2482 N94-23673
MCCUNN, CARRIE J. p 2459 N94-24812

MCDONALD, M. J. .... p 2472 N94-23201
MCDONNELL, J. R. .... p 2490 N94-24921
MCDONNELL, JOHN R. .... p 2496 N94-24778
p 2475 N94-25139
MCELROY, JAMES F. .... p 2393 N94-23362
MCFADDEN, P. D. .... p 2353 N94-23178
MCGLADE, DESMOND P. .... p 2173 N94-24781
MCGRAW, MARVIN E., JR. .... p 2169 N94-24311
MCGUIRK, JAMES P. .... p 2408 N94-23577
p 2408 N94-23619
p 2409 N94-23621
MCHARGUE, C. J. .... p 2543 N94-23458
MCINTOSH, ROBERT E. .... p 2419 N94-24944
MCINTYRE, C. M. .... p 2202 N94-24121
MCINTYRE, DAVID .... p 2536 N94-24717
MCINTYRE, JAMES .... p 2520 N94-23966
MCKAY, MICHAEL H. .... p 2517 N94-23951
MCKEE, SANDRA D. .... p 2434 N94-24191
MCKENNA, VICTORIA JONES .... p 2196 N94-24309
MCKENZIE, A. J. .... p 2455 N94-24122
MCKNIGHT, ROBERT C. .... p 2153 N94-24100
MCKNIGHT, WILLIAM H. .... p 2312 N94-25042
MCLANE, P. J. .... p 2285 N94-22805
MCLAUCHLAN, PHILIP F. .... p 2593 N94-25326
p 2346 N94-25472
MCLEAN, A. N. .... p 2285 N94-22807
MCLEAN, DAVID .... p 2520 N94-23964
p 2520 N94-23966
MCLEAN, T. .... p 2629 N94-24695
MCMAHAN, ROBERT .... p 2439 N94-24835
p 2439 N94-24956
MCMANIGLE, A. P. .... p 2242 N94-23475
MCMANUS, HUGH L. .... p 2229 N94-24579
MCMASTERS, DALE .... p 2313 N94-25276
MCMATH, W. S. .... p 2370 N94-23421
MCMICHAEL, L. D. .... p 2229 N94-24632
MCMILLAN, SCOTT .... p 2438 N94-24667
MCMILLAN, W. WALLACE .... p 2620 N94-24893
MCMINN, JOHN D. .... p 2163 N94-25104
p 2164 N94-25113
MCNAMARA, BERNARD .... p 2580 N94-24435
MCNEIL, STEPHEN .... p 2276 N94-22753
MCNENNY, ROBERT .... p 2272 N94-23892
MCPETERS, RICHARD D. .... p 2410 N94-24355
MCQUARRIE, ALLAN D. .... p 2406 N94-25538
MCQUEEN, ROY D. .... p 2192 N94-24072
MCVEY, JOHN B. .... p 2234 N94-24565
MCWHORTER, P. .... p 2342 N94-22954
p 2343 N94-23200
MCWILLIAMS, DENNIS .... p 2205 N94-24702
MEAD, JAYLEE M. .... p 2600 N94-25387
MEADE, ANDREW J. .... p 2477 N94-25370
MEASURES, CHRIS .... p 2419 N94-25164
MEESTERS, GABRIEL MARINUS HENRICUS
p 2338 N94-25227
MEGSON, G. M. .... p 2474 N94-24544
MEGUID, S. A. .... p 2244 N94-24170
MEHOLIC, GREG .... p 2179 N94-24332
p 2190 N94-24551
p 2184 N94-25004
MEHROTRA, PIYUSH .... p 2448 N94-23092
MEHTA, NARINDER K. .... p 2264 N94-23243
MEHTA, S. .... p 2451 N94-23301
MELKO, JOSEPH P. .... p 2614 N94-24333
MELLQVIST, JOHAN .... p 2402 N94-24108
MELLSTROM, J. A. .... p 2292 N94-23268
MELSON, N. DUANE .... p 2482 N94-23673
MENDE, STEPHEN B. .... p 2550 N94-23565
MENDELBOIM, TAL .... p 2157 N94-24265
MENDOZA, SAUL .... p 2182 N94-24966
MENG, RUIBIN .... p 2534 N94-23806
MENOLASCINO, R. .... p 2277 N94-22760
MENON, M. M. .... p 2354 N94-23797
MENON, V. .... p 2263 N94-25409
MENSAH, S. Y. .... p 2568 N94-25447
MENU, JEAN-PIERRE .... p 2431 N94-23978
MEREDITH, T. .... p 2266 N94-23657
MERENICH, J. J. .... p 2212 N94-23040
MERKLE, CHARLES L. .... p 2210 N94-23033
p 2213 N94-23046
p 2214 N94-23050
p 2215 N94-23055
p 2215 N94-23060
p 2216 N94-23066
MERKLE, K. L. .... p 2558 N94-22990
MERMELSTEIN, MARC D. .... p 2545 N94-24722
MERMINGA, L. .... p 2540 N94-24662
MEROLLA, ANTHONY .... p 2395 N94-24071
MERSCH, G. B. .... p 2361 N94-24035
MESSER, DION D. .... p 2273 N94-22736
MESSER, JOHN .... p 2527 N94-24212
MESSINA, M. J. .... p 2473 N94-24518
METCALF, D. .... p 2390 N94-23295
METZGER, M. .... p 2235 N94-24784
MEYER, F. W. .... p 2532 N94-22956
MEYER, J. J. C. .... p 2478 N94-22984
p 2473 N94-23747
p 2473 N94-23748
MEYER, M. K. .... p 2227 N94-22977
MEYER, MICHAEL L. .... p 2213 N94-23049
MEYER, RUDOLF X. .... p 2614 N94-24333
MEYERS, C. .... p 2376 N94-23342
MEZAACHE, AHMED L. .... p 2417 N94-23291
MICAELLI, ALAIN .... p 2370 N94-23424
MICCI, M. M. .... p 2213 N94-23047
p 2216 N94-23065
MICCOLIS, LAWRENCE E. .... p 2186 N94-24774
MICHALSKE, T. A. .... p 2234 N94-24772
p 2565 N94-25086
MICHALUK, C. .... p 2242 N94-23541
MICHELS, JAMES H. .... p 2496 N94-24951
MICKELSEN, R. A. .... p 2560 N94-23205
MICOCCI, ANGELO .... p 2434 N94-24193
MIKLOSOVIC, DAVE .... p 2323 N94-23650
MIKOLAJEWICZ, U. .... p 2407 N94-23156
MIKROS, EFTHIMIOS .... p 2299 N94-24670
MIKROVAS, A. C. .... p 2247 N94-25127
MIKULAS, MARTIN M., JR. .... p 2376 N94-23560
MILES, GAINES E. .... p 2444 N94-25371
MILES, RALPH F., JR. .... p 2374 N94-23939
MILGRAM, PAUL .... p 2433 N94-24171
MILLER, CHRISTOPHER J. .... p 2187 N94-23545
MILLER, D. P. .... p 2607 N94-23387
MILLER, DAVID P. .... p 2464 N94-23410
p 2371 N94-23427
MILLER, ED .... p 2383 N94-23598
MILLER, GEORGE, III .... p 2534 N94-24487
MILLER, JOEL B. .... p 2537 N94-25047
MILLER, K. B. .... p 2397 N94-23016
MILLER, KEVIN J. .... p 2506 N94-23885
MILLER, MARK D. .... p 2249 N94-25142
MILLER, N. .... p 2275 N94-22746
MILLER, NEIL E. .... p 2426 N94-24102
MILLER, R. L. .... p 2553 N94-24628
MILLER, ROBERT A. .... p 2242 N94-23467
MILLIGAN, J. .... p 2522 N94-25014
MILLIKEN, SAMUEL .... p 2278 N94-22763
MILLS, D. M. .... p 2545 N94-24550
MILLS, W. J. .... p 2244 N94-23792
MIMIS, VASSILIOS .... p 2276 N94-22753
MIMURA, KOJIRO .... p 2345 N94-24977
MINAMISONO, KENICHI .... p 2284 N94-22797
MINECK, RAYMOND E. .... p 2169 N94-24586
MINNIX, JAY .... p 2520 N94-23965
MINTZER, S. .... p 2239 N94-22965
MINUCCI, MARCO A. S. .... p 2154 N94-24247
MINUTO, JUAN C. .... p 2299 N94-24669
MISCHLER, JOHN .... p 2321 N94-23643
MISHKINYUK, V. .... p 2370 N94-23420
MISHKINYUK, V. K. .... p 2369 N94-23374
MISIEWICZ, J. K. .... p 2486 N94-23758
MISRA, AJAY K. .... p 2243 N94-23556
MISTR, E. KIRK .... p 2180 N94-24479
MISTRETTA, I. .... p 2282 N94-22789
MITCHELL, CHRISTINE M. .... p 2443 N94-23929
p 2459 N94-24797
MITCHELL, DOMINIQUE .... p 2204 N94-24621
MITCHELL, KENNETH .... p 2413 N94-24385
MITCHELL, R. .... p 2438 N94-24706
MITCHELL, R. E. .... p 2342 N94-22989
MITCHELL, R. L. .... p 2389 N94-22888
MITCHELL, T. E. .... p 2563 N94-24517
MITO, TOSHIYUKI .... p 2271 N94-24459
MITROVICA, J. X. .... p 2405 N94-25205
MITSCHDOERFER, P. .... p 2502 N94-23858
MITSKEVICH, A. V. .... p 2369 N94-23374
MIURA, NOBORU .... p 2564 N94-24959
p 2568 N94-25515
MIURA, Y. .... p 2606 N94-23379
MIYAKAWA, Y. .... p 2360 N94-24021
MIYAKE, YOSHIAKI .... p 2188 N94-24490
MIZUKAMI, M. .... p 2326 N94-23670
MIZUSAWA, E. A. .... p 2541 N94-22722
MIZUTA, HIROSHI .... p 2510 N94-23906
MIZZI, JEAN-PAUL .... p 2352 N94-22885
MOCELLIN, ANNICK .... p 2239 N94-22972
MOCHRIE, S. G. J. .... p 2245 N94-24612
MOCIO, JIM .... p 2221 N94-24834
MOE, KAREN L. .... p 2520 N94-23965
MOEBIUS, E. .... p 2624 N94-22841
MOEHRING, W. .... p 2318 N94-23198
MOENG, CHIN-HOH .... p 2413 N94-24388
p 2414 N94-24396
MOERLAND, P. D. .... p 2454 N94-23768
MOFFA, P. J. .... p 2306 N94-25498
MOHR, D. L. .... p 2227 N94-23022
MOIN, PARVIZ .... p 2327 N94-24139
p 2171 N94-24143
MOK, B. K. K. .... p 2373 N94-25475
MOLENKAMP, E. .... p 2454 N94-23750
MOLINARI, JOHN .... p 2413 N94-24386
MOLLER, P. .... p 2277 N94-22758
MOLNAR, PETER H. .... p 2175 N94-24826
MOLZOW, M. .... p 2178 N94-24323
MONCRIEFF, MITCH .... p 2411 N94-24377
p 2413 N94-24386
MONDELLO, G. .... p 2357 N94-24002
MONDIER, J. B. .... p 2369 N94-23404
MONGAN, PHILIP T. .... p 2205 N94-24625
MONROE, D. K. .... p 2348 N94-23185
MONTAGUE, S. .... p 2343 N94-23200
MONTEMERLO, MEL .... p 2370 N94-23414
MONTENBRUCK, O. .... p 2464 N94-23927
MONTGOMERY, RONALD W. .... p 2426 N94-23623
MOODY, DAVID .... p 2204 N94-23828
MOODY, H. .... p 2278 N94-22766
MOOG, C. H. .... p 2475 N94-24755
MOONEY, G. D. .... p 2389 N94-22888
MOORE, C. .... p 2224 N94-24343
MOORE, C. E. .... p 2223 N94-24338
MOORE, ERVETTE P. .... p 2435 N94-24198
MOORE, FRANK G. .... p 2171 N94-25411
MOORE, J. D. .... p 2322 N94-23648
MOORE, LORETTA A. .... p 2198 N94-24436
MOORE, RICHARD K. .... p 2409 N94-24048
p 2409 N94-24087
p 2410 N94-24126
MOORE, WENDY A. .... p 2195 N94-24497
MORALES, WILFREDO .... p 2253 N94-23371
MORCHAT, RICHARD M. .... p 2266 N94-24728
p 2262 N94-25136
MORELIERE, M. .... p 2369 N94-23412
MORELLI, EUGENE A. .... p 2164 N94-25110
MORENO, J. C. .... p 2347 N94-22867
MORGAN, JOHN C. .... p 2529 N94-24220
MORGAN, R. G. .... p 2319 N94-23513
p 2320 N94-23532
MORGAN, STEVE .... p 2422 N94-24810
MORI, SHIGEYUKI .... p 2405 N94-24980
MORIARITY, DEBRA M. .... p 2422 N94-24437
MORIARTY, MICHAEL P. .... p 2219 N94-24061
MORIN, GREG .... p 2181 N94-24787
MORISHITA, SUSUMU .... p 2188 N94-24490
MORITSCH, HANS .... p 2448 N94-23092
MORLANS, R. .... p 2370 N94-23423
MORREN, SYBIL .... p 2210 N94-23030
MORRIS, JOSEPH H. .... p 2367 N94-25055
MORRISETT, GREG .... p 2467 N94-24692
MORRISON, ANDREW D. .... p 2389 N94-23840
MORRISON, DONALD A. .... p 2605 N94-23376
MORRISON, LARRY M. .... p 2301 N94-25040
p 2301 N94-25041
MORT, NIEL .... p 2476 N94-25307
MOSER, A. .... p 2492 N94-25310
MOSER, M. D. .... p 2212 N94-23040
MOSES, R. W. .... p 2218 N94-23283
MOSKALIK, STEVE .... p 2179 N94-24401
MOSLEHY, FAISSAL A. .... p 2201 N94-24919
MOTOJIMA, O. .... p 2553 N94-24623
MOTTADASILVA, JOSE R. .... p 2530 N94-25073
MOULDER, RON .... p 2259 N94-24788
MOULTON, MARC L. .... p 2312 N94-25039
MOUNT, FRANCIS E. .... p 2434 N94-24191
MOURA, D. .... p 2606 N94-23382
MOUYON, P. .... p 2474 N94-24627
MOYA, J. L. .... p 2268 N94-23000
MOYNIHAN, GARY P. .... p 2429 N94-24438
MUDAMBI, S. .... p 2420 N94-23468
MUEHLRATZER, A. .... p 2256 N94-24239
MUELLER, C. .... p 2305 N94-23909
MUELLER, D. C. .... p 2266 N94-24700
MUELLER, DONN C. .... p 2210 N94-23031
MUELLER, PETER .... p 2419 N94-24948
MUENCHOW, L. .... p 2539 N94-25477
MUGNUOLO, R. .... p 2369 N94-23399
MULHOLLAND, K. .... p 2589 N94-23126
MULLER, G. .... p 2359 N94-24016
MUNDY, J. L. .... p 2464 N94-25471
MUNOZ-GARCIA, SAMUEL G. .... p 2274 N94-22743
MUNOZ, M. E. .... p 2523 N94-25328
MUR, G. .... p 2294 N94-23727
p 2294 N94-23733
MUR, GERRIT .... p 2298 N94-24597
p 2298 N94-24637
MUR, TERRIT .... p 2298 N94-24593
MURAKAMI, AKINORI .... p 2235 N94-24984
MURAKAMI, M. .... p 2549 N94-22998
MURATORE, JOHN .... p 2305 N94-23838
MUROLO, A. .... p 2369 N94-23399
MURPHY, ELIZABETH D. .... p 2443 N94-23936
MURPHY, JAMES R. .... p 2621 N94-24894
p 2621 N94-24896
MURPHY, OLIVER J. .... p 2393 N94-23359
MURPHY, SEAN .... p 2298 N94-24582
MURPHY, SUSAN C. .... p 2506 N94-23885
MURRAY, DAVID W. .... p 2343 N94-23162
p 2346 N94-25472
MURRAY, DOUGLAS .... p 2457 N94-24626
MURRAY, J. .... p 2559 N94-23186

MURTHY, JAYATHI Y. p 2215 N94-23056
MURTHY, PAPPU L. N. p 2376 N94-23551
MUSIELAK, Z. E. p 2628 N94-25264
MUSSETTO, MICHAEL p 2306 N94-25494
MUSTAFA, DENIS p 2471 N94-23147
p 2472 N94-23163
p 2492 N94-25324
MUZYCHKA, A. YU. p 2567 N94-25425
MYERS, DONALD p 2204 N94-23828
MYERS, EDWARD R. p 2565 N94-25027
MYERS, ROGER M. p 2219 N94-24361
p 2553 N94-25190

N

NADAY, I. p 2556 N94-22921
NAGAMATSU, HENRY T. p 2154 N94-24247
NAGIB, HASSAN M. p 2336 N94-24793
NAGRONYK, V. p 2609 N94-23397
NAGWANEY, BHOJ p 2355 N94-23988
NAIK, DIPAK p 2439 N94-24857
NAIK, RAJIV A. p 2241 N94-23274
NAITO, HIDEYUKI p 2288 N94-22829
NAKAGAWARA, VAN B. p 2426 N94-23623
NAKAI, NAOMASA p 2603 N94-24985
NAKAMURA, S. p 2323 N94-23652
NAKANO, TAKENORI p 2603 N94-24976
p 2603 N94-24983
NAKATANI, I. p 2369 N94-23402
NALLEY, GREGORY M. p 2388 N94-24809
NANDI, S. p 2196 N94-23258
NAOR, D. p 2157 N94-24262
NAPOLITANO, MARCELLO R. p 2190 N94-24804
NARAYAN, RAMESH p 2629 N94-25091
NARAYANAN, S. p 2392 N94-23354
NARAYANAN, S. R. p 2393 N94-23361
NASCIMENTO, MARCO A. C. p 2154 N94-24247
NASH-STEVENSON, S. K. p 2233 N94-24073
NASH, ANTHONY R. p 2206 N94-25523
NASH, DENNIS C. p 2275 N94-22748
NASHASHIBI, FAWZI p 2471 N94-22908
NASSERI, M. p 2316 N94-22855
NATHAN, A. p 2157 N94-24261
NATION, ROBERT p 2527 N94-24211
NATKANIEC, I. p 2567 N94-25425
NAUMANN, CHARLES B. p 2196 N94-24309
NAVARD, SHARON E. p 2374 N94-25372
NAVARRETE, R. p 2591 N94-24607
NAVATHE, S. B. p 2592 N94-24691
NAWIJN, W. M. p 2478 N94-22710
p 2478 N94-22726
p 2467 N94-24524
NAZ, P. p 2528 N94-24214
NECSULESCU, D. p 2370 N94-23421
NEDELKO, S. N. p 2570 N94-25337
NEILSEN, M. K. p 2375 N94-23217
NEILSON, G. H. p 2552 N94-24502
NEJAD, ABDOLLAH S. p 2340 N94-25530
NELSON, JOEY L. p 2186 N94-23255
NELSON, NICK p 2181 N94-24591
NEMESURE, S. p 2386 N94-23779
NEMETH, NOEL N. p 2258 N94-24682
NEPSTAD, DANIEL C. p 2399 N94-24861
NEREM, R. S. p 2401 N94-23282
NES, E. p 2562 N94-23535
NESSLER, W. p 2557 N94-22929
NESTERENKO, V. V. p 2492 N94-25338
NEUENDORFFER, TOM p 2460 N94-24932
NEUFANG, RICH p 2184 N94-25021
NEVANLINNA, O. p 2479 N94-23106
NEVASMAA, PEKKA p 2251 N94-25419
NEVILL, GAIL E., JR. p 2422 N94-24810
NEWELL, O. J. p 2415 N94-24850
NEWMAN, D. E. p 2549 N94-22963
NEWMAN, J. C., JR. p 2228 N94-23279
NEWSOME, PENNY A. p 2197 N94-23907
NEWTON, R. p 2217 N94-23069
NG, TONY p 2206 N94-24916
NGUYEN, RICHARD p 2312 N94-25035
NGUYEN, SON p 2182 N94-24966
NGUYEN, VIET DUNG p 2491 N94-25214
NGUYENPHUONG, LAN p 2449 N94-23155
NI, S. p 2300 N94-24678
NIBOURG, J. M. p 2471 N94-23137
NICHOLS, DAVID A. p 2389 N94-23840
NICHOLS, S. p 2557 N94-22940
NICKELSON, JAMES p 2195 N94-24995
NICKUM, WILLIAM p 2516 N94-23943
NICOL, DAVID M. p 2451 N94-23341
NICOLLIN, F. p 2608 N94-23393
NIE, XIAO-BO p 2554 N94-25330
NIEDRA, JANIS M. p 2312 N94-24870
NIEH, T. G. p 2252 N94-22930
p 2229 N94-24547
NIELSON, GREG p 2200 N94-24065
NIEMANN, R. C. p 2559 N94-22993
NIEMEGEERS, I. G. p 2299 N94-24650
NIEMINEN, MARKKU p 2375 N94-23120
NIESSEN, L. p 2542 N94-23171
NIEUWKOOP, JURGEN ADAM WILLEM
p 2400 N94-25223
NIEWENHUIS, GERT p 2488 N94-24526
NIJMEIJER, H. p 2469 N94-22703
p 2447 N94-22711
p 2470 N94-22714
NIKITICHEV, ALEXEY A. p 2563 N94-24404
NIKOSKINEN, K. I. p 2524 N94-23110
NINOMIYA, KEIKEN p 2207 N94-23860
NIRANJANA, T. p 2164 N94-25111
NISHI, RYOICHI p 2603 N94-24976
NISHIHARA, KATSUHIRO p 2345 N94-24977
NISHIHATA, SEIJI p 2509 N94-23903
NISHIMURA, ARATA p 2271 N94-24459
NISHIMURA, M. p 2355 N94-23992
p 2360 N94-24021
NISHIZAWA, OSAMU p 2405 N94-24980
NITSCHE, W. p 2315 N94-22852
p 2316 N94-22855
NITSCHKE, MICHAEL D. p 2207 N94-23654
NITSCHKO, T. p 2361 N94-24031
NITTA, KAZUMASA p 2286 N94-22813
NIXON, MARK W. p 2378 N94-24839
p 2182 N94-24953
NOBLE, JOHN M. p 2528 N94-24218
NOBLE, VIVECA K. p 2306 N94-24439
NODOMI, Y. p 2360 N94-24021
NOERNBERG, CLEMM p 2182 N94-24966
NOGUCHI, HARUSHIGE p 2501 N94-23854
NOMOTO, KENICHI p 2602 N94-24867
NOOR, AHMED K. p 2177 N94-24314
NOORDIJK, A. C. p 2417 N94-24107
NORDINE, PAUL C. p 2248 N94-25129
NORDTVEDT, KENNETH p 2601 N94-23099
NORI, S. p 2301 N94-24707
NORMAN, CASSIDY p 2205 N94-24702
NORMAN, COLIN A. p 2601 N94-23537
NORMAN, TIMOTHY L. p 2206 N94-25007
NORMANDIN, FRANCIS p 2168 N94-24178
NOSKOV, V. p 2370 N94-23420
NOSSEIR, N. S. p 2338 N94-25140
NOTEBORN, HENRICUS JOSEPH MARIA F.
p 2565 N94-25059
NOULTY, R. A. p 2629 N94-24695
NOVAK, KEN p 2182 N94-24817
NOWELL, D. p 2379 N94-25478
NOWICKI, L. J. p 2238 N94-22718
p 2240 N94-23009
p 2240 N94-23194
NOYES, JAMES L. p 2469 N94-25454
NUALART, JAIME p 2209 N94-24840
NULL, CYNTHIA H. p 2428 N94-24855
NURMI, SALME p 2231 N94-25420
NYLUND, H. K. p 2241 N94-23446
NYMAN, L. A. p 2599 N94-24780

O

OAKS, ARNOLD p 2410 N94-24355
OBARA, NORIAKI p 2282 N94-22790
OBERAI, AVTAR S. p 2630 N94-23572
OBI, KINICHI p 2235 N94-24984
OBRIEN, T. KEVIN p 2228 N94-24083
OBUKHOV, YU. V. p 2263 N94-25404
OCHS, WILLIAM p 2520 N94-23964
OCONNOR, T. G. p 2549 N94-23013
p 2549 N94-23014
ODA, M. p 2607 N94-23389
ODA, MITSUSHIGE p 2608 N94-23390
ODERKERK, ROBERT PETER p 2538 N94-25259
ODONNELL, KEVIN J. p 2175 N94-24474
ODONOGHUE, DENNIS P. p 2153 N94-24100
OECAL, M. p 2398 N94-23818
OEDMAN, SVANTE p 2544 N94-23723
OERNHAGEN, HANS p 2430 N94-23743
OEZGUENER, UEMIT p 2195 N94-24482
OGASAWARA, HIROYUKI p 2207 N94-23910
OGBURN, MARILYN E. p 2164 N94-25107
OHASHI, NAGAYOSHI p 2604 N94-24987
OHDACHI, S. p 2554 N94-25327
OHERN, M. E. p 2543 N94-23458
OHKAMI, Y. p 2370 N94-23415
OHMAE, HIROKAZU p 2385 N94-23612
OHMORI, M. p 2508 N94-23898
OHMORI, SHINGO p 2288 N94-22829
OHN, MYO MYINT p 2544 N94-24466
OHTA, KAZUHIKO p 2419 N94-25435
OHTA, KAZUO p 2608 N94-23390
OJARD, G. C. p 2243 N94-23717
OKAMOTO, PAUL R. p 2560 N94-23189
OKAYAMA, SHIGEO p 2546 N94-24982
OKRASINSKI, RICHARD J. p 2527 N94-24210
OKU, YUKIO p 2476 N94-25345
OLAH, A. L. p 2467 N94-23752
OLAH, G. A. p 2393 N94-23361
OLDENBURG, C. M. p 2335 N94-24655
OLESON, STEVEN R. p 2219 N94-23555
OLIGER, JOSEPH p 2569 N94-24109
p 2631 N94-25003
OLIVAS, J. D. p 2245 N94-24747
OLMSTEAD, DEAN p 2288 N94-22828
OLOFSSON, H. p 2602 N94-23812
OLSEN, ROBERT p 2527 N94-24211
OLSEN, ROBERT O. p 2527 N94-24208
p 2527 N94-24210
OLSON, R. p 2450 N94-23207
OLSSON, PELLE p 2569 N94-24109
ONDAS, M. S. p 2211 N94-23036
ONDRUS, PAUL p 2505 N94-23881
ONEAL, MICHAEL p 2433 N94-24186
ONEIL, WILLIAM F. p 2306 N94-25503
ONIYAMA, AKIO p 2509 N94-23903
ONKEN, J. F. p 2505 N94-23878
ONO, A. p 2384 N94-23609
p 2385 N94-23610
ONSTOTT, ROBERT G. p 2418 N94-24918
OOST, W. p 2381 N94-23145
OPIELA, JOHN p 2205 N94-24702
OPLINGER, D. W. p 2230 N94-24779
p 2230 N94-24942
p 2230 N94-25163
OPSTAD, K. p 2268 N94-23450
ORAEVSKY, V. p 2625 N94-22847
ORANGE, THOMAS W. p 2377 N94-24715
ORDONIO, ROBERT R. p 2457 N94-24556
OREILLY, D. p 2372 N94-24174
ORLIN, JAMES p 2468 N94-24939
ORREN, SCOTT p 2182 N94-24915
ORTEGA, ED p 2181 N94-24711
ORTEGA, R. p 2376 N94-23342
OSBORNE, T. H. p 2551 N94-23782
OSHIMA, YASUHIRO p 2235 N94-24984
OSHMAN, YAAKOV p 2157 N94-24264
p 2157 N94-24265
OSINGA, H. M. p 2480 N94-23140
OTA, KOJI p 2603 N94-24985
OTRANTO, JOHN F. p 2197 N94-23907
OTTE, N. p 2490 N94-24727
OTTEN, G. D. p 2478 N94-22725
OTTER, ANDRIES p 2338 N94-25243
OUTLAW, R. A. p 2245 N94-25117
OVERBEEK, R. p 2420 N94-23468
OVERBURY, S. H. p 2532 N94-22956
OVERFELT, TONY p 2246 N94-25122
OVERMYER, SCOTT P. p 2588 N94-25373
OVSHINSKY, S. R. p 2391 N94-23352
OWENS, T. p 2394 N94-23365
OZARAPOGLU, VASIL p 2186 N94-23253

P

PAAR, GERHARD p 2608 N94-23394
PACK, GINGER p 2272 N94-23892
PADIN, S. p 2599 N94-23705
PADOVANI, C. p 2374 N94-23112
PAEZ, T. L. p 2371 N94-22918
PAGANO, NICHOLAS J. p 2255 N94-24232
PAGE, BRENDA p 2520 N94-23964
p 2520 N94-23966
PAI, S. P. p 2229 N94-24402
PAL, S. p 2212 N94-23040
p 2212 N94-23042
PALAMIDESE, P. p 2449 N94-23111
PALAZZOLO, ALAN B. p 2371 N94-24440
PALEY, MARK S. p 2225 N94-24347
PALMER, JAMES M. p 2383 N94-23598
PALMER, M. D. p 2519 N94-23958
PALMER, MATTHEW E. p 2180 N94-24479
PALMQUIST, R. D. p 2472 N94-23201
PALOMAEKI, AIJA p 2588 N94-22734
PAMADI, BANDU N. p 2164 N94-25111
PAN, H. p 2317 N94-23114
PAN, SI-MING p 2285 N94-22806
PANDYA, ABHILASH p 2437 N94-24205
p 2437 N94-24206
PANKAKOSKI, PEKKA H. p 2379 N94-25418
PANKONIN, JON p 2179 N94-24401
PANTON, DAVID M. p 2585 N94-22704
PAPADOPOULOS, LOUKAS p 2474 N94-24635
PAPE, U. p 2502 N94-23858
PARA, VICTOR p 2183 N94-24975
PARAYO, MANUEL p 2181 N94-24803
PARCHEN, RENE RAYMOND p 2339 N94-25248
PARIS, HENRY G. p 2220 N94-24595
PARIS, JOSEPH p 2517 N94-23951
PARISH, THOMAS R. p 2621 N94-24895

PARK, D. S. p 2338 N94-25140
PARK, INHAG p 2308 N94-23154
PARK, K. C. p 2203 N94-23618
PARKER, B. EUGENE, JR. p 2525 N94-23698
PARKER, F. T. p 2559 N94-22995
PARKER, JOEY K. p 2371 N94-24441
PARKER, ROBERT L. p 2405 N94-24854
PARKER, T. p 2589 N94-23127
PARKER, T. J. p 2589 N94-23126
PARKES, A. p 2203 N94-23954
PARKES, STEPHEN MAXWELL p 2370 N94-23422
PARKINSON, R. D. p 2229 N94-24632
PARLIAMENT, HUGH p 2455 N94-24116
p 2296 N94-24133
p 2455 N94-24134
p 2455 N94-24135
PARLIER, M. p 2256 N94-24233
PARLIER, MICHEL p 2254 N94-24129
PARLIER, RANDY p 2197 N94-23902
PARLOCK, ANDREW p 2206 N94-25007
PARMAR, DEVENDRA S. p 2375 N94-23308
PARSHIN, P. P. p 2567 N94-25424
PARSONS, E. L., JR. p 2394 N94-23781
PARSONS, KIERAN J. p 2275 N94-22747
PARTHASARATHY, R. p 2263 N94-25409
PARTHASARATHY, TRIPLICANE A.
p 2255 N94-24231
PARTIN, J. K. p 2382 N94-23492
PASCIAK, JOSEPH E. p 2482 N94-23677
PASCIUTO, MICHAEL P. p 2518 N94-23957
PASQUIER, HELENE p 2464 N94-23962
PASSI, RANJIT M. p 2418 N94-24671
PASSILLY, B. p 2256 N94-24233
PATEL, G. B. p 2401 N94-23282
PATIN, J. F. p 2359 N94-24014
PATNAIK, SURYA N. p 2378 N94-24845
PATT, FREDERICK S. p 2417 N94-23338
PATTEN, R. p 2472 N94-23201
PATTERSON, JAMES D. p 2631 N94-24493
PATTERSON, MICHAEL J. p 2218 N94-23372
p 2221 N94-24770
p 2222 N94-25201
PATTERSON, SARA p 2598 N94-25006
PAUFLER, DAVE p 2190 N94-24957
PAUFLER, DAVID p 2183 N94-24969
p 2184 N94-25021
PAUL, ANTHONY D. p 2389 N94-24442
PAULL, A. p 2319 N94-23513
PAVEL, M p 2441 N94-25500
PAVEL, M. p 2441 N94-25501
p 2443 N94-25514
PEACH, R. C. p 2275 N94-22746
PEARCE, C. E. M. p 2494 N94-23749
PEARL, JOHN C. p 2620 N94-24893
PEARSON, ANDREA p 2279 N94-22773
PEASE, R. F. p 2346 N94-25154
PECARIC, M. p 2437 N94-24299
PECCIA, N. M. p 2197 N94-23913
PECK, J. p 2376 N94-23342
PECORA, LOUIS M. p 2302 N94-25057
PEDERSEN, ALLISTER p 2279 N94-22773
PEDERSEN, K. S. p 2268 N94-23429
p 2269 N94-23506
PEDRAZZOLI, G. p 2362 N94-24039
PEDROVIEJOPOYATOS, JUAN JOSE
p 2252 N94-22910
PEEBLES, DIAMOND p 2249 N94-25133
PEEBLES, HENRY p 2249 N94-25133
PEETERS, J. C. H. p 2418 N94-24601
PEETERS, R. p 2479 N94-23107
PEKALA, R. W. p 2252 N94-22931
PELED, D. p 2158 N94-24269
PELL, BARNEY p 2591 N94-24552
PELTON, JOSEPH N. p 2293 N94-23622
p 2293 N94-23627
p 2293 N94-23628
PENA, M. T. p 2531 N94-22951
PENCIL, ERIC J. p 2221 N94-24766
PENDALWAR, SHEKHAR L. p 2262 N94-25145
PENETRANTE, B. M. p 2351 N94-22865
p 2351 N94-22866
PENG, JIAN p 2365 N94-24699
PENKO, PAUL F. p 2214 N94-23053
PENN, BENJAMIN G. p 2225 N94-24346
PENNARTZ, C. p 2420 N94-23454
PENNELL, BILL p 2411 N94-24379
PEPERZAK, L. p 2418 N94-24601
PEPI, MARC S. p 2263 N94-25410
PERAELAE, J. p 2382 N94-23224
PEREIRA, NINO R. p 2553 N94-24949
PERERA, L. p 2536 N94-24675
p 2537 N94-24940
PEREZ-DAVIS, MARLA E. p 2218 N94-23370
PEREZ, M. R. p 2599 N94-23334
PEREZ, RAUL GARCIA p 2502 N94-23863
PERKEY, DON p 2413 N94-24385
PERKINS, L. J. p 2553 N94-24628
PERLACK, R. D. p 2395 N94-24499
PERLWITZ, JUDITH p 2403 N94-24491
PEROT, J. BLAIR p 2171 N94-24143
PERRETTA, DAVE p 2181 N94-24787
PERRING, T. p 2557 N94-22925
PERRONE, D. p 2392 N94-23354
PERRONE, JOHN A. p 2442 N94-25510
PERRY, J. p 2540 N94-24662
PERRY, JOSEPH W. p 2226 N94-24354
PERRY, M. D. p 2348 N94-23181
PERRY, WILLIAM J. p 2596 N94-25066
PERSHING, DEAN p 2311 N94-24818
PERSOON, ANN M. p 2540 N94-23495
PERSSON, AAKE p 2437 N94-24292
PERSSON, GUNNAR p 2437 N94-24292
PERVUSHIN, V. N. p 2539 N94-25477
PESCHKE, WILLIAM T. p 2234 N94-24565
PESHEVA, N. C. p 2524 N94-25208
PETACH, MICHAEL p 2598 N94-23536
PETERS, H. C. p 2417 N94-24107
PETERS, MARC A. p 2480 N94-23144
PETERSON, D. L. p 2311 N94-24500
PETIAU, C. p 2179 N94-24327
PETRICH, L. p 2471 N94-23011
PETRIU, E. M. p 2370 N94-23421
PETROV, KONSTANTIN p 2391 N94-23353
PETROV, V. A. p 2538 N94-25341
PETROVIC, J. J. p 2563 N94-24517
PETTERSEN, G. p 2561 N94-23428
PETTERSSON, LEIF p 2294 N94-23742
PEURANEN, PASI p 2588 N94-22734
PEYTON, DERRICK R. p 2175 N94-24176
PFEFFER, RICHARD L. p 2404 N94-24674
PFEFFERLE, L. D. p 2233 N94-23736
PFEIFFER, F. p 2369 N94-23406
PHALIPPOU, JEAN p 2254 N94-24129
PHAN-THIEN, N. p 2316 N94-22870
PHANORD, DIEUDONNE D. p 2416 N94-24443
PHARAOH, M. W. p 2256 N94-24236
PHILIPPE, JEAN J. p 2176 N94-23254
PHILIPPE, PACHOLCZYK p 2500 N94-23846
PHILIPSEN, ALBERT p 2474 N94-24543
PHILLIPS, E. P. p 2228 N94-23279
PHILLIPS, J. C. p 2553 N94-24756
PHILLIPS, J. E. p 2389 N94-22862
PHILLIPS, MARY A. p 2251 N94-25531
PHILLIPS, ROGER J. p 2623 N94-24996
p 2623 N94-24997
PHILLIPS, T. G. p 2296 N94-24105
PICHERIT, F. p 2545 N94-24631
PICHKHAZE, K. p 2370 N94-23416
PICKARD, P. S. p 2348 N94-23185
PICKERING, KENNETH p 2413 N94-24390
PICKERING, THOMAS G. p 2426 N94-24102
PICKETT, MARK T. p 2192 N94-23091
PICKETT, TIM p 2182 N94-24966
PIDGEON, A. p 2203 N94-23954
PIELKE, ROGER p 2413 N94-24387
p 2413 N94-24388
p 2414 N94-24395
PIER, NICHOLAS F. p 2344 N94-24184
PIETRAS, JOHN p 2305 N94-23847
PIETRZAK, JOHN p 2460 N94-24935
PIILA, J. p 2374 N94-23113
PIJNENBURG, MARCUS JOHANNES PETRUS
p 2373 N94-25295
PILLAY, K. K. S. p 2535 N94-24505
PIN, J.-E. p 2518 N94-23956
PINARDI, K. p 2294 N94-23728
PINCK, DEBORAH p 2276 N94-22755
p 2277 N94-22757
PINCOSY, P. A. p 2307 N94-22950
PINDER, J. N. p 2207 N94-24018
PINDERA, M. Z. p 2212 N94-23041
PINDZOLA, M. S. p 2533 N94-23543
PINELLI, THOMAS E. p 2592 N94-24649
p 2592 N94-24660
p 2593 N94-24709
PINERO, LUIS R. p 2218 N94-23372
PINKERTON, J. T. p 2472 N94-23201
PINNINGTON, R. J. p 2363 N94-24076
PIRES, L. F. p 2454 N94-23751
p 2272 N94-24648
PIRI, JOHN L. p 2312 N94-25039
PIRK, R. p 2156 N94-24257
PITCHKHADZE, K. p 2609 N94-23397
PITTS, FELIX L. p 2162 N94-25099
p 2165 N94-25115
PITTS, PATRICIA S. p 2600 N94-25387
PLAGA, R. p 2629 N94-25459
PLATZER, M. F. p 2167 N94-23975
PLEIM, JOHN p 2413 N94-24390
PLENTOVICH, E. B. p 2169 N94-24464
PLESCIA, J. B. p 2607 N94-23387
PLETCHER, RICHARD H. p 2481 N94-23554
POCHARD, MARC p 2362 N94-24040
POELZLEITNER, WOLFGANG p 2608 N94-23394
POENSGEN, C. A. p 2315 N94-22854
POEPPEL, R. B. p 2563 N94-24624
POIARESBAPTISTA, J. P. V. p 2283 N94-22795
p 2284 N94-22798
POINSOT, THIERRY J. p 2237 N94-24155
POIRIER, DIANE p 2333 N94-24177
POJMAN, JOHN A. p 2226 N94-24352
POLITES, M. E. p 2269 N94-23574
POLKA, LESLEY A. p 2298 N94-24616
POLL, E. p 2454 N94-23817
POLLACK, JAMES B. p 2618 N94-24880
p 2621 N94-24896
POLLACK, JORDAN B. p 2468 N94-25030
POLLANO, G. p 2179 N94-24325
POLLARD, A. p 2341 N94-23675
POLLMEIER, VINCENT M. p 2305 N94-23922
POLYCARPOU, ANASTASIS C. p 2298 N94-24616
PONNUSAMY, RAVI p 2458 N94-24679
POON, C. p 2229 N94-24137
POOR, H. VINCENT p 2525 N94-23698
POROTOV, V. p 2609 N94-23397
PORTER, DAVID p 2520 N94-23963
PORTER, DAVID B. p 2173 N94-24718
PORTREE, DAVID S. F. p 2598 N94-24644
POSER, K. p 2361 N94-24028
POSKETT, PETER p 2282 N94-22788
POSKIE, T. J. p 2239 N94-22999
POSTON, CATHERINE A. p 2496 N94-25518
POTH, STEFAN p 2198 N94-24860
POTOTZKY, ANTHONY S. p 2164 N94-25113
POTTER, B. G. p 2542 N94-23202
POTTER, WILLIAM p 2520 N94-23964
POTTER, WILLIAM J. p 2459 N94-24797
POTTS, RICHARD G. p 2175 N94-24127
POTTS, SHERRILL S. p 2374 N94-23932
POTTS, SU K. p 2305 N94-23842
POULSEN, P. p 2307 N94-22950
POULTER, G. A. p 2270 N94-23790
POULTER, K. p 2508 N94-23897
POULTER, K. J. p 2197 N94-23849
POVINELLI, L. A. p 2333 N94-24460
POWER, J. L. p 2209 N94-23012
POWERS, LYNN M. p 2258 N94-24682
POZZI, E. p 2358 N94-24007
PRADINES, D. p 2196 N94-23919
PRAGER, S. C. p 2549 N94-22976
PRAKASH, G. K. SURYA p 2393 N94-23361
PRATT, J. RICHARD p 2252 N94-23079
PRATT, S. p 2569 N94-23453
PRESTON, G. A. p 2525 N94-22959
PRETTE, JOHN p 2184 N94-25017
PRICE, C. p 2408 N94-23471
PRICE, S. p 2622 N94-24903
PRICE, W. B. p 2358 N94-24011
p 2363 N94-24045
PRIDDY, T. G. p 2371 N94-22918
PRIEST, STACY MARIE p 2377 N94-24587
PRIMINI, FRANCIS A. p 2600 N94-25269
PRITZKOW, WALTER E. C. p 2396 N94-25464
p 2396 N94-25479
PRIVAT, M. p 2358 N94-24012
PROBE, JOHN D. p 2436 N94-24203
p 2436 N94-24204
PROCTOR, MARGARET P. p 2216 N94-23063
PROKOP, BORIS p 2244 N94-23802
PROVOST, CYNTHIA A. p 2206 N94-25532
PRUESS, K. p 2335 N94-24655
PUENTE, LAURA p 2182 N94-24817
PUIGVIDAL, MANUEL p 2556 N94-22905
PULSONETTI, M. V. p 2319 N94-23513
p 2320 N94-23532
PURCELL, C. W. p 2397 N94-23016
PURSCH, ANDREW p 2385 N94-23615
p 2385 N94-23616
PURWANTO, A. p 2239 N94-22939
PUSTOVITOV, V. D. p 2551 N94-24306
PUTNEY, BARBARA p 2196 N94-23920
PUZO, ANTOINE p 2313 N94-25421

Q

QI, HAI-HUA p 2566 N94-25332
QIN, XIAO p 2451 N94-23301
QU, D. p 2234 N94-24545
QUAN, A. G. p 2477 N94-23900
QUINLAN, DANIEL p 2469 N94-23697
QUINT, P. p 2257 N94-24562
QUINTANA, F. p 2358 N94-24008
QUINTANA, JORGE A. p 2201 N94-23567
QUIRK, ELENA p 2182 N94-24837

R

RACHO, C. S. p 2291 N94-23260
RACKLEY, MICHAEL p 2197 N94-23843
RADKE, GEORGE p 2323 N94-23650
RADKE, JEFFREY p 2429 N94-25492
RAHM, STEPHAN p 2547 N94-25305
RAHMAT-SAMII, YAHYA p 2289 N94-22834
RAJPUT, BALRAM p 2496 N94-25147
RAMACHANDRAN, N. p 2224 N94-24345
RAMASWAMY, BALA p 2341 N94-23693
RAMBAUT, JEAN PIERRE p 2601 N94-23378
RAMBAUT, JEAN-PIERRE p 2369 N94-23405
RAMEIKA, R. p 2626 N94-23515
RAMOHALLI, KUMAR p 2265 N94-24578
p 2204 N94-24621
RAMOND, P. p 2569 N94-24532
RAMSBOTTOM, W. p 2372 N94-24136
RAMSEIER, STEFAN p 2286 N94-22811
RANDJBAR-DAEMI, S. p 2491 N94-25213
RANEY, DAVID L. p 2164 N94-25113
RANNEY, J. W. p 2395 N94-24499
RAO, D. M. p 2164 N94-25111
RAPTIS, A. C. p 2371 N94-22872
RASH, JAMES L. p 2305 N94-23918
RASHKOV, R. CH. p 2570 N94-25336
RASMUSSEN, ARTHUR N. p 2508 N94-23895
RASPET, RICHARD p 2527 N94-24212
p 2569 N94-24777
RASSOUL, HAMID K. p 2631 N94-24493
RATEL, CHRISTOPHE p 2447 N94-22882
RATOWSKY, R. P. p 2541 N94-22868
RATVASKY, THOMAS P. p 2172 N94-23523
RAUCH, JEFFREY S. p 2521 N94-24302
RAUFASTE, N. J. p 2270 N94-23737
RAVELO, R. p 2374 N94-22871
RAVINDRAN, R. p 2318 N94-23198
RAY, E. R. p 2395 N94-23785
RAY, WILLIAM J. p 2428 N94-24799
RAYMOND, JOHN C. p 2600 N94-25178
RAYMOND, LEE H. p 2388 N94-24809
RAZZELL, A. G. p 2256 N94-24236
READ, PETER L. p 2619 N94-24886
p 2620 N94-24889
REAGAN, M. K. p 2325 N94-23662
RECK, R. A. p 2396 N94-22887
REDDY, B. R. p 2233 N94-24073
REED, BRIAN p 2210 N94-23030
p 2214 N94-23052
REED, DAVID W. p 2195 N94-24995
REEHORST, ANDREW L. p 2172 N94-23523
REHFELD, JAMES p 2209 N94-24840
REHSE, S. J. p 2348 N94-23203
REICHENBACH, H. p 2319 N94-23470
REICHERT, BRUCE A. p 2169 N94-24335
p 2170 N94-25182
REID, MARGARET A. p 2392 N94-23355
REILEY, DANIEL J. p 2345 N94-24852
REILLY, H. F. p 2291 N94-23261
REILLY, JAMES J. p 2391 N94-23353
REIMANIS, I. E. p 2563 N94-24517
REINKING, R. F. p 2396 N94-22913
REISMAN, JILL p 2221 N94-24979
REMER, DONALD S. p 2520 N94-23968
REMICK, R. J. p 2389 N94-22723
REMIS, R. p 2294 N94-23729
REN, LIN p 2566 N94-25297
REN, ZHAO-XING p 2555 N94-25333
RETTIG, C. L. p 2551 N94-23782
RETTMAN, PAUL L. p 2388 N94-24809
REUTER, JAMES D. p 2168 N94-24182
REYNAUD, P. p 2264 N94-24010
p 2256 N94-24234
REYNOLDS, JOHN R. p 2259 N94-24792
REYNOLDS, R. S. p 2189 N94-23658
RHEE, IN-SIK p 2261 N94-25029
RHEINFURTH, M. p 2376 N94-23342
RHIM, WON-KYU p 2238 N94-25135
RHOADS, RON W. p 2473 N94-24068
RICCITIELLO, SALVATORE R. p 2253 N94-23311
RICCO, A. J. p 2526 N94-23718
RICE, M. p 2285 N94-22807
RICE, SALLY A. p 2196 N94-24309
RICHARDS, B. p 2548 N94-22945
RICHARDS, EVAN E. p 2204 N94-24226
p 2205 N94-24710
RICHARDS, MERCEDES T. p 2602 N94-24557
RICHARDS, W. LANCE p 2376 N94-23487
RICHMOND, ELMER RAYDEAN p 2306 N94-25374
RICHTER, STEPHEN p 2456 N94-24470
RIECKE, E. p 2239 N94-22966
RIEMERSMA, S. p 2534 N94-23806
RIESTER, PETER p 2182 N94-24915
RIETDIJK, RACHEL HELOISE p 2570 N94-25257
RIGLEY, JACK p 2273 N94-22735
RIGSBEE, J. M. p 2235 N94-24784
RILEY, A. p 2398 N94-23818
RILEY, CLYDE p 2225 N94-24346
RILEY, DAVID R. p 2185 N94-25440
RILEY, G. N., JR. p 2556 N94-22886
RIND, D. p 2616 N94-24872
RINNOOYKAN, A. H. G. p 2468 N94-24764
RINOUS, P. p 2278 N94-22765
p 2289 N94-22833
RISTORCELLI, J. R. p 2319 N94-23302
p 2335 N94-24712
RITTI, MARIE-HELENE p 2254 N94-24129
RIVACOBA, J. p 2358 N94-24008
RIVERA, FRANCISCO p 2184 N94-25017
RIVERA, JORGE E. p 2200 N94-24577
RIVORD, G. p 2591 N94-24501
RIZKALLA, O. F. p 2336 N94-24771
ROBERTS, BARNEY B. p 2369 N94-23377
ROBERTS, BARRY p 2442 N94-25508
ROBERTS, E. W. p 2356 N94-23993
p 2363 N94-24044
p 2363 N94-24045
ROBERTS, G. T. p 2320 N94-23532
ROBERTS, I. p 2278 N94-22765
ROBERTS, R. G. p 2569 N94-24532
ROBERTS, RON p 2180 N94-24498
ROBERTSHAW, G. A. p 2301 N94-24926
ROBERTSON, BOBBY J. p 2444 N94-25375
ROBERTSON, JAMES A. p 2529 N94-24221
ROBINSON, A. p 2355 N94-23988
p 2209 N94-24006
ROBINSON, M. T. p 2243 N94-23715
ROCARD, F. p 2606 N94-23382
RODERICK, N. F. p 2311 N94-24500
RODGERS, MARK D. p 2175 N94-24472
RODIONOVA, J. F. p 2607 N94-23385
RODRIGUE, G. p 2448 N94-22980
RODRIGUEZ, AGUSTIN M. p 2249 N94-25171
RODRIGUEZ, DOMINIQUE p 2450 N94-23180
RODRIGUEZ, J. p 2342 N94-22954
p 2343 N94-23200
RODRIGUEZ, JOSE p 2422 N94-24810
ROEBELING, R. A. p 2386 N94-23734
ROEDERER, A. p 2278 N94-22765
ROEDSETH, O. J. p 2452 N94-23451
ROELVAG, TERJE p 2453 N94-23534
ROGARD, R. p 2282 N94-22789
ROGERS, A. E. E. p 2599 N94-23705
ROGERS, CHARLES p 2393 N94-23360
ROGERS, CLAIBORNE p 2180 N94-24479
ROGERS, JAMES p 2528 N94-24216
ROGERS, P. p 2490 N94-24727
ROGOVSKY, G. p 2607 N94-23384
p 2370 N94-23416
ROHR, DOUG p 2280 N94-22778
ROIG, DAVID p 2218 N94-23370
ROKHLIN, V. p 2491 N94-24947
ROLAND, CHARLES M. p 2258 N94-24737
ROM, JOSEPH p 2154 N94-24248
RONDEAU, KATHLEEN M. p 2458 N94-24684
ROOD, ROBERT p 2545 N94-24665
ROOIJACKERS, J. E. p 2447 N94-22731
ROOKE, S. P. p 2321 N94-23642
ROSA, FERDINAND p 2251 N94-23244
ROSADO, PEDRO J. p 2200 N94-24577
ROSE, M. FRANK p 2394 N94-23365
ROSEN, A. p 2161 N94-24285
p 2161 N94-24286
ROSENBAND, V. p 2159 N94-24275
ROSENBERG, SANDERS D. p 2154 N94-24243
ROSENBERGER, FRANZ p 2224 N94-24344
ROSENBLUTH, M p 2552 N94-24502
ROSENKILDE, CARL p 2488 N94-24503
ROSENQVIST, J. p 2621 N94-24897
ROSMAIT, RUSSELL L. p 2586 N94-25197
ROSNELL, S. p 2450 N94-23226
ROSQVIST, ROLAND p 2421 N94-24290
ROSS, C. B. p 2536 N94-24729
p 2346 N94-25151
ROSS, CLAUDIA B. p 2547 N94-25144
ROSS, G. G. p 2569 N94-24532
ROSS, I. p 2522 N94-25011
ROSS, S. p 2556 N94-22921
ROSSE, RODNEY p 2462 N94-25287
ROSSI, F. p 2519 N94-23959
ROSSITER, J. A. p 2476 N94-25428
p 2476 N94-25429
ROSSOW, VERNON J. p 2317 N94-23077
p 2319 N94-23306
ROSSOW, W. B. p 2616 N94-24872
ROTE, D. M. p 2352 N94-22991
p 2352 N94-22996
ROTH, DUANE p 2301 N94-25041
ROTHWELL, C. A. p 2464 N94-25471
ROUBY, D. p 2256 N94-24234
ROULET, MICHEL E. p 2610 N94-23408
ROUNS, T. N. p 2562 N94-23535
ROUSSEL, T. p 2278 N94-22764
ROWE, BRIAN H. p 2165 N94-25068
ROWNTREE, R. A. p 2358 N94-24009
p 2358 N94-24011
p 2362 N94-24042
p 2363 N94-24043
ROZEN, S. p 2155 N94-24252
ROZENFELD, PAWEL p 2429 N94-23933
ROZEVELD, S. J. p 2558 N94-22990
RUBIN, ALLAN M. p 2403 N94-24580
RUBIN, MARILYN p 2427 N94-25376
RUBINE, DEAN p 2460 N94-24932
RUBINSTEIN, D. p 2160 N94-24281
RUBY, EDWARD G. p 2422 N94-24791
RUDD, E. J. p 2393 N94-23363
RUDISILL, MARIANNE p 2433 N94-24187
RUEGER, A. p 2402 N94-23516
RUETTINGER, A. p 2178 N94-24319
RUF, J. H. p 2214 N94-23054
RUFFLES, PHILIP p 2187 N94-23570
RUGGIERI, M. p 2277 N94-22761
RUGGIERO, A. J. p 2265 N94-23778
RUIZ, A. C. p 2469 N94-22703
RUIZ, JAVIER BENEDICTO p 2274 N94-22743
RUPAR, MICHAEL A. p 2303 N94-25089
RUSCH, DAVID W. p 2626 N94-23626
RUSHBY, JOHN p 2466 N94-23293
RUSSELL, JOHN M. p 2237 N94-23245
RUSSELL, STEPHEN D. p 2546 N94-25043
RUTH, DUANE p 2301 N94-25040
RUTHER, W. E. p 2242 N94-23457
RUTLEDGE, SHARON K. p 2218 N94-23370
p 2534 N94-23825
RUTTAN, ARDEN p 2484 N94-23686
RUTTEN, R. J. p 2625 N94-22848
RUTTKAY, SOFIA p 2489 N94-24643
RUTTKAY, Z. p 2486 N94-23762
p 2497 N94-23764
p 2487 N94-23765
RUUSKANEN, PEKKA p 2250 N94-25316
RUYMGAART, FRITZ H. p 2495 N94-24508
RYAN, H. M. p 2212 N94-23042
RYDER, GRAHAM p 2613 N94-24058
RYE, ROBERT p 2249 N94-25133
RYJACEK, Z. p 2487 N94-24053
RYUM, N. p 2241 N94-23446

S

SABA, JULIA L. R. p 2626 N94-23276
SABERI, ALI p 2473 N94-24542
SABOUNI, IMAD p 2308 N94-23165
SACHER, P. W. p 2177 N94-24316
SADDOUGHI, SEYED G. p 2332 N94-24166
SAEAESKI, J. p 2449 N94-23117
p 2374 N94-23118
SAELTHUN, NILS ROAR p 2399 N94-24633
SAGER, GARRETT L. p 2180 N94-24498
SAGGIO, JOSEPH, JR. p 2222 N94-25201
SAHAY, VISHNU p 2276 N94-22753
SAHOO, N. K. p 2347 N94-22967
SAIF, A. G. p 2525 N94-25389
p 2566 N94-25390
p 2566 N94-25391
p 2566 N94-25392
SAIKKONEN, HEIKKI p 2449 N94-23103
SAITO, GUNJI p 2564 N94-24978
SAITO, K. p 2369 N94-23402
SAITO, MAMORU p 2603 N94-24985
SALAZAR, A. J. p 2501 N94-23853
SALEM, ASHRAF MOHAMMED EL-FARGHLY
p 2306 N94-22883
SALPEKAR, SATISH A. p 2228 N94-24083
SALPINI, D. P. p 2280 N94-22776
SALT, JONATHAN G. p 2364 N94-24128
SALTZ, JOEL p 2458 N94-24679
p 2458 N94-24740
SAMADANI, RAMIN p 2400 N94-23084
SAMANIEGO, J.-M. p 2237 N94-24156
SAMEC, T. p 2306 N94-25498
SAMPAIO, CARLOS E. p 2436 N94-24199
p 2436 N94-24200
SAMSON, CLAUDE p 2475 N94-24963
SAMUELSEN, G. S. p 2481 N94-23593
SANDFORD, S. P. p 2349 N94-24488
SANDHOLM, RONALD G. p 2175 N94-24127
SANDVIG, ANNE M. p 2244 N94-23802
SANECKI, J. E. p 2242 N94-23457
SANKARAN, S. N. p 2245 N94-25117
SANKOVIC, JOHN M. p 2219 N94-23531
p 2219 N94-23630
p 2221 N94-25189
SANTAVICCA, D. A. p 2211 N94-23036
SANTEE, MICHELLE p 2622 N94-24898

SANTER, B. D. p 2407 N94-23156
SANTI, L. MICHAEL p 2222 N94-24444
SANTORO, R. J. p 2212 N94-23040
p 2212 N94-23042
SANTUCCI, F. p 2277 N94-22761
SANUKI, H. p 2552 N94-24456
SANYAL, S. P. p 2567 N94-25423
SAPHIER, D. p 2155 N94-24252
SARABURA, M. p 2569 N94-23453
SARGENT, STEVE p 2384 N94-23607
SARICK, JOHN p 2206 N94-25007
SARIG, N. p 2161 N94-24284
SARIKAYA, M. p 2257 N94-24677
SARKIMO, MATTI p 2379 N94-25418
SARMIENTO, CHARLES J. p 2219 N94-23531
SARYCHEVA, L. I. p 2539 N94-25476
SASABE, H. p 2257 N94-24562
p 2261 N94-24930
SASAKI, A. p 2360 N94-24021
SASAKI, MINORU p 2603 N94-24985
SASAKI, S. p 2552 N94-24456
SASAKI, SATOSHI p 2568 N94-25515
SASAKI, SUSUMU p 2207 N94-23860
SASHIN, I. L. p 2567 N94-25425
SASSON, N. p 2156 N94-24259
SATHYAPRAKASH, B. S. p 2604 N94-25211
p 2604 N94-25212
SATO, MASAKI p 2287 N94-22821
SATOH, SADAO p 2271 N94-24459
SATTERWHITE, VINCENT E. p 2218 N94-23372
SATYANARAYANAN, M. p 2593 N94-24946
SAUVE, DUANE A. p 2547 N94-25533
SAVELEV, A. E. p 2570 N94-25207
SAVIJARVI, H. p 2622 N94-24899
SAVINELL, ROBERT p 2393 N94-23360
SAXEN, B. p 2472 N94-23463
SAXON, J. B. p 2376 N94-24359
SAYEGH, SOHEIL p 2304 N94-25266
SAYOOD, KHALID p 2301 N94-24707
SCAFFIDI, CHARLES p 2464 N94-23893
SCHAEFFER, J. p 2621 N94-24896
SCHAFER, K. J. p 2531 N94-22869
SCHAFER, LAUREN E. p 2436 N94-24204
SCHAFFAR, M. p 2176 N94-23146
p 2340 N94-25463
SCHEFFERS, BERNARDUS CORNELIS
p 2404 N94-24647
SCHEMM, J. p 2407 N94-23132
SCHEMMANN, M. E. C. p 2348 N94-23168
SCHEPS, RICHARD p 2350 N94-25044
p 2350 N94-25216
SCHERPEN, J. M. A. p 2469 N94-22705
SCHERRER, JOHN p 2209 N94-23484
SCHERRER, PHILLIP H. p 2591 N94-24099
SCHERSON, DANIEL p 2393 N94-23360
SCHERSON, DANIEL A. p 2391 N94-23347
SCHEUER, J. T. p 2218 N94-23283
SCHICHL, K. p 2316 N94-22858
SCHIELOW, N. p 2502 N94-23858
SCHIERMEYER, I. p 2487 N94-24053
SCHIMMEL, C. p 2178 N94-24322
SCHKOLNIK, GERARD S. p 2188 N94-24106
SCHLEICH, D. p 2551 N94-23703
SCHLESINGER, BARRY M. p 2410 N94-24355
SCHLOSSER, HERBERT p 2243 N94-23578
SCHMEICHEL, E. p 2478 N94-22715
SCHMID, M. p 2361 N94-24032
SCHMIDT, JERRY p 2412 N94-24384
SCHMIDT, W. p 2177 N94-24316
SCHMITZ, MARION p 2600 N94-25387
SCHMITZ, STEFAN p 2515 N94-23937
SCHNEIDER, KARL M. p 2504 N94-23875
SCHNEIDER, R. P. p 2350 N94-24659
SCHNEIDER, STEVE p 2184 N94-25268
SCHNEIDER, STEVEN p 2211 N94-23038
p 2214 N94-23052
SCHNEIDER, STEVEN P. p 2167 N94-23625
SCHNIEDER, GEORGE p 2190 N94-24957
p 2183 N94-24969
SCHOCK, MICHAEL R. p 2244 N94-23802
SCHOEN, DAVID C. p 2281 N94-22782
SCHOENBERG, K. F. p 2218 N94-23283
SCHOENMAKERS, LAMBERTUS ADRIANUS M.
p 2476 N94-25290
SCHOENWALD, D. A. p 2293 N94-23473
SCHOER, J. K. p 2536 N94-24729
p 2346 N94-25151
SCHOER, JONATHAN K. p 2547 N94-25144
SCHOFIELD, B. E. p 2179 N94-24324
SCHOLS, HUBERT MARIE JEAN-LOUIS
p 2304 N94-25303
SCHOLTEN, HUIBERT FRANK p 2263 N94-25299
SCHONFELD, F. W. p 2245 N94-24747
SCHOTMAN, A. H. M. p 2254 N94-23763
SCHOUTEN, GERARD p 2428 N94-25298
SCHOWALTER, LEO p 2563 N94-23972
SCHRAGE, DEAN S. p 2323 N94-23651
SCHRECKENGHOST, DEBRA L. p 2473 N94-24068
SCHREUR, BARBARA p 2465 N94-24445
SCHRYVER, J. C. p 2429 N94-22997
SCHUBERT, S. p 2407 N94-23132
SCHULTZ, J. A. p 2562 N94-23805
SCHULTZ, ROBERT G. p 2297 N94-24554
SCHULZE, ROLF p 2505 N94-23877
SCHULZE, W. A. p 2254 N94-23720
SCHUMANN, ROBIN p 2416 N94-25271
SCHUMANN, ROBIN S. p 2408 N94-23576
SCHUMM, JEFFRY S. p 2537 N94-25087
SCHURMEIER, H. p 2370 N94-23416
SCHUTT, J. p 2603 N94-24964
SCHUTZ, R. E. p 2207 N94-23259
SCHUWER, ROBERT VICTOR p 2477 N94-25431
SCHWARTZ, S. E. p 2386 N94-23779
SCHWARZ-VANMANEN, ADRIANA DYMPHENA
p 2339 N94-25291
SCHWARZ, RICARDO B. p 2391 N94-23353
SCHWEE, LEONARD J. p 2446 N94-24724
SCHWENDEMAN, ROBERT J. p 2297 N94-24183
SCHWENTERLY, S. W. p 2307 N94-23019
SCHWER, DOUGLAS A. p 2216 N94-23066
SCHWUTTKE, URSULA M. p 2477 N94-23900
p 2197 N94-23902
SCIALDONE, JOHN J. p 2218 N94-23343
SCOKAERT, PIERRE O. M. p 2477 N94-25469
SCOON, GEORGE E. N. p 2608 N94-23391
SCOTT, CAROL J. p 2429 N94-23934
SCOTT, J. N. p 2323 N94-23652
SCOTT, JAMES N. p 2326 N94-23672
SCOTT, JEFF W. p 2348 N94-23123
SCOTT, RANDALL C. p 2461 N94-25074
SCOTTI, STEPHEN J. p 2376 N94-23368
SCRIVENS, WALTER A. p 2235 N94-24925
SECCI, G. p 2362 N94-24039
SECHOVSKY, V. p 2239 N94-22939
SEGAL, A. p 2157 N94-24260
SEGAL, LEON D. p 2430 N94-23527
SEINMANN, LAURA p 2426 N94-23544
SEKI, K. p 2360 N94-24021
SELA, N. p 2158 N94-24269
SELLERS, PIERS p 2413 N94-24387
SELLERS, R. p 2389 N94-22888
SENAPATI, NAGA p 2259 N94-24788
SENAY, HIKMET p 2452 N94-23507
SENJANOVIC, G. p 2532 N94-22970
SEPANIAK, M. J. p 2233 N94-23716
SEPPAELAE, J. p 2254 N94-23561
SEPPAENEN, J. p 2444 N94-23754
SEPULVEDA, JOSE A. p 2574 N94-23246
SEREGELYI, J. S. p 2193 N94-24117
p 2193 N94-24123
SERGENT, DAN p 2183 N94-24971
SERRANZANA, RAY p 2183 N94-24972
SETH, KAMAL K. p 2540 N94-23791
SETH, SHASHI p 2280 N94-22775
SETTIMO, F. p 2277 N94-22760
SEVAT, P. p 2193 N94-24117
SEVERANCE, KURT p 2166 N94-23512
SEVERIJNS, CAMILLUS ADRIANUS
p 2537 N94-25082
SEVERING, A. p 2557 N94-22925
SEWARD, FREDERICK D. p 2600 N94-25269
SFORZA, M. p 2283 N94-22795
p 2283 N94-22796
p 2284 N94-22798
SHABBIR, A. p 2333 N94-24460
SHABBIR, AAMIR p 2326 N94-24063
p 2336 N94-24713
SHAFAI, L. p 2289 N94-22830
SHAFARMAN, W. N. p 2389 N94-22862
SHAH, SUNIL p 2261 N94-24937
SHAHABUDDIN, PERWEZ p 2457 N94-24638
SHAIK, K. p 2292 N94-23269
SHAKER, A. W. p 2341 N94-23689
SHALEV, D. p 2157 N94-24260
p 2161 N94-24288
SHALKHAUSER, MARY JO p 2201 N94-23567
SHANAHAN, DENNIS F. p 2174 N94-25141
SHANNON, SAMUEL G. p 2174 N94-25141
SHAPIRO, DAVID p 2426 N94-24102
SHAPIRO, I. I. p 2405 N94-25205
SHAPIRO, S. p 2307 N94-22955
SHARBER, JIM p 2209 N94-23484
SHARMA, A. p 2547 N94-25209
SHASHIDAR, R. p 2262 N94-25159
SHAUGHNESSY, JOHN D. p 2163 N94-25104
SHAW, A. L. p 2178 N94-24318
SHAW, PETER R. p 2419 N94-25165
SHAY, M. p 2158 N94-24268
SHEEN, SHUH-HAW p 2371 N94-22872
SHEINMAN, Y. p 2157 N94-24260
SHELDON, DAVID W. p 2192 N94-23091
SHELEY, ELIZABETH p 2630 N94-23572
SHELTON, ARTEMUS p 2195 N94-24995
SHEN, BA-ZHONG p 2491 N94-25079
SHEN, D. p 2392 N94-23354
SHEN, F. p 2238 N94-25132
SHENDOCK, ROBERT p 2203 N94-23947
SHENG, YAN-YA p 2555 N94-25333
SHENG, ZHENG-MING p 2555 N94-25344
SHEPHARD, MARK S. p 2466 N94-23483
SHEPHERD, CHIP p 2434 N94-24192
p 2306 N94-24194
SHER, E. p 2155 N94-24252
p 2155 N94-24253
SHERBAUM, VALERY p 2155 N94-24251
SHERER, SCOTT E. p 2326 N94-23672
SHERIF, JOSEF p 2520 N94-23968
SHERIFF, R. E. p 2288 N94-22827
SHERVAIS, JOHN W. p 2614 N94-24363
p 2614 N94-24364
p 2614 N94-24365
p 2614 N94-24366
p 2615 N94-24367
p 2615 N94-24368
p 2615 N94-24369
p 2615 N94-24370
p 2615 N94-24371
p 2616 N94-24372
p 2616 N94-24373
SHI, JIAN p 2523 N94-25480
SHI, YI-CAI p 2555 N94-25333
SHIAO, MICHAEL C. p 2378 N94-25188
SHIBATA, KATSUNORI M. p 2604 N94-24986
SHIH, M. P. p 2279 N94-22770
SHIH, T.-H. p 2333 N94-24460
SHIH, TSAN-HSING p 2326 N94-24063
p 2336 N94-24713
SHIMABUKURO, RANDY L. p 2312 N94-25050
SHIMADA, TOSHIO p 2446 N94-24981
SHIMKAVEG, G. M. p 2541 N94-22868
SHIN, JAIWON p 2166 N94-23522
SHINONAGA, HIDEYUKI p 2288 N94-22825
SHIOKAWA, TAKAYASU p 2284 N94-22797
SHIRBACHEH, M. p 2314 N94-23401
SHIVAKUMAR, K. N. p 2228 N94-24083
SHOEMAKER, PATRICK A. p 2312 N94-25050
SHOJI, T. p 2554 N94-25327
SHOKAIR, I. R. p 2198 N94-23210
SHORSHI, G. p 2156 N94-24258
SHORT, OWEN G. p 2516 N94-23941
SHOUCRI, MERIT M. p 2306 N94-25494
SHPILBERG, I. p 2160 N94-24282
SHRUSTER, I. p 2158 N94-24268
SHU, CHI-WANG p 2480 N94-23278
SHUB, Y. p 2158 N94-24266
SHUI, XIAOPING p 2394 N94-23367
SHULTS, W. D. p 2234 N94-24548
SHUMAKER, GERALD C. p 2177 N94-24315
SHUMWAY, ROBERT H. p 2406 N94-25538
SHVETS, N. R. p 2492 N94-25338
SICRE, J. p 2264 N94-24010
SIDI, MARCEL p 2158 N94-24271
SIEBEN, A. p 2388 N94-24636
SIEBER, M. p 2571 N94-25340
SIEGMUND, DAVID p 2475 N94-24943
SIEKHAUS, W. J. p 2232 N94-23298
SIERA, J. p 2232 N94-23482
SIGALOVSKY, J. p 2255 N94-24223
SIGMUND, WOLFGANG M. p 2259 N94-24792
p 2261 N94-24930
SIHVOLA, A. p 2524 N94-23131
p 2290 N94-23225
SIILI, TERO p 2622 N94-24899
SILIN, I. N. p 2463 N94-25432
SILVA, JAY M. p 2462 N94-25287
SILVA, WALTER A. p 2164 N94-25112
SILVER, R. N. p 2569 N94-24516
SIMMONDS, BORIS G. p 2322 N94-23649
SIMMONS, J. M. p 2319 N94-23513
SIMOENS, SERGE p 2317 N94-22971
SIMON-GILLO, J. p 2569 N94-23453
SIMON, A. p 2156 N94-24259
SIMON, FREDERICK F. p 2320 N94-23525
SIMON, MARVIN K. p 2287 N94-22819
SIMONEAU, ROBERT J. p 2334 N94-24481
SIMONIS, A. W. p 2242 N94-23475
SIMONS, RAINEE N. p 2310 N94-24308
SIMONSON, S. p 2426 N94-23575
SIMROCK, S. p 2540 N94-24662
SIMS, J. R. p 2307 N94-22987
SIMS, JAMES p 2172 N94-23523
SINCLAIR, J. C. p 2269 N94-23582
SINCLAIR, M. B. p 2542 N94-23202
SINGER, J. p 2160 N94-24280
SINGER, MICHAEL p 2179 N94-24332
p 2190 N94-24551
p 2184 N94-25004
SINGH, JAG J. p 2375 N94-23308

SINGH, M. p 2222 N94-23500
SINGH, N. B. p 2225 N94-24348
SINGHAL, S. N. p 2177 N94-24317
p 2179 N94-24326
SINGLE, THOMAS G. p 2204 N94-24620
SINHA, K. K. p 2604 N94-25210
SIRMAN, MELINDA p 2195 N94-24995
SITENKO, I. p 2370 N94-23417
SIVOKLOKOV, S. YU. p 2539 N94-25476
SIX, FRANK p 2574 N94-24405
SJOEBLOM, J. p 2254 N94-23561
SKAMAROCK, WILLIAM p 2414 N94-24392
SKELLY, MICHAEL p 2182 N94-24915
SKINNER, D. p 2390 N94-23295
SKOCYPEC, R. D. p 2268 N94-23000
SLACK, D. S. p 2549 N94-23013
SLATTERY, KERRY T. p 2231 N94-24446
SLATTERY, RHONDA p 2174 N94-25272
SLATTON, CLINT p 2205 N94-24702
SLOAN, G. C. p 2406 N94-25535
SLOOFF, W. p 2242 N94-23496
p 2397 N94-23497
SMALBRUGGE, E. p 2348 N94-23168
SMEETS, G. p 2318 N94-23160
SMENTKOWSKI, V. S. p 2565 N94-25160
SMIALEK, JAMES L. p 2343 N94-23826
SMIGIELSKI, P. p 2343 N94-24054
SMILANSKY, U. p 2571 N94-25340
SMITH, BARRY p 2465 N94-22973
SMITH, BYRON p 2182 N94-24915
SMITH, C. E. p 2187 N94-24082
SMITH, C. R. p 2335 N94-24689
SMITH, CHARLES R. p 2364 N94-24175
SMITH, CHRIS p 2413 N94-24387
SMITH, D. BARTON p 2543 N94-23461
SMITH, D. E. p 2401 N94-23282
SMITH, D. L. p 2238 N94-22718
p 2240 N94-23009
p 2240 N94-23194
SMITH, DEAN LANCE p 2447 N94-25377
SMITH, DEBORAH K. p 2419 N94-25165
SMITH, G. A. p 2217 N94-23069
SMITH, GENE p 2517 N94-23948
SMITH, GRANT D. p 2565 N94-25093
SMITH, H. p 2282 N94-22791
p 2508 N94-23897
SMITH, H. N. p 2197 N94-23849
SMITH, JAMES P. p 2374 N94-22960
SMITH, JOSEPH G. p 2253 N94-23305
SMITH, K. p 2282 N94-22788
SMITH, PAUL p 2591 N94-24337
SMITH, PAUL L. p 2415 N94-24705
SMITH, PHILLIP N. p 2441 N94-25505
p 2442 N94-25506
SMITH, R. D. p 2417 N94-23517
SMITH, RANDY L. p 2435 N94-24195
p 2435 N94-24198
p 2436 N94-24199
p 2436 N94-24201
p 2436 N94-24202
SMITH, ROBERT S. p 2443 N94-24447
SMITH, RUTH S. p 2594 N94-25541
SMITH, STEVE p 2413 N94-24385
SMITH, TODD V. p 2543 N94-23461
SMITHRICK, JOHN J. p 2392 N94-23356
SMITS, A. p 2337 N94-24929
SMOLDERS, A. B. p 2290 N94-22876
SMOOKE, M. D. p 2233 N94-23736
SNEIDERMAN, GARY p 2361 N94-24029
SNOEIJ, P. p 2381 N94-23145
SNOOK, JOHN p 2412 N94-24384
SNOW, GLENN A. p 2204 N94-24620
SNOW, RUSS p 2184 N94-25021
SNOW, RUSS M. p 2190 N94-24957
p 2183 N94-24969
SNYDER, A. L. p 2301 N94-24926
SOARES-FILHO, WILLIAM p 2530 N94-25073
SOCCI, E. P. p 2567 N94-25441
SOETHOUDT, JOHANNES MARIA
p 2492 N94-25277
SOH, WOO-YUNG p 2153 N94-23553
SOHN, CHANG W. p 2336 N94-24821
SOKOLOV, RADOMIR p 2528 N94-24216
SOLER, CHRISTIAN p 2508 N94-23899
SOLOGUB, P. S. p 2370 N94-23418
SOLOMON, G. p 2292 N94-23265
SOLOMON, L. p 2158 N94-24269
SOMANI, ARUN K. p 2451 N94-23340
SONG, KYO-DONG p 2534 N94-24487
SONG, Y.-H. p 2211 N94-23036
SONI, BHARAT K. p 2170 N94-24849
SONI, NITIN J. p 2201 N94-23567
p 2295 N94-24101
SONNEMANS, PETRUS JOHANNES MARIA
p 2340 N94-25484
SONNENFELD, GERALD p 2425 N94-23331
SOO, S. L. p 2325 N94-23663
SOONG, SU TZAI p 2413 N94-24387
SOONG, SU-TZAI p 2414 N94-24392
SOPRANO, C. p 2285 N94-22810
SORATHIS, USMAN A. p 2230 N94-24735
SORENSEN, E. M. p 2503 N94-23866
p 2305 N94-23909
SORENSEN, N. R. p 2270 N94-23790
SORETS, EUGENE p 2456 N94-24535
SORGE, H. p 2569 N94-23453
SOTKOV, G. p 2478 N94-22969
SOULAS, GEORGE C. p 2553 N94-25190
SOULIAC, M. p 2359 N94-24016
SOWA, W. A. p 2481 N94-23593
SOWELS, TERRI p 2181 N94-24803
SOWERS, C. H. p 2559 N94-22995
SPAGNUOLO, JOELLE M. p 2190 N94-24804
SPALL, ROBERT E. p 2324 N94-23659
SPANIOL, CRAIG p 2303 N94-25191
p 2303 N94-25192
SPASOJEVIC, MIRJANA p 2593 N94-24946
SPEAR, K. E. p 2231 N94-22933
SPEARING, ROBERT p 2519 N94-23961
SPEECE, ROBERT F. p 2200 N94-24577
SPEGAR, T. D. p 2211 N94-23036
SPENCER, R. E. p 2599 N94-24521
SPEYER, J. L. p 2198 N94-24752
SPICCI, V. p 2359 N94-24013
SPIESBERGER, JOHN L. p 2418 N94-24719
SPIJKER, N. M. p 2487 N94-23786
SPINHIRNE, JAMES D. p 2294 N94-23827
SPITALE, JOSEPH N. p 2504 N94-23875
SPITZER, CHRISTOPHER J. p 2282 N94-22787
SPIVEY, R. A. p 2322 N94-23648
SPRAGUE, JAMES A. p 2350 N94-24952
SPRINGER, P. T. p 2549 N94-22949
SPROTT, J. C. p 2549 N94-22963
SPRUNCK, MARTIN p 2184 N94-25017
SQUIRES, KYLE D. p 2330 N94-24152
SRAJER, G. p 2545 N94-24550
SRIDHAR, BANAVAR p 2441 N94-25505
SRINIVASAN, S. p 2389 N94-22962
SRINIVASAN, SUPRAMANIAM p 2391 N94-23353
SRIVASTAVA, P. P. p 2568 N94-22968
ST.CLAIR, TERRY L. p 2252 N94-23079
ST.JOHN, PAT p 2598 N94-25006
STACY, KATHRYN p 2166 N94-23512
STAELIN, DAVID H. p 2614 N94-24328
STAFFA, EUGENE p 2280 N94-22779
STAHL, H. PHILIP p 2343 N94-23285
STALKER, R. J. p 2319 N94-23513
p 2320 N94-23532
STALLARD, B. W. p 2209 N94-23012
STALLINGS, ROBERT L., JR. p 2169 N94-24464
STAN-LOTTER, HELGA p 2422 N94-24807
p 2422 N94-24811
STANBERY, B. J. p 2560 N94-23205
STANGLE, G. C. p 2254 N94-23720
STANIFORTH, ANDREW p 2413 N94-24391
p 2414 N94-24392
STANISHKOV, M. p 2478 N94-22969
STANTON, N. p 2626 N94-23515
STANTON, P. H. p 2291 N94-23261
STAPLETON, G. p 2540 N94-24662
STAPPAERTS, EDDY A. p 2344 N94-24360
STARK, KENNETH W. p 2367 N94-25046
STARKE, J. p 2417 N94-24107
STAROPOLI, F. p 2179 N94-24325
STARR, DAVID p 2411 N94-24378
p 2413 N94-24385
STARR, T. L. p 2227 N94-23022
STARRETT, WILLIAM DAVID, JR.
p 2200 N94-24112
STARSKI, J. PIOTR p 2294 N94-23773
STASSINOPOULOS, E. G. p 2540 N94-23273
STAUFFER, C. A. p 2540 N94-23273
STAUFFER, DAVID p 2412 N94-24384
STAUFFER, LARRY p 2365 N94-24806
STAVNES, MARK W. p 2203 N94-23632
STEAKLEY, MICHAEL F. p 2601 N94-23537
STEED, ALLAN J. p 2384 N94-23607
STEELE, D. p 2529 N94-25026
STEELE, W. G. p 2306 N94-25498
STEELE, W. GLENN p 2320 N94-23637
STEIN, MATTHEW D. p 2181 N94-24591
STEINBACH, BILL p 2180 N94-24498
STEINHAEUSER, RAFAEL p 2281 N94-22781
STEN, J. C. E. p 2308 N94-23105
STENGER, ANTHONY J. p 2306 N94-25497
STENGER, GREGORY J. p 2463 N94-25453
STENIUS, P. p 2308 N94-23130
STEPHENS, CRAIG A. p 2334 N94-24495
STEPHENS, ERIC B. p 2257 N94-24558
p 2259 N94-24789
p 2260 N94-24863
STERL, ANDREAS p 2401 N94-23159
STERN, DAN p 2209 N94-24840
STERN, KURT H. p 2258 N94-24720
STERN, M. p 2390 N94-23295
STEUTEL, F. W. p 2495 N94-24571
STEVENS, B. p 2394 N94-23365
STEVENS, R. p 2457 N94-24566
STEWARD, MICHAEL E. p 2312 N94-25050
STEWART, D. S. p 2326 N94-23809
STEWART, ERIC C. p 2163 N94-25102
STEWART, HELEN p 2453 N94-23568
STEWART, J. M. p 2560 N94-23205
STEYAERT, LOU p 2413 N94-24387
STIEGLMEIER, M. p 2316 N94-22856
STIKVOORT, EDUARD FERDINAND
p 2530 N94-25220
STINSON, MICHAEL p 2528 N94-24219
STIXRUD, THOMAS E. p 2345 N94-25037
STOAKLEY, DIANE M. p 2252 N94-23079
STODDARD, FRANK J. p 2212 N94-23043
STOEREN, S. p 2241 N94-23447
STOESSEL, A. p 2407 N94-23156
STOFANAK, R. J. p 2239 N94-22999
STOHR, J. F. p 2255 N94-24229
STOJKOVIC, I. p 2278 N94-22765
STOLARSKI, RICHARD S. p 2398 N94-24104
STONE, BARBARA A. p 2194 N94-23710
STONE, HOWARD p 2162 N94-25098
STONE, LELAND p 2442 N94-25510
STONE, THOMAS A. p 2399 N94-24861
STONE, W. C. p 2194 N94-23819
STONE, WILLIAM C. p 2194 N94-23770
STONER, G. E. p 2238 N94-22932
STONEY, ROBERT p 2180 N94-24581
STOORVOGEL, A. A. p 2489 N94-24608
p 2474 N94-24609
STOORVOGEL, ANTON A. p 2473 N94-24542
STOREY, C. p 2236 N94-25427
STORI, A. p 2254 N94-23431
STOSS, F. W. p 2397 N94-23794
STOUT, CYNTHIA S. p 2420 N94-23088
STOVALL, JOHN R. p 2590 N94-23289
p 2199 N94-23571
STRAFACCI, D. J. p 2156 N94-24257
STRATHDEE, J. p 2491 N94-25213
STRAUCH, R. G. p 2381 N94-23001
STRAWN, ROGER p 2529 N94-24307
STRAYER, M. R. p 2525 N94-23206
STRAZNICKY, P. V. p 2229 N94-24137
STRELTSOV, V. N. p 2539 N94-25481
STRENG, MARTIN p 2568 N94-22709
STRICKER, J. N. M. p 2407 N94-23129
STRICKLAND, J. H. p 2318 N94-23220
STRIZENEC, P. p 2536 N94-24844
STROH, K. R. p 2392 N94-23357
STROUD, DAVID p 2248 N94-25130
STRUIK, PIETER p 2468 N94-25278
STUART, MARK A. p 2435 N94-24197
p 2435 N94-24198
p 2436 N94-24199
p 2436 N94-24200
p 2436 N94-24201
p 2436 N94-24202
STUBBS, SANDY M. p 2177 N94-24304
STUMM, ALBERT p 2184 N94-25002
STUNAULT, DIDIER p 2589 N94-23150
STURROCK, W. R. p 2372 N94-24136
STUTZMAN, W. L. p 2301 N94-25005
SU, S. L. p 2279 N94-22770
SU, Y. T. p 2279 N94-22770
SU, ZHAO-BIN p 2538 N94-25388
p 2567 N94-25426
SUBOTIC, NIKOLA S. p 2546 N94-24731
SUBRAMANIAM, RAM p 2280 N94-22779
SUDHOFF, F. p 2390 N94-23212
SUDRE, O. p 2256 N94-24233
SUEMATSU, H. p 2563 N94-24517
SUGAYA, F. p 2567 N94-25412
SUGAYA, FUMITAKA p 2564 N94-24958
SUKAMTO, L. p 2289 N94-22832
SUKHANOV, K. G. p 2502 N94-23861
SULLIVAN, D. J. p 2216 N94-23065
SULLIVAN, DENNIS p 2481 N94-23547
p 2488 N94-24536
SULLIVAN, J. P. p 2569 N94-23453
SULLIVAN, JOHN p 2184 N94-25268
SULLIVAN, THOMAS A. p 2194 N94-23292
SUN, CHEN-KUO p 2312 N94-25042
SUN, L. p 2535 N94-24555
p 2536 N94-24729
SUN, WEIMIN p 2365 N94-24699
SUO-ANTTILA, A. p 2217 N94-23193
SUOKAS, ESA p 2231 N94-25420
SUORSA, RAYMOND E. p 2441 N94-25505
SURAMPUDI, S. p 2392 N94-23354
p 2393 N94-23361
SURAMPUDI, SUBBARAO p 2310 N94-23823

SUREK, T. p 2395 N94-24512
SURRATT, M. p 2217 N94-23069
SURVANSHI, S. S. p 2427 N94-24950
SUSAN, S. p 2561 N94-23214
SUSSMAN, ALAN p 2458 N94-24740
SUTHERLAND, H. J. p 2394 N94-23472
SUTHERLAND, S. p 2256 N94-24236
SUTTON, JOHN F. p 2303 N94-25192
SUZUKI, M. p 2355 N94-23992
SUZUKI, RYUTARO p 2283 N94-22793
SUZUKI, Y. p 2627 N94-24961
SVENNERUS, GOERAN p 2294 N94-23742
SVENSSON, T. p 2378 N94-24742
SWAIN, GREG M. p 2391 N94-23351
SWEBY, PETER K. p 2454 N94-24110
SWEET, B. p 2441 N94-25500
SWEET, BARBARA T. p 2439 N94-25490
p 2176 N94-25495
SWEETIN, MAURY p 2374 N94-23931
SWELDENS, WIM p 2485 N94-23691
SWENSON, D. p 2307 N94-23008
SWETITS, J. J. p 2350 N94-24851
SWETTE, LARRY L. p 2392 N94-23358
SWISSLER, TOM p 2410 N94-24355
SYDOR, JOHN p 2285 N94-22804
p 2289 N94-22836
SYGULLA, D. p 2256 N94-24239
SYKES, G. B. p 2244 N94-23792
SYM, A. p 2452 N94-23518
SYMONDS, BETH A. p 2459 N94-24812
SYROMIATNIKOV, V. S. p 2357 N94-24004
SZALAI, S. p 2370 N94-23417
SZEREDI, P. p 2420 N94-23468
SZILAGYI, MARIA p 2421 N94-24294

T

TAEHTINEN, SEPPO p 2571 N94-25416
p 2396 N94-25417
TAFAZOLLI, R. p 2277 N94-22759
TAFAZOLLI, RAHIM p 2288 N94-22826
TAFT, BRETT p 2204 N94-24621
TAHERZADEH, SHAHRAM p 2527 N94-24213
TAISANT, J.-P. p 2278 N94-22764
TAKABATAKE, SATOSHI p 2564 N94-24958
TAKAHASHI, HITOSHI p 2181 N94-24803
TAKAHASHI, TAKASHI p 2287 N94-22821
TAKAHASHI, TETSUO p 2501 N94-23854
TAKAHATA, KAZUYA p 2271 N94-24459
TAKAI, H. p 2532 N94-23007
TAKAMIZAWA, K. p 2301 N94-25005
TAKAMURA, S. p 2552 N94-24456
TAKAO, MASARU p 2347 N94-22922
TAKATS, P. p 2278 N94-22766
TAKEUCHI, MAKOTO p 2287 N94-22821
p 2288 N94-22829
TALAGRAND, O. p 2619 N94-24884
TALIA, GEORGE E. p 2251 N94-24448
TALLEY, D. G. p 2211 N94-23039
TALMAN, A. J. J. p 2596 N94-24477
TAMAGNO, JOSE p 2192 N94-23564
TAMAI, H. p 2554 N94-25327
TAMBOUR, Y. p 2159 N94-24274
p 2160 N94-24283
TAMURA, SHINICHI p 2604 N94-24986
TANAKA, A. K. p 2592 N94-24691
TANAKA, KAZUHIRO p 2501 N94-23854
TANAKA, KENJI p 2282 N94-22790
TANDY, P. C. p 2532 N94-22952
p 2406 N94-25535
TANG, Y. p 2241 N94-23446
TANG, YUAN-LIANG p 2442 N94-25507
TANGUAY, ARMAND R. p 2474 N94-24622
TANGYUNYONG, P. p 2234 N94-24772
p 2565 N94-25086
TANIGUCHI, MASAKI p 2345 N94-24977
TANIGUCHI, Y. p 2553 N94-24623
TANNER, J. E. p 2220 N94-24511
TANRIVERDI, TIMOR p 2544 N94-23723
TANSEL, I. N. p 2368 N94-25436
TAO, RONGJIA p 2337 N94-25032
TAO, W. C. p 2265 N94-23807
TAO, WEI-KUO p 2413 N94-24390
TAPIA, JOSE p 2221 N94-24979
TARICCO, G. p 2450 N94-23228
TARVER, C. M. p 2265 N94-23778
p 2265 N94-23807
TASK, H. LEE p 2432 N94-23982
p 2432 N94-23983
TATARCHUK, BRUCE J. p 2391 N94-23351
p 2393 N94-23364
TATENO, SATOSHI p 2305 N94-23835
TATTAR, MARC J. p 2170 N94-25173
TAUB, SUSAN R. p 2313 N94-25170
TAUR, R. R. p 2279 N94-22770
TAVERNIER, GILLES p 2202 N94-23925
TAYLOR, ARTHUR C., III p 2265 N94-24301
TAYLOR, BRUCE C. p 2427 N94-25378
TAYLOR, E. JENNINGS p 2394 N94-23366
TAYLOR, GREGORY p 2416 N94-25271
TAYLOR, GREGORY E. p 2408 N94-23576
TAYLOR, LESLIE A. p 2276 N94-22750
TAYLOR, MIKE p 2183 N94-24972
TAYLOR, R. E. p 2248 N94-25128
TAYLOR, R. M. p 2521 N94-25010
TAYLOR, ROBERT P. p 2320 N94-23637
TAYLOR, STEVEN L. p 2410 N94-24355
TAYLOR, W., IV p 2523 N94-24658
TCHANTCHANE, A. p 2448 N94-23024
TCHON, KRZYSZTOF p 2469 N94-22712
TEANEY, P. E. p 2243 N94-23784
TEDESCO, MARK p 2205 N94-24702
TEERINK, W. p 2361 N94-24035
TEEUW, W. B. p 2465 N94-22986
TELEMAN, NICOLAS p 2488 N94-24536
TELLA, GUSTAVO p 2179 N94-24332
p 2190 N94-24551
p 2184 N94-25004
TEMAM, ROGER p 2327 N94-24139
TENTHIJEBOONKAMP, J. H. M. p 2491 N94-24954
TENTHIJEBOONKKAMP, J. H. M. p 2334 N94-24574
TERAKURA, KIYOYUKI p 2564 N94-24960
TERDAN, FRED p 2222 N94-25201
TERKUILE, W. M. p 2417 N94-23176
TERRY, J. p 2407 N94-23132
TERRY, P. W. p 2533 N94-23435
THANG, NGUYEN TOAN p 2492 N94-25334
THANG, TRAN QUYET p 2493 N94-25433
THE, P. S. p 2599 N94-23334
THEILER, J. p 2557 N94-22940
THEIS, GERHARD p 2305 N94-23847
THEODORE, B. p 2622 N94-24900
THEOFYLAKTOS, NOULIE p 2280 N94-22780
THIBAULT, JEAN-PHILIPPE p 2471 N94-22907
THIBODEAUX, A. F. p 2262 N94-25159
THIEMANN, J. G. F. p 2481 N94-23442
THILL, D. C. p 2173 N94-24864
THOM, A. J. p 2227 N94-22977
THOMAS, CHARLES P. p 2345 N94-24831
THOMAS, GREG p 2181 N94-24787
THOMAS, R. C. p 2234 N94-24772
p 2565 N94-25086
THOMAS, R. K. p 2268 N94-23000
THOMAS, STAN J. p 2477 N94-23247
THOMPSON, ANNE p 2413 N94-24390
p 2414 N94-24398
THOMPSON, C. D. p 2238 N94-22936
THOMPSON, J. D. p 2557 N94-22925
THOMPSON, JOHN F. p 2249 N94-25142
THOMPSON, MICHAEL W. p 2306 N94-25379
THOMPSON, ROGER C. p 2208 N94-24449
THOMPSON, STEVEN R. p 2251 N94-25531
THOMSON, DENNIS W. p 2528 N94-24217
THORN, KAREN E. p 2203 N94-23949
THORN, R. J. p 2556 N94-22912
p 2561 N94-23432
THORNTON, STEPHEN V. p 2168 N94-24295
THORWALD, GREGORY p 2376 N94-23560
THUAN, NGUYEN NGOC p 2492 N94-25334
TIBBITTS, SCOTT F. p 2361 N94-24034
TIESINGA, EITE p 2537 N94-25239
TIETSWORTH, STEVEN C. p 2302 N94-25049
TIITTA, A. T. p 2566 N94-25347
TILBROOK, I. R. p 2590 N94-23190
TIMMINS, S. P. p 2388 N94-24757
TIRKAS, PANAYIOTIS A. p 2365 N94-24699
TISCHLER, DAYNA S. p 2180 N94-24479
TISCHLER, MARC E. p 2420 N94-24124
TISDALE, WILLIAM R. H. p 2281 N94-22784
TISTAD, LENA p 2437 N94-24292
TITLE, A. p 2600 N94-22850
TITRAN, ROBERT H. p 2242 N94-23550
TIVANOV, GENADI p 2154 N94-24248
TIWARI, S. N. p 2530 N94-25177
TOBBECHE, S. p 2448 N94-23024
TODD, BETH A. p 2427 N94-25380
TOEPFER, GEORGE p 2183 N94-24975
TOGNARELLI, MICHAEL p 2182 N94-24837
TOKARZEWSKI, STANISLAW p 2490 N94-24768
TOLSON, ROBERT H. p 2474 N94-24635
TOMASELLI, CLARE MARIE p 2426 N94-23530
TOMITA, AKIHIKO p 2603 N94-24985
TOMSIA, ANTONI P. p 2244 N94-23811
TONETTI, N. p 2357 N94-24002
TOP, JAAP p 2479 N94-23139
TORGERSON, SHAD p 2184 N94-25268
TORO, E. F. p 2340 N94-25486
TORRENCE, GEOFFREY W. p 2283 N94-22792
TORRES, S. G. p 2240 N94-23017
TOSCANO, WILLIAM B. p 2426 N94-24102
TOTSUKA, YOJI p 2627 N94-24962
TOUR, JAMES M. p 2257 N94-24558
p 2259 N94-24789
p 2260 N94-24815
p 2260 N94-24863
p 2260 N94-24922
p 2260 N94-24924
p 2235 N94-24925
p 2537 N94-25087
p 2262 N94-25145
TOUZENE, ABDEREZAK p 2444 N94-22900
TOWELL, TIMOTHY W. p 2252 N94-23076
TOWNSEND, J. p 2376 N94-23342
TOWNSEND, JAMES C. p 2457 N94-24603
TOWNSEND, LAWRENCE W. p 2540 N94-23509
p 2540 N94-24305
TRACY, M. B. p 2169 N94-24464
TRAN, THO C. p 2545 N94-24730
TRAUB, WESLEY A. p 2404 N94-24738
TRAVERS, M. N. p 2289 N94-22833
TRAVIS, L. D. p 2616 N94-24872
TRESSER, CHARLES p 2481 N94-23548
TRESSLER, R. E. p 2231 N94-22933
TREUR, J. p 2486 N94-23762
p 2487 N94-23765
TREUR, JAN p 2474 N94-24543
p 2489 N94-24643
TRINCHIERI, GINEVRA p 2600 N94-25269
TRIPATHY, S. K. p 2260 N94-24813
TRIPOLI, GREG p 2413 N94-24385
TRIVEDI, KISHOR S. p 2451 N94-23340
p 2458 N94-24680
TROENDLY, GREGORY p 2516 N94-23943
TROPEA, C. p 2316 N94-22856
TROUVE, A. p 2237 N94-24158
TRUE, B. p 2188 N94-24594
TRUMBORE, SUSAN E. p 2399 N94-24853
TRUONG, THE p 2272 N94-23892
TRUSZKOWSKI, WALTER F. p 2443 N94-23936
TRY, PAUL p 2411 N94-24376
TRYK, DONALD p 2393 N94-23360
TRYK, DONALD A. p 2391 N94-23347
TSANG, K. M. p 2463 N94-25321
TSENG, WU-YANG p 2186 N94-23255
p 2188 N94-24180
TSO, JIN p 2165 N94-22894
TSUEI, HSIN-HUA p 2210 N94-23033
TUAN, HOANG ANH p 2492 N94-25334
TUCHMAN, ALAN p 2520 N94-23964
p 2520 N94-23966
TUECKE, S. p 2450 N94-23207
TULINTSEFF, A. p 2289 N94-22832
TUMURA, KAORU p 2207 N94-23910
TUNBRIDGE, D. p 2362 N94-24041
TUNBRIDGE, D. E. L. p 2207 N94-24018
TUNG, C. p 2171 N94-25187
TURNER, FRANK p 2187 N94-23519
p 2595 N94-23580
TURNER, GREG p 2275 N94-22744
TURNER, JOYCE E. p 2590 N94-24079
TURNER, LAWRENCE L., JR. p 2372 N94-24553
TURNER, M. H. p 2397 N94-23016
TURNER, ROBERT H. p 2322 N94-23646
TURNS, S. R. p 2266 N94-24700
TURNS, STEPHEN R. p 2210 N94-23031
TUTTLE, B. A. p 2542 N94-23202
TUTTLE, BRUCE A. p 2565 N94-25027
TUTTLE, S. p 2320 N94-23532
TUTTLE, S. L. p 2319 N94-23513
TYREE, GERALD W. p 2364 N94-24175
TZENG, FORREST F. p 2274 N94-22741
TZONG, G. T. J. p 2179 N94-24324

U

UCHIDA, SEISHI p 2188 N94-24490
UCKAN, T. p 2548 N94-22945
UEDA, TAKASHI p 2286 N94-22813
UEDA, YOSHIFUMI p 2345 N94-24977
UENK, D. p 2382 N94-23177
UESUGI, Y. p 2552 N94-24456
UHRIC, TOM p 2321 N94-23643
ULJON, LINDA p 2305 N94-23838
ULMER, LON p 2306 N94-25493
ULVKLO, M. p 2388 N94-24741
ULVSAND, THOMAS p 2437 N94-24292
UMEBAYASHI, TOYOHARU p 2603 N94-24976
UNGER, A. p 2161 N94-24288
UPPERMAN, PIETER MARTINUS p 2462 N94-25237
URAMOTO, JOSHIN p 2536 N94-24868
URBANSKI, E. p 2390 N94-23295
URISTA, JUAN p 2477 N94-23916
URTIEW, P. A. p 2265 N94-23807
UUTTU, TERO p 2379 N94-25418
UZ, MEHMET p 2242 N94-23550

V

V.COSSART, GOETZ p 2402 N94-24108
VAARKAMP, MARINUS p 2236 N94-25250
VAGOV, A. V. p 2567 N94-25424
VAISNYS, A. p 2273 N94-22739
VALDES, CAROL p 2571 N94-23230
VALENTA, LISA p 2184 N94-25002
VALLENTGOED, M. p 2555 N94-22730
VALTONEN, M. p 2308 N94-23130
VAMOS, E. p 2392 N94-23354
p 2393 N94-23361
VANAMELSVOORT, PETRUS J. L. M.
p 2586 N94-25076
VANANDEL-SCHEFFER, PIETERDINA J. M.
p 2236 N94-25296
VANBEEK, P. p 2486 N94-23757
VANBENNEKOM, P. p 2542 N94-23171
VANBRUGGEN-KERKHOF, MARIA JOHANNA
p 2554 N94-25285
VANCE, VICKI L. p 2271 N94-24473
VANDAM, G. C. p 2418 N94-24600
VANDEGOOR, ANTONIUS ALBERTUS A. M.
p 2236 N94-25233
VANDEMORTEL-FRONCZAK, JOANNA MARIA
p 2468 N94-25226
VANDENBERG, JOEREN p 2585 N94-22704
VANDENBOOM, ANTONIUS JOSEPHUS J.
p 2476 N94-25262
VANDENBOOM, H. p 2542 N94-23171
VANDENBOOM, T. J. J. p 2470 N94-22873
VANDENBOSCH, J. F. M. p 2357 N94-24005
VANDENHEUVEL, J. P. p 2478 N94-22715
VANDENHEUVEL, J. P. M. p 2478 N94-22727
VANDERAALST, WILLIBRORDUS M. P.
p 2522 N94-25293
VANDERAAR, MARK p 2202 N94-25095
VANDERBORGH, N. E. p 2392 N94-23357
VANDERHOEK, W. p 2478 N94-22984
p 2473 N94-23747
p 2473 N94-23748
VANDERHOFF, JOHN W. p 2225 N94-24350
VANDERLAAN, J. F. p 2550 N94-23182
VANDERLAAN, PAUL p 2494 N94-23546
p 2494 N94-23798
p 2487 N94-23799
p 2490 N94-24763
VANDERLEEUW, J. p 2495 N94-23814
VANDERLUGT, HERMEN JASPER
p 2541 N94-25256
VANDERMAAREL, H. T. M. p 2317 N94-22985
VANDERMAST, C. p 2592 N94-24642
VANDERPUTTEN, P. H. A. p 2308 N94-23136
VANDERSANDEN, J. J. p 2386 N94-23755
VANDERSCHAFT, A. J. p 2469 N94-22706
p 2469 N94-22707
VANDERSCHOOT, H. p 2459 N94-24758
VANDERVEEN, W. A. p 2404 N94-24598
VANDERZANDEN, ANTONIUS JOHANNUS J.
p 2339 N94-25247
VANDEVEL, M. p 2479 N94-23093
p 2486 N94-23708
VANDEVEN, A. A. F. p 2562 N94-23769
VANDEVORST, G. A. L. p 2336 N94-24761
VANDEWAKKER, ANTONIUS MARIA
p 2587 N94-25283
VANDEWALL, R. E. p 2325 N94-23663
VANDIJK, ALBERT P. H. p 2445 N94-23170
VANDIJK, GERARDUS JOHANNES W.
p 2468 N94-25062
VANDOOREN, G. A. J. p 2283 N94-22795
VANDRESAR, NEIL T. p 2346 N94-25202
VANEEDEN, CONSTANCE p 2494 N94-23546
p 2494 N94-23798
p 2487 N94-23799
VANETTEN, W. p 2347 N94-22874
p 2542 N94-23171
VANFOSSEN, G. JAMES p 2334 N94-24481
p 2338 N94-25183
VANGILS, M. J. p 2470 N94-22877
VANGISBERGEN, S. J. C. H. M. p 2243 N94-23714
VANGRIETHUYSEN, VALERIE J. p 2320 N94-23636
VANGROENENDAAL, WILLEM p 2495 N94-24634
VANHALSEMA, E. p 2381 N94-23145
VANHECKE, H. p 2569 N94-23453
VANHEE, K. M. p 2268 N94-23476
p 2271 N94-24475
p 2456 N94-24513
p 2489 N94-24615
VANHEIJST, EUGENE JOSEPHUS L. J.
p 2446 N94-25081
VANHIMBEECK, CARL p 2284 N94-22801
VANHOESEL, C. P. M. p 2468 N94-24764
VANHOESEL, STAN p 2459 N94-24765
VANJOOLINGEN, WOUTER REINDER
p 2462 N94-25219
VANLANGEVELDE, IZAK p 2474 N94-24543
VANLEEUWEN, H. J. C. p 2382 N94-23177
VANLINDER, B. p 2473 N94-23747
VANOMMEREN, J. C. W. p 2493 N94-22724
VANOOSTROM, V. p 2453 N94-23707
p 2457 N94-24570
VANRAAMSDONK, F. p 2457 N94-24570
VANROSENDALE, JOHN p 2490 N94-24914
VANRYN, PERCY p 2184 N94-25004
VANSCHEVICOVEN, HENK JAN p 2565 N94-25280
VANSINDEREN, M. p 2454 N94-23751
p 2272 N94-24648
VANSTEENWYK, BRETT p 2472 N94-23332
VANSUCH, GREGORY J. p 2351 N94-25445
VANSWEDE, V. p 2589 N94-23095
VANVELDHUIZEN, E. M. p 2268 N94-23174
VANVLIET, J. C. p 2589 N94-23095
VANWIJNEN, PAUL JACQUES p 2313 N94-25253
VARAR, T. p 2390 N94-23295
VARGAS, PEDRO M. p 2378 N94-25143
VARMETTE, PETER G. p 2585 N94-24455
VATALARO, F. p 2277 N94-22761
VAUGHAN, J. D. p 2568 N94-22719
VAULES, DAVID, JR. p 2507 N94-23890
VEAL, B. p 2557 N94-22929
VEAUX, JACQUES p 2176 N94-24181
VEENHOF, R. J. p 2533 N94-23746
VEERS, P. S. p 2371 N94-22918
VEGTER, G. p 2480 N94-23140
VEGTER, GERT p 2479 N94-23138
VEIJALAINEN, JARI p 2588 N94-22734
VELDEN, CHRISTOPHER S. p 2410 N94-24125
VELDHORST, M. p 2451 N94-23441
VELDMAN, H. J. p 2478 N94-22727
VELTMAN, B. p 2467 N94-23756
p 2467 N94-23767
VELTMAN, BART p 2468 N94-25221
VENKATESAN, S. p 2391 N94-23352
VENKATESWARAN, S. p 2216 N94-23066
VENKATESWARAN, SANKARAN p 2213 N94-23046
p 2215 N94-23055
VENKATESWARLU, P. p 2233 N94-24073
VERA, V. J. p 2523 N94-25328
VERAIN, M. A. P. p 2315 N94-23989
VERBEEK, ADRIAAN THOMAS JACQUES
p 2555 N94-25439
VERDON, JOSEPH M. p 2169 N94-24606
VERDURMEN, EDWIN MARIA F. J.
p 2262 N94-25236
VEREGGE, J. R. p 2477 N94-23900
VERES, JOSEPH P. p 2215 N94-23059
VERFAILLIE, GERARD p 2520 N94-23967
VERGNE, P. p 2264 N94-24010
VERHEIJDEN, SANDRA M. L. p 2382 N94-23148
VERHEUL, E. p 2486 N94-23708
VERLINDE, HANS p 2412 N94-24383
VERLINDEN, JOUKE p 2592 N94-24642
VERNUCCI, A. p 2278 N94-22767
p 2279 N94-22768
VERSFELD, NICOLAUS JACOBUS
p 2530 N94-25289
VERWEIJ, M. D. p 2524 N94-23731
VESS, T. M. p 2234 N94-24549
VEST, GERRY W. p 2409 N94-23621
VESTERHEIM, VEGARD p 2453 N94-23534
VETTER, SCOTT K. p 2614 N94-24365
p 2614 N94-24366
p 2615 N94-24367
p 2615 N94-24370
p 2615 N94-24371
p 2616 N94-24372
p 2616 N94-24373
VIALLEFONT, PIERRE p 2464 N94-23911
VIETINGHOFF, H. p 2229 N94-24137
VIGUE, Y. p 2207 N94-23259
VIHERKANTO, KAI p 2357 N94-24000
VILLEDIEU, E. p 2369 N94-23403
VILPAS, MARTTI p 2251 N94-25419
VINCENT, BRETT T. p 2207 N94-23653
VINCENT, DAYTON G. p 2415 N94-24485
VINCENT, F. p 2185 N94-25301
VINE, M. K. p 2362 N94-24042
VIOLA, R. p 2273 N94-22737
p 2286 N94-22816
VIONNET, CARLOS A. p 2325 N94-23668
VISINTIN, ARNALDO p 2391 N94-23353
VISSCHER, MARNIX p 2261 N94-25078
VISSERS, C. A. p 2454 N94-23751
p 2272 N94-24648
VISSERS, M. A. M. p 2386 N94-23755
VITERBI, ANDREW J. p 2282 N94-22786
VO, DINH PHUOC p 2508 N94-23899
VOGEL, CHRISTINE p 2184 N94-25017
VOGEL, WOLFHARD J. p 2283 N94-22792
VOGELZANG, J. p 2381 N94-23145
VOLLTRAUER, H. p 2390 N94-23295
VONBOKERN, GREG J. p 2172 N94-23288
VONDERHAAR, THOMAS H. p 2415 N94-24705
VONLAVEN, G. M. p 2589 N94-23127
p 2589 N94-23128
VOORHIES, COERTE V. p 2403 N94-24465
VORTAC, O. U. p 2176 N94-25444
VOSS, R. p 2407 N94-23156
VRANISH, JOHN M. p 2352 N94-23078
p 2352 N94-23082
p 2354 N94-23969
VUCHIC, B. L. p 2558 N94-22990
VUIK, C. p 2335 N94-24641
VUILLET, ALAIN E. p 2176 N94-23254
VUL, ALEXANDER p 2158 N94-24267

W

WAAGEN, D. p 2490 N94-24921
WAAGEN, DON p 2496 N94-24778
p 2475 N94-25139
WAAS, S. p 2381 N94-23145
WADE, M. R. p 2354 N94-23797
WADSWORTH, J. p 2252 N94-22930
p 2239 N94-22958
p 2229 N94-24547
WAGELMANS, A. P. M. p 2468 N94-24764
WAGENER, R. p 2386 N94-23779
WAGNER, J. p 2252 N94-22992
WAGNER, L. M. p 2241 N94-23434
WAGNER, LEONARD S. p 2303 N94-25089
WAGNER, MICHAEL p 2182 N94-24915
WAGNER, PETER M. p 2316 N94-22857
WAGNER, W. J. p 2625 N94-22845
WAHLEN, MARTIN p 2399 N94-25092
WAINRIGHT, JESSE p 2393 N94-23360
WAKANA, HIROMITSU p 2282 N94-22790
p 2283 N94-22793
p 2287 N94-22821
WAKIZOE, MASANOBU p 2389 N94-22962
WALCEK, CHRISTOPHER p 2413 N94-24390
WALF, K. p 2270 N94-23587
WALGEMOED, H. p 2178 N94-24322
WALGREN p 2599 N94-24051
WALKER, C. K. p 2296 N94-24105
WALKER, D. W. p 2446 N94-24538
WALKER, J. D. p 2335 N94-24689
WALL, M. A. p 2241 N94-23297
WALL, S. D. p 2519 N94-23960
WALL, STEPHEN D. p 2505 N94-23880
WALLACE, CLARK E. p 2320 N94-23636
WALLACE, J. F. p 2349 N94-23286
WALLACE, T. C., SR. p 2348 N94-23203
WALLACE, TIM L. p 2453 N94-23624
WALLING, R. W. p 2541 N94-22868
WALLSTROM, T. p 2569 N94-24516
WALSH, R. P. p 2307 N94-22987
WALSH, THOMAS D. p 2617 N94-24875
WALTER, P. B. p 2217 N94-23071
WALTERBOS, RENE A. M. p 2601 N94-23537
WAN, A. S. p 2347 N94-22867
WANCZUK, G. p 2500 N94-23845
WANDER, JOHN p 2365 N94-24842
WANDZURA, S. p 2491 N94-24947
WANG, C. JEFF p 2231 N94-24450
WANG, CHI R. p 2337 N94-25119
WANG, CHUI-LIN p 2538 N94-25388
WANG, G. p 2270 N94-23589
WANG, JAI-CHING p 2267 N94-24451
WANG, JUNMING p 2367 N94-25249
WANG, LUI p 2202 N94-23921
WANG, MAO-QUAN p 2554 N94-25329
WANG, MENG p 2332 N94-24163
WANG, Q. p 2296 N94-24132
p 2300 N94-24697
WANG, Q. DANIEL p 2601 N94-23537
WANG, SHI-HONG p 2554 N94-25330
WANG, W. J. p 2353 N94-23178
WANG, WEI-XING p 2554 N94-25330
WANG, WEN-ZHENG p 2538 N94-25388
WANG, Y. M. p 2300 N94-24678
WANGLER, T. G. p 2350 N94-24851
WANTUCK, P. J. p 2348 N94-23203
WARD, SUSAN E. p 2196 N94-24820
WARE, A. S. p 2533 N94-23435
WARE, GEORGE M. p 2170 N94-24716
WARK, CANDACE E. p 2336 N94-24793
WARNER, TOM p 2412 N94-24383
p 2413 N94-24391
WARREN, W. L. p 2542 N94-23202
WATANABE, K. Y. p 2553 N94-24623
WATERS, WILLIAM M. p 2301 N94-25045
WATKINS, SETH p 2204 N94-24334
WATSON, ANDREW B. p 2442 N94-25509

WATSON, G. M. .... p 2245 N94-24612
WATSON, JOHN C. .... p 2306 N94-25381
WATSON, WILLIAM .... p 2457 N94-24626
WATTS, C. .... p 2549 N94-22963
WATTS, C. A. .... p 2550 N94-23211
WATTS, D. R. .... p 2418 N94-24795
WAVRE, N. .... p 2355 N94-23988
p 2315 N94-24036
p 2315 N94-24037
WAWRZYNEK, PAUL .... p 2246 N94-25118
WAYDA, MICHAEL E. .... p 2426 N94-24093
WEATHERFORD, CHARLES A. .... p 2536 N94-24798
WEATHERS, JOHN M. .... p 2196 N94-24309
WEAVER, ELLEN C. .... p 2387 N94-24403
WEAVER, STEVEN .... p 2203 N94-23947
WEBB, MIKE .... p 2460 N94-24933
WEBBER, MATT .... p 2182 N94-24915
WEBER, RICHARD .... p 2238 N94-25125
WEDDENDORF, BRUCE C. .... p 2203 N94-23824
WEEKS, WILFORD F. .... p 2419 N94-25088
WEFEL, JOHN P. .... p 2628 N94-25031
WEI, JIAN .... p 2565 N94-25160
WEIDEMANN, H.-J. .... p 2369 N94-23406
WEIHS, T. P. .... p 2241 N94-23297
WEINER, K. H. .... p 2309 N94-23520
WEINER, M. M. .... p 2301 N94-24926
WEINSTEIN, ARNOLD .... p 2179 N94-24401
WEINSTOCK, B. .... p 2376 N94-23342
WEISBIN, C. R. .... p 2370 N94-23414
WEISS, JONATHAN M. .... p 2215 N94-23056
WEISS, R. S. .... p 2395 N94-24563
WEISS, ROSANNE M. .... p 2193 N94-24559
WEISSBERG, I. .... p 2161 N94-24285
WEISSBERG, V. .... p 2160 N94-24278
WELCH, GERARD E. .... p 2189 N94-25185
WELD, KATHRYN R. .... p 2305 N94-23870
WELLEN, J. S. .... p 2348 N94-23168
WELLER, T. .... p 2157 N94-24260
p 2160 N94-24280
WELLIVER, ALBERTUS D. .... p 2185 N94-25069
WELP, U. .... p 2557 N94-22929
WELZ, LINDA L. .... p 2374 N94-23932
WEN, HAI-HU .... p 2555 N94-25333
WENDT, B. J. .... p 2166 N94-23465
WENDT, BRUCE J. .... p 2170 N94-25182
WENSINK, G. J. .... p 2417 N94-24107
WERBY, M. F. .... p 2525 N94-23206
WERLEY, K. A. .... p 2552 N94-24519
WERNER, R. .... p 2178 N94-24320
WERNERT, P. .... p 2165 N94-23149
p 2165 N94-23161
p 2171 N94-25461
WERNLUND, LARS-DAVID .... p 2297 N94-24530
WERT, K. L. .... p 2213 N94-23045
WERTHEIM, A. H. .... p 2542 N94-22895
WERTHMAN, W. LANCE .... p 2217 N94-23069
WERY, BRUNO .... p 2284 N94-22801
WESOKY, HOWARD L. .... p 2398 N94-24104
WESSELS, JAAP .... p 2477 N94-25526
WESSEN, RANDII R. .... p 2504 N94-23871
WESTBROOK, E. .... p 2556 N94-22921
WESTBROOK, M. .... p 2556 N94-22921
WESTERHUIJS, PETER .... p 2537 N94-25228
WESTFALL, B. A. .... p 2241 N94-23434
WESTON, R. J. .... p 2529 N94-25026
WESTON, ROBERT P. .... p 2457 N94-24603
WESTWATER, E. R. .... p 2381 N94-23001
WETZEL, PETER .... p 2413 N94-24387
WHEADON, J. .... p 2506 N94-23887
p 2508 N94-23896
WHEELER, JAMES R. .... p 2391 N94-23350
WHEELER, MARK .... p 2416 N94-25271
WHEELER, MARK M. .... p 2408 N94-23576
WHEELER, R., IV .... p 2556 N94-22886
WHEELWRIGHT, CHARLES D. .... p 2435 N94-24195
WHEITNER, JEFFREY A. .... p 2373 N94-24769
WHIRLEY, R. G. .... p 2568 N94-23216
WHITAKER, KEVIN W. .... p 2477 N94-24452
WHITE, E. .... p 2559 N94-23186
WHITE, O. R. .... p 2629 N94-25260
WHITE, R. G. .... p 2363 N94-24076
WHITE, WARREN .... p 2365 N94-24703
WHITEHORNE, R. L. G. .... p 2202 N94-24121
WHITEHOUSE, D. A. .... p 2626 N94-23515
WHITEHURST, R. A. .... p 2460 N94-24935
WHITING, JEFFREY A. .... p 2417 N94-23291
WHITTAKER, W. .... p 2370 N94-23414
WHITTAKER, WILLIAM .... p 2367 N94-25274
WICZYNSKI, P. D. .... p 2258 N94-24753
WIEDEMAN, ROBERT A. .... p 2282 N94-22786
WIEDEMANN, M. .... p 2178 N94-24320
WIESEMAN, CAROL D. .... p 2163 N94-25105
WIETRICH, F. .... p 2165 N94-23149
p 2165 N94-23161
WIGHT, J. S. .... p 2300 N94-24694
WIGHUS, R. .... p 2268 N94-23430
WIJCKMANS, P. M. E. J. .... p 2481 N94-23455
WILCOX, LAWRENCE M. .... p 2465 N94-25382
WILDIN, MAURICE W. .... p 2336 N94-24821
WILEMSKI, GERALD .... p 2394 N94-23366
WILHELM, J. M. .... p 2375 N94-23294
WILHELM, M. .... p 2292 N94-23269
WILHELM, RENE .... p 2537 N94-25231
WILHELMSON, ROBERT .... p 2414 N94-24392
WILK, M. .... p 2271 N94-23793
WILKINSON, AMIE .... p 2481 N94-23548
WILKINSON, B. M. .... p 2501 N94-23853
WILKINSON, BELINDA .... p 2514 N94-23930
WILKINSON, S. P. .... p 2254 N94-23486
WILKS, D. .... p 2430 N94-23290
WILLEMS, HENRICUS XAVIER .... p 2263 N94-25281
WILLIAMS, ADAM P. .... p 2197 N94-23940
WILLIAMS, D. .... p 2559 N94-23186
WILLIAMS, GLENN L. .... p 2345 N94-25116
WILLIAMS, J. M. .... p 2543 N94-23458
p 2519 N94-23958
WILLIAMS, L. R. .... p 2446 N94-25438
WILLIAMS, M. C. .... p 2390 N94-23212
p 2394 N94-23781
WILLIAMS, ROGER M. .... p 2309 N94-23820
WILLIAMS, TREVOR .... p 2208 N94-25383
WILLIAMSEN, JOEL E. .... p 2203 N94-23824
WILLIS, JERRY W. .... p 2585 N94-25384
WILLSHIRE, WILLIAM L., JR. .... p 2526 N94-24207
WILMINGTON, ROBERT P. .... p 2435 N94-24197
WILMS, R. J. G. .... p 2493 N94-23142
p 2494 N94-23440
p 2481 N94-23442
p 2495 N94-23815
WILSON, BRIAN .... p 2209 N94-24840
WILSON, DAVID J. .... p 2185 N94-25440
WILSON, GORDON R. .... p 2209 N94-24453
WILSON, JEFFREY D. .... p 2310 N94-24056
WILSON, R. JOHN .... p 2622 N94-24901
WILSON, T. M. .... p 2178 N94-24321
WIMER, J. .... p 2390 N94-23212
WINDLEY, PHILLIP J. .... p 2466 N94-23252
p 2467 N94-24075
p 2467 N94-24463
WINER, W. O. .... p 2254 N94-23783
WINKENS, A. .... p 2193 N94-24739
WINTER, TOM .... p 2184 N94-25002
WINTERKAMP, J. .... p 2407 N94-23284
WIRE, G. L. .... p 2239 N94-22999
WITKOWSKI, MONA M. .... p 2374 N94-23932
WITSCH, KRISTIAN .... p 2469 N94-23697
WITT, C. E. .... p 2389 N94-22888
WITT, L. ALAN .... p 2429 N94-25442
WITTE, LARRY C. .... p 2267 N94-23594
WITTENAUER, J. P. .... p 2239 N94-22958
WLAD, FRANK .... p 2184 N94-25021
WNEK, G. E. .... p 2223 N94-24341
WOFSY, STEVEN C. .... p 2404 N94-24738
WOHLMAN, RICHARD A. .... p 2416 N94-23248
WOJCIK, Z. ALEX .... p 2371 N94-23841
WOLD, E. .... p 2561 N94-23445
p 2544 N94-23629
WOLF-WATZ, HANS .... p 2421 N94-24290
WOLF, D. .... p 2558 N94-22990
WOLF, PETER .... p 2252 N94-23075
WOLF, STEPHEN N. .... p 2530 N94-25073
WOLFF, MICHAEL .... p 2598 N94-23536
WOLFF, RICHARD S. .... p 2276 N94-22755
WOLFF, T. .... p 2503 N94-23866
WONG, R. L. .... p 2549 N94-23013
WONG, YEN F. .... p 2305 N94-23918
WONICA, D. .... p 2292 N94-23269
WOO, KEN .... p 2289 N94-22831
WOOD, KATHRYN J. .... p 2426 N94-23623
WOOD, M. LOREN .... p 2175 N94-24127
WOOD, R. F. .... p 2556 N94-22864
p 2556 N94-22919
WOODS, D. .... p 2285 N94-22805
WOODWARD, JOE .... p 2181 N94-24787
WOODWARD, ROGER .... p 2210 N94-23029
WOODWORTH, E. .... p 2540 N94-24662
WOODY, C. .... p 2532 N94-23007
WOOLEY, CHRISTINE L. .... p 2164 N94-25113
WOOLFORD, BARBARA .... p 2435 N94-24196
p 2437 N94-24205
p 2437 N94-24206
WORKMAN, GARY L. .... p 2597 N94-24829
WORTMAN, MICHAEL .... p 2205 N94-24702
WOUTERS, MARCUS JOHANNES F.
p 2587 N94-25279
WRAY, RICHARD B. .... p 2199 N94-23571
WRAY, RICK L. .... p 2172 N94-23288
WRIGHT, ANTHONY .... p 2221 N94-24979
WRIGHT, JOSEPH .... p 2253 N94-23335
WRIGHT, M. C. H. .... p 2599 N94-23705
WRIGHT, S. I. .... p 2557 N94-22938
p 2240 N94-23021
WRIGLEY, ROBERT .... p 2387 N94-24403
WRONA, DANIEL J. .... p 2180 N94-24479
WU, C. T. .... p 2563 N94-24624
WU, CHAO-C. .... p 2312 N94-25042
WU, K. H. .... p 2368 N94-25436
WU, RUILIAN .... p 2260 N94-24815
WU, S. T. .... p 2627 N94-24461
p 2627 N94-24484
WU, S.-C. .... p 2196 N94-23257
WU, SEAN F. .... p 2334 N94-24605
WU, T. K. .... p 2289 N94-22831
p 2289 N94-22835
WUBS, F. W. .... p 2404 N94-24598
WUEBBLES, D. J. .... p 2397 N94-23700
WUJEK, BRETT .... p 2183 N94-25001
WUNDERLICH, BERNHARD .... p 2226 N94-24353
WYATT, CLAIR L. .... p 2384 N94-23607
WYMAN, DOUGLAS J. .... p 2280 N94-22777
WYNGAARD, JOHN .... p 2413 N94-24388
WYNNE, ELEANOR C. .... p 2169 N94-24576
WYSOCK, BARBARA M. .... p 2244 N94-23802

X

XIA, YUAN-FU .... p 2566 N94-25332
XIANG, NONG .... p 2555 N94-25344
XIAO, F. .... p 2319 N94-23460
XIAODAN, LI .... p 2297 N94-24179
XIAODONG, ZHANG .... p 2226 N94-22890
XIONG, Y. .... p 2229 N94-24137
XU, C. .... p 2535 N94-24555
XU, CHUANJING .... p 2526 N94-23718
XU, LIN-BAO .... p 2554 N94-25330
XU, ZHONG LING .... p 2366 N94-24846
p 2490 N94-24847
XUE, CHANGQIN .... p 2404 N94-24738

Y

YABE, T. .... p 2319 N94-23460
YAGLEY, JENNIFER A. .... p 2214 N94-23050
YAHNKE, C. J. .... p 2545 N94-24550
YAMADA, KOJI .... p 2564 N94-24959
YAMADA, SHIGEO .... p 2509 N94-23903
YAMADA, SHUICHI .... p 2271 N94-24459
YAMADA, SIGEO .... p 2207 N94-23910
YAMADA, TAKAHIRO .... p 2207 N94-23860
YAMAGUCHI, M. .... p 2567 N94-25412
YAMAGUCHI, MASUHIRO .... p 2564 N94-24958
YAMAGUCHI, S. .... p 2553 N94-24623
YAMAGUCHI, YASUSHI .... p 2385 N94-23611
YAMAMOTO, I. .... p 2567 N94-25412
YAMAMOTO, ISAO .... p 2564 N94-24958
YAMAMOTO, JUNYA .... p 2271 N94-24459
YAMAMOTO, MINORU .... p 2287 N94-22821
YAMAMOTO, SHIN-ICHI .... p 2282 N94-22790
YAMAMOTO, YOSHIKATSU .... p 2509 N94-23903
p 2207 N94-23910
YAMAMURA, HIDEMASA .... p 2271 N94-24459
YAMAYA, K. .... p 2508 N94-23898
YAMAYA, KOUSAKU .... p 2501 N94-23854
YAMAZAKI, K. .... p 2553 N94-24623
YAMAZAKI, KOZO .... p 2552 N94-24458
YAMBE, M. .... p 2508 N94-23898
YAN, JERRY .... p 2452 N94-23510
YAN, QI-JIE .... p 2566 N94-25332
YAN, Y. .... p 2448 N94-23073
YANDLE, BARBARA .... p 2365 N94-24806
YANG, A. S. .... p 2211 N94-23035
YANG, TAH-TEH .... p 2324 N94-23660
YANG, VIGOR .... p 2211 N94-23034
YANG, YII-CHING .... p 2374 N94-24454
YANG, YUEMEI L. .... p 2235 N94-24790
YANG, ZHIGANG .... p 2336 N94-24713
YATES, J. T., JR. .... p 2565 N94-25160
YATES, LESLIE A. .... p 2165 N94-25169
YEAGER, ERNEST .... p 2393 N94-23360
YEE, HELEN C. .... p 2454 N94-24110
YEH, BRUCE .... p 2221 N94-24834
YEN, J. L. .... p 2297 N94-24296
YEN, WEN .... p 2520 N94-23966
YERSAVICH, ANN .... p 2416 N94-25271
YERSAVICH, ANN M. .... p 2408 N94-23576
YEUNG, K. K. .... p 2455 N94-24122
YEUNG, S. K. .... p 2370 N94-23421
YIH, T. C. .... p 2368 N94-25436
YOKIMCUS, T. A. .... p 2389 N94-22862
YOKOMIZO, MASATO .... p 2207 N94-23910
YONG, L. .... p 2240 N94-23119
YONGACOGLU, A. .... p 2287 N94-22820
YOON, M. .... p 2245 N94-24612
YOON, TAE-WOONG .... p 2477 N94-25470
YOSHIDA, FUMIYOSHI .... p 2501 N94-23854
YOSHIDA, SHOUSEI .... p 2285 N94-22809

YOSHIDA, T. .... p 2370 N94-23415
YOST, FRED .... p 2249 N94-25133
YOU, CHULSOO .... p 2528 N94-24215
YOUNG, JACK H. .... p 2326 N94-23669
YOUNG, JOAN A. .... p 2426 N94-23544
YOUNG, L. E. .... p 2196 N94-23258
YOUNG, PAUL .... p 2313 N94-25170
YOUNG, R. E. .... p 2618 N94-24881
YOUNG, R. J. .... p 2286 N94-22815
YOUNG, S. K. .... p 2306 N94-25498
YOUNG, STEPHEN K. .... p 2306 N94-25494
YU, GUO-YANG .... p 2555 N94-25344
YU, LAI PAUL K. .... p 2312 N94-25042
YU, LU .... p 2538 N94-25388
p 2567 N94-25426
YUEN, JOSEPH H. .... p 2290 N94-23256
YUJIRI, LARRY .... p 2306 N94-25494

Z

ZABLE, MIKE .... p 2183 N94-24974
ZACK, JOHN .... p 2412 N94-24384
ZAGWIJN, P. M. .... p 2561 N94-23222
ZAKRAJSEK, JAMES J. .... p 2364 N94-24483
ZAKS, C. .... p 2283 N94-22794
ZALZALA, ALI M. S. .... p 2446 N94-25312
p 2446 N94-25313
p 2368 N94-25322
ZAMAN, K. B. M. Q. .... p 2167 N94-23592
ZAMBRESKY, LIANA .... p 2416 N94-25071
ZAMEL, JAMES M. .... p 2598 N94-23536
ZANDER, JENS .... p 2297 N94-24531
ZAOUCHE, G. .... p 2197 N94-23856
ZAPOTOSKY, J. E. .... p 2299 N94-24676
ZAVADIL, K. R. .... p 2555 N94-22717
ZAVOSH, FRANK .... p 2365 N94-24699
ZBASNIK, J. P. .... p 2549 N94-23013
ZECCHETTO, S. .... p 2381 N94-23145
ZEE, RALPH .... p 2244 N94-24066
ZEE, WARNER .... p 2181 N94-24591
ZEHNER, D. M. .... p 2532 N94-22956
p 2245 N94-24612
ZEIERMAN, MEIR .... p 2158 N94-24270
ZEIJLMANSVANEMMICHOVEN, P. A.
p 2532 N94-22956
ZEISCHKA, J. .... p 2207 N94-24017
ZELENKA, JIM .... p 2460 N94-24932
ZELENSKY, NIKITA .... p 2196 N94-23920
ZELESNIK, DONNA .... p 2214 N94-23053
ZELLER, REINHARDT R. .... p 2484 N94-23686
ZEMAN, O. .... p 2171 N94-24142
ZEMLYANOV, M. G. .... p 2567 N94-25424
ZENSUS, A. .... p 2599 N94-23705
ZENT, AARON P. .... p 2622 N94-24902
ZEYTINOGLU, NURI .... p 2199 N94-23249
ZGRAGGEN, CRAIG .... p 2182 N94-24915
ZHAI, YA .... p 2566 N94-25332
ZHANG, F. J. .... p 2599 N94-24521
ZHANG, GUO-QI .... p 2377 N94-24645
ZHANG, H. .... p 2476 N94-25308
p 2462 N94-25311
p 2492 N94-25318
ZHANG, JIA-TAI .... p 2554 N94-25330
ZHANG, SHU-GUI .... p 2554 N94-25330
ZHONG, W. .... p 2559 N94-22994
ZHOU, GUI AN .... p 2366 N94-24846
ZHOU, GUOHUI .... p 2340 N94-25466
ZHOU, S.-X. .... p 2561 N94-23428
ZHOU, W. .... p 2616 N94-24872
ZHOU, X. .... p 2310 N94-24070
ZHU, JIAN .... p 2336 N94-24713
ZHU, Q. M. .... p 2492 N94-25306
p 2492 N94-25318
ZHUANG, W. .... p 2287 N94-22820
ZIEGLER, CONRAD .... p 2413 N94-24387
ZIEMANN, A. .... p 2316 N94-22858
ZILBERMAN, M. .... p 2158 N94-24268
ZILBERMAN, MOSHE .... p 2155 N94-24250
ZIMA, HANS .... p 2448 N94-23092
ZIMKAS, CHUCK .... p 2598 N94-25006
ZIMMERMAN, G. A. .... p 2291 N94-23264
ZIMMERMAN, M. L. .... p 2300 N94-24678
ZIMMERMANN, H. .... p 2178 N94-24323
ZISSERMAN, A. .... p 2464 N94-25471
ZOBRIST, GEORGE W. .... p 2447 N94-23250
ZOLE, ARIE .... p 2161 N94-24287
ZOLENSKY, MICHAEL E. .... p 2386 N94-24095
ZOMBECK, MARTIN V. .... p 2600 N94-25269
ZOU, JIANSHENG .... p 2382 N94-23158
ZUBER, M. T. .... p 2401 N94-23282
ZUBRIN, R. .... p 2622 N94-24903
ZUNIGA, FANNY A. .... p 2381 N94-22961
ZUPANC, FRANK J. .... p 2210 N94-23032
ZUPANSKI, MILIJA .... p 2412 N94-24383
ZUREK, RICHARD W. .... p 2617 N94-24876
p 2623 N94-24904
ZUTAUT, S. .... p 2224 N94-24343
ZWANENBURG, R. .... p 2356 N94-23994
ZWEBEN, MONTE .... p 2510 N94-23904
ZWECKER, STELLA .... p 2445 N94-22903

CORPORATE SOURCE INDEX

Typical Corporate Source Index Listing

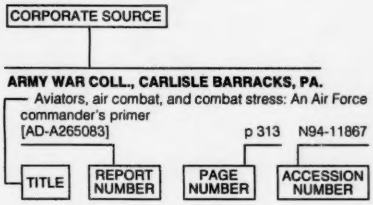

ARMY WAR COLL., CARLISLE BARRACKS, PA.
Aviators, air combat, and combat stress: An Air Force commander's primer
[AD-A265083] p 313 N94-11867

Listings in this index are arranged alphabetically by corporate source. The title of the document provides the user with a brief description of the subject matter. The report number helps to indicate the type of document cited (e.g., NASA report, translation, NASA contractor report). The accession number denotes the number by which the citation is identified. The page number helps you locate the citation in the abstract section. The titles are arranged under each corporate source in ascending accession number order.

A

ABLE ENGINEERING CO., INC., SANTA BARBARA, CA.
A novel rotary actuator for spacecraft
p 2361 N94-24034

ACADEMIA SINICA, BEIJING (CHINA).
LHCD (low hybrid current drive) experiment on the HT-6B tokamak
[DE93-613720] p 2555 N94-25331
Activities of Academia Sinica
[DE93-614529] p 2541 N94-25335

ACADEMY OF SCIENCES (USSR), ALMA-ATA.
Nearly uniform deployment/retrieval strategy for space tether systems p 2156 N94-24256

ACADEMY OF SCIENCES (USSR), MOSCOW.
Solar physics and the Coronas project
p 2625 N94-22847
Mars 96 small rover: Mission strategy
p 2606 N94-23381
Mars 96 rover: Science, instrumentation, and control
p 2369 N94-23395
Balloon experiments at Mars 96 project
p 2608 N94-23396
Results of the Mojave tests of the Mars 96 rover
p 2370 N94-23416
Mars 96 rover: Technical vision and navigation
p 2370 N94-23417

ACADEMY OF SCIENCES (USSR), SAINT PETERSBURG.
Soviet developments of planet rovers in period of 1964 - 1990 p 2369 N94-23374
Machines for moving in soil p 2369 N94-23411
Marsohkod movement control p 2370 N94-23418
Perspective of creation of means for collecting information concerning transport situation
p 2370 N94-23420

ACOUSTICAL SOCIETY OF AMERICA, NEW YORK, NY.
US tag for ISO/TC 108 mechanical vibration and shock: Minutes of the accredited Standards Committee on Mechanical Vibration and Shock, S2
[AD-A273015] p 2376 N94-23789

ADVANCED RESEARCH AND APPLICATIONS CORP., SUNNYVALE, CA.
Demonstration of the feasibility of an integrated x ray laboratory for planetary exploration
[NASA-CR-177631] p 2598 N94-24832

ADVISORY GROUP FOR AEROSPACE RESEARCH AND DEVELOPMENT, NEUILLY-SUR-SEINE (FRANCE).
Cardiopulmonary Aspects in Aerospace Medicine
[AGARD-LS-189] p 2423 N94-23313
Visual Problems in Night Operations
[AGARD-LS-187] p 2431 N94-23976
Aircraft flight safety: A bibliography
[AGARD-R-805] p 2173 N94-24091
Introduction of Ceramics into Aerospace Structural Composites
[AGARD-R-795] p 2255 N94-24228
Integrated Airframe Design Technology
[AGARD-R-794] p 2177 N94-24313
New Advances in Mission Planning and Rehearsal Systems
[AGARD-LS-192] p 2521 N94-25008

AERO-DESIGN AND DEVELOPMENT LTD., REHOVOTH (ISRAEL).
Aerodynamic models for performance calculations of modern technology propellers p 2161 N94-24285

AEROJET-GENERAL CORP., AZUSA, CA.
Earth Observing System (EOS) Advanced Microwave Sounding Unit-A (AMSU-A) schedule plan
[NASA-CR-194856] p 2585 N94-23563

AERONAUTICAL RESEARCH LABS., MELBOURNE (AUSTRALIA).
Proceedings of Workshop on Laser Diagnostics in Fluid Mechanics and Combustion
[AD-A272808] p 2347 N94-22914

AEROSPACE CORP., EL SEGUNDO, CA.
Optical spin polarization and state-sensitive detection of a cesium atomic beam
[ATR-92(8436)-1] p 2534 N94-24077

AEROSPACE MEDICAL RESEARCH LABS., BROOKS AFB, TX.
Artificial gravity in space flight
[AD-A273420] p 2427 N94-24928

AEROSPACE MEDICAL RESEARCH LABS., WILLIAMS AFB, AZ.
Night operations p 2431 N94-23977
Night vision goggle illusions and visual training
p 2432 N94-23984

AEROSPACE MEDICAL RESEARCH LABS., WRIGHT-PATTERSON AFB, OH.
Night vision devices and characteristics
p 2432 N94-23982
Cockpit/NVG visual integration issues
p 2432 N94-23983

AEROSPATIALE, CANNES (FRANCE).
Rover: Autonomous concepts for Mars exploration
p 2369 N94-23400
Data relay system satellite: The development of an antenna pointing mechanism for the inter-orbit link antenna p 2359 N94-24015

AI SIGNAL RESEARCH, INC., HUNTSVILLE, AL.
Develop advanced nonlinear signal analysis topographical mapping system
[NASA-CR-195128] p 2388 N94-24827
Develop advanced nonlinear signal analysis topographical mapping system
[NASA-CR-194785] p 2389 N94-24856

AIR FORCE FLIGHT DYNAMICS LAB., WRIGHT-PATTERSON AFB, OH.
Nonlinear equations of motion for a panel subject to external loads
[AD-A273142] p 2170 N94-24773

AIR FORCE FLIGHT TEST CENTER, EDWARDS AFB, CA.
Analysis of the effects of wake passage on heat transfer in a linear turbine cascade
[AD-A273729] p 2339 N94-25446

AIR FORCE INST. OF TECH., WRIGHT-PATTERSON AFB, OH.
Transient studies of capillary-induced flow
p 2325 N94-23662
Third Annual Foreign Acquisitions Workshop: Improving Access to Foreign Gray Literature
[NASA-TM-109683] p 2593 N94-24759
Infrared fluorescence studies of electronic-to-vibrational energy transfer in a Br2:NO system
[AD-A273727] p 2539 N94-25443
The effects of optical feedback on polarization of vertical cavity surface emitting lasers
[AD-A273728] p 2351 N94-25445
Analysis and characteristics of compressor stall precursor signals in forward and AFT swept high speed compressor
[AD-A273820] p 2171 N94-25517
Solving the ranking and selection indifference-zone formulation for normal distributions using computer software
[AD-A273821] p 2496 N94-25518
Experimental characterization of the AFIT Neutron Facility
[AD-A273822] p 2539 N94-25519
Numerical analysis of the motion of a rigid body with an attached spring-mass-damper
[AD-A273825] p 2379 N94-25520
Diffusion in electronegative discharges with magnetic fields
[AD-A273826] p 2304 N94-25521
Automatic pressure control system for the Wright Laboratory Compressor Research Facility
[AD-A273827] p 2194 N94-25522
Modeling of a large undamped space structure using time domain techniques
[AD-A273828] p 2206 N94-25523
Effect of longitudinal vibration on the capillary limit of a wrapped screen wick copper/water heat pipe
[AD-A273830] p 2571 N94-25524
Flight controller design using mixed H2/H infinity optimization with a singular H infinity constraint
[AD-A273831] p 2191 N94-25525
Steady motions of rigid body satellites in a central gravitational field
[AD-A273742] p 2206 N94-25532
A theoretical investigation of electrically tunable birefringent optical filters as the special discriminator in hyperspectral imaging systems
[AD-A273743] p 2547 N94-25533
Off-design performance of crenulated blades in a linear compressor cascade
[AD-A273744] p 2340 N94-25534
Shielded Coil Electrodynamic Propulsion (SCEP). A feasibility study
[AD-A273824] p 2314 N94-25539

AIR FORCE MATERIALS LAB., WRIGHT-PATTERSON AFB, OH.
Aircraft digital flight control technical review
p 2163 N94-25106

AIR FORCE OFFICE OF SCIENTIFIC RESEARCH, BOLLING AFB, WASHINGTON, DC.
Research interests and broad agency announcement 94-1 of the Air Force Office of Scientific Research
[AD-A273410] p 2632 N94-25075

AIR FORCE SYSTEMS COMMAND, BROOKS AFB, TX.
Screening for asymptomatic coronary heart disease
p 2423 N94-23315
Aeromedical disposition for coronary artery disease
p 2423 N94-23316
Primary prevention of coronary heart disease
p 2423 N94-23317
Aeromedical disposition of Arrhythmias and electrocardiographic findings in aircrew
p 2423 N94-23318
Echocardiographic findings in trained aircrew: The effect of +Gz on cardiac structure (working group 18)
p 2424 N94-23320
Aeromedical implications of mitral valve prolapse
p 2424 N94-23323

AIR FORCE TEST PILOT SCHOOL, EDWARDS AFB, CA.
Carbon monoxide fuel cells as a source for Mars rover electric power p 2314 N94-23409

AKRON UNIV., OH.

Study of transient behavior of finned coil heat exchangers p 2321 N94-23642

Evaluation of bioimpedance for the measurement of physiologic variables as related to hemodynamic studies in space flight p 2427 N94-25378

ALABAMA A & M UNIV., HUNTSVILLE.

A study of the core module simulator floor capability p 2380 N94-24418

Effects of thermal-solutal convection on temperature and solutal fields under various gravitational orientations p 2267 N94-24451

ALABAMA AGRICULTURAL AND MECHANICAL COLL., NORMAL.

Direct observation of crystal growth from solution using optical investigation of a growing crystal face [NASA-CR-195141] p 2563 N94-24617

ALABAMA UNIV., HUNTSVILLE.

Design of a new high-performance pointing controller for the Hubble Space Telescope [NASA-CR-193891] p 2364 N94-24088

Excitation of XUV radiation in solar flares [NASA-CR-193703] p 2627 N94-24094

Temperature dependence of protein solubility-determination, application to crystallization, and growth kinetics studies p 2224 N94-24344

Nonlinear optical thin films p 2225 N94-24349

The 1993 NASA/ASEE Summer Faculty Fellowship Program [NASA-CR-193862] p 2574 N94-24405

Interoperability through standardization: Electronic mail, and X Window systems p 2575 N94-24406

Risk identification and reduction in integrated product teams p 2497 N94-24407

Viscoelastic analysis of seals for extended service life p 2371 N94-24408

Finite element based electric motor design optimization p 2315 N94-24411

Foil bearings p 2371 N94-24415

Design and specification of a centralized manufacturing data management and scheduling system p 2577 N94-24416

Technology utilization office data base analysis and design p 2577 N94-24417

A compilation of technology spinoffs from the US Space Shuttle Program p 2578 N94-24424

Measuring the dynamics of structural changes in biological macromolecules from light scattering data p 2422 N94-24426

J-integral patch for finite element analysis of dynamic fracture due to impact of pressure vessels p 2381 N94-24429

CFD simulation of coaxial injectors p 2342 N94-24430

Evaluation of ovostatin and ovostatin assay p 2422 N94-24437

Evaluation of computer-aided instruction techniques for the crew interface coordination position p 2429 N94-24438

Controller modeling and evaluation for PCV electro-mechanical actuator p 2371 N94-24441

LRAT: Lightning Radiative Transfer p 2416 N94-24443

The Far Ultraviolet (FUV) auroral imager for the Inner Magnetospheric Imager (IMI) mission: Options p 2209 N94-24453

Scientific study in solar and plasma physics relative to rocket and balloon projects [NASA-CR-193885] p 2627 N94-24461

Model development for Ulysses and SOHO [NASA-CR-193884] p 2627 N94-24484

Investigate zero-stress replicated optics [NASA-CR-193889] p 2545 N94-24665

NASA tech brief evaluations [NASA-CR-195150] p 2597 N94-24829

Polarization analysis of a balloon-borne solar magnetograph [NASA-CR-193908] p 2345 N94-24852

Analysis of SOFCAL calibration data [NASA-CR-193910] p 2345 N94-25000

An analysis of gamma ray burst time histories [NASA-CR-195191] p 2629 N94-25199

On the physics of waves in the solar atmosphere: Wave heating and wind acceleration [NASA-CR-195197] p 2628 N94-25264

Loading, electromyograph, and motion during exercise p 2427 N94-25380

ALABAMA UNIV., TUSCALOOSA.

The 1993 NASA/ASEE Summer Faculty Fellowship Program [NASA-CR-193862] p 2574 N94-24405

Impact damage in filament wound composite bottles p 2231 N94-24421

Access to space studies p 2199 N94-24434

Using neural networks to assist in OPAD data analysis p 2477 N94-24452

Design and application of electromechanical actuators for deep space missions [NASA-CR-195134] p 2365 N94-24842

Use of photostress to characterize the mechanical behavior of weldments [NASA-CR-195201] p 2378 N94-25267

ALASKA UNIV., FAIRBANKS.

WISPER: Wirless Space Power Experiment [NASA-CR-195538] p 2396 N94-24701

National Academy of Sciences-Academy of Sciences of the USSR Workshop on the Mechanics of Ice and its Applications [AD-A273338] p 2419 N94-25088

ALCATEL ESPACE, TOULOUSE (FRANCE).

Rover: Autonomous concepts for Mars exploration p 2369 N94-23400

ALENIA AERONAUTICA, TORINO (ITALY).

The integration of design and manufacturing processes at Alenia DVD p 2179 N94-24325

ALGIERS UNIV. (ALGERIA).

VTGRAPH:Computer graphics program using ReGIS mode [DE94-600342] p 2448 N94-23024

ALLIED-SIGNAL AEROSPACE CO., PHOENIX, AZ.

The 3-D CFD modeling of gas turbine combustor-integral bleed flow interaction p 2189 N94-23658

AMARILLO COLL., TX.

Modeling of the ground-to-SSFMB link networking features using SPW p 2306 N94-25381

AMERICAN MOBILE SATELLITE CORP., WASHINGTON, DC.

US domestic and international regulatory issues p 2275 N94-22748

AMES LAB., IA.

Evaluation of A5Si3Z(x) intermetallics for use as high temperature structural materials [DE93-041127] p 2227 N94-22977

New extensions in the development of deformation processed metal-metal matrix composites [DE94-000692] p 2227 N94-23004

Creep deformation characteristics of ductile discontinuous fiber reinforced composites [DE94-000697] p 2227 N94-23005

A numerical analysis of crack propagation in microcracking ceramic and ceramic composites [DE94-001192] p 2253 N94-23183

Density functional studies: First principles and semi-emperical calculations of clusters and surfaces [DE94-002836] p 2561 N94-23214

Large-scale production of Si(0.8)Ge(0.2) thermoelectric alloys by mechanical alloying [DE94-000695] p 2243 N94-23753

AMSTERDAM UNIV. (NETHERLANDS).

Local grid refinement method for the euler equations [PB93-223329] p 2317 N94-22985

Application of maximum entropy and irreducible cluster integrals to joint probability distributions for x ray structure determination [PB93-224152] p 2559 N94-23109

Ga delta-doping layers in silicon [PB93-224632] p 2561 N94-23222

Magnetic resonance study of zinc-related defects in silicon with optimized EPR spectrometer [PB93-224640] p 2561 N94-23223

Electrophysiology of the rat nucleus accumbens: Local circuitry, neuromodulation and synaptic plasticity [PB93-232254] p 2420 N94-23454

Medians and steiner trees [PB94-110616] p 2486 N94-23708

Reactivity of ambident anions in the gas phase [PB93-232189] p 2533 N94-23713

Magnetic resonance studies of 3d transition metal impurities in compound semiconductors [PB93-232197] p 2243 N94-23714

Low mass muon pair production in 450 GeV p-Be collisions [PB94-110699] p 2533 N94-23746

Sequential composition, action prefixes and process prefix [PB94-101433] p 2488 N94-24539

Real-time process logic [PB94-101441] p 2446 N94-24540

The L3 visualization system and its use in the Z(zero) line shape analysis [ETN-94-95382] p 2537 N94-25231

The state space method for integro-differential equations of convolution type with rational matrix symbols [ETN-94-95379] p 2491 N94-25244

Wiener-Hopf factorization of rational matrix functions in terms of realizations: An alternative version [ETN-94-95380] p 2491 N94-25245

The determination of the branching ratios of the Z(zero) boson into heavy quarks using neural networks [ETN-94-95381] p 2538 N94-25246

Bottom quark production at the Z resonance [ISBN-9-09-006217-3] p 2538 N94-25255

The data-acquisition and second level trigger system for ZEUS calorimeter [ETN-94-95384] p 2541 N94-25256

Applications of supersymmetric quantum mechanics [ETN-94-95385] p 2570 N94-25257

On BRST quantization of constrained systems [ETN-94-95386] p 2570 N94-25258

Relativistic hadrons in an external field [ETN-94-95387] p 2538 N94-25259

ANACAPA SCIENCES, INC., FORT RUCKER, AL.

Aviation system safety risk management tool analysis. Volume 2: Appendices [AD-A273502] p 2173 N94-24864

ANALEX CORP., BROOK PARK, OH.

Phase linearity of the 914H coupled-cavity traveling wave tube [NASA-CR-191056] p 2290 N94-23087

ANGLIN AND GIACCHERINI, PLAYA DEL REY, CA.

International organizations to enable world-wide mobile satellite services p 2275 N94-22749

APPLIED RESEARCH, INC., HUNTSVILLE, AL.

New Ways Of Doing Business (NWODB) cost quantification analysis [NASA-CR-195186] p 2586 N94-25197

APPLIED RESEARCH CORP., LANDOVER, MD.

Observational studies of the clearing phase in proto-planetary disk systems [NASA-CR-195182] p 2604 N94-25265

APPLIED SILICON, INC., OTTAWA (ONTARIO).

ASPT software source code: ASPT application software package, host component [CTN-94-60907] p 2455 N94-24116

ASPT software source code: ASPT signal excision software package [CTN-94-60904] p 2296 N94-24133

ASPT software source code: Development system package, library component [CTN-94-60905] p 2455 N94-24134

ASPT software source code: ASPT application software package, VME-C30 component [CTN-94-60906] p 2455 N94-24135

ARGONNE NATIONAL LAB., IDAHO FALLS, ID.

Electrical transport in La(2-x)Sr(x)CuO(4-y) [DE93-040885] p 2556 N94-22912

Grain-boundary microchemistry and intergranular cracking of irradiated austenitic stainless steel [DE94-000466] p 2242 N94-23457

ARGONNE NATIONAL LAB., IL.

Relationship of microstructure and mechanical properties for V-Cr-Ti alloys [DE94-001431] p 2238 N94-22718

Theoretical studies of wave propagation in multilayered piezoelectric media [DE93-040273] p 2371 N94-22872

Heavy ion irradiation of Bi-2223 silver-clad tapes for superconducting current density enhancement [DE93-017416] p 2556 N94-22886

Overview of global greenhouse effects [DE93-041165] p 2396 N94-22887

The de Haas-van Alphen measurements in Ba(0.6)K(0.4)BiO3 [DE93-041169] p 2556 N94-22920

Characterization of CCD-based imaging x ray detectors for diffraction experiments [DE93-041343] p 2556 N94-22921

The elastic and electromechanical properties of BaTiO3 single crystal through the ferroelectric transition [DE94-001437] p 2557 N94-22927

Anisotropic uniaxial pressure effects in YBa2Cu3O(7-delta) [DE94-001456] p 2557 N94-22929

Proceedings of the Fifth Users Meeting for the Advanced Photon Source [DE93-040692] p 2531 N94-22948

Users manual for the Chameleon parallel programming tools [DE94-001934] p 2465 N94-22973

Atomic-scale structure of grain boundaries: Correlations to grain boundary properties [DE94-001289] p 2558 N94-22990

Vehicle/guideway interaction and ride comfort in maglev systems [DE94-001319] p 2352 N94-22991

The structure and spin dynamics of lanthanide-bearing silicate glasses [DE94-001320] p 2252 N94-22992

Design of microchannels for cryostabilization of high temperature superconducting magnets [DE94-001324] p 2559 N94-22993

Processing of YBCO superconductors for improved levitation force [DE94-001326] p 2559 N94-22994

Photo-induced antiferromagnetic interlayer coupling in Fe superlattices with iron silicide spacers [DE94-001345] p 2559 N94-22995

Performance analysis of the combined EDS maglev propulsion, levitation, and guidance system
[DE94-001346] p 2352 N94-22996

Effects of neutron irradiation and hydrogen on ductile-brittle transition temperatures of V-Cr-Ti alloys
[DE94-001466] p 2240 N94-23009

Modifications to 8x8 dynamical theory: Polarizations redefined according to x ray diffraction convention
[DE94-001290] p 2560 N94-23187

Proposed additions to the SHADOW ray-tracing code for general-asymmetric perfect-crystal optics
[DE94-001291] p 2560 N94-23188

Generalized melting criterion for beam-induced amorphization
[DE94-001333] p 2560 N94-23189

A system for managing information at ATLAS
[DE94-001337] p 2590 N94-23190

Effect of neutron irradiation on tensile properties of V-Cr-Ti alloys
[DE94-001433] p 2240 N94-23194

Programming in Fortran M
[DE94-000541] p 2450 N94-23207

Asymptotic analysis: Working note no. 3, boundary layers
[DE94-002299] p 2318 N94-23213

Conductors with small Fermi energies and small gap energies
[DE93-040887] p 2561 N94-23432

Applications of the Aurora parallel PROLOG system to computational molecular biology
[DE93-041166] p 2420 N94-23468

Computational model of surface ablation from tokamak disruptions
[DE94-002204] p 2550 N94-23474

Exact transformation of the anisotropic Ginzburg-Landau model and its consequences
[DE94-002208] p 2562 N94-23795

Pulsed Ion Beam Surface Analysis (PIBSA) as a means of in-situ real-time analysis of thin films during growth
[DE94-001276] p 2562 N94-23805

B-quark production at hadron colliders
[DE94-001459] p 2534 N94-23806

Germanium x ray phase plates for the production of circularly polarized x rays
[DE94-002908] p 2545 N94-24550

High-performance computing and communications
[DE94-002215] p 2457 N94-24566

Thermomechanical processing of Ag-clad Bi2Sr2CaCu2O(x) superconductors
[DE94-002347] p 2563 N94-24624

Superconducting energy storage
[DE94-002248] p 2395 N94-24654

ARIZONA STATE UNIV., TEMPE.

On the numeric integration of dynamic attitude equations
[NASA-CR-194788] p 2448 N94-23073

The explicit computation of integration algorithms and first integrals for ordinary differential equations with polynomials coefficients using trees
[NASA-CR-194787] p 2448 N94-23074

High-frequency techniques for RCS prediction of plate geometries and a physical optics/equivalent currents model for the RCS of trihedral corner reflectors, parts 1 and 2
[NASA-CR-195140] p 2298 N94-24616

Advanced electromagnetic methods for aerospace vehicles
[NASA-CR-195111] p 2365 N94-24699

UV extinction and IR emission in diffuse H2 regions
[NASA-CR-195194] p 2600 N94-25270

ARIZONA UNIV., TUCSON.

Eos cross-calibration radiometers
p 2383 N94-23601

An application of small-gap equations in sealing devices p 2325 N94-23668

Skeletal muscle metabolism in hypokinetic rats
[NASA-CR-195082] p 2420 N94-24124

Solid rocket combustion simulator technology using the hybrid rocket for simulation
[NASA-CR-195142] p 2265 N94-24578

Autonomous Space Processor for Orbital Debris (ASPOD)
[NASA-CR-195521] p 2204 N94-24621

Mars dust-driven tides and their impact on the thermosphere p 2617 N94-24876

ARMSTRONG STATE COLL., SAVANNAH, GA.

A review of ISEAS design p 2465 N94-24410

ARMY AEROMEDICAL RESEARCH LAB., FORT RUCKER, AL.

Projected effectiveness of airbag supplemental restraint systems in US Army helicopter cockpits
[AD-A273250] p 2174 N94-25141

ARMY ARMAMENT RESEARCH, DEVELOPMENT AND ENGINEERING CENTER, WATERVLIET, NY.

X ray diffraction analysis of electrodeposited beta-tantalum
[AD-A273254] p 2249 N94-25142

ARMY AVIATION SYSTEMS COMMAND, MOFFETT FIELD, CA.

The future of rotary-wing aircraft p 2185 N94-25070

ARMY BELVOIR RESEARCH AND DEVELOPMENT CENTER, FORT BELVOIR, VA.

Investigation of the ultrafiltration technique using military greases
[AD-A273633] p 2261 N94-25029

ARMY CONSTRUCTION ENGINEERING RESEARCH LAB., CHAMPAIGN, IL.

Electrochemical behavior of ion-plated TiN and Cu-Cr coatings
[AD-A273411] p 2235 N94-24784

The use of design automation software by government-contracted architect/engineer firms: A status report
[AD-A273181] p 2459 N94-24812

Demonstration of polyscann ultrasonic butt-fusion inspection system for polyethylene pipes
[AD-A273279] p 2373 N94-24814

Flow and temperature distribution in a naturally stratified thermal storage tank
[AD-A273511] p 2336 N94-24821

Aqueous alkaline cleaners: An alternative to organic solvents
[AD-A273510] p 2260 N94-24848

Declarative Object Manipulation Environment (DOME): Alpha version
[AD-A273233] p 2460 N94-24935

ARMY ELECTRONIC PROVING GROUND, FORT HUACHUCA, AZ.

Analog communication transmitter and receiver test procedures
[AD-A273423] p 2300 N94-24687

ARMY ENGINEER WATERWAYS EXPERIMENT STATION, VICKSBURG, MS.

Joint Acoustic Propagation Experiment (JAPE)
p 2527 N94-24208

Analysis of passive acoustic ranging of helicopters from the joint acoustic propagation experiment
p 2529 N94-24220

Preliminary analysis of the JAPE ground vehicle test data with an artificial neural network classifier
p 2529 N94-24222

ARMY RESEARCH LAB., ABERDEEN PROVING GROUND, MD.

A comparison of in-bore projectile motion from an electromagnetic railgun versus that of a conventional cannon barrel
[AD-A273473] p 2198 N94-24690

ARMY RESEARCH LAB., WATERTOWN, MA.

A preliminary evaluation of the phosphazene resin PPZ
[AD-A273674] p 2263 N94-25410

ARMY RESEARCH LAB., WHITE SANDS MISSLE RANGE, NM.

Comparison between 1-minute and 15-minute averages of turbulence parameters p 2528 N94-24218

ARMY TOPOGRAPHIC ENGINEERING CENTER, FORT BELVOIR, VA.

Hyperspectral imagery classification using a backpropagation neural network
[AD-A273615] p 2545 N94-24730

Edge detection using a complex wavelet
[AD-A273699] p 2493 N94-25452

ATLAS ELEKTRONIK G.M.B.H., BREMEN (GERMANY).

Some results gained from JAPE: An overview
p 2527 N94-24209

ATR OPTICAL AND RADIO COMMUNICATIONS RESEARCH LABS., KYOTO (JAPAN).

Study of LEO-SAT microwave link for broad-band mobile satellite communication system p 2279 N94-22769

AUBURN UNIV., AL.

Spatial and temporal variability of soil temperature, moisture and surface soil properties
[NASA-CR-194109] p 2401 N94-23337

High surface area, low weight composite nickel fiber electrodes p 2391 N94-23351

Composite fiber structures for catalysts and electrodes
p 2393 N94-23364

Limiting factors for carbon based chemical double layer capacitors p 2394 N94-23365

Theoretical atomic physics for fusion
[DE94-000712] p 2533 N94-23543

Hot hydrogen testing of metallic turbo pump materials
[NASA-CR-193880] p 2244 N94-24066

Update of GRASP/Ada reverse engineering tools for Ada
[NASA-CR-193890] p 2455 N94-24111

Numerical modeling of physical vapor transport under microgravity conditions: Effect of thermal creep and stress p 2223 N94-24340

Validation of a nonintrusive optical technique for the measurement of liquid mass distribution in a two-phase spray p 2548 N94-24420

Octave: A MARSYAS post-processor for computer-aideed control system design
p 2465 N94-24422

Weld fracture criteria for computer simulation
p 2251 N94-24425

Integration and evaluation of a simulator designed to be used within a dynamic prototyping environment
p 2198 N94-24436

Influence of backup bearings and support structure dynamics on the behavior of rotors with active supports
[NASA-CR-195106] p 2365 N94-24751

Thermophysical property sensitivity effects in steel solidification p 2246 N94-25122

An extended laser flash technique for thermal diffusivity measurement of high-temperature materials
p 2238 N94-25132

AUTOMETRIC CORP., INC., ALEXANDRIA, VA.

Image analysis technology applied to problems in crystallography
[AD-A273516] p 2566 N94-25288

B

BABAKIN ENGINEERING AND RESEARCH CENTER, MOSCOW (RUSSIA).

Prospects for using mobile vehicles in missions to Mars and other planets p 2607 N94-23384

Rover in the Mars 96 mission p 2609 N94-23397

BARNES ENGINEERING CO., SHELTON, CT.

Worst case analysis: Earth sensor assembly for the tropical rainfall measuring mission observatory
[NASA-CR-189320] p 2311 N94-24754

BARRON ASSOCIATES, INC., STANDARDSVILLE, VA.

Adaptive nonlinear polynomial neural networks for control of boundary layer/structural interaction
[NASA-CR-189645] p 2525 N94-23698

BATTELLE NORTHWEST LABS., RICHLAND, WA.

Atmospheric Radiation Measurement (ARM)/CART site p 2411 N94-24379

BEI MOTION SYSTEMS CO., LITTLE ROCK, AR.

High resolution encoder-motor used in the orbital spin scan radiometer, GOES VAS satellites
p 2209 N94-24038

BELEIDSCOMMISSIE REMOTE SENSING, DELFT (NETHERLANDS).

VIERS-1, phase 3
[BCRS-92-24] p 2381 N94-23145

Literature study on: Remote Fraunhofer luminescence detection of algal bloom in marine environments
[BCRS-92-25] p 2417 N94-23176

Optical component MAC Europe ground truth report: Flevoland 1991 (Netherlands)
[BCRS-92-27] p 2382 N94-23177

HERACLITUS, phase 1. Harbour Entrance of Rotterdam Radar based Current Related Information for Traffic Guidance of Ships: Feasibility of deriving current profile data from sea surface observations in the Rotterdam (Netherlands) port entrance
[BCRS-93-04] p 2417 N94-24107

BEN GURION UNIV. OF THE NEGEV, BEERSHEVA (ISRAEL).

The effect of high altitude pressure on the power and efficiency of an airborne two-stroke engine
p 2155 N94-24253

BENDIX FIELD ENGINEERING CORP., SEABROOK, MD.

The FOT tool kit concept p 2507 N94-23889

BERKELEY RESEARCH ASSOCIATES, INC., CA.

X ray simulator theory support
[AD-A273613] p 2553 N94-24949

BERN UNIV. (SWITZERLAND).

Prospects for future solar-wind missions
p 2624 N94-22841

BERTIN ET CIE., PLAISIR (FRANCE).

Microwelding due to random vibration
p 2359 N94-24019

BETTIS ATOMIC POWER LAB., WEST MIFFLIN, PA.

Irradiation damage behavior of low alloy steel wrought and weld materials
[DE94-000519] p 2239 N94-22999

Thermally activated low temperature creep and primary water stress corrosion cracking of NiCrFe alloys
[DE94-001756] p 2241 N94-23219

Effect of irradiation on the stress corrosion cracking behavior of Alloy X-750 and Alloy 625
[DE94-001759] p 2244 N94-23792

BEVILL STATE COMMUNITY COLL., FAYETTE, AL.

Investigating pyrolysis/incineration as a method of resource recovery from solid waste
p 2444 N94-25375

BHABHA ATOMIC RESEARCH CENTRE, BOMBAY (INDIA).
A new automatic design method to develop multilayer thin film devices for high power laser applications [DE93-632490] p 2347 N94-22967
Design refinement of multilayer optical thin film devices with two optimization techniques [DE93-634228] p 2542 N94-22979

BOEING CO., SEATTLE, WA.
High-order technology: Applying technical excellence to new airplane development p 2185 N94-25069

BOEING COMMERCIAL AIRPLANE CO., SEATTLE, WA.
Airport surface operations requirements analysis [NASA-CR-191508] p 2172 N94-23288

BOEING DEFENSE AND SPACE GROUP, SEATTLE, WA.
Research on polycrystalline thin-film CuInGaSe2 solar cells [DE94-000203] p 2560 N94-23205
Towards the formal specification of the requirements and design of a processor interface unit: HOL listings [NASA-CR-191465] p 2466 N94-23252
Towards the formal verification of the requirements and design of a processor interface unit [NASA-CR-4522] p 2467 N94-24075
Towards the formal specification of the requirements and design of a processor interface unit [NASA-CR-4521] p 2467 N94-24463

BORDEAUX 1 UNIV., TALENCE (FRANCE).
A comparison of locally adaptive multigrid methods: LDC, FAC and FIC p 2485 N94-23692
White-light, pressure, and temperature interferopolarimetric sensor featuring optical fibers [PB93-199792] p 2545 N94-24631

BOSTON COLL., CHESTNUT HILL, MA.
The CRRES time history data base: All sensors [AD-A273737] p 2207 N94-25542

BOWLING GREEN STATE UNIV., OH.
A mixed method Poisson solver for three-dimensional self-gravitating astrophysical fluid dynamical systems p 2484 N94-23684

BRADFORD UNIV. (ENGLAND).
Measurements on the satellite-mobile channel at L and S bands p 2282 N94-22791
Low earth orbit satellite/terrestrial mobile service compatibility p 2288 N94-22827

BRISTOL UNIV. (ENGLAND).
Broadband linearisation of high-efficiency power amplifiers p 2275 N94-22747
Handover aspects for a Low Earth Orbit (LEO) CDMA Land Mobile Satellite (LMS) system p 2288 N94-22824

BRITISH AEROSPACE DEFENCE LTD., PRESTON (ENGLAND).
Frameworks for integrated airframe design p 2178 N94-24318

BRITISH AEROSPACE DEFENSE LTD., FARNBOROUGH (ENGLAND).
Human factors of mission planning systems: Applications and implementation p 2522 N94-25011

BRITISH AEROSPACE PUBLIC LTD. CO., BRISTOL (ENGLAND).
Towards real-time stereovision systems for planetary missions p 2370 N94-23422
Primary deployment mechanism for the European Polar Platform p 2207 N94-23995

BRITISH AEROSPACE PUBLIC LTD. CO., STEVENAGE (ENGLAND).
Applicability of different onboard routing and processing techniques to mobile satellite systems p 2278 N94-22767

BRITISH BROADCASTING CORP., KINGSWOOD (ENGLAND).
The HDTV digital audio matrix [BBC-RD-1993/9] p 2295 N94-24085
An introduction to digital modulation and OFDM techniques [BBC-RD-1993/10] p 2295 N94-24086

BRITISH RAILWAY TECHNICAL CENTRE, DERBY (ENGLAND).
A rail corrugation theory which allows for contact patch size p 2269 N94-23582

BROOKE ARMY MEDICAL CENTER, FORT SAM HOUSTON, TX.
Annual research progress report, fiscal year 1992. Volume 2: Department of Clinical Investigation [AD-A273584] p 2427 N94-24945

BROOKHAVEN NATIONAL LAB., UPTON, NY.
The status of glueballs [DE93-040040] p 2531 N94-22923
A novel method for determination of transport parameters of H2 and O2 in PEMFCs [DE94-001492] p 2389 N94-22962
Low p(sub T) photon production in proton-nucleus collisions at 18 GeV/c [DE94-001380] p 2532 N94-23007
Cloud-free aerosol optical depth determination over oceans from satellite radiometry [DE94-001897] p 2386 N94-23779
In situ and ex situ spectroelectrochemical and x ray absorption studies on rechargeable, chemically-modified and other MnO2 materials [DE94-001387] p 2234 N94-24545

BSO/AEROSPACE AND SYSTEMS B.V., NIEUWEGEIN (NETHERLANDS).
Integrating payload design, planning, and control in the Dutch Utilisation Centre p 2207 N94-23869

BUBBLE TECHNOLOGY INDUSTRIES, INC., CHALK RIVER (ONTARIO).
To perform a proof-of-concept study on the use of superheated drop detectors for the measurement of LET spectra in space environments [BTI-92/3-31] p 2629 N94-24695

BUCHAREST POLYTECHNIC INST. (ROMANIA).
Arc consistency problem: An exercise in parallel programming with shared objects [PB94-110590] p 2466 N94-23706

C

CAEN UNIV. (FRANCE).
Mechanical behavior of CMCs: Crack growth resistance and creep aspects p 2256 N94-24235

CALIAN COMMUNICATIONS, KANATA (ONTARIO).
Detection and analysis of unbalanced QPSK in Gaussian noise, version 1.0 [DREO-12-020.1] p 2296 N94-24131

CALIFORNIA INST. OF TECH., PASADENA.
Correlated petrographic, electron microprobe, and ion microprobe studies of selected primitive and processed phase assemblages in meteorites [NASA-CR-194827] p 2601 N94-23499
Skin friction measurement in complex flows using thin oil film techniques [NASA-CR-194872] p 2327 N94-24098
A low noise 665 GHz SIS quasi-particle waveguide receiver [NASA-CR-194735] p 2296 N94-24105
Optimal gains for a single polar orbiting satellite p 2208 N94-24873
Symposium on diffusion in ordered alloys [AD-A273643] p 2245 N94-25033

CALIFORNIA POLYTECHNIC STATE UNIV., SAN LUIS OBISPO.
An experimental investigation of the effect of upper surface blowing on dynamic stall [NASA-CR-194863] p 2165 N94-22894
An experimental study of the flow field surrounding a subsonic jet in a cross flow [NASA-CR-194770] p 2317 N94-23072
Tools reference manual for a Requirements Specification Language (RSL), version 2.0 [NASA-CR-191461] p 2445 N94-23125
Lift augmentation on a delta wing via leading edge fences and the Gurney flap [NASA-CR-194793] p 2168 N94-24103
JB-300: An advanced medium size transport for 2005 [NASA-CR-195499] p 2179 N94-24401
Implementation of the Baldwin-Barth turbulence model into the ZETA code and its diagnosis [NASA-CR-194795] p 2335 N94-24640
The cetaceopteryx: A global range military transport aircraft [NASA-CR-195519] p 2181 N94-24711
VLCT-13: A commercial transport for the 21st Century [NASA-CR-195492] p 2181 N94-24803
The AC-120: The advanced commercial transport [NASA-CR-195491] p 2182 N94-24966
A global range military transport: The ostrich [NASA-CR-195494] p 2183 N94-24972
Weasel works SA-150: Design study of a 100 to 150 passenger transport aircraft [NASA-CR-195489] p 2183 N94-24975

CALIFORNIA UNIV., BERKELEY.
100 GHz map of 3C 446 [PB94-104882] p 2599 N94-23705
Quantum optical aspects of topological phases, such as Berry's phase [AD-A273632] p 2570 N94-25028

CALIFORNIA UNIV., BERKELEY. LAWRENCE BERKELEY LAB.
Physics with chemically and isotopically pure semiconductors [DE93-040120] p 2557 N94-22926
High-resolution soft x ray photoionization studies of selected molecules [DE94-000568] p 2532 N94-23002
Towards a theory of quark and lepton masses [DE94-001726] p 2533 N94-23218
A two-dimensional dispersion module for the TOUGH2 simulator [DE94-002262] p 2335 N94-24655
The use of harmonics in 3-D magnetic fields [DE94-002274] p 2299 N94-24656
Ge-Au eutectic bonding of Ge (100) single crystals [DE94-002281] p 2564 N94-24657
Coadjoint orbits and conformal field theory [DE94-002285] p 2523 N94-24658

CALIFORNIA UNIV., DAVIS.
A comparison between coherent and noncoherent mobile systems in large Doppler shift, delay spread, and C/I environment p 2287 N94-22818
Parametric and nonparametric discriminants for regional earthquakes and explosions [AD-A273807] p 2406 N94-25538

CALIFORNIA UNIV., IRVINE.
Investigation of evolution-related aspects of bacterial rhodopsins [NASA-CR-194826] p 2420 N94-23501
On the dynamics of approximating schemes for dissipative nonlinear equations p 2332 N94-24168
Effect of land use change on the carbon cycle in Amazon soils [NASA-CR-195168] p 2399 N94-24853

CALIFORNIA UNIV., LOS ANGELES.
Isolated and coupled superquadric loop antennas for mobile communications applications p 2289 N94-22834
Multigrid methods for differential equations with highly oscillatory coefficients p 2484 N94-23685
Heat pipe vapor dynamics [NASA-CR-194217] p 2327 N94-24096
Aeroelastic, aeromechanical and vibration problems in helicopters p 2154 N94-24244
Planetary and asteroid missions. Getting there: Anchoring spacecraft to asteroids [NASA-CR-195493] p 2614 N94-24333
Approximate optimal guidance for the advanced launch system [NASA-CR-4568] p 2198 N94-24752

CALIFORNIA UNIV., SAN DIEGO.
Progress report for the UCSD experimental HEP group [DE94-001357] p 2533 N94-23699
Geomagnetic field models incorporating physical constraints on the secular variation [NASA-CR-195165] p 2405 N94-24854

CALIFORNIA UNIV., SAN DIEGO, LA JOLLA.
The role of radiation in mesoscale flows: Physics, parameterizations, codes p 2413 N94-24389
Session on modeling of radiative transfer processes p 2414 N94-24397
Carbon and hydrogen isotope composition and C-14 concentration in methane from sources and from the atmosphere: Implications for a global methane budget [NASA-CR-195166] p 2399 N94-25092

CALIFORNIA UNIV., SANTA BARBARA.
Ceramic matrix composites: Challenges and opportunities p 2255 N94-24230

CAMBRIDGE UNIV. (ENGLAND).
Turbulence modeling for non-equilibrium flows p 2328 N94-24144

CANADIAN SPACE AGENCY, OTTAWA (ONTARIO).
Sensing and modelling concepts for autonomous and remote mobile robot control p 2370 N94-23421

CANADIAN SPACE AGENCY, VANIER (ONTARIO).
Ground operation of robotics on Space Station Freedom p 2371 N94-23841

CANON INFORMATION SYSTEMS, INC., PALO ALTO, CA.
Some background information on perceptual color matching pertinent to computer applications [PB93-200327] p 2445 N94-23788

CARLETON UNIV., OTTAWA (ONTARIO).
Analysis of time-diversity combining methods for frequency-hopped signals [CU-DOE-92-09] p 2300 N94-24694
Composite sequences for rapid acquisition of direct-sequence spread spectrum signals [CTN-94-60901] p 2300 N94-24696

CARNEGIE-MELLON UNIV., PITTSBURGH, PA.
Optimizing parallelization [AD-A273565] p 2467 N94-24692
A type-theoretic approach to higher-order modules with sharing [AD-A273566] p 2458 N94-24693
Performance measurements of the multimedia testbed on Mach 3.0: Experience writing real-time device drivers, servers, and applications [AD-A273600] p 2460 N94-24932
Analyzing the properties of user interface software [AD-A273601] p 2460 N94-24933
A usage profile and evaluation of a wide-area distributed file system [AD-A273590] p 2593 N94-24946

Design of a walking robot
[NASA-CR-195200] p 2367 N94-25274

CASE WESTERN RESERVE UNIV., CLEVELAND, OH.
Laser light scattering instrument advanced technology development
[NASA-CR-194803] p 2349 N94-23286
Applications of x ray absorption fine structure to the in situ study of the effect of cobalt in nickel hydrous oxide electrodes for fuel cells and rechargeable batteries
p 2391 N94-23347
The electrolyte challenge for a direct methanol-air polymer electrolyte fuel cell operating at temperatures up to 200 C p 2393 N94-23360
The effects of anisotropy on the nonlinear behavior of bridged cracks in long strips
[NASA-CR-194453] p 2377 N94-24604
Surface chemistry of liquid metals
p 2249 N94-25133

CENTENARY COLL. OF LOUISIANA, SHREVEPORT.
Whole rock major element chemistry of KREEP basalt clasts in lunar breccia 15205: Implications for the petrogenesis of volcanic KREEP basalts
p 2614 N94-24365

CENTER FOR INDUSTRIAL RESEARCH, OSLO (NORWAY).
Selective hydrogen separation by palladium-based composite membranes
[PB93-201671] p 2254 N94-23431

CENTER FOR MATHEMATICS AND COMPUTER SCIENCE, AMSTERDAM (NETHERLANDS).
The computation of R(sub 0) for discrete-time epidemic models with dynamic heterogeneity
[CWI-AM-R9301] p 2420 N94-23521
Multiprocessor scheduling with communication delays
[ETN-94-95346] p 2468 N94-25221

CENTRAL INTELLIGENCE AGENCY, WASHINGTON, DC.
Third Annual Foreign Acquisitions Workshop: Improving Access to Foreign Gray Literature
[NASA-TM-109683] p 2593 N94-24759

CENTRE D'ENSEIGNEMENT ET DE RECHERCHES DE MEDECINE AERONAUTIQUE, PARIS (FRANCE).
Physical aspects of the visual stimulus
p 2431 N94-23978
Mental images p 2429 N94-23980
Multi-sensoral approach to night flight: Perceptive and Cognitive limitations p 2432 N94-23981

CENTRE D'ETUDES ET DE RECHERCHES, TOULOUSE (FRANCE).
Asymptotic correctors: The LTR
[PB93-199701] p 2474 N94-24627

CENTRE EUROPEEN RECHERCHE ET DE FORMATION ADVANCE EN CALCUL SCIENTIFIC, TOULOUSE (FRANCE).
The combustion program at CTR
p 2237 N94-24155

CENTRE NATIONAL D'ETUDES SPATIALES, TOULOUSE (FRANCE).
Missions, Technologies, and Design of Planetary Mobile Vehicles
[ISBN-2-85428-331-7] p 2605 N94-23373
Mission and system design of a long range rover mission p 2608 N94-23392
Rover: Autonomous concepts for Mars exploration
p 2369 N94-23400
Planetary rover locomotion mechanisms
p 2369 N94-23404
The Mars 96 balloon guiderope: An autonomous system in extreme environment conditions p 2369 N94-23412
The space operations at CNES p 2498 N94-23837
SPOT satellite family: Past, present, and future of the operations in the mission and control center
p 2500 N94-23846
SPOT4 Operational Control Center (CMP)
p 2197 N94-23856
CNES organization for station positioning of geostationary satellites p 2501 N94-23857
AGENDA: A task organizer and scheduler
p 2504 N94-23876
Distributed computing environments for future space control systems p 2464 N94-23911
Real-time on-board orbit determination with DORIS
p 2196 N94-23919
Mars 1994/1996: The French navigation tasks
p 2195 N94-23924
MERCATOR: Methods and Realization for Control of the Attitude and the Orbit of spacecraft
p 2202 N94-23925
HISPASAT launch and early operations phases: Computation and monitoring of geostationary satellite positioning p 2514 N94-23928
From requirements to acceptance tests
p 2464 N94-23962
Planning: Management of predictability and uncertainty and keeping abreast of developments
p 2520 N94-23967
Tribological characterization of spatial wet lubricants under vacuum p 2264 N94-24010
Interferometer scan unit mechanism definition
p 2358 N94-24012

CENTRE NATIONAL DE LA RECHERCHE SCIENTIFIQUE, CAEN (FRANCE).
A reference Martian mission for a long range rover
p 2606 N94-23382

CENTRE NATIONAL DE LA RECHERCHE SCIENTIFIQUE, TOULOUSE (FRANCE).
Compression for an effective management of telemetry data p 2518 N94-23956

CENTRE NATIONAL DE LA RECHERCHE SCIENTIFIQUE, VERRIERES-LE BUISSON (FRANCE).
Prospects for very-high-resolution solar physics with the Simuris inteferometric mission p 2625 N94-22848
Mars subsurface sounding with a ground penetrating radar p 2608 N94-23393
Periscope mechanism for SWAN instrument
p 2357 N94-24000
Cloud, dust, and ozone vertical profiles from solar occultation measurements: Implications for dynamics
p 2617 N94-24877
Two-dimensional modeling of thermal inversion layers in the middle atmosphere of Mars p 2622 N94-24900

CENTRO BRASILEIRO DE PESQUISAS FISICAS, RIO DE JANEIRO.
On spontaneous symmetry breaking mechanism in light-front quantized field theory
[DE93-633211] p 2568 N94-22968

CENTRO NAZIONALE UNIV. PER IL CALCOLO ELETTRONICO, PISA (ITALY).
Software for scientific visualization: State of the art and experiences
[PB93-225183] p 2449 N94-23111
Control of the internal stresses in plane elasticity
[PB93-225514] p 2374 N94-23112

CENTRO TECNICO AEROSPACIAL, SAN JOSE DOS CAMPOS (BRAZIL).
Modal test of the Brazilian satellite launcher (VLS) configuration burn-out of the first stage
p 2156 N94-24257

CHALMERS UNIV. OF TECHNOLOGY, GOETEBORG (SWEDEN).
100 GHz map of 3C 446
[PB94-104882] p 2599 N94-23705

CHINA NUCLEAR INFORMATION CENTRE, BEIJING.
The anomalous transport caused by particles transverse drift
[DE93-613685] p 2554 N94-25329
Numerical simulation and analysis of experimental results on stimulated Raman scattering in laser-plasma Hohlraum targets
[DE93-613719] p 2554 N94-25330
LHCD (low hybrid current drive) experiment on the HT-6B tokamak
[DE93-613720] p 2555 N94-25331
Investigation of the solid-solid surface adsorption of Eu2O3 on amorphous Al2O3
[DE93-613824] p 2566 N94-25332
Investigation and application of microwave electron cyclotron resonance plasma physical vapour deposition
[DE93-613909] p 2555 N94-25333
Effect of LHCD (low hybrid current drive) on tearing mode instability
[DE93-613700] p 2555 N94-25344

CHRISTIAN BROTHERS COLL., MEMPHIS, TN.
Space Shuttle Main Engine performance analysis
p 2222 N94-24444

CHRISTOPHER NEWPORT COLL., NEWPORT NEWS, VA.
Investigation of the optical and laser properties of Tm and Ho in YAG anf YLF
[REPT-94-001] p 2563 N94-24404
Computer modeling of nonlinearities
p 2458 N94-24661
Excited state dynamics of thulium ions in yttrium aluminum garnets
[NASA-CR-195159] p 2564 N94-25024
Two micron stimulated emission of activated insulating crystals
[REPT-94-002] p 2565 N94-25025

CINCINNATI UNIV., OH.
Design of a lunar propellant processing facility. NASA/USRA advanced program
[NASA-CR-195502] p 2266 N94-24618
Space Station flexible dynamics under plume impingement p 2208 N94-25383

CITY COLL. OF THE CITY UNIV. OF NEW YORK, NY.
The status of glueballs
[DE93-040040] p 2531 N94-22923

CIVIL AEROMEDICAL INST., OKLAHOMA CITY, OK.
Vision impairment and corrective considerations of civil airmen
[DOT/FAA/AM-93/21] p 2426 N94-23623
Index to FAA Office of Aviation Medicine Reports: 1961 through 1993
[DOT/FAA/AM-94/1] p 2426 N94-24093
An examination of the operational error database for air route traffic control centers
[DOT/FAA/AM-93/22] p 2175 N94-24472

CLARKSON UNIV., POTSDAM, NY.
An adaptive multigrid model for hurricane track prediction p 2416 N94-23687
Relaxation schemes for Chebyshev spectral multigrid methods p 2484 N94-23688

CLEMSON UNIV., SC.
On the estimation of the correlation dimension and its application to radar reflector discrimination
[NASA-CR-4564] p 2309 N94-23304
The 3-D numerical study of airflow in the compressor/combustor prediffuser and dump diffuser of an industrial gas turbine p 2324 N94-23660

COAST GUARD, GROTON, CT.
A multilevel cost-space approach to solving the balanced long transportation problem p 2483 N94-23678

CODECHAMP S.A., CHAMPAGNAT (FRANCE).
Encoders for space applications p 2363 N94-24046

COLLEGE DE FRANCE, PARIS.
Interferometric astronomy on the Moon
p 2601 N94-23378

COLORADO SCHOOL OF MINES, GOLDEN.
Dynamic ray tracing and its application in triangulated media
[DE94-000875] p 2402 N94-23516

COLORADO STATE UNIV., FORT COLLINS.
Study of improved methods for predicting chemical equilibria
[DE94-001647] p 2568 N94-22719
Scientific goals of the Cooperative Multiscale Experiment (CME) p 2411 N94-24381
Joint sessions on moisture processes and cumulus parameterization p 2414 N94-24393
Session on coupled land surface/hydrological/atmospheric models
p 2414 N94-24395
Template synthesis of electronically conductive polymers
[AD-A273673] p 2263 N94-25409

COLORADO UNIV., BOULDER.
Evolution of large-scale plasma structures in comets: Kinematics and physics
[NASA-CR-194777] p 2601 N94-23251
Extending substructure based iterative solvers to multiple load and repeated analyses
[NASA-CR-194822] p 2466 N94-23504
A structural design methodology for large angle articulated trusses considering realistic joint modeling
p 2376 N94-23560
OASIS-CC presentation p 2385 N94-23613
Real-time dynamics and control strategies for space operations of flexible structures
[NASA-CR-194794] p 2203 N94-23618
An analysis of solar mesospheric temperatures for the upper stratosphere and mesosphere
[NASA-CR-194861] p 2626 N94-23626
Supersonic minimum length nozzle design for dense gases p 2171 N94-23656
Sound radiation due to boundary layer transition
p 2332 N94-24163
Weld joint concepts for on-orbit repair of Space Station Freedom fluid system tube assemblies
p 2371 N94-24427
Particle sizes and composition of Mars atmospheric dust based upon Viking and Mariner 9 observations
p 2618 N94-24878
Temporal and spatial mapping of surface albedo and atmospheric dust opacity on Mars p 2619 N94-24887

COLORADO UNIV., COLORADO SPRINGS.
Conceptual communications system design in the 25.25-27.5 and 37.0-40.5 GHz frequency bands
p 2306 N94-25379

COLUMBIA STATE COMMUNITY COLL., TN.
CAPE for CaPE p 2416 N94-24409

COLUMBIA UNIV., NEW YORK, NY.
A complete public archive for the Einstein IPC
[NASA-CR-189316] p 2453 N94-23559
Inverse free electron laser beat-wave accelerator research
[DE94-002597] p 2349 N94-23702
On the large eddy simulation of turbulent flows in complex geometry p 2329 N94-24148
Computation of large-scale statistics in decaying isotropic turbulence p 2332 N94-24167
Tensoral for post-processing users and simulation authors p 2333 N94-24169

COM DEV LTD., CAMBRIDGE (ONTARIO).
SAW based systems for mobile communications satellites p 2275 N94-22746

COMISION NACIONAL DE ENERGIA ATOMICA, BUENOS AIRES (ARGENTINA).

Influence of sintering atmospheres on the aluminum sintering characteristics
[DE93-632412] p 2239 N94-22965

Diffusion of hydrogen in iron oxides
[DE93-632430] p 2239 N94-22966

COMMISSARIAT A L'ENERGIE ATOMIQUE, FONTENAY-AUX-ROSES (FRANCE).

Mechanical design of a planetary rover
p 2369 N94-23403

COMMUNICATIONS RESEARCH CENTRE, OTTAWA (ONTARIO).

Proceedings of the Third International Mobile Satellite Conference (IMSC 1993)
[NASA-CR-194516] p 2273 N94-22735

Canadian aeronautical mobile data trials
p 2279 N94-22773

Direct digital RF synthesis and modulation for MSAT mobile applications p 2285 N94-22804

Theoretical and simulated performance for a novel frequency estimation technique p 2285 N94-22808

Separable concatenated codes with iterative map decoding for Rician fading channels
p 2286 N94-22815

Aeronautical satellite antenna steering using magnetic field sensors p 2289 N94-22836

COMMUNICATIONS SATELLITE CORP., CLARKSBURG, MD.

Aeronautical audio broadcasting via satellite
p 2274 N94-22741

A study of satellite motion-induced multipath phenomena p 2283 N94-22794

System services and architecture of the TMI satellite mobile data system p 2286 N94-22817

Modulation and synchronization technique for MF-TDMA system
[NASA-CR-194448] p 2304 N94-25266

COMPAGNIA ITALIANA SERVIZI TECNICI, ROME.

Operational characterisation of requirements and early validation environment for high demanding space systems p 2519 N94-23959

COMPUTATIONAL FLUID DYNAMICS RESEARCH CORP., HUNTSVILLE, AL.

Numerical parametric studies of spray combustion instability p 2212 N94-23041

COMPUTER RESOURCES INTERNATIONAL A/S (DENMARK).

The ESIS query environment pilot project
p 2518 N94-23952

COMPUTER SCIENCES CORP., GREENBELT, MD.

UV spectral variability in the Herbig Ae star HR 5999. 11: The accretion interpretation
[NASA-CR-189313] p 2599 N94-23334

COMPUTER SCIENCES CORP., LANHAM, MD.

Long term trending of engineering data for the Hubble Space Telescope p 2516 N94-23942

COMPUTER SOFTWARE MANAGEMENT AND INFORMATION CENTER, ATHENS, GA.

COSMIC monthly progress report
[NASA-CR-195153] p 2460 N94-25023

COMPUTER TECHNOLOGY ASSOCIATES, INC., ROCKVILLE, MD.

The advanced orbiting systems testbed program: Results to date p 2197 N94-23907

Reliable transfer of data from ground to space
p 2305 N94-23908

CONSEJO SUPERIOR DE INVESTIGACIONES CIENTIFICAS, MADRID (SPAIN).

Microstrip monopulse antenna for land mobile communications p 2289 N94-22833

CONSTRUCCIONES AERONAUTICAS S.A., MADRID (SPAIN).

GOLF mechanisms p 2357 N94-24003

CONTINUOUS ELECTRON BEAM ACCELERATOR FACILITY, NEWPORT NEW, VA.

Gauge invariance and the electromagnetic current of composite pions
[DE93-040869] p 2532 N94-22952

The CEBAF beam loss sensors
[CEBAF-PR-93-032] p 2540 N94-24662

Polarized structure functions of the nucleon in the resonance region
[CEBAF-PR-94-001] p 2540 N94-24663

CONTRAVES ITALIANA, ROME.

Recharge mechanism based on shape memory alloy
p 2362 N94-24039

CORNELL UNIV., ITHACA, NY.

Uniform convergence of multigrid V-cycle iterations for indefinite and nonsymmetric problems
p 2482 N94-23677

FRANC2D: A two-dimensional crack propagation simulator. Version 2.7: User's guide
[NASA-CR-4572] p 2246 N94-25118

CRANFIELD INST. OF TECH., BEDFORD (ENGLAND).

Arbitrary-order numerical schemes for linear hyperbolic systems
[CRANFIELD-AERO-9211] p 2523 N94-25480

Factors influencing perceived usability and utility of LIBERTAS at Cranfield: Implications for system modification and user education
[CRANFIELD-AERO-9212] p 2594 N94-25485

A numerical investigation of the artificial compressibility method for the solution of the Navier-Stokes equations
[CRANFIELD-AERO-9213] p 2340 N94-25486

CRAY SYSTEMS, BRISTOL (ENGLAND).

The Ulysses spacecraft control and monitoring concepts and realities p 2502 N94-23862

Mission planning for an Earth observation low Earth orbiter: ERS-1 p 2503 N94-23868

SIMSAT: An object oriented architecture for real-time satellite simulation p 2197 N94-23940

CRYOLIFE, INC., MARIETTA, GA.

Cellular and tissue injury during nonfreezing cold injury and frostbite
[AD-A270883] p 2423 N94-22732

CUMMINS ENGINE CO., INC., COLUMBUS, IN.

Development of high temperature liquid lubricants for low-heat rejection: Heavy duty diesel engines
[NASA-CR-191197] p 2258 N94-24753

D

DANISH METEOROLOGICAL INST., COPENHAGEN.

High latitude cusp signature observations for southward IMF B sub Z
[AD-A273801] p 2406 N94-25536

DASSAULT (E. M.) CO., SAINT CLOUD (FRANCE).

Trends of design methodology of airframe
p 2179 N94-24327

DASSAULT-BREGUET AVIATION, SAINT CLOUD (FRANCE).

A DTM-based path planning method for planetary rovers p 2370 N94-23423

In flight mission planning in the Copilote Electronique
p 2522 N94-25015

DAVID SARNOFF RESEARCH CENTER, PRINCETON, NJ.

Enhanced image capture through fusion
p 2346 N94-25502

DAYTON UNIV., OH.

Life cycle cost modeling of conceptual space vehicles
[NASA-CR-194813] p 2203 N94-23329

Ultrasonic process for curing adhesives
[AD-A273175] p 2259 N94-24788

Birdstrike resistant crew enclosure program
[AD-A273700] p 2463 N94-25453

DEFENCE AND CIVIL INST. OF ENVIRONMENTAL MEDICINE, DOWNSVIEW (ONTARIO).

Physiological protection for aircrew at high altitudes: A review of the literature
[DCIEM-93-13] p 2432 N94-24114

Operation Friction: Development and introduction of personal cooling for CH124 Sea King aircrew
[DCIEM-93-06] p 2433 N94-24119

Computer control of an electro-mechancial regulator for providing positive pressure breathing and an electronic G-valve for human +Gz research
[DCIEM-93-05] p 2437 N94-24299

DEFENCE AND CIVIL INST. OF ENVIRONMENTAL MEDICINE, TORONTO (ONTARIO).

Cardiovascular and pulmonary disease in NATO aircrew: An overview p 2423 N94-23314

Echocardiographic screening of aircrew candidates
p 2424 N94-23319

Asthma in aircrew p 2425 N94-23327

DEFENCE RESEARCH AGENCY, FARNBOROUGH (ENGLAND).

Earth observation archive activities at DRA Farnborough p 2519 N94-23958

Mission planning and mission rehearsal systems: Displays and other interactive techniques
p 2522 N94-25013

Sub-sonic flow about a slender profile in a tunnel having perforated walls
[AD-A273184] p 2170 N94-25137

DEFENCE RESEARCH ESTABLISHMENT ATLANTIC, DARTMOUTH (NOVA SCOTIA).

Experimental verification of an acoustic telemetry link between an Aurora and CFAV quest
[DREA-TC-93-304] p 2202 N94-24121

PROPWR: A versatile tool for 1/3 octave processing and narrowband line tracking
[DREA-TC-93-303] p 2297 N94-24298

Isothiazolone volatility study of a water bottom from fuel treated with Kathon (tm) FP1.5 biocide
[AD-A273165] p 2266 N94-24728

The effects of zinc borate addition on the flammability characteristics of polyester, vinyl ester, and epoxy glass reinforced plastics
[AD-A273164] p 2262 N94-25136

DEFENCE RESEARCH ESTABLISHMENT, OTTAWA (ONTARIO).

Safety guidelines for the operation of the DREO 10 m EMP simulator DREMPS
[DREO-TN-93-5] p 2193 N94-24117

CF-18 AN/ALQ-126B-MG 13 IIP interface to the DREO Electronic Warfare Engagement Simulation Facility
[DREO-TN-93-4] p 2296 N94-24118

TEM cell safety report
[DREO-TN-93-9] p 2193 N94-24123

DEFENCE RESEARCH ESTABLISHMENT PACIFIC, VICTORIA (BRITISH COLUMBIA).

A colour image processing algorithm to identify copper-based particles in filter debris samples
[DREP-TM-93-19] p 2455 N94-24122

The detection performance of a long-term spectral integrator using normalized and quantized data
[DREP-TM-93-11] p 2455 N94-24130

An evaluation of Compton scatter imaging using COMSCAN
[DREP-TM-93-38] p 2372 N94-24136

DELAWARE UNIV., NEWARK.

Polycrystalline thin film materials and devices
[DE93-018213] p 2389 N94-22862

DEPARTMENT OF COMMUNICATIONS, OTTAWA (ONTARIO).

The provision of spectrum for feeder links of non-geostationary mobile satellites
p 2276 N94-22751

Use of the 30/20 GHz band by multipurpose satellite systems p 2276 N94-22753

DEPARTMENT OF DEFENSE, FORT MEADE, MD.

Transparent data service with multiple wireless access
p 2276 N94-22754

DEPARTMENT OF ENERGY, MORGANTOWN, WV.

Mathematical modeling of MCFC cells/stacks and networks
[DE94-001914] p 2390 N94-23212

Overview of molten carbonate fuel cell technology development
[DE94-001911] p 2394 N94-23781

DEPARTMENT OF ENERGY, WASHINGTON, DC.

Federal alternative fuel program light duty vehicle operations
[DE93-040663] p 2264 N94-22878

Electric and hybrid vehicles program
[DE93-040664] p 2352 N94-22881

Fusion plasma theory project summaries
[DE94-001712] p 2551 N94-23808

DEPARTMENT OF THE NAVY, WASHINGTON, DC.

Molten salt reactor for potentiostatic electroplating
[AD-D016020] p 2258 N94-24720

Curing phthalonitrile resins with acid and amine
[AD-D016021] p 2258 N94-24721

Heterodyne array for measurement of target velocity
[AD-D016025] p 2545 N94-24722

Method of fabricating a receptor-based sensor
[AD-D016026] p 2344 N94-24723

Crosstie random access memory element having associated read/write circuitry
[AD-D016027] p 2446 N94-24724

Method and apparatus for the non-invasive measurement of pressure inside pipes using a fiber optic interferometer sensor
[AD-D016013] p 2344 N94-24734

Fire-resistant barriers for composite materials
[AD-D016014] p 2230 N94-24735

Field emitter array memory device
[AD-D016015] p 2311 N94-24736

High temperature adhesive
[AD-D016019] p 2258 N94-24737

Laser-deposited biocompatible films and methods and apparatuses for producing same
[AD-D016017] p 2350 N94-24952

High speed electronic analog computers using low-gain amplifiers
[AD-D015974] p 2446 N94-25034

Method for fabricating self-aligned gate diffused junction field effect transistor
[AD-D015975] p 2312 N94-25035

Laser energized high voltage direct current power supply
[AD-D015977] p 2312 N94-25036

Thermistor controlled current source versatile temperature sensor
[AD-D015979] p 2345 N94-25037

Conveying digital data in noisy, unstable, multipath environments
[AD-D015980] p 2301 N94-25038

Solid state Time Base Corrector (TBC)
[AD-D015981] p 2312 N94-25039

Radar target discrimination by spectrum analysis [AD-D015982] p 2301 N94-25040
Radar target discrimination systems using artificial neural network topology [AD-D015984] p 2301 N94-25041
Bridge type optoelectronic sample and hold circuit [AD-D015986] p 2312 N94-25042
Conformal method of fabricating and optical waveguide on a semiconductor substrate [AD-D015988] p 2546 N94-25043
Tunable lasers pumped by visible laser diodes [AD-D016000] p 2350 N94-25044
Layered parallel interface for an active antenna array [AD-D016002] p 2301 N94-25045
Precision drive and speed reduction device [AD-D016004] p 2367 N94-25046
Nuclear magnetic resonance imaging with short gradient pulses [AD-D016006] p 2537 N94-25047
Preprocessor and adaptive beamformer for linear-frequency modulation active signals [AD-D016008] p 2302 N94-25048
Very low frequency and low frequency transmitting antenna parameter monitoring system [AD-D015989] p 2302 N94-25049
MOS analog memory with injection capacitors [AD-D015990] p 2312 N94-25050
Regulated drag area parachute [AD-D015992] p 2170 N94-25051
Generic drone control system [AD-D015993] p 2184 N94-25052
System for cancelling phase noise in an interferometric fiber optic sensor arrangement [AD-D015994] p 2345 N94-25053
Curing phthalonitriles with acid [AD-D015996] p 2261 N94-25054
Electro-rheological control valve [AD-D015997] p 2367 N94-25055
Method and apparatus of generating sum or difference signals corresponding to an apparent beam in a monopulse radar system [AD-D015998] p 2302 N94-25056
System for producing synchronized signals [AD-D016003] p 2302 N94-25057
Method and apparatus for determining target elevation angle, altitude and range, and the like in a monopulse radar system with reduced multipath errors [AD-D016005] p 2302 N94-25058
Field emitter array [AD-D016023] p 2303 N94-25150
Internally folded scalable laser [AD-D015978] p 2350 N94-25216
Wide bandwidth differential amplifier [AD-D015985] p 2303 N94-25217

DEUTSCHE AEROSPACE A.G., MUNICH (GERMANY).
Applications of CFD codes and supercomputers to aircraft design activities p 2177 N94-24316
The process network in the design and manufacturing of aircraft p 2178 N94-24319

DEUTSCHE AIRBUS G.M.B.H., HAMBURG (GERMANY).
Integrated stress and strength analysis of airplane structures using the data processing tool ISSY p 2178 N94-24320
Influence of active controls on the design process of a large transport aircraft p 2178 N94-24323

DEUTSCHE BUNDESBAHN, MUNICH (GERMANY).
A rail joint: The possible initiator of corrugation? p 2269 N94-23583

DEUTSCHE FORSCHUNGS- UND VERSUCHSANSTALT FUER LUFT- UND RAUMFAHRT, STUTTGART (GERMANY).
CMC design consequences p 2256 N94-24238

DEUTSCHE FORSCHUNGSANSTALT FUER LUFT- UND RAUMFAHRT, OBERPFAFFENHOFEN (GERMANY).
Manned Space-laboratories Control Center (MSCC) operations concept p 2505 N94-23882
The geo-control system for station keeping and colocation of geostationary satellites p 2464 N94-23927
Large-eddy simulation of flow in a plane, asymmetric diffuser p 2328 N94-24147
Improvement of system properties of a pulsed laser Doppler anemometer with respect to an optical amplifier [DLR-FB-93-19] p 2547 N94-25305
ROSAT mission planning using artificial intelligence methods [DLR-FB-93-14] p 2476 N94-25345
Collection and evaluation of numerical models with the aim to investigate the impact of aircraft emissions [DLR-MITT-93-06] p 2400 N94-25414

DEUTSCHE FORSCHUNGSANSTALT FUER LUFT- UND RAUMFAHRT, STUTTGART (GERMANY).
Microwave excitation of pulsed high pressure gas discharge lasers [DLR-FB-93-12] p 2351 N94-25304
The hexagonal compound parabolic concentrator design and construction [DLR-MITT-93-03] p 2396 N94-25464
The pressure loaded volumetric ceramic receiver 500 kW version design and construction [DLR-MITT-93-02] p 2396 N94-25479

DIRECTION DES RECHERCHES, ETUDES ET TECHNIQUES, PARIS (FRANCE).
Exciplex laser study: Discharge and magnetic switching systems [PB93-199768] p 2349 N94-24629

DORNIER SYSTEM G.M.B.H., FRIEDRICHSHAFEN (GERMANY).
Investigations into deployment complications of the ERS-1 SAR antenna p 2305 N94-23996
Development steps on the basis of test with the LOCSTAR reflector deployment mechanism p 2356 N94-23998
Development of a Low-Temperature Gear Motor (LOG) p 2361 N94-24032

DOUGLAS AIRCRAFT CO., INC., LONG BEACH, CA.
Current and future design methods for large transport aircraft p 2179 N94-24324

DRAPER (CHARLES STARK) LAB., INC., CAMBRIDGE, MA.
Overall system concepts in mission planning p 2521 N94-25009
Computing techniques in mission planning p 2522 N94-25012

DUESSELDORF UNIV. (GERMANY).
An object-oriented approach for parallel self adaptive mesh refinement on block structured grids p 2469 N94-23697

DUKE UNIV., DURHAM, NC.
Magnetic shielding of interplanetary spacecraft against solar flare radiation [NASA-CR-195539] p 2204 N94-24334

E

EAGLE-PICHER INDUSTRIES, INC., COLORADO SPRINGS, CO.
Review of super Ni/Cd cell designs and performance p 2391 N94-23348

EAGLE-PICHER INDUSTRIES, INC., JOPLIN, MO.
High specific energy, high capacity nickel-hydrogen cell design p 2391 N94-23350

EAST CAROLINA UNIV., GREENVILLE, NC.
Spatial interpretation of NASA's Marshall Space Flight Center Payload Operations Control Center using virtual reality technology p 2198 N94-24432

ECOLE CENTRALE DE LYON (FRANCE).
Method for simulating a vehicle shock test: Design and realization of the required implementation tools [ECL-92-14] p 2352 N94-22885
Image analysis applications to mixing phenomena and turbulent dispersions [ECL-92-29] p 2317 N94-22971
An analytical ultra-high vacuum tribometer for solid lubricant studies p 2361 N94-24033
Contribution to the study of HF converters radiated disturbances [ECL-92-34] p 2313 N94-25421

ECOLE CENTRALE DE PARIS (FRANCE).
Stretch-induced quenching in flame-vortex interactions p 2237 N94-24156
The production of premixed flame surface area in turbulent shear flow p 2237 N94-24158

ECOLE POLYTECHNIQUE FEDERALE DE LAUSANNE (SWITZERLAND).
Power attenuation characteristics as switch-over criterion in personal satellite mobile communications p 2277 N94-22756

EDGERTON, GERMESHAUSEN AND GRIER, INC., IDAHO FALLS, ID.
Novel fringe scanning/Fourier transform method of synthetic imaging [DE93-018936] p 2542 N94-22917
Imaging System (INEL) T805 prototype [DE94-002807] p 2382 N94-23492
Measurement of interfacial tension by use of pendant drop video techniques [DE93-000168] p 2345 N94-24831

EDGEWOOD ARSENAL, ABERDEEN PROVING GROUND, MD.
The transputer [AD-A273688] p 2446 N94-25438

EDWARDS UNDERGROUND WATER DISTRICT, SAN ANTONIO, TX.
Evaluation of the use of remote-sensing data to identify crop types and estimate irrigated acreage, Uvalde and Medina Counties, Texas, 1989 [PB93-193159] p 2388 N94-24809

EG AND G MOUND APPLIED TECHNOLOGIES, MIAMISBURG, OH.
Development testing of the two-watt RTG heat source and Hastelloy-S/T-111 alloy compatibility studies [DE94-002875] p 2243 N94-23784

EG AND G ROCKY FLATS, INC., GOLDEN, CO.
JBK-75 stainless steel machinability study [DE94-002268] p 2242 N94-23475

EIDGENOESSISCHE TECHNISCHE HOCHSCHULE, ZURICH (SWITZERLAND).
A mixed map/variable structure observer for target tracking p 2157 N94-24263

ELECTROTECHNICAL LAB., TSUKUBA (JAPAN).
Study on fine grain dynamic dataflow computer [REPT-946] p 2446 N94-24981
A study on electrostatic quadrupole lenses and their application technologies [REPT-948] p 2546 N94-24982

ELORET CORP., PALO ALTO, CA.
Simulation studies for surfaces and materials strength [NASA-CR-195185] p 2565 N94-25093
Advanced ballistic range technology [NASA-CR-195198] p 2165 N94-25169

ELTECH SYSTEMS, INC., FAIRPORT HARBOR, OH.
High energy density aluminum-oxygen cell p 2393 N94-23363

EMBRY-RIDDLE AERONAUTICAL UNIV., DAYTONA BEACH, FL.
Aircraft empennage structural detail design [NASA-CR-195496] p 2179 N94-24332
Aircraft wing structure detail design [NASA-CR-195485] p 2180 N94-24498
Cockpit control system conceptual design [NASA-CR-195543] p 2190 N94-24551
Cockpit control system [NASA-CR-195488] p 2190 N94-24957
Aircraft empennage structural detail design [NASA-CR-195486] p 2183 N94-24969
Aircraft wing structural detail design (wing, aileron, flaps, and subsystems) [NASA-CR-195487] p 2183 N94-24974
The Triton: Design concepts and methods [NASA-CR-195542] p 2184 N94-25004
Design project: Viper [NASA-CR-195484] p 2184 N94-25021

EMORY UNIV., ATLANTA, GA.
LPCVD of InN on GaAs(110) using HN3 and TMIn: Comparison with Si(100) results [AD-A273555] p 2235 N94-24917

ENGINEERING SOCIETIES LIBRARY, NEW YORK.
The 5th Engineering Foundation Conference: Advanced Heterostructure Transistors [AD-A273508] p 2312 N94-24819

ENSCO, INC., MELBOURNE, FL.
Implementation and evaluation of the new wind algorithm in NASA's 50 MHz doppler radar wind profiler [NASA-CR-194880] p 2408 N94-23576
The evaluation of ASOS for the Kennedy Space Center's Shuttle Landing Facility [NASA-CR-195685] p 2416 N94-25271

ENVIRONMENTAL PROTECTION AGENCY, ANN ARBOR, MI.
EPA's survey of in-use driving patterns: Implications for mobile source emission inventories [PB94-118502] p 2399 N94-24525

ENVIRONMENTAL PROTECTION AGENCY, CINCINNATI, OH.
Statistical procedures for corrosion studies [PB93-199412] p 2244 N94-23802

ENVIRONMENTAL PROTECTION AGENCY, RESEARCH TRIANGLE PARK, NC.
Alternative control techniques document: NOx emissions from stationary reciprocating internal combustion engines [PB94-104494] p 2398 N94-24476

ENVIRONMENTAL RESEARCH INST. OF MICHIGAN, ANN ARBOR.
Optical wavelet transform processor [AD-A273625] p 2546 N94-24731
Examination of the physical, electrical, and microwave evolution of water into young sea ice [AD-A273559] p 2418 N94-24918

ERASMUS UNIV., ROTTERDAM (NETHERLANDS).
Sensitivity analysis of list scheduling heuristics [PB93-237766] p 2468 N94-24764

ERLANGEN-NUREMBERG UNIV. (GERMANY).
SFOLDA: A semiconductor LDA for measurements in complex flows p 2316 N94-22856
Relativistic hadrons in an external field [ETN-94-95387] p 2538 N94-25259

ERNO RAUMFAHRTTECHNIK G.M.B.H., BREMEN (GERMANY).
Mission activities planning for a Hermes mission by means of AI-technology p 2502 N94-23858
Micro-gravity compatible drive (MGCD) p 2355 N94-23988

Reliable redundant device for mechanisms p 2361 N94-24030

EROS DATA CENTER, SIOUX FALLS, SD.
The AGRHYMET data communications project p 2280 N94-22776

ESSEX CORP., ORLANDO, FL.
Transfer of perceptual adaptation to space sickness: What enhances an individual's ability to adapt? [NASA-CR-188256] p 2427 N94-24227

ETEL S.A., MOTIERS (SWITZERLAND).
Low noise electric motor p 2315 N94-23989
Sensorless, brushless motor to drive a sealed freon-ammonia pump p 2315 N94-24036
Design and performances of electromagnetic initiators for space mechanisms: An alternative to pyrotechnic system p 2315 N94-24037

ETREMA PRODUCTS, INC., AMES, IA.
Improved magnetostrictive transducer drive elements achieved by reduction of crystalline defects and improved crystalline orientation [AD-A273391] p 2313 N94-25276

EUROCONTROL EXPERIMENTAL CENTRE, BRETIGNY (FRANCE).
Harmonisation of man-machine interface experiments in the context of the development of PHARE advanced tools [PB93-204725] p 2430 N94-23744

EUROPEAN SPACE AGENCY, PARIS (FRANCE).
Scientific Requirements for Future Solar-Physics Space Missions [ESA-SP-1157] p 2623 N94-22837
The TOPSIM 4 graphic user interface [ESA-STM-247] p 2450 N94-23228
Mission and system concepts for Mars robotic precursor missions p 2608 N94-23391
The Fifth European Space Mechanisms and Tribology Symposium [ESA-SP-334] p 2355 N94-23985

EUROPEAN SPACE AGENCY. EUROPEAN SPACE OPERATIONS CENTER, DARMSTADT (GERMANY).
Commonality of flight control systems for support of European telecommunications missions p 2304 N94-23834
A user view of the EURECA ground segment p 2499 N94-23844
SCOS2: ESA's new generation of mission control systems p 2197 N94-23851
Ulysses log 1992 p 2502 N94-23863
A review of mission planning systems p 2503 N94-23866
AMFESYS: Modelling and diagnosis functions for operations support p 2506 N94-23887
ESSOPE: Towards S/C operations with reactive schedule planning p 2508 N94-23896
The Advanced Technology Operations System: ATOS p 2508 N94-23897
Automatic tools for system testing p 2197 N94-23913
An engineering database management system for spacecraft operations p 2517 N94-23951
The European Space Agency standard for space packet utilisation p 2203 N94-23954

EUROPEAN SPACE AGENCY. EUROPEAN SPACE RESEARCH AND TECHNOLOGY CENTER, ESTEC, NOORDWIJK (NETHERLANDS).
ESA personal communications and digital audio broadcasting systems based on non-geostationary satellites p 2273 N94-22737
Adaptive digital beamforming for a CDMA mobile communications payload p 2274 N94-22743
The possibilities for mobile and fixed services in the 20/30 GHz frequency bands p 2276 N94-22752
Geostationary payload concepts for personal satellite communications p 2278 N94-22765
The European Mobile System (EMS) p 2282 N94-22789
Propagation model for the Land Mobile Satellite channel in urban environments p 2283 N94-22796
Global coverage Mobile Satellite Systems: System availability versus channel propagation impairments p 2284 N94-22798
First satellite mobile communication trials using BLQS-CDMA p 2284 N94-22801
A CDMA synchronisation scheme p 2285 N94-22810
Diversity reception for advanced multi-satellite networks: A CDMA approach p 2286 N94-22816
The design and networking of dynamic satellite constellations for global mobile communication systems p 2288 N94-22826
Solar physics within ESA's planning p 2624 N94-22844
Guide to software configuration management [ESA-PSS-05-09-ISSUE-1] p 2450 N94-23229
Automation technology for remote sample acquisition p 2369 N94-23407
Accuracy control in Monte Carlo radiative calculations p 2321 N94-23639
Numerical simulation of Ulysses nutation p 2207 N94-24017
The Olympus PAX, measurement of mechanism induced vibration p 2362 N94-24041

EUROPEAN SPACE TRIBOLOGY LAB., RISLEY (ENGLAND).
The tribology of some MoS2-lubricated engineering ceramics p 2356 N94-23993
Thermal vacuum performance of cycloid and harmonic gearboxes with solid (MoS2) and liquid (Braycote 601) lubrication p 2358 N94-24009
In-vacuum performance of Fomblin Z25-lubricated, 52100 steel bearings with TiC-coated balls p 2358 N94-24011
BLAST, a new lubricant screening tester for space oils and greases p 2362 N94-24042
Static adhesion in preloaded contacts subjected to long-term vacuum exposure p 2363 N94-24043
An assessment of solid lubricant films for use in high temperature space applications p 2363 N94-24044
The development of dry-lubricated ceramic cages p 2363 N94-24045

EUTELSAT, PARIS (FRANCE).
EUTELTRACS: The European experience on mobile satellite services p 2281 N94-22781

EVANS AND SUTHERLAND COMPUTER CORP., SALT LAKE CITY, UT.
Mission rehearsal in the SOF-ATS program p 2522 N94-25016

EXOS, INC., WOBURN, MA.
Development of a force feedback anthropomorphic teleoperation input device for control of robot hands [NASA-CR-195109] p 2437 N94-24329

F

FAIRCHILD SPACE CO., GERMANTOWN, MD.
Manned Mars mission on-orbit operations FTS capabilities assessment [NASA-CR-189328] p 2430 N94-23080

FEDERAL AVIATION ADMINISTRATION, ATLANTIC CITY, NJ.
Initial evaluation of burn characteristics of phenolic foam runway brake arrestor material [DOT/FAA/CT-TN93/7] p 2253 N94-23335
Combined 1991 and 1992 Robinson-22B (R-22) parking test results [AD-A273550] p 2193 N94-24559
Full-scale fire testing of seat component materials [AD-A273499] p 2174 N94-24941

FEDERAL AVIATION ADMINISTRATION, OKLAHOMA CITY, OK.
Perceptions of organizational support and affectivity as predictors of job satisfaction [DOT/FAA/AM-94/2] p 2429 N94-25442

FEDERAL AVIATION ADMINISTRATION, WASHINGTON, DC.
The FAA satellite communications program p 2279 N94-22772
General aviation activity survey [AD-A273284] p 2162 N94-24923

FEDERAL AVIATION AGENCY, OKLAHOMA CITY, OK.
Automation and cognition in air traffic control: An empirical investigation [DOT/FAA/AM-94/3] p 2176 N94-25444

FERMI NATIONAL ACCELERATOR LAB., BATAVIA, IL.
The current status of observational constraints on cosmic strings [DE94-001505] p 2601 N94-23010
Search for the top quark and other new particles at D0 [DE94-001220] p 2535 N94-24515
Electro-weak, QCD and top physics at the Tevatron [DE94-002304] p 2535 N94-24611
Welding of niobium to stainless [DE94-003365] p 2365 N94-24614

FIAT SPAZIO, ROME (ITALY).
Feasibility study of an automatic vehicle for planetary exploration p 2369 N94-23399

FIBER MATERIALS, INC., BIDDEFORD, ME.
Humidity effects on soluble core mechanical and thermal properties (polyvinyl alcohol/microballoon composite) type CG extendospheres, volume 2 [NASA-CR-193893] p 2229 N94-24224

FINNISH ARTIFICIAL INTELLIGENCE SOCIETY, HELSINKI.
Neural network research in Finland. Symposium [PB93-224822] p 2472 N94-23463
SETI: Search for extraterrestrial intelligence. An international interdisciplinary seminar, star days [PB93-230597] p 2444 N94-23754

FINNISH METEOROLOGICAL INST., HELSINKI.
Periscope mechanism for SWAN instrument p 2357 N94-24000
Martian mesoscale circulations induced by variations in surface optical and thermal characteristics: A numerical study p 2622 N94-24899

FLIR SYSTEMS, INC., PORTLAND, OR.
Infrared sensors and systems for enhanced vision/autonomous landing applications p 2439 N94-25491

FLORENCE UNIV. (ITALY).
Architectures and protocols for an integrated satellite-terrestrial mobile system p 2277 N94-22760
Keys to understanding the corona p 2624 N94-22839

FLORIDA AGRICULTURAL AND MECHANICAL UNIV., TALLAHASSEE.
A framework for SFC/DC system data analysis p 2523 N94-23234
Application and development of the Schwinger multichannel scattering theory and the partial differential equation theory of electron-molecule scattering [NASA-CR-194774] p 2536 N94-24798

FLORIDA INST. OF TECH., MELBOURNE.
Interpretation of discrepancies in mass spectroscopy data obtained from different experimental configurations p 2237 N94-23245
JOVE NASA-FIT program: Microgravity and aeronomy projects [NASA-CR-195121] p 2631 N94-24493

FLORIDA INTERNATIONAL UNIV., MIAMI.
Research experience for undergraduates in robotics and materials [AD-A273659] p 2368 N94-25436

FLORIDA STATE UNIV., TALLAHASSEE.
Nonlinear dynamics applied to atmospheric prediction [AD-A273437] p 2404 N94-24674
Considerations regarding the deployment of hypermedia at JSC p 2595 N94-25366

FLORIDA UNIV., GAINESVILLE.
Mass properties measurement system dynamics p 2368 N94-23235
Mass properties measurement system: Dynamics and statics measurements p 2368 N94-23236
STM studies of LB deposited alkyl substituted polyaniline and its corresponding monomer [AD-A273553] p 2257 N94-24562
Electrochemically mediated polymerization of 2-pentadecylaniline confined to a planar liquid-liquid interface [AD-A273541] p 2259 N94-24792
Bioregenerative life support systems for microgravity [NASA-CR-195516] p 2422 N94-24810
The 2-D polymerized Langmuir-Blodgett films studied by STM [AD-A273542] p 2261 N94-24930
Surface-induced static undulations in multilayer films of liquid-crystalline polymers [AD-A273517] p 2262 N94-25159

FLUENT, INC., LEBANON, NH.
Computation of propulsion-related flowfields using unstructured adaptive meshes p 2215 N94-23056

FMT INTERNATIONAL TRADE A.B. (SWEDEN).
System for automatic transportation of aircraft on the ground [CA-PATENT-1-322-361] p 2193 N94-24785

FOKKER B.V., SCHIPOL-OOST (NETHERLANDS).
Some practical problems in multidisciplinary design and optimisation p 2178 N94-24322

FOKKER SPACE AND SYSTEMS, AMSTERDAM (NETHERLANDS).
The Columbus solar array mechanisms p 2356 N94-23994
HERA (Hermes robot arm) overview p 2357 N94-24005
The development of the HERA Test Facility (HTF) p 2197 N94-24020

FOOD AND AGRICULTURE ORGANIZATION OF THE UNITED NATIONS, ROME (ITALY).
Manual on measurement of methane and nitrous oxide emissions from agriculture [DE93-616429] p 2399 N94-25167

FRANCE TELECOM INTERNATIONAL, ISSY-LES-MOULINEAUX.
Optimizing space constellations for mobile satellite systems p 2278 N94-22764

FUJITSU LTD., KAWASAKI (JAPAN).
ASTER TIR subsystem and calibration p 2385 N94-23612

G

GALAXY SCIENTIFIC CORP., PLEASANTVILLE, NJ.
Pilot-vehicle interface [DOT/FAA/CT-92/21] p 2430 N94-23083

Airport pavement test machine design and cost study [DOT/FAA/CT-93/51] p 2192 N94-24072

Pilot-vehicle interface handbook, chapter 19. Volume 2: Digital systems validation [DOT/FAA/CT-88/10-VOL-2] p 2438 N94-24830

GAS RESEARCH INST., CHICAGO, IL.

Development of durable high-temperature catalysts for natural gas combustion [PB93-226447] p 2232 N94-23477

GEC AVIONICS LTD., ROCHESTER (ENGLAND).

Ground based mission planning systems p 2522 N94-25014

GENERAL ACCOUNTING OFFICE, WASHINGTON, DC.

Space operations: Archiving space science data needs further management improvements. Report to the Chairman, Subcommittee on Investigations and Oversight, Committee on Science, Space, and Technology, House of Representatives [GAO/NSIAD-94-25] p 2591 N94-24092

B-2 bomber: Assessment of DOD's response to mandated certifications and reports [AD-A273179] p 2184 N94-25152

C-17 lot 3 production contract [AD-A273180] p 2174 N94-25153

GENERAL APPLIED SCIENCE LABS., INC., RONKONKOMA, NY.

Calibration of HYPULSE for hypervelocity air flows corresponding to flight Mach numbers 13.5, 15, and 17 [NASA-CR-191578] p 2192 N94-23564

HYPULSE combustor analysis [NASA-CR-191579] p 2336 N94-24771

GENERAL ATOMICS TECHNOLOGIES CORP., SAN DIEGO, CA.

CAMAC throughput of a new RISC-based data acquisition computer at the DIII-D tokamak [DE94-001113] p 2550 N94-23182

The role of the radial electric field in confinement and transport in H-mode and VH-mode discharges in the DIII-D tokamak [DE94-002746] p 2551 N94-23782

Performance characteristics of the DIII-D advanced divertor cryopump [DE94-002745] p 2354 N94-23797

Measurement of electron temperature and density in the DIII-D neutral beam ion source arc chamber [DE94-001099] p 2553 N94-24746

Investigation of the heat handling capabilities of DIII-D neutral beamline internal components [DE94-001107] p 2553 N94-24756

GENERAL DYNAMICS CORP., SAN DIEGO, CA.

Prediction of three sigma maximum dispersed density for aerospace applications p 2207 N94-23654

GENERAL ELECTRIC CO., CINCINNATI, OH.

Aviation: The timeless industry p 2165 N94-25068

GENERAL ELECTRIC CO., FAIRFIELD, CT.

Vibration isolating engine mount [CA-PATENT-1-320-710] p 2353 N94-23215

Counterrotating aircraft propulsor blades [CA-PATENT-1-319-357] p 2186 N94-23255

Seal assembly [CA-PATENT-163126888] p 2364 N94-24128

Wing mounted unducted fan engine [CA-PATENT-1323353] p 2188 N94-24180

GENERAL ELECTRIC CO., SCHENECTADY, NY.

Fatigue crack growth rate studies of medium sulfur low alloy steels tested in high temperature water [DE93-040437] p 2238 N94-22861

Analysis of Alloy 600 and X-750 stress corrosion cracks [DE94-001578] p 2238 N94-22936

Evaluation of reducing gas turbine emissions through hydrogen-enhanced steam-injected combustion [PB94-109873] p 2187 N94-23709

GENERAL MOTORS CORP., INDIANAPOLIS, IN.

Wear reduction in ceramic bearings by surface generated pyrolytic carbon continuously replenished by ethylene gas [NASA-CR-189214] p 2364 N94-24090

GEOLOGICAL SURVEY, MENLO PARK, CA.

Science strategy for Mars exploration p 2606 N94-23380

GEOLOGICAL SURVEY OF JAPAN, IBARAKI.

In-flight cross-calibration of ASTER/TIR and MODIS-N p 2385 N94-23611

GEORGE WASHINGTON UNIV., WASHINGTON, DC.

Supercomputer networking for space science applications [NASA-CR-194876] p 2465 N94-23085

A knowledge based system for scientific data visualization [NASA-CR-194879] p 2452 N94-23507

Development and application of new algorithms for the simulation of viscous compressible flows with moving bodies in three dimensions [AD-A273514] p 2338 N94-25157

GEORGIA INST. OF TECH., ATLANTA.

Theory and computation of optimal low- and medium-thrust transfers [NASA-CR-194812] p 2217 N94-23275

Robust stability of second-order systems [NASA-CR-195175] p 2488 N94-24564

Assessment of impact damage of composite rocket motor cases [NASA-CR-195143] p 2220 N94-24595

Modeling of database constraints in active databases [AD-A273484] p 2592 N94-24691

Investigation of passive atmospheric sounding using millimeter and submillimeter wavelength channels [NASA-CR-194858] p 2404 N94-24843

Integrated design and manufacturing for the high speed civil transport [NASA-CR-195511] p 2182 N94-24968

GINER, INC., WALTHAM, MA.

PEM regenerative fuel cells p 2392 N94-23358

GOETTINGEN UNIV. (GERMANY).

A method for recognition of frequency cells in a cylinder flow influenced by wall effects p 2316 N94-22860

GORCA SYSTEMS, INC., CHERRY HILL, NJ.

Adaptive array antenna for satellite cellular and direct broadcast communications p 2275 N94-22745

GOSUDARSTVENNYI KOMITET PO ISPOLZOVANIYU ATOMNOI ENERGII, SERPUKHOV (USSR).

Proton spin: The role of quark-gluon and hadron degrees of freedom [DE93-616867] p 2538 N94-25341

GRENOBLE-1 UNIV. (FRANCE).

An information retrieval logical model applied to the formalism of conceptual graphs: The ELEN prototype and its experimentation on a corpus of software components [ETN-94-95162] p 2588 N94-22879

A general model for dynamic and complex information management: The ELEN prototype object manager for software engineering [ETN-94-95163] p 2588 N94-22880

Definition and realization of a formal verification tool of LUSTRE programs: The LESAR system [ETN-94-95164] p 2447 N94-22882

Formal verification of digital circuits described in VHDL [ETN-94-95165] p 2306 N94-22883

Artificial neural networks: Application to the optical recognition of music partitions [ETN-94-95166] p 2470 N94-22884

Specifications of ETS, the Enhanced Transport Service [RR-907-I] p 2589 N94-23150

Mixed analog-digital description and simulation: Proposition for VHDL-analogue [RR-908-I] p 2450 N94-23180

Physical modeling and dynamic simulation of planet vehicles: Application to the motion prediction p 2371 N94-23426

Optimization of techniques to reconstruct images disturbed by atmospheric turbulence in the near infra-red [PB93-199784] p 2298 N94-24630

GRONINGEN RIJKSUNIV. (NETHERLANDS).

The Hamiltonian double-zero eigenvalue [W-9304] p 2479 N94-23138

A rational elliptic surface related to the question of expressing squares as sum of consecutive squares [W-9305] p 2479 N94-23139

On the numerical computation of invariant manifolds [W-9306] p 2480 N94-23140

The cusp horseshoe and its bifurcations in the unfolding of an inclination-flip homoclinic orbit [W-9307] p 2480 N94-23141

Atmospheric flow in heterogeneous vegetated regions [W-9303] p 2401 N94-23175

Comparison of time integration methods for the evolution of galaxies [PB94-111671] p 2602 N94-24522

Hamiltonian approach to fairly low and long gravity waves [PB94-111119] p 2404 N94-24598

Signatures of selfadjoint pencils [PB94-111127] p 2457 N94-24599

H

HARRIS CORP., MELBOURNE, FL.

A homotopy algorithm for digital optimal projection control GASD-HADOC [NASA-CR-193881] p 2456 N94-24470

HARRIS GOVERNMENT AEROSPACE SYSTEMS DIV., MELBOURNE, FL.

Electrical performance of wire mesh for spacecraft deployable reflector antennas p 2275 N94-22744

HARVARD COLL. OBSERVATORY, CAMBRIDGE, MA.

Neutron star mergers and gamma-ray bursts [NASA-CR-195176] p 2629 N94-25091

HARVARD UNIV., CAMBRIDGE, MA.

Bounds and asymptotic expansions for solutions of the free boundary problems related to sequential decision versions of a bioequivalence problem [AD-A273551] p 2495 N94-24560

Microbial biofilm formation and its consequences for the CELSS program [NASA-CR-195146] p 2438 N94-24706

HAWAII UNIV., HONOLULU.

Statistical methods in physical oceanography [AD-A273612] p 2419 N94-24948

HAWAII UNIV., MANOA.

Reactive trace metals as indicators of subduction and ventilation processes in the ocean [AD-A273585] p 2419 N94-25164

HEIDELBERG UNIV. (GERMANY).

An adaptive streamline diffusion finite element method for hyperbolic systems in gas dynamics [PREPRINT-688] p 2340 N94-25466

HELSINKI UNIV. OF TECHNOLOGY, ESPOO (FINLAND).

Acoustic and optical investigations of superfluid He-3 [PB93-224889] p 2523 N94-23101

Modelling of solid polymer and direct methanol fuel cells: Phenomenological equations and analytical solutions [PB93-224897] p 2390 N94-23102

Distributed Operating Systems and Mach. Proceedings of the Spring 1992 Graduate Seminar on Distributed Systems [PB93-224905] p 2449 N94-23103

Lectures on magnetohydrodynamical drives [PB93-224962] p 2308 N94-23104

Static image method for computing the electric potential due to sources in a layered sphere [PB93-224970] p 2308 N94-23105

Incomplete corrections in nonlinear problems [PB93-225746] p 2479 N94-23106

Transient analysis of conducting half-plane problem with noncausal scattering image [PB93-225027] p 2524 N94-23110

Energy estimates and asymptotic analysis in the theory of shells [PB93-225738] p 2374 N94-23113

Two-dimensional Navier-Stokes computations of subsonic and supersonic flows through turbine cascades [PB93-226223] p 2317 N94-23114

POISs3: A 3D poisson smoother of structured grids [PB93-226231] p 2318 N94-23115

Computational study of GA(W)-1: Airfoil near stall [PB93-226249] p 2165 N94-23116

Hypermedia support for engineering design system [PB93-226256] p 2449 N94-23117

Fundamentals of fatigue analysis [PB93-226264] p 2374 N94-23118

Internal friction associated with dislocation relaxations in virgin martensite [PB93-226280] p 2240 N94-23119

Thermal fatigue: A literature review [PB93-226306] p 2375 N94-23120

Transient analysis of circuits including frequency-dependent components using transgyrator and convolution [PB93-225001] p 2308 N94-23130

Polarizability of gyrotropic sphere [PB93-225019] p 2524 N94-23131

Application of ERS-1 active microwave instrumentation data to remote sensing of snow [PB93-224756] p 2382 N94-23224

Proceedings of the 1993 Bi-Isotropics Workshop on Novel Microwave Materials [PB93-224772] p 2290 N94-23225

APLAC: An object-oriented analog circuit simulator and design tool. 6.1 system simulations manual [PB93-224871] p 2450 N94-23226

Surface and interfacial properties of polymer blends. A literature survey [PB93-230191] p 2254 N94-23561

SETI: Search for extraterrestrial intelligence. An international interdisciplinary seminar, star days [PB93-230597] p 2444 N94-23754

HEWLETT-PACKARD CO., PALO ALTO, CA.

SATCOM simulator speeds MSS deployment and lowers costs p 2287 N94-22822

HIGH TECHNOLOGY CORP., HAMPTON, VA.

Relationship between transition and modes of instability in supersonic boundary layers [NASA-CR-4562] p 2336 N94-24725

HITACHI LTD., YOKOHAMA (JAPAN).

The robotic Mars rover p 2608 N94-23390

HONEYWELL, INC., MINNEAPOLIS, MN.

Intelligent tutoring and aiding in satellite ground control p 2443 N94-23929

Synthetic vision system flight test results and lessons learned p 2429 N94-25492

Image processing for flight crew enhanced situation awareness p 2442 N94-25508

HOUSTON UNIV., CLEAR LAKE, TX.

Measuring track densities in lunar grains by image analysis p 2623 N94-25355

Design and testing of a unique randomized gravity, continuous flow bioreactor p 2423 N94-25368

HOUSTON UNIV., TX.

Studies of two phase flow [NASA-CR-195099] p 2267 N94-23594

Integrated risk management p 2588 N94-25361

Image remapping strategies applied as protheses for the visually impaired p 2444 N94-25363

Near surface analysis p 2407 N94-25364

A multimedia adult literacy program: Combining NASA technology, instructional design theory, and authentic literacy concepts p 2585 N94-25384

HUGHES AIRCRAFT CO., LOS ANGELES, CA.

Trends in mobile satellite communication p 2278 N94-22763

A practical system for regional mobile satellite services p 2288 N94-22828

Low melting temperature alloy deployment mechanism p 2356 N94-23997

HUGHES AIRCRAFT CO., SAN DIEGO, CA.

CADBIT 2: Computer-aided design for built-in test, volume 1 [AD-A273702] p 2463 N94-25455

CADBIT 2: Computer-aided design for built-in test, volume 2 [AD-A273703] p 2463 N94-25456

HUGHES STX, INC., GREENBELT, MD.

Voyager observations of globular clusters [NASA-CR-194806] p 2598 N94-23330

HUGHES STX, INC., LANHAM, MD.

UV-bright stars in globular clusters [NASA-CR-189324] p 2599 N94-24666

HULBURT (E. O.) CENTER FOR SPACE RESEARCH, WASHINGTON, DC.

Requirements for future solar-physics missions that include UV instrumentation p 2625 N94-22851

HYDROLOGIC ENGINEERING CENTER, DAVIS, CA.

The HEC NexGen software development project [AD-A273512] p 2460 N94-24822

I

IDAHO UNIV., MOSCOW.

Design of a wheeled articulating land rover [NASA-CR-195520] p 2365 N94-24806

IIT RESEARCH INST., CHICAGO, IL.

ELF communications system ecological monitoring program [AD-A273456] p 2299 N94-24676

IIT RESEARCH INST., DAYTON, OH.

Acoustic target detection and classification using neural networks p 2529 N94-24221

ILLINOIS INST. OF TECH., CHICAGO.

Interactive control in turbulent shear layers [AD-A273544] p 2336 N94-24793

ILLINOIS UNIV., CHICAGO.

Viewing hybrid systems as products of control systems and automata [NASA-CR-194792] p 2472 N94-23300

Path planning by querying persistent stores of trajectory segments [NASA-CR-194789] p 2451 N94-23301

ILLINOIS UNIV., URBANA.

Performance of prefabricated geocomposite subdrainage system in an airport runway [DOT/FAA/RD-93/23] p 2192 N94-23303

Investigations on detonation shock dynamics and related topics [DE94-002570] p 2326 N94-23809

Integrated reflector antenna design and analysis [NASA-CR-195164] p 2300 N94-24678

Three-dimensional, inelastic response of single-edge notch bend specimens subjected to impact loading [AD-A273302] p 2378 N94-25143

ILLINOIS UNIV., URBANA-CHAMPAIGN.

On the determination of local instantaneous averages in particulate flow measurements p 2325 N94-23663

IN-SPACE PROPULSION LTD., SACRAMENTO, CA.

Liquid rocket propulsion: Retrospective and prospects p 2154 N94-24243

INDIANA UNIV. OF PENNSYLVANIA, INDIANA, PA.

Diffusion on Cu surfaces p 2251 N94-24428

INSTITUT DES HAUTES ETUDES SCIENTIFIQUES, BURES-SUR-YVETTE (FRANCE).

Tensor-scalar cosmological models and their relaxation toward general relativity [PB93-220796] p 2601 N94-23099

Lacunary series as quadratic differentials in conformal dynamics [PB93-238061] p 2481 N94-23547

When an infinitely-renormalizable endomorphism of the interval can be smoothed [PB93-238087] p 2481 N94-23548

Periodic nonlinear Schroedinger equation and invariant measures [PB93-238012] p 2487 N94-23775

Cauchy problem for periodic KDV-type equations [PB93-238020] p 2487 N94-23776

Quasiconformal mappings, operators on Hilbert space, and local formulae for characteristic classes [PB93-238079] p 2488 N94-24536

Stable non-Gaussian diffusive profiles [PB93-238053] p 2489 N94-24610

INSTITUT FRANCO-ALLEMAND DE RECHERCHES, SAINT-LOUIS (FRANCE).

Computation of the loads on the AH-1/OLS model rotor in forward flight and comparison with wind tunnel tests [ISL-CO-230/92] p 2176 N94-23146

A new experimental apparatus for the study of the unsteady flowfield over an airfoil in pitching and heaving motions using laser Doppler anemometry [ISL-CO-229/92] p 2165 N94-23149

Interferometry in rarefied gas flows [ISL-CO-207/92] p 2318 N94-23160

LDA measurements of the unsteady near wake behind an airfoil undergoing transient and periodic pitching motions [ISL-CO-215/92] p 2165 N94-23161

Real-time holographic endoscopy [ISL-CO-203/92] p 2343 N94-24054

JAPE 91: Influence of terrain masking of the acoustic propagation of helicopter noise p 2528 N94-24214

Validation of the ROTAC code for the rotor noise prediction [PB93-204311] p 2529 N94-24514

The ISL rotor bench [ISL-R-108/92] p 2185 N94-25301

Study of a system for producing a pulsed magnetic field (B 2T) with a frequency of 50 Hz [ISL-N-601/92] p 2314 N94-25460

Detailed description of two calculation programs for incompressible, steady state boundary layer flows, applied to determine the aerodynamic characteristics of NACA12 and OA312 foils at low Reynolds numbers [ISL-N-604/92] p 2171 N94-25461

Measurement of the volume mass by spontaneous Raman scattering. Study of turbulent fluctuations of mixing in a subsonic free jet. Measurements in supersonic wind tunnels [ISL-R-102/92] p 2339 N94-25462

Study of the blade/vortex interaction: Acoustics, aerodynamics and models [ISL-R-104/92] p 2340 N94-25463

INSTITUT NATIONAL DE RECHERCHE D'INFORMATIQUE ET D'AUTOMATIQUE, VALBONNE (FRANCE).

Preliminary results on time-varying feedback stabilization of a nonholonomic car-like mobile robot [INRIA-RR-1512] p 2475 N94-24963

INSTITUT NATIONAL DES SCIENCES APPLIQUEES, LYON (FRANCE).

Role of interfaces on the cyclic fatigue behaviour of ceramic matrix composites p 2256 N94-24234

INSTITUT NATIONAL DES SCIENCES APPLIQUEES DE LYON, VILLEURBANNE (FRANCE).

Damage under monotonic or cyclic loads of new AlSiFe alloys prepared by the Osprey (tm) process [ISAL-93-0008] p 2239 N94-22972

Contribution to the interface micromechanical study and to the damage fundamental phenomena in glass fiber epoxy resin model composites [ISAL-93-0027] p 2227 N94-23133

INSTITUT NATIONAL POLYTECHNIQUE, GRENOBLE (FRANCE).

Motion planning for a non-holonomic mobile in a dynamic workspace [ETN-94-95180] p 2470 N94-22898

Verification of synchronous sequential numerical material systems: Application of the LUSTRE language and of the LESAR verification tool [ETN-94-95181] p 2447 N94-22899

Resolution of Markov models on distributed memory machines [ETN-94-95182] p 2444 N94-22900

Design of integrated architectures for low level image processing [ETN-94-95183] p 2445 N94-22901

Modeling parallelism and synchronization [ETN-94-95179] p 2465 N94-23134

Logic synthesis on programmable networks [ETN-94-95174] p 2449 N94-23151

Installation of an artificial neural network on distributed memory microprocessors [ETN-94-95175] p 2471 N94-23152

Contribution to the evaluation of efficiency of a microprocessor functional test [ETN-94-95176] p 2445 N94-23153

AMICAL: An aid for architectural synthesis and exploration of control circuits [ETN-94-95177] p 2308 N94-23154

A type declarative system for PROLOG [ETN-94-95178] p 2449 N94-23155

Generation of modules for control communication circuits: A design study used in the framework of the safe vehicle PROMETHEUS [ETN-94-95171] p 2308 N94-23165

Structures of tetrahedrization: A mathematical and algorithmical point of view [ETN-94-95172] p 2480 N94-23166

A parallel PROLOG system for distributed memory multiprocessor [ETN-94-95173] p 2465 N94-23167

INSTITUTE FOR AEROSPACE RESEARCH, OTTAWA (ONTARIO).

A prediction method for the compressive strength of impact damaged composite laminates [CTN-94-60925] p 2229 N94-24137

INSTITUTE FOR COMPUTER APPLICATIONS IN SCIENCE AND ENGINEERING, HAMPTON, VA.

Flames in dusty mixtures: Their structure and stability [NASA-CR-191567] p 2317 N94-23089

On the Daubechies-based wavelet differentiation matrix [NASA-CR-191583] p 2479 N94-23090

Dynamic data distributions in Vienna Fortran [NASA-CR-191575] p 2448 N94-23092

The theoretical accuracy of Runge-Kutta time discretizations for the initial boundary value problem: A careful study of the boundary error [NASA-CR-191561] p 2480 N94-23272

On the Gibbs phenomenon 3: Recovering exponential accuracy in a sub-interval from a spectral partial sum of a piecewise analytic function [NASA-CR-191560] p 2480 N94-23278

A representation for the turbulent mass flux contribution to Reynolds-stress and two-equation closures for compressible turbulence [NASA-CR-191569] p 2319 N94-23302

Phased-mission system analysis using Boolean algebraic methods [NASA-CR-191564] p 2451 N94-23340

Automated parallelization of timed Petri-net simulations [NASA-CR-191574] p 2451 N94-23341

Experience with parametric binary dissection [NASA-CR-191552] p 2473 N94-23558

On the differentiation matrix for Daubechies-based wavelets on an interval [NASA-CR-191582] p 2487 N94-24291

The acoustic and instability waves of jets confined inside an acoustically lined rectangular duct [NASA-CR-191586] p 2334 N94-24602

Responses of a finite baffled plate subject to turbulent and mean flow excitations [NASA-CR-191570] p 2334 N94-24605

Fast simulation of packet loss rates in a shared buffer communications switch [NASA-CR-191556] p 2457 N94-24638

Runtime support and compilation methods for user-specified data distributions [NASA-CR-191587] p 2458 N94-24679

A comparison of approximate interval estimators for the Bernoulli parameter [NASA-CR-191585] p 2458 N94-24680

Carrying the mass flux terms exactly in the first and second moment equations of compressible turbulence [NASA-CR-191568] p 2335 N94-24712

An integrated runtime and compile-time approach for parallelizing structured and block structured applications [NASA-CR-191554] p 2458 N94-24740

Projection techniques for iterative solution of A(bar x) equals (bar b) with successive right-hand sides [NASA-CR-191571] p 2490 N94-24836

Vortex generation and wave-vortex interaction over a concave plate with roughness and suction [NASA-CR-191589] p 2337 N94-24869

Triangular spectral elements for incompressible fluid flow [NASA-CR-191588] p 2490 N94-24914

Research in progress and other activities of the Institute for Computer Applications in Science and Engineering [NASA-CR-191576] p 2444 N94-25090

INSTITUTE FOR PERCEPTION RVO-TNO, SOESTERBERG (NETHERLANDS).

Validation of a second generation conspicuity meter [IZF-1993-A-11] p 2542 N94-22895

INSTITUTE OF PLASMA PHYSICS, PRAGUE (CZECHOSLOVAKIA).

IPP Prague Contributions to the IAEA Technical Committee Meeting on Research Using Small Tokamaks
[IPPCZ-329] p 2551 N94-24293

INSTITUTO DE ESTUDOS AVANCADOS, SAO JOSE DOS CAMPOS (BRAZIL).

An investigation on a new technique to improve the performance of the shock tube/tunnel testing in the equilibrium interface condition p 2154 N94-24247

INSTITUTO DE FISICA TEORICA, SAO PAULO (BRAZIL).

Off-critical W(infinity) and Virasoro algebras as dynamical symmetries of the integrable models
[DE93-633215] p 2478 N94-22969

INSTITUTO DE PESQUISAS ESPACIAIS, SAO JOSE DOS CAMPOS (BRAZIL).

Operational training for the mission operations at the Brazilian National Institute for Space Research (INPE)
p 2429 N94-23933

INSTITUUT TNO VOOR BOUWMATERIALEN EN BOUWCONSTRUCTIES, DELFT (NETHERLANDS).

Hydro-elastic analysis using a selection of commercial analysis programs
[PB94-118734] p 2376 N94-24478

INTEGRATED SYSTEMS, INC., SANTA CLARA, CA.

Intelligent control of chemical vapor deposition processes
[AD-A273356] p 2261 N94-24937

INTERNATIONAL ATOMIC ENERGY AGENCY, VIENNA (AUSTRIA).

Manual on measurement of methane and nitrous oxide emissions from agriculture
[DE93-616429] p 2399 N94-25167

INTERNATIONAL CENTRE FOR THEORETICAL PHYSICS, TRIESTE (ITALY).

Flavor changing strings and domain walls
[DE93-633217] p 2532 N94-22970

Vacancy formation energy of Li(H, D) and Na(H, D) systems
[DE93-633452] p 2558 N94-22978

Super Beltrami differentials and N equal to 4 superconformal anomalies
[DE93-613047] p 2491 N94-25166

An attempt at a macrorealistic quantum worldview
[DE93-616821] p 2570 N94-25206

Derivation of the macroscopic rate equations for the driven diffusive Ising model at pair level of approximation
[DE93-616839] p 2524 N94-25208

Solutions of the 2-D Helmoholtz equation for optical waveguides
[DE93-616840] p 2547 N94-25209

A brief history of the universe
[DE93-616843] p 2604 N94-25210

Choice of filters for the detection of gravitational waves from coalescing binaries. 2: Detection in coloured noise
[DE93-616844] p 2604 N94-25211

A parallel algorithm for filtering gravitational waves from coalescing binaries
[DE93-616845] p 2604 N94-25212

The renormalization group for flag manifolds
[DE93-616846] p 2491 N94-25213

The fundamental group of the complement of complexified real arrangements
[DE93-616847] p 2491 N94-25214

Cosmic wake fields
[DE93-616849] p 2604 N94-25215

A scalar-vector model of quark-antiquark interaction under linear confinement
[DE93-616871] p 2538 N94-25317

On the continuity of limit capacity of central Cantor sets
[DE93-613022] p 2523 N94-25328

On a new functional integral formalism for Hubbard model
[DE93-614017] p 2492 N94-25334

The 2D supergravity and integrable systems
[DE93-616848] p 2570 N94-25336

Modification in the kinetic solution for magnetized plasmas
[DE93-613687] p 2555 N94-25343

Localized excitations in competing bond-order-wave, charge-density-wave and spin-density-wave systems. 2: Competing charge-density-wave and spin-density-wave
[DE93-617131] p 2538 N94-25388

A vibrating wire parallel to a type 2 superconducting slab of arbitrary thickness
[DE93-617134] p 2525 N94-25389

The effect of a transport current on the surface barrier of a uniaxial anisotropic superconducting slab
[DE93-617135] p 2566 N94-25390

Effects of a vibrating wire carrying DC current on a moving type 2 superconducting slab of arbitrary thickness
[DE93-617136] p 2566 N94-25391

Surface barrier of a uniaxial anisotropic type 2 superconducting cylinder
[DE93-617137] p 2566 N94-25392

Simulation of the vortex motion in the high T(c) superconductors
[DE93-617138] p 2567 N94-25403

Electronic structure and high pressure phase transition in LaSb and CeSb
[DE93-617051] p 2567 N94-25423

The Haldane energy gap of a doped linear-chain Heisenberg antiferromagnet
[DE93-617130] p 2567 N94-25426

Extension problem for generalized multi-monogenic functions in Clifford analysis
[DE93-616818] p 2493 N94-25433

The least energy critical set
[DE93-616820] p 2493 N94-25434

Effect of high frequency field on the transport properties of superlattice
[DE93-617047] p 2568 N94-25447

Orbit spaces over commutative rings and projectives as semi-isomorphisms
[DE93-616822] p 2493 N94-25473

A quark structure of hadrons and nuclei
[DE93-616872] p 2539 N94-25474

Excitation mechanisms for XUV and x ray lasers
[DE93-617006] p 2351 N94-25482

Contribution of all excited states to ZFS of a (sup 6) S-state
[DE93-617007] p 2568 N94-25483

INTERNATIONAL MARITIME SATELLITE ORGANIZATION, LONDON (ENGLAND).

Evolution of INMARSAT systems and applications: The land mobile experience p 2280 N94-22779

INMARSAT's personal communicator system
p 2282 N94-22788

INTERNATIONAL SOLAR ELECTRIC TECHNOLOGY, INGLEWOOD, CA.

Novel two-stage selenization methods for fabrication of thin-film CIS cells and submodules
[DE94-000220] p 2390 N94-23296

INTERRACIAL COUNCIL FOR BUSINESS OPPORTUNITY, NEW YORK, NY.

Activities involving aeronautical, space science, and technology support for minority institutions
[NASA-CR-195095] p 2574 N94-24225

INTERSONICS, INC., NORTHBROOK, IL.

Containerless measurements on liquids at high temperatures p 2238 N94-25125

Liquidus temperature and optical properties measurement by containerless techniques
p 2247 N94-25126

Optical properties and emissivities of liquid metals and alloys p 2248 N94-25129

IOWA STATE UNIV. OF SCIENCE AND TECHNOLOGY, AMES.

Development of small punch testing technique and its application to evaluation of mechanical properties degradation
[DE94-001193] p 2375 N94-23184

Modelling TOVS radiances of synoptic systems
[NASA-CR-194847] p 2408 N94-23620

Strength, acoustic evaluation and metallurgy of diffusion bonds
[DE94-001804] p 2243 N94-23717

Iowa satellite project ISAT-1
[NASA-CR-195517] p 2206 N94-24838

IOWA UNIV., IOWA CITY.

Multi-ion, multi-event test of ion cyclotron resonance heating
[NASA-CR-194859] p 2540 N94-23495

ISRAEL AIRCRAFT INDUSTRIES LTD., BEN-GURION AIRPORT.

UAV current technology and future trends
p 2154 N94-24245

Repair of cracked aluminum aircraft structure with composite patches p 2156 N94-24259

Post buckling behaviour of stiffened composite panels loaded in cyclic compression and shear
p 2157 N94-24260

Nonlinear analysis using a modal based reduction technique p 2161 N94-24288

ISRAEL AIRCRAFT INDUSTRIES LTD., LOD.

S-2E Tracker maritime patrol aircraft re-engine and system upgrade program p 2158 N94-24270

ISRAEL AIRCRAFT INDUSTRIES LTD., TASHAN.

New features in Computational Fluid Dynamics (CFD) technology at the TASHAN Engineering Center at IAI
p 2155 N94-24249

On the effect of the damping coefficients on the trajectories of symmetric and non-symmetric stores
p 2155 N94-24250

Development of a damage tolerance tool to analyze multiple-site damage in aircraft structure
p 2157 N94-24261

Computer based expert system for battle damage repair of composite structures p 2157 N94-24262

Pilot evaluation system p 2158 N94-24266

Attachment methods in composite joints - analysis of test results by controlled experiments method
p 2158 N94-24269

Evaluation of the fracture resistance and durability of adhesive bonded joints p 2160 N94-24278

ISRAEL AIRCRAFT INDUSTRIES LTD., YEHUD.

Reactive thrust cruise for a geosynchronous satellite with minimum fuel consumption p 2158 N94-24271

Momentum management and torque distribution
p 2159 N94-24272

ISRAEL ATOMIC ENERGY COMMISSION, BEERSHEBA.

Transient flows occurring during the accelerated crucible rotation technique
[DE93-617049] p 2567 N94-25422

ISRAEL SOCIETY OF AERONAUTICS AND ASTRONAUTICS, TEL AVIV.

The 33rd Israel Annual Conference on Aviation and Astronautics
[ITN-94-85227] p 2153 N94-24241

ISRAELI AIR FORCE, ZAHAL.

Comparison of c.t.s. based prediction of store trajectory with flight test data p 2158 N94-24268

ITALIAN SPACE AGENCY, ROME.

DS-SSMA capacity for a mobile satellite system
p 2286 N94-22814

The Columbus logistics support at the APMC: Requirements and implementation aspects
p 2515 N94-23935

ITHACO, INC., ITHACA, NY.

A combined Earth scanner and momentum wheel for attitude determination and control of small spacecraft
p 2208 N94-24022

J

JAPAN ATOMIC ENERGY RESEARCH INST., TOKYO.

Properties of the transfer matrices of deflecting magnet systems for free electron laser
[DE93-508257] p 2347 N94-22922

Report of the Joint Seminar on Solid State Physics, Atomic and Molecular Physics, and Materials Science in the Energy Region of Tandem Accelerators
[DE93-508268] p 2548 N94-22924

JAYCOR, VIENNA, VA.

Investigation of Raman beam cleanup and phase conjugation
[AD-A273157] p 2545 N94-24672

JET PROPULSION LAB., CALIFORNIA INST. OF TECH., PASADENA.

Proceedings of the Third International Mobile Satellite Conference (IMSC 1993)
[NASA-CR-194516] p 2273 N94-22735

Direct broadcast satellite-radio, space-segment/receiver tradeoffs p 2273 N94-22738

Direct broadcast satellite-radio, receiver development
p 2273 N94-22739

Internetworking satellite and local exchange networks for personal communications applications
p 2276 N94-22755

Integration of mobile satellite and cellular systems
p 2277 N94-22757

ACTS broadband aeronautical experiment
p 2279 N94-22771

ACTS mobile SATCOM experiments
p 2280 N94-22774

ACTS advanced system concepts and experimentation p 2280 N94-22780

Channel and terminal description of the ACTS mobile terminal p 2284 N94-22802

Pseudo-coherent demodulation for mobile satellite systems p 2287 N94-22819

K- and Ka-band mobile-vehicular satellite-tracking reflector antenna system for the NASA ACTS mobile terminal p 2289 N94-22831

An active K/Ka-band antenna array for the NASA ACTS mobile terminal p 2289 N94-22832

L-band mobile terminal antennas for helicopters
p 2289 N94-22835

The Telecommunications and Data Acquisition Report
[NASA-CR-194766] p 2290 N94-23256

A review of GPS-based tracking techniques for TDRS orbit determination p 2196 N94-23257

New approaches for tracking earth orbiters using modified GPS ground receivers p 2196 N94-23258

Improved thermal force modeling for GPS satellites
p 2207 N94-23259

Experimental modification and identification of the DSS-13 antenna control system model
p 2291 N94-23260

Performance of the X-/Ka/KABLE-band dichroic plate in the DSS-13 beam waveguide antenna
p 2291 N94-23261

Cryogenic, low-noise high electron mobility transistor amplifiers for the Deep Space Network p 2291 N94-23262
Analysis of open-loop conical scan pointing error and variance estimators p 2291 N94-23263
Spur-reduced digital sinusoid synthesis p 2291 N94-23264
Box codes of lengths 48 and 72 p 2292 N94-23265
Integer cosine transform compression for Galileo at Jupiter: A preliminary look p 2292 N94-23266
Link monitor and control operator assistant: A prototype demonstrating semiautomated monitor and control p 2292 N94-23267
Beam-waveguide antenna servo design issues for tracking low earth-orbiting satellites p 2292 N94-23268
Optical subnet concepts for the deep space network p 2292 N94-23269
Dual frequency optical carrier technique for transmission of reference frequencies in dispersive media [NASA-CASE-NPO-18007-2-CU] p 2543 N94-23270
Status of the development of rechargeable lithium cells p 2392 N94-23354
Advances in direct oxidation methanol fuel cells p 2393 N94-23361
Past US studies and developments for planetary rovers p 2369 N94-23375
Lunar rover navigation concepts p 2607 N94-23386
Unmanned lunar rovers: Utilization for exploration p 2607 N94-23387
The new family of JPL planetary surface vehicles p 2369 N94-23398
The mass of massive rover software p 2464 N94-23410
Mobility analysis, simulation, and scale model testing for the design of wheeled planetary rovers p 2370 N94-23425
Experiments with a small behaviour controlled planetary rover p 2371 N94-23427
Definitions in use by the visible and near-infrared, and thermal working groups p 2383 N94-23598
Cross-calibration survey (VISNIR) p 2383 N94-23599
Diffuse panel studies: Conclusions p 2384 N94-23606
GEWEX p 2385 N94-23614
Validating a large geophysical data set: Experiences with satellite-derived cloud parameters p 2385 N94-23615
Non-volatile, solid state bistable electrical switch [NASA-CASE-NPO-17621-1-CU] p 2309 N94-23820
Planar varactor frequency multiplier devices with blocking barrier [NASA-CASE-NPO-18428-1-CU] p 2310 N94-23821
Overcharge and overdischarge protection of ambient temperature secondary lithium cells [NASA-CASE-NPO-18343-1-CU] p 2310 N94-23823
SpaceOps 1992: Proceedings of the Second International Symposium on Ground Data Systems for Space Mission Operations [NASA-CR-194486] p 2497 N94-23832
ASTER, a multinational Earth observing concept p 2389 N94-23840
Mission planning for Shuttle Imaging Radar-C (SIR-C) with a real-time interactive planning software p 2305 N94-23842
Development of the Cassini Ground Data System in a multimission environment p 2500 N94-23845
An OSI architecture for the deep space network p 2305 N94-23848
Distributed science operations for JPL planetary missions p 2500 N94-23850
Operations concepts for Mars missions with multiple mobile spacecraft p 2501 N94-23852
Preparing the DSN operations concepts p 2501 N94-23853
Radioastron flight operations p 2502 N94-23861
Galileo spacecraft anomaly and safing recovery p 2207 N94-23864
The Mars mapper science and mission planning tool p 2503 N94-23867
Voyager uplink planning in the interstellar mission era p 2305 N94-23870
Science planning and sequencing for Cassini p 2504 N94-23871
Techniques and software for optimum and efficient mission science sequence development p 2504 N94-23872
The instant sequencing task: Toward constraint-checking a complex spacecraft command sequence interactively p 2504 N94-23875
A MOS for all seasons p 2505 N94-23879
Making adaptable systems work for mission operations: A case study p 2506 N94-23883
An approach to the design of operations systems p 2506 N94-23884
Object-oriented technologies in a multi-mission data system p 2506 N94-23885
Management of information for mission operations using automated keyword referencing p 2506 N94-23886
Mars Observer screen display design for a multimission environment p 2197 N94-23888
Combining real-time monitoring and knowledge-based analysis in MARVEL p 2477 N94-23900
Making tomorrow's mistakes today: Evolutionary prototyping for risk reduction and shorter development time p 2197 N94-23902
Digital test signal generation: An accurate SNR calibration approach for the DSN p 2305 N94-23912
Representing operations procedures using temporal dependency networks p 2305 N94-23914
Situation management in the Link Monitor and Control Operator Assistant (LMCOA) p 2305 N94-23915
Using Mach threads to control DSN operational sequences p 2477 N94-23916
Deep Space Network (DSN), Network Operations Control Center (NOCC) computer-human interfaces p 2447 N94-23917
XRTD: An X-Windows based, real-time radiometric display and analysis system p 2305 N94-23922
Navigation of space VLBI missions: Radioastron and VSOP p 2513 N94-23926
Operability engineering in the Deep Space Network p 2514 N94-23930
Mission operations and command assurance: Instilling quality into flight operations p 2374 N94-23932
Training: Plugging the information gaps p 2429 N94-23934
Specifying design conservatism: Worst case versus probabilistic analysis p 2374 N94-23939
Expert diagnostics system as a part of analysis software for power mission operations p 2516 N94-23944
The evolving trend in spacecraft health analysis p 2202 N94-23946
Using the SPICE system to help plan and interpret space science observations p 2517 N94-23950
Mars Observer data production, transfer, and archival: The data production assembly line p 2518 N94-23953
Multimission image processing and science data visualization p 2518 N94-23955
Resource allocation planning with international components p 2520 N94-23963
Estimating the Deep Space Network modification costs to prepare for future space missions by using major cost drivers p 2520 N94-23968
Method of forming silicon structures with selectable optical characteristics [NASA-CASE-NPO-18625-1-CU] p 2563 N94-23972
The Jet Propulsion Laboratory space exploration: Past, present and future p 2153 N94-24242
Optimization of microscopic and macroscopic second order optical nonlinearities p 2226 N94-24354
Results of the 1993 NASA/JPL balloon flight solar cell calibration program [NASA-CR-195158] p 2395 N94-24563
Evidence for dust transport in Viking IR thermal mapper opacity data p 2620 N94-24892
Diagnostic calculations of the circulation in the Martian atmosphere p 2622 N94-24898
Mars Observer: Applications to atmospheric transport p 2623 N94-24904
Microwave techniques for physical property measurements p 2238 N94-25134
Electrostatic levitation technology for thermophysical properties of molten materials p 2238 N94-25135

JET PROPULSION LAB., CALIFORNIA INST. OF TECH., WRIGHTWOOD.
Science objectives for short-range rovers on Mars p 2606 N94-23383

JOANNEUM RESEARCH CENTRE, GRAZ (AUSTRIA).
Descent and landing phase: Vision based robust spacecraft motion estimation and elevation modeling p 2608 N94-23394

JOHNS HOPKINS UNIV., LAUREL, MD.
K-band mobile propagation measurements using ACTS p 2283 N94-22792
Multi-grid domain decomposition approach for solution of Navier-Stokes equations in primitive variable form p 2341 N94-23693
A packet-based concept for spacecraft command planning p 2504 N94-23873
Connecting science and operations: The operations coordinator p 2504 N94-23874

JOINT INST. FOR ADVANCEMENT OF FLIGHT SCIENCES, HAMPTON, VA.
X-31 aerodynamic characteristics determined from flight data p 2164 N94-25109

JOINT INST. FOR NUCLEAR RESEARCH, DUBNA (USSR).
New evaluation of hadronic contributions to the anomalous magnetic moment of charged leptons [DE93-634394] p 2536 N94-24844
On the connection of classical mechanics, physical kinetics and quantum theory [DE93-616823] p 2570 N94-25207
Phase structure of the two-dimensional phi(4) field theory within thermo-field dynamics [DE93-616850] p 2570 N94-25337
The Casimir energy of the rigid string with massive ends [DE93-616851] p 2492 N94-25338
Deviation equations of Synge and Schild in spaces with affine connection and metric, and equations for gravitational waves detectors [DE93-616852] p 2571 N94-25339
Critical currents in YBaCuO-ceramics [DE93-617140] p 2263 N94-25404
Lattice dynamics of Ba(1-x)K(x)BiO3 as studied by neutron scattering and computer simulation [DE93-617053] p 2567 N94-25424
Crystal field in Nd2CuO4 [DE93-617054] p 2567 N94-25425
New algorithm for minimizing (chi)(sup 2) functionals with constraints [DE93-616800] p 2463 N94-25432
Weak interactions in a bilocal chiral theory [DE93-616887] p 2539 N94-25477
On the transverse size of a fast moving nucleon [DE93-616891] p 2539 N94-25481

JOINT PUBLICATIONS RESEARCH SERVICE, ARLINGTON, VA.
JPRS report: Science and technology. Central Eurasia: Space [JPRS-USP-93-006] p 2194 N94-23015

K

KANSAS STATE UNIV., MANHATTAN.
Pushing technology to satisfy world applications [DE94-001365] p 2353 N94-23191

KANSAS UNIV., LAWRENCE.
Synthesis of passive microwave and radar altimeter data for estimating accumulation rates of polar snow [NASA-CR-194864] p 2382 N94-23573
Precipitation measurement using SIR-C: A feasibility study [NASA-CR-195104] p 2409 N94-24048
The effect of sub-surface volume scattering on the accuracy of ice-sheet altimeter retracking algorithms [NASA-CR-194825] p 2386 N94-24060
Estimation of the rain signal in the presence of large surface clutter [NASA-CR-195105] p 2409 N94-24087
Precipitation measurement using SIR-C: A feasibility study. Investigation at nadir [NASA-CR-195103] p 2410 N94-24126

KARLSRUHE UNIV. (GERMANY).
Turbulent separated flows above an obstacle in an open channel p 2316 N94-22859

KATHOLIEKE UNIV., NIJMEGEN (NETHERLANDS).
Number of moduli of families of curves on toric surfaces [PB93-230381] p 2479 N94-23121

KENT STATE UNIV., OH.
Application of multigrid methods to the solution of liquid crystal equations on a SIMD computer p 2484 N94-23686

KIEPENHEUER-INST. FUER SONNENPHYSIK, FREIBURG (GERMANY).
Goals of ground-based solar observations p 2624 N94-22840

KOKUSAI DENSHIN DENWA CO. LTD., SAITAMA (JAPAN).
A prediction model of signal degradation in LMSS for urban areas p 2284 N94-22797
Study on networking issues of medium earth orbit satellite communications systems p 2288 N94-22825

KYOTO UNIV., SAKYOKU (JAPAN).
On superconductivity of alpha-(BEDT-TTF)2KHg(SCN)4 [REPT-A-2660] p 2564 N94-24978
CO-to-H2 conversion factor in dwarf irregular galaxies [REPT-333] p 2603 N94-24985

L

LA SALLE UNIV., PHILADELPHIA, PA.
Cost benefits of advanced software: A review of methodology used at Kennedy Space Center p 2464 N94-23240

LABORATOIRE D'AUTOMATIQUE ET D'ANALYSE DES SYSTEMES, TOULOUSE (FRANCE).
Pyroelectric sensors in copolymer integrated on silicon [LAAS-93044] p 2342 N94-22902

Representation and specification of architectures for heterogeneous internetworking: Using a knowledge based approach
[LAAS-93088] p 2445 N94-22903

Contribution to geometric and dynamic modeling of parallel robots
[LAAS-93089] p 2470 N94-22904

Floating well based design methodology aimed to improve latch-up immunity in a CMOS/DMOS smart power technology
[LAAS-93093] p 2556 N94-22905

An architecture for teleprogramming autonomous mobile robots at task level
[LAAS-93107] p 2470 N94-22906

Interpretation of evolutive environment by a multisensory perception machine
[LAAS-93111] p 2471 N94-22907

Perception and 3D environment modeling for mobile robot autonomous navigation
[LAAS-93117] p 2471 N94-22908

Microwave analog frequency dividers: Design, modeling and realization
[LAAS-93139] p 2307 N94-22909

Disilane LPCVD deposited silicon films: Deposition mechanisms, properties and capability of making transistors on thin films
[LAAS-93156] p 2252 N94-22910

Causal labeled transition systems: A new approach for describing the behavior of concurrent systems
[LAAS-93179] p 2447 N94-22911

The remote-operated autonomous-robot concept: From deep sea to outer space applications
p 2370 N94-23413

LABORATOIRE DE METEOROLOGIE DYNAMIQUE, PARIS (FRANCE).

The annual pressure cycle on Mars: Results from the LMD Martian atmospheric general circulation model
p 2619 N94-24884

LASER DATA TECHNOLOGY, INC., SAINT LOUIS, MO.

Multi-access laser communications terminal
[NASA-CR-191251] p 2295 N94-23830

LAVAL UNIV. (QUEBEC).

Experimental study of a turbulent boundary layer in presence of external manipulators of NACA 0009 profile in the transonic regime
[ISBN-0-315-57633-2] p 2333 N94-24177

LAWRENCE LIVERMORE NATIONAL LAB., CA.

Thermoelectric cooled, purge-and-trap device for enhancing the utility of fiber optic VOC sensors
[DE94-001772] p 2541 N94-22722

Economics of electron beam and electrical discharge processing for post-combustion NO(x) control in internal combustion engines
[DE93-019574] p 2351 N94-22865

Fundamental limitations of non-thermal plasma processing for internal combustion engine NO(x) control
[DE93-019622] p 2351 N94-22866

Characterization of germanium stripe x ray lasers
[DE93-019629] p 2347 N94-22867

Ray and wave optics modeling of laboratory x ray lasers
[DE93-019940] p 2541 N94-22868

Limits on high-order harmonic generation from single-atom calculations
[DE93-019950] p 2531 N94-22869

Gas-pressure forming of superplastic ceramic sheet
[DE94-001520] p 2252 N94-22930

Carbon aerogels: An update on structure, properties, and applications
[DE94-001528] p 2252 N94-22931

Structure and flow of data through an environmental data management system
[DE93-040487] p 2589 N94-22934

Analysis of a proposed Compton backscatter imaging technique
[DE93-040537] p 2371 N94-22935

High pressure Hugoniot of sapphire
[DE94-001048] p 2558 N94-22946

Imaging XUV spectroscopy of a Z-pinch plasma in the former Soviet Union
[DE93-040849] p 2549 N94-22949

Picosecond High Pressure Gas Switch experiment
[DE93-040853] p 2307 N94-22950

The history of development of molybdenum alloys for structural applications
[DE94-000389] p 2239 N94-22958

A geometric weighted elliptic grid regeneration method for 3D unstructured ALE hydrodynamics
[DE94-000309] p 2448 N94-22980

Relativistic configuration interaction calculation of the correlation energies of highly-charged ions
[DE94-001055] p 2532 N94-22988

Customizable VLSI artificial neural network chips based on a novel technology
[DE94-001418] p 2307 N94-23008

A novel process monitoring and control system based on a neural manufacturing concept
[DE94-001516] p 2471 N94-23011

Analysis and experiments of a whistler-wave plasma thruster
[DE94-001533] p 2209 N94-23012

Superconducting magnet system for the TPX Tokamak
[DE94-001535] p 2549 N94-23013

Structural analysis of a superconducting central solenoid for the Tokamak Physics Experiment
[DE94-001536] p 2549 N94-23014

Tensile properties of 21-6-9 stainless steel at elevated temperatures
[DE94-001852] p 2240 N94-23017

High-order sum and difference-frequency generation in helium
[DE94-001064] p 2348 N94-23181

Fully coupled nonlinear thermomechanical analysis including general contact in PALM2D
[DE94-001661] p 2568 N94-23216

Phase transformations in Cu-Zr multilayers
[DE94-000393] p 2241 N94-23297

Condensed-phase thermal decomposition of TATB investigated by Atomic Force Microscopy (AFM) and Simultaneous Thermogravimetric Modulated Beam Mass Spectrometry (STMBMS)
[DE94-000396] p 2232 N94-23298

Determination of the compatibility between structural alloys and molten metals at high temperatures
[DE94-000954] p 2241 N94-23434

The ignition temperature of solid explosives exposed to a fire
[DE94-001047] p 2265 N94-23436

Shock-induced turbulent flow in baffle systems
[DE94-001532] p 2319 N94-23470

Lightning, atmospheric electricity, and climate change
[DE94-002003] p 2408 N94-23471

Sodium-layer laser guide stars
[DE93-019621] p 2349 N94-23490

Materials Science and Engineering
[DE94-003018] p 2228 N94-23493

Remote sensing, imaging, and signal engineering
[DE94-003021] p 2382 N94-23494

Fabrication of sub-40-nm p-n junctions for 0.18 micron MOS device applications using a cluster-tool-compatible, nanosecond thermal doping technique
[DE94-001608] p 2309 N94-23520

A multilevel adaptive projection method for unsteady incompressible flow p 2341 N94-23690

Radiative forcing calculations for SF6 and CH4 using a correlated k-distribution transmission model
[DE94-001855] p 2397 N94-23700

Inertial confinement fusion
[DE94-002602] p 2551 N94-23703

Physics of iron
[DE94-002002] p 2402 N94-23721

Energy transfer in solid explosives
[DE94-001523] p 2265 N94-23778

A matrix analysis of conjugate gradient algorithms
[DE94-002546] p 2454 N94-23796

Multiple shock initiation of LX-17
[DE94-001524] p 2265 N94-23807

Stabilization of the external kink and other MHD issues
[DE94-001541] p 2552 N94-24502

Studies on the implementation of normals and curvatures. Part 1: The first or mean curvature
[DE94-001546] p 2488 N94-24503

High strain rate superplasticity in metals and composites
[DE94-001521] p 2229 N94-24547

Nondestructive evaluations
[DE94-003020] p 2373 N94-24613

Tokamak Physics Experiment (TPX) cost and performance trade studies using supercode
[DE94-002720] p 2553 N94-24628

Crashworthiness analysis using advanced material models in DYNA3D
[DE94-002988] p 2229 N94-24632

LEAR ASTRONICS CORP., SANTA MONICA, CA.

The 94 GHz MMW imaging radar system
p 2306 N94-25493

LEHIGH UNIV., BETHLEHEM, PA.

Feasibility study: Monodisperse polymer particles containing laser-excitable dyes p 2225 N94-24350

Heat transfer and flow structure in end-wall boundary layers
[AD-A273470] p 2335 N94-24689

Robotic weld overlay coatings for erosion control
[DE94-002665] p 2258 N94-24749

LEIDEN UNIV. (NETHERLANDS).

Reduction of nitric oxide over platinum, rhodium and platinum-rhodium single crystal surfaces
[PB93-230092] p 2232 N94-23482

Error due to the stopping of the Newton iteration in implicit linear multistep methods
[PB94-101425] p 2487 N94-23786

Rao-Blackwell theorem in stereology and some counterexamples
[PB94-111713] p 2496 N94-24639

On finding optimal policies for Markov decision chains: A unifying framework for mean-variance-tradeoffs
[TW-92-13] p 2497 N94-25528

LETOURNEAU COLL., LONGVIEW, TX.

Data analysis and interpretation of lunar dust exosphere p 2623 N94-25349

LIEGE UNIV. (BELGIUM).

Tribological behaviour of fluorinated resins and polyimide resins sliding over a metallic surface in liquid nitrogen
p 2355 N94-23991

LIMBURG STATE UNIV., MAASTRICHT (NETHERLANDS).

Sensitivity analysis of list scheduling heuristics
[PB93-237766] p 2468 N94-24764

LITTON SYSTEMS, INC., MINNEAPOLIS, MN.

Integrated accelerometer assembly
[CA-PATENT-1322107] p 2344 N94-24184

LIVERPOOL UNIV. (ENGLAND).

Design of novel catalysts for the partial oxidation of methane to methanol
[PB94-114212] p 2235 N94-24920

LOCKHEED AIRCRAFT CORP., PALO ALTO, CA.

Why put visible solar telescopes in space?
p 2600 N94-22850

LOCKHEED CORP., BURBANK, CA.

Flush head fastener
[CA-PATENT-1308581] p 2364 N94-24175

LOCKHEED ENGINEERING AND SCIENCES CO., HAMPTON, VA.

A parametric study of harmonic rotor hub loads
[NASA-CR-4558] p 2181 N94-24726

Nonlinear aerodynamic modeling using multivariate orthogonal functions p 2164 N94-25110

LOCKHEED ENGINEERING AND SCIENCES CO., HOUSTON, TX.

Space Station Freedom (SSF) Data Management System (DMS) performance model data base
[NASA-CR-188270] p 2590 N94-23289

Implementing the space shuttle data processing system with the space generic open avionics architecture
[NASA-CR-188254] p 2199 N94-23571

Spacecraft crew procedures from paper to computers
p 2433 N94-24186

Automated system function allocation and display format: Task information processing requirements
p 2434 N94-24189

The use of analytical models in human-computer interface design p 2434 N94-24190

Use of infrared telemetry as part of a nonintrusive inflight data collection system to collect human factors data
p 2434 N94-24193

Performing speech recognition research with hypercard p 2306 N94-24194

Programmable display pushbuttons on the Space Station's telerobot control panel p 2435 N94-24198

Speech versus manual control of camera functions during a telerobotic task p 2436 N94-24199

Space Station Freedom coupling tasks: An evaluation of their telerobotic and EVA compatibility
p 2436 N94-24200

The effects of spatially displaced visual feedback on remote manipulator performance p 2436 N94-24201

Simulation of the human-telerobot interface on the Space Station p 2436 N94-24202

Quantitative assessment of human motion using video motion analysis p 2436 N94-24203

LOCKHEED ENGINEERING AND SCIENCES CO., MOFFETT FIELD, CA.

Simulation of a passive millimeter wave sensor
p 2346 N94-25499

LOCKHEED MISSILES AND SPACE CO., PALO ALTO, CA.

Coronal abundances and their variation
[NASA-CR-194811] p 2626 N94-23276

Artificial plasma experiments. Chemical release observations associated with the CRRES program
[NASA-CR-194871] p 2550 N94-23565

LOCKHEED SANDERS, INC., NASHUA, NH.

Effects of atmospheric variations on acoustic system performance p 2527 N94-24211

New Technologies for Space Avionics, 1993
[NASA-CR-195157] p 2272 N94-25193

Appendix A: Proposed statement of work, 1994
p 2272 N94-25194

Appendix B: Rapid development approaches for system engineering and design p 2272 N94-25195

Appendix C: Rapid development approaches for system engineering and design p 2272 N94-25196

LOGICA LTD., LONDON (ENGLAND).
ATOS-1: Designing the infrastructure for an advanced spacecraft operations system p 2197 N94-23849

LOGICA SPACE AND COMMUNICATIONS LTD., LONDON (ENGLAND).
ATOS-1: Designing the infrastructure for an advanced spacecraft operations system p 2197 N94-23849
The EURECA telecommanding chain: Experience with packet telecommand and telemetry systems p 2305 N94-23909

LOGICON CONTROL DYNAMICS CO., HUNTSVILLE, AL.
LSS systems planning and performance program [NASA-CR-193862] p 2196 N94-24309

LORAL AEROSPACE CORP., PALO ALTO, CA.
The Globalstar mobile satellite system for worldwide personal communications p 2282 N94-22786
Development of a multilayer interference simulation program for MSS systems p 2287 N94-22823

LOS ALAMOS NATIONAL LAB., NM.
Nonlocal models in continuum mechanics [DE93-040146] p 2316 N94-22870
Fracture simulations via massively parallel molecular dynamics [DE93-040159] p 2374 N94-22871
Spin-hole doping in the Kondo insulator Ce3Bi4Pt3 studied by neutron scattering [DE93-040107] p 2557 N94-22925
Pions and neutrinos as probes of the nucleon and nuclear few-body system [DE93-040127] p 2531 N94-22928
Discontinuous phase formation and selective attack of SiC materials exposed to low oxygen partial pressure environments [DE93-040161] p 2231 N94-22933
Orientation imaging microscopy: New possibilities for microstructural investigations using automated BKD analysis [DE94-000777] p 2557 N94-22938
Magnetic phases in UNiGe [DE94-000793] p 2239 N94-22939
Coherence lost? Not-so-fast escapes from the in-phase attractor of a set of globally coupled nonlinear oscillators [DE94-000799] p 2557 N94-22940
Anomalous magnetoresistance behavior of superconducting Nd(2-x)Ce(x)CuO(4-y) single crystal [DE94-000806] p 2558 N94-22941
A valence-fluctuation theory of cuprate superconductivity [DE94-000887] p 2558 N94-22942
Thermochemistry of the actinides [DE94-000895] p 2231 N94-22943
Developments in materials for high-field magnets [DE94-000761] p 2307 N94-22987
Interplay of magnetic and superconducting heavy fermion ground states [DE94-000680] p 2240 N94-23003
Muon spin relaxation studies of the interplay between magnetism and superconductivity in heavy fermion systems [DE94-000700] p 2559 N94-23006
Recent results from the Soviet-American Gallium Experiment [DE94-000677] p 2626 N94-23020
Texture gradient effects in tantalum [DE94-000689] p 2240 N94-23021
Advanced nuclear thermal propulsion concepts p 2217 N94-23068
Vaporization behavior of non-stoichiometric refractory carbide materials and direct observations of the vapor phase using laser diagnostics [DE93-040094] p 2348 N94-23203
The internal structure and dynamics of the railgun plasma armature between infinitely wide ablating rails [DE94-001473] p 2196 N94-23208
Reduction of the anode fall in a coaxial plasma thruster with an applied magnetic nozzle [DE94-000670] p 2218 N94-23283
On testing two major cumulus parameterization schemes using the CSU regional atmospheric modeling system [DE94-000703] p 2407 N94-23284
Primary and secondary electrical space power based on advanced PEM systems p 2392 N94-23357
Assessment of an SP-100 bi-modal propulsion and power system [DE94-000889] p 2218 N94-23433
SP-100 heat transport technology development [DE94-000769] p 2218 N94-23452
Calculations of Bose-Einstein correlations from Relativistic Quantum Molecular Dynamics [DE94-000794] p 2569 N94-23453
Accelerator-based neutrino oscillation searches [DE94-000818] p 2626 N94-23515
Global ocean modeling on the Connection Machine [DE94-000888] p 2417 N94-23517
The effects of texture and strain on the r-va lue of heavy gauge tantalum plate [DE94-000690] p 2242 N94-23541
Radar stimulator interface protocol, preliminary interface design and Doppler Beam Sharpening implementation [DE94-002567] p 2453 N94-23701
Investigations on detonation shock dynamics and related topics [DE94-002570] p 2326 N94-23809
Computer modeling of plasma flow switches-high current switching on Procyon [DE93-040189] p 2311 N94-24500
Effects of ionizing radiation on modern ion exchange materials [DE94-001569] p 2535 N94-24505
Density estimation by maximum quantum entropy [DE94-002626] p 2569 N94-24516
The mechanical properties of single crystal (alpha)-Si3N4 [DE94-002632] p 2563 N94-24517
Diagnosing process faults using neural network models [DE94-002633] p 2473 N94-24518
Start-up simulations of the PULSAR pulsed tokamak reactor [DE94-002634] p 2552 N94-24519
Procedures for determining MATMOD-4V material constants [DE94-002638] p 2245 N94-24520
The experimental physics and industrial control system architecture: Past, present, and future [DE94-002639] p 2457 N94-24626
Tokamak Physics Experiment (TPX) cost and performance trade studies using supercode [DE94-002720] p 2553 N94-24628
A survey of metallurgical research on several actinides [DE94-002643] p 2245 N94-24747

LOUGHBOROUGH UNIV. OF TECHNOLOGY (ENGLAND).
Liapunov stability in chemical engineering [MATHS-REPT-A-184] p 2236 N94-25427
Kernels of anti-causal operators and the multivariable generalized predictive control problem [MATHS-REPT-A-191] p 2476 N94-25428
Advances in generalized and constrained generalized predictive control with application to a dynamometer model [MATHS-REPT-A-192] p 2476 N94-25429
The scattering and collision of gravitational waves in Friedmann-Robertson-Walker open universes [MATHS-REPT-A-193] p 2406 N94-25430

LOUISIANA STATE UNIV., BATON ROUGE.
Theoretical investigation of variable periodicity (graded) multilayers for hard x ray applications [NASA-CR-194824] p 2543 N94-23502
Solar flares and magnetospheric particles: Investigations based upon the ONR-602 and ONR-604 experiments [AD-A273639] p 2628 N94-25031

LOUISIANA TECH UNIV., RUSTON.
Parallel processing methods for space based power systems p 2222 N94-25352

LOUISVILLE UNIV., KY.
Cytokines and immune surveillance in humans [NASA-CR-194801] p 2425 N94-23331

LOWELL OBSERVATORY, FLAGSTAFF, AZ.
A study of cloud motions on Mars. 2: Some examples of observations and analyses since 1969 p 2620 N94-24891

LOYOLA COLL., BALTIMORE, MD.
Advanced display technologies in Russia, Ukraine, and Belarus. Viewgraphs p 2630 N94-22893
Satellite communications systems and technology. Executive Summary [NASA-TM-109388] p 2293 N94-23622
Satellite communications systems and technology. Volume 1: Analytical chapters [NASA-TM-109398] p 2293 N94-23627
Satellite communications systems and technology. Volume 2: Site reports [NASA-TM-109399] p 2293 N94-23628

LUNAR AND PLANETARY INST., HOUSTON, TX.
Catalog of Apollo 17 rocks. Volume 1: Stations 2 and 3 (South Massif) [NASA-CR-194854] p 2613 N94-24058
Workshop on Atmospheric Transport on Mars [NASA-CR-194855] p 2616 N94-24871
Antarctic Meteorite Location and Mapping Project (AMLAMP): Antarctic meteorite location map series explanatory text and user's guide to AMLAMP data [NASA-CR-194841] p 2603 N94-24964

LYNNTECH, INC., COLLEGE STATION, TX.
High power density proton exchange membrane fuel cells p 2393 N94-23359

M

M-C POWER CORP., BURR RIDGE, IL.
Advanced research and technology development of MCFCs [DE94-001918] p 2389 N94-22723

MACNEAL-SCHWENDLER CORP., GOUDA (NETHERLANDS).
The plastic response of a cylindrical shell subjected to an internal blast wave with a finite width shock front p 2154 N94-24246

MADRID UNIV. (SPAIN).
Energy transfer and constrained simulations in isotropic turbulence p 2330 N94-24153

MAINE UNIV., ORONO.
An analytic study of a two-phase laminar airfoil in simulated heavy rain p 2171 N94-23661

MANITOBA UNIV., WINNIPEG.
Low cost antennas for MSAT vehicular applications p 2289 N94-22830

MARITIME ADMINISTRATION, WASHINGTON, DC.
Worldwide vessel locating and tracking system, volume 1 [PB93-193217] p 2175 N94-24474

MARQUETTE UNIV., MILWAUKEE, WI.
Characteristics of products generated by selective sintering and stereolithography rapid prototyping processes p 2264 N94-24412

MARTIN MARIETTA ASTRO SPACE, PHILADELPHIA, PA.
GPHS-RTG's in support of the Cassini mission [DE94-001445] p 2218 N94-23459

MARTIN MARIETTA CORP., DENVER, CO.
Task 1: Health management demonstration. Task 2: Process management environment and support of enterprise integration. Task 3: New algorithm development in the PME [NASA-CR-188268] p 2430 N94-23290
Magellan spacecraft and memory state tracking: Lessons learned, future thoughts p 2207 N94-23865
VMPLOT: A versatile analysis tool for mission operations p 2507 N94-23891
Using SFOC to fly the Magellan Venus mapping mission p 2516 N94-23941
Space transfer vehicle concepts and requirements. Volume 4: Summary of special studies [NASA-CR-193918] p 2201 N94-24970

MARTIN MARIETTA LABS., BALTIMORE, MD.
Collocated tunable wavenumber sensor/actuators for smart structures [AD-A273697] p 2314 N94-25488

MARYLAND UNIV., COLLEGE PARK.
A protocol for satellite access via use of spot-beams p 2286 N94-22811
Aeroelastic response and stability of tiltrotors with elastically-coupled composite rotor blades [NASA-TM-108758] p 2182 N94-24953
A comparison of Boolean-based retrieval to the WAIS system for retrieval of aeronautical information [NASA-CR-4569] p 2594 N94-25487
NACA collections: A directory of significant collections of the documents of the National Advisory Committee for Aeronautics [NASA-CR-195686] p 2594 N94-25541

MASCHINENFABRIK AUGSBURG-NUERNBERG A.G., MUNICH (GERMANY).
Integrated approach in modelling, testing, and design of gradient-CVI derived CMC components p 2256 N94-24239

MASSACHUSETTS INST. OF TECH., CAMBRIDGE.
Massachusetts Institute of Technology Plasma Fusion Center 1992-1993 report to the President [DE94-001725] p 2548 N94-22721
The mass of massive rover software p 2464 N94-23410
Walking, jumping, and tumbling: More than one way to get around Mars p 2370 N94-23419
Selection of polymer binders and fabrication of SiC fiber-reinforced reaction-bonded silicon nitride matrix composites [NASA-CR-194874] p 2255 N94-24223
Voyager planetary radio astronomy studies [NASA-CR-194776] p 2614 N94-24328
Processing of semicrystalline polymers p 2226 N94-24351
Plasma initiation in a tokamak with conducting superstructure: First results from Alcator C-MOD [DE94-001565] p 2552 N94-24504
Prediction of thermal cycling induced cracking in polmer matrix composites [NASA-CR-195135] p 2229 N94-24579
Damage tolerance of pressurized graphite/epoxy tape cylinders under uniaxial and biaxial loading [NASA-CR-195101] p 2377 N94-24587

Thermal phase behavior of metal surfaces: X-ray scattering studies of Pt(001)
[DE94-002991] p 2245 N94-24612

Control of nonlinear systems represented in quasilinear form
[NASA-CR-194840] p 2475 N94-24760

GPS survey of the western Tien Shan
[NASA-CR-195174] p 2175 N94-24826

Compact free electron lasers for medical applications
[AD-A273609] p 2350 N94-24934

New directions in network flows
[AD-A273467] p 2468 N94-24939

Morphology of highly textured polyethylene/polyethylene- propylene semicrystalline diblock copolymers
[AD-A273683] p 2263 N94-25413

MASSACHUSETTS INST. OF TECH., LEXINGTON.

Analysis and surveillance performance at Chicago O'Hare Airport
[DOT/FAA/RD-92/29] p 2175 N94-24127

ASR-9 microburst detection algorithm
[AD-A273591] p 2415 N94-24850

MASSACHUSETTS UNIV., AMHERST.

Ultrastructure processing of macromolecular materials
[AD-A273413] p 2258 N94-24782

Center for advanced electrical and structural polymers
[AD-A273415] p 2259 N94-24783

Use of microwave polarimetry to enhance SAR images of the ocean surface
[AD-A273568] p 2419 N94-24944

MASSACHUSETTS UNIV., LOWELL.

Dipolar relaxation in a second-order nonlinear optical interpenetrating polymer network
[AD-A273626] p 2258 N94-24732

Polythiophene derivative with a side chain chromophore as photovoltaic and photorefractive materials
[AD-A273245] p 2260 N94-24813

MATERIALS RESEARCH LABS., ASCOT VALE (AUSTRALIA).

Interaction of tacrine at M(1) and M(2) cholinoceptors in guinea pig brain p 2421 N94-24294

MATERIALS RESEARCH SOCIETY, PITTSBURG, PA.

Ferroelectric thin films 3
[AD-A273394] p 2565 N94-25027

MATERIALS SCIENCES CORP., BLUE BELL, PA.

Test methods for composites: A status report. Volume 2: Compression test methods
[AD-A273522] p 2230 N94-24779

Test methods for composites: A status report. Volume 1: Tension test methods
[AD-A273501] p 2230 N94-24942

Test methods for composites: A status report. Volume 3: Shear test methods
[AD-A273561] p 2230 N94-25163

MATRA MARCONI SPACE, TOULOUSE (FRANCE).

Influence of a new generation of operations support systems on current spacecraft operations philosophy: The users feedback p 2507 N94-23894

A cross-disciplinary response to improve test activities: The corporate memory capitalization in Ariane4 test domain p 2508 N94-23899

Kalman filtering applied to real-time monitoring of apogee maneuvers p 2196 N94-23923

Inter orbit link antenna pointing mechanisms design using standard actuators p 2359 N94-24016

MAX-PLANCK-INST. FUER AERONOMIE, KATLENBURG-LINDAU (GERMANY).

Ultra-clean high-precision mechanisms for the SUMER EUV spectrometer on SOHO p 2356 N94-23999

The development of the SOHO SUMER mechanisms p 2361 N94-24028

MAX-PLANCK-INST. FUER METEOROLOGIE, HAMBURG (GERMANY).

Monte Carlo climate change forecasts with a global coupled ocean-atmosphere model
[MPIM-97] p 2407 N94-23156

Locally modified Bott-scheme for highly convective flows
[MPIM-99] p 2400 N94-23157

Modes of ocean variability in the tropical Pacific as derived from Geosat altimetry
[MPIM-103] p 2382 N94-23158

Climate variability in a coupled GCM. Part 2: The Indian Ocean and monsoon
[MPIM-104] p 2401 N94-23159

Modal structure of variations in the tropical climate system. Part 2: Origins of the low-frequency mode
[MPIM-96] p 2407 N94-23199

Tropospheric Ozone Lidar Intercomparison Experiment, TROLIX 1991
[MPIM-102] p 2402 N94-24108

Northern hemisphere tropospheric mid-latitude circulation after violent volcanic eruptions
[MPIM-107] p 2403 N94-24491

MAX-PLANCK-INST. FUER PHYSIK UND ASTROPHYSIK, GARCHING (GERMANY).

Examination of the response capacity of a silicon pixel detector for ions and molecules in the energy area 100 to 300 keV
[MPE-241] p 2346 N94-25415

CsI(Tl)-photodiode detectors for spectroscopy at low radiation levels
[MPI-PHE/92-22] p 2314 N94-25457

High energy gamma astronomy above 200 GeV
[MPI-PHE/93-04] p 2600 N94-25458

Superconducting cosmic strings near the electroweak scale and cosmic-ray propagation
[MPI-PHE/93-05] p 2629 N94-25459

MAX-PLANCK-INST. FUER STROEMUNGSFORSCHUNG, GOETTINGEN (GERMANY).

Forced vibrations of a non-viscous drop
[MPIS-24/1992] p 2318 N94-23198

MCDONNELL-DOUGLAS AEROSPACE, LONG BEACH, CA.

Variability of measured sonic boom signatures. Volume 1: Technical report
[NASA-CR-191483-VOL-1] p 2526 N94-24172

Variability of measured sonic boom signatures. Volume 2: Data report
[NASA-CR-191483-VOL-2] p 2526 N94-24173

Current and future design methods for large transport aircraft p 2179 N94-24324

MCDONNELL-DOUGLAS AEROSPACE INFORMATION SERVICES CO., SAINT LOUIS, MO.

Aircraft maneuvers for the evaluation of flying qualities and agility. Volume 2: Maneuver descriptions and section guide
[AD-A273665] p 2185 N94-25440

MCDONNELL-DOUGLAS CORP., SAINT LOUIS, MO.

Application of concurrent engineering principles to aircraft structural design p 2178 N94-24321

MCMASTER UNIV., HAMILTON (ONTARIO).

Automatic modulation recognition based on spatial pattern classification using artificial neural networks
[CTN-94-60897] p 2296 N94-24115

MECON B.V., DOETINCHEM (NETHERLANDS).

Multipurpose clamping device with electrical connector for in orbit attachment of payloads p 2361 N94-24035

MELBOURNE UNIV., PARKVILLE (AUSTRALIA).

Local isotropy in distorted turbulent boundary layers at high Reynolds number p 2332 N94-24166

MEMPHIS STATE UNIV., TN.

Digital data, composite video multiplexer and demultiplexer boards for an IBM PC/AT compatible computer p 2447 N94-25377

MESSIER-HISPANO-BUGATTI S.A., MONTROUGE (FRANCE).

Landing gear with swivelling beam
[CA-PATENT-1323020] p 2176 N94-24181

MICHIGAN STATE UNIV., EAST LANSING.

Extinguishment of combustible porous solids by water droplets
[PB93-198893] p 2270 N94-23740

The 7th Annual National Conference of Black Physics Students p 2524 N94-24583

MICHIGAN TECHNOLOGICAL UNIV., HOUGHTON.

Preliminary analysis of amplitude and phase fluctuations in the JAPE multiple tone data to distances of 500 meters p 2528 N94-24216

MICHIGAN UNIV., ANN ARBOR.

Reduced cost alternatives to premise wiring using ATM and microcellular technologies p 2314 N94-23239

Data analysis and theoretical studies of the upper mesosphere and lower thermosphere
[NASA-CR-195108] p 2402 N94-24089

Defects in electro-optically active polymer solids p 2223 N94-24342

Mesospheric and lower thermospheric winds, temperatures densities, and volume emission rates
[NASA-CR-195147] p 2403 N94-24486

Design of an airborne launch vehicle for an air launched space booster
[NASA-CR-195534] p 2198 N94-24860

GRYPHON: Air launched space booster
[NASA-CR-195497] p 2199 N94-25022

MIDWEST RESEARCH INST., GOLDEN, CO.

Polycrystalline thin film materials and devices
[DE93-018213] p 2389 N94-22862

Progress in phases 2 and 3 of the Photovoltaic Manufacturing Technology Project (PVMaT)
[DE94-000206] p 2389 N94-22888

Research on polycrystalline thin-film CuInGaSe2 solar cells
[DE94-000203] p 2560 N94-23205

Amorphous silicon PVMaT, phase 2A
[DE93-018221] p 2390 N94-23295

Novel two-stage selenization methods for fabrication of thin-film CIS cells and submodules
[DE94-000220] p 2390 N94-23296

A review of the Workshop on Fatigue Life Methodologies for Wind Turbines
[DE94-002039] p 2394 N94-23472

Thin film cadmium telluride photovoltaic cells
[DE94-000201] p 2395 N94-24509

Overview of the status and progress in photovoltaics research in the United States
[DE94-000981] p 2395 N94-24512

MINISTRY OF POSTS AND TELECOMMUNICATIONS, IBARAKI (JAPAN).

Adaptive data rate control TDMA systems as a rain attenuation compensation technique p 2287 N94-22821

MINISTRY OF POSTS AND TELECOMMUNICATIONS, KASHIMA (JAPAN).

Land mobile satellite propagation measurements in Japan using ETS-V satellite p 2282 N94-22790

Measurement of multipath delay profile in land mobile satellite channels p 2283 N94-22793

MINISTRY OF POSTS AND TELECOMMUNICATIONS, TOKYO (JAPAN).

Advanced mobile satellite communications using COMETS satellite in MM-wave and Ka-band p 2288 N94-22829

MINNESOTA MINING AND MFG. CO., SAINT PAUL.

Ordered organic thin films self-assembled from the vapor phase p 2223 N94-24339

MINNESOTA UNIV., MINNEAPOLIS.

Arc electrode interaction study
[NASA-CR-195096] p 2310 N94-24070

Lunar transportation system
[NASA-CR-195540] p 2365 N94-24805

Feedback control laws for highly maneuverable aircraft
[NASA-CR-195195] p 2190 N94-25176

Mechanisms of eye-hand coordination
[AD-A273687] p 2428 N94-25437

MINOT STATE UNIV., ND.

A comparative evaluation plan for the Maintenance, Inventory, and Logistics Planning (MILP) System Human-Computer Interface (HCI) p 2588 N94-25373

MISSION RESEARCH CORP., LOS ALAMOS, NM.

Radar stimulator interface protocol, preliminary interface design and Doppler Beam Sharpening implementation
[DE94-002567] p 2453 N94-23701

MISSION RESEARCH CORP., NEWINGTON, VA.

Design and testing of ubitron amplifier tubes
[AD-A273297] p 2311 N94-24818

MISSISSIPPI STATE UNIV., MISSISSIPPI STATE.

Uncertainty analysis of diffuse-gray radiation enclosure problems: A hypersensitive case study p 2320 N94-23637

Numerical flow simulation for complete vehicle configurations
[AD-A273588] p 2170 N94-24849

MISSISSIPPI STATE UNIV., STATE COLLEGE.

Structure in gamma ray burst time profiles: Correlations with other observables p 2579 N94-24431

Using contour maps to search for red-shifted 511 keV features in BATSE GRB spectra p 2585 N94-24455

MISSISSIPPI UNIV., UNIVERSITY.

Comparison of measured and predicted pure tone propagation levels from JAPE-1: An evaluation of the performance of ASOPRAT p 2527 N94-24212

Comparisons of calculated and measured helicopter noise near instrument hill p 2528 N94-24215

A study of element interaction in thermoacoustic engines
[AD-A273228] p 2569 N94-24777

MISSOURI UNIV., ROLLA.

Switch configuration for migration to optical fiber network p 2447 N94-23250

MITRE CORP., BEDFORD, MA.

Electromagnetic interference impact of the proposed emitters for the High Frequency Active Auroral Research Program (HAARP)
[AD-A273401] p 2301 N94-24926

MITRE CORP., GREENBELT, MD.

A reference model for space data system interconnection services p 2305 N94-23847

MITRE CORP., HOUSTON, TX.

PILOT: An intelligent distributed operations support system p 2508 N94-23895

MITSUBISHI HEAVY INDUSTRIES LTD., TOKYO (JAPAN).

Gas turbine and operating method of the same
[CA-PATENT-APPL-SN-2043039] p 2188 N94-24490

MONTREAL UNIV. (QUEBEC).

Three dimensional study of an airplane wing and its wake in the subsonic regime
[ISBN-0-315-58963-9] p 2168 N94-24178

MOSCOW STATE UNIV. (RUSSIA).

Behavior of the intermittency exponents and a quark-gluon plasma formation in the heavy ion collisions
[DE93-616869] p 2541 N94-25342

On the hadron formation time in pion-nucleus interaction [DE93-616879] p 2539 N94-25476

MOTOROLA, INC., CHANDLER, AZ.

Systems implications of L-band fade data statistics for LEO mobile systems p 2284 N94-22799

MOTOROLA, INC., MCLEAN, VA.

The Iridium (tm) system: Personal communications anytime, anyplace p 2281 N94-22785

MOTOROLA, INC., PHOENIX, AZ.

Satellite communications system [CA-PATENT-APPL-SN-2053597] p 2297 N94-24183

MOUNT HOLYOKE COLL., SOUTH HADLEY, MA.

The role of visual context in manual target localization p 2429 N94-25351

MPR TELTECH LTD., OTTAWA (ONTARIO).

Interworking evolution of mobile satellite and terrestrial networks p 2277 N94-22758

MULLARD SPACE SCIENCE LAB., DORKING (ENGLAND).

Requirements for future solar-physics missions with x ray instrumentation p 2625 N94-22849

MURRAY STATE UNIV., KY.

Multigrid method for integral equations and automatic programs p 2464 N94-23696

M2A ENGINEERING, PARIS (FRANCE).

Bond graph modeling, simulation, and reflex control of the Mars planetary automatic vehicle p 2370 N94-23424

N

NAGOYA UNIV. (JAPAN).

Solar-terrestrial environmental laboratory p 2630 N94-23336

NATIONAAL INST. VOOR KERNFYSICA EN HOGE ENERGIEFYSICA, AMSTERDAM (NETHERLANDS).

Low mass muon pair production in 450 GeV p-Be collisions [PB94-110699] p 2533 N94-23746

Applications of supersymmetric quantum mechanics [ETN-94-95385] p 2570 N94-25257

On BRST quantization of constrained systems [ETN-94-95386] p 2570 N94-25258

Relativistic hadrons in an external field [ETN-94-95387] p 2538 N94-25259

Heavy flavour physics at LEP [NIKHEF-H/92-19] p 2539 N94-25465

NATIONAL ACADEMY OF ENGINEERING, WASHINGTON, DC.

The Future of Aerospace: Proceedings of a symposium held in honor of Alexander H. Flax [LC-93-83945] p 2631 N94-25065

NATIONAL ACADEMY OF SCIENCES - NATIONAL RESEARCH COUNCIL, WASHINGTON, DC.

The national geomagnetic initiative [LC-93-85739] p 2401 N94-23344

Panel to review EOSDIS plans [NASA-CR-195088] p 2387 N94-24303

Women scientists and engineers employed in industry: Why so few? A report based on a conference [ISBN-0-309-04991-1] p 2585 N94-24698

A biological survey for the nation [LC-93-85920] p 2421 N94-24704

Information technology in the service society: A twenty-first century lever [ISBN-0-309-04876-1] p 2593 N94-24833

NATIONAL AERONAUTICS AND SPACE ADMINISTRATION, WASHINGTON, DC.

Solar physics within NASA's planning p 2625 N94-22845

The birth of NASA: The diary of T. Keith Glennan [NASA-SP-4105] p 2630 N94-23333

Aerospace applications of batteries p 2390 N94-23346

Evolving directions in NASA's planetary rover requirements and technology p 2370 N94-23414

Space tourism: A flight of fantasy or the next major space product? Paper session 3: Products [NASA-TM-109385] p 2194 N94-23710

Aeronautical engineering: A continuing bibliography with indexes (supplement 298) [NASA-SP-7037(298)] p 2153 N94-23711

NASA patent abstracts bibliography: A continuing bibliography. Section 2: Indexes (supplement 44) [NASA-SP-7039(44)-SECT-2] p 2590 N94-23712

Strategies in transition p 2498 N94-23833

Future trends in NASA space operations p 2498 N94-23836

An operations concept methodology to achieve low-cost mission operations p 2505 N94-23880

Space Station Freedom ground data system: Design and operations p 2518 N94-23957

Toward lowering the cost of mission operations p 2519 N94-23960

NASA printing, duplicating, and copying management handbook [NASA-NHB-1490.5] p 2590 N94-23971

Aeronautical engineering: A continuing bibliography with indexes (supplement 299) [NASA-SP-7037(299)] p 2153 N94-23973

NASA high performance computing and communications program [NASA-TM-4554] p 2591 N94-24337

Japanese aerospace science and technology 1992. A bibliography with indexes [NASA-SP-7104] p 2631 N94-24585

Human-like robots for space and hazardous environments [NASA-CR-195549] p 2365 N94-24703

Management. A bibliography for NASA managers [NASA-SP-7500(27)] p 2586 N94-24708

Third Annual Foreign Acquisitions Workshop: Improving Access to Foreign Gray Literature [NASA-TM-109683] p 2593 N94-24759

A white paper: NASA virtual environment research, applications, and technology [NASA-TM-109682] p 2428 N94-24855

Ultraviolet, visible, and gravity astrophysics: A plan for the 1990's [NASA-NP-152] p 2603 N94-24973

Spinoff 1993 [NASA-NP-211] p 2597 N94-25018

NASA STI program database: Journal coverage (1990-1992) [NASA-TM-109720] p 2593 N94-25168

NATIONAL AERONAUTICS AND SPACE ADMINISTRATION. AMES RESEARCH CENTER, MOFFETT FIELD, CA.

Probe shapes that measure time-averaged streamwise momentum and cross-stream turbulence intensity [NASA-CASE-ARC-11934-1] p 2317 N94-23077

Increasing accuracy in the assessment of motion sickness: A construct methodology [NASA-TM-108797] p 2420 N94-23088

Probe systems for measuring static pressure and turbulence intensity in fluid streams [NASA-CASE-ARC-11935-1] p 2319 N94-23306

Output optics for laser velocimeters [NASA-CASE-ARC-11889-1-SB] p 2543 N94-23309

Deployable video conference table [NASA-CASE-ARC-11950-1] p 2192 N94-23310

Ceramic silicon-boron-carbon fibers from organic silicon-boron-polymers [NASA-CASE-ARC-11956-1-SB] p 2253 N94-23311

Head related transfer function pseudo-stereophony [NASA-CASE-ARC-11919-1-NP] p 2525 N94-23312

Summary of lift and lift/cruise fan powered lift concept technology [NASA-CR-177619] p 2176 N94-23489

The Automated Instrumentation and Monitoring System (AIMS) reference manual [NASA-TM-108795] p 2452 N94-23510

LinAir: A multi-element discrete vortex Weissinger aerodynamic prediction method [NASA-TM-108786] p 2167 N94-23557

A review of European applications of artificial intelligence to space [NASA-TM-108789] p 2453 N94-23568

Exercise, exercise training, and the immune system. A compendium of research (1902-1991) [NASA-TM-108778] p 2426 N94-23575

Constraint-based scheduling p 2510 N94-23904

Reducing video frame rate increases remote optimal focus time [NASA-TM-104018] p 2431 N94-23970

Evaluation of visual acuity with Gen 3 night vision goggles [NASA-TM-108792] p 2431 N94-23974

Compressibility effects on dynamic stall of airfoils undergoing rapid transient pitching motion [NASA-TM-109681] p 2167 N94-23975

Autogenic-feedback training: A potential treatment for post-flight orthostatic intolerance in aerospace crews [NASA-TM-108785] p 2426 N94-24102

Investigation of the asymptotic state of rotating turbulence using large-eddy simulation p 2330 N94-24152

On streak spacing in wall-bounded turbulent flows p 2331 N94-24159

Transition to turbulence in an elliptic vortex p 2331 N94-24161

Factors affecting the identification of phytoplankton groups by means of remote sensing [NASA-TM-108799] p 2387 N94-24403

The evolution of energy-transducing systems. Studies with an extremely halophilic archaebacterium [NASA-CR-193803] p 2422 N94-24807

The evolution of energy-transducing systems. Studies with archaebacteria [NASA-CR-195129] p 2422 N94-24811

Impact of the CO2 and H2O clouds of the Martian polar hood on the polar energy balance p 2618 N94-24880

Multiannual simulations with the Mars climate model p 2618 N94-24881

Regarding tracer transport in Mars' winter atmosphere in the presence of nearly stationary, forced planetary waves p 2618 N94-24882

Dust transport in the Martian atmosphere p 2621 N94-24894

The role of atmospheric heat transport in the seasonal carbon dioxide cycle p 2621 N94-24896

Vertical transport of water in the Martian boundary layer p 2622 N94-24902

The Mars Aerial Platform (MAP) mission p 2622 N94-24903

Effect of an extendable slat on the stall behavior of a VR-12 airfoil [NASA-TP-3407] p 2171 N94-25187

Conflict-free trajectory planning for air traffic control automation [NASA-TM-108790] p 2174 N94-25272

Proceedings of the Workshop on Augmented Visual Display (AVID) Research [NASA-CP-10128] p 2439 N94-25490

Application of aircraft navigation sensors to enhanced vision systems p 2176 N94-25495

Engineering workstation: Sensor modeling p 2441 N94-25500

Image fusion p 2441 N94-25501

Expansion-based passive ranging p 2176 N94-25504

Multiple-camera/motion stereoscopy for range estimation in helicopter flight p 2441 N94-25505

Validation of vision-based range estimation algorithms using helicopter flight data p 2442 N94-25506

DCT quantization matrices visually optimized for individual images p 2442 N94-25509

Extracting heading and temporal range from optic flow: Human performance issues p 2442 N94-25510

Optical information in landing scenes p 2442 N94-25511

Sensor fusion display evaluation using information integration models in enhanced/synthetic vision applications p 2443 N94-25512

Quality metrics for sensor images p 2443 N94-25513

Evaluation of image quality p 2443 N94-25514

NATIONAL AERONAUTICS AND SPACE ADMINISTRATION. GODDARD INST. FOR SPACE STUDIES, NEW YORK, NY.

Rice cultivation and methane emission: Documentation of distributed geographic data sets [NASA-TM-104595] p 2381 N94-24800

The NASA/GISS Mars general circulation model: Preliminary experiments p 2616 N94-24872

NATIONAL AERONAUTICS AND SPACE ADMINISTRATION. GODDARD SPACE FLIGHT CENTER, GREENBELT, MD.

Spline screw multiple rotations mechanism [NASA-CASE-GSC-13452-1] p 2352 N94-23078

Split spline screw [NASA-CASE-GSC-13434-1] p 2352 N94-23082

Estimates of monthly mean soil moisture for 1979-1989 [NASA-TM-104571] p 2407 N94-23132

CRRES microelectronics package flight data analysis [NASA-TP-3423] p 2540 N94-23273

Modulation characteristics of a high-power semiconductor Master Oscillator Power Amplifier (MOPA) [NASA-TM-104577] p 2308 N94-23281

An improved gravity model for Mars: Goddard Mars Model-1 (GMM-1) [NASA-TM-104584] p 2401 N94-23282

SeaWiFS technical report series. Volume 9: The simulated SeaWiFS data set, version 1 [NASA-TM-104566-VOL-9] p 2417 N94-23291

SeaWiFS technical report series. Volume 11: Analysis of selected orbit propagation models for the SeaWiFS mission [NASA-TM-104566-VOL-11] p 2417 N94-23338

Contamination control and plume assessment of low-energy thrusters [NASA-TM-104585] p 2218 N94-23343

Instrument interface description for NOAA 2000 instruments with European morning spacecraft and/or NOAA-OPQ spacecraft [NASA-TM-109406] p 2208 N94-23478

Command/telemetry bus general specification for the NOAA-OPQ polar orbiting environmental satellites and EUMETSAT polar satellite systems [NASA-TM-109407] p 2208 N94-23479

Low rate data bus general specification for the NOAA-OPQ polar orbiting environmental satellites and EUMETSAT polar satellite systems [NASA-TM-109408] p 2208 N94-23480

High-rate data link general specification for the NOAA-OPQ polar orbiting environmental satellites and EUMETSAT satellite systems
[NASA-TM-109384] p 2208 N94-23481

The Fifth Calibration/Data Product Validation Panel Meeting
[NASA-TM-108270] p 2383 N94-23595

SPDB (science processing database): Quick reference guide p 2383 N94-23597

MODIS calibration p 2383 N94-23600

Experience of the JPL Exploratory Data Analysis Team at validating HIRS2/MSU cloud parameters
p 2385 N94-23616

An overview of the UARS data validation effort
p 2386 N94-23617

Micro pulse laser radar
[NASA-CASE-GSC-13493-1] p 2294 N94-23827

Magnetic power piston fluid compressor
[NASA-CASE-GSC-13565-1] p 2354 N94-23831

Mission operations update for the restructured Earth Observing System (EOS) mission p 2499 N94-23839

SAMPEX payload operation control center implementation p 2197 N94-23843

NASA/Goddard Space Flight Center's testbed for CCSDS compatible systems p 2197 N94-23855

A quick uplink, expandable executable for the NSSC-1 of the Hubble Space Telescope p 2305 N94-23859

Mission engineering p 2505 N94-23881

GSMS and space views: Advanced spacecraft monitoring tools p 2507 N94-23890

The mission events graphic generator software: A small tool with big results p 2464 N94-23893

Customizing graphical user interface technology for spacecraft control centers p 2510 N94-23905

A method for interference mitigation in space communications scheduling p 2305 N94-23918

TOPEX/Poseidon precision orbit determination production and expert system p 2196 N94-23920

Automating a human factors evaluation of graphical user interfaces for NASA applications: An update on CHIMES
p 2443 N94-23936

Mission and science activity scheduling language
p 2515 N94-23938

High performance, low cost, self-contained, multipurpose PC based ground systems
p 2516 N94-23943

GenSAA: A tool for advancing satellite monitoring with graphical expert systems p 2516 N94-23945

Orbital Signature Analyzer (OSA): A spacecraft health/safety monitoring and analysis tool
p 2203 N94-23947

EOS ground data systems: A description and interface overview p 2517 N94-23948

Telemetry ground system development via the component approach p 2203 N94-23949

New mission requirements methodologies for services provided by the Office of Space Communications
p 2519 N94-23961

An intelligent planning and scheduling system for the HST servicing missions p 2520 N94-23964

Scheduling the future NASA Space Network: Experiences with a flexible scheduling prototype
p 2520 N94-23965

Software reuse in spacecraft planning and scheduling systems p 2520 N94-23966

Electromagnetic brake/clutch device
[NASA-CASE-GSC-13502-1] p 2354 N94-23969

The Submillimeter Wave Astronomy Satellite (SWAS) solar array system p 2361 N94-24029

Participation in TOMS missions
[NASA-CR-195110] p 2398 N94-24078

The atmospheric effects of stratospheric aircraft: A third program report
[NASA-RP-1313] p 2398 N94-24104

Nimbus-7 Total Ozone Mapping Spectrometer (TOMS) data products user's guide
[NASA-RP-1323] p 2410 N94-24355

Report of the proceedings of the Colloquium and Workshop on Multiscale Coupled Modeling
[NASA-CP-3217] p 2410 N94-24374

GEWEX Water Vapor Project (GVaP)
p 2411 N94-24378

Grand challenge scientific questions in coupled modeling p 2412 N94-24382

Next generation initiation techniques
p 2412 N94-24383

Measurement and modeling of moist processes
p 2413 N94-24385

Parameterization of sub-grid scale convection
p 2413 N94-24386

Coupled land surface/hydrologic/atmospheric models
p 2413 N94-24387

Chemistry on the mesoscale: Modeling and measurement issues p 2413 N94-24390

Validation of mesoscale models p 2413 N94-24391

Session on coupled atmospheric/chemistry coupled models p 2414 N94-24398

Steady induction effects in geomagnetism. Part 1C: Geomagnetic estimation of steady surficial core motions: Application to the definitive geomagnetic reference field models
[NASA-TP-3272-PT-1C] p 2403 N94-24465

An Earth albedo model: A mathematical model for the radiant energy input to an orbiting spacecraft due to the diffuse reflectance of solar radiation from the Earth below
[NASA-TM-104596] p 2195 N94-24497

Intelligent systems and advanced user interfaces for design, operation, and maintenance of command management systems
[NASA-CR-195172] p 2459 N94-24797

Satellite situation report, volume 33, number 4
[NASA-TM-109677] p 2205 N94-24824

Retrieval of temperature profiles from Martian infrared spectra p 2620 N94-24893

An active antenna for ELF magnetic fields
p 2303 N94-25192

Catalog of infrared observations, third edition
[NASA-RP-1294] p 2600 N94-25387

NATIONAL AERONAUTICS AND SPACE ADMINISTRATION. HUGH L. DRYDEN FLIGHT RESEARCH CENTER, EDWARDS, CA.

Strain gage measurement errors in the transient heating of structural components
[NASA-TM-104274] p 2376 N94-23487

Mechanical and thermal buckling analysis of sandwich panels under different edge conditions
[NASA-TM-4535] p 2228 N94-23514

Reduction of structural loads using maneuver load control on the Advanced Fighter Technology Integration (AFTI)/F-111 mission adaptive wing
[NASA-TM-4526] p 2168 N94-24295

NATIONAL AERONAUTICS AND SPACE ADMINISTRATION. HUGH L. DRYDEN FLIGHT RESEARCH FACILITY, EDWARDS, CA.

A photogrammetric solution to a particular problem
[NASA-TP-3415] p 2381 N94-22961

Identification of integrated airframe: Propulsion effects on an F-15 aircraft for application to drag minimization
[NASA-TM-4532] p 2188 N94-24106

Thermal-fluid analysis of the fill and drain operations of a cryrogenic fuel tank
[NASA-TM-104273] p 2334 N94-24495

NATIONAL AERONAUTICS AND SPACE ADMINISTRATION. JOHN F. KENNEDY SPACE CENTER, COCOA BEACH, FL.

NASA/ASEE Summer Faculty Fellowship Program
[NASA-CR-194678] p 2571 N94-23230

Responses to LBNP in men with varying profiles of strength and aerobic capacity: Implications for flight crews
[NASA-TP-3346] p 2426 N94-23530

Debris/Ice/TPS assessment and integrated photographic analysis for Shuttle Mission STS-61
[NASA-TM-109195] p 2199 N94-24059

Debris/ice/TPS assessment and integrated photographic analysis for Shuttle mission STS-58
[NASA-TM-109194] p 2200 N94-24577

NATIONAL AERONAUTICS AND SPACE ADMINISTRATION. LYNDON B. JOHNSON SPACE CENTER, HOUSTON, TX.

Proof test of the computer program BUCKY for plasticity problems
[NASA-TP-3444] p 2374 N94-22960

Catalog of Apollo experiment operations
[NASA-RP-1317] p 2194 N94-23292

Lunar science strategy: Exploring the Moon with humans and machines p 2605 N94-23376

Rover requirements for the planet surface segment of the space exploration initiative p 2369 N94-23377

Fluid-loading solutions and plasma volume: Astro-ade and salt tablets with water
[NASA-TP-3456] p 2426 N94-23544

Fingered bola body, bola with same, and methods of use
[NASA-CASE-MSC-21967-1] p 2354 N94-23822

Common front end systems for Space Shuttle and Space Station control centers at Johnson Space Center
p 2305 N94-23838

Real-time automated failure identification in the Control Center Complex (CCC) p 2272 N94-23892

A real-time navigation monitoring expert system for the Space Shuttle Mission Control Center
p 2202 N94-23921

Making intelligent systems team players: Additional case studies
[NASA-TM-104786] p 2473 N94-24068

Analysis of impactor residues in tray clamps from the Long Duration Exposure Facility. Part 2: Clamps from Bay B of the satellite
[NASA-TM-104784] p 2386 N94-24095

Crew interface analysis: Selected articles on space human factors research, 1987 - 1991
[NASA-TM-104756] p 2433 N94-24185

Process and representation in graphical displays
p 2433 N94-24187

Using computer graphics to design Space Station Freedom viewing p 2434 N94-24191

A simulation system for Space Station extravehicular activity p 2434 N94-24192

Illumination requirements for operating a space remote manipulator p 2435 N94-24195

Previous experience in manned space flight: A survey of human factors lessons learned p 2435 N94-24196

Hand controller commonality evaluation process
p 2435 N94-24197

Reach performance while wearing the Space Shuttle launch and entry suit during exposure to launch accelerations p 2436 N94-24204

Development of biomechanical models for human factors evaluations p 2437 N94-24205

Establishing a relationship between maximum torque production of isolated joints to simulate EVA ratchet push-pull maneuver: A case study p 2437 N94-24206

Heterogeneity in small aliquots of Apolllo 15 olivine-normative basalt: Implications for breccia clast studies p 2616 N94-24373

Suddenly, tomorrow came... A history of the Johnson Space Center
[NASA-SP-4307] p 2631 N94-24584

Orbital docking system centerline color television camera system test
[NASA-TM-104783] p 2205 N94-24625

Orbital debris and near-Earth environmental management: A chronology
[NASA-RP-1320] p 2598 N94-24644

The future of manned spaceflight
p 2195 N94-25067

National Aeronautics and Space Administration (NASA)/American Society for Engineering Education (ASEE) Summer Faculty Fellowship Program, 1993, volume 1
[NASA-CR-188271-VOL-1] p 2632 N94-25348

National Aeronautics and Space Administration (NASA)/American Society for Engineering Education (ASEE) Summer Faculty Fellowship Program, 1993, volume 2
[NASA-CR-188271-VOL-2] p 2636 N94-25367

NATIONAL AERONAUTICS AND SPACE ADMINISTRATION. LANGLEY RESEARCH CENTER, HAMPTON, VA.

Di(hydroxyphenyl)- 1,2,4-triazole monomers
[NASA-CASE-LAR-14440-2] p 2252 N94-23075

Preparing polymeric matrix composites using an aqueous slurry technique
[NASA-CASE-LAR-14771-1] p 2252 N94-23076

Polyimide processing additives
[NASA-CASE-LAR-13669-2] p 2252 N94-23079

A dataflow analysis tool for parallel processing of algorithms
[NASA-TM-109054] p 2448 N94-23086

Determination of fiber-matrix interface failure parameters from off-axis tests
[NASA-TM-109043] p 2241 N94-23274

Fatigue life and crack growth prediction methodology
[NASA-TM-109044] p 2228 N94-23279

Time dependent behavior of a graphite/thermoplastic composite and the effects of stress and physical aging
[NASA-TM-109047] p 2228 N94-23280

Di(hydroxyphenyl)- benzimidazole monomers
[NASA-CASE-LAR-14643-2] p 2253 N94-23305

Phenylethynl-terminated poly(arylene ethers)
[NASA-CASE-LAR-14797-1] p 2253 N94-23307

Method of determining shear stress employing a monomer-polymer laminate structure
[NASA-CASE-LAR-14654-2] p 2375 N94-23308

Experimental investigation of generic three-dimensional sidewall-compression scramjet inlets at Mach 6 in tetrafluoromethane
[NASA-TM-4497] p 2319 N94-23339

A structural design decomposition method utilizing substructuring
[NASA-TM-107750] p 2376 N94-23368

Early lunar rover mission studies
p 2607 N94-23388

Composite material impregnation unit
[NASA-TM-107751] p 2254 N94-23486

Optical model analyses of galactic cosmic ray fragmentation in hydrogen targets
[NASA-TP-3404] p 2540 N94-23509

Leading-edge votex-system details obtained on F-106B aircraft using a rotating vapor screen and surface techniques
[NASA-TP-3374] p 2166 N94-23512

Flight solar calibrations using the Mirror Attenuator Mosaic (MAM): Low scattering mirror
p 2384 N94-23602

Some useful innovations with TRASYS and SINDA-85
p 2322 N94-23647

The Sixth Copper Mountain Conference on Multigrid Methods, part 1
[NASA-CP-3224-PT-1] p 2482 N94-23673

Analysis of local delaminations caused by angle ply matrix cracks
[NASA-TM-109052] p 2228 N94-24083

Joint Acoustic Propagation Experiment (JAPE-91) Workshop
[NASA-CP-3231] p 2526 N94-24207

Studies of Shuttle orbiter arrestment system
[NASA-TP-3370] p 2177 N94-24304

Momentum loss in proton-nucleus and nucleus-nucleus collisions
[NASA-TP-3405] p 2540 N94-24305

An experimental investigation of a Mach 3.0 high-speed civil transport at supersonic speeds
[NASA-TP-3365] p 2169 N94-24311

New computing systems, future computing environment, and their implications on structural analysis and design
p 2177 N94-24314

The radiated noise from isotropic turbulence revisited
[NASA-CR-191547] p 2333 N94-24356

Experimental cavity pressure measurements at subsonic and transonic speeds. Static-pressure results
[NASA-TP-3358] p 2169 N94-24464

Active control of buildings during earthquakes
[NASA-TM-109033] p 2271 N94-24473

Progress toward ultra-stable lasers for use in space
[NASA-TM-109678] p 2349 N94-24488

Structural dynamics division research and technology accomplishments for FY 1993 and plans for FY 1994
[NASA-TM-109036] p 2169 N94-24576

Aerodynamic characteristics and pressure distributions for an executive-jet baseline airfoil section
[NASA-TM-4529] p 2169 N94-24586

A programming environment for distributed complex computing. An overview of the Framework for Interdisciplinary Design Optimization (FIDO) project. NASA Langley TOPS exhibit H120b
[NASA-TM-109058] p 2457 N94-24603

Admittance model for the shuttle remote manipulator system in four configurations
[NASA-CR-4555] p 2474 N94-24635

NASA/DOD Aerospace Knowledge Diffusion Research Project. Report number 20: The use of selected information products and services by US aerospace engineers and scientists: Results of two surveys
[NASA-TM-109022] p 2592 N94-24649

NADA/DOD Aerospace Knowledge Diffusion Research Project. Report number 19: The US government technical report and the transfer of federally funded aerospace R/D: An analysis of five studies
[NASA-TM-109061] p 2592 N94-24660

NASA/DOD Aerospace Knowledge Diffusion Research Project. Report number 21: US aerospace industry librarians and technical information specialists as information intermediaries: Results of the phase 2 survey
[NASA-TM-109064] p 2593 N94-24709

Supersonic aerodynamic characteristics of a circular body Earth-to-Orbit vehicle
[NASA-TM-4533] p 2170 N94-24716

Dynamic analysis of pretwisted elastically-coupled rotor blades
[NASA-TM-109070] p 2378 N94-24839

Temporal model of an optically pumped co-doped solid state laser
[NASA-TM-109680] p 2350 N94-24851

NASA LaRC Workshop on Guidance, Navigation, Controls, and Dynamics for Atmospheric Flight, 1993
[NASA-CP-10127] p 2162 N94-25096

US general aviation: The ingredients for a renaissance. A vision and technology strategy for US industry, NASA, FAA, universities p 2162 N94-25097

Future space transportation system architecture avionics requirements p 2162 N94-25098

Highly-reliable fly-by-light/power-by-wire technology
p 2162 N94-25099

Differential GPS for air transport: Status
p 2162 N94-25100

Future directions in flight simulation: A user perspective p 2162 N94-25101

A simulation study of control and display requirements for zero-experience general aviation pilots
p 2163 N94-25102

Parametric uncertainty modeling for application to robust control p 2163 N94-25103

Hypersonic vehicle control law development using H(infinity) and micron-synthesis p 2163 N94-25104

On-line evaluation of multiloop digital controller performance p 2163 N94-25105

Development of high-angle-of-attack nose-down pitch control margin design guidelines for combat aircraft
p 2164 N94-25107

Modeling transonic aerodynamic response using nonlinear systems theory for use with modern control theory p 2164 N94-25112

Effect of aeroelastic-propulsive interactions on flight dynamics of a hypersonic vehicle p 2164 N94-25113

Optimal RTLS abort trajectories for an HL-20 personnel launch vehicle p 2165 N94-25114

Advanced Information Processing System (AIPS)
p 2165 N94-25115

Surface compositional variations of Mo-47Re alloy as a function of temperature
[NASA-TP-3402] p 2245 N94-25117

A model-based approach for detection of objects in low resolution passive-millimeter wave images
p 2442 N94-25507

NATIONAL AERONAUTICS AND SPACE ADMINISTRATION. LEWIS RESEARCH CENTER, CLEVELAND, OH.

Utilizing a TDRS satellite for direct broadcast satellite-radio propagation experiments and demonstrations p 2274 N94-22740

Small rocket flowfield diagnostic chambers
p 2210 N94-23030

Laser diagnostics for small rockets
p 2210 N94-23032

Small rocket research and technology
p 2211 N94-23038

Axisymmetric single shear element combustion instability experiment p 2213 N94-23044

Flow visualization study in high aspect ratio cooling channels for rocket engines p 2213 N94-23049

Advanced materials for radiation-cooled rockets
p 2214 N94-23052

Molecular gas dynamics applied to low-thrust propulsion p 2214 N94-23053

Two stage turbine for rockets p 2215 N94-23059

A technique to measure rotordynamic coefficients in hydrostatic bearings p 2215 N94-23061

Brush seals for cryogenic applications
p 2216 N94-23063

Flow quality studies of the NASA Lewis Research Center Icing Research Tunnel diffuser
[NASA-TM-106311] p 2192 N94-23091

Lewis Research Center R and D Facilities
[NASA-TM-109400] p 2630 N94-23135

An overview of a model rotor icing test in the NASA Lewis Icing Research Tunnel
[NASA-TM-106471] p 2166 N94-23299

Space Electrochemical Research and Technology
[NASA-CP-3228] p 2390 N94-23345

Impedance measurements on a spiral-wound nickel/metal hydride cell cycled in a simulated Leo orbit
p 2392 N94-23355

NASA Lewis advanced IPV nickel-hydrogen technology p 2392 N94-23356

Transparent conducting thin films for spacecraft applications
[NASA-TM-106466] p 2218 N94-23370

Infrared analysis of vapor phase deposited tricresylphosphate (TCP)
[NASA-TM-106423] p 2253 N94-23371

Power console development for NASA's electric propulsion outreach program
[NASA-TM-106428] p 2218 N94-23372

Electrical power technology for robotic planetary rovers p 2314 N94-23401

Refraction of high frequency noise in an arbitrary jet flow
[NASA-TM-106465] p 2525 N94-23464

Measurements and modeling of flow structure in the wake of a low profile wishbone vortex generator
[NASA-TM-106468] p 2166 N94-23465

Transient Ejector Analysis (TEA) code user's guide
[NASA-TM-106310] p 2186 N94-23466

Characterization and durability testing of plasma-sprayed zirconia-yttria and hafnia-yttria thermal barrier coatings. Part 2: Effect of spray parameters on the performance of several hafnia-yttria and zirconia-yttria coatings
[NASA-TP-3296] p 2242 N94-23467

Theoretical considerations for Reaction-Formed Silicon Carbide (RFSC) formation by molten silicon infiltration into slurry-derived preforms
[NASA-TM-106414] p 2222 N94-23500

Characteristics of surface roughness associated with leading edge ice accretion
[NASA-TM-106459] p 2166 N94-23522

Close-up analysis of inflight ice accretion
[NASA-TM-106457] p 2172 N94-23523

The use of transition region characteristics to improve the numerical simulation of heat transfer in bypass transitional flows
[NASA-TM-106445] p 2320 N94-23525

Investigation of a subsonic-arc-attachment thruster using segmented anodes
[NASA-TM-106419] p 2219 N94-23531

Holographic testing of composite propfans for a cruise missile wind tunnel model
[NASA-TM-105271] p 2187 N94-23545

Characterization of the microstructure of Nb-1wt.%Zr-0.1wt.%C tubes as affected by thermomechanical processing
[NASA-TM-106381] p 2242 N94-23550

Material data representation of hysteresis loops for Hastelloy X using artificial neural networks
[NASA-TM-105990] p 2376 N94-23551

An implicit numerical scheme for the simulation of internal viscous flows on unstructured grids
[NASA-TM-106437] p 2481 N94-23554

Effect of hydrogen exposure on a Cu-8 Cr-4 Nb alloy
[NASA-TM-106429] p 2243 N94-23556

Bibliography of Lewis Research Center technical publications announced in 1992
[NASA-TM-106035] p 2590 N94-23562

Fault tolerant onboard packet switch architecture for communication satellites: Shared memory per beam approach
[NASA-TM-106397] p 2201 N94-23567

Multilayer relaxation and surface structure of ordered alloys
[NASA-TM-106433] p 2243 N94-23578

A method to remove intercalates from bromine and iodine intercalated carbon fibers
[NASA-TM-106443] p 2222 N94-23591

Effect of delta tabs on mixing and axis switching in jets from asymmetric nozzles
[NASA-TM-106450] p 2167 N94-23592

Optimization of orifice geometry for cross-flow mixing in a cylindrical duct
[NASA-TM-106436] p 2481 N94-23593

Performance evaluation of the Russian SPT-100 thruster at NASA LeRC
[NASA-TM-106401] p 2219 N94-23630

The Fifth Annual Thermal and Fluids Analysis Workshop
[NASA-CP-10122] p 2320 N94-23634

A comparison of TSS and TRASYS in form factor calculation p 2321 N94-23638

Utilization of recently developed codes for high power Brayton and Rankine cycle power systems
p 2222 N94-23641

A comparative study of computational solutions to flow over a backward-facing step p 2326 N94-23670

Method and apparatus for producing a thermal atomic oxygen beam
[NASA-CASE-LEW-15614-1] p 2534 N94-23825

High temperature, oxidation resistant noble metal-Al alloy thermocouple
[NASA-CASE-LEW-15515-1] p 2343 N94-23826

Rime-, mixed- and glaze-ice evaluations of three scaling laws
[NASA-TM-106461] p 2173 N94-24047

Generalized three-dimensional simulation of ferruled coupled-cavity traveling-wave-tube dispersion and impedance characteristics
[NASA-TP-3389] p 2310 N94-24056

Reliability in second moment turbulence closures revisited
[NASA-TM-106469] p 2326 N94-24063

Miniature convection cooled plug-type heat flux gauges
[NASA-TM-106483] p 2344 N94-24069

A solar photovoltaic power system for use in Antarctica
[NASA-TM-106417] p 2395 N94-24071

Engine materials characterization and damage monitoring by using x ray technologies
[NASA-TP-3328] p 2372 N94-24074

CFD assessment of orifice aspect ratio and mass flow ratio on jet mixing in rectangular ducts
[NASA-TM-106434] p 2187 N94-24082

Evaluation of turbulence models in the PARC code for transonic diffuser flows
[NASA-TM-106391] p 2168 N94-24084

Roles, uses, and benefits of general aviation aircraft in aerospace engineering education
[NASA-TM-106463] p 2153 N94-24100

Integration and test of high-speed transmitter electronics for free-space laser communications
[NASA-TM-106295] p 2295 N94-24101

Discrete sensitivity derivatives of the Navier-Stokes equations with a parallel Krylov solver
[NASA-TM-106481] p 2265 N94-24301

Controllability of free-piston Stirling engine/linear alternator driving a dynamic load
[NASA-TM-106497] p 2521 N94-24302

Spatial frequency multiplier with active linearly tapered slot antenna array
[NASA-TM-106494] p 2310 N94-24308

Probabilistic simulation of concurrent engineering of propulsion systems p 2177 N94-24317

Multi-disciplinary coupling for integrated design of propulsion systems p 2179 N94-24326

Ethylene trace-gas techniques for high-speed flows
[NASA-TM-106491] p 2169 N94-24335

Center for modeling of turbulence and transition: Research briefs, 1993
[NASA-TM-106383] p 2333 N94-24336

Improved pressure measurement system for calibration of the NASA LeRC 10x10 supersonic wind tunnel
[NASA-TM-106470] p 2344 N94-24362

Workshop on Computational Turbulence Modeling
[NASA-CP-10130] p 2333 N94-24460

Stagnation region heat transfer: The influence of turbulence parameters, Reynolds number and body shape
[NASA-TM-106504] p 2334 N94-24481

Optimal Space Station solar array gimbal angle determination via radial basis function neural networks
[NASA-TM-106482] p 2195 N94-24482

Application of fault detection techniques to spiral bevel gear fatigue data
[NASA-TM-106467] p 2364 N94-24483

Mixing characteristics of directly opposed rows of jets injected normal to a crossflow in a rectangular duct
[NASA-TM-106477] p 2188 N94-24594

Power generation technology options for a Mars mission
[NASA-TM-106451] p 2220 N94-24681

Durability evaluation of ceramic components using CARES/LIFE
[NASA-TM-106475] p 2258 N94-24682

A vorticity dynamics based model for the turbulent dissipation: Model development and validation
[NASA-TM-106177] p 2336 N94-24713

Elevated temperature crack propagation
[NASA-TM-106490] p 2377 N94-24715

Preliminary far-field plume sputtering characterization of the Stationary Plasma Thruster (SPT-100)
[NASA-TM-106464] p 2221 N94-24766

Performance of the NASA cm ion thruster
[NASA-TM-106426] p 2221 N94-24770

Thermal control system for Space Station Freedom photovoltaic power module
[NASA-TM-105650] p 2205 N94-24825

Merits and limitations of optimality criteria method for structural optimization
[NASA-TP-3373] p 2378 N94-24845

Bounds and simulation results of 32-ary and 64-ary quadrature amplitude modulation for broadband-ISDN via satellite
[NASA-TM-106484] p 2202 N94-25095

VLSI-based video event triggering for image data compression
[NASA-TM-106500] p 2345 N94-25116

Turbulence models and Reynolds analogy for two-dimensional supersonic compression ramp flow
[NASA-TM-106474] p 2337 N94-25119

Workshop on the Thermophysical Properties of Molten Materials
[NASA-CP-10121] p 2246 N94-25120

Temperature dependent performance of Coplanar Waveguide (CPW) on substrates of various materials
[NASA-TM-106505] p 2313 N94-25170

Structure and energetics of high index Fe, Al, Cu and Ni surfaces using equivalent crystal theory
[NASA-TM-106408] p 2249 N94-25171

Fan noise research at NASA
[NASA-TM-106512] p 2530 N94-25172

A continuing search for a near-perfect numerical flux scheme. Part 1: AUSM+
[NASA-TM-106524] p 2338 N94-25180

NASA/Army rotorcraft transmission research, a review of recent significant accomplishments
[NASA-TM-106508] p 2367 N94-25181

Improving diffusing S-duct performance by secondary flow control
[NASA-TM-106492] p 2170 N94-25182

Measurements of the influence of integral length scale on stagnation region heat transfer
[NASA-TM-106503] p 2338 N94-25183

Temperature measurement using infrared imaging systems during turbine engine altitude testing
[NASA-TM-105871] p 2193 N94-25184

Two-dimensional CFD modeling of wave rotor flow dynamics
[NASA-TM-106261] p 2189 N94-25185

Matrix fatigue cracking mechanisms of alpha(2) TMC for hypersonic applications
[NASA-TM-106506] p 2230 N94-25186

Probabilistic assessment of smart composite structures
[NASA-TM-106358] p 2378 N94-25188

Power electronics development for the SPT-100 thruster
[NASA-TM-106488] p 2221 N94-25189

Development of a power electronics unit for the Space Station plasma contactor
[NASA-TM-106486] p 2222 N94-25201

Thermodynamic models for bounding pressurant mass requirements of cryogenic tanks
[NASA-TM-106476] p 2346 N94-25202

NATIONAL AERONAUTICS AND SPACE ADMINISTRATION. MARSHALL SPACE FLIGHT CENTER, HUNTSVILLE, AL.

SSME fuel preburner injector characterization
p 2211 N94-23037

Computational Fluid Dynamics (CFD) applications in rocket propulsion analysis and design
p 2214 N94-23054

Performance assessment of low pressure nuclear thermal propulsion p 2217 N94-23070

Analysis and test of low profile aluminum aerospace tank dome
[NASA-TP-3442] p 2375 N94-23294

Review of the probabilistic failure analysis methodology and other probabilistic approaches for application in aerospace structural design
[NASA-TP-3434] p 2376 N94-23342

Results of a laboratory experiment that tests rotating unbalanced-mass devices for scanning gimbaled payloads and free-flying spacecraft
[NASA-TP-3458] p 2269 N94-23574

Advanced X ray Astrophysics Facility-Imaging (AXAF-I) thermal analyses using Integrated Thermal Analysis System (ITAS) program p 2320 N94-23635

Pressure wall patch
[NASA-CASE-MFS-28724-1] p 2203 N94-23824

Generic mission planning concepts for space astronomy missions p 2505 N94-23878

Development of infrared sensors using energy transfer/energy upconversion processes: Study of laser excited fluorescence in rare Earth ion doped crystals
[NASA-TM-108437] p 2233 N94-24073

Fiscal year 1993 scientific and technical reports, articles, papers, and presentations
[NASA-TM-108423] p 2590 N94-24079

MAMS data for the Convection and Moisture Experiment (CAMEX)
[NASA-TM-108435] p 2409 N94-24080

Microgravity Studies of Organic and Polymeric Materials
[NASA-CP-3250] p 2223 N94-24338

Prediction of nonlinear optical properties of organic materials. General theoretical considerations
p 2224 N94-24343

Modeling of PCG fluid dynamics: Salient results
p 2224 N94-24345

Low-gravity electrodeposition and growth of polymer thin films with large third-order optical nonlinearities by electrochemical processes for devices: Thiophene-based polymers p 2225 N94-24346

Polydiacetylene thin films for nonlinear optical applications p 2225 N94-24347

CORSS: Cylinder Optimization of Rings, Skin, and Stringers
[NASA-TP-3457] p 2490 N94-24727

New Ways Of Doing Business (NWODB) cost quantification analysis
[NASA-CR-195186] p 2586 N94-25197

NATIONAL AERONAUTICS AND SPACE ADMINISTRATION. PASADENA OFFICE, CA.

Dual frequency optical carrier technique for transmission of reference frequencies in dispersive media
[NASA-CASE-NPO-18007-2-CU] p 2543 N94-23270

Non-volatile, solid state bistable electrical switch
[NASA-CASE-NPO-17621-1-CU] p 2309 N94-23820

Planar varactor frequency multiplier devices with blocking barrier
[NASA-CASE-NPO-18428-1-CU] p 2310 N94-23821

Overcharge and overdischarge protection of ambient temperature secondary lithium cells
[NASA-CASE-NPO-18343-1-CU] p 2310 N94-23823

Method of forming silicon structures with selectable optical characteristics
[NASA-CASE-NPO-18625-1-CU] p 2563 N94-23972

NATIONAL AERONAUTICS AND SPACE ADMINISTRATION. WALLOPS FLIGHT FACILITY, WALLOPS ISLAND, VA.

Development and application of an empirical probability distribution for the prediction error of re-entry body maximum dynamic pressure p 2207 N94-23653

NATIONAL AEROSPACE LAB., AMSTERDAM (NETHERLANDS).

Glossary knowledge engineering
[NLR-TP-91435-U] p 2471 N94-23137

NATIONAL AEROSPACE LAB., TOKYO (JAPAN).

Tribological characteristics of ball bearings lubricated with a sputtered molybdenum disulphide film in a vacuum under a high thrust load p 2355 N94-23992

NATIONAL ASSOCIATION OF CORROSION ENGINEERS, HOUSTON, TX.

Proceedings of the 12th International Congress: Corrosion Control for Low-Cost Reliability. Volume 4: Oil/Gas Pipeline
[AD-A273665] p 2250 N94-25405

Proceedings of the 12th International Congress: Corrosion Control for Low-Cost Reliability. Volume 5A: Corrosion: General issues
[AD-A273666] p 2250 N94-25406

Proceedings of the 12th International Congress: Corrosion Control for Low-Cost Reliability. Volume 5B: Corrosion: General issues
[AD-A273667] p 2250 N94-25407

Proceedings of the 12th International Congress: Corrosion Control for Low-Cost Reliability. Volume 6: Electric Power Industry
[AD-A273668] p 2250 N94-25408

Proceedings of the 12th International Congress: Corrosion Control for Low-Cost Reliability. Volume 1: Coatings
[AD-A273661] p 2251 N94-25448

Preceedings of the 12th International Congress: Corrosion Control for Low-Cost Reliability. Volume 2: Process Industries Plant Operations
[AD-A273662] p 2251 N94-25449

Preceedings of the 12th International Congress: Corrosion Control for Low-Cost Reliability. Volume 3A: Corrosion: Specific issues
[AD-A273663] p 2251 N94-25450

Proceedings of the 12th International Congress: Corrosion Control for Low-Cost Reliability. Volume 3B: Corrosion: Specific issues
[AD-A273664] p 2251 N94-25451

NATIONAL CENTER FOR ATMOSPHERIC RESEARCH, BOULDER, CO.

Some challenging problems of the structured and dynamical solar atmosphere p 2624 N94-22838

GEWEX Cloud Systems Study (GCSS)
p 2411 N94-24377

Aviation Weather Program (AWP)
p 2411 N94-24380

Incorporation of the planetary boundary layer in atmospheric models p 2413 N94-24388

Joint sessions on modeling of boundary layer and radiative transfer processes p 2414 N94-24396

Session on validation of coupled models
p 2414 N94-24399

The solar spectral irradiances from x ray to radio wavelengths
[NASA-CR-195203] p 2629 N94-25260

NATIONAL CENTRAL UNIV., CHUNG-LI (TAIWAN).

ROCSAT-1 telecommunication experiments
p 2279 N94-22770

NATIONAL DEFENCE HEADQUARTERS, OTTAWA (ONTARIO).

An overview of a generic multi-sensor integrated navigation system design
[CTN-94-60916] p 2174 N94-24120

NATIONAL DEFENCE RESEARCH ESTABLISHMENT, LINKOEPING (SWEDEN).

Intelligent Material Systems and Structures (IMSS). Part 5: Fiber optic registration of deformation in carbon laminates 91/92
[PB93-204600] p 2544 N94-23723

Study of methods and structures for handling of digitized maps for geographical information systems
[PB93-204402] p 2590 N94-23741

Radar signature related radome techniques for flush-mounted HF-, VHF- and, UHF communication antennas
[PB93-204618] p 2294 N94-23742

Survival suit for submarine personnel: Summary of evaluation studies
[PB93-204634] p 2430 N94-23743

Calibration block for digital beam forming antenna
[PB93-204550] p 2294 N94-23773

Fiber optical angular sensor: Literature study and experimental results
[PB93-204345] p 2545 N94-24529

Calibration network intended for phase-array antennas at 3 GHz
[PB93-204352] p 2297 N94-24530

Radio communication and wave propagation. A visit to the Netherlands in December 1992
[PB93-204360] p 2297 N94-24531

NATIONAL DEFENCE RESEARCH ESTABLISHMENT, UMEA (SWEDEN).

Microinjection of the Yersinia YopE cytotoxin in mammalian cells induces actin microfilament disruption
[FOA-B-40418-4.4] p 2421 N94-24290

Towards a new radiation protection organization
[FOA-C-40304-4.3] p 2437 N94-24292

NATIONAL GEOPHYSICAL DATA CENTER, BOULDER, CO.

Solar-geophysical data number 584, April 1993. Part 1: (Prompt reports). Data for February, March, 1993, and late data
[PB93-198323] p 2626 N94-23738

Solar-geophysical data number 584, April 1993. Part 2: (Comprehensive reports). Data for October 1992, and miscellaneous
[PB93-198331] p 2627 N94-23739

Solar-geophysical data number 587, July 1993. Part 1: (Prompt reports). Data for June, May 1993, and late data
[PB93-232874] p 2628 N94-24989

Solar-geophysical data number 587, July 1993. Part 2: (Comprehensive reports). Data for January 1993, and miscellaneous
[PB93-232882] p 2628 N94-24990

Solar-geophysical data number 588, August 1993. Part 1: (Prompt reports). Data for July, June 1993, and late data
[PB94-109089] p 2628 N94-24991

Solar-geophysical data number 588, August 1993. Part 2: (Comprehensive reports). Data for February 1993, and miscellaneous
[PB94-109105] p 2628 N94-24992

Solar-geophysical data number 589, September 1993. Part 1: (Prompt reports). Data for August, July 1993, and late data
[PB94-117082] p 2628 N94-24993

Solar-geophysical data number 589, September 1993. Part 2: (Comprehensive reports). Data for March 1993, and miscellaneous
[PB94-117405] p 2628 N94-24994

NATIONAL INST. FOR FUSION SCIENCE, NAGOYA (JAPAN).

Chaotic phenomena in plasma, 2
[DE93-508286] p 2549 N94-22964

Tracking sharp interface of two fluids by the CIP (Cubic-Interpolated Propagation) scheme
[DE93-508322] p 2319 N94-23460

Some theoretical problems of magnetic diagnostics in tokamaks and stellarators
[NIFS-262] p 2551 N94-24306

Pellet ablation in the large helical device
[NIFS-260] p 2551 N94-24358

Temporal behavior of the electron density profile during limiter biasing in the HYBTOK-2 tokamak
[NIFS-257] p 2552 N94-24456

A study of non-ideal focus properties of 30 deg parallel plate energy analyzers
[NIFS-263] p 2311 N94-24457

Proposal of Modular Heliotron: Advanced modular helical system compatible with closed helical divertor
[NIFS-261] p 2552 N94-24458

Reduction of hydrocarbon impurities in 200 l/h helium liquefier-refrigerator system
[NIFS-259] p 2271 N94-24459

Design of central control system for Large Helical Device (LHD)
[NIFS-258] p 2553 N94-24623

Nonequilibria in thermal emission from supernova remnants
[NIFS-264] p 2602 N94-24866

X ray enhancement of SN 1987A due to interaction with its ring-like nebula
[NIFS-265] p 2602 N94-24867

A research of possibility for negative muon production by a low energy electron beam accompanying ion beam
[NIFS-266] p 2536 N94-24868

NATIONAL INST. OF STANDARDS AND TECHNOLOGY, GAITHERSBURG, MD.

Activities of NIST (National Inst. of Standards and Technology) p 2384 N94-23605

Research for electric energy systems
[DE94-001839] p 2293 N94-23719

Zone fire modeling with natural building flows and a zero order shaft model
[PB94-112166] p 2270 N94-23735

Impacts: NIST Building and Fire Research Laboratory (technical and societal)
[PB94-113420] p 2270 N94-23737

Extinguishment of combustible porous solids by water droplets
[PB93-198893] p 2270 N94-23740

Proceedings of the NIST Conference on Reducing the Cost of Space Infrastructure and Operations: Part 1: Oral presentations and discussion
[PB94-111374] p 2194 N94-23770

Dispersion of fire suppression agents discharged from high pressure vessels: Establishing initial/boundary conditions for the flow outside the vessel
[PB94-103660] p 2172 N94-23810

National Institute of Standards and Technology Conference on Reducing the Cost of Space Infrastructure and Operations. Part 2: Topical papers
[PB94-113487] p 2194 N94-23819

Collaborating with our customers: NIST building and fire research laboratory
[PB94-110194] p 2272 N94-24955

Dynamic measurements of thermophysical properties of metals and alloys at high temperatures by subsecond pulse heating techniques p 2247 N94-25124

NATIONAL OCEANIC AND ATMOSPHERIC ADMINISTRATION, BOULDER, CO.

NOAA Federal/State Cooperative Program in Atmospheric Modification Research. Collected publication titles and abstracts
[PB93-198125] p 2396 N94-22913

A field evaluation of remote sensor measurements of wind, temperature, and moisture for ARM integrated sounding system research
[DE94-000565] p 2381 N94-23001

Evaluating NOAA satellite products for global climate monitoring p 2384 N94-23604

NATIONAL OCEANIC AND ATMOSPHERIC ADMINISTRATION, PRINCETON, NJ.

Three-dimensional numerical simulation of thermal tides in the Martian atmosphere p 2622 N94-24901

NATIONAL OCEANIC AND ATMOSPHERIC ADMINISTRATION, SILVER SPRING, MD.

United States Weather Research Program (USWRP)
p 2411 N94-24375

NATIONAL PHYSICAL LAB., TEDDINGTON (ENGLAND).

Exercise keevil: Noise levels of six military helicopters
[PB93-210722] p 2529 N94-25026

NATIONAL RADIO ASTRONOMY OBSERVATORY, SOCORRO, NM.

100 GHz map of 3C 446
[PB94-104882] p 2599 N94-23705

NATIONAL RESEARCH COUNCIL OF CANADA, OTTAWA (ONTARIO).

Beamforming in an acoustic shadow
p 2528 N94-24219

NATIONAL RESEARCH COUNCIL OF CANADA, VANCOUVER (BRITISH COLUMBIA).

Surface observations of stick-slip oscillations in tightly conformal wheel/rail contacts p 2270 N94-23588

NATIONAL RESEARCH LAB. OF METROLOGY, TOKYO (JAPAN).

Concept of ASTER calibration requirement
p 2384 N94-23609

VNIR and SWIR transfer radiometers developed at NRLM for preflight laboratory cross-calibration
p 2385 N94-23610

NATIONAL SPACE DEVELOPMENT AGENCY, TOKYO (JAPAN).

NASDA's view of ground control in mission operations
p 2305 N94-23835

NASDA knowledge-based network planning system
p 2508 N94-23898

NASDA's Advanced On-Line System (ADOLIS)
p 2509 N94-23903

Applications of CCSDS recommendations to Integrated Ground Data Systems (IGDS) p 2510 N94-23906

Verification of technical elements of the advanced spacecraft based upon the CCSDS recommendation
p 2207 N94-23910

NATIONAL SPACE DEVELOPMENT AGENCY, TSUKUBA (JAPAN).

NASDA satellite mission operation system and operations p 2501 N94-23854

NATIONAL SWEDISH ROAD AND TRAFFIC RESEARCH INST., LINKOEPING.

Estimation of delays and emissions at four-way junctions with different forms of regulation, principally four-way mandatory stop
[PB94-105236] p 2398 N94-23813

NATIONAL TRANSPORTATION SAFETY BOARD, WASHINGTON, DC.

Aircraft accident report: Inadvertent in-flight slat deployment, China Eastern Airlines Flight 583, McDonnell Douglas MD-11, B-2171, 950 nautical miles south of Shemya, Alaska, 6 April 1993
[PB93-910408] p 2172 N94-23579

Aircraft accident report: In-flight engine separation. Japan Airlines, Inc., flight 46E, Boeing 747-121, N473EV, Anchorage, Alaska, 31 March 1993
[PB93-410407] p 2173 N94-24062

Annual review of aircraft accident data. US general aviation calendar year 1990
[PB94-126869] p 2173 N94-24841

Aircraft accident report: In-flight loss of propeller blade and uncontrolled collision with terrain Mitsubishi MU-2B-60, N86SD, Zwingle, Iowa, 19 April 1993
[PB93-910409] p 2174 N94-25175

Aircraft accident/incident summary report: Controlled flight into terrain GP Express Airlines, Inc., N115GP Beechcraft C-99, Shelton, Nebraska, 28 April 1993
[PB94-910401] p 2174 N94-25273

NAVAL AIR SYSTEMS COMMAND, ARLINGTON, VA.

Advanced avionics architecture and technology review. Executive summary and volume 1: Avionics tech nology. Volume 2: Avionics systems engineering
[AD-A273630] p 2186 N94-24733

NAVAL COMMAND, CONTROL AND OCEAN SURVEILLANCE CENTER, SAN DIEGO, CA.

Evolving recurrent perceptrons
[AD-A273241] p 2496 N94-24778

Evolving neural network connectivity
[AD-A273134] p 2490 N94-24921

Determining neural network hidden layer size using evolutionary programming
[AD-A273242] p 2475 N94-25139

Active control of oscillatory lift forces on a circular cylinder
[AD-A273243] p 2338 N94-25140

NAVAL MEDICAL RESEARCH INST., BETHESDA, MD.

A statistical analysis of recent Naval Experimental Diving Unit (NEDU) single-depth human exposures to 100 percent oxygen at pressure
[AD-A273488] p 2427 N94-24950

NAVAL POSTGRADUATE SCHOOL, MONTEREY, CA.

Multigrid methods for a semilinear PDE in the theory of pseudoplastic fluids p 2341 N94-23689

An analysis of traditional operational testing to project how testing will be conducted in the future
[AD-A273189] p 2372 N94-24553

A simulation and evaluation of NATO Standardization Agreement (STANAG) 4214
[AD-A273195] p 2297 N94-24554

An automated tool to facilitate code translation for software fault tree analysis
[AD-A273205] p 2457 N94-24556

Design project: LONGBOW supersonic interceptor
[NASA-CR-195510] p 2180 N94-24581

NPS alternate techsat satellite, design project for AE-4871
[NASA-CR-195512] p 2204 N94-24590

Comparison of HF groundwave propagation models
[AD-A273146] p 2299 N94-24668

Simulation of adjacent channel interference in a UHF satellite system
[AD-A273147] p 2299 N94-24669

Mitigation of EMI/RFI produced by a 1.2 kW uninterruptible power supply
[AD-A273149] p 2299 N94-24670

SEMATECH, a case study: Analysis of a government-industry partnership
[AD-A273166] p 2586 N94-24683

An investigation of requirements traceability to support systems development
[AD-A273167] p 2458 N94-24684

Crosstalk analysis of synchronous and asynchronous optical chip interconnects with direct detection
[AD-A273261] p 2311 N94-24685

Free-surface/vorticity interaction
[AD-A273263] p 2335 N94-24686

A numerical study of airplanes flying in proximity
[AD-A273373] p 2173 N94-24718

Evaluation of the UH-1N instrument panel
[AD-A273145] p 2186 N94-24774

A methodology for software cost estimation using machine learning techniques
[AD-A273158] p 2459 N94-24775

Information systems strategy in air transport
[AD-A273125] p 2173 N94-24781

Conceptual design proposal: HUGO global range/mobility transport aircraft
[NASA-CR-195501] p 2181 N94-24787

Near Earth asteroid rendezvous
[NASA-CR-195518] p 2195 N94-24808

Object recognition through image understanding for an autonomous mobile robot
[AD-A273206] p 2475 N94-24862

Dumbo heavy lifter aircraft
[NASA-CR-195500] p 2182 N94-24915

Parametric uncertainty reduction in robust multivariable control
[AD-A273412] p 2460 N94-24927

Sabot high speed interceptor AE 4273 aircraft design
[NASA-CR-195495] p 2183 N94-24971

Observed and Navy operational global model climatologies of synoptic disturbances over the tropical western Pacific during winter 1991-1992
[AD-A273400] p 2416 N94-25071

An x ray diffraction investigation of alpha-Al2O2 addition to Yttria Stabilized Zirconia (YSZ) thermal barrier coatings subject to destabilizing vanadium pentoxide (V2O5) exposure
[AD-A273403] p 2261 N94-25072

Reengineering real-time software systems
[AD-A273408] p 2461 N94-25074

An implementation of the REpresentation and MAintenance of Process knowledge (REMAP) model in the knowledge-based software assistant concept demonstration system
[AD-A273207] p 2461 N94-25138
An exploratory stochastic model for toxic effects on cells
[AD-A273438] p 2422 N94-25146

NAVAL RESEARCH LAB., WASHINGTON, DC.
Measurements and modeling of multitone, low-frequency acoustic data from the Arraial do Cabo range
[AD-A273406] p 2530 N94-25073
Northern Exposure 1992: An investigation of transauroral HF radio skywave propagation
[AD-A273363] p 2303 N94-25089
An AVHRR cloud classification database typed by experts
[AD-A273560] p 2416 N94-25162

NAVAL SURFACE WARFARE CENTER, DAHLGREN, VA.
State-of-the-art engineering aeroprediction methods with emphasis on new semiempirical techniques for predicting nonlinear aerodynamics on complete missile configurations
[AD-A273680] p 2171 N94-25411

NEBRASKA UNIV., LINCOLN.
A constrained joint source/channel coder design and vector quantization of nonstationary sources
[NASA-CR-195145] p 2301 N94-24707

NEBRASKA UNIV., OMAHA.
Investigation of hand capabilities under a variety of performance conditions and an attempt to explain performance differences p 2444 N94-25354

NEVADA UNIV., RENO.
Second law analysis of a conventional steam power plant p 2322 N94-23646

NEW BRUNSWICK UNIV., FREDERICTON.
An investigation into acceleration determination for airborne gravimetry using the global positioning system
[ISBN-0-315-59470-5] p 2175 N94-24176
A constrained optimization technique for arbitrary antenna arrays and various performance indices
[ISBN-0-315-59455-1] p 2297 N94-24179

NEW ENERGY AND INDUSTRIAL TECHNOLOGY DEVELOPMENT ORGANIZATION, TOKYO (JAPAN).
Feasibility study on a CO2 global recycling system using natural energy
[DE94-714889] p 2397 N94-23026
Preliminary study concerning development of petroleum-substitution energy integration technology
[DE94-714902] p 2264 N94-23027

NEW MEXICO STATE UNIV., LAS CRUCES.
Momentum and coordinate space three-nucleon potentials
[DE93-040868] p 2531 N94-22951
The soft x ray halo of the spiral galaxy NGC4631
[NASA-CR-194820] p 2601 N94-23537
Intercomparison of remote and balloon-borne sensors operated at JAPE-91 p 2527 N94-24210
Flux measurements using the BATSE spectroscopic detectors p 2580 N94-24435
Influence of test configuration on the combustion characteristics of polymers as ignition sources
p 2238 N94-25365

NEW MEXICO UNIV., ALBUQUERQUE.
Interactions between organized, surface-confined monolayers and vapor-phase probe molecules. 7: Comparison of self-assemblying organomercaptan monolayers deposited on gold from liquid and vapor phases
[AD-A273196] p 2535 N94-24555
Synthesis and characterization of two-dimensional molecular recognition interfaces
[AD-A273177] p 2536 N94-24729
Chemically sensitive interfacial force microscopy: Contact potential measurements of self-assembling monolayer films
[AD-A273135] p 2234 N94-24772
The nanometer-scale mechanics of gold films
[AD-A273307] p 2565 N94-25086
Scanning probe lithography. 2: Selective chemical vapor deposition of copper into scanning tunneling microscope-defined patterns
[AD-A273304] p 2547 N94-25144
Scanning probe surface modification
[AD-A273178] p 2346 N94-25151

NEW ORLEANS UNIV., LA.
Experimental and analytical study of cryogenic propellant boiloff to develop and verify alternate pressurization concepts for Space Shuttle external tank using a scaled down tank p 2266 N94-23657

NEW YORK UNIV., NEW YORK.
Center for Analysis of Heterogeneous and Nonlinear Media
[AD-A273515] p 2230 N94-25158

NEWCASTLE-UPON-TYNE UNIV. (ENGLAND).
Systematic construction of trigonometric neural networks
[PB93-200228] p 2474 N94-24544

NIPPON ELECTRIC CO. LTD., KAWASAKI (JAPAN).
A pattern jitter free AFC scheme for mobile satellite systems p 2285 N94-22809

NIPPON TELEGRAPH AND TELEPHONE PUBLIC CORP., YOKOSUKA (JAPAN).
Performance of the unique-word-reverse-modulation type demodulator for mobile satellite communications
p 2286 N94-22813

NOBEYEMA SOLAR RADIO OBSERVATORY (JAPAN).
Magnetic field dissipation and contraction of molecular clouds
[REPT-337] p 2603 N94-24976
Protoplanetary disks: Theory and observation by millimeter and sub-millimeter arrays
[REPT-331] p 2603 N94-24983
High spatial resolution observations of CO in CRL 618
[REPT-334] p 2604 N94-24986
The Nobeyama millimeter array survey for protoplanetary disks around protostar candidates and T Tauri stars in Taurus
[REPT-336] p 2604 N94-24987

NOKIA DATA, HELSINKI (FINLAND).
APLAC: An object-oriented analog circuit simulator and design tool. 6.1 system simulations manual
[PB93-224871] p 2450 N94-23226

NORFOLK STATE UNIV., VA.
Radiative properties of molecular nitrogen ions produced by helium Penning ionization and argon effects
[NASA-CR-195126] p 2534 N94-24487

NORTH CAROLINA STATE UNIV., RALEIGH.
Numerical solutions of the complete Navier-Stokes equations
[NASA-CR-194780] p 2337 N94-24858
Computational fluid mechanics
[NASA-CR-194765] p 2337 N94-24859

NORTH CAROLINA UNIV., CHAPEL HILL.
Image pattern recognition supporting interactive analysis and graphical visualization
[NASA-CR-194878] p 2451 N94-23369
Free energy profiles for Li(+) and I(-) ions approaching Pt(100) surface: A molecular dynamics study
[AD-A273455] p 2536 N94-24675
Auditory spectro-temporal pattern analysis
[AD-A273554] p 2427 N94-24865
Structures of Cl(-)(H2O)(n) and F(-)(H2O)(n) (n equal to 2,3...15) clusters: Molecular dynamics computer simulations
[AD-A273474] p 2537 N94-24940

NORTH CAROLINA UNIV., CHARLOTTE.
Design and simulation of EVA tools for first servicing mission of HST
[NASA-CR-194784] p 2439 N94-24857

NORTHEAST RADIO OBSERVATORY CORP., WESTFORD, MASS. HAYSTACK OBSERVATORY.
100 GHz map of 3C 446
[PB94-104882] p 2599 N94-23705

NORTHEASTERN UNIV., BOSTON, MA.
Mixing and unmixedness in plasma jets 1: Near-field analysis p 2323 N94-23655

NORTHROP CORP., HAWTHORNE, CA.
Doppler global velocimetry: Development of a flight research instrumentation system for application to non-intrusive measurements of the flow field
[NASA-CR-191490] p 2344 N94-24360

NORTHWESTERN UNIV., EVANSTON, IL.
Strong interactions studies with medium energy probes
[DE94-001446] p 2540 N94-23791

NOTRE DAME UNIV., IN.
NASA/USRA University Advanced Design Program, 1992-1993. The Diamondback: A simulated commercial air transportation study
[NASA-CR-195523] p 2180 N94-24462
The Blue Emu
[NASA-CR-195535] p 2182 N94-24817
The airplane: A simulated commercial air transportation study
[NASA-CR-195525] p 2182 N94-24837
The Bunny: A simulated commercial air transportation study
[NASA-CR-195537] p 2183 N94-25001
The Gold Rush: A simulated commercial air transportation study
[NASA-CR-195528] p 2184 N94-25002
The RTL-46: A simulated commercial air transportation study
[NASA-CR-195524] p 2184 N94-25017

NUMEREX, ALBUQUERQUE, NM.
The internal structure and dynamics of the railgun plasma armature between infinitely wide ablating rails
[DE94-001473] p 2198 N94-23208

O

OAK RIDGE NATIONAL LAB., TN.
High-T(c) superconducting superlattices
[DE93-019200] p 2556 N94-22864
Catalog of data bases and reports
[DE93-040597] p 2588 N94-22875
Assessment of stellarators as reactors
[DE93-017775] p 2548 N94-22916
Spin-polaron theory of high-T(c) superconductivity. 2: Electronic structure of the CuO2 planes
[DE93-019197] p 2556 N94-22919
Active probing of plasma edge turbulence and feedback studies on the Texas Experimental Tokamak (TEXT)
[DE94-001017] p 2548 N94-22945
Electron spectroscopic studies of the neutralization of slow multicharged ions during interactions with a metal surface
[DE93-041046] p 2532 N94-22956
Low temperature diffusion of hydrogenic species in oxide crystals: Radiation induced diffusion
[DE94-000374] p 2558 N94-22957
Implementation and parallelization of fast matrix multiplication for a fast Legendre transform
[DE94-002184] p 2478 N94-22975
Eye-gaze control of the computer interface: Discrimination of zoom intent
[DE94-000480] p 2429 N94-22997
Fluctuations and confinement in ATF
[DE94-000485] p 2549 N94-22998
Simple estimate of stored energy and conductor insulation voltage-withstand requirements for advanced solenoid magnet designs
[DE93-041048] p 2307 N94-23019
Development of silicon nitride composites with continuous fiber reinforcement
[DE94-001996] p 2227 N94-23022
Classical scattering theory of waves from the view point of an eigenvalue problem and application to target identification
[DE94-000472] p 2525 N94-23206
Surface modification of sapphire for enhanced infrared window performance
[DE94-000333] p 2543 N94-23458
Fiber optic temperature sensor using a Y2O2S:Eu thermographic phosphor
[DE94-000331] p 2543 N94-23461
Overview of the ATF stellarator program
[DE94-000371] p 2550 N94-23462
System identification using a wavelet-based approach
[DE94-002191] p 2293 N94-23473
The statistics of sputtering
[DE94-001128] p 2243 N94-23715
Development of a theory of the wear of ceramics
[DE94-002773] p 2254 N94-23783
Enhanced absorption cycle computer model
[DE94-001997] p 2271 N94-23793
Performance of the Carbon Dioxide Information Analysis Center (CDIAC)
[DE94-002190] p 2397 N94-23794
Performance characteristics of the DIII-D advanced divertor cryopump
[DE94-002745] p 2354 N94-23797
Considerations in implementing integrated biomass energy systems in developing countries
[DE93-018720] p 2395 N94-24499
Experimental and theoretical features of strong suppression and shifting phenomena in odd-photon resonant excitations and stimulated emissions
[DE94-000341] p 2535 N94-24510
The design of a standard message passing interface for distributed memory concurrent computers
[DE94-002536] p 2446 N94-24538
Fifty years of continuous improvement: What has DOE done for analytical chemistry?
[DE94-002539] p 2234 N94-24548
Total light loss optic spectroscopy: Progress towards a fiber optic Raman organic vapor sensor
[DE94-002545] p 2234 N94-24549
The torsion space nucleic acids molecular mechanics program DUPLEX: Surveying conformation space by potential energy minimization
[DE94-002441] p 2563 N94-24567
Normal zone propagation and thermal hydraulic quenchback in a cable-in-conduit superconductor
[DE94-002457] p 2271 N94-24568
Integral equations for the microstructures of supercritical fluids
[DE94-002460] p 2535 N94-24569
Tokamak Physics Experiment (TPX) cost and performance trade studies using supercode
[DE94-002720] p 2553 N94-24628
Tools for visualizing landscape pattern for large geographic areas
[DE94-001121] p 2388 N94-24757

OAKWOOD COLL., HUNTSVILLE, AL.
The measurement and analysis of leaf spectral reflectance of two stands of loblolly pine populations p 2389 N94-24442
OAO CORP., ALTADENA, CA.
The application of automated operations at the Institutional Processing Center p 2509 N94-23901
The application of total quality management principles to spacecraft mission operations p 2374 N94-23931
OBSERVATOIRE DE PARIS-MEUDON (FRANCE).
Eddy mixing coefficient upper limit derived from the photochemical balance of O2 p 2621 N94-24897
OESTERREICHISCHE RAUMFAHRT- UND SYSTEMTECHNIK, VIENNA (AUSTRIA).
Viscous rotary damper p 2361 N94-24031
OFFICE NATIONAL D'ETUDES ET DE RECHERCHES AEROSPATIALES, PARIS (FRANCE).
Bent-tip blade for aircraft rotary-wing [CA-PATENT-1-315-259] p 2176 N94-23254
Glass-ceramic Li-Al-Si-O composition and process for its production [CA-PATENT-APPL-SN-2043757] p 2254 N94-24129
An overview on the main available ceramic composites and their processing routes p 2255 N94-24229
Micromechanical characterization of ceramic-matrix composites using the instrumented microindentation technique p 2256 N94-24233
OFFICE OF TECHNOLOGY ASSESSMENT, WASHINGTON, DC.
Making government work: Electronic delivery of Federal services [OTA-TCT-578] p 2290 N94-23081
Contributions of DOE weapons labs and NIST to semicondutor technology [OTA-ITE-585] p 2630 N94-23572
Proceedings of Technology and Governance in the 1990's [PB93-192904] p 2597 N94-24312
Aircraft evacuation testing: Research and technology issues [PB94-107620] p 2173 N94-24750
OFFICINE GALILEO S.P.A., FLORENCE (ITALY).
Width modulator mechanism for spectrometer entrance slits p 2357 N94-24002
High precision double four bar linkage mechanism for interferometric linear scanning p 2359 N94-24013
OHIO STATE UNIV., CLEVELAND.
Investigation of the effects of manufacturing variations and materials on fatigue crack detection methods in gear teeth [NASA-CR-195093] p 2373 N94-24769
OHIO STATE UNIV., COLUMBUS.
Simulation of unsteady flows through stator and rotor blades of a gas turbine using the Chimera method p 2323 N94-23652
Upwind MacCormack Euler solver with non-equilibrium chemistry p 2326 N94-23672
NASA/USRA advanced design program [NASA-CR-195548] p 2180 N94-24492
Configuration development study of the OSU 1 hypersonic research vehicle [NASA-CR-195522] p 2181 N94-24591
High-level connectionist models [AD-A273638] p 2468 N94-25030
A conceptual design of an unmanned test vehicle using an airbreathing propulsion system [NASA-CR-195550] p 2189 N94-25085
Thermophysical properties of simple liquid metals: A brief review of theory p 2248 N94-25130
Design and implementation of a distributed version of the NASA Engine Performance Program [NASA-CR-194475] p 2462 N94-25179
Mechanisms of anode power deposition in a low pressure free burning arc [NASA-CR-194442] p 2553 N94-25190
OHIO UNIV., ATHENS.
A minimum cost tolerance allocation method for rocket engines and robust rocket engine design p 2222 N94-24419
The in situ observation of epitaxial diamond thin film nucleation and growth using emission electron microscopy [AD-A273698] p 2263 N94-25489
OKLAHOMA UNIV., NORMAN.
Examples of data assimilation in mesoscale models p 2412 N94-24384
Techniques and resources for storm-scale numerical weather prediction p 2414 N94-24392
Session on techniques and resources for storm-scale numerical weather prediction p 2415 N94-24400
Performance of the engineering analysis and data system 2 common file system p 2576 N94-24413
Water cycle research associated with the CaPE hydrometeorology project (CHymP p 2416 N94-24414
OLD DOMINION UNIV., NORFOLK, VA.
Theoretical studies of a molecular beam generator [NASA-CR-194779] p 2540 N94-23485
Feasibility of detecting aircraft wake vortices using passive microwave radiometers [NASA-CR-191553] p 2343 N94-23498
Preliminary eddy current modelling for the large angle magnetic suspension test fixture [NASA-CR-194772] p 2192 N94-23539
Stability of premixed laminar flames in a stagnation point flow to general disturbances [AD-A273429] p 2234 N94-24673
The effects of profiles on supersonic jet noise [NASA-CR-195164] p 2530 N94-25177
OLTECH CORP., CHESTERLAND, OH.
A dual reciprocal boundary element formulation for viscous flows p 2325 N94-23666
ONSALA SPACE OBSERVATORY (SWEDEN).
Molecular abundances in the envelopes around evolved stars [PB94-104916] p 2602 N94-23812
The 1404+286: A non-ideal calibrator for VLBI observations [PB94-104908] p 2599 N94-24521
Infrared and SIO maser observations of OH/IR stars [PB94-104890] p 2599 N94-24780
First results from the Fennoscandian GPS networks p 2405 N94-25204
OPEN UNIV., MILTON (ENGLAND).
Ground characterization for JAPE p 2527 N94-24213
OPTICAL CONCEPTS, INC., LOMPOC, CA.
InGaAsP/InP based 1.3/1.55 micron vertical cavity surface emitting lasers for wavelength division multiplexed high speed distributed computing, phase 1 [AD-A271081] p 2348 N94-23123
OPTRA, INC., BEVERLY, MA.
Measuring electrically charged particle fluxes in space using a fiber optic loop sensor [NASA-CR-191328] p 2544 N94-23829
OPTUS COMMUNICATIONS, SYDNEY (AUSTRALIA).
Mobilesat (tm): A world first p 2281 N94-22783
ORBITAL SCIENCES CORP., FAIRFAX, VA.
The ORBCOMM data communications system p 2281 N94-22782
OREGON STATE UNIV., CORVALLIS.
Matter-wave interferometry with laser cooled atoms [AD-A273249] p 2536 N94-24717
A diagnostic model to estimate winds and small-scale drag from Mars Observer PMIRR data p 2617 N94-24874
Eddy mixing coefficient values derived from simulations with the NASA Ames Mars GCM p 2617 N94-24875
Topics in probability and dynamics [AD-A273543] p 2496 N94-24931
ORGANISATIE VOOR TOEGEPAST NATUURWETENSCHAPPELIJK ONDERZOEK, THE HAGUE (NETHERLANDS).
Results from the VISA project [AD-A273752] p 2406 N94-25540
ORGANIZATION FOR INDUSTRIAL RESEARCH, TNO, THE HAGUE (NETHERLANDS).
Remote vibration measurements at a sud aviation alouette 3 helicopter with a CW CO2-laser system [AD-A273818] p 2190 N94-25516
OSLO UNIV. (NORWAY).
Prospects for future ground-based solar observations p 2624 N94-22842
OTTAWA UNIV. (ONTARIO).
Transmission over EHF mobile satellite channels p 2287 N94-22820
Fracture kinetics analysis of empirical and semi-empirical corrosion fatigue relations p 2159 N94-24277
On the deformation kinetics constitutive law of plastic deformation: The rate equation p 2161 N94-24289
OVONIC BATTERY CO., TROY, MI.
Ovonic nickel metal hydride batteries for space applications p 2391 N94-23352
OWENS VALLEY RADIO OBSERVATORY, PASADENA, CA.
100 GHz map of 3C 446 [PB94-104882] p 2599 N94-23705
OXFORD UNIV. (ENGLAND).
How much integral action can a control system tolerate? [OUEL-1923/92] p 2471 N94-23147
Stereo for gazing and converging cameras. Part 1: Basic geometry [OUEL-1915/92] p 2343 N94-23162
Reduced-order modelling and control of a class of systems for which balanced truncation is Hankel-norm optimal [OUEL-1922/92] p 2472 N94-23163
The design of a turbine vane cooling system used in the topping cycle [OUEL-1963/92] p 2353 N94-23164
Time-frequency domain analysis of vibration signals for machinery diagnostics.(4): Interpretation using image processing techniques [OUEL-1953/92] p 2353 N94-23178
A tracking sonar sensor for vehicle guidance [OUEL-1956/92] p 2472 N94-23179
Multigrid and cyclic reduction applied to the Helmholtz equation p 2304 N94-23676
New methane chemistry synthesis of materials for reversible uptake and useful functionalization of methane [PB94-112786] p 2233 N94-23801
The influence of orography on the transport of atmospheric constituents p 2619 N94-24886
Modeling and data assimilation for Mars Observer p 2620 N94-24889
Balanced truncation is Hankel-norm optimal when used to approximate a finite-difference model of a parabolic PDE [OUEL-1921/92] p 2492 N94-25324
Ring nuclei of strain for bonded dissimilar elastic half spaces with particular application to axisymmetric crack problems [OUEL-1966/92] p 2379 N94-25325
Horatio: Libraries for vision applications, release 2.0 [OUEL-1967/92] p 2593 N94-25326
Fluid velocity and electromagnetic forces measured by a rotating Langmuir probe in the scrape off layer of JFT-2M [OUEL-1968/92] p 2554 N94-25327
A soft robot interface [OUEL-1948/92] p 2463 N94-25468
Stability questions in predictive control [OUEL-1970/93] p 2477 N94-25469
Adaptive predictive control of the benchmark plant [OUEL-1972/93] p 2477 N94-25470
Extracting projective information from single views of 3D point sets [OUEL-1973/93] p 2464 N94-25471
Active camera calibration for a head-eye platform using a variable state dimension filter [OUEL-1975/93] p 2346 N94-25472
Fault detection in HVAC systems using fuzzy models [OUEL-1977/93] p 2373 N94-25475
The complete stress field due to a dislocation located anywhere in two bonded quarter planes [OUEL-1990/93] p 2379 N94-25478

P

PACIFIC NORTHWEST LAB., RICHLAND, WA.
Translative interface for data sharing and integrating: A paradigm for distributed data systems [DE93-018790] p 2588 N94-22863
Evaluation of uranium transitions for isotopically-selective laser induced fluorescence with diode lasers (technical report for ST064) [DE94-002000] p 2347 N94-22974
US Department of Energy phaseout of CFC-refrigerants [DE94-001668] p 2397 N94-23016
PARIS VII UNIV. (FRANCE).
Conceptual design and architecture of hexapod robotic vehicles for the (L)OVLA project p 2369 N94-23405
PARIS XI UNIV., ORSAY (FRANCE).
Prospects for improved instrumentation on future solar space missions p 2624 N94-22843
PENNSYLVANIA STATE UNIV., ERIE.
Prediction of pressure drop in fluid tuned mounts using analytical and computational techniques p 2321 N94-23643
Solution of mixed convection heat transfer from isothermal in-line fins p 2321 N94-23644
Comparison of numerical simulation and experimental data for steam-in-place sterilization p 2326 N94-23669
PENNSYLVANIA STATE UNIV., UNIVERSITY PARK.
NASA Propulsion Engineering Research Center, volume 2 [NASA-CR-194719-VOL-2] p 2209 N94-23028
Measurement of intact-core length of atomizing liquid jets by image deconvolution p 2210 N94-23029
A theoretical evaluation of aluminum gel propellant two-phase flow losses on vehicle performance p 2210 N94-23031
CFD analyses of combustor and nozzle flowfields p 2210 N94-23033
LOX droplet vaporization in a supercritical forced convective environment p 2211 N94-23034
Evaporation and combustion of LOX under supercritical and subcritical conditions p 2211 N94-23035
Droplet turbulence interactions under subcritical and supercritical conditions p 2211 N94-23036

An experimental study of characteristic combustion-driven flows for CFD validation
p 2212 N94-23040
Spray formation processes of impinging jet injectors
p 2212 N94-23042
Development of a droplet breakup model considering aerodynamic and droplet collision effects
p 2213 N94-23045
Development of a computational testbed for numerical simulation of combustion instability
p 2213 N94-23046
Shear coaxial injector instability mechanisms
p 2213 N94-23047
Numerical investigation of two- and three-dimensional heat transfer in expander cycle engines
p 2213 N94-23048
CFD analyses of coolant channel flowfields
p 2214 N94-23050
Efficiency and reliability enhancements in propulsion flowfield modeling p 2215 N94-23055
Foil bearing research at Penn State
p 2215 N94-23058
Computational fluid dynamic modelling of cavitation
p 2215 N94-23060
Computation of flows in a turn-around duct and a turbine cascade using advanced turbulence models
p 2216 N94-23062
Reliability enhancement of Navier-Stokes codes through convergence enhancement p 2216 N94-23064
Optimization of energy transfer in microwave electrothermal thrusters p 2216 N94-23065
CFD modeling of microwave electrothermal thrusters
p 2216 N94-23066
An antiproton driver for ICF propulsion
p 2217 N94-23069
Nuclear propulsion control and health monitoring
p 2217 N94-23071
Lightning studies using LDAR and LLP data
p 2416 N94-23238
In situ detection of tropospheric OH, HO2, NO2, and NO by laser-induced fluorescence in detection chambers at reduced pressures
[NASA-CR-194810] p 2397 N94-23277
Thermodynamics of nickel-cadmium and nickel-hydrogen batteries p 2391 N94-23349
A direct approach to finding unknown boundary conditions in steady heat conduction
p 2322 N94-23645
Three-dimensional solidification and melting using magnetic field control p 2325 N94-23664
Unsteady three-dimensional thermal field prediction in turbine blades using nonlinear BEM
p 2325 N94-23665
Perception in flight: Shape and motion perception, space perception, spatial orientation, and visual vestibular interaction p 2429 N94-23979
Dimensional analysis of acoustically propagated signals p 2528 N94-24217
Session on cumulus parameterization
p 2414 N94-24394
Structural design criteria for filament-wound composite shells
[NASA-CR-195125] p 2229 N94-24402
Torque equilibrium attitudes for the Space Station
p 2208 N94-24449
A mission to Mercury and a mission to the moons of Mars
[NASA-CR-195530] p 2195 N94-24619
Ignition and combustion characteristics of metallized propellants, phase 2
[NASA-CR-195107] p 2266 N94-24700
EEG and chaos: Description of underlying dynamics and its relation to dissociative states
[NASA-CR-195171] p 2428 N94-24799

PHILIPS GLOEILAMPENFABRIEKEN N.V., EINDHOVEN (NETHERLANDS).
Some subjects in digital audio, noise shaping, sample rate conversion, dynamic range compression and testing
[ISBN-9-09-005162-7] p 2530 N94-25220
On the quality of synthetic speech evaluation and improvements
[ETN-94-95298] p 2304 N94-25234
Metallic multilayers: Experimental investigation of magnetic anisotropy and magnetic interlayer coupling
[ETN-94-95364] p 2250 N94-25242
On the characterization and optimization of high-speed silicon bipolar transistors
[ETN-94-95367] p 2313 N94-25253
A design method for parallel programs
[ETN-94-95331] p 2469 N94-25282
Laser ablation and deposition of metals
[ETN-94-95311] p 2351 N94-25294

PHILLIPS LAB., EDWARDS AFB, CA.
Fundamental rocket injector/spray programs at the Phillips Laboratory p 2211 N94-23039

PHILLIPS LAB., HANSCOM AFB, MA.
Report on operations of the Air Force Geophysics Laboratory infrared array spectrometer
[AD-A273800] p 2406 N94-25535
A nighttime structure model of atmospheric optical turbulence, c2(n), derived from thermosonde and high resolution rawinsonde measurements
[AD-A273803] p 2406 N94-25537

PHILLIPS LAB., KIRTLAND AFB, NM.
Thermal analysis of combinatorial solid geometry models using SINDA p 2323 N94-23650

PHYSICS AND ELECTRONICS LAB. TNO, THE HAGUE (NETHERLANDS).
Experimental evaluation of camouflage effectiveness in the thermal infrared
[FEL-93-A043] p 2381 N94-22896

PIONEER AEROSPACE CORP., MELBOURNE, FL.
Radially constructed cruciform parachute
[CA-PATENT-1323021] p 2168 N94-24182

PITTSBURGH UNIV., PA.
Selected bibliography 2: Diamond surface chemistry
[AD-A273518] p 2565 N94-25160

POLISH ACADEMY OF SCIENCES, WARSAW.
Two-point PADE approximants for Stieltjes series
p 2490 N94-24768

POLITECNICO DI TORINO (ITALY).
DS-SSMA capacity for a mobile satellite system
p 2286 N94-22814

PRATT AND WHITNEY AIRCRAFT, WEST PALM BEACH, FL.
Advanced Capability Exhaust Systems/Integrated Product Development for advanced nozzles (ACES/IPD)
[AD-A273209] p 2189 N94-24776
Advanced launch system. Advanced development oxidizer turbopump program
[NASA-CR-193920] p 2367 N94-25174

PRATT AND WHITNEY AIRCRAFT OF CANADA LTD., LONGUEUIL (QUEBEC).
Turbine engine with induced pre-swirl at the compressor inlet
[CA-PATENT-1-317-467] p 2186 N94-23253

PRINCETON UNIV., NJ.
Mechanism and enhancement of flame stabilization
[DE94-002181] p 2232 N94-23023
Model atmosphere analysis of selected luminous B stars
[NASA-CR-195098] p 2599 N94-24051
Photoinduced charge separation in solid state and molecular systems
[DE94-001727] p 2563 N94-24537
The transition from diapirism to dike intrusion: Implications for planetary volcanism
[NASA-CR-195133] p 2403 N94-24580
Nanodesigning of hierarchical multifunctional ceramics
[AD-A273466] p 2257 N94-24677
Three-dimensional numerical simulation of thermal tides in the Martian atmosphere p 2622 N94-24901
Development and validation of RNG methodology for compressible turbulence
[AD-A273469] p 2337 N94-24929

PSI TECHNOLOGY CO., ANDOVER, MA.
A high performance H2-Cl2 fuel cell for space power applications p 2394 N94-23366

PUERTO RICO UNIV., MAYAGUEZ.
FTIR quantification of industrial hydraulic fluids in perchloroethylene p 2264 N94-23243
Stress corrosion cracking properties of 15-5PH steel
p 2251 N94-23244
On the analysis of clear air radar echoes severely contaminated by clutter p 2306 N94-24423
Soft x ray optics by pulsed laser deposition
[NASA-CR-195139] p 2546 N94-24967

PULLMAN KELLOGG, HOUSTON, TX.
Evaluation of reducing gas turbine emissions through hydrogen-enhanced steam-injected combustion
[PB94-109873] p 2187 N94-23709

PURDUE UNIV., WEST LAFAYETTE, IN.
A prototype expert/information system for examining environmental risks of KSC activities
p 2400 N94-23237
Flame trench analysis of NLS vehicles
p 2199 N94-23249
Development of a code for wall contour design in the transonic region of axisymmetric and square nozzles
[NASA-CR-194857] p 2167 N94-23625
A regional analysis of cloudy mean spherical albedo over the marine stratocumulus region and the tropical Atlantic Ocean
[NASA-CR-194771] p 2409 N94-24049
Observational and modeling studies of heat, moisture, precipitation and global-scale circulation patterns
[NASA-CR-195148] p 2415 N94-24485
Establishment of computerized numerical databases on thermophysical and other properties of molten as well as solid materials and data evaluation and validation for generating recommended reliable reference data
p 2246 N94-25123
An overview of the measurements of thermophysical properties and some results on molten superalloys and semiconductors p 2248 N94-25128
High lift aerodynamics
[NASA-CR-195183] p 2184 N94-25268
Robotics in a controlled, ecological life support system
p 2444 N94-25371

Q

QUEENS UNIV., KINGSTON (ONTARIO).
Asynchronous timing and Doppler recovery in DSP based DPSK modems for fixed and mobile satellite applications p 2285 N94-22805
FAS multigrid calculations of three dimensional flow using non-staggered grids p 2341 N94-23675

QUEENSLAND UNIV., SAINT LUCIA (AUSTRALIA).
Shock tunnel studies of scramjet phenomena, supplement 7
[NASA-CR-191572] p 2319 N94-23513
Shock tunnel studies of scramjet phenomena, supplement 8
[NASA-CR-191573] p 2320 N94-23532

R

RAFAEL ARMAMENT DEVELOPMENT AUTHORITY, HAIFA (ISRAEL).
Altitude simulation facility for testing large space motors p 2156 N94-24255

RANDOLPH-MACON COLL., ASHLAND, VA.
Evaluation of inorganic zinc-rich primers using Electrochemical Impedance Spectroscopy (EIS)
p 2237 N94-23233

RANGE COMMANDERS COUNCIL, WHITE SANDS MISSILE RANGE, NM.
HORACE: Presentation-level protocol standard for digital transmission of monochrome television images
[AD-A273395] p 2197 N94-25064
IRIG radar calibration catalog. Version 2: The IRIG error model reference for radar calibrations
[AD-A273344] p 2303 N94-25155

RAYTHEON CO., TEWKSBURY, MA.
DARPA DICE manufacturing optimization
[AD-A273345] p 2461 N94-25156

READING UNIV. (ENGLAND).
Aspects of the Martian global circulation
p 2618 N94-24879

REMTECH, INC., HUNTSVILLE, AL.
Analysis and effects of the advanced solid rocket motor on the Space Shuttle elements
[NASA-CR-193879] p 2200 N94-24664

RENSSELAER POLYTECHNIC INST., TROY, NY.
Parallel unstructured grid generation for computational aerosciences
[NASA-CR-192244] p 2466 N94-23483
A random distribution reacting mixing layer model
[NASA-CR-194445] p 2187 N94-23552
Wear reduction in ceramic bearings by surface generated pyrolytic carbon continuously replenished by ethylene gas
[NASA-CR-189214] p 2364 N94-24090
Electric field-mediated processing of polymer blend solutions p 2223 N94-24341
Adsorption, desorption, and decomposition of HCl and HBr on Ge(100): Competitive pairingand near-first-order desorption kinetics
[AD-A273504] p 2235 N94-24790

RESEARCH INST. FOR ADVANCED COMPUTER SCIENCE, MOFFETT FIELD, CA.
Energy and maximum norm estimates for nonlinear conservation laws
[NASA-CR-195091] p 2569 N94-24109
On the dynamics of some grid adaption schemes
[NASA-CR-195092] p 2454 N94-24110
Unstructured adaptive mesh computations of rotorcraft high-speed impulsive noise
[NASA-CR-195090] p 2529 N94-24307
Increasing levels of assistance in refinement of knowledge-based retrieval systems
[NASA-CR-195144] p 2591 N94-24552
RIACS/USRA
[NASA-CR-195117] p 2631 N94-25003

RESEARCH INST. OF NATIONAL DEFENCE, LINKOEPING (SWEDEN).
Method for selection of wavelength bands for multispectral classification
[PB93-204378] p 2388 N94-24741

RESEARCH TRIANGLE INST., RESEARCH TRIANGLE PARK, NC.
Fundamental study of NO(x) control in catalytic combustion
[PB94-112323] p 2398 N94-23818
NASA technology applications team: Applications of aerospace technology
[NASA-CR-194775] p 2597 N94-24494

RHODE ISLAND UNIV., NARRAGANSETT.
Vertical motion in the SYNOP central array
[AD-A273593] p 2418 N94-24795

RICE UNIV., HOUSTON, TX.
Domain decomposition methods for nonconforming finite element spaces of Lagrange-type
p 2483 N94-23680
Designers' models of the human-computer interface
p 2433 N94-24188
Development of programmable artificial neural networks p 2477 N94-25370

RICHMOND UNIV., VA.
The Adam language: Ada extended with support for multiway activities
[NASA-CR-4565] p 2456 N94-24480

RIJKSINSTITUUT VOOR VOLKSGEZONDHEID EN MILIEUHYGIEENE, BILTHOVEN (NETHERLANDS).
Exploratory report nickel and nickel compounds
[PB93-223998] p 2242 N94-23496
Exploratory report antimony and antimony compounds
[PB93-224004] p 2397 N94-23497

RIJKSWATERSTAAT, THE HAGUE (NETHERLANDS).
Analysis of vulnerability to the impacts of sea level rise: A case study for The Netherlands
[PB94-111150] p 2399 N94-24573
Recent developments in the mathematical modelling and physical understanding of transport and dispersion in aquatic systems, with special reference to tidal waters
[PB94-111135] p 2418 N94-24600
Nutrients and light as factors controlling phytoplankton biomass on the Dutch continental shelf (North Sea), 1988-1990
[PB94-111143] p 2418 N94-24601

RMS ASSOCIATES, LINTHICUM HEIGHTS, MD.
A comparison of Boolean-based retrieval to the WAIS system for retrieval of aeronautical information
[NASA-CR-4569] p 2594 N94-25487
NACA collections: A directory of significant collections of the documents of the National Advisory Committee for Aeronautics
[NASA-CR-195686] p 2594 N94-25541

ROCHESTER UNIV., NY.
Dynamic localization and second-order subgrid-scale models in large eddy simulations of channel flow
p 2329 N94-24149

ROCKWELL INTERNATIONAL CORP., CANOGA PARK, CA.
Dual-bell altitude compensating nozzles
p 2215 N94-23057
Heat pipe cooled heat rejection subsystem modelling for nuclear electric propulsion
[NASA-CR-191132] p 2219 N94-24061
System for Anomaly and Failure Detection (SAFD) system development
[NASA-CR-193907] p 2372 N94-24174

ROCKWELL INTERNATIONAL CORP., CEDAR RAPIDS, IA.
Low cost coherent demodulation for mobile satellite terminals p 2284 N94-22803

ROCKWELL INTERNATIONAL CORP., HUNTSVILLE, AL.
Modeling dynamically coupled fluid-duct systems with finite line elements
[NASA-CR-193909] p 2376 N94-24359

ROLLS-ROYCE LTD., DERBY (ENGLAND).
Rolls-Royce in perspective: Past, present and future
[PNR-90882] p 2187 N94-23519
The RB211: The first 25 years
[PNR-90977] p 2187 N94-23570
Engineering for profitability
[PNR-90990] p 2595 N94-23580

ROME LAB., GRIFFISS AFB, NY.
Correlation function estimator performance in non-Gaussian spherically invariant random processes
[AD-A273498] p 2496 N94-24951

ROME UNIV. (ITALY).
Handover procedures in integrated satellite and terrestrial mobile systems p 2277 N94-22761
A working algorithm to isolate integrable surfaces in E cubed
[SSCL-PREPRINT-761] p 2452 N94-23518

ROSE-HULMAN INST. OF TECH., TERRE HAUTE, IN.
Design of a surface deformation measuring instrument for the Surface Tension Driven Convection Experiment (STDCE-2)
[NASA-CR-194758] p 2343 N94-23285

ROUEN UNIV. (FRANCE).
A transport equation for the scalar dissipation in reacting flows with variable density: First results
p 2331 N94-24157

ROYAL AIR FORCE, FARNBOROUGH (ENGLAND).
Human factors of mission planning systems: Theory and concepts p 2521 N94-25010

ROYAL AIR FORCE, LONDON (ENGLAND).
Left ventricular hypertrophy and athlete's heart
p 2424 N94-23321
Aortic valve disease p 2424 N94-23322
Chronic obstructive pulmonary disease
p 2425 N94-23324
Sarcoidosis and the aviator p 2425 N94-23325
Spontaneous pneumothorax, cysts and bullae
p 2425 N94-23326
Arterial hypertension and the aviator
p 2425 N94-23328

RUTGERS - THE STATE UNIV., PISCATAWAY, NJ.
Discrete applied mathematics
[AD-A273552] p 2488 N94-24561

RUTHERFORD APPLETON LAB., CHILTON (ENGLAND).
Stitching the Yukawa quilt
[PB93-204477] p 2569 N94-24532
Spin fluctuations in an ordered Heisenberg ferromagnet with dipolar interactions
[PB93-204493] p 2524 N94-24533
MERILL: An equational reasoning system in standard ML: A user guide (prerelease version 0.4)
[PB93-204501] p 2456 N94-24534

S

SAAB MISSLES A.B., LINKOEPING (SWEDEN).
Device for the selective detection of objects
[CA-PATENT-1-308-179] p 2544 N94-24489

SAAB-SPACE A.B., LINKOEPING (SWEDEN).
Opening mechanism for ISO/CVV cover release
p 2357 N94-24001

SAINT JOHN FISHER COLL., ROCHESTER, NY.
A chemical sensor and biosensor based totally automated water quality monitor for extended space flight: Step 1 p 2443 N94-24447

SAINT LOUIS UNIV., MO.
Development of a model to assess orthostatic responses p 2427 N94-25376

SAITAMA UNIV., URAWA (JAPAN).
The role of emitter states in magnetotunneling through double-barrier resonant-tunneling diodes at high magnetic fields
[REPT-A-2658] p 2564 N94-24959

SANDIA NATIONAL LABS., ALBUQUERQUE, NM.
Ultraviolet photosulfidation of III-V compound semiconductors for electronic passivation
[DE94-001417] p 2555 N94-22717
Probabilistic analysis of mechanical systems
[DE93-041145] p 2371 N94-22918
Chromate-free talc chemical conversion coatings for aluminum alloys
[DE94-001567] p 2238 N94-22932
Bridgman's concern
[DE93-040900] p 2558 N94-22953
Robust, wide-range hydrogen sensor for use in commercial, space, and government applications
[DE93-040902] p 2342 N94-22954
Development and experimental validation of computational methods to simulate abnormal thermal and structural environments
[DE94-000554] p 2268 N94-23000
Bibliographic Retrieval System (BARS), Sandia Shock Compression (SSC) database Shock Physics Index
[DE94-001679] p 2589 N94-23126
Bibliographic Retrieval System (BARS). Sandia Shock Compression (SSC) database Shock Physics Index (SPHINX) database. Volume 1: UNIX version query guide customized application for INGRES
[DE94-001703] p 2589 N94-23127
Bibliographic Retrieval System (BARS), Sandia Shock Compression (SSC) database, Shock Physics Index (SPHINX) database, Volume 2: UNIX version user's guide
[DE94-001704] p 2589 N94-23128
Power beaming to space using a nuclear reactor-pumped laser
[DE94-001208] p 2348 N94-23185
A qualified radiation hardened nonvolatile memory for space and tactical weapons applications
[DE94-001211] p 2559 N94-23186
Generic microelectronic smart sensor platform for detection of toxic, hazardous, and flammable gases
[DE93-017626] p 2343 N94-23200
Graphical programming: A systems approach for telerobotic servicing of space assets
[DE93-019016] p 2472 N94-23201
Photo-induced and electrooptic properties of (Pb,La)(Zr,Ti)O3 films for optical memories
[DE93-019820] p 2542 N94-23202
Sensors for process control Focus Team report
[DE93-040897] p 2560 N94-23204
Characterization of heat transport and radiation hydrodynamics in collisional laser plasmas using collective Thomson scattering
[DE94-001502] p 2349 N94-23209
Projectile transverse motion and stability in electromagnetic induction launchers
[DE94-001557] p 2198 N94-23210
Continuum representations of cellular solids
[DE94-001706] p 2375 N94-23217
A method to simulate viscous diffusion of vorticity by convective transport of vortices at a non-solenoidal velocity
[DE94-001777] p 2318 N94-23220
Lunar exploration rover program developments
[DE93-040759] p 2613 N94-23469
A review of the Workshop on Fatigue Life Methodologies for Wind Turbines
[DE94-002039] p 2394 N94-23472
Object oriented simulation implementation in support of robust system design
[DE93-011687] p 2452 N94-23488
A lower bound for routing on a completely connected optical communication parallel computer
[DE93-040752] p 2466 N94-23491
Thermal control system for SSF sensor/electronics
[SAND-92-0652C] p 2321 N94-23640
Control algorithms for effective operation of variable-speed wind turbines
[DE94-002607] p 2394 N94-23704
Chemically sensitive interfaces on SAW devices
[DE94-001832] p 2526 N94-23718
The Electronics Quality/Reliability Center: Lessons learned from partnering with industry
[DE94-001501] p 2309 N94-23777
Laser soldering of Sn plated brass integrator assembly housings
[DE94-001149] p 2270 N94-23790
Disorder effects on small-polaron formation and hopping
[DE94-001205] p 2534 N94-23804
Metal-mullite reactions
[DE94-002038] p 2244 N94-23811
Fact-based enterprise information management using NIAM
[DE93-041135] p 2591 N94-24501
Ozone depletion, paradigms, and politics
[DE94-001600] p 2398 N94-24506
The chemistry of particulate formation in fluorocarbon plasmas
[DE94-001500] p 2552 N94-24546
Waste minimization/pollution prevention at R/D facilities: A cradle-to-grave tracking and information system that will be implemented at Sandia National Laboratories
[DE93-040330] p 2591 N94-24607
Electrochemical sulfur passivation of visible (approximately 670nm) AlGaInP lasers
[DE94-002293] p 2350 N94-24659
Carbon supercapacitors
[DE94-002652] p 2311 N94-24748

SCHWARTZ ELECTRO-OPTICS, INC., ORLANDO, FL.
Nonlinear dynamical control of lasers
[AD-A273359] p 2350 N94-24938

SCIENCE AND TECHNOLOGY CORP., WASHINGTON, DC.
GEWEX Continental-scale International Project (GCIP)
p 2411 N94-24376

SCIENCE APPLICATIONS INTERNATIONAL CORP., ALBUQUERQUE, NM.
An F2D analysis of the Flow Instability Test (FIT) experiment
[DE94-001420] p 2217 N94-23193

SCIENCE APPLICATIONS INTERNATIONAL CORP., GLENDORA, CA.
The possible effects of the natural and induced space environment on the optical and thermal properties of EOS surfaces p 2207 N94-23596

SECA, INC., HUNTSVILLE, AL.
Heat transfer in rocket combustion chambers
p 2214 N94-23051
Heat transfer in rocket engine combustion chambers and regeneratively cooled nozzles
[NASA-CR-195094] p 2220 N94-24471

SED SYSTEMS, INC., SASKATOON (SASKATCHEWAN).
Improved frame synchronization schemes for INMARSAT-B/M SCPC and TDM channels
p 2285 N94-22806

SELSKAPET FOR INDUSTRIELL OG TEKNISK FORSKNING, TRONDHEIM (NORWAY).
Magnetic properties and transmission electron microscopy investigations of Nd-Fe-B-Co-Al melt spun ribbons
[PB93-201531] p 2561 N94-23428
Fire safety engineering research in Norway
[PB93-201630] p 2268 N94-23429
Extinguishment of enclosed gas fires with water sprays
[PB93-201663] p 2268 N94-23430
Selective hydrogen separation by palladium-based composite membranes
[PB93-201671] p 2254 N94-23431
Visualization of results from meteorological simulations on CRAY
[PB93-201358] p 2451 N94-23443
GLview user's guide
[PB93-201366] p 2452 N94-23444
Spectroscopic IR ellipsometry of 100 and 001 oriented YBa2Cu3O(7-delta) films
[PB93-201481] p 2561 N94-23445
Quantitative analysis in the Al-Mg-Si system with small amounts of Mg and Si
[PB93-201499] p 2241 N94-23446
Theory of extrusion: Advances and challenges
[PB93-201572] p 2241 N94-23447
Weld cladding of hard surfaces
[PB93-201598] p 2353 N94-23448
Plasma ARC keyhole welding of aluminum
[PB93-201606] p 2353 N94-23449
Calculation of flame spread on lining materials by the field model KAMELEON. Project 5 of the EUREFIC fire research programme
[PB93-201614] p 2268 N94-23450
MITS architecture V1.0
[PB93-201762] p 2452 N94-23451
Observation of non-centrosymmetry and determination of polarity in III-V semiconductors
[PB93-201416] p 2561 N94-23503
Perturbation theory in electron diffraction
[PB93-201424] p 2533 N94-23505
Field models: Their present and future application in fire safety engineering
[PB93-201622] p 2269 N94-23506
Source spacing in B-ISDN
[PB93-201747] p 2293 N94-23508
Simultaneous simulation and visualization using DGL
[PB93-201341] p 2453 N94-23534
Characterization of 3-D particle distributions and effects on recrystallization studied by computer simulation
[PB93-201408] p 2562 N94-23535
Mueller matrix analysis of infrared ellipsometry
[PB93-201549] p 2544 N94-23629
Snow modeling, water resources, climate change
[PB93-201770] p 2399 N94-24633

SENER S.A., LAS ARENAS (SPAIN).
Docking mechanisms: An overview of different systems p 2357 N94-24004
Preloaded launch locking devices for SILEX
p 2358 N94-24008
Precision Displacement Mechanism (PDM)
p 2360 N94-24026
An opening mechanism for the scientific airlock outer hatch p 2360 N94-24027

SHEFFIELD UNIV. (ENGLAND).
Approximation to nonlinear equations using nonlinear rational models
[RR-448] p 2492 N94-25306
On-line control of dynamic systems using feedforward neural networks
[RR-457] p 2476 N94-25307
The phase response of nonlinear systems
[RR-458] p 2476 N94-25308
Fixed points and shift cycles in cellular automata
[RR-459] p 2492 N94-25309
On the inversion of the n-dimensional Laplace transform
[RR-461] p 2492 N94-25310
Unwrapping the phase response functions for nonlinear systems
[RR-465] p 2462 N94-25311
Transputer benchmarks and performance comparisons with other computing machines
[RR-467] p 2446 N94-25312
Advanced control structures: A transputer-based multi-robot system
[RR-468] p 2446 N94-25313
Validating identified nonlinear models with chaotic dynamics
[RR-469] p 2523 N94-25314
Genetic algorithms in control systems engineering
[RR-470] p 2463 N94-25315
Frequency response functions for nonlinear rational models
[RR-471] p 2492 N94-25318
Adaptive noise cancellation using recurrent radial basis function networks
[RR-472] p 2313 N94-25319
Relationship between the structure and performance of identified nonlinear polynomial models
[RR-474] p 2492 N94-25320
Two-dimensional pattern analysis and classification using a complex orthogonal estimation algorithm
[RR-475] p 2463 N94-25321
Genetic-based motion planning for articulated robotic manipulators
[RR-476] p 2368 N94-25322
Controlling regular and chaotic dynamics in the Duffing-Ueda oscillator
[RR-477] p 2523 N94-25323

SHIZUOKA UNIV. (JAPAN).
GGA study of the magnetic and cohesive properties of bcc, fcc and hcp Mn
[REPT-A-2662] p 2564 N94-24960

SIEGEN UNIV., (GERMANY).
Turbulence sensors for separated flows: Current capabilities, future requirements p 2315 N94-22853

SKODA WORKS, PILSEN (CZECHOSLOVAKIA).
New welding and finishing procedures
[DE94-602022] p 2352 N94-23025

SMITHSONIAN ASTROPHYSICAL OBSERVATORY, CAMBRIDGE, MA.
The calculation of theoretical chromospheric models and the interpretation of solar spectra from rockets and spacecraft
[NASA-CR-195083] p 2626 N94-23569
SAO mission support software and data standards, version 1.0
[NASA-CR-193906] p 2454 N94-24050
The resonance lines of MG2 as diagnostics of the upper solar chromosphere
[NASA-CR-195084] p 2627 N94-24300
Measurement of HO2 and other trace gases in the stratosphere using a high resolution far-infrared spectrometer
[NASA-CR-195173] p 2404 N94-24738
Shocked clouds in the Cygnus Loop
[NASA-CR-195190] p 2600 N94-25178
ROSAT observations of the x ray binary HD 154791
[NASA-CR-195189] p 2600 N94-25198
Measurement and Interpretation of Crustal Deformation Rates Associated with Postglacial Rebound
[NASA-CR-195193] p 2405 N94-25203
Investigation relative to the Roentgen Satellite (ROSAT)
[NASA-CR-195192] p 2600 N94-25269

SOCIETE ANONYME D'ETUDES ET REALISATIONS NUCLEAIRES, LIMEIL-BREVANNES (FRANCE).
A fifteen years lifetime mechanism for an infrared Earth sensor p 2362 N94-24040

SOCIETE D'APPLICATIONS GENERALES D'ELECTRICITE ET DE MECANIQUE, CERGY-PONTOISE (FRANCE).
An Earth observation telescope refocusing mechanism
p 2359 N94-24014

SOCIETE D'APPLICATIONS GENERALES D'ELECTRICITE ET DE MECANIQUE, PARIS (FRANCE).
Rover: Autonomous concepts for Mars exploration
p 2369 N94-23400

SOCIETE EUROPEENNE DE PROPULSION, SAINT-MEDARD-EN-JALLES (FRANCE).
Ceramic matrix composite parts design
p 2256 N94-24237

SOCIETE GENERALE DE CONSTRUCTIONS ELECTRIQUES ET MECANIQUES ALSTHOM, MASSY (FRANCE).
Rover: Autonomous concepts for Mars exploration
p 2369 N94-23400

SOCIETE NATIONALE INDUSTRIELLE AEROSPATIALE, PARIS (FRANCE).
Internal combustion engine with a central crankshaft and integral tandem annular pistons
[CA-PATENT-1-320-878] p 2363 N94-24055

SOFTWARE KINETICS LTD., STITTSVILLE (ONTARIO).
ACES spectral display software: Software description
[SK-1600-99-003] p 2455 N94-24297

SOFTWARE PRODUCTIVITY CONSORTIUM, HERNDON, VA.
Reuse-Driven Software Processes Guidebook, version 02.00.03
[AD-A273644] p 2461 N94-25148
Reuse Adoption Guidebook, version 02.00.05
[AD-A273652] p 2461 N94-25149

SOLAR PHYSICS RESEARCH CORP., TUCSON, AZ.
Solar magnetic cycle
[NASA-CR-195202] p 2628 N94-25275

SOREQ RESEARCH ESTABLISHMENT, ISRAEL ATOMIC ENERGY COMMISSION, YAVNEH.
Burning rate of double-base propellant in the presence of plasma p 2155 N94-24252

SOURIAU, PARAY (FRANCE).
Connector mechanisms in compliance with extreme space conditions p 2360 N94-24025

SOUTH CAROLINA UNIV., COLUMBIA.
Wavelet multiresolution analyses adapted for the fast solution of boundary value ordinary differential equations
p 2485 N94-23691
Basaltic Volcanism and Ancient Planetary Crusts
[NASA-CR-193151] p 2614 N94-24363
Highland crust at the Apollo 14 site: A review
p 2614 N94-24364
Major element chemistry of Apollo 14 mare basalt clasts and highland plutonic clasts from lunar breccia 14321: Comparison with neutron activation results
p 2614 N94-24366
Auto-metasomatism of the western lunar highlands: Result of closed system fractionation and mobilization of a KREEPy trapped liquid p 2615 N94-24367
Polytopic vector analysis in igneous petrology: Application to lunar petrogenesis p 2615 N94-24368
The western highland province at the Apollo 14 site
p 2615 N94-24369
Lunar mare volcanism: Mixing of distinct, mantle source regions with KREEP-like component
p 2615 N94-24370
A dynamic melting model for the origin of Apollo 15 olivine-normative and quartz-normative mare basalts
p 2615 N94-24371
Melt rock components in KREEPy breccia 15205: Petrography and mineral chemistry of KREEP basalts and quartz-normative mare basalts p 2616 N94-24372
Synthesis of soluble halogenated polyphenylenes: Mechanism for the coupling halogenated lithiobenzenes
[AD-A273547] p 2257 N94-24558
Metal-catalyzed alkynylation of brominated polyphenylenes: Thermoset precursors of high density monolithic glassy carbon
[AD-A273232] p 2259 N94-24789
Electrochemical and electronic properties of neural and oxidized soluble orthogonally-fused thiophene oligomers
[AD-A273283] p 2260 N94-24815
Metal-catalyzed alkynylation of (Bromophenyl)Oligophenylenes: A rapid route to thermoset precursors of high density monolithic glass-like carbon
[AD-A273219] p 2260 N94-24863
Planar poly(p-phenylene) derivatives: Ladder formation for maximization of extended conjugation
[AD-A273220] p 2260 N94-24922
Synthesis of polyphenylenes via Bergman cyclization of enediyne monomers
[AD-A273298] p 2260 N94-24924
Potent solvents for C60 and their utility for the rapid acquisition of 13CNMR data for fullerenes
[AD-A273349] p 2235 N94-24925
Synthesis of molecular wires by a novel divergent/convergent approach
[AD-A273332] p 2537 N94-25087
Dispersion of Rh/Cu in a sol-gel matrix. Highly chemo- and stereoselective catalyst for the reduction of alkynes to Z-alkenes
[AD-A273306] p 2262 N94-25145

SOUTH DAKOTA SCHOOL OF MINES AND TECHNOLOGY, RAPID CITY.
Further studies to extend and test the area-time-integral technique applied to satellite data
[NASA-CR-195132] p 2415 N94-24705

SOUTHAMPTON UNIV. (ENGLAND).
A modelling of the noise from simple co-axial jets. Part 2: In a simulated flightstream
[ISVR-TR-226] p 2525 N94-22959
Spacecraft vibrations due to mechanisms; measurements from Olympus on-station
p 2207 N94-24018
Vibrational power transmission analysis of machinery installations in ships with the objective of noise reduction
[ISVR-TR-216] p 2363 N94-24076

SOUTHEASTERN OKLAHOMA STATE UNIV., DURANT.
Software engineering methodologies and tools
p 2465 N94-25382

SOUTHERN METHODIST UNIV., DALLAS, TX.
Tectonic Evolution of Mars
[NASA-CR-194714] p 2623 N94-24996
The geophysical signal of the martian global dichotomy p 2623 N94-24997

SOUTHERN VITAL RECORDS CENTER, INC., FLORA, MS.
A prototype to automate the video subsystem routing for the video distribution subsystem of Space Station Freedom p 2306 N94-25353

SOUTHWEST RESEARCH INST., SAN ANTONIO, TX.
PULSAUR 2
[NASA-CR-194832] p 2209 N94-23484
SO2 on Venus: A final cross-calibration with Pioneer Venus
[NASA-CR-195162] p 2599 N94-24988

SPACE APPLICATIONS SERVICES, BRUSSELS (BELGIUM).
Columbus system support for telescience operations
p 2505 N94-23877

SPACE ENGINEERING, ROME (ITALY).
A European mobile satellite system concept exploiting CDMA and OBP p 2279 N94-22768

SPACE FOUNDATION, COLORADO SPRINGS, CO.
Space technology: A study of the significance of recognition for innovators of spinoff technologies. 1993 activities/1994, 1995 plans
[NASA-CR-194836] p 2596 N94-23526
Space technology: A study of the significance of recognition for innovators of spinoff technologies. Commercial Space Expo-USA, 1993
[NASA-CR-194833] p 2596 N94-23528
Prototype Space Technology Hall of Fame exhibit at Technology 2003: Analysis of data from computer-based questionaire
[NASA-CR-194834] p 2596 N94-23540
Space Technology: A study of the significance of recognition for innovators of spinoff technologies. A case study on the impact of the space technology hall of fame award
[NASA-CR-194835] p 2597 N94-24496
The Ninth National Space Symposium
[ISBN-0-9616962-7-3] p 2598 N94-25006

SPACE PHYSICS RESEARCH INST., SUNNYVALE, CA.
Analyzing Martian winds and tracer concentrations using Mars Observer data p 2619 N94-24883

SPAR AEROSPACE LTD., SAINTE-ANNE-DE-BELLEVUE (QUEBEC).
A system architecture for an advanced Canadian wideband mobile satellite system p 2278 N94-22766
The down, release, and deployment of the RADARSAT SAR antenna p 2305 N94-23986

SRI INTERNATIONAL CORP., MENLO PARK, CA.
Formal methods and digital systems validation for airborne systems
[NASA-CR-4551] p 2466 N94-23293
Development of durable high-temperature catalysts for natural gas combustion
[PB93-226447] p 2232 N94-23477
SALI chemical analysis of provided samples
[NASA-CR-194138] p 2232 N94-23524
In vitro system for studying metabolism of environmental chemicals in human cells
[AD-A273427] p 2421 N94-24688

STANFORD LINEAR ACCELERATOR CENTER, CA.
Progress on the design of a data push architecture for an array of optimized time tagging pixels
[DE93-041011] p 2307 N94-22955
Photon-photon collisions at the next linear collider: Theory
[DE93-041025] p 2534 N94-23803

STANFORD UNIV., CA.
A pressurized thermogravimetric analyzer for use in studies of gas/solid systems
[DE94-001224] p 2342 N94-22989
Computer assisted analysis of auroral images obtained from high altitude polar satellites
[NASA-CR-194873] p 2400 N94-23084
AstroMail: Electronic mail for the astrophysics community
[NASA-CR-194877] p 2591 N94-24099
Annual research briefs, 1993
[NASA-CR-194755] p 2327 N94-24138
Optimal feedback control of turbulent channel flow
p 2327 N94-24139
Drag reduction at a plane wall p 2327 N94-24140
Boundary layer receptivity and control
p 2327 N94-24141
Toward modeling wingtip vortices
p 2171 N94-24142
New concepts for Reynolds stress transport equation modeling of inhomogeneous flows p 2171 N94-24143
Large eddy simulation of a boundary layer with concave streamwise curvature p 2328 N94-24146
Toward large eddy simulation of turbulent flow over an airfoil p 2172 N94-24150
Unstructured grid large eddy simulation of wall bounded turbulent flows p 2329 N94-24151
Numerical simulation of non-Newtonian free shear flows p 2331 N94-24160
Direct simulation of isothermal-wall supersonic channel flow p 2172 N94-24164
Effects of shock strength on shock turbulence interaction p 2332 N94-24165
Change-point detection and adaptive control of time-varying systems
[AD-A273509] p 2475 N94-24943
High precision x ray lithographic masks
[AD-A273342] p 2346 N94-25154

STARSYS RESEARCH CORP., BOULDER, CO.
Metal band drives in spacecraft mechanisms
p 2355 N94-23987

STATCOM, INC., MCLEAN, VA.
Computerized testing system software conversion and development: Identifying software and hardware portability issues and solutions
[AD-A273489] p 2462 N94-25287

STATE AGRICULTURAL UNIV., WAGENINGEN (NETHERLANDS).
Urban/rural application of weather radar for flow forecasting. Proceedings of the Informal CEc -Workshop
[PB93-220135] p 2407 N94-23129

STATE UNIV. OF NEW YORK, ALBANY.
Observational case studies and diagnostic analyses of long-lived large-amplitude inertia-gravity waves
[AD-A273545] p 2404 N94-24794

STATE UNIV. OF NEW YORK, ALFRED.
Combustion synthesis and engineering of nanoparticles for electronic, structural and superconductor applications
[DE94-001865] p 2254 N94-23720

STATE UNIV. OF NEW YORK, BUFFALO.
Hairy carbon electrodes studied by cyclic voltammetry and battery discharge testing p 2394 N94-23367
Vortical structure in a forced plane mixing layer
p 2331 N94-24162
LES, DNS and RANS for the analysis of high-speed turbulent reacting flows
[NASA-CR-195196] p 2337 N94-25094

STATE UNIV. OF NEW YORK, STONY BROOK.
A large eddy simulation scheme for turbulent reacting flows p 2330 N94-24154

STERNBERG ASTRONOMICAL INST., MOSCOW (USSR).
The morphology of the lunar surface parts in the region of work of the mobile geological laboratory vehicle in Mare Imbrium p 2607 N94-23385

STOCKTON STATE COLL., POMONA, NJ.
A geochemical study of acapulcoite and lodranite meteorites p 2605 N94-25358

SURREY UNIV., GUILDFORD (ENGLAND).
Interworking and integration of the Inmarsat Standard-M with Pan-European GSM system p 2277 N94-22759
A high quality voice coder with integrated echo canceller and voice activity detector for mobile satellite applications p 2286 N94-22812

SVERDRUP TECHNOLOGY, INC., BROOK PARK, OH.
Advanced space propulsion concepts
p 2216 N94-23067
Simplified, inverse, ejector design tool
[NASA-CR-194438] p 2166 N94-23511
Unsteady jet flow computation towards noise prediction
[NASA-CR-194449] p 2153 N94-23553
Low power ground-based laser illumination for electric propulsion applications
[NASA-CR-194444] p 2219 N94-23555
A comparison of two multi-variable integrator windup protection schemes
[NASA-CR-194436] p 2190 N94-23590
A review of wiring system safety in space power systems
[NASA-CR-194439] p 2203 N94-23632
Convection equation modeling: A non-iterative direct matrix solution algorithm for use with SINDA
p 2323 N94-23651
Stationary plasma thruster plume characteristics
[NASA-CR-194454] p 2219 N94-24361
Numerical simulation of cylindrical, self-field MPD thrusters with multiple propellants
[NASA-CR-194458] p 2220 N94-24714
Comparative M-H characteristics of 1-5 and 2-17 type samarium-cobalt permanent magnets to 300 C
[NASA-CR-194440] p 2312 N94-24870
Analytical skin friction and heat transfer formula for compressible internal flows
[NASA-CR-191185] p 2170 N94-25173
Effect of power system technology and mission requirements on high altitude long endurance aircraft
[NASA-CR-194455] p 2189 N94-25200

SVERDRUP TECHNOLOGY, INC., HUNTSVILLE, AL.
Features of a SINDA/FLUINT model of a liquid oxygen supply line p 2322 N94-23649
Microbiological analysis of debris from Space Transportation System (STS)-55 Spacelab D-2
[NASA-CR-193883] p 2421 N94-24310

SWARTHMORE COLL., PA.
The three-dimensional structure of the infrared cirrus
[NASA-CR-194870] p 2410 N94-24097

SWEDISH INST. FOR MATERIALS TESTING, BORAS.
Variable amplitude fatigue, modelling and testing
[PB93-204469] p 2376 N94-24742

SWISS CENTER FOR ELECTRONICS AND MICROTECHNOLOGY, INC., NEUCHATEL.
Electronic payloads for Martian missions: A preliminary assessment of technologies p 2610 N94-23408
New tribocoating combination for vacuum operation
p 2355 N94-23990
New pin-on-disk equipment for vacuum tribometry
p 2360 N94-24023

SYNETICS CORP., WAKEFIELD, MA.
Worldwide vessel locating and tracking system, volume 1
[PB93-193217] p 2175 N94-24474

T

TALLINN POLYTECHNIC INST. (USSR).
Lectures on magnetohydrodynamical drives
[PB93-224962] p 2308 N94-23104

TARRANT COUNTY JUNIOR COLL., FORT WORTH, TX.
Modeling and analysis of selected space station communications and tracking subsystems
p 2306 N94-25374

TAYLOR (LESLIE A.) ASSOCIATES, BETHESDA, MD.
Use of negotiated rulemaking in developing technical rules for low-Earth orbit mobile satellite systems
p 2276 N94-22750

TECHNICAL RESEARCH CENTRE OF FINLAND, ESPOO.
Open EDI
[VTT-TIED-1353] p 2588 N94-22734
Periscope mechanism for SWAN instrument
p 2357 N94-24000
Solid state synthesis of Fe-B-Si alloys
[VTT-PUBS-118] p 2250 N94-25316
Use of scanning tunneling microscope in corrosion studies
[VTT-TIED-1416] p 2250 N94-25346
Dual-purpose RTOF diffractometer facility at the ET-RR-1 reactor
[VTT-TIED-1425] p 2566 N94-25347
Constitutive modelling of fiber-reinforced concrete under uniaxial tensile loading
[VTT-JULK-774] p 2379 N94-25385
Alternatives for reinforcement: Fiber composites
[VTT-TIED-1412] p 2230 N94-25386
Hydride thermodynamic machines
[VTT-JULK-768] p 2571 N94-25416
Metal hydride storage
[VTT-JULK-769] p 2396 N94-25417
Strength and life of pressure vessels subjected to impacts and thermomechanical GFRP loading
[VTT-JULK-771] p 2379 N94-25418
Weldability of Accelerated-Cooled (AcC) high strength TMCP steel X80
[VTT-TIED-1413] p 2251 N94-25419
Composites and textile reinforcement
[VTT-TIED-1424] p 2231 N94-25420
Frost effects on the microstructure of high strength concrete, and methods for their analysis
[VTT-PUBS-126] p 2379 N94-25529

TECHNICAL UNIV. OF DENMARK, LYNGBY.
Reburning rich-lean kinetics
[PB93-220887] p 2232 N94-23100

TECHNION - ISRAEL INST. OF TECH., HAIFA.
Enhanced absorption cycle computer model
[DE94-001997] p 2271 N94-23793
Stability of hypersonic flow of a detonable gas mixture in the stagnation region of a blunt body and a forward facing step p 2154 N94-24248
Thrust vectoring theory, laboratory and flight tests
p 2155 N94-24251
Design considerations of hybrid rockets
p 2156 N94-24254
Satellite autonomous navigation and orbit determination using magnetometers p 2156 N94-24258
Decentralized autonomous attitude determination using an inertially stabilized payload p 2157 N94-24264
Maximum likelihood modal parameter identification and realization of stochastic systems p 2157 N94-24265
Failure-proof estimation under conditions of lack of information p 2158 N94-24267
Modelling the ignition of boron/titanium particles
p 2159 N94-24273
On the stability of the process of formation of combustion generated particles by coagulation and simultaneous shrinkage due to particle oxidation p 2159 N94-24274
Experimental investigation of ignition of boron/titanium composite particles p 2159 N94-24275
Mean stress models for low cycle fatigue of a nickel-base superalloy p 2159 N94-24276
Vibrations of variable cross section Timoshenko beams p 2160 N94-24279
Global dynamic stability of a shallow arch by poincare-like simple cell mapping p 2160 N94-24280
Inverse dynamics of a rigid rod system as a simplified model of flexible beam p 2160 N94-24281
Transient phenomena in laminar spray combustion
p 2160 N94-24282
Effect of initial droplet-size distributions on fuel-vapor profiles in a shear-layer flow p 2160 N94-24283

Multiple flames in counterflow spray combustion p 2161 N94-24284
The influence of elastic pitch variations on helicopter flight mechanics p 2161 N94-24286
Continuous gust response and sensitivity derivatives using state-space models p 2161 N94-24287
TECHNISCHE HOCHSCHULE, AACHEN (GERMANY).
Measurement of kinematically unstationary separated flows p 2315 N94-22854
TECHNISCHE HOGESCHOOL, DELFT (NETHERLANDS).
Nested Krylov methods and preserving the orthogonality p 2483 N94-23681
TECHNISCHE HOGESCHOOL, TWENTE (NETHERLANDS).
Compressible turbulent flow simulation with a multigrid multiblock method p 2342 N94-23694
TECHNISCHE HOGESCHOOL TWENTE, ENSCHEDE (NETHERLANDS).
Relational algebra and equational proofs [PB94-110822] p 2486 N94-23724
Multi-set extended relational algebra: A formal approach to a practical issue [PB94-110830] p 2486 N94-23725
Mean-value of product-form stochastic Petri net models of slotted-ring systems [PB94-110871] p 2494 N94-23749
Micro SIL-1 simulator [PB94-110889] p 2454 N94-23750
Advanced design concepts for open distributed systems development [PB94-110897] p 2454 N94-23751
Design and implementation issues of end-to-end protocols in high-speed networks [PB94-110905] p 2467 N94-23752
Non-trivial examples of real isolated singularity at the origin [PB94-110939] p 2487 N94-23787
Concepts and techniques for an active database approach to office procedure support [PB94-110749] p 2590 N94-23816
TECHNISCHE PHYSISCHE DIENST TNO-TH, DELFT (NETHERLANDS).
The pre-development of the Aristoteles calibration mechanism p 2209 N94-24006
TECHNISCHE UNIV., BERLIN (GERMANY).
Experimental Methods in Separated Flows [ILR-MITT-260(1991)] p 2315 N94-22852
Pressure oscillation measurements in turbulent flows p 2316 N94-22855
The use of near-wall hot-wire probes for time-resolved skin-friction measurements p 2316 N94-22857
Image processing for acquisition of fluid rest time in the running of an artificial heart valve p 2316 N94-22858
Rail Corrugations [ILR-BER-59] p 2269 N94-23581
A linear model for corrugation and its limit of validity p 2269 N94-23584
Wear characteristics of technical dry rolling/sliding systems with relations to corrugation problems p 2269 N94-23586
Surface analysis of corrugated rail treads p 2270 N94-23587
Contact analysis of rough rail surfaces p 2270 N94-23589
TECHNISCHE UNIV., BRUNSWICK (GERMANY).
Lateral high frequency oscillations and stability of a wheel rolling on a flexible track p 2269 N94-23585
TECHNISCHE UNIV., DELFT (NETHERLANDS).
Plan generation for flexible assembly systems [PB93-217974] p 2267 N94-22981
Particle formation in a laser-heated aerosol reactor. Application to silicon and silicon nitride synthesis [PB93-217982] p 2347 N94-22982
Integrated hydrometallurgical jarosite treatment [PB93-217990] p 2232 N94-22983
Shell buckling research at Delft, 1976 - 1992 [PB93-224442] p 2375 N94-23221
Diffraction analysis of transient acoustic waves: Half-plane in a layered medium [PB94-110988] p 2526 N94-23726
Compatibility relations and the finite-element formulation of electromagnetic field problems [PB94-110996] p 2294 N94-23727
Study of a local absorbing boundary condition for the modeling of an infinite external domain in the time-domain finite-element package FEMAXT [PB94-111002] p 2294 N94-23728
Electromagnetic scattering by inhomogeneous objects. Solution methods based upon reciprocity theorems of time-convolution and time-correlation type [PB94-111010] p 2294 N94-23729
Similarity in wave propagation under a global relaxation law [PB94-111028] p 2524 N94-23730
Analysis of time-domain acoustic wavefields in horizontally continuously layered configurations based on the modified Cagniard method [PB94-111044] p 2524 N94-23731
Analysis for the computational modeling of finite cladding and lossy coating effects in fibers [PB94-111085] p 2544 N94-23732
FEMAX finite-element package for computing three-dimensional time-domain electromagnetic fields in inhomogeneous media [PB94-111093] p 2294 N94-23733
Efficient interpolation of velocity and flux components defined on 2- and 3-dimensional non-cartesian grids [PB94-118619] p 2486 N94-23757
Logarithm of probability measures and infinite divisibility of sub-stable random vectors [PB94-118627] p 2486 N94-23758
Reaction of isocyanates with carboxylic acids and its application to polymer synthesis [PB94-118858] p 2254 N94-23763
Particle size measurement for the control of industrial crystallizers [PB94-119104] p 2562 N94-23766
Polynomials orthogonal with respect to an inner product involving differences [PB94-110731] p 2489 N94-24572
Time-domain analysis of conduction and displacement current distributions in inhomogeneous and anisotropic layered media [PB94-111036] p 2403 N94-24592
Edge elements, their advantages and disadvantages [PB94-111069] p 2298 N94-24593
Finite-element modelling of three-dimensional electromagnetic fields using edge and nodal elements [PB94-111077] p 2298 N94-24597
Hydraulics and morphology of mountain rivers: A literature survey. Communications on hydraulic and geotechnical engineering [PB94-110772] p 2388 N94-24636
Finite-element method for computing three-dimensional electromagnetic fields in inhomogeneous media (1993) [PB94-111101] p 2298 N94-24637
Solution of the discretized incompressible Navier-Stokes equations with iterative methods [PB94-118635] p 2335 N94-24641
World processor: An interface for textual display and manipulation in virtual reality [PB94-118643] p 2592 N94-24642
Stability analysis of anisotropic conical shells [PB94-119054] p 2377 N94-24645
RITL: An information system for application reuse-in-the-large [PB94-119088] p 2592 N94-24646
Near-surface seismic imaging [PB94-119096] p 2404 N94-24647
Pre-design study of a general purpose vehicle simulator platform [PB93-215366] p 2193 N94-24739
Buckling of circular cylindrical shells subjected to combined loads (axial compression, normal pressure, bending and transverse shear loading) [PB93-215358] p 2378 N94-24745
Mechanisms of droplet formation [ISBN-9-06-275765-0] p 2338 N94-25227
Microscopic dynamics in dense helium-neon mixtures: Neutron scattering, kinetic theory and computer simulations [ISBN-9-07-386105-5] p 2537 N94-25228
Downward extrapolation of multi-component seismic data [ISBN-9-09-005213-5] p 2405 N94-25229
Decomposition of multi-component measurements into P and S waves [ISBN-9-09-005197-X] p 2405 N94-25251
On chain coding of line drawings [ISBN-9-06-275778-2] p 2462 N94-25252
On the characterization and optimization of high-speed silicon bipolar transistors [ETN-94-95367] p 2313 N94-25253
Hydrodynamics of stirred gas-liquid dispersions [ETN-94-95368] p 2339 N94-25254
Mesoscopic phenomena in metallic point contacts [ETN-94-95371] p 2313 N94-25286
Coherent structures over grooved surfaces [ETN-94-95308] p 2339 N94-25291
TECHNISCHE UNIV., EINDHOVEN (NETHERLANDS).
Algorithms for speech coding systems based on linear prediction [EUT-92-E-260] p 2447 N94-22731
Electromagnetic field strength prediction in an urban environment: A useful tool for the planning of LMSS p 2283 N94-22795
Identification for robust control using an H(sub infinity) norm [EUT-92-E-261] p 2470 N94-22873
Laser linewidth measurement in the presence of RIN and using the recirculating self heterodyne method [EUT-92-E-262] p 2347 N94-22874
Rigorous analysis of thick microstrip antennas and wire antennas embedded in a substrate [EUT-92-E-263] p 2290 N94-22876
The adaptive resonance theory network: (Clustering-) behaviour in relation with brainstem auditory evoked potential patterns [EUT-92-E-264] p 2470 N94-22877
Multidisciplinary specification and design of microelectronics in products [EUT-93-E-269] p 2308 N94-23136
On the asymptotically uniform distribution modulo 1 of extreme order statistics [MEMO-COSOR-91-38-REV] p 2493 N94-23142
On non-informativeness in a classical Bayesian inference problem [MEMO-COSOR-92-35] p 2494 N94-23143
A mixed H2/H(infinity) function for a discrete time system [MEMO-COSOR-92-33] p 2480 N94-23144
Manufacturing and characterization of GaAs/AlGaAs multiple quantumwell ridge waveguide lasers [EUT-92-E-265] p 2348 N94-23168
Using genetic algorithms for scheduling data flow graphs [EUT-92-E-266] p 2449 N94-23169
A method for the general simultaneous full decomposition of sequential machines: Algorithms and implementation [EUT-92-E-267] p 2445 N94-23170
An optical ASK and FSK phase diversity transmission system [EUT-92-E-268] p 2542 N94-23171
PROGRIL: A language for the definition of protocol grammars [EUT-93-E-270] p 2449 N94-23172
Code generation for the attribute evaluator of the protocol engine grammar processor unit [EUT-93-E-271] p 2450 N94-23173
Flue gas cleaning by pulse corona streamer [EUT-93-E-272] p 2268 N94-23174
Note on the use of spherical vectorfields in Clifford analysis [PB93-237667] p 2480 N94-23437
Mathematical addenda to Hopper's model of plane stokes flow driven by capillarity on a free surface [PB93-237691] p 2480 N94-23438
Stability behavior of systems obtained by index-reduction [PB93-237709] p 2481 N94-23439
Limiting distribution of fractional parts of extreme order statistics [PB93-237733] p 2494 N94-23440
Linear time algorithm to schedule trees with communication delays optimally on two machines [PB93-237782] p 2451 N94-23441
Characterizations of shift-invariant distributions based on summation modulo one [PB93-237824] p 2481 N94-23442
Differential algebraic equations [PB93-237618] p 2481 N94-23455
Bayesian decision theory with imprecise prior probabilities applied to replacement problems [PB93-237634] p 2481 N94-23456
Systems engineering: A formal approach. Part 1: System concepts [PB93-225308] p 2268 N94-23476
Subset selection for the best of two populations: Tables of the expected subset size [PB93-237857] p 2494 N94-23546
Preemptive scheduling in a two-stage multiprocessor flow shop is Np-hard [PB94-111648] p 2467 N94-23756
Three, four, five, six or the complexity of scheduling with communication delays [PB94-111630] p 2467 N94-23767
Exercises in multiprogramming [PB94-101458] p 2454 N94-23768
Review of a variational method applied to magnetoelastic buckling problems [PB94-111184] p 2562 N94-23769
Maximal type test statistics based on conditional processes [PB94-111614] p 2494 N94-23771
Decision making with imprecise probabilities [PB94-111622] p 2494 N94-23772
Asymptotic confidence intervals for the length of the shortt under random censoring [PB93-237816] p 2494 N94-23774
Subset selection with a generalized selection goal based on a loss function [PB94-111192] p 2494 N94-23798
Some generalized subset selection procedures [PB94-111655] p 2487 N94-23799

Infinite divisible and stable distributions modulo 1
[PB94-110640] p 2495 N94-23815
Typechecker for bijective pure type systems
[PB94-110814] p 2454 N94-23817
Systems engineering: A formal approach. Part 4: Analysis methods
[PB94-101417] p 2271 N94-24475
Tail processes under heavy random censorship with applications
[PB94-110632] p 2495 N94-24508
Systems engineering: A formal approach. Part 3: Modeling methods
[PB94-101409] p 2456 N94-24513
Sequential composition, action prefixes and process prefix
[PB94-101433] p 2488 N94-24539
Real-time process logic
[PB94-101441] p 2446 N94-24540
Discrete-time H(infinity) control problem with strictly proper measurement feedback
[NASA-CR-195089] p 2473 N94-24542
Probabilistic methods in problems of applied analysis
[PB94-110681] p 2495 N94-24571
Conservation equations for reacting gas flow
[PB94-111168] p 2334 N94-24574
Some maximality results for effect-valued measures
[PB94-111176] p 2569 N94-24575
Squaring-down and the problems of almost-zeros for continuous-time systems
[PB93-237758] p 2489 N94-24608
Discrete time minimum entropy H(infinity) control problem
[PB93-237808] p 2474 N94-24609
Systems engineering: A formal approach. Part 2: Frameworks
[PB94-101391] p 2489 N94-24615
Controlled invariance of nonlinear systems: Nonexact forms speak louder than exact forms
[PB93-237790] p 2475 N94-24755
BEM solution for the simulation of axisymmetric viscous sintering
[PB93-237717] p 2336 N94-24761
Genericity of stabilizability for time-delay systems
[PB93-237725] p 2475 N94-24762
Efficiency of subset selection of an epsilon-best uniform population relative to selection of the best one
[PB93-237741] p 2490 N94-24763
Sensitivity analysis of list scheduling heuristics
[PB93-237766] p 2468 N94-24764
Class of strong valid inequalities for the discrete iot-sizing and scheduling problem
[PB93-237774] p 2459 N94-24765
Characteristic method for one-dimensional scalar hyperbolic conservation laws with stiff source terms
[PB93-237675] p 2491 N94-24954
Quantum tunneling transport of electrons in double-barrier heterostructures: Theory and modeling
[ETN-94-95332] p 2565 N94-25059
The influence of flow type, particle type and gravity on orthokinetic coagulation
[ETN-94-95333] p 2267 N94-25060
Generalized linear mixed models and their application in plant breeding research
[ETN-94-95335] p 2460 N94-25061
The design of the EMPS multiprocessor executive for distributed computing
[ETN-94-95336] p 2468 N94-25062
Binary block codes for correcting asymmetric or unidirectional errors
[ETN-94-95337] p 2460 N94-25063
The increase of the controllability of production organizations
[ISBN-9-03-860161-1] p 2586 N94-25076
Psychophysical and signal-processing aspects of speech representation
[ETN-94-95292] p 2302 N94-25077
The measurement of the film thickness and the roughness deformation of lubricated elastomers
[ETN-94-95293] p 2261 N94-25078
Algebraic-geometric codes and their decoding algorithms
[ETN-94-95294] p 2491 N94-25079
Area-power-delay trade-off in logic synthesis
[ISBN-9-09-005332-8] p 2461 N94-25080
Special signature schemes
[ETN-94-95296] p 2446 N94-25081
Computer simulation of low energy scattering
[ETN-94-95326] p 2537 N94-25082
PLANET: A hierarchical network simulator
[ISBN-9-09-005693-9] p 2313 N94-25083
The reaction mechanism of W-CVD in Si
[ETN-94-95329] p 2261 N94-25084
The evolution of the laser: A systems perspective on science, technology and society
[ETN-94-95319] p 2351 N94-25218
Understanding and facilitating discovery learning in computer-based simulation environment
[ISBN-9-03-860242-1] p 2462 N94-25219
Some subjects in digital audio, noise shaping, sample rate conversion, dynamic range compression and testing
[ISBN-9-09-005162-7] p 2530 N94-25220
Multiprocessor scheduling with communication delays
[ETN-94-95346] p 2468 N94-25221
The nanostructure of multilayered films: A NMR study
[ETN-94-95347] p 2262 N94-25222
Soil pollution at former industrial sites, the heritage of 150 years of industrial development in Noord-Brabant, The Netherlands
[ISBN-9-09-005758-7] p 2400 N94-25223
Practical evaluation of robust control for a class of nonlinear mechanical dynamic systems
[ISBN-9-03-860092-5] p 2475 N94-25224
Microstructure of styrene methyl methacrylate copolymers grafted onto polybutadiene seeds
[ETN-94-95360] p 2262 N94-25225
Models of trace theory systems
[ETN-94-95361] p 2468 N94-25226
Electrophoresis in open capillaries: Some fundamental aspects
[ETN-94-95290] p 2236 N94-25232
Capillary electrophoresis of biomolecules: Theory, instrumentation and applications
[ETN-94-95297] p 2236 N94-25233
On the quality of synthetic speech evaluation and improvements
[ETN-94-95298] p 2304 N94-25234
Production control and demand management in capacitated flow process industries
[ISBN-9-03-860211-1] p 2586 N94-25235
Particle nucleation and growth in butadiene emulsion polymerization
[ETN-94-95300] p 2262 N94-25236
Designs with a small number of runs for factorial experiments
[ISBN-9-03-860162-X] p 2462 N94-25237
On the mechanism of action of 3',5'-cyclic adenosine monophosphate: A study of four- and five-coordinated phosphorus compounds, modelling the activated state of cAMP
[ISBN-9-03-860222-7] p 2226 N94-25238
Ultracold atoms in traps and fountains
[ETN-94-95325] p 2537 N94-25239
Intramultiplet mixing for Ne(**)(3p)+He at superthermal energies
[ETN-94-95327] p 2538 N94-25240
Excitation balances and transport in an inductively coupled plasma
[ETN-94-95330] p 2554 N94-25241
Metallic multilayers: Experimental investigation of magnetic anisotropy and magnetic interlayer coupling
[ETN-94-95364] p 2250 N94-25242
The hydrodynamics of a moving fluid-liquid contact line
[ETN-94-95352] p 2339 N94-25247
Decay of swirl in turbulent pipe flows
[ETN-94-95353] p 2339 N94-25248
Design of gas bearing systems for precision applications
[ISBN-9-03-860112-3] p 2367 N94-25249
The structure and catalytic properties of supported platinum catalysts
[ETN-94-95357] p 2236 N94-25250
Wind climate and urban geometry
[ISBN-9-03-860132-8] p 2416 N94-25261
MIMO system identification for H(infinity) robust control: A frequency domain approach with minimum error bounds
[ETN-94-95354] p 2476 N94-25262
From circuit to signal: Development of a piecewise linear simulator
[ISBN-9-09-005713-7] p 2462 N94-25263
Introduction to a behavioral approach for continuous time systems
[ETN-94-95301] p 2492 N94-25277
Designing parallel programs of parameterized granularity
[ETN-94-95302] p 2468 N94-25278
Relevant costs or full costs? Explaining why managers use capacity cost allocations for short term decisions
[ISBN-9-06-215364-X] p 2587 N94-25279
Tunnelling in metallic contacts on high-T(c) superconductors: A story of charge carriers in YBa2Cu3O(7-delta) and Bi2CaSr2Cu2O(8+delta)
[ISBN-9-03-860142-5] p 2565 N94-25280
Preparation and properties of translucent gamma-aluminium oxynitride
[ETN-94-95305] p 2263 N94-25281
A design method for parallel programs
[ETN-94-95331] p 2469 N94-25282
Throughput time control and due date reliability in tool and die shops
[ISBN-9-03-860182-4] p 2587 N94-25283
Modelling of premixed laminar flames
[ETN-94-95317] p 2236 N94-25284
A relativistic theory on wave propagation in inhomogeneous magnetoplasmas
[ETN-94-95322] p 2554 N94-25285
On the auditory discrimination of spectral shape
[ETN-94-95306] p 2530 N94-25289
Data structures and amortized complexity in a functional setting
[ETN-94-95307] p 2476 N94-25290
Coherent structures over grooved surfaces
[ETN-94-95308] p 2339 N94-25291
Linear and nonlinear adaptive filtering and their application to speech intelligibility enhancement
[ISBN-9-09-005342-5] p 2304 N94-25292
Timed coloured Petri nets and their application to logistics
[ETN-94-95310] p 2522 N94-25293
Laser ablation and deposition of metals
[ETN-94-95311] p 2351 N94-25294
Reliability analysis of a repairable dependent parallel system
[ETN-94-95312] p 2373 N94-25295
The electrochemistry of the solvated electron: A study of its properties and of its applications
[ETN-94-95313] p 2236 N94-25296
On the origin of 1/f noise in epitaxial GaAs
[ISBN-9-09-006067-7] p 2566 N94-25297
Luminance-brightness mapping: The missing decades
[ETN-94-95351] p 2428 N94-25298
Evaluation of multiaxial fracture models for technical ceramics
[ISBN-9-03-860192-1] p 2263 N94-25299
Modelling of thermal argon plasmas
[ETN-94-95363] p 2554 N94-25300
Drying deformable media: Kinetics, shrinkage and stresses
[ETN-94-95314] p 2236 N94-25302
Delay-insensitive communication
[ETN-94-95315] p 2304 N94-25303
The use of knowledge systems
[ETN-94-95318] p 2477 N94-25431
Plasma sprayed thermal barrier coatings: Production, characterization and testing
[ISBN-9-03-860082-8] p 2555 N94-25439
Application of body fitted-coordinates in heat conduction problems
[ETN-94-95338] p 2340 N94-25484
Product forms as a solution base for queueing systems
[MEMO-COSOR-92-37] p 2477 N94-25526
A reachability test for systems over polynomial rings using Groebner bases
[MEMO-COSOR-92-38] p 2493 N94-25527

TECHNISCHE UNIV., MUNICH (GERMANY).
Walking machines for space p 2369 N94-23406

TECHNISCHE UNIV., TWENTE (NETHERLANDS).
ACOS: The performance based approach to build a parallel complex object server
[PB93-223816] p 2465 N94-22986
Simple calculus of finite probabilistic processes
[PB93-223782] p 2493 N94-23108
The Third Twente Workshop on Graphs and Combinatorial Optimization
[PB94-110947] p 2486 N94-23722
Egalitarian non-average contribution method for cooperative games
[PB94-111705] p 2497 N94-23800
Reduced game properties of egalitarian division rules for cooperative games
[PB94-111689] p 2521 N94-24523
Tool sharing, part 3
[PB94-111697] p 2467 N94-24524
Investigation on interval edge-coloring of graphs
[PB94-110913] p 2488 N94-24541
What makes industries believe in formal methods
[PB94-110848] p 2272 N94-24648
Service description of communication systems supporting multi-media multi-user applications
[PB94-110855] p 2299 N94-24650
Criterion for some Hamiltonian graphs to be hamilton-connected
[PB94-110921] p 2489 N94-24651
The Third Twente Workshop on Graphs and Combinatorial Optimization: Abstracts and late extended abstracts
[PB94-110954] p 2489 N94-24652
Irreducible core of a minimum cost spanning tree game
[PB94-110962] p 2489 N94-24653
Correct and efficient interface for logical query languages with complex objects
[PB93-211175] p 2593 N94-24743

Validation activities for LOTOS based on static data flow analysis
[PB94-110863] p 2459 N94-24758

TECHNISCHER UERBERWACHUNGS-VEREIN RHEINLAND E.V., COLOGNE (GERMANY).
Security aspects of space operations data
p 2515 N94-23937

TECHNOLOGY SERVICE CORP., SANTA MONICA, CA.
The IRGen infrared data base modeler
p 2440 N94-25496
The Radar Image Generation (RIG) model
p 2306 N94-25497

TECHNOLOGY STRATEGIES AND ALLIANCES, MENLO PARK, CA.
Defense aerospace and the new world order
p 2596 N94-25066

TECNOSPAZIO S.P.A., MILAN (ITALY).
A system for the challenging task of collecting samples from a comet surface p 2358 N94-24007

TELDIX LUFTFAHRT-AUSRUESTUNGS G.M.B.H., HEIDELBERG (GERMANY).
The low noise momentum wheel MW-X: EM design and predicted properties p 2360 N94-24024

TELEDYNE BROWN ENGINEERING, HUNTSVILLE, AL.
Analysis of high vacuum systems using SINDA'85
p 2322 N94-23648

TELESAT CANADA, GLOUCESTER (ONTARIO).
The MSAT spacecraft of Telesat Mobile Inc.
p 2207 N94-22742

TELESAT MOBILE, INC., OTTAWA (ONTARIO).
Design and implementation considerations of a MSAT packet data network p 2280 N94-22778

TENNESSEE UNIV., KNOXVILLE.
Capillary electrokinetic separations with optical detection
[DE94-001639] p 2233 N94-23716
Synthesis and in-vivo detection of boronated compounds for use in BNCT
[DE94-001899] p 2233 N94-23780
Polymer morphologh p 2226 N94-24353
Infinitely divisible processes and their nonlinear functionals; a study of their structural, statistical and sample path properties and their prediction problems
[AD-A273468] p 2496 N94-25147

TEXAS A&I UNIV., KINGSVILLE.
Evaluation of the efficiency and fault density of software generated by code generators p 2465 N94-24445

TEXAS A&M UNIV., COLLEGE STATION.
Alloys for hydrogen storage in nickel/hydrogen and nickel/metal hydride batteries p 2391 N94-23353
Uncertainties in climate data sets
[NASA-CR-194848] p 2408 N94-23577
Convective organization in the Pacific ITCZ: Merging OLR, TOVS, and SSM/I information
[NASA-CR-194850] p 2408 N94-23619
Diagnostic budgets of analyzed and modelled tropical plumes
[NASA-CR-194853] p 2409 N94-23621
Thermohydrodynamic analysis of cryogenic liquid turbulent flow fluid film bearings
[NASA-CR-194869] p 2363 N94-24081
Computation of turbulent flows over backward and forward-facing steps using a near-wall Reynolds stress model p 2172 N94-24145
Neural network-based control using Lyapunov functions p 2477 N94-24433
Simulation of cryogenic turbopump annular seals
p 2371 N94-24440
A finite-element-based perturbation model for the rotordynamic analysis of shrouded pump impellers: Part 1: Model development and applications
[NASA-CR-193916] p 2366 N94-24998
A finite-element-based perturbation model for the rotordynamic analysis of shrouded pump impellers: Part 2: User's guide
[NASA-CR-193917] p 2366 N94-24999
Non-invasive optical detection of glucose in cell culture nutrient medium p 2422 N94-25357

TEXAS A&M UNIV., GALVESTON.
Unified approach for incompressible flows
p 2342 N94-25356

TEXAS SOUTHERN UNIV., HOUSTON.
Strategies for recruiting additional African Americans into the NASA JSC summer faculty fellows program
p 2585 N94-25362

TEXAS TECHNOLOGICAL UNIV., LUBBOCK.
Modelling the Shuttle Remote Manipulator System: Another flexible model p 2371 N94-25350

TEXAS UNIV., AUSTIN.
Conceptual design of a device to measure hand swelling in a micro-gravity environment
[NASA-CR-195509] p 2437 N94-24330
NASA project 1: Full-body dynamometer
[NASA-CR-195507] p 2438 N94-24331
Concepts and embodiment design of a reentry recumbent seating system for the NASA Space Shuttle
[NASA-CR-195504] p 2438 N94-24667
A small satellite design for deep space network testing and training
[NASA-CR-195526] p 2205 N94-24702
Design of a recumbent seating system
[NASA-CR-195503] p 2438 N94-24786
Design of orbital debris shields for oblique hypervelocity impact
[NASA-CR-195152] p 2205 N94-24828
Embodiment design for a multipropellant resistojet
[NASA-CR-195505] p 2221 N94-24834
Specification list and function structure for a full-body dynamometer to be used aboard Space Station Freedom
[NASA-CR-195508] p 2439 N94-24835
Preliminary design of a satellite observation system for Space Station Freedom
[NASA-CR-195514] p 2209 N94-24840
Extended duration lunar lander
[NASA-CR-195527] p 2206 N94-24916
Conceptual design of an astronaut hand anthropometry device
[NASA-CR-195490] p 2439 N94-24956
Design of a resistojet for Space Station Freedom
[NASA-CR-195506] p 2221 N94-24979
PERCIVAL mission to Mars
[NASA-CR-195541] p 2195 N94-24995

TEXAS UNIV., BROWNSVILLE.
The H(sub infinity) optimal controller design and reduction for the inertial hold mode of the attitude control system of the XTE spacecraft
[NASA-CR-195137] p 2366 N94-24846
Exploiting structure: Introduction and motivation
[NASA-CR-195136] p 2490 N94-24847

TEXAS UNIV., SAN ANTONIO.
Monoclonal antibodies directed against surface molecules of multicell spheroids
[NASA-CR-195102] p 2420 N94-23633

THARSYS (FRANCE).
The Mars 96 balloon guiderope: An autonomous system in extreme environment conditions p 2369 N94-23412

THIOKOL CORP., BRIGHAM CITY, UT.
Postflight hardware evaluation RSRM-29 (STS-54). Appendix D: Nozzle postfire data
[NASA-CR-193898] p 2199 N94-24057
Postflight hardware evaluation RSRM-29 (STS-54). Appendix C: Nozzle PFORs
[NASA-CR-193894] p 2219 N94-24064
Final postflight hardware evaluation report RSRM-32 (STS-57)
[NASA-CR-193903] p 2200 N94-24065
Postflight hardware evaluation RSRM-29 (STS-54). Appendix E: Insulation postfire data
[NASA-CR-193897] p 2200 N94-24067
Final postflight hardware evaluation report RSRM-28 (STS-53)
[NASA-CR-193902] p 2200 N94-24112
Flex bearing UUEC, volume 2
[NASA-CR-193901] p 2365 N94-24588
Postflight hardware evaluation (RSRM-29, STS-54)
[NASA-CR-193895] p 2201 N94-24802
Postflight hardware evaluation 360T021 (RSRM-21, STS-45), revision A
[NASA-CR-193904] p 2201 N94-24965
Postflight hardware evaluation RSRM-29 (STS-54). Case, seals, and joints PFORs, appendix B
[NASA-CR-193899] p 2367 N94-25020

TILBURG UNIV. (NETHERLANDS).
The p-ranks of Latin square graphs
[PB93-230498] p 2479 N94-23107
Temporal aggregation in a periodically integrated autoregressive process
[PB93-230480] p 2479 N94-23122
Algorithm on addition chains with restricted memory
[PB94-118692] p 2454 N94-23759
Coordinate-free interpretations of the optimal costs for Lq problems subject to implicit systems
[PB94-118700] p 2473 N94-23760
First order conditions for the maximum likelihood estimation of an exact ARMA model
[PB94-110533] p 2495 N94-23814
Simplicial variable dimension restart algorithm to find economic equilibria on the unit simplex using n(n+1) rays
[PB94-110541] p 2596 N94-24477
Verification and validation of models
[PB94-110566] p 2456 N94-24507
Uniform limit theorems for marked point processes
[PB94-118726] p 2488 N94-24526
Two-stage versus sequential sample-size determination in regression analysis of simulation experiments
[PB94-110558] p 2495 N94-24634

TOKUYAMA COLL. OF TECHNOLOGY (JAPAN).
Performance of inverse photoemission spectrometer with a new bandpass photon detector of narrow bandwidth and high sensitivity
[REPT-A-2659] p 2345 N94-24977

TOKYO ASTRONOMICAL OBSERVATORY, MITAKA (JAPAN).
The next Japanese solar satellite
p 2625 N94-22846

TOKYO INST. OF TECH. (JAPAN).
Dual rover concept for Mars exploration
p 2370 N94-23415
Laboratory detection of C5S by pulsed-discharge-nozzle Fourier-transform microwave spectroscopy
[JTN-94-80519] p 2235 N94-24984

TOKYO INST. OF TECH., YOKAHAMA (JAPAN).
Electromagnetic field changes as a precursory phenomena of earthquakes and volcanic eruptions
[REPT-157] p 2405 N94-24980

TOKYO UNIV. (JAPAN).
Magnetic properties of NdCo3 and its gamma phase hydride NdCo3H(4.1)
[REPT-A-2655] p 2567 N94-25412
Magnetic field-induced saddle point in GaAs/AlGaAs short period superlattices
[REPT-A-2656] p 2568 N94-25515

TOKYO UNIV., SAGAMIHARA (JAPAN).
Development/drilling test of auger boring machine on board Mars rover for Mars exploration
p 2369 N94-23402
Ground data system for Space Flyer Unit (SFU)
p 2207 N94-23860

TOKYO UNIV., TANASHI (JAPAN).
Kamiokande results on solar neutrinos and a supernova search
[ICRR-REPT-294-93-6] p 2627 N94-24961
Solar neutrinos: Real-time experiments
[ICRR-REPT-293-93-5] p 2627 N94-24962

TOLEDO UNIV., OH.
Semiempirical studies of atomic structure
[DE94-001588] p 2531 N94-22937
Northern hemisphere dust storms on Mars
p 2619 N94-24885

TORONTO UNIV. (ONTARIO).
Operating the Daisy facility to perform control experiments
[ISBN-0-315-83554-0] p 2196 N94-22889
The use of expanding monomers in carbon fibre composites
[ISBN-0-315-83550-8] p 2226 N94-22890
Fiber optic detection of laser generated ultrasound for materials characterization
[ISBN-0-315-83541-9] p 2541 N94-22891
Optimization of laminate orientation to enhance failure properties
[ISBN-0-315-83539-7] p 2227 N94-22892
Feasibility study of shot-peening modeling
[CTN-94-60926] p 2244 N94-24170
Investigation of time and intensity effects in operator workload and performance
[CTN-94-60927] p 2433 N94-24171
Evaluation of EHF multi-beam adaptive arrays
[CTN-94-60898] p 2297 N94-24296
Fiber optic detection of ultrasound and its application to cure monitoring
[ISBN-0-315-83424-2] p 2544 N94-24466
Predictive head movement tracking using innovations generated by Kalman filters
[ISBN-0-315-83371-8] p 2427 N94-24467
Structural characterization and thermal cycling behaviour of EB-PVD thermal barrier coating systems
[ISBN-0-315-83365-3] p 2257 N94-24468
Detection of velocity in high temperature liquid metals
p 2247 N94-25127
Constraining proposed combinations of ice history and Earth rheology using VLBI determined baseline length rates in North America p 2405 N94-25205

TOSHIBA CORP., KAWASAKI (JAPAN).
Development of gears for space use
p 2360 N94-24021

TOVS PATHFINDER SCIENTIFIC WORKING GROUP.
TOVS Pathfinder product validation and intercomparison p 2384 N94-23603

TOWSON STATE UNIV., MD.
Wide band fiber-optic communications
p 2304 N94-23231

TRACER TECHNOLOGIES, INC., SOMERVILLE, MA.
New method for increasing machine service-life, phase 2
[PB93-200707] p 2354 N94-23533

TRIANGLE RESEARCH AND DEVELOPMENT CORP., RESEARCH TRIANGLE PARK, NC.
Telerobotic rendezvous and docking vision system architecture
[NASA-CR-191329] p 2204 N94-23828

TRW, INC., REDONDO BEACH, CA.
High energy collimating fine grids for HESP program
[NASA-CR-189317] p 2209 N94-24767
Passive millimeter-wave imaging p 2306 N94-25494
Advanced radiometric and interferometric milimeter-wave scene simulations p 2306 N94-25498
TRW DEFENSE AND SPACE SYSTEMS GROUP, REDONDO BEACH, CA.
Inherent stability of central element coaxial liquid-liquid injectors p 2212 N94-23043
TRW SPACE AND DEFENSE SECTOR, REDONDO BEACH, CA.
Odyssey personal communications satellite system p 2282 N94-22787
TRW SPACE TECHNOLOGY LABS., REDONDO BEACH, CA.
Gas-grain simulation experiment module conceptual design and gas-grain simulation facility breadboard development
[NASA-CR-177632] p 2598 N94-23536
TSUKUBA SPACE CENTER (JAPAN).
The study of the mobile lunar explorer p 2607 N94-23389
TULANE UNIV., NEW ORLEANS, LA.
Loading, electromyograph, and motion during exercise p 2427 N94-25359
TUSKEGEE INST., AL.
Rack Insertion End Effector (RIEE) automation p 2368 N94-23242
Error coding simulations p 2306 N94-24439
Properties and processing characteristics of low density carbon cloth phenolic composites p 2231 N94-24450
Evaluation of advanced materials through experimental mechanics and modelling p 2374 N94-24454

U

UNITED STATES INFORMATION AGENCY, WASHINGTON, DC.
Worldwide survey of direct-to-listener digital audio delivery systems development since WARC-1992 p 2273 N94-22736
UNITED TECHNOLOGIES CORP., HUNTSVILLE, AL.
Lightning tests and analyses of tunnel bond straps and shielded cables on the Space Shuttle solid rocket booster
[NASA-CR-193921] p 2200 N94-24801
UNITED TECHNOLOGIES CORP., STRATFORD, CT.
Wind tunnel test of a variable-diameter tiltrotor (VDTR) model
[NASA-CR-177629] p 2181 N94-24796
UNITED TECHNOLOGIES CORP., WEST PALM BEACH, FL.
STE thrust chamber technology: Main injector technology program and nozzle Advanced Development Program (ADP)
[NASA-CR-193919] p 2221 N94-25019
UNITED TECHNOLOGIES CORP., WINDSOR LOCKS, CT.
Recent advances in SPE (tm) water electrolyzer p 2393 N94-23362
UNITED TECHNOLOGIES RESEARCH CENTER, EAST HARTFORD, CT.
Study of streamwise vorticity-stirred combustion
[NASA-CR-194450] p 2234 N94-24565
An analysis for high Reynolds number inviscid/viscid interactions in cascades
[NASA-CR-4519] p 2169 N94-24606
The importance of properties in modeling p 2246 N94-25121
UNIVERSITAET DER BUNDESWEHR MUENCHEN, NEUBIBERG (GERMANY).
Response of an anchored annular cylindrical liquid layer to various axial excitations in zero-gravity
[LRT-WE-9-FB-3-1992] p 2266 N94-23195
Coupled frequencies of a hydroelastic rectangular system
[LRT-WE-9-FB-4-1992] p 2375 N94-23196
Liquid oscillations in a spherical system with sliding edges boundary by two conical solid surfaces in zero-gravity
[LRT-WE-9-FB-5-1992] p 2318 N94-23197
Applications of the homogenization method to flow and transport in porous media
[BER-9110] p 2340 N94-25467
UNIVERSITEIT TWENTE, ENSCHEDE (NETHERLANDS).
On some approximately balanced combinatorial cooperative games
[MEMO-1113] p 2493 N94-22702
Decoupling problems around a trajectory: From linearity to nonlinearity
[MEMO-1115] p 2469 N94-22703
Personnel shift assignment: Existence conditions and network models
[MEMO-1116] p 2585 N94-22704
Balancing for unstable nonlinear systems
[MEMO-1118] p 2469 N94-22705
Nonlinear state space H(sub infinity) control theory
[MEMO-1119] p 2469 N94-22706
Nonlinear systems which have finite-dimensional H(sub infinity) suboptimal central controllers
[MEMO-1120] p 2469 N94-22707
Generalized concavity in cooperative game theory: Characterizations in terms of the core
[MEMO-1121] p 2497 N94-22708
Quantum mechanics, locality and realism
[MEMO-1117] p 2568 N94-22709
Tool sharing: An application of max-algebra, part 2
[MEMO-1122] p 2478 N94-22710
On dynamic input-output linearization of discrete-time nonlinear systems
[MEMO-1123] p 2447 N94-22711
Normal forms of kinematic singularities of 3R robot manipulators
[MEMO-1124] p 2469 N94-22712
A multigrid multiblock solver for compressible turbulent flow
[MEMO-1125] p 2315 N94-22713
Feedback linearization of parametrized nonlinear time-varying systems
[MEMO-1126] p 2470 N94-22714
Toughness and triangle-free graphs
[MEMO-1127] p 2478 N94-22715
On the reduced game property for and the axiomatization of the tau-value
[MEMO-1128] p 2497 N94-22716
Loss probabilities in batch-arrival bulk-service queues with finite capacity
[MEMO-1106] p 2493 N94-22724
Setting test limits under prescribed consumer loss
[MEMO-1107] p 2478 N94-22725
Tool sharing: An application of max-algebra, part 1
[MEMO-1108] p 2478 N94-22726
Long cycles in graphs with prescribed toughness and minimum degree
[MEMO-1109] p 2478 N94-22727
Nonlinear smoothing for random fields
[MEMO-1110] p 2493 N94-22728
The characterization of reaction-convection-diffusion processes by travelling waves
[MEMO-1111] p 2273 N94-22729
A nonlinear degenerating parabolic problem from the theory of type 2 superconductors
[MEMO-1112] p 2555 N94-22730
Toughness in Hamiltonicity in almost claw-free graphs
[MEMO-1114] p 2487 N94-24053
Lubrication in cold rolling: Numerical simulation using multigrid techniques
[ISBN-9-09-005313-1] p 2262 N94-25230
Forces on an oscillating cylinder and related fluid flow phenomena
[ISBN-9-09-005589-4] p 2338 N94-25243
UNIVERSITIES SPACE RESEARCH ASSOCIATION, HUNTSVILLE, AL.
Atmospheric numerical modeling resource enhancement and model convective parameterization/scale interaction studies
[NASA-CR-194769] p 2400 N94-23124
Scientific investigations of atmospheric processes
[NASA-CR-194805] p 2401 N94-23271
Microgravity sciences application visiting scientist program
[NASA-CR-194804] p 2267 N94-23287
UNIVERSITY OF CENTRAL FLORIDA, ORLANDO.
NASA/ASEE Summer Faculty Fellowship Program
[NASA-CR-194678] p 2571 N94-23230
Control of a serpentine manipulator with collision avoidance p 2368 N94-23232
Chemical characterization of some aerobic liquids in CELSS p 2422 N94-23241
KSC management training system project p 2574 N94-23246
Development of a nondestructive vibration technique for bond assessment of Space Shuttle tiles
[NASA-CR-195163] p 2201 N94-24919
UNIVERSITY OF SOUTH ALABAMA, MOBILE.
Numerical analysis of a vortex controlled diffuser p 2324 N94-23659
UNIVERSITY OF SOUTH AUSTRALIA, POORAKA.
Estimation of frequency offset in mobile satellite modems p 2285 N94-22807
UNIVERSITY OF SOUTH FLORIDA, SAINT PETERSBURG.
Algorithm-development activities
[NASA-CR-193225] p 2420 N94-23538
UNIVERSITY OF SOUTHERN CALIFORNIA, LOS ANGELES.
Photonic technology for implementation of generalizable neural networks: A synthetic approach
[AD-A273497] p 2474 N94-24622
Symbiosis in marine luminous bacteria
[AD-A273540] p 2422 N94-24791
UNIVERSITY OF SOUTHERN ILLINOIS, CARBONDALE.
A theorem regarding roots of the zero-order Bessel function of the first kind p 2325 N94-23667
Electro-rheology fluids and liquid fuel flow
[AD-A273640] p 2337 N94-25032
UNIVERSITY OF SOUTHERN MISSISSIPPI, BAY SAINT LOUIS.
An efficient data assimilation algorithm with a gaussian covariance structure
[AD-A273152] p 2418 N94-24671
UNIVERSITY OF SOUTHERN MISSISSIPPI, HATTIESBURG.
Convective instabilities in traveling fronts of addition polymerization p 2226 N94-24352
UNIVERSITY OF SOUTHWESTERN LOUISIANA, LAFAYETTE.
Vectorization and parallelization of the finite strip method for dynamic Mindlin plate problems p 2483 N94-23679
UNIVERSITY OF WESTERN CAROLINA, CULLOWHEE, NC.
Hurricane risk assessment: Rollback or ride out p 2416 N94-23248
UNIVERSITY OF WESTERN ONTARIO, LONDON.
Segregation and oxidation studies of Al-Li and Al-Mg alloys
[ISBN-0-315-83993-7] p 2244 N94-24469
UTAH STATE UNIV., LOGAN.
Calibration of a helium-cooled infrared spatial radiometer and grating spectrometer p 2384 N94-23607
Infrared calibration p 2384 N94-23608
Mapping Tomorrow's Resources: A symposium on the uses of remote sensing, Geographic Information Systems (GIS), and Global Positioning Systems (GPS) for natural resources management p 2387 N94-24357
UTILITY POWER GROUP, CHATSWORTH, CA.
Amorphous silicon PVMaT, phase 2A
[DE93-018221] p 2390 N94-23295
UTRECHT STATE UNIV. (NETHERLANDS).
Sequential composition, action prefixes and process prefix
[PB94-101433] p 2488 N94-24539
Real-time process logic
[PB94-101441] p 2446 N94-24540

V

VACHON (WILLIAM A.) AND ASSOCIATES, INC., MANCHESTER, MA.
Control algorithms for effective operation of variable-speed wind turbines
[DE94-002607] p 2394 N94-23704
VANDERBILT UNIV., NASHVILLE, TN.
Stiffening of deployable space booms: Automated Protein Crystal Growth Facility
[NASA-CR-195547] p 2196 N94-24820
VIABLE SYSTEMS, INC., MEDFIELD, MA.
The study of dopant segregation behavior during the growth of GaAs in microgravity
[NASA-CR-193905] p 2267 N94-23549
VICTORIA UNIV. (BRITISH COLUMBIA).
Coding for frequency hopped spread spectrum satellite communications
[ECE-91-1] p 2296 N94-24132
Coding for frequency hopped spread spectrum satellite communications
[ECE-92-1] p 2300 N94-24697
VIGYAN RESEARCH ASSOCIATES, INC., HAMPTON, VA.
Cockpit weather graphics using mobile satellite communications p 2280 N94-22775
A study of roll attractor and wing rock of delta wings at high angles of attack p 2164 N94-25111
VIRGINIA COMMONWEALTH UNIV., RICHMOND.
Modelling early failures in Space Station Freedom p 2374 N94-25372
VIRGINIA POLYTECHNIC INST. AND STATE UNIV., BLACKSBURG.
Spatiotemporal behavior and nonlinear dynamics in a phase conjugate resonator
[NASA-CR-4567] p 2543 N94-23529
Issac, Jason Cherian ses in transonic flow
[NASA-CR-194837] p 2167 N94-24052
Design of a vehicle based system to prevent ozone loss
[NASA-CR-195498] p 2180 N94-24479
LOLA: Lunar Optical Long-baseline Array. 1992-1993 space design
[NASA-CR-195533] p 2298 N94-24582
LOITA: Lunar Optical/Infrared Telescope Array
[NASA-CR-195532] p 2546 N94-24816

Feasibility study of a synthesis procedure for array feeds to improve radiation performance of large distorted reflector antennas
[NASA-CR-195167] p 2301 N94-25005

VIRGINIA UNIV., CHARLOTTESVILLE.

Out of plane gradients in laminated composites
[NASA-CR-194875] p 2228 N94-23566

Chromospheric activity in agol binaries
[AD-A273546] p 2602 N94-24557

Environmentally assisted cracking of high strength beta titanium alloys
[AD-A273598] p 2245 N94-24823

VON KARMAN INST. FOR FLUID DYNAMICS, RHODE-SAINT-GENESE (BELGIUM).

Activities report to NATO
[ETN-94-95047] p 2318 N94-23227

VRIJE UNIV., AMSTERDAM (NETHERLANDS).

Making some issues of implicit knowledge explicit
[PB93-220606] p 2478 N94-22984

Median stabilization degree of a median algebra
[PB93-220010] p 2479 N94-23093

Characterization of measures with a convex range: A generalization of Lyapounov's theorem
[PB93-220523] p 2523 N94-23094

Flexible framework for contingent information systems modelling
[PB93-220549] p 2589 N94-23095

Asynchronous rendezvous in distributed logic programming
[PB93-220614] p 2448 N94-23096

Linear algorithm for flattening list graphs
[PB93-220648] p 2448 N94-23097

Characterization of measures with a convex matrix-k-range
[PB93-220655] p 2479 N94-23098

Transition system specifications in stalk format with bisimulation as a congruence
[PB94-110608] p 2453 N94-23707

Object distribution in orca using compile-time and run-time techniques
[PB94-110574] p 2453 N94-23745

Logic of capabilities
[PB94-110715] p 2473 N94-23747

Epistemic logic for defeasible reasoning using a meta-level architecture metaphor
[PB94-110723] p 2473 N94-23748

Extension of the critical path method
[PB94-118817] p 2488 N94-24527

Modular approach to project management
[PB94-118833] p 2586 N94-24528

Compositional architecture for simple design formally specified in DESIRE
[PB94-119013] p 2474 N94-24543

Combinatory reduction systems: Introduction and survey
[PB94-110582] p 2457 N94-24570

Non-brittleness of a DESIRE-model for an office assignment task
[PB94-119021] p 2489 N94-24643

General optimal stopping theorems for semi-Markov processes
[PB93-214989] p 2496 N94-24744

VRIJE UNIV., BRUSSELS (BELGIUM).

Arc consistency problem: An exercise in parallel programming with shared objects
[PB94-110590] p 2466 N94-23706

Framework for interactive solving of meta-constraint satisfaction problems
[PB94-118825] p 2585 N94-23761

Design and specification of a generic task model for solving boolean constraint satisfaction problems
[PB94-118841] p 2486 N94-23762

Structured constraint satisfaction
[PB94-119039] p 2497 N94-23764

Two applications of a generic task model for solving boolean constraint satisfaction problems
[PB94-119047] p 2487 N94-23765

W

WAGENINGEN AGRICULTURAL UNIV. (NETHERLANDS).

Methodology for the assessment of surface resistance and soil water storage variability at mesoscale based on remote sensing measurements. A case study with HAPEX-EFEDA data. UNESCO-International Hydrological Program 4
[PB94-111721] p 2386 N94-23734

Groundtruth collection for the JPL-SAR and ERS-1 campaign in Flevoland and Veluwe, Netherlands, 1991
[PB93-230654] p 2386 N94-23755

WAKE FOREST UNIV., WINSTON-SALEM, NC.

Expanding the KATE toolbox p 2477 N94-23247

WALLACE (T. L.), NASHVILLE, TN.

Development of an analytical-numerical model to predict radiant emission or absorption
[NASA-CR-194860] p 2453 N94-23624

WARWICK UNIV., COVENTRY (ENGLAND).

Microstructure and micromechanical behaviour of CMCs p 2256 N94-24236

WASHINGTON STATE PATROL, BELLEVUE.

Using satellite communications for a mobile computer network p 2280 N94-22777

WASHINGTON UNIV., SAINT LOUIS, MO.

Two populations and models of gamma ray bursts
[NASA-CR-194762] p 2629 N94-22947

Micromechanical simulation of damage progression in carbon phenolic composites p 2231 N94-24446

WASHINGTON UNIV., SEATTLE.

Atomic probes of surface structure and dynamics
[DE94-001651] p 2530 N94-22720

A reliable algorithm for optimal control synthesis
[NASA-CR-194809] p 2472 N94-23332

Dynamics of the atmosphere of Mars: Review of some outstanding problems p 2620 N94-24888

WEIZMANN INST. OF SCIENCE, REHOVOTH (ISRAEL).

Correlations in the actions of periodic orbits derived from quantum chaos
[DE93-616866] p 2571 N94-25340

WEST VIRGINIA STATE COLL., CHARLESTON.

Magnetic Earth Ionosphere Resonant Frequencies
[NASA-CR-195131] p 2303 N94-25191

WEST VIRGINIA UNIV., MORGANTOWN.

Determination of the stability and control derivatives of the NASA F/A-18 HARV using flight data
[NASA-CR-194838] p 2190 N94-24804

Preliminary design of a universal Martian lander
[NASA-CR-195529] p 2206 N94-25007

WESTERN AEROSPACE LABS., INC., MONTE SERENO, CA.

Activity Catalog Tool (ACT) user manual, version 2.0
[NASA-CR-177634] p 2430 N94-23527

WESTINGHOUSE ELECTRIC CORP., BALTIMORE, MD.

MSAT and cellular hybrid networking
p 2278 N94-22762

Implementation of a system to provide mobile satellite services in North America p 2281 N94-22784

The Westinghouse Series 1000 Mobile Phone: Technology and applications p 2284 N94-22800

Advanced technology for a satellite multichannel demultiplexer/demodulator
[NASA-CR-194435] p 2202 N94-23631

WESTINGHOUSE ELECTRIC CORP., PITTSBURGH, PA.

Contaminant effects in solid oxide fuel cells
[DE94-002963] p 2395 N94-23785

WESTINGHOUSE ELECTRIC CORP., SUNNYVALE, CA.

Radar E-O image fusion p 2306 N94-25503

WESTINGHOUSE IDAHO NUCLEAR CO., INC., IDAHO FALLS.

Quality data validation: Comprehensive approach to environmental data validation
[DE94-000925] p 2589 N94-22944

Improved gas core propulsion model
[DE94-000929] p 2220 N94-24511

WESTINGHOUSE SCIENCE AND TECHNOLOGY CENTER, PITTSBURGH, PA.

Crystal growth of organics for nonlinear optical applications p 2225 N94-24348

WICHITA STATE UNIV., KS.

Microstructural analysis of the 2195 aluminum-lithium alloy welds p 2251 N94-24448

WINAND STARING CENTRE, WAGENINGEN (NETHERLANDS).

Integrated use of hydrological modelling and remote sensing in the province of Drenthe (The Netherlands): Possibilities and restrictions
[REPT-61] p 2382 N94-23148

WISCONSIN UNIV., MADISON.

Organometallic chemistry of bimetallic compounds
[DE94-002313] p 2238 N94-22897

Chaos in plasma simulation and experiment
[DE94-001574] p 2549 N94-22963

Plasma research in the Madison Symmetric Torus (MST)
[DE94-002318] p 2549 N94-22976

A measurement of the forward-backward asymmetry and sin(sup 2)(theta)(sub W) from the process Z(sup 0) (yields) (mu)(sup +)(mu)(sup (minus)) at (radical)s = 1.8 TeV
[DE94-001908] p 2532 N94-23018

1993 annual report for the Phaedrus-T RF current drive experiments
[DE94-001369] p 2550 N94-23192

Chaos and simple determinism in reversed field pinch plasmas: Nonlinear analysis of numerical simulation and experimental data
[DE94-001575] p 2550 N94-23211

Nonlinear ion-mixing-mode particle transport in the dissipative trapped electron regime
[DE94-000989] p 2533 N94-23435

Atmospheric moisture fields derived by satellite observations over the tropical Pacific Ocean
[NASA-CR-194852] p 2408 N94-23542

A nonconforming multigrid method using conforming subspaces p 2485 N94-23695

Implementation of a state of the art automated system for the production of cloud/water vapor motion winds from geostationary satellites
[NASA-CR-195087] p 2410 N94-24125

Hubble Space Telescope high speed photometer orbital verification
[NASA-CR-189333] p 2204 N94-24226

An investigation of current and future satellite and in-situ data for the remote sensing of the land surface energy balance
[NASA-CR-195138] p 2387 N94-24596

Hubble Space Telescope high speed photometer science verification test report
[NASA-CR-189322] p 2205 N94-24710

Mars Operational Environmental Satellite (MOES): A post-Mars Observer discovery mission
p 2620 N94-24890

A thermodynamic approach to obtain materials properties for engineering applications
p 2248 N94-25131

WISCONSIN UNIV., MILWAUKEE.

Inelastic electron scattering from surfaces
[DE94-001368] p 2531 N94-22733

WISCONSIN UNIV., PLATTEVILLE.

Response-coefficient method for heat-conduction transients with time-dependent inputs
p 2326 N94-23671

WOODS HOLE OCEANOGRAPHIC INST., MA.

Global acoustic mapping of ocean temperatures (GAMOT)
[AD-A273387] p 2418 N94-24719

Seafloor characterization/Galapagos propagating rift
[AD-A273586] p 2419 N94-25165

Analysis of modal evolution caused by a weakly range-dependent seabed in shallow water and its application to inversion for geoacoustic properties
[AD-A273656] p 2419 N94-25435

WOODS HOLE RESEARCH CENTER, MA.

Human impacts on soil carbon dynamics of deep-rooted Amazonian forests
[NASA-CR-195127] p 2399 N94-24861

WORCESTER POLYTECHNIC INST., HOLDEN, MA.

NASA advanced design program. Design and analysis of a radio-controlled flying wing aircraft
[NASA-CR-195515] p 2180 N94-24589

WORCESTER POLYTECHNIC INST., MA.

Conceptual design of a two stage to orbit spacecraft
[NASA-CR-195536] p 2204 N94-24620

WRIGHT LAB., WRIGHT-PATTERSON AFB, OH.

A fully automated stage for optical waveguide measurements
[AD-A273042] p 2542 N94-22915

An engineering code to analyze hypersonic thermal management systems p 2320 N94-23636

Ultrasonic nondestructive evaluation as a tool for the development of aerospace structural ceramic composites p 2257 N94-24240

Early manufacturing considerations in design
p 2177 N94-24315

Robust, nonlinear, high angle-of-attack control design for a supermaneuverable vehicle p 2164 N94-25108

A comparison of free-space and fiber mixer performances
[AD-A273558] p 2547 N94-25161

Structure of cholesteryl-4-vinylbenzoate
[AD-A273686] p 2567 N94-25441

Expert system rule-base evaluation using real-time parallel processing
[AD-A273701] p 2469 N94-25454

Direct measurement of turbulent dissipation rate using dual laser doppler velocimeters
[AD-A273740] p 2340 N94-25530

The mechanical property data base from an Air Force/Industry Cooperative Test Program on advanced aluminum alloys (7064 and CW67)
[AD-A273741] p 2251 N94-25531

WRIGHT RESEARCH DEVELOPMENT CENTER, WRIGHT-PATTERSON AFB, OH.

Interface evaluation in ceramic composites
p 2255 N94-24231

Micromechanical failure modes in brittle matrix composites p 2255 N94-24232

WYOMING UNIV., LARAMIE.

Three-dimensional numerical simulation of near-surface flows over the Martian north polar cap
p 2621 N94-24895

Failure detection and recovery in the assembly/contingency subsystem p 2306 N94-25360

An evaluation of three-dimensional sensors for the extravehicular activity helper/retreiver
p 2444 N94-25369

X

XSIRIUS SCIENTIFIC, INC., CAMARILLO, CA.
New concepts for HgI2 scintillator gamma ray spectroscopy
[NASA-CR-194819] p 2233 N94-24113

Y

YALE UNIV., NEW HAVEN, CT.
Implementing abstract multigrid or multilevel methods
p 2483 N94-23682
Numerical solution of flame sheet problems with and without multigrid methods p 2237 N94-23683
Fundamental and experimental studies on the catalytic combustion of methane
[PB94-112661] p 2233 N94-23736
Fast fourier transforms of piecewise constant functions
[AD-A272648] p 2456 N94-24535
Fractal geometry in physics
[AD-A273271] p 2523 N94-24936
Generalized Gaussian quadrature rules for systems of arbitrary functions
[AD-A273610] p 2491 N94-24947

YAMAGUCHI UNIV. (JAPAN).
Robotic exploration of Moon and Mars
p 2606 N94-23379

YOKOHAMA NATIONAL UNIV. (JAPAN).
Influences of nitrogen absorption on the magnetic properties of YFe2, YFe3 and Y6Fe23
[REPT-A-2654] p 2564 N94-24958

Z

ZURICH UNIV. (SWITZERLAND).
A multigrid solver for the semiconductor equations
p 2482 N94-23674

REPORT NUMBER INDEX

SCIENTIFIC AND TECHNICAL AEROSPACE REPORTS VOLUME 32 NUMBER 6

Typical Report Number Index Listing

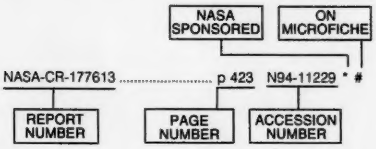

Listings in this index are arranged alphanumerically by report number. The accession number denotes the number by which the citation is identified. The page number helps to locate the citation in the abstract section. An asterisk (*) indicates that the item is a NASA report. A pound sign (#) indicates that the item is available on microfiche.

AF PROJ. 2304 .... p 2496 N94-24951
AF PROJ. 2305 .... p 2542 N94-22915
AF PROJ. 2307 .... p 2167 N94-23975
AF PROJ. 2401 .... p 2170 N94-24773
AF PROJ. 2422 .... p 2567 N94-25441
AF PROJ. 7930 .... p 2427 N94-24928
AF-AFOSR-0004-92 .... p 2167 N94-23975
AF-AFOSR-0007-91 .... p 2167 N94-23975
AF-AFOSR-0012-90 .... p 2167 N94-23975
AF-AFOSR-0040-91 .... p 2257 N94-24677
AF-AFOSR-0090-90 .... p 2230 N94-25158
AF-AFOSR-0090-93 .... p 2480 N94-23278
p 2487 N94-24291
AF-AFOSR-0150-90 .... p 2259 N94-24783
AF-AFOSR-0168-90 .... p 2496 N94-25147
AF-AFOSR-0171-90 .... p 2336 N94-24793
AF-AFOSR-0180-91 .... p 2234 N94-24673
AF-AFOSR-0218-91 .... p 2335 N94-24689
AF-AFOSR-0251-90 .... p 2496 N94-24931
AF-AFOSR-0261-90 .... p 2337 N94-24929
AF-AFOSR-0276B-89 .... p 2472 N94-23163
AF-AFOSR-0336-91 .... p 2212 N94-23042
AF-AFOSR-0364-89 .... p 2565 N94-25160
AF-AFOSR-0455-89 .... p 2485 N94-23691
AF-AFOSR-0459-89 .... p 2406 N94-25536
AF-AFOSR-0466-89 .... p 2474 N94-24622
AF-AFOSR-0512-89 .... p 2488 N94-24561
ARPA ORDER 8313 .... p 2458 N94-24693
ARPA ORDER 8363 .... p 2461 N94-25156
A90/KL/656 .... p 2381 N94-22896
A92/KLU/325 .... p 2542 N94-22895
BMFT-ITR-900689 .... p 2469 N94-23697
BMFT-07-KFT-86/2 .... p 2403 N94-24491
BMFT-13-N-55-45 .... p 2351 N94-25304
BU-4426-301 .... p 2421 N94-24290
CNPQ-200597/90-6 .... p 2523 N94-25314
p 2492 N94-25320
p 2523 N94-25323
DA PROJ. X15-96 .... p 2416 N94-25162
DA PROJ. 1L1-62211-A-47-A .... p 2364 N94-24483
p 2367 N94-25181
DA PROJ. 1L1-62618-AH-80 .... p 2198 N94-24690
DA PROJ. 1O1-62622-A-553 .... p 2446 N94-25438
DA PROJ. 2Q1-62785-A-791 .... p 2462 N94-25287
DA PROJ. 3M1-62787-A-878 .... p 2174 N94-25141
DA PROJ. 4A1-62784-AT-41 .... p 2460 N94-24935
DAAB07-92-R-C977 .... p 2289 N94-22834
DAAL03-89-C-0018 .... p 2234 N94-24565
DAAL03-91-G-0123 .... p 2480 N94-23278
DAAL03-91-G-0162 .... p 2484 N94-23685
DAAL03-92-2-60205 .... p 2393 N94-23364
DAAL04-89-C-0023 .... p 2230 N94-24779
p 2230 N94-24942
p 2230 N94-25163
DASG60-93-C-0048 .... p 2348 N94-23123
DE-AC02-76CH-00016 .... p 2531 N94-22923
p 2389 N94-22962
p 2532 N94-23007
p 2482 N94-23677
p 2386 N94-23779
p 2234 N94-24545
p 2245 N94-24612
DE-AC02-76CH-03000 .... p 2601 N94-23010
p 2535 N94-24515
p 2535 N94-24611
p 2365 N94-24614
DE-AC02-76ER-00881 .... p 2532 N94-23018
DE-AC02-76ER-01545 .... p 2533 N94-23218
DE-AC02-78ET-51013 .... p 2548 N94-22721
p 2552 N94-24504
DE-AC02-83CH-10093 .... p 2389 N94-22862
p 2389 N94-22888
p 2560 N94-23205
p 2390 N94-23295
p 2390 N94-23296
p 2395 N94-24509
p 2395 N94-24512
DE-AC03-76SF-00098 .... p 2557 N94-22926
p 2532 N94-23002
p 2533 N94-23218
p 2335 N94-24655
p 2299 N94-24656
p 2564 N94-24657
p 2523 N94-24658
DE-AC03-76SF-00515 .... p 2307 N94-22955
p 2534 N94-23803
DE-AC03-89ER-51114 .... p 2550 N94-23182
p 2551 N94-23782
p 2354 N94-23797
p 2553 N94-24746
p 2553 N94-24756
DE-AC03-91SF-18852 .... p 2218 N94-23459
DE-AC04-76DP-00789 .... p 2371 N94-22918
p 2558 N94-22953
p 2342 N94-22954
p 2268 N94-23000
p 2348 N94-23185
p 2559 N94-23186
p 2343 N94-23200
p 2472 N94-23201
p 2542 N94-23202
p 2560 N94-23204
p 2613 N94-23469
p 2394 N94-23472
p 2452 N94-23488
p 2466 N94-23491
p 2321 N94-23640
p 2270 N94-23790
p 2534 N94-23804
p 2244 N94-23811
p 2591 N94-24501
p 2591 N94-24607
DE-AC04-88DP-43495 .... p 2243 N94-23784
DE-AC04-94AL-85000 .... p 2555 N94-22717
p 2238 N94-22932
p 2589 N94-23126
p 2589 N94-23127
p 2589 N94-23128
p 2217 N94-23193
p 2349 N94-23209
p 2198 N94-23210
p 2375 N94-23217
p 2318 N94-23220
p 2394 N94-23472
p 2394 N94-23704
p 2526 N94-23718
p 2309 N94-23777
p 2244 N94-23811
p 2398 N94-24506
p 2552 N94-24546
p 2350 N94-24659
p 2311 N94-24748
DE-AC05-76OR-00033 .... p 2429 N94-22997
DE-AC05-84ER-40150 .... p 2531 N94-22951
p 2532 N94-22952
p 2540 N94-24662
p 2540 N94-24663
DE-AC05-84OR-21400 .... p 2556 N94-22864
p 2588 N94-22875
p 2548 N94-22916
p 2556 N94-22919
p 2548 N94-22945
p 2532 N94-22956
p 2558 N94-22957
p 2478 N94-22975
p 2429 N94-22997
p 2549 N94-22998
p 2307 N94-23019
p 2227 N94-23022
p 2525 N94-23206
p 2543 N94-23458
p 2543 N94-23461
p 2550 N94-23462
p 2293 N94-23473
p 2243 N94-23715
p 2254 N94-23783
p 2271 N94-23793
p 2397 N94-23794
p 2354 N94-23797
p 2395 N94-24499
p 2535 N94-24510
p 2446 N94-24538
p 2234 N94-24548
p 2563 N94-24567
p 2271 N94-24568
p 2535 N94-24569
p 2553 N94-24628
p 2388 N94-24757
DE-AC06-76RL-01830 .... p 2588 N94-22863
p 2347 N94-22974
p 2397 N94-23016
p 2386 N94-23779
DE-AC07-76ID-01570 .... p 2542 N94-22917
p 2382 N94-23492
p 2345 N94-24831
DE-AC07-84ID-12435 .... p 2589 N94-22944
p 2220 N94-24511
DE-AC11-89PN-38014 .... p 2239 N94-22999
p 2244 N94-23792
DE-AC11-93PN-38195 .... p 2241 N94-23219
DE-AC11-93PN38195 .... p 2244 N94-23792
DE-AC12-76SN-00052 .... p 2238 N94-22861
p 2238 N94-22936
DE-AC21-89MC-26355 .... p 2395 N94-23785
DE-AC21-90MC-27394 .... p 2389 N94-22723
DE-AC34-90DP-62349 .... p 2242 N94-23475
DE-AC35-89ER-40486 .... p 2457 N94-24626
DE-AI01-91CE-50306 .... p 2258 N94-24753
DE-AI06-91RL-12089 .... p 2381 N94-23001
DE-AI06-91RL-12090 .... p 2381 N94-23001
DE-AI06-91RL-12092 .... p 2381 N94-23001
DE-FC02-86CH-10311 .... p 2394 N94-23472
DE-FC07-91ID-13074 .... p 2353 N94-23191
DE-FG02-84ER-45076 .... p 2531 N94-22733
DE-FG02-85ER-13406 .... p 2238 N94-22897
DE-FG02-85ER-13438 .... p 2563 N94-24537
DE-FG02-85ER-25001 .... p 2483 N94-23679
DE-FG02-85ER-53198 .... p 2549 N94-22963
p 2549 N94-22976
p 2550 N94-23211
DE-FG02-86ER-13582 .... p 2568 N94-22719
DE-FG02-86ER-53218 .... p 2533 N94-23435
DE-FG02-87ER-40344 .... p 2540 N94-23791
DE-FG02-88ER-53264 .... p 2550 N94-23192
DE-FG02-89ER-13988 .... p 2232 N94-23023
DE-FG02-89ER-14079 .... p 2402 N94-23516
DE-FG02-90ER-60931 .... p 2563 N94-24567
DE-FG02-91ER-40669 .... p 2349 N94-23702
DE-FG02-93ER-12128 .... p 2254 N94-23720
DE-FG03-90ER-40546 .... p 2533 N94-23699
DE-FG03-91ER-40674 .... p 2307 N94-22955
DE-FG05-86ER-13613 .... p 2233 N94-23716
DE-FG05-86ER-40272 .... p 2569 N94-24532
DE-FG05-86ER-53217 .... p 2533 N94-23543
DE-FG05-87ER-52141 .... p 2553 N94-24628
DE-FG05-88ER-13958 .... p 2531 N94-22937
DE-FG05-89ER-60892 .... p 2233 N94-23780
DE-FG05-92ER-79119 .... p 2342 N94-22989
DE-FG06-91ER-14224 .... p 2530 N94-22720
DE-FG22-92PC-92542 .... p 2258 N94-24749
DE-2103-86SF-16310 .... p 2242 N94-23550
DEN3-373 .... p 2258 N94-24753
DL-H-418511 .... p 2472 N94-23163
DLA900-86-C-0022 .... p 2529 N94-24221
DMR89-20147 .... p 2484 N94-23686
DNA001-85-C-0183 .... p 2393 N94-23364
DNA001-88-C-0006 .... p 2553 N94-24949

DNA001-90-C-0127 p 2393 N94-23364
DNA001-91-C-0127 p 2394 N94-23365
DRET-86-156 p 2165 N94-23149
p 2165 N94-23161
DRET-88-201 p 2339 N94-25462
DRET-88-214 p 2340 N94-25463
DSS-9F011-2-0923 p 2370 N94-23421
DSS-9F011-2-0976 p 2370 N94-23421
DTFA-01-93-Z-02018 p 2175 N94-24127
DTFAC1-87-Z-02015 p 2192 N94-23303
DTFA01-89-Z-0203 p 2415 N94-24850
DTFA01-93-Y-1021 p 2162 N94-24923
DTFA02-91-C-91089 p 2176 N94-25444
DTFA03-88-A-0029 p 2230 N94-24779
p 2230 N94-24942
p 2230 N94-25163
DTFA03-89-C-00043 p 2430 N94-23083
p 2192 N94-24072
DTFA03-89-C-0043 p 2438 N94-24830
DTMA91-91-C-10038 p 2175 N94-24474
EEC-SCI-CT91-0695 p 2489 N94-24610
EEL66.1206 p 2462 N94-25263
ESTEC-8741/90/NL/JG(SC) p 2370 N94-23422
ESTEC-9195/90/NL/SF p 2608 N94-23394
ESTEC-9239/90/NL/PP p 2315 N94-23989
EV5V-CT92-0121 p 2382 N94-23158
p 2401 N94-23159
FRG-1244 p 2321 N94-23642
F04611-90-C-0095 p 2393 N94-23359
F19628-89-C-0001 p 2301 N94-24926
F19628-90-C-0002 p 2175 N94-24127
F19628-90-K-0028 p 2207 N94-25542
F19628-90-L-0003 p 2460 N94-24933
F19628-91-C-0168 p 2458 N94-24693
F19628-91-K-0033 p 2406 N94-25538
F30602-90-C-0116 p 2463 N94-25455
p 2463 N94-25456
F30602-92-C-0092 p 2592 N94-24691
F33615-84-C-3404 p 2463 N94-25453
F33615-89-C-5612 p 2257 N94-24240
F33615-89-C-5643 p 2259 N94-24788
F33615-90-C-3600 p 2185 N94-25440
F33615-90-C-3608 p 2472 N94-23163
F33615-91-C-5733 p 2189 N94-24776
F33615-91-C-5737 p 2368 N94-25436
F40620-93-1-0045 p 2427 N94-24865
F49620-90-C-0019 p 2258 N94-24782
F49620-90-C-0027 p 2170 N94-24849
F49620-90-C-0066 p 2261 N94-24937
F49620-91-C-0050 p 2421 N94-24688
F49620-91-C-0058 p 2566 N94-25288
F49620-91-C-0084 p 2491 N94-24947
F49620-92-J-0024 p 2602 N94-24557
F49620-92-J-0058 p 2338 N94-25157
F49620-92-J-0116 p 2468 N94-24939
F49620-92-J-0411 p 2475 N94-24943
F49620-92-J-0498 p 2404 N94-24674
F49620-93-1-0002 p 2404 N94-24794
F49620-93-1-0078 p 2327 N94-24139
GRI-5086-260-1325 p 2233 N94-23801
GRI-5091-260-2126 p 2232 N94-23100
GRI-5091-260-2141 p 2235 N94-24920
GRI-5091-260-2206 p 2233 N94-23736
GRI-5091-260-2233 p 2232 N94-23477
GRI-5091-293-2188 p 2187 N94-23709
GRI-5092-260-2333 p 2398 N94-23818
IACRO-93-817 p 2341 N94-23690
IC-EEL-88.036 p 2313 N94-25083
INMARSAT-92-798/BK p 2284 N94-22797
IOP-TK-86.B051 p 2555 N94-25439
IOP-TK-88A022 p 2263 N94-25281
IOP-TK-88B040 p 2263 N94-25299
JPL-958733 p 2292 N94-23269
JPL-958734 p 2292 N94-23269
MA000-MA999/4476-4479 p 2483 N94-23678
MDA903-91-D-0024 p 2462 N94-25287
MDA903-92-D-0025 p 2173 N94-24864
MDA904-84-H-2008 p 2478 N94-22727
MDA972-90-C-0036 p 2593 N94-24946
MDA972-91-C-0040 p 2393 N94-23363
MDA972-92-C-0020 p 2461 N94-25156
MDA972-92-J-1018 p 2461 N94-25148
p 2461 N94-25149
MDA972-93-1-0004 p 2418 N94-24719
NAGW-0758 p 2401 N94-23337
NAGW-107 p 2296 N94-24105
NAGW-1085 p 2623 N94-24996
NAGW-1192 p 2238 N94-25132
NAGW-1356 p 2209 N94-23028
NAGW-1387 p 2601 N94-23251
NAGW-1858 p 2387 N94-24596
NAGW-212 p 2420 N94-23501
NAGW-2130 p 2626 N94-23626
NAGW-227 p 2420 N94-24124
NAGW-2542 p 2399 N94-25092
NAGW-2579 p 2624 N94-22841
NAGW-2667 p 2401 N94-23344
NAGW-2729 p 2399 N94-25092
NAGW-2748 p 2399 N94-24853
NAGW-2750 p 2399 N94-24861
NAGW-2814 p 2627 N94-24300
NAGW-2918 p 2629 N94-22947
NAGW-2966 p 2405 N94-24854
NAGW-3150 p 2409 N94-24049
NAGW-3322 p 2596 N94-23526
p 2596 N94-23528
p 2596 N94-23540
p 2597 N94-24496
NAGW-3346 p 2382 N94-23573
p 2386 N94-24060
NAGW-3457 p 2402 N94-24089
NAGW-3576 p 2540 N94-23495
NAGW-3589 p 2403 N94-24580
NAGW-674 p 2319 N94-23513
p 2320 N94-23532
NAGW-843 p 2399 N94-25092
NAG1-060 p 2451 N94-23341
NAG1-1056 p 2192 N94-23539
NAG1-1057 p 2397 N94-23277
NAG1-1082 p 2365 N94-24699
NAG1-1090 p 2198 N94-24752
NAG1-1122 p 2337 N94-25094
NAG1-1132 p 2451 N94-23341
NAG1-1133 p 2167 N94-23625
NAG1-1145 p 2480 N94-23278
NAG1-1184 p 2246 N94-25118
NAG1-1210 p 2473 N94-24542
NAG1-126 p 2475 N94-24760
NAG1-1315 p 2403 N94-24486
NAG1-1327 p 2203 N94-23329
NAG1-1363 p 2543 N94-23529
NAG1-1371 p 2442 N94-25507
NAG1-1380 p 2190 N94-25176
NAG1-1397 p 2488 N94-24564
NAG1-1411 p 2167 N94-24052
NAG1-1424 p 2540 N94-23485
NAG1-1441 p 2428 N94-24799
NAG1-1485 p 2458 N94-24679
p 2458 N94-24740
NAG1-1493 p 2229 N94-24579
NAG1-1513 p 2534 N94-24487
NAG1-1581 p 2530 N94-25177
NAG1-244 p 2337 N94-24858
NAG1-562 p 2298 N94-24616
NAG1-774 p 2456 N94-24480
NAG1-787 p 2451 N94-23341
NAG1-796 p 2564 N94-25024
NAG1-841 p 2228 N94-23566
NAG1-859 p 2301 N94-25005
NAG1-928 p 2309 N94-23304
NAG1-955 p 2564 N94-25024
NAG1-982 p 2229 N94-24402
NAG1-991 p 2377 N94-24587
NAG10-117 p 2201 N94-24919
NAG2-261 p 2327 N94-24098
NAG2-384 p 2420 N94-24124
NAG2-513 p 2448 N94-23073
p 2448 N94-23074
p 2472 N94-23300
p 2451 N94-23301
NAG2-691 p 2472 N94-23332
NAG2-819 p 2420 N94-23633
NAG2-827 p 2466 N94-23504
NAG2-832 p 2466 N94-23483
NAG2-854 p 2184 N94-25268
NAG3-LL54 p 2391 N94-23351
NAG3-1044 p 2266 N94-24700
NAG3-1147 p 2373 N94-24769
NAG3-1300 p 2343 N94-23285
NAG3-1332 p 2310 N94-24070
NAG3-1369 p 2462 N94-25179
NAG3-1429 p 2563 N94-24617
NAG3-1434 p 2363 N94-24081
NAG3-1507 p 2365 N94-24751
NAG3-845 p 2255 N94-24223
NAG3-856 p 2377 N94-24604
NAG3-899 p 2327 N94-24096
NAG5-1152 p 2410 N94-24097
NAG5-1267 p 2303 N94-25191
NAG5-1490 p 2404 N94-24843
NAG5-1536 p 2600 N94-25269
NAG5-1612 p 2301 N94-24707
NAG5-1696 p 2398 N94-24078
NAG5-1743 p 2600 N94-25270
NAG5-1769 p 2599 N94-24051
NAG5-1870 p 2600 N94-25178
NAG5-1904 p 2629 N94-25091
NAG5-1913 p 2599 N94-24988
NAG5-1924 p 2601 N94-23537
NAG5-1930 p 2405 N94-25203
NAG5-1941 p 2175 N94-24826
NAG5-1947 p 2175 N94-24826
NAG5-1980 p 2600 N94-25198
NAG5-2038 p 2439 N94-24857
NAG5-2188 p 2546 N94-24967
NAG5-2210 p 2366 N94-24846
p 2490 N94-24847
NAG5-2226 p 2459 N94-24797
NAG5-386 p 2415 N94-24705
NAG5-500 p 2627 N94-24094
NAG5-537 p 2614 N94-24328
NAG5-671 p 2209 N94-23484
NAG8-1016 p 2220 N94-24595
NAG8-195 p 2631 N94-24493
NAG8-212 p 2586 N94-25197
p 2629 N94-25199
p 2378 N94-25267
NAG8-240 p 2365 N94-24842
NAG8-836 p 2415 N94-24485
NAG8-839 p 2628 N94-25264
NAG8-845 p 2408 N94-23542
p 2408 N94-23577
p 2408 N94-23619
p 2408 N94-23620
p 2409 N94-23621
NAG8-883 p 2265 N94-24578
NAG8-921 p 2217 N94-23275
NAG8-974 p 2410 N94-24125
NAG9-169 p 2614 N94-24363
NAG9-185 p 2601 N94-23499
NAG9-485 p 2425 N94-23331
NAG9-546 p 2267 N94-23594
NAG9-574 p 2203 N94-23618
NAG9-586 p 2205 N94-24828
NANB8D0861 p 2270 N94-23740
NASA ORDER A-25364-D p 2176 N94-23489
NASA ORDER H-13034-D p 2543 N94-23502
NASA ORDER H-18070-D p 2453 N94-23624
NASA ORDER S-97230-E p 2598 N94-23330
p 2599 N94-24666
NASW-4367 p 2597 N94-24494
NASW-4435 p 2437 N94-24330
p 2438 N94-24331
p 2179 N94-24332
p 2614 N94-24333
p 2204 N94-24334
p 2179 N94-24401
p 2180 N94-24462
p 2180 N94-24479
p 2180 N94-24492
p 2180 N94-24498
p 2190 N94-24551
p 2180 N94-24581
p 2298 N94-24582
p 2180 N94-24589
p 2204 N94-24590
p 2181 N94-24591
p 2266 N94-24618
p 2195 N94-24619
p 2204 N94-24620
p 2204 N94-24621
p 2438 N94-24667
p 2396 N94-24701
p 2205 N94-24702
p 2365 N94-24703
p 2181 N94-24711
p 2438 N94-24786
p 2181 N94-24787
p 2181 N94-24803
p 2365 N94-24805
p 2365 N94-24806
p 2195 N94-24808
p 2422 N94-24810
p 2546 N94-24816
p 2182 N94-24817
p 2196 N94-24820
p 2221 N94-24834
p 2439 N94-24835
p 2182 N94-24837
p 2206 N94-24838
p 2209 N94-24840
p 2198 N94-24860
p 2182 N94-24915
p 2206 N94-24916
p 2439 N94-24956
p 2190 N94-24957
p 2182 N94-24966
p 2182 N94-24968
p 2183 N94-24969
p 2183 N94-24971
p 2183 N94-24972
p 2183 N94-24974
p 2183 N94-24975
p 2221 N94-24979
p 2195 N94-24995
p 2183 N94-25001
p 2184 N94-25002
p 2184 N94-25004

p 2206 N94-25007
p 2184 N94-25017
p 2184 N94-25021
p 2199 N94-25022
p 2189 N94-25085
NASW-4574 p 2613 N94-24058
p 2616 N94-24871
p 2603 N94-24964
NASW-4584 p 2594 N94-25487
p 2594 N94-25541
NASW-4627 p 2387 N94-24303
NASW-4670 p 2460 N94-25023
NASW-4721 p 2629 N94-25260
p 2628 N94-25275
NASW-4756 p 2604 N94-25265
NASW-4814 p 2626 N94-23276
NAS1-18027 p 2172 N94-23288
NAS1-18450 p 2192 N94-23564
p 2336 N94-24771
NAS1-18586 p 2445 N94-23125
p 2466 N94-23252
p 2467 N94-24075
p 2467 N94-24463
NAS1-18605 p 2451 N94-23341
NAS1-18606 p 2469 N94-23697
NAS1-18969 p 2466 N94-23293
NAS1-19000 p 2181 N94-24726
NAS1-19060 p 2526 N94-24172
p 2526 N94-24173
NAS1-19271 p 2525 N94-23698
NAS1-19299 p 2336 N94-24725
NAS1-19440 p 2344 N94-24360
NAS1-19480 p 2317 N94-23089
p 2479 N94-23090
p 2448 N94-23092
p 2480 N94-23272
p 2480 N94-23278
p 2319 N94-23302
p 2451 N94-23340
p 2451 N94-23341
p 2473 N94-23558
p 2487 N94-24291
p 2333 N94-24356
p 2334 N94-24602
p 2334 N94-24605
p 2457 N94-24638
p 2458 N94-24679
p 2458 N94-24680
p 2335 N94-24712
p 2458 N94-24740
p 2490 N94-24836
p 2337 N94-24869
p 2490 N94-24914
p 2444 N94-25090
NAS1-19595 p 2280 N94-22775
NAS1-19858 p 2343 N94-23498
NAS10-11844 p 2408 N94-23576
p 2416 N94-25271
NAS2-13408 p 2598 N94-23536
NAS2-13416 p 2598 N94-24832
NAS2-13484 p 2181 N94-24796
NAS2-13721 p 2569 N94-24109
p 2454 N94-24110
p 2529 N94-24307
p 2591 N94-24552
p 2631 N94-25003
NAS3-24635 p 2392 N94-23358
NAS3-24816 p 2172 N94-23523
NAS3-25266 p 2166 N94-23299
p 2525 N94-23464
p 2242 N94-23467
p 2166 N94-23511
p 2153 N94-23553
p 2219 N94-23555
p 2243 N94-23556
p 2190 N94-23590
p 2203 N94-23632
p 2395 N94-24071
p 2153 N94-24100
p 2521 N94-24302
p 2310 N94-24308
p 2219 N94-24361
p 2344 N94-24362
p 2220 N94-24714
p 2312 N94-24870
p 2202 N94-25095
p 2170 N94-25173
p 2553 N94-25190
p 2189 N94-25200
NAS3-25425 p 2169 N94-24606
NAS3-25776 p 2290 N94-23087
p 2243 N94-23578
NAS3-25808 p 2219 N94-24061
NAS3-25865 p 2202 N94-23631
NAS3-25933 p 2304 N94-25266
NAS3-25950 p 2364 N94-24090
NAS3-25954 p 2188 N94-24594
NAS3-25967 p 2187 N94-24082
NAS3-27186 p 2202 N94-25095
NAS5-24487 p 2204 N94-24226
p 2205 N94-24710
NAS5-27772 p 2520 N94-23964
p 2520 N94-23966
NAS5-28575 p 2443 N94-23929
NAS5-29386 p 2410 N94-24355
NAS5-30189 p 2430 N94-23080
NAS5-30428 p 2400 N94-23084
p 2465 N94-23085
p 2451 N94-23369
p 2452 N94-23507
p 2591 N94-24099
NAS5-30680 p 2443 N94-23936
NAS5-30709 p 2204 N94-23828
NAS5-30883 p 2544 N94-23829
NAS5-31170 p 2295 N94-23830
NAS5-31716 p 2420 N94-23538
NAS5-31841 p 2599 N94-23334
NAS5-32059 p 2599 N94-23334
NAS5-32063 p 2453 N94-23559
NAS5-32314 p 2585 N94-23563
NAS5-32463 p 2311 N94-24754
NAS5-32529 p 2209 N94-24767
NAS7-1204 p 2233 N94-24113
NAS7-918 p 2273 N94-22735
p 2497 N94-23832
p 2409 N94-24048
p 2409 N94-24087
p 2410 N94-24126
NAS8-36123 p 2454 N94-24050
NAS8-36300 p 2200 N94-24801
NAS8-36630 p 2550 N94-23565
NAS8-36670 p 2196 N94-24309
NAS8-37140 p 2401 N94-23271
NAS8-37141 p 2400 N94-23124
NAS8-37490 p 2221 N94-25019
NAS8-37595 p 2367 N94-25174
NAS8-37800 p 2229 N94-24224
NAS8-37814 p 2421 N94-24310
NAS8-37821 p 2366 N94-24998
p 2366 N94-24999
NAS8-37856 p 2201 N94-24970
NAS8-37858 p 2267 N94-23549
NAS8-38100 p 2199 N94-24057
p 2219 N94-24064
p 2200 N94-24065
p 2200 N94-24067
p 2200 N94-24112
p 2365 N94-24588
p 2201 N94-24802
p 2201 N94-24965
p 2367 N94-25020
NAS8-38550 p 2376 N94-24359
NAS8-38575 p 2456 N94-24470
NAS8-38609 p 2364 N94-24088
p 2627 N94-24461
p 2627 N94-24484
p 2545 N94-24665
p 2345 N94-24852
p 2345 N94-25000
NAS8-38785 p 2267 N94-23287
NAS8-38961 p 2220 N94-24471
NAS8-39131 p 2244 N94-24066
p 2455 N94-24111
NAS8-39235 p 2200 N94-24664
NAS8-39364 p 2437 N94-24329
NAS8-39393 p 2388 N94-24827
p 2389 N94-24856
NAS8-40000 p 2372 N94-24174
NAS9-17900 p 2590 N94-23289
p 2199 N94-23571
p 2433 N94-24186
p 2433 N94-24188
p 2435 N94-24195
p 2435 N94-24196
p 2435 N94-24198
p 2436 N94-24199
p 2436 N94-24200
p 2436 N94-24201
p 2436 N94-24202
NAS9-18035 p 2427 N94-24227
NAS9-18873 p 2272 N94-25193
NAS9-18879 p 2430 N94-23290
NATO-CRG-910397 p 2495 N94-24508
NATO-CRG-921251 p 2478 N94-22715
p 2478 N94-22727
NCA2-722 p 2335 N94-24640
NCA2-811 p 2165 N94-22894
NCCW-11 p 2177 N94-24314
NCCW-26 p 2574 N94-24225
NCC1-104 p 2474 N94-24635
NCC1-22 p 2337 N94-24859
NCC2-297 p 2565 N94-25093
NCC2-486 p 2430 N94-23527
p 2441 N94-25501
NCC2-492 p 2536 N94-24798
NCC2-578 p 2422 N94-24807
p 2422 N94-24811
NCC2-583 p 2165 N94-25169
NCC2-628 p 2438 N94-24706
NCC2-730 p 2168 N94-24103
NCC2-731 p 2317 N94-23072
NCC2-759 p 2190 N94-24804
NCC3-156 p 2300 N94-24678
NCC3-19 p 2218 N94-23370
NCC3-213 p 2187 N94-23552
NCC3-233 p 2326 N94-24063
p 2265 N94-24301
p 2333 N94-24336
p 2333 N94-24460
p 2336 N94-24713
NCC3-297 p 2367 N94-25274
NCC3-74 p 2349 N94-23286
NCC8-18 p 2597 N94-24829
NGT-01-008-021 p 2574 N94-24405
NGT-44-001-800 p 2632 N94-25348
p 2636 N94-25367
NGT-50346 p 2350 N94-24851
NGT-60002 p 2571 N94-23230
NMRI PROJ. M00-99 p 2427 N94-24950
NR PROJ. LR0-330244 p 2303 N94-25089
NSERC-STR-0100720 p 2287 N94-22820
NSF ASC-88-19373 p 2451 N94-23341
NSF ASC-91-07674 p 2490 N94-24836
NSF ASC-92-13821 p 2458 N94-24679
p 2458 N94-24740
NSF ASC-92-17394 p 2466 N94-23504
NSF AST-90-15755 p 2296 N94-24105
NSF AST-91-23777 p 2601 N94-23537
NSF ATM-88-14571 p 2407 N94-23199
NSF ATM-91-18966 p 2416 N94-23687
p 2484 N94-23688
NSF CCR-92-01195 p 2451 N94-23341
NSF CCR-92-10372 p 2451 N94-23341
NSF CCR-93-57840 p 2458 N94-24679
NSF CDA-90-24618 p 2485 N94-23695
NSF CTS-90-14914 p 2325 N94-23663
NSF DMS-89-03041 p 2489 N94-24610
NSF DMS-90-07185 p 2482 N94-23677
NSF DMS-90-12135 p 2456 N94-24535
NSF DMS-91-01089 p 2448 N94-23073
p 2472 N94-23300
p 2451 N94-23301
NSF DMS-91-03104 p 2484 N94-23685
NSF DMS-91-12847 p 2483 N94-23680
NSF DMS-92-03502 p 2485 N94-23695
NSF DMS-92-06991 p 2478 N94-22715
NSF DMS-92-11820 p 2480 N94-23278
p 2487 N94-24291
NSF EAR-91-15159 p 2175 N94-24826
NSF EAR-91-17889 p 2175 N94-24826
NSF ECS-92-09347 p 2490 N94-24914
NSF ENG-91-11333 p 2293 N94-23627
NSF MSM-85-00195 p 2354 N94-23533
NSG-5175 p 2404 N94-24738
NSG-7054 p 2626 N94-23569
NWO-611-306-523 p 2480 N94-23140
NWO-611-307-018 p 2480 N94-23140
N00014-82-K-0612 p 2263 N94-25409
N00014-85-C-2141 p 2311 N94-24818
N00014-86-K-0753 p 2255 N94-24230
N00014-88-K-0126 p 2570 N94-25028
N00014-89-C-2146 p 2545 N94-24672
N00014-89-J-1021 p 2419 N94-25165
N00014-89-J-1169 p 2536 N94-24675
p 2537 N94-24940
N00014-89-J-1235 p 2235 N94-24917
N00014-89-J-1527 p 2491 N94-24947
N00014-89-J-3062 p 2257 N94-24558
p 2259 N94-24789
p 2260 N94-24815
p 2260 N94-24863
p 2260 N94-24922
p 2260 N94-24924
p 2235 N94-24925
p 2537 N94-25087
p 2262 N94-25145
N00014-89-J-3230 p 2419 N94-24944
N00014-90-J-1026 p 2523 N94-24936
N00014-90-J-1148 p 2258 N94-24732
p 2260 N94-24813
N00014-90-J-1343 p 2485 N94-23691
N00014-90-J-1466 p 2628 N94-25031
N00014-90-J-1681 p 2419 N94-25164
N00014-90-J-1695 p 2465 N94-22973
N00014-90-J-4041 p 2337 N94-25032
N00014-90-J-4130 p 2350 N94-24934
N00014-90-K-2000 p 2346 N94-25154
N00014-91-C-0044 p 2423 N94-22732

N00014-91-J-1005 .... p 2495 N94-24560
N00014-91-J-1045 .... p 2263 N94-25413
N00014-91-J-1198 .... p 2536 N94-24717
N00014-91-J-1379 .... p 2419 N94-25435
N00014-91-J-1550 .... p 2235 N94-24790
N00014-91-J-1596 .... p 2263 N94-25489
N00014-91-J-1655 .... p 2257 N94-24562
p 2259 N94-24792
p 2261 N94-24930
p 2262 N94-25159
N00014-91-J-1991 .... p 2535 N94-24555
p 2536 N94-24729
p 2234 N94-24772
p 2565 N94-25086
p 2547 N94-25144
p 2346 N94-25151
N00014-91-J-4016 .... p 2480 N94-23278
p 2487 N94-24291
N00014-91-J-4134 .... p 2419 N94-25088
N00014-91-J-4164 .... p 2245 N94-24823
N00014-92-C-0140 .... p 2418 N94-24918
N00014-92-C-0210 .... p 2313 N94-25276
N00014-92-C-0214 .... p 2314 N94-25488
N00014-92-J-1716 .... p 2422 N94-24791
N00014-92-J-1848 .... p 2393 N94-23360
N00014-92-J-1890 .... p 2484 N94-23685
N00014-92-J-1905 .... p 2428 N94-25437
N00014-92-J-1921 .... p 2245 N94-25033
N00014-92-J-4013 .... p 2418 N94-24795
N00014-92-J-4112 .... p 2418 N94-24671
N00014-93-C-0053 .... p 2350 N94-24938
N00014-93-C-0108 .... p 2546 N94-24731
N00014-93-I-0400 .... p 2565 N94-25027
N00014-93-1-0059 .... p 2468 N94-25030
N00014-93-1-0077 .... p 2569 N94-24777
N00014-93-1-0125 .... p 2312 N94-24819
N00014-93-1-0156 .... p 2419 N94-24948
N00024-91-C-4067 .... p 2393 N94-23359
N00039-91-C-0001 .... p 2341 N94-23693
p 2504 N94-23873
N00039-93-C-0001 .... p 2299 N94-24676
N61533-88-C-0035 .... p 2378 N94-25143
ONR-SC-282-1-22813 .... p 2458 N94-24679
p 2458 N94-24740
ORSSP-R2444 .... p 2321 N94-23642
RSG/323 .... p 2368 N94-25322
RTOP 199-14-12-06 .... p 2426 N94-24102
RTOP 199-18-12-07 .... p 2426 N94-23575
RTOP 199-30-92-14 .... p 2387 N94-24403
RTOP 199-45-16-11 .... p 2540 N94-23509
p 2540 N94-24305
RTOP 199-52-82 .... p 2395 N94-24071
RTOP 199-70-12-14 .... p 2420 N94-23088
RTOP 232-01-04-05 .... p 2198 N94-24752
RTOP 233-01-01 .... p 2254 N94-23486
RTOP 233-01-03 .... p 2448 N94-23086
RTOP 233-02-0B .... p 2220 N94-24681
RTOP 233-03-01-01 .... p 2543 N94-23529
RTOP 235-01-04 .... p 2202 N94-23631
p 2202 N94-25095
RTOP 235-01-08 .... p 2313 N94-25170
RTOP 310-10-61-84-02 .... p 2207 N94-23259
RTOP 310-10-61-92-01 .... p 2196 N94-23257
RTOP 310-10-61-92-91 .... p 2196 N94-23258
RTOP 310-20-64-83-02 .... p 2291 N94-23261
RTOP 310-20-65-63-00 .... p 2291 N94-23260
p 2291 N94-23263
RTOP 310-20-66-09-01 .... p 2291 N94-23262
RTOP 310-30-70-87-02 .... p 2291 N94-23264
RTOP 310-30-71-83-02 .... p 2292 N94-23265
p 2292 N94-23266
RTOP 310-40-73-90-01 .... p 2292 N94-23267
RTOP 314-30-50-12-80 .... p 2292 N94-23268
RTOP 315-91-30-20-03 .... p 2292 N94-23269
RTOP 323-57-4A .... p 2203 N94-23632
RTOP 324-01-00 .... p 2525 N94-23698
RTOP 474-46-10 .... p 2205 N94-24825
RTOP 476-14-03 .... p 2431 N94-23970
RTOP 505-41-41 .... p 2222 N94-23591
RTOP 505-59-10-09 .... p 2344 N94-24360
RTOP 505-59-10-30 .... p 2169 N94-24586
RTOP 505-59-20-01 .... p 2169 N94-24311
RTOP 505-59-20 .... p 2167 N94-23557
RTOP 505-59-30-03 .... p 2166 N94-23512
RTOP 505-59-53-01 .... p 2482 N94-23673
RTOP 505-59-53-08 .... p 2457 N94-24603
RTOP 505-61-51 .... p 2171 N94-25187
RTOP 505-62-10 .... p 2364 N94-24483
p 2189 N94-25185
RTOP 505-62-30 .... p 2186 N94-23466
RTOP 505-62-36 .... p 2367 N94-25181
RTOP 505-62-50 .... p 2190 N94-23590
p 2344 N94-24069
RTOP 505-62-52 .... p 2166 N94-23465
p 2320 N94-23525
p 2187 N94-23552
p 2481 N94-23554
p 2169 N94-24335
p 2334 N94-24481
p 2337 N94-25119
p 2338 N94-25180
p 2170 N94-25182
p 2338 N94-25183
RTOP 505-62-84 .... p 2192 N94-23091
p 2344 N94-24362
p 2193 N94-25184
RTOP 505-63-1A .... p 2230 N94-25186
RTOP 505-63-1C .... p 2378 N94-24845
RTOP 505-63-10-02 .... p 2177 N94-24304
RTOP 505-63-36 .... p 2181 N94-24726
RTOP 505-63-40 .... p 2228 N94-23514
RTOP 505-63-5A .... p 2253 N94-23371
p 2242 N94-23467
RTOP 505-63-5B .... p 2376 N94-23551
p 2377 N94-24604
p 2377 N94-24715
RTOP 505-63-50-04 .... p 2241 N94-23274
p 2228 N94-23280
RTOP 505-63-50-08 .... p 2376 N94-23368
RTOP 505-63-50-13 .... p 2169 N94-24576
RTOP 505-63-50-15 .... p 2378 N94-24839
RTOP 505-63-50 .... p 2168 N94-24295
RTOP 505-63-70-02 .... p 2526 N94-24207
RTOP 505-64-10-07 .... p 2445 N94-23125
p 2466 N94-23252
p 2467 N94-24075
p 2467 N94-24463
RTOP 505-64-10-13 .... p 2466 N94-23293
RTOP 505-64-10 .... p 2456 N94-24480
RTOP 505-64-12-02 .... p 2309 N94-23304
RTOP 505-64-12-04 .... p 2343 N94-23498
RTOP 505-64-13-01 .... p 2172 N94-23288
RTOP 505-64-13 .... p 2174 N94-25272
RTOP 505-64-36 .... p 2439 N94-25490
RTOP 505-64-52-01 .... p 2162 N94-25096
RTOP 505-68-10 .... p 2166 N94-23522
p 2172 N94-23523
p 2173 N94-24047
RTOP 505-68-11 .... p 2166 N94-23299
RTOP 505-68-70-08 .... p 2169 N94-24464
RTOP 505-68-71 .... p 2381 N94-22961
RTOP 505-69-50 .... p 2166 N94-23511
p 2170 N94-25173
p 2462 N94-25179
RTOP 505-70-62-02 .... p 2319 N94-23513
RTOP 505-70-62-09 .... p 2192 N94-23564
RTOP 505-70-62-16 .... p 2320 N94-23532
RTOP 505-70-63 .... p 2376 N94-23487
p 2334 N94-24495
RTOP 505-90-00 .... p 2592 N94-24649
p 2592 N94-24660
p 2593 N94-24709
RTOP 505-90-5K .... p 2326 N94-24063
p 2265 N94-24301
p 2333 N94-24336
p 2333 N94-24460
p 2336 N94-24713
RTOP 505-90-52-01 .... p 2317 N94-23089
p 2479 N94-23090
p 2448 N94-23092
p 2480 N94-23272
p 2480 N94-23278
p 2319 N94-23302
p 2451 N94-23340
p 2451 N94-23341
p 2473 N94-23558
p 2487 N94-24291
p 2333 N94-24356
p 2334 N94-24602
p 2334 N94-24605
p 2457 N94-24638
p 2458 N94-24679
p 2458 N94-24680
p 2335 N94-24712
p 2458 N94-24740
p 2490 N94-24836
p 2337 N94-24869
p 2490 N94-24914
p 2444 N94-25090
RTOP 505-90-53 .... p 2243 N94-23578
p 2249 N94-25171
RTOP 506-40-41-02 .... p 2319 N94-23339
RTOP 506-40-61-01 .... p 2170 N94-24716
RTOP 506-41-21 .... p 2390 N94-23345
RTOP 506-41-41 .... p 2218 N94-23370
RTOP 506-42-31 .... p 2218 N94-23372
p 2219 N94-23531
p 2219 N94-23555
p 2219 N94-23630
p 2219 N94-24361
p 2221 N94-24766
p 2221 N94-24770
p 2221 N94-25189
p 2553 N94-25190
p 2222 N94-25201
RTOP 506-42-73 .... p 2346 N94-25202
RTOP 506-42-81 .... p 2220 N94-24714
RTOP 506-44-2C .... p 2310 N94-24308
RTOP 506-59-11 .... p 2465 N94-23085
p 2451 N94-23369
p 2452 N94-23507
p 2591 N94-24099
RTOP 506-72-00 .... p 2290 N94-23087
p 2310 N94-24056
RTOP 506-72-21 .... p 2201 N94-23567
p 2295 N94-24101
p 2304 N94-25266
RTOP 509-10-33 .... p 2452 N94-23510
RTOP 510-01-50 .... p 2372 N94-24074
RTOP 510-02-12 .... p 2378 N94-25188
RTOP 533-02-39 .... p 2188 N94-24106
RTOP 535-03-10 .... p 2187 N94-23545
RTOP 537-02-20 .... p 2481 N94-23593
RTOP 537-02-21 .... p 2188 N94-24594
RTOP 537-02-22 .... p 2153 N94-23553
p 2167 N94-23592
RTOP 537-02-23 .... p 2525 N94-23464
p 2168 N94-24084
RTOP 537-03-21-03 .... p 2526 N94-24172
p 2526 N94-24173
RTOP 537-03-23-03 .... p 2336 N94-24725
RTOP 537-04-20 .... p 2222 N94-23500
RTOP 537-10-20 .... p 2189 N94-25200
RTOP 538-02-10-01 .... p 2228 N94-23279
p 2228 N94-24083
p 2246 N94-25118
RTOP 538-03-11 .... p 2530 N94-25172
RTOP 583-02-01 .... p 2242 N94-23550
RTOP 583-02-21 .... p 2312 N94-24870
RTOP 584-03-11 .... p 2243 N94-23556
p 2169 N94-24606
RTOP 585-03-11-01 .... p 2271 N94-24473
RTOP 586-02-11 .... p 2474 N94-24635
RTOP 586-02-21 .... p 2453 N94-23568
RTOP 590-13-11 .... p 2521 N94-24302
RTOP 674-27-05 .... p 2246 N94-25120
RTOP 685-00-00 .... p 2600 N94-25387
RTOP 694-03-OC .... p 2345 N94-25116
RTOP 763-23-21 .... p 2336 N94-24771
RTOP 763-23-45 .... p 2245 N94-25117
RTOP 778-34-2A .... p 2258 N94-24753
RTOP 900-00-00 .... p 2540 N94-23273
RTOP 916-00-00 .... p 2410 N94-24355
SBIR-02.10-4400 .... p 2525 N94-23698
SBIR-05.01-2878 .... p 2204 N94-23828
SBIR-08.13-7670 .... p 2544 N94-23829
SBIR-14.02-2250 .... p 2295 N94-23830
SERC-GR/F-2417.7 .... p 2492 N94-25306
SERC-GR/F-8564.2 .... p 2476 N94-25308
p 2462 N94-25311
p 2492 N94-25318
SERC-GR/G-30003 .... p 2346 N94-25472
SERC-GR/H-35286 .... p 2523 N94-25314
p 2492 N94-25320
p 2523 N94-25323
SMRC-07-490-5A .... p 2421 N94-24290
SRI PROJ. PYH-2976 .... p 2232 N94-23477
SRI PROJ. 3557 .... p 2232 N94-23524
SRI-1-1EH-46755 .... p 2232 N94-23524
STUF-90-005-770 .... p 2421 N94-24290
STW-DTN-40.0566 .... p 2339 N94-25254
ST2J-0451-C(GDF) .... p 2381 N94-23145
SWRI PROJ. 15-3822 .... p 2209 N94-23484
SWRI PROJ. 15-5301 .... p 2599 N94-24988
USGS-AFR-0973-P-IC-9014 .... p 2280 N94-22776
W-31-109-ENG-38 .... p 2238 N94-22718
p 2371 N94-22872
p 2556 N94-22886
p 2396 N94-22887
p 2556 N94-22912
p 2556 N94-22920
p 2556 N94-22921
p 2557 N94-22927
p 2557 N94-22929
p 2531 N94-22948
p 2465 N94-22973
p 2558 N94-22990
p 2352 N94-22991
p 2252 N94-22992
p 2559 N94-22993
p 2559 N94-22994
p 2559 N94-22995
p 2352 N94-22996
p 2240 N94-23009
p 2560 N94-23187
p 2560 N94-23188
p 2560 N94-23189
p 2590 N94-23190

p 2240 N94-23194
p 2450 N94-23207
p 2318 N94-23213
p 2561 N94-23432
p 2569 N94-23453
p 2242 N94-23457
p 2420 N94-23468
p 2550 N94-23474
p 2562 N94-23795
p 2562 N94-23805
p 2534 N94-23806
p 2545 N94-24550
p 2457 N94-24566
p 2563 N94-24624
p 2457 N94-24626
p 2395 N94-24654
W-7405-ENG-36 .... p 2316 N94-22870
p 2374 N94-22871
p 2556 N94-22920
p 2557 N94-22925
p 2531 N94-22928
p 2231 N94-22933
p 2371 N94-22935
p 2557 N94-22938
p 2239 N94-22939
p 2557 N94-22940
p 2558 N94-22941
p 2558 N94-22942
p 2231 N94-22943
p 2307 N94-22987
p 2240 N94-23003
p 2559 N94-23006
p 2626 N94-23020
p 2240 N94-23021
p 2348 N94-23203
p 2198 N94-23208
p 2218 N94-23283
p 2407 N94-23284
p 2218 N94-23433
p 2218 N94-23452
p 2569 N94-23453
p 2626 N94-23515
p 2417 N94-23517
p 2242 N94-23541
p 2453 N94-23701
p 2326 N94-23809
p 2311 N94-24500
p 2535 N94-24505
p 2569 N94-24516
p 2563 N94-24517
p 2473 N94-24518
p 2552 N94-24519
p 2245 N94-24520
p 2457 N94-24626
p 2553 N94-24628
p 2245 N94-24747
W-7405-ENG-48 .... p 2541 N94-22722
p 2351 N94-22865
p 2351 N94-22866
p 2347 N94-22867
p 2541 N94-22868
p 2531 N94-22869
p 2252 N94-22930
p 2252 N94-22931
p 2589 N94-22934
p 2558 N94-22946
p 2549 N94-22949
p 2307 N94-22950
p 2239 N94-22958
p 2448 N94-22980
p 2532 N94-22988
p 2307 N94-23008
p 2471 N94-23011
p 2209 N94-23012
p 2549 N94-23013
p 2549 N94-23014
p 2240 N94-23017
p 2348 N94-23181
p 2349 N94-23209
p 2568 N94-23216
p 2241 N94-23297
p 2232 N94-23298
p 2241 N94-23434
p 2265 N94-23436
p 2319 N94-23470
p 2408 N94-23471
p 2349 N94-23490
p 2228 N94-23493
p 2382 N94-23494
p 2309 N94-23520
p 2341 N94-23690
p 2397 N94-23700
p 2551 N94-23703
p 2402 N94-23721
p 2265 N94-23778
p 2454 N94-23796
p 2265 N94-23807
p 2552 N94-24502
p 2488 N94-24503
p 2229 N94-24547
p 2234 N94-24549
p 2373 N94-24613
p 2553 N94-24628
p 2229 N94-24632
W-7405-ENG-82 .... p 2227 N94-22977
p 2227 N94-23004
p 2227 N94-23005
p 2253 N94-23183
p 2375 N94-23184
p 2561 N94-23214
p 2243 N94-23717
p 2243 N94-23753
W7714-0-9393/01-ST .... p 2629 N94-24695
W7714-9-9213/01-SS .... p 2300 N94-24696
ZZ867-ZZ899/5986 .... p 2341 N94-23689
36001-0-3503/01-SS .... p 2300 N94-24697

CONTRACT NUMBER INDEX

SCIENTIFIC AND TECHNICAL AEROSPACE REPORTS VOLUME 32 NUMBER 6

Typical Contract Number Index Listing

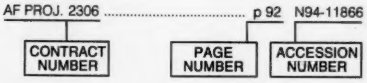

Listings in this index are arranged alphanumerically by contract number. Under each contract number the accession numbers denoting documents that have been produced as a result of research done under that contract are arranged in ascending order. The page number helps to locate the citation in the abstract section. The accession number denotes the number by which the citation is identified.

A-93056 .... p 2171 N94-25187 * #
A-93075 .... p 2431 N94-23970 * #
A-93091 .... p 2426 N94-23575 * #
A-93109 .... p 2426 N94-24102 * #
A-93111 .... p 2167 N94-23557 * #
A-93113 .... p 2176 N94-23489 * #
A-93123 .... p 2439 N94-25490 * #
A-93127 .... p 2453 N94-23568 * #
A-93132 .... p 2174 N94-25272 * #
A-93134 .... p 2431 N94-23974 * #
A-94012 .... p 2452 N94-23510 * #
A-94014 .... p 2420 N94-23088 * #
A-94018 .... p 2181 N94-24796 * #
A-94022 .... p 2387 N94-24403 * #
A-94033 .... p 2598 N94-24832 * #
A-94034 .... p 2598 N94-23536 * #
A-94046 .... p 2430 N94-23527 * #

AD-A235276 .... p 2197 N94-25064 #
AD-A258806 .... p 2632 N94-25075 #
AD-A270883 .... p 2423 N94-22732 #
AD-A271081 .... p 2348 N94-23123 #
AD-A272648 .... p 2456 N94-24535 #
AD-A272808 .... p 2347 N94-22914 #
AD-A273015 .... p 2376 N94-23789 #
AD-A273042 .... p 2542 N94-22915 #
AD-A273125 .... p 2173 N94-24781 #
AD-A273134 .... p 2490 N94-24921 #
AD-A273135 .... p 2234 N94-24772 #
AD-A273142 .... p 2170 N94-24773 #
AD-A273145 .... p 2186 N94-24774 #
AD-A273146 .... p 2299 N94-24668 #
AD-A273147 .... p 2299 N94-24669 #
AD-A273149 .... p 2299 N94-24670 #
AD-A273152 .... p 2418 N94-24671 #
AD-A273157 .... p 2545 N94-24672 #
AD-A273158 .... p 2459 N94-24775 #
AD-A273164 .... p 2262 N94-25136 #
AD-A273165 .... p 2266 N94-24728 #
AD-A273166 .... p 2586 N94-24683 #
AD-A273167 .... p 2458 N94-24684 #
AD-A273175 .... p 2259 N94-24788
AD-A273177 .... p 2536 N94-24729 #
AD-A273178 .... p 2346 N94-25151 #
AD-A273179 .... p 2184 N94-25152 #
AD-A273180 .... p 2174 N94-25153 #
AD-A273181 .... p 2459 N94-24812 #
AD-A273184 .... p 2170 N94-25137 #
AD-A273189 .... p 2372 N94-24553 #
AD-A273195 .... p 2297 N94-24554 #
AD-A273196 .... p 2535 N94-24555 #
AD-A273205 .... p 2457 N94-24556 #
AD-A273206 .... p 2475 N94-24862 #
AD-A273207 .... p 2461 N94-25138 #
AD-A273209 .... p 2189 N94-24776 #
AD-A273219 .... p 2260 N94-24863
AD-A273220 .... p 2260 N94-24922
AD-A273228 .... p 2569 N94-24777 #
AD-A273232 .... p 2259 N94-24789
AD-A273233 .... p 2460 N94-24935
AD-A273241 .... p 2496 N94-24778 #
AD-A273242 .... p 2475 N94-25139 #
AD-A273243 .... p 2338 N94-25140 #
AD-A273245 .... p 2260 N94-24813
AD-A273249 .... p 2536 N94-24717 #
AD-A273250 .... p 2174 N94-25141 #
AD-A273254 .... p 2249 N94-25142 #
AD-A273261 .... p 2311 N94-24685 #
AD-A273263 .... p 2335 N94-24686 #
AD-A273271 .... p 2523 N94-24936
AD-A273279 .... p 2373 N94-24814
AD-A273283 .... p 2260 N94-24815
AD-A273284 .... p 2162 N94-24923
AD-A273297 .... p 2311 N94-24818
AD-A273298 .... p 2260 N94-24924
AD-A273302 .... p 2378 N94-25143
AD-A273304 .... p 2547 N94-25144 #
AD-A273306 .... p 2262 N94-25145 #
AD-A273307 .... p 2565 N94-25086 #
AD-A273332 .... p 2537 N94-25087 #
AD-A273338 .... p 2419 N94-25088 #
AD-A273342 .... p 2346 N94-25154 #
AD-A273344 .... p 2303 N94-25155
AD-A273345 .... p 2461 N94-25156
AD-A273349 .... p 2235 N94-24925
AD-A273356 .... p 2261 N94-24937
AD-A273359 .... p 2350 N94-24938
AD-A273363 .... p 2303 N94-25089 #
AD-A273373 .... p 2173 N94-24718
AD-A273387 .... p 2418 N94-24719
AD-A273391 .... p 2313 N94-25276 #
AD-A273394 .... p 2565 N94-25027
AD-A273395 .... p 2197 N94-25064 #
AD-A273400 .... p 2416 N94-25071 #
AD-A273401 .... p 2301 N94-24926
AD-A273403 .... p 2261 N94-25072 #
AD-A273406 .... p 2530 N94-25073
AD-A273408 .... p 2461 N94-25074 #
AD-A273410 .... p 2632 N94-25075 #
AD-A273411 .... p 2235 N94-24784
AD-A273412 .... p 2460 N94-24927
AD-A273413 .... p 2258 N94-24782
AD-A273415 .... p 2259 N94-24783
AD-A273420 .... p 2427 N94-24928
AD-A273423 .... p 2300 N94-24687 #
AD-A273427 .... p 2421 N94-24688
AD-A273429 .... p 2234 N94-24673
AD-A273437 .... p 2404 N94-24674
AD-A273438 .... p 2422 N94-25146 #
AD-A273455 .... p 2536 N94-24675
AD-A273456 .... p 2299 N94-24676
AD-A273466 .... p 2257 N94-24677
AD-A273467 .... p 2468 N94-24939
AD-A273468 .... p 2496 N94-25147
AD-A273469 .... p 2337 N94-24929
AD-A273470 .... p 2335 N94-24689
AD-A273473 .... p 2198 N94-24690 #
AD-A273474 .... p 2537 N94-24940
AD-A273484 .... p 2592 N94-24691 #
AD-A273488 .... p 2427 N94-24950 #
AD-A273489 .... p 2462 N94-25287 #
AD-A273497 .... p 2474 N94-24622
AD-A273498 .... p 2496 N94-24951 #
AD-A273499 .... p 2174 N94-24941 #
AD-A273501 .... p 2230 N94-24942 #
AD-A273502 .... p 2173 N94-24864 #
AD-A273504 .... p 2235 N94-24790 #
AD-A273508 .... p 2312 N94-24819 #
AD-A273509 .... p 2475 N94-24943 #
AD-A273510 .... p 2260 N94-24848 #
AD-A273511 .... p 2336 N94-24821 #
AD-A273512 .... p 2460 N94-24822 #
AD-A273514 .... p 2338 N94-25157 #
AD-A273515 .... p 2230 N94-25158 #
AD-A273516 .... p 2566 N94-25288 #
AD-A273517 .... p 2262 N94-25159 #
AD-A273518 .... p 2565 N94-25160 #
AD-A273522 .... p 2230 N94-24779 #
AD-A273540 .... p 2422 N94-24791 #
AD-A273541 .... p 2259 N94-24792 #
AD-A273542 .... p 2261 N94-24930 #
AD-A273543 .... p 2496 N94-24931 #
AD-A273544 .... p 2336 N94-24793 #
AD-A273545 .... p 2404 N94-24794 #
AD-A273546 .... p 2602 N94-24557 #
AD-A273547 .... p 2257 N94-24558 #
AD-A273550 .... p 2193 N94-24559 #
AD-A273551 .... p 2495 N94-24560 #
AD-A273552 .... p 2488 N94-24561 #
AD-A273553 .... p 2257 N94-24562
AD-A273554 .... p 2427 N94-24865
AD-A273555 .... p 2235 N94-24917
AD-A273558 .... p 2547 N94-25161
AD-A273559 .... p 2418 N94-24918
AD-A273560 .... p 2416 N94-25162
AD-A273561 .... p 2230 N94-25163
AD-A273565 .... p 2467 N94-24692 #
AD-A273566 .... p 2458 N94-24693 #
AD-A273568 .... p 2419 N94-24944 #
AD-A273584 .... p 2427 N94-24945 #
AD-A273585 .... p 2419 N94-25164
AD-A273586 .... p 2419 N94-25165
AD-A273588 .... p 2170 N94-24849
AD-A273590 .... p 2593 N94-24946 #
AD-A273591 .... p 2415 N94-24850
AD-A273593 .... p 2418 N94-24795
AD-A273598 .... p 2245 N94-24823
AD-A273600 .... p 2460 N94-24932
AD-A273601 .... p 2460 N94-24933
AD-A273609 .... p 2350 N94-24934
AD-A273610 .... p 2491 N94-24947
AD-A273612 .... p 2419 N94-24948 #
AD-A273613 .... p 2553 N94-24949 #
AD-A273615 .... p 2545 N94-24730
AD-A273625 .... p 2546 N94-24731
AD-A273626 .... p 2258 N94-24732
AD-A273630 .... p 2186 N94-24733
AD-A273632 .... p 2570 N94-25028
AD-A273633 .... p 2261 N94-25029
AD-A273638 .... p 2468 N94-25030
AD-A273639 .... p 2628 N94-25031
AD-A273640 .... p 2337 N94-25032 #
AD-A273643 .... p 2245 N94-25033
AD-A273644 .... p 2461 N94-25148 #
AD-A273652 .... p 2461 N94-25149 #
AD-A273656 .... p 2419 N94-25435 #
AD-A273659 .... p 2368 N94-25436 #
AD-A273661 .... p 2251 N94-25448 #
AD-A273662 .... p 2251 N94-25449 #
AD-A273663 .... p 2251 N94-25450 #
AD-A273664 .... p 2251 N94-25451 #
AD-A273665 .... p 2250 N94-25405 #
AD-A273666 .... p 2250 N94-25406 #
AD-A273667 .... p 2250 N94-25407 #
AD-A273668 .... p 2250 N94-25408 #
AD-A273673 .... p 2263 N94-25409 #
AD-A273674 .... p 2263 N94-25410 #
AD-A273680 .... p 2171 N94-25411 #
AD-A273683 .... p 2263 N94-25413 #
AD-A273685 .... p 2185 N94-25440 #
AD-A273686 .... p 2567 N94-25441 #
AD-A273687 .... p 2428 N94-25437 #
AD-A273688 .... p 2446 N94-25438 #
AD-A273697 .... p 2314 N94-25488 #
AD-A273698 .... p 2263 N94-25489 #
AD-A273699 .... p 2493 N94-25452 #
AD-A273700 .... p 2463 N94-25453 #
AD-A273701 .... p 2469 N94-25454 #
AD-A273702 .... p 2463 N94-25455 #
AD-A273703 .... p 2463 N94-25456 #
AD-A273727 .... p 2539 N94-25443 #
AD-A273728 .... p 2351 N94-25445 #
AD-A273729 .... p 2339 N94-25446 #
AD-A273737 .... p 2207 N94-25542 #
AD-A273740 .... p 2340 N94-25530 #
AD-A273741 .... p 2251 N94-25531 #
AD-A273742 .... p 2206 N94-25532 #
AD-A273743 .... p 2547 N94-25533 #
AD-A273744 .... p 2340 N94-25534 #
AD-A273752 .... p 2406 N94-25540 #
AD-A273800 .... p 2406 N94-25535 #

AD-A273801 p 2406 N94-25536 #
AD-A273803 p 2406 N94-25537 #
AD-A273807 p 2406 N94-25538 #
AD-A273818 p 2190 N94-25516 #
AD-A273820 p 2171 N94-25517 #
AD-A273821 p 2496 N94-25518 #
AD-A273822 p 2539 N94-25519 #
AD-A273824 p 2314 N94-25539 #
AD-A273825 p 2379 N94-25520
AD-A273826 p 2304 N94-25521
AD-A273827 p 2194 N94-25522
AD-A273828 p 2206 N94-25523
AD-A273830 p 2571 N94-25524
AD-A273831 p 2191 N94-25525

AD-D015974 p 2446 N94-25034
AD-D015975 p 2312 N94-25035
AD-D015977 p 2312 N94-25036
AD-D015978 p 2350 N94-25216
AD-D015979 p 2345 N94-25037
AD-D015980 p 2301 N94-25038
AD-D015981 p 2312 N94-25039
AD-D015982 p 2301 N94-25040
AD-D015984 p 2301 N94-25041
AD-D015985 p 2303 N94-25217
AD-D015986 p 2312 N94-25042
AD-D015988 p 2546 N94-25043
AD-D015989 p 2302 N94-25049
AD-D015990 p 2312 N94-25050
AD-D015992 p 2170 N94-25051
AD-D015993 p 2184 N94-25052
AD-D015994 p 2345 N94-25053
AD-D015996 p 2261 N94-25054
AD-D015997 p 2367 N94-25055
AD-D015998 p 2302 N94-25056
AD-D016000 p 2350 N94-25044
AD-D016002 p 2301 N94-25045
AD-D016003 p 2302 N94-25057
AD-D016004 p 2367 N94-25046
AD-D016005 p 2302 N94-25058
AD-D016006 p 2537 N94-25047
AD-D016008 p 2302 N94-25048
AD-D016013 p 2344 N94-24734
AD-D016014 p 2230 N94-24735
AD-D016015 p 2311 N94-24736
AD-D016017 p 2350 N94-24952
AD-D016019 p 2258 N94-24737
AD-D016020 p 2258 N94-24720
AD-D016021 p 2258 N94-24721
AD-D016023 p 2303 N94-25150
AD-D016025 p 2545 N94-24722
AD-D016026 p 2344 N94-24723
AD-D016027 p 2446 N94-24724

AD-E201703 p 2406 N94-25536 #
AD-E201709 p 2406 N94-25538 #
AD-E201725 p 2406 N94-25535 #

ADXC-E201701 p 2406 N94-25537 #

AFIT/DS/ENP/93-08 p 2304 N94-25521

AFIT/GA/ENY/93D-7 p 2206 N94-25523
AFIT/GA/ENY/93D-8 p 2206 N94-25532 #

AFIT/GAE/ENY/93D-14 p 2171 N94-25517 #
AFIT/GAE/ENY/93D-18 p 2571 N94-25524
AFIT/GAE/ENY/93D-19 p 2194 N94-25522
AFIT/GAE/ENY/93D-21 p 2191 N94-25525
AFIT/GAE/ENY/93D-2 p 2339 N94-25446 #
AFIT/GAE/ENY/93D-8 p 2379 N94-25520
AFIT/GAE/ENY/93D-9 p 2340 N94-25534 #

AFIT/GAP/ENP/93D-03 p 2539 N94-25443 #
AFIT/GAP/ENP/93D-06 p 2539 N94-25519 #
AFIT/GAP/ENP/93D-09 p 2351 N94-25445 #

AFIT/GEO/ENP/93D-02 p 2547 N94-25533 #

AFIT/GSO/ENS/ENC/93D-12 p 2496 N94-25518 #

AFIT/GSO/ENY/93D-6 p 2314 N94-25539 #

AFOSR-PAM-70-1 p 2632 N94-25075 #

AFOSR-TR-93-0848 p 2632 N94-25075 #

AFOSR-93-0847TR p 2261 N94-24937
AFOSR-93-0850TR p 2565 N94-25160 #
AFOSR-93-0853TR p 2404 N94-24794 #
AFOSR-93-0854TR p 2421 N94-24688
AFOSR-93-0856TR p 2427 N94-24865
AFOSR-93-0857TR p 2404 N94-24674
AFOSR-93-0858TR p 2602 N94-24557 #
AFOSR-93-0860TR p 2475 N94-24943 #
AFOSR-93-0861TR p 2338 N94-25157 #
AFOSR-93-0862TR p 2468 N94-24939
AFOSR-93-0863TR p 2170 N94-24849
AFOSR-93-0864TR p 2258 N94-24782
AFOSR-93-0865TR p 2566 N94-25288 #
AFOSR-93-0866TR p 2259 N94-24783
AFOSR-93-0867TR p 2230 N94-25158 #
AFOSR-93-0868TR p 2337 N94-24929
AFOSR-93-0870TR p 2257 N94-24677
AFOSR-93-0871TR p 2496 N94-25147
AFOSR-93-0872TR p 2234 N94-24673
AFOSR-93-0873TR p 2496 N94-24931 #
AFOSR-93-0875TR p 2335 N94-24689
AFOSR-93-0876TR p 2336 N94-24793 #
AFOSR-93-0877TR p 2488 N94-24561 #
AFOSR-93-0878TR p 2474 N94-24622

AGARD-LS-187 p 2431 N94-23976 #
AGARD-LS-189 p 2423 N94-23313 #
AGARD-LS-192 p 2521 N94-25008 #

AGARD-R-794 p 2177 N94-24313 #
AGARD-R-795 p 2255 N94-24228 #
AGARD-R-805 p 2173 N94-24091 #

AIAA PAPER 93-1899 p 2219 N94-23531 * #
AIAA PAPER 93-3764 p 2188 N94-24106 * #
AIAA PAPER 93-3812 p 2190 N94-23590 * #
AIAA PAPER 93-4359 p 2529 N94-24307 * #
AIAA PAPER 94-0091 p 2265 N94-24301 * #
AIAA PAPER 94-0138 p 2153 N94-23553 * #
AIAA PAPER 94-0139 p 2525 N94-23464 * #
AIAA PAPER 94-0186 p 2167 N94-23592 * #
AIAA PAPER 94-0217 p 2188 N94-24594 * #
AIAA PAPER 94-0218 p 2187 N94-24082 * #
AIAA PAPER 94-0219 p 2481 N94-23593 * #
AIAA PAPER 94-0306 p 2481 N94-23554 * #
AIAA PAPER 94-0365 p 2170 N94-25182 * #
AIAA PAPER 94-0375 p 2218 N94-23370 * #
AIAA PAPER 94-0582 p 2168 N94-24084 * #
AIAA PAPER 94-0620 p 2166 N94-23465 * #
AIAA PAPER 94-0716 p 2166 N94-23299 * #
AIAA PAPER 94-0718 p 2173 N94-24047 * #
AIAA PAPER 94-0733 p 2169 N94-24335 * #
AIAA PAPER 94-0799 p 2166 N94-23522 * #
AIAA PAPER 94-0804 p 2172 N94-23523 * #
AIAA PAPER 94-0852 p 2153 N94-24100 * #
AIAA PAPER 94-1101 p 2201 N94-23567 * #
AIAA PAPER 94-1158 p 2295 N94-24101 * #

AL/CF-PC-1993-0040 p 2427 N94-24928

ANL-HEP-CP-93-66 p 2534 N94-23806

ANL-93/23 p 2465 N94-22973 #
ANL-93/26 p 2450 N94-23207

ANL/APS/CP-5 p 2531 N94-22948 #

ANL/CHM/CP-80915 p 2562 N94-23805 #

ANL/CHM/PP-77001 p 2561 N94-23432 #
ANL/CHM/PP-77691 p 2556 N94-22912 #

ANL/ECT/CP-80138 p 2556 N94-22921

ANL/EP/CP-79902 p 2550 N94-23474 #

ANL/ER/CP-80457 p 2396 N94-22887 #

ANL/ES/CP-80771 p 2352 N94-22996

ANL/ES/RP-81001 p 2395 N94-24654 #

ANL/ET/CP-78614 p 2563 N94-24624 #
ANL/ET/CP-78724 p 2559 N94-22994
ANL/ET/CP-79670 p 2371 N94-22872
ANL/ET/CP-80643 p 2352 N94-22991 #
ANL/ET/CP-80756 p 2242 N94-23457 #
ANL/ET/CP-80862 p 2238 N94-22718 #
ANL/ET/CP-80863 p 2240 N94-23194 #
ANL/ET/CP-80889 p 2240 N94-23009

ANL/IPNS/CP-79847 p 2252 N94-22992

ANL/MCS-TM-181 p 2318 N94-23213 #

ANL/MCS/CP-80305 p 2420 N94-23468
ANL/MCS/CP-81094 p 2457 N94-24566 #

ANL/MCT/CP-78916 p 2559 N94-22993
ANL/MCT/CP-80158 p 2556 N94-22886 #

ANL/MSD/CP-78506 p 2557 N94-22927 #
ANL/MSD/CP-79360 p 2559 N94-22995 #
ANL/MSD/CP-79942 p 2560 N94-23189 #
ANL/MSD/CP-80681 p 2556 N94-22920
ANL/MSD/CP-80905 p 2558 N94-22990
ANL/MSD/CP-80962 p 2557 N94-22929 #
ANL/MSD/CP-81086 p 2562 N94-23795 #

ANL/PHY/CP-80830 p 2590 N94-23190 #

ANL/XFD/CP-80250 p 2560 N94-23188
ANL/XFD/CP-80251 p 2560 N94-23187
ANL/XFD/CP-81131 p 2545 N94-24550

AN25/UK/151092/1.1 p 2373 N94-25475 #

ARCCB-TR-93031 p 2249 N94-25142 #

ARI-TR-990 p 2462 N94-25287 #

ARL-CR-120-VOL-2 p 2173 N94-24864 #
ARL-CR-141 p 2234 N94-24565 * #

ARL-MR-138 p 2367 N94-25181 * #

ARL-TR-223 p 2263 N94-25410 #
ARL-TR-295 p 2198 N94-24690 #
ARL-TR-345 p 2364 N94-24483 * #

ASIPP-0027 p 2555 N94-25333
ASIPP-0028 p 2554 N94-25329 #
ASIPP-0029 p 2555 N94-25344 #
ASIPP-0030 p 2555 N94-25331 #

ATC-193 p 2175 N94-24127 #
ATC-197 p 2415 N94-24850

ATCOM-TR-93-A-002 p 2171 N94-25187 * #

ATR-92(8436)-1 p 2534 N94-24077

AU-5-34046 p 2401 N94-23337 * #

AVSCOM-TR-92-C-032 p 2364 N94-24090 * #

B-254957 p 2591 N94-24092 #

BARC-1992/E/042 p 2542 N94-22979 #
BARC-1992/E/047 p 2347 N94-22967

BBC-RD-1993/10 p 2295 N94-24086
BBC-RD-1993/9 p 2295 N94-24085

BC-ISR-03 p 2207 N94-25542 #

BCRS-92-24 p 2381 N94-23145 #
BCRS-92-25 p 2417 N94-23176 #
BCRS-92-27 p 2382 N94-23177 #
BCRS-93-04 p 2417 N94-24107 #

BER-570-97 p 2378 N94-25267 * #
BER-605-163 p 2365 N94-24842 * #
BER-9110 p 2340 N94-25467 #

BNL-49416 p 2531 N94-22923 #
BNL-49453 p 2532 N94-23007 #
BNL-49477 p 2234 N94-24545 #
BNL-49483 p 2245 N94-24612 #
BNL-49530 p 2386 N94-23779 #
BNL-49537 p 2389 N94-22962 #

BRA-92-WO24R p 2553 N94-24949 #

BRDEC-TR/2544 p 2261 N94-25029

BTI-92/3-31 p 2629 N94-24695

CA-PATENT-APPL-SN-2043039 p 2188 N94-24490
CA-PATENT-APPL-SN-2043757 p 2254 N94-24129
CA-PATENT-APPL-SN-2053597 p 2297 N94-24183

CA-PATENT-1-308-179 p 2544 N94-24489
CA-PATENT-1-315-259 p 2176 N94-23254
CA-PATENT-1-317-467 p 2186 N94-23253
CA-PATENT-1-319-357 p 2186 N94-23255
CA-PATENT-1-320-710 p 2353 N94-23215
CA-PATENT-1-320-878 p 2363 N94-24055
CA-PATENT-1-322-361 p 2193 N94-24785
CA-PATENT-1308581 p 2364 N94-24175 #
CA-PATENT-1322107 p 2344 N94-24184
CA-PATENT-1323020 p 2176 N94-24181
CA-PATENT-1323021 p 2168 N94-24182
CA-PATENT-1323353 p 2188 N94-24180
CA-PATENT-163126888 p 2364 N94-24128

CAL-2145 p 2453 N94-23559 * #

CAR-94-06 p 2597 N94-24829 * #

CARDIVNSWC-TR-61-CR-93-02 p 2378 N94-25143

CBPF-NF-004/92 .... p 2568 N94-22968

CDDF-92-02 .... p 2269 N94-23574 * #

CDRL-12B .... p 2311 N94-24754 * #

CEBAF-PR-93-032 .... p 2540 N94-24662 #
CEBAF-PR-94-001 .... p 2540 N94-24663 #

CEBAF-TH-93-05 .... p 2532 N94-22952
CEBAF-TH-93-09 .... p 2531 N94-22951 #

CERL-FEAP-TR-FM-93/06 .... p 2373 N94-24814

CERL-IR-FF-93/06 .... p 2459 N94-24812 #

CERL-TR-FF-93/12 .... p 2460 N94-24935

CERT-2/7766-DERA .... p 2474 N94-24627

CIS-N-93-742 .... p 2445 N94-23788

CMOTT-93-08 .... p 2336 N94-24713 * #
CMOTT-93-16 .... p 2333 N94-24336 * #
CMOTT-93-17 .... p 2333 N94-24460 * #
CMOTT-93-18 .... p 2326 N94-24063 * #

CMU-CS-93-171 .... p 2467 N94-24692 #
CMU-CS-93-197 .... p 2458 N94-24693 #
CMU-CS-93-201 .... p 2460 N94-24933
CMU-CS-93-205 .... p 2460 N94-24932

CNIC-00511 .... p 2555 N94-25333
CNIC-00513 .... p 2554 N94-25330 #
CNIC-00567 .... p 2566 N94-25332 #
CNIC-00569 .... p 2554 N94-25329 #
CNIC-00576 .... p 2555 N94-25344 #
CNIC-00577 .... p 2555 N94-25331 #

COAM-TR-2/94 .... p 2418 N94-24671 #

COMPUTING SCIENCE NOTES-93/07 .... p 2454 N94-23768
COMPUTING SCIENCE NOTES-93/10 .... p 2489 N94-24615
COMPUTING SCIENCE NOTES-93/11 .... p 2456 N94-24513
COMPUTING SCIENCE NOTES-93/12 .... p 2271 N94-24475
COMPUTING SCIENCE NOTES-93/14 .... p 2488 N94-24539
COMPUTING SCIENCE NOTES-93/15 .... p 2446 N94-24540
COMPUTING SCIENCE NOTES-93/22 .... p 2454 N94-23817 #
COMPUTING SCIENCE NOTES-93/23 .... p 2486 N94-23724 #

CONF-9101168 .... p 2548 N94-22924 #
CONF-9210290 .... p 2531 N94-22948 #
CONF-9210401 .... p 2352 N94-23025
CONF-921188-2 .... p 2471 N94-23011
CONF-921188-3 .... p 2307 N94-23008 #
CONF-921261-4 .... p 2533 N94-23218
CONF-921277-3 .... p 2234 N94-24545 #
CONF-9301119-3 .... p 2348 N94-23181 #
CONF-9302103-5 .... p 2239 N94-22958 #
CONF-9303221-2 .... p 2265 N94-23436 #
CONF-9303237-1 .... p 2454 N94-23796 #
CONF-930367-9 .... p 2556 N94-22920
CONF-930389-22 .... p 2531 N94-22923 #
CONF-930389-24 .... p 2626 N94-23515 #
CONF-930405-43 .... p 2241 N94-23297 #
CONF-9304145-3 .... p 2240 N94-23003 #
CONF-9304146-2 .... p 2241 N94-23219 #
CONF-9304146-3 .... p 2238 N94-22936 #
CONF-9304174 .... p 2239 N94-22965
CONF-9304174 .... p 2239 N94-22966
CONF-9304191-3 .... p 2556 N94-22864
CONF-9304191-4 .... p 2556 N94-22919 #
CONF-9304197-2 .... p 2542 N94-23202
CONF-9304201-1 .... p 2588 N94-22863
CONF-9304206-1 .... p 2589 N94-22934 #
CONF-930445-26 .... p 2525 N94-23206 #
CONF-930449-5 .... p 2534 N94-23803
CONF-9305199-2 .... p 2601 N94-23010 #
CONF-9305210-2 .... p 2548 N94-22916 #
CONF-9305210-4 .... p 2550 N94-23462 #
CONF-9305210-5 .... p 2549 N94-22998 #
CONF-9305280-1 .... p 2557 N94-22926 #
CONF-930540-11 .... p 2389 N94-22888 #
CONF-930571-27 .... p 2389 N94-22962 #
CONF-930571-28 .... p 2238 N94-22932 #
CONF-9306125-4 .... p 2531 N94-22869 #
CONF-930616-38 .... p 2311 N94-24500 #
CONF-930616-39 .... p 2307 N94-22950 #
CONF-9306176-12 .... p 2535 N94-24611 #
CONF-9306200-1 .... p 2535 N94-24510 #
CONF-9306221-5 .... p 2535 N94-24515 #
CONF-9306237-4 .... p 2563 N94-24567 #
CONF-9306245-1 .... p 2349 N94-23490 #
CONF-9306254-1 .... p 2342 N94-22954 #
CONF-9306256-1 .... p 2307 N94-22955 #
CONF-9306258-3 .... p 2534 N94-23806
CONF-9306267-1 .... p 2552 N94-24502 #
CONF-930636-4 .... p 2569 N94-23453
CONF-930636-6 .... p 2532 N94-23007 #
CONF-930637-5 .... p 2626 N94-23020
CONF-930676-SUPPL .... p 2402 N94-23721 #
CONF-930676-51 .... p 2558 N94-22953 #
CONF-930676-59 .... p 2558 N94-22946
CONF-930703-34 .... p 2307 N94-23019 #
CONF-930703-37 .... p 2271 N94-24568 #
CONF-930703-9 .... p 2556 N94-22886 #
CONF-930710-4 .... p 2557 N94-22929 #
CONF-930711-1 .... p 2532 N94-22956 #
CONF-930712-7 .... p 2243 N94-23715 #
CONF-930713-27 .... p 2232 N94-23298 #
CONF-930713-30 .... p 2265 N94-23807
CONF-930713-32 .... p 2265 N94-23778 #
CONF-9307140-1 .... p 2560 N94-23204 #
CONF-930720-22 .... p 2552 N94-24504 #
CONF-930722-32 .... p 2347 N94-22867 #
CONF-930722-34 .... p 2541 N94-22868 #
CONF-930722-38 .... p 2549 N94-22949 #
CONF-930722-43 .... p 2542 N94-22917 #
CONF-930738-1 .... p 2562 N94-23795 #
CONF-930751-1 .... p 2564 N94-24657 #
CONF-930776-3 .... p 2535 N94-24569 #
CONF-930788-6 .... p 2319 N94-23470 #
CONF-930802-15 .... p 2390 N94-23212
CONF-930802-16 .... p 2526 N94-23718 #
CONF-930804-20 .... p 2243 N94-23753 #
CONF-930804-21 .... p 2394 N94-23781 #
CONF-9308106-1 .... p 2395 N94-24499 #
CONF-9308122-10 .... p 2558 N94-22990
CONF-9308122-11 .... p 2244 N94-23811
CONF-9308122-13 .... p 2229 N94-24547 #
CONF-9308122-7 .... p 2543 N94-23458 #
CONF-9308122-9 .... p 2558 N94-22957
CONF-9308145-1 .... p 2351 N94-22865
CONF-9308149-1 .... p 2351 N94-22866
CONF-9308150-4 .... p 2591 N94-24607
CONF-9308151-2 .... p 2552 N94-24546 #
CONF-9308154-2 .... p 2245 N94-24612 #
CONF-9308158-3 .... p 2252 N94-22931 #
CONF-9308159-1 .... p 2472 N94-23201 #
CONF-9308159-2 .... p 2613 N94-23469 #
CONF-9308163-1 .... p 2348 N94-23203
CONF-9308163-2 .... p 2231 N94-22933 #
CONF-9308164-1 .... p 2531 N94-22928 #
CONF-9308167-1 .... p 2371 N94-22872
CONF-9308172-1 .... p 2448 N94-22980
CONF-9308173-2 .... p 2558 N94-22941
CONF-9308183-3 .... p 2551 N94-23782 #
CONF-9308188-1 .... p 2569 N94-24516 #
CONF-930824-13 .... p 2560 N94-23187
CONF-930824-14 .... p 2560 N94-23188
CONF-930824-20 .... p 2545 N94-24550
CONF-930824-6 .... p 2556 N94-22921
CONF-930825-11 .... p 2244 N94-23792
CONF-930825-6 .... p 2238 N94-22861 #
CONF-930825-7 .... p 2239 N94-22999 #
CONF-930825-9 .... p 2242 N94-23457 #
CONF-930838-2 .... p 2395 N94-24512 #
CONF-930852-3 .... p 2557 N94-22927 #
CONF-930865-11 .... p 2558 N94-22942
CONF-930865-4 .... p 2557 N94-22925 #
CONF-930879-1 .... p 2534 N94-23804 #
CONF-930893-16 .... p 2395 N94-23785 #
CONF-930893-6 .... p 2389 N94-22723 #
CONF-930905-10 .... p 2231 N94-22943 #
CONF-930905-11 .... p 2239 N94-22939 #
CONF-930905-20 .... p 2245 N94-24747 #
CONF-930905-6 .... p 2559 N94-23006 #
CONF-9309137-1 .... p 2397 N94-23016
CONF-9309139-9 .... p 2589 N94-22944 #
CONF-9309185-2 .... p 2557 N94-22940 #
CONF-9309199-10 .... p 2541 N94-22722 #
CONF-9309199-11 .... p 2234 N94-24549 #
CONF-9309199-5 .... p 2543 N94-23461 #
CONF-9309215-3 .... p 2268 N94-23000 #
CONF-9309230-2 .... p 2388 N94-24757 #
CONF-9309231-2 .... p 2557 N94-22938
CONF-9309231-3 .... p 2242 N94-23541 #
CONF-9309231-4 .... p 2240 N94-23021
CONF-9309238-2 .... p 2591 N94-24501 #
CONF-9309251-1 .... p 2560 N94-23189 #
CONF-930926-13 .... p 2307 N94-22987
CONF-930926-15 .... p 2549 N94-23013
CONF-930926-17 .... p 2549 N94-23014
CONF-930926-18 .... p 2299 N94-24656 #
CONF-9309262-1 .... p 2590 N94-23190 #
CONF-9309264-1 .... p 2309 N94-23520 #
CONF-9309272-1 .... p 2473 N94-24518 #
CONF-930928-7 .... p 2240 N94-23194 #
CONF-930928-8 .... p 2240 N94-23009
CONF-930928-9 .... p 2238 N94-22718 #
CONF-930948-1 .... p 2209 N94-23012
CONF-931009-3 .... p 2227 N94-22977 #
CONF-931009-4 .... p 2227 N94-23005
CONF-931009-5 .... p 2375 N94-23184 #
CONF-931009-6 .... p 2243 N94-23717 #
CONF-931009-8 .... p 2563 N94-24624 #
CONF-9310100-3 .... p 2429 N94-22997 #
CONF-9310145-2 .... p 2397 N94-23794 #
CONF-9310164-3 .... p 2371 N94-22935 #
CONF-9310167-2 .... p 2371 N94-22918 #
CONF-9310172-1 .... p 2420 N94-23468
CONF-9310173-1 .... p 2396 N94-22887 #
CONF-931018-11 .... p 2550 N94-23182 #
CONF-931018-17 .... p 2553 N94-24756 #
CONF-931018-36 .... p 2550 N94-23474 #
CONF-931018-42 .... p 2553 N94-24628 #
CONF-931018-4 .... p 2553 N94-24746 #
CONF-931018-55 .... p 2354 N94-23797 #
CONF-931018-56 .... p 2552 N94-24519 #
CONF-9310194-1 .... p 2270 N94-23790 #
CONF-9310195-1 .... p 2349 N94-23209 #
CONF-9310203-1 .... p 2398 N94-24506 #
CONF-931023-6 .... p 2457 N94-24626 #
CONF-931081-5 .... p 2234 N94-24548 #
CONF-931102-1 .... p 2352 N94-22996
CONF-931102-2 .... p 2352 N94-22991 #
CONF-931103-3 .... p 2227 N94-23004
CONF-931103-4 .... p 2559 N94-22994
CONF-9311101-1 .... p 2559 N94-23186 #
CONF-9311101-4 .... p 2309 N94-23777 #
CONF-9311104-1 .... p 2562 N94-23805 #
CONF-9311104-2 .... p 2555 N94-22717 #
CONF-9311104-6 .... p 2350 N94-24659 #
CONF-9311115-1 .... p 2311 N94-24748 #
CONF-9311117-1 .... p 2457 N94-24566 #
CONF-931121-21 .... p 2316 N94-22870 #
CONF-931121-22 .... p 2374 N94-22871 #
CONF-931121-27 .... p 2568 N94-23216 #
CONF-931121-28 .... p 2559 N94-22993
CONF-931121-29 .... p 2245 N94-24520 #
CONF-931121-30 .... p 2229 N94-24632 #
CONF-931133-4 .... p 2252 N94-22992
CONF-931133-5 .... p 2559 N94-22995 #
CONF-931142-1 .... p 2253 N94-23183 #
CONF-931142-3 .... p 2563 N94-24517 #
CONF-931208-1 .... p 2452 N94-23488 #
CONF-931215-1 .... p 2343 N94-23200 #
CONF-931233-2 .... p 2293 N94-23473 #
CONF-940101-11 .... p 2218 N94-23452 #
CONF-940101-13 .... p 2220 N94-24511 #
CONF-940101-4 .... p 2218 N94-23433 #
CONF-940101-5 .... p 2348 N94-23185 #
CONF-940101-6 .... p 2217 N94-23193 #
CONF-940101-8 .... p 2218 N94-23283 #
CONF-940113-2 .... p 2394 N94-23472 #
CONF-940115-3 .... p 2407 N94-23284 #
CONF-940115-7 .... p 2386 N94-23779 #
CONF-940130-1 .... p 2466 N94-23491 #
CONF-940131-1 .... p 2417 N94-23517 #
CONF-940139-1 .... p 2408 N94-23471 #

CRANFIELD-AERO-9211 .... p 2523 N94-25480 #
CRANFIELD-AERO-9212 .... p 2594 N94-25485 #
CRANFIELD-AERO-9213 .... p 2340 N94-25486 #

CSN-93/09 .... p 2268 N94-23476

CTN-94-60868 .... p 2544 N94-24489
CTN-94-60869 .... p 2364 N94-24128
CTN-94-60870 .... p 2188 N94-24490
CTN-94-60871 .... p 2254 N94-24129
CTN-94-60872 .... p 2364 N94-24175 #
CTN-94-60873 .... p 2175 N94-24176
CTN-94-60874 .... p 2333 N94-24177
CTN-94-60875 .... p 2168 N94-24178
CTN-94-60876 .... p 2297 N94-24179
CTN-94-60893 .... p 2455 N94-24130
CTN-94-60895 .... p 2432 N94-24114
CTN-94-60896 .... p 2296 N94-24131
CTN-94-60897 .... p 2296 N94-24115
CTN-94-60898 .... p 2297 N94-24296
CTN-94-60899 .... p 2300 N94-24694
CTN-94-60900 .... p 2629 N94-24695
CTN-94-60901 .... p 2300 N94-24696
CTN-94-60902 .... p 2300 N94-24697
CTN-94-60903 .... p 2296 N94-24132
CTN-94-60904 .... p 2296 N94-24133
CTN-94-60905 .... p 2455 N94-24134
CTN-94-60906 .... p 2455 N94-24135
CTN-94-60907 .... p 2455 N94-24116

CTN-94-60908 p 2455 N94-24297
CTN-94-60911 p 2297 N94-24298
CTN-94-60912 p 2437 N94-24299
CTN-94-60913 p 2193 N94-24117
CTN-94-60914 p 2296 N94-24118
CTN-94-60915 p 2433 N94-24119
CTN-94-60916 p 2174 N94-24120
CTN-94-60917 p 2202 N94-24121
CTN-94-60918 p 2455 N94-24122
CTN-94-60919 p 2193 N94-24123
CTN-94-60921 p 2372 N94-24136
CTN-94-60922 p 2186 N94-23253
CTN-94-60923 p 2176 N94-23254
CTN-94-60924 p 2186 N94-23255
CTN-94-60925 p 2229 N94-24137
CTN-94-60926 p 2244 N94-24170
CTN-94-60927 p 2433 N94-24171
CTN-94-60928 p 2363 N94-24055
CTN-94-60929 p 2353 N94-23215
CTN-94-60930 p 2188 N94-24180
CTN-94-60931 p 2176 N94-24181
CTN-94-60932 p 2168 N94-24182
CTN-94-60933 p 2193 N94-24785
CTN-94-60934 p 2297 N94-24183
CTN-94-60935 p 2344 N94-24184
CTN-94-60944 p 2196 N94-22889
CTN-94-60945 p 2226 N94-22890
CTN-94-60946 p 2541 N94-22891
CTN-94-60947 p 2227 N94-22892
CTN-94-60956 p 2544 N94-24466
CTN-94-60957 p 2427 N94-24467
CTN-94-60958 p 2257 N94-24468
CTN-94-60959 p 2244 N94-24469

CU-CSSC-93-16 p 2203 N94-23618 * #

CU-DOE-92-09 p 2300 N94-24694

CWI-AM-R9301 p 2420 N94-23521 #

CWP-139 p 2402 N94-23516 #

CWRU-342-7658 p 2349 N94-23286 * #

DCIEM-93-05 p 2437 N94-24299
DCIEM-93-06 p 2433 N94-24119
DCIEM-93-13 p 2432 N94-24114

DCN-1-3-EB-29681 p 2453 N94-23624 * #

DE93-000168 p 2345 N94-24831 #
DE93-011687 p 2452 N94-23488 #
DE93-017416 p 2556 N94-22886 #
DE93-017626 p 2343 N94-23200 #
DE93-017775 p 2548 N94-22916 #
DE93-018213 p 2389 N94-22862 #
DE93-018221 p 2390 N94-23295 #
DE93-018720 p 2395 N94-24499 #
DE93-018790 p 2588 N94-22863
DE93-018936 p 2542 N94-22917 #
DE93-019016 p 2472 N94-23201 #
DE93-019197 p 2556 N94-22919 #
DE93-019200 p 2556 N94-22864
DE93-019574 p 2351 N94-22865
DE93-019621 p 2349 N94-23490 #
DE93-019622 p 2351 N94-22866
DE93-019629 p 2347 N94-22867 #
DE93-019820 p 2542 N94-23202
DE93-019940 p 2541 N94-22868 #
DE93-019950 p 2531 N94-22869 #
DE93-040040 p 2531 N94-22923 #
DE93-040094 p 2348 N94-23203
DE93-040107 p 2557 N94-22925 #
DE93-040120 p 2557 N94-22926 #
DE93-040127 p 2531 N94-22928 #
DE93-040146 p 2316 N94-22870 #
DE93-040159 p 2374 N94-22871 #
DE93-040161 p 2231 N94-22933 #
DE93-040189 p 2311 N94-24500 #
DE93-040273 p 2371 N94-22872
DE93-040330 p 2591 N94-24607
DE93-040437 p 2238 N94-22861 #
DE93-040487 p 2589 N94-22934 #
DE93-040537 p 2371 N94-22935 #
DE93-040597 p 2588 N94-22875
DE93-040663 p 2264 N94-22878 #
DE93-040664 p 2352 N94-22881 #
DE93-040692 p 2531 N94-22948 #
DE93-040752 p 2466 N94-23491 #
DE93-040759 p 2613 N94-23469 #
DE93-040849 p 2549 N94-22949 #
DE93-040853 p 2307 N94-22950 #
DE93-040868 p 2531 N94-22951 #
DE93-040869 p 2532 N94-22952
DE93-040885 p 2556 N94-22912 #
DE93-040887 p 2561 N94-23432 #
DE93-040897 p 2560 N94-23204 #
DE93-040900 p 2558 N94-22953 #
DE93-040902 p 2342 N94-22954 #
DE93-041011 p 2307 N94-22955 #
DE93-041025 p 2534 N94-23803
DE93-041046 p 2532 N94-22956 #
DE93-041048 p 2307 N94-23019 #
DE93-041127 p 2227 N94-22977 #
DE93-041135 p 2591 N94-24501 #
DE93-041145 p 2371 N94-22918 #
DE93-041165 p 2396 N94-22887 #
DE93-041166 p 2420 N94-23468
DE93-041169 p 2556 N94-22920
DE93-041343 p 2556 N94-22921
DE93-508257 p 2347 N94-22922 #
DE93-508268 p 2548 N94-22924 #
DE93-508286 p 2549 N94-22964 #
DE93-508322 p 2319 N94-23460 #
DE93-613022 p 2523 N94-25328 #
DE93-613047 p 2491 N94-25166
DE93-613685 p 2554 N94-25329 #
DE93-613687 p 2555 N94-25343 #
DE93-613700 p 2555 N94-25344 #
DE93-613719 p 2554 N94-25330 #
DE93-613720 p 2555 N94-25331 #
DE93-613824 p 2566 N94-25332 #
DE93-613909 p 2555 N94-25333
DE93-614017 p 2492 N94-25334 #
DE93-614529 p 2541 N94-25335 #
DE93-616429 p 2399 N94-25167
DE93-616800 p 2463 N94-25432
DE93-616818 p 2493 N94-25433
DE93-616820 p 2493 N94-25434
DE93-616821 p 2570 N94-25206
DE93-616822 p 2493 N94-25473
DE93-616823 p 2570 N94-25207
DE93-616839 p 2524 N94-25208
DE93-616840 p 2547 N94-25209 #
DE93-616843 p 2604 N94-25210
DE93-616844 p 2604 N94-25211
DE93-616845 p 2604 N94-25212
DE93-616846 p 2491 N94-25213
DE93-616847 p 2491 N94-25214
DE93-616848 p 2570 N94-25336
DE93-616849 p 2604 N94-25215 #
DE93-616850 p 2570 N94-25337
DE93-616851 p 2492 N94-25338 #
DE93-616852 p 2571 N94-25339
DE93-616866 p 2571 N94-25340
DE93-616867 p 2538 N94-25341
DE93-616869 p 2541 N94-25342
DE93-616871 p 2538 N94-25317
DE93-616872 p 2539 N94-25474
DE93-616879 p 2539 N94-25476
DE93-616887 p 2539 N94-25477
DE93-616891 p 2539 N94-25481
DE93-617006 p 2351 N94-25482 #
DE93-617007 p 2568 N94-25483
DE93-617047 p 2568 N94-25447
DE93-617049 p 2567 N94-25422
DE93-617051 p 2567 N94-25423
DE93-617053 p 2567 N94-25424
DE93-617054 p 2567 N94-25425
DE93-617130 p 2567 N94-25426
DE93-617131 p 2538 N94-25388
DE93-617134 p 2525 N94-25389
DE93-617135 p 2566 N94-25390
DE93-617136 p 2566 N94-25391
DE93-617137 p 2566 N94-25392
DE93-617138 p 2567 N94-25403
DE93-617140 p 2263 N94-25404
DE93-632412 p 2239 N94-22965
DE93-632430 p 2239 N94-22966
DE93-632490 p 2347 N94-22967
DE93-633211 p 2568 N94-22968
DE93-633215 p 2478 N94-22969
DE93-633217 p 2532 N94-22970
DE93-633452 p 2558 N94-22978
DE93-634228 p 2542 N94-22979 #
DE93-634394 p 2536 N94-24844 #
DE94-000201 p 2395 N94-24509 #
DE94-000203 p 2560 N94-23205 #
DE94-000206 p 2389 N94-22888 #
DE94-000220 p 2390 N94-23296
DE94-000309 p 2448 N94-22980
DE94-000331 p 2543 N94-23461 #
DE94-000333 p 2543 N94-23458 #
DE94-000341 p 2535 N94-24510 #
DE94-000371 p 2550 N94-23462 #
DE94-000374 p 2558 N94-22957
DE94-000389 p 2239 N94-22958 #
DE94-000393 p 2241 N94-23297 #
DE94-000396 p 2232 N94-23298 #
DE94-000466 p 2242 N94-23457 #
DE94-000472 p 2525 N94-23206 #
DE94-000480 p 2429 N94-22997 #
DE94-000485 p 2549 N94-22998 #
DE94-000519 p 2239 N94-22999 #
DE94-000541 p 2450 N94-23207
DE94-000554 p 2268 N94-23000 #
DE94-000565 p 2381 N94-23001 #
DE94-000568 p 2532 N94-23002 #
DE94-000670 p 2218 N94-23283 #
DE94-000677 p 2626 N94-23020
DE94-000680 p 2240 N94-23003 #
DE94-000689 p 2240 N94-23021
DE94-000690 p 2242 N94-23541 #
DE94-000692 p 2227 N94-23004
DE94-000695 p 2243 N94-23753 #
DE94-000697 p 2227 N94-23005
DE94-000700 p 2559 N94-23006 #
DE94-000703 p 2407 N94-23284 #
DE94-000712 p 2533 N94-23543
DE94-000761 p 2307 N94-22987
DE94-000769 p 2218 N94-23452 #
DE94-000777 p 2557 N94-22938
DE94-000793 p 2239 N94-22939 #
DE94-000794 p 2569 N94-23453
DE94-000799 p 2557 N94-22940 #
DE94-000806 p 2558 N94-22941
DE94-000818 p 2626 N94-23515 #
DE94-000875 p 2402 N94-23516 #
DE94-000887 p 2558 N94-22942
DE94-000888 p 2417 N94-23517 #
DE94-000889 p 2218 N94-23433 #
DE94-000895 p 2231 N94-22943 #
DE94-000925 p 2589 N94-22944 #
DE94-000929 p 2220 N94-24511 #
DE94-000954 p 2241 N94-23434 #
DE94-000981 p 2395 N94-24512 #
DE94-000989 p 2533 N94-23435 #
DE94-001017 p 2548 N94-22945 #
DE94-001047 p 2265 N94-23436 #
DE94-001048 p 2558 N94-22946
DE94-001055 p 2532 N94-22988
DE94-001064 p 2348 N94-23181 #
DE94-001099 p 2553 N94-24746 #
DE94-001107 p 2553 N94-24756 #
DE94-001113 p 2550 N94-23182 #
DE94-001121 p 2388 N94-24757 #
DE94-001128 p 2243 N94-23715 #
DE94-001149 p 2270 N94-23790 #
DE94-001192 p 2253 N94-23183 #
DE94-001193 p 2375 N94-23184 #
DE94-001205 p 2534 N94-23804 #
DE94-001208 p 2348 N94-23185 #
DE94-001211 p 2559 N94-23186 #
DE94-001220 p 2535 N94-24515 #
DE94-001224 p 2342 N94-22989 #
DE94-001276 p 2562 N94-23805 #
DE94-001289 p 2558 N94-22990
DE94-001290 p 2560 N94-23187
DE94-001291 p 2560 N94-23188
DE94-001319 p 2352 N94-22991 #
DE94-001320 p 2252 N94-22992
DE94-001324 p 2559 N94-22993
DE94-001326 p 2559 N94-22994
DE94-001333 p 2560 N94-23189 #
DE94-001337 p 2590 N94-23190 #
DE94-001345 p 2559 N94-22995 #
DE94-001346 p 2352 N94-22996
DE94-001357 p 2533 N94-23699 #
DE94-001365 p 2353 N94-23191 #
DE94-001368 p 2531 N94-22733 #
DE94-001369 p 2550 N94-23192
DE94-001380 p 2532 N94-23007 #
DE94-001387 p 2234 N94-24545 #
DE94-001417 p 2555 N94-22717 #
DE94-001418 p 2307 N94-23008 #
DE94-001420 p 2217 N94-23193 #
DE94-001431 p 2238 N94-22718 #
DE94-001433 p 2240 N94-23194 #
DE94-001437 p 2557 N94-22927 #
DE94-001445 p 2218 N94-23459 #
DE94-001446 p 2540 N94-23791 #
DE94-001456 p 2557 N94-22929 #
DE94-001459 p 2534 N94-23806
DE94-001466 p 2240 N94-23009
DE94-001473 p 2198 N94-23208 #
DE94-001492 p 2389 N94-22962 #
DE94-001500 p 2552 N94-24546 #
DE94-001501 p 2309 N94-23777 #
DE94-001502 p 2349 N94-23209 #
DE94-001505 p 2601 N94-23010 #
DE94-001516 p 2471 N94-23011
DE94-001520 p 2252 N94-22930 #
DE94-001521 p 2229 N94-24547 #
DE94-001523 p 2265 N94-23778 #
DE94-001524 p 2265 N94-23807
DE94-001528 p 2252 N94-22931 #
DE94-001532 p 2319 N94-23470 #
DE94-001533 p 2209 N94-23012

DE94-001535 .... p 2549 N94-23013
DE94-001536 .... p 2549 N94-23014
DE94-001541 .... p 2552 N94-24502 #
DE94-001546 .... p 2488 N94-24503 #
DE94-001557 .... p 2198 N94-23210 #
DE94-001565 .... p 2552 N94-24504 #
DE94-001567 .... p 2238 N94-22932 #
DE94-001569 .... p 2535 N94-24505 #
DE94-001574 .... p 2549 N94-22963 #
DE94-001575 .... p 2550 N94-23211 #
DE94-001578 .... p 2238 N94-22936 #
DE94-001588 .... p 2531 N94-22937 #
DE94-001600 .... p 2398 N94-24506 #
DE94-001608 .... p 2309 N94-23520 #
DE94-001639 .... p 2233 N94-23716 #
DE94-001647 .... p 2568 N94-22719 #
DE94-001651 .... p 2530 N94-22720 #
DE94-001661 .... p 2568 N94-23216 #
DE94-001668 .... p 2397 N94-23016
DE94-001679 .... p 2589 N94-23126 #
DE94-001703 .... p 2589 N94-23127 #
DE94-001704 .... p 2589 N94-23128 #
DE94-001706 .... p 2375 N94-23217 #
DE94-001712 .... p 2551 N94-23808
DE94-001725 .... p 2548 N94-22721 #
DE94-001726 .... p 2533 N94-23218
DE94-001727 .... p 2563 N94-24537
DE94-001756 .... p 2241 N94-23219 #
DE94-001759 .... p 2244 N94-23792
DE94-001772 .... p 2541 N94-22722 #
DE94-001777 .... p 2318 N94-23220 #
DE94-001804 .... p 2243 N94-23717 #
DE94-001832 .... p 2526 N94-23718 #
DE94-001839 .... p 2293 N94-23719 #
DE94-001852 .... p 2240 N94-23017
DE94-001855 .... p 2397 N94-23700 #
DE94-001865 .... p 2254 N94-23720 #
DE94-001897 .... p 2386 N94-23779 #
DE94-001899 .... p 2233 N94-23780 #
DE94-001908 .... p 2532 N94-23018 #
DE94-001911 .... p 2394 N94-23781 #
DE94-001914 .... p 2390 N94-23212
DE94-001918 .... p 2389 N94-22723 #
DE94-001934 .... p 2465 N94-22973 #
DE94-001996 .... p 2227 N94-23022 #
DE94-001997 .... p 2271 N94-23793 #
DE94-002000 .... p 2347 N94-22974 #
DE94-002002 .... p 2402 N94-23721 #
DE94-002003 .... p 2408 N94-23471 #
DE94-002038 .... p 2244 N94-23811
DE94-002039 .... p 2394 N94-23472 #
DE94-002181 .... p 2232 N94-23023 #
DE94-002184 .... p 2478 N94-22975 #
DE94-002190 .... p 2397 N94-23794 #
DE94-002191 .... p 2293 N94-23473 #
DE94-002204 .... p 2550 N94-23474 #
DE94-002208 .... p 2562 N94-23795 #
DE94-002215 .... p 2457 N94-24566 #
DE94-002248 .... p 2395 N94-24654 #
DE94-002262 .... p 2335 N94-24655 #
DE94-002268 .... p 2242 N94-23475
DE94-002274 .... p 2299 N94-24656 #
DE94-002281 .... p 2564 N94-24657 #
DE94-002285 .... p 2523 N94-24658 #
DE94-002293 .... p 2350 N94-24659 #
DE94-002299 .... p 2318 N94-23213 #
DE94-002304 .... p 2535 N94-24611 #
DE94-002313 .... p 2238 N94-22897 #
DE94-002318 .... p 2549 N94-22976 #
DE94-002347 .... p 2563 N94-24624 #
DE94-002441 .... p 2563 N94-24567 #
DE94-002457 .... p 2271 N94-24568 #
DE94-002460 .... p 2535 N94-24569 #
DE94-002536 .... p 2446 N94-24538 #
DE94-002539 .... p 2234 N94-24548 #
DE94-002545 .... p 2234 N94-24549 #
DE94-002546 .... p 2454 N94-23796 #
DE94-002567 .... p 2453 N94-23701 #
DE94-002570 .... p 2326 N94-23809 #
DE94-002597 .... p 2349 N94-23702 #
DE94-002602 .... p 2551 N94-23703 #
DE94-002607 .... p 2394 N94-23704 #
DE94-002626 .... p 2569 N94-24516 #
DE94-002632 .... p 2563 N94-24517 #
DE94-002633 .... p 2473 N94-24518 #
DE94-002634 .... p 2552 N94-24519 #
DE94-002638 .... p 2245 N94-24520 #
DE94-002639 .... p 2457 N94-24626 #
DE94-002643 .... p 2245 N94-24747 #
DE94-002652 .... p 2311 N94-24748 #
DE94-002665 .... p 2258 N94-24749 #
DE94-002720 .... p 2553 N94-24628 #
DE94-002745 .... p 2354 N94-23797 #
DE94-002746 .... p 2551 N94-23782 #
DE94-002773 .... p 2254 N94-23783 #
DE94-002807 .... p 2382 N94-23492 #
DE94-002836 .... p 2561 N94-23214 #
DE94-002875 .... p 2243 N94-23784 #
DE94-002908 .... p 2545 N94-24550
DE94-002963 .... p 2395 N94-23785 #
DE94-002988 .... p 2229 N94-24632 #
DE94-002991 .... p 2245 N94-24612 #
DE94-003018 .... p 2228 N94-23493 #
DE94-003020 .... p 2373 N94-24613 #
DE94-003021 .... p 2382 N94-23494 #
DE94-003365 .... p 2365 N94-24614 #
DE94-600342 .... p 2448 N94-23024
DE94-602022 .... p 2352 N94-23025
DE94-714889 .... p 2397 N94-23026 #
DE94-714902 .... p 2264 N94-23027 #

DGW-93.004 .... p 2418 N94-24601
DGW-93.034 .... p 2399 N94-24573

DLR-FB-93-12 .... p 2351 N94-25304 #
DLR-FB-93-14 .... p 2476 N94-25345 #
DLR-FB-93-19 .... p 2547 N94-25305 #

DLR-MITT-93-02 .... p 2396 N94-25479 #
DLR-MITT-93-03 .... p 2396 N94-25464 #
DLR-MITT-93-06 .... p 2400 N94-25414 #

DNA-TR-92-6 .... p 2553 N94-24949 #

DODA-AR-008-393 .... p 2347 N94-22914 #

DOE/EE-0003 .... p 2352 N94-22881 #
DOE/EE-0004 .... p 2264 N94-22878 #

DOE/ER-00881/T4 .... p 2532 N94-23018 #
DOE/ER-0603T .... p 2551 N94-23808
DOE/ER-12128/2 .... p 2254 N94-23720 #
DOE/ER-13406/8 .... p 2238 N94-22897 #
DOE/ER-13438/T1 .... p 2563 N94-24537
DOE/ER-13582/T3 .... p 2568 N94-22719 #
DOE/ER-13613/45 .... p 2233 N94-23716 #
DOE/ER-13958/43 .... p 2531 N94-22937 #
DOE/ER-13988/T2 .... p 2232 N94-23023 #
DOE/ER-14079/27 .... p 2402 N94-23516 #
DOE/ER-14224/T1 .... p 2530 N94-22720 #
DOE/ER-40150/236 .... p 2531 N94-22951 #
DOE/ER-40150/240 .... p 2532 N94-22952
DOE/ER-40344/7 .... p 2540 N94-23791 #
DOE/ER-40546/T3 .... p 2533 N94-23699 #
DOE/ER-40669/3 .... p 2349 N94-23702 #
DOE/ER-45076/T2 .... p 2531 N94-22733 #
DOE/ER-53198/223 .... p 2549 N94-22963 #
DOE/ER-53198/224 .... p 2550 N94-23211 #
DOE/ER-53198/226 .... p 2549 N94-22976 #
DOE/ER-53217/T2 .... p 2533 N94-23543
DOE/ER-53264/4 .... p 2550 N94-23192
DOE/ER-60892/4 .... p 2233 N94-23780 #
DOE/ER-79119/1 .... p 2342 N94-22989 #

DOE/ET-51013/302 .... p 2548 N94-22721 #
DOE/ET-51013/303 .... p 2552 N94-24504 #

DOE/ID-01570/T170 .... p 2345 N94-24831 #
DOE/ID-13074/T9 .... p 2353 N94-23191 #

DOE/MC-26355/94/C0254 .... p 2395 N94-23785 #
DOE/MC-27394/94/C0263 .... p 2389 N94-22723 #

DOE/METC-C/94/7109 .... p 2390 N94-23212
DOE/METC-C/94/7110 .... p 2394 N94-23781 #

DOE/NASA/0373-1 .... p 2258 N94-24753 * #
DOE/NASA/16310-21 .... p 2242 N94-23550 * #

DOE/PC-92542/T3 .... p 2258 N94-24749 #

DOE/RL-12089/T2 .... p 2381 N94-23001 #

DOE/SF-18852/T31 .... p 2218 N94-23459 #

DOT/FAA/AM-93/21 .... p 2426 N94-23623 #
DOT/FAA/AM-93/22 .... p 2175 N94-24472 #
DOT/FAA/AM-94/1 .... p 2426 N94-24093 #
DOT/FAA/AM-94/2 .... p 2429 N94-25442 #
DOT/FAA/AM-94/3 .... p 2176 N94-25444 #

DOT/FAA/CT-TN93/13 .... p 2174 N94-24941 #
DOT/FAA/CT-TN93/6 .... p 2193 N94-24559 #
DOT/FAA/CT-TN93/7 .... p 2253 N94-23335 #

DOT/FAA/CT-88/10-VOL-2 .... p 2438 N94-24830 #
DOT/FAA/CT-92/21 .... p 2430 N94-23083 #
DOT/FAA/CT-93/17-VOL-1 .... p 2230 N94-24942 #
DOT/FAA/CT-93/17-VOL-2 .... p 2230 N94-24779 #
DOT/FAA/CT-93/17-VOL-3 .... p 2230 N94-25163
DOT/FAA/CT-93/51 .... p 2192 N94-24072 #

DOT/FAA/NR-93/2 .... p 2415 N94-24850

DOT/FAA/RD-92/29 .... p 2175 N94-24127 #
DOT/FAA/RD-93/23 .... p 2192 N94-23303 #
DOT/FAA/RD-93/41 .... p 2309 N94-23304 * #

DRA-LIBRARY-TRANS-2202 .... p 2170 N94-25137 #

DREA-TC-93-303 .... p 2297 N94-24298
DREA-TC-93-304 .... p 2202 N94-24121

DREA-TM-93/214 .... p 2262 N94-25136 #
DREA-TM-93/216 .... p 2266 N94-24728 #

DREO-TN-93-4 .... p 2296 N94-24118
DREO-TN-93-5 .... p 2193 N94-24117
DREO-TN-93-9 .... p 2193 N94-24123

DREO-12-020.1 .... p 2296 N94-24131

DREP-TM-93-11 .... p 2455 N94-24130
DREP-TM-93-19 .... p 2455 N94-24122
DREP-TM-93-38 .... p 2372 N94-24136

E-7014 .... p 2205 N94-24825 * #
E-7152 .... p 2242 N94-23467 * #
E-7301 .... p 2376 N94-23551 * #
E-7325 .... p 2378 N94-24845 * #
E-7336 .... p 2193 N94-25184 * #
E-7549 .... p 2372 N94-24074 * #
E-7602 .... p 2590 N94-23562 * #
E-7790 .... p 2219 N94-23531 * #
E-7830 .... p 2290 N94-23087 * #
E-7851 .... p 2169 N94-24606 * #
E-7877 .... p 2336 N94-24713 * #
E-7977 .... p 2310 N94-24056 * #
E-8033 .... p 2295 N94-24101 * #
E-8050 .... p 2186 N94-23466 * #
E-8051 .... p 2192 N94-23091 * #
E-8060 .... p 2310 N94-24308 * #
E-8069 .... p 2246 N94-25120 * #
E-8075 .... p 2390 N94-23345 * #
E-8094 .... p 2320 N94-23634 * #
E-8096 .... p 2170 N94-25173 * #
E-8145 .... p 2378 N94-25188 * #
E-8194 .... p 2242 N94-23550 * #
E-8201 .... p 2333 N94-24460 * #
E-8202 .... p 2333 N94-24336 * #
E-8203 .... p 2187 N94-23545 * #
E-8216 .... p 2168 N94-24084 * #
E-8224 .... p 2201 N94-23567 * #
E-8235 .... p 2219 N94-23630 * #
E-8245 .... p 2249 N94-25171 * #
E-8250 .... p 2222 N94-23500 * #
E-8254 .... p 2395 N94-24071 * #
E-8260 .... p 2253 N94-23371 * #
E-8268 .... p 2221 N94-24770 * #
E-8270 .... p 2218 N94-23372 * #
E-8271 .... p 2243 N94-23556 * #
E-8275 .... p 2243 N94-23578 * #
E-8276 .... p 2187 N94-24082 * #
E-8278 .... p 2481 N94-23593 * #
E-8279 .... p 2481 N94-23554 * #
E-8283 .... p 2190 N94-23590 * #
E-8287 .... p 2222 N94-23591 * #
E-8289 .... p 2166 N94-23511 * #
E-8290 .... p 2320 N94-23525 * #
E-8291 .... p 2203 N94-23632 * #
E-8303 .... p 2553 N94-25190 * #
E-8308 .... p 2167 N94-23592 * #
E-8310 .... p 2220 N94-24681 * #
E-8315 .... p 2187 N94-23552 * #
E-8317 .... p 2202 N94-23631 * #
E-8318 .... p 2172 N94-23523 * #
E-8320 .... p 2166 N94-23522 * #
E-8323 .... p 2173 N94-24047 * #
E-8324 .... p 2304 N94-25266 * #
E-8326 .... p 2153 N94-24100 * #
E-8328 .... p 2221 N94-24766 * #
E-8329 .... p 2153 N94-23553 * #
E-8330 .... p 2525 N94-23464 * #
E-8332 .... p 2218 N94-23370 * #
E-8333 .... p 2364 N94-24483 * #
E-8334 .... p 2166 N94-23465 * #
E-8336 .... p 2326 N94-24063 * #
E-8338 .... p 2344 N94-24362 * #
E-8340 .... p 2166 N94-23299 * #
E-8349 .... p 2337 N94-25119 * #
E-8388 .... p 2377 N94-24604 * #
E-8402 .... p 2258 N94-24682 * #
E-8403 .... p 2346 N94-25202 * #
E-8404 .... p 2189 N94-25185 * #
E-8405 .... p 2188 N94-24594 * #
E-840626 .... p 2219 N94-24361 * #
E-8408 .... p 2189 N94-25200 * #
E-8411 .... p 2265 N94-24301 * #

E-8412 .... p 2195 N94-24482 * #
E-8420 .... p 2344 N94-24069 * #
E-8470 .... p 2202 N94-25095 * #
E-8473 .... p 2222 N94-25201 * #
E-8475 .... p 2221 N94-25189 * #
E-8477 .... p 2377 N94-24715 * #
E-8478 .... p 2169 N94-24335 * #
E-8479 .... p 2170 N94-25182 * #
E-8481 .... p 2220 N94-24714 * #
E-8481 .... p 2312 N94-24870 * #
E-8488 .... p 2521 N94-24302 * #
E-8512 .... p 2345 N94-25116 * #
E-8532 .... p 2338 N94-25183 * #
E-8534 .... p 2334 N94-24481 * #
E-8583 .... p 2313 N94-25170 * #
E-8610 .... p 2230 N94-25186 * #
E-8616 .... p 2367 N94-25181 * #
E-8619 .... p 2462 N94-25179 * #
E-8623 .... p 2530 N94-25172 * #

ECE-91-1 .... p 2296 N94-24132
ECE-92-1 .... p 2300 N94-24697

ECL-92-14 .... p 2352 N94-22885 #
ECL-92-29 .... p 2317 N94-22971 #
ECL-92-34 .... p 2313 N94-25421 #

ECU-8200-150 .... p 2466 N94-23293 * #

EDR-16732 .... p 2364 N94-24090 * #

EEC-256 .... p 2430 N94-23744

EGG-EE-10723 .... p 2382 N94-23492 #

EGG-M-93041 .... p 2542 N94-22917 #

EMTL-REPT-1539 .... p 2229 N94-24224 * #

EPA/453/R-93/032 .... p 2398 N94-24476
EPA/600/A-93/118 .... p 2244 N94-23802

ERDEC-TR-123 .... p 2446 N94-25438 #

ERIM-248500-1-F .... p 2418 N94-24918
ERIM-254400-1-P .... p 2546 N94-24731

ERP-1119 .... p 2406 N94-25537 #

ESA-PSS-05-09-ISSUE-1 .... p 2450 N94-23229 #

ESA-SP-1157 .... p 2623 N94-22837 #
ESA-SP-334 .... p 2355 N94-23985 #

ESA-STM-247 .... p 2450 N94-23228 #

ESDP-4048 .... p 2588 N94-22875

ET/EM-1993-01 .... p 2294 N94-23727 #
ET/EM-1993-02 .... p 2294 N94-23729 #
ET/EM-1993-03 .... p 2294 N94-23728 #
ET/EM-1993-04 .... p 2403 N94-24592
ET/EM-1993-05 .... p 2524 N94-23730 #
ET/EM-1993-06 .... p 2524 N94-23731 #
ET/EM-1993-09 .... p 2298 N94-24593
ET/EM-1993-10 .... p 2298 N94-24597
ET/EM-1993-11 .... p 2294 N94-23733 #
ET/EM-1993-12 .... p 2544 N94-23732 #
ET/EM-1993-13 .... p 2298 N94-24637
ET/EM-1993-15 .... p 2526 N94-23726 #

ETN-93-93653 .... p 2452 N94-23518
ETN-93-93707 .... p 2187 N94-23570
ETN-93-93708 .... p 2187 N94-23519
ETN-93-93709 .... p 2595 N94-23580
ETN-93-93710 .... p 2475 N94-24963
ETN-93-93763 .... p 2421 N94-24290 #
ETN-93-94176 .... p 2269 N94-23581 #
ETN-93-94490 .... p 2437 N94-24292 #
ETN-93-94996 .... p 2589 N94-23150 #
ETN-93-94997 .... p 2450 N94-23180 #
ETN-94-94439 .... p 2605 N94-23373
ETN-94-94475 .... p 2588 N94-22734 #
ETN-94-94712 .... p 2420 N94-23521 #
ETN-94-94742 .... p 2493 N94-22724 #
ETN-94-94743 .... p 2478 N94-22725 #
ETN-94-94744 .... p 2478 N94-22726 #
ETN-94-94745 .... p 2478 N94-22727 #
ETN-94-94746 .... p 2493 N94-22728 #
ETN-94-94747 .... p 2273 N94-22729 #
ETN-94-94748 .... p 2555 N94-22730 #
ETN-94-94749 .... p 2487 N94-24053 #
ETN-94-94750 .... p 2493 N94-22702 #
ETN-94-94751 .... p 2469 N94-22703 #
ETN-94-94752 .... p 2585 N94-22704 #
ETN-94-94753 .... p 2469 N94-22705 #
ETN-94-94754 .... p 2469 N94-22706 #
ETN-94-94755 .... p 2469 N94-22707 #
ETN-94-94756 .... p 2497 N94-22708 #
ETN-94-94757 .... p 2568 N94-22709 #
ETN-94-94758 .... p 2478 N94-22710 #
ETN-94-94759 .... p 2447 N94-22711 #
ETN-94-94760 .... p 2469 N94-22712 #
ETN-94-94761 .... p 2315 N94-22713 #
ETN-94-94762 .... p 2470 N94-22714 #
ETN-94-94763 .... p 2478 N94-22715 #
ETN-94-94764 .... p 2497 N94-22716 #
ETN-94-94767 .... p 2447 N94-22731 #
ETN-94-94768 .... p 2470 N94-22873 #
ETN-94-94769 .... p 2347 N94-22874 #
ETN-94-94770 .... p 2290 N94-22876 #
ETN-94-94771 .... p 2470 N94-22877 #
ETN-94-94772 .... p 2348 N94-23168 #
ETN-94-94773 .... p 2449 N94-23169 #
ETN-94-94774 .... p 2445 N94-23170 #
ETN-94-94775 .... p 2542 N94-23171 #
ETN-94-94776 .... p 2308 N94-23136 #
ETN-94-94777 .... p 2449 N94-23172 #
ETN-94-94778 .... p 2450 N94-23173 #
ETN-94-94779 .... p 2268 N94-23174 #
ETN-94-94784 .... p 2471 N94-23137
ETN-94-94788 .... p 2401 N94-23175 #
ETN-94-94789 .... p 2479 N94-23138 #
ETN-94-94790 .... p 2479 N94-23139 #
ETN-94-94791 .... p 2480 N94-23140 #
ETN-94-94792 .... p 2480 N94-23141 #
ETN-94-94793 .... p 2493 N94-23142 #
ETN-94-94796 .... p 2494 N94-23143 #
ETN-94-94797 .... p 2480 N94-23144 #
ETN-94-94798 .... p 2477 N94-25526 #
ETN-94-94799 .... p 2493 N94-25527 #
ETN-94-94831 .... p 2497 N94-25528
ETN-94-94862 .... p 2355 N94-23985 #
ETN-94-94928 .... p 2542 N94-22895
ETN-94-94953 .... p 2381 N94-22896
ETN-94-95037 .... p 2381 N94-23145 #
ETN-94-95038 .... p 2417 N94-23176 #
ETN-94-95039 .... p 2382 N94-23177 #
ETN-94-95040 .... p 2417 N94-24107 #
ETN-94-95041 .... p 2382 N94-23148 #
ETN-94-95046 .... p 2539 N94-25465 #
ETN-94-95047 .... p 2318 N94-23227 #
ETN-94-95077 .... p 2315 N94-22852 #
ETN-94-95084 .... p 2340 N94-25466
ETN-94-95086 .... p 2340 N94-25467 #
ETN-94-95088 .... p 2266 N94-23195 #
ETN-94-95089 .... p 2375 N94-23196 #
ETN-94-95090 .... p 2318 N94-23197 #
ETN-94-95104 .... p 2318 N94-23198 #
ETN-94-95106 .... p 2407 N94-23199 #
ETN-94-95107 .... p 2407 N94-23156 #
ETN-94-95108 .... p 2400 N94-23157 #
ETN-94-95109 .... p 2402 N94-24108 #
ETN-94-95110 .... p 2382 N94-23158 #
ETN-94-95111 .... p 2401 N94-23159 #
ETN-94-95112 .... p 2403 N94-24491 #
ETN-94-95113 .... p 2314 N94-25457
ETN-94-95114 .... p 2600 N94-25458
ETN-94-95115 .... p 2629 N94-25459
ETN-94-95116 .... p 2314 N94-25460
ETN-94-95117 .... p 2171 N94-25461 #
ETN-94-95118 .... p 2339 N94-25462
ETN-94-95119 .... p 2340 N94-25463 #
ETN-94-95120 .... p 2185 N94-25301
ETN-94-95122 .... p 2343 N94-24054 #
ETN-94-95123 .... p 2318 N94-23160 #
ETN-94-95124 .... p 2165 N94-23161 #
ETN-94-95126 .... p 2165 N94-23149 #
ETN-94-95127 .... p 2176 N94-23146 #
ETN-94-95128 .... p 2492 N94-25306 #
ETN-94-95129 .... p 2476 N94-25307 #
ETN-94-95130 .... p 2476 N94-25308 #
ETN-94-95131 .... p 2492 N94-25309
ETN-94-95132 .... p 2492 N94-25310 #
ETN-94-95133 .... p 2462 N94-25311 #
ETN-94-95134 .... p 2446 N94-25312 #
ETN-94-95135 .... p 2446 N94-25313 #
ETN-94-95136 .... p 2523 N94-25314 #
ETN-94-95137 .... p 2463 N94-25315 #
ETN-94-95138 .... p 2492 N94-25318 #
ETN-94-95139 .... p 2313 N94-25319 #
ETN-94-95140 .... p 2492 N94-25320 #
ETN-94-95141 .... p 2463 N94-25321 #
ETN-94-95142 .... p 2368 N94-25322 #
ETN-94-95143 .... p 2523 N94-25323 #
ETN-94-95144 .... p 2343 N94-23162 #
ETN-94-95145 .... p 2492 N94-25324 #
ETN-94-95146 .... p 2472 N94-23163 #
ETN-94-95147 .... p 2471 N94-23147
ETN-94-95148 .... p 2353 N94-23178 #
ETN-94-95149 .... p 2472 N94-23179 #
ETN-94-95150 .... p 2353 N94-23164 #
ETN-94-95152 .... p 2379 N94-25325 #
ETN-94-95153 .... p 2593 N94-25326 #
ETN-94-95154 .... p 2554 N94-25327 #
ETN-94-95155 .... p 2463 N94-25468 #
ETN-94-95156 .... p 2477 N94-25469 #
ETN-94-95157 .... p 2477 N94-25470 #
ETN-94-95158 .... p 2464 N94-25471 #
ETN-94-95159 .... p 2346 N94-25472 #
ETN-94-95160 .... p 2373 N94-25475 #
ETN-94-95161 .... p 2379 N94-25478 #
ETN-94-95162 .... p 2588 N94-22879 #
ETN-94-95163 .... p 2588 N94-22880 #
ETN-94-95164 .... p 2447 N94-22882 #
ETN-94-95165 .... p 2306 N94-22883 #
ETN-94-95166 .... p 2470 N94-22884 #
ETN-94-95167 .... p 2352 N94-22885 #
ETN-94-95168 .... p 2317 N94-22971 #
ETN-94-95169 .... p 2239 N94-22972 #
ETN-94-95170 .... p 2227 N94-23133 #
ETN-94-95171 .... p 2308 N94-23165 #
ETN-94-95172 .... p 2480 N94-23166
ETN-94-95173 .... p 2465 N94-23167 #
ETN-94-95174 .... p 2449 N94-23151
ETN-94-95175 .... p 2471 N94-23152
ETN-94-95176 .... p 2445 N94-23153 #
ETN-94-95177 .... p 2308 N94-23154 #
ETN-94-95178 .... p 2449 N94-23155
ETN-94-95179 .... p 2465 N94-23134 #
ETN-94-95180 .... p 2470 N94-22898 #
ETN-94-95181 .... p 2447 N94-22899
ETN-94-95182 .... p 2444 N94-22900
ETN-94-95183 .... p 2445 N94-22901 #
ETN-94-95184 .... p 2342 N94-22902 #
ETN-94-95185 .... p 2445 N94-22903
ETN-94-95186 .... p 2470 N94-22904 #
ETN-94-95187 .... p 2556 N94-22905 #
ETN-94-95188 .... p 2470 N94-22906 #
ETN-94-95189 .... p 2471 N94-22907 #
ETN-94-95190 .... p 2471 N94-22908 #
ETN-94-95191 .... p 2307 N94-22909 #
ETN-94-95192 .... p 2252 N94-22910 #
ETN-94-95193 .... p 2447 N94-22911 #
ETN-94-95194 .... p 2623 N94-22837 #
ETN-94-95195 .... p 2450 N94-23228 #
ETN-94-95196 .... p 2450 N94-23229 #
ETN-94-95200 .... p 2313 N94-25421 #
ETN-94-95201 .... p 2351 N94-25304 #
ETN-94-95202 .... p 2476 N94-25345 #
ETN-94-95203 .... p 2547 N94-25305 #
ETN-94-95204 .... p 2396 N94-25479 #
ETN-94-95205 .... p 2396 N94-25464 #
ETN-94-95207 .... p 2400 N94-25414 #
ETN-94-95208 .... p 2346 N94-25415 #
ETN-94-95218 .... p 2523 N94-25480 #
ETN-94-95219 .... p 2594 N94-25485 #
ETN-94-95220 .... p 2340 N94-25486 #
ETN-94-95227 .... p 2236 N94-25427 #
ETN-94-95228 .... p 2476 N94-25428 #
ETN-94-95229 .... p 2476 N94-25429 #
ETN-94-95230 .... p 2406 N94-25430 #
ETN-94-95234 .... p 2250 N94-25316 #
ETN-94-95236 .... p 2379 N94-25529 #
ETN-94-95241 .... p 2571 N94-25416 #
ETN-94-95242 .... p 2396 N94-25417 #
ETN-94-95243 .... p 2379 N94-25418 #
ETN-94-95248 .... p 2379 N94-25385 #
ETN-94-95253 .... p 2230 N94-25386 #
ETN-94-95254 .... p 2251 N94-25419 #
ETN-94-95255 .... p 2250 N94-25346 #
ETN-94-95256 .... p 2231 N94-25420 #
ETN-94-95257 .... p 2566 N94-25347 #
ETN-94-95290 .... p 2236 N94-25232
ETN-94-95291 .... p 2586 N94-25076 #
ETN-94-95292 .... p 2302 N94-25077 #
ETN-94-95293 .... p 2261 N94-25078 #
ETN-94-95294 .... p 2491 N94-25079 #
ETN-94-95295 .... p 2461 N94-25080 #
ETN-94-95296 .... p 2446 N94-25081 #
ETN-94-95297 .... p 2236 N94-25233 #
ETN-94-95298 .... p 2304 N94-25234 #
ETN-94-95299 .... p 2586 N94-25235 #
ETN-94-95300 .... p 2262 N94-25236 #
ETN-94-95301 .... p 2492 N94-25277 #
ETN-94-95302 .... p 2468 N94-25278 #
ETN-94-95303 .... p 2587 N94-25279 #
ETN-94-95304 .... p 2565 N94-25280 #
ETN-94-95305 .... p 2263 N94-25281 #
ETN-94-95306 .... p 2530 N94-25289 #
ETN-94-95307 .... p 2476 N94-25290 #
ETN-94-95308 .... p 2339 N94-25291 #
ETN-94-95309 .... p 2304 N94-25292 #
ETN-94-95310 .... p 2522 N94-25293 #
ETN-94-95311 .... p 2351 N94-25294 #
ETN-94-95312 .... p 2373 N94-25295 #
ETN-94-95313 .... p 2236 N94-25296 #
ETN-94-95314 .... p 2236 N94-25302 #

ETN-94-95315 .... p 2304 N94-25303 #
ETN-94-95316 .... p 2555 N94-25439 #
ETN-94-95317 .... p 2236 N94-25284 #
ETN-94-95318 .... p 2477 N94-25431 #
ETN-94-95319 .... p 2351 N94-25218 #
ETN-94-95320 .... p 2462 N94-25219 #
ETN-94-95321 .... p 2530 N94-25220 #
ETN-94-95322 .... p 2554 N94-25285
ETN-94-95323 .... p 2462 N94-25237 #
ETN-94-95324 .... p 2226 N94-25238 #
ETN-94-95325 .... p 2537 N94-25239 #
ETN-94-95326 .... p 2537 N94-25082 #
ETN-94-95327 .... p 2538 N94-25240 #
ETN-94-95328 .... p 2313 N94-25083 #
ETN-94-95329 .... p 2261 N94-25084 #
ETN-94-95330 .... p 2554 N94-25241 #
ETN-94-95331 .... p 2469 N94-25282 #
ETN-94-95332 .... p 2565 N94-25059 #
ETN-94-95333 .... p 2267 N94-25060 #
ETN-94-95334 .... p 2566 N94-25297
ETN-94-95335 .... p 2460 N94-25061 #
ETN-94-95336 .... p 2468 N94-25062 #
ETN-94-95337 .... p 2460 N94-25063 #
ETN-94-95338 .... p 2340 N94-25484 #
ETN-94-95346 .... p 2468 N94-25221 #
ETN-94-95347 .... p 2262 N94-25222 #
ETN-94-95348 .... p 2400 N94-25223 #
ETN-94-95349 .... p 2587 N94-25283 #
ETN-94-95350 .... p 2416 N94-25261 #
ETN-94-95351 .... p 2428 N94-25298
ETN-94-95352 .... p 2339 N94-25247 #
ETN-94-95353 .... p 2339 N94-25248 #
ETN-94-95354 .... p 2476 N94-25262 #
ETN-94-95355 .... p 2367 N94-25249
ETN-94-95356 .... p 2462 N94-25263 #
ETN-94-95357 .... p 2236 N94-25250
ETN-94-95359 .... p 2475 N94-25224
ETN-94-95360 .... p 2262 N94-25225 #
ETN-94-95361 .... p 2468 N94-25226
ETN-94-95362 .... p 2263 N94-25299
ETN-94-95363 .... p 2554 N94-25300 #
ETN-94-95364 .... p 2250 N94-25242 #
ETN-94-95365 .... p 2405 N94-25251
ETN-94-95366 .... p 2462 N94-25252
ETN-94-95367 .... p 2313 N94-25253
ETN-94-95368 .... p 2339 N94-25254
ETN-94-95369 .... p 2338 N94-25227 #
ETN-94-95370 .... p 2537 N94-25228 #
ETN-94-95371 .... p 2313 N94-25286 #
ETN-94-95373 .... p 2405 N94-25229 #
ETN-94-95376 .... p 2262 N94-25230 #
ETN-94-95377 .... p 2338 N94-25243
ETN-94-95379 .... p 2491 N94-25244
ETN-94-95380 .... p 2491 N94-25245 #
ETN-94-95381 .... p 2538 N94-25246
ETN-94-95382 .... p 2537 N94-25231 #
ETN-94-95383 .... p 2538 N94-25255 #
ETN-94-95384 .... p 2541 N94-25256
ETN-94-95385 .... p 2570 N94-25257
ETN-94-95386 .... p 2570 N94-25258 #
ETN-94-95387 .... p 2538 N94-25259

EUT-92-E-260 .... p 2447 N94-22731 #
EUT-92-E-261 .... p 2470 N94-22873 #
EUT-92-E-262 .... p 2347 N94-22874 #
EUT-92-E-263 .... p 2290 N94-22876 #
EUT-92-E-264 .... p 2470 N94-22877 #
EUT-92-E-265 .... p 2348 N94-23168 #
EUT-92-E-266 .... p 2449 N94-23169 #
EUT-92-E-267 .... p 2445 N94-23170 #
EUT-92-E-268 .... p 2542 N94-23171 #
EUT-93-E-269 .... p 2308 N94-23136 #
EUT-93-E-270 .... p 2449 N94-23172 #
EUT-93-E-271 .... p 2450 N94-23173 #
EUT-93-E-272 .... p 2268 N94-23174 #
EUT-93-WSK-01 .... p 2334 N94-24574

FAA-APO-93-10 .... p 2162 N94-24923

FEL-93-A043 .... p 2381 N94-22896
FEL-93-A058 .... p 2406 N94-25540 #
FEL-93-A183 .... p 2190 N94-25516 #

FEW-571 .... p 2456 N94-24507
FEW-572 .... p 2495 N94-24634
FEW-599 .... p 2479 N94-23122
FEW-600 .... p 2479 N94-23107
FEW-603 .... p 2454 N94-23759 #
FEW-604 .... p 2473 N94-23760 #
FEW-606 .... p 2488 N94-24526
FEW-608 .... p 2596 N94-24477
FEW-611 .... p 2495 N94-23814

FMI-EMTL-W/A-3111 .... p 2229 N94-24224 * #

FNAL-TM-1831 .... p 2365 N94-24614 #

FNAL/C-93/196-A .... p 2601 N94-23010 #
FNAL/C-93/279-E .... p 2535 N94-24515 #
FNAL/C-93/286 .... p 2535 N94-24611 #

FOA-A-50014-5.1 .... p 2430 N94-23743

FOA-B-40418-4.4 .... p 2421 N94-24290 #

FOA-C-30688-3.1 .... p 2388 N94-24741
FOA-C-30689-3.1 .... p 2545 N94-24529
FOA-C-306960-3.1-PT-5 .... p 2544 N94-23723
FOA-C-306960-8.4-PT-5 .... p 2544 N94-23723
FOA-C-30699-3.2 .... p 2297 N94-24530
FOA-C-30699-8.4 .... p 2297 N94-24530
FOA-C-30700-3.2 .... p 2294 N94-23773
FOA-C-30700-8.4 .... p 2294 N94-23773
FOA-C-30701-8.3 .... p 2297 N94-24531
FOA-C-30703-3.2 .... p 2294 N94-23742
FOA-C-40304-4.3 .... p 2437 N94-24292 #

FOA-30078-3.4 .... p 2590 N94-23741

FPR8-TLW-01794 .... p 2453 N94-23624 * #

FR-23115 .... p 2367 N94-25174 * #
FR-23116 .... p 2221 N94-25019 * #

GA-A-21398 .... p 2553 N94-24746 #
GA-A-21409 .... p 2553 N94-24756 #
GA-A-21412 .... p 2354 N94-23797 #
GA-A-21415 .... p 2551 N94-23782 #
GA-A-21416 .... p 2550 N94-23182 #

GAO/NSIAD-93-301R .... p 2174 N94-25153 #
GAO/NSIAD-94-25 .... p 2591 N94-24092 #
GAO/NSIAD-94-75 .... p 2184 N94-25152 #

GRI-92/0521 .... p 2232 N94-23477
GRI-92/0523 .... p 2233 N94-23736 #
GRI-93/0076 .... p 2398 N94-23818
GRI-93/0190 .... p 2233 N94-23801
GRI-93/0206 .... p 2232 N94-23100
GRI-93/0267 .... p 2235 N94-24920 #
GRI-93/0272 .... p 2187 N94-23709

GSFC-S-480-53-REV-B .... p 2208 N94-23478 *
GSFC-S-480-72 .... p 2208 N94-23479 *
GSFC-S-480-73 .... p 2208 N94-23480 *
GSFC-S-480-74 .... p 2208 N94-23481 *

GSO-TR-93-2 .... p 2418 N94-24795

H-1888 .... p 2381 N94-22961 * #
H-1940 .... p 2168 N94-24295 * #
H-1946 .... p 2188 N94-24106 * #
H-1953 .... p 2228 N94-23514 * #
H-1960 .... p 2376 N94-23487 * #
H-1961 .... p 2334 N94-24495 * #

HEC-TP-138 .... p 2460 N94-24822 #

HMSC-CADBIT-FR-93-1 .... p 2463 N94-25455 #
HMSC-CADBIT-FR-93-2 .... p 2463 N94-25456 #

HUPHY-01-93 .... p 2532 N94-22952

IAEA-TECDOC-674 .... p 2399 N94-25167

IAPCM-0018 .... p 2554 N94-25330 #

IC-92/183 .... p 2491 N94-25166
IC-92/200 .... p 2538 N94-25317
IC-92/201 .... p 2539 N94-25474
IC-92/264 .... p 2523 N94-25328 #
IC-92/274 .... p 2555 N94-25343 #
IC-92/276 .... p 2492 N94-25334 #
IC-92/287 .... p 2567 N94-25423
IC-92/299 .... p 2568 N94-25447
IC-92/336 .... p 2604 N94-25210
IC-92/343 .... p 2493 N94-25433
IC-92/345 .... p 2604 N94-25211
IC-92/346 .... p 2604 N94-25212
IC-92/348 .... p 2568 N94-25483
IC-92/350 .... p 2524 N94-25208
IC-92/354 .... p 2491 N94-25213
IC-92/355 .... p 2491 N94-25214
IC-92/358 .... p 2525 N94-25389
IC-92/360 .... p 2566 N94-25390
IC-92/361 .... p 2566 N94-25391
IC-92/362 .... p 2566 N94-25392
IC-92/363 .... p 2493 N94-25434
IC-92/372 .... p 2570 N94-25336
IC-92/373 .... p 2567 N94-25403
IC-92/378 .... p 2567 N94-25426
IC-92/380 .... p 2538 N94-25388
IC-92/392 .... p 2570 N94-25206
IC-92/396 .... p 2604 N94-25215 #
IC-92/400 .... p 2493 N94-25473
IC-93/130 .... p 2558 N94-22978
IC-93/77 .... p 2532 N94-22970

ICASE-IR-25 .... p 2473 N94-23558 * #

ICASE-93-100 .... p 2490 N94-24914 * #
ICASE-93-101 .... p 2337 N94-24869 * #
ICASE-93-75 .... p 2333 N94-24356 * #
ICASE-93-77 .... p 2458 N94-24740 * #
ICASE-93-79 .... p 2457 N94-24638 * #
ICASE-93-83 .... p 2480 N94-23272 * #
ICASE-93-84 .... p 2451 N94-23340 * #
ICASE-93-86 .... p 2317 N94-23089 * #
ICASE-93-87 .... p 2335 N94-24712 * #
ICASE-93-88 .... p 2319 N94-23302 * #
ICASE-93-89 .... p 2334 N94-24605 * #
ICASE-93-90 .... p 2490 N94-24836 * #
ICASE-93-91 .... p 2451 N94-23341 * #
ICASE-93-92 .... p 2448 N94-23092 * #
ICASE-93-94 .... p 2487 N94-24291 * #
ICASE-93-95 .... p 2479 N94-23090 * #
ICASE-93-97 .... p 2458 N94-24680 * #
ICASE-93-98 .... p 2334 N94-24602 * #
ICASE-93-99 .... p 2458 N94-24679 * #

ICOMP-93-20 .... p 2336 N94-24713 * #
ICOMP-93-44 .... p 2333 N94-24336 * #
ICOMP-93-46 .... p 2333 N94-24460 * #
ICOMP-93-48 .... p 2481 N94-23554 * #
ICOMP-93-51 .... p 2326 N94-24063 * #
ICOMP-94-2 .... p 2265 N94-24301 * #

ICRR-REPT-293-93-5 .... p 2627 N94-24962 #
ICRR-REPT-294-93-6 .... p 2627 N94-24961 #

IEPC-93-052 .... p 2222 N94-25201 * #
IEPC-93-094 .... p 2219 N94-23630 * #
IEPC-93-098 .... p 2221 N94-24766 * #
IEPC-93-108 .... p 2221 N94-24770 * #
IEPC-93-194 .... p 2553 N94-25190 * #
IEPC-93-208 .... p 2219 N94-23555 * #
IEPC-93-250 .... p 2218 N94-23372 * #

IEPEC-93-044 .... p 2221 N94-25189 * #

IFT-P-001/93 .... p 2478 N94-22969

IFVE-OTF-91-171 .... p 2538 N94-25341

IHES/M/93/28 .... p 2487 N94-23775
IHES/M/93/29 .... p 2487 N94-23776
IHES/M/93/37 .... p 2481 N94-23547 #
IHES/M/93/38 .... p 2488 N94-24536
IHES/M/93/39 .... p 2481 N94-23548 #

IHES/P/93/16 .... p 2601 N94-23099 #
IHES/P/93/36 .... p 2489 N94-24610

IITRI-D06205-3 .... p 2299 N94-24676

ILR-BER-59 .... p 2269 N94-23581 #

ILR-MITT-260(1991) .... p 2315 N94-22852 #

INIS-AR-012 .... p 2239 N94-22966
INIS-AR-013 .... p 2239 N94-22965

INIS-MF-13429 .... p 2541 N94-25335 #
INIS-MF-13691 .... p 2448 N94-23024
INIS-MF-13703 .... p 2352 N94-23025

INP-MSU-91-42-236 .... p 2541 N94-25342
INP-MSU-91-45-249 .... p 2539 N94-25476

INRIA-RR-1512 .... p 2475 N94-24963

INT-PATENT-CLASS-A47B-77/10 p 2192 N94-23310 *

INT-PATENT-CLASS-B25J-11/00 p 2352 N94-23082 *
INT-PATENT-CLASS-B64C-025/34 p 2176 N94-24181
INT-PATENT-CLASS-B64C-11/20 p 2186 N94-23255
INT-PATENT-CLASS-B64C-11/48 p 2186 N94-23255
INT-PATENT-CLASS-B64C-27/46 p 2176 N94-23254
INT-PATENT-CLASS-B64D-017/02 p 2168 N94-24182
INT-PATENT-CLASS-B64D-027/02 p 2188 N94-24180
INT-PATENT-CLASS-B64D-027/10 p 2188 N94-24180
INT-PATENT-CLASS-B64D-27/26 p 2353 N94-23215
INT-PATENT-CLASS-B64F-001/22 p 2193 N94-24785
INT-PATENT-CLASS-B64G-1/64 . p 2354 N94-23822 *

INT-PATENT-CLASS-C03B-003/08
5 .... p 2254 N94-24129
INT-PATENT-CLASS-C03B-014/00 p 2254 N94-24129
INT-PATENT-CLASS-C04B-35/52 p 2253 N94-23311 *

INT-PATENT-CLASS-C07D-235/18 p 2253 N94-23305 *
INT-PATENT-CLASS-C07D-249/08 p 2252 N94-23075 *
INT-PATENT-CLASS-C09J-5/02 p 2252 N94-23076 *
INT-PATENT-CLASS-C30B-23/02 p 2563 N94-23972 *

INT-PATENT-CLASS-E02D-37/00 p 2203 N94-23824 *

INT-PATENT-CLASS-F01D-1/12 p 2186 N94-23253
INT-PATENT-CLASS-F012C-7/28 p 2364 N94-24128
INT-PATENT-CLASS-F02B-75/26 p 2363 N94-24055
INT-PATENT-CLASS-F02C-007/04
2 p 2188 N94-24490
INT-PATENT-CLASS-F02C-7/20 p 2353 N94-23215
INT-PATENT-CLASS-F04B-37/00 p 2354 N94-23831 *
INT-PATENT-CLASS-F16B-19/00 p 2364 N94-24175 #
INT-PATENT-CLASS-F16B-3/00 p 2352 N94-23082 *
INT-PATENT-CLASS-F16B-31/00 p 2364 N94-24175 #
INT-PATENT-CLASS-F16D-1/00 p 2352 N94-23078 *
INT-PATENT-CLASS-F16F-15/04 p 2353 N94-23215
INT-PATENT-CLASS-F16H-25/20 p 2352 N94-23078 *
INT-PATENT-CLASS-F16J-15/44 p 2364 N94-24128

INT-PATENT-CLASS-G01C-3/08 p 2294 N94-23827 *
INT-PATENT-CLASS-G01C-3/08 p 2544 N94-24489
INT-PATENT-CLASS-G01F-1/46 p 2317 N94-23077 *
INT-PATENT-CLASS-G01F-1/46 p 2319 N94-23306 *
INT-PATENT-CLASS-G01P-015/02 p 2344 N94-24184
INT-PATENT-CLASS-G01P-015/08 p 2344 N94-24184
INT-PATENT-CLASS-G01P-3/36 p 2543 N94-23309 *
INT-PATENT-CLASS-G01P-5/165 p 2319 N94-23306 *
INT-PATENT-CLASS-G01S-13/95 p 2294 N94-23827 *
INT-PATENT-CLASS-G01S-3/78 p 2544 N94-24489

INT-PATENT-CLASS-H01L-35/12 p 2343 N94-23826 *
INT-PATENT-CLASS-H01M-10/48 p 2310 N94-23823 *
INT-PATENT-CLASS-H04B-10/00 p 2543 N94-23270 *
INT-PATENT-CLASS-H04R-5/00 p 2525 N94-23312 *
INT-PATENT-CLASS-H05H-3/00 p 2534 N94-23825 *

IP-345 p 2406 N94-25535 #

IPPCZ-329 p 2551 N94-24293 #

IR-290 p 2478 N94-22984 #
IR-300 p 2448 N94-23097
IR-304 p 2448 N94-23096 #
IR-310 p 2589 N94-23095
IR-311 p 2488 N94-24527
IR-312 p 2585 N94-23761 #
IR-313 p 2586 N94-24528
IR-314 p 2486 N94-23762 #
IR-315 p 2487 N94-23765 #
IR-316 p 2497 N94-23764 #
IR-317 p 2489 N94-24643
IR-318 p 2474 N94-24543
IR-328 p 2453 N94-23745
IR-329 p 2473 N94-23748 #
IR-330 p 2473 N94-23747 #
IR-331 p 2466 N94-23706 #
IR-332 p 2453 N94-23707 #

IRIG-STANDARD-210-93 p 2197 N94-25064 #

IS-M-753 p 2227 N94-22977 #
IS-M-763 p 2227 N94-23004
IS-M-767 p 2243 N94-23753 #
IS-M-768 p 2227 N94-23005
IS-M-771 p 2253 N94-23183 #
IS-M-772 p 2375 N94-23184 #
IS-M-773 p 2243 N94-23717 #

IS-T-1649 p 2561 N94-23214 #

ISAL-93-0008 p 2239 N94-22972 #
ISAL-93-0027 p 2227 N94-23133 #

ISBN-0-16-041936-0 p 2630 N94-23333 * #
ISBN-0-16-042080-6 p 2290 N94-23081 #
ISBN-0-16-042095-4 p 2630 N94-23572 #
ISBN-0-16-042100-4 p 2597 N94-25018 * #
ISBN-0-309-04876-1 p 2593 N94-24833
ISBN-0-309-04881-8 p 2631 N94-25065
ISBN-0-309-04977-6 p 2401 N94-23344 * #
ISBN-0-309-04984-0 p 2421 N94-24704
ISBN-0-309-04991-1 p 2585 N94-24698
ISBN-0-315-57633-2 p 2333 N94-24177
ISBN-0-315-58963-9 p 2168 N94-24178
ISBN-0-315-59455-1 p 2297 N94-24179
ISBN-0-315-59470-5 p 2175 N94-24176
ISBN-0-315-83365-3 p 2257 N94-24468
ISBN-0-315-83371-8 p 2427 N94-24467
ISBN-0-315-83424-2 p 2544 N94-24466
ISBN-0-315-83539-7 p 2227 N94-22892
ISBN-0-315-83541-9 p 2541 N94-22891
ISBN-0-315-83550-8 p 2226 N94-22890
ISBN-0-315-83554-0 p 2196 N94-22889
ISBN-0-315-83993-7 p 2244 N94-24469
ISBN-0-9616962-7-3 p 2598 N94-25006
ISBN-1-87-156449-2 p 2523 N94-25480 #
ISBN-1-87-156450-6 p 2594 N94-25485 #
ISBN-1-87-156455-7 p 2340 N94-25486 #
ISBN-1-877914-65-7 p 2250 N94-25405 #
ISBN-1-877914-65-7 p 2250 N94-25406 #
ISBN-1-877914-65-7 p 2250 N94-25407 #
ISBN-1-877914-65-7 p 2250 N94-25408 #
ISBN-1-877914-65-7 p 2251 N94-25448 #
ISBN-1-877914-65-7 p 2251 N94-25449 #
ISBN-1-877914-65-7 p 2251 N94-25450 #
ISBN-1-877914-65-7 p 2251 N94-25451 #
ISBN-1-883712-26-2 p 2293 N94-23627 * #
ISBN-1-883712-27-0 p 2293 N94-23628 * #
ISBN-2-85428-331-7 p 2605 N94-23373
ISBN-3-7983-1505-1 p 2269 N94-23581 #
ISBN-9-03-860082-8 p 2555 N94-25439 #
ISBN-9-03-860092-5 p 2475 N94-25224
ISBN-9-03-860112-3 p 2367 N94-25249
ISBN-9-03-860132-8 p 2416 N94-25261 #
ISBN-9-03-860142-5 p 2565 N94-25280 #
ISBN-9-03-860161-1 p 2586 N94-25076 #
ISBN-9-03-860162-X p 2462 N94-25237 #
ISBN-9-03-860182-4 p 2587 N94-25283 #
ISBN-9-03-860192-1 p 2263 N94-25299
ISBN-9-03-860211-1 p 2586 N94-25235 #
ISBN-9-03-860222-7 p 2226 N94-25238 #
ISBN-9-03-860242-1 p 2462 N94-25219 #
ISBN-9-05-411068-6 p 2381 N94-23145 #
ISBN-9-05-411070-8 p 2417 N94-23176 #
ISBN-9-05-411072-4 p 2382 N94-23177 #
ISBN-9-05-411079-1 p 2417 N94-24107 #
ISBN-9-06-144260-5 p 2447 N94-22731 #
ISBN-9-06-144261-3 p 2470 N94-22873 #
ISBN-9-06-144262-1 p 2347 N94-22874 #
ISBN-9-06-144263-X p 2290 N94-22876 #
ISBN-9-06-144264-8 p 2470 N94-22877 #
ISBN-9-06-144265-6 p 2348 N94-23168 #
ISBN-9-06-144266-4 p 2449 N94-23169 #
ISBN-9-06-144267-2 p 2445 N94-23170 #
ISBN-9-06-144268-0 p 2542 N94-23171 #
ISBN-9-06-144269-9 p 2308 N94-23136 #
ISBN-9-06-144270-2 p 2449 N94-23172 #
ISBN-9-06-144271-0 p 2450 N94-23173 #
ISBN-9-06-144272-9 p 2268 N94-23174 #
ISBN-9-06-215364-X p 2587 N94-25279 #
ISBN-9-06-275765-0 p 2338 N94-25227 #
ISBN-9-06-275778-2 p 2462 N94-25252
ISBN-9-07-386105-5 p 2537 N94-25228 #
ISBN-9-09-005162-7 p 2530 N94-25220 #
ISBN-9-09-005197-X p 2405 N94-25251
ISBN-9-09-005213-5 p 2405 N94-25229 #
ISBN-9-09-005313-1 p 2262 N94-25230 #
ISBN-9-09-005332-8 p 2461 N94-25080 #
ISBN-9-09-005342-5 p 2304 N94-25292 #
ISBN-9-09-005589-4 p 2338 N94-25243
ISBN-9-09-005693-9 p 2313 N94-25083 #
ISBN-9-09-005713-7 p 2462 N94-25263 #
ISBN-9-09-005758-7 p 2400 N94-25223 #
ISBN-9-09-006067-7 p 2566 N94-25297
ISBN-9-09-006217-3 p 2538 N94-25255 #
ISBN-9-29-092065-3 p 2623 N94-22837 #
ISBN-9-29-092178-1 p 2355 N94-23985 #
ISBN-9-29-092212-5 p 2450 N94-23228 #
ISBN-9-51-384236-5 p 2250 N94-25316 #
ISBN-9-51-384244-4 p 2379 N94-25529 #
ISBN-9-51-384310-6 p 2250 N94-25346 #
ISBN-9-51-384319-X p 2566 N94-25347 #
ISBN-90-369-0272-X p 2418 N94-24601
ISBN-90-370-0073-8 p 2232 N94-22983
ISBN-90-370-0081-9 p 2267 N94-22981 #
ISBN-90-6275-790-1 p 2562 N94-23766 #
ISBN-90-6275-871-1 p 2592 N94-24646
ISBN-90-6275-876-2/CIP p 2377 N94-24645
ISBN-90-9004155-9 p 2479 N94-23121
ISBN-90-9006108-8 p 2404 N94-24647
ISBN-90-9006115-0 p 2347 N94-22982
ISBN-92-835-0676-6 p 2431 N94-23976 #
ISBN-92-835-0722-3 p 2423 N94-23313 #
ISBN-92-835-0723-1 p 2521 N94-25008 #
ISBN-92-835-0728-2 p 2255 N94-24228 #
ISBN-92-835-0729-0 p 2177 N94-24313 #
ISBN-92-835-0730-4 p 2173 N94-24091 #
ISBN-951-22-1428-8 p 2479 N94-23106
ISBN-951-22-1442-3 p 2290 N94-23225 #
ISBN-951-22-1449-0 p 2254 N94-23561
ISBN-951-22-1455-5 p 2308 N94-23105 #
ISBN-951-22-1478-4 p 2375 N94-23120 #
ISBN-951-22-1482-2 p 2317 N94-23114 #
ISBN-951-22-1494-6 p 2308 N94-23130
ISBN-951-22-1499-7 p 2374 N94-23118 #
ISBN-951-22-1500-4 p 2449 N94-23117
ISBN-951-22-1501-2 p 2524 N94-23131
ISBN-951-22-1523-3 p 2240 N94-23119
ISBN-951-22-1524-1 p 2524 N94-23110
ISBN-951-22-1564-0 p 2374 N94-23113
ISBN-951-22-1601-9 p 2450 N94-23226 #
ISBN-951-38-4116-2 p 2571 N94-25416 #
ISBN-951-38-4117-0 p 2396 N94-25417 #
ISBN-951-38-4119-7 p 2379 N94-25418 #
ISBN-951-38-4122-7 p 2379 N94-25385 #
ISBN-951-38-4166-9 p 2588 N94-22734 #
ISBN-951-38-4306-8 p 2230 N94-25386 #
ISBN-951-38-4307-6 p 2251 N94-25419 #
ISBN-951-38-4318-1 p 2231 N94-25420 #
ISBN-951-650-188-5 p 2472 N94-23463
ISBN-951-96735-0-4 p 2444 N94-23754

ISL-CO-203/92 p 2343 N94-24054 #
ISL-CO-207/92 p 2318 N94-23160 #
ISL-CO-215/92 p 2165 N94-23161 #
ISL-CO-228/92 p 2529 N94-24514
ISL-CO-229/92 p 2165 N94-23149 #
ISL-CO-230/92 p 2176 N94-23146 #

ISL-N-601/92 p 2314 N94-25460
ISL-N-604/92 p 2171 N94-25461 #

ISL-R-102/92 p 2339 N94-25462
ISL-R-104/92 p 2340 N94-25463 #
ISL-R-108/92 p 2185 N94-25301

ISVR-TR-216 p 2363 N94-24076
ISVR-TR-226 p 2525 N94-22959

ITN-94-85227 p 2153 N94-24241

ITOP-6-2-242 p 2300 N94-24687 #

IZF-1993-A-11 p 2542 N94-22895

JAERI-M-92-202 p 2548 N94-22924 #
JAERI-M-92-211 p 2347 N94-22922 #

JINR-E-14-91-519 p 2567 N94-25424
JINR-E-17-91-438 p 2263 N94-25404
JINR-E-2-91-464 p 2570 N94-25337
JINR-E-2-91-531 p 2539 N94-25481
JINR-E-2-91-566 p 2492 N94-25338 #
JINR-E-2-92-19 p 2571 N94-25339
JINR-E-2-92-281 p 2536 N94-24844 #
JINR-E-4-92-9 p 2539 N94-25477

JINR-R-10-91-482 p 2463 N94-25432
JINR-R-17-91-269 p 2570 N94-25207
JINR-R-3-91-450 p 2567 N94-25425

JPL-PUBL-93-009 p 2273 N94-22735 * #
JPL-PUBL-93-30 p 2395 N94-24563 * #
JPL-PUBL-93-5 p 2497 N94-23832 * #

JPRS-USP-93-006 p 2194 N94-23015 #

JTN-94-80510 p 2405 N94-24980 #
JTN-94-80515 p 2446 N94-24981 #
JTN-94-80516 p 2546 N94-24982 #
JTN-94-80518 p 2603 N94-24983 #
JTN-94-80519 p 2235 N94-24984 #
JTN-94-80520 p 2603 N94-24985 #
JTN-94-80521 p 2604 N94-24986 #
JTN-94-80522 p 2604 N94-24987 #
JTN-94-80523 p 2603 N94-24976 #
JTN-94-80525 p 2564 N94-24958 #
JTN-94-80526 p 2567 N94-25412 #
JTN-94-80527 p 2568 N94-25515 #
JTN-94-80529 p 2564 N94-24959 #
JTN-94-80530 p 2345 N94-24977 #
JTN-94-80531 p 2564 N94-24978 #
JTN-94-80533 p 2564 N94-24960 #
JTN-94-80540 p 2627 N94-24961 #
JTN-94-80542 p 2627 N94-24962 #

KAPL-4760 p 2238 N94-22936 #
KAPL-4761 p 2238 N94-22861 #

L-17133 p 2319 N94-23339 * #
L-17150 p 2166 N94-23512 * #
L-17157 p 2169 N94-24464 * #
L-17171 p 2169 N94-24311 * #
L-17186 p 2177 N94-24304 * #
L-17228 p 2169 N94-24586 * #
L-17275-PT-1 p 2482 N94-23673 * #
L-17278 p 2245 N94-25117 * #
L-17286 p 2170 N94-24716 * #
L-17304 p 2540 N94-24305 * #
L-17306 p 2540 N94-23509 * #
L-17331 p 2526 N94-24207 * #

LA-SUB-93-178 p 2198 N94-23208 #
LA-SUB-93-236 p 2453 N94-23701 #
LA-SUB-93-299 p 2326 N94-23809 #

LA-UR-93-2942 p 2348 N94-23203
LA-UR-93-2949 p 2557 N94-22925 #
LA-UR-93-3006 p 2531 N94-22928 #
LA-UR-93-3070 p 2311 N94-24500 #
LA-UR-93-3124 p 2316 N94-22870 #
LA-UR-93-3127 p 2556 N94-22920
LA-UR-93-3144 p 2558 N94-22941
LA-UR-93-3184 p 2374 N94-22871 #
LA-UR-93-3189 p 2231 N94-22933 #
LA-UR-93-3241 p 2557 N94-22940 #
LA-UR-93-3268 p 2557 N94-22938
LA-UR-93-3304 p 2231 N94-22943 #
LA-UR-93-3324 p 2218 N94-23433 #
LA-UR-93-3327 p 2417 N94-23517 #
LA-UR-93-3329 p 2558 N94-22942
LA-UR-93-3334 p 2569 N94-23453
LA-UR-93-3350 p 2239 N94-22939 #
LA-UR-93-3361 p 2218 N94-23452 #
LA-UR-93-3391 p 2307 N94-22987
LA-UR-93-3408 p 2626 N94-23515 #
LA-UR-93-3439 p 2407 N94-23284 #
LA-UR-93-3449 p 2559 N94-23006 #
LA-UR-93-3453 p 2242 N94-23541 #
LA-UR-93-3454 p 2240 N94-23021
LA-UR-93-3473 p 2240 N94-23003 #
LA-UR-93-3488 p 2626 N94-23020
LA-UR-93-3518 p 2218 N94-23283 #
LA-UR-93-3531 p 2563 N94-24517 #
LA-UR-93-3550 p 2569 N94-24516 #
LA-UR-93-3584 p 2245 N94-24520 #
LA-UR-93-3598 p 2473 N94-24518 #
LA-UR-93-3599 p 2552 N94-24519 #
LA-UR-93-3628 p 2245 N94-24747 #
LA-UR-93-3640 p 2457 N94-24626 #
LA-UR-93-3677 p 2553 N94-24628 #

LA-12655-MS p 2535 N94-24505 #

LAAS-93044 p 2342 N94-22902 #
LAAS-93088 p 2445 N94-22903
LAAS-93089 p 2470 N94-22904 #
LAAS-93093 p 2556 N94-22905 #
LAAS-93107 p 2470 N94-22906 #
LAAS-93111 p 2471 N94-22907 #
LAAS-93117 p 2471 N94-22908 #
LAAS-93139 p 2307 N94-22909 #
LAAS-93156 p 2252 N94-22910 #
LAAS-93179 p 2447 N94-22911 #

LAMP-92/2 p 2547 N94-25209 #
LAMP-92/4 p 2351 N94-25482 #

LBL-32505 p 2335 N94-24655 #
LBL-33432 p 2299 N94-24656 #
LBL-33677 p 2533 N94-23218
LBL-34280 p 2557 N94-22926 #
LBL-34447 p 2564 N94-24657 #
LBL-34481 p 2532 N94-23002 #
LBL-34507 p 2523 N94-24658 #

LC-92-85596 p 2593 N94-24833
LC-93-31238 p 2630 N94-23333 * #
LC-93-83945 p 2631 N94-25065
LC-93-85739 p 2401 N94-23344 * #
LC-93-85920 p 2421 N94-24704
LC-93-86012 p 2631 N94-24584 * #
LC-93-86930 p 2585 N94-24698

LESC-30753 p 2199 N94-23571 * #
LESC-30966 p 2590 N94-23289 * #

LPI-CONTRIB-805 p 2613 N94-24058 * #

LPI-TR-93-05 p 2616 N94-24871 * #
LPI-TR-93-07 p 2603 N94-24964 * #

LRT-WE-9-FB-3-1992 p 2266 N94-23195 #
LRT-WE-9-FB-4-1992 p 2375 N94-23196 #
LRT-WE-9-FB-5-1992 p 2318 N94-23197 #

M-614 p 2375 N94-23221
M-662 p 2193 N94-24739
M-663 p 2378 N94-24745
M-734 p 2376 N94-23342 * #
M-736 p 2223 N94-24338 * #
M-737 p 2375 N94-23294 * #
M-740 p 2490 N94-24727 * #
M-741 p 2269 N94-23574 * #

MA-RD-840-93000-VOL-1 p 2175 N94-24474

MATHS-REPT-A-184 p 2236 N94-25427 #
MATHS-REPT-A-191 p 2476 N94-25428 #
MATHS-REPT-A-192 p 2476 N94-25429 #
MATHS-REPT-A-193 p 2406 N94-25430 #

MCR-93-1362-VOL-4 p 2201 N94-24970 * #
MCR-93-5013 p 2430 N94-23290 * #

ME-ANA-TSTO p 2204 N94-24620 * #

MEMO-COSOR-91-38-REV p 2493 N94-23142 #
MEMO-COSOR-92-35 p 2494 N94-23143 #
MEMO-COSOR-92-36 p 2480 N94-23144 #
MEMO-COSOR-92-37 p 2477 N94-25526 #
MEMO-COSOR-92-38 p 2493 N94-25527 #
MEMO-COSOR-93-01 p 2494 N94-23546 #
MEMO-COSOR-93-02 p 2481 N94-23442 #
MEMO-COSOR-93-03 p 2494 N94-23774
MEMO-COSOR-93-05 p 2474 N94-24609
MEMO-COSOR-93-06 p 2475 N94-24755
MEMO-COSOR-93-07 p 2451 N94-23441 #
MEMO-COSOR-93-08 p 2459 N94-24765
MEMO-COSOR-93-09 p 2481 N94-23456 #
MEMO-COSOR-93-10 p 2468 N94-24764
MEMO-COSOR-93-11 p 2489 N94-24608
MEMO-COSOR-93-12 p 2490 N94-24763
MEMO-COSOR-93-13 p 2494 N94-23440 #
MEMO-COSOR-93-14 p 2475 N94-24762
MEMO-COSOR-93-15 p 2494 N94-23798
MEMO-COSOR-93-16 p 2473 N94-24542 *
MEMO-COSOR-93-17 p 2494 N94-23771
MEMO-COSOR-93-18 p 2494 N94-23772
MEMO-COSOR-93-19 p 2467 N94-23767
MEMO-COSOR-93-20 p 2467 N94-23756
MEMO-COSOR-93-21 p 2487 N94-23799
MEMO-COSOR-93-22 p 2495 N94-23815 #
MEMO-COSOR-93-23 p 2495 N94-24508
MEMO-COSOR-93-24 p 2495 N94-24571

MEMO-INF-93-02 p 2593 N94-24743
MEMO-INF-93-11 p 2465 N94-22986 #
MEMO-INF-93-25 p 2590 N94-23816 #
MEMO-INF-93-31 p 2486 N94-23725 #
MEMO-INF-93-33 p 2272 N94-24648
MEMO-INF-93-38 p 2454 N94-23750 #

MEMO-1106 p 2493 N94-22724 #
MEMO-1107 p 2478 N94-22725 #
MEMO-1108 p 2478 N94-22726 #
MEMO-1109 p 2478 N94-22727 #
MEMO-1110 p 2493 N94-22728 #
MEMO-1111 p 2273 N94-22729 #
MEMO-1112 p 2555 N94-22730 #
MEMO-1113 p 2493 N94-22702 #
MEMO-1114 p 2487 N94-24053 #
MEMO-1115 p 2469 N94-22703 #
MEMO-1116 p 2585 N94-22704 #
MEMO-1117 p 2568 N94-22709 #
MEMO-1118 p 2469 N94-22705 #
MEMO-1119 p 2469 N94-22706 #
MEMO-1120 p 2469 N94-22707 #
MEMO-1121 p 2497 N94-22708 #
MEMO-1122 p 2478 N94-22710 #
MEMO-1123 p 2447 N94-22711 #
MEMO-1124 p 2469 N94-22712 #
MEMO-1125 p 2315 N94-22713 #
MEMO-1126 p 2470 N94-22714 #
MEMO-1127 p 2478 N94-22715 #
MEMO-1128 p 2497 N94-22716 #
MEMO-1129 p 2487 N94-23787
MEMO-1130 p 2488 N94-24541
MEMO-1131 p 2489 N94-24651
MEMO-1132A p 2489 N94-24652
MEMO-1132 p 2486 N94-23722
MEMO-1133 p 2489 N94-24653
MEMO-1134 p 2467 N94-24524
MEMO-1135 p 2497 N94-23800
MEMO-1136 p 2521 N94-24523

MISC-2514 p 2187 N94-23519
MISC-2665 p 2187 N94-23570
MISC-2693 p 2595 N94-23580

MIT-OSP-99857 p 2255 N94-24223 * #

MLM-3786 p 2243 N94-23784 #

MML-TM-93-25 p 2314 N94-25488 #

MP-93-164 p 2232 N94-23524 * #

MPE-241 p 2346 N94-25415 #

MPI-PHE/92-22 p 2314 N94-25457
MPI-PHE/93-04 p 2600 N94-25458
MPI-PHE/93-05 p 2629 N94-25459

MPIM-102 p 2402 N94-24108 #
MPIM-103 p 2382 N94-23158 #
MPIM-104 p 2401 N94-23159 #
MPIM-107 p 2403 N94-24491 #
MPIM-96 p 2407 N94-23199 #
MPIM-97 p 2407 N94-23156 #
MPIM-99 p 2400 N94-23157 #

MPIS-24/1992 p 2318 N94-23198 #

MRC/WDC-R-316 p 2311 N94-24818

M93B0000044RI p 2301 N94-24926

NAS 1.15:104018 p 2431 N94-23970 * #
NAS 1.15:104273 p 2334 N94-24495 * #
NAS 1.15:104274 p 2376 N94-23487 * #
NAS 1.15:104566-VOL-11 p 2417 N94-23338 * #
NAS 1.15:104566-VOL-9 p 2417 N94-23291 * #
NAS 1.15:104571 p 2407 N94-23132 * #
NAS 1.15:104577 p 2308 N94-23281 * #
NAS 1.15:104584 p 2401 N94-23282 * #
NAS 1.15:104585 p 2218 N94-23343 * #
NAS 1.15:104595 p 2381 N94-24800 * #
NAS 1.15:104596 p 2195 N94-24497 * #
NAS 1.15:104756 p 2433 N94-24185 * #
NAS 1.15:104783 p 2205 N94-24625 * #
NAS 1.15:104784 p 2386 N94-24095 * #
NAS 1.15:104786 p 2473 N94-24068 * #
NAS 1.15:105271 p 2187 N94-23545 * #
NAS 1.15:105650 p 2205 N94-24825 * #
NAS 1.15:105871 p 2193 N94-25184 * #
NAS 1.15:105990 p 2376 N94-23551 * #
NAS 1.15:106035 p 2590 N94-23562 * #
NAS 1.15:106177 p 2336 N94-24713 * #
NAS 1.15:106261 p 2189 N94-25185 * #
NAS 1.15:106295 p 2295 N94-24101 * #
NAS 1.15:106310 p 2186 N94-23466 * #
NAS 1.15:106311 p 2192 N94-23091 * #
NAS 1.15:106358 p 2378 N94-25188 * #
NAS 1.15:106381 p 2242 N94-23550 * #
NAS 1.15:106383 p 2333 N94-24336 * #
NAS 1.15:106391 p 2168 N94-24084 * #
NAS 1.15:106397 p 2201 N94-23567 * #
NAS 1.15:106401 p 2219 N94-23630 * #
NAS 1.15:106408 p 2249 N94-25171 * #
NAS 1.15:106414 p 2222 N94-23500 * #
NAS 1.15:106417 p 2395 N94-24071 * #
NAS 1.15:106419 p 2219 N94-23531 * #
NAS 1.15:106423 p 2253 N94-23371 * #
NAS 1.15:106426 p 2221 N94-24770 * #
NAS 1.15:106428 p 2218 N94-23372 * #
NAS 1.15:106429 p 2243 N94-23556 * #
NAS 1.15:106433 p 2243 N94-23578 * #
NAS 1.15:106434 p 2187 N94-24082 * #
NAS 1.15:106436 p 2481 N94-23593 * #
NAS 1.15:106437 p 2481 N94-23554 * #
NAS 1.15:106445 p 2320 N94-23525 * #
NAS 1.15:106450 p 2167 N94-23592 * #
NAS 1.15:106451 p 2220 N94-24681 * #
NAS 1.15:106457 p 2172 N94-23523 * #
NAS 1.15:106459 p 2166 N94-23522 * #
NAS 1.15:106461 p 2173 N94-24047 * #
NAS 1.15:106463 p 2153 N94-24100 * #
NAS 1.15:106464 p 2221 N94-24766 * #
NAS 1.15:106465 p 2525 N94-23464 * #
NAS 1.15:106466 p 2218 N94-23370 * #
NAS 1.15:106467 p 2364 N94-24483 * #
NAS 1.15:106468 p 2166 N94-23465 * #
NAS 1.15:106469 p 2326 N94-24063 * #
NAS 1.15:106470 p 2344 N94-24362 * #
NAS 1.15:106471 p 2166 N94-23299 * #
NAS 1.15:106474 p 2337 N94-25119 * #
NAS 1.15:106475 p 2258 N94-24682 * #
NAS 1.15:106476 p 2346 N94-25202 * #
NAS 1.15:106477 p 2188 N94-24594 * #
NAS 1.15:106481 p 2265 N94-24301 * #
NAS 1.15:106482 p 2195 N94-24482 * #
NAS 1.15:106483 p 2344 N94-24069 * #
NAS 1.15:106484 p 2202 N94-25095 * #
NAS 1.15:106486 p 2222 N94-25201 * #
NAS 1.15:106488 p 2221 N94-25189 * #
NAS 1.15:106490 p 2377 N94-24715 * #
NAS 1.15:106491 p 2169 N94-24335 * #
NAS 1.15:106492 p 2170 N94-25182 * #
NAS 1.15:106494 p 2310 N94-24308 * #
NAS 1.15:106497 p 2521 N94-24302 * #
NAS 1.15:106500 p 2345 N94-25116 * #
NAS 1.15:106503 p 2338 N94-25183 * #
NAS 1.15:106504 p 2334 N94-24481 * #
NAS 1.15:106505 p 2313 N94-25170 * #
NAS 1.15:106506 p 2230 N94-25186 * #
NAS 1.15:106508 p 2367 N94-25181 * #
NAS 1.15:106512 p 2530 N94-25172 * #
NAS 1.15:106524 p 2338 N94-25180 * #
NAS 1.15:107750 p 2376 N94-23368 * #
NAS 1.15:107751 p 2254 N94-23486 * #
NAS 1.15:108270 p 2383 N94-23595 * #
NAS 1.15:108423 p 2590 N94-24079 * #
NAS 1.15:108435 p 2409 N94-24080 * #

NAS 1.15:108437 .... p 2233 N94-24073 * #
NAS 1.15:108758 .... p 2182 N94-24953 * #
NAS 1.15:108778 .... p 2426 N94-23575 * #
NAS 1.15:108785 .... p 2426 N94-24102 * #
NAS 1.15:108786 .... p 2167 N94-23557 * #
NAS 1.15:108789 .... p 2453 N94-23568 * #
NAS 1.15:108790 .... p 2174 N94-25272 * #
NAS 1.15:108792 .... p 2431 N94-23974 * #
NAS 1.15:108795 .... p 2452 N94-23510 * #
NAS 1.15:108797 .... p 2420 N94-23088 * #
NAS 1.15:108799 .... p 2387 N94-24403 * #
NAS 1.15:109022 .... p 2592 N94-24649 * #
NAS 1.15:109033 .... p 2271 N94-24473 * #
NAS 1.15:109036 .... p 2169 N94-24576 * #
NAS 1.15:109043 .... p 2241 N94-23274 * #
NAS 1.15:109044 .... p 2228 N94-23279 * #
NAS 1.15:109047 .... p 2228 N94-23280 * #
NAS 1.15:109052 .... p 2228 N94-24083 * #
NAS 1.15:109054 .... p 2448 N94-23086 * #
NAS 1.15:109058 .... p 2457 N94-24603 * #
NAS 1.15:109061 .... p 2592 N94-24660 * #
NAS 1.15:109064 .... p 2593 N94-24709 * #
NAS 1.15:109070 .... p 2378 N94-24839 * #
NAS 1.15:109194 .... p 2200 N94-24577 * #
NAS 1.15:109195 .... p 2199 N94-24059 * #
NAS 1.15:109384 .... p 2208 N94-23481 *
NAS 1.15:109385 .... p 2194 N94-23710 * #
NAS 1.15:109388 .... p 2293 N94-23622 * #
NAS 1.15:109398 .... p 2293 N94-23627 * #
NAS 1.15:109399 .... p 2293 N94-23628 * #
NAS 1.15:109400 .... p 2630 N94-23135 * #
NAS 1.15:109406 .... p 2208 N94-23478 *
NAS 1.15:109407 .... p 2208 N94-23479 *
NAS 1.15:109408 .... p 2208 N94-23480 *
NAS 1.15:109677 .... p 2205 N94-24824 * #
NAS 1.15:109678 .... p 2349 N94-24488 * #
NAS 1.15:109680 .... p 2350 N94-24851 * #
NAS 1.15:109681 .... p 2167 N94-23975 * #
NAS 1.15:109682 .... p 2428 N94-24855 * #
NAS 1.15:109683 .... p 2593 N94-24759 * #
NAS 1.15:109720 .... p 2593 N94-25168 * #
NAS 1.15:16443 .... p 2222 N94-23591 * #
NAS 1.15:4497 .... p 2319 N94-23339 * #
NAS 1.15:4526 .... p 2168 N94-24295 * #
NAS 1.15:4529 .... p 2169 N94-24586 * #
NAS 1.15:4532 .... p 2188 N94-24106 * #
NAS 1.15:4533 .... p 2170 N94-24716 * #
NAS 1.15:4535 .... p 2228 N94-23514 * #
NAS 1.15:4554 .... p 2591 N94-24337 * #
NAS 1.18:1490.5 .... p 2590 N94-23971 * #
NAS 1.21:4105 .... p 2630 N94-23333 * #
NAS 1.21:4307 .... p 2631 N94-24584 * #
NAS 1.21:7037(298) .... p 2153 N94-23711 *
NAS 1.21:7037(299) .... p 2153 N94-23973 *
NAS 1.21:7039(44)-SECT-2 .... p 2590 N94-23712 *
NAS 1.21:7104 .... p 2631 N94-24585 * #
NAS 1.21:7500(27) .... p 2586 N94-24708 *
NAS 1.26:177619 .... p 2176 N94-23489 * #
NAS 1.26:177629 .... p 2181 N94-24796 * #
NAS 1.26:177631 .... p 2598 N94-24832 * #
NAS 1.26:177632 .... p 2598 N94-23536 * #
NAS 1.26:177634 .... p 2430 N94-23527 * #
NAS 1.26:188254 .... p 2199 N94-23571 * #
NAS 1.26:188256 .... p 2427 N94-24227 * #
NAS 1.26:188268 .... p 2430 N94-23290 * #
NAS 1.26:188270 .... p 2590 N94-23289 * #
NAS 1.26:188271-VOL-1 .... p 2632 N94-25348 * #
NAS 1.26:188271-VOL-2 .... p 2636 N94-25367 * #
NAS 1.26:189214 .... p 2364 N94-24090 * #
NAS 1.26:189313 .... p 2599 N94-23334 * #
NAS 1.26:189316 .... p 2453 N94-23559 * #
NAS 1.26:189317 .... p 2209 N94-24767 * #
NAS 1.26:189318 .... p 2430 N94-23080 * #
NAS 1.26:189320 .... p 2311 N94-24754 * #
NAS 1.26:189322 .... p 2205 N94-24710 * #
NAS 1.26:189324 .... p 2599 N94-24666 * #
NAS 1.26:189333 .... p 2204 N94-24226 * #
NAS 1.26:189645 .... p 2525 N94-23698 * #
NAS 1.26:191056 .... p 2290 N94-23087 * #
NAS 1.26:191132 .... p 2219 N94-24061 * #
NAS 1.26:191185 .... p 2170 N94-25173 * #
NAS 1.26:191197 .... p 2258 N94-24753 * #
NAS 1.26:191251 .... p 2295 N94-23830 * #
NAS 1.26:191328 .... p 2544 N94-23829 * #
NAS 1.26:191329 .... p 2204 N94-23828 * #
NAS 1.26:191461 .... p 2445 N94-23125 * #
NAS 1.26:191465 .... p 2466 N94-23252 * #
NAS 1.26:191483-VOL-1 .... p 2526 N94-24172 * #
NAS 1.26:191483-VOL-2 .... p 2526 N94-24173 * #
NAS 1.26:191490 .... p 2344 N94-24360 * #
NAS 1.26:191508 .... p 2172 N94-23288 * #
NAS 1.26:191547 .... p 2333 N94-24356 * #
NAS 1.26:191552 .... p 2473 N94-23558 * #
NAS 1.26:191553 .... p 2343 N94-23498 * #
NAS 1.26:191554 .... p 2458 N94-24740 * #
NAS 1.26:191556 .... p 2457 N94-24638 * #
NAS 1.26:191560 .... p 2480 N94-23278 * #
NAS 1.26:191561 .... p 2480 N94-23272 * #
NAS 1.26:191564 .... p 2451 N94-23340 * #
NAS 1.26:191567 .... p 2317 N94-23089 * #
NAS 1.26:191568 .... p 2335 N94-24712 * #
NAS 1.26:191569 .... p 2319 N94-23302 * #
NAS 1.26:191570 .... p 2334 N94-24605 * #
NAS 1.26:191571 .... p 2490 N94-24836 * #
NAS 1.26:191572 .... p 2319 N94-23513 * #
NAS 1.26:191573 .... p 2320 N94-23532 * #
NAS 1.26:191574 .... p 2451 N94-23341 * #
NAS 1.26:191575 .... p 2448 N94-23092 * #
NAS 1.26:191576 .... p 2444 N94-25090 * #
NAS 1.26:191578 .... p 2192 N94-23564 * #
NAS 1.26:191579 .... p 2336 N94-24771 * #
NAS 1.26:191582 .... p 2487 N94-24291 * #
NAS 1.26:191583 .... p 2479 N94-23090 * #
NAS 1.26:191585 .... p 2458 N94-24680 * #
NAS 1.26:191586 .... p 2334 N94-24602 * #
NAS 1.26:191587 .... p 2458 N94-24679 * #
NAS 1.26:191588 .... p 2490 N94-24914 * #
NAS 1.26:191589 .... p 2337 N94-24869 * #
NAS 1.26:192244 .... p 2466 N94-23483 * #
NAS 1.26:193151 .... p 2614 N94-24363 * #
NAS 1.26:193225 .... p 2420 N94-23538 * #
NAS 1.26:193703 .... p 2627 N94-24094 * #
NAS 1.26:193803 .... p 2422 N94-24807 * #
NAS 1.26:193862 .... p 2574 N94-24405 * #
NAS 1.26:193879 .... p 2200 N94-24664 * #
NAS 1.26:193880 .... p 2244 N94-24066 * #
NAS 1.26:193881 .... p 2456 N94-24470 * #
NAS 1.26:193882 .... p 2196 N94-24309 * #
NAS 1.26:193883 .... p 2421 N94-24310 * #
NAS 1.26:193884 .... p 2627 N94-24484 * #
NAS 1.26:193885 .... p 2627 N94-24461 * #
NAS 1.26:193889 .... p 2545 N94-24665 * #
NAS 1.26:193890 .... p 2455 N94-24111 * #
NAS 1.26:193891 .... p 2364 N94-24088 * #
NAS 1.26:193893 .... p 2229 N94-24224 * #
NAS 1.26:193894 .... p 2219 N94-24064 * #
NAS 1.26:193895 .... p 2201 N94-24802 * #
NAS 1.26:193897 .... p 2200 N94-24067 * #
NAS 1.26:193898 .... p 2199 N94-24057 * #
NAS 1.26:193899 .... p 2367 N94-25020 * #
NAS 1.26:193901 .... p 2365 N94-24588 * #
NAS 1.26:193902 .... p 2200 N94-24112 * #
NAS 1.26:193903 .... p 2200 N94-24065 * #
NAS 1.26:193904 .... p 2201 N94-24965 * #
NAS 1.26:193905 .... p 2267 N94-23549 * #
NAS 1.26:193906 .... p 2454 N94-24050 * #
NAS 1.26:193907 .... p 2372 N94-24174 * #
NAS 1.26:193908 .... p 2345 N94-24852 * #
NAS 1.26:193909 .... p 2376 N94-24359 * #
NAS 1.26:193910 .... p 2345 N94-25000 * #
NAS 1.26:193916 .... p 2366 N94-24998 * #
NAS 1.26:193917 .... p 2366 N94-24999 * #
NAS 1.26:193918 .... p 2201 N94-24970 * #
NAS 1.26:193919 .... p 2221 N94-25019 * #
NAS 1.26:193920 .... p 2367 N94-25174 * #
NAS 1.26:193921 .... p 2200 N94-24801 * #
NAS 1.26:194109 .... p 2401 N94-23337 * #
NAS 1.26:194138 .... p 2232 N94-23524 * #
NAS 1.26:194217 .... p 2327 N94-24096 * #
NAS 1.26:194435 .... p 2202 N94-23631 * #
NAS 1.26:194436 .... p 2190 N94-23590 * #
NAS 1.26:194438 .... p 2166 N94-23511 * #
NAS 1.26:194439 .... p 2203 N94-23632 * #
NAS 1.26:194440 .... p 2312 N94-24870 * #
NAS 1.26:194442 .... p 2553 N94-25190 * #
NAS 1.26:194444 .... p 2219 N94-23555 * #
NAS 1.26:194445 .... p 2187 N94-23552 * #
NAS 1.26:194448 .... p 2304 N94-25266 * #
NAS 1.26:194449 .... p 2153 N94-23553 * #
NAS 1.26:194450 .... p 2234 N94-24565 * #
NAS 1.26:194453 .... p 2377 N94-24604 * #
NAS 1.26:194454 .... p 2219 N94-24361 * #
NAS 1.26:194455 .... p 2189 N94-25200 * #
NAS 1.26:194458 .... p 2220 N94-24714 * #
NAS 1.26:194475 .... p 2462 N94-25179 * #
NAS 1.26:194486 .... p 2497 N94-23832 * #
NAS 1.26:194516 .... p 2273 N94-22735 * #
NAS 1.26:194678 .... p 2571 N94-23230 * #
NAS 1.26:194714 .... p 2623 N94-24996 * #
NAS 1.26:194719-VOL-2 .... p 2209 N94-23028 * #
NAS 1.26:194735 .... p 2296 N94-24105 * #
NAS 1.26:194755 .... p 2327 N94-24138 * #
NAS 1.26:194758 .... p 2343 N94-23285 * #
NAS 1.26:194762 .... p 2629 N94-22947 * #
NAS 1.26:194765 .... p 2337 N94-24859 * #
NAS 1.26:194766 .... p 2290 N94-23256 * #
NAS 1.26:194769 .... p 2400 N94-23124 * #
NAS 1.26:194770 .... p 2317 N94-23072 * #
NAS 1.26:194771 .... p 2409 N94-24049 * #
NAS 1.26:194772 .... p 2192 N94-23539 * #
NAS 1.26:194774 .... p 2536 N94-24798 * #
NAS 1.26:194775 .... p 2597 N94-24494 * #
NAS 1.26:194776 .... p 2614 N94-24328 * #
NAS 1.26:194777 .... p 2601 N94-23251 * #
NAS 1.26:194779 .... p 2540 N94-23485 * #
NAS 1.26:194780 .... p 2337 N94-24858 * #
NAS 1.26:194784 .... p 2439 N94-24857 * #
NAS 1.26:194785 .... p 2389 N94-24856 * #
NAS 1.26:194787 .... p 2448 N94-23074 * #
NAS 1.26:194788 .... p 2448 N94-23073 * #
NAS 1.26:194789 .... p 2451 N94-23301 * #
NAS 1.26:194792 .... p 2472 N94-23300 * #
NAS 1.26:194793 .... p 2168 N94-24103 * #
NAS 1.26:194794 .... p 2203 N94-23618 * #
NAS 1.26:194795 .... p 2335 N94-24640 * #
NAS 1.26:194801 .... p 2425 N94-23331 * #
NAS 1.26:194803 .... p 2349 N94-23286 * #
NAS 1.26:194804 .... p 2267 N94-23287 * #
NAS 1.26:194805 .... p 2401 N94-23271 * #
NAS 1.26:194806 .... p 2598 N94-23330 * #
NAS 1.26:194809 .... p 2472 N94-23332 * #
NAS 1.26:194810 .... p 2397 N94-23277 * #
NAS 1.26:194811 .... p 2626 N94-23276 * #
NAS 1.26:194812 .... p 2217 N94-23275 * #
NAS 1.26:194813 .... p 2203 N94-23329 * #
NAS 1.26:194819 .... p 2233 N94-24113 * #
NAS 1.26:194820 .... p 2601 N94-23537 * #
NAS 1.26:194822 .... p 2466 N94-23504 * #
NAS 1.26:194824 .... p 2543 N94-23502 * #
NAS 1.26:194825 .... p 2386 N94-24060 * #
NAS 1.26:194826 .... p 2420 N94-23501 * #
NAS 1.26:194827 .... p 2601 N94-23499 * #
NAS 1.26:194832 .... p 2209 N94-23484 * #
NAS 1.26:194833 .... p 2596 N94-23528 * #
NAS 1.26:194834 .... p 2596 N94-23540 * #
NAS 1.26:194835 .... p 2597 N94-24496 * #
NAS 1.26:194836 .... p 2596 N94-23526 * #
NAS 1.26:194837 .... p 2167 N94-24052 * #
NAS 1.26:194838 .... p 2190 N94-24804 * #
NAS 1.26:194840 .... p 2475 N94-24760 * #
NAS 1.26:194841 .... p 2603 N94-24964 * #
NAS 1.26:194847 .... p 2408 N94-23620 * #
NAS 1.26:194848 .... p 2408 N94-23577 * #
NAS 1.26:194850 .... p 2408 N94-23619 * #
NAS 1.26:194852 .... p 2408 N94-23542 * #
NAS 1.26:194853 .... p 2409 N94-23621 * #
NAS 1.26:194854 .... p 2613 N94-24058 * #
NAS 1.26:194855 .... p 2616 N94-24871 * #
NAS 1.26:194856 .... p 2585 N94-23563 * #
NAS 1.26:194857 .... p 2167 N94-23625 * #
NAS 1.26:194858 .... p 2404 N94-24843 * #
NAS 1.26:194859 .... p 2540 N94-23495 * #
NAS 1.26:194860 .... p 2453 N94-23624 * #
NAS 1.26:194861 .... p 2626 N94-23626 * #
NAS 1.26:194863 .... p 2165 N94-22894 * #
NAS 1.26:194864 .... p 2382 N94-23573 * #
NAS 1.26:194869 .... p 2363 N94-24081 * #
NAS 1.26:194870 .... p 2410 N94-24097 * #
NAS 1.26:194871 .... p 2550 N94-23565 * #
NAS 1.26:194872 .... p 2327 N94-24098 * #
NAS 1.26:194873 .... p 2400 N94-23084 * #
NAS 1.26:194874 .... p 2255 N94-24223 * #
NAS 1.26:194875 .... p 2228 N94-23566 * #
NAS 1.26:194876 .... p 2465 N94-23085 * #
NAS 1.26:194877 .... p 2591 N94-24099 * #
NAS 1.26:194878 .... p 2451 N94-23369 * #
NAS 1.26:194879 .... p 2452 N94-23507 * #
NAS 1.26:194880 .... p 2408 N94-23576 * #
NAS 1.26:195082 .... p 2420 N94-24124 * #
NAS 1.26:195083 .... p 2626 N94-23569 * #
NAS 1.26:195084 .... p 2627 N94-24300 * #
NAS 1.26:195087 .... p 2410 N94-24125 * #
NAS 1.26:195088 .... p 2387 N94-24303 * #
NAS 1.26:195089 .... p 2473 N94-24542 *
NAS 1.26:195090 .... p 2529 N94-24307 * #
NAS 1.26:195091 .... p 2569 N94-24109 * #
NAS 1.26:195092 .... p 2454 N94-24110 * #
NAS 1.26:195093 .... p 2373 N94-24769 * #
NAS 1.26:195094 .... p 2220 N94-24471 * #
NAS 1.26:195095 .... p 2574 N94-24225 * #
NAS 1.26:195096 .... p 2310 N94-24070 * #
NAS 1.26:195098 .... p 2599 N94-24051 * #
NAS 1.26:195099 .... p 2267 N94-23594 * #
NAS 1.26:195101 .... p 2377 N94-24587 * #
NAS 1.26:195102 .... p 2420 N94-23633 * #
NAS 1.26:195103 .... p 2410 N94-24126 * #
NAS 1.26:195104 .... p 2409 N94-24048 * #
NAS 1.26:195105 .... p 2409 N94-24087 * #
NAS 1.26:195106 .... p 2365 N94-24751 * #
NAS 1.26:195107 .... p 2266 N94-24700 * #
NAS 1.26:195108 .... p 2402 N94-24089 * #
NAS 1.26:195109 .... p 2437 N94-24329 * #
NAS 1.26:195110 .... p 2398 N94-24078 * #
NAS 1.26:195111 .... p 2365 N94-24699 * #
NAS 1.26:195117 .... p 2631 N94-25003 * #
NAS 1.26:195121 .... p 2631 N94-24493 * #
NAS 1.26:195125 .... p 2229 N94-24402 * #
NAS 1.26:195126 .... p 2534 N94-24487 * #

NAS 1.26:195127 .... p 2399 N94-24861 * #
NAS 1.26:195128 .... p 2388 N94-24827 * #
NAS 1.26:195129 .... p 2422 N94-24811 * #
NAS 1.26:195131 .... p 2303 N94-25191 * #
NAS 1.26:195132 .... p 2415 N94-24705 * #
NAS 1.26:195133 .... p 2403 N94-24580 * #
NAS 1.26:195134 .... p 2365 N94-24842 * #
NAS 1.26:195135 .... p 2229 N94-24579 * #
NAS 1.26:195136 .... p 2490 N94-24847 * #
NAS 1.26:195137 .... p 2366 N94-24846 * #
NAS 1.26:195138 .... p 2387 N94-24596 * #
NAS 1.26:195139 .... p 2546 N94-24967 * #
NAS 1.26:195140 .... p 2298 N94-24616 * #
NAS 1.26:195141 .... p 2563 N94-24617 * #
NAS 1.26:195142 .... p 2265 N94-24578 * #
NAS 1.26:195143 .... p 2220 N94-24595 * #
NAS 1.26:195144 .... p 2591 N94-24552 * #
NAS 1.26:195145 .... p 2301 N94-24707 * #
NAS 1.26:195146 .... p 2438 N94-24706 * #
NAS 1.26:195147 .... p 2403 N94-24486 * #
NAS 1.26:195148 .... p 2415 N94-24485 * #
NAS 1.26:195150 .... p 2597 N94-24829 * #
NAS 1.26:195152 .... p 2205 N94-24828 * #
NAS 1.26:195153 .... p 2460 N94-25023 * #
NAS 1.26:195157 .... p 2272 N94-25193 * #
NAS 1.26:195158 .... p 2395 N94-24563 * #
NAS 1.26:195159 .... p 2564 N94-25024 * #
NAS 1.26:195162 .... p 2599 N94-24988 * #
NAS 1.26:195163 .... p 2201 N94-24919 * #
NAS 1.26:195164 .... p 2300 N94-24678 * #
NAS 1.26:195165 .... p 2405 N94-24854 * #
NAS 1.26:195166 .... p 2399 N94-25092 * #
NAS 1.26:195167 .... p 2301 N94-25005 * #
NAS 1.26:195168 .... p 2399 N94-24853 * #
NAS 1.26:195171 .... p 2428 N94-24799 * #
NAS 1.26:195172 .... p 2459 N94-24797 * #
NAS 1.26:195173 .... p 2404 N94-24738 * #
NAS 1.26:195174 .... p 2175 N94-24826 * #
NAS 1.26:195175 .... p 2488 N94-24564 * #
NAS 1.26:195176 .... p 2629 N94-25091 * #
NAS 1.26:195182 .... p 2604 N94-25265 * #
NAS 1.26:195183 .... p 2184 N94-25268 * #
NAS 1.26:195184 .... p 2530 N94-25177 * #
NAS 1.26:195185 .... p 2565 N94-25093 * #
NAS 1.26:195186 .... p 2586 N94-25197 * #
NAS 1.26:195189 .... p 2600 N94-25198 * #
NAS 1.26:195190 .... p 2600 N94-25178 * #
NAS 1.26:195191 .... p 2629 N94-25199 * #
NAS 1.26:195192 .... p 2600 N94-25269 * #
NAS 1.26:195193 .... p 2405 N94-25203 * #
NAS 1.26:195194 .... p 2600 N94-25270 * #
NAS 1.26:195195 .... p 2190 N94-25176 * #
NAS 1.26:195196 .... p 2337 N94-25094 * #
NAS 1.26:195197 .... p 2628 N94-25264 * #
NAS 1.26:195198 .... p 2165 N94-25169 * #
NAS 1.26:195200 .... p 2367 N94-25274 * #
NAS 1.26:195201 .... p 2378 N94-25267 * #
NAS 1.26:195202 .... p 2628 N94-25275 * #
NAS 1.26:195203 .... p 2629 N94-25260 * #
NAS 1.26:195484 .... p 2184 N94-25021 * #
NAS 1.26:195485 .... p 2180 N94-24498 * #
NAS 1.26:195486 .... p 2183 N94-24969 * #
NAS 1.26:195487 .... p 2183 N94-24974 * #
NAS 1.26:195488 .... p 2190 N94-24957 * #
NAS 1.26:195489 .... p 2183 N94-24975 * #
NAS 1.26:195490 .... p 2439 N94-24956 * #
NAS 1.26:195491 .... p 2182 N94-24966 * #
NAS 1.26:195492 .... p 2181 N94-24803 * #
NAS 1.26:195493 .... p 2614 N94-24333 * #
NAS 1.26:195494 .... p 2183 N94-24972 * #
NAS 1.26:195495 .... p 2183 N94-24971 * #
NAS 1.26:195496 .... p 2179 N94-24332 * #
NAS 1.26:195497 .... p 2199 N94-25022 * #
NAS 1.26:195498 .... p 2180 N94-24479 * #
NAS 1.26:195499 .... p 2179 N94-24401 * #
NAS 1.26:195500 .... p 2182 N94-24915 * #
NAS 1.26:195501 .... p 2181 N94-24787 * #
NAS 1.26:195502 .... p 2266 N94-24618 * #
NAS 1.26:195503 .... p 2438 N94-24786 * #
NAS 1.26:195504 .... p 2438 N94-24667 * #
NAS 1.26:195505 .... p 2221 N94-24834 * #
NAS 1.26:195506 .... p 2221 N94-24979 * #
NAS 1.26:195507 .... p 2438 N94-24331 * #
NAS 1.26:195508 .... p 2439 N94-24835 * #
NAS 1.26:195509 .... p 2437 N94-24330 * #
NAS 1.26:195510 .... p 2180 N94-24581 * #
NAS 1.26:195511 .... p 2182 N94-24968 * #
NAS 1.26:195512 .... p 2204 N94-24590 * #
NAS 1.26:195514 .... p 2209 N94-24840 * #
NAS 1.26:195515 .... p 2180 N94-24589 * #
NAS 1.26:195516 .... p 2422 N94-24810 * #
NAS 1.26:195517 .... p 2206 N94-24838 * #
NAS 1.26:195518 .... p 2195 N94-24808 * #
NAS 1.26:195519 .... p 2181 N94-24711 * #
NAS 1.26:195520 .... p 2365 N94-24806 * #
NAS 1.26:195521 .... p 2204 N94-24621 * #
NAS 1.26:195522 .... p 2181 N94-24591 * #
NAS 1.26:195523 .... p 2180 N94-24462 * #
NAS 1.26:195524 .... p 2184 N94-25017 * #
NAS 1.26:195525 .... p 2182 N94-24837 * #
NAS 1.26:195526 .... p 2205 N94-24702 * #
NAS 1.26:195527 .... p 2206 N94-24916 * #
NAS 1.26:195528 .... p 2184 N94-25002 * #
NAS 1.26:195529 .... p 2206 N94-25007 * #
NAS 1.26:195530 .... p 2195 N94-24619 * #
NAS 1.26:195532 .... p 2546 N94-24816 * #
NAS 1.26:195533 .... p 2298 N94-24582 * #
NAS 1.26:195534 .... p 2198 N94-24860 * #
NAS 1.26:195535 .... p 2182 N94-24817 * #
NAS 1.26:195536 .... p 2204 N94-24620 * #
NAS 1.26:195537 .... p 2183 N94-25001 * #
NAS 1.26:195538 .... p 2396 N94-24701 * #
NAS 1.26:195539 .... p 2204 N94-24334 * #
NAS 1.26:195540 .... p 2365 N94-24805 * #
NAS 1.26:195541 .... p 2195 N94-24995 * #
NAS 1.26:195542 .... p 2184 N94-25004 * #
NAS 1.26:195543 .... p 2190 N94-24551 * #
NAS 1.26:195547 .... p 2196 N94-24820 * #
NAS 1.26:195548 .... p 2180 N94-24492 * #
NAS 1.26:195549 .... p 2365 N94-24703 * #
NAS 1.26:195550 .... p 2189 N94-25085 * #
NAS 1.26:195685 .... p 2416 N94-25271 * #
NAS 1.26:195686 .... p 2594 N94-25541 * #
NAS 1.26:4519 .... p 2169 N94-24606 * #
NAS 1.26:4521 .... p 2467 N94-24463 * #
NAS 1.26:4522 .... p 2467 N94-24075 * #
NAS 1.26:4551 .... p 2466 N94-23293 * #
NAS 1.26:4555 .... p 2474 N94-24635 * #
NAS 1.26:4558 .... p 2181 N94-24726 * #
NAS 1.26:4562 .... p 2336 N94-24725 * #
NAS 1.26:4564 .... p 2309 N94-23304 * #
NAS 1.26:4565 .... p 2456 N94-24480 * #
NAS 1.26:4567 .... p 2543 N94-23529 * #
NAS 1.26:4568 .... p 2198 N94-24752 * #
NAS 1.26:4569 .... p 2594 N94-25487 * #
NAS 1.26:4572 .... p 2246 N94-25118 * #
NAS 1.55:10121 .... p 2246 N94-25120 * #
NAS 1.55:10122 .... p 2320 N94-23634 * #
NAS 1.55:10127 .... p 2162 N94-25096 * #
NAS 1.55:10128 .... p 2439 N94-25490 * #
NAS 1.55:10130 .... p 2333 N94-24460 * #
NAS 1.55:3217 .... p 2410 N94-24374 * #
NAS 1.55:3224-PT-1 .... p 2482 N94-23673 * #
NAS 1.55:3228 .... p 2390 N94-23345 * #
NAS 1.55:3231 .... p 2526 N94-24207 * #
NAS 1.55:3250 .... p 2223 N94-24338 * #
NAS 1.60-3272-PT-1C .... p 2403 N94-24465 * #
NAS 1.60:3296 .... p 2242 N94-23467 * #
NAS 1.60:3328 .... p 2372 N94-24074 * #
NAS 1.60:3346 .... p 2426 N94-23530 * #
NAS 1.60:3358 .... p 2169 N94-24464 * #
NAS 1.60:3365 .... p 2169 N94-24311 * #
NAS 1.60:3370 .... p 2177 N94-24304 * #
NAS 1.60:3373 .... p 2378 N94-24845 * #
NAS 1.60:3374 .... p 2166 N94-23512 * #
NAS 1.60:3389 .... p 2310 N94-24056 * #
NAS 1.60:3402 .... p 2245 N94-25117 * #
NAS 1.60:3404 .... p 2540 N94-23509 * #
NAS 1.60:3405 .... p 2540 N94-24305 * #
NAS 1.60:3407 .... p 2171 N94-25187 * #
NAS 1.60:3415 .... p 2381 N94-22961 * #
NAS 1.60:3423 .... p 2540 N94-23273 * #
NAS 1.60:3434 .... p 2376 N94-23342 * #
NAS 1.60:3442 .... p 2375 N94-23294 * #
NAS 1.60:3444 .... p 2374 N94-22960 * #
NAS 1.60:3456 .... p 2426 N94-23544 * #
NAS 1.60:3457 .... p 2490 N94-24727 * #
NAS 1.60:3458 .... p 2269 N94-23574 * #
NAS 1.61:1294 .... p 2600 N94-25387 * #
NAS 1.61:1313 .... p 2398 N94-24104 * #
NAS 1.61:1317 .... p 2194 N94-23292 * #
NAS 1.61:1320 .... p 2598 N94-24644 * #
NAS 1.61:1323 .... p 2410 N94-24355 * #
NAS 1.83:152 .... p 2603 N94-24973 * #
NAS 1.83:211 .... p 2597 N94-25018 * #

NASA-CASE-ARC-11889-1-SB ..... p 2543 N94-23309 *
NASA-CASE-ARC-11919-1-NP .... p 2525 N94-23312 *
NASA-CASE-ARC-11934-1 .... p 2317 N94-23077 *
NASA-CASE-ARC-11935-1 .... p 2319 N94-23306 *
NASA-CASE-ARC-11950-1 .... p 2192 N94-23310 *
NASA-CASE-ARC-11956-1-SB ..... p 2253 N94-23311 *

NASA-CASE-GSC-13434-1 .... p 2352 N94-23082 *
NASA-CASE-GSC-13452-1 .... p 2352 N94-23078 *
NASA-CASE-GSC-13493-1 .... p 2294 N94-23827 *
NASA-CASE-GSC-13502-1 .... p 2354 N94-23969 *
NASA-CASE-GSC-13565-1 .... p 2354 N94-23831 *

NASA-CASE-LAR-13669-2 .... p 2252 N94-23079 *
NASA-CASE-LAR-14440-2 .... p 2252 N94-23075 *
NASA-CASE-LAR-14643-2 .... p 2253 N94-23305 *
NASA-CASE-LAR-14654-2 .... p 2375 N94-23308 *
NASA-CASE-LAR-14771-1 .... p 2252 N94-23076 *
NASA-CASE-LAR-14797-1 .... p 2253 N94-23307 *

NASA-CASE-LEW-15515-1 .... p 2343 N94-23826 *
NASA-CASE-LEW-15614-1 .... p 2534 N94-23825 *

NASA-CASE-MFS-28724-1 .... p 2203 N94-23824 *

NASA-CASE-MSC-21967-1 .... p 2354 N94-23822 *

NASA-CASE-NPO-17621-1-CU .... p 2309 N94-23820 *
NASA-CASE-NPO-18007-2-CU .... p 2543 N94-23270 *
NASA-CASE-NPO-18343-1-CU .... p 2310 N94-23823 *
NASA-CASE-NPO-18428-1-CU .... p 2310 N94-23821 * #
NASA-CASE-NPO-18625-1-CU .... p 2563 N94-23972 *

NASA-CP-10121 .... p 2246 N94-25120 * #
NASA-CP-10122 .... p 2320 N94-23634 * #
NASA-CP-10127 .... p 2162 N94-25096 * #
NASA-CP-10128 .... p 2439 N94-25490 * #
NASA-CP-10130 .... p 2333 N94-24460 * #
NASA-CP-3217 .... p 2410 N94-24374 * #
NASA-CP-3224-PT-1 .... p 2482 N94-23673 * #
NASA-CP-3228 .... p 2390 N94-23345 * #
NASA-CP-3231 .... p 2526 N94-24207 * #
NASA-CP-3250 .... p 2223 N94-24338 * #

NASA-CR-177619 .... p 2176 N94-23489 * #
NASA-CR-177629 .... p 2181 N94-24796 * #
NASA-CR-177631 .... p 2598 N94-24832 * #
NASA-CR-177632 .... p 2598 N94-23536 * #
NASA-CR-177634 .... p 2430 N94-23527 * #
NASA-CR-188254 .... p 2199 N94-23571 * #
NASA-CR-188256 .... p 2427 N94-24227 * #
NASA-CR-188268 .... p 2430 N94-23290 * #
NASA-CR-188270 .... p 2590 N94-23289 * #
NASA-CR-188271-VOL-1 .... p 2632 N94-25348 * #
NASA-CR-188271-VOL-2 .... p 2636 N94-25367 * #
NASA-CR-189214 .... p 2364 N94-24090 * #
NASA-CR-189313 .... p 2599 N94-23334 * #
NASA-CR-189316 .... p 2453 N94-23559 * #
NASA-CR-189317 .... p 2209 N94-24767 * #
NASA-CR-189320 .... p 2311 N94-24754 * #
NASA-CR-189322 .... p 2205 N94-24710 * #
NASA-CR-189324 .... p 2599 N94-24666 * #
NASA-CR-189328 .... p 2430 N94-23080 * #
NASA-CR-189333 .... p 2204 N94-24226 * #
NASA-CR-189645 .... p 2525 N94-23698 * #
NASA-CR-191056 .... p 2290 N94-23087 * #
NASA-CR-191132 .... p 2219 N94-24061 * #
NASA-CR-191185 .... p 2170 N94-25173 * #
NASA-CR-191197 .... p 2258 N94-24753 * #
NASA-CR-191251 .... p 2295 N94-23830 * #
NASA-CR-191328 .... p 2544 N94-23829 * #
NASA-CR-191329 .... p 2204 N94-23828 * #
NASA-CR-191461 .... p 2445 N94-23125 * #
NASA-CR-191465 .... p 2466 N94-23252 * #
NASA-CR-191483-VOL-1 .... p 2526 N94-24172 * #
NASA-CR-191483-VOL-2 .... p 2526 N94-24173 * #
NASA-CR-191490 .... p 2344 N94-24360 * #
NASA-CR-191508 .... p 2172 N94-23288 * #
NASA-CR-191547 .... p 2333 N94-24356 * #
NASA-CR-191552 .... p 2473 N94-23558 * #
NASA-CR-191553 .... p 2343 N94-23498 * #
NASA-CR-191554 .... p 2458 N94-24740 * #
NASA-CR-191556 .... p 2457 N94-24638 * #
NASA-CR-191560 .... p 2480 N94-23278 * #
NASA-CR-191561 .... p 2480 N94-23272 * #
NASA-CR-191564 .... p 2451 N94-23340 * #
NASA-CR-191567 .... p 2317 N94-23089 * #
NASA-CR-191568 .... p 2335 N94-24712 * #
NASA-CR-191569 .... p 2319 N94-23302 * #
NASA-CR-191570 .... p 2334 N94-24605 * #
NASA-CR-191571 .... p 2490 N94-24836 * #
NASA-CR-191572 .... p 2319 N94-23513 * #
NASA-CR-191573 .... p 2320 N94-23532 * #
NASA-CR-191574 .... p 2451 N94-23341 * #
NASA-CR-191575 .... p 2448 N94-23092 * #
NASA-CR-191576 .... p 2444 N94-25090 * #
NASA-CR-191578 .... p 2192 N94-23564 * #
NASA-CR-191579 .... p 2336 N94-24771 * #
NASA-CR-191582 .... p 2487 N94-24291 * #
NASA-CR-191583 .... p 2479 N94-23090 * #
NASA-CR-191585 .... p 2458 N94-24680 * #
NASA-CR-191586 .... p 2334 N94-24602 * #
NASA-CR-191587 .... p 2458 N94-24679 * #
NASA-CR-191588 .... p 2490 N94-24914 * #
NASA-CR-191589 .... p 2337 N94-24869 * #
NASA-CR-192244 .... p 2466 N94-23483 * #
NASA-CR-193151 .... p 2614 N94-24363 * #
NASA-CR-193225 .... p 2420 N94-23538 * #
NASA-CR-193703 .... p 2627 N94-24094 * #
NASA-CR-193803 .... p 2422 N94-24807 * #
NASA-CR-193862 .... p 2574 N94-24405 * #
NASA-CR-193879 .... p 2200 N94-24664 * #

NASA-CR-193880 .... p 2244 N94-24066 * #
NASA-CR-193881 .... p 2456 N94-24470 * #
NASA-CR-193882 .... p 2196 N94-24309 * #
NASA-CR-193883 .... p 2421 N94-24310 * #
NASA-CR-193884 .... p 2627 N94-24484 * #
NASA-CR-193885 .... p 2627 N94-24461 * #
NASA-CR-193889 .... p 2545 N94-24665 * #
NASA-CR-193890 .... p 2455 N94-24111 * #
NASA-CR-193891 .... p 2364 N94-24088 * #
NASA-CR-193893 .... p 2229 N94-24224 * #
NASA-CR-193894 .... p 2219 N94-24064 * #
NASA-CR-193895 .... p 2201 N94-24802 * #
NASA-CR-193897 .... p 2200 N94-24067 * #
NASA-CR-193898 .... p 2199 N94-24057 * #
NASA-CR-193899 .... p 2367 N94-25020 * #
NASA-CR-193901 .... p 2365 N94-24588 * #
NASA-CR-193902 .... p 2200 N94-24112 * #
NASA-CR-193903 .... p 2200 N94-24065 * #
NASA-CR-193904 .... p 2201 N94-24965 * #
NASA-CR-193905 .... p 2267 N94-23549 * #
NASA-CR-193906 .... p 2454 N94-24050 * #
NASA-CR-193907 .... p 2372 N94-24174 * #
NASA-CR-193908 .... p 2345 N94-24852 * #
NASA-CR-193909 .... p 2376 N94-24359 * #
NASA-CR-193910 .... p 2345 N94-25000 * #
NASA-CR-193916 .... p 2366 N94-24998 * #
NASA-CR-193917 .... p 2366 N94-24999 * #
NASA-CR-193918 .... p 2201 N94-24970 * #
NASA-CR-193919 .... p 2221 N94-25019 * #
NASA-CR-193920 .... p 2367 N94-25174 * #
NASA-CR-193921 .... p 2200 N94-24801 * #
NASA-CR-194109 .... p 2401 N94-23337 * #
NASA-CR-194138 .... p 2232 N94-23524 * #
NASA-CR-194217 .... p 2327 N94-24096 * #
NASA-CR-194435 .... p 2202 N94-23631 * #
NASA-CR-194436 .... p 2190 N94-23590 * #
NASA-CR-194438 .... p 2166 N94-23511 * #
NASA-CR-194439 .... p 2203 N94-23632 * #
NASA-CR-194440 .... p 2312 N94-24870 * #
NASA-CR-194442 .... p 2553 N94-25190 * #
NASA-CR-194444 .... p 2219 N94-23555 * #
NASA-CR-194445 .... p 2187 N94-23552 * #
NASA-CR-194448 .... p 2304 N94-25266 * #
NASA-CR-194449 .... p 2153 N94-23553 * #
NASA-CR-194450 .... p 2234 N94-24565 * #
NASA-CR-194453 .... p 2377 N94-24604 * #
NASA-CR-194454 .... p 2219 N94-24361 * #
NASA-CR-194455 .... p 2189 N94-25200 * #
NASA-CR-194458 .... p 2220 N94-24714 * #
NASA-CR-194475 .... p 2462 N94-25179 * #
NASA-CR-194486 .... p 2497 N94-23832 * #
NASA-CR-194516 .... p 2273 N94-22735 * #
NASA-CR-194678 .... p 2571 N94-23230 * #
NASA-CR-194714 .... p 2623 N94-24996 * #
NASA-CR-194719-VOL-2 .... p 2209 N94-23028 * #
NASA-CR-194735 .... p 2296 N94-24105 * #
NASA-CR-194755 .... p 2327 N94-24138 * #
NASA-CR-194758 .... p 2343 N94-23285 * #
NASA-CR-194762 .... p 2629 N94-22947 * #
NASA-CR-194765 .... p 2337 N94-24859 * #
NASA-CR-194766 .... p 2290 N94-23256 * #
NASA-CR-194769 .... p 2400 N94-23124 * #
NASA-CR-194770 .... p 2317 N94-23072 * #
NASA-CR-194771 .... p 2409 N94-24049 * #
NASA-CR-194772 .... p 2192 N94-23539 * #
NASA-CR-194774 .... p 2536 N94-24798 * #
NASA-CR-194775 .... p 2597 N94-24494 * #
NASA-CR-194776 .... p 2614 N94-24328 * #
NASA-CR-194777 .... p 2601 N94-23251 * #
NASA-CR-194779 .... p 2540 N94-23485 * #
NASA-CR-194780 .... p 2337 N94-24858 * #
NASA-CR-194784 .... p 2439 N94-24857 * #
NASA-CR-194785 .... p 2389 N94-24856 * #
NASA-CR-194787 .... p 2448 N94-23074 * #
NASA-CR-194788 .... p 2448 N94-23073 * #
NASA-CR-194789 .... p 2451 N94-23301 * #
NASA-CR-194792 .... p 2472 N94-23300 * #
NASA-CR-194793 .... p 2168 N94-24103 * #
NASA-CR-194794 .... p 2203 N94-23618 * #
NASA-CR-194795 .... p 2335 N94-24640 * #
NASA-CR-194801 .... p 2425 N94-23331 * #
NASA-CR-194803 .... p 2349 N94-23286 * #
NASA-CR-194804 .... p 2267 N94-23287 * #
NASA-CR-194805 .... p 2401 N94-23271 * #
NASA-CR-194806 .... p 2598 N94-23330 * #
NASA-CR-194809 .... p 2472 N94-23332 * #
NASA-CR-194810 .... p 2397 N94-23277 * #
NASA-CR-194811 .... p 2626 N94-23276 * #
NASA-CR-194812 .... p 2217 N94-23275 * #
NASA-CR-194813 .... p 2203 N94-23329 * #
NASA-CR-194819 .... p 2233 N94-24113 * #
NASA-CR-194820 .... p 2601 N94-23537 * #
NASA-CR-194822 .... p 2466 N94-23504 * #
NASA-CR-194824 .... p 2543 N94-23502 * #
NASA-CR-194825 .... p 2386 N94-24060 * #
NASA-CR-194826 .... p 2420 N94-23501 * #
NASA-CR-194827 .... p 2601 N94-23499 * #
NASA-CR-194832 .... p 2209 N94-23484 * #
NASA-CR-194833 .... p 2596 N94-23528 * #
NASA-CR-194834 .... p 2596 N94-23540 * #
NASA-CR-194835 .... p 2597 N94-24496 * #
NASA-CR-194836 .... p 2596 N94-23526 * #
NASA-CR-194837 .... p 2167 N94-24052 * #
NASA-CR-194838 .... p 2190 N94-24804 * #
NASA-CR-194840 .... p 2475 N94-24760 * #
NASA-CR-194841 .... p 2603 N94-24964 * #
NASA-CR-194847 .... p 2408 N94-23620 * #
NASA-CR-194848 .... p 2408 N94-23577 * #
NASA-CR-194850 .... p 2408 N94-23619 * #
NASA-CR-194852 .... p 2408 N94-23542 * #
NASA-CR-194853 .... p 2409 N94-23621 * #
NASA-CR-194854 .... p 2613 N94-24058 * #
NASA-CR-194855 .... p 2616 N94-24871 * #
NASA-CR-194856 .... p 2585 N94-23563 * #
NASA-CR-194857 .... p 2167 N94-23625 * #
NASA-CR-194858 .... p 2404 N94-24843 * #
NASA-CR-194859 .... p 2540 N94-23495 * #
NASA-CR-194860 .... p 2453 N94-23624 * #
NASA-CR-194861 .... p 2626 N94-23626 * #
NASA-CR-194863 .... p 2165 N94-22894 * #
NASA-CR-194864 .... p 2382 N94-23573 * #
NASA-CR-194869 .... p 2363 N94-24081 * #
NASA-CR-194870 .... p 2410 N94-24097 * #
NASA-CR-194871 .... p 2550 N94-23565 * #
NASA-CR-194872 .... p 2327 N94-24098 * #
NASA-CR-194873 .... p 2400 N94-23084 * #
NASA-CR-194874 .... p 2255 N94-24223 * #
NASA-CR-194875 .... p 2228 N94-23566 * #
NASA-CR-194876 .... p 2465 N94-23085 * #
NASA-CR-194877 .... p 2591 N94-24099 * #
NASA-CR-194878 .... p 2451 N94-23369 * #
NASA-CR-194879 .... p 2452 N94-23507 * #
NASA-CR-194880 .... p 2408 N94-23576 * #
NASA-CR-195082 .... p 2420 N94-24124 * #
NASA-CR-195083 .... p 2626 N94-23569 * #
NASA-CR-195084 .... p 2627 N94-24300 * #
NASA-CR-195087 .... p 2410 N94-24125 * #
NASA-CR-195088 .... p 2387 N94-24303 * #
NASA-CR-195089 .... p 2473 N94-24542 *
NASA-CR-195090 .... p 2529 N94-24307 * #
NASA-CR-195091 .... p 2569 N94-24109 * #
NASA-CR-195092 .... p 2454 N94-24110 * #
NASA-CR-195093 .... p 2373 N94-24769 * #
NASA-CR-195094 .... p 2220 N94-24471 * #
NASA-CR-195095 .... p 2574 N94-24225 * #
NASA-CR-195096 .... p 2310 N94-24070 * #
NASA-CR-195098 .... p 2599 N94-24051 * #
NASA-CR-195099 .... p 2267 N94-23594 * #
NASA-CR-195101 .... p 2377 N94-24587 * #
NASA-CR-195102 .... p 2420 N94-23633 * #
NASA-CR-195103 .... p 2410 N94-24126 * #
NASA-CR-195104 .... p 2409 N94-24048 * #
NASA-CR-195105 .... p 2409 N94-24087 * #
NASA-CR-195106 .... p 2365 N94-24751 * #
NASA-CR-195107 .... p 2266 N94-24700 * #
NASA-CR-195108 .... p 2402 N94-24089 * #
NASA-CR-195109 .... p 2437 N94-24329 * #
NASA-CR-195110 .... p 2398 N94-24078 * #
NASA-CR-195111 .... p 2365 N94-24699 * #
NASA-CR-195117 .... p 2631 N94-25003 * #
NASA-CR-195121 .... p 2631 N94-24493 * #
NASA-CR-195125 .... p 2229 N94-24402 * #
NASA-CR-195126 .... p 2534 N94-24487 * #
NASA-CR-195127 .... p 2399 N94-24861 * #
NASA-CR-195128 .... p 2388 N94-24827 * #
NASA-CR-195129 .... p 2422 N94-24811 * #
NASA-CR-195131 .... p 2303 N94-25191 * #
NASA-CR-195132 .... p 2415 N94-24705 * #
NASA-CR-195133 .... p 2403 N94-24580 * #
NASA-CR-195134 .... p 2365 N94-24842 * #
NASA-CR-195135 .... p 2229 N94-24579 * #
NASA-CR-195136 .... p 2490 N94-24847 * #
NASA-CR-195137 .... p 2366 N94-24846 * #
NASA-CR-195138 .... p 2387 N94-24596 * #
NASA-CR-195139 .... p 2546 N94-24967 * #
NASA-CR-195140 .... p 2298 N94-24616 * #
NASA-CR-195141 .... p 2563 N94-24617 * #
NASA-CR-195142 .... p 2265 N94-24578 * #
NASA-CR-195143 .... p 2220 N94-24595 * #
NASA-CR-195144 .... p 2591 N94-24552 * #
NASA-CR-195145 .... p 2301 N94-24707 * #
NASA-CR-195146 .... p 2438 N94-24706 * #
NASA-CR-195147 .... p 2403 N94-24486 * #
NASA-CR-195148 .... p 2415 N94-24485 * #
NASA-CR-195150 .... p 2597 N94-24829 * #
NASA-CR-195152 .... p 2205 N94-24828 * #
NASA-CR-195153 .... p 2460 N94-25023 * #
NASA-CR-195157 .... p 2272 N94-25193 * #
NASA-CR-195158 .... p 2395 N94-24563 * #
NASA-CR-195159 .... p 2564 N94-25024 * #
NASA-CR-195162 .... p 2599 N94-24988 * #
NASA-CR-195163 .... p 2201 N94-24919 * #
NASA-CR-195164 .... p 2300 N94-24678 * #
NASA-CR-195165 .... p 2405 N94-24854 * #
NASA-CR-195166 .... p 2399 N94-25092 * #
NASA-CR-195167 .... p 2301 N94-25005 * #
NASA-CR-195168 .... p 2399 N94-24853 * #
NASA-CR-195171 .... p 2428 N94-24799 * #
NASA-CR-195172 .... p 2459 N94-24797 * #
NASA-CR-195173 .... p 2404 N94-24738 * #
NASA-CR-195174 .... p 2175 N94-24826 * #
NASA-CR-195175 .... p 2488 N94-24564 * #
NASA-CR-195176 .... p 2629 N94-25091 * #
NASA-CR-195182 .... p 2604 N94-25265 * #
NASA-CR-195183 .... p 2184 N94-25268 * #
NASA-CR-195184 .... p 2530 N94-25177 * #
NASA-CR-195185 .... p 2565 N94-25093 * #
NASA-CR-195186 .... p 2586 N94-25197 * #
NASA-CR-195189 .... p 2600 N94-25198 * #
NASA-CR-195190 .... p 2600 N94-25178 * #
NASA-CR-195191 .... p 2629 N94-25199 * #
NASA-CR-195192 .... p 2600 N94-25269 * #
NASA-CR-195193 .... p 2405 N94-25203 * #
NASA-CR-195194 .... p 2600 N94-25270 * #
NASA-CR-195195 .... p 2190 N94-25176 * #
NASA-CR-195196 .... p 2337 N94-25094 * #
NASA-CR-195197 .... p 2628 N94-25264 * #
NASA-CR-195198 .... p 2165 N94-25169 * #
NASA-CR-195200 .... p 2367 N94-25274 * #
NASA-CR-195201 .... p 2378 N94-25267 * #
NASA-CR-195202 .... p 2628 N94-25275 * #
NASA-CR-195203 .... p 2629 N94-25260 * #
NASA-CR-195484 .... p 2184 N94-25021 * #
NASA-CR-195485 .... p 2180 N94-24498 * #
NASA-CR-195486 .... p 2183 N94-24969 * #
NASA-CR-195487 .... p 2183 N94-24974 * #
NASA-CR-195488 .... p 2190 N94-24957 * #
NASA-CR-195489 .... p 2183 N94-24975 * #
NASA-CR-195490 .... p 2439 N94-24956 * #
NASA-CR-195491 .... p 2182 N94-24966 * #
NASA-CR-195492 .... p 2181 N94-24803 * #
NASA-CR-195493 .... p 2614 N94-24333 * #
NASA-CR-195494 .... p 2183 N94-24972 * #
NASA-CR-195495 .... p 2183 N94-24971 * #
NASA-CR-195496 .... p 2179 N94-24332 * #
NASA-CR-195497 .... p 2199 N94-25022 * #
NASA-CR-195498 .... p 2180 N94-24479 * #
NASA-CR-195499 .... p 2179 N94-24401 * #
NASA-CR-195500 .... p 2182 N94-24915 * #
NASA-CR-195501 .... p 2181 N94-24787 * #
NASA-CR-195502 .... p 2266 N94-24618 * #
NASA-CR-195503 .... p 2438 N94-24786 * #
NASA-CR-195504 .... p 2438 N94-24667 * #
NASA-CR-195505 .... p 2221 N94-24834 * #
NASA-CR-195506 .... p 2221 N94-24979 * #
NASA-CR-195507 .... p 2438 N94-24331 * #
NASA-CR-195508 .... p 2439 N94-24835 * #
NASA-CR-195509 .... p 2437 N94-24330 * #
NASA-CR-195510 .... p 2180 N94-24581 * #
NASA-CR-195511 .... p 2182 N94-24968 * #
NASA-CR-195512 .... p 2204 N94-24590 * #
NASA-CR-195514 .... p 2209 N94-24840 * #
NASA-CR-195515 .... p 2180 N94-24589 * #
NASA-CR-195516 .... p 2422 N94-24810 * #
NASA-CR-195517 .... p 2206 N94-24838 * #
NASA-CR-195518 .... p 2195 N94-24808 * #
NASA-CR-195519 .... p 2181 N94-24711 * #
NASA-CR-195520 .... p 2365 N94-24806 * #
NASA-CR-195521 .... p 2204 N94-24621 * #
NASA-CR-195522 .... p 2181 N94-24591 * #
NASA-CR-195523 .... p 2180 N94-24462 * #
NASA-CR-195524 .... p 2184 N94-25017 * #
NASA-CR-195525 .... p 2182 N94-24837 * #
NASA-CR-195526 .... p 2205 N94-24702 * #
NASA-CR-195527 .... p 2206 N94-24916 * #
NASA-CR-195528 .... p 2184 N94-25002 * #
NASA-CR-195529 .... p 2206 N94-25007 * #
NASA-CR-195530 .... p 2195 N94-24619 * #
NASA-CR-195532 .... p 2546 N94-24816 * #
NASA-CR-195533 .... p 2298 N94-24582 * #
NASA-CR-195534 .... p 2198 N94-24860 * #
NASA-CR-195535 .... p 2182 N94-24817 * #
NASA-CR-195536 .... p 2204 N94-24620 * #
NASA-CR-195537 .... p 2183 N94-25001 * #
NASA-CR-195538 .... p 2396 N94-24701 * #
NASA-CR-195539 .... p 2204 N94-24334 * #
NASA-CR-195540 .... p 2365 N94-24805 * #
NASA-CR-195541 .... p 2195 N94-24995 * #
NASA-CR-195542 .... p 2184 N94-25004 * #
NASA-CR-195543 .... p 2190 N94-24551 * #
NASA-CR-195547 .... p 2196 N94-24820 * #
NASA-CR-195548 .... p 2180 N94-24492 * #
NASA-CR-195549 .... p 2365 N94-24703 * #
NASA-CR-195550 .... p 2189 N94-25085 * #
NASA-CR-195685 .... p 2416 N94-25271 * #
NASA-CR-195686 .... p 2594 N94-25541 * #
NASA-CR-4519 .... p 2169 N94-24606 * #
NASA-CR-4521 .... p 2467 N94-24463 * #

NASA-CR-4522 .... p 2467 N94-24075 * #
NASA-CR-4551 .... p 2466 N94-23293 * #
NASA-CR-4555 .... p 2474 N94-24635 * #
NASA-CR-4558 .... p 2181 N94-24726 * #
NASA-CR-4562 .... p 2336 N94-24725 * #
NASA-CR-4564 .... p 2309 N94-23304 * #
NASA-CR-4565 .... p 2456 N94-24480 * #
NASA-CR-4567 .... p 2543 N94-23529 * #
NASA-CR-4568 .... p 2198 N94-24752 * #
NASA-CR-4569 .... p 2594 N94-25487 * #
NASA-CR-4572 .... p 2246 N94-25118 * #

NASA-NHB-1490.5 .... p 2590 N94-23971 * #

NASA-NP-152 .... p 2603 N94-24973 * #
NASA-NP-211 .... p 2597 N94-25018 * #

NASA-RP-1294 .... p 2600 N94-25387 * #
NASA-RP-1313 .... p 2398 N94-24104 * #
NASA-RP-1317 .... p 2194 N94-23292 * #
NASA-RP-1320 .... p 2598 N94-24644 * #
NASA-RP-1323 .... p 2410 N94-24355 * #

NASA-SP-4105 .... p 2630 N94-23333 * #
NASA-SP-4307 .... p 2631 N94-24584 * #
NASA-SP-7037(298) .... p 2153 N94-23711 *
NASA-SP-7037(299) .... p 2153 N94-23973 *
NASA-SP-7039(44)-SECT-2 .... p 2590 N94-23712 *
NASA-SP-7104 .... p 2631 N94-24585 * #
NASA-SP-7500(27) .... p 2586 N94-24708 *

NASA-TM-104018 .... p 2431 N94-23970 * #
NASA-TM-104273 .... p 2334 N94-24495 * #
NASA-TM-104274 .... p 2376 N94-23487 * #
NASA-TM-104566-VOL-11 .... p 2417 N94-23338 * #
NASA-TM-104566-VOL-9 .... p 2417 N94-23291 * #
NASA-TM-104571 .... p 2407 N94-23132 * #
NASA-TM-104577 .... p 2308 N94-23281 * #
NASA-TM-104584 .... p 2401 N94-23282 * #
NASA-TM-104585 .... p 2218 N94-23343 * #
NASA-TM-104595 .... p 2381 N94-24800 * #
NASA-TM-104596 .... p 2195 N94-24497 * #
NASA-TM-104756 .... p 2433 N94-24185 * #
NASA-TM-104783 .... p 2205 N94-24625 * #
NASA-TM-104784 .... p 2386 N94-24095 * #
NASA-TM-104786 .... p 2473 N94-24068 * #
NASA-TM-105271 .... p 2187 N94-23545 * #
NASA-TM-105650 .... p 2205 N94-24825 * #
NASA-TM-105871 .... p 2193 N94-25184 * #
NASA-TM-105990 .... p 2376 N94-23551 * #
NASA-TM-106035 .... p 2590 N94-23562 * #
NASA-TM-106177 .... p 2336 N94-24713 * #
NASA-TM-106261 .... p 2189 N94-25185 * #
NASA-TM-106295 .... p 2295 N94-24101 * #
NASA-TM-106310 .... p 2186 N94-23466 * #
NASA-TM-106311 .... p 2192 N94-23091 * #
NASA-TM-106358 .... p 2378 N94-25188 * #
NASA-TM-106381 .... p 2242 N94-23550 * #
NASA-TM-106383 .... p 2333 N94-24336 * #
NASA-TM-106391 .... p 2168 N94-24084 * #
NASA-TM-106397 .... p 2201 N94-23567 * #
NASA-TM-106401 .... p 2219 N94-23630 * #
NASA-TM-106408 .... p 2249 N94-25171 * #
NASA-TM-106414 .... p 2222 N94-23500 * #
NASA-TM-106417 .... p 2395 N94-24071 * #
NASA-TM-106419 .... p 2219 N94-23531 * #
NASA-TM-106423 .... p 2253 N94-23371 * #
NASA-TM-106426 .... p 2221 N94-24770 * #
NASA-TM-106428 .... p 2218 N94-23372 * #
NASA-TM-106429 .... p 2243 N94-23556 * #
NASA-TM-106433 .... p 2243 N94-23578 * #
NASA-TM-106434 .... p 2187 N94-24082 * #
NASA-TM-106436 .... p 2481 N94-23593 * #
NASA-TM-106437 .... p 2481 N94-23554 * #
NASA-TM-106443 .... p 2222 N94-23591 * #
NASA-TM-106445 .... p 2320 N94-23525 * #
NASA-TM-106450 .... p 2167 N94-23592 * #
NASA-TM-106451 .... p 2220 N94-24681 * #
NASA-TM-106457 .... p 2172 N94-23523 * #
NASA-TM-106459 .... p 2166 N94-23522 * #
NASA-TM-106461 .... p 2173 N94-24047 * #
NASA-TM-106463 .... p 2153 N94-24100 * #
NASA-TM-106464 .... p 2221 N94-24766 * #
NASA-TM-106465 .... p 2525 N94-23464 * #
NASA-TM-106466 .... p 2218 N94-23370 * #
NASA-TM-106467 .... p 2364 N94-24483 * #
NASA-TM-106468 .... p 2166 N94-23465 * #
NASA-TM-106469 .... p 2326 N94-24063 * #
NASA-TM-106470 .... p 2344 N94-24362 * #
NASA-TM-106471 .... p 2166 N94-23299 * #
NASA-TM-106474 .... p 2337 N94-25119 * #
NASA-TM-106475 .... p 2258 N94-24682 * #
NASA-TM-106476 .... p 2346 N94-25202 * #
NASA-TM-106477 .... p 2188 N94-24594 * #
NASA-TM-106481 .... p 2265 N94-24301 * #
NASA-TM-106482 .... p 2195 N94-24482 * #
NASA-TM-106483 .... p 2344 N94-24069 * #
NASA-TM-106484 .... p 2202 N94-25095 * #
NASA-TM-106486 .... p 2222 N94-25201 * #
NASA-TM-106488 .... p 2221 N94-25189 * #
NASA-TM-106490 .... p 2377 N94-24715 * #
NASA-TM-106491 .... p 2169 N94-24335 * #
NASA-TM-106492 .... p 2170 N94-25182 * #
NASA-TM-106494 .... p 2310 N94-24308 * #
NASA-TM-106497 .... p 2521 N94-24302 * #
NASA-TM-106500 .... p 2345 N94-25116 * #
NASA-TM-106503 .... p 2338 N94-25183 * #
NASA-TM-106504 .... p 2334 N94-24481 * #
NASA-TM-106505 .... p 2313 N94-25170 * #
NASA-TM-106506 .... p 2230 N94-25186 * #
NASA-TM-106508 .... p 2367 N94-25181 * #
NASA-TM-106512 .... p 2530 N94-25172 * #
NASA-TM-106524 .... p 2338 N94-25180 * #
NASA-TM-107750 .... p 2376 N94-23368 * #
NASA-TM-107751 .... p 2254 N94-23486 * #
NASA-TM-108270 .... p 2383 N94-23595 * #
NASA-TM-108423 .... p 2590 N94-24079 * #
NASA-TM-108435 .... p 2409 N94-24080 * #
NASA-TM-108437 .... p 2233 N94-24073 * #
NASA-TM-108758 .... p 2182 N94-24953 * #
NASA-TM-108778 .... p 2426 N94-23575 * #
NASA-TM-108785 .... p 2426 N94-24102 * #
NASA-TM-108786 .... p 2167 N94-23557 * #
NASA-TM-108789 .... p 2453 N94-23568 * #
NASA-TM-108790 .... p 2174 N94-25272 * #
NASA-TM-108792 .... p 2431 N94-23974 * #
NASA-TM-108795 .... p 2452 N94-23510 * #
NASA-TM-108797 .... p 2420 N94-23088 * #
NASA-TM-108799 .... p 2387 N94-24403 * #
NASA-TM-109022 .... p 2592 N94-24649 * #
NASA-TM-109033 .... p 2271 N94-24473 * #
NASA-TM-109036 .... p 2169 N94-24576 * #
NASA-TM-109043 .... p 2241 N94-23274 * #
NASA-TM-109044 .... p 2228 N94-23279 * #
NASA-TM-109047 .... p 2228 N94-23280 * #
NASA-TM-109052 .... p 2228 N94-24083 * #
NASA-TM-109054 .... p 2448 N94-23086 * #
NASA-TM-109058 .... p 2457 N94-24603 * #
NASA-TM-109061 .... p 2592 N94-24660 * #
NASA-TM-109064 .... p 2593 N94-24709 * #
NASA-TM-109070 .... p 2378 N94-24839 * #
NASA-TM-109194 .... p 2200 N94-24577 * #
NASA-TM-109195 .... p 2199 N94-24059 * #
NASA-TM-109384 .... p 2208 N94-23481 *
NASA-TM-109385 .... p 2194 N94-23710 * #
NASA-TM-109388 .... p 2293 N94-23622 * #
NASA-TM-109398 .... p 2293 N94-23627 * #
NASA-TM-109399 .... p 2293 N94-23628 * #
NASA-TM-109400 .... p 2630 N94-23135 * #
NASA-TM-109406 .... p 2208 N94-23478 *
NASA-TM-109407 .... p 2208 N94-23479 *
NASA-TM-109408 .... p 2208 N94-23480 *
NASA-TM-109677 .... p 2205 N94-24824 * #
NASA-TM-109678 .... p 2349 N94-24488 * #
NASA-TM-109680 .... p 2350 N94-24851 * #
NASA-TM-109681 .... p 2167 N94-23975 * #
NASA-TM-109682 .... p 2428 N94-24855 * #
NASA-TM-109683 .... p 2593 N94-24759 * #
NASA-TM-109720 .... p 2593 N94-25168 * #
NASA-TM-4497 .... p 2319 N94-23339 * #
NASA-TM-4526 .... p 2168 N94-24295 * #
NASA-TM-4529 .... p 2169 N94-24586 * #
NASA-TM-4532 .... p 2188 N94-24106 * #
NASA-TM-4533 .... p 2170 N94-24716 * #
NASA-TM-4535 .... p 2228 N94-23514 * #
NASA-TM-4554 .... p 2591 N94-24337 * #

NASA-TP-3272-PT-1C .... p 2403 N94-24465 * #
NASA-TP-3296 .... p 2242 N94-23467 * #
NASA-TP-3328 .... p 2372 N94-24074 * #
NASA-TP-3346 .... p 2426 N94-23530 * #
NASA-TP-3358 .... p 2169 N94-24464 * #
NASA-TP-3365 .... p 2169 N94-24311 * #
NASA-TP-3370 .... p 2177 N94-24304 * #
NASA-TP-3373 .... p 2378 N94-24845 * #
NASA-TP-3374 .... p 2166 N94-23512 * #
NASA-TP-3389 .... p 2310 N94-24056 * #
NASA-TP-3402 .... p 2245 N94-25117 * #
NASA-TP-3404 .... p 2540 N94-23509 * #
NASA-TP-3405 .... p 2540 N94-24305 * #
NASA-TP-3407 .... p 2171 N94-25187 * #
NASA-TP-3415 .... p 2381 N94-22961 * #
NASA-TP-3423 .... p 2540 N94-23273 * #
NASA-TP-3434 .... p 2376 N94-23342 * #
NASA-TP-3442 .... p 2375 N94-23294 * #
NASA-TP-3444 .... p 2374 N94-22960 * #
NASA-TP-3456 .... p 2426 N94-23544 * #
NASA-TP-3457 .... p 2490 N94-24727 * #
NASA-TP-3458 .... p 2269 N94-23574 * #

NEDO-GET-9210-2 .... p 2397 N94-23026 #
NEDO-P-9219 .... p 2264 N94-23027 #

NIFS-MEMO-7 .... p 2549 N94-22964 #

NIFS-206 .... p 2319 N94-23460 #
NIFS-257 .... p 2552 N94-24456 #
NIFS-258 .... p 2553 N94-24623 #
NIFS-259 .... p 2271 N94-24459 #
NIFS-260 .... p 2551 N94-24358 #
NIFS-261 .... p 2552 N94-24458 #
NIFS-262 .... p 2551 N94-24306 #
NIFS-263 .... p 2311 N94-24457 #
NIFS-264 .... p 2602 N94-24866 #
NIFS-265 .... p 2602 N94-24867 #
NIFS-266 .... p 2536 N94-24868 #

NIKHEF-H/92-19 .... p 2539 N94-25465 #

NIST-GCR-93-621 .... p 2270 N94-23740 #

NIST/SP-838/3 .... p 2272 N94-24955
NIST/SP-838/4 .... p 2270 N94-23737 #

NISTIR-5219 .... p 2172 N94-23810
NISTIR-5251 .... p 2270 N94-23735 #
NISTIR-5255 .... p 2194 N94-23770
NISTIR-5256-PT-2 .... p 2194 N94-23819
NISTIR-5268 .... p 2293 N94-23719 #

NLR-TP-91435-U .... p 2471 N94-23137

NMRI-93-59 .... p 2427 N94-24950 #

NOAA-TM-ERL-WPL-231 .... p 2396 N94-22913 #

NPL-RSA(EXT)0042 .... p 2529 N94-25026

NPS-MR-93-003 .... p 2416 N94-25071 #

NPS-OR-93-104 .... p 2422 N94-25146 #

NRCN-533 .... p 2567 N94-25422

NREL/TP-411-5501 .... p 2389 N94-22888 #
NREL/TP-411-5739-PHASE-2A ... p 2390 N94-23295 #
NREL/TP-413-5835 .... p 2560 N94-23205 #
NREL/TP-413-5844 .... p 2390 N94-23296
NREL/TP-451-5755 .... p 2389 N94-22862 #
NREL/TP-451-5813 .... p 2395 N94-24509 #

NRL/FR/5554-93-9575 .... p 2303 N94-25089 #
NRL/FR/7127-93-9580 .... p 2530 N94-25073

NRL/MR/7531-93-7207 .... p 2416 N94-25162

NSF/ISI-92005 .... p 2354 N94-23533 #

NSWCDD/TR-93/551 .... p 2171 N94-25411 #

NTSB/AAR-93/06 .... p 2173 N94-24062 #
NTSB/AAR-93/07 .... p 2172 N94-23579 #
NTSB/AAR-93/08 .... p 2174 N94-25175 #
NTSB/AAR-94/01/SUM .... p 2174 N94-25273 #

NTSB/ARG-93/02 .... p 2173 N94-24841 #

NU-0007 .... p 2566 N94-25332 #

ONR-TR-26 .... p 2537 N94-25087 #

ORNL/CDIAC-34/R3 .... p 2588 N94-22875

ORNL/SUB-87-00184/04 .... p 2227 N94-23022 #
ORNL/SUB-91-SH641/1 .... p 2271 N94-23793 #
ORNL/SUB-93-07802 .... p 2254 N94-23783 #

ORNL/TM-12285 .... p 2478 N94-22975 #
ORNL/TM-12424 .... p 2548 N94-22945 #
ORNL/TM-12512 .... p 2446 N94-24538 #

OSURF-726944 .... p 2468 N94-25030
OSURF-760388 .... p 2468 N94-25030

OTA-A-565 .... p 2597 N94-24312 #

OTA-ITE-585 .... p 2630 N94-23572 #

OTA-TCT-578 .... p 2290 N94-23081 #

OUEL-1915/92 .... p 2343 N94-23162 #
OUEL-1921/92 .... p 2492 N94-25324 #
OUEL-1922/92 .... p 2472 N94-23163 #
OUEL-1923/92 .... p 2471 N94-23147
OUEL-1948/92 .... p 2463 N94-25468 #
OUEL-1953/92 .... p 2353 N94-23178 #
OUEL-1956/92 .... p 2472 N94-23179 #

OUEL-1963/92 .... p 2353 N94-23164 #
OUEL-1966/92 .... p 2379 N94-25325 #
OUEL-1967/92 .... p 2593 N94-25326 #
OUEL-1968/92 .... p 2554 N94-25327 #
OUEL-1970/93 .... p 2477 N94-25469 #
OUEL-1972/93 .... p 2477 N94-25470 #
OUEL-1973/93 .... p 2464 N94-25471 #
OUEL-1975/93 .... p 2346 N94-25472 #
OUEL-1977/93 .... p 2373 N94-25475 #
OUEL-1990/93 .... p 2379 N94-25478 #

PARGUM-93-04 .... p 2569 N94-24777 #

PB93-192904 .... p 2597 N94-24312 #
PB93-193159 .... p 2388 N94-24809 #
PB93-193217 .... p 2175 N94-24474
PB93-198125 .... p 2396 N94-22913 #
PB93-198323 .... p 2626 N94-23738
PB93-198331 .... p 2627 N94-23739
PB93-198893 .... p 2270 N94-23740 #
PB93-199412 .... p 2244 N94-23802
PB93-199701 .... p 2474 N94-24627
PB93-199768 .... p 2349 N94-24629
PB93-199784 .... p 2298 N94-24630
PB93-199792 .... p 2545 N94-24631
PB93-200228 .... p 2474 N94-24544
PB93-200327 .... p 2445 N94-23788
PB93-200707 .... p 2354 N94-23533 #
PB93-201341 .... p 2453 N94-23534
PB93-201358 .... p 2451 N94-23443
PB93-201366 .... p 2452 N94-23444
PB93-201408 .... p 2562 N94-23535
PB93-201416 .... p 2561 N94-23503
PB93-201424 .... p 2533 N94-23505
PB93-201481 .... p 2561 N94-23445
PB93-201499 .... p 2241 N94-23446
PB93-201531 .... p 2561 N94-23428
PB93-201549 .... p 2544 N94-23629
PB93-201572 .... p 2241 N94-23447
PB93-201598 .... p 2353 N94-23448
PB93-201606 .... p 2353 N94-23449
PB93-201614 .... p 2268 N94-23450
PB93-201622 .... p 2269 N94-23506
PB93-201630 .... p 2268 N94-23429
PB93-201663 .... p 2268 N94-23430
PB93-201671 .... p 2254 N94-23431
PB93-201747 .... p 2293 N94-23508 #
PB93-201762 .... p 2452 N94-23451
PB93-201770 .... p 2399 N94-24633
PB93-204303 .... p 2176 N94-23146 #
PB93-204311 .... p 2529 N94-24514
PB93-204345 .... p 2545 N94-24529
PB93-204352 .... p 2297 N94-24530
PB93-204360 .... p 2297 N94-24531
PB93-204378 .... p 2388 N94-24741
PB93-204402 .... p 2590 N94-23741
PB93-204469 .... p 2378 N94-24742
PB93-204477 .... p 2569 N94-24532
PB93-204493 .... p 2524 N94-24533
PB93-204501 .... p 2456 N94-24534
PB93-204550 .... p 2294 N94-23773
PB93-204600 .... p 2544 N94-23723
PB93-204618 .... p 2294 N94-23742
PB93-204634 .... p 2430 N94-23743
PB93-204725 .... p 2430 N94-23744
PB93-209815 .... p 2293 N94-23627 * #
PB93-210722 .... p 2529 N94-25026
PB93-211175 .... p 2593 N94-24743
PB93-214989 .... p 2496 N94-24744
PB93-215358 .... p 2378 N94-24745
PB93-215366 .... p 2193 N94-24739
PB93-217974 .... p 2267 N94-22981 #
PB93-217982 .... p 2347 N94-22982
PB93-217990 .... p 2232 N94-22983
PB93-220010 .... p 2479 N94-23093
PB93-220135 .... p 2407 N94-23129
PB93-220523 .... p 2523 N94-23094
PB93-220549 .... p 2589 N94-23095
PB93-220606 .... p 2478 N94-22984 #
PB93-220614 .... p 2448 N94-23096 #
PB93-220648 .... p 2448 N94-23097
PB93-220655 .... p 2479 N94-23098
PB93-220796 .... p 2601 N94-23099 #
PB93-220887 .... p 2232 N94-23100
PB93-223329 .... p 2317 N94-22985 #
PB93-223782 .... p 2493 N94-23108 #
PB93-223816 .... p 2465 N94-22986 #
PB93-223998 .... p 2242 N94-23496
PB93-224004 .... p 2397 N94-23497 #
PB93-224152 .... p 2559 N94-23109
PB93-224442 .... p 2375 N94-23221
PB93-224632 .... p 2561 N94-23222
PB93-224640 .... p 2561 N94-23223 #
PB93-224756 .... p 2382 N94-23224 #
PB93-224772 .... p 2290 N94-23225 #
PB93-224822 .... p 2472 N94-23463
PB93-224871 .... p 2450 N94-23226 #
PB93-224889 .... p 2523 N94-23101
PB93-224897 .... p 2390 N94-23102
PB93-224905 .... p 2449 N94-23103
PB93-224962 .... p 2308 N94-23104
PB93-224970 .... p 2308 N94-23105 #
PB93-225001 .... p 2308 N94-23130
PB93-225019 .... p 2524 N94-23131
PB93-225027 .... p 2524 N94-23110
PB93-225183 .... p 2449 N94-23111
PB93-225308 .... p 2268 N94-23476
PB93-225514 .... p 2374 N94-23112
PB93-225738 .... p 2374 N94-23113
PB93-225746 .... p 2479 N94-23106
PB93-226223 .... p 2317 N94-23114 #
PB93-226231 .... p 2318 N94-23115
PB93-226249 .... p 2165 N94-23116
PB93-226256 .... p 2449 N94-23117
PB93-226264 .... p 2374 N94-23118 #
PB93-226280 .... p 2240 N94-23119
PB93-226306 .... p 2375 N94-23120 #
PB93-226447 .... p 2232 N94-23477
PB93-227023 .... p 2208 N94-23478 *
PB93-227031 .... p 2208 N94-23479 *
PB93-227049 .... p 2208 N94-23480 *
PB93-227056 .... p 2208 N94-23481 *
PB93-230092 .... p 2232 N94-23482
PB93-230191 .... p 2254 N94-23561
PB93-230381 .... p 2479 N94-23121
PB93-230480 .... p 2479 N94-23122
PB93-230498 .... p 2479 N94-23107
PB93-230597 .... p 2444 N94-23754
PB93-230654 .... p 2386 N94-23755
PB93-231116 .... p 2293 N94-23622 * #
PB93-232189 .... p 2533 N94-23713
PB93-232197 .... p 2243 N94-23714
PB93-232254 .... p 2420 N94-23454 #
PB93-232874 .... p 2628 N94-24989
PB93-232882 .... p 2628 N94-24990
PB93-237618 .... p 2481 N94-23455 #
PB93-237634 .... p 2481 N94-23456 #
PB93-237667 .... p 2480 N94-23437 #
PB93-237675 .... p 2491 N94-24954
PB93-237691 .... p 2480 N94-23438 #
PB93-237709 .... p 2481 N94-23439 #
PB93-237717 .... p 2336 N94-24761
PB93-237725 .... p 2475 N94-24762
PB93-237733 .... p 2494 N94-23440 #
PB93-237741 .... p 2490 N94-24763
PB93-237758 .... p 2489 N94-24608
PB93-237766 .... p 2468 N94-24764
PB93-237774 .... p 2459 N94-24765
PB93-237782 .... p 2451 N94-23441 #
PB93-237790 .... p 2475 N94-24755
PB93-237808 .... p 2474 N94-24609
PB93-237816 .... p 2494 N94-23774
PB93-237824 .... p 2481 N94-23442 #
PB93-237857 .... p 2494 N94-23546 #
PB93-238012 .... p 2487 N94-23775
PB93-238020 .... p 2487 N94-23776
PB93-238053 .... p 2489 N94-24610
PB93-238061 .... p 2481 N94-23547 #
PB93-238079 .... p 2488 N94-24536
PB93-238087 .... p 2481 N94-23548 #
PB93-410407 .... p 2173 N94-24062 #
PB93-910408 .... p 2172 N94-23579 #
PB93-910409 .... p 2174 N94-25175 #
PB94-100187 .... p 2293 N94-23628 * #
PB94-101391 .... p 2489 N94-24615
PB94-101409 .... p 2456 N94-24513
PB94-101417 .... p 2271 N94-24475
PB94-101425 .... p 2487 N94-23786
PB94-101433 .... p 2488 N94-24539
PB94-101441 .... p 2446 N94-24540
PB94-101458 .... p 2454 N94-23768
PB94-103660 .... p 2172 N94-23810
PB94-104494 .... p 2398 N94-24476
PB94-104882 .... p 2599 N94-23705 #
PB94-104890 .... p 2599 N94-24780
PB94-104908 .... p 2599 N94-24521
PB94-104916 .... p 2602 N94-23812
PB94-105236 .... p 2398 N94-23813
PB94-107620 .... p 2173 N94-24750 #
PB94-109089 .... p 2628 N94-24991 #
PB94-109105 .... p 2628 N94-24992 #
PB94-109873 .... p 2187 N94-23709
PB94-110194 .... p 2272 N94-24955
PB94-110533 .... p 2495 N94-23814
PB94-110541 .... p 2596 N94-24477
PB94-110558 .... p 2495 N94-24634
PB94-110566 .... p 2456 N94-24507
PB94-110574 .... p 2453 N94-23745
PB94-110582 .... p 2457 N94-24570
PB94-110590 .... p 2466 N94-23706 #
PB94-110608 .... p 2453 N94-23707 #
PB94-110616 .... p 2486 N94-23708 #
PB94-110632 .... p 2495 N94-24508
PB94-110640 .... p 2495 N94-23815 #
PB94-110681 .... p 2495 N94-24571
PB94-110699 .... p 2533 N94-23746 #
PB94-110715 .... p 2473 N94-23747 #
PB94-110723 .... p 2473 N94-23748 #
PB94-110731 .... p 2489 N94-24572 #
PB94-110749 .... p 2590 N94-23816 #
PB94-110772 .... p 2388 N94-24636
PB94-110814 .... p 2454 N94-23817 #
PB94-110822 .... p 2486 N94-23724 #
PB94-110830 .... p 2486 N94-23725 #
PB94-110848 .... p 2272 N94-24648
PB94-110855 .... p 2299 N94-24650
PB94-110863 .... p 2459 N94-24758
PB94-110871 .... p 2494 N94-23749 #
PB94-110889 .... p 2454 N94-23750 #
PB94-110897 .... p 2454 N94-23751 #
PB94-110905 .... p 2467 N94-23752 #
PB94-110913 .... p 2488 N94-24541
PB94-110921 .... p 2489 N94-24651
PB94-110939 .... p 2487 N94-23787
PB94-110947 .... p 2486 N94-23722
PB94-110954 .... p 2489 N94-24652
PB94-110962 .... p 2489 N94-24653
PB94-110988 .... p 2526 N94-23726 #
PB94-110996 .... p 2294 N94-23727 #
PB94-111002 .... p 2294 N94-23728 #
PB94-111010 .... p 2294 N94-23729 #
PB94-111028 .... p 2524 N94-23730 #
PB94-111036 .... p 2403 N94-24592
PB94-111044 .... p 2524 N94-23731 #
PB94-111069 .... p 2298 N94-24593
PB94-111077 .... p 2298 N94-24597
PB94-111085 .... p 2544 N94-23732 #
PB94-111093 .... p 2294 N94-23733 #
PB94-111101 .... p 2298 N94-24637
PB94-111119 .... p 2404 N94-24598
PB94-111127 .... p 2457 N94-24599
PB94-111135 .... p 2418 N94-24600
PB94-111143 .... p 2418 N94-24601
PB94-111150 .... p 2399 N94-24573
PB94-111168 .... p 2334 N94-24574
PB94-111176 .... p 2569 N94-24575
PB94-111184 .... p 2562 N94-23769
PB94-111192 .... p 2494 N94-23798
PB94-111200 .... p 2473 N94-24542 *
PB94-111374 .... p 2194 N94-23770
PB94-111614 .... p 2494 N94-23771
PB94-111622 .... p 2494 N94-23772
PB94-111630 .... p 2467 N94-23767
PB94-111648 .... p 2467 N94-23756
PB94-111655 .... p 2487 N94-23799
PB94-111663 .... p 2480 N94-23140 #
PB94-111671 .... p 2602 N94-24522
PB94-111689 .... p 2521 N94-24523
PB94-111697 .... p 2467 N94-24524
PB94-111705 .... p 2497 N94-23800
PB94-111713 .... p 2496 N94-24639
PB94-111721 .... p 2386 N94-23734 #
PB94-112166 .... p 2270 N94-23735 #
PB94-112323 .... p 2398 N94-23818
PB94-112661 .... p 2233 N94-23736 #
PB94-112786 .... p 2233 N94-23801
PB94-113420 .... p 2270 N94-23737 #
PB94-113487 .... p 2194 N94-23819
PB94-114212 .... p 2235 N94-24920 #
PB94-117082 .... p 2628 N94-24993 #
PB94-117405 .... p 2628 N94-24994 #
PB94-118502 .... p 2399 N94-24525
PB94-118619 .... p 2486 N94-23757 #
PB94-118627 .... p 2486 N94-23758 #
PB94-118635 .... p 2335 N94-24641 #
PB94-118643 .... p 2592 N94-24642 #
PB94-118692 .... p 2454 N94-23759 #
PB94-118700 .... p 2473 N94-23760 #
PB94-118726 .... p 2488 N94-24526
PB94-118734 .... p 2376 N94-24478 #
PB94-118817 .... p 2488 N94-24527
PB94-118825 .... p 2585 N94-23761 #
PB94-118833 .... p 2586 N94-24528
PB94-118841 .... p 2486 N94-23762 #
PB94-118858 .... p 2254 N94-23763 #
PB94-119013 .... p 2474 N94-24543
PB94-119021 .... p 2489 N94-24643
PB94-119039 .... p 2497 N94-23764 #
PB94-119047 .... p 2487 N94-23765 #
PB94-119054 .... p 2377 N94-24645
PB94-119088 .... p 2592 N94-24646
PB94-119096 .... p 2404 N94-24647
PB94-119104 .... p 2562 N94-23766 #
PB94-126588 .... p 2493 N94-25527 #
PB94-126596 .... p 2477 N94-25526 #
PB94-126869 .... p 2173 N94-24841 #
PB94-910401 .... p 2174 N94-25273 #

PFC/CP-93-1 p 2552 N94-24504 #

PFC/IR-93-1 p 2548 N94-22721 #

PL-TR-93-2012 p 2406 N94-25535 #
PL-TR-93-2016 p 2406 N94-25537 #
PL-TR-93-2068 p 2406 N94-25536 #
PL-TR-93-2114 p 2301 N94-24926
PL-TR-93-2146 p 2207 N94-25542 #
PL-TR-93-2164 p 2406 N94-25538 #

PNL-SA-21755 p 2588 N94-22863
PNL-SA-23021 p 2397 N94-23016

PNL-8864 p 2347 N94-22974 #

PNR-90882 p 2187 N94-23519
PNR-90977 p 2187 N94-23570
PNR-90990 p 2595 N94-23580

PREPRINT-688 p 2340 N94-25466

PW/GESP-FR-22402 p 2189 N94-24776 #

RAL-93-010 p 2569 N94-24532
RAL-93-013 p 2524 N94-24533
RAL-93-026 p 2456 N94-24534

RANA-92-16 p 2336 N94-24761
RANA-93-01 p 2481 N94-23439 #
RANA-93-02 p 2481 N94-23455 #
RANA-93-03 p 2480 N94-23438 #
RANA-93-05 p 2491 N94-24954
RANA-93-06 p 2480 N94-23437 #
RANA-93-08 p 2569 N94-24575
RANA-93-09 p 2562 N94-23769

RB-5459 p 2340 N94-25467 #

RCC-256-93 p 2303 N94-25155

REPT-A-2654 p 2564 N94-24958 #
REPT-A-2655 p 2567 N94-25412 #
REPT-A-2656 p 2568 N94-25515 #
REPT-A-2658 p 2564 N94-24959 #
REPT-A-2659 p 2345 N94-24977 #
REPT-A-2660 p 2564 N94-24978 #
REPT-A-2662 p 2564 N94-24960 #

REPT-10392 p 2585 N94-23563 * #
REPT-157 p 2405 N94-24980 #
REPT-1993/39 p 2308 N94-23104
REPT-26 p 2407 N94-23129
REPT-31 p 2386 N94-23755
REPT-331 p 2603 N94-24983 #
REPT-333 p 2603 N94-24985 #
REPT-334 p 2604 N94-24986 #
REPT-336 p 2604 N94-24987 #
REPT-337 p 2603 N94-24976 #
REPT-38 p 2386 N94-23734 #
REPT-61 p 2382 N94-23148 #
REPT-6 p 2382 N94-23224 #
REPT-92-81 p 2489 N94-24572 #
REPT-93-4 p 2388 N94-24636
REPT-93-52 p 2486 N94-23757 #
REPT-93-53 p 2486 N94-23758 #
REPT-93-54 p 2335 N94-24641 #
REPT-93-55 p 2592 N94-24642 #
REPT-93/67 p 2599 N94-23705 #
REPT-93/70 p 2599 N94-24780
REPT-93/71 p 2599 N94-24521
REPT-93/75 p 2602 N94-23812
REPT-93A00689 p 2600 N94-25387 * #
REPT-93B00006 p 2407 N94-23132 * #
REPT-93B00016 p 2308 N94-23281 * #
REPT-93B00077 p 2401 N94-23282 * #
REPT-93B00083 p 2410 N94-24374 * #
REPT-93B00086-VOL-9 p 2417 N94-23291 * #
REPT-93B00097-VOL-11 p 2417 N94-23338 * #
REPT-94-001 p 2563 N94-24404 #
REPT-94-001 p 2416 N94-25271 * #
REPT-94-002 p 2565 N94-25025 #
REPT-94B00007 p 2540 N94-23273 * #
REPT-94B00008-PT-1C p 2403 N94-24465 * #
REPT-94B00013 p 2410 N94-24355 * #
REPT-94B00030 p 2381 N94-24800 * #
REPT-94B00034 p 2195 N94-24497 * #
REPT-946 p 2446 N94-24981 #
REPT-948 p 2546 N94-24982 #

RFP-4627 p 2242 N94-23475

RIACS-TR-93-10 p 2529 N94-24307 * #
RIACS-TR-94-01 p 2569 N94-24109 * #
RIACS-TR-94-02 p 2454 N94-24110 * #
RIACS-TR-94-03 p 2591 N94-24552 * #

RIVM-710401017 p 2242 N94-23496
RIVM-710401020 p 2397 N94-23497 #

RL-TR-93-117-VOL-1 p 2463 N94-25455 #
RL-TR-93-117-VOL-2 p 2463 N94-25456 #
RL-TR-93-179 p 2496 N94-24951 #
RL-TR-93-189 p 2592 N94-24691 #

RR-448 p 2492 N94-25306 #
RR-457 p 2476 N94-25307 #
RR-458 p 2476 N94-25308 #
RR-459 p 2492 N94-25309
RR-461 p 2492 N94-25310 #
RR-465 p 2462 N94-25311 #
RR-467 p 2446 N94-25312 #
RR-468 p 2446 N94-25313 #
RR-469 p 2523 N94-25314 #
RR-470 p 2463 N94-25315 #
RR-471 p 2492 N94-25318 #
RR-472 p 2313 N94-25319 #
RR-474 p 2492 N94-25320 #
RR-475 p 2463 N94-25321 #
RR-476 p 2368 N94-25322 #
RR-477 p 2523 N94-25323 #
RR-907-I p 2589 N94-23150 #
RR-908-I p 2450 N94-23180 #

RSL-TR-17 p 2309 N94-23304 * #
RSL-TR-8370-1 p 2409 N94-24048 * #
RSL-TR-8370-2 p 2410 N94-24126 * #
RSL-TR-8730-3 p 2409 N94-24087 * #

RTI/4321/Q4-93 p 2597 N94-24494 * #

RTR-250-01 p 2200 N94-24664 * #

R93-217 p 2604 N94-25265 * #

S-697 p 2433 N94-24185 * #
S-738 p 2194 N94-23292 * #
S-743 p 2205 N94-24625 * #
S-747 p 2598 N94-24644 * #
S-748 p 2386 N94-24095 * #
S-752 p 2473 N94-24068 * #
S-753 p 2374 N94-22960 * #
S-756 p 2426 N94-23544 * #

SAND-90-7112 p 2394 N94-23704 #
SAND-92-0652C p 2321 N94-23640 * #
SAND-93-0547C p 2542 N94-23202
SAND-93-0549C p 2244 N94-23811
SAND-93-0922C p 2452 N94-23488 #
SAND-93-1107C p 2555 N94-22717 #
SAND-93-1127C p 2350 N94-24659 #
SAND-93-1138 p 2270 N94-23790 #
SAND-93-1211C p 2591 N94-24501 #
SAND-93-1287 p 2375 N94-23217 #
SAND-93-1296C p 2398 N94-24506 #
SAND-93-1351 p 2198 N94-23210 #
SAND-93-1375C p 2394 N94-23472 #
SAND-93-1391 p 2589 N94-23126 #
SAND-93-1400C p 2558 N94-22953 #
SAND-93-1420C p 2613 N94-23469 #
SAND-93-1422-VOL-1 p 2589 N94-23127 #
SAND-93-1422-VOL-2 p 2589 N94-23128 #
SAND-93-1617C p 2343 N94-23200 #
SAND-93-1648C p 2238 N94-22932 #
SAND-93-1750C p 2560 N94-23204 #
SAND-93-1763 p 2318 N94-23220 #
SAND-93-1835C p 2472 N94-23201 #
SAND-93-1866C p 2466 N94-23491 #
SAND-93-1965C p 2559 N94-23186 #
SAND-93-2031C p 2591 N94-24607
SAND-93-2046C p 2534 N94-23804 #
SAND-93-2057C p 2552 N94-24546 #
SAND-93-2081C p 2371 N94-22918 #
SAND-93-2100C p 2309 N94-23777 #
SAND-93-2155C p 2342 N94-22954 #
SAND-93-2182C p 2349 N94-23209 #
SAND-93-2215C p 2268 N94-23000 #
SAND-93-2244C p 2348 N94-23185 #
SAND-93-2265C p 2526 N94-23718 #
SAND-93-2421C p 2311 N94-24748 #
SAND-93-7080C p 2217 N94-23193 #

SAO-AXAF-DR-93-059 p 2454 N94-24050 * #

SATCOM-93-20 p 2301 N94-25005 * #

SECA-FR-93-18 p 2220 N94-24471 * #

SER-B-93-41 p 2165 N94-23116
SER-B-93-42 p 2318 N94-23115

SGD-584-PT-1 p 2626 N94-23738
SGD-584-PT-2 p 2627 N94-23739

SGD-587-PT-1 p 2628 N94-24989
SGD-587-PT-2 p 2628 N94-24990
SGD-588-PT-1 p 2628 N94-24991 #
SGD-588-PT-2 p 2628 N94-24992 #
SGD-589-PT-1 p 2628 N94-24993 #
SGD-589-PT-2 p 2628 N94-24994 #

SI-93-2679 p 2200 N94-24801 * #

SK-1600-99-003 p 2455 N94-24297

SLAC-PUB-6249 p 2307 N94-22955 #

SP-RAPP-1993:13 p 2378 N94-24742

SPC-92019-CMC p 2461 N94-25148 #
SPC-92051-CMC p 2461 N94-25149 #

SR-2 p 2406 N94-25538 #

SSCL-PREPRINT-761 p 2452 N94-23518

STF10-A92018 p 2453 N94-23534
STF10-A92019 p 2451 N94-23443
STF10-A93002 p 2452 N94-23444
STF19-A91017 p 2562 N94-23535
STF19-A92018 p 2561 N94-23503
STF19-A92019 p 2533 N94-23505
STF19-A92030 p 2561 N94-23445
STF19-A92031 p 2241 N94-23446
STF19-A92035 p 2561 N94-23428
STF19-A93003 p 2544 N94-23629
STF20-A92187 p 2241 N94-23447
STF20-A93022 p 2353 N94-23448
STF20-A93032 p 2353 N94-23449
STF25-A92016 p 2268 N94-23450
STF25-A92041 p 2269 N94-23506
STF25-A92042 p 2268 N94-23429
STF25-A92051 p 2268 N94-23430
STF28-A93013 p 2254 N94-23431
STF40-A92145 p 2293 N94-23508 #
STF48-A93001 p 2452 N94-23451
STF60-A92023 p 2399 N94-24633

SU-SLAC-PUB-6314 p 2534 N94-23803

S2/251 p 2376 N94-23789 #

TDA-PR-42-115 p 2290 N94-23256 * #

TDCK-TD-93-0756 p 2406 N94-25540 #

TDCK-TD93-2777 p 2190 N94-25516 #

TD93-0373 p 2542 N94-22895
TD93-0749 p 2381 N94-22896

TEC-R-199 p 2545 N94-24730
TEC-R-200 p 2493 N94-25452 #

TELAC-93-19 p 2377 N94-24587 * #

TIOS-93/08 p 2493 N94-23108 #
TIOS-93/20 p 2299 N94-24650
TIOS-93/21, p 2459 N94-24758
TIOS-93/22 p 2494 N94-23749 #
TIOS-93/23 p 2454 N94-23751 #
TIOS-93/24 p 2467 N94-23752 #

TKK-F-C149 p 2390 N94-23102

TKO-C61 p 2449 N94-23103

TNO-IMW-R-92/396 p 2417 N94-23176 #

TNO-93-CMC-R0210-2 p 2376 N94-24478 #

TR-ME/ES-93-2 p 2439 N94-24857 * #

TR-ONR-C-15 p 2495 N94-24560 #

TR-073093-357OP p 2309 N94-23304 * #
TR-10 p 2262 N94-25159 #
TR-11 p 2259 N94-24792 #
TR-11 p 2263 N94-25413 #
TR-12 p 2547 N94-25144 #
TR-14 p 2536 N94-24675
TR-14 p 2262 N94-25145 #
TR-15 p 2260 N94-24863
TR-20-ONR p 2235 N94-24790 #
TR-21 p 2259 N94-24789
TR-22 p 2235 N94-24917
TR-23 p 2257 N94-24558 #
TR-24 p 2260 N94-24924
TR-26 p 2537 N94-25087 #
TR-27 p 2235 N94-24925

TR-335 ..... p 2192 N94-23564 * #
TR-352 ..... p 2336 N94-24771 * #
TR-4002-93-12 ..... p 2389 N94-24856 * #
TR-4002-94-01 ..... p 2388 N94-24827 * #
TR-7 ..... p 2565 N94-25086 #
TR-8 ..... p 2257 N94-24562
TR-94-01 ..... p 2260 N94-24813
TR-94-02 ..... p 2258 N94-24732
TR-94-4 ..... p 2300 N94-24676 * #
TR-9 ..... p 2261 N94-24930 #

TRC-EM-CAB-9401 ..... p 2365 N94-24699 * #
TRC-EM-CAB-9402 ..... p 2298 N94-24616 * #

TRS-416 ..... p 2474 N94-24544

TW-90-10 ..... p 2497 N94-25528
TW-92-13 ..... p 2497 N94-25528
TW-93-05 ..... p 2487 N94-23786
TW-93-07 ..... p 2496 N94-24839

TWR-60695 ..... p 2201 N94-24965 * #
TWR-64216 ..... p 2200 N94-24112 * #
TWR-64222 ..... p 2199 N94-24057 * #
TWR-64222 ..... p 2219 N94-24064 * #
TWR-64222 ..... p 2200 N94-24067 * #
TWR-64222 ..... p 2201 N94-24802 * #
TWR-64222 ..... p 2367 N94-25020 * #
TWR-64240 ..... p 2200 N94-24065 * #
TWR-64983-VOL-2 ..... p 2365 N94-24588 * #

UAH-5-30163 ..... p 2586 N94-25197 * #
UAH-5-30166 ..... p 2629 N94-25199 * #
UAH-5-33020 ..... p 2364 N94-24088 * #
UAH-5-33127 ..... p 2545 N94-24665 * #

UCB-PTH-93/04 ..... p 2533 N94-23218
UCB-PTH-93/26 ..... p 2523 N94-24658 #

UCID-ID-112778 ..... p 2382 N94-23494 #

UCRL-CR-114189 ..... p 2252 N94-22930 #

UCRL-ID-112775 ..... p 2228 N94-23493 #
UCRL-ID-112777 ..... p 2373 N94-24613 #
UCRL-ID-114590 ..... p 2240 N94-23017
UCRL-ID-114706 ..... p 2241 N94-23434 #
UCRL-ID-115042 ..... p 2397 N94-23700 #
UCRL-ID-115168-PT-1 ..... p 2488 N94-24503 #

UCRL-JC-110366 ..... p 2307 N94-23008 #
UCRL-JC-110367 ..... p 2471 N94-23011
UCRL-JC-111342 ..... p 2265 N94-23807
UCRL-JC-111343 ..... p 2265 N94-23778 #
UCRL-JC-111732 ..... p 2589 N94-22934 #
UCRL-JC-112339 ..... p 2307 N94-22950 #
UCRL-JC-112553 ..... p 2347 N94-22867 #
UCRL-JC-112765 ..... p 2549 N94-23014
UCRL-JC-113254 ..... p 2371 N94-22935 #
UCRL-JC-113299 ..... p 2558 N94-22946
UCRL-JC-113309 ..... p 2319 N94-23470 #
UCRL-JC-113560 ..... p 2454 N94-23796 #
UCRL-JC-113810 ..... p 2241 N94-23297 #
UCRL-JC-114003 ..... p 2309 N94-23520 #
UCRL-JC-114025 ..... p 2348 N94-23181 #
UCRL-JC-114109 ..... p 2232 N94-23298 #
UCRL-JC-114114 ..... p 2239 N94-22958 #
UCRL-JC-114187 ..... p 2229 N94-24547 #
UCRL-JC-114192 ..... p 2252 N94-22931 #
UCRL-JC-114201 ..... p 2265 N94-23436 #
UCRL-JC-114363 ..... p 2448 N94-22980
UCRL-JC-114367 ..... p 2532 N94-22988
UCRL-JC-114438 ..... p 2349 N94-23490 #
UCRL-JC-114493 ..... p 2541 N94-22868 #
UCRL-JC-114579 ..... p 2229 N94-24632 #
UCRL-JC-114643 ..... p 2209 N94-23012
UCRL-JC-114679 ..... p 2549 N94-23013
UCRL-JC-114754 ..... p 2552 N94-24502 #
UCRL-JC-114803 ..... p 2549 N94-22949 #
UCRL-JC-114852 ..... p 2351 N94-22866
UCRL-JC-114857 ..... p 2531 N94-22869 #
UCRL-JC-114927 ..... p 2351 N94-22865
UCRL-JC-115005 ..... p 2541 N94-22722 #
UCRL-JC-115035 ..... p 2408 N94-23471 #
UCRL-JC-115046 ..... p 2234 N94-24549 #
UCRL-JC-115418 ..... p 2568 N94-23216 #

UCRL-LR-105821-93-3 ..... p 2551 N94-23703 #

UDR-TR-92-87 ..... p 2463 N94-25453 #

UFIFT-93-06 ..... p 2569 N94-24532

UH-BUDGET-1-5-54282 ..... p 2267 N94-23594 * #

UILU-ENG-93/2006 ..... p 2378 N94-25143

US-PATENT-,5,229,961 ..... p 2446 N94-24724

US-PATENT-APPL-CLASS-188-82.2 ..... p 2354 N94-23969 *

US-PATENT-APPL-SN-000902 ..... p 2543 N94-23270 *
US-PATENT-APPL-SN-008026 ..... p 2534 N94-23825 *
US-PATENT-APPL-SN-014960 ..... p 2375 N94-23308 *
US-PATENT-APPL-SN-024971 ..... p 2354 N94-23831 *
US-PATENT-APPL-SN-045336 ..... p 2253 N94-23307 *
US-PATENT-APPL-SN-084064 ..... p 2252 N94-23079 *
US-PATENT-APPL-SN-086584 ..... p 2343 N94-23826 *
US-PATENT-APPL-SN-361471 ..... p 2253 N94-23311 *
US-PATENT-APPL-SN-414820 ..... p 2309 N94-23820 *
US-PATENT-APPL-SN-546817 ..... p 2311 N94-24736
US-PATENT-APPL-SN-615832 ..... p 2446 N94-24724
US-PATENT-APPL-SN-619567 ..... p 2537 N94-25047
US-PATENT-APPL-SN-636808 ..... p 2312 N94-25042
US-PATENT-APPL-SN-639500 ..... p 2312 N94-25050
US-PATENT-APPL-SN-643629 ..... p 2253 N94-23311 *
US-PATENT-APPL-SN-650336 ..... p 2252 N94-23075 *
US-PATENT-APPL-SN-654439 ..... p 2309 N94-23820 *
US-PATENT-APPL-SN-656330 ..... p 2302 N94-25057
US-PATENT-APPL-SN-660473 ..... p 2317 N94-23077 *
US-PATENT-APPL-SN-666125 ..... p 2303 N94-25217
US-PATENT-APPL-SN-690437 ..... p 2345 N94-25053
US-PATENT-APPL-SN-690440 ..... p 2319 N94-23306 *
US-PATENT-APPL-SN-691602 ..... p 2543 N94-23309 *
US-PATENT-APPL-SN-702540 ..... p 2344 N94-24734
US-PATENT-APPL-SN-703238 ..... p 2543 N94-23270 *
US-PATENT-APPL-SN-713658 ..... p 2302 N94-25049
US-PATENT-APPL-SN-718034 ..... p 2303 N94-25150
US-PATENT-APPL-SN-720129 ..... p 2301 N94-25038
US-PATENT-APPL-SN-721821 ..... p 2312 N94-25039
US-PATENT-APPL-SN-730620 ..... p 2367 N94-25046
US-PATENT-APPL-SN-738362 ..... p 2350 N94-24952
US-PATENT-APPL-SN-745045 ..... p 2312 N94-25036
US-PATENT-APPL-SN-751479 ..... p 2446 N94-25034
US-PATENT-APPL-SN-783039 ..... p 2230 N94-24735
US-PATENT-APPL-SN-788403 ..... p 2252 N94-23076 *
US-PATENT-APPL-SN-790730 ..... p 2253 N94-23305 *
US-PATENT-APPL-SN-818575 ..... p 2258 N94-24721
US-PATENT-APPL-SN-818672 ..... p 2261 N94-25054
US-PATENT-APPL-SN-820123 ..... p 2344 N94-24723
US-PATENT-APPL-SN-826749 ..... p 2525 N94-23312 *
US-PATENT-APPL-SN-829839 ..... p 2192 N94-23310 *
US-PATENT-APPL-SN-841945 ..... p 2258 N94-24737
US-PATENT-APPL-SN-842297 ..... p 2310 N94-23821 * #
US-PATENT-APPL-SN-849612 ..... p 2375 N94-23308 *
US-PATENT-APPL-SN-850107 ..... p 2258 N94-24720
US-PATENT-APPL-SN-866649 ..... p 2170 N94-25051
US-PATENT-APPL-SN-876615 ..... p 2546 N94-25043
US-PATENT-APPL-SN-880856 ..... p 2253 N94-23311 *
US-PATENT-APPL-SN-887202 ..... p 2350 N94-25216
US-PATENT-APPL-SN-889806 ..... p 2302 N94-25058
US-PATENT-APPL-SN-889920 ..... p 2302 N94-25056
US-PATENT-APPL-SN-892053 ..... p 2354 N94-23822 *
US-PATENT-APPL-SN-892058 ..... p 2252 N94-23079 *
US-PATENT-APPL-SN-894508 ..... p 2350 N94-25044
US-PATENT-APPL-SN-903316 ..... p 2301 N94-25045
US-PATENT-APPL-SN-905708 ..... p 2252 N94-23075 *
US-PATENT-APPL-SN-906649 ..... p 2545 N94-24722
US-PATENT-APPL-SN-912961 ..... p 2563 N94-23972 *
US-PATENT-APPL-SN-918747 ..... p 2352 N94-23082 *
US-PATENT-APPL-SN-923867 ..... p 2184 N94-25052
US-PATENT-APPL-SN-929216 ..... p 2294 N94-23827 *
US-PATENT-APPL-SN-937916 ..... p 2312 N94-25035
US-PATENT-APPL-SN-941816 ..... p 2253 N94-23305 *
US-PATENT-APPL-SN-942491 ..... p 2310 N94-23823 *
US-PATENT-APPL-SN-946111 ..... p 2352 N94-23078 *
US-PATENT-APPL-SN-947591 ..... p 2367 N94-25055
US-PATENT-APPL-SN-957544 ..... p 2302 N94-25048
US-PATENT-APPL-SN-957563 ..... p 2345 N94-25037
US-PATENT-APPL-SN-961293 ..... p 2203 N94-23824 *
US-PATENT-APPL-SN-976048 ..... p 2301 N94-25040
US-PATENT-APPL-SN-977301 ..... p 2301 N94-25041
US-PATENT-APPL-SN-986632 ..... p 2354 N94-23969 *

US-PATENT-CLASS-102-504 ..... p 2354 N94-23822 *
US-PATENT-CLASS-108-3 ..... p 2192 N94-23310 *
US-PATENT-CLASS-108-59 ..... p 2192 N94-23310 *
US-PATENT-CLASS-114-227 ..... p 2203 N94-23824 *
US-PATENT-CLASS-136-236.1 ..... p 2343 N94-23826 *
US-PATENT-CLASS-136-241 ..... p 2343 N94-23826 *
US-PATENT-CLASS-137-807 ..... p 2367 N94-25055
US-PATENT-CLASS-156-307.4 ..... p 2252 N94-23076 *
US-PATENT-CLASS-156-330.9 ..... p 2252 N94-23076 *
US-PATENT-CLASS-156-613 ..... p 2563 N94-23972 *
US-PATENT-CLASS-188-163 ..... p 2354 N94-23969 *
US-PATENT-CLASS-188-171 ..... p 2354 N94-23969 *
US-PATENT-CLASS-188-82.3 ..... p 2354 N94-23969 *
US-PATENT-CLASS-188-82.84 ..... p 2354 N94-23969 *
US-PATENT-CLASS-192-44 ..... p 2354 N94-23969 *
US-PATENT-CLASS-192-45.1 ..... p 2354 N94-23969 *
US-PATENT-CLASS-204-241 ..... p 2258 N94-24720
US-PATENT-CLASS-244-152 ..... p 2170 N94-25051
US-PATENT-CLASS-244-161 ..... p 2352 N94-23078 *
US-PATENT-CLASS-244-161 ..... p 2354 N94-23822 *
US-PATENT-CLASS-244-190 ..... p 2184 N94-25052
US-PATENT-CLASS-250-227.19 ..... p 2344 N94-24734
US-PATENT-CLASS-250-251 ..... p 2534 N94-23825 *
US-PATENT-CLASS-250-551 ..... p 2312 N94-25042
US-PATENT-CLASS-257-15 ..... p 2310 N94-23821 * #
US-PATENT-CLASS-257-199 ..... p 2310 N94-23821 * #
US-PATENT-CLASS-257-2 ..... p 2309 N94-23820 *
US-PATENT-CLASS-257-476 ..... p 2310 N94-23821 * #
US-PATENT-CLASS-257-480 ..... p 2310 N94-23821 * #
US-PATENT-CLASS-257-482 ..... p 2310 N94-23821 * #
US-PATENT-CLASS-257-486 ..... p 2310 N94-23821 * #
US-PATENT-CLASS-257-506 ..... p 2310 N94-23821 * #
US-PATENT-CLASS-257-528 ..... p 2309 N94-23820 *
US-PATENT-CLASS-264-DIG.19 ..... p 2253 N94-23311 *
US-PATENT-CLASS-273-84R ..... p 2354 N94-23822 *
US-PATENT-CLASS-294-66.1 ..... p 2354 N94-23822 *
US-PATENT-CLASS-294-86.1 ..... p 2354 N94-23822 *
US-PATENT-CLASS-307-201 ..... p 2309 N94-23820 *
US-PATENT-CLASS-310-83 ..... p 2367 N94-25046
US-PATENT-CLASS-312-282 ..... p 2192 N94-23310 *
US-PATENT-CLASS-322-2R ..... p 2312 N94-25036
US-PATENT-CLASS-324-309 ..... p 2537 N94-25047
US-PATENT-CLASS-338-13 ..... p 2309 N94-23820 *
US-PATENT-CLASS-338-38 ..... p 2309 N94-23820 *
US-PATENT-CLASS-342-149 ..... p 2302 N94-25056
US-PATENT-CLASS-342-149 ..... p 2302 N94-25058
US-PATENT-CLASS-342-159 ..... p 2301 N94-25041
US-PATENT-CLASS-342-160 ..... p 2301 N94-25040
US-PATENT-CLASS-342-26 ..... p 2294 N94-23827 *
US-PATENT-CLASS-342-368 ..... p 2301 N94-25045
US-PATENT-CLASS-342-54 ..... p 2294 N94-23827 *
US-PATENT-CLASS-356-28.5 ..... p 2543 N94-23309 *
US-PATENT-CLASS-356-28.5 ..... p 2294 N94-23827 *
US-PATENT-CLASS-356-28.5 ..... p 2545 N94-24722
US-PATENT-CLASS-356-32 ..... p 2375 N94-23308 *
US-PATENT-CLASS-356-342 ..... p 2294 N94-23827 *
US-PATENT-CLASS-356-345 ..... p 2345 N94-25053
US-PATENT-CLASS-356-5 ..... p 2294 N94-23827 *
US-PATENT-CLASS-357-68 ..... p 2303 N94-25150
US-PATENT-CLASS-358-149 ..... p 2312 N94-25039
US-PATENT-CLASS-359-154 ..... p 2543 N94-23270 *
US-PATENT-CLASS-359-158 ..... p 2543 N94-23270 *
US-PATENT-CLASS-359-173 ..... p 2543 N94-23270 *
US-PATENT-CLASS-359-183 ..... p 2543 N94-23270 *
US-PATENT-CLASS-359-189 ..... p 2543 N94-23270 *
US-PATENT-CLASS-359-276 ..... p 2303 N94-25217
US-PATENT-CLASS-359-362 ..... p 2543 N94-23309 *
US-PATENT-CLASS-359-67 ..... p 2375 N94-23308 *
US-PATENT-CLASS-361-500 ..... p 2309 N94-23820 *
US-PATENT-CLASS-364-481 ..... p 2302 N94-25049
US-PATENT-CLASS-364-807 ..... p 2446 N94-25034
US-PATENT-CLASS-365-225.6 ..... p 2311 N94-24736
US-PATENT-CLASS-365-45 ..... p 2312 N94-25050
US-PATENT-CLASS-365-87 ..... p 2446 N94-24724
US-PATENT-CLASS-367-103 ..... p 2302 N94-25048
US-PATENT-CLASS-372-20 ..... p 2350 N94-25044
US-PATENT-CLASS-372-93 ..... p 2350 N94-25216
US-PATENT-CLASS-374-173 ..... p 2345 N94-25037
US-PATENT-CLASS-375-38 ..... p 2301 N94-25038
US-PATENT-CLASS-380-48 ..... p 2302 N94-25057
US-PATENT-CLASS-381-17 ..... p 2525 N94-23312 *
US-PATENT-CLASS-381-24 ..... p 2525 N94-23312 *
US-PATENT-CLASS-381-26 ..... p 2525 N94-23312 *
US-PATENT-CLASS-403-13 ..... p 2352 N94-23078 *
US-PATENT-CLASS-403-24 ..... p 2352 N94-23078 *
US-PATENT-CLASS-403-348 ..... p 2352 N94-23082 *
US-PATENT-CLASS-403-359 ..... p 2352 N94-23082 *
US-PATENT-CLASS-417-48 ..... p 2354 N94-23831 *
US-PATENT-CLASS-417-50 ..... p 2354 N94-23831 *
US-PATENT-CLASS-426-191 ..... p 2310 N94-23823 *
US-PATENT-CLASS-427-2 ..... p 2350 N94-24952
US-PATENT-CLASS-428-1 ..... p 2375 N94-23308 *
US-PATENT-CLASS-428-213 ..... p 2230 N94-24735
US-PATENT-CLASS-428-367 ..... p 2252 N94-23076 *
US-PATENT-CLASS-428-408 ..... p 2252 N94-23076 *
US-PATENT-CLASS-428-409 ..... p 2375 N94-23308 *
US-PATENT-CLASS-428-457 ..... p 2258 N94-24737
US-PATENT-CLASS-428-480 ..... p 2375 N94-23308 *
US-PATENT-CLASS-428-913 ..... p 2375 N94-23308 *
US-PATENT-CLASS-429-194 ..... p 2310 N94-23823 *
US-PATENT-CLASS-429-218 ..... p 2310 N94-23823 *
US-PATENT-CLASS-429-91 ..... p 2310 N94-23823 *
US-PATENT-CLASS-437-105 ..... p 2563 N94-23972 *
US-PATENT-CLASS-437-200 ..... p 2563 N94-23972 *
US-PATENT-CLASS-437-225 ..... p 2344 N94-24723
US-PATENT-CLASS-437-231 ..... p 2546 N94-25043
US-PATENT-CLASS-439-362 ..... p 2352 N94-23078 *
US-PATENT-CLASS-501-90 ..... p 2253 N94-23311 *
US-PATENT-CLASS-501-92 ..... p 2253 N94-23311 *
US-PATENT-CLASS-501-95 ..... p 2253 N94-23311 *
US-PATENT-CLASS-52-514 ..... p 2203 N94-23824 *
US-PATENT-CLASS-524-538 ..... p 2252 N94-23076 *
US-PATENT-CLASS-524-608 ..... p 2252 N94-23076 *
US-PATENT-CLASS-525-362 ..... p 2261 N94-25054

US-PATENT-CLASS-528-125 .... p 2253 N94-23307 *
US-PATENT-CLASS-528-126 .... p 2253 N94-23307 *
US-PATENT-CLASS-528-151 .... p 2253 N94-23307 *
US-PATENT-CLASS-528-152 .... p 2253 N94-23307 *
US-PATENT-CLASS-528-153 .... p 2253 N94-23307 *
US-PATENT-CLASS-528-155 .... p 2253 N94-23307 *
US-PATENT-CLASS-528-170 .... p 2252 N94-23079 *
US-PATENT-CLASS-528-171 .... p 2252 N94-23079 *
US-PATENT-CLASS-528-173 .... p 2252 N94-23079 *
US-PATENT-CLASS-528-174 .... p 2252 N94-23079 *
US-PATENT-CLASS-528-176 .... p 2252 N94-23079 *
US-PATENT-CLASS-528-219 .... p 2253 N94-23307 *
US-PATENT-CLASS-528-353 .... p 2252 N94-23079 *
US-PATENT-CLASS-528-362 .... p 2258 N94-24721
US-PATENT-CLASS-548-145 .... p 2253 N94-23305 *
US-PATENT-CLASS-548-267.4 .... p 2252 N94-23075 *
US-PATENT-CLASS-548-267.8 .... p 2252 N94-23075 *
US-PATENT-CLASS-548-268.6 .... p 2252 N94-23075 *
US-PATENT-CLASS-548-269.4 .... p 2252 N94-23075 *
US-PATENT-CLASS-548-305.4 .... p 2253 N94-23305 *
US-PATENT-CLASS-548-305.7 .... p 2253 N94-23305 *
US-PATENT-CLASS-73-147 .... p 2317 N94-23077 *
US-PATENT-CLASS-73-147 .... p 2319 N94-23306 *
US-PATENT-CLASS-73-170.14 .... p 2317 N94-23077 *
US-PATENT-CLASS-73-180 .... p 2317 N94-23077 *
US-PATENT-CLASS-73-861.65 .... p 2319 N94-23306 *
US-PATENT-CLASS-73-861.66 .... p 2317 N94-23077 *
US-PATENT-CLASS-74-89.15 ...... p 2352 N94-23078 *
US-PATENT-CLASS-901-30 .... p 2352 N94-23082 *

US-PATENT-5,150,192 .... p 2303 N94-25150
US-PATENT-5,173,944 .... p 2525 N94-23312 *
US-PATENT-5,218,197 .... p 2344 N94-24734
US-PATENT-5,223,461 .... p 2253 N94-23311 *
US-PATENT-5,225,374 .... p 2344 N94-24723
US-PATENT-5,227,725 .... p 2537 N94-25047
US-PATENT-5,227,857 .... p 2345 N94-25053
US-PATENT-5,231,606 .... p 2311 N94-24736
US-PATENT-5,233,354 .... p 2301 N94-25040
US-PATENT-5,233,403 .... p 2545 N94-24722
US-PATENT-5,233,420 .... p 2312 N94-25039
US-PATENT-5,233,537 .... p 2302 N94-25049
US-PATENT-5,233,865 .... p 2319 N94-23306 *
US-PATENT-5,235,339 .... p 2301 N94-25041
US-PATENT-5,235,455 .... p 2303 N94-25217
US-PATENT-5,236,773 .... p 2230 N94-24735
US-PATENT-5,237,045 .... p 2258 N94-24721
US-PATENT-5,237,526 .... p 2446 N94-25034
US-PATENT-5,238,877 .... p 2546 N94-25043
US-PATENT-5,239,181 .... p 2312 N94-25042
US-PATENT-5,239,560 .... p 2301 N94-25038
US-PATENT-5,240,207 .... p 2184 N94-25052
US-PATENT-5,241,315 .... p 2294 N94-23827 *
US-PATENT-5,241,317 .... p 2302 N94-25058
US-PATENT-5,241,318 .... p 2302 N94-25056
US-PATENT-5,241,866 .... p 2317 N94-23077 *
US-PATENT-5,241,991 .... p 2367 N94-25055
US-PATENT-5,242,563 .... p 2258 N94-24720
US-PATENT-5,242,706 .... p 2350 N94-24952
US-PATENT-5,242,755 .... p 2258 N94-24737
US-PATENT-5,245,043 .... p 2252 N94-23075 *
US-PATENT-5,245,044 .... p 2253 N94-23305 *
US-PATENT-5,247,060 .... p 2261 N94-25054
US-PATENT-5,247,310 .... p 2301 N94-25045
US-PATENT-5,248,117 .... p 2170 N94-25051
US-PATENT-5,248,626 .... p 2312 N94-25035
US-PATENT-5,248,931 .... p 2312 N94-25036
US-PATENT-5,249,189 .... p 2350 N94-25044
US-PATENT-5,249,196 .... p 2350 N94-25216
US-PATENT-5,251,186 .... p 2302 N94-25048
US-PATENT-5,252,168 .... p 2252 N94-23076 *
US-PATENT-5,253,196 .... p 2312 N94-25050
US-PATENT-5,253,938 .... p 2345 N94-25037
US-PATENT-5,261,735 .... p 2192 N94-23310 *
US-PATENT-5,261,758 .... p 2352 N94-23082 *
US-PATENT-5,264,907 .... p 2543 N94-23309 *
US-PATENT-5,267,072 .... p 2543 N94-23270 *
US-PATENT-5,268,444 .... p 2253 N94-23307 *
US-PATENT-5,270,781 .... p 2375 N94-23308 *
US-PATENT-5,271,286 .... p 2352 N94-23078 *
US-PATENT-5,272,248 .... p 2252 N94-23079 *
US-PATENT-5,273,617 .... p 2563 N94-23972 *
US-PATENT-5,275,261 .... p 2354 N94-23969 *
US-PATENT-5,275,537 .... p 2354 N94-23831 *
US-PATENT-5,275,670 .... p 2343 N94-23826 *
US-PATENT-5,278,000 .... p 2310 N94-23823 *
US-PATENT-5,278,444 .... p 2310 N94-23821 * #
US-PATENT-5,278,636 .... p 2309 N94-23820 *
US-PATENT-5,279,092 .... p 2203 N94-23824 *
US-PATENT-5,279,482 .... p 2354 N94-23822 *
US-PATENT-5,280,174 .... p 2534 N94-23825 *

USACERL-TR-EP-93/05 .... p 2260 N94-24848 #

USACERL-TR-FE-94/01 .... p 2336 N94-24821 #

USACERL-TR-FM-93/16 .... p 2235 N94-24784

USGS/WRI-92-4117 .... p 2388 N94-24809 #

UTRC-R93-958160-1 .... p 2234 N94-24565 * #

UW-CPTC-93-5 .... p 2533 N94-23435 #

VPI-AOE-210 .... p 2167 N94-24052 * #

VTI/MEDDELANDE-700 .... p 2398 N94-23813

VTT-JULK-768 .... p 2571 N94-25416 #
VTT-JULK-769 .... p 2396 N94-25417 #
VTT-JULK-771 .... p 2379 N94-25418 #
VTT-JULK-774 .... p 2379 N94-25385 #

VTT-PUBS-118 .... p 2250 N94-25316 #
VTT-PUBS-126 .... p 2379 N94-25529 #

VTT-TIED-1353 .... p 2588 N94-22734 #
VTT-TIED-1412 .... p 2230 N94-25386 #
VTT-TIED-1413 .... p 2251 N94-25419 #
VTT-TIED-1416 .... p 2250 N94-25348 #
VTT-TIED-1424 .... p 2231 N94-25420 #
VTT-TIED-1425 .... p 2566 N94-25347 #

W-9303 .... p 2401 N94-23175 #
W-9304 .... p 2479 N94-23138 #
W-9305 .... p 2479 N94-23139 #
W-9306 .... p 2480 N94-23140 #
W-9307 .... p 2480 N94-23141 #
W-9313 .... p 2457 N94-24599
W-9314 .... p 2404 N94-24598
W-9316 .... p 2602 N94-24522

WAPD-T-2990 .... p 2244 N94-23792
WAPD-T-2991 .... p 2239 N94-22999 #
WAPD-T-3008 .... p 2241 N94-23219 #

WHOI-93-35 .... p 2419 N94-25435 #

WINCO-11968 .... p 2589 N94-22944 #
WINCO-11981 .... p 2220 N94-24511 #

WIS-PH-92-73 .... p 2571 N94-25340

WL-TM-93-308 .... p 2170 N94-24773 #

WL-TR-93-1136 .... p 2547 N94-25161
WL-TR-93-2053 .... p 2340 N94-25530 #
WL-TR-93-3082-VOL-2 .... p 2185 N94-25440 #
WL-TR-93-3088 .... p 2463 N94-25453 #
WL-TR-93-3098 .... p 2469 N94-25454 #
WL-TR-93-4037 .... p 2259 N94-24788
WL-TR-93-4088 .... p 2567 N94-25441 #
WL-TR-93-4090 .... p 2251 N94-25531 #
WL-TR-93-4092 .... p 2542 N94-22915 #
WL-TR-93-8021 .... p 2368 N94-25436 #
WL-TR-93-8030 .... p 2189 N94-24776 #

WS-394 .... p 2523 N94-23094
WS-396 .... p 2479 N94-23098
WS-405 .... p 2479 N94-23093
WS-406 .... p 2496 N94-24744
WS-412 .... p 2486 N94-23708 #

XC-PL/HANSCOM .... p 2406 N94-25535 #
XC-PL/HANSCOM .... p 2406 N94-25537 #

YALEU/DCS/RR-986 .... p 2456 N94-24535 #
YALEU/DCS/RR-990 .... p 2491 N94-24947

93E01024 .... p 2218 N94-23343 * #

APPENDIX

NASA SCIENTIFIC AND TECHNICAL INFORMATION PROGRAM PRODUCTS AND SERVICES

The NASA Scientific and Technical Information (STI) Program provides for the collection and announcement of aerospace-related reports and literature obtained worldwide through agreements and exchanges. The result of the collection is the comprehensive NASA STI Database that covers aeronautics, space, and supporting disciplines.

The STI Database, documents generated or obtained by NASA, and products and services derived from or supporting the database are made available to the NASA research community and to the public. Descriptions and sources of these items are presented in the following pages.

Scientific and Technical Aerospace Reports (STAR) is an abstract journal, listing citations with abstracts for aerospace-related reports obtained from worldwide sources. *STAR* is issued on the first of each month, and announces current documents that have been entered into the NASA STI Database during the previous month. The reports are of the following types:

- NASA, NASA contractor, and NASA grantee reports;
- Reports issued by other U.S. Government agencies, domestic and foreign institutions, universities, and private firms;
- Translations in report form;
- NASA-owned patents and patent applications
- Other U.S. Government agency and foreign patents and patent applications
- Domestic and foreign dissertations and theses.

Journal, book, and conference literature, journal translations, and certain foreign dissertations having the same subject scope as *STAR* are announced in a companion journal, *NASA Open Volumes on Aerospace (NOVA). NOVA* is issued on the 15th of each month and is available from the NASA Center for AeroSpace Information, at the address below.

ELIGIBILITY AND REGISTRATION FOR NASA STI PRODUCTS AND SERVICES

Organizations of the type listed below that have registered with NASA can receive products and services.

- NASA offices and installations, contractors, subcontractors, grantees, and consultants;
- Other U.S. Government agencies and their contractors;
- Libraries in the United States that have arrangements with NASA to maintain collections of NASA documents for public reference;
- Other organizations in the United States having a need for NASA documents in work related to aeronautics and space research;
- Organizations abroad that have established reciprocal documents exchange arrangements with NASA.

The central service points—central points of document acquisition and control within qualified organizations—or individuals are eligible to register for NASA STI products and services. Domestic organizations or individuals may be eligible to receive various classes of NASA publications and services and should address their requests for registration or further information to:

ATTN: Registration Services
NASA Center for AeroSpace Information
800 Elkridge Landing Road
Linthicum Heights, MD 21090-2934
301-621-0390

Organizations abroad should direct requests to:

National Aeronautics and Space Administration
Scientific and Technical Information Program (JTT)
International STI Program
Washington, DC 20546-0001
USA
703-271-5640

SUBJECT SCOPE

The subject scope of *STAR* and *NOVA* includes all aspects of aeronautics and space research and development, supporting basic and applied research, and applications. Aerospace aspects of Earth resources, energy development, conservation, oceanography, environmental protection, urban transportation, and other topics of high national priority are also covered.

HOW TO USE *STAR* SUBJECT CATEGORIES

Abstracts in *STAR* are categorized by 10 major subject divisions that are divided further into 76 specific subject categories. The subject divisions and categories are listed in the Table of Contents together with a note for each that defines its scope and provides any cross-references. For example:

> **16 SPACE TRANSPORTATION**
>
> Includes passenger and cargo space transportation, e.g., shuttle operations; and space rescue techniques. For related information see also *03 Air Transportation and Safety* and *18 Spacecraft Design, Testing and Performance*. For space suits see *54 Man/System Technology and Life Support.*

CROSS-REFERENCES

Individual *STAR* abstracts are not ordinarily cross-referenced, except for certain conference reports or book translations that have had separate abstracts written for their component papers or chapters. Citations and abstracts of the components follow immediately after those of the parent document. When the subject content of a component differs sufficiently from the general content of the parent, a cross-reference citation also is printed at the end of the category to which it normally would have been assigned if it were independent.

DOCUMENTS ON MICROFICHE

Documents available on microfiche are designated by a pound sign (#) following the accession number.

LIMITED REPRODUCIBILITY

A note of limited reproducibility appears in the citation, if there are factors affecting the reproducibility of more than 20% of the document. These factors include faint or broken type, color photographs, black and white photographs, foldouts, dot matrix print, or some other factor that limits the reproducibility of the document. This notation also appears on the microfiche header.

COLOR COPIES

An increasing number of NASA scientific and technical reports are being produced with color graphs, charts, illustrations, and photographs. An indication that a document has color pages follows the source and pricing (SAP) information in the *STAR* citation.

Registered users of the NASA Scientific and Technical Information Program will receive ordered documents with color at no additional cost, as long as stock copies of the document are available. Otherwise, an additional fee of $2.00 per color page will be charged. The NASA Center for AeroSpace Information staff will contact registered users to determine individual user's needs.

NASA PATENTS AND PATENT APPLICATIONS

Patents and patent applications owned by NASA are announced in *STAR* under appropriate subject categories and are referenced in the *STAR* indexes. In the Report Number Index, patents are indexed by the NASA Case Number, and the U.S. Patent Class. Patent applications are indexed by the NASA Case Number and the U.S. Patent Application Serial Number.

Printed copies of patents (which are not microfiched) are available for purchase from the U.S. Patent and Trademark Office.

When ordering patents, the U.S. Patent Number should be used, and payment must be remitted in advance, by money order or check payable to the Commissioner of Patents and Trademarks. Prepaid purchase coupons for ordering are also available from the U.S. Patent and Trademark Office.

NASA patent application specifications are sold in both paper copy and microfiche by the NASA Center for AeroSpace Information (CASI). The N accession number should be used in ordering either paper copy or microfiche from CASI.

The patents and patent applications announced in *STAR* are owned by NASA and are available for royalty-free licensing. Requests for licensing terms and further information should be addressed to:

National Aeronautics and Space Administration
Associate General Counsel for Intellectual Property
Code GP
Washington, DC 20546-0001

SOURCES FOR DOCUMENTS

One or more sources from which a document announced in *STAR* is available to the public is ordinarily given on the last line of the citation. The most commonly indicated sources and their acronyms or abbreviations are listed below, and their addresses are listed on page A-6. If the publication is available from a source other than those listed, the publisher and his address will be displayed on the availability line or in combination with the corporate source line.

Avail: CASI. Sold by the NASA Center for AeroSpace Information. Prices for hard copy (HC) and microfiche (MF) are indicated by a price code following the letters HC or MF in the *STAR* citation. Current values for the price codes are given in the tables on page A-7.

NOTE ON ORDERING DOCUMENTS: When ordering publications from CASI, use the N accession number or other report number. It is also advisable to cite the title and other bibliographic identification.

Avail: SOD (or GPO). Sold by the Superintendent of Documents, U.S. Government Printing Office, in hard copy.

Avail: BLL (formerly NLL): British Library Lending Division, Boston Spa, Wetherby, Yorkshire, England. Photocopies available from this organization at the price shown. (If none is given, inquiry should be addressed to the BLL.)

Avail: DOE Depository Libraries. Organizations in U.S. cities and abroad that maintain collections of Department of Energy reports, usually in microfiche form, are listed in *Energy Research Abstracts*. Services available from the DOE and its depositories are described in a booklet, *DOE Technical Information Center - Its Functions and Services* (TID-4660), which may be obtained without charge from the DOE Technical Information Center.

Avail: ESDU. Pricing information on specific data, computer programs, and details on Engineering Sciences Data Unit (ESDU) topic categories can be obtained from ESDU International Ltd. Requesters in North America should use the Virginia address while all other requesters should use the London address, both of which are on page A-6.

Avail: Fachinformationszentrum Karlsruhe. Gesellschaft für wissenschaftlich-technische Information mbH 76344 Eggenstein-Leopoldshafen, Germany.

Avail: HMSO. Publications of Her Majesty's Stationery Office are sold in the U.S. by Pendragon House, Inc. (PHI), Redwood City, CA. The U.S. price (including a service and mailing charge) is given, or a conversion table may be obtained from PHI.

Avail: Issuing Activity, or Corporate Author, or no indication of availability. Inquiries as to the availability of these documents should be addressed to the organization shown in the citation as the corporate author of the document.

Avail: NASA Public Document Rooms. Documents so indicated may be examined at or purchased from the National Aeronautics and Space Administration (JBD-4), Public Documents Room (Room 1H23), Washington, DC 20546-0001, or public document rooms located at NASA installations, and the NASA Pasadena Office at the Jet Propulsion Laboratory.

Avail: NTIS. Sold by the National Technical Information Service. Initially distributed microfiche under the NTIS SRIM (Selected Research in Microfiche) are available. For information concerning this service, consult the NTIS Subscription Section, Springfield, VA 22161.

Avail: Univ. Microfilms. Documents so indicated are dissertations selected from *Dissertation Abstracts* and are sold by University Microfilms as xerographic copy (HC) and microfilm. All requests should cite the author and the Order Number as they appear in the citation.

Avail: US Patent and Trademark Office. Sold by Commissioner of Patents and Trademarks, U.S. Patent and Trademark Office, at the standard price of $1.50 each, postage free. (See discussion of NASA patents and patent applications on page A-3.)

Avail: (US Sales Only). These foreign documents are available to users within the United States from the National Technical Information Service (NTIS). They are available to users outside the United States through the International Nuclear Information Service (INIS) representative in their country, or by applying directly to the issuing organization.

Avail: USGS. Originals of many reports from the U.S. Geological Survey, which may contain color illustrations, or otherwise may not have the quality of illustrations preserved in the microfiche or facsimile reproduction, may be examined by the public at the libraries of the USGS field offices whose addresses are listed on page A-6. The libraries may be queried concerning the availability of specific documents and the possible utilization of local copying services, such as color reproduction.

FEDERAL DEPOSITORY LIBRARY PROGRAM

In order to provide the general public with greater access to U.S. Government publications, Congress established the Federal Depository Library Program under the Government Printing Office (GPO), with 53 regional depositories responsible for permanent retention of material, inter-library loan, and reference services. At least one copy of nearly every NASA and NASA-sponsored publication, either in printed or microfiche format, is received and retained by the 53 regional depositories. A list of the regional GPO libraries, arranged alphabetically by state, appears on page A-8. These libraries are *not* sales outlets. A local library can contact a regional depository to help locate specific reports, or direct contact may be made by an individual.

PUBLIC COLLECTION OF NASA DOCUMENTS

An extensive collection of NASA and NASA-sponsored publications is maintained by the British Library Lending Division, Boston Spa, Wetherby, Yorkshire, England for public access. The British Library Lending Division also has available many of the non-NASA publications cited in *STAR*. European requesters may purchase facsimile copy or microfiche of NASA and NASA-sponsored documents, those identified by both the symbols # and * from ESA — Information Retrieval Service European Space Agency, 8-10 rue Mario-Nikis, 75738 CEDEX 15, France.

SUBMITTING DOCUMENTS

All users of this abstract service are urged to forward reports to be considered for announcement in *STAR*. This will aid NASA in its efforts to provide the fullest possible coverage of all scientific and technical publications that might support aeronautics and space research and development. If you have prepared relevant reports (other than those you will transmit to NASA, DOD, or DOE through the usual contract- or grant-reporting channels), please send them for consideration to the NASA Center for AeroSpace Information, 800 Elkridge Landing Road, Linthicum Heights, MD 21090-2934.

Reprints of journal articles, book chapters, and conference papers are also welcome. These will be considered for announcement in *STAR's* companion journal, *NOVA*.

You may specify a particular source to be included in a report announcement if you wish; otherwise the report will be placed on a public sale at the NASA Center for AeroSpace Information. Copyrighted publications will be announced but not distributed or sold.

PURCHASE OF *STAR*

STAR is publicly available on annual subscription from the NASA Center for AeroSpace Information (CASI) at $94.00/domestic, $117.00/foreign. Single copy prices: $33.00/domestic, $41.00/foreign.

An annual, cumulative *STAR Index* is also available at $54.00/domestic, $65.00/foreign.

STAR is available to registered users on annual subscription from the NASA Center for AeroSpace Information, ATTN: Registration Services, 800 Elkridge Landing Road, Linthicum Heights, MD 21090-2934.

ADDRESSES OF ORGANIZATIONS

British Library Lending Division
Boston Spa, Wetherby, Yorkshire
England

Commissioner of Patents and Trademarks
U.S. Patent and Trademark Office
Washington, DC 20231

Department of Energy
Technical Information Center
P.O. Box 62
Oak Ridge, TN 37830

European Space Agency-
Information Retrieval Service ESRIN
Via Galileo Galilei
00044 Frascati (Rome) Italy

Engineering Sciences Data Unit International
P.O. Box 1633
Manassas, VA 22110

Engineering Sciences Data Unit
International, Ltd.
251-259 Regent Street
London, W1R 7AD, England

Fachinformationszentrum Karlsruhe
Gesellschaft für wissenschaftlich-technische
Information mbH
76344 Eggenstein-Leopoldshafen, Germany

Her Majesty's Stationery Office
P.O. Box 569, S.E. 1
London, England

NASA Center for AeroSpace Information
800 Elkridge Landing Road
Linthicum Heights, MD 21090-2934

National Aeronautics and Space Administration
Scientific and Technical Information Program
(JTT)
Washington, DC 20546-0001

National Technical Information Service
5285 Port Royal Road
Springfield, VA 22161

Pendragon House, Inc.
899 Broadway Avenue
Redwood City, CA 94063

Superintendent of Documents
U.S. Government Printing Office
Washington, DC 20402

University Microfilms
A Xerox Company
300 North Zeeb Road
Ann Arbor, MI 48106

University Microfilms, Ltd.
Tylers Green
London, England

U.S. Geological Survey Library National Center
MS 950
12201 Sunrise Valley Drive
Reston, VA 22092

U.S. Geological Survey Library
2255 North Gemini Drive
Flagstaff, AZ 86001

U.S. Geological Survey
345 Middlefield Road
Menlo Park, CA 94025

U.S. Geological Survey Library
Box 25046
Denver Federal Center, MS914
Denver, CO 80225

CASI PRICE TABLES

(Effective August 1, 1993)

STANDARD PRICE DOCUMENTS

PRICE CODE	NORTH AMERICAN PRICE	FOREIGN PRICE
A01	$ 9.00	$ 18.00
A02	12.50	25.00
A03	17.50	35.00
A04-A05	19.50	39.00
A06-A09	27.00	54.00
A10-A13	36.50	73.00
A14-A17	44.50	89.00
A18-A21	52.00	104.00
A22-A25	61.00	122.00
A99	Call For Price	Call For Price

MICROFICHE

PRICE CODE	NORTH AMERICAN PRICE	FOREIGN PRICE
A01	$ 9.00	$ 18.00
A02	12.50	25.00
A03	17.50	35.00
A04	19.50	39.00
A06	27.00	54.00
A10	36.50	73.00

IMPORTANT NOTICE

CASI Shipping and Handling Charges
U.S.—ADD $3.00 per TOTAL ORDER
Canada and Mexico—ADD $3.50 per TOTAL ORDER
All Other Countries—ADD $7.50 per TOTAL ORDER
Does NOT apply to orders
requesting CASI RUSH HANDLING.
CASI accepts most credit/charge cards.

NASA Center for AeroSpace Information
800 Elkridge Landing Road
Linthicum Heights, MD 21090-2934
Telephone: (301) 621-0390
E-mail: help@sti.nasa.gov
Fax: (301) 621-0134

FEDERAL REGIONAL DEPOSITORY LIBRARIES

ALABAMA
AUBURN UNIV. AT MONTGOMERY LIBRARY
Documents Dept.
7300 University Dr.
Montgomery, AL 36117-3596
(205) 244-3650 Fax: (205) 244-0678

UNIV. OF ALABAMA
Amelia Gayle Gorgas Library
Govt. Documents
Box 870266
Tuscaloosa, AL 35487-0266
(205) 348-6046 Fax: (205) 348-8833

ARIZONA
DEPT. OF LIBRARY, ARCHIVES, AND PUBLIC RECORDS
Federal Documents
Third Floor State Capitol
1700 West Washington
Phoenix, AZ 85007
(602) 542-4121 Fax: (602) 542-4400, 542-4500

ARKANSAS
ARKANSAS STATE LIBRARY
State Library Services
One Capitol Mall
Little Rock, AR 72201
(501) 682-2869

CALIFORNIA
CALIFORNIA STATE LIBRARY
Govt. Publications Section
914 Capitol Mall - P.O. Box 942837
Sacramento, CA 94237-0001
(916) 322-4572 Fax: (916) 324-8120

COLORADO
UNIV. OF COLORADO - BOULDER
Norlin Library
Govt. Publications
Campus Box 184
Boulder, CO 83309-0184
(303) 492-8834 Fax: (303) 492-2185

DENVER PUBLIC LIBRARY
Govt. Publications Dept. BS/GPD
1357 Broadway
Denver, CO 80203
(303) 571-2135

CONNECTICUT
CONNECTICUT STATE LIBRARY
231 Capitol Avenue
Hartford, CT 06106
(203) 566-4971 Fax: (203) 566-3322

FLORIDA
UNIV. OF FLORIDA LIBRARIES
Documents Dept.
Library West
Gainesville, FL 32611-2048
(904) 392-0366 Fax: (904) 392-7251

GEORGIA
UNIV. OF GEORGIA LIBRARIES
Govt. Documents Dept.
Jackson Street
Athens, GA 30602
(404) 542-8949 Fax: (404) 542-6522

HAWAII
UNIV. OF HAWAII
Hamilton Library
Govt. Documents Collection
2550 The Mall
Honolulu, HI 96822
(808) 948-8230 Fax: (808) 956-5968

IDAHO
UNIV. OF IDAHO LIBRARY
Documents Section
Moscow, ID 83843
(208) 885-6344 Fax: (208) 885-6817

ILLINOIS
ILLINOIS STATE LIBRARY
Reference Dept.
300 South Second
Springfield, IL 62701-1796
(217) 782-7596 Fax: (217) 524-0041

INDIANA
INDIANA STATE LIBRARY
Serials/Documents Section
140 North Senate Avenue
Indianapolis, IN 46204
(317) 232-3678 Fax: (317) 232-3728

IOWA
UNIV. OF IOWA LIBRARIES
Govt. Publications Dept.
Washington & Madison Streets
Iowa City, IA 52242
(319) 335-5926 Fax: (319) 335-5830

KANSAS
UNIV. OF KANSAS
Govt. Documents & Map Library
6001 Malatt Hall
Lawrence, KS 66045-2800
(913) 864-4660 Fax: (913) 864-5380

KENTUCKY
UNIV. OF KENTUCKY LIBRARIES
Govt. Publications/Maps Dept.
Lexington, KY 40506-0039
(606) 257-3139 Fax: (606) 257-1563, 257-8379

LOUISIANA
LOUISIANA STATE UNIV.
Middleton Library
Govt. Documents Dept.
Baton Rouge, LA 70803
(504) 388-2570 Fax: (504) 388-6992

LOUISIANA TECHNICAL UNIV.
Prescott Memorial Library
Govt. Documents Dept.
305 Wisteria Street
Ruston, LA 71270-9985
(318) 257-4962 Fax: (318) 257-2447

MAINE
TRI-STATE DOCUMENTS DEPOS.
Raymond H. Fogler Library
Govt. Documents & Microforms Dept.
Univ. of Maine
Orono, ME 04469
(207) 581-1680

MARYLAND
UNIV. OF MARYLAND
Hornbake Library
Govt. Documents/Maps Unit
College Park, MD 20742
(301) 454-3034 Fax: (301) 454-4985

MASSACHUSETTS
BOSTON PUBLIC LIBRARY
Govt. Documents Dept.
666 Boylston Street
Boston, MA 02117
(617) 536-5400 ext. 226
Fax: (617) 267-8273, 267-8248

MICHIGAN
DETROIT PUBLIC LIBRARY
5201 Woodward Avenue
Detroit, MI 48202-4093
(313) 833-1440, 833-1409
Fax: (313) 833-5039

LIBRARY OF MICHIGAN
Govt. Documents Unit
P.O. Box 30007
Lansing, MI 48909
(517) 373-0640 Fax: (517) 373-3381

MINNESOTA
UNIV. OF MINNESOTA
Wilson Library
Govt. Publications Library
309 19th Avenue South
Minneapolis, MN 55455
(612) 624-5073 Fax: (612) 626-9353

MISSISSIPPI
UNIV. OF MISSISSIPPI
J.D. Williams Library
Federal Documents Dept.
106 Old Gym Bldg.
University, MS 38677
(601) 232-5857 Fax: (601) 232-5453

MISSOURI
UNIV. OF MISSOURI - COLUMBIA
Ellis Library
Govt. Documents
Columbia, MO 65201
(314) 882-6733 Fax: (314) 882-8044

MONTANA
UNIV. OF MONTANA
Maureen & Mike Mansfield Library
Documents Div.
Missoula, MT 59812-1195
(406)243-6700 Fax: (406) 243-2060

NEBRASKA
UNIV. OF NEBRASKA - LINCOLN
D.L. Love Memorial Library
Documents Dept.
Lincoln, NE 68588
(402) 472-2562

NEVADA
UNIV. OF NEVADA
Reno Library
Govt. Publications Dept.
Reno, NV 89557
(702) 784-6579 Fax: (702) 784-1751

NEW JERSEY
NEWARK PUBLIC LIBRARY
U.S. Documents Div.
5 Washington Street - P.O. Box 630
Newark, NJ 07101-0630
(201) 733-7812 Fax: (201) 733-5648

NEW MEXICO
UNIV. OF NEW MEXICO
General Library
Govt. Publications Dept.
Albuquerque, NM 87131-1466
(505) 277-5441 Fax: (505) 277-6019

NEW MEXICO STATE LIBRARY
325 Don Gaspar Avenue
Santa Fe, NM 87503
(505) 827-3826 Fax: (505) 827-3820

NEW YORK
NEW YORK STATE LIBRARY
Documents/Gift & Exchange Section
Federal Depository Program
Cultural Education Center
Albany, NY 12230
(518) 474-5563 Fax: (518) 474-5786

NORTH CAROLINA
UNIV. OF NORTH CAROLINA - CHAPEL HILL
CB#3912, Davis Library
BA/SS Dept. - Documents
Chapel Hill, NC 27599
(919) 962-1151 Fax: (919) 962-0484

NORTH DAKOTA
NORTH DAKOTA STATE UNIV. LIB.
Documents Office
Fargo, ND 58105
(701) 237-8886 Fax: (701) 237-7138
In cooperation with Univ. of North Dakota, Chester Fritz Library Grand Forks

OHIO
STATE LIBRARY OF OHIO
Documents Dept.
65 South Front Street
Columbus, OH 43266
(614) 644-7051 Fax: (614) 752-9178

OKLAHOMA
OKLAHOMA DEPT. OF LIBRARIES
U.S. Govt. Information Div.
200 NE 18th Street
Oklahoma City, OK 73105-3298
(405) 521-2502, ext. 252, 253
Fax: (405) 525-7804

OKLAHOMA STATE UNIV.
Edmon Low Library
Documents Dept.
Stillwater, OK 74078
(405) 744-6546 Fax: (405) 744-5183

OREGON
PORTLAND STATE UNIV.
Millar Library
934 SW Harrison - P.O. Box 1151
Portland, OR 97207
(503) 725-3673 Fax: (503) 725-4527

PENNSYLVANIA
STATE LIBRARY OF PENN.
Govt. Publications Section
Walnut St. & Commonwealth Ave. - P.O. Box 1601
Harrisburg, PA 17105
(717) 787-3752

SOUTH CAROLINA
CLEMSON UNIV.
Cooper Library
Public Documents Unit
Clemson, SC 29634-3001
(803) 656-5174 Fax: (803) 656-3025
In cooperation with Univ. of South Carolina, Thomas Cooper Library, Columbia

TENNESSEE
MEMPHIS STATE UNIV. LIBRARIES
Govt. Documents
Memphis, TN 38152
(901) 678-2586 Fax: (901) 678-2511

TEXAS
TEXAS STATE LIBRARY
United States Documents
P.O. Box 12927 - 1201 Brazos
Austin, TX 78711
(512) 463-5455 Fax: (512) 463-5436

TEXAS TECH. UNIV. LIBRARY
Documents Dept.
Lubbock, TX 79409
(806) 742-2268 Fax: (806) 742-1920

UTAH
UTAH STATE UNIV.
Merrill Library & Learning Resources Center, UMC-3000
Documents Dept.
Logan, UT 84322-3000
(801) 750-2684 Fax: (801) 750-2677

VIRGINIA
UNIV. OF VIRGINIA
Aldermman Library
Govt. Documents
Charlottesville, VA 22903-2498
(804) 824-3133 Fax: (804) 924-4337

WASHINGTON
WASHINGTON STATE LIBRARY
Document Section
MS AJ-11
Olympia, WA 98504-0111
(206) 753-4027 Fax: (206) 753-3546

WEST VIRGINIA
WEST VIRGINIA UNIV. LIBRARY
Govt. Documents Section
P.O. Box 6069
Morgantown, WV 26506
(304) 293-3640

WISCONSIN
ST. HIST. SOC. OF WISCONSIN LIBRARY
Govt. Publications Section
816 State Street
Madison, WI 53706
(608) 262-2781 Fax: (608) 262-4711
In cooperation with Univ. of Wisconsin - Madison, Memorial Library

MILWAUKEE PUBLIC LIBRARY
Documents Div.
814 West Wisconsin Avenue
Milwaukee, WI 53233
(414) 278-2167 Fax: (414) 278-2137

* U.S. GOVERNMENT PRINTING OFFICE: 1994-301-249/00005

POSTMASTER
Address Correction Requested
(Sections 137 and 159 Post Manual)

National Aeronautics and
Space Administration
Code JTT
Washington, DC 20546-0001

Official Business
Penalty for Private Use, $300

BULK RATE
POSTAGE & FEES PAID
NASA
PERMIT No. G-27

NASA

POSTMASTER: If Undeliverable (Section 158
Postal Manual) Do Not Return

Please circulate this publication to other colleagues within your organization.

NASA
STI PROGRAM
SCIENTIFIC &
TECHNICAL
INFORMATION